Can. J. Chem. Downloaded from www.nrcresearchpress.com by 69.46.99.164 on 09/04/12
For personal use only.

Canadian Journal of Chemistry

Issued by THE NATIONAL RESEARCH COUNCIL OF CANADA

VOLUME 38 JANUARY 1960 NUMBER 1

THE MECHANISM OF ORGANOMERCURIAL OXIDATION BY MERCURIC SALTS[1,2]

J. H. ROBSON AND GEORGE F WRIGHT

ABSTRACT

It has been shown that the oxidation of organomercuric salts by inorganic mercuric salts is inhibited by oxygen, accelerated to some extent by acids, and will form esters as products even in the presence of much water. Moreover, the system will polymerize acrylonitrile. These evidences of free radical participation are substantiated by the formation of the same products when pernitrous acid replaces inorganic mercuric salt in the system. Kinetic studies show that radicals are involved in a self-regenerating chain in which active monomeric mercurous salt seems to be the carrier.

It has been shown previously (1) that the oxidation of organomercuric salts in which the anion is nitrato is much more facile than maintains for systems in which the salts are acetates. Because of this difference in reactivity we have found it convenient to discuss the nitrato and acetato systems separately.

THE OXIDATION OF ORGANOMERCURIC NITRATES

In the earlier publication (1) it was shown that the reaction of benzylmercuric nitrate with mercuric nitrate in methanol led to benzyl methyl ether and benzyl nitrate. Additional examples have now been sought. Although *n*-butylmercuric nitrate will not react, cyclohexylmercuric nitrate in methanol containing mercuric nitrate gives an 8% yield of methoxycyclohexane and a 31% yield of cyclohexyl nitrate.

Of greater interest is the observation that benzylmercuric nitrate with mercuric nitrate in water yields not only benzyl alcohol, benzaldehyde, and benzoic acid but also benzyl nitrate. Similarly cyclohexylmercuric nitrate with mercuric nitrate in water gives not only a 40% yield of cyclohexanol and a trace of formylcyclopentane (to be explained in a forthcoming publication) but also a 21% yield of cyclohexyl nitrate. The formation of these nitrate esters in aqueous solution is unusual even though these reaction systems are not entirely homogeneous. To be sure benzylmercuric chloride has been found (2) to yield benzyl nitrite and nitrate in nitric acid but little water was present in that system. Certainly cyclohexanol with mercuric nitrate in dilute nitric acid does not form cyclohexyl nitrate according to infrared spectral examination. Indeed the formation of appreciable amounts of nitrate esters under conditions where they should be absent or minimal if they were constituents of heteropolar or ionic equilibria indicates strongly that these nitrate esters are formed by a homopolar or free-radical mechanism.

[1]*Manuscript received July 16, 1959.*
Contribution from the Department of Chemistry, University of Toronto, Toronto, Ontario.
[2]*Presented at the 136th meeting of the American Chemical Society, Atlantic City, 1959.*

Can. J. Chem. Downloaded from www.nrcresearchpress.com by 69.46.99.164 on 09/04/12
For personal use only.

Of course the generality of the reaction whereby organomercuric nitrates are oxidized by mercuric nitrate is not established by the reactions in aqueous solutions, especially since the second-order kinetics of the non-aqueous reaction (1) cannot be demonstrated in the aqueous systems because of their inhomogeneity. Therefore, direct evidence for the participation of radicals in the methanolic systems has been sought. In the first instance this investigation has involved methanolic mercuric nitrate alone.

It has been shown by Waters and Merz (3, 4) and by Uri (5) that mercuric salts are reduced to the mercurous state in aqueous sulphuric acid containing various organic substrates when Fenton's reagent (6, 7) is added. The significance of the substrate is shown by the absence of reduction when mercuric nitrate in aqueous solution is treated with Fenton's reagent. As was expected, we find that methanolic mercuric nitrate is rapidly reduced to the mercurous level when hydrogen peroxide is added, if, also, a trace of ferrous salt is present. Methanolic mercuric nitrate also is reduced to mercurous nitrate when isobutyryl peroxide is added. The mercurous salt is quite stable in these media and metallic mercury is never detected.*

The reduction of mercuric to mercurous nitrate implies oxidation of the methanolic medium. Since the over-all reaction of mercuric nitrate with an organomercuric nitrate causes oxidation of the latter, it is reasonable to presume that reduction of the inorganic salt forms free radicals from the substrate which in turn act upon the organomercurial. In order to test this presumption we have treated alkylmercuric nitrates (which are stable toward demercuration in acids) with a peracid instead of mercuric nitrate. Although *n*-butylmercuric nitrate is so inert under these conditions that eventual reaction does not lead to recognizable products, we have been successful with cyclohexylmercurials.

Thus pernitrous acid (8, 9, 10, 11) is formed from sodium nitrite and hydrogen peroxide in aqueous medium. When cyclohexylmercuric nitrate is added to this system (together with some methanol for solubilization) mercurous salt is formed. The mercurous salt yield (52%) is not meaningful because Hg^+ is partly oxidized by this medium but it indicates that accompanying radicals are involved in the 30% yield of cyclohexanol and the 25% yield of cyclohexyl nitrate, which are obtained together with some cyclohexanone.

FORMATION AND PERSISTENCE OF RADICALS IN THE MERCURIC NITRATE - ORGANOMERCURIC NITRATE SYSTEM

Although a radical source such as pernitrous acid will convert cyclohexylmercuric nitrate to cyclohexanol and its nitrate ester, and Fenton's reagent will reduce mercuric nitrate in a manner which should produce radicals in and from the substrate, it remains to prove that radicals are formed and do persist in the actual system of organomercuric salt and inorganic mercuric salt.

There is some evidence that the initiation of the radical reaction may arise in the organomercurial itself, since a methanol solution of diphenylpicrylhydrazyl is bleached by each of a series of organomercuric nitrates. When the mercurial is present in large excess the bleaching of the hydrazyl proceeds at a first-order rate (Fig. 1). A series of such hydrazyl bleaching rates are shown in Table I together with the second-order rates for reaction of the same mercurials with mercuric nitrate. It may be seen that there is a rough correlation. Complete agreement cannot be expected because the first-order rate of hydrazyl bleaching would only be the first, inducing, step in the reactions that comprise

**It may be noted that mercuric acetate is not reduced under comparable conditions. Of course a complete reduction would not be expected since mercurous acetate is oxidized by peroxides. However, in the absence of any reduction one recalls Waters' observation that a radical chain reaction does not ordinarily proceed via acetato radicals.*

the second-order oxidation. Nevertheless, the correspondence in relative rates for 6 of 10 entries in this table indicates that radicals are involved in the second-order oxidation.*

If radicals are involved in the oxidation of organomercuric nitrates by mercuric nitrate then these radicals ought to be detectable. To this end we first prepared 2-hydroxycyclohexylmercuric nitrate *in situ* by treatment of cyclohexene with 1 equivalent of mercuric

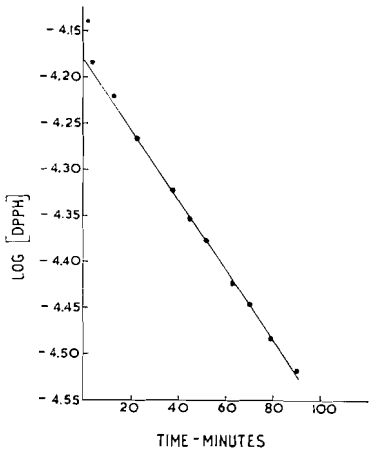


FIG. 1. The reaction of benzylmercuric nitrate (0.01 *M*) and diphenylpicrylhydrazyl (0.000081 *M*) in methanol at 25° C.

TABLE I

Comparison of reaction rates of nitratomercurials with diphenylpicrylhydrazyl and with mercuric nitrate

Nitratomercurial	1st order DPPH reaction ($k\times10^3$)	2nd order oxidation reaction ($k\times10^2$)
1. α-1-Nitratomercuri-2-methoxy-1,2-diphenylethane	21.4	30.0
2. Cyclohexylmercuric nitrate	17.1	2.11
3. Benzylmercuric nitrate	8.85	1.79
4. Isopropylmercuric nitrate	7.60	1.79
5. β-2-Methoxycyclohexylmercuric nitrate	3.03	—[a]
6. *n*-Propylmercuric nitrate	2.78	—[a]
7. α-2-Methoxycyclohexylmercuric nitrate	2.66	0.055
8. *n*-Butylmercuric nitrate	2.63	—[a]
9. 1-Phenyl-1-nitratomercuri-2-methyl-2-methoxypropane	2.44	1.74
10. β-1-Nitratomercuri-2-methoxy-1,2-diphenylethane	0.76	1.47

[a]Too slow to be measured.

It is of interest that since submission of this manuscript a monomeric mercurous salt has been postulated (Weinmayer, V. J. Am. Chem. Soc. **81, 3590 (1959)) as an intermediate in the photolysis of oxyalkylmercuric halides. The specificity of methanol or water as the substrate is remindful of the reactions which we have described in the present publication. Moreover the coupling reaction which Weinmayer describes must have been preceded by a homolytic fission into radicals the presence of which are implied in any explanation of the hydrazyl bleaching reaction.*

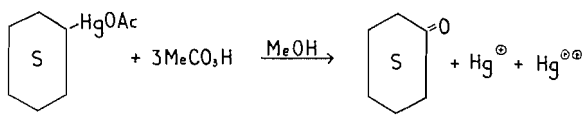
Can. J. Chem. Downloaded from www.nrcresearchpress.com by 69.46.99.164 on 09/04/12
For personal use only.

nitrate in aqueous solution and then added acrylonitrile. No polymer was formed during 24 hours. On the other hand, when another equivalent of mercuric nitrate was added together with the polyacrylonitrile polyarylonitrile, the system became turbid after 40 minutes and a 4% yield of acrylonitrile was obtained after 3 hours. Moreover, the turbidity appeared immediately and the yield of polymer was 7% when the system was deaerated before addition of mercuric nitrate and acrylonitrile. Finally the yield of polymer was increased to 24% by inclusion of 4 mole per cent of N,N′-methylene-bis-acrylamide as a cross-linking agent. These yields of polyacrylonitrile (with characteristically diffuse X-ray diffraction pattern) persuade us (12) that radical-induced polymerization has occurred, especially since the same behavior was observed with acrylonitrile and Fenton's reagent in an aqueous medium.

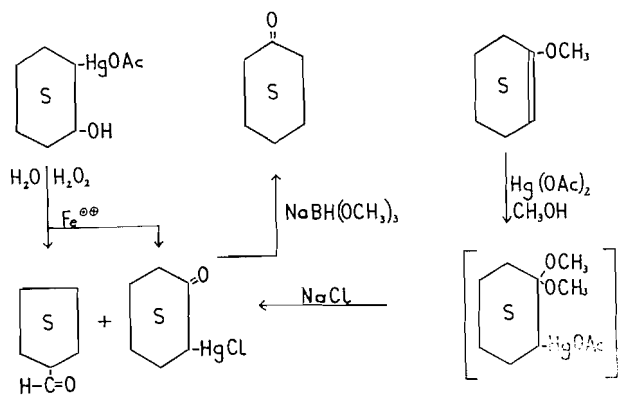
THE OXIDATION OF ORGANOMERCURIC ACETATES

More critical for a study of the oxidation are the reactions of organomercuric acetates with mercuric acetate. The rates of reaction are much slower (sometimes immeasurably so) than are the comparable reaction rates with nitrate salts. Variations which induce or accelerate reaction are more definitive for the systems containing acetate than they are for the system containing nitrate salts. However, the same type of product is obtained in either circumstance.

For example, cyclohexylmercuric acetate in methanol reacts with peracetic acid to give some (8%) mercurous acetate together with the mercuric acetate (73%) which would be expected to be formed by peracetic acid oxidation of mercurous salt. To be sure the organic product is not the expected cyclohexanol but, instead, is cyclohexanone in 75% yield. However, it would appear from the next paragraph that a secondary alcohol can be oxidized by peroxidic reagents in systems containing salts of mercury.



The participation of radicals is more apparent in the reaction of 2-hydroxycyclohexylmercuric acetate with Fenton's reagent. The expected products are mercurous salt and formylcyclopentane if the reaction proceeds like that of 2-hydroxycyclohexylmercuric nitrate with mercuric nitrate in water. Both of these products are obtained. The yields are low because of a by-product, 2-acetoxymercuricyclohexanone (isolated as its chloromercurial), which would appear to have been formed by the action of hydrogen peroxide



Can. J. Chem. Downloaded from www.nrcresearchpress.com by 69.46.99.164 on 09/04/12
For personal use only.

on the original 2-hydroxycyclohexylmercuric acetate in the system containing metallic salts. The identity of the ketomercurial, which has been reported previously (13), has been established by its reduction to cyclohexanone by means of sodium trimethoxyborohydride and by its synthesis from 1-methoxycyclohexene. Parenthetically it is of interest that sodium trimethoxyborohydride reduces the chloromercuri group preferentially with respect to the carbonyl group.

If the action of peroxy compounds on organomercuric salts leads to products like those obtained by action of mercuric salts in primary alcohols then it is reasonable to postulate that mercuric salts in alcohols are sources of radicals which act upon the organomercurials. The postulation is supported by the observation (Table II) that mercuric acetate and mercuric nitrate in methanol undergo reduction to the mercurous salts to the extent of 14% and 36% respectively at 50° in 80 to 90 hours. Since formaldehyde cannot be detected during these reductions, one may assume that the oxidation of the substrate leads to radicals which decompose to a multiplicity of simple fragments that have not been characterized.

TABLE II

The effect of acids on the reduction of mercuric salts in methanol at 50°

Expt. No.	Salt	Acid	Time (hours)	% reduction
1	0.2 *M* $Hg(OAc)_2$	None	82	14
2	0.2 *M* $Hg(OAc)_2$	0.2 *M* $BF_3{\cdot}Et_2O$	24	100
3	0.2 *M* $Hg(OAc)_2$	0.2 *M* p-$MeC_6H_4SO_3H$	85	46
4	0.2 *M* $Hg(OAc)_2$	0.2 *M* HNO_3	85	42
5	0.2 *M* $Hg(OAc)_2$	0.34 *M* $HClO_4$	70	60
6	0.2 *M* $Hg(NO_3)_2$	None	88	36
7	0.2 *M* $Hg(NO_3)_2$	0.2 *M* HNO_3	88	13

As may be seen in Table II these slow reductions are accelerated by acids, of which the most effective is boron fluoride. At first glance one might presume that the accelerations involve ionic rather than radical reactions. However, the effective participation of ionic species is doubtful in view of earlier studies of the over-all oxidation (1).

These earlier studies, involving variations in salt concentration, indicated that ionic species were not directly involved. Moreover, the effectiveness of the acid used in the over-all reaction seemed to be unrelated to its extent of dissociation insofar as acid strengths in methanol are known. The same divergence may be observed in Table II. Indeed a comparison of experiments 4, 6, and 7 leads to a suspicion that the rate of reduction depends upon the extent to which a basic salt of a relatively strong acid is present. This suspicion may be expressed in terms of the following formulation of competing equilibria.

$$\begin{array}{ccccccc} HgX_2 & \rightleftharpoons & HX & \rightleftharpoons & HX & \rightleftharpoons & MeOH \\ + & & + & \pm HY & + & & + \\ MeOH & & MeOHgX & & MeOHgY & & HgY_2 \end{array}$$

It is evident that the maximum amount of the most reactive basic salt (say MeOHgY) will be dependent upon the strengths and concentrations of HX and HY.

There ought to be kinetic significance from the evidence of Table II, and from that of Shearer and Wright (1), that the mercuric acetate – methanol system is affected by acids in the same way as is the organomercuric acetate – methanol – mercuric acetate system.

Can. J. Chem. Downloaded from www.nrcresearchpress.com by 69.46.99.164 on 09/04/12
For personal use only.

This significance is not easily apparent in the kinetically second-order reaction of organomercuric acetates with mercuric acetate in methanol because these reactions are very slow. However, as Shearer and Wright (1) showed, the oxidation is accelerated by addition of an acid like boron trifluoride to a rate that is satisfactory for kinetic study. The catalyzed reaction is kinetically first order.

Shearer and Wright specified the catalyzed reaction as first order in respect of the organomercurial and this opinion would seem to be at variance with the present evidence that the over-all oxidation is directly dependent upon the behavior of mercuric acetate in methanol. However, we have found the conclusion of Shearer and Wright to be incorrect. The over-all oxidation of organomercuric acetate by mercuric acetate in methanol containing boron trifluoride is first order with respect to mercuric acetate and not to the organomercurial.

The rate of reaction of mercuric acetate with methanol is negligible within a reasonable time in absence of boron trifluoride. The rate becomes measurable when 20 mole% of this catalyst is added. This rate is higher when 40 mole% of boron trifluoride is included but (see Fig. 2) is not increased by further addition of catalyst. The rate of disappearance

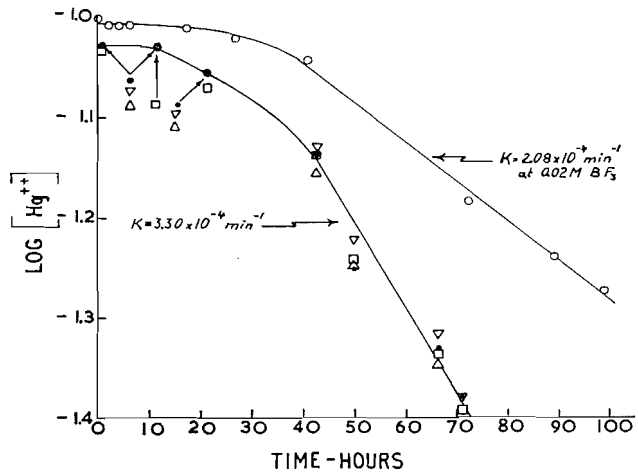
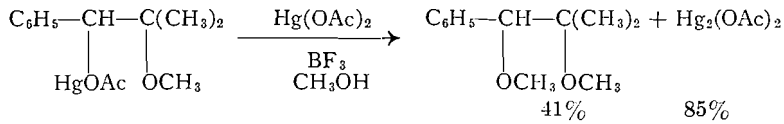


FIG. 2. Boron fluoride etherate catalysis of reduction of mercuric acetate (0.10 *M*) in methanol at 25° C. [$BF_3 \cdot Et_2O$]: ○, 0.02 *M*; □, 0.04 *M*; △, 0.06 *M*; ●, 0.08 *M*; ▽, 0.10 *M*.

of mercuric salt with 20 mole% of catalyst is found to be identical ($k = 2.08 \times 10^{-4}$) with the rate of appearance of mercurous salt, as it was determined in a separate experiment. Moreover (see Table III), this rate is unaltered when the methoxymercurials of *trans*-stilbene (in several concentrations) and of β,β-dimethylstyrene are included.*



**The products from experiments 1–6 inclusive have been described previously. We have now found the expected phenylisobutane diether by a separate experiment which includes the reagents of experiment 7, Table III. Except for the fact that these reactions of acetate salts yield only ethers and not esters they are similar to the reaction of the analogous nitrates.*

Can. J. Chem. Downloaded from www.nrcresearchpress.com by 69.46.99.164 on 09/04/12
For personal use only.

TABLE III

System: Mercuric acetate (0.10 *M*), boron fluoride etherate (0.02 *M*), and additive in methanol at 25°

Expt. No.	Additive	$k\times10^{-4}$ min^{-1}
1	None	2.08
2	0.0025 *M* β-2-methoxy-1,2-diphenylethylmercuric acetate	1.98
3	0.050 *M* β-2-methoxy-1,2-diphenylethylmercuric acetate	1.90
4	0.050 *M* β-2-methoxy-1,2-diphenylethylmercuric acetate	2.04
5	0.075 *M* β-2-methoxy-1,2-diphenylethylmercuric acetate	2.08
6	0.100 *M* β-2-methoxy-1,2-diphenylethylmercuric acetate	2.08
7	0.050 *M* 2-methoxy-2-methyl-1-phenylpropylmercuric acetate	2.03

Both Table III and Fig. 3 (in which the rate, 2.04×10^{-4} min^{-1}, of an experiment from

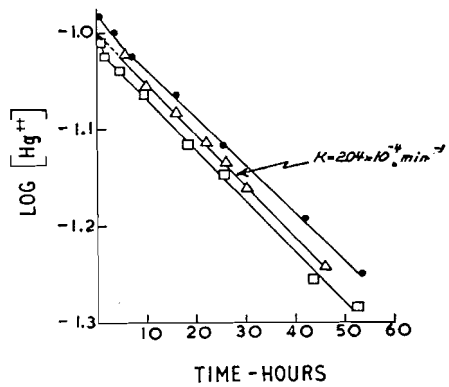


FIG. 3. System: Mercuric acetate (0.10 *M*) and boron fluoride etherate (0.02 *M*) in methanol at 25° C. ●, 0.05 *M trans*-stilbene (as alkene); △, 0.05 *M trans*-stilbene (as mercurial); □, 0.05 *M* β,β-dimethylstyrene (as mercurial).

reference 1 is included as the line drawn through squares) show that the reaction is first order with respect to mercuric acetate and is independent of the concentration of the organomercurial. Thus it is understandable, as is shown in Table IV, that the oxidation rates of the mercurials prepared *in situ* (1) from *cis*- and *trans*-stilbenes are practically identical. Of course these rates are greater than those shown in Table III because the boron fluoride concentration is higher relative to the molarity of mercurial.

TABLE IV

Summary of *cis*- and *trans*-stilbene oxidation rates with mercuric acetate in methanol with boron fluoride etherate added, reference 1

	Molarities after mercuration				1st order
	Stilbene		Mercuric acetate	$BF_3\cdot Et_2O$	$k\times10^{-4}$ min^{-1}
1	*cis*	0.05*	0.05	0.02	5.68±0.30
2	*cis*	0.05	0.05	0.02	5.05±0.25
3	*trans*	0.05*	0.05	0.02	5.05±0.30
4	*trans*	0.05	0.05	0.02	5.05±0.30
5	*trans*	0.05	0.10	0.02	5.35±0.30
6	*trans*	0.10	0.10	0.04	5.56

*The alkene and excess mercuric acetate were used to give the concentrations shown.

Can. J. Chem. Downloaded from www.nrcresearchpress.com by 69.46.99.164 on 09/04/12
For personal use only.

Can. J. Chem. Downloaded from www.nrcresearchpress.com by 69.46.99.164 on 09/04/12
For personal use only.

It would appear from these results that the rate-determining step in the acid-catalyzed oxidation of organomercuric acetates by mercuric acetate is the oxidation–reduction of mercuric acetate in methanol. But the over-all reaction seems to involve radicals, so one may speculate that a homopolar fission of the methoxymercuric salt is occurring

$$\mathrm{MeOHgX} \longrightarrow \mathrm{MeO}\cdot + \cdot\mathrm{HgX}.$$

Evidence for radicals in the mercuric acetate – methanol system is afforded because an induction period occurs before mercurous salt appears. It may be seen in Fig. 4 that this induction period may be shortened markedly by removal of dissolved oxygen from the system. Of course the inhibition by oxygen also indicates that radicals are involved in the induction step.

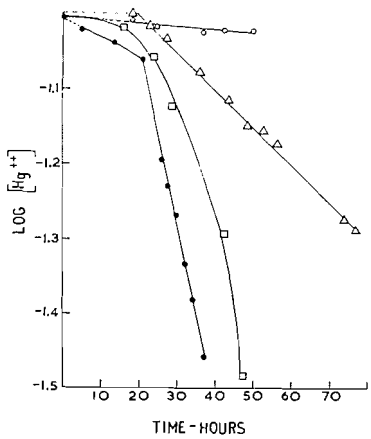


FIG. 4. System: Mercuric acetate (0.10 *M*) and boron fluoride etherate (0.02 *M*) in methanol at 25° C. ○, under oxygen; △, under air; □, deaerated three times; ●, deaerated four times.

Since the long period of induction does not occur in the over-all oxidation, it seems probable that inducing radicals are more prevalent in the presence of an organomercuric salt than they are in its absence. This supposition is borne out by the evidence of Fig. 5.

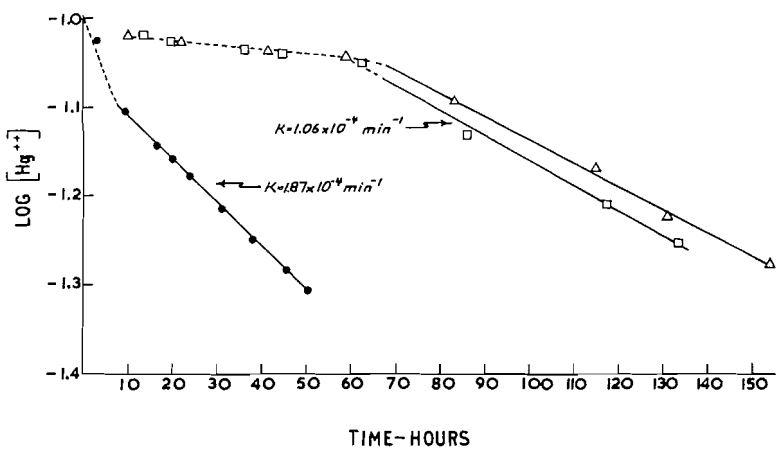


FIG. 5. System: Mercuric acetate (0.10 *M*) and boron fluoride (0.02 *M*) in methanol at 25° C. Additive: 0.05 *M* α-2-methyl-2-methoxycyclohexylmercuric acetate, ●; 0.05 *M* *n*-butylmercuric acetate, △; 0.05 *M* α-2-methoxycyclohexylmercuric acetate, □.

Here it is shown by the inclusion of organomercurials that *n*-butylmercuric acetate, which cannot be oxidized in the mercuric acetate – boron fluoride – methanol system, does not alter the inhibition. Neither does α-2-methoxycyclohexylmercuric acetate, the reaction of which is very slow in this system. On the other hand, the addition of 2-methyl-2-methoxycyclohexylmercuric acetate (which is oxidized rapidly in systems where the reagent concentration is stoichiometric) markedly shortens the induction period. Evidently it is acting here as a scavenger for oxygen.

THE MECHANISM OF THE OXIDATION

In summary of the evidence which now has been presented it is suggested that for several reasons mercuric salt in methanol very slowly undergoes a homopolar fission into anionomercury radicals and a radical (acetato, nitrato, methoxy, or hydroxy) deriving from the salt or its solvolysis product in water or methanol. This behavior is expressed in equations [i], [ii], and [iii]. The radical population generated by any one of these three reactions must be so low at room temperature (especially when mercuric acetate without boron fluoride is involved) that "breeding" of a chain reaction is largely prevented by oxygen. The decomposition of some organomercuric salts into radicals, as is expressed by equation [iv], should be more extensive according to the rate at which diphenylpicrylhydrazine is bleached (Fig. 1). The elimination of inhibition by oxygen seems to be confirmatory.

$$HgX_2 \rightleftarrows X\cdot + \cdot HgX \quad [i]$$

$$HgX_2 + ROH \rightleftarrows ROHgX + HX \quad [ii]$$

$$ROHgX \rightleftarrows RO\cdot + \cdot HgX \quad [iii]$$

$$R'HgX \rightleftarrows R'\cdot + \cdot HgX \quad [iv]$$

$$\cdot HgX + ROHgX \rightarrow RO\cdot + Hg_2X_2 \quad [v]$$

$$RO\cdot + R'HgX \rightarrow R'OR + \cdot HgX \quad [vi]$$

$$\cdot HgX + HgX_2 \rightarrow X\cdot + Hg_2X_2 \quad [vii]$$

$$X\cdot + R'HgX \rightarrow R'X + \cdot HgX \quad [viii]$$

$$RO\cdot \rightarrow H\cdot + (R \text{ minus } H)O \quad [ix]$$

$$H\cdot + ROHgX \rightarrow ROH + \cdot HgX \quad [x]$$

$$RO\cdot + H\cdot \rightarrow ROH \quad [xi]$$

$$2\cdot HgX \rightarrow Hg_2X_2 \quad [xii]$$

$$2\cdot HgX + O_2 \rightarrow XHg{-}O{-}O{-}HgX \quad [xiii]$$

These meager reactions ([i]–[iv]) cannot account for the rates at which organomercuric salts can be oxidized by mercuric salts. However, an explanation is afforded by consideration of a novel particle, anionomercury radical. If this half of a mercurous salt reacts with a basic mercuric salt according to equation [v] or with the non-solvolyzed mercuric salt by equation [vii], then stable (dimeric?) mercurous salt is formed together with a radical. This radical may be RO· (R = H or Me) from the solvolyzed salt in water or an alcohol, say methyl alcohol, or it may be X· (nitrato from mercuric nitrate or else the dead radical, acetato). If the live radicals, RO· or NO_3· were to react with the organomercuric salt according to reaction [vi] or [viii], products such as alcohols, methyl ethers, or nitrate esters would be obtained together with the anionomercury radical. But this radical would then promote reactions [v] and [vii], thus establishing a self-sustaining chain. The continuation of this radical chain would therefore depend upon a supply of new anionomercury radical according to equations [i], [iii], and [iv] in order to compensate for depletion of the radical according to equations [xii] and [xiii]. Other radical-depletion reactions are suggested by equations [ix], [x], and [xi].

Can. J. Chem. Downloaded from www.nrcresearchpress.com by 69.46.99.164 on 09/04/12
For personal use only.

The anionomercury radical which is postulated here is envisaged as an active form of monomeric mercurous salt. The idea of this monomer is not unprecedented. A low concentration in equilibrium with the dimer has been postulated on the basis of spectroscopic evidence (14), and an apparent contradiction in favor of the dismutation into mercuric ion and free mercury (15) may only show that the monomer itself is an unstable species which may dismutate.

$$Hg_2X_2 \rightleftharpoons 2HgX \longrightarrow HgX_2 + Hg^0.$$

Certainly the dismutation reaction is well known. The intermediacy of the monomer has been suggested as a boundary state in the calomel electrode (16, 17), and the position of mercury in the periodic classification of elements is appropriate for the P → O electron shell transition which would allow of the temporal active state, ·HgX. Actually an unspecified active mercurous state has been suggested for the radical-like behaviors of the Eder reaction (18), which resembles closely the reaction that we have reported here and which we have described as a regenerative radical chain.

In our opinion the catalytic effect of acids does not conflict with our conception of a regenerative radical chain. Of course electron attraction within a group does so weaken a bond that ionic dissociation occurs. But such electrical field deformation may also equalize electron sharing in a bond, so that it becomes amenable to homopolar fission. Perhaps the best known example of this equalization influence is found in the effect of acidity upon redox potentials. Also it is significant that some of the homopolar reactions of diazotized amines are promoted by boron fluoride.

There remains the necessity to explain why the accelerating effect of boron fluoride on the organomercuric acetate – methanol – mercuric acetate system shifts the kinetic behavior from the second order observed for the uncatalyzed reaction (or for the reaction of the nitrate salts) to a first-order rate. An explanation may be offered in terms of equations [v] and [vi]. In absence of the accelerating action of boron fluoride the reaction according to equation [vi] will be rate controlling and hence will require both basic mercuric salt and organomercuric salt, each as first-order participants. But if boron fluoride catalyzes the reaction of equation [vi] (by labilization of the C—Hg bond in the organomercurial) then the anionomercury radical will be ample for the reaction of equation [v]. In this circumstance the regenerative chain ([v] and [vi]) will depend only on the concentration of the basic mercuric salt.

One might question why the co-ordinative tendency of boron fluoride ought not also labilize the basic mercuric salt of equation [v]. If this labilization occurred to an appreciable extent the explanation presented above would not be valid. We believe it to be fortuitous that the difference in co-ordination of boron fluoride with methanolic mercuric acetate versus the organomercuric acetates that we used was sufficiently great as not to vitiate the first-order kinetics. But we would not expect to be so fortunate with other organomercuric salts. Indeed, the poor kinetic studies of the earlier report (1) may in retrospect be explained on this basis.

STEREOCHEMICAL ASPECTS OF THE OXIDATION

If this oxidation of organomercurials is indeed homopolar then the unique characteristic is its stereospecificity. Moreover, the stereospecific reaction occurs with inversion if the recent assignment of configurations for 2-methoxy-1,2-diphenylethylmercuric salts is correct (19). In terms of the Werner concept of substitution (commonly called Sn_2) the stereospecific substitution via radicals may seem to be anomalous in the sense that nucleophilic attraction is absent in the neutral radical.

Can. J. Chem. Downloaded from www.nrcresearchpress.com by 69.46.99.164 on 09/04/12
For personal use only.

Of course the original Werner concept of concise co-ordination as an intermediate state of substitution by inversion has now largely been superseded by the idea of a dynamic transition. In the latter view the assignment of electrical polarity is much less significant than is required by co-ordination, even if it is ephemeral. Indeed a transition state for equation [vi] in which radicals are involved may be described as a concerted coupling and decoupling of spin, exemplified in Fig. 6.

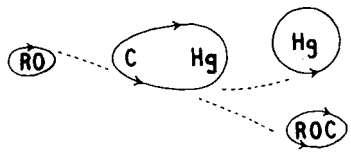


FIG. 6.

Of course it is surprising that the necessity for specification of this mechanism has not arisen previously among examples of Walden inversion. Perhaps the complexity of the usual radical reaction has disguised any stereospecificity. Indeed, the mechanism (Fig. 6) which we have proposed may turn out to be exemplified among the stereospecific polymerizations which are radical-induced and propagated.

The authors wish to thank the National Research Council of Canada for funds in aid of this investigation.

EXPERIMENTAL*

Reagents and Equipment

Mercuric acetate was purified by crystallization from dilute acetic acid. Mercuric nitrate (Merck reagent) was used as such; analysis showed that it contained 105.56% (gravimetric) and 104.94% (volumetric) of mercuric ion assuming anhydrous mercuric nitrate. Thus it was actually a basic salt. Absolute nitric acid (better than 99%) was distilled, water-white. Dry methanol (from magnesium methoxide) contained less than 0.002% water (Karl Fischer titration). Spectra were determined with Beckman DK-1, IR-4, and IR-5 instruments. Kinetic studies at 25° were controlled to ±0.1°.

The Reduction of Mercuric Acetate in Methanol with Boron Fluoride Etherate

(*a*) *Kinetics*

The rate of disappearance of mercuric acetate was determined by volumetric analysis for mercuric salt using the method of titration with potassium iodide and mercuric nitrate. This was necessitated by the fact that mercurous salts were not completely removed as the acetate when appreciable amounts of boron fluoride were present in the methanol solutions and would have interfered with analysis by thiocyanate titration. The rate data are plotted in Fig. 2, from which the first-order rate constants were calculated. The experiment involving 1 mole equivalent of boron fluoride is given as representative.

Mercuric acetate (3.1876 g, 0.01 mole) was dissolved in 75 ml of dry methanol, and 1.260 ml (0.01 mole) of freshly distilled boron fluoride etherate added. The volume was made up to 100.00 ml and the sample thermostatted at 25±0.1°. Aliquots (4.00 ml) were added to 10 ml of 2 *M* hydrochloric acid and filtered through Celite to remove mercurous chloride. The filtrate and washings were diluted to 70 ml with water, 10.00 ml of 0.2 *M*

**Melting points have been corrected against reliable standards. X-Ray diffraction patterns are reported using* Cu(K_α) Ni-*filtered radiation in Angstroms at relative intensities* [I/I_1].

Can. J. Chem. Downloaded from www.nrcresearchpress.com by 69.46.99.164 on 09/04/12
For personal use only.

standard potassium iodide solution added, and then titrated with mercuric nitrate solution. The latter, used as the primary standard, was freshly prepared each 24 hours by dissolving 5.4152 g of mercuric oxide in 6.3 ml of concentrated nitric acid and diluting to 500 ml.

The rate of this reaction, using 0.02 *M* boron fluoride, was checked by analyzing gravimetrically for mercurous salt. A series of solutions containing 0.7950 g (0.0025 mole) of mercuric acetate and 0.070 g (0.0005 mole) of boron fluoride was made up to 25.00 ml in methanol and held at 25°. Periodically samples were rinsed out of the volumetric flasks with 25 ml of water containing 2 ml of 8 *M* nitric acid and then 2.0 ml of 5 *M* sodium chloride added. The mercurous chloride was recovered by filtration, using about 0.5 g of previously dried and accurately weighed Celite to facilitate the operation. The filtrate was made basic and mercuric oxide separated in the same manner. The precipitates were dried 4 hours at 50°/1 mm, giving the following data.

TABLE V

Gravimetric rate data

Time (hours)	Wt. Hg_2Cl_2 (g)	Wt. HgO (g)	Total [Hg] (*M*)
0	0.0000	0.5402	0.0998
11.50	0.0078	0.5365	0.1002
33.50	0.0461	0.4989	0.0998
41.25	0.0548	0.4893	0.0995
57.25	0.1320	0.4195	0.0999
67.25	0.2062	0.3348	0.0969
81.75	0.2744	0.2764	0.0976
129.75	0.3925	0.1598	0.0960

When this data was plotted similarly to that shown in Fig. 2, the rates, based on the mercurous and mercuric determinations respectively, were 2.08×10^{-4} min^{-1} and 2.14×10^{-4} min^{-1}.

Kinetics of the Oxidation of trans-Stilbene and its Methoxymercurial with Mercuric Acetate and Boron Fluoride Etherate in Methanol

(*a*) *Initially Alkene*

A suspension of 0.450 g (0.0025 mole) of *trans*-stilbene and 2.3902 g (0.0075 mole) of mercuric acetate in 40 cc of dry methanol was shaken 1 hour, causing nearly complete solution of the solids. Boron fluoride etherate (0.126 ml, 0.001 mole) was added and the volume made up to 50.00 ml, whereupon a brief shaking caused complete solution. This was then thermostatted at 25°, zero time being taken as that of boron fluoride addition.

(*b*) *Initially Mercurial*

Quantities of 2.235 g (0.005 mole) of β-2-methoxy-1,2-diphenylethylmercuric chloride (20) and 0.835 g (0.005 mole) of silver acetate were shaken with 25 ml of dry methanol for 1 hour then filtered to remove 0.716 g (100%) of silver chloride. To the filtrate was added 1.593 g (0.005 mole) of mercuric acetate and 0.126 ml (0.001 mole) of boron fluoride etherate. After it was diluted to 50.00 ml, the whole was shaken a few minutes to cause complete solution and kept at 25°.

In both cases (*a*) and (*b*) the analytical procedure used was the mercuric nitrate titration described above.

The Oxidation of 1-Phenyl-2-methoxy-2-methyl-propylmercuric Acetate with Mercuric Acetate and Boron Fluoride

(*a*) *Kinetics*

The rate of oxidation of this mercurial was determined by the method described above

Can. J. Chem. Downloaded from www.nrcresearchpress.com by 69.46.99.164 on 09/04/12
For personal use only.

and is given in Table II. The actual rate data is plotted in Fig. 3 together with the comparable experiments with stilbenes described above.

(*b*) *Products of the Reaction*

A 10.0-g (0.025 mole) quantity of 1-phenyl-2-methoxy-2-methylpropylmercuric chloride (21) was converted to its acetato analogue with 4.17 g (0.025 mole) of silver acetate in 200 ml of dry methanol (yield of silver chloride 99%). To the acetatomercurial was added 15.9 g (0.05 mole) of mercuric acetate and 6.3 ml (0.05 mole) of boron fluoride etherate, and the solution kept at 50° for 24 hours. After it was cooled to 0° and filtered from 6.02 g of solid (presumed to be mercurous acetate and testing black with alkali). the solution was concentrated to 40 ml by distillation at 15–20° under reduced pressure, and diluted with 200 ml of water. After the addition of just sufficient 8 *M* nitric acid to dissolve all solids, the suspension was extracted with chloroform (3×50 ml). The aqueous phase gave 9.51 g of chloroform-insoluble mercurous chloride when excess sodium chloride was added. Distillation of the chloroform extract yielded 2.01 g (41%) of crude 1-phenyl-1,2-dimethoxy-2-methylpropane, b.p. 94–96°/8 mm, m.p. −4.0 to +1.5°, n_D^{20} 1.4972. Literature values for this compound (1) are b.p. 94–100°/8 mm, m.p. 8–11°, n_D^{20} 1.4980.

Inhibition of Mercuric Acetate – Methanol Reaction

The data of Fig. 3 were obtained by the analytical methods described above with solutions of 1.5935 g (0.005 mole) of mercuric acetate in 100 ml of dry methanol to which 0.126 ml of boron fluoride etherate was added at zero time in a magnetically stirred flask at 26–27°. Duration of experiment was 50 hours. The reaction under oxygen was maintained at 17–19 lb absolute pressure and a yellow turbidity was observable at termination. Deaeration experiments were conducted by flushing system and solution with nitrogen, cooling by liquid air bath to incipient solidification, evacuation at 0.1 mm until cessation of bubbling, followed by complete solidification with 10 minutes of continued evacuation. The system was then warmed to 25° and pure nitrogen was admitted, followed by boron fluoride etherate. The relative first-order rates are: under oxygen, negligible; under air, $k = 1.97\times10^{-4}$ min^{-1}; after four deaerations, $k = 9.28\times10^{-4}$ min^{-1}.

Acceleration of Mercuric Acetate – Methanol Reaction

The experiment recorded in Table IV for acceleration by nitric acid is typical. A solution containing 0.935 g (0.0029 mole) of mercuric acetate, 0.120 ml of absolute nitric acid, and 15.0 ml of dry methanol was kept at 50° for 85 hours. After the solution was cooled to 0°, sufficient 8 *M* nitric acid was added to dissolve any precipitated solid, and excess sodium chloride solution (5 *M*) was added to precipitate 0.289 g (42%) of mercurous chloride. When the filtrate was basified, 0.272 g (58%) of mercuric oxide was obtained. The combined recovery of mercury salts was always 100±2%.

The Ultraviolet Absorption Spectra of Mercury Salts in Methanol

(*a*) *Mercuric Nitrate*

A solution of mercuric nitrate (2×10^{-4} *M*) in dry methanol showed no absorption maxima above 230 mμ. At shorter wave lengths total absorption occurred. Over a period of 100 hours an absorption peak appeared at 242 mμ, which was shown to be due to mercurous nitrate. When 4 mole equivalents of sodium acetate were added to this solution, the peak at 242 mμ was immediately replaced by one at 236 mμ due to mercurous acetate.

When a solution of mercuric nitrate (2×10^{-4} *M*) and absolute nitric acid (8×10^{-4} *M*) was freshly prepared it showed no absorption maxima above 230 mμ, but after 24 hours a peak had appeared at 290 mμ, and there was no absorption at 242 mμ attributable to mercurous nitrate. The addition of 4 mole equivalents of mercurous acetate to this solu-

Can. J. Chem. Downloaded from www.nrcresearchpress.com by 69.46.99.164 on 09/04/12
For personal use only.

tion shifted the 290-mμ absorption to 275 mμ. This latter absorption region was not observed in any of the mercuric and mercurous acetate solutions.

These spectra of mercurous nitrate solutions, showing only the maxima at 242 mμ, are not changed upon addition of 2 equivalents of sodium acetate. However, when the solutions had been left standing 100 hours the appearance of absorption at 290 mμ was observed.

(*b*) *Mercuric Acetate*

A solution of mercuric acetate (2×10^{-4} *M*) showed no maxima below 230 mμ when freshly prepared. Over a period of 9 days a peak appeared at 236 mμ, identical with that found with mercurous acetate (2×10^{-4} *M*). When a similar solution containing nitric acid (4×10^{-4} *M*) was aged 10 days, only the absorptions appeared due to mercurous nitrate (242 mμ) and the unidentified mercuric species (290 mμ).

The 236-mμ peak found for mercurous acetate was shifted to 242 mμ (mercurous nitrate) upon addition of 2 equivalents of nitric acid.

Oxidation of Cyclohexylmercuric Nitrate with Mercuric Nitrate

(*a*) *In Methanol*

A 10.00-g (0.0313 mole) quantity of the chloromercurial was converted to the nitrato analogue with silver nitrate in 450 ml of methanol. To this solution was added 10.18 g (0.0313 mole) of mercuric nitrate and 1.32 ml (0.0313 mole) of absolute nitric acid. After 38 hours, the solution was cooled to 0°, diluted with 400 ml of water, and 15 ml of 5 *M* sodium chloride added. Filtration gave 12.79 g (87%) of chloroform-insoluble mercurous chloride. The filtrate was extracted with ether (6×75 ml) which was washed with dilute base, water, dried, and distilled, giving a fraction, b.p. 25–41°/2–3 mm, n_D^{20} 1.4522, wt. 1.06 g. This material gave a positive nitrate ester test with benzidine (22) and a negative test for carbonyl compounds. A chromatoplate analysis was made on silicic acid, eluting with commercial hexane; comparison with pure compounds showed that methoxycyclohexane and cyclohexyl nitrate were present. When these pure compounds and the product mixture were submitted for infrared spectral analysis (courtesy of Canadian Armaments Research and Development Establishment, Quebec) the mixture was found to represent yields of 31% of cyclohexyl nitrate and 8% of methyl cyclohexyl ether.

(*b*) *In Water*

A 20.00-g (0.0627 mole) quantity of the chloromercurial and 10.65 g (0.0627 mole) of silver nitrate in 500 ml of dry methanol were stirred 1 hour, filtered from 8.98 g (100%) of silver chloride, and the filtrate taken to dryness as rapidly as possible at 20–25°. The grey residue was dissolved in 100 ml of chloroform, filtered from 0.58 g of grey solid, and again concentrated at reduced pressure to give 20.00 g (0.058 mole) of white crystals presumed to be the nitratomercurial. To this was added 140 ml of water, 18.82 g (0.058 mole) of mercuric nitrate, and 7.5 ml of 8 *M* nitric acid (0.060 mole). After it was stirred 16 hours the mixture was extracted with ether (6×50 ml), and 2.51 g (0.0125 mole) of metallic mercury separated from the aqueous phase. Addition of excess sodium chloride to the aqueous phase gave 24.5 g (0.103 mole) of mercurous chloride, which was totally insoluble in chloroform.

The ether extracts, washed with dilute sodium hydroxide which produced some mercuric oxide, then with water till neutral, were dried and distilled to give two fractions: (1) b.p. 15–40°/37 mm, wt. 0.38 g; and (2) b.p. 65–84°/42–3 mm, wt. 4.14 g. The infrared spectra of both fractions were nearly identical and indicated them to be mainly a mixture of cyclohexanol and cyclohexyl nitrate. Fraction 2 was analyzed by this means, using the

Can. J. Chem. Downloaded from www.nrcresearchpress.com by 69.46.99.164 on 09/04/12
For personal use only.

hydroxyl band at 3450 cm^{-1} (ϵ = 98.1) for the alcohol and the strong covalent nitrate band at 1650 cm^{-1} (ϵ = 1090) for the ester. Each of these bands is free from contribution of the other component. Solution spectra in cyclohexane were used at concentrations of about 0.1 g/ml for the alcohol and 0.015 g/ml for the ester. Fraction 2 was thus found to be 43% by weight of ester and 55% alcohol. Hence fractions 1 and 2 represent yields of 40% and 21% respectively of cyclohexanol and cyclohexyl nitrate. The following principal absorption bands (cm^{-1}) were observed. Cyclohexanol: 3450, 2910, 1458, 1375, 1338, 1290, 1239, 1145, 1095, 1052, 1011, 991, 952, 930. Cyclohexyl nitrate: 3050, 2900, 1650, 1465, 1325, 1283, 1240, 993, 941, 915, 862.

A portion of fraction 2 (0.10 g) was treated with dinitrophenylhydrazine reagent to give 12 mg of the hydrazone of formylcyclopentane, m.p. 149–152°, which melting point was raised by mixture with an authentic sample.

Another portion of fraction 2 (1.92 g) was reduced with zinc and iron in acetic acid by the method of Dewar and Fort (23) to give 1.17 g of only one fraction, b.p. 158–160°, m.p. 16–22°. A test with diphenylamine was negative for nitrate ester. When this cyclohexanol (0.57 g, 0.0057 mole) was treated with 1.2 g (0.0057 mole) of α-naphthylisocyanate, there was obtained 1.53 g (100% crude yield) of urethane, m.p. 126–130°; this melting point was raised upon admixture with authentic urethane of m.p. 130–131°.

Under otherwise comparable conditions (except that the system was homogeneous) replacement of the mercurial by cyclohexanol did not lead to any cyclohexyl nitrate.

Oxidation of Benzylmercuric Nitrate with Mercuric Nitrate in Water

Benzylmercuric chloride (10.00 g, 0.0306 mole) was converted to the nitrate salt with silver nitrate in 90 ml of methanol. After filtration of silver chloride (100%), the filtrate was rapidly concentrated at reduced pressure to dryness. To this was added a clear solution prepared from 60 ml of water, 6.63 g (0.0306 mole) of mercuric oxide, and 11.15 ml (0.0918 mole) of 8.2 *M* nitric acid. After the solution was stirred for 10 hours, the reaction mixture was extracted with ether (5×25 ml). Then excess sodium chloride (5 *M*) was added to the aqueous phase to precipitate 11.63 g (81%) of mercurous chloride, which tested black with alkali and was chloroform-insoluble. The ethereal extracts were water-washed until neutral, dried, and concentrated to 2.46 g of yellow oil. Now, 1.000 g of this oil was chromatographed on a 10×250-mm column, using a 2:1 silicic acid:Celite adsorbent which had been activated at 150°. Two main fractions were obtained, one of which, wt. 0.360 g, tested positively for both a carbonyl and a nitrate ester (diphenylamine test) component. The second fraction contained no nitrate ester. The first fraction was dissolved in 15.0 ml of dry ethanol, and then 1.43 ml (0.025 mole) of glacial acetic acid and 0.59 g (0.0034 mole) of Girard's P reagent was added. After standing 15 hours the solution was poured into 50 ml of cold water containing 1.19 g (0.0112 mole) of sodium carbonate and was extracted in the cold with chloroform (4×20 ml). These extracts were washed with water, dried over magnesium sulphate, and concentrated to give 0.288 g of benzyl nitrate, m.p. −23 to −17.5°, n_D^{20} 1.5192. A mixed melting point with authentic benzyl nitrate (m.p. −17 to −15°, n_D^{20} 1.5205) was raised to −19 to −16°. The yield of benzyl nitrate was 15%.

In an identical experiment the oil obtained by ether extraction was distilled, taking a 2.36-g fraction, b.p. 65–100° (mostly boiling at 90–100°) at 30 mm. Treatment of 0.47 g of this oil with phenylisocyanate gave 0.39 g of the phenylurethane of benzyl alcohol, m.p. 76–78° (lit. value, m.p. 78° (24)). This indicates a 16% yield of the alcohol. From the oil there was also obtained a trace amount of benzaldehyde, separated as its dinitro-

Can. J. Chem. Downloaded from www.nrcresearchpress.com by 69.46.99.164 on 09/04/12
For personal use only.

phenylhydrazone, and identified by mixture melting point. Upon standing 2 days the oil also deposited about 20 mg of benzoic acid crystals, also identified by mixture melting point.

Reactions of Mercuric Nitrate with Radical Sources

(*a*) *With Hydrogen Peroxide*

When 0.01 mole each of mercuric nitrate and hydrogen peroxide (Becco 90%) were added to 40 ml of dry methanol a test showed no formation of mercurous salt (test with sodium chloride) after 4 hours, but the addition of 3–4 mg of ferrous sulphate heptahydrate initiated an exothermic reaction. After the solution was stirred for 20 hours, 7 ml of 8 *M* nitric acid was added to give complete solution and mercurous chloride and mercuric oxide were recovered using sodium chloride and sodium hydroxide respectively, in 60% and 40% yield. When the above was repeated using 0.10 g of ferrous salt, a nearly explosive reaction resulted. However, the same amounts of reagents, in water instead of methanol, using 5 mg of ferrous salt, produced no mercurous salt after 10 hours. It was shown that mercurous nitrate in methanol was unchanged by hydrogen peroxide and ferrous salt.

(*b*) *With Isobutyryl Peroxide in Methanol*

A 0.83-mmole quantity of mercuric nitrate in 5.0 ml of dry methanol was stirred for 12 hours with 5.0 ml of an 0.17 *M* solution of isobutyryl peroxide (25) in methanol. This system was analyzed by the method of Price (26). A test for peroxide was now negative. Addition of water, sufficient nitric acid to dissolve solids, and excess sodium chloride gave 0.12 g (62%) of mercurous chloride. Addition of excess base now gave no mercuric oxide.

Reactions of Mercury Acetates with Radical Sources

No mercurous salt was formed when 0.01 mole each of mercuric acetate and hydrogen peroxide in 40 ml of methanol was treated with 5 mg of ferrous sulphate. Indeed a 36% conversion to mercuric salt was observed when a solution of 0.005 mole of mercurous acetate and 0.01 mole of 90% hydrogen peroxide in 40 ml of methanol containing 5 mg of ferrous sulphate was stirred for 5 hours. This conversion was detected by subsequent addition of 90 ml of water and 10 ml of 5 *M* aqueous sodium chloride, then sufficient 8 *M* nitric acid to just dissolve the orange-colored solid. After filtration of 1.76 g (64%) of mercurous salt the filtrate was basified to yield 0.77 g of mercuric oxide. The conversion to mercuric salt was complete when 0.05 mole of peracetic acid in 10 ml of chloroform was refluxed with 0.01 mole of mercurous acetate in 20 ml of methanol during 4 hours.

Reaction of Cyclohexylmercuric Nitrate with Pernitrous Acid in Water–Methanol

A system was prepared at 0° containing 300 ml of dry methanol, 300 ml of water, 0.06 mole of the nitrato–mercurial, 0.009 mole of 8 *M* nitric acid, and 0.09 mole of 90% hydrogen peroxide. This suspension was warmed to and maintained at 25° while a solution of 4.56 g (0.066 mole) of sodium nitrite in 60 ml of water was added dropwise during 20 minutes. Now the serial addition of the same amounts of nitric acid, hydrogen peroxide, and then (slowly and dropwise) sodium nitrite was repeated thrice, and the mixture cooled to maintain the temperature at 25°. The reaction mixture was then extracted with ether (8×50 ml), the extracts dried and distilled to give 5.51 g of oil. Treatment of a sample of this oil with dinitrophenylhydrazine gave the derivative of cyclohexanone, m.p. 150–153°, identified by mixture melting point. Infrared analysis of the oil was made by the method described above for analysis of the products of oxidation of cyclohexylmercuric nitrate with mercuric nitrate. Thus the crude product contained 32% and 39% by weight

Can. J. Chem. Downloaded from www.nrcresearchpress.com by 69.46.99.164 on 09/04/12
For personal use only.

respectively of cyclohexanol and cyclohexylnitrate. These results indicate respective yields of 30% and 25% for these products in the pernitrous acid oxidation.

The original reaction mixture, after ether extraction, was treated with excess sodium chloride solution to yield 7.41 g (52%) of chloroform-insoluble mercurous chloride (black with alkali).

Reaction of α-2-Hydroxycyclohexylmercuric Acetate and Fenton's Reagent in Water

A solution containing 0.10 mole of cyclohexene, 0.10 mole of mercuric acetate, and 200 ml of water was stirred 2 hours, at which time a test with base indicated that no mercuric salt was present. Now, over a 2-hour period, there was added, simultaneously and equivalently, 10 ml of water containing 0.10 mole of hydrogen peroxide and 0.10 mole of ferrous sulphate heptahydrate. The resulting suspension was stirred 68 hours, then extracted with ether (4×50 ml). Distillation of the dried ethereal extracts gave one fraction, b.p. 90–140°, which upon redistillation yielded 1.19 g of product, b.p. 130–138°, n_D^{20} 1.4390. It was identified as formylcyclopentane (23%) via its dinitrophenylhydrazone, m.p. 153–155°, whose mixture melting point with an authentic specimen was not depressed.

To the aqueous phase was added 0.10 mole of 5 *M* sodium chloride. The precipitate, after drying, was extracted with 150 ml of hot chloroform to give 7.07 g of chloroform-soluble solid. This solid melted at 138–140° with decomposition, and could be recrystallized from acetone without change in melting point. Assuming it to be 2-chloromercuricyclohexanone, the yield was 23%. This compound has been reported by Nesmeyanov (13) to melt at 134–135°. The X-ray diffraction pattern was: [10] 6.70, 5.05, 4.99; [8] 3.49; [7] 2.99; [5] 2.36; [2] 3.78, 3.29, 3.11. Calc. for C_6H_9ClHgO: C, 21.62; Found: C, 22.1.

Oxymercuration of 1-Methoxycyclohexene

After 5 hours a system comprised of 1.12 g (0.01 mole) of 1-methoxycyclohexene (27) (n_D^{20} 1.4569, b.p. 140–141° at 750 mm), 3.18 g (0.01 mole) of mercuric acetate, and 25 ml of methanol was treated with 3.8 ml of 10% aqueous sodium hydroxide. After filtration the solvent was removed under reduced pressure. The residue was treated with 5 ml of saturated aqueous sodium chloride and alkali was added to pH 6. After 1 day the precipitated oil had solidified, 2.64 g, m.p. 99–102°. This crude material was dissolved in chloroform and diethyl ether was added. Further purification (difficult because decomposition occurred slowly with deposition of calomel) was effected by solution in dioxane and reprecipitation by addition of water, 0.25 g, m.p. 128–129.5° (with decomp.). Although the sample is impure its X-ray diffraction pattern shows identity with 2-chloromercuricyclohexanone.

Although cyclohexanone in dilute alkali is reduced to cyclohexanol by sodium trimethoxyborohydride it was possible to convert chloromercuricyclohexanone (m.p. 134–135°) to cyclohexanone, b.p. 150–160° (760 mm), n_D^{20} 1.4477, in 53% yield. A solution of 1.66 g (0.005 mole) of the mercurial in 1 ml of 6 *M* alkali at 0° was treated with 0.64 g (0.005 mole) of sodium trimethoxyborohydride during 1 hour. Distillation of the ether extract yielded 0.26 g which was converted to the 2,4-dinitrophenylhydrazone, m.p. 156–158°, not depressed by admixture with an authentic sample.

Kinetics of the Reaction of Diphenylpicrylhydrazyl (DPPH) with Nitratomercurials in Methanol

The first-order rates listed in Table I were obtained from plots of log [DPPH] versus time, an example of which is shown in Fig. 1. The reaction of DPPH and cyclohexylmercuric nitrate is given here as an example of the method.

Can. J. Chem. Downloaded from www.nrcresearchpress.com by 69.46.99.164 on 09/04/12
For personal use only.

A quantity of 1.595 g (0.005 mole) of cyclohexylmercuric chloride (freshly recrystallized, m.p. 162–163° decomp.) and 0.850 g (0.005 mole) of silver nitrate in 40 ml of methanol was shaken for 30 minutes, then filtered to remove silver chloride (0.714 g, 100%). The filtrate was added to a freshly prepared solution of 16.0 mg of DPPH in 400 ml of methanol and the whole made up to 500 ml. The per cent transmittance at 510 mμ was then measured at appropriate time intervals, using a new sample of the stock reaction solution for each measurement. The molecular extinction coefficient mentioned above (ϵ = 10,220) was determined for a solution of DPPH (32.0 mg/l.) and used for calculation of the DPPH concentration. The spectrum of the solution in which the absorption maxima of DPPH had completely decayed was identical with that of a solution of diphenylpicrylhydrazine in the 440- to 800-mμ region.

Kinetics of the Oxidation of Nitratomercurials with Mercuric Nitrate in Methanol

The second-order rate constants (calculated on the basis of the rate of loss of mercuric nitrate) are presented in Table I. In each case the nitratomercurial was used. To exemplify the procedure, the experiment with cyclohexylmercuric nitrate is described.

A quantity of 0.998 g (0.00313 mole) of cyclohexylmercuric chloride was converted in the usual manner to its nitrato analogue in 25 ml of dry methanol. (If any additive was to be present, it was dissolved in this solution at this point.) The nitratomercurial solution was then added to 1.016 g (0.00313 mole) of mercuric nitrate in 10 ml of dry methanol which had been shaken for 10 minutes previously to disintegrate the lumps. Upon adding 0.260 ml (0.00626 mole) of absolute nitric acid the solution became homogeneous and was immediately diluted to 50.00 ml with dry methanol. From this there were removed 5.00-ml samples which were placed in tared centrifuge tubes. These rubber-stoppered samples were thermostatted at 25° and analyzed as follows.

Four milliliters of 2 *M* hydrochloric acid was added, the sample allowed to stand 10 minutes with occasional stirring to allow complete deoxymercuration of any oxymercurial present, then centrifuged. The precipitate was then thoroughly washed successively with 5-ml portions of water, methanol, and twice with chloroform. A slender glass rod (3 mm diameter) was found to be satisfactory for stirring in these operations and was easily rinsed free of particles with methanol. When solid particles tended to remain at the liquid–air interface, they were readily centrifuged down by first floating a layer of methanol or ether on the top. The sample was dried at 110°, then finally at 56°/1 mm, and weighed as mercurous chloride.

The rate data was plotted as the reciprocal of $[Hg^{++}]$, the latter referring to the mercuric nitrate concentration. Values for $[Hg^{++}]$ were calculated from the relationship

$$[Hg^{++}] = 0.0625 - [Hg_2Cl_2],$$

it being assumed that for each equivalent of mercuric nitrate which had reacted 1 equivalent of dimeric Hg_2Cl_2 was formed.

Formation of Polyacrylonitrile in the Oxidation System: Acrylonitrile – Cyclohexene – Mercuric Nitrate – Nitric Acid – Water

(*a*) *In Air*

A solution of 2.71 g (0.0125 mole) of mercuric oxide, 3.14 ml of concentrated nitric acid (0.050 mole), and 23 ml of water was prepared. To this was added 0.51 g (0.00625 mole) of cyclohexene and the mixture shaken 5 minutes to dissolve the alkene, whereupon 0.66 g (0.0125 mole) of freshly distilled acrylonitrile was added. After 40 minutes the solution became turbid and at 60 minutes the suspended material coagulated upon swirling. After

Can. J. Chem. Downloaded from www.nrcresearchpress.com by 69.46.99.164 on 09/04/12
For personal use only.

3 hours there was filtered 0.026 g (4% of monomer) of solid. This material gave a diffuse X-ray pattern having no diffraction lines. A sample was decomposed in hot concentrated nitric acid and then the solution made basic; there was no precipitate, indicating that the material contained no mercury.

(*b*) *Deaerated*

The above procedure was repeated except that the solution of mercuric nitrate, nitric acid, and water was deaerated three times prior to addition of the other reagents. After 3 hours the yield of insoluble polymer was 7%, which material had a similarly diffuse X-ray pattern.

(*c*) *With Methylene-bis-acrylamide Added*

This reaction was repeated a third time as outlined in the first procedure, adding 0.10 g (0.65 mmole) of methylene-bis-acrylamide. Within 5 minutes the solution had become opaque and after 3 hours it had set to a gel. Centrifugation gave 0.176 g (24% yield based on total available monomer) of solid which did not contain mercury (demonstrated by decomposition with a sulphuric – nitric acid mixture). The product gave a diffuse X-ray pattern.

Polyacrylonitrile

To a solution of 0.65 ml (0.01 mole) of acrylonitrile in 20 ml of water was added 0.10 ml of 90% hydrogen peroxide and 1–2 mg of ferrous sulphate heptahydrate. After 1 hour there was no visible change so 2 ml of 8 *M* nitric acid was added. The solution rapidly became turbid and after 12 hours, filtration gave 0.28 g (43%) of polyacrylonitrile. This polymer corresponded to those produced as is described above, in that it was insoluble in most common solvents, had no melting point but charred above 300°, and gave no distinct X-ray diffraction pattern after 8 hours' exposure.

Attempted Polymerization of Acrylonitrile in the Presence of 2-Hydroxycyclohexylmercuric Nitrate

A solution was prepared of 1.352 g (0.00625 mole) of mercuric oxide, 1.57 ml of concentrated nitric acid, and 23 ml of water. Cyclohexene (0.63 ml, 0.00625 mole) was added and the whole shaken for 30 minutes, at which time the homogeneous solution gave a negative test with base for mercuric ion. To this was added 0.81 ml (0.0125 mole) of acrylonitrile. A faint opalescence slowly developed, but after 1 day this had not increased to a degree which allowed separation of a solid phase.

Cyclohexylmercuric Acetate and Peracetic Acid in Methanol

A solution of 0.05 mole of peracetic acid in chloroform was added to 0.01 mole of cyclohexylmercuric acetate in 20 ml of dry methanol. After 7 hours of reflux a peroxide test was negative. The mercurous acetate was filtered off and was converted by treatment with sodium chloride to 0.20 g (8%) of calomel. The filtrate was diluted to 80 ml with water and was 4 times extracted with a total of 80 ml of chloroform. The aqueous phase yielded 1.58 g (73%) of mercuric oxide when it was treated with alkali. The chloroform phase was distilled to yield only the solvent and then 0.74 g (75%) of cyclohexanone, b.p. 150–55°, n_D^{20} 1.4497, which was characterized as the 2,4-dinitrophenylhydrazone m.p. 154–5°, mixture m.p. not depressed.

REFERENCES

1. SHEARER, D. A. and WRIGHT, G. F. Can. J. Chem. **33**, 1002 (1955).
2. TITOV, A. I. and RUSANOV, D. E. Doklady Akad. Nauk S.S.S.R. **82**, 65 (1952); Chem. Abstr. **47**, 2688 (1953).
3. MERZ, J. H. and WATERS, W. A. J. Chem. Soc. 15 (1949).

Can. J. Chem. Downloaded from www.nrcresearchpress.com by 69.46.99.164 on 09/04/12
For personal use only.

4. MERZ, J. H. and WATERS, W. A. J. Chem. Soc. 2427 (1949).
5. URI, N. Chem. Revs. **50**, 375 (1952).
6. DHAR, H. J. Chem. Soc. 690 (1917).
7. WEISS, J. Discussions Faraday Soc. **2**, 188 (1941).
8. ABEL, E. Monatsh. **83**, 111 (1952).
9. HALFPENNY, E. and ROBINSON, P. J. Chem. Soc. 928 (1952).
10. HESLOP, R. and ROBINSON, P. J. Chem. Soc. 1271 (1954).
11. LAVILLE, J. and WATERS, W. A. J. Chem. Soc. 400 (1954).
12. CRAMER, R. J. Am. Chem. Soc. **79**, 6125 (1957).
13. NESMEYANOV, A. N., LUTSENKO, I., and KHOMUTOV, R. Doklady Akad. Nauk S.S.S.R. **88**, 837 (1953). NESMEYANOV, A. N., LUTSENKO, I., and LUMANOVA, Z. Izvest. Akad. Nauk S.S.S.R. Otdel. Khim. Nauk, 601 (1949).
14. HIGGINSON, W. C. E. J. Chem. Soc. 1438 (1951).
15. MOSER, H. C. and VOIGT, A. F. J. Am. Chem. Soc. **79**, 1837 (1957).
16. HILLS, J. C. and IVES, D. J. G. J. Chem. Soc. 311 (1951).
17. DIBBS, H. P., IVES, D. J. G., and PITTMAN, R. W. J. Chem. Soc. 3370 (1957).
18. CARTLEDGE, G. H. J. Am. Chem. Soc. **63**, 906 (1941).
19. ABERCROMBIE, M., BHARUCHA, K. R., RODGMAN, A., and WRIGHT, G. F. Can. J. Chem. **37**, 1328 (1959).
20. BIRKS, A. M. and WRIGHT, G. F. J. Am. Chem. Soc. **62**, 2412 (1940).
21. BERMAN, L., HALL, R. H., PYKE, R. G., and WRIGHT, G. F. Can. J. Research, **30**, 541 (1952).
22. FEIGL, F. Spot tests in organic analysis. Elsevier Press, Inc., New York. 1956. p. 168.
23. DEWAR, J. and FORT, G. J. Chem. Soc. 492 (1944).
24. SHRINER, R. L. and FUSON, R. C. Identification of organic compounds. John Wiley & Sons, Inc., New York. 1940. p. 186.
25. KHARASCH, M. S., KANE, S. S., and BROWN, H. C. J. Am. Chem. Soc. **63**, 526 (1941).
26. PRICE, C. and MORITA, H. J. Am. Chem. Soc. **75**, 3686 (1953).
27. WIELAND, H. and GARBASCH, P. Ber. **59**, 2490 (1926).

Can. J. Chem. Downloaded from www.nrcresearchpress.com by 69.46.99.164 on 09/04/12
For personal use only.

Can. J. Chem. Downloaded from www.nrcresearchpress.com by 69.46.99.164 on 09/04/12
For personal use only.

THE AUTOOXIDATION OF ORGANOMERCURIC SALTS[1]

J. H. Robson and George F Wright

ABSTRACT

It has been found that besides the homopolar bimolecular oxidation of alkylmercuric salts which has been reported previously an alternative unimolecular reaction of heteropolar character may occur. The product of this heteropolar reaction is the alkene, but it probably proceeds through an alkylmercury cation since reaction in benzene leads to the Friedel–Crafts type of product. Like the homopolar reaction, the heteropolar reaction is accelerated by electron withdrawal of the anionic part of the salt. Indeed, it is believed that both mechanisms are operative among many of the mercuric salt oxidations of alkenes which previously have been reported.

The oxidation of organomercuric salts by means of mercuric nitrate and mercuric acetate plus boron fluoride (1) has recently been re-examined (2). This reaction is now believed to involve a self-sustaining radical chain in which anionomercury radical (monomeric mercurous salt) is the chain carrier. The expectation that such a reaction would be inhibited by oxygen is in fact realized. This inhibition is exemplified by an induction period which occurs especially when the system comprised of mercuric acetate and boron fluoride in methanol is used as the oxidizing medium. It is evident that if there were an oxidation reaction of different mechanism, which was not inhibited by oxygen, then this latter alternative reaction would occur preferentially. Although the alternative is not observed when the mercurial to be oxidized is sufficiently reactive (as is the case with many oxymercurials), it has been observed with simple alkylmercurials.

The reaction under present consideration differs from the homopolar reaction (1, 2) in several respects. First, it does not require an inorganic mercuric salt and therefore may be classed as an autooxidation of an alkylmercuric salt. Secondly, mercury rather than mercurous salt seems to be one product while the other is the alkene to be expected if the elements of hydrogenmercuric salt were to be eliminated from the mercurial. The reaction is not entirely a general one (we have been unable yet to oxidize a primary alkylmercuric salt), but the secondary and, especially, the tertiary mercurials are oxidized with relative ease.

Typical is the reaction of cyclohexylmercuric acetate with boron trifluoride in methanol. After 90 hours at 25° the system yields 90% of the mercury as the metal. After removal

TABLE I

Autooxidation of cyclohexylmercuric salts (0.10 mole) to cyclohexene (isolated by subsequent conversion to 2-methoxycyclohexylmercuric chloride) at 50° with catalysts (0.04 mole) in several media

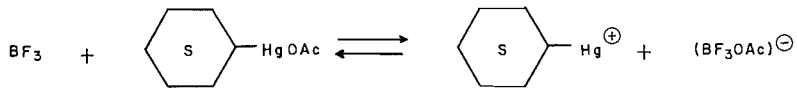
				Yields, %		
Salt	Catalyst	Time (hours)	Medium	C_6H_{10}	Hg^0	Recovered salt
OAc	None	24	Methanol	0	0	96
OAc	BF_3Et_2O	21	Methanol	88	90	0
OAc	Same	15	Benzene	73	87	0
OAc	Same	160	2,5-Dioxahexane	73	71	21
OAc	CF_3COOH	70	Methanol	72	92	0
CF_3COO	None	22	Same	79	90	0
Cl	HCl	168	Same	0	0	100
NO_3	None	24	Same	73	97	0

[1]*Manuscript received July 15, 1959.*
Contribution from the Department of Chemistry, University of Toronto, Toronto, Ontario.

of this metal, the presence of cyclohexene in 89% yield may be demonstrated by its conversion to α-2-methoxycyclohexylmercuric chloride when mercuric acetate is added.

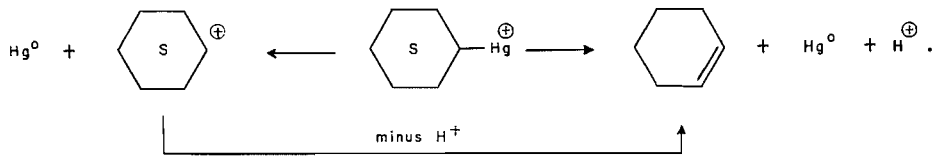
Although the autooxidation of the secondary alkylmercuric salt described above does not occur in absence of boron fluoride (expt. 1, Table I) it may be seen from this table that the Lewis acid must function only by increasing the polarity of the cyclohexylmercuric acetate. Thus the trifluoroacetate and the nitrate undergo the reaction without any boron fluoride. The reaction of the nitrate is especially notable because this salt reacts readily in the presence of an equivalent of mercuric nitrate in methanol by the homopolar path (2) to yield cyclohexyl nitrate and methoxycyclohexane. Contrariwise, the chloride does not undergo reaction, as might be expected in view of the stability of organomercuric chlorides.

The autooxidation reactions of Table I might be described in terms of an ionization



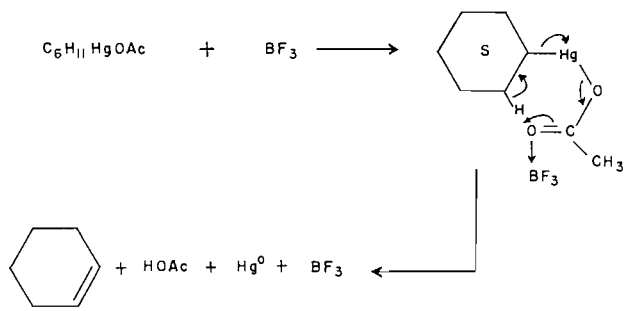
[i]

in which the cation is unstable and decomposes according to the following alternative modes



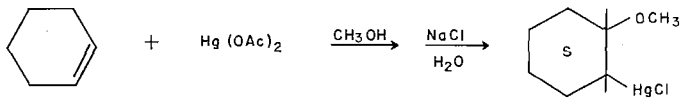
[ii]

However it is probably significant that neither phenylmercuric acetate nor *n*-butylmercuric acetate in methanol precipitate metallic mercury in presence of boron fluoride. It is possible that a stereomechanism such as is shown below is operative rather than reaction via free ions.



It might be expected, if mercuric acetate were added to the cyclohexylmercuric acetate system in methanol, that the homopolar reaction would occur to give methoxycyclohexane and mercurous acetate as the products. When 2 equivalents of mercuric acetate are included the organic product is α-2-methoxycyclohexylmercuric acetate, indicating that cyclohexene is the initial product. Thus initial excess of mercuric salt does not appreciably diminish the catalytic effect of boron fluoride.

Can. J. Chem. Downloaded from www.nrcresearchpress.com by 69.46.99.164 on 09/04/12
For personal use only.



To be sure, the other product is not elemental mercury but, rather, mercurous salt. However this is not surprising because the metal ought to react rapidly with mercuric acetate according to the known dismutation (3, 4).

$$Hg^0 + Hg(OAc)_2 \rightleftarrows Hg_2(OAc)_2 \xrightarrow{NaCl} Hg_2Cl_2$$

The maintenance of the heteropolar reaction under the conditions of the homopolar reaction may be explained in two ways. First, cyclohexylmercuric acetate, unlike the analogous nitrate salt, is not sufficiently reactive toward radicals. Secondly, the heteropolar reaction is not inhibited by oxygen. Therefore no induction period is involved such as is found in systems of mercuric acetate and unreactive organomercuric salts when the homopolar reaction occurs. This lack of an induction period is seen in Fig. 1 where the

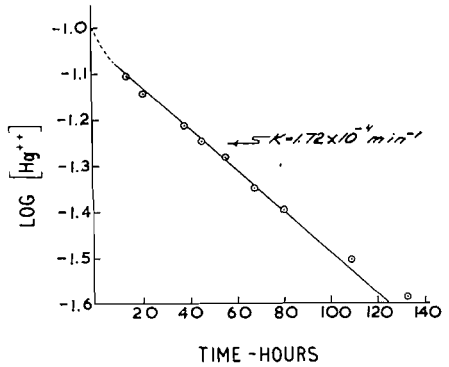


FIG. 1. System: mercuric acetate (0.10 m), cyclohexylmercuric acetate (0.05 m), and boron fluoride etherate (0.02 m) in methanol at 25° C.

actual concentration of mercuric acetate at a certain time is defined as the difference between twice the experimentally determined value and the initial value.

$$[Hg(OAc)_2]_t = 2[Hg^{++}\text{obs.}] - [Hg(OAc)_2]_0$$

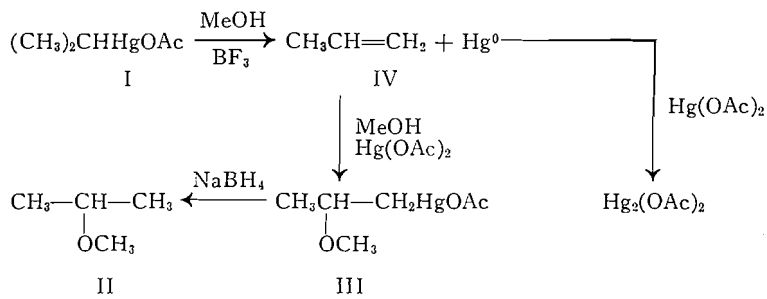
This calculation is valid because the oxymercurial formed *in situ* is decomposed prior to titration.

Inspection of Fig. 1 shows that the experimental data do not justify the first order slope that is drawn through part of the points. An attempt to fit the data to second order kinetics has been equally unsatisfactory. These discrepancies are not unexpected since the yield of α-2-methoxycyclohexylmercuric salt is only 75% while the yield of mercurous salt is 105%. Indeed it would be expected that upon the termination of its induction period the reaction of mercuric acetate plus boron fluoride in methanol (2) would commence to form mercurous salt and radicals. If a reactive organomercurial were present the homopolar reaction would then proceed concomitantly with the heteropolar reaction. This duality does not occur with the unreactive cyclohexylmercuric acetate but an example will be seen later in this report.

Can. J. Chem. Downloaded from www.nrcresearchpress.com by 69.46.99.164 on 09/04/12
For personal use only.

Of course it might be postulated that the oxidation of organomercuric salts proceeds by three rather than two mechanisms. It has been assumed that free alkene is formed and then oxymercurated when mercuric acetate is included in the organomercuric acetate – boron fluoride – methanol system. Alternatively, a third mechanism might be postulated in which oxidation occurred at the carbon adjacent to the acetatomercuri group. In this circumstance the formation of an oxymercurial would not be presumptive for initial formation of an alkene.

This alternative is not valid according to the reaction of 2-propylmercuric acetate (I) with boron fluoride and 2 equivalents of mercuric acetate in methanol. The product has been shown (by its reduction using sodium trimethoxyborohydride to 2-methoxypropane, II) to be 2-methoxy-1-propylmercuric salt (III) rather than 1-methoxy-2-propylmercuric salt, which would be the product of oxidation of 2-propylmercuric salt at the neighboring carbon atom. The over-all reaction may be formulated as follows.



Therefore it would seem that the recognizable product from this type of oxidation derives from the alkene such as IV rather than by a third mechanism involving α-oxidation of the alkylmercuric salt.

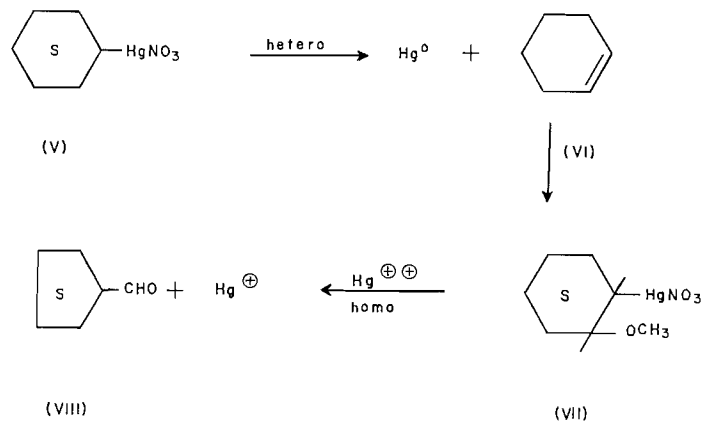
The actual experiment, which was not terminated until all of the 2 equivalents of mercuric acetate had been consumed, does not conform stoichiometrically with the formulation outlined above. The yield of mercurous salt is 130% of that expected by this formulation, while the yield of 2-methoxypropylmercuric chloride is only 32%. A similar discrepancy has been observed in the less-definitive oxidation of 3-pentylmercuric acetate. No definite kinetic order can be specified for these reactions. While no products other than the methoxymercurials are present in sufficient quantity for isolation it is significant that none of the original alkylmercuric salt is recoverable.

These deviations from stoichiometry may be attributed to the concomitant decomposition of mercuric acetate plus boron fluoride in methanol which establishes a radical chain if a susceptible organomercuric salt is present. While 2-propylmercuric acetate does not possess this susceptibility any more than does the cyclohexyl analogue it may be expected that the products of alkene oxymercuration (and especially the oxymercurials of pentene-2) will resemble 2-methoxy-2-methyl-1-phenylpropylmercuric acetate (2) more than they do the relatively stable α-2-methoxycyclohexylmercuric salt. The homopolar side reaction therefore consumes the oxymercurial derived from the alkene which is the initial product of the heteropolar reaction. It is evident that these homopolar side reactions may be minimized by deliberate oxygen inhibition.

A typical example of simultaneous reaction involving the two mechanisms has been reported in the previous publication (2) since it involves the opposite situation—where the homopolar reaction is the major one and the heteropolar reaction is minor. A small

Can. J. Chem. Downloaded from www.nrcresearchpress.com by 69.46.99.164 on 09/04/12
For personal use only.

amount of formylcyclopentane (VIII) has been observed (2), besides the main products, cyclohexanol and its nitrate ester, when cyclohexylmercuric nitrate (V) is homolytically oxidized by mercuric nitrate. Undoubtedly this trace of aldehyde (1) is formed by a separate homopolar oxidation of 2-methoxycyclohexylmercuric nitrate (VII) which is derived *in situ* from cyclohexene (VI). This alkene will be formed by the heteropolar oxidation of V such as is reported in Table I.



The simultaneous homopolar and heteropolar process on a single mercurial is shown also in the single instance of reaction with a tertiary alkylmercuric salt which we have been able to carry out. With this 1-methyl-1-cyclohexylmercuric salt no boron fluoride is required. Even the chloride survives only a few hours at 25° before it decomposes to metallic mercury and an oil. The acetatomercurial (IX) cannot be isolated but we have prepared it *in situ* by addition of silver acetate to a slurry of 1-methyl-1-chloromercuricyclohexane in a solution of mercuric acetate (2 equivalents) in methanol. It is evident from the rapidity of reaction that electron repulsion in the alkyl group precludes the necessity for electron attraction by a Lewis acid.

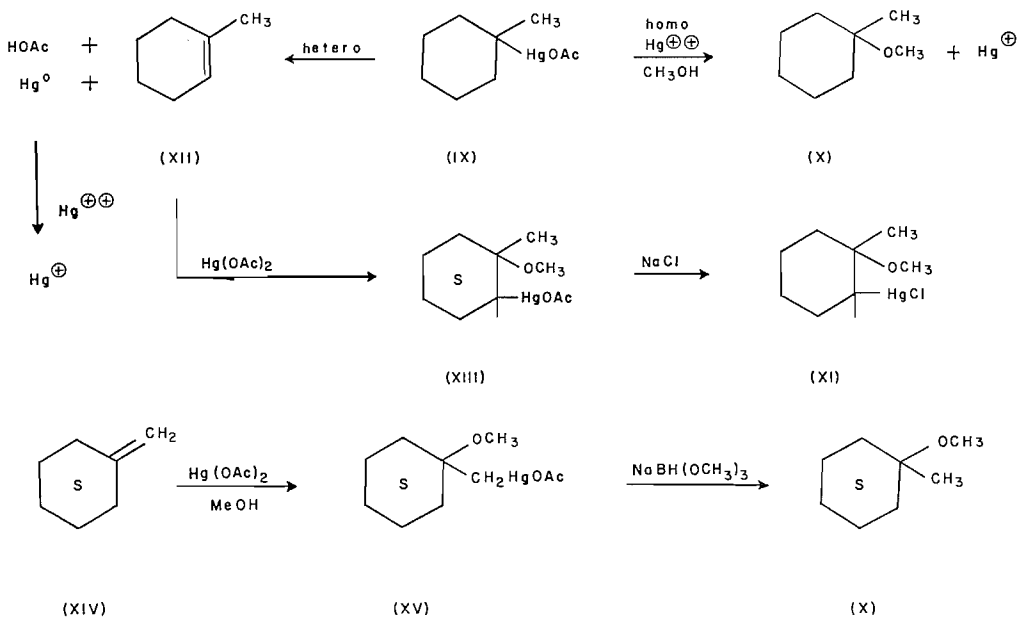
Three products have been isolated from a complex mixture. The isolated non-mercurial has been shown to be 1-methoxy-1-methylcyclohexane (X, estimated yield 25%) by comparison of its physical constants (5) and its R_f on a chromatoplate (6). This product is the expected one from the homolytic oxidation described in earlier reports (1, 2).

Not all of the substances containing mercury have been separated from the mixture of products, and the yields of substances which have been isolated are not significant because of the difficulties of separation. Several per cent of 2-methoxy-2-methylcyclohexylmercuric chloride (XI) has been isolated, which indicates that the heterolytic autooxidation also has been taking place via XII and XIII.

Another organomercuric salt was also isolated but it has not been identified. It is not 1-chloromercurimethyl-1-methoxycyclohexane (XV) because this substance has been synthesized for the purpose of comparison from methylenecyclohexane (XIV) (7) and its structure has been proved by reduction to 1-methoxy-1-methylcyclohexane.

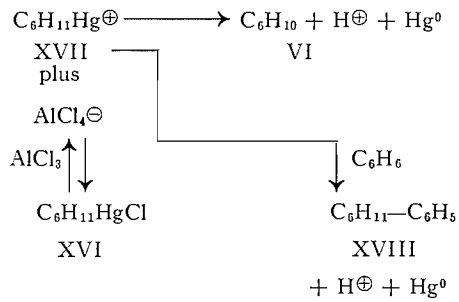
This non-identity should not be construed as evidence that XV is not present in the mixture of products obtained from 1-methylchloromercuricyclohexane. It does show that the oxidation is more complex than may be shown by the formulation which is outlined above. But of prime significance is the evidence that when the C—Hg linkage is sufficiently weak the electron-withdrawing action of a Lewis acid is not required. Moreover, the

Can. J. Chem. Downloaded from www.nrcresearchpress.com by 69.46.99.164 on 09/04/12
For personal use only.



reaction shows that the lability of the C—Hg bond is specifically neither homo- nor hetero-polar, but rather is responsive to the environment in which it exists.

Nevertheless, the effect of the electron-withdrawing agent is profound. Thus it may be seen in Table I that cyclohexylmercuric chloride (XVI) is stable in methanol in presence of hydrochloric acid; also it is stable in benzene – hydrogen chloride. However the addition of 0.4 equivalent of aluminum chloride induces reaction in benzene to a 75% yield of cyclohexylbenzene (XVIII).



The reaction may proceed via the cyclohexylmercuri cation (XVII), or else cyclohexene (VI) may be an intermediate. Certainly the same product is obtained by treatment of cyclohexene in benzene with aluminum chloride. On the other hand the product is not cyclohexene but, rather, a polymer when the reaction is carried out in cyclohexane rather than benzene. Neither cyclohexene nor bicyclohexyl is detectable. In further extensions of the reaction *sec*-butylmercuric chloride yields *sec*-butylbenzene, but *n*-butylmercuric chloride does not react.

Can. J. Chem. Downloaded from www.nrcresearchpress.com by 69.46.99.164 on 09/04/12
For personal use only.

Can. J. Chem. Downloaded from www.nrcresearchpress.com by 69.46.99.164 on 09/04/12
For personal use only.

DISCUSSION

Although the heteropolar autooxidation of organomercurials has not been reported previously there are numerous papers dealing with the oxidation of alkenes by mercuric salts. In our opinion all of these oxidations involve an oxymercurial as an intermediate. Only one of these, the reaction of safrole with mercuric acetate (8, 9), may be explained as a homopolar oxidation of the intermediate. The remainder (references 10–17 inclusive) may be explained on the basis of the products in terms of heteropolar autooxidation of an intermediate oxymercurial. To be sure a concomitant homopolar oxidation cannot be precluded in these oxidations. The yield of product typical of heteropolar autooxidation is not high, so the unidentified by-products may well be the result of homopolar oxidation. Indeed it is possible that the yield of the desired products might be augmented by sufficient oxygen concentration to inhibit the homopolar reaction. In this instance a single equivalent of mercuric acetate per mole of alkene ought to be sufficient, especially if boron fluoride were added as well.

The authors acknowledge financial aid from the National Research Council of Canada, which has been used to support this investigation.

EXPERIMENTAL*

Autooxidation of Cyclohexylmercuric Acetate

(*a*) *In Methanol*

A solution of cyclohexylmercuric acetate (0.005 mole) was prepared by filtration of silver chloride (quantitative) after a solution of cyclohexylmercuric chloride (0.005 mole, 1.60 g) in 50 ml of methanol was treated with 0.005 mole (0.84 g) of silver acetate. The filtrate was then treated with 0.002 mole (0.25 ml) of boron fluoride etherate and was maintained at 50° for 24 hours. Then the cooled system was filtered to remove metallic mercury (0.99 g, 99%) and the filtrate was treated with 1.60 g (0.005 mole) of mercuric acetate. After 30 minutes the system, chilled to 0°, was treated with 100 ml of water and 2.5 ml of 5 *M* aqueous sodium chloride. Filtration gave 88% (1.52 g) of α-2-methoxycyclohexylmercuric chloride, m.p. 112–113°, identified by mixture melting point. When the same experiment was carried out at 25° during 72 hours the yield of mercury was 90%, and 84% of the organomercurial was obtained. Expt. 5, Table I, shows an identical experiment except that trifluoroacetic acid was used instead of boron fluoride etherate.

(*b*) *In Methanol with 2 Equivalents of Mercuric Acetate*

This reaction was followed kinetically. A solution of 0.005 mole of cyclohexylmercuric acetate in 50 ml of methanol was prepared from 1.595 g (0.005 mole) of cyclohexylmercuric chloride and 0.834 g (0.005 mole) of silver acetate. After quantitative removal of silver chloride, 0.252 ml (0.002 mole) of boron trifluoride etherate and 3.188 g (0.01 mole) of mercuric acetate were added. The solution was made up to 100 ml with methanol and was maintained at 25°. Analyses were made by removal of mercurous salt and unchanged cyclohexylmercurial by dilute hydrochloric acid according to the method described previously (2). We used 3-ml aliquots and allowed the solution before filtration to stand 30 minutes to ensure complete decomposition of the 2-methoxycyclohexylmercuric salt. The filtrate was titrated for unchanged and regenerated mercuric salt. The results are shown in Fig. 1.

**Melting points have been corrected by reference to reliable standards. X-ray patterns are reported in Å at intensities $[I/I_1]$ using* Cu K_α *(Ni-filtered) radiation.*

A duplicate reaction system was maintained *in toto* for 37 hours at 50° and then was filtered to remove 5.48 g (105%) of mercurous acetate. The filtrate was diluted with 200 ml of water plus 10 ml of 5 *N* aqueous sodium chloride, and then was five times extracted with 25-ml portions of chloroform. Evaporation of the extracts left 2.62 g (75%) of α-2-methoxycyclohexylmercuric chloride, m.p. 113–114°, identified by mixture melting point. The absence of β diastereomer was shown by solution of 0.5 g in 8 ml of methanol to which 0.2 ml of concentrated hydrochloric acid was added. After the solution was swirled for exactly 1 minute 1 ml of 6 *M* aqueous sodium hydroxide and then 8 ml of water were added quickly. After filtration through Celite the filtrate was acidified by carbon dioxide and finally by acetic acid. There was no precipitation of β diastereomer.

(*c*) *In Benzene*

The solution of cyclohexylmercuric acetate (0.005 mole) in methanol was evaporated to dryness under reduced pressure and then was dissolved in 50 ml of benzene containing 0.002 mole (0.25 ml) of boron fluoride etherate. After 15 hours at 50° the system was cooled and filtered to remove 0.87 g (87%) of metallic mercury. The filtrate distilled totally, showing that no mercurial remained. The distillate was treated with 100 ml of methanol and 1.60 g (0.005 mole) of mercuric acetate. After 15 hours the system was evaporated under reduced pressure (20–25°) and the residue, dissolved in water–methanol, was treated with sodium chloride to yield 1.27 g (73%) of α-2-methoxycyclohexylmercuric chloride, m.p. 108–111°, identified by mixture melting point.

(*d*) *In 2,5-Dioxahexane*

In an otherwise identical system dioxahexane replaced benzene. After 160 hours at 50° the cooled system was filtered to remove 0.71 g (71%) of metallic mercury. Vacuum distillation at 20° left 15 ml which, treated with aqueous sodium chloride, yielded 0.34 g (21%) of cyclohexylmercuric chloride. The distillate, treated with 60 ml of methanol and 0.005 mole of mercuric acetate for 30 minutes, was again vacuum-evaporated. Treatment of the residue with aqueous sodium chloride yielded 1.01 g (73%) of α-2-methoxycyclohexylmercuric chloride, identified by mixture melting point.

Autooxidation of Cyclohexylmercuric Trifluoroacetate

The silver trifluoroacetate used in this experiment was prepared from silver oxide and trifluoroacetic acid (0.354 mole). After evaporation at 0.1 mm the residue was dissolved in benzene (75 ml), and 50 ml of hexane was added. The precipitate was evidently a complex with benzene since 25.2 g, finely ground, was reduced in weight to 22.2 g at 55° (0.1 mm). The X-ray diffraction pattern was: [10] 6.10, 3.60; [8] 2.33; [7] 2.58; [5] 3.00; [4] 2.70; [2] 3.31, 2.50; [1] 4.74, 3.95, 3.11. Calc. for $C_2F_3O_2Ag$: Ag, 48.84. Found: Ag, 48.55, 48.68.

The mercurial was prepared from 0.005 mole (1.60 g) of cyclohexylmercuric chloride and 0.005 mole (1.11 g) of silver trifluoroacetate in 50 ml of methanol; the silver chloride was filtered off. After 22 hours at 50° the system was processed as was described for the acetate – boron fluoride experiments to yield mercury (92%) and α-2-methoxycyclohexylmercuric chloride (70%).

Autooxidation of Cyclohexylmercuric Nitrate

A solution of 0.005 mole of cyclohexylmercuric chloride in 50 ml of methanol was treated with 0.005 mole (0.85 g) of silver nitrate and the silver chloride was filtered off. Subsequent processing, like the acetate, after 1 day at 50° yielded mercury (97%) and α-2-methoxycyclohexylmercuric chloride (73%).

Can. J. Chem. Downloaded from www.nrcresearchpress.com by 69.46.99.164 on 09/04/12
For personal use only.

Reaction of Organomercurials with Hydrogen Chloride

A 94% recovery of isopropylmercuric chloride was effected after 1-hour reflux with 4 ml concentrated hydrochloric acid in 15 ml of methanol; similarly with cyclohexylmercuric chloride. The same behavior was observed at 25° for 1 day with hydrogen-chloride-saturated methanol. In none of these instances was inorganic mercury detectable. On the other hand, 1 g (0.0031 mole) of benzylmercuric chloride in 15 ml of hydrogen-chloride-saturated methanol at 50° for 24 hours yielded only 0.39 g (39%) of unchanged chloromercurial (mixture melting point) upon dilution with water. The basified filtrate yielded 0.35 g (53%) of mercuric oxide.

Reaction of Phenylmercuric Acetate with Boron Fluoride

A solution of 0.005 mole of phenylmercuric acetate, 0.002 mole of boron fluoride etherate, and 50 ml of dry methanol was held at 50° for 24 hours but no metal precipitated. Subsequently 98% of the original mercurial was recovered as phenylmercuric chloride, m.p. 250–251°, mixture melting point not lowered.

Isopropylmercuric Chloride

This preparation is reported as typical for alkylmercuric halides since the procedure is simplified beyond others reported in the literature, while the yields are oftentimes better, especially for some unstable halogenomercurials.

The filtered Grignard reagent from 0.20 mole of isopropyl chloride in 120 ml of dry ether was stirred while 0.24 mole (64.8 g) of dried mercuric chloride was added in portions during 2 hours. The resulting suspension was stirred for 24 hours, more dry ether being added if necessary to ensure efficient stirring. Then 250 ml of water was added cautiously and the ether was removed while the system (below 10°) was stirred under reduced pressure. The final slurry was filtered, air-dried, and dissolved with trituration in 400 ml of chloroform at 25°. After a final brief temperature increase to 45° the solution was filtered and the filtrate was evaporated under reduced pressure leaving 47.6 g (86%) of isopropylmercuric chloride, m.p. 94.5–95.5°, not raised by recrystallization from commercial hexane or 85% aqueous methanol. Calc. for C_3H_7HgCl: C, 12.9; H ,2.53. Found: C, 13.0; H, 2.71. This product in methanol could be converted to the nitrate salt by means of silver nitrate and thence by treatment with sodium bromide to isopropylmercuric bromide, m.p. 90.5–91.5°. A mixture melting point with the chloromercurial was depressed to 77–82°.

Cyclohexylbenzene

A solution of 1.59 g (0.005 mole) of cyclohexylmercuric chloride, 0.27 g (0.002 mole) of aluminum chloride, and 50 ml of benzene was stirred for 6 hours and then was decanted from 0.77 g (77%) of metallic mercury. The solution was then washed with water until it was neutral, during which time 0.22 g (19%) of mercurous chloride separated. The non-aqueous layer was distilled up to 80° to prove that the distillate contained no cyclohexene (test with mercuric acetate and methanol) and then was distilled further, b.p. 108–110° at 12 mm, 0.66 g (75%), m.p. 4.5–6.5°. This product was identified by mixture melting point with an authentic sample prepared from cyclohexene, hydrogen chloride, aluminum chloride, and benzene (18).

When this experiment was carried out in cyclohexane rather than benzene, 92% of the mercury was precipitated as metal, but only a gummy mass with no cyclohexene or bicyclohexyl was obtained as the organic product.

Can. J. Chem. Downloaded from www.nrcresearchpress.com by 69.46.99.164 on 09/04/12
For personal use only.

sec-Butylbenzene

A slurry of 8.00 g (0.027 mole) of *sec*-butylmercuric chloride (19), 1.49 g (0.0112 mole) of aluminum chloride, and 100 ml of dry benzene was stirred for 15 hours and then decanted onto ice. The metallic mercury was separated (3.66 g, 67%). The benzene phase, washed with dilute alkali and then water, was dried (magnesium sulphate) and distilled, b.p. 170–173° (750 mm), 2.74 g (75%), n_D^{20} 1.4908 (20). When *n*-butylmercuric chloride was used instead of the secondary isomer it was recovered quantitatively.

2-Methoxypropylmercuric Chloride

(*a*) *From Isopropylmercuric Acetate*

A quantity of 2.79 g (0.01 mole) of isopropylmercuric chloride in 50 ml of methanol was converted to the acetate by means of silver acetate (0.01 mole). After filtration of the silver chloride, 6.38 g (0.02 mole) of mercuric acetate and 0.50 ml (0.004 mole) of boron fluoride etherate were added together with methanol to a total volume of 100 ml. After 37 hours at 50°, 6.26 g of mercurous acetate was filtered off and the chilled filtrate was diluted with 120 ml of water to which 10 ml of 5 *M* aqueous sodium chloride was then added. The resulting suspension was 5 times extracted with chloroform (125 ml total), and the aqueous phase was then filtered to remove 0.52 g of mercurous chloride (total Hg_2^{++}, 0.0132 mole or 132%). Vacuum evaporation of the chloroform left 1.00 g (32%) of yellow oil, m.p. −15° to −12.5°. Three crystallizations from methanol (2.5 ml per g) raised the melting point (−9 to −7.5°), and a mixture melting point with the authentic specimen described below was not lowered.

(*b*) *From Propene*

Propene gas was bubbled into a stirred suspension of 15.9 g (0.05 mole) of mercuric acetate in 75 ml of methanol at 0° at such a rate that a slight positive pressure was maintained in the closed system. When the pressure rose sharply and the test for mercuric ion was negative, the system was poured into 150 ml of cold water and 15 ml of 5 *M* aqueous sodium chloride was added. The oil was taken up by four extractions with a total of 120 ml of chloroform. The extract was dried (calcium chloride) and vacuum-evaporated, 15.24 g (99%), m.p. −7 to −4°. Three crystallizations from methanol (3 cc per g) left 10.4 g, m.p. −5.5 to −4.5°. After several days at −10° this substance started to decompose, yielding calomel. The organomercurial was analyzed by a micro method (21). Calc. for C_4H_9ClHgO: Hg, 64.9; Cl, 11.47. Found: Hg, 64.8; Cl, 11.63.

2-Methoxypropane

(*a*) *From 2-Methoxypropylmercuric Chloride*

A solution of 7.15 g (0.025 mole) of 2-methoxypropylmercuric chloride in 35 ml of water plus 5 ml of 6 *M* aqueous sodium hydroxide was chilled to 0° while 6.39 g (0.05 mole) of sodium trimethoxyborohydride was added during 1 hour. The system was then warmed to 60° to distil the ether into an ice-cold receiver. Redistillation gave 1.20 g (65%) of 2-methoxypropane, b.p. 32–33°, d_4^{25} 0.720, n_D^{20} 1.3532.

(*b*) *From 2-Propanol*

Sodium (0.16 g-atom, 3.68 g) was dissolved in 125 ml of dry 2-propanol. Then 17 g (0.12 mole) of methyl iodide was added and the solution was refluxed for 1 hour. Distillation gave 6.7 g (75%), b.p. 32–33°, d_4^{25} 0.719, n_D^{20} 1.3532. A similar preparation of 1-methoxypropane gave constants as follows: b.p. 38°, d_4^{25} 0.727, n_D^{20} 1.3584.

Can. J. Chem. Downloaded from www.nrcresearchpress.com by 69.46.99.164 on 09/04/12
For personal use only.

3-Chloromercuripentane

This substance was prepared from 3-chloropentane (22) by the general method for alkyl chloromercurials outlined above, 79% crude yield, m.p. 18–20°. Crystallization from commercial hexane (3 ml per g) raised the melting point to 21.3–21.7°. The substance was unstable and formed calomel slowly at 25°. Mercury analysis was effected by Walton's method (23). Calc. for $C_5H_{11}ClHg$: C, 19.5; H, 3.62; Hg, 65.3. Found C, 18.9; H, 3.61; Hg, 65.1.

Mixture of Vicinal Methoxypentylmercuric Chlorides

(*a*) *From 2-Pentene*

A solution of 2-pentene (b.p. 36–36.5°, n_D^{20} 1.3816) (24) and 4.47 g (0.014 mole) of mercuric acetate in 12 ml of dry methanol gave a negative test for mercuric ion within 15 minutes. The solution was poured into 24 ml of water containing 4 ml of 6 *M* aqueous alkali and the whole was filtered through Celite for clarification. To the chilled filtrate was added 3 ml of 5 *M* aqueous sodium chloride and then gaseous carbon dioxide was added until precipitation of oil was complete. The oil was collected in chloroform and the extract was evaporated leaving 3.36 g (71%) of non-crystallizable oil. The infrared spectrum (2–15 μ) showed the following absorption bands (cm^{-1}): 2950(s), 1465(m), 1382(m), 1326(m), 1196(m), 1185(m), 1152(m), 1080(s), 1028(w), 992(w), 921(w), 886(w), 832(w), 802(w), 758(w).

(*b*) *By Autooxidation of 3-Acetatomercuripentane*

A solution of 3-chloromercuripentane (3.07 g, 0.01 mole) in 30 ml of dry methanol was converted to the acetatomercurial by treatment with an equivalent of silver acetate. After removal of silver chloride (100%), 6.38 g (0.02 mole) of mercuric acetate and 0.50 ml of boron fluoride etherate were added. The system was made up to 100 ml with methanol and maintained for 44 hours at 50°. Then 5.81 g of mercurous acetate was filtered off, and the chilled filtrate was diluted with 120 ml of cold water followed by 10 ml of 5 *M* aqueous sodium chloride. Five extractions with chloroform removed the oxymercurials leaving 0.13 g of calomel filterable from the aqueous phase (total Hg_2X_2 0.012 mole, 120%).

The crude oxychloromercurial was purified by solution in aqueous alkali followed by treatment of the filtered solution with gaseous carbon dioxide. The product, recovered by chloroform extraction, gave an infrared spectrum superimposable upon that obtained by the product of procedure (*a*).

1-Methylcyclohexylmercuric Chloride

Fractionally distilled 1-methyl-1-chlorocyclohexane (25) (b.p. 77.5–78.0° at 73 mm, n_D^{20} 1.5484), 0.5 g in 5 ml of dry ethyl ether was stirred with 0.73 g (0.03 g-atom) of magnesium. This metal (stored under dry ether until it was used) had previously been activated by treatment with bromobenzene from which it was subsequently freed by thorough washing by dry ether.

After the reaction had commenced (cloudiness) a solution of 3.2 g of the chloride (total 0.027 mole) in 30 ml of dry diethyl ether was added during 8 hours. After 12 hours of further stirring 7.60 g (0.028 mole) of mercuric chloride was added rapidly. The suspension was stirred for another 7 hours, then was diluted with 70 ml of chloroform and the whole was filtered. Vacuum evaporation of the filtrate left a crystalline mass which was dissolved at 25° in 25 ml of acetone. This solution at −80° precipitated 0.92 g of white needles. A second similar crystallization from acetone gave 0.79 g (9.4%) of 1-methyl-

Can. J. Chem. Downloaded from www.nrcresearchpress.com by 69.46.99.164 on 09/04/12
For personal use only.

cyclohexylmercuric chloride, no definite melting point. The X-ray diffraction pattern was [10] 9.50; [6] 4.02; [5] 3.70; [4] 4.60, 3.49; [3] 4.89, 3.29, 2.85; [2] 4.44, 4.29. Calc. for $C_7H_{13}ClHg$: C, 25.2; H, 3.93; Hg, 60.2. Found: C, 25.3; H, 3.70; Hg, 60.2, where the analysis for mercury was that of Whitmore and Sobatzki (26). The substance decomposed quickly at 25° but was stable for a few days at −70°.

1-Methylcyclohexylmercuric Acetate with Mercuric Acetate in Methanol

A slurry was prepared by dissolving 5.83 g (0.0183 mole) of mercuric acetate in 45 ml of dry methanol, then adding 1.55 g (0.0093 mole) of silver acetate and finally 3.09 g (0.0093 mole) of 1-methyl-1-chloromercuricyclohexane. The system was stirred 4 hours and then a gray solid was filtered off. This solid was shaken with 40 ml of 13% aqua ammonia to dissolve the silver chloride and leave 3.70 g (0.0178 mole) of mercurous oxide.

The methanolic filtrate at 0° was diluted with 100 ml of water, and 3 ml of 5 *M* aqueous sodium chloride was added. This diluate was extracted seven times with a total of 175 ml of ether. The extract was washed four times with a total of 120 ml of 1 *M* aqueous sodium hydroxide and then with water until the non-aqueous phase was neutral.

The combined alkaline and aqueous washing was filtered to remove 0.83 g (0.0038 mole) of mercuric oxide. The filtrate was acidified with carbon dioxide and then four times extracted with a total of 100 ml of chloroform. Vacuum evaporation of this extract left 1.52 g, m.p. 70–120°. Extraction with 3 ml of commercial hexane left an insoluble fraction which was crystallized from 3:7 water–methanol (8 ml per g), 0.57 g, m.p. 122–124°. This unidentified mercurial is base-soluble and easily demercurated by the action of methanolic hydrogen chloride. It is not 2-methoxy-2-methylcyclohexylmercuric chloride, described below.

The hexane-soluble part of the crude product extraction was evaporated and the residue was crystallized repeatedly from commercial hexane (20 ml per g), 0.06 g (3%), m.p. 79–80°, which was identified by mixture melting point with an authentic specimen (27).

The ether phase from which the alkaline phase containing the mercurials was separated was dried with magnesium sulphate and then distilled, 0.29 g, b.p. 130–140°. Redistillation gave 0.11 g (25% crude, 9% redistilled) of 1-methoxy-1-methylcyclohexane, b.p. 140–150°, n_D^{20} 1.4422. The identity with an authentic sample (b.p. 147–149°, n_D^{20} 1.4427) prepared according to Triebs' procedure (5) was established by a chromatoplate analysis in which silicic acid was the adsorbent and benzene was the eluant. The chromatogram was developed by use of a nitric – sulphuric acid spray.

1-Chloromercurimethyl-1-methoxycyclohexane

Hexahydrobenzyl acetate was pyrolyzed to methylenecyclohexane by Arnold's method (7). This alkene (0.96 g, 0.01 mole) and 3.19 g (0.01 mole) of mercuric acetate were shaken for 1 hour in 12 ml of dry methanol, then the system was chilled, diluted by 35 ml of cold water, and 3.0 cc of 5 *M* aqueous sodium chloride was added. The 3.33-g (91% crude) yield, m.p. 59–64°, was thrice crystallized from commercial hexane (8 ml per g), m.p. 68.3–69.0°. Calc. for $C_8H_{15}ClHgO$: C, 26.5; H, 4.16. Found: C, 26.6; H, 4.30.

A solution of 6.9 g (0.019 mole) of this mercurial in 4 ml of 6 *M* aqueous sodium hydroxide plus 35 ml of water was stirred at 0° while 4.85 g (0.038 mole) of sodium trimethoxyborohydride was added during 30 minutes. The ether extract of this system was then dried with magnesium sulphate and distilled, 1.73 g (71%), b.p. 145–148°, n_D^{20} 1.4414. This 1-methoxy-1-methylcyclohexane was identified by chromatoplate and also by comparison with the sample prepared by Triebs' method (5) according to the following

Can. J. Chem. Downloaded from www.nrcresearchpress.com by 69.46.99.164 on 09/04/12
For personal use only.

infrared spectra: 3120, 2700, 1425, 1334, 1308, 1265, 1245, 1180–1020, 953, 918, 875, 845, 810, 697 cm^{-1}.

REFERENCES

1. SHEARER, D. A. and WRIGHT, G. F. Can. J. Chem. **33**, 1002 (1955).
2. ROBSON, J. H. and WRIGHT, G. F. Can. J. Chem. **38**, 1 (1960).
3. SCHWARZENBACH, G. and ANDEREGG, G. Helv. Chim. Acta, **37**, 1289 (1954).
4. MOSER, H. G. and VOIGT, A. F. J. Am. Chem. Soc. **79**, 1837 (1957).
5. TRIEBS, W. Ber. B, **70**, 589 (1937).
6. ALLENTOFF, N. and WRIGHT, G. F. Can J. Chem. **35**, 900 (1957).
7. ARNOLD, R. T. and DOWDALL, J. F. J. Am. Chem. Soc. **70**, 2590 (1948).
8. BALBIANO, L. and PAOLINI, V. Ber. **35**, 2994 (1902).
9. BALBIANO, L. and PAOLINI, V. Ber. **36**, 3775 (1903).
10. TRIEBS, W. and BAST, H. Ann. **561**, 165 (1949).
11. KARRER, P. Helv. Chim. Acta, **34**, 1400 (1950).
12. JEFFRIES, P., MACBETH, A., and MILLIGAN, B. J. Chem. Soc. 705 (1954).
13. WINDAUS, A. and LINSERT, O. Ann. **465**, 157 (1928).
14. WINDAUS, A. Ann. **552**, 135, 142 (1942).
15. BARTON, D. J. Chem. Soc. 516 (1946).
16. BARTON, D. and ROSENFELDER, W. J. Chem. Soc. 2381 (1951).
17. RUYLE, W. *et al.* J. Am. Chem. Soc. **75**, 2604 (1953).
18. KURSSANOW, N. Ann. **318**, 309 (1901).
19. MARVEL, C. S. and CALVERY, H. O. J. Am. Chem. Soc. **45**, 820 (1923).
20. KLAGES, A. Ber. **35**, 3506 (1902).
21. STONESTREET, G. and WRIGHT, G. F. Can. J. Research, B, **18**, 246 (1940).
22. WHITMORE, F. C. and KARNATZ, F. A. J. Am. Chem. Soc. **60**, 2536 (1938).
23. WALTON, H. F. and SMITH, H. A. Anal. Chem. **28**, 406 (1956).
24. ORG. SYNTHESES. John Wiley & Sons, Inc., New York. Coll. Vol. I. p. 430. 1932.
25. GUTT, J. Ber. **40**, 2061 (1907).
26. WHITMORE, F. C. and SOBATZKI, R. J. J. Am. Chem. Soc. **55**, 1128 (1933).
27. PARK, W. R. R. and WRIGHT, G. F. Can. J. Chem. **35**, 1088 (1957).

Can. J. Chem. Downloaded from www.nrcresearchpress.com by 69.46.99.164 on 09/04/12
For personal use only.

Can. J. Chem. Downloaded from www.nrcresearchpress.com by 69.46.99.164 on 09/04/12
For personal use only.

HYDROGEN BONDING IN THE AMINE HYDROHALIDES

II. THE INFRARED SPECTRUM FROM 4000 TO 2200 CM^{-1} [1]

C. BRISSETTE AND C. SANDORFY

ABSTRACT

The infrared spectra of a number of amine hydrohalides have been measured in the lithium fluoride region.

Hydrogen bonding and the torsional oscillations of the $\overset{+}{N}H_3$ groups influence these spectra characteristically. The $\overset{+}{N}$—H - - - X^- stretching frequencies give broad or fairly broad bands. They are near 3000 cm^{-1} for aliphatic primary amine salts. The corresponding band lies at somewhat lower frequencies for secondary amine salts and much lower for tertiary ones. The aromatic amine hydrohalides exhibit these bands at lower frequencies than do the aliphatic amine salts of the same order. There is a shift to higher frequencies in the series hydrochloride, hydrobromide, hydriodide.

All these spectra contain a number of sharper bands which may or may not coincide with the hydrogen-bonded stretching bands. These are combination bands involving mainly deformation vibrations, and they shift to lower frequencies, throughout the series hydrochloride, hydrobromide, hydriodide.

The importance of electrical anharmonicity for the appearance of these bands is stressed. The hydrogen bonds in amine hydrohalides appear to be largely electrostatic in character.

INTRODUCTION

The infrared spectra of ammonium halides were investigated by Wagner and Hornig (1, 2) and by Plumb and Hornig (3, 4). A primary aliphatic amine hydrohalide, methylamine hydrochoride, was treated by Waldron (5). Tertiary amine hydrohalides were discussed by Lord and Merrifield (6). More recently Chenon and Sandorfy (7) discussed some general aspects of the infrared spectra of amine hydrohalides measuring the spectra of a number of aliphatic and aromatic primary, secondary, and tertiary amine hydrochlorides, hydrobromides, and hydriodides. (This paper will be referred to henceforth as I.)

This series of compounds offers particular advantages for the study of hydrogen bonding. By studying the different hydrohalides of the same amine we can introduce a gradual change in hydrogen bond energy and by considering the amines of different order we can vary from one to three the number of hydrogen atoms which may be affected by hydrogen bonding. The effect of the more distant molecular environment may be studied by taking various aromatic and aliphatic amines. The effect of the net charges on the end atoms may also be examined.

In paper I, a general review of the subject was given. At present we intend to consider the high frequency part of the infrared spectrum (4000 to 2200 cm^{-1}) in more detail. This will lead us to a closer look at the nature of hydrogen bonding in these cases.

EXPERIMENTAL

A Perkin–Elmer model 112 single beam – double pass instrument was used with a lithium fluoride prism.

The whole instrument was put under a dry nitrogen atmosphere in order to eliminate atmospheric water and CO_2 absorption. All the spectra were taken in both nujol and fluorocarbon oil mulls. No significant differences were observed between the spectra taken in these two media.

[1]*Manuscript received August 20, 1959.*
Contribution from Département de Chimie, Université de Montréal, Montréal, Québec.

Can. J. Chem. Downloaded from www.nrcresearchpress.com by 69.46.99.164 on 09/04/12
For personal use only.

RESULTS

The spectra of the three hydrohalides of the following amines were measured.

(*a*) Aliphatic primary amines: ethylamine, *n*-butylamine, *sec*-butylamine, isobutylamine, *tert*-butylamine, cyclohexylamine.

(*b*) Aliphatic secondary amines: diethylamine, di-*n*-butylamine, piperidine.

(*c*) Aliphatic tertiary amines: triethylamine, tri-*n*-butylamine.

(*d*) Aromatic primary amines: aniline, α-naphthylamine, β-naphthylamine.

(*e*) Aromatic secondary amines: diphenylamine, N-methylaniline.

(*f*) Aromatic tertiary amines: pyridine, N,N-dimethylaniline, N-methyl diphenylamine.

Tables I and II give one typical example for each of classes (*a*) to (*f*). The data concerning the bands located between 2200 and 1900 cm^{-1} are taken from paper I (sodium chloride prism).

INTERPRETATION OF THE SPECTRA

(*A*) *Aliphatic Primary Amine Salts*

It was not possible under the low resolution of the sodium chloride prism and with a number of CH_3 and CH_2 groups present in the molecules to disentangle the coincident CH_3, CH_2, and $\overset{+}{N}H_3$ or $\overset{+}{N}H_2$ absorption near 3000 cm^{-1}. This remains difficult using the lithium fluoride prism. It is quite clear, however, that in the case of aliphatic primary and secondary amine salts there is a strong and fairly broad band system in partial coincidence with CH_3 and CH_2 bands. This band system must contain the two $\overset{+}{N}H_2$ or $\overset{+}{N}H_3$ stretching bands or, in the case of the latter, the three stretching bands if the symmetry is lower than C_{3v}.

The spectra of the aliphatic primary amine salts, shown in Table I, bear a great resemblance to those of the ammonium halides (1, 2, 3, 4) and seem to be quite analogous to the spectrum of methylamine hydrochloride discussed by Waldron (5), who measured this spectrum at 300° K, 90° K, and 230° K. At each of these temperatures the compound exists in a different phase designated α, β, and γ in this order. In the α-phase he found the two $\overset{+}{N}H_3$ and the two CH_3 stretching frequencies near 3000 cm^{-1} giving a broad feature in the spectrum and only two or three bands down to 2000 cm^{-1}. The band near 2000 cm^{-1} which we found in all the primary aliphatic amine hydrohalides is significantly absent from the spectrum in the α-phase.

Waldron was able to assign practically all the bands using the analogy with ethane. Under C_{3v} symmetry the antisymmetrical $\overset{+}{N}H_3$ and CH_3 stretching and bending vibrations and the $\overset{+}{N}H_3$ and CH_3 rocking vibrations are doubly degenerate and the torsional oscillation is forbidden, though it might appear in combinations. Actually in the α-phase no splitting of the degenerate bands occurs and the torsional oscillation is absent, indicating threefold symmetry. In the β-phase the torsional oscillation was found by Waldron at 487 cm^{-1}, a strong band appears at 2075 cm^{-1} and a series of sharp bands appear between 2800 and 2400 cm^{-1}. In the γ-phase the situation was similar but the torsional oscillation band was not actually found. The main point is that the low temperature phases have no threefold axis and therefore the degenerate bands split.

Now, it is very interesting that all our primary amine hydrohalide spectra closely resemble Waldron's low temperature spectra although they have all been measured at room temperature. The natural explanation is that because of the bulky groups linked to the nitrogen atom none of our compounds possesses C_{3v} symmetry nor a threefold axis.

Can. J. Chem. Downloaded from www.nrcresearchpress.com by 69.46.99.164 on 09/04/12
For personal use only.

TABLE I

(*a*) Cyclohexylamine				(*b*) Di-*n*-butylamine				(*c*) Triethylamine			
Free amine, liquid	Hydrochloride	Hydrobromide	Hydriodide	Free amine, liquid	Hydrochloride	Hydrobromide	Hydriodide	Free amine, liquid	Hydrochloride	Hydrobromide	Hydriodide
3355 m	3211 vw	3202 vw	3178 w		3173 sh	3138 sh	3146 sh			3169 vw	
3277 m	3106 vw	3093 vw	3070 w		2986 sh, broad	2988 sh, broad	3027 sh, broad			3049 vw	
3178 w	2975 sh } broad	2980sh, broad	2987 vs, broad	2950 s	2950 s	2950 s	2950 vs		2989 sh	2992 m	2988 sh
3088 vw	2948 sh }	2952 sh	2963 s	2915 s	2923 s	2923 s	2915 vs	2960 vs	2967 s	2963 s	2961 s
2915 vs, broad	2920 vs }	2920 s	2925 sh	2865 s	2860 s	2860 s	2865 vs	2929 vs	2945 s	2926 vs	2926 s
2846 s	2900 }	2897 s	2899 s, broad	2853 s	2792 sh	2789 s	2789 s	2890 s	2874 s	2868 vs	2878 s
2740 vw	2850 s	2850 s	2848 s	2800 s	2780 m			2868 s			2815 vw
2714 vw	2828 m	2821 m	2804 m		2754 m	2744 sh	2735 sh	2805 }	2803 m	2796 s	2787 m
2696 vw	2775 m	2765 m	2752 m		2730 m	2730 sh	2698 sh	2794 } vs	2761 m	2746 s	2745 s
2660 w	2722 m	2714 m	2698 m		2705 sh	2699 sh	2682 sh	2786 }	2731 m	2731 s	2730 s } *
2589 vw	2668 m	2660 m	2642 m		2655 sh	2651 sh		2751 sh	2660 sh }	2668 vs } broad	2667 s } broad
	2611 m	2599 m	2576 m		2626 sh	2620 sh	2620 sh	2716 s	2633 sh }	2647 sh* }	2643 sh }
	2564 m	2555 m	2537 m		2562 sh	2555 sh	2547 w	2706 sh	2613 s } *		
			2505 vw		2548 m	2537 m	2518 m	2662 m	2594 s, broad }	2590 w	2575 vw
	2507 m	2498 m	2474 m		2531 sh	2516 sh	2492 m	2638 m	2561 m }	2562 vw	2557 vw
			2454 w		2448 s	2431 s	2413 s	2566 w			
	2050 m	2030 m	1957 m		2385 m	2370 m	2359 m		2520 m	2519 vw	2516 vw
	1965 w	1950 w							2486 s	2482 s	2468 m
										2425 w	2420 w
									2270 vw	2267 vw	2252 vw
									2248 vw	2131 vw	2126 vw

Can. J. Chem. Downloaded from www.nrcresearchpress.com by 69.46.99.164 on 09/04/12
For personal use only.

TABLE II

(*a*) Aniline				(*b*) Diphenylamine				(*c*) Pyridine			
Free amine, liquid	Hydrochloride	Hydrobromide	Hydriodide	Free amine, solid	Hydrochloride	Hydrobromide	Hydriodide	Free amine, liquid	Hydrochloride	Hydrobromide	Hydriodide
3433 vs				3400 vs	3104 vw	3082 w	3095 vw				3228 sh, m
				3377 vs	3071 vw	3063 vw					
3350 vs	3168 sh			3175 m	3052 vw	3044 vw	3036 vw	3067 w	3208 w	3200 w	3200 m
				3096 s	3038 w	3030 w					
3214 vs	3149 w			3046 vs	3015 w	3011 w	3013 vw	3046 w	3160 sh	3135 sh	3137 w
				3028 vs	2895 m	2880 m	2865 w				
3100 sh	3093 m						2843 w	3015 w	3124 w	3119 sh	3114 sh, w
				2747 m	2842 m	2832 m	2820 w				
3088 m	3036 m	3000 sh	2990 sh	2720 m			2799 w	2992 w	3092 vw	3085 sh	3075 w
				2651 m	2795 m	2775 m	2770 w				
3063 s	2810 s, broad*	2830 s, broad*	2870 s, broad*	2532 m	2749 sh	2738 sh		2901 w		3061 sh	
				2476 w	2743 m	2723 m	2724 sh				
3025 vs	2631 sh	2600 sh, w		2390 w	2722 w	2713 sh	2717 m	2846 w	3043 m	3030 sh	3040 m
					2698 m	2686 m					
2999 s	2583 m	2572 m	2555 m				2663 sh		3010 m		
					2673 m	2662 m	2658 m*				
2949 w	2558 m	2546 m	2529 m		2648 m	2638 m			2920 m	2908 w	2925 m, broad*
					2607 sh	2605 sh	2592 m				
2921 w	2418 w				2589 s	2575 s	2576 m				2870 sh
					2572 s	2550 s					
2900 w	2280 w						2510 w		2846 m	2842 w	2850 m, broad*
						2498 m	2498 w				
2765 w	2263 m				2474 sh	2464 sh	2452 m*		2713 w	2708 w	2718 w

Can. J. Chem. Downloaded from www.nrcresearchpress.com by 69.46.99.164 on 09/04/12
For personal use only.

TABLE II (*concluded*)

(*a*) Aniline				(*b*) Diphenylamine				(*c*) Pyridine			
Free amine, liquid	Hydrochloride	Hydrobromide	Hydriodide	Free amine, solid	Hydrochloride	Hydrobromide	Hydriodide	Free amine, liquid	Hydrochloride	Hydrobromide	Hydriodide
					2455 vs	2447 m	2440 m				
							2417 m			2655 sh	2685 sh
							2401 sh				
2727 w	2201 w										
					2405 sh	2385 sh				2605 s, broad*	2560 w
2652 w	2163 w					2354 sh					
					2344 sh, vs	2331 s			2589 sh	2582 sh	2553 w
2620 w	2055 m				2331 vs	2320 s*					
					2322 vs				2519 sh		2498 vw
	2015 m				2280 vs*	2279 s	2283 vs				
					2245 sh						2460 vw
	1990 m				2218 sh						
					2174 m	2167 w			2422 s, broad*	2417 w	2402 w
					2156 m	2146 w					
					2082 w	2071 w			2240 w	2233 w	2226 w
					2045 m	2030 m	1990 m				
					1985 m	1945 m	1935 m		2159 vw		2152 vw
											2099 vw
									2091 m		2071 vw
									2005 m		

vs = very strong. s = strong. m = medium. w = weak. vw = very weak. * = "centre of gravity".

The band near 2075 cm^{-1} was assigned by Waldron to a combination band between the torsional oscillation (487 cm^{-1}) and the antisymmetrical bending vibration of the $\overset{+}{N}H_3$ group (1580 cm^{-1}); the sharp bands between 2800 and 2400 cm^{-1} were assigned to combinations between various $\overset{+}{N}H_3$ and other deformation bands. This can now be generalized to all the aliphatic primary amine hydrohalides whose spectra are reported here.

The sharp bands between 2800 and 2400 cm^{-1} generally accompany the strong combination band near 2000 cm^{-1}. The splitting of the former and the high intensity of the latter both appear to be connected with the lowering of symmetry, although the combination tone near 2000 cm^{-1} is allowed under C_{3v} symmetry. The lowering of the intensity of the bending bands in the 1600–1500 cm^{-1} area found by Waldron seems to be a related phenomenon.

The characteristic shift toward lower frequencies of the bands between 2800 and 2400 cm^{-1} in the order Cl→Br→I is definitely confirmed by our new measurements and is explained making use of the above assignments. This shift is in the $\overset{+}{N}H_3$ *deformation* bands. The $\overset{+}{N}H_3$ stretching bands should then shift in the opposite direction giving the strongest hydrogen bond with the chloride ion and the weakest with the iodide ion. Unfortunately it is quite impossible to establish this prediction because of the considerable amount of band overlap which takes place in the 3000 cm^{-1} region. The cyclohexylamine salts give relatively the best chance of resolving the $\overset{+}{N}H_3$ stretching bands since there we have only CH_2 groups, and no CH_3 groups. In fact the cyclohexylamine hydriodide has the $\overset{+}{N}H_3$ bands well separated from the CH_2 bands while the hydrobromide and hydrochloride give only strong shoulders. A consideration of the spectra of the N-deuterated and perfluoro-alkyl analogs could solve this problem and work is going on in this laboratory in this direction.

The above interpretation is, however, in line with our findings on amine salts of other classes and therefore seems very probably correct (see below).

The band near 2000 cm^{-1} shifts in the same direction but more rapidly in the hydrohalide series Cl→Br→I than do the upper sharp bands. This must be due to the fact that its two components shift individually in the same direction.

There are two or three weak bands above the $\overset{+}{N}H_3$ stretching bands up to about 3200 cm^{-1}. These can be readily assigned to the first overtones of the bending vibrations located in the 1600–1500 cm^{-1} area or to a combination of them.

The interpretation of the sharp bands between 2800 and 2400 cm^{-1} as combination tones involving deformation modes (which differs from the assignment suggested in paper I) appears to be the key to the understanding of these spectra. Indeed, their characteristic shifting with different hydrohalides provides us with a method of distinguishing between $\overset{+}{N}$—H--X^- stretching bands and deformation bands. Combinations involving C—H or C—C vibrations should be distinguishable as well, since these should shift very little, or not at all, when the type of hydrohalide is varied from hydrochloride to hydriodide.

(*B*) *Aliphatic Secondary Amine Salts*

In the spectra of the secondary amine salts the $\overset{+}{N}H_2$ stretching bands are found at lower frequencies overlapping the CH_3 and CH_2 stretching bands from the low frequency side.

Can. J. Chem. Downloaded from www.nrcresearchpress.com by 69.46.99.164 on 09/04/12
For personal use only.

The situation is not entirely clear, however, because of the high degree of overlapping.

There are no bands near 2000 cm^{-1} in the spectra of diethylamine and di-*n*-butylamine hydrohalides. In piperidine hydrohalides there are two or three weak bands in this part of the spectrum and at the same time a greater number of sharp bands appear in the 2800–2400 cm^{-1} region. The bands near 2000 cm^{-1} are probably due to combinations between the $\overset{+}{N}H_2$ bending vibration below 1600 cm^{-1} and some low frequency vibration. Proof should come from the low frequency part of the spectrum.

The bands of the secondary amine hydrohalides tend to be somewhat broader than those of the primary amine hydrohalides.

(*C*) *Aliphatic Tertiary Amine Salts*

As was stated in paper I, the center of gravity of the broad $\overset{+}{N}H$ absorption region of the hydrohalides of a given tertiary amine shifts towards higher frequencies in the order Cl→Br→I. This shift is in the reverse direction to that of the sharp bands between 2800 and 2400 cm^{-1} in the primary and secondary amine salts.

In all likelihood this absorption region is due to the $\overset{+}{N}H$ stretching band. Then it can be seen that since the hydrochloride has the lowest $\overset{+}{N}H$ stretching frequency the chloride ion gives the strongest hydrogen bonds.

The centers of the bands are at considerably lower frequencies than are the $\overset{+}{N}H$ stretching frequencies in the primary and secondary amine hydrohalides, being found at about 2600 and 2450 for the hydrochlorides of triethylamine and tri-*n*-butylamine respectively. Although we do not know exactly the frequency range of the unassociated $\overset{+}{N}H$ stretching band, it is quite clear that tertiary amine hydrohalides form stronger hydrogen bonds than do the primary and secondary amine salts. This is consistent with the fact that in this case the positive charge is distributed only between the nitrogen atom and one hydrogen atom, rather than two or three hydrogen atoms.

No broad bands appear in superposition with the CH_3 and CH_2 stretching bands in the tertiary amine salt spectra and this further confirms the assignment of the $\overset{+}{N}H$ stretching band in all these cases.

There are a great number of sharp bands superimposed on both sides of the main band center, and it is significant that those sharp bands which can be followed hydrochloride to hydrobromide to hydriodide exhibit a slight shift toward lower frequencies in the order Cl → Br → I just as do the sharp bands in the primary and secondary aliphatic salts. This shows again that these are combination bands involving $\overset{+}{N}H$ deformation bands and that the broad stretching band shifts in the opposite direction. Other bands of similar origin are in coincidence with the broader $\overset{+}{N}H$ stretching bands and it is difficult to follow their shifting.

As expected, no band appears near 2000 cm^{-1}, since there is no possibility of torsional oscillations of the tertiary amine group.

(*D*) *Aromatic Primary Amine Hydrochlorides*

The two main bands in aniline hydrochloride have their maxima at 2810 and 2570 cm^{-1} respectively, the upper one having a strong shoulder on the high frequency side. In the two other salts the separation is even larger. Since in the aliphatic case the antisym-

Can. J. Chem. Downloaded from www.nrcresearchpress.com by 69.46.99.164 on 09/04/12
For personal use only.

Can. J. Chem. Downloaded from www.nrcresearchpress.com by 69.46.99.164 on 09/04/12
For personal use only.

metrical and symmetrical $\overset{+}{N}H_3$ stretching vibrations are almost coincident, it seems to be unlikely that the two main maxima in aniline hydrochloride correspond to these bands.

The upper maximum of aniline hydrochloride shifts toward higher frequencies in the order $Cl \rightarrow Br \rightarrow I$ but less than in the case of the tertiary amine hydrohalides. The lower maximum (with two peaks), however, shifts toward lower frequencies showing that these are not $\overset{+}{N}H_3$ stretching bands but combination bands involving fundamentals of $\overset{+}{N}H_3$ deformation vibrations and that the upper band which is stronger and broader must contain the two or three $\overset{+}{N}H_3$ stretching frequencies. There is a close analogy here with the "satellite" bands of carboxylic acid dimers discussed by Bratož, Hadži, and Sheppard (9).

As was pointed out in paper I, since aniline is a very weak base, it is possible that we have two potential minima of comparable depths for the hydrogen-bonded $\overset{+}{N}H_3$ stretching motions with a low barrier between them. If this is the situation, tunnelling of the proton may occur and the $\overset{+}{N}H_3$ stretching bands (or rather only the antisymmetrical one) (see ref. 3) may split. Blinc and Hadži (10) interpreted in this fashion the spectra of KH_2PO_4-type compounds and Detoni and Hadži (11) those of sulphinic acid.

A similar explanation, however, could hardly explain the two main bands of the aniline hydrohalides. It would be contradicted by the above described shifting of these bands and it is rendered improbable, too, by the large separation between them. A splitting by double-well mechanism is still possible if both bands resulting from the splitting are contained in the broad upper band. There is more indication for this in the spectra of α and β naphthylamine salts which otherwise resemble the spectrum of aniline. More work is needed to elucidate this problem.

The main point is that these spectra actually resemble the aliphatic analogues more closely than it may appear at first sight and follow the same general pattern.

In all the aromatic primary amine *hydrochlorides* there is a strong combination tone near 2000. Comparison with the amines themselves shows that these are unlikely to belong to the well-known combination bands of the aromatic compounds (12). However, torsional oscillations should be again possible in these cases.

(*E*) *Aromatic Secondary Amine Hydrohalides*

Diphenylamine hydrohalides have interesting spectra. The main band is at much lower frequencies than it is in aniline. Again the center of gravity shows the upward shift in going from Cl^- to I^- but the other sharp bands show the downward shift.

Surprisingly there is a well-formed doublet in the 2000 cm^{-1} area. This may be a combination between some low frequency vibration and the $\overset{+}{N}H_2$ bending band near 1550 cm^{-1}.

The N-methylaniline hydrohalide spectra show the same general features but the $\overset{+}{N}H_2$ stretching bands are in the 2800 cm^{-1} region.

(*F*) *Aromatic Tertiary Amine Hydrohalides*

N-Methyl diphenylamine and pyridine give very strong hydrogen bonds; N,N-dimethylaniline gives somewhat weaker ones, probably for steric reasons.

The centers of gravity of the $\overset{+}{N}H$ stretching bands move upwards (except in the case

of N,N-dimethylaniline where the hydrochloride and hydrobromide have $\overset{+}{N}H$ stretching bands at about the same place), and the sharp bands show the above described slight downward shift.

The $\overset{+}{N}H$ stretching bands in this group of salts are at rather low frequencies and this shows again that weak bases and tertiary bases form the strongest hydrogen bonds and that this is accompanied by greatly broadened bands.

The two bands in pyridine salts near 2000 cm^{-1} constitute a difficult problem. We tentatively assign them to combination tones usually found in spectra of aromatic compounds.

We see that the spectra of aromatic amine hydrochlorides differ from the aliphatic salts inasmuch as the hydrogen bonds are usually stronger and the bands are broader in the former, but the differences are not really of a fundamental nature.

DISCUSSION AND CONCLUSIONS

Among the factors which determine the energy of a hydrogen bond are the following: attractive electrostatic forces operating in an X—H---Y system, repulsions between the end atoms, and delocalization of the Y lone pair and X—H bonding electrons (13, 14, 15). The usually high intensity of hydrogen-bonded X—H stretching bands is explained by considering the variation of bond polarity during the vibrational motion and the increasing amount of delocalization when the bond is shortening (16, 17).

Concerning the energy of the hydrogen bond we suggest that in the case of amine hydrohalides it is largely electrostatic as would be expected because of the presence of net charges. The amount of positive charge left on the hydrogen-bonded protons is important in determining shifts going from hydrochlorides to hydrobromides and hydriodides. This was treated in more detail in paper I.

Although the absolute intensities were not measured, it was observed that the amine hydriodides have usually the weakest spectra. Since delocalization would give them the highest intensity this is further evidence that these hydrogen bonds are largely electrostatic in character.

The width of the bands and the appearence of many bands when hydrogen bonding is present are certainly the most interesting of the related problems and have received much attention. It has been suggested that the great anharmonicity of the potential surfaces is the cause of the appearance of many overtones and combination tones (18). The importance of anharmonicity for the various phenomena connected to hydrogen bonding cannot be overestimated. It is, however, very likely, as Bratož and Hadži pointed out, that only the parts of the potential surface pertaining to the XH stretching vibrations are very anharmonic and that the parts pertaining to the bending vibrations are only slightly anharmonic. It might, therefore, be suggested that those combination bands which are found in the XH stretching region accompanying the "real" XH stretching bands should be combinations between the latter and some other bands of lower frequency. This is, however, obviously not the case. In Waldron's interpretation of methylamine hydrochloride all the bands around the broad "real" stretching bands are overtones or combination tones involving bending vibrations. This is confirmed by the present results and especially by the direction of the frequency shift from hydrochloride to hydrobromide to hydriodide of all the sharper bands, which is in the opposite sense from that occurring for the broad true $\overset{+}{N}H$ stretching bands. Bratož, Hadži, and Sheppard (9) reached similar conclusions for carboxylic acid dimers and Newman and Badger for certain amides (19).

Combination tones due to deformation vibrations may coincide with the "real"

Can. J. Chem. Downloaded from www.nrcresearchpress.com by 69.46.99.164 on 09/04/12
For personal use only.

hydrogen-bonded stretching band and broaden and complicate it further. This is the case in the spectra of many secondary and tertiary amine hydrohalides. In other cases they may appear non-coincident giving a clearer spectrum as in ammonium salts and primary aliphatic amine hydrohalides.

If the sharp bands which appear in the $\overset{+}{N}H$ stretching region were interpreted as combinations between the "real" stretching bands and some low frequency band (possibly the series of harmonics of the XY bridge frequency) then they would have to be difference tones and thus they should disappear or become very weak at low temperatures. Waldron's work shows quite clearly, however, that this does not happen.

The pronounced ability of the bending bands to form combination tones may appear unusual because of the low mechanical anharmonicity of the deformation vibrations involved. (Fermi resonance could only be involved to explain their relatively high intensities where they fall close to the $\overset{+}{N}H$ stretching bands; this, however, is very often not the case.) It is interesting to note in this respect that the free amines, which form only weak hydrogen bonds, exhibit a few such bands in the 2800–2400 cm^{-1} area (see Tables I and II). It seems likely, therefore, that the mechanical anharmonicity of the potential curve due to hydrogen bonding is not the main cause of the appearance of these combination bands. Since the only other factor which might cause them to appear is electrical anharmonicity, we conclude that this latter effect must be very important in hydrogen-bonded molecules especially for bending vibrations, and that it is responsible for much of the fine structure. W. E. Thompson and Pimentel (20) reached similar conclusions in a study of the association between chloroform and cyclohexylamine.

RÉSUMÉ

Les spectres infrarouges d'un certain nombre d'halogénures d'amine ont été mesurés.

La formation de liaisons hydrogène et les oscillations torsionnelles des groupements $\overset{+}{N}H_3$ influencent ces spectres d'une manière charactéristique. Les vibrations de valence du groupe $\overset{+}{N}$—H---Y^- donnent des bandes larges ou assez larges. Elles se trouvent autour de 3000 cm^{-1} chez les sels des amines aliphatiques primaires. Elles apparaissent à des fréquences un peu plus basses chez les sels d'amines secondaires et beaucoup plus basses chez les tertiaires. Les sels halogènes des amines aromatiques ont ces bandes à des fréquences plus basses que les sels d'amines aliphatiques de la même catégorie.

Il y a un déplacement vers les hautes fréquences dans l'ordre chlorhydrate, bromhydrate, iodhydrate.

Tous ces spectres contiennent un certain nombre de bandes plus minces qui coincident ou non avec les bandes de valence $\overset{+}{N}$—H---Y^-. Ce sont des tons de combinaison faisant intervenir des modes de déformation. Ils se déplacent vers les fréquences basses dans l'ordre chlorhydrate, bromhydrate, iodhydrate.

L'importance de l'anharmonicité électrique faisant apparaître ces bandes est soulignée.

L'énergie de la liaison hydrogène vient surtout de contributions électrostatiques.

ACKNOWLEDGMENTS

We are indebted to the National Research Council of Canada and to Imperial Oil Limited of Sarnia for financial help.

We express our thanks to Dr. K. L. McEwen for help in improving the English of our manuscript.

Can. J. Chem. Downloaded from www.nrcresearchpress.com by 69.46.99.164 on 09/04/12
For personal use only.

REFERENCES

1. WAGNER, E. L. and HORNIG, D. F. J. Chem. Phys. **18**, 296 (1950).
2. WAGNER, E. L. and HORNIG, D. F. J. Chem. Phys. **18**, 305 (1950).
3. PLUMB, R. C. and HORNIG, D. F. J. Chem. Phys. **21**, 366 (1953).
4. PLUMB, R. C. and HORNIG, D. F. J. Chem. Phys. **23**, 947 (1955).
5. WALDRON, R. D. J. Chem. Phys. **21**, 734 (1953).
6. LORD, R. C. and MERRIFIELD, R. E. J. Chem. Phys. **21**, 166 (1953).
7. CHENON, B. and SANDORFY, C. Can. J. Chem. **36**, 1181 (1958).
8. WADDINGTON, T. C. J. Chem. Soc. 4340 (1958).
9. BRATOŽ, S., HADŽI, D., and SHEPPARD, N. Spectrochim. Acta, **8**, 249 (1956).
10. BLINC, R. and HADŽI, D. Molecular Physics, **1**, 391 (1958).
11. DETONI, S. and HADŽI, D. J. Chem. Soc. 3163 (1955).
12. WHIFFEN, D. H. Spectrochim. Acta. **7**, 253 (1955).
13. COULSON, C. A. and DANIELSSON, U. Arkiv Fysik, **8**, 239, 245 (1954).
14. TSUBOMURA, H. Bull. Chem. Soc. Japan, **27**, 445 (1954).
15. NAGAKURA, S. and GOUTERMAN, M. J. Chem. Phys. **26**, 881 (1957).
16. BARROW, G. M. J. Phys. Chem. **59**, 1129 (1955).
17. COULSON, C. A. Research, **10**, 149 (1957).
18. BRATOˇ, S. and HADŽI, D. J. Chem. Phys. **27**, 991 (1957).
19. NEWMAN, R. and BADGER, R. M. J. Chem. Phys. **19**, 1147 (1951).
20. THOMPSON, W. E. and PIMENTEL, G. C. Symposium on molecular structure and spectroscopy. Columbus, Ohio. 1958.

Can. J. Chem. Downloaded from www.nrcresearchpress.com by 69.46.99.164 on 09/04/12
For personal use only.

Can. J. Chem. Downloaded from www.nrcresearchpress.com by 69.46.99.164 on 09/04/12
For personal use only.

COMPLEX COBALT PERIODATES[1]

M. W. LISTER AND Y. YOSHINO[2]

ABSTRACT

A number of complex cobalt periodates have been prepared. Sodium periodatocobaltate (III) $Na_5H_2Co(IO_6)_2.10H_2O$ is obtained as green crystals when cobaltous and periodate ions react in the presence of alkaline sodium hypochlorite. Somewhat similar potassium, barium, and lanthanum salts are described. Various methods of demonstrating that the cobalt is trivalent, including the observation that sodium periodatocobaltate (III) is diamagnetic, are described. The free acid $H_7Co(IO_6)_2$ can be obtained in solution, and measurements have been made on its ionization constants. Observations have been made on the stability of these compounds, and the stability constant of the periodatocobaltic ion (in alkaline solution at 60° C) has been shown to be in the neighborhood of 10^{18}.

Some years ago one of the writers of this paper noted that complex periodates of trivalent copper could be prepared by oxidizing divalent copper to trivalent copper by means of sodium hypochlorite in the presence of sodium or potassium periodate (1). The compounds so obtained were the same as those prepared earlier by Malatesta, using persulphate oxidation (2). Evidence for the existence of the copper complexes and measurements on their stability were obtained from the fact that copper was a much less efficient catalyst for the decomposition of sodium hypochlorite if periodate was present; the complex salt did not catalyze this reaction while uncomplexed copper did. It was noted at the same time that the catalysis by cobalt salts was also much decreased if periodate was present, and this suggested that a similar cobalt compound might be formed. The present paper describes the preparation of compounds of this sort, and gives a description of some of their properties.

(*1*) *Preparation of Compounds*

(*i*) *Sodium Periodatocobaltate* (III)

The general method used to prepare sodium periodatocobaltate (III) was as follows: cobalt sulphate (or chloride) solution was mixed with sodium periodate and enough dilute sulphuric acid to dissolve this relatively insoluble salt. The mixture was then poured into a considerable excess of alkaline sodium hypochlorite with vigorous stirring. A dark green precipitate formed, which was centrifuged off, washed with a little cold water, and then largely redissolved in dilute sodium hydroxide. The solution was filtered, and the complex periodate reprecipitated by adding alcohol. It was then filtered off, washed, and dried.

In some cases the initial precipitate was small in size and almost black (probably containing mostly cobalt (III) hydroxide). If this was filtered off, the filtrate was dark green and slowly deposited green crystals of the complex periodate. In every preparation, considerable loss of yield was caused by precipitation of cobalt (III) hydroxide, and it was essential to recrystallize the product to free it from this compound.

In a typical preparation, 14 g of sodium periodate, $Na_2H_3IO_6$, was dissolved in 75–100 ml of water with a minimum of nitric acid present to effect solution. Five grams of cobalt chloride hexahydrate was added. Meanwhile, 15 g of sodium hydroxide was dissolved in 50 ml of 1.5 *M* sodium hypochlorite. The two solutions were mixed, and the green precipitate was separated by centrifuging. The precipitate was washed with a little cold water, and then stirred into 400 ml of dilute (about 0.1 *M*) sodium hydroxide. The

[1]*Manuscript received August 18, 1959.*
Contribution from the Department of Chemistry, University of Toronto, Toronto, Ontario.
[2]*National Research Council Postdoctorate Fellow.*

insoluble portion was filtered off, and alcohol was added to the filtrate. The sodium periodatocobaltate (III) precipitated. The yield after a further recrystallization was 3.7 g.

(*ii*) *Analysis*

The method of analysis was as follows. A weighed sample was dissolved in water, and enough sulphur dioxide was bubbled in to cause complete reduction to iodide. The solution was briefly boiled to remove excess sulphur dioxide, and silver nitrate was added in excess. The precipitated AgI was filtered off, dried at 100° C, and weighed. This gives the iodine content. Excess potassium iodide was added to the filtrate, and silver iodide was filtered off. Cobalt was precipitated from the filtrate, either as cobalt anthranilate or as cobalt sulphide by ammonium carbonate and hydrogen sulphide. In the latter case the precipitate was digested with sulphuric acid, evaporated, and the residue of $CoSO_4$ was weighed. For sodium, a sample was dissolved in aqueous sulphur dioxide as before, and the cobalt removed as sulphide. The filtrate was evaporated with a little sulphuric acid, and the residue (after treatment with ammonium carbonate to remove $NaHSO_4$) was weighed as Na_2SO_4.

A second, more convenient, method was developed later. The sample was reduced by sulphur dioxide, the excess being boiled off as before. The solution was passed through a column of a cation exchange resin (14 cm long by 1 cm diameter of Dowex 50S-X8 in 50–100 mesh) in its hydrogen form. The effluent contains the iodide, which was estimated as AgI as before. The resin was eluted with 0.4 *N* HCl which removes the sodium. This liquid was then evaporated, and the residue of NaCl weighed. Finally the resin was eluted with 2 *N* HCl which removes the cobalt, and this was converted to the anthranilate or sulphate for weighing.

The water in the sample was measured by the loss in weight at 150° C.

The result of a typical analysis follows. Found: Na, 14.3; Co, 7.33; I, 31.25; H_2O, 22.3%. Theoretical for $Na_5H_2Co(IO_6)_2.10H_2O$: Na, 14.34; Co, 7.35; I, 31.65; H_2O, 22.47%.

In many samples the cobalt was a little high (up to about 8%), presumably because of contamination by cobalt hydroxide.

Another check on the sodium content was made by passing a solution of sodium periodatocobaltate (III) through an anion exchange resin in its chloride form. The complex displaces chloride into the effluent solution, and by using known amounts of the complex it was found that five chlorides (measured by silver nitrate titration) were displaced by 1 molecule of complex.

$$5RCl + Na_5H_2Co(IO_6)_2 \rightarrow R_5H_2Co(IO_6)_2 + 5HCl$$

where R represents the ion exchange resin.

Further evidence supporting this formula will be given later.

(*iii*) *Potassium Periodatocobaltate* (III)

A very similar compound was obtained using the potassium instead of the sodium salts in the method given above. The potassium compound, however, is more soluble than the sodium salt, so it needed more alcohol to precipitate it. The salt, after being dried over calcium chloride, is hygroscopic, and readily picks up water, at least in humid weather. An alternative method was to pass the sodium salt in solution through a cation exchange resin in its hydrogen form, when free periodatocobaltic acid is obtained. This was then neutralized by potassium hydroxide, and precipitated with alcohol.

The analysis, done by the same methods as for the sodium salt, gave as follows. Found: K, 22.6; Co, 8.60; I, 32.8; H_2O, 7.45%. Calc. for $K_4H_3Co(IO_6)_2.3H_2O$: K, 21.8; Co, 8.21; I, 35.3; H_2O, 7.52%. This preparation was made in somewhat less alkaline solution than

Can. J. Chem. Downloaded from www.nrcresearchpress.com by 69.46.99.164 on 09/04/12
For personal use only.

Can. J. Chem. Downloaded from www.nrcresearchpress.com by 69.46.99.164 on 09/04/12
For personal use only.

for the sodium salt, which may account for the lower alkali metal content. Like the sodium salt, this compound gave small green crystals.

(*iv*) *Barium Periodatocobaltate* (III)

The barium salt was prepared in various ways, and gave different compounds depending on the conditions. Firstly, the sodium salt was converted into the free acid by passing through a cation exchange resin in its hydrogen form. The free acid was neutralized to pH = 11.5 by carbonate-free sodium hydroxide, and then barium chloride solution was added. This was done under nitrogen to avoid contamination with barium carbonate. A green precipitate formed which was filtered off, washed, and dried. The analysis was as described above, except that the barium was weighed as $BaSO_4$. The results were as follows. Found: Ba, 37.5; Co, 6.55; I, 25.8; H_2O, 9.58%. Calc. for $Ba_5[H_2Co(IO_6)_2]_2.10H_2O$: Ba, 36.5; Co, 6.27; I, 26.9; H_2O, 9.51%.

In acid solutions a different precipitate was obtained. If the free complex acid (pH about 2.5) was mixed with barium chloride solution, a green precipitate was formed of rather variable composition. It gave a Ba/Co ratio of close to one, but the iodine content was lower than that expected if the I/Co ratio is 2 as in the compounds described above. Several samples gave analyses close to $Ba_2H_5Co_2(IO_6)_3.5H_2O$. However, the results were sufficiently variable that it cannot be considered that this has been established as a definite compound.

(*v*) *Lanthanum Periodatocobaltate* (III)

This compound was prepared by converting 1.6 g of the sodium salt to the free acid by cation exchange, and adding 50 ml of 0.1 *M* lanthanum nitrate. The green precipitate analyzed as follows. Found: La, 21.0; Co, 9.28; I, 29.7; H_2O, 16.4%. Calc. for $La_2Co_2H_3(IO_6)_3.12H_2O$: La, 21.6; Co, 9.18; I, 29.7; H_2O, 16.8%.

It is interesting to note that another iodine-to-cobalt ratio is present. Possibly the lanthanum as another trivalent atom is capable of taking the place of cobalt in the compound.

At high pH (by adding lanthanum nitrate to the sodium complex) the green precipitate, however, had approximately the 2:1 ratio for iodine to cobalt found in the sodium complex. The analyses most nearly agreed with $La_4[H_3Co(IO_6)_2]_3.18H_2O$. However, no way of recrystallizing this compound (or the barium compounds) was found, for it is insoluble in water, and decomposed by acids.

(*2*) *Valency of Cobalt*

In the formulae quoted above it was assumed that the cobalt was trivalent. This is certainly the valency that one would expect for cobalt complexes formed under oxidizing conditions. However, these formulae are supported by various experimental results, which will now be given.

(*i*) *Oxidation of Iodide*

It was found that the corresponding copper compounds oxidized iodide ions in acid solution. The amount of iodine liberated depended on whether the acid was added before or after the iodide. If the iodide was added first, the copper was reduced by it from copper (III) to copper (I). If acid was added first, it decomposed the compound to give copper (II), and later addition of iodide only reduced copper (II) to copper (I). Hence, in the latter case less iodine was liberated, and from the ratio of the amounts the valency of the copper in the original compound could be deduced.

The same method was applied to sodium periodatocobaltate (III). The difficulty here is that the complex acid is so stable that prolonged boiling with acid is needed to decompose

it. However, it can be done, and then on adding iodide the cobalt remains as Co(II) and only periodate is reduced. If iodide is added first, the equivalent weight of sodium periodatocobaltate (III) is 1/17 of its molecular weight (eight iodines are liberated for each periodate, and one for Co(III) to Co(II)).

The observed equivalent weights were:

(1) Potassium iodide added first, obs. equivalent weight = 47.0, calc. equivalent weight = 47.15 (mol. wt./17).

(2) Acid added first, obs. equivalent weight = 50.7, calc. equivalent weight = 50.1 (mol. wt./16).

These results support a formula with trivalent cobalt.

(ii) Reduction by Sulphur Dioxide

A rather similar experimental confirmation comes from the reduction of the compound by aqueous sulphur dioxide. Here the sulphur dioxide is oxidized to sulphuric acid, and after unused sulphur dioxide has been boiled out, the acid can be titrated with sodium hydroxide. If bromcresol green is used as indicator, the cobalt ions do not interfere in the titration. It was found that 1 g-equivalent of sulphuric acid was produced by 67.0 g of the compound. The weights calculated for different cobalt valencies are: Co(II) 73.0; Co(III) 66.8; Co(IV) 61.6. Hence these results support trivalent cobalt, and the equation for the reduction is:

$$2Na_5H_2Co(IO_6)_2 \cdot 10H_2O + 17SO_2 \rightarrow 5Na_2SO_4 + CoI_2 + 10H_2O + 12H_2SO_4.$$

(iii) Reduction by Ferrous Sulphate

Sodium periodatocobaltate (III) can be titrated with ferrous sulphate in acid solution. A solution of the complex salt in about 1.0 *N* sulphuric acid was used, and the titration was followed potentiometrically. The cell used was: $Pt/Na_5H_2Co(IO_6)_2$ in acid/Hg_2Cl_2 in saturated KCl/Hg. With more dilute sulphuric acid (about 0.1 *N*), some precipitate formed in the early part of the titration, and the results were somewhat erratic. Sodium periodate also gives a similar titration, and it is then reduced to sodium iodate; some results of this titration are given for comparison. The results given below are the voltages relative to the saturated calomel electrode, so −0.242 v (3) must be added for voltages relative to the standard hydrogen electrode.

(*a*) Titration of 0.00503 *M* sodium periodatocobaltate (III) in 1.0 *N* sulphuric acid against 0.0913 *M* ferrous sulphate at 25° C. Moles Fe^{++}/moles $Na_5H_2Co(IO_6)_2$ and e.m.f. (volts): 0 (−1.023), 0.91 (−1.023), 1.82 (−1.019), 2.72 (−1.006), 3.18 (−1.002), 3.63 (−0.996), 3.99 (−0.987), 4.36 (−0.962), 4.72 (−0.889), 5.08 (−0.770), 5.45 (−0.675), 5.81 (−0.617), 6.17 (−0.584), 6.53 (−0.569), 7.26 (−0.556), 9.08 (−0.549).

(*b*) Titration of sodium periodate in 1.0 *N* sulphuric acid at 25° C. Moles Fe^{++}/moles $Na_2H_3IO_6$ and e.m.f. (volts): 0 (−1.045), 0.49 (−1.041), 0.98 (−1.031), 1.38 (−1.002), 1.57 (−1.016), 1.77 (−1.012), 1.97 (−0.732), 2.16 (−0.619), 2.36 (−0.588), 2.56 (−0.577), 2.95 (−0.570), 4.91 (−0.560).

In the second titration the voltage at the point where the periodate is half reduced is −1.033, or −1.275 relative to a standard hydrogen electrode. This is lower than Abel and Smetana's (4) result for this potential (−1.51 v), or Latimer's (5) estimate of it from the chemical behavior of periodic acid. Only about 0.05 v of this discrepancy can be attributed to partial ionization of the periodic acid. It seems probable that the electrode did not take up the true equilibrium potential for this system. Similarly, the apparent standard electrode potential for the reduction of the complex ion is between −1.19 and

Can. J. Chem. Downloaded from www.nrcresearchpress.com by 69.46.99.164 on 09/04/12
For personal use only.

Can. J. Chem. Downloaded from www.nrcresearchpress.com by 69.46.99.164 on 09/04/12
For personal use only.

-1.20 v relative to hydrogen, but again this may not be the true equilibrium potential. A reaction of this sort involving transfer of oxygen may well be a slow reaction.

However, the number of molecules of ferrous sulphate reacting is quite definite. The inflection occurs at 2 molecules for sodium periodate (i.e. reduction to iodate) and 5 for sodium periodatocobaltate (III). This is what is required for trivalent cobalt:

$$2Na_5H_2Co(IO_6)_2 + 10FeSO_4 + 10H_2SO_4 \rightarrow 4NaIO_3 + 5Fe_2(SO_4)_3 + 3Na_2SO_4 + 2CoSO_4 + 12H_2O.$$

(iv) Magnetic Properties

Measurements were made of the magnetic susceptibility of the sodium compound, by means of a Goüy apparatus of the conventional type. Both the solid and an aqueous solution were used. The results in aqueous solution cannot be very accurate, since the sodium periodatocobaltate (III) is not very soluble in water, and hence a dilute solution had to be used. The results made $\chi = -570(\pm 100)\times 10^{-6}$ per g-molecule of compound, from the solution measurements.

In the solid state, the degree of purity of the sample had a considerable effect on the result, the sample becoming more diamagnetic as it was recrystallized. It is evident that most samples contain traces of a paramagnetic impurity, probably cobalt oxide. The purest sample gave a susceptibility of -290×10^{-6}/g-molecule. It is difficult to make a precise theoretical calculation for this number, since the contributions of the atoms, particularly the iodine in this valency state, are not too certain. However, Angus's expression (6) predicts a value of about -350×10^{-6}/g-molecule. In any case it is clear that the compound is diamagnetic, as is generally found for Co(III) compounds.

(3) Spectrum of Sodium Cobalt Periodate and of Periodate-cobaltic Acid

Solutions of sodium periodatocobaltate (III) are green. The absorption spectrum shows a maximum at 625 mμ, and a minimum at 535 mμ. The absorption rises steadily towards the violet and falls towards the red. Values for the extinction coefficients, measured on a 5×10^{-3} *M* aqueous solution by means of a Beckmann D.U. spectrophotometer, are for sodium periodatocobaltate (III), λ (ϵ): 320 (2340), 340 (1440), 360 (1085), 380 (687), 400 (550), 420 (389), 440 (275), 460 (206), 480 (153), 500 (100), 510 (79.5), 520 (69), 530 (64), 540 (64.5), 550 (68.5), 560 (75.5), 580 (93), 600 (108), 610 (111.5), 620 (112.5), 630 (113), 640 (109), 650 (103), 675 (75.5), 700 (47), 750 (17), 800 mμ (11). The absorption in the violet starts at much longer wave lengths than does the similar absorption of periodate ions alone. KH_4IO_6, λ (ϵ): 260 (320), 280 (236), 300 (150), 320 (45), 340 mμ (4). $K_3H_2IO_6$, λ (ϵ): 290 (395), 300 (272), 310 (182), 320 (113), 340 (35), 360 mμ (8).

In acid solution the spectrum is somewhat altered. This change seems to take place in at least two stages. If acid ($HClO_4$) is added, and the spectrum is rapidly measured, it is found to be as follows, 3.35×10^{-3} *M* sodium periodatocobaltate (III) in 3.35×10^{-2} *M* perchloric acid, λ (ϵ): 450 (193), 460 (162.5), 480 (116.5), 500 (87.5), 520 (70.5), 540 (67.5), 560 (73), 580 (85), 590 (88), 600 (90.5), 610 (91), 620 (90.5), 630 (87.5), 650 (76), 675 (57), 700 (38), 750 (18), 800 mμ (12). The maximum is shifted to 610 mμ, and the maximum and minimum are less well marked. After this initial rapid change a slow further change occurs which will be considered in the next section on the stability of these compounds.

(4) Stability of Sodium Periodatocobaltate (III) *and of Periodatocobaltic Acid*

(i) Stability of Free Acid

If sodium copper (III) periodate is acidified, decomposition rapidly occurs to give Cu^{++} ions. It was expected that a similar reaction might occur with cobalt. However, the

acid proved much more stable, and required at least several hours of boiling with dilute sulphuric acid to give fairly complete decomposition to Co^{++} ions. At room temperature, solutions of periodatocobaltic acid (obtained by passing a solution of the sodium periodatocobaltate (III) through the hydrogen form of a cation exchange resin) can be kept for months.

As mentioned above, the absorption spectrum at first changes very rapidly if a solution of the sodium salt is acidified with perchloric acid. After this there is a further, moderately slow, change, taking place over a time of the order of 100 minutes at room temperature. This second stage in the decomposition is not simply decomposition to Co^{++} ions, as the spectrum after it has occurred is still fairly similar to that of sodium periodatocobaltate, and the rate of the process is much faster than that of the formation of Co^{++}. The rate of this second stage was examined a little more closely. Since the color change at any wave length is quite small (e.g. in one sample the color density changed from 0.381 to 0.353), it was only possible to get a rough measurement of the rate. If we assume that one colored species is slowly turning into another, and that the extent of the change is proportional to the change in the optical density, then the results indicate that this is a first-order reaction, with a rate constant about 0.03 min^{-1} at 30° C. The rate is very little affected by the hydrogen ion concentration, and has a fairly low temperature coefficient. Since the precise nature of this change is unknown, it did not seem to be worth while to get more than a rough estimate of its speed.

(*ii*) *Dissociation of Sodium Periodatocobaltate* (III)

In the work on the copper complexes referred to above it was possible to measure the stability of the complex (i.e. the equilibrium constant of the reaction: complex $\rightleftharpoons$ copper +periodate ions) by measuring the rate of oxygen evolution from sodium hypochlorite solution containing various amounts of copper and periodate. It was assumed that only the simple copper ions acted as a catalyst of this decomposition, and this assumption led to consistent values of the equilibrium constant.

An attempt to make similar measurements with the cobalt compound encountered difficulties. In the first place, if relatively small amounts of a cobalt salt and a periodate are added separately to a solution of sodium hypochlorite, some of the cobalt always remains as the black insoluble cobaltic oxide. This causes relatively rapid oxygen evolution. This cannot be considered to prove that the equilibrium is much in favor of the simple ions, since, if sodium periodatocobaltate (III) solution is added, almost no gas is evolved as a result. It seems reasonable to assume that the very insoluble cobaltic oxide reacts so slowly that equilibrium is not reached. With copper, on the other hand, the metal is present as the soluble $NaCu(OH)_4$. Whether equilibrium is reach when a solution of sodium periodatocobaltate (III) is added is uncertain; that is equilibrium for the reaction: $Co(HIO_6)_2^{-5} \rightleftharpoons Co^{+3} + 2HIO_6^{-4}$. The most that can be said is that no precipitate appears, and the rate of oxygen evolution does not rise appreciably with time.

The increase in the rate of gas evolution when the cobalt complex was added is so small that only a very rough value for this equilibrium constant can be obtained by this method. For instance, a solution containing an average concentration (during the measurement) of sodium hypochlorite of 1.495 *M* evolved oxygen at the rate of 0.1778 ml (at S.T.P.)/min per liter of solution, when its temperature was 60° C. When the solution was made 6.52×10^{-5} *M* in sodium periodatocobaltate (III), the rate of evolution was 0.1696 ml (S.T.P.)/min per liter; the average concentration of sodium hypochlorite was 1.416 *M*. The rate/$[ClO^-]$ is 0.1189 without sodium periodatocobaltate (III), and 0.1199 with it. The weight of cobalt which would produce this increase can be

Can. J. Chem. Downloaded from www.nrcresearchpress.com by 69.46.99.164 on 09/04/12
For personal use only.

calculated from earlier data (7), and is 7.5×10^{-7} g of uncomplexed cobalt. From the volume of solution (767 ml) the concentration can be obtained, and as two periodates are combined with each cobalt, the equilibrium constant can be calculated. The result is K = [complex]/[Co(III)].[periodate]^2 = 3×10^{18}. Other measurements gave somewhat lower values (down to 3×10^{17}); the cause of this lack of consistency is undoubtedly the very small differences (e.g. 0.004 ml/min) in the rate of oxygen evolution due to the cobalt compound.

However, it is plain that the cobalt compound is more stable than the copper compound where the corresponding equilibrium constant is 1.25×10^{10} at 40° C. For sodium periodatocobaltate the constant is in the neighborhood of 10^{18} at 60° C. These measurements are for dilute alkaline (about 0.1 M) solution, in which the precise chemical form of the uncomplexed cobalt is uncertain.

(*5*) pH *Measurements*

Since periodatocobaltic acid is reasonably stable, measurements were made to discover its ionization constants, and its general behavior in acid base titrations.

A solution of the free complex acid was prepared by passing the sodium salt through the hydrogen form of a cation exchange resin. The solution was 3.35×10^{-3} M and had a pH of 2.25 measured on a Beckmann pH meter with glass electrode. This makes the hydrogen ion concentration (or activity) 5.6×10^{-3}. This is not far off two hydrogen ions per molecule, so the first two ionization constants must be fairly large (if the first two ionization constants were the same, they would both have to be 1.0×10^{-2} to give the above pH). This conclusion is supported by the fact that when a solution of the free complex acid was run through an anion exchange resin (Dowex 1-X4) in its chloride form, slightly above two chlorides were displaced per molecule of periodatocobaltic acid:

$$[H_3O^+]_2[H_5Co(IO_6)_2^{--}] + 2RCl \rightarrow R_2[H_5Co(IO_6)_2] + 2H_3O^+ + 2Cl^-.$$

Under similar conditions phosphoric acid liberated 0.90 chloride per molecule ($pK_1 = 2.12$).

On titrating periodatocobaltic acid with sodium hydroxide the curve in Fig. 1 was obtained. This has inflections at 2 and at 4NaOH added per molecule. The first inflection

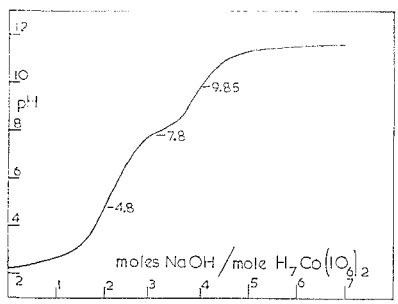


FIG. 1.

(2NaOH) is at a pH of 4.8, and the most horizontal part of the curve, between 2 and 4NaOH is at a pH of 7.8. Since the pH at an inflection point is the mean of the pK_a values on either side of it, the inflection at 2NaOH makes pK_3 = 7.6 (taking pK_2 to be 2.0 as found above). This agrees reasonably with the pH of 7.8 at 3NaOH. pK_3 and pK_4 must be fairly similar, and their average value is about 7.7. The inflection at 4NaOH has a pH of 9.85, making pK_5 = 12.0.

An almost identical titration curve was obtained by adding perchloric acid to a solution

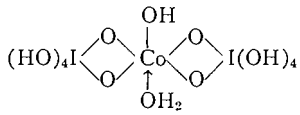
Can. J. Chem. Downloaded from www.nrcresearchpress.com by 69.46.99.164 on 09/04/12
For personal use only.

of $Na_5H_2Co(IO_6)_2$ and titrating the liberated acid with sodium hydroxide; or (in reverse) by titrating $Na_5H_2Co(IO_6)_2$ with perchloric acid.

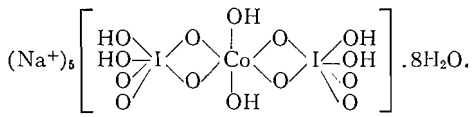
To sum up, pH measurements do not distinguish between the first and second ionization constants of periodatocobaltic acid, or between the third and fourth. The first two hydrogens ionize easily with an average pK value of 2.0; the next two pK values average 7.7. The fifth ionization constant is small with $pK_5 = 12.0$. These values are not very different from those for periodic acid ($pK_1 = 1.6$, pK_2 about 7). The jump in pK is very much what is generally found for ionization of successive OH groups attached to a central atom (compare phosphoric acid with successive pK values of 2.1, 7.2, and 12.3). It is, of course, to be expected that pK_1 and pK_2 should be similar, since this presumably involves ionization of two hydrogens from remote, but identical, parts of the molecule.

(6) General Remarks

It is not yet possible to write a detailed formula for sodium periodatocobaltate (III). There can be little doubt that it contains a complex ion, but it is uncertain whether each periodate is attached by three or two oxygens to the cobalt. Since the co-ordination of cobalt (III) is generally six, in the latter case the other places would have to be taken by water, or OH^-. The acid–base behavior indicates that the two periodate groups are identical in the free acid, and if each periodate is attached by three oxygens it is difficult to write a symmetrical formula. Hence it is perhaps a little more likely that each periodate is attached through two oxygens. This would make the free periodatocobaltic acid:



and the sodium periodatocobaltate (III):



It must be admitted that these formulae are quite speculative; but it is worth noting that the pH behavior can be explained by formulae such as the above, while, if each periodate is attached by three oxygens, it seems impossible to do so.

REFERENCES

1. LISTER, M. W. Can. J. Chem. **31**, 638 (1953).
2. MALATESTA, L. Gazz. chim. ital. **71**, 467, 580 (1941).
3. LATIMER, W. M. Oxidation potentials. 2nd ed. Prentice-Hall, Inc., New York. 1952. p. 177.
4. ABEL, E. and SMETANA, O. Monatsh. **60**, 181 (1932).
5. LATIMER, W. M. Oxidation potentials. 2nd ed. Prentice-Hall, Inc., New York. 1952. p. 66.
6. ANGUS, W. R. Proc. Roy. Soc. A, **136**, 569 (1932).
7. LISTER, M. W. Can. J. Chem. **34**, 479 (1956).

Can. J. Chem. Downloaded from www.nrcresearchpress.com by 69.46.99.164 on 09/04/12
For personal use only.

Can. J. Chem. Downloaded from www.nrcresearchpress.com by 69.46.99.164 on 09/04/12
For personal use only.

SOME PROPERTIES OF SILICA DISPERSIONS[1]

A. F. Sirianni, F. W. Meadus, and I. E. Puddington

ABSTRACT

When silicic acid sols are formed from solutions of sodium silicate by acid neutralization, a pronounced minimum in the time required for the sol–gel transformation is observed if the titration is stopped near pH 8. If the sol is prepared by electrodialysis, a similar minimum is obtained when the operation is stopped at about pH 5.5. Intermediate values for the minimum are found if the original silicate solution is partially dialyzed followed by neutralization with acid. When the water content of the gels is replaced by liquid hydrocarbons, maximum interaction between the silica particles occurs when the aqua gel has been formed or conditioned at pH 5.5 regardless of the method of preparation of the sol. A minimum in electrophoretic mobility and a maximum in sedimentation rate of the particles are observed at a similar pH value. These properties are modified considerably if the system is thoroughly dehydrated.

INTRODUCTION

A previous investigation (1) of the flow properties of dispersions of finely divided silica in hydrocarbon oils revealed a pronounced and unexpected maximum in the yield value when the silica used had been gelled or conditioned in aqueous solutions of about pH 5 prior to its suspension in oil. Both maximum yield values in suspensions and minimum times for sol–gel transformations might normally be expected to be associated with the maximum degree of interaction between the solid particles of the dispersion. It was surprising, therefore, that the minimum time of set for silica sols, which occurs at about pH 8 when sodium silicate solutions are neutralized with acid (2, 3, 4), did not coincide with the isoelectric point of silicic acid, which is about pH 5 (5). Since minimum gelation times for silica sols prepared by different methods have been variously reported in the pH range 5 to 8 (6), it seemed worth while to re-examine some of the conditions that may influence both this phenomenon and the flow properties of non-aqueous suspensions of the gels.

EXPERIMENTAL

Two types of sodium silicate were used: N grade containing about 28.7% SiO_2, 8.9% Na_2O, with 62.4% water and Metso Granular containing 28.3% SiO_2, 29.4% Na_2O, and 42.3% water. Both of these silicates are produced by the Philadelphia Quartz Co. Concentrated solutions were centrifuged to optical clarity prior to dilution to suitable concentrations for experimental purposes.

Substantially cation-free silica sols were prepared by electrodialysis using an American Instrument Co. electrodialyzer fitted with screen platinum electrodes of equal area and a cellophane #600 semipermeable membrane. The cathode compartment of the cell was washed continuously with fresh water to suppress electrolysis owing to a build-up of sodium hydroxide in the compartment. The cathode was positioned about 6 mm from the cellophane membrane to keep the cell resistance as low as possible. Changes in pH in the anode compartment as dialysis proceeded were followed by periodic measurements with a Beckman meter. When the desired pH was reached, the sol in the anode compartment was drained into a clean 600-cc Pyrex beaker prior to shutting off of the current. The beakers containing the sol were sealed with saran wrap.

Sols were also prepared by titrating the sodium silicate solutions to desired pH values with sulphuric acid solution. These sols necessarily contained the sodium sulphate formed during the titration.

[1]*Manuscript received July 7, 1959.*
Contribution from the Division of Applied Chemistry, National Research Council, Ottawa, Canada. Issued as N.R.C. No. 5450.

The time of set of the sol was taken as the period between the sol preparation and the time when polymerization and flocculation had proceeded sufficiently for the system to adhere to the sides of the beaker when it was tilted through 45°.

In a number of instances the flow properties of dispersions of particular gels were examined when the water of the aqua gel had been replaced by liquid hydrocarbon. These dispersions were prepared by adding to the mechanically broken gel, after as much water as possible had been removed by vacuum filtration, a mutual solvent for oil and water in an amount slightly in excess of the quantity required to form an azeotrope with the water that remained. The desired quantity of oil was then added and the water and residual solvent removed by evaporation, the final temperature being raised to 125° C for several hours to reduce the free water and solvent content of the system to a minimum. The operation was completed by mechanically homogenizing the system to produce a uniform paste of the silica in the oil. The aqua gels were normally aged for 24 hours prior to displacing their water content with oil. *n*-Propyl alcohol was a satisfactory mutual solvent for oil and water and the final product contained about 5% by weight of silica dispersed in an oil with a viscosity of about 0.6 poise. Viscometric measurements were carried out as previously described (1).

Gels prepared by acid titration were in most instances washed virtually free from salts with distilled water before dispersing them in the oil.

Electrophoretic measurements were conducted on portions of the pastes used for the rheological work diluted with medicinal oil to give a silica concentration of about one per cent. The measurements were carried out as described by Agius and Mulvey (7). The mobility was taken as the plateau in the velocity vs. time curve that appeared within 24 hours after starting the experiment.

Sedimentation experiments were carried out in vertical Pyrex tubes of 20 mm i.d. The suspensions were portions of the samples used in the electrophoretic determinations.

RESULTS AND DISCUSSION

Typical data relating gelation time for dialyzed sodium silicate and the pH of the sol are shown in Fig. 1. A pronounced minimum occurred at about pH 5.5, and this was substantially independent of the type of sodium silicate used, the concentration range explored, or the source of the water used in washing the cathode compartment of the cell. Softer gels with no odor of chlorine and gelation times up to 500 times longer were obtained when conductivity water was substituted for tap water in the washing procedure. The minimum time of set increased from 9 to 22 hours when the silica concentration was reduced from 4.15 to 2.92% and conductivity water was used to wash the cathode compartment. With a tap water wash the minimum time of set for a sol containing 3.6% SiO_2 was 4 minutes. These observations are consistent with those of Hurd and co-workers (8) on the effect of impurities and solids concentration on the time of set.

Since the behavior of a series of gels prepared by titration of sodium silicate solutions with sulphuric acid agreed with the results of previous investigations in that the minimum gelation time was about 4 seconds at a pH of 7.9 for a sol containing 3.6% SiO_2, it is apparent that the difference in the pH for minimum gelation time for these sols is owing to the presence of electrolytes from the reagents used in their preparation. It is quite possible, however, that the ions from different acids could modify the magnitude of the effect.

Two further series of gels prepared by partial electrodialysis, followed by titration with sulphuric acid to the desired end points, showed that the pH of minimum gelation time decreased regularly as the amount of electrolyte in the final sol was reduced.

The flow properties of 5% by weight dispersions of silica in hydrocarbon oil are

Can. J. Chem. Downloaded from www.nrcresearchpress.com by 69.46.99.164 on 09/04/12
For personal use only.

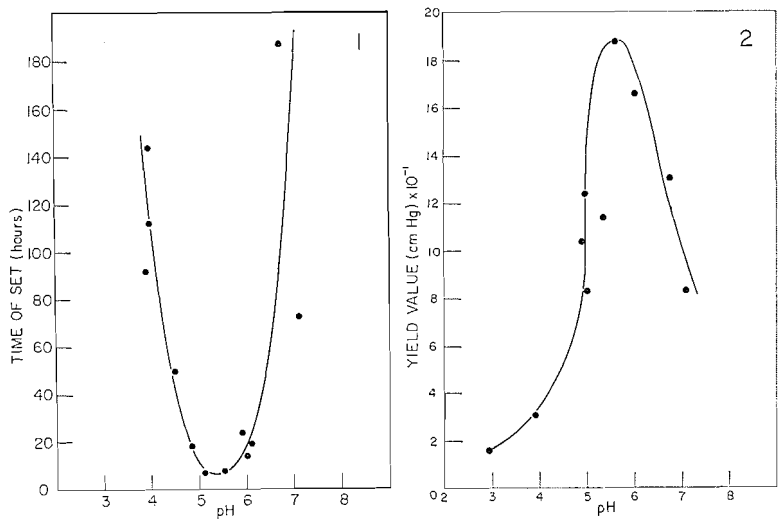


FIG. 1. Dependence of gelation times for dialyzed sodium silicate solutions on the pH of the sol.
FIG. 2. Yield values of 5% dispersions of silica in hydrocarbon oils as a function of the pH at which the silica was prepared.

indicated in Fig. 2. This shows the change in yield value of the dispersion as a function of the pH at which the sol–gel transformation occurred. A very pronounced maximum in the yield value was found at about pH 5.5 and this was independent of the method of gel preparation. Since the yield value of the pastes and the setting of gels both indicate interaction between the solid particles forming the structure, it seems that the behavior of silica in oil and in aqueous media is rather similar. The yield value of the silica-oil pastes was modified only slightly by the presence of sodium sulphate, and comparable flow properties were found when the gels were prepared by dialysis and by acid precipitation with or without the removal of the sodium sulphate. On the other hand, the aqua gels were considerably softer when prepared by dialysis using a conductivity water wash of the cathode cell and it would appear that electrolytes exert a strong flocculating influence on the polymerized silicic acid. Their inertness in oil is probably owing to their almost complete insolubility in that medium. A maximum in the elastic properties has also been observed for silica gels prepared near the point of minimum gelation time when the sols were formed by acid neutralization (9). This, too, is indicative of a high degree of adhesion between the flocculated particles.

The sedimentation rates and electrophoretic mobility of silica dispersed in oil are shown in Fig. 3. The maximum sedimentation rate which occurs at the same pH value as the maximum yield value in the more concentrated pastes strongly suggests a high degree of flocculation, and this, in turn, is indicative of higher particle interaction at this point. That the improved stability of the sols containing silica prepared above and below pH 5.5 is probably electrical in origin is suggested by the electrophoretic behavior. The mobility is essentially zero at the pH of maximum particle interaction in an electric field of about 70 v per cm with a velocity of migration rising sharply on either side of this minimum. The direction of particle motion indicates opposite charge on the silica on either side of the minimum and this is supported by the fact that the mixtures prepared from equal quantities of positively and negatively charged sols showed flocculation properties similar to those of the neutral sols. However, since some agitation is necessary to prepare the suspensions, and the oil has a very high electrical resistance, the possibility of the charges

Can. J. Chem. Downloaded from www.nrcresearchpress.com by 69.46.99.164 on 09/04/12
For personal use only.

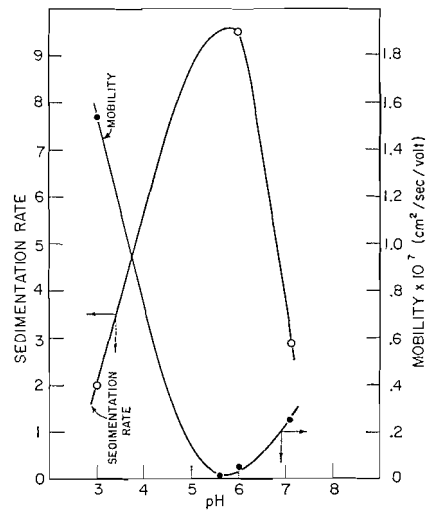


FIG. 3. Sedimentation rates and electrophoretic mobilities of finely divided silica prepared at different pH values in liquid hydrocarbons.

arising from the relative motion of the solid and the liquid cannot be ruled out completely. In those systems showing the highest mobilities there was a tendency for the velocity of migration to decrease after about 40 hours in the electrophoretic cell. No corresponding change in the sedimentation velocity of the more stable suspensions was observed, however, and the adsorption of oil-soluble ionic substances such as traces of hydrocarbon oxidation products is perhaps a more reasonable explanation for the apparent particle charge.

Although the amounts of water in these preparations must be small, traces of water have been observed to exert an influence on the electrical properties of non-aqueous systems (10), and the amounts desorbed from container walls may be important. To assess this point, the suspensions used in the sedimentation and in the electrophoretic work were diluted in their containers with 10% of toluene, which was then removed by boiling off at atmospheric pressure. This treatment had the general effect of making the sedimentation and electrical properties more uniform and similar in magnitude to those at the isoelectric point. It would thus appear that traces of water may exert an appreciable influence on the electrical properties of non-aqueous suspensions probably because of the enhanced ionizing power of the organic liquid containing it. No significant changes in the flow properties of more concentrated suspensions could be observed, however, after a similar treatment. The increased particle interaction is thus not sufficient to have an appreciable effect on the yield value.

REFERENCES

1. SIRIANNI, A. F. and PUDDINGTON, I. E. Can. J. Chem. **33**, 391 (1955).
2. MERRILL, R. C. and SPENCER, R. W. J. Phys. Chem. **59**, 806 (1950).
3. MUNRO, L. A. and PEARCE, J. A. Can. J. Research, B, **17**, 266 (1939).
4. HURD, C. B. and MARATTA, A. J. J. Am. Chem. Soc. **62**, 2767 (1940).
5. BATCHELOR, H. W. J. Phys. Chem. **42**, 575 (1938).
6. ILER, R. K. The colloid chemistry of silica and silicates. Cornell Univ. Press, Ithaca, N.Y. 1955. p. 47.
7. AGIUS, P. J. and MULVEY, D. J. Inst. Petrol. **44**, 229 (1958).
8. HURD, C. B., RHOADES, J. W., GORMLEY, W. G., and SANTORA, A. C. J. Phys. Chem. **62**, 882 (1958).
9. MUNRO, L. A., MCNAB, J. G., and OTT, W. L. Can. J. Research, B, **27**, 781 (1949).
10. HUMPHRY, R. H. and JANE, R. S. Trans. Faraday Soc. **22**, 420 (1926).

Can. J. Chem. Downloaded from www.nrcresearchpress.com by 69.46.99.164 on 09/04/12
For personal use only.

Can. J. Chem. Downloaded from www.nrcresearchpress.com by 69.46.99.164 on 09/04/12
For personal use only.

THE RELATIVE ENTHALPIES OF CONCENTRATED POTASSIUM HYDROXIDE SOLUTIONS[1]

WENDELL J. BIERMANN

ABSTRACT

Measurements were made of the heats of neutralization of concentrated solutions of potassium hydroxide with hydrochloric acid, with an estimated accuracy better than one part per thousand. From this information it was possible to calculate relative enthalpy data for potassium hydroxide solutions up to 16 molal.

INTRODUCTION

The relative enthalpies of potassium hydroxide solutions have been measured calorimetrically in the relatively dilute range by Richards and Rowe (1), and over an extended concentration range by Bender and Akerlof (2), using an electromotive force method similar to the work of Akerlof and Kegeles (3) with sodium hydroxide solutions, and presumably of comparable accuracy. Because, as aptly pointed out by Harned and Owen (4), electromotive force data must be regarded as hypothetical until substantiated by other evidence, it appeared desirable to verify these high concentration values by calorimetric measurement.

As has been previously established (5, 6), heat of neutralization measurements can supply data from which relative enthalpy values can be derived conveniently and reliably, provided necessary auxiliary data are available. Because of the availability of both suitable equipment and the prerequisite data, the heats of neutralization of potassium hydroxide solutions by hydrochloric acid solutions were measured over a wide concentration range. This information was utilized in the computation of the relative enthalpies of potassium hydroxide solutions over a concentration range of 3 to 16 molal.

EXPERIMENTAL AND RESULTS

The calorimetric equipment and general method of operation have been described previously (5, 7). Reagent grade potassium hydroxide was freed of carbonate by standard procedures, and reagent grade hydrochloric acid was used without further treatment. Stock solutions were diluted as required with conductivity water and the diluted solutions analyzed gravimetrically by the precipitation of an equivalent amount of silver chloride.

The heat liberated in the bomb reaction differs from the desired quantity, the heat of neutralization of potassium hydroxide solution by hydrochloric acid solution, both at the same molal concentration m and 25.00° C, because of simultaneous heat effects, the most important being caused by:

(1) The solution of hydrogen chloride from the vapor phase after completion of the reaction.

(2) Dilution effects due to the impracticability of adjusting the concentrations of the reactants to exactly the same molality.

(3) A slight excess of one reactant being experimentally unavoidable; hydrochloric acid was therefore added in slight excess, thus minimizing the error due to any residual carbonate in the base. An enthalpy change is involved in the dilution of this excess acid.

[1]*Manuscript received August 25, 1959.*
Contribution from the Department of Chemistry, University of Manitoba, Winnipeg, Canada.

TABLE I

Heats of neutralization of potassium hydroxide solutions by hydrochloric acid as observed experimentally

Reactant concentration (moles solute/kg solvent)	Observed heat of neutralization (defined calories at 25.00° C)	Reactant concentration (moles solute/kg solvent)	Observed heat of neutralization (defined calories at 25.00° C)
15.985	−21,448	10.126	−17,693
	21,437		17,692
14.961	20,838	9.034	17,213
14.915	20,816		17,194
	20,817		17,186
12.960	15,593	7.000	16,255
	15,596		16,257
12.023	18,963	6.987	16,251
	18,965		16,260
11.005	18,195	4.990	15,383
	18,212		15,378
10.969	18,181	3.113	14,605
	18,177		14,616

(4) A reaction temperature other than 25.00° C, except in the fortuitous case of the calorimeter being exactly 25.00° C when the reaction is initiated.

The heats of neutralization reported in Table I have been computed from the heats of the bomb reactions by "correcting" them for the above-mentioned heat effects. Experimental conditions were carefully controlled so that these corrections were small and the uncertainties involved in their calculation are negligible compared to experimental errors. Smoothed values of the heats of neutralization at integral values of the concentration are shown in Table II.

TABLE II

Smoothed values of the heats of neutralization of potassium hydroxide by hydrochloric acid

Molality	Heat of neutralization (defined calories)	Molality	Heat of neutralization (defined calories)	Molality	Heat of neutralization (defined calories)
3	−14,560	8	−16,715	12	−18,945
4	14,965	9	17,185	13	19,620
5	15,390	10	17,635	14	20,255
6	15,815	10.56	17,885	15	20,865
7	16,260	11	18,200	16	21,450

The only auxiliary data whose reliability could significantly affect the accuracy of the heats of neutralization are the specific heats of the product solutions, which were used in computing the heat capacity of the system. Values of the specific heats of potassium chloride solutions over the pertinent concentration range are available from Randall and Bison (8), Bousfield and Bousfield (9), and Galagoleva-Cherbou (10). When compared graphically, the average deviation of the experiment points was less than 0.1% from the mean curve, an insignificant error with respect to the use.

Calculation of the relative enthalpies of potassium hydroxide solutions from the smoothed heat of neutralization data involves the use of the relationship:

$$\Delta H_N = \Delta H^\circ_N + [L_2(KCl)_{m'} - L_2(KOH)_m - L_2(HCl)_m] + (55.51/m) \times [(m/m' L_1(KCl)_{m'} - L_1(KOH)_m - L_1(HCl)_m]$$

Can. J. Chem. Downloaded from www.nrcresearchpress.com by 69.46.99.164 on 09/04/12
For personal use only.

at concentrations below the saturation concentration of potassium chloride. When the solubility of potassium chloride is exceeded, the enthalpy relationship takes the form:

$$\Delta H_N = \Delta H^\circ_N + [L_2(KCl)_{sat} - L_2(KOH)_m - L_2(HCl)_m] + \{(1 - m_{sat})/m'\} \times [H_{solid} - H_2(KCl)_{sat}] + (55.51/m)\,[m/m'\,L_1(KCl)_{sat} - L_1(KOH)_m - L_1(HCl)_m]$$

where "m" is used to designate the molality of the reactants, m' is used for $(55.51\ m)/(111.02+m)$, and m_{sat} is used to indicate the molality of saturated potassium chloride solution, 10.56 moles per kilogram of solvent. ΔH_N refers to the heat of neutralization at a reactant molality m, and ΔH°_N the heat of neutralization at infinite dilution. Supplementary data used were: heat of dilution data for potassium chloride solutions from Lange *et al.* (11), relative enthalpy data for hydrochloric acid solutions from Akerlof and Teare (12) and Sturtevant (13), and the heat of neutralization at infinite dilution was taken as −13.32 defined kilocalories (7). Differential heat of solution of potassium chloride was taken from Wüst and Lange (14); as macrocrystalline potassium chloride was produced in the present work, their initial and final states correspond to those encountered here.

Table III contains the relative partial molal enthalpies of solvent and solute, and the relative enthalpies per mole of solute for potassium hydroxide solutions at integral values of the solute concentration over the range 3 to 16 molal, calculated as described above.

TABLE III

Relative enthalpies of potassium hydroxide solution, defined kilocalories at 25.00° C

m	L_1	L_2	L	m	L_1	L_2	L
3	−.018	+ .63	+ .30	10	−.370	+3.43	+1.38
4	.035	.91	.42	11	.475	4.02	1.57
5	.061	1.24	.56	12	.612	4.67	1.84
6	.098	1.59	.69	13	.690	5.01	2.07
7	.146	2.00	.84	14	.771	5.36	2.29
8	.206	2.45	1.02	15	.855	5.67	2.51
9	.280	2.93	1.20	16	.942	5.98	2.71

DISCUSSION

Analysis of the results and a consideration of the contributing sources of error lead to the conclusion that the heat of neutralization values obtained are uncertain to less than 0.1%.

Further confidence in the reliability of the heat of neutralization data is obtained from a study of the discontinuity in the heat of neutralization versus concentration curve. At a reactant concentration of 10.56 molal, a discontinuity appears due to the precipitation of potassium chloride. The experimentally determined upper and lower sections of the curve fall within 5 calories of each other when extended to this point, and the change of slope is 283 units, compared with the calculated value of 270 units.

The average deviation between these relative molar enthalpies and those reported by Akerlof and Bender is about 100 calories, which is similar to the discrepancy between the Akerlof and Kegeles values and the calorimetric values of Bertetti and McCabe (16) for sodium hydroxide solutions.

REFERENCES

1. Richards, T. W. and Rowe, R. A. J. Am. Chem. Soc. **44**, 684 (1922).
2. Bender, P. and Akerlof, G. J. Am. Chem. Soc. **63**, 1085 (1941).
3. Akerlof, G. and Kegeles, G. J. Am. Chem. Soc. **61**, 1027 (1939).

Can. J. Chem. Downloaded from www.nrcresearchpress.com by 69.46.99.164 on 09/04/12
For personal use only.

4. HARNED, H. and OWEN, B. The physical chemistry of electrolytic solutions. 3rd ed. Reinhold Publishing Corp., New York. 1958. p. 429.
5. BIERMANN, W. J. and WEBER, N. J. Am. Chem. Soc. **76**, 4289 (1954).
6. BIERMANN, W. J. and BIDINOSTI, D. R. Can. J. Chem. **34**, 1591 (1956).
7. BENDER, P. and BIERMANN, W. J. J. Am. Chem. Soc. **74**, 322 (1952).
8. RANDALL, M. and BISON, C. S. J. Am. Chem. Soc. **42**, 347 (1920).
9. BOUSFIELD, W. W. and BOUSFIELD, W. M. Trans. Roy. Soc. London, A, **218**, 119 (1919).
10. GALAGOLEVA-CHERBOU, P. G. Trudy Kazan. Khim. Tekhnol. Inst. im S. M. Kirova, **4–5**, 29 (1935).
11. HARNED, H. S. and OWEN, B. B. The physical chemistry of electrolytic solutions. 3rd ed. Reinhold Publishing Corp., New York. 1958. p. 707.
12. AKERLOF, G. and TEARE, J. J. Am. Chem. Soc. **59**, 1855 (1937).
13. STURTEVANT, J. M. J. Am. Chem. Soc. **62**, 3265, 2276 (1940).
14. WÜST, J. and LANGE, E. Z. physik. Chem. **116**, 161 (1925).
15. BERTETTI, J. W. and MCCABE, W. L. Ind. Eng. Chem. **28**, 375 (1935).

Can. J. Chem. Downloaded from www.nrcresearchpress.com by 69.46.99.164 on 09/04/12
For personal use only.

Can. J. Chem. Downloaded from www.nrcresearchpress.com by 69.46.99.164 on 09/04/12
For personal use only.

A DETAILED STUDY OF THE SAMUEL–MAGEE MODEL FOR THE RADIATION CHEMISTRY OF WATER

PART II. KINETICS OF RADICAL REACTIONS IN THE TRACKS OF DENSELY IONIZING PARTICLES[1]

P. J. Dyne and J. M. Kennedy

ABSTRACT

The kinetics of recombination of H and OH radicals, formed in liquid water along the track of a densely ionizing particle in the manner suggested by Samuel and Magee, have been studied using an electronic computer. The variation in yields with track density is in good qualitative agreement with experiment. Arguments are advanced to show that the energy required to produce one effective radical pair in liquid water is about 20 ev. Discussions are presented of the effects of scavenger concentration and its depletion at the center of the track, track diameter, the value of the rate constant for the recombination of H atoms and OH radicals, and the value of $G(-H_2O)$ as a function of track density.

1. INTRODUCTION

This paper presents calculations performed on the Chalk River Datatron Computer on the kinetics of diffusion and recombination of H and OH radicals formed in water along the track of a densely ionizing particle, such as a proton or an α-particle. According to the model suggested by Samuel and Magee (1) these radicals are formed by the dissociation of excited water molecules which, in turn, result from the ionization and excitation brought about by the ionizing particle. These radicals have similar spatial distributions, lying in a uniform column along the track of the particle. The concentration of these radicals falls off rapidly across the axis of the column according to a Gaussian or some similar distribution. The diffusion processes are, accordingly, described in a cylindrical co-ordinate system.

In the tracks of lightly ionizing particles (fast electrons) the excitation is localized into small clusters or spurs containing a few (four to eight) radical pairs. These spurs have spherical symmetry and the diffusion process is described in a spherical co-ordinate system. In a previous paper (2), which will be referred to as Part I or (I), we presented calculations of the kinetics of recombination of H and OH radicals in these small spurs. The present paper is an extension of the techniques and arguments used in Part I to cylindrical tracks. The reader is referred to Sections 1 and 2 of Part I for a more detailed introduction to the topic.

2. THE TRACK EQUATION

We adopt the convention that the hydrogen atom is species 1, with diffusion constant D_1, recombination rate constant k_{11}, and concentration C_1, which is a function of time and space. The OH radical is species 2 with constants D_2, k_{22}, C_2, etc. The rate constant for recombination of H and OH radicals is k_{12}. The radical scavenger is species 3, with diffusion constant D_3; the rate constants for reaction of scavenger with radicals 1, 2 are k_{13}, k_{23} respectively.

The track equations governing the kinetics of reaction and diffusion are:

$$[1] \qquad \partial C_1/\partial t = D_1\nabla^2 C_1 - 2k_{11}C_1^2 - k_{12}C_1C_2 - k_{13}C_1C_3$$

$$[2] \qquad \partial C_2/\partial t = D_2\nabla^2 C_2 - 2k_{22}C_2^2 - k_{12}C_1C_2 - k_{23}C_2C_3$$

$$[3] \qquad \partial C_3/\partial t = D_3\nabla^2 C_3 - k_{13}C_1C_3 - k_{23}C_2C_3.$$

[1]*Manuscript received August 19, 1959.*
Contribution from Research Chemistry and Theoretical Physics Branches, Atomic Energy of Canada Limited, Chalk River, Ontario.
Issued as A.E.C.L. No. 920.

Can. J. Chem. Downloaded from www.nrcresearchpress.com by 69.46.99.164 on 09/04/12
For personal use only.

These equations differ from those used for γ-ray spurs in three respects.

(*a*) The Laplacian refers to cylindrical, not spherical co-ordinates.

(*b*) There is no weighting function in front of the terms $k_{11}C_1^2$ and $k_{22}C_2^2$. In a γ-ray spur containing, say, five radicals, the bimolecular rate is given by $4/5\ k_{11}C_1^2$, since one radical can only react with four others. The cylindrical tracks are long and so N, the number of radicals in the track, is large and the weighting function $(N-1)/N$ is not significantly different from unity.

(*c*) The introduction of equation [3], which describes the depletion of scavenger at the center of the track and its replacement by diffusion from the bulk of the liquid.

The yields of hydrogen and hydrogen peroxide are the values of

$$\int_0^\infty\int_0^\infty k_{11}C_1^{\,2}\,dv.dt \quad \text{and} \quad \int_0^\infty\int_0^\infty k_{22}C_2^{\,2}\,dv.dt,$$

respectively, while

$$\int_0^\infty\int_0^\infty k_{12}C_1C_2\,dv.dt$$

is the amount of H_2O re-formed in the track. The numerical method is described in the Appendix.

3. THE CHOICE OF CONSTANTS

Rate constants and diffusion constants are chosen essentially as in Part I. They are $D_2 = 2\times10^{-5}$ cm²/sec, $D_1 = 8\times10^{-5}$ cm²/sec, $k_{11} = 6.0\times10^{-12}$, $k_{12} = 15\times10^{-12}$, $k_{22} = 4.5\times10^{-12}$ cc/molecule sec.[2] Constants k_{13} were taken as 1.0×10^{-11} cc/molecule sec, D_3 was taken as 2×10^{-5} cm²/sec. If it is assumed that the radicals have a Gaussian distribution, the track radius is expressed by the parameters β_1, β_2 where $C_1(r) = (N_1\beta_1^2/\pi)\exp(-\beta_1^2r^2)$. N_1 is the number of radicals/Å. For initial studies we have taken $1/\beta = 10^{-7}$cm = 10 Å for species 1 and 2. In the following discussion it is, at times, more illustrative to use the parameter $R = 1/\beta$, which can be visualized as the "radius" of the track. The "concentration" of scavenger in the initial calculation is $10^{-3}\ M$ (6.0×10^{17} molecules/cc). As experimental rate constants of scavengers are nearer 10^{-10} cc/molecule sec rather than the value of 10^{-11} which we use in the calculation, the equivalent experimental concentration of scavenger is nearer $10^{-4}\ M$.

The track density is expressed by the parameters N_1 and N_2, the number of radicals/Å. Cases were examined over the range 0.1–10 radicals/Å. We have converted the number of radicals/Å to L.E.T. (Linear Energy Transfer) (ev/Å) using the arbitrary figure of an energy deposition of 10 ev to give one radical pair. This value is derived from Firestone's measurement of $G(-H_2O) = 11\pm1$ (3) for the decomposition of water vapor (Part I, Section 4). If, for instance, $N_1 = N_2 = 0.2$ radicals/Å then this corresponds to a particle track with an L.E.T. of 2 ev/Å. Our L.E.T. values should not be used too literally because, as will be shown in subsequent discussion, the value of 10 ev/radical pair is a minimum value. The effective value in liquid water may be nearer 20 ev/radical pair.

[2]*The rate constants k_{11}, k_{22} were defined in an inconsistent manner in Part I. The value of k_{11}, for instance, in the normal chemical definition gives the number of reactions* $H + H \rightarrow H_2$. *The value of k_{11} used in the program was used to calculate the number of hydrogen atoms removed by recombination and is therefore a factor of 2 greater than the rate constant defined "chemically". The rate constants k_{11} and k_{22} tabulated in Table I of Part I are just twice the "chemical rate constants" for each case, e.g. the initial case "A" has "true" chemical rate constants, $k_{11} = 6\times10^{-12}$, $k_{22} = 4.5\times10^{-12}$, $k_{12} = 30\times10^{-12}$. This differs essentially from the initial case defined in Part II in that k_{12} is larger by a factor of two. This error in definition does not affect the results and conclusions of Part I.*

Can. J. Chem. Downloaded from www.nrcresearchpress.com by 69.46.99.164 on 09/04/12
For personal use only.

4. THE CALCULATIONS

The detailed results of the calculations are presented in Table I. The numbers to the left of the double line are the constants which specify the individual case: those to the right are the yields of molecular products and scavenged radicals. These are expressed as fractions of one initial radical pair. The yields of H_2 and H_2O_2 are expressed as the number of atoms or radicals which have recombined to give these molecular products. The numbers of molecules, H_2 and H_2O_2, formed are half these numbers. The number of water molecules re-formed is $[H_2O^*]$, the net decomposition of H_2O is $[-H_2O]$. The yields defined in this manner, symbolized by enclosure in square brackets, obey these stoichiometric relationships:

$$[H_2] + [H_2O^*] + [H] = [H_2O_2] + [H_2O^*] + [OH] = [H_2O^*] + [-H_2O] = 1.$$

(The yields for γ-ray spurs in Part I were expressed as the number of radicals, etc., per spur. They are identical with the yields defined above when divided by the number of radical pairs/spur.)

The final yields at infinite time are estimated numerically as follows. If the number of radicals recombined at times t_A and t_B are N_A and $N_B(t_B > t_A)$ then the number of radicals recombined at infinite time is $N_\infty = N_B + 9.5(N_B - N_A)$. This formula is justified in the Appendix. The yields of radicals which escape recombination are small and obtained by difference between two larger numbers, e.g. $[OH] = [-H_2O] - [H_2O_2]$. Small errors in estimating the molecular yields make larger errors in the radical yields. The radical yields, particularly at high L.E.T., have consequently rather low numerical precision.

The results of a typical calculation are shown in Fig. 1. The features of interest are firstly, the time scale during which significant reaction takes place—four orders of magnitude are plotted—and secondly, the large amount of total recombination which occurs in 10^{-9} seconds as compared with the extent of recombination in γ-ray spurs (Fig. 1, Part I). The effects of diffusion control are shown by the crossing of the curves for $[H_2]$ and $[H_2O_2]$. Initially $[H_2]$ is greater than $[H_2O_2]$ because $k_{11} > k_{22}$. After 10^{-10} seconds, however, hydrogen atoms have been removed from the center of the track so that $k_{11}[H]^2$ is less than $k_{22}[OH]^2$, and the yield of H_2O_2 becomes greater than that of H_2.

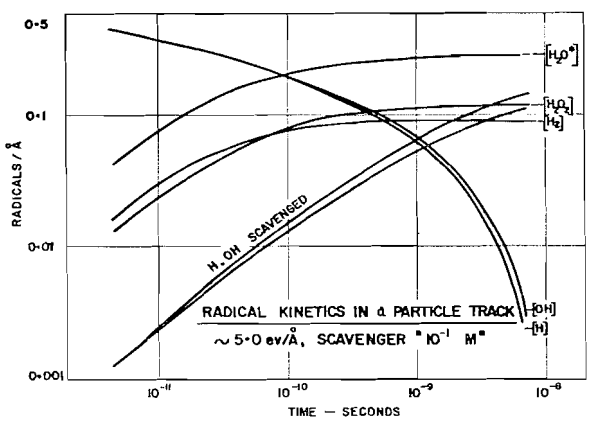


FIG. 1. Kinetics of recombination in a cylindrical track for case I.

Can. J. Chem. Downloaded from www.nrcresearchpress.com by 69.46.99.164 on 09/04/12
For personal use only.

TABLE I

Computed molecular and radical yields for cylindrical tracks

Case		k_{11} $\times 10^{12}$	k_{22} $\times 10^{12}$	k_{12} $\times 10^{12}$	$k_{13}=k_{23}$ $\times 10^{12}$	D_1 $\times 10^5$	D_2 $\times 10^5$	D_3 $\times 10^5$	$N_1=N_2$	β_1 $\times 10^{-7}$	β_2 $\times 10^{-7}$	$C_3\div 6$ $\times 10^{17}$	$[H_2]$	$[H_2O_2]$	$[H_2O^*]$	[H]	[OH]	$[-H_2O]$
A	Variation of track	6.0	4.5	15.0	10.0	8.0	2.0	2.0	0.1	1.0	1.0	1.0	0.208	0.370	0.338	0.454	0.292	0.662
B	density	"	"	"	"	"	"	"	0.2	"	"	"	0.272	0.412	0.418	0.307	0.168	0.580
C		"	"	"	"	"	"	"	0.5	"	"	"	0.338	0.438	0.494	0.168	0.068	0.506
D		"	"	"	"	"	"	"	1.0	"	"	"	0.371	0.438	0.531	0.098	0.031	0.469
E		"	"	"	"	"	"	"	2.0	"	"	"	0.391	0.427	0.550	0.059	0.023	0.450
F		"	"	"	"	"	"	"	10.0	"	"	"	0.408	0.418	0.578	0.013	0.004	0.422
G	Variation of	6.0	4.5	30.0	"	"	"	"	0.5	"	"	1	0.224	0.290	0.651	0.122	0.056	0.346
H	scavenger con-	"	"	"	"	"	"	"	"	"	"	10	0.214	0.279	0.634	0.152	0.087	0.369
I	centration	"	"	"	"	"	"	"	"	"	"	10^2	0.185	0.237	0.554	0.262	0.210	0.446
J		"	"	"	"	"	"	"	"	"	"	10^3	0.134	0.150	0.390	0.476	0.460	0.610
K	No diffusion of scavenger	"	"	"	10^{-2}	"	"	"	"	"	"	10^6	0.128	0.138	0.370	0.502	0.492	0.630
L	D_3 reduced	"	"	"	10.0	"	"	0.5	"	"	"	10^3	0.132	0.151	0.391	0.476	0.456	0.608
M	Varying k_{12}	"	"	10	"	"	"	2.0	"	"	"	1.0	0.408	0.522	0.368	0.206	0.092	0.614
N		"	"	3.0	"	"	"	"	"	"	"	"	0.576	0.724	0.166	0.258	0.110	0.834
O		"	"	90	"	"	"	"	"	"	"	"	0.098	0.123	0.850	0.050	0.026	0.149
P	Varying spur	"	"	30.0	"	"	"	"	"	0.5	0.5	"	0.220	0.288	0.650	0.130	0.062	0.350
Q	diameter	"	"	"	"	"	"	"	"	1.0	1.0	"	0.224	0.290	0.651	0.122	0.056	0.346
R		"	"	"	"	"	"	"	"	2.0	2.0	"	0.224	0.294	0.660	0.116	0.046	0.340
S	Varying β_1	"	"	"	"	"	"	"	"	0.65	1.0	"	0.228	0.344	0.620	0.152	0.036	0.380
T		"	"	"	"	"	"	"	"	0.4	"	"	0.258	0.434	0.538	0.204	0.028	0.462

NOTE: The columns to the left of the double line refer to the parameters of the track and are explained in Sections 3 and 4. The columns to the right of the double line give the computed yields defined in Section 4.

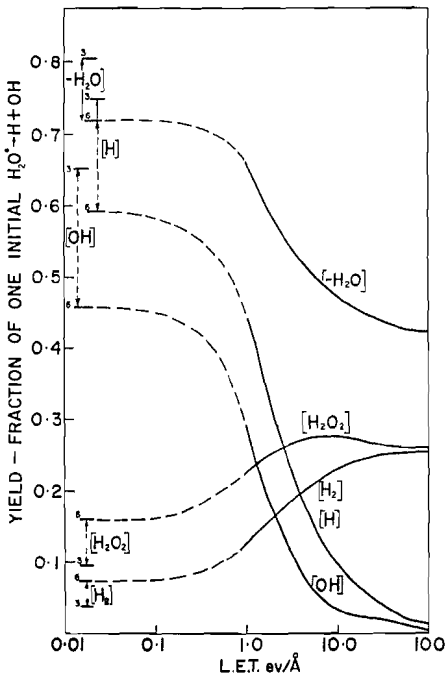


FIG. 2. Variation in yields with track density. The solid lines at the right of the figure are obtained from cases A–F. The yields at the left of the figure, plotted at L.E.T. of 0.02 ev/Å are for spherical spurs with three or six radical pairs/spur. The dotted lines are interpolations; no calculations have been made in this region. The scale of L.E.T. is arbitrary and can only be compared qualitatively with Fig. 3. For further details see text.

5. VARIATION IN YIELDS WITH TRACK DENSITY

The variation in yield with track density is shown in Fig. 2. The solid curves cover the range 0.1–10 radical pairs/Å and are derived from cases A–F (Table I). These cases use the rate constants, diffusion constants, and other parameters chosen for the "initial case" in the previous section. Note again that the scale of linear energy transfer in ev/Å is obtained from the track density using the arbitrary value of 10 ev/radical pair. Yields for γ-ray spurs for the same choice of rate constants and diffusion constants are plotted at a value of 0.02 ev/Å (corresponding to Compton recoils generated by ~1-Mev γ-rays). Values for both three and six radical pairs/spur are shown.

The yields are expressed as the number of molecules or radicals formed per initial H_2O dissociated. These are identical with the figures given in Table I except that the values of $[H_2]$ and $[H_2O_2]$ are divided by two. The yields as plotted are proportional to G-values (molecules/100 ev). The dotted portions of the curves in Fig. 2 lie in the region where the track expands partly in spherical and partly in cylindrical geometry. The present calculations do not cover this range and the curves have been drawn on the assumption that there is an asymptotic approach of the yields to the values for isolated spurs.

The calculations have been carried over the extreme range for which the cylindrical approximation is valid; at a track density as low as 0.1 radicals/Å and with a value of 10 Å for the modulus of the Gaussian, the track may be more correctly visualized as a series of spherical spurs which are just overlapping or touching. The errors involved are probably small because of the short time which elapses before such a track expands to a

Can. J. Chem. Downloaded from www.nrcresearchpress.com by 69.46.99.164 on 09/04/12
For personal use only.

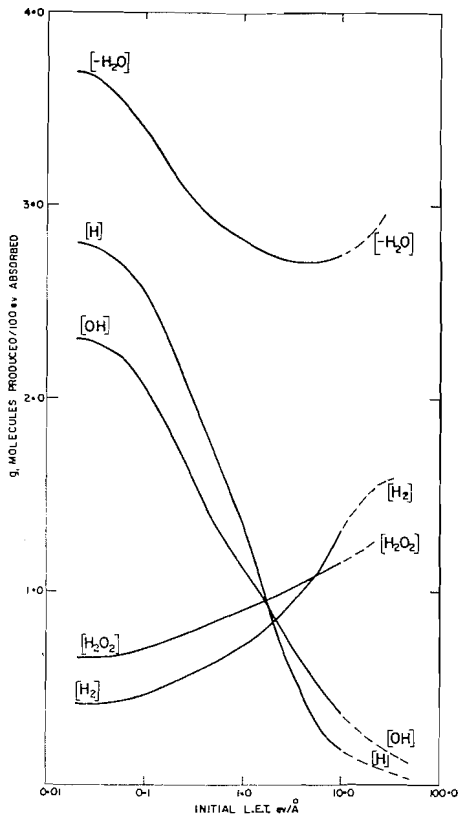


FIG. 3. Experimental variation in yields with initial track density. The figure shows smoothed, idealized curves based largely on the data of Schwarz, Caffrey, and Scholes.

uniform cylinder and because of the relative insensitivity of the yield to the initial track diameter. The errors will be in the direction of underestimating the amount of recombination.

Figure 2 is qualitatively in good agreement with experiment and may be compared with Fig. 3, which presents the experimental data for pure water in a somewhat idealized fashion. Figure 2 should also be compared with Figs. 2–16, reference 13, which present similar curves for acid solutions. The experimental curves are similar and differ mainly in numerical details.

Both in theory and experiment the yields of radicals decrease and the molecular yields increase with increasing L.E.T. In very dense tracks the radical yields are virtually zero. At the same time the ratio of the molecular yields $[H_2O_2]/[H_2]$ decreases. At low L.E.T. $[H_2O_2] > [H_2]$ but at high L.E.T. they approach equality. In the calculation the inequality arises because of the greater diffusion constant chosen for hydrogen atoms; this removes hydrogen atoms more rapidly from the high-density region of the track where the bulk of bimolecular recombination takes place. In the highest-density cylindrical tracks the effects of diffusion are reduced and the yields are not very different from those predicted by homogeneous kinetics.

The small maximum in the calculated value of $[H_2O_2]$ is another consequence of the more rapid diffusion of hydrogen atoms. The studies in Part I showed that $[H_2O_2]$ was strongly influenced by the availability of hydrogen atoms which compete for OH radicals

Can. J. Chem. Downloaded from www.nrcresearchpress.com by 69.46.99.164 on 09/04/12
For personal use only.

by the $H + OH \rightarrow H_2O$ recombination. The maximum in $[H_2O_2]$ occurs where the diffusion of H atoms is becoming significant, their removal from the center of the track increases the availability of OH for recombination to H_2O_2, and consequently $[H_2O_2]$ shows a slight maximum. The effect is quite small and would be difficult to observe experimentally. The calculated maximum is only significant in illustrating the kinetic complexities of the system and the somewhat unexpected effects of competing processes.

It is possible that the experimentally observed increase in $G(H_2)$ at high L.E.T. (see Fig. 3 and ref. 4) making $G(H_2) > G(H_2O_2)$ could be the result of similar kinetic effects if k_{11} were made much larger than the values chosen here. A few calculations (not specified in Table I) showed, however, that the changes in the constants required to produce such an effect were too drastic to be reasonable.

(a) The Energy Scale

The calculated value of $[-H_2O]$ varies from ~0.8 for a γ-ray spur containing initially three radical pairs to ~0.5 for a track having 0.5 radical pairs/Å. Combining these figures with the value of ~10 ev/initial radical pair we find $G(-H_2O)$ (molecules/100 ev) to be ~8 for γ-rays and ~5 for a particle track with L.E.T. of 5 ev/Å. These values are greater, by a factor ~2, than the experimental values. $G(-H_2O)$ for γ-rays in neutral water is 3.7 (2). For 11-Mev α-particles in neutral water $G(-H_2O)$ is 2.57 (4). The energy required to produce one radical pair must be ~20 ev/radical pair (essentially double our initial estimate) to give agreement with experiment.

The same conclusion has been reached by both Schwarz, Caffrey, and Scholes (4) and Burton and Kurien (5). Both these groups of workers estimated *initial* values of $G(-H_2O)$, designated G^0, from experimentally determined values of $G(-H_2O)$, $G(H_2)$, and $G(H_2O_2)$. This was done by putting

$$G(H_2O^*) = G(H_2) + G(H_2O_2). \qquad [4]$$

$G(H_2O^*)$ is the yield of water re-formed in the track and is equivalent to $[H_2O^*]$ in our terminology.[3] The values of G^0 are obtained by putting

$$G^0 = G(-H_2O) + G(H_2O^*).$$

The assumption of equation [4] is equivalent, in these calculations, to putting $k_{11} = k_{12} = k_{22}$ and $D_1 = D_2$. The constants used in this paper would make $G(H_2O^*) \simeq 1.3(G(H_2) + G(H_2O_2))$ so that the approximation is not unreasonable. With these assumptions Schwarz *et al.* found $G^0 = 4.4$–4.7 in neutral solution for Co-60 γ-rays increasing to 6.1 for 3.5-Mev α's. In acid solution Burton and Kurien found $G^0 = 6.3$–6.7 for Co-60 γ-rays and 50-kev X-rays, and $G^0 = 7.3$ for α-rays with an average energy of 3.4 Mev.

The constancy of G^0-values over a fair energy range in both series of experiments supports the validity of the calculation. A value of $G^0 \simeq 5$ corresponds again to an energy requirement of ~20 ev/radical pair. It follows, therefore, that the value of ~10 ev/radical pair, obtained experimentally by Firestone (3) from studies in water vapor, is not directly applicable to liquid water.

The gas-phase and liquid values of the initial radical yield may be reconciled if it is assumed that there is a very high initial probability of an H, OH pair recombining in the first few diffusion steps. The effective radical pair yield is then less than the instantaneous initial value (4).

[3]*Burton and Kurien use a modified relation* $G(H_2O^*) = (N-1)/N\,(G(H_2) + G(H_2O_2))$ *for* γ*-ray spurs where N is the number of radical pairs/spur.*

Can. J. Chem. Downloaded from www.nrcresearchpress.com by 69.46.99.164 on 09/04/12
For personal use only.

Can. J. Chem. Downloaded from www.nrcresearchpress.com by 69.46.99.164 on 09/04/12
For personal use only.

(*b*) *The Variation of* $G(-H_2O)$ *with L.E.T.*

The value of $[-H_2O]$ falls with increasing L.E.T. as do the experimental values of $G(-H_2O)$ in pure water. The experimental ratio $G(-H_2O)$ γ-rays/$G(-H_2O)$ 11.5-Mev α-rays is 1.4 (4). The calculated ratio using the "initial" rate constants and diffusion constants for a track with 0.5 radicals/Å is 1.4 if the γ-ray spur contains six radical pairs and 1.6 if the spur contains three radical pairs. This we regard as being in qualitative agreement with experiment. The values obtained in acid solution are in less satisfactory agreement. Burton and Kurien (5) report a value of 1.12 for the ratio of $G(-H_2O)$ γ-rays/$G(-H_2O)$ 5.3-Mev α-rays in 0.8 N H_2SO_4; significantly different from the values in neutral water and from our quoted calculations.

The calculated value of this ratio is, however, a sensitive function of the value chosen for k_{12}. A plot of the ratio of $[-H_2O]$ for a γ-ray spur containing six radical pairs to $[-H_2O]$ for cylindrical tracks with $N_1 = N_2 = 0.5$ radical pairs/Å, is shown in Fig. 4. A value of 1.1 for this ratio is obtained with $k_{12} = 0.5\times10^{-11}$, 1/8 of the value chosen in the initial series of calculations. This figure is derived from cases M, N, and O and some calculations on γ-ray spurs not published in Part I.

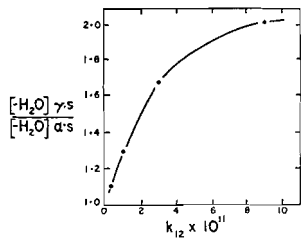


FIG. 4. The variation in $[-H_2O]$ as a function of k_{12}, expressed as the ratio $[-H_2O]$ γ's/$[-H_2O]$ α's for spherical spurs with six radical pairs/spur and cylindrical tracks with $N_1 = N_2 = 0.5$/Å.

The kinetic scheme used here to describe the Samuel–Magee model does, therefore, predict a reduction in $[-H_2O]$ in pure water with increasing L.E.T. which is qualitatively in agreement with experiment. The change in this and other yields with pH shows, however, that this kinetic scheme is incomplete. The observed pH effects may, *inter alia*, be equivalent to processes which, in effect, change the value of k_{12} in the simple kinetic scheme.

An increase in $G(-H_2O)$ at high L.E.T. has been observed by several workers. This has been qualitatively explained by Schwarz, Caffrey, and Scholes (4). It is supposed that the H and OH radicals from the dissociation of 1 water molecule are initially so close together that there is a fairly high probability of these two radicals recombining. At very high ionization densities however, the density of excited water molecules, and hence of H and OH radicals, is so high that one hydrogen atom is more likely to recombine with another hydrogen atom than to recombine with the OH from which it was dissociated. If this competing reaction for formation of H_2O_2 and H_2 is at all favorable then $G(-H_2O)$ will increase at high track densities.[4] This process could also explain the difference between the initial radical yields in the gas and liquid phases; in the gas phase the recombination of H and OH formed from 1 individual water molecule would

[4]*This explanation neglects the opposite effect where* H *atoms are closer to* OH *radicals produced from neighboring excited water molecules. This effect would decrease* $G(-H_2O)$ *as the track density increases and could exactly counterbalance the effect described above. This comment underlines the complexity of radical correlation effects.*

be less probable. Effects of this nature could be formally incorporated into the kinetic scheme of the model by the introduction of time-dependent rate constants. A procedure for doing this has been advanced by Monchick, Samuel, and Magee (11).

6. THE EFFECT OF SCAVENGER CONCENTRATION

The reduction in yields of molecular products as the concentration of scavenger is increased is calculated in cases G, H, I, J. The changes in the yields, expressed relative to the yield at the lowest concentration of scavenger, are shown in Fig. 5. The curve is qualitatively very similar to that for γ-ray spurs (I, Fig. 12) but the quantitative effect is somewhat smaller for cylindrical tracks than for the γ-ray spurs. This difference is also shown in the calculations of Ganguly and Magee (6). This arises because of the competition between the scavenging processes and the recombination processes. In the cylindrical tracks the recombination reaction occurs to a greater extent, and a given concentration of scavenger will have less effect here than in a spherical spur.

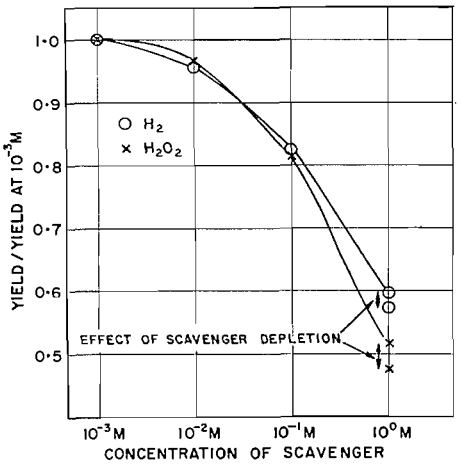


FIG. 5. Effects of scavenger concentration on the molecular yield. The abscissa is the ratio of $[H_2]$, $[H_2O_2]$ at the plotted scavenger concentration to the yield at "10^0 M". $k_{1S} = k_{2S} = 1\times10^{-11}$ (cases G, H, I, J). The two lower points at 10^0 M represent the relative yields obtained if depletion of scavenger at the center of the track is neglected (case K).

Schwarz, Caffrey, and Scholes (4), Burton and Kurien (5), and Senvar and Hart (10) have made extensive studies of yields as a function of scavenger concentration and have found good agreement with the one-radical calculations of Ganguly and Magee and those of Fricke and Flanders (8). These simpler calculations are, at the present time, more suitable for experimental comparison than our two-radical calculations because of the smaller number of parameters in the calculation.

Figure 5 shows that the yields of $[H_2]$ and $[H_2O_2]$ are changed at varying rates by the addition of scavenger. The curve for $[H_2]$ is at first lower than that for $[H_2O_2]$, but rises above it again at higher scavenger concentrations. This effect is numerically small and barely significant. In comparing these results with experiment it should be noted that, in these calculations, the scavenger reacts with both species simultaneously. In many experimental cases the scavenger reacts primarily with one species (e.g. halide ion with OH) and the other radical is removed by a secondary product (e.g. hydrogen atom by halogen atom). The over-all scavenger effects will also be affected by the competition

Can. J. Chem. Downloaded from www.nrcresearchpress.com by 69.46.99.164 on 09/04/12
For personal use only.

between the primary recombination steps. For these reasons a detailed study of effects of scavenger concentration with variation in track density and differing values of k_{13} and k_{23} has been deferred until more experimental data is available.

The effect of depletion of scavenger can be seen from case K. Here k_{13} and k_{23} and C_3 have been chosen in such a way that the effective concentration of scavenger—measured by the products $k_{13}C_3$ and $k_{23}C_3$—is the same as in case J even though C_3 is greater by a factor of 10^3. The recombination is, in effect, taking place in a constant concentration of scavenger so that there is no significant depletion of the scavenger. As expected, the effect of scavenger is greater if depletion at the center of the track is neglected, i.e. the values of $[H_2]$ and $[H_2O_2]$ are less in K than they are in J. The effect is, however, small, changing the yields by only 5–10%. Qualitative arguments, comparing the initial concentration of radicals in the spur ($\sim$10 M) with the concentration of scavenger, suggest that the effect would be quite large. The direct comparison of the initial concentration of radicals is therefore somewhat misleading. It should be noted that the major fraction of recombination takes place before much scavenging has taken place, i.e. the two reactions are not competing on an equal basis until some appreciable time has elapsed. During this time the track has expanded and reduced the concentration of radicals quite sharply. At longer times the effect of depletion at the center of the track is counteracted by the diffusion of radicals to regions of higher scavenger concentration.

The relatively small effects due to diffusion of scavenger are also demonstrated by comparing L and J. The diffusion constant for the scavenger D_3 is reduced by a factor 4 in L, and the yields are unchanged within the numerical accuracy of the calculation.

7. VARIATION IN YIELDS WITH TRACK DIAMETER

The geometrical factors in the diffusion process for spherical spurs and cylindrical tracks make a considerable difference in the sensitivity of yields to spur or track radius. In spherical spurs the yields are quite sharply reduced when R_1 and R_2 ($R = 1/\beta$ where β is the modulus of the Gaussian, see Section 3) are increased by a factor of 2. In cylindrical tracks, however, the yields are relatively insensitive to the initial track radius. The molecular yields change by only about 3% in cases P, Q, and R where R_1, R_2 change from 5 Å to 20 Å. For spherical spurs the yields are reduced by 60–80% over the same range (A, S, T, Table I, Part I). In spherical spurs where R_1 only is increased, R_2 being kept constant, $[H_2]$ decreases and $[H_2O_2]$ increases. A different effect is observed for cylindrical tracks. Here $[H_2]$, $[H_2O_2]$, and $[-H_2O]$ all increase as R_1 increases (Q, S, T). At the same time [H] increases and [OH] decreases. These effects arise because of the insensitivity of the yield to the initial spur radius and to the behavior of the recombination term $k_{12}(H)(OH)$, which affects the yields of $[H_2]$ and $[H_2O_2]$ strongly. By making R_1 greater than R_2 the value of this term is decreased and more like radicals are available for recombination. A comparison between γ-ray spurs and cylindrical tracks is made in Table II.

TABLE II

Ratio of yields for R_1 = 10 Å to R_1 = 25 Å, (R_2 = 10 Å)
(cases A, Z, Part I; cases Q, T, Part II)

	$[H_2]$	$[H_2O_2]$	$[-H_2O]$
γ-Ray spurs	2.0	0.65	0.70
Cylindrical tracks	0.84	0.67	0.75

Can. J. Chem. Downloaded from www.nrcresearchpress.com by 69.46.99.164 on 09/04/12
For personal use only.

These results are of considerable interest in connection with the interpretation of the different yields in light and heavy water. The most recent experimental work on the system is summarized by Dainton (7). For γ-rays it appears that $G(H_2) > G(D_2)$, $G(-D_2O) > G(-H_2O)$, and G(radicals D_2O) > G(radicals H_2O). The discussion in Part I on these isotope effects was related to earlier experimental work which suggested that $G(-D_2O) < G(-H_2O)$ and is consequently superseded by the experimental work reported by Dainton and his co-workers.

Dainton suggests that the change in yields can be explained by assuming that, initially, D atoms are more widely dispersed than H atoms, i.e. $R_1(D) > R_1(H)$. The first line in Table I shows that a change in this direction does decrease $[H_2]$ and increase $[-H_2O]$ for γ-ray spurs. The effect is, however, partially inverted for cylindrical tracks, $[H_2]$ is increased as R_1 is increased. Measurement of D_2 yields for densely ionizing particles may therefore shed some light on the origin of isotope effects in water. It should also be noted that this change in R_1 affects the yield of $[H_2O_2]$ as well so that one would expect $G(H_2O_2) < G(D_2O_2)$. This inequality is found experimentally in some, but not all, of the aqueous systems which have been studied.

The mechanism proposed by Dainton to account for the larger displacement of D atoms requires some hydrogen atoms to be formed by the process: $e^-_{aq} + H_2O \rightarrow H + OH^-$. The Samuel–Magee model as originally proposed discounts this type of process.

8. GENERAL CRITIQUE OF THE SAMUEL–MAGEE MODEL

The original model proposed by Samuel and Magee can be modified in many ways without, in principle, changing the basic idea, namely that the radical and molecular yields arise from a bimolecular, diffusion-controlled reaction of H and OH. The inclusion of reactions between radicals and molecules and the concept of spatial correlation of the radicals (leading to time-dependent rate constants) are minor modifications to the kinetic scheme of the model. The principal criticism of the model is still that the mechanism of formation of free radicals H and OH from the initial ionized state ($H_2O^+ + e$(100 ev)) is neither established nor understood (12).

The model was originally advanced to explain the separation between radical and molecular yields of water. The relative values of these yields have been shown to be correctly predicted in a qualitative sense in the one-radical calculations cited elsewhere in this paper (1, 6, 8). The relative values of the yields of H_2O, H_2O_2, H, OH are qualitatively predicted in the two-radical versions of the model described in this series of papers. The variation of molecular yields with scavenger concentration has been predicted semiquantitatively in several treatments (6, 8, 9). The variation in yields with ionization density is, in its broad features, correctly predicted in the calculations of Ganguly and Magee and the two-radical model in this paper. These successes of the model are powerful arguments in favor of its validity. To be more specific, one can conclude from the comparison of theory and experiment that H_2 and H_2O_2 are formed by kinetically similar mechanisms and that these are bimolecular diffusion-controlled reactions, probably simple recombinations H + H, OH + OH, and H + OH.

On the other hand, the model, in the simple formulation discussed here, predicts neither the variations in yield with pH, nor the details of the yields at high-track density (inversion of the relations $[H_2] < [H_2O_2]$ and the increase in $G(-H_2O)$) and does not explain the isotope effects. (We reject large *ad hoc* variations in rate constants as "explanations" of such effects.) Variations in yields with pH require the introduction of reactions involving hydrogen ions. These, however, are an elaboration of the kinetic

Can. J. Chem. Downloaded from www.nrcresearchpress.com by 69.46.99.164 on 09/04/12
For personal use only.

scheme and so do not alter its essence. Variations in yield at high-track density may also be explained by radical–molecule reactions, and/or by taking into account the spatial correlation of free radicals. These, again, elaborate the kinetic scheme, but do not, in principle, alter the model. The isotope effects cannot apparently be explained without some significant change in the kinetic scheme or of the constants and parameters in the system.

One of the more significant conclusions of these papers is that the use of gas-phase data to deduce the initial structure of spurs and tracks is, at best, misleading. Even after exercising the caution necessary when deducing a mechanism from kinetics, the qualitative successes of the model are very striking and lead us to believe that it describes correctly the majority of processes occurring in the life history of spurs and tracks. The model only does this, however, for spur sizes and radical densities that are significantly different from those deduced from gas-phase data. In Part I arguments are developed, from gas-phase data, showing that the "average" spur resulted from an energy deposition of 65 ± 10 ev and contained $\sim$6 radical pairs/spur. The calculations in this part show, however, that an energy deposition of $\sim$20 ev is required to produce one "effective" radical pair. This invalidates the use of Firestone's measurements on the radiolysis of water vapor to estimate the energy required to produce a radical pair in liquid water and, further, makes either the validity or the relevance of cloud-chamber data to determine the energy deposition/spur open to question. The discussions to be found in ref. 12 are still very pertinent to the present state of knowledge.

ACKNOWLEDGMENT

It is a pleasure to acknowledge the benefit of helpful and critical discussions with Dr. R. H. Betts.

REFERENCES

1. SAMUEL, A. H. and MAGEE, J. L. J. Chem. Phys. **21**, 1080 (1953).
2. DYNE, P. J. and KENNEDY, J. M. Can. J. Chem. **36**, 1518 (1958).
3. FIRESTONE, R. F. J. Am. Chem. Soc. **78**, 3226 (1956); **79**, 5593 (1957).
4. SCHWARZ, H. A., CAFFREY, J. M., and SCHOLES, G. J. Am. Chem. Soc. **81**, 1801 (1959).
5. BURTON, M. and KURIEN, K. C. J. Phys. Chem. **63**, 899 (1959).
6. GANGULY, A. K. and MAGEE, J. L. J. Chem. Phys. **25**, 129 (1956).
7. DAINTON, F. S. Radiation Research (Suppl. 1), 1, (1959).
8. FRICKE, H. and FLANDERS, D. A. J. Chem. Phys. **28**, 1126 (1958).
9. SCHWARZ, H. A. J. Am. Chem. Soc. **77**, 4960 (1955).
10. SENVAR, C. B. and HART, E. J. Proceedings 2nd United Nations Conference on Atomic Energy, Geneva, **29**, 19 (1958).
11. MONCHICK, L., MAGEE, J. L., and SAMUEL, A. H. J. Chem. Phys. **26**, 935 (1957).
12. MAGEE, J. L., KAMEN, M. D., and PLATZMAN, R. L. (*Editors*) Physical and chemical aspects of basic mechanisms in radiobiology. U.S. Natl. Research Council, Publ. No. 305 (1953).
13. PLATZMAN, R. L. Basic mechanisms of biological reaction to radiation. *In* Radiation biology and medicine. *Edited by* W. D. Claus. Addison-Wesley Publishing Co., Inc., Cambridge, Mass. 1958. p. 58.

APPENDIX

DIFFUSION WITH RECOMBINATION IN CYLINDRICAL GEOMETRY

(*1*) *The Equations*

The concentrations C_i of three types of particles are given by

$$[1] \qquad \frac{\partial C_i}{\partial t} = D_i\nabla^2 C_i - \sum_j k_{ij}C_iC_j,$$

Can. J. Chem. Downloaded from www.nrcresearchpress.com by 69.46.99.164 on 09/04/12
For personal use only.

where the D_i are diffusion constants and the k_{ij} are rate constants for recombination reactions. The operator ∇^2 is the cylindrical Laplacian:

$$\nabla^2 \equiv \frac{\partial^2}{\partial r^2}+\frac{1}{r}\frac{\partial}{\partial r}.$$

Initially the particles of types 1 and 2 are confined to a small cylindrical region, while those of type 3 are uniformly distributed through all space:

$$C_i(r,0) = \frac{N_i\beta_i^2}{\pi} e^{-\beta_i^2 r^2}$$

for $i = 1, 2$.

[2] $$C_3(r,0) = C_3,$$

where N_i is the number of particles per unit length and β_i the range parameter for type i.

We assume throughout that $k_{33} \equiv 0$.

The problem is the evaluation of the losses of particles (per unit length) due to the various modes of recombination:

[3] $$L_{ij}(t) = \int_0^t dt \int_0^\infty 2\pi k_{ij} C_i C_j r\, dr = \int_0^t \lambda_{ij}(t)\, dt.$$

(2) Co-ordinate Transformations

Before attempting the numerical solution of the system [1] it is useful to make several changes of variable. We define new dependent variables by

[4] $$X_i = t^{\frac{3}{4}} r^{\frac{1}{2}} C_i,$$

and introduce the expanding radial co-ordinate by

[5] $$\rho = r/(D_1 t)^{\frac{1}{2}}$$

where (by convention) D_1 is the larger of D_1 and D_2.

Equation [1] is transformed into

[6] $$t\frac{\partial X_i}{\partial t} = \Delta_i\left[\frac{\partial^2 X_i}{\partial \rho^2}+\frac{1}{4\rho^2}X_i\right]+\tfrac{3}{4}X_i+\frac{\rho}{2}\frac{\partial X_i}{\partial \rho}-\frac{1}{\rho^{\frac{1}{2}}D_1^{\frac{1}{4}}}\sum_j k_{ij}X_iX_j.$$

These transformations are similar to the ones used previously in spherical geometry. Their utility arises from the fact that in the absence of recombination terms the solution that is initially

$$C_1(r,t_0) = A\, e^{-\beta_1^2 r^2}$$

at time t_0 makes the right side of (6) vanish provided t_0 is chosen so that

$$4\beta_1^2 D_1 t_0 = 1.$$

Thus the numerical work is devoted to examination of that part of the behavior that is not simple outward diffusion.

Can. J. Chem. Downloaded from www.nrcresearchpress.com by 69.46.99.164 on 09/04/12
For personal use only.

It is straightforward to verify that in the absence of recombination the equation for X_3 reduces to

$$t(\partial X_3/\partial t) = X_3$$

or

$$[7] \qquad X_3 = \frac{t}{t_0} X_3(t_0).$$

The increase in X_3 is a consequence of the fact that in real space C_1 and C_2 at any point decrease like $1/t$ due to outward diffusion, so that the transformation that keeps these constant gives an apparent increase in X_3 corresponding to constant C_3.

Finally, it is expeditious to introduce a new time variable x such that equal increments in x correspond to expanding steps in t. This is related to the physical fact that as time proceeds the concentrations and their gradients decrease, and we can afford to pursue them more vigorously. After some numerical experiments the choice made for spherical geometry was adopted.

$$[8] \qquad t = t_0 e^x.$$

The final form of [6] is

$$[9] \qquad \frac{\partial X_i}{\partial x} = \Delta_i\left[\frac{\partial^2 X_i}{\partial \rho^2}+\frac{1}{4\rho^2}X_i\right]+\frac{3}{4}+\frac{\rho}{2}\frac{\partial X_i}{\partial \rho}-\frac{1}{\rho^{\frac{1}{2}}D_1^{\frac{1}{2}}}\sum_j k_{ij}X_iX_j.$$

(3) Solution of the Equations

The method of integration follows closely the method used for spherical geometry. Tables of X_1, X_2, X_3 at 40 values of ρ were used, and the space derivatives evaluated using the relations

$$\frac{\partial^2 X^{(n)}}{\partial \rho^2}+\frac{1}{4\rho^2}X^{(n)} = \frac{1}{h^2}[X^{(n+1)}-T_nX^{(n)}+X^{(n-1)}]$$

$$[10] \qquad \frac{\rho}{2}\frac{\partial X^{(n)}}{\partial \rho} = \frac{nT_n}{8}[X^{(n+1)}-X^{(n-1)}]$$

where h is the interval in the variable ρ, and

$$T_n = \left(1-\frac{1}{n}\right)^{\frac{1}{2}}+\left(1+\frac{1}{n}\right)^{\frac{1}{2}}.$$

The choice of T_n is related to a quirk of cylindrical geometry. The usual formula for the second derivative is

$$\frac{\partial^2 X^{(n)}}{\partial \rho^2} = \frac{1}{h^2}[X^{(n+1)}-2X^{(n)}+X^{(n-1)}].$$

Now for large n,

$$T_n = 2-\frac{1}{4n^2}+\text{terms of order } \frac{1}{n^4};$$

hence the use of T_n in place of 2 compensates for the inclusion of $(1/4\rho^2)X$ in the Laplacian. Also, for small n, $X \sim \rho^{\frac{1}{2}}$, and its derivatives are not well represented by finite difference formulas due to the singularity at $\rho = 0$. The choice of T_n makes the formulas exact for the function $X = \rho^{\frac{1}{2}}$, and hence compensates for this difficulty.

Can. J. Chem. Downloaded from www.nrcresearchpress.com by 69.46.99.164 on 09/04/12
For personal use only.

When [12] is substituted into [11], we are left with a set of 120 first-order differential equations for $X_i^{(n)}(x)$ for $i = 1, 2, 3$, and $n = 0, 1, \ldots.39$. The integration is carried out by the second-order "midpoint" method already used for spherical geometry.

The initial conditions and boundary conditions are obtained from [2], applying the co-ordinate transformations [4] and [5].

$$X_i^{(n)}(0) = t^{\frac{3}{4}} r^{\frac{1}{2}} \frac{N_i \beta_i^2}{\pi} e^{-\beta_i^2 r^2}$$

for $i = 1, 2$. With $t = t_0$ and $\rho = nh$

$$X_i^{(n)}(0) = \frac{N_i \beta_i^2 t_0}{\pi} (nh)^{\frac{1}{2}} (D_1)^{\frac{1}{4}} e^{-\beta_i^2 D_1 t_0 n^2 h^2}. \tag{11}$$

It follows that $X_1^{(0)} = X_2^{(0)} = 0$ for all time, and we also impose the condition that $X_1^{(39)} = X_2^{(39)} = 0$ for all time. Naturally, h must be large enough that this cutoff at "infinity" leads to negligible error.

The initial condition for X_3 is

$$\begin{aligned} X_3^{(n)}(0) &= t^{\frac{3}{4}} r^{\frac{1}{2}} C_3 \\ &= t_0 (nh)^{\frac{1}{2}} D_1^{\frac{1}{4}} C_3. \end{aligned} \tag{12}$$

Again $X_3^{(0)} = 0$ for all time. For the outer point $X_3^{(39)}$ we note that since X_1 and X^2 vanish here and $k_{33} \equiv 0$ there is no recombination. Thus equation [8] applies at the outer point, and

$$\begin{aligned} X_3^{(39)} &= X_3^{(39)}(t_0)\, t/t_0 \\ &= X_3^{(39)}(t_0)\, e^x. \end{aligned} \tag{13}$$

(4) The Integrals

For the loss integrals, we use

$$L_{ij} = \sum_x \lambda_{ij}(x),$$

where the loss during any interval Δx is

$$\begin{aligned} \lambda_{ij} &= \frac{dt}{dx} (\Delta x) \int_0^\infty 2\pi k_{ij} C_i C_j r\, dr \\ &= 2\pi D^{\frac{1}{2}} (\Delta x) \int_0^\infty k_{ij} X_i X_j\, d\rho \end{aligned} \tag{14}$$

after applying the transformation [4], [5], [8].

Similarly, the current values of the numbers of particles per unit length may be obtained from

$$\begin{aligned} N_i(x) &= 2\pi \int_0^\infty C_i r\, dr \\ &= 2\pi D_1^{\frac{1}{2}} \int_0^\infty X_i^{\frac{1}{2}} D_1^{\frac{1}{4}}\, d\rho. \end{aligned} \tag{15}$$

The integrands in [14] and [15] are available as tables obtained during the solution of the equations. The integrals are evaluated by Simpson's rule.

Can. J. Chem. Downloaded from www.nrcresearchpress.com by 69.46.99.164 on 09/04/12
For personal use only.

(5) Input and Output

The input data are defined by a choice of

$$\begin{array}{lllll} & t_0, & h = \Delta\rho, & \Delta x, & \\ k_{11}, & k_{22}, & k_{12}, & k_{13}, & k_{23}, \\ D_1, & D_2, & D_3, & & \\ N_1, & N_2, & \beta_1, & \beta_2, & C_3. \end{array}$$

It has been found that $\Delta x = 0.02$ is about the largest value that avoids instability in the solutions; $h = 0.3$ is a convenient choice. The value of t_0 depends on the physical parameters; it must set the pace of the co-ordinate system expansion to the pace of the actual diffusion. The "theoretically best" value is

$$t_0 = \tfrac{1}{4}\beta_1^2 D_1,$$

but it has been found that a rather smaller value

$$t \approx \tfrac{1}{6}\beta_1^2 D_1$$

avoids certain difficulties arising from the outer boundary conditions.

After every few steps in x (10 steps in most of the production runs), the following quantities are printed.

Elapsed time

$$\begin{array}{lllll} L_{11} & L_{12} & L_{13} & N_1 & \Sigma_1 \\ L_{22} & L_{12} & L_{23} & N_2 & \Sigma_2, \end{array}$$

where Σ_i is the sum of the four other quantities in its row. Σ_i should be independent of t, and its constancy is a check on the stability of the solution.

(6) Extrapolation to $t = \infty$

The printed results emerge at equal increments in x. It turns out that if the results for L_{11}, L_{12}, L_{22} are plotted as a function of the variable

$$y = e^{-x/2} = \sqrt{t_0/(T+t_0)}\ ,$$

where T is the elapsed time, they lie very nearly on a straight line for small y (large T). Thus for any of these terms,

$$L_\infty = L_F + \frac{y_F}{y_{F-1} - y_F}(L_F - L_{F-1})$$

$$= L_F + \frac{1}{(y_{F-1}/y_F) - 1}(L_F - L_{F-1}),$$

where L_F and L_{F-1} are the last and the penultimate values.

Now $y_{F-1}/y_F = e^{\frac{1}{2}\Delta x}$, and we have used $\Delta x = 0.2$. Thus

[16] $$L_\infty = L_F + 9.5\,(L_F - L_{F-1}).$$

It should be remarked that there is no particular justification for this recipe other than the empirical straightness of a line. At best, L_∞ given by [16] may contain one more significant figure than would be obtained by taking $L_\infty = L_F$.

Can. J. Chem. Downloaded from www.nrcresearchpress.com by 69.46.99.164 on 09/04/12
For personal use only.

Can. J. Chem. Downloaded from www.nrcresearchpress.com by 41.223.56.140 on 09/04/12
For personal use only.

THE RADIOLYSIS OF SOME ORGANIC HALOGEN COMPOUNDS IN AQUEOUS SOLUTION[1]

R. J. Woods and J. W. T. Spinks

ABSTRACT

Dilute aqueous solutions of some halogen-substituted ethanols, acetaldehydes, and acetates have been irradiated with Co^{60} gamma rays, and the yield of acid products determined. Irradiations were carried out using air-saturated solutions and also solutions from which the air had been displaced by nitrogen or hydrogen. The acid yields are correlated with the structure of the organic compounds.

INTRODUCTION

The action of ionizing radiations on certain organic chloro-compounds has been studied extensively, both in aqueous solution and as two-phase systems with water, with a view to their use as chemical dosimeters, though little consideration has been given to the chemical reactions taking place (1). Two-phase systems of chloroform or tetrachloroethylene with water have received most attention; when irradiated in the presence of air both give high yields of hydrochloric acid which are directly proportional to the dose of radiation received. The acid is formed by a chain reaction and the yields are dependent on the temperature, dose rate, and energy of the incident radiation, and are lowered by traces of impurities. These variables curtail the usefulness of the systems for dosimetry; their effect may be reduced by increasing the proportion of water in the system, for example by using dilute aqueous solutions of the organic compounds, though the amount of acid formed by a given dose of radiation falls if this is done. However, the ease with which acid can be determined in an aqueous solution suggested that it would be worth while to measure the acid formed from solutions of other organic halogen compounds on irradiation, and attempt to correlate the yield of acid with the structure of the compound. The halogen-substituted hydrocarbons are normally only slightly soluble in water but by substituting a suitable group, which for convenience will be referred to as the functional group, in the molecule, water-soluble compounds can be obtained. The present study employs a series of halogen-substituted ethanols, acetaldehydes, and acetates in which the functional groups are hydroxymethyl, aldehyde, and carboxylate respectively.

The compounds were irradiated as 0.1 molar solutions of the neutral compounds and 0.1 normal solutions of the barium salts of the substituted acids. Yields of acid were determined by titration with aqueous alkali and yields of halide ion, other than fluoride, by titration with silver nitrate solution; fluoride was estimated by a colorimetric method. Results are given to show the effect upon the acid yield of varying the dose rate and of displacing the air normally present by nitrogen or hydrogen, since previous work had shown that the yield from trichloroacetaldehyde (chloral) (2) and tribromoacetaldehyde (bromal) (3) was dependent upon the dose rate and the presence of oxygen. Some estimates of the oxygen consumed during radiolysis are given.

Experiment showed that the halogen was liberated as halide from every compound examined, though the yields of fluoride from fluorine-substituted compounds were generally

[1]*Manuscript received August 31, 1959.*
Contribution from the Department of Chemistry, University of Saskatchewan, Saskatoon, Saskatchewan.

low. The acid yields are discussed with reference to the structure of the compounds irradiated. The use of these halogen-substituted compounds in chemical dosimetry is discussed briefly.

EXPERIMENTAL

Materials

The distilled water used was redistilled from alkaline permanganate and then from acid dichromate solutions and stored in Pyrex bottles.

Reagent grade chemicals were used when these were available commercially. Materials of lower grade, and products prepared in the laboratory, were purified by crystallization to constant melting point or by repeated distillation, until the main fraction had a boiling range of less than 2° C. The purity of several of the bromo-compounds could be checked by treating them (10–20 mg) with excess 0.1 *N* sodium hydroxide solution and titrating the excess of alkali after a suitable interval (see Table VI) (cf. ref. 3). Equivalent weights determined in this way are given after the preparation of the appropriate compound. Whenever possible the radiolysis yields from two separate batches of a given compound were compared; in no case were there serious differences in yield between the different samples.

Reagent grade chloroform was washed 10 times by shaking with distilled water, distilled, and stored under water, in the dark.

Trifluoroacetaldehyde

Trifluoroacetaldehyde hydrate (fluoral hydrate), prepared from trifluoroacetic acid (4), was fractionated and the fraction, b.p. 103–105° C, dehydrated with hot, concentrated sulphuric acid. The gaseous fluoral was absorbed in a little less than the theoretical amount of water and the crystalline hydrate, which separated, filtered off, and dried over phosphorus pentoxide, m.p. 66–66.5° C.

Bromoacetaldehydes

The bromoacetaldehydes were prepared by brominating paraldehyde (5); omitting the sulphur catalyst, since this increased the quantity of tarry residue formed without markedly improving the yield of products, and distilling the volatile products from the reaction vessel under reduced pressure and as rapidly as possible when the reaction was complete. The distillate was carefully fractionated under reduced pressure to give monobromoacetaldehyde, b.p. 52–53° C/57–62 mm, dibromoacetaldehyde, b.p. 61–64° C/58–62 mm, and tribromoacetaldehyde (bromal), b.p. 43–45° C/4–5 mm.

The proportions of the three bromoacetaldehydes formed varied with the proportions of the reactants used and with the conditions of the bromination. For example, when 1360 g bromine (8.5 moles) was added dropwise to 193 g paraldehyde (equivalent to 4.4 moles of acetaldehyde) diluted with 400 ml carbon tetrachloride over a period of 4 hours and the mixture warmed to 50° C for a further 1 hour the products were 124 g monobromoacetaldehyde (1.0 mole), 300 g dibromoacetaldehyde (1.5 moles), and 179 g bromal (0.65 mole). The theoretical quantity of bromine, added to the paraldehyde – carbon tetrachloride mixture while it was being cooled with a cold-water bath, gave monobromoacetaldehyde in 80% yield. The proportion of bromal in the products could be increased by using a molar ratio of bromine to paraldehyde of 3:1 and stirring the reaction mixture at 50° C for several hours after adding the bromine: the products always included some dibromoacetaldehyde.

Both monobromoacetaldehyde and dibromoacetaldehyde polymerized on standing

Can. J. Chem. Downloaded from www.nrcresearchpress.com by 41.223.56.140 on 09/04/12
For personal use only.

and, for convenience, were converted into the stable hydrates immediately after distillation by being stirred with a small excess of water. Seed crystals to initiate crystallization of monobromoacetaldehyde hydrate were obtained by distilling a portion of the aldehyde–water mixture; the distillate (b.p. 97°/720 mm) crystallized in the condenser. Monobromoacetaldehyde hydrate crystallized from water as needles; m.p. between 61 and 95° C, depending upon the rate of heating. Dibromoacetaldehyde hydrate crystallized from water as needles, m.p. 61–61.5° C. (Found: equiv. wt., 75.1. Calc. for $C_2H_4O_2Br_2$: equiv. wt., 73.3.) Bromal hydrate, m.p. 54° C. (Found: equiv. wt., 294. Calc. for $C_2H_3O_2Br_3$: equiv. wt., 299.)

Tribromoacetic Acid

Fuming nitric acid (30 ml) was added dropwise, through a reflux condenser, to bromal (100 g) which was warmed to about 70° C with a warm-water bath. When the addition was complete (15 minutes) the temperature of the water bath was raised to 90–100° C and the reaction mixture kept at this temperature for 3 hours. Removal of the volatile materials by distillation under reduced pressure (90° C/30 mm) left a residue of white crystals which were recrystallized from a mixture of benzene and light petroleum to give tribromoacetic acid as white plates (88 g), m.p. 127.5° C, unchanged by further recrystallization. Found: equiv. wt., 291. Calc. for $C_2HO_2Br_3$: equiv. wt., 297. A further quantity of pure acid was recovered from the mother liquors (5 g; total yield 88% theoretical).

Dibromoacetic Acid

(*a*) Fuming nitric acid (15 ml) was added cautiously to dibromoacetaldehyde hydrate (26 g) contained in a flask fitted with a reflux condenser and heated in a boiling-water bath. The heating was continued for 1 hour after the acid had been added. The products were fractionated under reduced pressure, and the fraction collected, b.p. 123–125° C/17 mm (20.4 g; 77% theoretical). Found: equiv. wt., 221. Calc. for $C_2H_2O_2Br_2$: equiv. wt., 218. The acid solidified on standing (m.p. about 36° C) and could be crystallized, with difficulty, from light petroleum. The crystals were very deliquescent and the acid was more conveniently purified by distillation.

(*b*) (Cf. ref. 6, which gives the preparation of dichloroacetic acid from chloral hydrate.) To a solution of bromal hydrate (45 g) in water (45 ml), warmed to 50° C, were added calcium carbonate (15.3 g) and a solution of sodium cyanide (1 g) in water (3 ml). The mixture was shaken and allowed to stand at room temperature until its temperature, which slowly rose to 74° C after the cyanide had been added, started to fall. Isopropanol (1–2 ml) was added to curb frothing and the mixture gently refluxed for 20–30 minutes, cooled, and extracted with ether. The ether extract was dried over magnesium sulphate, the ether evaporated, and the residue fractionated under reduced pressure to give dibromoacetic acid, b.p. 109–111° C/10 mm (24.9 g; 76% theoretical) as a colorless liquid which rapidly solidified. Found: equiv. wt., 222.

Substituted Ethanols

2,2,2-Trichloroethanol was prepared by reducing chloral with either aluminum isopropoxide (7) or lithium aluminum hydride (8); both reactants gave the pure alcohol, b.p. 148° C/705 mm, 73° C/35 mm, in about 65% yield.

Reduction of bromal in a similar manner with either aluminum isopropoxide or lithium aluminum hydride gave 2,2,2-tribromoethanol as colorless crystals, m.p., after recrystallization from water or a mixture of benzene and light petroleum, 78° C. Found: equiv. wt., 93.5. Calc. for $C_2H_3OBr_3$: equiv. wt., 94.3. The yields of pure alcohol were about 60% and 20% respectively.

Can. J. Chem. Downloaded from www.nrcresearchpress.com by 41.223.56.140 on 09/04/12
For personal use only.

Reduction of dibromoacetaldehyde with aluminum isopropoxide gave 2,2-dibromoethanol, b.p. 66–67° C/3 mm (57% theoretical). Found: equiv. wt., 101. Calc. for $C_2H_4OBr_2$: equiv. wt., 102.

Chlorodifluoroacetic Acid and Dichlorofluoroacetic Acid

These acids were obtained from L. Light and Co. Ltd., Poyle Trading Estate, Colnbrook, Bucks, England, and were redistilled before use. The chlorodifluoroacetic acid had b.p. 124–126° C and the dichlorofluoroacetic acid b.p. 156–158° C.

Barium Salts

The acids were generally irradiated as solutions of the barium salt so that the pH of the solutions would be comparable to those of the neutral halogen compounds. The salt solutions were prepared either from the pure crystalline salt or by making up a standard solution of the acid in the presence of an excess of pure barium carbonate, subsequently filtering off the excess carbonate, and drawing a current of moisture-saturated air through the solution to bring it into equilibrium with the atmosphere. The crystalline salts were prepared by adding an excess of pure barium carbonate to aqueous solutions of the pure (chloroacetic) acids, filtering off the excess carbonate, and allowing the neutral solutions partially to evaporate at room temperature; higher temperatures caused some decomposition. The crystals deposited were collected, washed with water, and dried over phosphorus pentoxide; the barium content was determined gravimetrically by precipitation with dilute sulphuric acid. Found: Ba, 30.3, 30.3. Calc. for $C_4O_4Cl_6Ba$: Ba, 29.7%. Found: Ba, 35.8, 35.6. Calc. for $C_4H_2O_4Cl_4Ba$: Ba, 34.95%. Found: Ba, 41.0, 41.0. Calc. for $C_4H_4O_4Cl_2Ba$: Ba, 42.35%. The yield of acid obtained on irradiation was the same by whichever method the salt solution was prepared.

The calcium salts of dibromo- and tribromo-acetic acids and of trichloroacetic acid, prepared by adding calcium carbonate to a standard solution of the acid, were also irradiated, with results in good agreement with those obtained using solutions of the barium salts.

Irradiations

Irradiations were carried out using Co^{60} sources of about 1 and 90 curies, respectively. Dose rates were measured using the ferrous sulphate dosimeter (9), assuming a G value of 15.5 for the formation of ferric ion.

As far as possible solutions were prepared immediately before use; the pH of the solutions was measured using a Beckman model M pH meter. Aliquots (3.0 ml) were irradiated at room temperature in stoppered glass test tubes, 13×100 mm, supported in lucite blocks arranged concentrically about the 90-curie source or else supported in a water bath surrounding the 1-curie source.

The acid formed on irradiation was determined as described earlier (3), by titration with either 0.1 N sodium hydroxide solution (bromophenol blue) or 0.01 N silver nitrate solution (eosin). Occasionally the bromophenol blue was partially bleached when added to solutions which had been irradiated for a long time, the color change making it difficult to decide when the irradiated solution being titrated matched the color of the blank. The difficulty could be partly overcome by allowing the irradiated solution to stand for 1 or 2 hours before being titrated, and may be caused by peroxides formed on irradiation; neither bromine nor chlorine have been detected in the irradiated solutions. It was noted previously (3) that solutions of bromal might be titrated up to 24 hours after irradiation without change in the titer. When potassium iodide was added to solutions of bromal which had been irradiated, a little iodine was liberated immediately and larger amounts

Can. J. Chem. Downloaded from www.nrcresearchpress.com by 41.223.56.140 on 09/04/12
For personal use only.

Can. J. Chem. Downloaded from www.nrcresearchpress.com by 41.223.56.140 on 09/04/12
For personal use only.

were liberated on standing; the iodine was estimated by titration with 0.1 *N* sodium thiosulphate solution using a starch indicator. Iodine formed in solutions of iodoacetate by irradiation was estimated in the same way.

If the compound being irradiated was relatively stable to alkali, for example the substituted acetates, the acid formed could be titrated using an indicator changing color at a higher pH than bromophenol blue; bromocresol purple, bromothymol blue, and phenolphthalein were used to determine acid products that would not be neutralized at the bromophenol blue end point. However, difficulty was sometimes experienced in reaching a stable end point with these indicators, when it appeared that alkali-labile products were being slowly hydrolyzed by the alkali added; stable end points could be reached eventually by adding alkali as required, over a period of several minutes.

Fluoride was estimated by its action in bleaching a zirconium–alizarin red lake, measured with a photoelectric colorimeter (Megregian–Maier method) (10).

Solutions irradiated in the absence of air were treated before irradiation by passing a stream of either nitrogen or hydrogen through aliquots of the solution contained in irradiation tubes sealed with rubber serum-bottle caps. The gases were introduced into the tubes through a glass capillary which was pushed through the rubber cap, and escaped through a hypodermic needle inserted in the cap; a piece of adhesive tape effectively sealed the small holes left when the capillary and needle were removed. Traces of oxygen were removed from the nitrogen by passage through an alkaline solution of sodium hydrosulphite containing a catalytic amount of anthraquinone 2-sulphonate and from the hydrogen by passing it through a catalytic deoxidizer. Both gases were washed with water before being passed into the aliquots, which were purged for from 10 to 20 minutes; the shortest period of purging to ensure consistent results was about 5 minutes. An air-saturated solution of bromal gave the same yield of acid when irradiated in tubes sealed with glass stoppers or rubber serum-bottle caps.

Fluoral hydrate solutions were irradiated in both glass test tubes and in lusteroid tubes; the same acid yield was found in both cases.

The acid produced, in terms of microequivalents per liter, was plotted against the dose in kilorads and the slope of the straight line measured to give the acid yield in microequivalents per liter per kilorad. Each point on the graph was the average value of the acid produced for two or three duplicate irradiations; from 6 to 10 points were used to determine the slope of the line. Acid yields were found to be reproducible to $\pm 10\%$, or better, with different batches of material and for duplicate determinations at intervals of several months.

RESULTS

Acid yields in terms of microequivalents per liter per kilorad were multiplied by 0.945 to convert them to *G* values; the factor was derived in a similar manner to the factor used previously (3) to convert acid yields from microequivalents per liter per kiloroentgen to *G* values; it also includes a small correction for the difference in energy absorption of the ferrous sulphate dosimeter solution and the solutions of the halogen compounds. The errors introduced by using a single, average, value of the conversion factor for the solutions of slightly different density and electron density were estimated to be not more than 1% and may be discounted in view of the larger experimental uncertainty already present.

Acid Yield from Air-saturated Solutions

Table I gives the yield of acid from the compounds studied, determined by titration with sodium hydroxide solution, and, in parentheses, the yield of halide ion.

Can. J. Chem. Downloaded from www.nrcresearchpress.com by 41.223.56.140 on 09/04/12
For personal use only.

The indicator used in the acid–base titrations, bromophenol blue, was such that strongly acid products, for example the halogen-substituted acetic acids, would be neutralized while weak acids, acetic acid and carbon dioxide, would not. When both acid yield and halide yield (other than fluoride) were determined for the same compound it was found that the acid yield was the larger for the substituted aldehydes and alcohols and the smaller for the substituted acids. The acid yield was greater than the halide yield by about 18% for air-saturated solutions of bromal hydrate (cf. ref. 11) and tribromoethanol and by about 25% for solutions of dibromoacetaldehyde, showing that besides hydrobromic acid appreciable quantities of other strongly acid products are formed from these compounds; these products are probably bromine-substituted acetic acids. It has been reported that the yield of acid from aqueous solutions of chloral hydrate is about 30% greater than the yield of chloride when they are irradiated with either Co^{60} gamma rays (12, 13) or Sr^{90} beta rays (13). No systematic attempt has been made to determine weakly acid products from our irradiations; a single determination of the acid formed from a solution of bromal hydrate (1020 rads/min) using both bromophenol blue and bromocresol purple as indicators gave a 17% greater yield with the latter indicator; carbon dioxide was removed from the solution before titrating. The yield of acid from the bromoacetates was from 30 to 50% lower than the yield of bromide, part of the organic acid originally present being converted to neutral products during the irradiation; carbon dioxide in the products was estimated approximately and was found sufficient to account for the loss of the acid groups by decarboxylation. Irradiated solutions of dibromoacetate and tribromoacetate, freed of carbon dioxide and titrated with alkali, gave the same titer when either bromophenol blue or phenolphthalein was used as indicator; thus weakly acid products were not formed and the bromoacetic acid originally present was not, in effect, neutralized by being converted to a much weaker acid. The negative G value shown for trifluoroacetate means that more acid was lost by decarboxylation than was formed by breakage of the carbon–fluorine bond.

Poor results were obtained when monobromoacetate was irradiated at low dose rates because of partial hydrolysis of the acid during the long periods of irradiation; at higher dose rates the irradiation times were shorter and the hydrolysis less important. Iodine liberated from monoiodoacetate appeared partly as iodide ion and partly as molecular iodine; the G values for each are given in Table I.

Hayon and Weiss (14) have irradiated monochloroacetic acid solutions with X-rays and report G_{Cl^-} values from 2 to 8 for air-saturated solutions (0.01 to 1 M) and 0.9 for deaerated solutions (0.1 M). They also report G_{Cl^-} 6 to 16 for deaerated solutions of trichloroacetic acid over the concentration range 10^{-2} to 1 molar (cf. Table III).

The concentration of the chloroform solution was limited to that of a saturated solution at the temperature of the experiment, i.e. 0.07 molar. However, both 0.07 molar and 0.1 molar solutions gave the same acid yield in the following instances: trichloroethanol, irradiated at 1020 and 17 rads/min, and chloral hydrate and trichloroacetate, irradiated at 1020 rads/min, and the G values for chloroform are directly comparable with the other values in Table I. Taplin (1) gives G_{acid} 25.5 and Teplý and Bednář (15) G_{Cl^-} 25.8 ± 1.3 for air-saturated chloroform solutions irradiated under conditions comparable to those for the values in Table I; the latter authors determined the acid produced in several ways and it appears that for chloroform the yield of acid and the yield of chloride are the same. Teplý and Bednář also give G_{CO_2} 8.4 for air-saturated chloroform solutions and G_{Cl^-} 6.3 for solutions from which the air had been displaced by nitrogen.

Acid Yield in the Absence of Oxygen

When the amount of acid produced was plotted against the dose of radiation received

TABLE I

Yield of acid from aqueous solutions of organic halogen compounds on irradiation*

Compound	G_{acid} dose rate 1020 rads/min	450 rads/min	17 rads/min
Aldehydes			
$Br_3C.CH(OH)_2$	80 (69)	114 (98)	440 (360)
$Br_2CH.CH(OH)_2$	24.5 (21)	25.5 (21.5)	51.5 (35)
$BrCH_2.CH(OH)_2$			(34)
$Cl_3C.CH(OH)_2$	43	50	112
$F_3C.CH(OH)_2$	6.7 (~1.5)		7.1
Alcohols			
$Br_3C.CH_2OH$	36.5 (31)	38 (32)	104 (89)
$Br_2CH.CH_2OH$			(31.5)
$BrCH_2.CH_2OH$			(9.5)
$Cl_3C.CH_2OH$	24.5		27
Hydrocarbon			
Cl_3CH	27†		27†
Acids			
$ICH_2.COOH$	(2.6) (G_{I_2}, 1.4)		(9.2) (G_{I_2}, 0.6)
$Br_3C.COOH$	23 (41)	17.5 (38)	21 (39)
$Br_2CH.COOH$	9.2 (17.5)		15.5 (20.5)
$BrCH_2.COOH$	4.2 (6.6)		18? (27?)
$Cl_3C.COOH$	16		15.5
$Cl_2CH.COOH$	12		12
$ClCH_2.COOH$	4.2		8.9
$Cl_2CF.COOH$	7.2 (F^-, 0.8)	7.3	7.3
$ClCF_2.COOH$	5.1 (F^-, 2.9)	4.9	6.8
$F_3C.COOH$	−1.9 (0.04)		

Values of $G_{halide\ ion}$ are given in parentheses.
*Air-saturated 0.1 molar solutions, pH 3.5–5, 21±2° C. The acids were irradiated as 0.1 normal solutions of the barium salt.
†A saturated aqueous solution of chloroform was used; 0.07 *M*.

a straight line was obtained whose slope was a measure of the yield of acid. If the irradiation was continued long enough a rather abrupt change in the slope of the line occurred, the slope after the break corresponding to a lower yield, or *G* value, than that found initially. The break has been correlated with the point at which oxygen originally present in the solution has been used up (2, 3), the rather abrupt nature of the change in slope showing that the concentration of oxygen is not important. After the break was reached the yield of acid was that from a solution deficient in oxygen; the break did not appear with irradiations in which the acid was formed very slowly, for example solutions of monochloroacetate irradiated at low dose rates, when sufficient oxygen could diffuse into the solution to meet the needs of the reaction. Apart from such cases the break was found with solutions of all of the halogen compounds studied.

Table II gives the acid yield from solutions of bromal hydrate both before and after the break corresponding to exhaustion of the oxygen present; the latter yields were variable, from experiment to experiment, since the rate at which oxygen diffused into the solutions was not controlled. For comparison acid yields are included for solutions from which the air had been displaced by nitrogen; these yields were lower than those for the oxygen-depleted solutions, though the difference became smaller as the dose rate was increased, increasing the rate of the radiolysis reactions but not the rate of oxygen diffusion. In Table III are given acid yields from solutions saturated with either air or nitrogen.

Acid yields obtained from nitrogen-saturated and hydrogen-saturated solutions are

Can. J. Chem. Downloaded from www.nrcresearchpress.com by 41.223.56.140 on 09/04/12
For personal use only.

compared in Table IV. In the presence of hydrogen the ratio of hydroxyl radicals to hydrogen atoms, formed initially in definite proportions by the action of the radiation upon the water, may be altered in favor of the hydrogen atoms by the reaction (16),

$$OH + H_2 \rightarrow H + H_2O. \qquad [1]$$

TABLE II

The effect of oxygen depletion on the yield of acid from bromal hydrate solutions*

Dose rate (rads/min)	G_{acid} Air-saturated solutions	Oxygen depleted	Air displaced by nitrogen
17	440 (360)	63–87 (87–130)	27.5 (20.5)
166	138	32	19.5
450	114	34	16
1020	82.5 (69.5)	17.5–20.5 (14)	16 (12)

Values of $G_{halide\ ion}$ are given in parentheses.
*0.1 molar solutions, pH 3.5–5, 21±2° C.

TABLE III

Yield of acid from organic halogen compounds irradiated in solutions saturated with either air or nitrogen*

Compound	G_{acid} Air-saturated solutions (17 rads/min)	Nitrogen-saturated solutions (17 rads/min)	Nitrogen-saturated solutions (1020 rads/min)
$Br_3C.CH(OH)_2$	440 (360)	27.5 (20.5)	16 (12)
$Br_2CH.CH(OH)_2$	51.5 (35)	(16)	
$Cl_3C.CH(OH)_2$	112	19.5	
$Br_3C.CH_2OH$	104 (89)	(18)	
$Cl_3C.CH_2OH$	27	13.5	
$Br_3C.COOH$	21 (39)	(14)	(10)
$Br_2CH.COOH$	15.5 (20.5)	9.1 (16.5)	6.0
$Cl_3C.COOH$	15.5	7.2	7.4
$Cl_2CH.COOH$	12	5.4	4.5
$ClCH_2.COOH$	8.9	5.6	3.2
$Cl_2CF.COOH$	7.3	8.2	6.9 (F^-, 0.25)
$ClCF_2.COOH$	6.8	3.7	4.0 (F^-, 0.7)
$F_3C.COOH$			−4.9

Values of $G_{halide\ ion}$ are given in parentheses.
*0.1 molar solutions, pH 3.5–5, 21±2° C. The acids were irradiated as 0.1 normal solutions of the barium salt.

TABLE IV

Yield of acid from organic halogen compounds irradiated in solutions saturated with either nitrogen or hydrogen*

Compound	G_{acid} Nitrogen-saturated solutions	Hydrogen-saturated solutions
$Br_3C.CH(OH)_2$	(20.7)	(19.8)
$Br_2CH.CH(OH)_2$	(15.8)	(15.0)
$Br_3C.CH_2OH$	(18.2)	(19.1)
$Br_3C.COOH$	(13.9)	(13.6)
$Br_2CH.COOH$	6.0† (10.0†)	6.0† (9.9†)
$Cl_3C.COOH$	7.2	6.9
$Cl_2CH.COOH$	5.4	5.1
$ClCH_2.COOH$	5.6	5.5

Values of $G_{halide\ ion}$ are given in parentheses.
*0.1 molar solutions, pH 3.5–5, 21±2° C. The acids were irradiated as 0.1 normal solutions of the barium salt. Dose rate, 17 rads/min.
†Solutions irradiated at a dose rate of 1020 rads/min.

Can. J. Chem. Downloaded from www.nrcresearchpress.com by 41.223.56.140 on 09/04/12
For personal use only.

Hydrogen atoms and hydroxyl radicals would be expected to react differently with the halogen compounds and the absence of any marked difference between the yields for nitrogen- and hydrogen-saturated solutions suggests that at the low hydrogen concentrations used (about 10^{-3} M) the hydroxyl radicals react with the organic molecules in preference to hydrogen.

The ratio of the acid produced to the oxygen consumed could be estimated approximately from the position of the break in the graph, assuming that the solutions irradiated contained dissolved oxygen equal in amount to that in water under the same conditions of temperature and pressure; Table V gives some values estimated in this way. The values are the average for four or five experiments except for bromal hydrate when 30 values, distributed between the three dose-rate ranges shown, were available; the values were generally reproducible to within ± 0.5 unit, though they were not precise enough to show a consistent difference in a ratio when it was determined from the yield of acid and the yield of bromide separately. For bromal hydrate the ratio increased as the dose rate was increased; increasing the dose rate lowers the chain length of the chain-reaction forming acid and it may be inferred that less oxygen was consumed, relative to the amount of acid produced, in the chain-terminating steps than in the propagating steps. The values given in Table V show a tendency for less acid to be formed, relative to the oxygen used up, as the functional group was changed from $-CH(OH)_2$ (or H) to $-CH_2OH$ and —COOH. The ratio was also lowered when a bromine atom of bromal hydrate was replaced by hydrogen to give dibromoacetaldehyde. Teplý and Bednář (15) give a ratio for chloroform of 3.9–4.7 equivalents of hydrochloric acid formed per molecule of oxygen used up, estimated in the same way.

TABLE V

Ratio of the acid produced to the oxygen used up*

Compound	Acid groups estimated	Dose rate (rads/min)	Equivalents of acid gained / Molecules of oxygen used up
$Br_3C.CH(OH)_2$	HBr and total acid	9–18	3.0 ± 0.5
		160–450	3.6
		880–1460	4.0
$Cl_3C.CH(OH)_2$	Total acid	1020	4.1
Cl_3CH	Total acid	1020	4.2
$Br_3C.CH_2OH$	HBr and total acid	9–1020	3.6
$Cl_3C.CH_2OH$	Total acid	1020	3.1
$Br_3C.COOH$	HBr	1020	2.8
$Cl_3C.COOH$	Acid change	1020	2.3
$Br_2CH.CH(OH)_2$	HBr and total acid	390–1020	2.2

*Air-saturated 0.1 molar solutions, pH 3.5–5, $21 \pm 2°$ C. The acids were irradiated as 0.1 normal solutions of the barium salt.

Peroxides have been detected in irradiated solutions of the substituted acetates and of bromal hydrate; potassium iodide added to the latter solutions gave some iodine immediately and a greater amount on standing for several hours, the iodine formed immediately corresponded to hydrogen peroxide present in solution and that formed on standing to organic peroxides present. The concentration of hydrogen peroxide in the bromal solutions (dose rate 1020 rads/min) reached a low equilibrium value and then remained constant, but the concentration of organic peroxide increased in proportion to the dose of radiation received with a G value of about 12.

Can. J. Chem. Downloaded from www.nrcresearchpress.com by 41.223.56.140 on 09/04/12
For personal use only.

Effect of Dose Rate

The effect of changing the dose rate upon the yield of acid products has been examined by determining yields at two or three standard dose rates (cf. Tables I, II, and III). In the absence of oxygen, changes in dose rate had only a slight effect; a larger effect was observed in the presence of oxygen but only for those compounds which gave a high yield of acid products, indicative of a chain reaction, and then only at those dose rates at which the chain reaction was postulated. Dibromoacetaldehyde (Fig. 1) and tribromoethanol, for example, showed a dose rate dependency at dose rates in the region of 17 rads/min, but the acid yields were almost independent of dose rate between 450 and 1020 rads/min.

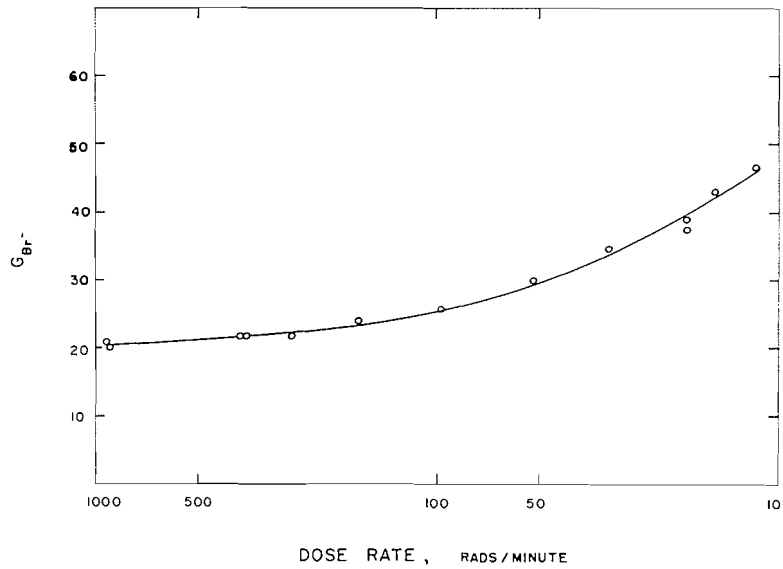


FIG. 1. Variation in G_{Br^-} with dose rate. Irradiation of 0.1 molar dibromoacetaldehyde hydrate solution, pH 4.2, 19° C.

Other work has shown that for dose rates in the range 1 to 60 rads/min G_{acid} for chloral hydrate (2) and bromal hydrate (3) was inversely proportional to the square root of the dose rate. The present work shows that this relationship is not obeyed closely at higher dose rates and it is possible that the yield of acid becomes independent of the dose rate as this is increased still further. The square root relationship was explained by postulating a chain reaction in which the termination step was the combination of two of the chain-propagating free radical intermediates to give a stable product; as the dose rate is increased the concentration of free radicals becomes greater and the chain length shorter. When the concentration of radicals becomes sufficiently high the chain length will approach unity and, unless the radicals interfere with the propagating steps, the acid yield will approach a constant value as the dose rate is increased. It is noteworthy that G_{acid} values for dibromoacetaldehyde and tribromoethanol, when they have reached the stage of being almost independent of dose rate, and some other dose rate independent G_{acid} values in Table I are greater than the sum of the probable G_H and G_{OH} values for water (about 5–6) and hence, if these inorganic radicals are responsible for the chemical changes occurring upon irradiation, each inorganic radical must be able to initiate reactions leading to the formation of several molecules of acid.

Can. J. Chem. Downloaded from www.nrcresearchpress.com by 41.223.56.140 on 09/04/12
For personal use only.

Action of Alkali on the Halogen Compounds

Most of the halogen compounds listed in Table I react readily with dilute aqueous alkali and these reactions were used as the basis for estimating the purity of several of the bromo-compounds (cf. ref. 3); a summary of the results is given in Table VI.

TABLE VI

Reaction of bromo-compounds with aqueous alkali*

Compound	Equiv. NaOH neutralized / Mole of compound	Estimated time for complete reaction
$Br_3C.CH(OH)_2$	1.0	Less than 1 minute
$Br_2CH.CH(OH)_2$	3.0	3–5 minutes
$BrCH_2.CH(OH)_2$	About 1.5	1–2 hours
$Br_3C.CH_2OH$	3.0	5 hours
$Br_2CH.CH_2OH$	2	5 hours
$BrCH_2.CH_2OH$	1	5–10 minutes
$Br_3C.COOH$	1.0	Neutralized immediately, about 3% hydrolysis and fission in 4 hours
$Br_2CH.COOH$	1.0	Neutralized immediately, about 1% hydrolysis in 18 hours
$BrCH_2.COOH$	2.0	Less than 1 minute

*Excess 0.1 *N* sodium hydroxide solution, titrated after reaction using phenolphthalein as indicator.

DISCUSSION

Effect of Structure on Acid Yield

Table I shows that for air-saturated solutions of the compounds studied the acid yield falls as (*i*) a halogen atom is replaced by hydrogen or by a more electronegative halogen, and (*ii*) as the functional group is changed from $-CH(OH)_2$ to $-CH_2OH$, to $-COO^-$. The acid yield from the one substituted hydrocarbon included, chloroform, is the same as that from the corresponding alcohol, trichloroethanol, in which the hydrogen is replaced by a hydroxymethyl group. Although acid yields may be changed by altering the dose rate, the relative position of the compounds if arranged in order of increasing acid yield is, in general, the same at any dose rate. Displacement of oxygen from the solutions by either nitrogen or hydrogen (Tables III and IV) lowers the acid yields but the relative position of the compounds is almost unchanged.

The carbon–halogen bond dissociation energy for the halogen-substituted methanes (Table VII) falls as the number of halogen substituents is increased and is lower for the less electronegative halogens. It is reasonable to assume that the carbon–halogen bond strength in the three groups of compounds studied, aldehydes, alcohols, and acid anions, will vary within each group in the same manner as in the substituted methanes as the number and nature of the substituting halogen atoms is changed. Thus, the greatest yields of acid are obtained on irradiation of the compounds which would be expected to have the lowest carbon–halogen bond dissociation energies, based upon the structure of the substituted methyl group present.

Chemical evidence leads to a similar conclusion; it is found that the compounds giving the greatest yield of acid on irradiation are those from which the halogen can be removed most readily by chemical reduction, and changes in halogen substitution which were found to lead to greater acid yields on irradiation also facilitate the removal of halogen by reduction. The effect of increasing halogen substitution, for example, upon the ease of reduction is shown by the action of zinc upon the chloroacetic acids (18); with this

Can. J. Chem. Downloaded from www.nrcresearchpress.com by 41.223.56.140 on 09/04/12
For personal use only.

reagent the chlorine atoms in trichloroacetic acid may be replaced one at a time by hydrogen, but each succeeding replacement requires longer or more vigorous treatment. A similar stepwise reduction of trichloroacetic acid can be achieved electrochemically by using cathodes with increasing hydrogen overpotential or by using progressively greater cathode potentials (ref. 19, pp. 47, 91). This is well illustrated by the polarography of trichloroacetic acid (Table VIII). The acid shows two waves corresponding to the removal of first one, and then a second, chlorine atom; the second wave, at the more negative half-wave potential, being the same as that obtained with dichloroacetic acid. The final chlorine could not be reduced under the conditions used though all three bromine atoms could be removed from tribromoacetic acid, the increasing half-wave potential for each succeeding step showing that reduction is progressively more difficult. The table also shows that bromine may be removed from a bromoacetic acid more readily than chlorine from the analogous chloroacetic acid.

The postulate that substituents influence the acid yield on irradiation through their effect upon the strength of the carbon–halogen bond would require the acid yield to increase with the following changes in the functional group, $-COO^- < H < -CH_2OH < -CH(OH)_2 < -COOH$, in accordance with the increasing electron attraction shown by these groups, and similar to their effect on the ease of removal of halogen from a trichloromethyl group, as demonstrated by polarography (Table IX). In practice it was found that the carboxylate ion gave lower yields of acid than the alcohols and these, in turn, lower yields than the aldehydes. However, isolated irradiations of the free substituted acids have indicated that though these give higher yields than the anions they give lower yields than the alcohols and aldehydes, despite the predicted lower carbon–halogen bond strength in the acids. It seems clear that the functional group may affect the acid yield in other ways besides its indirect action upon the strength of the carbon–halogen bond. The explanation probably lies in the possibility of radical attack at either of the two carbon groups present; the susceptibility of the functional group to such attack and the nature

TABLE VII

Carbon–halogen bond dissociation energies for halogen-substituted methane (ref. 17, pp. 20, 24)

Substituted methane	Halogen substituents, R			
	F	Cl	Br	I
		kcal/mole		
$H_3C—R$	118	81	67.5	54
$H_2RC—R$		78.5	62.5	
$HR_2C—R$		73.5	55.5	
$R_3C—R$		68	49	

TABLE VIII

Half-wave potentials for the reduction of halogen-substituted acetates*

Halogen, X	$XCH_2.COOH$	$X_2CH.COOH$	$X_3C.COOH$
		volt	
Cl	—	−1.57	−1.57
			−0.85
Br	−1.33	−1.35	−1.31
		−0.42	−0.42
			−0.32
I	−0.49		

*Refs. 20, 21. Saturated calomel reference electrode, pH 7.7–7.9, 25° C.

Can. J. Chem. Downloaded from www.nrcresearchpress.com by 41.223.56.140 on 09/04/12
For personal use only.

of the radical formed from it might then be more important than its indirect effect through the neighboring carbon group. The lower ratio of acid (or halide) produced to oxygen consumed as the functional group is changed from —$CH(OH)_2$ to —CH_2OH and —COO^- (Table V) suggests that more oxygen is used up through attack at the functional group with the latter compounds. The radicals formed from the acid groups, R.COO· and, by decarboxylation, R·, would also be expected to be less reactive than those formed from the alcohol and aldehyde, R.ĊHOH and R.Ċ$(OH)_2$.

TABLE IX

Half-wave potentials for the reduction of the trichloromethyl group*

Compound	Half-wave potential, volt	Ref.
$Cl_3C.COOH$	−0.45	22
$Cl_3C.Cl$	−0.75	23
$Cl_3C.COO^-$	−1.00	22
$Cl_3C.CH(OH)_2$	−1.35	24
$Cl_3C.CH_2OH$	−1.45	25
$Cl_3C.H$	−1.7	23

*Saturated calomel reference electrode, pH 7–8, other than $Cl_3C.COOH$, 25° C.

Mechanism

The first step in the interaction of ionizing radiation and a dilute aqueous solution is the absorption of the radiation by the water to give both molecular and free radical products. For Co^{60} gamma irradiation the molecular products, hydrogen and hydrogen peroxide, are formed with G values of about 0.4 and 0.8 respectively (26); they are unreactive, compared to the free radical products, and the low concentrations produced are not likely to react directly with the organic solutes used here. The radical products are formed with higher G values, about 2.7 and 2.0 for hydrogen atoms and hydroxyl radicals respectively (26; neutral solutions), and are believed to be responsible for most of the chemical action observed.

For convenience the initial reactions between the primary radicals and the solute may be divided into attack at either the substituted methyl group or the functional group. Attack at the substituted methyl group might be as follows;

$$X_2HC.R' + H \rightarrow HX + XH\dot{C}.R' \quad [2]$$

$$+ OH \rightarrow HOX + XH\dot{C}.R' \quad [3]$$

$$+ OH \rightarrow H_2O + X_2\dot{C}.R' \quad [4]$$

$$+ H \rightarrow H_2 + X_2\dot{C}.R' \quad [5]$$

where X is a halogen atom and R′ either —CH_2OH, —$CH(OH)_2$, or —COO^-. A disubstituted halogen compound is shown for the purposes of illustration; this could equally be a mono- or tri-substituted group, though in the latter case reactions involving hydrogen abstraction, reactions [4] and [5], would not be possible.

Breaking of the carbon–halogen bond during the initial reactions is supported by the relationship between the strength of this bond and the yield of halide on irradiation, particularly in those cases where a chain reaction is not postulated. The removal of halogen by hydrogen atoms (reaction [2]) is analogous to the reduction of halogen compounds at a cathode and during polarography, for which hydrogen atoms have been suggested as the active intermediates (cf. ref. 19, p. 47, and ref. 27). Removal of the halogen by

Can. J. Chem. Downloaded from www.nrcresearchpress.com by 41.223.56.140 on 09/04/12
For personal use only.

hydroxyl radicals (reaction [3]) is less likely and it has been shown (15) that carbon tetrachloride does not react with chemically produced hydroxyl radicals though chloroform does, presumably by hydrogen abstraction (reaction [4]). Polarographic data (Table VIII) suggest that hydrogen atoms are more likely to abstract halogen (reaction [2]) than hydrogen (reaction [5]) unless the halogen is firmly bound.

The primary inorganic radicals will also react with the functional groups present, the most probable reaction being hydrogen abstraction by the hydroxyl radicals. Most of the hydrogen atoms would be expected to react with the halogen-substituted group; polarography of the halogen-substituted aldehydes (28) shows that the halogen group is reduced in preference to the aldehyde group, both acids and alcohols are reduced less readily than the aldehydes. Hydrogen abstraction from an alcohol and an aldehyde hydrate would give the radicals $R.\dot{C}HOH$ and $R.\dot{C}(OH)_2$ respectively and electron transfer between an anion and a hydroxyl radical the carboxylate radical, $R.COO\cdot$.

The subsequent reactions of the organic radicals are uncertain. If oxygen is not present they may combine in pairs to give stable products or react with the solute, though the yields of acid products are relatively low and the extent of the reaction must be limited. The products obtained by irradiating solutions of the substituted acetic acids appear to be similar to those formed by anodic oxidation, in which carboxylate radicals are believed to be intermediates (ref. 19, p. 97, and refs. 29, 30). For example the products formed by irradiating an aqueous solution of monochloroacetic acid in the absence of air include carbon dioxide, carbon monoxide, formaldehyde, and hydrochloric acid (14), all of which are formed at the anode when the solution is electrolyzed (31, 32); in addition glyoxylic acid was identified among the radiolysis products and small amounts of chlorine, methylene chloride, and chloromethyl chloroacetate among the electrolysis products.

Oxygen markedly increases the yields of acid obtained on irradiation and is believed to add to the organic radicals, $R'\cdot$, to give relatively unreactive peroxy radicals, $R'O_2\cdot$, which may be unstable and break down to give a mixture of products or be converted to a more reactive alkoxy-type radical, $R'O\cdot$. The radical $R'O\cdot$ may itself be unstable and break down to give a mixture of products. The higher acid yields in the presence of oxygen can arise from the breakdown of oxygenated radicals and products to give acid materials or from the formation of reactive radicals which are able to sustain a chain reaction. The active radicals might be of the type $R'O\cdot$ or be inorganic radicals formed by the breakdown of unstable organic radicals.

Some evidence for the formation and subsequent breakdown of peroxy radicals during radiolysis arises from the formation of free fluoride from the fluorine-substituted acetates. Very little fluoride is formed from trifluoroacetate, even in the presence of oxygen (Table I), showing that the carbon–fluorine bond is not readily broken under the conditions of the irradiations. Chlorodifluoroacetate gives a greater yield of both fluoride and acid on irradiation (Table I); the yield of fluoride falls when the oxygen is absent (Table III). The carbon–fluorine bond can be broken chemically by substituting a hydroxyl group onto the carbon carrying the fluorine, when hydrolysis of the fluorine takes place in the presence of water, or by forming a free radical with the free electron on the fluorine-substituted carbon atom and allowing this to add oxygen to form a peroxy radical which will break down in the presence of water to give the fluorine as hydrogen fluoride (33). The chlorine present in chlorodifluoroacetate offers a point of attack not present in trifluoroacetate, and loss of the chlorine gives a radical which may react with either a hydroxyl radical or

Can. J. Chem. Downloaded from www.nrcresearchpress.com by 41.223.56.140 on 09/04/12
For personal use only.

oxygen and subsequently break down, i.e.,

$$\cdot CF_2.COO^- + OH \xrightarrow{H_2O} HOOC.COO^- + 2HF \quad [6]$$

or

$$\cdot CF_2.COO^- \xrightarrow{O_2,\ H_2O} HOOC.COO^-,\ 2HF. \quad [7]$$

The lower yield of fluoride in the absence of oxygen suggests that the changes represented by reaction [7] occur.

Iodoacetate gives a lower yield of acid (measured by $G_{I^-} + G_{I_2}$) than either monobromoacetate or monochloroacetate, though a higher yield might be expected in view of its weaker carbon–halogen bond. The concurrent formation of molecular iodine from the iodoacetate suggests that some of the initiating radicals (H and OH) are converted to less reactive iodine atoms by reaction with iodide ions or molecular iodine and so prevented from reacting with the iodoacetate. An equimolar amount of potassium iodide added to a bromal hydrate solution before irradiation prevented the formation of any acid products but gave molecular iodine with a G value of about 10. This is higher than the value for solutions of iodide alone (G_{I_2} about 1.7) and suggests that some organic radicals are formed and converted to peroxides before reaction with iodide or iodine occurs to terminate the reaction. Bromide and chloride are without effect since the chain reactions involved in the radiolysis of bromal and chloral hydrates are not hindered by the increasing concentrations of bromide and chloride ions respectively as the irradiations progress.

Organic Halogen Compounds in Dosimetry

The liberation of acid from organic halogen compounds upon irradiation has been used as the basis for methods of detecting and measuring ionizing radiation (1). The compounds most generally studied have been chloroform and tetrachloroethylene, usually in the form of the pure organic liquid overlayered with water. If a pH indicator dye is added to the aqueous layer the acid formed may be estimated visually or by means of a photoelectric colorimeter, or it may be estimated by any of the standard methods for determining strong acids. However, before the water-soluble acid can be estimated in the aqueous layer it is necessary to hydrolyze acid-precursors, generally acid chlorides, dissolved in the organic phase and extract the acid formed into the aqueous layer, a procedure that may require shaking or stirring for periods ranging from minutes to hours (cf. ref. 34). By using carefully purified materials the two-phase systems can be made sensitive to small doses of radiation of the order of 1.0 to 10 rads. The integral dose that such a system can measure is limited by the amount of oxygen present, and once this has been used up by the radiolysis reactions the yield of acid falls to a small value. Larger doses of radiation can be measured by adding small quantities of inhibitors, generally aliphatic or aromatic hydroxy compounds, which lower the amount of acid formed, and of oxygen used up, for a given dose of radiation received by the system. Exhaustion of the oxygen present still imposes an upper limit to the dose that can be measured unless steps are taken to introduce fresh oxygen while the irradiation is in progress.

The two-phase systems suffer from the disadvantage of being rather dependent upon the energy of the incident radiation. This may be largely overcome by using dilute aqueous solutions of organic halogen compounds, for example, chloral hydrate (12). The

Can. J. Chem. Downloaded from www.nrcresearchpress.com by 41.223.56.140 on 09/04/12
For personal use only.

greatest yields of acid have been obtained from aqueous solutions of chloral hydrate, bromal hydrate, and tribromoethanol; the yields shown in Table I may be increased by using more concentrated solutions (cf. refs. 3, 12) but they are generally lower than the yields from the two-phase systems. These solutions, in common with the two-phase systems, are broken down by chain reactions initiated by the radiation. The reactions are very susceptible to traces of impurities and the chain length, and hence the yield of acid is dependent on the dose rate and the temperature. These features associated with the chain reaction are undesirable in chemical dosimetry, though almost impossible to avoid, since the chain reaction itself is essential if small doses of radiation are to lead to the relatively large quantities of product that are required for a convenient determination. Among the water-soluble compounds, traces of impurity have proved particularly troublesome with bromal hydrate; chloral hydrate and tribromoethanol are available commercially for drug use and little difficulty would be expected, or has been experienced, in obtaining reproducible results with them.

If the greatest sensitivity is not required, it is possible to choose a system for which the acid yield is independent of dose rate; chloroform, in aqueous solution, is undoubtedly the first choice on the grounds of availability, ease of purification, and ease of preparation of the solution, though the acid yield is low compared to that from chloral or bromal hydrates, or the two-phase systems. Aqueous solutions have the advantage that any acid-precursors formed are hydrolyzed immediately and the acid products can be titrated to a sharp end point as soon as the irradiation is finished. In addition, chloroform has the advantage over the two-carbon compounds listed in Table I that only one acid product is formed, thus avoiding confusion that might arise between the yield of halide and the total yield of acid.

Acid formed from the non-polar compounds when they are irradiated in aqueous solution can be determined conveniently from the electrical conductivity of the solution (12, 15). By this means the acid formed can be measured continuously, at a distance, while an irradiation is in progress and the integral dose confirmed after the irradiation by titrating the acid formed.

ACKNOWLEDGMENTS

Grateful acknowledgment is made to the Atomic Energy Control Board for continued financial support and to Mr. E. C. Bailey for the fluoride analyses.

REFERENCES

1. TAPLIN, G. V. Radiation dosimetry. *Edited by* G. J. Hine and G. L. Brownell. Academic Press, Inc., New York. 1956. Chap. 8.
2. FREEMAN, G. R., VAN CLEAVE, A. B., and SPINKS, J. W. T. Can. J. Chem. **31**, 1164 (1953).
3. WOODS, R. J. and SPINKS, J. W. T. Can. J. Chem. **35**, 1475 (1957).
4. BRAID, M., ISERSON, H., and LAWLOR, F. E. J. Am. Chem. Soc. **76**, 4027 (1954).
5. LONG, F. A. and HOWARD, J. W. Org. Syntheses, **17**, 18 (1937).
6. COPE, A. C., CLARK, J. R., and CONNOR, R. Org. Syntheses, **19**, 38 (1939).
7. CHALMERS, W. Org. Syntheses, **15**, 80 (1935).
8. BROWN, W. G. Org. Reactions, **6**, 489 (1951).
9. WEISS, J., ALLEN, A. O., and SCHWARZ, H. A. Proc. Intern. Conf. Peaceful Uses Atomic Energy, **14**, 179 (1956).
10. STANDARD METHODS FOR THE EXAMINATION OF WATER, SEWAGE, AND INDUSTRIAL WASTES. 10th ed. American Public Health Assoc., New York. 1955. p. 101.
11. HEUSINGER, H., WOODS, R. J., and SPINKS, J. W. T. Can. J. Chem. **37**, 1127 (1959).
12. ANDREWS, H. L. and SHORE, P. A. J. Chem. Phys. **18**, 1165 (1950).
13. PLATFORD, R. F. Thesis, University of Saskatchewan, Saskatoon, Sask. 1958.
14. HAYON, E. and WEISS, J. Proc. Second Intern. Conf. Peaceful Uses Atomic Energy, **29**, 80 (1958).
15. TEPLÝ, J. and BEDNÁŘ, J. Proc. Second Intern. Conf. Peaceful Uses Atomic Energy, **29**, 71 (1958).
16. DAINTON, F. S. and HARDWICK, T. J. Trans. Faraday Soc. **53**, 333 (1957).

Can. J. Chem. Downloaded from www.nrcresearchpress.com by 41.223.56.140 on 09/04/12
For personal use only.

17. SEMENOV, N. N. Some problems in chemical kinetics and reactivity. *Translated by* M. Boudart. Princeton Univ. Press, Princeton, New Jersey. 1958.
18. DOUGHTY, H. W. and LACOSS, D. A. J. Am. Chem. Soc. **51**, 852 (1929).
19. ALLEN, M. J. Organic electrode processes. Chapman and Hall, Ltd., London. 1958.
20. ELVING, P. J. and TANG, C.-S. J. Am. Chem. Soc. **72**, 3244 (1950).
21. ELVING, P. J., ROSENTHAL, I., and KRAMER, M. K. J. Am. Chem. Soc. **73**, 1717 (1951).
22. ROSENTHAL, I., TANG, C.-S., and ELVING, P. J. J. Am. Chem. Soc. **74**, 6112 (1952).
23. KOLTHOFF, I. M., LEE, T. S., STOCESOVA, D., and PARRY, E. P. Anal. Chem. **22**, 521 (1950).
24. ELVING, P. J. and BENNETT, C. E. Anal. Chem. **26**, 1572 (1954).
25. ELVING, P. J. and BENNETT, C. E. J. Am. Chem. Soc. **76**, 4473 (1954).
26. HOCHANADEL, C. J. and LIND, S. C. Ann. Rev. Phys. Chem. **7**, 83 (1956).
27. HICKLING, A. Quart. Revs. **3**, 95 (1949).
28. KIRRMANN, A. and FEDERLIN, P. Bull. soc. chim. France, 944 (1958). FEDERLIN, P. Bull. soc. chim. France, 949 (1958).
29. WEEDON, B. C. L. Quart. Revs. **6**, 380 (1952).
30. WATERS, W. A. The chemistry of free radicals. Oxford at the Clarendon Press. 1946. p. 142.
31. KAUFLER, F. and HERZOG, C. Ber. **42**, 3858 (1909).
32. TROEGER, J. and EWERS, E. J. prakt. Chem. **58**, 121 (1898).
33. FRANCIS, W. C. and HASZELDINE, R. N. J. Chem. Soc. 2151 (1955). HASZELDINE, R. N. and NYMAN, F. J. Chem. Soc. 387 (1959).
34. SUTHERLAND, J. W. and SPINKS, J. W. T. Can. J. Chem. **37**, 79 (1959).

Can. J. Chem. Downloaded from www.nrcresearchpress.com by 41.223.56.140 on 09/04/12
For personal use only.

Can. J. Chem. Downloaded from www.nrcresearchpress.com by 69.46.99.164 on 09/04/12
For personal use only.

CYCLIALKYLATIONS OF ALKYL BENZENES WITH OLEFINS AND ALKYL HALIDES[1]

L. Ross C. Barclay, J. W. Hilchie, A. H. Gray, and (in part) N. D. Hall

ABSTRACT

A revised mechanism is given for the formation of octamethyloctahydroanthracene from 1,3,5-tri-*t*-butylbenzene and *t*-butyl chloride. 1,3,5-Tri-*t*-butylbenzene reacts with isopropyl chloride to yield an octamethylhydrindacene which also forms when 1,3,5-triisopropylbenzene is cyclialkylated with isobutene. 1,3,5-Triisopropylbenzene is cyclialkylated with 2-methyl-2-butene to yield a decamethylhydrindacene. Treatment of 1,3,5-triisopropylbenzene with 2-chloro-2,4,4-trimethylpentane yields a hydrocarbon, $C_{23}H_{38}$, most probably 1,1,3-trimethyl-5,6-diisopropyl-3-neopentylindan. Structures assigned to the cyclialkylation products are based on ultraviolet, infrared, and mass spectroscopic data, and in some instances classical syntheses. Mechanisms are suggested to account for these reactions.

INTRODUCTION

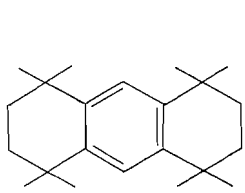
In this paper, a revision is presented for a mechanism to account for cyclialkylation of 1,3,5-tri-*t*-butylbenzene with *t*-butyl chloride to form octamethyloctahydroanthracene (I). In addition, similar cyclialkylations are applied to some other systems. For example, treatment of 1,3,5-tri-*t*-butylbenzene with isopropyl chloride under Friedel–Crafts conditions yielded an octamethylhydrindacene (III). 1,3,5-Triisopropylbenzene reacted with isobutene in the presence of isopropyl chloride also to produce III. Under similar conditions, triisopropylbenzene and 2-methyl-2-butene yielded a decamethylhydrindacene (IV). Treatment of triisopropylbenzene with 2-chloro-2,4,4-trimethylpentane yielded another new compound, $C_{23}H_{38}$, which also was formed by cyclialkylation of triisopropylbenzene with 2,4,4-trimethyl-1-pentene in the presence of isopropyl chloride. The compound $C_{23}H_{38}$ apparently is 1,1,3-trimethyl-5,6-diisopropyl-3-neopentylindan (V). The structures given to the cyclialkylation products are based on ultraviolet, infrared, and mass spectroscopic data, and in some instances on classical syntheses. Mechanisms are suggested to account for the cyclialkylations.

DISCUSSION

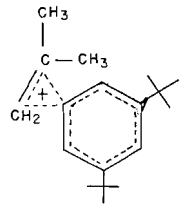
In an earlier publication (1), a mechanism was proposed for the formation of 1,1,4,4,-5,5,8,8-octahydroanthracene (I) from 1,4-di-*t*- or 1,3,5-tri-*t*-butylbenzene and *t*-butyl chloride involving the formation of a primary tri-*t*-butylbenzene carbonium ion and cyclialkylation with isobutene. Condon (2) proposed an alternative mechanism for the formation of I. His mechanism requires that this cyclialkylation takes place through the 2,4,4-trimethylpentyl carbonium ion which apparently rearranges through a protonated cyclopropyl carbonium ion to the dimethylhexyl carbonium ion. It has been demonstrated by Barclay and Hilchie (3) that this dimethylhexyl system can displace *t*-butyl groups from 1,4-di-*t*-butylbenzene to produce I. However, a more adequate test of Condon's mechanism would be to carry out alkylations of aromatics with 2-chloro-2,4,4-trimethylpentane to find if the initial 2,4,4-trimethylpentyl ion rearranges to the required 2,5-dimethylhexyl system under conditions favorable for the formation of I. According to Condon's mechanism, it would be expected that I should form from benzene or the *t*-butylated benzenes and 2-chloro-2,4,4-trimethylpentane in at least as good a yield as reported (4) for the preparation of I from the *t*-butylated benzenes and *t*-butyl

[1]*Manuscript received September 8, 1959.*
Contribution from the Department of Chemistry, Mount Allison University, Sackville, New Brunswick.

chloride. Benzene and 1,4-di-*t*-butylbenzene were therefore treated with 2-chloro-2,4,4-trimethylpentane under a variety of conditions which might be expected to cause cyclialkylation. However, no cyclialkylation products such as I could be detected in the reaction products. These negative results cannot be entirely conclusive but it does appear unlikely that this cyclialkylation proceeds via the 2,4,4-trimethylpentyl ion. The only objection to the initial mechanism proposed by Barclay and Betts (1) is that it involves a high energy primary carbonium ion. However, this neophyl ion could have a more stable bridged structure (II) where the neighboring phenyl group participates in the displacement of the hydride ion from a primary carbon.



(I)



(II)

Similar cyclic bridged phenonium ions have been postulated by Cram (5) for a variety of reactions and by Schmerling and co-workers (6) to explain aluminum-chloride-catalyzed isomerizations of alkyl benzenes. Recently, Douglas and Roberts (7) postulated removal of a hydride ion from the β-carbon of propyl benzene with "anchimeric assistance from the phenyl group" to produce a phenonium ion intermediate analogous to II. In our reactions the ion II would be expected to react with isobutene at the unsubstituted CH_2 group rather than at the more hindered branched position of II and therefore I is the octamethyloctahydroanthracene which forms.

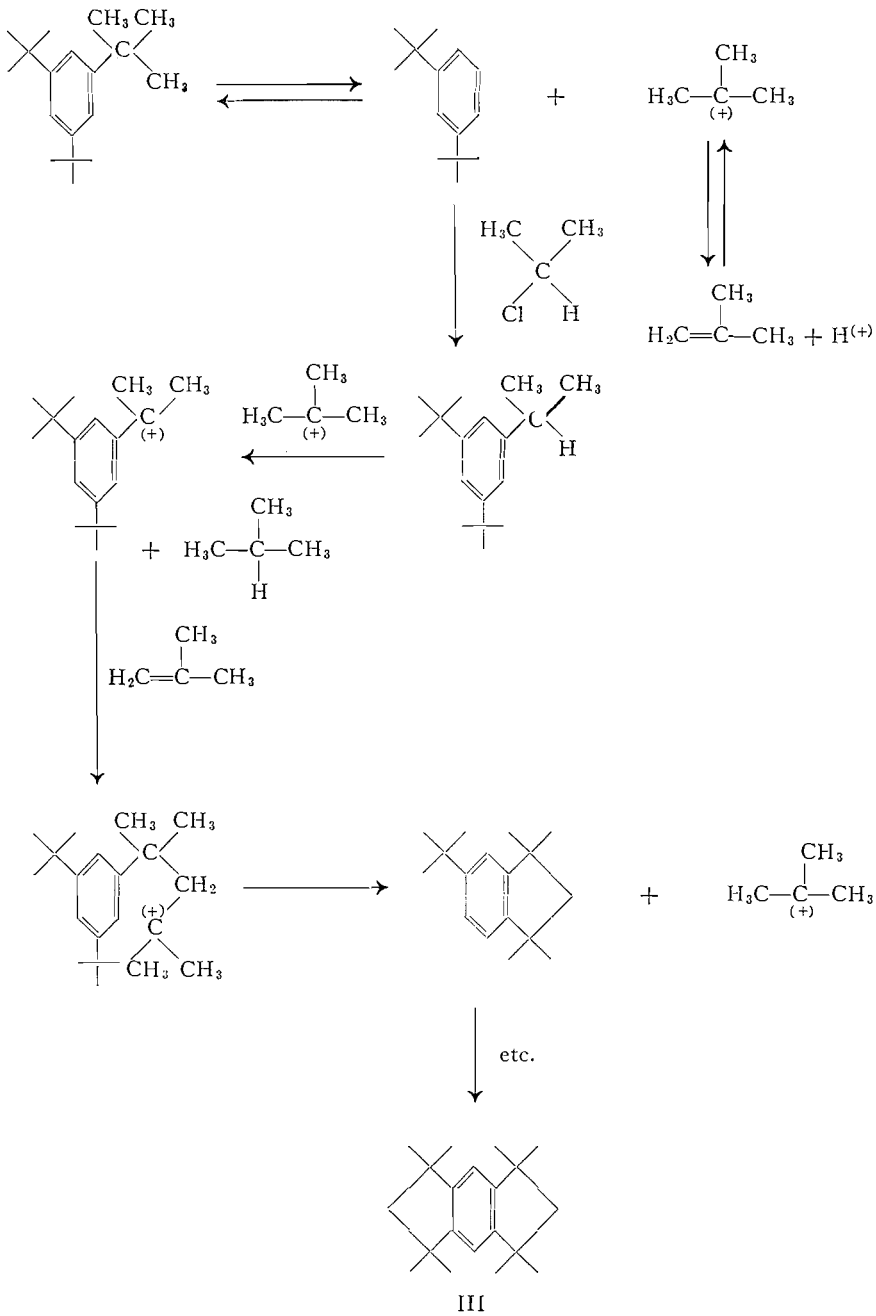
In an effort to extend these cyclialkylations to other systems, 1,3,5-tri-*t*-butylbenzene was treated with isopropyl chloride under Friedel–Crafts conditions. A compound of parent mass 270 was isolated corresponding to $C_{20}H_{30}$. This compound was dehydrogenated to yield an anthracene derivative, indicating that $C_{20}H_{30}$ is tricyclic. The infrared spectrum showed bands attributed to *t*-butyl groups and a band of 11.35 microns attributed to 1,2,4,5-tetrasubstitution. From this evidence it was proposed that this compound is 1,1,3,3,5,5,7,7-octamethylhydrindacene (III). The structure suggested for $C_{20}H_{30}$ was confirmed by a classical synthesis by the alkylation of 1,1,3,3-tetramethylindan with 2,4-dimethyl-2,4-pentanediol.

A general mechanism to account for the formation of III from 1,3,5-tri-*t*-butylbenzene and isopropyl chloride is outlined on page 96.

It is proposed that isopropyl groups replace *t*-butyl groups by a dealkylation–alkylation reaction. Then a hydride ion transfer from an isopropyl group to a *t*-butyl carbonium ion sets up a carbonium ion on a side chain which is alkylated with isobutene. The resulting cation will then cyclize with the elimination of an ortho *t*-butyl group. The remaining *t*-butyl group is replaced by isopropyl which in turn is cyclialkylated so that III is the final product. This interpretation is supported by the fact that 1,3,5-triisopropylbenzene is cyclialkylated with isobutene in the presence of isopropyl chloride (as a hydride ion acceptor) to give a good yield of III.

The mechanism for the formation of III might also be described by the condensation of isobutene and an isopropyl cation to form the 2,4-dimethylpentyl carbon skeleton.

Can. J. Chem. Downloaded from www.nrcresearchpress.com by 69.46.99.164 on 09/04/12
For personal use only.



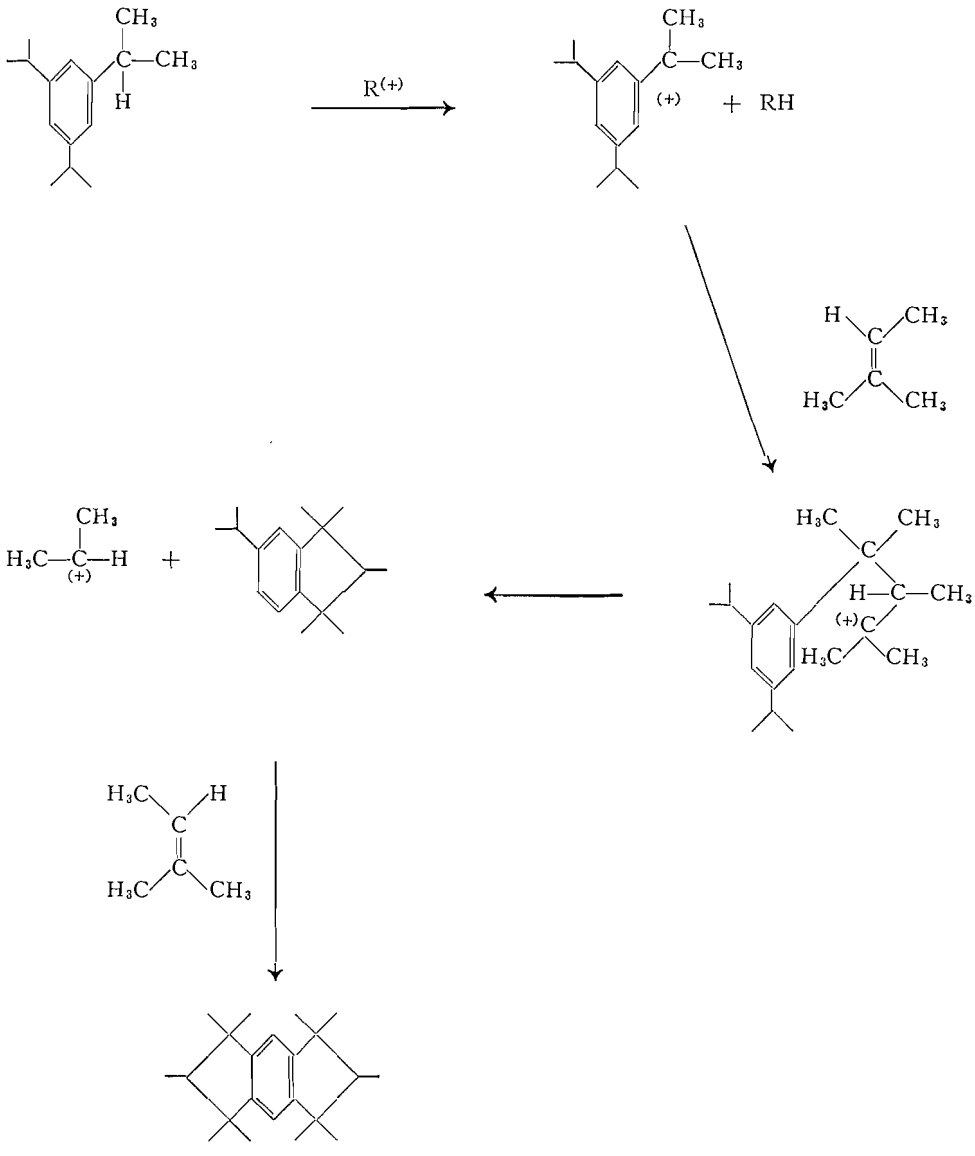
III

The latter could possibly replace isopropyl or *t*-butyl groups and form III. However, attempts to prepare III in this way by the alkylation of 1,4-di-*t*-butylbenzene with 2-chloro-2,4-dimethylpentane failed. It is therefore unlikely that the reaction proceeds by this alternative mechanism.

The formation of polymethylhydrindacenes was extended to another system by cyclialkylating 1,3,5-triisopropylbenzene with 2-methyl-2-butene in the presence of isopropyl chloride. In this case a high melting (245–245.6°) hydrocarbon ($C_{22}H_{34}$) was

Can. J. Chem. Downloaded from www.nrcresearchpress.com by 69.46.99.164 on 09/04/12
For personal use only.

obtained with an ultraviolet spectrum practically identical with that of III. The infrared spectra of these hydrocarbons were also very similar. Both had bands at 7.75, 8.10, and near 8.5 microns attributed to *t*-butyl groups. The main difference was due to bands appearing in the spectrum of the higher melting sample at 8.9 microns and in the 9.4- to 10-micron region which were absent in III. Both compounds had a strong band at 11.35 microns attributed to 1,2,4,5-tetrasubstitution. Therefore, the higher melting compound most probably has the decamethylhydrindacene structure IV and would form from 1,3,5-triisopropylbenzene as follows.



IV

The cyclialkylations outlined above have some similarity to the reaction discovered by Ipatieff, Pines, and Olberg (8) for the formation of 1,3,3,6-tetramethyl-1-*p*-tolylindan

Can. J. Chem. Downloaded from www.nrcresearchpress.com by 69.46.99.164 on 09/04/12
For personal use only.

from *p*-cymene and a number of different olefins in the presence of sulphuric acid or hydrogen fluoride. Schlatter also reported similar reactions in the formation of 1,1,3,3,5-pentamethylindan by the *t*-butylation of *p*-cymene (9) and of the side product 1,1,3,3,-5,6-hexamethylindan from the alkylation of 1,2-dimethyl-4-*t*-butylbenzene (10). All of these cyclialkylations illustrate how highly branched, condensed ring systems can be produced in essentially a one-step process from relatively simple starting materials. The so-called classical syntheses of these hydrocarbons on the other hand often involve many steps which often proceed in poor yields. That these processes must have practical significance is evident in some recent patents (11, 12, 13) on the production of polyalkyl indans from styrene compounds. Many of these branched hydrocarbons are of practical importance to the perfume industry and the petroleum industry.

Although 2-chloro-2,4,4-trimethylpentane failed to cyclialkylate benzene or 1,4-di-*t*-butylbenzene, it reacted with 1,3,5-triisopropylbenzene to give an interesting unexpected result. A crystalline product was isolated from which two compounds were separated. The main component was a compound of m.p. 101–102° (V). A small amount of another compound, m.p. 203–205° (VI), was also separated.

The mass spectrum analysis of V showed that it consists mainly of a compound of mass 314. There was also a large peak at mass 243 which corresponds to a loss of C_5H_{11} from the compound of mass 314. The infrared spectrum of V showed bands attributed to isopropyl groups and to tetrasubstitution. Dehydrogenation of this compound in a sealed tube at a high temperature yielded a product whose ultraviolet spectrum indicated the presence of a substituted naphthalene.

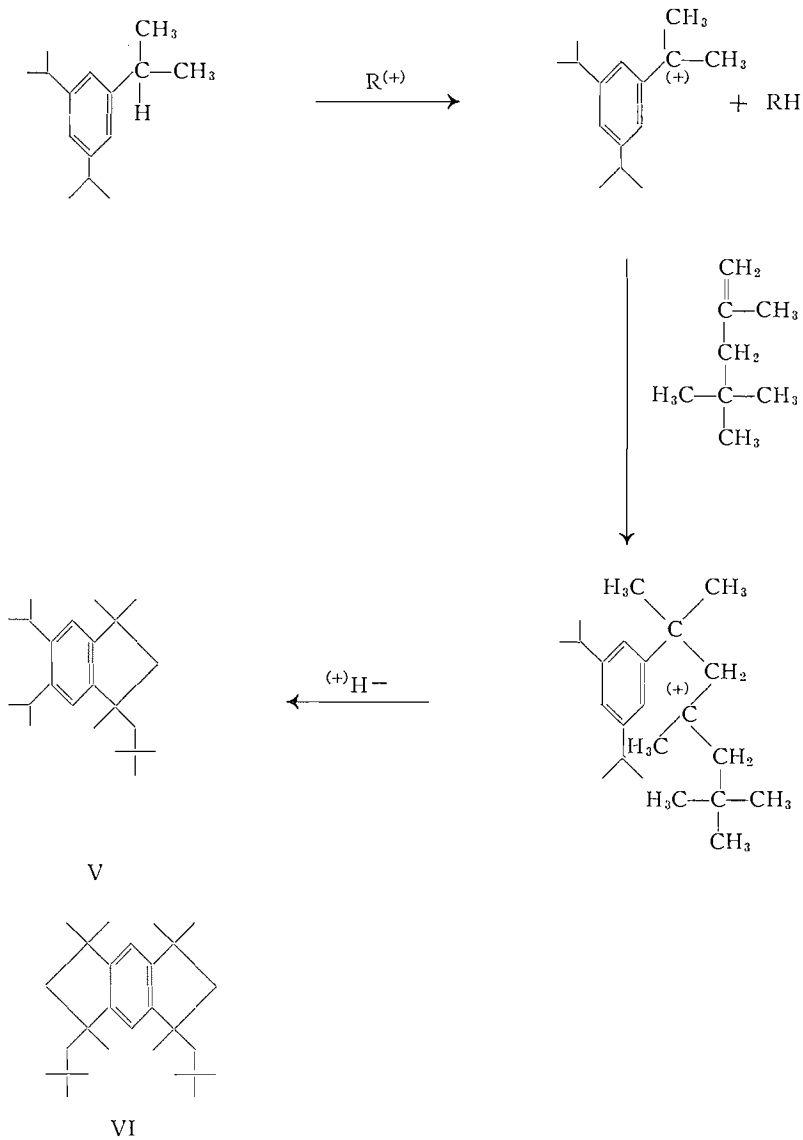
Although VI was not available in sufficient amount for a complete analysis, the mass spectrum indicated a parent mass of 383 and a peak at mass 311 corresponded to the loss of a C_5H_{11} group from a compound of mass 383. The ultraviolet spectrum of VI was practically identical with that of octamethylhydrindacene indicating that VI is most probably a similar polyalkyl hydrindacene.

The structures shown on page 99 for V and VI seem logical to explain the analyses discussed above. Reaction mechanisms are illustrated to account for the formation of these compounds.

In the reactions outlined on page 99 the olefin involved in the cyclialkylation is 2,4,4-trimethyl-1-pentene since only this isomer would lead to structures V and VI which lose a neopentyl fragment during the mass spectroscopic analysis. This olefin is not the expected one according to the classical Saytzeff rule by which the proton is expected to be eliminated from the CH_2 group to form 2,4,4-trimethyl-2-pentene. However, Whitmore and Rohrmann (14) have found that the corresponding alcohol, dimethyl-neopentylcarbinol, dehydrates to yield 2,4,4-trimethyl-1-pentene. In both cases the neopentyl group does not take part in the elimination. Both of these "unusual" eliminations can be explained if one assumes that the factor governing the course of elimination here is inhibition of close approach of a proton acceptor to the hindered CH_2 group.

The 1,2,4,5-formulation for V makes it possible to offer an explanation of why this dicyclic compound forms in better yields than the tricyclic compound, VI. Usually in these cyclialkylation experiments the tricyclic compound forms very readily and it is difficult to isolate dicyclic compounds analogous to V. However, further cyclialkylation of V in this case would not readily take place because the bulky olefin (trimethyl-1-pentene) would be hindered from alkylating an isopropyl group by an adjacent isopropyl group. The 1,2,4,5-orientation for V is also favored by its ultraviolet spectrum which is very similar to the spectrum of 1,2,4,5-tetraisopropylbenzene. The latter showed bands

Can. J. Chem. Downloaded from www.nrcresearchpress.com by 69.46.99.164 on 09/04/12
For personal use only.



V

VI

at λ_{max} 2770 Å, ϵ = 649 and λ_{max} 2682 Å, ϵ = 586, while V had bands at λ_{max} 2760 Å, ϵ = 749 and λ_{max} 2677 Å, ϵ = 690.

As a check for the structure suggested for V and the mechanism involving the postulated olefin 2,4,4-trimethyl-1-pentene, experiments were carried out on the alkylation of 1,3,5-triisopropylbenzene with this olefin in the presence of isopropyl chloride. This reaction did produce a compound identical with V and in high yield.

EXPERIMENTAL

The melting points were obtained with a Fisher–Johns apparatus equipped with a microscope, and are uncorrected. Ultraviolet spectra were recorded on a Beckman DK-2 ratio recording spectrophotometer using spectro-grade cyclohexane as the solvent.

Can. J. Chem. Downloaded from www.nrcresearchpress.com by 69.46.99.164 on 09/04/12
For personal use only.

Can. J. Chem. Downloaded from www.nrcresearchpress.com by 69.46.99.164 on 09/04/12
For personal use only.

The infrared spectra were recorded on a Perkin–Elmer Model 137 instrument using purified carbon disulphide as the solvent. Some of the infrared spectra were determined by an independent laboratory. The mass spectroscopic measurements were made in another laboratory on a special high temperature inlet mass spectrometer. The ultimate analyses were determined by the Schwarzkopf Microanalytical Laboratory, New York.

In all of the cyclialkylation experiments the progress of the reactions was followed by means of the recording ultraviolet spectrophotometer. Aliquots were taken from the reaction mixtures at short time intervals, the aluminum chloride complexes decomposed in water, and spectra were recorded immediately. In this way the course of the reaction was followed with a time lag of not more than a few minutes. Significant changes, such as changes in positions of alkyl groups on the benzene ring, the formation of di- or tricyclic products, and in some instances the introduction of a conjugated double bond were quite easily detected. Thus the reaction could be terminated at an appropriate time to permit isolation of the desired products or intermediates.

The Reaction of 1,3,5-Tri-t-butylbenzene with Isopropyl Chloride

Isopropyl chloride was prepared almost quantitatively by heating isopropyl alcohol with an equal volume of a saturated solution of zinc chloride in concentrated hydrochloric acid while passing through hydrogen chloride. The product was distilled off the top of a reflux condenser on formation.

1,3,5-Tri-*t*-butylbenzene, prepared as described by Barclay and Betts (4), (6.6 g, 0.027 mole) and isopropyl chloride (5.8 g, 0.074 mole) were stirred together and cooled to below 0°. Nine grams of aluminum chloride (0.067 mole) was added in small portions over a period of 2 hours. After 7 hours reaction time, the brown complex which formed was decomposed in cold water. A white solid (4.6 g) was formed which was filtered and recrystallized from ethanol–benzene. After five recrystallizations the melting point was 220–222.5°. Calc. for $C_{20}H_{30}$: C, 88.84; H, 11.16; molecular weight, 270. Found: C, 88.53, 88.64, 88.61, 88.96; H, 11.04, 11.10, 10.78, 11.04.

This compound showed a peak in the mass spectrometer corresponding to a parent mass of 270. There was also a large peak at 255 attributed to the loss of a methyl fragment.

The infrared spectrum of this compound, both in carbon disulphide solution and in potassium bromide pellets, showed a series of bands in the 1200- to 1500-cm^{-1} region attributed to *t*-butyl groups. In the ultraviolet spectrum there were bands at λ_{max} 2810 Å, ϵ = 4725; λ_{max} 2760 Å, ϵ = 4243; λ_{max} 2715 Å, ϵ = 3760; and λ_{max} 2670 Å, ϵ = 2700.

This compound was dehydrogenated by heating 1 g of it with 2 g of selenium powder in a sealed tube for 40 hours at 400°. The product fluoresced under an ultraviolet light. The ultraviolet spectrum indicated that it is a substituted anthracene.

A solution of 0.55 g of this hydrocarbon in a mixture of 25 ml of glacial acetic acid and 15 ml of acetic anhydride was treated with 1 ml of fuming nitric acid and heated at 70° for 3 hours. Distillation of the solvent mixture left a crude nitro derivative which was contaminated with some unreacted hydrocarbon. Repeated recrystallizations from acetone yielded colorless crystals, m.p. 275–277°.

Cyclialkylation of 1,3,5-Triisopropylbenzene with Isobutene

Isobutene was generated by dropping 85% phosphoric acid on warm *t*-butyl alcohol. The gas thus produced was passed through an ice trap, a bubbler containing 85% phosphoric acid, and a calcium chloride tube. This was then bubbled into the reaction mixture which contained 12.5 g of 1,3,5-triisopropylbenzene, prepared as described by

Gustavson (15), 9.6 g of isopropyl chloride (0.122 mole) as a hydrogen acceptor, and 16.3 g of aluminum chloride (0.122 mole). The reaction was cooled to below 0° in an ice–salt bath and the gas was allowed to pass through for 5½ hours. The reaction was decomposed on water and allowed to stand overnight. The organic material was extracted with ether. The ether was distilled off and the residue recrystallized from ethanol–benzene. A solid was obtained which weighed 9.8 g (59% yield). After five recrystallizations the melting point was 218–220°. The melting point was not lowered when the product was mixed with the product of alkylation of 1,3,5-tri-*t*-butylbenzene with isopropyl chloride.

Synthesis of 1,1,3,3,5,5,7,7-Octamethylhydrindacene (II)

1,1,3,3-Tetramethylindane was prepared, as described by Bogert and Davidson (16), starting with diacetone alcohol and benzene. Diacetone alcohol was prepared as described in ref. 17. 2,4-Dimethyl-2,4-pentanediol was prepared as described by Franke and Kohn (18) from diacetone alcohol and methyl magnesium iodide.

The indane (1.24 g, 0.007 mole) and the diol (0.94 g, 0.007 mole) were dissolved in 4 ml of carbon disulphide. Aluminum chloride (0.95 g, 0.007 mole) was added in small portions over a period of ½ hour. A complex began to form almost immediately after the addition of aluminum chloride. The mixture was stirred for 15 minutes, and then another 0.95 g of aluminum chloride was added slowly. The reaction was allowed to proceed for a total of 4 hours. It was then poured into water and the organic material was extracted with ether. On concentration of the ether, 1.75 g (88% yield) of crude crystals was obtained. These crystals were purified by recrystallization from ethanol–benzene three times to yield a material of m.p. 218.5–220°.

The melting point of the synthetic hydrindacene did not lower when mixed with the product of the cyclialkylation reactions described in previous sections. The ultraviolet absorption spectrum of the synthetic compound, II, was identical with the spectrum of the cyclialkylation product. The X-ray diffraction patterns of the synthetic product and the cyclialkylation product were also identical.

Cyclialkylation of 1,3,5-Triisopropylbenzene with 2-Methyl-2-butene

Isopropyl chloride (5.0 g, 0.05 mole) was cooled to −5° in a three-neck flask. Then aluminum chloride (3.33 g, 0.025 mole), and a mixture of 2-methyl-2-butene (4.0 g, 0.05 mole) and 1,3,5-triisopropylbenzene (5.0 g, 0.025 mole), were added slowly to the cooled reaction mixture. At the end of 4 hours, the reaction mixture was decomposed in cold water and allowed to stand overnight. The semisolid hydrocarbon layer was filtered to yield 4 g of crude product. Four recrystallizations from ethanol–benzene produced colorless crystals, m.p. 245–245.6°. Calc. for $C_{22}H_{34}$: C, 88.51; H, 11.49. Found: C, 88.10, 87.96; H, 11.08, 11.24. In the mass spectroscope, this compound showed a parent mass of 298 corresponding to $C_{22}H_{34}$.

The ultraviolet spectrum of this material had bands at λ_{max} 2800 Å, $\epsilon = 4760$; λ_{max} 2747 Å, $\epsilon = 4170$; λ_{max} 2705 Å, $\epsilon = 3680$; λ_{max} 2660, $\epsilon = 2680$.

The Reaction of 1,3,5-Triisopropylbenzene with 2-Chloro-2,4,4-trimethylpentane

1,3,5-Triisopropylbenzene (5.2 g, 0.025 mole) and 2-chloro-2,4,4-trimethylpentane (7.5 g, 0.050 mole) were placed in a three-neck flask and cooled to below 0° in an ice–salt bath. Aluminum chloride (6.7 g, 0.050 mole) was added in small portions with stirring over a period of 1½ hours. After 8 hours reaction time, the reaction mixture was poured into water and allowed to stand overnight. The solid material which separated was

Can. J. Chem. Downloaded from www.nrcresearchpress.com by 69.46.99.164 on 09/04/12
For personal use only.

filtered and recrystallized from benzene–ethanol. Forty milligrams of a compound with a melting point of 203–205° separated out in the first crop of crystals. The melting point of this compound was lowered when mixed with octamethyloctahydroanthracene (I) or when mixed with octamethylhydrindacene (III). The ultraviolet spectrum of the compound of m.p. 203–205° showed maxima at the same wavelengths as observed for III. In the mass spectrometer this compound showed a parent mass of 383 with a peak at mass 311 corresponding to the loss of a C_5H_{11} fragment.

On concentration of the original benzene–ethanol solution, 1.2 g of a second compound with m.p. 101–102° separated. Calc. for $C_{23}H_{38}$: C, 87.82; H, 12.18; molecular weight, 314. Found: C, 88.44, 88.53; H, 11.87, 11.88.

The mass spectrum of the lower melting compound showed a parent mass of 314. There was also a large peak at mass 243, corresponding to the loss of a C_5H_{11} fragment. The infrared spectrum of this compound in a potassium bromide pellet showed two strong bands of equal intensity at 7.28 and 7.37 microns attributed to isopropyl groups. There was also a strong band at 11.45 microns attributed to 1,2,4,5-tetrasubstitution. The ultraviolet spectrum of this compound showed bands at λ_{max} 2760 Å, $\epsilon = 749$ and λ_{max} 2677 Å, $\epsilon = 690$.

A sample of the compound of m.p. 101–102° (0.2 g) was dehydrogenated by heating with an equal weight of selenium powder in a sealed tube at 320° for 10 hours. The crude product was dissolved in cyclohexane and chromatographed on alumina using cyclohexane as eluant. The chromatograph fractions all showed a strong band in the ultraviolet spectrum at 2280 Å with weak absorption in the 2800 Å region containing some fine structure much like the alkyl naphthalenes.

Cyclialkylation of 1,3,5-Triisopropylbenzene with 2,4,4-Trimethyl-1-pentene

The 2,4,4-trimethyl-1-pentene used in these experiments was obtained from Matheson, Coleman and Bell, East Rutherford, N.J. It was also prepared by fractionating diisobutylene (η_D^{20} 1.4102) in a Podbielniak column. The diisobutylene was prepared by the procedure of Whitmore and co-workers (19). The 2,4,4-trimethyl-1-pentene isomer was removed in the fraction which boiled at 101° (760 mm), η_D^{20} 1.4090. The literature values (19) are 101.2° (760 mm) and η_D^{20} 1.4082.

1,3,5-Triisopropylbenzene (10 g, 0.05 mole) was dissolved in 25 ml of carbon disulphide and cooled in an ice–salt bath to −10°. A mixture of isopropyl chloride (5.6 g, 0.06 mole) and 2,4,4-trimethyl-1-pentene (5.6 g, 0.05 mole) was slowly added to the cooled, stirred solution over a period of 2 hours. Aluminum chloride (1.5 g, 0.01 mole) was added in small portions over the same period. From ultraviolet spectra run on various aliquots, the reaction product appeared to be formed in high yield after approximately 1 hour. After 2 hours reaction time, the carbon disulphide layer was poured into crushed ice and the organic layer extracted with ether. In concentrations of the ether extract, there was obtained 2 g of crystals and 5 g of semisolid material. The latter showed approximately the same ultraviolet spectrum as the crystalline material. The crude material was recrystallized from ethanol to yield colorless needles, m.p. 105–106.5°. This product was found to be identical with the product from alkylation of 1,3,5-triisopropylbenzene with 2-chloro-2,4,4-trimethylpentane by mixed melting points and ultraviolet spectra.

ACKNOWLEDGMENT

Financial assistance provided by the National Research Council in the form of grants in aid of research is gratefully acknowledged.

Can. J. Chem. Downloaded from www.nrcresearchpress.com by 69.46.99.164 on 09/04/12
For personal use only.

REFERENCES

1. BARCLAY, L. R. C. and BETTS, E. E. J. Am. Chem. Soc. **77**, 5735 (1955).
2. CONDON, F. E. J. Org. Chem. **21**, 761 (1956).
3. BARCLAY, L. R. C. and HILCHIE, J. W. J. Org. Chem. **22**, 633 (1957).
4. BARCLAY, L. R. C. and BETTS, E. E. Can. J. Chem. **33**, 672 (1955).
5. CRAM, D. J. J. Am. Chem. Soc. **75**, 332 (1953).
6. SCHMERLING, L., WELCH, R. W., and LUVISI, J. P. J. Am. Chem. Soc. **79**, 2636 (1957).
7. DOUGLASS, J. E. and ROBERTS, R. M. Chem. & Ind. (No. 29), 926 (1959).
8. IPATIEFF, V. N., PINES, H., and OLBERG, R. C. J. Am. Chem. Soc. **70**, 2123 (1948).
9. SCHLATTER, M. J. Symposium on petrochemicals in the postwar years. Am. Chem. Soc. Div. Petrol. Chem. Sept. 6–11, 1953. p. 79.
10. SCHLATTER, M. J. Joint symposium on synthetic fuels and chemicals. Am. Chem. Soc. Div. Petrol. Chem. Sept. 12–15, 1955.
11. POLAK'S FRUTAL WORKS, INC. Brit. Patent No. 790,129.
12. POLAK'S FRUTAL WORKS, INC. Brit. Patent No. 796,130.
13. POLAK'S FRUTAL WORKS, INC. U.S. Patent No. 2,851,501.
14. WHITMORE, F. C. and ROHRMANN, E. J. Am. Chem. Soc. **63**, 2033 (1941).
15. GUSTAVSON, G. Compt. rend. **140**, 940 (1905).
16. BOGERT, M. T. and DAVIDSON, D. J. Am. Chem. Soc. **56**, 185 (1934).
17. ORGANIC SYNTHESES. Collective Vol. I. John Wiley & Sons, Inc., New York. 1932. p. 199.
18. FRANKE, A. and KOHN, M. Ber. **37**, 4730 (1904).
19. TONGBERG, C. O., PICKENS, J. D., FENSKE, M. R., and WHITMORE, F. C. J. Am Chem. Soc. **54** 3706 (1932).

Can. J. Chem. Downloaded from www.nrcresearchpress.com by 69.46.99.164 on 09/04/12
For personal use only.

Can. J. Chem. Downloaded from www.nrcresearchpress.com by 69.46.99.164 on 09/04/12
For personal use only.

THE PHOTOLYSIS AND THE FLUORESCENCE OF PERFLUORO DIETHYL KETONE[1]

G. GIACOMETTI,[2] H. OKABE,[3] S. J. PRICE,[4] AND E. W. R. STEACIE

ABSTRACT

The photolysis and the fluorescence of $C_2F_5COC_2F_5$ have been studied at various temperatures, concentrations, and wavelengths. There is a strong dependence of the photochemical yield and to a lesser extent of the relative fluorescence yield on these factors. The reaction products are solely CO and C_4F_{10}. The fluorescence is excited by light of the wavelength region between 2537 Å and 3650 Å. The fluorescence band lies in almost the same wavelength region as that of CF_3COCF_3 and the relative fluorescence yield is slightly less in the higher concentration region. This behavior closely follows the pattern for CF_3COCF_3 and, hence, may be discussed by the same mechanism. A comparison is made of the primary photochemical reaction among fluorinated ketones.

INTRODUCTION

The photolyses of CF_3COCF_3 (1) and $C_3F_7COC_3F_7$ (2) have been investigated earlier in this laboratory. It was found that the dissociation takes place via an electronically excited species and that CO and fluorocarbons, formed by recombination of CF_3 and C_3F_7 radicals, are the sole products. The primary photochemical yield can be obtained directly from the rate of CO formation.

The fluorescence efficiency of CF_3COCF_3 has been studied in connection with the photolysis and a mechanism of the primary process has been presented (3, 4). Fluorescence has been observed also during the photolysis of $C_3F_7COC_3F_7$ but to such a small extent that no measurements have yet been made (unpublished observation by H. Okabe). In view of the simplicity of the mechanism it seems of interest to extend the investigation to other fluorinated ketones. The main purpose of this work is to study the photolysis and the fluorescence of $C_2F_5COC_2F_5$ and to see if the proposed mechanism (4) can be applied to this compound.

EXPERIMENTAL

The apparatus and experimental procedure have already been described (2, 3, 4). The quartz reaction cells used were 10 cm in length for photolysis and 15 cm for fluorescence experiments. The light source was a Hanovia S-500 lamp operated on a regulated supply. Radiation of 2640 Å was isolated for the photolysis experiments by means of a Corning 9863 filter and 5 cm of chlorine (100 mm Hg). The transparency band of this combination has a maximum at 2640 Å. Light in the 2537 Å region is also transmitted but is negligibly absorbed by the ketone. The $C_2F_5COC_2F_5$ was supplied by Dr. Leitch of this laboratory and later by Merck and Co. of Canada. The ketone was carefully distilled on a Podbielniak column (b.p. 26° C) and dried on P_2O_5. It was then degassed by bulb-to-bulb distillation under vacuum. A typical mass spectrometric cracking pattern is shown in Table I. Samples supplied for the early stages of this work showed the same mass spectro-

[1]*Manuscript received September 24, 1959.*
Contribution from the Division of Pure Chemistry, National Research Council, Ottawa, Canada.
Issued as N.R.C. No. 5449.
[2]*National Research Council Postdoctorate Fellow 1956–58. Present address: Istituto Di Chimica Fisica Dell' Universita, Padova, Italy.*
[3]*National Research Council Postdoctorate Fellow 1956–58. Present address: National Bureau of Standards, Washington, D.C.*
[4]*National Research Council Postdoctorate Fellow 1958–59. Present address: Chemistry Department, Essex College, Assumption University, Windsor, Ontario.*

TABLE I
Mass spectrum of $C_2F_5COC_2F_5$*

Mass number	Rel. height	Probable positive ion	Mass number	Rel. height	Probable positive ion
197	0.38	$C_2F_5COCF_2$	97	1.75	†
193	0.26	C_3F_8	93	3.14	C_3F_3
181	0.29	C_4F_7	85	0.5–2.5	† (from SiF_4)
162	0.28	C_4F_6	81	3.80	C_2F_3
149	0.29	†	78	4.73	CF_2CO
147	100	C_2F_5CO	74	0.64	C_3F_2
144	0.76	†	71	0.69	†
131	1.49	C_3F_5	69	130	CF_3
128	3.40	C_2F_4CO	62	0.77	C_2F_2
124	0.42	C_4F_4	50	10.2	CF_2
119	284	C_2F_5	47	0.34	†
112	0.60	C_3F_4	44	1.20	†
109	4.00	C_2F_3CO	31	20.0	CF
100	22.9	C_2F_4	28	9.0	CO

*The isotope peaks are not recorded.
†These peaks are not attributed. They are usually found in mass spectra of fluorinated hydrocarbons (see N.B.S. Reports).

graph except for relative amounts of trace impurities. Later samples contained significant quantities of benzene and some unidentified bromine compound. These were removed by partition chromatography using a fluoroester column (Fluid 316, Fluoroester Lubricant, Petroleum Chemicals Division, E.I. DuPont De Nemours and Co., 30% by weight on Fisher Scientific Company Columpak) maintained at −15° C. On a 200-cm column, 10 mm i.d., with a hydrogen flow rate of 120 cc/min the appearance time of the ketone was 17 minutes.

Following photolysis runs, carbon monoxide was pumped from the products at −210° C. The unreacted ketone and other photolysis products were collected together owing to the impossibility of a separation by low temperature distillation. In the later stages of the photolysis work the condensable products were analyzed by gas chromatography using a 3-foot alumina column (80–100 mesh) at 25° C. The ketone appears to be completely adsorbed by the column. The retention volume of C_4F_{10} is about 600 cc but this varies considerably with the amount of ketone on the column and with the moisture content of the alumina used. All quantum yields were determined using acetone as an actinometer.

The fluorescence spectrum was taken with a Hilger intermediate quartz spectrograph on a Kodak 103_a-B plate. The relative fluorescence yield, Q, in arbitrary units, is obtained from the following equation (4).

$$Q = \frac{D_f - D_f^0}{D_t^0 - D_t} \frac{S_t T}{\lambda_t}$$

where D_f is the galvanometer deflection for the fluorescence light emerging from the center of the cell, D_f^0 is the deflection for scattered light from the empty cell, D_t and D_t^0 are the deflection for the transmitted light with and without the gas in the cell respectively, S_t is the spectral sensitivity of the phototube to the transmitted light of wavelength λ, and T is the % transmission of an exit window. This equation is approximately valid when the absorption of the gas is not large.

RESULTS

The absorption spectrum was recorded with a Cary spectrometer. The spectrum

Can. J. Chem. Downloaded from www.nrcresearchpress.com by 69.46.99.164 on 09/04/12
For personal use only.

extends over a wavelength region between 2500 Å and 3600 Å. Some structure is observed between 3000 Å and 3500 Å. The molar extinction coefficient, k, in l. mole^{-1} cm^{-1} is shown in Table II.

TABLE II

The molar extinction coefficient, k, (l. mole^{-1} cm^{-1}) of $C_2F_5COC_2F_5$ at various wavelengths

Wavelength (Å)	k at 23° C
2640	3.50
3130	22.3
3340	14.3

The coefficient at 3130 Å is about three times as large as that of CF_3COCF_3.

Photolysis

The results of runs in which the condensable products were analyzed by adsorption chromatography are shown in Table III. Within experimental error the quantum yields based on CO and on C_4F_{10} are identical. Hence CO and C_4F_{10} would appear to be the sole products of the photolysis. As an additional check runs have been performed at room temperature up to 50% decomposition and the products, after elimination of CO, analyzed on the mass spectrometer. The peak at mass 147 was used for the ketone and peaks at masses 150 and 169 for C_4F_{10}. The total spectrum was that predictable from the sum of the two pure samples except for very minor discrepancies (for instance the ratio 150/169 was slightly altered in the presence of the ketone). The quantity of C_4F_{10} was equal within 5% to the CO produced. No peaks attributable to other products were noticed. Furthermore, the total number of moles of gas collected from the cell after the long runs was always found, after removal of CO, to be equal to the initial number of moles of ketone introduced. All this is in agreement with the exclusive formation of CO and C_4F_{10}.

The primary photochemical yield, based on the rate of CO production, was measured at various temperatures, concentrations, and wavelengths. Figure 1 illustrates quantum yield vs. concentration at four temperatures. Light of wavelength 3130 Å was used for

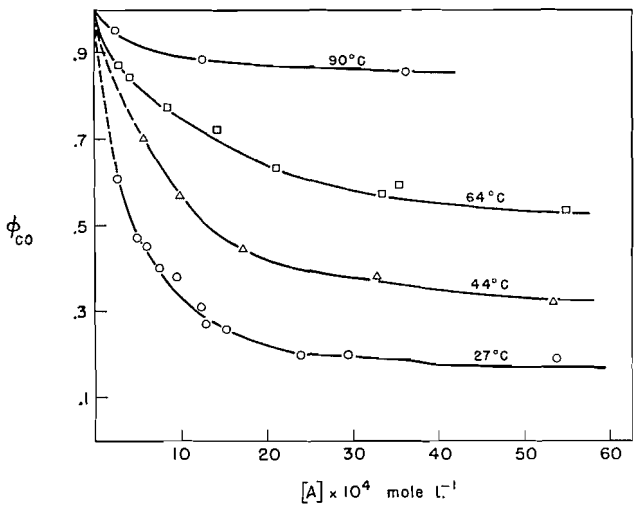


FIG. 1. The photochemical yield at various temperatures vs. concentration at 3130 Å.

Can. J. Chem. Downloaded from www.nrcresearchpress.com by 69.46.99.164 on 09/04/12
For personal use only.

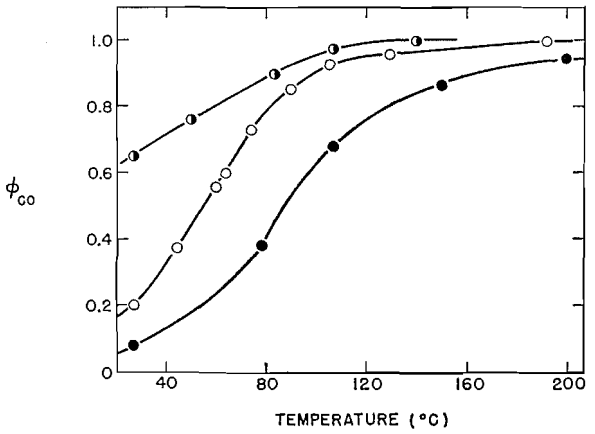


FIG. 2. The effect of temperature on quantum yield for production of carbon monoxide; ○ perfluoro di-*n*-propyl ketone, ◑ perfluoro diethyl ketone, ● hexafluoroacetone. Concentration approximately 26×10^{-4} mole $l.^{-1}$, λ = 3130 Å.

excitation. Figure 2 shows the quantum yield as a function of temperature. The points shown are taken in part from Fig. 1 at a concentration of 26×10^{-4} mole $l.^{-1}$, additional points being obtained from runs at other temperatures using approximately this concentration. The curves for perfluoro di-*n*-propyl ketone and hexafluoroacetone under similar conditions are included for comparison. Figure 3 shows quantum yield as a

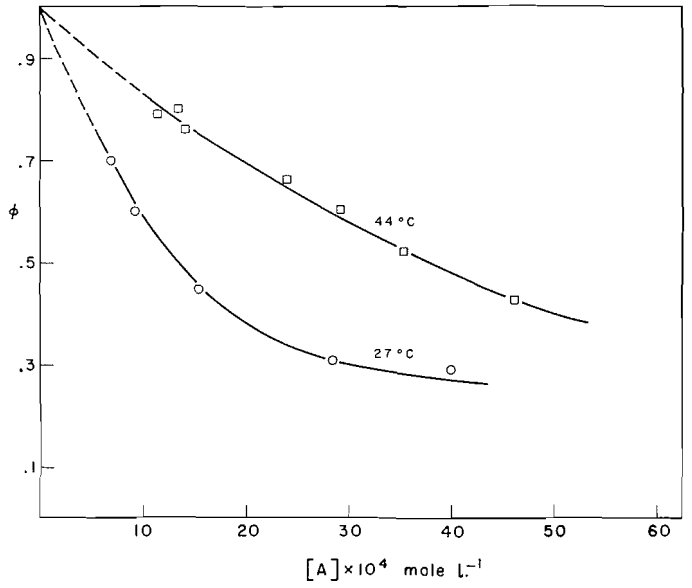


FIG. 3. The photochemical yield at various temperatures vs. concentration at 2640 Å.

function of concentration at two different temperatures when light of 2640 Å was used for excitation.

Fluorescence

The fluorescence is observed with light of any wavelength between 2537 Å and

Can. J. Chem. Downloaded from www.nrcresearchpress.com by 69.46.99.164 on 09/04/12
For personal use only.

TABLE III

A comparison of quantum yields based on carbon monoxide and on perfluorobutane

Temp. (° C)	Concentration (10^{-4} mole/l.)	ϕ_{CO}	$\phi_{C_4F_{10}}$
192	8.1	1.00	0.99
106	26.7	0.93	0.93
90	33.1	0.85	0.84
	12.4	0.87	0.85
74	27.8	0.73	0.73
60	26.0	0.56	0.57

3650 Å. The fluorescence band extends over the wavelength region between 3500 Å and 5000 Å with a broad maximum at about 4100 Å. There is little effect of temperature on the position and the apparent intensity distribution of the band.

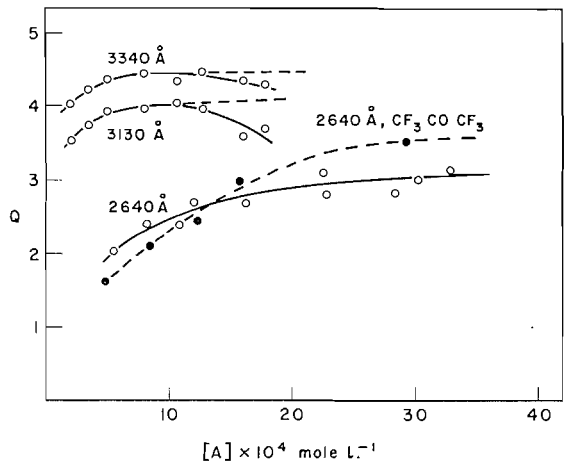


FIG. 4. The relative fluorescence yield at various wavelengths vs. concentration at room temperature; the curves are those of $C_2F_5COC_2F_5$ unless otherwise noted.

Figure 4 shows the concentration dependence at room temperature of Q at various wavelengths. For comparison Q for CF_3COCF_3 at 2640 Å is added. The apparent decrease of Q beyond the concentration of 10×10^{-4} moles per l. at 3130 Å and 3340 Å is undoubtedly due to the invalidity of the equation used in its calculation, which holds only when the absorption is less than 50%. The temperature dependence of the fluorescence yield was measured over the range from room temperature to 190° C. The fluorescence yield decreases with an increase of temperature with a negative temperature coefficient of about 0.7 kcal per mole, when light of 3130 Å and a concentration of 52×10^{-4} mole per l. are used.

DISCUSSION

The photochemical and the fluorescence behavior of $C_2F_5COC_2F_5$ as a function of temperature, concentration, and wavelength closely resembles that of CF_3COCF_3, namely:

(1) The mechanism of the photolysis is obviously the general one accepted for the other fluorinated ketones.

Can. J. Chem. Downloaded from www.nrcresearchpress.com by 69.46.99.164 on 09/04/12
For personal use only.

(2) The photochemical yield, ϕ, increases and approaches unity as the concentration decreases. It increases with an increase of temperature and excitation energy. The yield has a larger concentration dependence at shorter wavelength over the moderate (10×10^{-4} mole per l.) and higher concentration range at the same temperature (Figs. 1 and 3).

(3) The fluorescence band extends over almost the same wavelength region. The relative fluorescence yield increases with an increase of concentration and with a decrease of excitation energy, approaching almost 70% that of CF_3COCF_3. The increase is larger at shorter wavelength (Fig. 4). The yield decreases as the temperature increases and the negative temperature coefficient is of the same order of magnitude. The mechanism may therefore be expressed by equations previously proposed (4).

[1] $$K + h\nu \rightarrow K_n$$

[2] $$K_n \rightarrow D$$

[3] $$K_n + K \rightarrow K_0 + K$$

[4] $$K_0 \rightarrow h\nu + K$$

[5] $$K_0 \rightarrow Z_0$$

[6] $$Z_0 \rightarrow D$$

[7] $$Z_0 \rightarrow K$$

where K, K_n, and K_0 designate the ground electronic state of $C_2F_5COC_2F_5$ and the nth and 0th vibrational levels of a singlet excited state from which the fluorescence originates. D denotes the dissociation products; Z_0 represents a molecule in the lowest vibrational level of another excited (probably triplet) state, from which dissociation and possibly internal conversion take place but not emission. From the above mechanism, the following equation is obtained:

[8] $$\frac{\phi}{1-\phi} = \frac{\alpha}{1-\alpha} + \frac{k_2}{k_3[K](1-\alpha)}$$

where α is the photochemical yield at infinite concentration. Figure 5 shows the relationship between $\phi/(1-\phi)$ and the reciprocal of the concentration at various temperatures and wavelengths. The data fit the equation well at 3130 Å, whereas at 2640 Å the equation is obeyed only approximately. In Fig. 5 the data at 3130 Å enable a reliable extrapolation to be made to $1/[A] = 0$, and hence the intercepts can be established with some certainty. Unfortunately, since the lines at 2640 Å are curved it is impossible to establish the value of the intercepts with any degree of certainty. The mechanism suggests that the intercepts should have the same values at both wavelengths, and the curves have been drawn in this way. It should be emphasized, however, that while the data are entirely consistent with common intercepts, they do not in any way establish this point. The rate of dissociation from upper vibrational levels of the singlet excited state, k_2, obtained from the slopes, is larger at the shorter wavelength. The values of α obtained from the intercept are given in Table IV. For comparison, α for CF_3COC_3F and $C_3F_7COC_3F_7$ are also given.

As can be seen from Table IV, α at the same temperature increases in the order CF_3COCF_3, $C_2F_5COC_2F_5$, $C_3F_7COC_3F_7$. If a plot is made of $\log\{(1/\alpha)-1\}$ vs. $1/T$ for

Can. J. Chem. Downloaded from www.nrcresearchpress.com by 69.46.99.164 on 09/04/12
For personal use only.

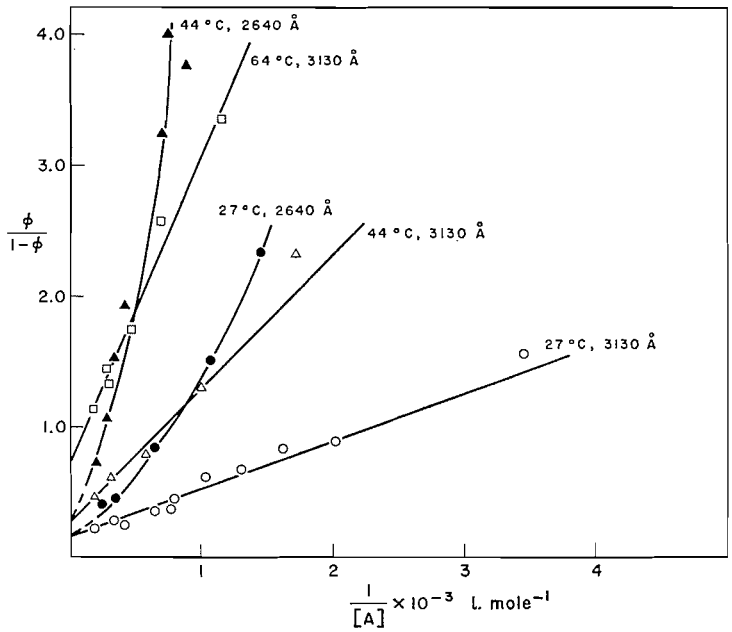


FIG. 5. The relationship between $\phi/(1-\phi)$ and the reciprocal of concentration at various temperatures and wavelengths.

TABLE IV

The photochemical yield at infinite concentration, α, at various temperatures for fluorinated ketones at 3130 Å

Compound	Temperature (° C)	α
$C_2F_5COC_2F_5$	27	0.15
	44	0.27
	64	0.43
	90	0.83
CF_3COCF_3*	27	0.04
	53	0.18
	78	0.37
	107	0.63
	219	1.0
$C_3F_7COC_3F_7$†	27	0.55
	50	0.78
	80	0.90
	107	1.0

*Reference 1. †Reference 2.

these compounds, apparent negative activation energies of 9.2, 8.9, and 7.8 kcal per mole are obtained for CF_3COCF_3, $C_2F_5COC_2F_5$, and $C_3F_7COC_3F_7$ respectively. If the mechanism is correct these energies correspond approximately to the activation energy differences between the dissociation and the internal conversion from the (triplet) state.

If a comparison is made of the photolysis at 27° C between $C_2F_5COC_2F_5$ and CF_3COCF_3 at 2640 Å, where the dissociation would mainly originate from higher vibrational levels, it is evident that ϕ for $C_2F_5COC_2F_5$ is smaller in the lower concentration region, but larger at higher concentrations. In other words, ϕ for $C_2F_5COC_2F_5$ has a smaller con-

Can. J. Chem. Downloaded from www.nrcresearchpress.com by 69.46.99.164 on 09/04/12
For personal use only.

centration dependence at this wavelength. From equation [8] this gives for $C_2F_5COC_2F_5$ a value of k_2/k_3 less than half that for CF_3COCF_3. Assuming the same rate of deactivation for both compounds, k_2 is much smaller in $C_2F_5COC_2F_5$. This suggests that since there are more vibrational degrees of freedom for $C_2F_5COC_2F_5$, there will be less probability that the energy will concentrate in the particular bond leading to dissociation.

Corresponding to the smaller concentration dependence of ϕ for $C_2F_5COC_2F_5$ at 27° C and 2640 Å, there is also less concentration dependence of Q at this temperature and wavelength (Fig. 4). It would be of great interest to find direct evidence of the two close-lying excited states of these molecules. It is possible that ultraviolet spectroscopy, performed under conditions such that no dissociation would occur (low temperature and moderate pressures), may supply the answer.

ACKNOWLEDGMENTS

The authors are indebted to Dr. L. C. Leitch of this laboratory for the supply of ketone, to Miss A. B. Thornton for the mass spectrometric analyses, and to Dr. K. O. Kutschke for much advice and discussion.

REFERENCES

1. AYSCOUGH, P. B. and STEACIE, E. W. R. Proc. Roy. Soc. A, **234**, 476 (1956).
2. MILLER, G. H., PRITCHARD, G. O., and STEACIE, E. W. R. Z. physik. Chem. **15**, 262 (1958).
3. OKABE, H. and STEACIE, E. W. R. Can. J. Chem. **36**, 137 (1958).
4. GIACOMETTI, G., OKABE, H., and STEACIE, E. W. R. Proc. Roy. Soc. A, **250**, 287 (1959).

Can. J. Chem. Downloaded from www.nrcresearchpress.com by 69.46.99.164 on 09/04/12
For personal use only.

Can. J. Chem. Downloaded from www.nrcresearchpress.com by 69.46.99.164 on 09/04/12
For personal use only.

THE POLYSACCHARIDES OF FURCELLARIA FASTIGIATA

I. ISOLATION AND PARTIAL MERCAPTOLYSIS OF A GEL-FRACTION[1]

T. J. PAINTER

ABSTRACT

Addition of potassium chloride to an aqueous extract of the red alga *Furcellaria fastigiata* precipitated a polysaccharide containing residues of D-galactose and 3,6-anhydro-D-galactose in the approximate ratio 1.3:1. Approximately two monomer units in five bore sulphate half-ester groups. The fraction gave a single, sharp peak in the analytical ultracentrifuge. Partial mercaptolysis afforded the crystalline diethyl mercaptals of D-galactose, 3,6-anhydro-D-galactose, and 4-*O*-β-D-galactopyranosyl-3,6-anhydro-D-galactose (A); the respective yields were 27%, 20%, and 42% w/w of the recovered mercaptolysate. The polysaccharide resembles κ-carregeenin.

The red alga *Furcellaria fastigiata* (Huds.) Lamour. contains a hydrocolloid which is similar in properties to carrageenin (1, 2). The alga grows in the Baltic Sea, and is particularly abundant in the adjacent Kattegatt, where it is harvested for the manufacture of "Danish agar", or "furcellaran" (3). It is also reported to grow in the Gulf of St. Lawrence, Canada (4), in commercial quantities (5).

In 1943, Kylin showed that residues of D-galactose, and sulphate half-ester groups were present in the mucilage (6). More recently, Dillon, O'Colla, and co-workers found that residues of 3,6-anhydro-galactose were also present (7). The unfractionated mucilage was subjected to acetylative desulphation; examination of the degraded, sulphate-free product by methylation showed that the galactose residues were linked mainly through positions 1 and 3, but occasionally also through position 6 (7). In the present study, an attempt has been made to isolate a homogeneous polysaccharide from the mucilage, and to examine its structure by partial mercaptolysis.

In the first series of experiments, the milled alga was extracted with acetone, and then stirred for 2 hours with hot aqueous sodium acetate at pH 7. After three successive extractions of the residue in the same way, 73% of the dry weight of the alga had been removed as water-soluble products. Extraction in this manner appeared to be impeded by the presence of protein, of which the alga may contain 17–18% (N, 2.8%) (8). Furthermore, the extracts were contaminated with a brown pigment which could be removed only in part with decolorizing charcoal. In later experiments, when it was unnecessary to avoid slight degradation of the polysaccharides, both difficulties were overcome as described below.

A slurry of the alga in water, stirred at 75° C, was treated with dilute chlorous acid, added dropwise over a period of 30 minutes. During this time, the pH of the mixture fell slowly to 3.5. The pH was then brought immediately to 7 with sodium acetate, and extraction at 75° C was continued for 1 hour. In these cases, a single treatment caused dissolution of 88% of the alga, and the recovered polysaccharides were free from colored contaminants.

When potassium chloride (9, 10) was added to the aqueous extracts obtained by either method, a gelatinous precipitate was obtained of the potassium salt of a sulphated polysaccharide. This was collected and converted into the sodium salt by dialysis against aqueous sodium acetate. After three reprecipitations with potassium chloride in the same

[1]*Manuscript received October 5, 1959.*
Contribution from the National Research Council, Atlantic Regional Laboratory, Halifax, Nova Scotia. Issued as N.R.C. No. 5448.

Can. J. Chem. Downloaded from www.nrcresearchpress.com by 69.46.99.164 on 09/04/12
For personal use only.

way, the purified product (sodium salt) had $[\alpha]_D$ $+75° \pm 2°$ in water. It contained residues of galactose (43.1%), 3,6-anhydro-galactose (30.3%), and half-ester sulphate (as SO_3Na) (20.1%).

When a solution of the polysaccharide in 0.1 *M* sodium chloride was examined in the analytical ultracentrifuge, a single, sharp peak was observed. Chromatography of an acid-hydrolyzate of the material indicated the presence of galactose, a trace of xylose, and a component having an R_f similar to that of 5-hydroxymethyl-2-furaldehyde. Upon isolation, the galactose crystallized extensively; the crystals were of D-galactose.

Total mercaptolysis of the polysaccharide with ethyl mercaptan and concentrated hydrochloric acid gave a high yield of the crystalline diethyl mercaptals of D-galactose and 3,6-anhydro-D-galactose, in the molar ratio 1.3:1. These compounds were further characterized by conversion, respectively, into crystalline D-galactose, and into 3,6-anhydro-D-galactose phenylosazone.

Mercaptolysis for a shorter period of time afforded the above-named mercaptals (47%), together with a large amount (42%) of a disaccharide mercaptal (A). This component (A) was isolated by chromatography of the mixture on a column of cocoanut charcoal (11), followed by preparative paper chromatography. It crystallized, and was identical with an authentic specimen of 4-*O*-β-D-galactopyranosyl-3,6-anhydro-D-galactose diethyl mercaptal, as prepared by the partial mercaptolysis of κ-carrageenin (12). The identity of the two compounds was confirmed by comparison of their crystalline hexa-*O*-acetyl derivatives.

Demercaptallation of (A) with mercuric chloride and cadmium carbonate in water afforded a reducing disaccharide (B), from which a crystalline phenylosazone was prepared. Reduction of (B) with aqueous sodium borohydride yielded a crystalline glycitol (C), which formed a crystalline hepta-*O*-acetyl derivative (D). The physical constants of (C) and (D) agreed well with those recently reported by Clingman and Nunn (13) for 4-*O*-β-D-galactopyranosyl-3,6-anhydro-D-galactitol, and for its hepta-*O*-acetate, respectively.

These results suggest that a part of the mucilage of *Furcellaria fastigiata* is made up of a homogeneous polysaccharide which consists essentially of residues of D-galactose and 3,6-anhydro-D-galactose. The traces of xylose detected in hydrolyzates of the polysaccharide may have arisen from contaminating xylan. No evidence for the presence of monomer units derived from the L-series of sugars was obtained.

The high yield of the disaccharide mercaptal (A) indicates that the two types of sugar residue must be very evenly distributed throughout the macromolecule. As an idealized picture, the polysaccharide could be considered to consist entirely of repeating units represented by the disaccharide (B); the 30% molar excess of D-galactose residues might have arisen from a contaminating galactan which escaped detection in the ultracentrifuge. It is equally probable, however, that the polymer has a rather less highly ordered structure, with occasional small groups of contiguous D-galactose residues in the chains; a small proportion of the 3,6-anhydro-D-galactose residues may be similarly grouped.

As a result of the highly labile nature of 3,6-anhydro-galactosidic linkages, an investigation of the present type provides little information about them, beyond the fact that most of them must be directed towards D-galactose residues in the polysaccharide. However, when these results are considered together with the methylation studies of Dillon, O'Colla, and co-workers (7), it appears probable that most of the 3,6-anhydro-D-galactose residues are linked to position 3 of D-galactose residues. The positive specific rotation of the polysaccharide suggests, moreover, that most of these linkages are in the α-configuration.

It would follow that the polysaccharide is similar to κ-carrageenin, although the sulphate content is somewhat lower. Another polysaccharide of this type was recently isolated from *Hypnea specifera* by Clingman and Nunn (13).

EXPERIMENTAL

Paper chromatography was carried out on Whatman No. 1 filter paper. For preparative work, large sheets (57×46 cm) of Whatman No. 3MM paper were used; in these cases, the solvent was supplied to the sheets through short strips (57×8 cm) of Whatman No. 1 paper, which were attached to the main sheets with staples. The irrigant was either (*a*) butan-1-ol–ethanol–water (3:1:1 v/v) or (*b*) butan-1-ol–pyridine–water (6:4:3 v/v). Reducing sugars were located on the chromatograms by spraying with *p*-anisidine hydrochloride in butan-1-ol (14). Sugar mercaptals were located by spraying with silver nitrate in acetone, followed by ethanolic sodium hydroxide (15). Chromatographic mobilities are calculated relative to the solvent front (R_f).

Optical rotations were measured at 21°±2° C; unless otherwise stated, the solvent was water. Melting points were determined with a Kofler block. Solvents were evaporated under diminished pressure at 30–45° C. X-Ray powder photography was carried out using chromium radiation and a vanadium filter; the powdered samples were mounted in the camera on lead-free glass fibers, to which they were attached with silicone grease. For sedimentation, a 0.2% w/v solution of the polysaccharide in 0.1 *M* sodium chloride was used. The ultracentrifuge, a Spinco Model E instrument, was operated at 59,780 r.p.m.

Sulphate was determined gravimetrically, after complete hydrolysis of the polysaccharide with 0.5 *N* hydrochloric acid (20 hours at 95° C), by precipitation as barium sulphate. Galactose and 3,6-anhydro-galactose were estimated by a modification (16, 17) of a method (18) for the simultaneous estimation of glucose and fructose. In an independent method, 3,6-anhydro-galactose was estimated selectively by a modification (16, 17) of the resorcinol method (19) for fructose. The results agreed well, and the figures given are averages.

Preparation of the Polysaccharide

The alga was collected near Pictou, Nova Scotia, in November, 1958. It was dried in a current of air at 45° C for 3 hours, and ground in a Wiley mill to pass a 20-mesh sieve. The product was extracted exhaustively with hot acetone, dried at room temperature, and used as follows.

Method (a)

The alga (100 g: 10% w/w moisture) was stirred in water (3 l.) containing sodium acetate (15 g) at 80° C for 2 hours. The mixture was then centrifuged while hot. The residue was extracted twice more in the same way, and then subjected to a final extraction for 6 hours. The final residue, when isolated and dried, weighed 21 g. The combined centrifugates (ca. 12 l.) were dialyzed against aqueous sodium acetate (0.1% w/v) for 24 hours. The solution was heated at 80° C with decolorizing charcoal (100 g) for 1 hour, and then filtered through Celite in a heated, sintered-glass funnel. To the clear, pale brown filtrate was added potassiun chloride (400 g) in water (2 l.); the solution was allowed to cool slowly to 4° C, while being vigorously stirred. The gelatinous precipitate was collected by centrifugation, and dispersed in aqueous sodium acetate (0.1% w/v; 5 l.). This mixture was dialyzed against aqueous sodium acetate until the gel had dissolved (60 hours). The solution was diluted to 10 l. with water, heated with charcoal, and filtered as before, and again treated with potassium chloride. The gel was collected and reprecipitated twice more in the same way. It was finally dispersed in water (3 l.) and

Can. J. Chem. Downloaded from www.nrcresearchpress.com by 69.46.99.164 on 09/04/12
For personal use only.

dialyzed against aqueous sodium acetate until it had redissolved. The solution was poured into ethanol saturated with sodium acetate (10 l.). The precipitate was collected, washed thoroughly with aqueous ethanol (80% v/v), followed by absolute ethanol, then by ether, and dried over silica gel in a vacuum desiccator. The yield of light brown, fibrous polysaccharide (F-1) was 15.0 g.

Method (b)

The alga (50 g; 10% w/w moisture) was stirred in water (2 l.) at 75° C for 10 minutes. A solution of chlorous acid was prepared by treating aqueous sodium chlorite (4% w/v) with an excess of Amberlite resin IR-120. This solution (150 ml) was added, uniformly and dropwise, to the above slurry over a period of 30 minutes. At 5-minute intervals, aliquot portions were withdrawn and cooled, and the pH was measured with a Beckman pH meter.

Time (minutes)	0	5	10	15	20	25	30
pH	7.2	6.7	6.3	5.7	5.0	4.3	3.5

The mixture was then neutralized with sodium acetate (30 g) and sodium carbonate (4 g), and stirring at 75° C was continued for 1 hour. Water (3 l.) was added, and the mixture was centrifuged at 40–50° C. The residue, when isolated and dried, weighed 5.4 g. The centrifugate was filtered through Celite at 80° C, and then treated with potassium chloride (200 g) in water (1 l.), and allowed to cool. The gelatinous precipitate was collected and purified as described in method (*a*), with the exception that no charcoal was used. The final yield of white, fibrous polysaccharide (Na salt) (F-2) was 10.5 g.

Preliminary Examination of the Polysaccharide (F-1)

The following analytical values were obtained: $[\alpha]_D$ +75°±2° (*c*, 0.2); ash, 14.6%; sulphated ash, 15.0%; SO_3Na, 20.1%; galactose (as $C_6H_{10}O_5$), 43.1%; 3,6-anhydrogalactose (as $C_6H_8O_4$), 30.3%. In the ultracentrifuge, a single, sharp peak was obtained which showed only slight spreading of the boundary.

A portion (1 g) was hydrolyzed with *N* sulphuric acid at 100° C for 12 hours. The solution was neutralized with barium carbonate, filtered, deionized (resins), and concentrated to a syrup (350 mg). Chromatography of the hydrolyzate in solvent (*a*) or (*b*) indicated the presence of galactose, a trace of xylose, and a component similar to 5-hydroxymethyl-2-furaldehyde. Separation of the galactose on a large chromatogram gave a syrup (260 mg) which had $[\alpha]_D$ +78° (*c*, 2.6). It crystallized from methanol, and after one recrystallization from the same solvent, the yield of pure crystals was 190 mg. They had m.p. 165–166° C, unchanged on admixture with pure α-D-galactose, and $[\alpha]_D$ +139° (by extrapolation) → +79° (24 hours) (*c*, 1.0).

Total Mercaptolysis of the Polysaccharide

The polysaccharide (F-2; 10 g) was stirred with concentrated hydrochloric acid (70 ml) at 0° C for 10 minutes. Ethyl mercaptan (25 ml) was added over a period of 1 hour. The mixture was then allowed to warm slowly to 10° C, and stirring at this temperature was continued. The flask was kept closed to minimize evaporation of ethyl mercaptan. After 24 hours, more ethyl mercaptan (25 ml) was added. After a total time of 96 hours, the mixture was cooled to 0° C, and ice-cold methanol (800 ml) was added. The resulting homogeneous solution was neutralized with lead carbonate, filtered, and the filtrate and washings were concentrated to a syrup. This was dissolved in absolute methanol (300 ml); the solution was cooled to 0° C, and the small deposit of inorganic salt was removed by filtration. The filtrate was concentrated to a syrup (11.5 g). Chromatography of this product in solvent (*a*), followed by the use of the silver nitrate spray reagent, indicated

Can. J. Chem. Downloaded from www.nrcresearchpress.com by 69.46.99.164 on 09/04/12
For personal use only.

an intense black spot, R_f 0.65, corresponding to galactose diethyl mercaptal, and a light brown spot, R_f 0.90, corresponding to 3,6-anhydro-galactose diethyl mercaptal. Also detected were small spots corresponding to xylose diethyl mercaptal (R_f 0.77), to ethyl 1-thio-galactopyranoside (R_f 0.50), to free galactose (R_f 0.15), and to traces of reducing oligosaccharides (R_f 0–0.05).

(*i*) D-*Galactose Diethyl Mercaptal*

The above mercaptolysate was dissolved in water (100 ml), and the solution was cooled to 0° C, whereupon it solidified to a crystalline mass. This was lixiviated with ice-cold water. The crystals were collected (yield, 3.5 g), and recrystallized twice from methanol–ether. The pure product had $[\alpha]_D$ $-3.7°\mp0.5°$ (*c*, 0.7), and m.p. 141–141.5° C, unchanged on admixture with synthetic D-galactose diethyl mercaptal. The crystals (1 g), mercuric chloride (5 g), and cadmium carbonate (10 g) were heated in water (100 ml) for 2 hours at 50° C. The mixture was cooled and filtered, and the filtrate was saturated with hydrogen sulphide. Precipitated material was removed, and the solution was then neutralized with Amberlite resin IR-45. It was concentrated to a syrup (0.5 g), which was dissolved in a minimum of hot methanol. On cooling, crystals separated, and after recrystallization from methanol, the compound had m.p. and mixed m.p. with α-D-galactose, 165.5–166.5° C, and $[\alpha]_D$ +142° (by extrapolation) → +80° (14 hours) (*c*, 1.1).

(*ii*) *3,6-Anhydro*-D-*galactose Diethyl Mercaptal*

After collection of the D-galactose diethyl mercaptal, the aqueous filtrate was diluted to 500 ml with water, and then shaken 10 times with ether (10×200 ml) in a separatory funnel. The combined ether extracts (2 l.) were dried with Drierite, filtered, and concentrated to 200 ml. When ligroin (b.p. 35–60° C) (100 ml) was added, a flocculent mass of crystals separated; they were collected by filtration (yield, 2.4 g), and recrystallized twice from ether–ligroin. From the filtrate, a second crop (1.1 g) of crystals was obtained. The pure crystals had $[\alpha]_D$ $-9.8°\mp0.5°$ (*c*, 0.4), and m.p. 111.5–112.5° C, unchanged on admixture with a synthetic specimen (12) of 3,6-anhydro-D-galactose diethyl mercaptal. A mixture with 3,6-anhydro-L-galactose diethyl mercaptal (m.p. 110–111° C), prepared by the mercaptolysis of agar (20), had a melting range of 109–134° C.

A sample of the compound (100 mg) was heated in water (15 ml) with mercuric chloride (500 mg) and cadmium carbonate (1 g) at 50° C for 2 hours. The mixture was cooled and filtered, and the filtrate was extracted exhaustively with ether. It was then heated with phenylhydrazine (0.2 ml), sodium acetate (1 g), and acetic acid (1 ml) at 80° C for 2 hours. The flocculent yellow precipitate was collected and recrystallized from methanol. The product had m.p. 217° C, unchanged on admixture with 3,6-anhydro-D-galactose phenylosazone (12), and $[\alpha]_D$ +75° (15 minutes) → +54° (20 hours, constant) (*c*, 0.2 in methanol). For 3,6-anhydro-L-galactose phenylosazone, Araki and Hirase (21) report $[\alpha]_D$ −75° (initial) → −53° (24 hours) (in methanol–pyridine).

(*iii*) *Ethyl 1-Thio-*α-D-*galactopyranoside*

The aqueous solution remaining after the extraction of 3,6-anhydro-D-galactose diethyl mercaptal was concentrated to a syrup (3.2 g). Chromatography indicated the presence of three major constituents. The mixture was separated on large chromatograms, to yield D-galactose (0.5 g), D-galactose diethyl mercaptal (1.2 g), and the other component, having R_f 0.50 in solvent (*a*), (0.6 g). This last component was obtained as a syrup having $[\alpha]_D$ +280° (*c*, 2.5). It crystallized slowly on standing, and after three recrystallizations from butan-1-ol, it had $[\alpha]_D$ $+318°\pm2°$ (*c*, 0.6), and m.p. 152–153.5° C. For ethyl 1-thio-α-D-galactopyranoside, Fried and Walz (22) report $[\alpha]_D$ +320°, and m.p. 153.5–154° C. Calculated for $C_8H_{16}O_5S$: S, 14.3%. Found: S, 12.7%. Demercaptallation in the usual

Can. J. Chem. Downloaded from www.nrcresearchpress.com by 69.46.99.164 on 09/04/12
For personal use only.

way afforded D-galactose, $[\alpha]_D$ +78°, characterized by conversion into its 1-methyl-1-phenylhydrazone, m.p. 189° C.

Partial Mercaptolysis of the Polysaccharide

The polysaccharide (F-1; 10 g) was stirred at 0° C with concentrated hydrochloric acid (70 ml) for 10 minutes. Ethyl mercaptan (30 ml) was then added, and stirring at 0° C was continued for 20 hours. The mixture was then stirred at 10° C for a further 24 hours. The mercaptolysate (10.5 g) was recovered as described above. It was dissolved in water (50 ml) and the solution was cooled to 0° C. Crystals (1.2 g) of D-galactose diethyl mercaptal separated, and were collected by filtration. The filtrate was diluted with water, and extracted by shaking with ether. From the extract, 3,6-anhydro-D-galactose diethyl mercaptal (1.8 g) was recovered. The remaining aqueous solution was then extracted exhaustively with ether in a liquid–liquid extractor for 3 days. From the extract, a further quantity of D-galactose diethyl mercaptal (0.8 g) was recovered. The aqueous layer was then concentrated to a syrup (6.0 g). On chromatograms developed in solvent (*a*), and sprayed with the silver nitrate reagent, the presence was shown of (*i*) a small, black spot, R_f 0.67, corresponding to galactose diethyl mercaptal; (*ii*) a very large, light brown spot having R_f 0.60; (*iii*) a dark brown spot, R_f 0.50, corresponding to ethyl 1-thio-galactopyranoside; (*iv*) three very small spots having R_f 0.42, 0.30, and 0.27 respectively; (*v*) a spot, R_f 0.15, corresponding to free galactose; and (*vi*) spots corresponding to traces of reducing oligosaccharides.

Isolation of 4-O-β-D-Galactopyranosyl-3,6-anhydro-D-galactose Diethyl Mercaptal (A)

Owing to overlapping of the spots, it was not possible to isolate the major component (A; R_f 0.60 in solvent *a*) of the mixture directly by paper chromatography. The mixture (6.0 g) was therefore adsorbed on a column (14×4 cm) of cocoanut charcoal (11). Elution with aqueous ethanol (5% v/v; 2 l.) displaced D-galactose (0.8 g). Aqueous ethanol (7.5% v/v) then displaced ethyl 1-thio-D-galactopyranoside (0.6 g in 8 l.), followed by D-galactose diethyl mercaptal (0.4 g in 10 l.). Elution with 20% v/v aqueous ethanol then displaced traces of reducing oligosaccharides, and the components with R_f 0.30 and 0.27 in solvent (*a*) (0.2 g in 5 l.). Finally, aqueous ethanol (50% v/v; 6 l.) eluted a mixture (3.8 g) containing ca. 90% of component (A). This last fraction was purified by preparative paper chromatography, to yield a viscous, colorless syrup having $[\alpha]_D$ +14° (*c*, 2.0). It was indistinguishable on chromatograms developed in solvent (*a*) or (*b*) from an authentic specimen of 4-*O*-β-D-galactopyranosyl-3,6-anhydro-D-galactose diethyl mercaptal, which was prepared from κ-carrageenin, and characterized by the late Dr. A. N. O'Neill (12). After drying over phosphorus pentoxide, it crystallized from absolute ethanol–ether, and had m.p. 116–117° C, undepressed on admixture with the authentic specimen.

A portion (100 mg) was heated at 80° C with pyridine (15 ml) and acetic anhydride (10 ml) for 1 hour. Excess of these reagents was then removed by distillation *in vacuo*, and the residue was washed by decantation with water. The residue crystallized from ethanol–water, and after three recrystallizations from the same solvents, the product had $[\alpha]_D$ +12° (*c*, 0.4 in chloroform), and m.p. 121.0–121.5° C, unaltered on addition of authentic 4-*O*-(2,3,4,6-tetra-*O*-acetyl-β-D-galactopyranosyl)-2,5-di-*O*-acetyl-3,6-anhydro-D-galactose diethyl mercaptal (12). X-ray powder photographs of the two hexa-*O*-acetates were identical.

4-O-β-D-Galactopyranosyl-3,6-anhydro-D-galactose (B)

A portion (1 g) of the disaccharide mercaptal (A) was demercaptallated with mercuric

Can. J. Chem. Downloaded from www.nrcresearchpress.com by 69.46.99.164 on 09/04/12
For personal use only.

chloride and cadmium carbonate in water in the usual way. Excess of mercuric chloride was removed by extraction with ether. The syrupy product (B; 0.7 g) reduced Fehling's solution in the cold, and restored the color to Schiff's reagent. Calculated for $C_{11}H_{19}O_9(CHO)$: reducing equivalent weight, 162. Found (by iodometric titration): 155.

A part of the syrup (25 mg) was heated in water (5 ml) with phenylhydrazine (0.1 ml), sodium acetate (0.5 g), and acetic acid (0.5 ml) at 80° C for 2 hours. On cooling, yellow crystals separated; they were collected, and after recrystallization from ethanol–ether, the product had m.p. 211–213° C, and $[\alpha]_D$ +110°±8° (*c*, 0.4 in methanol).

*4-O-β-*D*-Galactopyranosyl-3,6-anhydro-*D*-galactitol (C)*

The remainder of the above syrup (B), dissolved in water (20 ml), was treated with sodium borohydride (1 g), and the solution was allowed to stand overnight at room temperature. It was then treated with excess of Amberlite resin IR-120, and filtered. The filtrate and washings were concentrated to dryness, and boric acid was then removed by the repeated distillation of added methanol. The final residue (C; 0.6 g) crystallized spontaneously on cooling, and after recrystallization from methanol–ether, it had m.p. 172.5–173.5° C, and $[\alpha]_D$ +12.7°±1.0° (*c*, 0.12). For 4-*O*-β-D-galactopyranosyl-3,6-anhydro-D-galactitol, Clingman and Nunn (13) report m.p. 173–174° C, and $[\alpha]_D$ +15°. Calculated for $C_{12}H_{22}O_{10}$: C, 44.2%; H, 6.75%. Found: C, 44.64%; H, 6.80%.

A part of the product (C; 100 mg) was acetylated with pyridine and acetic anhydride in the same way as for (A). The product (D) crystallized from ethanol as strongly birefringeant needles, having m.p. 145.5–146.0° C and $[\alpha]_D$ −6.2°∓1.0° (*c*, 0.2 in chloroform). For 4-*O*-(2,3,4,6-tetra-*O*-acetyl-β-D-galactopyranosyl)-1,2,5-tri-*O*-acetyl-3,6-anhydro-D-galactitol, Clingman and Nunn (13) report m.p. 144–145° C, and $[\alpha]_D$ −7.6° (in chloroform). Calculated for $C_{26}H_{36}O_{17}$: C, 50.3%; H, 5.8%; Ac, 48.5%. Found: C, 50.02%; H, 6.01%; Ac, 48.10%.

ACKNOWLEDGMENTS

The author is indebted to Dr. J. W. Lorimer for help and advice in operating the ultracentrifuge, to Dr. O. Knop and Mr. R. D. McDonald of the Nova Scotia Technical College for X-ray powder photography, and to Dr. W. Yaphe for the colorimetric estimation of galactose and 3,6-anhydro-galactose. He is also grateful to Dr. Yaphe for his interest in this work.

REFERENCES

1. YAPHE, W. and BAXTER, B. Appl. Microbiol. **3** (6), 380 (1955).
2. YAPHE, W. Can. J. Botany, **37**, 751 (1959).
3. SCHACHAT, R. E. and GLICKSMAN, M. *Quoted in* Chem. Eng. News, **36** (38), 32 (1958).
4. BELL, H. P. and MACFARLANE, C. Can. J. Research, **9**, 265 (1933).
5. MACFARLANE, C. Third Intern. Seaweed Symposium, Galway, 1958.
6. KYLIN, H. Kgl. Fysiograf. Sällskap. Lund, Förh. **13**, 51 (1943); Chem. Abstr. **42**, 4247*e* (1948).
7. CLANCY, M. J., WALSH, K., O'COLLA, P. S., and DILLON, T. Third Intern. Seaweed Symposium, Galway, 1958.
8. ROSS, A. G. J. Sci. Food Agr. **4**, 333 (1953).
9. SMITH, D. B. and COOK, W. H. Arch. Biochem. Biophys. **45** (1), 232 (1953).
10. SMITH, D. B., COOK, W. H., and NEAL, J. L. Arch. Biochem. Biophys. **53** (1), 192 (1954).
11. BARTH, F. W. and TIMELL, T. E. Can. J. Chem. **36**, 1321 (1958).
12. O'NEILL, A. N. J. Am. Chem. Soc. **77**, 2837, 6324 (1955).
13. CLINGMAN, A. L. and NUNN, J. R. J. Chem. Soc. 493 (1959).
14. HOUGH, L., JONES, J. K. N., and WADMAN, W. H. J. Chem. Soc. 1702 (1950).
15. TREVELYAN, W. E., PROCTER, D. P., and HARRISON, J. S. Nature, **166**, 444 (1950).
16. YAPHE, W. Nature, **183**, 44 (1959).
17. YAPHE, W. To be published.
18. BROWN, W. L., YOUNG, M. K., and SERAILE, L. G. J. Lab. Clin. Med. **49** (4), 630 (1957).
19. ROE, J. H., EPSTEIN, J. H., and GOLDSTEIN, N. P. J. Biol. Chem. **178**, 839 (1949).
20. O'NEILL, A. N. and STEWART, D. K. R. Can. J. Chem. **34**, 1700 (1956).
21. ARAKI, C. and HIRASE, S. Bull. Chem. Soc. Japan, **26**, 463 (1953).
22. FRIED, J. and WALZ, D. E. J. Am. Chem. Soc. **71**, 140 (1949).

Can. J. Chem. Downloaded from www.nrcresearchpress.com by 69.46.99.164 on 09/04/12
For personal use only.

Can. J. Chem. Downloaded from www.nrcresearchpress.com by 69.46.99.164 on 09/04/12
For personal use only.

CHEMISTRY OF THE TRIFLUOROMETHYL GROUP

PART I. COMPLEX FORMATION BY PHOSPHINES CONTAINING THE TRIFLUOROMETHYL GROUP[1, 2]

M. A. A. Beg and H. C. Clark

ABSTRACT

The formation of co-ordination compounds of $(CH_3)_3P$, $(CH_3)_2PCF_3$, $CH_3P(CF_3)_2$, and $P(CF_3)_3$, with boron trifluoride and platinum (II) chloride has been studied. The properties of the new compounds $(CH_3)_2PCF_3.BF_3$, $[(CH_3)_2PCF_3]_2PtCl_2$, $[CH_3P(CF_3)_2]_2PtCl_2$ are described, and it is hence concluded that the stabilities of the boron trifluoride compounds decrease in the order

$$(CH_3)_3P.BF_3 > (CH_3)_2PCF_3.BF_3 > (CH_3P(CF_3)_2BF_3 > P(CF_3)_3.BF_3),$$

while for the platinum (II) complexes the order of stability is

$$[(CH_3)_3P]_2PtCl_2 < [(CH_3)_2PCF_3]_2PtCl_2 > [CH_3P(CF_3)_2]_2PtCl_2 > ([P(CF_3)_3]_2PtCl_2).$$

These two orders are related to the electronegativity of the trifluoromethyl group and its influence on the bonding properties of the phosphorus atoms.

INTRODUCTION

While a range of organometallic and organometalloidal trifluoromethyl compounds has been prepared, little quantitative information is so far available for the trifluoromethyl group. Since its electronegativity will differ widely from that of a normal alkyl or aryl group, these organometalloidal compounds may be expected to show unusual properties. A study has therefore been made of the effect of the trifluoromethyl group on the donor properties of substituted phosphines. Two types of addition products may be formed: (*a*) those containing only a σ-bond from phosphorus to the acceptor atom, as for example in $F_3P.BH_3$, and (*b*) those in which both σ- and π-bonding occurs, usually between phosphorus and a transition metal, e.g. $(R_3P)_2PtCl_2$. The effect of the electronegative trifluoromethyl group on the formation of σ- and π-bonds will vary and may be investigated by examining the properties of these two classes of compounds.

EXPERIMENTAL

Preparation of the Phosphines

Trimethylphosphine was prepared by the method of Mann and Wells (1). This reaction normally gives low yields, but it was found that, with strong cooling of the reaction vessel in an acetone–solid CO_2 mixture, yields of 60% could be regularly obtained. The phosphine was isolated as the silver iodide complex, which, when warmed *in vacuo*, readily evolved the phosphine.

The reaction of trimethylphosphine with trifluoroiodomethane, as described by Haszeldine and West (2), was used to prepare dimethyl trifluoromethylphosphine, but yields higher than 33% based on CF_3I could not be obtained. The reaction appeared to commence below −78° and was virtually complete after the mixture had stood at room temperature for about 30 minutes. Apart from the desired product and an involatile residue of tetramethylphosphonium iodide, a volatile white solid identified as dimethyl bis(trifluoromethyl)phosphonium iodide, m.p. 60°, was also found. The latter compound (0.472 g) reacted with excess aqueous sodium hydroxide at room temperature to give fluoroform (0.235 g) corresponding to the loss of two CF_3 groups. Purification of the

[1]*Manuscript received August 20, 1959.*
Contribution from the Chemistry Department, University of British Columbia, Vancouver 8, B.C.
[2]*Presented at the International Conference on Co-ordination Chemistry, London, April 1959.*

dimethyl trifluoromethylphosphine was best achieved by thermal decomposition of its silver iodide complex as described by Haszeldine and West.

Methyl bis(trifluoromethyl)phosphine was prepared by reacting tris-trifluoromethylphosphine with methyl iodide as described by Haszeldine and West (3).

The preparation of tris(trifluoromethyl)phosphine from phosphorus and trifluoroiodomethane followed the methods of earlier workers (4).

Commercial boron trifluoride was used after purification by vacuum distillation. Platinum (II) chloride was prepared by heating chloroplatinic acid to 325° in an atmosphere of nitrogen. The complexes described below were prepared by reacting the phosphines with boron trifluoride or platinum (II) chloride in sealed, evacuated tubes. The identities of the boron trifluoride derivatives were determined from the ratios of the reactants and those of the platinum (II) chloride complexes by standard methods of analysis. Saturation pressures were measured with an isoteniscope, the boron trifluoride compounds being prepared directly in its bulb in order to avoid decomposition with moisture.

Compounds with Boron Trifluoride

(*a*) *Trimethylphosphine.*—The phosphine (0.1995 g, 2.60 mmoles) reacted immediately with boron trifluoride (0.1927 g, 2.79 mmoles) to give a white solid. The recovery of excess trifluoride (0.0031 g) gave a ratio phosphine:boron trifluoride of 1:1. The compound $(CH_3)_3P.BF_3$ has been reported previously (5) but few of its properties have been described. It is decomposed slowly in moist air, and rapidly in water, acetone, and ethanol. It is only slightly soluble in chloroform and insoluble in carbon tetrachloride and carbon disulphide. The melting point is 126–130° (decomp.) and the saturation pressure is given by the equation $\log_{10} p$ (mm) $= 8.460-(2627/T)$ in the range 25°–100°, whence the heat of sublimation is 11.98 kcal mole^{-1}.

(*b*) *Dimethyl trifluoromethylphosphine.*—The phosphine (0.2952 g, 2.27 mmole) reacted with boron trifluoride (0.1589 g, 2.27 mmole) to give a white solid which melted below room temperature to a viscous liquid. The compound showed the same behavior towards moist air and polar solvents as its trimethylphosphine analogue. The melting or freezing point could not be precisely determined since supercooling to a glass occurred. Softening of the glass took place at approximately −9° C. The vapor pressure of the compound is given by the equation $\log_{10} p$ (mm) $= 10.354-(2146/T)$ whence the heat of vaporization is 9.68 kcal mole^{-1}.

(*c*) *Methyl bis(trifluoromethyl)phosphine.*—In this case, no reaction occurred after 120 hours at room temperature between the phosphine (0.2690 g) and boron trifluoride (0.0938 g). Cooling to −78° still allowed the boron trifluoride to be recovered and there was no sign of complex formation. Similarly, the treatment of tris(trifluoromethyl)-phosphine (0.3106 g) with boron trifluoride (0.1934 g) failed to reveal the formation of any complex.

Compounds with Platinum (II) *Chloride*

(*a*) *Trimethylphosphine.*—The complex $[(CH_3)_3P]_2PtCl_2$ has been prepared previously (6) but it was here prepared for comparison with its trifluoromethyl analogues. Direct reaction between the phosphine and platinum (II) chloride in the absence of a solvent was very slow. In a benzene suspension, reaction was more rapid although the yield was still low. Thus trimethylphosphine (0.195 g) shaken for 24 hours with platinum (II) chloride (0.3345 g) in benzene gave only 0.10 g of the complex, a 20% yield. Higher yields could be obtained by using the method described by Jensen (7) for the preparation of the

Can. J. Chem. Downloaded from www.nrcresearchpress.com by 69.46.99.164 on 09/04/12
For personal use only.

Can. J. Chem. Downloaded from www.nrcresearchpress.com by 69.46.99.164 on 09/04/12
For personal use only.

corresponding triethylphosphine complex. This involved shaking an aqueous solution of potassium chloroplatinite (1.20 g) with the phosphine (0.43 g). The mixture was heated on a steam bath for 30 minutes, and the white complex was filtered, and washed with water, alcohol, and ether. Recrystallization from methanol gave a yield of 0.51 g, a 41% yield of bis(trimethylphosphine)dichloroplatinum (II). Found: Pt, 45.5; Cl, 17.0. Calc. for $[(CH_3)_3P]_2PtCl_2$: Pt, 44.7; Cl, 16.1%. The melting point is 324–326° and the dissociation pressure in the range 155–190° is given by the equation $\log_{10} p$ (mm) $= 6.510 - (2108/T)$, whence the heat of dissociation is 9.59 kcal mole^{-1}. The complex dissolves readily in chloroform, is sparingly soluble in ethanol, and almost insoluble in ether, benzene, and carbon tetrachloride. In water, particularly when heated, decomposition occurs and the free phosphine is evolved.

(*b*) *Dimethyl trifluoromethylphosphine.*—The reaction of the phosphine (0.412 g, 3.17 mmoles) with platinum (II) chloride (0.425 g, 1.59 mmoles) at room temperature for 48 hours in a sealed tube gave a pale yellow product, which was recrystallized from methanol to give white, needle-shaped crystals of bis(dimethyl (trifluoromethyl)-phosphine)dichloroplatinum (II). Found: Pt, 37.2; Cl, 13.2. Calc. for $[(CH_3)_2PCF_3]_2PtCl_2$: Pt, 37.1; Cl, 13.5%. The complex melted at 188–190° with decomposition and the dissociation pressure over the range 90–130° is given by the equation $\log_{10} p$ (mm) $= 7.969 - (2438/T)$ whence the heat of dissociation is 11.31 kcal mole^{-1}. It is soluble in alcohol, chloroform, and carbon disulphide and insoluble in ether, benzene, and carbon tetrachloride. It is not soluble in cold water, but reacts slowly with hot water to evolve fluoroform. Almost complete conversion (90%) to fluoroform is obtained on heating to 80° with 25% aqueous sodium hydroxide.

(*c*) *Methyl bis(trifluoromethyl)phosphine.*—This phosphine and platinum (II) chloride in a 2:1 ratio reacted only slowly and unreacted phosphine was always recovered from the reaction tubes. Extraction of the solid reaction product with carbon tetrachloride or methanol and evaporation of the extract gave yellow crystals of bis(methyl bis(trifluoromethyl)-phosphine)dichloroplatinum (II). Found: Pt, 29.9; Cl, 11.2. Calc. for $[CH_3P(CF_3)_2]_2$-$PtCl_2$: Pt, 30.7; Cl, 11.2%. The melting point is 85–87° and the dissociation pressure in the range 80–140° may be expressed as $\log_{10} p$ (mm) $= 4.885 - (1258/T)$ whence the heat of dissociation is 5.76 kcal mole^{-1}. The complex is soluble in carbon tetrachloride, ether, acetone, and alcohol, but is insoluble in water. Hydrolysis (50% approx.) to fluoroform occurs with 25% aqueous sodium hydroxide at 80°.

(*d*) *Tris(trifluoromethyl)phosphine.*—The following experiments were performed in attempts to prepare a platinum (II) complex. In all cases the reactants were completely recovered and no sign of complex formation was observed. (*i*) Direct reaction of the phosphine (0.175 g) and platinum (II) chloride (0.132 g) at room temperature. (*ii*) The passage of the phosphine in a stream of nitrogen over platinum (II) chloride heated to 200°. (*iii*) Reaction of the phosphine and platinum (II) chloride in methanol. Several experiments were performed under this last set of conditions and in all cases the methanol acquired a yellow color and a few colorless crystals appeared to be formed. All attempts to isolate a product were unsuccessful, apparently because of decomposition.

Dipole Moments

Because of the low solubility of the platinum complexes and also their tendency, in certain cases, to decompose slowly in the presence of moisture, accurate dipole moments were not calculated. The dielectric constants were measured with a simple Ebarch dielectric constant meter and dipole moments were calculated using Jensen's formula (8) for dilute solutions. The accuracy of the dipole moments is ± 0.5 D.

TABLE

Molar concentration	ϵ_{soln}	P_m	μ (D)
$[(CH_3)_3P]_2PtCl_2$ measured in chloroform:benzene (1:1) solution (ϵ_{mix} = 3.380)			
0.000466	3.426	3320	
0.000977	3.441	3780	13.1±0.5
$[(CH_3)_2PCF_3]_2PtCl_2$ measured in chloroform solution (ϵ_{CHCl_3} = 4.947)			
0.00985	4.982	1667	
0.00189	5.007	1806	9.2±0.5
$[CH_3P(CF_3)_2]_2PtCl_2$ measured in carbon tetrachloride solution (ϵ_{CCl_4} = 2.261)			
0.00297	2.261		
0.00525	2.261		0

DISCUSSION

The addition compounds formed by phosphines with boron trifluoride result from dative σ-bond formation from phosphorus to boron. Smaller secondary effects such as back co-ordination may also be involved but these are of only minor importance. Evidence from other series of BF_3 derivatives (9), comparable to that described here, reveals that a decrease in the electron-donating power of the co-ordinating base produces a corresponding decrease in the stability of the molecular addition compound. As a qualitative measure of stability, we have here employed relative volatilities. The vapor pressure equations quoted above show the lower volatility and greater stability of $(CH_3)_3P.BF_3$ as compared with $(CH_3)_2PCF_3.BF_3$. The trifluoromethyl group thus markedly reduces the donor properties of the phosphorus atom. This is in accordance with a higher electronegativity and a smaller inductive effect for the trifluoromethyl in contrast to the methyl group.

Since the adduct $(CF_3)_3P.BH_3$ does not exist (10) and since borine adducts are generally more stable than their boron trifluoride analogues, it is not surprising that methyl bis(trifluoromethyl)phosphine– and tris(trifluoromethyl)phosphine–boron trifluoride adducts could not be isolated.

The possibility that steric interaction by the much larger CF_3 group is responsible for the observed decrease in stability must also be considered, although the extent of such interaction is difficult to determine accurately. The steric requirements will certainly be greatest for tris(trifluoromethyl)phosphine for which Bowen (11) has shown the CPC angles to be 100° and the CF_3 groups all to lie on the same side of the phosphorus atom. Also since there is some rearrangement of the planar BF_3 molecule towards a tetrahedral configuration on formation of the co-ordinate bond, it would appear that steric interaction between the CF_3 groups and F atoms must be comparatively small. For the other phosphines with fewer CF_3 groups, steric interactions will be of even less significance. The observed decrease in stability of the BF_3 adducts is therefore not due to steric effects.

The infrared spectra of $(CH_3)_3P.BF_3$ and $(CH_3)_2PCF_3.BF_3$ could not be completely resolved so that full interpretation is not possible. However, in both cases the B—F stretching frequencies at 1450 and 1505 cm^{-1} in BF_3 were shifted to the 1175–1200 cm^{-1}. This is similar to the shifts observed for ketone–BF_3 complexes by Susz *et al.* (12). There is also a considerable shifting of bands in the 650–750 cm^{-1} region. Since both the BF_3 bending and P—C (aliphatic) stretching frequencies occur in this region and since no other similar spectra are available for comparison, assignments have not been made.

In phosphine – platinum (II) co-ordination compounds, in addition to the formation of dative σ-bonds from phosphorus to platinum, strong $d\pi$–$d\pi$-bonding is also possible and appears to be of considerable importance in determining relative stabilities. As an extreme

Can. J. Chem. Downloaded from www.nrcresearchpress.com by 69.46.99.164 on 09/04/12
For personal use only.

Can. J. Chem. Downloaded from www.nrcresearchpress.com by 69.46.99.164 on 09/04/12
For personal use only.

case, consider bis(trifluorophosphine)dichloroplatinum (II) $(F_3P)_2PtCl_2$ (13). Here the highly electronegative fluorine atoms reduce the electron donor properties of phosphorus, but at the same time cause considerable π-bonding which appears to involve the unshared *d*-electron pairs of platinum and the vacant 3*d* orbitals of the phosphorus atoms. The extent of this electron drift from platinum back to phosphorus is shown by the small dipole moment of 4.4 D. This indicates a *cis*-configuration and must be compared with values of 11–12 D for the *cis*-isomers of bis(trialkylphosphine)dichloroplatinum (II) complexes. Similarly, the substitution of trifluoromethyl for methyl groups may tend to give increased π-bonding between platinum and phosphorus although not to the same extent as phosphorus trifluoride.

The configurations of the complexes described earlier can be deduced from their colors, solubilities in polar and non-polar solvents, and their dipole moments. Bis(trimethylphosphine)dichloroplatinum (II) and bis(dimethyl trifluoromethylphosphine)dichloroplatinum (II) are obtained as the *cis*-isomers since they are white solids and have large dipole moments. Bis(methyl bis(trifluoromethyl)phosphine)dichloroplatinum (II) is isolated in the *trans*-form which is yellow-orange and has a zero dipole moment. It must be emphasized that these are the major components of reaction products prepared and recrystallized under the same conditions. In all three cases there were indications that the other isomer was also formed but only to the extent of less than about 5%. Since it is known that the isomer obtained under a given set of conditions may depend to some extent on relative solubilities, it would clearly be necessary to study in detail the *cis–trans* equilibria in order to determine unambiguously the relative stabilities of the isomers of the various complexes. However, since all our complexes could be prepared under identical conditions in the absence of solvents, the fact that different isomers are obtained with dimethyl trifluoromethylphosphine and methyl bis(trifluoromethyl)phosphine is significant and is discussed later.

The relative stabilities of these new phosphine complexes may be examined in several ways. Chemically, the trimethylphosphine complex appears the least stable since decomposition always occurs to a small extent during recrystallization from methanol, and to a much larger extent on reaction with warm water. Also, the solid compound always smells strongly of the free phosphine. In contrast the other two complexes were odorless solids which could be recrystallized without decomposition and which reacted only slowly with hot water. An accurate index of thermal stability is seen in the heats of dissociation calculated from the observed dissociation pressures, the values being 6.7 kcal $mole^{-1}$ for *cis*-$[(CH_3)_3P]_2PtCl_2$, 11.3 kcal $mole^{-1}$ for *cis*-$[(CH_3)_2PCF_3]_2PtCl_2$, and 5.8 kcal $mole^{-1}$ for *trans*-$[CH_3P(CF_3)_2]_2PtCl_2$. The process of dissociation probably involves the loss of a phosphine molecule and the formation of a dimeric bridged complex,

$$2(\text{phosphine})_2PtCl_2 \rightarrow 2\text{phosphine} + (\text{phosphine})_2Pt_2Cl_4$$

but it could alternatively result in the simultaneous loss of both phosphine molecules to give free platinum (II) chloride. Although the actual course of dissociation is unknown, the above values are considered a reasonable guide to relative stabilities of the platinum complexes and they show the order to be

$$(CH_3)_3P < (CH_3)_2PCF_3 > CH_3P(CF_3)_2[> P(CF_3)_3].$$

Points of particular interest are: (*a*) the increase and then decrease in stability in the series as CF_3 is substituted for CH_3; (*b*) the non-existence, under the conditions so far studied, of a Pt(II) complex of tris(trifluoromethyl)phosphine; and (*c*) the fact that, under

the same conditions, dimethyl (trifluoromethyl)phosphine gives the *cis*-isomer, while methyl bis(trifluoromethyl)phosphine produces the *trans*-isomer. In platinum (II) complexes the greatest degree of π-bonding is obtained when the two π-bonding ligands are *cis* to one another (14). Substitution of the first methyl group by the more electronegative CF_3 group thus appears to give greater stability to the complex by causing a greater increase in π-bonding than is offset by the reduction in strength of the σ-bond. This can also be seen by a comparison of the dipole moment of 13.1 D for $[(CH_3)_3P]_2PtCl_2$ with that of 9.2 D for $[(CH_3)_2PCF_3]_2PtCl_2$. For the complex of methyl bis(trifluoromethyl) phosphine there might be expected to occur one of only two possibilities: (*a*) introduction of the second CF_3 group on each phosphine might produce even greater stability; or (*b*) the reduction in strength of the σ-bond may more than offset any increase in π-bonding so as to give a less stable complex. In either case, one might expect that the *cis*-isomer would be obtained. The occurrence of the *trans*-isomer is therefore unexpected, and can satisfactorily be explained, together with the non-existence of a tris(trifluoromethyl)-phosphine complex, in terms of steric hindrance. When models are drawn using the usual values of atomic radii, it can be shown that 2 trimethyl(or indeed any alkyl)phosphine molecules can be placed *cis* to one another about a platinum atom, but not 2 tris(trifluoromethyl)phosphine molecules. The observed effects are certainly not just due to the decreased donor properties of the phosphines since the *cis*-isomer of bis(trifluorophosphine)-dichloroplatinum (II) is known and is more stable than its *trans*-isomer. The importance of steric effects for the trifluoromethylphosphines is also shown by the fact that nickel carbonyl derivatives have been obtained (15) in which no more than 2 of the carbon monoxide molecules can be replaced by tris(trifluoromethyl)phosphine. In contrast, the more electronegative and more weakly electron-donating but much smaller PF_3 molecule can occupy all four positions to give $Ni(PF_3)_4$ (16).

Although these stability orders for the boron trifluoride and platinum (II) chloride derivatives might well be investigated further by the determination of thermodynamic values, particularly the thermodynamic differences between *cis*- and *trans*-isomers, the present information does emphasize the high electronegativity of the trifluoromethyl group, as well as the importance of π-bonding in transition metal complexes.

ACKNOWLEDGMENTS

We gratefully acknowledge the support of the National Research Council, and one of us (M. A. A. B.) expresses thanks for a scholarship received from C. S. I. R. (Pakistan) under the auspices of the Colombo Plan.

REFERENCES

1. MANN, F. G. and WELLS, A. F. J. Chem. Soc. 702 (1938).
2. HASZELDINE, R. N. and WEST, B. O. J. Chem. Soc. 3631 (1956).
3. HASZELDINE, R. N. and WEST, B. O. J. Chem. Soc. 3880 (1957).
4. BENNETT, F. W., EMELEUS, H. J., and HASZELDINE, R. N. J. Chem. Soc. 1565 (1953); BURG, A. B. and MAHLER, W. J. Am. Chem. Soc. **79**, 247 (1957).
5. GRAHAM, W. A. G. and STONE, F. G. A. J. Inorg. & Nuclear Chem. **3**, 164 (1956).
6. CAHOURS, A. Ann. **156**, 302 (1870).
7. JENSEN, K. A. Z. anorg. Chem. **229**, 225 (1936).
8. JENSEN, K. A. and NYGAARD, B. Acta Chem. Scand. **3**, 479 (1949).
9. STONE, F. G. A. Chem. Rev. **58**, 101 (1958).
10. BURG, A. B. and BRENDEL, G. J. Am. Chem. Soc. **80**, 3198 (1958).
11. BOWEN, H. J. M. Trans. Faraday Soc. **50**, 463 (1954).
12. CHALANDON, P. and SUSZ, B. P. Helv. Chim. Acta, **41**, 697 (1958).
13. CHATT, J. and WILLIAMS, A. A. J. Chem. Soc. 3061 (1951).
14. CHATT, J. and WILKINS, R. G. J. Chem. Soc. 273 (1952).
15. EMELEUS, H. J. and SMITH, J. D. J. Chem. Soc. 527 (1958).
16. WILKINSON, G. J. Am. Chem. Soc. **73**, 5501 (1951).

Can. J. Chem. Downloaded from www.nrcresearchpress.com by 69.46.99.164 on 09/04/12
For personal use only.

Can. J. Chem. Downloaded from www.nrcresearchpress.com by 69.46.99.164 on 09/04/12
For personal use only.

HYDROGEN BONDING IN DIASTEREOISOMERIC α-β AMINOALCOHOLS: A REINVESTIGATION OF THE EPHEDRINES BY N.M.R.[1]

JAMES B. HYNE[2]

ABSTRACT

The results of an n.m.r. study of the diastereoisomeric ephedrine and ψ-ephedrine molecules in non-polar solvents are interpreted and discussed in terms of the relative stabilities of the intramolecularly hydrogen-bonded conformers.

INTRODUCTION

The presence of two different asymmetric centers in the ephedrine molecule accounts for the existence of four optically active forms of the molecule. Previous configurational analysis of the ephedrines (1, 2, 3) has established the configuration of the two centers in all four forms of ephedrine as summarized in Table I. Considerable chemical evidence has accumulated which suggests that there is preferred spatial distribution of the hydroxyl and amino functional groups in the ψ-ephedrines which differs from that in the ephedrines.

TABLE I

Configuration of the ephedrines

$C_6H_5\underset{\uparrow}{C}H(OH)\underset{\uparrow}{C}H(NHCH_3)CH_3$

C_O C_N

(+)-ψ-ephedrine	$C_O(+)C_N(+)$	(−)-ephedrine	$C_O(-)C_N(+)$
(−)-ψ-ephedrine	$C_O(-)C_N(-)$	(+)-ephedrine	$C_O(+)C_N(-)$

C_O, center configuration related to (+)- and (−)-mandelamide.
C_N, center configuration related to (+)- and (−)-alanine.

Emde (1) first suggested that this conformational difference existed and the work of Welsh (4), Nagai and Kanoa (5), and Fodor and Koczka (6) further suggested that in the ψ-ephedrines the hydroxyl and amino functional groups were spatially in a preferred gauche conformation, while in the ephedrines the *trans* disposition about the C_O—C_N bond was preferred. Close (7) explained the production of an oxazolidone from ψ-ephedrine on fusion with urea compared with an imidazolidone on similar treatment of ephedrine on the basis of a preferred gauche disposition of the hydroxyl and amino groups in ψ-ephedrine compared with *trans* in ephedrine. This conformational difference is reflected in the mechanism of ring closure to form the oxazolidone or imidazolidone, in the former case by elimination of ammonia and in the latter case of water. Everett and Hyne (8) reported approximate calculations of the energetically most favorable conformations for the two forms of ephedrine based on the repulsive interactions between non-bonded groups on the C_O and C_N centers and ignoring specific interactions between the hydroxyl and amino groups. These rough calculations give surprisingly good agreement with the chemical evidence showing that in the ψ-ephedrine the angle between the C_O—OH and C_N—$NHCH_3$ bonds, looking down the C_O—C_N axis, is 60° and in the ephedrine case 180°.

Phillips (9) has reported the X-ray crystallographic data on both ephedrine and ψ-ephedrine hydrochlorides. In these crystal lattices the hydroxyl and amino functional

[1]*Manuscript received October 6, 1959.*
Contribution No. 1554 from the Sterling Chemistry Laboratory, Yale University, New Haven, Conn., U.S.A.
[2]*Present address: Department of Chemistry, Dartmouth College, Hanover, N.H., U.S.A.*

groups were found to be gauche to one another in both forms of the hydrochloride. However, as Phillips points out, the presence of the chloride ion in the lattice probably constrains these groups to adopt a gauche conformation, but this need not apply under other conditions of aggregation of the ephedrine molecules. Kanzawa (10) has recently reported that the infrared spectra of (−)-ephedrine and (+)-ψ-ephedrine indicate a greater predominance of intramolecularly hydrogen-bonded species in solutions of the ψ-isomer in non-polar solvents, and interprets this observation in terms of the preferred gauche conformation of the hydroxyl and amino groups.

The development of high resolution n.m.r. techniques provides a further tool for the investigation of this type of problem, and although in the case of the ephedrines the conformational differences have already been convincingly demonstrated by other methods a reinvestigation by n.m.r. serves to establish the applicability of this technique to such problems. Various n.m.r. studies of the chemical shift associated with hydroxylic hydrogens have shown that the chemical shift depends upon the degree to which these hydrogens are involved in hydrogen bonding (11, 12, 13, 14). None of the previous n.m.r. studies of this kind, however, have considered the case where intramolecular hydrogen bonding is only possible in a particular conformer and the various conformers are separated by relatively low energy barriers resulting from steric hindrance to free rotation about a single bond. Clearly, the application of n.m.r. techniques to such problems would be of particular value in the many conformational problems associated with the stereochemistry of aminoalcohols, diols, and related systems. An additional advantage of the n.m.r. method over the infrared method lies in the fact that the n.m.r. technique involves measurement of the peak *position* which can be determined with considerably greater precision than the *areas* of infrared absorption peaks, which frequently overlap to a considerable extent.

If the conformational difference suggested by previous work is real then the ψ-ephedrine isomer should show a much higher degree of intramolecular hydrogen bonding which should be less sensitive to breakdown as a result of dilution compared with the ephedrine diastereoisomer in which there is a greater degree of intermolecular hydrogen bonding. A study of the chemical shift associated with the hydroxyl and amino hydrogens as a function of concentration should, therefore, reveal a difference in behavior in the two ephedrine forms. Furthermore, the intermolecular hydrogen bond might be expected to be more sensitive to temperature changes than the intramolecular bond. The results of the study of both the concentration and temperature dependence of the resonance frequency of the hydroxyl and amino hydrogens are reported in this paper.

N.M.R. SPECTRA

Spectra were measured with a Varian V 4300 spectrometer operated at a fixed frequency of 40 megacycles. Samples were spun in 12-mm inside diameter tubes and temperature maintained at 20°±1° except where otherwise specified. Chemical shifts, in c.p.s. from benzene as an external standard, were measured by standard side-band techniques with an accuracy of ±2 c.p.s. or better. Solutions were prepared by dilution of a master solution prepared by weight. Attempts to measure spectra in carbon tetrachloride as solvent were unsuccessful due to reaction of the ephedrines with the solvent and precipitation of hydrochlorides. A similar reaction was found to take place in chloroform but only after several weeks of standing and could not be detected when the solution was stored in the dark. Even under conditions of normal illumination no evidence could be found of reaction of this type during the normal period required to prepare solutions and take spectra.

Can. J. Chem. Downloaded from www.nrcresearchpress.com by 69.46.99.164 on 09/04/12
For personal use only.

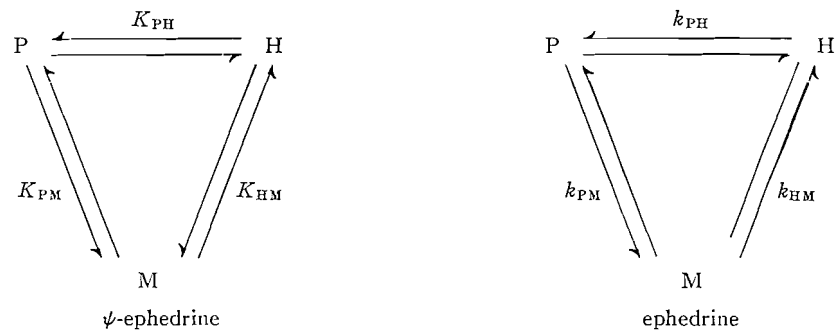
A single peak only was observed for both the NH and OH hydrogens (ν_{obs}) at all except very low concentrations at which it was difficult to distinguish between real splitting and noise effects. The single peak probably arises from rapid exchange of the hydrogens catalyzed by trace amounts of acid in the solvent.

Concentration Dependence of ν_{obs}

Figure 1 shows the dependence of the chemical shift associated with the NH and OH hydrogens on the concentration, c, in chloroform expressed in moles per liter of solvent. The observed difference in behavior for the two diastereoisomeric forms can be summarized as: (*a*) at any given concentration the frequency observed (ν_{obs}) for ψ-ephedrine is always lower than that for ephedrine; (*b*) the rate of increase of ν_{obs} with dilution is initially greater in the ψ-ephedrine case; (*c*) the ν_{obs} for ψ-ephedrine appears to approach a limiting value at the lowest concentrations measured, but that for ephedrine shows no such behavior within the experimental range of concentrations studied.

Huggins, Pimentel, and Shoolery (12) have previously reported chemical shift behavior of a similar type in the n.m.r. spectra of *o*-, *m*-, and *p*-chlorophenol. The concentration dependence of the *o*-chlorophenol OH resonance frequency reaches a maximum value for the frequency at low concentrations, while that of the *m*- and *p*-chlorophenol continues to increase throughout the dilution range studied. These authors attribute the differing behavior to the ability of the *o*-chlorophenol to hydrogen-bond intramolecularly, a phenomenon which is prohibited in the *m*- and *p*-chlorophenols for steric reasons.

In the ephedrine systems we consider a cyclic equilibrium between three species: P, an intermolecularly hydrogen-bonded polymer characterized by an NH/OH frequency ν_P; H, an intramolecularly hydrogen-bonded monomer with frequency ν_H; and M, an unhydrogen-bonded monomer with frequency ν_M. Clearly, we could consider various types of polymer, but as was shown previously by Saunders and Hyne (14) a model of this type involving equilibria between various types of n-mers leads to a result which is experimentally indistinguishable from one assuming a monomer–dimer equilibrium only. Assuming that the frequencies associated with the various species P, H, and M are



approximately equal for both forms (i.e. $\nu_P(\psi\text{-ephedrine}) = \nu_P(\text{ephedrine})$ etc.) a knowledge of the values of these frequencies would enable a quantitative interpretation of the observed data in terms of the equilibria postulated. Unfortunately, however, these values are not available from the data since the limiting value of ν_{obs} in either case can not be assumed to be the value for any single species of monomer. Despite the lack of this precise information we can interpret the data qualitatively in terms of the relative values of the equilibrium constants for the various processes in the cyclic equilibrium.

From the data in Fig. 1 we can deduce the relative magnitudes of ν_P, ν_H, and ν_M. It is known that the frequency associated with hydrogen-bonded hydrogen is lower than that

Can. J. Chem. Downloaded from www.nrcresearchpress.com by 69.46.99.164 on 09/04/12
For personal use only.

for unhydrogen-bonded hydrogen, therefore ν_P and ν_H must be less than ν_M. The relative values of ν_P and ν_H can be estimated from the observed slopes of the frequency versus concentration curves and the low concentration behavior. If ν_P and ν_H were equal, dissociation to hydrogen-bonded monomer H would not affect ν_{obs} and the observed greater slope of the ψ-ephedrine curve would be due entirely to easier dissociation to unhydrogen-bonded monomer M compared to the ephedrine case. This easier dissociation to unhydrogen-bonded monomer in the ψ-ephedrine system, however, is not in keeping with the observed behavior at low concentration. The approach to a limiting ν_{obs} which is considerably less than that observed for ephedrine clearly indicates that ψ-ephedrine does not dissociate more readily to the highest frequency monomer M. We therefore conclude that the relative order of magnitude of the frequencies must be $\nu_P < \nu_H < \nu_M$.

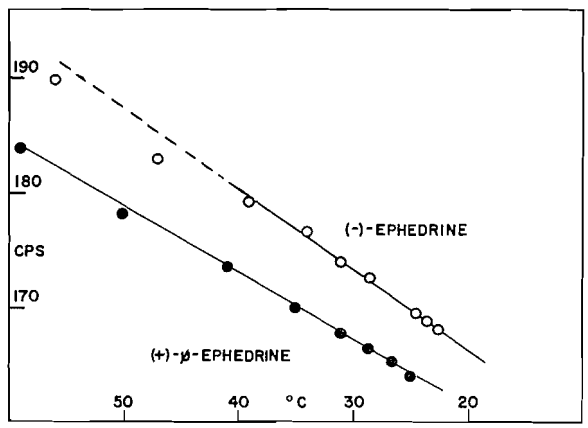


FIG. 1. The concentration dependence of resonance frequency for NH/OH hydrogens in c.p.s. from benzene (external) for ephedrine and ψ-ephedrine in chloroform solution. Concentration, c, in moles/liter.

The polymeric forms P of both ephedrines may dissociate to either one of two species, H or M. The data show that on initial dilution the ψ-ephedrine polymer dissociates more easily to the hydrogen-bonded monomer H with intermediate ν_H value. This will account for the greater observed slope and also the fact that at low concentrations the ν_{obs} tends to a limiting value which must be intermediate between that for ν_H and ν_M since both forms of the monomer exist in equilibrium. In terms of the dissociation constants this means that $K_{PH} > k_{PH}$ and $k_{PM} > K_{PM}$. That is, the hydrogen-bonded monomer of ψ-ephedrine is more stable relative to the unhydrogen-bonded monomer than the ephedrine counterpart, or $K_{HM} < k_{HM}$.

The concentration dependence of the NH/OH chemical shift for the two ephedrines therefore provides convincing evidence of the greater stability of the intramolecularly hydrogen-bonded ψ-ephedrine species, a conclusion which can only be rationalized in terms of the preferred gauche conformation of the hydroxyl and amino groups in the ψ-ephedrine diastereoisomer.

The Temperature Dependence of ν_{obs}

If, as has been suggested above, the ψ-ephedrine hydrogen-bonded species in the equilibrium mixture contain a greater proportion of intramolecularly hydrogen-bonded monomer than the ephedrine system at the same concentration, then the temperature dependence of ν_{obs} should differ in the two forms. This will only be true if the strengths of the inter- and intra-molecular bonds are different, but it seems reasonable to assume

Can. J. Chem. Downloaded from www.nrcresearchpress.com by 69.46.99.164 on 09/04/12
For personal use only.

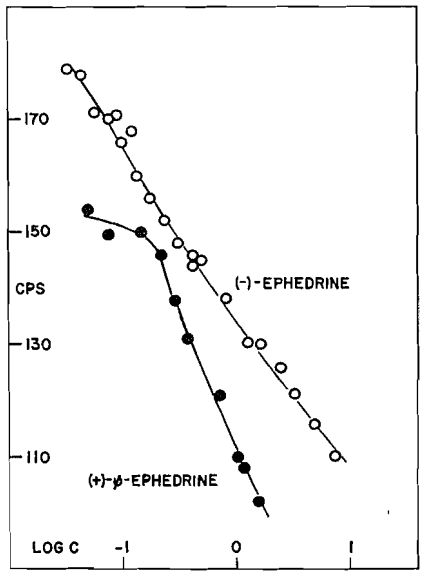


FIG. 2. The temperature dependence of resonance frequency for NH/OH hydrogens in c.p.s. from benzene (internal) for ephedrine and ψ-ephedrine in benzene solution.

that the intramolecular hydrogen bond will be less sensitive to temperature change than the intermolecular hydrogen bond. Figure 2 shows the temperature dependence of ν_{obs} for the two diastereoisomers in benzene solution. Benzene was used as a solvent rather than chloroform to avoid complication at higher temperatures arising from the reaction with solvent mentioned previously and in order to obtain a higher boiling solvent. Any shifts due to the anisotropy of the benzene will not seriously affect an argument based on the comparison of two isomers in the same solvent. The observed difference in temperature dependence is small but there is evidence at lower temperatures of a somewhat greater sensitivity to temperature in the case of ephedrine. Since only a proportion of the ψ-ephedrine hydrogen-bonded species will be intramolecularly hydrogen bonded and only these species will contribute to the reduction in temperature dependence compared with ephedrine the small observed difference is explicable. Furthermore, the intra- and intermolecular hydrogen bond strengths may differ by less than a kilocalorie and at most by no more than three or four. Although, in itself, the temperature dependence cannot be considered strong evidence for the preferred gauche conformation of the functional groups in ψ-ephedrine the small difference noted is in the direction to be expected on the basis of other evidence.

CONCLUSIONS

The concentration dependence of the chemical shift associated with the amino and hydroxyl hydrogens in the diastereoisomeric ephedrines provides good evidence for preferential residence of the ψ-ephedrine in the gauche form compared with the ephedrine isomer. Although the temperature dependence of the shift does not provide convincing evidence, the small effect noted does support the same conclusion. The work of Huggins, Pimentel, and Shoolery (12) on the chlorophenols has established the value of n.m.r. studies of intramolecular hydrogen-bonding phenomena where the hydrogen-bonded groups are not free to rotate by virtue of the order of the bond joining them. This work shows that

Can. J. Chem. Downloaded from www.nrcresearchpress.com by 69.46.99.164 on 09/04/12
For personal use only.

the method can be extended to systems where the restriction arises from steric factors rather than bond order. Therefore, studies of the dilution effect on chemical shift can provide additional criteria for establishing preferred conformations arising out of rotation about a single bond where the degree and type of hydrogen bonding vary with the conformation.

ACKNOWLEDGMENT

The author expresses his thanks to Dr. Martin Saunders of this laboratory for his helpful discussion during the course of this work.

REFERENCES

1. EMDE, H. Helv. Chim. Acta, **12**, 365 (1929).
2. FREUDENBERG, K. and NIKOLAI, F. Ann. **510**, 223 (1934).
3. FREUDENBERG, K., SCHOEFFEL, E., and BRAUN, E. J. Am. Chem. Soc. **54**, 234 (1932).
4. WELSH, L. H. J. Am. Chem. Soc. **71**, 3500 (1949).
5. NAGAI, W. N. and KANOA, S. Ann. **470**, 157 (1929).
6. FODOR, G. and KOCZKA, K. J. Chem. Soc. 850 (1952).
7. CLOSE, W. J. J. Org. Chem. **15**, 1131 (1950).
8. EVERETT, D. H. and HYNE, J. B. J. Chem. Soc. 1636 (1958).
9. PHILLIPS, G. D. Acta Cryst. **7**, 159 (1954).
10. KANZAWA, T. Bull. Chem. Soc. Japan, **29**, 398 (1956).
11. BECKER, E., LIDDEL, U., and SHOOLERY, J. J. Mol. Spectroscopy, **2**, 1 (1958).
12. HUGGINS, C., PIMENTEL, G., and SHOOLERY, J. J. Phys. Chem. **60**, 1311 (1956).
13. COHEN, A. and REID, C. J. Chem. Phys. **25**, 790 (1956).
14. SAUNDERS, M. and HYNE, J. B. J. Chem. Phys. **29**, 1319 (1958).

Can. J. Chem. Downloaded from www.nrcresearchpress.com by 69.46.99.164 on 09/04/12
For personal use only.

Can. J. Chem. Downloaded from www.nrcresearchpress.com by 69.46.99.164 on 09/04/12
For personal use only.

THE STRUCTURE OF 2-*p*-DIMETHYLAMINOBENZYLIDENEINDOXYL AND ITS SALTS[1]

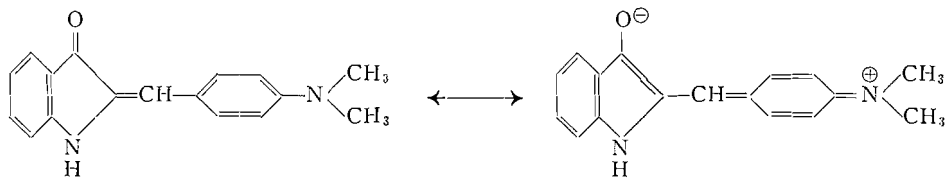
R. A. ABRAMOVITCH[2] AND A. M. MARKO[3]

ABSTRACT

2-*p*-Dimethylaminobenzylideneindoxyl has been shown to have mainly the dipolar quinonoid structure (II), though quaternization takes place at the dimethylamino nitrogen atom in the unperturbed structure (I). This has been established by a study of its infrared and ultraviolet absorption spectra and by a comparison of these with those of its monohydrochloride, its methiodide, and of 2-benzylideneindoxyl.

A quantitative method of analysis of indican in urine has been devised (1) which involves the reaction of the indican-containing solution with *p*-dimethylaminobenzaldehyde and spectrophotometric measurement of the red color developed. The color was shown to be due to 2-*p*-dimethylaminobenzylideneindoxyl (I), which could be isolated as a purple crystalline solid exhibiting dichroism, and which was identical with the product prepared by Noelting (2) from indoxyl-2-carboxylic acid and *p*-dimethylaminobenzaldehyde. This compound is reported (2) to be a dyestuff and the deep color of the crystals was noteworthy. The ultraviolet absorption spectrum in 95% ethanol exhibited an intense band at 510 mμ (ϵ = 21,300) which did not seem to be compatible with the unperturbed structure (I). In dilute hydrochloric acid the color of the solution is a light orange-yellow, the intense band in the ultraviolet at 510 mμ being replaced by a weaker one at 497 mμ (ϵ = 15,620).

The deep color of 2-*p*-dimethylaminobenzylideneindoxyl would be understandable if canonical structure (II) was the main contributor to the resonance hybrid:



(I) (II)

Support of this suggestion was readily obtained from a consideration of the infrared and ultraviolet spectra of the base and some of its derivatives. In fact, the infrared spectrum of the solid dyestuff showed a medium-to-weak band at 1655 cm^{-1}. Because of the low intensity ($\Delta\nu_{\frac{1}{2}}$ for most of the bands in this region mentioned here are nearly comparable) and the position of this band, the band was considered unlikely to be due to the carbonyl group in (I). In fact, the ketonic carbonyl group in N-acetylindoxyl gives rise to a strong band at 1716 cm^{-1} and that in 1-methylindoxyl to a band near 1750 cm^{-1} (3). For the purpose of comparison the spectrum of 2-benzylideneindoxyl was recorded, and exhibited a strong conjugated carbonyl band at 1680 cm^{-1}. On the other hand, Edwards, Clarke, and Douglas (4) and Habgood and Marion (5*a*) have assigned a medium intensity band at 1668–1682

[1]*Manuscript received September 29, 1959.*
Contribution from the University of Saskatchewan, Saskatoon, Saskatchewan.
[2]*Department of Chemistry, University of Saskatchewan, Saskatoon, Saskatchewan.*
[3]*Departments of Biochemistry and Paediatrics, University of Saskatchewan, Saskatoon, Saskatchewan.*

cm^{-1} to the grouping $C{=}\overset{\oplus}{N}\!\!<$ (see also Witkop and Patrick (5*b*)); such a grouping (conjugated in this case) is present in structure (II). The other bands observed in the 6-μ region may also be interpreted on the basis of structure (II): thus the strong bands at 1617 (sh) and 1607 cm^{-1} may be attributed to the conjugated C=C bonds and the band at 1558 cm^{-1} (s) to the highly conjugated enolate anion $\left(\begin{array}{c} O^{\ominus} \\ | \\ C{=}C \end{array}\right)$ (the enolate anion grouping is reported to give rise to a strong band at 1604 cm^{-1} (6)). Braunholtz, Ebsworth, Mann, and Sheppard (7) have shown that compounds containing an NMe or an $N\!<^{Me}_{Me}$ grouping exhibit a strong-to-medium band between 2760 and 2820 cm^{-1}. Salt formation or quaternization causes the disappearance of this band. No such band was observed in the infrared spectrum (KBr disk or hexachlorobutadiene mull) of 2-*p*-dimethylaminobenzylideneindoxyl. Evidence from ultraviolet absorption spectra also backs up the suggestion that (II) is the main contributory structure to the resonance hybrid. This evidence is as follows.

When a solution of 2-*p*-dimethylaminobenzylideneindoxyl in ethanol was treated with dilute hydrochloric acid, a marked change in color took place from reddish purple to yellowish orange. This was also accompanied by a change in the ultraviolet absorption spectrum (see Fig. 1). Thus, the intense band at 510 mμ underwent a hypsochromic shift

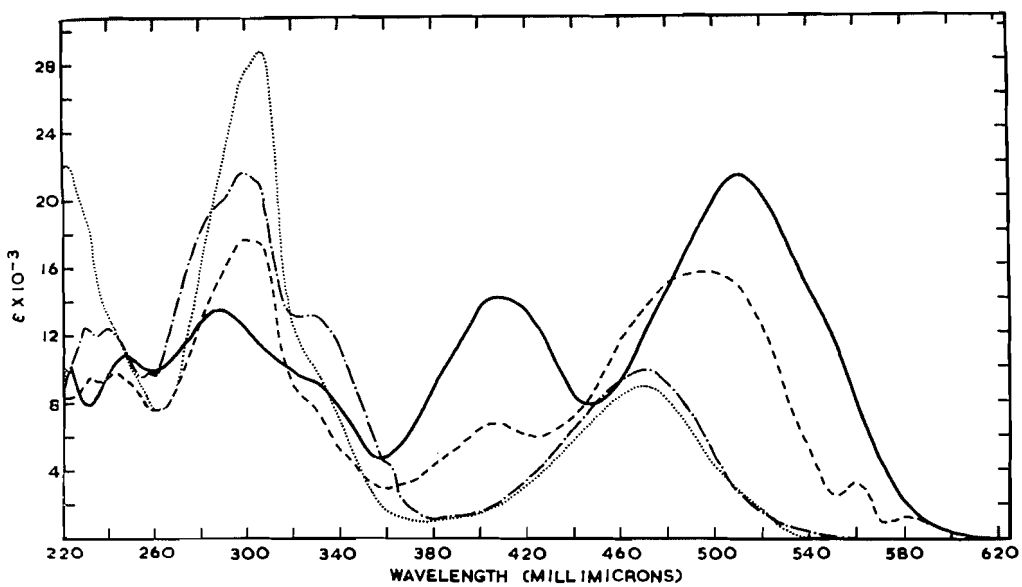
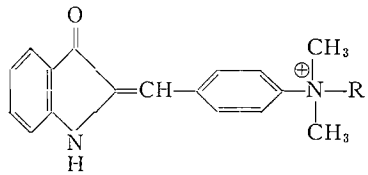


FIG. 1. ——— 2-*p*-Dimethylaminobenzylideneindoxyl in 95% ethanol. – – – 2-*p*-Dimethylaminobenzylideneindoxyl in 95% ethanol containing a small amount of HCl. —·—·— 2-Benzylideneindoxyl in 95% ethanol. ..... 2-*p*-Dimethylaminobenzylideneindoxyl methiodide in 95% ethanol.

to 497 mμ as well as a decrease in intensity. The intensity of the 407-mμ band also decreased, whereas the 288-mμ band underwent a bathochromic shift to 300 mμ as well as an increase in intensity. Since the monohydrochloride could not be isolated in a pure state and it was felt to be important to determine which atom had been protonated

Can. J. Chem. Downloaded from www.nrcresearchpress.com by 69.46.99.164 on 09/04/12
For personal use only.

(the $-O^{\ominus}$ in (II) or the $-N(CH_3)_2$ in (I)), the crystalline methiodide was prepared instead. This showed a similar ultraviolet absorption to that of the hydrochloride with the changes above even more intensified, i.e. a stronger hypsochromic shift and decrease in intensity in the longer wavelength band, and an increase in the intensity of the shorter wavelength band. It is possible that the hydrochloride is only partially formed in solution and exists in equilibrium with the free base, or that there exists a tautomeric equilibrium between the N and O protonated forms, both of which hypotheses could explain the smaller hypsochromic shift observed.* This would indicate that in the formation of the salt, attachment of the proton or of the methyl group took place preferentially at the dimethylamino group of (I), thus resulting in a decrease in color due to the loss of the quinonoid structure, and to the fact that no resonating structures similar to (I) ↔ (II) can be written for (III) without invoking an inadmissible pentacovalent nitrogen atom.



(R = H or CH_3)

(III)

Support for structure (III; R = CH_3) was adduced from its infrared absorption spectrum which, unlike that of the parent 2-*p*-dimethylaminobenzylideneindoxyl, exhibited a strong band at 1686 cm^{-1} characteristic of the conjugated carbonyl group.

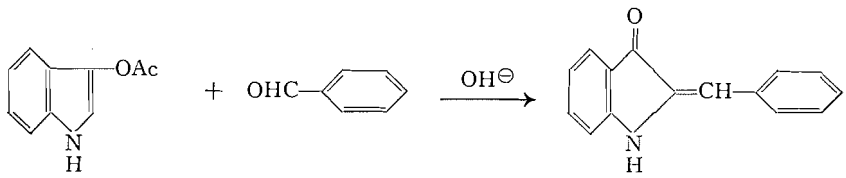
Conclusive supporting evidence for structures (II) (predominantly) and (III) assigned to the free base and salts respectively was obtained by a comparison of their ultraviolet absorption spectra with that of 2-benzylideneindoxyl (IV). Similar comparisons have very recently been carried out between *p*-dimethylaminoazobenzene and its methiodide, and azobenzene (9). Here the mesomeric effect of the dimethylamino group upon the ultraviolet absorption spectrum of the unsubstituted azobenzene is virtually nullified by quaternization, with the result that the spectra of azobenzene and *p*-trimethylammonium-azobenzene iodide are almost superimposable, whereas that of *p*-dimethylaminoazobenzene shows the expected bathochromic shift and increase in intensity due to the +M effect of the $-N(CH_3)_2$ group. When the ultraviolet absorption spectra of 2-*p*-dimethylaminobenzylideneindoxyl, its monohydrochloride, and its methiodide in ethanol were compared with that of 2-benzylideneindoxyl a comparable result to that reported (9) in the azobenzene series was observed (see Fig. 1). It is, therefore, concluded that though the quinonoid structure (II) is the main contributor to the structure of 2-*p*-dimethylaminobenzylideneindoxyl, quaternization occurs preferentially at the dimethylamino nitrogen atom.

When formation of the second conjugate acid of (II) was effected by dissolving the base in concentrated hydrochloric acid, the ultraviolet absorption spectrum changed markedly; the bands at 407 and 510 mμ in the base, and at 407 and 497 mμ in the monohydrochloride, disappeared and were replaced by a band at 380 mμ. This solution was unstable and the color soon faded.

2-Benzylideneindoxyl (IV) had previously been prepared by Baeyer by heating indoxylic acid with benzaldehyde at 120° (10). In the present work it was found more

**Yeh and Jaffé (8) have recently presented evidence that the formally related first conjugate acid of p-dimethylaminoazobenzene consists of a tautomeric mixture of the ammonium and azonium-quinoid forms.*

Can. J. Chem. Downloaded from www.nrcresearchpress.com by 69.46.99.164 on 09/04/12
For personal use only.



(IV)

convenient to obtain this compound by the condensation of indoxyl-*O*-acetate with benzaldehyde in aqueous alkali, the yield of product being nearly theoretical.

EXPERIMENTAL

The infrared spectra were measured in potassium bromide disks and in Nujol mulls using a Perkin–Elmer Model 21 double beam spectrometer with sodium chloride optics. Ultraviolet absorption spectra were determined using a Beckman DK 2 recording spectrophotometer.

2-p-Dimethylaminobenzylideneindoxyl

A filtered solution of crude indican (0.7 g) (from the oxidation of indole with potassium persulphate (11)) in water (150 ml) was treated with a 3% ethanolic solution of *p*-dimethylaminobenzaldehyde (75 ml), followed by 6 *N* hydrochloric acid (100 ml) whereupon the solution turned dark brown. After it was stirred for 1 hour the mixture was filtered and the purple solid (0.3 g) discarded (this may arise due to the presence of impurities in the crude indican). The filtrate was neutralized with 10% sodium hydroxide (25 ml) and saturated aqueous sodium acetate solution (200 ml), the precipitate (2.2 g) filtered, washed with water, and then with light petroleum. Unreacted *p*-dimethylaminobenzaldehyde was removed by washing with hot light petroleum (4×30 ml) and then once with hot ethyl acetate (20 ml). The last procedure resulted in the loss of some of the desired product. The product was recrystallized from benzene–cyclohexane giving long needles, m.p. 236–238°, which were green by reflected and red by transmitted light. Crystallization from alcohol gave purple needles. Noelting (2) reports m.p. 226°–227° for this compound while Gossner (12) reports 231–232°. Calc. for $C_{17}H_{16}ON_2$: C, 77.30; H, 6.11; N, 10.60. Found: C, 77.50; H, 6.08; N, 10.52. λ_{max} 248, 288, 407, 510, λ_{infl} 324 mμ; $\epsilon\times10^{-3}$ 10.89, 13.61, 14.21, 21.30, 9.54 (in 95% ethanol). λ_{max} 232, 244, 300, 407, 497, λ_{infl} 324 mμ; $\epsilon\times10^{-3}$ 9.48, 9.79, 17.70, 6.66, 15.62, 8.44 (in ethanolic hydrogen chloride).

Infrared spectrum (KBr disk) (main peaks only): 3240, 1655 (mw) (C=$\overset{\oplus}{\text{N}}$<, 1617 (sh) (s), 1607 (s) (conjugated C=C), 1558 (s) (C=C(–$O^{\ominus}$)–), 1545 (NH), 1526 cm^{-1}. Identical values were observed when the measurement was carried out on a Nujol mull.

Attempted Preparation of 2-p-Dimethylaminobenzylidene-N-acetylindoxyl

N-Acetylindoxyl (1.75 g) and *p*-dimethylaminobenzaldehyde (1.6 g) were boiled under reflux in 80% ethanol (25 ml) with 5 drops of concentrated hydrochloric acid for 5 hours. On cooling, the solution deposited crystals of 2-*p*-dimethylaminobenzylideneindoxyl, identical with those obtained above from indican. Working up the mother liquors only led to the isolation of intractable tars which, on chromatography on neutral alumina, could only be resolved into a number of tarry fractions which could not be induced to crystallize. When the reaction was carried out using piperidine as the catalyst instead of

Can. J. Chem. Downloaded from www.nrcresearchpress.com by 69.46.99.164 on 09/04/12
For personal use only.

hydrochloric acid, similar results were obtained. The use of absolute instead of aqueous ethanol did not result in the isolation of any 2-*p*-dimethylaminobenzylideneindoxyl nor of any identifiable product.

2-p-Dimethylaminobenzylideneindoxyl Methiodide

This was prepared by adding an excess of methyl iodide to a suspension of 2-*p*-dimethylaminobenzylideneindoxyl in 95% ethanol; the flask was stoppered, shaken occasionally for 3 hours and left overnight. The purple solid gradually went into solution and the methiodide separated overnight as golden platelets which were recrystallized from ethanol after being washed with acetone. The product had m.p. 217–218° (after darkening at 204–205°). Calc. for $C_{18}H_{19}ON_2I$: C, 53.21; H, 4.68. Found: C, 53.02; H, 4.76. λ_{max} 306, 470, λ_{infl} 294, 326 mμ; $\epsilon \times 10^{-3}$ 28.70, 8.90, 24.50, 10.91 (in 95% ethanol). Infrared spectrum (Nujol mull) (main peaks only): 3300, 1686 (s) (>C=O) 1622 (s) (C=C), 1605 (s) (aromatic), 1589 (s), 1575 cm^{-1} (sh) (w).

2-Benzylideneindoxyl

Indoxyl-*O*-acetate (0.22 g) and benzaldehyde (0.135 g) in water (10 ml) containing 10 drops of 4 *N* sodium hydroxide were warmed on a water bath. A flocculent yellow precipitate began to separate immediately and the warm mixture was shaken until no more dark brown oil remained. The cooled product was extracted repeatedly with ether, the extract concentrated to a small volume, and cooled in a freezer at −17°. The crystals, which were obtained in nearly theoretical yield, were filtered and recrystallized at a low temperature from ether, yielding orange rods, m.p. 177–178°. Baeyer (10) reports m.p. 176° for this compound. λ_{max} 231, 241, 299, 470, λ_{infl} 284, 326, 358 mμ; $\epsilon \times 10^{-3}$ 12.50, 12.42, 21.60, 9.88, 19.10, 13.19, 4.60. Infrared spectrum (Nujol mull) (main peaks only): 3260, 1680 (s) (>C=O), 1625 (s) (C=C), 1604 (s), 1590 (s), 1560 cm^{-1} (sh) (m).

2-*p*-Dimethylaminobenzylideneindoxyl may be prepared conveniently and in high yield by substituting *p*-dimethylaminobenzaldehyde for benzaldehyde in this procedure.

ACKNOWLEDGMENTS

Financial support from the National Research Council (to R.A.A.) and from the Department of Public Health, Ottawa (to A.M.M.) are gratefully acknowledged. The authors are also indebted to Dr. L. Vining for the use of a recording ultraviolet spectrophotometer and to Mr. L. D. Johnson for technical assistance.

REFERENCES

1. MARKO, A. M. and REYNOLDS, F. B. Can. J. Biochem. and Physiol. To be published.
2. NOELTING, E. Bull. Soc. ind. Mulhouse, **72**, 236 (1902); Chem. Zentr. **I**, 34 (1903).
3. HOLT, S. J., KELLIE, A. E., O'SULLIVAN, D. G., and SADLER, P. W. J. Chem. Soc. 1217 (1958).
4. EDWARDS, O. E., CLARKE, F. H., and DOUGLAS, B. Can. J. Chem. **32**, 235 (1954).
5. (*a*) HABGOOD, T. and MARION, L. Can. J. Chem. **34**, 604 (1955). (*b*) WITKOP, B. and PATRICK, J. B. J. Am. Chem. Soc. **75**, 4474 (1953).
6. BENDER, M. L. and FIGUERAS, J. J. Am. Chem. Soc. **75**, 6304 (1953).
7. BRAUNHOLTZ, J. T., EBSWORTH, E. A. V., MANN, F. G., and SHEPPARD, N. J. Chem. Soc. 2780 (1958).
8. YEH, S.-Y. and JAFFÉ, H. H. J. Am. Chem. Soc. **81**, 3283 (1959).
9. PENTIMALLI, L. Tetrahedron, **5**, 27 (1959).
10. BAEYER, A. Ber. **16**, 2188 (1883).
11. BOYLAND, E., SIMS, P., and WILLIAMS, D. C. Biochem. J. **62**, 546 (1956).
12. GOSSNER, W. Z. physiol. Chem. **282**, 262 (1947).

Can. J. Chem. Downloaded from www.nrcresearchpress.com by 69.46.99.164 on 09/04/12
For personal use only.

Can. J. Chem. Downloaded from www.nrcresearchpress.com by 69.46.99.164 on 09/04/12
For personal use only.

THE PREFERENTIAL TOSYLATION OF THE *ENDO*-5-HYDROXYL GROUP OF 1,4;3,6-DIANHYDRO-D-GLUCITOL[1]

R. U. LEMIEUX AND A. G. MCINNES

ABSTRACT

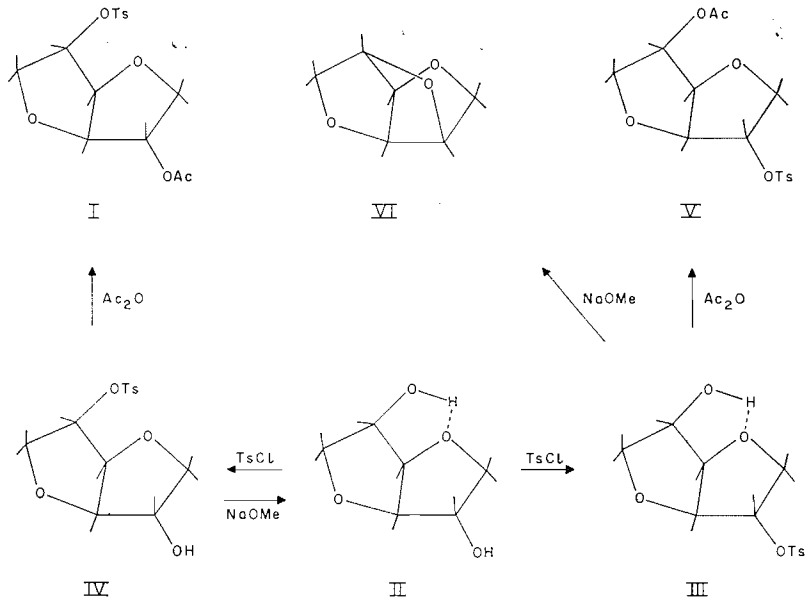
Reaction of 1,4;3,6-dianhydro-D-glucitol (isosorbide) with an equimolar amount of tosyl chloride in pyridine gave a fourfold greater yield of the *endo*-5-tosylate (IV) than of the *exo*-2-tosylate (III). Compound III reacted about 1.4 times more rapidly with tosyl chloride than did IV. The structures of III and IV were established by infrared spectroscopy and by their reaction with sodium methoxide. The *exo*-tosyloxy group of the monoacetate of III resists replacement by iodide ion.

Cope and Shen (1) reported the preparation of a mono-*O*-tosyl mono-*O*-acetyl 1,4;3,6-dianhydro-D-glucitol (mono-*O*-tosyl mono-*O*-acetyl isosorbide). Since the compound was converted (1) to 1,4;2,5;3,6-trianhydro-D-mannitol (VI) on treatment with sodium *t*-butoxide, it was concluded that the tosyl group in I was situated at the *exo*-2-position (compound V). However, Cope and Shen (1) reported unequivocal evidence that a transtosylation reaction can take place under these conditions and, consequently, the monotosylate may have had the tosyl group at the *endo*-5-position as shown in structure I. Recently, Jackson and Hayward (2) have shown the compound to undergo replacement of the tosyloxy group when heated with sodium iodide dissolved in acetic anhydride. This observation was taken as proof that the tosyloxy group was at the *endo*-5-position. It is conceivable, however, that the *endo*-acetoxy group of 2-*O*-tosyl 5-*O*-acetyl isosorbide (V) can participate in the solvolysis of the tosyloxy group to lead to a 2,5-bridged acetoxonium ion, which could then react with iodide ion to give the iodoacetate isolated by Jackson and Hayward (2). Thus, the reaction of the compound with sodium iodide could not be taken as unequivocal evidence that it possesses the structure I.

A consideration of a molecular model for isosorbide (II) shows that the *endo*-5-hydroxyl group is eclipsed with the oxygen atom which bridges the 1- and 4-positions, whereas the *exo*-2-hydroxyl is eclipsed only with hydrogen atoms. The non-bonded interaction between the eclipsed oxygen atoms should be especially unfavorable since it brings into close opposition carbon-to-oxygen bonds polarized in the same direction. This contention is supported by the fact that D-glucitol is converted more readily to the 1,4-anhydride which possesses a 2,3-*trans*-glycol, then to the 3,6-anhydride which possesses a 4,5-*cis*-glycol (3). It could be anticipated that the *endo*-5-hydroxyl group of isosorbide would be intramolecularly hydrogen bonded to the eclipsing 4-oxygen atom. This conclusion was supported by the observation (see below) that the *endo*-5-hydroxyl group of 2-*O*-tosyl isosorbide (III) in fact is involved in an intramolecular hydrogen bond.

Therefore, one might expect (1) that the *exo*-2-hydroxyl group of isosorbide (II) would undergo tosylation substantially more rapidly than the sterically shielded and hydrogen-bonded *endo*-5-hydroxyl group. *The main purpose of this communication is to show that precisely the opposite is in fact the case.* This observation clearly has an important bearing on the general subject of preferential esterification of alcoholic hydroxyl groups in the field of carbohydrate chemistry and in particular on the hazards of introducing

[1]*Manuscript received August 25, 1959.*
Contribution from the Department of Chemistry, University of Ottawa, Ottawa, Ontario. This paper is to be a portion of a thesis to be submitted by A. G. McInnes for the Ph.D. degree.



notions on the subject derived from studies of simple alicyclic alcohols into the field of carbohydrate chemistry.

Isosorbide (II) was reacted with 1 mole equivalent of tosyl chloride in pyridine at 5° for 40 hours (1, 2). The ditosyl derivative was obtained in 17.1% yield. The syrupy residue was chromatographed on silicic acid with chloroform as developing phase to yield a crystalline monotosylate (III) in 11.7% yield and an isomer (IV), which has resisted crystallization, in 45.4% yield. Acetylation of IV yielded the monotosyl monoacetate (I) previously prepared by Cope and Shen (1). Acetylation of the crystalline monotosylate (III) led to a mono-*O*-tosyl mono-*O*-acetyl derivative of II which has not crystallized. The structures of the monotosylates III and IV were readily established through their behavior in presence of sodium methoxide. Compound III consumed the base about 40 times more rapidly than IV at room temperature and led to the formation of 1,4;2,5;3,6-trianhydro-D-mannitol (VI). On the other hand, IV when heated in the presence of sodium methoxide was converted to isosorbide (II) in excellent yield. Clearly, therefore, compounds III and IV have the structures shown. This conclusion was supported by the fact that the compounds III and IV showed absorption maxima for the hydroxyl groups, in the infrared, at 3564 and 3624 cm^{-1}, respectively, when 0.0025 *M* in carbon tetrachloride. These results indicate intramolecular hydrogen bonding in compound III which can only be possible with the hydroxyl group at the *endo*-5-position. The *O*-acetyl derivative of III (V) was recovered in high yield after treatment with sodium iodide in refluxing acetic anhydride for 2.5 hours. Consequently, the acetoxy group of V is in fact not well disposed for participation in the dissociation of the tosyloxy group. We have confirmed the observation (2) that I undergoes facile replacement of the tosyloxy group by iodine under these conditions. It is of interest that compound I resisted refluxing in 4:1 acetic acid – acetic anhydride containing potassium acetate for 24 hours.

The phenomenon of the preferential tosylation of the *endo*-hydroxyl group of I was

Can. J. Chem. Downloaded from www.nrcresearchpress.com by 69.46.99.164 on 09/04/12
For personal use only.

further substantiated by a study of the rates of tosylation of the monotosylates III and IV. The compound with the *endo*-hydroxyl group (III) reacted with tosyl chloride in pyridine at 25° approximately 1.4 times more rapidly than the isomer with the *exo*-hydroxyl group. It is not known whether or not this phenomenon is unique for the isosorbide structure. However, the literature suggests it may be of general importance in the esterification of polyhydric compounds. This matter is receiving further attention in this laboratory.

EXPERIMENTAL

Isosorbide (II) was prepared by the procedure of Montgomery and Wiggins (4). The white crystalline product melted at 62–63.5° (uncorr.) with $[\alpha]_D$ +44.6° (*c*, 1.78 in water) and +65° (*c*, 2.94 in pyridine). The reported values are m.p. 61.9–64°, $[\alpha]_D$ +44.8° (*c*, 2.22 in water) and +64.9° (*c*, 2.32 in pyridine) (5).

Reaction of Isosorbide (II) *with Tosyl Chloride*

Isosorbide, 13.2 g (0.905 mole), was dissolved in 100 ml pyridine and cooled to −5°. An equimolar amount of tosyl chloride (*p*-toluenesulphonyl chloride) was added and the reaction mixture stored at 5° for 46 hours. Any tosyl chloride present at the end of the reaction time was destroyed by the addition of 5 ml of distilled water to the reaction mixture, which was subsequently poured into 250 ml of distilled water and extracted with three 150-ml aliquots of chloroform. The combined chloroform extract was washed with concentrated hydrochloric acid to remove pyridine and then washed free of acid with distilled water. After drying over anhydrous sodium sulphate the chloroform solution was evaporated under reduced pressure at 50° to yield 22.6 g of a syrupy residue. The residue was dissolved in 100 ml 95% aqueous ethanol, and after the solution was left to stand overnight at 5°, 5.02 g of a white crystalline compound, m.p. 96–97° (uncorr.), was precipitated. The melting point and infrared spectrum of the substance were consistent with those expected for 2,5-di-*O*-tosyl isosorbide (6). The filtrate on evaporation under reduced pressure yielded 17.53 g of syrup.

The syrupy residue was chromatographed on 400 g silicic acid (Mallinckrodt) which had previously been activated at 120° for 24 hours. When the chromatogram was developed with chloroform, three fractions were cleanly separated in the following order: (*a*) a white crystalline compound, 2.00 g, the infrared spectrum of which was identical with that of 2,5-di-*O*-tosyl isosorbide; (*b*) a white crystalline compound (III), 3.18 g (11.7% of theory based on isosorbide), which after recrystallization from ethyl acetate melted at 108–109° with $[\alpha]_D$ +47.7° (*c*, 1.86 in chloroform); and (*c*) a colorless syrup (IV), 12.31 g (45.4% of theory), $[\alpha]_D$ +57.9° (*c*, 4.27 in chloroform). The total yield of ditosylate was 17.1% of theory.

A study, using a Beckman DK2 spectrometer, of the infrared spectra in the O—H stretching region of 0.0025 molar solutions of III and IV in carbon tetrachloride showed absorption at 3564 cm^{-1} and 3624 cm^{-1}, respectively. The latter is characteristic of the stretching vibration of a non-bonded secondary hydroxyl group, whereas the former shows a shift to lower frequency of 60 cm^{-1} which is characteristic of hydroxyl groups forming intramolecular hydrogen bonds.

Acetylation of 2-O-Tosyl (III) *and 5-O-Tosyl Isosorbide* (IV)

Samples of III, 1.74 g, and of IV, 5.31 g, were acetylated in pyridine with acetic anhydride at 5° to yield 1.80 g (90% theory) of 2-*O*-tosyl 5-*O*-acetyl isosorbide (V) and

Can. J. Chem. Downloaded from www.nrcresearchpress.com by 69.46.99.164 on 09/04/12
For personal use only.

5.70 g (94% theory) of 2-*O*-acetyl 5-*O*-tosyl isosorbide (I), respectively. V was a colorless oil, $[\alpha]_D$ +83.6° (*c*, 3.43 in chloroform), whereas I crystallized from methanol, 5.0 g (83% theory), m.p. 65.5–66° (uncorr.), and $[\alpha]_D$ +79.2° (*c*, 3.54 in chloroform). Reported (2) for 2-*O*-acetyl 5-*O*-tosyl isosorbide (I), m.p. 64–65° and $[\alpha]_D$ +77.9° (in chloroform). The nuclear magnetic resonance spectra of compounds I and V were in agreement with those expected for mono-*O*-acetyl mono-*O*-tosyl derivatives of isosorbide; furthermore, the infrared spectra were very similar. There could therefore be no doubt as to the composition of I.

Reaction of (III) *and* (IV) *with Sodium Methoxide*

The compounds III, 0.345 g (1.15 mmoles), and IV, 0.2905 g (0.97 mmole), were dissolved in 10 ml of methanol approximately 0.2 *N* in sodium methoxide and left standing at room temperature. At intervals, over a period of 72 hours, 1-ml aliquots were taken and titrated with 0.064 *N* hydrochloric acid. At the end of the reaction period, III had consumed 0.108 milliequivalent (94% theory) and IV 0.065 milliequivalent (17% theory) of the sodium methoxide. Assuming second-order kinetics, the ratio of the rate constants, k_{III}/k_{IV}, was approximately 40.

Compounds III, 0.2005 g (0.667 mmole), and IV, 0.4585 g (1.53 mmoles), were refluxed with 2 ml and 4 ml, respectively, of methanol approximately 1 *N* in sodium methoxide for 8 hours. After cooling to room temperature, the excess sodium methoxide was neutralized with solid carbon dioxide. The reaction mixtures were taken to dryness at room temperature under reduced pressure and the residues extracted with ether and acetone, respectively. After solvent removal, the residues were distilled under reduced pressure. Compound III yielded 0.0689 g (81% theory) of a crystalline compound, m.p. 68–68.6° the infrared spectrum of which showed no absorption in the O—H stretching or aromatic skeletal vibration regions and was consistent with that expected for 1,4;2,5;3,6-trianhydro-D-mannitol (VI). The trianhydride (VI) was reported (1) to melt at 66.5–67.2°. On the other hand, IV yielded 0.1566 g (70% theory) of a crystalline compound whose infrared spectrum was identical with that of isosorbide (II).

Rates of Tosylation

The rates of tosylation of III and IV were compared by reacting 0.2256 g (0.75 mmole) of the compounds with 2 mmoles of tosyl chloride in 5 ml of pyridine at 25°. One-milliliter aliquots of the solutions were taken at intervals and added to 5 ml of 90% aqueous pyridine and left standing for 5 minutes. Ten milliliters of distilled water was then added and the free acid determined by titration with 0.0882 *N* sodium hydroxide using phenolphthalein as indicator. A solution containing only tosyl chloride in the same molar concentration was used as control. The reaction of III was complete after 28 hours, whereas IV had reacted to the extent of 72% of theory after this time. Assuming second-order kinetics the ratio of the rate constants for the two reactions, k'_{III}/k'_{IV}, was approximately 1.4.

Reaction of Sodium Iodide with I *and* V

The compounds V, 1.43 g (4.2 mmoles), and I, 3.43 g (10 mmoles), were refluxed with 20 ml and 50 ml, respectively, of a 0.5 *M* solution of sodium iodide in acetic anhydride. After 2.5 hours the solutions were cooled to room temperature and the sodium tosylate was recovered by filtration and weighed as described by Jackson and Hayward (2). Compound V yielded 0.060 g (7.4% theory) and I yielded 1.78 g (92% theory) of sodium *p*-toluenesulphonate.

Can. J. Chem. Downloaded from www.nrcresearchpress.com by 69.46.99.164 on 09/04/12
For personal use only.

ACKNOWLEDGMENT

The research was in part sponsored by the Sugar Research Foundation, New York, on Project No. 88.

REFERENCES

1. COPE, A. C. and SHEN, T. Y. J. Am. Chem. Soc. **78**, 5912 (1956).
2. JACKSON, M. and HAYWARD, L. D. Can. J. Chem. **37**, 1048 (1959).
3. SOLTZBERG, S., GOEPP, R. M., JR., and FREUDENBERG, W. J. Am. Chem. Soc. **68**, 919 (1946).
4. MONTGOMERY, R. and WIGGINS, L. F. J. Chem. Soc. 390 (1946).
5. FLETCHER, H. G., JR. and GOEPP, R. M., JR. J. Am. Chem. Soc. **67**, 1042 (1945).
6. HOCKETT, R. C., FLETCHER, H. G., JR., SHEFFIELD, E. L., GOEPP, R. M., JR., and SOLTZBERG, S. J Am. Chem. Soc. **68**, 930 (1946).

Can. J. Chem. Downloaded from www.nrcresearchpress.com by 69.46.99.164 on 09/04/12
For personal use only.

Can. J. Chem. Downloaded from www.nrcresearchpress.com by 69.46.99.164 on 09/04/12
For personal use only.

ADSORPTION EQUILIBRIA OF HYDROGEN, DEUTERIUM, AND THEIR MIXTURES. PART I[1]

D. BASMADJIAN[2]

ABSTRACT

Adsorption isotherms of hydrogen and deuterium have been measured at temperatures of 75–90° K and pressures up to 760 mm Hg on the following six adsorbents: charcoal (2), silica gel, and Linde molecular sieves type 4A, 5A, and 13X.

Deuterium was found to be adsorbed to a greater extent than hydrogen in all cases investigated, its isosteric heat of adsorption exceeding that of hydrogen by 50 to 300 cal/mole.

Binary adsorption isotherms were determined on the same adsorbents in the range 10–90% D_2 at temperatures of 75 and 90° K and a total pressure π of 750 and 200 mm Hg. The analyses were performed by the thermal conductivity method using thermistor sensing elements in a static system at atmospheric pressure. The device proved of exceptional stability, requiring no recalibrations and yielding an analytical accuracy of better than 0.02% deuterium content. The binary separation factors α were found to be constant over the concentration range investigated, with values for α varying from about 1.25 on charcoal to 2.54 on type 4A molecular sieves at 75° K and 750 mm Hg. The results suggest that the variations in α are due mainly to differences in chemical composition of the adsorbents rather than pore size, surface area, or origin of the materials.

INTRODUCTION

Among isotopes of the same element or compound the heavier species are usually preferentially adsorbed. The effect becomes more pronounced with decreasing molecular weight and experiments in this field have therefore mostly dealt with low molecular weight substances such as the neon (1, 2) and hydrogen isotopes. Separation of the latter by means of sorption has been investigated by a number of workers (Table I).

TABLE I

Summary of literature data on deuterium enrichment by sorption

Adsorbent	Temp., ° K	Pressure, mm Hg	Separation factor*	Ref.
(1) Binary equilibria				
Silica gel	20	10^{-5}	20–25	2
	78		4.5	
	90		3.0	
Silica gel	50–55	10^{-3}	~20	3
Charcoal	65	10^{-3}	~2–5	3
Charcoal	77	760	1.2	4
Alumina	20	?	~30	5
(2) Enrichment by desorption				
Charcoal	Liquid air	?	Pure fractions obtained	6.7
Charcoal	Liquid air	50–0	~1.15	8
Charcoal	65	$\sim 10^{-3}$	2–5	3
Silica gel	49–55	$\sim 10^{-3}$	4–40	3
Silica gel	78–90	10^{-5}	7.8–5	2
Silica gel	20	10^{-3}–10^{-5}	40±10	2
Silica gel	20	10^{-3}–10^{-5}	"Up to 100"	9

*The separation factor is defined as the ratio of adsorbed phase to gas phase mole fractions, $\alpha = (X_{D_2}/X_{H_2})/(Y_{D_2}/Y_{H_2})$.

[1]*Manuscript received July 7, 1959.*

Contribution from the Department of Applied Chemistry and Chemical Engineering, University of Toronto, Toronto, Ontario. Excerpts from thesis submitted in partial fulfillment of requirements for the degree of Doctor of Philosophy.

[2]*Present address: Assistant Professor, Department of Chemical Engineering, University of Ottawa, Ottawa, Ontario.*

The measurements usually consist in determining equilibrium separation factors (relative adsorptivities) α or analyzing the fractions obtained by slow desorption. A number of authors have also dealt with the gas chromatographic separation of the isotopes using supported palladium (10, 11) and type 5A Linde molecular sieves (12) as adsorbent.

From the results published so far, three major trends may be distinguished.

(*a*) Equilibrium separation factors show a marked increase with decreasing temperature and pressure, particularly at low values of the latter.

(*b*) By using the process of slow desorption, the equilibrium enrichment may be increased by factors as high as 1.7 (2).

The majority of data have been measured under conditions designed to yield maximum separations, i.e. pressures of 1 micron Hg or less and temperatures as low as 20° K. There are no published values of separation factors measured at temperatures and pressures suitable for use in the large-scale recovery of deuterium from natural hydrogen (75 to 100° K, 1 atm and above). The low values of α on charcoal at 77° K and 1 atm reported by Strange (4) give little reason to expect spectacular separations at these conditions and raise the problem of obtaining improved enrichments by means other than those mentioned above. The best prospects for achieving this appear to be in varying the adsorbent composition. Melkonian and Reps (2) have reported the enrichment on silica gel to be higher than on charcoal and it was thought to be of interest to measure separation factors on these and a number of other high capacity adsorbents at temperatures of liquid air and atmospheric pressure. In addition to charcoal and silica gel, measurements were made on the newly developed synthetic zeolites, Linde molecular sieves, which afford a means for determining any possible effects due to pore size. Single component isotherms of hydrogen and deuterium were also measured to provide additional data for the interpretation of the binary isotherms.

EXPERIMENTAL

The apparatus used is shown schematically in Fig. 1. Binary equilibria were determined by circulating hydrogen–deuterium mixtures of varying composition over the cooled adsorbent, equilibrium being assumed when the conductivity readings showed no further change (within $\pm 0.02\%$ D_2) over a period of $\frac{1}{2}$ hour. This was usually achieved within 2 to 3 hours after circulation was started. The adsorbed gases were then removed by means of the Toepler pump, and after the total volume was measured a sample was admitted to the conductivity cell for analysis. Single component isotherms were determined in the usual manner by admitting successive portions of the gases from a calibrated burette to the adsorbent. Pressures were measured by means of a McLeod gauge (below 5 mm Hg) and a U-tube manometer read to 0.05 mm Hg with a kathetometer. Constant readings were usually obtained within $\frac{1}{2}$ hour after the gases were admitted.

Liquid oxygen served as thermostat liquid, the appropriate temperature ($\pm 0.05°$) being maintained by pumping down the charge by means of aspirators through manually operated control valves. Temperatures were measured with calibrated oxygen and nitrogen manometers.

The binary gas mixtures were circulated by means of an oscillating mercury column contained in a side-arm between two ground-in glass valves. The reciprocating motion was generated by the alternating action of a vacuum pump and a solenoid relief valve.

Analytical Procedure

Analysis of the deuterium–hydrogen mixtures was carried out by the thermal conductivity method (13). Figure 2 shows a schematic diagram of the analysis cell and

Can. J. Chem. Downloaded from www.nrcresearchpress.com by 69.46.99.164 on 09/04/12
For personal use only.

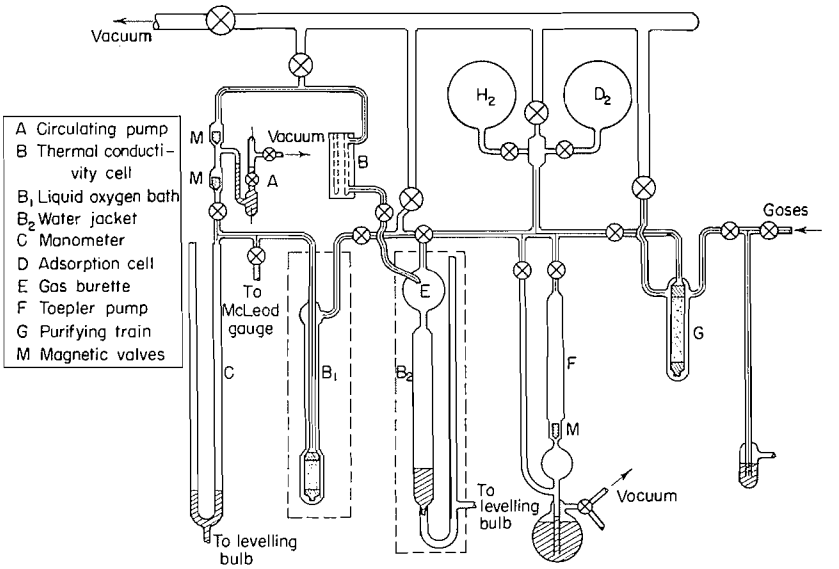


FIG. 1. Apparatus for the measurement of adsorption equilibria.

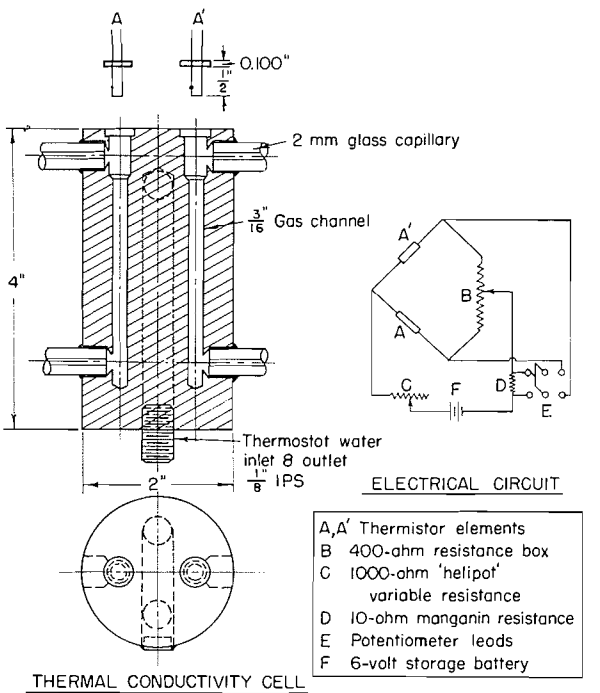


FIG. 2. Apparatus for the analysis of deuterium–hydrogen mixtures.

Wheatstone bridge circuit. Considerable difficulty was experienced in eliminating the drift caused by the instability of the sensing elements and ambient temperature fluctuations. Platinum or tungsten wires used by previous workers (2, 6, 13–17) proved unsatisfactory as they required constant recalibration or elaborate precautions which resulted only in partial elimination of the drift (16). The danger, in addition, of a possible

Can. J. Chem. Downloaded from www.nrcresearchpress.com by 69.46.99.164 on 09/04/12
For personal use only.

reaction of the isotopes to HD in contact with the hot filaments led to the adoption of thermistors as sensing elements. These units, consisting of tiny, glass-coated beads of semiconducting oxides, could be completely stabilized by annealing at 100° C for a period of 3 weeks. The small size and low operating temperature of the elements makes it unnecessary to analyze at accurate reduced pressures, in order to minimize convection currents, as suggested by Trenner and others (14, 16). The bridge was balanced with both sides of the cell containing pure hydrogen at 1 atm and the current input set at approximately 5 ma. A Leeds Northrup type K-2 precision potentiometer was used to measure bridge unbalance, which varied almost linearly with deuterium content of the sample, ranging up to a maximum of 150 mv for pure deuterium. Current input was controlled within 10^{-6} amp by adjusting the potential drop measured across a standard resistance, and the cell was kept at constant temperature by pumping water thermostated to 1/50° C through the cell body. The analytical accuracy attained in this manner was better than $\pm 0.02\%$ deuterium content, the readings being reproducible over a period of several months. The performance exceeds that of previous units described in the literature and could quite possibly be improved even further if the device is used in a flow system (11, 12) where convection and ambient temperature changes become less important.

Since all the adsorbents used were found to catalyze ortho–para conversion, the calibrations were carried out with hydrogen which had previously been equilibrated over charcoal at the temperature to be used. An increase of 1% in para-hydrogen content was found to correspond to a decrease of 0.1% in deuterium concentration. Ortho–para deuterium conversion is small at the adsorption temperatures used and the difference in heat capacity at room temperature negligible (13). No change in the conductivity readings could therefore be detected. Prior to a series of runs each adsorbent was tested for possible preferential adsorption of ortho-hydrogen as suggested in a number of recent papers (5, 18, 19). A charge of pure equilibrated hydrogen was fractionally desorbed and the fractions analyzed. Conductivity measurements in all cases agreed within $\pm 0.02\%$ in terms of deuterium content. A number of tests were also made to establish the absence of catalytic HD-formation. It can be shown from calculations made by Trenner (16) that the formation of 1% HD from an equimolar mixture of hydrogen and deuterium should cause a change in conductivity reading corresponding to about 0.1% D_2. Mixtures of the isotopes were accordingly left in contact with various parts of the apparatus for a period of 12 hours. No change in the conductivity readings was observed. This is in agreement with the results reported by Gould *et al.* (8), who tested mercury, activated charcoal, and glass surfaces for possible catalytic effects. Burstein (20), however, has found rapid conversion of hydrogen and deuterium to occur on charcoal previously evacuated for 1 month at 950° C. The effect was attributed to the baring of active spots. As a precaution all the adsorbents used in this work were evacuated for no longer than 24 hours at a temperature of 180–200° C.

Materials Used

Deuterium.—Supplied by Stuart Oxygen Co., San Francisco. Purity better than 99.5%; used without further purification.

Hydrogen.—Supplied by Dominion Oxygen Co., Toronto. Purified over charcoal at liquid air temperature.

Helium.—Supplied by Dominion Oxygen Co., Toronto. Used without further purification in dead-space determination.

Can. J. Chem. Downloaded from www.nrcresearchpress.com by 69.46.99.164 on 09/04/12
For personal use only.

Can. J. Chem. Downloaded from www.nrcresearchpress.com by 69.46.99.164 on 09/04/12
For personal use only.

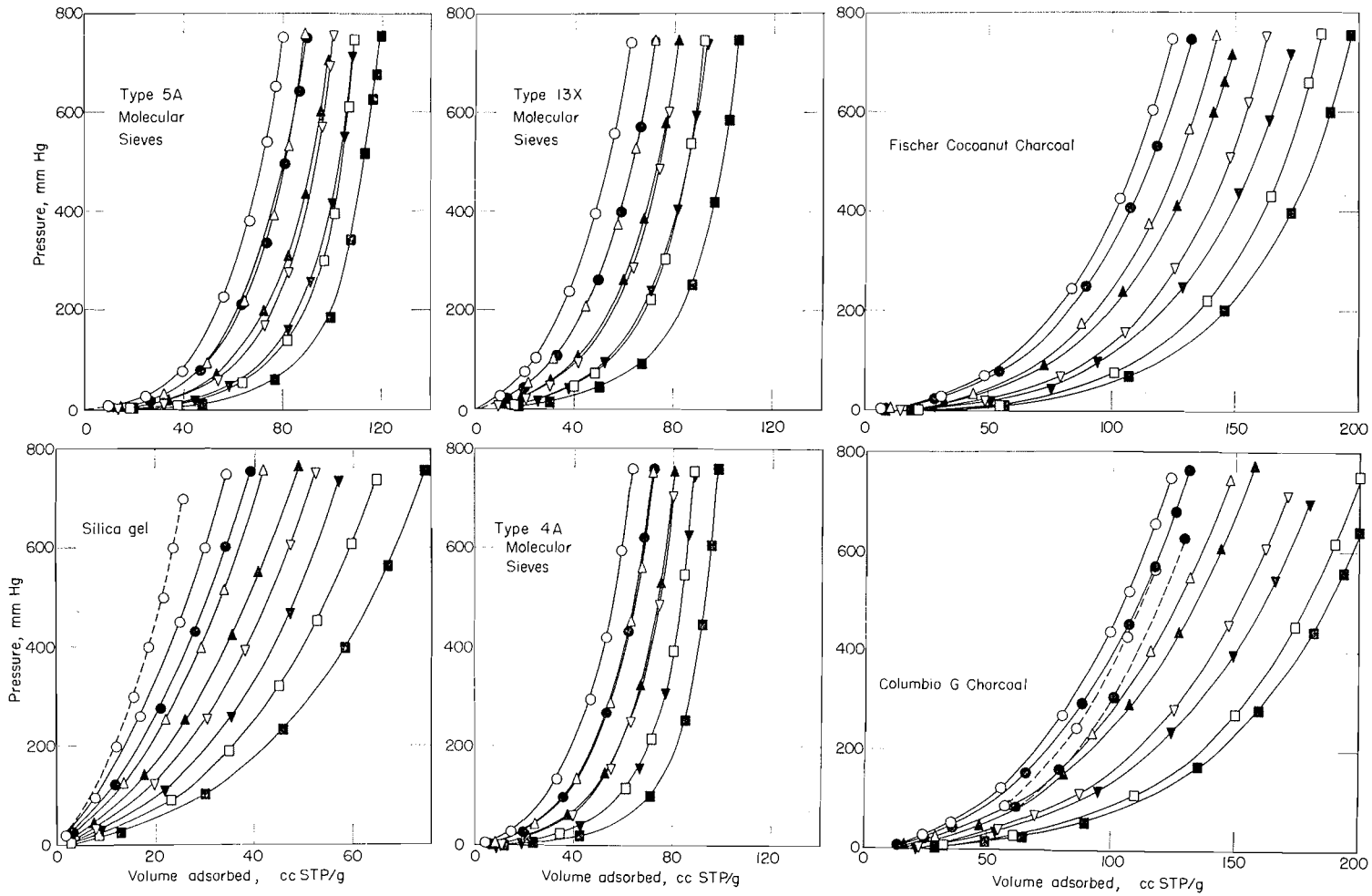


FIG. 3. Single component adsorption isotherms. Open symbols are for H_2, closed for D_2. Temperature (°K) for ○ and ●, 90; △ and ▲, 85; ▽ and ▼, 80; □ and ■, 75.---Ref. 22 (charcoal) and Ref. 23 (silica gel).

Adsorbents.—Columbia 'G' Charcoal, 12–20 mesh, 1250 sq. m/g, Carbide and Carbon Chemicals Co., New York. Fischer Cocoanut Charcoal, 12–20 mesh, 1100 sq. m/g. Supplied by Fischer Scientific Co., Toronto. Silica gel, 6–16 mesh, 750 sq. m/g, Fischer Scientific Co., Toronto. Molecular sieves type 4A, 5A, and 13X, 1/16-inch pellets containing approximately 20% inorganic binder, all 700–800 sq. m/g. Supplied by Linde Air Products Co., Tonawanda, N.Y.

Approximate formulae (21).—Type 4A: 0.96 $Na_2O \cdot 1.00\ Al_2O_3 \cdot 1.92\ SiO_2 \cdot xH_2O$ Type 13X: 0.83 $Na_2O \cdot 1.00\ Al_2O_3 \cdot 2.48\ SiO_2 \cdot xH_2O$. Type 5A is produced from type 4A through ion exchange of about 75% of the sodium ions by calcium ions. For a discussion of molecular sieve crystal structure, see Barrer (25).

Thermistors.—Type A33 matched thermistors, 2000-ohm nominal resistance. Supplied by Victory Engineering Corporation, Union, N.J.

RESULTS

Pure component adsorption isotherms of hydrogen and deuterium on the six adsorbents are shown in Fig. 3. Deuterium was found to be adsorbed to a greater extent than hydrogen in all cases investigated and both gases yield type I isotherms. The Freundlich and Langmuir equations were applied to the data but neither gave satisfactory agreement over the entire pressure range. The data of van Itterbeek and van Dingenen (22) (hydrogen and deuterium on "Carbotox" charcoal) and van der Waarden (23, hydrogen on silica gel) confirm the general trend of our isotherms.

Isosteric heats of adsorption were calculated from plots of log p versus $1/T$ at constant volume adsorbed. Straight lines were obtained in all cases over the entire temperature range. The heat of adsorption for deuterium was found to exceed that of hydrogen on all adsorbents, the difference tending to increase toward lower coverages (Fig. 4). The values found on charcoal compare well with the difference of 100 cal/mole calculated from the data of van Itterbeek and van Dingenen (22) and 80 cal/mole found by Beggerow (quoted by Melkonian and Reps (2)).

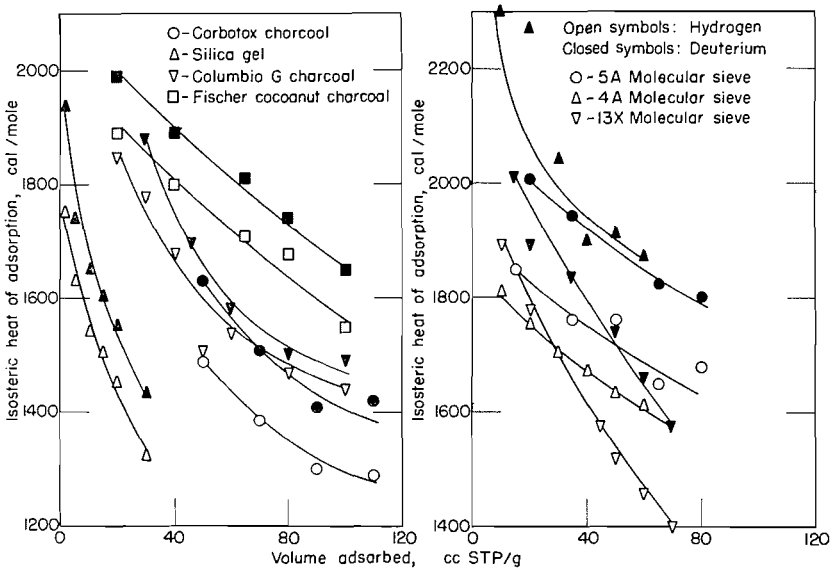


FIG. 4. Isosteric heats of adsorption of hydrogen and deuterium.

Can. J. Chem. Downloaded from www.nrcresearchpress.com by 69.46.99.164 on 09/04/12
For personal use only.

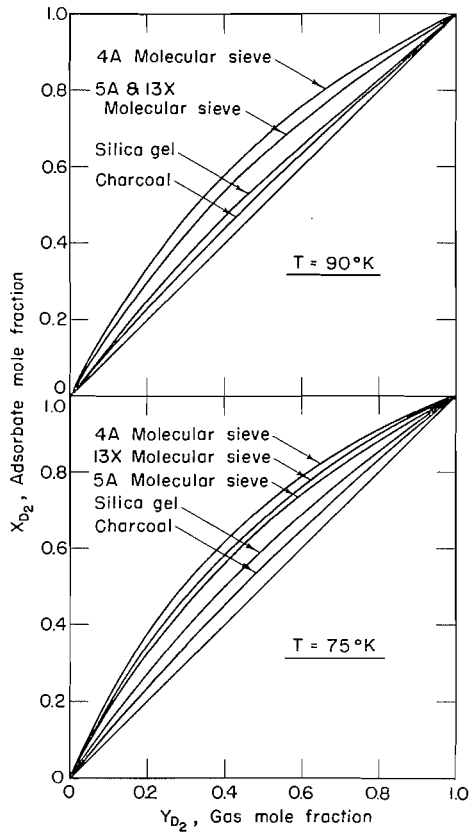


FIG. 5. Summary of binary adsorption equilibria (π = 750 mm Hg).

The binary data obtained in this work are summarized in Table II and Fig. 5. The results have been expressed in terms of the relative adsorptivity α which was found to be essentially constant over the entire concentration range investigated. More detailed graphs are given in Part II of this paper, where a comparison is made with values of α obtained directly from the single component data.

TABLE II

Summary of measured hydrogen–deuterium separation factor*

Adsorbent	T = 90° K π = 750 mm Hg	T = 90° K π = 200 mm Hg	T = 75° K π = 750 mm Hg
Columbia 'G' Charcoal	1.149 (±0.013)	1.145 (±0.004)	1.23 (±0.013)
Fischer Cocoanut Charcoal	1.17 (±0.008)	1.17 (±0.011)	1.28 (±0.013)
Silica gel	1.33 (±0.023)	1.38 (±0.029)	1.47 (±0.097)
Type 4A molecular sieves	2.06 (±0.12)	2.01 (±0.10)	2.54 (±0.07)
Type 5A molecular sieves	1.77 (±0.12)	1.82 (±0.18)	2.00 (±0.18)
Type 13X molecular sieves	1.77 (±0.08)	1.78 (±0.015)	2.16 (±0.10)

*Maximum deviations in parentheses.

Can. J. Chem. Downloaded from www.nrcresearchpress.com by 69.46.99.164 on 09/04/12
For personal use only.

A number of qualitative conclusions may be drawn from the results:

(1) There seems to be little variation in the separation factors measured on chemically identical adsorbents of different origin. Values determined by us on two different charcoals are nearly the same as that reported by Strange (4) on a sample of unidentified origin and, as will be shown in a subsequent paper (II), similar values can be derived from the single component data measured on Carbotox charcoal by van Itterbeek and van Dingenen (22) and on sugar charcoal by Barrer and Rideal (24).

(2) The relatively high separation factors obtained on the molecular sieves do not appear to be due to any screening effect of the pores. Type 13X sieves with a nominal pore diameter of 13 angstrom give similar enrichment as type 4A, the pore size of which is close to the van der Waals diameter of hydrogen (2.4 angstrom).* A sample of 3A molecular sieves was also investigated but proved to have a negligible capacity for the two isotopes.

(3) The chemical composition of the adsorbent appears to have a marked effect on the separation factor, greater chemical heterogeneity tending to yield increased enrichment. The relative magnitude of α obtained on silica gel and charcoal agrees with the data of Melkonian and Reps (2), whose measurements at pressures of 1 micron Hg and less showed charcoal to be less effective than silica gel.

(4) The trend of increasing α with a decrease in temperature is confirmed by our results, but the lowest pressure used here (200 mm) was apparently not sufficiently small to reveal any effect on the separation factor.

The assistance received through a Research Foundation of Ontario Fellowship and grants by the School of Engineering Research, University of Toronto, is gratefully acknowledged. The author also expresses his appreciation to Dr. R. McIntosh and Dr. W. F. Graydon of the University of Toronto for a number of valuable discussions.

REFERENCES

1. Glueckauf, E. *et al.* Discussions Faraday Soc. **7**, 199 (1949).
2. Melkonian, G. A. and Reps, B. Z. Elektrochem. **58**, 616 (1954).
3. Edse, R. and Harteck, P. Angew, Chem. **53**, 210 (1940).
4. Strange, S. A.E.R.E., Harwell, Berks., England. Private communication.
5. White, D. and Haubach, W. J. J. Chem. Phys. **27**, 1368 (1959).
6. Keier, N. and Roginskii, S. Z. Doklady Akad. Nauk S.S.S.R. **57**, 157 (1947).
7. Peters, R. and Lohmar, W. Z. physik. Chem. A, **180**, 51 (1937).
8. Gould, A. J. *et al.* J. Chem. Phys. **2**, 362 (1934).
9. Harteck, P. and Melkonian, G. A. Naturwis. **19**, 450 (1950).
10. Glueckauf, E. and Kitt, G. P. *In* Vapour phase chromatography. D. H. Desty. Butterworth Scientific Publications, London. 1947.
11. Thomas, C. O. and Smith, H. A. J. Phys. Chem. **63**, 427 (1959).
12. Ohkoshi, S. *et al.* J. Chem. Soc. Japan, **31**, 770 (1958).
13. Farkas, A. Orthohydrogen, parahydrogen and heavy hydrogen. The University Press, Cambridge, Eng. 1935.
14. Sachsse, H. and Bratzler, K. Z. physik. Chem. A, **171**, 331 (1934).
15. Gross, P. H. and Steiner, H. Mikrochemie, **17**, 43 (1935).
16. Trenner, N. R. J. Chem. Phys. **5**, 382 (1937).
17. Maybury, P. C. and Koski, W. S. J. Chem. Phys. **21**, 742 (1953).
18. Sandler, Y. C. J. Phys. Chem. **58**, 58 (1954).
19. Cunningham, C. M. *et al.* J. Am. Chem. Soc. **80**, 2382 (1958).
20. Burstein, R. Acta Physicochim U.R.S.S. **8**, 857 (1938).
21. Linde Air Products Co., Tonawanda, N.Y. Form 9947.
22. van Itterbeek, A. and van Dingenen, W. Physica, **6**, 49 (1939).
23. van der Waarden, M. and Scheffer, F. E. C. Rec. trav. chim. **71**, 689 (1952).
24. Barrer, R. M. and Rideal, E. K. Proc. Roy. Soc. London, A, **149**, 231 (1935).
25. Barrer, R. M. Brit. Chem. Eng. **4**, 267 (1959).
26. *(a)* van Cleave, A. B. and Maass, O. Can. J. Research, **12**, 57 (1935). *(b)* van Cleave, A. B. and Maass, O. Can. J. Research, **12**, 372 (1935).

**The van der Waals diameter of deuterium obtained from thermal conductivity and viscosity measurements at 20° C is identical with that of hydrogen (26 a, b).*

Can. J. Chem. Downloaded from www.nrcresearchpress.com by 69.46.99.164 on 09/04/12
For personal use only.

Can. J. Chem. Downloaded from www.nrcresearchpress.com by 69.46.99.164 on 09/04/12
For personal use only.

ADSORPTION EQUILIBRIA OF HYDROGEN, DEUTERIUM, AND THEIR MIXTURES. PART II[1]

D. BASMADJIAN[2]

ABSTRACT

An investigation has been made of the fundamental factors which determine isotope separation factors on adsorbents, based on hydrogen and deuterium isotherms reported in Part I. Through the use of a semiempirical thermodynamic approach, the binary separation factors α have been related to the single component isotherms ($p = f(v)$), and these in turn broken down into a number of terms involving the isosteric heat of adsorption q, temperature T, and surface coverage. If the less important contributions are neglected, the treatment leads to the following sequence of approximate relations:

$$[1] \quad \log \alpha \doteq \underset{[I]}{\frac{1}{(v_{H_2})_\pi} \int_0^{(v_{H_2})_\pi} \log\left(\frac{p_{H_2}}{p_{D_2}}\right)_v dv} \doteq \underset{[II]}{\frac{0.11}{(v_{H_2})_\pi} \int_0^{(v_{H_2})_\pi} \frac{q_{D_2} - q_{H_2}}{T} dv} \propto \underset{[III]}{\frac{\epsilon^0_{H_2} - \epsilon^0_{D_2}}{T}}$$

where ϵ^0 = total vibrational zero-point energy of adsorbed molecules.

The rigorous form of equation [I] agrees well with the experimental results, and semi-quantitative agreement with the data is shown by equation [II]. A qualitative discussion of [III] is given. It is suggested that the horizontal zero-point vibrations of the adsorbed species in some cases constitute an important contributing factor in addition to the vertical vibrations previously thought to be solely responsible for differences in isotope behavior.

INTRODUCTION

In a previous paper (1) we had reported data obtained from measurements of binary and single component adsorption isotherms of hydrogen and deuterium on a number of adsorbents. The surprisingly high separation factors which were obtained, particularly on type 4A molecular sieves, have led us to examine the fundamental factors which determine adsorption equilibria involving isotopes.

Differences in the sorption of isotopes are frequently attributed solely to zero-point energy effects. Sherman and Eyring (2) derived the expression

$$[2] \quad \frac{r_{H_2}}{r_{D_2}} = e^{(q_{D_2} - q_{H_2})/RT} = e^{(\epsilon^0_{H_2} - \epsilon^0_{D_2})/RT},$$

where r = rate of desorption, to explain the deuterium enrichment obtained by Gould *et al.* (3) by desorption from charcoal. Barrer and Rideal (4) obtained linear isotherms for hydrogen and deuterium on charcoal at a few millimeters of Hg and expressed their results in terms of the equation

$$[3] \quad \left(\frac{p_{H_2}}{p_{D_2}}\right)_v = e^{(q_{D_2} - q_{H_2})/RT} = e^{(\epsilon^0_{H_2} - \epsilon^0_{D_2})/RT},$$

where p = equilibrium pressure, v = volume adsorbed.

A more quantitative approach is achieved by the use of partition functions, but the advantages of this method are offset by the assumptions which have to be made in formulating the energy states of the adsorbed phase. Wheeler (5) applied the method to single component equilibria of the isotopes, assuming the adsorbed molecules to be

[1]*Manuscript received July 7, 1959.*

Contribution from the Department of Applied Chemistry and Chemical Engineering, University of Toronto, Toronto, Ontario. Excerpts from thesis submitted in partial fulfillment of requirements for the degree of Doctor of Philosophy.

[2]*Present address: Assistant Professor, Department of Chemical Engineering, University of Ottawa, Ottawa, Ontario.*

localized with 5 vibrational degrees of freedom relative to the surface. The result is described by the equation

$$[4] \qquad \left(\frac{p_{H_2}}{p_{D_2}}\right)_v = \frac{v_{m_{D_2}} - v_{H_2}}{v_{m_{H_2}} - v_{H_2}}$$

where v_m = monolayer volume.

In a recent note, White and Haubach (6) propose extending this treatment to the calculation of binary separation factors. The authors apparently assume Langmuir's mixed isotherm (7) to apply, postulating vertical vibrations as well as hindered rotation in the adsorbed phase. As a first approximation, zero-point energies only are considered, leading to qualitative agreement with some results obtained on alumina at 20° K.

One immediate difficulty in applying the above treatments arises from the fact that our data do not obey Langmuir's isotherm. Even if this were the case, it would not necessarily indicate that we are dealing with an energetically homogeneous surface justifying the use of the simple partition functions proposed by Wheeler, and White and Haubach. The formulation of more complex functions, on the other hand, would require a knowledge of surface energy distributions and other fundamental data which are difficult to obtain (see e.g. ref. 8). In the treatment given below we have sought to avoid these difficulties by employing a semiempirical thermodynamic approach involving variables which are easily obtained or estimated from the measured isotherms. The stepwise procedure consists in relating the binary separation factor α to the single component pressure ratio at constant volume adsorbed $(p_{H_2}/p_{D_2})_v$; this ratio is in turn expressed in terms of the difference in heat of adsorption of the two isotopes, system temperature, and surface coverage. The more significant of these, the heat of adsorption difference, is further broken down into the zero-point energies, adsorbent/adsorbate interaction potentials, and heat capacity integrals of the adsorbed isotopes. Each of these terms is discussed qualitatively as to its contribution to the total separation factor.

(a) Correlation of Binary and Single Component Data

Most theoretical treatments of this problem stipulate single component data which conform to a given isotherm equation, e.g., the Langmuir (7), Freundlich (9), or BET (10) isotherms. Our own data, which do not obey any of these equations, are represented by a modification of the correlation given by Lewis *et al.* (11):

$$[5] \qquad \frac{(v_{H_2})_\pi(\alpha-1)}{\alpha(v_{H_2}/v_{D_2})_\pi - 1} \log \alpha\left(\frac{v_{H_2}}{v_{D_2}}\right)_\pi = (v_{D_2} - v_{H_2})_\pi \log \pi + \int_0^{(v_{H_2})_\pi} \log p_{H_2}\, dv - \int_0^{(v_{D_2})_\pi} \log p_{D_2}\, dv.$$

The equation is based on the assumption that (*a*) α is independent of concentration, (*b*) the total binary adsorbate volume v_T is related to the adsorbate mole fraction X as follows:

$$[6] \qquad \frac{1}{v_T} = \frac{X_{H_2}}{(v_{H_2})_\pi} + \frac{X_{D_2}}{(v_{D_2})_\pi}.$$

The first of these was found to hold in the region 10–90% D_2 and will be assumed valid over the entire concentration range. The second assumption can be shown by an appropriate plot to be a close approximation of the linear relation found experimentally for our system:

$$[7] \qquad v_T = (v_{D_2} - v_{H_2})_\pi X_{D_2} + (v_{H_2})_\pi.$$

Can. J. Chem. Downloaded from www.nrcresearchpress.com by 69.46.99.164 on 09/04/12
For personal use only.

The derivation given by Lewis *et al.* was repeated using equation [7] instead of [6]. The result, although considerably more complex, was found to be fully equivalent to the Lewis correlation.

For the purposes of this work it was found best to combine the two single component integrals in equation [5] into the pressure ratio $(p_{H_2}/p_{D_2})_v$, the residual term being evaluated by assuming log p to vary linearly with v over the short range in question. Thus:

$$[8] \qquad \frac{(\alpha-1)(v_{D_2}/v_{H_2})_\pi}{\alpha-(v_{D_2}/v_{H_2})_\pi}\log\frac{\alpha}{(v_{D_2}/v_{H_2})_\pi} = \frac{1}{(v_{H_2})_\pi}\int_0^{(v_{H_2})_\pi}\log\left(\frac{p_{H_2}}{p_{D_2}}\right)_v dv + \tfrac{1}{2}(v_{D_2}/v_{H_2}-1)_\pi \log\left(\frac{p_{H_2}}{p_{D_2}}\right)_{(v_{H_2})_\pi}.$$

It can be shown that for $\alpha < 4$ and $(v_{D_2}/v_{H_2})_\pi < 1.5$, the equation reduces to the approximate expression

$$[9] \qquad \log\alpha \doteq \frac{1}{(v_{H_2})_\pi}\int_0^{(v_{H_2})_\pi}\log\left(\frac{p_{H_2}}{p_{D_2}}\right)_v dv.$$

Plots of the ratio $(p_{H_2}/p_{D_2})_v$ versus v for the single component data reported previously are presented in Fig. 1. The curves show an initial sharp drop and appear to pass through a minimum at higher pressures. The general trend of the curves is confirmed by the data of van Itterbeek and van Dingenen (12) for hydrogen and deuterium on "Carbotox" charcoal. In terms of equation [9] the plots of Fig. 1 predict an increase in the separation factor α with decreasing total pressure π and temperature. This is confirmed by the high separations obtained by various authors on silica gel and charcoal at extremely low pressures and temperatures (see Part I, Table I). Our own binary data generally show excellent agreement with values of α calculated from equation [8] (see Fig. 2). The deviations observed in the case of the 4A molecular sieves are partly due

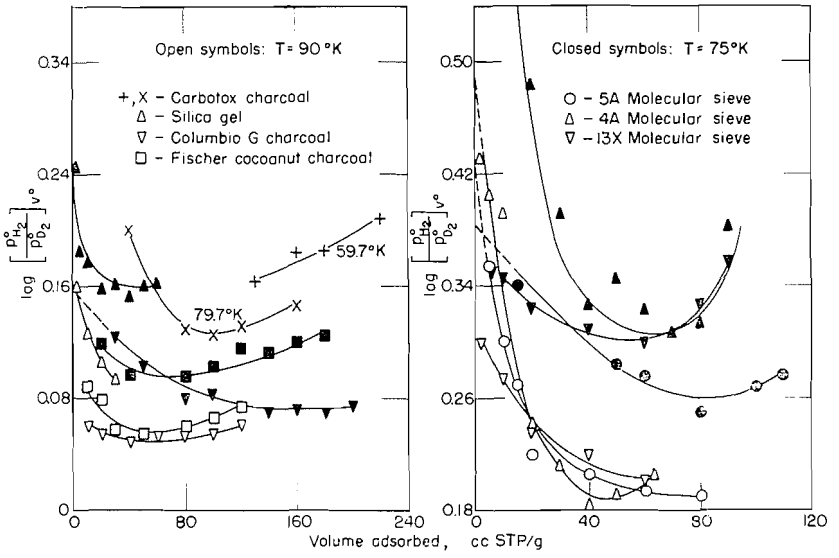


FIG. 1. Ratio of pure component adsorption pressure of hydrogen and deuterium versus volume adsorbed.

Can. J. Chem. Downloaded from www.nrcresearchpress.com by 69.46.99.164 on 09/04/12
For personal use only.

Can. J. Chem. Downloaded from www.nrcresearchpress.com by 69.46.99.164 on 09/04/12
For personal use only.

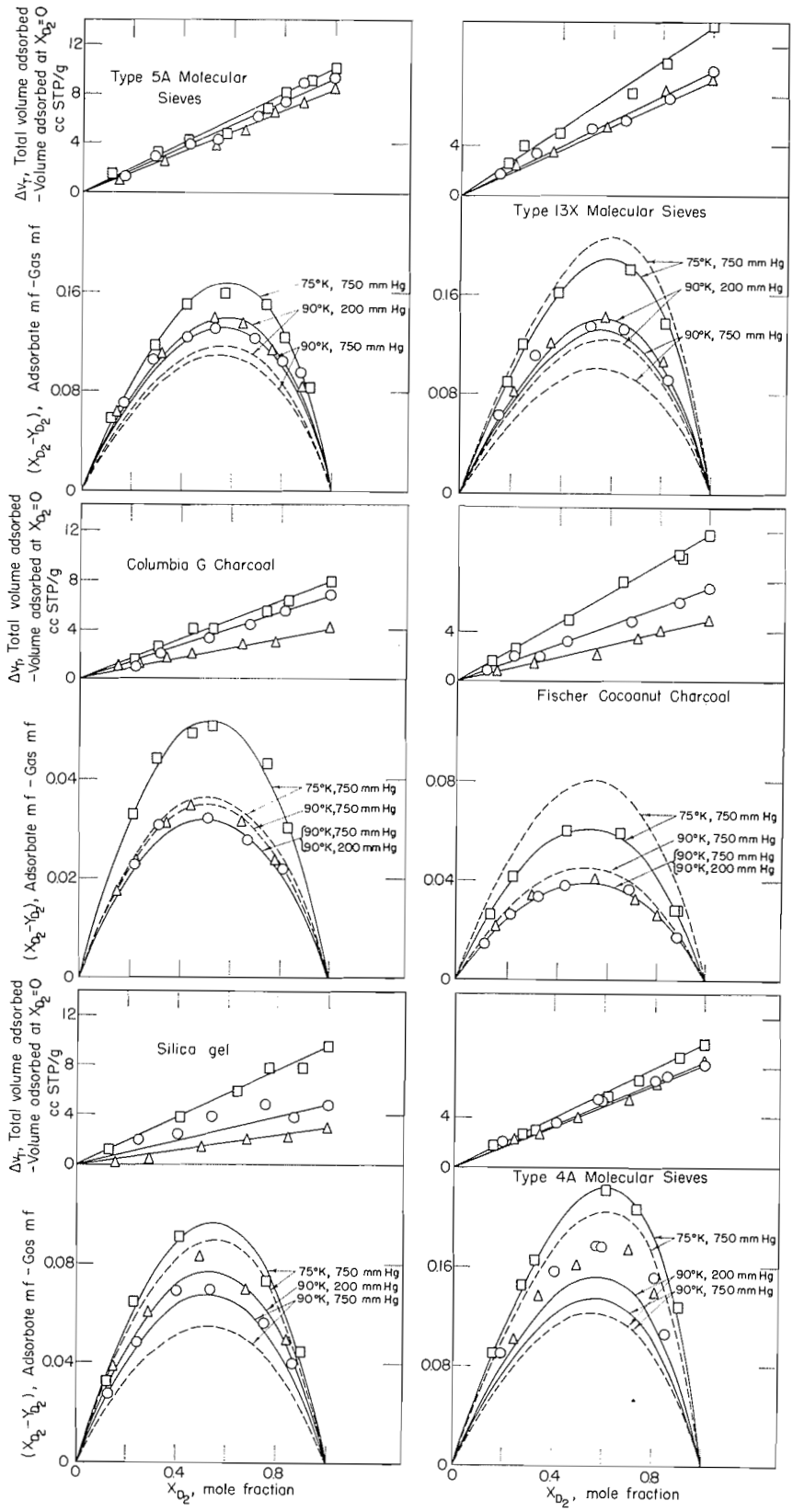


FIG. 2. Comparison of binary adsorption equilibria with equation [8] (———) and [9] (– – – – –). ○ $T = 90°$ K $\pi = 750$ mm Hg, △ $T = 90°$ K $\pi = 200$ mm Hg, □ $T = 75°$ K $\pi = 750$ mm Hg.

to the difficulty in extrapolating the pressure ratio to $v = 0$, and possibly also to a variation of α with composition at low concentrations.

Equation [9] is seen to be very similar to Raoult's Law for ideal liquid solutions, to which in fact it reduces by assuming p_{H_2}/p_{D_2} to be constant for all values of v. A slightly different form of this equation may be derived by postulating proportionality between gas and adsorbed phase mole fractions, Y and X, as follows:

$$[10] \qquad \begin{matrix} Y_{D_2}\pi = X_{D_2}(p_{D_2})_{v_T} \\ Y_{H_2}\pi = X_{H_2}(p_{H_2})_{v_T} \end{matrix} \quad \text{whence} \quad \frac{Y_{H_2}\cdot X_{D_2}}{Y_{D_2}\cdot X_{H_2}} = \alpha = \left(\frac{p_{H_2}}{p_{D_2}}\right)_{v_T}.$$

Values of α obtained from equation [10] agree less well with the experimental results than those calculated from the more accurate equation [8] (see Fig. 2). This underlines the importance of making allowance for the variation in the pressure ratio $(p_{H_2}/p_{D_2})_v$ with coverage.

(*b*) *The Pure Component Pressure Ratio*

We next proceed to express the pure component equilibrium pressure in terms of conventional thermodynamic functions. In the first instance this leads to the equation

$$[11] \qquad \Delta\mu = RT \ln p = \Delta H - T\Delta S.$$

(For an exact definition of the functions see, e.g., ref. 13*a*.)

The enthalpy term is in this case equivalent to the isosteric heat of adsorption q (13*a*), which is determined in the usual manner from a plot of $\log p$ versus $1/T$ at constant volume adsorbed. The entropy term is most conveniently evaluated by making use of a semiempirical correlation proposed by Everett (13*b*):

$$[12] \qquad \Delta S = \Delta S^* - R \ln \frac{\theta}{1-\theta}$$

where

$$[13] \qquad \Delta S^* = A \cdot q + B.$$

For a large number of gases on charcoal at 300° K, A was found to be equal to $0.38/T$ (14). Other systems give values of A between $0.45/T$ and $0.55/T$ (28), particularly at low temperatures, and a partial theoretical justification of this has been given by Drain and Morrison (14). Following Young (28), we have chosen the value of $0.50/T$ for A; B appears to be essentially independent of temperature below 90° K (13*b*), although this conclusion is based on rather scant data. The isotope pressure ratio then becomes:

$$[14] \qquad \log\left(\frac{p_{H_2}}{p_{D_2}}\right)_v = 0.11\,\frac{q_{D_2}-q_{H_2}}{T} + \log\frac{v_{m_{D_2}}/v_{m_{H_2}} - \theta_{H_2}}{1-\theta_{H_2}}$$

and

$$[15] \qquad \log\alpha = \frac{0.11}{(v_{H_2})_\pi}\int_0^{(v_{H_2})_\pi}\frac{q_{D_2}-q_{H_2}}{T}\,dv + \frac{1}{(v_{H_2})_\pi}\int_0^{(v_{H_2})_\pi}\log\frac{v_{m_{D_2}}/v_{m_{H_2}} - \theta_{H_2}}{1-\theta_{H_2}}\,dv.$$

A quantitative comparison with our data is rendered difficult by the high accuracy required in evaluating the heat of adsorption integral. Table I shows the results of some calculations based on approximate average values of $q_{D_2}-q_{H_2}$. The monolayer volume ratio was taken as 1.10 based on the low temperature isotherms of van Itterbeek and van Dingenen (12). Liquid molar volumes give a value of 1.20, solid molar volumes

Can. J. Chem. Downloaded from www.nrcresearchpress.com by 69.46.99.164 on 09/04/12
For personal use only.

one of about 1.15 (15). The pure component hydrogen coverage Θ_{H_2} was estimated from surface area measurements to vary from 0 to 0.3 for the cases investigated.

It is apparent that the term $(q_{D_2}-q_{H_2})/T$ constitutes the main contribution to the separation factor. Hence, as a first approximation:

$$\log \alpha \doteq \frac{0.11}{(v_{H_2})_\pi}\int_0^{(v_{H_2})_\pi}\frac{q_{D_2}-q_{H_2}}{T}\,dv. \qquad [16a]$$

Equations of a similar form

$$\alpha = A\cdot e^{\Delta q/RT} \qquad [16b]$$

have been suggested by several authors on a purely empirical basis (e.g. 16, 17). The experimental results of these workers are unfortunately difficult to interpret in terms of equations [14] and [15] due to the lack of data on single component isotherms.

(*c*) *The Heat of Adsorption Difference*

Having established that the separation factor is largely determined by the heat of adsorption difference, it is of interest to examine the factors which cause the large variation of $q_{D_2}-q_{H_2}$ on the various adsorbents investigated. The difference is conveniently broken down into a number of separate terms, following the treatment of Orr (18):

$$(q_{D_2}-q_{H_2})_T = \phi_{D_2}-\phi_{H_2}-(\epsilon^0_{D_2}-\epsilon^0_{H_2}) -\int_0^T C_{a_{D_2}}dT+\int_0^T C_{g_{D_2}}dT+\int_0^T C_{a_{H_2}}dT-\int_0^T C_{g_{H_2}}dT \qquad [17]$$

where ϕ = total interaction energy, C_a = adsorbate heat capacity, C_g = ideal gas heat capacity. Due to a lack of data, it is not possible to present more than qualitative conclusions on the contribution made by each term. Most authors are inclined to emphasize the importance of the zero-point energy difference. There is in fact some reason to believe that neither of the other two terms contributes appreciably to $q_{D_2}-q_{H_2}$. The intermolecular potentials of gaseous hydrogen and deuterium are known to be identical (19). Calculations based on the Kirkwood–Mueller equation (7) have shown the interaction potential of the isotopes with adsorbent surfaces to be nearly identical. Thus, as a first approximation, $\Delta\phi$ may be set = 0.

No measurements have been made of the heat capacities of either hydrogen or deuterium in the adsorbed state. A number of authors have, however, reported values for nitrogen (20, 22), oxygen (22), krypton (21), and argon (23) adsorbed on rutile over a temperature range extending from near 0° K to well above the normal boiling point. The results indicate that the difference of the heat capacity integrals

$$-\int C_a dT+\int C_g dT$$

for these gases does not exceed 100–200 cal/mole. On this basis, the algebraic sum of the isotopic heat capacity integrals (equation [17]) may be expected to be even smaller, if not completely negligible. At any rate, it would seem difficult to attribute heat of adsorption differences as high as 300 cal/mole solely to heat capacity effects.

(*d*) *The Zero-point Energy Difference*

The zero-point energy of a harmonic oscillator vibrating vertically to a surface is given by:

$$\epsilon^0_v = \frac{Nh}{\pi}\left(\frac{\phi}{4mr_0^2}\right)^{\frac{1}{2}} \qquad [18]$$

Can. J. Chem. Downloaded from www.nrcresearchpress.com by 69.46.99.164 on 09/04/12
For personal use only.

h = Planck's constant and N = Avogadro's constant, where r_0 = equilibrium distance from surface and m = mass of isotope. Hence,

$$[19] \qquad q_{D_2} - q_{H_2} \doteq \frac{N \cdot h}{2\pi} \left\{ \left(\frac{\phi_{H_2}}{2mr_{0_{H_2}}^2} \right)^{\frac{1}{2}} - \left(\frac{\phi_{D_2}}{2mr_{0_{D_2}}^2} \right)^{\frac{1}{2}} \right\}.$$

While the order of magnitude of this expression agrees well with observed values of the heat of adsorption difference, it is difficult to account for its large variation with adsorbent composition solely on the basis of equation [19]. This would require a change in ϕ and r_0 incompatible with observed heats of adsorption or intermolecular van der Waals distances. It appears likely that other modes of energy may be involved, such as zero-point vibrations parallel to the surface or hindered rotation (6). Hill (24) has derived the following expression for horizontal vibrations on a surface with sinusoidal potential gradient:

$$[20] \qquad \epsilon_h^0 = Nh \left(\frac{V}{4ms^2} \right)^{\frac{1}{2}}$$

where V = maximum potential barrier, s = distance between potential minima.

Equations of similar form may be expected to hold for more complex surfaces.

In the case of charcoal at higher coverages, the horizontal contribution is probably negligible, calculations having yielded a surface potential periodicity for argon on graphite of only about 50 cal/mole (25). Silica gel has been shown to give lower surface diffusivities than charcoal, in spite of higher heats of adsorption on the latter (26). This is interpreted as proof that the former has higher surface heterogeneity, possibly due to its chemical structure, and horizontal zero-point vibrations may partly account for the higher α values observed.

Surface heterogeneity may also be used to explain in part the high separation factors measured on the molecular sieves. This may again be due to the presence of different types of atoms and ions in the adsorbent surface. In addition, however, it is to be expected that the small size of the intercrystalline voids (11A diameter, ref. 27) in which the main adsorption occurs will cause a considerable increase of the horizontal potential barrier. The large enrichment factors obtained by Melkonian and Reps (17), and others, at extremely low pressures can be similarly accounted for if the adsorption sites at these coverages are visualized as very narrow cracks.

The contribution due to hindered rotation (vertically to the surface) has been discussed briefly by White and Haubach (6). The ortho-hydrogen enrichment in the adsorbed phase reported by various authors (see Part I) indicates that the adsorbed

TABLE I

Qualitative test of equation [15] (π = 750 mm Hg)

Adsorbent	$q_{D_2} - q_{H_2}$	$(\log \alpha)^a$ calc.		$(\log \alpha)$ exp.	
		T = 90°	T = 75° K	T = 90°	T = 75° K
Columbia Charcoal	50	0.11	0.12	0.055	0.089
Fisher Cocoanut Charcoal	75	0.14	0.16	0.068	0.11
Silica gel	100	0.17	0.20	0.12	0.17
Type 4A molecular sieves	300	0.42	0.49	0.32	0.40
Type 5A molecular sieves	150	0.23	0.27	0.25	0.30
Type 13X molecular sieves	175	0.26	0.31	0.25	0.33

[a] $\log (v_{m_{D_2}}/v_{m_{H_2}} - \theta_{H_2})/(1-\theta_{H_2})$ varies from 0.04 to 0.06 for θ_{H_2} = 0 to 0.3. An average value of 0.05 was used in all calculations.

Can. J. Chem. Downloaded from www.nrcresearchpress.com by 69.46.99.164 on 09/04/12
For personal use only.

isotopes do in fact possess some form of hindered rotational motion. It would be difficult, however, to explain the observed variation of $q_{D_2}-q_{H_2}$ with adsorbent composition solely on this basis, since this would again require a change in r_0 or the vertical potential barrier incompatible with the physical facts. The measurement of surface diffusivities suggests itself as a possible means for confirming the importance of surface heterogeneity, as compared to potential barriers affecting the vertical rotation of the molecule.

REFERENCES

1. BASMADJIAN, D. Can. J. Chem. **38**, 141 (1960).
2. EYRING, H. and SHERMAN, A. J. J. Chem. Phys. **1**, 345 (1933).
3. GOULD, A. J. *et al.* J. Chem. Phys. **2**, 362 (1934).
4. BARRER, R. M. and RIDEAL, E. K. Proc. Roy. Soc. London, A, **149**, 231 (1935).
5. WHEELER, A. J. Chem. Phys. **6**, 746 (1938).
6. WHITE, D. and HAUBACH, W. J. J. Chem. Phys. **27**, 1368 (1959).
7. BRUNAUER, S. The adsorption of gases and vapors. Princeton Univ. Press, Princeton, N.J. 1945.
8. TOMPKINS, F. C. Trans. Faraday Soc. **46**, 569 (1950).
9. TOMPKINS, F. C. and YOUNG, D. M. Trans. Faraday Soc. **47**, 88 (1951).
10. WHITE, C. and SCHNEIDER, G. H. J. Am. Chem. Soc. **71**, 2593 (1949).
11. LEWIS, W. K. *et al.* Ind. Eng. Chem. **42**, 1319 (1950).
12. VAN ITTERBEEK, A. and VAN DINGENEN, W. Physica, **6**, 49 (1939).
13. *(a)* EVERETT, D. H. Trans. Faraday Soc. **46**, 942 (1950). *(b)* EVERETT, D. H. Trans. Faraday Soc. **46**, 957 (1950).
14. DRAIN, L. and MORRISON, J. A. Trans. Faraday Soc. **48**, 316 (1952).
15. WOOLLEY, H. W. *et al.* J. Research Nat. Bur. Standards, **41**, 379 (1948).
16. BEGGEROW, G. Z. physik. Chem. **193**, 265 (1944).
17. MELKONIAN, G. A. and REPS, B. Z. Elektrochem. **58**, 616 (1954).
18. ORR, W. J. C. Trans. Faraday Soc. **35**, 1247 (1939).
19. HIRSCHFELDER, J. O. *et al.* Molecular theory of gases and liquids. John Wiley & Sons, Inc., New York. 1954.
20. ASTON, G. *et al.* J. Am. Chem. Soc. **73**, 1937 (1951).
21. PAGE, E. C. *et al.* J. Am. Chem. Soc. **78**, 1531 (1956).
22. DRAIN, L. and MORRISON, J. A. Trans. Faraday Soc. **49**, 654 (1953).
23. MORRISON, J. A. *et al.* Trans. Faraday Soc. **47**, 1023 (1951).
24. HILL, T. J. Chem. Phys. **16**, 181 (1948).
25. YOUNG, D. M. and CROWELL, A. D. Trans. Faraday Soc. **49**, 1080 (1953).
26. CARMAN, P. C. and MALHERBE, P. LER. Proc. Roy. Soc. London, A, **203**, 165 (1950).
27. LINDE AIR PRODUCTS CO., Tonawanda, N.Y. Form 9947.
28. YOUNG, D. M. Trans. Faraday Soc. **47**, 1228 (1951).

Can. J. Chem. Downloaded from www.nrcresearchpress.com by 69.46.99.164 on 09/04/12
For personal use only.

Can. J. Chem. Downloaded from www.nrcresearchpress.com by 69.46.99.164 on 09/04/12
For personal use only.

IODINE COMPLEXES IN INERT SOLVENTS

XI. CRYOSCOPIC STUDY OF THE IODINE – NAPHTHALENE COMPLEX DISSOLVED IN CYCLOHEXANE[1]

P. A. D. DE MAINE AND P. J. SANTIAGO

ABSTRACT

Here is reported cryoscopic evidence of the specific interaction between naphthalene and iodine dissolved together in cyclohexane. Cryoscopic constants accurate to within 2% are given for iodine and naphthalene dissolved separately in cyclohexane or in benzene.

INTRODUCTION

Since publication of the work of Benesi and Hildebrand (2), many researchers have used their spectrophotometric method, or modifications like those proposed by Ketelaar *et al.* (9) or Andrews and Keefer (1), to show that iodine molecules react reversibly with many aromatic and aliphatic compounds to form one-to-one complexes in solution. In many cases, the spectrophotometric method has been used to determine the heats of formation of these complexes. However, except for the calorimetric work reported by Hartley and Skinner (7) and the determination of solubilities by Kortüm and Vogel (10) there appears to be no direct non-spectrophotometric evidence of specific interaction between iodine and aromatic molecules in solution.

De Maine and Peone (4) have reported that the heat of formation ($\Delta H = -1.63 \pm 0.25$ kcal/mole) of the complex, naphthalene–I_2, is independent of the inert diluent used. Solvents used were carbon tetrachloride, cyclohexane, *n*-heptane, *n*-hexane, and chloroform.

In the present work we report cryoscopic evidence for the specific interaction between naphthalene and iodine in cyclohexane.

EXPERIMENTAL

(*i*) *Chemicals*

Fisher reagent grade anhydrous magnesium sulphate was heated for 6 hours at 150° C. Mallinckrodt A.R. grade benzene and Fisher spectrograde cyclohexane were stored in glass-stoppered bottles containing magnesium sulphate for at least 1 week before use. Solvents were removed with a "propipette" from the storage bottles immediately before the start of the experiment.

Fisher resublimed iodine and certified reagent grade naphthalene were used without further purification.

(*ii*) *Procedure*

Before each experiment the cell and its glass attachments (described below) were soaked in concentrated nitric acid for at least 6 hours, then were washed with copious amounts of water, and finally were rinsed with anhydrous acetone or methanol. Then the clean cell and attachments were heated at 55–65° C for not less than 1 hour and then were blown with pure nitrogen (dew point less than −40° C). Twenty-five milliliters of the anhydrous solvent was pipetted into the assembled cell, which was placed in the modified, Precision Scientific Co., cryoscopic molecular weight apparatus. The Beckman

[1]*Manuscript received September 11, 1959.*
Contribution from the Chemistry Department, New York State College for Teachers, New York State University, Albany 3, New York, U.S.A.

Differential thermometer was transferred from an ice-water bath to the cell after the solvent was cool. Care was taken to avoid transfer of moisture. The freezing point of the solvent was determined by the procedure described in the operating instructions of Precision Scientific Co. (3737 Cortland St., Chicago 47, Illinois. Index TS-65920-1). Special care was taken to maintain a constant tube-stirrer velocity, to cool at a rate less than 0.1° C per minute, and to seed the solution at a fixed temperature below the freezing point. The maximum amount of supercooling permissible for each solution was determined separately.

The freezing point of each aliquot of solvent was determined at least three times. Then the solution was heated approximately four degrees centigrade above the freezing point, and an accurately weighed portion of the desired solid was introduced into the cell by means of a polyethylene, long-stemmed funnel and an adapted Burgess Vibra-Tool. One hour after addition of the solid the new freezing point was determined. (In separate experiments we have shown that all the iodine and naphthalene were dissolved in both solvents within 45 minutes.) This procedure was repeated with further addition of the solid materials.

All the operations described above were performed in a dry, cool atmosphere (relative humidity less than 20%, temperature 15° C), and precautions were taken to exclude moisture from the freezing solutions at all times. The relative freezing point could be reproduced to within 0.001° C.

(*iii*) *Instrumentation*

(*a*) *Description of Cell and Attachments*

The cell supplied by the manufacturers was replaced by one modified as follows. The stainless-steel tube-stirrer and brass stirrer-bearing were replaced by an all-glass assembly, which was fitted with a $CaCl_2$ drying tube. The thermometer was replaced by a Beckman Differential thermometer fitted with a male 24-40 ground glass joint, and an electromagnetic vibrator clamped to the metal ferrule. The vibrator was switched on a few minutes before measurement of the freezing point in order to obtain the quoted accuracy (within 0.001° C). We also found that glass dust from the stirrer-bearing could effect changes as large as 0.010° C over several hours. Special design of the stirrer assembly and lubricating techniques was necessary to eliminate this source of error.

(*b*) *Modifications of the Precision-shell, Cryoscopic Molecular Weight Apparatus*

To insure continuous operation of the instrument for periods up to 24 hours, modifications were made as follows. The small-bore, copper cooling-coil which surrounds the cell cavity and is immersed in the coolant was replaced by a cooling-coil made of $\frac{3}{8}$-inch internal diameter copper tubing. Ice water was pumped with a high capacity pump (greater than 1 gallon per minute) through the cooling-coil from a 5-gallon bath equipped with a high speed stirrer. The ice-bath pump and cooling-coil feed tubes were thoroughly insulated to minimize condensation. The coolant was commercial "Antifreeze".

RESULTS

More than 120 freezing points were each determined in duplicate with the instrument and procedure described above. With proper precautions to prevent moisture contamination of the solutions or hysteresis of the mercury in the Beckman Differential thermometer (13), the freezing points could be easily determined to within 0.001° C. The reproducibility obtained by us is considerably better than the 0.005° C quoted by the manufacturers (13).

Can. J. Chem. Downloaded from www.nrcresearchpress.com by 69.46.99.164 on 09/04/12
For personal use only.

In other experiments we have shown that the freezing point for solutions with single or mixed solutes does not change measurably even after several hours. The freezing points of fresh portions of each pure solvent did not vary by more than 0.002° C.

Cryoscopic constants (K_f = ° C for 1 mole dissolved in 100 g) for both solutes dissolved in each solvent were calculated with the standard formula (5). In these calculations the exact weights of solvent used were computed with densities estimated from published temperature–density equations (8). Such calculations have shown that K_f can be determined to high precision with small weights of the solute (Table I).

Typical data and K_f values for naphthalene dissolved separately in solutions of iodine plus cyclohexane are given in Table II.

TABLE I

Cyclohexane						Benzene					
Iodine			Naphthalene			Iodine			Naphthalene		
w (g)	Δt° C	K_f	w (g)	Δt° C	K_f	w (g)	Δt° C	K_f	w (g)	Δt° C	K_f
0.0315	0.109	170.1	0.0573	0.499	217.3	0.1040	0.066	35.4	0.1295	0.236	51.3
0.0279	0.094	165.7	0.0636	0.569	223.2	0.1051	0.063	33.5	0.1009	0.187	52.2
0.0323	0.111	169.2	0.0498	0.439	220.0	0.1015	0.063	35.0	0.1036	0.184	50.0
0.0447	0.154	170.1	0.1209	1.068	220.4	0.1031	0.064	35.0	0.1027	0.190	52.1
0.0276	0.093	166.0	0.1707	1.507	220.0	0.2087	0.129	34.5	0.1049	0.194	52.1
0.0723	0.252	171.8	0.0558	0.481	215.1	0.3127	0.195	34.8	0.1066	0.189	49.9
0.0331	0.112	168.4	0.0470	0.408	216.6	0.4178	0.258	34.5	0.2386	0.445	52.5
0.0281	0.101	178.8	0.1028	0.889	215.8	0.5226	0.319	34.1	0.2045	0.371	51.1
						0.6241	0.382	34.2	0.3072	0.561	51.4
0.0247	0.088	176.1				0.7272	0.446	34.2	0.4121	0.755	51.6
0.0420	0.142	167.7							0.5187	0.944	51.3
0.0671	0.242	178.8									
0.0723	0.247	168.5									
0.0603	0.205	167.5									
Arithmetic mean		171.1			218.6			34.5			51.4
Square root–mean square deviation		4.3			2.4			0.5			0.8

NOTE: Cryoscopic constants (K_f) for iodine and naphthalene dissolved separately in cyclohexane or in benzene. Δt° C is the measured depression of the freezing point of the pure solvent by the indicated weight (w (g)) of solute added to 25 cc of solvent. The units for K_f are degrees centigrade for 1 mole of solute added to 100 g of solvent.

TABLE II

w_{I_2} (g)	w_N (g)	Δt° C	K_f	w_{I_2} (g)	w_N (g)	Δt° C	K_f
0.0289	—	0.000	—	0.0723	—	0.000	—
0.0289	0.0493	0.402	202.5	0.0723	0.0557	0.444	198.4
0.0315	—	0.000	—	0.0723	0.1040	0.831	198.0
0.0315	0.0608	0.502	204.8	0.0723	0.1632	1.292	197.0
0.0315	0.1206	1.011	207.8	0.0723	0.2147	1.681	194.7
0.0315	0.1789	1.482	205.4	0.0723	0.2778	2.146	191.1
0.0315	0.2351	1.932	203.8	0.0723	0.3290	2.523	190.7

NOTE: Cryoscopic constants (K_f) for naphthalene dissolved in iodine plus cyclohexane. Δt° C is the depression of the freezing point of the iodine solution observed on addition of the indicated weight of napthalene (w_N (g)) to 25 cc of the pure solvent with w_{I_2} g of iodine. K_f is in degrees centigrade for 1 mole dissolved in 100 g of solvent. K_f for napthalene alone is 218.6.

DISCUSSION

The new K_f value for naphthalene dissolved in benzene (51.4±0.7) is in good agreement with the accepted value of 51.2 (6, 11). However, the new value of K_f for cyclohexane (218.6±2.4) is significantly larger than the published values of 200 to 204 (6, 8, 11). The significantly lower K_f values reported for iodine in both solvents (Table I) cannot be

Can. J. Chem. Downloaded from www.nrcresearchpress.com by 69.46.99.164 on 09/04/12
For personal use only.

attributed to partial polymerization of the solute, as has been suggested for other compounds in cyclohexane (12), because the K_f values are independent of the iodine concentration (Table I). Thus these low K_f values must be due to formation of solid solutions (5).

The significant decrease observed in the K_f values for naphthalene for the mixed-solute system (Table II) cannot be attributed to "salting-out" of either component because absorption spectra of these solutions show no sudden break when the temperature is lowered to near the freezing point. Also the saturation concentrations for both components dissolved separately in the pure solvent are significantly greater than the concentrations we studied. Thus the observed decrease for K_f must be due to specific interactions between iodine and naphthalene molecules in solution. This conclusion is in accord with published spectrophotometric work (3, 4, 14).

Calculations with data for naphthalene dissolved in iodine plus benzene solutions show that K_f decreases only slightly in the presence of iodine. (The maximum decrease observed was 2.5 for 0.7000 g of naphthalene dissolved in 21.98 g of benzene and 0.3000 g of iodine.) Calculations with spectrophotometrically determined values for the equilibrium constants for the separate reactions between iodine and benzene (2) or naphthalene (3, 14) show that in the competitive system less than 2% of the iodine will combine with the naphthalene. Thus the small decrease in K_f values can be understood.

No attempt has been made to calculate the equilibrium constant and hence ΔH for the reaction between iodine and naphthalene because of the different K_f values for iodine and naphthalene in cyclohexane.

ACKNOWLEDGMENTS

P. A. D. de Maine gratefully acknowledges financial assistance in the form of grants from the Research Corporation and the Research Foundation, State University of New York. Thanks are also due to Mr. Wilt of Wilt Glassblowing Company, Watervleit, N.Y., for valuable suggestions in the cell design.

REFERENCES

1. Andrews, L. J. and Keefer, R. M. J. Am. Chem. Soc. **73**, 4169 (1951).
2. Benesi, H. A. and Hildebrand, J. H. J. Am. Chem. Soc. **71**, 2703 (1949).
3. Blake, N. W., Winston, H., and Patterson, J. A. A. J. Am. Chem. Soc. **73**, 4437 (1951).
4. de Maine, P. A. D. and Peone, J., Jr. J. Mol. Spectroscopy. In press. (1959).
5. Glasstone, S. Textbook of physical chemistry. 2nd ed. D. Van Nostrand Company, Inc., New York. 1946.
6. Handbook of Chemistry and Physics. 35th ed. Chemical Rubber Publishing Co., Cleveland, Ohio. 1954.
7. Hartley, K. and Skinner, H. A. Trans. Faraday Soc. **46**, 621 (1950).
8. International Critical Tables. 1st ed. McGraw-Hill Book Co. Inc., New York. 1926.
9. Ketelaar, J. A. A., Van de Stolpe, C., Goudsmit, A., and Dzcubas, W. Rec. trav. chim. **71**, 1104 (1952).
10. Kortüm, G. and Vogel, W. M. Z. Elektrochem. **59**, 16 (1955).
11. Lange, N. A. Handbook of chemistry. 9th ed. Handbook Publ. Inc., Sandusky, Ohio. 1956.
12. Mascarelli, L. and Musatty, I. Atti accad. Lincei, **18**, II, 195 (1909).
13. Precision Scientific Company. 3737 Cortland St., Chicago 47, Illinois. Index TS-65920-1 (1950).
14. Van de Stolpe, C. Solvatie van Jodium in Organische Oplosmiddelen. Ph.D. Thesis, Amsterdam. 1953.

Can. J. Chem. Downloaded from www.nrcresearchpress.com by 69.46.99.164 on 09/04/12
For personal use only.

Can. J. Chem. Downloaded from www.nrcresearchpress.com by 69.46.99.164 on 09/04/12
For personal use only.

CALCULATION OF HEATS OF SOLUTION IN SATURATED MIXED ELECTROLYTES[1]

Y. IYENGAR[2]

ABSTRACT

Theoretical equations have been derived for calculating heats of solutions of an electrolyte in its saturated system comprising one or more electrolytes. These expressions involve the application of "Harned's rule" concerning activity coefficients in mixed electrolytic solutions to an extension of van't Hoff's equation dealing with the temperature coefficient of solubility product in non-ideal systems. The commonly occurring case of mixed electrolytic pairs has been considered in detail. Application of theoretical equations to calculate the heats of solutions KCl, NaCl, and KNO_3 in the saturated systems KCl–NaCl–H_2O and KCl–KNO_3–H_2O is briefly discussed.

I. INTRODUCTION

A knowledge of the heats of solution of an electrolyte in its saturated system comprising one or more co-solutes is very useful in the computation of heat balances in processes involving steps such as the dissolution and crystallization of the electrolyte in these systems. Particularly of interest is the fact that the heat of crystallization of a salt is identified with its negative heat of solution at saturation.

Experimental data on heats of solutions in saturated solutions of mixed electrolytes are conspicuous by their absence. Even the data in fairly concentrated solutions are scarce (1–3). Such measurements are extremely difficult and tedious owing to the very slow rate of dissolution of a solute in a nearly saturated solution.

By a thermodynamic treatment involving the extension of van't Hoff's equation to non-ideal solutions, Williamson (4) derived expressions for calculating heats of solution of electrolytes at saturation in water. However, the influence of the presence of other electrolytes was not considered in his work.

The present work offers a theoretical method of calculating the heats of solution of a salt in saturated mixed electrolyte systems. The lack of experimental data in such systems lends considerable value to the theoretical solution.

II. GENERAL EQUATION FOR A PAIR OF ELECTROLYTES

(a) No Common Ions

Consider a system comprising a saturated solution of a pair of electrolytes having no ions in common between them. Let the properties of the species A and B be designated by the subscripts "1" and "2". The problem now is to derive expressions for evaluating heats of solutions of either A or B in a solution saturated with respect to both A and B.

From solubility relationships for component A

$$[1] \qquad P_1\gamma_1^{\nu_1} = P_{1(W)}\gamma_{1(W)}^{\nu_1}$$

where $P_{1(W)}$ and P_1 are the stoichiometrical solubility products of electrolyte A in water and in a solution saturated with respect to both A and B respectively, and $\gamma_{1(W)}$ and γ_1 are the corresponding mean activity coefficients. ν_1 is the total number of ions in 1 molecule of the electrolyte A.

[1]*Manuscript received August 19, 1959.*
Contribution from U.S. Borax Research Corporation, Anaheim, California, U.S.A.
[2]*Present address: Industrial Products Research Laboratory, Textile Fibers Department, E. I. du Pont de Nemours Co., Water Street, Newport, Delaware, U.S.A.*

Extending van't Hoff's equation to non-ideal systems of component A in the saturated A–B–H_2O system,

$$[2] \qquad \frac{d \ln P_1 {\gamma_1}^{\nu_1}}{dT} = \frac{\Delta H_{1(0)}}{RT^2},$$

where $\Delta H_{1(0)}$ is the differential heat of solution of A in pure water. Now, in the absence of a common ion,

$$[3] \qquad P_1 = (\nu_+{}^{\nu_+}\nu_-{}^{\nu_-}){m_1}^{\nu},$$

where ν_+ and ν_- are the number of cations and anions respectively in 1 molecule of the electrolyte and m_1 is the molality of A. Combining eqs. [3] and [2]

$$[4] \qquad \frac{d \ln m_1}{dT} + \left(\frac{d \ln \gamma_1}{dT}\right)_{\text{sat}} = \frac{\Delta H_{1(0)}}{\nu_1 RT^2},$$

where the subscript "sat" stands for "solution saturated with respect to both A and B".

Since the variation of γ_1 with temperature is also accompanied by changes in the ionic strengths μ_1 and μ_2 of A and B respectively,

$$\partial \ln \gamma_1 = \left(\frac{\partial \ln \gamma_1}{dT}\right)_{\mu_1,\mu_2} dT + \left(\frac{\partial \ln \gamma_1}{\partial \mu_1}\right)_{\mu_2,T} d\mu_1 + \left(\frac{\partial \ln \gamma_1}{\partial \mu_2}\right)_{\mu_1,T} d\mu_2,$$

whence

$$[5] \qquad \left(\frac{d \ln \gamma_1}{dT}\right)_{\text{sat}} = \left(\frac{\partial \ln \gamma_1}{\partial T}\right)_{\mu_1,\mu_2} + \left(\frac{\partial \ln \gamma_1}{\partial \mu_1}\right)_{\mu_2,T} \frac{d\mu_1}{dT} + \left(\frac{\partial \ln \gamma_1}{\partial \mu_2}\right)_{\mu_1,T} \frac{d\mu_2}{dT}.$$

Now,

$$[6] \qquad \left(\frac{\partial \ln \gamma_1}{\partial T}\right)_{\mu_1,\mu_2} = -\frac{\bar{L}_1}{\nu_1 RT^2},$$

where $\bar{L}_1$ is the relative partial molal heat content of A in a solution saturated with respect to both A and B. Combining eqs. [4], [5], and [6],

$$[7] \qquad \frac{d \ln m_1}{dT} + \left(\frac{\partial \ln \gamma_1}{\partial \mu_1}\right)_{\mu_2,T} \frac{d\mu_1}{dT} + \left(\frac{\partial \ln \gamma_1}{\partial \mu_2}\right)_{\mu_1,T} \frac{d\mu_2}{dT} = \frac{(\Delta H_{1(0)} + \bar{L}_1)}{\nu_1 RT^2}.$$

The variation of activity coefficients of salts in mixed electrolytes has been extensively investigated by Harned (5). Harned's rule, which has been successfully applied to several electrolyte pairs, can be written in the present context as

$$[8a] \qquad \ln \gamma_1 = \ln \gamma_{1(0)} - \alpha_1 \mu_2$$

$$[8b] \qquad \ln \gamma_2 = \ln \gamma_{2(0)} - \alpha_2 \mu_1,$$

where α_1, α_2 are constants at a given temperature, μ_1, μ_2 are the ionic strengths of A and B, and $\gamma_{1(0)}$, $\gamma_{2(0)}$ are the activity coefficients of A and B in their respective solutions in *water* at the *total* ionic strength $\mu = (\mu_1 + \mu_2)$.

Using eq. [8*a*],

$$[9] \qquad \left(\frac{\partial \ln \gamma_1}{\partial \mu_1}\right)_{\mu_2,T} = \left(\frac{\partial \ln \gamma_{1(0)}}{\partial \mu_1}\right)_{\mu_2,T} - \mu_2 \left(\frac{\partial \alpha_1}{\partial \mu_1}\right)_{\mu_2,T} = \left(\frac{\partial \ln \gamma_{1(0)}}{\partial \mu}\right)_T - \mu_2 \left(\frac{\partial \alpha_1}{\partial \mu}\right)_T.$$

Also

$$[10] \qquad \left(\frac{\partial \ln \gamma_1}{\partial \mu_2}\right)_{\mu_1,T} = \left(\frac{\partial \ln \gamma_{1(0)}}{\partial \mu}\right)_T - \mu_2 \left(\frac{\partial \alpha_1}{\partial \mu}\right)_T - \alpha_1.$$

Can. J. Chem. Downloaded from www.nrcresearchpress.com by 69.46.99.164 on 09/04/12
For personal use only.

The activity coefficient $\gamma_{1(0)}$ of A in water at high ionic strengths (even exceeding the solubility of the salt in water) may be obtained by the empirical rule of Åkerlöf and Thomas (6), according to which

$$\ln \gamma_{1(0)} - \ln \gamma_{R(0)} = \beta_1 \mu, \qquad [11]$$

where $\gamma_{R(0)}$ is the mean activity coefficient of a reference electrolyte, and β_1 is a constant at a given temperature. The above relationship has been confirmed (6) for various electrolytes in concentrated solutions even up to saturation. Hydrochloric acid is generally used as the reference solute (R) since its activity coefficient is known over a very wide range of concentration (3–16 m) (7).

Differentiation of eq. [11] with respect to μ gives,

$$\left(\frac{\partial \ln \gamma_{1(0)}}{\partial \mu}\right)_T = \left(\frac{\partial \ln \gamma_{R(0)}}{\partial \mu}\right)_T + \beta_1. \qquad [12]$$

Substituting eqs. [9], [10], and [12] in eq. [7], and also using the mathematical identity,

$$\frac{d \ln m_1}{dT} = \frac{1}{m_1}\frac{dm_1}{dT},$$

$$\frac{1}{m_1}\frac{dm_1}{dT} + \frac{d\mu_1}{dT}\left[\left(\frac{\partial \ln \gamma_{R(0)}}{\partial \mu}\right)_T + \beta_1 - \mu_2\left(\frac{\partial \alpha_1}{\partial \mu}\right)_T\right] + \frac{d\mu_2}{dT}\left[\left(\frac{\partial \ln \gamma_{R(0)}}{\partial \mu}\right)_T + \beta_1 - \mu_2\left(\frac{\partial \alpha_1}{\partial \mu}\right)_T - \alpha_1\right] = \frac{(\Delta H_{1(0)} + \bar{L}_1)}{\nu_1 RT^2}. \qquad [13]$$

β_1 can be determined from eq. [11] if the activity coefficients of electrolyte A and the reference electrolyte R at the same ionic strengths are known. Accurate values of β_1 may be obtained by plotting $\ln \gamma_{1(0)} - \ln \gamma_{R(0)}$ against μ and evaluating β_1 as the slope of this line.

α_1 may be evaluated from solubility data as follows.
Equation [1] may be written in the form,

$$\ln P_1/\nu_1 + \ln \gamma_1 = \ln P_{1(W)}/\nu_1 + \ln \gamma_{1(W)}. \qquad [14]$$

Substituting for

$$P_{1(W)} = (\nu_+^{\nu_+}\nu_-^{\nu_-})m_{1(W)}^{\nu},$$

$$P_1 = (\nu_+^{\nu_+}\nu_-^{\nu_-})m_1^{\nu},$$

$$\ln \gamma_{1(W)} = \ln \gamma_{R(W_1)} + \beta_1 \mu_{1(W)},$$

and for $\ln \gamma_1$ from eqs. [8a] and [11], where $m_{1(W)}$ is the solubility of A in water, and $\mu_{1(W)}$ the ionic strength of A at saturation in water, and $\gamma_{R(W_1)}$ is the activity coefficient of the reference electrolyte (R) at ionic strength $\mu_{1(W)}$, eq. [14] now becomes,

$$\ln m_1 + \ln \gamma_{R(0)} + \beta_1 \mu - \alpha_1 \mu_2 = \ln m_{1(W)} + \ln \gamma_{R(W_1)} + \beta_1 \mu_{1(W)},$$

whence

$$\alpha_1 = \frac{1}{\mu_2}[\ln (m_1/m_{1(W)}) + \ln (\gamma_{R(0)}/\gamma_{R(W_1)}) + \beta_1(\mu - \mu_{1(W)})]. \qquad [15]$$

Extending van't Hoff's equation to the non-ideal system of component B in saturated A–B–H_2O, the following expression analogous to eq. [13] may be derived going through similar steps.

Can. J. Chem. Downloaded from www.nrcresearchpress.com by 69.46.99.164 on 09/04/12
For personal use only.

[16] $$\frac{1}{m_2}\frac{dm_2}{dT}+\frac{d\mu_2}{dT}\left[\left(\frac{\partial \ln \gamma_{R(0)}}{\partial \mu}\right)_T+\beta_2-\mu_1\left(\frac{\partial \alpha_2}{\partial \mu}\right)_T\right]+\frac{d\mu_1}{dT}\left[\left(\frac{\partial \ln \gamma_{R(0)}}{\partial \mu}\right)_T+\beta_2-\mu_1\left(\frac{\partial \alpha_2}{\partial \mu}\right)_T-\alpha_2\right]=\frac{(\Delta H_{2(0)}+\bar{L}_2)}{\nu_2 RT^2},$$

where ν_2 is the total number of ions in 1 molecule of electrolyte B, and where β_2, α_2, $\Delta H_{2(0)}$, and $\bar{L}_2$ of B correspond to β_1, α_1, $\Delta H_{1(0)}$, and $\bar{L}_1$ of A.

β_2 and α_2 are given by expressions similar to eqs. [11] and [15]:

[17] $$\ln \gamma_{2(0)}/\ln \gamma_{R(0)} = \beta_2\mu$$

[18] $$\alpha_2 = \frac{1}{\mu_1}[\ln (m_2/m_{2(W)})+\ln (\gamma_{R(0)}/\gamma_{R(W_2)})+\beta_2(\mu-\mu_{2(W)})].$$

Further simplifications of eqs. [13] and [16] are possible by considering certain relationships between α_1 and α_2.

Harned and Owen (5) applied the Gibbs–Duhem equation to their rule (eqs. [8*a*], [8*b*]) and obtained, on the basis of Åkerlöf and Thomas' rule, eq. [11],

[19] $$\alpha_1-\alpha_2 = \text{constant},$$

whereas Glueckauf, McKay, and Mathieson (8, 9) obtained by thermodynamic considerations,

[20] $$\alpha_1+\alpha_2 = \text{constant}.$$

Equations [19] and [20] reveal that both α_1 and α_2 are constants independent of ionic strength of solution in concentrated solutions where Harned's rule is applicable. Since α_1 and α_2 are independent of μ,

$$(\partial\alpha_1/\partial\mu)_T = 0,$$

and

$$(\partial\alpha_2/\partial\mu)_T = 0,$$

whence eq. [13] becomes

[21] $$\frac{1}{m_1}\frac{dm_1}{dT}+\frac{d\mu_1}{dT}\left[\left(\frac{\partial \ln \gamma_{R(0)}}{\partial \mu}\right)_T+\beta_1\right]+\frac{d\mu_2}{dT}\left[\left(\frac{\partial \ln \gamma_{R(0)}}{d\mu}\right)_T+\beta_1-\alpha_1\right]=\frac{(\Delta H_{1(0)}+\bar{L}_1)}{\nu_1 RT^2}$$

and eq. [16] becomes

[22] $$\frac{1}{m_2}\frac{dm_2}{dT}+\frac{d\mu_2}{dT}\left[\left(\frac{\partial \ln \gamma_{R(0)}}{\partial \mu}\right)_T+\beta_2\right]+\frac{d\mu_1}{dT}\left[\left(\frac{\partial \ln \gamma_{R(0)}}{\partial \mu}\right)_T+\beta_2-\alpha_2\right]=\frac{(\Delta H_{2(0)}+\bar{L}_2)}{\nu_2 RT^2}.$$

Denoting the left-hand sides of eqs. [21] and [22] by X and Y respectively, the equations can be rewritten as

[23] $$\nu_1 RT^2 X = \Delta H_{1(0)}+\bar{L}_1$$

[24] $$\nu_2 RT^2 Y = \Delta H_{2(0)}+\bar{L}_2.$$

Now, the heat of solution ΔH_{12} of A in a solution saturated with respect to both A and B is given by

$$\Delta H_{12} = (\bar{H}_{1(0)}-H_{1(s)})-(\bar{H}_1-\bar{H}_{1(0)}),$$

Can. J. Chem. Downloaded from www.nrcresearchpress.com by 69.46.99.164 on 09/04/12
For personal use only.

where $\bar{H}_{1(0)}$ is the partial molal enthalpy of A in an infinitely dilute solution of A in water, $H_{1(s)}$ is the molal enthalpy of A in the solid state, and $\bar{H}_1$ is the partial molal enthalpy of A in a solution saturated with respect to both A and B.

Since

$$(\bar{H}_{1(0)}-H_{1(s)}) = \Delta H_{1(0)}$$

and

$$(\bar{H}_1-H_{1(0)}) = \bar{L}_1,$$

therefore

[24*a*] $$\Delta H_{12} = \Delta H_{1(0)}+\bar{L}_1$$

and similarly

[24*b*] $$\Delta H_{21} = \Delta H_{2(0)}+\bar{L}_2,$$

where ΔH_{21} is the heat of solution of B in a solution saturated with respect to both A and B. Combining eqs. [23], [24], [24*a*], and [24*b*]

[25] $$\Delta H_{12} = \nu_1 RT^2 X$$

[26] $$\Delta H_{21} = \nu_2 RT^2 Y.$$

Equations [25] and [26] indicate that the heats of solutions of either one of the components in a solution saturated with respect to the electrolyte pair A, B can be simultaneously calculated by knowing X and Y from the solubility and thermodynamic data of the saturated system A–B–H_2O.

(b) Common Ion Effect

For the case of an electrolytic pair with a common ion eqs. [21] and [22] become slightly modified. If the anion is assumed to be common between the two electrolytes A and B, P_1 (see eq. [3]) is now given by

[27] $$\begin{aligned} P_1 &= m_+^{\nu_+} m_-^{\nu_-} \\ &= ({}_1\nu_+ m_1)^{{}_1\nu_+}({}_1\nu_- m_1+{}_2\nu_- m_2)^{{}_1\nu_-}, \end{aligned}$$

where ${}_1\nu_+$ and ${}_1\nu_-$ are the number of cations and anions in 1 molecule of the electrolyte A respectively and ${}_2\nu_-$ is the number of anions in 1 molecule of B. Instead of eq. [4] we now have

[28] $$\frac{1}{\nu_1}[{}_1\nu_+ d\ln m_1/dT+{}_1\nu_- d\ln({}_1\nu_- m_1+{}_2\nu_- m_2)/dT]+(d\ln\gamma_1/dT)_{\text{sat}} = \Delta H_{1(0)}/\nu_1 RT^2.$$

Equation [21] now becomes

[29] $$\begin{aligned} \frac{1}{\nu_1}[{}_1\nu_- d\ln({}_1\nu_- m_1+{}_2\nu_- m_2)/dT+(dm_1/dT)({}_1\nu_+/m_1)]+(d\mu_1/dT)[(\partial\ln\gamma_{R(0)}/\partial\mu)_T+\beta_1] \\ +(d\mu_2/dT)[(\partial\ln\gamma_{R(0)}/\partial\mu)_T+\beta_1-\alpha_1] = (\Delta H_{1(0)}+\bar{L}_1)/\nu_1 RT^2 \end{aligned}$$

Can. J. Chem. Downloaded from www.nrcresearchpress.com by 69.46.99.164 on 09/04/12
For personal use only.

and eq. [22] becomes

$$[30]\quad \frac{1}{\nu_2}\left[{}_2\nu_- d\ln({}_1\nu_-m_1+{}_2\nu_-m_2)/dt+\left(\frac{dm_2}{dT}\right)\left(\frac{{}_2\nu_+}{m_2}\right)\right]+\frac{d\mu_2}{dT}\left[\left(\frac{\partial \ln \gamma_{R(0)}}{\partial\mu}\right)_T+\beta_2\right]$$
$$+\frac{d\mu_1}{dT}\left[\left(\frac{\partial \ln \gamma_{R(0)}}{\partial\mu}\right)_T+\beta_2-\alpha_2\right]=\frac{(\Delta H_{2(0)}+\bar{L}_1)}{\nu_2 RT^2}.$$

Also from eqs. [14] and [27],

$$[31]\quad \alpha_1=\frac{1}{\mu_2}\left[\frac{{}_1\nu_+}{\nu_1}\ln m_1+\frac{{}_1\nu_-}{\nu_1}\ln({}_1\nu_-m_1+{}_2\nu_-m_2)-\ln m_{1(W)}+\ln(\gamma_{R(0)}/\gamma_{R(W_1)})\right.$$
$$\left.+\beta_1(\mu-\mu_{1(W)})\right].$$

Similarly,

$$[32]\quad \alpha_2=\frac{1}{\mu_1}\left[\frac{{}_2\nu_+}{\nu_2}\ln m_2+\frac{{}_2\nu_-}{\nu_2}\ln({}_1\nu_-m_1+{}_2\nu_-m_2)-\ln m_{2(W)}+\ln(\gamma_{R(0)}/\gamma_{R(W_2)})\right.$$
$$\left.+\beta_2(\mu-\mu_{2(W)})\right].$$

ΔH_{12} and ΔH_{21} may be calculated as before, by substituting X and Y for the left-hand side of eqs. [29] and [30] and using the eqs. [25] and [26].

III. 1:1 ELECTROLYTE PAIR

Equations [21], [22], [29], and [30] become considerably simple for the case of a pair of 1:1 electrolytes.

(a) No Common Ion

Consider the case when the 1:1 electrolytes A and B have no ions in common. Equations [11], [15], [17], [18], [21], and [22] remain practically unchanged except that ionic strengths (μ) become molalities (m)

$$\mu = m, \qquad \mu_1 = m_1, \qquad \mu_2 = m_2,$$

$$\mu_{1(W)} = m_{1(W)}, \qquad \mu_{2(W)} = m_{2(W)}.$$

Also

$$\nu = 2.$$

With these modifications and substitutions, ΔH_{12} and ΔH_{21} may be evaluated by eqs. [25] and [26].

(b) Common Ion Effect

Assume the anion to be common between the 1:1 electrolytes A and B. Since

$${}_1\nu_- = {}_2\nu_- = {}_1\nu_+ = {}_2\nu_+ = 1,$$
$$\mu_{1(W)} = m_{1(W)},$$
$$\mu_{2(W)} = m_{2(W)},$$

and

$$m = m_1+m_2,$$

Can. J. Chem. Downloaded from www.nrcresearchpress.com by 69.46.99.164 on 09/04/12
For personal use only.

eqs. [29] and [30] become greatly simplified to

$$[33]\quad \left(\frac{dm_1}{dT}\right)\left[\frac{1}{2m_1}+\frac{1}{2m}+\left(\frac{\partial \ln \gamma_{R(0)}}{\partial m}\right)_T+\beta_1\right]+\left(\frac{dm_2}{dT}\right)\left[\frac{1}{2m}+\left(\frac{\partial \ln \gamma_{R(0)}}{\partial m}\right)_T+\beta_1-\alpha_1\right] = \frac{(\Delta H_{1(0)}+\bar{L}_1)}{2RT^2}$$

and

$$[34]\quad \left(\frac{dm_2}{dT}\right)\left[\frac{1}{2m_2}+\frac{1}{2m}+\left(\frac{\partial \ln \gamma_{R(0)}}{\partial m}\right)_T+\beta_2\right]+\left(\frac{dm_1}{dT}\right)\left[\frac{1}{2m}+\left(\frac{\partial \ln \gamma_{R(0)}}{\partial m}\right)_T+\beta_2-\alpha_2\right] = \frac{(\Delta H_{2(0)}+\bar{L}_2)}{2RT^2}.$$

As before, the left-hand sides of these equations may be equated to X and Y respectively so that ΔH_{12} and ΔH_{21} may be evaluated from eqs. [25] and [26].

The expressions for α_1 and α_2 (eqs. [31] and [32]) also become greatly simplified to

$$[35]\quad \alpha_1 = (1/m_2)[\ln (m_1 m)^2 - \ln m_{1(W)} + \ln (\gamma_{R(0)}/\gamma_{R(W1)}) + \beta_1(m - m_{1(W)})]$$

$$[36]\quad \alpha_2 = (1/m_1)[\ln (m_2 m)^2 - \ln m_{2(W)} + \ln (\gamma_{R(0)}/\gamma_{R(W2)} + \beta_2(m - m_{2(W)})].$$

The expressions for β_1 and β_2 are similar to eq. [11] with μ being equal to molality.

IV. APPLICATION OF THEORY TO EXPERIMENTAL RESULTS

The above theoretical treatment has been applied to the saturated KCl–NaCl–H_2O and KCl–KNO_3–H_2O systems for calculating heats of solutions of both salts in each of the saturated systems.

Since both these are 1:1 electrolyte systems with common ions, eqs. [33] and [34] along with eqs. [25] and [26] are to be applied for calculation of heats of solutions. The data and calculations are given in Tables I and II.

TABLE I

Data for the saturated systems KCl–NaCl–H_2O and KCl–KNO_3–H_2O

$t°$ C	m_1	m_2	dm_1/dT	dm_2/dT	$m_{1(W)}$	$m_{2(W)}$	$\ln \gamma_{R(W1)}$	$\ln \gamma_{R(W2)}$	$\ln \gamma_{R(0)}$
(*i*) KCl–NaCl–H_2O (subscript "1" refers to KCl and "2" to NaCl)									
18	1.93[a]	5.16[a]	.0319[a]	−.0128[a]	4.48[b]	6.14[b]	.737[c]	1.264[c]	1.568[c]
25	2.17	5.08	.0336	−.0111	4.83	6.17	.803	1.216	1.550
40	2.69	4.94	.0336	−.0078	5.37	6.23	.857	1.108	1.503
(*ii*) KCl–KNO_3–H_2O (subscript "1" refers to KCl and "2" to KNO_3)									
25	4.42[b]	2.14[b]	.0227[b]	.0636[b]	4.83[b]	3.69[b]	.803[c]	.461[c]	1.193[c]

[a]Unpublished results from Palestine Potash Co., Jerusalem, communicated by Dr. Martin Wilson, now with the U.S. Borax Research Corporation.

[b]A. Seidell. Solubilities of inorganic and metal organic compounds. Vol. I. D. Van Nostrand Company, Inc., New York. 1940.

[c]Reference 5, p. 577.

V. DISCUSSION OF RESULTS

No experimental data are yet available on heats of solutions in nearly saturated salt pairs. However, the influence of added electrolytes on the heats of solutions of salts has been experimentally investigated (1, 2). Our calculations in saturated systems may be qualitatively reviewed in relation to the data in the unsaturated systems. Drucker's

Can. J. Chem. Downloaded from www.nrcresearchpress.com by 69.46.99.164 on 09/04/12
For personal use only.

TABLE II

Heats of solutions in the saturated systems KCl–NaCl–H_2O and KCl–KNO_3–H_2O

t° C	β_1	β_2	α_1	α_2	$\Delta H_{1(0)}$	$\Delta H_{2(0)}$	ΔH_{12}	ΔH_{21}
(*i*) KCl–NaCl–H_2O (subscript "1" refers to KCl and "2" to NaCl)								
18	−.286[a]	−.210[a]	−.0206	.0461	4.44[b]	1.28[b]	3.33	0.19
25	−.275[c]	−.198[c]	−.0228[f]	.0468[f, g]	4.12[d]	1.07[d]	3.42	0.43
40	−.250[a]	−.172[a]	−.0182	.0532	3.68[e]	0.68[e]	3.34	0.73
(*ii*) KCl–KNO_3–H_2O (subscript "1" refers to KCl and "2" to KNO_3)								
25	−.275[c]	−.520[c]	.0780	−.137	4.12[d]	8.38[d]	2.59	2.31

[a]Calculated from interpolated data in reference 5, pp. 557, 558.
[b]International Critical Tables. Vol V. Natl. Research Council U.S. 1929. pp. 200, 203.
[c]Calculated from data tabulated by R. A. Robinson and R. H. Stokes. Trans. Faraday Soc. **45**, 612 (1949).
[d]Reference 3.
[e]N. K. Voskrenskaya and K. S. Ponomareva. Compt. rend. acad. sci. U.R.S.S. **45**, 188 (1944).
[f]$\alpha_1 = -.02$ and $\alpha_2 = .059$, at a total molality of 5, obtained from e.m.f. studies (reference 9, p. 179).
[g]$\alpha_2 = .048$ from solubility studies of G. Åkerlöf. J. Phys. Chem. **41**, 1053 (1937).

work on KCl–NaCl–H_2O system indicates that the heat of solution of KCl was depressed from 4.4 kcal/mole in water (18° C) to 3.2 kcal/mole on the addition of 4.0 molar NaCl. This depression of 1.2 kcal/mole may be compared with the value of $\bar{L}_1$ (eq. [23]) which represents the relative partial molal heat content of NaCl in a solution saturated with respect to both KCl and NaCl.

$$\bar{L}_1 = 2RT^2X - \Delta H_{1(0)}$$
$$= 3.33 - 4.44 = -1.11 \text{ at } 18° \text{ C},$$

which is close to the observed depression. Since the system investigated by Drucker had about 0.2 molal KCl in it, it appears that $\bar{L}_1$ does not alter very much between this concentration and saturation (1.93 m). The data (2) on KCl–KNO_3–H_2O system are not extensive enough to evaluate heats of solutions at concentrations nearing saturation even by extrapolation. However, the high negative value of

$$\bar{L}_2 = 2RT^2Y - \Delta H_{2(0)} = -6.07 \text{ kcal/mole}$$

predicted by theory for a saturated KCl–KNO_3–H_2O system is justified by the trend of experimental results according to which (3) $\bar{L}_2$ in a solution containing 2.7 m KNO_3 and 0.27 m KCl is considerably large and negative ($\bar{L}_2 = 4.14 - 8.59 = -4.45$ kcal/mole).

ACKNOWLEDGMENT

The author wishes to thank the U.S. Borax Research Corporation for permission to publish this work.

REFERENCES

1. Drucker, C. Arkiv Kemi, Mineral. Geol. **2**, 1 (1934).
2. Voskrenskaya, N. K. and Ponomareva, K. S. J. Phys. Chem. U.S.S.R. **20**, 433 (1946).
3. Kaganovich, Yu. Ya. and Mishchenko, K. P. J. Gen. Chem. U.S.S.R. (English Translation) **21**, 29 (1951).
4. Williamson, A. T. Trans. Faraday Soc. **40**, 421 (1944).
5. Harned, H. S. and Owen, B. B. The physical chemistry of electrolytic solutions. 2nd ed. (ACS Monograph Series No. 95.) Reinhold Publishing Corp., New York. 1950. pp. 444–479.
6. Åkerlöf, G. and Thomas, H. C. J. Am. Chem. Soc. **56**, 593 (1934).
7. Åkerlöf, G. and Teare, J. W. J. Am. Chem. Soc. **59**, 1855 (1937).
8. Glueckauf, E., McKay, H. A. C., and Mathieson, A. R. J. Chem. Soc. S299 (1949).
9. Robinson, R. A. *In* Electrochemical constants. Natl. Bur. Standards Circ. No. 524. 1953. pp. 171–192.

Can. J. Chem. Downloaded from www.nrcresearchpress.com by 69.46.99.164 on 09/04/12
For personal use only.

APPENDIX

Heats of Solutions in Saturated Multicomponent Systems

The present treatment may be extended to multicomponent systems as follows: Consider a saturated system of 'n' components A_1, A_2, ... A_n. Extending van't Hoff's equation with respect to component A_1, whose properties are designated by subscript "1",

$$[A1] \qquad d \ln P_1\gamma_1^{\nu_1}/dT = \Delta H_{1(0)}/RT^2,$$

whence

$$[A2] \qquad \frac{1}{\nu_1}\frac{d \ln P_1}{dT}+\left(\frac{d \ln \gamma_1}{dT}\right)_{sat} = \frac{\Delta H_{1(0)}}{\nu_1 RT^2}.$$

Now,

$$[A3] \qquad \left(\frac{d \ln \gamma_1}{dT}\right)_{sat} = \left(\frac{\partial \ln \gamma_1}{\partial T}\right)_{\mu_1,\mu_2,\ldots\ldots\mu_n} +\left(\frac{\partial \ln \gamma_1}{\partial \mu_1}\right)_{\mu_2,\mu_3,\ldots\ldots\mu_n,T}\left(\frac{d\mu_1}{dT}\right)$$
$$+\left(\frac{\partial \ln \gamma_1}{\partial \mu_2}\right)_{\mu_1,\mu_3,\ldots\ldots\mu_n,T}\left(\frac{d\mu_2}{dT}\right)+\ldots\ldots+\left(\frac{\partial \ln \gamma_1}{\partial \mu_n}\right)_{\mu_1,\mu_2,\ldots\ldots\mu_{n-1},T}\left(\frac{d\mu_n}{dT}\right),$$

where $\mu_1, \mu_2, \ldots\ldots \mu_n$ are the ionic strengths of $A_1, A_2, \ldots\ldots A_n$ respectively. Now, assuming validity of Harned's rule (see eqs. [8*a*], [8*b*] of text)

$$[A4] \qquad \begin{aligned} \ln \gamma_1 &= \ln \gamma_{1(0)} - \alpha_1(\mu-\mu_1) \\ \ln \gamma_2 &= \ln \gamma_{2(0)} - \alpha_2(\mu-\mu_2) \\ \ln \gamma_n &= \ln \gamma_{n(0)} - \alpha_n(\mu-\mu_n), \end{aligned}$$

where μ, the total ionic strength $= (\mu_1+\mu_2+\ldots\ldots\mu_n)$. From [A4], equations analogous to [9] and [10] of text follow:

$$[A5] \qquad \left(\frac{\partial \ln \gamma_1}{\partial \mu_1}\right)_{\mu_2,\mu_3,\ldots\ldots\mu_n,T} = \left(\frac{\partial \ln \gamma_{1(0)}}{\partial \mu}\right)_T - (\mu-\mu_1)\left(\frac{\partial \alpha_1}{\partial \mu}\right)_T$$

and

$$[A6_1] \qquad \left(\frac{\partial \ln \gamma_1}{\partial \mu_2}\right)_{\mu_1,\mu_3,\ldots\ldots\mu_n,T} = \left(\frac{\partial \ln \gamma_{1(0)}}{\partial \mu}\right)_T - (\mu-\mu_1)\left(\frac{\partial \alpha_1}{\partial \mu}\right)_T - \alpha_1$$

$$[A6_n] \qquad \left(\frac{\partial \ln \gamma_1}{\partial \mu_n}\right)_{\mu_1,\mu_2,\ldots\ldots\mu_{n-1},T} = \left(\frac{\partial \ln \gamma_{1(0)}}{\partial \mu}\right)_T - (\mu-\mu_1)\left(\frac{\partial \alpha_1}{\partial \mu}\right)_T - \alpha_1.$$

Further,

$$[A7] \qquad \left(\frac{\partial \ln \gamma_{1(0)}}{\partial \mu}\right)_T = \left(\frac{\partial \ln \gamma_{R(0)}}{\partial \mu}\right)_T + \beta_1$$

analogous to eq. [12] of text.

Substituting eqs. [A7], [A6$_1$]–[A6$_n$], and [A5] in eq. [A3] and also noting that

$$(\partial \alpha_1/\partial \mu)_T = 0$$

and

$$\left(\frac{\partial \ln \gamma_1}{\partial T}\right)_{\mu_1,\mu_2,\ldots\ldots\mu_n} = -\frac{\bar{L}_1}{\nu_1 RT^2},$$

Can. J. Chem. Downloaded from www.nrcresearchpress.com by 69.46.99.164 on 09/04/12
For personal use only.

where $\bar{L}_1$ is the relative partial molal heat content of A_1 in the saturated multicomponent system,

$$[A8_1] \qquad \frac{1}{\nu_1}\frac{d\ln P_1}{dT}+\frac{d\mu_1}{dT}\left[\left(\frac{\partial \ln \gamma_{R(0)}}{\partial \mu}\right)_T+\beta_1\right]+\frac{d(\mu-\mu_1)}{dT}\left[\left(\frac{\partial \ln \gamma_{R(0)}}{\partial \mu}\right)_T+\beta_1-\alpha_1\right] = \frac{(\Delta H_{1(0)}+\bar{L}_1)}{\nu_1 RT^2}.$$

Equations similar to $[A8_1]$ may be written for the other components. In general,

$$[A8_n] \qquad \frac{1}{\nu_n}\frac{d\ln P_n}{dT}+\frac{d\mu_n}{dT}\left[\left(\frac{\partial \ln \gamma_{R(0)}}{\partial \mu}\right)_T+\beta_n\right]+\frac{d(\mu-\mu_n)}{dT}\left[\left(\frac{\partial \ln \gamma_{R(0)}}{\partial \mu}\right)_T+\beta_n-\alpha_n\right] = \frac{(\Delta H_{n(0)}+\bar{L}_n)}{\nu_n RT^2},$$

where, $P_1, P_2, \ldots . P_n$ are the stoichiometric solubility products and $\Delta H_{1(0)}, \Delta H_{2(0)}, \ldots . \Delta H_{n(0)}$ are the differential heats of solutions in water of $A_1, A_2, \ldots . A_n$ respectively. A knowledge of $\beta_1, \beta_2, \ldots . \beta_n$ and $\alpha_1, \alpha_2, \ldots . \alpha_n$ is necessary to evaluate the left-hand sides of eqs. $[A8_1]$ to $[A8_n]$. Now $\beta_1, \beta_2, \ldots . \beta_n$ are given by the equations of the type,

$$[A9] \qquad \ln \gamma_{n(0)} = \ln \gamma_{R(0)}+\mu\beta_n.$$

$\alpha_1, \alpha_2, \ldots . \alpha_n$ are evaluated as follows.

For the species A_n, the solubility relationship gives

$$[A10] \qquad \ln P_n/\nu_n+\ln \gamma_n = \ln P_{n(W)}/\nu_n+\ln \gamma_{n(W)}$$

where the subscript (w) indicates "solution in pure water". Substituting for $\ln \gamma_n$ from eqs. [A4] and [A9] and remembering that

$$\ln \gamma_{n(W)} = \ln \gamma_{R(W)}+\beta_n\mu_{n(W)},$$

where $\mu_{n(W)}$ is the ionic strength of A_n, we get on rearranging,

$$[A11] \qquad \alpha_n = [(1/\nu_n)\ln(P_n/P_{n(W)})+\ln(\gamma_{R(0)}/\gamma_{R(Wn)})+\beta_n(\mu-\mu_{n(W)})]/(\mu-\mu_n).$$

Now, denoting the left-hand sides of eqs. $[A8_1]$ to $[A8_n]$ by $X_1, X_2, \ldots . X_n$, respectively

$$[A12_1] \qquad \nu_1 X_1 RT^2 = \Delta H_{1(0)}+\bar{L}_1$$

$$[A12_2] \qquad \nu_2 X_2 RT^2 = \Delta H_{2(0)}+\bar{L}_2$$

$$[A12_n] \qquad \nu_n X_n RT^2 = \Delta H_{n(0)}+\bar{L}_n.$$

Now, if $\Delta H_1, \Delta H_2, \ldots . \Delta H_n$ are the heats of solutions of $A_1, A_2, \ldots . A_n$, respectively, in a system saturated with all the components

$$[A13_1] \qquad \Delta H_1 = \Delta H_{1(0)}+\bar{L}_1 = \nu_1 RT^2 X_1$$

$$[A13_2] \qquad \Delta H_2 = \Delta H_{2(0)}+\bar{L}_2 = \nu_2 RT^2 X_2$$

and in general

$$[A13_n] \qquad \Delta H_n = \Delta H_{n(0)}+\bar{L}_n = \nu_n RT^2 X_n.$$

Thus, knowing $X_1, X_2, \ldots . X_n$ from eqs. $[A8_1]$ to $[A8_n]$ it is possible to calculate the heats of solutions $\Delta H_1, \Delta H_2, \ldots . \Delta H_n$ of components $A_1, A_2, \ldots . A_n$ in their saturated multicomponent systems by means of eqs. $[A13_1]$ to $[A13_n]$.

Can. J. Chem. Downloaded from www.nrcresearchpress.com by 69.46.99.164 on 09/04/12
For personal use only.

Can. J. Chem. Downloaded from www.nrcresearchpress.com by 69.46.99.164 on 09/04/12
For personal use only.

ELECTRICAL EFFECTS ON THE C–O–C ASYMMETRICAL STRETCHING VIBRATION IN ANISOLES

G. K. GOLDMAN, H. LEHMAN, AND, C. N. R. RAO*

The infrared vibrational frequencies and the band intensities of several groups in related series of organic molecules have been found to be influenced systematically by substituents (1–4). In benzene derivatives of the type RC_6H_4X, where X is the functional group and R is a meta- or a para-substituent, linear relations have been found between reactivity constants of R with the vibrational frequency of X and also with the logarithm of the band intensity of X (1–4). Among the electron-donating groups, only the hydroxy and the amino groups have been studied in detail. Little is known about the electrical effects of substituents on the ether linkage (C–O–C) in anisoles. The 1200-cm^{-1} band in esters assigned to the C–O stretching vibration has been studied in a number of alkyl esters (5), but the results do not throw any light on the substituent effects. We have now investigated the electrical effects of substituents on the asymmetrical C–O–C stretching vibration (6) in parasubstituted anisoles.

All the compounds were purified before use. The infrared spectra were recorded in carbon tetrachloride solutions using a Perkin–Elmer, Model 21, spectrophotometer. The molarities of the solutions were kept constant at about 0.05 for all the compounds. The apparent molecular extinction coefficients (ϵ) at the maximal frequencies were calculated from the Beer's law.

The C–O–C asymmetrical stretching frequency in *p*-substituted anisoles increases with the electron withdrawing power of the *p*-substituent. The plot of the frequency

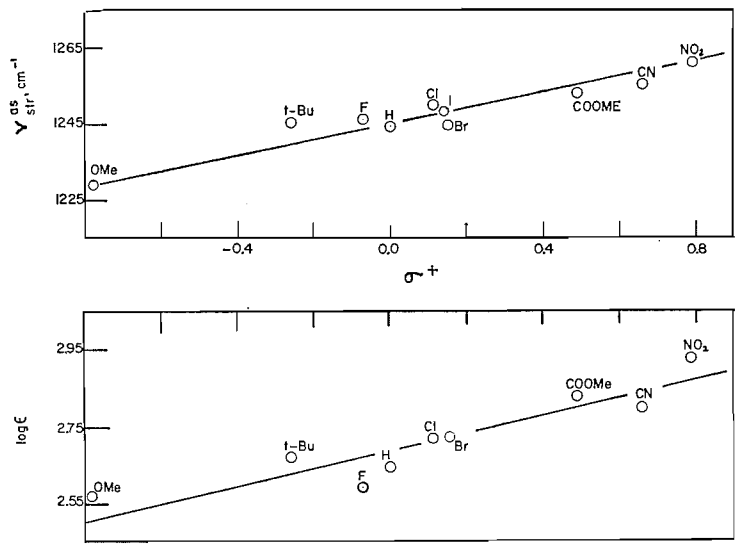
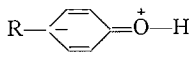


FIG. 1. Correlation of the C–O–C asymmetrical stretching frequency and the band intensity in para-substituted anisoles with the electrophilic substituent constants.

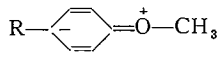
**To whom all the correspondence should be addressed at: Department of Physical Chemistry, Indian Institute of Science, Bangalore, India.*

against Brown–σ^+ values (7) is found to be linear (Fig. 1). The slope of the ν–σ^+ plot is about 21.

The plot of the logarithm of the apparent molecular extinction coefficients of the C–O–C asymmetric stretching frequency against the σ^+ values is also found to be fairly linear (Fig. 1). The band intensity increases with the electron-attracting ability of the *p*-substituent. The apparent half band widths did not seem to show any regular trend. It is interesting to note that the OH band intensity in substituted phenols also shows a similar behavior (8, 9). Since the band intensity of a stretching vibration is directly related to the electrical properties of the particular bond in question (i.e. bond moment and its direction), it appears reasonable that the prominent resonance structures in phenols (I) and in anisoles (II) should be similar:



I



II

The OH stretching frequency in *p*-substituted phenols (unlike the C–O–C stretching frequency in *p*-substituted anisoles) decreases with the increasing electron-withdrawing ability of the *p*-substituent. Of course, it is true that if two functional groups show similar trends of the band intensities with the reactivity constants, it does not follow that the trends of the frequencies will be similar.

ACKNOWLEDGMENT

The authors wish to thank Professor Herbert C. Brown for his kind encouragement.

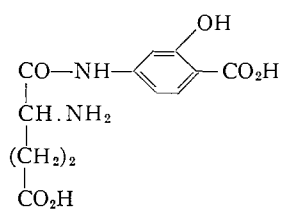
1. Rao, C. N. R. and Silverman, G. B. Current Sci. India, **26**, 375 (1957), and the references listed there.
2. Brown, T. L. Chem. Revs. **58**, 581 (1958).
3. Thompson, H. W. and James, D. A. Spectrochim. Acta, **13**, 236 (1958).
4. Krueger, P. J. and Thompson, H. W. Proc. Roy. Soc. London, A, **250**, 22 (1959).
5. Russell, R. A. and Thompson, H. W. J. Chem. Soc. 479 (1955).
6. Jones, R. N. and Sandorfy, C. *In* Chemical applications of spectroscopy. *Edited by* A. Weissberger. Interscience Publishers, Inc., New York. 1956.
7. Brown, H. C. and Okamoto, Y. J. Am. Chem. Soc. **80**, 4979 (1958).
8. Brown, T. L. J. Phys. Chem. **61**, 820 (1957).
9. Stone, P. J. and Thompson, H. W. Spectrochim. Acta, **10**, 17 (1957).

Received September 8, 1959.
Department of Chemistry,
Purdue University,
West Lafayette, Indiana, U.S.A.

DERIVATIVES OF *p*-AMINOSALICYLIC ACID

M. H. Fisher and T. F. Massiah

Darrach and Polglase (1) have described the preparation of N-(α-L-glutamyl)-*p*-aminosalicylic acid (I). They claim that it is a useful antituberculous drug and that it does not cause the toxic side effects associated with *p*-aminosalicylic acid itself. This report

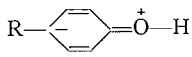


(I)

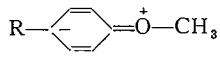
Can. J. Chem. Downloaded from www.nrcresearchpress.com by 69.46.99.164 on 09/04/12
For personal use only.

against Brown–σ^+ values (7) is found to be linear (Fig. 1). The slope of the ν–σ^+ plot is about 21.

The plot of the logarithm of the apparent molecular extinction coefficients of the C–O–C asymmetric stretching frequency against the σ^+ values is also found to be fairly linear (Fig. 1). The band intensity increases with the electron-attracting ability of the *p*-substituent. The apparent half band widths did not seem to show any regular trend. It is interesting to note that the OH band intensity in substituted phenols also shows a similar behavior (8, 9). Since the band intensity of a stretching vibration is directly related to the electrical properties of the particular bond in question (i.e. bond moment and its direction), it appears reasonable that the prominent resonance structures in phenols (I) and in anisoles (II) should be similar:



I



II

The OH stretching frequency in *p*-substituted phenols (unlike the C–O–C stretching frequency in *p*-substituted anisoles) decreases with the increasing electron-withdrawing ability of the *p*-substituent. Of course, it is true that if two functional groups show similar trends of the band intensities with the reactivity constants, it does not follow that the trends of the frequencies will be similar.

ACKNOWLEDGMENT

The authors wish to thank Professor Herbert C. Brown for his kind encouragement.

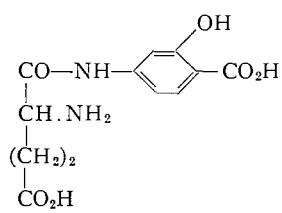
1. Rao, C. N. R. and Silverman, G. B. Current Sci. India, **26**, 375 (1957), and the references listed there.
2. Brown, T. L. Chem. Revs. **58**, 581 (1958).
3. Thompson, H. W. and James, D. A. Spectrochim. Acta, **13**, 236 (1958).
4. Krueger, P. J. and Thompson, H. W. Proc. Roy. Soc. London, A, **250**, 22 (1959).
5. Russell, R. A. and Thompson, H. W. J. Chem. Soc. 479 (1955).
6. Jones, R. N. and Sandorfy, C. *In* Chemical applications of spectroscopy. *Edited by* A. Weissberger. Interscience Publishers, Inc., New York. 1956.
7. Brown, H. C. and Okamoto, Y. J. Am. Chem. Soc. **80**, 4979 (1958).
8. Brown, T. L. J. Phys. Chem. **61**, 820 (1957).
9. Stone, P. J. and Thompson, H. W. Spectrochim. Acta, **10**, 17 (1957).

Received September 8, 1959.
Department of Chemistry,
Purdue University,
West Lafayette, Indiana, U.S.A.

DERIVATIVES OF *p*-AMINOSALICYLIC ACID

M. H. Fisher and T. F. Massiah

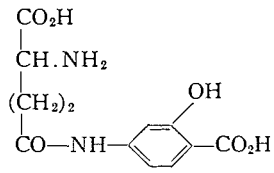
Darrach and Polglase (1) have described the preparation of N-(α-L-glutamyl)-*p*-aminosalicylic acid (I). They claim that it is a useful antituberculous drug and that it does not cause the toxic side effects associated with *p*-aminosalicylic acid itself. This report



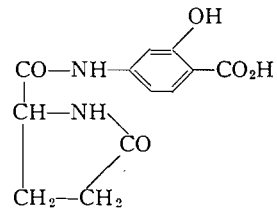
(I)

Can. J. Chem. Downloaded from www.nrcresearchpress.com by 41.223.56.140 on 09/04/12
For personal use only.

describes the synthesis of N-(γ-DL-glutamyl)-*p*-aminosalicylic acid (II) and N-(L-pyroglutamyl)-*p*-aminosalicylic acid (III). The γ-compound (II) was prepared by treatment



(II)



(III)

of *p*-aminosalicylic acid with N-phthalyl-DL-glutamic anhydride (2), followed by hydrolysis of the intermediate with hydrazine. The reaction of phthalylglutamic anhydride with amines was known to give γ-derivatives (2) and additional evidence for this structure was furnished by the formation of a thiohydantoin when the product was warmed with ammonium thiocyanate and acetic anhydride (3).

The pyroglutamyl-derivative (III) was prepared either by treatment of *p*-aminosalicylic acid with L-pyroglutamyl chloride or by dehydration of N-(α-L-glutamyl)-*p*-aminosalicylic acid when heated above its melting point. Alkaline hydrolysis under a variety of conditions always resulted in cleavage of the side chain amide in preference to the cyclic amide linkage.

EXPERIMENTAL

N-(N-*Phthalyl*-γ-DL-*glutamyl*)-*p*-*aminosalicylic Acid*

A suspension of N-phthalyl-DL-glutamic anhydride (110 g) and *p*-aminosalicylic acid (65 g) in ethyl acetate (2 l.) was stirred at room temperature for 24 hours. The reactants slowly dissolved and then the product separated (120 g) m.p. 227–228° (decomp.). Crystallization from ethyl acetate yielded white needles, m.p. 229° (decomp.). Anal. Calc. for $C_{20}H_{16}N_2O_8$: C, 58.3; H, 3.9; N, 6.8. Found: C, 58.0; H, 4.0; N, 6.7.

N-(γ-DL-*Glutamyl*)-*p*-*aminosalicylic Acid* (II)

N-(N-Phthalyl-γ-DL-glutamyl)-*p*-aminosalicylic acid (41.2 g) in 1 *N* hydrazine hydrate (200 cc) was refluxed for 30 minutes and then cooled. Phthalyl hydrazide was filtered off and the filtrate evaporated to dryness under reduced pressure. The white residue which remained was crystallized from aqueous ethanol yielding the hydrazinium salt of the product (16 g), m.p. 172° (decomp.). Anal. Calc. for $C_{12}H_{18}N_4O_6$: C, 45.9; H, 5.8; N, 17.8. Found: C, 45.9; H, 5.7; N, 17.6.

The salt was treated with 1 equivalent of hydrochloric acid to yield the desired product, m.p. 225° (decomp.). Anal. Calc. for $C_{12}H_{14}N_2O_6$: C, 51.1; H, 5.0; N, 9.9. Found: C, 51.2; H, 5.1; N, 9.9.

1-Acetyl-2-thiohydantoyl-5-β-(3-acetoxy-4-carboxypropionanilide)

A mixture of N-(γ-DL-glutamyl)-*p*-aminosalicylic acid (1 g), ammonium thiocyanate (0.3 g), acetic anhydride (10 cc), and glacial acetic acid (1 cc) was warmed on a hot plate for ½ hour until a clear solution was obtained, and then evaporated under reduced pressure. The residual gum solidified after it was rubbed with water and a little ethanol. Two crystallizations from aqueous ethanol yielded white needles (0.3 g), m.p. 190° (decomp.). Anal. Calc. for $C_{17}H_{17}N_3O_7S$: C, 50.1; H, 4.2; N, 10.3; S, 7.8. Found: C, 49.5; H, 4.2; N, 10.1; S, 7.4.

Can. J. Chem. Downloaded from www.nrcresearchpress.com by 41.223.56.140 on 09/04/12
For personal use only.

N-(L-*Pyroglutamyl*)-*p-aminosalicylic Acid* (III)

(*a*) L-Pyroglutamic acid (38.7 g) was added to thionyl chloride (65 cc) and the mixture stirred at room temperature for 5 hours. The excess of thionyl chloride was evaporated under reduced pressure. Dry benzene was added to the residue and then evaporated under reduced pressure to remove the last traces of thionyl chloride. The crude acid chloride was dissolved in tetrahydrofuran (150 cc) and slowly added to a stirred suspension of *p*-aminosalicylic acid (45.9 g) in tetrahydrofuran (150 cc). The mixture was stirred at room temperature for 18 hours, and then the product (76.7 g) was filtered off. Purified material, m.p. 237–238° (decomp.) was obtained by dissolution in aqueous sodium bicarbonate, carbon treatment, and precipitation with hydrochloric acid. Crystallization from water yielded white needles, m.p. 242°–244° (decomp.). Anal. Calc. for $C_{12}H_{12}N_2O_5$: C, 54.6; H, 4.6; N, 10.6. Found: C, 54.7; H, 4.6; N, 10.4. $[\alpha]_D^{21}$ −7.5° (*c*, 5.0 in water).

(*b*) N-(α-L-Glutamyl)-*p*-aminosalicylic acid (4.3 g) was heated at 170° for 4 hours in an oil bath. The starting material melted at 160° and then resolidified. Crystallization from water yielded white needles (1.1 g), m.p. 242–243° (decomp.). The melting point was not depressed by admixture with the product from preparation (*a*).

1. DARRACH, M. and POLGLASE, W. J. Federation Proc. **18**, 303 (1959).
2. KING, F. E. and KIDD, D. A. A. J. Chem. Soc. 3315 (1949).
3. SWAN, J. M. Australian J. Sci. Research, A, **5**, 721 (1952).

RECEIVED SEPTEMBER 25, 1959.
RESEARCH DEPARTMENT,
MERCK & CO. LIMITED,
P.O. BOX 899,
MONTREAL 3, QUEBEC.

6-*O*-ETHYL-D-GALACTOSE

G. G. MCKEOWN AND L. D. HAYWARD

In connection with some other work 6-*O*-ethyl-D-galactose was prepared as a sirup by ethylation of 1,2;3,4-di-*O*-isopropylidene-D-galactose followed by dilute acid hydrolysis of the isopropylidene groups. After standing for more than a year at room temperature this new sugar derivative crystallized and the opportunity was taken to record its melting point, equilibrium specific rotation, paper chromatographic behavior, and infrared spectrum.

The 6-*O*-ethyl-D-galactose appeared as a distinct, brown, non-fluorescent spot on paper chromatograms sprayed with *p*-anisidine hydrochloride reagent. This behavior appeared to be characteristic of 6-*O*-alkyl derivatives of galactose since it was shown by 6-*O*-methyl-D-galactose but not by the mono-1,2,3, or 4-*O*-methyl ethers (1). In the glucopyranose series the 2- and 6-mono-*O*-methyl ethers showed this same color reaction which was also distinct from the behavior of the 3- and 4-*O*-methyl compounds (2).

EXPERIMENTAL

Paper chromatograms were prepared with 1-butanol–ethanol–water (5:1:4 v/v) and were sprayed with *p*-anisidine hydrochloride reagent.

*6-O-Ethyl-1,2;3,4-di-O-isopropylidene-*D*-galactose*

Diacetone-D-galactose (1,2;3,4-di-*O*-isopropylidene-D-galactopyranose) was prepared from D-galactose in 34% yield (3), $[\alpha]_D^{20}$ −55.0° (*c*, 6.66 in chloroform) and gave a single

Can. J. Chem. Downloaded from www.nrcresearchpress.com by 41.223.56.140 on 09/04/12
For personal use only.

N-(L-*Pyroglutamyl*)-*p-aminosalicylic Acid* (III)

(*a*) L-Pyroglutamic acid (38.7 g) was added to thionyl chloride (65 cc) and the mixture stirred at room temperature for 5 hours. The excess of thionyl chloride was evaporated under reduced pressure. Dry benzene was added to the residue and then evaporated under reduced pressure to remove the last traces of thionyl chloride. The crude acid chloride was dissolved in tetrahydrofuran (150 cc) and slowly added to a stirred suspension of *p*-aminosalicylic acid (45.9 g) in tetrahydrofuran (150 cc). The mixture was stirred at room temperature for 18 hours, and then the product (76.7 g) was filtered off. Purified material, m.p. 237–238° (decomp.) was obtained by dissolution in aqueous sodium bicarbonate, carbon treatment, and precipitation with hydrochloric acid. Crystallization from water yielded white needles, m.p. 242°–244° (decomp.). Anal. Calc. for $C_{12}H_{12}N_2O_5$: C, 54.6; H, 4.6; N, 10.6. Found: C, 54.7; H, 4.6; N, 10.4. $[\alpha]_D^{21}$ −7.5° (*c*, 5.0 in water).

(*b*) N-(α-L-Glutamyl)-*p*-aminosalicylic acid (4.3 g) was heated at 170° for 4 hours in an oil bath. The starting material melted at 160° and then resolidified. Crystallization from water yielded white needles (1.1 g), m.p. 242–243° (decomp.). The melting point was not depressed by admixture with the product from preparation (*a*).

1. DARRACH, M. and POLGLASE, W. J. Federation Proc. **18**, 303 (1959).
2. KING, F. E. and KIDD, D. A. A. J. Chem. Soc. 3315 (1949).
3. SWAN, J. M. Australian J. Sci. Research, A, **5**, 721 (1952).

RECEIVED SEPTEMBER 25, 1959.
RESEARCH DEPARTMENT,
MERCK & CO. LIMITED,
P.O. BOX 899,
MONTREAL 3, QUEBEC.

6-*O*-ETHYL-D-GALACTOSE

G. G. MCKEOWN AND L. D. HAYWARD

In connection with some other work 6-*O*-ethyl-D-galactose was prepared as a sirup by ethylation of 1,2;3,4-di-*O*-isopropylidene-D-galactose followed by dilute acid hydrolysis of the isopropylidene groups. After standing for more than a year at room temperature this new sugar derivative crystallized and the opportunity was taken to record its melting point, equilibrium specific rotation, paper chromatographic behavior, and infrared spectrum.

The 6-*O*-ethyl-D-galactose appeared as a distinct, brown, non-fluorescent spot on paper chromatograms sprayed with *p*-anisidine hydrochloride reagent. This behavior appeared to be characteristic of 6-*O*-alkyl derivatives of galactose since it was shown by 6-*O*-methyl-D-galactose but not by the mono-1,2,3, or 4-*O*-methyl ethers (1). In the glucopyranose series the 2- and 6-mono-*O*-methyl ethers showed this same color reaction which was also distinct from the behavior of the 3- and 4-*O*-methyl compounds (2).

EXPERIMENTAL

Paper chromatograms were prepared with 1-butanol–ethanol–water (5:1:4 v/v) and were sprayed with *p*-anisidine hydrochloride reagent.

*6-O-Ethyl-1,2;3,4-di-O-isopropylidene-*D*-galactose*

Diacetone-D-galactose (1,2;3,4-di-*O*-isopropylidene-D-galactopyranose) was prepared from D-galactose in 34% yield (3), $[\alpha]_D^{20}$ −55.0° (*c*, 6.66 in chloroform) and gave a single

Can. J. Chem. Downloaded from www.nrcresearchpress.com by 69.46.99.164 on 09/04/12
For personal use only.

yellow spot, R_f 0.88, on a paper chromatogram. A mixture of diacetone-D-galactose (5.04 g), acetone (10 ml), water (25 ml), and sodium hydroxide pellets (10 g) was heated to 55° C with vigorous stirring, and diethyl sulphate (13 ml) was added dropwise over a period of 45 minutes. The mixture was then heated at 85° C for 1 hour, cooled, and extracted with chloroform. The chloroform extract was dried (anhydrous sodium carbonate) and evaporated and the residue was distilled under reduced pressure from sodium carbonate (yield, 3.68 g, 66%). Hydrolysis of a sample with boiling 70% acetic acid and paper chromatography of the hydrolyzate showed that the sirupy distillate contained some unreacted diacetone-D-galactose. The developed chromatogram had a distinct, brown, non-fluorescent spot, R_f 0.40, for 6-*O*-ethyl-D-galactose plus a faint, yellow-brown, fluorescent spot, R_f 0.11, which corresponded to D-galactose. The sirup was redistilled from sodium hydroxide (b.p. 101–103° C at 0.2 mm) to give 2.63 g of a colorless product, $[\alpha]_D^{27}$ −57.6° (*c*, 4.90 in ethanol), which failed to crystallize.

6-O-Ethyl-D-galactose

6-*O*-Ethyl-1,2;3,4-di-*O*-isopropylidene-D-galactopyranose (783 mg) was dissolved in 80% acetic acid (10 ml) and heated on a steam bath for 15 hours. The hydrolyzate was evaporated to dryness *in vacuo* and the residue was refluxed with water (10 ml) for 5 hours to reverse any acetate formation. A chromatogram showed a trace of D-galactose in the product which was removed by passage through a cellulose column developed with butanol–water. The appropriate fractions when combined yielded a colorless glass (358 mg, 63.3%) which crystallized in pentagonal plates after standing at room temperature for 15 months. The reducing sugar derivative was recrystallized from anhydrous ethyl acetate to a constant melting point (104.5–105.0° C); $[\alpha]_D^{27}$ +88.6° (23 minutes) changing to +69.0° (constant at 148 minutes) (*c*, 2.10 in water). Anal. Calc. for $C_8H_{16}O_6$: C, 46.1; H, 7.7; OC_2H_5, 21.6%. Found: C, 45.8; H, 7.5; OC_2H_5, 21.8%.* The infrared spectrum of the compound (potassium bromide window) exhibited absorption maxima at the following frequencies (cm^{-1}): 3430, 2900, 1635, 1390, 1240, 1100, 970, 830, 800, 775.

We thank the National Research Council of Canada and the Sugar Research Foundation, New York, for research grants.

1. BOUVENG, H. and LINDBERG, B. Acta Chem. Scand. **10**, 1283 (1956).
2. MCKEOWN, G. G., SERENIUS, R. S. E., and HAYWARD, L. D. Can. J. Chem. **35**, 28 (1957).
3. VAN GRUNENBERG, H., BREDT, C., and FREUDENBERG, W. J. Am. Chem. Soc. **60**, 1507 (1938).

RECEIVED AUGUST 4, 1959.
DEPARTMENT OF CHEMISTRY,
UNIVERSITY OF BRITISH COLUMBIA,
VANCOUVER, B.C.

**Microanalyses by A. Bernhardt, Kaiser Wilhelm Platz, Mulheim (Ruhr), Germany.*

Can. J. Chem. Downloaded from www.nrcresearchpress.com by 69.46.99.164 on 09/04/12
For personal use only.

Can. J. Chem. Downloaded from www.nrcresearchpress.com by 69.46.99.164 on 09/04/12
For personal use only.

Canadian Journal of Chemistry

Issued by THE NATIONAL RESEARCH COUNCIL OF CANADA

VOLUME 38 FEBRUARY 1960 NUMBER 2

THE CHEMICAL COMPOSITION OF THE HEARTWOOD EXTRACTIVES OF LARIX LYALLII PARL.[1]

G. V. NAIR[2] AND E. VON RUDLOFF

ABSTRACT

The heartwood of Canadian Alpine larch was found to contain 4.8% acetone-soluble material. From this extract taxifolin and aromadendrin were isolated in 26% and 17% yield, as well as conidendrin in a small amount. About one-quarter of the extract was composed of esters of phthalic, ferulic, and fatty acids. After saponification β-sitosterol, nonan-2-ol, phthalic acid, and a mixture of fatty acids were isolated. Gas–liquid chromatography indicated the presence of palmitic, an unidentified C_{16}, stearic, oleic, linoleic, linolenic, an unidentified C_{20} acid, and two unidentified alcohols.

Recently we have reported on the chemical composition of the heartwood extractives of *Larix laricina* (Du Roi) K. Koch (tamarack) (1). This paper deals with the results obtained with a similar extract of another Canadian larch species, *L. lyallii Parl.* (alpine larch). This medium-sized tree is found in the high mountains of Western Canada, usually at an altitude of 5000 to 6000 feet. Botanical sources do not mention any particular resistance to decay of this wood, nor has it found any extensive commercial use. Acetone extraction of the heartwood of a mature tree from the Minnewanka district, Banff National Park, Alberta, gave a yield of about 4.8% soluble extractives. The fractionation scheme and yields of the various compounds isolated are shown in Fig. 1.

The two flavanonols (nomenclature (2)), taxifolin and aromadendrin, were isolated in 1.25% and 0.82% yield respectively (based on the dry weight of the wood). Thus, *L. lyallii* is an excellent source for these two compounds, especially so for the less common aromadendrin. Both flavanonols have previously been found in *L. decidua*, *L. leptolepis*, and *L. occidentalis* (3, 4, 5*a*, 5*b*), and Gripenberg (3) has shown that the distylin of *L. kaempferi* (5, 6) is a mixture of these two compounds. The isolation of these two flavanonols in the Canadian larch species *L. lyallii* and *L. laricina* (1) provides additional support to Erdtman's hypothesis (7) that closely related species of conifers have certain characteristic heartwood constituents in common, irrespective of geography, which are therefore of value in taxonomic classifications.

A small amount of conidendrin (0.03%) was also isolated. This lignan is widespread amongst conifers and other plants (2, 7) but has not previously been found in the wood of larches. The lignan lariciresinol has been isolated from the resin produced by *L. decidua* (7, 8).

About one-fourth of the extract of *L. lyallii* was found to consist of β-sitosterol, nonan-2-ol, and unidentified alcohols esterified with phthalic, ferulic, and a complex mixture of

[1]*Manuscript received October 5, 1959.*
Contribution from the National Research Council of Canada, Prairie Regional Laboratory, Saskatoon, Saskatchewan.
Issued as N.R.C. No. 5466.
[2]*National Research Council of Canada Postdoctorate Fellow 1958–60.*

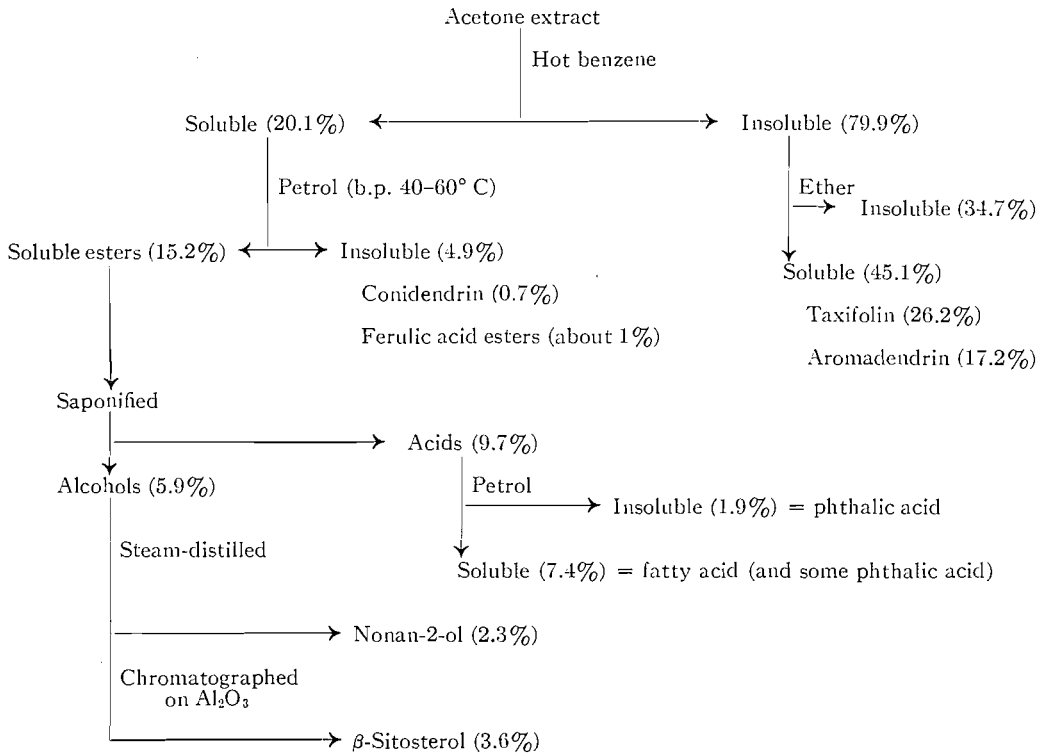


FIG. 1. Fractionation scheme and yields of components (based on the dry weight of acetone extract).

fatty acids. A mixture of esters composed of ferulic acid, nonan-2-ol, and an unknown alcohol of similar molecular weight was isolated from the petrol-insoluble portion (see Fig. 1). It hydrolyzed with difficulty, causing considerable degradation of the ferulic acid moiety, and its infrared absorption spectrum was similar to that of the eicosanyl ferulate isolated from the heartwood of *L. laricina* (1). The non-saponifiable portion was composed of a mixture of alcohols which failed to crystallize and which could not be resolved by distillation. Gas–liquid partition chromatography (GLPC) showed two peaks of about equal intensity corresponding to nonan-2-ol and an unidentified alcohol in the C_9-to-C_{10} region. Higher alcohols appeared to be absent.

The petrol-soluble esters were saponified and, from the resulting mixture of acids, phthalic acid was isolated by crystallization. The presence of phthalic acid in *L. lyallii* and *L. laricina* is noteworthy, since this aromatic acid is found only rarely in nature (1, 9, 10). The residual acid mixture was resolved by GLPC and peaks corresponding to palmitic, oleic, linoleic, phthalic, linolenic, and unidentified C_{16} and C_{20} acids were obtained. From the non-saponifiable portion, nonan-2-ol was obtained by steam distillation and β-sitosterol by chromatography on neutral alumina and crystallization. GLPC of the total non-saponifiable portion gave a major peak corresponding to nonan-2-ol and two minor peaks in the C_9-to-C_{10} and C_{16} region.

The extract contained no resin acids nor neutral terpenoid compounds, and differed from that of *L. laricina* in that free sugars and eicosanol were absent.

EXPERIMENTAL

Melting points were obtained with a Leitz hot stage microscope. All known compounds

Can. J. Chem. Downloaded from www.nrcresearchpress.com by 69.46.99.164 on 09/04/12
For personal use only.

Can. J. Chem. Downloaded from www.nrcresearchpress.com by 69.46.99.164 on 09/04/12
For personal use only.

were identified by mixed melting point and by comparing infrared spectra with those of authentic samples. Infrared spectra were recorded on a Perkin–Elmer model 21 double beam recording spectrophotometer, using the KBr disk method or the film technique. Gas–liquid partition chromatograms were obtained with a Beckman GC 2 chromatograph on $\frac{1}{4}$-inch columns of either washed silicone (11) or polyester (12) on C-22 firebrick, unless otherwise indicated.

Extraction of the Wood

The air-dried, milled wood (3.9 kg) (moisture content about 4.5%) was extracted with acetone in a Soxhlet extractor for 36 hours. The acetone extract was reduced to dryness in a rotary evaporator at about 50° C giving dark brown viscous material. The crude concentrated extract was dried *in vacuo* for several hours and then re-extracted with dry acetone and filtered. The filtrate was concentrated and dried as above to yield 178 g of acetone-soluble material (4.8% yield, based on the dry weight of the wood).

Preliminary color tests on the crude extract for flavanonols were positive, but precipitation tests with digitonin for sterols and cyclohexylamine for resin acids were negative. Paper chromatography (with impregnated paper (13), using petrol (b.p. 40–60° C) as the mobile phase and diazotized benzidine spray) provided no evidence for tropolones. Gripenberg's (3) chromatographic technique on paper using chloroform:ethanol:water (8:2:1, v/v) with addition of 2% acetic acid (1) showed spots corresponding to taxifolin and aromadendrin. A portion of the extract, after saponification, showed the presence of sterols, volatile constituents, and fatty acids, but no resin acids.

Separation of the Constituents

The crude extract (10.55 g) was triturated with hot benzene and filtered. The benzene-soluble matter (2.18 g) was further separated into petrol-soluble (b.p. 40–60° C) (1.65 g) and -insoluble (0.53 g) portions. The benzene-insoluble matter (8.6 g) was extracted with ether to yield 4.9 g of a phenolic mixture. The residue was ethanol-soluble and failed to yield crystalline material.

Isolation and Identification of Taxifolin and Aromadendrin

The ethereal extract of the benzene-insoluble portion was soluble in alkali but insoluble in bicarbonate. A paper chromatogram, using chloroform:ethanol:water (8:2:1 v/v) containing 2% acetic acid to prevent tailing (1), showed spots corresponding to aromadendrin (R_f 0.8) and taxifolin (R_f 0.6) when sprayed with bis-diazotized benzidine (14). The mixture (2.27 g) was resolved on a cellulose powder column (50×4.5 cm) using the same solvent mixture as eluent. Fractions of 20 ml were collected and tested individually by paper chromatography. Tubes 1–20 contained aromadendrin (0.44 g), m.p. 236–237° C (from chloroform), $[\alpha]_D^{25.4}$ +44.5 (*c*, 0.21; acetone–water) and tubes 41–153 gave taxifolin (0.89 g), m.p. 238–240° C (from water), $[\alpha]_D^{25.4}$ +45.21 (*c*, 0.11; water–acetone). Tubes 30–41 (0.845 g) contained about equal quantities of aromadendrin and taxifolin, bringing the over-all yield to about 17% and 26% respectively.

Isolation and Identification of Conidendrin and Ferulic Esters

The benzene-soluble portion (2.18 g) was evaporated to dryness and triturated with cold petrol (b.p. 40–60° C). The powdery, insoluble residue was filtered off, washed thoroughly with cold petrol, and dried. The crude product was crystallized from ethanol to give conidendrin (0.073 g), m.p. 238–239° C (lit. 255–256° C and 238° C (15)); $[\alpha]_D^{25.4}$ −59.43 (*c*, 1.1, acetone). It gave a green coloration with aqueous ferric chloride. Found: C, 67.08%; H, 5.95%. Calculated for $C_{20}H_{20}O_6$: C, 67.40; H, 5.66%. The mother liquor was chromatographed on a column of neutral alumina (M. Woelm, Eschwege,

activity grade I). Elution with ether produced a small amount of a mixture of fatty acid esters (infrared spectrum). When elution was continued with mixtures of petrol–ethanol (1:1 v/v) and benzene–ethanol (1:1 v/v) a liquid fraction was obtained, which had a well-defined infrared absorption spectrum which was similar to those of ferulic acid esters. The intensity of the C—H absorption in the 3000 to 2800 cm^{-1} region was relatively weaker than that for eicosanyl ferulate, but considerably stronger than that for methyl ferulate, indicating that the aliphatic chain of the alcohol moiety was of intermediate length. The material was hydrolyzed under reflux in a 2 *N* solution of potassium hydroxide in ethylene glycol monomethyl ether. Ferulic acid was identified in the saponifiable portion by paper chromatography. Attempts to crystallize the acid failed due to the presence of a considerable amount of degradation products. The non-saponifiable portion failed to yield a pure compound on distillation and crystallization attempts. GLPC on a polyethylene glycol column at 160° C gave two peaks of about equal area with retention times corresponding to nonan-2-ol and a C_9-to-C_{10} alcohol. Washing the column of neutral alumina with alcohol produced a small amount of conidendrin.

Petrol Extract

The petrol-soluble portion (1.65 g) was saponified under reflux with potassium hydroxide (3.4 g) in ethyleneglycol monomethyl ether (30 ml) for 3 hours. The reaction mixture was reduced in volume and worked up in the usual manner to give the non-saponifiable (0.64 g) and saponifiable (1.005 g) portions.

The non-saponifiable portion was steam-distilled and the distillate (1 liter) was saturated with sodium chloride and extracted thrice with ether. The ether extract was dried over Drierite and the solvent was distilled off to yield 0.25 g (2.3%) of a sweet-smelling, colorless liquid alcohol, b.p. 81–83° C at 15 mm, n_D^{25} 1.4390. The retention time of this alcohol on gas chromatograms was identical with that of nonan-2-ol. The non-volatile residue was extracted with ether and the ethereal solution evaporated after drying to give 0.4 g of a semisolid residue. This was chromatographed on a column of neutral alumina and eluted first with a 1:1 mixture of petrol (b.p. 40–60° C) and ether to yield a trace of unsaponified esters of fatty acid. Elution with a 1:1 mixture of ethanol–ether gave 0.39 g (3.6%) of a steroid material (positive Liebermann–Buchard reaction). Crystallization from alcohol gave β-sitosterol, having m.p. 136–137°.

Acid Mixture

The thoroughly dried acidic residue obtained after saponification of the esters was triturated with warm petrol (b.p. 40–60° C) and filtered. The petrol-insoluble portion (0.2 g, 1.9%) was crystallized from acetone, and gave phthalic acid, m.p. 201–202° C. The petrol-soluble portion (0.8 g, 7.6%) was re-esterified with diazomethane, and the methyl esters were analyzed by GLPC using the polyester column. Peaks corresponding to the following acids (in order of their retention times) were obtained: palmitic (5.9%); an unidentified C_{16} (5.7%); stearic (1.5%); oleic (18.2%); linoleic (34.7%); phthalic (22.1%); linolenic (3.4%); and an unidentified C_{20} acid (5.5%). The percentage composition was obtained by determining the area under the curve of each peak by the triangulation method.

ACKNOWLEDGMENTS

The authors wish to express their gratitude to Mr. M. Granat for technical assistance, to Mr. M. Mazurek for the microanalyses, and to Miss I. M. Gaffney for the infrared spectra. We also wish to thank Professor H. Erdtman for authentic samples of flavanonols

Can. J. Chem. Downloaded from www.nrcresearchpress.com by 69.46.99.164 on 09/04/12
For personal use only.

and conidendrin, and Dr. J. C. Hopkins and Mr. E. Stenton for obtaining the alpine larch wood.

REFERENCES

1. NAIR, G. V. and RUDLOFF, E. VON. Can. J. Chem. **37**, 1608 (1959).
2. ERDTMAN, H. *In* Perspectives in organic chemistry. *Edited by* A. Todd. Interscience Publishers, Inc., New York. 1956. p. 453.
3. GRIPENBERG, J. Acta Chem. Scand. **6**, 1153 (1952).
4. BREWERTON, H. V. New Zealand J. Sci. Technol. B, **37**, 626 (1956).
5. (*a*) HASEGAWA, M. and SHIRATO, T. J. Chem. Soc. Japan, **72**, 223 (1951). (*b*) BARTON, G. M. and GARDNER, J. A. F. Anal. Chem. **30**, 279 (1958).
6. MIGITA, N., NAKANO, J., and TOROI, T. J. Japan Tech. Assoc. Pulp Paper Ind. **5**, 399 (1951); Chem. Abstr. **46**, 1254*g* (1952).
7. ERDTMAN, H. *In* Progress in organic chemistry. Vol. 1. *Edited by* J. W. Cook. Butterworth Scientific Publications, London. 1952. pp. 22–63.
8. BAMBERGER, M. and LANDSIEDL, A. Monatsh. **18**, 481 (1897); **20**, 647, 755 (1899).
9. HAAGEN-SMIT, A. J., HIROSAWA, F. N., and WANG, T. H. Food Research, **14**, 472 (1949).
10. KOHLBRENNER, P. J. and SCHUERCH, C. J. Org. Chem. **24**, 166 (1959).
11. CRAIG, B. M. and MURTY, N. L. Can. J. Chem. **36**, 1297 (1958).
12. CRAIG, B. M. and MURTY, N. L. J. Am. Oil Chemists' Soc. **36**, 549 (1959).
13. WACHTMEISTER, C. A. and WICKBERG, B. Acta Chem. Scand. **12**, 1335 (1958).
14. LINDSTEDT, G. Acta Chem. Scand. **4**, 448 (1950).
15. PEARL, I. A. J. Org. Chem. **10**, 219 (1945).

Can. J. Chem. Downloaded from www.nrcresearchpress.com by 69.46.99.164 on 09/04/12
For personal use only.

Can. J. Chem. Downloaded from www.nrcresearchpress.com by 41.223.56.140 on 09/04/12
For personal use only.

THE ACTIVATION ENERGY FOR THE RECOMBINATION OF TRIFLUOROMETHYL RADICALS[1]

G. O. PRITCHARD[2] AND J. R. DACEY

ABSTRACT

By photolyzing mixtures of acetone and hexafluoroacetone, and measuring the rates of formation of the three ethanes, we have found $E_1 - \frac{1}{2}E_2 - \frac{1}{2}E_3 = -1070 \pm 100$ cal, which means that the activation energy for the recombination of CF_3 radicals is 2140 ± 200 cal, assuming zero activation energies for the other two radical recombinations, and that none of the ethanes is formed except by radical recombination.

INTRODUCTION

Although Ayscough (1) has shown that CF_3 radicals recombine on nearly every collision with a rate almost identical with that found for CH_3 radicals, he was unable to determine whether the recombination was temperature dependent or not. This problem is of theoretical interest since it has been suggested that due to the marked polarity of the C—F bond a potential barrier to CF_3 radical combination could exist, with a consequent small positive activation energy for the reaction (2). There is no such restriction for the recombination of simple alkyl radicals, and they are assumed to recombine with zero activation energy.

We have photolyzed mixtures of acetone and hexafluoroacetone over a temperature range from 29° to 169° C to see if we could detect any variation in the relative rates of formation of the three ethanes with temperature. Writing these rates as $R_{CH_3CF_3}$, $R_{C_2H_6}$, and $R_{C_2F_6}$ for the reactions

$$CH_3 + CF_3 \xrightarrow{k_1} CH_3CF_3 \qquad [1]$$

$$CH_3 + CH_3 \xrightarrow{k_2} C_2H_6 \qquad [2]$$

and

$$CF_3 + CF_3 \xrightarrow{k_3} C_2F_6, \qquad [3]$$

and assuming the activation energies for reactions [1] and [2] to be zero, i.e. $E_1 = E_2 = 0$, any variation in the ratio $R_{CF_3CH_3}/R^{\frac{1}{2}}_{C_2H_6} R^{\frac{1}{2}}_{C_2F_6} = k_1/k_2^{\frac{1}{2}}k_3^{\frac{1}{2}}$ (for steady-state conditions) will be caused by $E_3 \neq 0$, provided the above reactions are the only source of the ethanes in the system. (If $E_1 = E_2 = E_3$, and the steric factors for the three reactions are identical, the ratio reduces to 2.30, assuming $\sigma_{CH_3} = 3.5$ Å and $\sigma_{CF_3} = 4.0$ Å.)

EXPERIMENTAL

Hexafluoroacetone was obtained from the Merck Chemical Company as the hydrate. It was dehydrated with P_2O_5 and purified by low temperature fractionation. The acetone used was A.R. grade; it also was thoroughly dried and outgassed.

Mixtures of the ketones were photolyzed in the more or less standard high vacuum apparatus for experiments of this type. The light source was a B.T.H. high pressure lamp (ME/D, 250 watts), operated at constant intensity over the time of a run. The light beam was collimated by a single quartz lens and a stop. No filtering system, which would

[1]*Manuscript received August 31, 1959.*
Contribution from the Royal Military College of Canada, Department of Chemistry, Kingston, Ontario.
[2]*Present address: Department of Chemistry, University of California at Santa Barbara, Goleta, California.*

Can. J. Chem. Downloaded from www.nrcresearchpress.com by 41.223.56.140 on 09/04/12
For personal use only.

have reduced the light intensity considerably, was employed to isolate the 3130 Å radiation. With this arrangement it was found that convenient quantities of the ethanes were produced. The 175-cc cylindrical quartz reaction vessel was mounted in a furnace the temperature of which was held within ±1.5° C of the desired temperature.

Analysis of the reaction products was by low temperature fractionation, using a solid nitrogen trap and two Ward–LeRoy stills, a small Hg diffusion pump, and a combined Toepler pump and gas buret. CO and CH_4 were pumped off at −210° C. The C_2H_6, C_2F_6, and CF_3H were collected with the stills carefully regulated at −161° and −156° C respectively whilst the system was pumped in intermittent bursts of about 5 seconds in duration until a constant pressure of 10^{-3} mm Hg was obtained. After measurement, this mixture was analyzed mass spectrographically. (Reference gases were obtained commercially and purified if necessary.) The amount of CF_3CH_3 carried over using this technique was found to be less than 2% of the sample, although CO_2 was found to be present as well. The remainder of the reaction mixture was condensed in a tube containing carefully outgassed distilled water. The contents were allowed to warm up to room temperature, and shaken vigorously. The CF_3CH_3 was then distilled off at −130° C. This procedure removed all the CF_3COCF_3, which would otherwise contaminate the CF_3CH_3 samples. Trial experiments proved this method to be quantitative. Pure CF_3CH_3 was prepared by the reaction of SbF_3 on CH_3CCl_3 in a sealed bomb (3); this also served as a mass spectrometer standard. Mass spectrographic analysis of the CF_3CH_3 samples showed that they were essentially pure, but they also contained some CO_2.

RESULTS

The relevant data is collected in Table I. The quantities of CO_2 are the total amounts found; this was usually evenly divided between the two samples. They represent a 1%

TABLE I

Pressure reactants cm_{Hg} and moles of product $\times 10^6$

Run	Time (min)	Temp. (° C)	CH_3COCH_3	CF_3COCF_3	C_2F_6	C_2H_6	CF_3H	CF_3CH_3	CO_2	$\frac{k_1}{k_2^{\frac{1}{2}}k_3^{\frac{1}{2}}}$	$\frac{k_4}{k_3^{\frac{1}{2}}}$ (mole/cc)
1	120	29	9.30	5.05	4.76	3.09	1.56	13.1	1.79	3.46	0.127
2	60	30	6.90	6.80	5.22	2.34	0.864	8.92	1.50	2.55	0.129
3	60	30	13.10	8.90	3.48	1.27	1.41	6.80	2.84	3.23	0.135
4	60	30	7.85	6.25	4.87	2.35	1.81	9.60	1.96	2.84	0.245
5	70	89	10.95	6.20	40.1	4.18	22.2	29.2	5.35	2.26	0.845
6	60	89	13.30	4.70	30.2	5.83	18.6	29.2	3.55	2.20	0.715
7	70	96	8.05	8.15	73.2	2.87	20.0	31.2	1.27	2.16	0.765
8	70	129	10.10	5.45	61.3	17.8	63.9	71.0	3.41	2.15	2.34
9	15	169	10.15	5.45	49.9	2.29	56.3	18.9	0.66	1.77	5.43

CO_2 impurity in the hexafluoroacetone (detected in the mass spectrometer), but repeated treatment of the ketones with slaked lime failed to eliminate CO_2 altogether. The other volatile products, CO and CH_4, are not included in the table.

Assuming steady-state conditions, $R_{CF_3CH_3}/R^{\frac{1}{2}}_{C_2H_6}\ R^{\frac{1}{2}}_{C_2F_6} = k_1/k_2^{\frac{1}{2}}k_3^{\frac{1}{2}}$. An Arrhenius plot of the data is given in Fig. 1. A least squares treatment results in $(E_1 - \frac{1}{2}E_2 - \frac{1}{2}E_3) = -(1070 \pm 100)$ cal with the pre-exponential ratio $A_1/A_2^{\frac{1}{2}}A_3^{\frac{1}{2}} = 0.52 \pm 0.06$. Assuming $E_1 = E_2 = 0$, we have $E_3 = 2140 \pm 200$ cal. On the same graph are some identical measurements obtained by Sieger and Calvert (4) from the photolysis of CH_3COCF_3. They, however, consider these results to be unreliable, mainly due to the extremely small amounts of C_2F_6 which were obtained in the experiments.

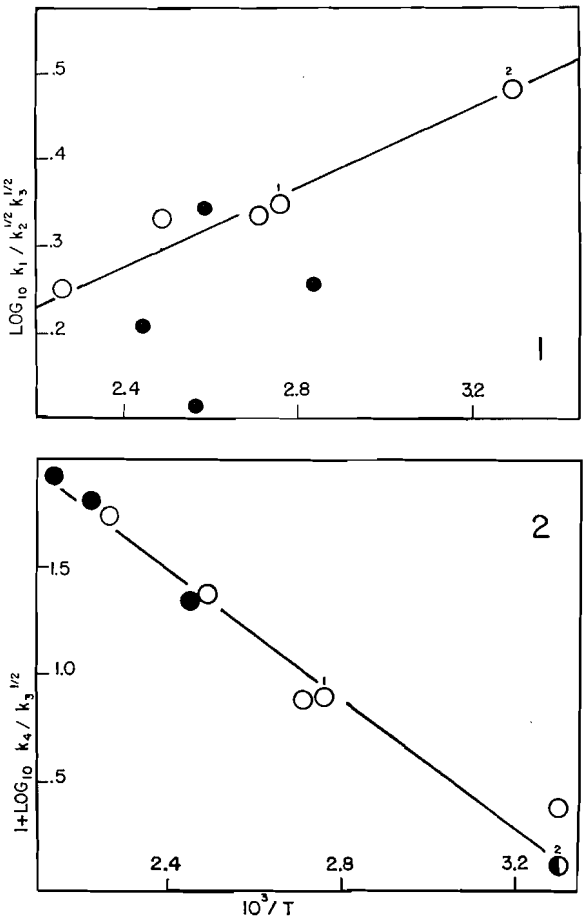


FIG. 1. Arrhenius plot of $k_1/k_2^{\frac{1}{2}}k_3^{\frac{1}{2}}$ versus $1/T$. (1) Average of two experiments. (2) Average of four experiments. ● Data of Sieger and Calvert from photolysis of CF_3COCH_3.

FIG. 2. Arrhenius plot of $k_4/k_3^{\frac{1}{2}}$ versus $1/T$. (1) Average of two experiments. (2) Average of six experiments. Shaded data not reported in Table I.

If all the CF_3H collected in our system is formed in the reaction

$$CF_3 + CH_3COCH_3 \rightarrow CF_3H + CH_2COCH_3 \qquad [4]$$

we have $k_4/k_3^{\frac{1}{2}} = R_{CF_3H}/R^{\frac{1}{2}}_{C_2F_6}$ [acetone]. Using the original acetone concentration in this expression, a least squares treatment of the Arrhenius plot of the function (Fig. 2) gives $k_4/k_3^{\frac{1}{2}} = 1.24\times10^4 \exp[-(6.9\pm0.1)\times10^3/RT]$ (mole/cc)$^{-\frac{1}{2}}$ sec$^{-\frac{1}{2}}$. This agrees well with a previous value of $E_4-\frac{1}{2}E_3$ of 8.0 kcal/mole (2), as it is possible from the manner in which it was computed that this latter figure is high by 1.5 kcal.

The shaded points in Fig. 2 represent six experiments not recorded in Table I because of the comparatively small amounts of C_2H_6 formed in these runs, which rendered the data unreliable. This was due to the fact that insufficient acetone was used, especially so at the higher temperatures, as the rate of photolysis of hexafluoroacetone is markedly temperature dependent up to 200° C (5). The point marked "2" represents the average of six experiments, half of which are recorded in Table I. The values of $k_4/k_3^{\frac{1}{2}}$ (excepting run 4, which is shown separately) obtained for all the six experiments were so close as to make them indistinguishable on the scale of the graph.

Can. J. Chem. Downloaded from www.nrcresearchpress.com by 41.223.56.140 on 09/04/12
For personal use only.

Can. J. Chem. Downloaded from www.nrcresearchpress.com by 41.223.56.140 on 09/04/12
For personal use only.

One remarkable feature of these experiments was that at room temperature the pressure dropped during the reaction and the total ethanes plus small quantity of methanes was only equal to about one-half the CO formed. Above 100° C the balance of radical products to CO was normal. No dark reaction occurs between the two ketones at 30° C, but when equal quantities (about 5 cm each) were illuminated for a period of hours the final pressure was approximately half the original pressure. The addition of CH_3 radicals to the carbonyl double bond in hexafluoroacetone has been discussed previously (6). The species $[CF_3CH_3COCF_3]$ could be stabilized at low temperatures by the addition of, rather than by the expulsion of, a radical, resulting in a loss in radical products. The participation of the CH_3CO radical, which is relatively stable up to a 100° C, cannot be precluded, but this would tend to give excess radical products. We are investigating this further.

Due to this effect it is difficult to estimate the exact percentage decomposition of the individual ketones in the experiments at room temperature, but about 5% of each was consumed. Material balance showed that about 5% or less acetone was decomposed in all the runs, but the decomposition of hexafluoroacetone increased to 10% at 100° C, and to 20% at 170° C. This latter figure is high for the application of steady-state conditions, so that the high temperature runs are probably less accurate.

The radical disproportionation reactions

$$CH_3 + CH_3 \rightarrow CH_4 + CH_2 \quad [5]$$

and

$$CF_3 + CH_3 \rightarrow CF_3H + CH_2 \quad [6]$$

have not been considered. Evidence for [5] is scant (7), but the occurrence of [6] cannot be ruled out. In some of the CF_3CH_3 analyses peaks at mass numbers 29 and 81 were obtained for which there appears to be no suitable explanation. Mass number 29 could possibly be from propane, but the residual at 43 was not really large enough to recommend propane as a constituent. It is worth speculating that propane could arise from the reaction of methylene with ethane if reaction [6] occurred.

DISCUSSION

If Ayscough's value (1) for k_3 at 400° K of 2.34×10^{13} $(mole/cc)^{-1}$ sec^{-1} is compared with the value calculated from collision theory of 1.5×10^{14} $(mole/cc)^{-1}$ sec^{-1} at 400° K, assuming $E_3 = 0$, the steric factor for reaction [3] is 0.16. If the steric factor is taken as unity E_3 becomes 1500 cal.

At the pressures used in our system there is no likelihood of third body restrictions affecting the radical recombination reactions and therefore no possibility of them exhibiting negative temperature coefficients (8, 9). If $E_1 \geqslant 0$, from the relationship $E_1-\frac{1}{2}E_2-\frac{1}{2}E_3 = -1070$ cal we have $E_2+E_3 \geqslant 2140$ cal. If $E_1 = 0$, and $E_2 = 700$ cal (the upper limit of Gomer and Kistiakowsky (10)), $E_3 = 1440$ cal. It is evident that many other combinations are possible; obviously all three activation energies cannot be identical, nor can they all be zero. If E_1 and E_2 are zero, or very nearly so, E_3 is of the order of 2 kcal. However, it is improbable that either E_1 or E_2 (and for that matter E_3) can be zero due to the slight temperature dependence of the collision number for a given reaction and the consequent small activation energy associated with it, which amounts to some 350 cal over the temperature range of our experiments. A value of E_1, E_2, or E_3 less than this could only occur if there was some third body restriction.

Shepp and Kutschke (11) have found an activation energy of 2.0 ± 1 kcal for ethyl radical recombination which they consider to be real, as they rate the possibility that there will be mutual repulsion of the C—H bond orbitals during C—C bond formation involving an energy barrier of the order of that due to hindered rotation, about 2 to 3 kcal. They suggest that CH_3 radical recombination is more favorable sterically, and that

the known temperature independence of the reaction (12) puts an upper limit of about 1 kcal on the activation energy, which could be due to the fact that the CH_3 radical is planar (13). The adjustment of two CH_3 radicals to the near tetrahedral arrangement in C_2H_6 could result in $E_2 > 0$. This is also true for E_3, if CF_3 is planar.

It is apparent in reactions where there is no significant potential energy barrier that the temperature dependence is due to several small factors of similar magnitude, which will tend to cancel each other if they are of differing sign. Thus the concept of "activation energy" is becoming more indeterminate in these cases. The most general conclusion that can be drawn is that all the three radical recombination reactions discussed here have a small positive temperature dependence, the greatest being attributable to reaction [3]. It is not clear what the effect, if any, of the C—F bond polarity is on this reaction, although the fact that E_3 is larger than E_1 or E_2 indicates that it could be of some consequence.

ACKNOWLEDGMENTS

We are greatly indebted to Dr. H. I. Schiff of McGill University, Montreal, for the mass spectrographic analyses, and to the Defence Research Board of Canada, under Grant 9530/13, for generous financial assistance.

REFERENCES

1. AYSCOUGH, P. B. J. Chem. Phys. **24**, 944 (1956).
2. PRITCHARD, G. O., PRITCHARD, H. O., SCHIFF, H. I., and TROTMAN-DICKENSON, A. F. Trans. Faraday Soc. **52**, 849 (1956).
3. HENNE, A. L. and RENOLL, M. W. J. Am. Chem. Soc. **58**, 889 (1936).
4. SIEGER, R. A. and CALVERT, J. G. J. Am. Chem. Soc. **76**, 5197 (1954).
5. AYSCOUGH, P. B. and STEACIE, E. W. R. Proc. Roy. Soc. A, **234**, 476 (1956).
6. PRITCHARD, G. O. and STEACIE, E. W. R. Can. J. Chem. **35**, 1216 (1957).
7. STEACIE, E. W. R. Atomic and free radical reactions. 2nd ed. Reinhold Publishing Corp., New York. 1954.
8. INGOLD, K. U., HENDERSON, I. H. S., and LOSSING, F. P. J. Chem. Phys. **21**, 2239 (1953).
9. HUSAIN, D. and PRITCHARD, H. O. J. Chem. Phys. **30**, 1101 (1959).
10. GOMER, R. and KISTIAKOWSKY, G. B. J. Chem. Phys. **19**, 85 (1951).
11. SHEPP, A. and KUTSCHKE, K. O. J. Chem. Phys. **26**, 1020 (1957).
12. SHEPP, A. J. Chem. Phys. **24**, 939 (1956).
13. COLE, T., PRITCHARD, H. O., DAVIDSON, N. R., and MCCONNELL, H. M. Mol. Phys. **1**, 406 (1958).

Can. J. Chem. Downloaded from www.nrcresearchpress.com by 41.223.56.140 on 09/04/12
For personal use only.

Can. J. Chem. Downloaded from www.nrcresearchpress.com by 41.223.56.140 on 09/04/12
For personal use only.

THE INFRARED ABSORPTION SPECTRA OF UREA–HYDROCARBON ADDUCTS[1]

P. H. H. Fischer and C. A. McDowell

ABSTRACT

The infrared absorption spectra of the adducts formed between urea and hydrocarbons from *n*-heptane to *n*-hexadecane have been measured in the range 600 cm^{-1} to 4000 cm^{-1}. From a consideration of the crystal symmetries of urea and the urea–hydrocarbon adducts it has been possible to assign the various vibration frequencies. The band shifts observed are explained in terms of changes in bond lengths and bond angles.

INTRODUCTION

Urea forms adducts, or clathrates, with a variety of organic molecules such as hydrocarbons, esters, and organosilanes. X-Ray studies (1) have revealed the general details of the structures of hydrocarbon–urea adducts. There have also been infrared studies (2, 3, 4) which have supplemented this structural information. The results available show that whereas pure urea crystallizes with a tetragonal structure, when it forms an adduct it adopts a hexagonal crystal structure. In this way long channels are formed which allow the enclathrated hydrocarbon, or other molecule, to be located inside a cage of urea molecules held together by hydrogen bonds. Until quite recently little information was available concerning the physical state of the enclathrated hydrocarbon in these urea–hydrocarbon adducts. Nuclear magnetic resonance studies in these laboratories (5) have shown that the enclathrated hydrocarbon molecules have some vibrational and rotational, or torsional, freedom within the urea channels. We here report studies of the infrared absorptions spectra of a series of urea–hydrocarbon complexes. The aim of this work is to obtain information on the molecular motions of the trapped hydrocarbons, the stabilities of the complexes, and the structure of the hexagonal form of urea.

Apart from work by Stuart (2), who studied the N—H stretching frequencies of the urea–cetane adduct, and by Barlow and Corish (4) on the same adduct (among other classes of adducts), no other investigations of the homologous hydrocarbon–urea adducts seem to have been undertaken.

EXPERIMENTAL

The preparation of the adducts was accomplished by two different methods. (*a*) 1.25 g of A. R. grade urea (recrystallized), very finely powdered, was shaken with 15 ml of the respective hydrocarbon (Phillips, research grade) for periods ranging from 12 to 48 hours. Decantation, vacuum filtration for 30 seconds, and drying in filter paper gave a finely crystalline product. (*b*) 300 mg of hydrocarbon were placed in a vial with 10 ml of saturated urea–methanol solution and brought to boil. Cooling of the stoppered vial in a well-insulated Dewar flask yielded hexagonal crystals up to 35 mm in length.

The spectroscopic measurements were carried out on a Perkin–Elmer infrared spectrophotometer, model 21. The crystalline hydrocarbon–urea adducts were examined either by the potassium bromide disk method, or as Nujol and hexachlorobutadiene mulls.

[1]*Manuscript received September 8, 1959.*
Contribution from the Department of Chemistry, University of British Columbia, Vancouver 8, B.C., Canada.

Can. J. Chem. Downloaded from www.nrcresearchpress.com by 41.223.56.140 on 09/04/12
For personal use only.

RESULTS AND DISCUSSION

The spectra obtained (as KBr disks) are shown in Fig. 1. All complex spectra show similar changes from the spectrum of tetragonal urea, although in varying degree. Table I lists urea frequencies, both of the tetragonal and hexagonal structures.

TABLE I

Urea frequencies (cm^{-1})

Urea	Present study	Urea complex (lit.)	Assignment
3436*	3420	3420‡	ν(NH) b_2
3333*	3220	3225‡	ν(NH) b_2
3268 (sh)*	—	—	
1686†	1676	4 bands between 1675 and 1590§	ν(CO) a_1
	1654		
1629†	1630		$\delta(NH_2)$ b_2
1603†	1595		δ(NH) a_1
1464†	1492	1485§	ν(CN) b_2
1150†	1160	1160§	ρ(NH) a_1
1000†	1014	1011§	ν(CN) a_1
789†	793	791§	β(OCNN) b_1
717†	721	—	ω(NH) b_1

*Ref. 6. †Ref. 7. ‡Ref. 2. §Ref. 4.

Infrared studies (6, 8, 9) of urea have indicated that the molecule is planar and this has been confirmed by proton magnetic resonance studies (10). Thus the isolated urea molecule belongs to symmetry group C_{2v}. Ordinary urea crystallizes in a lattice of symmetry V_d^3 with 2 molecules per unit cell. Hence the site symmetry of the planar C_{2v} urea molecule is still C_{2v}, and the selection rules for the free molecule apply to the crystal as well (11). A free urea molecule with a planar C_{2v} structure has the following fundamental vibrational frequencies; $7a_1+2a_2+3b_1+6b_2$. All the vibrations are Raman active, but the two a_2 vibrations, a NH_2 wagging, and a NH_2 torsional oscillation are forbidden in the infrared spectrum. The hexagonal form of urea crystallizes with lattice symmetry $C_{6,2}$–D_6^2 (2) having 6 molecules per unit cell. There are consequently two distinct sets of sites having symmetry C_2 (with six equivalent sites per set). The selection rules of the free molecule do not apply to the crystal and an assignment of the vibrations based on C_2 symmetry is indicated (11). In this case, in contrast with the C_{2v} case above, all 18 fundamental vibrations are allowed in both the Raman and infrared spectra. The change in lattice symmetry from tetragonal to hexagonal allows the two formerly forbidden a_2 (NH_2) vibrations to appear in the infrared spectrum of the hexagonal structure.

TABLE II

Vibrational frequencies of the trapped hydrocarbons (cm^{-1})

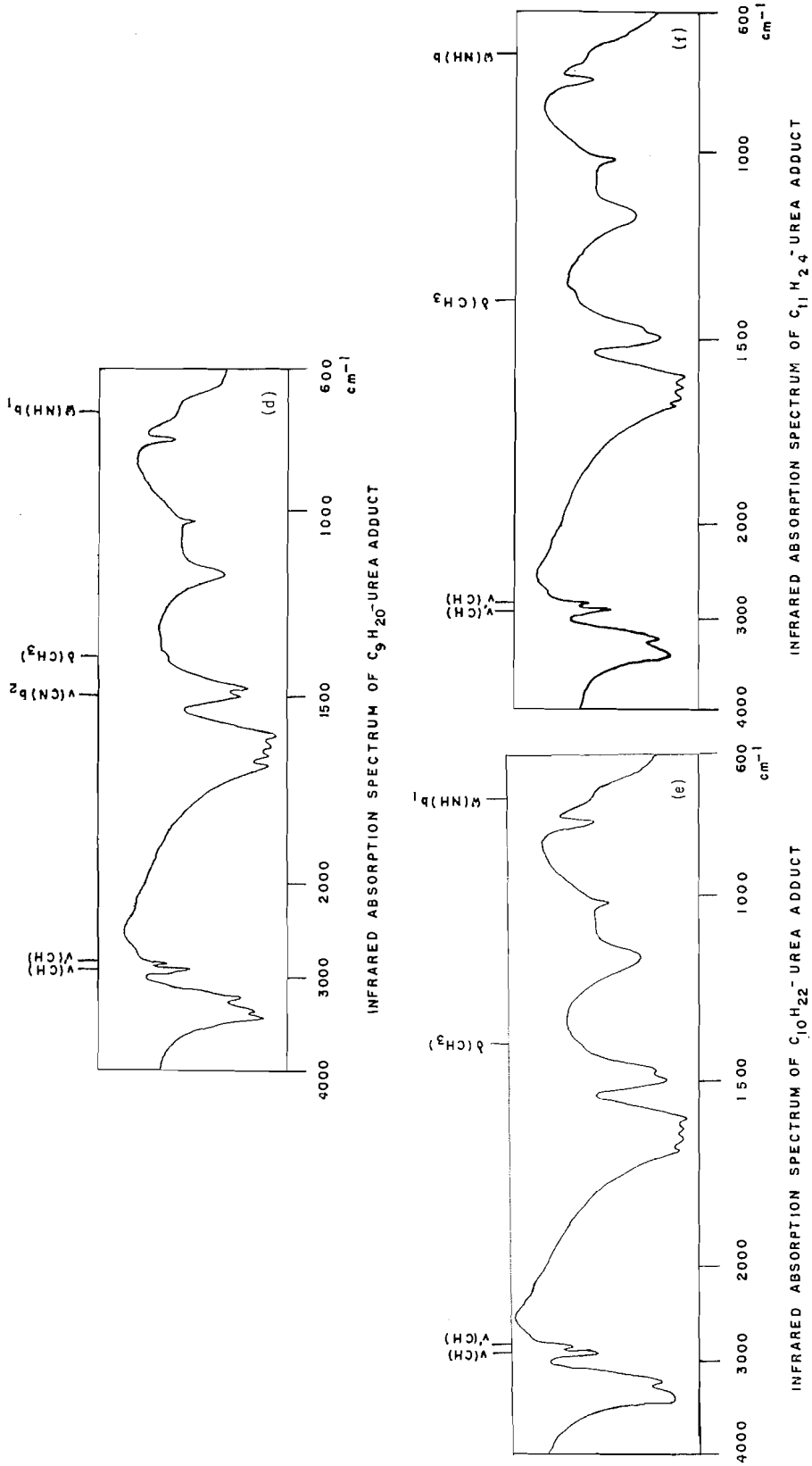
Present study	Lit. (4)	Assignment
2920	2920	Asym. CH stretch
2850	2850	Sym. CH stretch
1463 (sh)	ca. 1465	CH_2 bend*
1380	—	Sym. CH_3 bend

*There may also be a contribution from the CH_3 asymmetrical bending vibration.

Can. J. Chem. Downloaded from www.nrcresearchpress.com by 41.223.56.140 on 09/04/12
For personal use only.

FIG. 1 (*a*), (*b*), (*c*).

Can. J. Chem. Downloaded from www.nrcresearchpress.com by 41.223.56.140 on 09/04/12
For personal use only.



INFRARED ABSORPTION SPECTRUM OF C_9H_{20}-UREA ADDUCT

INFRARED ABSORPTION SPECTRUM OF $C_{10}H_{22}$-UREA ADDUCT

INFRARED ABSORPTION SPECTRUM OF $C_{11}H_{24}$-UREA ADDUCT

FIG. 1 (*d*), (*e*), (*f*).

Can. J. Chem. Downloaded from www.nrcresearchpress.com by 41.223.56.140 on 09/04/12
For personal use only.

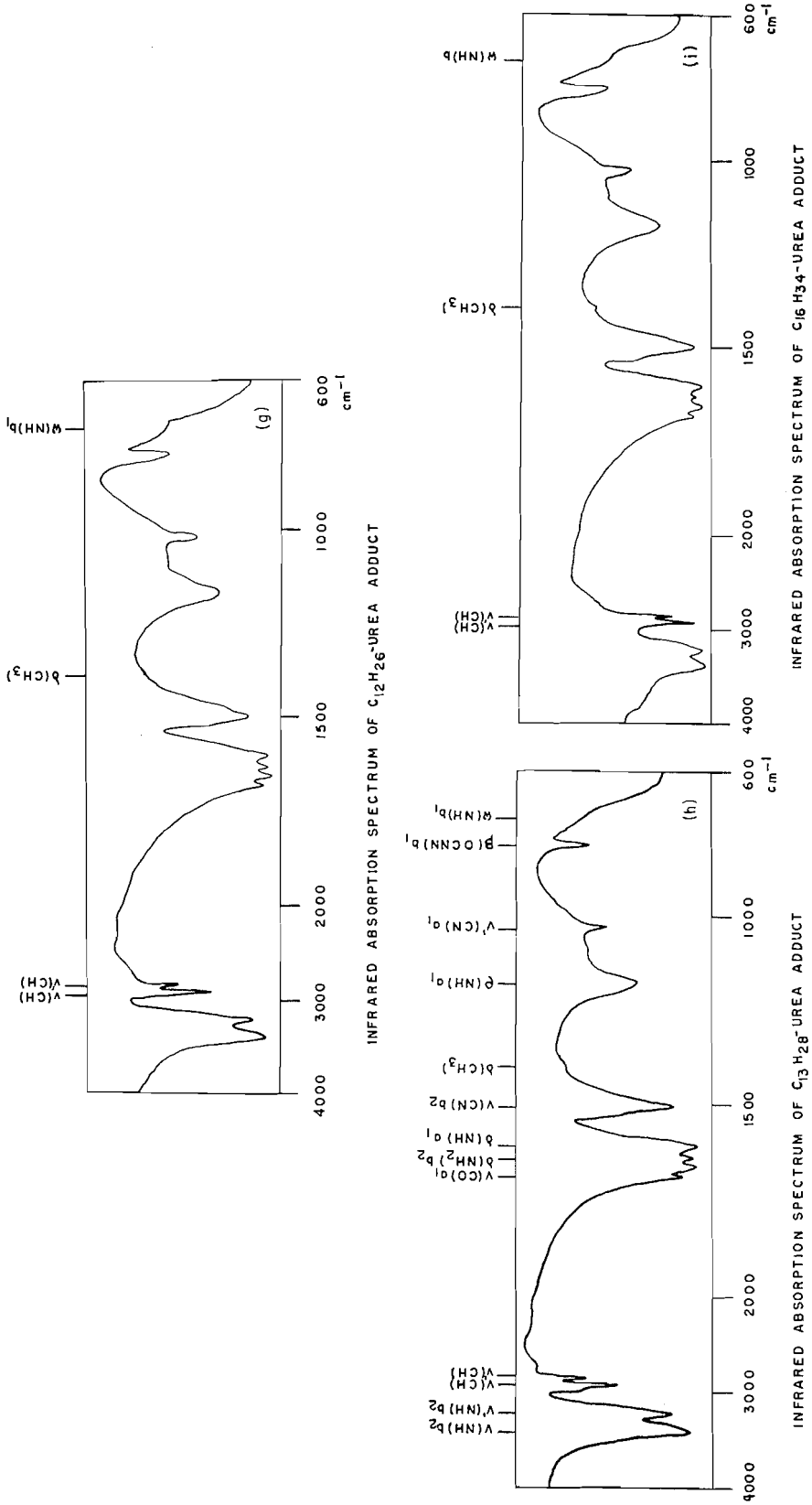


FIG. 1 (*g*), (*h*), (*i*).

The most striking change in the adduct spectra occurs in the N—H stretching frequency region. The out-of-phase vibration occurring at 3436 cm^{-1} in the tetragonal urea is lowered to 3420 cm^{-1}, whereas the in-phase vibration is shifted from 3333 cm^{-1} to 3220 cm^{-1} in going from tetragonal to hexagonal unit cell. An increase in the strength of the hydrogen bonds is apparent.

TABLE III

Bond distances in urea (1)

Bond	Hexagonal urea	Tetragonal urea
C—O	1.28 Å	1.25 Å
C—N	1.33	1.37 (ref.1) 1.335 (ref.12)
N—N	2.30	2.31
$N_1H \ldots O$	2.93	2.99
$N_2H \ldots O$	3.04	3.04

It seems reasonable to assume that the shorter hydrogen bonds of the tetragonal structure are situated in a much more favorable position for hydrogen bonding to occur during complex formation and that the stability of the adducts is mainly due to these bonds. Although crystallographic data shows no shortening of bond length of the longer hydrogen bonds, spectral analysis indicates a slight shortening.

The band at 1676 cm^{-1} is identified with the CO vibration and is explained by the lengthening of the C—O bond length. In this connection it may perhaps be mentioned that Krimm (13) found a correlation between the CO stretching frequencies in polypeptides and proteins, and the CO . . . NH angles. The raising of the C—N vibration frequency from 1464 cm^{-1} to 1492 cm^{-1} may be explained by the shortening of the C—N bond if the data of Smith (1) are accepted. However, Vaughan and Donohue (12) give a value of 1.335 Å for the C—N bond length in tetragonal urea; this value is very close to that given by Smith for hexagonal urea. Similar remarks apply to the finding that the symmetric C—N frequency is increased from 1000 cm^{-1} to 1014 cm^{-1}. It will be noticed that the intensity of the 1014 cm^{-1} band is greatly increased in the complex. The CO and CNH_2 groups have similar masses and due to resonance similar force constants. The CO group in the complex will be more highly polarized due to the stronger hydrogen bonding, and the C—O vibration, in phase with the C—N vibration, will tend to increase the intensity of the latter.

The slight raising of the skeletal out-of-phase bending frequency at 793 cm^{-1} (789 cm^{-1} in tetragonal urea) is explained by a somewhat larger deformational force constant, resulting from the decrease in the N—N distance. Other very small changes in the complex spectra are due to changes in the permanent dipole of the new structure.

From a study of Fig. 1 it is concluded that the spectra of the urea–tridecane and urea–hexadecane represent spectra of the pure complex, since only weak shoulders near 1465 cm^{-1} due to (CH_2) bending vibrations are present, and other bands found in tetragonal urea have been shifted, leaving no trace of the old band. In the case of the spectra of the heptane to dodecane adducts, it is noticed that a regular transition of intensity and degree of shift of bands has occurred. The continuous transition from the spectrum of pure urea to that of the pure complex is due probably to the instability of the lower hydrocarbon complexes. If the adduct had not been subjected to grinding, pressure, and vacuum during the pellet-making process, spectra resembling those of the pure complex would undoubtedly have been obtained. As some of the complex was presumably destroyed under

Can. J. Chem. Downloaded from www.nrcresearchpress.com by 41.223.56.140 on 09/04/12
For personal use only.

such vigorous conditions, the spectra are likely those of varying proportions of pure urea and complex. Later experiments, using mulling techniques with Nujol and/or hexachlorobutadiene confirmed this, as spectra obtained resembled those of urea–tridecane and urea–hexadecane much more closely.

Although it would be expected that the spectrum of the octene-1 complex should resemble that of the octane complex, such was not the case. Rather, the spectrum of a more stable complex was obtained. An explanation for the greater stability may be that the labile electrons of the π-bond give the octene molecule enough polar character to permit dipole–dipole interactions. In an extreme case, there exists even the possibility of weak hydrogen bonding to the surrounding structure.

ACKNOWLEDGMENT

This work was supported by grants from The National Research Council of Canada and we wish to thank that body for its generosity.

REFERENCES

1. SMITH, A. E. Acta Cryst. **5**, 224 (1952).
2. STUART, V. Rec. trav. chim. **75**, 906 (1956).
3. RODELL, J. and HUNT, P. D. J. Am. Chem. Soc. **80**, 2683 (1958).
4. BARLOW, G. R. and CORISH, P. J. J. Chem. Soc. 1706 (1959).
5. GILSON, D. F. R. and McDOWELL, C. A. Nature, **183**, 1183 (1959).
6. STEWART, J. E. J. Chem. Phys. **26**, 248 (1957).
7. YAMAGUCHI, A., MIYAGAWA, T., SHIMANOUCHI, T., and MIZUSHIMA, S. Spectrochim. Acta, **10**, 170 (1957).
8. KELLER, W. E. J. Chem. Phys. **16**, 1003 (1948).
9. WALDRON, R. D. and BADGER, R. M. J. Chem. Phys. **18**, 566 (1950).
10. ANDREW, E. R. and HYNDMAN, D. Discussions Faraday Soc. No. 19, 195 (1955).
11. HALFORD, R. S. J. Chem. Phys. **14**, 8 (1946).
12. VAUGHAN, P. and DONOHUE, J. Acta Cryst. **5**, 530 (1952).
13. KRIMM, S. J. Chem. Phys. **23**, 1371 (1955).

Can. J. Chem. Downloaded from www.nrcresearchpress.com by 41.223.56.140 on 09/04/12
For personal use only.

Can. J. Chem. Downloaded from www.nrcresearchpress.com by 41.223.56.140 on 09/04/12
For personal use only.

HALF-LIVES OF THE NUCLIDES Au^{195}, Pt^{195m}, AND Pt^{197} [1]

M. BRESESTI[2] AND J. C. ROY

ABSTRACT

The half-lives of Au^{195}, Pt^{195m}, and Pt^{197} have been measured. The radionuclides were produced by neutron irradiation in the NRX reactor at Chalk River and were radiochemically purified after the irradiation. The decay of the X rays and γ-radiations from Au^{195} and Pt^{195m} was observed with a NaI (Tl) detector, and the β-decay of Pt^{197} was observed with an anthracene detector. The half-lives are:

Au^{195}	199 ±3 days,
Pt^{195m}	4.08 ±0.12 days,
Pt^{197}	20.00 ±0.12 hours.

The errors quoted are the estimated reliability of the measurement and include the statistical counting error plus an estimated systematic error.

INTRODUCTION

Values differing by nearly a factor of two have been reported for the half-lives of both Au^{195} and the isomeric state of Pt^{195} whereas no precise measurement of the half-life of Pt^{197} has been made heretofore.

The half-life of Au^{195} has been reported to be 185±3 days by Wilkinson (1), who followed the decay of the radiations of Au^{195} with an end-window Geiger counter for 2 years. In a similar study Steffen *et al.* (2) obtained a value of 180±15 days after observing the decay of a source for 14 months. In contrast to these measurements, Cressman and Wilkinson (3) found a value of 90±10 days by following the decay of the conversion electron lines of the gamma rays of Au^{195}; the length of time of observation of the decay of the source is not mentioned by the authors.

DeShalit *et al.* (4), who followed the decay of the conversion electron lines of the gamma radiations of Pt^{195m}, reported a half-life of 3.8 days. Cork *et al.* (5) on examination of the conversion electron lines in a magnetic photographic spectrometer have deduced a half-life of about 6 days. Also a radioactivity in platinum observed by McMillan (6) ($t_{\frac{1}{2}}$ = 3.3 days), Hole (7) ($t_{\frac{1}{2}}$ = 3.5 days), and Haldar (8) ($t_{\frac{1}{2}}$ = 4.4 days) has been assigned to Pt^{195m} in the "Table of Isotopes" of Strominger *et al.* (9). Unquestionably these three values were obtained from sources containing Pt^{191}, Pt^{193m}, and Pt^{195m}, and in one case Au^{199} (6) and they cannot therefore be assigned with certainty to Pt^{195m}.

Earlier measurements on the half-life of Pt^{197} were done with sources contaminated with the other radionuclides of platinum and in some cases with a long-lived activity now known to be the 71-day Ir^{192} (10). The values reported by different workers are 18 (6, 4, 11); 17.4 (12); and 19 hours (8).

The present work was undertaken to reduce the uncertainties recorded in the earlier literature.

EXPERIMENTAL

(*a*) *Irradiation*

Au^{195}, Pt^{195m}, and Pt^{197} were produced by neutron irradiation of suitable targets in the NRX reactor at Chalk River.

Gold-195 was obtained by a $(n,3n)$ reaction on Au^{197}, the observation of which has

[1]*Manuscript received September 30, 1959.*
Contribution from Research Chemistry Branch, Atomic Energy of Canada Limited, Chalk River, Ontario. Issued as A.E.C.L. No. 931.
[2]*Visiting Research Chemist. Present address: Gruppo Radioelementi, Via Mecenatte 84, Milano, Italy.*

Can. J. Chem. Downloaded from www.nrcresearchpress.com by 41.223.56.140 on 09/04/12
For personal use only.

been reported recently by Eastwood and Roy (13). Early in the measurement of the radioactivity of Au^{195}, it was found that the source was radiochemically pure and that it could be used for half-life determination. Observations of the decay were begun 5 months after the end of the irradiation. Other gold isotopes produced in the irradiation, Au^{196}, Au^{198}, and Au^{199} had decayed to insignificance by this time.

The isomeric state of Pt^{195} was produced by the irradiation of platinum enriched to 60% in Pt^{195}. A filter of 0.076 cm of cadmium was used and under these conditions Pt^{195m} was produced by the (n,n') reaction on Pt^{195} and the (n,γ) reactions on Pt^{194}; the former is believed to be the more important reaction. The observations of the decay started about 15 days after the end of the irradiation; the Pt^{197} activities had decayed to a negligible level by this time.

Platinum-197 was obtained by a (n,γ) reaction on platinum metal enriched to 66% in Pt^{196}. Observations of the decay started 3 days after the end of the irradiation.

From the abundance of the other platinum isotopes and the values of the neutron cross sections (14) one can calculate that irradiations under cadmium of platinum enriched in Pt^{195} should give predominantly Pt^{195m} and correspondingly, irradiation of enriched Pt^{196} should give predominantly Pt^{197}. This arrangement substantially reduces the uncertainties associated with earlier work.

(*b*) *Purification*

The purification of the gold has already been described (13). The platinum metal was dissolved in aqua regia and the solution was evaporated to dryness. The residue was dissolved in 3 *N* HCl and washed 10 times with equal volumes of ethyl acetate containing gold carrier. The HNO_3 was eliminated from the aqueous solution by repeated evaporation and addition of concentrated HCl. The chloroplatinate in 3 *N* HCl was reduced to the platinic form with stannous chloride followed by an extraction with ethyl acetate. The ethyl acetate solution was washed five times with 3 *N* HCl and was then evaporated to a small volume (15). The sources of platinum were prepared by drying a few drops of the solution on an aluminum tray. Similarly, the gold source was prepared by deposition of the gold metal on an aluminum tray. All the sources were covered with a layer of Scotch tape to avoid loss of material.

(*c*) *Counting Techniques*

The decay schemes of Au^{195} (3) and Pt^{195m} (5, 16) are well known. The prominent radiation of these radionuclides is the 67-kev *K* X ray which arises mainly from *K*-capture and internal conversion of the 98-kev γ-ray in Au^{195} and from internal conversion of the 98- and 130-kev γ-rays in Pt^{195m}. In these measurements, the half-lives were obtained by following the decay of the *K* X ray and the 98-kev radiation with a 1 in. $\times$ 1 in. NaI (Tl) crystal coupled to an RCA 5919 photomultiplier tube. The γ-ray spectrum was displayed on a multichannel analyzer using an AEP-type 1444 linear amplifier with a resolving time of 0.5 μsec (17). The γ-ray spectra of Au^{195} and Pt^{195m} are shown on Fig. 1. Readings were taken about twice a month for Au^{195} and once or twice daily for Pt^{195m}. Before or after each reading the stability of the apparatus was checked with a source of Am^{241} ($t_{\frac{1}{2}}$ = 458 years). The strong 59.6-kev γ-ray of Am^{241} makes it a convenient and reliable standard. For the period over which the data were accumulated, the variations in the counting rate of the source of Am^{241} were random and fluctuated around a mean value. The standard deviation from this mean for the entire set of data was taken as a measure of the error due to the stability of the counter. It was 1.9% and 1.3% for the gold and platinum measurements respectively. There was no measurable counting loss due to the resolving time of the amplifier.

Can. J. Chem. Downloaded from www.nrcresearchpress.com by 41.223.56.140 on 09/04/12
For personal use only.

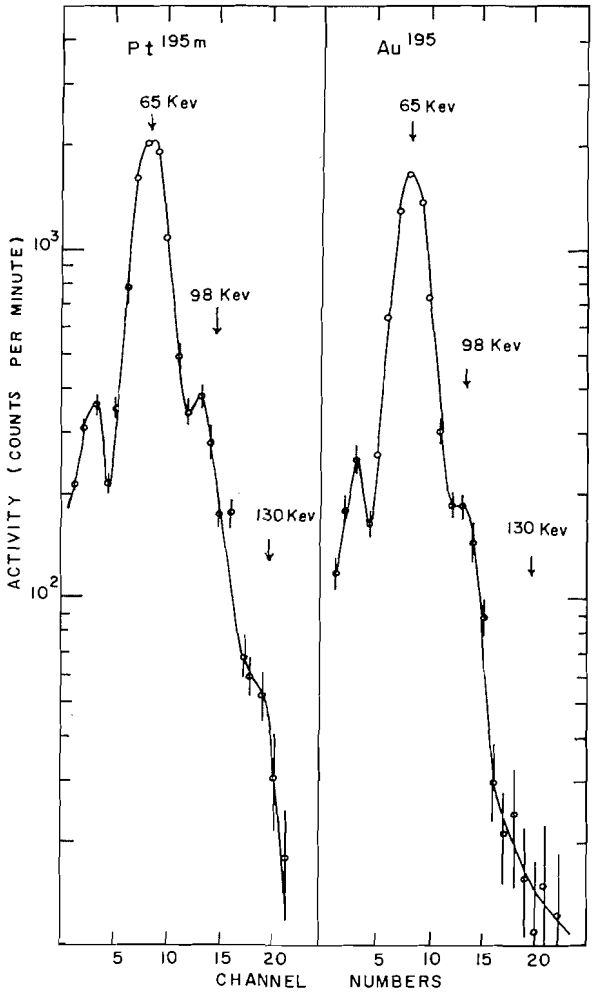


FIG. 1. Pulse-height distribution of Pt^{195m} and Au^{195} taken with 1 in. × 1 in. NaI (Tl) crystal.

The Pt^{197} activities were measured with an anthracene beta counter. The distance between source and window was 2.0 cm of air. The thickness of the window was 2.16 mg/cm² of aluminum, that of the Scotch tape covering the source was 9.0 mg/cm², and that of the source was a few mg/cm². These materials will absorb the conversion electrons emitted by other radionuclides of platinum present in small amount in the sources of Pt^{197}. The anthracene crystal was coupled to an RCA 6199 photomultiplier tube used with a linear amplifier–discriminator combination. The standard error due to the stability of the counter was measured to be ±0.5% by counting a source of Cs^{137} several days before and after the measurement. No dead time correction was applied because, for the highest initial counting rate obtained in the measurement, 1000 counts/sec, the counting loss was less than 0.3%. One half-life determination was also made using a conventional 2π-proportional counter.

RESULTS AND DISCUSSION

One source of Au^{195}, three sources of Pt^{195m} from two separate irradiations, and five

sources of Pt^{197} from four separate irradiations were used in the measurement. A study of the gamma-ray spectrum and of the absorption of the beta rays in aluminum was made for each source in order to detect the presence of possible impurities and to determine also the degree of interference of the other platinum activities.

In the range 25 kev to 2 Mev, only the radiations characteristic of the nuclide being measured could be observed. Platinum-191 has several gamma rays above 160 kev (16) which, if present in the sources of Pt^{195m}, could have been detected easily. Their absence in the sources of Pt^{195m} shows that the activity of Pt^{191} was less than 0.3%. The activity of Pt^{193m} was calculated to be less than 2% of that of Pt^{195m}. No beta rays could be observed in the sources of Au^{195} and Pt^{195m}. The soft conversion electrons emitted by these radionuclides were absorbed in the sources and Scotch tape covering them. The decay of the sources of Pt^{195m} and Pt^{197} were followed until the counting rate was just 1/10th of the background and in all cases no deviation from a linearity could be detected in the usual semilogarithmic plot. The backgrounds of the γ- and β-detectors were 50 ± 10 and 10 ± 1 counts/minute respectively. A further check was provided by dividing in two the time over which the decay of each source was observed and calculating the half-life for both parts. For the three radionuclides, the half-life calculated from each half of the data agreed with that calculated from the full data within the experimental error.

In the computation of the data each point was assigned an internal error formed by combining quadrically the statistical counting error and the error due to the stability of the counter. The half-life for decay of each source was calculated by the method of least squares, each point being weighted by the reciprocal of the squares of the assigned error. The data and the results of the computation are assembled in Table I. The external error

TABLE I

Summary of the half-life determinations

Radio-nuclide		Initial counting rate, counts/min	No. of points	No. of half-lives followed	Half-life	Internal error	External error
Au^{195}		6,000	34	2.1	199.04	1.54	1.05 days
Pt^{195m}	(1)	16,000	17	5.2	4.178	0.015	0.022 days
	(2)	9,300	14	3.1	3.998	0.024	0.012 days
	(3)	19,400	9	2.4	4.028	0.035	0.015 days
			Weighted average		4.083	0.015	0.060 days
Pt^{197}	(1)	54,200	62	6	20.113	0.018	0.019 hours
	(2)	43,200	50	5	19.930	0.019	0.025 hours
	(3)	62,300	44	6.3	19.977	0.016	0.023 hours
	(4)	49,200	30	4.5	19.661	0.027	0.050 hours
	(5)*	59,600	31	3.6	19.895	0.010	0.054 hours
			Weighted average		19.998	0.012	0.057 hours

*Half-life measured with a proportional counter.

listed in the last column is a measure of the deviation of the data from a least-squares fit. The weighted mean value is taken as the final half-life value and the larger of the internal or external error is taken as the final statistical error. The presence of other platinum activities, although in low abundance, could cause a small systematic error. It follows from the discussion that such a systematic error could be of the order of the statistical error. Therefore the statistical error is doubled and the half-lives are given as

Au^{195} 199 ± 3 days,
Pt^{195m} 4.08 ± 0.12 days,
Pt^{197} 20.00 ± 0.12 hours.

Can. J. Chem. Downloaded from www.nrcresearchpress.com by 41.223.56.140 on 09/04/12
For personal use only.

The values of the half-lives of Au^{195} and Pt^{195m} found in this work are in fair agreement with those reported by Wilkinson (1), Steffen *et al.* (2), and deShalit (4) respectively. However, the present work does not support the values of 90 days (3) for Au^{195} and 6 days (5) for Pt^{195m}. The earlier approximate values of 18 (6, 4, 11), 17.4 (12), and 19 hours (8) are in reasonable agreement with the more precise value of 20.0 $\pm$0.12 hours recorded in this paper.

ACKNOWLEDGMENT

The authors would like to express their thanks to Dr. J. M. Kennedy for programming the Chalk River Datatron upon which the computations were carried out.

REFERENCES

1. Wilkinson, G. Phys. Rev. **75**, 1019 (1949).
2. Steffen, R. M., Huber, O., and Humbel, F. Helv. Phys. Acta, **22**, 167 (1949).
3. Cressman, P. J. and Wilkinson, R. G. Phys. Rev. **109**, 872 (1958).
4. deShalit, A., Huber, O., and Schneider, H. Helv. Phys. Acta, **25**, 279 (1952).
5. Cork, J. M., Brice, M. K., Schmid, L. C., Hickman, G. D., and Nine, H. Phys. Rev. **94**, 1218 (1954).
6. McMillan, E. M., Kamen, M., and Ruben, S. Phys. Rev. **52**, 375 (1937).
7. Hole, N. Arkiv Mat. Astron. Fysik, **36**, A, No. 9 (1949).
8. Haldar, B. C. Phys. Rev. **87**, 158 (1952).
9. Strominger, D., Hollander, J. M., and Seaborg, G. T. Revs. Modern Phys. **30**, 585 (1958).
10. Warren, G. W. and Fink, R. W. Bull. Am. Phys. Soc. Ser. II, **1**, 171 (1956).
11. Schneider, H., Huber, O., Humbel, F., deShalit, A., and Zunti, W. Helv. Phys. Acta, **25**, 259 (1952).
12. Cork, J. M., Stoddard, A. E., Rutledge, W. C., Branyan, C. E., and Leblanc, J. M. Phys. Rev. **77**, 843 (1950).
13. Eastwood, T. A. and Roy, J. C. Can J. Phys. **37**, 815 (1959).
14. Hughes, D. J. and Schwartz, R. B. U.S. Atomic Energy Commission. Report BNL-325. 2nd ed. (1958).
15. Meinke, W. W. U.S. Atomic Energy Commission. Report AECD-2738.
16. Potnis, V. R., Mandeville, C. E., and Burlew, J. S. Phys. Rev. **101**, 753 (1956).
17. Moody, N. F., Howell, W. D., Battell, W. J., and Taplin, R. H. Atomic Energy of Canada Limited. Report CREL-464.

Can. J. Chem. Downloaded from www.nrcresearchpress.com by 41.223.56.140 on 09/04/12
For personal use only.

Can. J. Chem. Downloaded from www.nrcresearchpress.com by 41.223.56.140 on 09/04/12
For personal use only.

A METHOD OF INTEGRATION OF THE GIBBS–DUHEM EQUATION WHEN ACTIVITIES OF A SOLUTE ARE REQUIRED FROM THOSE OF THE SOLVENT[1]

M. L. LAKHANPAL[2] AND B. E. CONWAY

ABSTRACT

A new graphical method has been developed for integrating the Gibbs–Duhem equation for the case where activities of the solute are required from experimentally determined values of the activity of the solvent in a binary solution. This method has been applied to the determination of the activities of fractions of polyoxypropylene glycols in methanolic solutions. The accuracy of the procedure is discussed.

When partial thermodynamic functions are required for solute and solvent in a binary mixture from measurements of the vapor pressure of the solvent, it is necessary to utilize an integrated form of the Gibbs–Duhem equation. Whilst the integration of this equation by graphical or other means is easy when activities of the solvent are to be calculated from those of the solute, e.g. in the Tl–Hg case (1, 4) the reverse procedure, which is more often required, presents considerable difficulties since the function for integration then rises asymptotically to high values as the activity coefficient of the solvent tends to unity in dilute solutions and an unambiguous integration cannot then be carried out. For this case where activities of the solute are to be calculated from those of the solvent, approximate analytical methods (1) have been suggested but these can give erroneous results (1) for dilute solutions. It is therefore the purpose of this paper to report a new semiempirical graphical procedure for integration of the Gibbs–Duhem equation when *solute* activities are required. The method is illustrated by reference to thermodynamic measurements on the system polyglycol(mol. wt. 1955)–methanol, which we have recently carried out.

The Gibbs–Duhem equation

$$[1] \qquad \sum_i x_i d\mu_i = 0$$

gives, for a two-component system, the familiar relationship

$$[2] \qquad x_2 \, d \ln \frac{a_2}{x_2} = -x_1 \, d \ln \frac{a_1}{x_1},$$

where x_1, x_2 are the mole fractions; a_1, a_2 are the activities and μ_1 and μ_2 are the chemical potentials of the solvent and solute, respectively. Upon integrating equation [2] from the limit $x_2 = 0$ where a_2 is zero to any point $x_2 = x$, where a_2 is finite, the expression

$$[3] \qquad \ln \frac{a_2}{x_2} = -\int_{x_2=0}^{x_2=x} \frac{x_1}{x_2} d \ln \frac{a_1}{x_1}$$

is obtained. In the analytical method, the activities of the solute are determined by obtaining an empirical relationship by which the activities of the solvent can be expressed as a function of the composition of the two-component system (1, 2) so that [3] can be directly integrated and the activities of the solute calculated at various compositions. This procedure, however, necessitates very accurate knowledge of the experimental

[1]*Manuscript received October 2, 1959.*
Contribution from the Department of Chemistry, University of Ottawa, Ottawa, Canada, and the Department of Chemistry, University of Panjab, Panjab, India.
[2]*On leave of absence from the University of Panjab, Panjab, India.*

activities of the solvent over a range of concentrations (particularly at low concentrations) sufficient to enable an empirical equation to be formulated which can be relied upon to represent the experimental behavior of limitingly dilute solutions. The graphical method consists in plotting the values of x_1/x_2 against log a_1/x_1 and determining the area under the curve between the limits indicated in equation [3]. The graph of the function x_1/x_2 vs. log a_1/x_1 is shown in Fig. 1 for solutions in methanol of a polyoxypropylene glycol fraction (number average mol. wt. = 1955), the experimental data for which have been obtained by differential vapor-pressure measurements which will be described in detail elsewhere (3). Since the curve of x_1/x_2 against log a_1/x_1 (see Fig. 1) is asymptotic*

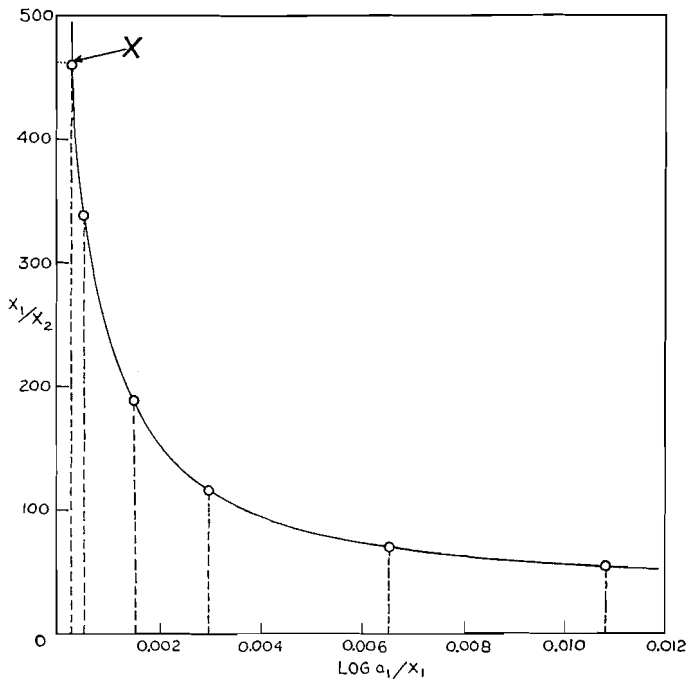


FIG. 1. Plot of the mole fraction ratio x_1/x_2 vs. log a_1/x_1 for solutions of polyoxypropylene glycol (mol. wt. 1955) in methanol.

to the axis of the ordinate x_1/x_2, it has to be extrapolated to an infinite value of x_1/x_2 in order to obtain the total area under the curve. The accurate assessment of the integral by measurement of the area under the extrapolated curve presents a practical difficulty particularly in the asymptotic region of the curve. Usually a rough approximation of this area is made or an extrapolation function is devised (1) which is often unsatisfactory in the dilute solution region.

In view of these difficulties, we have developed an alternative method for obtaining the integral to an infinite value of x_1/x_2 as log a_1/x_1 tends to zero. As in the graphical method mentioned above, the values of x_1/x_2 are first plotted against log a_1/x_1 (see Fig. 1). The area under the curve from a point X in the asymptotic region to an infinite value of x_1/x_2 is considered to be equal to an unknown constant C, so that the total integral up to

*When the activity of the "solute" is measured and it is desired to obtain the corresponding activity of the "solvent", for example in the system Tl–Hg (4), this difficulty does not arise since the function for integration becomes zero when $x_2/x_1 = 0$.

Can. J. Chem. Downloaded from www.nrcresearchpress.com by 41.223.56.140 on 09/04/12
For personal use only.

any point on the curve is equal to C plus the area under the curve from the point X to that point. If C is first considered to be equal to zero, we obtain apparent first approximation values of log a_2/x_2. The values of x_2/x_1 are now plotted against the apparent values of log a_2/x_2 as shown in Fig. 2. It is found that the value of log a_2/x_2 for a value x_2/x_1

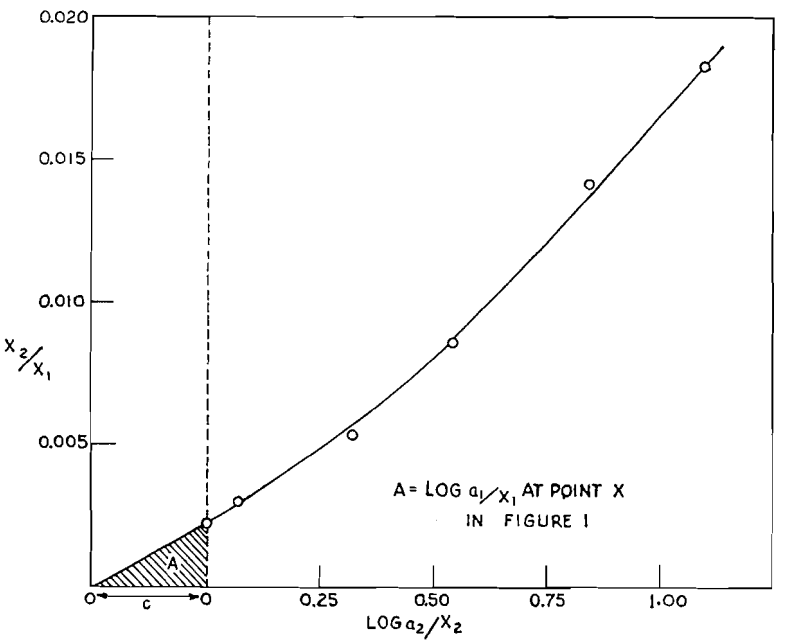


FIG. 2. Plot of the mole fraction ratio x_2/x_1 vs. log of the first approximation values of a_2/x_2 for solutions of polyoxypropylene glycol (mol. wt. 1955) in methanol.

corresponding to the point X in Fig. 1 is zero, so that the curve in Fig. 2 does not pass through the origin as it should do. This suggests that if we smoothly extend the curve back to the axis of abscissae, the point at which the curve meets that axis should be the actual origin. Hence all the apparent values of log a_2/x_2 must be increased by the constant C equal to the shift of the origin along the horizontal axis. Without any further information about the course of the curve in the region covered by extrapolation, there may be some uncertainty in the value of the constant C thus estimated. However, in order to make a more correct extrapolation it is possible to utilize the fact that the area A under the curve in Fig. 2 must be equal to log a_1/x_1 at the point X in Fig. 1, and this is known experimentally.

The above method makes it possible to compute the value of C and hence allows the determination of the values of a_2, the activity of the solute, corresponding to the various experimental values of a_1. The values of the constant C may be determined with an accuracy better than $\pm 5\%$ so that the values of log a_2/x_2 may be obtained with an accuracy increasing from about $\pm 4\%$ to better than $\pm 1\%$ for increasing values of the concentration of the solute. This enables the calculation of the activities of the solute to be made with an accuracy of better than $\pm 0.5\%$ in a_2. The accuracy of the above method of integration may be illustrated by applying it to the data on aqueous sucrose solutions discussed by Lewis and Randall (ref. 1, pp. 275–276). From the given values (1) of molal concentrations and ln a_1, we have calculated the values of ln a_1/x_1 shown in column 4,

Can. J. Chem. Downloaded from www.nrcresearchpress.com by 41.223.56.140 on 09/04/12
For personal use only.

TABLE I

Calculations of the activities of sugar in aqueous sugar solutions

m	x_1/x_2	ln a_1	ln a_1/x_1	ln a_2/x_2	ln a_1/x_1	ln a_1
0.050	1110	−0.00053	0.00037	−0.035±20%	−0.00002	−0.00092
0.172	322.7	−0.00013	−0.00013	−0.090±5%	−0.00013	−0.00324
0.454	122.3	−0.00871	−0.00056	−0.167±1%	−0.00055	−0.00870
1.009	55.01	−0.02002	−0.00201	−0.274±1%	−0.00194	−0.01995

Data taken from Lewis and Randall (ref. 1, p. 275).

Table I. The positive value of ln a_1/x_1 for the first concentration indicates that the value of a_1 is incorrect (as also concluded by Lewis and Randall). The last three concentrations (see Table I) were therefore used for the calculation of ln a_2/x_2 by the method described above and these values are given in column 5 of Table I. In order to test the validity of these calculated values of ln a_2/x_2, the values of ln a_1/x_1 were back-calculated from those of ln a_2/x_2 and are given in column 6. Considering that only three concentrations are available for these calculations the agreement of the values of ln a_1/x_1 in columns 4 and 6 of the table is very satisfactory. An estimate of the accuracy with which the values of ln a_2/x_2 can be obtained is also recorded in column 5.

An attempt has also been made to assess the approximate value of ln a_1/x_1 for the first concentration. The value obtained is −0.00002; the value of ln a_1 is therefore 0.00092 and it can be seen from Table I that this figure is accurate to about ±1%.

The above case has been examined in order to indicate the convenience and accuracy of this method of integration as applied to previously determined data which have also been treated by other methods of integration (1). The procedure reported here has some advantages in that it is convenient and not very sensitive to small inaccuracies in the determination of the experimental points for solutions in the region of low concentrations, whilst the special analytical extrapolation method described by Lewis and Randall is.

The method has enabled us to calculate the values of the activities of a number of different molecular weight fractions of polyoxypropylene glycol in methanolic solutions of various concentrations. The values of the activities of the solvent, a_1, and the corresponding activities of the solute, a_2, in solutions of the polymer of mol. wt. 1955 are reported in columns 3 and 4 of Table II as an example of the application of the method

TABLE II

The activities of the solute and the solvent in a polyoxypropylene glycol – methanol system at 15° C

Polymer molecular weight	Polymer mole fraction	Activity of solvent, a_1	Activity of solute, a_2
1955	0.00219	0.9972	0.004
	0.00299	0.9959	0.006
	0.00527	0.9913	0.019
	0.0085	0.9847	0.052
	0.0139	0.9714	0.179
	0.0179	0.9579	0.244

using Figs. 1 and 2. A more complete treatment of the thermodynamic properties of these systems will be communicated shortly.

Can. J. Chem. Downloaded from www.nrcresearchpress.com by 41.223.56.140 on 09/04/12
For personal use only.

ACKNOWLEDGMENTS

One of the authors (M. L. L.) wishes to express his gratitude to the Defence Research Board for financial support during his leave of absence. Grateful acknowledgment is also made to the Defence Research Board, Department of National Defence (Canada) for their support of the project under Grant No. D.R.B. 9530-15.

REFERENCES

1. LEWIS, G. N. and RANDALL, M. Thermodynamics. McGraw-Hill Book Co., Inc., New York. 1926.
2. GLASSTONE, S. Thermodynamics for chemists. D. Van Nostrand Co., Inc., New York. 1947.
3. LAKHANPAL, M. and CONWAY, B. E. J. Polymer Sci. In press.
4. LEWIS, G. N. and RANDALL, M. J. Am. Chem. Soc. **43**, 233 (1921).

Can. J. Chem. Downloaded from www.nrcresearchpress.com by 41.223.56.140 on 09/04/12
For personal use only.

Can. J. Chem. Downloaded from www.nrcresearchpress.com by 41.223.56.140 on 09/04/12
For personal use only.

THE OXYGENATED FATTY ACIDS OF THE OIL OF WHEAT STEM RUST UREDOSPORES[1]

A. P. TULLOCH

ABSTRACT

The principal oxygenated acid present in the oil of wheat stem rust is *cis*-9,10-epoxyoctadecanoic acid, and is accompanied by a small proportion of (+) *threo*-9,10-dihydroxyoctadecanoic acid.

INTRODUCTION

The component fatty acids of the oil from uredospores of *Puccinia graminis* var. *tritici*, race 15B, were described previously (1), and the present paper reports chemical evidence for the structure of the *cis*-9,10-epoxyoctadecanoic acid which was found in the oil. After preliminary experiments (1) had shown the presence of an epoxy acid in the mixture, the free fatty acids were treated with acetic acid according to Gunstone's procedure (2) and the acetoxy acid, produced from the epoxide, was hydrolyzed. A dextrorotatory dihydroxyoctadecanoic acid was isolated and separated into racemic and (+) *threo*-9,10-dihydroxyoctadecanoic acids by fractional crystallization. The melting point and rotation of the latter were practically the same as those reported by McGhie *et al.* (3) for the synthetic (+) acid. The dihydroxy acid obtained initially was oxidized with the permanganate–periodate reagent (4, 5), which afforded only azelaic and pelargonic acids. These results, and those reported before (1), establish that the acid contains a *cis* epoxy group at the 9,10 position, but some of the dihydroxy acid isolated could have been present in the original oil. Therefore, a fresh sample of oil was fractionated by countercurrent distribution as the methyl esters and found to contain 1.3% of (+) *threo*-9,10-dihydroxyoctadecanoic acid and about 27% of the epoxy acid. Oil from other spores collected in the field in 2 different years contained 4–5% of the (+) dihydroxy acid and 20–22% of the epoxy acid.

threo-9,10-Dihydroxyoctadecanoic acid has been found in small amounts in the oil of *Lycopodium clavatum* spores (6, 7) but not in conjunction with an epoxy acid. However, Bharucha and Gunstone (8) found that the seed oil of *Cephalocroton cordofanus* (Muell Arg.) contained, in addition to 62% of *cis*-12,13-epoxyoleic acid, 4% of *threo*-12,13-dihydroxyoleic acid. King (9) has prepared a *cis*-9,10-epoxyoctadecanoic acid (m.p. 59.5° C, $[\alpha]_D$ +0.29°) from the naturally occurring form of *erythro*-9,10-dihydroxyoctadecanoic acid; however, the epoxy acid isolated in the present work melts at 58.5–59.5° C and has $[\alpha]_D$ −0.25°, and is probably the enantiomorphic form.

Bharucha and Gunstone (10) and Gunstone and Morris (11) found that acetolysis of *cis*-12,13-epoxyoleic acid and of *cis*-15,16-epoxylinoleic acid is, to some extent at least, stereospecific giving dextrorotatory *threo*-dihydroxy acids. With the 9,10-epoxy acid a completely stereospecific ring opening would give either the (+) or (−) 9,10-dihydroxy acid with a specific rotation of ±26°. However, acetic acid treatment of the epoxy acid followed by hydrolysis gave only a very weakly dextrorotatory product showing that, for this type of reaction, when the epoxide group is in the central 9,10-position the two C—O bonds are broken with almost equal ease. Therefore, samples of oil which yielded appreci-

[1]*Manuscript received October 19, 1959.*
Contribution from the National Research Council of Canada, Prairie Regional Laboratory, Saskatoon, Saskatchewan.
Issued as N.R.C. No. 5478.

able amounts of (+) dihydroxy acid on acetolysis were assumed to have contained this acid before the reaction was carried out. In particular, the fatty acids from the 1951 spores, which gave a dihydroxy acid with a specific rotation of +12.4°, must have contained more (+) acid than usual, perhaps because of the age of the spores.

EXPERIMENTAL

Extraction of the oil was carried out as previously described (1, 12). Melting points were measured with a Leitz heating stage microscope. Infrared spectra were recorded in the manner described earlier (1). All rotations were measured in ethanol in a 1-dm tube.

Acetolysis of the Fatty Acids of the Oil

The oil, extracted from rust spores which had been collected in 1951, was saponified by refluxing with 5% ethanolic potassium hydroxide for 1 hour and the free fatty acids isolated in the usual way. The fatty acids (3.800 g) were refluxed with glacial acetic acid (50 ml) for 4 hours, the acetic acid taken off, the product hydrolyzed with 5% alcoholic potash, acidified, and the acids extracted with ether. Removal of the ether gave a mixture of acids (3.760 g) which was distributed between 100-ml portions of 80% methanol and petroleum (b.p. 40–60° C) in five stages. The two most polar fractions contained 1.230 g of gum which, on crystallization from ethyl acetate, gave *threo*-9,10-dihydroxyoctadecanoic acid (0.818 g), $[\alpha]_D^{24}$ +12.4° (*c*, 1.7). The methyl ester prepared by diazomethane treatment gave colorless prisms from acetone/petroleum (b.p. 60–80° C), m.p. 68–70° C. Calculated for $C_{19}H_{38}O_4$: C, 69.04%; H, 11.59%. Found: C, 68.77%; H, 11.31%. Five further crystallizations of the acid from ethyl acetate gave racemic *threo*-9,10-dihydroxyoctadecanoic acid (0.200 g), m.p. 96–97° C, not depressed by admixture with the synthetic acid (13) of m.p. 95–96° C. Calculated for $C_{18}H_{36}O_4$: C, 68.31%; H, 11.47%. Found: C, 68.59%; H, 11.54%. The infrared spectrum was indistinguishable from that of the synthetic material. The acid recovered from the mother liquor of the first two ethyl acetate crystallizations was crystallized four times from acetone, yielding (+) *threo*-9,10-dihydroxyoctadecanoic acid (0.062 g), m.p. 98.5–99.5° C; $[\alpha]_D^{26}$ +25.60° (*c*, 0.6) (lit. (3) gives m.p. 99.5° C and $[\alpha]_D$ +23.5° in methanol). Calculated for $C_{18}H_{36}O_4$: C, 68.31%; H, 11.47%. Found: C, 68.31%; H, 11.49%. The infrared spectrum showed some small differences from that of the racemic acid.

Oxidation of the Dihydroxy Acid

The acid (0.127 g) was dissolved in a solution of potassium carbonate (0.174 g in 132 ml water), and sodium periodate (0.360 g) and potassium permanganate (0.004 g) in water (64 ml) were added. After it was shaken for 24 hours the solution was acidified (dilute sulphuric acid), saturated with sodium chloride, and extracted seven times with ether. Evaporation of the ether gave a mixture of acids (0.156 g) which, on stirring with petroleum, b.p. 40–60° C, gave azelaic acid (0.079 g), m.p. 104–106° C, after crystallization from ethyl acetate, which was not depressed by authentic azelaic acid, m.p. 105–107° C. Distillation of the petroleum-soluble fraction gave pelargonic acid, b.p. 95–100° C (air bath)/0.1 mm, the infrared spectrum of which was indistinguishable from that of an authentic specimen. The *p*-bromophenacyl ester had m.p. 63.5–64.0° C, undepressed by the synthetic derivative, m.p. 63.5–64.5° C. Calculated for $C_{17}H_{23}O_3Br$: C, 57.47%; H, 6.52%. Found: C, 57.68%; H, 6.59%. The mother liquors of both fractions were converted to methyl esters and, examined by gas liquid phase chromatography using the apparatus described previously (1), appeared to contain only pelargonic and azelaic esters.

Can. J. Chem. Downloaded from www.nrcresearchpress.com by 41.223.56.140 on 09/04/12
For personal use only.

Can. J. Chem. Downloaded from www.nrcresearchpress.com by 41.223.56.140 on 09/04/12
For personal use only.

Isolation of the Oxygenated Acids

Spores were collected from rusted Stewart wheat grown in the greenhouse (controlled to temperatures of 60–75° F) in July 1959 and the oil was extracted. Methyl esters of the fatty acids were prepared by treating the oil (4.327 g) with diazomethane to esterify traces of free acids, and then refluxing with methanolic sodium methoxide (70 ml, from 0.5 g of sodium in 1 liter of methanol) for 50 minutes. The solution was poured off from the insoluble residue (0.194 g), acetic acid (0.15 ml) added, the methanol distilled off, water added to the residue, and the product extracted with ether. After the solvent was removed, the esters (3.995 g) were separated by 120-tube distribution between petroleum (b.p. 60–80° C) and 85% ethanol using a modified E.C. Apparatus Co. fractionator with 100 tubes and 20-ml capacity each phase. Fractions 16–35 (0.100 g) after crystallization from petroleum, b.p. 60–80° C, gave methyl (+) *threo*-9,10-dihydroxyoctadecanoate, m.p. 59–61° C, $[\alpha]_D^{24}$ +23.9° (*c*, 1.65) (lit. (3) gives m.p. 62° C and $[\alpha]_D$ +22.5° in methanol). Calculated for $C_{19}H_{38}O_4$: C, 69.04%; H, 11.59%. Found: C, 68.82%; H, 11.47%. Saponification of the sample gave (+) *threo*-9,10-dihydroxyoctadecanoic acid (0.053 g, 1.3%), m.p. 98–99° C, $[\alpha]_D^{23}$ +26.6° (*c*, 1.3).

Fractions 68–85 (1.087 g) consisted almost entirely of methyl *cis*-9,10-epoxyoctadecanoate, and crystallization from acetone at 0° C gave the pure ester as leaflets, m.p. 24.5–25.5° C. Calculated for $C_{19}H_{36}O_3$: C, 73.03%; H, 11.61%. Found: C, 72.98%; H, 11.73%. $[\alpha]_D^{26}$ +1.1° (*c*, 5.25). The infrared spectrum showed a *cis* epoxide peak at 825 cm^{-1}; synthetic methyl *cis*-9,10-epoxyoctadecanoate had a very similar spectrum with a peak at 826 cm^{-1} (14). The ester (1.087 g) was refluxed with 2% ethanolic potassium hydroxide for 30 minutes, water (200 ml) was added, followed by hydrochloric acid (*N*/2) until the mixture was just acidic, the solid product was filtered off and washed thoroughly with water. On drying, *cis*-9,10-epoxyoctadecanoic acid (0.989 g) was obtained and crystallized from acetone as colorless platelets, m.p. 58.5–59.5° C (lit. (9) 59.5° C) depressed to 53–56° C on admixture with the synthetic racemic acid (13), m.p. 58.3–58.8° C. Calculated for $C_{18}H_{34}O_3$: C, 72.43%; H, 11.48%. Found: C, 72.51%; H, 11.56%. $[\alpha]_D^{24}$ −0.25° (*c*, 17.00) (lit. (9) gives $[\alpha]_D^{19}$ +0.29°). The infrared spectrum had a *cis* epoxide peak at 845 cm^{-1} compared to 842 cm^{-1} for the racemic acid (14, 15). Fractions 86–112 contained the methyl esters of the other fatty acids of the oil (C_{12}–C_{18}) (1) (2.511 g), and the other fractions contained only very small quantities of material.

Conversion of the Epoxy Acid to threo-9,10-Dihydroxyoctadecanoic Acid

The *cis*-9,10-epoxyoctadecanoic acid (0.400 g) was refluxed with glacial acetic acid (25 ml) for 4 hours and the acetic acid removed under vacuum. The residual syrup (0.487 g) $[\alpha]_D^{24}$ +0.71° (*c*, 6.30) was hydrolyzed with alcoholic sodium hydroxide (3%) and the product (0.411 g) isolated in the usual way. Without purification the $[\alpha]_D^{25}$ was +1.11° (*c*, 5.60); one crystallization from ethyl acetate (15 ml) gave racemic *threo*-9,10-dihydroxyoctadecanoic acid (0.270 g), m.p. 94–95.5° C, which had an infrared spectrum closely similar to that of an authentic sample.

ACKNOWLEDGMENTS

The author wishes to thank Dr. G. A. Ledingham and Dr. H. J. Reisener for gifts of spores and Mr. L. L. Hoffman and Mr. T. M. Mallard for assistance with the collection of spores and the extraction of the oil. Microanalyses were by Mr. M. Mazurek and infrared absorption spectra by Miss I. M. Gaffney.

REFERENCES

1. TULLOCH, A. P., CRAIG, B. M., and LEDINGHAM, G. A. Can. J. Microbiol. **5**, 485 (1959).
2. GUNSTONE, F. D. J. Chem. Soc. 1611 (1954).
3. MCGHIE, J. F., ROSS, W. A., and POLTON, D. J. Chem. & Ind. 353 (1956).
4. LEMIEUX, R. U. and VON RUDLOFF, E. Can. J. Chem. **33**, 1701 (1955).
5. VON RUDLOFF, E. Can. J. Chem. **34**, 1413 (1956).
6. RIEBSOMER, J. L. and JOHNSON, J. R. J. Am. Chem. Soc. **55**, 3352 (1933).
7. HIRAI, H. and TOYAMA, Y. J. Chem. Soc. Japan, Ind. Chem. Sect. **52**, 212 (1949).
8. BHARUCHA, K. E. and GUNSTONE, F. D. J. Sci. Food Agr. **7**, 606 (1956).
9. KING, G. J. Chem. Soc. 387 (1942).
10. BHARUCHA, K. E. and GUNSTONE, F. D. J. Chem. Soc. 1611 (1956).
11. GUNSTONE, F. D. and MORRIS, L. J. J. Chem. Soc. 2127 (1959).
12. HOUGEN, F. W., CRAIG, B. M., and LEDINGHAM, G. A. Can. J. Microbiol. **4**, 521 (1958).
13. SWERN, D. *In* Organic reactions. Vol. 7. *Edited by* R. Adams. John Wiley & Sons, Inc., New York. 1953. p. 378.
14. SHREVE, O. D., HEETHER, M. R., KNIGHT, H. B., and SWERN, D. Anal. Chem. **23**, 277 (1951).
15. O'CONNOR, R. T., MACK, C. H., DUPRÉ, E. F., and BICKFORD, W. G. J. Org. Chem. **18**, 693 (1953).

Can. J. Chem. Downloaded from www.nrcresearchpress.com by 41.223.56.140 on 09/04/12
For personal use only.

Can. J. Chem. Downloaded from www.nrcresearchpress.com by 41.223.56.140 on 09/04/12
For personal use only.

THE GAS HYDRATE OF BROMOCHLORODIFLUOROMETHANE[1]

D. N. Glew

ABSTRACT

An experimental study has been made of the saturation pressure – temperature lines of liquid bromochlorodifluoromethane, liquid bromochlorodifluoromethane – water, bromochlorodifluoromethane hydrate – water, and bromochlorodifluoromethane hydrate – ice systems, for which the characteristic equations are given. Two quadruple points for the hydrate systems have been located and solubilities of water in bromochlorodifluoromethane and bromochlorodifluoromethane in water determined. A systematic treatment of gas hydrate saturation pressure data to yield thermodynamic equations is indicated, and the thermodynamic functions for bromochlorodifluoromethane hydrate and its phase reactions are tabulated. Bromochlorodifluoromethane hydrate is shown to be a stoichiometric compound, and its thermodynamic functions are considered in relation to those of other gas hydrates.

INTRODUCTION

The gas hydrate clathrates, in which hydrate-formers are included in three-dimensional hydrogen-bonded water lattices, are of considerable interest in their own right and in the direct indication that they provide on the nature of the hydration shells confining aqueous non-electrolytes at lower temperatures (1, 2, 3).

Although the gas hydrates have been known for approximately 150 years their chemical formulae remained uncertain until 1951, when the structural work of Claussen (4) and the X-ray work of v. Stackelberg and Müller (5) elucidated the crystallographic structures of two distinct gas hydrate families based on two different fundamental water lattices. Recently two independent theoretical treatments (6, 7) have indicated that the formulae for the small molecule gas hydrates (Structure I) should change with temperature as a result of varying partial occupancy by the hydrate-former of available co-ordination sites within the hydrate water lattice.

It was therefore of interest to examine whether this partial occupancy obtained in the hydrates of larger molecules (Structure II) having the ideal crystallographic formula $M.17H_2O$. Furthermore, theoretical models for the gas hydrates have always assumed that the thermodynamic functions for the lattice water were little different from ice, in spite of the considerable difference of both hydrogen bond angles and separations (8). To obtain evidence for this assumption it was desirable to determine the heat capacity changes for hydrate formation, which would be considerably different from theoretical values for Structure II hydrates if the lattice water contributions were very different from ice, and/or if these hydrates were to exhibit significant changes of occupancy with temperature.

EXPERIMENTAL

Bromochlorodifluoromethane was purified in a Podbielniak low temperature distillation column and was analyzed as 99.9 mole% pure by mass spectrometry, the impurities being closely related halofluoromethanes. All water used was laboratory-once-distilled which had been passed through a mixed bed, demineralizing column.

The saturation pressure measurements were carried out with the condensed phases contained in either a simple unstirred 40-ml-capacity glass cell or a 100-ml glass cell equipped with a rotating paddle, which was driven magnetically. The pressure from the

[1]*Manuscript received September 17, 1959.*
Contribution No. 22 from the Exploratory Research Laboratory of Dow Chemical of Canada, Limited, Sarnia, Ontario, Canada.

saturation cell was transmitted via small bore glass tubing to a 1-cm I.D., U-type mercury manometer on which pressures were measured by cathetometer comparison with a stainless steel length standard accurate to ±0.02 mm at 100 mm and to ±0.04 mm at 1000 mm. All pressures were corrected to, and are quoted in, International mm Hg.

The vapor pressure cells were maintained at constant temperature using baths of melting methylene chloride −95°, subliming carbon dioxide −79°, melting chlorobenzene −45°, or a large capacity ethylene glycol – water thermostat between −30 and +10° C, the temperature of the vapor pressure cell being measured concurrently with the saturation pressure determinations. Temperatures were determined with a calibrated 65-ohm platinum resistance thermometer and standardized Müller bridge using a total bridge current of 2 ma and photoelectric amplifier–galvanometer as null detector. In the temperature range −20 to +10° C the precision of temperature difference measurement was ±0.001°, which, including ice-point errors and thermostat fluctuations, gives the temperatures reported an absolute accuracy of ±0.003° on the centigrade scale.

For vapor pressure measurement a 20-ml middle-fraction, from an original 40-ml freeze-outgassed sample of bromochlorodifluoromethane, was distilled into the evacuated vapor pressure cell, the sample was further freeze-outgassed and the cell was then isolated by mercury cutoff valve. For the experiments below −30° C the unstirred 40-ml cell immersed in the various cooling baths was used; the pressure and temperature were measured at regular intervals for periods of 4–10 hours, and some 20–30 independent readings were averaged in obtaining each of the experimental values recorded. Between −21 and 10° C, vapor pressure measurements were conducted in the 100-ml capacity cell immersed in the thermostat which maintained temperatures constant to ±0.002° C. The use of stirrer was unnecessary since the vapor pressure attained equilibrium within 1 hour, after which time a series of 4–6 pressure–temperature readings were taken to define each reported result.

In the preparation of the two-component water–bromochlorodifluoromethane systems, approximately 50 ml of freeze-outgassed water was transferred to the evacuated 100-ml cell maintained by the thermostat at +0.5° C. The stirrer was put into operation, the stirred water evacuated a further 30 minutes, the pumps isolated, and a 5-ml sample of freeze-outgassed bromochlorodifluoromethane distilled from a cold finger into the cell at 900 mm Hg pressure. After a short period gas hydrate formed and after the pressure had decreased to 600 mm Hg the cell and its contents were isolated by mercury cutoff valve.

Equilibrium measurements of (l_1l_2v), see Glossary of Symbols, were found to be most rapidly and reproducibly obtained by approaching equilibrium from higher temperatures, since removal of supersaturation was faster than attainment of saturation from the unsaturated condition. Thus, in obtaining equilibrium at a given temperature the thermostat was raised 0.7° C above this and the cell contents stirred rapidly for 4 hours, after which time the temperature was lowered to the required value and the stirring progressively moderated over a 6-hour period. The system was allowed to equilibrate a further 6 hours and then 4–6 equilibrium measurements were taken over a 4-hour period.

Kinetic measurements on (hl_1v) showed that equilibrium was generally attained with stirring after about 24 hours when approached from lower temperatures and pressures, as opposed to 48 hours when approached from higher temperatures. It was further observed that although the kinetic rates in different experiments varied irreproducibly, presumably due to uncontrolled factors such as hydrate crystallite size, proximity of crystals to liquid surface, quantity of freely suspended crystals in liquid phase, etc., equilibrium was attained in any single experiment with constant (or no) stirring according to a first-order

Can. J. Chem. Downloaded from www.nrcresearchpress.com by 41.223.56.140 on 09/04/12
For personal use only.

rate law. When equilibrium measurements, which were approached from both lower and higher temperatures, were taken, the vapor pressure cell contents were stirred for 24–48 hours to come near to equilibrium, the stirrer was stopped, and the system left for a further 24 hours, after which 7–20 pressure–temperature readings were taken at regular intervals for a period 2–6 days, depending on the variability observed. To allow for the diurnal temperature variation of the unthermostatted mercury manometer and connecting tubing, all observed pressures were corrected to the average ambient temperature by applying a dead-volume correction. The precision of measurement of the pressures is essentially that of the length standard; however, the accuracy achieved over the 0–10° C range is certainly inferior, and is probably still due to lack of attainment of equilibrium.

Measurements on the solid (hs_1v), for which the stirrer was inoperative, showed that equilibrium was reached faster, 1–3 days, by approach from lower temperatures in which the hydrate decomposition reaction was involved. However, to confirm equilibrium, experiments from -5 to $-20°$ C were conducted starting both from below and above the required equilibrium temperatures, and the readings reported for each temperature represent averages of 25–42 separate measurements conducted over periods of 1 week or longer. The remaining results were derived from experiments approaching equilibrium from lower temperatures in which some 15 measurements were taken over 3-day periods. The improved absolute accuracy of the pressures measured for (hs_1v) is due both to the large number of readings taken at each temperature and to the reduced effect of ambient temperature variation. The apparent agreement shown in Table IV below $-10°$ C is fortuitous and cannot be considered significant since it is far beyond the ultimate accuracy ± 0.02 mm of the calibrated length standard.

The saturation pressure at $Q(hs_1l_1v)$ was determined by kinetic analysis of the first-order change of pressure with time exhibited when (hs_1v) initially at $-0.2°$ C was maintained in the thermostat set at $+0.013°$ C. The rate of melting of s_1 to l_1 was sufficiently slow that (hs_1l_1v) was observed for 30 hours, and the recorded pressure is an average of the "infinite time" pressures derived from six experimental measurements taken between 24 and 30 hours.

Liquid Bromochlorodifluoromethane – Vapor System

In Table I are presented experimental values for the saturation vapor pressure, p_2^0 International mm Hg, of liquid bromochlorodifluoromethane between -100 and $+10°$ C. In conjunction with the critical constants (9) the least-squares equation is derived,

$$[1] \qquad \log_{10} p_2^0 = -2106.200/T - 12.25100 \log_{10} T + 0.007417\, T + 38.47978$$

which is valid in the range -100 to $+154°$ C with $T°\,K = 273.16 + t°$ C. In the third column are shown back-calculated values using [1], from which a standard deviation of $\pm 0.0635\%$ is assigned to individual measurements. This error is unrealistically large for pressures between 366 and 1260 mm Hg and must be ascribed to inadequacy of the four-constant equation [1].

The normal boiling point derived from [1] is $-4.01 \pm 0.01°$ C. A liquid molar volume of 85 ml and a second virial coefficient of -722 ml, obtained respectively from the liquid densities (9, 10) and from the law of corresponding states (*vide infra*), lead to a compressibility factor of 0.9635, a heat content of vaporization of 5339 ± 30 cal_{15}/mole or 32.28 cal/g, and a Trouton constant of 19.8 cal/deg-mole. The statistical heat capacity of the ideal vapor from Gelles and Pitzer (11) yield heat capacities of 17.2 ± 0.1 and 23.1 ± 0.7 cal/deg-mole for the real vapor and liquid respectively at $-4.01°$ C.

Can. J. Chem. Downloaded from www.nrcresearchpress.com by 41.223.56.140 on 09/04/12
For personal use only.

Hydrate Molar Volume and Bromochlorodifluoromethane Second Virial Coefficient

In the calculation of the thermodynamic functions for bromochlorodifluoromethane hydrate from the saturation data to be presented, a knowledge of the associated phase volume changes and the bromochlorodifluoromethane vapor imperfections is essential.

TABLE I

Vapor pressure of liquid bromochlorodifluoromethane

t (° C)	p_2^0 obs. (Int. mm Hg)	p_2^0 calc. (Int. mm Hg)
−95.335	2.45	2.45
−78.798	11.19	11.15
−45.305	110.29	110.28
−21.531	366.06	366.55
−20.002	392.03	392.46
−17.398	439.49	439.91
−15.034	486.39	486.82
−12.447	542.26	542.58
−10.049	598.46	598.64
− 7.455	664.05	664.29
− 5.074	701.64	701.71
− 4.161	755.85	755.62
− 4.078	758.14	758.03
− 3.957	761.71	761.58
− 3.860	764.59	764.42
− 2.080	818.57	818.16
− 0.093	882.05	881.57
+ 1.914	949.98	949.42
3.909	1020.9	1020.8
5.925	1097.6	1097.1
7.907	1177.0	1176.3
9.890	1260.8	1259.8
153.8[a]	30770.	30800.

[a]Critical point reference 9.

The molar volumes of liquid water $V_1^{l_1}$ and of solid ice $V_1^{s_1}$ have been taken from the critical compilation of Dorsey (12), whilst the derived values for the hydrate molar volume V^h and the bromochlorodifluoromethane second virial coefficient B_2 are presented here. Taken in order $t°$ C, V^h ml/mole, B_2 ml/mole; −20, 390.5, −816; −15, 391, −786; −10, 391, −757; −5, 391.5, −728; 0, 392, −701; +5, 392, −675; and +10, 392.5, −650. Values for V^h have been calculated from the cubic lattice spacing $a = 17.33$ Angstrom units at 0° C, measured by v. Stackelberg *et al.* (8, 13) for similar hydrates of CH_2Cl_2, $CHCl_3$, CCl_2F_2, and CCl_3F, using a coefficient of expansion for hydrate assumed equal to the volume coefficient $\beta = 153 \times 10^{-6}$ deg^{-1} for ice (12). Values for B_2 have been obtained from an assumed similarity with the second virial coefficients of CCl_2F_2 and CCl_3F (14), invoking the principle of corresponding states as applied to the reduced second virial coefficients (15), using the bromochlorodifluoromethane critical constants (9), $V_c = 232$ ml/mole at $t_c = 153.8°$ C.

Liquid Water – Liquid Bromochlorodifluoromethane – Vapor System

The liquid water (l_1) – liquid bromochlorodifluoromethane (l_2) – vapor (v), (l_1l_2v), three-phase system attains equilibrium at constant temperature according to the equation,

[2] $$H_2O\ (l_1) + CBrClF_2\ (l_2) \rightleftharpoons H_2O\ (v) + CBrClF_2\ (v)$$

$x_1^{l_1}$ $x_1^{l_2}$ $p_1(l_1l_2v)$

$x_2^{l_1}$ $x_2^{l_2}$ $p_2(l_1l_2v)$

Can. J. Chem. Downloaded from www.nrcresearchpress.com by 41.223.56.140 on 09/04/12
For personal use only.

in which $x_1^{l_1}$ and $x_1^{l_2}$ are the mole fractions of component 1, water, in phases l_1 and l_2; $x_2^{l_1}$ and $x_2^{l_2}$ are the mole fractions of component 2, bromochlorodifluoromethane, in l_1 and l_2; and $p_1(l_1l_2v)$ and $p_2(l_1l_2v)$ are the component 1 and 2 saturation partial pressures for the (l_1l_2v) equilibrium. Since $x_1^{l_2} \simeq 10^{-3}$ and $x_2^{l_1} \simeq 10^{-4}$ (*vide infra*), the experimental total pressure $P(l_1l_2v)$ is accurately represented by the sum of the Raoult law terms

$$[3] \qquad P(l_1l_2v) = p_1(l_1l_2v)+p_2(l_1l_2v) = p_1^0+p_2^0\,x_2^{l_2}$$

in which $p_1^0\,x_1^{l_1}$ is replaced by p_1^0 for pure l_1.
Rearrangement of [3], noting that $x_1^{l_2}+x_2^{l_2} = 1$, yields

$$[4] \qquad x_1^{l_2} = [p_1^0 + p_2^0 - P(l_1l_2v)]/p_2^0 = 1-p_2(l_1l_2v)/p_2^0$$

from which the saturation solubility of water in liquid bromochlorodifluoromethane is derived.

Calculation of $x_1^{l_2}$ from [4] requires values of p_2^0 at temperatures corresponding to the (l_1l_2v) measurements, and although equation [1] would appear suitable for this purpose its long temperature range and small number of constants make it a forcing equation, from which the experimental p_2^0 values show systematic deviations between -21 and 10° C. To provide a better representation of the experimental p_2^0 values between 4 and 10° C, and a relation for $p_2(l_1l_2v)$ between 9.4 and 10.4° C, the equations

$$[5] \qquad \log_{10} p_2(l_1l_2v) = -1197.8701/T+7.332245\pm0.000018$$

$$[6] \qquad \log_{10} p_2^0 = -1197.8701/T+7.332552\pm0.000070,$$

shown with their standard errors, have been derived as best fits of the data presented in Table II, using a slope factor defined by [1] at 7° C. In the fourth column of Table II are

TABLE II

Solubility of water in liquid bromochlorodifluoromethane

t (° C)	$p_2(l_1l_2v)$ (Int. mm Hg)	p_2^0 (Int. mm Hg)	$x_1^{l_2}$ ($\times10^4$)
10.362	1279.99		8.8
10.266	1275.65		9.8
10.096	1268.51		7.5
9.968	1263.06		6.6
9.906[a]	1260.37		6.5
9.890	—	1260.79	—
9.846	1257.70		7.1
9.773	1254.50		7.4
9.766	1254.29		6.7
9.589	1246.65		6.7
9.416	1239.36		5.7
9.412	1239.28		4.9
7.907	—	1176.97	—
7.882	1175.15		4.9
5.925	—	1097.60	—
5.910	1096.18		7.1
3.909	—	1020.90	—

[a]Below 9.96° (l_1l_2v) metastable with respect to $(hl_{IV}v)$.

shown values of $x_1^{l_2}$, derived from $p_2(l_1l_2v)$ and p_2^0 from [6], on which there is a standard deviation ±0.00021. At an average temperature 9.86° C, which is near to $Q(hl_1l_2v)$ at 9.96° C (*vide infra*), equations [5] and [6] yield $x_1^{l_2} = 0.000707\pm0.000165$.

Although no comparable solubility measurement is available for water in liquid bromochlorodifluoromethane, this value is of the same magnitude although slightly larger than the mole fractions 0.00029 and 0.00042 reported (16) for water in the similar dichlorodifluoromethane and trichlorofluoromethane liquids.

Can. J. Chem. Downloaded from www.nrcresearchpress.com by 41.223.56.140 on 09/04/12
For personal use only.

Hydrate – Liquid Water – Vapor System

When the (l_1l_2v) system containing excess l_1 is cooled below 10° C it becomes metastable with respect to the (hl_1v) three-phase equilibrium, which is established according to the equation

[7] $$CBrClF_2.nH_2O\ (h) \rightleftharpoons nH_2O(l_1) + CBrClF_2\ (v)$$
$$p_1(hl_1v) \quad p_2(hl_1v)$$
$$x_1^{l_1}\ x_2^{l_1}$$

in which a solid bromochlorodifluoromethane hydrate phase h coexists with a dilute aqueous solution phase and a vapor phase. At constant temperature the system becomes invariant and its total pressure $P(hl_1v)$ attains a saturation equilibrium value, often called the "hydrate vapor pressure". This total pressure is adequately expressed by the relation

[8] $$P(hl_1v) = p_1^0 + p_2(hl_1v)$$

(cf. equation [3]) in which $p_2(hl_1v)$ is the saturation partial pressure of 2 for the (hl_1v) equilibrium.

In Table III are shown values for $p_2(hl_1v)$ and back-calculated values from the relation

[9] $$\log_{10} p_2(hl_1v) = 9963.8593/T + 144.056871 \log_{10} T - 385.31498$$

which has been derived by the method of least squares. The theory of errors indicates a standard error of ±0.0806% on individual pressure measurements which is significantly

TABLE III

Vapor pressure of bromochlorodifluoromethane hydrate with water

t (° C)	$p_2(hl_1v)$ (Int. mm Hg)	$p_2(hl_1v)$ calc. (Int. mm Hg)
9.960[a]	—	1262.6
9.777	1213.2	1212.4
9.244	1076.9	1076.7
8.740	962.85	962.67
8.723	958.33	958.92
8.255	864.41	864.20
7.779	776.58	777.49
7.658	756.32	756.87
7.284	695.50	696.56
6.772	620.70	621.72
6.275	557.39	556.86
6.254	553.49	554.26
5.764	498.09	497.24
5.757	496.89	496.46
5.273	446.05	445.98
5.264	445.17	445.08
4.764	398.61	398.45
4.267	356.97	356.97
3.773	320.34	320.03
3.270	286.44	286.37
2.767	256.25	256.26
2.268	229.47	229.54
1.766	205.43	205.49
1.256	183.54	183.64
0.755	164.43	164.47
0.244	146.98	146.97
0.235	146.71	146.68
0.092	142.30	142.14
0.023	139.96	140.00
0.019	139.80	139.87
0.013	139.69	139.68
-0.001_4[b]	139.18	139.25

[a] = $Q(hl_1l_2v)$. [b] = $Q(hs_1l_1v)$.

Can. J. Chem. Downloaded from www.nrcresearchpress.com by 41.223.56.140 on 09/04/12
For personal use only.

larger than the precision of ±0.02 mm on the pressure measurement. At low pressures the standard error derives approximately equally from pressure measurement and effect of dead space, whilst at higher pressures the error is predominantly due to lack of attainment of equilibrium through diurnal temperature variation of the dead space.

Hydrate–Ice–Vapor System

When the (hl_1v) system is cooled below 0° C all excess l_1 freezes to give a solid ice phase s_1 and the (hs_1v) equilibrium is then established according to the equation

$$[10] \qquad \underset{}{CBrClF_2.nH_2O(h)} \rightleftharpoons \underset{p_1(hs_1v)}{nH_2O(s_1)} + \underset{p_2(hs_1v).}{CBrClF_2(v)}$$

At constant temperature the total pressure $P(hs_1v)$ attains a constant saturation value, equal to the sum of $p_2(hs_1v)$ and $p_1(hs_1v)$, of which the latter is the saturation sublimation pressure of ice (12).

In Table IV are presented values for $p_2(hs_1v)$ between 0 and −20° C which are represented by the equation

$$[11] \qquad \log_{10} p_2(hs_1v) = -1809.4253/T + 0.034379 \log_{10} T + 8.68372$$

with a standard error of ±0.0860% on single pressure determinations. In the third column of the table are shown back-calculated values for $p_2(hs_1v)$ from [11] using the experimental temperatures. Although few experimental values are given, each result represents multiple determinations approaching equilibrium from pressures above and below the saturation value.

Quadruple Points

In the present two-component system the end points of the (hl_1v) stability range at approximately 10 and 0° C are the respective invariant quadruple points $Q(hl_1l_2v)$ and $Q(hs_1l_1v)$, corresponding to the equilibrium coexistence of the four-phase systems (hl_1l_2v) and (hs_1l_1v).

The cut of the (l_1l_2v) and (hl_1v) three-phase lines (equations [5] and [9]) defines $Q(hl_1l_2v)$, with $p_2(hl_1l_2v)$ = 1262.65±0.58 mm Hg at $t(hl_1l_2v)$ = 9.96±0.03° C, above which temperature the hydrate cannot exist in the presence of a vapor phase. $Q(hl_1l_2v)$ is

TABLE IV

Vapor pressure of bromochlorodifluoromethane hydrate with ice

t (° C)	$p_2(hs_1v)$ (Int. mm Hg)	$p_2(hs_1v)$ calc. (Int. mm Hg)
− 0.001_4[b]	139.18	139.13
− 0.292	136.79	136.87
− 1.083	131.06	130.92
− 5.066	104.15	104.23
−10.067	77.548	77.518
−15.070	56.991	56.990
−19.993	41.606	41.608

[b] = $Q(hs_1l_1v)$.

sometimes called the "hydrate critical point" which is a misnomer since, although this point is located at the highest temperature of coexistence of phases h and v, it does not necessarily represent the highest temperature at which hydrate can exist under hydrostatic pressure in the absence of a vapor phase (17).

Can. J. Chem. Downloaded from www.nrcresearchpress.com by 41.223.56.140 on 09/04/12
For personal use only.

Direct experimental determination of the invariant point $Q(hs_1l_1v)$ has been made through kinetic analysis of the total pressure change observed during the isothermal phase reaction $(hs_1v) \rightarrow (hl_1v)$. These experiments gave a total pressure $P(hs_1l_1v) = 143.757 \pm 0.010$ mm Hg or $p_2(hs_1l_1v) = 139.181$ mm Hg. Substitution of this value for $p_2(hs_1l_1v)$ into equations [9] and [11] yields the temperatures $-0.003_6°$ and $+0.006_3°$ C respectively for the four-phase point, whilst the intersection of the (hl_1v) and (hs_1v) curves (equations [9] and [11]) gives $-0.006_9°$ C. On consideration of the lack of agreement of these three results, on which there are standard errors of $\pm 0.005°$ C, the experimentally determined four-phase temperature is taken as their mean $-0.001_4 \pm 0.005°$ C. Quantitative analysis of the l_1 phase at the termination of the experiment showed the presence of halogen acids depressing the experimental four-phase point by $0.001_4°$ C, from which the true quadruple temperature $t(hs_1l_1v) = 0.000 \pm 0.005°$ C.

Solubility of Bromochlorodifluoromethane in Water

The triple point of water (12), corrected for hydrostatic pressure, taken in conjunction with $Q(hs_1l_1v)$ at $0.000 \pm 0.005°$ C indicates a freezing point depression of $0.0084 \pm 0.005°$ C due to a mole fraction $x_2^{l_1} = 8.2 \times 10^{-5}$, which yields a Henry's law constant $H_2 = p_2(hs_1l_1v)/x_2^{l_1} = 1.7 \pm 1.0 \times 10^6$ mm Hg at 0° C for the solubility of bromochlorodifluoromethane in water. No other solubility determination is available for direct comparison, but the present value compares favorably with 4.1×10^6 mm Hg for dichlorodifluoromethane at 0° C extrapolated from the work of Parmelee (18). If it is assumed that the heat functions for the solubility of component 2 in l_1 are the same (3) as those for dichlorodifluoromethane (18), the temperature variation of H_2 in mm Hg is expressed by

$$\log_{10} H_2 = -10920/T - 72 \log_{10} T + 221.6298. \quad [12]$$

This equation is used to evaluate the solubility correction terms in [18].

Quantitative analysis of bromide and chloride ion concentration in phase l_1, by the mercuric nitrate – diphenyl carbazone method, showed hydrolysis of a mole fraction of 1.72×10^{-6} of bromochlorodifluoromethane over a period of 124 days, from which an upper limit of 2×10^{-9} (sec^{-1}) is set on the first-order velocity constant for hydrolysis of dissolved aqueous bromochlorodifluoromethane at 0° C.

Thermodynamic Functions for Hydrate Phase Reactions

Scheffer and Meyer (19) first indicated the exact use of the Clapeyron equation for obtaining the heat changes along the (hs_1v) and (hl_1v) saturation lines making due allowance for the small attendant vaporization heats of ice and water and solution heat of hydrate-forming gas. These workers, however, restricted their consideration to heat changes, being primarily interested in determination of the hydrate formula number n (*vide infra*, equation [23]). Here, in uniformity with modern usage, it was deemed desirable to indicate the systematic incorporation of correction terms necessary in obtaining other thermodynamic functions from hydrate equilibrium line data, and to define standard states in a manner convenient for comparison and conjunction with existent thermochemical tabulations. In this and other work the standard thermodynamic functions refer to condensed phases at 1 normal atmosphere pressure and to gaseous phases at 1 atmosphere fugacity; these standard functions are denoted by the usual superscript zero followed by a characteristic indication of phase. Standard changes of thermodynamic functions are represented in the normal way except that the phase reaction direction is included in parenthesis.

Consider the (hl_1v) equilibrium for which G_1, G_2, and G^h are the respective molar free

Can. J. Chem. Downloaded from www.nrcresearchpress.com by 41.223.56.140 on 09/04/12
For personal use only.

Can. J. Chem. Downloaded from www.nrcresearchpress.com by 41.223.56.140 on 09/04/12
For personal use only.

energies of components 1 and 2 and of h throughout the system at absolute temperature T and total saturation pressure $P(\mathrm{hl_1v})$. At equilibrium, the molar free energy change for [7], denoted by $\Delta G(\mathrm{h} \rightarrow \mathrm{l_1v})$, is given by

$$\Delta G(\mathrm{h} \rightarrow \mathrm{l_1v}) = nG_1 + G_2 - G^{\mathrm{h}} = 0 \qquad [13]$$

in which the individual molar free energy terms are defined by

$$G_1 = G_1^{0\,\mathrm{l_1}} + RT \ln x_1^{\mathrm{l_1}} + [P(\mathrm{hl_1v}) - 1] V_1^{\mathrm{l_1}}, \qquad [14]$$

$$G_2 = G_2^{0\mathrm{v}} + RT \ln p_2(\mathrm{hl_1v}) + p_2(\mathrm{hl_1v}) B_2, \qquad [15]$$

and

$$G^{\mathrm{h}} = G^{0\,\mathrm{h}} + [P(\mathrm{hl_1v}) - 1] V^{\mathrm{h}}. \qquad [16]$$

In [14] and [16] $G_1^{0\,\mathrm{l_1}}$ and $G^{0\,\mathrm{h}}$ are the free energies for the condensed phases of pure $\mathrm{l_1}$ and of h at 1 atmosphere pressure, whilst $G_2^{0\mathrm{v}}$ is the free energy for an ideal gaseous component 2 having a fugacity of 1 atmosphere. Substitution of [14], [15], and [16] into [13] with replacement of $RT \ln x_1^{\mathrm{l_1}}$ by $-RTp_2(\mathrm{hl_1v})/H_2$ yields

$$-\Delta G^0(\mathrm{h} \rightarrow \mathrm{l_1v}) = RT \ln p_2(\mathrm{hl_1v}) + RT \ln \gamma(\mathrm{hl_1v}) \qquad [17]$$

with

$$RT \ln \gamma(\mathrm{hl_1v}) = p_2(\mathrm{hl_1v})[B_2 - nRT/H_2] + [P(\mathrm{hl_1v}) - 1][n V_1^{\mathrm{l_1}} - V^{\mathrm{h}}] \qquad [18]$$

where $\Delta G^0(\mathrm{h} \rightarrow \mathrm{l_1v})$ is the standard free energy change at 1 atmosphere for reaction [7] and $\gamma(\mathrm{hl_1v})$ is the over-all reaction activity coefficient.

A similar treatment applied to the $(\mathrm{hs_1v})$ equilibrium yields the parallel relations

$$\begin{aligned} -\Delta G^0(\mathrm{h} \rightarrow \mathrm{s_1v}) &= -(nG_1^{0\,\mathrm{s_1}} + G_2^{0\mathrm{v}} - G^{0\,\mathrm{h}}) \\ &= RT \ln p_2(\mathrm{hs_1v}) + RT \ln \gamma(\mathrm{hs_1v}) \end{aligned} \qquad [19]$$

and

$$RT \ln \gamma(\mathrm{hs_1v}) = p_2(\mathrm{hs_1v}) B_2 + [P(\mathrm{hs_1v}) - 1][n V_1^{\mathrm{s_1}} - V^{\mathrm{h}}] \qquad [20]$$

in which $\Delta G^0(\mathrm{h} \rightarrow \mathrm{s_1v})$ is the standard free energy change for reaction [10] and $\gamma(\mathrm{hs_1v})$ is the corresponding reaction activity coefficient.

In order to evaluate [18] and [20] n must be determined; the hydrate structural work of Claussen (4) and of v. Stackelberg (8, 13), together with the uncorrected heat content changes derived from [9] and [11] taken in [23], indicates that $n = 17$ for bromochlorodifluoromethane hydrate. With this preliminary value for n, $\gamma(\mathrm{hl_1v})$ and $\gamma(\mathrm{hs_1v})$ are calculated at each experimental temperature and the $p_2(\mathrm{hl_1v}).\gamma(\mathrm{hl_1v})$ and $p_2(\mathrm{hs_1v}).\gamma(\mathrm{hs_1v})$ terms (atmospheres) evaluated. The common logarithms of the reaction activity functions are fitted by the method of least squares to yield

$$\log_{10} p_2(\mathrm{hl_1v}).\gamma(\mathrm{hl_1v}) = 1156.5003/T + 69.766909 \log_{10} T - 174.95407 \qquad [21]$$

$$\log_{10} p_2(\mathrm{hs_1v}).\gamma(\mathrm{hs_1v}) = -1876.5722/T - 0.607407 \log_{10} T + 7.61080 \qquad [22]$$

from which the standard thermodynamic function changes are derived.

In Table V are presented the thermodynamic functions at 273.16° K for $(\mathrm{h} \rightarrow \mathrm{l_1v})$ and $(\mathrm{h} \rightarrow \mathrm{s_1v})$ derived from [21] and [22] using the gas constant $R = 1.986467$ $\mathrm{cal_{15}}$/deg-mole. The quoted limits of error are standard errors including variances from random error, solubility error, and a 5% uncertainty on the second virial coefficient. Although the free

energy, heat content, and entropy terms at 273.16° K are only slightly affected by variation of solubility and compressibility corrections, $\Delta Cp^0(h \rightarrow l_1v)$ is a sensitive function depending strongly on these corrections (cf. coefficients of $\log_{10} T$ in [9] and [21]), the errors on which contribute more than half the standard error quoted. The standard error on $\Delta Cp^0(h \rightarrow s_1v)$ is reduced, although based on fewer points, since this function is derived from lower pressure data independent of any solubility correction.

Derived indirectly from the heat content change relation

[23] $$\Delta H^0(h \rightarrow l_1v) - \Delta H^0(h \rightarrow s_1v) = n\Delta H^0(s_1 \rightarrow l_1)$$

in which $\Delta H^0(s_1 \rightarrow l_1)$ is the heat of fusion of water (12) (1435.7 cal_{15}/mole at 273.16° K); the hydrate formula number n is found respectively at −5, 0, and +5° C to be 16.99, 16.94, and 16.90±0.34 within a 90% confidence limit of error.

TABLE V

Thermodynamic functions for $CBrClF_2.17H_2O$ at 273.16° K

	$(h \rightarrow l_1v)$		$(h \rightarrow s_1v)$	
ΔG^0 cal/mole	923.3±0.5		923.3±0.5	
ΔH^0 cal/mole	32,567±70		8,254±29	
ΔS^0 cal/deg-mole	115.8±0.3		26.8±0.1	
ΔCp^0 cal/deg-mole	138.6±10.9		−1.2±5.9	
$17S_1^{0\,l_1} + S_2^{0\,v}$	332.4±0.3	$17S_1^{0\,s_1} + S_2^{0\,v}$		243.1±0.3
$S^{0\,h}$ cal/deg-mole	216.6±0.4	$S^{0\,h}$ cal/deg-mole		216.2±0.3
$17Cp_1^{0\,l_1} + Cp_2^{0\,v}$	324.9±0.1	$17Cp_1^{0\,s_1} + Cp_2^{0\,v}$		165.9±0.1
$Cp^{0\,h}$ cal/deg-mole	186.3±10.9	$Cp^{0\,h}$ cal/deg-mole		167.1±5.9
$d(17Cp_1^{0\,s_1} + Cp_2^{0\,v})/dT$		0.60±0.01		
$d(Cp^{0\,h})/dT$ cal/deg²-mole		1.29±0.83		

The hydrate standard entropy values presented are derived from Gordon's (20) spectroscopic entropy for water and from Gelles and Pitzer's (11) spectroscopic values for bromochlorodifluoromethane with n taken as 17.00. The two values of $Cp^{0\,h}$ quoted are strictly mean values at 278.05 $(h \rightarrow l_1v)$ and at 263.16° K $(h \rightarrow s_1v)$ and are derived from the properties of the pure components (11, 12, 20) at these temperatures.

DISCUSSION

The experimental value determined for n between −5 and +5° C for the present hydrate is equal to the ideal crystallographic value of 17 given by Claussen (4) and by v. Stackelberg (8, 13) the deviation being well within the 90% confidence limit of error. It had been expected that this work would show a possible significant deviation of n greater than 17, similar to the deviations discussed by Platteeuw and van der Waals (6) for the gas hydrates (Structure I) of small molecules: this, however, is apparently not the case for bromochlorodifluoromethane hydrate (Structure II).

The thermodynamic functions for the $(h \rightarrow s_1v)$ reaction are somewhat remarkable in their similarity with those for normal liquid evaporation, in spite of the complex nature of the hydrate decomposition process involving an environmental change of 17 moles of hydrogen-bonded lattice water. With our present structural knowledge of the hydrogen-bonded gas hydrate lattices (Structures I and II) the simplest interpretation of this similarity, always assuming that it is not fortuitous, is that the thermodynamic functions for the water within the hydrate lattices are little different from ice, whilst those for hydrate-former escape are comparable with liquid evaporation. Notwithstanding the

Can. J. Chem. Downloaded from www.nrcresearchpress.com by 41.223.56.140 on 09/04/12
For personal use only.

differences, the analogy is further extended on recognition that the hydrate-former leaves a confining cell of high and nearly spherical symmetry, whereas in liquid evaporation the escape is from a cell with statistical spherical symmetry.

On the assumption of identity of the water functions, $\Delta H^0(\text{h} \rightarrow \text{s}_1\text{v})$ gives a direct measure of the over-all attractive energy of the hydrate-former with its lattice, primarily arising from interaction with its immediate 28-member water co-ordination shell and to a smaller extent with more distant water and hydrate-former neighbors. Consideration of the force field exerted at the hydrate-former by the hydrogen-bonded water co-ordination shell shows that the attractive energy derives predominantly from central fields of the α_1–α_2 dispersion type on which a smaller $\mu_2-\alpha_1$ induction effect is superimposed. The angularly dependent $\mu_1-\mu_2$ orientation and $\mu_1-\alpha_2$ induction effects do not arise because of high co-ordination shell symmetry and water dipole neutralization through hydrogen bonding, which reduces μ_1 to zero or to a higher multipole. For such a model it is reasonably expected that the nearly spherical bromochlorodifluoromethane hydrate-former should rotate classically within the approximately central force field of its water co-ordination shell, and that the interaction energy should be accurately calculable from theoretical considerations.

As early as 1902 de Forcrand (21), to evaluate $\Delta H(\text{h} \rightarrow \text{s}_1\text{v})$ for a number of unmeasured hydrate-formers, used an empirical gas hydrate entropy rule similar to the Trouton rule for liquids. Recently v. Stackelberg (22) demonstrated that $\Delta S^0(\text{h} \rightarrow \text{s}_1\text{v})$ at 0° C was approximated by the entropy of sublimation of the hydrate-former, ascribing a constant value of 22 cal/deg-mole; agreement with experimental data, however, was only moderate. Platteeuw and van der Waals (6) pointed out the failure of a constant valued $\Delta S^0(\text{h} \rightarrow \text{s}_1\text{v})$, and in their partially occupied lattice treatment, based on the Lennard-Jones and Devonshire cell model, achieved better agreement with experiment.

Here analogy is maintained with liquid evaporation as in the v. Stackelberg approximation (22) and $\Delta S^0(\text{h} \rightarrow \text{s}_1\text{v})$ is taken as an evaporation entropy term plus a further $R \ln e$ for the lack of communal entropy in the hydrate. However, the evaporation entropy term is not considered to be constant, but rather a function of hydrate former molar volume, which is geometrically related to the hydrate-former free volume within its nearly constant-volume co-ordination shell. Figure 1 illustrates such a relationship for the small molecule (Structure I) and large molecule (Structure II) gas hydrates, for which $\Delta S^0(\text{h} \rightarrow \text{s}_1\text{v})$ at 0° C has been plotted against V, the hydrate-former molar volume at the normal boiling point. From the figure it is immediately apparent that the hydrates fall into two distinct groups which present linear and parallel entropy change – volume relationships running over the range 22–27 cal/deg-mole. Furthermore, the hydrate-formers smallest with respect to their co-ordination polyhedra, H_2S, CH_4 (Structure I), and CH_3I (Structure II), all present $\Delta S^0(\text{h} \rightarrow \text{s}_1\text{v})$ values near to 22 cal/deg-mole, whilst the relatively larger hydrate formers C_2H_6, CH_3Br, and $CBrClF_2$, associated with smaller free volumes within their confining polyhedra, present larger values of 27 cal/deg-mole. The only real anomaly for the Structure I hydrates is the large entropy change for sulphur dioxide which might arise from specific interaction with its water co-ordination shell. For the Structure II hydrates the position of ethyl chloride is unexpectedly high, but here an experimental uncertainty of ± 3.5 cal/deg-mole on the entropy change could cover the discrepancy.

On the basis of stoichiometric hydrate formulae, using a simple, smoothed potential, hard sphere, free volume model, similar to the Eyring and Hirschfelder (23) treatment of liquids, and on the assumption that the thermodynamic functions for the hydrate lattice

Can. J. Chem. Downloaded from www.nrcresearchpress.com by 41.223.56.140 on 09/04/12
For personal use only.

water remain unchanged irrespective of hydrate-former size, it can be shown that two different cavity sizes should give rise to two linear and parallel ΔS^0–V relations, similar to those shown in Fig. 1, for hydrate-former, hard sphere volumes between 3 and 73% of the cavity volume.

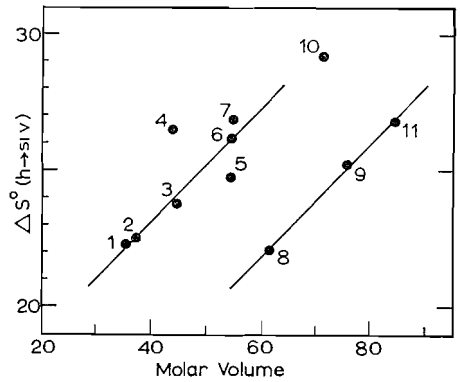


FIG. 1. Entropy change – volume correlation for gas hydrates.

	Key	Error on ΔS^0(h → s$_1$v)	Source		Key	Error on ΔS^0(h → s$_1$v)	Source
1.	H_2S	±0.7	Ref. 19	7.	CH_3Br	±3.7	Ref. 26
2.	CH_4	±0.7	Ref. 25	8.	CH_3I	±1.8	Ref. 26
3.	Cl_2	±1.8	Ref. 26	9.	C_3H_8	±0.7	Ref. 25
4.	SO_2	±1.1	Ref. 26	10.	C_2H_5Cl	±1.8	Ref. 26
5.	Br_2	±1.5	Ref. 26	11.	$CBrClF_2$	±0.1	This work
6.	C_2H_6	±0.7	Ref. 25				

Molar volumes at normal boiling point from International Critical Tables. McGraw-Hill Book Co., Inc., New York. 1933.

Consideration of the hydrate heat capacity is made on the basis of Pople's (24) theoretical analysis of the kinetic and potential energy terms contributing to the specific heat of a classical cell model liquid, as applied to the hydrate former within its co-ordination shell. If this analysis is used, assuming that the internal degrees of bromochlorodifluoromethane remain sensibly unchanged in the hydrate and that the lattice water has the same heat capacity as ice, ΔCp^0(h → s$_1$v) is given by $R(7/2-9/2$ or $7/2-10/2)$, i.e. -2 or -3 cal/deg-mole, which is in agreement with the experimental value. The error on the measured value is too large to consider the agreement better than satisfactory, but it should be considered that a variation of ±0.5 cal/deg-mole per hydrate water mole would change the experimental ΔCp^0(h → s$_1$v) to +6 or −10 cal/deg-mole. It is thus possible to state that, assuming the bromochlorodifluoromethane hydrate-former to behave as a classical rotator, the heat capacity of the hydrate lattice water does not differ from that of ice by more than ±0.3 cal/deg-mole, or alternatively assuming that the lattice water heat capacity is identical with ice, the hydrate-former behaves as a classical entrapped rotator within its co-ordination shell. With the second statement the increase of ΔS^0(h → s$_1$v) will derive mainly from reduction of translational free volume within its co-ordination shell, as implied by Fig. 1, rather than from increased hindered rotation.

Although not of great absolute significance the value of $d(Cp^{0\ h})/dT$ is positive indicating experimental consistency, and within experimental error is comparable with that of its components.

Can. J. Chem. Downloaded from www.nrcresearchpress.com by 41.223.56.140 on 09/04/12
For personal use only.

Can. J. Chem. Downloaded from www.nrcresearchpress.com by 41.223.56.140 on 09/04/12
For personal use only.

GLOSSARY OF SYMBOLS

Component 1, water:

l_1 liquid water phase

s_1 solid ice phase.

Component 2, bromochlorodifluoromethane:

l_2 liquid bromochlorodifluoromethane phase

h solid gas hydrate phase

v vapor phase.

$x_1^{l_1}$ mole fraction of component 1 in phase l_1.

$x_2^{l_1}$ mole fraction of component 2 in phase l_1.

$x_1^{l_2}$ mole fraction of component 1 in phase l_2.

$x_2^{l_2}$ mole fraction of component 2 in phase l_2.

(l_1l_2v) three-phase system consisting of l_1, l_2, and v.

(hs_1l_1v) four-phase system consisting of h, s_1, l_1, and v.

p_1^0 and p_2^0 saturation vapor pressures of pure components 1 and 2 respectively.

$P(l_1l_2v)$, $P(hl_1v)$, and $P(hs_1v)$, equilibrium total pressures exerted respectively by (l_1l_2v), (hl_1v), and (hs_1v).

$p_1(l_1l_2v)$, $p_1(hl_1v)$, and $p_1(hs_1v)$, component 1 partial pressures exerted respectively by (l_1l_2v), (hl_1v), and (hs_1v), in all cases taken equal to p_1^0.

$p_2(l_1l_2v)$, $p_2(hl_1v)$, and $p_2(hs_1v) \equiv P(l_1l_2v) - p_1^0$, $P(hl_1v) - p_1^0$, and $P(hs_1v) - p_1^0$, component 2 partial pressures exerted by (l_1l_2v), (hl_1v), and (hs_1v) respectively.

$Q(hl_1l_2v)$ and $Q(hs_1l_1v)$ invariant points for (hl_1l_2v) and (hs_1l_1v).

H_2 Henry's law constant for solubility of component 2 in l_1.

B_2 second virial coefficient of gaseous component 2.

X_1, X_2, and X^h, molar thermodynamic property X of components 1, 2, and of gas hydrate.

$X_1^{0\ l_1}$ and $X_1^{0\ s_1}$, standard molar thermodynamic property X of component 1, as pure l_1 and s_1 at 1 atmosphere pressure.

$X^{0\ h}$, standard thermodynamic property X of h at 1 atmosphere pressure.

$X_2^{0\ v}$, standard thermodynamic property of component 2 as vapor at 1 atmosphere fugacity.

$\Delta X(h \rightarrow l_1v)$ and $\Delta X(h \rightarrow s_1v)$, molar thermodynamic property change for reactions in the direction $(h \rightarrow l_1v)$ and $(h \rightarrow s_1v)$ respectively.

$\Delta X^0(h \rightarrow l_1v)$ and $\Delta X^0(h \rightarrow s_1v)$, molar thermodynamic property change for respective phase reactions with reactants and products in standard states.

REFERENCES

1. ELEY, D. D. Trans. Faraday Soc. **35**, 1281 (1939).
2. CLAUSSEN, W. F. and POLGLASE, M. F. J. Am. Chem. Soc. **74**, 4817 (1952).
3. GLEW, D. N. and MOELWYN-HUGHES, E. A. Discussions Faraday Soc. **15**, 150, 261 (1953).
4. CLAUSSEN, W. F. J. Chem. Phys. **19**, 259, 662, 1425 (1951).
5. v. STACKELBERG, M. and MÜLLER, H. R. J. Chem. Phys. **19**, 1319 (1951).
6. PLATTEEUW, J. C. and VAN DER WAALS, J. H. Mol. Phys. **1**, 91 (1958).
7. BARRER, R. M. and STUART, W. I. Proc. Roy. Soc. A, **243**, 172 (1957).
8. v. STACKELBERG, M. and MÜLLER, H. R. Z. Elektrochem. **58**, 25 (1954).
9. KINETIC TECHNICAL BULLETIN. B-4. E. I. DuPont de Nemours and Co.
10. BARNHART, W. S. Brit. Patent No. 713522 (1954).
11. GELLES, E. and PITZER, K. S. J. Am. Chem. Soc. **75**, 5259 (1953).
12. DORSEY, N. E. Properties of ordinary water-substance. Reinhold Publishing Corp., New York. 1940.
13. v. STACKELBERG, M. and JAHNS, W. Z. Elektrochem. **58**, 162 (1954).
14. HIRSCHFELDER, J. O., MCCLURE, F. T., and WEEKS, I. F. J. Chem. Phys. **10**, 201 (1942).
15. GUGGENHEIM, E. A. and MCGLASHAN, M. L. Proc. Roy. Soc. A, **206**, 448 (1951).
16. KINETIC TECHNICAL BULLETIN. RT-11. E. I. DuPont de Nemours and Co.
17. ROOZEBOOM, H. W. B. Rec. trav. chim. **3**, 36 (1884).

18. PARMALEE, H. M. Refrig. Eng. **61**, 1341 (1953).
19. SCHEFFER, F. E. C. and MEYER, G. Verslag Gewone Vergader. Afdeel. Natuurk. Ned. Akad. Wetenschap. **27**, 1104, 1305 (1919).
20. GORDON, A. R. J. Chem. Phys. **2**, 65 (1934).
21. DE FORCRAND, M. Compt. rend. **135**, 959 (1902).
22. v. STACKELBERG, M. Z. Elektrochem. **58**, 104 (1954).
23. EYRING, H. and HIRSCHFELDER, J. O. J. Phys. Chem. **41**, 249 (1937).
24. POPLE, J. A. Discussions Faraday Soc. **15**, 257 (1953).
25. DEATON, W. M. and FROST, E. M., JR. Gas hydrates and their relation to the operation of natural-gas pipe lines. U.S. Bureau of Mines. Monograph 8. 1946.
26. v. STACKELBERG, M. Naturwiss. **36**, 359 (1949).

Can. J. Chem. Downloaded from www.nrcresearchpress.com by 41.223.56.140 on 09/04/12
For personal use only.

Can. J. Chem. Downloaded from www.nrcresearchpress.com by 41.223.56.140 on 09/04/12
For personal use only.

SOME DEUTERIUM ISOTOPE EFFECTS

I. WATER SOLVOLYSIS OF METHYL-d_3 ESTERS[1]

J. A. LLEWELLYN,[2] R. E. ROBERTSON, AND J. M. W. SCOTT[2]

ABSTRACT

The α-deuterium isotope effect has been examined for the solvolysis of a series of esters containing a fully deuterated methyl group. The possible sources of the effect have been divided into "thermodynamic" effects which appear to favor more rapid reaction of the protium compound and "zero point" effects where stiffening of out-of-plane vibrations may account for the direction of the observed isotope effects. It appears that the inverse isotope effect may be a measure of the spatial restrictions placed on the hydrogen atoms on the carbon atom in the activated complex.

The substitution of deuterium for α-hydrogen in alkyl halides and substituted sulphonates has been shown to produce varying effects on reaction rates. Thus the solvolysis of methyl *p*-bromobenzenesulphonate in methanol and the reaction with methoxide ion are accelerated by α-deuteration (1). Isopropyl bromide reacting with ethoxide ion is apparently unaffected by this substitution (2), and phenyl ethyl toluenesulphonate solvolyzes in formic acid at a reduced rate when isotopically substituted at the α-hydrogen (3). Johnson and Lewis systematized these changes, suggesting that they were the consequence of the sensitivity of the C—H bending vibrations to the presence of entering and leaving groups and noted a decrease in the isotope effect, k_H/k_D, with increasing necessity for nucleophilic attack from the rear (1). From information available at the time they were unable to choose between several possible sources for the inverse isotope effect observed for methyl esters.

Streitwieser and co-workers (4) have observed a reduction in the acetolysis rate for cyclopentyl *p*-toluenesulphonate following α-deuteration. They have attributed this to the change in vibrational frequencies involving the α-hydrogen, produced by the difference in hybridization between initial and transition states, together with the effect of the leaving group which was postulated to stiffen the out-of-plane vibrations of the hydrogen.

Thus there appear to be three factors for consideration in assessing the zero-point contribution to the change in rate for nucleophilic displacements caused by α-deuterium substitution. These factors are: (*a*) the effect of the incoming group, (*b*) the effect of the leaving group, and (*c*) the change in hybridization.

Factors (*a*) and (*b*) will be related, inasmuch as bulky entering or leaving groups will be expected to stiffen the out-of-plane C—H bending modes. This effect will be modified by distance, but clearly, stiffening will increase the disparity in the energy levels of deuterium and hydrogen compounds in the transition state, and will produce changes tending to reduce the free energy of activation for the deuterium compound, compared with that of the protium compound. Reactions having the highest degree of nucleophilic interaction with large entering groups will presumably have the most stiffening.

The change in hybridization will also affect the characteristic frequencies but presents a problem in that even a qualitative decision concerning the effect is not simple. If we examine the force constants for molecules which can be considered to have C—H bonds analogous to those in the transition state, then we have a choice from a fairly wide range

[1]*Manuscript received September 23, 1959.*
Contribution from the Division of Pure Chemistry, National Research Council, Ottawa, Canada.
Issued as N.R.C. No. 5493.
[2]*National Research Council of Canada Postdoctorate Fellow.*

Can. J. Chem. Downloaded from www.nrcresearchpress.com by 41.223.56.140 on 09/04/12
For personal use only.

of values. Added to this is the difficulty of deciding the hybridization of the transition state. If we reject the idea of an intermediate for the S_N2[3] reaction, the transition state will probably have three C—H bonds as sp^2 hybrids with entering and leaving groups interacting with the remaining p orbital.[4] The transition state of the S_N1 reaction will presumably occur before complete flattening of the carbon center linkages has occurred, and it might be considered that the C—H bonds are in a state between sp^3 and sp^2 with structure closer to tetrahedral when internal charge stabilization is more effective. Lower degrees of internal stabilization will mean that transition state C—H bonds are probably closer to sp^2 hybridization (6). From an examination of the force constants it appears that the stretching constants increase and bending constants decrease when hybridization changes from sp^3 to sp^2, although this is not invariably so. Some crude calculations which we have made indicate that the consequences of decreasing bending constants may outweigh the increase in stretching constant in terms of the zero-point energies, so that the change favors more rapid reaction of the protium compound. Since the hybridization change is most marked in the S_N2 reaction the effect should be pronounced in this case, but it will be offset by the closeness of the stiffening entering and leaving groups.

In the course of the present work we have examined the effect of deuteration on the reaction rates of a series of methyl esters solvolyzing in water (Table I). In the discussion

TABLE I

Rate data illustrating effects for methyl compounds hydrolyzing in water

X	CD_3 (k sec^{-1})	CH_3 (k sec^{-1})	$T°$ C	k_H/k_D
p-Methyl benzenesulphonate	9.75×10^{-4}	9.33×10^{-4}*	70.05	0.96
	9.73×10^{-4}	9.25×10^{-4}*		
	9.72×10^{-4}	9.36×10^{-4}*		
Chloride		5.49×10^{-5}*	89.995	
		5.46×10^{-5}*		
		5.49×10^{-5}*		
		5.47×10^{-5} (18)		
	5.81×10^{-5}	5.38×10^{-5} (18)	89.794	0.92
	5.84×10^{-5}			
	5.88×10^{-5}			
Bromide	2.99×10^{-4}	2.70×10^{-4} (18)	79.94	0.90
	2.99×10^{-4}			
Iodide	3.24×10^{-5}	2.82×10^{-5}*	70.05	0.87
	3.24×10^{-5}	2.81×10^{-5}*		
		2.800×10^{-5} (18)		
Nitrate	3.396×10^{-5}	3.109×10^{-5}*	100.005	0.92
	3.399×10^{-5}	3.109×10^{-5}*		
	3.400×10^{-5}	3.122×10^{-5}*		
		3.105×10^{-5} (24)		
Methane sulphonate	2.398×10^{-4}	2.257×10^{-4} (26)	60.067	0.96
	2.382×10^{-4}			
	2.390×10^{-4}			
Methoxy sulphonate	1.616×10^{-4}	1.572×10^{-4}*	24.64	0.97
	1.616×10^{-4}	1.569×10^{-4}*		
		1.59×10^{-4} (26)		

*Values to check previous results. See experimental section.

preceding this section it has been assumed that the only effective term in isotopic rate changes is the difference in zero-point energy change produced by the deuteration, but for the simpler esters and especially the methyl halides, this is not the case and other factors

[3]*The molecularity refers to the number of molecules undergoing covalent change and completely neglects the solvating molecules (5).*

[4]*The four original sp^3 hybrids become three coplanar sp^2 hybrids and the remaining p orbital combines with entering and leaving groups to give three M.O.'s two of which contain the four available electrons.*

must be considered. The problem of the alteration in reactivity for gas phase reactions has been dealt with extensively by Bigeleisen and co-workers (7). We have not adopted this treatment for our discussion because we are not sure of its application to reactions occurring in the liquid phase although other workers have made use of it as a basis for discussion (8, 4). We feel that discussion on a more naïve basis simplifies calculation of the effect of different models. Difficulties arise over the nature of the partition functions to be used in the description of the liquid systems, especially with respect to the transition state. Melander (9) uses the normal transition state equation with an added factor $\alpha/\alpha^{\neq}$ to compensate for the altered chemical potentials in the solution. This activity coefficient ratio is then considered as an increment ($\Delta F^{\neq}_{ex}$) to the free energy of activation. If a solute is strongly solvated, as in an ionic transition state, the alteration in chemical potential will be large and negative, and the stronger the interaction with the solvent the less will be $\Delta F^{\neq}$, so that reaction will be promoted for the species which is most strongly solvated in the transition state. A model for this interaction would be the C—H···O(H)(H) hydrogen bond, and the maximum value for this alteration would be the difference between hydrogen bonds involving deuterium and hydrogen in water.

Because of this difficulty we have proceeded by assessing the differences in the initial state of reaction, assuming that the gas phase differences which are calculated will be retained in the solution. Some justification for this is contained in a discussion of the nature of the solution. The free energy of the solution process may be considered in terms of the solute–solvent and solvent–solvent interactions. When a non-polar molecule is dissolved in water there is, in general, an increase in solvent–solvent interaction in the immediate vicinity of the solute, and the solute may be regarded as occupying a cavity in the solvent. The energy changes resulting from this process are more dependent on the properties of water than on those of the solute, and within a series, for example, alkanes, alkyl halides, alcohols, the free energy of solution is sensibly constant. Changes in enthalpy and entropy of solution oppose each other within the series and appear to be largely dependent on molecular volume so that the changes resulting from isotopic substitution would be expected to be negligible in the initial state. If we assume that the solute molecule rotates freely in the cavity in the water structure, and that the principal effect of solution is a reduction in the free volume available for translation, we arrive at the same conclusions. By factorizing the partition function into translational, rotational, and vibrational terms and making use of the relationships between the partition function and the thermodynamic properties, the following equations may be derived to represent the influence of isotope change on the initial state.

Translation

$$\delta F/T = 6.8635 \log M_D/M_H \text{ cal/mole deg}$$

(M = mass of compound in a.w.u.). δ is used to denote changes produced by isotopic substitution, and suffix D refers to the deuterium compound.

$$\delta H = 0$$

Rotation

$$\delta F/T = 2.2878 \log (ABC)_D/(ABC)_H \text{ cal/mole deg.}$$

$$\delta H = 0 \qquad A, B, C, \text{ moments of inertia.}$$

Can. J. Chem. Downloaded from www.nrcresearchpress.com by 41.223.56.140 on 09/04/12
For personal use only.

Vibration

There will be a thermodynamic contribution, and an additional contribution from the decrease in zero-point energy. The thermodynamic terms will be:

$$\frac{\delta F}{T} = 1.9872\left(\sum \ln\left(1-e^{-hc\omega_D/kT}\right)-\sum \ln\left(1-e^{-hc\omega_H/kT}\right)\right)$$

$$\frac{\delta H}{T} = 1.9872\left(\sum \frac{hc\omega_H}{kT(e^{-hc\omega_H/kT}-1)}-\sum \frac{hc\omega_D}{kT(e^{-hc\omega_D/kT}-1)}\right).$$

The zero-point change will affect free energy and enthalpy in the same way and will be $\sum \frac{1}{2}hc\omega_H - \sum \frac{1}{2}hc\omega_D$ where ω_H and ω_D are the frequencies of the fundamental modes in wave numbers per cm for the two isotopic species.

Calculations for methyl halides yield the values in Table III from the data in Table II. For more complex molecules the following considerations will apply.

TABLE II

Data for calculation of initial state differences

Compound	Mass(a.w.u.)	Moments of inertia (a.w.u./Å) A	$B = C$
CH_3Cl*	50.5	3.31	38.48
CD_3Cl*	53.5	6.62	47.36
CH_3Br (19)	94.9	3.313	53.07
CD_3Br (19)	97.9	6.625	66.85
CH_3I (20, 21)	141.9	3.31	67.34
CD_3I (20, 22)	144.9	6.62	83.65

*Calculated from values of: Miller, S. L., Aamodt, L. C., Dousmanis, A., Townes, C. H., and Craitchman, J. J. Chem. Phys. 20, 1112 (1952). B value for CH_3Cl is in agreement with that of Gelles, E. and Pitzer, K. S. J. Am. Chem. Soc. 75, 5259 (1953), and a value given by Moelwyn-Hughes, E. A. Physical chemistry. The Pergamon Press, Ltd., London. 1957. p. 499, but disagrees with that given by Herzberg (ref. 12, p. 437).

TABLE III

Initial state differences calculated from data in Table II

Compound	Translational δF	Rotational δF
CH_3Cl	56	378
CH_3Br	32	394
CH_3I	21	384

(*a*) Deuteration will have little effect on the mass so that translational terms will be virtually unaffected.

(*b*) The moments of inertia will also be little affected by isotopic substitution so that rotational free energy will be unchanged. Deuteration will double the moment of inertia of the CH_3 grouping about a central axis perpendicular to the plane of the hydrogens, so that the possibility of contributions from internal rotation must be examined. A crude estimate may be made by considering the CH_3 group to be rotating with respect to a large mass (as in the *p*-toluenesulphonate ester).

The partition function for free rotation about a bond is

$$Q = \frac{(8\pi^3 I_r kT)^{\frac{1}{2}}}{\sigma h}$$

where I_r is the reduced moment of inertia for the system and σ the symmetry number.

Can. J. Chem. Downloaded from www.nrcresearchpress.com by 41.223.56.140 on 09/04/12
For personal use only.

For symmetrical coaxial tops, with moments of inertia I_A and I_B

$$I_r = (I_A I_B)/(I_A I_B)$$

(this is obviously a crude approximation for the system being examined)

$$F = -RT \ln Q$$
$$\delta F = RT \ln Q_D/Q_H = \tfrac{1}{2}RT \ln I_{r(D)}/I_{r(H)}$$

identifying CH_3 and CD_3 in turn with I_A

$$\delta F = \frac{RT}{2} \frac{I_{CH_3}(I_{CD_3}+I_B)}{I_{CD_3}(I_{CH_3}+I_B)}$$

when $I_B \gg I_{CD_3}$

$$\delta F = \frac{RT}{2} \ln \tfrac{1}{2}$$

which will be about -238 cal/mole at 343° K.

In most cases the inequality above does not hold and rotation will not be free so that this value will be considerably reduced. More accurate assessment is probably not possible even if the height of the potential barrier hindering rotation was known (10). In the transition state the charge development may also hinder rotation despite the extension of the ester linkage and the net contribution to $\delta\Delta F^{\ddagger}$ will be the difference between two very small terms so that we feel justified in neglecting this issue.

The thermodynamic contribution of the vibrations is small so that inaccuracies here are probably unimportant, but the zero-point energy differences are the largest factor in the initial state differences so that this will be the principal source of error. The fundamental frequencies of the methyl and deuteromethyl halides have been established and using the values of Table IV the free energy and enthalpy changes have been calculated. From

TABLE IV

Fundamentals for methyl halides (cm^{-1})

	Degeneracy	CH_3Cl (12)	CD_3Cl (19)	CH_3Br (19)	CD_3Br	CH_3I (20)	CD_3I (20)
ν_1	(1)	2966	2161	2972	2157	2975	2135
ν_2	(1)	1355	1029	1305	993	1252	948
ν_3	(1)	732	695	611	578	533	493
ν_4	(2)	3042	2286	3057	2293	3061	2285
ν_5	(2)	1455	1058	1444	1056	1449	1070
ν_6	(2)	1015	775	955	712	882	665

these calculations it appears that initial state conditions strongly favor more rapid reaction of the protium compounds, although it is of interest to note that the thermodynamic enthalpy difference favors more rapid reaction of the deuterium compound by about 200 cal/mole for the alkyl halides.

In order to evaluate the consequences of isotopic substitution in the transition state, it is necessary to postulate a model or models for the calculation. The S_N1–S_N2 classification of the reaction will provide information concerning covalent interaction between the solvolyzing ester and a specific water molecule acting as a nucleophile, but will not specify the transition state. The experimental observations show that $\Delta H^{\ddagger}$, the enthalpy of activation, varies with temperature and this is interpreted as a consequence of the

Can. J. Chem. Downloaded from www.nrcresearchpress.com by 41.223.56.140 on 09/04/12
For personal use only.

Can. J. Chem. Downloaded from www.nrcresearchpress.com by 41.223.56.140 on 09/04/12
For personal use only.

change in heat capacity[5] on passing from initial to transition state. For many reactions this change does not appear to be readily detectable and in this case, it is largely attributable to the changes in the water molecules in the immediate vicinity of the reaction substrate. Current ideas suggest that these molecules are ordered (compared to the bulk of the water) in the initial state and less ordered (compared to the bulk of the water) in the quasi-ionic or ionic transition state. The magnitude of the heat capacity change suggests that more than one water molecule is involved in this disordering process (11, 18). Because these molecules have effect in determining the value of the heat capacity of the transition state it is not possible to disregard their presence in the calculations of the changes produced by isotopic substitution. For the evaluation of the thermodynamic changes caused by alterations in mass, a model containing a single water molecule will provide us with a maximum value and it may be stated with reasonable confidence that these contributions will actually be smaller. Proceeding on this basis a series of calculations reveal that the effect of mass increase on the translational contribution to $\delta F^{\ddagger}$ produces changes, which considered with the initial state values of δF, have very small, almost negligible, contributions to $\delta\Delta F^{\ddagger}$. The calculations for the effect of rotational contribution alterations were made for a series of models using different C—O, C—X distances, with the methyl hydrogens coplanar and carbon set at the C—H distance in ethylene (corresponding to sp^2 hybridization). The calculations indicated that alteration over a reasonable range of configurations did not seriously affect the outcome which showed $\delta\Delta F^{\ddagger}$ again in favor of the more rapid reaction of the protium compound. In the discussion of the initial state the possibility of internal rotation was considered and it appears that if a partial bond between carbon and oxygen has occurred, this effect may arise. Because of the symmetry of the system the potential energy will not be sensitive to the orientation of the two rotors CH_3 and H_2O and it seemed that for the case of the methyl halides, where the anionic moiety would have no moment of inertia about the internal axis, there might be an appreciable contribution. The model in Fig. 1 was

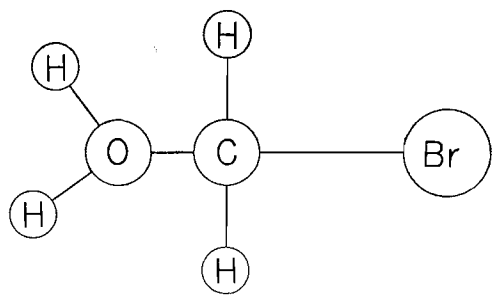


FIG. 1. Transition state model used for calculation of internal rotation contributions. O—H, 0.955 Å HOH 105°6′; C—H, 1.071 Å CH_3 coplanar; C—O, incipient bond formation; C—Br, incipient bond rupture

adopted, and assuming free rotation, a value close to -50 cal/mole at 343° K was calculated as a contribution to $\delta\Delta F^{\ddagger}$, i.e. reducing the free energy of activation for the deuterium compound. Generally speaking the calculations show that initial state differences favor more rapid reaction of the light compound. The effect of increased mass on the thermo-

[5]*$\Delta H^{\ddagger}$ is determined by identifying the gradient $(d \ln K)^{\ddagger}/(d\ 1/T)$ with $\Delta H^{\ddagger}/R$ and from the basic equation of transition state theory it can be readily shown that $\Delta H^{\ddagger} = E_0 + \int_0^T C_p^{\ddagger} dT - \int_0^T C_p dT$, where E_0 is the difference between the zero-point energy levels in initial and transition states.*

dynamic properties of the initial state will be paralleled in the transition state but will be reduced in size compared with the less massive initial state. Thus these transition state changes will tend to cancel the initial state changes, but will be less effective as the model postulated for the transition state becomes more complicated, and might be quite small where several water molecules are involved. Thus it seems that all these factors will increase the activation free energy of the deuterium compound relative to that of the protium compound with the exception of the internal rotation mentioned above.

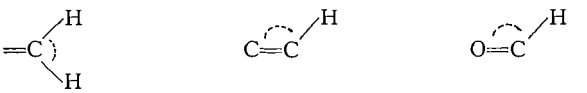
We have omitted the part played by the vibrational contributions to $\delta\Delta F^{\ddagger}$ so that the nature of the vibrations of the transition state complex may be discussed separately. The results of our calculations indicate that the principal source of the inverse isotope effect probably lies in the altered vibrational frequencies which characterize the transition state. A substantial difference in the free energy of activation is present as a consequence of the initial state alterations in a direction which favors more rapid reaction of the protium compound. The direction of the isotope effect implies that the frequency sum for the transition state must exceed that of the initial state. The calculations which we mentioned earlier indicate that the simple hybridization change alters the frequencies downwards, that is, in a direction contrary to that expected from the rate alteration. If this is so, alternate sources of stiffening of the carbon–hydrogen vibrations must be sought, such as those proposed by Lewis and Johnson (1) and Streitwieser (4).

The presence of a nucleophile in close proximity to the coplanar methyl grouping, together with an additional contribution from the leaving group, appears to be a reasonable source of hindrance to out-of-plane carbon–hydrogen vibrations. As an extension of this hypothesis a correlation of the type noted by Lewis and Johnson would be expected. Since the hybridization change alone produces vibrational changes which would lead to isotope effects with $k_H/k_D > 1$, one would expect that with increasing hindrance to bending from increased nucleophilic interaction that the isotope effect would steadily decrease, pass through unity where α-deuteration would apparently have no consequences, and become less than one where the stiffening was extreme. The magnitude of the changes required to account for the experimental observations can be assessed if the frequencies of the fundamental vibrations of the transition state are estimated. The usual transition state theory represents the system as a mass point moving over a potential energy hypersurface. Translation along one co-ordinate in this hyperspace is associated with reaction and this translation is identified with one of the modes of vibration of the transition state complex. It seems a necessary condition that an incoming water molecule will be close to the carbon atom in the transition state and presumably the ester linkage will be extended so that movement in these two linkages will form part of the reaction co-ordinate. The effect that we have observed is small and thus it may be concluded that the reaction mode of vibration does not involve a normal mode which includes the movement of hydrogen in an important way so that the consequences of deuterium substitution on this mode will not be severe.[6] If it is concluded that the important changes will be those involving only the central CH_3 grouping then the problem is that of estimating the frequencies of the vibrations associated with this group. The bonds to the ester grouping and the incoming water molecule are assumed to be weak so that the effect of these groups on the in-plane vibrations can be neglected. The frequency sum for these vibrations for a coplanar CH_3 group was calculated assuming simple valence forces (12), and the effect of deuterium

[6]*An analogy can be drawn by considering the* ν_2 *and* ν_3 *vibrations of methyl iodide which can be described as the symmetrical* CH_3 *deformation frequency and the* C—I *stretching frequency, respectively. Deuteration produces an alteration of the frequency by factors of 0.76 where the vibration involves hydrogens in an important way, and only 0.92 where this is not so.*

Can. J. Chem. Downloaded from www.nrcresearchpress.com by 41.223.56.140 on 09/04/12
For personal use only.

assessed by using a modified mass correction (12, 4). By assuming that the isotope effect is derived from the large value of the frequency associated with out-of-plane bending, a force constant for this motion can be calculated for comparison with those encountered normally. These calculations are detailed in the Appendix. The fundamentals are ν_1, 2930; ν_2, 3120; ν_4, 1290 cm^{-1}, and the stiffened mode will have a value 2135 cm^{-1} to account for the observed isotope effect for methyl bromide. Calculating backwards, a value of $3.1\times10^5\ r^2$ dyne cm^2 can be derived for the out-of-plane bending force constant. This can be compared with the following values for bending modes in other molecules.



0.46 r^2 0.51 r^2 1.5 r^2 $\times10^5$ dynes/cm.

(N.B. These are all in-plane modes.)

The value that we have calculated is considerably higher than those above but does not render the stiffening hypothesis untenable since it represents a maximum where all the effect has been attributed to the stiffening of one mode. The presence of increments of charge on the constituent atoms of the group would increase the force constants for in-plane bending and stretching modes so that the aplanar bending need not be so stiff in order to account for the observed rate change.

CONCLUSIONS

The possibility that the deuterium compound is more strongly solvated in the transition state, and thus reacts more rapidly, is rejected because it fails to apply in cases where the opposing thermodynamic change (resulting from mass alterations) is quite small. Halevi's (13) suggestion that the potential surface is not invariant with respect to isotopic change cannot be dismissed (see below) but represents an unknown factor which does not appear essential in discussions concerning other systems where more precise statistical mechanics can be applied (17). It appears therefore that the observed inverse isotope effect can be attributed to stiffening of the C—H vibrations in the transition state which produces a decrease in the zero-level energy difference for the deuterium compound compared to the protium compound. This alteration counterbalances the change in the thermodynamic properties (arising from mass changes) which favors more rapid reaction of the light compound. The isotope effect varies with the nature of the group attached to the methyl group, but it is not clear whether the variation is a consequence of altered stiffening derived from changing size of the leaving group or changing degree of nucleophilic interaction by the entering water molecule. The sulphonates will presumably have similar effects in steric terms and do not show a variation in k_H/k_D which lies outside experimental error. The alteration in the methyl halide series follows the increase in leaving group size which is also the order of increase in the degree of nucleophilic attack if the rate ratio comparing OH^- attack in water with water solvolysis is accepted as a measure of this interaction (27).

The postulate that the alteration in $\Delta F^{\ddagger}$ is a consequence of opposing $\Delta H^{\ddagger}$ and $\Delta S^{\ddagger}$ changes leads to consideration of the possibility of experimental verification.

The temperature dependence of $\Delta H^{\ddagger}$ for methyl halide solvolysis has been examined by Heppolette and Robertson (18). Detailed examination of the Arrhenius E_a vs. T relationship indicated that the root mean square deviation of E_a from the derived smooth curve was ±90 cal for the methyl iodide solvolysis. If this value is taken as an index of the

Can. J. Chem. Downloaded from www.nrcresearchpress.com by 41.223.56.140 on 09/04/12
For personal use only.

precision with which $\Delta H^{\ddagger}$ can be measured, then experiments over a temperature range $t°$ will not reveal changes in $\Delta S^{\ddagger}$ which are less than $90/t$. The difference in gas phase entropies between CH_3I and CD_3I is slightly less than 2 e.u. in the range of experimental temperatures so that experiments 50° apart would just detect this change, but when the transition state difference is considered it is almost certain that the effect will not be detectable at the present level of experimental sensitivity.

Differential electron release would produce a reduction in E_0[7] favoring the heavy compounds we have examined here. Although there is considerable evidence to show that the substitution of deuterium for protium changes the ground state electron density configuration, it is uncertain whether these changes always imply differences in reactivity. Halevi (13–16) has measured isotope effects and interpreted them on the basis of electron release but some of these effects may be explicable in terms of the more usual phenomena associated with isotopic substitution discussed earlier, so that the significance of this factor in the cases discussed here is doubtful. Reasoning on the basis of electronegativity, isotope effects would be expected to increase along the series I, Br, Cl, sulphonates, and we find the reverse, but do not rule out this effect because a rapid saturation of this electron-releasing process might lead to the order observed in the experiments.

The thermodynamic contributions, which favor reduced reactivity of the deuterium compound, are greatest for the methyl halides and yet the inverse isotope effect is greatest for these compounds. A similar trend exists within the halides themselves and it is concluded that the more important factor is the vibration change produced by altered hybridization and stiffening by entering and leaving groups.

EXPERIMENTAL

The deuterated methyl methanesulphonate and methyl tosylate were synthesized according to the method of Morgan and Cretcher from CD_3OH (99.5%) supplied by Merck and Co. Ltd. of Montreal. The dimethyl sulphate was a pure sample supplied by Dr. Leitch of these laboratories. The methyl bromide and iodide were obtained from Merck and Co. Ltd. and were better than 99% isotopic purity.

Samples of both the normal and isotopic methyl chloride were prepared by heating the corresponding tosylate with an equal weight of anhydrous $CaCl_2$ in a suitable apparatus and collecting the evolved gas. The kinetic rates of hydrolysis for the normal material were shown to be identical with those previously obtained in a more extensive study in this laboratory (23).

Methyl nitrate was synthesized by the method previously used by Robertson and Laughton (24) and shown to be at least 95% isotopically pure by mass spectrometry.

Rate determination and other details of the kinetic studies were the same as those previously described by us (25).

REFERENCES

1. Johnson, R. R. and Lewis, E. S. Proc. Chem. Soc. 52 (1958).
2. Shiner, V. J. J. Am. Chem. Soc. **74**, 5285 (1952).
3. Saunders, W. H., Asperger, S., and Edison, D. H. Chem. & Ind. 1417 (1957).
4. Streitwieser, A., Jr., Jagow, R. H., Fahey, R. C., and Suzuki, S. J. Am. Chem. Soc. **80**, 2326 (1958).
5. Ingold, C. K. Structure and mechanism in organic chemistry. Cornell Univ. Press, Ithaca, N.Y. 1953. Chap. 7.
6. *Discussed with references by* Streitweiser, A., Jr. Chem. Revs. **56**, 571 (1956).
7. Bigeleisen, J. and Wolfsberg, M. *In* Advances in chemical physics. Vol. I. *Edited by* I. Prigogine. Interscience Publishers, Inc., New York. 1958. Chap. II.

[7]*Note that this is E_0, the difference between zero-point energy levels and not Arrhenius' E_a.*

Can. J. Chem. Downloaded from www.nrcresearchpress.com by 41.223.56.140 on 09/04/12
For personal use only.

8. SHINER, V. J. Tetrahedron, **5**, 243 (1959).
9. MELANDER, L. Arkiv Kemi, **2**, 211 (1950).
10. STOCKMAYER, J. H. J. Chem. Phys. **27**, 321 (1957).
11. MOELWYN-HUGHES, E. A. Proc. Roy. Soc. **164**, 295 (1938).
12. HERZBERG, G. Infrared and Raman spectra of polyatomic molecules. D. Van Nostrand Co., Inc., New York. 1945. Chap. 3.
13. HALEVI, E. A. Tetrahedron, **1**, 174 (1957).
14. HALEVI, E. A. Tetrahedron, **5**, 352 (1959).
15. HALEVI, E. A. and NUSSIM, M. Bull. Research Council Israel, A, **7**, 230 (1958).
16. HALEVI, E. A. Trans. Faraday Soc. **54**, 1441 (1958).
17. WESTON, R. E. Tetrahedron, **6**, 31 (1959).
18. HEPPOLETTE, R. L. and ROBERTSON, R. E. Proc. Roy. Soc. A, **252**, 273 (1959).
19. WEISSMANN, H. B., BERNSTEIN, R. B., ROSSER, S. E., MEISTER, A. G., and CLEVELAND, F. F. J. Chem. Phys. **23**, 544 (1955).
20. FENLON, P. F., CLEVELAND, F. F., and MEISTER, A. G. J. Chem. Phys. **19**, 1561 (1951).
21. GORDY, W., SIMMONS, J. W., and SMITH, A. G. Phys. Rev. **74**, 243 (1948).
22. SIMMONS, J. W. Phys. Rev. **76**, 686 (1949).
23. ROBERTSON, R. E., HEPPOLETTE, R. L., and SCOTT, J. M. W. Can. J. Chem. **37**, 803 (1959).
24. LAUGHTON, P. M. and ROBERTSON, R. E. Can. J. Chem. **35**, 1319 (1957).
25. ROBERTSON, R. E. Can. J. Chem. **33**, 1536 (1955).
26. ROBERTSON, R. E. Unpublished work.
27. FELLS, I. and MOELWYN-HUGHES, E. A. J. Chem. Soc. 1326 (1958).

APPENDIX

Calculations on the basis of a transition state model which contains only 1 water molecule interacting with methyl bromide and the deuterated analogue produce thermodynamic changes giving $\delta\Delta F^{\ddagger}$ 40 cal/mole at 343° K. The experimental value of $\delta\Delta F^{\ddagger}$ is -175 cal/mole so that if the transition state alteration in zero-point energy is the source of the inverse isotope effect then deuteration must account for this 215 cal/mole in addition to the 5647 cal/mole arising from the initial state zero-point differences.

For these vibrational calculations we consider only the ν_1, ν_2, ν_4, and ν_5 modes for the initial state which are those involving C—H bond vibrations in an important way (see Table IV). The ν_3 and ν_6 vibrations are strongly dependent on the X grouping and it is assumed that the errors involved in neglecting these in the initial state will be balanced by similar terms in the transition state, for vibrations involving bending with respect to the principal axis and stretching the C—O, C—X linkages. The purpose of this calculation is to show that the stiffening which must be postulated to account for the experimental observations does not lead to unreasonable values for the force constants involved. The model consists of a coplanar CH_3 group with the hydrogen atoms set at the C—H distance in ethylene with the stretching and in-plane bending force constants taken from the ethylene molecule.

A simple valence force treatment was then applied and the frequencies for the in-plane modes were calculated. By assuming that a mass correction can be applied to these vibrators the effect of deuterium substitution was assessed. From this information and the results of previous calculations a frequency for the out-of-plane bending mode was calculated which would account for the observations. Evaluation of the corresponding force constant enabled compromise with other systems.

A simple valence force treatment of the coplanar XY_3 molecule gives the following expressions for the fundamental frequencies.

$$\lambda_1 = k/m_y \quad [1]$$

$$\lambda_2 = (1+3m_y/m_x)\, k_\Delta/m_y r^2 \quad [2]$$

$$\lambda_4+\lambda_3 = (1+3m_y/2m_x)(k/m_y+3k_\delta/m_y r^2) \quad [3]$$

$$\lambda_3+\lambda_4 = 3(1+3m_y/m_x)(k/m_y^2 . k/r^2) \quad [4]$$

Can. J. Chem. Downloaded from www.nrcresearchpress.com by 41.223.56.140 on 09/04/12
For personal use only.

x = C; y = H; k, C—H stretching constant; k_Δ, aplanar bending constant; k_δ, HCH angle bending constant.

N.B. $4\pi c^2 M\nu^2 = 5.8894 . 10^{-2} . \nu^2 = \lambda$. This is treated in detail in Herzberg (12).

Using the values C—H stretch 5.1×10^5 dyne/cm, planar bend $0.3\times10^5 r^2$ dyne/cm, m_x = 12.011 a.w.u., m_y = 1.0008 a.w.u., r = 1.07 Å we may calculate ν_1, ν_3, and ν_4 leaving ν_2 the aplanar bending mode for later consideration.

The values obtained are

$$\nu_1\ 2930\ \text{cm}^{-1},$$

$$\nu_3\ 3120\ \text{cm}^{-1},$$

$$\nu_4\ 1290\ \text{cm}^{-1}.$$

Denoting the missing frequency by ν_2

$$\text{zero point energy} = \frac{1}{2}\left(\sum_i \nu_i\right) = (11750+\nu_2)/2\ \text{cm}^{-1}.$$

The initial state sums (for the frequencies mentioned earlier) are 13279 and 9830 cm^{-1} for protium and deuterium compounds respectively so that the zero-point change will be 1725 cm^{-1} ($\frac{1}{2}\sum_i \Delta\nu_i$). If the ν_2 vibration is to account for the effect then the zero point change in the transition state must be equal to the initial state zero point change plus the calculated thermodynamic changes plus the experimentally observed difference.

Applying the approximation $\nu_H = 1.35\nu_D$ the transition state zero point change is given by

$$\frac{1}{2}\sum\Delta\nu = \frac{11750+\nu_2}{2} - \frac{11750+\nu_2}{2\times1.35}$$

so that

$$\frac{11750+\nu_2}{2} - \frac{11750+\nu_2}{2.7} = 1725+75+22$$

where the second term (75 cm^{-1}) on the right-hand side represents the maximum value of the thermodynamic differences for methyl bromide and the third term (22 cm^{-1}) represents the experimental difference in $\Delta F^{\neq}$. The frequency of the stiffened mode is given by ν_2 = 2565 cm^{-1}, whence the force constant $k_\Delta r^2 = 3.12\times10^5$ dynes/cm for the out-of-plane vibration can be calculated using equation [2]. The only significance that we attach to these calculations is the more or less qualitative concept that the hybridization change produces a frequency sum decrease and that some degree of stiffening is required to change the zero-point energy in the appropriate direction to account for the observed effect.

It may be argued that a complete analysis of the transition state vibrations would be more effective but aside from the difficulty of carrying out such analyses for possible models, there remains the basic difficulty of definition of the reaction co-ordinate for a system such as this, superimposed upon the doubt whether it is capable of being identified with any of the normal modes of the transition state.

Can. J. Chem. Downloaded from www.nrcresearchpress.com by 41.223.56.140 on 09/04/12
For personal use only.

Can. J. Chem. Downloaded from www.nrcresearchpress.com by 41.223.56.140 on 09/04/12
For personal use only.

THE LUMINESCENCE OF COMPLEX MOLECULES IN RELATION TO THE INTERNAL CONVERSION OF EXCITATION ENERGY

PART II. N-HETEROAROMATICS[1]

ROBIN M. HOCHSTRASSER

ABSTRACT

The relative fluorescence and/or phosphorescence yields of a number of methyl- and halogeno-quinolines, isoquinolines, and acridines have been measured as a function of the wavelength of the exciting light. In all cases the solvent was absolute ethanol. The results show that the efficiency of internal conversion processes between excited singlet states is extremely high in comparison to other intramolecular steps. The effect of substituted heavy atoms is discussed, as well as the fluorescence of the conjugate acids of the bases.

INTRODUCTION

In general, the fluorescence and phosphorescence quantum yields of aromatic molecules do not depend on which electronic state of the molecule is initially excited (6, 8, 9, 13, 25). In Part I of this series (9) some exceptional cases were reported and it was shown that this is not necessarily true if the excited molecule is free to isomerize. In these cases it was found that the quantum yield of fluorescence was considerably lower when the higher electronic states of the molecule were excited. Other exceptions are found with certain substances at very low pressure in the vapor phase. Under these conditions the molecule may photodissociate before the excess of vibrational energy is removed by collision. Consequently the fluorescence yield depends on the initial vibrational energy content which in turn is determined by the excitation energy. Another possible exception is that intramolecular energy transfer processes might occur within very short times (10^{-12} second). Should such a process as intersystem crossing, for example, occur at this rate it would probably compete favorably with the internal conversion process between electronic states. The result would be that the quantum yield of fluorescence would decrease and the quantum yield of phosphorescence would increase when the excitation energy was increased and successively higher electronic states were populated. An investigation of halogenated anthracenes (6) suggested that the last reason may be of importance. In particular, it was found that the fluorescence yield of dibromoanthracene was reduced to half its value when the excitation was directly into the higher electronic states.

The spectral similarity of anthracenic and naphthalenic systems to the analogous N-heteroaromatic molecules acridine and the quinoline isomers prompted the present experiments. The relative fluorescence and/or phosphorescence yields of a group of halogenated quinolines, isoquinolines, and acridines have been measured over a wide range of excitation wavelengths. Previous investigations of this type on heterocyclic molecules were mainly concerned with the larger molecular systems of biology and photosynthesis (7, 21), although more recently Weber and Teale (25) measured the quantum yield of fluorescence of 9-aminoacridine and found this to be constant over the range of exciting wavelengths 2100–4700 Å.

EXPERIMENTAL

The experimental arrangement, which was designed by Ferguson (6) and modified by the author (9), was essentially the same as that described in Part I. The excitation spectrum and absorption spectrum of each substance was determined before proceeding

[1]*Manuscript received September 14, 1959.*
Contribution from the Chemistry Department, the University of British Columbia, Vancouver, B.C.

to the yield determinations. In this way there was reasonable certainty as to the nature of the emitting species because luminescent impurities would have been readily detected in these experiments. Unless noted, the specimens were not examined in the long wavelength tail of the absorption band but from the wavelength of the first absorption maximum towards shorter wavelengths. Light from the hydrogen lamp was passed through a Beckman monochromater onto the sample, contained in a silica cell, and the luminescence was detected by a photomultiplier (RCA 5819). A filter was used to prevent the exciting light from reaching the photomultiplier. The filters used were benzyl alcohol (1.5 cm) or sodium nitrite (1.5 cm, saturated in water). The former cut off at approximately 3400 Å and the latter at 4000 Å. No luminescence could be detected from either filter. The benzyl alcohol filter was used for the fluorescence of the quinolines and isoquinolines, and the sodium nitrite filter for the green phosphorescence from these compounds and for the blue-green fluorescence from the acridines. Measurements were made of the excitation spectra of luminescence and of the relative quantum yields of fluorescence at different excitation energies. The experimental error in relative yields was about 3%. The concentration of the compounds investigated was sufficiently large that at least 99.9% of the exciting light was absorbed at each exciting wavelength. Thus any slight spectral shifts or sharpening of the spectra on cooling to liquid nitrogen temperatures would not have affected the quantum yield curves. In a few cases the separation of the phosphorescence and fluorescence emission was checked by using a Corning filter (No. 3486, cut off at about 4500 Å under the present conditions) in addition to the benzyl alcohol filter, and was found satisfactory.

RESULTS

(*A*) *Quinoline and Isoquinoline Derivatives*

Two emissions of different spectral location and apparent lifetime were observed for most of the compounds. The short-lived luminescence occurred in the region 3400–4000 Å. The longer-lived component, which appeared beyond 4000 Å, was observed only in rigid solutions. There was no doubt that each emission originated through the absorption of the incident radiation by the substance (of known absorption spectrum) under consideration. In the halogenated derivatives the phosphorescence and fluorescence could not be distinguished by qualitative observations of the apparent lifetime of the emission. This was to be expected by analogy with the corresponding naphthalenes where the phosphorescence lifetime decreases considerably as the atomic number of the substituted halogen is increased (14). However, there was no reason to suppose that the spectral location of the emissions would change by more than 1000–2000 cm^{-1} throughout the series, so the same filters were employed in these cases.

The compounds listed in Table I were investigated at room temperature and at the temperature of boiling nitrogen (−196° C). The range of excitation wavelengths over which the efficiencies remain constant are given in Table I.

(*B*) *Acridines*

The fluorescence from acridine is intense and lies in the visible region of the spectrum. The phosphorescence, on the other hand, is weak and probably lies in the near infrared. Craig and Ross (5) could find no triplet–triplet absorption of acridine although their experiments suggested that it is photochemically stable in a rigid glass. The weakness of the phosphorescence, its awkward spectral location, and the uncertain photochemical

Can. J. Chem. Downloaded from www.nrcresearchpress.com by 41.223.56.140 on 09/04/12
For personal use only.

TABLE I

Substances for which the fluorescence and phosphorescence yields are constant throughout the investigated range of exciting wavelengths

Substance	Exciting wavelength, mμ	
	Fluorescence	Phosphorescence
Quinoline	220–315	260–315
2-Methylquinoline	220–315	260–320
4-Methylquinoline	220–315	260–320
2-Chloroquinoline	250–320	260–320
6-Chloroquinoline	250–320	260–320
6-Bromoquinoline	250–320	260–320
Isoquinoline	220–315	260–315
3-Methylisoquinoline	220–315	260–315
4-Chloroisoquinoline	250–315	260–315
4-Bromoisoquinoline	250–315	260–315

behavior of the halogen derivatives suggested that with the present experimental arrangements no conclusive evidence could be obtained from the excitation spectra of phosphorescence. However, certain useful results were nevertheless obtained from the following fluorescence experiments.

The relative fluorescence yields of acridine, 9-chloroacridine, and 9-bromoacridine were determined as a function of the energy of the exciting light. The first two had constant yields over the range 230–395 mμ. The yield of 9-bromoacridine was considerably less than that of the other compounds. This may be contrasted with observations on the fluorescence yields of the bromoanthracenes, which suggested that there is no significant difference in yield between anthracene and 9,10-dibromoanthracene (19). The yield is so low for 9-bromoacridine that the excitation spectrum at room temperature resembles the *inverted* absorption spectrum. Presumably the bulk of the molecules in solution act as an inner filter to the incident light and the luminescing species is a minute amount of a photoproduct. At liquid nitrogen temperatures the fluorescence of 9-bromoacridine completely obscured the impurity luminescence, as indicated by the spectra of excitation and fluorescence. The fluorescence yield remained constant in a rigid ethanol glass over the range of exciting wavelengths 250–395 mμ. This result is in disagreement with that previously reported by the author (11) which appears to have been caused by the presence of a diacridinic photoproduct.

The absorption spectra of the halogenoacridines have not previously been examined in detail, although Zanker (28) determined the absorption and fluorescence spectra of acridine and the aminoacridines, and Mataga (15) computed the energy levels of acridine. The main difference in the spectra of anthracene and acridine is the intensity of the ^1L_b band in acridine and its feebleness in anthracene (2). It is of interest to compare the relative shifts of the ^1L_a and ^1L_b states and also the intensities of the bands on substitution of electron-donating halogen atoms. The energy of the 0–0 transition to the lowest ^1L_a state decreases through the series 9, X-acridine (X=H, =Cl, =Br) in the order 26,100 cm^{-1}, 25,150 cm^{-1}, and 24,140 cm^{-1} while the intensity does not change appreciably. On the other hand the energy of the transition $^1L_b \leftarrow {}^1A$ scarcely changes through the series while the intensity changes considerably. These results agree with those on the protonated and non-protonated N-heterocyclics (17, 28) and are similar to results obtained with the analogous substituted anthracenes (12).

Can. J. Chem. Downloaded from www.nrcresearchpress.com by 41.223.56.140 on 09/04/12
For personal use only.

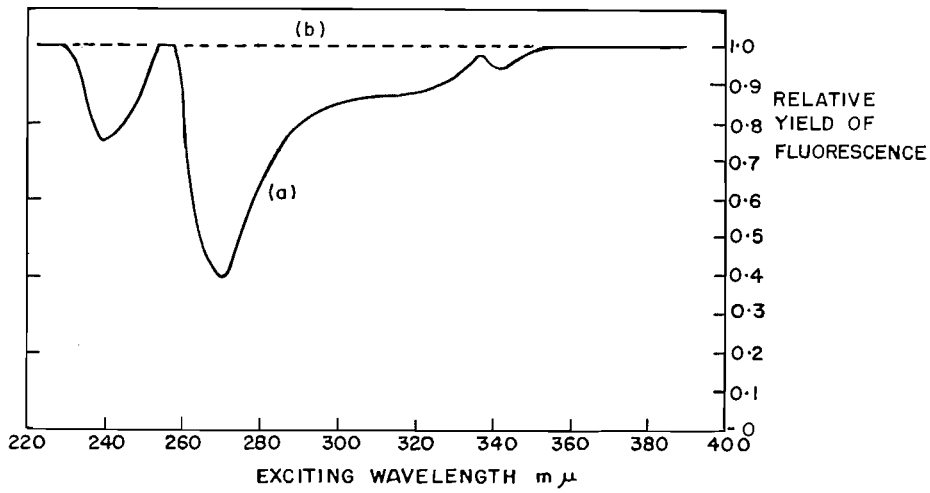


FIG. 1. The variation of the fluorescence yield of acridine conjugate acid with the wavelength of the exciting light. (*a*) No additional free acid. (*b*) Excess acid added.

(C) Luminescence of Conjugate Acids

A few experiments on the conjugate acids of all of the aforementioned bases were carried out. These included measurements of the absorption spectra, fluorescence spectra, and excitation spectra at room temperature and at liquid nitrogen temperature. In each case the quantum yield of fluorescence and/or phosphorescence was independent of the wavelength of exciting light over the same ranges as given in the previous section.

Some results which at first appeared anomalous were obtained for acridine conjugate acid. The excitation spectrum of fluorescence is shown in Fig. 1. In this experiment (concentration of acridine conjugate acid, 10^{-2} mole/liter; cell length, 1 cm; solvent, water) the curve would have been a straight line of zero slope and unit intercept if there had been only one emitting species. Consequently the curve shape must arise because there are two emitting species. These are the conjugate acid and the base with which it is in equilibrium.

As acid is added to this solution the yield becomes independent of excitation wavelength and eventually shows that only the conjugate acid is emitting with constant yield throughout the complete absorption range. The fluorescence of the base and its conjugate acid lie in slightly different spectral regions but both occur in a region where the photomultiplier response is not strongly wavelength dependent.

The results given in sections (*A*) and (*B*) indicate that the rule of the emitting level being the lowest of a given multiplicity is generally applicable to N-heterocyclic aromatic molecules. In each case the emitting level is the thermally equilibrated level of the lowest excited electronic state.

Quinolines and Isoquinolines

In alcohol solution it is likely that the fluorescent level is a $^1(\pi,\pi^*)$ state lying just below a $^1(n,\pi^*)$ state (22). The measurements, which extended throughout the absorption region of very concentrated solutions (that is, to energies comparable with the probable 0–0 transition), confirmed that internal conversion between these two states occurs with very high efficiency. The constancy of the yield also indicated that there is only one emitting species. This is an important observation in the light of recent work by Kasha and Mostafa

Can. J. Chem. Downloaded from www.nrcresearchpress.com by 41.223.56.140 on 09/04/12
For personal use only.

Can. J. Chem. Downloaded from www.nrcresearchpress.com by 41.223.56.140 on 09/04/12
For personal use only.

Amr Sayed (22), who showed that the orbital excitation types of the lowest electronic states of 2-ring N-heterocyclics may interchange on solvation. These authors found that the ratio of the phosphorescence to fluorescence yields was greatest when quinoline was dissolved in a non-hydroxylic (hydrocarbon) solvent and smallest when the solvent was an alcohol. This effect was attributed to hydrogen bonding. The fluorescence yields of hydrogen-bonded and non-hydrogen-bonded heteroaromatics are normally quite different (1, 16), the fluorescence yield of the latter being considerably greater since the emitting level is a $^1(\pi,\pi^*)$ state in which the probability of intersystem crossing is usually less than for a $^1(n,\pi^*)$ state (3, 23). As a hydroxylic solvent was used in this case all the emission presumably comes from hydrogen-bonded molecules.

The effect of small quantities of hydroxylic molecules on the relative fluorescence yield of quinolines, which will be discussed in detail in Part III, should be mentioned. When the excitation wavelength is longer than 3150 Å (beyond the first absorption maximum at 3140 Å) the quantum yield of fluorescence is no longer independent of the exciting energy. The yield *increases* as the excitation wavelength increases to 3300 Å and then remains constant at the higher value for longer exciting wavelengths. The amount of the increase is a function of the hydroxylic concentration. It is believed that this results from the dissociation of hydrogen-bonded molecules in the excited state. It appears that efficient mixing of the $^1(n,\pi^*)$ and $^1(\pi,\pi^*)$ states can occur when the solvent contains hydroxylic groups, that is to say when the lowest excited state is $^1(\pi,\pi^*)$ and the excitation is to levels beyond the first absorption maximum (3140 Å) as in the present work.

The phosphorescence in all cases was a $^3(\pi,\pi^*) \rightarrow {}^1A$ transition. It may also be concluded that the introduction of a bromine substituent into the ring system does not enhance intersystem crossing sufficiently for the process to compete favorably with internal conversion between excited states. The same general conclusions are known to be true for the analogous naphthalenes (6).

Internal Conversion

It may be asked why the internal conversion efficiency is independent of the excitation energy for bromoacridine but not for dibromoanthracene (6). These molecules are so similar that such a result is unexpected. An increase in spin orbital interaction due to the presence of a heavy atom could be brought about by altering the nodal distribution of π-electrons and hence the π-electron density in the region of the heavy atom. In most molecules this effect is not experimentally observable since the rate of intersystem crossing is much less than the rate of internal conversion between excited states (13, 20). The probability of intersystem crossing from the fluorescent state is measured by the ratio of the phosphorescence to fluorescence yield (13) while the probability of crossing from an upper state is given by the ratio of the phosphorescence to the internal conversion yield. For the cases under discussion this is presumed different from unity. The rate of upper state crossing k is given by

$$k = k_i \frac{(1-\phi)}{\phi} \geqslant 10^{13}/1 = 10^{13}\ \text{seconds}^{-1}$$

for 9,10-dibromoanthracene where the ratio $(1-\phi)/\phi$ is nearly unity (6) and where ϕ is the relative fluorescence yield. This value for k is much greater than that for most molecules. For example in the halogenated naphthalenes where heavy atom induced intersystem crossing is known to occur (14) the rate of intersystem crossing has a maximum value of about 10^{10} seconds^{-1}. There is no reason to believe that intersystem crossing via the upper states of molecules will be any more rapid than crossing from the first excited singlet state

in molecules where spin–orbit interaction is large. It is known that the fluorescent state of anthracenic molecules is particularly insensitive to heavy atom perturbation (18) so some enhancement is to be expected on excitation to a higher state. Also it has been shown that the process responsible for the reduction in the number of internal conversions when the excitation is in the upper state must occur at least 400 times faster than the apparent rate of fluorescence emission from the lowest singlet state (10). Thus the rate of removal of quanta from the upper state must be just below 10^{13} seconds^{-1}. Consequently, the phenomenon may not be explained as due to a slower rate of internal conversion due to unfavorable crossing of the excited state potential energy surfaces, as has been postulated in the case of azulene (24). It is possible that the increased efficiency of internal conversion in bromoacridine is connected with the presence of $^1(n,\pi^*)$ states. Theoretically these states lie quite close to each $^1(\pi,\pi^*)$ state, thus permitting internal conversion to occur through mixing of (n,π^*) and (π,π^*) electronic states.

Acridine Conjugate Acid

Although the base strengths of heterocyclic molecules differ in the ground and excited states (26), it is interesting that for acridine conjugate acid the constancy of the quantum yield of fluorescence throughout the regions where most of the light is absorbed by the conjugate acid (e.g. 2200–2300 Å, 2500–2600 Å, and 3500–3900 Å in Fig. 1) indicates that the base strength in the upper excited states is not much less than in the fluorescent state. The bimolecular rate constants for proton recombinations and additions in such systems (27) indicate that an excited acid molecule would probably lose its proton within 10^{-12} seconds. This implies that proton loss could compete favorably with internal conversion in such molecules if the base strength were low enough in the upper states. For acridine, the base strengths of the excited states are probably in the order ^1L_a > ground > ^1L_b, ^1B_b. This order was deduced from the electron densities at the N atom of the base in each excited state, using the Coulson definition of bond orders and charge densities (4). Alternatively one may consider the relative polarization directions of the transitions to these states, which are predicted to be short axis, short axis permanent, long axis, and long axis respectively (15). It is reasonable to assign a higher electron density at the nitrogen atom, hence a higher base strength, for the short axis polarized states. Thus it should be fairly simple to observe effects such as described above if the molecule chosen has greatly different base strengths in each of its electronic states. Of course it is also necessary that the proton recombination times for excited base molecules be of approximately the same magnitude as (or larger than) the fluorescence lifetimes of the base and its conjugate acid. Investigations of such systems will be important in order to determine the role of internal conversion. A more detailed discussion will be given in Part III, with special reference to quinoline.

The measurement of the fluorescence efficiency as a function of exciting light energy for a solution containing a base in equilibrium with its conjugate acid can make possible a calculation of the acid–base equilibrium constant of the acid–base reaction if the absorption spectra of the acid and of the base are known. The relative yield values such as these of Fig. 1 may be used in such calculations.

REFERENCES

1. Bowen, E. J. and Sahu, J. J. Chem. Soc. 3716 (1958).
2. Clar, E. Aromatische Kohlenwasserstoffe. Zweite Auflage. Springer-Verlag, Berlin. 1952. p. 37.
3. Clementi, E. and Kasha, M. J. Mol. Spectroscopy, **2**, 297 (1958).
4. Coulson, C. A. and Longuet-Higgins, H. C. Proc. Roy. Soc. (London), A, **191**, 39 (1947).
5. Craig, D. P. and Ross, I. J. Chem. Soc. 1589 (1954).

Can. J. Chem. Downloaded from www.nrcresearchpress.com by 41.223.56.140 on 09/04/12
For personal use only.

6. FERGUSON, J. J. Mol. Spectroscopy, **3**, 177 (1959).
7. FRENCH, C. S. and YOUNG, V. M. K. *In* Radiation biology. Vol. 3. *Edited by* A. Hollaender. McGraw-Hill Book Co., Inc., New York. 1956. p. 37.
8. GILMORE, E. H., GIBSON, G. E., and MCLURE, D. S. J. Chem. Phys. **20**, 829 (1952).
9. HOCHSTRASSER, R. M. Can. J. Chem. **37**, 1367 (1959).
10. HOCHSTRASSER, R. M. To be published.
11. HOCHSTRASSER, R. M. *In a paper entitled* Internal conversion in polyatomic molecules *presented at the* Symposium on Molecular Structure and Spectroscopy, the Ohio State University, Columbus, Ohio. June, 1959.
12. JONES, R. N. Chem. Revs. **41**, 353 (1947).
13. KASHA, M. Discussions Faraday Soc. **9**, 14 (1950).
14. MCLURE, D. S. J. Chem. Phys. **17**, 905 (1949); see also ref. 13.
15. MATAGA, N. Z. physik. Chem. **18**, 19 (1958).
16. MATAGA, N. and TSUNE, S. Bull. Chem. Soc. Japan, **30**, 368 (1957).
17. MATAGA, S. and MATAGA, N. Z. physik. Chem. **19**, 231 (1959).
18. PADHYE, M. R., MCGLYNN, S. T., and KASHA, M. J. Chem. Phys. **24**, 588 (1956).
19. POLOVIKOV, F. I. Doklady Akad. Nauk S.S.S.R. **71**, 453 (1950).
20. PLATT, J. *In* Radiation biology. Vol. 3. *Edited by* A. Hollaender. McGraw-Hill Book Co., Inc., New York. 1956. Chap. 2.
21. RABINOWITZ, E. Photosynthesis and related processes. Vol. 2. Interscience Publishers Inc., New York. 1951.
22. SAYED, M. A. and KASHA, M. *In a paper entitled* Interchange of orbital excitation types of the lowest electronic states of 2-ring N-heterocyclics by solvation *presented at the* Symposium on Molecular Structure and Spectroscopy, the Ohio State University, Columbus, Ohio. June, 1959.
23. SIDMAN, J. W. Chem. Revs. **58**, 704 (1958).
24. VISWANETH, G. and KASHA, M. J. Chem. Phys. **24**, 574 (1956).
25. WEBER, G. and TEALE, F. W. J. Trans. Faraday Soc. **54**, 640 (1958).
26. WELLER, A. Z. Elektrochem. **61**, 956 (1957).
27. WELLER, A. Discussions Faraday Soc. **27**, 2135 (1959).
28. ZANKER, V. Z. physik. Chem. **2**, 50 (1954).

Can. J. Chem. Downloaded from www.nrcresearchpress.com by 41.223.56.140 on 09/04/12
For personal use only.

Can. J. Chem. Downloaded from www.nrcresearchpress.com by 41.223.56.140 on 09/04/12
For personal use only.

STUDIES IN THE WAGNER–MEERWEIN REARRANGEMENT

PART IV. DERIVATIVES OF BENZ[b]FLUORENE[1]

F. A. L. ANET AND P. M. G. BAVIN[2]

ABSTRACT

10-Methyl-10-benz[b]fluorenylmethyl tosylate[3] gave mainly 5-methylbenz[a]anthracene on formolysis, but the related alcohol gave a mixture of the 5- and 6-methyl isomers by reaction with phosphorus pentoxide. Reaction of benz[b]fluorenone with excess diazomethane gave 5-methoxybenz[a]anthracene as the only isolable product. The alkylation of methyl benz[b]-fluorene-10-carboxylate was studied.

Collins and his co-workers have employed ^{14}C to study migratory aptitudes in Wagner–Meerwein rearrangements of polycyclic systems (1, 2, 3, 4). In particular, 10-benz[b]-fluorenylmethanol-11-^{14}C (I) was dehydrated by phosphorus pentoxide in boiling xylene to benz[a]anthracene (II), in which ^{14}C was found at carbon atoms 5 and 6 in the ratio 48:52 (3).

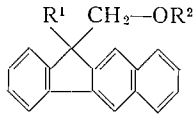
It seemed to us that similar information could be obtained without the use of ^{14}C, by using 10-methyl-10-benz[b]fluorenylmethyl tosylate (III), in which the carbon is labelled with a methyl group. On formolysis III gave almost pure 5-methylbenz[a]anthracene in about 60% yield. Examination of infrared spectra suggested the presence of traces of 6-methylbenz[a]anthracene (V) in the mother liquors from IV. However, the infrared spectra of IV and V were not sufficiently different to enable an accurate analysis to be made.

The greater migrating power of the naphthelenic over the benzenic ring in the formolysis of III is in contrast to the reaction of I with phosphorus pentoxide, where the two rings have about equal migrating powers. This may be due to the different experimental conditions leading in the case of Collins' work to a transition state more nearly approximating to a free carbonium ion which should have a low selectivity. In the case of the tosylate (III), formation of the benzanthracene probably occurs with participation of the aromatic ring in the ionization step, as in simpler systems studied by Cram (5). However, the reaction of 10-methyl-10-benz[b]fluorenylmethanol with phosphorus pentoxide gave nearly equal proportions of IV and V, in agreement with the results of Collins.

By reaction of benz[b]fluorenone with excess diazomethane, 5-methoxybenz[a]anthracene (VI) was obtained as the only isolable product, but in only fair yield (38%). The intermediate involved is almost certainly VII or a close approximation to it (6), so that this reaction is similar mechanistically to the Wagner–Meerwein rearrangement. A similar ring-expansion of benz[a]fluorenone has been reported (7), the only product isolated being 6-methoxychrysene. Thus in both of these examples the naphthalenic ring appears to have the greater migratory power.

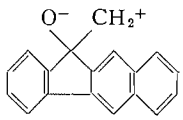
Methyl benz[b]fluorene-10-carboxylate was not alkylated as smoothly as the fluorene analogue (8), the reaction failing with *t*-butyl bromide, though the methyl and isopropyl derivatives were readily obtainable.

[1]*Manuscript received September 23, 1959.*
Contribution from the Department of Chemistry, University of Ottawa, Ottawa, Canada.
[2]*National Research Council Postdoctorate Fellow, 1954–56. Present address: the University, Kingston-upon-Hull, East Yorkshire, England.*
[3]*Ring Index nomenclature and numbering are used throughout.*

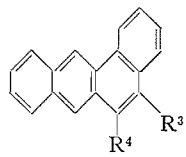


(I) $R^1 = R^2 = H$

(III) $R^1 = CH_3$
$R^2 = CH_3C_6H_4.SO_2$



(VII)



(II) $R^3 = R^4 = H$

(IV) $R^3 = CH_3$
$R^4 = H$

(V) $R^3 = H$
$R^4 = CH_3$

(VI) $R^3 = OCH_3$
$R^4 = H$

EXPERIMENTAL

Methyl Benz[b]fluorene-10-carboxylate

Benz[b]fluorene (10 g) in warm benzene (150 ml) was added to a vigorously stirred solution of phenyl lithium (from 10.5 g bromobenzene and 1 g lithium) in ether (500 ml) under an atmosphere of dry nitrogen. The solution rapidly assumed a deep purple color. After half an hour it was poured onto powdered Dry Ice (500 g). Next day the mixture was acidified with dilute hydrochloric acid and steam-distilled to remove solvents. After cooling, the solid was collected, washed, and dissolved in hot 5% sodium carbonate solution (400 ml). Filtration with Norite and subsequent acidification gave the acid as a white solid. Esterification was effected by boiling for 4 hours with dry methanol previously saturated with hydrogen chloride. Concentration to 600 ml and cooling gave pale yellow prismatic needles of methyl benz[b]fluorene-10-carboxylate (8.7 g, 70%), m.p. 124–125°, raised to 126–126.5° by a further crystallization from acetone–methanol. (Lit. m.p. 117–118° (2).) Found: C, 83.23; H, 5.71. Calculated for $C_{19}H_{14}O_2$: C, 83.20; H, 5.15%.

Methyl 10-Methylbenz[b]fluorene-10-carboxylate

The preceding ester (5 g) was dissolved in methanol (100 ml) containing sodium methoxide (from 1 g sodium) to give a deep orange solution. Addition of excess methyl iodide caused a rapid change of color to pale yellow. Isolation of the product in the usual way and crystallization from acetone–methanol gave pale yellow prisms (4.07 g) m.p. 141.5–142.5°, raised to 142–143° by a further crystallization. Found: C, 83.23; H, 5.23%. Calculated for $C_{20}H_{16}O_2$: C, 83.31; H, 5.59%.

Concentration of the original mother liquors gave a second crop (9.4 g) of almost pure material, raising the yield to 87%.

10-Methyl-10-benz[b]fluorenylmethyl Tosylate

The preceding ester (3 g) was reduced with an excess of ethereal lithium aluminum hydride. 10-Methyl-10-benz[b]fluorenylmethanol was obtained as a difficultly crystallizable oil, slow evaporation of a benzene–hexane solution affording small well-defined rhombs, m.p. 108.5–110°. The bulk of the oil was esterified with tosyl chloride (2.6 g) in dry pyridine. The product crystallized from benzene–hexane as small white needles (2.95 g), m.p. 118–119°; concentration of the mother liquors afforded a further 0.16 g. An analytical sample was obtained after a further crystallization, m.p. 118.5–119.5°. Found: C, 75.33; H, 5.35%. Calculated for $C_{26}H_{22}O_3S$: C, 75.35; H, 5.35%.

Can. J. Chem. Downloaded from www.nrcresearchpress.com by 41.223.56.140 on 09/04/12
For personal use only.

5-Methylbenz[a]anthracene

(*a*) In the best of several experiments, the once-crystallized tosylate (0.82 g) and 95% formic acid (100 ml) were boiled under reflux for 1 hour. Isolation of the product with chloroform gave a yellow gum, which was dissolved in hexane containing a little benzene and the solution passed through a column of activated alumina. Further elution with hexane and evaporation of the combined eluants gave crude 5-methylbenz[a]anthracene which crystallized from methanol as small white needles (0.28 g, 64%), m.p. 152–153°. (Lit. m.p. 155.9–156.9°, corr. (9).) The identity was confirmed by a mixed melting point with a sample of m.p. 154° and by comparison of infrared spectra. The melting point was strongly depressed by adding 6-methylbenz[a]anthracene.

Evaporation of the mother liquors gave material of m.p. 92–100° (0.08 g). The infrared spectrum showed a weak peak at 11.85 μ indicating the presence of a small proportion of the 6-methyl isomer, but attempts to isolate this through the picrate or by careful chromatography were unsuccessful.

(*b*) 10-Methyl-10-benz[b]fluorenylmethanol (0.5 g) and phosphorus pentoxide (1 g) in xylene (10 ml) were boiled under reflux for 4 hours. Purification of the product and examination of the infrared spectrum showed that there was present a mixture of about equal amounts of 5- and 6-methylbenz[a]anthracene.

Methyl 10-Isopropylbenz[b]fluorene-10-carboxylate

Methyl benz[b]fluorene-10-carboxylate (0.5 g) was alkylated using 3 equivalents each of isopropyl bromide and methanolic sodium methoxide. The product was a yellow oil which failed to crystallize, but passage of a hexane solution through a column of activated alumina and crystallization of the colorless fractions from acetone–methanol gave prisms, (0.4 g), m.p. 150–151°. Found: C, 83.40; H, 6.37%. Calculated for $C_{22}H_{20}O_2$: C, 83.51; H, 6.37%.

Further elution of the chromatogram gave a yellow oil (0.09 g) which formed a vermilion 2,4-dinitrophenylhydrazone. This was not characterized.

Attempts were made to *t*-butylate methyl benz[b]fluorene-10-carboxylate, as described for the fluorene analogue (8). The product was always contaminated with orange material which could not be removed by chromatography. Saponification to an acid followed by esterification with diazomethane also failed to yield a pure compound, so these experiments were discontinued.

5-Methoxybenz[a]anthracene

Benz[b]fluorene (1 g) was oxidized with sodium dichromate in acetic acid and a solution of the products in hexane passed through a column of activated alumina. Elution of the yellow band and crystallization from methanol gave yellow needles, m.p. 151–152° (0.7 g). (Lit. m.p. 152° (10).)

The pure ketone (0.5 g) was dissolved in methanol (100 ml) to which was added a large excess of ethereal diazomethane. Next morning the solvent was removed and the residue dissolved in hot heptane. The solution was passed through a column of activated alumina, elution being continued with the solvent until a fluorescent colorless band had been eluted. Evaporation and crystallization from benzene–hexane gave colorless needles (0.22 g) (38%), m.p. 165–166°. (Lit. m.p. 167–168° (11).) The melting point was not depressed on mixing with an authentic specimen, prepared by methylating 5-hydroxybenz[a]anthracene with diazomethane.

The only other material recovered from the chromatogram was unreacted ketone (0.11 g).

Can. J. Chem. Downloaded from www.nrcresearchpress.com by 41.223.56.140 on 09/04/12
For personal use only.

ACKNOWLEDGMENTS

The authors are indebted to Professor L. F. Fieser for a sample of 5-hydroxybenz[a]-anthracene and to Professor M. S. Newman for the methylbenz[a]anthracene isomers.

REFERENCES

1. BENJAMIN, B. M. and COLLINS, C. J. J. Am. Chem. Soc. **75**, 402 (1953).
2. COLLINS, C. J., BURR, J. G., and HESS, D. H. J. Am. Chem. Soc. **73**, 5176 (1951).
3. COLLINS, C. J., HESS, D. H., MAYOR, R. H., TOFFEL, G. M., and JONES, A. R. J. Am. Chem. Soc. **75**, 397 (1953).
4. COLLINS, C. J. and BENJAMIN, B. M. J. Am. Chem. Soc. **75**, 1644 (1953).
5. CRAM, D. and *co-workers*. J. Am. Chem. Soc. **74**, 2129, 2159, 5839, (1952); **75**, 339, 3189 (1953).
6. GUTSCHE, C. D. Organic reactions. Vol. VIII. John Wiley & Sons, Inc., New York. 1954. Chap. 8.
7. COOK, J. W. and SCHOENTAL, R. J. Chem. Soc. 288 (1945).
8. ANET, F. A. L. and BAVIN, P. M. G. Can. J. Chem. **34**, 991 (1956).
9. NEWMAN, M. S. and GAERTNER, R. J. Am. Chem. Soc. **72**, 264 (1950).
10. THIELE, J. and SCHNEIDER, J. Ann. **369**, 287 (1909).
11. FIESER, L. F., HERSHBERG, E. B., LONG, L., and NEWMAN, M. S. J. Am. Chem. Soc. **59**, 475 (1937).

Can. J. Chem. Downloaded from www.nrcresearchpress.com by 41.223.56.140 on 09/04/12
For personal use only.

Can. J. Chem. Downloaded from www.nrcresearchpress.com by 69.46.99.164 on 09/04/12
For personal use only.

A SURVEY OF AMINO ACID CONTENT OF THE UREDOSPORES OF SOME RACES OF WHEAT RUST (PUCCINIA GRAMINIS)[1]

M. E. McKillican

ABSTRACT

The free and combined amino acids of seven samples of wheat rust were analyzed quantitatively by paper and column chromatography and compared with the amino acids present in uninfected wheat leaves. All races studied contained different proportions of free amino acids.

INTRODUCTION

The physiology of *Puccinia graminis* has been studied in some detail. For example, investigations of wheat leaf metabolism have indicated that diffusible substances spread from the fungal mycelium (1) and, as the parasite developed, the rise in oxygen consumption in the tissue of non-resistant wheat was found to occur later than in rust-resistant plants (2). This increase in respiration proved to be not merely an additive effect of the fungus respiration, but to be due to respiratory changes in the host tissues (3). In rust-susceptible wheat, decreased glycolic acid oxidase activity was shown to accompany the increased respiratory rate (4).

In contrast, the chemical constitution of the uredospores of *P. graminis* has been little investigated. The carotenoid pigments of the uredospores have been described (5) and studies made of a substance (6) or substances (7) that cause differentiation of infection structures. An examination of four races of wheat rust has shown a different total amino acid and sugar content for each race (8).

In the present work, the free and combined amino acids of seven samples of wheat stem rust uredospores are analyzed quantitatively by paper and column chromatography and compared with the free amino acids present in uninfected wheat leaves.

MATERIALS AND METHODS

The original rust cultures were obtained from the Plant Pathology laboratory in Winnipeg. The two-race mixtures and one sample of race 29, as well as the samples of field-collected wheat rust spores, were grown in Winnipeg. All races except the field-collected mixtures were grown on Little Club wheat in a greenhouse. Spores of all races were harvested when they reached maturity.

The free amino acids were obtained from the spores in the following manner: The uredospores were first extracted with ethyl ether for 20 hours to facilitate penetration of the aqueous solvent. Boiling water (20 ml per g) was then added to the sample and refluxed for 1 hour. The mixture was filtered, the filtrate cooled and poured into two volumes of ethanol. Any precipitate was removed by filtration. The extract was taken to small volume under reduced pressure, and the concentrate placed on a short (20 g) column of Dowex 50, 4% cross-linked, (50X4), 50–100 mesh, prepared according to Partridge (9, 10), and washed with 200 ml water. Acidic and neutral fractions were thus washed through, and the amino acid fraction (plus other weakly basic compounds) was then eluted from the Dowex 50X4 column with 0.2 *N* ammonium hydroxide. The ammonia was removed under reduced pressure and then *in vacuo* at 50° C.

[1]*Manuscript received June 22, 1959.*
Contribution No. 2 from the Genetics and Plant Breeding Research Institute, Research Branch, Canada Department of Agriculture, Ottawa, Canada.

A sample of uninfected leaves of Little Club wheat was freeze-dried and extracted in the same manner as the spores.

Individual amino acids were identified qualitatively by two-dimensional chromatography on Whatman No. 1 chromatographic paper. The sample was developed first with 80% phenol containing 0.04% 8-hydroxyquinoline, a small beaker of dilute ammonia being placed in the cylinder (11). The second solvent system was *n*-butanol – acetic acid – water 4:1:1 (12). The chromatogram was sprayed with 0.25% ninhydrin in *n*-butanol (13) to develop the color, or with isatin (14) to show proline and hydroxyproline and to help identify other amino acids by color differences between the effects of the two sprays.

The amino acid composition of the various races was determined as described by Moore and Stein (15). The concentration of amino acid in each fraction was estimated colorimetrically according to Moore and Stein (16) and Chinard (17).

Bound amino acids were released from the residue of the aqueous extraction by a 20-hour hydrolysis in 6 *N* hydrochloric acid used in the proportion of 25 ml per g of original sample (18, 19). The hydrolyzate was filtered and the hydrochloric acid removed from the filtrate by evaporation under reduced pressure. After the removal of most of the hydrochloric acid, a small amount of fine precipitate was present in the aqueous solution. This substance was slightly soluble in the Moore and Stein buffer pH 3.42 used initially on the column and, unless it was removed, the separation of the amino acids was not distinct. The hydrolyzate, after filtration (or centrifugation), was taken to dryness and stored over sodium hydroxide pellets to remove any remaining traces of free acid. An aliquot of suitable size (representing 0.2-g uredospores) was dissolved in buffer pH 3.42 and placed on the Moore and Stein column as in the case of the extract.

The individual amino acids in both the extract and hydrolyzate were identified by paper chromatography and by their position in the series of fractions from the Moore and Stein column. To calculate the percentage composition of a mixture of amino acids, the weight of each acid was expressed as a percentage of the total weight of the amino acids recovered from the column. This procedure was adopted to give a uniform basis of comparison among races.

After the over-all pattern of amino acid distribution had been noted, a synthetic mixture of amino acids was analyzed chromatographically to determine any limitations in the analytical methods.

RESULTS AND DISCUSSION

Each amino acid component of the synthetic mixture is recovered in essentially the same percentage of the total weight of amino acids in which it was present in the original mixture. When 10 mg of amino acids were applied to the column, 10.49 mg were recovered for an over-all efficiency of 104.9%.

By summing the weights of the amino acids in the fractions collected, the following information on over-all amino acid composition of *P. graminis* uredospores was obtained. Free amino acids made up approximately 0.5% of the original weight of spores and acid hydrolysis released a further 11% by weight of combined amino acids.

The proportions of free amino acids in the various races of rust studied are shown in Table I. Using the precision of recovery of the synthetic mixture as a model, appreciable differences in free amino acids were found between races. The variations in glycine and α-alanine contents separately, however, should be viewed with caution as the large amount of α-alanine present caused an overlapping of the peaks. There is also lack of resolution on the column of the peaks of tyrosine and phenylalanine.

Can. J. Chem. Downloaded from www.nrcresearchpress.com by 69.46.99.164 on 09/04/12
For personal use only.

TABLE I
Free amino acids

Amino acid	Race 11	11+15B	15B	15B+87	29	48	56	A*	B*	Little Club leaves
Methionine sulphoxide	—	—	—	—	—	—	—	4.4	—	—
Cysteic acid	8.2	9.9	9.3	5.8	9.7	8.4	12.4	6.3	10.2	—
Aspartic acid	5.2	5.3	5.0	7.1	8.4	5.0	12.6	17.8	4.9	3.8
Threonine	—	—	—	2.7	—	2.5	—	—	—	3.2
Serine	13.0	7.0	6.6	4.5	7.0	10.5	1.5	6.4	7.8	9.1
Glutamic acid	10.6	3.9	1.2	7.1	3.0	17.0	—	1.9	5.7	5.6
Proline	Trace	—	—	—	—	—	Trace	—	—	5.6
Glycine	5.2	1.8	10.4	0.2	0.3	3.3	0.6	0.6	1.3	0.8
α-Alanine	22.0	37.6	28.0	31.2	29.7	18.6	41.3	19.4	18.2	17.6
Valine	4.1	2.3	3.0	4.0	4.3	4.0	2.8	3.6	4.0	4.9
Methionine	2.5	1.8	—	1.0	1.3	1.7	0.6	—	0.5	2.0
Isoleucine	1.7	1.3	1.3	1.5	1.6	1.7	0.7	1.2	1.2	2.3
Leucine	2.1	1.5	1.4	1.6	2.1	2.0	3.0	1.6	1.4	3.3
Tyrosine	2.6	1.5	1.8	4.0	2.6	3.5	1.7	2.2	3.4	3.8
Phenylalanine	2.6	1.7	2.7	2.8	4.0	2.3	3.8	3.0	2.0	6.2
γ-Aminobutyric acid	13.1	18.6	22.6	22.0	18.0	11.4	12.7	29.1	29.3	21.1
Histidine	2.7	1.8	Trace	2.4	4.4	2.7	2.8	0.9	3.1	3.9
Lysine	3.0	2.0	2.8	0.7	1.8	2.1	2.3	1.5	1.3	4.7
Arginine	1.4	2.0	4.1	1.6	1.8	3.4	1.4	Trace	5.3	2.2

*A Stem rust, field-collected and stored before analysis.
*B Stem rust, field-collected.

The greatest variation is shown by glutamic acid and aspartic acid. α-Alanine and glycine together show considerable variation although less is shown by the other α-amino-monocarboxylic acids, i.e. valine and the leucines. The other main constituent, γ-amino-butyric acid varies considerably as does serine while somewhat less variation is shown by the basic amino acids and those containing a benzene nucleus.

In contrast to the free amino acids, the bound amino acids in *P. graminis* uredospores are remarkably constant in composition from race to race.

On the basis of the results presented here, it would appear that the free amino acid content of uredospores, although its quantitative determination is tedious, might be considered a useful method for differentiating among races of wheat rust. For example, race 56 might be identified through its lack of glutamic acid and high content of aspartic acid and α-alanine. Similarly, the presence of large amounts of glutamic acid and low content of α-alanine and γ-aminobutyric acid might be used to identify race 48.

ACKNOWLEDGMENTS

The author appreciates the gift of rust cultures and samples from the Plant Pathology laboratory in Winnipeg; the co-operation of the Cereal Division, Central Experimental Farm, in providing greenhouse space; and the assistance of Miss S. G. Howsam and Mr. A. D. Gordon in carrying out the analytical work.

REFERENCES

1. SHAW, M., BROWN, S. A., and JONES, D. R. Nature, **173**, 768 (1954).
2. SHAW, M. and SAMBORSKI, D. J. Can. J. Botany, **35**, 389 (1957).
3. FARKAS, F. L. and KIRALY, Z. Physiol. Plantarum, **8**, 877 (1955).
4. FARKAS, F. L. and KIRALY, Z. Növénytermelés, **6**, 131 (1957); Chem. Abstr. **52**, 8291*a* (1958).
5. IRVINE, G. N., GOLUBCHUK, M., and ANDERSON, J. A. Can. J. Agr. Sci. **34**, 234 (1954).
6. ALLEN, P. J. Plant Physiol. **32**, 385 (1957).

Can. J. Chem. Downloaded from www.nrcresearchpress.com by 69.46.99.164 on 09/04/12
For personal use only.

7. FRENCH, R. C., MASSEY, L. M., Jr., and WEINTRAUB, R. L. Plant Physiol. **32**, 389 (1957).
8. BROYLES, J. W. Phytopathology, **42**, 3 (1952).
9. PARTRIDGE, S. M. and WESTALL, R. G. Biochem. J. **44**, 418 (1949).
10. ALLENTOFF, N. J. Sci. Food & Agr. **5**, 231 (1954).
11. BLOCK, R. J., DURRUM, E. L., and ZWEIG, G. A manual of paper chromatography. Academic Press, Inc., New York. 1955. p. 77.
12. REID, L. J. J. Biol. Chem. **183**, 451 (1950).
13. BLOCK, R. J., DURRUM, E. L., and ZWEIG, G. A manual of paper chromatography. Academic Press, Inc., New York. 1955. p. 88.
14. SMITH, I. Nature, **171**, 43 (1953).
15. MOORE, S. and STEIN, W. H. J. Biol. Chem. **192**, 663 (1951).
16. MOORE, S. and STEIN, W. H. J. Biol. Chem. **211**, 893 (1954).
17. CHINARD, F. P. J. Biol. Chem. **199**, 91 (1952).
18. BLOCK, R. J., DURRUM, E. L., and ZWEIG, G. A manual of paper chromatography. Academic Press, Inc., New York. 1955. p. 80.
19. BLOCK, R. J. J. Dairy Sci. **34**, 1 (1951).

Can. J. Chem. Downloaded from www.nrcresearchpress.com by 69.46.99.164 on 09/04/12
For personal use only.

Can. J. Chem. Downloaded from www.nrcresearchpress.com by 41.223.56.140 on 09/04/12
For personal use only.

PHYSICOCHEMICAL STUDIES OF ALKALI LIGNINS

I. PREPARATION AND PROPERTIES OF FRACTIONS[1]

P. R. GUPTA[2] AND D. A. I. GORING

ABSTRACT

Alkali lignin was prepared by cooking periodate lignin with sodium hydroxide. Fractionation by gradual decrease of pH was not possible as most of the lignin was precipitated sharply at pH 4.4. Fractionation could be achieved by addition of non-solvents such as acetone, dioxane, or ethanol to an alkaline aqueous solution of the lignin, but the initial fractions when separated could not be redissolved. This difficulty was overcome by using barium chloride as a precipitant when all the fractions remained soluble. X-Ray analysis revealed no difference between the insoluble and soluble fractions.

The intrinsic viscosity of the fractions ranged from 0.027 to 0.585 g^{-1} dl. Reduced viscosities were considerably increased at lower ionic strength indicating that the molecule was a polyelectrolyte. The fractions possessed nearly constant methoxyl content (13%), visible absorption (0.28 cm^{-1} l. g^{-1} at 5460 Å), U.V. absorption (18 cm^{-1} l. g^{-1} at 2800 Å), neutralization equivalent (1.3 meq g^{-1}), and electrophoretic mobility (-12.6×10^{-5} cm^2 v^{-1} sec^{-1}). The partial specific volumes of a high and a low molecular weight fraction were 0.63 and 0.68 g^{-1} ml respectively.

INTRODUCTION

Various methods have been used to fractionate lignins and lignin derivatives. Attempts to fractionate lignin include fractional precipitations (1–6), fractional solution (7–9), dialysis (10–12), partitioning between two immiscible solvents (13, 14), chromatographic separation (15, 16), molecular distillation (17), and ultrafiltration (12).

Several early investigations on the isolation and purification of alkali lignin have been reviewed by Brauns (18) and Hägglund (19). In general, these workers were interested mainly in determining elementary composition and chemical constituents and no serious attempt was made to fractionate the lignin preparations as to particle size.

As far as is known, there have been no systematic studies of the solution properties of alkali lignins analogous to the work of Gardon and Mason (20), Goring *et al.* (21, 22), and McCarthy *et al.* (23, 24) on lignin sulphonates. The present investigation deals with the fractionation and subsequent physicochemical characterization of the fractions. In this paper, the development of the method of fractionation is described and measurements of U.V. and visible absorption, methoxyl content, neutralization equivalent, electrophoresis, viscosity, and X-ray diffraction are reported. Succeeding papers (25, 26) will deal with ultracentrifugal sedimentation analysis and the size and shape of the macromolecule.

Throughout the present work, emphasis has been laid on relatively mild treatment and careful purification. Cooking times were kept to the minimum required to render most of the lignin soluble. Ion exchange procedures, dialysis, and ultracentrifugation were used to purify the fractions from excess ions or colloidal debris. The difficulty of separating the alkali lignin from the soluble wood components was overcome by using periodate lignin as a starting material. Ritchie and Purves (27) have shown that the behavior of periodate lignin is similar to that of protolignin in many important respects, e.g., ethanolysis, hydrogenation, nitrobenzene oxidation, and bisulphite cooking. It is known that some methoxyl is lost but the phenyl propane chain is probably not broken.

[1]*Manuscript received August 4, 1959.*
Contribution from the Physical Chemistry Division, Pulp and Paper Research Institute of Canada, and the Department of Chemistry, McGill University, Montreal, Que.
[2]*Holder of the Anglo Paper Research Fellowship, the Alexander McFee Fellowship, and a Studentship from the National Research Council of Canada.*

Periodate lignin was, therefore, regarded as a suitable starting material for physicochemical investigations although comparison with lignins prepared directly from wood is planned as a subsequent extension of the work.

EXPERIMENTAL AND RESULTS

Materials

Periodate lignin was isolated from white spruce by a method similar to that of Purves and co-workers (27–29). The preparation has been described in a previous publication (21).

The sodium hydroxide solution was prepared from chemically pure reagent. Solvents were redistilled. Prior to distillation, dioxane was refluxed with sodium hydroxide pellets until no further brown precipitate was formed. The sodium bicarbonate – sodium hydroxide buffer was prepared by the method of Bates and Bower (30) to have an ionic strength, $\Gamma/2$, of 0.1 and pH 9.65.

Preparation of Alkali Lignin

About 100 g of the periodate lignin was homogenized manually in an agate mortar to pass a 150-mesh sieve.

Digestion was carried out in a stainless steel autoclave of 1.2-liter capacity fitted with a motor stirrer (21). The digestion was of 15-minute duration at 162° C with 10% NaOH solution. The lignin to liquor ratio was 1:50. The autoclave was heated to 162° C in 18 minutes, and cooled to room temperature in 5 minutes by immersing in cold water. The periodate lignin was first soaked with the cooking liquor in the autoclave for 17 hours. The reaction mixture was deaerated by evacuation prior to soaking and autoclaving. After digestion, it was centrifuged at 2000 r.p.m. for 30 minutes to separate the insoluble residue.

Lignin was precipitated from the centrifuged liquor by neutralizing with 20% HCl to pH 1.0. The precipitated lignin was washed with distilled water to pH 3.0, at which point it started dispersing in the wash water. The dispersed lignin was recovered using a Sharples ultracentrifuge. The lignin was then neutralized with NaOH to pH 7.0, when it dissolved giving a clear solution. The neutralized solution was filtered through a medium, sintered glass crucible, freeze-dried, and finally desiccated over magnesium perchlorate to give flakes of alkali lignin which were soluble in distilled water and in dilute sodium hydroxide.

The mother liquor from the acid precipitation of alkali lignin was light yellow in color and evidently contained some degraded lignin. This liquor was not investigated further.

Two batches of the alkali lignin were prepared. The second of these batches was obtained from three successive cooks. About 20 g of the periodate lignin was used for each cook. The yields of the insoluble residue, precipitated lignin, and lignin soluble at pH 1.0 are given in Table I. The neutralization equivalent, N_E (meq of Na per g of the precipitated lignin required for neutralizing to pH 7.0), is also included.

TABLE I

Recovery of alkali lignin

Lignin batch	Insoluble residue (%)	Precipitated (%)	Soluble at pH 1.0 (%)	N_E (meq g^{-1})
1	13	68	19	1.09
2	28	60	12	1.06

Can. J. Chem. Downloaded from www.nrcresearchpress.com by 41.223.56.140 on 09/04/12
For personal use only.

By Mohr's titration, the chloride content of the precipitated lignin was less than 0.1%, and N_E by flame spectrophotometric determination of Na was 1.03 meq g^{-1}.

Fractionation

An attempt to fractionate the alkali lignin dissolved in the buffer by gradual decrease of pH with HCl failed. Most of the lignin precipitated sharply at pH 4.4 and could not be separated into fractions. The precipitated lignin could be redissolved and reprecipitated with an increase and decrease in pH respectively.

The lignin was then fractionated by adding non-solvents such as acetone, dioxane, or ethyl alcohol to aqueous solutions of the alkali lignin. A 2% solution of alkali lignin (batch 1, Table I) in the $NaHCO_3$–NaOH buffer was thermostated at 25° C. Fractions were obtained by progressive addition of the non-solvents and centrifuging the lignin off at 2000 r.p.m. for 30 minutes. The last fraction was recovered by evaporating the mother liquor under vacuum at 40° C. The fractions were redissolved in water, purified by ion-exchange (Dowex 1X-8 and 50X-8), neutralized to pH 7.0, freeze-dried, and desiccated over magnesium perchlorate. The data on fractionation with acetone and dioxane are given in Tables II and III respectively.

TABLE II

Fractionation by addition of acetone

Fraction	Acetone concn. (%)	Wt. of fraction (g)	Yield (%)	Fraction	Acetone concn. (%)	Wt. of fraction (g)	Yield (%)
A-1[a]	75	0.49	9.8	A-6	87	0.75	15.0
A-2[a]	76	0.10	2.0	A-7	90	0.21	4.2
A-3[a]	77	0.17	3.4	A-8	94	0.45	9.0
A-4[a]	79	1.50	30.0	A-9	—	0.90	18.0
A-5	82	0.33	6.6	Loss (by difference)		0.10	2.0

[a]Insoluble.

TABLE III

Fractionation by addition of dioxane

Fraction	Dioxane concn. (%)	Wt. of fraction (g)	Yield (%)	$[\eta]$ (g^{-1} dl)	k'
D-1[a]	75	0.12	1.6	—	—
D-2[a]	79	1.93	26.0	—	—
D-3[b]	—	0.86	16.5	0.073	0.78
D-4	83	1.23	11.5	0.080	1.08
D-5	85	0.48	6.4	0.051	1.16
D-6	88	0.67	9.0	0.036	3.17
D-7	—	1.85	24.8	0.027	7.66
Loss (by difference)		0.31	4.2	—	—

[a]Insoluble.

[b]D-3 was obtained by extracting D-1 and D-2 with dilute NaOH solution.

Invariably, the fractions initially precipitated by addition of non-solvents could not be redissolved in water or dilute NaOH. Fractionations with ethanol, similar to those in Tables II and III, produced insoluble initial fractions. Many variations of the procedure were tried. These include (*a*) addition of excess salt, (*b*) addition of diatomaceous earth to prevent aggregate formation, (*c*) decrease or increase pH, and (*d*) rigorous exclusion of oxygen. In all cases, part of the lignin was rendered insoluble by the fractionation procedure.

Can. J. Chem. Downloaded from www.nrcresearchpress.com by 41.223.56.140 on 09/04/12
For personal use only.

Can. J. Chem. Downloaded from www.nrcresearchpress.com by 41.223.56.140 on 09/04/12
For personal use only.

It was then found that fractionation by addition of barium chloride was possible and that the initial fractions were no longer insoluble. The barium chloride fractionation was carried out at 25° C on 11 g of alkali lignin (batch 2, Table I) dissolved in 500 ml of 0.02 *N* sodium hydroxide solution and centrifuged at 40×10^3 g for 20 minutes. *N*/10 $BaCl_2$ was then slowly added to the continuously stirred solution until a turbidity developed. The mixture was stirred for 30 minutes after which the precipitate was separated by ultracentrifugation and dissolved in 0.1 *N* sodium hydroxide solution. A series of such fractions was obtained by progressive addition of barium chloride solution. The last fraction B-9 was obtained by evaporating the mother liquor. The fractions in solution were converted into neutral freeze-dried powders as described earlier. The data are given in Table IV.

TABLE IV

Fractionation by addition of barium chloride

Fraction	0.1 *N* $BaCl_2$ added (ml)	Wt. of fraction (g)	Yield (%)	$[\eta]$ (g^{-1} dl)	k'
B-0[a]	—	—	—	0.105	2.02
B-1	100	0.31	2.8	0.208	1.36
B-2	50	0.40	3.6	0.234	1.48
B-3	25	0.17	1.5	0.164	0.97
B-4	25	1.43	13.0	0.136	1.26
B-5	25	1.93	17.5	0.105	1.24
B-6	25	1.85	16.8	0.084	1.56
B-7	25	1.03	9.4	0.075	1.45
B-8	50	1.06	9.6	0.066	1.54
B-9	—	0.35	3.2	0.033	6.88
Loss (by difference)	—	2.47	22.5	—	—

[a]B-0 unfractionated.

Subfractionations of fractions B-4 and B-5 (Table V) were carried out by similar methods using the lower lignin concentrations of 0.13% and 0.2% respectively.

TABLE V

Subfractionation of B-4 and B-5 by addition of barium chloride

Fraction	0.1 *N* $BaCl_2$ added (ml)	Wt. of fraction (g)	Yield (%)
B-4-I[a]	—	0.25	32.5
B-4-II	50	0.29	37.7
B-4-III	—	0.23	29.8
B-5-I	70	0.17	13.5
B-5-II	40	0.48	38.1
B-5-III	70	0.23	18.3
B-5-IV	—	0.38	30.1

[a]Obtained by prolonged ultracentrifugation (2 hours at 150,000 *g*) of fraction B-4.

Finally, a series of fractions was made from the fractions shown in Tables IV and V. Low molecular weight material was removed by dialysis through cellophane tubing against successive changes of buffer and distilled water. Very high molecular weight material was eliminated by prolonged ultracentrifugation. In some cases fractions were blended to give enough material for study. The fractions thus obtained were designated the F-series and are shown in Table VI. Fractions F-1, F-2, and F-9 were prepared

TABLE VI

Fractions obtained by ultracentrifugal purification and dialysis

Fraction	$[\eta]$ (g^{-1} dl)	k'	Source
F-1	0.585	6.51	Described in the text
F-2	0.294	2.48	Described in the text
PF-2	0.20	—	Described in the text
F-3	0.133	1.59	B-1 and B-2
F-4	0.125	0.86	B-4-II
F-5	0.150	1.26	B-5-II and B-5-III
F-6	0.083	2.02	B-6
F-7	0.071	2.61	B-7
F-8	0.059	2.54	B-8
F-9	0.042	5.68	Described in the text

directly from the unfractionated material; F-2 and F-1 were obtained by two consecutive extractions with buffer of the sediment produced by ultracentrifugation at 150×10^3 g for 1 hour of a solution which had been centrifuged at 40×10^3 g for 1 hour; PF-2 was obtained on subsequent purification of F-2 by centrifugation and dialysis; F-9 was recovered from the dialyzate of the unfractionated material. In all cases (except F-1, F-2, and PF-2) fractions were neutralized and freeze-dried to give soluble powders. The purpose of more rigorous purification of the F-series was to prepare a series of fractions for light-scattering measurements to be described in a subsequent paper (26).

Viscosity

Intrinsic viscosity determinations were made in the $NaHCO_3$–NaOH buffer at $25\pm0.01°$ C with Ubbelohde-type viscometers as described by Craig and Henderson (31). The precision of the data is illustrated by the graphs of η_{sp}/c vs. c for the B-series shown in Fig. 1. From the "least square", lines $[\eta]$ and the Huggins' slope constant k' were

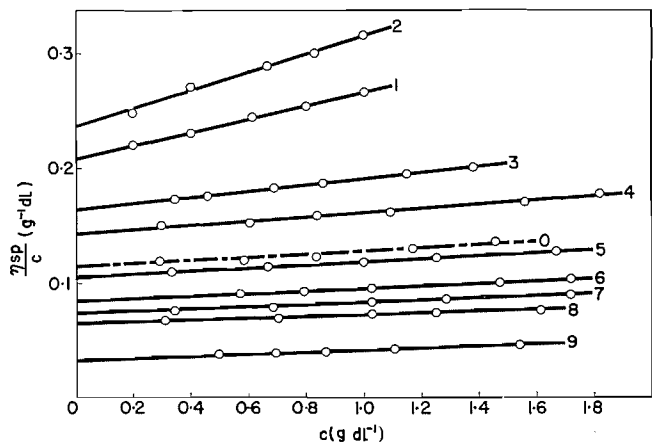


FIG. 1. η_{sp}/c vs. c in the $NaHCO_3$–NaOH buffer ($\Gamma/2 = 0.1$: pH = 9.65) for fractions of B-series.

obtained. Values of $[\eta]$ and k' for the various fractions are given in Tables III, IV, and VI. The intrinsic viscosity is given here as a convenient method of characterizing the fractions. Detailed interpretation of $[\eta]$ and k' is reserved for a later paper (26).

Although no barium could be detected in the purified fractions, it was considered possible that minute residual quantities of Ba^{++} might cause an anomalous increase in

Can. J. Chem. Downloaded from www.nrcresearchpress.com by 41.223.56.140 on 09/04/12
For personal use only.

[η] by promoting aggregation. Accordingly the intrinsic viscosity of B-0 was redetermined in buffer with a small amount of $BaCl_2$ added. Instead of an increase, [η] was reduced by 13% in the presence of barium probably because of the increased cationic strength of the buffer. This proved that if traces of Ba^{++} were present they would not cause erroneously high values of [η].

Polyelectrolyte Behavior

Reduced viscosities were considerably increased with decrease in ionic strength and the characteristic polyelectrolyte upsweep of η_{sp}/c at low concentration was found for fractions dissolved in buffer of ionic strength 10^{-5} (Fig. 2). However, the effect was

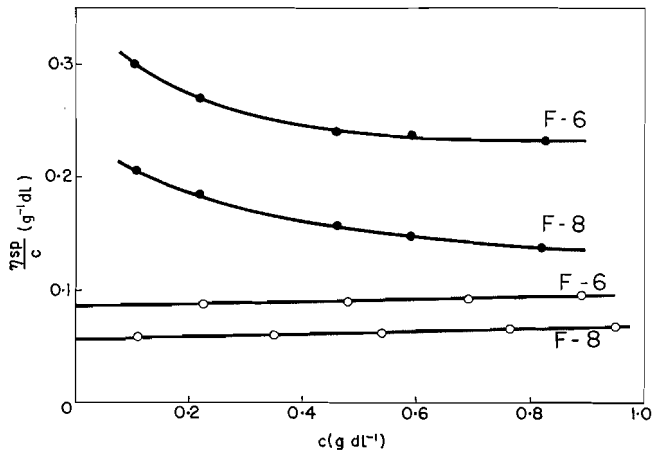


FIG. 2. η_{sp}/c vs. c in $NaHCO_3$–NaOH buffer at ionic strengths of 0.1 (open circles) and 10^{-5} (closed circles).

less than that found with lignin sulphonates by Rezanowich and Goring (32). Therefore the use of $\Gamma/2 = 0.1$ buffer was considered appropriate to depress the polyelectrolyte behavior, but a further small decrease in η_{sp}/c would be likely if the ionic strength was further increased.

Methoxyl, Neutralization Equivalent, and Light Absorption

Methoxyl estimations were made by Tappi Standard Method 2M43.

The neutralization equivalent was calculated from the sulphated ash obtained by igniting the samples with sulphuric acid at 750° C.

Optical densities were measured with a Beckman DU spectrophotometer as previously described (21). Measurements were made at wavelengths of 5460 Å and 2800 Å using concentrations of 0.2 and 0.002 g dl^{-1} respectively. The solvent was the $NaHCO_3$–NaOH buffer. Absorption was expressed in terms of the coefficient, ϵ, given by

$$\epsilon = D/cd \qquad [1]$$

where D is the optical density, c the concentration, and d the cell length. Values of ϵ together with methoxyl content and neutralization equivalent are given in Table VII.

Electrophoresis

Moving boundary electrophoresis was carried out in a Spinco Tiselius apparatus as previously described (22). The temperature of the bath was 0.8° C. Lignin fractions were dissolved directly in the $NaHCO_3$–NaOH buffer. The electrical conductivity of the

Can. J. Chem. Downloaded from www.nrcresearchpress.com by 41.223.56.140 on 09/04/12
For personal use only.

TABLE VII

Data on methoxyl content, neutralization equivalent, and light absorption

Fraction	OCH_3 (%)	N_E (meq g^{-1})	ϵ_{2800} (cm^{-1} l. g^{-1})	ϵ_{5460} (cm^{-1} l. g^{-1})
B-0	12.8	1.03	—	—
B-1	12.7	—	—	—
B-2	12.5	—	—	—
B-3	12.7	—	—	—
B-4	13.2	—	—	—
B-5	13.4	—	—	—
B-6	13.2	—	—	—
B-7	13.1	—	—	—
B-8	13.0	—	—	—
B-9	11.3	1.12	18.4	0.22
F-3	13.1	1.76	17.8	0.20
F-4	13.0	1.68	16.5	0.17
F-5	13.0	1.40	17.5	0.19
F-6	13.3	1.06	18.7	0.21
F-7	13.4	1.12	18.6	0.21
F-8	13.5	1.06	18.5	0.22
F-9	11.0	1.12	18.5	0.26

solutions and buffer agreed within 2%. The duration of the run was about 2 hours. Peaks were clearly defined, though the patterns showed considerable spreading of the boundaries. The velocity, dx/dt, of the maximum ordinate was determined with respect to the ϵ or δ "stationary" boundaries. Electrophoresis diagrams are given in Fig. 3 and mobilities

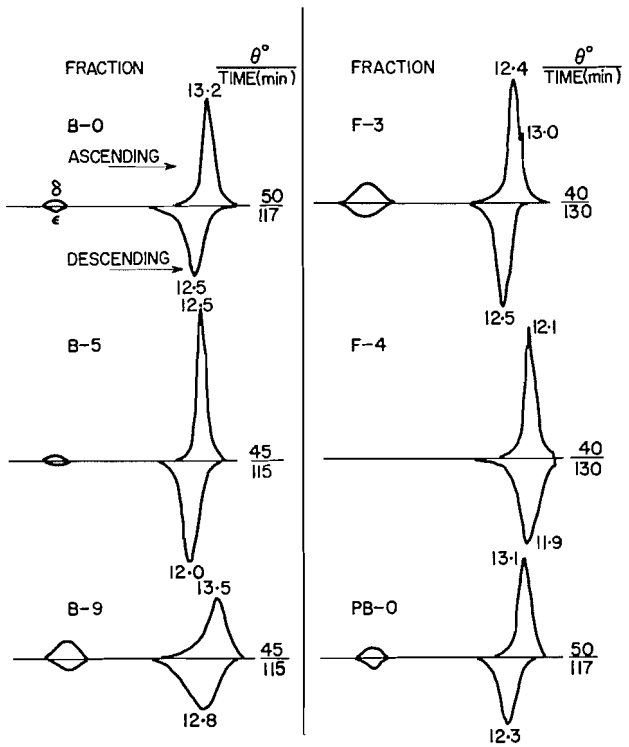


FIG. 3. Electrophoresis diagrams for some of the fractions; $\Gamma/2 = 0.1$; pH = 9.65; $c = 0.50\%$ (except F-3 and F-4 with $c = 0.41\%$).

Can. J. Chem. Downloaded from www.nrcresearchpress.com by 41.223.56.140 on 09/04/12
For personal use only.

calculated in the usual manner (33) are shown in the diagram near the appropriate peaks.

X-Ray Analysis

It was possible that the insolubility of initially precipitated fractions could be ascribed to the development of crystallinity by polymerization (34). This would be revealed by X-ray diffraction, as more ordered patterns would be expected in the insoluble fractions.

X-Ray measurements were made using the technique described by Kouris, Ruck, and Mason (35). Exposures were of 4-hour duration with Cu K_α radiation. Broad diffuse rings, indicating an amorphous structure, were obtained and there was no difference in the diagram for the soluble and insoluble fractions. Therefore, the insolubility could not be associated with the development of crystallinity.

Partial Specific Volume

The classical pycnometer method (36) was used to determine the partial specific volume, $\bar{v}$, of the lignin fractions B-1 and B-6 in the buffer. A 5-ml Lipkin pycnometer (37) gave reproducible results with the usual precautions (38). Values of $\bar{v}$ for B-1 and B-6 were 0.63 and 0.68 g^{-1} ml respectively. The reported values of $\bar{v}$ range from 0.61 to 0.74 g^{-1} ml (5, 39, 40).

DISCUSSION

The fact that the alkali lignin could be fractionated into a series of fractions with progressively decreasing viscosity demonstrates its polydisperse macromolecular character. The intrinsic viscosities range from 0.027 to 0.585 g^{-1} dl. Such high $[\eta]$ values have not been reported earlier for alkali lignin. Recently, Goring and Rezanowich (21) obtained a similar range of $[\eta]$ for lignin sulphonates prepared by fractional solution under relatively mild cooking conditions. It is very interesting that two entirely different processes for making the lignin soluble yield macromolecular solutes similar as to particle size. This would support the concept that lignin exists as a three-dimensional network structure (41, 42) which, when made soluble by a comparatively mild treatment, yields a wide range of molecular weights.

The fractions were quite similar with regard to methoxyl content 13.1 ($\pm$0.3)% excluding B-9 and F-9. Constancy of methoxyl content has also been noted by Goring and Rezanowich (21), McCarthy and co-workers for non-dialyzable lignin sulphonates (24), and by Hess for fractionated native lignins (43). Values of methoxyl reported in the present work are higher as compared to lignin sulphonates but similar to native lignins. Gardon and Mason (12) reported low methoxyl contents in low molecular weight lignin sulphonates but further work showed that this was due to the presence of a small quantity of non-lignin organic impurity. The low values of 11.3% and 11.0% in B-9 and F-9 respectively may have been due to this effect. In agreement with results for other series of lignins (4, 6, 21, 23) the U.V. absorption was also constant. Though there was a greater variation in visible light absorption from fraction to fraction, no clear maximum was found as in the case of lignin sulphonates (21). The average value of ϵ_{2800} was 18.1 ($\pm$0.6) cm^{-1} l. g^{-1} which is considerably greater than the corresponding value of 13.8 cm^{-1} l. g^{-1} for the sulphonates (21) and nearly equal to the absorption noted by Hess for fractionated native black spruce lignin (43). These results suggest that the quick alkali treatment did not destroy the essential structure of the lignin. The high U.V. absorption seems also to have some bearing on the question of degradation of the lignin by the periodate treatment. In the oxidation by periodate some methoxyl is lost (27). As suggested by Adler (44), if this is accompanied by opening of the aromatic

Can. J. Chem. Downloaded from www.nrcresearchpress.com by 41.223.56.140 on 09/04/12
For personal use only.

ring, then the proportion of aromatic to aliphatic carbon in the molecule will decrease, thereby altering the U.V. absorption. The good agreement of ϵ_{2800} with the values for spruce native lignin indicates that periodate degradation of the aromatic portion of the molecule must be small.

With one minor exception, single electrophoretic peaks were obtained (Fig. 3) similar to those for lignin sulphonate from a mild cook (21). Schubert *et al.* (45) found the native and enzymatically liberated lignins from oak, maple, and cork electrophoretically homogeneous while Scots pine lignin showed only small secondary components. This is in contrast to the marked electrophoretic heterogeneity of lignin sulphonates degraded by prolonged cooking (21). Similarly, McCarthy and co-workers (46) have found several electrophoretically distinguishable components in the alkali degradation products of lignin sulphonates. Evidently, separation into electrophoretically distinct components is characteristic of degraded lignins and the homogeneity found in the present work is a further support for the relatively undegraded character of the fractions studied.

The electrophoretic mobilities of the fractions studied were fairly constant. Migration was anodic and the mean U for the ascending and descending peaks were -12.8 (± 0.4) $\times 10^{-5}$ and -12.4 (± 0.3) $\times 10^{-5}$ cm^2 v^{-1} sec^{-1} respectively. Constant mobilities have also been observed by Goring *et al.* (22) for lignin sulphonates with a wide range of intrinsic viscosities. In a later report (26) it is demonstrated that the alkali lignin macromolecule is compact and not free-draining. Thus the ionizing charge groups which produce electrophoresis are probably near the surface of the macromolecule. Consistency of mobility suggests, therefore, identical surface charge densities, in spite of a large variation in size of the macromolecule. A fairly uniform charge distribution is indicated also by the failure to fractionate the lignin by addition of acid. A gradual decrease of pH caused most of the lignin to precipitate sharply at pH 4.4. This was probably due to the association of acidic groups on the molecule eliminating formal charges, the hydrophilic nature of which made the molecule soluble. The sharpness of the effect indicated that the ionizing groups were all of the same type and were probably —COO^- since the pK values of many carboxylic acids lie around pH 4–5. The charged nature of the molecule was verified also by its polyelectrolyte behavior although the effect was less than that produced by —SO_3^- groups in lignin sulphonate (32).

Fractional precipitation with non-solvents was intriguing as the initial few fractions became partially or completely insoluble. With acetone and dioxane about 45% and 27% respectively of the lignin was rendered insoluble. The later soluble fractions appeared to be effectively differentiated with respect to molecular weights because [η] decreased in the usual manner. Thus the material which became insoluble was probably of a higher molecular weight. Schuerch (13) has found in ethanol lignin that the initial fraction (supposedly the highest molecular weight fraction), when precipitated from chloroform–ethanol mixture on adding aqueous ethanolic alkali, gave an insoluble product. A higher dilution and a better aqueous solvent system was suggested by him for the partitioning of higher molecular weight fractions in order to avoid insolubilization.

In the present study an irreversible aggregation was considered as a possible cause for the insolubility of the initial fractions. To eliminate this, several variations of the technique were tried but without success. The precipitation was carried out in the presence of materials with large surface area such as diatomaceous earth, anion exchange resin (Dowex 1X-8; 200–400 mesh), or ball-milled glass. The idea was to provide nuclei for the precipitating lignin and decrease lignin–lignin contacts supposedly responsible for the aggregation. Diatomaceous earth absorbed lignin completely. Initially precipi-

Can. J. Chem. Downloaded from www.nrcresearchpress.com by 41.223.56.140 on 09/04/12
For personal use only.

tated lignin still became insoluble in the presence of the powdered glass or resin. It was also considered possible that some oxidation (18) would occur during fractionation in alkaline medium rendering part of the lignin insoluble. Insoluble fractions still resulted when the lignin solution was deaerated and fractionation was carried out under a nitrogen atmosphere. Anyway, polymerization would not be likely in the mild alkaline conditions of the experiments as the sample had already been subjected to strong alkali at 162° C during its preparation from periodate lignin.

During the non-solvent fractionations it was noted that if the freshly precipitated lignin was removed immediately from the solution, it was still soluble. When the fractionation was carried out allowing time for equilibrium, the initially precipitated lignin was rendered insoluble. This result suggested that under the dehydrating conditions producing precipitation, irreversible lignin–lignin bonding developed with time in the high molecular weight material. Such an effect did not occur with the low molecular weight fractions even though the environment contained a greater proportion of non-solvent in the solution. X-Ray analysis revealed no greater order in the insoluble material, which showed that the insolubility was not associated with any tendency to crystallinity.

Whatever the cause of this interesting effect, it is quite evident that, under certain conditions, alkali lignin tends to adhere to itself. Also the material which behaves in this way is the high molecular fraction which, analogous to the sulphonates (21), is probably extracted at the final stage of cooking. Partial delignification of wood with alkali would therefore be expected to leave some of this "sticky" lignin on the cellulose which may effect considerably the subsequent bonding properties of the fiber.

Fractionation with Ba^{++} as precipitant was comparatively successful as the initially precipitated lignin was no longer rendered insoluble and there was a regular decrease in viscosity of the fractions. Fischer and co-workers (18) while studying alkaline oxidation of lignin were able to precipitate lignin with barium and separated it into readily soluble and slightly soluble fractions. Fractionation with Ba^{++} is not particularly selective and the fractions had a wide polydispersity as discussed in the following paper of the present series (25). Perhaps the polydispersity contributes to the solubility of the initial high molecular weight fractions with Ba^{++} as precipitant, assuming that the low molecular weight molecules peptize or disperse the high molecular weight material.

Finally, it is worth while to consider how representative the fractions were of the lignin in the wood. The periodate lignin was 64% of the Klason lignin content of the white spruce used (21). However, the lignin lost in the periodate preparation was mostly colloidal material which should be representative of the protolignin. With careful recovery on a small scale, Purves and co-workers (27) have obtained a 97% yield based on Klason lignin. From the data in Table I, it is evident that the material fractionated comprised about 65% of the periodate lignin. After the lignin was cooked with sodium hydroxide about 20% remained insoluble and about 15% could not be precipitated at the low pH. The latter would probably have a low intrinsic viscosity, while the insoluble portion if dissolved by longer digestion may have a somewhat higher $[\eta]$ than the values reported in this paper. The fractions used, therefore, corresponded to about 42% of the Klason lignin of the original wood and probably represented a "middle cut" with respect to molecular weight produced in the cooking process.

ACKNOWLEDGMENTS

The authors wish to thank Dr. R. St. J. Manley for the X-ray diffraction measurements and Dr. A. H. Sehon for use of the electrophoresis apparatus.

Can. J. Chem. Downloaded from www.nrcresearchpress.com by 41.223.56.140 on 09/04/12
For personal use only.

Can. J. Chem. Downloaded from www.nrcresearchpress.com by 41.223.56.140 on 09/04/12
For personal use only.

REFERENCES

1. STAUDINGER, H. and DREHER, E. Ber. **69**, 1729 (1936).
2. PATTERSON, R. F. *et al.* J. Am. Chem. Soc. **63**, 2065 (1941).
3. JONES, E. J. Tappi, **32**, 167 (1949).
4. MARKHAM, A. E., PENISTON, Q. P., and MCCARTHY, J. L. J. Am. Chem. Soc. **71**, 3599 (1949).
5. OLLEMAN, E. D., PENNINGTON, D. E., and RITTER, D. M. J. Colloid Sci. **3**, 185 (1948).
6. MOACANIN, J., FELICETTA, V. F., HALLER, W., and MCCARTHY, J. L. J. Am. Chem. Soc. **77**, 3470 (1955).
7. STUMF, W. and FREUDENBERG, K. A. Angew. Chem. **62**, 537 (1950).
8. ERDTMAN, H. Svensk Papperstidn. **45**, 374 (1942); **45**, 392 (1942).
9. ERDTMAN, H. Svensk Kem. Tidskr. **53**, 201 (1941).
10. ERNSBERGER, F. M. and FRANCE, W. G. J. Phys. & Colloid Chem. **52**, 267 (1948).
11. SCHWABE, K. and HASNER, L. Cellulosechemie, **20**, 61 (1942).
12. GARDON, J. L. and MASON, S. G. Can. J. Chem. **33**, 1477 (1955).
13. SCHUERCH, C. J. Am. Chem. Soc. **74**, 5061 (1952).
14. LOVELL, E. L. and HIBBERT, H. J. Am. Chem. Soc. **63**, 2070 (1941).
15. BLAND, D. E. and GATLEY, F. M. Nature, **173**, 32 (1954).
16. GOLDSCHMID, G. Tappi, **38**, 728 (1955).
17. BAILEY, A. J. Paper Trade J. **111**, 27 (1940).
18. BRAUNS, F. E. Chemistry of lignin. Academic Press, Inc., New York. 1952.
19. HÄGGLUND, E. Chemistry of wood. Academic Press, Inc., New York. 1951.
20. GARDON, J. L. and MASON, S. G. Can. J. Chem. **33**, 1491 (1955).
21. GORING, D. A. I. and REZANOWICH, A. Can. J. Chem. **36**, 1653 (1958).
22. GORING, D. A. I., WEBB, T., and SEHON, A. H. Svensk Papperstidn. **61**, 1010 (1958).
23. NOKIHARA, E., TUTTLE, M. J., FELICETTA, V. F., and MCCARTHY, J. L. J. Am. Chem. Soc. **79**, 4495 (1957).
24. FELICETTA, V. F. and MCCARTHY, J. L. J. Am. Chem. Soc. **79**, 4499 (1957).
25. GUPTA, P. R., ROBERTSON, R. F., and GORING, D. A. I. Can. J. Chem. **38**, 259 (1960).
26. GUPTA, P. R. and GORING, D. A. I. Can. J. Chem. **38**, 270 (1960).
27. RITCHIE, P. F. and PURVES, C. B. Pulp Paper Mag. Can. **48**, 74 (1947).
28. WALD, W. J., RITCHIE, P. F., and PURVES, C. B. J. Am. Chem. Soc. **69**, 1371 (1947).
29. SMITH, D. M. and PURVES, C. B. Ind. Eng. Chem. **49**, 1394 (1957).
30. BATES, R. G. and BOWER, V. E. Anal. Chem. **28**, 1322 (1956).
31. CRAIG, A. W. and HENDERSON, D. A. J. Polymer Sci. **19**, 215 (1956).
32. REZANOWICH, A. and GORING, D. A. I. To be published.
33. LONGSWORTH, L. G. and MACINNES, D. A. J. Am. Chem. Soc. **62**, 705 (1940).
34. FLORY, P. J. Principles of polymer chemistry. Cornell Univ. Press, Ithaca, N.Y. 1953.
35. KOURIS, M., RUCK, H., and MASON, S. G. Can. J. Chem. **36**, 931 (1958).
36. SVEDBERG, T. and PEDERSON, K. O. The ultracentrifuge. Oxford Univ. Press, London. 1940.
37. LIPKIN, M. R., DAVISON, J. A., HARVEY, W. T., and KURTZ, S. S., JR. Ind. Eng. Chem. **16**, 55 (1944).
38. BAUER, N. *In* Physical methods of organic chemistry. Interscience Publishers, Inc., New York. 1949.
39. GRALEN, N. J. Colloid Sci. **1**, 453 (1946).
40. IVARSSON, B. Svensk Papperstidn. **54**, 1 (1951).
41. JAHN, E. C., HOLMBERG, C. V., and SCHUERCH, C. Chem. in Can. **5**, 35 (1953).
42. BJÖRKMAN, A. Ind. Eng. Chem. **49**, 1395 (1957).
43. HESS, C. L. Tappi, **35**, 312 (1952).
44. ADLER, E., HERNESTAM, S., and WALLDEN, I. Svensk Papperstidn. **61**, 641 (1958).
45. SCHUBERT, W. J., PASSANNANTE, A., DE STEVENS, G., BIER, M., and NORD, F. F. J. Am. Chem. Soc. **75**, 1869 (1953).
46. FELICETTA, V. F., AHOLA, A., and MCCARTHY, J. L. J. Am. Chem. Soc. **78**, 1899 (1956).

Can. J. Chem. Downloaded from www.nrcresearchpress.com by 41.223.56.140 on 09/04/12
For personal use only.

PHYSICOCHEMICAL STUDIES OF ALKALI LIGNINS

II. ULTRACENTRIFUGAL SEDIMENTATION ANALYSIS[1]

P. R. GUPTA,[2] R. F. ROBERTSON, AND D. A. I. GORING

ABSTRACT

Ultracentrifugal sedimentation of alkali lignin fractions revealed marked boundary spreading at low and high centrifugal fields. An analysis of the gradient diagrams indicated a wide distribution of sedimentation coefficients ranging from 0.5 to over 400×10^{-13} second. There was only a small decrease in the polydispersity on subfractionation. The distributions were continuous with a single peak and positive skewness. A linear relationship was found between the intrinsic viscosity and the standard deviation of the weight-average sedimentation coefficient. The sedimentation coefficient based on the movement of the maximum ordinate at a field of 11.5×10^3 *g* was several times greater than the corresponding coefficient for the same fraction at 200×10^3 *g*. A qualitative interpretation of this phenomenon is given in terms of the Faxen and the Archibald solution to the Lamm equation.

INTRODUCTION

To interpret the physicochemical behavior of a macromolecule, a knowledge of the molecular weight distribution is a prerequisite. Theoretically, the sedimentation velocity method offers a direct measure of size distribution without recourse to fractionation. In practice, the technique is often unsatisfactory because marked concentration dependence in the sedimentation coefficient, *s*, masks the boundary spreading due to distribution in *s*. However in certain biological systems, e.g., enzymatically degraded glycogen (1, 2), there is only a small dependence of *s* on concentration and boundary spreading experiments can yield useful data on the molecular size distribution of a given sample. The present investigation deals with such an ultracentrifugal analysis of the fractionated alkali lignins described in the preceding paper of the present series (3).

We could find only one previous report on the sedimentation of lignins and this was by Gralen (4). Diffuse single peaks were obtained for thio- and hypo-bromide lignins. Sedimentation coefficients calculated from the movement of the maximum ordinate were from 1.0 to 3.0×10^{-13} second for the various fractions. The sedimentation diagrams were not analyzed for distribution of *s*, but Gralen noted that the fractions were polydisperse because the peak spreading in sedimentation was greater than observed in diffusion.

Recently, several workers (5–11) have reported wide polydispersity in lignin sulphonates fractionated by a variety of methods, and molecular weights as high as 138,000 were found. In contrast, the reported molecular weights of alkali lignin and other lignin derivatives are relatively low, i.e., up to 11,000 (12). Anticipating low molecular weights, the use of Archibald's (13) modification of Svedberg's (14) sedimentation equilibrium method was explored initially. To examine the applicability of this procedure, preliminary ultracentrifugal experiments were made at the lowest available rotor speed. It was found that even in this low field, sharp peak formation occurred indicating the presence of high molecular weight material. At centrifugal speeds, commonly used in velocity sedimentation experiments, a more diffuse peak was formed. A comparison of the movement of the peaks at the two speeds revealed an interesting discrepancy. Sedimentation coefficients based on the velocity of the maximum ordinate differed widely for the same

[1]*Manuscript received August 4, 1959.*
Contribution from the Physical Chemistry Division, Pulp and Paper Research Institute of Canada, and the Department of Chemistry, McGill University, Montreal, Que.
[2]*Holder of the Anglo Paper Research Fellowship, the Alexander McFee Fellowship, and a Studentship from the National Research Council of Canada.*

fraction at two speeds. A technique was then developed in which the same solution was run successively at two speeds thereby providing a more complete picture of the distribution of sedimentation coefficients.

The calculation of sedimentation coefficient distribution is an extremely laborious operation and the amount of labor depends on the degree of refinement used in the computations. The present study is the first of its kind to be made on any type of lignin. Therefore, it was decided to adopt certain approximations to permit the analysis of as many fractions as possible in the time available. The simplifying assumptions necessary for this are reported and discussed in the following sections.

EXPERIMENTAL AND RESULTS

The preparation and properties of the fractions studied are described in the first paper of the present series (3). Sedimentation measurements were made with Spinco Model E ultracentrifuge. The temperature was 26 (±0.5)° C. A double sector cell was used. One sector contained the solution while the other contained buffer which provided an accurate base line. A small quantity of methyl blue was added to the buffer to make its transmission at 5460 Å equal to that of the lignin solution. Phase plate optics were used and the schlieren angle was 45°. Unless otherwise stated, fractions were run at a concentration of 0.5 (±0.02) g dl^{-1} in $NaHCO_3$–NaOH buffer (pH = 9.65: $\Gamma/2 = 0.1$).

Measurements were made at 12,600 and 52,600 r.p.m. corresponding to 11.5×10^3 *g* and 200×10^3 *g* respectively. To allow for sedimentation during acceleration, one-third the acceleration time (15) was added to the time at the selected r.p.m. It was found possible to make the low and high speed measurements successively without stopping the ultracentrifuge. Usually six exposures at 4- or 8-minute intervals were taken at 12,600 r.p.m. The rotor was then accelerated to 52,600 r.p.m. and six more pictures at 8-minute intervals were recorded. Sedimentation diagrams obtained in this manner at the high speed were identical with diagrams at the equivalent time based on uninterrupted acceleration from 0 to 52,600 r.p.m.

Examples of sedimentation boundary gradient curves are shown in Fig. 1. The sedimentation coefficient, s_m, defined by the velocity of the maximum ordinate, was obtained

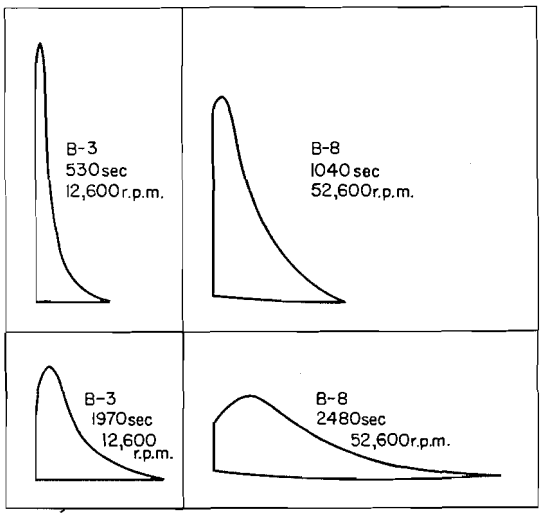


FIG. 1. Examples of sedimentation boundary gradient curves for fractions B-3 and B-8. The solvent was $NaHCO_3$–NaOH buffer (pH = 9.65; $\Gamma/2 = 0.1$).

Can. J. Chem. Downloaded from www.nrcresearchpress.com by 41.223.56.140 on 09/04/12
For personal use only.

from linear plots of $\log_{10} x_m$ vs. t (Fig. 2) where x_m is the distance of the maximum ordinate from the center of the rotor and t is the time. The origin was not used as a

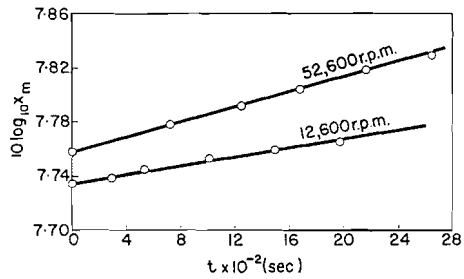


FIG. 2. Plot of log x_m vs. time for fraction B-3.

point in order to eliminate the error due to the interval of time at which the peak remains at the meniscus (16). The small correction required to normalize s_m to the viscosity and density of pure water at 25° C was neglected. Sedimentation coefficients, s_{m1} and s_{m2}, corresponding respectively to 12,600 r.p.m. and 52,600 r.p.m. are given in Table I.

TABLE I

Sedimentation coefficients of the fractions at a concentration of 0.5 (±0.02) g dl^{-1} in $NaHCO_3$–NaOH buffer (pH = 9.65; $\Gamma/2$ = 0.1)

Fraction	$s_{m1}\times10^{13}$ (sec)	$s_{m2}\times10^{13}$ (sec)	Fraction	$s_{m1}\times10^{13}$ (sec)	$s_{m2}\times10^{13}$ (sec)
B-0	18.7	2.2	B-5-I	42.1	[a]
B-1	27.6	1.4	B-5-II	23.9	2.6
B-2	26.5	1.7	B-5-III	17.9	2.6
B-3	18.4	2.0	B-5-IV	No peak	2.2
B-4	17.6	2.2			
B-5	16.3	2.4	F-3	19.9	2.3
B-6	13.8	2.7	F-4	17.0	2.7
B-7	11.4	2.6	F-5	18.0	2.8
B-8	4.5	2.6	F-6	15.3	2.8
B-9	No peak	0.7	F-7	13.3	2.5
			F-8	5.2	2.5
B-4-I	39.2	[a]	F-9	No peak	No peak
B-4-II	17.0	2.4			
B-4-III	No peak	No peak			

[a]Material sediments completely to the cell bottom.

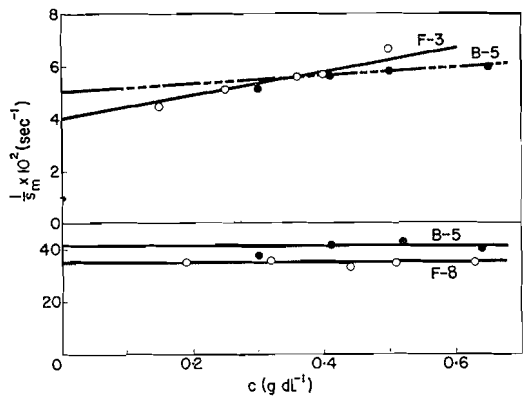


FIG. 3. Reciprocal s_m (Svedberg units) vs. c at 12,600 r.p.m. (top) and 52,600 r.p.m. (bottom). The solvent was $NaHCO_3$–NaOH buffer (pH = 9.65; $\Gamma/2$ = 0.1).

Can. J. Chem. Downloaded from www.nrcresearchpress.com by 41.223.56.140 on 09/04/12
For personal use only.

The concentration dependence of sedimentation coefficients measured in a few selected fractions is shown in Fig. 3. It is evident that for the high speed runs, s_m is independent of concentration, c, within the experimental error imposed by the diffuse shape of the peaks. At the low speed, some dependence exists, partially due to the changing viscosity of the solution (of the low molecular weight material) through which the heavier particles sediment. In B-5 and F-3, the least square lines were given by the empirical relationship (17–20).

$$1/s = (1/s_m)_{c=0}(1+k_s c)$$

where the constant k_s was 0.53 and 1.61 g^{-1} dl respectively. If s_m is corrected for the viscosity of the solution, these values of k_s change to 0.37 and 1.21 g^{-1} dl. No correction was made for the concentration dependence of s in the low speed experiments, an approximation justified by the small ratio (15% on the average) of the material sedimenting at 12,600 r.p.m. to that sedimenting at the higher speed.

Distribution of Sedimentation Coefficients

The distribution of sedimentation coefficients was determined by the method of Williams and others (17, 18, 21–26), from the progressive spreading of the boundary with time. The distribution function $g(s)$ was obtained as a quantity such that the weight fraction of the material with sedimentation coefficients between s and $(s+ds)$ was given by $g(s)ds$. An apparent distribution function $g^*(s)$, corresponding to discrete

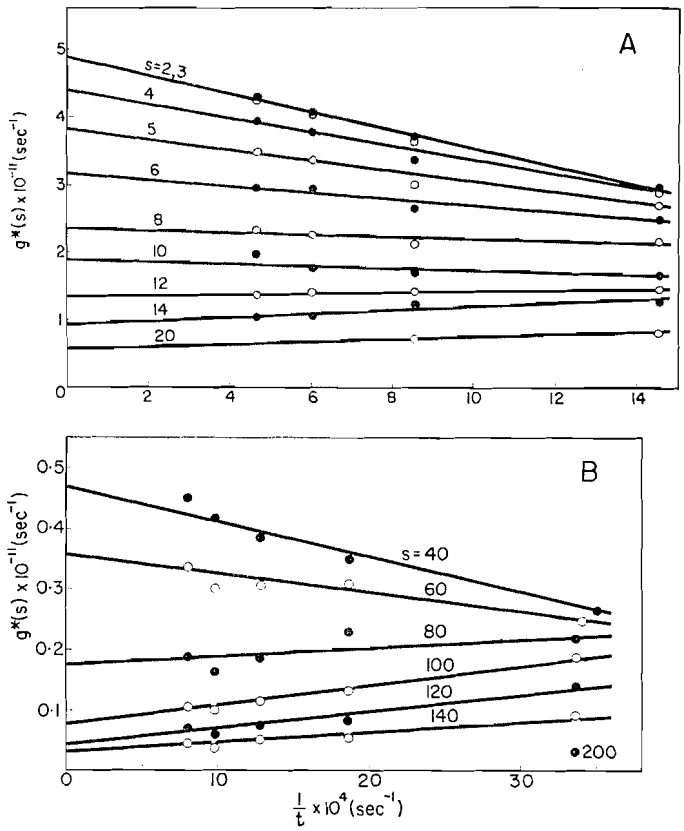


FIG. 4. Extrapolation of $g^*(s)$ to infinite time for fraction B-1 at 52,600 r.p.m. (A) and at 12,600 r.p.m. (B).

Can. J. Chem. Downloaded from www.nrcresearchpress.com by 41.223.56.140 on 09/04/12
For personal use only.

values of x, was computed from (27)

[1] $$g^*(s) = (dc/dx)(\omega^2 t x^3)(c_0^{-1} x_0^{-2})$$

where x, x_0, ω, and c_0 are respectively the distance from the center of rotor, the position of the meniscus, the angular velocity, and the initial concentration. Each value of x corresponds to a definite sedimentation coefficient, s, given by

[2] $$s - s_m = 2(x - x_m)/\omega^2 t(x + x_m).$$

In eq. [1], dc/dx and c_0 were replaced respectively by the refractive index gradient, dn/dx, and Δn, the difference in refractive index between solution and solvent.

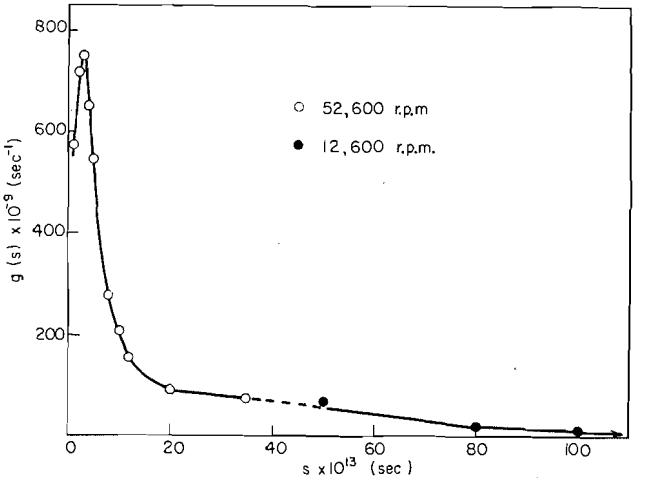


FIG. 5. Combination of distributions at 52,600 r.p.m. and 12,600 r.p.m. to give a single distribution curve for B-5.

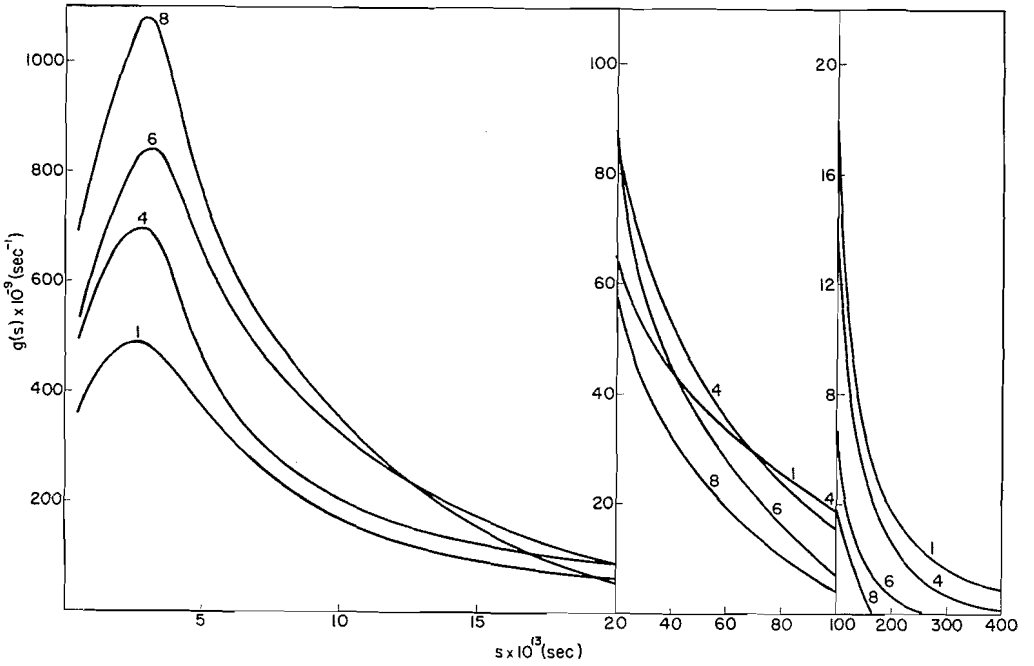


FIG. 6. Distribution of sedimentation coefficients for fractions B-1, B-4, B-6, and B-8 respectively (bottom to top). The solvent was $NaHCO_3$–NaOH buffer (pH = 9.65; $\Gamma/2$ = 0.1).

Can. J. Chem. Downloaded from www.nrcresearchpress.com by 41.223.56.140 on 09/04/12
For personal use only.

In the initial experiments, the effect of diffusion was eliminated by plotting $g^*(s)$ (derived for discrete values of s) against $1/t$ as shown in Fig. 4. Such graphs were extrapolated as being linear (1) and from the intercepts at $1/t = 0$, values of $g(s)$ (i.e., $g^*(s)_{t=\infty}$) were obtained (21, 22).

From the data at the two speeds, two separate distributions of sedimentation coefficients were found. These did not overlap, which suggested that the material sedimenting at the low speed was spun quickly to the bottom of the cell in the 16 times stronger field at the high speed. The two graphs of $g(s)$ vs. s could, therefore, be combined to give single smooth curves shown in Fig. 5 for fraction B-5.

The distributions were all of the same type as shown in Fig. 6. They were characterized by a single maximum with positive skewness and varying proportions of heavy material in a wide range of s values. Curves were analyzed with an Amsler integrator (28). The null axis parallel to the ordinate gave the weight-average sedimentation coefficient, s_w; the square root, σ, of the second moment about the null axis was taken as a measure of the polydispersity (23).

As noted by others (1, 2, 29, 30), the procedure of computing the distribution in s is very time-consuming. Even with the use of an electronic computer, about 40 man-hours were required to process the data at two speeds for one sample. In order to simplify the procedure, extrapolation to infinite time was abandoned. Instead an analysis was done on a single sedimentation diagram at each speed. The second or third picture at the slow speed and the final picture at the high speed were found most suitable. The distribution for the two pictures were combined and analyzed as described above. The two methods were compared for several fractions and except for fractions heavier than B-3, the distributions obtained by the simplified method were nearly identical with those obtained by the detailed extrapolation method. The good agreement between s_w and σ obtained by the two methods for five fractions is given in Table II. A fivefold reduction in time was achieved by this method.

TABLE II

Comparison of s_w and σ computed by the detailed and simplified methods

	$s_w \times 10^{13}$ (sec)		$\sigma \times 10^{13}$ (sec)	
Fraction	Detailed	Simplified	Detailed	Simplified
B-4	53	68	60	60
B-5	32	28	43	42
B-6	20	21	29	27
B-7	15	15	22	22
B-8	14	14	21	17

In Table III, the value of σ, s_w, and $[\eta]$ are given for the fractions studied. Included is the most probable value of the sedimentation coefficient, s_p, corresponding to $g(s_p)$, the maximum value of $g(s)$ in the distribution curve. Fractions B-5-II and B-5-III (obtained by subfractionation of B-5) and F-3 to F-8 were analyzed by the simplified method.

With the exception of fractions B-1 to B-3, the integral $\int_0^\infty g(s)ds$ as measured by the area under a distribution curve was approximately unity. This represents a confirmation of the somewhat empirical technique of combining the distributions since the concentration term used in eq. [1] was not based on the sedimentation diagram but on the

Can. J. Chem. Downloaded from www.nrcresearchpress.com by 41.223.56.140 on 09/04/12
For personal use only.

known refractive index difference between solution and solvent. In the heavier fractions, the integral was less than unity, probably because even at the low speed some material sedimented quickly to the base of the cell.

TABLE III

Values of σ, s_w, s_p, $g(s_p)$ and $[\eta]$ for the fractions at 0.5 ($\pm$0.02) g dl^{-1}

Fraction	$\sigma\times10^{13}$ (sec)	$s_w\times10^{13}$ (sec)	$s_p\times10^{13}$ (sec)	$g(s_p)\times10^{-10}$	$[\eta]$ (g^{-1} dl)
B-1	59	46	2.5	50	0.208
B-2[a]	59	46	2.5	50	0.234
B-3	70	45	2.2	63	0.164
B-4	60	53	2.7	70	0.136
B-5	43	32	2.8	75	0.105
B-6	29	20	3.0	85	0.085
B-7	22	15	3.0	85	0.075
B-8	21	14	3.0	108	0.066
B-9	1	2.2	1.0	164	0.033
B-5-II	32	32	3.8	40	—
B-5-III	21	19	3.8	93	—
F-3	54	35	2.5	69	0.134
F-4	27	24	4.4	53	0.125
F-5	44	30	3.7	63	0.150
F-6	30	20	2.8	95	0.083
F-7	28	17	2.8	112	0.071
F-8	17	11	2.8	112	0.060

[a]The sedimentation diagrams of B-2 were identical with those of B-1. No analysis was made of B-2 and the values of σ, s_w, s_p, and $g(s_p)$ were assumed to be equal in the two fractions.

To avoid excessive computation, the distributions were not corrected for the concentration dependence of s or the related Johnston–Ogston effect (31). The error caused by such an approximation would be expected to be relatively small because of the small dependence of s on c quoted earlier. This point was further tested by measuring distributions on B-5 at four concentrations between 0.3 and 0.7 g dl^{-1}. The results in Table IV

TABLE IV

Concentration dependence of s_w and σ for fraction B-5

Concentration (g dl^{-1})	$s_w\times10^{13}$ (sec)	$\sigma\times10^{13}$ (sec)
0.65	23	30
0.50	32	42
0.41	25	44
0.30	32	48

show no clear trend in s_w and the mean deviation is $\pm$14%. This large error is probably due to the fact that s_w is a weight average and the difficultly measurable values of $g(s)$ at large s_w affect the result considerably. An increase in σ with decrease in c is noted but the effect is small for the three low concentrations. The results confirm that the change in s_w and σ between concentrations of 0.5 g dl^{-1} and zero is not gross and legitimate comparison can be made in data for different fractions obtained at the same concentration of 0.5 g dl^{-1}.

DISCUSSION

The results indicate that the alkali lignins prepared in the present study had an

Can. J. Chem. Downloaded from www.nrcresearchpress.com by 41.223.56.140 on 09/04/12
For personal use only.

exceptionally wide range of particle size. Sedimentation coefficients from 0.5 to over 400×10^{-13} second were recorded. Polydispersity was not unexpected since other lignin preparations (4–12) have been shown to be polydisperse. But such a wide range as indicated by the sedimentation data has not previously been reported. Probably the extremely high molecular weight species were obtained as a result of the mild method of preparation. However, strikingly similar results have been obtained in degradation studies of glycogen (1, 2, 30), amylopectin (30), and dextran (32–35). It has been shown by a number of workers (34, 36–39) that a random degradation of a branched or cross-linked network will produce a broad size distribution in the degradation products. Thus the data support the concept that lignin exists in wood as an extensive three-dimensional structure which undergoes random scission during the process of delignification.

The data in Table III show that the B-series with barium ion as precipitant had a gradation in s_w as in $[\eta]$. In this respect the fractionation was successful. Fractions were highly polydisperse although there was no indication of a discontinuous distribution in any of the fractions. It is further interesting that not only was the form of the distribution the same in all the fractions but s_p was approximately constant at $2.9\ (\pm0.5)\times10^{-13}$ second. In contrast the value of $g(s_p)$ decreased in the heavier fractions and empirically $1/g(s_p)$ vs. $[\eta]$ gave a roughly linear graph (Fig. 7). This result suggested that the low

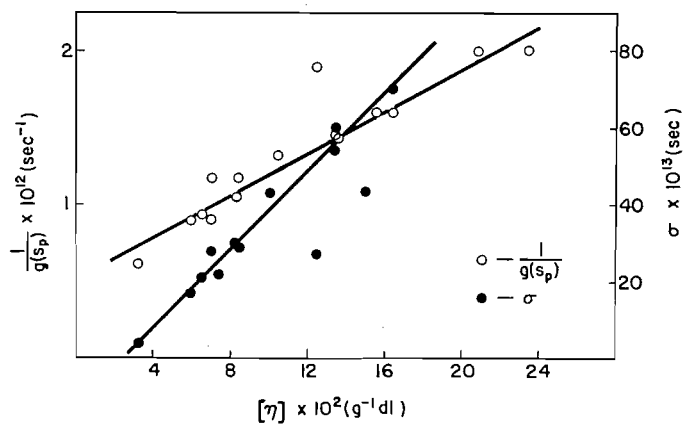


FIG. 7. Graphs of $1/\{g(s_p)\}$ vs. $[\eta]$ and σ vs. $[\eta]$ for fractions shown in Table III.

molecular weight, more soluble material was distributed relatively closely about a sedimentation coefficient of 2.9×10^{-13} second. In contrast, the high molecular weight, less soluble particles existed in an extreme range of size. Fractional precipitation produced successive fractions with decreasing amount of the heavy material. Therefore, in addition to a gradation in $[\eta]$, the initial fractions were more polydisperse as illustrated in Fig. 7 (except for B-1, B-2, and B-3) where σ shows a regular increase with an increase in $[\eta]$. In the case of B-1, B-2, and B-3 $\int_0^\infty g(s)\,ds$ was significantly less than unity which indicated that about 15% (on the average) of the material sedimented quickly to the bottom of the cell and did not contribute to the sedimentation diagrams. This may explain the reversal of the trend of increasing s and σ with $[\eta]$ for B-1, B-2, and B-3 (Table III). If an approximate correction is made based on the assumption that the proportion lost by rapid sedimentation had s values equal to the highest recorded in the

Can. J. Chem. Downloaded from www.nrcresearchpress.com by 41.223.56.140 on 09/04/12
For personal use only.

distributions, σ increases to 105, 105,[3] and 92×10^{-13} second and s_w increases to 133, 133,[3] and 133×10^{-13} second for B-1, B-2,[3] and B-3 respectively.

There was a small decrease in polydispersity on subfractionation as shown by the lower values of σ for F-4 and F-5 (Table III and Fig. 7) which were the subfractions of B-4 and B-5 respectively. It seems that fractionation with barium is not particularly selective as to particle size. Moreover, the initial heterogeneity of the material is so great that extensive refractionation may be needed to give homogeneous fractions. It is interesting that similar results, as to wide polydispersity and limited subfractionation, have been reported for glycogen by Bryce and co-workers (2, 30) and Stetten *et al.* (35). Purification of fractions B-6 to B-9 by dialysis and ultracentrifugation did not decrease the polydispersity significantly. Such treatment was, however, essential in order to prepare fractions for the light-scattering experiments (40) described in the following paper of the present series (41).

The values of s_m (Table I) obtained at the two centrifugal fields used differed by an order of magnitude. As far as is known this behavior has not yet been reported in any other system. It is probably not specifically associated with the lignin molecule but is a general phenomenon to be found in any widely polydisperse system in which the sedimentation rate is not dependent on the concentration. Roughly, one may say that at low speed, the high molecular weight material sediments through a constant concentration of the low molecular weight component. At the higher speed, the heavy particles sediment rapidly to the cell bottom and the moving boundary is made up of smaller molecules. The foregoing analysis of the data is based on such a picture. More correctly, the phenomenon is probably due to the simultaneous presence of particles, some of which are large enough to obey the Faxen (42) solution to the Lamm (43) sedimentation equation while the others are smaller and are more appropriately described by Archibald's solution (13). The resulting gradient pattern will then be a combination of the classical sedimentation equilibrium distribution in which the gradient decreases from the meniscus and the sedimentation velocity distribution in which a Gaussian peak moves down the cell. High speed will favor peak formation of smaller molecules and thus yield the smaller values of s_{m2}.

The wide difference in s_{m1} and s_{m2} at the two speeds is in marked contrast to the sedimentation behavior in certain other systems. In the case of naturally occurring polyelectrolytes such as sodium desoxyribonucleate, sodium alginate, and sodium carrageenate, Goring and Chepeswick (44) found sedimentation coefficients constant to $\pm1\%$ for changes in the field from 44×10^3 *g* to 260×10^3 *g*. Similarly, Huque (45) noted no change in the sedimentation coefficient of cellulose trinitrate for a change in field from 39×10^3 *g* to 260×10^3 *g*. The above examples are those of linear extended macromolecules which show a considerable concentration dependence. Thus the peak spreading due to diffusion and polydispersity necessary to produce the effect would be masked by the familiar peak sharpening (46) due to concentration dependence of *s*. It is probable that the difference between s_{m1} and s_{m2} would be found in systems such as the glycogens in which the concentration dependence of *s* is small. A more detailed study of this effect will be reported in a later publication in which changes of s_m with rotor speed are compared with similar data for a macromolecule known to be monodisperse.

Finally, it is worth while to consider the limitations in the present method of obtaining the distribution in *s*. Although used by others on similar systems (1, 2, 30), it is questionable whether the Singer–Gross relationship (eq. [1]) can be applied under the conditions

[3]*See Table III.*

Can. J. Chem. Downloaded from www.nrcresearchpress.com by 41.223.56.140 on 09/04/12
For personal use only.

described above. An analysis based on an exact theoretical treatment would be preferable. Such a treatment has never been presented and is beyond the scope of the present investigation. The approximate correctness of the results obtained by the present method is supported by the following:

(1) The agreement between the results obtained by extrapolation to infinite time (detailed procedure) and the simplified method.

(2) The fact that the slow and fast speed distributions did not overlap.

(3) The value of unity found for the integral $\int_0^\infty g(s)\,ds$ after use of the refractive index differences corresponding to gravimetric concentration in eq. [1].

Further confirmation of the method was obtained by comparing the distribution of s for the original alkali lignin, B-0, with a combined distribution of all the B-series. As shown in Fig. 8, the agreement was reasonable in spite of losses during fractionation and purification.

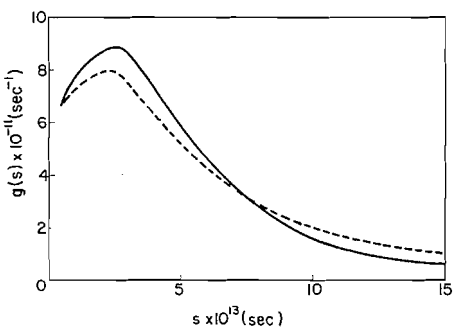


FIG. 8. Comparison of the distribution obtained by summation of $g(s)$ values of B-series fractions (dotted curve) with the distribution of the unfractionated lignin, B-0 (solid curve).

From the above, it is clear that future work in this field should include measurements with the synthetic boundary cell (47). Complications at the meniscus would be avoided and theoretical treatment of the boundary spreading would then be simplified. Also, values of s_m could be measured more accurately because of the initial sharp boundary.

Discussion of the relationship between s_w and $[\eta]$ is included in the following paper of the present series (41).

ACKNOWLEDGMENTS

The authors wish to thank Mr. Rankowicz for his extremely efficient operation of the ultracentrifuge.

REFERENCES

1. LARNER, J., RAY, B. R., and CRANDALL, H. F. J. Am. Chem. Soc. **78**, 5890 (1956).
2. BRYCE, W. A. J., GREENWOOD, C. T., and JONES, I. G. J. Chem. Soc. 3845 (1958).
3. GUPTA, P. R. and GORING, D. A. I. Can. J. Chem. **38**, 248 (1960).
4. GRALEN, N. J. Colloid Sci. **1**, 453 (1946).
5. GARDON, J. L. and MASON, S. G. Can. J. Chem. **33**, 1477 (1955).
6. FELICETTA, V. F., AHOLA, A., and MCCARTHY, J. L. J. Am. Chem. Soc. **78**, 1899 (1956).
7. NOKIHARA, E., TUTTLE, J., FELICETTA, V. F., and MCCARTHY, J. L. J. Am. Chem. Soc. **79**, 4495 (1957).
8. FELICETTA, V. F. and MCCARTHY, J. L. J. Am. Chem. Soc. **79**, 4499 (1957).
9. GORING, D. A. I. and REZANOWICH, A. Can. J. Chem. **36**, 1653 (1958).
10. MOACANIN, J., FELICETTA, V. F., and MCCARTHY, J. L. J. Am. Chem. Soc. **81**, 2052 (1959).

Can. J. Chem. Downloaded from www.nrcresearchpress.com by 41.223.56.140 on 09/04/12
For personal use only.

11. MOACANIN, J., NELSON, H., BACK, E., FELICETTA, V. F., and MCCARTHY, J. L. J. Am. Chem. Soc. **81**, 2054 (1959).
12. GORING, D. A. I. Pulp Paper Mag. Can. **58**, 165 (1957).
13. ARCHIBALD, W. J. J. Phys. & Colloid Chem. **51**, 1204 (1947).
14. SVEDBERG, T. and PEDERSEN, K. O. The ultracentrifuge. Oxford University Press, London. 1940.
15. DE LALLA, O. and GOFMAN, J. W. UCRL-2427. Univ. of California. 1953.
16. FUJITA, H. and MACCOSHAM, V. J. J. Chem. Phys. **30**, 291 (1959).
17. WILLIAMS, J. W. and SAUNDERS, W. M. J. Phys. Chem. **58**, 854 (1954).
18. WILLIAMS, J. W., SAUNDERS, W. M., and CICIRELLI, J. S. J. Phys. Chem. **58**, 774 (1954).
19. SCHUMAKER, V. N. and SCHACHMAN, H. K. Biochim. et Biophys. Acta, **23**, 628 (1957).
20. SHOOTER, K. V. and BUTLER, J. A. V. Trans. Faraday Soc. **52**, 734 (1956).
21. BALDWIN, R. L. and WILLIAMS, J. W. J. Am. Chem. Soc. **72**, 4325 (1950).
22. GOSTING, L. J. J. Am. Chem. Soc. **74**, 1548 (1952).
23. WILLIAMS, J. W., BALDWIN, R. L., SAUNDERS, W. M., and SQUIRE, P. G. J. Am. Chem. Soc. **74**, 1542 (1952).
24. BALDWIN, R. L. J. Am. Chem. Soc. **76**, 402 (1954).
25. BALDWIN, R. L. J. Phys. Chem. **58**, 1081 (1954).
26. WILLIAMS, J. W., VAN HOLDE, K. E., BALDWIN, R. L., and FUJITA, H. Chem. Revs. **58**, 715 (1958).
27. SINGER, R. and GROSS, H. Helv. Chim. Acta, **17**, 726 (1934).
28. JENSEN, R. J. Polymer Sci. **12**, 401 (1954).
29. MARK, H. Paper Trade J. **113**, 28 (1941).
30. BRYCE, W. A. J., COWIE, J. M. G., GREENWOOD, C. T., and JONES, I. G. J. Chem. Soc. 3558 (1958).
31. JOHNSTON, J. P. and OGSTON, A. G. Trans. Faraday Soc. **42**, 789 (1946).
32. STACY, C. J. and FOSTER, J. F. J. Polymer Sci. **20**, 57 (1956).
33. STACY, C. J., FOSTER, J. F., and ERLANDER, S. R. Makromol. Chem. **17**, 181 (1956).
34. SENTI, F. R., *et al.* J. Polymer Sci. **17**, 527 (1955).
35. STETTEN, M. R., KATZEN, H. M., and STETTEN, D. J. Biol. Chem. **222**, 587 (1956); **232**, 475 (1958).
36. ERLANDER, S. R. and FRENCH, D. J. Polymer Sci. **32**, 291 (1958).
37. FLORY, P. J. Principles of polymer chemistry. Cornell Univ. Press, Ithaca, N.Y. 1953.
38. JAHN, E. C., HOLMBERG, C. V., and SCHUERCH, C. Chem. in Can. **5**, 35 (1953).
39. ARLT, H. G., JR. and SCHUERCH, C. Tappi, **41**, 481 (1958).
40. HUQUE, M. M., JAWORZYN, J., and GORING, D. A. I. J. Polymer Sci. **39**, 9 (1959).
41. GUPTA, P. R. and GORING, D. A. I. Can. J. Chem. **38**, 270 (1960).
42. FAXEN, H. Arkiv Mat. Astron. Fysik, B, **21**, No. 3 (1929).
43. LAMM, O. Arkiv Mat. Astron. Fysik, B, **21**, No. 2 (1929).
44. GORING, D. A. I. and CHEPESWICK, C. J. Phys. Chem. **60**, 506 (1956).
45. HUQUE, M. M. Ph.D. Thesis, McGill University, Montreal, Que. 1957.
46. ALEXANDER, A. E. and JOHNSON, P. Colloid Science. The Clarendon Press, Oxford. 1949.
47. KEGELES, G. J. Am. Chem. Soc. **74**, 5532 (1952).

Can. J. Chem. Downloaded from www.nrcresearchpress.com by 41.223.56.140 on 09/04/12
For personal use only.

Can. J. Chem. Downloaded from www.nrcresearchpress.com by 69.46.99.164 on 09/04/12
For personal use only.

PHYSICOCHEMICAL STUDIES OF ALKALI LIGNINS

III. SIZE AND SHAPE OF THE MACROMOLECULE[1]

P. R. GUPTA[2] AND D. A. I. GORING

ABSTRACT

Light-scattering measurements were made on the alkali lignin fractions described in a previous paper. The range of molecular weights found was from 50,000 to 48×10^6. The usual logarithmic graph of intrinsic viscosity and molecular weight was linear and gave a value of 0.32 for the exponent. From the logarithmic sedimentation coefficient – molecular weight relationship, the exponent was found as 0.52. Flory's hydrodynamic parameter Φ^1P^{-1} was 2.3×10^6. These results suggested that the configuration of the alkali lignin macromolecule conformed to a structure between that of a random coil and an Einstein's sphere impenetrable to solvent. The branching parameter, g, introduced by Zimm and Stockmayer, decreased with an increase in molecular weight as expected. Most of the values of Huggins' constant, k,' were between 1 and 2 which indicated a compact particle. A marked increase in k' was noted for fractions of low or very high molecular weight. The significance of the data is discussed and a model tentatively suggested for the macromolecule.

INTRODUCTION

Molecular weights of lignin derivatives reported in the early literature are usually between 250 and 11,000 (1, 2, 3). In contrast, McCarthy and co-workers (4) have recently obtained molecular weights as high as 138,000 in a light-scattering study of fractionated lignin sulphonates. Similarly, Gardon and Mason (5) reported M values as high as 58,000 in lignin sulphonates fractionated by ultrafiltration and dialysis. In another study, Gralen (6) found molecular weights up to 34,000 for thioglycolic acid lignins by sedimentation and diffusion. In considering the discrepancy it must be noted that the low molecular weights were all obtained by one or other of the number-average methods. In addition to this, the earlier investigators used highly degraded lignin samples.

The present paper deals with the light-scattering determination of molecular weights of alkali lignin fractions. As described in an earlier paper of the current series (7), the alkali lignin was prepared from a periodate lignin of white spruce by a relatively mild treatment and its properties may be regarded as being fairly close to those of the protolignin in the wood. Fractionation was achieved by precipitation with $BaCl_2$.

Several proposals exist as to the chemical structure of lignin, but little information is available about its configurational behavior in solution. Recently, McCarthy *et al.* (4) and Gardon and Mason (5) both tentatively suggested a random coil for the lignin sulphonates. On the other hand, lignin in wood has been regarded (but not proved) to be a three-dimensional network structure. In the present investigation the relationships between the molecular weight, intrinsic viscosity (7), and weight-average sedimentation coefficient (8) are analyzed and a possible configuration for the alkali lignin macromolecule is proposed. Certain hydrodynamic parameters are also derived and correlated with the size and shape of the macromolecule.

EXPERIMENTAL AND RESULTS

The alkali lignin fractions (except PB-0) investigated here are fully described in the first paper of the present series (7). Fraction PB-0 represented the remainder of un-

[1]*Manuscript received August 4, 1959.*
Contribution from the Physical Chemistry Division, Pulp and Paper Research Institute of Canada, and the Department of Chemistry, McGill University, Montreal, Que.
[2]*Holder of the Anglo Paper Research Fellowship, the Alexander McFee Fellowship, and a Studentship from the National Research Council of Canada.*

Can. J. Chem. Downloaded from www.nrcresearchpress.com by 69.46.99.164 on 09/04/12
For personal use only.

fractionated lignin, B-0, from which the large and small molecular weight material was removed by ultracentrifugation (2 hours at 150,000 *g*) and dialysis respectively.

Light-scattering measurements were made with a Brice–Phoenix (9) photometer as modified by Huque *et al.* (10). Fractions were dissolved in $NaHCO_3$–NaOH buffer (pH = 9.65; $\Gamma/2 = 0.1$) and a series of five concentrations was obtained by diluting aliquot portions. Solutions were spun in the light-scattering cells in the SW 25.1 swinging bucket rotor of a Spinco Model L ultracentrifuge. The centrifugation times were from 30 to 60 minutes at 2000 to 35,000 *g*. After light-scattering measurements, concentrations were measured spectrophotometrically. Usually there was no appreciable change from the initial gravimetric concentration except in F-3, F-4, and F-5 where there was a decrease of nearly 10%. The spectrophotometric concentration was used in light scattering.

The photometer was calibrated with Ludox colloidal silica taking the precautions described in an earlier paper (11). The calibration was checked by a measurement of the molecular weight of bovine serum albumin (Armour Lot No. S 68004) in 0.1 *N* sodium chloride. A value of 68,500 was obtained which was in good agreement with published data (12–15).

The refractive index increment, dn/dc, of the alkali lignin fractions was measured with a Brice–Phoenix differential refractometer for $\lambda = 5460$ Å at 25° C. The instrument was calibrated with sucrose solutions using sodium light ($\lambda = 5890$ Å). The calibration was checked and found correct with an aqueous potassium chloride solution. The data on dn/dc are given in Table I. For the nine fractions studied dn/dc is fairly constant with a mean value of 0.218 (± 0.004) g^{-1} ml. In calculating the molecular weight of F-1, F-2, PF-2, and PB-0, the mean value of dn/dc was used.

TABLE I

Light scattering and viscometric data for the fractions of alkali lignin dissolved in $NaHCO_3$–NaOH buffer (pH = 9.65; $\Gamma/2 = 0.1$)

Fraction	$M_w \times 10^{-3}$	$[z]$ $(i_{45}/i_{135})_{c=0}$	$\bar{s}$ (Å)	$[\eta]$ (g^{-1} dl)	dn/dc (g^{-1} ml)
F-1	48,000[a]	3.5	1700[a]	0.585	—
F-2	47,000[a]	3.4	2600[a]	0.294	—
PF-2	10,000[a]	2.3	1350[a]	0.20	—
F-3	1200	1.9	520	0.133	0.211
F-4	1800	1.5	420	0.125	0.224
F-5	1860	1.6	440	0.150	0.210
F-6	610	1.6	440	0.083	0.222
F-7	550	1.6	440	0.071	0.221
F-8	290	1.5	420	0.059	0.219
F-9	80	1.9	520	0.042	0.219
B-0	2000	2.2	580	0.105	0.217
B-9	50	1.8	500	0.033	0.215
PB-0	450	1.6	440	—	—

[a]These were calculated from Zimm plots and therefore $\bar{s}$ is the *Z*-average radius of gyration. For fractions F-1, F-2, and PF-2, values of $\bar{s}$ computed from dissymmetry for a spherical model are 700 Å, 700 Å, and 590 Å respectively.

For most fractions molecular weights were determined by using Debye's equation (16)

$$[1] \qquad Hc/\tau = 1/M_w + 2A_2c$$

where $H = 32\pi^3n^2(dn/dc)^2/3N\lambda^4$ and the symbols have their usual significance. The turbidity was evaluated from 90° scattering measurements by means of a calibration factor. Linear plots of Hc/τ vs. c were extrapolated to zero concentration as shown for

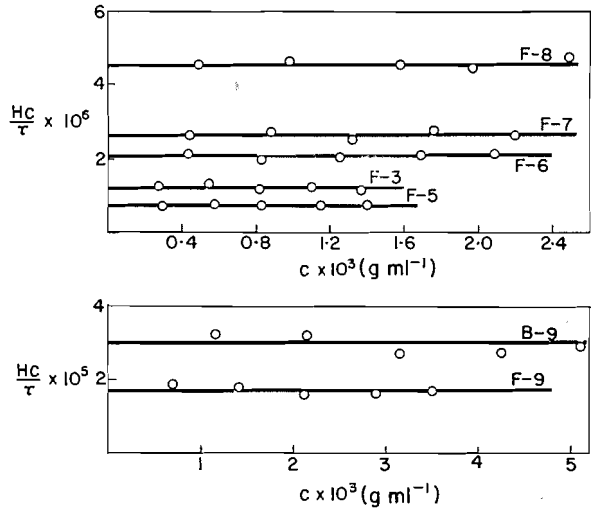


FIG. 1. Hc/τ vs. c for fractions of alkali lignin dissolved in $NaHCO_3$–NaOH buffer (pH = 9.65; $\Gamma/2 = 0.1$). The abscissa scale for B-9 is shown ×5.

some of the fractions in Fig. 1. The dissymmetry, z, was also measured at each concentration and extrapolation to zero concentration gave the intrinsic dissymmetry, $[z]$. The reciprocal of $(Hc/\tau)_{c=0}$ gave the weight-average molecular weight, M_w, which was then corrected for dissymmetry assuming a spherical model. For dissymmetries of about 1.9 or less the choice of model does not alter the correction factor by more than 10% (17). Data on M_w, $[z]$, and the radius of gyration, $\bar{s}$, computed from $[z]$ for a spherical molecule are given in Table I.

The dissymmetry was large in the case of fractions F-1, F-2, and PF-2. Zimm plots, an example of which is shown in Fig. 2, were obtained for these fractions by plotting Kc/R_θ vs. $\sin^2\theta/2+kc$, where $K = 2\pi^2n^2(dn/dc)^2/N\lambda^4$ and the symbols have their usual meanings. The molecular weight was then obtained from the reciprocal of $(Kc/R_\theta)_{c,\theta=0}$. From the slope and intercept of the extrapolated zero concentration line, the radius of gyration, $\bar{s}$,

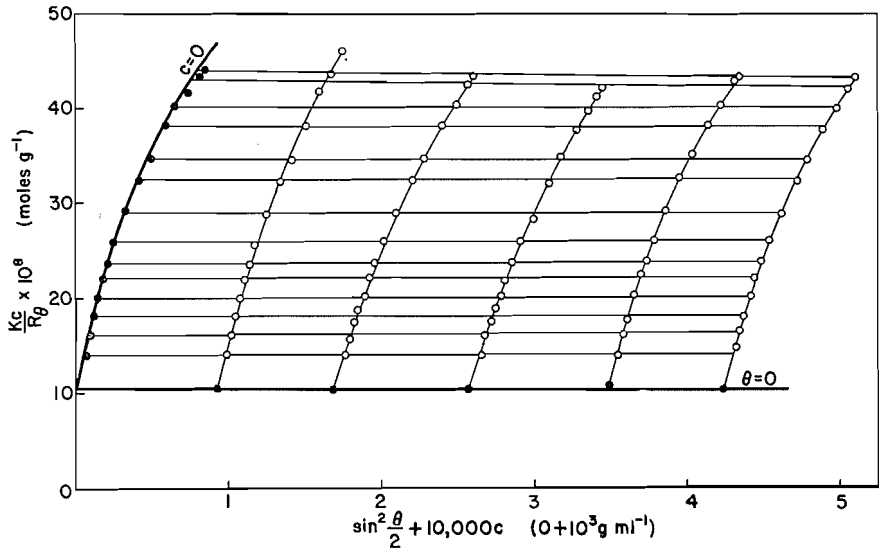


FIG. 2. Light-scattering Zimm plot for fraction PF-2 dissolved in $NaHCO_3$–NaOH buffer (pH = 9.65; $\Gamma/2 = 0.1$).

Can. J. Chem. Downloaded from www.nrcresearchpress.com by 69.46.99.164 on 09/04/12
For personal use only.

was calculated to give the values included in Table I. In all cases, either from the Zimm graphs or the turbidity plots, the second virial coefficient, A_2, was zero within the limits of experimental accuracy.

Also included in Table I are the intrinsic viscosities of the various fractions as reported in the first paper of the present series (7).

Absorption, Fluorescence, and Depolarization

The alkali lignin solutions were all amber colored because of strong absorption of visible light. Correction for absorption was not required; attenuation of transmitted and scattered beams were equal because of the symmetry of the cell.

The solutions were found to show considerable fluorescence which in some cases amounted to 20% of the emitted light. A high degree of fluorescence has also been noted for lignin sulphonates by McCarthy and collaborators (4) and Goring *et al.* (18). Rather than adopt the lengthy procedure described by Brice *et al.* (19) a filter was sought which would eliminate from the emitted beam the longer wavelength component due to fluorescence. The most suitable was a combination of blue-green (Corning No. 4305; C.S. 4-71) and didynium (Corning No. 5120; C.S. 1-60), called henceforth the blue–didynium filter. This filter combination was found to transmit 26.5% of the 5460 Å light and only 0.8% of the fluorescence. All light-scattering measurements were made with the blue–didynium filter in the analyzing nosepiece of the photometer. The proportion of 90° scattering due to fluorescent light was thus reduced to less than 1%. No correction was made for this effect.

Measurements were also made with the red filter (Corning No. 2424; C.S. 2-63, supplied with the instrument) which passes only fluorescent light. The galvanometer deflection, G_f, due to fluorescence alone is given by $G_f = G_r/T_r$ where G_r is the galvanometer reading with the red filter in the nosepiece of the phototube and T_r is the transmission of the red filter to fluorescent light. T_r was determined at the 90° position with a polaroid horizontal in the nosepiece, by the ratio of the galvanometer deflections with and without the red filter. From G_f and the calibration factor, a "turbidity", τ_f, equivalent to the fluorescent emission was computed. Therefore, τ_f may be regarded as a measure of the fluorescent intensity of a particular solution and τ_f/c becomes the fluorescence per gram of a given fraction. In Table II, values of τ_f/c for several of the fractions are compared with τ/c due only to scattering. Since the fractions were of different molecular weights, there is a considerable spread in τ/c. This is in contrast to τ_f/c which was relatively constant with a mean value of 5.2 ± 0.9.

TABLE II

Comparison of scattered and fluorescent light for alkali lignin fractions dissolved in $NaHCO_3$–NaOH buffer (pH = 9.65; $\Gamma/2 = 0.1$)

Fraction	$M_w \times 10^{-3}$	τ/c (g^{-1} ml cm^{-1})	τ_f/c (g^{-1} ml cm^{-1})
F-3	1200	52.7	3.7
F-4	1800	102.6	6.0
F-5	1860	90.9	7.4
F-6	610	33.5	5.5
F-7	550	26.3	4.9
F-8	290	15.2	4.1
PB-0	450	23.8	5.0

Depolarization of scattered light was small and no correction was made for this effect (20).

Can. J. Chem. Downloaded from www.nrcresearchpress.com by 69.46.99.164 on 09/04/12
For personal use only.

Can. J. Chem. Downloaded from www.nrcresearchpress.com by 69.46.99.164 on 09/04/12
For personal use only.

DISCUSSION

In most of the early work (1, 2), soluble lignins have been regarded as low molecular weight compounds with M values lying between 250 and 11,000. The weight-average molecular weights given in Table I show that the above concept is quite inaccurate. Values of M_w ranged from 50,000 to 48×10^6 proving that the alkali lignin of this investigation is definitely a macromolecule. There are two main reasons for this discrepancy. In the present study emphasis was placed on milder conditions of lignin solubilization whereas previous investigators used highly degraded samples. Perhaps the more important reason lies in the wide polydispersity of the fractions as shown by the spread in sedimentation coefficients (8). As many of the earlier workers computed the molecular weights by number-average methods, their values would be lower than the weight averages obtained by light scattering, particularly in highly polydisperse preparations. In amylopectin and glycogen where a wide polydispersity similar to the alkali lignins is common, Erlander and French showed theoretically that the ratio M_w/M_n may easily be as high as 100 and this has been verified experimentally (21).

Although no measurements similar to the present work have been reported for alkali lignins, support for their high molecular weight is to be found in several recent papers on the lignin sulphonates. Gardon and Mason (5) have reported number-average molecular weights up to 58,000 while McCarthy *et al.* (4) found light-scattering molecular weights as high as 138,000 for lignin sulphonates obtained by the usual acid sulphite procedure. Goring and Rezanowich (22) made soluble sulphonates by fractional solution of periodate lignin. The intrinsic viscosity of these fractions ranged from 0.035 to 0.34 g^{-1} dl (22), and light-scattering molecular weights of over 1×10^6 were found (18). It appears, therefore, that alkali lignins as well as lignin sulphonates can be very high molecular weight substances.

An important question concerns the origin of these soluble macromolecules. Does the lignin *in situ* exist as a high molecular weight network structure which gives soluble macromolecules on random degradation (2, 23, 24), or are the macromolecules produced by polymerization of relatively low molecular weight lignin during isolation (5)? The fact that the alkali lignins and the sulphonates both possess high molecular weights supports the concept of an infinite network broken down by alkali or acid treatment. It seems unlikely that an initial polymerization could occur in both the alkaline and acidic conditions of lignin solubilization. The network structure of protolignin would explain its well-recognized insolubility and difficulty of separation from the carbohydrate moiety. Wardrop has shown that lignification takes place at a comparatively late stage in the development of the cell wall (25). If the protolignin is laid down as a three-dimensional network, part of this material is likely to grow around individual carbohydrate molecules. The resulting entanglement of molecular chains could make separation difficult or impossible as in the case of the synthetic "snake cage" polymer mixtures (26). Thus it is not necessary to postulate chemical linkages between lignin and carbohydrate to explain their difficulty of separation (24).

At this stage a reservation should be made because of the nature of the starting material in the present investigation. This was periodate lignin. It is possible that the periodate oxidation polymerizes the lignin during its isolation although all the properties of periodate lignin suggest that this is not the case. For example, Purves *et al.* (2) showed that periodate lignin was chemically similar to protolignin in respect of ethanolysis, hydrogenation, and nitrobenzene oxidation. It is also sulphonatable under the conditions of a standard bisulphite treatment (22). Moreover, in the present study 80% of the lignin was

made soluble in 15 minutes, which is a considerably shorter time than usually used in commercial delignification of wood under comparable conditions. If the lignin was polymerized by the periodate treatment, the reverse would have been expected. However, it is recognized that the present work should be supplemented with a similar study on lignin made soluble directly from wood to settle this point.

The fluorescence measurements, as far as is known, are the first reported for a soluble lignin derivative. Fluorescence of organic compounds is a fundamental property, determined by the presence and configuration of π-electrons in the molecule (27). In lignosulphonic acid, Hägglund (1) proposed that fluorescence may be due to a carbonyl group. However, if the lignin fractions form a polymeric series, the fluorescence being an intrinsic property should be identical from fraction to fraction per unit weight of the material. The data in Table II roughly support this concept where τ_f/c over a wide range of molecular weight is constant within $\pm 17\%$. The variation could be due to experimental error introduced in measuring the small galvanometer deflections involved.

The refractive index increment also has a similar characteristic value for a series of fractions. As shown in Table I, dn/dc was essentially constant for the nine fractions studied. This may be compared with the previously obtained constancy of methoxyl content and U.V. absorption (7) and is a further proof of the chemical homogeneity of the fractions. It is interesting to note that the mean value of 0.218 g^{-1} ml was higher than the usual values (28) for proteins ($\simeq$ 0.19 g^{-1} ml) or polysaccharides ($\simeq$ 0.11 g^{-1} ml) but similar to polystyrene (0.22 g^{-1} ml). According to Freudenberg (1, 29), this may be due to the high proportion of aromatic nuclei in the alkali lignin.

We may now consider a somewhat detailed interpretation of the quantitative relationships obtainable from the present data. The customary double logarithmic plot of intrinsic viscosity versus molecular weight is shown in Fig. 3. The graph is roughly linear with no

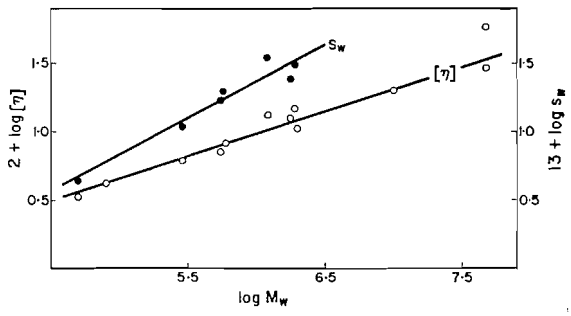


FIG. 3. Double logarithmic plot of intrinsic viscosity and weight-average sedimentation coefficient versus molecular weight.

indication of regions of different slope. Also plotted logarithmically against the molecular weight is the weight-average sedimentation coefficient, s_w, described in the preceding paper of the present series (8). From the two least square lines in Fig. 3

$$[\eta] = 1.16\times10^{-3}\, M_w^{0.32} \qquad [2]$$

$$s_w = 1.63\times10^{-15}\, M_w^{0.52}. \qquad [3]$$

The compact nature of the alkali lignin macromolecule may be inferred directly from eq. [2]. For a molecular weight of 10^6, $[\eta]$ = 0.1 g^{-1} dl, which is small compared with the approximate values of 20 and 2 g^{-1} dl respectively for nitrocellulose and polystyrene fractions of similar molecular weight. In eq. [2] the theoretical value of the exponent for linear coiled molecules is somewhat greater than 0.5 (30) while for Einstein spheres it is

Can. J. Chem. Downloaded from www.nrcresearchpress.com by 69.46.99.164 on 09/04/12
For personal use only.

zero (31). Similarly in eq. [3], the exponents expected for spheres (32) and random coils (33) are 0.66 and 0.44 respectively. In the present study it is clear that in both sedimentation and viscosity, the hydrodynamic properties of the fractions fall between those of a random coil and a rigid sphere. This point may be further illustrated by computing the combined hydrodynamic parameter $\Phi^{\frac{1}{3}}P^{-1}$ of Flory *et al.* (30) which is given by

$$[4] \qquad \Phi^{\frac{1}{3}}P^{-1} = s_w[\eta]^{\frac{1}{3}}N\,\eta_0/M_w^{\frac{2}{3}}\,(1-\bar{v}\rho_0)$$

in which the symbols have their usual significance. There was some spread in the data corresponding to individual fractions. If smoothed values for $[\eta]$, s_w, and M_w from Fig. 3 are substituted in eq. [4], $\Phi^{\frac{1}{3}}P^{-1}$ is found to be independent of molecular weight and equal to 2.3×10^6 which lies between 2.1×10^6 and 2.6×10^6, these being the expected values for sphere and Gaussian coil respectively.

The results described above may profitably be compared with similar data for systems which would be expected to be analogous to alkali lignin. For example, Granath (34) has found in a highly branched dextran, an exponent of 0.34 in the viscosity – molecular weight relationship which suggests a compact type of molecule. Bryce *et al.* (35) obtained an exponent of 0.63 in eq. [3] and concluded that glycogen molecules were essentially spherical. Further, they observed only a very small increase in viscosity with a large increase in molecular weight, thus giving additional confirmation of the compact nature of the particles. In an earlier investigation on lignin sulphonates, Gardon and Mason (5) found an exponent of 0.47 in eq. [2]. Interestingly, the point for their highest molecular weight fraction was considerably below the log–log line of 0.47 slope and indicated a lower exponent for the higher molecular weights. These fractions were prepared from a commercially spray-dried waste sulphite liquor and were of fairly low molecular weight compared with the fractions in the present study.

The intrinsic viscosity and molecular weight data may also be analyzed in terms of the branching parameter, g, introduced by Zimm and Stockmayer (36). This factor represents the ratio of the squares of the unperturbed radii of gyration of branched and unbranched molecules having the same molecular weight and is given by

$$[5] \qquad [\eta] = K^*g^{3/2}M^{\frac{1}{2}}\alpha^3$$

where α is the expansion factor arising from the polymer–solvent interaction and K^* is a constant for a given polymer series. Equation [5] is theoretically valid when the solution obeys van't Hoff's law, i.e., when $\alpha = 1$ (37). Such conditions of ideality hold at the θ-temperature or when the second virial coefficient, A_2, is independent of concentration in light scattering. In the present work, A_2 was zero for all the fractions studied. Thus the expansion factor is unity and g may be computed from eq. [5] if K^* is known. To

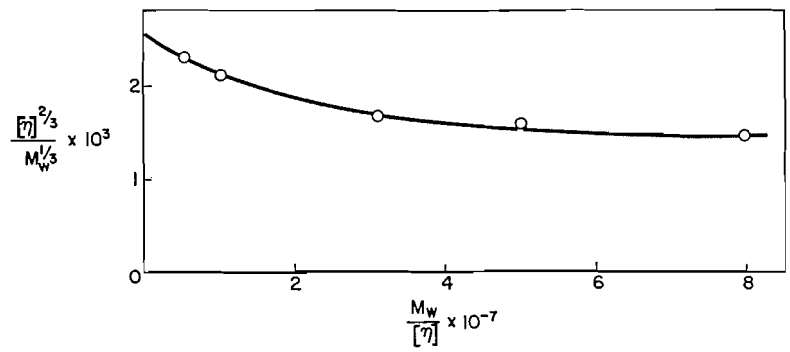


FIG. 4. Graph of $[\eta]^{\frac{1}{3}}/M_w^{\frac{1}{3}}$ vs. $M_w/[\eta]$ using smoothed values of intrinsic viscosity and molecular weight.

Can. J. Chem. Downloaded from www.nrcresearchpress.com by 69.46.99.164 on 09/04/12
For personal use only.

derive K^*, a plot of $[\eta]^{\frac{1}{3}}/M^{\frac{1}{3}}$ vs. $M/[\eta]$ was made as suggested by Wales *et al.* (38). Figure 4 shows such a plot with the present data. In the limit $M/[\eta] \rightarrow 0$, g becomes unity and $[\eta]^{\frac{1}{3}}/M^{\frac{1}{3}}$ approaches $K^{*\frac{1}{3}}$. From the intercept, K^* was found to be 1.25×10^{-4} and values of g computed for smoothed values of $[\eta]$ and M_w are given in Table III. The factor g is seen to decrease with increase of molecular weight as anticipated for a branched polymer (37).

TABLE III

Values of g computed from smoothed $[\eta]$ and M_w data

$[\eta]$ (g^{-1} dl)	$M_w \times 10^{-3}$	g
0.251	20,000	0.59
0.20	10,000	0.64
0.145	4,500	0.67
0.096	1,000	0.85
0.066	360	0.92

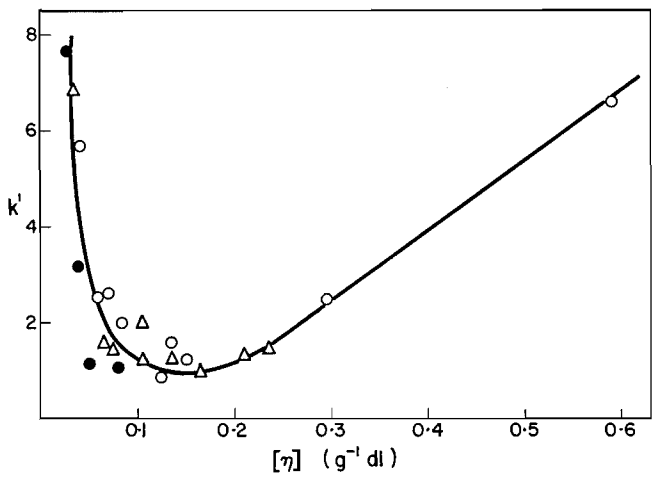


FIG. 5. Variation of Huggins' constant k' with intrinsic viscosity for alkali lignin fractions dissolved in $NaHCO_3$–NaOH buffer (pH = 9.65; $\Gamma/2$ = 0.1). The fractions are described in detail in the initial paper of the present series (7).

The variation of viscosity with concentration as expressed by the Huggins' coefficient k' (39) has been used as an indication of branching in a macromolecule (40–42) though recently some doubt has been expressed as to the validity of this interpretation (43). However, because of its widespread use, it may be worth while to consider the changes in k'. The values of k' (cf. Tables III, IV, and VI in the first paper of the present series (7)) are plotted against $[\eta]$ in Fig. 5 for 22 fractions of alkali lignin. For most of the fractions, k' lies between 1 and 2. According to Eirich and Riseman (44), such values of k' would suggest a compact structure for the lignin macromolecule. Recently Arlt and Schuerch (45) suggested branching in ethanol lignins based on k' values.

As shown in Fig. 5, considerably higher k' values were found for the lowest and the highest molecular weight fractions. It is interesting that a similar minimum in k' was obtained by Senti *et al.* (46) with acid-hydrolyzed dextran but no explanation was given. The increase at different ends of the molecular weight range is probably due to different phenomena. According to Cragg and Manson (47), for the fractions of a given polymer sample containing cross-linked species, cross-linking should be most intensive in the

Can. J. Chem. Downloaded from www.nrcresearchpress.com by 69.46.99.164 on 09/04/12
For personal use only.

fractions of highest intrinsic viscosity and k' should be highest when $[\eta]$ is highest. On the other hand, an increase in k' for very low molecular weight can be attributed to the transition from a random coil to the rigid linear form (48, 49). It may be noted, in passing, that for a polyelectrolyte, k' is a function of the ionic strength of the solution. Goring and Rezanowich (50) have found k' for a lignin sulphonate to increase from 1 to 400 for change in the ionic strength of 1 M to 2×10^{-5} M. In the present investigation, $\Gamma/2$ was maintained constant at 0.1, an ionic strength which would suppress the polyelectrolyte effect almost completely. Therefore the changes in Huggins' coefficient k' are probably related to change in the configuration or rigidity of the alkali lignin macromolecule at the extremes of molecular weight.

The radii of gyration (Table I) show that some of the fractions contained particles of appreciable size. There appeared to be no regular trend of $\bar{s}$ with molecular weight. Similar observations have been reported for glycogen by Stetten *et al.* (51). A probable reason for this is that the Z-average dimension obtained by light scattering is sensitive to the wide polydispersity of the fractions. Therefore the values of $\bar{s}$ in Table I are to be regarded as giving only an approximate measure of the dimension of the macromolecule. A more detailed consideration of the size must await data obtained for sharper fractions.

The alkali lignin molecule, thus, emerges as a polydisperse entity with the hydrodynamic behavior between that of a solid sphere and a Gaussian coil. These molecules are probably formed by random degradation of a three-dimensional network, i.e., protolignin. If the network is cross-linked, protolignin can then be regarded as a gel. Solubilization consists of breaking down the gel by hydrolytic degradation into microgel particles and at the same time producing hydrophilic groups on the gel. In the case of alkali lignin, these may be carboxylic or phenolic groups while in lignin sulphonate, the sulphonic acid group would supply a hydrophilic character. According to this picture, lignin derivatives made soluble by a mild procedure consist of particles of microgel, some of which would be large enough to correspond to the high molecular weights noted. In the loosening of a particular piece of gel from the mother matrix, links between the chains near the edge may be broken and the chains frayed apart. These loose chains would also bear most of the hydrophilic groups of the molecule. The microgel particle would be surrounded by a layer of loosely coiling chains which would be free to move about in the liquid. This halo of randomly coiling material would impart to the molecule a partly Gaussian character. It would also permit a certain degree of polyelectrolyte expansion as noted both in the alkali lignin (7) and the lignin sulphonates (18).

It must be emphasized that the results described above do not define the system unambiguously. The model proposed is therefore only tentative. It is possible that changes in axial ratio occur, particularly at the extremes of molecular weight. Here, an electron micrograph study of the high molecular weight material might be useful. Such a study is planned. It should also be pointed out that the variation of the sedimentation constant and the intrinsic viscosity with the molecular weight can be affected by the polydispersity of the fractions. However, M_w and s_w are both weight averages while the viscosity average is usually regarded as being equivalent to weight average. Thus the conclusions based on a comparison of these quantities are probably qualitatively valid although any further detailed interpretation must be postponed until more critical fractionation procedures have been developed.

ACKNOWLEDGMENTS

The authors wish to thank Mr. J. Jaworzyn for his help in developing the fluorescence technique in light scattering.

Can. J. Chem. Downloaded from www.nrcresearchpress.com by 69.46.99.164 on 09/04/12
For personal use only.

Can. J. Chem. Downloaded from www.nrcresearchpress.com by 69.46.99.164 on 09/04/12
For personal use only.

REFERENCES

1. Brauns, F. E. Chemistry of lignin. Academic Press, Inc., New York. 1952.
2. Goring, D. A. I. Pulp Paper Mag. Can. **58**, 165 (1957).
3. Gross, S. J., Sarkanen, K., and Schuerch, C. Anal. Chem. **30**, 518 (1958).
4. Moacanin, J., Felicetta, V. F., Haller, W., and McCarthy, J. L. J. Am. Chem. Soc. **77**, 3470 (1955).
5. Gardon, J. L. and Mason, S. G. Can. J. Chem. **33**, 1477 (1955); **33**, 1491 (1955).
6. Gralen, N. J. Colloid Sci. **1**, 453 (1946).
7. Gupta, P. R. and Goring, D. A. I. Can. J. Chem. **38**, 248 (1960).
8. Gupta, P. R., Robertson, R. F., and Goring, D. A. I. Can. J. Chem. **38**, 259 (1960).
9. Brice, B. A., Halwer, M., and Speiser, R. J. Opt. Soc. Am. **40**, 768 (1950).
10. Huque, M. M., Jaworzyn, J., and Goring, D. A. I. J. Polymer Sci. **39**, 9 (1959).
11. Goring, D. A. I., Senez, M., Melanson, B., and Huque, M. M. J. Colloid Sci. **12**, 412 (1957).
12. Scatchard, G., Batchelder, A. C., and Brown, A. J. Am. Chem. Soc. **68**, 2320 (1946).
13. Oncley, J. L., Scatcherd, G., and Brown, A. J. Phys. & Colloid Chem. **51**, 184 (1947).
14. McClure, L. E., Schieler, L., and Dunn, M. S. J. Am. Chem. Soc. **75**, 1980 (1953).
15. Gutfreund, H. Trans. Faraday Soc. **50**, 628 (1954).
16. Debye, P. J. Phys. & Colloid Chem. **51**, 18 (1947).
17. Doty, P. and Steiner, R. F. J. Chem. Phys. **18**, 1211 (1950).
18. Rezanowich, A. and Goring, D. A. I. To be published.
19. Brice, B. A., Nutting, G. C., and Halwer, M. J. Am. Chem. Soc. **75**, 824 (1953).
20. Doty, P. and Stein, S. J. J. Polymer Sci. **3**, 750 (1948).
21. Erlander, S. and French, D. J. Polymer Sci. **20**, 7 (1956); J. Am. Chem. Soc. **80**, 4413 (1958).
22. Goring, D. A. I. and Rezanowich, A. Can. J. Chem. **36**, 1653 (1958).
23. Jahn, E. C., Holmberg, C. V., and Schuerch, C. Chem. in Can. **5**, 35 (1953).
24. Björkman, A. Ind. Eng. Chem. **49**, 1395 (1957).
25. Wardrop, A. B. Tappi, **40**, 225 (1957).
26. Hatch, M. J., Dillon, J. A., and Smith, H. B. Ind. Eng. Chem. **49**, 1812 (1957).
27. Birks, J. B. and Cameron, A. J. Proc. Roy. Soc. A, **249**, 297 (1959).
28. Brice, B. A. and Halwer, M. J. Opt. Soc. Am. **41**, 1033 (1951).
29. Freudenberg, K., Sohns, F., Dürr, W., and Niemann, C. Cellulosechemie, **12**, 263 (1931).
30. Flory, P. J. Principles of polymer chemistry. Cornell Univ. Press, Ithaca, N.Y. 1953.
31. Alexander, A. E. and Johnson, P. Colloid science. Clarendon Press, Oxford. 1949.
32. Kuhn, W. and Kuhn, H. Helv. Chim. Acta, **26**, 1394 (1943).
33. Mandelkern, L., Krigbaum, W. R., Scheraga, H. A., and Flory, P. J. J. Chem. Phys. **20**, 1392 (1952).
34. Granath, K. A. J. Colloid Sci. **13**, 308 (1958).
35. Bryce, W. A. J., Greenwood, C. T., and Jones, I. G. J. Chem. Soc. 3845 (1958).
36. Zimm, B. H. and Stockmayer, W. H. J. Chem. Phys. **17**, 1301 (1949).
37. Thurmond, C. D. and Zimm, B. H. J. Polymer Sci. **8**, 477 (1952).
38. Wales, M., Marshall, P. A., and Weissberg, S. G. J. Polymer Sci. **10**, 229 (1953).
39. Huggins, M. L. J. Am. Chem. Soc. **64**, 2716 (1942).
40. Henderson, D. A. and Legge, N. R. Can. J. Research, **27**, 666 (1949).
41. Speiser, R. and Whittenberger, R. T. J. Chem. Phys. **13**, 349 (1945).
42. Manson, J. A. and Cragg, L. H. Can. J. Chem. **30**, 482 (1952).
43. Manson, J. A. and Cragg, L. H. Can. J. Chem. **36**, 858 (1958).
44. Eirich, F. and Riseman, J. J. Polymer Sci. **4**, 417 (1949).
45. Arlt, H. B. and Schuerch, C. Tappi, **41**, 481 (1958).
46. Senti, F. R. *et al.* J. Polymer Sci. **17**, 527 (1955).
47. Cragg, L. H. and Manson, J. A. J. Polymer Sci. **9**, 265 (1952).
48. Pepper, D. C. Sci. Proc. Roy. Dublin Soc. **25**, 239 (1951).
49. Rybnikar, F. J. Polymer Sci. **29**, 519 (1958).
50. Goring, D. A. I. and Rezanowich, A. To be published.
51. Stetten, M. R., Katzen, H. M., and Stetten, D., Jr. J. Biol. Chem. **222**, 587 (1956).
52. Baker, W. O. Ind. Eng. Chem. **41**, 511 (1949).
53. Medalia, A. I. J. Polymer Sci. **6**, 423 (1950).

Can. J. Chem. Downloaded from www.nrcresearchpress.com by 41.223.56.140 on 09/04/12
For personal use only.

STRUCTURE OF AN ARABOGALACTAN FROM TAMARACK (LARIX LARICINA)[1, 2]

G. A. ADAMS

ABSTRACT

A water-soluble polysaccharide containing L-arabinose and D-galactose in a molar ratio 1:3.8 was isolated from tamarack. Fractionation with ethanol from aqueous solution yielded one main component which was judged to be homogeneous on the basis of electrophoresis and sedimentation data. Hydrolysis of the fully methylated polysaccharide yielded, 2,3,5-tri-*O*-methyl-L-arabinose (2 moles); 2,3,4,6-tetra-*O*-methyl-D-galactose (16 moles); 2,5-di-*O*-methyl-L-arabinose (5 moles); 2,3,4-tri-*O*-methyl-L-arabinose (5.5 moles); 2,3,4-tri-*O*-methyl-D-galactose (11 moles); 2,4,6-tri-*O*-methyl-D-galactose (3 moles); 2,6-di-*O*-methyl-D-galactose (1 mole); 2,4-di-*O*-methyl-D-galactose (20 moles); 2-*O*-methyl-D-galactose (3 moles).

Possible structures for the arabogalactan are proposed and discussed on the basis of these results.

Complex polysaccharides composed of galactose and arabinose units occur abundantly in the larches (1–6) and to a lesser extent in several other coniferous trees (7–11). Among those occurring in larches the structure of the arabogalactan of the western larch (*Larix occidentalis*) has been studied by White (5, 12–14) and that of the ϵ-galactan of European larch (*Larix decidua*) by Campbell *et al.* (15) and Aspinall *et al.* (16). Arabogalactans from the coniferous trees Jeffrey pine (*Pinus jeffreyi*), jack pine (*Pinus banksiana*), and white spruce (*Picea glauca*) have been studied by Wadman *et al.* (9), Bishop (10), and Adams (11) respectively.

Structural studies, to be meaningful, require a homogeneous polysaccharide, and the problem of isolating such a material and establishing its homogeneity is a difficult one. The heterogeneity of the arabogalactan from western larch was demonstrated by Peterson *et al.* (17), and the ϵ-galactan of European larch was shown to be heterogeneous by Campbell *et al.* (15). White made a detailed structural study of the arabogalactan of western larch and regarded his material as homogeneous (5). However, Campbell *et al.* claim that the data could be interpreted as indicating heterogeneity of the original polysaccharide (15). On the other hand, the arabogalactans isolated from Jeffrey pine (9), jack pine (10), and white spruce (11) were shown to be homogeneous by all acceptable criteria.

This investigation was concerned with the isolation and structural features of an arabogalactan isolated from tamarack (*Larix laricina* (Du Roi) Koch).

The crude polysaccharide was extracted from extractive-free tamarack wood in 5.6% yield with water at room temperature. Purification was achieved by fractional precipitation from aqueous solutions with ethanol. The results were plotted graphically and the curve obtained is shown in Fig. 1. The shape of the curve is indicative of a single main component which was precipitated when the solution had attained an ethanol concentration of 50–60%. Further evidence of the homogeneity of the polysaccharide was provided by electrophoretic and sedimentation patterns shown in Fig. 2. Single, relatively sharp peaks in both the electrophoresis and sedimentation curves are indicative of a single homogeneous component.

[1]*Manuscript received October 2, 1959.*
Contribution from the Division of Applied Biology, National Research Council, Ottawa, Canada. Issued as N.R.C. No. 5483.
[2]*Presented before the Symposium on Wood Hemicelluloses, Division of Cellulose Chemistry, 136th Meeting, American Chemical Society, Atlantic City, N.J., 1959.*

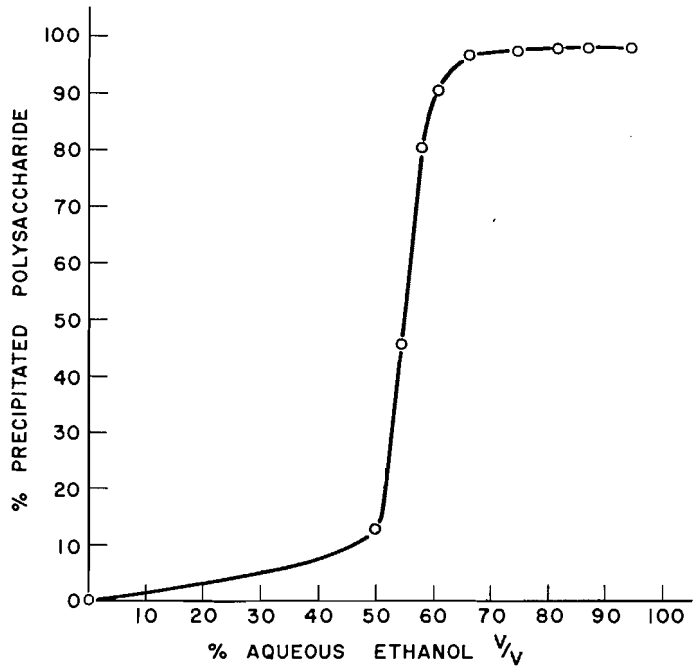


FIG. 1. Ethanol fractionation of water-soluble polysaccharide from tamarack.

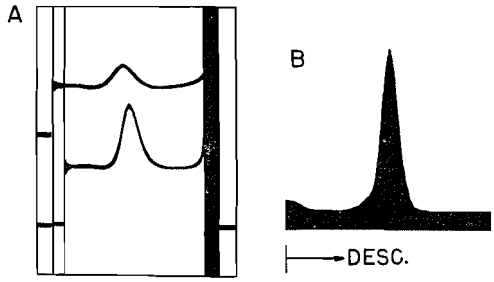


FIG. 2. (A) Sedimentation diagram of tamarack arabogalactan. Upper curve 0.5% solution (borate buffer 0.05 *M*), lower curve 1.0% solution, rotor speed 59,780 r.p.m., photograph taken 83 minutes after attaining full speed, direction of sedimentation left to right.
(B) Electrophoresis diagram of tamarack arabogalactan. Polysaccharide solution, 1.0% in 0.05 *M* borate buffer. Photograph taken 67 minutes after appearance of initial boundary.

The purified polysaccharide comprised 84% of the crude polysaccharide and contained arabinose and galactose in a molar ratio of 1:3.8. The specific rotation $[\alpha]_D^{25}$ +11° corresponded closely to those reported for larch arabogalactan $[\alpha]_D^{20}$ +11° to +15° (17). However, the molar ratio of the two component sugars is considerably different from the 1:6 L-arabinose to D-galactose ratio reported for the arabogalactans from larches (2, 14, 16, 17).

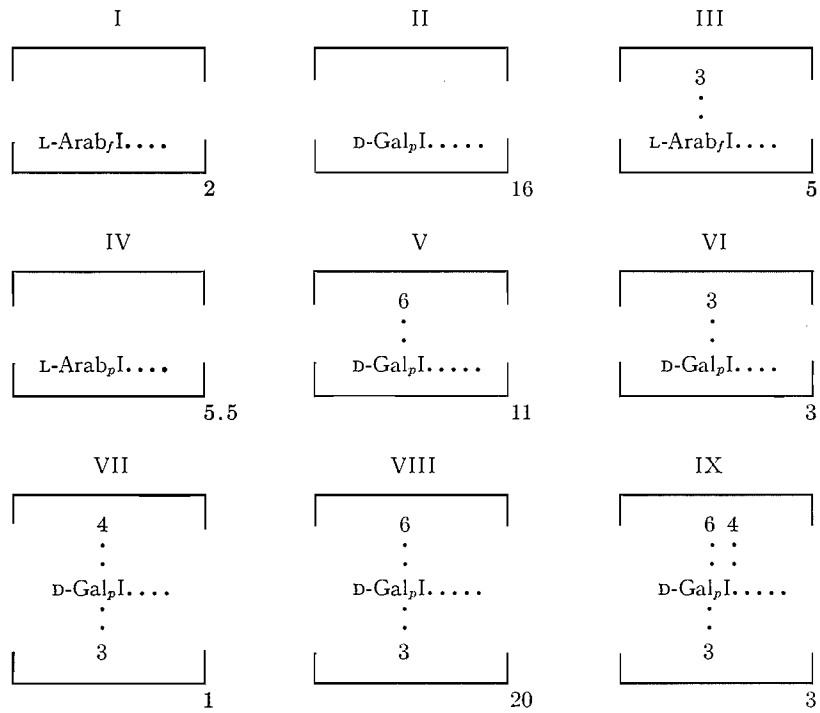
Sedimentation data as determined in the ultracentrifuge gave an approximate molecular weight of 50,000. Reported molecular weight values by Mosiman and Svedberg (18) on the component polysaccharides of ϵ-galactan showed that two polysaccharides were present having approximate molecular weights of 16,000 and 100,000 respectively. Examination of ϵ-galactan in the ultracentrifuge by Aspinall *et al.* (16) showed only one

Can. J. Chem. Downloaded from www.nrcresearchpress.com by 41.223.56.140 on 09/04/12
For personal use only.

molecular species but no molecular weight estimations were made. The molecular weight of the arabogalactan of Jeffrey pine was approximately 100,000 and the polysaccharide was markedly polydisperse as determined from sedimentation data (9). It seems clear that considerable variation occurs in the molecular dimensions of arabogalactans from different species of wood.

The tamarack arabogalactan was methylated and the methyl ether was subjected to methanolysis and hydrolysis. The methylated sugars were separated chromatographically on a Celite column (19). Fractions that were still mixtures were refractionated by repeated column and paper chromatography. The purified methylated sugars were characterized by their physical properties and preparation of characteristic crystalline derivatives. The amounts and molar ratios of the various methylated sugar components are given in Table III. Comparison of the ratio of methylated arabinose to methylated galactose (1:4.5) with that of the arabinose to galactose ratio (1:3.8) in the original polysaccharide showed that some galactose units were lost during methylation and hydrolysis

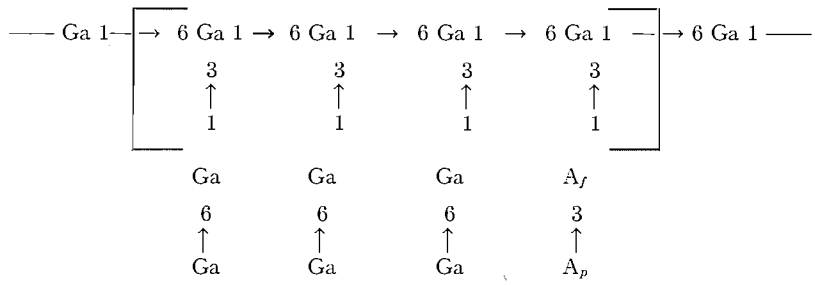
On the basis of the methylation studies, the arabogalactan must contain the following units:



There are a number of ways in which these units may be joined together and no unique structural formula can be deduced from these data. However, certain constitutional features become evident, and on the basis of these some possible structures are proposed.

The large proportion of VIII showed that there was a predominance of 1→3 and 1→6 linkages between the galactose units of the molecule. It is possible to envisage repeating units composed of 1→6 linked units or 1→3 linked units or a combination of both. Possible structures involving the main components are shown in A, B, and C. Structure A would have a predicted periodate consumption of 1.17 moles, and a formic acid production

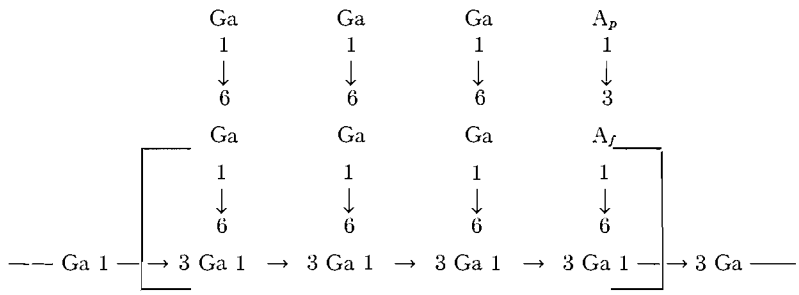
Can. J. Chem. Downloaded from www.nrcresearchpress.com by 41.223.56.140 on 09/04/12
For personal use only.



		Methylated sugars moles, found
2,3,4 Me_3Ga	3×5 = 15 moles	11.0
2,3,4,6 Me_4Ga	3×5 = 15 moles	16.0
2,4 Me_4Ga	4×5 = 20 moles	20.0
2,5 Me_2Ar	1×5 = 5 moles	5.0
2,3,4 Me_3Ar	1×5 = 5 moles	5.5

Periodate consumed 1.17 moles/mole
Formic acid produced 0.6 mole/mole

STRUCTURE A.



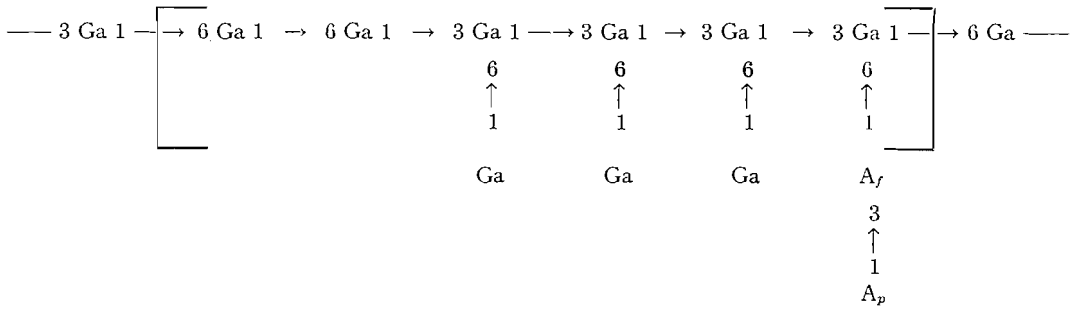
		Methylated sugars, moles, found
2,4 Me_2Ga	4×5 = 20 moles	20.0
2,3,4 Me_3Ga	3×5 = 15 moles	11.0
2,3,4,6 Me_4Ga	3×5 = 15 moles	16.0
2,5 Me_2Ar	1×5 = 5 moles	5.0
2,3,4 Me_3Ar	1×5 = 5 moles	5.5

Periodate consumed 1.17 moles/mole
Formic acid produced 0.6 mole/mole

STRUCTURE B.

of 0.6 mole per anhydrohexose unit. These values are in close agreement with the experimental values of 1.16 moles of periodate and 0.51 mole of formic acid. However, the amount of 2,3,4-tri-*O*-methyl-D-galactose produced on hydrolysis of the fully methylated polysaccharide would be 50% greater than the amount found by experiment. Structure B, which is based on a main core of 1→3 linked D-galactose units, has the same objections as that of Structure A. Structure C, which combines 1→3 and 1→6 linked D-galactose units in the same chain, also gives values for calculated periodate consumption and formic acid production which agree closely with the experiment values. In addition, the proportions of methylated sugars are in reasonably good agreement with those found experimentally. It seems likely that the repeating units of the polysaccharide have a generalized structure similar to that of C. More details will have to await the results of fragmentation studies now in progress.

Can. J. Chem. Downloaded from www.nrcresearchpress.com by 41.223.56.140 on 09/04/12
For personal use only.



		Methylated sugars, moles, found
2,4 Me_2Ga	4×5 = 20 moles	20.0
2,3,4 Me_3Ga	2×5 = 10 moles	11.0
2,3,4,6 Me_4Ga	3×5 = 15 moles	16.0
2,5 Me_2Ar	1×5 = 5 moles	5.0
2,3,4 Me_3Ar	1×5 = 5 moles	5.5

Periodate consumed 1.09 moles/mole
Formic acid produced 0.5 mole/mole

STRUCTURE C.

Branching occurs in the 1→3 linked D-galactopyranose units also at $C_{(4)}$ (as shown by the presence of 2,6-di-*O*-methyl-D-galactose), although with a frequency of 1 in 20 compared with the branching through $C_{(6)}$. In addition, a small number of 1→3 linked D-galactose units are unbranched as shown by the presence of a small proportion of 2,4,6-tri-*O*-methyl-D-galactose. The presence of 2-*O*-methyl-D-galactose showed the presence of triply branched D-galactose units IX. Although incomplete methylation of the polysaccharide and demethylation on hydrolysis may contribute to the presence of a monomethyl galactose, the presence of a relatively large amount suggests that it has a structural significance and actually originated from triply branched galactose units in the polysaccharide.

The number of units (27) forming branch points (VII, VIII, and IX) are in only fair agreement with the number of terminal units (23.5) (I, II, and IV) and indicate that some end group has been lost.

Jones (20) has identified the disaccharide 3-*O*-L-arabopyranosyl-L-arabinose as a product of partial hydrolysis of larch β-galactan. Although this disaccharide was not isolated from the partial hydrolyzate of tamarack arabogalactan, chromatographic examination showed a disaccharide containing arabinose units and having the same mobility on paper as that reported by Jones (20). It seems reasonable, therefore, that this unit is present in this arabogalactan and that it would give rise to approximately equimolar amounts of 2,3,4-tri-*O*-methyl-L-arabinose and 2,5-di-*O*-methyl-L-arabinose.

Single terminal arabofuranose units I attached to the galactose structure were released as free arabinose on acid hydrolysis and appeared as 2,3,5-tri-*O*-methyl-L-arabinose after methylation and hydrolysis of the polysaccharide.

Estimation of the periodate consumed and formic acid produced by the polysaccharide on the basis of the linkages found by methylation gave a value of 1.01 moles of the former and 0.49 mole of the latter per mole of anhydro-D-galactose residue. The experimental values (1.16 moles of periodate and 0.51 mole of formic acid) were somewhat higher than the calculated values and indicated that some end group or 1,6 linked D-galactose residues had been lost. Hydrolysis and chromatography of the periodate-oxidized polysaccharide

Can. J. Chem. Downloaded from www.nrcresearchpress.com by 41.223.56.140 on 09/04/12
For personal use only.

showed that a large number of galactose units and some arabinose units had not been oxidized. Galactose units which were linked 1→3 and also 1→6 linked units which were branched at C_3 would account for the unoxidized galactose. The unoxidized arabinose units must have been those which gave rise to 2,5-di-*O*-methyl-L-arabinose after methylation and which presumably were substituted in the C_3 position by an arabopyranose unit in the polysaccharide.

The change in specific rotation on hydrolysis of the methylated polysaccharide from $[\alpha]_D^{25}$ −45° to +85° indicated that the glycoside bonds were mainly in the β configuration.

The tamarack arabogalactan has structural features that are very similar to those from other woods, particularly the other larches (5, 15, 16). The main characteristics are a high degree of branching through positions 3 and 6 of the anhydro-D-galactose units. The tamarack arabogalactan resembled most closely the ϵ-galactan of European larch (16) in which most of the arabinose units are in the pyranose form. The arabinose units in arabogalactan from western larch (13), jack pine (10), and white spruce (11) are all in the furanose form and are terminal in the molecule. Recently, however, the presence of 3-*O*-β-L-arabopyranosyl-L-arabinose has been reported in western larch arabogalactan (21).

EXPERIMENTAL

All specific rotations are equilibrium values unless otherwise stated, melting points are corrected, and all evaporations were done at 35° C or less.

Paper Chromatography

Chromatographic separations were carried out using the following solvent systems (v/v ratios): (*A*) pyridine:ethyl acetate:water (2:1:2); (*B*) methyl ethyl ketone:water (2:1); (*C*) ethanol:benzene:water (47:200:15); (*D*) *n*-butanol:ethanol:water (40:11:19); (*E*) ethyl acetate:acetic acid:formic acid:water (18.3:1:4); and (*F*) ethylacetate:acetic acid:water (3:1:3). Separations were made by the descending technique on Whatman No. 1 filter paper. Sugars were located on the paper by *p*-anisidine hydrochloride spray reagent (22).

Preparation of the Polysaccharide

A 47-year-old log of tamarack (*Larix laricina* (Du Roi) Koch) was stripped of its bark and planed into shavings which were passed through a Wiley mill. The milled wood was screened, and the fraction passing through 40 mesh and retained on 100 mesh was used. This material was exhaustively extracted with benzene:ethanol (2:1), then with ethanol, and was dried in air. The extracted wood meal (807 g) was added to water (14 liters) and stirred continuously for 24 hours at room temperature. At the end of the extraction period the wood residue was removed by filtration through fine filter cloth on a Buchner funnel and re-extracted twice more by the same procedure. Following the last extraction, the residue was washed with water. The aqueous extracts and washings were clarified by centrifuging in a Sharples supercentrifuge and were concentrated in a Majonnier evaporator at 26° C to about 1/16 of the original volume. The concentrated solution was dialyzed against distilled water for a period of 48 hours and the non-dialyzable portion was concentrated at 35°. Freeze drying yielded 45.5 g of polysaccharide (5.63% yield) sulphated ash, 0.55%, Klason lignin, 0.97%.

The polysaccharide dissolved in water to give a slightly opalescent solution, $[\alpha]_D^{25}$ +11, (*c*, 1% in water). Hydrolysis of a 10-mg sample by *N* sulphuric acid for 12 hours at 100° C and chromatographic examination of the sugars (solvents *A*, *D*, and *F*) showed the presence of arabinose and galactose. Quantitative estimation of the sugars was made by

Can. J. Chem. Downloaded from www.nrcresearchpress.com by 41.223.56.140 on 09/04/12
For personal use only.

separating them from an acid hydrolyzate (200 mg) on a Celite column (19). The weights of arabinose and galactose were in a ratio of 1:4.6. Examination of the acid hydrolyzate by paper electrophoresis in 0.025 *N* sodium bicarbonate for 1 hour at 900 v showed no trace of sugar acid components.

Fractionation of the Polysaccharide

The crude polysaccharide (995 mg) was dissolved in water (100 ml) with stirring, and a small amount of insoluble material removed by centrifuging. The soluble polysaccharides were then fractionally precipitated from the aqueous solution by gradient addition of ethanol. The fractions were collected, washed, and dried by solvent exchange with ethanol and ether. Samples (10 mg) were hydrolyzed by acid and the resulting sugars were examined by paper chromatography (solvent *A*). The fractionation curve is shown in Fig. 1. The results indicated the presence of one main component, approximately 90% of the material being insoluble in 60% ethanol. There were small differences in the arabinose: galactose ratios, the first fractions being relatively richer in galactose than in the main fraction, while the later fractions were richer in arabinose. On the basis of this preliminary experiment a main lot of polysaccharide (16 g) was fractionated in the same way. The material precipitated by ethanol (53–63%) comprised 84% of the crude polysaccharide. The specific rotation $[\alpha]_D^{25}$ was +11 (*c*, 1.1% in water) and the weight ratio of arabinose:galactose was 1:4.6 (molar ratio, 1:3.8). All subsequent investigations were done on this fraction.

Graded Hydrolysis

Polysaccharide (27 mg) was heated in a boiling water bath for 5 hours with 5 ml of oxalic acid (0.025 *N*). Chromatography of the hydrolyzate showed arabinose and galactose in a ratio of 6:1. Degraded polysaccharide was recovered by precipitation with ethanol and washed thoroughly with methanol. The precipitate was hydrolyzed by *N* sulphuric acid and the sugars chromatographed in solvent *A*. Although the predominant sugar was galactose, some arabinose still remained. The precipitate was small (8 mg) and indicated that the galactan portion of the molecule was severely degraded. In another experiment, polysaccharide (100 mg) was heated on a boiling water bath in 10 ml of hydrochloric acid (0.01 *N*). Within 2 hours, galactose and arabinose were present in large amounts, and, in addition, four other spots were detected on the paper chromatogram having R_{xylose} values of 0.21, 0.40, 0.49, and 0.60 respectively in solvent *A*. The spot having R_{xylose} 0.60 increased in intensity up to 20 hours and then gradually disappeared. Chromatographic evidence indicated that it was a disaccharide of arabinose and was probably identical with 3-*O*-β-L-arabopyranosyl-L-arabinose ($R_{galactose}$ 0.70, solvent *E*) isolated by Jones (20) from larch ϵ-galactan. After about 10 hours heating the amount of galactose was almost equal to that of arabinose. The galactose continued to increase slowly throughout the experiment (53 hours). Precipitation of a small amount of degraded polysaccharide with ethanol after 53 hours heating and chromatographic examination of its acid hydrolyzate showed that the material was a galactan containing a trace of arabinose.

Periodate Oxidation

Duplicate samples of the polysaccharide (101.4, 101.3 mg) were dissolved in water (50 ml) and oxidized by 0.1 *M* sodium metaperiodate (50 ml) in the dark at 16° C. Appropriate blanks were prepared under the same conditions. At the intervals noted in the table below analyses were made for periodate consumption and formic acid production (23). The results given in moles per mole anhydro-D-galactose unit were as follows:

Can. J. Chem. Downloaded from www.nrcresearchpress.com by 41.223.56.140 on 09/04/12
For personal use only.

Time (hours)	7	24	32	48	56
Periodate consumption	1.14	1.16	1.16	1.17	1.18
Formic acid production	0.45	0.46	0.47	0.49	0.51

In a separate experiment the polysaccharide (52 mg) was oxidized with periodate for 48 hours as described above. The excess periodate was destroyed by the addition of ethylene glycol and the solution was dialyzed. The non-dialyzable material was recovered by freeze-drying and hydrolyzed with *N* sulphuric acid. Chromatographic examination of the sugars showed galactose to be present in large amounts along with a small amount of arabinose.

Methylation

The polysaccharide (7.0 g) was dissolved in 20% sodium hydroxide (40 ml) and methylated by the dropwise addition of dimethyl sulphate (75 ml) and 45% sodium hydroxide (125 ml) with vigorous stirring. The reagent additions required a period of 4 hours and the solution was kept alkaline at all times. The addition of methylating reagents was repeated four more times. The methylation mixture was heated for 30 minutes at 80° C, then cooled and neutralized with sulphuric acid. The precipitated salts were dissolved in water, and the partly methylated polysaccharide was extracted continuously by chloroform for 48 hours. The recovered methylated polysaccharide (7.73 g) showed a definite hydroxyl band at 3500–3600 cm^{-1} in its infrared spectrum. The partially methylated polysaccharide was dissolved in methyl iodide (75 ml) and methylated on the addition of silver oxide (10 g) in portions of 2 g every hour. The solution was heated under reflux for 18 hours. The methylated product was recovered by extraction with acetone. Five additional methylations by this same procedure were required to yield a product having only a trace of hydroxyl band at 3500–3600 cm^{-1} in its infrared spectrum. The yield of methylated polysaccharide was 7.14 g, $[\alpha]_D^{25}$ −38.8° (*c*, 0.6% in chloroform), OMe 42.3% (theoretical value for the arabogalactan 43.0%).

Fractionation of Methylated Polysaccharide

The methylated polysaccharide (7.0 g) was fractionally extracted with various solvent mixtures of chloroform and petroleum ether (b.p. 30–60°). The solvents were removed and the residues dried to constant weight *in vacuo*. Specific rotation and methoxyl content

TABLE I

Fractionation of methylated polysaccharide

Fraction No.	Chloroform: pet. ether	Yield (g)	$[\alpha]_D^{25}$	OMe
1	0:100	0.0326	− 5.2	18.3
2	10:90	0.2015	−22.8	39.7
3	12.5:87.5	0.5296	−26.1	40.6
4	15:85	1.4430*	−44.9	42.2
5	17.5:82.5	3.9725	−44.6	42.3
6	20:80	0.1021	−45.9	42.5

*Approximately 800 mg lost by accident.

of each of the six fractions were measured and are given in Table I. On the basis of similar values, fractions 4, 5, and 6 were combined and used in subsequent investigations.

Can. J. Chem. Downloaded from www.nrcresearchpress.com by 41.223.56.140 on 09/04/12
For personal use only.

Can. J. Chem. Downloaded from www.nrcresearchpress.com by 41.223.56.140 on 09/04/12
For personal use only.

Hydrolysis of Methylated Polysaccharide

The methylated arabogalactan (5.17 g) was refluxed in 8% methanolic hydrogen chloride (60 ml) in a boiling water bath for 10 hours. The methanolic hydrogen chloride was then removed by a stream of air at room temperature and the residue was taken up in 0.5 *N* hydrochloric acid (35 ml) and refluxed for 10 hours. A small amount of insoluble precipitate was filtered off and the acidic solution was neutralized with Amberlite resin IR-45 (OH). The neutral solution was concentrated to a thin syrup, taken up in 50% aqueous ethanol, clarified with charcoal, and concentrated to a thick syrup. After drying *in vacuo* over calcium chloride the mixture of free methylated sugars weighed 5.07 g and had $[\alpha]_D^{25}$ +85° (*c*, 1.05% in water). Examination of the syrup by paper chromatography (solvent *D*) indicated the presence of the following methylated sugars:

2,3,5-tri-*O*-methyl-L-arabinose, (R_g 0.96);
2,3,4,6-tetra-*O*-methyl-D-galactose, (R_g 0.92);
2,3,4-tri-*O*-methyl-D-galactose, (R_g 0.76);
2,4-di-*O*-methyl-D-galactose, (R_g 0.58);
2,6-di-*O*-methyl-D-galactose, (R_g 0.62);
2,3,4-tri-*O*-methyl-L-arabinose, (R_g 0.83);
2,5-di-*O*-methyl-L-arabinose, (R_g 0.88); and monomethyl galactose (R_g 0.40).

(R_g, movement relative to that of 2,3,4,6-tetra-*O*-methyl-D-glucose).

Separation of Methylated Sugars

The mixture of methylated sugars (5.0 g) was separated on a Celite column using *n*-butanol saturated with water as the developing phase (19). The eluate was collected by an automatic fraction collector in 15-ml quantities. Chromatographic examination of every fifth tube on paper strips (solvent *D*) permitted grouping of fractions of similar composition. The combined samples were evaporated to dryness, taken up in water, filtered, and dried to constant weight. Results of the preliminary separation are given in Table II with the identification of the sugars being based tentatively on chromatographic evidence. The yields and molar ratio of the purified sugars are shown in Table III.

TABLE II

Chromatographic separation of methylated sugars

Fractions from column		Methylated sugar	Yield (mg)
1	(Tube 0–73)	2,3,5-Tri-*O*-methyl-L-arabinose	164
2	(Tube 74–123)	2,3,4,6-Tetra-*O*-methyl-galactose 2,5-Di-*O*-methyl-arabinose 2,3,4-Tri-*O*-methyl arabinose	1545
3	(Tube 124–155)	2,3,4-Tri-*O*-methyl arabinose 2,5-Di-*O*-methyl arabinose	362
4	(Tube 156–218)	2,3,4-Tri-*O*-methyl-galactose	973
5	(Tube 219–235)	2,3,4-Tri-*O*-methyl galactose 2,6-Di-*O*-methyl galactose	86
6	(Tube 236–280)	2,3,4-Tri-*O*-methyl galactose 2,4-Di-*O*-methyl galactose	280
7	(Tube 281–360)	2,4-Di-*O*-methyl galactose	1159
8	(Tube 361–460)	Monomethyl galactose	214
9	Column washed with 50% ethanol	Unknowns	188

TABLE III

Yield of methylated sugars

Methylated sugar	Weight (mg)	Milli-moles	Molar ratio
2,3,5-Tri-*O*-methyl arabinose	130	0.68	2.0
2,3,4,6-Tetra-*O*-methyl galactose	1255	5.32	16.0
2,5-Di-*O*-methyl arabinose	290	1.62	5.0
2,3,4-Tri-*O*-methyl arabinose	352	1.83	5.5
2,3,4-Tri-*O*-methyl galactose	798	3.60	11.0
2,4,6-Tri-*O*-methyl galactose	225	1.01	3.0
2,6-Di-*O*-methyl galactose	64	0.31	1.0
2,4-Di-*O*-methyl galactose	1409	6.78	20.0
2-*O*-Methyl galactose	204	1.05	3.0

Identification of Methylated Sugars

Fraction 1

This methylated sugar was dissolved in water, clarified with charcoal, and dried to constant weight (130 mg). Chromatographic examination in solvents *B*, *C*, and *E* showed that the sugar had an identical rate of movement with 2,3,5-tri-*O*-methyl-L-arabinose. The specific rotation $[\alpha]_D^{25}$ was $-33°$ and the methoxyl content was 47.4% (calculated for $C_8H_{16}O_5$: OMe, 48.4%). A portion of the syrup (114 mg) was dissolved in water (3 ml) and oxidized with bromine (0.5 ml) for 72 hours. Bromine was removed by aeration and the acid solution was neutralized with silver carbonate. The filtrate was deionized with Amberlite IR-120 resin and evaporated to yield syrupy 2,3,5-tri-*O*-methyl-L-arabonic acid. The acid was lactonized by distillation (bath temp., 120–145° C at 0.025 mm), and the lactone was dissolved in methanol saturated with ammonia at 0° C. After 24 hours, the solvent was removed and the amide crystallized on nucleation. Recrystallization from methanol–ether solution yielded pure 2,3,5-tri-*O*-methyl-L-arabonamide, m.p. 136° C (undepressed with an authentic sample) and $[\alpha]_D^{25}$ $-18°$ (*c*, 1% in water), these values agree with those reported for this compound (24).

Fraction 2

Chromatographic examination of this syrup in solvents *C* and *D* showed a mixture of three sugars. The main component (R_g 0.92, solvent *D*) corresponded to 2,3,4,6-tetra-*O*-methyl-D-galactose, the next fastest moving component corresponded to 2,5-di-*O*-methyl-L-arabinose (R_g 0.88, solvent *D*), and the slowest moving component corresponded to 2,3,4-tri-*O*-methyl-L-arabinose (R_g 0.84, solvent *D*).

Fraction 3

Chromatographic examination in solvents *C* and *D* showed two components which corresponded to the tentatively identified 2,5-dimethyl arabinose and 2,3,4-trimethyl arabinose found in fraction 2.

Since fractions 2 and 3 were mixtures, they were fractionated chromatographically on a cellulose column using the solvent benzene:ethanol:water:ammonium hydroxide (200:47:14:1). The column was washed thoroughly first with the aqueous phase and then with the organic phase of the solvent and the separation was made by irrigating with the organic phase. Three separate sugars were recovered and corresponded chromatographically with those found in the original fractions.

2,3,4,6-Tetra-O-methyl-D-galactose

The sugar (1255 mg) had $[\alpha]_D^{25}$ $+118°$ (*c*, 1.12% in water) and MeO 52.3% (theoretical value for $C_{10}H_{20}O_6$, 52.5%). A portion of the syrup (110 mg) was refluxed with aniline

Can. J. Chem. Downloaded from www.nrcresearchpress.com by 41.223.56.140 on 09/04/12
For personal use only.

(49 mg) in ethanol (5 ml) for 3 hours. The solution was slowly evaporated in a desiccator leaving a crystalline residue which was recrystallized from ethanol to yield 72 mg of 2,3,4,6-tetra-*O*-methyl-N-phenyl-D-galactosylamine (25), m.p. and mixed m.p. 196–198° C, $[\alpha]_D^{25}$ −137° (*c*, 1.5% in pyridine).

2,5-Di-O-methyl-L-arabinose

The sugar (290 mg) had $[\alpha]_D^{25}$ −26° (*c*, 1% in water); OMe, 33.7% (calculated for $C_7H_{14}O_5$: OMe, 34.8%) and gave only one spot on chromatographic examination (R_g 0.88–0.89, solvent *D*). Demethylation by 47% hydrobromic acid yielded only one sugar which was identified as arabinose on paper chromatograms. Oxidation of the sugar (105 mg) with bromine for 72 hours at room temperature yielded the corresponding 2,5-di-*O*-methyl-L-arabonic acid (82 mg). Distillation of the acid (bath temp., 130–135° C, at 0.05 mm) yielded the lactone which crystallized on seeding with 2,5-di-*O*-methyl-L-arabonolactone, m.p. and mixed m.p. 60° C. To a portion of the lactone (28 mg) phenylhydrazine (20 mg) in methanol (5 ml) was added and the mixture was refluxed for 2 hours. On removal of the solvent the product crystallized (16 mg) and was recrystallized from ethanol:ether solution to give pure 2,5-di-*O*-methyl-L-arabonophenylhydrazide, m.p. and mixed m.p. 165–167° C.

2,3,4-Tri-O-methyl-L-arabinose

The syrup (362 mg) gave one spot on chromatographic examination (R_g 0.83–0.85, solvent *D*). Demethylation yielded only arabinose as detected on paper chromatograms. Specific rotation $[\alpha]_D^{25}$ was +120° (*c*, 1.2% in water) and the OMe 47.3% (calculated for $C_8H_{10}O_5$: OMe, 48.4%). A portion of the syrup (65 mg) was oxidized in aqueous solution (3 ml) with bromine (0.05 ml) for 50 hours at room temperature. The excess bromine was removed by aeration and the 2,3,4-tri-*O*-methyl-L-arabonic acid extracted with chloroform in a continuous extractor for 24 hours. The chloroform was evaporated and the acid lactonized by distilling (bath temp., 100–118° C, at 0.04–0.05 mm). The lactone (41 mg) was heated with phenylhydrazine (26 mg) in methanol (5 ml) for 3 hours. Removal of the solvent yielded 2,3,4-tri-*O*-methyl-L-arabonophenylhydrazide which crystallized on nucleation. Recrystallization from methanol–ether – petroleum ether yielded the pure product, m.p. and mixed m.p. 158° C. The reported value is 156° C (26).

Fraction 4

The syrup (973 mg) was chromatographically identical in solvents *B* and *D* with 2,3,4-tri-*O*-methyl-D-galactose, had $[\alpha]_D^{25}$ +114° (*c*, 0.79% in water) and OMe, 39.8% (calculated for $C_9H_{18}O_6H_{20}$: OMe, 38.7%). A portion of the fraction (118 mg) was refluxed with aniline (58 mg) in methanol (5 ml) for 2 hours. Evaporation of the solvent yielded crystals which on recrystallization from ethyl acetate proved to be 2,3,4-tri-*O*-methyl-N-phenyl-D-galactosylamine, m.p. and mixed m.p. 165–166° C and $[\alpha]_D^{25}$ +40° (*c*, 1.1% in methanol). Another portion of the syrup (125 mg) in water solution was oxidized with bromine (0.6 ml) for 72 hours at room temperature. Bromine was removed by aeration and the acid was neutralized with silver carbonate. The silver salts were filtered off and the excess silver ions were removed as sulphide. The 2,3,4-tri-*O*-methyl-D-galactonic acid was lactonized by distillation (bath temp., 150–160° C at 0.025 mm). Addition of methanolic ammonia and storage at 5° C for 24 hours yielded 2,3,4-tri-*O*-methyl-D-galactonamide, m.p. 166–167° C, and $[\alpha]_D^{25}$ +33 (*c*, 1% in water). These values are in good agreement with those previously reported (27).

Chromatographic examination of fraction 4 in solvent *C* showed a spot which was slightly slower in movement than 2,3,4-tri-*O*-methyl-D-galactose and which appeared to

Can. J. Chem. Downloaded from www.nrcresearchpress.com by 41.223.56.140 on 09/04/12
For personal use only.

Can. J. Chem. Downloaded from www.nrcresearchpress.com by 41.223.56.140 on 09/04/12
For personal use only.

be 2,4,6-tri-*O*-methyl-D-galactose. Separation of the two sugars was made according to the method described by White (13). A portion of fraction 4 (475 mg) was dissolved in pyridine (3 ml), triphenylchloromethane (654 mg) was added, and the reaction mixture was kept at room temperature for 2 days. A small amount of water was then added and the solution was poured into ice water. The insoluble trityl derivative precipitated as a gum and was removed by centrifugation. The solution and washings were neutralized with Amberlite IR-45, extracted with benzene to remove triphenylcarbinol, and the sugar was recovered as a yellow syrup (96 mg) OMe, 40.0% (calculated for $C_9H_{18}O_6$: OMe, 41.9%) and $[\alpha]$ +90 (*c*, 1.72 in water). The syrup (20 mg) was refluxed in methanol (5 ml) with aniline (10 mg) and yielded 2,4,6-tri-*O*-methyl-N-phenyl-D-galactosylamine, m.p. 176° (reported value 178°) (13). The amount of 2,4,6-tri-*O*-methyl galactose mixed with 2,3,4-tri-*O*-methyl galactose in the original fraction 4 was estimated to be 225 mg.

Fraction 5

This fraction (84 mg) was a mixture of two sugars which on paper chroamtograms in solvents *E* and *D* moved at the same rate as 2,3,4-tri-*O*-methyl-D-galactose (R_g 0.74–0.76, solvent *D*) and 2,6-di-*O*-methyl-D-galactose (R_g 0.59–0.60, solvent *D*). Separation on paper strips using solvent *E* yielded 2,6-di-*O*-methyl-D-galactose (64 mg). Oxidation of this sugar with bromine (0.3 ml) in water (5 ml) for 60 hours at room temperature yielded 2,6-di-*O*-methyl-D-galactonic acid. Distillation of the acid (bath temp., 100°–120° C/0.010 mm) yielded 2,6-di-*O*-methyl-D-galactonic acid lactone (15 mg). The lactone (15 mg) was refluxed with phenylhydrazine for 2 hours in methanol (5 ml) and yielded crystalline 2,6-di-*O*-methyl-D-galactonophenylhydrazide. Recrystallization from methanol–ether solution yielded a pure product, m.p. 144° C unchanged when admixed with an authentic sample.

Fraction 6

The syrup (280 mg) on chromatographic examination in solvent *D* showed a small amount of 2,3,4-tri-*O*-methyl-D-galactose (R_g 0.74–0.76) with the main component being 2,4-di-*O*-methyl-D-galactose (R_g 0.58). Separation of the two sugars was made chromatographically on paper sheets (Whatman No. 1) using solvent *D*. The yields were 2,3,4-tri-*O*-methyl-D-galactose (30 mg) and 2,4-di-*O*-methyl-D-galactose (230 mg).

Fraction 7

This fraction (1159 mg) crystallized spontaneously and was chromatographically identical in solvents *B* and *D* with 2,4-di-*O*-methyl-D-galactose. Recrystallization from ethyl ether yielded 2,4-di-*O*-methyl-D-galactose monohydrate m.p. 100–101° C with sintering at 73–76° C; $[\alpha]_D^{25}$ +125° (5 minutes) → 85° (18 hours) (*c*, 0.8% in water) and OMe 26.7% (theoretical value for $C_8H_{16}O_6.H_2O$: OMe, 27.4%). Dehydration of the monohydrate by heating at 55° C at 0.1 mm over phosphorus pentoxide for 18 hours yielded anhydrous 2,4-di-*O*-methyl-D-galactose, m.p. and mixed m.p. 103–104° C in good agreement with reported values (10). A portion of the pure sugar (85 mg) was refluxed with aniline (44 mg) in methanol (5 ml) for 3 hours. The solution was evaporated in a desiccator and the crystalline sugar was recrystallized from ethyl acetate yielding 2,4-di-*O*-methyl-N-phenyl-D-galactosylamine and having a m.p. and mixed m.p. 218–220° C and $[\alpha]_D^{25}$ −181 (*c*, 1.1% in pyridine).

Fraction 8

This fraction (204 mg) had an R_g of 0.40 (solvent *D*); $[\alpha]_D^{25}$ +88° (*c*, 1% in water) (reported value (29) for 2-*O*-methyl-D-galactose +86°); OMe 15.9%. The indication that the sugar was 2-*O*-methyl-D-galactose was confirmed by the preparation of its anilide by

the method already described. The product was crystalline, and on recrystallization from acetone solution yielded 2-*O*-methyl-N-phenyl-D-galactosylamine, m.p. 163° in good agreement with the reported value of 165° (25).

Fraction 9

This fraction (108 mg) on chromatographic examination (solvent *D*) showed two faint spots, one of which moved at a slower rate than 2-*O*-methyl galactose and the other, a bright red spot, was located near the starting line. The latter component appeared to be a methylated uronic acid although no uronic was detected in the hydrolyzate of the original polysaccharide. The components were separated on filter paper (solvent *D*) and the slower moving component recovered (60 mg), OMe 13.2% (calculated for $C_7H_{12}O_7$: OMe, 14.9%) and $[\alpha]_D^{25}$ +49°. In solvent *E*, the unknown had the same mobility as 4-*O*-methyl-D-glucuronic acid and on the basis of the foregoing properties was tentatively identified as 4-*O*-methyl-D-glucuronic acid.

Molecular Weight

Molecular weight was determined in the Spinco Model E ultracentrifuge by Archibald's method (30) as modified by Klainer and Kegeles (31). The methods of computation were those developed by Smith (32). The centrifuge was run at 8225 r.p.m., the temperature was controlled at 20° C, and a bar angle of 80° was used. A single run was made on a 1.0% arabogalactan solution in 0.05 *M* borate buffer. Measurements were made at the base and meniscus of five photographs taken over a period of 27 minutes to 51 minutes from the time of attaining full speed. A value of 0.60 for partial specific volume was used (9).

The weight average molecular weight measured at the meniscus was approximately 50,000 and at the base was approximately 67,000. These observations indicated a small degree of molecular weight heterogeneity.

Sedimentation Coefficient

Sedimentation coefficients were measured in a Spinco Model E ultracentrifuge at concentrations of 1.0, 0.75, 0.50, and 0.25% in 0.05 *M* borate buffer. The sedimentation coefficients ($S_{20,w}$) were calculated in the usual way and the results are:

Concn., %	$S_{20,w,10^{13}}$
1.0	4.87±.235
0.75	5.27±.193
0.50	4.73±.207
0.25	5.02±.256

There was no evidence of concentration dependence in the sedimentation rate. The absence of concentration dependence may be interpreted as indicating a relatively globular molecule and confirms the highly branched structure proposed on the basis of methylation data. Figure 1 shows the single peak obtained on ultracentrifugation and indicates that the arabogalactan was homogeneous.

Electrophoresis

Polysaccharide (151 mg) was dissolved in 0.05 *M* borate buffer (15 ml) and dialyzed against the buffer at 4° C for 24 hours. The electrophoretic separation was made in a Spinco apparatus Model H and the arabogalactan moved as a single peak with $\mu = 10.50 \times 10^{-5}$ cm^2/v^{-1}/sec^{-1}. The peak is shown in Fig. 1.

ACKNOWLEDGMENTS

The author wishes to acknowledge the valuable technical assistance of W. R. Rowsome throughout this work. Thanks are due to Professor J. K. N. Jones, Queen's University,

Can. J. Chem. Downloaded from www.nrcresearchpress.com by 41.223.56.140 on 09/04/12
For personal use only.

Kingston, for a gift of 2,3,4-tri-*O*-methyl-L-arabonophenylhydrazide and also to Dr. D. J. Bell, Agricultural Research Council, Edinburgh, for a sample of 2,6-di-*O*-methyl-D-galactonophenylhydrazide. The author also gratefully acknowledges the help of Dr. D. B. Smith of this Division in obtaining and interpreting the sedimentation data.

REFERENCES

1. SCHORGER, A. W. and SMITH, D. F. Ind. Eng. Chem. **8**, 494 (1916).
2. WISE, L. E. and PETERSON, F. C. Ind. Eng. Chem. **22**, 362 (1930).
3. WISE, L. E. and UNKAUF, H. C. Cellulosechemie, **14**, 20 (1933).
4. NIKITIN, N. I. and SOLOVIEV, I. A. J. Appl. Chem. U.S.S.R. **8**, 1016 (1935).
5. WHITE, E. V. J. Am. Chem. Soc. **63**, 2871 (1941).
6. HIRST, E. L., JONES, J. K. N., and CAMPBELL, W. G. Nature, **147**, 25 (1941).
7. BRAUNS, F. E. Science, **102**, 155 (1945).
8. FOREMAN, E. L. and ENGLES, D. T. Ind. Eng. Chem. **23**, 415 (1931).
9. WADMAN, W. H., ANDERSON, A. B., and HASSID, W. Z. J. Am. Chem. Soc. **76**, 4097 (1954).
10. BISHOP, C. T. Can. J. Chem. **35**, 1010 (1957).
11. ADAMS, G. A. Can. J. Chem. **36**, 755 (1958).
12. WHITE, E. V. J. Am. Chem. Soc. **64**, 302 (1942).
13. WHITE, E. V. J. Am. Chem. Soc. **64**, 1507 (1942).
14. WHITE, E. V. J. Am. Chem. Soc. **64**, 2838 (1942).
15. CAMPBELL, W. G., HIRST, E. L., and JONES, J. K. N. J. Chem. Soc. 774 (1948).
16. ASPINALL, G. O., HIRST, E. L., and RAMSTAD, E. J. Chem. Soc. 593 (1958).
17. PETERSON, F. C., BARRY, A. J., UNKAUF, H., and WISE, L. E. J. Am. Chem. Soc. **62**, 2361 (1940).
18. MOSIMAN, VON. H. and SVEDBERG, T. Kolloid-Z. **100**, 99 (1942).
19. LEMIEUX, R. U., BISHOP, C. T., and PELLETIER, G. E. Can. J. Chem. **34**, 1365 (1956).
20. JONES, J. K. N. J. Chem. Soc. 1617 (1:53).
21. BOUVENG, H. and LINDBERG, B. Acta Chem. Scand. **10**, 1515 (1956).
22. HOUGH, L., JONES, J. K. N., and WADMAN, W. H. J. Chem. Soc. 1702 (1950).
23. CHANDA, S. K., HIRST, E. L., JONES, J. K. N., and PERCIVAL, E. G. V. J. Chem. Soc. 1289 (1950).
24. HUMPHREYS, R. W., PRYDE, J., and WATERS, E. T. J. Chem. Soc. 1298 (1931).
25. MCCREATH, D. and SMITH, F. J. Chem. Soc. 387 (1939).
26. SMITH, F. J. Chem. Soc. 744 (1939).
27. SMITH, F. J. Chem. Soc. 1724 (1939).
28. BELL, D. J. J. Chem. Soc. 692 (1945).
29. OLDHAM, J. W. H. and BELL, D. J. J. Am. Chem. Soc. **60**, 323 (1938).
30. ARCHIBALD, W. J. J. Phys. Chem. **57**, 1204 (1947).
31. KLAINER, S. M. and KEGELES, G. J. Phys. Chem. **59**, 952 (1955).
32. SMITH, D. B. Personal communication.

Can. J. Chem. Downloaded from www.nrcresearchpress.com by 41.223.56.140 on 09/04/12
For personal use only.

Can. J. Chem. Downloaded from www.nrcresearchpress.com by 41.223.56.140 on 09/04/12
For personal use only.

THE BIOGENESIS OF ALKALOIDS

XXIV. THE ROLE OF CITRIC ACID IN THE BIOGENESIS OF HYOSCYAMINE[1]

A. V. Robertson[2] and Léo Marion

ABSTRACT

It is known that ornithine is a precursor of the pyrrolidine ring present in hyoscyamine. It was assumed that citric acid might be the precursor of the remaining three carbons that complete the tropine ring structure. To test this assumption 3-^{14}C-citric acid was fed to *Datura stramonium* plants. The hyoscyamine isolated from these plants was radioactive, but the activity was very low. It must be concluded that citric acid, although it can be used to a small extent, is not the normal precursor of the chain of three carbons attached to the pyrrolidine ring in hyoscyamine.

Tracer work in these laboratories on the biosynthesis of the tropane alkaloids in mature *Datura stramonium* has shown that ornithine is an efficient precursor of the pyrrolidine ring in hyoscyamine and that the N-methyl group arises from methionine (1, 2). The radioactivity of labelled putrescine was not incorporated in hyoscyamine (3). Hyoscine in the above experiments was never radioactive, suggesting that this alkaloid was not being synthesized during the time the plants were in contact with the radiotracers. Derivation of the "acetone" fragment of tropine from acetone, acetoacetic acid, acetone dicarboxylic acid, or from citric acid in the presence of an oxidase has been suggested (e.g. Robinson (4), Birch (5)). Wenkert has emphasized that the direct intervention of acetone dicarboxylic acid is unlikely in biochemical processes (6), despite the very successful use of this compound in laboratory syntheses under "physiological conditions".

We have fed 3-^{14}C-citric acid to mature *D. stramonium* plants. Radioactivity in the nutrient solution decreased rapidly. The plants were harvested after 2 days to minimize randomization due to the various pathways available for citric acid metabolism. The alkaloids were isolated by established methods. Paper chromatographic assay of the crude basic fraction showed that neither hyoscyamine nor hyoscine had measurable radioactivity and that only a small proportion of the latter alkaloid was present. Separation of the bases by partition chromatography, usually employed, was therefore not undertaken. Instead the mixture was treated with gold chloride and the hyoscyamine aurichloride was purified by recrystallization and conversion to the picrate. Pure hyoscyamine picrate had an activity of 10 d.p.m./mg, unchanged by recrystallization. This measurement, just detectable with certainty, may represent a real though insignificant incorporation of radioactivity in the molecule. The activity was not sufficient to be detected at the concentrations used on paper chromatograms or to make degradations of the compound worth while. Hence citric acid is not a satisfactory "acetone equivalent" in *D. stramonium*. Feeding experiments with labelled acetoacetic acid are in progress.

Citric acid-1,5-^{14}C has been prepared by Rothchild and Fields (7), who improved the original synthesis of citric acid by Grimaux and Adam (8) which started from 1,3-dichloroacetone. 3-^{14}C-Citric acid required for the present experiment was obtained by synthesizing 2-^{14}C-1,3-dichloroacetone from 1-^{14}C-acetate and then following the method of Rothchild and Fields (7) except for the use of inactive cyanide in the last stage. The

[1]*Manuscript received November 4, 1959.*
Contribution from the Division of Pure Chemistry, National Research Council, Ottawa, Canada.
Issued as N.R.C. No. 5495.
[2]*National Research Council of Canada Postdoctoral Fellow, 1957–59.*

dichloroacetone was prepared in good yield by the reaction sequence: acetic acid, chloroacetic acid, chloroacetyl chloride, 1,3-dichloroacetone. Of these steps only the last has not been described in the literature. Treatment of chloroacetyl chloride with diazomethane and hydrogen chloride gave an almost quantitative yield of dichloroacetone. The diazoketone was not isolated. Purity of intermediates at all stages was critical. The radioactive citric acid was purified by ion exchange chromatography (9) and via the trimethyl ester (7).

Feeding of 3-^{14}C-citric acid to *D. stramonium* was expected to give rise to hyoscyamine with the radioactivity located at carbon-3 of the tropine skeleton. The degradative scheme chosen to isolate this carbon atom in high yield was as follows. Tropine, obtained by alkaline hydrolysis of hyoscyamine, was oxidized to tropinone by the method of Willstätter (10). Interaction of tropinone with phenyl-lithium gave 3-phenyltropan-3-ol (10*a*) from which the required carbon atom was obtained by permanganate oxidation to benzoic acid.

Because of the low activity of the hyoscyamine isolated, however, the base was not degraded.

EXPERIMENTAL

Melting points are corrected. Radioactivities were determined with a Radiation Counters Laboratory "Nucleometer" counting 50% of disintegrations. Infrared spectra were measured in carbon disulphide solution on a Perkin–Elmer double beam spectrometer model 21B.

Synthesis of 3-^{14}C-*Citric Acid*

Sodium acetate-1-^{14}C (2 mc, 50 mg) was dissolved in acetic acid (3.25 g) and chlorinated using the method of Ostwald (11), yield of sublimed chloroacetic acid, 3.95 g (76%). Of the various methods available for preparing the acid chloride, the most readily adapted for small-scale work and ease of separation of product proved to be halide exchange with benzoyl chloride following the procedure of Brown (12), yield of distilled chloroacetyl chloride, 3.59 g (76%). This acyl chloride was added dropwise to an excess of a sodium-dried ethereal solution (200 ml) of diazomethane (prepared from 25 g of nitrosomethylurea). Thirty minutes later hydrogen chloride was passed through until the yellow color was discharged. The solution was concentrated *in vacuo* to 50 ml and washed with saturated aqueous sodium bicarbonate (2×5 ml). The residue obtained by evaporation of the ether was sublimed at 1 mm/50° onto a cold finger condenser containing dry ice and acetone; yield of white crystalline 2-^{14}C-1,3-dichloroacetone, 4.02 g (99%). The method of Rothchild and Fields (7) was followed for the rest of the synthesis. Failure to remove acid impurities in the dichloroacetone by washing with bicarbonate resulted in poor yields in the next step, presumably because of the influence of acid on the cyanohydrin equilibrium. Even so, small quantities of black oil or tar separated during the acid hydrolysis to bischloromethylglycollic acid. After reaction of potassium bischloromethylglycollate with radioinactive potassium cyanide and acid hydrolysis, the organic fraction in the dry residue was separated from inorganic material by several extractions with hot acetone. Most of the impurities in the crude citric acid were removed by ion exchange chromatography on Amberlite IRA-400 resin in the acetate form (9). Elution with 0.1 *N* hydrochloric acid and removal of solvent *in vacuo* at 30° gave a partly crystalline orange residue. The product was further purified through the trimethyl ester (7) which was crystallized from cyclohexane.

Can. J. Chem. Downloaded from www.nrcresearchpress.com by 41.223.56.140 on 09/04/12
For personal use only.

Can. J. Chem. Downloaded from www.nrcresearchpress.com by 41.223.56.140 on 09/04/12
For personal use only.

Administration of 3-^{14}C-Citric Acid and Isolation of Alkaloids

D. stramonium plants were grown from seed in soil for 8 weeks with transplantations as required. The almost mature plants were then transferred to a hydroponic setup (1). Nutrient solution as described by Leete (13) was used except for substituting ferrous ammonium sulphate (36 mg/l. of nutrient solution, added in dilute aqueous versenol) as the source of iron. Additional iron was added as required to suppress incipient chlorosis. The plants grew vigorously and in the 15th week 3-^{14}C-citric acid (434 mg, total activity 1.46×10^8 d.p.m.) in water (100 ml) was distributed evenly between 11 plants (total nutrient solution, 9 liters). Each plant had at least four seed pods, and several flowers and developing buds. Five per cent of the original activity remained in the nutrient solution after 1 day and less than 1% after 2 days, at which time the plants were harvested. After overnight drying at 110°, the entire plants were ground to 20 mesh, and the total activity, obtained by extracting a small sample with methanol, was 1.4×10^7 d.p.m. The ground material (234 g) was moistened overnight with water (150 ml) in a closed container and then triturated with powdered calcium hydroxide (50 g) after the method of Evans and Partridge (14). The mixture was extracted with water-saturated ether (1500 ml) by vigorous mechanical stirring (1 hour) in a beaker at room temperature. The extract was decanted and the process was repeated until no further radioactivity was removed (10 times). The combined ether extracts (total activity 1.14×10^6 d.p.m.) were evaporated to 200 ml and the basic material present was completely extracted into 2 *N* hydrochloric acid (5×20 ml). Separation of the emulsified phases was achieved by centrifugation. The crude alkaloids were obtained as a dark gum (237 mg, total activity 1.4×10^4 d.p.m.) by collection in ether after rendering the acid fraction alkaline with ammonia. Paper chromatography in butanol – concentrated hydrochloric acid (100:10) saturated with water (Bc 10 solvent of Munier and Macheboeuf (15)) showed the presence of hyoscyamine, R_F 0.90 and a comparatively smaller quantity of hyoscine, R_F 0.79. Neither spot had measureable radioactivity. The gum was treated with gold chloride (250 mg) in hot dilute hydrochloric acid. Hyoscyamine aurichloride (144 mg) crystallized on cooling of the solution, and after recrystallization had m.p. 163–165°, not depressed on admixture with an authentic specimen. The recrystallized sample had an activity of 16 d.p.m./mg. The aurichloride was decomposed with hydrogen sulphide and the free base (40 mg) which was isolated in the usual way was treated with picric acid (50 mg). The hyoscyamine picrate was crystallized from water and had m.p. 164–165° and radioactivity of 10 d.p.m./mg, unchanged by further recrystallization.

Degradation to Isolate Carbon-3 of Tropine

Tropinone, obtained by chromic acid oxidation of tropine (10), was purified via the picrate. Tropinone (565 mg) in ether (2 ml) was added dropwise to a solution of phenyllithium (2 mole equiv.) in refluxing ether (10 ml) under nitrogen. Five minutes later the reaction was cooled in ice and stirred magnetically while *N* hydrochloric acid (10 ml) was slowly added. The separated acid layer was washed with a little ether and basified with sodium hydroxide. Ether extraction of the alkaline solution gave 3-phenyltropan-3-ol (720 mg, 82%) which crystallized from hexane in rosettes of spears having m.p. 162–163° and infrared absorption at 3570 cm^{-1} (hydroxyl), 752 and 693 cm^{-1} (monosubstituted benzene), and having no absorption in the carbonyl region. Found: C, 77.3; H, 8.6; N, 6.5. $C_{14}H_{14}NO$ requires: C, 77.4; H, 8.8; N, 6.5%.

3-Phenyltropan-3-ol (200 mg), suspended in water (20 ml), was treated with potassium permanganate (2 g) and the mixture was refluxed (1 hour). Precipitated manganese

dioxide was dissolved by passage of sulphur dioxide and the solution was acidified with hydrochloric acid and extracted with ether. The acid fraction in the ether was separated from neutral material in the usual way, giving benzoic acid (102 mg, 91%) which had m.p. and mixed m.p. 121–122° after recrystallization from water. The infrared spectrum was indistinguishable from that of authentic benzoic acid.

REFERENCES

1. LEETE, E., MARION, L., and SPENSER, I. D. Can. J. Chem. **32**, 1116 (1954).
2. MARION, L. and THOMAS, A. F. Can. J. Chem. **33**, 1853 (1955).
3. DIAPER, D. G. M., KIRKWOOD, S., and MARION, L. Can. J. Chem. **29**, 964 (1951).
4. ROBINSON, R. The structural relations of natural products. Clarendon Press, Oxford. 1955. p. 60.
5. BIRCH, A. J. *In* Perspectives in organic chemistry. *Edited by* A. Todd. Interscience Publishers, Inc., New York. 1956. p. 141.
6. WENKERT, E. Experientia, **15**, 165 (1959).
7. ROTHCHILD, S. and FIELDS, M. J. Am. Chem. Soc. **74**, 2401 (1952).
8. GRIMAUX, E. and ADAM, P. Bull soc. chim. France, **36**, 18 (1881).
9. ANET, E. F. L. J. and REYNOLDS, T. M. Australian J. Chem. **8**, 267 (1955).
10. WILLSTÄTTER, R. Ber. **29**, 396 (1896).

10*a*. COPE, A. C. and D'ADDIECO, A. A. J. Am. Chem. Soc. **73**, 3419 (1951).

11. OSTWALD, R. J. Biol. Chem. **173**, 207 (1948).
12. BROWN, H. C. J. Am. Chem. Soc. **60**, 1325 (1938).
13. LEETE, E. J. Am. Chem. Soc. **78**, 3520 (1956).
14. EVANS, W. C. and PARTRIDGE, M. W. J. Pharm. Pharmacol. **4**, 729 (1952).
15. MUNIER, R. and MACHEBOEUF, M. Bull. soc. chim. biol. **33**, 846 (1951).

Can. J. Chem. Downloaded from www.nrcresearchpress.com by 41.223.56.140 on 09/04/12
For personal use only.

Can. J. Chem. Downloaded from www.nrcresearchpress.com by 41.223.56.140 on 09/04/12
For personal use only.

KINETICS OF THE THERMAL DECOMPOSITION OF TETRAMETHYLTETRAZEN[1]

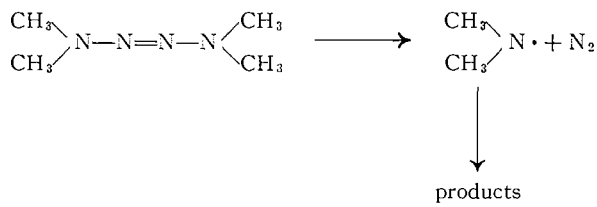
J. S. WATSON AND A. J. WARING[2]

ABSTRACT

The kinetics of the thermal decomposition of tetramethyltetrazen (T.M.T.) have been studied in a static system at pressures up to 1.8×10^{-2} mm and temperatures between 125.5 and 147.5° C by measuring the rate of production of nitrogen. The results show that the decomposition is first order in T.M.T. at the pressures used and give approximate values for the Arrhenius parameters.

The present study of the kinetics of the thermal decomposition of tetramethyltetrazen was undertaken as a continuation of the work published previously by one of the authors (1). It was also intended to supplement the kinetic measurements by detailed analysis of the reaction products but, because of the death of Dr. J. S. Watson during the early stages of the experiments, the product analyses were not performed. Since this project is now terminated as a result of Dr. Watson's death, it is considered worth while to report briefly the results of the kinetic study.

The previous work (1) shows that thermal decomposition of tetramethyltetrazen proceeds by a radical mechanism involving $(CH_3)_2N\cdot$ radicals which react further. Thus, following the reaction by pressure change is inaccurate and the most satisfactory method seems to be by measurement of the nitrogen produced.



The previous work also shows that no H_2 is produced, so all products apart from the nitrogen can be trapped by liquid N_2.

Tetramethyltetrazen was prepared by Renouf's method (2) from 1,1-dimethyl hydrazine, the procedure being identical with that used previously (1). The apparatus used for pyrolysis consisted of a removable glass reaction vessel (volume approximately 100 ml) fitted with a teflon seat valve, attached to a vacuum system with Toepler pump, and calibrated gas burette with a mercury-sealed, one-way valve. The sample was introduced by micro syringe and frozen into the reaction vessel. Then the whole apparatus was evacuated to better than 10^{-3} mm and the teflon seat valve closed. Heating was carried out in an oil bath, the temperature of which was controlled by a Canlab magnetic control-type, mercury-metal thermoregulator. After the required time, the reaction was quenched with iced water and the products completely transferred, by the Toepler pump, through a liquid nitrogen trap into the gas burette where the nitrogen was measured.

[1]*Manuscript received October 23, 1959.*
Contribution from the Division of Applied Chemistry, National Research Council, Ottawa, Canada. Issued as N.R.C. No. 5494.
[2]*National Research Council exchange summer student, 1959. Present address: Department of Organic and Inorganic Chemistry, Cambridge University, Cambridge, England.*

Fifty-four runs were carried out at six different temperatures. Typical set of values is:

Temp., 147.5° C. Start with 75×10^{-5} mole T.M.T.

Time (minutes)	5	10	15	20	$24\frac{3}{4}$	$32\frac{1}{2}$
Moles N_2 produced $\times10^5$	0.68	1.64	2.39	2.86	4.14	5.30

Plots were made of $-\log_{10}$ (moles unchanged T.M.T.) against the time of heating. The values of the first order rate constants K_1 derived from the graphs were:

Temp., ° C	125.5	132.5	136.0	141	145	147.5
$K_1\times10^6$ (sec^{-1})	0.91	1.35	2.43	3.15	4.49	7.33
Error $\times10^6$ (sec^{-1})	0.02	0.09	0.08	0.28	0.33	0.07

Plot of $-\log_{10} K_1$ against the reciprocal absolute temperature is shown in the figure. It gives the following Arrhenius parameters:

$$E = (31.9\pm3.0) \text{ kcal/mole}, \qquad \log_{10} A = 11.4\pm1.65$$

i.e.

$$\log_{10} K_1 = (11.4\pm1.65) - \frac{(31.9\pm3.0)1000}{2.303\,RT} \qquad (K_1 \text{ in sec}^{-1}).$$

Within the experimental uncertainty the value of the pre-exponential factor is normal for a unimolecular reaction.

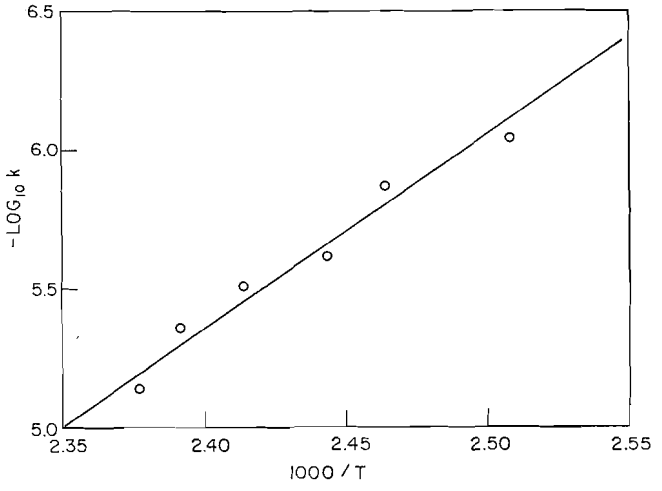


FIG. 1.

ACKNOWLEDGMENTS

One of the authors (A. J. W.) would like to express his thanks to the National Research Council for the opportunity of doing this work as a summer student and to the staff of the Division of Applied Chemistry, especially to Dr. R. J. Cvetanović, for their help and encouragement.

REFERENCES

1. WATSON, J. S. J. Chem. Soc. 3677 (1956).
2. RENOUF, E. Ber. **13**, 2173 (1880).

Can. J. Chem. Downloaded from www.nrcresearchpress.com by 41.223.56.140 on 09/04/12
For personal use only.

Can. J. Chem. Downloaded from www.nrcresearchpress.com by 41.223.56.140 on 09/04/12
For personal use only.

CHEMICAL SHIFTS IN THE NUCLEAR MAGNETIC RESONANCE SPECTRA OF MOLECULES CONTAINING POLAR GROUPS[1]

A. D. BUCKINGHAM[2]

ABSTRACT

It is shown that the electric field at a particular nucleus arising from polar groups in other parts of a molecule can lead to chemical shifts proportional to the first power of the field strength. The change $\Delta\sigma$ in the proton screening constant of an X—H bond when it is subjected to an electric field E is approximately given by

$$\Delta\sigma = -2\times10^{-12}E_z - 10^{-18}E^2$$

where E_z is the component of E in the bond direction. A field along the X—H bond draws the electrons in the enriched region between the nuclei away from the proton, thereby causing its resonance to occur at lower magnetic field strengths, while a field in the H—X direction leads to resonance at higher fields. The electric field produced by the polarization of neighboring solvent molecules may also be important and lead to a solvent shift related to the dielectric constant of the solvent. The direction of the internal field, and that due to the solvent, can easily be estimated when the molecule is rigid, so that the model can be useful in assigning spectra. It gives a simple and reasonably accurate account of the observed spectra of substituted benzenes and of some solvent effects on the proton resonances of *cis*- and *trans*-1,2-dichloroethene.

INTRODUCTION

In nuclear magnetic resonance experiments, nuclei with magnetic moments are effectively used as probes to measure the actual magnetic field, H_{local}, at the nucleus.

[1] $$H_{\text{local}} = (1-\sigma)H$$

where H is the applied magnetic field strength and σ is the *screening constant*. Owing to rapid molecular motion in gases and liquids, the observed screening constant corresponds to an average for all molecular orientations. The molecules which are far removed from the one with the resonant nucleus interact with it as if they formed a continuum having the bulk properties of the fluid, and they may contribute to σ a term proportional to the volume susceptibility; this term depends on the sample shape, and vanishes for a spherical specimen. The screening constants quoted in this paper have all been "corrected" so as to remove this bulk susceptibility effect.

Progress in understanding observed screening constants has largely been based on models in which σ is split up into atomic contributions (see Pople, Schneider, and Bernstein (1) and Saika and Slichter (2)). Thus,

[2] $$\sigma = \sigma_d+\sigma_p+\sigma_o+\sigma_c$$

where σ_d and σ_p are the dia- and para-magnetic shielding of the nucleus whose total screening constant is σ; σ_d is proportional to the magnetic field produced at the nucleus by the moment induced through the rotation of the electrons about the nucleus with the Larmor precessional frequency $eH/2mc$. The paramagnetic shielding σ_p arises from the hindrance to the Larmor precession produced by the lack of axial symmetry about the field H; in a linear molecule, σ_p is zero when H is along the molecular axis, but in general it is non-zero for an atom in a molecule. σ_o is the shielding constant proportional to the field produced by the magnetic moments induced in other atoms, and σ_c is the contribution

[1]*Manuscript received September 18, 1959.*
Contribution from Division of Pure Chemistry, National Research Council of Canada, Ottawa.
Issued as N.R.C. No. 5530.
[2]*Permanent address: Inorganic Chemistry Laboratory, University of Oxford, Oxford, England.*

Can. J. Chem. Downloaded from www.nrcresearchpress.com by 41.223.56.140 on 09/04/12
For personal use only.

from interatomic currents (3); σ_o is zero in a tumbling molecule if the other atoms have isotropic susceptibilities.

A uniform electric field E_z distorts an atom in an S-state, and this distortion affects σ_d and σ_p. σ_d is diminished in both the z and x (or y) directions, the diminution being greater in the z-direction; σ_p is zero in the z-direction, but is negative in the x- and y-directions. The change in σ due to E_z is proportional to E_z^2, for the symmetry of the atom requires the shielding to be unaffected by a reversal of E_z. For a hydrogen atom in its ground state, Marshall and Pople (4) showed that, neglecting the effect of electron spin,

$$\sigma_{zz} = \frac{e^2}{3mc^2a}\left\{1-\frac{439}{40}\frac{a^4E_z^2}{e^2}\right\}$$

[3]

$$\sigma_{xx} = \sigma_{yy} = \frac{e^2}{3mc^2a}\left\{1-\frac{193}{15}\frac{a^4E_z^2}{e^2}\right\}$$

for weak electric fields ($E_z \ll e/a^2$), where e is the protonic charge (4.803×10^{-10} e.s.u.) and a the Bohr radius (0.5292 Å).

If the resonant nucleus is not at a molecular center of inversion, the screening for a fixed orientation of the molecule may be affected by a reversal of E_z, so that in weak fields σ may be proportional to E_z, rather than E_z^2. If E_z is a fixed external field, the shielding proportional to E_z averages to zero in a gas or liquid, but if E_z arises from a polar group within the molecule itself, or from neighboring solvent molecules polarized by the solute, then the mean value of E_z at a particular nucleus may be non-zero. A screening constant proportional to E_z, in addition to one proportional to E_z^2, is therefore possible. Thus in an X—H bond, σ for the proton will be proportional to the first power of the component of the field along the bond, and to the second power of the field perpendicular to it.

The purpose of this paper is to investigate the influence of this "internal field" effect on proton screening constants in gaseous molecules, and to discuss changes in σ arising from fields due to the presence of a solvent; the latter part extends Stephen's approach (5) to the problem of solvent effects.

GENERAL THEORY

In the presence of a primary uniform magnetic field **H**, there will be, at a particular nucleus, an induced secondary magnetic field **H′**, and the screening constant tensor $\sigma_{\alpha\beta}$ for this nucleus is defined by

$$H'_\alpha = -\sigma_{\alpha\beta}H_\beta \qquad [4]$$

where the Greek subscripts denote tensor components (α and β can be x, y, or z, and repeated subscripts indicate a summation over x, y, and z components; thus $\sigma_{\alpha\beta}H_\beta = \sigma_{\alpha x}H_x+\sigma_{\alpha y}H_y+\sigma_{\alpha z}H_z$). It is supposed that if the molecule is in a uniform electric field **E**, the screening is affected in such a way that σ can be expanded as a power series in E

$$\sigma_{\alpha\beta} = \sigma^{(0)}_{\alpha\beta}+\sigma^{(1)}_{\alpha\beta\gamma}E_\gamma+\tfrac{1}{2}\sigma^{(2)}_{\alpha\beta\gamma\delta}E_\gamma E_\delta+\ldots \qquad [5]$$

If the molecule is symmetric in x (that is, if $\sigma_{\alpha\beta}$ is unaffected by an inversion in the yz plane), then $\sigma^{(1)}_{\alpha\beta x} = 0$. Thus $\sigma^{(1)} = 0$ for an atom; for a molecule which is symmetrical about the z-axis (an X—H bond is usually approximately symmetric about the bond direction) $\sigma^{(1)}_{\alpha\beta x} = \sigma^{(1)}_{\alpha\beta y} = 0$. The observed screening constant σ for a molecule in a gas or liquid corresponds to an average of $\sigma_{\alpha\beta}$ over all orientations. Averaging over all molecular

orientations is equivalent to fixing the molecule (and in this case the electric field) and averaging over all directions of the magnetic field. Thus,

$$[6] \qquad \sigma = \frac{1}{H^2}\sigma_{\alpha\beta}\overline{H_\alpha H_\beta} = \tfrac{1}{3}\sigma_{\alpha\alpha} = \tfrac{1}{3}\{\sigma^{(0)}_{\alpha\alpha}+\sigma^{(1)}_{\alpha\alpha\gamma}E + \tfrac{1}{2}\sigma^{(2)}_{\alpha\alpha\gamma\delta}E_\gamma E_\delta + \ldots\}.$$

For an atom in an S-state $\sigma^{(1)} = 0$ and there are two independent $\sigma^{(2)}$ tensor components. For a hydrogen atom in a uniform field E_z, [5] yields

$$\sigma_{zz} = \sigma^{(0)}+\tfrac{1}{2}\sigma^{(2)}_{zzzz}E_z{}^2+\ldots$$
$$\sigma_{xx} = \sigma^{(0)}+\tfrac{1}{2}\sigma^{(2)}_{xxzz}E_z{}^2+\ldots$$

whence, from [3],

$$[7] \qquad \sigma^{(0)} = \frac{e^2}{3mc^2a}; \qquad \sigma^{(2)}_{zzzz} = \sigma^{(2)}_{||} = -\frac{439}{60}\frac{a^3}{mc^2}$$
$$\sigma^{(2)}_{xxzz} = \sigma^{(2)}_{\perp} = -\frac{386}{45}\frac{a^3}{mc^2}.$$

The $\sigma^{(2)}$ tensor is given by

$$[8] \qquad \sigma^{(2)}_{\alpha\beta\gamma\delta} = \sigma^{(2)}_{\perp}\delta_{\alpha\beta}\delta_{\gamma\delta}+\tfrac{1}{2}(\sigma^{(2)}_{||}-\sigma^{(2)}_{\perp})(\delta_{\alpha\gamma}\delta_{\beta\delta}+\delta_{\alpha\delta}\delta_{\beta\gamma})$$

where $\delta_{\alpha\beta}$ is the substitution tensor ($= 1$ if $\alpha = \beta$, $= 0$ if $\alpha \neq \beta$).

In an axially symmetric X—H bond there can be no screening proportional to the first power of the field at right angles to the bond. Thus $\sigma^{(1)}_{\alpha\beta x} = \sigma^{(1)}_{\alpha\beta y} = 0$, and there are two independent $\sigma^{(1)}$ tensors, $\sigma^{(1)}_{zzz} = \sigma^{(1)}_{||}$ and $\sigma^{(1)}_{xxz} = \sigma^{(1)}_{yyz} = \sigma^{(1)}_{\perp}$. From [6] and [8]

$$[9] \qquad \sigma = \sigma^{(0)}+\sigma^{(1)}E_z+\tfrac{1}{2}\sigma^{(2)}E^2+\ldots$$

where

$$\sigma^{(0)} = \tfrac{1}{3}(\sigma^{(0)}_{||}+2\sigma^{(0)}_{\perp}) \qquad \text{and} \qquad \sigma^{(1)} = \tfrac{1}{3}(\sigma^{(1)}_{||}+2\sigma^{(1)}_{\perp}).$$

To estimate the importance of the proton shielding proportional to E and to E^2 in an X—H bond, use can be made of the results of Marshall and Pople (4) for the E^2 effect on an H-atom. Consider a model in which an H-atom is at a distance R from a point charge λ. In the presence of a uniform electric field **E**, the total electric field **F** acting on the atom is

$$[10] \qquad \mathbf{F} = \{E_x, E_y, E_z+(\lambda/R^2)\}$$

and hence an effect proportional to F^2 will involve terms of the first and second order in E. The screening constant for the proton in this "molecule" is given by [5] and [8] and is

$$[11] \qquad \sigma_{\alpha\beta} = \frac{e^2}{3mc^2a}\delta_{\alpha\beta}-\frac{193}{45}\frac{a^3F^2}{mc^2}\delta_{\alpha\beta}+\frac{227}{360}\frac{a^3}{mc^2}F_\alpha F_\beta.$$

Because of the form of F (see [10]), [11] leads to screening proportional to E_z and to E^2, and it can be shown that

$$\sigma^{(1)}_{||} = \frac{\lambda}{R^2}\sigma^{(2)}_{||} \qquad \text{and} \qquad \sigma^{(1)}_{\perp} = \frac{\lambda}{R^2}\sigma^{(2)}_{\perp}.$$

Can. J. Chem. Downloaded from www.nrcresearchpress.com by 41.223.56.140 on 09/04/12
For personal use only.

Thus [9] becomes

$$\sigma = \frac{e^2}{3mc^2a} - \frac{881}{108}\frac{a^3}{mc^2}\frac{\lambda}{R^2}E_z - \frac{881}{216}\frac{a^3}{mc^2}E^2 - \ldots$$

$$[12] \qquad = \sigma^{(0)} + \sigma^{(2)}\left\{\frac{\lambda}{R^2}E_z + \tfrac{1}{2}E^2\right\} + \ldots$$

where

$$\sigma^{(2)} = \tfrac{1}{3}(\sigma_{||}^{(2)} + 2\sigma_{\perp}^{(2)}).$$

From [7], $\sigma^{(0)} = 17.8\times10^{-6}$, $\sigma^{(2)} = -1.5\times10^{-18}$ e.s.u., $\lambda = 10^{-10}$ e.s.u., and typical parameters are $R = 10^{-8}$ cm, whence

$$[13] \qquad \sigma = 2\times10^{-5} - 2\times10^{-12}E_z - 10^{-18}E^2 - \ldots$$

Thus for $E = 10^5$ e.s.u. (the field 7 Å from a proton), the shielding proportional to E is $\sim$0.2 p.p.m., and is $\sim$20 times that proportional to E^2.

The sign of $\sigma^{(1)}$ is opposite to that of λ. However, in most X—H bonds, it is reasonable to assume that there is an increased electronic charge between the nuclei (as for a positive λ), so that an electric field in the X—H direction will tend to draw this excess charge further away from the proton, thereby decreasing its shielding constant. Equation [13] indicates that the change in σ arising from the action of an electric field on an XH bond is approximately $-2\times10^{-12}E_z - 10^{-18}E^2$, and the measurements discussed later in this paper confirm this result in the case of CH bonds.

SOLVENT EFFECTS

When a polar molecule is dissolved, it polarizes the surrounding medium, and this polarization leads to an electric field—the "reaction field"—at the solute. If the molecule is sufficiently symmetrical, the mean reaction field is parallel and proportional to its dipole moment. For the Onsager model (6), in which the solute molecule is represented by a sphere of radius r containing a point dipole of moment μ at its center, and the solvent by a continuum of dielectric constant ϵ, the reaction field $\mathbf{R}$ is

$$[14] \qquad \mathbf{R} = \frac{2(\epsilon-1)}{2\epsilon+1}\frac{\mathbf{m}}{r^3} = \frac{2(\epsilon-1)(n^2-1)}{3(2\epsilon+n^2)}\frac{\mathbf{\mu}}{\alpha}$$

where $\mathbf{m} = \mathbf{\mu} + \alpha\mathbf{R}$ is the total dipole moment of the solute in the medium, $\alpha = \frac{n^2-1}{n^2+2}r^3$ being the polarizability of the sphere, and n the refractive index of the pure solute (as a liquid or solid). Thus $n^2 \sim 2.5$, and

$$[15] \qquad \mathbf{R} = \frac{\epsilon-1}{2\epsilon+2.5}\frac{\mathbf{\mu}}{\alpha}.$$

Protons are normally on the "surface" of a molecule and are therefore exposed to direct contact with the surrounding molecules, so that the Onsager field [14] is probably frequently a poor approximation to the actual reaction field acting on a proton, although it might adequately describe the field at a nucleus in the interior of a molecule. (Thus the C^{13} screening constants in substituted methanes $C^{13}X_nY_{4-n}$ should be approximately linearly dependent on $(\epsilon-1)/(2\epsilon+2.5)$.) Local solvent effects due to polar groups near a proton are probably important; thus in the non-dipolar molecule 1,4-dinitrobenzene, fields arising from the induced charges on the solvent molecules near the highly polar

Can. J. Chem. Downloaded from www.nrcresearchpress.com by 41.223.56.140 on 09/04/12
For personal use only.

nitro groups probably lead to electric fields at the protons, even though $\mu = 0$. The reaction field gradient R' for a model similar to Onsager's is (7)

$$R' = \frac{6(\epsilon-1)}{3\epsilon+2}\frac{\Theta}{r^5} \qquad [16]$$

where Θ is the molecular quadrupole moment; for a molecule with two opposed dipolar groups of moment μ separated by a distance d, $\Theta = 2\,\mu d$. Figure 1 shows the probable

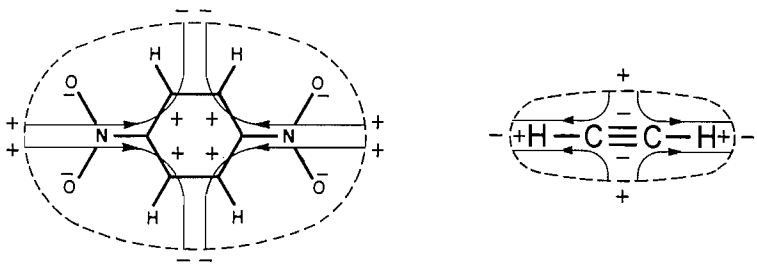


FIG. 1. Quadrupolar reaction fields in 1,4-dinitrobenzene and in acetylene.

form of the reaction field in 1,4-dinitrobenzene and in acetylene. If one of the protons in acetylene were replaced by an electronegative group (e.g., F, Cl, CN) a larger solvent shift would be expected, for in this case the shifts due to R and to R' are both to lower magnetic field strengths. When both R and R' are important, [15] and [16] indicate that σ should be approximately linearly dependent on $(\epsilon-1)/(\epsilon+1)$.

DISCUSSION

Although the well-known inductive and mesomeric effects undoubtedly play an important part in determining charge distributions in substituted aromatic molecules, the protons are isolated from the ring by sigma bonds, making it dangerous to try to correlate proton signals with pi-electron densities on the associated carbon atoms, or with Hammett acidity functions. In fact, it is shown in this section that the general pattern of proton screening constants in mono- and poly-substituted benzenes can be largely explained in terms of [13] and "internal" and "reaction" fields.

Consider a substituted benzene C_6H_5X, in which there is a "bond-dipole" μ as shown. If μ is situated at a point distant half-way along the X—C bond, and if the benzene ring is a regular hexagon, then the electric fields at the five protons, in the directions of the various CH bonds, are (if μ is the only significant contributor to the field)

$$E_{CH_2} = E_{CH_6} = \frac{4\mu\{10l_{CC}^2-8l_{CH}^2-2l_{CX}^2+10l_{CC}l_{CH}+5l_{CC}l_{CX}+13l_{CH}l_{CX}\}}{\{4l_{CC}^2+4l_{CH}^2+l_{CX}^2+4l_{CC}l_{CH}+2l_{CC}l_{CX}-2l_{CH}l_{CX}\}^{5/2}}$$

$$E_{CH_3} = E_{CH_5} = \frac{4\mu\{42l_{CC}^2+8l_{CH}^2+2l_{CX}^2+42l_{CC}l_{CH}+21l_{CC}l_{CX}+13l_{CH}l_{CX}\}}{\{12l_{CC}^2+4l_{CH}^2+l_{CX}^2+12l_{CC}l_{CH}+6l_{CC}l_{CX}+2l_{CH}l_{CX}\}^{5/2}} \qquad [17]$$

$$E_{CH_4} = \frac{16\mu}{\{4l_{CC}+2l_{CH}+l_{CX}\}^3}$$

where l_{AB} is the length of the A—B bond. For $l_{CC} = 1.39$ Å, $l_{CH} = 1.07$ Å, $l_{CX} = 2.0$ Å

$$\begin{aligned} E_{CH_2} &= 8.74\times10^{22}\,\mu; & E_2^2 &= 82.8\times10^{44}\,\mu^2, \\ E_{CH_3} &= 2.32\times10^{22}\,\mu; & E_3^2 &= 5.88\times10^{44}\,\mu^2, \\ E_{CH_4} &= 1.75\times10^{22}\,\mu; & E_4^2 &= 3.07\times10^{44}\,\mu^2. \end{aligned} \qquad [18]$$

Can. J. Chem. Downloaded from www.nrcresearchpress.com by 41.223.56.140 on 09/04/12
For personal use only.

Thus for an isolated nitrobenzene molecule, $\mu \sim 4\times10^{-18}$ e.s.u., so that [13] leads to the following contributions to σ arising from E_z and E^2

$$\begin{aligned}\sigma_{H_2} = \sigma_{H_6} &= -0.70\times10^{-6}-0.13\times10^{-6},\\ \sigma_{H_3} = \sigma_{H_5} &= -0.19\times10^{-6}-0.01\times10^{-6},\\ \sigma_{H_4} &= -0.14\times10^{-6}-0.005\times10^{-6}.\end{aligned} \qquad [19]$$

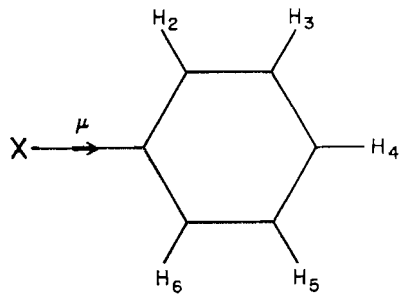
From [19], it is clear that the approximately isotropic E^2 effect is of secondary importance, and is negligible except where the "source" of the electric field is close to the proton (as, for example, in hydrogen bonds (8)). If the electric field effects are the only significant contributors to the relative chemical shifts, [19] indicates that in gaseous nitrobenzene, for example, the *o*-protons should have the largest shift to low field (relative to benzene itself), followed by the *m*- and *p*-hydrogens. Unfortunately, there are no data on gaseous substituted benzenes, but in solution in cyclohexane (9) the *o*-proton in $C_6H_5NO_2$ is shifted by -0.97, the *m*, -0.30, and the *p*, -0.42 p.p.m. relative to benzene in the same solvent.

The reaction field R of [15] tends to shift the H_3 and H_4 signals to low field (H_3 being influenced less than H_4) and H_2 to high field. These data (9) were obtained in a solvent which was a mixture of equal volumes of cyclohexane and nitrobenzene, for which $\epsilon = 16$, so that for $\mu/\alpha = 4.0\times10^5$, $R = 1.7\times10^5$ e.s.u. When E_z in [13] is put equal to $R\cos\phi$, where ϕ is the angle between **R** and a C—H axis, the following solvent shifts are obtained:

$$(\sigma_{H_2})_s = 0.14\times10^{-6},\quad (\sigma_{H_3})_s = -0.20\times10^{-6},\quad (\sigma_{H_4})_s = -0.37\times10^{-6}. \qquad [20]$$

Combining [19] and [20], it is found that the *o*-, *m*-, and *p*-protons should be shifted by -0.69, -0.40, and -0.51 p.p.m. relative to benzene, in qualitative agreement with the above facts. If this is a valid interpretation of the $C_6H_5NO_2$ spectrum, polar aliphatic solvents (e.g., acetone, acetonitrile) should increase the separation between the *m*- and *p*-proton signals, and bring the *o*-peak closer to the *p*-one (relative to the situation in a non-polar solvent like CCl_4).

If the sign of μ is changed (as, for example, in $C_6H_5NH_2$) E is reversed and shifts to higher field are expected. Also, since the E and E^2 effects now act in opposite directions, the *o*-signal should be closer to the *m*- and *p*-ones. These expectations are in accord with the facts (10).



The proton resonance spectrum of di- and tri-substituted benzenes should be interpretable in terms of the model. Thus in 1,2-dichlorobenzene, the difference between the electric fields acting along the CH_3 and CH_4 axes is (from [18]) $6.99\times10^{22}\,\mu$, and for a C—Cl bond dipole moment of 1.7×10^{-18} e.s.u., [13] leads to a difference in the resonance

Can. J. Chem. Downloaded from www.nrcresearchpress.com by 41.223.56.140 on 09/04/12
For personal use only.

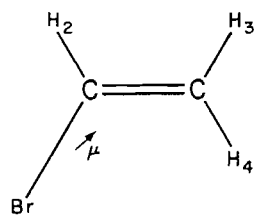
frequencies of the H_3 and H_4 protons of -0.24 p.p.m. The observed value is -0.25 p.p.m. for a solution in CCl_4 (11). The model predicts that increasing the polarity of the solvent will not affect H_3, but will shift the H_4 signal to lower field. Similarly, in 1,2,3-trichlorobenzene in CCl_4, the signal from H_4 and H_6 should be shifted -0.22 p.p.m. relative to that from H_5, but this difference should decrease as the polarity of the solvent increases. The observed shift in CCl_4 is -0.23 p.p.m. (11).

The effects of solvents on the chemical shifts of the protons in the 2- and 3-positions in some 1,4-disubstituted benzenes have been investigated by Schaefer and Schneider (12). They found that in *p*-methyl nitrobenzene the *m*-proton screening constant is shifted by -0.29 p.p.m. on changing the solvent from *n*-hexane to acetone. The corresponding shift for the *o*-proton is -0.06 p.p.m. Thus, although the *o*-proton is closer to the polar NO_2 group, its solvent shift is smaller. Our model is capable of explaining this, for the reaction field **R** is parallel to the 1-4 axis and therefore leads to a *m*-proton screening constant of $\frac{1}{2}\sigma^{(1)}R$ (that is, a shift to lower field, for $\sigma^{(1)}$ is negative) and an ortho shift of the same magnitude to higher field. (The small observed negative solvent shift (-0.06 p.p.m.) for the *o*-proton is partly due to an R^2 effect (this leads to a relative shift of -0.02 p.p.m.) but chiefly to the inadequacy of [15] for describing the reaction field in the immediate neighborhood of a highly polar group.) The difference between the *o*- and *m*-proton shifts in changing the solvent from *n*-hexane to acetone (-0.23×10^{-6}) should be approximately given by

$$\left\{\left(\frac{\epsilon-1}{2\epsilon+2.5}\right)_{\text{acetone}}-\left(\frac{\epsilon-1}{2\epsilon+2.5}\right)_{\text{hexane}}\right\}\frac{\mu}{\alpha}\sigma^{(1)}.$$

Taking $\mu/\alpha = 3.3\times10^5$ e.s.u., this leads to $\sigma^{(1)} = -2.6\times10^{-12}$ (confirming the order of magnitude of the estimate in [13]). However, our model cannot explain the large positive shift of the *m*-proton relative to the *o*-proton on changing the solvent from *n*-hexane to benzene. It is clear that some other type of interaction between *p*-methyl nitrobenzene and benzene must exist; Schaefer and Schneider (12) postulated hydrogen bonding between the *m*-proton and the π-electrons of the neighboring benzene molecule.

The model should sometimes be helpful in assigning observed peaks to particular protons. Thus in vinyl bromide, the direction of the "bond" dipole moment is probably approximately along the line joining the bromine nucleus to the mid-point of the C=C bond. The reaction field is therefore approximately parallel to the CH_3 and

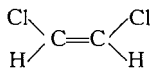


perpendicular to the CH_4 bonds. Hence, it can be anticipated that the H_3 resonance signal will be shifted more (to low field) than that of H_4 on increasing the dielectric constant of the aliphatic solvent.

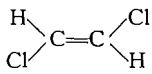
In *cis*- and *trans*-1,2-dichloroethene (I and II) "local" effects are probably approximately the same for all protons, whereas only I has an effect due to a dipolar reaction field. Thus the protons in I should have a larger low-field shift on changing the solvent

Can. J. Chem. Downloaded from www.nrcresearchpress.com by 41.223.56.140 on 09/04/12
For personal use only.

from hexane to acetone; since μ/α for I is 2.3×10^5, the expected difference is -0.07 p.p.m.; the experimental value is -0.08 p.p.m. (13).



I



II

Equation [16] for the quadrupolar reaction field implies that appreciable solvent shifts will occur in non-dipolar molecules like 1,4-dinitrobenzene, for which $\Theta \sim -20\times10^{-26}$ e.s.u. The four protons will experience a reaction field $R = -(R'r \cos 30°)/2$ along the C—H bonds, and this should lead to a shift of -0.15 p.p.m. on changing the solvent from *n*-hexane to acetone. In NNN′N′-tetramethyl *p*-phenylene diamine Θ will be positive, so the corresponding shift should be positive. For acetylene, $\Theta \sim 3\times10^{-26}$ e.s.u. and $R = R'r$, so that the corresponding shift in the proton signals should be -0.19 p.p.m. Thus protons near polar groups experience "local" solvent electric fields which may be comparable to those due to the reaction fields of polar molecules. Fortunately both are approximately proportional to $(\epsilon-1)/(\epsilon+1)$, so that if other solvent influences (such as shape effects coupled with diamagnetic anisotropy, as in benzene or diacetylene, or strong van der Waals forces, as in CH_2I_2, or strong specific interactions, as in hydrogen bonded substances (14)) are absent σ should vary approximately linearly with this solvent parameter.

ACKNOWLEDGMENTS

The author is grateful to Dr. W. G. Schneider for a number of very helpful discussions and for inviting him to spend the summer of 1959 in Ottawa, and to Dr. T. Schaefer for communicating experimental results to him.

REFERENCES

1. Pople, J. A., Schneider, W. G., and Bernstein, H. J. High resolution nuclear magnetic resonance. McGraw-Hill Book Co., Inc., New York. 1959. Section 7.4.
2. Saika, A. and Slichter, C. P. J. Chem. Phys. **22**, 26 (1954).
3. Reference 1. Section 7.5 *b*.
4. Marshall, T. W. and Pople, J. A. Mol. Phys. **1**, 199 (1958).
5. Stephen, M. J. Mol. Phys. **1**, 223 (1958).
6. Onsager, L. J. Am. Chem. Soc. **58**, 1486 (1936).
7. Buckingham, A. D. J. Chem. Phys. **30**, 1580 (1959).
8. Schneider, W. G., Bernstein, H. J., and Pople, J. A. J. Chem. Phys. **28**, 601 (1958).
9. Corio, P. L. and Dailey, B. P. J. Am. Chem. Soc. **78**, 3043 (1956).
10. Reference 1. p. 260. Figs. 11–15.
11. Reference 1. p. 263.
12. Schaefer, T. and Schneider, W. G. J. Chem. Phys. In press.
13. Schaefer, T. University of Manitoba, Winnipeg, Man. Personal communication.
14. Buckingham, A. D., Schaefer, T., and Schneider, W. G. J. Chem. Phys. To be published.

Can. J. Chem. Downloaded from www.nrcresearchpress.com by 41.223.56.140 on 09/04/12
For personal use only.

Can. J. Chem. Downloaded from www.nrcresearchpress.com by 41.223.56.140 on 09/04/12
For personal use only.

NOTES

THE REACTION OF SODIUM METAPERIODATE WITH SOME NITROGEN DERIVATIVES OF CARBOHYDRATES

M. J. Abercrombie and J. K. N. Jones

Methods which might be used in the chemical degradation of carbon-14-labelled carbohydrates required an investigation of the reaction of sodium metaperiodate with certain nitrogen-containing carbohydrate derivatives. The aim of these experiments was to convert specific carbon atoms of the carbohydrates to formic acid, which could then be oxidized to carbon dioxide with mercuric acetate. The carbon dioxide was then converted to barium carbonate and its activity determined.

The oxidation of phenylosazones (1) and phenylosotriazoles (2) by sodium metaperiodate resulted in the rapid consumption of the theoretical quantity of metaperiodate. This was followed, in the case of the phenylosazones, by a slow overoxidation by the metaperiodate. Recently the metaperiodate oxidation of some phenylhydrazones has been reported by O'Donnel and Percival (3), who found that the consumption of oxidant corresponded to the amount required for an acyclic structure. They did not determine the quantities of formaldehyde and formic acid produced during the oxidation.

D-Mannose phenylhydrazone and D-xylose 2,4-dinitro-phenylhydrazone have been oxidized with sodium metaperiodate in aqueous ethanol; the metaperiodate consumed, the formic acid and formaldehyde produced were then measured.

The experimental and theoretical results, for an acyclic structure are shown in Table I (mole/mole).

TABLE I

	Theoretical			Experimental		
	IO_4	HCHO	HCOOH	IO_4	HCHO	HCOOH
D-Mannose phenylhydrazone	4.00	1.00	3.00	4.05	1.05	2.96
D-Xylose 2,4-dinitro-phenylhydrazone	3.00	1.00	2.00	3.02	1.01	2.06

These phenylhydrazones probably exist in solution as cyclic structures. On oxidation they form unstable intermediates which break down further.

The metaperiodate uptake and the formic acid released were determined using the procedure quoted by Hough (1). The formaldehyde was determined by the method of Perry and Pietak (4). The experimental results show that both of the compounds are oxidized in the open chain form by metaperiodate.

The metaperiodate oxidation of two other nitrogen derivatives was studied; these were 6-*O*-toluene-*p*-sulphonyl-(tosyl)-D-glucose phenylosotriazole and 6-*O*-benzoyl-D-glucose phenylosotriazole. The metaperiodate uptake and formaldehyde produced were determined as described above. Table II shows the theoretical and experimental results.

The experimental results show that only the hydroxyl group on position 6 has been substituted thus the periodate oxidation releases carbon 4 as formic acid. This carbon atom of D-mannose is difficult to isolate by standard procedure.

TABLE II

	Theoretical		Experimental	
	IO_4	HCHO	IO_4	HCHO
6-*O*-Tosyl-D-glucose phenylosotriazole	2.00	0.00	2.05	0.07
6-*O*-Benzoyl-D-glucose phenylosotriazole	2.00	0.00	1.98	0.00

EXPERIMENTAL

The 2,4-dinitro-phenylhydrazone of D-xylose was prepared by the method of Lloyd (5) and the mannose phenylhydrazone by the standard method (6).

6-O-Toluene-p-sulphonyl-D-glucose Phenylosotriazole

D-Glucose phenylosotriazole was prepared by the method of Hudson (2). To 0.5 g of the D-glucose phenylosotriazole dissolved in 15 ml of pyridine was added 0.39 g of toluene-*p*-sulphonyl chloride (1:1.2 mole). The solution was kept overnight at room temperature and was then added to 50 ml of crushed ice. The white precipitate thus produced was collected and the product washed with dilute acetic acid, water, and ethanol. The product was crystallized from ethanol (yield 0.52 g, 70%), m.p. 149–150°. Calc. for $C_{19}H_{21}O_6N_3S$: C, 54.50%; H, 5.10%. Found: C, 54.54%; H, 5.17%.

6-O-Benzoyl-D-glucose Phenylosotriazole

This was prepared in a manner similar to that of the previous compound. The product was recrystallized from ethanol by the addition of water until the solution became turbid. When the solution was left standing, long, white, needle-shaped crystals were obtained (yield 45%), m.p. 166–167°. Calc. for $C_{19}H_{19}O_5N_3$: C, 61.70%; H, 5.15%. Found: C, 61.95%; H, 5.39%.

ACKNOWLEDGMENTS

The authors wish to thank Miss T. Pietak for technical assistance, and one of us (M.J.A.) thanks the National Research Council for a scholarship.

1. Hough, L., Powell, D. B., and Woods, B. M. J. Chem. Soc. 4799 (1956). Chargaff, E. and Magansanik, B. J. Am. Chem. Soc. **69**, 1459 (1947). Courtois, J. E., Wickstrom, A., and Le Dizet, P. Bull. soc. chim. France, 1006 (1952).
2. Haskins, W. T., Hann, R. M., and Hudson, C. S. J. Am. Chem. Soc. **67**, 939 (1945); **68**, 1766 (1946); **69**, 1050 (1947).
3. O'Donnel, J. J. and Percival, E. J. Chem. Soc. 2312 (1959).
4. Perry, M. B. and Pietak, T. (Personal communication.) To be published.
5. Lloyd, E. A. and Doherty, D. G. J. Am. Chem. Soc. **74**, 4214 (1952).
6. Butler, C. L. and Cretcher, L. H. J. Am. Chem. Soc. **53**, 4358 (1931).

Received October 13, 1959.
Department of Chemistry,
Queen's University,
Kingston, Ontario.

ELECTRON SPIN RESONANCE ABSORPTION OF BORO-ULTRAMARINE

Yoshio Matsunaga*

The color of ultramarine has been known to be associated with the presence of regulated amounts of alkali and polysulphide sulphur. Gardner and Fraenkel (1) found that ultra-

**N.R.C. Postdoctoral Fellow 1957–59. On leave of absence from Department of Chemistry, University of Tokyo, Tokyo, Japan.*

Can. J. Chem. Downloaded from www.nrcresearchpress.com by 41.223.56.140 on 09/04/12
For personal use only.

TABLE II

	Theoretical		Experimental	
	IO_4	HCHO	IO_4	HCHO
6-*O*-Tosyl-D-glucose phenylosotriazole	2.00	0.00	2.05	0.07
6-*O*-Benzoyl-D-glucose phenylosotriazole	2.00	0.00	1.98	0.00

EXPERIMENTAL

The 2,4-dinitro-phenylhydrazone of D-xylose was prepared by the method of Lloyd (5) and the mannose phenylhydrazone by the standard method (6).

6-O-Toluene-p-sulphonyl-D-glucose Phenylosotriazole

D-Glucose phenylosotriazole was prepared by the method of Hudson (2). To 0.5 g of the D-glucose phenylosotriazole dissolved in 15 ml of pyridine was added 0.39 g of toluene-*p*-sulphonyl chloride (1:1.2 mole). The solution was kept overnight at room temperature and was then added to 50 ml of crushed ice. The white precipitate thus produced was collected and the product washed with dilute acetic acid, water, and ethanol. The product was crystallized from ethanol (yield 0.52 g, 70%), m.p. 149–150°. Calc. for $C_{19}H_{21}O_6N_3S$: C, 54.50%; H, 5.10%. Found: C, 54.54%; H, 5.17%.

6-O-Benzoyl-D-glucose Phenylosotriazole

This was prepared in a manner similar to that of the previous compound. The product was recrystallized from ethanol by the addition of water until the solution became turbid. When the solution was left standing, long, white, needle-shaped crystals were obtained (yield 45%), m.p. 166–167°. Calc. for $C_{19}H_{19}O_5N_3$: C, 61.70%; H, 5.15%. Found: C, 61.95%; H, 5.39%.

ACKNOWLEDGMENTS

The authors wish to thank Miss T. Pietak for technical assistance, and one of us (M.J.A.) thanks the National Research Council for a scholarship.

1. Hough, L., Powell, D. B., and Woods, B. M. J. Chem. Soc. 4799 (1956). Chargaff, E. and Magansanik, B. J. Am. Chem. Soc. **69**, 1459 (1947). Courtois, J. E., Wickstrom, A., and Le Dizet, P. Bull. soc. chim. France, 1006 (1952).
2. Haskins, W. T., Hann, R. M., and Hudson, C. S. J. Am. Chem. Soc. **67**, 939 (1945); **68**, 1766 (1946); **69**, 1050 (1947).
3. O'Donnel, J. J. and Percival, E. J. Chem. Soc. 2312 (1959).
4. Perry, M. B. and Pietak, T. (Personal communication.) To be published.
5. Lloyd, E. A. and Doherty, D. G. J. Am. Chem. Soc. **74**, 4214 (1952).
6. Butler, C. L. and Cretcher, L. H. J. Am. Chem. Soc. **53**, 4358 (1931).

Received October 13, 1959.
Department of Chemistry,
Queen's University,
Kingston, Ontario.

ELECTRON SPIN RESONANCE ABSORPTION OF BORO-ULTRAMARINE

Yoshio Matsunaga*

The color of ultramarine has been known to be associated with the presence of regulated amounts of alkali and polysulphide sulphur. Gardner and Fraenkel (1) found that ultra-

**N.R.C. Postdoctoral Fellow 1957–59. On leave of absence from Department of Chemistry, University of Tokyo, Tokyo, Japan.*

Can. J. Chem. Downloaded from www.nrcresearchpress.com by 41.223.56.140 on 09/04/12
For personal use only.

marines show electron spin resonance absorption with a g-value of 2.029. On the basis of the similarity of the g-value of the radicals in ultramarine, in liquid sulphur 2.024 (2), and in the blue solution of sulphur in oleum 2.016 and 2.026 (3), they have suggested that the paramagnetism of ultramarine arises from some type of sulphur radical. Previously we have observed that the color, the intensity, and the g-value of resonance absorption of ultramarine change almost reversibly with the replacement of sodium ion by silver ion and vice versa (4). This observation can be explained by the assumption that unpaired electrons are associated with polysulphide ions and can interact with each other through cations. Here we wish to present further results which support this view.

It has been known that the fusion of borax, boric acid, and sodium sulphite gives a stable blue product (5). The presence of alkali and excess of boric acid is required to produce blue color. Sulphite can be replaced by sulphur or polysulphides. This system seemed to be more easily controllable than ordinary ultramarine, therefore we examined the electron spin resonance absorption of this so-called boro-ultramarine. The mixture of borax, boric acid, and sodium sulphite was heated to 750° C in an electric furnace. At this temperature sodium sulphite decomposes to sulphate and sulphide (6).

The electron spin resonance absorption spectrum of boro-ultramarine is not simple and seems to consist of three peaks, namely a main peak with a g-value of 2.209 and shoulders at both sides as shown in Fig. 1. This pattern does not depend on the composition of the starting mixture. The g-value of the main absorption is in good agreement with that

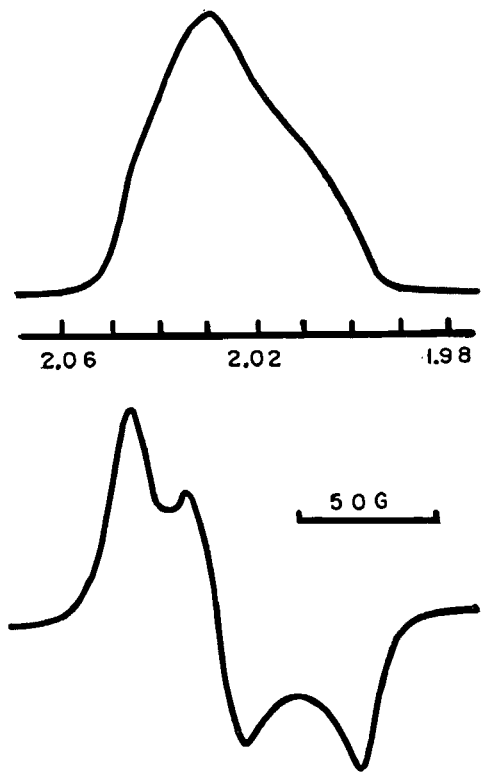


FIG. 1. Electron spin resonance absorption of boro-ultramarine at 9 kMc/s and at room temperature. Lower curve is derivative as recorded and upper curve is the integrated one.

Can. J. Chem. Downloaded from www.nrcresearchpress.com by 41.223.56.140 on 09/04/12
For personal use only.

of ordinary blue alkali-ultramarine. Ingram and Symons (7, 8) studied in more detail the resonance absorption of the sulphur–oleum system and postulated that the resonance absorption with a high *g*-value is caused by brown polymeric sulphur radicals similar to those in liquid sulphur. The difference of color and *g*-value of these sulphur radicals can be attributed to the effect of the medium as seen in the case of substituted ultramarines. Therefore, we may conclude that the blue color and the unpaired electrons in ordinary and boro-ultramarines arise from polysulphide sulphur in coexistence with alkali ions. The shoulder with a *g*-value of about 2.01 may correspond to the blue radical in the sulphur–oleum system. The latter was assigned to monomeric sulphur sesquioxide by Symons (8). The formation of the same compound at high temperature in our borax – boric oxide system containing sulphate and sulphide seems to be likely. The other shoulder has a *g*-value of about 2.04. The nature of this radical is not clear and such a high *g*-value has not been found in the other radicals containing sulphur.

We also examined the boro-ultramarine containing selenium instead of sulphur, but no electron spin resonance absorption was detected with the red product.

Thanks are due to Professor C. A. McDowell for his interest and encouragement throughout this work. The research was supported by grants from the National Research Council of Canada, and thanks are due to that body for its generosity.

1. Gardner, D. M. and Fraenkel, G. K. J. Am. Chem. Soc. **77**, 6399 (1955).
2. Gardner, D. M. and Fraenkel, G. K. J. Am. Chem. Soc. **78**, 3279 (1956).
3. Gardner, D. M. and Fraenkel, G. K. J. Am. Chem. Soc. **78**, 6411 (1956).
4. Matsunaga, Y. Can. J. Chem. **37**, 994 (1959).
5. Hoffmann, J. Z. anorg. u. allgem. Chem. **183**, 37 (1929), and his previous papers cited therein.
6. Foerster, F. and Kubel, K. Z. anorg. u. allgem. Chem. **139**, 261 (1924).
7. Ingram, D. J. E. and Symons, M. C. R. J. Chem. Soc. 2437 (1957).
8. Symons, M. C. R. J. Chem. Soc. 2440 (1957).

Received October 16, 1959.
Department of Chemistry,
University of British Columbia,
Vancouver 8, B.C.

A CHEMICAL SYNTHESIS OF 4-*O*-METHYL-D-GLUCURONIC ACID

W. D. S. Bowering and T. E. Timell

A chemical synthesis of 4-*O*-methyl-D-glucuronic acid has so far not been reported (1), although the compound has been obtained from numerous polysaccharides and a method for its large-scale preparation has been developed (2). This note is concerned with the synthesis of 4-*O*-methyl-D-glucuronic acid from methyl α-D-glucopyranoside.

Methyl 4-*O*-methyl-α-D-glucoside was prepared from methyl α-D-glucopyranoside in a yield of 18.5%, essentially according to the method of McGilvray (3, 4). Contrary to all expectations, oxidation of the 2,3-di-*O*-benzyl derivative of this compound with permanganate (5) failed to produce the expected uronic acid, nor was it possible to introduce a carboxyl group at C_6 in the methyl 4-*O*-methyl-α-D-glucoside by oxidation with air or oxygen in the presence of a platinum catalyst (6, 7). Oxidation of the glucoside with sodium nitrite in phosphoric acid (8), followed by hydrolysis, yielded a mixture of sugars, the acid portion of which was resolved on an anion exchange resin, resulting in the isolation of chromatographically pure 4-*O*-methyl-D-glucuronic acid in a yield of 1–2%. The compound was identified by reduction of its methyl ester – methyl glycoside, followed

Can. J. Chem. Downloaded from www.nrcresearchpress.com by 41.223.56.140 on 09/04/12
For personal use only.

of ordinary blue alkali-ultramarine. Ingram and Symons (7, 8) studied in more detail the resonance absorption of the sulphur–oleum system and postulated that the resonance absorption with a high *g*-value is caused by brown polymeric sulphur radicals similar to those in liquid sulphur. The difference of color and *g*-value of these sulphur radicals can be attributed to the effect of the medium as seen in the case of substituted ultramarines. Therefore, we may conclude that the blue color and the unpaired electrons in ordinary and boro-ultramarines arise from polysulphide sulphur in coexistence with alkali ions. The shoulder with a *g*-value of about 2.01 may correspond to the blue radical in the sulphur–oleum system. The latter was assigned to monomeric sulphur sesquioxide by Symons (8). The formation of the same compound at high temperature in our borax – boric oxide system containing sulphate and sulphide seems to be likely. The other shoulder has a *g*-value of about 2.04. The nature of this radical is not clear and such a high *g*-value has not been found in the other radicals containing sulphur.

We also examined the boro-ultramarine containing selenium instead of sulphur, but no electron spin resonance absorption was detected with the red product.

Thanks are due to Professor C. A. McDowell for his interest and encouragement throughout this work. The research was supported by grants from the National Research Council of Canada, and thanks are due to that body for its generosity.

1. Gardner, D. M. and Fraenkel, G. K. J. Am. Chem. Soc. **77**, 6399 (1955).
2. Gardner, D. M. and Fraenkel, G. K. J. Am. Chem. Soc. **78**, 3279 (1956).
3. Gardner, D. M. and Fraenkel, G. K. J. Am. Chem. Soc. **78**, 6411 (1956).
4. Matsunaga, Y. Can. J. Chem. **37**, 994 (1959).
5. Hoffmann, J. Z. anorg. u. allgem. Chem. **183**, 37 (1929), and his previous papers cited therein.
6. Foerster, F. and Kubel, K. Z. anorg. u. allgem. Chem. **139**, 261 (1924).
7. Ingram, D. J. E. and Symons, M. C. R. J. Chem. Soc. 2437 (1957).
8. Symons, M. C. R. J. Chem. Soc. 2440 (1957).

Received October 16, 1959.
Department of Chemistry,
University of British Columbia,
Vancouver 8, B.C.

A CHEMICAL SYNTHESIS OF 4-*O*-METHYL-D-GLUCURONIC ACID

W. D. S. Bowering and T. E. Timell

A chemical synthesis of 4-*O*-methyl-D-glucuronic acid has so far not been reported (1), although the compound has been obtained from numerous polysaccharides and a method for its large-scale preparation has been developed (2). This note is concerned with the synthesis of 4-*O*-methyl-D-glucuronic acid from methyl α-D-glucopyranoside.

Methyl 4-*O*-methyl-α-D-glucoside was prepared from methyl α-D-glucopyranoside in a yield of 18.5%, essentially according to the method of McGilvray (3, 4). Contrary to all expectations, oxidation of the 2,3-di-*O*-benzyl derivative of this compound with permanganate (5) failed to produce the expected uronic acid, nor was it possible to introduce a carboxyl group at C_6 in the methyl 4-*O*-methyl-α-D-glucoside by oxidation with air or oxygen in the presence of a platinum catalyst (6, 7). Oxidation of the glucoside with sodium nitrite in phosphoric acid (8), followed by hydrolysis, yielded a mixture of sugars, the acid portion of which was resolved on an anion exchange resin, resulting in the isolation of chromatographically pure 4-*O*-methyl-D-glucuronic acid in a yield of 1–2%. The compound was identified by reduction of its methyl ester – methyl glycoside, followed

Can. J. Chem. Downloaded from www.nrcresearchpress.com by 69.46.99.164 on 09/04/12
For personal use only.

by hydrolysis, when there was obtained 4-*O*-methyl-D-glucose, characterized through its crystalline phenylosazone derivative (9).

EXPERIMENTAL

Preparation of Methyl 4-O-Methyl-α-D-glucoside

Methyl 2,3-di-*O*-benzyl-6-*O*-trityl-α-D-glycopyranoside (3, 4), $[\alpha]_D^{21}$ +14° (*c*, 4.6 in chloroform), was converted to methyl 2,3-di-*O*-benzyl-4-*O*-methyl-6-*O*-trityl-α-D-glucoside in an almost quantitative yield by one methylation according to Kuhn *et al.* (10). Anal. calc. for $C_{41}H_{42}O_6$:OCH_3, 9.8%. Found: OCH_3, 10.4%; $[\alpha]_D^{20}$ +30° (*c*, 1.6 in chloroform). Detritylation with aqueous acetic acid, followed by reductive debenzylation (3, 11), gave sirupy methyl 4-*O*-methyl-α-D-glucoside, which, after distillation *in vacuo*, was obtained in an over-all yield of 18.5%. Anal. calc. for $C_8H_{16}O_6$:OCH_3, 29.8%. Found: OCH_3, 28.6%; $[\alpha]_D^{20}$ +145° (*c*, 4.2 in ethanol). Hydrolysis gave 4-*O*-methyl-D-glucose, $[\alpha]_D^{22}$ +51° (*c*, 3.0 in water). Anal. calc. for $C_7H_{14}O_6$:OCH_3, 16.0%. Found: OCH_3, 15.5%. The osazone derivative had m.p. and mixed m.p. 159–160° (corr.).

Oxidation of Methyl 4-O-Methyl-α-D-glucoside

Methyl 4-*O*-methyl-α-D-glucoside (8.7 g) was dissolved in 85% phosphoric acid (200 ml) containing sodium nitrite (10 g) (8). After 17 hours at room temperature, water was added (25 ml) and the sirup obtained on evaporation was boiled under reflux for 5 hours in 0.5 *N* sulphuric acid (100 ml). The sirup obtained after neutralization (barium carbonate) contained approximately equal quantities of 4-*O*-methylglucuronic acid, glucuronic acid, 4-*O*-methylglucose, and glucose. The sugar mixture was resolved on a column of Dowex 1X4 (acetate form) anion exchange resin by elution with water, followed by 2 *N* acetic acid. The fractions containing 4-*O*-methylglucuronic acid only were concentrated to a sirup (0.12 g, 1.3%), $[\alpha]_D^{18}$ +35° (*c*, 1.3 in water). Anal. calc. for $C_7H_{12}O_7$:OCH_3, 14.9%. Found: OCH_3, 14.6%.

Characterization of 4-O-Methyl-D-glucuronic Acid

Chromatographically pure 4-*O*-methyl-D-glucuronic acid (73 mg) was converted to the methyl ester – methyl glycoside which was reduced with lithium aluminum hydride (0.5 g) in anhydrous tetrahydrofuran (30 ml). The sirup obtained after hydrolysis (40 mg) was chromatographically identical with 4-*O*-methyl-D-glucose, $[\alpha]_D^{19}$ +50° (*c*, 1.2 in water). Anal. Calc. for $C_7H_{14}O_6$:OCH_3, 16.0%. Found: OCH_3, 15.7%. The phenylosazone derivative had m.p. and mixed m.p. 158–159° C and gave an infrared spectrum indistinguishable from that of an authentic specimen.

1. Aspinall, G. O. Advances in Carbohydrate Chem. **9**, 131 (1954).
2. Gorin, P. A. J. Can. J. Chem. **35**, 595 (1957).
3. Dennison, J. C. and McGilvray, D. I. J. Chem. Soc. 1616 (1951).
4. McGilvray, D. I. J. Chem. Soc. 3648 (1952).
5. Edington, R. A., Hirst, E. L., and Percival, E. E. J. Chem. Soc. 2281 (1955).
6. Mehltretter, C. L., Alexander, B. H., Mellies, R. L., and Rist, C. E. J. Am. Chem. Soc. **73**, 2424 (1951).
7. Marsh, C. A. J. Chem. Soc. 1578 (1952).
8. Machida, S., Uchino, N., and Inano, M. Bull. Fac. Text. Fibers, Kyoto Univ. **1**, No. 3, 459 (1956).
9. Schinle, R. Ber. **65**, 315 (1932).
10. Kuhn, R., Trischmann, H., and Löw, I. Angew. Chem. **67**, 32 (1955).
11. Bell, D. J. and Lorber, J. J. Chem. Soc. 453 (1940).

Received October 15, 1959.
McGill University and
Pulp and Paper Research Institute of Canada,
Montreal, Que.

Can. J. Chem. Downloaded from www.nrcresearchpress.com by 69.46.99.164 on 09/04/12
For personal use only.

Can. J. Chem. Downloaded from www.nrcresearchpress.com by 69.46.99.164 on 09/04/12
For personal use only.

ARSENIDES OF THE TRANSITION METALS
III. A NOTE ON THE HIGHER ARSENIDES OF IRON, COBALT, AND NICKEL*

R. D. Heyding and L. D. Calvert

The metal-rich binary compounds formed by arsenic and the transition metals, iron, cobalt, and nickel, have been discussed in the first two papers of this series (1, 2). In continuation of these studies, the arsenic-rich regions of the binary phase diagrams have been investigated, and the compounds observed are described in this note.

The materials and experimental methods employed were similar to those recorded in the earlier papers. The alloys were prepared by direct combination of metal sponge containing less than 10 p.p.m. total impurities, and metallic arsenic containing less than 0.01% antimony. The latter was obtained by reduction of reagent grade arsenic trioxide with sugar charcoal and subsequent double or triple vacuum sublimation.

In general, the alloys formed readily at moderate temperatures. Since the decomposition pressures of the higher arsenides are appreciable, annealing temperatures were not allowed to exceed 900° C, consequently only the nickel alloys were fused. The quantities of arsenic which separated on quenching from temperatures above 700° C were prohibitive except for the cobalt alloys. Again, because of the high arsenic vapor pressures, no attempts were made to study these systems in the high temperature diffraction camera. Room temperature diffraction patterns were obtained in 11.46-cm Norelco Debye–Scherrer cameras using copper K_α (λ = 1.5405 Å) and cobalt K_α (λ = 1.7889 Å) radiation.

Synthesis of the minerals skutterudite ($CoAs_3$), loellingite ($FeAs_2$), rammelsbergite and pararammelsbergite ($NiAs_2$) has been reported by Holmes (3, 4). We have confirmed the appearance of these compounds in the binary phase systems; we were able to detect only one other compound, $CoAs_2$. There is no evidence to support the formation of the compound Co_2As_3 discussed in the literature (5), nor of any of the higher arsenides previously supposed to exist.

The Iron/Arsenic System

One arsenic-rich compound, $Fe(Fe_xAs_{2-x})$, is formed in this system. The terminal composition determined by sublimation of excess arsenic from an alloy/arsenic mixture in a small temperature gradient at 400° C corresponded to an As/Fe ratio of 1.93. No variation in interplanar spacing with alloy composition was observed, and we conclude that the homogeneity range is narrow. The compound is isostructural with loellingite (orthorhombic V_h^{12}, *Pmnn* (6, 7)), with unit cell dimensions a_0 = 2.882, b_0 = 5.300, c_0 = 5.982 Å. The dimensions reported for the mineral are a = 2.85, b = 5.25, c = 5.92 Å. The observed density of the terminal alloy was 7.35 g/cc; the crystallographic densities for $Fe_2As_{3.86}$, $Fe_2(Fe_{0.08}As_{3.92})$, and $Fe_{2.08}As_4$ would be 7.28, 7.44, and 7.55 g/cc, respectively. It appears most probable that the unit cell contains $2(Fe(Fe_xAs_{2-x}))$, x = 0.04, and that some iron atoms occupy arsenic lattice positions, which is the arrangement proposed for the mineral itself (7).

The Cobalt/Arsenic System

In this system two compounds, $CoAs_2$ and $CoAs_3$, are formed. The latter is isostructural with skutterudite (cubic T_h^5, *Im*3, Z = 8 (8)) with a unit cell edge of 8.206±0.002 Å; D_m = 6.71, D_x = 6.79 g/cc. This cell edge is somewhat greater than Holmes' value of

Issued as N.R.C. No. 5496.

8.187 Å for synthetic skutterudite (4). The unit cell of the mineral varies from 8.187 Å to 8.311 Å, depending on the extent of substitution of other transition metals for cobalt in the lattice.

The low order diffraction pattern of the compound $CoAs_2$ is recorded in Table I. This pattern is unaltered by any heat treatment below 900° C, and is unchanged in the presence of CoAs or $CoAs_3$.

TABLE I

Low order diffraction pattern of $CoAs_2$

I/I_0	d_{obs}	d_{calc}	hkl	I/I_0	d_{obs}	d_{calc}	hkl
3	3.81	3.81	102	80	1.656	1.657	320
6	2.92	2.94	200			1.654	205
11	2.78	2.75	120	13	1.635	1.634	321
51	2.66	2.66	210	13	1.623	1.624	224
		2.65	121	21	1.612	1.612	016
51	2.64	2.64	023	13	1.572	1.573	322
		2.63	113	26	1.559	1.556	040
100	2.53	2.53	202	33B	1.332	1.328	420
100B	2.41	2.41	122	33B	1.326	1.325	242
41	2.31	2.30	104			1.321	044
13	2.04	2.03	031	9	1.316	1.316	421
21	1.959	1.956	130			1.315	226
33	1.907	1.902	015	17	1.313	1.314	413
51	1.866	1.867	310	17	1.289	1.291	206
51	1.848	1.851	124			1.289	144
41	1.821	1.821	132	51	1.267	1.269	127
6	1.700	1.694	230			1.266	404
3	1.668	1.668	006	21	1.232	1.234	423

Fe-filtered Co radiation, $\lambda = 1.7889$ Å; camera diameter, 11.46 cm; cutoff, 20 Å; temperature, 24° C.
Tentative orthorhombic cell: $a_0 = 5.87$, $b_0 = 6.22$, $c_0 = 10.01$ Å; $D_{obs} = 7.56$; $Z = 8$.

In view of the similarity of the other compounds in these binary systems to those found in mineral systems, one might expect $CoAs_2$ and the corresponding mineral, safflorite, to be isostructural. Although there is some confusion in the literature with respect to the diffraction pattern of safflorite, it is shown quite clearly in Fig. 1 that the pattern of $CoAs_2$ is unlike any safflorite pattern. Moreover, safflorite invariably contains considerable quantities of iron, and is more accurately represented by the formula $(Fe,Co)As_2$. According to Peacock (7), the safflorite structure is similar to, but not isostructural with, the loellingite structure due to non-equivalence of Fe and Co positions. Accepting Peacock's crystal structure as the definition of the mineral, the synthetic counterpart of safflorite will be found only in the ternary Fe/Co/As system as $Fe_{1-x}Co_xAs_2$, in which the range of homogeneity may commence at $x = 0$, but will not extend to $x = 1$.

The orthorhombic unit cell proposed for $CoAs_2$ in Table I is offered only as a tentative solution obtained by the usual trial and error methods applied to powder diffraction patterns. Although de Jong's study (9) of the mineral diarsenides has been largely discredited, and although there is little apparent similarity in the pattern of $CoAs_2$ and de Jong's safflorite pattern (Fig. 1), our unit cell dimensions and those proposed by de Jong appear to be related by the transformation 001/100/020.

The Nickel/Arsenic System

One higher arsenide, $NiAs_2$, is formed in this system. It is dimorphic; the low temperature modification, α-$NiAs_2$, is isostructural with pararammelsbergite, while the high temperature modification, β-$NiAs_2$, is isostructural with rammelsbergite.

Can. J. Chem. Downloaded from www.nrcresearchpress.com by 69.46.99.164 on 09/04/12
For personal use only.

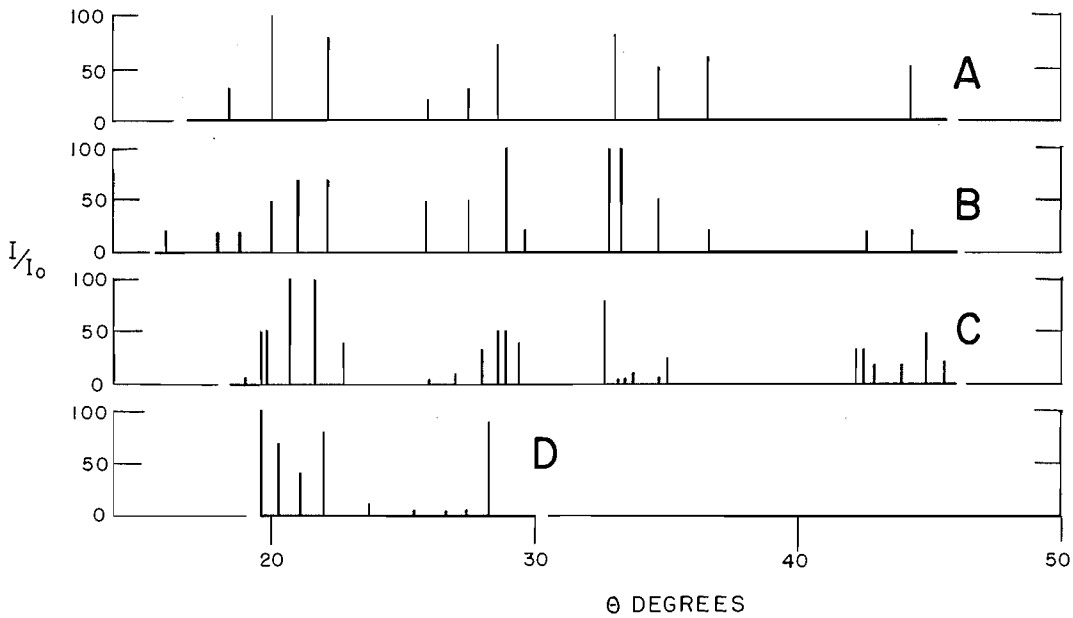


FIG. 1. Comparison of the low order diffraction patterns of safflorite and $CoAs_2$. (A) Safflorite; X-ray Powder Data File, card 2-0986. (B) Safflorite; X-ray Powder Data File, card 2-1317. (C) $CoAs_2$; this work. (D) Safflorite; de Jong (9).

Above 600° C nickel and arsenic in the proper proportions react to form β-$NiAs_2$. Unfortunately, the decomposition pressure is very appreciable, and we were unable to avoid disproportionation on cooling. However, small single crystals were recovered from the surface of several melts, and the patterns were identical with that of rammelsbergite (orthorhombic V_h^{12}, *Pmnn* (9, 10)). The unit cell dimensions are $a_0 = 3.54$, $b_0 = 4.76$, $c_0 = 5.79$ Å, in good agreement with Peacock's values of 3.53, 4.78, and 5.78 kX for the mineral. Terminal composition and density could not be determined. No variation in interplanar spacings with over-all sample composition could be detected.

Of all the compounds formed in these binary systems, α-$NiAs_2$ was the most difficult to obtain, and in fact was never obtained pure. Arsenic and nickel react rapidly to form NiAs even at an ambient temperature of 350° C, the heat of formation being sufficient to fuse the specimen. The subsequent attack of NiAs by excess arsenic is exceedingly slow below 500° C. The pattern of the product obtained by repeated grinding and reheating was identical with that of pararammelsbergite (10, 11, 12) in the presence of NiAs and As. Similarly, the transformation of β-$NiAs_2$ to α-$NiAs_2$ is exceptionally slow. In 6 weeks at 450° C the transformation was less than 20% complete judging from the relative intensities of the two patterns. The transformation of the α form to the β form occurs rapidly at 600° C.

Alloys containing As/Ni atomic ratios greater than two, when heated at 700° C and annealed at 450° C, exhibited only patterns of α- and β-$NiAs_2$ and arsenic, while alloys with As/Ni ratios less than two showed only the patterns of α- and β-$NiAs_2$ and NiAs. Consequently, although the precise constitution of the compound cannot be given, it cannot lie far from the simple 1:2 stoichiometric ratio. The orthorhombic unit cell dimensions are essentially identical with those proposed by Thompson (13) for pararammelsbergite: $a_0 = 5.75$, $b_0 = 5.82$, $c_0 = 11.43$ Å.

Can. J. Chem. Downloaded from www.nrcresearchpress.com by 69.46.99.164 on 09/04/12
For personal use only.

Detailed powder diffraction data for $Fe(Fe_xAs_{2-x})$, $CoAs_3$, $CoAs_2$, and β-$NiAs_2$ have been submitted to the X-ray Powder Data File.

We are indebted to Miss Theresa Clarke for assistance in obtaining Debye–Scherrer patterns, and to Mr. D. S. Russell for analysis of reactants and alloys.

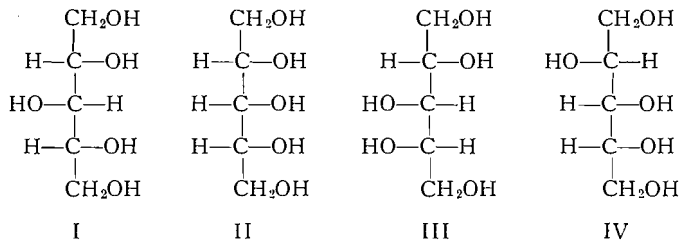
1. HEYDING, R. D. and CALVERT, L. D. Can. J. Chem. **35**, 449 (1957).
2. HEYDING, R. D. and CALVERT, L. D. Can. J. Chem. **35**, 1205 (1957).
3. HOLMES, R. J. Science, **96**, 90 (1942).
4. HOLMES, R. J. Bull. Geol. Soc. Am. **58**, 299 (1947).
5. KOCHNEV, M. I. J. Appl. Chem. (U.S.S.R.), **35**, 595 (1950).
6. BUERGER, M. J. Z. Krist. **82**, 165 (1932).
7. PEACOCK, M. A. Proc. Roy. Soc. Can. **38**, 155 (1944).
8. OFTEDAL, I. Z. Krist. **66**, 517 (1928).
9. DE JONG, W. F. Physica, **6**, 325 (1926).
10. PEACOCK, M. A. and DADSON, A. S. Am. Mineralogist, **25**, 561 (1940).
11. KAIMAN, S. Univ. of Toronto Studies, Geol. Ser. **51**, 49 (1946).
12. PEACOCK, M. A. and MICHENER, C. E. Univ. of Toronto Studies, Geol. Ser. **42**, 95 (1939).
13. THOMPSON, R. M. X-ray Powder Data File, Card 9-8.

RECEIVED OCTOBER 22, 1959.
DIVISION OF APPLIED CHEMISTRY,
NATIONAL RESEARCH COUNCIL,
OTTAWA, CANADA.

THE PENTITOL PENTANITRATES*

I. G. WRIGHT AND L. D. HAYWARD

In connection with a study of the selective denitration of polynitrate esters (1, 2, 3) we have prepared and characterized the crystalline, fully nitrated derivatives of the three isomeric pentitols, xylitol (I), ribitol (adonitol) (II), and L-(−)-arabinitol (III). The only previous references to the pentitol nitrates in the literature dated from the end of the last century and described xylitol pentanitrate (4) and the pentanitrate of D-(+)-arabinitol (IV) (5) as explosive, non-crystallizable sirups.



In the present work the stable, crystalline form of xylitol (I) was synthesized in 62% yield by the sodium borohydride reduction of D-xylose and was further identified through conversion to the known penta-*O*-acetyl derivative (6). The other two pentitols (II and III) were commercially available in crystalline form.†

Direct nitration of the pure pentitols in a mixture of fuming nitric acid and acetic anhydride at 0° C (7) gave the crystalline pentanitrate esters in excellent yield (Table I).

Presented in part at the Symposium on the Chemistry, Technology, and Pharmacology of Nitric Acid Esters, 132nd meeting, American Chemical Society, New York, September 8–13, 1957.

†*Nutritional Biochemicals Corporation, Cleveland 28, Ohio.*

Can. J. Chem. Downloaded from www.nrcresearchpress.com by 69.46.99.164 on 09/04/12
For personal use only.

Detailed powder diffraction data for $Fe(Fe_xAs_{2-x})$, $CoAs_3$, $CoAs_2$, and β-$NiAs_2$ have been submitted to the X-ray Powder Data File.

We are indebted to Miss Theresa Clarke for assistance in obtaining Debye–Scherrer patterns, and to Mr. D. S. Russell for analysis of reactants and alloys.

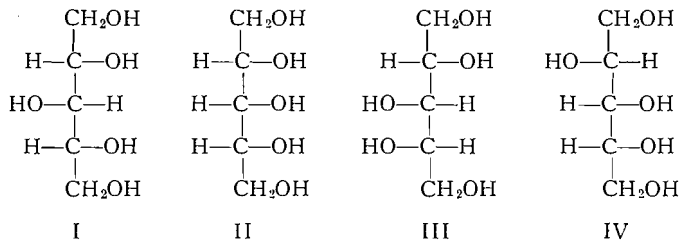
1. HEYDING, R. D. and CALVERT, L. D. Can. J. Chem. **35**, 449 (1957).
2. HEYDING, R. D. and CALVERT, L. D. Can. J. Chem. **35**, 1205 (1957).
3. HOLMES, R. J. Science, **96**, 90 (1942).
4. HOLMES, R. J. Bull. Geol. Soc. Am. **58**, 299 (1947).
5. KOCHNEV, M. I. J. Appl. Chem. (U.S.S.R.), **35**, 595 (1950).
6. BUERGER, M. J. Z. Krist. **82**, 165 (1932).
7. PEACOCK, M. A. Proc. Roy. Soc. Can. **38**, 155 (1944).
8. OFTEDAL, I. Z. Krist. **66**, 517 (1928).
9. DE JONG, W. F. Physica, **6**, 325 (1926).
10. PEACOCK, M. A. and DADSON, A. S. Am. Mineralogist, **25**, 561 (1940).
11. KAIMAN, S. Univ. of Toronto Studies, Geol. Ser. **51**, 49 (1946).
12. PEACOCK, M. A. and MICHENER, C. E. Univ. of Toronto Studies, Geol. Ser. **42**, 95 (1939).
13. THOMPSON, R. M. X-ray Powder Data File, Card 9-8.

RECEIVED OCTOBER 22, 1959.
DIVISION OF APPLIED CHEMISTRY,
NATIONAL RESEARCH COUNCIL,
OTTAWA, CANADA.

THE PENTITOL PENTANITRATES*

I. G. WRIGHT AND L. D. HAYWARD

In connection with a study of the selective denitration of polynitrate esters (1, 2, 3) we have prepared and characterized the crystalline, fully nitrated derivatives of the three isomeric pentitols, xylitol (I), ribitol (adonitol) (II), and L-(−)-arabinitol (III). The only previous references to the pentitol nitrates in the literature dated from the end of the last century and described xylitol pentanitrate (4) and the pentanitrate of D-(+)-arabinitol (IV) (5) as explosive, non-crystallizable sirups.



In the present work the stable, crystalline form of xylitol (I) was synthesized in 62% yield by the sodium borohydride reduction of D-xylose and was further identified through conversion to the known penta-*O*-acetyl derivative (6). The other two pentitols (II and III) were commercially available in crystalline form.†

Direct nitration of the pure pentitols in a mixture of fuming nitric acid and acetic anhydride at 0° C (7) gave the crystalline pentanitrate esters in excellent yield (Table I).

**Presented in part at the Symposium on the Chemistry, Technology, and Pharmacology of Nitric Acid Esters, 132nd meeting, American Chemical Society, New York, September 8–13, 1957.*
†Nutritional Biochemicals Corporation, Cleveland 28, Ohio.

Can. J. Chem. Downloaded from www.nrcresearchpress.com by 41.223.56.140 on 09/04/12
For personal use only.

The structure and configuration of these high-explosive compounds were established through their nitrogen contents (Table I) and infrared spectra and by nearly quantitative conversion to the parent alcohols on catalytic hydrogenation (Table II).

TABLE I

The pentitol pentanitrates

Pentanitrate	Yield (%)	m.p. (° C)	Nitrogen content (%)[a]
Ribitol	90.2	33.5–34.0	18.2[b]
Xylitol	95.6	37–40	17.8[c]
L-(−)-Arabinitol	97.5	26.5–27.5	18.0[c]

[a]Theoretical value = 18.6%.
[b]Modified semimicro Kjeldahl method (10).
[c]Ultramicro procedure based on the Kjeldahl method and involving Nesslerization of the distilled ammonia (11, 12).

TABLE II

Hydrogenation products of the pentitol pentanitrates

Pentanitrate	Ribitol	Xylitol	L-(−)-Arabinitol
% Yield	97.5	95.5	97.5
M.p., ° C	99–101	92–94[a]	101–103
Mixed m.p., ° C	99–102	92.0–94.5	101–103
Reported m.p., ° C	102	93.0–94.5	102
Reference	(9)	(8)	(9)

[a]Stable modification.

The infrared spectra of the pentanitrates of ribitol and xylitol in nujol mull and the spectrum of L-arabinitol pentanitrate as a liquid film showed closely similar peaks near 1650, 1265, and 750 cm^{-1}. The very strong peaks at 1650 and 1265 cm^{-1} were characteristic of covalent nitrate groups (14) and this was probably also true of the medium-to-weak peak near 750 cm^{-1} which has also been observed in a series of other nitrate esters in this laboratory (15). No peaks occurred in the frequency ranges for hydroxyl and carbonyl stretching in saturated acyclic compounds. A strong peak at 2910 cm^{-1} in the spectrum of L-arabinitol pentanitrate was attributed to the methylene group and was not observed in the other spectra since they were compensated with nujol.

The three pentitol pentanitrates reacted with dry pyridine at 20–24° C in much the same manner as D-mannitol hexanitrate (1, 2). The xylitol derivative evolved more gas and the pyridine solution became darker in color than with the arabinitol and ribitol compounds. Partially nitrated sirups were recovered in good yield from the pyridine solutions on dilution with water. The nitrogen contents, solubility, and infrared spectra of these products indicated that they were probably partially nitrated anhydropentitols. Further study of their constitution is in progress.

EXPERIMENTAL

Xylitol

A solution of D-xylose (66.0 g, m.p. 145–6° C, $[\alpha]_D^{22.5}$ +18.9±0.2°) in 400 ml of water was cooled in an ice bath, and a solution of 16.5 g of sodium borohydride in 100 ml of water was added dropwise. The temperature of the mixture rose to 45° C during the addition, the rate of evolution of hydrogen slowly decreased, and the solution became alkaline (pH 9). After the mixture had been standing for 1.5 hours at room temperature

Can. J. Chem. Downloaded from www.nrcresearchpress.com by 41.223.56.140 on 09/04/12
For personal use only.

reduction was complete as shown by Fehling's test. Excess borohydride was destroyed with 6 *N* acetic acid and the solution was deionized and concentrated to a sirup under reduced pressure. The sirupy xylitol was freed of boric acid by repeated evaporations with methanol and crystallized after seeding with a sample obtained through the courtesy of Dr. M. L. Wolfrom, Ohio State University. After recrystallization from ethanol the xylitol (41.3 g, 61.5%) melted correctly at 93.0–94.5° C (8).

Acetylation of 3.8 g of the xylitol with acetic anhydride and sodium acetate yielded 3.7 g of pure xylitol pentaacetate melting at 62.0–63.5° C after recrystallization from methanol (6).

Nitration of the Pentitols

A suspension of the pentitol (1.0 g) in acetic anhydride (4 ml) was cooled in an ice–salt bath and a cooled solution of fuming nitric acid (5 ml) in acetic anhydride (5 ml) was added slowly with stirring. After 1 hour the reaction mixture was allowed to warm to room temperature during 30 minutes by which time all of the pentitol had dissolved. The mixture was then poured into ice water and the colorless, semisolid product was separated and dried *in vacuo* at 0° C for several days. The pentitol pentanitrate was recrystallized from five parts of dry toluene at about −40° C and was recovered on a glass funnel jacketed with melting chlorobenzene (m.p. −45° C) and fitted with a drying tube. Yields and melting points of the pentitol pentanitrates are shown in Table I together with the nitrogen analyses. The nitrates detonated under the hammer and were not decomposed after they were stored in a desiccator at 0–5° C for 3 years.

Hydrogenation of the Pentitol Pentanitrates

The pentitol pentanitrate (0.5 g) was dissolved in 95% ethanol (100 ml) and hydrogenated over palladium-on-charcoal catalyst (0.5–1.0 g) as previously described (1, 13). The yields, melting points, and mixed melting points of the recovered pentitols are shown in Table II.

The Action of Pyridine on the Pentitol Pentanitrates

The pentitol pentanitrate (100 mg) dissolved readily at 20° C in pyridine (6.2 ml) freshly distilled from barium oxide (b.p. 114.5–116.0° C). Within 2 minutes the initially colorless solution became yellow and evolved a colorless gas while the temperature increased to 24° C. After 6 hours at 20° C the solution was warmed to 50° C for 30 minutes which caused no apparent change in color or rate of gas evolution. The reaction mixture was then diluted with water (8 ml) and extracted with ether. Evaporation of the washed and dried ether extract yielded 50 to 65 mg of a colorless, viscous sirup.

The nitrogen contents of the thoroughly dried products from ribitol, xylitol, and arabinitol pentanitrates were 15.0, 14.5, and 12.5% respectively. These products were insoluble in water, *n*-hexane, and carbon tetrachloride and readily soluble in ethyl acetate, ether, and acetone. The infrared spectra (potassium bromide windows) showed the presence of covalent nitrate groups (1635–1650 cm^{-1} and 1273–1287 cm^{-1} and 747–750 cm^{-1}) and no carbonyl groups. An hydroxyl stretching frequency (3420 cm^{-1}) appeared only in the spectrum of the product from L-arabinitol pentanitrate.

We thank Mr. I. G. Csizmadia for nitrogen analyses and the Defence Research Board of Canada for funds in support of this research.

1. HAYWARD, L. D. J. Am. Chem. Soc. **73**, 1974 (1951).
2. BROWN, J. R. and HAYWARD, L. D. Can. J. Chem. **33**, 1735 (1955).
3. MCKEOWN, G. G. and HAYWARD, L. D. Can. J. Chem. **33**, 1392 (1955).

Can. J. Chem. Downloaded from www.nrcresearchpress.com by 41.223.56.140 on 09/04/12
For personal use only.

4. BERTRAND, G. Bull. soc. chim. (3), **5**, 740 (1891).
5. VIGNON, L. and GERIN, F. Compt. rend. **133**, 641 (1901).
6. WOLFROM, M. L. and KOHN, E. J. J. Am. Chem. Soc. **64**, 1739 (1942).
7. HONEYMAN, J. and MORGAN, J. W. W. J. Chem. Soc. 3660 (1955).
8. CARSON, J. F., WAISBROT, S. W., and JONES, F. T. J. Am. Chem. Soc. **65**, 1777 (1943).
9. LOHMAR, R. L. *In* The carbohydrates, chemistry, biochemistry, physiology. *Edited by* W. Pigman. Academic Press, Inc., New York. 1957. p. 243.
10. BROWN, R. K. and PURVES, C. B. Pulp Paper Mag. Can. **48**, No. 6, 100 (1947).
11. TOURTELLOTTE, W. W., PARKER, J. A., ALVING, R. E., and DEJONG, R. N. Anal. Chem. **30**, 1563 (1958).
12. HAWK, P. B., OSER, B. L., and SUMMERSON, W. H. Practical physiological chemistry. 13th ed. McGraw-Hill Book Co., Inc., New York. 1954.
13. HAYWARD, L. D. and PURVES, C. B. Can. J. Chem. **32**, 19 (1954).
14. BELLAMY, L. J. The infrared spectra of complex molecules. 2nd ed. Methuen & Co. Ltd., London. 1958.
15. HAYWARD, L. D. To be published.

RECEIVED OCTOBER 23, 1959.
DEPARTMENT OF CHEMISTRY,
UNIVERSITY OF BRITISH COLUMBIA,
VANCOUVER 8, B.C.

A TEST OF TRANSITION STATE THEORY

G. O. PRITCHARD,* H. O. PRITCHARD,† G. H. MILLER,* AND J. R. DACEY‡

The transition state theory of the radical combination reactions $CX_3 + CX_3 \rightarrow C_2X_6$ has not yet been satisfactorily formulated because the concept of the transition state itself in the reactions is so indeterminate. Nor is the situation made any easier by the lack of good data on the frequency factors of such combination reactions and of the reverse decompositions. It has, however, been assumed that whatever the transition state may be, there must be free rotation of the CX_3 groups about the incipient C—C bond (1). A further difficulty arises in the calculation of frequency factors because the major contribution to the entropy of activation is dependent on the unknown pressure of the free radicals, since there is a change in the number of species in these reactions (2). Recently, Pritchard and Dacey (3) have obtained a ratio of frequency factors for CX_3 radical combination reactions which can be used as a test of transition state theory because the uncertainties in the formulation of the respective transition states cancel out.

Pritchard and Dacey studied the competition of the three reactions

$$CH_3 + CH_3 \xrightarrow{k_{11}} C_2H_6$$
$$CH_3 + CF_3 \xrightarrow{k_{12}} CH_3CF_3$$
$$CF_3 + CF_3 \xrightarrow{k_{22}} C_2F_6$$

by photolyzing mixtures of CH_3COCH_3 and CF_3COCF_3, and found that the ratio $k_{12}/(k_{11}k_{22})^{\frac{1}{2}} = 0.52 \pm 0.06 \exp[(1070 \pm 100)/RT]$ at pressures where three body restrictions were absent.

Considering the scheme

$$2 \text{ radicals} \xrightarrow{\Delta S^*} \text{transition state} \xleftarrow{\Delta S'} \text{ethane},$$

*Chemistry Department, University of California at Santa Barbara, Goleta, California.
†Department of Chemistry, University of Manchester, Manchester 13, England.
‡Chemistry Department, Royal Military College of Canada, Kingston, Ontario.

Can. J. Chem. Downloaded from www.nrcresearchpress.com by 41.223.56.140 on 09/04/12
For personal use only.

4. BERTRAND, G. Bull. soc. chim. (3), **5**, 740 (1891).
5. VIGNON, L. and GERIN, F. Compt. rend. **133**, 641 (1901).
6. WOLFROM, M. L. and KOHN, E. J. J. Am. Chem. Soc. **64**, 1739 (1942).
7. HONEYMAN, J. and MORGAN, J. W. W. J. Chem. Soc. 3660 (1955).
8. CARSON, J. F., WAISBROT, S. W., and JONES, F. T. J. Am. Chem. Soc. **65**, 1777 (1943).
9. LOHMAR, R. L. *In* The carbohydrates, chemistry, biochemistry, physiology. *Edited by* W. Pigman. Academic Press, Inc., New York. 1957. p. 243.
10. BROWN, R. K. and PURVES, C. B. Pulp Paper Mag. Can. **48**, No. 6, 100 (1947).
11. TOURTELLOTTE, W. W., PARKER, J. A., ALVING, R. E., and DEJONG, R. N. Anal. Chem. **30**, 1563 (1958).
12. HAWK, P. B., OSER, B. L., and SUMMERSON, W. H. Practical physiological chemistry. 13th ed. McGraw-Hill Book Co., Inc., New York. 1954.
13. HAYWARD, L. D. and PURVES, C. B. Can. J. Chem. **32**, 19 (1954).
14. BELLAMY, L. J. The infrared spectra of complex molecules. 2nd ed. Methuen & Co. Ltd., London. 1958.
15. HAYWARD, L. D. To be published.

RECEIVED OCTOBER 23, 1959.
DEPARTMENT OF CHEMISTRY,
UNIVERSITY OF BRITISH COLUMBIA,
VANCOUVER 8, B.C.

A TEST OF TRANSITION STATE THEORY

G. O. PRITCHARD,* H. O. PRITCHARD,† G. H. MILLER,* AND J. R. DACEY‡

The transition state theory of the radical combination reactions $CX_3 + CX_3 \rightarrow C_2X_6$ has not yet been satisfactorily formulated because the concept of the transition state itself in the reactions is so indeterminate. Nor is the situation made any easier by the lack of good data on the frequency factors of such combination reactions and of the reverse decompositions. It has, however, been assumed that whatever the transition state may be, there must be free rotation of the CX_3 groups about the incipient C—C bond (1). A further difficulty arises in the calculation of frequency factors because the major contribution to the entropy of activation is dependent on the unknown pressure of the free radicals, since there is a change in the number of species in these reactions (2). Recently, Pritchard and Dacey (3) have obtained a ratio of frequency factors for CX_3 radical combination reactions which can be used as a test of transition state theory because the uncertainties in the formulation of the respective transition states cancel out.

Pritchard and Dacey studied the competition of the three reactions

$$CH_3 + CH_3 \xrightarrow{k_{11}} C_2H_6$$
$$CH_3 + CF_3 \xrightarrow{k_{12}} CH_3CF_3$$
$$CF_3 + CF_3 \xrightarrow{k_{22}} C_2F_6$$

by photolyzing mixtures of CH_3COCH_3 and CF_3COCF_3, and found that the ratio $k_{12}/(k_{11}k_{22})^{\frac{1}{2}} = 0.52 \pm 0.06 \exp[(1070 \pm 100)/RT]$ at pressures where three body restrictions were absent.

Considering the scheme

$$2 \text{ radicals} \xrightarrow{\Delta S^*} \text{transition state} \xleftarrow{\Delta S'} \text{ethane},$$

*Chemistry Department, University of California at Santa Barbara, Goleta, California.
†Department of Chemistry, University of Manchester, Manchester 13, England.
‡Chemistry Department, Royal Military College of Canada, Kingston, Ontario.

Can. J. Chem. Downloaded from www.nrcresearchpress.com by 41.223.56.140 on 09/04/12
For personal use only.

where ΔS^* and $\Delta S'$ are the entropies of activation in the senses indicated, we may express the observed frequency factor ratio of $A^*_{12}/(A^*_{11}\,A^*_{22})^{\frac{1}{2}} = 0.52\pm0.06$ in the form

$$\Delta S^*_{12}-\tfrac{1}{2}(\Delta S^*_{11}+\Delta S^*_{22}) = -1.30\pm0.2 \text{ e.u.}$$

Rewriting this in terms of the absolute entropies S^*_{11}, S^*_{22}, and S^*_{12} of the activated complexes, we have

$$S^*_{12}-\tfrac{1}{2}(S^*_{11}+S^*_{22}) = -1.30\pm0.2 \text{ e.u.},$$

the absolute entropies of the free radicals having cancelled out.

This entropy difference expression can also be written in terms of the absolute entropies, S_{11}, S_{22}, and S_{12}, of the three ethanes, i.e.,

$$S^*_{12}-\tfrac{1}{2}(S^*_{11}+S^*_{22}) = [S_{12}-\tfrac{1}{2}(S_{11}+S_{22})]+[\Delta S'_{12}-\tfrac{1}{2}(\Delta S'_{11}+\Delta S'_{22})]$$

making, of course, the tacit assumption that the transition states for the forward and reverse reactions are identical.

At 298.15° K and 1 atmosphere, the absolute entropy of ethane is $S_{11} = 54.85$ e.u. (4), that of trifluoroethane is $S_{12} = 66.87$ e.u. (5), and that of hexafluoroethane can be calculated from the data of Pace and Aston (6) to be $S_{22} = 81.85$ e.u. Thus the first bracket becomes -1.48 e.u. In the evaluation of the second bracket we are not critically dependent on an exact formulation of the transition state. We infer that the restricted rotation which exists in each molecule must be freed (1), and that there will be some change in the nature of the vibrations in each ethane, principally associated with the stretching of the C—C bond. The changes in vibrational entropy in the three cases must be so similar as to cancel out when substituted in the second bracket, so that the only significant terms will be changes in entropy associated with the freeing of the restricted rotations. These changes were calculated using the tables of Pitzer (7) and the following experimental data (4, 5, and 6).

	C_2H_6	CH_3CF_3	C_2F_6	
Barrier height	2850	3450	4350	cal/mole
Reduced moment of inertia	2.65×10^{-40}	5.12×10^{-40}	76.7×10^{-40}	g cm^2

They are $(S_t-S_{rr})_{11} = 1.22$ e.u., $(S_t-S_{rr})_{12} = 1.50$ e.u., and $(S_t-S_{rr})_{22} = 1.92$ e.u. and the second bracket becomes -0.07 e.u. We therefore have to compare the experimental data for $[S^*_{12}-\tfrac{1}{2}(S^*_{11}+S^*_{22})]$ of -1.30 ± 0.2 e.u. with the calculated value of -1.55 e.u. (with a possible error at least as large as the experimental one).

The agreement between the two figures is well within the limits of error and provides an excellent over-all test of transition state theory as applied to these combination reactions. Because of the smallness of the rotational term we are unable to discriminate between a transition state with or without free rotation, and can say little more about the frequency factors for the ethane decompositions, other than to note that A'_{12} will be approximately the geometric mean of A'_{11} and A_{22}'.

Two of us, G.O.P. and G.H.M., acknowledge a grant from the National Science Foundation.

Can. J. Chem. Downloaded from www.nrcresearchpress.com by 41.223.56.140 on 09/04/12
For personal use only.

1. TROTMAN-DICKENSON, A. F. Free radicals. Methuen & Co. Ltd., London. 1959.
2. BEVINGTON, J. C. Trans. Faraday Soc. **48**, 1045 (1952).
3. PRITCHARD, G. O. and DACEY, J. R. To be published.
4. BRICKWEDDE, F. G., MOSKOW, M., and ASTON, J. G. J. Research Natl. Bur. Standards, **37**, 263 (1946).
5. RUSSELL, H., JR., GOLDING, D. R. V., and YOST, D. M. J. Am. Chem. Soc. **66**, 16 (1944).
6. PACE, E. L. and ASTON, J. G. J. Am. Chem. Soc. **70**, 566 (1948).
7. PITZER, K. S. Quantum chemistry. Constable & Co. Ltd., London. 1953.

RECEIVED SEPTEMBER 24, 1959.
DEPARTMENT OF PHYSICAL SCIENCES,
UNIVERSITY OF CALIFORNIA AT SANTA BARBARA,
GOLETA, CALIFORNIA, U.S.A.

Can. J. Chem. Downloaded from www.nrcresearchpress.com by 41.223.56.140 on 09/04/12
For personal use only.

Can. J. Chem. Downloaded from www.nrcresearchpress.com by 41.223.56.140 on 09/04/12
For personal use only.

Canadian Journal of Chemistry

Issued by THE NATIONAL RESEARCH COUNCIL OF CANADA

VOLUME 38 MARCH 1960 NUMBER 3

MAGNETIC PROPERTIES OF MESONAPHTHODIANTHRENE[1]

YOSHIO MATSUNAGA[2]

ABSTRACT

Electron spin resonance absorption was detected in mesonaphthodianthrene and mesonaphthodianthrone. The spectra of both of these compounds consist of, at least, seven lines with a separation of 4.4 oersteds and the central line has a *g*-value of 2.0024±0.0002. The growth of the central line by admission of air was observed in the case of the hydrocarbon. Some suggestions are presented as to the nature of the unpaired electrons in these compounds. The magnitude of the molar diamagnetic susceptibility of mesonaphthodianthrene, after correction for the paramagnetic contribution from the unpaired electrons, is discussed in relation to the molecular structure.

INTRODUCTION

The appearance of unpaired electrons has been reported in crystals of some highly conjugated molecules, namely metal-free phthalocyanine (1, 2), violanthrone (3, 4), violanthrene (3, 4), and binaphthoquinones (5). Here we wish to present the results of a study of mesonaphthodianthrene (I) and mesonaphthodianthrone (II) by the electron spin resonance method. The hydrocarbons studied are compounds which have anomalously small values of diamagnetic susceptibility (6). This anomaly was found to be characteristic of perylene (III) and its analogues. In the sense of the valence-bond theory the central single bonds in perylene, violanthrone (IV), and mesonaphthodianthrene can be doubled only in the excited states.

EXPERIMENTAL

Mesonaphthodianthrone was prepared by photodehydrogenation of bianthraquinone dissolved in pyridine (7). The hydrocarbon was obtained by the zinc-dust fusion of the quinone (8). The latter was found to be reactive towards oxygen, therefore our sample was stored in an evacuated tube after repeated sublimation in high vacuum.

The electron spin resonance was examined at a frequency of 9 kMc/s at room temperature, and at 77° K.

RESULTS

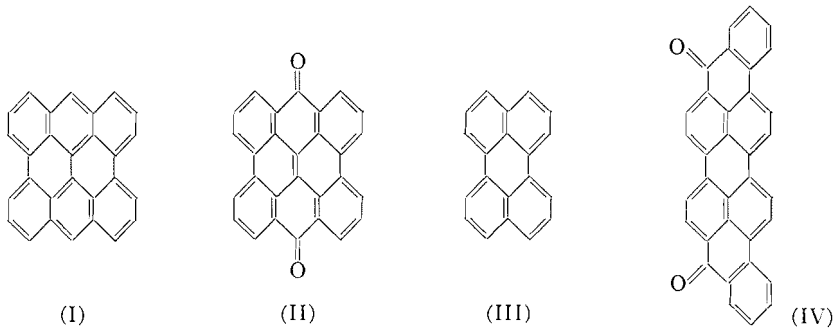
Unlike the spectra of the other paramagnetic polycyclic aromatic compounds, the spectra of mesonaphthodianthrene and its quinone show some structure and this can be modified by admission of air. The spectra of these two compounds consist of at least seven lines with a separation of 4.4 oersteds and spread over 50 oersteds as shown in Fig. 1. The *g*-value of the central peak, estimated by comparison with D.P.P.H. (2.0036), was found to be 2.0024±0.0002. The spin concentration was about 3×10^{21} per mole

[1]*Manuscript received October 16, 1959.*
Contribution from Department of Chemistry, University of British Columbia, Vancouver 8, B.C., Canada.
[2]*N.R.C. Postdoctoral Fellow 1957–59. On leave of absence from Department of Chemistry, University of Tokyo, Tokyo, Japan.*

in the hydrocarbon. This value was not affected by further sublimation nor by cooling to liquid-nitrogen temperature. The spin concentration in the quinone was about one-third of that of the hydrocarbon.

In contact with air the central peak in the spectrum of mesonaphthodianthrene grew slowly. After a few days the intensity of this sharp absorption reached its maximum. The line width of the signal from this oxygen-containing radical was about one oersted at half height. In Fig. 2, a higher magnetic-field modulation was used to detect the broad main absorption, so the central line is artificially broadened. The ratio of the number of unpaired electrons contributing to the sharp absorption to that contributing to the broad one was estimated as about one-tenth at its maximum. By evacuation for a few minutes the intensity of this sharp absorption was decreased considerably; however, only a slow decrease was observed by further prolonged evacuation at room temperature.

No electron spin resonance absorption was detected in bianthraquinone. However, samples heated to 194° C or higher show resonance absorption (9). No structure was observed and the line width at a half height was about twelve oersteds.



(I) (II) (III) (IV)

DISCUSSION

The nature of the broad absorption found in the hydrocarbon and quinone seems not to be simple. Winslow *et al.* (2) suggested that enough thermal energy is absorbed at room temperature to produce unpaired electrons in crystals of highly conjugated, metal-free phthalocyanine. Although the electron spin resonance absorption of naphthalene in a triplet state is too broad to be observed in a randomly orientated system (10), the dipolar interaction, which contributes to line broadening, is proportional to the inverse cube of the electron–electron distance, therefore the resonance absorption of the unpaired electrons in excited states might be detectable in large aromatic molecules like the present hydrocarbon. However, the spin concentration in our samples was found to be independent of temperature as in violanthrone (4).

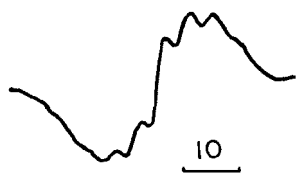


FIG. 1. Derivative of electron spin resonance absorption of mesonaphthodianthrene in vacuum.

Polycyclic aromatic compounds have been known as intrinsic semiconductors and the activation energy for semiconduction was considered as the energy gap between the full

Can. J. Chem. Downloaded from www.nrcresearchpress.com by 41.223.56.140 on 09/04/12
For personal use only.

band and the empty band (11, 12, 13). Consequently the unpaired electrons in the present compounds cannot be considered charge carriers and must be trapped somewhere. It has been shown that crystals of highly conjugated aromatic molecules contain the imperfections which can behave as traps for charge carriers. Although the nature of the imperfections in molecular crystals is not well known, this term includes not only chemical impurities but also some kinds of lattice defects (14, 15). Because our hydrocarbon and quinone give the same hyperfine structure in resonance absorption, the unpaired electrons must be in a common situation in these compounds. The presence of hyperfine structure can be attributed to the dipolar interaction between an unpaired electron and several ring protons. The line splitting can be given approximately by $28/r^3$ where r is the electron–proton distance (16). The presence of seven or more lines with a separation of 4.4 oersteds suggests that the unpaired electron is surrounded by six or more protons at a distance of about 1.8 Å.

It seems highly likely that the unpaired electrons in our compounds are associated with some common impurity. If the impurity molecule has originally an unpaired electron, this free-radical molecule must be extraordinarily stable and survive through the processes of zinc-dust fusion and repeated vacuum sublimations. Besides, it seems to be unlikely that such a free-radical molecule, which must be formed in the process of photodehydrogenation of bianthraquinone, has six nearly equivalent protons at a distance of about 1.8 Å from the unpaired electron. It is more probable that the impurity molecules which have originally no unpaired electrons can create favorable sites to trap electrons by interaction with the semiconductive host lattice. In this case an unpaired electron may be shared by neighboring molecules and find six or more nearly equivalent protons at a distance as small as 1.8 Å. This situation may be similar to that in aromatic hydrocarbon – iodine complexes which show strong resonance absorption. Therefore, we extended our low-temperature measurements to molecular complexes. For example, perylene–iodine (2 : 3) complex gives a resonance absorption with a g-value of 2.0033. At room temperature the line width at a half power was about eight oersteds and the ratio of the number of unpaired electrons to that of perylene molecules was about 0.07 (17). On cooling to 77° K the line width decreases to about 2.5 oersteds and the spin concentration is estimated as 0.06. Similar decreases of line width were observed in pyranthrene– and violanthrene–iodine complexes. The spin concentration in the latter two is also found to be independent of temperature within the limit of experimental error. If unpaired electrons in these highly conductive molecular complexes are charge carriers, the spin concentration must be decreased by a factor of hundreds by cooling to liquid-nitrogen temperature (18). The appearance of unpaired electrons in hydrocarbon–iodine complexes is apparently related to the complex formation by strong intermolecular charge-transfer forces. However, the whole mechanism is not yet clear.

It is interesting to point out that if we compare the spin concentrations in violanthrone and its hydrocarbon (3, 4) and mesonaphthodianthrene and its quinone, in each pair the member which is of perylene type shows stronger resonance absorption than the other. This fact suggests the importance of the role of the host molecules in the appearance of unpaired electrons. Therefore, it might be possible that without impurity molecules the host molecules associated with some kind of lattice defects can form traps for unpaired electrons; however, at present we have no detailed knowledge of such lattice defects in molecular crystals.

The nature of the unpaired electrons in the other polycyclic aromatic compounds may be similar to those in the present hydrocarbon and quinone. We can hope to resolve

Can. J. Chem. Downloaded from www.nrcresearchpress.com by 41.223.56.140 on 09/04/12
For personal use only.

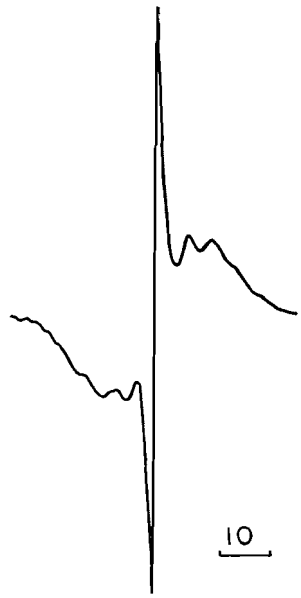


FIG. 2. Derivative of electron spin resonance absorption of mesonaphthodianthrene in air.

broad component lines from dipolar interaction in a randomly orientated solid sample only when the interaction is with equivalent protons. The absence of hyperfine structure in resonance absorption in the other cases may be due to non-equivalence of the interacting protons.

Oxygen molecules, which contribute to the appearance of a sharp line, seem to be combined loosely on the surface of crystals of the hydrocarbon, but the presence of slow diffusion in the formation and dissociation of this free radical is likely. Absence of detectable asymmetry in the sharp absorption line suggests that the new free radical has no axial symmetry; therefore the formation of a peroxide radical is not probable. The effect of oxygen on electron spin resonance absorption has been observed in a number of organic free radicals and carbonaceous materials; however, the effect in most cases is line broadening or disappearance. Similar appearance of a symmetric absorption by admission of air or oxygen has been reported only in the case of tri-*p*-nitrophenylmethyl where the *g*-value is as high as 2.006 (19). Therefore, the present case seems to be an entirely new kind of oxygen effect. Our oxygen-containing free radical, which gives a sharp line with a *g*-value as low as 2.0024, may be some kind of molecular complex formed by interaction between oxygen and the hydrocarbon molecule.

The effect of oxygen on the semiconductivity and the photoconductivity of some highly conjugated aromatic compounds is known (20, 21). Therefore, a study of the effect on the electrical properties of mesonaphthodianthrene might be fruitful in order to elucidate the nature of the oxygen-containing free radical. The semiconductivity of the present hydrocarbon was studied by Inokuchi but the oxygen effect was not considered (12).

Using London's molecular orbital theory for diamagnetic anisotropy of aromatic molecules, Hazato predicted that the conjugation between two naphthalene nuclei in a perylene molecule brings about a decrease of diamagnetic anisotropy from twice that of naphthalene (22). This prediction is qualitatively in agreement with the experimental results. We shall examine here whether or not the same relation is valid for mesonaph-

Can. J. Chem. Downloaded from www.nrcresearchpress.com by 41.223.56.140 on 09/04/12
For personal use only.

thodianthrene and violanthrone after the correction for the paramagnetic contribution from the unpaired electrons. The diamagnetic anisotropy ΔK is defined by the following equation,

$$\Delta K = 3(\chi_m - K_I),$$

where χ_m is the mean molar susceptibility and K_I is the isotropic part of molar susceptibility. The latter can be estimated by empirical rules (23, 24). Following our previous paper (6), the isotropic part will be estimated by

$$K_I \times 10^6 = -3.36 \times N_C - 2.93 \times N_H + 1.73 \times N_O,$$

where N_C, N_H, N_O are the numbers of aromatic carbon atoms, hydrogen atoms, and quinone oxygen atoms in a molecule. The results are summarized in Table I. All the

TABLE I

Diamagnetic susceptibilities and anisotropies of mesonaphthodianthrene and related compounds

Compound	Molar susceptibility (multiplied by 10^6)				
	Total by static method	Paramagnetic part by ESR	Diamagnetic part	Isotropic part	Anisotropy
Naphthalene	−91.9	0	−91.9	−57.0	−105
Perylene	−166.8	0	−166.8	−102.4	−193
Anthracene	−129.4	0	−129.4	−76.3	−159
Mesonaphthodianthrene	−214.6	+6	−220.6	−135.1	−257
Benzanthrone	−142.9	0	−142.9	−84.7	−175
Violanthrone	−204.8	+25 to +63*	−230 to −268	−157.7	−217 to −331

*See reference 4.

necessary values of susceptibility were taken from our previous paper. Although there is uncertainty in the values of the total molar susceptibility and the paramagnetic part because different preparations were used for the measurements with a Gouy balance and with an electron spin resonance spectrometer, it appears that the diamagnetic anisotropy of mesonaphthodianthrene is far less than twice that of anthracene even after the correction for the paramagnetic contribution from the unpaired electrons. A similar relation was found in violanthrone. The large difference between the anisotropy of mesonaphthodianthrene and twice that of anthracene suggests the presence of strong conjugation between two anthracene nuclei in a mesonaphthodianthrene molecule. This conclusion is in accordance with the fact that the difference between the calculated π-electron energy for mesonaphthodianthrene and twice that for anthracene is nearly twice as large as the similar difference for perylene and naphthalene as cited in Table II (25).

TABLE II

Total π-electron energies and average radii of π-electron orbitals in mesonaphthodianthrene and related compounds

Compound	Total π-electron energy by LCAO*	Average radius of π-electron orbital (Å)
Naphthalene	3.68 β	1.57
Perylene	8.24 β	1.51
Anthracene	5.31 β	1.64
Mesonaphthodianthrene	12.1 β	1.47

*See reference 25.

Can. J. Chem. Downloaded from www.nrcresearchpress.com by 41.223.56.140 on 09/04/12
For personal use only.

The diamagnetic anisotropy is correlated with the average radius of the π-electron orbital $\sqrt{\bar{r}^2}$ by the two-dimensional Langevin's equation,

$$\Delta K = -(Ne^2/4mc^2) \sum \bar{r}^2 = -4.248\times10^{10}\, p\bar{r}^2,$$

where p is the number of π-electrons in a molecule and the other symbols have the usual physical meanings (26). Therefore, as shown in Table II, we must conclude that, on the average, the π-electrons in the mesonaphthodianthrene molecule are less mobile than those in the anthracene molecule.

ACKNOWLEDGMENTS

The author would like to thank Professor C. A. McDowell for his interest and guidance throughout the course of this research. This work was supported by grants from the National Research Council of Canada, and we wish to thank that body for its generosity.

REFERENCES

1. D. J. E. Ingram and J. E. Bennett. J. Chem. Phys. **22**, 1136 (1954).
2. F. H. Winslow, W. O. Baker, and W. A. Yager. J. Am. Chem. Soc. **77**, 4751 (1955).
3. Y. Yokozawa and I. Tatsuzaki. J. Chem. Phys. **22**, 2087 (1954).
4. H. Akamatu, S. Mrozowski, and D. Wobschall. Proceedings of the Third Conference on Carbon. Pergamon Press, Inc., New York. 1959. p. 129.
5. Y. Matsunaga. Can. J. Chem. **37**, 1003 (1959).
6. H. Akamatu and Y. Matsunaga. Bull. Chem. Soc. Japan, **26**, 364 (1953).
7. H. Brockmann and R. Mühlmann. Chem. Ber. **82**, 348 (1949).
8. E. Clar. Ber. **72**, 1645 (1939).
9. W. G. Nielsen and G. K. Fraenkel. J. Chem. Phys. **21**, 1619 (1953).
10. C. A. Hutchison and B. W. Mangum. J. Chem. Phys. **29**, 952 (1958).
11. H. Akamatu and H. Inokuchi. J. Chem. Phys. **18**, 810 (1950); **20**, 1481 (1952).
12. H. Inokuchi. Bull. Chem. Soc. Japan, **24**, 222 (1951); **27**, 22 (1954).
13. D. D. Eley and G. D. Parfitt. Trans. Faraday Soc. **51**, 1529 (1955).
14. J. Kommandeur and W. G. Schneider. J. Chem. Phys. **28**, 590 (1958).
15. D. M. J. Compton, W. G. Schneider, and T. C. Waddington. J. Chem. Phys. **28**, 741 (1958).
16. D. J. E. Ingram. Free radicals as studied by electron spin resonance. Butterworth Scientific Publications, London. 1958. p. 117.
17. Y. Matsunaga. J. Chem. Phys. **30**, 855 (1959).
18. H. Akamatu, H. Inokuchi, and Y. Matsunaga. Bull. Chem. Soc. Japan, **29**, 213 (1956).
19. F. M. Schimmel and F. W. Heineken. Physica, **28**, 781 (1957).
20. H. Pick and W. Wissman. Z. Physik, **138**, 436 (1954).
21. T. C. Waddington and W. G. Schneider. Can. J. Chem. **36**, 789 (1958); and references cited there.
22. G. Hazato. Bull. Chem. Soc. Japan, **22**, 151 (1949).
23. H. Shiba and G. Hazato. Bull. Chem. Soc. Japan, **22**, 92 (1949).
24. A. Pacault. Bull. soc. chim. France, D, 40 (1949).
25. C. A. Coulson, L. J. Schaad, and L. Burnelle. Proceedings of the Third Conference on Carbon. Pergamon Press, Inc., New York. 1959. p. 27.
26. K. Lonsdale. Proc. Roy. Soc. (London), A, **159**, 149 (1937).

Can. J. Chem. Downloaded from www.nrcresearchpress.com by 41.223.56.140 on 09/04/12
For personal use only.

Can. J. Chem. Downloaded from www.nrcresearchpress.com by 41.223.56.140 on 09/04/12
For personal use only.

THE REACTIONS OF ACTIVE NITROGEN WITH CYANOGEN AND CN RADICALS[1]

CATHERINE HAGGART[2] AND C. A. WINKLER

ABSTRACT

Cyanogen is destroyed by active nitrogen at temperatures of 80° to 400° C, and nitrogen pressures of 0.34 to 3.1 mm, with the formation of polymer. At 400° C and sufficiently high flow rates of cyanogen, a constant amount is destroyed, which apparently corresponds to practically complete consumption of the available nitrogen atoms.

The formation of CN radicals in the reaction of cyanogen with active nitrogen was established by the production of HCN and CH_3CN when hydrogen or methane was added to the reaction mixture. The rate of destruction of cyanide radicals, when they were transported through a reaction vessel, was determined by introducing hydrogen below the site of reaction, and found to follow first order kinetics.

INTRODUCTION

The reactions of active nitrogen with saturated and unsaturated hydrocarbons have been studied and found generally to produce small amounts of cyanogen in addition to hydrogen cyanide as the main product. The behavior of cyanogen with active nitrogen has therefore been investigated, to assess, if possible, the significance of its presence in the reaction products, in relation to the mechanism of formation of hydrogen cyanide in the hydrocarbon – active nitrogen systems.

EXPERIMENTAL

The apparatus used in this investigation was similar to those described in previous papers from this laboratory (1, 2). A spherical reaction vessel was employed in preliminary experiments to study the reactions of CN radicals, but subsequently a cylindrical vessel made of 28-mm O.D. pyrex tubing was used. Since the results were essentially similar, regardless of the reaction vessel employed, only those results obtained with the cylindrical vessel are reported in detail.

Three nitrogen flow rates were used, 14, 130, and 315 μmoles per second, corresponding to nitrogen pressures of 0.34, 1.4, and 3.1 mm in the reaction vessel. In the experiments in which the nitrogen flow rate was 14 μmoles per second, the total pressure in the reaction vessel was maintained constant at 1.43 mm, by the addition of argon to the nitrogen prior to its introduction into the discharge tube.

As in previous studies, the active nitrogen concentration in the system (assumed to be nitrogen atoms) was estimated from the maximum amount of HCN produced in the ethylene – active nitrogen reaction at 300° C (3).

Cyanogen was analyzed by hydrolysis followed by estimation of the cyanide thus formed. Since the hydrolysis proceeds slowly in water but rapidly and almost quantitatively in sodium hydroxide (4) to produce sodium cyanide and sodium cyanate, the unreacted cyanogen was collected in 10 to 20 ml 10% NaOH and the cyanide was then analyzed by the Liebig–Dénigès method (5).

When methane was added to the cyanogen – active nitrogen reaction mixture, the

[1]*Manuscript received November 4, 1959.*
Contribution from the Upper Atmosphere Chemistry Research Group, the Physical Chemistry Laboratory, McGill University, Montreal, with financial assistance from Canadian Industries Limited and the National Research Council of Canada.
[2]*Holder of a C.I.L. Fellowship 1958–59.*

HCN and CH_3CN formed, as well as the unreacted cyanogen, were collected in a known volume of 10% NaOH which was then separated into three equal portions. The cyanide content of the first portion, consisting of HCN and the cyanide from the hydrolysis of cyanogen, was determined by the Liebig–Dénigès method. To the second portion, dilute sulphuric acid was added to expel the HCN, and after this solution was heated for 2 hours, the nitrogen content was determined by a Kjeldahl distillation (5). The value so obtained corresponded to the amount of cyanate present in the original solution due to the hydrolysis of the cyanogen. The difference between the amounts of cyanide and cyanate was equal to the HCN present in the original solution. Since Ouillemard (6) reported that methyl cyanide was quantitatively hydrolyzed by the action of concentrated sulphuric acid to form ammonia and acetic acid, concentrated sulphuric acid was carefully added to the third portion, which had been previously frozen in liquid air, and then the solution was digested at 150° C for 8 hours. After the digestion, the total nitrogen content of the solution was determined by a Kjeldahl distillation. The difference between the total nitrogen content of this last solution and the total cyanide content of the first portion of the original solution provided a measure of the methyl cyanide formed in the reaction.

In the experiments in which hydrogen was added as a second reactant, HCN and cyanogen were present in the reaction products and were separated and analyzed by the method described by Wallis (7) and Rhodes (8). Since HCN, but not cyanogen, reacts with acidified silver nitrate solution, both products were collected in a known volume of standard silver nitrate solution to which a few drops of dilute nitric acid had been added. Cyanogen was quantitatively recovered from the mixture by bubbling nitrogen through the absorber and then into three scrubbers (Wallis bubblers), one containing acidified silver nitrate and two containing 10% sodium hydroxide solution. The excess silver nitrate was titrated with potassium thiocyanate using ferrous ammonium sulphate indicator (5) and the amount of cyanide in the last two bubblers was estimated by the Liebig–Dénigès method (5).

RESULTS AND DISCUSSION

The introduction of even small amounts of cyanogen into the stream of yellow active nitrogen immediately quenched the afterglow and caused the emission of a bright red reaction flame accompanied by the accumulation of a black polymer.

The extent to which cyanogen was destroyed by active nitrogen was determined under various conditions of temperature and pressure and over a wide range of cyanogen flow rates, Fig. 1. At 100° C, and a nitrogen pressure of 1.4 mm, with an active nitrogen concentration of 19.5 μmoles per second, the amount of cyanogen destroyed increased slowly to a constant or plateau value of about 9.5 μmoles per second when the cyanogen flow rate was 90 μmoles per second. Although an increase of temperature to 400° C increased somewhat the rate of destruction of cyanogen, the plateau value, which approximated one-half the nitrogen atom concentration, still was reached only at cyanogen flow rates greater than 85 μmoles per second.

To substantiate these observations, the nitrogen pressure was decreased to 0.34 mm and 7.6 μmoles per second respectively, with the total pressure in the system maintained at 1.4 mm by the addition of argon to the nitrogen prior to its introduction into the discharge tube. The results obtained were similar to those outlined previously, i.e. the amount of cyanogen destroyed increased slowly as the cyanogen flow rate was increased and at 400° C the plateau value for the amount of cyanogen destroyed corresponded to one-half the nitrogen atom concentration.

Can. J. Chem. Downloaded from www.nrcresearchpress.com by 41.223.56.140 on 09/04/12
For personal use only.

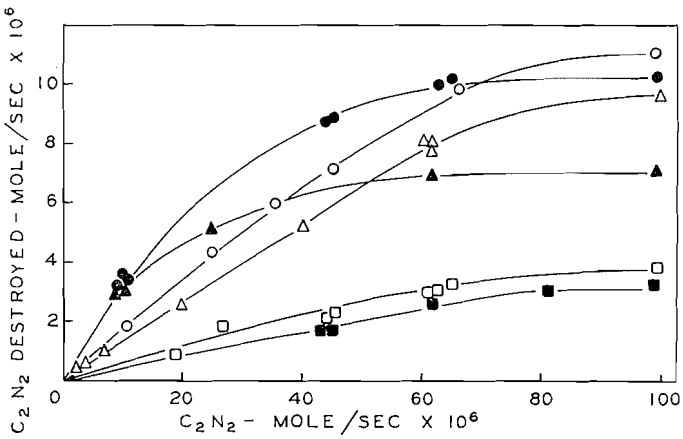


FIG. 1. Relation between amount of cyanogen destroyed by active nitrogen and the cyanogen flow rate. ○ P_{N_2} = 1.4 mm; T = 405° C. ● P_{N_2} = 3.1 mm; T = 410° C. △ P_{N_2} = 1.4 mm; T = 100° C. ▲ P_{N_2} = 3.1 mm; T = 115° C. □ P_{N_2} = 0.34 mm; T = 395° C. ■ P_{N_2} = 0.34 mm; T = 80° C.

The results obtained under the various experimental conditions suggested that NC radicals were formed in the cyanogen – active nitrogen reaction mixture. Since the NC radical, but not cyanogen itself, apparently reacts with hydrogen to produce HCN (9), while hydrogen does not react appreciably with active nitrogen, it seemed that the presence of CN radicals might be detected by the addition of hydrogen to the reaction mixture. Similarly, the addition of methane, which also reacts to a negligible extent with active nitrogen at lower temperatures, might be expected to cause reaction with CN radicals to produce HCN and CH_3CN.

A constant flow rate of hydrogen, 10 μmoles per second, was added to cyanogen prior to its introduction into the stream of active nitrogen. HCN was isolated from the reaction products in amounts which increased with increase of temperature. At flow rates of cyanogen below 6 μmoles per second, all the CN radicals produced in the cyanogen – active nitrogen mixture reacted with hydrogen to form HCN, and polymer formation was virtually eliminated. There was no evidence of a chain reaction, since the amount of HCN isolated was never greater than the amount of CN radicals formed, assuming that two CN radicals were produced for each cyanogen molecule destroyed. As the flow rate of cyanogen was increased, the presence of hydrogen was no longer able to eliminate the formation of polymer at either 124° or 440° C and the yield of HCN reached a plateau value, corresponding to about 30% reaction of the CN radicals with hydrogen.

To determine the amount of hydrogen necessary to react completely with all the CN radicals formed, experiments were made in which the cyanogen flow rate was maintained constant and the flow rate of hydrogen was varied. In this way it was found that at least 90% of the CN radicals produced could be isolated at 100° C as HCN when the hydrogen flow rate was some twenty-five times that of the flow rate of CN radicals, while at 400° C the hydrogen flow rate had to be about fifteen times that of the CN radicals for their complete conversion to HCN.

As an alternative to the large amounts of hydrogen necessary to react effectively with all the CN radicals formed, the use of methane as addend was investigated, since the abstraction of a hydrogen atom by a CN radical would result in the formation of a CH_3 radical which might be expected to combine easily with a second CN radical. When a constant flow rate of 40 μmoles per second of methane was added to the cyanogen at room

Can. J. Chem. Downloaded from www.nrcresearchpress.com by 41.223.56.140 on 09/04/12
For personal use only.

temperature, prior to its introduction into the reaction vessel, both HCN and CH_3CN were isolated from the reaction products. Both products attained plateau values at sufficiently high flow rates of cyanogen when about 60% of the CN radicals were consumed by methane. Unfortunately, the reaction of CN radicals with methane was limited to lower temperatures since the reaction of methane with active nitrogen becomes significant at temperatures above about 250° C.

Since the use of hydrogen permitted a measure of the CN radicals present in the cyanogen – active nitrogen mixture, it was possible to study the rate at which CN radicals were lost in being transported through the reaction vessel. A cylindrical reaction vessel was used so that cyanogen could be introduced into the active nitrogen stream through one inlet and hydrogen through other inlets placed at various distances, 3.1, 7.3, 11.3, and 26.6 cm, below the cyanogen inlet.

When 90 μmoles per second of hydrogen was added to the active nitrogen – cyanogen mixture through the second inlet, it was found that, at low flow rates of cyanogen, the majority of the CN radicals formed reacted with hydrogen to produce HCN. Hence, this amount of hydrogen was introduced through the third, fourth, and fifth inlets and the amount of HCN produced was determined to follow the destruction of CN radicals as they were transported through the reaction vessel.

The rate of destruction of CN radicals appears to follow first order kinetics, Table I. The rate constant at 95° C was 220 ± 10 sec^{-1} and at 400° C 125 ± 10 sec^{-1}. On this basis,

TABLE I

Rate of destruction of CN radicals

N_2 pressure (mm)	T (° C)	Flow rate (μmoles/sec)					
		C_2N_2	CN produced	HCN produced (inlet) 1	2	3	4
1.4	100	2.0	0.8	0.8	0.25	0.09	Nil
		5.5	1.6	1.6		0.15	0.1
		6.0	1.6	1.6	0.7	0.18	0.1
0.34	80	20.0	1.6	1.5		0.3	Traces
		45.0	3.5	1.7		0.3	0.02
1.4	400	5.0	2.2	2.1	1.1	0.8	0.2
		11.5	4.6	4.4		1.3	0.2
0.34	400	44.1	4.4	4.3		2.2	0.68
		45.0	4.3	4.3		2.2	0.7
3.1	410	9.0	6.4	4.5		1.0	Nil

$k_{av} = 220\pm10$ sec^{-1} at low temperature. $k_{av} = 125\pm10$ sec^{-1} at 400° C.

the process responsible for the destruction of CN radicals would have a negative activation energy of roughly -1.5 kcal and might be assumed to involve a wall reaction.

Since small amounts of cyanogen were sufficient to quench the active nitrogen afterglow, it was of interest to determine, if possible, the extent to which nitrogen atoms were destroyed in the process. Since ethylene is known to react rapidly with active nitrogen (3) to produce HCN, the introduction of ethylene into the reaction vessel below the site of the cyanogen – active nitrogen reaction should produce substantial amounts of HCN if relatively little destruction of nitrogen atoms by cyanogen occurred, whereas the formation of relatively small amounts of HCN should indicate that practically all the nitrogen atoms were destroyed by cyanogen. Cyanogen at the rate of 10 μmoles per second was

Can. J. Chem. Downloaded from www.nrcresearchpress.com by 41.223.56.140 on 09/04/12
For personal use only.

admitted into the reaction vessel and the amount of ethylene was varied from 20 to 50 μmoles per second. HCN was formed but the amount isolated was always less than the amount of CN radicals produced, corresponding to reaction of not more than 5% of the nitrogen atoms with ethylene.

Some, at least, of this HCN might have been formed by reaction of CN radicals with ethylene, since a small amount of liquid, possibly acrylonitrile, was formed during the reaction, perhaps by abstraction of a hydrogen atom from ethylene by CN radicals. It may therefore be assumed that at least 95% of the nitrogen atoms were destroyed by small amounts of cyanogen, even though only about 10% of the cyanogen was destroyed in the reaction.

The following series of reaction can account for the observed behavior of the cyanogen – active nitrogen reactions.

$$C_2N_2 + N \rightarrow [C_2N_2 . N] \rightarrow CN + CN_2 \quad (I)$$

$$CN_2 + N \rightarrow CN + N_2 \quad (II)$$

$$2[C_2N_2 . N] \rightarrow 2CN + C_2N_2 + N_2 \quad (III)$$

in competition with the catalytic recombination of nitrogen atoms

$$[C_2N_2 . N] + N \rightarrow C_2N_2 + N_2 \quad (IV)$$

The competition between reactions (I), (II), and (IV) can account for the slow rate at which cyanogen is destroyed by active nitrogen. At high temperatures, the rates of reactions (I) and (II) would be expected to increase, thus using more nitrogen atoms at the expense of reaction (IV), and the concentration of CN radicals would then approach the nitrogen atom concentration.

If only reactions (I), (II), and (IV) are considered, an increase in nitrogen pressure, up to 3.1 mm, would be expected to result in an increase in the rates of all three reactions and no difference should be noted in the rate at which cyanogen was destroyed (Fig. 1). However, it was found that an increase in pressure effected a more rapid rate of destruction of cyanogen and it is then necessary to include reaction (III) which would be expected to occur more readily as the total pressure in the reaction vessel was increased.

It may be noted that the present study does not support the view that the formation of HCN in the reactions of active nitrogen with hydrocarbons involves the initial formation of CN radicals, since such relatively large amounts of hydrogen or hydrocarbon are required to react with one cyanide radical. Furthermore, the results when methane was added indicate that, since hydrocarbon free radicals are presumably formed in the active nitrogen – hydrocarbon reactions, the formation of nitriles would be expected if CN radicals were present in significant amounts, and this behavior is not noted experimentally.

REFERENCES

1. J. H. GREENBLATT and C. A. WINKLER. Can. J. Research, B, **27**, 721 (1949).
2. P. A. GARTAGANIS and C. A. WINKLER. Can. J. Chem. **34**, 1457 (1956).
3. J. VERSTEEG and C. A. WINKLER. Can. J. Chem. **31**, 1 (1953).
4. R. VON NAUMAN. Z. Elektrochem. **16**, 772 (1910).
5. I. M. KOLTHOFF and E. B. SANDELL. Textbook of quantitative inorganic chemistry. Rev. ed. The Macmillan Co., New York. 1948.
6. H. OUILLEMARD. Bull. soc. chim. **I**(4), 196 (1907).
7. T. WALLIS. Ann. **345**, 352 (1906).
8. F. N. RHODES. Ind. Eng. Chem. **4**, 652 (1912).
9. C. HAGGART and C. A. WINKLER. Can. J. Chem. **37**, 1791 (1959).

Can. J. Chem. Downloaded from www.nrcresearchpress.com by 41.223.56.140 on 09/04/12
For personal use only.

Can. J. Chem. Downloaded from www.nrcresearchpress.com by 41.223.56.140 on 09/04/12
For personal use only.

THE REACTIONS OF ACTIVE NITROGEN WITH HYDROGEN SULPHIDE AND CARBON DISULPHIDE[1]

R. A. WESTBURY[2] AND C. A. WINKLER

ABSTRACT

The destruction of either hydrogen sulphide or carbon disulphide by active nitrogen appears to be minimal at some temperature in the range 200–250° C. Both reactions yield large amounts of polymer.

It is postulated that the main reactions involve destruction of the reactant as it acts as a third body for recombination of nitrogen atoms. As the temperature is increased, dissociation of the nitrogen atom – reactant complex apparently increases. To account for the observed temperature effects, it is assumed that reactions also occur to regenerate reactant.

INTRODUCTION

In his pioneering work with active nitrogen, Strutt (1) found it to react with both hydrogen sulphide and carbon disulphide and suggested that the respective reactions were

$$N + H_2S \rightarrow NS + H_2$$

and

$$N + CS_2 \rightarrow NS + CS$$

with subsequent polymerization of the NS and CS radicals. The N–H_2S reaction yielded a light yellow deposit, which was suggested to consist, "at all events in part", of nitrogen sulphide. Two separate polymers were produced in the N–CS_2 reaction. A blue deposit, which formed on the wall of the reaction vessel, was attributed to polymerized NS radicals. A brown-colored deposit, which appeared on the chilled surface of a liquid-air trap, was thought to be the polymeric carbon monosulphide described previously by Dewar and Jones (2).

The reactions have been studied spectroscopically by Strutt and Fowler (3) and by Fowler and Vaidya (4). A banded deep blue reaction flame was observed in both reactions, and Christy and Naude have shown (5) that this spectrum is derived from an allowed transition of the sulphur molecule, corresponding to the Schumann–Runge bands of oxygen. In the N–CS_2 reaction the only evidence for the presence of carbon was afforded by a weak band of the CN radical at λ 3883 Å.

EXPERIMENTAL

The apparatus used in the present study was of the fast-flow type described previously (6, 7).

Hydrogen sulphide (98.5% pure, Matheson) was twice partially fractionated, the first and last portions being rejected each time. This was followed by three complete cycles of thawing, freezing, and pumping to remove residual air, which was followed in turn by distillation from a bath at −78° C, (acetone – dry ice slurry). The gas finally obtained was sufficiently dry that it gave no indication of reaction with a clean mercury surface, while titration with standard alkali showed that, within experimental error, the gas was free of ammonia.

[1]*Manuscript received November 10, 1959.*
Contribution from the Upper Atmosphere Chemistry Research Group, the Physical Chemistry Laboratory, McGill University, with financial assistance from the National Research Council of Canada, Ottawa.
[2]*Holder of research grants, 1956–58, from the Scientific Research Bureau, Province of Quebec, Quebec.*

Ethylene (99%, Ohio Chemical Co.) was also given two bulb-to-bulb fractionations, followed by distillation from a bath at −78° C.

Carbon disulphide (reagent grade, Merck) was cycled four times through a treatment which consisted of cooling it to −78° C, followed by partial evacuation (10 minutes) and warming (to room temperature) to remove air and other possible volatile impurities. It was then dried by passage as a vapor through a column of activated alumina.

In the temperature range −23° C to +6° C, the purified carbon disulphide had a vapor pressure that agreed, within experimental error, with published data (8). To prevent its attack upon stopcock grease when experiments were not in progress, the purified carbon disulphide was stored at liquid-air temperature.

Unreacted hydrogen sulphide, after being absorbed into 15% NaOH solution, was analyzed by acidifying the solution, adding excess standard iodine solution, and then back-titrating with standard thiosulphate solution (9). Blank experiments showed that this scheme of analysis was quite satisfactory.

Ammonia, produced in the N–H_2S reaction, was absorbed in standard acid, which was then back-titrated with standard alkali after the acid solution had been heated to drive off residual hydrogen sulphide.

Hydrogen cyanide, produced in the high-temperature active nitrogen – ethylene reaction as a measure of nitrogen atom concentration, was titrated according to the Liebig–Dénigès method (10).

Unreacted carbon disulphide was estimated by distillation into a small glass bulb, which could then be weighed on an analytical balance. A graph was established to relate the amount of CS_2 to its pressure in a standard volume at room temperature, in order that reactant flow rates might be calculated from pressure–volume measurements.

RESULTS

The N–H_2S *Reaction*

The only reaction flame observed in the reaction was a deep blue glow that appeared to fill the entire upper half of the reaction vessel. This flame was almost invisible under normal artificial illumination, but could be seen clearly in a darkened room.

In conformity with the early qualitative studies of Strutt, a good deal of dark brown polymer was found to result from this reaction. Much of this polymer deposited on the wall of the reaction vessel when the reaction vessel was not heated externally, although a small amount was carried along in the gas stream, and deposited on the connecting tube to the cold trap. When the reaction vessel was heated externally, polymer was not deposited on the wall but on the cooler connecting tube, which gradually became quite black.

A reaction vessel in which polymer had been deposited at lower temperatures could be cleaned by heating it for 2 to 3 hours at 350° C.

The polymer that deposited on the wall of the reaction vessel was not stable. While it deposited as an unbroken layer, it began to evolve gas almost immediately, and after the polymer had been standing under vacuum for 4–5 days a number of "gas pockets", ranging in size from 5 mm to 20 mm, tended to force the polymer layer off the wall. Several attempts were made to remove the polymer layer intact for analysis, but all were unsuccessful. A dilute solution of ammonia, presumably because of its ability to attack the underlying phosphoric acid wall poison, quickly separated the polymer from the wall, while the solution itself became a deep violet color. However, the brown flakes and shreds almost as quickly hydrolyzed to sulphur.

Can. J. Chem. Downloaded from www.nrcresearchpress.com by 41.223.56.140 on 09/04/12
For personal use only.

Several attempts to remove the polymer layer from the reaction vessel by organic solvents, of which CS_2 appeared to be the most promising, gave unsatisfactory results. Only a small amount of material was ever recovered, much less than by using aqueous ammonia solution. The product obtained upon solvent evaporation was usually a reddish-brown sticky substance, which dried to a hard mass. Attempts to fractionate this substance yielded only oils, but qualitative tests showed it to contain both nitrogen and free sulphur.

When present on the wall of the reaction vessel, the polymer markedly affected the decay of the active nitrogen. It appeared to act as a more efficient poison than the 2% metaphosphoric acid normally used, since the nitrogen afterglow was perceptibly brighter after some polymer had been deposited on the wall. It might be noted that Strutt found hydrogen sulphide to be the most effective of a number of substances that he introduced with the nitrogen to poison the walls of the discharge tube and reaction vessel (11).

Special precautions, which need not be detailed here, were taken to ensure that this poisoning effect did not vitiate the experimental results (12).

The amounts of H_2S destroyed at different flow rates, over a range of temperatures,

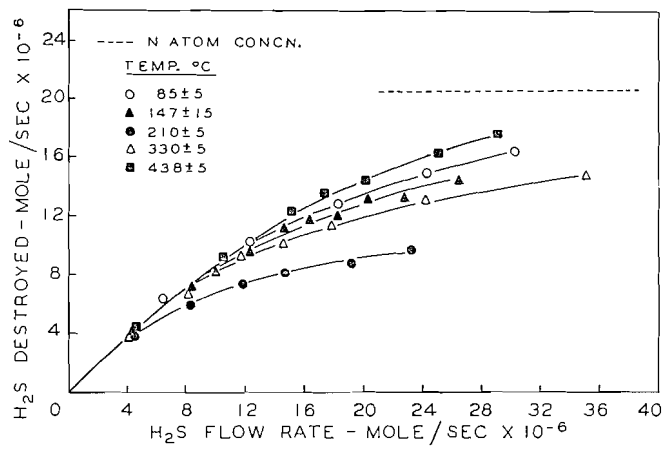


FIG. 1. Relation between H_2S flow rate and amount of H_2S destroyed by active nitrogen at different temperatures.

are shown in Fig. 1. Further experiments using a new discharge tube showed that the reaction was quite reproducible in its behavior with increase in temperature. The amount of ammonia recovered as a product of the reaction was virtually independent of temperature, and accounted for only about 3% of the nitrogen atom concentration, as estimated from the maximum HCN production in the active nitrogen – ethylene reaction.

The N–CS_2 *Reaction*

In this reaction, a pale blue flame was observed to fill the entire reaction vessel at high reactant flow rates, and continue some distance along the connecting tube to the pump. Examination with a small spectroscope (1-in. prism) showed this flame to be a continuum (within the resolution of the instrument) with its limits lying roughly between

Can. J. Chem. Downloaded from www.nrcresearchpress.com by 41.223.56.140 on 09/04/12
For personal use only.

λ 4200 Å and λ 6400 Å. At very low flow rates of CS_2, however, this apparent continuum disappeared, to be replaced by what appeared to be the red and violet band systems of the CN radical.

Preliminary work showed that the reaction deposited a good deal of brown polymer on the wall of an unheated reaction vessel. This polymer was similar in appearance to that produced in the N–H_2S reaction, and it, too, slowly evolved gas upon standing. Most, but not all, of this polymer could be removed from the wall of the reaction vessel by heating it strongly. No analysis of the polymer was attempted, owing to the difficulty of removing it and its ease of hydrolysis, in which respects it resembled the polymer from the N–H_2S reaction.

The reaction was complicated by the appearance of a second polymer, of brownish-black color, which spread as a thin dark film on the tube connecting the reaction vessel to the pump, but deposited mainly on the wall of the first trap cooled with liquid air. This second polymer would seem to be the polymeric carbon monosulphide first described by Dewar and Jones (2), since its deposition, if continued long enough (50–100 seconds, depending upon the flow rate of CS_2) almost invariably resulted in an explosion in the trap.

It was quickly realized that the N–CS_2 reaction could be studied successfully only if the explosions could be prevented. This was necessary, since the reaction was followed by recovery and estimation of the unreacted CS_2 at various reactant flow rates, and it was obvious that the explosions might vitiate the results, apart from possible damage to the apparatus. (On several occasions, at the conclusion of an experiment, a vacuum could not be attained prior to distillation of the trapped CS_2, because the explosion had cracked the wall of the trap).

There are a number of references in the literature to this polymerized carbon monosulphide, but no information was available on possible methods of moderating or eliminating the explosions. Experiments showed that coolants at −112° C or −130° C were only partially successful, in that they did not prevent entirely the explosions that occurred in a following trap cooled with liquid air. However, a slurry of isopentane (approximately −160° C) was completely successful in allowing the reaction products to be condensed without subsequent explosion, and as a consequence a slurry of isopentane was usually used to trap excess CS_2 from the flowing gas stream. No explosion was ever observed with such trapping conditions, and blank experiments showed that CS_2 vapor was trapped quantitatively.

The actual character of the explosions is difficult to describe. During an experiment there would be a sudden sharp "click", a flash of light from the tube, and the liquid-air coolant would bubble vigorously for several seconds, indicative of a quite exothermic reaction. On several occasions the discharge faltered for a few tenths of a second, as if there had been a sudden rise of pressure within the discharge tube. Occasionally, the expected explosion did not occur during the deposition of the CS radical, but did take place 1 to 2 minutes after an experiment had been completed, with the discharge shut off, and no gas flowing through the system.

Analysis of the black polymer deposited at −160° C showed it to be a mixture of paracyanogen and $(CS)x$.

In Fig. 2 are shown the relations between the CS_2 flow rates and the amounts of CS_2 destroyed at different temperatures. These data were quite reproducible. The "Prussian blue" test gave no qualitative indication of cyanogen in the condensible products at any of the three reaction temperatures used.

Can. J. Chem. Downloaded from www.nrcresearchpress.com by 41.223.56.140 on 09/04/12
For personal use only.

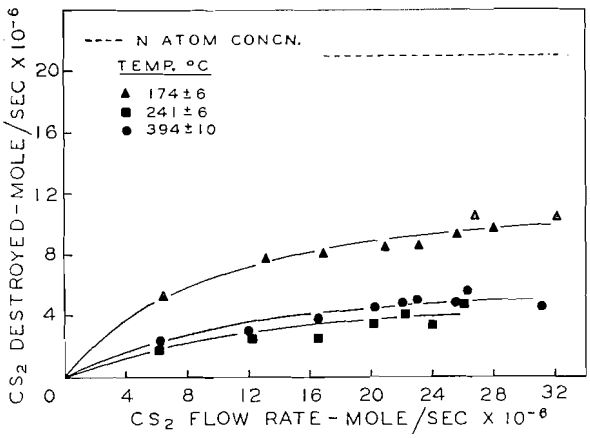


FIG. 2. Relation between CS_2 flow rate and amount of CS_2 destroyed by active nitrogen at different temperatures.

DISCUSSION

It is readily apparent from Figs. 1 and 2 that in both the N–H_2S and N–CS_2 reactions the amount of reactant destroyed passes through a minimum as the temperature is raised. It is tempting to explain this behavior in a similar manner for the two substances, and it will be seen that the proposed mechanisms do have a good deal in common.

The N–H_2S *Reaction*

The initial step involved in this reaction must certainly be the formation of a transition complex

$$N + H_2S \rightarrow N.H_2S. \qquad [1]$$

Decomposition of the complex by the reaction

$$N.H_2S \rightarrow NH + HS \qquad [2]$$

would seem to be improbable, not only because hydrogenation of the imino radical might be expected to yield ammonia in rather larger quantities than those found, but the fast reaction observed does not seem compatible with an activation energy of at least 7 kcal/mole for reaction [2].[3]

The complex might well decompose in the manner suggested by Strutt, i.e.

$$N.H_2S \rightarrow NS(^2\Pi) + H_2 \text{ (see footnote 4)} \qquad [3]$$

since the over-all change represented by reactions [1] and [3] is exothermic to the extent of 44 kcal/mole. However, it does not seem possible to account for the experimental results solely by these reactions.

Decomposition of the $N.H_2S$ complex by reaction [3] involves a change of spin, as well as the splitting of two bonds, and, as such, is likely to require a significant activation energy (13). It is suggested, therefore, that at lower temperatures this complex will have

[3]*Heats of reaction have been calculated on the basis of the following bond energies.* $D(H_2)$, *103.2;* $D(N_2)$, *225.0;* D(NH), *85; (T. L. Cottrell. The strength of chemical bonds. 2nd ed. Butterworth Scientific Publications, London. 1958).* $D(S_2)$, *101.5;* D(NS), *115; (A. G. Gaydon. Dissociation energies and spectra of diatomic molecules. 2nd ed. Chapman & Hall, Ltd., London. 1953).* D(H–SH), *92; (D. P. Stevenson. Trans. Faraday Soc.* **49**, *867 (1953)).* D(S=CS), *90; (L. P. Blanchard and P. LeGoff. Can. J. Chem.* **35**, *89 (1957)).* D(SH), *82;* D(CS), *184; (calculated).*

Can. J. Chem. Downloaded from www.nrcresearchpress.com by 41.223.56.140 on 09/04/12
For personal use only.

a lifetime long enough that it might suffer a collision with a second nitrogen atom at low flow rates, or with another $N.H_2S$ complex, at higher flow rates of H_2S, to induce catalytic recombination of nitrogen atoms, with concomitant dissociation of the H_2S molecule. This may be represented at low flow rates of H_2S by

$$N + N.H_2S \rightarrow N_2 + H + HS + 133 \text{ kcal} \quad [4]$$

$$\rightarrow N_2 + 2H + S + 51 \text{ kcal} \quad [5]$$

and at higher flow rates by

$$N.H_2S + N.H_2S \rightarrow N_2 + H_2S + H + HS + 133 \text{ kcal} \quad [6]$$

$$\rightarrow N_2 + H_2S + 2H + S + 51 \text{ kcal} \quad [7]$$

$$\rightarrow N_2 + 2H + 2HS + 41 \text{ kcal.} \quad [8]$$

The hydrogen atoms formed in reactions [4] to [8] should destroy H_2S by the fast reaction

$$H + H_2S \rightarrow H_2 + HS + 11 \text{ kcal} \quad [9]$$

while the HS radicals probably interact by

$$2HS \rightarrow H_2S + S + 10 \text{ kcal} \quad [10]$$

$$\rightarrow H_2 + S_2 + 40 \text{ kcal.} \quad [11]$$

Darwent and Roberts (14) have found, by a steady-state approximation, that at room temperature 87% of the effective collisions of two HS radicals result in reaction [10], and the remaining 13% in reaction [11]. These authors concluded that reactions [10] and [11] occurred rapidly, and without appreciable activation energy. Some, though probably slight, regeneration of H_2S at 35° C might also result from hydrogen atom reaction with sulphur, since experiments showed that hydrogen atoms removed sulphur from the wall of the reaction vessel at room temperature.

The decrease in destruction of H_2S as the temperature is increased to 210° C may now be attributed to the increased recombination of hydrogen atoms at the higher temperature, together with increased regeneration of H_2S from attack of hydrogen atoms on sulphur, perhaps in the gas phase, or as a wall reaction. The apparent increase in destruction of H_2S at still higher temperatures may be explained by assuming that at these higher temperatures, decomposition of the $N.H_2S$ complex by reaction [3] becomes predominant. This follows from the earlier suggestion that this reaction probably has an appreciable activation energy. Decomposition of the $N.H_2S$ complex by reaction [3] would immediately result in a decrease in the production of H atoms and HS radicals, and this in turn should accentuate the decrease in the back reaction [10].

The small amounts of ammonia recovered probably had their origin in the known reaction of nitrogen atoms with hydrogen atoms (15), followed by hydrogenation of the NH radical.

The appearance of polymer is readily understood by polymerization of the NS radical. The monomer might also be produced, particularly at low flow rates of H_2S, by additional reactions such as

$$N + HS \rightarrow NS + H + 33 \text{ kcal,} \quad [12]$$

$$N + S_2 \rightarrow NS + S + 14 \text{ kcal,} \quad [13]$$

[4]*The ground state of the* NS *radical is* $^2\Pi$; *cf. R. F. Barrow, G. Drummond, and P. B. Zeeman. Proc. Phys. Soc. (London), A,* **67**, *365 (1954).*

Can. J. Chem. Downloaded from www.nrcresearchpress.com by 41.223.56.140 on 09/04/12
For personal use only.

and

$$N + S + M \rightarrow NS + M + 115 \text{ kcal.} \quad [14]$$

In addition to a number of nitrogen sulphides in various degrees of polymerization, free sulphur might also be expected to deposit, as observed, on the wall of the reaction vessel or on the connecting tubing.

The N–CS_2 *Reaction*

As for the N–H_2S reaction, it is suggested that the initial step by which carbon disulphide is destroyed by active nitrogen is formation of a complex

$$N + CS_2 \rightarrow N.CS_2 \quad [15]$$

which might be expected to decompose according to

$$N.CS_2 \rightarrow NS(^2\Pi) + CS. \quad [16]$$

Reactions [15] and [16], considered as a whole, are of course equivalent to the over-all reaction suggested by Strutt,

$$N + CS_2 \rightarrow NS + CS.$$

However, this reaction involves a change of spin if, as seems probable from its relatively long lifetime, the CS radical is formed in the singlet state. This relatively long lifetime is clearly indicated since about 0.3 second was required for the CS radical to pass from the reaction vessel to the trap where explosions occurred. Moreover, Parker has found (16) by flash photolysis of CS_2, that the half life of the reaction

$$n\text{CS} \rightarrow (\text{CS})_n \quad [17]$$

was 60 seconds, and he concluded that a half life of this magnitude implied that the CS radical was in the singlet state. Dyne and Ramsay (17) have concluded that, in the gas phase, CS shows the chemical stability of a normal molecule, and this again is consistent only with the singlet state of the radical.

By analogy, then, with H_2S, it is suggested that the destruction of the $N.CS_2$ complex by reaction [16] requires an activation energy, so that, at lower temperatures, the complex may have sufficient lifetime to suffer collision with a further nitrogen atom, at low flow rates of CS_2, or with another complex, at higher reactant flow rates. At low reactant flow rates, the reaction would be

$$N + N.CS_2 \rightarrow N_2 + CS + S + 135 \text{ kcal} \quad [18]$$

while at higher flow rates it would be

$$N.CS_2 + N.CS_2 \rightarrow N_2 + CS_2 + CS + S + 135 \text{ kcal} \quad [19]$$

$$\rightarrow N_2 + 2CS + 2S + 45 \text{ kcal.} \quad [20]$$

It will be noted that the similarity to the mechanism suggested for the N–H_2S reaction is not complete, because there is not enough energy available to break both bonds in the CS_2 molecule.

Again, the results indicate that a reaction to regenerate the parent sulphur compound is an important factor in the mechanism. It might also be inferred from Fig. 2 that this regeneration reaction requires some activation energy, since otherwise more regeneration of CS_2, hence less apparent destruction of it, might have been expected than was actually found at 174° C.

The regeneration step might well be

$$CS + S \rightarrow CS_2^* \rightarrow CS_2 + h\nu \quad [21]$$

Can. J. Chem. Downloaded from www.nrcresearchpress.com by 41.223.56.140 on 09/04/12
For personal use only.

in which the collision complex is probably in a triplet state to conserve spin. This is by analogy with the reactions

$$CO + O \rightarrow CO_2^* \rightarrow CO_2 + h\nu \text{ (continuous spectrum)} \quad [22]$$

and

$$CO + O + M \rightarrow CO_2^{**} + M \quad [23]$$

followed by

$$CO_2^{**} \rightarrow CO_2 + h\nu \text{ (band spectrum)} \quad [24]$$

by which the CO flame spectrum may be interpreted (18).

Broida and Gaydon (19) have recently concluded, from studies of the oxygen atom – carbon monoxide reaction, that reaction [22] has an appreciable activation energy, while [23] followed by [24], which occurred rapidly at room temperature, was suggested to require little or no activation energy. It is quite possible that reaction [21] might require rather less activation energy than [22], since the CS radical is probably more reactive than CO.

The analogue of reaction [23] is also possible as a regenerative reaction i.e.

$$CS + S + M \rightarrow CS_2^{**} + M \quad [25]$$

followed of course by

$$CS_2^{**} \rightarrow CS_2 + h\nu \quad [26]$$

and by reasoning similar to the above, reaction [25] should have virtually no activation energy.

Choice between [21] and [25] as the main reaction for regeneration of CS_2 probably can be made only on the basis of spectroscopic data, and a spectroscope of sufficient resolution was not available. As indicated earlier, examination of the N–CS_2 flame with a small glass spectroscope revealed the spectrum to be a continuum, but this is scarcely an adequate basis on which to distinguish between the two reactions.

It is apparent that reactions [18] to [21], the last with a small but significant activation energy, are able to explain both the high rate of destruction of CS_2 by active nitrogen at 174° C, and the apparent decrease in the amount of CS_2 destroyed as the temperature is raised. The increase destruction of CS_2 at 394° C relative to that at 241° C can be explained by assuming that, at the higher temperature, the rate of destruction of CS_2 by reaction [16] becomes important relative to its destruction by reactions [18] to [20] and its regeneration by reaction [21]. This explanation is similar to that suggested for the corresponding behavior of the N–H_2S reaction at high temperatures.

The suggestion that reaction [21] has an activation energy raises a question concerning those sulphur atoms and CS radicals, produced at 174° C, that do not react further by [21]. The fate of these entities must be to deposit eventually on the wall of the reaction vessel, although they may also react by reactions [11] and [12], or by

$$N + CS \rightarrow CN + S + 4 \text{ kcal} \quad [27]$$

followed by

$$2CN + M \rightarrow (CN)_2 + M. \quad [28]$$

Reactions [27] and [28] are consistent both with the small amount of paracyanogen present in the CS matrix, and with the appearance of CN bands in the N–CS_2 reaction flame at very low CS_2 flow rates.

Can. J. Chem. Downloaded from www.nrcresearchpress.com by 41.223.56.140 on 09/04/12
For personal use only.

REFERENCES

1. R. J. STRUTT. Proc. Roy. Soc. (London), A, **88**, 539 (1913).
2. SIR JAMES DEWAR and H. O. JONES. Proc. Roy. Soc. (London), A, **85**, 574 (1911).
3. R. J. STRUTT and A. FOWLER. Proc. Roy. Soc. (London), A, **86**, 105 (1912).
4. A. FOWLER and W. H. VAIDYA. Proc. Roy. Soc. (London), A, **132**, 310 (1931).
5. A. CHRISTY and S. M. NAUDE. Phys. Rev. **37**, 490, 903 (1931).
6. J. H. GREENBLATT and C. A. WINKLER. Can. J. Research, B, **27**, 721 (1949).
7. P. GARTAGANIS and C. A. WINKLER. Can. J. Chem. **34**, 1475 (1956).
8. D. R. STULL. Ind. Eng. Chem. **39**, 517 (1947).
9. W. W. SCOTT. Standard methods of chemical analysis. 5th ed. *Edited by* N. H. Furman. D. Van Nostrand, Co., Inc., New York. 1939.
10. I. M. KOLTHOFF and E. B. SANDELL. Textbook of quantitative inorganic analysis. 3rd ed. The Macmillan Co., New York. 1952.
11. R. J. STRUTT. Proc. Roy. Soc. (London), A, **91**, 303 (1915).
12. R. A. WESTBURY. Thesis, McGill University, Montreal, Que. 1959.
13. H. G. V. EVANS and C. A. WINKLER. Can. J. Chem. **34**, 1217 (1956).
14. B. DE B. DARWENT and R. ROBERTS. Proc. Roy. Soc. (London), A, **216** (1953).
15. B. LEWIS. J. Am. Chem. Soc. **50**, 27 (1928).
16. G. PARKER. Proc. Roy. Soc. (London), A, **200**, 284 (1950).
17. P. J. DYNE and D. A. RAMSAY. J. Chem. Phys. **20**, 1055 (1952).
18. A. G. GAYDON. The spectroscopy of flames. Chapman & Hall, Ltd., London. 1957.
19. H. P. BROIDA and A. G. GAYDON. Trans. Faraday Soc. **49**, 1190 (1953).

Can. J. Chem. Downloaded from www.nrcresearchpress.com by 41.223.56.140 on 09/04/12
For personal use only.

Can. J. Chem. Downloaded from www.nrcresearchpress.com by 41.223.56.140 on 09/04/12
For personal use only.

BACTERIOSTATS

III. OXYAMINES AND THEIR DERIVATIVES[1]

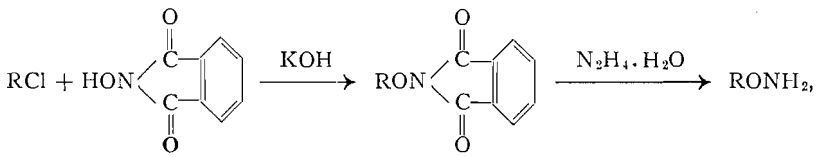
A. F. McKay, D. L. Garmaise, G. Y. Paris, and S. Gelblum

ABSTRACT

A number of benzyloxyamines were prepared for conversion into urea and thiourea derivatives. The benzyloxyamine hydrochlorides on treatment with phosgene gave a mixture of the corresponding benzyl 4-(benzyloxy)-allophanate and benzyloxycarbamyl chloride. Triethylamine converted the benzyloxycarbamyl chlorides into the corresponding 1,3,5-tri-(benzyloxy)-isocyanuric acids. The reactions of the allophanates with amines and sodium hydroxide are described.

A series of oxyamine derivatives has been examined for bacteriostatic activity. These O-substituted oxyamines were prepared by one of the following three routes;

$$RCl + HONHCOOC_2H_5 \xrightarrow{KOH} RONHCOOC_2H_5 \xrightarrow[H_2O]{KOH} RONH_2, \qquad [1]$$



[2]

$$RCl + HON(SO_3K)_2 \xrightarrow{KOH} RON(SO_3K)_2 \xrightarrow[H_2O]{H_2SO_4} RONH_2. \qquad [3]$$

The majority of the urea and thiourea derivatives listed in Table I were obtained by the addition of isocyanates or isothiocyanates to a solution of the oxyamine in an inert solvent such as ether or benzene. 1-(β-Hydroxyethyl)-2-(2,4-dichlorobenzyloxyamino)-2-imidazoline was formed by the reaction of 2,4-dichlorobenzyloxyamine with 1-(β-hydroxyethyl)-2-methylmercapto-2-imidazolinium chloride. β-Aminoethylamine dihydrochloride, γ-aminopropyloxyamine, N-(α-naphthylmethyloxy)-urethane, and N,N′-dicarbethoxy-α,α′-di-(aminoöxy)-p-xylene also were prepared during this investigation.

All of the oxythiourea derivatives were unstable. The white crystalline products, after standing at room temperature for several weeks, changed into a mixture of crystals and red, viscous oil. The product from 1-(3,4-dichlorobenzyloxy)-3-(3,4-dichlorobenzyl)-thiourea was separated into free sulphur, 1,3,5-tri-(3,4-dichlorobenzyl)-isomelamine, and unchanged thiourea. In 1891 Voltmer found that heating 1-ethoxy-3-phenyl-thiourea in solution split it into sulphur, ethanol, and phenylcyanamide according to the following equation

$$C_6H_5NHC(S)NHOCH_3 \rightarrow C_6H_5NHCN + S + C_2H_5OH.$$

The scission of crystalline oxythioureas undoubtedly follows a similar course but in this case the generated 3,4-dichlorobenzylcyanamide trimerized to 1,3,5-tri-(3,4-dichlorobenzyl)-isomelamine (m.p. 171–172° C). N^2,N^4,N^6-Tri-(3,4-dichlorobenzyl)-melamine

[1]*Manuscript received November 10, 1959.*
Contribution No. 25 from the L. G. Ryan Research Laboratories of Monsanto Canada Limited, LaSalle, Que.

Can. J. Chem. Downloaded from www.nrcresearchpress.com by 41.223.56.140 on 09/04/12
For personal use only.

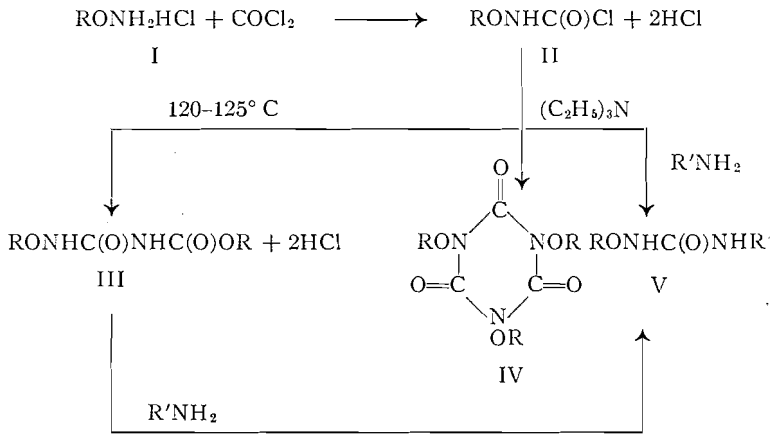
TABLE I

R	R′	X	M.p. (°C)	Yield (%)	Formula	C		H		Cl		N	
						Calc.	Found	Calc.	Found	Calc.	Found	Calc.	Found
(*A*) Urea and thiourea derivatives RONHC(X)NHR′													
4-$ClC_6H_4CH_2$	4-ClC_6H_4	O	154–155[a]	74[g]	$C_{14}H_{12}Cl_2N_2O_2$	54.03	54.02	3.89	3.84	22.79	22.97	9.00	9.26
4-$ClC_6H_4CH_2$	4-BrC_6H_4	O	158–159[a]	98[g]	$C_{14}H_{12}BrClN_2O_2$[i]	47.30	47.25	3.40	3.32			7.88	8.32
4-$ClC_6H_4CH_2$	2,5-$Cl_2C_6H_3$	O	135–136[a]	94[g]	$C_{14}H_{11}Cl_3N_2O_2$	48.66	48.84	3.21	3.18	30.78	30.88	8.11	8.50
4-$ClC_6H_4CH_2$	$CH_3(CH_2)_{10}$—	O	81–82[b]	77.5[g]	$C_{19}H_{31}ClN_2O_2$	64.30	64.56	8.81	8.86	9.99	10.02	7.89	7.64
4-$ClC_6H_4CH_2$	CH_2=$CH(CH_2)_8$—	O	70–71[b]	80[g]	$C_{18}H_{27}ClN_2O_2$	63.79	63.72	8.03	7.80	10.46	10.83	8.27	8.40
4-$ClC_6H_4CH_2$	$C_{10}H_7$	O	165–166[c]	86[g]	$C_{18}H_{15}ClN_2O_2$	66.13	66.18	4.63	4.81	10.85	10.74	8.57	8.84
4-$ClC_6H_4CH_2$	4-$ClC_6H_4CH_2$	O	123–124[d]	88.5[h]	$C_{15}H_{14}Cl_2N_2O_2$	55.40	55.43	4.34	4.44	21.81	21.69	8.62	8.61
4-$ClC_6H_4CH_2$	3,4-$Cl_2C_6H_3CH_2$	O	140–141[d]	78[h]	$C_{15}H_{13}Cl_3N_2O_2$	50.09	50.48	3.64	3.63	29.57	29.64	7.79	8.00
4-$ClC_6H_4CH_2$	C_6H_5	S	120–121[d]	100[g]	$C_{14}H_{13}ClN_2OS$[j]	57.42	57.02	4.47	4.44	12.11	12.19	9.57	9.77
4-$ClC_6H_4CH_2$	4-$ClC_6H_4CH_2$	S	115–116[d]	99[g]	$C_{15}H_{14}Cl_2N_2OS$[k]	52.78	53.09	4.13	4.44	20.78	20.46	8.21	8.28
4-$ClC_6H_4CH_2$	3,4-$Cl_2C_6H_3CH_2$	S	116–117[d]	100[g]	$C_{15}H_{13}Cl_3N_2OS$[l]	47.95	47.96	3.49	3.58	28.31	28.51	7.46	7.59
2,4-$Cl_2C_6H_3CH_2$	2,5-$Cl_2C_6H_3$	O	173–174[a]	73.5	$C_{14}H_{10}Cl_4N_2O_2$	44.24	44.20	2.65	2.71	37.32	37.25	7.37	7.49
2,4-$Cl_2C_6H_3CH_2$	4-$ClC_6H_4CH_2$	O	115–116	44[h]	$C_{15}H_{13}Cl_3N_2O_2$	50.09	50.43	3.64	3.53	29.52	29.46	7.78	7.57
2,4-$Cl_2C_6H_3CH_2$	3,4-$Cl_2C_6H_3CH_2$	S	86–87[e]	48.7[g]	$C_{15}H_{12}Cl_4N_2OS$[m]	43.91	44.01	2.95	3.07	34.58	34.30	6.83	6.82
3,4-$Cl_2C_6H_3CH_2$	4-ClC_6H_4	O	141–142[a]	89.5[g]	$C_{14}H_{11}Cl_3N_2O_2$	48.66	48.60	3.21	3.45	30.78	31.01	8.11	8.33
3,4-$Cl_2C_6H_3CH_2$	4-BrC_6H_4	O	148–149[a]	90.8	$C_{14}H_{11}BrCl_2N_2O_2$[n]	43.10	43.13	2.84	2.95			7.18	7.38
3,4-$Cl_2C_6H_3CH_2$	2,5-$Cl_2C_6H_3$	O	153–154[f]	92[g]	$C_{14}H_{10}Cl_4N_2O_2$	44.24	44.37	2.65	2.75	37.32	37.71	7.37	7.60
3,4-$Cl_2C_6H_3CH_2$	4-$ClC_6H_4CH_2$	O	119–120	100[h]	$C_{15}H_{13}Cl_3N_2O_2$	50.09	50.35	3.64	3.64	29.52	29.42	7.78	7.74
3,4-$Cl_2C_6H_3CH_2$	4-$ClC_6H_4CH_2$	S	121–122[d]	96[g]	$C_{15}H_{13}Cl_3N_2OS$[o]	47.95	48.40	3.49	3.50	28.31	28.45	7.46	7.80
3,4-$Cl_2C_6H_3CH_2$	3,4-$Cl_2C_6H_3CH_2$	S	107–108[d]	100[g]	$C_{15}H_{12}Cl_4N_2OS$[p]	43.91	43.93	2.95	2.95	34.58	34.60	6.83	6.75
3,4-$Cl_2C_6H_3CH_2$	CH_3	S	129–130[a]	25[g]	$C_9H_{10}Cl_2N_2OS$[q]	40.77	40.90	3.80	3.91	26.74	26.42	10.52	10.67
4-$NO_2C_6H_4CH_2$	4-$ClC_6H_4CH_2$	O	170–171	50.5[h]	$C_{15}H_{15}ClN_3O_4$	53.66	53.88	4.20	3.90	10.52	10.48	12.53	12.37
(*B*) Diurea derivatives R(NHC(O)NHOR′)$_2$													
$(CH_2)_6$	4-$ClC_6H_4CH_2$		142–143[f]	83.5	$C_{22}H_{28}Cl_2N_4O_2$	54.65	54.62	5.84	5.83	14.67	15.01	11.59	11.54
2,4-Tolyl	4-$ClC_6H_4CH_2$		141–142[r]	81.0	$C_{23}H_{22}Cl_2N_4O_2$	56.44	56.78	4.83	4.65	14.49	14.15	11.45	11.52

[a]Crystallized from ethyl acetate – petroleum ether. [b]From petroleum ether. [c]From acetone–water. [d]From absolute ethanol. [e]From ether – petroleum ether. [f]From ethyl acetate. [g]Prepared from the corresponding isocyanates and isothiocyanates. [h]Prepared from the corresponding allophanates and amines. [i]Halogen: calc., 32.46; found, 32.22. [j]S: calc., 10.95; found, 11.68. [k]S: calc., 9.39; found, 9.01. [l]S: calc., 8.53; found, 8.68. [m]S: calc., 7.82; found, 7.73. [n]Halogen: calc., 38.67; found, 38.53. [o]S: calc., 7.82; found, 7.85. [p]S: calc., 8.53; found, 8.55. [q]S: calc., 12.09; found, 11.78. [r]From ethyl acetate – petroleum ether (1:1) solution.

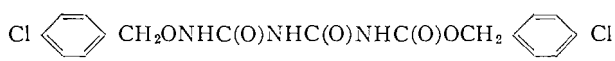
(m.p. 217–218° C) was prepared from the reaction of cyanuric chloride with 3,4-dichlorobenzylamine for comparison with the isomelamine derivative.

Earlier attempts (2, 3, 4) to prepare esters or salts of the hypothetical acid HONCO have been described in the literature. We also were unsuccessful in preparing the monomeric esters but the corresponding allophanates III and trimers IV were isolated. Phosgene combined with the substituted oxyamines to give the corresponding crude oxycarbamyl chlorides (II).



R = $C_6H_5CH_2$; 4-$ClC_6H_4CH_2$; 4-$NO_2C_6H_4CH_2$; 2,4-$Cl_2C_6H_3CH_2$; 3,4-$Cl_2C_6H_3CH_2$.
R′ = 3,4-$Cl_2C_6H_3$; 4-$ClC_6H_4CH_2$.

4-Chlorobenzyloxycarbamyl chloride (II, R = 4-$ClC_6H_4CH_2$—) on treatment with 2 equivalents of 3,4-dichloroaniline gave the calculated yield of 3,4-dichloroaniline hydrochloride and a 51% yield of 1-(4-chlorobenzyloxy)-3-(3,4-dichlorophenyl)-urea (V, R = 4-$ClC_6H_4CH_2$, R′ = 3,4-$Cl_2C_6H_3$). When 4-chlorobenzylamine was added to crude 4-chlorobenzyloxycarbamyl chloride (II, R = 4-$ClC_6H_4CH_2$) in ether, small amounts of 1,5-di-(4-chlorobenzyl)- and 1-(4-chlorobenzyloxy)-5-(4-chlorobenzyl)-biurets were obtained together with the expected 1-(4-chlorobenzyloxy)-3-(4-chlorobenzyl)-urea (V, R and R′ = 4-$ClC_6H_4CH_2$). This indicates that part of the oxycarbamyl chloride and/or the oxyamine hydrochloride is converted into carbamyl chloride and the corresponding benzyl alcohol under the conditions of the phosgene reaction. The benzyl alcohol could be expected to combine with phosgene or carbamyl chloride to yield 4-chlorobenzyl chloroformate or 4-chlorobenzyl carbamate. These products and the unchanged oxycarbamyl chloride supply the components required in the formation of the allophanates (III). The allophanates in turn combine with amines to give derivatives of biuret (5, 6, 7). When non-anhydrous chlorobenzene was used as a solvent in the reaction of phosgene with 4-chlorobenzyloxyamine hydrochloride, a low yield (11.5%) of 4-chlorobenzyl 4-(4-chlorobenzyloxycarbamyl)-allophanate (VI) was



VI

isolated.

If the oxyamine hydrochlorides (I) are heated to 120–125° in anhydrous chlorobenzene

Can. J. Chem. Downloaded from www.nrcresearchpress.com by 41.223.56.140 on 09/04/12
For personal use only.

during the reaction with phosgene, they are converted mainly into the corresponding benzyl 4-(benzyloxy)-allophanates (III). When benzyloxyamine hydrochloride was treated with phosgene under these conditions, the benzyl group was chlorinated and 4-chlorobenzyl 4-(4-chlorobenzyloxy)-allophanate (III, R = 4-$ClC_6H_4CH_2$) was obtained. Some unchanged oxycarbamyl chlorides remained in solution after the allophanates were recovered by precipitation with ether. The ether solutions on treatment with triethylamine yielded the corresponding 1,3,5-tribenzyloxy-isocyanuric acids (IV). Several of the oxyurea derivatives (V) described in Table I(*A*) were obtained by heating the aralkyl 4-aralkyloxy-allophanates (III) with amines in chlorobenzene under reflux. The main product from the reaction of 4-chlorobenzylamine with 4-chlorobenzyl 4-(4-chlorobenzyloxy)-allophanate was 1-(4-chlorobenzyloxy)-3-(4-chlorobenzyl)-urea (88% yield) but small quantities of *O*-(4-chlorobenzyl)-4-chlorobenzaldoxime and 1,5-di-(4-chlorobenzyl)-biuret also were isolated.

The products from the treatment of 4-chlorobenzyl 4-(4-chlorobenzyloxy)-allophanate (III, R = 4-$ClC_6H_4CH_2$) with alkali indicate that a rather complex series of reactions occur. The allophanate splits partly into 4-chlorobenzyl alcohol, 4-chlorobenzyloxyamine, 4-chlorobenzaldehyde, and 1-(4-chlorobenzyloxy)-urea. Then 4-chlorobenzyloxyamine condenses with the original allophanate to give 1,5-di-(4-chlorobenzyloxy)-biuret. It also could be considered to combine with 4-chlorobenzaldehyde to produce the isolated *O*-(4-chlorobenzyl)-4-chlorobenzaldoxime. When 3,4-dichlorobenzyl 4-(3,4-dichlorobenzyloxy)-allophanate was treated with methanolic sodium hydroxide solution, 3,4-dichlorobenzaldehyde was isolated from the products as its 2,4-dinitrophenylhydrazone. The other product, which was isolated from this reaction, was 1,5-di-(3,4-dichlorobenzyloxy)-biuret.

Absorption Spectra

The infrared absorption bands associated with the N—H and C=O groups are given in Table II. The infrared absorption bands assigned to the C=O stretching modes in the oxyurea derivatives agree with those assigned in the urea series (8). When an aryl group is attached directly to a nitrogen atom of the urea then the absorption band of the C=O group shifts from 1642–1653 cm^{-1} to 1666–1678 cm^{-1}. In the carbamates, the C=O absorption band occurs between the frequencies associated with the ester and amide C=O group (9). Allophanates display two absorption peaks between 1700 and 1718 cm^{-1} which would be expected from the two C=O groups existing in different environments. The biuret derivatives also give two distinct absorption bands at ca. 1703–1710 cm^{-1} and 1672–1687 cm^{-1}. 4-Chlorobenzyl 4-(4-chlorobenzyloxycarbamyl)-allophanate, which contains three C=O groups, displays three strong absorption peaks at 1788, 1760, and 1735 cm^{-1} and another peak at 1688 cm^{-1} on the shoulder of the 1735 cm^{-1} band. In the cyclic isocyanuric acid derivatives three absorption peaks are also discernible. These absorption bands occur at 1794, 1750, and 1738 cm^{-1} with 1,3,5-tri-(4-chlorobenzyloxy)-isocyanuric acid but in the other isocyanuric acids the latter two bands are not resolved distinctly.

Bacteriostatic Activities

None of the compounds listed in Table I(*A*) nor the allophanates displayed strong bacteriostatic activity. The most active compound of this series, i.e., 1-(3,4-dichlorobenzyloxy)-3-(2,5-dichlorophenyl)-urea, inhibited the growth of the following organisms at the minimal inhibitory concentrations given in parentheses; *M. pyogenes* var. *aureus* (Penicillin sensitive) (1:80,000), *Sarcina lutea* (1:80,000), *Streptococcus faecalis* (1:40,000),

Can. J. Chem. Downloaded from www.nrcresearchpress.com by 41.223.56.140 on 09/04/12
For personal use only.

TABLE II

Infrared absorption band (cm^{-1}) assignments

Compound	N—H Stretching modes	C=O Stretching modes	N—H Bending modes
1-(4-Chlorobenzyloxy)-3-(3,4-dichlorobenzyl)-urea	3360, 3240	1650	1540
1-(4-Chlorobenzyloxy)-3-(4-chlorobenzyl)-urea	3300, 3260	1653	1555
1-(3,4-Dichlorobenzyloxy)-3-(4-chlorobenzyl)-urea	3350, 3175	1644	1550
1-(2,4-Dichlorobenzyloxy)-3-(4-chlorobenzyl)-urea	3360, 3160	1642	1544
1-(4-Chlorobenzyloxy)-3-(4-chlorophenyl)-urea	3370, 3170	1673	1539
1-(3,4-Dichlorobenzyloxy)-3-(2,4-dichlorophenyl)-urea	3380, 3135	1686	1527
1-(4-Chlorobenzyloxy)-3-(3,4-dichlorophenyl)-urea	3360, 3170	1672	1526
1-(4-Chlorobenzyloxy)-3-(4-bromophenyl)-urea	3370, 3170	1673	1539
4-Chlorobenzyl carbamate	3440, 3360, 3305, 3212	1695	1622
4-Chlorobenzyl 3,4-dichlorobenzylcarbamate	3305	1691	1539
1,5-Di-(4-chlorobenzyl)-biuret	3320, 3190	1703, 1687	1518
1,5-Di-(4-chlorobenzyloxy)-biuret	3320, 3190	1703, 1687	1518
1,5-Di-(3,4-dichlorobenzyloxy)-biuret	3355, 3150	1712, 1672	1519
4-Nitrobenzyl 4-(4-nitrobenzyloxy)-allophanate	3320	1718, 1700[a,b]	
4-Chlorobenzyl 4-(4-chlorobenzyloxy)-allophanate	3320, 3170	1706[c]	1542
2,4-Dichlorobenzyl 4-(2,4-dichlorobenzyloxy)-allophanate	3320, 3170	1708[c]	1560
3,4-Dichlorobenzyl 4-(3,4-dichlorobenzyloxy)-allophanate	3290, 3190	1718, 1710	1572
4-Chlorobenzyl 4-(4-chlorobenzyloxycarbamyl)-allophanate	3298, 3160	1788, 1760, 1735, 1688	1608, 1503
1,3,5-Tri-(4-chlorobenzyloxy)-isocyanuric acid		1794, 1750, 1738	
1,3,5-Tri-(4-nitrobenzyloxy)-isocyanuric acid		1794(w) 1730[c,d]	
1,3,5-Tri-(benzyloxy)-isocyanuric acid		1796(w), 1730[c]	

(w) indicates weak absorption bands. The remainder are strong absorption bands. [a]NO_2 group asymmetric and symmetric absorption bands at 1520 cm^{-1} and 1348 cm^{-1}. [b]Strong absorption band at 1610 cm^{-1} which could be a combination of N—H bending and aryl absorption bands. [c]Doublets. [d]NO_2 group absorption bands at 1530 cm^{-1} and 1350 cm^{-1}.

E. coli No. 198 (1:20,000), *A. aerogenes* (1:20,000), *S. pullorum* (1:20,000), *P. aeruginosa* (1:40,000), and *P. vulgaris* (1:20,000).

EXPERIMENTAL[2]

Benzyl Isothiocyanates

The preparation and properties of the benzyl isothiocyanates, which were used in the preparation of the thiourea derivatives listed in Table I(*A*), have been described (10).

Hydroxyurethan

Hydroxyurethan was prepared in 77% yield by the method of Fuller and King (11).

N,N′-*Dicarbethoxy-α,α′-di-(aminoöxy)-p-xylene*

α,α'-Dichloro-*p*-xylene (8.75 g, 0.05 mole), hydroxyurethan (21.2 g, 0.2 mole), and 85% potassium hydroxide (8.05 g) in absolute ethanol (300 ml) were refluxed for 4.5 hours. The precipitated potassium chloride was removed by filtration and the clear filtrate was neutralized with concentrated hydrochloric acid. Evaporation of the filtrate gave 24.2 g of residue. This residue on treatment with ether – petroleum ether solution gave 13.7 g (71.5%) of solid melting at 90–94°. Several crystallizations from the same solution raised the melting point to 103–104°. Anal. Calc. for $C_{14}H_{20}N_2O_6$: C, 53.84; H, 6.45; N, 8.97. Found: C, 53.92; H, 6.41; N, 8.73.

[2]*All melting points are uncorrected. Microanalyses were determined by Micro-Tech Laboratories, Skokie, Ill. and Schwarzkopf Microanalytical Laboratory, Woodside, New York.*

Can. J. Chem. Downloaded from www.nrcresearchpress.com by 41.223.56.140 on 09/04/12
For personal use only.

α-Chloromethylnaphthalene

α-Chloromethylnaphthalene (n_D^{25} 1.63827) was prepared in 44.5% yield by the method of Cambron (12).

α-Naphthylmethyloxyurethan

An absolute ethanol (100 ml) solution of α-chloromethylnaphthalene (27.7 g, 0.16 mole), hydroxyurethan (10.5 g, 0.1 mole), and potassium hydroxide (6.6 g, 85% pure) was refluxed for 4.5 hours. After removal of the potassium chloride (7.7 g) the filtrate was evaporated to dryness, yield 27.7 g. The residue was dissolved in ether (50 ml) and a solid (m.p. 90–92°) was precipitated by the addition of petroleum ether (50 ml), yield 12.58 g, (51.2%). Crystallization from petroleum ether raised the melting point to 93–94°. Anal. Calc. for $C_{14}H_{15}NO_3$: C, 68.54; H, 6.61; N, 5.71. Found: C, 68.60; H, 5.84; N, 5.83.

2-Bromoethylurethan

2-Bromoethylurethan (b.p. 90°/0.6 mm) was prepared in 80% yield by the method of Katchalski and Ishai (13).

2-(N-Carbethoxyamino)-ethyloxyurethan

A solution of β-bromoethylurethan (9.8 g, 0.05 mole), hydroxyurethan (5.8 g, 0.05 mole), and potassium hydroxide (2.8 g, 0.05 mole) in methanol (50 ml) was refluxed for 15 minutes. The precipitate (5.38 g, 90.4%) of potassium bromide was removed and the filtrate was evaporated to dryness. The residue (9.38 g) was distilled *in vacuo*. The second fraction (b.p. 133°/0.18 mm; n_D^{25} 1.45459, d_4^{26} 1.137) weighed 5.23 g (56.8%). Anal. Calc. for $C_8H_{16}N_2O_5$: C, 43.62; H, 7.33; N, 12.73. Found: C, 43.61; H, 7.20; N, 12.88.

2-Aminoethyloxyamine

2-(N-Carbethoxyamino)-ethyloxyurethan (4.4 g, 0.02 mole) and barium hydroxide (10.29 g, 0.06 mole) in water (250 ml) were heated under reflux for 1 hour. The cooled solution was saturated with carbon dioxide and the precipitated barium carbonate was removed by filtration through Celite. The filtrate was acidified with hydrochloric acid and taken to dryness *in vacuo*. The residue (m.p. 165–169° decomp.) on crystallization from methanol–ether solution gave 1.54 g (51.7%) of crystalline hydrochloride melting at 187° with decomposition.

A large-scale preparation gave a 58.6% yield of the dihydrochloride of 2-aminoethyloxyamine melting at 189° C (decomp.). Anal. Calc. for $C_2H_{10}Cl_2N_2O$: C, 16.11; H, 6.77; Cl, 47.58; N, 18.80. Found: C, 16.38; H, 6.87; Cl, 47.53; N, 18.74.

4-Chlorobenzyloxyurethan

A solution of hydroxyurethan (14.2 g, 0.135 mole) and potassium hydroxide (85% grade) (8.9 g, 0.135 mole) in isopropanol (140 ml) was treated with 4-chlorobenzyl chloride (21.6 g, 0.135 mole) in isopropanol (10 ml). After the solution was refluxed for 4.5 hours, the precipitated potassium chloride was removed by filtration and the filtrate was evaporated to dryness. The yield of crude 4-chlorobenzyloxyurethan (m.p. 73–78°) was 21.6 g (69.7%). Crystallization from petroleum ether (b.p. 65–110°) raised the melting point to 85–86°. Anal. Calc. for $C_{10}H_{12}ClNO_3$: C, 52.27; H, 5.27; Cl, 15.44; N, 6.10. Found: C, 52.46; H, 5.26; Cl, 15.75; N, 6.34.

3,4-Dichlorobenzyloxyurethan

Hydroxyurethan (15.4 g, 0.146 mole), 3,4-dichlorobenzyl chloride (28.7 g, 0.146 mole), and potassium hydroxide (9.6 g) in absolute ethanol (150 ml) were refluxed for 4.5 hours.

Can. J. Chem. Downloaded from www.nrcresearchpress.com by 41.223.56.140 on 09/04/12
For personal use only.

The potassium chloride was removed by filtration and the filtrate on evaporation gave 35.5 g (91.5%) of white solid (m.p. 57–62° C). Two crystallizations from petroleum ether (b.p. 65–110° C) raised the melting point to 82–83° C. Anal. Calc. for $C_{10}H_{11}Cl_2NO_3$: C, 45.46; H, 4.20; Cl, 27.85; N, 5.30. Found: C, 45.69; H, 4.21; Cl, 27.67; N, 5.58.

N-*Hydroxyphthalimide*

N-Hydroxyphthalimide (m.p. 220–225° C) was prepared in 83% yield by the method of Orndorff and Pratt (14). These authors report a melting point of 220–226° C.

3-N-*Phthalimidopropyloxy*-N-*phthalimide*

A stirred solution of γ-bromopropylphthalimide (150 g, 0.56 mole), N-hydroxyphthalimide (91.7 g, 0.56 mole), and triethylamine (121 g, 1.2 mole) in dimethylformamide (700 ml) was gradually heated to 90° C over a period of 1 hour and maintained at this temperature for another 30 minutes. The cooled reaction mixture was diluted with water (2 l.) and the precipitate (m.p. 177–179° C) was removed by filtration, yield 176 g (89.3%). Two crystallizations from glacial acetic acid (8 ml/g) raised the melting point to 178–180° C. Anal. Calc. for $C_{19}H_{14}N_2O_5$: C, 65.32; H, 4.03; N, 7.99. Found: C, 64.98; H, 4.20; N, 7.96.

3-Aminopropyloxyamine

Hydrazine hydrate (20 g, 0.4 mole) was added to a solution of 3-N-phthalimidopropyloxy-N-phthalimide (35.0 g, 0.1 mole) in dimethylformamide (200 ml) at 70° C. This solution was allowed to cool over a period of 1 hour after which it was diluted with water (300 ml) and the pH was lowered to 3 with hydrochloric acid. The phthalylhydrazide was removed and the filtrate was evaporated *in vacuo* at 40–50°. The residue was dissolved in methanol (1 l.) and the solution was passed through a column of IRA 400 resin (1 l. in OH form previously treated with methanol). The column was washed with methanol (1.5 l.) and the combined eluates were evaporated. Distillation of the residue gave 3.0 g (45%) of product (b.p. 110–115°/3 mm). Redistillation gave pure material (b.p. 99°/40 mm, n_D^{25} 1.4614; d_4^{25} 0.999), yield 2.06 g. Anal. Calc. for $C_3H_{10}N_2O$: C, 39.97; H, 11.19; N, 31.09; M_R 24.75. Found: C, 39.86; H, 11.11; N, 30.83; M_R 24.58.

A portion (0.32 g) of 3-aminopropyloxyamine in methanol was neutralized with dry hydrogen chloride. Ether was added to the mixture and the precipitated dihydrochloride (m.p. 207–208° decomp.) was recovered by filtration, yield 0.46 g (71.2%). One crystallization from methanol–ether solution raised the melting point to 208–209° with decomposition. Anal. Calc. for $C_3H_{12}Cl_2N_2O$: C, 22.10; H, 7.42; Cl, 43.48; N, 17.19. Found: C, 22.25; H, 7.39; Cl, 43.71; N, 16.85.

The dipicrate (m.p. 208–209° decomp.) was formed in the usual manner from aqueous solution. Anal. Calc. for $C_{15}H_{16}N_8O_{15}\cdot H_2O$: C, 31.79; H, 3.20; N, 19.77. Found: C, 32.00; H, 3.73; N, 20.04.

N-(*4-Chlorobenzyloxy*)-*phthalimide*

A methanolic solution of potassium hydroxide (20.2 ml of 4.95 *N* KOH) was added dropwise to a solution of N-hydroxyphthalimide (16.3 g, 0.1 mole) and 4-chlorobenzyl chloride (16.1 g, 0.1 mole) in dimethylformamide (300 ml) at 65° over a period of 1 hour. When the addition was complete, the solution was cooled and diluted with water (1 l.). The precipitate (m.p. 125–130°) was removed by filtration, yield 20.4 g (70.8%). Crystallization from ethanol (60 ml) raised the melting point to 137–138° C. Anal. Calc. for $C_{15}H_{10}ClNO_3$: C, 62.62; H, 3.50; Cl, 12.33; N, 4.87. Found: C, 62.60; H, 3.37; Cl, 12.68; N, 4.76.

Can. J. Chem. Downloaded from www.nrcresearchpress.com by 41.223.56.140 on 09/04/12
For personal use only.

Can. J. Chem. Downloaded from www.nrcresearchpress.com by 41.223.56.140 on 09/04/12
For personal use only.

N-(3,4-Dichlorobenzyloxy)-phthalimide

N-Hydroxyphthalimide (90.0 g, 0.05 mole) was added portionwise to a stirred solution of 3,4-dichlorobenzyl chloride (108 g, 0.55 mole) and triethylamine (120 g, 1.19 mole) in dimethylformamide (500 ml) at 70° C. When one-half of the N-hydroxyphthalimide was added, a massive precipitate prevented further stirring. The remainder of the phthalimide was added in one portion and the precipitate dissolved while the product separated from solution. The stirring was continued at 70° C for 2 hours. The cooled solution on dilution with water (3 l.) yielded crude N-(3,4-dichlorobenzyloxy)-phthalimide (m.p. 167–171° C), yield 133 g, (74.7%). Recrystallization from methanol raised the melting point to 182–183° C. Anal. Calc. for $C_{15}H_9Cl_2NO_3$: C, 55.92; H, 2.82; Cl, 22.02; N, 4.35. Found: C, 55.97; H, 2.97; Cl, 22.12; N, 4.30.

Dipotassium Hydroxylamine Disulphonate

Solid dipotassium hydroxylamine disulphonate was prepared in 77% yield by the method of Rollefson and Oldershaw (15).

4-Chlorobenzyloxyamine

Method A

A solution of dipotassium hydroxylamine disulphonate (300 g, 0.985 mole) in potassium hydroxide solution (83.7 g, in 560 ml water) was treated with 4-chlorobenzyl chloride (161 g, 1 mole). The stirred mixture was heated on a steam bath for 1.75 hours. After cooling the solid was removed and then refluxed in 1.5 *N* sulphuric acid solution (1000 ml) for 3 hours. The mixture was cooled and made strongly alkaline with 15% sodium hydroxide solution. The mixture was extracted with ether and the dried ethereal extract was taken to dryness. The solid residue (m.p. 35–38°) weighed 80 g (51.5%). Schroeter and Peschkes (16) reported a melting point of 38°. The solid in ether (1 l.) was treated with anhydrous hydrogen chloride and the precipitated 4-chlorobenzyloxyamine hydrochloride (m.p. 243–244° decomp.) was removed by filtration, yield 59 g (60%).

Method B

Potassium hydroxide (10.7 g, 0.19 mole) in water (25 ml) was added to 4-chlorobenzyloxyurethan (10.95 g, 0.098 mole) in isopropanol (60 ml) and this solution was refluxed for 1 hour. Additional water (50 ml) was added and the oily layer was extracted with ether (70 ml). Evaporation of the ether gave 6.5 g (84.2%) of an oil. Fractional distillation *in vacuo* gave 5.53 g (71.6%) of 4-chlorobenzyloxyamine (b.p. 100°/1 mm; m.p. 32–38°) and a second fraction of 1 g (b.p. 150°/1 mm; m.p. 66–71°). The second fraction, after two crystallizations from ethanol (10 ml), melted at 113–114°, yield 0.13 g. The analytical values of this by-product agreed with those calculated for *O*-(4-chlorobenzyl)-4-chlorobenzaldoxime. Anal. Calc. for $C_{14}H_{11}Cl_2NO$: C, 60.00; H, 3.93; Cl, 25.36; N, 5.00. Found: C, 59.81; H, 3.92; Cl, 25.71; N, 5.11. Schroeter and Peschkes (16) reported a melting point of 114° for *O*-(4-chlorobenzyl)-4-chlorobenzaldoxime.

Method C

N-(4-chlorobenzyloxy)-phthalimide (16 g, 0.056 mole) was dissolved in a solution of dimethylformamide (30 ml) in methanol (300 ml). Hydrazine hydrate (6.1 g, 0.123 mole) was added to the solution at 60° and the whole was allowed to stand for 3 hours. The suspension was acidified to pH 2 with 2 *N* hydrochloric acid and the phthalylhydrazide was removed by filtration. The filtrate was taken to dryness and 2 *N* sodium hydroxide solution (75 ml) was added to the residue. This suspension was extracted with ether

(2×40 ml) and the ether extract was distilled to give 3.8 g (57.6%) of 4-chlorobenzyloxyamine (b.p. 95–100°/2 mm; m.p. 38°).

3,4-Dichlorobenzyloxyamine

3,4-Dichlorobenzyloxyamine (b.p. 95–105°/1 mm) was prepared in 88% yield from 3,4-dichlorobenzyloxyurethan by method B described above for the preparation of 4-chlorobenzyloxyamine. A portion (b.p. 121°/3.6 mm; n_D^{25} 1.57140), which had been redistilled in a collar flask, was submitted for analysis. Anal. Calc. for $C_7H_7Cl_2NO$: C, 43.78; H, 3.67; Cl, 36.93; N, 7.29. Found: C, 43.87; H, 3.73; Cl, 36.70; N, 7.55.

A sample of 3,4-dichlorobenzyloxyamine was converted into its picrate in 45.5% yield by treatment with a saturated ether solution of picric acid. Two crystallizations from absolute ethanol – petroleum ether (1:5) solution raised the melting point from 173–175° to 175–176°. Anal. Calc. for $C_{13}H_{10}Cl_2N_4O_8$: C, 37.08; H, 2.39; Cl, 16.84; N, 13.30. Found: C, 37.26; H, 2.48; Cl, 16.96; N, 13.62.

3,4-Dichlorobenzyloxyamine also was prepared in 52% yield from N-(3,4-dichlorobenzyloxy)-phthalimide (method C).

3,4-Dichlorobenzyloxyamine Hydrochloride

3,4-Dichlorobenzyl chloride (190 g, 0.965 mole), dipotassium hydroxylamine disulphonate (303 g, 0.995 mole), and potassium hydroxide (83.7 g) in water (560 ml) were heated on a steam bath for 5 hours. The solid was removed from the cooled solution by filtration, washed with ethanol, and then refluxed in 1.5 *N* sulphuric acid solution (1 l.) for 3 hours. The mixture was made alkaline with 15% sodium hydroxide solution after which it was extracted with ether. Anhydrous hydrogen chloride was bubbled into the dried ether solution and the precipitated 3,4-dichlorobenzyloxyamine hydrochloride was recovered by filtration, yield 58 g (25.4%). Four crystallizations from ethanol raised the melting point from 195–198° C (decomp.) to 200° C (decomp.). Anal. Calc. for $C_7H_8Cl_3NO$: C, 36.78; H, 3.58; Cl, 46.54; N, 6.13. Found: C, 37.00; H, 3.66; Cl, 46.44; N, 6.16.

The hydrochlorides of benzyloxyamine (17), 4-chlorobenzyloxyamine (16), 4-nitrobenzyloxyamine (18), and 2,4-dichlorobenzyloxyamine were prepared similarly in yields of 34.5, 31, 39.5, and 16.5% respectively.

2,4-Dichlorobenzyloxyamine hydrochloride was converted into its free base by treatment with 10% sodium hydroxide. The oil was extracted with ether and distilled *in vacuo* in a collar flask. A sample of the 2,4-dichlorobenzyloxyamine (b.p. 120–121° C/4.6 mm; n_D^{25} 1.57168) was submitted for analysis. Anal. Calc. for $C_7H_7Cl_2NO$: C, 43.78; H, 3.67; Cl, 36.93; N, 7.29. Found: C, 43.91; H, 3.63; Cl, 36.60; N, 7.56.

The picrate formed in 50% yield in the usual manner from ether solution melted at 176–182°. Anal. Calc. for $C_{13}H_{10}Cl_2N_4O_8$: C, 37.08; H, 2.39; Cl, 16.84; N, 13.30. Found: C, 37.10; H, 2.70; Cl, 16.82; N, 13.28.

Reaction of 4-Chlorobenzyloxyamine Hydrochloride with Phosgene

4-Chlorobenzyloxyamine hydrochloride (5.82 g, 0.03 mole) in anhydrous chlorobenzene (60 ml) was saturated with phosgene at room temperature. Phosgene was bubbled through the reaction mixture while the temperature was increased to 95–100° and maintained at this level for 1 hour. Then the excess phosgene was removed by bubbling nitrogen through the reaction mixture and the chlorobenzene was removed *in vacuo*. An oil remained which was considered to be N-(4-chlorobenzyloxy)-carbamyl chloride, yield 6.6 g (100%). Anal. Calc. for $C_8H_7Cl_2NO_2$: N, 6.37; Cl, 32.23. Found: N, 6.98; Cl, 29.87.

Can. J. Chem. Downloaded from www.nrcresearchpress.com by 41.223.56.140 on 09/04/12
For personal use only.

The analysis indicated that the oil was not pure. However a part (2.58 g, 0.011 mole) of the oil in ether (100 ml) was treated with 3,4-dichloroaniline (3.80 g, 0.023 mole). The solid 3,4-dichloroaniline hydrochloride was removed by filtration, yield 2.36 g (50% based on added 3,4-dichloroaniline). The filtrate was evaporated to dryness and the residue was crystallized from ethanol, yield 2.07 g (51.2%). One crystallization from ethyl acetate – petroleum ether solution raised the melting point of the 1-(4-chlorobenzyloxy)-3-(3,4-dichlorophenyl)-urea from 135–140° to 150–151°. Anal. Calc. for $C_{14}H_{11}Cl_3N_2O_2$: C, 48.61; H, 3.21; Cl, 30.78; N, 8.11. Found: C, 48.68; H, 3.28; Cl, 30.71; N, 8.48.

4-Chlorobenzyl 4-(4-Chlorobenzyloxy)-allophanate and 1,3,5-Tri-(4-chlorobenzyloxy)-isocyanuric Acid

A suspension of 4-chlorobenzyloxyamine hydrochloride (50 g, 0.257 mole) in chlorobenzene (300 ml) was saturated with phosgene. This reaction mixture was heated at 120–125° for 3.5 hours (until the suspended solid dissolved) while phosgene was bubbled through the reaction mixture. Removal of the chlorobenzene *in vacuo* left a mixed solid and oil residue which was extracted with ether (150 ml). The ether-insoluble 4-chlorobenzyl 4-(4-chlorobenzyloxy)-allophanate (m.p. 147–149° C decomp.) was recovered by filtration, yield 19.55 g (41%). Crystallization from glacial acetic acid raised the melting point to 148–149° with decomposition. Anal. Calc. for $C_{16}H_{14}Cl_2N_2O_4$: C, 52.05; H, 3.82; Cl, 19.21; N, 7.59; mol. wt., 369.20. Found: C, 52.49; H, 3.63; Cl, 19.55; N, 7.90; mol. wt., 398 (Rast).

The ether solution was made alkaline with triethylamine at room temperature. The precipitated solid (m.p. 225–235° decomp.) was removed by filtration and washed with water until the filtrate gave a negative chloride ion test, yield 6 g (12.7%). The melting point of this crude 1,3,5-tri-(4-chlorobenzyloxy)-isocyanuric acid was raised to 248–249° with decomposition by crystallizing from glacial acetic acid. Anal. Calc. for $C_{24}H_{18}Cl_3N_3O_6$: C, 52.34; H, 3.29; Cl, 19.31; N, 7.63; mol. wt., 550.77. Found: C, 52.41; H, 3.22; Cl, 19.20; N, 7.71; mol. wt., 575 (Rast).

When benzyloxyamine hydrochloride was heated with phosgene under the above conditions a 68% yield of 4-chlorobenzyl 4-(4-chlorobenzyloxy)-allophanate (m.p. 148–149° decomp.) and a 4.8% yield of 1,3,5-tri-(4-chlorobenzyloxy)-isocyanuric acid (m.p. 248–249°) were obtained. These compounds were identified by mixed melting point determinations.

In another experiment a suspension of 4-chlorobenzyloxyamine hydrochloride (23.29 g, 0.12 mole) in commercial chlorobenzene (180 ml), which was not dried, was saturated with phosgene at room temperature. Phosgene was bubbled in while the reaction mixture was heated at 95–100° for 1.5 hours and 108–110° for 3 hours. Evaporation of the solution *in vacuo* left a semisolid residue which was triturated with ether (200 ml). The ether-insoluble 4-chlorobenzyl 4-(4-chlorobenzyloxycarbamyl)-allophanate, m.p. 230–260°, was recovered by filtration, yield 2.53 g (11.5% from 2 moles of 4-chlorobenzyloxyamine hydrochloride). Repeated recrystallization from methanol raised the melting point to 271–272°. Anal. Calc. for $C_{17}H_{15}Cl_2N_3O_5$: C, 49.54; H, 3.67; Cl, 17.20; N, 10.20. Found: C, 49.76; H, 3.47; Cl, 17.10; N, 10.50.

Reaction of 4-Chlorobenzylamine with Crude 4-Chlorobenzyloxycarbamyl Chloride

A solution of 4-chlorobenzylamine (11.0 g, 0.078 mole) in ether (50 ml) was added to crude 4-chlorobenzyloxycarbamyl chloride (8.35 g, 0.039 mole) at room temperature. The precipitate of 4-chlorobenzylamine hydrochloride was removed by filtration, yield 5.19 g (75.0%). The filtrate was evaporated and the residue was crystallized from ether, giving

Can. J. Chem. Downloaded from www.nrcresearchpress.com by 41.223.56.140 on 09/04/12
For personal use only.

a precipitate of 5.10 g, m.p. 113–115°. Recrystallization from chloroform and from ethanol gave 1-(4-chlorobenzyloxy)-3-(4-chlorobenzyl)-urea, m.p. 123–124°, yield 4.34 g, 24.3%. Elementary analysis of this product is given in Table I(*A*). The mother liquors from this crystallization were evaporated (0.65 g, m.p. 130–140° C) and the residue was recrystallized twice from ethanol, giving 1,5-di-(4-chlorobenzyl)-biuret (m.p. 177–178°), yield 0.043 g (0.3%). Anal. Calc. for $C_{16}H_{15}Cl_2N_3O_2$: C, 54.57; H, 4.29; Cl, 20.14; N, 11.93. Found: C, 54.64; H, 4.54; Cl, 19.91; N, 11.64.

The combined mother liquors were evaporated to dryness and dissolved in ether. Anhydrous hydrogen chloride was passed through the ether solution, causing the separation of additional 4-chlorobenzylamine hydrochloride, yield 2.20 g (31.8%). The total recovery of 4-chlorobenzylamine hydrochloride was 53.4% (based on added 4-chlorobenzylamine).

The filtrate was evaporated to dryness and the residue (5.81 g), in benzene, was chromatographed on alumina (240 g). The fraction eluted by ether (1.79 g) was recrystallized from ethanol – petroleum ether. The crystals melted at 84–85°, yield 0.25 g. The analytical values agree with the calculated for ethyl 4-chlorobenzyloxycarbamate. This apparently arose from presence of ethanol in the ether used as solvent. Anal. Calc. for $C_{10}H_{12}ClNO_3$: C, 52.29; H, 5.27; Cl, 15.44; N, 6.10. Found: C, 52.21; H, 5.02; Cl, 15.34; N, 6.14.

A 2% solution of methanol in absolute ether removed a fraction (1.79 g, m.p. 100–110°) from the column which was recrystallized from ethanol to give additional 1-(4-chlorobenzyloxy)-3-(4-chlorobenzyl)-urea, m.p. 123–124°, yield 0.72 g, 5.7%. The total yield of pure urea was 30.0%.

The fraction eluted by 4% methanol in ether consisted of crude 1-(4-chlorobenzyl)-5-(4-chlorobenzyloxy)-biuret (m.p. 140–145°), yield 0.59 g (0.52%). Crystallization from ethanol raised the melting point to 149–150°. Anal. Calc. for $C_{16}H_{15}Cl_2N_3O_3$: C, 52.20; H, 4.11; Cl, 19.26; N, 11.42. Found: C, 52.14; H, 4.22; Cl, 19.35; N, 11.91.

Reactions of 4-Chlorobenzyl 4-(4-Chlorobenzyloxy)-allophanate

A. Alkaline Hydrolysis

A solution of the allophanate (3.69 g, 0.01 mole) in 1,2-dimethoxyethane (100 ml) was added to sodium hydroxide (0.40 g, 0.01 mole) in water (10 ml). After standing at room temperature for 18 hours, the solution was neutralized with hydrochloric acid and evaporated almost to dryness. The residue was diluted with water (30 ml) and extracted with chloroform (2×100 ml). Evaporation of the dried chloroform extract yielded an oily residue (3.4 g) which on crystallization from chloroform gave 1,5-di-(4-chlorobenzyloxy)-biuret (m.p. 173–175°), yield 0.60 g (31.3%). Crystallizations from chloroform and ethyl acetate raised the melting point to 174.5–175.5°. Anal. Calc. for $C_{16}H_{15}Cl_2N_3O_4$: C, 50.02; H, 3.94; Cl, 18.46; N, 10.94. Found: C, 50.02; H, 4.10; Cl, 18.46; N, 11.04.

Repeated recrystallization of the mother liquors from ether yielded a small quantity (0.07 g) of unchanged allophanate (m.p. 148–149°).

Alumina chromatography of the combined mother liquors gave, in the petroleum ether:benzene (1:1) eluate, *O*-(4-chlorobenzyl)-4-chlorobenzaldoxime (108 mg, 7.8% yield) melting at 113–114°. A mixed melting point determination with a known sample of *O*-(4-chlorobenzyl)-4-chlorobenzaldoxime gave no depression. 4-Chlorobenzyl alcohol, melting point and mixed melting point 71–72°, was isolated from the ether:benzene (1:1) eluate, yield 0.238 g (16.7%).

A 10% methanol in ether solution removed 4-chlorobenzyloxyurea from the column.

Can. J. Chem. Downloaded from www.nrcresearchpress.com by 41.223.56.140 on 09/04/12
For personal use only.

This urea melted at 165–166° after recrystallization from ethanol and petroleum ether, yield 0.255 g (12.8%). This product was identified by a mixed melting point determination with a known sample which was prepared as follows: A solution of 4-chlorobenzyloxyamine hydrochloride (1.0 g, 0.0051 mole) and potassium cyanate (0.42 g, 0.0051 mole) in water (25 ml) was refluxed for 5 hours. 4-Chlorobenzyloxyurea (m.p. 163–165°), separated from the cooled solution, yield 0.82 g (86.3%). Crystallization from ethanol – petroleum ether solution raised the melting point to 165–166°. Anal. Calc. for $C_8H_9ClN_2O_2$: C, 47.82; H, 4.52; Cl, 17.65; N, 13.95. Found: C, 47.96; H, 4.52; Cl, 17.93; N, 14.16.

B. Reaction with 4-Chlorobenzylamine

A solution of the allophanate (1.93 g, 0.0052 mole) and 4-chlorobenzylamine (1.47 g, 0.0104 mole) in chlorobenzene (20 ml) was refluxed for 90 minutes. The solution was evaporated to dryness and the residue was crystallized from chloroform, giving 1-(4-chlorobenzyl)-3-(4-chlorobenzyloxy)-urea (m.p. 123–124°), yield 1.51 g, (88.5%). The urea was identified by a mixed melting point determination.

The mother liquors were combined and evaporated to dryness, and the residue on crystallization from petroleum ether weighed 0.55 g (2.1%). It did not depress the melting point of a known sample of 1,5-di-(4-chlorobenzyl)-biuret (m.p. 177–178°).

Chromatography of the remaining mother liquors gave crystals of *O*-(4-chlorobenzyl)-4-chlorobenzaldoxime (m.p. 113–114°), yield 0.073 g (10.0%), and a very small quantity of a substance which sublimed readily to give crystals melting at 90–91°. The aldoxime was identified by a mixed melting point determination.

The other allophanates described in this paper were treated with 4-chlorobenzylamine in the same way. The resulting unsymmetrical ureas are described in Table I(*A*).

4-Chlorobenzyl Chloroformate

4-Chlorobenzyl alcohol (21.4 g, 0.15 mole) and quinoline (19.4 g, 0.15 mole) were added to a stirred solution of phosgene (61 g, 0.165 mole) in toluene (75 ml), and the mixture was allowed to stand for 36 hours. The quinoline hydrochloride was removed by filtration, and the filtrate was evaporated to dryness at 40–45°. An attempt to distill the crude chloroformate resulted in the isolation of 4-chlorobenzyl chloride, b.p. 72–74° (1.4 mm) (hexamethylenetetramine salt, melting point and mixed melting point 200° decomp). The undistilled chloroformate (2.05 g, 0.01 mole) in ether (50 ml) was added to 3,4-dichlorobenzylamine (3.52 g, 0.02 mole) in ether (50 ml) at room temperature. The precipitated 3,4-dichlorobenzylamine hydrochloride (1.10 g, 52%) was filtered, and the filtrate was concentrated to 10 ml. Addition of petroleum ether caused the separation of 4-chlorobenzyl N-3,4-dichlorobenzylcarbamate (m.p. 94–96°), yield 1.55 g, (45%).

Recrystallization from ethanol – petroleum ether raised the melting point to 95–96°. Anal. Calc. for $C_{15}H_{12}Cl_3NO_2$: C, 52.28; H, 3.51; Cl, 30.87; N, 4.06. Found: C, 52.16; H, 3.80; Cl, 30.68; N, 3.95.

The reaction of 4-chlorobenzyl chloroformate with potassium cyanate and potassium thiocyanate did not yield any identifiable products.

1,3-Di-(4-chlorobenzyloxy)-urea

A solution of phosgene (0.2 g, 0.002 mole) in toluene (7.5 ml) was added to a stirred and cooled solution of 4-chlorobenzyloxyamine (1.1 g, 0.007 mole) in benzene (25 ml). The precipitate of 4-chlorobenzyloxyamine hydrochloride was removed by filtration and the filtrate was evaporated to dryness. 1,3-Di-(4-chlorobenzyloxy)-urea (m.p. 116–118°) was

Can. J. Chem. Downloaded from www.nrcresearchpress.com by 41.223.56.140 on 09/04/12
For personal use only.

obtained from a solution of the residue in chloroform by addition of petroleum ether, yield 0.418 g (68%). One crystallization from ethanol raised the melting point to 117–118°. Anal. Calc. for $C_{15}H_{14}Cl_2N_2O_3$: C, 52.80; H, 4.14; Cl, 20.78; N, 8.21. Found: C, 52.74; H, 4.11; Cl, 20.68; N, 8.21.

4-Chlorobenzylcarbamate

A mixture of 4-chlorobenzyl alcohol (2.84 g, 0.02 mole), urea (0.60 g, 0.01 mole), and stannic chloride (0.04 g, 0.00015 mole) was stirred at 150° for 8 hours. The cooled reaction mixture was triturated with ether, giving 4-chlorobenzyl carbamate (m.p. 134–137°), yield 1.03 g (55.6%). Crystallization from ethanol raised the melting point to 136.5–137.5°. Anal. Calc. for $C_8H_8ClNO_2$: C, 51.76; H, 4.34; Cl, 19.11; N, 7.55. Found: C, 51.62; H, 4.37; Cl, 19.09; N, 7.25.

3,4-Dichlorobenzyl 4-(3,4-Dichlorobenzyloxy)-allophanate and its Treatment with Methanolic Sodium Hydroxide

3,4-Dichlorobenzyloxyamine hydrochloride was treated with phosgene in anhydrous chlorobenzene at 120–125° as described above in the preparation of 4-chlorobenzyl 4-(4-chlorobenzyloxy)-allophanate. 3,4-Dichlorobenzyl 4-(3,4-dichlorobenzyloxy)-allophanate (m.p. 121–123°) was obtained in 75.5% yield. Crystallization from glacial acetic acid raised the melting point to 125–126° (decomp.). Anal. Calc. for $C_{16}H_{12}Cl_4N_2O_4$: C, 43.87; H, 2.76; Cl, 32.38; N, 6.32; mol. wt., 438.11. Found: C, 44.19; H, 2.61; Cl, 32.67; N, 6.65; mol. wt., 430 (Rast).

A solution of the allophanate (2.19 g, 0.005 mole) and sodium hydroxide (0.2 g, 0.005 mole) in methanol (250 ml) was heated to boiling and then allowed to stand for 3 days. The solution was concentrated almost to dryness and then diluted with water. It gave an oily solid which was filtered and washed with ether. The crystalline residue of 1,5-di-(3,4-dichlorobenzyloxy)-biuret, melted at 156–158°, yield 0.83 g (57%). Crystallization from methanol raised the melting point to 157–158°. Anal. Calc. for $C_{16}H_{13}Cl_4N_3O_4$: C, 42.42; H, 2.89; Cl, 31.31; N, 9.28. Found: C, 42.30; H, 3.09; Cl, 31.36; N, 9.04.

The ether washings were evaporated and the residue was treated with an excess of 2,4-dinitrophenylhydrazine in ethanol. The 2,4-dinitrophenylhydrazone of 3,4-dichlorobenzaldehyde, (m.p. 308–309°) was recovered by filtration, yield 0.45 g (25%). It was identified by a mixed melting point determination with a known sample of the 2,4-dinitrophenylhydrazone of 3,4-dichlorobenzaldehyde.

4-Nitrobenzyl 4-(4-Nitrobenzyloxy)-allophanate and 1,3,5-Tri-(4-nitrobenzyloxy)-isocyanuric Acid

4-Nitrobenzyloxyamine hydrochloride on treatment with phosgene under the conditions described above for 4-chlorobenzyloxyamine hydrochloride gave an 81% yield of 4-nitrobenzyl 4-(4-nitrobenzyloxy)-allophanate (m.p. 183–185° decomp.). Crystallization from glacial acetic acid raised the melting point to 184–185° (decomp.). Anal. Calc. for $C_{16}H_{12}N_4O_8$: C, 49.01; H, 3. 61; N, 14.36; mol. wt., 390.30. Found: C, 49.18; H, 3.62; N, 14.60; mol. wt., 395 (Rast).

Treatment of the ether extract with triethylamine gave a 2.9% yield of 1,3,5-tri-(4-nitrobenzyloxy)-isocyanuric acid (m.p. 183–220° decomp.). The melting point was raised to 251–252° (decomp.) by crystallization from glacial acetic acid, yield 0.8%. Anal. Calc. for $C_{24}H_{18}N_6O_{12}$: C, 49.49; H, 3.12; N, 14.43. Found: C, 49.75; H, 3.04; N, 14.15.

Can. J. Chem. Downloaded from www.nrcresearchpress.com by 41.223.56.140 on 09/04/12
For personal use only.

2,4-Dichlorobenzyl 4-(2,4-Dichlorobenzyloxy)-allophanate and 1,3,5-Tri-(2,4-dichlorobenzyloxy)-isocyanuric Acid

When 2,4-dichlorobenzyloxyamine hydrochloride was treated with phosgene under the same conditions, a 34.5% yield of 2,4-dichlorobenzyl 4-(2,4-dichlorobenzyloxy)-allophanate (m.p. 95–98° decomp.) was obtained. Crystallization from glacial acetic acid raised the melting point to 97–98° (decomp.). Anal. Calc. for $C_{16}H_{10}Cl_4N_2O_4$: C, 43.87; H, 2.76; Cl, 32.38; N, 6.32; mol. wt., 438.11. Found: C, 44.28; H, 2.50; Cl, 32.62; N, 6.38; mol. wt., 438 (Rast).

The ether extract on addition of triethylamine gave 0.5% yield of 1,3,5-tri-(2,4-dichlorobenzyloxy)-isocyanuric acid (m.p. 198–200° decomp.). It melted at 201–202° (decomp.) after crystallization from glacial acetic acid. Anal. Calc. for $C_{24}H_{15}Cl_3N_3O_6$: C, 44.07; H, 2.31; Cl, 32.53; N, 6.43. Found: C, 44.25; H, 2.37; Cl, 32.41; N, 6.27.

1,3,5-Tribenzyloxy-isocyanuric Acid

A suspension of benzyloxyamine hydrochloride (9.57 g, 0.060 mole) in chlorobenzene (81 ml) was saturated with phosgene at room temperature. The flow of phosgene was continued while the reaction mixture was heated at 105–110° for 2 hours. The clear solution was evaporated *in vacuo* and the residual oil was dissolved in ether (40 ml). This solution was made basic with triethylamine and the precipitate was filtered and washed with water, yield 4.6 g (51.5%). The melting point was raised from 225–235° (decomp.) to 239–241° (decomp.) by crystallization from glacial acetic acid. Anal. Calc. for $C_{24}H_{21}N_3O_6$: C, 64.29; H, 4.73; N, 9.39; mol. wt., 447.42. Found: C, 64.45; H, 4.61; N, 9.59; mol. wt., 449 (Rast).

Urea and Thiourea Derivatives

The urea and thiourea derivatives prepared by the reaction of isocyanates and isothiocyanates with substituted oxyamines are described in Table I. The following procedure was used in the preparation of all of these derivatives.

4-Chlorobenzyl isothiocyanate (0.82 g, 0.004 mole) in ether (5 ml) was added to 4-chlorobenzyloxyamine (0.71 g, 0.004 mole). The ether on evaporation gave a crystalline residue (m.p. 107–111°), yield 1.51 g (99%). Crystallization from absolute ethanol raised the melting point to 115–116° C.

1-(β-Hydroxyethyl)-2-methylmercapto-2-imidazolinium Chloride

A mixture of 1-(β-hydroxyethyl)-2-imidazolidinethione (19) (612 g, 4.3 moles), methyl chloride (660 g, 13 moles), and isopropanol (1450 ml) was heated at 55–60° C under 30–70 p.s.i. in an autoclave with stirring for 6 hours. A quantitative gravimetric estimation of chloride ion at the end of the reaction period indicated a 92% conversion of the cyclic thiourea to 1-(β-hydroxyethyl)-2-methylmercapto-2-imidazolinium chloride. The autoclave was emptied and washed with isopropanol (2×200 ml). The combined washings and reaction mixture on cooling at 0° C for several hours deposited crystals. These crystals (m.p. 104–106° C) were recovered by filtration, yield 394 g (48%). The remainder of the product was obtained by evaporation of the filtrate *in vacuo*. Crystallization of the crude product from isopropanol raised the melting point to 105–106° C. Anal. Calc. for $C_6H_{13}ClN_2OS$: C, 36.63; H, 6.66; Cl, 18.02; N, 14.24; S, 16.29. Found: C, 37.02; H, 6.95; Cl, 17.92; N, 14.10; S, 15.91.

1-(β-Hydroxyethyl)-2-(2,4-dichlorobenzyloxyamine)-2-imidazoline

1-(β-Hydroxyethyl)-2-methylmercapto-2-imidazolinium chloride (19.67 g, 0.1 mole) and 2,4-dichlorobenzyloxyamine (19.20 g, 0.1 mole) in isopropanol (100 ml) were heated

Can. J. Chem. Downloaded from www.nrcresearchpress.com by 41.223.56.140 on 09/04/12
For personal use only.

under reflux for 2 hours. Methyl mercaptan was evolved during the reaction. After the solution stood at 25° C overnight some solid (m.p. 124–125° C), precipitated, yield 2.09 g (11.9%). The melting point was raised to 125–126° C by crystallization from isopropanol. The analyses agree with the calculated values for *O*-(2,4-dichlorobenzyl)-2,4-dichlorobenzaldoxime. Anal. Calc. for $C_{14}H_9Cl_4NO$: C, 48.18; H, 2.60; Cl, 40.64; N, 4.01. Found: C, 48.37; H, 2.61; Cl, 40.46; N, 4.03.

The residue obtained on evaporation of the filtrate to dryness was treated with excess sodium hydroxide solution and the basic solution was extracted with ether. The ether extract was washed with water and dried over anhydrous sodium sulphate. Evaporation of the ether gave a solid melting at 103–105°, yield 18.04 g (59.2%). Crystallization from absolute ethanol – petroleum ether solution raised the melting point to 109–110°. Anal. Calc. for $C_{12}H_{15}Cl_2N_2O_2$: C, 47.37; H, 4.97; Cl, 23.31; N, 13.81. Found: C, 47.67; H, 5.11; Cl, 23.60; N, 14.05.

Isolation of 1,3,5-Tri-(3,4-dichlorobenzyl)-isomelamine

An analytical sample of 1-(3,4-dichlorobenzyloxy)-3-(3,4-dichlorobenzyl)-thiourea (m.p. 107–108°) on standing at room temperature for 2 weeks changed into a mixture of red oil and crystals. A portion (3.95 g) of this mixture was triturated with ether (50 ml) and the insoluble material (m.p. 151–156°) recovered. The solid was taken up in acetone (30 ml) and the insoluble free sulphur (0.11 g, m.p. 116°) was removed by filtration. The filtrate on dilution with water gave 0.72 g of product melting at 168–170°. Two crystallizations from acetone–water solution raised the melting point to 171–172°. Anal. Calc. for $C_{24}H_{18}Cl_6N_6$: C, 47.78; H, 3.01; Cl, 35.27; N, 13.93; mol. wt., 603.18. Found: C, 47.78; H, 3.19; Cl, 35.90; N, 13.82; mol. wt., 580 (Rast).

N^2,N^4,N^6-*Tri-(3,4-dichlorobenzyl)-melamine*

3,4-Dichlorobenzylamine hydrochloride (12.66 g, 0.06 mole) was treated with an excess of 25% sodium hydroxide solution and the free amine was extracted with ether (100 ml). The dried ether solution was treated with cyanuric chloride (1.84 g, 0.01 mole). An exothermic reaction occurred and the ether solution began to reflux. The ether was replaced with *o*-xylene and the mixture was refluxed for 4 hours. The solvent was removed *in vacuo* and the semisolid residue was triturated with acetone (50 ml). The insoluble material (m.p. 210–215°) was removed by filtration, yield 7 g. One crystallization from water raised the melting point to 244°. This solid was identified as 3,4-dichlorobenzylamine hydrochloride by a mixed melting point determination.

The acetone filtrate on dilution with petroleum ether (50 ml) gave crystals which melted at 203–214°, yield 1.84 g (20.9%). Crystallization from absolute ethanol raised the melting point to 217–218°. Anal. Calc. for $C_{24}H_{18}Cl_6N_6$: C, 47.78; H, 3.01; Cl, 35.27; N, 13.93; mol. wt., 603. Found: C, 47.66; H, 3.39; Cl, 35.77; N, 14.11; mol. wt., 643 (Rast).

ACKNOWLEDGMENTS

The bacteriostatic activities reported in this paper were determined by Dr. H. A. Baker of Ayerst, McKenna and Harrison Limited, Montreal, Quebec. The infrared spectra were run by Dr. C. Sandorfy of the University of Montreal, Montreal, Quebec.

REFERENCES

1. L. VOLTMER. Ber. **24**, 378 (1891).
2. J. U. NEF. Ann. **280**, 263 (1894).
3. L. W. JONES. Am. Chem. J. **20**, 1 (1898).
4. L. W. JONES and L. NEUFFER. J. Am. Chem. Soc. **39**, 652 (1917).

Can. J. Chem. Downloaded from www.nrcresearchpress.com by 41.223.56.140 on 09/04/12
For personal use only.

5. H. BILTZ and A. JELTSCH. Ber. **56**, 1914 (1923).
6. F. H. S. CURD, D. G. DAVEY, and D. N. RICHARDSON. J. Chem. Soc. 1732 (1949).
7. E. S. GATEWOOD. J. Am. Chem. Soc. **47**, 407 (1925).
8. A. F. MCKAY, G. Y. PARIS, and D. L. GARMAISE. J. Am. Chem. Soc. **80**, 6276 (1958).
9. L. J. BELLAMY. The infrared spectra of complex molecules. 2nd ed. John Wiley & Sons, Inc., New York, N.Y. 1958.
10. A. F. MCKAY, D. L. GARMAISE, R. GAUDRY, H. A. BAKER, G. Y. PARIS, R. W. KAY, G. E. JUST, and R. SCHWARTZ. J. Am. Chem. Soc. **81**, 4328 (1959).
11. A. T. FULLER and H. KING. J. Chem. Soc. 963 (1947).
12. A. CAMBRON. Can. J. Research, B, **17**, 10 (1939).
13. E. KATCHALSKI and D. B. ISHAI. J. Org. Chem. **15**, 1067 (1950).
14. W. R. ORNDORFF and D. S. PRATT. Am. Chem. J. **47**, 89 (1912).
15. G. K. ROLLEFSON and C. F. OLDERSHAW. J. Am. Chem. Soc. **54**, 977 (1932).
16. G. SCHROETER and M. PESCHKES. Ber. **33**, 1975 (1900).
17. A. MICHAELIS and G. SHROETER. Ber. **26**, 2155 (1893).
18. O. L. BRADY and L. KLEIN. J. Chem. Soc. 874 (1927).
19. A. F. MCKAY and G. R. VAVASOUR. Can. J. Chem. **32**, 59 (1954).

Can. J. Chem. Downloaded from www.nrcresearchpress.com by 41.223.56.140 on 09/04/12
For personal use only.

Can. J. Chem. Downloaded from www.nrcresearchpress.com by 41.223.56.140 on 09/04/12
For personal use only.

PROTON MAGNETIC RESONANCE ABSORPTION IN THE C-FORM OF STEARIC ACID[1]

R. F. GRANT[2] AND B. A. DUNELL

ABSTRACT

The proton magnetic resonance absorption in the C-form of stearic acid has been measured over a temperature range from −78° C to the melting point. The results suggest that the methyl end groups may be free to rotate about their triad axes throughout this temperature range, and that premelting becomes significant above 40° C.

INTRODUCTION

Proton magnetic resonance absorption measurements are sometimes useful for determining the nature and extent of molecular motion in solid organic compounds. This method has been successfully employed in the study of several long chain hydrocarbon compounds. For instance, it has been shown that the methyl groups at the ends of *n*-pentane and *n*-hexane molecules may undergo reorientation about their triad axes at temperatures well below the melting points of these compounds (1). Moreover, considerable reorientation of whole molecules has been reported in the high temperature phases of solid octacosane, *n*-dotriacontane, and lauryl alcohol (2). With the onset of molecular motion, there is a decrease of the proton magnetic resonance line width, if the rate of molecular reorientation is comparable to or greater than the line width expressed in frequency units. The extent of the narrowing will depend upon the rate and nature of the reorientation. Rapid reorientation of the whole molecule about many axes, which may occur in liquids, leads to very narrow line widths.

No extensive motion of stearic acid molecules in the solid has been reported. However, stearic acid exhibits a large, anomalous increase in volume between 60° C and the melting point, 69.6° C (3). Such behavior in long chain hydrocarbon compounds has sometimes been attributed to premelting (4). The following is an investigation of this possibility.

EXPERIMENTAL

The stearic acid used in this investigation was Eastman Kodak white label grade with a freezing point of 68.1° C. The stearic acid was purified by numerous crystallizations at −20° C from freshly distilled acetone, after the method outlined by Brown and Kolb (5). The freezing point of the purified stearic acid was 69.3° C obtained from the plateau of a time – temperature cooling curve run on a 6-g sample of the purified acid using a calibrated thermometer. This value agrees very well with the best setting points (s.p.) obtained by Francis and his co-workers (6, 7), viz., 69.35 and 69.32° C for stearic acid, and indicates that at most a very small amount of impurity was present in our sample. Indeed, Francis, Collins, and Piper found that 1% of palmitic acid impurity added to pure stearic acid (s.p. 69.32° C) lowered the setting point to 69.08° (7).

Narrow proton magnetic resonance line widths from molten stearic acid were recorded with a Varian V-4300 high resolution spectrometer operating at 40 Mc/sec. The broad line widths from solid stearic acid were measured with an oscillating detector spectrometer of conventional design (8), operating at 28 Mc/sec. A Varian electromagnet with

[1]*Manuscript received November 9, 1959.*
Contribution from the Department of Chemistry, University of British Columbia, Vancouver 8, B.C.
[2]*Holder of National Research Council Studentships. Present address: Division of Applied Chemistry, National Research Council of Canada, Ottawa.*

6-in. pole faces and a 1.75-in. gap supplied the magnetic field, which was swept linearly in time and modulated at 27 c/sec.

The samples were placed in 10-mm O.D. Pyrex test tubes. These were maintained at the higher temperatures by arranging the sample container in a glass tube through which hot air was passed from an external heater. Low temperatures were obtained by immersing the sample container in a mixture of dry ice and acetone in a narrow glass dewar. The temperature was measured with a copper–constantan thermocouple placed directly in the sample. The temperature variation during the recording of a magnetic resonance signal was about $\pm 0.5°$ C. The widths of the proton magnetic resonance absorption lines were taken as the separation in gauss of the points of maximum and minimum slope, which are the maximum and minimum of the recorded derivative signal. The second moments of the resonance absorption lines (9) were obtained from the experimental derivative curves by numerical integration (10) and were corrected for the broadening effects of modulation (11).

RESULTS

Although the proton magnetic resonance signal of stearic acid showed no fine structure from $-77°$ C to about room temperature, at about 24° C the derivative absorption line began to show a narrow peak along with the usual broad peak expected for a solid paraffin. Above 24° C this narrow peak became more and more prominent until finally the broad peak almost disappeared. The selection of first derivative lines in Fig. 1 serves to illustrate this behavior. The variation of line width with temperature for the broad peak of the resonance curve from the purified stearic acid is given by Fig. 2. Over the temperature range from $-77°$ C to 66° C, the line width remains approximately constant with values ranging from 14.0 gauss to 14.6 gauss. At 67° C the broad component of the resonance curve is so weak that its width is difficult to measure accurately. A trace of the broad component remains, however, until 69° C.

The true width of the narrow component of the resonance line was not obtained directly. The line width of 0.1 gauss obtained with the broad line spectrometer was

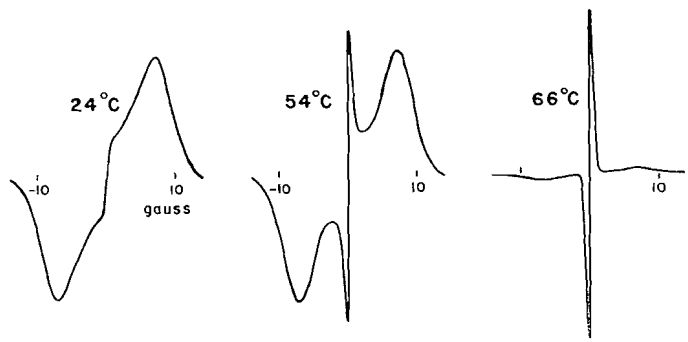


FIG. 1. Examples of derivative absorption curves showing growth of narrow component.

considered to be due to the inhomogeneity of the magnetic field over the sample and to modulation broadening. High resolution spectra from stearic acid were therefore obtained as the molten acid slowly solidified. No proton magnetic resonance absorption could be observed below the freezing point with the high resolution spectrometer, but just before freezing the line width was 0.01 gauss. The true widths of the narrow peaks of the resonance lines are, then, somewhere between 0.1 and 0.01 gauss.

Can. J. Chem. Downloaded from www.nrcresearchpress.com by 41.223.56.140 on 09/04/12
For personal use only.

The second moments of the proton magnetic resonance absorption lines decreased as the temperature approached the melting point if one took the second moment of the total curve, including the narrow peak. However, when the narrow peaks on the broad resonance lines were removed by a procedure first employed by Wilson and Pake (12), the second moment values remained almost constant throughout the whole temperature range. These second moment results from stearic acid are given as a function of temperature in Fig. 2.

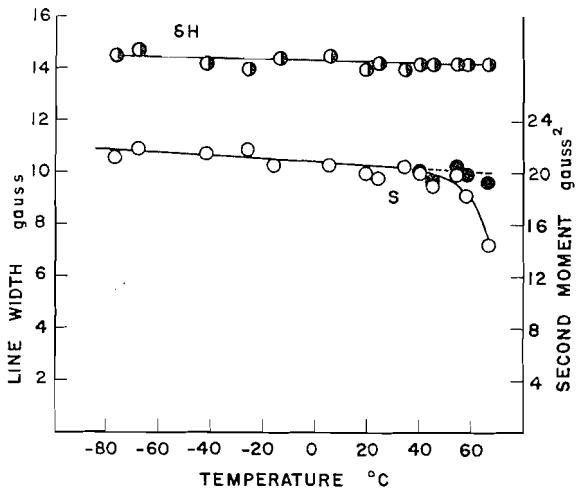


FIG. 2. Line width of broad portion of signal and second moment of stearic acid as functions of temperature. Half-filled circles, line width; open circle, second moment of the entire resonance line; filled circle, second moment calculated after the narrow component of the resonance line has been removed.

DISCUSSION

The second moment of the proton magnetic resonance of stearic acid can be calculated from structural parameters by means of Van Vleck's formula (9). For a polycrystalline sample the second moment, S, of an assembly of protons is

$$S = \frac{716}{N} \sum_{j>k} r_{jk}^{-6}$$

where N is the number of protons whose interactions are considered and r_{jk} is the distance in Å between any two protons j and k (1). We have assumed in using this formula that the crystal lattice is rigid, which in this case means that molecular reorientation occurs at a rate less than about 60 kc/sec, the low temperature experimental line width, expressed as a frequency. We have also assumed that nuclei with non-zero magnetic moments, other than protons, are absent. This is not exactly so, for C^{13} and O^{17} will be present in natural abundance. Their concentrations, however, are too small to have a significant effect on the proton second moment. The calculation of the rigid lattice second moment requires in principle a knowledge of the interproton distances throughout the crystal lattice, but because their contribution to the second moment is very small proton pairs whose separation r_{jk} is greater than 6 Å have been included in the second moment calculation by integration. The distances between pairs can be considered in two categories, namely, the intramolecular and intermolecular distances, which for convenience have been treated separately.

The intramolecular distances have been taken from the model of a long hydrocarbon

Can. J. Chem. Downloaded from www.nrcresearchpress.com by 41.223.56.140 on 09/04/12
For personal use only.

chain described by Müller (13). This model represents the molecules as planar zigzag chains of carbon atoms with tetrahedral angles of 109°28′ between the bonds. The C—H bond lengths have been taken as 1.094 Å and the C—C bond distances as 1.54 Å (14). With those parameters, the intramolecular second moment was found to be 18.4 gauss^2. The dimensions of the monoclinic unit cell used to calculate the intermolecular distances in the C-form of stearic acid are from the X-ray diffraction results of Abrahamsson and von Sydow (15). The tilt of the hydrocarbon chains has been assumed to be the same as that of lauric acid, 54°52′ to the basal (001) plane containing the carboxyl groups (16). The packing of the hydrocarbon chains is such that there are two acid dimers per unit cell. The arrangement of these carboxyl dimers has also been assumed to be the same as in lauric acid (16). The O—H bond length of the carboxyl group has been taken as 1.04 Å (17) and hence the interproton distance in the carboxyl dimer as 2.40 Å. The hydrocarbon chains are arranged end-to-end such that the distance between the planes passing through the carbon atoms of opposing methyl end groups is about 2.18 Å. From these data, the intermolecular second moment was found to be 6.0 gauss^2. The total rigid lattice second moment is therefore 24.4 gauss^2.

Since this calculated rigid lattice second moment is 3 gauss^2 larger than the mean experimental value of 21.5 gauss^2 found below −30° C, some molecular motion must be present below −30° C. It has already been mentioned that the methyl end groups might be free to reorient about their triad axes in the solid, even at low temperatures. Moreover, the low moment of inertia of the methyl group makes a tunnelling mechanism quite probable (18). If the methyl end groups reorient freely about their triad axes, the reduction in the theoretical second moment can be calculated following Gutowsky and Pake (19). The intramolecular contribution decreases by 1.92 gauss^2, and if we assume the intermolecular contribution changes proportionately (2), the total decrease is 2.6 gauss^2 and the theoretical second moment of stearic acid with rotating methyl groups is 21.8 gauss^2. This new value agrees within experimental error with the results obtained below −20° C. It is possible, therefore, that the broad portion of the resonance curve represents an almost rigid lattice and that the existing molecular motion probably concerns only the methyl-group ends of the molecules.

On the other hand, there is the possibility that the 3-gauss^2 difference between the experimental second moment below −30° C and the calculated rigid lattice value may be largely due to zero-point vibrational motions of the protons.* A detailed calculation of the importance of this effect would be difficult, but we may obtain an indication of its significance from the following considerations. An analysis of the reduction of the second moment resulting from zero-point motions has been made for ammonium halides and hydrazine fluoride (20–23). Gutowsky, Pake, and Bersohn found that the intramolecular contribution to the second moment of the ammonium ion was reduced by its zero-point torsional oscillations by a factor

$$1-\epsilon \cong \left(\left\langle 1-\frac{3}{2}\theta^2 \right\rangle\right)^2 \qquad [1]$$

where θ is the angle of torsional oscillation (20). If we consider that the significant motions in stearic acid are CH_2 twisting and rocking modes, we might use equations [34] and [35] of Ibers and Stevenson (23) to obtain

$$\theta^2 = (h/8\pi^2 c)\left(\frac{1}{I_1\nu_1}+\frac{1}{I_2\nu_2}\right) \qquad [2]$$

We are indebted to the referee for raising this question.

Can. J. Chem. Downloaded from www.nrcresearchpress.com by 41.223.56.140 on 09/04/12
For personal use only.

Can. J. Chem. Downloaded from www.nrcresearchpress.com by 41.223.56.140 on 09/04/12
For personal use only.

where ν and I are the torsional frequency and moment of inertia for each mode. Taking $\nu_1 = 720$ cm^{-1} for the rocking mode (24) and I_1 as the moment of inertia of both CH_2 protons about a fixed carbon, and $\nu_2 = 1200$ cm^{-1} for the twisting mode (24) and I_2 as the moment of inertia of both CH_2 protons about the center of the line joining them, one obtains $1-\epsilon = 0.946$ from equations [1] and [2]. This value will apply to the reduction of the second moment contribution of the methylene groups. If we now assume that the whole second moment is reduced by a similar factor we find a reduction of 1.3 gauss^2. The uncertainties involved in this estimation are very large. Ibers and Stevenson (23) suggest that the reduction of the intermolecular contribution may be larger than the reduction of the intramolecular contribution (in this case the CH_2 contribution). On the other hand, we have used the smallest possible values of moments of inertia, and if the methylene carbon is involved in the 720 cm^{-1} rocking mode or the 1180–1350 cm^{-1} band progression assigned to the wagging and twisting modes, the larger moments of inertia which would be appropriate would bring $1-\epsilon$ closer to unity. That these modes do involve the carbon atom is suggested by the fact that the 720 cm^{-1} band appears only in chains —$(CH_2)_n$— where $n \geqq 4$ (25), and that the 1180 cm^{-1} band progression exists only in the solid state and depends on chain length (26). There is, then, doubt as to whether the end methyl groups rotate. However, lack of an obvious reason for difference between the behavior of the methyl end groups in the fatty acid and in *n*-pentane and *n*-hexane studied by Rushworth (1), together with the uncertainties of the zero-point motional corrections, suggest to us that rotation of the methyl groups is the more probable explanation.

As we have reported above, the narrow component of the proton magnetic resonance line, which exists above about 20° C, does not correspond to a liquid condition, for which a line width of about 10^{-4} gauss might be expected. The observed line width of between 0.1 and 0.01 gauss does suggest, however, rapid molecular motion about several axes. The over-all line shape is similar to the proton magnetic resonance lines obtained from some high polymers for which the narrow component represents an amorphous phase and the broad component a crystalline one (10). In an important respect, however, the comparison with polymer systems breaks down. In polymers, the width of the narrow line is temperature dependent, being comparable to the width of the broad component at low temperatures (12, 27). In stearic acid the width of the narrow line is less than 0.1 gauss regardless of temperature, the change with temperature being in the amplitude of the narrow line. This increasing amplitude suggests that more and more molecules begin to move rapidly as the temperature rises. Since the percentage area under the narrow component corresponds approximately to the percentage of the hydrogen nuclei that are in rapid motion, a comparison of the integrated areas under the broad and narrow components of some of the proton resonance lines has been given in Table I. Although

TABLE I

Fraction of the protons involved in rapid motion

Temp. (° C)	Percentage area of narrow component
40	0.9
45	1.1
54	2.5
58	5.9
66	27.4

parts of molecules rather than entire molecules might be in rapid motion at temperatures above 20° C, it is unlikely that if 27% of each molecule is in rapid motion at 66° C, the remaining portion of each molecule would be rigidly constrained in the lattice as the high second moment of the broad component suggests. It seems more likely that solid stearic acid is present in two phases. One phase, as we have shown, has a rigid, ordered structure, possibly with only end methyl groups rotating and the other has a rather flexible and disordered structure. The amount of disordered phase increases as the temperature rises. This increase in the disordered phase below the melting point could account for the anomalous volume increase in stearic acid between 60° and 69° C (3).

Premelting in some cases has been thought to be due to rotation of molecules below the melting point. It might also be a co-operative increase in the number of holes and interstitial molecules in the solid which leads to the break up of long-range order at the melting point (28). It has been reported that the number of holes in equilibrium with the lattice is abnormally large near the melting points in some long chain hydrocarbons (29). These results suggest that such a process occurs in stearic acid. Lattice defects due to dislocations and impurities in the crystal might allow a few stearic acid molecules to flex and rotate. This could correspond to motion about many axes and lead to the observed narrow component of the proton magnetic resonance line. As the temperature rises these zones of motion and disorder grow in size at the expense of the surrounding ordered structure, until just below the melting point the entire crystal structure is completely disordered or amorphous.

ACKNOWLEDGMENTS

The authors are indebted to Dr. T. M. Connor for the high resolution measurements and to Professor C. A. McDowell for his interest in this problem. We thank the National Research Council for a studentship awarded to one of us (R.F.G.) and for a grant-in-aid of the research.

REFERENCES

1. F. A. Rushworth. Proc. Roy. Soc. (London), A, **222**, 526 (1954).
2. E. R. Andrew. J. Chem. Phys. **18**, 607 (1950).
3. W. S. Singleton, T. L. Ward, and F. G. Dollear. J. Am. Oil Chemists' Soc. **27**, 143 (1950).
4. A. R. Ubbelohde. Trans. Faraday Soc. **34**, 282 (1938).
5. J. B. Brown and D. K. Kolb. Progress in the chemistry of fats and other lipids. The Pergamon Press, Ltd., London. Vol. 3. 1955. p. 58.
6. F. Francis and F. J. E. Collins. J. Chem. Soc. 137 (1936).
7. F. Francis, F. J. E. Collins, and S. H. Piper. Proc. Roy. Soc. (London), A, **158**, 691 (1937).
8. H. S. Gutowsky, L. H. Meyer, and R. E. McClure. Rev. Sci. Instr. **24**, 644 (1953).
9. J. H. Van Vleck. Phys. Rev. **74**, 1168 (1948).
10. G. E. Pake and E. M. Purcell. Phys. Rev. **74**, 1184 (1948).
11. E. R. Andrew. Phys. Rev. **91**, 425 (1953).
12. C. W. Wilson and G. E. Pake. J. Chem. Phys. **27**, 115 (1957).
13. A. Müller. Proc. Roy. Soc. (London), A, **154**, 624 (1936).
14. L. Pauling. The nature of the chemical bond. Cornell Univ. Press, Ithaca, N.Y. 1948. p. 161.
15. S. Abrahamsson and E. von Sydow. Acta Cryst. **7**, 591 (1954).
16. V. Vand, W. M. Morley, and T. R. Lomer. Acta Cryst. **4**, 324 (1951).
17. M. M. Davies and G. B. B. M. Sutherland. J. Chem. Phys. **6**, 755 (1938).
18. T. P. Das. J. Chem. Phys. **27**, 763 (1957).
19. H. S. Gutowsky and G. E. Pake. J. Chem. Phys. **18**, 162 (1950).
20. H. S. Gutowsky, G. E. Pake, and R. Bersohn. J. Chem. Phys. **22**, 643 (1954).
21. L. E. Drain. Discussions Faraday Soc. **19**, 200 (1955).
22. C. M. Deeley and R. E. Richards. Trans. Faraday Soc. **50**, 560 (1954).
23. J. A. Ibers and D. P. Stevenson. J. Chem. Phys. **28**, 929 (1958).
24. R. G. Sinclair, A. F. McKay, and R. N. Jones. J. Am. Chem. Soc. **74**, 2570 (1952).
25. L. J. Bellamy. The infrared spectra of complex molecules. Methuen & Co., Ltd., London. 1954. p. 26.
26. R. N. Jones, A. F. McKay, and R. G. Sinclair. J. Am. Chem. Soc. **74**, 2575 (1952).
27. D. W. McCall and W. P. Slichter. J. Polymer Sci. **27**, 171 (1957).
28. J. E. Lennard-Jones and A. F. Devonshire. Proc. Roy. Soc. (London), A, **170**, 464 (1939).
29. J. W. H. Oldham and A. R. Ubbelohde. Trans. Faraday Soc. **35**, 328 (1939); Proc. Roy. Soc. (London), A, **176**, 50 (1940).

Can. J. Chem. Downloaded from www.nrcresearchpress.com by 41.223.56.140 on 09/04/12
For personal use only.

Can. J. Chem. Downloaded from www.nrcresearchpress.com by 41.223.56.140 on 09/04/12
For personal use only.

ELECTRONIC POTENTIAL SURFACES OF ACETYLENE IN LCAO/MO APPROXIMATION[1]

G. W. KING

ABSTRACT

A digital computer has been programmed to carry out 6-electron LCAO/ASMO calculations for linear and *trans*-bent acetylene, with the following input variables; coefficients of the LCAO/MOs, carbon–carbon bond length, and effective nuclear charge on the carbon atoms. The effect of varying these parameters upon the calculated electronic energy levels is discussed, and approximations to "best" MOs are obtained for various states of the molecule, leading to values of hybridization parameters for the carbon atoms. Certain assumptions enable the electronic energies to be related to the C—C—H bending angle; from this it is concluded the ground state is linear and the lowest A_u excited state is bent, in accordance with experiment. Values are given for electronic transition energies and hydrogen-bending force constants.

INTRODUCTION

In the LCAO/MO method for calculating the electronic energies of molecules, an orthogonal set of single-electron molecular orbitals[2] ϕ_i are formed by linear combination of n atomic orbitals χ_n:

$$\phi_i = \sum_n c_{in}\,\chi_n. \qquad [1]$$

These are combined in determinantal form to give ASMO wave functions:

$$\Phi_p = (N!)^{-\frac{1}{2}}|\phi_0(q_0)\ \phi_1(q_1)\ \ldots\ldots\ \phi_N(q_N)|. \qquad [2]$$

In general, the eigenvalues of the system have the expectation value

$$\int {\Psi_k}^{S*} H\, {\Psi_k}^{S}\, d\tau \qquad [3]$$

where the ${\Psi_k}^S$ are linear combinations of the ASMO functions:

$${\Psi_k}^S = \sum_p d_{kp}\,\Phi_p. \qquad [4]$$

If a large number of suitable Φ_p are taken in each such linear combination [4] (i.e., allowed to interact configurationally), and the stationary states of the system are found by solving the corresponding secular determinantal equations of high order, then the forms of the ϕ_i in [1] are of secondary importance. But if only a few Φ_p are taken in [4], it is necessary that the ϕ_i resemble the "best" MOs for a given electronic state as closely as possible, that is, the eigenfunctions of the Hartree–Fock operator for that state. The variational way to achieve this is an iterative one that becomes extremely complex for configurations comprising partly filled molecular orbitals, in which Ψ_k must be constructed from at least two suitably chosen Φ_p in order to be in accord with the Pauli principle.

For simple and highly symmetric molecules, the ϕ_i in [1] are usually chosen to transform like irreducible representations of the appropriate symmetry point group. This

[1]*Manuscript received November 9, 1959.*
Contribution from the Burke Chemical Laboratories, Hamilton College, McMaster University, Hamilton, Ontario.
[2]*The notation follows that of Howard and King, reference 1.*

often fixes values for certain of the c_{in}, and some of the remaining coefficients in [1] may be interrelated by orthogonality requirements between the MOs, leaving only a small number of coefficients c_j as independent parameters defining the whole set. Instead of attempting to find the best values of these by a cyclic self-consistent procedure, a more direct approach is used here in evaluating [3] for a wide range of values of the parameters c_j and locating the position of minimum energy for a given electronic state graphically, by plotting electronic energy [3] as a function of these parameters. This method is well suited to computer calculation, since a basic program can be written to evaluate concurrently the energies of different electronic states, with the c_j as the variable input parameters. Furthermore, it can be applied to configurations with partly filled orbitals.

It must be noted, however, that the various configurational wave functions for states of the same symmetry class are not necessarily orthogonal in the approximation used below. The only orthogonality present is due to differences in symmetry class, and a configuration interaction treatment would improve the values obtained for the energies.

APPLICATION TO ACETYLENE

The electronic states of *trans*-acetylene are considered here as a 6-electron problem, in LCAO/MO approximation. This example has certain disadvantages owing to the approximations it is necessary to make, especially those concerning the carbon–hydrogen bonds. On the other hand, there is considerable spectroscopic data available for the linear ground Σ_g^+ state (2) and for the lowest excited A_u *trans*-bent state (3, 4), which differ widely in geometry. LCAO/MO/CI calculations have been carried out by Ross (5) for the linear states with $r_{CC} = 1.203$ Å, corresponding to the observed ground state value, and by Howard and King (1) for bent states with $r_{CC} = 1.383$ Å and $\angle CCH = 120°$, corresponding to the observed values for the A_u state. The computer program closely followed the procedures used by Howard and King to obtain the diagonal elements E' of their equation [7], except that the coefficients listed in their paper[3] for the hybrid AOs χ_1–χ_8 were replaced by the general forms given below. Orthogonality was maintained between MOs of the same symmetry class.[4]

Let Cartesian axes be attached to each carbon atom with the z-axes pointing towards each other and with parallel y-axes in the molecular plane. Then the hybrid AOs on the carbon nuclei a and b may be written:

$$\chi_1 = t^{-1}(\lambda \cos\theta . a_s + r . a_z) \qquad \chi_2 = t^{-1}(\lambda \cos\theta . b_s + r . b_z)$$
$$\chi_3 = a_x \qquad \chi_4 = b_x$$
$$\chi_5 = t^{-1}(r\lambda \sin\theta . a_s - 2^{-1}\lambda^2 \sin 2\theta . a_z + t^2 . a_y)$$
$$\chi_6 = t^{-1}(r\lambda \sin\theta . b_s - 2^{-1}\lambda^2 \sin 2\theta . b_z - t^2 . b_y)$$
$$\chi_7 = r . a_s - \lambda \cos\theta . a_z - \lambda \sin\theta . a_y \qquad \chi_8 = r . b_s - \lambda \cos\theta . b_z + \lambda \sin\theta . b_y$$

where $t = (1-\lambda^2 \sin^2\theta)^{\frac{1}{2}}$ and $r = (1-\lambda^2)^{\frac{1}{2}}$, $0 < \theta < 90°$.

All the coefficients are expressed here in terms of two independent parameters, θ and λ. θ is the acute angle between the orbitals χ_7 or χ_8 and a line through the carbon nuclei,

[3]*See ref. 1, p. 703.*

[4]*Strictly, the electronic energies would be independent of the actual forms chosen for such* MOs *only if they were exact solutions of the Hartree-Fock equations. We note that in the calculations both of Ross and of Howard and King, the introduction of* CI *had only a small effect on the energies of many of the electronic states, indicating that the* MOs *they used were reasonably good approximations for these states.*

Can. J. Chem. Downloaded from www.nrcresearchpress.com by 41.223.56.140 on 09/04/12
For personal use only.

and λ is the amount of p character in each of these orbitals when they are written in the vectorial form

$$\chi_{7,8} = \eta s + \lambda p, \qquad 0 < \lambda < 1.$$

In previous calculations (1, 5), the hydrogen atoms were formally attached to χ_7 and χ_8 respectively, making θ the complement of the C—C—H bond angle. The validity of this assumption is discussed in a later section. Inserting $\theta = 60°$ and $\lambda = (2/3)^{\frac{1}{2}}$, we obtain the AOs used by Howard and King in which three equivalent sp^2 hybrids are centered on each carbon atom; $\theta = 0$ and $\lambda = 2^{-\frac{1}{2}}$ gives the sp hybrid AOs used by Ross for the linear molecule. Situations such as $\theta = 0$, $\lambda = 0$, for example, in which the H atoms are bound by pure $2s$ carbon orbitals are highly improbable, and the calculations show that very high energies are associated with such states. In general, one would not expect the C—H bond to have less p character than it does in the linear state, and it will be seen that the minima of potential surfaces fall within the anticipated range of values for λ.

χ_3 and χ_4 are pure p orbitals above and below the molecular plane, and remain unchanged as θ is varied. This is similar to the qualitative approach used by Walsh (6).

A Bendix D-15G computer, using the "Intercom 1000 Double Precision" interpretative subroutine was programmed to calculate energies of all the low-lying electronic states of *trans*-acetylene over all permissible (θ,λ) values at intervals of (10°, 0.1). The E' for each (θ,λ) value was computed in 12 minutes. These are simply the values of the diagonal elements of the secular determinants: limitations in the storage capacity of the computer prevented evaluation of the off-diagonal elements and the calculation of configuration interaction between states of the same symmetry. However, the program included interpolation in the tables of molecular integrals of Kotani (7), enabling the effective nuclear charge for $n = 2$ and also the separation of the carbon atoms to be included as additional variable parameters. The effective nuclear charge for $1s$ carbon atomic orbitals, to which the $2s$ orbitals were made orthogonal, was kept at 5.70.

The program was readily checked by comparison at different stages with results obtained by Ross and by Howard and King, using the appropriate (θ,λ) values. Excellent agreement was obtained.

Once a potential minimum for a given state had been located approximately, its position was accurately fixed by a "fine" scan over the region at (1°, 0.01) intervals.

RESULTS

Figure 1 shows energy contours, relative to the minimum value, for the lowest A_g state of acetylene, with $r_{CC} = 1.203$ Å. The contours were obtained by graphical interpolation of the computer results. This A_g state correlates with the ground Σ_g^+ state of the linear molecule. The potential minimum occurs at (0°, 0.643), λ having a slightly lower value than that of 0.707 for simple sp-type hybridization. Thus the C—H bond has slightly more, and the C—C bond slightly less, $2s$ character than is commonly supposed. Moffitt (8), on the basis of fairly general arguments, has predicted slight effects in the opposite direction.

Figure 2 is a similar diagram for the lowest A_u state, calculated for $r_{CC} = 1.383$ Å. This is the spectroscopically observed state. The potential minimum, indicated by a cross, is at the point (44°, 0.81). λ is fairly close to the value for ordinary sp^2-type

Can. J. Chem. Downloaded from www.nrcresearchpress.com by 41.223.56.140 on 09/04/12
For personal use only.

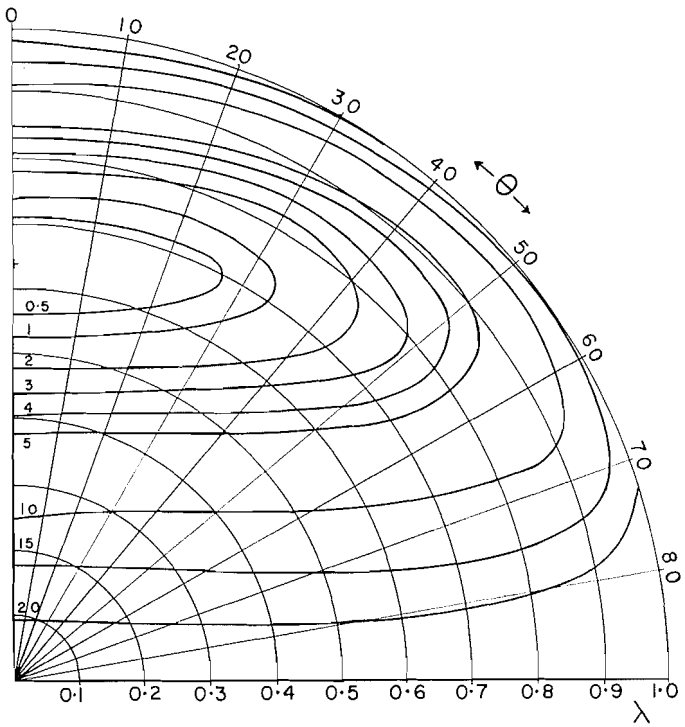


FIG. 1. Energy contours in ev for ground A_g (Σ_g^+) electronic state of *trans*-acetylene. r_{CC} = 1.203 Å, Z_{eff} = 3.18.

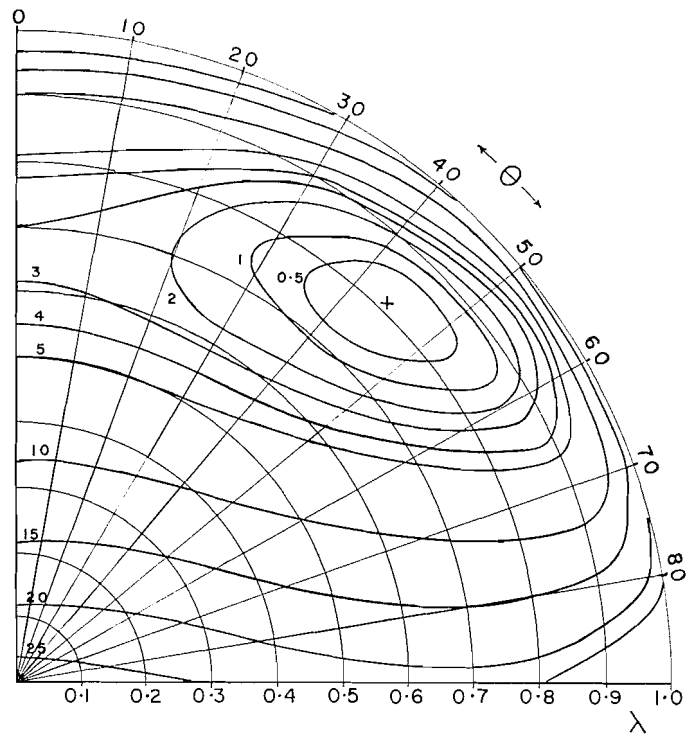


FIG. 2. Energy contours in ev for lowest A_u electronic state of *trans*-acetylene. r_{CC} = 1.383 Å, Z_{eff} = 3.18.

Can. J. Chem. Downloaded from www.nrcresearchpress.com by 41.223.56.140 on 09/04/12
For personal use only.

hybridization; this agrees with the observation (3) that the molecule in this state resembles ethylene with two *trans*-hydrogen atoms missing.

In these two figures, the effective nuclear charge Z_{eff} on the carbon atoms for $n = 2$ in the Slater AOs, is 3.18. In Fig. 3, the calculations of Fig. 2 have been repeated with

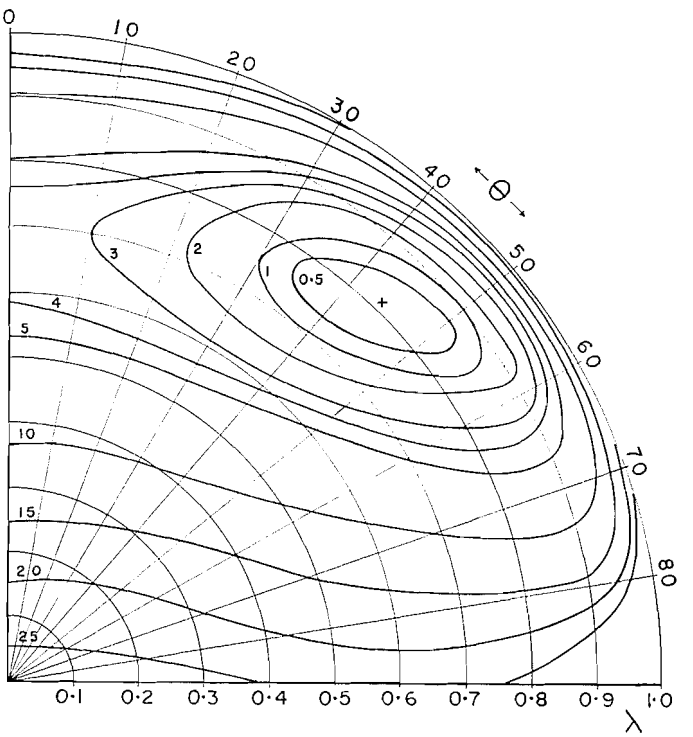


FIG. 3. Energy contours in ev for lowest A_u electronic state of *trans*-acetylene. $r_{CC} = 1.383$ Å, $Z_{eff} = 3.50$.

$Z_{eff} = 3.50$. Only small differences in the position of the energy minimum (44°, 0.82) and in the shapes of the energy contours are observed. This was found to be true generally for similar calculations with Z_{eff} ranging down to a 2.80. The relative energy levels for a given (θ,λ) in the region of minimum energy only changed slightly on varying Z_{eff}. Shull and Ellison (9) found this to hold also for benzene. Consequently, in subsequent calculations reported here, Z_{eff} was fixed at the free atom value of 3.18. Minimization of all potential energies with respect to Z_{eff} would have represented an unjustifiably large increase in the amount of computation.

TABLE I

Positions of electronic energy minima for the lowest A_u state for various C—C distances to nearest (1°, 0.01) intervals of (θ,λ)

r_{CC} (Å)	1.34	1.36	1.383	1.40	1.42
θ	44	44	44	45	45
λ	0.81	0.81	0.81	0.82	0.82

Can. J. Chem. Downloaded from www.nrcresearchpress.com by 41.223.56.140 on 09/04/12
For personal use only.

TABLE II

Positions of electronic energy minima for the ground Σ_g^+ state for various C—C distances, to nearest 0.001 intervals of λ, $\theta = 0°$

r_{CC} (Å)	1.18	1.203	1.22
λ	0.638	0.643	0.647

Tables I and II show the positions of potential minima for the A_u and A_g states respectively for different values of r_{CC}. Very little change occurs in each case. Table II indicates a slight increase in p character of the σ-type C—C bond as r_{CC} decreases.

In order to minimize the energy with respect to r_{CC}, and also to calculate the energy of the A_u–Σ_g^+ transition, it is necessary to evaluate energies of repulsion between the carbon nuclei. These have a magnitude of several hundred ev, and are very sensitive to small changes in the value for the nuclear charge, which depends on the extent of electron screening. In addition, variation of r_{CC} will affect electrostatic contributions to the energy due to any polarity in the C—H bonds, which is an unknown factor. In the circumstances, we merely report the value of 2.5 ev for transition between the potential minima of the two states, assuming a carbon nuclear charge of +4. The experimental value is 5.24 ev. The agreement is not as good as that obtained by Howard and King. It must, however, be remembered that the calculated figure is a difference between two quantities each of magnitude of some 250 ev.

The positions of minimum energy for the lowest states of the four symmetry classes of point group C_{2h} are summarized in Table III. These are all values for $r_{CC} = 1.383$ Å.

TABLE III

Electronic configurations and positions of minimum energy for lowest states of each symmetry class

State	Configuration	(θ,λ)
A_g	$(a_g\sigma_g 2sp^2)^2(a_u\pi_u 2p)^2(b_u 2sp^2)^2$	(0, 0.67)
A_u	$(a_g\sigma_g 2sp^2)^2(a_u\pi_u 2p)(b_u 2sp^2)^2(a_g 2sp^2)$	(44, 0.81)
B_g	$(a_g\sigma_g 2sp^2)^2(a_u\pi_u 2p)(b_u 2sp^2)(a_g 2sp^2)^2$	(50, 0.8)
B_u	$(a_g\sigma_g 2sp^2)^2(a_u\pi_u 2p)^2(b_u 2sp^2)(a_g 2sp^2)$	(0, 0.65)

The B_g state has $\theta > 0$. The B_u state is apparently linear, but this conclusion is invalid for the following reason. Certain of the lower excited states of bent acetylene correlate with degenerate species of the linear molecule; thus, $A_u + B_u \rightarrow \Delta_u$ (see ref. 3, Part III, Table 7). However, the calculated energies of such states do not converge in pairs upon the corresponding degenerate linear states as $\theta \rightarrow 0$; on the contrary, for example, the lowest pair of A_u states converge on each other, as do the lowest pair of B_u states, and each species would require a proper CI treatment to sort them in accordance with correlation relationships. Thus energy values for $\theta = 0$ for such states as calculated here are in error, which decreases as θ increases and states of the same symmetry move apart in energy. This does not apply to the lowest A_g state, which correlates with a single Σ_g^+ state; the next A_g state lies some 18 ev higher in the linear molecule for $\lambda = 0.643$, but this separation does decrease somewhat as θ increases to 90°.

THE CARBON-HYDROGEN BONDS

Two assumptions are made here: that the potentials of the hydrogen atoms can be neglected, and that they can be regarded as attached to orbitals χ_7 and χ_8 respectively,

Can. J. Chem. Downloaded from www.nrcresearchpress.com by 41.223.56.140 on 09/04/12
For personal use only.

with complete localization of the C—H bond electrons. A refined calculation would include these in MOs extending over all four atoms of the molecule; and the coefficients of the carbon AOs in the "best" MOs, in the Hartree–Fock sense, need not bear a simple relationship to the C—C—H bond angles (although a suitable unitary transformation could be made to localize charge in the C—H bond directions).

On the other hand, it may be argued that for linear and moderately bent models, there is quite a small overlap between symmetry MOs formed purely from the well-separated C—H bond orbitals and the MOs of the C—C bond, and hence little interaction between them. There will also be a very small charge concentration of C—C bond electrons in the neighborhood of the hydrogen nuclei. The overlap would be greater if the C—H symmetry MOs contained several modes, but states in which such MOs are occupied will be high in energy and unlikely to affect the energies of low-lying electronic states. Hence in a first approximation θ can be correlated with the C—C—H angle; this becomes increasingly in error both as $\theta \rightarrow 90°$ and as $\lambda \rightarrow 0$, as interactions between C—C and C—H bond electrons increase. Since in general such interactions will lower the energies of our electronic states, it follows that the values calculated here are too high for small λ and large θ values; the necessary correction would shift the positions of the potential minima for bent states in the direction of these, and thus, for example, improve agreement with the observed 120° bending angle in the A_u state.

Ellison and Shull (10) have obtained SCF/MOs for the water molecule at different bond angles, and converted these by unitary transformations into equivalent orbitals directed towards the hydrogen atoms. They found that localization of electrons in O—H bond equivalent orbitals was not a justifiable assumption, as had been supposed by Pople (11) in his original treatment. Similar conclusions follow from the calculations of Higuchi (12) on the NH_2 radical. In these molecules, however, one would expect large interactions between electrons in any orbital representations directed along the X—H axes, owing to their proximity. This is not the case in acetylene.

If θ is identified with the acute C—C—H angle, some interesting conclusions emerge. The A_g (Σ_g^+) state in Fig. 1 is predicted to be linear and the A_u state in Fig. 2 to be *trans*-bent, in accordance with observation. The lowest B_u state is also expected to be bent.

Bending force constants can be derived for the C—H bonds. The two hydrogen atoms are approximated by a point executing small harmonic oscillations about the potential minimum at constant λ. This gives a bending constant of 0.24×10^{-11} erg/radian^2 for the A_g state, identical with the value derived from the known vibrational frequencies (13). The value for the A_u state is 4×10^{-11} erg/radian^2, which is much larger than would be expected; for example, the force constant for the comparable hydrogen-bending motion in benzene (3) is 0.8×10^{-11} erg/radian^2. The potential well for the A_u state is, however, very anharmonic, and the assumption of constant λ for this motion is somewhat provisional.

It would be helpful if λ could be related to r_{CH} and some estimate obtained for C—H stretching force constants. Various empirical expressions for the dependence of r_{CH} on degree of hybridization at a carbon atom are to be found in the literature (14, 15, 16). It was found that stretching constants several hundred times too large were obtained if any of these were used. Apart from the fact that none of them provides a good fit to experimental data, and that those methods based on addition of covalent bond radii are open to criticism (17), such expressions are derived using series of molecules in which both θ and λ vary with carbon atom hybridization, and cannot be readily employed here.

Can. J. Chem. Downloaded from www.nrcresearchpress.com by 41.223.56.140 on 09/04/12
For personal use only.

In conclusion, a 6-electron, two-center approximation seems to give a better picture of the linear ground state of acetylene than of the bent excited states. The assumptions inherent in the treatment give only a qualitative significance to the results, but nevertheless avoid the troublesome calculation of three- and four-center integrals that would be entailed in more precise calculations.

ACKNOWLEDGMENT

Financial support for this work was provided by the National Research Council.

REFERENCES

1. H. HOWARD and G. W. KING. Can. J. Chem. **37**, 700 (1959).
2. B. D. SAKSENA. J. Chem. Phys. **20**. 95 (1952).
3. C. K. INGOLD and G. W. KING. J. Chem. Soc. 2702 (1953).
4. K. K. INNES. J. Chem. Phys. **22**, 863 (1954).
5. I. G. ROSS. Trans. Faraday Soc. **48**, 973 (1952).
6. A. D. WALSH. J. Chem. Soc. 2288 (1953).
7. M. KOTANI, A. AYAO, I. EIICHI, and K. TOSAKU. Tables of molecular integrals. Maruzen Co., Ltd., Tokyo. 1955.
8. W. MOFFITT. Proc. Roy. Soc. (London), A, **202**, 548 (1950).
9. H. SHULL and F. O. ELLISON. J. Chem. Phys. **19**, 1595 (1951).
10. F. O. ELLISON and H. SHULL. J. Chem. Phys. **23**, 2348 (1955).
11. J. A. POPLE. Proc. Roy. Soc. (London), A, **202**, 323 (1950).
12. J. HIGUCHI. J. Chem. Phys. **24**, 535 (1956).
13. J. W. LINNETT, D. F. HEATH, and P. J. WHEATLEY. Trans. Faraday Soc. **45**, 832 (1949).
14. L. PAULING, H. D. SPRINGALL, and K. J. PALMER. J. Am. Chem. Soc. **61**, 927 (1939).
15. M. G. BROWN. Trans. Faraday Soc. **55**, 694 (1959).
16. H. J. BERNSTEIN. J. Phys. Chem. **63**, 567 (1959).
17. M. J. S. DEWAR and H. N. SCHWEISING. Tetrahedron, **5**, 166 (1959).

Can. J. Chem. Downloaded from www.nrcresearchpress.com by 41.223.56.140 on 09/04/12
For personal use only.

Can. J. Chem. Downloaded from www.nrcresearchpress.com by 41.223.56.140 on 09/04/12
For personal use only.

TRITIUM EXCHANGE BETWEEN CELLULOSE AND WATER: ACCESSIBILITY MEASUREMENTS AND EFFECTS OF CYCLIC DRYING[1]

A. R. G. LANG[2] AND S. G. MASON

ABSTRACT

Tritium exchange between cellulose and water vapor was used to measure the accessibilities of amylopectin, amylose, regenerated cellulose, wood pulp, bacterial and Valonia cellulose, and cellulose trinitrate using both gas counting and solid counting techniques. The results compare satisfactorily with other accessibility and crystallinity measurements.

The incomplete reversibility of the exchange reaction was used to study directly changes in the accessibility of regenerated cellulose which occurred during repeated wetting and drying from water. The results indicated that a partial interchange of accessible and inaccessible regions occurs during wetting and drying.

INTRODUCTION

This paper describes preliminary experiments which use the exchange reaction of tritium between cellulose and water to study the "accessibility" of cellulose to water vapor, and to measure directly the formation of new inaccessible regions in cellulose during successive wetting and drying cycles.

Deuterium has been used extensively as a tracer in the exchange of hydrogen isotopes between cellulose and water (1–11), but only the more recent studies of Frilette, Hanle, and Mark (3), Almin (5), and Mann and Marrinan (8–11) are of value in accessibility studies. The exchange reaction, which was almost complete in 1 hour, was attributed to exchange with the hydroxyl hydrogens of the cellulose units in the amorphous regions and on the faces of the crystallites. The ratio of the cellulose participating in the reaction to the total, calculated by assuming that 3 hydroxyl groups reacted per anhydroglucose unit, was taken as a quantitative measure of the accessibility. These accessibilities were in good agreement with other accessibility and crystallinity measurements.

In the present work tritium (H^3), which, being radioactive, has the advantage that it may be easily, accurately, and sensitively determined, was introduced as a tracer in the exchange reaction

$$R.OH + HTO \rightleftharpoons R.OT + H_2O \qquad [1]$$

where R.OH is a carbohydrate containing accessible hydroxyls. The extent of this reaction was used to determine the accessibility of the carbohydrate. Measurements were made on a variety of samples in two ways.

1. By a gas counting technique in which cellulose and tritiated water vapor were reacted together, and the adsorbed and vapor-phase water removed and analyzed by gas counting. The extent of the reaction was calculated from the stoichiometry of the system and the dilution of the tritium in the water.

2. A radioactivity counting method for solid samples was used in which cellulose was exchanged with tritiated water vapor, the water removed, and the tritium in the cellulose measured by counting the solid sample. This method required a special apparatus, the Vacuum Transfer Counter (VTC), described elsewhere (12).

The gas counting method was used chiefly for calibration and corroboration of the solid counting method.

[1]*Manuscript received October 29, 1959.*
Contribution from Physical Chemistry Division, Pulp and Paper Research Institute of Canada, and Department of Chemistry, McGill University, Montreal, Que.
[2]*Holder, Frank J. Sensenbrenner Fellowship 1956–57, and National Research Council of Canada Studentships 1957–58 and 1958–59.*

Confirming the observations of Mann and Marrinan (9) with deuterated water, it was found that the exchange of the accessible regions was not completely reversible; cellulose dried from tritiated water contained some tritium which could not be removed by soaking in water, i.e. some of the cellulose was rendered inaccessible by the wetting and drying. This newly formed inaccessibility is believed to be due to the formation of new interchain bonds during drying.

A number of additional experiments were conducted in which this newly created inaccessibility was used to study changes in cellulose caused by alternate wetting and drying. Two quantities were measured.

1. The amount of inaccessible material, $\delta\omega_n$, formed during the nth cycle, was determined by alternately wetting and drying the cellulose from ordinary water $(n-1)$ times, followed by a single wetting and drying from tritiated water for the nth cycle. The labile tritium was removed by soaking in ordinary water, and the amount of inaccessible cellulose formed in the nth cycle determined by counting the solid cellulose sample in the VTC. This quantity is analogous to the "resistant OD groups" of Mann and Marrinan (9).

2. The net inaccessible cellulose, W_n, formed during n cycles was determined by wetting and drying cellulose from tritiated water (n) times. The labile tritium was removed and the sample counted as before.

Both $\delta\omega_n$ and W_n were expressed as percentages of the total cellulose.

EXPERIMENTAL PART

Samples

(*a*) Amylopectin (Ramelin-G from Stein Hall and Co., Inc.) was dissolved in cold water and evaporated on a mercury surface to form a film with a superficial density of about 3 mg per sq. cm.

(*b*) Amylose (Superlose from Stein Hall) was dissolved in water at 160° C. A film (about 3 mg per sq. cm) was formed by evaporation of the solution on a mirror-finished stainless steel plate.

(*c*) Air-dried cellulose film (Dupont of Canada Ltd.) made from viscose was used, having a superficial density of 3.0 mg per sq. cm (about 23 μ thick). It had been neither plasticized nor coated.

(*d*) Acetate-grade softwood dissolving pulp having an α-cellulose (Tappi method) content of 96% was formed into sheets of superficial density 7.8 and 3 mg per sq. cm on a British sheet machine, pressed, and air-dried against a glazing plate.

(*e*) Bacterial cellulose grown from *Acetobacter xylinum* (kindly supplied by Dr. J. R. Colvin, National Research Council) was made into a sheet of superficial density 3 mg per sq. cm on a British sheet machine, pressed, and air-dried against a glazing plate.

(*f*) Valonia cellulose, obtained in a water–formaldehyde mixture from the General Biological Supply House, was purified by the method of Ranby (13), i.e. refluxed in 1.0% sodium hydroxide for 6 hours with a solvent change after 3 hours, then washed in dilute acetic acid and water.

(*g*) Ramie cellulose trinitrate (N content 13.80% corresponding to 97.7% complete nitration) was cast into a film (3 mg per sq. cm) from ethyl acetate on a mirror-finished stainless steel sheet.

Accessibility by Gas Counting

A dry sample containing exchangeable hydrogens was reacted with tritiated water and

Can. J. Chem. Downloaded from www.nrcresearchpress.com by 41.223.56.140 on 09/04/12
For personal use only.

then all the water was recovered by distillation. The accessibility of the sample was calculated from the resultant dilution of the radioactivity in the water and the stoichiometry of the system.

The apparatus used is shown in Fig. 1. The reaction vessel (C), which has a removable top (B) sealed with an O-ring, was fitted with a Pirani gauge (Edwards MA-5) (A), a

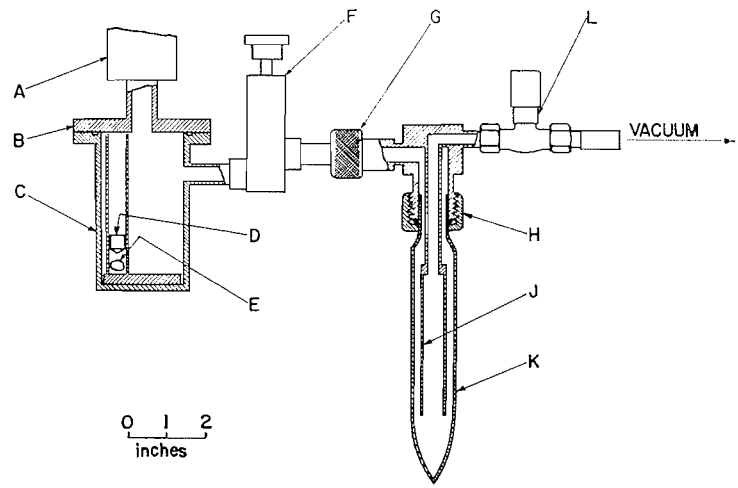


FIG. 1. Gas counting method apparatus. A, Pirani gauge; B, reaction vessel top; C, reaction vessel; D, ampoule breaker; E, ampoule; F, vacuum valve; G and H, vacuum couplings; J, trap inner tube; K, trap jacket; L, vacuum valve.

special ampoule breaker (D), and a Veeco high vacuum valve (L38S) (F). It could either be joined directly to the high vacuum system consisting of a liquid air trap, a two-stage oil diffusion pump, and a mechanical pump, or to the trap (K) by a Veeco quick coupling (G). The trap, which accommodated a special syringe (not shown) within the inner tube (J), could be dismantled by loosening another quick coupling (H) and was connected through a Hoke bellows seal-valve (L) to the vacuum system. The apparatus was, except for the Pyrex glass jacket of the trap (K), made of copper and brass, with connections either soldered or sealed with rubber O-rings. The metal and glass syringe with Teflon gaskets was made as described by Robinson (14).

About 0.4 ml of tritiated water with an activity of 0.5 microcurie (μc) per g was syringed into a weighed, thin-walled, Pyrex ampoule; freed of air by freezing, evacuating, and melting several times; then sealed and reweighed. Cellulose samples *a*, *c*, and *d* were used, of superficial densities 3, 3, and 7.8 mg per sq. cm, respectively. The ampoule, and a 2-g sample cut into strips about 7.5 cm wide and folded to expose as much surface as possible, were placed into the reaction vessel (C). This was sealed, and then evacuated for at least 11 hours at 70° C or for 43 hours at room temperature, and then isolated by closing valve F. The reaction was started by shaking until the ampoule was broken by the plunger (D) and continued at room temperature for an arbitrary period of 7 hours for amylopectin, and 1 hour for all other samples since this period was found adequate by other workers (3, 9).

Meanwhile the trap was assembled with the syringe, set to contain 0.2 ml, inside the central tube (J) so that the needle rested in the bottom of the jacket (K), and the isolated

Can. J. Chem. Downloaded from www.nrcresearchpress.com by 41.223.56.140 on 09/04/12
For personal use only.

reaction vessel was coupled to the trap, which was then evacuated. After the reaction the water was recovered by cooling the trap with liquid air, closing valve L and opening valve F during the first rapid distillation, then opening valve L to the vacuum and heating the reaction vessel to 70° C for 4 to 46 hours. Valves F and L were closed, the water in the trap was melted and collected in the bottom of the jacket (K); then air, let in through valve L, forced the water into the still-evacuated syringe. This procedure prevented dilution of the radioactivity in the water by exposure to the water vapor in the atmosphere. Table I lists the experimental details.

The water in the syringe was analyzed for tritium by the method of Robinson (15), i.e. by reacting it with methyl grignard in butyl ether to form radioactive methane under carefully controlled conditions, fractionating the methane, metering it into a gas counting tube, and measuring the radioactivity with a suitable scaler. Several improvements or modifications were made to the apparatus described by Robinson.

1. A Kjeldahl flask was used for the reaction.
2. The burner heating the water bath was replaced by an annular electrical heater to ensure temperature uniformity.
3. Commercial glass, gas counting tubes patterned on those of Bernstein and Ballentine (16) replaced the metal gas counters.

The method of assay was found to be very satisfactory.

Accessibility by Solid Counting

A variety of samples (*b*, *c*, *d*, *e*, *f*, and *g*) were measured using the Vacuum Transfer Counter (VTC) and following procedures described earlier (12). Briefly stated, the sample was mounted on a suitable holder, evacuated in the VTC, treated with tritiated water vapor at a relative humidity of 79 to 97% at about 25° C for 1 hour, evacuated again, transferred while under vacuum to a counter, and the radioactivity of the sample measured. Corrections were made for contamination of the counter and absorption of radiation by the counter window.

It was shown (12) that a 1-hour reaction was sufficient for replication of results, and that the time for completion of the reaction probably depended upon the establishment of isotopic equilibrium throughout the apparatus after the dilution of activity by the cellulose; therefore, the mass of sample was kept constant by using a superficial density of 3 mg per sq. cm. The only exception was Valonia (1.1 mg per sq. cm) since there was insufficient material.

All samples were "infinitely" thick; i.e. their thicknesses exceeded the range of tritium β-particles (1 mg per sq. cm) (17, 18).

Amylopectin films could not be measured because they buckled and broke when exposed to the water vapor.

Cyclic Drying Experiments

Gel cellulose of the same stock as sample *c*, but which had never been dried, was used in all of these experiments.

(*i*) *Determination of* $\delta\omega$

Samples were placed in a vacuum desiccator containing anhydrous magnesium perchlorate or deaerated saturated sodium chloride solution to provide relative humidities of 0 and 75% respectively, evacuated for about 10 minutes, then isolated. After the 23 hours required for moisture equilibrium (19), the desiccator was opened and a sample removed. The remainder was soaked for 1 hour in distilled water at about 25° C, then

Can. J. Chem. Downloaded from www.nrcresearchpress.com by 41.223.56.140 on 09/04/12
For personal use only.

replaced in the desiccator. Each drying and wetting cycle was repeated to 30 and 56 times for the 0 and 75% r.h. experiments respectively, with periodic removal of samples. The dried samples together with a piece of the original undried sample were mixed for 7 hours in a 50-ml flask with at least 1 ml tritiated water (about 8 μc per mg) per 80 mg of sample. Then the water was poured into a trap and the remaining water removed by vacuum distillation and collected in the same trap cooled with liquid air. Samples cycled at 0% r.h. were dried as quickly as possible with the flask surrounded by a water bath at 25° C; the 75% r.h. samples were distilled at a vapor pressure equivalent to 75% r.h. as measured with a mercury manometer, by throttling the vapor flow to the trap. Distillations at 0% r.h. were made in 3 batches and at 75% in 2 batches. The water removed from the samples was assayed for tritium by the gas counting method already described.

Labile tritium was removed from the cellulose by soaking in distilled water for at least 2 days with four changes of water. The wet sample was mounted on a holder (ref. 12, Fig. 4) dried in the air for 1 hour, evacuated in the VTC for 1 hour, then counted. The background determined immediately before counting was subtracted directly from the observed count rate, which was then corrected for window absorption (12).

(*ii*) *Determination of W*

An inverted U-tube of 15-mm o.d. Pyrex glass tubing with sealed arms 20 cm and 14 cm long was used in each experiment. One milliliter of tritiated water (about 8 μc per mg) was added to a sheet of undried gel cellulose (2.5×5 cm) held in the 20-cm arm by glass fingers. The tube, after being evacuated through a 5-mm o.d. side arm for 15 seconds so that water vapor purged the air from the apparatus, was sealed off with a torch. The sample and liquid water were mixed by shaking the tube and equilibrated for 7 hours, then the free water was poured from the sample into the 14-cm arm. The arm containing the cellulose was put in a water bath at 25.0±0.1° C and the other arm either in dry ice – acetone mixture or a water bath at 20.0±0.2° C for distillations at 0 and 75% r.h. respectively. After 23 hours the U-tube was removed from the baths, and the water poured back onto the cellulose for 1 hour, then the drying cycle repeated. The number of cycles was varied up to 28 corresponding to 0% r.h. and 57 to 75% r.h. Finally the U-tube was broken open, the water assayed for tritium, the labile tritium was removed from the sample by soaking in water, and the sample counted as before.

(*iii*) *Control Experiments*

Gel cellulose samples were soaked in tritiated water (6.5 μc per mg) for 1 hour, 12 hours, and 31 days, then, without drying, soaked in distilled water to remove the labile tritium and counted as before.

RESULTS AND DISCUSSION

Accessibility by Gas Counting

The results are summarized in Table I.

The per cent accessibility, A'_g, was calculated from the relation

$$[2] \qquad A'_g = 600\,\frac{m}{M}\left(\frac{N_0}{N_\tau}-1\right)$$

where m is the mass of water in the ampoule (g), M is the mass of the sample on an over-dry (105° C) basis (g), N_0 and N_τ are the original and final activities in the water in the same units; the factor 600 converts the masses m and M to molecular equivalents and the results to a percentage. This expression assumes that:

Can. J. Chem. Downloaded from www.nrcresearchpress.com by 41.223.56.140 on 09/04/12
For personal use only.

TABLE I

Accessibility by the gas counting method

Expt.	Sample	Evacuation: Time (hours)	Evacuation: Temp. (° C)	Water recovery (hours)	m/M	Accessibility (%): A_g'	Accessibility (%): A_g corrected for isotope effects
1	Cellulose film	11	70	9	0.192	89	
2	Cellulose film	11	70	11	0.192	87	
3	Cellulose film	44	25	46	0.192	89	
4	Cellulose film	43	25	25	0.196	85	
					Mean	87.5	71
5	Wood pulp	12	70	15	0.185	69	
6	Wood pulp	13	70	11	0.195	66	
7	Wood pulp	12	70	12	0.179	62	
					Mean	66	54
8	Amylopectin	20	70	4	0.207	129	
9	Amylopectin	37	70	5	0.197	117	
					Mean	123	100

NOTE: Pressure after water recovery was < 0.1 μ Hg except for expts. 8 and 9 which were 5 and 3 μ respectively.

$$\frac{m}{M} = \frac{\text{mass of water in ampoule}}{\text{mass of dry cellulose}}.$$

1. There are three exchangeable hydrogens per anhydroglucose unit.

2. There is no adsorbed water on the cellulose prior to the reaction. Work described elsewhere (20) showed that under the conditions of the experiment the residual adsorbed water was generally zero and always less than 4 mg per g, corresponding to an apparent accessibility of 2.4%.

3. There is no isotope effect in eq. [1]; i.e.

$$[3] \qquad k_1 = \frac{\text{T/H in accessible part of carbohydrate}}{\text{T/H in adsorbed water}} = 1.$$

4. There is no change in the tritium concentration in the carbohydrate during the recovery of adsorbed water.

Equation [2] is equally applicable to linear and branched chain molecules of anhydroglucose units, provided that the D.P. is sufficiently high that the additional exchangeable end group per molecule may be neglected, since with branched chains the loss of one hydroxyl at the branch is exactly balanced by the gain in the additional end unit.

Since amylopectin, the highly branched fraction of starch, has been shown (21) to have a completely amorphous X-ray diffraction pattern (an observation which we have confirmed) all its hydroxyl hydrogens should be accessible to exchange with water. However, A_g' (expts. 8 and 9, Table I) exceeded the expected value of 100%. This suggested that some of the C—H linked hydrogens in addition to the hydroxyls were participating in the exchange. However, infrared measurements on cellulose (8) and the accessibility measurements on cellulose nitrate described later showed that no exchange occurred between hydrocarbon hydrogens of cellulose and water. It was concluded that the abnor-

Can. J. Chem. Downloaded from www.nrcresearchpress.com by 41.223.56.140 on 09/04/12
For personal use only.

mally high A'_g was due to two isotope effects, one in the exchange reaction (eq. [1]) and the other in the recovery of tritiated water.

The reported values of the isotope distribution factor k_1 (eq. [3]) for the exchange equilibria between alcohols and deuterated water vary from 0.96 to 1.25 (22–28); of these the value of Hobden *et al.* (27) of 1.09 is probably the best. Although no data are available it is probable that similar effects exist for alcohols and tritiated water.

An isotope effect probably occurred in the recovery of the tritiated water from the sample because the equilibrium vapor pressure of HTO is lower than H_2O. From direct measurements of liquid/vapor equilibria, Price (29) has reported ratios of the vapor pressures of HTO and H_2O which may be expressed by the separation factor

$$\alpha = \frac{\text{T/H in liquid}}{\text{T/H in vapor}}. \qquad [4]$$

At 26° C, $\alpha = 1.29$. Therefore during a simple distillation, the distillate is deficient in HTO, while the water being distilled is correspondingly enriched. When all the water is distilled it has, of course, the same average composition as the original liquid; all distillations were, therefore, taken to completion. However, a complication probably occurred during the distillations from solids containing exchangeable hydrogens: as the tritium concentration in the adsorbed water increased, the equilibrium in eq. [1] was probably driven to the right, so that more tritium became attached to the hydroxyl oxygens to cause an additional decrease of tritium in the distillate. This would cause the accessibility calculated by eq. [2] to be high.

The possible magnitude of such an effect is indicated by first considering the equilibrium distillation of a mixture of H_2O and HTO. At low concentrations of tritium the molecular species T_2O may be neglected, so that the problem becomes the simple distillation of a mixture of two volatile components HTO and H_2O, and the expression

$$\log_e \frac{L_1}{L_2} = \frac{1}{k-1} \log_e \frac{x_1}{x_2} \qquad [5]$$

derived by Perry (30) is applicable, where L_1 is the number of moles of original water, L_2 is moles of residual water, x_1 and x_2 are the mole fractions of HTO in the original water and the residual water respectively, and

$$k = \frac{\text{mole fraction HTO in vapor}}{\text{mole fraction HTO in liquid}} \text{ at equilibrium.}$$

Note that the original derivation was made in terms of the more volatile component, but eq. [5] is equally applicable to the less volatile component, i.e., HTO.

When the concentration of T $\ll$ H, as in the conditions studied,

$$k \simeq \frac{\text{HTO/H}_2\text{O in vapor}}{\text{HTO/H}_2\text{O in liquid}} \simeq \frac{1}{\alpha} \qquad [6]$$

and

$$\frac{x_1}{x_2} \simeq \frac{\text{T/H in original water}}{\text{T/H in residual water}} = \frac{t_0}{t} \qquad [7]$$

i.e., replacing the mole fraction of HTO by the atom fraction of T. Using eqs. [6] and [7], the approximate value of $\alpha = 1.3$, and putting $L_1/L_2 = 1/m$, where m is the fraction of original liquid which has not been distilled, eq. [5] becomes

Can. J. Chem. Downloaded from www.nrcresearchpress.com by 41.223.56.140 on 09/04/12
For personal use only.

[8] $$\log_e m = \frac{1.3}{0.3} \log_e \frac{t_0}{t}.$$

This expression gives the ratio of the atom fractions of tritium in the original to the residual water at any stage during the distillation.

By making a material balance this can be re-expressed to give the ratio F of the atom fraction in the original liquid to the average atom fraction in the distillate at any stage

[9] $$F = (1-m^{1/1.3})/(1-m).$$

If equilibrium is maintained between amylopectin and tritiated water at all times, the complete distillation of water from amylopectin may be considered as a partial liquid distillation in which the amylopectin corresponds to the residual liquid. Thus assuming that $k_1 = 1$ (eq. [3]), the value of m corresponding to 2 g amylopectin and 0.4 g water is 0.453, and by substitution in eq. [8], $F = 0.834$. If the correction for such a fractionation were neglected the accessibility, A'_g, calculated from eq. [2] would be 142%. While this value represents an upper limit, it serves to show the importance of this isotope effect.

The isotope effects in this exchange reaction are of some interest and will be discussed in a subsequent paper. For the present work the values in Table I were used as reference values for the accessibility of cellulose films which were subsequently measured in the solid counter (VTC). The measured accessibility values, A'_g, in Table I were corrected by multiplying by the factor 100/123 on the assumptions that amylopectin was 100% accessible and the correction for the isotope effect was given by a single factor which was the same for all samples, and hence cancelled out of the calculations.

Table II shows that this method of obtaining the corrected values, A_g, gave good agreement with comparable values obtained by other methods (3, 9–11, 31, 32).

TABLE II

Accessibility of samples by solid counting and comparison of data

	Accessibility (%)						
	Liquid D_2O		D_2O vapor,	HTO vapor		Amorphous cellulose (%)†	
Sample	Frilette *et al.*	Mann and Marrinan	Mann and Marrinan	Gas counting (A_g)	Solid counting* (A_s)	By X-ray diffraction	By density measurements
Amylopectin				100			
Amylose					100±3 (2)		
Cellulose film	81	83	75	71	71±5 (4)	60	60
Cellulose film dried at 75% r.h. 56 times					73±1.5 (2)		
Wood pulp	54–68			54	60±0.3 (2)	35	50
Bacterial cellulose		39	30		42±2.5 (2)	60	
Valonia purified					27 (1)	30–35	29
Cellulose trinitrate					0±3 (2)		—

*Number of replicates given in parentheses and range by limits.
†Values of Hermans (31) except for underlined value (32).

The advantages of the gas counting method are good reproducibility, relatively simple apparatus, and the fact that the surface roughness of the sample does not affect the results. The principal disadvantage is the uncertain magnitude of the isotope effects; these must be known in order to yield absolute values of the accessibilities.

Can. J. Chem. Downloaded from www.nrcresearchpress.com by 41.223.56.140 on 09/04/12
For personal use only.

Accessibility by Solid Counting

Table II contains a summary of the results obtained in the VTC. The percentage accessibility, A_s, of a sample was calculated from the relation

$$[10] \qquad A_s = \frac{\text{count rate of sample}}{\text{count rate of cellulose film}} \times 71$$

where 71 is the accessibility (A_g) of the cellulose film determined by the gas counting method. As in the gas counting method it is probable that isotope effects occurred in the exchange reaction and during the removal of water. It is assumed that the correction for the isotope effects was given by a single factor, which was the same for all the samples and hence cancelled out of eq. [10].

In this calculation no consideration has been given to differences in relative humidity during the reactions in the gas counting and solid counting methods. In the gas counting method the relative humidity for sample *c* was estimated from the sorption isotherm for viscose rayon given in the literature (33) as about 80%, while the measured relative humidity for the solid counting method ranged from 79 to 97%. The effect of relative humidity on the accessibility has not been studied, but it is believed that at high relative humidities it is not great.

Since radioactive water remaining adsorbed on the cellulose would contribute to the count rate, it was necessary to estimate the amount adsorbed under the experimental conditions. Separate experiments using oxygen isotope exchange between water vapor and cellulose sample *c*, which are described elsewhere (20), showed that the adsorbed water remaining on cellulose under the conditions of the present experiment, i.e. after 23 hours evacuation, was 6.5 mg per g, equivalent to an accessibility of 4%. Although a different apparatus was used, the value should be approximately the same for the VTC. However, the amount of adsorbed water in the other samples was roughly proportional to the accessibility (34), so that the total activity from the sample, arising from exchanged hydroxyls in the accessible regions and the small contribution from adsorbed water, remained proportional to the accessibility of the sample. Since only relative total activities are used to calculate A_s, the actual error introduced by the adsorbed water was less than 4%.

The amount of water which passed from the sample in the VTC into the vapor phase between isolation of the sample and the completion of counting (30 minutes) was calculated to be 0.016 μg from the pressure rise in separate adsorption experiments (20), and by making allowance for the much smaller sample in the VTC. This amount of water corresponded to 44 counts per minute which was negligible. Therefore, any errors caused by extraneous water were well within the experimental accuracy and may be neglected.

Table II shows that the accessibility values agreed reasonably with the D_2O vapor accessibilities of Mann and Marrinan (9–11). Although accessibilities and amorphous cellulose determined by X-ray diffraction and density methods measured different quantities, both methods graded the samples in the same order, except for bacterial cellulose. The X-ray values for bacterial cellulose were respectively twice and one and one-half times as high as the accessibility values of Mann and Marrinan and those of the present work. In making the comparisons the difference in the samples as well as the experimental methods should be borne in mind.

Amylose sheets have given an indication of an oriented X-ray diffraction pattern (35); however, the 100% accessibility of amylose (Table II) showed that the crystalline fraction was very small, or that the crystallites were unstable in the presence of water vapor. The

Can. J. Chem. Downloaded from www.nrcresearchpress.com by 41.223.56.140 on 09/04/12
For personal use only.

100±2% value also gave excellent confirmation of the self-consistency of the solid counting method. The 98% nitrated cellulose had the expected accessibility of zero since practically all its hydroxyl groups were replaced, and showed convincingly that only hydroxyl hydrogens take part in the exchange.

Because of the short range of tritium β-particles (about 6 μ in cellulose) and the difficulty of preparing reproducible samples (18, 36), it was expected that surface roughness might have a large effect on the accuracy of the measurements with the VTC, and so normally only smooth-surfaced samples were used. However, a sheet of acetate grade dissolving pulp having a fluffy surface, gave an accessibility only 6% higher than the value by the gas counting method, which is independent of surface roughness. This indicated that the VTC may also be used to compare paper samples with similar surfaces.

These results show that the solid counting method, once calibrated, provides reliable accessibilities for starch and cellulosic samples. It is believed that the simplicity of the method will make it useful for characterizing various kinds of cellulose and other substances.

Cyclic Drying Experiments

The results of these experiments are plotted in Figs. 2 and 3. The percentage of in-

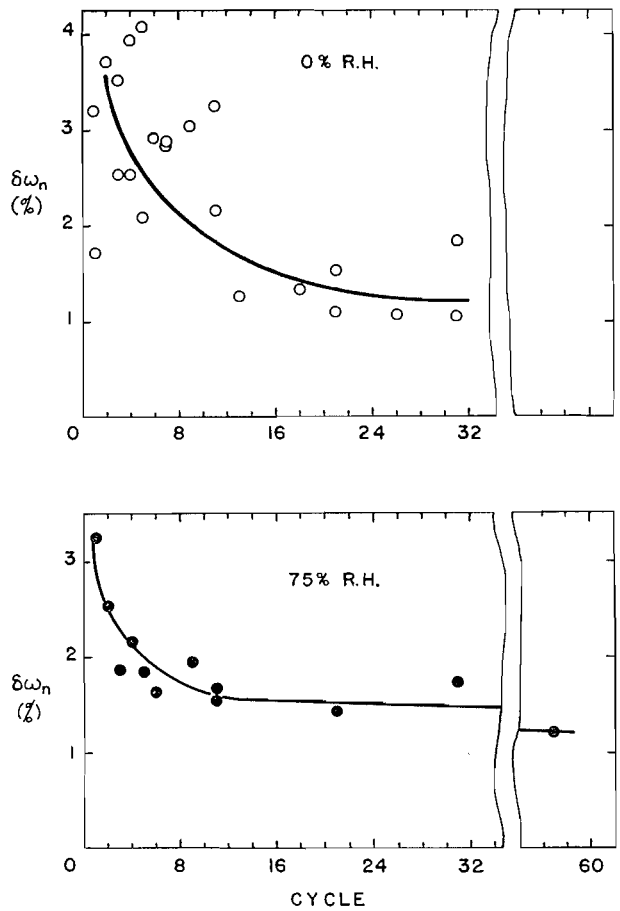


FIG. 2. Inaccessible cellulose formed during each wetting and drying cycle ($\delta\omega_n$). Top graph, 0% relative humidity. Bottom graph, 75% relative humidity.

Can. J. Chem. Downloaded from www.nrcresearchpress.com by 41.223.56.140 on 09/04/12
For personal use only.

accessible cellulose, $\delta\omega_n$ or W_n, formed by drying tritiated water was calculated from the equation

$$[11] \qquad \delta\omega_n \quad \text{or} \quad W_n = \frac{N}{13{,}200} \times \frac{1.20}{S} \times 100$$

where N is the corrected counts per minute from the cycled sample, 13,200 the counts per minute for a completely exchanged sample calculated from the observed count rate of cellulose film (9400 per minute) and its known accessibility (71%), and 1.20 and S are the specific activities in μc per mg of the tritiated water used in the accessibility measurements and the cyclic experiments respectively. Each point on Fig. 2 was obtained from a separate piece of cellulose, but some of the pieces had common distillation steps from tritiated water. Because of the possibility of irregular temperature variations from one distillation to another, particularly at 0% r.h., the experimental points cannot strictly be considered as representing completely separate experiments. On the other hand, each point on Fig. 3 was obtained from a completely independent experiment. The newly formed inaccessibilities of the control samples soaked in tritiated water, but not dried, were only 0.2, 0, and 2.3% for the 1-hour, 12-hour, and 31-day soakings respectively, showing that only changes occurring during the wetting and drying need be considered for the interpretation of the values of $\delta\omega_n$ or W_n.

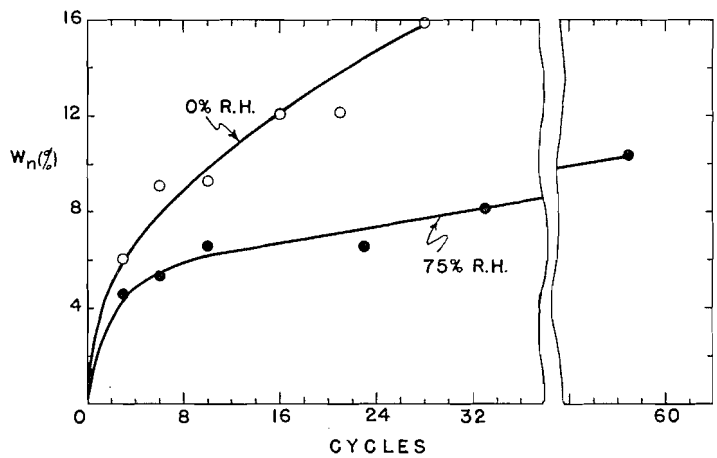


FIG. 3. Net inaccessibility formed during a number of wetting and drying cycles (W_n). At 0% and 75% relative humidity.

The values of $\delta\omega_n$ at both 0% and 75% r.h. decreased to a limiting value of 1.3% with increasing number of cycles. The corresponding W_n (Fig. 3) showed an initial rapid increase followed by a slower rise, but there was no indication of a limiting value at either 0% or 75% r.h. up to 28 and 57 cycles respectively. Somewhat unexpectedly the values of W_n for 0% r.h. were always greater than those at 75% r.h., since previous values of the liquid water permeability (19) and dimensional swelling (37) of cellulose cyclically dried at different relative humidities were interpreted to mean that more cross-linking occurred on drying at higher humidities. However, in the present experiments at 0% r.h. the temperature decreased during the rapid removal of water from the cellulose, and the influence of temperature on the processes is at present unknown. No difference was definable for the values of $\delta\omega_n$ at 0% and 75% r.h., possibly because of the scatter of the 0% r.h. results.

Can. J. Chem. Downloaded from www.nrcresearchpress.com by 41.223.56.140 on 09/04/12
For personal use only.

The value of $\delta\omega_n$ is the inaccessibility to liquid water caused by the nth cycle alone, and that of W_n the net inaccessibility resulting from n cycles. Therefore, if the inaccessible material is formed irreversibly it follows that

$$[12] \qquad \sum_{1}^{n} \delta\omega_n = W_n.$$

Figure 4 shows that this is not so, but that $\sum\delta\omega_n$ at 75% r.h. increasingly exceeded W_n. Some of the newly formed inaccessible cellulose represented by $\delta\omega_n$ must therefore have become accessible during subsequent wettings and dryings. Furthermore, W_n at 10 and 28 cycles at 0% r.h. and 10 and 33 cycles at 75% r.h. decreased by 1.6, 4.5, 2.2, and 1.6 respectively when the samples were cycled four more times using ordinary water and drying at the relative humidity of their preparation.

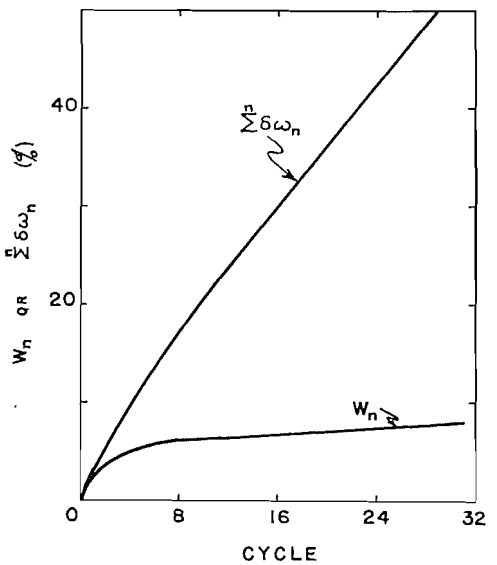


FIG. 4. Comparison of $\Sigma\delta\omega_n$ and W_n at 75% relative humidity.

It is believed that these experiments give the first direct evidence of the conversion of inaccessible to accessible cellulose by wetting and drying. In view of this it should be noted that all measurements were made after the samples had an additional wetting and drying cycle using ordinary water to remove labile tritium and to mount the sample on the holder. It is interesting to note that decreases of 0.5 to 1 in $\delta\omega_n$ and W_n occurred immediately after removal from the VTC, presumably by exchange between the atmospheric water and the inaccessible cellulose rendered accessible by the drying in the VTC. However, since exactly the same techniques of soaking, mounting, and drying were carefully followed in the measurements of $\delta\omega_n$ and W_n, the preceding observation does not affect the comparison made in Fig. 4.

After the initial small loss of activity immediately after removal from the VTC, the sample was stable for weeks, showing that the anhydroglucose units in the inaccessible part of the dried cellulose did not become accessible; otherwise the tritium would have exchanged with the atmospheric water (5).

The results discussed so far have shown that part of the newly formed inaccessible cellulose becomes once again accessible after further wetting and drying, but they give

Can. J. Chem. Downloaded from www.nrcresearchpress.com by 41.223.56.140 on 09/04/12
For personal use only.

Can. J. Chem. Downloaded from www.nrcresearchpress.com by 41.223.56.140 on 09/04/12
For personal use only.

no direct information about the stability of the inaccessible cellulose present in the original wet sample either while standing in water or on wetting and drying. However, the small inaccessibilities formed in the control experiments mentioned previously showed quantitatively that in the swollen state any formation of inaccessible cellulose was very slow. Nevertheless the 2.3% value showed that, in time, changes do occur which may be caused by (*a*) an increase in the total accessibility (which is, however, unlikely since the accessibility probably reached a constant value during the 6 months of soaking which preceded the experiment), (*b*) by penetration of tritiated water into the crystallites, or (*c*) by a slow process of interconversion of accessible and inaccessible regions. Thus there is the possibility that the inaccessible regions in the original undried gel may not be stable to prolonged soaking in water.

If the original inaccessible cellulose becomes accessible during the cyclic treatment then W_n should be greater than the decrease in accessibility caused by the corresponding number of cycles. The increase of W_n during 28 cycles at 0% r.h. and 57 cycles at 75% r.h. was not reflected by a decrease in the accessibility, A_s, between 1 and 56 cycles at 75% r.h. (Table II). However Mann and Marrinan (10, 11) reported a decrease of 3% and 5% in accessibility during the second wetting and drying of viscose film. D_2O accessibility measurements by Brickman *et al.* (6) of cyclically dried samples gave erratic results.

A net decrease in accessibility of cellulose on wetting and drying is consistent with many of the published experimental values which are believed to be related to the extent of the cross-bonding in cellulose. Thus irreversible decreases occurred in the dimensional swelling (37), permeability of water (19), moisture regain (6, 31), and heat of wetting (6). On the other hand, the X-ray crystallinity of cellulose was almost constant during drying from the gel state (38) and on cyclically drying (39). However, the experimental difficulties of the X-ray measurements and the relative small changes occurring in the cyclic experiments may account for these conflicting results. Under some experimental conditions the accessibility of cellulose to nitration (6, 40) and hydrolysis (41) showed a small but definite increase with successive wetting and drying; this appears to be at variance with the notion of lower accessibility after wetting and drying. It was not possible to decide definitely from this partly conflicting data whether or not inaccessible regions in the original cellulose are rendered accessible by wetting and drying.

CONCLUDING REMARKS

The unexpected difference between $\sum\delta\omega_n$ and W_n may be explained by the following hypothesis.

1. Cellulose chain molecules are continually moving, particularly when wet, and undergo segmental jumping, as shown by dielectric measurements (42). Thus an arrangement of chains, once formed, does not necessarily remain unchanged. The stability of a particular molecular configuration depends upon the attraction between chains resulting from van der Waals' forces and, more important, hydrogen bonding. For example in a crystalline configuration, which requires the greatest energies to separate the chains and is thus the most stable, there are one or two interchain hydrogen bonds per anhydroglucose unit (43, 44). Less regular arrangements having fewer interchain bonds are less stable, so that a spectrum of stabilities exists.

2. A configuration may be disrupted by (*i*) the formation of hydrogen bonds between cellulose and water at the expense of cellulose–cellulose interchain bonds, (*ii*) mechanical stresses resulting from the effort of neighboring molecules to arrange themselves into more stable configurations, and (*iii*) segmental thermal motion. In a very stable arrangement

Can. J. Chem. Downloaded from www.nrcresearchpress.com by 41.223.56.140 on 09/04/12
For personal use only.

of cellulose chains such as in the crystalline regions, weakening of interchain bonds by water molecules alone is energetically unfavorable: the water molecule forms hydrogen bonds with the cellulose which may be equal in energy to those which are replaced; but the chains have to separate to accommodate the water molecule which stretches and weakens the neighboring interchain bonds, so that an increase in energy is required. However a stable configuration may be rendered less stable if the competition of water molecules for interchain hydrogen bond positions occurs simultaneously with the disruptive action of a number of mechanical stresses which act by chance in co-operation.

3. When cellulose is very wet, the water forms hydrogen bonds with all hydroxyl groups attached to *mobile* chains and the formation of new more stable configurations from these mobile chains is almost completely prevented. Furthermore, under these conditions no mechanical stresses arise to disrupt existing stable configurations. At the other extreme, in dry cellulose the mobility of the chains is decreased by the greater number of interchain bonds, so that rearrangement into new stabler configurations almost ceases. Therefore, new stable configurations do not form in very wet or very dry cellulose, but only at some intermediate, possibly narrow, range of moisture content. At this critical moisture content some of the stable regions are being continually disrupted while new stable configurations are being formed.

4. From simple statistical considerations, the rate of formation of the stabler configurations will decrease, and the rate of destruction increase, as the quantity of cellulose in stable configurations becomes larger. Thus, at the critical moisture content, the amount of cellulose in the stable configurations slowly increases with time until an equilibrium value is reached.

The mechanical stresses mentioned above are believed to be identical with those which cause cellulose to shrink when it is dried.

The hypothesis is now considered in terms of wetting and drying. Stable configurations which form and are not broken by the next wetting and drying cycle are measured as newly formed inaccessible regions by the cyclic drying experiments. Note that the critical moisture content which is favorable to the formation of stable configurations is traversed once on wetting and once on drying, so that inaccessible regions should form twice during a cycle but not necessarily in identical amounts.

The only reliable data which do not appear to be consistent with this hypothesis are the nitration of cyclically dried cellulose (6, 40), and the hydrolysis of dried cellulose (41). No reasons can be cited, but it may be significant that the hydrolysis measurements were made on samples dried from ethanol instead of water.

The hypothesis also explains the formation of "resistant OD groups" in the experiments of Mann and Marrinan (9), which are closely analogous to the $\delta\omega$ values. A careful study of their results showed that a necessary, and, except for one experiment involving a rapid treatment of a cyclically dried sample, a sufficient condition for the formation of resistant OD groups is that the cellulose be passed through the intermediate moisture range in the presence of D_2O, either by being wet or dried. Similarly their "deuteration of crystalline regions" (11), in which a higher accessibility was found with liquid D_2O than with the vapor, can be attributed to the deuteration by the liquid of cellulose which was accessible at any stage during the wetting and drying cycle, i.e. the cellulose originally available to the vapor, as well as the inaccessible cellulose which was rendered accessible during the wetting and drying processes. It follows also that the difference between this quantity (8% of the total viscose film) and the decrease in accessibility (3%) measured by their D_2O vapor method (11) after wetting and drying should be comparable with $\delta\omega_n$ for the

second cycle. The actual difference of about 5% is, considering the differences in technique, in very good agreement with the direct measurement of 2.5% in the present experiments.

The new feature of this hypothesis is the reversible interconversion of accessible (and possibly amorphous) and inaccessible (and possibly crystalline) regions on repeated wetting and drying. Thus it may be possible to completely deuterate the hydroxyl groups of cellulose by using a sufficient number of wetting and drying cycles with liquid D_2O.

It is proposed to continue these experiments.

REFERENCES

1. K. F. Bonhoeffer. Z. Elektrochem. **40**, 469 (1934).
2. G. Champetier and E. Viallard. Bull. soc. chim. France, Ser. 5, **5**, 1042 (1938).
3. V. J. Frilette, J. Hanle, and H. Mark. J. Am. Chem. Soc. **70**, 1107 (1948).
4. J. W. Rowen and E. K. Plyler. J. Research Natl. Bur. Standards, **44**, 313 (1950).
5. K. E. Almin. Svensk Papperstidn. **55**, 767 (1952).
6. W. J. Brickman, H. B. Dunford, E. M. Tory, J. L. Morrison, and R. K. Brown. Can. J. Chem. **31**, 550 (1953).
7. H. Corte and H. Schaschek. Das Papier, **9**(21/22), 519 (1955).
8. H. J. Marrinan and J. Mann. J. Appl. Chem. **4**, 204 (1954).
9. J. Mann and H. J. Marrinan. Trans. Faraday Soc. **52**, 481 (1956).
10. J. Mann and H. J. Marrinan. Trans. Faraday Soc. **52**, 487 (1956).
11. J. Mann and H. J. Marrinan. Trans. Faraday Soc. **52**, 492 (1956).
12. A. R. G. Lang and S. G. Mason. Intern. J. Appl. Radiation and Isotopes. In press. 1960.
13. B. G. Ranby. Inaugural dissertation, University of Uppsala. 1952.
14. C. V. Robinson. Anal. Chem. **26**, 1100 (1954).
15. C. V. Robinson. Nucleonics, **13** (11), 90 (1955).
16. W. Bernstein and R. Ballentine. Rev. Sci. Instr. **21**, 158 (1950).
17. W. F. Libby. Anal. Chem. **19**, 2 (1947).
18. M. L. Eidinoff and J. E. Knoll. Science, **112**, 250 (1950).
19. J. M. Kuzmak. Ph.D. thesis, McGill University, Montreal. 1953.
20. A. R. G. Lang and S. G. Mason. Can. J. Chem. **37**, 1829 (1959).
21. F. L. Bates, D. French, and R. E. Rundle. J. Am. Chem. Soc. **65**, 142 (1943).
22. W. J. C. Orr. Trans. Faraday Soc. **23**, 1033 (1936).
23. M. Harada and T. Titani. Bull. Chem. Soc. Japan, **11**, 465 (1936).
24. M. Koizumi and T. Titani. Bull. Chem. Soc. Japan, **13**, 427 (1938).
25. C. K. Ingold and C. L. Wilson. Z. Elektrochem. **44**, 62 (1938).
26. J. O. Halford and B. Pecherer. J. Chem. Phys. **6**, 571 (1938).
27. F. W. Hobden, E. F. Johnston, L. H. P. Weldon, and C. L. Wilson. J. Chem. Soc. 61 (1939).
28. J. Hine and C. H. Thomas. J. Am. Chem. Soc. **75**, 739 (1953).
29. A. H. Price. Nature, **181**, 262 (1958).
30. J. H. Perry. Chemical engineers' handbook. 3rd ed. McGraw-Hill Book Co., Inc., New York. 1950. p. 580.
31. P. H. Hermans. Physics and chemistry of cellulose fibres. Elsevier Pub. Co. Inc., Amsterdam. 1949.
32. R. D. Preston, E. Nicolai, R. Reed, and A. Millard. Nature, **162**, 665 (1948).
33. E. Ott and H. M. Spurlin. Cellulose and cellulose derivatives. Part I. 2nd ed. Interscience Publishers, Inc., New York. 1954. p. 420.
34. L. Valentine. Chem. & Ind. **43**, 1279 (1956).
35. R. E. Rundle, L. Daasch, and D. French. J. Am. Chem. Soc. **66**, 130 (1944).
36. F. L. Jackson and H. W. Lampe. Anal. Chem. **28**, 1735 (1956).
37. E. Hubert, A. Matthes, and K. Weisbrod. Kolloid-Z. **98**, 173 (1942).
38. P. H. Hermans and A. Weidinger. Makromol. Chem. **18/19**, 75 (1956).
39. M. Kouris, H. Ruck, and S. G. Mason. Can. J. Chem. **36**, 931 (1958).
40. T. P. Yin and R. K. Brown. Can. J. Chem. **37**, 444 (1959).
41. B. G. Ranby. *In* Fundamentals of papermaking fibres. The British Paper and Board Makers Association, Inc. Technical Section. 1958. p. 52.
42. R. Seidman and S. G. Mason. Can. J. Chem. **32**, 744 (1954).
43. J. Mann and H. J. Marrinan. J. Polymer Sci. **32**, 357 (1958).
44. D. W. Jones. J. Polymer Sci. **32**, 371 (1958).

Can. J. Chem. Downloaded from www.nrcresearchpress.com by 41.223.56.140 on 09/04/12
For personal use only.

Can. J. Chem. Downloaded from www.nrcresearchpress.com by 41.223.56.140 on 09/04/12
For personal use only.

SEPARATION OF CARBOHYDRATE DERIVATIVES BY GAS–LIQUID PARTITION CHROMATOGRAPHY[1]

C. T. Bishop and F. P. Cooper

ABSTRACT

Gas–liquid partition chromatography has been used to separate all of the possible tetra- and tri-*O*-methyl ethers of methyl α- and β-D-glucopyranoside. Anomeric methyl glycosides of each isomer were well separated except those of 3,4,6-tri-*O*-methyl-D-glucose. The six di-*O*-methyl-D-glucopyranoses were partially resolved as their methyl glycosides. The four possible mono-*O*-methyl-D-glucopyranoses were completely resolved after conversion to the corresponding mono-*O*-methyl-penta-*O*-acetyl-D-glucitols, a series of compounds which, except for the 6-*O*-methyl isomer, have not been reported previously. Quantitative estimations of mixtures containing varying amounts of methyl-2,3,4-tri-*O*-methyl-β-D-xylopyranoside and methyl-2,3,4,6-tetra-*O*-methyl-α-D-glucopyranoside showed that molar ratios of components in a mixture could be determined with a mean deviation of ±0.5 in 100.

Since its development by James and Martin (1) in 1952, gas–liquid partition chromatography has been used to separate a wide variety of volatile organic compounds. The first report of its application to carbohydrates dealt with the separation of fully methylated methyl glycosides of some monosaccharides (2). Good separations were obtained and it was also established that the compounds were stable under the conditions used because they could be recovered unchanged from the effluent gas stream. These results encouraged further investigation to see if gas–liquid partition chromatography could be extended to more general use in carbohydrate chemistry. This paper describes the separation of methyl ethers of glucose and also deals with the accuracy of gas–liquid partition chromatography in quantitative estimations of carbohydrate derivatives.

All separations shown in the figures were obtained on an apparatus employing an ionization detector (3). The high sensitivity of this detector permitted the use of small samples (2–4 γ) and this resulted in a considerable increase in resolution of components over that obtained in the apparatus previously described (2), which contained a thermal conductivity cell as a detector. However, the latter apparatus was used when it was necessary to collect samples from the effluent gas stream.

Retention volumes of the compounds used were dependent on the composition of the stationary liquid phase. It was advantageous to use two columns, one containing a polar liquid phase, the other a non-polar, because separations of some isomeric methyl ethers could be obtained on one and not on the other. Butanediol succinate polyester and Apiezon M were used as the polar and non-polar stationary liquid phases respectively. A number of other liquid phases were tried in preliminary work including Dow Corning silicone grease, carbowax 4000, zinc stearate, D-mannitol, partially benzylated raffinose, methyl cellulose (methoxyl, 27.9%), and mannitol hexastearate. The silicone gave separations comparable with those obtained on Apiezon M but was less convenient to use because a solvent extraction was required to remove low molecular weight material from the liquid phase. Most separations on carbowax were similar to those obtained on butanediol succinate polyester but the carbowax was not as suitable for general use. Mannitol, mannitol hexastearate, and zinc stearate gave columns having poor resolving power. The benzylated raffinose was unstable and the columns bled excessively at operating tempera-

[1]*Manuscript received November 30, 1959.*
Contribution from the Division of Applied Biology, National Research Council of Canada. Presented at the 136th meeting of the American Chemical Society, Atlantic City, N.J., September 1959.
Issued as N.R.C. No. 5522.

tures of 150–200° C; the methyl cellulose was not liquid at these temperatures. The carbohydrate derivatives mentioned were tested as liquid phases because their structural similarities to the components to be separated might be expected to give enhanced separations. Although none of the carbohydrate derivatives tested here were useful as liquid phases, Kircher (4) has reported recently the separation of fully methylated methyl glycosides of monosaccharides by gas–liquid partition chromatography using fully methylated hydroxyethyl cellulose as the liquid phase.

Alkali-washed Celite 545 was chosen as the inert support for the liquid phase because the alkali washing decreased the tendency of those compounds which passed easily through the column to give asymmetrical peaks (due to adsorption). However, the number of derivatives that could be eluted from the columns was reduced considerably by the use of alkali-washed Celite because of increased adsorption of sugars in which the anomeric hydroxyl group was free or substituted by an acetyl group and in which there were a large number of free hydroxyls. These derivatives which were adsorbed by alkali-washed Celite could be eluted, but with poor resolution, from columns in which the inert support was acid-washed Celite, firebrick, powdered glass, or sodium chloride. The alkali-washed Celite was sieved to give narrow screen fractions which facilitated even packing of the columns but the particle size appeared to have little effect on resolving power.

Because 1-*O*-acetyl- and free reducing sugars were adsorbed by alkali-washed Celite it was necessary to block the reducing group by formation of methyl glycosides. The diethyl mercaptals and *N*-phenyl glycosylamines were also tested but these derivatives, even when formed from fully methylated sugars, were not sufficiently volatile. The first publication (2) concerning this work reported that the anomeric methyl glycosides of 2,3,4-tri-*O*-methyl-L-arabinose and of 2,3,4,6-tetra-*O*-methyl-D-galactose were not separated under the conditions used. However, this was either a property of the particular conformations of these sugars or was caused by the lower resolving power of the instrument used in that work because it has now been found that anomeric methyl glycosides of methyl ethers of glucose can be separated.

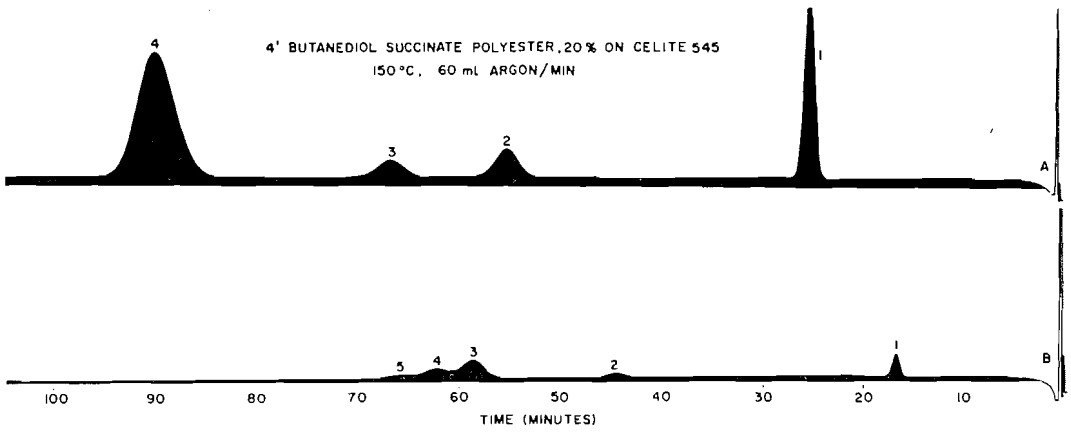


FIG. 1. Separation of tetra- and tri-*O*-methyl ethers of methyl α- and β-D-glucopyranosides.

(A) α-Methyl glycosides of:
(1) 2,3,4,6-Tetra-*O*-methyl-D-glucose.
(2) 2,3,4-Tri-*O*-methyl-D-glucose.
(3) 3,4,6-Tri-*O*-methyl-D-glucose.
(4) 2,3,6- and 2,4,6-Tri-*O*-methyl-D-glucose.

(B) β-Methyl glycosides of:
(1) 2,3,4,6-Tetra-*O*-methyl-D-glucose.
(2) 2,3,4-Tri-*O*-methyl-D-glucose.
(3) 2,4,6-Tri-*O*-methyl-D-glucose.
(4) 2,3,6-Tri-*O*-methyl-D-glucose.
(5) 3,4,6-Tri-*O*-methyl-D-glucose.

Can. J. Chem. Downloaded from www.nrcresearchpress.com by 41.223.56.140 on 09/04/12
For personal use only.

The largest number of possible methyl ethers of glucose was best obtained by partial methylation and, because anomers were separable, methyl-α-D-glucopyranoside and methyl-β-D-glucopyranoside were partially methylated separately. Figure 1 shows the separation of the tetra- and tri-*O*-methyl ethers that resulted from these partial methylations. Identities were assigned to these peaks as described in the experimental section. All of the anomeric methyl-D-glucopyranosides were separated except those of 3,4,6-tri-*O*-methyl-D-glucose; isomers within an anomeric series were clearly distinguishable except for the methyl 2,3,6- and 2,4,6-tri-*O*-methyl-α-D-glucopyranosides which were both under peak 4, line A, in Fig. 1. This peak was collected from the effluent gas stream and rechromatographed on the non-polar Apiezon M column. As shown by Fig. 2 the two components were separated completely and it was possible therefore, by using the polar and non-polar liquid phases, to separate all of the isomeric tri-*O*-methyl-D-glucopyranosides. Table I gives the retention volumes of each of these components relative to that of methyl-2,3,4,6-tetra-*O*-methyl-α-D-glucopyranoside as a standard. An empirical observation based on these results is that in the glucose series the α-methyl glycosides, in which the anomeric methoxyl occupies the axial position, always had higher retention volumes than the corresponding β-methyl glycosides where the anomeric methoxyl is equatorial; this indicated a greater solubility of the axially oriented anomers in both the polar and non-polar phases. These relative retention volumes are much more reproducible than *R* values in paper chromatography and, although not obviating the necessity for preparing crystalline derivatives, constitute a much more sensitive and reliable criterion of purity and identification than any other chromatographic method.

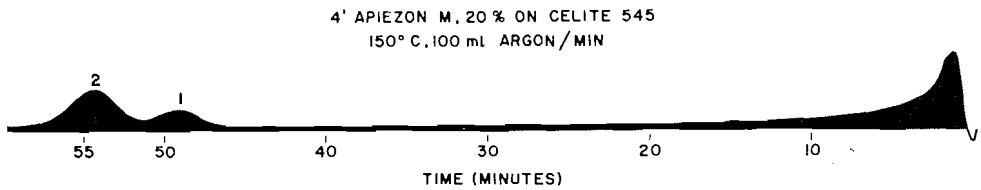


FIG. 2. Separation of methyl 2,3,6- and 2,4,6-tri-*O*-methyl-α-D-glucopyranosides. α-Methyl glycosides of: (1) 2,3,6-Tri-*O*-methyl-D-glucose. (2) 2,4,6-Tri-*O*-methyl-D-glucose.

TABLE I

Retention volumes of methyl ethers of methyl α- and β-D-glucopyranoside relative to methyl-2,3,4,6-tetra-*O*-methyl-α-D-glucopyranoside

On butanediol succinate polyester		On Apiezon M
β-2,3,4,6	0.67	0.82
α-2,3,4,6	1.000 (standard)	1.000 (standard)
β-2,3,4	1.78	0.98
α-2,3,4	2.19	1.12
β-2,4,6	2.34	1.09
β-2,3,6	2.48	1.12
β-3,4,6	2.62	1.13
α-3,4,6	2.65	1.13
α-2,3,6	3.56	1.26
α-2,4,6	3.56	1.38

Conditions: 20% liquid phase on alkali-washed Celite 545; 4-ft column, 150° C, 60 ml argon/min.

Can. J. Chem. Downloaded from www.nrcresearchpress.com by 41.223.56.140 on 09/04/12
For personal use only.

The di-*O*-methyl ethers of glucose were not resolved as well as the tri-*O*-methyl ethers. Figure 3 shows a separation of the products from partial methylation of methyl-β-D-glucopyranoside and presumably all six of the di-*O*-methyl isomers should be present. Crystalline methyl-2,4-di-*O*-methyl-β-D-glucopyranoside was isolated from peak 4 but a

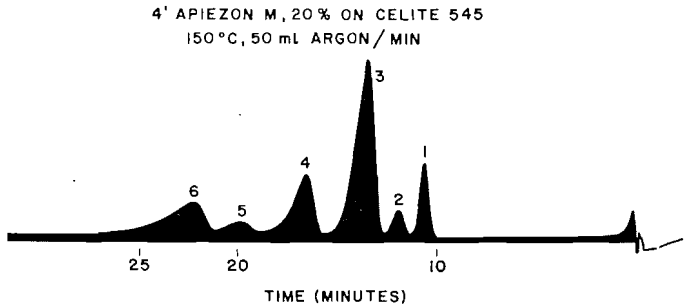


FIG. 3. Separation showing methyl di-*O*-methyl-β-D-glucopyranosides. β-Methyl glycosides of: (1) 2,3,4,6-Tetra-*O*-methyl-D-glucose. (2) 2,3,4-Tri-*O*-methyl-D-glucose. (3) Tri-*O*-methyl-D-glucoses (mainly 2,4,6-). (4), (5), and (6) Di-*O*-methyl-D-glucoses.

lack of standards has prevented assignments to the other peaks. Under the conditions used in this work it was found that skewed peaks invariably indicated heterogeneity and it is therefore almost certain that peaks 4, 5, and 6 in Fig. 3 each represent more than one component. This separation was done on Apiezon M in which the methyl-di-*O*-methyl α- and β-D-glucopyranosides moved quite rapidly but were not resolved sufficiently. On the butanediol succinate polyester column these compounds were retarded considerably because of the extra polar hydroxyl group and a useful separation was not feasible. A more selective liquid phase, or possibly one that is intermediate in polarity between those used here, is obviously needed to achieve a complete separation of all the possible methyl-di-*O*-methyl α- and β-glucopyranosides. However, Fig. 3 shows that the methyl glycosides of di-*O*-methyl hexoses are sufficiently volatile to be analyzed by gas–liquid partition chromatography. It should be mentioned that on freshly prepared columns, using alkali-washed Celite 545, the first few samples of methyl-di-*O*-methyl hexosides were irreversibly adsorbed. The columns were conditioned by running a few samples which presumably covered the active sites and no further adsorption of these compounds was encountered. There was no evidence of exchange or displacement of the samples used to condition the columns. Practically, the lack of complete separation of as complex a mixture of di-*O*-methyl hexoses as just described is not too serious because methanolysis of a methylated polysaccharide seldom yields more than three di-*O*-methyl hexoses. Work to be published on application of this technique to the structural investigation of polysaccharides has shown that the di-*O*-methyl hexoses in these less complex mixtures can be separated and identified easily (5).

The methyl mono-*O*-methyl-D-glucopyranosides were not sufficiently volatile to be separated by gas–liquid partition chromatography. Methyl mono-*O*-methyl hexopyranosides, and indeed methyl hexopyranosides, passed through columns that were conditioned as described for the methyl-di-*O*-methyl glucopyranosides. However, their retention volumes were so great that resolution of a mixture was not possible. The following sequence of reactions was therefore applied to the mono-*O*-methyl-D-glucose to give derivatives that were sufficiently volatile to be separated by gas–liquid partition chromatography. The mono-*O*-methyl-D-glucoses were reduced to the corresponding mono-*O*-methyl-D-

Can. J. Chem. Downloaded from www.nrcresearchpress.com by 41.223.56.140 on 09/04/12
For personal use only.

glucitols which were then acetylated. The resolution of these mono-*O*-methyl-penta-*O*-acetyl-D-glucitols is shown in Fig. 4. It appears that the only one of these isomeric compounds to be reported previously was the 1,2,3,4,5-penta-*O*-acetyl-6-*O*-methyl-D-glucitol (6). Because anomeric methyl glycosides were separable by gas–liquid partition chromatography it appeared that this procedure of reduction and acetylation was a good way to

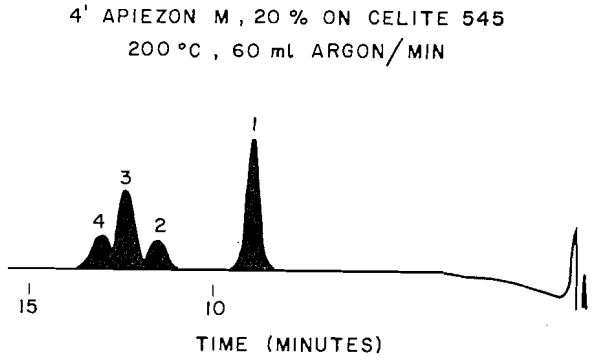


FIG. 4. Separation of mono-*O*-methyl-penta-*O*-acetyl-D-glucitols. (1) 6-*O*-methyl-D-sorbitol pentaacetate. (2) 2-*O*-Methyl-D-sorbitol pentaacetate. (3) 3-*O*-Methyl-D-sorbitol pentaacetate. (4) 4-*O*-Methyl-D-sorbitol pentaacetate.

avoid the complex mixture of anomers that might be expected in the methanolysis products from a methylated polysaccharide. However, there could be difficulty in deciding on the location of a methyl group in the original sugar when the resulting sugar alcohol was symmetrical and, in practice, it was found that methanolysis of methylated polysaccharides did not yield as complex mixtures as had been anticipated.

Gas–liquid partition chromatography affords a quick and accurate means of estimating the relative amounts of individual components in a mixture of methylated sugars. Table II gives the results from estimations of various molar ratios of two components and the mean deviation in the estimation was ±0.5 in 100. The argon ionization detector used in the

TABLE II

Molar ratios of two methylated monosaccharides as determined by gas–liquid partition chromatography

Calculated		Found	
A	*B*	*A*	*B*
60.7	39.3	60.5	39.5
50.6	49.4	50.0	50.0
33.8	66.2	33.1	66.9
20.3	79.7	20.6	79.4
0.9	99.1	1.3	98.7
		Mean deviation = ±0.5	

A, methyl-2,3,4-tri-*O*-methyl-β-D-xyloside. B, methyl-2,3,4,6-tetra-*O*-methyl-α-D-glucoside.

present work was developed by Lovelock (3) and shown to respond on a molar basis. It was therefore possible to obtain a molar ratio of components in a mixture directly from the separation curve simply by measuring the areas under the peaks. The method can also be used for measuring absolute quantities provided that a known percentage of an internal standard can be added to the mixture. The technique has proved extremely

Can. J. Chem. Downloaded from www.nrcresearchpress.com by 41.223.56.140 on 09/04/12
For personal use only.

Can. J. Chem. Downloaded from www.nrcresearchpress.com by 41.223.56.140 on 09/04/12
For personal use only.

useful in examining the methanolysis products of methylated polysaccharides. Although methyl mono-*O*-methyl hexosides and methyl hexosides are not sufficiently volatile to permit the separation of individual isomers, it is possible to obtain an estimate of these components, as one peak, relative to the more highly methylated products. Ratios of isomers within that one peak can then be determined by the procedure described for the mono-*O*-methyl glucoses. Other methods for estimating relative amounts of methylated sugars in a mixture depend on separation of the components by paper chromatography, elution from the paper, and estimation of the individual components by stoichiometric reaction of the reducing groups (e.g., 7) or spectrophotometric measurement of the color produced with specific reagents (e.g., 8, 9). Accuracies in these methods ranged from $\pm 0.8\%$ to $\pm 10\%$ and are, of course, influenced by impurities eluted from the paper; spectrophotometric methods require standard absorption curves for each component. Gas–liquid partition chromatography is therefore at least as accurate, much faster, and more convenient than any of those methods for estimating methylated sugars in a mixture. Each separation of the two components given in Table II required about 10 minutes and for quantitative estimation the peaks were simply cut from the chart and weighed.

EXPERIMENTAL

Apparatus

The apparatus with ionization detector was a "Pye Argon Chromatograph"* and some of its pertinent characteristics are listed below.

Column size, 4 ft, 5 mm I.D.
Detector, ionization (80 μc radium D).
Carrier gas, argon.
Sample size, 2–4 γ.
Resolution, up to 1000 theoretical plates/ft.
Limit of detection, 0.01 γ.
Temperatures used, 150° C and 200° C.

Column Packing

Celite 545 was screened to remove fines and material retained on the 100-mesh sieve was stirred with 5% methanolic potassium hydroxide for 2 hours. The solid was filtered and dried, first by air sucked through the filter and finally in an oven at 100° C. This dried material was used to prepare the columns described below.

Apiezon M vacuum grease (2 g/8 g Celite) was dissolved in petroleum ether (30–60° C) and added to the Celite in an open beaker. Sufficient solvent was used to give a mobile slurry, which was stirred during evaporation of the solvent at room temperature by a stream of air. Last traces of solvent were removed in an oven at 100° C, the mixture being stirred intermittently during this process. The dried material was then used to pack the columns and any traces of volatile material remaining were removed by equilibration of the column under operating conditions for 6–7 hours.

The butanediol succinate polyester was prepared (10) from succinic acid (50 g) and 1,4-butanediol (50 g) using zinc chloride (0.1 g) as catalyst. The mixture was stirred and heated for 3 hours at 160° C then for 2 hours at 190° C. The water formed during esterification was removed through an air condenser by a stream of nitrogen. Heating was continued for another 2 hours during which 1,4-butanediol was removed *in vacuo*. The mixture was then cooled to room temperature to give a white, crystalline solid which softened at 90° C and was completely melted at 96° C. To remove catalyst the mixture

**Obtained from Technical Service Laboratories, Toronto, Ont.*

was dissolved in chloroform and poured through a short column of Amberlite IR-120 ion exchange resin. Columns containing this liquid phase were prepared as described for those containing Apiezon M, except that chloroform was used as solvent instead of petroleum ether.

Partial Methylation

Methyl-α-D-glucopyranoside and methyl-β-D-glucopyranoside were methylated separately with 30% sodium hydroxide and dimethyl sulphate using one-third of the amount of dimethyl sulphate theoretically required for complete methylation. The reactions were stirred for 6 hours after the dropwise addition of dimethyl sulphate had been completed and the products were then isolated by extraction with chloroform.

Identification of Components

To assign identities to the peaks on the separation curves authentic samples of the various glucose methyl ethers were converted individually into glucosides by refluxing with 2% methanolic hydrogen chloride. These derivatives were then separated by gas chromatography each one giving two peaks, one of which coincided with the peak of that particular isomer in the α-series, the other with a peak in the β-series. It was not possible to establish the separations reported in this paper by using only authentic samples of glucose methyl ethers because, after methyl glycoside formation, each sample gave two peaks and it could not be proved which one was the α-anomer and which the β-. This could only be done by preparing the methyl ethers of each anomeric methyl glycoside as just described.

Mono-O-methyl-penta-O-acetyl-D-glucitols

Authentic samples of 2-, 3-, 4-, and 6-*O*-methyl-D-glucose were reduced separately with an equal weight of potassium borohydride in aqueous solutions. To assure complete reduction the reactions were allowed to stand at room temperature for 24 hours. Amberlite IR-120 ion exchange resin was then added until gas evolution ceased. The resin was then filtered, washed with methanol, and the combined filtrates and washings were evaporated under diminished pressure at 35° C. Repeated evaporation from methanol removed borate and the sirupy mono-*O*-methyl-D-glucitols were acetylated with acetic anhydride and sulphuric acid. The acetylation reactions were added directly to silica gel columns and the products were eluted with chloroform. Evaporation of the chloroform eluates left the isomeric mono-*O*-methyl-penta-*O*-acetyl-D-glucitols; the 6-*O*-methyl isomer crystallized on evaporation of the solvent and the 2-*O*-methyl isomer crystallized after being stored for 1 week in an evacuated desiccator over sodium hydroxide. The 3- and 4-*O*-methyl isomers have not crystallized. Anal. Calc. for $C_{17}H_{26}O_{11}$: C, 50.24%; H, 6.45%; acetyl, 52.9%. Found:

(*a*) 2-*O*-methyl-1,3,4,5,6-penta-*O*-acetyl-D-glucitol; m.p. 53–54° C (recrystallized from ether:hexane), $[\alpha]_D^{24} = +24° \pm 1°$ (*c*, 1.6% in chloroform). C, 50.15%; H, 6.64%; acetyl, 52.8%.

(*b*) 3-*O*-methyl-1,2,4,5,6-penta-*O*-acetyl-D-glucitol; $[\alpha]_D^{24} = +3° \pm 1°$ (*c*, 1.85% in chloroform). C, 50.52%; H, 6.75%; acetyl, 53.04%.

(*c*) 4-*O*-methyl-1,2,3,5,6-penta-*O*-acetyl-D-glucitol; $[\alpha]_D^{24} = +5° \pm 1°$ (*c*, 1.5% in chloroform). C, 49.92%; H, 6.71%; acetyl, 52.5%.

(*d*) 6-*O*-methyl-1,2,3,4,5-penta-*O*-acetyl-D-glucitol; m.p. 109–110° C (recrystallized from methanol:water), $[\alpha]_D^{24} = +6° \pm 1°$ (*c*, 1.71% in chloroform). C, 50.21%; H, 6.49%; acetyl, 53.07%. Vargha and Puskas (6) reported m.p. 105° C and $[\alpha]_D^{20} = +7.6°$ (*c*, 2.624% in chloroform) for this compound.

Can. J. Chem. Downloaded from www.nrcresearchpress.com by 41.223.56.140 on 09/04/12
For personal use only.

Quantitative Estimations

Solutions of known concentration were made up in methanol of methyl-2,3,4-tri-*O*-methyl-β-D-xylopyranoside and methyl-2,3,4,6-tetra-*O*-methyl-α-D-glucopyranoside. Samples were pipetted accurately from these standard solutions and mixed to give the molar mixtures listed in Table II. Aliquots from these mixtures were then analyzed by gas–liquid partition chromatography and the peaks on the separation curve were cut out and weighed giving the results shown in Table II.

ACKNOWLEDGMENTS

The authors wish to thank Mr. A. G. McInnes for many valuable discussions about this work. We would also like to thank Dr. B. M. Craig for making available detailed directions for preparing the butanediol succinate polyester prior to publication. A generous donation of many of the authentic samples of glucose methyl ethers by Dr. T. E. Timell is gratefully acknowledged, and our thanks are due to Dr. A. Wickstrom for a sample of 3,4,6-tri-*O*-methyl-D-glucose. Microanalyses were done by Mr. A. E. Castagne.

REFERENCES

1. A. T. JAMES and A. J. P. MARTIN. Biochem. J. **50**, 679 (1952).
2. A. G. MCINNES, D. H. BALL, F. P. COOPER, and C. T. BISHOP. J. Chromatog. **1**, 556 (1958).
3. J. E. LOVELOCK. J. Chromatog. **1**, 35 (1958).
4. H. W. KIRCHER. Am. Chem. Soc., 136th meeting. Atlantic City. 1959. Abstr. p. 18D.
5. C. T. BISHOP and F. P. COOPER. Unpublished results.
6. L. VARGHA and T. PUSKAS. Chem. Ber. **76**, 859 (1943).
7. E. L. HIRST, L. HOUGH, and J. K. N. JONES. J. Chem. Soc. 928 (1949).
8. J. K. N. JONES and J. B. PRIDHAM. Biochem. J. **58**, 288 (1954).
9. T. A. TIMELL, C. P. J. GLAUDEMENS, and A. L. CURRIE. Anal. Chem. **28**, 1916 (1956).
10. B. M. CRAIG and N. L. MURTY. J. Am. Oil Chemists' Soc. **36**, 549 (1959).

Can. J. Chem. Downloaded from www.nrcresearchpress.com by 41.223.56.140 on 09/04/12
For personal use only.

Can. J. Chem. Downloaded from www.nrcresearchpress.com by 41.223.56.140 on 09/04/12
For personal use only.

THE BIOGENESIS OF ALKALOIDS

XXV. THE ROLE OF HYGRIC ACID IN THE BIOGENESIS OF STACHYDRINE[1]

A. V. ROBERTSON[2] AND LÉO MARION

ABSTRACT

In alfalfa 2–3 weeks old neither labelled ornithine nor labelled proline act as precursors of stachydrine. It has been shown, however, that the methyl group of methionine becomes incorporated into the alkaloid so that the biogenesis appears to occur at that time of growth. It is now shown that hygric acid (N-methylproline) is a precursor of stachydrine. The implications of the results obtained are discussed.

It has been shown previously that in alfalfa seedlings, the activity of administered proline labelled with ^{14}C in the carboxyl group or at position 2 is not incorporated in the stachydrine subsequently isolated (1–4). Nevertheless, radioactive stachydrine is produced at the same plant age by feeding Me-^{14}C-methionine (4). The implications of these results have been discussed and several alternatives were suggested to circumvent the most obvious conclusion that proline is not a precursor of stachydrine (4). One of these hypotheses was that only processes involving the formation of the second N-methyl group of stachydrine were taking place in alfalfa 2–3 weeks old, the heterocyclic ring having been formed from proline at some other time. For example, the final step in the biosynthesis of stachydrine might be a methylation of already preformed hygric acid (N-methylproline). Possibly one of the methyl groups of stachydrine is dynamically involved in alfalfa transmethylation reactions, in which case the methylation of hygric acid to stachydrine would be reversible. Leete and Bell (5) have shown that the methyl group of nicotine is in equilibrium with methyl acceptors in tobacco plants.

Information has now been obtained about the role of hygric acid in stachydrine biosynthesis from experiments in which carboxyl-^{14}C-hygric acid was fed to alfalfa seedlings 17 days old. The plants were harvested 4 days later at which time most of the radioactivity in the nutrient solution had disappeared. The alkaloids were isolated by established methods (6), and the crystalline mixture of pure stachydrine and homostachydrine hydrochlorides obtained was highly radioactive. Paper chromatographic assay showed that there was no contamination due to hygric acid, and that all of the activity was present in the stachydrine. Although homostachydrine has been obtained pure from the mixture of betaine hydrochlorides (7), it has not yet proved possible to separate pure stachydrine on a preparative scale. Decarboxylation to isolate the radioactive carbon as barium carbonate was therefore performed on the mixture. Appropriate corrections were made for the relative proportions of the compounds in the mixture, and for the yields of barium carbonate obtained from either component in separate experiments with inactive material. Within the limits of experimental error, all of the activity in the stachydrine was present in the carboxyl group. Therefore hygric acid serves as an efficient precursor for the heterocyclic ring of this alkaloid.

All attempts so far to show the role of ornithine or proline in the biogenesis of stachydrine have failed (1–4), and the only definite precursor of the alkaloid that has been found is hygric acid. It is conceivable that the formation of proline and its conversion to hygric acid take place at an earlier stage of growth of the plant, but since some of the

[1]*Manuscript received November 9, 1959.*
Contribution from the Division of Pure Chemistry, National Research Council, Ottawa, Canada.
Issued as N.R.C. No. 5532.
[2]*National Research Council of Canada Postdoctoral Fellow, 1957–59.*

experiments previously reported were done after only 12 days of growth this does not seem too probable. Further, since ornithine can be converted to proline in the plant in the presence of pyridoxal (2), it also seems improbable that the failure of proline to give rise to stachydrine at the same period of growth could be attributable to the possibility that the proline might not get to the site of synthesis. The observation of Abelson and Vogel (8) concerning the difference in behavior between exogenous and endogenous ornithine in *Neurospora crassa*, however, supports such a possibility. If hygric acid were formed from proline one would have to conclude that proline was synthesized in two different sites, and that neither the ornithine nor proline from one site could find its way to the other site. The concept of multiple sites is not in itself reluctant, but it is difficult to accept that the required precursors existing in one part of the plant could not be translocated to the site where they are needed when hygric acid is. Although the suggestion is made with hesitancy, the results obtained so far could best be explained if hygric acid were synthesized not from proline, but directly from smaller fragments. Further work will be necessary to prove or disprove such a suggestion, but it becomes impossible to ignore the repeated failures to implicate ornithine or proline in the pathway to stachydrine.

EXPERIMENTAL

Synthesis of Carboxyl-^{14}C-DL-*hygric Acid*

Carboxyl-^{14}C-DL-proline (0.1 mc, sp. act. 2.7 mc/mmole) was diluted with DL-proline (44 mg) and monomethylated by the method of Ingram (9) (see also Bowman and Stroud (10)). The product was sublimed at 140°/1 mm giving a quantitative yield of pure hygric acid.

Feeding Experiment and Extraction of Alkaloids

Alfalfa seed (240 g) was grown in 8 trays as previously described (6) and on the 18th day, carboxyl-^{14}C-DL-hygric acid (54 mg, total activity 1.8×10^8 d.p.m.) in water (80 ml) was divided evenly among the trays. The radioactivity in the nutrient solution decreased as follows: 9% remained after 1 day, 4% after 2 days, 3% after 3 days, less than 2% after 4 days. The plants were harvested on the 22nd day and the alkaloids were isolated by the usual extraction procedure (6). In this experiment the crude betaine hydrochlorides obtained by ion exchange of the reineckates were discolored and oily. The oil was removed by ether extraction of an aqueous acid solution of the hydrochlorides before purification through the mercuric chloride complex. The crystalline mixture of pure homostachydrine and stachydrine hydrochlorides had an activity of 2.82×10^3 d.p.m./mg. Paper chromatography in 95% ethanol – concentrated aqueous ammonia (95:5) showed that all of the activity was confined to the stachydrine spot, R_F 0.45, and that homostachydrine, R_F 0.54, was the only other component. Hygric acid had R_F 0.51 on the same paper. Hygric acid does not give a satisfactory reaction with Dragendorff's reagent or iodine vapor, so the orcinol – sulphuric acid method of Ingram (9) was used. The betaines are also developed by this reagent. The mixture was estimated by the intensity of spots on paper chromatograms (developed with Dragendorff's reagent) to contain 60 ± 5% (w/w) of stachydrine hydrochloride. The activity of the stachydrine hydrochloride is therefore 4.7×10^3 d.p.m./mg and sp. act. 8.4×10^5 d.p.m./mmole.

Degradation to Isolate Radioactivity

Fifty milligrams of the mixture of betaine hydrochlorides in quinoline (2 ml) was heated with copper powder (100 mg) and the temperature was gradually raised from 210–250° (1 hour). A slow stream of purified nitrogen was passed through the reaction

Can. J. Chem. Downloaded from www.nrcresearchpress.com by 41.223.56.140 on 09/04/12
For personal use only.

flask and the nitrogen and evolved gases were bubbled through barium hydroxide solution. The precipitated barium carbonate (42 mg) had an activity of 2.70×10^3 d.p.m./mg. In separate experiments with inactive stachydrine hydrochloride, homostachydrine hydrochloride, and mixtures of the two compounds, the weight of barium carbonate obtained under the above conditions was $86\pm2\%$ of the weight of starting material. Hence the ratio of the weights of barium carbonate arising from stachydrine to that from homostachydrine is equal (within $\pm2\%$) to the ratio of stachydrine to homostachydrine (w/w) in the mixture which was decarboxylated. The weight of barium carbonate arising from stachydrine is thus 60% of the total weight of the radioactive barium carbonate sample. Therefore barium carbonate formed by decarboxylation of radioactive stachydrine has an activity of 4.5×10^3 d.p.m./mg and sp. act. 8.9×10^5 d.p.m./mmole.

REFERENCES

1. E. LEETE, L. MARION, and I. D. SPENSER. J. Biol. Chem. **214**, 71 (1955).
2. A. MORGAN and L. MARION. Can. J. Chem. **34**, 1704 (1956).
3. G. WIEHLER and L. MARION. J. Biol. Chem. **231**, 799 (1958).
4. A. V. ROBERTSON and L. MARION. Can. J. Chem. **37**, 1197 (1959).
5. E. LEETE and V. M. BELL. J. Am. Chem. Soc. **81**, 4358 (1959).
6. A. V. ROBERTSON and L. MARION. Can. J. Chem. **37**, 1043 (1959).
7. G. WIEHLER and L. MARION. Can. J. Chem. **36**, 339 (1958).
8. P. H. ABELSON and H. J. VOGEL. J. Biol. Chem. **213**, 355 (1955).
9. V. M. INGRAM. J. Biol. Chem. **202**, 193 (1953).
10. R. E. BOWMAN and H. H. STROUD. J. Chem. Soc. 1342 (1950).

Can. J. Chem. Downloaded from www.nrcresearchpress.com by 41.223.56.140 on 09/04/12
For personal use only.

Can. J. Chem. Downloaded from www.nrcresearchpress.com by 41.223.56.140 on 09/04/12
For personal use only.

THE ACIDITY OF SOME AROMATIC FLUORO ALCOHOLS AND KETONES[1]

ROSS STEWART AND R. VAN DER LINDEN[2]

ABSTRACT

A series of five trifluoroacetophenones and five phenyl trifluoromethyl carbinols have been synthesized and their ionization constants in water measured. They are the unsubstituted, *p*-methoxy, *p*-methyl, *m*-bromo, and *m*-nitro compounds. The ketones exist as hydrates in aqueous solution and each is about two pK units stronger than the corresponding alcohol. The acidities of both series are correlated by the Hammett relation with ρ values of 1.11 and 1.01 for the ketone hydrates and alcohols respectively. The acid strengths vary from a pK_a of 9.18 for *m*-nitro-α,α,α-trifluoroacetophenone to 12.24 for *p*-methoxyphenyl trifluoromethyl carbinol.

In connection with an investigation of the mechanism of the permanganate oxidation of alcohols (1) we have examined a series of trifluoromethyl carbinols (2). These were chosen because their enhanced acidity permitted measurements to be made of the concentration of the alkoxide ion believed to be the intermediate in the oxidation mechanism. The trifluoromethyl carbinols and the ketones from which they are prepared are interesting compounds in their own right because of their acidities, the hydrates of the latter being of similar strength to phenols. We would like to report herein the synthesis of a series of substituted phenyl trifluoromethyl alcohols and ketones and the determination of their acidities.

EXPERIMENTAL

Reagents

α,α,α-Trifluoroacetophenone was obtained from Columbia Organic Chemicals and was fractionally distilled before use. All other reagents used were of reagent grade.

p-Methyl-α,α,α-trifluoroacetophenone

p-Tolylmagnesium bromide was prepared in the usual way from *p*-bromotoluene (34.7 g, 0.203 mole) and an equivalent amount of magnesium. Trifluoroacetic acid (7.5 g, 0.066 mole) dissolved in ether was added dropwise with vigorous stirring over a period of 2 hours at room temperature. After refluxing for 1 hour the reaction mixture was poured onto a 10% sulphuric acid – ice mixture and extracted several times with ether. The ether extracts were dried and distilled and a clear fraction boiling at 69° at 13 mm was obtained; yield, 30–50%, $n_D^{25} = 1.4710$ (lit., $n_D^{20} = 1.4693$ (3)); 2,4-dinitrophenylhydrazone, m.p. 133–136°. Calc. for $C_9H_7OF_3$: C, 57.4; H, 3.7; F, 30.3. Found: C, 57.8; H, 3.9; F, 26.8. This compound has been synthesized previously using a different procedure (3).

m-Bromo-α,α,α-trifluoroacetophenone

To a Carius tube of approximately 100 ml volume was added α,α,α-trifluoroacetophenone (20 g, 0.115 mole), anhydrous ferric chloride (0.1 g), and bromine (9 ml, 0.168 mole). The mixture was cooled in liquid nitrogen, the tube was sealed and then heated in a furnace for 6 days at 130°.

After reaction the liquid was extracted with aqueous sodium bromide and then fractionally distilled giving a small amount of unreacted ketone, a solid residue, and a clear liquid, b.p. 83.5° at 12 mm, $n_D^{24} = 1.5030$; yield, 50%. Calc. for $C_8H_4OF_3Br$: C, 38.0; H, 1.5; F, 22.5. Found: C, 38.2; H, 1.6; F, 20.6. 2,4-Dinitrophenylhydrazone, m.p.

[1]*Manuscript received November 18, 1959.*
Contribution from the Department of Chemistry, University of British Columbia, Vancouver, B.C.
[2]*Present address: Imperial Oil Limited, Sarnia, Ontario.*

121.5–123°. Calc. for $C_{14}H_8O_4N_4F_3Br$: C, 38.6; H, 1.9; N, 12.9; F, 13.2. Found: C, 38.8; H, 2.5; N, 12.0; F, 12.0.

As a check on the identity of this compound a sample was hydrolyzed with aqueous base and gave *m*-bromobenzoic acid, identical with an authentic sample.

m-Nitro-α,α,α-trifluoroacetophenone

Sixty milliliters of concentrated sulphuric acid was added slowly with stirring to trifluoroacetophenone (27.2 ml, 0.2 mole) with the temperature kept at 0° or below. A nitrating mixture (made up from 12 ml concentrated nitric acid, 4 ml fuming nitric acid, and 24 ml concentrated sulphuric acid) was added dropwise with cooling to keep the temperature from rising above 0°. A yellow solid began to precipitate after part of the nitrating mixture had been added. The mixture was poured onto crushed ice and extracted with ether. The latter was dried and on removal of the ether gave a yellow oil which on fractional distillation gave a pale yellow, low melting solid, b.p. 113° at 12 mm; yield, 75%. Calc. for $C_8H_4O_3F_3N$: C, 43.8; H, 1.8; F, 26.0; N, 6.4. Found: C, 43.4; H, 1.9; F, 24.3; N, 6.6. 2,4-Dinitrophenylhydrazone, m.p. 128–132°. Calc. for $C_{14}H_8O_5N_5F_3$: C, 42.2; H, 2.0; N, 17.6; F, 14.3. Found: C, 43.1; H, 2.8; N, 17.0; F, 13.4.

Alkaline hydrolysis of the ketone gave *m*-nitrobenzoic acid, identical with an authentic sample.

p-Methoxy-α,α,α-trifluoroacetophenone

This compound was prepared by the Grignard procedure essentially as described for *p*-methyl-α,α,α-trifluoroacetophenone. B.p. 64° at 0.5 mm; $n_D^{23} = 1.5051$. Calc. for $C_9H_7F_3O_2$: C, 52.9; H, 3.5. Found: C, 51.9; H, 3.6. 2,4-Dinitrophenylhydrazone, m.p. 104–105° (decomp.).

Phenyl Trifluoromethyl Carbinols

The unsubstituted, *m*-bromo, and *p*-methyl compounds were prepared by a lithium aluminum hydride reduction of the corresponding ketones by a standard method. Data are listed in Table I. The yields of crude product before purification were of the order of 80–90%.

TABLE I

Physical properties and analytical data for the fluoro alcohols

$YC_6H_4CHOHCF_3$	B.p.	Refractive index	Phenylurethan m.p.	Analysis*	
				Calculated	Found
H	82° (13 mm)	$1.4590^{25°}$	103–104°	C, 61.0; H, 4.1; F, 19.3	C, 61.2; H, 4.2; F, 19.0
p-CH_3O	80° (0.5 mm)	$1.4780^{23°}$		C, 52.4; H, 4.4	C, 52.2; H, 4.6
p-CH_3	94.5° (12 mm)	$1.4650^{24°}$		C, 56.9; H, 4.7; F, 30.0	C, 57.1; H, 5.0; F, 26.6
			104–105°	C, 62.1; H, 4.5; F, 18.4; N, 4.5	C, 62.1; H, 4.5; F, 16.7; N, 5.1
m-Br	115° (12 mm)	$1.5005^{27°}$		C, 37.1; H, 2.4; F, 22.4; Br, 31.4	C, 38.0; H, 2.5; F, 20.0; Br, 31.6
m-NO_2	106° (2 mm) (m.p. = 47–48°)			C, 43.5; H, 2.7; F, 25.8; N, 6.3	C, 43.7; H, 3.1; F, 23.7; N, 6.4
			102–103°	C, 53.0; H, 3.2; F, 16.8; N, 8.2	C, 53.1; H, 3.6; F, 16.3; N, 8.3

*Analysis by A. Bernhardt, Mulheim, West Germany.

m-Nitrophenyl Trifluoromethyl Carbinol

m-Nitro-α,α,α-trifluoroacetophenone (10 g, 0.045 mole) and aluminum isopropoxide

Can. J. Chem. Downloaded from www.nrcresearchpress.com by 41.223.56.140 on 09/04/12
For personal use only.

(8.2 g, 0.04 mole) dissolved in 40 ml of dry isopropyl alcohol were distilled slowly for 2 hours with the alcohol being replaced as it distilled. The mixture was poured onto a 3 *M* HCl–ice mixture and extracted with ether. Distillation yielded a viscous oil, b.p. 106° at 2 mm, which crystallized on standing. Recrystallization from benzene – petroleum ether gave pale yellow needles, m.p. 47–48°.

p-Methoxyphenyl Trifluoromethyl Carbinol

This compound was prepared by essentially the method described for *m*-nitrophenyl trifluoromethyl carbinol. See Table I for physical constants.

pK_a *Measurements*

Stock solutions of the alcohols and ketones of appropriate concentration were prepared by weighing out the pure liquids (purified in most cases by gas chromatography), and dissolving them with shaking in distilled water. Usually 10 ml of these solutions and 10 ml of phosphate buffer were added to a 25-ml volumetric flask which was then made up to volume with distilled water. The buffer consisted of 0.02 *M* Na_2HPO_4 solution to which 1 *N* NaOH or 1 *N* H_2SO_4 was added to produce approximately the desired pH. Solutions more basic than pH 13 were obtained by using NaOH directly rather than the buffer. The pH of these solutions was obtained directly from the concentration of NaOH present. The optical density of a few milliliters of the buffered ketone or alcohol solution was then measured using a Beckman DU spectrophotometer at a suitable wavelength. The latter was located by measuring the entire spectrum of the ketone or alcohol in neutral and basic solution (usually pH 4.0 and 13.6) using a Cary model 14 recording spectrophotometer. The absorption maxima are listed in Tables I and II. The cell compartment of the DU spectrophotometer was kept at 25° by means of thermospacers.

TABLE II

Ultraviolet spectral data for trifluoroacetophenone and derivatives

Trifluoro-acetophenone	Neutral aqueous solution		Basic aqueous solution		Cyclohexane solution	
	λ_{max}	ϵ	λ_{max}	ϵ	λ_{max}	ϵ
Unsubstituted	267	350	266	144	253	13,300
	260	474	260	237	288	1000
	255	427	256	278		
	250	345	250	247		
m-Br	274.5	342	273.5	213	254	10,500
	267.5	451	267	306	302	1520
	261.5	358	261	258		
	255 (sh)	250	255 (sh)	200		
m-NO_2	263	14,000	269	13,600	233	20,800
					302	900
					292	1050
p-CH_3	265	590	294	73	264	15,700
	259	607	260	356		
			253	390		
			243	410		
p-CH_3O	300	1360	276	980	289	15,900
	277	1530	270	1080	231	9300
	270	1390			225	11,000

After the optical density readings were made the pH of the remainder of the solution was measured using a Beckman model G pH meter which was standardized against

Can. J. Chem. Downloaded from www.nrcresearchpress.com by 41.223.56.140 on 09/04/12
For personal use only.

buffer at pH 7.00 and 10.00. It has been reported (4) that trifluoroacetophenones are decomposed by alkali to CHF_3 and the corresponding benzoic acid. The alkaline solutions we used were stable during the time of the measurements but it was noted that decomposition was occurring in some cases after a few hours.

Calculations

For all the compounds studied a plot of optical density against pH gave a typical titration curve. The ionization constants were calculated using the equation,

$$pK_a = pH \pm \log [(D - D_{A^-})/(D_{HA} - D)]$$

where D is the optical density of the solution at the selected wavelength, D_{A^-} that at complete ionization obtained by measuring the optical density of a 0.6 N NaOH solution of the compound (corrected in the case of the alcohols for incomplete ionization), and D_{HA} that of the completely unionized form obtained by a measurement at pH 4. A minimum of three values in the vicinity of half ionization was obtained for each compound and these values averaged to obtain the values listed in Table III. The probable error varies from compound to compound because of the differences in spectra but is generally of the order of ± 0.06 pK units.

The wavelengths in millimicrons used for the pK measurements were as follows, with the alcohol listed first and the ketone second: H (260, 260); p-CH_3O (280, 276); p-CH_3 (269, 260); m-Br (274, 274.5 and 267.5); m-NO_2 (330, 320).

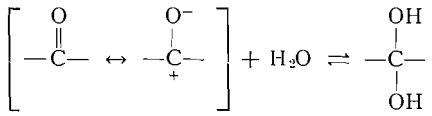
TABLE III

Ultraviolet spectral data for phenyl trifluoromethyl carbinol and derivatives

Phenyl trifluoromethyl carbinol	Neutral aqueous solution		Basic aqueous solution	
	λ_{max}	ϵ	λ_{max}	ϵ
Unsubstituted	266	140	262	149
	260	210	257	200
	256	224	251	165
	250	163	247	130
m-Br	274	254	274	162
	267	340	267	244
	261	286		
m-NO_2	264	7600	270	7000
p-CH_3	265	156	271	192
	260	225	262	275
	254	194	256	230
p-CH_3O	278	1130	277	1080
	272	1320	271	1240

RESULTS

Polyfluorinated ketones exist in the hydrated form in aqueous solution (5, 6) presumably because of the strongly electron-withdrawing group which raises the energy of the dipolar canonical structure and shifts the following equilibrium to the right.



Can. J. Chem. Downloaded from www.nrcresearchpress.com by 41.223.56.140 on 09/04/12
For personal use only.

The trifluoroacetophenones reported herein are all hydrated in aqueous solution as can be seen from an examination of their ultraviolet spectra. Table II which lists the absorption maxima of the ketones in cyclohexane and in water and Fig. 1 which shows the spectrum of *m*-bromo-α,α,α-trifluoroacetophenone in water reveal the absence of the usual phenyl ketone absorption in aqueous solution. The latter spectrum appears when these compounds are dissolved in cyclohexane. (The absorption of the *p*-methoxy ketone

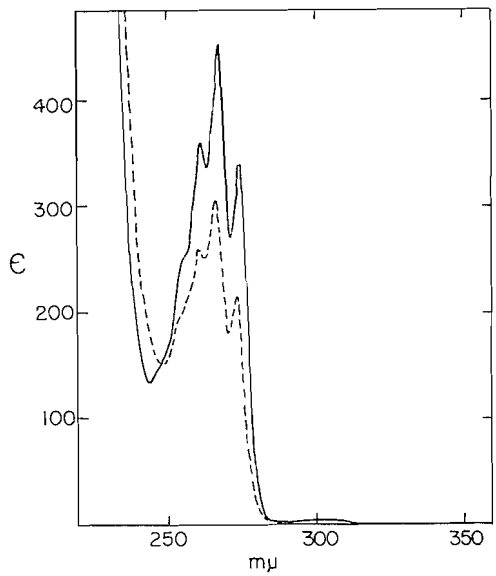


FIG. 1. The ultraviolet spectrum of *m*-bromo-α,α,α-trifluoroacetophenone in water: solid line, pH 4; broken line, pH 13.

at 300 mμ is probably due to the presence of some unhydrated ketone since this ketone is the one expected to be least hydrated in water.) When trifluoroacetophenone is dissolved in ethanol the characteristic phenyl ketone absorption at 253 mμ rapidly decays until the spectrum resembles that in aqueous solution.

The ultraviolet spectrum of the hydrate of trifluoroacetophenone is essentially a benzene spectrum modified by the side chain. When one of the hydroxyls in the side chain is ionized in basic solution the spectrum is sufficiently altered to enable measurements of the concentrations of the two forms to be made (Fig. 1).

The same applies to the alcohols, and in fact the spectra of the ketone hydrates and their anions were found to be very similar to those of the corresponding alcohols and their anions. Tables II and III reveal the close similarity in the wavelength maxima in the two series. The extinction coefficients are, however, somewhat larger for the ketone hydrates than for the alcohols.

Comparison of Acidities in the Two Series

The ionization constants of the alcohols and ketone hydrates are listed in Table IV; Fig. 2 shows the pK values plotted against σ, the Hammett substituent constant (7, 8). A satisfactory linear relation is obtained for both series. It can be seen that the ketone hydrates are about 2 pK units more acidic than the alcohols. This 100-fold increase in

Can. J. Chem. Downloaded from www.nrcresearchpress.com by 41.223.56.140 on 09/04/12
For personal use only.

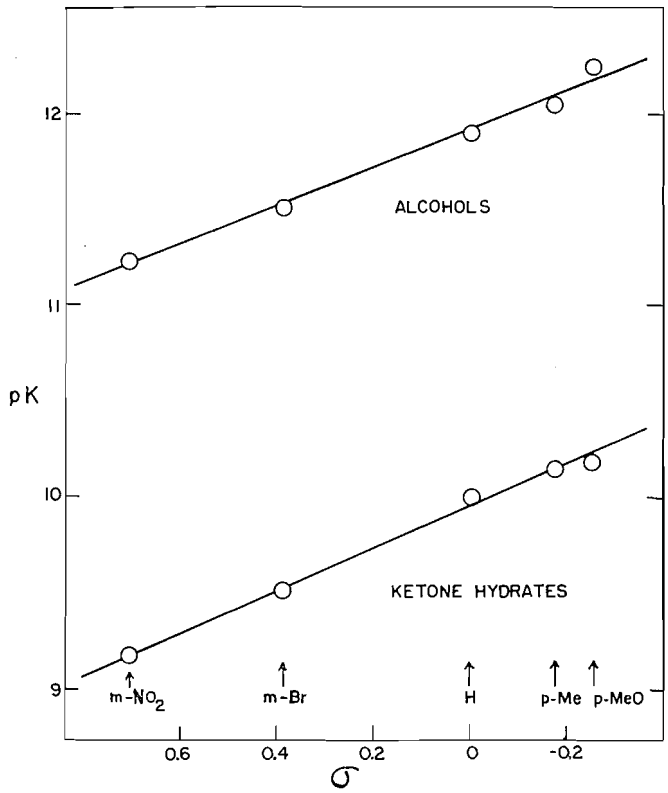


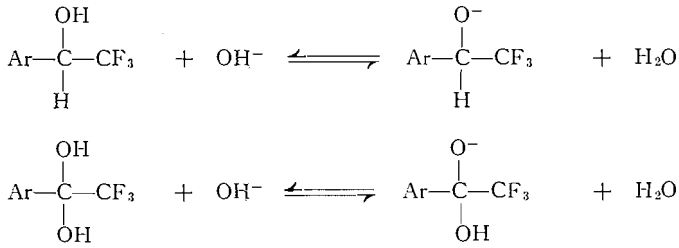
FIG. 2. Hammett plots for the ionization of phenyl trifluoromethyl carbinols (alcohols) and ketones.

TABLE IV

Acidities of substituted phenyl trifluoromethyl carbinols and ketone hydrates

Substituent	Carbinol (pK)	Ketone hydrate (pK)
H	11.90	10.00
p-CH_3O	12.24	10.18
p-CH_3	12.04	10.15
m-Br	11.50	9.51
m-NO_2	11.23	9.18

ionization constant (50-fold if a statistical correction is made for the extra ionizable proton in the ketone hydrate) is due entirely to the electronegative nature of the additional oxygen atom in the former.



Can. J. Chem. Downloaded from www.nrcresearchpress.com by 41.223.56.140 on 09/04/12
For personal use only.

In these two systems resonance effects on the ionization are completely absent and it is worth comparing the effect of the additional oxygen atom on the acidity of the hydroxyl group with that in analogous cases. Table V shows that the addition of an oxygen atom

TABLE V
Effect of oxidation on acidities

Acid	K_I	Acid	K_{II}	K_{II}/K_I	Reference
$C_6H_5C(OH)(H)CF_3$	1.2×10^{-12}	$C_6H_5C(OH)(OH)CF_3$	1.0×10^{-10}	80	Herein
$HC(=O)OH$	1.8×10^{-4}	$HOC(=O)OH$	2×10^{-4}*	~1	(9)
$HP(OH)_2$	1×10^{-2}	$HOP(OH)_2$	1.6×10^{-2}	1.6	(10)
$C_6H_5C(OH)H$	1.2×10^{7}	$C_6H_5C(OH)_2$	1.8×10^{7}	1.5†	(11, 12)

*Corrected for incomplete hydration of CO_2.

†This ratio varies with the substituent in the ring. The p-CH_3O substituent reduces the importance of resonance *within* the carbonyl group and raises this ratio to a value of 13.

to formic acid, hypophosphorous acid, and benzaldehyde conjugate acid produces much smaller charges in acidity than the addition of an oxygen atom to phenyl trifluoromethyl carbinol. In the former cases the electron-withdrawing inductive effect of oxygen is largely cancelled by its electron-donating resonance effect, assuming in the case of phosphorous acid that resonance occurs with the expanded valence shell of phosphorus. Resonance involving the oxygen atoms is not possible in the case of the ketone hydrates.

The Reaction Constant

The values of the reaction constant, ρ (the slopes in Fig. 2) (7, 8), are 1.01 for the alcohols and 1.11 for the ketone hydrates. Values close to 1.0 are expected for ionizations in which the proton is removed from the second atom of the side chain (13) as in both the present cases.*

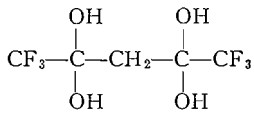
Rate of Ionization of the Fluoroketones

When the fluoroketones reported herein are dissolved in water they react rapidly to form the hydrates since the spectrum taken immediately after solution is effected is identical with that taken after long standing. The ionization of these weak acids is essentially instantaneous as expected for hydroxylic compounds. This rather obvious point is referred to here because certain fluorinated ketone hydrates have been shown to ionize only slowly with base. Thus hexafluoroacetylacetone which exists in solution as

*NOTE ADDED IN PROOF: *Since there is no conjugation between the sidechain and the substituents in these series one should obtain a better correlation with the recently derived σ^0 values (R. W. Taft, Jr., S. Ehrenson, I. C. Lewis, and R. Glick. J. Am. Chem. Soc. **81**, 5352 (1959)) than with the standard sigma values. Even though σ and σ^0 are not greatly different for the substituents studied in this work it does appear that the correlation is slightly better for σ^0 than for σ.*

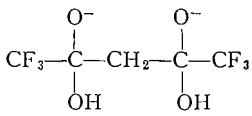
Can. J. Chem. Downloaded from www.nrcresearchpress.com by 41.223.56.140 on 09/04/12
For personal use only.

the dihydrate, I,

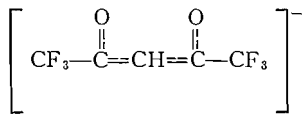


I

although a much stronger acid ($pK = 4.35$) than trifluoroacetophenone hydrate ($pK = 10.0$) ionizes at a relatively slow rate requiring over 3 hours for neutralization with 1 *M* NaOH (14, 15). A similar situation exists with thenoyltrifluoroacetone (14). The reason for the apparent discrepancy is the following. The stable anion of I is undoubtedly not ion II, but ion III.



II



III

The slow neutralization by base is due to ion II, which is almost certainly formed immediately by the action of strong base, having to revert to the unhydrated form and then eliminate a proton from the central carbon to form the more stable ion III. Such an enolate anion is, of course, not possible with aromatic ketones so that the further, slow, ionization does not take place.

ACKNOWLEDGMENT

The financial support of the National Research Council is gratefully acknowledged.

REFERENCES

1. R. STEWART. J. Am. Chem. Soc. **79**, 3057 (1957).
2. R. STEWART and R. VAN DER LINDEN. To be published.
3. J. D. PARK, H. A. BROWN, and J. R. LACKER. J. Am. Chem. Soc. **73**, 709 (1951).
4. J. H. SIMONS and E. O. RAMLER. J. Am. Chem. Soc. **65**, 389 (1943).
5. A. L. HERNE, J. W. SHEPHARD, and E. J. YOUNG. J. Am. Chem. Soc. **72**, 3577 (1950).
6. E. H. COOK and R. W. TAFT, JR. J. Am. Chem. Soc. **74**, 6103 (1952).
7. L. P. HAMMETT. Physical organic chemistry. McGraw-Hill Book Co., Inc., New York. 1940. Chap. VII.
8. H. H. JAFFÉ. Chem. Revs. **53**, 191 (1953).
9. W. W. LATIMER and J. H. HILDEBRAND. Reference book of inorganic chemistry. Macmillan Co., New York. 1951. p. 282, 285.
10. W. W. LATIMER and J. H. HILDEBRAND. Reference book of inorganic chemistry. Macmillan Co., New York. 1951. p. 229.
11. K. YATES and R. STEWART. Can. J. Chem. **37**, 664 (1959).
12. K. YATES. Ph.D. Thesis, The University of British Columbia, Vancouver, B.C.
13. R. W. TAFT, JR. and I. C. LEWIS. J. Am. Chem. Soc. **80**, 2436 (1958).
14. R. W. TAFT, JR. and E. H. COOK. J. Am. Chem. Soc. **81**, 46 (1959).
15. L. G. VAN UITART. M.Sc. Thesis. The Pennsylvania State College. 1951. Referred to in ref. 14.

Can. J. Chem. Downloaded from www.nrcresearchpress.com by 41.223.56.140 on 09/04/12
For personal use only.

Can. J. Chem. Downloaded from www.nrcresearchpress.com by 41.223.56.140 on 09/04/12
For personal use only.

THE IONIZATION AND DISSOCIATION OF SOME HALOGEN MOLECULES BY ELECTRON IMPACT[1]

D. C. Frost and C. A. McDowell

ABSTRACT

The ionization and dissociation of chlorine, bromine, iodine, iodine monochloride, and iodine monobromide by electron impact have been studied in a mass spectrometer which uses a monoenergetic electron source. Many ionization potentials have been observed for these molecules which, of course, refer to the formation of the parent molecular ions in different excited states. These experimental results are discussed in terms of simple molecular orbital theories of the electronic structures of the different halogen molecules.

Electron-induced dissociative ionization processes for the different substances have also been studied. Where possible, appearance potentials of both the positive and negative ions have been determined. These results have been used to construct potential energy diagrams illustrating the origin of some of the negative ion and dissociation processes observed.

INTRODUCTION

Modern electron impact methods (1, 2, 5, 6) which use monoenergetic electron sources can provide much information concerning the excited states of molecular ions. The data so obtained are of importance in understanding the electronic structure of the molecules studied. They also can be used to provide means of assessing quantum mechanical calculations. Frequently these data are the only source of information about the energy levels and excited states of the molecular ions of quite common molecules. This is so because in many cases little or nothing is known about the spectra of the molecular ions concerned.

In this paper we present the results of a detailed study of the ionization and dissociation of some halogen molecules. We have used the retarding potential difference (R.P.D.) method to obtain essentially monoenergetic electrons. The molecules studied are chlorine, bromine, iodine, iodine monochloride, and iodine monobromide.

EXPERIMENTAL

The mass spectrometer used was that described in our earlier publications (2, 3). Krypton was used as a calibrating gas for the measurements on positive ions; its ionization potential is 112,914.5 cm^{-1} (7) or 13.997 ev. For negative ions, the appearance potential of SF_6^- from sulphur hexafluoride at 0.03 ev (9) and the appearance potentials of O^- from oxygen at 4.53 ev (4) and 17.26 ev (8) were taken as standards.

In the sections dealing with resonance capture processes allowance has been made for the electron energy distribution (see reference 10) in the quoted capture energies.

Where ICl and IBr are concerned, we present results on the parent ions only, since the dissociative ionization was complicated through large contributions to the fragment ion currents from I_2 and Cl_2 or Br_2 impurities which could not be completely eliminated. Owing to the corrosive nature of the vapors studied, it was frequently necessary to remove the ion source for cleaning to retain an electron energy bandwidth of less than 0.2 ev.

[1]*Manuscript received October 30, 1959.*
Contribution from the Department of Chemistry, University of British Columbia, Vancouver 8, B.C., Canada.

Can. J. Chem. Downloaded from www.nrcresearchpress.com by 41.223.56.140 on 09/04/12
For personal use only.

RESULTS AND DISCUSSION

(A) The Ionization of Chlorine, Bromine, and Iodine

(i) Chlorine

The electronic structure of Cl_2, Br_2, and I_2 may be represented (11) by the formula:

$$[1] \qquad \text{-----}\,(\sigma_g ns)^2(\sigma_u ns)^2(\sigma_g np)^2(\pi_u np)^4(\pi_g np)^4,\ {}^1\Sigma_g^+$$

where $n = 3$, 4, or 5 for Cl_2, Br_2, and I_2 respectively. The inner electrons are omitted and the orbitals are written in order of decreasing binding energy.

The outer $(\pi_g np)^4$ and $(\pi_u np)^4$ orbitals are mainly atomic in character, and the energies necessary to remove an electron from either of them would not be expected to be too different. The ion formed by the removal of an electron from one of these π orbitals would be expected to have the configuration $\text{-----}(\pi_u)^4(\pi_g)^3$, $^2\Pi_g$, or at a higher energy, $\text{-----}(\pi_u)^3(\pi_g)^4$, $^2\Pi_u$, and each of these $^2\Pi$ states would be a doublet ($^2\Pi_{3/2}$, $^2\Pi_{1/2}$) with an energy separation somewhat less than that existing in the relevant halogen atom ion ground state. The energy separations for the doublet ground states of the halogen atoms are 0.11 ev for Cl, 0.46 ev for Br, and about 0.7 ev for I. The actual energy difference between the $^2\Pi_u$ and $^2\Pi_g$ states will depend on the overlap between the wave functions for the $(np\pi)^4$ and $(np\pi)^3$ atomic groups. Mulliken (11) predicted that the overlap should be quite small, perhaps small enough to give the order of ionic electronic states as:

$$^2\Pi_{3/2,\,g};\ ^2\Pi_{3/2,\,u};\ ^2\Pi_{1/2,\,g};\ ^2\Pi_{1/2,\,u}.$$

We will now consider the case of chlorine. Watanabe (12), using a photoionization technique, measured the first Cl_2 ionization potential to be 11.48 ± 0.01 ev. Morrison and Nicholson (13) and Thorburn (14) found a value of 11.8 ev by electron impact. The value obtained in our work is 11.63 ± 0.04 (standard deviation) ev. It will be noted that the electron impact figures are considerably higher than Watanabe's, and this is no doubt due to a low ionization cross section at the threshold. The Cl_2^+ ground state potential energy curve will be displaced in equilibrium internuclear distance from the $Cl_2(^1\Sigma^+)$ since primary ionization involves the removal of an antibonding electron.

The only spectroscopic observations on the chlorine molecular ion Cl_2^+ have been of the high frequency emission spectrum. This consists of ultraviolet continua and red-degraded bands from 3400 to at least 5500 Å. Ota and Uchida (15) arranged these bands into three systems, and later Elliott and Cameron (16) remeasured them and were unable to accept the former workers' analysis. Elliott and Cameron in 1938 (17) further analyzed the rotational structure of 18 bands and concluded that they belonged to $^2\Pi$–$^2\Pi$ transitions with system origins at approximately 20,800 and 20,600 cm^{-1}. This placed the $^2\Pi$ states about 2.55 ev apart.

Howell (18) disagreed with Elliott and Cameron's interpretation of their analysis, and put forward strong arguments in favor of assigning the bands to transitions with a common lower state deriving from $^2\Pi$, and the upper state from separate $^2\Sigma$ type levels. It will be shown later that this most recent interpretation fits in with our new electron impact data.

In the present work, there appear to be several ionic energy levels within about 0.6 ev of the ionization threshold (Fig. 1), and it seems very probable that within this energy range the Cl_2^+ ion is being formed in its $^2\Pi_g$ and $^2\Pi_u$ electronic states, each with an expected doublet separation of about 0.1 ev. This would explain the inability of the instrument to resolve any breaks in this neighborhood. Furthermore, since the curvature extends over

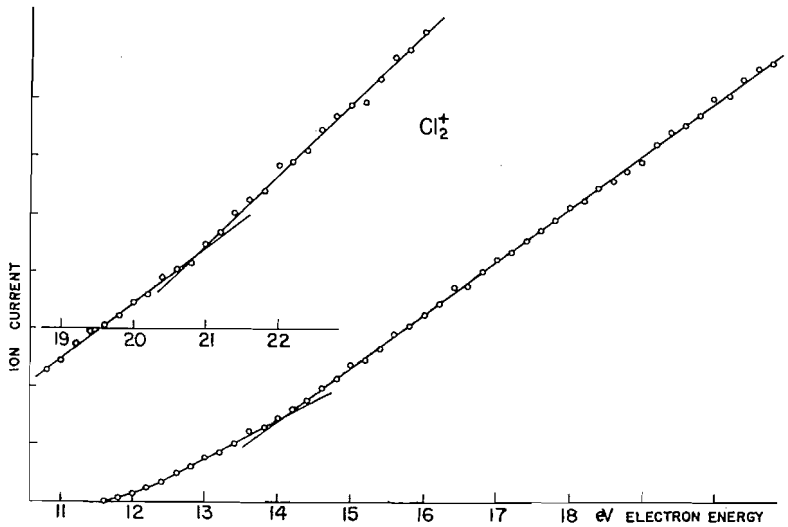


FIG. 1. The ionization efficiency curve for the formation of Cl_2^+ from chlorine by electron impact.

as great an energy as 0.6 ev, it appears probable that the $^2\Pi$ doublets do not overlap. The order of the $^2\Pi$ states would then be

$$^2\Pi_{3/2,\,g};\ ^2\Pi_{1/2,\,g};\ ^2\Pi_{3/2,\,u};\ ^2\Pi_{1/2,\,u}$$

in order of increasing energy. If the $^2\Pi_{3/2,\,u}$ did overlap the $^2\Pi_{1/2,\,g}$ level then the curvature in the ionization efficiency curve tail would be unlikely to spread over more than 0.3 or 0.4 ev.

The next inner ionization potential would be expected to refer to the removal of an electron from the strongly bonding $(\sigma_g 3p)^2$ orbital to leave the ion with the configuration;

[2] $$KKLL\ (\sigma_g 3s)^2(\sigma_u 3s)^2(\sigma_g 3p)(\pi_u 3p)^4(\pi_g 3p)^4,\ ^2\Sigma_g^+.$$

The $^2\Sigma_g^+$ ion formed by this process would therefore be expected to have a dissociation energy much less and an equilibrium internuclear distance greater than the Cl_2 molecule in the ground state.

The lowest Cl_2^+ dissociation limit, at 15.434 ev where $Cl^+(^3P)$ and $Cl(^2P)$ are the products, correlates with the molecular states Σ^+, Σ^- (2), Π (2), and Δ as doublets and quartets. These include the observed $^2\Pi_u$ and $^2\Pi_g$ and also a $^2\Sigma^+$. The next highest dissociation limit for Cl_2^+ occurs at 24.35 ev (giving at infinite separation $Cl^+(^4P) + Cl(^3P)$) and it is most unlikely that this limit is associated with the $^2\Sigma_g^+$ state of expression [2] since the corresponding ionization potential would be of the order of 22 ev. The energy required for the removal of a $Cl_2(\sigma_g 3p)$ electron would be expected to be much less than this.

It is fairly certain, then, that the Cl_2^+ ion represented by configuration [2] will have 15.434 ev as the dissociation limit; and for the following reasons it is proposed to assign the electron impact ionization potential at 14.09 ev to the process giving rise to this ion species. First, having assumed that ionization from the chlorine $(\pi_u)^4$ and $(\pi_g)^4$ orbitals takes place near the threshold, one would expect from expression [2] the first break in the curve (above the commencement of linearity) to refer to the removal of a $(\sigma_g 3p)$ electron. Secondly, Howell's (18) interpretation of the available spectroscopic data places

Can. J. Chem. Downloaded from www.nrcresearchpress.com by 41.223.56.140 on 09/04/12
For personal use only.

the $^2\Sigma_g^+$ state 2.55 ev above the $^2\Pi$, and this is in good agreement with the electron impact separation of 2.46 ev between the first ionization potential at 11.63 ev and the one at 14.09 ev. Thirdly, the vertical ionization potential at 14.09 ev infers that the ionic state has a dissociation energy of about 1 ev less than that for $Cl_2(^1\Sigma_g^+)$ (2.475 ev). This means the ionic state arises through the removal of a bonding electron. Lastly, Cl^+ fragment ions are observed to be formed at 15.51 ev (see below), this is strong evidence that at this energy vertical transitions are taking place to an upper stable state of Cl_2^+, having an internuclear distance r_e greater than that for $Cl_2(^1\Sigma_g^+)$, and to a region on the ionic potential energy curve opposite to the dissociation limit of 15.434 ev. It is fairly reasonable then to conclude that the electron impact ionization potential at 14.09 ev refers to the removal of a $(\sigma_g 3p)$ bonding electron to leave the ion with the configuration [2].

The next inner ionization potential would be expected to refer to the removal of a $(\sigma_u 3s)$ electron. This orbital is likely to have a somewhat antibonding nature, and so the energy necessary to remove an electron from it would be less than 24.46 ev, the binding energy of a Cl $3s$ electron. It seems reasonable to assign the electron impact ionization potential at 20.51 ev to a process which leaves the Cl_2^+ ion with the configuration

[3] $$KKLL\ (\sigma_g 3s)^2(\sigma_u 3s)(\sigma_g 3p)^2(\pi_u 3p)^4(\pi_g 3p)^4,\ ^2\Sigma_g^+.$$

(ii) Iodine

For iodine, five distinct processes leading to ion formation were observed, and they were found to occur at 9.35±0.03 ev, 9.97±0.02 ev, 10.91±0.04 ev, 11.72±0.04 ev, and 13.64±0.06 ev, quoted with standard deviations. Watanabe found the first ionization potential to be 9.28 ev (12).

A typical ion efficiency curve for the I_2^+ ion is shown in Fig. 2. The electronic structure of the iodine molecule may be written in a similar way to that for chlorine:

[4] $$KKLLMM(N)(N)(\sigma_g 5s)^2(\sigma_u 5s)^2(\sigma_g 5p)^2(\pi_u 5p)^4(\pi_g 5p)^4,\ ^1\Sigma_g^+.$$

The outer two π orbitals will be largely atomic iodine $5p$, and the main bonding orbital is the $(\sigma_g 5p)^2$. As with chlorine, each of the ionic states formed when an electron is removed from either of the two outer orbitals will be split into two owing to spin–orbit interaction.

The magnitude of the splitting is expected to be somewhat less than 0.7 ev. That is just what is found in our work. The first two ionization potentials at 9.35 and 9.97 ev are 0.62 ev apart, and the second two at 10.91 and 11.72 ev are 0.81 ev apart.

The ionization potentials at 9.35 and 9.97 ev therefore refer to the removal of an electron from the outer $(\pi_g 5p)^4$ orbital to form the I_2^+ ion with the electronic configuration

[5] $$\text{-----}\ (\sigma_g 5p)^2(\pi_u 5p)^4(\pi_g 5p)^3,\ ^2\Pi_{g;\ 3/2,\ 1/2}$$

and the third and fourth ionization potentials will refer to ionization from the $(\pi_u 5p)^4$ orbital to form the I_2^+ ion in the $^2\Pi_{u,\ 3/2}$ and $^2\Pi_{u,\ 1/2}$ states.

A fifth ionization potential is observed at 13.64 ev, and from the molecular orbital formula for I_2 this should be the energy necessary to ionize from the bonding $(\sigma_g 5p)^2$ orbital to leave the I_2^+ ion in the $^2\Sigma_g^+$ electronic state. It would be expected that the $(\sigma_g 5p)^2$ iodine ionization potential is less than that of the chlorine $(\sigma_g 3p)^2$, previously found to be 14.09±0.03 ev, since $D(I_2) < D(Cl_2)$. It is therefore reasonable to assume that the 13.64 ev ionization potential arises through the removal of a $(\sigma_g 5p)$ electron to leave the ionic configuration:

[6] $$\text{-----}\ (\sigma_g 5p)(\pi_u 5p)^4(\pi_g 5p)^4,\ ^2\Sigma_g^+.$$

Can. J. Chem. Downloaded from www.nrcresearchpress.com by 41.223.56.140 on 09/04/12
For personal use only.

(iii) Bromine

In the case of bromine we find that there are five distinct processes giving rise to ion formation within the energy range used. They occur at 10.69±0.03, 11.05±0.05, 11.97±0.03, 12.36±0.04, and 13.72±0.04 ev. An ion efficiency curve for the Br_2^+ ion is shown in Fig. 3.

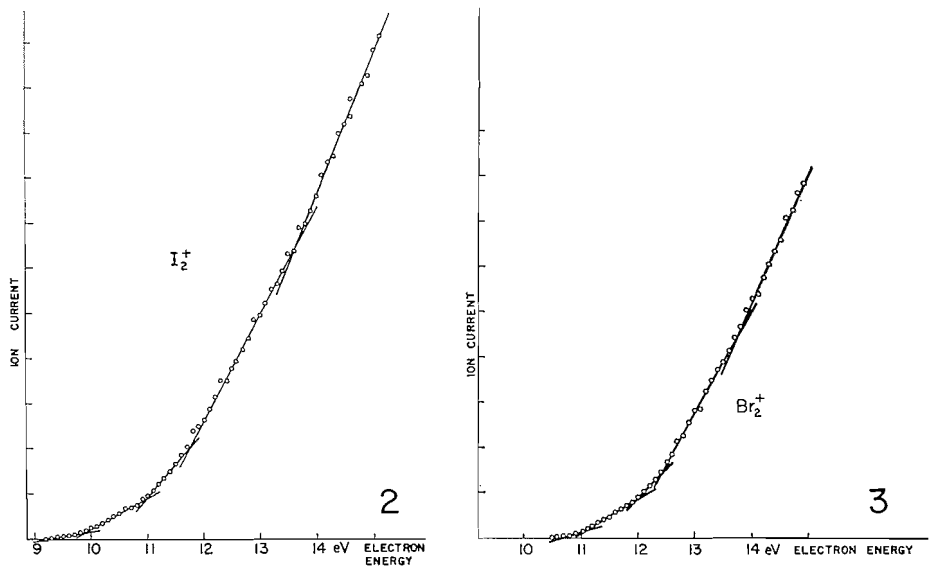


FIG. 2. The ionization efficiency curve for the formation of I_2^+ from iodine by electron impact.
FIG. 3. The ionization efficiency curve for the formation of Br_2^+ from bromine by electron impact.

Previous determinations of the first ionization potential of Br_2 have been made by Watanabe (12) (10.55 ev) and Morrison and Nicholson (13) (10.92 ev). The figure of 10.69 ev we obtain may be due to a low ionization cross section near the threshold as with chlorine.

As with iodine and chlorine, we expect four ionization potentials to lie near the ionization threshold, but here the separation of the components of each set of two is expected to be somewhat less than 0.45 ev. The first four experimental ionization potentials for bromine, quoted above, bear out this expectation. The components of each set are about 0.4 ev apart, and so we infer that at the energies of the first four processes Br_2^+ are being formed in the $^2\Pi_{g,\,3/2}$, $^2\Pi_{g,\,1/2}$, $^2\Pi_{u,\,3/2}$, and $^2\Pi_{u,\,1/2}$ electronic states. From expression [1], the next inner ionization potential would be expected to arise through the removal of one of the main bonding $(\sigma_g 4p)$ electrons. It has been shown above that similar processes in Cl_2 and I_2 require 14.09 and 13.64 ev respectively. Since $D(I_2) < D(Br_2) < D(Cl_2)$, the bromine (σ_g) ionization potential should lie between the chlorine and iodine (σ_g) values, i.e. 14.09 and 13.64 ev. The next innermost bromine ionization potential does lie between these values, at 13.72 ev, and will therefore refer to the formation of Br_2^+ with the structure

$$[7] \qquad \text{-----}(\sigma_g 4p)(\pi_u 4p)^4(\pi_g 4p)^4,\ ^2\Sigma_g^+.$$

(B) The Ionization of Iodine Monochloride and Monobromide

Figures 4 and 5 show the ion efficiency curves for ICl^+ and IBr^+ respectively, and

Can. J. Chem. Downloaded from www.nrcresearchpress.com by 41.223.56.140 on 09/04/12
For personal use only.

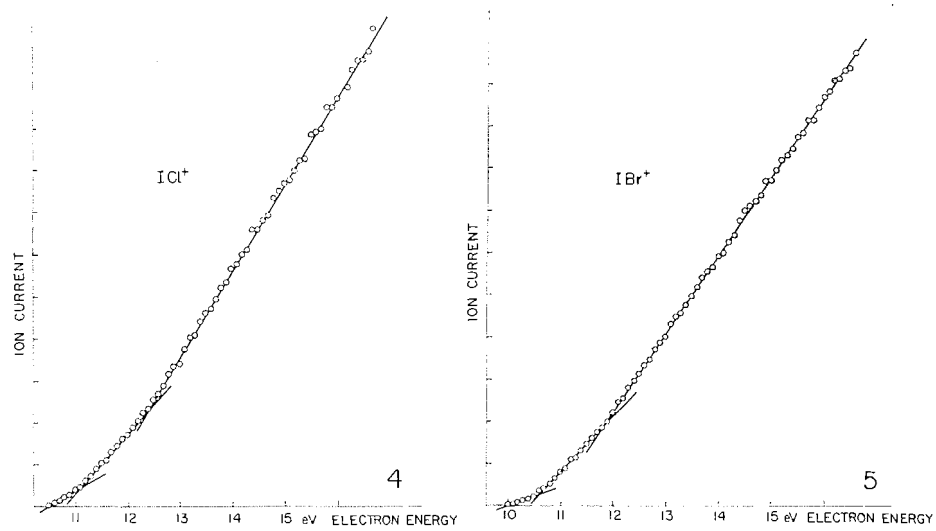


FIG. 4. The ionization efficiency curve for the formation of ICl^+ from iodine monochloride by electron impact.

FIG. 5. The ionization efficiency curve for the formation of IBr^+ from iodine monobromide by electron impact.

clearly they both exhibit three ionization processes. They occur, for ICl at 10.31 ± 0.02, 10.79 ± 0.03, and 12.13 ± 0.04 ev and for IBr at 9.98 ± 0.03, 10.49 ± 0.03, and 11.59 ± 0.05 ev.

The electronic configuration of ICl and IBr may be written, in order of decreasing binding energy (see reference 11)

[8] $$\text{-----}\,(np\sigma_X+5p\sigma_I,\,\sigma)^2(np\pi_X)^4(5p\pi_I)4,\ ^1\Sigma^+$$

where X refers to either Cl or Br. The outer two orbitals are mainly atomic X (X = Cl, or Br) and I π-type, whilst the $(\sigma+\sigma,\,\sigma)$ is mainly bonding. The first ionization potential should therefore correspond to the removal of a $(5p\pi_I)$ electron leaving the ionic structure

[9] $$\text{-----}\,(np\sigma_X+5p\sigma_I,\,\sigma)^2(np\pi_X)^4(5p\pi_I)^3,\ ^2\Pi_{3/2,\,1/2}.$$

The $^2\Pi$ states should be inverted, with a doublet separation mainly determined by the $(5p\pi_I)^3$ group and therefore similar to the spin–orbit splitting of the I^+ ground state. This splitting is about 0.7 ev, however the $^2\Pi$ splitting in ICl^+ and IBr^+ is expected to be less than this. The difference will depend on the degree of mixing of the outer (π_X) and (π_I) orbitals, and how much of the initial ionization occurs at the expense of the X atom. The evidence of this work is that for both ICl and IBr the splitting is less than the estimated value by about 0.2 ev (see Table I).

TABLE I

Electron impact ionization potentials of Cl_2, Br_2, I_2, ICl, and IBr

Proposed electronic state of ion	Ionization potentials, ev				
	Cl_2	Br_2	I_2	ICl	IBr
$^2\Pi_{g,\,3/2}$	$11.48\pm.01$	$10.69\pm.03$	$9.35\pm.03$	$10.31\pm.02$	$9.98\pm.03$
$^2\Pi_{g,\,1/2}$	~11.6	$11.05\pm.05$	$9.97\pm.02$	$10.79\pm.03$	$10.49\pm.03$
$^2\Pi_{u,\,3/2}$	~11.8	$11.97\pm.03$	$10.91\pm.04$	$12.13\pm.04$	$11.59\pm.05$
$^2\Pi_{u,\,1/2}$	~11.9	$12.36\pm.04$	$11.72\pm.04$	~12.2	~11.7
$^2\Sigma_g^+$	$14.09\pm.03$	$13.72\pm.04$	$13.64\pm.06$	—	—
$^2\Sigma_u^+$	$20.61\pm.06$	—	—	—	—

Can. J. Chem. Downloaded from www.nrcresearchpress.com by 41.223.56.140 on 09/04/12
For personal use only.

Can. J. Chem. Downloaded from www.nrcresearchpress.com by 41.223.56.140 on 09/04/12
For personal use only.

The first ionization potential of iodine monochloride is found to be 10.31 ev, and the second at 10.79 ev. Since these are 0.48 ev apart, i.e. less than 0.7 ev, we can reasonably assume that they refer to the formation of ICl^+ in the $^2\Pi_{3/2}$ and $^2\Pi_{1/2}$ states respectively.

Similar processes would seem to be responsible for the first two IBr ionization potentials we observe at 9.98 and 10.49 ev. The splitting here is 0.51 ev. We observe one additional increase in ion efficiency for each species, at 12.13 ev for ICl and at 11.59 ev for IBr. From expression [8] we would expect these ionization potentials to refer to the removal of, in each case, an $(np\pi_X)$ electron to leave the electronic configuration

[10] $$\text{-----}\ (np\sigma_X+5p\sigma_I,\ \sigma)^2(np\pi_X)^3(5p\pi_I)^4,\ ^2\Pi_{3/2,\ 1/2}.$$

The $^2\Pi$ splitting is expected to be 0.08 ev for ICl or 0.35 ev for IBr. It is clear, however, from Figs. 4 and 5 that we have been unable to resolve these doublets.

No further breaks are observed in the ion efficiency curves up to an electron energy of 18 ev, which infers that the cross sections for formation of ICl^+ and IBr^+ in their $^2\Sigma^+$ states through ionization from the σ bond are too small to be detected here. Probably the ion with the structure $\text{-----}\ (\sigma+\sigma,\ \sigma)(\pi)^4(\pi)^4$ immediately dissociates.

(C) The Dissociative Ionization of Chlorine, Bromine, and Iodine

(i) Chlorine

The Cl^- resonance capture peak is observed to have an onset energy of 1.60 ± 0.05 ev, a peak maximum at 2.4 ± 0.1 ev, and an over-all width of 1.6 ± 0.2 ev. It is most probable that the Cl^- ions are being produced by transitions to a repulsive Cl_2^- state, of dissociation limit equal to $D(Cl_2)-EA(Cl)$, or -1.055 ev with respect to the Cl_2 ground state. The process occurring is clearly

[11] $$Cl_2+e \rightarrow Cl^-+Cl+K+E$$

where K and E are respectively the total kinetic and excitation energies of the fragments.

The potential energy diagram illustrating the formation of Cl^- by process [11] is sketched in Fig. 7, and a typical Cl^- capture peak with a SF_6^- calibration peak is shown in Fig. 6.

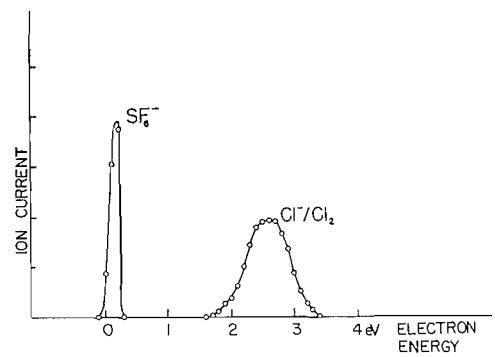


FIG. 6. The resonance capture peak for the formation of Cl^- from chlorine by electron impact.

Figure 8 shows the ion efficiency curve for Cl^+ from Cl_2. There are clearly only two processes here, and their onset energies are 11.86 ± 0.04 ev and 15.51 ± 0.03 ev. The former is identified with an ion pair process since Cl^- is observed to appear at the similar energy of 11.93 ± 0.06 ev (Fig. 9).

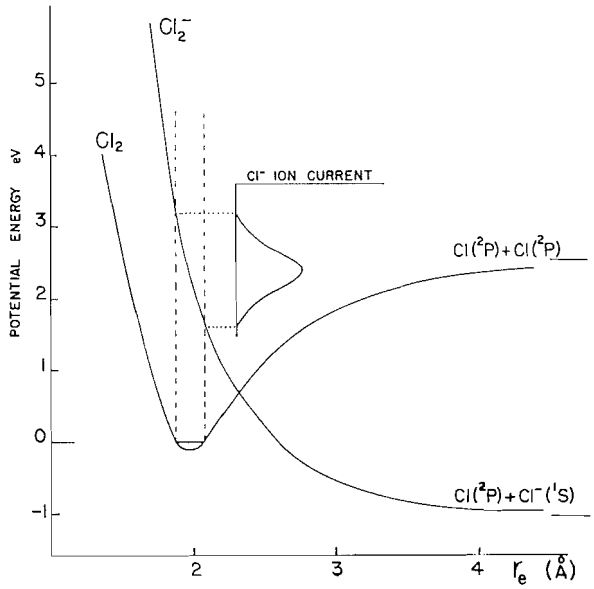


FIG. 7. Potential energy diagram to illustrate the formation of Cl^- from chlorine by a resonance capture process.

The lowest dissociation limit involving a Cl^+ and Cl^- ion pair is at 11.96 ev, assuming $EA(Cl) = 3.53$ ev (19), $D(Cl_2) = 2.48$ ev (20), and $I(Cl) = 13.01$ ev (21). The observed appearance potentials are very close to this limit, and so it is most probable that transitions are occurring from $Cl_2(^1\Sigma_g^+)$ to a stable excited state of Cl_2 having its dissociation limit at 11.96 ev.

The only other Cl^+ appearance potential detected below 23 ev is at 15.51 ev, and this clearly refers to vertical transitions from $Cl_2(^1\Sigma_g^+)$ to $Cl_2^+(^2\Sigma_g^+)$. Transitions to the ionic state will be likely to occur near the energy of the dissociation limit since the internuclear distance, r_e, for the $^2\Sigma_g^+$ is expected to be appreciably greater than r_e for the Cl_2 ground state.

These results on Cl^+ and Cl^- are in good agreement with Thorburn's (14) except that we do not detect the process producing Cl^- ions which he observed to occur at 4.4 ev.

(ii) Bromine

At low electron energies Br^- is observed to be formed with maximum probability at 0.03 ± 0.03 ev, and the ion current rapidly decreases to zero at 0.72 ± 0.05 ev. The process occurring is obviously

$$[12] \qquad Br_2+e \rightarrow Br^-+Br+K+E.$$

Assuming the fragments to be formed in their ground states, Fig. 10 shows the form of the potential energy curves involved here. The Br^- and SF_6^- resonance capture peaks are shown in Fig. 11.

Figure 12 shows an ion efficiency curve for Br^+ formation from Br_2. Several of the breaks are shallow, but repeated observations indicate that processes occur at energies of 10.38 ± 0.05, 12.30 ± 0.06, 14.31 ± 0.03, 15.88 ± 0.04, 17.06 ± 0.04, 17.97 ± 0.06, and 19.98 ± 0.06 ev.

Figure 13 concerns Br^- formation through processes other than resonance capture.

Can. J. Chem. Downloaded from www.nrcresearchpress.com by 41.223.56.140 on 09/04/12
For personal use only.

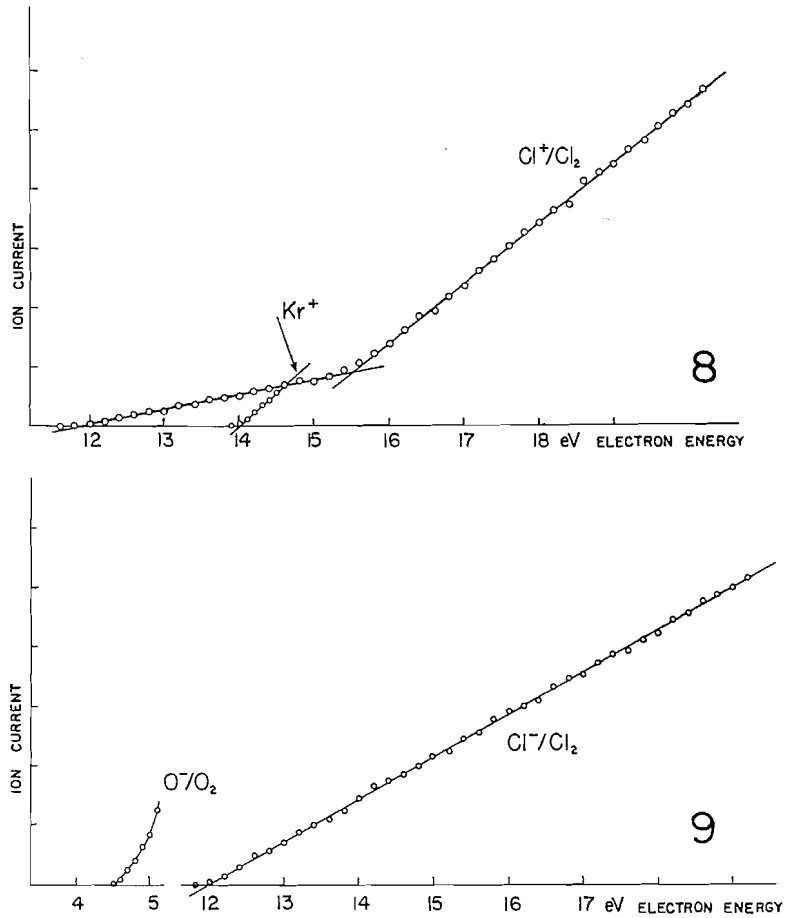


FIG. 8. The ionization efficiency curve for the formation of Cl^+ from chlorine by electron impact.
FIG. 9. The ionization efficiency curve for the formation of Cl^- from chlorine by an ion pair process as the result of electron impact.

There are two, and they occur at 10.34±0.04 and 12.27±0.05 ev. The first two appearance potentials for Br^- agree closely with the first two for Br^+, and so it is probable that these result from ion pair processes:

$$[13] \qquad Br_2 + e \rightarrow Br^+ + Br^- + K + E + e.$$

The average observed Br^+ and Br^- appearance potentials are 10.36 and 12.28 ev. Assuming $EA(Br) = 3.49$ ev (21), $D(Br_2) = 1.97$ ev (20), and $I(Br) = 11.80$ ev (21), the energy necessary to form Br^+ and Br^- in their ground states from $Br_2(^1\Sigma^+)$ is 10.28 ev. The ion pair process at 10.36 ev would therefore seem to be occurring through transitions to the potential curve of an excited Br_2 state at points opposite to the dissociation limit to give $Br^+(^2P_{3/2}) + Br^-(^1S)$. A repulsive Br_2 excited state is unlikely to be involved here as the observed appearance potential is very close to the dissociation limit energy.

The first excited state of the Br atom is the $^2P_{1/2}$ state, 0.457 ev above the ground $^2P_{3/2}$ state, and there is the possibility of a dissociation limit 10.74 ev above the ground $Br_2(^1\Sigma^+)$ state. The second ion pair process at 12.28 ev could therefore be occurring

Can. J. Chem. Downloaded from www.nrcresearchpress.com by 41.223.56.140 on 09/04/12
For personal use only.

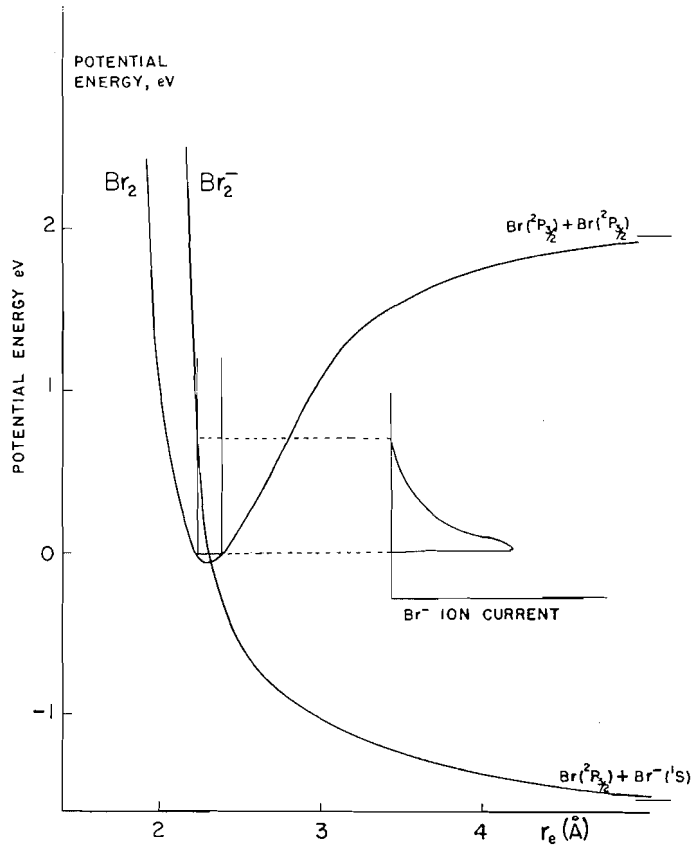


FIG. 10. Potential energy diagram to illustrate the formation of Br^- from bromine by a resonance capture process.

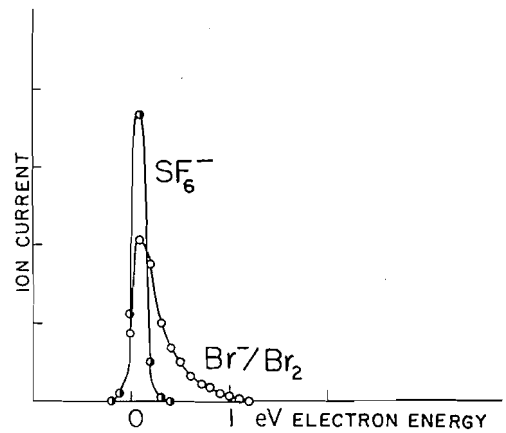
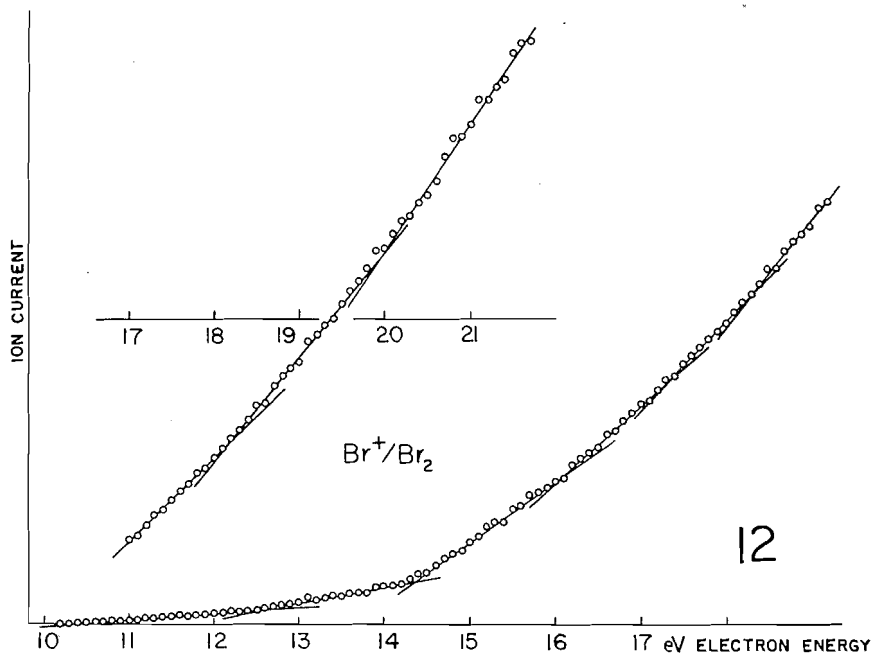


FIG. 11. The resonance capture peak for the formation of Br^- from bromine by electron impact.

through transitions to an excited unstable Br_2 state having a dissociation limit at 10.28 ev or at 10.74 ev. No further breaks in the Br^- ion efficiency curve were observed up to 18 ev.

The Br^+ ion is next formed at 14.31 ev, and from Fig. 12 it is evident that this process is easily the most important for Br^+ production. There are dissociation limits for Br_2^+ at

Can. J. Chem. Downloaded from www.nrcresearchpress.com by 41.223.56.140 on 09/04/12
For personal use only.



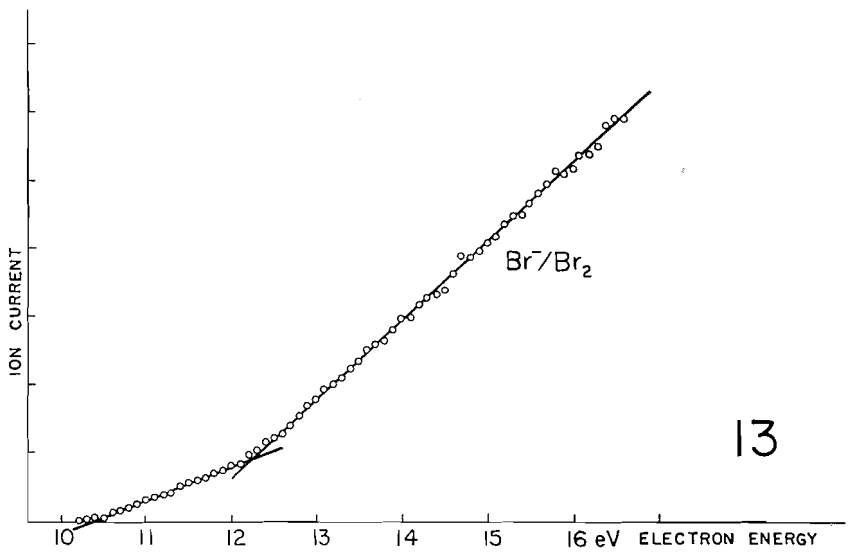


FIG. 12. The ionization efficiency curve for the formation of Br^+ from bromine by electron impact.
FIG. 13. The ionization efficiency curve for the formation of Br^- from bromine by ion pair processes as the result of electron impact.

13.77 and 14.23 ev, and we have observed a stable state (probably $^2\Sigma^+$) of Br_2^+ at 13.72 ev which probably dissociates into normal fragments at 13.77 ev. The $^2\Sigma^+$ state could, however, dissociate to $Br^+(^5S)+Br(^2P_{1/2})$ at 14.23 ev, and if this is so then the Br^+ ion group at 14.31 ev could be formed by transitions to the $^2\Sigma_g^+$ state just above the dissociation limit—a possibility since the internuclear distance, r_e, for this state is likely to be appreciably greater than that for $Br_2(^1\Sigma_g^+)$. Otherwise, the Br^+ ion formation here must result from transitions to a repulsive Br_2^+ state associated with the 13.77 ev dissociation limit.

Can. J. Chem. Downloaded from www.nrcresearchpress.com by 41.223.56.140 on 09/04/12
For personal use only.

Br^+ ions are next observed to appear at 15.88 ev, and must be formed through transitions to a repulsive Br_2^+ state associated with the fragments $Br^+(^5S)+Br(^2P_{3/2})$ or $+Br(^2P_{1/2})$ mentioned above, or with a $Br(^2P)+Br^+(^5D)$ limit a few hundredths of a volt above the $Br^+(^5S)$ one.

At 17.06, 17.97, and 19.98 ev Br^+ ions are formed, and it is possible to write down the many possible processes in each case. However, little is to be gained by this since the kinetic energy with which the fragments are endowed upon formation is unknown and therefore it is not possible to make other than tentative suggestions regarding the processes occurring.

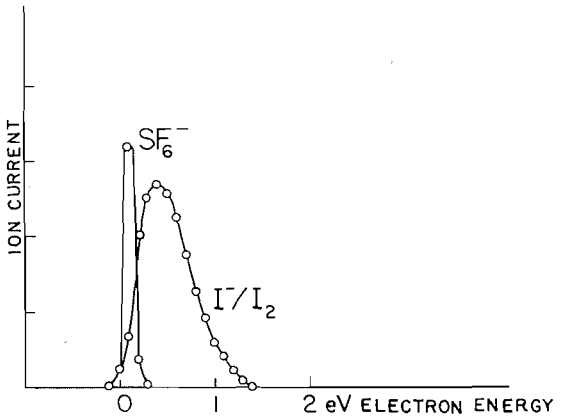


FIG. 14. The resonance capture peak for the formation of I^- from iodine by electron impact.

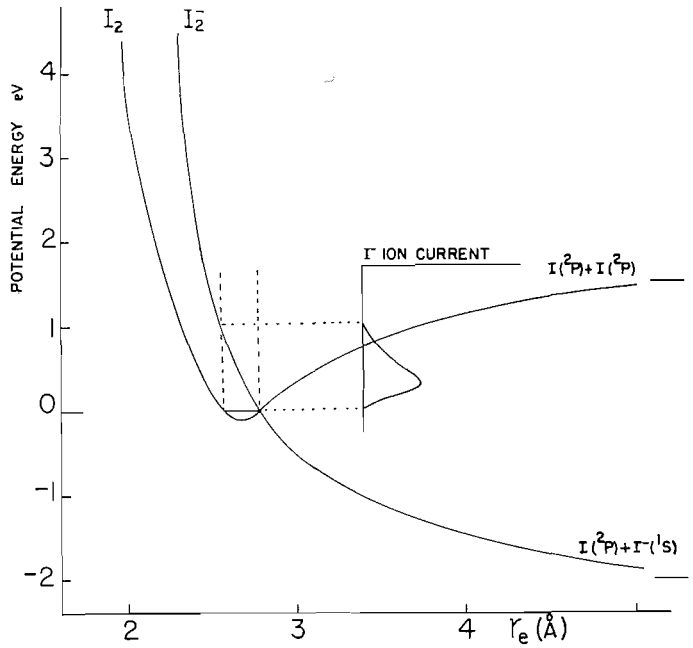


FIG. 15. Potential energy diagram to illustrate the formation of I^- from iodine by a resonance capture process.

Can. J. Chem. Downloaded from www.nrcresearchpress.com by 41.223.56.140 on 09/04/12
For personal use only.

(iii) Iodine

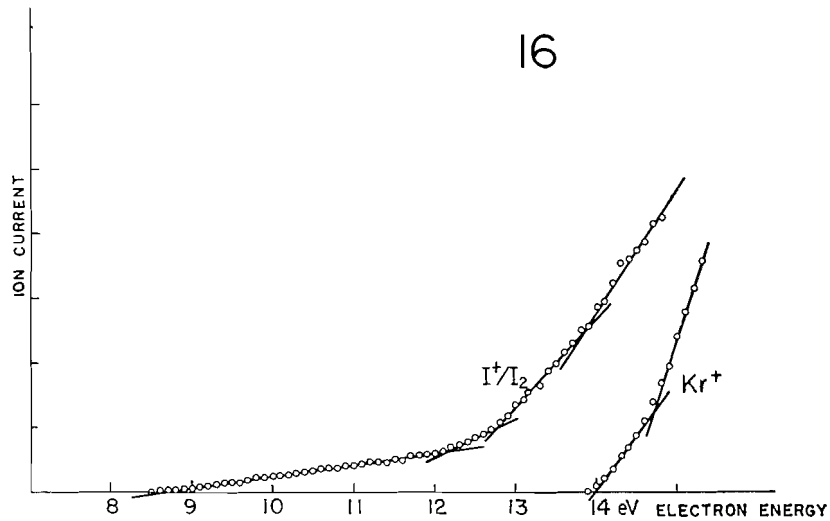
We find the I^- resonance capture process onset energy to be 0.03 ± 0.03 ev, the upper energy limit to be 1.08 ± 0.04 ev, and the energy for maximum capture cross section to be 0.34 ± 0.07 ev. A typical I^- capture peak, with the one for SF_6^-, is shown in Fig. 14.

The process responsible for I^- formation here will be

$$I_2+e \rightarrow I^-+I+K+E \qquad [14]$$

and is illustrated in Fig. 15 where the relevant potential curves are sketched. We have described the formation of I^- from I_2 by resonance capture in more detail elsewhere (10).

Figure 16 shows the ion efficiency curve for I^+ from I_2 at electron energies between 8 and 17 ev. There are clearly four different processes possible for I^+ formation that have been resolved, and these are found to occur at 8.62 ± 0.06, 12.02 ± 0.04, 12.72 ± 0.04, and



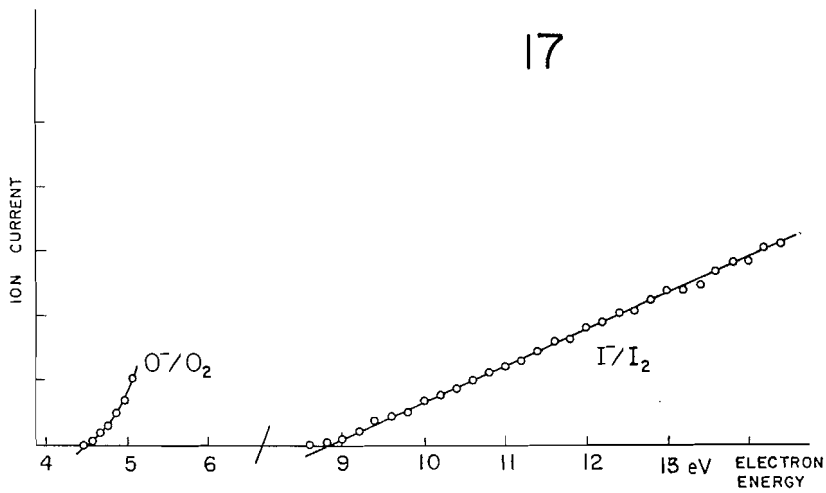


FIG. 16. The ionization efficiency curve for the formation of I^+ from iodine by electron impact.
FIG. 17. The ionization efficiency curve for the formation of I^- from iodine by ion pair processes as the result of electron impact.

Can. J. Chem. Downloaded from www.nrcresearchpress.com by 41.223.56.140 on 09/04/12
For personal use only.

13.71 ± 0.06 ev. A typical ion efficiency curve for I^- is shown in Fig. 17, and there is evidence for only one process—found to occur at 8.68 ± 0.07 ev.

The first appearance potentials for I^+ and I^- are very close together and we assume that the ion pair process

$$[15] \qquad I_2 + e \rightarrow I^+(^3P_2) + I^-(^1S) + K + E + e$$

is responsible for their formation. Assuming no kinetic energy to be involved the minimum appearance potential for the pair would be 8.84 ev, since $EA(I) = 3.14$ ev (22), $I(I) = 10.44$ ev (21), and $D(I_2) = 1.542$ ev (20).

The excited I_2 upper state involved here must be stable because if it were not then the I^+ and I^- appearance potentials would be expected to considerably exceed the minimum energy required for their formation.

The second I^+ appearance potential occurs at 12.02 ev, and the upper state involved is almost certainly the $I_2^+(^2\Pi_u)$—of r_e greater than r_e of $I_2(^1\Sigma_g^+)$ and shown above to have components at 10.91 and 11.72 ev above the $I_2(^1\Sigma_g^+)$. This $^2\Pi_u$ state should dissociate to normal $I^+(^3P_2) + I(^2P_{3/2})$ at 11.98 ev.

I^+ ions are next formed at 12.72 ev, probably through transitions to a repulsive I_2^+ state associated with the dissociation limit just mentioned at 11.98 ev.

At 13.71 ev a further process giving rise to I^+ ions occurs, and it is probable that the $I_2^+(^2\Sigma_g^+)$ state is concerned here. We have deduced this state to lie 13.64 ev above the I_2 ground state, and it is likely to have an internuclear distance r_e much greater than r_e of the $I_2(^1\Sigma_g^+)$ since it arises through the removal of a strongly bonding σ electron. The I_2^+ ion in the $^2\Sigma_g^+$ state will therefore have a much lower dissociation energy than $I_2(^1\Sigma_g^+)$, and could dissociate to $I^+(^1D_2) + I(^2P_{3/2})$ at 13.68 ev. In this case, vertical transitions to $I_2^+(^2\Sigma_g^+)$ would be expected to produce not only I_2^+ but also I^+ ions, and this process is suggested to account for the I^+ observed to occur at 13.71 ev.

This work was supported in part by the Geophysical Research Directorate of the United States Air Force Cambridge Research Centre, Air Research and Development Command, under Contract No. AF19-(604)-2275, and by grants from the National Research Council of Canada.

REFERENCES

1. R. E. Fox, W. M. Hickam, T. Kjeldaas, Jr., and D. J. Grove. Phys. Rev. **84**, 859 (1951).
2. D. C. Frost and C. A. McDowell. Proc. Roy. Soc. A, **232**, 227 (1955).
3. D. C. Frost and C. A. McDowell. Proc. Roy. Soc. A, **236**, 278 (1956).
4. D. C. Frost and C. A. McDowell. J. Am. Chem. Soc. **80**, 6183 (1958).
5. D. C. Frost and C. A. McDowell. J. Chem. Phys. **29**, 503 (1958).
6. D. C. Frost and C. A. McDowell. Can. J. Chem. **36**, 39 (1958).
7. R. F. Becker and S. Goudsmit. Atomic energy states. McGraw-Hill Book Co., Inc., New York.
8. L. M. Branscomb. J. Chem. Phys. **29**, 452 (1958).
9. W. M. Hickam and R. E. Fox. J. Chem. Phys. **25**, 642 (1956).
10. D. C. Frost and C. A. McDowell. J. Chem. Phys. **29**, 964 (1958).
11. R. S. Mulliken. Phys. Rev. **46**, 549 (1934).
12. K. Watanabe. J. Chem. Phys. **26**, 542 (1957).
13. J. D. Morrison and A. J. Nicholson. J. Chem. Phys. **20**, 1021 (1952).
14. R. Thorburn. Proc. Phys. Soc. **123**, 122 (1959).
15. Y. Ota and Y. Uchida. Japan. J. Phys. **5**, 53 (1928).
16. A. Elliott and W. H. B. Cameron. Proc. Roy. Soc. A, **158**, 681 (1937).
17. A. Elliott and W. H. B. Cameron. Proc. Roy. Soc. A, **164**, 531 (1938).
18. H. G. Howell. Proc. Phys. Soc. A, **66**, 759 (1953).
19. H. O. Pritchard and H. A. Skinner. Chem. Revs. **55**, 745 (1955).
20. G. Herzberg. Spectra of diatomic molecules. D. Van Nostrand Co., Inc., New York. 1950.
21. G. Herzberg. Atomic spectra and atomic structure. Dover Publications, New York. 1944.
22. P. P. Sutton and J. E. Meyer. J. Chem. Phys. **3**, 20 (1935).

Can. J. Chem. Downloaded from www.nrcresearchpress.com by 41.223.56.140 on 09/04/12
For personal use only.

Can. J. Chem. Downloaded from www.nrcresearchpress.com by 41.223.56.140 on 09/04/12
For personal use only.

ABSOLUTE THERMAL NEUTRON FISSION YIELDS OF U^{233} [1]

D. C. SANTRY[2] AND L. YAFFE

ABSTRACT

The absolute fission yields of 22 nuclides formed in the thermal neutron fission of U^{233} have been measured radiochemically. Disintegration rates were measured by 4π β-proportional counting techniques. The identity of each nuclide was established by chemical separations and decay characteristics as determined by 4π β-counting and γ-ray scintillation spectrometry. The reaction $Co^{59}(n,\gamma)Co^{60}$ was used as a neutron flux monitor. Yields were calculated on the basis of $\sigma_f^{U^{233}}/\sigma_c^{Co^{59}} = 524/36.3$.

INTRODUCTION

Although the thermal neutron fission yields for U^{235} have been investigated extensively, yields reported for the fission products of U^{233} are few and inconsistent. Relative radiochemical yields for U^{233} fission have been measured by Grummitt and Wilkinson (1), and Steinberg *et al.* (2, 3). The yields given by the latter groups were determined relative to their absolute yield value of 6.0% for Ba^{140} which had been measured by direct fission counting (2). The uncertainty in the application of correction factors to observed counting rates of fission products in order to obtain disintegration rates accounted for most of the large errors (10% to 20%) associated with radiochemical yields.

In applying the mass-spectrometric method to isotope abundance measurements of U^{233} fission products, Steinberg *et al.* (4), Fleming *et al.* (5), and Melaika *et al.* (6) were able to measure relative yields believed reliable to 3% to 5%. These relative yields were often normalized with the aid of radiochemical yields (7, 8). Such mass-spectrometric data were then no more accurate on an absolute basis than the yields to which they were normalized.

Isotope dilution techniques have more recently been used in mass spectrometry by Anikina *et al.* (9), Kukavadze *et al.* (10), and Ivanov *et al.* (11) to measure the absolute yields of some stable and long-lived fission products in U^{233} fission. These investigators determined the number of fission events which occurred by measuring the depletion of U^{233} in a heavily irradiated sample. The errors associated with these measurements range from 2% to 15%.

Thus all fission yields for the thermal neutron fission of U^{233} previously measured possess rather large experimental errors. Such errors obscure the presence or absence of fine structure in the fission product, mass distribution curve.

The purpose of this work was to establish, radiochemically, accurate yields for various nuclides along the yield–mass curve. It was felt that by using 4π β-counting techniques, and by determining absolute rather than relative yields, the errors associated with radiochemical yields could be greatly reduced.

The $Co^{59}(n,\gamma)Co^{60}$ reaction was used to measure the neutron flux. Absolute yields could then be expressed in terms of the known values for the thermal neutron capture and fission cross sections for Co^{59} and U^{233} respectively.

It can be shown that, if U_0 atoms of U^{233} were irradiated in a thermal flux I of a nuclear

[1]*Manuscript received in original form April 27, 1959, and, as revised, December 9, 1959.*
Contribution from the Radiochemistry Laboratory, Department of Chemistry, McGill University, Montreal, Que., with financial assistance from the National Research Council of Canada, Atomic Energy Control Board, and the Defence Research Board.
[2]*Holder of a National Research Council Studentship, 1956–57. Present address: Chemistry Branch, Atomic Energy of Canada Limited, Chalk River, Ontario.*

reactor for a time T, then at some time t, after removal from the reactor, the following equation would apply:

$$[1] \qquad N\lambda = U_0 I\sigma_f Y_f(1-e^{-\lambda T})e^{-\lambda t}.$$

In the above equation λ is the disintegration constant of the fission product being studied and N is the number of atoms of that nuclide present at time t. Thus $N\lambda$ is the disintegration rate. The fission cross section of U^{233} is represented by σ_f, and Y_f is the probability of formation, or the fission yield of the nuclide under study.

If some cobalt were irradiated simultaneously with and under the same conditions as the U^{233}, then the following equation would obtain:

$$[2] \qquad N_1\lambda_1 = N_{Co} I\sigma_c(1-e^{-\lambda_1 T})e^{-\lambda_1 t}.$$

As before, $N_1\lambda_1$ would be the disintegration rate of Co^{60}, N_{Co} the number of cobalt atoms placed in the reactor, and σ_c the thermal neutron cross section for the reaction $Co^{59}(n,\gamma)Co^{60}$.

If equations [1] and [2] are now divided, the term I cancels, all other quantities are easily measurable, and Y_f, the fission yield, can be determined in terms of σ_f/σ_c.

EXPERIMENTAL AND RESULTS

(a) Irradiation

Accurately weighed amounts (2.30 to 6.18 mg) of uranium oxide (U_3O_8) were sealed into thin quartz tubes. Isotopic analysis of the uranium used indicated 97.746% U^{233},* the remainder being U^{238}. A spectrographic analysis showed that the level of impurities was too low to form any of the fission products by (n,γ) reactions. Into similar tubes were sealed weighed amounts (1.00 to 1.50 mg) of "spec-pure" cobalt wire (0.005-in. diameter). The tubes containing the fissile uranium and the cobalt wire were irradiated together in a "self-serve" position of the NRX reactor at Chalk River for a period of 24 hours. The position chosen was one where the neutron spectrum was predominantly thermal.

(b) Disintegration Rate Determinations

All disintegration rates were determined with good precision, using the 4π β-counters described by Pate and Yaffe (12–16). Sources were deposited on calibrated gold-plated VYNS films (10–19 $\mu g/cm^2$). Pretreatment of the films with a 5% insulin solution ensured an even deposition of the source over a known area. Sources were dried under infrared radiation.

Corrections for loss of the radiation in the exceedingly thin source-mount were obtained from the data of Pate and Yaffe (14) and were very small. Self-absorption losses were determined by combining the results of Pate and Yaffe (15) with those of Fishman and Yaffe (17) into a plot of self-absorption as a function of β-end-point energy and source thickness. The sources were all of high specific activity, so that the correction factors were usually small and accurately known.

(c) Treatment of Flux Monitor

The irradiated cobalt wire was removed from its quartz capsule, dissolved in nitric acid, and made up to a known volume. The fraction of Co^{60} activity lost by recoil into the quartz vial was measured on a γ-ray scintillation counter and found to be 0.31%.

Aliquots of the master solution were removed for disintegration rate determination.

*We wish to acknowledge with thanks the fact that this material was obtained on loan from A.E.C.L., Chalk River, Ontario.

Can. J. Chem. Downloaded from www.nrcresearchpress.com by 41.223.56.140 on 09/04/12
For personal use only.

The source superficial density was always less than 10 $\mu g/cm^2$. The self-absorption correction was 0.6% while that for source-mount absorption was 0.1%.

The neutron attenuation in the sample was calculated, using the formula

$$I = I_0 e^{-N\sigma\rho d/A}$$

where I and I_0 are the final and initial fluxes, N is Avogadro's number, σ is the total cross section of the sample for neutrons, ρ is the density of the sample, A the atomic weight, and d the thickness.

The attenuation factor was found to be 0.979* for a wire of 0.0064-cm radius.

The cobalt thermal neutron capture cross section and the half-life used were 36.3 barns (18, 19) and 5.24 years (20) respectively.

The epi-thermal contribution in the irradiation position used was determined by shielding the cobalt wire during one irradiation with $\frac{1}{2}$-mm cadmium. The epi-cadmium contribution was determined to be 1.76%.

(d) Treatment of U^{233}

The fissile sample was dissolved by crushing the irradiated vial under a warm nitric acid solution. To reduce the loss of activities by adsorption effects, 1 mg each of appropriate inactive ions (Cs^+, Ba^{++}, La^{+++}, and I^-) had been added to the nitric acid solution as "carriers". The dissolved uranium and fission products were transferred to a volumetric flask. The finely crushed remains of the vial were washed several times with small portions of nitric acid to recover fission products imbedded in the quartz. Measured aliquots of the fission product stock solution were removed and added to known amounts (10 to 20 mg) of inactive carriers of the elements to be separated. Standard methods (21, 22, 23) were used for the separation of fission product elements. In many cases slight modifications to reported procedures were used to ensure radiochemical purity. After decontamination, the element of interest was precipitated in a suitable chemical form, dissolved, and made up to a known volume. Aliquots of the solution were removed periodically for activity measurements and later for the determination of chemical recovery, using standard analytical techniques.

After the chemical separation, the radiochemical purity and identity of each nuclide was confirmed by the presence or absence of γ-radiation. A sodium iodide crystal spectrometer was used to measure gamma energies and half-lives.

The very high stability of the 4π β-counting equipment enabled the accurate measurement of both half-lives and disintegration rates.

The amount of Ba^{140} and Sr^{89} formed in cadmium-covered and -uncovered samples, irradiated under otherwise identical conditions, was measured. The epi-cadmium contribution was found to be 2.10%.

The neutron attenuation in the uranium oxide was calculated for all samples. The values ranged from 0.975 for the heaviest sample to 0.997 for the lightest.

Data given for the various nuclides include the half-life and other factors involving time. This was done so that corrections could be made later by others should more accurate nuclear constants be obtained.

(e) Individual Elements

(1) Bromine

The method of Glendenin *et al.* (24) was used to separate bromine. The activity of the

**This is in excellent agreement with that determined experimentally by Dr. R. E. Jervis, A.E.C.L., Chalk River, and we are grateful to him for making available to us the results of his determination.*

Can. J. Chem. Downloaded from www.nrcresearchpress.com by 41.223.56.140 on 09/04/12
For personal use only.

sample was measured for 100 hours and showed a pure 34.5-hour half-life corresponding to Br^{82}. Since the extraction was carried out 40 hours after the end of the irradiation, one would not expect to find any 2.3-hour Br^{83}.

Br^{82} is a shielded nuclide produced only by direct formation, so that measurement of its fission yield constitutes an independent yield determination. The relevant data are given in Table I.

TABLE I

Fission yield data for 36-hour Br^{82}

Time in reactor	24 hours
Time after irradiation	40.6 hours
Activity at saturation	1.694×10^{5} disintegrations/sec
Fission rate	2.270×10^{10} fissions/sec
Fission yield	$(7.46\pm0.17)\times10^{-4}\%$

(2) Strontium

A slight modification to the method of Glendenin (25) was used for this separation. Strontium and barium carriers were added and precipitated with fuming nitric acid. Further purifications were effected by scavenging with ferric hydroxide. Barium was removed by a chromate precipitation in a buffered solution. Strontium was precipitated as the oxalate, dissolved in nitric acid, and reprecipitated with fuming nitric. The nitrate precipitate was washed with ethanol before being dissolved in water and made up to volume.

Isotopes of strontium likely to be detected in this work are Sr^{89}, Sr^{90}, and Sr^{91}.

Each strontium separation showed the presence of a 50.0- to 50.5-day activity corresponding to Sr^{89} and a long-lived component. One separation performed shortly after the end of the irradiation exhibited the 9.7-hour Sr^{91} activity in addition to these. No γ-photopeaks were observed on the scintillation spectrometer except when the 9.7-hour activity was present. A plot of γ-counting rate vs. time showed that the 750- and 1020-kev peaks decayed with a 9.7-hour half-life. The initial growth and decay of the 550-kev peak indicated the formation of the 51-minute Y^{91m} daughter of Sr^{91}. The apparent purity of the sample was indicated by the absence of other γ-rays and the consistent half-lives obtained from the β- and γ-ray measurements allowed the assignment of the long-lived component to Sr^{90} (27.7 years).

When in equilibrium, the disintegration rates of Sr^{90} and Y^{90} are equal. Therefore one-half of the observed residual counting rate, after applying absorption corrections, could be attributed to the Sr^{90}. On this basis, the fission yield of Sr^{90} was calculated. As a further check on this yield, a separated strontium sample was allowed to decay and the yttrium which formed was separated and counted. The fission yield of Sr^{90}, calculated in this way from the Y^{90} daughter, agreed well with that in which the Sr^{90} was counted directly.

The counting rate of 50-day Sr^{89} was determined in the usual way by subtracting the amount of long-lived activity observed.

It is not possible to obtain the amount of Sr^{91} activity by direct analysis of the gross decay curve owing to the formation of Y^{91}. However, from the following considerations, it is possible to determine the amount of Sr^{89} and Sr^{91} present. At the end of the strontium separation there is no yttrium, therefore the total observed activity (N_T^0) is

$$N_T^0 = Sr^{89^0}+Sr^{91^0}+Sr^{90}.$$

Can. J. Chem. Downloaded from www.nrcresearchpress.com by 41.223.56.140 on 09/04/12
For personal use only.

At a time later when the Sr^{91} has completely decayed to form Y^{91}, the total observed counting rate (N_T^1) is

$$N_T^1 = Sr^{89^0}\exp(-\lambda_1 T)+\frac{\lambda_3}{\lambda_2-\lambda_3}Sr^{91^0}\exp(-\lambda_3 t)+(Sr^{90}+Y^{90^1})$$

where λ_1, λ_2, and λ_3 are the decay constants for Sr^{89}, Sr^{91}, and Y^{91} respectively, and t is the time from the end of separation until the time when N_T^1 is measured. Since N_T^0, N_T^1, $(Sr^{90}+Y^{90^1})$ can be measured, it is possible to solve for Sr^{89^0} and Sr^{91^0}. Since the decay of Sr^{91} involves delayed γ-emission, i.e. γ-emission from the Y^{91m} state, it is necessary to know the efficiency of the counting unit for the detection of Y^{91m} disintegrations. The important factors involved are: (*i*) the γ-detection efficiency, (*ii*) the amount of internal conversion, and (*iii*) the efficiency for detection of internal conversion electrons. By means of growth and decay equations and starting with pure Sr^{91}, the relative counting rates for Sr^{91}, Y^{91}, and Y^{91m} were calculated for various decay times. The calculated rates were then compared to the observed relative counting rates at the same decay times. The observed relative counting rates were obtained by dividing the observed counting rate at time t by the counting rate obtained by extrapolating the initial portion of the strontium decay curve to the time at which the separation had ended. This extrapolation procedure is justified if counting had begun soon after the separation, before Y^{91m} reached equilibrium with Sr^{91}. The observed relative counting rate agreed very well with that calculated for Sr^{91} plus Y^{91}, indicating that the efficiency for counting Y^{91m} in the 4π-proportional counter is very low.

The relevant data for the fission yields of the strontium isotopes are given in Tables II, III, and IV.

TABLE II

Fission yield data for 50.4-day Sr^{89}

Irradiation No.	A 1	A 2	B 1	C 1	D_a 1	D_a 2	D_b 1	D_b 2	E	F
Time in reactor (hours)	24	24	24	24	18.5	18.5	18.5	18.5	23.83	24.17
Time after irradiation (days)	17.35	29.10	9.90	3.75	15.44	95.44	73.25	115.41	27.0	1.5
Activity at saturation (d/s)	6.279×10^8	6.010×10^8	1.199×10^9	1.637×10^9	7.936×10^9	7.904×10^8	4.079×10^8	4.091×10^8	1.295×10^7	1.406×10^9
Fission rate (f/s)			2.270×10^{10}	2.885×10^{10}	1.464×10^{10}	1.464×10^{10}	7.225×10^9	7.225×10^9	Fast fission	2.587×10^{10}
Fission yield (%)	*	*	5.28 ± 0.14	5.67 ± 0.07	5.42 ± 0.18	5.40 ± 0.08	5.65 ± 0.06	5.66 ± 0.06	—	5.43 ± 0.08

*All fission yields calculated for irradiation A were determined relative to Sr^{89} since no cobalt monitor was bombarded. The value for the fission yield of Sr^{89}, which will be discussed later, was taken as 5.56% for that irradiation.

TABLE III

Fission yield data for 27.7-year Sr^{90}

Irradiation No.	A 1	D_a 2*	D_b 2*
Time in reactor (hours)	24	18.5	18.5
Time after irradiation (days)	17.35	106	115.41
Activity at saturation (d/s)	6.867×10^8	9.025×10^8	4.481×10^8
Fission rate (f/s)	(Relative yield)	1.464×10^{10}	7.225×10^9
Fission yield (%)	6.16 ± 0.12	6.16 ± 0.07	6.20 ± 0.09

*Determined by counting 64.3-hour Y^{90}.

Can. J. Chem. Downloaded from www.nrcresearchpress.com by 41.223.56.140 on 09/04/12
For personal use only.

TABLE IV

Fission yield data for 9.7-hour Sr^{91}

Irradiation No.	F 1
Time in reactor	24.16 hours
Time after irradiation	36.0 hours
Activity at saturation	1.246×10^{9} d/s
Fission rate	2.587×10^{10} f/s
Fission yield	$(4.82\pm0.25)\%$

(3) Yttrium

The yttrium was separated by the method given by Ballou (26). Sufficient time was allowed to elapse after the strontium was separated, so that the 65-hour Y^{90} had decayed. The yttrium fraction was followed for a period of 400 days and decayed cleanly with a half-life of 59 days, corresponding to Y^{91}. The data are presented in Table V.

TABLE V

Fission yield data for 59-day Y^{91}

Irradiation No.	B 1	C 1
Time in reactor	24 hours	24 hours
Time after irradiation	158 days	137.64 days
Activity at saturation	7.897×10^{8} d/s	1.039×10^{9} d/s
Fission rate	2.269×10^{10} f/s	2.885×10^{10} f/s
Fission yield	$(3.48\pm0.18)\%$	$(3.60\pm0.11)\%$

(4) Zirconium

The separation used was essentially a combination of procedures given by Hume (27) and Moore (23). The zirconium was extracted with 2-thenoyl-trifluoroacetone (TTA) and back-extracted from the organic phase with a nitric – hydrofluoric acid mixture. The zirconium was precipitated as barium zirconyl fluoride, dissolved in a boric acid – nitric acid mixture and passed through a Dowex-1 anion exchanger to remove borate and fluoride ions. The zirconium was precipitated with ammonia, dissolved in nitric acid, and made to volume.

The measurements in the 4π β-proportional counter indicated an initial growth and subsequent decay with a 65-day half-life. A 740-kev γ-photopeak, observed on the scintillation spectrometer, was a combination of the 722- and 754-kev γ-rays emitted by Zr^{95}. This peak also showed an initial increase and tailed off with a half-life of 65 days. The growth of this peak was due to the formation of the 770-kev γ-emitter Nb^{95} which is a daughter of Zr^{95}.

The counting rate for Zr^{95} was obtained by measuring sources immediately after the separation and by making a short extrapolation back to the end of separation where no niobium activity was present. A correct counting rate for Zr^{95} in the presence of niobium activities was not obtained due to incomplete knowledge of the decay schemes involved and the detection efficiency of radiations emitted. The fission yield data for Zr^{95} are given in Table VI.

TABLE VI

Fission yield data for 65-day Zr^{95}

Irradiation No.	A 1	B 1
Time in reactor	24 hours	24 hours
Time after irradiation	13.1 days	28.63 days
Activity at saturation	5.365×10^{8} d/s	1.309×10^{8} d/s
Fission rate	Relative yield	2.270×10^{10} f/s
Fission yield	$(4.82\pm0.50)\%$	$(5.77\pm1.44)\%$

Can. J. Chem. Downloaded from www.nrcresearchpress.com by 41.223.56.140 on 09/04/12
For personal use only.

(5) Niobium

The separation of niobium from other fission products was based on the specific precipitation of Nb_2O_5 from an oxalate solution with chloric acid (28).

Sources of the niobium activity were counted in the 4π-proportional counter. All sources which had been separated at least 33 days after the end of the irradiation were followed for at least 200 days and decayed with a half-life of 35 days. A sample of the niobium when analyzed on the scintillation spectrometer indicated the presence of a nuclide emitting a 770-kev γ-ray with a half-life of about 35 days. No 90-hour Nb^{95m} could be detected, indicating that the amount of this isomer formed from the decay of Zr^{95} must indeed be small as is indicated by the decay scheme.

The β-end-point energy for Nb^{95} is 0.160 Mev. The calculation of a disintegration rate for this nuclide involves rather large self-absorption corrections ($\sim$25%). To keep the niobium in solution, it was necessary to add an excess of oxalic acid which increased the superficial density of the source. The total source thickness was determined by weighing an aliquot of the sample which had been evaporated on a known area.

The data for the fission yield of Nb^{95} are given in Table VII.

TABLE VII

Fission yield data for 35-day Nb^{95}

Irradiation No.	F 1	F 2
Time in reactor	24.17 hours	24.17 hours
Time after irradiation	87.1 days	114.25 days
Activity at saturation	1.281×10^{9} d/s	1.561×10^{9} d/s
Fission rate	2.587×10^{10} f/s	2.587×10^{10} f/s
Fission yield	(4.94 ± 0.29)%	(6.03 ± 0.99)%

(6) Ruthenium

Carriers of ruthenium (Ru^{+3}), iodide, and bromide were added to an aliquot of the fission product stock solution. After an oxidation with sodium bismuthate and perchloric acid, ruthenium was separated from the other fission products by distilling the volatile RuO_4 into a sodium hydroxide solution (29). Ruthenium oxide was precipitated several times in the presence of sodium hydroxide by reduction with ethanol. The final oxide separated was dissolved in 6 *M* hydrochloric acid, and made up to volume.

The decay of ruthenium was measured in the 4π-proportional counter. A drop of dilute lithium hydroxide was added to the active sources on VYNS films to aid in drying. A 40-day activity and a longer-lived component ($\sim$1 year) were observed. A γ-spectrum was obtained showing the presence of a 500-kev γ-ray which decayed with a half-life of 40 days. The 40-day activity could then be conclusively attributed to Ru^{103}.

The residual activity with a half-life of about 1 year was assigned to Ru^{106}, a known fission product with a half-life of 1.02 years (30) and a β-end-point energy of 39.2 kev (31).

The measurement of a disintegration rate for both Ru^{103} and Ru^{106} is difficult due to the low energy of the radiation and the presence of short-lived daughter activities.

For Ru^{103} it was necessary to consider the effects of the delayed γ-emitter Rh^{103m}. The total internal conversion coefficient (α_T) for the 40.2-kev γ-ray is about 484 (32). From this value can be calculated N_{e^-}, the number of conversion electrons emitted.

$$N_{e^-} = \alpha_T/(1+\alpha_T) = 0.998.$$

Therefore, 99.8% of Rh^{103m} disintegrations involve conversion electron emission. The

Can. J. Chem. Downloaded from www.nrcresearchpress.com by 41.223.56.140 on 09/04/12
For personal use only.

energies of these electrons are low enough so that only 5% are not absorbed in the source and source-mount and are detected by the counter.

The observed 1-year activity represents an equilibrium counting rate for Ru^{106} and Rh^{106}. Absorption losses are to be expected for the Ru^{106} radiation but not for Rh^{106} since the latter has maximum β-energies of 3.5 (82%) and 2.3 (18%) Mev (33).

Fission yield data are presented for Ru^{103} and Ru^{106} in Tables VIII and IX respectively.

TABLE VIII

Fission yield data for 40-day Ru^{103}

Irradiation No.	B 1
Time in reactor	24 hours
Time after irradiation	22.53 days
Activity at saturation	4.581×10^{8} d/s
Fission rate	2.269×10^{10} f/s
Fission yield	$(2.02\pm0.08)\%$

TABLE IX

Fission yield data for 1.02-year Ru^{106}

Irradiation No.	B 1
Time in reactor	24 hours
Time after irradiation	22.53 days
Activity at saturation	5.881×10^{7} d/s
Fission rate	2.269×10^{10} f/s
Fission yield	$(0.259\pm0.03)\%$

(7) Rhodium

The separation of rhodium was based on its extraction into pyridine from a strongly alkaline solution (34).

Sources, when counted in the 4π-proportional counter, were observed to give a 36-hour decay curve, and the presence of a 320-kev photopeak in the γ-spectrum for this activity helped establish its identity as Rh^{105}.

The fission yield data for Rh^{105} are given in Table X.

TABLE X

Fission yield data for 36.5-hour Rh^{105}

Irradiation No.	F 1
Time in reactor	24.16 hours
Time after irradiation	144.6 hours
Activity at saturation	3.770×10^{7} d/s
Fission rate	2.587×10^{10} f/s
Fission yield	$(0.146\pm0.037)\%$

(8) Silver

Silver was separated from other fission products by precipitating silver chloride. Additional decontamination was achieved, as suggested by Glendenin (35), by alternative ferric hydroxide scavengings and silver sulphide precipitations from an ammoniacal solution.

The silver decay curves were obtained with the 4π β-proportional counter. The length of time from the end of the irradiation to the silver separation was such that any Ag^{112}

Can. J. Chem. Downloaded from www.nrcresearchpress.com by 41.223.56.140 on 09/04/12
For personal use only.

present had been formed from the decay of the parent Pd^{112}. Because of this, the Ag^{112} data have been presented in Table XIII with the fission yield data for Pd^{112}. The fission yield calculated for Ag^{111} is given in Table XI.

TABLE XI

Fission yield data for 7.6-day Ag^{111}

Irradiation No.	B 1	D 1
Time in reactor	24 hours	18.5 hours
Time after irradiation	1.91 days	2.5 days
Activity at saturation	4.28×10^6 d/s	2.701×10^6 d/s
Fission rate	2.270×10^{10} f/s	1.464×10^{10} f/s
Fission yield	$(0.0188\pm0.0003)\%$	$(0.0185\pm0.0007)\%$

(9) Palladium

The separation of palladium from other fission products was accomplished by the precipitation of palladium dimethylglyoxime from an acid solution. Scavenging with ferric hydroxide and silver iodide was performed for additional purification. Palladium was finally precipitated with dimethylglyoxime, dissolved in hot concentrated nitric acid and made up to volume.

The decay curves for palladium were measured on the 4π-proportional counter. They were found to contain a 65-day (probably Zr^{95}) and a 9-day impurity. A 21-hour activity was resolved by analyzing the initial portion of the gross decay curve. This activity was taken as Pd^{112} (36) and a fission yield was calculated (Table XII). The peaks observed on the scintillation spectrometer were not sufficiently resolved to permit an identification of nuclides present. If the 65-day activity represented Zr^{95}, then 17-hour Zr^{97} might also be present and add to the counting rate of Pd^{112}. As a further check on the Pd^{112} yield, the daughter activity Ag^{112} was counted and from its measurements the yield for Pd^{112} was indirectly determined (Table XIII). The values obtained for the yield of Pd^{112} by both methods agreed favorably.

TABLE XII

Fission yield data for 21-hour Pd^{112}

Irradiation No.	B 1	F 1
Time in reactor	24 hours	24 hours
Time after irradiation	69.5 hours	76.2 hours
Activity at saturation	2.776×10^6 d/s	3.180×10^6 d/s
Fission rate	2.270×10^{10} f/s	2.587×10^{10} f/s
Fission yield	$(0.0122\pm0.0001)\%$	$(0.0123\pm0.0001)\%$

TABLE XIII

Fission yield data for 21-hour Pd^{112}*

Irradiation No.	B 1	D 1
Time in reactor	24 hours	18.5 hours
Time after irradiation	44.8 hours	58.7 hours
Activity at saturation	2.938×10^6 d/s	1.729×10^6 d/s
Fission rate	2.270×10^{10} f/s	1.464×10^{10} f/s
Fission yield	$(0.0129\pm0.0001)\%$	$(0.0118\pm0.0005)\%$

*Determined from the daughter 3.2-hour Ag^{112}.

Can. J. Chem. Downloaded from www.nrcresearchpress.com by 41.223.56.140 on 09/04/12
For personal use only.

(10) Antimony

The method of Boldridge and Hume (37) was used to separate antimony from other fission products. The decay of antimony activities, as measured by the 4π-proportional counter, yielded half-lives of 3.79 days and 75 days. An intense 245-kev γ-photopeak was observed on the scintillation spectrometer which also decayed with a 3.6-day half-life. Two less-defined γ-peaks were observed at 740 and 480 kev. These peaks appeared to be associated with the 75-day activity. The shorter-lived activity was assigned to Sb^{127}. Half-lives reported recently for this nuclide are 88 hours (38) and 93 hours (39). The value used in this work was the observed 91 hours. The γ-peaks at 480 and 740 kev appeared to correspond to the reported 463- and 772-kev energies of Sb^{127} but decayed with a 75-day half-life. No observed 75-day antimony activity has been reported in fission. The only antimony nuclide positively identified in this work is that of mass number 127 and the data for this are given in Table XIV. A fission yield was calculated for the observed longer-lived antimony activity, using a half-life of 75 days, and the data are shown in Table XV.

TABLE XIV

Fission yield data for 91-hour Sb^{127}

Irradiation No.	B 1	D 1
Time in reactor	24 hours	18.5 hours
Time after irradiation	14.82 days	3.23 days
Activity at saturation	1.524×10^{8} d/s	7.511×10^{7} d/s
Fission rate	2.270×10^{10} f/s	1.464×10^{10} f/s
Fission yield	$(0.67\pm0.13)\%$	$(0.51\pm0.12)\%$

TABLE XV

Fission yield data for "75-day Sb"

Irradiation No.	B 1
Time in reactor	24 hours
Time after irradiation	14.82 days
Activity at saturation	1.121×10^{8} d/s
Fission rate	2.270×10^{10} f/s
Fission yield	$(0.53\pm0.14)\%$

(11) Tellurium

A direct separation of radiochemically pure tellurium was obtained by using a method reported by Glendenin (40).

The decay of tellurium was measured in the 4π-proportional counter. The curve could be resolved into activities with half-lives of 3.2 days, 37 days, and 105 days corresponding to Te^{132}, Te^{129m}, and Te^{127m} respectively. A freshly separated tellurium sample analyzed on the scintillation spectrometer at first showed only a 220-kev γ-photopeak corresponding to Te^{132}. Then the 670- and 780-kev γ-peaks of the I^{132} daughter grew in and later decayed. In equilibrium, all three peaks decayed with a half-life of 3.2 days.

The data involved in the calculation of a fission yield for Te^{132} are given in Table XVI. An additional yield measurement for Te^{132} was obtained by separating and measuring 2.3-hour I^{132}. Data for the latter measurements are listed in Table XVII.

(12) Iodine

A rapid solvent extraction method for the separation of iodine has been reported by Glendenin and Metcalf (41) and has been used in this work. To the final iodine, separated

Can. J. Chem. Downloaded from www.nrcresearchpress.com by 41.223.56.140 on 09/04/12
For personal use only.

TABLE XVI

Fission yield data for 77-hour Te^{132}

Irradiation No.	A 1	C 1
Time in reactor	24 hours	24 hours
Time after irradiation	28.65 days	16.84 days
Activity at saturation	5.227×10^{8} d/s	1.215×10^{8} d/s
Fission rate	Relative yield	2.885×10^{9} f/s
Fission yield	$(4.70\pm0.94)\%$	$(4.21\pm0.63)\%$

TABLE XVII

Fission yield data for 77-hour Te^{132}*

Irradiation No.	A 3	B 1	C 1	F 1
Time in reactor (hours)	24	24	24	24.16
Time after irradiation (hours)	15.76	87.01	301.9	433.4
Activity at saturation (d/s)	5.266×10^{8}	9.56×10^{8}	1.320×10^{9}	1.073×10^{8}
Fission rate (f/s)	Relative yield	2.270×10^{10}	2.885×10^{10}	2.587×10^{10}
Fission yield (%)	4.71 ± 0.14	4.21 ± 0.13	4.57 ± 0.16	4.15 ± 0.05

*Determined from the daughter 2.3-hour I^{132}.

in the form of iodide, was added a small amount of lithium hydroxide and the solution was diluted to volume.

The method used for source preparation was that suggested by Bartholomew *et al.* (42), in which the iodide solution was added to a drop of very dilute silver nitrate already present on the prepared VYNS film. The purpose of the silver is to prevent the oxidation and subsequent volatilization of iodine. Prior to each measurement, each iodine source was heated for 15 minutes under an infrared lamp. This technique was used to remove xenon decay products formed from iodine. The half-lives observed by 4π-counting were 2.3-hour I^{132}, 20.9-hour I^{133}, and 8.0-day I^{131}. All γ-photopeaks observed on the scintillation spectrometer decayed with similar half-lives. Peaks at 670, 780, 980, and 1400 kev decayed with a half-life of 2.2 hours. The 520-kev peak decayed with a half-life of 20.3 hours and the 360- and 640-kev peaks with a half-life of 8.4 days. No attempt was made to remove xenon decay products from the sources used on the scintillation spectrometer.

Iodine separations were performed at a time after the irradiation when any independently formed I^{132} had completely decayed. The observed I^{132} activity resulted from the decay of Te^{132} and consequently its disintegration rate was used to calculate the yield of Te^{132} (Table XVII). The fission yields of I^{131} and I^{132} are given in Tables XVIII and XIX.

TABLE XVIII

Fission yield data for 8.05-day I^{131}

Irradiation No.	A 3	B 1	C 1
Time in reactor	24 hours	24 hours	24 hours
Time after irradiation	15.81 days	88 hours	12.6 days
Activity at saturation	3.420×10^{8} d/s	6.866×10^{8} d/s	8.833×10^{8} d/s
Fission rate	Relative yield	2.270×10^{10} f/s	2.885×10^{10} f/s
Fission yield	$(3.06\pm0.10)\%$	$(3.02\pm0.09)\%$	$(3.06\pm0.09)\%$

(13) Cesium

The procedure used for the isolation of cesium activity from other fission products was that given by Glendenin and Nelson (43).

Can. J. Chem. Downloaded from www.nrcresearchpress.com by 41.223.56.140 on 09/04/12
For personal use only.

TABLE XIX

Fission yield data for 20.9-hour I^{133}

Irradiation No.	B 1	D 1
Time in reactor	24 hours	18.5 hours
Time after irradiation	87.01 hours	62.6 hours
Activity at saturation	8.31×10^{8} d/s	4.504×10^{8} d/s
Fission rate	2.270×10^{10} f/s	1.464×10^{10} f/s
Fission yield	$(3.66\pm0.10)\%$	$(3.08\pm0.10)\%$

An activity of 13 days was found attributable to Cs^{136}. This is a shielded nuclide and is therefore produced directly in fission as a primary fragment. After 80 days of counting, the cesium activity remained constant at a value well above the background counting rate for the counter due to the presence of long-lived Cs^{137}. The data for the independent fission yield of Cs^{136} are given in Table XX. By assuming that the residual cesium activity was due to Cs^{137}, calculations were made for the fission yield of this nuclide.

In the decay, 95% of the transitions go to the 2.6-minute Ba^{137m} state. Corrections for the contribution to the 4π β-counting rate were made, using the following data:

$$\alpha_K = 0.097$$

$$K/L = 4.9.$$

Therefore

$$\alpha_L = .02.$$

Assume

$$\alpha_M+\alpha_N+\ldots = 0.004.$$

Therefore

$$\alpha_T = .121.$$

The efficiency of the 661-kev γ-ray in our counter has been found to be 0.45%.

The total number of conversion electrons

$$N_e = \alpha_T/(1+\alpha_T)\ \text{(total } \gamma\text{-transitions)}.$$

The number of unconverted γ's

$$N = 1/(1+\alpha_T)\ \text{(total } \gamma\text{-transitions)}.$$

Therefore counts registered equal

$$\frac{\alpha_T}{1+\alpha_T}(0.95)n+0.0045\,\frac{1}{1+\alpha_T}(0.95)n+n$$

where n = true disintegration rate. Therefore counts registered = $1.106\,n$. The counting rate registered was divided by this number.

The half-life of Cs^{137} has recently been reported as 30.0 years (44) and 26.6 years (45). The fission yield for Cs^{137} is given in Table XXI using both half-lives.

(14) Barium

After the separation of barium from the strontium by a chromate precipitation, as described previously, the barium was dissolved and reprecipitated twice by means of a

Can. J. Chem. Downloaded from www.nrcresearchpress.com by 41.223.56.140 on 09/04/12
For personal use only.

TABLE XX

Fission yield data for 12.9-day Cs^{136}

Irradiation No.	D 1
Time in reactor	18.5 hours
Time after irradiation	31.3 days
Activity at saturation	1.244×10^{7} d/s
Fission rate	1.464×10^{10} f/s
Fission yield	$(0.0849\pm0.0022)\%$

TABLE XXI

Fission yield data for Cs^{137}

Irradiation No.	D 1	
Reported half-life	30.0 years	26.6 years
Time in reactor	18.5 hours	18.5 hours
Time after irradiation	31.3 days	31.3 days
Activity at saturation	7.887×10^{8} d/s	7.100×10^{8} d/s
Fission rate	1.464×10^{10} f/s	1.464×10^{10} f/s
Fission yield	$(5.39\pm0.11)\%$	$(4.85\pm0.10)\%$

cold hydrochloric acid – ether mixture. The final barium chloride precipitate was dissolved in water and made to volume.

Barium sources were mounted and counted as soon after the end of a separation as possible. The counting rate, as measured by the 4π-proportional counter, increased with time reaching a maximum value at about 4 days, and then decreased with a half-life of 12.8 days. For the first few hours after a barium separation the growth of La^{140} is linear with respect to time. Therefore a plot of the total counting rate vs. time can be accurately extrapolated back to the time at which barium was separated. By using growth and decay equations, it is also possible to calculate the amount of Ba present initially from a measured Ba plus La counting rate at a known time after the separation. The calculated values agreed with those obtained by back-extrapolating the initial portions of the growth and decay curves.

Barium sources counted were about 30 $\mu g/cm^2$ thick. A decrease in the thickness by a factor of 100 showed no change in the source specific activity. This observation, together with the agreement between calculated and observed growth and decay curves, indicated that absorption effects, as described by Grummitt *et al.* (46), were not significant in this work.

Each barium separation was analyzed on the scintillation spectrometer. No extraneous γ-peaks were observed. A plot of peak heights against time produced a curve similar to the net growth and decay as obtained in the 4π β-counter. The fission yield data for Ba^{140} are given in Table XXII.

TABLE XXII

Fission yield data for 12.8-day Ba^{140}

Irradiation No.	A 1	A 2	B 1	B 2	C 1	C 2	D_a 1	D_a 2	E 2	F 1
Time in reactor (hours)	24	24	24	24	24	24	18.5	18.5	23.8	24.16
Time after irradiation (days)	17.0	23.83	4.69	10.69	3.56	56.71	16.01	67.06	5.0	13.08
Activity at saturation (d/s)	5.300×10^{8}	5.913×10^{8}	1.214×10^{9}	1.121×10^{9}	1.548×10^{9}	1.567×10^{9}	7.247×10^{8}	7.552×10^{8}	1.217×10^{7}	1.318×10^{9}
Fission rate (f/s)	Relative yield		2.269×10^{10}	2.269×10^{10}	2.885×10^{10}	2.885×10^{10}	1.464×10^{10}	1.464×10^{10}	Fast fission	2.587×10^{10}
Fission yield (%)	4.76 ± 0.66	5.31 ± 0.13	5.35 ± 0.23	4.94 ± 0.16	5.37 ± 0.16	5.43 ± 0.22	4.95 ± 0.05	5.16 ± 0.11		5.09 ± 0.05

Can. J. Chem. Downloaded from www.nrcresearchpress.com by 41.223.56.140 on 09/04/12
For personal use only.

(15) Cerium

Two procedures were used for the separation of cerium activity. The first was similar to that used for the separation of yttrium (26). After Ce, Y, and the rare earths were isolated from other fission products, cerium was oxidized and precipitated twice as the iodate. The precipitate was dissolved in a nitric acid – hydrogen peroxide mixture and further purified by zirconium iodate scavenging. Precipitations of ceric hydroxide, cerous hydroxide, and cerous oxalate produced radiochemically pure cerium. The final precipitate was washed with water, dissolved in a minimum of nitric acid, and made up to a known volume.

The second method used for the separation of cerium was described by Glendenin *et al.* (22). Cerium carrier and sodium bromate were added to an aliquot of the fission product stock solution. Cerium was extracted into methylisobutyl ketone. The organic layer was separated and washed with dilute nitric acid containing sodium bromate. Cerium was back-extracted into water containing a little 30% hydrogen peroxide. An oxalate precipitation was used to recover cerium from the aqueous layer. The cerium was then dissolved in dilute nitric acid, diluted, and reprecipitated with oxalic acid. The final oxalate precipitate was dissolved and made up to volume.

Cerium activities detected in this work were 33-day Ce^{141}, 33-hour Ce^{143}, and 285-day Ce^{144}. A 290-kev photopeak, attributed to Ce^{143}, was observed on the scintillation spectrometer to decay with a 33-hour half-life.

The data, for which the fission yields for Ce^{141}, Ce^{143}, and Ce^{144} were calculated, are given in Tables XXIII, XXIV, and XXV respectively.

TABLE XXIII

Fission yield data for 33-day Ce^{141}

Irradiation No.	A 1	B 2	C 1	C 2
Time in reactor (hours)	24	24	24	24
Time after irradiation (days)	61.0	35.51	5.0	124.1
Activity at saturation (d/s)	2.966×10^{8}	1.236×10^{9}	1.553×10^{9}	1.555×10^{9}
Fission rate (f/s)	Relative yield	2.270×10^{10}	2.885×10^{10}	2.885×10^{10}
Fission yield (%)	5.22 ± 0.04	5.44 ± 0.16	5.38 ± 0.23	5.39 ± 0.48

TABLE XXIV

Fission yield data for 33-hour Ce^{143}

Irradiation No.	C 1
Time in reactor	24 hours
Time after irradiation	5.0 days
Activity at saturation	2.018×10^{8} d/s
Fission rate	2.885×10^{10} f/s
Fission yield	$(6.99\pm0.35)\%$

TABLE XXV

Fission yield data for 285-day Ce^{144}

Irradiation No.	B 2	C 1
Time in reactor	24 hours	24 hours
Time after irradiation	35.51 days	5.0 days
Activity at saturation	8.724×10^{9} d/s	9.999×10^{8} d/s
Fission rate	2.269×10^{10} f/s	2.885×10^{10} f/s
Fission yield	$(3.84\pm0.11)\%$	$(3.47\pm0.15)\%$

Can. J. Chem. Downloaded from www.nrcresearchpress.com by 41.223.56.140 on 09/04/12
For personal use only.

The errors in these experiments are as follows:

(*a*) Systematic errors. These, such as weighing, dilutions, pipetting, were less than 0.5% due to the use of a sensitive microbalance, calibrated glassware, etc. The major error lies in the chemical yield determinations. In order to minimize source self-absorption corrections, minimal amounts of carriers were used. This made chemical yield determinations difficult, and this is reflected in the limits placed on the determinations.

(*b*) The fast fission correction was small ($\sim$2%) and the error in correcting for this is $\pm$0.2%.

(*c*) Loss of activity by fission recoil $\pm$0.2%.

(*d*) Source-mount absorption $\pm$0.2%.

(*e*) Self-absorption in the sample, 0.1 $\rightarrow$ 2%, depending on the energy of the β-emitter and sample thickness.

(*f*) Saturation activity calculations. The pile power was constant during all but one irradiation. In this latter irradiation, the saturation factor was obtained by use of an analogue computer.*

(*g*) External errors. Errors in reported decay schemes and decay constants may greatly influence the results. Each fission yield is given in terms of the half-life as observed and the decay schemes as discussed.

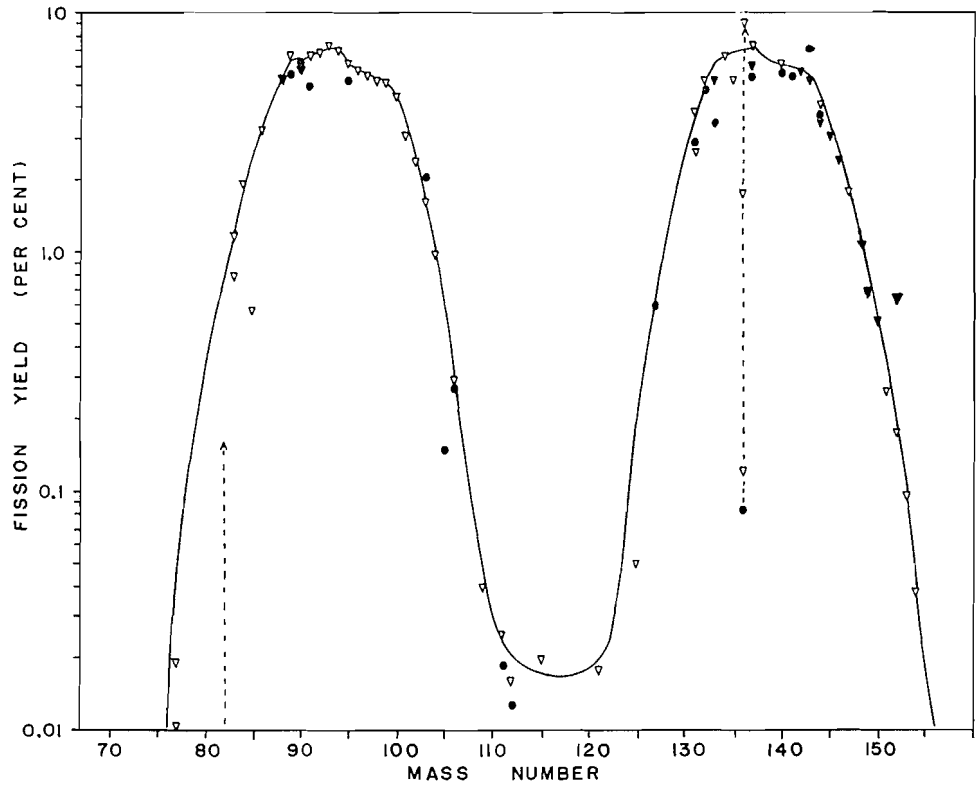


FIG. 1. Yield–mass distribution in the thermal neutron fission of U^{233}.
▽ Relative yields} previously reported.
▼ Absolute yields}
● Absolute yields, this work.
Broken line represents the correction for chain yield.

*We are grateful to Dr. J. G. Bayly, Reactor Physics Branch, A.E.C.L., for performing these calculations.

Can. J. Chem. Downloaded from www.nrcresearchpress.com by 41.223.56.140 on 09/04/12
For personal use only.

All yields were calculated relative to σ_t/σ_{Co} and can be renormalized should the necessity arise.

When several determinations were made for one nuclide, an average fission yield was calculated by weighing each individual value according to the reciprocal of its own experimental error. The error quoted finally is the root-mean-square deviation.

DISCUSSION

The absolute yields obtained are presented in Table XXVI. Included in this table are values measured by other investigators. Those listed in column 3 do not necessarily represent total chain yields, but merely refer to the cumulative yield for the nuclide given. No attempt was made to correct any of the values for delayed neutron emission, and no corrections were required for loss or gain due to neutron capture among the

TABLE XXVI

Thermal neutron fission yields for U^{233}

			This work					This work	
	Nuclide	Literature values (%)	Absolute yield of nuclide (%)	Estimated isobaric yield (%)		Nuclide	Literature values (%)	Absolute yield of nuclide (%)	Estimated isobaric yield (%)
12-*h*	Ge^{77}	0.010			Mass	115	0.020		
39-*h*	As^{77}	0.019			27.5-*h*	Sn^{121}	0.018		
36-*h*	Br^{82}		0.000746±0.000017	0.158	9.6-*d*	Sn^{125}	0.05		
2.4-*h*	Br^{83}	0.79			91-*h*	Sb^{127}		0.59±0.08	0.59
Stable	Kr^{83}	1.14			8.05-*d*	I^{131}	2.7	2.84±0.20	2.84
Stable	Kr^{84}	1.90			Stable	Xe^{131}	3.74		
10.3-*y*	Kr^{85}	0.56			77-*h*	Te^{132}		4.32±0.25	4.64
Stable	Kr^{86}	3.18			Stable	Xe^{132}	5.10		
Stable	Sr^{88}	5.3*			20.9-*h*	I^{133}		3.37±0.29	3.40
50.4-*d*	Sr^{89}	6.5	5.56±0.15	5.56	Stable	Cs^{133}	5.20†		
27.7-*y*	Sr^{90}	5.8*	6.19±0.03	6.19	Stable	Xe^{134}	6.54		
9.7-*h*	Sr^{91}		4.82±0.25	4.82	6.7-*h*	I^{135}	5.1		
59-*d*	Y^{91}		3.55±0.06	3.55	3×10^6-*y*	Cs^{135}	4.9		
Stable	Zr^{91}	6.53			12.9-*d*	Cs^{136}	0.12	0.0849±0.0022	8.5
Stable	Zr^{92}	6.70			86-*s*	I^{136}	1.7		
10^6-*y*	Zr^{93}	7.10			Stable	Xe^{136}	8.9		
Stable	Zr^{94}	6.82			30-*y*	Cs^{137}	7.16	5.39±0.11	5.39
65-*d*	Zr^{95}	5.9	5.01±0.56	5.01			5.80†		
35-*d*	Nb^{95}		5.16±0.64	5.16	12.8-*d*	Ba^{140}	6.0	5.21±0.27	5.48
Stable	Mo^{95}	6.1			Stable	Ce^{140}	5.45†		
Stable	Zr^{96}	5.6			33-*d*	Ce^{141}		5.30±0.10	5.30
Stable	Mo^{97}	5.35			Stable	Ce^{142}	5.50†		
Stable	Mo^{98}	5.18			33-*h*	Ce^{143}		6.99±0.35	6.99
67-*h*	Mo^{99}	4.8			Stable	Nd^{143}	5.00†		
Stable	Mo^{100}	4.40			285-*d*	Ce^{144}	4.1	3.69±0.18	3.69
Stable	Ru^{101}	3.00			Stable	Nd^{144}	3.80†		
Stable	Ru^{102}	2.37			Stable	Nd^{145}	2.82†		
40-*d*	Ru^{103}	1.6	2.02±0.08	2.02	Stable	Nd^{146}	2.20†		
Stable	Ru^{104}	0.96			Stable	Sm^{147}	1.71		
36.5-*h*	Rh^{105}		0.146×0.037	0.146	Stable	Nd^{148}	1.03†		
1.02-*y*	Ru^{106}	0.28	0.259±0.030	0.264	Stable	Sm^{149}	0.66†		
13.4-*h*	Pd^{109}	0.040			Stable	Nd^{150}	0.51†		
7.6-*d*	Ag^{111}	0.025	0.0187±0.0002	0.0187	80-*y*	Sm^{151}	0.26		
21-*h*	Pd^{112}	0.016	0.0125±0.0004	0.0128	Stable	Sm^{152}	0.60†		
43-*d*	Cd^{115m}	0.001			47-*h*	Sm^{153}	0.095		
53-*h*	Cd^{115}	0.019			Stable	Sm^{154}	0.037		

*Most recent values by Anikina *et al.* (48) published after this work was complete.

†Most recent values by Ivanov *et al.* (49) published after this work was complete.

All other values are as listed by Katcoff (7).

The relative yields of Bartholomew *et al.* (50) were published after this paper had been compiled. A renormalization of their yields to our value of 5.21% for Ba^{140} gives Sr^{89} = 5.46, Sr^{91} = 5.22, Ba^{139} = 5.20, and La^{141} = 5.74%.

Can. J. Chem. Downloaded from www.nrcresearchpress.com by 41.223.56.140 on 09/04/12
For personal use only.

fission products themselves. The same fast fission factor has been applied to all values determined. This correction will certainly apply to values on or near the peaks of the yield–mass curve. The effect on the mass distribution of increasing the neutron energy above the thermal region is to increase the probability of symmetric fission. For this reason the yields of nuclides in the trough of the curve (Ag^{111} and Pd^{112}) are to be considered maximum values. However, the position of the sample inside the reactor was such that the epi-cadmium neutrons detected could not have possessed high energy. Recent investigations on the fission of U^{235} with energies as high as 9.5 ev show no significant change in the trough yields from that produced by thermal neutrons (47), so that little change in the trough yields is to be expected.

In the last column are estimated mass yields for the chains studied. These were calculated by determining the most probable nuclear charge of a particular mass number from the curves given by Katcoff (51). A chain correction factor is then obtained for a value of the displacement from the most probable charge. The cumulative yield can then be estimated from the product of the actual measured fission yield and its cumulative fractional chain yield.

The agreement between yields measured in this work and other absolute yields determined mass spectrometrically is good. However, yields which were determined earlier either radiochemically or normalized to radiochemical values are generally higher.

There appears to be a discrepancy between the observed yields of 4.82% for Sr^{91} and 3.55% for Y^{91}. A decrease in cumulative yield along a chain is not to be expected. Such a difference might well be due to an incomplete knowledge of the mass 91 chain. Other investigators have also reported irregularities in this chain (52, 53). The low yield of I^{133} obtained appeared real since I^{131} and Te^{132} yields, calculated on the same samples, gave normal results. The high yield at mass 143 was based on one measurement and has not been confirmed. The absolute yield measured mass spectrometrically does not agree with this value. However, the mass 141 yield, determined on the same sample, seems to give a reasonable result.

Absolute yields for Sr^{90} on the light mass peak and Ce^{140} on the heavy mass peak, which were reported by Anikina and Ershler (9) and Kukavadze *et al.* (10), respectively, were not dependent on cross-section values. The agreement with this work indicated that the value of σ_t/σ_c used appears correct.

The yield values in Table XXVI are plotted in Fig. 1. The curve drawn is that suggested by Katcoff (7) for the thermal neutron fission of U^{233} and is such that the sum of the yields is the required 200%. The measured independent yields of Br^{82} and Cs^{136} have been corrected to chain yields as indicated by the broken arrows.

REFERENCES

1. W. E. Grummitt and G. Wilkinson. Nature, **161**, 520 (1948).
2. E. P. Steinberg, J. A. Seiler, A. Goldstein, and L. Dudley. U.S. Atomic Energy Rept. MDDC-1632 1948.
3. L. E. Glendenin and E. P. Steinberg. Intern. Conf. on the Peaceful Uses of Atomic Energy, **7**, 3 (1956).
4. E. P. Steinberg, L. E. Glendenin, M. G. Inghram, and R. J. Hayden. Phys. Rev. **95**, 867 (1954).
5. W. F. Fleming, R. H. Tomlinson, and H. G. Thode. Can. J. Phys. **32**, 522 (1954).
6. E. A. Melaika, M. J. Parker, J. A. Petruska, and R. H. Tomlinson. Can. J. Chem. **33**, 830 (1955).
7. S. Katcoff. Nucleonics, **16**, 78 (1958).
8. S. Peterson. U.S. Atomic Energy Comm. ORNL Rept. 55-6-144. 1955.
9. M. P. Anikina and B. V. Ershler. J. Nuclear Energy, **6**, 169 (1957).
10. G. M. Kukavadze, M. P. Anikina, L. L. Goldin, and B. V. Ershler. Conf. Acad. Sci. S.S.S.R. on Peaceful Uses of Atomic Energy, 125 (1955).
11. R. N. Ivanov, V. K. Gorshkov, M. P. Anikina, G. M. Kukavadze, and B. V. Ershler. Atomnaya Energ. **3**, 546 (1957).

Can. J. Chem. Downloaded from www.nrcresearchpress.com by 41.223.56.140 on 09/04/12
For personal use only.

12. B. D. PATE and L. YAFFE. Can. J. Chem. **33**, 15 (1955).
13. B. D. PATE and L. YAFFE. Can. J. Chem. **33**, 610 (1955).
14. B. D. PATE and L. YAFFE. Can. J. Chem. **33**, 929 (1955).
15. B. D. PATE and L. YAFFE. Can. J. Chem. **33**, 1656 (1955).
16. B. D. PATE and L. YAFFE. Can. J. Chem. **34**, 265 (1956).
17. J. B. FISHMAN and L. YAFFE. Unpublished data.
18. R. S. CARTER, H. PALEVSKY, V. W. MYERS, and D. J. HUGHES. Phys. Rev. **92**, 716 (1953).
19. L. YAFFE, R. C. HAWKINGS, W. F. MERRITT, and J. H. CRAVEN. Phys. Rev. **82**, 553 (1951).
20. K. W. GEIGER. Phys. Rev. **105**, 1539 (1957).
21. C. D. CORYELL and N. SUGARMAN. (*Editors*). Radiochemical studies: The fission products. National nuclear energy series. Div. IV. McGraw-Hill Book Co., Inc., New York. 1951. Paper 9.
22. L. E. GLENDENIN, K. F. FLYNN, R. F. BUCHANAN, and E. P. STEINBERG. Anal. Chem. **27**, 59 (1955).
23. F. L. MOORE. Anal. Chem. **28**, 997 (1956).
24. L. E. GLENDENIN, R. R. EDWARDS, and H. GEST. *In* Radiochemical studies: The fission products. *Edited by* C. D. Coryell and N. Sugarman. National nuclear energy series. Div. IV. McGraw-Hill Book Co., Inc., New York. 1951. Paper 232.
25. L. E. GLENDENIN. *In* Radiochemical studies: The fission products. *Edited by* C. D. Coryell and N. Sugarman. National nuclear energy series. Div. IV. McGraw-Hill Book Co., Inc., New York. 1951. Paper 236.
26. N. E. BALLOU. *In* Radiochemical studies: The fission products. *Edited by* C. D. Coryell and N. Sugarman. National nuclear energy series. Div. IV. McGraw-Hill Book Co., Inc., New York. 1951. Paper 292.
27. D. N. HUME. *In* Radiochemical studies: The fission products. *Edited by* C. D. Coryell and N. Sugarman. National nuclear energy series. Div. IV. McGraw-Hill Book Co., Inc., New York. 1951. Paper 245.
28. L. E. GLENDENIN. *In* Radiochemical studies: The fission products. *Edited by* C. D. Coryell and N. Sugarman. National nuclear energy series. Div. IV. McGraw-Hill Book Co., Inc., New York. 1951. Paper 253.
29. L. E. GLENDENIN. *In* Radiochemical studies: The fission products. *Edited by* C. D. Coryell and N. Sugarman. National nuclear energy series. Div. IV. McGraw-Hill Book Co., Inc., New York. 1951. Paper 260.
30. W. F. MERRITT, P. J. CAMPION, and R. C. HAWKINGS. Can. J. Phys. **35**, 16 (1957).
31. H. M. AGNEW. Phys. Rev. **77**, 655 (1950).
32. P. AVIGNON, A. MICHALOWICZ, and R. BOUCHEZ. J. phys. radium, **16**, 404 (1955).
33. W. C. PEACOCK. Phys. Rev. **72**, 1049 (1947).
34. N. E. BALLOU. *In* Radiochemical studies: The fission products. *Edited by* C. D. Coryell and N. Sugarman. National nuclear energy series. Div. IV. McGraw-Hill Book Co., Inc., New York. 1951. Paper 263.
35. L. E. GLENDENIN. *In* Radiochemical studies: The fission products. *Edited by* C. D. Coryell and N. Sugarman. National nuclear energy series. Div. IV. McGraw-Hill Book Co., Inc., New York. 1951. Paper 267.
36. J. A. SEILER. *In* Radiochemical studies: The fission products. *Edited by* C. D. Coryell and N. Sugarman. National nuclear energy series. Div. IV. McGraw-Hill Book Co., Inc., New York. 1951. Paper 119.
37. W. F. BOLDRIDGE and D. N. HUME. *In* Radiochemical studies: The fission products. *Edited by* C. D. Coryell and N. Sugarman. National nuclear energy series. Div. IV. McGraw-Hill Book Co., Inc., New York. 1951. Paper 272.
38. H. BOSCH and H. MUNCZEK. Phys. Rev. **106**, 983 (1957).
39. M. C. DAY and A. F. VOIGT. Phys. Rev. **101**, 1784 (1956).
40. L. E. GLENDENIN. *In* Radiochemical studies: The fission products. *Edited by* C. D. Coryell and N. Sugarman. National nuclear energy series. Div. IV. McGraw-Hill Book Co., Inc., New York. 1951. Paper 274.
41. L. E. GLENDENIN and R. P. METCALF. *In* Radiochemical studies: The fission products. *Edited by* C. D. Coryell and N. Sugarman. National nuclear energy series. Div. IV. McGraw-Hill Book Co., Inc., New York. 1951. Paper 278.
42. R. M. BARTHOLOMEW, F. BROWN, R. C. HAWKINGS, and L. YAFFE. Can. J. Chem. **31**, 120 (1953).
43. L. E. GLENDENIN and C. M. NELSON. *In* Radiochemical studies: The fission products. *Edited by* C. D. Coryell and N. Sugarman. National nuclear energy series. Div. IV. McGraw-Hill Book Co., Inc., New York. 1951. Paper 283.
44. F. BROWN, G. R. HALL, and A. J. WALTERS. J. Inorg. & Nuclear Chem. **1**, 241 (1955).
45. D. M. WILES and R. H. TOMLINSON. Phys. Rev. **99**, 188 (1955).
46. W. E. GRUMMITT, J. GUERON, G. WILKINSON, and L. YAFFE. Can. J. Research, B, **25**, 357 (1947).
47. R. NASUHOGLU, S. RABOY, G. R. RINGO, L. E. GLENDENIN, and E. P. STEINBERG. Phys. Rev. **108**, 1522 (1957).
48. M. P. ANIKINA, R. N. IVANOV, G. M. KUKAVADZE, and B. V. ERSHLER. J. Nuclear Energy, **9**, 167 (1959).
49. R. N. IVANOV, V. K. GORSHKOV, M. P. ANIKINA, G. M. KUKAVADZE, and B. V. ERSHLER. J. Nuclear Energy, **9**, 46 (1959).
50. R. M. BARTHOLOMEW, J. S. MARTIN, and A. P. BAERG. Can. J. Chem. **37**, 660 (1959).
51. S. KATCOFF. Low-energy induced fission. Handbook of nuclear engineering. Addison-Wesley Pub. Co., Inc., Cambridge, Mass. 1956.
52. W. E. GRUMMITT and G. M. MILTON. J. Inorg. & Nuclear Chem. **5**, 93 (1957).
53. A. P. BAERG and R. M. BARTHOLOMEW. Can. J. Chem. **35**, 980 (1957).

Can. J. Chem. Downloaded from www.nrcresearchpress.com by 41.223.56.140 on 09/04/12
For personal use only.

Can. J. Chem. Downloaded from www.nrcresearchpress.com by 41.223.56.140 on 09/04/12
For personal use only.

PERFLUOROALKYL ARSENICALS

PART I. THE PREPARATION OF ALKYL PERFLUOROALKYL ARSENICALS[1]

W. R. CULLEN

ABSTRACT

The reaction of tetramethyldiarsine with trifluoroiodomethane gives dimethyltrifluoromethylarsine. Trifluoroiodomethane and iodomethane similarly react with the compounds $(CF_3)_2M—M(CF_3)_2$ to give the compounds $(CF_3)_3M$ and $(CF_3)_2MCH_3$ respectively (M = As or P). Trifluoroiodomethane reacts with iododimethylarsine and diiodomethylarsine in the presence of mercury to give dimethyltrifluoromethylarsine and methylbistrifluoromethylarsine respectively. Heptafluoropropyldimethylarsine can be isolated from a similar reaction using heptafluoroiodopropane.

INTRODUCTION

Trifluoromethyl derivatives of phosphorus and arsenic are prepared by the action of trifluoroiodomethane on the elements, a mixture of products being obtained (1, 2).

$$M + CF_3I \rightarrow (CF_3)_3M + (CF_3)_2MI + CF_3MI_2 + MI_3 \qquad (M = As \text{ or } P)$$

Alkyl-trifluoromethyl-arsines and -phosphines can be obtained from Grignard reactions using trifluoromethyl-iodo-arsines (3, 4) and from exchange reactions using the compounds $(CF_3)_3M$ and $(CH_3)_3M$ (4, 5, 6).

$$(CF_3)_3M + CH_3I \rightarrow (CH_3)_2MCH_3 + CF_3I$$

$$2(CH_3)_3M + CF_3I \rightarrow (CH_3)_2MCF_3 + (CH_3)_4MI$$

In this paper new methods of preparing alkyl-perfluoroalkyl-arsines and -phosphines are described.

DISCUSSION AND RESULTS

Organometallic compounds containing metal—metal bonds are known to be highly reactive. Tetramethyldiarsine spontaneously inflames in air and the As—As bond is readily split by halogens (7) or alkyl halides (8). The tin—tin bond is similarly reactive (9) and hexamethylditin has been recently found to react at 80° with trifluoroiodomethane to give trimethyltrifluoromethyltin (10).

$$(CH_3)_3Sn—Sn(CH_3)_3 + CF_3I \rightarrow (CH_3)_3SnCF_3 + (CH_3)_3SnI$$

It has now been found that tetramethyldiarsine reacts at room temperature with trifluoroiodomethane to give dimethyltrifluoromethylarsine.

$$(CH_3)_2As—As(CH_3)_2 + CF_3I \rightarrow (CH_3)_2AsCF_3 + (CH_3)_2AsI$$

When excess trifluoroiodomethane is used the reaction appears to be complete. Trifluoroiodomethane reacts less readily with tetrakistrifluoromethyldiarsine to give tristrifluoromethylarsine and iodobistrifluoromethylarsine.

$$(CF_3)_2As—As(CF_3)_2 + CF_3I \rightarrow (CF_3)_3As + (CF_3)_2AsI$$

At 75° with excess trifluoroiodomethane the reaction is 60% complete after 14 hours and could probably be brought to completion if the conditions were adjusted appropriately. Tetrakistrifluoromethyldiarsine reacts also with iodomethane to give methylbistrifluoromethylarsine and iodobistrifluoromethylarsine.

$$(CF_3)_2As—As(CF_3)_2 + CH_3I \rightarrow (CF_3)_2AsCH_3 + (CF_3)_2AsI$$

[1]*Manuscript received October 5, 1959.*
Contribution from the Chemistry Department, University of British Columbia, Vancouver, B.C.

The reaction in this case seems to be slower, as at 75° with excess diarsine very little reaction takes place and even after 14 hours at 105° the reaction is only 10% complete.

Tetrakistrifluoromethyldiphosphine reacts similarly with both trifluoroiodomethane and iodomethane. After 20 hours at 70° the reaction with excess trifluoroiodomethane is 60% complete. However the diphosphine, like the diarsine, reacts more slowly with iodomethane and after 20 hours at 70°, using excess diphosphine, only a trace of methylbistrifluoromethylphosphine is formed, and at 105° there is little reaction after 18 hours. At 150° the reaction goes further, resulting in the conversion of up to 76% of the iodomethane after 48 hours.

It has also been found that perfluoroalkyl iodides will react at room temperature with a mixture of alkyl-iodo-arsines and mercury to give perfluoroalkyl-alkyl-arsines. Thus dimethyltrifluoromethylarsine and heptafluoropropyldimethylarsine are obtained from iododimethylarsine, and methylbistrifluoromethylarsine is obtained from diiodomethylarsine.

$$(CH_3)_2AsI + Hg + IR \rightarrow (CH_3)_2AsR + HgI_2 \qquad (R = CF_3 \text{ or } C_3F_7)$$

$$CH_3AsI_2 + 2Hg + 2CF_3I \rightarrow CH_3As(CF_3)_2 + 2HgI_2$$

The reaction of iododimethylarsine with trifluoroiodomethane is much faster than the reaction of the arsine with heptafluoroiodopropane Similarly the reaction of trifluoroiodomethane with iododimethylarsine is much faster than with the diiodo-arsine. The reaction of trifluoroiodomethane with chlorodimethylarsine in the presence of mercury is very slow.

Further work is in progress in an attempt to elucidate the exact nature of these reactions in view of their great synthetic potential.

Heptafluoropropyldimethylarsine is the first compound to be isolated with the As—C_3F_7 link. The reaction of heptafluoroiodopropane with arsenic appears to produce heptafluoropropyl arsenicals but these cannot be separated from by-products (11). As would be expected this new arsenical is similar to dimethyltrifluoromethylarsine in being unattacked by water and in being difficult to hydrolyze with base (5, 6). It is only 26% hydrolyzed by 10% sodium hydroxide solution after 3 days at 100°. Methylbistrifluoromethylarsine is only 9% hydrolyzed by 20% aqueous sodium hydroxide after 3 days at room temperature, whereas tristrifluoromethylarsine is completely hydrolyzed in less than 24 hours under the same conditions (6).

EXPERIMENTAL

Apparatus and Technique

Conventional vacuum techniques were used for the manipulation of reactants and products out of contact with moisture and oxygen. Molecular weights were determined by Regnault's method. Reactions were carried out in sealed Pyrex tubes in the absence of air and light. The infrared spectra of the trifluoromethyl derivatives of phosphorus and arsenic were used extensively for the identification of pure compounds and the constituents of mixtures impossible to separate by trap-to-trap distillation. These spectra have been reported previously (1, 3, 4, 12) and the very strong C—F stretching bands in the region 1050–1250 cm^{-1} together with the C—F deformation bands at ca. 700 cm^{-1} enabled ready characterization. The spectra were measured in the gas phase on a Perkin–Elmer Model 21 double-beam instrument with rock-salt optics.

Reaction of Tetramethyldiarsine with Trifluoroiodomethane

Tetramethyldiarsine was prepared by the reaction of chlorodimethylarsine with zinc

Can. J. Chem. Downloaded from www.nrcresearchpress.com by 41.223.56.140 on 09/04/12
For personal use only.

dust at 100° (13). The diarsine (1.627 g) and trifluoroiodomethane (5.359 g) were mixed in a sealed tube (100 ml). A yellow solid was produced which was soluble in the trifluoroiodomethane giving a green solution. The tube was opened after 28 days at room temperature. All the products were volatile and trap-to-trap distillation gave unchanged trifluoroiodomethane (3.866 g) identified spectroscopically and by its molecular weight (mol. wt.: found 197, calc. 196), a fraction condensing at −98° (1.198 g, 88%) identified spectroscopically as dimethyltrifluoromethylarsine, and a fraction condensing at −64° (1.435 g). This fraction was a relatively involatile red liquid which did not react with excess iodomethane at room temperature indicating that no unreacted diarsine was present (8). With iodomethane at 105° for 1 hour in a sealed tube (5 ml) crystals of tetramethylarsonium triiodide were obtained (m.p.: found 133°, lit. value 133° (8)). This identified the fraction as iododimethylarsine (8) (80% yield).

Reaction of Tetrakistrifluoromethyldiarsine with Trifluoroiodomethane

Tetrakistrifluoromethyldiarsine was obtained from the reaction of iodobistrifluoromethylarsine with mercury (4). The diarsine (1.125 g) and trifluoroiodomethane (1.991 g) in a sealed tube (30 ml) were heated to 75° for 14 hours. All the products were volatile and trap-to-trap distillation gave unreacted trifluoroiodomethane (1.681 g; mol. wt.: found 197, calc. 196), a fraction condensing at −98° which was identified spectroscopically and by molecular weight determination as nearly pure tristrifluoromethylarsine (0.475 g; mol. wt.: found 284, calc. 282; 61% yield based on the diarsine), and a fraction condensing at −64° (0.950 g). This fraction was shown by spectroscopic examination to be a mixture of iodobistrifluoromethylarsine and tetrakistrifluoromethyldiarsine. After the fraction was shaken with mercury at room temperature for 24 hours in a sealed tube (20 ml) spectroscopic examination showed it then contained only tetrakistrifluoromethyldiarsine. The loss of weight was 0.212 g corresponding to the formation of iodobistrifluoromethylarsine in 63% yield (based on the diarsine).

Reaction of Tetrakistrifluoromethyldiarsine with Iodomethane

The diarsine (0.975 g) and iodomethane (0.280 g) in a sealed tube (20 ml) were heated to 75° for 24 hours after which spectroscopic examination of the contents of the tube showed that only a very small amount of methylbistrifluoromethylarsine had been produced. The reaction mixture was then heated in a sealed tube (20 ml) for 14 hours at 105°. Trap-to-trap distillation and spectroscopic examination of the fractions showed that only a little more methylbistrifluoromethylarsine had been produced. All the fractions were combined and shaken with excess mercury in a sealed tube (20 ml) for 24 hours at room temperature to convert the iodobistrifluoromethylarsine to tetrakistrifluoromethyldiarsine. The loss of weight was 0.026 g corresponding to reaction of 10% of the iodomethane.

Reaction of Tetrakistrifluoromethyldiphosphine with Trifluoroiodomethane

Tetrakistrifluoromethyldiphosphine was prepared by the reaction of iodobistrifluoromethylphosphine with mercury (1). The diphosphine (0.848 g) and trifluoroiodomethane (3.072 g) in a sealed tube (20 ml) were heated to 70° for 20 hours. All the products were volatile and trap-to-trap distillation gave unreacted trifluoroiodomethane (2.800 g; mol. wt.: found 195, calc. 196), a fraction condensing at −112° which was identified spectroscopically and by molecular weight determination as nearly pure tristrifluoromethylphosphine (0.363 g; mol. wt.: found 236, calc. 238; 61% yield based on the diphosphine), and a fraction condensing at −78° (0.761 g). This fraction was shaken with

Can. J. Chem. Downloaded from www.nrcresearchpress.com by 41.223.56.140 on 09/04/12
For personal use only.

excess mercury in a sealed tube (20 ml) at room temperature for 3 days, to convert the iodobistrifluoromethylphosphine to tetrakistrifluoromethyldiphosphine. The loss of weight was 0.217 g corresponding to the formation of the iodo-phosphine in 58% yield (based on the diphosphine).

Reaction of Tetrakistrifluoromethyldiphosphine with Iodomethane

The diphosphine (1.516 g) and iodomethane (0.452 g) in a sealed tube (30 ml) were heated to 70° for 20 hours after which spectroscopic examination of the contents of the tube showed that only a trace of methylbistrifluoromethylphosphine had been produced. The reaction mixture was next heated to 105° for 18 hours. Spectroscopic examination then showed that more methylbistrifluorophosphine had been formed; iodobistrifluoromethylphosphine was also present. The reaction mixture was shaken with mercury for 3 days in a sealed tube (30 ml) to convert the iodobistrifluoromethylphosphine to the diphosphine. The loss of weight was 0.084 g corresponding to reaction of not more than 2% of the iodomethane. The recovered reactants and products were finally heated to 150° for 48 hours. All the products were volatile and trap-to-trap distillation combined with spectroscopic examination of the fractions showed that a considerable quantity of methylbistrifluoromethylphosphine was present; tristrifluoromethylphosphine was also found but only a trace of unreacted iodomethane remained. The loss of weight on shaking the combined fractions with excess mercury for 3 days at room temperature was 0.308 g corresponding to an over-all reaction up to 76% of the iodomethane.

There is much uncertainty in estimating the extent of the reactions of the diphosphine, especially at higher temperatures, owing to the tendency of the iodo-phosphines to disproportionate (1).

$$2(CF_3)_2PI \leftrightarrow (CF_3)_3P + CF_3PI_2$$

Reactions of this kind would then increase the expected yield of tristrifluoromethylphosphine. The presence of tristrifluoromethylphosphine in the products of the reaction of the diphosphine with iodomethane indicates such disproportionation has taken place as it is unlikely that methylbistrifluoromethylphosphine would disproportionate within the temperature range used for the reactions (6). Similarly estimating the extent of the reactions by loss of weight of iodine can at best be only approximate as the reaction of iodobistrifluoromethylphosphine with mercury is not quantitative (1), and the reaction of diiodotrifluoromethylphosphine with mercury gives involatile polymers, $(CF_3P)_x$, as well as mercuric iodide (14) resulting in a greater loss of weight than would occur if only the mercuric iodide remained in the reaction tube.

Reaction of Iododimethylarsine with Trifluoroiodomethane in the Presence of Mercury

Iododimethylarsine was prepared by the reduction of a solution of cacodylic acid in hydrochloric acid with sulphur dioxide, in the presence of potassium iodide (15). The iodo-arsine (15 g), trifluoroiodomethane (37.99 g), and mercury (200 g) in a sealed tube (150 ml) were shaken for 3 days at room temperature. Trap-to-trap distillation of the volatile contents of the tube gave unreacted trifluoroiodomethane (28.35 g) and a fraction condensing at −98°. This fraction was distilled in a nitrogen atmosphere at 760 mm in a low temperature still to give dimethyltrifluoromethylarsine (4.52 g, 40%; b.p.: found 58°, lit. value 58° (5)).

Reaction of Diiodomethylarsine with Trifluoroiodomethane in the Presence of Mercury

Diiodomethylarsine was prepared by the reduction of a solution of methylarsonic acid

Can. J. Chem. Downloaded from www.nrcresearchpress.com by 41.223.56.140 on 09/04/12
For personal use only.

in hydrochloric acid with sulphur dioxide, in the presence of potassium iodide (16). The iodo-arsine (38.9 g), trifluoroiodomethane (81.7 g), and mercury (300 g) in a sealed tube (150 ml) were shaken for 1 week at room temperature. Trap-to-trap distillation of the volatile products gave methylbistrifluoromethylarsine (3.689 g, 14%) which was identified spectroscopically and by molecular weight determination (mol. wt.: found 224, calc. 228).

Reaction of Chlorodimethylarsine with Trifluoroiodomethane in the Presence of Mercury

Chlorodimethylarsine was prepared by the reduction of a solution of cacodylic acid in hydrochloric acid with hypophosphorous acid (17). The arsine (7.2 g), trifluoroiodomethane (23.32 g), and mercury (150 g) in a sealed tube (150 ml) were shaken for 3 days at room temperature. Spectroscopic examination of the various fractions isolated by trap-to-trap distillation showed that only a trace of dimethyltrifluoromethylarsine had been produced. The recovery of trifluoroiodomethane was almost quantitative (23.19 g).

Reaction of Iododimethylarsine with Heptafluoroiodopropane in the Presence of Mercury

The iodo-arsine (8.2 g), heptafluoroiodopropane (33.5 g), and mercury (250 g) in a sealed tube (150 ml) were shaken at room temperature for 5 days. Fractionation of the volatile products gave unreacted heptafluoroiodopropane (19.9 g) and a fraction condensing at −64°. This fraction was distilled in a nitrogen atmosphere to give a further 11.1 g of heptafluoroiodopropane (b.p. 42°) and heptafluoropropyldimethylarsine (b.p. 93°) (1.6 g, 16%). Anal. calc. for $C_5H_6AsF_7$: C, 21.9; H, 2.19; As, 27.4; F, 48.5%; mol. wt., 274. Found: C, 22.2; H, 2.42; As, 27.5; F, 47.2%; mol. wt., 271.

The infrared spectrum showed the following absorption bands: vapor phase: 3010(vw), 2930(w), 2830(vw), 1427(w), 1345(vs), 1232(vs), 1224(vs), 1180(vs), 1157(s), 1129(vs), 1114(vs), 1070(m), 1042(s), 905(m), 882(m), 855(s), 822(s), 737(vs), 670(s).

Hydrolysis of Heptafluoropropyldimethylarsine

The arsine (0.168 g) and water (10 ml) were immiscible in a sealed tube (40 ml). Fractionation of the contents of the tube after 11 days at room temperature showed that no heptafluoropropane had been produced. The arsine (0.246 g) and 10% sodium hydroxide solution (10 ml) in a sealed tube (40 ml) were heated to 100° for 3 days. Fractionation of the contents of the tube gave heptafluoropropane (0.040 g, 26%) which was identified spectroscopically.

ACKNOWLEDGMENTS

The author wishes to acknowledge financial assistance from the National Research Council of Canada. He is also indebted to Drs. H. C. Clark and C. J. Willis for helpful discussions. Microanalyses for C, H, As, and F were carried out by Dr. Alfred Bernhardt.

REFERENCES

1. F. W. Bennett, H. J. Emeléus, and R. N. Haszeldine. J. Chem. Soc. 1565 (1953).
2. G. R. A. Brandt, H. J. Emeléus, and R. N. Haszeldine. J. Chem. Soc. 2552 (1952).
3. H. J. Emeléus, R. N. Haszeldine, and R. C. Paul. J. Chem. Soc. 881 (1954).
4. H. J. Emeléus, R. N. Haszeldine, and E. G. Walachewski. J. Chem. Soc. 1552 (1953).
5. R. N. Haszeldine and B. O. West. J. Chem. Soc. 3631 (1956).
6. R. N. Haszeldine and B. O. West. J. Chem. Soc. 3880 (1957).
7. A. Cahours. Ann. **122**, 192 (1862). C. J. Mortimer and H. A. Skinner. J. Chem. Soc. 4331 (1952).
8. W. Steinkopf and G. Schwenn. Ber. **54**, 1437 (1921).
9. C. A. Kraus and W. V. Sessions. J. Am. Chem. Soc. **47**, 2361 (1925). G. Gruttner. Ber. **50**, 1808 (1917).
10. H. C. Clark and C. J. Willis. J. Am. Chem. Soc. In press.
11. H. J. Emeléus and J. D. Smith. J. Chem. Soc. 375 (1959).

Can. J. Chem. Downloaded from www.nrcresearchpress.com by 41.223.56.140 on 09/04/12
For personal use only.

12. B. O. WEST. Ph.D. Thesis, Cambridge. 1954.
13. R. W. BUNSEN. Ann. **42**, 14 (1842).
14. W. MAHLER and A. B. BURG. J. Am. Chem. Soc. **80**, 6161 (1958).
15. G. J. BURROWS and E. E. TURNER. J. Chem. Soc. 1373 (1920).
16. G. J. BURROWS and E. E. TURNER. J. Chem. Soc. 426 (1921).
17. W. STEINKOPF and W. MIEG. Ber. **53**, 1013 (1920).

Can. J. Chem. Downloaded from www.nrcresearchpress.com by 41.223.56.140 on 09/04/12
For personal use only.

Can. J. Chem. Downloaded from www.nrcresearchpress.com by 41.223.56.140 on 09/04/12
For personal use only.

PERFLUOROALKYL ARSENICALS

PART II. THE PREPARATION AND PROPERTIES OF ARYL PERFLUOROALKYL ARSENICALS[1]

W. R. CULLEN

ABSTRACT

The reaction of iododiphenylarsine with trifluoroiodomethane in the presence of mercury produces diphenyltrifluoromethylarsine. Phenylbistrifluoromethylarsine and methylphenyltrifluoromethylarsine are prepared from similar reactions using diiodophenylarsine and iodomethylphenylarsine respectively. The properties of these new trifluoromethyl arsenicals are compared with those of related compounds.

DISCUSSION AND RESULTS

Although alkyl-trifluoromethyl-arsines have been known for some time (1, 2) no method of preparing aryl-trifluoromethyl-arsines was available. The reaction of trifluoroiodomethane with methyl-iodo-arsines in the presence of mercury has been recently found to yield methyl-trifluoromethyl-arsines (3) and by extending this reaction it has now been found that aryl-trifluoromethyl-arsines can be similarly prepared from aryl-iodo-arsines. Thus diphenyltrifluoromethylarsine is prepared by the reaction of trifluoroiodomethane with iododimethylarsine in the presence of mercury, phenylbistrifluoromethylarsine is prepared from diiodophenylarsine, and methylphenyltrifluoromethylarsine from iodomethylphenylarsine.

$$(C_6H_5)RAsI + Hg + ICF_3 \rightarrow (C_6H_5)RAsCF_3 + HgI_2 \qquad R = C_6H_5 \text{ or } CH_3$$

$$C_6H_5AsI_2 + 2Hg + 2ICF_3 \rightarrow C_6H_5As(CF_3)_2 + 2HgI_2.$$

The aryl-trifluoromethyl-arsines are involatile, colorless liquids of faint odor; they are stable to oxygen and moisture at ordinary temperatures. Table I gives their boiling points and those of related compounds, and it is apparent that the usual increase in volatility found on replacing all the hydrogens of methyl groups by fluorine is shown by these new compounds.

TABLE I

Compound	B.p.	Compound	B.p.
$(C_6H_5)_3As$	>360°	$C_6H_5As(CH_3)_2$	193–200°
$(C_6H_5)_2AsCH_3$	100–101 (10^{-3} mm)	$C_6H_5As(CF_3)_2$	160
$(C_6H_5)_2AsCF_3$	86–88 (10^{-3} mm)	$C_6H_5(CH_3)AsCF_3$	186

Diphenyltrifluoromethylarsine is less stable thermally than triphenylarsine, being decomposed slowly at 250° and at a much faster rate at 300°. The main volatile decomposition products are fluoroform and benzene. Triphenylarsine is stable above 360° and tristrifluoromethylarsine is unstable at 350° (4).

Diphenyltrifluoromethylarsine is stable to concentrated hydrochloric acid at 85° and is only slowly hydrolyzed to fluoroform by 10% aqueous sodium hydroxide at the same temperature. It is, however, unstable to alcoholic potassium hydroxide at 85°. The rate of hydrolysis of the aryl-trifluoromethyl-arsines increases as the number of trifluoromethyl groups is increased. A similar trend is shown by the rates of hydrolysis of the compounds $(CF_3)_nM(CH_3)_{3-n}$ (M = P, As, or Sb) (2). Methylphenyltrifluoromethylarsine is

[1]*Manuscript received November 23, 1959.*
Contribution from the Chemistry Department, University of British Columbia, Vancouver, B.C.

hydrolyzed much faster than is diphenyltrifluoromethylarsine indicating that alkyl-trifluoromethyl-arsines would be hydrolyzed more easily than the aryl-trifluoromethyl-arsines. When liquid ammonia is the solvolytic agent both diphenyltrifluoromethyl- and methylphenyltrifluoromethyl-arsine are only slowly attacked. The ammonolysis of phenylbistrifluoromethylarsine is faster as would be expected since ammonolysis of trifluoromethyl compounds parallels hydrolysis (5).

Diphenyltrifluoromethylarsine reacts with bromine in carbon tetrachloride solution to give diphenyltrifluoromethylarsenic dibromide. This compound, m.p. 110° (decomp.), is unstable to moisture and is easily hydrolyzed by aqueous sodium hydroxide to fluoroform (cf. the stability of diphenyltrifluoromethylarsine). In this case the fluoroform could easily be produced by elimination from an initially formed hydroxybromide. At 120° it decomposes to bromotrifluoromethane and bromodiphenylarsine. Bromination of methylphenyltrifluoromethylarsine under similar conditions appears to produce the pentavalent dibromide but this is unstable and decomposes to give mainly bromomethane, together with bromotrifluoromethane.The involatile liquid produced by the reaction is probably mainly bromophenyltrifluoromethylarsine. Although phenylbistrifluoromethyl-arsine was decomposed by bromine no evidence was obtained for the intermediate formation of a pentavalent dibromide; at 20° no decolorization of the bromine solution took place on addition to a solution of the arsine and no solid was obtained from the reaction. Tristrifluoromethylarsine is also decomposed by bromine without the formation of a pentavalent compound (6). Tertiary arsine dihalides containing both aromatic and alkyl groups decompose on heating to an alkyl halide and a secondary halogenated arsine (7).

$$RR_2'AsX_2 \rightarrow R_2'AsX + RX \qquad R = \text{alkyl group}$$
$$R_2R'AsX_2 \rightarrow RR'AsX + RX \qquad R' = \text{aryl group}$$

Thus the ease of loss of groups from the pentavalent dibromides seems to be in the order $C_6H_5 < CF_3 < CH_3$.

The aryl-trifluoromethyl-arsines do not easily form -onium compounds with iodomethane. No reaction occurs when ether solutions of the arsines and iodomethane are mixed and the reaction of diphenyltrifluoromethylarsine with excess iodomethane at 150° produces trifluoroiodomethane and fluoroform. Both tristrifluoromethylarsine and methyl-bistrifluoromethylarsine behave similarly (6, 2), but dimethyltrifluoromethylarsine reacts directly with iodomethane to give trimethyltrifluoromethylarsonium iodide (1). Dimethyl-trifluoromethylarsine is also the only arsine containing trifluoromethyl groups which is known to form a complex with mercuric chloride (8) since the aryl-trifluoromethyl-arsines failed to react on mixing solutions of mercuric chloride with solutions of the arsines.

The infrared spectra of the aryl trifluoromethyl arsenicals show the usual strong C—F stretching bands in the region 1050–1250 cm^{-1}. The compounds with only one trifluoromethyl group in the molecule show only two bands in this region, a feature which has been observed for other trifluoromethyl compounds (9, 10). The bands associated with the phenyl groups show little variation in intensity or position from compound to compound. The ultraviolet spectra of these and related compounds have been studied and the results will be published later.

Radical exchange reactions have previously been used to prepare alkyl-trifluoromethyl-arsines, as follows (1, 2, 6):

$$2(CH_3)_3As + CF_3I \rightarrow (CH_3)_2AsCF_3 + (CH_3)_4AsI,$$
$$(CF_3)_3As + CH_3I \rightarrow (CF_3)_2AsCH_3 + CF_3I.$$

Can. J. Chem. Downloaded from www.nrcresearchpress.com by 41.223.56.140 on 09/04/12
For personal use only.

In the present work it was found that analogous reactions do not produce aryl-trifluoromethyl-arsines. There is no reaction between tristrifluoromethylarsine and iodobenzene at 240°, and the reaction of trifluoroiodomethane with triphenylarsine at 210° gives a mixture of products including fluoroform, benzotrifluoride, benzene, and arsenic triodide. Neither phenylbistrifluoromethyl- nor diphenyltrifluoromethyl-arsine is produced.

EXPERIMENTAL

Apparatus and Technique

Conventional vacuum techniques were used for the manipulation of volatile reactants and products out of contact with moisture and oxygen. Reactions were carried out in sealed Pyrex tubes in the absence of air and light. Gas phase molecular weights were determined by Regnault's method. Infrared spectra were measured on a Perkin–Elmer Model 21 double-beam instrument with rock-salt optics.

Reaction of Iododiphenylarsine with Trifluoroiodomethane in the Presence of Mercury

Iododiphenylarsine was prepared by the action of hydriodic acid on bis-diphenylarsenic oxide (11). The oxide was prepared from phenylmagnesium bromide and arsenious oxide (12). The iodo-arsine (19.5 g), trifluoroiodomethane (41.2 g), and mercury (200 g) in a sealed tube (150 ml) were shaken at 20° for 3 days. Trap-to-trap distillation of the volatile contents of the tube gave only trifluoroiodomethane (30.6 g). The remaining contents of the tube were extracted with benzene which was then removed by distillation at 760 mm in a nitrogen atmosphere leaving a colorless involatile liquid. The liquid was distilled at 10^{-3} mm and the fraction boiling at 86–88° collected. This fraction (12.4 g) was identified as *diphenyltrifluoromethylarsine* (76% yield). Anal. calc. for $C_{13}H_{10}AsF_3$: C, 52.4; H, 3.4; As, 25.2; F, 19.1%; mol. wt., 298. Found: C, 52.3; H, 3.5; As, 25.4; F, 19.4%; mol. wt., 286. The infrared spectrum showed the following absorption bands: liquid film: 3075(m), 2220(w), 1963(w), 1882(w), 1813(w), 1755(w), 1650(w), 1584(w), 1490(m), 1443(m), 1387(w), 1340(w), 1311(w), 1272(w), 1257(w), 1190(w), 1137(vs), 1105(vs), 1028(m), 1003(m), 974(w), 916(w), 848(w), 738(s), 726(m), 696(s) cm^{-1}.

Reaction of Diiodophenylarsine with Trifluoroiodomethane in the Presence of Mercury

Diiodophenylarsine was prepared from phenylarsineoxide and hydriodic acid (13). The iodo-arsine (41.7 g) trifluoroiodomethane (80 g), and mercury (350 g) in a sealed tube (150 ml) were shaken for 7 days at 20°. The excess trifluoroiodomethane was removed by trap-to-trap distillation and the remaining contents of the tube were extracted with benzene. Distillation of the benzene extracts at 760 mm in an atmosphere of nitrogen gave *phenylbistrifluoromethylarsine*, b.p. 160° (2.9 g, 10% yield). Anal. calc. for $C_8H_5AsF_6$: C, 33.1; H, 1.7; As, 25.8; F, 39.3%; mol. wt., 290. Found: C, 33.2; H, 1.7; As, 26.3; F, 39.0%; mol. wt., 276. A small amount of an unidentified substance which boiled at 90–95° (10^{-3} mm) was also isolated. Qualitative tests showed that this substance did not contain any As—I bonds. The infrared spectrum of phenylbistrifluoromethylarsine showed the following absorption bands: liquid film: 3085(w), 2220(w), 1970(w), 1908(w), 1889(w), 1833(w), 1815(w), 1759(w), 1658(w), 1584(w), 1492(m), 1447(m), 1390(w), 1342(w), 1264(w), 1168(vs), 1126(vs), 1100(vs), 1064(m), 1051(m), 1030(m), 1005(m), 975(w), 922(w), 850(w), 828(w), 792(m), 765(m), 742(s), 733(s), 695(s).

Reaction of Iodomethylphenylarsine with Trifluoroiodomethane in the Presence of Mercury

Iodomethylphenylarsine was prepared by the reduction of a hydrochloric acid solution of methylphenylarsinic acid with sulphur dioxide in the presence of potassium iodide. The

Can. J. Chem. Downloaded from www.nrcresearchpress.com by 41.223.56.140 on 09/04/12
For personal use only.

arsinic acid was prepared from iodomethane and phenylarsenoxide (14). The iodo-arsine (11 g), trifluoroiodomethane (40 g), and mercury (200 g) in a sealed tube (150 ml) were shaken for 5 days at 20°. The contents of the tube were worked up in the same manner as described for the preparation of phenylbistrifluoromethylarsine and *methylphenyltrifluoromethylarsine*, b.p. 186° (760 mm), was isolated in 67% yield. Anal. calc. for $C_8H_8AsF_3$: C, 40.7; H, 3.4; F, 24.2%; mol. wt., 236. Found: C, 41.0; H, 3.6; F, 24.5%; mol. wt., 235. The infrared spectrum showed the following absorption bands: liquid film: 3080(w), 3025(w), 2925(w), 2240(w), 1985(w), 1965(w), 1900(w), 1879(w), 1810(w), 1753(w), 1648(w), 1585(w), 1490(m), 1443(m), 1423(m), 1388(w), 1337(w), 1309(w), 1264(w), 1252(w), 1189(w), 1141(vs), 1098(vs), 1073(s), 1027(m), 1003(m), 971(w), 913(w), 891(w), 852(m), 815(w), 740(s), 725(m), 696(s).

Solvolysis of the Aryl Trifluoromethyl Arsenicals

The results of a number of solvolysis experiments which were carried out in sealed tubes (40 ml) are given below. The identity and purity of the fluoroform isolated by trap-to-trap distillation from these reactions was checked spectroscopically and, where possible, by molecular weight measurement. Fluoride ion was not detected as a product from any of the reactions.

TABLE II

Compound	mmoles	Solvolysis reagent	Time	Temp.	Yield of fluoroform
$(C_6H_5)_2AsCF_3$	1.12	10% aqueous NaOH (5 ml)	5 days	85°	11.5%
$(C_6H_5)_2AsCF_3$	1.37	Liquid NH_3 (3.59 g)	5 days	20°	Trace[a]
$(C_6H_5)_2AsCF_3$	1.03	Conc. HCl (10 ml)	2 days	85°	None
$(C_6H_5)_2AsCF_3$	1.52	10% ethanolic KOH (5 ml)	3 hours	85°	94.5%
$C_6H_5As(CF_3)_2$	0.641	10% aqueous NaOH (5 ml)	5 days	85°	98%
$C_6H_5As(CF_3)_2$	0.934	Liquid NH_3 (3.51 g)	10 days	20°	56.5%[b]
$C_6H_5As(CF_3)CH_3$	0.779	10% aqueous NaOH (5 ml)	5 days	85°	60%
$C_6H_5As(CF_3)CH_3$	0.943	Liquid NH_3 (3.96 g)	10 days	20°	Trace[c]
$(C_6H_5)_2CF_3AsBr_2$	0.146	10% aqueous NaOH (5 ml)	4 days	20°	94%

[a]Recovered 1.36 mmoles of $(C_6H_5)_2AsCF_3$.

[b]A white hygroscopic crystalline solid, soluble in ammonia but insoluble in ether was left in the tube after the volatile contents had been removed. The solubility in ether precludes the possibility that the compound was $C_6H_5As{=}NH$ (15). The infrared spectrum of the solid suggested that it was $(C_6H_5AsCF_3)_2NH$ since only one N—H stretching band and only two C—F stretching bands were present (9, 10).

[c]No solid was produced and the involatile liquid remaining in the reaction tube after removal of the more volatile NH_3 and CF_3H was identified spectroscopically as unchanged $(C_6H_5)CH_3AsCF_3$.

Reactions of Diphenyltrifluoromethylarsine

(a) Preparation of Diphenyltrifluoromethylarsenic Dibromide

A solution of bromine (1 g, 6.24 mmoles) in carbon tetrachloride (5 ml) was slowly added to a solution of diphenyltrifluoromethylarsine (1.174 g, 3.94 mmoles) in the same solvent (5 ml). The bromine was decolorized until excess was present. The solvent and excess bromine were removed *in vacuo* at 20° to give a pale yellow solid (1.836 g), the increase in weight corresponding to the addition of bromine to the arsine in the mole ratio of 1.05 to 1. The solid was recrystallized from ether to give colorless, hygroscopic rhombohedrons which melted at 110° with decomposition. Analysis identified the solid as *diphenyltrifluoromethylarsenic dibromide*. Anal. calc. for $C_{13}H_{10}AsBr_2F_3$: Br, 34.9%. Found: Br, 35.1%. The infrared spectrum showed the following absorption bands: Nujol mull and KBr disk: 3395(w), 2330(w), 1570(w), 1559(w), 1480(m), 1460(w), 1442(m), 1380(w), 1330(w), 1304(w), 1273(w), 1187(s), 1171(s), 1158(s), 1082(s), 1019(w), 966(w), 828(w),

Can. J. Chem. Downloaded from www.nrcresearchpress.com by 41.223.56.140 on 09/04/12
For personal use only.

744(s), 736(s), 681(s). The dibromide (0.065 g) in a sealed tube (5 ml) was heated to 120° for 18 hours. Trap-to-trap distillation of the volatile products together with spectroscopic examination and molecular weight determination showed that only bromotrifluoromethane had been produced (0.0204 g, 97%; mol. wt.: found 153, calc. 149). A white solid which remained in the tube was identified as impure bromodiphenylarsine (m.p.: found 48–50°, lit. value 54–56° (11)).

(b) Thermal Decomposition of Diphenyltrifluoromethylarsine

The arsine (0.121 g) in a sealed tube (5 ml) was heated to 247° for 20 hours. Trap-to-trap distillation and spectroscopic examination of the very small amount of volatile product (1 mg) showed that this was mainly fluoroform. The liquid which remained in the reaction tube when examined spectroscopically was found to be mainly unchanged arsine. The arsine (0.113 g) in a sealed tube (5 ml) was heated to 302° for 48 hours. A black solid was deposited on the tube walls and no liquid remained. Trap-to-trap distillation of the volatile products gave a fraction which condensed at −196° (0.026 g) which was identified spectroscopically as a mixture of fluoroform, silicon tetrafluoride, and carbon dioxide, and a fraction which condensed at −98° (0.035 g) which was identified spectroscopically as benzene.

(c) Reaction with Methyl Iodide

The arsine (0.229 g) in ether solution (3 ml) was mixed with a solution of methyl iodide (1 g) in ether (5 ml). No precipitate was formed and after removal of the volatile materials the arsine (0.229 g) was recovered. The arsine (0.276 g) and methyl iodide (2.27 g) in a sealed tube (10 ml) were heated to 112° for 12 days; a very small amount of solid was formed. The tube was then left at 150° for a further 10 days. Trap-to-trap distillation of the volatile products gave a fraction condensing at −196° (0.019 g) which was identified spectroscopically as a mixture of fluoroform and trifluoroiodomethane, and a fraction condensing at −132° (0.099 g) which was shown spectroscopically and by molecular weight measurement to be slightly impure trifluoroiodomethane (mol. wt.: found 190, calc. 196). The remaining volatile fractions and the tarry material remaining in the reaction tube were not further investigated.

(d) Reaction with Mercuric Chloride and Cadmium Chloride

The arsine failed to give a complex with mercuric chloride when alcohol or ether solutions of the two reactants were mixed. Similarly, no complex was obtained from alcohol or ether solutions of the arsine and cadmium chloride.

Reaction of Methylphenyltrifluoromethylarsine with Bromine

A solution of bromine (1 g) in carbon tetrachloride (5 ml) was added to a solution of the arsine (0.721 g) in the same solvent (3 ml). The bromine was decolorized until excess was present. The volatile materials were removed *in vacuo* at 20° and a pale yellow solid remained which on standing for 2 hours at 20° decomposed to a colorless liquid (0.240 g). Spectroscopic examination of this liquid showed that trifluoromethyl and phenyl groups were still present and that no bromobenzene had been produced. The volatile products of the reaction were shaken with mercury in a sealed tube to remove the excess bromine. Trap-to-trap distillation of the contents of the tube gave a fraction (0.377 g), which had a molecular weight of 107, and which was found spectroscopically to be a mixture of bromomethane and bromotrifluoromethane. On the basis of the molecular weight this corresponds to loss of up to 100% of the methyl groups and loss of ca. 19% of the trifluoromethyl groups from the starting material. Thus the liquid formed in the initial reaction was probably mainly bromophenyltrifluoromethylarsine.

Can. J. Chem. Downloaded from www.nrcresearchpress.com by 41.223.56.140 on 09/04/12
For personal use only.

Reactions of Phenylbistrifluoromethylarsine

(a) Reaction with Bromine

A solution of bromine (0.7 g) in carbon tetrachloride (25 ml) was added to a solution of the arsine (0.652 g) in the same solvent; the bromine was not decolorized. The reaction mixture was left for 30 minutes at 20° after which the volatile materials were removed *in vacuo* at 20°. No solid was formed and an involatile liquid (0.374 g) was left in the reaction vessel. Qualitative tests showed that the liquid contained bromine and spectroscopic examination showed that the material contained no bromobenzene and was probably mainly bromophenyltrifluoromethylarsine.

(b) Reactions with Iodomethane and Mercuric Chloride

When ether solutions of iodomethane and the arsine were mixed no precipitate was obtained and after removal of the volatile materials the arsine was recovered. No precipitate was obtained on mixing ethanol solutions of the arsine and mercuric chloride.

Reaction of Tristrifluoromethylarsine with Iodobenzene

Tristrifluoromethylarsine was obtained from the reaction of trifluoroiodomethane with arsenic (6). The arsine (0.989 g) and iodobenzene (2.654 g) in a sealed tube (20 ml) were heated to 220° for 36 hours. Spectroscopic examination of the products of the reaction showed that no fluoroform or trifluoroiodomethane had been formed. The tristrifluoromethylarsine was recovered quantitatively (0.982 g; mol. wt: found 281, calc. 282).

Reaction of Triphenylarsine with Trifluoroiodomethane

The arsine (3.81 g) and trifluoroiodomethane (26.02 g) in a sealed tube (100 ml) were left at 20°. The arsine was completely soluble and there was no sign of reaction. After 7 days trifluoroiodomethane (25.89 g) was recovered unchanged. Similarly, there was no reaction between the arsine (2.05 g) and trifluoroiodomethane (4.932 g) after 4 days at 85°. The arsine (4.5 g) and trifluoroiodomethane (10.15 g) in a sealed tube (150 ml) were heated to 210° for 12 hours. Trap-to-trap distillation of the volatile products gave impure trifluoroiodomethane (4.62 g) which spectroscopic examination showed to contain fluoroform and a fraction condensing at −98° (2.69 g) which was identified spectroscopically as a mixture of benzene and benzotrifluoride. A yellow involatile liquid and a yellow solid remained in the tube. The liquid was extracted from the tube with ether which was then removed by distillation in a nitrogen atmosphere. Spectroscopic examination of the involatile residue showed the absence of either phenylbistrifluoromethylarsine or diphenyltrifluoromethylarsine. The solid (1.7 g) was identified as arsenic triiodide (m.p.: found 145°, lit. value 146°).

ACKNOWLEDGMENTS

The author wishes to acknowledge financial assistance from the National Research Council of Canada. He is also indebted to Dr. C. J. Willis for helpful discussions. Microanalyses for C, H, As, F and determinations of molecular weight were carried out by Dr. Alfred Bernhardt.

REFERENCES

1. R. N. Haszeldine and B. O. West. J. Chem. Soc. 3631 (1956).
2. R. N. Haszeldine and B. O. West. J. Chem. Soc. 3880 (1957).
3. W. R. Cullen. Can. J. Chem. **38**, 439 (1960).
4. P. B. Ayscough and H. J. Emeléus. J. Chem. Soc. 3381 (1954).
5. W. R. Cullen and H. J. Emeléus. J. Chem. Soc. 372 (1959).
6. H. J. Emeléus, R. N. Haszeldine, and E. G. Walachewski. J. Chem. Soc. 1552 (1953).

Can. J. Chem. Downloaded from www.nrcresearchpress.com by 41.223.56.140 on 09/04/12
For personal use only.

7. C. W. RAIZISS and J. L. GAVRON. Organic arsenical compounds. The Chemical Catalog Co., Inc., New York. 1923.
8. H. J. EMELÉUS, R. N. HASZELDINE, and R. C. PAUL. J. Chem. Soc. 881 (1954).
9. F. W. BENNETT, H. J. EMELÉUS, and R. N. HASZELDINE. J. Chem. Soc. 1565 (1953).
10. W. MAHLER and A. B. BURG. J. Am. Chem. Soc. **80**, 6161 (1958).
11. W. J. POPE and E. E. TURNER. J. Chem. Soc. 1447 (1920).
12. F. F. BLICKE and F. D. SMITH. J. Am. Chem. Soc. **51**, 1558 (1929).
13. A. MICHAELIS and C. SCHULTE. Ber. **14**, 912 (1881).
14. G. J. BURROWS and E. E. TURNER. J. Chem. Soc. 426 (1921).
15. A. MICHAELIS. Ann. **320**, 271 (1902).

Can. J. Chem. Downloaded from www.nrcresearchpress.com by 41.223.56.140 on 09/04/12
For personal use only.

Can. J. Chem. Downloaded from www.nrcresearchpress.com by 41.223.56.140 on 09/04/12
For personal use only.

STEROIDS AND RELATED PRODUCTS

XIII. THE SYNTHESIS OF 6α-FLUORO-17α-BROMOPROGESTERONE[1, 2]

CH. R. ENGEL AND R. DEGHENGHI

ABSTRACT

The synthesis of 6α-fluoro-17α-bromoprogesterone, a new potent gestogen, from pregnenolone acetate, is reported.

In a previous publication of this series (2) our group reported the synthesis and marked progestational activity of 17α-bromoprogesterone. Revesz *et al.* (3) further investigated the biological properties of this compound and established *inter alia* that unlike progesterone, 11-dehydroprogesterone, and 17α-methylprogesterone, it exhibited oral luteoid activity and that it showed no oestrogenic or androgenic side effects. Recently, a number of laboratories reported that certain substitutions in position 6α of the steroid nucleus markedly increased the progestational effect, especially the oral activity, of the parent compound (4–14, compare also 15). Among the biologically most interesting substances of this kind were 6α-halogenated steroids (compare 9, 10, 14, and 15).

It seemed attractive to combine the work in these two fields by preparing 6-substituted 17-halogenated progesterone derivatives, since, in addition to producing compounds of potential biological interest, this would allow us to broaden our investigation of the influence of 17-substituents, especially of a large size, on the progestational activity. It was hoped that this study would ultimately lead to a better understanding of the mechanism by which such groups exert their activity-enhancing action.

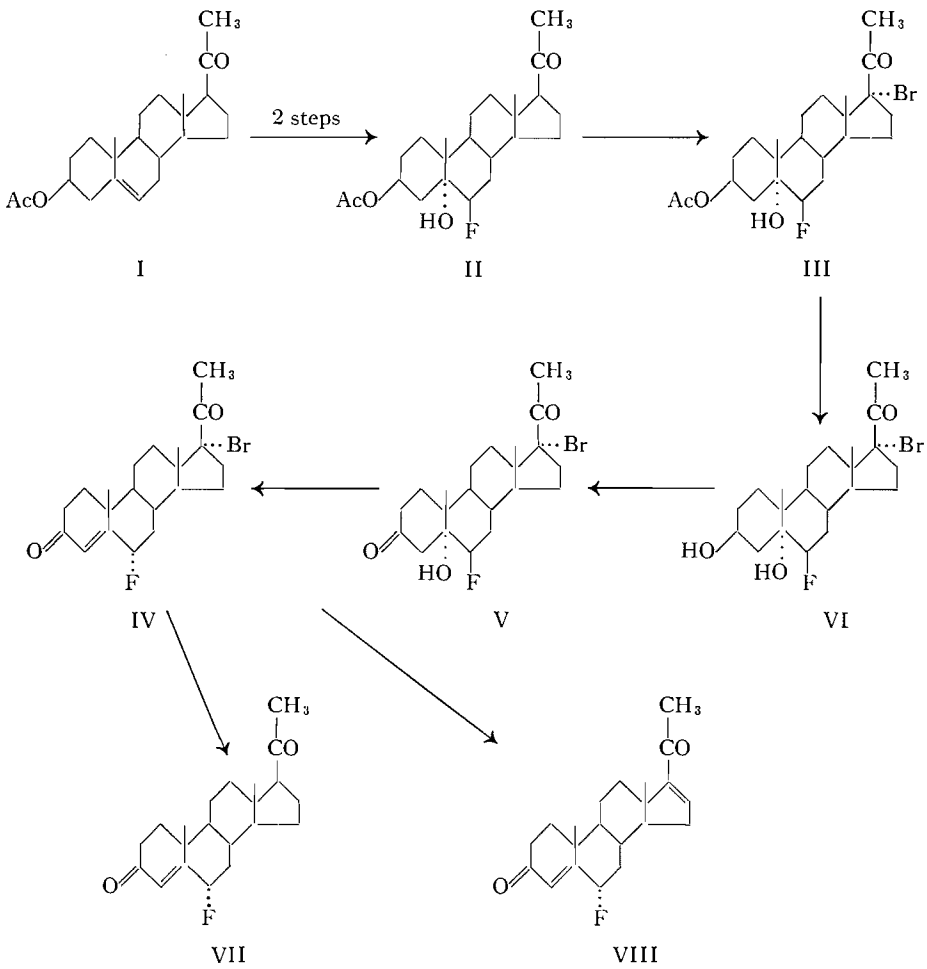
In the present paper we report the synthesis of 6α-fluoro-17α-bromoprogesterone (IV), the first 6,17-dihalogenated progesterone derivative.

Pregnenolone acetate (I) served as starting material. We transformed it, according to the procedure of Bowers and Ringold (16) [compare also the article by Henbest and Wrigley (17)], via the 5α,6α-epoxide, to 6β-fluoro-3β-acetoxy-5α-hydroxy-20-oxopregnane (II) which, upon treatment with N-bromosuccinimide under illumination (compare 18), gave in 80–85% yield the corresponding 17α-bromide III. The assignment of location of the bromine substituent to position 17α is in accord with analogous brominations (1, 18, 19) and was confirmed by the conversion of the derivative IV to the 16-unsaturated diketone VIII (*vide infra*). The typical levorotatory shift produced by bromination of 20-ketones in 17α (1, 2, 21) was observed.

Hydrolysis with perchloric acid in methanol (2, 20) gave in high yield the 3-hydroxy derivative VI which was oxidized with chromic acid and sulphuric acid in acetone (compare 16, 22, 23) to 6β-fluoro-17α-bromo-5α-hydroxy-3,20-dioxopregnane (V) in 60–70% yield. Dehydration with concomitant epimerization in 6 by treatment with hydrogen chloride in acetic acid (compare 16) gave the desired 6α-fluoro-17α-bromoprogesterone (IV) in approximately 70% yield.

The configuration of the 6-fluoro substituent was ascertained by the comparison of its molecular rotation (+50°) with the calculated value. Indeed, if, in accordance with the results in the 6-unsubstituted series (2), one assumes that the decrement of molecular rotation upon bromination in position 17α is −560°, one obtains from the rotations of the

[1]*Manuscript received November 19, 1959.*
Contribution from the Department of Chemistry, Laval University, Quebec, Que.
[2]*For Paper XII of this series see reference 1.*



6α- and 6β-fluoroprogesterones reported in the literature (10, 16) the values for the 6α- and 6β-fluoro-17α-bromoprogesterones, given in Table I. It can be clearly seen that the configuration of the 6-substituent of our 6,17-dihalogenated progesterone must be α. Comparable results are obtained when the decrements of molecular rotation, obtained upon bromination in 17α, are chosen from other series of experiments (compare i.e. 1, 21).

TABLE I

Molecular rotations of 6α- and 6β-fluoro-17α-bromoprogesterones[a]

Compound	$[M]_D$ calc.	$[M]_D$ found
6α-Fluoro-17α-bromoprogesterone	+35°[b] +75°[c]	+50°
6β-Fluoro-17α-bromoprogesterone	−290°[b] −215°[c]	

[a]The molecular rotations were calculated to the nearest 5°.

[b]Calculated from the values of the 17-unsubstituted products reported by Hogg *et al.* (10).

[c]Calculated from the values of the 17-unsubstituted products reported by Bowers and Ringold (16).

Can. J. Chem. Downloaded from www.nrcresearchpress.com by 41.223.56.140 on 09/04/12
For personal use only.

The structure of the new progesterone derivative IV was confirmed both by reduction with hydriodic acid (under the reaction conditions described by Zimmerman and Wen-Hsuan Cheng (24)), to 6α-fluoroprogesterone (VII) (10, 16) and by elimination of hydrogen bromide with dimethylformamide and lithium chloride (compare 25), leading to 16-dehydro-6α-fluoroprogesterone (VIII), which showed the typical spectral characteristics of the Δ^4-3-keto and Δ^{16}-20-keto moieties.

According to preliminary biological assays, for which we are indebted to Drs. M. Eisler and P. Perlman, 6α-fluoro-17α-bromoprogesterone (IV) exhibits marked progestational activity. A detailed account of the biological results will be published elsewhere.*

EXPERIMENTAL [3, 4, 5]

6β-Fluoro-17α-bromo-3β-acetoxy-5α-hydroxy-20-oxopregnane (III)

Following the procedure of Bowers and Ringold (16), pregnenolone acetate (I) was converted, via the 5α,6α-epoxide, to *6β-fluoro-3β-acetoxy-5α-hydroxy-20-oxopregnane* (II). The product crystallized from acetone–hexane in two modifications, one in leaflets melting at 186.5–187°, the other in prisms melting at 214–216°;[6] $[\alpha]_D^{22}$ +36° (*c*, 1.17 in $CHCl_3$); ν_{max}^{KBr} 1255 and 1730 cm^{-1} (acetate), 1692 cm^{-1} (20-ketone), 3360 cm^{-1} (hydroxy). Anal. Calc. for $C_{23}H_{35}O_4F$: C, 70.02; H, 8.94; F, 4.82. Found: C, 70.10; H, 9.00; F, 5.00.

To a solution of 1.082 g of 6β-fluoro-3β-acetoxy-5α-hydroxy-20-oxopregnane (II), m.p. 210–214°, in 18 cc of dichloromethane, 620 mg of N-bromosuccinimide and, subsequently, 36 cc of carbon tetrachloride were added. The solution was refluxed over a photoflood lamp for 10 minutes, cooled to room temperature, diluted with further quantities of dichloromethane, and washed with a cold 10% sodium bisulphite solution. The solution was dried with sodium sulphate, the solvent was removed *in vacuo*, and the residue (1.549 g) was crystallized from acetone to give 680 mg of bromoketone III, m.p. 159–160° decomp. The mother liquors were chromatographed on 30 g of silica gel. Benzene, containing 4% of ethyl acetate, eluted 401 mg of pure III, m.p. 168° decomp. (total yield 83%). A sample was recrystallized from methylene chloride – ether for analysis; colorless needles, m.p. 165° decomp., $[\alpha]_D^{24}$ −60.2° (*c*, 0.85 in $CHCl_3$); ν_{max}^{KBr} 1250 and 1720 cm^{-1} (acetate), 1692 cm^{-1} (20-ketone), 3400 cm^{-1} (5α-hydroxy). Anal. Calc. for $C_{23}H_{34}O_4FBr$: C, 58.35; H, 7.24; F, 3.92; Br, 16.88. Found: C, 58.06; H, 7.15; F, 4.22; Br, 16.79.

6β-Fluoro-17α-bromo-3β,5α-dihydroxy-20-oxopregnane (VI)

To a solution of 680 mg of 6β-fluoro-17α-bromo-3β-acetoxy-5α-hydroxy-20-oxopregnane (III), m.p. 159–160° decomp., in 90 cc of methanol was added, at room temperature, 4.5 cc of 70% aqueous perchloric acid. The solution was stored for 22 hours at 25° and was subsequently poured into iced dilute sodium bicarbonate solution. The precipitate was extracted with dichloromethane and the organic solution was washed with water, and was dried over sodium sulphate. Evaporation of the solvent *in vacuo* gave 670 mg of a foamy residue which, upon crystallization from acetone–hexane, afforded 530 mg (85% yield) of

[3] *The melting points were taken in evacuated capillaries and the temperatures were corrected.*

[4] *The microanalyses were performed by Dr. O. Schwarzkopf and his associates, New York, N.Y., to whom we express our sincere appreciation.*

[5] *For chromatography, Davison's silica gel No. 923 and non-alkaline aluminum oxide Woelm, activity II–III, were used.*

[6] *Bowers and Ringold (16) reported only the higher melting modification.*

*NOTE ADDED IN PROOF. — *Dr. R. Gaudry, Ayerst, McKenna & Harrison, Ltd., Montreal, informed us that his group also synthesized 6α-fluoro-17α-bromoprogesterone and that he intends to publish the results of his team shortly.*

Can. J. Chem. Downloaded from www.nrcresearchpress.com by 41.223.56.140 on 09/04/12
For personal use only.

crystalline hydroxy ketone VI, m.p. 156–158° decomp. A sample was recrystallized from acetone–hexane for analysis; needles, m.p. 165° decomp., $[\alpha]_D^{26}$ −66.6° (*c*, 1.05 in $CHCl_3$); ν_{max}^{KBr} 1695 cm^{-1} (20-ketone), 3380 cm^{-1} (5α-hydroxy), 3500 cm^{-1} (3β-hydroxy). Anal. Calc. for $C_{21}H_{32}O_3FBr$: C, 58.47; H, 7.47; F, 4.41; Br, 18.52. Found: C, 58.57; H, 7.25; F, 3.91; Br, 18.42.

6β-Fluoro-17α-bromo-5α-hydroxy-3,20-dioxopregnane (V)

To a solution of 608 mg of 6β-fluoro-17α-bromo-3β,5α-dihydroxy-20-oxopregnane (VI), m.p. 156–158° decomp., in 50 cc of absolute acetone, was added dropwise and with stirring, at 0–5°, 1 cc of an 8 *N* solution of chromic acid. The stirring was continued for 2.5 minutes and subsequently the mixture was poured into ice water and the colorless precipitate was filtered, washed to neutral, and dried. There was obtained 590 mg of a white solid which, upon crystallization from acetone–ether, gave 400 mg (65% yield) of V, m.p. 171° decomp. A sample was recrystallized from acetone–ether for analysis; prisms, m.p. 160° decomp., $[\alpha]_D^{24}$ −34.4° (*c*, 0.758 in $CHCl_3$); ν_{max}^{KBr} 1690 cm^{-1} (20-ketone), 1705 cm^{-1} (3-ketone), 3380 cm^{-1} (5α-hydroxy). Anal. Calc. for $C_{21}H_{30}O_3BrF$: C, 58.74; H, 7.04; F, 4.42; Br, 18.61. Found: C, 58.48; H, 7.10; F, 4.24; Br, 18.80.

Δ⁴-6α-Fluoro-17α-bromo-3,20-dioxopregnene (6α-Fluoro-17α-bromopregesterone) (IV)

At 10°, a stream of dry hydrogen chloride was passed for a period of 2 hours through a stirred solution of 470 mg of 6β-fluoro-17α-bromo-5α-hydroxy-3,20-dioxopregnane (V), in 47 cc of acetic acid. The solution was kept for 19 hours at 5–10° and was subsequently poured into ice water. The precipitate was filtered, washed to neutral, and dried. The resulting product (406 mg) was chromatographed on 45 g of silica gel. Benzene – ethyl acetate (97:3) eluted 312 mg (69% yield) of crystalline Δ⁴-6α-fluoro-17α-bromo-3,20-dioxopregnene (6α-fluoro-17α-bromoprogesterone) (IV), m.p. 157° decomp. A sample was recrystallized from acetone–hexane for analysis; fine needles, m.p. 169–170° decomp., $[\alpha]_D^{24}$ +12.1° (*c*, 2.46 in $CHCl_3$); λ_{max}^{EtOH} 236–237 mμ (log ε 4.2), ν_{max}^{KBr} 1621 and 1680 cm^{-1} (Δ⁴-3-ketone doublet), 1704 cm^{-1} (20-ketone). Anal. Calc. for $C_{21}H_{28}O_2FBr$: C, 61.31; H, 6.86; F, 4.62; Br, 19.43. Found: C, 61.33; H, 6.98; F, 4.40; Br, 19.63.

Reduction [6α-Fluoroprogesterone (VII)]

To a solution of 200 mg of 6α-fluoro-17α-bromoprogesterone (IV), m.p. 169–170° decomp., in 8 cc of absolute acetone was added, dropwise and with stirring, within 1.5 minutes, a solution of 1 cc of 55% hydriodic acid in 5 cc of absolute acetone. The mixture was poured into iced dilute sodium bisulphite solution, and the precipitate was extracted with dichloromethane. The organic solution was washed with dilute sodium bicarbonate solution and with water and was dried over sodium sulphate. Upon removal of the solvent there was obtained 150 mg of an oil, which crystallized from acetone–hexane to give colorless needles, m.p. 135–139°. A sample was recrystallized twice for analysis; long, silky needles, m.p. 143°, $[\alpha]_D^{26}$ +175° (*c*, 0.8 in $CHCl_3$); ν_{max}^{KBr} 1620 and 1680 cm^{-1} (Δ⁴-3-keto doublet), 1701 cm^{-1} (20-ketone); λ_{max}^{EtOH} 236 mμ (log ε 4.1). Anal. Calc. for $C_{21}H_{29}O_2F$: C, 75.87; H, 8.79; F, 5.71. Found: C, 76.16; H, 8.91; F, 5.63.

Dehydrobromination [6α-Fluoro-16-dehydroprogesterone (VIII)]

A solution of 144 mg of 6α-fluoro-17α-bromoprogesterone (IV), m.p. 162–164° decomp., in 25 cc of dimethylformamide was refluxed with 25 mg of lithium chloride for 1 hour. The cooled mixture was extracted with ether, the ethereal solution was washed with dilute hydrochloric acid, sodium bicarbonate solution, and water and dried over sodium sulphate. Removal of the solvent gave 108 mg of yellowish crystals, m.p. 142–146°. The product

Can. J. Chem. Downloaded from www.nrcresearchpress.com by 41.223.56.140 on 09/04/12
For personal use only.

was dissolved in benzene – ethyl acetate (97:3) and filtered through 4 g of silica gel. The colorless crystalline fractions (70 mg) were recrystallized twice from ether to afford pure $\Delta^{4,16}$-6α-fluoro-3,20-dioxopregnadiene (VIII), m.p. 162–163°, $[\alpha]_D^{26}$ +158.4° (*c*, 0.5 in $CHCl_3$), λ_{max}^{EtOH} 238 mμ (log ϵ 4.34); ν_{max}^{KBr} 1592 and 1662 cm^{-1} (Δ^{16}-20-ketone doublet), 1628 and 1678 cm^{-1} (Δ^4-3-ketone doublet). Anal. Calc. for $C_{21}H_{27}O_2F$: C, 76.33; H, 8.24; F, 5.75. Found: C, 76.22; H, 8.34; F, 5.61.

ACKNOWLEDGMENTS

We express our sincere thanks to Mr. D. Capitaine and Mrs. J. Capitaine for their devoted assistance in these experiments and to Drs. M. Eisler and P. Perlman, Bloomfield, New Jersey, for the preliminary biological tests. We are greatly indebted to the National Research Council of Canada, the Schering Corporation, Bloomfield, New Jersey, and the Schering Corporation Ltd., Montreal, for financial support of this project.

REFERENCES

1. R. Deghenghi and Ch. R. Engel. J. Am. Chem. Soc. In press. (1960).
2. Ch. R. Engel and H. Jahnke. Can. J. Biochem. and Physiol. **35**, 1047 (1957).
3. K. Revesz, R. Herné, and C. I. Chappel. Proc. Can. Federation Biol. Socs. **1**, 41 (1958); and personal communications by the authors.
4. A. David, F. Hartley, D. R. Millson, and V. Petrow. J. Pharm. and Pharmacol. **9**, 929 (1957).
5. H. J. Ringold, E. Batres, and G. Rosenkranz. J. Org. Chem. **22**, 99 (1957).
6. J. C. Babcock, E. S. Gutsell, M. E. Herr, J. A. Hogg, J. C. Stucki, L. E. Barnes, and W. E. Dulin. J. Am. Chem. Soc. **80**, 2904 (1958).
7. J. A. Campbell, J. C. Babcock, and J. A. Hogg. J. Am. Chem. Soc. **80**, 4717 (1958).
8. H. J. Ringold, J. Pérez Ruelas, E. Batres, and C. Djerassi. J. Am. Chem. Soc. **81**, 3712 (1959).
9. A. Bowers and H. J. Ringold. J. Am. Chem. Soc. **80**, 4423 (1958).
10. J. A. Hogg, G. B. Spero, J. L. Thompson, B. J. Magerlein, W. P. Schneider, D. H. Peterson, O. K. Sebek, H. C. Murray, J. C. Babcock, R. L. Pederson, and J .A. Campbell. Chem. & Ind. 1002 (1958).
11. A. Bowers, L. C. Ibànez, and H. J. Ringold. J. Am. Chem. Soc. **81**, 3707 (1959).
12. S. P. Barton, B. Ellis, and V. Petrow. J. Chem. Soc. 478 (1959).
13. P. B. Sollman, R. L. Elton, and R. M. Dodson. J. Am. Chem. Soc. **81**, 4435 (1959).
14. H. J. Ringold, E. Batres, A. Bowers, and J. Zederic. J. Am. Chem. Soc. **81**, 3485 (1959).
15. L. Fieser and M. Fieser. Steroids. Reinhold Publishing Corp., New York; and Chapman and Hall, Ltd., London. 1959. pp. 564–566.
16. A. Bowers and H. J. Ringold. Tetrahedron, **3**, 14 (1958).
17. H. B. Henbest and T. I. Wrigley. J. Chem. Soc. 4765 (1957).
18. R. U. Schock and W. J. Karpel. U.S. Patent No. 2,684,963 (1954).
19. Ch. R. Engel, G. Just, and R. G. Buttery. Unpublished data from this laboratory.
20. J. Fried and F. Sabo. J. Am. Chem. Soc. **74**, 3849 (1952).
21. H. Heusser, Ch. R. Engel, P. Th. Herzig, and Pl. A. Plattner. Helv. Chim. Acta, **33**, 2229 (1950).
22. K. Bowden, J. M. Heilbron, E. R. H. Jones, and B. C. L. Weedon. J. Chem. Soc. 3911 (1946).
23. C. Djerassi, R. R. Engle, and A. Bowers. J. Org. Chem. **21**, 1547 (1956).
24. H. E. Zimmerman and Wen-Hsuan Cheng. J. Am. Chem. Soc. **81**, 3634 (1959).
25. R. P. Holysz. J. Am. Chem. Soc. **75**, 4432 (1953).

Can. J. Chem. Downloaded from www.nrcresearchpress.com by 41.223.56.140 on 09/04/12
For personal use only.

Can. J. Chem. Downloaded from www.nrcresearchpress.com by 41.223.56.140 on 09/04/12
For personal use only.

REACTION OF *syn*-BENZALDOXIME WITH CARBON MONOXIDE AND HYDROGEN TO YIELD SUBSTITUTED UREAS

A. ROSENTHAL AND J. P. O'DONNELL

Our previous successful application of a modified oxo reaction to aromatic ketoximes (1) led us to subject an aromatic aldoxime to the action of carbon monoxide and hydrogen in the presence of preformed dicobalt octacarbonyl. Although *syn*-benzaldoxime is generally known to be resistant to dehydration, there is mention in the recent literature (2) that this isomer, when subjected to a pressure of 38,400 atm at a temperature of 200°, underwent an explosive decomposition to ammonia and a carbonaceous material.

When a benzene solution of *syn*-benzaldoxime was subjected to a mixture of carbon monoxide and hydrogen (98.5:1.5) at 300 atm and at about 220° in the presence of a high concentration of preformed dicobalt octacarbonyl, *sym*-dibenzylurea and monobenzylurea were formed. The ureas were accompanied by a small amount of benzaldehyde, as well as two crystalline compounds (A and B) which possessed no carbonyl (by infrared analyses).

$$\mathrm{Ph{-}C(=N{-}OH){-}H} \xrightarrow{CO + H_2} \underset{(C)\ 35\%}{\mathrm{PhCH_2NHCONHCH_2Ph}} + \underset{(D)\ 10\%}{\mathrm{PhCH_2NHCONH_2}} + \underset{3\%}{\mathrm{PhCHO}} + \mathrm{A} + \mathrm{B}$$

The reaction mixture was separated chromatographically on alumina. Gas-chromatographic fractionation of the gaseous product of the reaction showed that all of the hydrogen had been consumed, and only unused carbon monoxide was present.

By analogy with our previously described work (1), phthalimidine could be expected as a product of this reaction. That this was not realized is further proof that aromatic aldoximes are more unstable than aromatic ketoximes. The presence of benzaldehyde in the product implies that some hydrolysis might have taken place, though it does not preclude the possibility that a complex formed by the reaction of *syn*-benzaldoxime with dicobalt octacarbonyl might have decomposed to yield benzaldehyde. In support of this speculation, it is to be noted that Greenfield and co-workers (3) have found that diphenylacetylene formed an unstable complex with dicobalt octacarbonyl, which decomposed at room temperature to yield benzil. Unfortunately, our attempts to form a complex of the aldoxime and the catalyst in open systems at moderate temperatures were fruitless. An unstable cobalt-containing material was isolated chromatographically from the original reaction mixture.

Monobenzyl and *sym*-dibenzylurea were identified by mixed melting point using authentic samples (4). These compounds also possessed infrared spectra identical with those of the authentic samples. *sym*-Dibenzylurea was also characterized by oxidation with sodium dichromate in glacial acetic acid to yield *sym*-dibenzoylurea.

The only tentative mechanism which the authors are able to advance in order to explain the formation of dibenzylurea is one deduced from the work of Natta and co-workers (5). When styrene, aniline, and carbon monoxide were reacted, the latter authors reported the presence of an abnormally high amount of diphenylurea and the reduction of styrene to ethylbenzene.

It was suggested that the cobalt carbonyl acted as a hydrogen-transfer agent by formation and decomposition of the hydrocarbonyl. Such a hypothesis might also apply to our reaction. Part of the *syn*-benzaldoxime might be expected to be reduced to benzylamine by the hydrogen present in the original gaseous reactants. The latter primary amine might then react with carbon monoxide and unreacted oxime in some type of hydrogen-transfer process to yield dibenzylurea.

$$PhCH{=}NOH + H_2 \rightarrow PhCH_2NH_2 + H_2O$$

$$2PhCH_2NH_2 + CO + PhCH{=}NOH \rightarrow PhCH_2NHCONHCH_2Ph + PhCH_2NH_2 + H_2O$$

EXPERIMENTAL

General Considerations

The equipment was described previously (1).

Reaction of syn-Benzaldoxime with Carbon Monoxide and Hydrogen

A mixture of 6.5 g (0.054 mole) of *syn*-benzaldoxime (6), 85 ml of catalyst solution containing 0.02 mole of dicobalt octacarbonyl in benzene and carbon monoxide containing 1.5% by volume of hydrogen (2300 p.s.i. at 11°) was placed in the high pressure bomb. The reactants were heated with rocking at 190–220° for 40 minutes. An observed pressure drop of 210 p.s.i. at 11° (2.1 moles per mole of substrate) was obtained. Vapor phase chromatography of the product gases showed carbon monoxide only to be present. After decomposition of the catalyst and removal of the benzene under vacuum, the residue was dissolved in 51 ml of benzene. A 3-ml aliquot of this solution was placed on an alumina column (125×30 mm diameter) for chromatography. The following mixtures of developer were then added consecutively.

(1) 125 ml of benzene gave 0.040 g of crystalline A which was recrystallized from light petroleum ether, m.p. 239–242°. Infrared (KBr): 3050 (w), 1589 (w), 1523 (s).

(2) 50 ml of benzene yielded nothing.

(3) 150 ml of benzene eluted 0.040 g of crystalline B which after two recrystallizations from light petroleum ether melted at 280–282°. Infrared (KBr): 3055 (w), 1601 (w), 1579 (w), 1507 (w).

(4) 450 ml of benzene removed no material.

(5) 300 ml of benzene–ethanol (99:1) yielded 0.120 g of compound C.

(6) 150 ml of benzene–ethanol (98:2) eluted no material.

(7) 50 ml of benzene–ethanol (98:2) gave 0.027 g of compound D.

Chromatography of an aliquot of the original reaction mixture on alumina using benzene eluted a red zone (not dicobalt octacarbonyl) which decomposed rapidly on standing. Addition of light petroleum ether to the red material produced a benzene-insoluble brown substance.

All attempts to form a complex between *syn*-benzaldoxime and preformed dicobalt octacarbonyl in benzene in open systems at different temperatures from 20° to 45° were fruitless.

Extraction of Benzaldehyde from the Reaction Mixture

After evaporation of the benzene from the reaction mixture under reduced pressure at 40°, the residue was extracted with light petroleum ether. Removal of the petroleum ether yielded impure benzaldehyde which was purified by conversion to the bisulphite salt. Reaction of the purified benzaldehyde with 2,4-dinitrophenylhydrazine gave the hydrazone (0.54 g), m.p. 235–237°, undepressed on admixture with an authentic sample of benzaldehyde 2,4-dinitrophenylhydrazone.

Can. J. Chem. Downloaded from www.nrcresearchpress.com by 41.223.56.140 on 09/04/12
For personal use only.

Characterization of Compound C (*sym-Dibenzylurea*)

Compound C was twice recrystallized from benzene – light petroleum ether, m.p. 168–169°. The mixed melting point of compound C and an authentic sample of *sym*-dibenzylurea (4) was 167–169°. The infrared spectra of both compounds were identical. Anal. Found: C, 74.87; H, 6.79; N, 11.91; mol. wt. (Rast), 263. Calc. for $C_{15}H_{16}N_2O$: C, 75.00; H, 6.67; N, 11.67; mol. wt., 240. Infrared of C (KBr): 3337 (s), 3043 (w), 2922 (w), 1625 (s), 1591 (s), 1575 (s), 1497 (w).

Oxidation of sym-Dibenzylurea (Compound C*) to sym-Dibenzoylurea*

Compound C (63 mg) was dissolved in 25 ml of glacial acetic acid, and sodium dichromate (0.3 g) was added to the solution. After the solution was refluxed for 4 hours, the reaction mixture was poured into 50 ml of water. Extraction of the aqueous solution with chloroform gave on evaporation 42 mg of product. Recrystallization of the latter from ethanol yielded *sym*-dibenzoylurea, m.p. 202–203°. The literature (7) melting point of *sym*-dibenzoylurea is 203°. Infrared spectrum (KBr): 3240 (w), 1753 (s), 1670 (s), 1603 (w), 1577 (w), 1534 (m), 1506 (m), 1480 (m), 1288 (m), 1266 (s), 1200 (m).

Characterization of Compound D *(Monobenzylurea)*

Several recrystallizations of compound D from benzene – light petroleum ether gave pure monobenzylurea, m.p. 147–149°. The mixed melting point of an authentic sample of monobenzylurea (4) and compound D was 147–149°. The infrared spectrum of compound D was identical with that of the authentic sample. Infrared of D (KBr): 3440 (s), 3328 (s), 3035 (w), 2922 (w), 1651 (s), 1601 (s), 1564 (s), 1499 (w), 1471 (m), 1458 (m).

ACKNOWLEDGMENTS

Grateful acknowledgment is made to the National Research Council for financial support of this work.

This research was also supported in part by a grant from the Petroleum Research Fund administered by the American Chemical Society. Grateful acknowledgment is hereby made to the donors of said fund.

The authors wish to thank Dr. S. Ryce and Mr. S. Ruzicka of this department for vapor phase chromatography.

1. A. Rosenthal, R. F. Astbury, and A. Hubscher. J. Org. Chem. **23**, 1037 (1958).
2. I. S. Bengelsdorf. J. Am. Chem. Soc. **80**, 1442 (1958).
3. H. Greenfield, H. W. Sternberg, R. A. Friédel, J. H. Wotiz, R. Markby, and I. Wender. J. Am. Chem. Soc. **78**, 120 (1956).
4. T. L. Davis and K. C. Blanchard. J. Am. Chem. Soc. **45**, 1819 (1923).
5. G. Natta, P. Pino, and R. Ercoli. J. Am. Chem. Soc. **74**, 4496 (1952).
6. E. Beckmann. Ber. **23**, 1685 (1890).
7. H. Biltz. Ber. **40**, 2635 (1907).

Received October 23, 1959.
Department of Chemistry,
University of British Columbia,
Vancouver 8, B.C.

SEPARATION OF SOME HEAVY METALS BY SOLVENT EXTRACTION AND BY PAPER CHROMATOGRAPHY

Gerhard Weidmann*

The partition of the chlorides of Fe, Co, and Cu between tri-*n*-butyl phosphate and an aqueous HCl solution of different concentrations was determined. Tri-*n*-butyl phosphate

**Present address: Coburg, Kanonenweg 33, West Germany.*

Can. J. Chem. Downloaded from www.nrcresearchpress.com by 41.223.56.140 on 09/04/12
For personal use only.

Characterization of Compound C (*sym-Dibenzylurea*)

Compound C was twice recrystallized from benzene – light petroleum ether, m.p. 168–169°. The mixed melting point of compound C and an authentic sample of *sym*-dibenzylurea (4) was 167–169°. The infrared spectra of both compounds were identical. Anal. Found: C, 74.87; H, 6.79; N, 11.91; mol. wt. (Rast), 263. Calc. for $C_{15}H_{16}N_2O$: C, 75.00; H, 6.67; N, 11.67; mol. wt., 240. Infrared of C (KBr): 3337 (s), 3043 (w), 2922 (w), 1625 (s), 1591 (s), 1575 (s), 1497 (w).

Oxidation of sym-Dibenzylurea (Compound C*) to sym-Dibenzoylurea*

Compound C (63 mg) was dissolved in 25 ml of glacial acetic acid, and sodium dichromate (0.3 g) was added to the solution. After the solution was refluxed for 4 hours, the reaction mixture was poured into 50 ml of water. Extraction of the aqueous solution with chloroform gave on evaporation 42 mg of product. Recrystallization of the latter from ethanol yielded *sym*-dibenzoylurea, m.p. 202–203°. The literature (7) melting point of *sym*-dibenzoylurea is 203°. Infrared spectrum (KBr): 3240 (w), 1753 (s), 1670 (s), 1603 (w), 1577 (w), 1534 (m), 1506 (m), 1480 (m), 1288 (m), 1266 (s), 1200 (m).

Characterization of Compound D *(Monobenzylurea)*

Several recrystallizations of compound D from benzene – light petroleum ether gave pure monobenzylurea, m.p. 147–149°. The mixed melting point of an authentic sample of monobenzylurea (4) and compound D was 147–149°. The infrared spectrum of compound D was identical with that of the authentic sample. Infrared of D (KBr): 3440 (s), 3328 (s), 3035 (w), 2922 (w), 1651 (s), 1601 (s), 1564 (s), 1499 (w), 1471 (m), 1458 (m).

ACKNOWLEDGMENTS

Grateful acknowledgment is made to the National Research Council for financial support of this work.

This research was also supported in part by a grant from the Petroleum Research Fund administered by the American Chemical Society. Grateful acknowledgment is hereby made to the donors of said fund.

The authors wish to thank Dr. S. Ryce and Mr. S. Ruzicka of this department for vapor phase chromatography.

1. A. Rosenthal, R. F. Astbury, and A. Hubscher. J. Org. Chem. **23**, 1037 (1958).
2. I. S. Bengelsdorf. J. Am. Chem. Soc. **80**, 1442 (1958).
3. H. Greenfield, H. W. Sternberg, R. A. Friédel, J. H. Wotiz, R. Markby, and I. Wender. J. Am. Chem. Soc. **78**, 120 (1956).
4. T. L. Davis and K. C. Blanchard. J. Am. Chem. Soc. **45**, 1819 (1923).
5. G. Natta, P. Pino, and R. Ercoli. J. Am. Chem. Soc. **74**, 4496 (1952).
6. E. Beckmann. Ber. **23**, 1685 (1890).
7. H. Biltz. Ber. **40**, 2635 (1907).

Received October 23, 1959.
Department of Chemistry,
University of British Columbia,
Vancouver 8, B.C.

SEPARATION OF SOME HEAVY METALS BY SOLVENT EXTRACTION AND BY PAPER CHROMATOGRAPHY

Gerhard Weidmann*

The partition of the chlorides of Fe, Co, and Cu between tri-*n*-butyl phosphate and an aqueous HCl solution of different concentrations was determined. Tri-*n*-butyl phosphate

**Present address: Coburg, Kanonenweg 33, West Germany.*

Can. J. Chem. Downloaded from www.nrcresearchpress.com by 41.223.56.140 on 09/04/12
For personal use only.

was also used as an extraction agent to separate the chlorides of Fe, Ni, and Co or Fe, Ni, and Cu. The R_F values of Mn, Fe, Co, Ni, and Cu were determined using as a solvent tri-*n*-butyl phosphate adjusted with HCl of different concentrations.

Tri-*n*-butyl phosphate (TBP) is well known as an extraction agent for uranium, plutonium, and some other actinides from nitrate solutions (1, 2).

Other authors have investigated the extraction of zirconium (3), copper, and cobalt (4) from concentrated chloride or aqueous solutions using TBP. McKay and Hesford (5) and Healy and Kennedy (6) reported the extraction of nitrates of metals. Peppard and co-workers (7, 8) first showed that a feasible extraction of actinides, lanthanides, scandium, and zirconium from HCl solutions is possible using TBP and TBP – dibutyl ether mixtures and aqueous solutions of different HCl concentration.

In this work we have investigated the dependence of the partition of $FeCl_3$, $CoCl_2$, and $CuCl_2$ between pure TBP and aqueous HCl solutions as a function of HCl concentration. Referring to the obtained distribution coefficients and the fact that Ni is not extracted by pure TBP, a separation of Ni, Fe, and Co or Ni, Fe, and Cu can be realized. TBP was also used as a solvent in paper chromatography to separate a mixture of $MnCl_2$, $FeCl_3$, $CoCl_2$, $NiCl_2$, and $CuCl_2$.

Determination of the Distribution Coefficients of Fe, Co, Cu

Commercially available TBP was purified by washing with a 5% sodium carbonate solution and then by distillation at about 178° C, 25 mm Hg. All other reagents were of analytical grade.

Previous qualitative tests have shown that the chlorides of Fe, Co, Cu are extracted by TBP from an aqueous HCl solution, while Ni is not extracted.

EXPERIMENTAL

Before determination of the distribution coefficients the organic solvent was saturated with water. After separation 200-ml portions of the organic phase were shaken at 20° C with the following molarities of HCl: 1, 2, 3, 4, 5, 6, 7, 8, 9, 10, 11. Each portion was shaken so often with quantities of the corresponding HCl molarity that finally the HCl concentration in the aqueous phase remained constant. For this reason the distribution coefficients and R_F values in the following figures and tables are plotted as a function not of the actual HCl concentration in TBP but of the HCl concentration in the aqueous solution.

The chlorides corresponding to about 100 mg of each element were separately dissolved in 50 ml HCl of different molarity and shaken with an equal volume of TBP adjusted with HCl of the corresponding molarity. After the separation of the two phases, aliquots were taken and analyzed. Before analysis, the metals dissolved in the TBP phase were re-extracted completely by water. Concentrations higher than about 10 mg per 100 ml water of Co and Cu were transformed into sulphates and were determined by electrolysis. Fe was determined by redox titrations. Lower concentrations of Fe, Co, and Cu were determined colorimetrically using sulphosalicylate ($5HO \cdot C_6H_3 \cdot (COOH)SO_3H$) for Fe, ammonium thiocyanate for Co, and tetramine copper-II-chloride for Cu (10). Measurements were made with an ELKO Photo II colorimeter.*

Figure 1 shows the distribution coefficients (D) of $FeCl_3$, $CoCl_2$, and $CuCl_2$ and Fig. 2

*Carl Zeiss, Oberkochem/Württ.

Can. J. Chem. Downloaded from www.nrcresearchpress.com by 41.223.56.140 on 09/04/12
For personal use only.

shows the per cent of metal extracted ($\%E$) as a function of the molarity of aqueous HCl. $\%E$ is related to D by the following equation:

$$\%E = \frac{100D}{D+(V_{aq}/V_{TBP})},$$

where V_{TBP} and V_{aq} represent respectively the volumes of the organic and the aqueous phases.

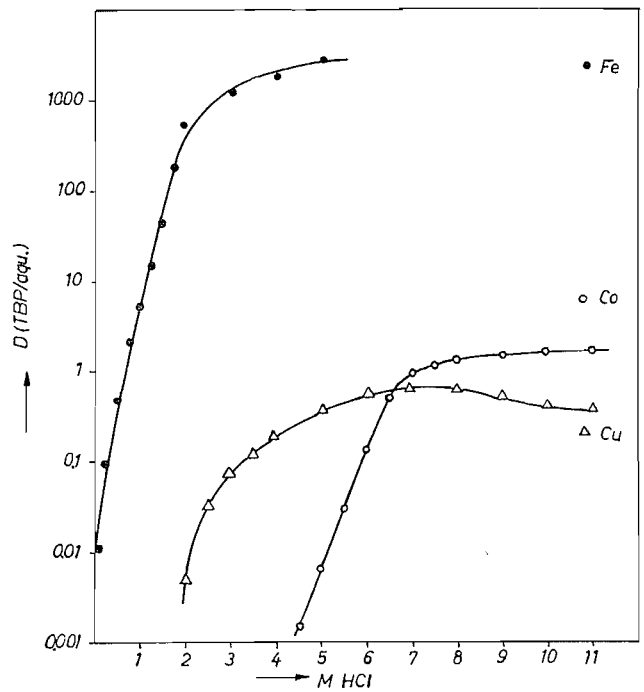


FIG. 1. Distribution of $FeCl_3$, $CoCl_2$, and $CuCl_2$ into TBP using HCl solutions of different molarity.

Separation of Ni, Fe, *and* Co *or* Ni, Fe, *and* Cu *Using* TBP *as an Extraction Agent*

As seen from Figs. 1 and 2 Fe can be easily separated from Co and Cu at about 2 *M* HCl, while a separation of Co and Cu is possible in the range from 2 to 4, 5 *M* HCl at a distribution coefficient$_{max}$ of Cu 0.288. The distribution coefficients of Co and Cu are greatest at high acid concentrations.

Procedure

The chlorides of Ni, Fe, and Co or Ni, Fe, and Cu each in portions of about 100 mg metal were dissolved in 2 *M* HCl. Fe was extracted quantitatively by adding TBP adjusted with 2 *M* HCl as described before, whereas Co(Cu), under these conditions, remains in the aqueous phase. After the acidity of the aqueous solution was increased to 10 *M* HCl for Co, or 8 *M* HCl for Cu, Co(Cu) was separated from Ni in stages by adding 30-ml portions of TBP. As mentioned before, Ni remains nearly completely in the aqueous phase. The chlorides of the metals in the TBP were re-extracted by water and were determined as described before. The procedure was repeated with four single samples and averages of the four results obtained for each element are recorded in Table I for Ni, Fe, Co and for Ni, Fe, Cu in Table II.

Can. J. Chem. Downloaded from www.nrcresearchpress.com by 41.223.56.140 on 09/04/12
For personal use only.

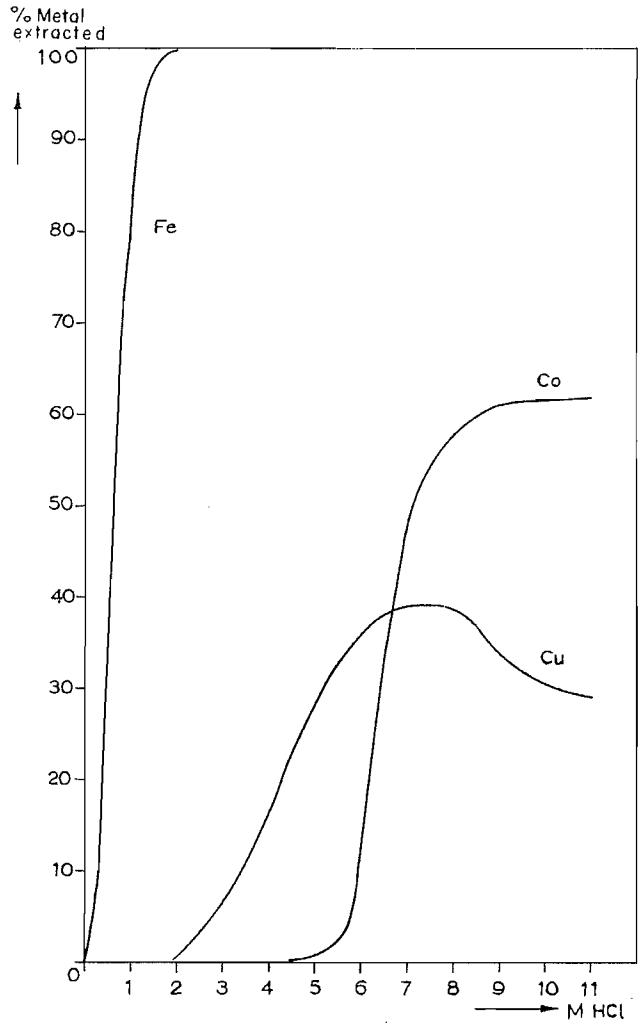


FIG. 2. Effect of hydrochloric acid concentration on the extractability of Fe-, Co-, and Cu-chlorides by TBP.

TABLE I

Separation of Ni, Fe, Co using TBP as an extraction agent

Solution of chlorides	Micrograms applied	Metal found	Recovery (%)
Ni	100.0	98.9	98.9
Fe	99.5	98.7	99.2
Co	98.9	98.0	99.1

Separation of Mn, Fe, Co, Ni, *and* Cu *by Paper Chromatography*

In another publication the author stated that TBP served as a solvent in paper chromatography to separate Ni and Co (11). Further on, TBP was tested also for other elements.

Can. J. Chem. Downloaded from www.nrcresearchpress.com by 41.223.56.140 on 09/04/12
For personal use only.

Can. J. Chem. Downloaded from www.nrcresearchpress.com by 41.223.56.140 on 09/04/12
For personal use only.

PLATE I

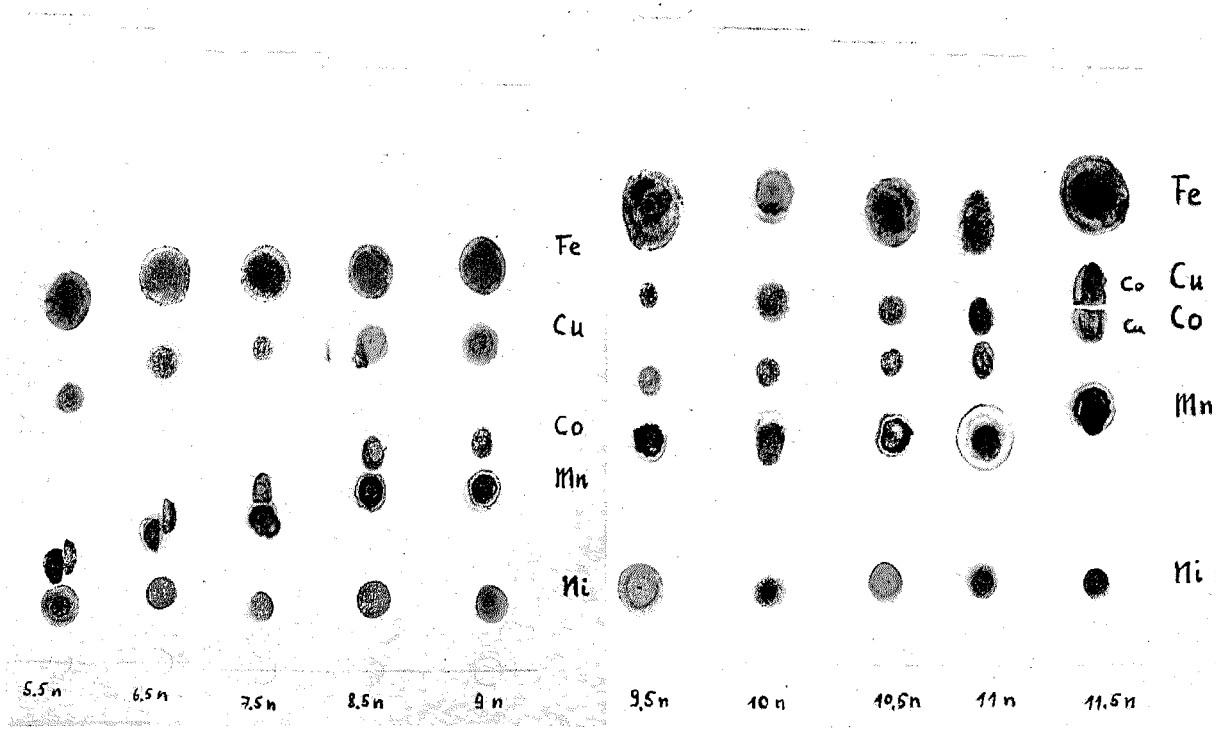


FIG. 3. Flow of Mn, Fe, Co, Ni, and Cu using a TBP/methanol mixture in the ratio 2:1 as a solvent.

The efficiency of TBP proved to be at least equal to that of other agents in the separation of Mn, Fe, Co, Ni, and Cu (12, 13, 14).

TABLE II

Separation of Ni, Fe, Cu using TBP as an extraction agent

Solution of chlorides	Micrograms applied	Metal found	Recovery (%)
Ni	100.0	98.9	98.9
Fe	99.5	98.6	99.0
Cu	101.2	100.1	98.9

Before use TBP was purified and then adjusted with HCl of different molarity as described above. The organic phase was separated and mixed with methanol (reagent grade) in the ratio of two volumes of TBP to one volume of methanol.

Procedure

The chromatograms were developed by ascending chromatography. The paper used was Schleicher and Schüll No. 4023*b* (Whatmann No. 1). Solutions of Mn-, Fe-, Ni-, Co-, and Cu-chlorides each in quantities of about 10 γ per 1 mm^3 were put on the paper. The process took 4 hours at a temperature of 22° C. Fe and Cu were easily identified by their yellow color and Co by its blue color.

In Fig. 3, Fe was marked with $K_4Fe(CN)_6$, Cu with an acetic acid – α-benzoinoxime solution, and Co with α-nitroso-β-naphthol. Ni was identified with an alcoholic solution of dimethyl glyoxime; Mn was first oxidized with sodium peroxide then marked with an acetic acid – benzidine solution (15).

RESULTS

The R_F values of Co, Mn, and Cu recorded in Table III show a significant dependence on the concentration of HCl used to equilibrate TBP. Increasing the concentration of HCl reduces the distance of Co, Mn, and Cu from the liquid front, i.e. the R_F values increase.

TABLE III

R_F values of Mn, Co, and Cu using TBP/methanol mixtures in the ratio 2:1

		TBP adjusted with HCl (molarity)									
		5.5	6.5	7.5	8.5	9.0	9.5	10.0	10.5	11.0	11.5
R_F	Mn	0.15	0.20	0.24	0.30	0.31	0.34	0.35	0.36	0.38	0.42
R_F	Co	0.16	0.23	0.28	0.35	0.38	0.43	0.46	0.48	0.51	0.61
R_F	Cu	0.42	0.48	0.52	0.54	0.56	0.57	0.57	0.57	0.58	0.59

At low concentrations of HCl similar R_F values are obtained for Co and Mn. However, this is optimum for the separation of Cu from Co and Mn. Increasing the concentration of HCl reduces the distance of Co from Cu and at a concentration of 11.5 *M* HCl the R_F value of Co is a little higher than the R_F of Cu.

The flow rates of Ni and Fe are independent of the HCl concentration and roughly proportional to the quantity of methanol present. Fe is always next to the liquid front (see Fig. 3).

Can. J. Chem. Downloaded from www.nrcresearchpress.com by 41.223.56.140 on 09/04/12
For personal use only.

SUMMARY

The chlorides of Fe, Co, and Cu were extracted by TBP from an aqueous HCl solution, while Ni was not extracted. Because of the different distribution coefficients of Fe, Co, and Cu, a separation of Ni, Fe, and Co or Ni, Fe, and Cu was possible. Fe can be easily separated from Ni, Co, and Cu at about 2 *M* HCl. After the acidity of the aqueous solution is increased to 10 *M* HCl for Co or 8 *M* HCl for Cu, Co or Cu can be separated from Ni.

TBP also served in paper chromatography as a solvent. Sharp chromatographic separations of the chlorides of Mn, Fe, Co, Ni, and Cu can be obtained using HCl-adjusted TBP. It is recommended that TBP is to be treated with 9 to 10 *M* HCl and mixed with methanol in the proportion 2:1.

With acknowledgments to Diplom-Chemiker H. G. Zimmermann and G. J. Weidmann for their help in translation and scientific discussion and to Mr. U. Mattern for experimental work.

1. K. ALCOCK, G. F. BEST, E. HESFORD, and H. A. C. MCKAY. J. Inorg. & Nuclear Chem. **6**, 328 (1958).
2. H. A. C. MCKAY and T. V. HEALY. Tri-*n*-butyl phosphate as an extracting agent. Anon. Progress in nuclear energy, Series 3, 546–556. Pergamon Press. 1959.
3. A. E. LEVITT and H. FREUND. J. Am. Chem. Soc. **78**, 1545 (1956).
4. M. CHATELETT and C. NICAUD. Chem. Revs. **242**, 1471, 1891 (1956).
5. E. HESFORD, E. E. JACKSON, and H. A. C. MCKAY. J. Inorg. & Nuclear Chem. **9**, 279 (1959).
6. T. V. HEALY, J. KENNEDY, and G. M. WAIND. J. Inorg. & Nuclear Chem. **10**, 137 (1959).
7. D. F. PEPPARD *et al.* J. Phys. Chem. **57**, 294 (1953).
8. D. F. PEPPARD, G. W. MASON, and J. L. MAIER. J. Inorg. & Nuclear Chem. **3**, 215 (1956).
9. J. J. GAL and A. RUVARAC. Bull. Inst. Nuclear Sci. "Boris Kidrich", **8**, 67 (1958).
10. B. LANGE. Kolorimetrische Analyse. Verlang Chemie G.m.b.H., Weinheim/Bergstr. 1956.
11. G. R. WEIDMANN. Can. J. Chem. **37**, 830 (1959).
12. W. J. FRIERSON and D. A. REARICK. Anal. Chem. **30**, 468 (1958).
13. F. H. BURSTALL *et al.* J. Chem. Soc. (London), 1497 (1952).
14. R. A. GUEDES DE CARVALHO. Anal. Chim. Acta, **16**, 555 (1957).
15. F. FEIGL. Spot tests in inorganic analysis. Elsevier Press, Inc., New York. 1958.

RECEIVED JUNE 19, 1959.
PRIVATE CONTRIBUTION.

THE YIELD OF Ba^{140} IN THE THERMAL NEUTRON FISSION OF U^{235} *

D. C. SANTRY† AND L. YAFFE

The fission product Ba^{140} has often been used as a standard in fission yield determinations. These determinations were usually subject to a large error due to uncertainties in the measurement of the various disintegration rates. In 1954, Yaffe *et al.* (1), using 4π β-counting methods, reported a value of $(6.32\pm0.24)\%$ for the yield of Ba^{140} in the thermal neutron fission of U^{235}.

The measurement consisted of a simultaneous, long-term irradiation of natural uranium and boron trifluoride. The Ba^{140} was estimated radiochemically and the depletion in the B^{10} content of the boron was determined mass spectrometrically. The Ba^{140} yield was estimated relative to a value of $\sigma_f/\sigma_B = 0.1456$ where σ_f is the fission cross section of U^{235} and σ_B is the cross section for the reaction $B^{10}(n,\alpha)Li^7$.

**Financial assistance was received from the Atomic Energy Control Board of Canada and the Defence Research Board.*

†*Present address: Chemistry Branch, Atomic Energy of Canada Limited, Chalk River, Ontario.*

Can. J. Chem. Downloaded from www.nrcresearchpress.com by 41.223.56.140 on 09/04/12
For personal use only.

SUMMARY

The chlorides of Fe, Co, and Cu were extracted by TBP from an aqueous HCl solution, while Ni was not extracted. Because of the different distribution coefficients of Fe, Co, and Cu, a separation of Ni, Fe, and Co or Ni, Fe, and Cu was possible. Fe can be easily separated from Ni, Co, and Cu at about 2 *M* HCl. After the acidity of the aqueous solution is increased to 10 *M* HCl for Co or 8 *M* HCl for Cu, Co or Cu can be separated from Ni.

TBP also served in paper chromatography as a solvent. Sharp chromatographic separations of the chlorides of Mn, Fe, Co, Ni, and Cu can be obtained using HCl-adjusted TBP. It is recommended that TBP is to be treated with 9 to 10 *M* HCl and mixed with methanol in the proportion 2:1.

With acknowledgments to Diplom-Chemiker H. G. Zimmermann and G. J. Weidmann for their help in translation and scientific discussion and to Mr. U. Mattern for experimental work.

1. K. ALCOCK, G. F. BEST, E. HESFORD, and H. A. C. MCKAY. J. Inorg. & Nuclear Chem. **6**, 328 (1958).
2. H. A. C. MCKAY and T. V. HEALY. Tri-*n*-butyl phosphate as an extracting agent. Anon. Progress in nuclear energy, Series 3, 546–556. Pergamon Press. 1959.
3. A. E. LEVITT and H. FREUND. J. Am. Chem. Soc. **78**, 1545 (1956).
4. M. CHATELETT and C. NICAUD. Chem. Revs. **242**, 1471, 1891 (1956).
5. E. HESFORD, E. E. JACKSON, and H. A. C. MCKAY. J. Inorg. & Nuclear Chem. **9**, 279 (1959).
6. T. V. HEALY, J. KENNEDY, and G. M. WAIND. J. Inorg. & Nuclear Chem. **10**, 137 (1959).
7. D. F. PEPPARD *et al.* J. Phys. Chem. **57**, 294 (1953).
8. D. F. PEPPARD, G. W. MASON, and J. L. MAIER. J. Inorg. & Nuclear Chem. **3**, 215 (1956).
9. J. J. GAL and A. RUVARAC. Bull. Inst. Nuclear Sci. "Boris Kidrich", **8**, 67 (1958).
10. B. LANGE. Kolorimetrische Analyse. Verlang Chemie G.m.b.H., Weinheim/Bergstr. 1956.
11. G. R. WEIDMANN. Can. J. Chem. **37**, 830 (1959).
12. W. J. FRIERSON and D. A. REARICK. Anal. Chem. **30**, 468 (1958).
13. F. H. BURSTALL *et al.* J. Chem. Soc. (London), 1497 (1952).
14. R. A. GUEDES DE CARVALHO. Anal. Chim. Acta, **16**, 555 (1957).
15. F. FEIGL. Spot tests in inorganic analysis. Elsevier Press, Inc., New York. 1958.

RECEIVED JUNE 19, 1959.
PRIVATE CONTRIBUTION.

THE YIELD OF Ba^{140} IN THE THERMAL NEUTRON FISSION OF U^{235} *

D. C. SANTRY† AND L. YAFFE

The fission product Ba^{140} has often been used as a standard in fission yield determinations. These determinations were usually subject to a large error due to uncertainties in the measurement of the various disintegration rates. In 1954, Yaffe *et al.* (1), using 4π β-counting methods, reported a value of $(6.32\pm0.24)\%$ for the yield of Ba^{140} in the thermal neutron fission of U^{235}.

The measurement consisted of a simultaneous, long-term irradiation of natural uranium and boron trifluoride. The Ba^{140} was estimated radiochemically and the depletion in the B^{10} content of the boron was determined mass spectrometrically. The Ba^{140} yield was estimated relative to a value of $\sigma_f/\sigma_B = 0.1456$ where σ_f is the fission cross section of U^{235} and σ_B is the cross section for the reaction $B^{10}(n,\alpha)Li^7$.

**Financial assistance was received from the Atomic Energy Control Board of Canada and the Defence Research Board.*

†*Present address: Chemistry Branch, Atomic Energy of Canada Limited, Chalk River, Ontario.*

Can. J. Chem. Downloaded from www.nrcresearchpress.com by 41.223.56.140 on 09/04/12
For personal use only.

Petruska *et al.* (2) introduced an additional self-shielding correction to the above value which they suggested should raise the value of the Ba^{140} yield to 6.55%. The uranium in the above-mentioned irradiation was in fairly massive form. This, coupled with the unpredictable nature of the geometrical arrangement, suggested to the present authors that the experiment be repeated under more favorable circumstances.

Accordingly, an irradiation was performed in a No. 1 self-serve position in the NRX Chalk River nuclear reactor. The uranium trioxide (63.67 mg) was placed in a quartz vial. Into similar tubes were sealed weighed amounts (1.348 and 1.174 mg) of "spec-pure" cobalt wire (0.005-in. diameter) which acted as flux monitors. The material was irradiated for 2.247 days. The neutron attenuations in the uranium and cobalt samples were calculated to be 1.0 and 2.1% respectively. The latter agreed with a similar value which R. E. Jervis of A.E.C.L., Chalk River, was kind enough to give to us for the same type of wire.

On removal from the reactor, the cobalt wires were dissolved and made up to a known volume. Measurements of the quartz vials after the removal of the cobalt wire indicated that the loss by recoil was negligible. A small aliquot of the cobalt solution was placed on a VYNS film and the Co^{60} disintegration rate determined in a 4π β-counter (3). Very small corrections were necessary for absorption in the very thin source and thin VYNS film. A thermal neutron flux value of 9.42×10^{11} n/cm^2 sec was obtained using 36.3 barns (4, 5) for the cross section of the reaction $Co^{59}(n,\gamma)Co^{60}$. Auxiliary measurements showed that the contribution by epicadmium neutrons in this irradiation position to the production of both Co^{60} and Ba^{140} was less than $\frac{1}{2}$%. The fission rate was then determined to be 5.220×10^8 fissions per second using σ_f equal to 571 barns (6). The reactor power was constant during this irradiation, so the normal saturation correction could be used.

The uranium trioxide was dissolved in dilute nitric acid and Ba^{140} was separated using standard methods. Agreement between theoretical and experimental growth and decay curves attested to the fact that both Ba^{140} with its soft β-component and La^{140}, the daughter with its hard β-component, were being measured with equal efficiency.

It can be shown that, if U_0 atoms of U^{235} were irradiated in a thermal flux I of a nuclear reactor for a time T, then at some time t, after removal from the reactor, the following equation would apply:

$$[1] \qquad N\lambda = U_0 I\sigma_f Y_f(1-e^{-\lambda T})e^{-\lambda t}.$$

In the above equation λ is the disintegration constant of the fission product being studied and N is the number of atoms of that nuclide present at time t. Thus $N\lambda$ is the disintegration rate. The fission cross section of U^{235} is represented by σ_f, and Y_f is the probability of formation, or the fission yield of the nuclide under study.

If some cobalt were irradiated simultaneously with and under the same conditions as the U^{235}, then the following equation would obtain:

$$[2] \qquad N_1\lambda_1 = N_{Co} I\sigma_c(1-e^{-\lambda_1 T})e^{-\lambda_1 t}.$$

As before, $N_1\lambda_1$ would be the disintegration rate of Co^{60}, N_{Co} the number of cobalt atoms placed in the reactor, and σ_c the thermal neutron cross section for the reaction $Co^{59}(n,\gamma)Co^{60}$.

If equations [1] and [2] are now divided, the term I cancels, all other quantities are easily measurable, and Y_f, the fission yield, can be determined in terms of σ_f/σ_c.

The fission yield of Ba^{140} was calculated in this manner and found to be (6.36 ± 0.12)%, in excellent agreement with that obtained earlier (1).

Can. J. Chem. Downloaded from www.nrcresearchpress.com by 41.223.56.140 on 09/04/12
For personal use only.

ACKNOWLEDGMENT

One of us (D.C.S.) gratefully acknowledges the receipt of a National Research Council Studentship.

1. L. YAFFE, H. G. THODE, W. F. MERRITT, R. C. HAWKINGS, F. BROWN, and R. M. BARTHOLOMEW. Can. J. Chem. **32**, 1017 (1954).
2. J. A. PETRUSKA, H. G. THODE, and R. H. TOMLINSON. Can. J. Phys. **33**, 693 (1955).
3. B. D. PATE and L. YAFFE. Can. J. Chem. **33**, 610 (1955).
4. R. S. CARTER, H. PALEVSKY, V. W. MYERS, and D. J. HUGHES. Phys. Rev. **92**, 716 (1953).
5. L. YAFFE, R. C. HAWKINGS, W. F. MERRITT, and J. A. CRAVEN. Phys. Rev. **82**, 553 (1951).
6. G. J. SAFFORD and E. MELKONIAN. Phys. Rev. Letters, **2**, 189 (1959).

RECEIVED NOVEMBER 27, 1959.
RADIOCHEMISTRY LABORATORY,
DEPARTMENT OF CHEMISTRY,
MCGILL UNIVERSITY,
MONTREAL, QUE.

THE PRIMARY PROCESS IN THE MERCURY-6($^3P_1$)-PHOTOSENSITIZED POLYMERIZATION OF ACETYLENE

ALDEN G. SHERWOOD AND HARRY E. GUNNING

In the reaction of Hg 6($^3P_1$) atoms with acetylene, LeRoy and Steacie (1) have suggested the following possible primary processes:

$$\text{Hg } 6(^3P_1) + C_2H_2 \rightarrow \text{Hg } 6(^1S_0) + H + C_2H \quad [1]$$

$$\rightarrow HgH + C_2H \quad [2]$$

$$\rightarrow HgC_2H + H. \quad [3]$$

An excited molecule mechanism has also been recently suggested (2). However such a sequence could not explain the observed consumption of mercury during the reaction. In the present study, the technique of monoisotopic mercury photosensitization in natural mercury vapor (3, 4, 5, 6, 7, 8) has been employed to determine the extent to which mercury consumption occurs in the primary reaction.

The apparatus used for the investigation was similar to that described in reference 5. The mercury in the electrodeless discharge source contained 95.0% ^{202}Hg. All runs were made at an acetylene pressure of 6.7 mm of Hg. The solid product of the reaction was a yellow deposit which formed on the walls of the spiral quartz reaction cell. The yellow product was treated in separate runs with a variety of reagents to convert the chemically combined mercury to a solution of mercuric ion, from which the mercury was extracted, after neutralization, by electrodeposition. Isotopic analysis of the mercury was carried out on a Metropolitan–Vickers, type MS-2, mass spectrometer. The results are summarized below:

Run No.	Treatment of product	% ^{202}Hg in recovered mercury
A	Solution in hot HNO_3–H_2SO_4	39.3
B	Solution in hot, conc. HCl	33.8
C	Solution in 0.1 *N* HCl	64.0
D	Solution in boiling water	62.7
E	Evacuation for 8 hours followed by solution in hot HNO_3–H_2SO_4	63.0
F	Solution in 2 *N* KI, 0.1 *N* in $Na_2S_2O_3$	32.4
	Natural abundance	29.8

Can. J. Chem. Downloaded from www.nrcresearchpress.com by 41.223.56.140 on 09/04/12
For personal use only.

ACKNOWLEDGMENT

One of us (D.C.S.) gratefully acknowledges the receipt of a National Research Council Studentship.

1. L. YAFFE, H. G. THODE, W. F. MERRITT, R. C. HAWKINGS, F. BROWN, and R. M. BARTHOLOMEW. Can. J. Chem. **32**, 1017 (1954).
2. J. A. PETRUSKA, H. G. THODE, and R. H. TOMLINSON. Can. J. Phys. **33**, 693 (1955).
3. B. D. PATE and L. YAFFE. Can. J. Chem. **33**, 610 (1955).
4. R. S. CARTER, H. PALEVSKY, V. W. MYERS, and D. J. HUGHES. Phys. Rev. **92**, 716 (1953).
5. L. YAFFE, R. C. HAWKINGS, W. F. MERRITT, and J. A. CRAVEN. Phys. Rev. **82**, 553 (1951).
6. G. J. SAFFORD and E. MELKONIAN. Phys. Rev. Letters, **2**, 189 (1959).

RECEIVED NOVEMBER 27, 1959.
RADIOCHEMISTRY LABORATORY,
DEPARTMENT OF CHEMISTRY,
MCGILL UNIVERSITY,
MONTREAL, QUE.

THE PRIMARY PROCESS IN THE MERCURY-6($^3P_1$)-PHOTOSENSITIZED POLYMERIZATION OF ACETYLENE

ALDEN G. SHERWOOD AND HARRY E. GUNNING

In the reaction of Hg 6($^3P_1$) atoms with acetylene, LeRoy and Steacie (1) have suggested the following possible primary processes:

$$\text{Hg } 6(^3P_1) + C_2H_2 \rightarrow \text{Hg } 6(^1S_0) + H + C_2H \quad [1]$$

$$\rightarrow HgH + C_2H \quad [2]$$

$$\rightarrow HgC_2H + H. \quad [3]$$

An excited molecule mechanism has also been recently suggested (2). However such a sequence could not explain the observed consumption of mercury during the reaction. In the present study, the technique of monoisotopic mercury photosensitization in natural mercury vapor (3, 4, 5, 6, 7, 8) has been employed to determine the extent to which mercury consumption occurs in the primary reaction.

The apparatus used for the investigation was similar to that described in reference 5. The mercury in the electrodeless discharge source contained 95.0% ^{202}Hg. All runs were made at an acetylene pressure of 6.7 mm of Hg. The solid product of the reaction was a yellow deposit which formed on the walls of the spiral quartz reaction cell. The yellow product was treated in separate runs with a variety of reagents to convert the chemically combined mercury to a solution of mercuric ion, from which the mercury was extracted, after neutralization, by electrodeposition. Isotopic analysis of the mercury was carried out on a Metropolitan–Vickers, type MS-2, mass spectrometer. The results are summarized below:

Run No.	Treatment of product	% ^{202}Hg in recovered mercury
A	Solution in hot HNO_3–H_2SO_4	39.3
B	Solution in hot, conc. HCl	33.8
C	Solution in 0.1 *N* HCl	64.0
D	Solution in boiling water	62.7
E	Evacuation for 8 hours followed by solution in hot HNO_3–H_2SO_4	63.0
F	Solution in 2 *N* KI, 0.1 *N* in $Na_2S_2O_3$	32.4
	Natural abundance	29.8

Can. J. Chem. Downloaded from www.nrcresearchpress.com by 41.223.56.140 on 09/04/12
For personal use only.

The results show conclusively that there is a primary process involving the formation of a mercury compound. The effects of the various methods of product treatment on the ^{202}Hg-content of the recovered mercury is instructive. In run A the hot HNO_3–H_2SO_4 reagent dissolved both the mercury compound and the cuprene polymer, together with any adsorbed natural mercury. The enrichment in ^{202}Hg was 32%. In run E the system, after reaction, was evacuated for 8 hours to pump off adsorbed natural mercury. The mercury recovered from this run, using the same reagent as in run A, was found to be enriched by 111% in ^{202}Hg. Previous experience has shown that it is very unlikely that all of the adsorbed natural mercury could be removed by this simple evacuation technique. The isotope-diluting effect of adsorbed natural mercury is also shown in run B. The hot, concentrated HCl reagent dissolved only the mercury compound and the adsorbed natural mercury. The cuprene was found to be insoluble under these conditions. The highest ^{202}Hg-enrichment was obtained by treating the product with dilute HCl as in run C. It is likely, however, that exchange reactions are occurring to some extent between dissolved natural mercury and $^{202}Hg^{+2}$ ions in the treatment with dilute HCl in run C and with boiling water in run D. The isotope-diluting effect of adsorbed natural mercury is obviously very extensive in the KI reagent used in run F.

The fact that mercury can be recovered from solution of the mercury product in boiling water would suggest that the primary product is readily hydrolyzed by water. This behavior is in consonance with the primary formation of a mercury carbide, as proposed in step [3].

As a result of this preliminary study it can be said that a mercury compound, probably a mercury carbide, is formed in the primary reaction between Hg $6(^3P_1)$ atoms and acetylene. A detailed investigation is currently underway in this laboratory to determine the specific primary processes operative in the acetylene reaction, and their relative importance.

The authors are indebted to The National Research Council, for financial assistance, and to the Associated Electrical Industries Export, Ltd., for performing the Mass Spectrometric Analyses.

1. D. J. LeRoy and E. W. R. Steacie. J. Chem. Phys. **12**, 117 (1944).
2. S. Shida, Z. Kuri, and T. Furuoya. J. Chem. Phys. **28**, 131 (1958).
3. K. R. Osborn, C. C. McDonald, and H. E. Gunning. J. Chem. Phys. **26**, 124 (1957).
4. H. E. Gunning. Can. J. Chem. **36**, 89 (1958).
5. R. Pertel and H. E. Gunning. Can. J. Chem. **37**, 35 (1959).
6. C. C. McDonald, J. R. McDowell, and H. E. Gunning. Can. J. Chem. **37**, 930 (1959).
7. K. R. Osborn and H. E. Gunning. Can. J. Chem. **37**, 1315 (1959).
8. J. R. McDowell, C. C. McDonald, and H. E. Gunning. Can. J. Chem. **37**, 1432 (1959).

Received November 16, 1959.
Department of Chemistry,
University of Alberta,
Edmonton, Alberta.

SENSITIVE FREQUENCIES. V. THE SENSITIVE AMMINE FREQUENCIES AND ELECTRONEGATIVITIES OF COMPLEX TRANSITION METAL ION RADICALS

J. K. Wilmshurst

The internal vibrational frequencies of the methyl group in the CH_3X derivatives are known to vary (1, 2, 3, 4) with the nature of the substituent X and as these variations are greater than those due to mass effects alone (5), they can be considered to reflect

Can. J. Chem. Downloaded from www.nrcresearchpress.com by 41.223.56.140 on 09/04/12
For personal use only.

The results show conclusively that there is a primary process involving the formation of a mercury compound. The effects of the various methods of product treatment on the ^{202}Hg-content of the recovered mercury is instructive. In run A the hot HNO_3–H_2SO_4 reagent dissolved both the mercury compound and the cuprene polymer, together with any adsorbed natural mercury. The enrichment in ^{202}Hg was 32%. In run E the system, after reaction, was evacuated for 8 hours to pump off adsorbed natural mercury. The mercury recovered from this run, using the same reagent as in run A, was found to be enriched by 111% in ^{202}Hg. Previous experience has shown that it is very unlikely that all of the adsorbed natural mercury could be removed by this simple evacuation technique. The isotope-diluting effect of adsorbed natural mercury is also shown in run B. The hot, concentrated HCl reagent dissolved only the mercury compound and the adsorbed natural mercury. The cuprene was found to be insoluble under these conditions. The highest ^{202}Hg-enrichment was obtained by treating the product with dilute HCl as in run C. It is likely, however, that exchange reactions are occurring to some extent between dissolved natural mercury and $^{202}Hg^{+2}$ ions in the treatment with dilute HCl in run C and with boiling water in run D. The isotope-diluting effect of adsorbed natural mercury is obviously very extensive in the KI reagent used in run F.

The fact that mercury can be recovered from solution of the mercury product in boiling water would suggest that the primary product is readily hydrolyzed by water. This behavior is in consonance with the primary formation of a mercury carbide, as proposed in step [3].

As a result of this preliminary study it can be said that a mercury compound, probably a mercury carbide, is formed in the primary reaction between Hg $6(^3P_1)$ atoms and acetylene. A detailed investigation is currently underway in this laboratory to determine the specific primary processes operative in the acetylene reaction, and their relative importance.

The authors are indebted to The National Research Council, for financial assistance, and to the Associated Electrical Industries Export, Ltd., for performing the Mass Spectrometric Analyses.

1. D. J. LeRoy and E. W. R. Steacie. J. Chem. Phys. **12**, 117 (1944).
2. S. Shida, Z. Kuri, and T. Furuoya. J. Chem. Phys. **28**, 131 (1958).
3. K. R. Osborn, C. C. McDonald, and H. E. Gunning. J. Chem. Phys. **26**, 124 (1957).
4. H. E. Gunning. Can. J. Chem. **36**, 89 (1958).
5. R. Pertel and H. E. Gunning. Can. J. Chem. **37**, 35 (1959).
6. C. C. McDonald, J. R. McDowell, and H. E. Gunning. Can. J. Chem. **37**, 930 (1959).
7. K. R. Osborn and H. E. Gunning. Can. J. Chem. **37**, 1315 (1959).
8. J. R. McDowell, C. C. McDonald, and H. E. Gunning. Can. J. Chem. **37**, 1432 (1959).

Received November 16, 1959.
Department of Chemistry,
University of Alberta,
Edmonton, Alberta.

SENSITIVE FREQUENCIES. V. THE SENSITIVE AMMINE FREQUENCIES AND ELECTRONEGATIVITIES OF COMPLEX TRANSITION METAL ION RADICALS

J. K. Wilmshurst

The internal vibrational frequencies of the methyl group in the CH_3X derivatives are known to vary (1, 2, 3, 4) with the nature of the substituent X and as these variations are greater than those due to mass effects alone (5), they can be considered to reflect

Can. J. Chem. Downloaded from www.nrcresearchpress.com by 41.223.56.140 on 09/04/12
For personal use only.

changes in the potential energy of the system. However, of the eight internal methyl group modes only three, the symmetrical deformation and the rocking modes, vary by a sufficiently large factor with changing X to make any empirical correlations meaningful and it has been shown in a previous publication (4) that the squares of these "sensitive" frequencies depend linearly on the electronegativity of X. Similar results would be expected for other series of the type MH_3X and, in fact, have been observed for the silyl (SiH_3X) derivatives (4).

In the present paper empirical plots of the squares of the symmetrical deformation and rocking frequencies in the ammine series (NH_3X) have been obtained against the electronegativity of X. The sensitive frequencies in the complex transition metal ammine ions have been fitted to these plots and estimates made for the electronegativity of the transition metal in its particular environment. A number of internal and external frequency relations in the MH_3X series are discussed and two are illustrated.

The Electronegativity Relation

In the ammine series, just as in the methyl and silyl series, only the symmetrical deformation (ν_d) and rocking frequency (ν_r) vary by a sufficiently large factor to warrant any reliable empirical correlation to be made. Only two simple NH_3—X molecules, in which the electronegativity of X is known (6) and for which the vibrational spectrum has been completely analyzed (7), are known, $[NH_3 \cdot OH]Cl$ and $[NH_3 \cdot NH_2]Cl$. If the assumption is made that the electronegativity of the mercury atom in $[Hg(NH_3)_2]Cl_2$ is

TABLE I

The ammine rocking and symmetrical deformation frequencies[a]

Compound	ν_d	ν_r	χ_X[b]	Ref.
$[NH_3 \cdot OH]Cl$	1478	1195, 1171	3.83[c]	7
$[NH_3 \cdot NH_2]Cl$	1414	1125, 1105	3.47[c]	7
$[Hg(NH_3)_2]Cl$	1268	719	1.93[d]	8
$[Co(NH_3)_6]Cl_2$	1158	650	1.39	10
$[Co(NH_3)_6]Cl_3$	1325	827	2.32	10
$[Co(NH_3)_5OH]Br_2$	1303	806	(2.19)	10
$[Co(NH_3)_5Cl]Br_2$	1310	840	(2.29)	10
$[Co(NH_3)_5Br]Br_2$	1312	832	(2.29)	10
$[Co(NH_3)_5H_2O]Cl_3$	1325	835	(2.33)	10
$[Co(NH_3)_5NO_2]Cl_2$	1315	850	2.33	10
Trans-$[Co(NH_3)_4(NO_2)_2]Cl$	1300	840	2.25	10
$[Co(NH_3)_3(NO_2)_3]$	1290	815	2.16	10
$K[Co(NH_3)_2(NO_2)_4]$	1265	790	2.02	10
$[Cr(NH_3)_6]Cl_3$	1314	757	(2.13)	10
$[Cr(NH_3)_5Cl]Cl_2$	1290	724	(2.07)	10
$[Cr(NH_3)_5NO_2]Cl_2$	1305	768	(2.11)	10
$[Ni(NH_3)_6]Cl_2$	1175	678	1.50	10
$[Cu(NH_3)_4]SO_4 \cdot H_2O$	1285	732	2.10	10
$[Pt(NH_3)_4]Cl_2$	1350	850	2.46	10
$[Pt(NH_3)_5Cl]Cl_2$	1355	935	2.70	10
Trans-$[Pt(NH_3)_2Cl_2]$	1295	815	(2.21)	10
$[Pd(NH_3)_4]Cl_2$	1304	827	2.25	10
Trans-$[Pd(NH_3)_2Cl_2]$	1250	756	1.90	10
$[Ag(NH_3)_2]_2SO_4$	1215	738	1.74	10
$[Na(NH_3)_4]Cl$	1105	500	1.00	[e]

[a]In cm^{-1}.

[b]Unless otherwise noted, electronegativity values were derived by fitting the sensitive frequencies to Fig. 1. Parentheses imply that compound is not shown in Fig. 1.

[c]Mean value of observed (refs. 9, 13) and calculated (ref. 11).

[d]Assumed the same as that for $Hg(CH_3)$.

[e]G. W. Leonard, E. R. Lippincott, R. D. Nelson, and D. E. Sellers. J. Am. Chem. Soc. 77, 2029 (1955).

Can. J. Chem. Downloaded from www.nrcresearchpress.com by 41.223.56.140 on 09/04/12
For personal use only.

the same as that in $Hg(CH_3)_2$, then the infrared spectral data for $[Hg(NH_3)_2]Cl_2$, which have been analyzed (8), can also be used. One further point at zero electronegativity is available if the effect of decreasing electronegativity (χ_x) of X on the rocking frequency in NH_3—X is considered. As $\chi_x \rightarrow 0$ the N—X bond strength must go to zero, the molecule falling apart and the rocking frequency going over into a pure rotation. The corresponding deformation frequency is just that for the ammonia molecule (9). The sensitive frequencies, ν_d, ν_r, for these molecules are given in Table I, together with the electronegativity, χ_x, of X.

As discussed elsewhere (4), the pair of lines ν_d^2 versus χ_x and ν_r^2 versus χ_x should be parallel and they are fitted to the four sets of points above* under this condition, the resulting plots being shown in Fig. 1. The analytical expressions for the pair of lines are

$$\nu_d^2 = 3.66\chi + 8.12$$

$$\nu_r^2 = 3.66\chi - 0.78$$

and these can be compared with the expressions for the corresponding lines obtained in the methyl (4), silyl (4), and germanyl† series:

$$CH_3X\begin{cases}\nu_d^2 = 4.21\chi+5.72\\ \nu_r^2 = 4.05\chi-1.78\end{cases}$$

$$SiH_3X\begin{cases}\nu_d^2 = 1.41\chi+4.83\\ \nu_r^2 = 1.40\chi+0.20\end{cases}$$

$$GeH_3X\begin{cases}\nu_d^2 = 1.22\chi+3.54\\ \nu_r^2 = 1.22\chi.\end{cases}$$

If the sensitive ammine frequencies observed (10) in the complex transition metal ions (Table I) are plotted on Fig. 1 in such a way that the deviation of ν_d^2 and ν_r^2 from their respective lines is equal for any molecule, estimates of the electronegativity of the transition metal ion in that configuration can be obtained‡ and these are given in Table I. Of interest is the fact that the electronegativity of the transition metal ion increases with increasing charge, e.g. cobalt and platinum, and that in the series $[Co(NH_3)_n(NO_2)_{6-n}]$ the electronegativity of the cobalt ion increases smoothly as n increases. Electronegativities of the transition metals and ions are only poorly known at present (11) and the method of calculating electronegativities for these elements from a consideration of the nuclear charge at the covalent boundary (12) is not applicable without some modification. Likewise, the method of calculation of group electronegativities (6) would not be applicable to the complex transition metal radicals without modification.

The scatter of the experimental points about the two lines in Fig. 1 is greater than that observed (4) in the methyl and silyl series. However, it must be remembered that in the latter two cases all compounds discussed were in the gaseous state whereas here all the ammines are solid. Thus, in the present case, the sensitive frequencies do not depend on electronegativity alone, but will also depend, though to a much lesser extent, on the type

*For molecules of symmetry C_{3v} the rocking modes are degenerate. For molecules of lower symmetry the average of the squares of the two rocking frequencies is plotted.

†The pair of lines for the germanyl series was obtained from the data of R. C. Lord and C.M. Steese (J. Chem. Phys. **22**, 542 (1954)) for GeH_3Cl with the consideration that in GeH_3^- ($\chi_x = 0$) the rocking frequency is zero. The line for ν_d^2 versus χ_x was drawn parallel to that for ν_r^2 versus χ_x and gave a deformation frequency for GeH_3^- of 595 cm^{-1}.

‡The meaning of such group electronegativities is, of course, dependent upon the reality of the empirical correlation (but see reference 5 for a more complete discussion).

Can. J. Chem. Downloaded from www.nrcresearchpress.com by 41.223.56.140 on 09/04/12
For personal use only.

Can. J. Chem. Downloaded from www.nrcresearchpress.com by 41.223.56.140 on 09/04/12
For personal use only.

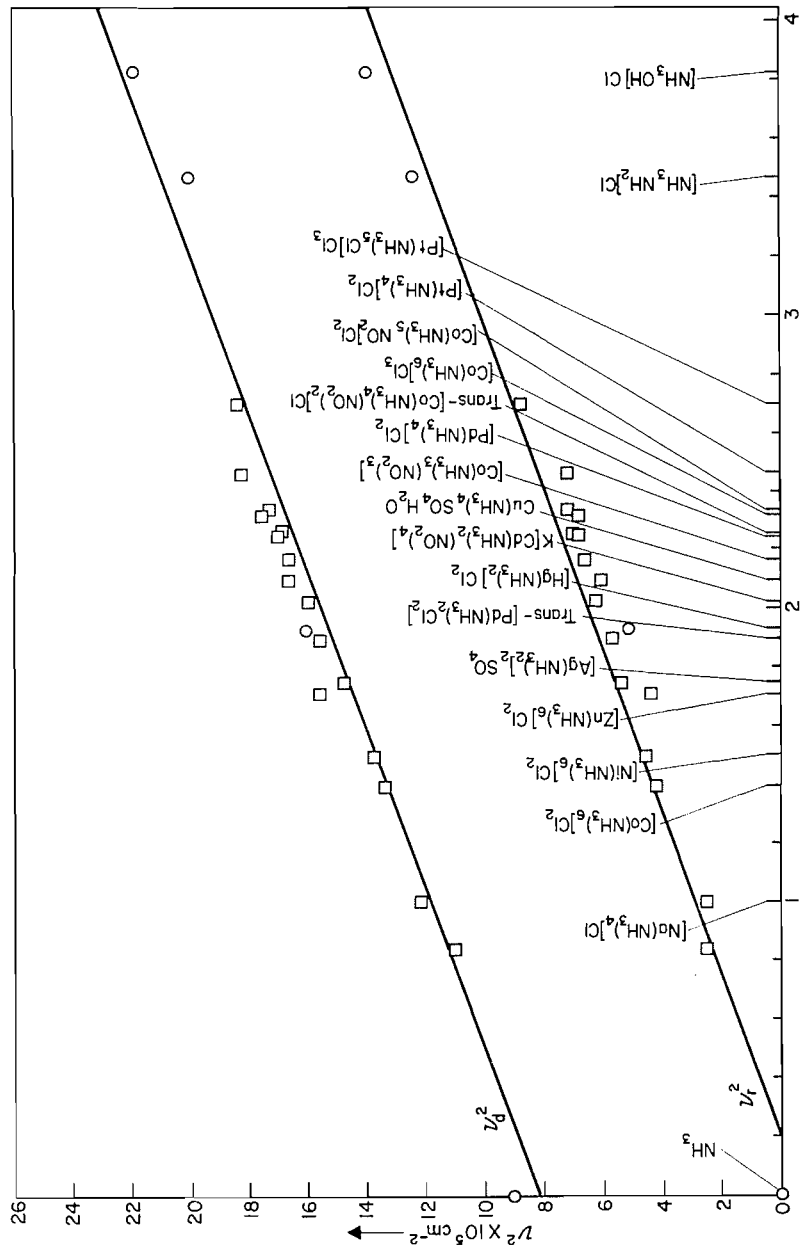


FIG. 1. The plot of ν_r^2 and ν_d^2 against electronegativity for the series of ammine derivatives. ○ Points to which the pair of parallel lines were fitted. □ Points that were fitted to the pair of lines.

Can. J. Chem. Downloaded from www.nrcresearchpress.com by 41.223.56.140 on 09/04/12
For personal use only.

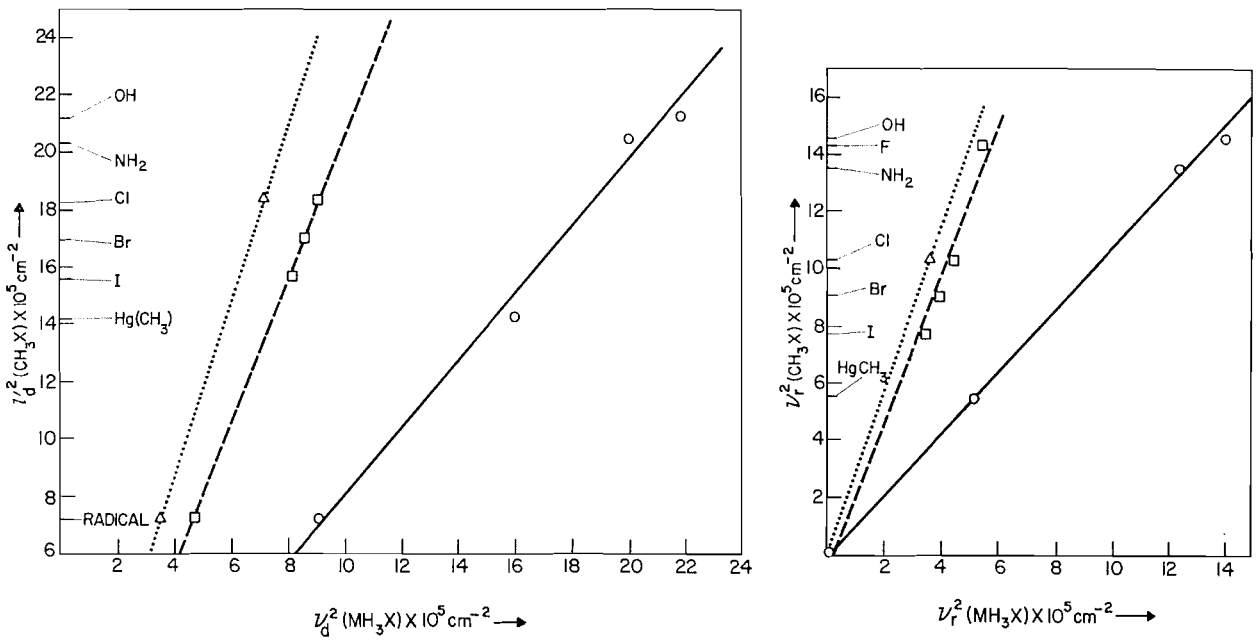


FIG. 2. Plots of ν_d^2 (CH_3X) against ν_d^2 (MH_3X) and of ν_r^2 (CH_3X) against ν_r^2 (MH_3X). —— Ammine frequencies. – – – – Silyl frequencies. . . . . Germanyl frequencies.

of inter- and intra-molecular bonding occurring. As this bonding will not, in general, be the same in every system the agreement obtained in Fig. 1 is considered reasonable.*

Frequency–Frequency Relations

It was illustrated in the methyl series that since both ν_d^2 and ν_r^2 depended linearly on electronegativity they would be linearly related to each other. Similar relations must hold between ν_r^2 and ν_d^2 in other MH_3X series.

Since the H—X stretching frequency depends (13) on the electronegativity of X, it would be expected that external relationships exist between it and the internal frequencies of the MH_3-group in the MH_3X series and this has been shown to hold true for the eight internal methyl group frequencies in the CH_3X series (1). Similar relationships would also be expected for the silyl, germanyl, and ammine series. Again, of course, since all the internal frequencies in the MH_3-groups are related to electronegativity, relations must exist between the internal frequencies of one MH_3-group with those of any other and this is illustrated in Fig. 2 for the symmetrical deformation and rocking frequencies.

It can be appreciated that the frequency–frequency relations suggested here are of use to the spectroscopist enabling him to predict the internal vibrational frequencies of any MH_3-group in MH_3X if the internal frequencies of the YH_3-group in YH_3X are known, or even more simply, if the HX stretching frequency is known.

1. L. J. Bellamy and R. L. Williams. J. Chem. Soc. 2753 (1956).
2. G. Herzberg. Infrared and Raman spectra of polyatomic molecules. D. Van Nostrand Company, Inc., New York. 1951. p. 315.
3. J. K. Wilmshurst. J. Chem. Phys. **23**, 2463 (1955).
4. J. K. Wilmshurst. J. Chem. Phys. **26**, 426 (1957).
5. J. K. Wilmshurst. Can. J. Chem. **37**, 1896 (1959).
6. J. K. Wilmshurst. J. Chem. Phys. **27**, 1129 (1957).
7. J. K. Wilmshurst. To be published.
8. E. P. Bertin, I. Nakagawa, S. Mizushima, J. J. Lane, and J. V. Quagliano. J. Am. Chem. Soc. **80**, 525 (1958).
9. G. Herzberg. Infrared and Raman spectra of polyatomic molecules. D. Van Nostrand Company, Inc., New York. 1951. p. 295.
10. G. F. Svatos, D. M. Sweeny, S. Mizushima, C. Curran, and J. V. Quagliano. J. Am. Chem. Soc. **79**, 3313 (1957).
11. W. Gordy and W. J. O. Thomas. J. Chem. Phys. **24**, 439 (1956).
12. W. Gordy. Phys. Rev. **69**, 604 (1946).
13. J. K. Wilmshurst. J. Chem. Phys. **28**, 733 (1958).

Received September 14, 1959.
Research Laboratories,
Parma, P.O. Box 6116,
Union Carbide Corporation,
Cleveland 1, Ohio.

DECARBOXYLATION OF DIMETHYLTRIFLUOROACETOXYARSINE

W. R. Cullen and L. G. Walker

This paper includes the preparation of the new compound dimethyltrifluoroacetoxyarsine and the characterization of fluorodimethylarsine. These compounds are best obtained as follows:

$$(CH_3)_2AsCl + AgOOCCF_3 \rightarrow (CH_3)_2AsOOCCF_3 + AgCl,$$

$$(CH_3)_2AsI + AgF \rightarrow (CH_3)_2AsF + AgI.$$

**Further, some coupling might be expected between the rocking modes when more than one ammine group is attached to the same metal atom, although this would, in general, be slight for the rather large central metal atoms experienced here.*

Can. J. Chem. Downloaded from www.nrcresearchpress.com by 41.223.56.140 on 09/04/12
For personal use only.

of inter- and intra-molecular bonding occurring. As this bonding will not, in general, be the same in every system the agreement obtained in Fig. 1 is considered reasonable.*

Frequency–Frequency Relations

It was illustrated in the methyl series that since both ν_d^2 and ν_r^2 depended linearly on electronegativity they would be linearly related to each other. Similar relations must hold between ν_r^2 and ν_d^2 in other MH_3X series.

Since the H—X stretching frequency depends (13) on the electronegativity of X, it would be expected that external relationships exist between it and the internal frequencies of the MH_3-group in the MH_3X series and this has been shown to hold true for the eight internal methyl group frequencies in the CH_3X series (1). Similar relationships would also be expected for the silyl, germanyl, and ammine series. Again, of course, since all the internal frequencies in the MH_3-groups are related to electronegativity, relations must exist between the internal frequencies of one MH_3-group with those of any other and this is illustrated in Fig. 2 for the symmetrical deformation and rocking frequencies.

It can be appreciated that the frequency–frequency relations suggested here are of use to the spectroscopist enabling him to predict the internal vibrational frequencies of any MH_3-group in MH_3X if the internal frequencies of the YH_3-group in YH_3X are known, or even more simply, if the HX stretching frequency is known.

1. L. J. Bellamy and R. L. Williams. J. Chem. Soc. 2753 (1956).
2. G. Herzberg. Infrared and Raman spectra of polyatomic molecules. D. Van Nostrand Company, Inc., New York. 1951. p. 315.
3. J. K. Wilmshurst. J. Chem. Phys. **23**, 2463 (1955).
4. J. K. Wilmshurst. J. Chem. Phys. **26**, 426 (1957).
5. J. K. Wilmshurst. Can. J. Chem. **37**, 1896 (1959).
6. J. K. Wilmshurst. J. Chem. Phys. **27**, 1129 (1957).
7. J. K. Wilmshurst. To be published.
8. E. P. Bertin, I. Nakagawa, S. Mizushima, J. J. Lane, and J. V. Quagliano. J. Am. Chem. Soc. **80**, 525 (1958).
9. G. Herzberg. Infrared and Raman spectra of polyatomic molecules. D. Van Nostrand Company, Inc., New York. 1951. p. 295.
10. G. F. Svatos, D. M. Sweeny, S. Mizushima, C. Curran, and J. V. Quagliano. J. Am. Chem. Soc. **79**, 3313 (1957).
11. W. Gordy and W. J. O. Thomas. J. Chem. Phys. **24**, 439 (1956).
12. W. Gordy. Phys. Rev. **69**, 604 (1946).
13. J. K. Wilmshurst. J. Chem. Phys. **28**, 733 (1958).

Received September 14, 1959.
Research Laboratories,
Parma, P.O. Box 6116,
Union Carbide Corporation,
Cleveland 1, Ohio.

DECARBOXYLATION OF DIMETHYLTRIFLUOROACETOXYARSINE

W. R. Cullen and L. G. Walker

This paper includes the preparation of the new compound dimethyltrifluoroacetoxyarsine and the characterization of fluorodimethylarsine. These compounds are best obtained as follows:

$$(CH_3)_2AsCl + AgOOCCF_3 \rightarrow (CH_3)_2AsOOCCF_3 + AgCl,$$

$$(CH_3)_2AsI + AgF \rightarrow (CH_3)_2AsF + AgI.$$

**Further, some coupling might be expected between the rocking modes when more than one ammine group is attached to the same metal atom, although this would, in general, be slight for the rather large central metal atoms experienced here.*

Can. J. Chem. Downloaded from www.nrcresearchpress.com by 41.223.56.140 on 09/04/12
For personal use only.

Dimethyltrifluoroacetoxyarsine is a colorless mobile liquid stable in nitrogen at its boiling point of 136 to 137°. It is moderately stable in the absence of air at 150° but decomposes at 205° to give, among other products, the known compound dimethyltrifluoromethylarsine (1) and carbon dioxide.

$$(CH_3)_2AsOOCCF_3 \rightarrow (CH_3)_2AsCF_3 + CO_2$$

Organometallic haloacetates have been prepared by this method previously (2, 3) and the trifluoroacetates are unusually stable in comparison with other haloacetates (3, 4), probably because of the stability of the C—F bond. The actual mode of decomposition of the haloacetates has been incompletely studied and such decarboxylation reactions may be useful in synthesizing other perfluoroalkyl derivatives of the metals and metalloids. This is now being investigated.

Fluorodimethylarsine is a very reactive liquid isolated by Bunsen (5) but not characterized. The fluorodimethylarsine attacks glass very readily and is unstable to oxygen and moisture. It boils in a nitrogen atmosphere at 75°, a value in good agreement with the estimated 72° (6). The yield of the fluorodimethylarsine from silver fluoride and chlorodimethylarsine is very low. The reaction of iododimethylarsine with the appropriate silver salt gives good yields of dimethylchloro-, dimethylbromo-, and dimethylcyanoarsine. The bromide is not obtainable from the chloride by this method. Similar reactions are known in the bis(trifluoromethyl)arsine series (6) and previous workers have obtained cyanodimethylarsine from chlorodimethylarsine and silver cyanide in benzene solution (7).

A reinvestigation of the reaction between chlorodimethylarsine and dimethylamine has led to the characterization of dimethylaminodimethylarsine, first isolated by Cullen and Emeléus (8).

$$(CH_3)_2AsCl + 2HN(CH_3)_2 \rightarrow (CH_3)_2As—N(CH_3)_2 + (CH_3)_2NH_2Cl$$

The amino compound boils at 112° and is unstable to oxygen and moisture. The compounds $(CH_3)_2P—N(CH_3)_2$ and $(CF_3)_2M—N(CH_3)_2$ (M = As or P) are obtained by similar reactions (8, 9, 10).

EXPERIMENTAL

Apparatus and Technique

Conventional vacuum techniques were used for the manipulation of volatile reactants and products out of contact with moisture and oxygen. Reactions were carried out in sealed Pyrex tubes (50-ml capacity) in the absence of air and light. Infrared spectra were measured on a Perkin–Elmer Model 21 double-beam instrument with rock-salt optics.

Dimethyltrifluoroacetoxyarsine

Chlorodimethylarsine (10.5 g) and silver trifluoroacetate (22 g) were heated to 60° for 15 hours. Trap-to-trap distillation of the volatile products followed by distillation of the least volatile fraction in a nitrogen atmosphere at 760 mm gave dimethyltrifluoroacetoxyarsine, b.p. 136–137° (4.5 g, 32% yield). Anal. calc. for $C_4H_6AsF_3O_2$: As, 34.3%. Found: As, 33.7%.

Decarboxylation of Dimethyltrifluoroacetoxyarsine

The arsine (1.919 g) was heated to 150° for 17 hours and little decomposition was detected. When the same sample was heated to 205° a black solid was slowly deposited, and after 17 hours at this temperature trap-to-trap distillation of the volatile products

Can. J. Chem. Downloaded from www.nrcresearchpress.com by 41.223.56.140 on 09/04/12
For personal use only.

gave a fraction condensing at −196° (0.194 g), a fraction condensing at −98° (0.354 g), and a fraction condensing at −64°. Spectroscopic examination showed the most volatile fraction to be mainly carbon dioxide together with traces of silicon tetrafluoride and fluoroform, and the least volatile fraction to contain no unchanged dimethyltrifluoroacetoxyarsine. The middle fraction was dimethyltrifluoromethylarsine (23% yield). Anal. found: mol. wt., 173. Calc.: mol. wt., 174. The infrared spectrum was identical with that of the pure compound (11, 12).

Preparation of Fluorodimethylarsine

Iododimethylarsine (12.5 g) and silver fluoride (12 g) were left at 20° for 48 hours. Distillation of the volatile products in a nitrogen atmosphere at 760 mm gave a 1-g (15% yield) fraction, b.p. 75°, identified as fluorodimethylarsine. Anal. calc. for C_2H_6AsF: As, 60.6%. Found: As, 61.2%.

Reaction of Iododimethylarsine with Silver Chloride

The arsine (8.5 g) and silver chloride (28 g) were heated to 60° for 14 hours. The volatile products were distilled in a nitrogen atmosphere to give 4.5 g (90% yield) of chlorodimethylarsine, b.p. 107° (published b.p. 106.5–107° (13)).

Reaction of Iododimethylarsine with Silver Bromide

The arsine (9.0 g) and silver bromide (38 g) were heated to 60° for 14 hours. The contents of the tube gave in the usual manner 6.0 g (81% yield) of bromodimethylarsine, b.p. 129° (published b.p. 128–129° (13)).

Reaction of Iododimethylarsine with Silver Cyanide

The arsine (12 g) and silver cyanide (13 g) were left at 20° for 48 hours. The solid cyanodimethylarsine (5 g, 76% yield) was sublimed *in vacuo* from the reaction tube. On distillation in a nitrogen atmosphere, the cyanodimethylarsine boiled at 162° (770 mm) (published b.p. 158–160° (730 mm) (7)).

Reaction of Chlorodimethylarsine with Dimethylamine

The arsine (4.8 g) and anhydrous dimethylamine (5.6 g) were left at 20° for 7 days. After removal of the excess dimethylamine by trap-to-trap distillation the least volatile fraction was distilled at 760 mm in a nitrogen atmosphere at 112°, with a middle cut of 2.1 g. This 2.1-g fraction on redistillation again boiled at 112° and was dimethylaminodimethylarsine. Anal. calc. for $C_4H_{12}AsN$: As, 50.3%. Found: As, 50.8%. The infrared spectrum showed the following absorption bands: liquid film: 2980(s), 2890(s), 2860(s), 2820(s), 2780(s), 2480(w), 1453(s), 1423(s), 1259(m), 1237(m), 1177(vs), 1140(m), 1095(w), 1054(s), 946(vs), 880(s), 813(s), 805(m), 775(w), 735(m) cm^{-1}.

ACKNOWLEDGMENT

The authors wish to acknowledge financial assistance from the National Research Council of Canada.

1. R. N. Haszeldine and B. O. West. J. Chem. Soc. 3631 (1954).
2. H. H. Anderson and H. Fischer. J. Org. Chem. **19**, 1296 (1954).
3. H. H. Anderson. J. Org. Chem. **20**, 536 (1955).
4. H. H. Anderson. J. Org. Chem. **22**, 147 (1957).
5. R. W. Bunsen. Ann. **37**, 1 (1841).
6. H. J. Emeléus, R. N. Haszeldine, and E. G. Walachewski. J. Chem. Soc. 1552 (1953).
7. C. S. Hamilton *et al.* J. Am. Chem. Soc. **69**, 927 (1947).
8. W. R. Cullen and H. J. Emeléus. J. Chem. Soc. 372 (1959).

Can. J. Chem. Downloaded from www.nrcresearchpress.com by 41.223.56.140 on 09/04/12
For personal use only.

9. G. S. HARRIS. J. Chem. Soc. 512 (1958).
10. A. B. BURG and P. J. SLOTA. J. Am. Chem. Soc. **80**, 1107 (1958).
11. H. J. EMELÉUS, R. N. HASZELDINE, and R. C. PAUL. Chemical Society No. 93.
12. B. O. WEST. Ph.D. Thesis, Cambridge. 1954.
13. G. W. RAIZISS and J. L. GAVRON. Organic arsenical compounds. The Chemical Catalog Co., Inc., New York. 1923.

RECEIVED NOVEMBER 17, 1959.
CHEMISTRY DEPARTMENT,
UNIVERSITY OF BRITISH COLUMBIA,
VANCOUVER, B.C.

Can. J. Chem. Downloaded from www.nrcresearchpress.com by 41.223.56.140 on 09/04/12
For personal use only.

Can. J. Chem. Downloaded from www.nrcresearchpress.com by 41.223.56.140 on 09/04/12
For personal use only.

Canadian Journal of Chemistry

Issued by THE NATIONAL RESEARCH COUNCIL OF CANADA

VOLUME 38 APRIL 1960 NUMBER 4

AMINO ACID DISTRIBUTION IN BIOLOGICALLY ACTIVE PEPTIDES[1]

SAUL B. NEEDLEMAN,[2] R. QUENTIN BLACKWELL, AND LEONARD S. FOSDICK

ABSTRACT

A group of biologically active peptides were examined for possible favored chain positions exhibited by some of the 21 constituent amino acids as well as for the unusual occurrence of specific peptide linkages. High levels of significance were revealed for certain amino acid couplets when they were subjected to chi-square analyses.

The work of Scheraga (1), Koshland (2), and others dealing with the spatial orientation and sequential arrangement of amino acids has engendered much speculation as to the nature of the active sites of biologically significant peptides. The extremely detailed study of Sorm *et al.* (3) represents one novel approach to the study of amino acid sequences.

The present work deals with a statistical evaluation of peptide structure in which a group of peptides with totally established amino acid sequences were examined for the occurrence of relative chain position preferences of the individual constituent amino acids and for statistically significant repeating amino acid sequences (4).

A list of all of the dipeptide couplets which appear in the peptides included in this analysis was prepared by recording each succeeding pair of amino acid residues beginning at the N-terminus and proceeding along the chain, one residue at a time.

RESULTS

In the primary peptides, 21 different amino acids occurred a total of 184 times. The combined amino acid percentage composition of the group of peptides is not strikingly different from that of numerous general proteins. Although the study was restricted to biologically active peptides because of the availability of complete sequence analyses, there is no reason to believe that these data would differ significantly from that which will be found when the sequence of many "structural" as well as "biologically active" proteins are known (3). There is no unusual concentration of one or more specific amino acids to be noted in the individual peptides. In general, it would appear that the amino acid content of these peptides being studied does not account for their special biological action. The only point of difference distinguishing these peptides from numerous proteins, so far as amino acid composition is concerned, is the occurrence of certain D-configuration amino acids in bacitracin A and of ornithine only in some antibiotics.

A principal concern of the present study is the relative position in the peptide chain occupied by the individual amino acids. Examination of the amino acid distribution in the peptides investigated for this study reveals an interesting tendency towards adventi-

[1]*Manuscript received July 31, 1959.*
Contribution from the Chemistry Department, Northwestern University, Evanston, Illinois, and the Chemistry Department, Northwestern University Dental School, Chicago, Illinois.
[2]*Present address: Nalco Chemical Company, Bedford Park, Illinois.*

tious positional concentrations. By plotting each amino acid in terms of its numerical position within the peptide chain as well as according to its fractional distance from the amino end, it was possible to draw certain conclusions. Figure 1 depicts the relative or

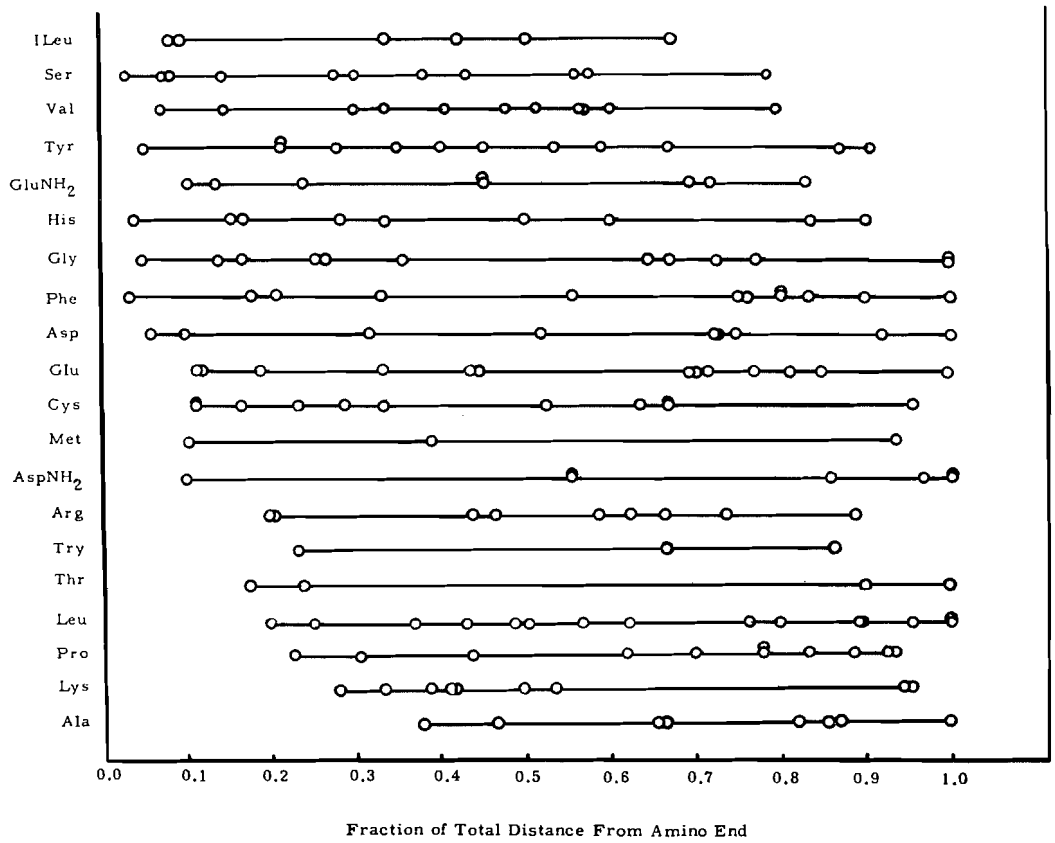


FIG. 1.

fractional distance of the individual amino acid moiety along the peptide chain. Our data show that certain acids, including glycine, glutamic acid, phenylalanine, and aspartic acid, are widely distributed from N- to C-terminal moieties. A few amino acids appear mainly in the interior: glutamine, methionine, tryptophan, and lysine. Cysteine predominates near the ends of the peptide chains. Others are found to tend toward one end of the molecule. For example, isoleucine, serine, valine, and histidine are associated more with the N-terminus while alanine, leucine, threonine, and proline are closer to the C-terminus. The remainder of the amino acids present do not fit well into any of the above groupings.

Some of the relationships may be seen best in terms of actual numerical positions within the peptide. For example, isoleucine does not appear in any of the peptides beyond the 8th moiety from the N-terminus, histidine not beyond the 10th, serine not beyond the 16th, although all of them occur in longer peptides and thus, presumably have the opportunity to occupy more distant positions. In the same way alanine is not found more than 14 positions from the C-terminus and leucine not more than 17. With two exceptions, all of the lysine moieties were clumped near the second quadrant of the peptide chains.

Can. J. Chem. Downloaded from www.nrcresearchpress.com by 41.223.56.140 on 09/04/12
For personal use only.

Of the total of 11 prolines present in the peptides, 4 were located in the third position from the C-terminus and 3 more were in the fourth position. Proline also was found to exhibit a periodicity of 12 in the corticotropins and the β–MSH hormones. It appears, at least, at the 12, 24, and 36 positions from the N-terminus of the three corticotropins (A, α, β); in the β–MSH molecules it appears at the 4 and 16 positions.

For the analysis of terminal amino acids a number of proteins and peptides were added to the peptides used in the remainder of the study. Sixteen of the 21 amino acids found to be present are found as N-terminal groups and 11 are found one or more times as the C-terminal groups. A total of 17 different amino acids are found at one or the other end; only methionine, tryptophan, ornithine, and glutamine were absent from terminal positions.

Another object of the present study was to compare the significance of occurrence of a number of dipeptide couplets making up the structure of a select group of peptides and proteins. It was desirable to determine whether a dipeptide sequence occurred more frequently or less frequently than could be predicted purely by chance based on the quantity of each of the amino acids making up the pool. The concept of chi-squares which considers the theoretical as well as the actual occurrence of each dipeptide moiety was used to compare the significance of uniquely occurring entities.

The dipeptide structures arise by removal from the metabolic pool of those amino acids necessary to synthesize the total host peptide. The metabolic pool may be different in different tissues. For the purpose of the present study, the metabolic pool arbitrarily was taken to consist of all the amino acids present in the peptides examined, in concentrations determined by the numbers present in each of these peptides. Although the resulting pool is derived from heterogeneous peptides, valid conclusions can be made from the corresponding chi-square values. That the pool bears no necessary relationship to its derivative peptides can be seen in the work of Ramachandran and Winnick (5), whose analysis of the very short peptides of the pituitary metabolic pool showed no sequential correlation to the peptide hormones derived from the pituitary.

For significance at the 10% level and for one degree of freedom, the chi-square for a dipeptide moiety should exceed a value of 2.706 (6). Table I lists all of the dipeptide couplets which were found to have significant chi-square values. Only four of the 122 couplets which occurred only once had a chi-square exceeding the requisite statistical limit; the occurrence ratio also indicated a much greater than expected existence. Two of these couplets make up one tripeptide fraction, –AspNH_2–Met–Met–, found in the protein, ribonuclease. Another dipeptide, –Orn–Ileu–, appears in bacitracin and closely resembles the related –Orn–Leu– occurring in other peptide antibiotics. The fourth couplet, –Try-D-Phe–, is in the tyrothricin B sequence but is in part of the peptide which differs from tyrothricin A.

For dipeptide couplets occurring more than once there was an expected increase in statistical significance. Thus, for couplets appearing twice, more than one-fifth (10 of 49) had significant chi-squares. In a few cases, the dipeptide occurred twice within the same protein molecule. Such moieties generally contained amino acids rich in functional groups rather than simple aliphatic types.

Since a total of 294 dipeptides form all the compounds included in this communication and since these are made up of 202 different types, it is evident that almost all dipeptide couplets as well as their parent peptides are unique structures.

It is evident that the mere occurrence of a particular combination of amino acid residues, even those having significant chi-square values, does not confirm a strict functional

Can. J. Chem. Downloaded from www.nrcresearchpress.com by 41.223.56.140 on 09/04/12
For personal use only.

TABLE I

Dipeptide couplets having significant chi-square values

Dipeptide couplet	Occurrence* ratio	χ^2†	Dipeptide couplet	Occurrence* ratio	χ^2†
Gly–Ileu	4.218	4.981	Tyr–Ileu	5.510	7.471
Ser	2.654	3.094	Ser	3.486	5.325
Ala–Glu	2.973	5.202	Lys–Asp	3.006	4.164
$GluNH_2$	3.090	2.804			
			Arg–Try	14.848	26.899
Leu–Phe	2.530	2.753	Arg	5.330	6.906
Val–Orn	12.642	31.740	Orn–Leu	12.005	30.250
Glu	2.686	4.228	Ileu	11.000	9.201
Ser–Met	6.217	8.820	Pro–Val	4.582	16.791
His	3.380	3.370	Lys	2.917	5.049
Arg	3.090	2.804			
Thr–Ser	3.988	6.750	Try–Phe	4.674	2.972
Cys–Cys	8.072	43.191	Asp–Asp	4.421	7.915
			Glu	3.529	7.289
Met–Met	11.731	9.200	$AspNH_2$–Met	5.331	3.453
Glu	4.718	5.949	$GluNH_2$	5.785	7.779
$AspNH_2$	5.333	3.451			
			Glu–Ala	2.974	5.280
His–Leu	5.835	2.747	Asp	2.650	3.095
Phe–His	3.380	3.370	$GluNH_2$–Cys	3.270	3.167
Arg	3.090	2.804			

*The expected "chance" frequency, C, may be calculated for the dipeptide couplet $X-Y$ from $(X/T) \times (Y/T-1)$, where X is the number of residues of the first amino acid comprising the couplet and Y is the number of units of the second amino acid. T represents the total of all amino acid units in the system.

The "actual" frequency, A, is found from the number of occurrences of $X-Y$ divided by the total number of dipeptide couplets.

The occurrence ratio is A/C.

†The chi-square value is calculated from the formula, $X^2 = (A-C)^2/C$, where A is the "actual" occurrence of a particular dipeptide unit and C is the "chance" occurrence of that couplet.

requirement for that combination of amino acids. Nevertheless, although couplets involved in other than activity functions may have chi-squares of significance, the technique may nevertheless be helpful for purposes of sequence characterization.

The existence of a number of significant chi-square values for certain couplets led to the reconstruction of the "characteristic" segments of some physiologically active peptide sequences. These sequences vary in length from five residues in the corticotropins to dipeptide couplets. In glucagon, in a span of nine residues, there are six hydroxyl-containing moieties. At least part of this unit is markedly characteristic through the –Thr–Ser– and –Tyr–Ser– couplets (Table I). Only one-third of the insulin A molecule, the portion at the N-terminus, showed non-random linkage frequencies by our test, while in the B chain, there was a continuous sequence of 12 residues, at the C-terminus, for which the chi-squares were not significant.

An interesting example which supports the possible usefulness of statistical evaluation of the dipeptide units can be noted from the specific biological activity of a synthetic peptide made up of the N-terminal portion of oxytocin and the C-terminus of vasopressin (7). This artificial hormone has a degree of activity of both natural peptides and contains only the statistically characteristic couplets of each.

Can. J. Chem. Downloaded from www.nrcresearchpress.com by 41.223.56.140 on 09/04/12
For personal use only.

Of the 441 unique dipeptidic arrangements which are possible for 21 different amino acids, 202 appeared in those compounds examined. Even under the best arrangements, it was not possible to find all 441 moieties since only a total of 294 dipeptide sequences comprised the pool. Assuming that naturally occurring proteins arise from metabolic pools similar to those yielding the peptides of this study, it would be reasonable to expect that certain of the missing couplets will yet appear as the sequence of additional proteins are unravelled. However, as has already been suggested in the work of Sorm (3), 897 couplets were examined and found to contain only 247 unique moieties. That is, by introducing an additional 603-couplet arrangement only 45 new and different dipeptide sequences were gained. One may further conclude that a natural barrier appears to exist for the occurrence of certain amino acid sequences in peptides. One might agree with Fox (8), who suggests that formation of peptides takes place by self-selection of the amino acid sequences, perhaps by a process akin to Darwinian selection which directs the synthesis of more adapted protein molecules from those of less value to the organism.

The authors are deeply indebted to Dr. Felix Haurowitz for his aid and helpful comments in the preparation of this manuscript.

REFERENCES

1. H. A. SCHERAGA, C. Y. CHA, J. HERMANS, JR., and C. L. SCHILDKRAUT. Abstr. 136th Meeting, Am. Chem. Soc., Atlantic City, N.J. (1959).
2. D. E. KOSHLAND, JR. and M. J. ERWIN. J. Am. Chem. Soc. **79**, 2657 (1957).
3. F. SORM, B. KEIL, V. HOLEYSOVSKI, V. KANESSLOVA, V. KOSTKA, P. MASIAR, B. MELOUN, O. MIKES, V. TOMASEK, and J. VANECEK. Collection Czechoslov. Chem. Commun. **22**, 1310 (1957).
4. S. B. NEEDLEMAN, R. Q. BLACKWELL, and L. S. FOSDICK. Abstr. 132nd Meeting, Am. Chem. Soc., New York, N.Y. (1957).
5. L. K. RAMACHANDRAN and T. WINNICK. Biochem. Biophys. Acta, **23**, 533 (1957).
6. G. W. SNEDECOR. Statistical methods applied to experiments in agriculture and biology. 5th ed. Iowa State College Press, Ames, Iowa. 1956. p. 28.
7. P. G. KATSOYANNIS. J. Am. Chem. Soc. **79**, 209 (1957).
8. S. W. FOX. Am. Scientist, **44**, 347 (1956).

Can. J. Chem. Downloaded from www.nrcresearchpress.com by 41.223.56.140 on 09/04/12
For personal use only.

Can. J. Chem. Downloaded from www.nrcresearchpress.com by 41.223.56.140 on 09/04/12
For personal use only.

SURFACE EFFECTS IN BUTANE OXIDATION[1]

M. Cherneskey and J. Bardwell

ABSTRACT

The oxidation of butane is considerably affected by the nature of the vessel surface. With a silica vessel, vigorous combustion accompanied by multiple cool flames occurs between 280° C and 320° C. These reactions are strongly inhibited when the vessel walls are coated with metal oxides or metal halides. Higher pressures are required for ignition at all temperatures. Of the compounds studied, lead monoxide is the most effective inhibitor. The results suggest that in the antiknock action of lead tetraethyl the true inhibitor is lead monoxide.

INTRODUCTION

There is considerable evidence that the oxidation of hydrocarbons is subject to surface effects. Kinetic experiments have revealed a dependence of rate on vessel diameter (1, 2) and on the previous treatment of the vessel walls (3, 4, 5). Although systematic investigations of surface effects have been made with hydrogen (6, 7, 8) and methane (4, 9) there is a lack of information about the role of the surface in the oxidation of the higher hydrocarbons, where mechanisms not found with methane come into play (10, 11). A better understanding of the part played by the surface in these reactions is desirable for several reasons: it would clarify some of the puzzling anomalies in the reaction kinetics (12, 13); it might suggest improvements in petrochemical processes; finally, it might help reveal the mechanism of "knock" and antiknock action in engines.

Although knock and its suppression have been subjected to much investigation (14, 15, 16) there is still considerable disagreement about the nature of the process. The work of King and co-workers (17, 18, 19) and of Walsh and co-workers (20, 21, 22) may be cited as illustrating both the lack of agreement on mechanism and the possible importance of heterogeneous processes.

King (17, 18) ascribes the action of antiknock agents such as iron carbonyl or lead tetraethyl to deposition of metals or metal oxides which are believed to promote the formation of steam and oxides of carbon; these gases may then dilute the combustible mixture and reduce its inflammability. Walsh and co-workers (20, 21, 22) ascribe the antiknock action of lead tetraethyl to the formation of a colloidal smoke of lead monoxide, which is assumed to inhibit the knocking reaction by virtue of a surface destruction of free radical chains. Each group of investigators claims supporting evidence from combustion experiments. The positive-catalyst theory favored by King is said to be supported by the results of flow experiments with fuels such as pentane and hydrogen (18, 19). The negative-catalyst theory favored by Walsh finds support from static experiments with fuels such as methane and ethers (21, 22).

The question of antiknock action has continued to be a contentious one (16, 23, 24). It appeared desirable to establish empirically the effects of various inorganic compounds on the combustion behavior of a typical hydrocarbon. For this investigation the fuel chosen was *n*-butane, which oxidizes at convenient rates between 250° C and 500° C. This compound's oxidation is accompanied by cool flames, two-stage ignition, and other phenomena associated with the low-temperature combustion of paraffin hydrocarbons and related substances (11, 25).

[1]*Manuscript received December 7, 1959.*
Contribution from the Department of Chemistry, University of Saskatchewan, Saskatoon, Saskatchewan. The research for this paper was supported in part by the National Research Council of Canada, and in part by the Defence Research Board of Canada, under Grant No. 5001-16.

Can. J. Chem. Downloaded from www.nrcresearchpress.com by 41.223.56.140 on 09/04/12
For personal use only.

EXPERIMENTAL

Apparatus

The apparatus used was a conventional one, consisting of a reaction vessel heated in a well-lagged furnace and connected to a manometer, a pumping system, and storage vessels for the reactants. The *n*-butane and oxygen were admitted separately to the vessel and the progress of reaction was followed by pressure measurements and by observation through a window. The reaction vessel was of clear silica, and was cylindrical in shape, 6 cm in diameter and 9 cm long. It was fitted with a capillary inlet tube and a ground joint.

Procedure for Modifying the Surface

Deposition of Soluble Salts

Sufficient salt solution (20% by weight) was transferred to the clean vessel, to leave, on drying, a salt coating of 2.5 mg per sq. cm. The vessel was heated to about 80° C by immersion in a water bath, and then connected to an aspirator for evaporation of solvent. During solvent evaporation, the vessel was continuously rotated in such a way as to bring the solution in contact with all parts of the inner surface.

Deposition of Insoluble Powders

The powder was screened and the portion that passed a 200-mesh screen was used. The fine powder was suspended in a small volume of water and transferred to the vessel. The water was evaporated as described above. Deposits amounting to 0.9 mg per sq. cm were used in most experiments; observations with other amounts are described below. It was found that the technique described yielded deposits that were reasonably uniform and that remained in place after numerous combustion experiments.

Cleaning the Vessel

On completion of combustion experiments with a given surface coating, the vessel was detached, washed with water and then with dilute nitric acid or other suitable solvent. For removal of possible contamination by organic matter, the vessel was left in contact for 1 hour with a freshly prepared mixture of concentrated nitric acid and concentrated sulphuric acid held at about 100° C. The vessel was then thoroughly rinsed with hot distilled water and dried. The vessel so treated will henceforth be referred to as "acid-cleaned".

When combustion experiments were done with the acid-cleaned vessel the rates found at first were similar to those with the new untreated vessel. These rates differed slightly, however, from those obtained subsequently with the same vessel. It is therefore necessary to distinguish two types of "clean" surface, the freshly acid-cleaned vessel and the "aged" vessel. The aged vessel showed slightly higher rates and improved reproducibility. Similar "aging" effects have been reported by other investigators (2, 4, 12) but their cause remains obscure.

Comparison of Results with Different Surfaces

It has been shown that with hydrocarbons such as propane and *n*-butane the pressure changes that accompany oxidation run roughly parallel with the consumption of reactants and the appearance of products (25, 26, 27). With *n*-butane the pressure–time curves show the usual shape: at first there is an induction period, ranging in duration from seconds to hours; at the beginning of the induction period the rate of pressure change is often immeasurably small, but it usually increases in an approximately exponential way, culminating in a period of more rapid reaction. During the latter period there may occur

pressure surges, which accompany luminescence in the vessel and indicate the occurrence of cool flames or ignition. Of the various criteria of reaction rate that may be used to evaluate the influence of the surface, the following will be employed in this paper:

(*a*) the length of the induction period which, for this purpose, will be defined as the time elapsing between the admission of the reactants to the vessel and the attainment of maximum reaction rate (or the passing of a cool flame);

(*b*) the magnitude of the maximum rate of pressure change for a given reaction mixture and vessel temperature;

(*c*) the pressure–temperature limits for the onset of ignition;

(*d*) the range of occurrence of cool flames.

RESULTS

Effect of Surface on Induction Period and on Maximum Rate

Table I illustrates the large differences in reaction rate encountered with different surface materials, under otherwise identical experimental conditions.

TABLE I

Induction period and maximum rate of pressure change in the oxidation of *n*-butane under different surface conditions

Surface treatment	Induction period, minutes	Maximum rate, mm/min
Clean silica (aged)	0.3	Ignition
KI coated	2	7
PbO coated	27	0.24

NOTE: Initial pressure of *n*-butane, 150 mm; initial pressure of oxygen, 150 mm; temperature of vessel, 292° C.

On the basis of these results, which are typical of many, the aged silica surface may be designated as "active", the KI-treated surface as "moderately inhibiting", and the PbO-treated surface as "strongly inhibiting".

Effect of Surface on Ignition Limits

The pressure–temperature limits for ignition of equimolar mixtures of *n*-butane and oxygen under different conditions of surface are shown in Fig. 1. The adverse effect of a

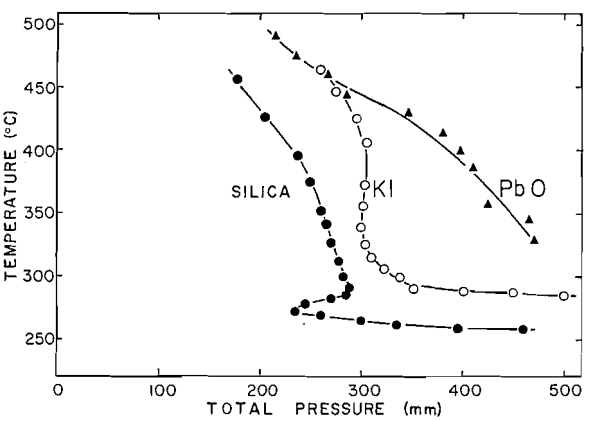


FIG. 1. Ignition limits for equimolar *n*-butane – oxygen mixtures with a silica vessel, untreated, and coated with KI and with PbO.

Can. J. Chem. Downloaded from www.nrcresearchpress.com by 41.223.56.140 on 09/04/12
For personal use only.

coating of KI or PbO on reaction rate is here revealed by an increase in the pressure required for ignition. Again it is clear that PbO is the more effective inhibitor, at least in the low-temperature region.

The results in Table I and Fig. 1 illustrate the difficulty of arriving at a satisfactory quantitative criterion of inhibition with a branching-chain reaction. The ratio of induction periods in Table I indicates that at 292° C reaction proceeds about 90 times faster in the aged vessel than in the PbO-coated vessel. On the other hand, the minimum pressures for ignition, in the low-temperature region, differ by a factor of a little less than two. This apparent discrepancy is believed to be related to the fact that reaction rate is strongly dependent on reactant pressure (1, 28, 29).

In subsequent sections of this paper, changes in ignition limits and cool flame limits will be used for assessing the magnitude of surface effects. It should be remembered that these limits are in general much less sensitive measures of inhibition than others that might have been employed, such as induction period or maximum rate. General use of the latter is made difficult or impossible by the marked changes in the nature of the reaction resulting from surface changes.

Ignition Diagram with an Active Surface

With *n*-butane, as with most hydrocarbons, intense reaction is frequently found even though the pressure is insufficient for ignition. Figure 2 shows, in a pressure–temperature

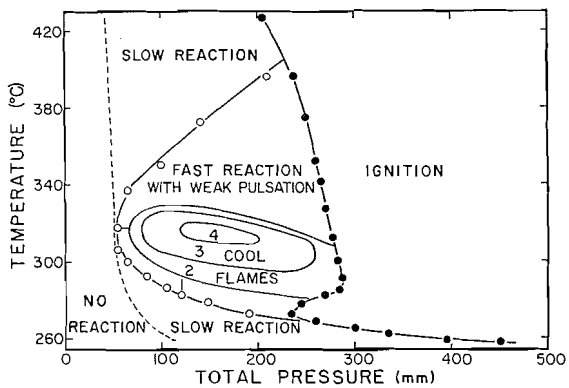


FIG. 2. Range of occurrence of combustion phenomena with equimolar *n*-butane – oxygen mixtures in a silica vessel, 6 cm in diameter. The numbers shown indicate the numbers of cool flames observed.

diagram, the range of occurrence of the various phenomena encountered when equimolar *n*-butane – oxygen mixtures were admitted to an aged silica vessel in the temperature range 250° C to 430° C. The phenomena include:

(*a*) No reaction: here the induction period is of infinite duration (28, 29).

(*b*) Slow reaction: the oxidation is accompanied by little if any luminescence, and the pressure increases without any surges or pulsations. This type of reaction occurs both at low temperatures and at high temperatures; for example, with a total pressure of 80 mm the maximum rate has a value of 10 mm/min at 287° C, at 380° C, and at 452° C (29).

(*c*) Single cool flame: the self-acceleration of the reaction is interrupted by a moderate pressure surge during which a bluish flame is seen in the vessel.

(*d*) Multiple cool flames: here a definite periodicity is present, the flames being separated by intervals of up to 100 seconds. The pressure–time record for this type of reaction is

Can. J. Chem. Downloaded from www.nrcresearchpress.com by 41.223.56.140 on 09/04/12
For personal use only.

illustrated in Fig. 3 (curve for 284° C). The passing of each flame brings about a marked deceleration of the reaction.

(*e*) Fast reaction with weak pulsation: As the vessel temperature is increased beyond about 320° C the periodic nature of the reaction becomes much less pronounced. The initial acceleration of the reaction is rapid, but the pressure surge is relatively weak and it is not followed by a substantial deceleration; instead reaction continues at a rapid rate. Figure 3 (curve for 360° C) illustrates the pressure–time record for this type of reaction and shows the contrast with the multiple cool flames that occur at lower temperatures.

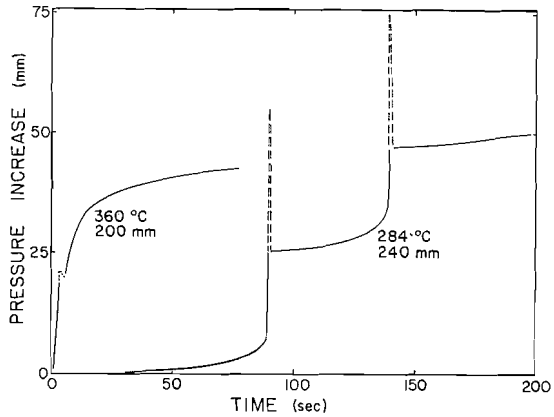


FIG. 3. Typical pressure–time record for double cool flame and for fast reaction with weak pulsation.

(*f*) Ignition: a bright blue or yellow flame traverses the reaction vessel and is associated with a large pressure increase. Below about 400° C, the ignition is a two-stage process, a cool flame preceding the hot flame. Many investigators have commented on the similarity of such ignition and the phenomenon of knock in engines (10, 11, 16).

The main features of the diagram in Fig. 2 are similar to those found by other investigators (using glass or silica vessels) with propane (26, 30), *n*-pentane (5), and butanone (31). As with these compounds the ignition limit is L-shaped with a peninsula at about 275° C.

As mentioned earlier, experiments with the acid-cleaned vessel gave somewhat slower reaction than those with the aged vessel. Examples are shown in Table II where some of the pressure–temperature limits are given. The differences, although appreciable, are evidently much smaller than those found between limits for the clean and the treated surfaces.

Ignition Diagram with a Moderately Inhibiting Surface

Typical results with a moderately inhibiting surface are shown in Fig. 4 which gives the ignition diagram for a NiO-coated surface. Comparison with Fig. 2 shows the following evidence of inhibition:

(*a*) A much larger region of no reaction.

(*b*) Elimination of multiple cool flames. The pressure–temperature conditions that usually give rise to these with the active surface, i.e., moderate pressures and temperatures in the range 280° C to 320° C now lead to either slow reaction or no reaction at all.

(*c*) Significantly higher ignition limits.

Can. J. Chem. Downloaded from www.nrcresearchpress.com by 41.223.56.140 on 09/04/12
For personal use only.

The ignition diagram in the low-temperature region was also determined with the surface coated in turn with the following metal oxides: Cu_2O, Fe_2O_3, Pb_3O_4, and PbO. The results are summarized in Table II. It is seen that Cu_2O, Fe_2O_3, and Pb_3O_4 give limits very similar to those for NiO. Furthermore, the ignition diagrams showed the same general features as found in Fig. 4, namely an L-shaped ignition boundary and a large area where the pressure–time record was similar to that in Fig. 3 (360° curve). In no case was the pressure–time record similar to the 284° C curve in Fig. 3, i.e., clearly marked multiple cool flames were not observed. The exceptionally strong inhibition found with PbO will be discussed below.

Table II also summarizes the results for the vessel coated with the following metal halides: $MnCl_2$, $NiCl_2$, $CuCl_2$, $PbCl_2$, KCl, and KI. With the exception of KCl, which appears to be a rather ineffective inhibitor, these metal halides also give limits that differ little from those for a NiO coating. The ignition diagrams again were found to resemble

TABLE II

Pressure–temperature limits for various surface treatments

Surface treatment	Minimum ignition temperature at 400 mm pressure, °C	Minimum temperature for pulsating reaction at 300 mm pressure, °C	Minimum pressure for pulsating reaction at 335° C	Minimum pressure for ignition at 335° C
Aged silica	259	265	65	267
Acid-cleaned silica	262	268	75	270
NiO	301	306	150	320
Cu_2O	296	302	140	315
Fe_2O_3	293	300	140	315
Pb_3O_4	303	308	125	295
$MnCl_2$	296	300	135	305
$NiCl_2$	295	302	130	300
$CuCl_2$	295	303	150	310
$PbCl_2$	305	312	130	295
KI	288	293	150	300
KCl	282	287	120	279
PbO	395	344	195	465

that in Fig. 4; the ignition boundary was L-shaped, no multiple cool flames were found, but fast reaction with weak pulsation took place above about 310° C.

Ignition Diagram with a Strongly Inhibiting Surface

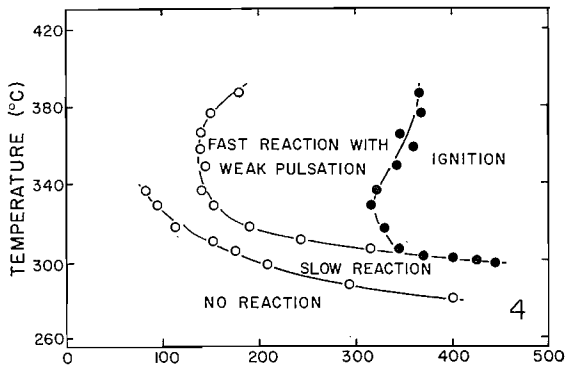
The exceptionally potent inhibition brought about by a PbO coating will now be presented in greater detail. Figure 5 shows the ignition behavior between 250° C and 435° C. The diagram is evidently much altered from that with the active surface (Fig. 2). Particularly noteworthy is the persistence of slow reaction in regions of pressure and temperature, e.g., 400 mm and 350° C, that lead to vigorous explosion with all the other surface treatments used.

Effect of Differences in Amount of Deposit

Some experiments were done to find out to what extent the inhibiting effect of PbO depends on the amount of it, present on the surface. Coatings amounting to 0.1, 0.9, and 2.2 mg per sq. cm were used.

The limit chosen for the comparison was the position of the upper boundary of the slow reaction zone, at 300 mm pressure, i.e., the temperature marking the transition from

Can. J. Chem. Downloaded from www.nrcresearchpress.com by 41.223.56.140 on 09/04/12
For personal use only.



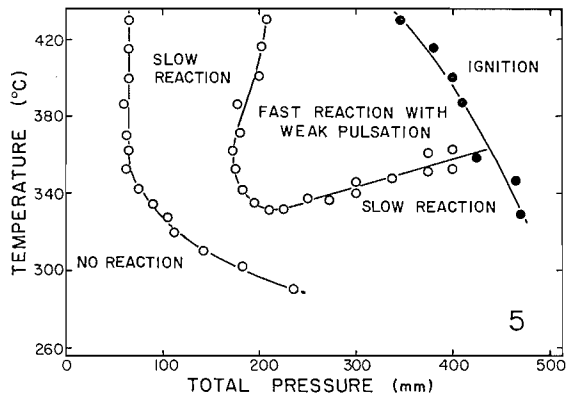


FIG. 4. Range of occurrence of combustion phenomena with equimolar *n*-butane – oxygen mixtures in a silica vessel coated with NiO.

FIG. 5. Range of occurrence of combustion phenomena with equimolar *n*-butane – oxygen mixtures in a silica vessel coated with PbO.

TABLE III

Effect of amount of PbO used on the degree of inhibition

Amount of PbO deposited, mg per sq. cm	Upper limit of slow reaction zone at 300 mm pressure, °C
0	268
0.1	321
0.9	344
2.2	343

non-pulsating reaction to reaction with pulsation. Table III shows that, by this criterion, the extent of inhibition increases sharply with the first addition of PbO (0.1 mg per sq. cm). When the coating is increased from 0.1 to 0.9 mg per sq. cm, there is some further inhibition, but increase beyond 0.9 mg per sq. cm is without effect.

Inert Gas Effects

The response of a free radical reaction to inert gas additions can provide a clue to the role of the surface. Attention will be confined to experimental conditions where the reaction proceeds without appreciable self-heating, since otherwise complications arise

Can. J. Chem. Downloaded from www.nrcresearchpress.com by 41.223.56.140 on 09/04/12
For personal use only.

because of heat capacity effects (25). The effects of inert gas additions on the slow development of the reaction in the induction period will therefore be considered.

With the aged silica vessel the rate of development of the reaction was found to be unaffected by inert gas additions. Measurements in the slow combustion region (270° C, 160 mm pressure) and in the cool flame region (284° C, 240 mm) showed that nitrogen additions of 200 mm had no effect on the length of the induction period. Additions of argon and of water vapor were also found to be without effect.

A different result was obtained when an acid-cleaned vessel was used. Inert gas additions at 300° C now had a moderate accelerating effect. For example, with a total reactant pressure of 160 mm, addition of 200 mm of nitrogen shortened the induction period from 130 seconds to 60 seconds. It is of interest that with the aged vessel under the same experimental conditions (300° C, 160 mm pressure, no inert gas) the induction period was only 24 seconds. On the basis of these results it might be anticipated that the differences in induction period between the acid-cleaned vessel and the aged vessel would disappear if experiments were done in the presence of sufficient inert gas.

Still greater effects were found with a PbO-coated vessel. Measurements were made in the slow combustion zone (312° C, 150 mm pressure). Addition of only 108 mm of nitrogen shortened the induction period from 20 minutes to only 2 minutes and increased the maximum rate from 0.34 mm/min to 1.0 mm/min.

DISCUSSION

There seems little reason to doubt that the large effects of the different surface materials on the rate have their origin in different efficiencies of these substances in destroying intermediates, probably free radicals. The chain-breaking efficiency of the aged silica vessel appears to be relatively low. This conclusion is supported by the observations that with this surface, lively reaction develops over a wide range of experimental conditions (Figs. 2 and 3), and its rate of development is not accelerated by inert gas additions. The latter observation shows that, under typical experimental conditions, there is no serious depletion of radicals by diffusion to the walls. Such depletion does apparently become significant, however, when the pressure is sufficiently reduced, as there is complete suppression of the reaction at pressures below about 50 mm (Fig. 2).

The acid-cleaned surface is evidently somewhat more efficient in breaking chains than is the aged surface; this is indicated by the longer induction period, the acceleration by inert gas, and the slightly higher pressure–temperature limits for cool flames and ignition (Table II).

Of the 11 inorganic compounds used as surface coatings, all but KCl and PbO lead to approximately the same degree of inhibition. For example, Table II shows that at 400 mm pressure the ignition temperatures show a range of 136° when all the surfaces are considered; these nine compounds, however, show a range of only 17°. It is interesting that KCl, which has frequently been used to provide an inhibiting surface in oxidation experiments (2, 3, 8), appears, from this investigation, to be the least effective of all the compounds tested.

It seems difficult to avoid the conclusion that PbO is an exceptionally efficient chain-breaking agent. Evidence of unusually strong inhibition by this substance has been presented in Tables I and II and in Fig. 5. Corroboration may be found in a comparison of the data in Tables II and III. It is seen that even a light coating of PbO (0.1 mg/sq. cm) leads to greater inhibition than the normal coating (0.9 mg/sq. cm) of the other metal oxides or even the heavy coating (2.5 mg/sq. cm) of the metal halides. The latter

Can. J. Chem. Downloaded from www.nrcresearchpress.com by 41.223.56.140 on 09/04/12
For personal use only.

comparison makes it unlikely that the observed difference between the results with PbO and with the other compounds is due to some unsuspected experimental factor such as differences in particle size distribution of the powders.

A complete discussion of surface effects would include identification of the radicals that suffer destruction at the walls. From indirect evidence Walsh and co-workers have suggested that the radical HO_2 plays such a role in the oxidation of methane at about 500° C (20, 22). In the oxidation of higher paraffins at low temperatures, many other radicals have been postulated as participating in the reaction mechanism (10, 27, 32). It is unlikely that some of the more complex of these radicals, e.g., C_4H_9OO, participate appreciably in wall reactions since there is evidence that they undergo rapid pyrolysis or isomerization reactions in the gas phase (27, 33). An additional possibility in the low-temperature range is the occurrence of heterogeneous side-reactions of intermediate molecules such as peroxides or aldehydes, whose normal reactions are believed responsible for chain-branching (12, 28).

Relation to Other Investigations

Although there appears to be no previous investigation of surface effects in the oxidation of *n*-butane, some information is available for propane and ethers. Day and Pease (30) determined cool flame limits and ignition limits for propane using three different surface treatments—cleaning with hot HNO_3, etching with HF, and rinsing with a KCl solution which was then drained out of the vessel. They found only small differences in the various limits and concluded that "the nature of the surface has no great effect on the cool flame and ignition characteristics of the reaction". In view of the results given above for *n*-butane and the general similarity of combustion behavior of propane and *n*-butane (25, 26), this generalization appears to be premature. A repetition of the work of Day and Pease, with thicker deposits and other compounds, would be desirable.

Chamberlain and Walsh (21) measured the ignition limits of diethyl ether using a silica vessel, with and without a coating of PbO. The PbO coating was found to raise the ignition pressure by 11% at 400° C and by 14% at 210° C. These results may be compared with those given above for *n*-butane, namely an increase of about 65% at 400° C and a slightly larger effect at lower temperatures, e.g., 75% at 330° C (Fig. 1). The lack of quantitative agreement is not surprising since ethers and hydrocarbons show other differences in their oxidation behavior (10, 33). There may also be a difference in amount of deposit used.

Relation to the Mechanism of Antiknock Action

The results given in this paper suggest that PbO may well be the true inhibitor when lead tetraethyl acts as an antiknock agent. It is worth while to compare the inhibition of the oxidation of *n*-butane by PbO with the known behavior of lead tetraethyl. As shown above in Tables I and II and in Figs. 1 and 5, the inhibition by PbO is pervasive; this substance greatly lengthens the induction period, it suppresses the phenomenon of multiple cool flames, and it raises ignition pressures by about 70%. Lead tetraethyl, on the other hand, has been found to have little effect on the induction period both with *n*-heptane (10, 16, 35) and with diethyl ether (34); its inhibiting effect apparently comes into play only at later stages of the reaction. The extent of inhibition by lead tetraethyl may be estimated from its effect on ignition pressures. Townend and Mandlekar found that this additive, when used in amounts similar to those required for satisfactory antiknock action (0.1%), brought about an increase in ignition pressure of about 5% with

Can. J. Chem. Downloaded from www.nrcresearchpress.com by 41.223.56.140 on 09/04/12
For personal use only.

n-butane and *n*-pentane (11, 36). It is interesting that, with some fuels, lead tetraethyl fails to give any antiknock effect and may even act as a proknock agent (10).

The complicated behavior of lead tetraethyl becomes more understandable if the true inhibitor is in fact PbO. The observation that the early stages of the reaction proceed at about the same rate whether lead tetraethyl is present or not (10, 16, 34) is explained if there is a delay in the formation of PbO; such a delay is to be expected if both chemical transformation of lead tetraethyl into PbO vapor and physical condensation of PbO vapor to solid particles are required. Furthermore, the chemical transformation is likely to release ethyl radicals into the combustion mixture and so cause some promoting action. An explanation is then available for the observation that lead tetraethyl has a net promoting effect under certain experimental conditions, for example, at very high temperatures (17) or with fuels that are believed to oxidize via very short chains (10, 20).

It has been suggested by Norrish and co-workers that in the inhibition of combustion reactions by lead compounds the processes are probably homogeneous and depend on vapor molecules, possibly including PbO vapor at very high temperatures (23, 24). The results reported in this paper, however, leave little doubt that heterogeneous processes are predominant in the temperature range considered here. The large influence of added inert gas on reaction rate points to surface breaking of chains. Furthermore, if vapor molecules were responsible for the inhibition, one would expect that the effect would be roughly proportional to the vapor pressure of PbO and so would increase markedly with increase of vessel temperature and would be independent of the amount of solid PbO on the surface. Figure 1 and Table III show that these expectations are not fulfilled.

While heterogeneous chain breaking at the vessel surface appears to be the predominant process responsible for the inhibition described in this paper, somewhat different mechanisms may be important under the higher pressure conditions found in engines when lead compounds exert an antiknock effect. The suggestion of Chamberlain and Walsh (21) that lead tetraethyl reacts with oxygen to form a colloidal smoke of PbO particles appears to be a plausible one. This mechanism makes possible heterogeneous chain breaking without, however, necessitating a long diffusion path.

REFERENCES

1. B. Aivazov and M. B. Neumann. Z. physik. Chem. (Leipzig), B, **33**, 349 (1936).
2. M. Prettre. Symposium on Combustion. 3rd Symposium, 1949. p. 397.
3. R. N. Pease. Chem. Revs. **21**, 279 (1937).
4. D. E. Hoare and A. D. Walsh. Symposium on Combustion. 5th Symposium, 1955. p. 467.
5. M. Lucquin and P. Laffitte. Compt. rend. **242**, 2944 (1956).
6. D. R. Warren. Proc. Roy. Soc. (London), A, **211**, 86 (1952).
7. D. R. Warren. Proc. Roy. Soc. (London), A, **211**, 96 (1952).
8. A. H. Willbourn and C. N. Hinshelwood. Proc. Roy. Soc. (London), A, **185**, 376 (1946).
9. D. E. Hoare and A. D. Walsh. Proc. Roy. Soc. (London), A, **215**, 454 (1952).
10. B. Lewis and G. von Elbe. Combustion, flames and explosions of gases. Academic Press Inc., New York. 1951. pp. 128–199.
11. D. T. A. Townend and M. R. Mandlekar. Proc. Roy. Soc. (London), A, **141**, 484 (1933).
12. M. F. Mulcahy and M. J. Ridge. Trans. Faraday Soc. **49**, 1297 (1953).
13. Z. G. Szabo. Symposium on Combustion. 7th Symposium, 1959. p. 118.
14. W. P. Hawthorne and E. J. Y. Scott. Advances in Chem. Ser. No. 20. 1958. p. 187.
15. J. D. B. Ogilvie, S. G. Davis, A. L. Thompson, W. T. Grummitt, and C. A. Winkler. Can. J. Research, F, **26**, 246 (1948).
16. A. J. Pahnke. Advances in Chem. Ser. No. 20. 1958. p. 202.
17. R. O. King. Can. J. Research, F, **25**, 326 (1947).
18. R. O. King. Can. J. Research, F, **26**, 228 (1948).
19. R. O. King, W. A. Wallace, and B. Mahapatra. Can. J. Research, F, **26**, 264 (1948).
20. G. H. N. Chamberlain, D. E. Hoare, and A. D. Walsh. Discussions Faraday Soc. No. 14, 89 (1953).
21. G. H. N. Chamberlain and A. D. Walsh. Proc. Roy. Soc. (London), A, **215**, 175 (1952).

Can. J. Chem. Downloaded from www.nrcresearchpress.com by 41.223.56.140 on 09/04/12
For personal use only.

22. D. E. CHEANEY, D. A. DAVIES, A. DAVIS, D. E. HOARE, J. PROSTHEROE, and A. D. WALSH. Symposium on Combustion. 7th Symposium, 1959. p. 183.
23. K. H. L. ERHARD and R. G. W. NORRISH. Proc. Roy. Soc. (London), A, **234**, 178 (1956).
24. R. G. W. NORRISH. Symposium on Combustion. 7th Symposium, 1959. p. 203.
25. J. BARDWELL. Symposium on Combustion. 5th Symposium, 1955. p. 529.
26. D. M. NEWITT and L. S. THORNES. J. Chem. Soc. 1656 (1937).
27. N. N. SEMENOV. Some problems of chemical kinetics and reactivity. Vol. I. Pergamon Press, New York. 1958. pp. 85–117.
28. F. E. MALHERBE and A. D. WALSH. Trans. Faraday Soc. **46**, 824 (1950).
29. NAN-CHIANG WU SHU and J. BARDWELL. Can. J. Chem. **33**, 1415 (1955).
30. R. A. DAY and R. N. PEASE. J. Am. Chem. Soc. **62**, 2234 (1940).
31. J. BARDWELL and C. N. HINSHELWOOD. Proc. Roy. Soc. (London), A, **205**, 375 (1951).
32. R. G. W. NORRISH. Discussions Faraday Soc. No. 10, 269 (1951).
33. C. E. BOORD. Advances in Chem. Ser. No. 20. 1958. p. 5.
34. L. OUELLET, E. LEGER, and C. OUELLET. J. Chem. Phys. **17**, 746 (1949).
35. A. J. PAHNKE, P. M. COHEN, and B. M. STURGIS. Ind. Eng. Chem. **46**, 1024 (1954).
36. D. T. A. TOWNEND and M. R. MANDLEKAR. Proc. Roy. Soc. (London), A, **143**, 168 (1934).

Can. J. Chem. Downloaded from www.nrcresearchpress.com by 41.223.56.140 on 09/04/12
For personal use only.

Can. J. Chem. Downloaded from www.nrcresearchpress.com by 41.223.56.140 on 09/04/12
For personal use only.

REMOVAL OF OXYGEN FROM METHANE AND THE USE OF NUCLEAR SPIN RELAXATION TO MEASURE OXYGEN CONCENTRATION[1]

H. S. SANDHU, J. LEES, AND M. BLOOM

ABSTRACT

Nuclear spin relaxation measurements are used to measure quantitatively the amount of oxygen present in methane. An upper limit of $2.5\times10^{-4}\%$ is placed on the amount of oxygen present in methane after treatment with a getter made of misch metal.

The proton spin relaxation time, T_1, in liquid and solid CH_4 has been found by us to be very sensitive to small amounts of oxygen in the sample, because of the fact that the O_2 molecule is paramagnetic. The effect of paramagnetic impurities on nuclear spin relaxation in diamagnetic liquids has long been known (1), and precautions must usually be taken to eliminate such impurities if one is interested in studying T_1 of the pure liquid (2). In our first measurements of T_1 in liquid CH_4 (3), T_1 was found to depend on the sample, the longest T_1 obtained being about 0.6 second while some "chemically pure" samples gave us T_1 values as low as 10^{-2} seconds. All samples used were obtained commercially, the purest samples being supplied by Phillips Petroleum Co.

Since the vapor pressure readings for such samples also disagreed with those published for pure CH_4 (4), it was considered necessary to find a reliable method of purifying our samples. Different techniques were used to remove oxygen. It may be noted that we plan to study T_1 in deuterated samples of methane, so that it is of importance that the purification method does not require very large quantities of the sample.

An attempt was first made to use the fact that the normal boiling point of oxygen (90° K) is lower than that of methane (112° K). The liquid was maintained at a temperature (106° K) such that most of the oxygen might boil off. The vapors were then pumped off. This process was repeated a number of times. Each time we pumped off the vapors and measured T_1 in the liquid, we obtained a longer relaxation time. Although T_1 values as long as 10 seconds were obtained, this technique for purification was finally dropped because T_1 values so obtained were not reproducible and the method was very wasteful of methane.

The second technique employed was to circulate methane over heated copper. This method was not satisfactory because the gas decomposed during the process.

The technique found to be most suitable for our purposes involved the use of a getter, misch metal, which consists of rare earths derived from monazite and alloyed with iron. This metal was selected because it was found by Ehrke and Slack (5) in their study of the gettering power of various metals like aluminum, magnesium, barium, and misch metal that misch metal is the most effective for removal of oxygen. As described in the following paragraph, our procedure is a slightly simplified version of that described by Ehrke and Slack (5).

A $\frac{1}{2}$-liter flask drawn into a long tube on one side is used as shown in Fig. 1. The end of the tube fits into an NMR probe to make T_1 measurements. A tungsten coil of five or six turns of 0.01-in. diameter, with two or three small pieces of misch metal in the coil, is sealed into the flask. The flask is then connected to a diffusion pump through a trap and evacuated to a pressure of the order of 10^{-6} cm. The flask is baked by flaming

[1]*Manuscript received December 14, 1959.*
Contribution from the Department of Physics, University of British Columbia, Vancouver, British Columbia.

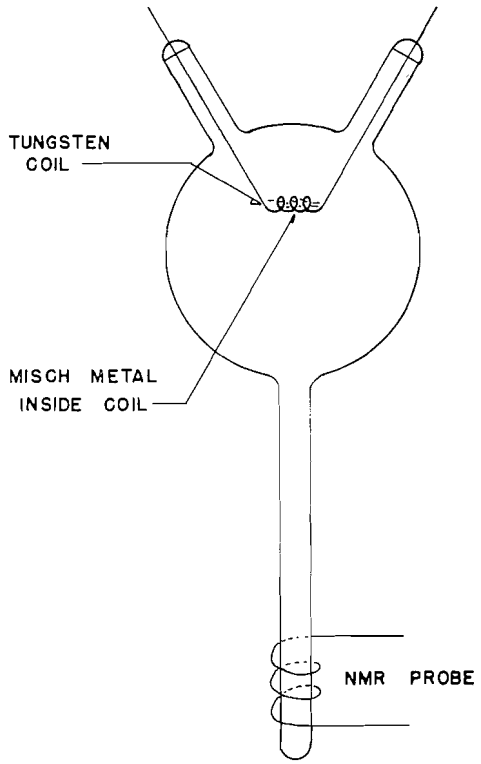


FIG. 1. Schematic drawing of the sample container.

several times during pumping to get rid of oxygen adsorbed on the walls. The tungsten coil is also degassed during pumping. When the flask has been thoroughly baked and pumped, it is filled with argon to a pressure of 1 to 2 mm. The getter is then flashed by passing current through the tungsten coil using a Variac to control the current, until a characteristic diffused layer of the deposit is produced. The presence of argon is necessary to produce a diffused deposit the gettering power of which is much higher than the bright shiny type (5). The argon is then pumped off, leaving an uncontaminated getter layer of high activity. Methane at 1-atmosphere pressure is introduced into the flask which is then sealed off from the system.

When this procedure was followed, T_1 was always found to increase to 14 seconds at 108° K, this value being reproduced whether the measurements were done on different samples or the same sample at different times during a period of several days. One of the samples studied had had approximately 0.5% oxygen purposely added as an impurity. The addition of nitrogen to the samples did not affect T_1.

In order to make quantitative measurements on the contribution of oxygen to T_1, a sample of CH_4 was prepared with approximately 1% oxygen. Mass spectrometer measurements performed at the Department of Chemistry, University of Washington, showed that the sample contained about 1.08% oxygen. T_1 was measured as a function of temperature and will be reported for this sample and other similarly prepared samples in a future publication. For purposes of using T_1 as a method of analyzing the oxygen concentration quantitatively, we give here only values of T_1 in CH_4 liquid under its

Can. J. Chem. Downloaded from www.nrcresearchpress.com by 41.223.56.140 on 09/04/12
For personal use only.

own vapor pressure at 108° K. The measurements were made using pulse techniques (3) and were accurate to about 5%.

For 1.08% O_2, we obtained $T_1 = 34\times10^{-3}$ sec. It is expected that $1/T_1^0 \propto f$ where T_1^0 is the contribution to T_1 due to the oxygen, and f is the percentage of oxygen molecules. This was borne out by studying a sample containing 2.54% oxygen, as measured by the mass spectrometer, which gave $T_1 = 15\times10^{-3}$ sec at 108° K.

Because of the oxygen background in the mass spectrometer, it was impossible to analyze the oxygen concentration with it in a region where T_1 measurements indicated that f was less than about 0.1%. Therefore, our T_1 measurements represent a more sensitive means of detecting oxygen than a mass spectrometer unless special steps are taken to cut down the oxygen background in the mass spectrometer.

If T_1^n represents the natural relaxation time of pure CH_4, we can write

$$\frac{1}{T_1} = \frac{1}{T_1^n} + \frac{1}{T_1^0}.$$

Our measurements indicate that $T_1^n = 14$ seconds at 108° K, since our measurements were reproducible from day to day and we would have been able to detect a change of less than 10% in T_1. If T_1^0 were about 14 seconds at 108° K, this would correspond to $f = 2.5\times10^{-3}$%. On the basis of the reproducibility of T_1 with time and in different samples, we are probably justified in saying that our purification procedure resulted in $f \lesssim 2.5\times10^{-4}$ %.

It would seem that the technique described here would be well suited to removal of oxygen from other hydrocarbons and this is being planned in connection with future measurements of T_1 of higher hydrocarbons in this laboratory.

This research was supported by a Research Grant from the National Research Council of Canada. We wish to thank Dr. L. Reeves for valuable suggestions and the mass spectrometer group at University of Washington for analyzing our samples.

REFERENCES

1. N. Bloembergen, E. M. Purcell, and R. V. Pound. Phys. Rev. **73**, 679 (1948).
2. J. H. Simpson and H. Y. Carr. Phys. Rev. **111**, 1201 (1958).
3. H. S. Sandhu and M. Bloom. Bull. Am. Phys. Soc. **3**, 324 (1958).
4. G. T. Armstrong, F. G. Brickwedde, and R. B. Scott. J. Research Natl. Bur. Standards, **55**, 39 (1955).
5. L. F. Ehrke and C. M. Slack. J. Appl. Phys. **11**, 129 (1940).

Can. J. Chem. Downloaded from www.nrcresearchpress.com by 41.223.56.140 on 09/04/12
For personal use only.

Can. J. Chem. Downloaded from www.nrcresearchpress.com by 41.223.56.140 on 09/04/12
For personal use only.

THE ACTION OF PYRIDINE ON THE DINITRATE ESTERS OF 1,4;3,6-DIANHYDROHEXITOLS[1]

M. JACKSON AND L. D. HAYWARD

ABSTRACT

In contrast to the rapid and selective replacement of a secondary *O*-nitro group by hydrogen in the hexitol hexanitrates at 25–50° C, the dinitrate esters of the 1,4;3,6-dianhydrides of D-mannitol, D-glucitol, and L-iditol (*cis*-isohexides) reacted slowly in anhydrous pyridine at 87–115° C. The chief products were a polymer, nitrogen oxides, and pyridinium nitrate; the yield of mononitrates did not exceed 10% and none of the parent diols were formed.

The relative rates of the first-order decomposition of the nitroxy groups in the isomeric dinitrates were in reverse order to that for S_N2 reaction at carbon in these compounds. Activation energies and frequency factors were determined and water was shown to have a retarding effect.

Thermal decomposition of the dinitrates in solution in nitrobenzene, *m*-xylene, or *sym*-tetrachloroethane was much slower than the pyridine reaction at the same temperature and was independent of the polarity of the solvent and the conformation of the ester.

INTRODUCTION

Dulcitol and D-mannitol hexanitrates have been shown to react selectively with pyridine to yield the corresponding 1,2,4,5,6-pentanitrates (1, 2). The rate of reaction was different for the two hexitol derivatives and the resulting pentanitrates were essentially stable to pyridine under the same conditions. Sorbitol hexanitrate reacted similarly with pyridine but the pentanitrate was not fully characterized (3). The reaction was inconveniently fast for kinetic studies even at 25° C and the multiplicity of nitroxy groups and molecular conformations further complicated the problem of sorting out the reaction mechanism.

The three known isomeric 1,4;3,6-dianhydrohexitols (the *cis*-isohexides) and their derivatives have been shown to behave characteristically in certain types of reactions due to differences in their restricted conformations (4, 5). In an attempt to determine the mechanism of the pyridine – nitrate ester reaction the dinitrates of the isohexides (I–III, Fig. 1) were selected for study since observation of similar steric effects in their reactions with pyridine would aid in diagnosis of the type of mechanism involved. The presence of only two, non-vicinal, secondary, nitroxy groups in these isomers was also expected to simplify analysis of the results.

RESULTS AND DISCUSSION

The three isohexide dinitrates (Fig. 1) were prepared in crystalline form and characterized through their nitrogen contents, infrared spectra, and nearly quantitative conversion to the parent diols. The physical constants and nitrogen contents of the isomers are shown in Table I. The dinitrates dissolved readily in pyridine and the colorless solutions were stable over several weeks at room temperature. No vigorous reaction occurred on heating under reflux; however, slow decomposition, accompanied by a red coloration of the solution and evolution of oxides of nitrogen, began at temperatures above 50° C.

At 115° C 0.424 *M* solutions of the isohexide dinitrates in anhydrous pyridine decomposed according to an apparent first-order rate law for loss of nitroxy groups (Fig. 2). Since pyridine, as solvent, was present in constant excess, it was likely that the reaction actually involved a second-order process which appeared to be first order because of this

[1]*Manuscript received December 23, 1959.*
Contribution from the Department of Chemistry, University of British Columbia, Vancouver, B.C. Abstracted from the Ph.D. thesis submitted by M. J. to the University in April, 1959.

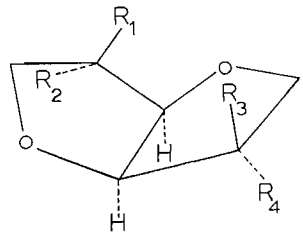


FIG. 1. 2,5-Dinitrates of 1,4;3,6-dianhydrohexitols.

I $R_1 = ONO_2$, $R_2 = H$, $R_3 = ONO_2$, $R_4 = H$: isomannide dinitrate
II $R_1 = ONO_2$, $R_2 = H$, $R_3 = H$, $R_4 = ONO_2$: isosorbide dinitrate
III $R_1 = H$, $R_2 = ONO_2$, $R_3 = H$, $R_4 = ONO_2$: isoidide dinitrate

TABLE I

1,4;3,6-Dianhydrohexitol dinitrates

	Isomannide dinitrate (I)	Isosorbide dinitrate (II)	Isoidide dinitrate (III)	Ref.
Melting point, ° C				
Found	64.5–65.5	50.5–51.5	68–69	
Reported	65.5	70	—	(6)
		71		(7)
		52		(8)
$[\alpha]_D$				
Found	+335	+141	+72.9	
Reported	—	+134	—	(8)
Nitrogen content (%)				
Found	11.8[a]	11.9[a]	11.8[a,b]	
Required	11.87	11.87	11.87	

[a]Modified micro-Kjeldahl method.
[b]Determined by Mr. I. G. Csizmadia. Found: C, 30.9; H, 3.95%. Calc. for $C_6H_8N_2O_8$: C, 30.5; H, 3.41%.

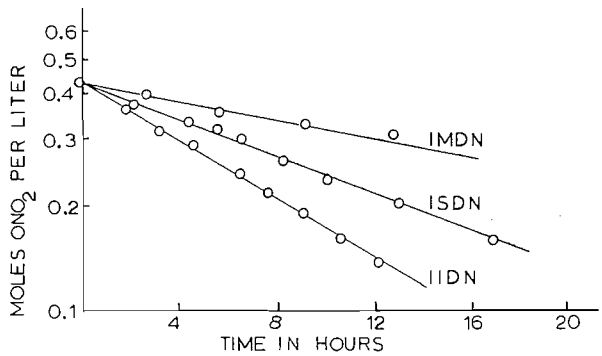


FIG. 2. Rate plots of isohexide dinitrate – pyridine reaction at 115° C. IMDN, isomannide dinitrate; ISDN, isosorbide dinitrate; IIDN, isoidide dinitrate.

limitation (9). The course of the reaction was followed by colorimetric determination of unreacted nitrate ester in aliquots of the reaction mixture. The rates were confirmed by quantitative isolation of the unreacted material followed by complete characterization. The rate of nitroxy group decomposition was also determined at 100° C and 87° C

Can. J. Chem. Downloaded from www.nrcresearchpress.com by 41.223.56.140 on 09/04/12
For personal use only.

TABLE II

Rates of decomposition of the isohexide dinitrates in pyridine

Conditions		Rate constants, $sec^{-1} \times 10^{-6}$		
Temperature, ° C	Moles water per mole nitroxy group	Isoidide dinitrate	Isosorbide dinitrate	Isomannide dinitrate
87	0	3.20	1.15	0.13
100	0	8.58	2.29	0.74
115	0	25.4	15.2	8.07
115	0.5	18.8	12.7	3.3
115	1.0	13.5	10.0	3.6
115	2.0	10.3	7.9	3.1

(Table II). From these results Arrhenius activation energies of 21, 24, and 41 kcal and log frequency factors of 7.6, 8.9, and 18.3 were found for isoidide, isosorbide, and isomannide dinitrates respectively.

None of the parent diols could be detected in the reaction products by chromatography. Isohexide mononitrates were isolated and characterized but accounted for a maximum of 10% of the decomposed dinitrate in runs with aqueous pyridine; with anhydrous pyridine only traces of mononitrate could be detected. Most of the weight of the reaction products was brown-black, polymeric material. In addition to pyridinium nitrate a small amount of an unidentified, optically active oil was also isolated.

For comparison with the pyridine reaction the rate of thermal decomposition of the dinitrates was determined in four solvents with boiling points above 115° C and dipole moments ranging from 0.37 to 3.98 Debye units. The slow decomposition of isosorbide dinitrate at 100° and 115° C in these solvents is shown in Table III. The other two

TABLE III

Thermal decomposition of isosorbide dinitrate in various solvents

		Decomposition, %			
		100° C		115° C	
Solvent	μ, Debyes	25 hours	50 hours	25 hours	50 hours
Nitrobenzene	3.98	2	5	18	37
m-Xylene	0.37	6	8	23	32
s-Tetrachloroethane	1.36	4	7	25	46
Diethylcarbinol	1.64	29	40	45	53

isomers decomposed at the same rate in *sym*-tetrachloroethane but were not tested in the other solvents.

The rates of decomposition of the nitroxy groups were very similar in nitrobenzene, *m*-xylene, and *sym*-tetrachloroethane with first-order rate constants of 0.41×10^{-6} and 2.7×10^{-6} sec^{-1} at 100° C and 115° C respectively. The more rapid reaction in diethylcarbinol was probably due to incursion of a transnitration reaction:

$$RONO_2 + R'OH \rightleftharpoons ROH + R'ONO_2.$$

It is well established that the first and rate-determining step in the thermal decomposition of nitrate esters in the gaseous state is the fission of the oxygen–nitrogen bond, generating a free alkoxyl radical (10, 11). A similar mechanism for the first-order thermal

Can. J. Chem. Downloaded from www.nrcresearchpress.com by 41.223.56.140 on 09/04/12
For personal use only.

Can. J. Chem. Downloaded from www.nrcresearchpress.com by 41.223.56.140 on 09/04/12
For personal use only.

decomposition of the esters in the condensed state seems probable (12). Thermal decomposition of the esters in solution, however, has not been previously investigated.

For the first-order decomposition of the isohexide nitrates in the non-hydroxylic solvents the activation energy of 37 kcal/mole and log frequency factor of 15 calculated from the data of Table III were in good agreement with the values quoted for gaseous and condensed nitrate esters (10, 11, 12). This suggested a free radical mechanism for this case also. Additional evidence of a free radical mechanism was the fact that the rates were independent of the polarity of the solvent (9). Since the rate of the thermal reaction was exceeded by a factor of 5.6 in the pyridine reaction with isosorbide dinitrate at both temperatures it was concluded that thermal decomposition did not play a major part in the pyridine reaction.

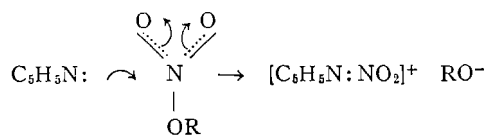
It was noted that the decomposition went faster with well-dried pyridine. To test the effect of water on the rate a series of runs was made with increasing amounts of water present. There was appreciable decrease in rate with increase in water content (Table II) but the nature of the products was not altered substantially. The rate law,

$$\text{rate} = \frac{k_1\,[\text{nitrate ester}]}{1+k_2[H_2O]},$$

was followed where k_1 was 2.54×10^{-5} and k_2 1.70 for isoidide dinitrate.

The S_N2 reactions at carbon of isohexide *O*-derivatives, such as the replacement of sulphonoxy group by iodine, had a characteristic order of rates due to steric hindrance at one face of the molecule (5). The *endo* group (as in isomannide) reacted several times faster than the *exo* group (as in isoidide). The order of the rates of the pyridine – nitrate ester reaction, however, was exactly the reverse and hence ruled out this mechanism.

On the other hand these results were consistent with nucleophilic attack by pyridine at the nitrogen of the nitroxy group resulting in heterolytic cleavage of the low energy O—NO_2 bond.



The approach of the bulky pyridine molecule to the *exo*-nitroxy group would be least hindered by the isohexide skeleton in this case. The unstable *N*-nitrated pyridine intermediate was recently synthesized by Oláh and co-workers by direct nitration of pyridine with nitronium tetrafluoroborate (13). This mechanism also agrees with retention of configuration at asymmetric carbons actually found with the hexitol hexanitrates. The subsequent reaction of the alkoxide ion led to polymer formation in the isohexide case. The failure to detect the parent diols was not due to their decomposition since they could be added to the reaction mixture and recovered quantitatively.

The nitroxy groups in the isohexide isomers were well separated on the carbon chain, and, except in the case of isomannide dinitrate (Fig. 1), were also well separated in space. These isolated groups reacted only slowly with pyridine. In the hexitol hexanitrates the secondary nitroxy groups were contiguous and closely packed; steric compression in the initial state was clearly indicated by the molecular models. The proximity of the α-nitroxy groups must therefore be of considerable importance in the activation of the center groups and in the lifetime of the alkoxide ion.

Can. J. Chem. Downloaded from www.nrcresearchpress.com by 41.223.56.140 on 09/04/12
For personal use only.

EXPERIMENTAL

1,4;3,6-Dianhydrohexitols (cis-Isohexides)

Isomannide and isosorbide were prepared from D-mannitol and sorbitol respectively by the method of Wiggins (14). Isoidide was most conveniently prepared, together with isosorbide, through hydrogenation of L-sorbose followed by dehydration.

L-Sorbose (50 g) in water (200 ml) was hydrogenated at 55 p.s.i. and 80° C for 4 hours with Raney nickel catalyst (from 10 ml of the alcoholic sludge). The catalyst and solvent were removed and the residue was dissolved in concentrated hydrochloric acid (300 ml). The solution was saturated with hydrogen chloride and refluxed for 24 hours. Hydrogen chloride was removed by repeated evaporation under reduced pressure alternated with addition of water, and the residual sirup was fractionally distilled under reduced pressure: fraction 1, b.p. 135–140° C at 0.18–0.20 mm, 8 g, crystallized (isosorbide); fraction 2, b.p. 140–143° C at 0.20–0.22 mm, 5 g, sirup (mixture); fraction 3, b.p. 143–155° C at 0.22–0.25 mm, 12 g, crystallized (isoidide). Fraction 3 after recrystallization from ethyl acetate had m.p. 44–46° C and specific rotation in water $[\alpha]_D^{23}$ +21.0° (*c*, 1.1). Cope and Shen (4) reported m.p. 43–45.5° C, $[\alpha]_D^{25}$ +18.7° (*c*, 2; water) for isoidide.

1,4;3,6-Dianhydrohexitol Dinitrates (I–III)

The nitrate esters were prepared from the isohexides by the method of Forman *et al.* (6) in a yield of about 50%; the yield was increased to 85–90% by nitration in acetic anhydride – nitric acid – acetic acid mixture.

Fuming nitric acid (sp. gr. 1.45, 5 ml) was slowly added to acetic acid – acetic anhydride (1:1, 15 ml) maintained at −2 to 5° C. The mixture was added dropwise, with stirring, to the isohexide (2 g) in acetic acid – acetic anhydride (2:1, 15 ml) maintained at 0° C. After standing for 2 hours at 5° C the mixture was poured into ice water (400 ml). Part of the nitrate ester (2.2 g) crystallized out on standing for 18 hours at 20° C and a further amount (0.6 g) was recovered by ether extraction of the mother liquor. The esters were recrystallized from methanol and analyzed for nitrate-nitrogen (Table I). The infrared spectra of the isomers (potassium bromide window) showed covalent nitrate group absorption at 1650, 1265, and 750 cm^{-1} and no hydroxyl or carbonyl peaks.

Hydrogenation of the nitrates in alcohol solution over palladium–charcoal (1) gave the parent diols in 90–98% yield.

Decomposition of Isohexide Dinitrates in Solution

(a) Solvents

Reagent grade pyridine was distilled and the middle fraction of 80% was collected and dried over calcium hydride for 48 hours, decanted, and redistilled immediately before use. Reagent grade nitrobenzene was dried over calcium chloride, distilled, redried over phosphorus pentoxide, and redistilled under reduced pressure. *m*-Xylene and *sym*-tetrachloroethane were dried over calcium chloride and distilled. Technical grade diethylcarbinol was dried over anhydrous sodium sulphate and distilled and the middle fraction was used.

(b) Decomposition in Pyridine

The reactions were conducted in glass bulbs (2.5-cm diameter) with long stems (30 cm) fitted with water jackets and closed by drying tubes containing Drierite. An initial concentration of 0.100 g of isohexide dinitrate in 2 ml pyridine was used (0.424 mole nitroxy group per liter). The bulbs were heated in an oil bath for reactions at 115° C (reflux temperature), in the vapor of boiling water (100° C), or in the vapor of a boiling two-layer mixture of 2-butanol and water (87° C).

Aliquots of the reaction mixture (0.100 or 0.200 ml) were removed at intervals, distilled water (2 ml) was added, and the mixture was extracted three times with 1-ml portions of ether. Tests with added amounts of the dinitrates showed that extraction was then complete. The combined ether extracts were made up to 10 ml and 1-ml samples were taken for colorimetric determination of nitrate ester (15, 16).

The nitrate sample, containing 10–80 μg nitrogen, was added to 15 ml of 70% (v/v) sulphuric acid in a 250-ml flask and 1 ml of a 1% solution of 3,4-dimethylphenol was added. After being mixed, the solution was let stand for 30–60 minutes at 30° C. Water (150 ml) was then added, boiling stones introduced, and the flask fitted with a U-shaped distilling tube leading into a 25-ml volumetric flask containing 2% sodium hydroxide solution (2.5 ml). Distillation was carried out with the volumetric flask cooled in ice water and 20 ml of distillate was collected. The distillate was made up to 25 ml and brought to 24.0±0.5° C before colorimetric estimation at 435 mμ in a Bausch and Lomb Spectronic 20 colorimeter. The nitrate–nitrogen content of the sample was given by O.D.×103 = μg nitrogen.

(c) Thermal Decomposition in Solution

The nitrate ester (50 mg) and solvent (1 ml) were placed in a reaction bulb as used in the pyridine studies and heated in the vapor of boiling diethylcarbinol (114–115° C). After the reaction period the contents of the bulb were transferred with ether to a 7.5 mm ×20 cm column of alumina (Alcoa Grade F-20, acid-washed, activated at 400° C for 4 hours). The column was eluated with ether followed by ether – ethyl acetate (9:1). Fractions of the eluate containing nitrate (diphenylamine test) were pooled and evaporated under reduced pressure. The residual sirupy dinitrates crystallized on seeding and were identified by their melting and mixed melting points.

(d) Reaction Products

Isohexide dinitrate (5 g) in pyridine (50 ml) was refluxed under anhydrous conditions until 50–90% decomposed. The mixture was poured into water (500 ml), extracted with ether (600 ml), and the solutions were filtered. The precipitate was a brown-black amorphous solid (product A, 0.5–1.5 g).

The ether solution was evaporated to dryness *in vacuo* to remove traces of pyridine and yielded a pale brown sirup (0.5–2.5 g). Samples of this sirup were chromatographed on paper in hexane–methanol solvent (17). Unreacted isohexide dinitrate and a faint nitrate-containing spot with lower R_f value were detected in the products from each reaction. Quantitative separation was obtained by chromatography on alumina columns developed with ether – ethyl acetate (9:1) followed by acetone–methanol (1:1). The ether – ethyl acetate fractions yielded unreacted isohexide dinitrate which was recrystallized and characterized by mixed melting point determinations.

The acetone–methanol fractions yielded a small amount of sirup which had R_f 0.05 on papergrams developed with hexane–methanol. The nitrate–nitrogen content was 5.6% (required for isohexide mononitrate, 7.3%). Complete nitration of the sirup gave a spot running parallel to isohexide dinitrate on papergrams.

The aqueous solution was evaporated *in vacuo* to a dark red sirup (0.5–1.5 g). Extraction of the sirup with hot ethanol (50 ml) left a brown, amorphous solid (product B, 0.5–1.0 g). A red-brown sirup (0.5–1.5 g) was recovered on evaporation of the ethanol solution. Celite column chromatography with 1-butanol – water as solvent (18) showed that this sirup contained no isohexide since the fractions had zero optical rotation. Isohexide added to the initial reaction mixture in some runs was recovered quantitatively from the Celite column by this technique.

Can. J. Chem. Downloaded from www.nrcresearchpress.com by 41.223.56.140 on 09/04/12
For personal use only.

The alcohol extract was subjected to ion-exchange and charcoal chromatography and pyridinium nitrate (0.2–0.8 g) was isolated together with a trace of an acidic, optically active oil.

Products A and B burned slowly in a Bunsen flame and were insoluble in organic solvents and water. Product A partially dissolved in 3 *N* sodium hydroxide solution and product B was soluble in aqueous pyridine and in 0.1 *N* sodium hydroxide solution. A brown-black solid was precipitated from the latter solution on acidification or addition of alcohol. Infrared spectra of the solid fractions thus obtained were very similar to each other and no functional groups could be identified. It was concluded that products A and B were polymers differing mainly in molecular weight.

ACKNOWLEDGMENTS

The authors gratefully acknowledge a research grant from the Defence Research Board of Canada and the award of a Studentship to one of us (M. J.) by the National Research Council of Canada.

REFERENCES

1. L. D. Hayward. J. Am. Chem. Soc. **73**, 1974 (1951).
2. G. G. McKeown and L. D. Hayward. Can. J. Chem. **33**, 1392 (1955).
3. T. Urbanski and S. Kwiatkowska. Roczniki Chem. **25**, 312 (1951).
4. A. C. Cope and T. Y. Shen. J. Am. Chem. Soc. **78**, 3177 (1956).
5. M. Jackson and L. D. Hayward. Can. J. Chem. **37**, 1048 (1959).
6. S. E. Formann, C. J. Carr, and J. C. Krantz. J. Am. Pharm. Assoc. **30**, 132 (1941).
7. L. F. Wiggins. Advances in Carbohydrate Chem. **5**, 206 (1950).
8. L. Goldberg. Acta Physiol. Scand. **15**, 173 (1948).
9. C. K. Ingold. Structure and mechanism in organic chemistry. Cornell Univ. Press, Ithaca, N.Y. 1953.
10. J. B. Levy. J. Am. Chem. Soc. **76**, 3254 (1954).
11. P. Gray and A. Williams. Chem. Revs. **59**, 239 (1959).
12. M. A. Cook. The science of high explosives. Reinhold Publishing Corp., New York. 1958.
13. G. Oláh, I. Kuhn, and A. Mlinkó. J. Chem. Soc. 4257 (1956).
14. L. F. Wiggins. J. Chem. Soc. 4 (1945).
15. H. Barnes. Analyst, **75**, 388 (1950).
16. A. C. Holler and R. V. Auch. Anal. Chem. **21**, 1385 (1949).
17. D. F. Meigh. Nature, **169**, 706 (1952).
18. R. U. Lemieux, C. T. Bishop, and G. E. Pelletier. Can. J. Chem. **34**, 1365 (1956).

Can. J. Chem. Downloaded from www.nrcresearchpress.com by 41.223.56.140 on 09/04/12
For personal use only.

Can. J. Chem. Downloaded from www.nrcresearchpress.com by 41.223.56.140 on 09/04/12
For personal use only.

THE ELECTRON SPIN RESONANCE SPECTRA OF THE POSITIVE AND NEGATIVE IONS OF DIPHENYLENE[1]

C. A. McDowell and J. R. Rowlands

ABSTRACT

The electron spin resonance spectra of the positive and negative ions of diphenylene have been measured. It has been found that these spectra consist of five lines showing that the observed hyperfine interaction is caused by four equivalent protons. The over-all extent of the positive ion spectrum is 18 gauss compared with that of 12.9 gauss for the negative ion. The hyperfine splittings observed are 4.0 gauss and 2.75 gauss respectively.

INTRODUCTION

The electron spin resonance spectra (e.s.r.) of both positive and negative ions of a number of alternant hydrocarbons have been measured in recent years (1). It has been shown that the qualitative features of the experimental spectra can be interpreted by use of unpaired electron spin densities calculated from the simple Hückel molecular orbital theory. The hyperfine interactions found in the e.s.r. spectra of these aromatic hydrocarbon ions are attributed to interactions between the odd electron spin and the nuclear spins of the protons attached to the carbon atoms. It has been shown that the hyperfine splitting produced by a proton attached to a given carbon atom is linearly proportional to the unpaired electron density on that carbon atom (2), i.e.,

$$\Delta H = Q\rho_\mu, \qquad [1]$$

where ΔH is the hyperfine splitting observed, and ρ_μ is the odd electron spin density on carbon atom μ.

From the properties of even alternant hydrocarbons it is evident that the odd electron spin densities on carbon atom μ, of an electron moving in a molecular orbital ϕ_i, are given by the equation

$$\rho_\mu = c_{i\mu}^2. \qquad [2]$$

It has been shown (3) that the atomic orbital coefficients $c_{i\mu}$ in paired orbitals are equal in magnitude, i.e. if orbitals ϕ_i and ϕ_j are paired in energy, then

$$c_{i\mu} = \pm c_{j\mu}. \qquad [3]$$

We can, therefore, expect that if ΔH^+ is the hyperfine splitting found in the monopositive ion, and ΔH^- that of the mononegative ion of a particular alternant hydrocarbon, and if Q is the same for both species, then

$$\Delta H^+ = \Delta H^-. \qquad [4]$$

It has been found experimentally for alternant hydrocarbons that although both species give the same number of components of hyperfine interaction, the over-all width of the monopositive ion spectra is in general about 4 gauss greater than the corresponding mononegative ions (1). The complexity of the spectra has made the determination of hyperfine splitting constants difficult. Where an analysis of the experimental spectra is possible, we have a choice of (*i*) assuming that the unpaired spin densities in both positive and negative ions are equal and are predicted accurately by the Hückel theory, and determining suitable values of the proportionality constant Q for the two species, or (*ii*)

[1]*Manuscript received December 22, 1959.*
Contribution from the Department of Chemistry, University of British Columbia, Vancouver 8, B.C.

assuming that this proportionality constant Q is the same for the two species, and is in fact constant for all even alternant hydrocarbons, and comparing the experimentally determined spin densities with those predicted from the Hückel molecular orbital theory.

In this paper on the ions of diphenylene the latter procedure has been followed.

EXPERIMENTAL

The mononegative ion of diphenylene was prepared by distilling dry tetrahydrofuran under vacuum into a bulb containing a freshly prepared sodium film. Attached to the bulb via a side arm was a narrow tube which held the diphenylene. The bulb was sealed off from the solvent source by freezing both sides with liquid nitrogen, pumping off any unfrozen tetrahydrofuran, and then sealing off at a constriction just above the neck of the bulb. When the solvent in the bulb was at room temperature the diphenylene was dissolved in it by shaking. The diphenylene then immediately reacted with the sodium to give a solution of the mononegative ion. Measurements of the e.s.r. spectra were then made by tipping the solution into the narrow tube, which was then placed in the cavity of the spectrometer operating in a TE012 mode. All the spectra were recorded on a high-resolution electron spin resonance spectrometer operating at 9000 Mc/sec. The magnetic field of approximately 3300 gauss was supplied by a Varian 6-in. magnet with shimmed pole faces. A modulating frequency of 10 kc/sec was used and the derivation of the spectra recorded on a Leeds & Northrup recorder as phase-sensitive detection was used. The monopositive ion of diphenylene was prepared by dissolving the hydrocarbon in concentrated sulphuric acid. Calibrations of all runs were made, by determining with the e.s.r. spectrum of Fremi's salt under identical sweep conditions.

RESULTS

The spectra of the negative and positive ions of diphenylene are shown in Figs. 1 and 2, together with the integrated absorption curves for each case. Each ion gives a spectrum containing five completely resolved lines with approximate intensity ratios of 1:4:6:4:1. No further hyperfine splitting could be detected for either ion, although the spectra were



FIG. 1. The electron spin resonance absorption spectrum of the diphenylene positive ion in concentrated sulphuric acid.

Can. J. Chem. Downloaded from www.nrcresearchpress.com by 41.223.56.140 on 09/04/12
For personal use only.

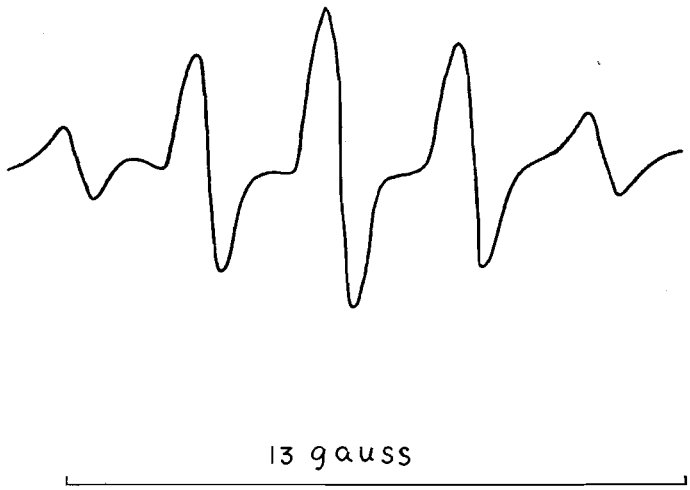


FIG. 2. The electron spin resonance absorption spectrum of the diphenylene negative ion in tetrahydrofuran.

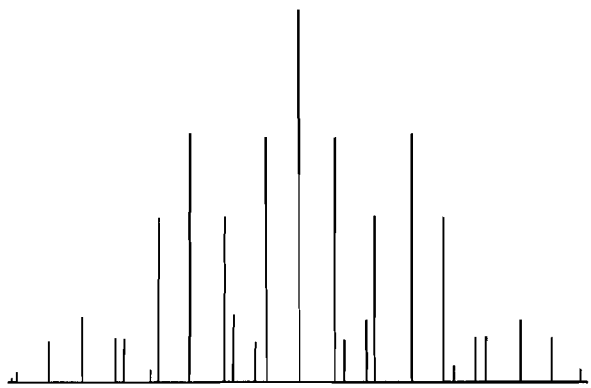


FIG. 3. Theoretical electron spin resonance absorption spectrum of diphenylene positive (or negative) ion on the Hückel molecular orbital approximation.

measured over a range of concentrations. Figure 3 is the theoretical spectrum built up using the calculated Hückel spin densities, assuming that all Coulomb integrals for the carbon atoms are the same and that all resonance integrals for the C—C bonds are also equal. The theoretical spectra of both positive and negative ions are of course identical on this picture.

DISCUSSION

It can be seen from Figs. 1 and 2 that the observed spectra consist of five lines. These lines are well resolved and there is no trace of any other fine structure on the spectra of either the positive or negative ion even when spectra have been taken with extreme care and very high resolution. The theoretical spectrum calculated from the Hückel electron densities indicates that there are 25 lines to be expected (see Fig. 3). Our observed spectra must, therefore, be interpreted on the assumption that there are only four equivalent protons contributing to the hyperfine splitting. These can be taken to be the protons attached to carbon atoms 2, 3, 6, and 7, which of the two sets of carbon atoms with protons

Can. J. Chem. Downloaded from www.nrcresearchpress.com by 41.223.56.140 on 09/04/12
For personal use only.

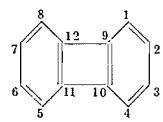
attached are those having the highest electron density on the Hückel theory. Carbon atoms 9, 10, 11, and 12 have no protons attached and for this reason the e.s.r. spectra of the ions of diphenylene extend only over about half the range observed for the ions of other alternant hydrocarbons. Thus the spectrum of the positive ion of diphenylene extends over only 18 gauss compared with about 33 gauss for the anthracene positive ion. The spin densities on carbon atoms 9, 10, 11, and 12 total about 54% of the total spin densities at all the carbon atoms in diphenylene; hence we would expect the e.s.r. spectrum of this substance to extend only over about half the range of spectrum of say the anthracene positive ion. This is in agreement with our observations.

Although the intensity distribution of the experimental spectra of the two ions is the same, there is a marked difference in the magnitude of the hyperfine interaction. The overall width of the positive ion spectrum is 18 gauss, with a splitting constant of 4.0 gauss. The corresponding figures for the negative ion are 12.9 gauss and 2.75 gauss respectively.

If we take the value of the proportionality constant Q to be the same for the two species, then there is a difference in the odd electron distribution in the two ions. In Table I we have listed the experimental spin densities for the two ions, obtained by using a value of Q derived from the benzene negative ion spectrum, which is the only alternant hydrocarbon

TABLE I

Electron spin densities for the mononegative and monopositive ions of diphenylene



		Expt.	Calc., Hückel theory	Calc., assuming $\alpha_{C_9} = \alpha_C + 1/5\beta$
Diphenylene$^+$ ion				
	ρ_1		0.0269	0.0179
	ρ_2	0.1739	0.0873	0.0906
	ρ_9	0.0000	0.1360	0.1414
Diphenylene$^-$ ion				
	ρ_1		0.0269	0.0372
	ρ_2	0.1195	0.0873	0.0853
	ρ_9	0.0000	0.1360	0.1274

for which accurate spin densities are known. Column 2 of Table I lists the spin densities calculated from the Hückel theory, with the assumption of equal Coulomb integrals for the carbon atoms. In column 3 of the table we have included spin densities obtained by assigning the four central carbon atoms with a Coulomb integral equal to the normal carbon Coulomb integral *plus one-fifth* the carbon–carbon resonance integral. It may be seen from the table that this makes the calculated spin densities of the positive ion different from those of the negative ion. Since in diphenylene we are studying a derivative of cyclobutadiene, it is quite plausible that we should treat it as containing two different types of carbon atom. It is quite obvious from the lack of agreement between experiment and theory that the simple Hückel molecular orbitals obtained by the assumption of equal Coulomb and resonance integrals are inadequate. It must, however, be recalled that other workers have previously noted that exact agreement between the electron densities calculated from the simple Hückel molecular orbital theory and the experimental values

Can. J. Chem. Downloaded from www.nrcresearchpress.com by 41.223.56.140 on 09/04/12
For personal use only.

is lacking. Further it has also been observed that in other alternant hydrocarbon systems there are significant differences between the positive and negative ion spectra which cannot be explained on the basis of the simple Hückel molecular orbital theory.

ACKNOWLEDGMENTS

We wish to thank the National Research Council and the Defence Research Board of Canada for grants-in-aid of this work. Our thanks are due to Drs. V. Rogers and J. F. McOmie for the gift of diphenylene.

REFERENCES

1. T. R. TUTTLE, Jr., R. L. WARD, and S. I. WEISSMAN. J. Chem. Phys. **25**, 189 (1956).
2. S. I. WEISSMAN and E. DE BOER. J. Am. Chem. Soc. **80**, 4549 (1958).
3. S. I. WEISSMAN. J. Chem. Phys. **25**, 890 (1956).
4. H. M. MCCONNELL. J. Chem. Phys. **24**, 764 (1956).
5. H. S. JARRETT. J. Chem. Phys. **25**, 1289 (1956).
6. C. A. COULSON and G. S. RUSHBROOKE. Proc. Cambridge Phil. Soc. **36**, 193 (1940).

Can. J. Chem. Downloaded from www.nrcresearchpress.com by 41.223.56.140 on 09/04/12
For personal use only.

Can. J. Chem. Downloaded from www.nrcresearchpress.com by 41.223.56.140 on 09/04/12
For personal use only.

THE CHEMISTRY OF THE "AMINOCHROMES"

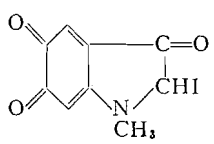
PART III. ON THE STRUCTURES OF "IODOÖXOADRENOCHROME" AND IODOEPINOCHROME[1,2]

R. A. HEACOCK AND B. D. SCOTT

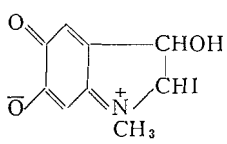
ABSTRACT

A substance prepared by the oxidation of adrenaline with iodic acid and described in the literature as 2-idoöxoadrenochrome appears, after consideration of a number of its physical and chemical properties to be identical with 2-iodoadrenochrome. The iodine atom in iodoepinochrome, obtained by the oxidation of epinine with potassium iodate, has been shown to be in the 2-position of the heterocyclic ring in the molecule.

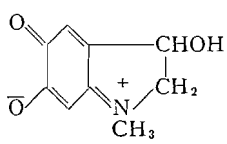
During the course of a study of the infrared spectra of the aminochromes and related compounds (1) it was observed that the spectrum of a substance described by Macciotta as 2-iodoöxoadrenochrome (formulated as I) (2) was identical with those obtained from



I



II



III

specimens of 2-iodoadrenochrome (usually formulated as II) prepared by the methods described in the literature (3, 4, 5, 6). The general form of the spectrum was more in keeping with a structure of type II than with one of type I. A definite hydrogen-bonded O—H stretching band was observed at 3410 cm^{-1} (microanalysis indicated that the compounds were anhydrous and therefore this peak could not have arisen from water of crystallization in I, and the "carbonyl" region was very similar to that of adrenochrome, usually formulated as III (cf. 7). It occurred to the authors that the possibility that Macciotta's compound was, in fact, merely 2-iodoadrenochrome (II) should be investigated, especially since no other "oxoaminochromes" have been isolated. The preparation, in solution, of "oxoadrenochrome" was reported (8), but this claim has since been disputed (9).

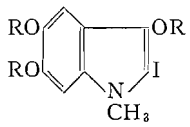
These compounds, which are very dark violet-brown in color, decompose on heating without melting and consequently melting point and mixed melting point determinations gave only inconclusive results. The analytical values obtained for carbon, hydrogen, and nitrogen were in good agreement in both cases with those calculated for II, although it must be admitted that only the hydrogen values are sufficiently different in the two cases to warrant drawing any conclusions. The ultraviolet and visible absorption spectra of I and II were identical and very similar to those of 2-iodoaminochromes in general (cf. 3). If I had the structure assigned to it by Macciotta it would contain a different chromophoric system to the 2-iodoaminochromes and would be expected to exhibit a different absorption spectrum.

Macciotta reported that reduction of I with sodium hydrosulphite gave 3,5,6-

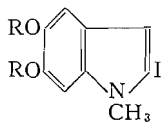
[1]*Manuscript received December 10, 1959.*
Contribution from the Psychiatric Research Unit, University Hospital, Saskatoon, Saskatchewan. This investigation was carried out under the auspices of the Saskatchewan Committee on Schizophrenia Research and supported by grants from the Department of National Health and Welfare (Ottawa) and the Rockefeller Foundation.

[2]*Part II: Can. J. Chem.* **36**, *1550 (1958).*

trihydroxy-2-iodoindole (IV: R = H), m.p. 116°, which gave a triacetyl derivative (IV: R = CH_3CO), m.p. 140°. In the hands of the authors the sodium hydrosulphite



IV



V

reduction products of I and II were identical. This was demonstrated by paper chromatography of the crude reaction mixtures and by the physical and chemical properties of the crystalline compounds isolated in each case. The infrared spectra of these products were much more consistent with their being 5,6-dihydroxy- rather than 3,5,6-trihydroxyindoles. In the latter case the product would be an indoxyl which would exist in the keto form in the solid state and consequently its infrared spectrum should show the indoxyl carbonyl peak (7, 10). However there are no peaks in the "carbonyl" region of the spectra of either of these substances. Their ultraviolet absorption spectra resemble that of 5,6-dihydroxy-*N*-methylindole more closely than that of adrenolutin, the corresponding 3,5,6-trihydroxy derivative. These products are considered by the present authors to be 5,6-dihydroxy-2-iodo-*N*-methylindole (V: R = H). The diacetyl derivatives of both reduction products were also identical; the m.p.'s of 151.5–152.5° and 152° (derived from I and II respectively) obtained by the authors for these products are very similar to the value quoted by Bergel and Morrison (153–155°) for a substance described as 5,6-diacetoxy-2-iodo-*N*-methylindole (V: R = CH_3CO) obtained by the direct acetylation of the crude sodium hydrosulphite reduction products of 2-iodoadrenochrome (11).

The reaction mixtures obtained from the reduction of I and II with several reducing agents including sodium hydrosulphite, sodium bisulphite, sodium borohydride, zinc and 2% acetic acid, ascorbic acid, B.A.L. (2,3-dimercapto-1-propanol), and glutathione were studied paper chromatographically (cf. 12). It can easily be seen by inspection of Table I that the chromatographic patterns obtained from I and II with each reducing agent were virtually identical. The main reduction product in all but two cases was 5,6-dihydroxy-2-iodo-*N*-methylindole (R_f ca. 0.20). (The standard R_f value for this substance was obtained from a specimen of the pure crystalline material isolated from the sodium hydrosulphite reduction products.) It was also noticed that with most of the reagents studied, greater or lesser amounts of 5,6-dihydroxy-*N*-methylindole ($R_f = 0.44 \pm 0.02$) were produced presumably by the elimination of the iodine atom during the process of reduction; when reduction was effected with zinc and dilute acetic acid, total deiodination occurred and no 5,6-dihydroxy-2-iodo-*N*-methylindole was detected among the products. The reduction of the aminochromes will be discussed in more detail in a later paper in this series (13); the results of the chromatographic studies are merely presented here to support the author's thesis of the similarity of I and II.

3,5,6-Triacetoxy-2-iodo-*N*-methylindole (IV: R = CH_3CO) was obtained from the action of acetic anhydride in pyridine on II (4), and an identical triacetyl derivative was prepared from I by the same experimental procedure.

The oxidation of epinine (3,4-dihydroxyphenylethylmethylamine) with potassium iodate in aqueous solution gives iodoepinochrome, a violet-brown crystalline solid (3, 14). There has been some disagreement in the literature as to the position of the iodine atom; Sobotka and Austin suggested the 2-position (3), whilst Bu'Lock and Harley-Mason proposed that the iodine atom was present in the 3-position (14), since the 5,6-diacetoxy-

Can. J. Chem. Downloaded from www.nrcresearchpress.com by 41.223.56.140 on 09/04/12
For personal use only.

TABLE I

Paper chromatography of some reduction products of 2-iodoöxoadrenochrome (I) and 2-iodoadrenochrome (II)

Reducing agents and chromogenic reagents	Average R_f values and color reactions† of major spots derived from the reduction products of I and II															
	2-Iodoadrenochrome (II)								2-Iodoöxoadrenochrome (I)							
Sodium hydrosulphite	21		45^{w}		82*^{w}		90*		20		44^{w}		80*^{w}		92*	
Ehr.	BV		BV		Y^{s}		RV^{s}		BV		BV		Y^{s}		RV^{s}	
DPNA	VBr		VBr		RBr		RBr		VBr		VBr		RBr		RBr	
F and C	BGy		BGy		BGy		BGy		BGy		BGy		BGy		BGy	
Gib.	Br		Br		Br		VBr		Br		Br		Br		VBr	
Sodium bisulphite			67^{w}		84*^{w}		90*				64^{w}		83*^{w}		90*	
Ehr.			V^{w}		Y^{s}		RV^{s}				V		Y^{s}		RV^{s}	
F and C			BGy		BGy		BGy				BGy		BGy		BGy	
Gib.			Br		Br		VBr				Br		Br		VBr	
Sodium borohydride	22		46^{vw}		87^{w}				20		46^{vw}		83^{w}			
Ehr.	BV		BV		RV^{s}				BV		BV		RV^{s}			
DPNA	VBr		VBr		—				VBr		VBr		—			
Gib.	Br		Br		Br				Br		Br		Br			
Zinc and dilute acetic acid		44			87^{w}						46		86^{w}			
Ehr.		BV			YBr^{s}						BV		YBr^{s}			
DPNA		VBr			Br^{s}						VBr		Br^{s}			
F and C		BGy			BGy						BGy		BGy			
Gib.		Br			Br						Br		Br			
Ascorbic acid	20	31	41^{w}		56^{w}		86		20	30	42^{w}		55^{w}		82	
Ehr.	BV	GBr	BV		BG		Y^{s}		BV	GBr	BV		BG		Y^{s}	
Fe.	B	B	B		B		B		B	B	B		B		B	
Gib.	Br	Br	Br		Br		VBr		Br	Br	Br		Br		VBr	
B.A.L.	21		44^{w}		72^{vw}		83		22		45^{w}		75^{vw}		83	
Ehr.	BV		BV		V		P^{s}		BV		BV		V		P^{s}	
DPNA	VBr		VBr		—		0		VBr		VBr		—		0	
F and C	BGy		BGy		B		B		BGy		BGy		B		B	
Glutathione	21		44^{w}		67		88		20		43^{w}		62		89	
Ehr.	BV		BV		V		Y^{s}		BV		BV		V		Y^{s}	
Cin.	P		OBr		O		OBr^{s}		P		OBr		O		OBr^{s}	
F and C	BGy		BGy		B		B		BGy		BGy		B		B	

REAGENTS: Ehr. = Ehrlich's reagent; Cin. = cinnamaldehyde; DPNA = diazotized *p*-nitroaniline; F and C = Folin and Ciocalteu's reagent; Fe = ferric chloride/potassium ferricyanide; Gib. = Gibb's reagent.

COLORS: BV = blue-violet; RV = red-violet; V = violet; B = blue; VBr = violet-brown; BGy = blue-grey; Br = brown; Y = yellow; BG = blue-green; GBr = green-brown; RBr = red-brown; YBr = yellow-brown; P = pink; O = orange; OBr = orange-brown.

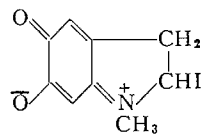
SUPERSCRIPTS: w = only weak color reactions obtained from this spot; vw = only a very weak color reaction obtained from this spot; * = there appear to be two substances produced both by $Na_2S_2O_4$ and by $NaHSO_3$ of high R_f which are not efficiently separated with this solvent system; s = color develops slowly. †Color observed after 24 hours.

iodo-*N*-methylindole obtained from the action of acetic anhydride and pyridine on iodoepinochrome had m.p. 146–147°, whereas the 5,6-diacetoxy-iodo-*N*-methylindole obtained from 2-iodoadrenochrome by Bergel and Morrison (11) had m.p. 153–155°. We have repeated the preparation of these two 5,6-diacetoxy-iodo-*N*-methylindoles from iodoepinochrome and iodoadrenochrome and obtained m.p.'s of 148–150° and 152° respectively; a mixed melting point showed no depression. The infrared spectra ("NUJOL" mulls and chloroform solutions), and the ultraviolet absorption spectra of the two 5,6-diacetoxy-iodo-*N*-methylindoles were identical, indicating that the iodine atom was in the same position in the heterocyclic ring in both cases; Harley-Mason is now also of this opinion (15). Preliminary paper chromatographic examination of the products obtained from the treatment of iodoepinochrome with a number of reducing agents indicated that a complex mixture of products was usually obtained, but that the internal rearrangement product,

Can. J. Chem. Downloaded from www.nrcresearchpress.com by 41.223.56.140 on 09/04/12
For personal use only.

i.e. 5,6-dihydroxy-2-iodo-*N*-methylindole ($R_f = 0.2$), was invariably detected among the products.

In conclusion it may be stated that: (*a*) the oxidation of adrenaline with iodic acid, carried out under the conditions described by Macciotta, gave, in the hands of the authors, a product that behaved identically to 2-iodoadrenochrome and did not exhibit the properties that would be expected for an oxoaminochrome; (*b*) the oxidation of epinine with potassium iodate gave an iodoepinochrome with the iodine atom in the 2-position in the nucleus (i.e. VI).



VI

EXPERIMENTAL

Oxidation of Adrenaline with Iodic Acid

Adrenaline (1.0 g) was oxidized with iodic acid according to the procedure of Macciotta (2). A brownish-violet crystalline solid (I) (1.1 g) was obtained (this was described as 2-iodoöxoadrenochrome by Macciotta). Found: C, 35.26; H, 2.62; N, 4.70. $C_9H_8NO_3I$ requires C, 35.43; H, 2.64; N, 4.59% (i.e. 2-iodoadrenochrome). $C_9H_6NO_3I$ requires C, 35.66; H, 1.99; N, 4.62% (i.e. 2-iodoöxoadrenochrome).

Oxidation of Adrenaline with Potassium Iodate

Adrenaline (1.0 g) was oxidized with potassium iodate according to the method of Sobotka and Austin (3) and 2-iodoadrenochrome (II) (1.5 g) was obtained in brownish-violet needles. Found: C, 35.11; H, 2.61; N, 4.76. $C_9H_8NO_3I$ requires C, 35.43; H, 2.64; N, 4.59%.

Reduction of I *and* II *with Sodium Hydrosulphite* (cf. Macciotta (2))

(*a*) A suspension of sodium hydrosulphite (2.0 g) in water (5 ml) was added to a suspension of freshly prepared I (1.0 g) in water (40 ml) and the reaction mixture stirred vigorously. The dark-violet solid dissolved with the formation of a cloudy yellow solution, from which a pale yellow flocculent precipitate separated, m.p. 96–97.5° (with decomposition), which gave pale yellow needles (product A, 0.22 g), m.p. 105–106° (with decomposition), on recrystallization from benzene – light petroleum (b.p. 80–100°).

(*b*) II (1.0 g) was reduced in the manner described above; the crude product, m.p. 94–95.5° (with decomposition), was recrystallized from benzene – light petroleum (b.p. 80–100°) and pale yellow needles (product B, 0.27 g), m.p. 105° (with decomposition), were obtained. A mixed melting point between the products A and B showed no depression (i.e. 105°, with decomposition). Found: product A: C, 37.66; H, 2.92%; product B: C, 37.63; H, 2.98%. $C_9H_8NO_2I$ requires C, 37.39; H, 2.79%. Macciotta, who considered product A to be 3,5,6-trihydroxy-2-iodo-*N*-methylindole ($C_9H_8NO_3I$ requires C, 35.43; H, 2.64), recorded a m.p. of 116°. However, consideration of the above analytical results, and those of the acetyl derivatives described below, together with the ultraviolet and infrared spectroscopic data strongly suggest that these substances are, in fact, 5,6-dihydroxy-2-iodo-*N*-methylindole.

Acetylation of Products A and B

The dihydroxy compound (i.e. product A or B) (0.2 g) was dissolved in acetic

Can. J. Chem. Downloaded from www.nrcresearchpress.com by 41.223.56.140 on 09/04/12
For personal use only.

anhydride (5 ml) and dry pyridine (5 ml); after standing overnight at room temperature the reaction mixture was poured into ice water and a white solid was obtained. The diacetyl derivatives were purified by recrystallization from benzene – light petroleum (b.p. 80–100°) and obtained as very pale yellow plates. Melting points: from A, 151–152.5°; from B, 152°; mixed m.p. (A+B), 151.5–152.5°. Found: C, 41.79; H, 3.30; N, 3.84; I, 33.91. $C_{13}H_{12}NO_4I$ requires C, 41.84; H, 3.24; N, 3.75; I, 34.01%. Macciotta obtained a substance, m.p. 140° (found: C, 41.52; H, 3.41; N, 3.30%), from the acetylation of the product he obtained by the reduction of I with sodium hydrosulphite which he erroneously considered to be 3,5,6-triacetoxy-2-iodo-*N*-methylindole. Bergel and Morrison obtained a substance, m.p. 153–155° (found: I, 33.9%), which they described as 5,6-diacetoxy-2-iodo-*N*-methylindole, from the acetylation of the crude sodium hydrosulphite reduction products of II (11). The substances obtained by the present authors by the acetylation of products A and B are in all probability both 5,6-diacetoxy-2-iodo-*N*-methylindole.

Paper Chromatographic Study of the Reduction Products of I *and* II

The method used was essentially the same as that employed by the authors for preliminary studies on the reduction of adrenochrome (12). I (or II) (0.01 g) was suspended in water (1.0 ml) and treated with a slight excess of the reducing agent at room temperature until no dark particles of the starting material remained in suspension, and the product filtered to obtain a clear solution. Spots, consisting of ca. 30 μl of the reaction mixture, were examined on Whatman No. 1 paper (previously washed for 48 hours with 2% acetic acid) using 2% acetic acid as running solvent. After drying, the developed chromatograms were examined for fluorescence in ultraviolet light and sprayed with Ehrlich's reagent, Gibb's reagent, diazotized *p*-nitroaniline, and Folin and Ciocalteu's reagent.

The results obtained with seven reducing agents, i.e. sodium hydrosulphite, sodium bisulphite, sodium borohydride, zinc and dilute acetic acid, ascorbic acid, B.A.L., and glutathione are given in Table I. It can be seen from the table the same reduction products are obtained from I and II in each case.

The Action of Acetic Anhydride in Pyridine on I *and* II

A solution of I (or II) (0.5 g) in a mixture of acetic anhydride (10 ml) and dry pyridine (10 ml) was allowed to stand overnight at room temperature. The reaction mixture was then poured into ice water and the white solid, which separated, recrystallized from light petroleum (b.p. 100–120°); the triacetyl derivatives were obtained in colorless prisms. Melting points: product from I, 150.5°; product from II, 148–149°; mixed m.p. 148.5–150.5°. (Found: C, 41.75; H, 3.30; N, 3.33; I, 29.42. $C_{15}H_{14}NO_6I$ requires C, 41.78; H, 3.27; N, 3.25; I, 29.44%.) In both cases the substance was 3,5,6-triacetoxy-2-iodo-*N*-methylindole. This substance had previously been obtained by Bu'Lock and Harley-Mason by the above procedure (m.p. 150°) (4).

The Action of Acetic Anhydride in Pyridine on Iodoepinochrome

Iodoepinochrome (0.4 g), prepared by the method of Sobotka and Austin (3), was dissolved in a mixture of acetic anhydride (10 ml) and dry pyridine (10 ml) and the solution allowed to stand at room temperature for 24 hours. The reaction mixture was then poured into ice water; a white solid separated, which gave 5,6-diacetoxy-2-iodo-*N*-methylindole as pale yellow prisms on recrystallization from benzene – light petroleum (b.p. 80–100°), m.p. 148–150°, undepressed on admixture with a sample prepared from 2-iodoadrenochrome by the method described above. Bu'Lock and Harley-Mason obtained a substance, m.p. 146–147°, from iodoepinochrome by the above procedure

Can. J. Chem. Downloaded from www.nrcresearchpress.com by 41.223.56.140 on 09/04/12
For personal use only.

which they considered to be 5,6-diacetoxy-3-iodo-*N*-methylindole (14), since its melting point differed from that (153–155°) previously reported by Bergel and Morrison for the corresponding 2-iodo compound (11).

Spectroscopic Studies

(a) Ultraviolet and Visible

The ultraviolet and visible absorption spectra of I and II, their sodium hydrosulphite reduction products (i.e. products A and B), the acetyl derivatives of A and B, the direct acetylation products of I, II, and iodoepinochrome were measured on a Warren Spectracord instrument. The results are given in Table II and it can easily be seen that

TABLE II

Ultraviolet and visible absorption spectra

Substance*	Solvent	Absorption maxima, mμ	Absorption minima, mμ
(1) "2-Iodoöxoadrenochrome" (I)	W	233; 303; 535	268; 385
(2) 2-Iodoadrenochrome (II)	W	233; 304; 535	268; 385
(3) Product A (from I)	M	282; 303; (313)†	256; 297
(4) Product B (from II)	M	282; 303; (313)	256; 296
(5) Diacetyl derivative of A	M	231; (280); 294; (303)	255
(6) Diacetyl derivative of B	M	231; (280); 293; (303)	255
(7) Product from direct acetylation of I	M	233; 302	263
(8) Product from direct acetylation of II	M	233; 301	263
(9) Product from direct acetylation of iodoepinochrome	M	231; (280); 293; (303)	254

NOTE: W = water; M = methanol.

*The above descriptions of the substances are given to indicate how each compound was obtained. In fact, (1) and (2) are both 2-iodoadrenochrome; (3) and (4) are both 5,6-dihydroxy-2-iodo-*N*-methylindole; (5), (6), and (9) are all 5,6-diacetoxy-2-iodo-*N*-methylindole; (7) and (8) are both 3,5,6-triacetoxy-2-iodo-*N*-methylindole.

†Figures in parentheses represent shoulders on the main peak.

the positions of the absorption maxima and minima are identical for corresponding pairs in the two series of compounds from I and II. It can also be seen that the absorption curve of the direct acetylation product of iodoepinochrome is the same as those of the diacetyl derivatives of products A and B.

(b) Infrared

The spectra were recorded on a Perkin–Elmer Infracord spectrophotometer. The spectra of I and II were obtained as "NUJOL" mulls and those of the various 5,6-dihydroxy- and 5,6-diacetoxy-indoles (i.e. compounds 3–9 in Table II) were obtained both as "NUJOL" mulls and in chloroform solution. The spectra of the corresponding pairs of substances in the two series of compounds from I and II were identical and that of the direct acetylation product of iodoepinochrome was the same as those of the diacetyl derivatives of the reduction products of I and II. The curves obtained from these last three substances together with those obtained from I and II are shown in Fig. 1.

Some of the more salient features of the infrared spectra are as follows. The products A and B (i.e. 5,6-dihydroxy-2-iodo-*N*-methylindole) showed a hydrogen-bonded O—H stretching band at 3240 cm^{-1} (in "NUJOL"). The ester carbonyl peak of the 5,6-diacetyl derivatives of A and B was observed at 1765 cm^{-1} (both in "NUJOL" and in chloroform). In the spectra of the direct acetylation products of I and II (i.e. 3,5,6-triacetoxy-2-iodo-*N*-methylindole), the main carbonyl absorption occurred at 1770 cm^{-1} in chloroform solution; in "NUJOL" the main peak was observed at 1757 cm^{-1} with a well-defined shoulder at ca. 1786 cm^{-1}.

Can. J. Chem. Downloaded from www.nrcresearchpress.com by 41.223.56.140 on 09/04/12
For personal use only.

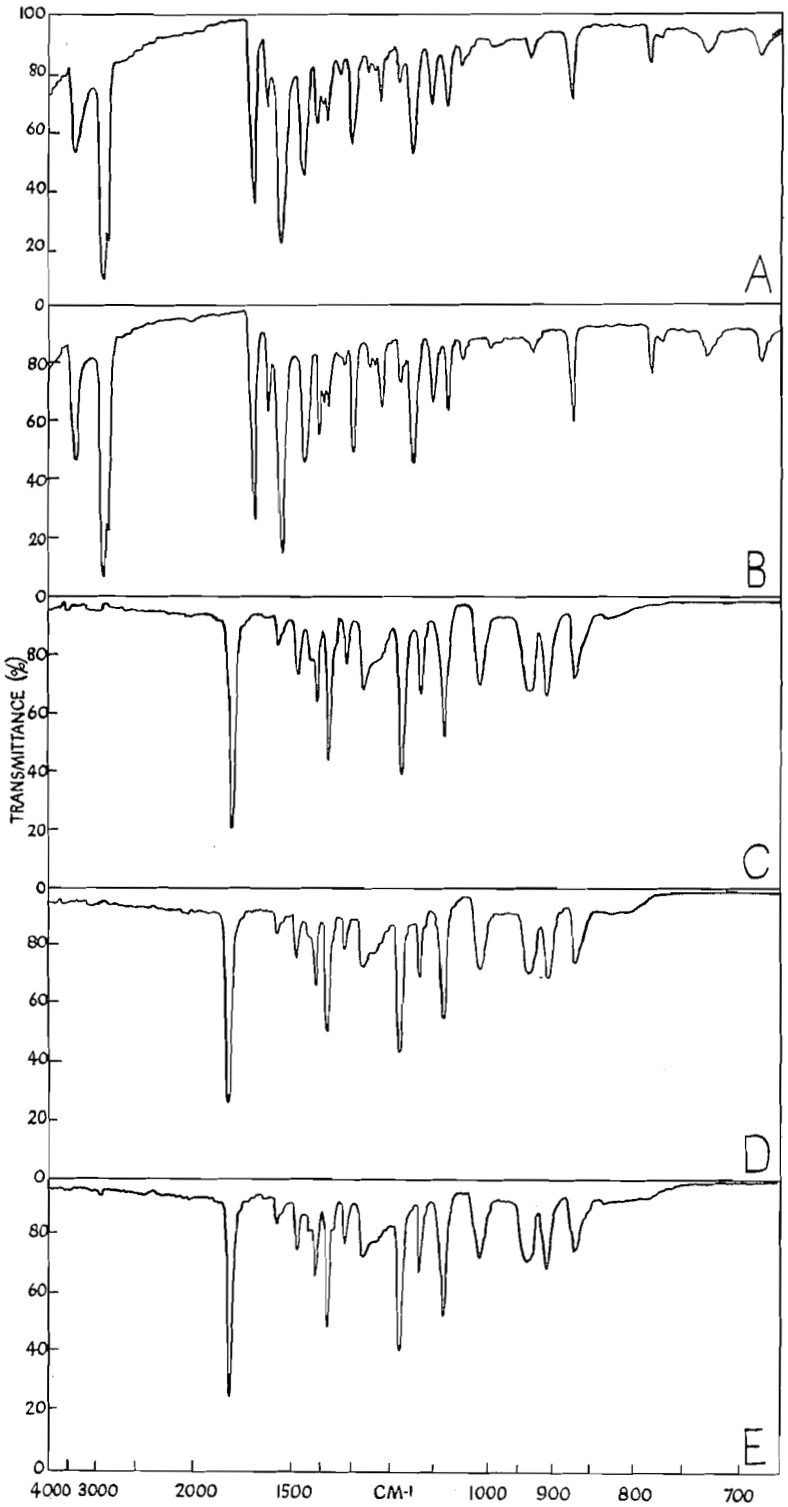


FIG. 1.

Can. J. Chem. Downloaded from www.nrcresearchpress.com by 41.223.56.140 on 09/04/12
For personal use only.

ACKNOWLEDGMENTS

The authors wish to express their thanks to Burroughs–Wellcome and Co. (Canada) Ltd. for a gift of epinine hydrochloride and to Mr. W. Irwin for recording the ultraviolet spectra.

REFERENCES

1. R. A. HEACOCK. In preparation.
2. E. MACCIOTTA. Gazz. chim. ital. **81**, 485 (1951).
3. H. SOBOTKA and J. AUSTIN. J. Am. Chem. Soc. **73**, 3077 (1951).
4. J. BU'LOCK and J. HARLEY-MASON. J. Chem. Soc. 712 (1951).
5. P. BOUVET. Ann. pharm. franc. **7**, 721 (1949).
6. D. RICHTER and H. BLASCHKO. J. Chem. Soc. 601 (1937).
7. R. A. HEACOCK and M. E. MAHON. Can. J. Chem. **36**, 1550 (1958).
8. G. N. COHEN. Compt. rend. **220**, 796, 927 (1945).
9. J. HARLEY-MASON. J. Chem. Soc. 1276 (1950).
10. S. J. HOLT, A. E. KELLIE, D. G. O'SULLIVAN, and P. W. J. SADLER. J. Chem. Soc. 1217 (1958).
11. F. BERGEL and A. L. MORRISON. J. Chem. Soc. 48 (1943).
12. R. A. HEACOCK and B. D. LAIDLAW. Chem. & Ind. (London), 1510 (1958).
13. R. A. HEACOCK and B. D. SCOTT. In preparation.
14. J. BU'LOCK and J. HARLEY-MASON. J. Chem. Soc. 2248 (1951).
15. J. HARLEY-MASON. Private communication. 1959.

FIG. 1. Infrared spectra of: A,* "2-iodoöxoadrenochrome" (I); B,* 2-iodoadrenochrome; C, diacetyl derivative of product A; D, diacetyl derivative of product B; E, product from the direct acetylation of iodoepinochrome.

Note: (*a*) A and B are both 2-iodoadrenochrome (spectra shown are of "NUJOL" mulls). (*b*) C, D, and E are 5,6-diacetoxy-2-iodo-*N*-methylindole (spectra shown are of solutions in chloroform).

*The letters A and B here refer o the infrared spectra of I and II and not to products A and B.

Can. J. Chem. Downloaded from www.nrcresearchpress.com by 41.223.56.140 on 09/04/12
For personal use only.

Can. J. Chem. Downloaded from www.nrcresearchpress.com by 41.223.56.140 on 09/04/12
For personal use only.

THE CHEMISTRY OF THE "AMINOCHROMES"

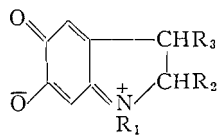
PART IV. SOME NEW AMINOCHROMES AND THEIR DERIVATIVES[1,2]

R. A. Heacock and B. D. Scott

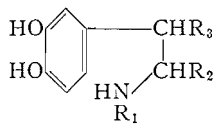
ABSTRACT

N-Ethylnoradrenochrome, *N*-isopropylnoradrenochrome, adrenochrome methyl ether, adrenochrome ethyl ether, and their 2-iodo derivatives have been prepared in crystalline form. The action of acetic anhydride in pyridine on these aminochromes has been studied; acetylated rearrangement products were obtained in each case. *N*-Ethylnoradrenochrome monosemicarbazone, *N*-ethylnoradrenolutin, 5,6-diacetoxy-*N*-ethyl-2-iodoindole, and 5,6-diacetoxy-2-iodo-*N*-isopropylindole have been prepared. The ultraviolet and visible absorption spectra of the aminochromes described above and several 5,6-diacetoxy- and 3,5,6-triacetoxy-*N*-alkylindoles have been measured and the paper chromatographic behavior of the unhalogenated aminochromes studied.

Adrenochrome (I: $R_1 = CH_3$; $R_2 = H$; $R_3 = OH$) (see 1 for list of references) and epinochrome (I: $R_1 = CH_3$; $R_2 = R_3 = H$) (2) are the only unhalogenated aminochromes



I



II

that have, so far, been fully characterized in the solid state. Noradrenochrome (I: $R_1 = R_2 = H$; $R_3 = OH$) has been described as "red rings on the side of the flask" (3) and *N*-isopropylnoradrenochrome (I: $R_1 = i\text{-}C_3H_7$; $R_2 = H$; $R_3 = OH$) is referred to in the patent literature as a purplish-red crystalline solid (4). A preliminary report on the isolation of solid adrenochrome methyl ether (I: $R_1 = CH_3$; $R_2 = H$; $R_3 = OCH_3$) has appeared recently (5). Adrenochrome is usually prepared by the oxidation of adrenaline (II: $R_1 = CH_3$; $R_2 = H$; $R_3 = OH$) in methanol with silver oxide. It has recently been demonstrated that contamination of the product with residual silver (colloidal and/or ionic) derived from the oxidizing agent was minimized by passage of the reaction mixture through a Dowex-1 (Cl^-) resin bed prior to crystallization (6); in this way a stable crystalline product was obtained. The apparent instability of some of the earlier preparations of adrenochrome may have been due to contamination with silver. This general technique has now been successfully utilized for the preparation of crystalline *N*-ethylnoradrenochrome (I: $R_1 = C_2H_5$; $R_2 = H$; $R_3 = OH$) from *N*-ethylnoradrenaline (II: $R_1 = C_2H_5$; $R_2 = H$; $R_3 = OH$) and *N*-isopropylnoradrenochrome (I: $R_1 = i\text{-}C_3H_7$; $R_2 = H$; $R_3 = OH$) from *N*-isopropylnoradrenaline (II: $R_1 = i\text{-}C_3H_7$; $R_2 = H$; $R_3 = OH$); these two aminochromes were obtained in somewhat higher yield than the corresponding yield of adrenochrome from adrenaline. *N*-Ethylnoradrenochrome has also been obtained in crystalline form by the oxidation of *N*-ethylnoradrenaline in 90% methanol with the calculated quantity of iodic acid (cf. preparation of adrenochrome by Macciotta (7)); the *N*-isopropyl analogue has been obtained in the solid state by oxidation of a suspension of *N*-isopropylnoradrenaline hydrochloride in dry acetonitrile with silver

[1]*Manuscript received December 10, 1959.*
Contribution from the Psychiatric Research Unit, University Hospital, Saskatoon, Saskatchewan. This investigation was carried out under the auspices of the Saskatchewan Committee on Schizophrenia Research and supported by grants from the Department of National Health and Welfare (Ottawa) and the Rockefeller Foundation.

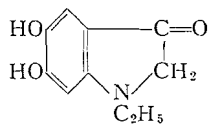
[2]*Part III: Can. J. Chem.* **38**, *508.*

oxide. These compounds are stable dark red-violet crystalline solids, decomposing without melting and exhibiting very similar physical and chemical properties to adrenochrome. The monosemicarbazone of *N*-ethylnoradrenochrome was obtained by a standard method for the preparation of semicarbazones; *N*-isopropylnoradrenochrome monosemicarbazone has previously been described (8); both are bright orange crystalline solids.

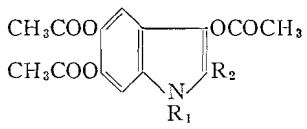
Although oxidation of the adrenaline ethers (II: $R_1 = CH_3$; $R_2 = H$; $R_3 = OCH_3$ or OC_2H_5) with silver oxide in methanol gave red solutions (from which the monosemicarbazones of the adrenochrome ethers have been isolated (9)) no solid could be isolated after cooling the solutions to $-20°$ (even after the addition of dry ether). However, oxidation of a suspension of adrenaline methyl ether hydrochloride in dry acetonitrile with silver oxide proceeded readily and crystalline adrenochrome methyl ether (I: $R_1 = CH_3$; $R_2 = H$; $R_3 = OCH_3$) could be obtained as a dark red solid on concentration of the solution (cf. 5). Adrenochrome ethyl ether (I: $R_1 = CH_3$; $R_2 = H$; $R_3 = OC_2H_5$) was prepared similarly.

When the oxidation of catecholamines is carried out with potassium iodate in aqueous solution (under acid conditions and with excess iodate) iodine-substituted aminochromes (e.g. 2-iodoadrenochrome, I: $R_1 = CH_3$; $R_2 = I$; $R_3 = OH$) are obtained (see 1 for references). *N*-Ethyl-2-iodonoradrenochrome (I: $R_1 = C_2H_5$; $R_2 = I$; $R_3 = OH$) and 2-iodo-*N*-isopropylnoradrenochrome (I: $R_1 = i\text{-}C_3H_7$; $R_2 = I$; $R_3 = OH$) have been obtained in good yield by the oxidation of *N*-ethylnoradrenaline and *N*-isopropylnoradrenaline respectively with potassium iodate, by an adaptation of the procedure described by Sobotka and Austin for the preparation of 2-iodoadrenochrome (2). The isopropyl derivative was obtained previously in lower yield by a slightly different procedure, the oxidation being carried out in more concentrated solution (8). The oxidation of adrenaline methyl and ethyl ethers with potassium iodate by the dilute solution technique (cf. 2) gave deep violet solutions but no precipitation of the iodoaminochrome occurred; however, when the reaction was carried out in more concentrated solution (cf. Bu'Lock and Harley-Mason's general procedure for the preparation of iodoaminochromes (8)) 2-iodoadrenochrome methyl ether (I: $R_1 = CH_3$; $R_2 = I$; $R_3 = OCH_3$) and 2-iodoadrenochrome ethyl ether (I: $R_1 = CH_3$; $R_2 = I$; $R_3 = OC_2H_5$) were obtained as brownish-purple crystalline solids.

The well-known hydroxyl ion catalyzed rearrangement of aminochromes to 5,6-dihydroxyindoles or 5,6-dihydroxyindoxyls (see 1 for references) has been extended to the preparation of *N*-ethyl-5,6-dihydroxyindoxyl (i.e. "*N*-ethylnoradrenolutin" (III)); the



III

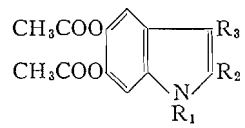


IV

N-isopropyl analogue has previously been described (8). Aqueous solutions of *N*-ethyl-5,6-dihydroxyindoxyl resemble those of the corresponding *N*-methyl and *N*-isopropyl compounds in exhibiting a very strong apple-green fluorescence, and also in being unstable in air, rapidly undergoing a destructive oxidation resulting in the disappearance of the fluorescence followed by the formation of a black melanitic precipitate. The treatment of an aminochrome with acetic anhydride in the presence of pyridine leads to the formation of acetylated rearrangement products (8, 10, 11) (e.g. adrenochrome gives 3,5,6-triacetoxy-*N*-methylindole (IV: $R_1 = CH_3$; $R_2 = H$)). 3,5,6-Triacetoxy-*N*-ethylindole

Can. J. Chem. Downloaded from www.nrcresearchpress.com by 41.223.56.140 on 09/04/12
For personal use only.

(IV: $R_1 = C_2H_5$; $R_2 = H$), 3,5,6-triacetoxy-*N*-isopropylindole (IV: $R_1 = i\text{-}C_3H_7$; $R_2 = H$), and 3,5,6-triacetoxy-*N*-ethyl-2-iodoindole (IV: $R_1 = C_2H_5$; $R_2 = I$) have been obtained in this manner from the corresponding aminochromes. Adrenochrome methyl and ethyl ethers and their 2-iodo derivatives appeared to behave similarly on treatment with acetic anhydride and pyridine. The products obtained analyzing well for 5,6-diacetoxy-3-methoxy-*N*-methylindole (V: $R_1 = CH_3$; $R_2 = H$; $R_3 = OCH_3$), 5,6-diacetoxy-3-ethoxy-*N*-methylindole (V: $R_1 = CH_3$; $R_2 = H$; $R_3 = OC_2H_5$), 5,6-diacetoxy-2-iodo-3-methoxy-*N*-methylindole (V: $R_1 = CH_3$; $R_2 = I$; $R_3 = OCH_3$), and 5,6-diacetoxy-3-ethoxy-2-iodo-*N*-methylindole (V: $R_1 = CH_3$; $R_2 = I$; $R_3 = OC_2H_5$)



V

respectively. The infrared spectra ("NUJOL" mulls) of the acetylated rearrangement products from adrenochrome methyl and ethyl ethers and from 2-iodoadrenochrome methyl ether exhibited a double ester "carbonyl" peak (e.g. the product from the methyl ether had two distinct peaks at 1770 and 1752 cm^{-1}). This behavior was in contrast to that observed in the spectra of several other 5,6-diacetoxy-*N*-alkylindoles available to the authors, which show only a single peak in the carbonyl region (e.g. 5,6-diacetoxy-2-iodo-*N*-methylindole has a single peak at 1765 cm^{-1}, cf. 12) and the product obtained from 2-iodoadrenochrome ethyl ether also showed only a single peak in this region at 1761 cm^{-1}.

5,6-Diacetoxy-2-iodo-*N*-methylindole (V: $R_1 = CH_3$; $R_2 = I$; $R_3 = H$) was obtained by Bergel and Morrison by the acetylation of the crude sodium hydrosulphite reduction products of 2-iodoadrenochrome (13); recently the intermediate 5,6-dihydroxy-2-iodo-*N*-methylindole has been isolated in crystalline form, and gave the same product (i.e. V: $R_1 = CH_3$; $R_2 = I$; $R_3 = H$) on acetylation (12). By an extension of this procedure 5,6-diacetoxy-*N*-ethyl-2-iodoindole (V: $R_1 = C_2H_5$; $R_2 = I$; $R_3 = H$) and 5,6-diacetoxy-2-iodo-*N*-isopropylindole (V: $R_1 = i\text{-}C_3H_7$; $R_2 = I$; $R_3 = H$) have been prepared by acetylation of the reduction products (obtained with sodium hydrosulphite or sodium borohydride) of *N*-ethyl-2-iodonoradrenochrome or 2-iodo-*N*-isopropylnoradrenochrome respectively.

It was reported in an earlier paper in this series that the paper chromatography of adrenochrome could be carried out satisfactorily on acid-washed paper using water or 2% acetic acid/water as running solvents, but that the employment of other common solvent systems usually resulted in decomposition of the adrenochrome (6). In the course of a chromatographic study of the reduction products of the aminochromes derived from "dopa" (3,4-dihydroxyphenylalanine, II: $R_1 = R_3 = H$; $R_2 = COOH$), dopamine (3,4-dihydroxyphenylethylamine, II: $R_1 = R_2 = R_3 = H$) and noradrenaline (II: $R_1 = R_2 = H$; $R_3 = OH$), Bouchilloux and Kodja reported the R_f's of dopachrome (I: $R_1 = R_3 = H$; $R_2 = COOH$), norepinochrome (I: $R_1 = R_2 = R_3 = H$), and noradrenochrome (I: $R_1 = R_2 = H$; $R_3 = OH$) as 0.92, 0.70, and 0.75 respectively on prewashed Whatman No. 1 paper with water as the running solvent (14). These authors also stated that the quinonoid pigments were unstable in butanol/acetic acid/water mixtures. Recently Bouchilloux has stressed the need to work with well-washed papers when studying the paper chromatography of the aminochromes, since traces of residual bisulphites in the paper combine with the aminochromes with great avidity to form

Can. J. Chem. Downloaded from www.nrcresearchpress.com by 41.223.56.140 on 09/04/12
For personal use only.

Can. J. Chem. Downloaded from www.nrcresearchpress.com by 41.223.56.140 on 09/04/12
For personal use only.

stable addition compounds (15). These products, which form bright yellow fluorescent spots, have high R_f's in water and 2% acetic acid/water, and low R_f's in butanol/aqueous acetic acid (cf. 16, 17). *N*-Ethylnoradrenochrome, *N*-isopropylnoradrenochrome, adrenochrome methyl ether, and adrenochrome ethyl ether behave similarly to adrenochrome and can be satisfactorily chromatographed on acid-washed paper with 10% acetic acid/water as running solvent; their R_f's were found to be: 0.79, 0.77, 0.81, and 0.82 respectively. The spots, being red in color, are self-indicating; however, the red color of the spots fades when the developed chromatograms are dried (cf. 6). The aminochrome spots give violet colors with Ehrlich's reagent. The aminochrome ethers are readily distinguished from aminochromes without the 3-alkoxy group by spraying the chromatograms with 10% zinc acetate solution, the "ethers" gave non-fluorescent dark blue spots and not the yellow "lutin" spots exhibiting the vivid apple-green fluorescence given by aminochromes with a 3-OH group. All attempts to chromatograph epinochrome solutions (in 2% acetic acid/water) gave in addition to the epinochrome spot (R_f ca. 0.8) an intense spot due to 5,6-dihydroxy-*N*-methylindole (the rearrangement product (cf. 11)) at $R_f = 0.44$ (cf. 17) and a spot due to an unknown substance (R_f = ca. 0.25) giving a violet color with Ehrlich's reagent. When the chromatograms were sprayed with 2% zinc acetate solution the red epinochrome spot was converted into a colorless spot, exhibiting a weak blue fluorescence, probably due to the formation of 5,6-dihydroxy-*N*-methylindole.

The ultraviolet and visible absorption spectra of adrenochrome and a few simple aminochromes have been reported in aqueous and alcoholic solutions (see 1, 18 for references). In general, with the unhalogenated aminochromes maxima occur at ca. 205–215, 300, and 470–500 mμ; with the iodoaminochromes the short wavelength maximum was observed at ca. 230 mμ, and the long wavelength maximum shifted to ca. 520–535 mμ; however, the position of the third peak remained unchanged in the region of 300 mμ (cf. 1, 2, 18). The spectra of the new aminochromes described in this paper have been measured in aqueous or methanolic solution, and in general the absorption maxima and minima occur at the wavelengths expected for this class of compounds. In all cases but one (2-iodoadrenochrome ethyl ether) the visible absorption peak was observed at a somewhat longer wavelength in water than in methanol; the same was true, to a lesser extent, of the peak near to 300 mμ. In the series adrenochrome, *N*-ethylnoradrenochrome, *N*-isopropylnoradrenochrome, there was a progressive small shift of the visible absorption peak towards lower frequencies with the increase in size of the alkyl group (i.e. 486, 490, 495 mμ, in water, respectively). This phenomenon was not observed in the case of their 2-iodo derivatives, the visible absorption peak in aqueous solution was observed at 535 mμ in each case. Adrenochrome methyl and ethyl ethers gave absorption curves similar to adrenochrome whilst that from 2-iodoadrenochrome methyl ether was very similar to that obtained from 2-iodoadrenochrome. 2-Iodoadrenochrome ethyl ether appeared to behave somewhat anomalously, the expected maximum was observed at 300 mμ but the high-frequency peak occurred at ca. 222 mμ and the long wavelength maximum was observed at 508 mμ in methanol and 505 mμ in water. In this case the wavelengths of these absorption maxima are about 10–20 mμ less than those usually observed for the iodoaminochromes. The ultraviolet spectra of several 5,6-diacetoxy- and 3,5,6-triacetoxy-*N*-alkylindoles have been measured in methanol solution; they all show the general form expected for a compound containing the indole chromophore. 5,6-Diacetoxy-*N*-methylindole and the *N*-ethyl and *N*-isopropyl analogues have maxima at 225 and 287–288 mμ ("shoulders" are present on the latter peak at 280 and 296 mμ). Iodination of these compounds in the 2-position results in a small shift (ca. 6 mμ) in the

position of all the peaks towards longer wavelengths. The 3,5,6-triacetoxy-*N*-alkylindoles show two main maxima, one in the region 225–229 mμ and the other at 292 mμ. Once again, the introduction of an iodine atom in the 2-position results in a slight shift in position of these maxima (i.e. to 233 and 301 mμ respectively).

EXPERIMENTAL

N-Ethylnoradrenochrome (cf. Preparation of Adrenochrome (*a*) by Heacock, Nerenberg, and Payza (6) and (*b*) by Macciotta (7))

(*a*) DL-*N*-Ethylnoradrenaline (5.0 g) was suspended in absolute methanol (150 ml) and 98% formic acid added dropwise, with stirring, until a clear solution was obtained. Freshly prepared silver oxide (20.0 g) was added portionwise to the well-stirred solution and the agitation continued for a further 3 minutes. The temperature of the reaction mixture was not allowed to exceed 25° during the oxidation. The product was filtered (with suction) through a Dowex-1 (Cl^-) resin bed (diam. = 6.5 cm; height = 1.8 cm),* and on cooling the deep red filtrate at −20° for 6 hours *N*-ethylnoradrenochrome separated in very dark red-violet (almost black) prisms (1.83 g) (decomposes without melting at 115°)†. Found: C, 62.24; H, 5.61; N, 7.20. $C_{10}H_{11}NO_3$ requires C, 62.16; H, 5.70; N, 7.31%. Dry ether (100 ml) was added to the filtrate and after cooling overnight at −20° a second crop of crystalline *N*-ethylnoradrenochrome (0.23 g) was obtained.

(*b*) DL-*N*-Ethylnoradrenaline (1.08 g) was suspended in methanol (50 ml) and just enough glacial acetic acid added to clarify the solution. A solution of iodic acid (0.5 g) in water (5 ml) was added and the solution, which rapidly became deep red in color, cooled to −20° for 6 hours; *N*-ethylnoradrenochrome (0.15 g) was obtained in dark red-violet prisms. A satisfactory second crop of crystalline material could not be obtained by the addition of dry ether and further cooling of the solution; only a black amorphous powder was obtained.

N-Ethylnoradrenochrome Monosemicarbazone

DL-*N*-Ethylnoradrenaline (1.05 g) was suspended in methanol (16.5 ml) and 98% formic acid added dropwise until a clear solution was obtained. Freshly prepared silver oxide (4.2 g) was added to the stirred solution and after the addition was complete, stirring was continued for 3 minutes. The reaction mixture was filtered through a Dowex-1 (Cl^-) resin bed (diam. = 2.5 cm; height = 1 cm) directly into a solution of semicarbazide hydrochloride (0.5 g) and sodium acetate (1 g) in water (6.5 ml). After standing at 0° for 4 hours bright orange-red needles of *N*-ethylnoradrenochrome monosemicarbazone (0.48 g) were obtained, m.p. 215° (with decomposition). Found: C, 52.67; H, 5.58; N, 22.32. $C_{11}H_{14}N_4O_3$ requires C, 52.80; H, 5.64; N, 22.40%. The ultraviolet and visible absorption spectra were measured in aqueous solution (λ_{max}: 354 with a shoulder at 435 mμ).

N-Isopropylnoradrenochrome

(*a*): (*i*) DL-*N*-Isopropylnoradrenaline (10.0 g) was suspended in absolute methanol (250 ml) and 98% formic acid added dropwise with stirring until a clear solution was obtained. Freshly prepared silver oxide (40.0 g) was added portionwise to the stirred solution and the stirring continued for a further 3 minutes. The reaction temperature was

**Unless otherwise stated the resin (200/400 mesh size) used in all the preparations described in this paper was prepared by extensive washing with: (1) 3 N hydrochloric acid, (2) with water until neutral to litmus, and (3) finally with dry methanol.*

†The decomposition points of all the aminochromes described in this paper were measured on a Leitz hot-stage instrument.

Can. J. Chem. Downloaded from www.nrcresearchpress.com by 41.223.56.140 on 09/04/12
For personal use only.

not allowed to rise above 25° during the oxidation. The product was filtered (with suction) through a Dowex-1 (Cl^-) resin bed (diam. = 6.5 cm; height = 3.5 cm) and the deep red filtrate allowed to crystallize slowly for 6 hours at −20°; *N*-isopropylnoradrenochrome was obtained in deep red-violet needles (2.0 g) (decomposes without melting at 123°). Found: C, 63.40; H, 6.36; N, 6.74. $C_{11}H_{13}NO_3$ requires C, 63.74; H, 6.32; N, 6.76%. Dry ether (150 ml) was added to the filtrate and after standing overnight at −20° a second crop (1.4 g) of *N*-isopropylnoradrenochrome was obtained.

(*a*): (*ii*) The above oxidation procedure was repeated except that DL-*N*-isopropylnoradrenaline hydrochloride (10 g), which was freely soluble in dry methanol (250 ml), was used in place of the free base and therefore in this instance the addition of formic acid was not required. A slightly better yield of crystalline *N*-isopropylnoradrenochrome (1st crop, 3.5 g; 2nd crop, 1.32 g) was obtained in this case.

(*b*) Freshly prepared silver oxide (4.0 g) was added to a well-stirred suspension of *N*-isopropylnoradrenaline hydrochloride (1.0 g) in dry acetonitrile (25 ml). An exothermic reaction ensued (the temperature rose to ca. 35–40°) and the red suspension was stirred for a further 5 minutes; the reaction mixture was filtered and after standing at −20° overnight the filtrate deposited deep red-violet needles of *N*-isopropylnoradrenochrome (0.20 g).

Like adrenochrome, when pure, these substances appear to be quite stable when kept in the dry state. They are readily soluble in water and other polar solvents to give deep red solutions, but are virtually insoluble in non-polar solvents. Similarly to adrenochrome, they form bright yellow solutions in concentrated sulphuric acid.

N-Ethyl-2-iodonoradrenochrome (cf. Preparation of 2-Iodoadrenochrome by Sobotka and Austin (2))

N-Ethylnoradrenaline (4.3 g) was suspended in water (3000 ml) and concentrated hydrochloric acid added, dropwise with stirring, until a clear solution was obtained. Potassium iodate (6.9 g) was added and the stirring continued until all the potassium iodate was in solution. After standing at room temperature for 4 hours *N*-ethyl-2-iodonoradrenochrome (5.9 g) was obtained as deep violet rods (decomposed without melting at 134.5°). Found: C, 37.73; H, 3.23; N, 4.37. $C_{10}H_{10}NO_3I$ requires C, 37.63; H, 3.16; N, 4.39%.

2-Iodo-N-isopropylnoradrenochrome (cf. Preparation of *N*-ethyl-2-iodonoradrenochrome (Above))

Potassium iodate (3.3 g) was added to a solution of *N*-isopropylnoradrenaline hydrochloride (2 g) in water (1600 ml); the solution was stirred until all the iodate was in solution. After standing at room temperature for 4 hours 2-iodo-*N*-isopropylnoradrenochrome (1.63 g) was obtained as deep violet-brown needles (completely decomposes without melting at 105.5°). Found: C, 39.68; H, 3.80; I, 38.21. $C_{11}H_{12}NO_3I$ requires C, 39.66; H, 3.63; I, 38.12%. (This substance had previously been obtained, in a lower yield, by Bu'Lock and Harley-Mason as the hemihydrate (8), who carried out the reaction in more concentrated solutions.)

Adrenochrome Methyl Ether

(*a*) Adrenaline methyl ether hydrochloride (1.0 g, prepared by the method of Hukki and Seppäläinen (9)) was dissolved in dry methanol (30 ml) and freshly prepared silver oxide (4.0 g) added. After standing for 5 minutes the bright red solution was filtered through a Dowex-1 (Cl^-) resin bed (diam. = 2.5 cm; height = 1 cm). No crystallization

Can. J. Chem. Downloaded from www.nrcresearchpress.com by 41.223.56.140 on 09/04/12
For personal use only.

occurred after allowing the solution to stand at −20° overnight and no solid product was obtained after the addition of dry ether (30 ml) and further cooling at −20°.

(*b*) Freshly prepared silver oxide (4.0 g) was added to a well-stirred suspension of adrenaline methyl ether hydrochloride (1 g) in dry acetonitrile (20 ml). The suspension rapidly developed a deep red color and the temperature rose to ca. 35–40°; the stirring was continued for 5 minutes. After filtration, the deep red filtrate was concentrated, *in vacuo* (with a nitrogen "leak"), below 35° to small bulk, dry ether (10 ml) was added and after cooling to −20°, adrenochrome methyl ether (0.46 g) was obtained as a deep red microcrystalline solid, m.p. 83° (with decomposition).* Found: C, 61.83; H, 5.61; N, 7.63. $C_{10}H_{11}NO_3$ required C, 62.16; H, 5.70; N, 7.31%.

Adrenochrome Ethyl Ether

Adrenaline ethyl ether hydrochloride (1.0 g, prepared by the method of Hukki and Seppäläinen (9)) was oxidized as described in section (*b*) above; adrenochrome ethyl ether (0.55 g) was obtained as a deep red microcrystalline powder, m.p. 70–72° (with decomposition).* Found: C, 63.25; H, 6.29. $C_{11}H_{13}NO_3$ requires C, 63.74; H, 6.32%.

The adrenochrome ethers were readily soluble in polar solvents to give deep red solutions; their solubility in non-polar solvents (e.g. chloroform), whilst being low, was considerably higher than that of adrenochrome. In this respect these compounds show a stronger resemblance to rubreserine than to adrenochrome.

2-Iodoadrenochrome Methyl Ether (cf. Preparation of Iodoaminochromes by Bu'Lock and Harley-Mason (8))

A solution of adrenaline methyl ether hydrochloride (2.0 g) in water (70 ml) was treated at 0° with a solution of potassium iodate (2.2 g) in water (70 ml). A dark violet tarry precipitate soon began to separate out and was removed by filtration after standing at 0° for 30 minutes and a further quantity of tar was filtered off after 1 hour; at this stage a crystalline precipitate began to form and after standing overnight at 0°, 2-iodoadrenochrome methyl ether (1.05 g) was obtained in violet-brown needles (completely decomposes without melting at 85°). Found: C, 38.07; H, 3.11; N, 4.15; I, 39.60. $C_{10}H_{10}NO_3I$ requires C, 37.63; H, 3.16; N, 4.39; I, 39.78%.

2-Iodoadrenochrome Ethyl Ether (cf. Preparation of Methyl Ether (Above))

A solution of adrenaline ethyl ether hydrochloride (2.0 g) in water (70 ml) was treated at 0° with potassium iodate (2.2 g) in water (70 ml). After filtration of the black tarry precipitates that formed during the first hour, a crystalline precipitate began to separate out and after standing overnight at 0°, 2-iodoadrenochrome ethyl ether (0.71 g) was obtained in violet-brown needles (decomposes without melting at 88°). Found: C, 39.92; H, 3.76. $C_{11}H_{12}NO_3I$ requires C, 39.66; H, 3.63%. These iodoadrenochrome ethers appear to be more soluble in water than 2-iodoadrenochrome and when the oxidation was carried out under more dilute conditions (cf. 2) deep violet solutions were obtained but no precipitation occurred even after standing at 0° for 24 hours.

N-Ethyl-5,6-dihydroxyindoxyl (*i.e. N-Ethylnoradrenolutin*) (cf. Preparation of Adrenolutin by Heacock and Mahon (20))

N-Ethylnoradrenaline (5 g) was suspended in water (150 ml) and concentrated hydrochloric acid was added dropwise until a clear solution was obtained. Freshly prepared silver oxide (20.0 g) was added to the well-stirred solution and the stirring continued for

**In contrast to the aminochromes without the 3-alkoxy group which decompose without melting, these substances appeared to actually form a liquid phase before decomposing.*

Can. J. Chem. Downloaded from www.nrcresearchpress.com by 41.223.56.140 on 09/04/12
For personal use only.

Can. J. Chem. Downloaded from www.nrcresearchpress.com by 41.223.56.140 on 09/04/12
For personal use only.

a further 3 minutes. The reaction mixture was then filtered through a Dowex-1 (Cl^-) resin bed (diam. = 6.5 cm; height = 1.5 cm)* and the filtrate cooled in ice. A stream of nitrogen was passed through the cooled filtrate, and 10% sodium hydroxide solution (50 ml) added. The brownish-green solution, which exhibited a typical "lutin" fluorescence was stirred and acidified by the dropwise addition of glacial acetic acid. *N*-Ethylnoradrenolutin (1.52 g) separated out as a bright yellow crystalline precipitate which was filtered off, washed with a little water, and rapidly dried *in vacuo* at room temperature. The product was obtained in very small yellow-orange prisms (m.p. indefinite, decomposes without melting at ca. 170°) on recrystallization from water (containing a little sodium hydrosulphite to prevent oxidation). In contrast to adrenolutin this product did not contain water of crystallization. Found: C, 62.01; H, 5.87; N, 7.21. $C_{10}H_{11}NO_3$ requires C, 62.16; H, 5.70; N, 7.31%. Although the crystalline material as prepared above tended to darken in color on keeping, a sample (decomposes without melting at 174–175°) which was purified by vacuum sublimation (190–200°/0.2 mm) and obtained in very small bright yellow rods showed no tendency to lose its bright yellow color. The ultraviolet and visible absorption spectra were measured in methanol solution (λ_{max}: 224, 259, 288 (with a shoulder at 308), 415 mμ; λ_{min}: 239, 274, 335 mμ).

The Action of Acetic Anhydride and Pyridine on the Aminochromes Described Above (cf. Bu'Lock and Harley-Mason (8))

The aminochrome (1.0 g) was dissolved in a mixture of acetic anhydride (15 ml) and dry pyridine (15 ml) and the solution allowed to stand at room temperature for 36 hours, after which time it was poured, with stirring, into ice water, when either an amorphous solid or an oil separated. If solid, the crude product was removed by filtration; if oily, it was extracted with peroxide-free ether (4×100 ml) (the ethereal extract washed with 5% sodium bicarbonate solution (4×100 ml) and with water (100 ml)) and concentration of the dried (Na_2SO_4) extract gave the crude product, usually as a greenish-yellow gum. In some instances it was possible to purify the product directly by recrystallization, but where this was not possible, chromatographic purification on silica gel columns was carried out.

N-Ethylnoradrenochrome gave 3,5,6-triacetoxy-*N*-ethylindole (0.61 g), m.p. 84.5–85.5°, in pale yellow prisms after chromatographic purification on silica gel using benzene as eluent and recrystallization from benzene – light petroleum (b.p. 80–100°). Found: C, 60.19; H, 5.41; N, 4.41. $C_{16}H_{17}NO_6$ requires C, 60.17; H, 5.37; N, 4.39%.

N-Isopropylnoradrenochrome gave 3,5,6-triacetoxy-*N*-isopropylindole (0.25 g), m.p. 85.5–87.5°, after chromatographic purification on silica gel using benzene as eluent. The product was initially obtained as a gum and only crystallized with difficulty after seeding with an authentic specimen. This compound had previously been prepared by Bu'Lock and Harley-Mason by the deiodination of 3,5,6-triacetoxy-2-iodo-*N*-isopropylindole (8), who reported a melting point of 87°. The product obtained by the authors did not depress the melting point of a sample prepared by Bu'Lock and Harley-Mason's method.

N-Ethyl-2-Iodonoradrenochrome gave 3,5,6-triacetoxy-*N*-ethyl-2-iodoindole (1.2 g) in pale yellow plates, m.p. 142–143.5°, after recrystallization from benzene – light petroleum (b.p. 80–100°). Found: C, 43.09; H, 3.45; I, 28.50. $C_{16}H_{16}NO_6I$ requires C, 43.15; H, 3.62; I, 28.51%.

Adrenochrome methyl ether gave 5,6-diacetoxy-3-methoxy-*N*-methylindole (0.4 g) in pale yellow prisms, m.p. 140–141°, after chromatographic purification on silica gel using

**This resin bed was prepared as previously described, except that the final washing with methanol was omitted.*

benzene as eluent and three recrystallizations from benzene – light petroleum (b.p. 80–100°). Found: C, 60.62; H, 5.41; N, 5.12; O—$COCH_3$, 31.5%; mol. wt., 311. $C_{14}H_{15}NO_5$ requires C, 60.64; H, 5.45; N, 5.05; O—$COCH_3$, 31.04%; mol. wt., 277. The peaks in the "carbonyl" region of the infrared spectrum* occur at 1770 and 1752 cm^{-1}.

Adrenochrome ethyl ether gave 5,6-diacetoxy-3-ethoxy-*N*-methylindole (0.47 g) in pale yellow-green elongated prisms, m.p. 84.5–85.5°, after chromatographic purification on silica gel using benzene as eluent and two recrystallizations from benzene – light petroleum (b.p. 80–100°). Found: C, 61.39; H, 5.86; N, 4.81%; mol. wt., 272. $C_{15}H_{17}NO_5$ requires C, 61.84; H, 5.88; N, 4.81%; mol. wt., 291. The peaks in the "carbonyl" region of the infrared spectrum occur at 1776 and 1755 cm^{-1}.

2-Iodoadrenochrome methyl ether gave 5,6-diacetoxy-2-iodo-3-methoxy-*N*-methylindole (0.57 g) in pale yellow plates, m.p. 191–192°, on recrystallization from benzene – light petroleum (b.p. 80–100°). Found: C, 41.88; H, 3.53; N, 3.20; I, 32.00; O—$COCH_3$, 21.66%; mol. wt., 406. $C_{14}H_{14}NO_5I$ requires C, 41.70; H, 3.49; N, 3.47; I, 31.48; O—$COCH_3$, 21.35%; mol. wt., 403. The peaks in the "carbonyl" region of the infrared spectrum occur at 1779 and 1767 cm^{-1}.

2-Iodoadrenochrome ethyl ether gave 5,6-diacetoxy-3-ethoxy-2-iodo-*N*-methylindole (0.61 g) in pale yellow prisms, m.p. 149.5°, on recrystallization from benzene – light petroleum (b.p. 80–100°). Found: C, 43.45; H, 3.86; N, 3.54; I, 30.29%; mol. wt., 400. $C_{15}H_{16}NO_5I$ requires C, 43.17; H, 3.86; N, 3.36; I, 30.42%; mol. wt., 417. There is apparently only one peak in the "carbonyl" region of the infrared spectrum of this compound occurring at 1761 cm^{-1}.

5,6-Diacetoxy-N-ethyl-2-iodoindole

A suspension of sodium hydrosulphite (2.0 g) in water (5 ml) was added to a stirred suspension of *N*-ethyl-2-iodonoradrenochrome (1.0 g) in water (40 ml). After being stirred at room temperature for 1 hour the reaction mixture was extracted with peroxide-free ether (6×50 ml). Concentration of the combined dried (Na_2SO_4) extracts in vacuum (nitrogen "leak"), below 35°, gave a greenish gum which was dissolved in a mixture of acetic anhydride (10 ml) and dry pyridine (10 ml). After standing overnight at room temperature the reaction mixture was poured into ice water; a pale yellow solid separated which afforded 5,6-diacetoxy-*N*-ethyl-2-iodoindole (0.5 g), m.p. 157.5–158.5°, in pale yellow small plates on recrystallization from benzene – light petroleum (b.p. 80–100°). Found: C, 43.00; H, 3.66; I, 32.30. $C_{14}H_{14}NO_4I$ requires C, 43.43; H, 3.65; I, 32.79%.

5,6-Diacetoxy-2-iodo-N-isopropylindole

(*a*) 2-Iodo-*N*-isopropylnoradrenochrome (1.0 g) was reduced with sodium hydrosulphite as described above for the *N*-ethyl analogue and gave 5,6-diacetoxy-2-iodo-*N*-isopropylindole (0.38 g), m.p. 111–112.5°, in white prisms after chromatographic purification on silica gel using benzene as eluent and recrystallization from light petroleum (b.p. 80–100°). Found: C, 45.04; H, 4.17; I, 31.60. $C_{15}H_{16}NO_4I$ requires C, 44.91; H, 4.02; I, 31.64%.

(*b*) 2-Iodo-*N*-isopropylnoradrenochrome (1.0 g) was suspended in water (25 ml) and solid sodium borohydride added very slowly to the stirred suspension until a clear yellow solution was obtained. After decomposition of the excess reducing agent by the cautious dropwise addition of 2 *N* sulphuric acid, the reaction mixture was immediately extracted with peroxide-free ether (4×100 ml). The combined dried (Na_2SO_4) extracts were

**The infrared spectra were recorded as "NUJOL" mulls on a Perkin–Elmer Infracord spectrophotometer using a sodium chloride prism.*

Can. J. Chem. Downloaded from www.nrcresearchpress.com by 41.223.56.140 on 09/04/12
For personal use only.

concentrated to dryness *in vacuo* (nitrogen "leak"), below 35°, and the residue dissolved in a mixture of acetic anhydride (10 ml) and dry pyridine (10 ml). After standing overnight at room temperature the acetylation mixture was poured into ice water and a yellow oil separated, which was extracted with peroxide-free ether (4×100 ml). After washing the combined ethereal extracts with 5% aqueous sodium bicarbonate (2×50 ml) and water (100 ml), the dried (Na_2SO_4) extract gave, on concentration, a yellowish-green gum which was purified chromatographically on a silica gel column using benzene as

TABLE I

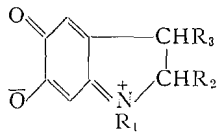
R_f's in 2% acetic acid and color reactions of some aminochromes

Aminochrome	R_f	Ehrlich*	DMCA*,†	10% zinc acetate	DPNA‡
Adrenochrome	0.78	BV	BG	Y^f	RBr
N-Ethylnoradrenochrome	0.79	BV	BG	Y^f	RBr
N-Isopropylnoradrenochrome	0.77	BV	BG	Y^f	RBr
Adrenochrome methyl ether	0.81	RV	GyG	B	YGy
Adrenochrome ethyl ether	0.82	RV	GyG	B	YGy

*The colors reported for Ehrlich's reagent and DMCA were those observed 12 hours after spraying the papers.
†DMCA = *p*-Dimethylaminocinnamaldehyde (cf. Harley-Mason and Archer (21)).
‡DPNA = diazotized *p*-nitroaniline.
NOTE: BV = blue-violet; RV = red-violet; BG = blue-green; GyG = grey-green; Y^f = yellow exhibiting a yellow-green fluorescence in ultraviolet light; B = blue; RBr = red-brown; YGy = yellow-grey.

TABLE II

Absorption spectra of some aminochromes (in the range 220–650 mμ)



Substance	R_1	R_2	R_3	Solvent	Absorption maxima, mμ			Absorption minima, mμ	
N-Ethylnoradrenochrome	C_2H_5	H	OH	M		301	472	262	380
				W		303	490	261	368
N-Isopropylnoradrenochrome*	*i*-C_3H_7	H	OH	M		301	482	263	364
				W		305	495	261	366
Epinochrome*	CH_3	H	H	E†		305	470	—	—
				W		308	480	257	364
Adrenochrome methyl ether	CH_3	H	OCH_3	M		297	480	270	372
				W		302	492	262	374
Adrenochrome ethyl ether	CH_3	H	OC_2H_5	M		297	478	272	377
				W		302	488	262	370
2-Iodoadrenochrome‡	CH_3	I	OH	M	233	302	528	268	385
				W	233	304	535	268	385
N-Ethyl-2-iodonoradrenochrome	C_2H_5	I	OH	M	232	303	525	270	400
				W	232	303	535	268	386
2-Iodo-*N*-isopropylnoradrenochrome	*i*-C_3H_7	I	OH	M	233	302	528	268	380
				W	232	306	535	268	390
2-Iodoadrenochrome methyl ether	CH_3	I	OCH_3	M	233	300	530	268	390
				W	233	302	535	267	388
2-Iodoadrenochrome ethyl ether	CH_3	I	OC_2H_5	M	222	300	508	265	375
				W	223	302	505	264	372

NOTE: M = methanol; W = water; E = ethanol.
*Beaudet oxidized *N*-isopropylnoradrenaline and epinine hydrochlorides in aqueous solution with silver oxide and recorded the absorption maxima of the products as 480, 300, and 220 mμ for the former and 470, 310, and 205 mμ for the latter (19).
†Results quoted by Sobotka *et al.* (18).
‡Sobotka *et al.* recorded the absorption maxima of 2-iodoadrenochrome in ethanolic solution as 530, 302, and 234 mμ (18). The maxima in aqueous solution have been reported to occur at 520, 305, and 233 mμ (22) and 525, 301, and 232 mμ (23).

Can. J. Chem. Downloaded from www.nrcresearchpress.com by 41.223.56.140 on 09/04/12
For personal use only.

eluent; 5,6-diacetoxy-2-iodo-*N*-isopropylindole (0.67 g), m.p. 111–113°, was obtained in white prisms after recrystallization of the product from light petroleum (b.p. 80–100°).

Paper Chromatography

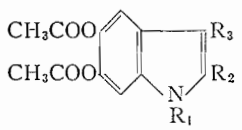
Whatman No. 1 paper was washed with (*a*) 2% acetic acid for 24 hours, and (*b*) water for 12 hours, and dried prior to use. The descending method of chromatography was employed in all cases and 2% acetic acid/water was used as the running solvent. The solvent was allowed to descend ca. 15 inches; this required about 2.5 to 3 hours running time. The R_f's (under these conditions) of *N*-ethylnoradrenochrome, *N*-isopropylnoradrenochrome, adrenochrome methyl ether, and adrenochrome ethyl ether were determined, ca. 20 μg of the compound being applied to the paper in each case. (The results are given in Table I). All four compounds are colored and therefore are self-indicating and location of the spots with spray reagents is not necessary; however, the colors developed by the aminochrome spots with a number of reagents are given in Table I.

Absorption Spectra

(*a*) The ultraviolet and visible absorption spectra of a number of aminochromes were measured in freshly prepared aqueous or methanol solutions of the pure crystalline aminochrome at a concentration of 1–2 mg/100 ml, using a Warren Spectracord instrument. The results are given in Table II.

TABLE III

Ultraviolet absorption spectra of some 5,6-diacetoxy- and 3,5,6-triacetoxy-*N*-alkylindoles (in methanol)



Substance	R_1	R_2	R_3	Absorption maxima, mμ	Absorption minima, mμ
5,6-Diacetoxy-*N*-methylindole*	CH_3	H	H	225; (279);† 287; (296)	252
5,6-Diacetoxy-*N*-ethylindole*	C_2H_5	H	H	225; (280); 288; (297)	252
5,6-Diacetoxy-*N*-isopropylindole*	i-C_3H_7	H	H	225; (281); 287; (297)	253
5,6-Diacetoxy-2-iodo-*N*-methylindole‡	CH_3	I	H	231; (280); 293; (303)	255
5,6-Diacetoxy-*N*-ethyl-2-iodoindole	C_2H_5	I	H	230; (280); 294; (303)	255
5,6-Diacetoxy-2-iodo-*N*-isopropylindole	i-C_3H_7	I	H	230; (282); 293; (303)	255
3,5,6-Triacetoxy-*N*-methylindole§	CH_3	H	$OCOCH_3$	225; 292	ca. 260
3,5,6-Triacetoxy-*N*-ethylindole	C_2H_5	H	$OCOCH_3$	228; 292	260
3,5,6-Triacetoxy-*N*-isopropylindole	i-C_3H_7	H	$OCOCH_3$	229; 292	260
3,5,6-Triacetoxy-2-iodo-*N*-methylindole‖	CH_3	I	$OCOCH_3$	233; 301	263
3,5,6-Triacetoxy-*N*-ethyl-2-iodoindole	C_2H_5	I	$OCOCH_3$	233; 301	263
5,6-Diacetoxy-3-methoxy-*N*-methylindole	CH_3	H	OCH_3	239; (286); 296	266
5,6-Diacetoxy-3-ethoxy-*N*-methylindole	CH_3	H	OC_2H_5	239; (285); 296	267
5,6-Diacetoxy-2-iodo-3-methoxy-*N*-methylindole	CH_3	I	OCH_3	242; (285); 314	272
5,6-Diacetoxy-3-ethoxy-2-iodo-*N*-methylindole	CH_3	I	OC_2H_5	242; (285); 313	272

*Prepared by a method to be described shortly (Part V of this series).
†Figures shown in parentheses indicate shoulders on the main peak.
‡Prepared by the method described in Part III of this series.
§Results quoted by Lund (24).
‖Prepared by the method of Bu'Lock and Harley-Mason (8).

Can. J. Chem. Downloaded from www.nrcresearchpress.com by 41.223.56.140 on 09/04/12
For personal use only.

(*b*) The ultraviolet absorption spectra of a number of 5,6-diacetoxy- and 3,5,6-triacetoxy-*N*-alkylindoles were measured in methanol at a concentration of 1–2 mg/100ml, using the apparatus described above. The results are given in Table III.

ACKNOWLEDGMENTS

The authors wish to express their thanks to Burroughs–Wellcome and Co. (Canada) Ltd. and Winthrop Laboratories of Canada Ltd. for generous gifts of chemicals, and to Dr. J. Harley-Mason of Cambridge University for kindly supplying an authentic sample of 3,5,6-triacetoxy-*N*-isopropylindole. Thanks are also accorded to Mr. W. Irwin, who recorded the ultraviolet spectra.

REFERENCES

1. R. A. HEACOCK. Chem. Revs. **59**, 181 (1959).
2. H. SOBOTKA and J. AUSTIN. J. Am. Chem. Soc. **73**, 3077 (1951).
3. P. MARQUARDT and E. CARL. Naturwissenschaften, **39**, 210 (1952).
4. H. SOBOTKA. U.S. Patent No. 2,655,510 (October, 1953); Chem. Abstr. **48**, 12809 (1954).
5. R. A. HEACOCK. Chem. & Ind. (London), 752 (1959).
6. R. A. HEACOCK, C. NERENBERG, and A. N. PAYZA. Can. J. Chem. **36**, 853 (1958).
7. E. MACCIOTTA. Gazz. chim. ital. **81**, 485 (1951).
8. J. BU'LOCK and J. HARLEY-MASON. J. Chem. Soc. 712 (1951).
9. J. HUKKI and N. SEPPÄLÄINEN. Acta. Chem. Scand. **12**, 1231 (1958).
10. J. HARLEY-MASON. J. Chem. Soc. 1276 (1950).
11. J. AUSTIN, J. D. CHANLEY, and H. SOBOTKA. J. Am. Chem. Soc. **73**, 2395, 5299 (1951).
12. R. A. HEACOCK and B. D. SCOTT. This issue.
13. F. BERGEL and A. L. MORRISON. J. Chem. Soc. 48 (1943).
14. S. BOUCHILLOUX and A. KODJA. Compt. rend. **247**, 2484 (1958).
15. S. BOUCHILLOUX. Compt. rend. soc. biol. **153**, 642 (1959).
16. J. VAN ESPEN. Pharm. Acta Helv. **33**, 207 (1958).
17. R. A. HEACOCK and B. D. LAIDLAW. Chem. & Ind. (London), 1510 (1958).
18. H. SOBOTKA, N. BARSEL, and J. D. CHANLEY. Fortschr. Chem. org. Naturstoffe, **14**, 217 (1957).
19. C. BEAUDET. Experientia, **7**, 291 (1951).
20. R. A. HEACOCK and M. E. MAHON. Can. J. Chem. **36**, 1550 (1958).
21. J. HARLEY-MASON and A. A. P. G. ARCHER. Biochem. J. **69**, 60P (1958).
22. F. G. STOCK and L. W. HINSON. J. Pharm. and Pharmacol. **7**, 512 (1955).
23. I. EHRLEN. Farm. Revy, **47**, 321 (1948); Chem. Abstr. **42**, 5075 (1948).
24. A. LUND. Acta Pharmacol. Toxicol. **5**, 121 (1949).

Can. J. Chem. Downloaded from www.nrcresearchpress.com by 41.223.56.140 on 09/04/12
For personal use only.

Can. J. Chem. Downloaded from www.nrcresearchpress.com by 41.223.56.140 on 09/04/12
For personal use only.

LYCOPODIUM ALKALOIDS

IX. CYCLIZED PRODUCTS FROM α- AND β-CYANOBROMOLYCOPODINE[1]

D. B. MacLean, Won-Ryul Song, and W. A. Harrison[2]

ABSTRACT

A study has been made of the products formed on treatment of α- and β-cyanobromolycopodine with potassium hydroxide in methanol and potassium acetate in ethanol, respectively. The product derived from the α-isomer is apparently formed in a cyclization reaction taking place alpha to the carbonyl group while that formed from the β-isomer may be an enol ether. The olefin expected from a normal dehydrobromination of α-cyanobromolycopodine has been prepared by an indirect method. Attempts to prepare the analogous olefin in the β-series led to the formation of a saturated cyclic ether. The hydrogenolysis product of β-cyanobromolycopodine has been prepared.

The reaction of lycopodine, $C_{16}H_{25}ON$, with cyanogen bromide to yield two isomeric bromocyanamides was first reported by MacLean, Manske, and Marion (1). A number of reactions of the bromocyanamides were reported at the same time. The study of their reactions has since been extended by Barclay and MacLean (2) and by MacLean and Harrison (3), and it is now known that both bromides are primary.

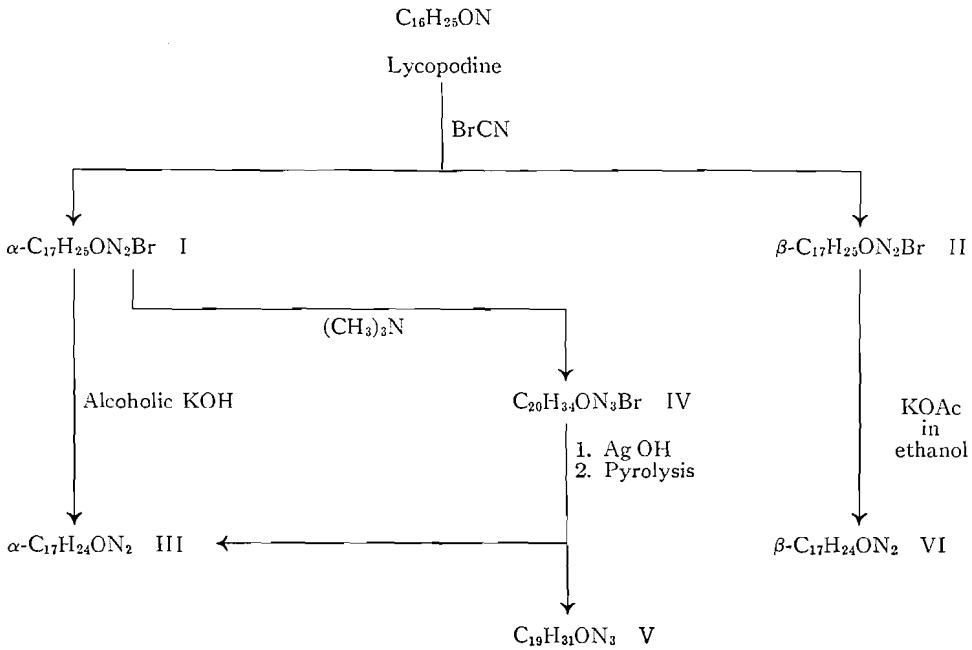
Among the reactions reported in the initial study were those leading to the formation of two isomeric compounds of the formula $C_{17}H_{24}ON_2$ from α-cyanobromolycopodine I, $C_{17}H_{25}ON_2Br$, and β-cyanobromolycopodine II, $C_{17}H_{25}ON_2Br$. Both isomers were formed in an elimination reaction with loss of hydrogen bromide. The α-isomer III was the product of the reaction of I with boiling methanolic potassium hydroxide. It also formed, along with a product of demethylation V, when α-cyanotrimethylaminolycopodine bromide IV was converted to the quaternary base and pyrolyzed. The β-isomer VI was obtained by the action of boiling ethanolic potassium acetate on the β-bromide II. Since neither compound displayed any evidence of unsaturation, it was suggested that III and VI were formed in cyclization reactions. This work is summarized below.

A more detailed study of the two compounds III and VI has now been undertaken and is reported here.

The product III, $C_{17}H_{24}ON_2$, was prepared from α-cyanobromolycopodine according to the method of MacLean, Manske, and Marion (1) and was examined by infrared and ultraviolet spectroscopy. The infrared spectrum of III showed a strong band at 1700 cm^{-1} in the carbonyl region but there was no absorption characteristic of an olefin linkage. The ultraviolet spectrum did not reveal the presence of a conjugated system in the molecule. The presence of the carbonyl group in III was confirmed chemically for it readily underwent reduction to the alcohol VII, $C_{17}H_{26}ON_2$, on treatment with sodium borohydride. Compound VII was in turn converted to III by oxidation with chromic acid.

Indirect evidence that a cyclization reaction had occurred adjacent to the carbonyl group came from the following observations. Compound III failed to react with benzaldehyde when it was treated under the same conditions that led to reaction with α-cyanolycopodine VIII (in α-cyanolycopodine the bromine atom of I has been replaced by hydrogen) (1, 2). When III was hydrolyzed to the secondary base and methylated

[1]*Manuscript received December 16, 1959.*
Contribution from the Burke Chemical Laboratories, Hamilton College, McMaster University, Hamilton, Ontario. Parts of this work were taken from theses submitted by W. R. Song in May, 1958, and W. A. Harrison in May, 1957, to the Faculty of Graduate Studies in partial fulfillment of the degree M.Sc.
[2]*Holder of National Research Council Studentship 1956–57, 1957–58, and 1958–59.*



to the tertiary base, the latter failed to react with phenyl lithium. The first observation suggests that the methylene group, which has been shown to be present in VIII (2), is absent or more hindered in III. The failure of III to form a benzylidene derivative cannot be taken as conclusive evidence for the absence of a methylene group for it has been reported that lycopodine, which must contain the methylene group found in α-cyanolycopodine, does not react with benzaldehyde (4). The second observation indicates that the carbonyl group in III is more hindered than in lycopodine, which reacts readily with phenyl lithium (1). Both observations lend support to a cyclization alpha to the carbonyl function. It has also been shown in the sequence outlined below, in which the olefin expected from a normal dehydrobromination of I has been prepared by an indirect method, that in the absence of the carbonyl group cyclization does not occur. One may conclude therefore that III is formed in a cyclization reaction and that, if cyclization is to occur, the carbonyl function must be present.

In the preparation of the olefin derived from compound I the following procedure was followed. The bromide I was treated with dimethylamine and yielded the dimethylamino compound V. Treatment of V with sodium borohydride yielded the dimethylamino alcohol IX, $C_{19}H_{33}ON_3$, which was in turn converted to its methiodide X. The Hofmann decomposition of X with potassium tertiary butoxide in boiling tertiary butanol proved the most satisfactory of a number of methods investigated. The product of this reaction was separated into a neutral and a basic fraction. The basic fraction was a mixture of V and IX which was separated by chromatography on alumina. The neutral fraction yielded two olefinic products XI, $C_{17}H_{24}ON_2$, and XII, $C_{17}H_{26}ON_2$. The olefin XI had absorption in the carbonyl region at 1700 cm^{-1} and in the olefin region at 1640 cm^{-1}, while the olefin XII showed no carbonyl absorption but had hydroxyl and olefin absorption. Both compounds had cyanamide absorption at 2200 cm^{-1}. The presence of the ketonic products

Can. J. Chem. Downloaded from www.nrcresearchpress.com by 41.223.56.140 on 09/04/12
For personal use only.

V and XI in this reaction is probably the result of oxidation catalyzed by potassium tertiary butoxide.

Compound XI was readily converted into XII on treatment with sodium borohydride. Treatment of XI with hydrogen over a platinum catalyst yielded α-cyanolycopodine VIII, indicating that rearrangement of the carbon skeleton had not occurred in the reaction. Ozonolysis of XII yielded formaldehyde, thus establishing the terminal character of the olefin linkage.

Compound VI, $C_{17}H_{24}ON_2$, was prepared originally by MacLean, Manske, and Marion (1) by treatment of β-cyanobromolycopodine II with potassium acetate in boiling ethanol. MacLean and Harrison (3) have found that it is also the main product formed on treatment of II with silver acetate in boiling benzene. In this laboratory it has been found that VI forms readily in a variety of basic media. For instance, it is the sole product formed on treatment of II with boiling methanolic potassium hydroxide. It is also formed when β-cyanobromolycopodine is treated with a solution of dimethylamine in methanol (5) and when a solution of II in ethanol is added to an excess of sodium borohydride in ethanol (6). In the latter case it is possible to induce the reaction to follow a different course and this is described in detail later.

Like its α-isomer, compound VI has been examined by infrared and ultraviolet spectroscopy. The infrared spectrum of VI has an absorption band at 1675 cm^{-1} which is less intense than that of the carbonyl absorption of lycopodine or of its α-isomer III and is shifted by about 25 cm^{-1}. There is no absorption in the 1600–1650 cm^{-1} region which might be expected of a compound with a terminal vinyl linkage. The ultraviolet spectrum is lacking in any absorption characteristic of a conjugated system. Chemically, the compound has proved to be peculiarly inert. It has been recovered unchanged after treatment with sodium borohydride under conditions which readily reduced its α-isomer III. Lithium aluminum hydride in boiling tetrahydrofuran converted VI into the secondary base XIII, $C_{16}H_{25}ON$, an oil which would not crystallize, and which was converted to its N-methyl base XIV, $C_{17}H_{27}ON$, which readily formed a crystalline perchlorate. Both XIII and XIV retained the characteristic absorption at 1675 cm^{-1} exhibited by VI. The N-methyl base XIV was recovered unchanged after treatment with phenyl lithium or further treatment with sodium borohydride or lithium aluminum hydride. This lack of reactivity toward hydride reducing agents makes it unlikely that there is a carbonyl function in VI, and accordingly, non-ketonic structures were considered.

The most reasonable alternative to a ketonic structure is one in which the oxygen is present in a cyclic enol ether linkage. This is compatible with the infrared spectrum of VI since some cyclic enol ethers have a strong band near 1675 cm^{-1} (7). The enol ether structure explains the inertness of XIV to hydrides and phenyl lithium, but inertness of this system to the addition of hydrogen as reported previously (1) and confirmed by us is not to be expected. Furthermore, an enol ether might be expected to cleave readily on treatment with acids, but the base XIV proved to be relatively stable under acidic conditions. It is true that treatment over prolonged periods with strong mineral acids yielded unidentified products which showed absorption in the carbonyl region at 1700 cm^{-1} and in the hydroxyl region. The fact that we were able to isolate the secondary base XIII by acid hydrolysis of VI is ample indication of the stability of the unsaturated function of VI, XIII, and XIV in an acidic medium.

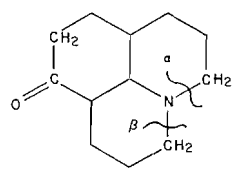
An attempt to form the normal product of dehydrobromination of β-cyanobromo-

Can. J. Chem. Downloaded from www.nrcresearchpress.com by 41.223.56.140 on 09/04/12
For personal use only.

lycopodine led instead to the formation of a cyclic saturated ether. A procedure analogous to that used in the preparation of the olefin XI in the α-series was employed. Although Barclay (6) has reported that compound VI is formed when β-cyanobromolycopodine is treated with an excess of sodium borohydride, we have been able to alter the reaction conditions so that the reaction follows a different course. When II was dissolved in ethanol, cooled to 0°, and treated with an ethanolic solution of sodium borohydride, the main reaction product was the hydroxybromide XV, $C_{17}H_{27}ON_2Br$. The hydroxybromide XV was readily converted to the quaternary salt XVI, $C_{20}H_{36}ON_3Br$, on treatment with trimethylamine. When the quaternary salt XVI was decomposed with potassium tertiary butoxide in boiling tertiary butanol, trimethylamine was liberated and a new compound XVII, $C_{17}H_{26}ON_2$, was isolated. This compound showed no hydroxyl or olefin absorption in its infrared spectrum and it can be concluded that an ether linkage formed in the reaction. This is substantiated by the appearance of a strong band in its infrared spectrum in the region characteristic of ethers. This is the third instance in which a cyclization involving the oxygen function has been observed in the β-series. Two of these have been discussed in this paper while the third was the formation of the lactone reported by MacLean and Harrison (3).

The ease with which the compound VI formed in a variety of basic media led us to investigate again the hydrogenolysis of the β-bromide II reported by MacLean, Manske, and Marion (1). We have found that under their conditions at least 90% of the reaction product was compound VI and not the expected hydrogenolysis product as they reported. If, however, the hydrogenolysis was carried out at dry ice temperature, and in the absence of a large excess of alkali, a normal reaction course was followed. The product of this reaction contained none of the cyclized compound VI but, instead, a new compound XVIII, $C_{17}H_{26}ON_2$, which had a normal carbonyl absorption in its infrared spectrum near 1700 cm^{-1}. Compound XVIII, designated β-cyanolycopodine, has also been prepared indirectly in the following manner. The hydroxybromide XV, $C_{17}H_{27}ON_2Br$, was treated with hydrogen over a palladium catalyst and underwent hydrogenolysis in a normal manner to give the compound XIX, $C_{17}H_{28}ON_2$, and that in turn was oxidized by the Oppenauer method to β-cyanolycopodine, identical in all respects with the compound prepared directly from II.

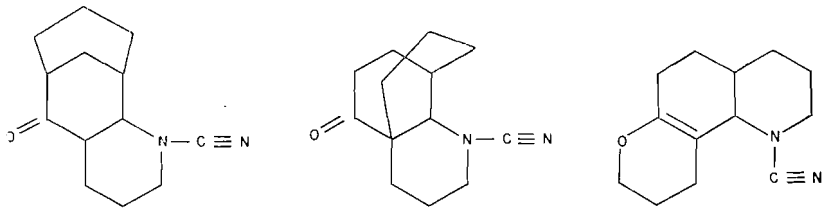
The reactions which have been discussed here can be accommodated by the partial formula A below which was recently proposed by MacLean and Harrison (3).



A

Compound III would form in a displacement reaction by the enolate ion involving C-alkylation to yield either structure B or C while compound VI would form in a displacement reaction by the enolate ion involving O-alkylation to give structure D. Partial structures of other compounds mentioned in the text can be deduced in a logical fashion from structure A.

Can. J. Chem. Downloaded from www.nrcresearchpress.com by 41.223.56.140 on 09/04/12
For personal use only.



B C D

The evidence in support of the cyclization reaction adjacent to the carbonyl group in the α-series is substantial, but we have been unable to differentiate between structures B and C. Support for structure D is meager but it appears to be the only plausible formulation for this peculiarly unreactive compound. The double bond has been assigned the position shown, rather than the alternative position, since this compound shows no =C—H stretching absorption in the region 3000–3120 cm^{-1} in its infrared spectrum.

EXPERIMENTAL

Treatment of α-Cyanobromolycopodine with Potassium Hydroxide in Methanol

The reaction was carried out and the product isolated according to the procedure of MacLean, Manske, and Marion (1). The infrared spectrum* of this product showed strong absorption at 1700 cm^{-1} in the carbonyl region and cyanamide absorption at 2200 cm^{-1}. The ultraviolet spectrum had no peaks characteristic of a conjugated system. This compound, III, would not form a benzylidene derivative under conditions which were successful with α-cyanolycopodine (2).

Reduction of III, $C_{17}H_{24}ON_2$, *with Sodium Borohydride*

Compound III (1.7 g) was added to a solution of 3.5 g of sodium borohydride in 80 ml of 95% ethanol and the solution was stirred for 3 hours and then allowed to stand overnight. The excess borohydride was destroyed with formaldehyde and the solution was made nearly neutral by the addition of mineral acid. The solvent was evaporated, water was added to the residue, and the resulting mixture was extracted with chloroform. The chloroform extract was evaporated to yield a residue which was purified by chromatography on alumina using chloroform as eluant. There was recovered 1.5 g of product VII which crystallized from ether and melted at 219°. Calc. for $C_{17}H_{26}ON_2$: C, 74.4; H, 9.55; N, 10.2%. Found: C, 74.5; H, 9.48; N, 10.0%.

The infrared spectrum had strong hydroxyl and cyanamide absorption but no absorption in the carbonyl region. The compound was converted to III upon treatment with chromic acid in pyridine.

Hydrolysis and Methylation of III, $C_{17}H_{24}ON_2$

Compound III (3.3 g) was dissolved in a mixture of 100 ml of 95% ethanol and 15 ml of 12 *M* hydrochloric acid. The solution was heated under reflux on a steam bath for 30 hours and then evaporated to dryness. The residue was dissolved in water, filtered, made basic with ammonia, and extracted with chloroform. The crude reaction product (2.3 g) was dissolved in acetone and acidified with perchloric acid. A crystalline perchlorate

**Infrared spectra were run in Nujol mull using a sodium chloride prism unless otherwise stated.*

Can. J. Chem. Downloaded from www.nrcresearchpress.com by 41.223.56.140 on 09/04/12
For personal use only.

separated which, after recrystallization from acetone, melted at 300°. Calc. for $C_{16}H_{25}ON.HClO_4$: C, 55.2; H, 7.53; N, 4.0%. Found: C, 55.3; H, 7.39; N, 4.1%.

The free base was liberated from the perchlorate and crystallized from petroleum ether. It melted at 105–106°. Calc. for $C_{16}H_{25}ON$: C, 77.7; H, 10.12; N, 5.7%. Found: C, 77.4; H, 9.97; N, 5.6%.

The infrared spectrum of the base had a sharp peak at 3330 cm^{-1} in the =NH region and a carbonyl peak at 1695 cm^{-1}.

The secondary base (2.0 g) obtained above was dissolved in a mixture of 40% formaldehyde (2.4 ml) and 90% formic acid (0.8 ml) and refluxed for a period of 33 hours. The mixture was quenched in water, made basic with ammonia, and extracted with ether. From the ether extract a residue was obtained on evaporation which was purified by chromatography on alumina using chloroform as eluant. There was obtained 1.6 g of tertiary base which was converted to its perchlorate in acetone solution. The crystalline perchlorate which separated was recrystallized from acetone and melted at 249–250°. Calc. for $C_{17}H_{27}ON.HClO_4$: C, 56.4; H, 7.80; N, 3.8%. Found: C, 56.6; H, 7.77; N, 3.9%.

The free base, regenerated from the perchlorate, crystallized in the absence of solvent and melted at 87–88°. Calc. for $C_{17}H_{27}ON$: C, 78.2; H, 10.33; N, 5.4%. Found: C, 78.0; H, 10.30; N, 5.4%.

This base was recovered unchanged after treatment with phenyl lithium under the same conditions which gave a successful reaction with lycopodine (1).

α-Cyanodimethylaminolycopodine V

This compound was prepared by the reaction of α-cyanobromolycopodine I with a saturated solution of dimethylamine in methanol. After removal of methanol the residue was dissolved in water, made basic with ammonia, and extracted with chloroform. Evaporation of the chloroform yielded the free base which was dissolved in acetone and treated with perchloric acid. A crystalline perchlorate separated which was recrystallized from boiling acetone. This compound proved to be identical with the compound isolated by MacLean, Manske, and Marion (1) from the pyrolysis of the quaternary base derived from the quaternary bromide IV. The melting point of a mixture of the two samples was not depressed and their infrared spectra were identical. The yield was virtually quantitative.

Reduction of V *with Sodium Borohydride*

α-Cyanodimethylaminolycopodine (1.90 g) was added to a solution of 0.95 g of sodium borohydride in 200 ml of 95% ethanol and the mixture was stirred for 3 hours. After standing overnight at room temperature the mixture was worked up in the manner previously described to yield 1.80 g of the reduced compound IX, which melted at 190–191° after recrystallization from acetone. Calc. for $C_{19}H_{33}ON_3$: C, 71.5; H, 10.34; N, 13.2%. Found: C, 71.2; H, 9.85; N, 13.0%.

Conversion of the Base IX *to its Methiodide* X

A solution of 0.43 g of IX in 10 ml of acetone was treated with methyl iodide and set aside in the refrigerator. A fine, crystalline precipitate, which was collected and recrystallized from acetone, separated after a few hours. It melted at 231–232°. Calc. for $C_{20}H_{36}ON_3I.H_2O$: C, 50.1; H, 7.52; N, 9.0%. Found: C, 50.6; H, 7.67; N, 9.0%.

Decomposition of the Quaternary Salt X *with Potassium Tertiary Butoxide*

Metallic potassium (7.4 g) was added in pieces over a period of 1 hour to 160 ml of dry

Can. J. Chem. Downloaded from www.nrcresearchpress.com by 41.223.56.140 on 09/04/12
For personal use only.

tertiary butyl alcohol. The methiodide X (6.7 g) was added to the above solution and the mixture was refluxed for 42 hours. The reaction mixture was taken to dryness under vacuum and the residue mixed with water and extracted with ether. From the ether extract 2.0 g of a basic fraction and 2.2 g of neutral fraction were obtained. The basic fraction proved to be a mixture of V and IX, in which the latter predominated. The neutral fraction was separated into two fractions by chromatography on alumina using chloroform as eluant. The first fraction eluted was recovered from the chloroform and purified by crystallization from ether. It melted at 112–113°. Calc. for $C_{17}H_{24}ON_2$: C, 75.0; H, 8.82; N, 10.3%. Found: C, 74.9; H, 8.84; N, 10.3%.

The infrared spectrum of compound XI had a strong carbonyl absorption at 1700 cm^{-1}, double-bond absorption at 3070, 1640, and 910 cm^{-1}, but no absorption in the hydroxyl region. The ultraviolet absorption spectrum showed no evidence of conjugation.

The more strongly adsorbed fraction was recovered from the chloroform and recrystallized from ether. It melted at 201–202°. Calc. for $C_{17}H_{26}ON_2$: C, 74.4; H, 9.55; N, 10.2%. Found: C, 74.6; H, 9.25; N, 10.5%.

The infrared spectrum of this compound showed olefin absorption at 3070 and 1640 cm^{-1} and hydroxyl absorption at 3400 cm^{-1}. Both compounds had the usual cyanamide absorption at 2200 cm^{-1}.

The keto-olefin XI was converted to the hydroxyolefin XII by reduction with sodium borohydride in 95% ethanol. Hydrogenation of the keto-olefin yielded α-cyanolycopodine (1) identified by a mixed melting point determination and by comparison of its infrared spectrum with an authentic sample.

Ozonolysis of the Hydroxyolefin XII

The hydroxyolefin XII (0.30 g) was dissolved in a solution of 10 ml of anhydrous ethyl acetate and 1 ml of glacial acetic acid and cooled to 20°. A stream of ozone-containing oxygen was passed through the mixture until absorption of ozone no longer occurred. The solution was then transferred to a 50-ml flask, 10 ml of glacial acetic acid and 0.4 g of zinc dust were added, and the mixture was heated under reflux for 5 minutes. The apparatus was then arranged for distillation and the mixture was distilled until the vapor temperature reached 97°. The distillate was collected in an ethanolic solution of 0.28 g of dimedone containing a drop of piperidine and the resulting mixture was allowed to stand for 1 hour. The solvent was then evaporated and the residue was allowed to crystallize from aqueous alcohol. There was obtained 0.13 g of white crystalline solid which melted at 189°, and which did not depress the melting point of an authentic sample of the dimedone derivative of formaldehyde.

Reaction of β-Cyanobromolycopodine II *with Potassium Hydroxide in Methanol*

A sample of II (0.5 g) was heated at reflux temperature with a mixture of 1 g of potassium hydroxide in 40 ml of methanol for 12 minutes. The solution was made slightly acid and evaporated to dryness under vacuum. The residue was treated with water and extracted with chloroform. Evaporation of the chloroform extract yielded 0.38 g of crystalline product which, when recrystallized from petroleum ether, melted at 98–100°. This compound, VI, proved to be identical with the product which MacLean, Manske, and Marion (1) obtained by treatment of II with ethanolic potassium acetate. The infrared spectrum of a solution of the compound in carbon tetrachloride had a strong absorption band at 1675 cm^{-1}, while the band at 1700 cm^{-1} in the starting compound had completely disappeared. The spectrum of crystalline VI in Nujol mull showed a slight shift of the band to 1680 cm^{-1}. The determination of the spectrum of VI in carbon

Can. J. Chem. Downloaded from www.nrcresearchpress.com by 41.223.56.140 on 09/04/12
For personal use only.

tetrachloride solution was repeated with a calcium fluoride prism in the spectrophotometer. No bands or inflections were detected in the region 3000–3120 cm^{-1} characteristic of the =C—H stretching absorption. The ultraviolet absorption spectrum showed no evidence of conjugation.

Acid Hydrolysis of Compound VI

A sample of the cyclized compound VI (0.60 g) was dissolved in a mixture of 6 ml of 1-propanol and 30 ml of 2 *M* hydrochloric acid. The mixture was heated for 20 hours on the steam bath and then evaporated to dryness under vacuum. The residue was partitioned between ether and dilute hydrochloric acid solution. The acid solution was then made basic with ammonia and extracted with ether to yield 0.33 g of acid-soluble material. This base was adsorbed on alumina and the column was eluted with chloroform. A fraction (0.24 g) was obtained which had strong infrared absorption at 1675 cm^{-1} and no cyanamide absorption. This semicrystalline fraction was converted to the hydrochloride in acetone solution. Recrystallization of the salt from acetone–ether yielded a sample which melted at 256–257°.

Reduction of Compound VI *with Lithium Aluminum Hydride*

A solution of VI (0.60 g) in anhydrous tetrahydrofuran was added to lithium aluminum hydride (1 g) in tetrahydrofuran (25 ml). The mixture was heated under reflux for 4 hours and then allowed to stand overnight. The excess hydride was destroyed with wet tetrahydrofuran and the tetrahydrofuran solution was filtered from inorganic residue. The precipitated hydroxides were washed well with warm chloroform and the combined filtrates were evaporated to dryness. The residue yielded 0.21 g of basic material which was dissolved in acetone and converted to the hydrochloride. The hydrochloride was identical with that obtained from the hydrolysis of VI in acid solution.

Methylation of the Secondary Base XIII

The secondary base XIII (0.2 g), derived from the hydrochloride above, was treated with a solution of 0.08 ml of 98% formic acid and 0.24 ml of formalin. The mixture was heated on the steam bath for 4 hours and allowed to stand overnight. The resulting solution was treated with dilute hydrochloric acid, filtered, made alkaline with ammonia, and extracted with ether. The dried ether extract yielded an oily residue (0.2 g) which was dissolved in acetone and treated with perchloric acid. The crystalline perchlorate, which separated, melted at 232° after recrystallization from acetone. Calc. for $C_{17}H_{27}ON.HClO_4$: C, 56.4; H, 7.80; N, 3.8%. Found: C, 56.5; H, 7.64; N, 3.7%.

Reduction of β-Cyanobromolycopodine II *with Sodium Borohydride*

A solution of 0.45 g of sodium borohydride in 95% ethanol was added dropwise over ½ hour to a stirred, ice-cooled solution of 0.50 g of β-cyanobromolycopodine in 95% ethanol. The reaction mixture was stirred for 7 hours at 0°, then made slightly acid with dilute hydrochloric acid and evaporated to dryness under reduced pressure. Water was added to the residue and the mixture extracted with ether. The ether extract was washed with dilute hydrochloric acid and with water, and dried over anhydrous sodium sulphate. Evaporation of the ether solution yielded a crystalline residue whose infrared spectrum exhibited strong hydroxyl and cyanamide absorption and very weak absorption in the carbonyl region. The presence of only a very small peak at 1675 cm^{-1} showed that little cyclization to form compound VI had taken place. Recrystallization of the product from ether gave 0.25 g of a compound, XV, which melted at 139–141° with decomposition. The

Can. J. Chem. Downloaded from www.nrcresearchpress.com by 41.223.56.140 on 09/04/12
For personal use only.

compound gave a positive Beilstein test for halogen. Calc. for $C_{17}H_{27}ON_2Br$: C, 57.5; H, 7.66; N, 7.9%. Found: C, 57.5; H, 7.66; N, 8.0%.

Preparation of the Quaternary Salt XVI

An ice-cold methanolic solution of 200 mg of the hydroxybromide XV was treated with an excess of a methanolic solution of trimethylamine. The solution was left overnight in the refrigerator. The solvent and excess amine were removed by evaporation under reduced pressure and the crystalline residue was washed with warm ether and then dissolved in acetone. Concentration of the acetone solution yielded a crop of crystals (135 mg) which melted at 271–272° with decomposition. The infrared spectrum exhibited strong cyanamide absorption at 2200 cm^{-1}, a band of medium strength at 1640 cm^{-1}, and three bands in the hydroxyl region: a strong band at 3315 cm^{-1} and medium bands at 3490 and 3550 cm^{-1}. When the sample was dried under vacuum at 56° for 4 hours a loss of weight of about 8% was observed, which corresponds to a loss of 2 moles of water. On exposure to the atmosphere the sample recovered about half of the weight loss in less than 5 minutes, but further gain in weight took place very much more slowly. The infrared spectrum of the material which had been dried and then exposed to the air showed cyanamide absorption as before, but only two bands in the hydroxyl region: a strong one at 3370 cm^{-1} and a very weak one at 3600 cm^{-1}. The band at 1640 cm^{-1} was no longer present but several very weak peaks were observed in the region 1600–1660 cm^{-1}. The analytical sample, which melted with decomposition at 271–272°, was taken from material which had been dried and then exposed to the atmosphere. Calc. for $C_{20}H_{36}ON_3Br.H_2O$: C, 55.5; H, 8.86; N, 9.7%. Found: C, 55.6; H, 8.62; N, 9.5%.

Decomposition of the Quaternary Salt XVI *with Potassium Tertiary Butoxide*

A solution of potassium tertiary butoxide was prepared by dissolving 0.35 g of potassium metal in 10 ml of tertiary butanol. To this solution was added 75 mg of the quaternary salt XVI. The reaction mixture was heated under reflux for 3 hours, then the solvent was removed under vacuum. The residue was treated with water and extracted with ether. The ether solution was washed with dilute hydrochloric acid and dried over anhydrous sodium sulphate. Evaporation of the ether yielded a crystalline residue (48 mg) which, after recrystallization from petroleum ether and a second recrystallization from ether, melted at 130–136°. An analytical sample, m.p. 135.5–137.5°, was prepared by sublimation of this material at a pressure of about 0.05 mm of mercury and at 75–110°. Calc. for $C_{17}H_{26}ON_2$: C, 74.4; H, 9.55%. Found: C, 74.1; H, 9.47%.

The infrared spectrum of the product showed strong cyanamide absorption, but no hydroxyl or olefin absorption. A strong band was observed at 1070 cm^{-1}, which is in the region where the ether C—O stretching absorption has been found to occur.

Reduction of the Hydroxybromide XV *with Hydrogen in an Alkaline Medium*

A pellet (ca. 50 mg) of potassium hydroxide and 30 mg of 2% palladium – calcium carbonate catalyst were added to a hydrogenation bottle containing a methanolic solution of 30 mg of the hydroxybromide. The mixture was shaken under hydrogen at a pressure of 24 lb/sq. in. for 4.5 hours, then filtered and the filtrate evaporated. The residue was treated with water and extracted several times with ether. The ether solution was dried over anhydrous sodium sulphate and filtered. Removal of the solvent by evaporation yielded a crystalline product, which melted at 183–185.5° after recrystallization from ether. The product XIX gave a negative Beilstein halogen test. Calc. for $C_{17}H_{28}ON_2$: C, 73.9; H, 10.21; N, 10.1%. Found: C, 73.9; H, 10.36; N, 9.8%.

Can. J. Chem. Downloaded from www.nrcresearchpress.com by 41.223.56.140 on 09/04/12
For personal use only.

Oppenauer Oxidation of β-Cyanodihydrolycopodine XIX

To a solution of 0.20 g of β-cyanodihydrolycopodine in 25 ml of anhydrous benzene were added 2.5 ml of acetone and 0.50 g of aluminum isopropoxide. The mixture was refluxed for 24 hours, then poured into water and the benzene layer separated and dried over anhydrous sodium sulphate. Evaporation of the benzene solution yielded a residue (0.20 g) which partially crystallized on standing. Recrystallization from ether – petroleum ether yielded 54 mg of unreacted XIX. The material recovered from evaporation of the mother liquor was dissolved in benzene and chromatographed on an alumina column using benzene as the eluant. The first fractions yielded 84 mg of crystalline material whose infrared spectrum showed carbonyl and cyanamide absorption at 1705 and 2210 cm^{-1}, respectively, and no hydroxyl absorption. Recrystallization from ether – petroleum ether yielded an analytical sample, m.p. 82.5–84°. Calc. for $C_{17}H_{26}ON_2$: C, 74.4; H, 9.55; N, 10.2%. Found: C, 74.6; H, 9.60; N, 10.5%.

After the band containing the oxidation product, designated β-cyanolycopodine XVIII, had been collected, elution of the column was continued with 99:1 benzene–methanol and a fraction yielding a further 40 mg of starting material was obtained.

Treatment of β-Cyanobromolycopodine II *with Hydrogen in Alkaline Medium*

β-Cyanobromolycopodine II (0.2 g) was dissolved in 25 ml of methanol containing 1 g of potassium hydroxide and 0.2 g of 2% palladium – calcium carbonate catalyst. The mixture was shaken with hydrogen at 40 lb/sq. in. for 6 hours and then worked up in the manner described in the account of the hydrogenolysis of the hydroxybromide XV. The reaction conditions are those which are given by MacLean, Manske, and Marion (1). The crude crystalline product gave a negative Beilstein test for halogen. The infrared spectrum of the product had a strong absorption band at 1675 cm^{-1} and only weak absorption at 1700 cm^{-1}. After recrystallization from petroleum ether the product melted at 98–100° and proved to be identical with that obtained by treatment of β-cyanobromolycopodine with methanolic potassium hydroxide. No β-cyanolycopodine XVIII was isolated.

The reaction was repeated under the same conditions and this time the crude product was treated with sodium borohydride in order to reduce any β-cyanolycopodine present to β-cyanodihydrolycopodine and thus facilitate chromatographic separation. The hydride reduction mixture was worked up in the usual way and the crude product was adsorbed on alumina and eluted with benzene–methanol. After the cyclized compound had passed through the column a fraction was collected which contained 15 mg of material whose infrared spectrum had absorption in the hydroxyl region and at 1630–1650 cm^{-1}. It could not be ascertained whether or not β-cyanodihydrolycopodine was present in this fraction. Further elution of the column failed to yield any more material.

A methanol solution of 0.25 g of β-cyanobromolycopodine was poured into a hydrogenation bottle containing a solution of 0.05 g of potassium hydroxide in methanol which had been cooled to about −60° by fitting the bottle with a jacket packed with dry ice. Palladium – calcium carbonate catalyst (0.2 g) was added to the solution and the mixture was shaken under hydrogen at 40 lb/sq. in. for 6 hours. During the first 1–2 hours of shaking, a low temperature was maintained by keeping the jacket filled with dry ice, but after this period the mixture was allowed to come to room temperature. The mixture was worked up by the usual procedure. The infrared spectrum of the crude product showed strong cyanamide absorption at 2210 cm^{-1} and a strong band at 1705 cm^{-1} in the carbonyl region. The 1675 cm^{-1} absorption characteristic of the cyclized compound was absent. The material was purified by chromatography on alumina using benzene–methanol as

Can. J. Chem. Downloaded from www.nrcresearchpress.com by 41.223.56.140 on 09/04/12
For personal use only.

eluant. The product (0.15 g) melted at 82–84° after recrystallization from ether – petroleum ether and was found to be identical with β-cyanolycopodine XVIII prepared by Oppenauer oxidation of compound XIX.

ACKNOWLEDGMENTS

We wish to acknowledge financial assistance from the National Research Council and the Ontario Research Foundation.

REFERENCES

1. D. B. MacLean, R. H. F. Manske, and L. Marion. Can. J. Research, B, **28**, 460 (1950).
2. L. R. C. Barclay and D. B. MacLean. Can. J. Chem. **34**, 1519 (1956).
3. D. B. MacLean and W. A. Harrison. Can. J. Chem. **37**, 1757 (1959).
4. B. Douglas, D. G. Lewis, and L. Marion. Can. J. Chem. **31**, 272 (1953).
5. W. R. Song. M.Sc. Thesis, McMaster University, Hamilton, Ont. May, 1958.
6. L. R. C. Barclay. Ph.D. Thesis, McMaster University, Hamilton, Ont. October, 1957.
7. G. D. Meakins. J. Chem. Soc. 4170 (1953).

Can. J. Chem. Downloaded from www.nrcresearchpress.com by 41.223.56.140 on 09/04/12
For personal use only.

Can. J. Chem. Downloaded from www.nrcresearchpress.com by 41.223.56.140 on 09/04/12
For personal use only.

RADIATION CHEMISTRY OF CYCLOHEXANE

I. ISOTOPIC COMPOSITION OF HYDROGEN EVOLVED FROM MIXTURES OF C_6D_{12} AND C_6H_{12}[1]

P. J. Dyne and W. M. Jenkinson

ABSTRACT

The yield of D_2 formed by a unimolecular process in the γ-ray irradiation of cyclohexane-d_{12} has been deduced from the isotopic composition of hydrogen evolved from C_6H_{12}–C_6D_{12} mixtures. A value of 0.25 molecule/100 ev is found for this "molecular" yield. This yield is only slightly reduced by iodine but is considerably reduced in the presence of biphenyl.

Hydrogen is the principal gaseous product formed in the fast-electron irradiation of cyclohexane, its initial yield being 5.5–5.8 molecules/100 ev. This yield is quite sharply reduced by small additions of solutes. Solutions containing $\sim 5 \times 10^{-3}$ moles/liter iodine, for instance, have $G(H_2) \sim 4.0$ (1); solutions of cyclohexane with benzene (1, 2), biphenyl, and terphenyls (3, 4) show a similar behavior. From a study of curves of $G(H_2)$ vs. iodine concentration, Burton *et al.* (1) conclude that hydrogen is produced by two mechanisms each with a yield of 2 to 3 molecules/100 ev, one of which is more rapidly suppressed by iodine than the other. Studies of $G(H_2)$ in biphenyl solutions lead to a similar conclusion (3, 4).

The two mechanisms could be (*a*) a bimolecular mechanism involving hydrogen-atom abstraction from the parent molecule and (*b*) a unimolecular mechanism in which molecular hydrogen is split off in one step from an excited parent molecule. These two types of mechanisms are sometimes referred to as "radical and molecular" or "intermolecular and intramolecular".

The existence of two such processes has been demonstrated by Dewhurst (5) in the radiolytic decomposition of *n*-hexane. The high probability of "molecular" processes in organic molecules is shown by Dorfman's work on the gas-phase radiolysis of ethane (6) where it was shown that 66% of the molecular hydrogen is formed by a molecular detachment process not involving free hydrogen atoms.

By examining the variation of the D_2 yield in C_6D_{12}–C_6H_{12} mixtures we have determined the value of the 'unimolecular' yield of D_2 from C_6D_{12}. Its value is low, $G(D_2)$ (unimolecular) being 0.25 molecule/100 ev.

THE METHOD OF SEPARATING UNIMOLECULAR AND BIMOLECULAR YIELDS

In a mixture of C_6H_{12}, (C_H), and C_6D_{12}, (C_D), the amount of D_2 produced by a unimolecular process will have a first-order dependence on the concentration of C_D and the amount produced by a bimolecular process will have a second-order dependence on C_D. For a precise development of the relation between the yield of D_2 and the relative amounts of C_H and C_D we symbolize the reactive intermediates in the bimolecular process as X_H and X_D and all other products by P. The symbols X_H and X_D are used for the reactive intermediates to stress the generality of the reasoning. The argument is independent of the identity of the intermediates. The unimolecular process is

$$C_H \rightsquigarrow H_2 + P \qquad \text{yield } G_1(H).$$

[1]*Manuscript received November 24, 1959.*
Contribution from Research Chemistry Branch, Atomic Energy of Canada Limited, Chalk River, Ontario. Issued as A.E.C.L. No. 973.

The bimolecular process consists of two steps. The first

$$C_H \rightsquigarrow X_H + P$$

has a yield $G_2(H)$ and is followed by

$$X_H + C_H \rightarrow H_2 + P$$

which has a specific rate constant k_1.

In mixtures of C_6H_{12} and C_6D_{12} the following additional reactions will occur:

$C_D \rightsquigarrow D_2 + P$	yield	$G_1(D)$
$C_D \rightsquigarrow X_D + P$	yield	$G_2(D)$
$X_D + C_H \rightarrow HD + P$	rate constant	k_2
$X_H + C_D \rightarrow HD + P$	rate constant	k_3
$X_D + C_D \rightarrow D_2 + P$	rate constant	k_4

In a mixture containing C_H and C_D gram-molecules of the two components the fraction of ionization energy absorbed by each species is proportional to the mole fractions $C_H/(C_H + C_D)$ and $C_D/(C_H + C_D)$. The number of species X_D formed on the absorption of 100 I ev is $I.G_2(D).C_D/(C_H + C_D)$. The fraction of these species which react to give D_2 is $k_4C_D/(k_2C_H + k_4C_D)$. The number of molecules of D_2 formed by the bimolecular process is therefore

$$\frac{I.G_2(D).k_4C_D^2}{(C_D+C_H)(k_2C_H+k_4C_D)}$$

which reduces to $I.G_2(D)\ (k_4/k_2)F^2$ where $F = C_D/C_H$ for mixtures in which $C_H \gg C_D$.

Similarly the number of molecules of D_2 formed by the unimolecular process is $IG_1(D).C_D/(C_D + C_H)$ which reduces to $I.G_1(D).F$ for mixtures in which $C_H \gg C_D$.

For these dilute solutions therefore we find that the yield of deuterium $G(D_2)$ based on the amount of energy absorbed in the mixture is given by

[1] $$G(D_2) = G_2(D).(k_4/k_2)F^2 + G_1(D)F$$

or

$$G(D_2)/F = G_2(D).(k_4/k_2)F + G_1(D).$$

A plot of the left side of equation 1 against F should give a straight line with an intercept of $G_1(D)$, the unimolecular yield.

The tacit assumption has been made that products P do not react with the intermediates X to any extent. This will only be generally true at low conversions.

EXPERIMENTAL

Cyclohexane-d_{12} was obtained from Merck and Co. The analysis given by the manufacturers was 94.8 mole % cyclohexane-d_{12}, 5.2 mole % cyclohexane-d_{11}, and 0.4% benzene-d_6 corresponding to an isotopic purity of 99.6%. Dilution of C_6D_{12} with C_6H_{12} was done in two stages. First, an accurate dilution by weighing was made to give a solution containing about 40% C_6D_{12}. Small amounts of this mixture (100–500λ) were added to 2-ml samples of light cyclohexane to give solutions containing up to 7% C_6D_{12}. These 2-ml samples were degassed by freezing, pumping, and thawing five times and were irradiated at room temperature under vacuum for 16 hours in glass vessels in a Co^{60} source at a dose rate of 8.5×10^{21} ev/lt hr. The residual vacuum above the frozen sample

Can. J. Chem. Downloaded from www.nrcresearchpress.com by 41.223.56.140 on 09/04/12
For personal use only.

was <0.1 micron before irradiation. Dosimetry is based on the Fricke dosimeter $G(Fe^{3+}) = 15.5$. The gas was pumped off, the amount measured in a conventional gas-analysis line and analyzed on a Consolidated 21-610 mass spectrometer. The mass spectrometer was calibrated against synthetic mixtures of H_2, HD, and D_2.

In blank experiments solutions of D_2 in C_6H_{12} were irradiated. No significant radiation-induced exchange was observed. This is to be expected when it is noted that the parent hydrocarbon, which can react with H atoms, is present in a very much higher concentration than the D_2.

THE YIELDS OF HD AND D_2

Results on mixtures of C_6D_{12} and C_6H_{12} are shown in Table I. They are plotted in the form required by equation 1 in Fig. 1. The experimental points extrapolate to give a value of $G_1(D)$, the unimolecular yield of 0.25 molecule/100 ev.

TABLE I

Isotopic composition of hydrogen from C_6H_{12}–C_6D_{12} mixtures

Mole % C_6D_{12}	$F = C_D/C_H \times 10^2$	G (hydrogen)*	% HD	% D_2	G(HD)	$G(D_2)\times 10^2$	$\frac{G(D_2)}{F}$
1.63	1.66	4.85	1.26	0.091_5	0.061_3	0.44_4	0.26_8
1.63	1.66	4.57	1.30	0.096_2	0.059_5	0.43_9	0.26_5
3.12	3.22	4.91	2.35	0.19_4	0.115	0.95_3	0.29_6
3.12	3.22	4.63	2.42	0.19_6	0.112	0.90_7	0.28_1
5.72	6.06	4.94	4.32	0.38_0	0.213	1.8_8	0.31_8
6.86	7.36	4.96	5.22	0.46_5	0.258	2.3_0	0.31_8

*This is total chemical hydrogen, i.e. (H_2 + HD + D_2).

Results on mixtures of C_6D_{12} and C_6H_{12} with added iodine or biphenyl are given in Table II and Table III and are also plotted in Fig. 1. The value of $G_1(D)$ in the presence of iodine is 0.22, approximately 10% lower than in the absence of iodine. The value of $G_1(D)$ is much more strongly reduced by biphenyl, the intercept being 0.12.

TABLE II

Isotopic composition of hydrogen from C_6H_{12}–C_6D_{12} mixtures saturated with I_2

Mole % C_6D_{12}	G (hydrogen)	% HD	% D_2	G(HD)	$G(D_2)\times 10^2$	$\frac{G(D_2)}{F}$
1.63	3.20	1.43	0.12_2	0.045	0.39	0.23_5
3.12	3.20	2.71	0.25	0.086	0.80	0.24_8
5.72	3.16	5.12	0.51_4	0.164	1.6_2	0.26_8
6.86	3.20	6.12	0.64	0.19_5	2.0_4	0.27_8

TABLE III

Isotopic composition of hydrogen from C_6H_{12}–C_6D_{12} mixtures with 10^{-1} M biphenyl

Mole % C_6D_{12}	Biphenyl moles/liter $\times 10^2$	G (hydrogen)	% HD	% D_2	G(HD)	$G(D_2)\times 10^2$	$\frac{G(D_2)}{F}$
1.63	9.76	2.51	1.4_8	0.09_7	0.037_1	0.24_3	0.14_6
3.12	9.32	2.55	2.8_4	0.20_4	0.072_4	0.52	0.16_1
5.72	8.54	2.63	5.21	0.43_4	0.13_7	1.1_4	0.18_8
6.86	8.20	2.65	6.24	0.53_9	0.16_5	1.4_3	0.19_4

Can. J. Chem. Downloaded from www.nrcresearchpress.com by 41.223.56.140 on 09/04/12
For personal use only.

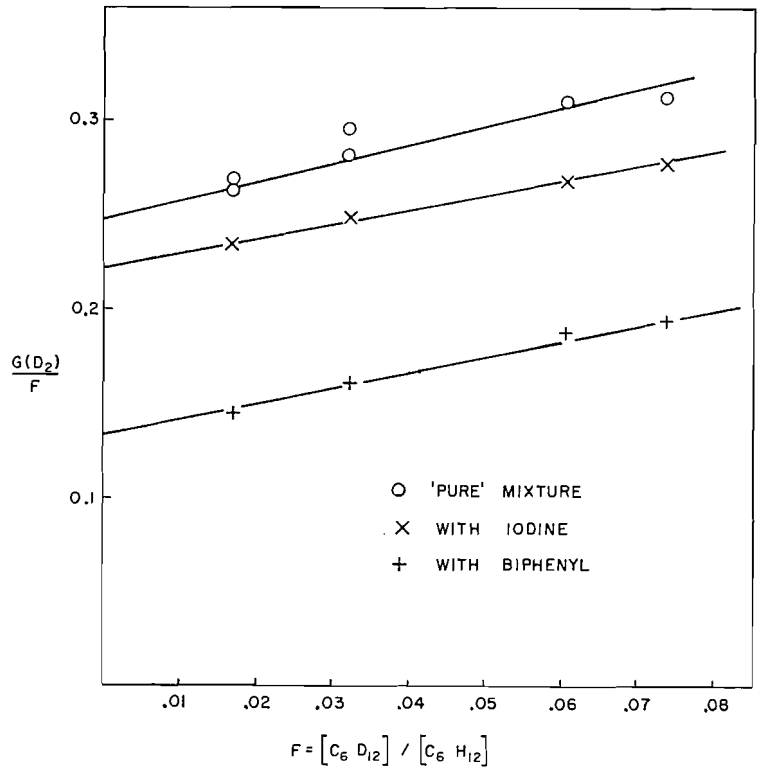


FIG. 1. The experimental results plotted in the form required by eq. 1. The intercept when $F = 0$ is the value of the "molecular" yield of D_2 from C_6D_{12} and from C_6D_{12} containing iodine and biphenyl.

DISCUSSION

The value of 0.25 for the unimolecular yield is for D_2 from C_6D_{12}. The corresponding yield for H_2 from C_6H_{12} will, in all probability, be considerably larger. This general prediction is borne out by Gordon and Burton's (7) measurements of $H_2(D_2)$ yields from benzene and benzene-d_6 and by Boyd's measurements of $H_2(D_2)$ and "polymer" yields from deuterated biphenyl and terphenyl (8). A value between 0.5 and 1.0 for $G_1(H)$ is reasonable. This estimate is in agreement with the limiting yield of cyclohexene observed by Dewhurst (9) in the presence of dissolved oxygen. A constant yield of 0.7 molecule C_6H_{10}/100 ev was observed which was assigned to the yield of the unimolecular process which would not be reduced by radical scavengers such as oxygen.

The small effect of iodine on the unimolecular yield in our experiments is consistent with our interpretation. The difference in the intercepts, which is of the order of 10%, may not be experimentally significant. While the isotopic measurements have a high degree of internal consistency the principal parameter determining the intercept is the total hydrogen yield. These experiments were not suited to the measurements of hydrogen yield to the highest accuracy and the values of $G(H_2) = 3.2$ are lower than the values we obtained for larger samples of cyclohexane and iodine, viz. 3.5.

The 50% reduction of the unimolecular yield by 10^{-1} M biphenyl is significant. If the mechanism of the "unimolecular" yield is

$$C_6H_{12} \rightsquigarrow C_6H_{12}^*$$

$$C_6H_{12}^* \rightsquigarrow C_6H_{10} + H_2$$

Can. J. Chem. Downloaded from www.nrcresearchpress.com by 41.223.56.140 on 09/04/12
For personal use only.

where $C_6H_{12}^*$ represents an excited intermediate state, then the reduction of the yield can only be due to quenching of the $C_6H_{12}^*$ by the biphenyl. This is an example of the energy-transfer process postulated by Manion and Burton (2).

The main conclusion to be drawn from these results is that the yield of "molecular" hydrogen from C_6H_{12} is a small fraction, 10–20%, of the total. If the balance of the hydrogen yield comes from two processes each with yields of between 2 and 3 molecules/100 ev as suggested in reference 1 it follows that both these processes are bimolecular.

A similar measurement of $G_1(H)$ using solutions of C_6H_{12} in C_6D_{12} was attempted. The isotopic purity of the C_6D_{12}, now the major constituent of the mixture, was not, however, sufficient to allow the application of the simple interpretation given above.

REFERENCES

1. M. BURTON, J. CHANG, S. LIPSKY, and M. P. REDDY. Radiation Research, **8**, 203 (1958).
2. J. P. MANION and M. BURTON. J. Phys. Chem. **56**, 560 (1952).
3. P. J. DYNE and J. W. FLETCHER. Unpublished.
4. J. H. BAXENDALE. Private communication.
5. H. A. DEWHURST. J. Phys. Chem. **62**, 15 (1958).
6. L. M. DORFMAN. J. Phys. Chem. **62**, 29 (1958).
7. S. GORDON and M. BURTON. Discussions Faraday Soc. **12**, 88 (1952).
8. A. W. BOYD. Private communication.
9. H. A. DEWHURST. J. Phys. Chem. **63**, 813 (1959).

Can. J. Chem. Downloaded from www.nrcresearchpress.com by 41.223.56.140 on 09/04/12
For personal use only.

Can. J. Chem. Downloaded from www.nrcresearchpress.com by 41.223.56.140 on 09/04/12
For personal use only.

FREE RADICALS BY MASS SPECTROMETRY

XIX. PRIMARY STEPS IN THE MERCURY-PHOTOSENSITIZED DECOMPOSITION OF FORMALDEHYDE[1]

A. G. HARRISON[2] AND F. P. LOSSING

ABSTRACT

In the Hg^3P, photosensitized decomposition of formaldehyde, evidence from deuterium labelling shows that 40% of the primary dissociation proceeds by way of an intramolecular elimination of H_2. The remainder dissociates by formation of H and HCO, or of 2H and CO. A clear distinction between these latter two processes cannot be made under the reaction conditions employed.

INTRODUCTION

Although the direct photolysis of formaldehyde has been rather extensively studied by a number of authors, no investigation of the mercury-photosensitized decomposition appears to have been made. One question of particular interest is whether the relative probability of occurrence of free radical and intramolecular rearrangement processes is dependent on the means of activation. If one uses the symbol HCHO* to designate a formaldehyde molecule which has been excited by a quantum, either by direct absorption or by collision with an excited mercury atom, the two primary dissociation processes of interest are

$$HCHO^* \rightarrow H + HCO, \quad [1]$$

$$\rightarrow H_2 + CO. \quad [2]$$

At wavelengths shorter than 2700 Å, a third reaction becomes energetically possible:

$$HCHO^* \rightarrow 2H + CO. \quad [3]$$

In this wavelength region reaction [1] might become indistinguishable from reaction [3] if the lifetime of the HCO radical were sufficiently shortened by energy carried over from the primary dissociation step.

Information as to the relative importance of these three primary steps in the direct photolysis at various wavelengths is rather ambiguous. Gorin (1) investigated the photolysis at 2537 Å, 3130 Å, and 3650 Å, using iodine as a radical trap. He concluded that at 2537 Å and 3130 Å reaction [1] is essentially the only process. Although reaction [3] is energetically possible at 2537 Å, he assigned an upper limit of 0.1 to its occurrence. He concluded that reaction [1] was still the major primary process at 3650 Å, although reaction [2] occurred to the extent of 0.3. These findings have been questioned by Steacie (2) in view of later work on the interfering effect of iodine in aldehyde photolyses.

Using the Paneth technique, Volman *et al.* (3) showed, by the removal of tellurium mirrors, that H atoms or HCO radicals must be formed in the photolysis at 2750 Å.

Calvert and Steacie (4) examined the photolysis at 3130 Å in some detail and found the mechanism to be consistent with the occurrence of reaction [1]. The extent to which reaction [2] occurred could not be determined from their results, however.

Klein and Schoen (5) photolysed mixtures of H_2CO and D_2CO at wavelengths from 3130 Å to 3750 Å. They found that at 3650 Å reaction [1] occurred, but to a smaller

[1]*Manuscript received December 17, 1959.*
Contribution from the Division of Pure Chemistry, National Research Council, Ottawa, Canada.
Issued as N.R.C. No. 5586.
[2]*National Research Council of Canada Postdoctorate Fellow, 1957–59.*

extent than reported by Gorin (1), and they concluded that reaction [2] was the major process. The occurrence of reaction [1] at this wavelength requires that D(H—CHO) be less than 78 kcal/mole, and consequently that D(H—CO) in formyl must be greater than 27 kcal/mole. This conclusion has been questioned by Calvert (6) on the grounds that the observed rate of reaction [1] at 3650 Å could result from absorption by vibrationally excited formaldehyde molecules. The interpretation of these results and their bearing on the bond dissociation energy in HCHO and HCO is still controversial (7, 8). For the present purpose, however, a significant finding of Klein and Schoen was that reactions [1] and [2] both occurred at 3130 Å, the latter with a greater probability. Concerning the occurrence of reaction [2] at 2537 Å, on the other hand, there seems to be no unambiguous evidence either for or against.

It was thought that a measurement of the relative probabilities of reactions [1] and [2] in the mercury-photosensitized reaction at 2537 Å would be of interest for comparison with the direct photolytic experiments at longer wavelengths. A similar investigation of the mercury-photosensitized decomposition of acetaldehyde (9) showed that the corresponding intramolecular reaction to form CH_4 and CO did not occur to any appreciable extent, although there is evidence in the literature for its participation in the direct photolytic decomposition.

EXPERIMENTAL

The mercury-photosensitized reaction was carried out at 55° C in a fast-flow reaction system coupled to a mass spectrometer (10). A portion of the stream of reaction products from the illuminated zone was allowed to flow directly into the ionization chamber. A modification to the original apparatus has been described recently (11), together with some considerations regarding the experimental conditions in the reactor. The partial pressure of formaldehyde was in the region of 1–6 microns, carried in a stream of helium at 8–10 mm. Addition of formaldehyde to the helium stream was controlled by means of metal needle valves leading to samples of liquid formaldehyde maintained at −78° C.

The sample of D_2CO, prepared for us through the kindness of Dr. L. C. Leitch, had an isotopic purity of about 99%.

RESULTS AND DISCUSSION

In preliminary experiments formaldehyde was found to have a relatively large cross section for reaction with Hg^3P_1 atoms. In a contact time of 0.001 second formaldehyde at a partial pressure of 6.0 microns was decomposed to the extent of 24.4%. At the same pressure and contact time acetone was decomposed to the extent of 21.9%. The yield of CO was found to be essentially quantitative (97%); consequently the polymerization of formaldehyde vapor was negligible. Using electrons of low energy, no increase in the mass 29 peak attributable to the HCO radical could be observed. Earlier experiments have indicated, however, that the sensitivity for detection of HCO radical in this instrument is quite low (9), presumably as a result of the dissociation of HCO on surfaces in the ionization chamber. No formation of the dimer, glyoxal, was observed.

The participation of reaction [2] was demonstrated using H_2CO–D_2CO mixtures in a manner similar to that previously employed for acetaldehyde (9). The results are given in Table I. In experiments using H_2CO alone, the yield of H_2 per H_2CO decomposed was 0.96 to 0.98, and independent of the partial pressure of H_2CO over the range 1.84–5.63 microns. When D_2CO was added to the reaction stream containing H_2CO, the yield of H_2 per H_2CO decomposed decreased progressively as the mole fraction of D_2CO was

Can. J. Chem. Downloaded from www.nrcresearchpress.com by 41.223.56.140 on 09/04/12
For personal use only.

TABLE I
Decomposition of H_2CO–D_2CO mixtures

Partial pressures (μ)				Decomposed						Mole fraction, H_2CO
Lamp off		Lamp on		μ		%		H_2 produced		
H_2CO	D_2CO	H_2CO	D_2CO	H_2CO	D_2CO	H_2CO	D_2CO	(μ)	$H_2/\Delta H_2CO$	$\frac{H_2CO}{H_2CO+D_2CO}$
1.84_2	—	1.20_5	—	0.63_7	—	34.5_8	—	0.61	0.96	1.00
3.22_2	—	2.20_3	—	1.02_7	—	31.8_2	—	1.00	0.97	1.00
5.62_8	—	3.97_6	—	1.65_2	—	29.3_5	—	1.62	0.98	1.00
5.38_3	1.70_2	3.91_8	1.24_7	1.46_5	0.45_5	27.2_1	26.7_3	1.23	0.84	0.76_0
5.62_8	2.77_0	4.12_9	2.05_1	1.49_9	0.71_9	26.6_3	25.9_6	1.17	0.78	0.67_0
2.75_0	2.78_2	2.01_6	2.05_1	0.73_4	0.73_1	26.6_9	26.2_8	0.52_7	0.72	0.49_7
2.93_0	5.06_1	2.14_5	3.77_0	0.78_5	1.29_1	26.7_9	25.5_0	0.46_4	0.59	0.36_7
1.71_7	5.23_1	1.26_1	3.86_7	0.45_6	1.36_4	26.5_5	26.0_7	0.25_3	0.55	0.24_7
1.03_7	5.59_7	0.76_4	4.13_5	0.27_3	1.46_2	26.3_2	26.1_2	0.13_8	0.49	0.15_6
4.60_4	4.55_4	3.54_5	3.50_9	1.05_9	1.04_5	22.9_8	22.9_6	0.72_9	0.69	0.50_8

increased. In these mixtures HD and D_2 were formed. It is evident that, as the ratio D_2CO/H_2CO is made very large, any H atoms produced in the primary dissociation step must result in the formation of HD rather than H_2. In this respect it makes no difference whether the H atoms are removed by any or all of the three possible reactions:

$$H + D\,(+ M) \rightarrow HD\,(+ M), \qquad [4]$$

$$H + DCO \rightarrow HD + CO, \qquad [5]$$

$$H + D_2CO \rightarrow HD + DCO. \qquad [6]$$

Any H_2 produced in mixtures containing a very large excess of D_2CO must therefore have been formed by the intramolecular process [2]. The yield of H_2 as a function of the mole fraction of H_2CO in the mixture, shown graphically in Fig. 1, was an approximately straight line. An extrapolation of the line to infinite dilution of H_2CO by D_2CO indicates that about 40% of the H_2CO must decompose to give H_2 in one step. One can therefore assign the relative probability of 0.40 ± 0.05 to reaction [2], leaving 0.6 ± 0.05 to be divided between reactions [1] and [3].

The relative probability of reaction [2] can also be calculated independently from HD production in mixtures of H_2CO and D_2CO. With the approximately equimolar mixture given in the last line of Table I, the partial pressure of HD formed was 0.660 micron. Neglecting possible interference from a very small amount of HDCO (see below), we may assume that all the HD was formed by reactions [4] and [5] and the isotopic equivalent of [5]:

$$D + HCO \rightarrow HD + CO. \qquad [7]$$

The amount of HD formed by reaction [6] is extremely small. That this reaction is negligibly slow under the reaction conditions employed is shown by the fact that the percentage of formaldehyde decomposed showed no increase with increasing partial pressure. With the further assumption that the fraction of formaldehyde dissociating by reaction [2] is the same for both isotopic species, and that consequently in this experiment [H] ≈ [D] and [HCO] ≈ [DCO], the amounts of H_2, HD, and D_2 formed by reactions [4], [5], and [6] and their isotopic equivalents would be in the ratio 1:2:1. The total amount of isotopic hydrogens formed as a consequence of the primary reactions [1] and [3] will then be twice the amount of HD observed, i.e. 1.32 microns. Since the total amount of formaldehyde decomposed was $1.059+1.045 = 2.104$ microns, reactions

Can. J. Chem. Downloaded from www.nrcresearchpress.com by 41.223.56.140 on 09/04/12
For personal use only.

[1] and [3] must account for 1.32/2.104 or 0.63 of the total reaction. The remainder, 0.37, is the relative probability of reaction [2]. This result agrees closely with the extrapolation in Fig. 1.

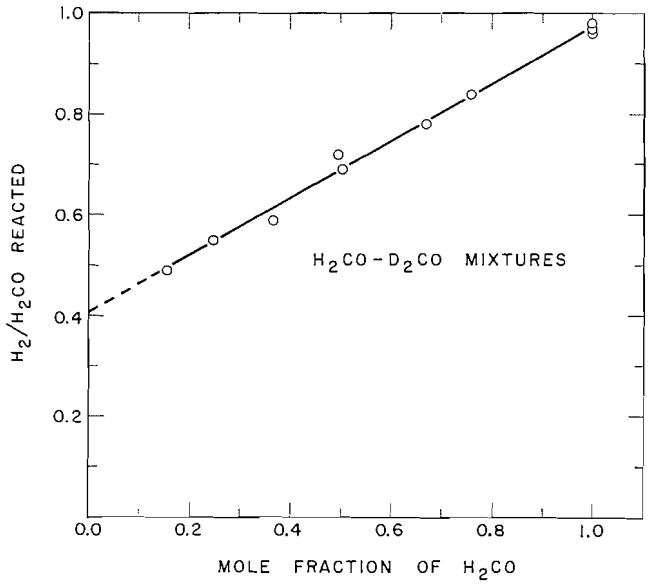


FIG. 1.

Although the data given above provide good evidence that about 40% of the total reaction goes by way of reaction [2], there remains the question as to whether the remainder of the reaction is better described by reaction [1] or reaction [3]. The energy available from $^3P_1$ mercury atoms, 112 kcal/mole, is more than sufficient to bring about reaction [3], for which the energy requirement is 105 kcal/mole. It is evident therefore that HCO radicals formed in reaction [1] would have sufficient excitation to dissociate spontaneously. Unless some effective means of deactivation is available, reactions [1] and [3] would consequently be indistinguishable. In the present experiments conditions would appear to be quite unfavorable for rapid deactivation, since helium at 8 mm pressure would be quite ineffective in this respect, and the partial pressure of formaldehyde was only a few microns. Nevertheless, some evidence for the presence of an appreciable concentration of formyl radicals in the reactor was obtained. It was observed that when mixtures of H_2CO and D_2CO were decomposed, a significant amount of the mixed aldehyde HDCO was formed. Possible modes of formation of HDCO are the following:

$$HCO + DCO \rightarrow HDCO + CO, \quad [8]$$

$$H + DCO \rightarrow HDCO, \quad [9]$$

$$H + D_2CO \rightarrow HDCO + D. \quad [10]$$

In a separate experiment in which the photosensitized decomposition of a mixture of H_2 and D_2CO in the reactor was carried out, no HDCO was formed. The formation of HD in this reaction showed, however, that H atoms were present either as a result of quenching of Hg^3P_1 atoms by H_2, or by exchange of D atoms with H_2. Since no HDCO

Can. J. Chem. Downloaded from www.nrcresearchpress.com by 41.223.56.140 on 09/04/12
For personal use only.

was formed, even though an appreciable quantity of H atoms was present, it may be concluded that reactions [9] and [10] are negligibly slow under the present reaction conditions. It would appear, then, that in mixtures of H_2CO and D_2CO, reaction [8] is the most probable source of the observed HDCO. In one such experiment, in which the amounts of H_2CO and D_2CO decomposed were 1.20 and 1.29 microns respectively, the partial pressure of HDCO formed was estimated to be 0.06 micron. (For this calculation the mass spectral sensitivity for HDCO at mass 31 was assumed to be the mean of the parent ion sensitivities for H_2CO and D_2CO.) If, as seems probable, the concentrations of HCO and DCO were not greatly different, the amounts of isotopic formaldehydes formed by disproportionation would be in the ratio 1:2:1. The total formaldehydes resulting from reaction [8] would then be 0.12 micron, and the total of formyl radicals involved equal to 0.24 micron. This amount corresponds to a lower limit of about 0.1 for reaction [1]. The fraction of primary reaction yielding such "stable" formyls is undoubtedly much greater than this, since formyls will be destroyed by other reactions. By analogy with the reaction of CH_3 with HCO (9), the abstraction reaction

$$H + HCO \rightarrow H_2 + CO \qquad [11]$$

is probably quite rapid. Some formyls may also be decomposed by reaction with a second excited mercury atom:

$$HCO + Hg^3P_1 \rightarrow H + CO + Hg^1S_0. \qquad [12]$$

From the present experiments, therefore, a lower limit for the occurrence of reaction [3] cannot be set. It might be expected that at higher pressures, where the possibility for deactivation of HCO radicals formed in [1] is increased, reaction [1] would be favored over reaction [3]. In the present reactor the effect of pressure could not be examined over a range wide enough to be significant.

In view of the large excess of energy available at 2537 Å, it is surprising that such a large part of the primary reaction proceeds by the almost thermoneutral formation of H_2 and CO rather than by rupture of a C—H bond. The substitution of CH_3 for H, as in acetaldehyde, is sufficient to reduce the similar intramolecular processes

$$CH_3CHO + Hg^3P_1 \rightarrow CH_4 + CO + Hg^1S_0 \qquad [13]$$

$$\rightarrow H_2 + CH_2 = CO \qquad [14]$$

to negligible proportions (9).

REFERENCES

1. E. Gorin. J. Chem. Phys. **7**, 256 (1939).
2. E. W. R. Steacie. Atomic and free radical reactions. 2nd. ed. Reinhold Publishing Corp., New York. 1954.
3. D. H. Volman, P. A. Leighton, F. E. Blacet, and R. K. Brinton. J. Chem. Phys. **18**, 203 (1950).
4. J. G. Calvert and E. W. R. Steacie. J. Chem. Phys. **19**, 176 (1951).
5. R. Klein and L. G. Schoen. J. Chem. Phys. **24**, 1094 (1956).
6. J. G. Calvert. J. Phys. Chem. **61**, 1206 (1957).
7. R. Klein and L. J. Schoen. J. Chem. Phys **29**, 953 (1958).
8. J. G. Calvert. J. Chem. Phys. **29**, 954 (1958).
9. F. P. Lossing. Can. J. Chem. **35**, 305 (1957).
10. F. P. Lossing, D. G. H. Marsden, and J. B. Farmer. Can. J. Chem. **34**, 701 (1956).
11. P. Kebarle and F. P. Lossing. Can. J. Chem. **37**, 389 (1956).

Can. J. Chem. Downloaded from www.nrcresearchpress.com by 41.223.56.140 on 09/04/12
For personal use only.

Can. J. Chem. Downloaded from www.nrcresearchpress.com by 41.223.56.140 on 09/04/12
For personal use only.

LONG-RANGE COUPLING CONSTANTS IN THE N.M.R. SPECTRA OF OLEFINES[1]

ROBERT R. FRASER

ABSTRACT

The spectra of tiglic and angelic acids and their methyl esters have been determined and analyzed by first-order perturbation theory. The magnitudes of the long-range coupling constants were found to be greater in each instance for *trans* oriented hydrogens than for *cis* hydrogens. All long-range coupling constants already reported have been examined and found to be consistent with the proposal that *trans* coupling constants are larger than *cis* coupling constants for hydrogens separated by more than three bonds.

Thus far, N.M.R. spectroscopy has been utilized in two ways to assign configuration to a pair of isomeric olefines. The magnitude of the coupling constant between the hydrogens attached to opposite ends of the double bond of a disubstituted olefine has been observed consistently to be larger for *trans* hydrogens than for *cis* hydrogens (1). These observations are in agreement with the theoretical calculation of coupling constants for olefines which were recently reported by Karplus (2). In symmetrically substituted olefines where coupling is not observable due to identical chemical shifts for the two protons on the double bond, the constant has been determined by examination of the peaks produced by interaction of the ethylenic hydrogens with the C^{13} nuclei present in natural abundance (3). The second method, proposed by Jackman and Wiley (4), assigns configuration to olefines on the basis of observations that a substituent β to a methoxycarbonyl group (each attached to one end of a double bond) will appear at a lower field strength when oriented *cis* to the ester group. A third method may be applicable by determination of the relative magnitude of long-range coupling constants between hydrogens *cis* or *trans* to each other.

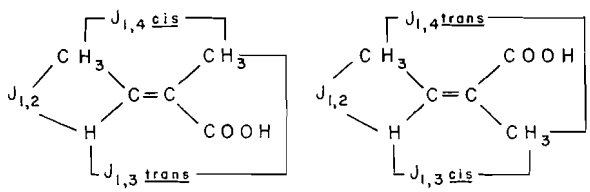


FIG. 1. Coupling constant nomenclature for tiglic (left) and angelic (right) acids.

Although the magnitude of spin–spin coupling decreases rapidly with increasing distance between the nuclei, the decrease is not so large when one of the intervening bonds possesses unsaturation. In olefines the size of the coupling constant between hydrogens separated by four bonds, hereafter called $J_{1,3}$, generally varies from 0.4 to 2.0 cycles per second (see Fig. 1 for nomenclature). Surprisingly we have observed equally large coupling constants between hydrogens separated by five bonds ($J_{1,4}$) as well. An examination of the literature revealed only relatively few cases where the spectra of a pair of *cis* and *trans* olefines are reported, including the $J_{1,3}$ values. We have measured the spectra of tiglic and angelic acids, and their methyl esters, to determine whether or not a simple relationship exists between the relative magnitude of 1,3 coupling constants and the geometrical relationship of the interacting nuclei. Should such a relationship obtain,

[1]*Manuscript received November 23, 1959.*
Contribution from the Department of Chemistry, University of Ottawa, Ottawa, Ontario.

assignment of configuration to trisubstituted olefines on this basis would be possible. Furthermore, as Muller and Pritchard have pointed out (5) such distant interaction indicates appreciable contribution of hitherto neglected structures to the ground-state wave function of the molecule. Thus the data obtained should be of use in estimating such contributions as was the case for ethylene (2).

TABLE I

Literature values for 1,3 coupling constants in cycles/sec

Compound	$J_{1,3}$ *trans*	$J_{1,3}$ *cis*	Reference
Butene-1	1.3	1.9	(6)
α-Methyl styrene	0.7	1.4	(7)
cis-Propenylbenzene	1.4	—	(7)
trans-Propenylbenzene	—	1.9	(8)
cis–cis-Dimethylmuconate	1.3	—	(9)
trans–trans-Dimethylmuconate	—	0.7	(9)
*trans**-1,2,3-Trichloropropene-1	0.8	—	(10)
cis-1,2,3-Trichloropropene-1	—	0.4	(10)
cis†-1,3-Dichloropropene-1	0.9	—	(10)
	1.2	—	(11)
trans-1,3-Dichloropropene-1		0.5	(10)
		1.2	(11)

**cis* and *trans* refer to the orientation of the two chlorine atoms on the double bond.

†*cis* and *trans* refer to the orientation of the two chlorine-containing groups.

The values of 1,3 coupling constants reported in the literature are given in Table I. At first glance no clear-cut relationship is obvious. Each set of values, however, must be critically appraised. The constants reported by Alexander (6) were obtained after a complete analysis of the spin wave functions for a system of five nuclei. The purpose of his analysis was to determine the relative signs of $J_{1,2}$ and $J_{1,3}$ and he found by testing various values for nine adjustable parameters that the best fit with the observed spectrum was obtained with the indicated values. An inversion of the magnitudes of $J_{1,3}$ *cis* and $J_{1,3}$ *trans* was not tested for comparison with the observed spectrum and could well be as acceptable. The relative magnitude of the coupling constants listed for α-methylstyrene depends on the assignment of peaks to the two ethylenic hydrogens. Pople, Bernstein, and Schneider (7) have only tentatively assigned the peak at high field to the hydrogen *cis* to the methyl group. The opposite assignment, perhaps even more acceptable,* would reverse the values for $J_{1,3}$ *trans* and $J_{1,3}$ *cis*. The results for the isomeric propenyl benzenes are more difficult to assess as details of the analysis of the *cis* isomer have not been reported. Should the values listed for the first three systems prove erroneous then the general rule $J_{trans} > J_{cis}$ would be obeyed.

Similar uncertainties exist in the remaining reported values in Table I with the exception of the trichloropropenes, which gave a simple spectrum. The most reliable values can only be obtained from spectra which can be analyzed by first-order perturbation theory. Such spectra have been obtained for tiglic and angelic acids and their methyl esters. The

**The effect of the benzene ring on its cis hydrogen can be either diamagnetic or paramagnetic depending on its orientation with respect to the rest of the molecule (12). The ultraviolet spectrum of α-methylstyrene shows a K-band maximum at lower wavelength with diminished intensity compared with that of styrene (13). Such a shift is most likely attributed to deviation of the aromatic ring from coplanarity with the ethylene system, the amount of which determines the strength of the paramagnetic effect.*

Can. J. Chem. Downloaded from www.nrcresearchpress.com by 41.223.56.140 on 09/04/12
For personal use only.

spectra for tiglic acid and methyl tiglate were first measured in carbon tetrachloride and showed complications in structure due to lack of a difference in chemical shift between the two methyl groups. When the spectra were measured on 10% solutions in benzene, solute–solvent interactions caused a preferential shift of the β-methyl group by 20 cycles/sec to high field thus allowing first-order analysis to be applied. Figure 2 shows the

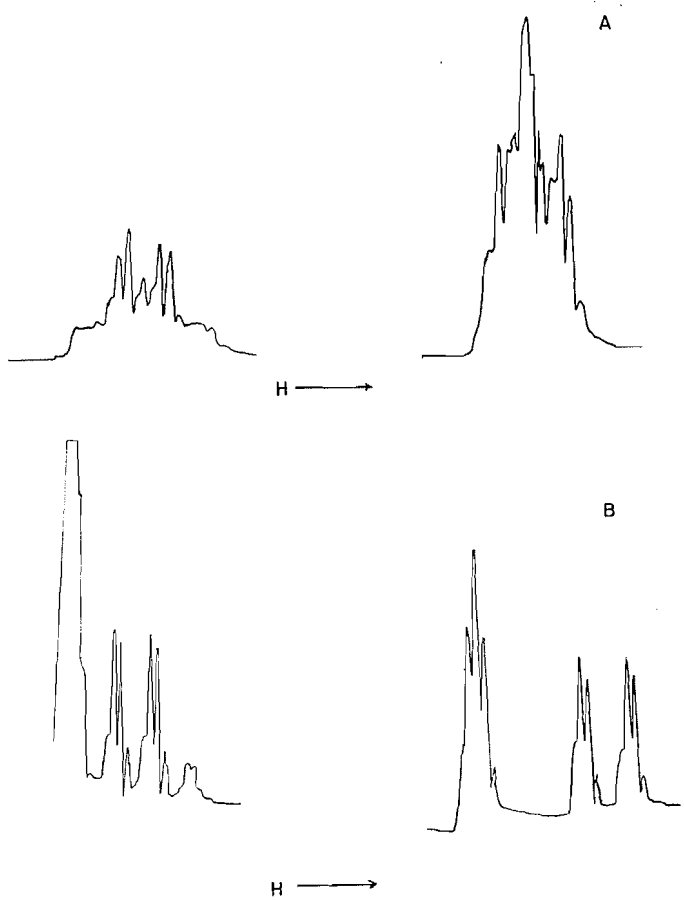


FIG. 2. Spectra due to ethylenic hydrogen (low-field peak) and methyl groups of tiglic acid. (A) 10% solution in carbon tetrachloride; (B) 10% solution in 93% deuterated benzene. (The 7% of benzene protons obscures the first quartet of the ethylenic absorption.)

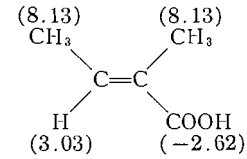
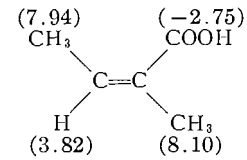
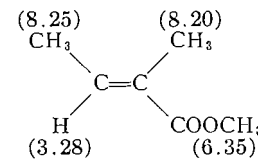
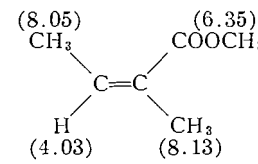
absorption peaks for the ethylenic hydrogen and the two methyl groups of tiglic acid in carbon tetrachloride and deuterobenzene solutions. Assignment of the two quartets at highest field to the β-methyl group is made on the basis of the assumption that the larger CH_3—C—H coupling will occur between hydrogens on adjacent carbon atoms. Exceptions to this assumption are known but are not likely here. The reverse assignment for the two methyl groups would require $J_{1,3}$ to be 7.11 cycles/sec and $J_{1,2}$ to be 1.43 cycles/sec, a highly improbable situation. Any doubt as to the structures of tiglic and angelic acids has recently been removed by the irrefutable evidence of X-ray analysis (14).

The measured values for the chemical shifts and coupling constants are given in Table II. The results obtained show $J_{1,3}$ *trans* > $J_{1,3}$ *cis* in both pairs of isomers. In addition $J_{1,4}$ *trans* > $J_{1,4}$ *cis*. The only other pair of geometrical isomers whose $J_{1,4}$ values have been

Can. J. Chem. Downloaded from www.nrcresearchpress.com by 41.223.56.140 on 09/04/12
For personal use only.

TABLE II

Chemical shifts* and coupling constants† for tiglic and angelic acids and their methyl esters

Compound	Formula	$J_{1,3}$	$J_{1,4}$	$J_{1,2}$
Tiglic acid		1.43 (σ = 0.03) σ = standard deviation	1.17 (σ = 0.06)	7.11 (σ = 0.05)
Angelic acid		1.28 (σ = 0.05)	1.46 (σ = 0.06)	7.16 (σ = 0.11)
Methyl tiglate		1.37 (σ = 0.04)	1.20 (σ = 0.04)	7.18 (σ = 0.14)
Methyl angelate		1.22 (σ = 0.03)	1.51 (σ = 0.05)	6.96 (σ = 0.14)

*Determined from 10% solutions in carbon tetrachloride containing 1% of tetramethylsilane and reported in parentheses as τ values (parts per million with tetramethylsilane assigned a value 10.00).

†In units of cycles per second.

determined are the butene-2 isomers. There, too, $J_{1,4}$ *trans* was found to be greater than $J_{1,4}$ *cis* (15). Demonstration that such a general relationship is true for long-range coupling constants in all olefines must await the accumulation of sufficient empirical and theoretical evidence. Work is continuing in this direction. Finally, it is interesting to note that our chemical shift data agree with the findings of Jackman and Wiley (4).

EXPERIMENTAL

The spectra were measured with a Varian V-4302 high resolution N.M.R. spectrometer. Peak separations in each multiplet were measured by the side band technique (16) employing a Hewlett–Packard wide-range oscillator. The accuracy of the oscillator was checked with a Hewlett–Packard standardized frequency counter and the error was found to be less than 0.5% in the range employed for coupling constant determinations and less than 0.75% when used for determination of chemical shifts. Each coupling constant is reported as the average of at least four determinations and the standard deviation is reported with each value. The spectrum of angelic acid was measured on a 10% solution in carbon tetrachloride. Those for tiglic acid and its methyl ester were obtained from 10% solutions in deuterobenzene and benzene respectively. Methyl angelate was run as the pure liquid. All chemical shifts were measured from 10% solutions in carbon tetrachloride containing 1% of tetramethylsilane as internal standard (17).

Can. J. Chem. Downloaded from www.nrcresearchpress.com by 41.223.56.140 on 09/04/12
For personal use only.

Tiglic Acid

This compound was prepared by the oxidation of tiglaldehyde by a modification of the method of Goldberg and Lindstead (18). A mixture of 52 g (0.6 mole) of tiglaldehyde, b.p. 114–115°, and 260 g (1.6 mole) of silver nitrate in 840 ml of 28% ethanol in a 3-l. flask was stirred for 4 hours. After standing for 12 hours the mixture was filtered. The filtrate was acidified and treated with 34 g (0.3 mole) of calcium chloride in 75 ml of water. The precipitated calcium salt was filtered off, and converted to the sodium salt by boiling with an excess of 10% sodium carbonate. The solution of the sodium salt was acidified, extracted with ether, and the dried extracts upon evaporation gave 32.5 g (53%) of tiglic acid, m.p. 64–65° (literature m.p. 64° (19)).

Methyl Tiglate

The methyl ester was obtained by esterification according to the method of Buckles and Mock (20). Methyl tiglate, b.p. 133–135°, n_D^{24} 1.4360 was obtained in 91% yield (literature b.p. 137.5–139°, n_D^{20} 1.4371 (20)).

Angelic Acid

Tiglic acid was converted to angelic acid by the procedure of Buckles and Mock (20). The over-all yield of angelic acid, m.p. 42–44°, was 39% (literature m.p. 44–45.2° (21)).

Methyl Angelate

Angelic acid was esterified by the procedure of Buckles and Mock (20). From 2.5 g of acid was obtained 1.5 g (52%) of methyl angelate, b.p. 125–126°, n_D^{24} 1.4307 (literature b.p. 127.2–128°, n_D^{20} 1.4330 (20)).

ACKNOWLEDGMENTS

The author gratefully acknowledges the financial assistance of the National Research Council of Canada. The author also thanks Professor F. A. L. Anet for helpful discussion and Mrs. L. Westland and Mrs. V. Nicholson for technical assistance.

REFERENCES

1. J. A. Pople, W. G. Schneider, and H. J. Bernstein. High resolution nuclear magnetic resonance. McGraw-Hill Book Co., Inc., New York. 1959. p. 194.
2. M. Karplus. J. Chem. Phys. **30**, 11 (1959).
3. A. D. Cohen, N. Sheppard, and J. J. Turner. Proc. Chem. Soc. 118 (1958).
4. L. M. Jackman and R. H. Wiley. Proc. Chem. Soc. 196 (1958).
5. N. Muller and D. E. Pritchard. J. Chem. Phys. **31**, 771 (1959).
6. S. Alexander. J. Chem. Phys. **28**, 358 (1958).
7. M. Karplus. J. Chem. Phys. **30**, 238 (1959).
8. R. W. Fessenden and J. S. Waugh. J. Chem. Phys. **30**, 944 (1959).
9. J. A. Elvidge and L. M. Jackman. Proc. Chem. Soc. 89 (1959).
10. F. S. Mortimer. J. Mol. Spectroscopy, **3**, 340 (1959).
11. C. N. Banwell, A. D. Cohen, N. Sheppard, and J. J. Turner. Proc. Chem. Soc. 266 (1959).
12. Reference 1, p. 180. J. Chem. Phys. **30**, 174 (1959).
13. R. T. Arnold and S. Searles. J. Am. Chem. Soc. **71**, 2022 (1949).
14. A. L. Porte and J. M. Robertson. J. Chem. Soc. 817 (1959).
15. F. A. L. Anet. Private communication.
16. Reference 1, p. 74.
17. G. V. D. Tiers. J. Phys. Chem. **62**, 1151 (1958).
18. A. A. Goldberg and R. P. Linstead. J. Chem. Soc. 2355 (1928).
19. I. Heilbron and H. M. Bunbury. Dictionary of organic compounds. Eyre & Spottiswoode Ltd., London. 1953. p. 510.
20. R. E. Buckles and G. V. Mock. J. Org. Chem. **15**, 680 (1950).
21. S. W. Pelletier and W. L. McLeish. J. Am. Chem. Soc. 74, 6292 (1952).

Can. J. Chem. Downloaded from www.nrcresearchpress.com by 41.223.56.140 on 09/04/12
For personal use only.

Can. J. Chem. Downloaded from www.nrcresearchpress.com by 41.223.56.140 on 09/04/12
For personal use only.

TRYPTAMINES, CARBOLINES, AND RELATED COMPOUNDS

PART V. 3-(α-ALKYL-β-AMINOETHYL)INDOLES[1,2]

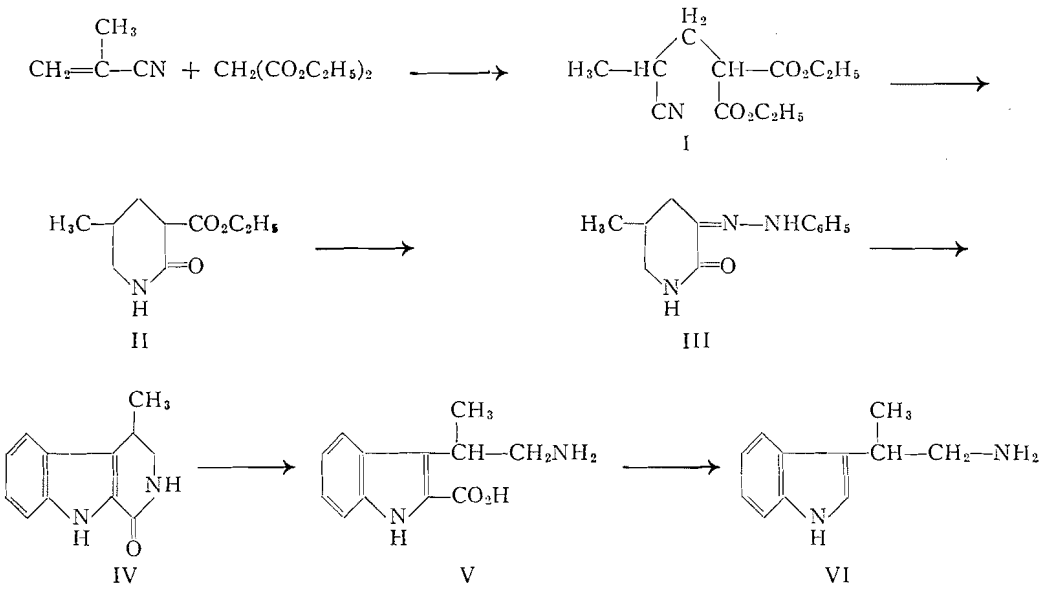
R. A. ABRAMOVITCH AND J. M. MUCHOWSKI

ABSTRACT

The scope of the tryptamine synthesis via 1-oxo-1,2,3,4-tetrahydro-β-carbolines has been extended to tryptamines bearing a side-chain α-alkyl group. The preparation of 3-(2-amino-1-methylethyl)indole by this procedure is described.

In a previous paper (1) an attempt was made to extend the method of synthesis of tryptamines via 1-oxo-1,2,3,4-tetrahydro-β-carbolines (2, 3) to the elaboration of the physostigmine ring system. The intermediate 4-methyl-2,3-dioxopiperidine 3-phenylhydrazone did not, however, undergo Fischer cyclization but instead rearranged to the geometrically isomeric phenylhydrazone. In order to examine the scope of this method of tryptamine synthesis the cyclization of 5-alkyl-substituted 2,3-dioxopiperidine 3-phenylhydrazones was examined, in particular that of 5-methyl-2,3-dioxopiperidine 3-phenylhydrazone (III). This reaction sequence should eventually lead to 3-(2-amino-1-methylethyl)indole (VI). This type of compound may be of physiological interest since Velluz (4) has shown that when a methyl substituent is introduced into the corresponding position in reserpine a more physiologically active compound is obtained.

The synthesis of the required indole was uneventful and followed the path described in the previous examples (2, 3):



Ethyl malonate was condensed with methacrylonitrile in the presence of sodium ethoxide giving diethyl 2-cyanopropylmalonate (I), which was hydrogenated to 3-ethoxycarbonyl-5-methyl-2-oxopiperidine (II). This underwent a Japp–Klingemann

[1]*Manuscript received December 14, 1959.*
Contribution from the Chemistry Department, University of Saskatchewan, Saskatoon, Saskatchewan.
[2]*Part IV: Can J. Chem.* **36**, *354 (1958).*

reaction with benzenediazonium chloride at pH 5 to give 5-methyl-2,3-dioxopiperidine 3-phenylhydrazone (III) which, unlike the corresponding 4-methyl-derivative, was cyclized quite smoothly to 4-methyl-1-oxo-1,2,3,4-tetrahydro-β-carboline (IV). Hydrolysis gave the amino acid (V). Decarboxylation of this acid takes place less readily than in the case of the unsubstituted tryptamine-2-carboxylic acid itself. Thus, whereas the latter yielded tryptamine in 75% yield after it was boiled for 1 hour with 10% hydrochloric acid, the methyl substituted acid only gave a 49% yield of 3-(2-amino-1-methylethyl)indole (VI) after it was boiled with 10% hydrochloric acid for 2 hours. In the latter case, an appreciable amount (44%) of unchanged acid is recovered. The methyltryptamine so obtained was identical with the product described by Noland and Lange (5) which these authors prepared from indole and 1-nitro-1-propene.

The method described above should be amenable to extension to the introduction of other alkyl groups, besides methyl, into the α-position of the tryptamine side chain, as well as to the preparation of such tryptamines bearing substituents in the benzene ring or on the nitrogen atoms (3).

EXPERIMENTAL

Melting points and boiling points are uncorrected. Infrared spectra were measured on a Perkin–Elmer Model 21 double-beam instrument using sodium chloride optics.

Diethyl 2-Cyanopropylmalonate (I)

To a cold solution of sodium (0.1 g) in absolute ethanol (10 ml) was added freshly distilled ethyl malonate (9.3 g). Methacrylonitrile (1.8 g) was added dropwise to the solution at such a rate that the temperature did not exceed 35°. The mixture was then stirred for 5 hours at room temperature, treated with acetic acid (0.3 g), diluted with water (15 ml), and extracted with ether (3×15 ml). The dried ($MgSO_4$) ether extract was evaporated and the residue distilled, ethyl malonate and any other low boiling products being collected below 130°. Vacuum distillation of the residual oil gave diethyl 2-cyanopropylmalonate (5.0 g, 84%) as a colorless liquid, b.p. 101–105°/0.23 mm. Calc. for $C_{10}H_{15}O_4N$: C, 58.16; H, 7.55. Found: C, 58.14; H, 7.79. Infrared spectrum (liquid film) (main bands only): 2240 (w), 1743 (s), 1728 cm^{-1} (s).

3-Ethoxycarbonyl-5-methyl-2-oxopiperidine (II)

Diethyl 2-cyanopropylmalonate (5.5 g) in absolute alcohol (100 ml) was hydrogenated over Raney nickel (0.2 g) at 80° and 1200 p.s.i. for 6 hours. The cooled solution was then filtered, evaporated on a steam bath, and the residue poured into 100 ml of light petroleum (b.p. 60–80°). The product crystallized immediately as a colorless solid (2.7 g, 60.2%). Recrystallization from light petroleum (b.p. 60–80°) containing a small amount of benzene gave colorless needles, m.p. 100–101°. Calc. for $C_9H_{15}O_3N$: C, 58.36; H, 8.16. Found: C, 58.47; H, 8.06. Infrared spectrum (Nujol mull) (main peaks only): 3196 (w), 1728 (s), 1674 (s), 1658 cm^{-1} (s).

5-Methyl-2,3-dioxopiperidine 3-Phenylhydrazone (III)

3-Ethoxycarbonyl-5-methyl-2-oxopiperidine (2.1 g) in water (25 ml) containing potassium hydroxide (0.7 g) was kept at room temperature overnight. The solution was cooled in an ice bath, stirred, and treated with a solution of benzenediazonium chloride (30 ml) (prepared from aniline (1.2 g), sodium nitrite (1.0 g), and concentrated hydrochloric acid (3 ml)). The mixture was immediately adjusted to pH 5 by the addition of cold 45% aqueous sodium acetate (25 ml). Stirring was continued at 0–10° for 4 hours, after which time the orange solid was filtered and dried, to give the phenylhydrazone

Can. J. Chem. Downloaded from www.nrcresearchpress.com by 41.223.56.140 on 09/04/12
For personal use only.

(2.0 g, 81.2%). Recrystallization from dilute alcohol gave light yellow needles, m.p. 238–239°. Calc. for $C_{12}H_{15}ON_3$: C, 66.34; H, 6.96. Found: C, 66.35; H, 7.05. Infrared spectrum (Nujol mull) (main peaks only): 3174 (m) (br), 1660 (s), 1603 (m), 1564 (s), 753 (m), 693 cm^{-1} (m).

4-Methyl-1-oxo-1,2,3,4-tetrahydro-β-carboline (IV)

The phenylhydrazone (2.2 g) was boiled under reflux with 90% formic acid (10 ml) for 1 hour, the hot solution diluted with water, and the brown oil which separated just brought into solution with hot absolute alcohol. The hot solution, on cooling, gave the oxocarboline (1.6 g, 80%) which, on recrystallization from absolute alcohol, gave white plates, m.p. 204–206°. Calc. for $C_{12}H_{12}ON_2$: C, 71.98; H, 6.04. Found: C, 71.58; H, 6.17. Infrared spectrum (Nujol mull)(main peaks only): 3195 (m) (br), 1649 (s), 1620 (m), 747 cm^{-1} (s). The picrate separated from alcohol as deep red rectangular rods, m.p. 185–187°.

3-(2-Amino-1-methylethyl)indole-2-carboxylic Acid (V)

4-Methyl-1-oxo-1,2,3,4-tetrahydro-β-carboline (0.45 g) in 50% aqueous ethanol (10 ml) containing potassium hydroxide (1.1 g) was boiled under reflux for 6 hours. The solvent was evaporated down to 5 ml, water (5 ml) was added, and the cooled solution filtered and acidified with acetic acid giving the amino acid (0.48 g, 96.8%). Recrystallization from dilute ethanol gave lustrous white plates, m.p. 242–243° (decomp.). Calc. for $C_{12}H_{14}O_2N_2$: C, 66.03; H, 6.47. Found: C, 65.65; H, 6.86. Infrared spectrum (Nujol mull) (main peaks only): 3420 (w), 2121 (w), 1642 (w) (br), 1624 (m), 1563 (m), 1544 (m) (br), 755 cm^{-1} (s).

3-(2-Amino-1-methylethyl)indole (VI)

3-(2-Amino-1-methylethyl)indole-2-carboxylic acid (0.30 g) was boiled under reflux with 10% hydrochloric acid (10 ml) for 2 hours. The cooled solution was made alkaline with dilute sodium hydroxide, extracted with ether, the ether layer dried ($MgSO_4$), and evaporated leaving the tryptamine (0.117 g, 48.8%) as a light brown oil. Neutralization of the aqueous layer with dilute hydrochloric acid resulted in the recovery of unreacted amino acid (0.133 g). The indole was converted to the picrate (from ether). Recrystallization from water gave the picrate as deep orange plates, m.p. 224–226° (decomp.). Noland and Lange (5) report m.p. 224–226° for this picrate. Calc. for $C_{11}H_{14}N_2$, $C_6H_3O_7N_3$: C, 50.62; H, 4.25. Found: C, 50.18; H, 3.90.

ACKNOWLEDGMENTS

This work was done during the tenure (by J. M. M.) of a Saskatchewan Research Council Scholarship, and with the financial assistance of the National Research Council.

REFERENCES

1. R. A. Abramovitch. Can. J. Chem. **36**, 354 (1958).
2. R. A. Abramovitch and D. Shapiro. J. Chem. Soc. 4589 (1956).
3. R. A. Abramovitch. J. Chem. Soc. 4593 (1956).
4. X. Velluz. *Quoted by* R. Robinson. Chem. and Ind. 964 (1959).
5. W. E. Noland and R. F. Lange. J. Am. Chem. Soc. **81**, 1203 (1959).

Can. J. Chem. Downloaded from www.nrcresearchpress.com by 41.223.56.140 on 09/04/12
For personal use only.

Can. J. Chem. Downloaded from www.nrcresearchpress.com by 41.223.56.140 on 09/04/12
For personal use only.

TRYPTAMINES, CARBOLINES, AND RELATED COMPOUNDS

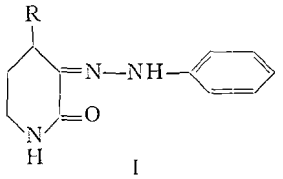
PART VI. STEREOCHEMISTRY OF THE MICHAEL ADDITION OF ETHYL MALONATE TO 1-CYCLOHEXENE CYANIDE[1,2]

R. A. ABRAMOVITCH AND J. M. MUCHOWSKI

ABSTRACT

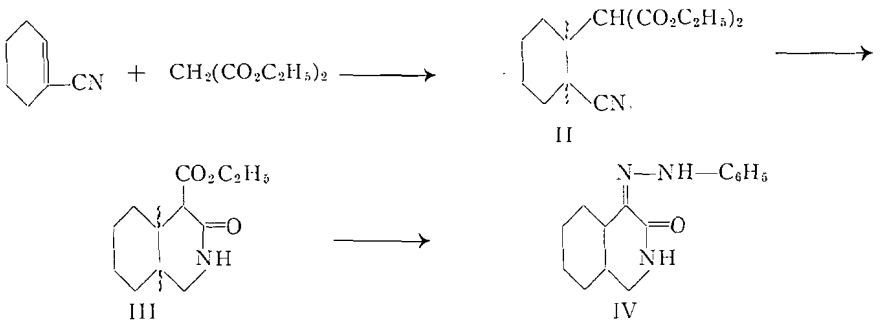
The Michael addition of diethyl malonate to 1-cyclohexene cyanide has been shown to give a mixture of the *cis*- and *trans*-diethyl 2-cyanocyclohexylmalonates in 72% and 28% yields respectively. The stereochemistry of the products was established by their unambiguous conversion to the respective *cis*- and *trans*-decahydroisoquinolines. Hydrogenation of a cyclohexane cyanide to the corresponding aminomethyl derivative takes place with retention of configuration. A number of substituted decahydroisoquinolines of known stereochemistry have been prepared. Decahydro-3,4-dioxoisoquinoline-4-phenylhydrazone underwent Fischer cyclization to a product assumed to be 2-oxo-octahydroindolo[2,3-d]isoquinoline indicating that the observation that 4-methyl-2,3-dioxopiperidine-3-phenylhydrazone did not undergo cyclization is not general for such 4-substituted piperidones.

It was shown in Part IV (1) that 4-methyl-2,3-dioxopiperidine-3-phenylhydrazone (I:R = CH_3) did not undergo Fischer cyclization to the indolenine but instead was rearranged to a geometrically isomeric phenylhydrazone. On the other hand, 5-methyl-2,3-dioxopiperidine-3-phenylhydrazone underwent smooth cyclization to the oxocarboline (2). It was, therefore, of interest to establish whether this limitation in what appears to be a widely applicable method of preparation of tryptamines was general for 2,3-dioxopiperidine-3-phenylhydrazones (I) having alkyl substituents at the 4-position. To this end it was decided to study the cyclization of decahydro-3,4-dioxoisoquinoline-4-phenylhydrazone (IV). The choice of that particular compound was of twofold interest:



I

(*i*) the generality of the limitation mentioned above could be tested, and (*ii*) little is definitely known concerning the steric route of nucleophilic additions of the Michael type to cyclohexene derivatives, and the preparation of the required phenylhydrazone would involve a study of the addition of ethyl malonate to 1-cyclohexene cyanide, as shown in the following scheme:



II

III

IV

[1]*Manuscript received December 14, 1959.*
Contribution from the Chemistry Department, University of Saskatchewan, Saskatoon, Saskatchewan.
[2]*Part V: Can. J. Chem.* **38**, *554 (1960).*

Can. J. Chem. Downloaded from www.nrcresearchpress.com by 41.223.56.140 on 09/04/12
For personal use only.

The work described in this paper involves mainly a study of the stereochemistry of the above Michael addition and eventually of the cyclization of the phenylhydrazone (IV).

Previous work in this field may be summarized briefly. Kon and Qudrat-I-Khuda (3) could only isolate *cis*-decahydro-4-carbethoxy-1,3-dioxonaphthalene from the condensation of 1-cyclohexenylmethyl ketone with ethyl malonate, whereas Ruzicka, Koolhaas, and Wind (4) and also Chuang and Tien (5) reported getting a mixture of the *cis*- and *trans*-isomers in this reaction. Boorman and Linstead (6) reported that 1-carbethoxycyclohexene yielded a triester of unspecified orientation on condensation with ethyl malonate. This ester, on hydrolysis with concentrated hydrochloric acid, yielded solely *trans*-hexahydrohomophthalic acid. Wohl and Losanitsch (7) carried out a similar reaction between ethyl malonate and 3-cyano-1,2,5,6-tetrahydropyridine and obtained a mixture of the *cis*- and *trans*-diethyl (3-cyano-4-piperidyl)malonates. Mixtures of stereoisomers were also obtained in the condensation of the sodio-derivative of 6-methoxy-1-tetralone with 1-acetylcyclopentene (8) and in the self-condensation of 1-acetylcyclohexene in the presence of sodamide (9, 10). On the other hand, Ginsburg and Pappo (11) condensed diethyl malonate with 2-phenyl-2-cyclohexenone; the orientation of the resulting malonate was not established, but after hydrolysis and decarboxylation to the acetic acid followed by Clemmensen reduction, *trans*-2-phenylcyclohexylacetic acid was obtained exclusively. As the authors rightly point out, isomerization to the more stable form may take place (particularly in the keto-malonate) so that the more stable form would be isolated after the sequence of reactions described. No conclusion can, therefore, be drawn concerning the steric mechanism of the addition reaction. The same comments would apply to the reactions studied by Bergmann and Szmuszkovicz (12). The above results do not provide conclusive evidence for the stereochemical course of addition. If, as seems likely, *trans*-addition predominates then the *cis*-isomer should be the one preferentially formed.

Addition of diethyl malonate to 1-cyanocyclohexene gave a mixture of the *cis*- and *trans*-diethyl 2-cyanocyclohexylmalonates (II). These could not be separated by fractional distillation so that a number of methods were explored to try and determine the relative proportions of the isomers. The mixture of cyano-esters was hydrolyzed to the corresponding mixture of hexahydrohomophthalic acids with boiling hydrochloric acid; it was hoped to separate these by fractional crystallization. This method of quantitative analysis of the cyano-esters was abandoned, however, when it was realized that the *cis*-acid may be converted to the more stable *trans*-form under the conditions used for the hydrolysis (13, 14). It is, therefore, not possible to assign any specific configuration to the triester obtained by Boorman and Linstead (6) which these authors hydrolyzed to *trans*-hexahydrohomophthalic acid using the above procedure.

The mixture of the stereoisomeric esters was hydrogenated to *cis*- and *trans*-decahydro-4-ethoxycarbonyl-3-oxoisoquinolines (V) which could be separated by chromatography on alumina into the two individual isomers: *cis*-68%, *trans*-32%. The configuration of each one of the isomers was established by converting it into the corresponding decahydroisoquinoline (VIII) of known geometry (15) by a series of reactions which could not effect inversion of configuration at the ring junctions. The method used is illustrated by the following equations:

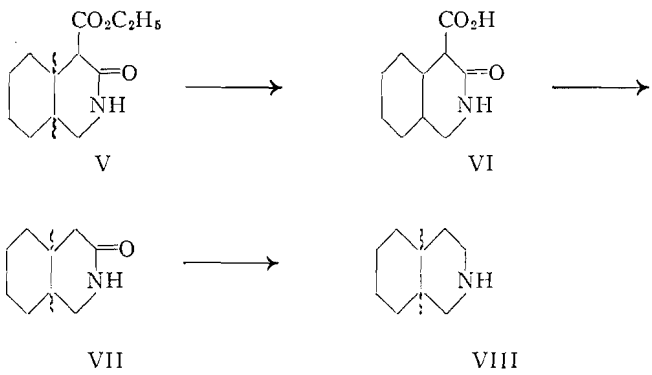


CHART I.

The pure amido-ester was saponified at room temperature to the decahydro-3-oxo-isoquinoline-4-carboxylic acid (VI) which, on being heated to its melting point, underwent decarboxylation to the decahydro-3-oxoisoquinoline (VII). This was reduced with lithium aluminum hydride to the known *cis-* or *trans*-decahydroisoquinoline thus establishing the conformation of the amido-ester. The same series of reactions was carried out on the mixture of *cis-* and *trans-* (V) before chromatography, final separation of the isomers being effected by fractional crystallization of the picrates of the secondary amines (VIII). This method gave the values *cis*-66%, *trans*-34%, which, though undoubtedly less reliable than the estimation by chromatographic separation, is in close agreement with it.

It should be emphasized at this stage that the stereospecificity of the reduction of a nitrile such as (II) to a cyclic amide via the primary amine seems to have had, up to this time, no experimental backing in the literature, and could therefore not be assumed. Unless such a reduction was stereospecific the quantitative data for the ratio of *cis*-to-*trans* amido-esters (V) could not be assumed to hold for the cyano-esters (II). It is theoretically possible that on hydrogenation the cyano-esters could pass through an intermediate such as (IX), and if one assumes, as is likely, that the larger malonate group is equatorial (16) in both cases, this intermediate will be the same for both geometrical isomers. Such being the case one would expect to get either the *same* geometrical isomer starting from the *cis-* or the *trans*-cyanide or the same mixture of geometrical isomers from each on hydrogenation of the cyano group. The absence of such an effect could be taken as evidence that an intermediate of the type IX was not involved and that reduction was indeed stereospecific.

At that stage two rather fortunate observations were made. A number of unsuccessful attempts had been made to resolve the mixture of cyano-esters by vapor phase chromatography using a variety of columns such as silicone on firebrick and polyesters on celite. It was now found that the geometrical isomers could be easily separated and estimated quantitatively using an Apiezon "M" column operated at 160°. The ratio of the two isomers was 72% to 28% as determined by this method. There was, however, no way of knowing which was which until it was observed that a sample of the mixed cyano-esters which had been standing for a few months deposited crystals of one of the isomers. These were filtered off and, after further recrystallization, shown to consist of a single isomer by vapor phase chromatography. The residual oil, on repeated distillation, gave a pure sample of the other geometrical isomer. Each one of these isomers was now catalytically

Can. J. Chem. Downloaded from www.nrcresearchpress.com by 41.223.56.140 on 09/04/12
For personal use only.

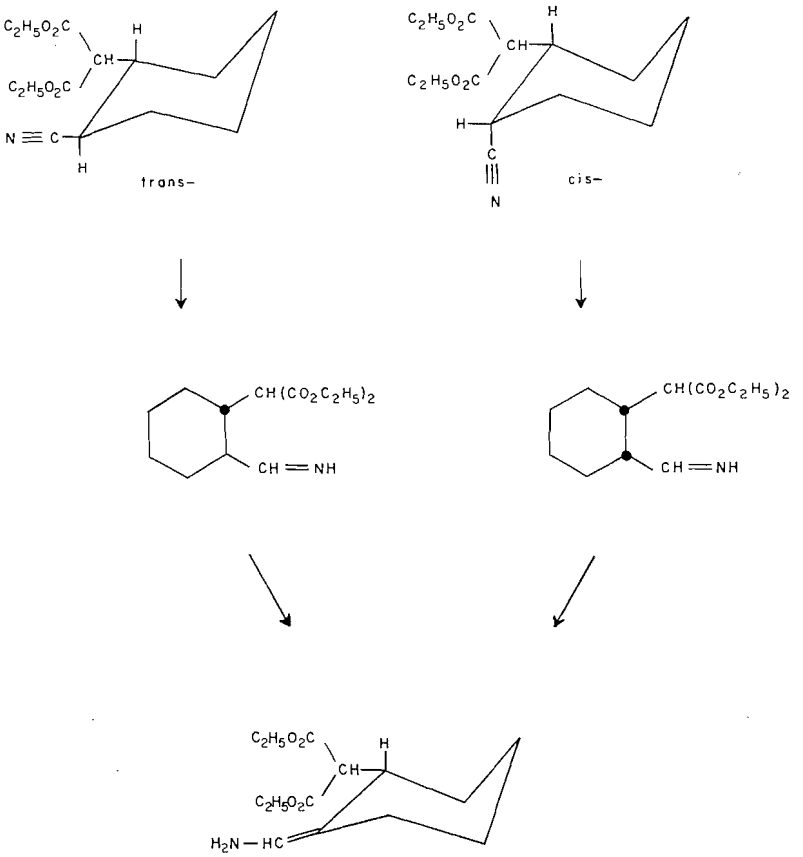


CHART II.

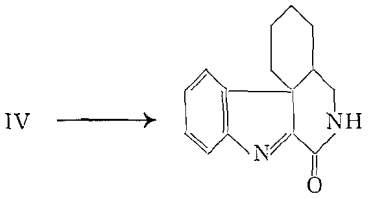
reduced individually and each one gave a single geometrical isomer of the corresponding amido-esters: the *trans*-form from the crystalline cyano-ester, and the *cis*-form from the liquid one. From the considerations outlined above it may be concluded that the catalytic reduction of the nitriles did not involve a change in the configuration so that the ratio of isomers obtained from the Michael addition is *cis*-72%, *trans*-28%. These figures are in close agreement with those obtained from the chromatography of the amido-esters on alumina, and it is felt that the difference between them falls within the experimental error expected for this type of estimation.

The results indicate that, as anticipated, the addition of diethyl malonate to 1-cyanocyclohexene gives predominently the *cis*-isomer, but that the *trans*-isomer is also formed in appreciable quantity. It should be emphasized that these results give the postequilibrium ratio of isomers. Work is at present under way to determine whether they apply also to pre-equilibrium conditions. If so, the mechanistic conclusion could be drawn that the Michael reaction proceeded, in this case, predominently by *trans*-addition. The equilibration of each of the cyano-esters is also being examined. The hydrogenation results indicate, however, that probably no equilibration of the cyano-esters takes place under vigorous treatment in the presence of base (the secondary amine is formed as a

Can. J. Chem. Downloaded from www.nrcresearchpress.com by 41.223.56.140 on 09/04/12
For personal use only.

by-product) so that predominent *trans*-addition might be tentatively assumed. As a by-product of the reactions a number of substituted decahydroisoquinolines (V, VI, VII) of known geometry have been obtained.

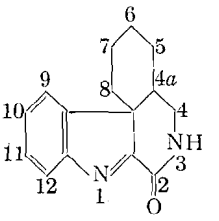
The mixture of amido-esters (V) was saponified and treated with benzenediazonium chloride to give a low yield of a single decahydro-3,4-dioxoisoquinoline-4-phenylhydrazone (IV). Since equilibration is possible at this stage one would expect the more stable of the two isomers, probably the *trans*-, to be formed. The geometry of the product was not determined though it is proposed to do so later. A red, tarry substance, assumed to be the phenylazo-derivative on the basis of its infrared spectrum, was also isolated but was not investigated further at this stage. When the phenylhydrazone was boiled with 90% formic acid a base was obtained which is tentatively assigned the structure 2-oxo-2,3,4,4*a*, 5,6,7,8-octahydroindolo[2,3-d]isoquinoline (X).* The evidence in support of this assign-



X

ment is based on the ultraviolet (see Fig. 1) and infrared spectra and on microanalytical data. The latter were not too good since, though the expected values were obtained in one instance, a somewhat lower value for carbon was obtained on a repeat analysis of a different sample. The nitrogen analysis also gave low values but indicated quite definitely that one nitrogen atom had been lost during the cyclization. There was not sufficient material on hand to repeat the purification of this compound, but this will be done as soon as possible. An interesting feature of the infrared spectrum of the cyclized product was the presence of *two* peaks in the 800–680 cm^{-1} region (765 and 685 cm^{-1}). This is unexpected, and might be due to some contamination which could perhaps be giving rise to the 685 cm^{-1} band, though the intensity of the latter seems to render this rather doubtful. The compound also exhibits two melting points, melting at 150°, resolidifying above that temperature, and melting again at 186–187°. After heating above 150°, the solid product only exhibited a *single* infrared peak in the aromatic C—H out-of-plane deformation region, at 758 cm^{-1}. Attempted hydrolysis of the amide (X) to an amino acid with ethanolic alkali gave rise instead to an isomeric product, m.p. 240–242°. The analysis of this substance agrees with the formula $C_{15}H_{16}ON_2$ but its infrared spectrum and particularly its ultraviolet absorption spectrum differ from those of X. The structure of this compound is presently under investigation.

**Proposed numbering for this ring system:*



Can. J. Chem. Downloaded from www.nrcresearchpress.com by 41.223.56.140 on 09/04/12
For personal use only.

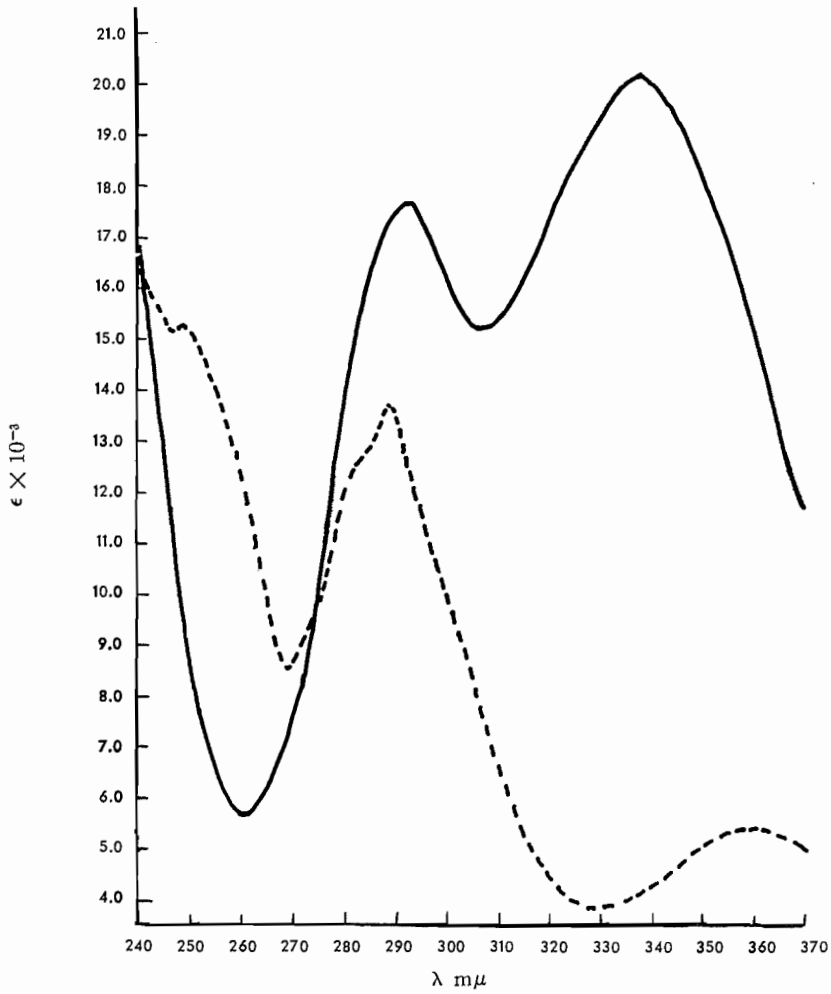


FIG. 1. —— Decahydro-3,4-dioxoisoquinoline-4-phenylhydrazone.
– – – 2-Oxo-2,3,4,4*a*,5,6,7,8-octahydroindolo[2,3-b]isoquinoline.

The results of the acid treatment of the phenylhydrazone (IV) indicate at least that the limitation reported (1) in the attempted cyclization of (I: R = CH_3) is not a general one for 4-substituted 2,3-dioxopiperidine-3-phenylhydrazones, since cyclization of some sort has occurred in the present case. Clearly, further work is necessary to clarify the identity of the cyclized product and of the isomeric amide it gives on prolonged alkali treatment. This will be reported on at a later date.

EXPERIMENTAL

Melting points and boiling points are uncorrected. Infrared spectra were measured with a Perkin–Elmer Model 21 spectrometer using sodium chloride optics. Ultraviolet absorption spectra were recorded on a Beckman DK2 spectrophotomer.

Diethyl 2-cyanocyclohexylmalonate

To a stirred solution of sodium ethoxide (from 16.9 g of sodium in 300 ml of absolute alcohol) was added freshly distilled diethyl malonate (170.5 g). To this solution was

Can. J. Chem. Downloaded from www.nrcresearchpress.com by 41.223.56.140 on 09/04/12
For personal use only.

Can. J. Chem. Downloaded from www.nrcresearchpress.com by 41.223.56.140 on 09/04/12
For personal use only.

added 1-cyclohexene cyanide (29.8 g), prepared by the procedure of McElvain and Starn (17) and the solution boiled under reflux for 24 hours when the initially colorless solution turned yellow. The solution was cooled, treated with glacial acetic acid (46.0 g), extracted with water (3×100 ml), and the aqueous solution extracted with ether (3×50 ml). The ether extract and the organic layer were combined, dried ($MgSO_4$), and the solvent removed. The residue was distilled up to 130° (bath temp.)/15 mm to remove excess diethyl malonate and any other low-boiling material and the residue distilled *in vacuo*, the fraction boiling at 125–135°/0.34 mm (53.0 g, 71% yield) being collected as the mixture of geometrically isomeric cyano-esters. This on redistillation had b.p. 119–125°/0.28 mm. Calc. for $C_{14}H_{21}O_4N$: C, 62.90; H, 7.92. Found: C, 62.35; H, 7.61.

Separation and Quantitative Analysis of the cis- and trans-Diethyl 2-Cyanocyclohexylmalonates by Vapor Phase Chromatography

A Beckman vapor phase chromatograph (Model GC-2) was used with a 4-ft Apiezon "M" on firebrick column operated at 160° and a helium inlet pressure of 20 p.s.i. The mixture (0.005 ml) was chromatographed and the areas under the curves for each isomer measured. The pure *trans*-isomer (0.005 ml) was then chromatographed and the area under the curve also measured.

% *trans*-diethyl 2-cyanocyclohexylmalonate: 27.6,

% *cis*-diethyl 2-cyanocyclohexylmalonate: 72.4 (by difference).

trans-Diethyl 2-Cyanocyclohexylmalonate

After standing for some months, *trans*-diethyl 2-cyanocyclohexylmalonate crystallized from the mixture as colorless needles. It was filtered and recrystallized from light petroleum (b.p. 60–80°) to give large, colorless, rectangular rods, m.p. 50–52°. Calc. for $C_{14}H_{21}O_4N$: C, 62.90: H, 7.92. Found: C, 63.26; H, 7.86. Infrared spectrum (liquid film) (main peaks only): 2242 (w), 1747 (s), 1732 cm^{-1} (s).

cis-Diethyl 2-Cyanocyclohexylmalonate

After removal of the *trans*-isomer by filtration from the above mixture the filtrate consisted almost entirely of *cis*-diethyl 2-cyanocyclohexylmalonate (as shown by vapor phase chromatography). Distillation under reduced pressure gave the pure *cis*-isomer, entirely free of the *trans*-form as far as could be detected by vapor phase chromatography, as a colorless mobile liquid, b.p. 118–120°/0.28 mm. Found: C, 62.56; H, 7.83. Infrared spectrum (liquid film) (main peaks only): 2242 (w), 1746(s), 1731 cm^{-1} (s).

cis- and trans-Hexahydrohomophthalic acid

The mixed diethyl 2-cyanocyclohexylmalonates (1.0 g) were boiled under reflux with 10% hydrochloric acid (30 ml) for 4 hours. The solvent was evaporated giving a brown oil (0.65 g, 93.2%) which solidified on cooling. Recrystallization of the product from water gave white rosettes of the mixture of the two isomeric acids, m.p. 90–130°. Infrared spectrum (Nujol mull) (main peaks only): 2645 (m)(br), 1705 (s), 1689 cm^{-1} (s). Windaus, Hückel, and Reverey (13) report m.p. 146° for *cis*- and m.p. 157° for *trans*-hexahydrohomophthalic acid respectively.

cis- and trans-Decahydro-4-ethoxycarbonyl-3-oxoisoquinoline

The mixture of stereoisomeric diethyl 2-cyanocyclohexylmalonates (5.5 g) in commercial absolute alcohol (50 ml) was hydrogenated over Raney nickel (0.2 g) at 110–120° and 1200 p.s.i. for 9 hours. The solution was filtered, the ethanol removed on a steam bath, and the residue distilled under reduced pressure to give the mixture of amido-esters as a very viscous liquid (3.1 g, 66.8%), b.p. 160–185°/0.4 mm. Calc. for $C_{12}H_{14}O_3N$: C, 63.97;

H, 8.50. Found: C, 63.74; H, 8.55. The mixture of esters (1.269 g) was chromatographed on a column of neutral alumina (3/4 in.×12 in.). Elution with ether–ethanol (200 ml) (20:1 v/v) gave the *trans*-isomer (0.406 g, 32.5%) identical with the product obtained as described below. Elution with hot alcohol (500 ml) gave the *cis*-isomer (0.843 g, 67.5%) identical with the product described below.

trans-Decahydro-4-ethoxycarbonyl-3-oxoisoquinoline

trans-Diethyl 2-cyanocyclohexylmalonate (3.0 g) was hydrogenated as described for the mixture of cyanides to give the pure *trans*-β-amido-ester (1.6 g, 63.3%) as a colorless, viscous liquid, b.p. 160–170°/0.04 mm, which slowly solidified. Crystallization from light petroleum (b.p. 60–80°) gave colorless needles, m.p. 114–115°. Calc. for $C_{12}H_{14}O_3N$: C, 63.97; H, 8.50. Found: C, 64.58; H, 7.95. Infrared spectrum (Nujol mull) (main peaks only): 3208 (w)(br), 1729 (s), 1673 cm^{-1} (s).

cis-Decahydro-4-ethoxycarbonyl-3-oxoisoquinoline

cis-Diethyl 2-cyanocyclohexylmalonate (4.8 g) treated in a manner analogous to the *trans*-compound yielded the *cis*-amido-ester (2.4 g, 59.4%) as a colorless viscous liquid, b.p. 136–140°/0.022 mm. Found: C, 64.25; H, 8.51. Infrared spectrum (liquid film) (main peaks only): 3187 (m)(br), 1724 (s), 1656 cm^{-1} (s).

trans-Decahydro-3-oxoisoquinoline-4-carboxylic Acid

trans-Decahydro-4-ethoxycarbonyl-3-oxoisoquinoline (0.62 g) in water (10 ml) containing potassium hydroxide (0.3 g) was shaken mechanically at room temperature for 12 hours, the solution filtered, acidified with concentrated hydrochloric acid, and set aside. After 2 hours the β-amido-acid had separated out (0.54 g, 100%) as short, colorless needles which on recrystallization from water had m.p. 113–115° (decomp.). Calc. for $C_{10}H_{15}O_3N$: C, 60.89; H, 7.67. Found: C, 60.37; H, 7.31. Infrared spectrum (Nujol mull) (main peaks only): 3297 (w)(sh), 3194 (m), 2590 (m)(br), 1735 (s), 1645 cm^{-1} (s).

trans-Decahydro-3-oxoisoquinoline

trans-Decahydro-3-oxoisoquinoline-4-carboxylic acid (0.180 g) was heated in an oil bath at 110–120° until effervescence ceased. The viscous oil remaining was sublimed at 110–120°/20 mm giving the colorless amide (0.060 g, 42.8%) which was recrystallized from light petroleum (b.p. 60–80°) containing a small amount of benzene and had m.p. 165–167°. Calc. for $C_9H_{15}ON$: C, 70.55; H, 9.87. Found: C, 70.61; H, 9.75. Infrared spectrum (Nujol mull) (main peaks only): 3216 (m), 3042 (m)(sh), 1654 cm^{-1} (s).

trans-Decahydroisoquinoline

trans-Decahydro-3-oxoisoquinoline (0.200 g) in dry dioxan (5 ml) was added to a suspension of lithium aluminum hydride (0.200 g) in dry ether (25 ml) at such a rate as to keep the ether boiling. When the addition was complete the mixture was boiled under reflux in an atmosphere of nitrogen for 5 hours. The suspension was cooled, the excess metal hydride decomposed by the careful addition of water, and the product extracted with ether (3×25 ml) and dried ($MgSO_4$). The solvent was evaporated, eventually under vacuum, to give the base (0.130 g, 71.4%) as a colorless oil. The amine was converted to its picrate (from ethanol); this, on recrystallization from methanol, gave *trans*-decahydroisoquinoline picrate, m.p. 172–174°. Gray and Heitmeier (18) report m.p. 173–174° for this picrate.

cis-Decahydro-3-oxoisoquinoline

cis-Decahydro-4-ethoxycarbonyl-3-oxoisoquinoline (2.83 g) in water (25 ml) containing potassium hydroxide (1.0 g) was mechanically shaken at room temperature for 12 hours.

Can. J. Chem. Downloaded from www.nrcresearchpress.com by 41.223.56.140 on 09/04/12
For personal use only.

The solution was filtered, acidified with concentrated hydrochloric acid, and kept in the refrigerator. After 24 hours a few crystals of the acid had separated as fine colorless needles. No attempt was made to purify this acid. The acidic solution was evaporated to dryness, the solid residue extracted with absolute alcohol (3×10 ml), the alcohol solution filtered and evaporated, and the residue heated in an oil bath at 100–110°. When effervescence had ceased the viscous oil obtained was sublimed at 100–110°/20 mm to give the *cis*-amide (1.05 g, 59.4%); this, on recrystallization from light petroleum (b.p. 60–80°), gave colorless flakes, m.p. 149–151°. Calc. for $C_9H_{15}ON$: C, 70.55; H, 9.87. Found: C, 70.60; H, 9.85. Infrared spectrum (Nujol mull) (main peaks only): 3214 (w), 3044 (w)(sh), 1654 cm^{-1} (s).

cis-Decahydroisoquinoline

The above amide (0.30 g) was treated with lithium aluminum hydride as described for the *trans*-amide to give the *cis*-base (0.20 g, 73.3%). The picrate, on recrystallization from methanol, gave pale yellow plates, m.p. 150–152°. Witkop (15) reported m.p. 150° for *cis*-decahydroisoquinoline picrate.

cis- and trans-Decahydro-3-oxoisoquinoline

The mixed decahydro-4-ethoxycarbonyl-3-oxoisoquinolines (0.219 g) were hydrolyzed and decarboxylated as described in the preparation of pure *cis*-decahydro-3-oxoisoquinoline. The mixture of amides (0.105 g, 70.5%), after sublimation at 100–110°/20 mm, had m.p. 65–95°.

cis- and trans-Decahydroisoquinoline

The mixture of *cis*- and *trans*-decahydro-3-oxoisoquinolines (0.585 g) in dry dioxan (10 ml) was reduced with lithium aluminum hydride (0.750 g) in dry ether (50 ml) as described for the preparation of *trans*-decahydroisoquinoline to give the mixture of bases (0.449 g, 84.5%) as a colorless oil. The picrates were prepared and fractionally crystallized as follows: The dried picrates (0.400 g) were washed five times with 1-ml portions of cold methanol. This removed mainly the *trans*-decahydroisoquinoline picrate. Recrystallization of the residue from methanol gave the *cis*-picrate (0.260 g, 66.2%), m.p. 150–152°. The combined cooled methanol extracts were slowly evaporated to give the *trans*-picrate as large, yellow, rectangular prisms which could easily be separated mechanically from some *cis*-picrate. After two recrystallizations from methanol the *trans*-picrate (0.133 g, 33.8%) had m.p. 172–174°.

Decahydro-3,4-dioxoisoquinoline-4-phenylhydrazone

Decahydro-4-ethoxycarbonyl-3-oxoisoquinoline (10.1 g, *cis* and *trans*) in water (50 ml) containing potassium hydroxide (2.6 g) was shaken mechanically at room temperature for 12 hours. The solution was cooled to 0° and adjusted to pH 5 with glacial acetic acid. To the stirred solution was added a solution of benzenediazonium chloride (70 ml) (prepared from 4.3 g of aniline, 3.4 g of sodium nitrite, and concentrated hydrochloric acid (7.0 ml)). The mixture was immediately adjusted to pH 5 by the addition of cold, 45% aqueous sodium acetate. Stirring was continued at 0–10° for 10 hours after which the suspension was kept in a refrigerator for 12 hours. The yellow brown solid (6.5 g) was filtered, dried, and extracted with benzene leaving behind the phenylhydrazone as a pale yellow solid (2.6 g, 22.6%). Recrystallization from dilute ethanol gave pale yellow needles, m.p. 214.5–215.5°. Calc. for $C_{15}H_{19}ON_3$: C, 70.00; H, 7.44. Found: C, 69.69; H, 7.68. Infrared spectrum (Nujol mull) (main peaks only): 3163 (w)(br), 1660 (s), 1602 (m), 1564 (m), 750 (m), 694 cm^{-1} (m). Ultraviolet absorption spectrum (in absolute ethanol), λ_{max}293, 338 mμ. $\epsilon \times 10^{-3}$ 17.67, 20.16.

Can. J. Chem. Downloaded from www.nrcresearchpress.com by 41.223.56.140 on 09/04/12
For personal use only.

Evaporation of the benzene washings above gave a red, tarry substance, assumed to be the phenylazo-derivative, which was not investigated further at this stage. Infrared spectrum (liquid film) (main peaks only): 3140 (s)(br), 1714 (m)(sh), 1639 (s), 1604 (s), 1547 (s), 752 (s), 692 cm^{-1} (s).

*2-Oxo-2,3,4,4a,5,6,7,8-octahydroindolo[2,3-*d*]isoquinoline*

The phenylhydrazone (0.993 g) was boiled under reflux with 90% formic acid (8 ml) for 1/2 hour, the solution cooled and filtered. The filtrate was made slightly alkaline (pH 8) with dilute sodium hydroxide, and the solid which separated (0.424 g, 45.7%) filtered and recrystallized from benzene, to give colorless needles, melting completely and sharply at 150°, resolidifying above that temperature, and melting again at 186–187°. Calc. for $C_{15}H_{16}ON_2$: C, 74.70; H, 6.72. Found: C, 74.97; H, 6.72. Infrared spectrum (Nujol mull) (main peaks only): 3192 (w)(br), 1672 (s), 1640 (m)(sh), 1599 (m), 765 (s), 685 cm^{-1} (m). Ultraviolet absorption spectrum (in absolute ethanol): λ_{max} 248 (infl.), 289, 360 mμ. $\epsilon \times 10^{-3}$ 15.27, 13.69, 5.4. After being heated to 150° and cooled again the compound exhibited the following peaks in the infrared: 3330 (w)(br), 1680 (s), 1602 (m), 758 cm^{-1} (m).

*Alkali Isomerization of 2-Oxo-2,3,4,4a,5,6,7,8-octahydroindolo[2,3-*d*]isoquinoline*

The indolenine (0.070 g) in 50% aqueous ethanol (5 ml) containing potassium hydroxide (0.5 g) was boiled under reflux for 6½ hours. The hot solution was filtered and gave, on cooling, a white crystalline solid (0.035 g). Acidification of the mother liquors with acetic acid did not give any of the expected amino acid. The solid obtained above was recrystallized from benzene to give colorless needles, m.p. 240–242° (decomp.). Calc. for $C_{15}H_{16}ON_2$: C, 74.97; H, 6.72. Found: C, 74.61; H, 7.21. Infrared spectrum (Nujol mull) (main peaks only): 3365 (m), 3182 (w)(br), 1667 (s), 1608 (m), 740 cm^{-1} (s). Ultraviolet absorption spectrum (in absolute ethanol): λ_{max} 235, 236 (infl.), 243, 248, 254, 260 mμ. $\epsilon \times 10^{-3}$ 13.66, 13.45, 12.79, 11.97, 11.20, 9.47.

ACKNOWLEDGMENTS

The authors are indebted to Dr. L. Vining for the use of a recording ultraviolet spectrophotometer. This work was carried out during the tenure (by J. M. M.) of a Saskatchewan Research Council Scholarship and with the financial support of the National Research Council.

REFERENCES

1. R. A. Abramovitch. Can. J. Chem. **36**, 354 (1958).
2. R. A. Abramovitch and J. M. Muchowski. Can. J. Chem. This issue.
3. G. A. R. Kon and M. Qudrat-i-Khuda. J. Chem. Soc. 3071 (1926).
4. L. Ruzicka, D. R. Koolhaas, and A. H. Wind. Helv. Chim. Acta, **14**, 1151 (1931).
5. Ch. K. Chuang and Y. L. Tien. Ber. **69**, 25 (1936).
6. E. J. Boorman and R. P. Linstead. J. Chem. Soc. 258 (1935).
7. A. Wohl and M. S. Losanitsch. Ber. **40**, 4698 (1907).
8. D. A. Peak and R. Robinson. J. Chem. Soc. 1581 (1937).
9. W. S. Rapson and R. Robinson. J. Chem. Soc. 1285 (1935).
10. E. R. H. Jones and H. P. Koch. J. Chem. Soc. 393 (1942).
11. D. Ginsburg and R. Pappo. J. Chem. Soc. 938 (1951).
12. E. D. Bergmann and J. Szmuszkovicz. J. Am. Chem. Soc. **75**, 3226 (1953).
13. A. Windaus, W. Hückel, and G. Reverey. Ber. **56**, 91 (1923).
14. S. S G. Sircar. J. Chem. Soc. 1252 (1927).
15. B. Witkop. J. Am. Chem. Soc. **70**, 2617 (1948).
16. E. J. Corey. J. Am. Chem. Soc. **77**, 1044 (1955).
17. S. M. McElvain and R. E. Starn, Jr. J. Am. Chem. Soc. **77**, 4571 (1955).
18. A. P. Gray and D. E. Heitmeier. J. Am. Chem. Soc. **80**, 6274 (1958).

Can. J. Chem, Downloaded from www.nrcresearchpress.com by 41.223.56.140 on 09/04/12
For personal use only.

Can. J. Chem. Downloaded from www.nrcresearchpress.com by 41.223.56.140 on 09/04/12
For personal use only.

THE KINETICS OF THE FORMATION OF THE MONO-FLUORO COMPLEX OF IRON (III) IN AQUEOUS SOLUTION[1]

D. POULI[2] AND W. MACF. SMITH[3]

ABSTRACT

The kinetics of the reactions involved in the formation of the mono-fluoro complex of iron (III) in aqueous solutions have been examined spectrophotometrically at ionic strength 0.5 and over the temperature interval 0.1 to 12.1° C. The results are interpretable on the assumption that the following two reactions contribute significantly to the rate $Fe^{+++} + F^- = FeF^{++}$ and $Fe^{+++} + HF = FeF^{++} + H^+$, the former having a heat of activation of 22.8 ± 2.5 kcal mole^{-1} and an entropy of activation of 35 ± 9 cal deg^{-1} mole^{-1}, the latter having a heat of activation of 8.7 ± 0.7 kcal mole^{-1} and an entropy of activation of -24.5 ± 3 cal deg^{-1} mole^{-1}.

INTRODUCTION

Reactions involving association of cations and anions may be considered displacement reactions in which the ligand displaced from the cation is a solvent molecule, e.g. $M(H_2O)_n^+ + X^- \rightarrow M(H_2O)_{n-1}X + H_2O$. Kinetic aspects of such reactions will reflect the nature of the path by which reaction occurs. The transition state associated with the prevailing path may involve loss of solvent molecules from the inner solvation spheres of the interacting ions (1) as well as reorganization of more distant solvent. It is also possible that protolytic changes in the co-ordinated solvent may be involved in some of the alternative mechanisms by which the net reactions may occur (2, 3, 4).

Although these so-called association reactions are among the simplest of those occurring in solution, experimental data relating to their kinetics are restricted. Eigen (5) is contributing valuable data about very fast reactions through his technique of relaxation spectrometry. The slow associations of chromic and thiocyanate have been studied by Postmus and King (2), of chromic and oxalate by Hamm and Davis (3). Below, Connick, and Coppel have recently published work on the ferric-thiocyanate association (4). Smith found that ferric and fluoride associates at a rate measurable with stop watch timing (6).

This paper deals with an extension of Smith's work to a wider range of acidities (and of necessity to a higher ionic strength) and to a range of temperatures. A spectrophotometric rather than the redox method used in the preliminary work has been used to follow the reaction, but the conditions studied have been restricted to those yielding rates measurable with stop watch timing.

EXPERIMENTAL

The course of the reaction was followed spectrophotometrically at 260 mμ using Beckman quartz cells of 1 cm path length as reaction vessels. At this wavelength there is a substantial increase in transmission accompanying the association reaction, ranging from about 25 to 300% under the range of conditions studied. The segment of a Beckman DU spectrophotometer normally housing the cell holder was replaced by an extended segment which housed a specially constructed holder for two quartz cells. This holder was machined from a brass block so that it had channels to carry thermostating water and demisting tubes which directed thermostated dry gas against the windows of the cells.

[1]*Manuscript received November 10, 1959.*
Contribution from the Department of Chemistry, Queen's University, Kingston, Ontario.
[2]*Holder of an Ontario Research Council Scholarship, 1958–59.*
[3]*Present address: The University Chemical Laboratory, Cambridge, England.*

Can. J. Chem. Downloaded from www.nrcresearchpress.com by 41.223.56.140 on 09/04/12
For personal use only.

During a kinetic run 2 ml of a solution containing ferric perchlorate, perchloric acid, and sodium perchlorate, previously brought close to reaction temperature in a thermostat bath, was pipetted into the reaction cell and also into a reference cell in the cell holder. The solution containing fluoride was added to the solution in the reaction vessel from a fine polythene tube connected to a 5-ml glass syringe. Prior to addition, the small volume (about 0.03 ml) of solution containing hydrogen fluoride, sodium perchlorate, and perchloric acid was in a length of the polythene tubing within the quartz cell. Pushing the plunger of the syringe introduced the solution of fluoride followed by a stream of gas which ensured mixing. The volume of solution introduced was reproducible to $\pm 2\%$. A small length of gas in the tubing between the fluoride solution and the exit of the tubing prevented loss of fluoride to the ferric solution prior to the pressing of the syringe.

Adequacy of mixing involved in this procedure was examined by adding acidified ferric perchlorate solution to dilute perchloric acid in the reaction vessel, using the same volumes as those involved during addition of fluoride, and noting the time required for attainment of a steady value for the transmission. It was found that a steady reading was attained within the time required to deliver the gas from a regular 5- or 10-ml syringe which was about three seconds. It should be noted that the values of the rate constant determined as indicated below are not dependent on knowledge of the exact time of mixing or the exact amount of reaction occurring during the mixing period and that some variability in the amount of reaction during the mixing procedure would not introduce an error in the rate constant. Trial kinetic runs carried out using various slit widths and wavelength settings of 240 mμ and 250 mμ as well as 260 mμ indicated no significant dependence between apparent reaction rate and slit width or wave length. The removal of fluoride by reaction with the wall of the reaction vessel was examined by gently agitating the equilibrium mixture containing ferric and fluoride for about thirty minutes (a period much in excess of that of a kinetic run) and noting the dependence of transmission on time. Four quartz vessels were examined and one only yielded a change of transmission with time. This vessel also gave irreproducible kinetic results. It was not used in further kinetic measurements and the data obtained during its use are not included in the results given below.

Initial and final transmittance readings were made on both reaction and reference cells but no attempt was made to correct the transmittance readings obtained with the reaction cell during the main course of the association which occupied periods ranging from about 150 down to 60 seconds after addition of fluoride.

All solutions were prepared from triply distilled water, the second distillation being from alkaline permanganate solution. Sodium perchlorate (anhydrous), perchlorate acid (70%), and ferric perchlorate were reagent grade chemicals obtained from G. Frederick Smith Chemical Company. The 50% hydrofluoric acid was Fisher reagent. The stock solutions of hydrofluoric acid were stored and manipulated in polythene ware and the concentrations of the diluted solutions which served as stocks were estimated by adding slight excess of sodium hydroxide and back titrating with hydrochloric acid using phenolphthalein as indicator. The stock solutions of sodium perchlorate were prepared from sodium perchlorate which had been heated for about two hours at 140° C prior to weighing. The stock solution of ferric perchlorate was prepared by dissolving the reagent in approximately 1 molar perchloric acid. Iron content of this solution was determined by redox titration (7) and gravimetry (8). Total acid plus iron (precipitated as $Fe(OH)_3$) was determined by titration with sodium hydroxide to phenolphthalein end point.

Can. J. Chem. Downloaded from www.nrcresearchpress.com by 41.223.56.140 on 09/04/12
For personal use only.

TREATMENT OF THE DATA

The data involving transmission were interpreted using the relation

$$[1] \qquad \frac{x}{c_e} = \frac{\log T_t - \log T_0}{\log T_\infty - \log T_0}$$

where x is the concentration of FeF^{++} at time t, c_e is that at equilibrium, and T_0, T_t, and T_∞ represent transmittance readings before association, at time t, and at equilibrium. In the lower range of acidities used in this work hydrolysis of ferric ion is appreciable and $FeOH^{++}$ as well as Fe^{+++} and FeF^{++} will contribute to the effective extinction coefficient. However, as the hydrogen ion concentration remained substantially constant during a single run, so will the ratio $[Fe^{+++}]/[FeOH^{++}]$ and consequently a single effective extinction coefficient may be associated with all Fe (III) in the forms Fe^{+++} and $FeOH^{++}$ at a given acidity and temperature, and the change in optical density will be proportional to concentration of FeF^{++} as long as the production of FeF_2^+ is negligible.

To estimate the value of x from the primary experimental data it was necessary to know the value of c_e for a given set of conditions. This may be calculated using the relationship

$$[2] \qquad \frac{c_e}{rs(m-c_e)(n-c_e)} = K_e$$

where $m = [Fe^{+++}]+[FeOH^{++}]+[FeF^{++}]$ = total iron (III) concentration,

$n = [F^-]+[HF]+[FeF^{++}]$ = total fluoride concentration,

$$r = \frac{[Fe^{+++}]}{[Fe^{+++}]+[FeOH^{++}]} = \frac{[H^+]}{K_h+[H^+]},$$

$$s = \frac{[F^-]}{[F^-]+[HF]} = \frac{K_a}{K_a+[H^+]}.$$

K_e is the association quotient for the reaction $Fe^{+++} + F^- \rightleftharpoons FeF^{++}$, e.g., K_e is the equilibrium value of $[FeF^{++}]/[Fe^{+++}][F^-]$ where [ ] signifies concentration in moles/per liter,

K_h is the hydrolysis quotient for the reaction $Fe^{+++} + H_2O \rightleftharpoons FeOH^{++} + H^+$;

K_a is the ionization quotient for the reaction $HF \rightleftharpoons H^+ + F^-$.

Our measurements were made at ionic strength 0.50 with sodium perchlorate the main contributor and consequently the equilibrium quotient for any one of these three reactions should have a unique value at one temperature.

The values of the various equilibrium quotients used in reducing our data are given in Table I. They were obtained by extrapolation of log K–$(1/T)$ plots of the values for

TABLE I

Equilibrium quotients used in reduction of kinetic data

Temperature (° C)	Ionic strength	$K_a \times 10^3$ (mole liter^{-1})	$K_h \times 10^4$	$K_e \times 10^{-5}$ (mole^{-1} liter)
0.11	0.50	1.96	5.02	1.07
7.16	0.50	1.67	7.47	1.19
12.10	0.50	1.52	10.1	1.28

K_a, K_e, and K_h for ionic strength 0.5 and temperatures 15°, 25°, and 35° C given by Connick and co-workers (9).

Substitution of the value of c_e appropriate to a given set of conditions along with values of transmittance readings obtained during a kinetic run in equation 1 allowed values of x at various times during approach to equilibrium to be estimated. These were interpreted to yield rate constants by the method described below.

It was initially assumed that the sole reaction involved in the formation of FeF^{++} was a second-order association opposed by a first-order dissociation as summarized by

$$Fe^{+++} + F^- \underset{k_{-I}}{\overset{k_I}{\rightleftharpoons}} FeF^{++}. \qquad (I)$$

To interpret the data obtained over a range of acid concentrations, it was necessary to assume that the second-order reactions

$$Fe + {}^{+++}HF \underset{k_{-II}}{\overset{k_{II}}{\rightleftharpoons}} FeF^{++} + H^+ \qquad (II)$$

are also contributing substantially at higher acidities. Since [HF] is proportional to $[H^+][F^-]$, kinetic data will not distinguish between II and a hydrogen ion catalyzed association.

If I is the sole set of reactions involved, then

$$[3] \qquad \frac{d}{dt}[FeF^{++}] = k_I[Fe^{+++}][F^-] - \frac{k_I}{K_e}[FeF^{++}]$$

or

$$\frac{dx}{dt} = k_I\left\{rs(m-x)(n-x) - \frac{1}{K_e}x\right\}$$

if the rates of ionization of hydrogen fluoride and of hydrolysis of ferric ion are relatively fast.

If reactions II are also involved,

$$\frac{d[FeF^{++}]}{dt} = k_I[Fe^{+++}][F^-] + k_{II}[Fe^{+++}][HF] - \frac{k_I}{K_e}[FeF^{++}] - \frac{k_{II}}{K_eK_a}[FeF^{++}][H^+].$$

This may be rewritten as

$$[4] \qquad \frac{dx}{dt} = \left(k_I + \frac{1-s}{s}k_{II}\right)\left\{rs(m-x)(n-x) - \frac{1}{K_e}x\right\}$$
$$= k'\left\{rs(m-x)(n-x) - \frac{1}{K_e}x\right\}.$$

The solution of [3] is

$$[5] \qquad \frac{1}{rs}\frac{1}{\sqrt{q}}\log\frac{2ax+b-\sqrt{q}}{2ax+b+\sqrt{q}} = k_It + \text{constant}$$

where

$$a = 1,$$
$$b = -m-n-\frac{1}{K_ers},$$
$$c = mn,$$
$$q = b^2-4ac.$$

The solution of [4] is the same except that k_I of [5] is replaced by k' where $k' = k_I + \{(1/s)-1\}k_{II}$.

Can. J. Chem. Downloaded from www.nrcresearchpress.com by 41.223.56.140 on 09/04/12
For personal use only.

If the above-mentioned assumptions are correct a plot of the values of the expression on the left of equation 5 against time should lie in a straight line. If reactions I are the sole contributors, the slope will be independent of $[H^+]$ and equal to k_I. If reactions II are also contributing then the slope will be dependent on $[H^+]$ and equal to k' $(= k_I + \{(1/s)-1\}\, k_{II})$. In the latter event a plot of k' against $1/s-1$ should yield a straight line with intercept at $1/s-1 = 0$ equal to k_I and slope equal to k_{II}.

EXPERIMENTAL RESULTS

Most of our measurements have been carried out at ionic strength 0.50, with acid concentrations ranging from 0.02 to 0.40 molar and the maximum Fe (III) concentration about 10^{-3} molar. The highest concentrations of Fe (III) which could be conveniently studied in the 1-cm cells were limited by the very high molecular extinction coefficient of ferric ion at 260 mμ (10) and also at lower acidities by complications which would be introduced due to the formation of condensed species such as $Fe_2(OH)_2^{4+}$ (10, 11). In all determinations the concentration of total fluoride was less than that of total ion, a condition particularly important at higher concentrations in maintaining a low value for the ratio $[FeF_2^+]/[FeF^{++}]$. We estimate, using values for the first and second association quotients derived from Connick's values (9), that the maximum equilibrium value for this ratio under any of our experimental conditions was less than 0.03.

The data obtained under each set of conditions which we examined were interpreted as indicated above and the quantity on the left of equation 5 when plotted against time yielded quite good straight lines regardless of the conditions. Figure 1 shows a plot of

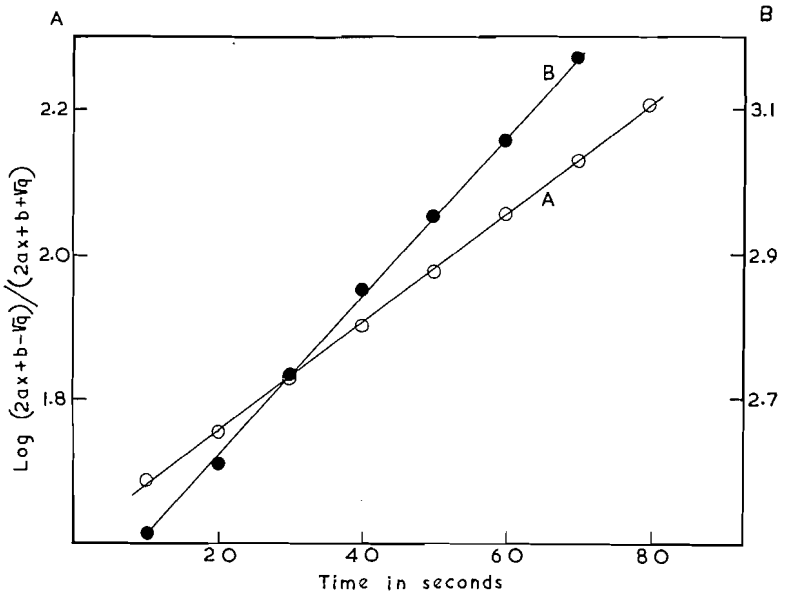


FIG. 1. Plot in accord with equation 5 using data from two runs at ionic strength 0.5 and temperature 0.11° C.

	$[HClO_4]$	[Total iron (III)]	[Total fluoride]
A	0.20 *M*	7.69×10^{-4}	1.50×10^{-4}
B	0.40	8.87×10^{-4}	0.89×10^{-4}

$\log\ (2ax + b - \sqrt{q})/(2\,ax + b + \sqrt{q})$ against time derived from data for two runs at 0.11° C. The plotted points involving the greatest time for each run refer to the formation of FeF^{++} to the extents of 0.92 and 0.85 of the amounts at equilibrium.

Can. J. Chem. Downloaded from www.nrcresearchpress.com by 41.223.56.140 on 09/04/12
For personal use only.

The values of k' obtained by this method from the data obtained at 0.1° C for three acid concentrations are given in Table II. Although the values obtained at any one acidity

TABLE II

Values of k^1 at 0.11° C and three acid concentrations

Hydrogen ion concn. (moles liter^{-1})	Total iron (III) concn.	Total fluoride concn.	k' (mole^{-1} liter second^{-1})	Hydrogen ion concn. (moles liter^{-1})	Total iron (III) concn.	Total fluoride concn.	k' (mole^{-1} liter second^{-1})
0.020	9.03	3.01	228	0.10	7.69	0.75	344
0.020	9.03	3.01	240	0.10	4.73	1.50	267
0.020	9.03	1.50	235	0.10	4.73	0.75	335
0.020	9.03	0.75	216				
				0.40	10.06	3.01	798
0.10	10.06	3.01	326	0.40	10.06	1.50	725
0.10	10.06	3.01	304	0.40	10.06	0.75	816
0.10	10.06	1.50	275	0.40	8.87	3.01	726
0.10	10.06	0.75	305	0.40	8.87	1.50	778
0.10	8.87	3.01	295	0.40	8.87	0.75	797
0.10	8.87	1.50	284	0.40	7.69	3.01	792
0.10	7.69	3.01	297	0.40	7.69	1.50	759
0.10	7.69	1.50	335	0.40	7.69	0.75	685

have a moderate scatter there is no significant dependence on the total concentration of iron (III) or of fluoride. However, there is a positive and significant dependence on the hydrogen ion concentration (which we take as identical with the concentration of perchloric acid). A 20-fold increase in hydrogen ion concentration leads to a 3-fold increase in the apparent rate constant on 0.1° C.

The values of k' plotted against $1/s-1$ ($= \{[H^+]/K_a\}$) for each of the three temperatures investigated (0.11, 7.16, and 12.10° C) are shown in Fig. 2. There appears to be the

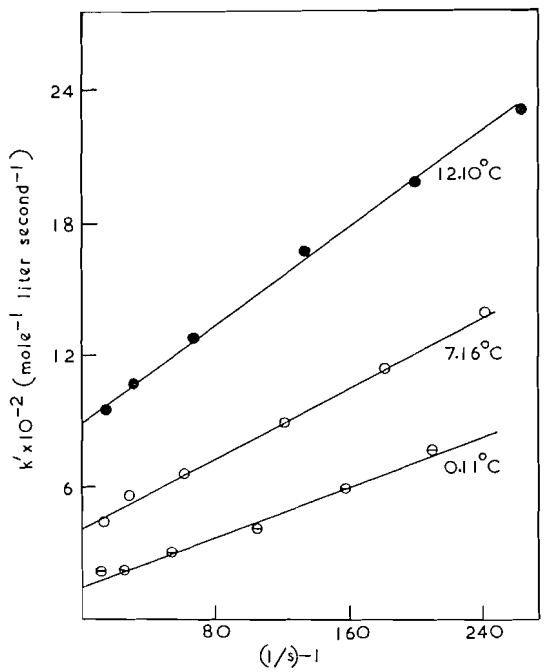


FIG. 2. Variation of effective rate constant k' with $1/s-1(= [H^+]/K_a)$.

Can. J. Chem. Downloaded from www.nrcresearchpress.com by 41.223.56.140 on 09/04/12
For personal use only.

linear relationship between k' and $\{(1/s)-1\}$ which would be expected if reactions I and II are involved. If a reaction involving $FeOH^{++}$ and fluoride ion were contributing appreciably to the rate, then the values of k' applying to the lower range of acidities should be greater than those indicated by the linear extrapolations of the points applying to the higher acidities. The data for 0.11° C may be consistent with a slight trend of this sort, but there is no evidence for such a trend at the higher temperatures.*

Values of k_I and k_{II} have been estimated from the intercepts and slopes of the lines of regression in Fig. 2 and are given in Table III. As can be seen from inspection of Fig. 2 the

TABLE III

The rate constants k_I and k_{II} in $mole^{-1}$ liter $second^{-1}$

Temperature (° C)	k_I	k_{II}
0.11	147	2.71
7.16	433	4.01
12.10	900	5.57

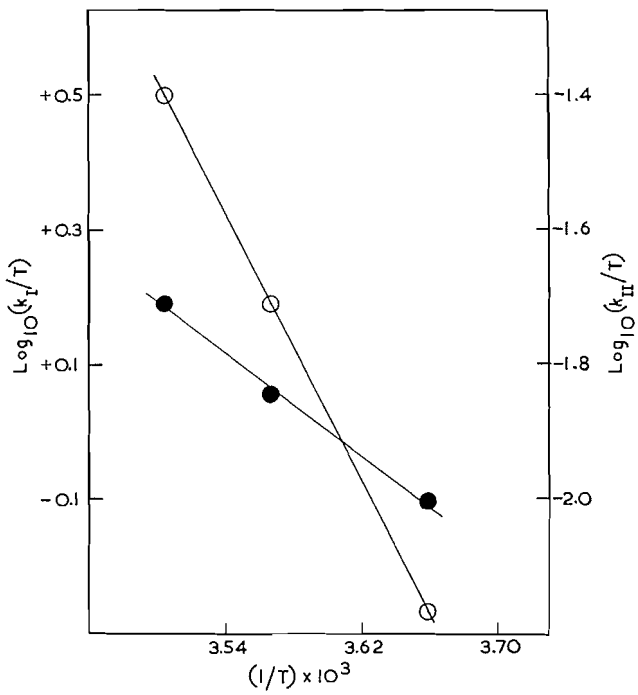


FIG. 3. Modified Arrhenius plots.

○ $\log(k_I/T)$ for reaction $Fe^{+++} + F^- \rightarrow FeF^{++}$,
● $\log(k_{II}/T)$ for reaction $Fe^{+++} + HF \rightarrow FeF^{++} + H^+$.

**We have made measurements at 0.1° C, at ionic strength 0.05, and perchloric acid concentrations down to 0.01 molar and find that the apparent rate constant at this acidity is not significantly different from that at acid concentration 0.045 molar. Smith's preliminary measurements suggested such a lack of dependence of rate on acidity over this range, but the values he found were about 30% lower than ours. The interpretation of the spectrophotometric measurements for lower acidities may be complicated by the formation of FeF_2^+ and $Fe_2(OH)_4^{4+}$ but this apparent lack of dependence of rate constant on acidity suggests that a significant contribution to the rate at acid concentration 0.01 by a reaction involving $FeOH^{++}$ cannot be definitely ruled out.*

Can. J. Chem. Downloaded from www.nrcresearchpress.com by 41.223.56.140 on 09/04/12
For personal use only.

uncertainties associated with the values of k_I are considerable and the third figure recorded in Table III for each value is of doubtful significance.

Plots of log (k_I/T) against $(1/T)$ and of log (k_{II}/T) against $(1/T)$ are given in Fig. 3. Heats and entropies of activation for the two reactions estimated from these plots are as follows:

For the reaction $Fe^{+++} + F^- \rightarrow FeF^{++}$

$$\Delta H_I^{\ddagger} = 22.8 \pm 2.5 \text{ kcal mole}^{-1} \text{ and } \Delta S_I^{\ddagger} = 35 \pm 9 \text{ cal deg}^{-1} \text{ mole}^{-1}.$$

For the reaction $Fe^{+++} + HF \rightarrow FeF^{++} + H^+$

$$\Delta H_{II}^{\ddagger} = 8.7 \pm 0.7 \text{ kcal mole}^{-1} \text{ and } \Delta S_{II}^{\ddagger} = -24 \pm 3 \text{ cal deg}^{-1} \text{ mole}^{-1}.$$

DISCUSSION

Below, Connick, and Coppel carried out their investigations of the ferric–thiocyanate association (4) at ionic strength 0.4 and obtained for the purely ionic association $Fe^{+++} + SCN^- \rightarrow Fe(SCN)^{++}$ a heat of activation of 13.0 ± 1.4 kcal per mole and an entropy of activation of -5 ± 5 cal deg^{-1} mole^{-1}. They did not detect any reaction catalyzed by hydrogen ions or involving any species protonated beyond that of triply charged ferric ion or singly charged thiocyanate, but they did find an increase of rate with decrease in acidity which they attributed to the reaction involving $Fe(OH)(H_2O)_5^{++}$ and the anion. The effect on the heat of activation or the entropy of activation of changing the ionic strength from 0.4 to 0.5 is small (12) and our values and those of Below, Connick, and Coppel may be considered comparable.

The values of $\Delta H^{\ddagger}$ and $\Delta S^{\ddagger}$ which we estimate for the forward reaction I are decidedly larger than those found for the ferric–thiocyanate association. This is possibly due to fluoride ion being much more firmly solvated than thiocyanate. If the attainment of the transition state involves marked desolvation of the anion then the reaction involving fluoride may be more demanding energetically and have a higher heat of activation. Likewise as has been pointed out by Below *et al.* (4) the entropy increase accompanying liberation of water from the anions will be more marked for fluoride than for thiocyanate.

Connick and co-workers have estimated the entropies of reaction for these two associations at ionic strength 0.4 and at 25° C. For the thiocyanate association $\Delta S°$ was given as 4.6 cal deg^{-1} mole^{-1} (4), and for the fluoride association as 30 cal deg^{-1} mole^{-1} (9). A moderate parallelism between the entropy of activation and the entropy of reaction for each of these reactions is apparent. The entropies of activation and reaction for the fluoride association are close in magnitude and positive. This supports the view that the organization of solvent in the transition state approaches that of the final state, even though the states are quite different energetically, and that the fluoride is actively involved in the transition state (i.e. the mechanism is S_N2). The entropies of activation and reaction for the thiocyanate association are both small and it appears that the entropy of activation is significantly more negative. However, in view of the weak solvation of thiocyanate ion and the lack of marked dependence of entropy change on the involvement or non-involvement of thiocyanate it is difficult to interpret these data as supporting either an S_N2 or an S_N1 mechanism.

The increase in apparent rate constant with acidity which we find could be attributed to either a hydrogen ion catalyzed reaction or to one involving HF. We favor the latter because it is difficult to envisage a likely mechanism for hydrogen ion catalysis, but possible to envisage a process where the reaction involving HF has a lower heat activation

Can. J. Chem. Downloaded from www.nrcresearchpress.com by 41.223.56.140 on 09/04/12
For personal use only.

than the mechanism involving fluoride. We consider that, relative to the conditions obtaining in the mechanism involving fluoride ion, the weaker solvation of HF may contribute more to the reduction of the heat of activation than does the reduced electrostatic interaction between ferric ion and hydrogen fluoride (relative to that between ferric and fluoride ions) contribute to its increase.

The values discussed above for the heats and entropies of activation for the reactions involving fluoride with ferric ions and thiocyanate with ferric ions were obtained from measurements made in solutions where the ionic strength was adjusted to 0.5 or 0.4 with sodium perchlorate and these values should be comparable. However, in view of the possibility of some association between ferric and perchlorate ions complicating the interpretation of the measurements at high ionic strength, it seems worth while to examine the kinetics of both the ferric–fluoride and ferric–thiocyanate associations over a wider range of ionic strengths and temperatures in an effort to obtain data applicable to limitingly low ionic strength and concentrations of competing ions.

ACKNOWLEDGMENTS

Financial support by the National Research Council of Canada is gratefully acknowledged. One of us (D. P.) wishes to thank the Ontario Research Council for a Scholarship.

REFERENCES

1. R. G. Pearson. J. Phys. Chem. **63**, 321 (1959).
2. C. Postmus and E. L. King. J. Phys. Chem. **59**, 1216 (1955).
3. R. E. Hamm and R. E. Davis. J. Am. Chem. Soc. **75**, 3085 (1953).
4. J. F. Below, Jr., R. E. Connick, and C. P. Coppel. J. Am. Chem. Soc. **80**, 2961 (1958).
5. M. Eigen. Discussions Faraday Soc. **17**, 194 (1954).
6. W. MacF. Smith. Proc. Chem. Soc. 207 (1957).
7. M. G. Mellon. Quantitative analysis. Thomas Y. Crowell Co., New York. 1955. p. 429.
8. A. I. Vogel. Quantitative inorganic chemistry. 2nd ed. Longmans Green & Co., Ltd., London. 1958. p. 408.
9. R. E. Connick, L. G. Hepler, Z. Z. Hugus, Jr., J. W. Kury, W. M. Latimer, and Maak-Sang Tsao. J. Am. Chem. Soc. **78**, 1827 (1956).
10. L. N. Mulay and P. W. Selwood. J. Am. Chem. Soc. **77**, 2693 (1955).
11. R. M. Milburn and W. C. Vosburgh. J. Am. Chem. Soc. **77**, 1352 (1955).
12. S. Glasstone, K. J. Laidler, and H. Eyring. The theory of rate processes. McGraw-Hill Book Co., Inc., New York. 1941. Chap. 8.

Can. J. Chem. Downloaded from www.nrcresearchpress.com by 41.223.56.140 on 09/04/12
For personal use only.

Can. J. Chem. Downloaded from www.nrcresearchpress.com by 41.223.56.140 on 09/04/12
For personal use only.

THEORY OF THE POLARIZATION CURVE TECHNIQUE FOR STUDYING CORROSION AND ELECTROCHEMICAL PROTECTION[1]

W. A. MUELLER

ABSTRACT

This study of the analysis of polarization curves is based on the identification of the partial currents of the single electrochemical reactions involved. The relationship between the gradient of polarization curves and the corrosion rate in uninhibited corrosion processes is investigated. The analysis of polarization curves is explained and two methods of using polarization curves in corrosion studies are compared. The conditions for stability of the active and the passive states are specified for application in anodic and cathodic protection.

I. INTRODUCTION

In the course of studies of the corrosion of steel in the presence of hot alkaline solutions (as in the kraft process of pulping of wood), some basic features of the electrochemical theory of corrosion were defined, and two methods for recording polarization curves were developed (1). The theory and experimental methods are expected to apply generally to the electrochemical reactions of any metal with any electrolyte. In this paper the practical corrosion problem, as studied previously, is considered only as an example of the general application of the theory and methods.

The practical problem concerned carbon-steel digesters attacked by alkaline pulping liquors in kraft mills. The cooking liquors contain 40 to 75% mill white liquor, the remainder being black liquor. The constituents of white liquor are about 100 g/liter sodium hydroxide and 35 g/liter sodium sulphide and minor quantities of sodium thiosulphate and polysulphides. Black liquor is the product of the reaction between the liquor mixture and wood (2).

The initial laboratory studies measured corrosion rates as a function of the liquor composition. Ruus and Stockman (3) found by laboratory experiments that sodium hydroxide, sodium sulphide, and sodium thiosulphate are main factors determining the corrosion rate in cooking liquor. This finding was corroborated by a Canadian field study (4). The role of polysulphide, thiosulphate, and dimethyldisulphide as depolarizers has also been described (5, 6, 7). However, two independent studies (3, 8) reported that the corrosion rates were not always reproducible even under presumably identical conditions. For instance, in an extreme case negligibly small corrosion rates of 10 or 20 M.P.Y. (milli-inches per year) were found alternating with rates of 650 and 750 M.P.Y. It appeared that the conditions were close to the border line between the stable active and passive states. Several series of potential–time curves revealed that steel immersed in white liquor at room temperature assumes either the active state at a potential of about -1.05 volt or the passive state at about -0.7 to -0.8 volt in reference to a saturated calomel cell (1) depending only on minor differences in the pretreatment of the steel. Another problem was provided by the observation that, during the heating period of the cook, the corrosion rate is high and falls unexpectedly during the later phase of the cook (3).

These observations, together with the problems connected with applying anodic or cathodic protection to steel in contact with these solutions, indicated a need for a basic study of the processes. The search for a theory and for experimental methods capable of

[1]*Manuscript received November 25, 1959.*
Contribution from the Physical Chemistry Division, Pulp and Paper Research Institute of Canada, Montreal, Que.

clarifying these problems was directed towards electrochemical methods for analyzing localized attack as well as general uniform corrosion. Electrochemical corrosion in the narrow meaning of the term requires that areas of anodic and cathodic reaction can be distinguished. The mechanism of extremely localized corrosion, characterized by complete separation of areas in which anodic or cathodic reactions occur, has been previously explained (9, 10) on this basis; but this principle does not apply in the case of general, uniform corrosion. However, a solution was found by assuming electrochemical reactions in the broad meaning of the term (11, 12, 13, 14, 15, 16) which implies the exchange of positive or negative electrical charges between metal and electrolyte, whereby anodic and cathodic reactions may occur on the same metal surfaces simultaneously. On this basis the general laws which govern the increase of corrosion resistance by means of alloying were examined by Tomashov (17).

Pourbaix (14) derived electrochemical equilibrium diagrams, which describe the effect of pH on electrochemical reactions at varied potentials. During recent years the "measurement of the corrosion rate of iron by the polarization curve techniques" has been studied by several workers (18, 19, 20) applying different principles. They showed empirically that the slope of the polarization curve of iron in certain solutions is related to the corrosion rate. This relationship was theoretically derived by Stern (21). It receives an improved and more detailed formulation in this paper on the basis of a different derivation.

However, the analysis of "current density – potential curves",* to determine their components, was considered to be an appropriate approach to the initially stated problem. This principle, introduced by Wagner and Traud (22) was applied by Bonhoeffer (23) to the analysis of the polarization curve of iron immersed in sulphuric acid. A very detailed account of the analysis was published by Schwarz (16). The analysis of polarization curves was recently discussed by Stern (15) and applied to criticize the "current–potential break" criterion as used in cathodic protection. The principle of the analysis has been extended, in an independent study (1), to cover both the active and passive states and particularly the potential range around the boundary between them. In this connection the studies of Edeleanu (24) are of particular interest.

This paper intends to clarify some basic problems of the polarization curve theory and its application in the study of corrosion problems. It shows how the polarization curve is combined from the waves of the single reactions (25) involved. Some new aspects are revealed of the relation between the corrosion rate, the slope of the polarization curve, and the diffusion conditions in the corrosive environment of the metal. Finally, the conditions of the stability of the active and passive states are explained.

II. ELECTROCHEMICAL ANALYSIS OF POLARIZATION CURVES

When the polarizing and the depolarizing reactions occur at separate electrodes, a cell is formed, causing corrosion of the anodic specimen (9) if it is in the active state. The corrosion rate is proportional to the strength of the current in agreement with Faraday's law. However, the total current is decreased when the partial reactions occur at the same electrode. When both reactions occur at equal rates all over the metal, there is no current flow, for as the partial currents are opposed, their sum is zero. The partial currents are governed by the same quantitative relationships, independently of the current distribution. An applied current causes a shift of the potential difference between metal and

*This term, which is normally used in continental Europe, implies that the potential is considered primarily as the independent variable, to be plotted on the abscissa, and the current or current density as the dependent variable, to be plotted on the ordinate. In this paper the expression polarization curve is used without discrimination and the potential is recorded on the abscissa as the independent variable.

Can. J. Chem. Downloaded from www.nrcresearchpress.com by 41.223.56.140 on 09/04/12
For personal use only.

electrolyte and this in turn causes an alteration of the partial currents. The potential shifts until the external current equals the sum of the partial currents (some of which may be negative). This quantitative relationship was experimentally proved by Bonhoeffer (23) for iron dissolving in sulphuric acid.

Identification of the single reactions is often possible when the current density is considered as the sum of partial currents, each of which is caused by one single reaction and represents an independent function of the potential difference between metal and electrolyte. The combination of single reactions with their respective reverse reaction has been discussed in another paper (25). This paper is concerned with polarization curves as combined from the single reactions which include their reverse reactions.

III. THE RELATIONSHIP BETWEEN THE POLARIZATION CURVE AND THE CORROSION RATE

In the introduction an empirical rule was mentioned which relates the corrosion rate to the slope of the polarization curve (20) and which can be formulated as:

$$[1] \qquad \frac{dE}{dI} = \frac{K}{-\left(\frac{dW}{dt}\right)^S}$$

where K = constant, $-dW/dt$ = corrosion rate, W = weight per unit area, S = exponent, $S > 1$. To avoid misunderstanding it may be pointed out that "the slope of the polarization curve" given by Skold and Larson (20) and by Stern (21) is defined as the reciprocal of the value used in this paper. The following derivation is based on the assumption that the partial currents are independent of one another. This implies that the corrosion rate is primarily related to the anodic dissolution current, but not to the polarization curve, which refers to the depolarization current in addition.

A method for determining corrosion rates from linear polarization data has been developed by Stern (21). In the following, a new derivation is given of this relation, and the deviations from Stern's equations are discussed. If the possible reverse reaction is included, the anodic dissolution current I_a on a metal surface free of a protective film can be formulated as a modified Tafel relation (25, 26)

$$[2] \qquad I_a = I_1 \exp \frac{a_a n_a F}{RT} (E - E_1)$$

where n_a = valency of ions formed in the dissolution process,

I_1 and E_1 are a couple of interconnected values of current density and potential,

a_a = apparent symmetry factor as defined and derived in a study of the transition from equilibrium conditions to single electrochemical reactions (25).

If I_a contains only the current caused by the forward reaction, a_a becomes identical with the symmetry factor α_a and eq. 2 becomes a conventional Tafel relation. If a reverse reaction is superposed on the forward reaction, the following relation is valid

$$[3] \qquad \alpha_a \leqq a_a \leqq 1$$

where $a_a = 1$ at equilibrium. Only in a limited potential range can "a" values be considered as constants. If "a_a" changes, I_1 and E_1 do so also.

Can. J. Chem. Downloaded from www.nrcresearchpress.com by 41.223.56.140 on 09/04/12
For personal use only.

If I_a equals the absolute value of the depolarizing current of an oxidizing reagent I_{ox}, $I_a = -I_{ox} = I_{corr}$ and the slope of I_a becomes

$$[4] \qquad \left(\frac{dI_a}{dE}\right)_{I_a=I_{corr}} = I_{corr}\frac{a_a n_a F}{RT}$$

where I_{corr} = corrosion current.

The current–potential relation referring to the depolarizing reaction represents a typical redox wave, caused by the reaction of an oxidizing reagent, which might be counteracted by the produced reducing reagent (25). This relation can be formulated

$$[5] \qquad \ln\frac{I_d - I_{ox}}{I_{ox}} = a_{ox}\frac{n_{ox}F}{RT}(E - E_{\frac{1}{2}})$$

where I_{ox} = current density of the depolarizing reaction of the oxidizing reagent,
I_d = current density of the diffusion current (I_d and I_{ox} are negative),
n_{ox} = valency involved in the depolarizing reaction,
$E_{\frac{1}{2}}$ = half wave potential of the depolarizing reaction,
a_{ox} = apparent symmetry factor of the depolarizing reaction of the oxidizing reagent. For an oxidizing reaction without reverse reaction $a_{ox} = \alpha_{ox}$ which is the symmetry factor of the oxidizing reaction. At equilibrium $a_{ox} = 1$.

This eq. 5 is basically different from Stern's corresponding eq. 2

$$[6] \qquad E_{conc} = 2.3\frac{RT}{nF}\log\left(1 - \frac{I}{I_L}\right)$$

where E_{conc} = change of potential caused by concentration polarization,

I_L = I_d of this paper.

Equation 6 is valid with respect to a metal in equilibrium with its ions in solution (27) as it has been derived from

$$[7] \qquad E_{conc} = 2.3\frac{RT}{nF}\log\frac{c}{c_b}$$

where c = concentration of the metal ions at the interface,
c_b = bulk concentration.

This is the overpotential of a metal in contact with a solution of its ions close to equilibrium; it is not the overpotential caused by a depolarizing reaction.

Differentiation of eq. 5 with respect to E results in

$$[8] \qquad -\frac{dI_{ox}}{dE}\frac{1}{I_d - I_{ox}} - \frac{dI_{ox}}{dE}\frac{1}{I_{ox}} = \frac{a_{ox}nF}{RT}.$$

Accordingly the slope of the partial current density of the depolarizing reaction under steady-state conditions ($I_a = -I_{ox} = I_{corr}$) is

$$[9] \qquad \left(\frac{dI_{ox}}{dE}\right)_{(I_a=I_{corr})} = I_{corr}\frac{a_{ox}n_{ox}F}{RT}\frac{-I_d - I_{corr}}{-I_d}.$$

Hence the relation between the slope of the polarization curve $dI/dE = (dI_a/dE) + (dI_{ox}/dE)$ and the corrosion rate can be expressed

$$[10] \qquad \left(\frac{dI}{dE}\right)_{(I_a=-I_{ox}=I_{corr})} = I_{corr}\frac{F}{RT}\left(a_a n_a + a_{ox}n_{ox}\frac{-I_d - I_{corr}}{-I_d}\right).$$

Can. J. Chem. Downloaded from www.nrcresearchpress.com by 41.223.56.140 on 09/04/12
For personal use only.

To show the meaning of eq. 10, the anodic dissolution current (ADC) and three polarigraphic waves (W1, W2, and W3) of oxidizing reagents are plotted in Fig. 1 as a schematic

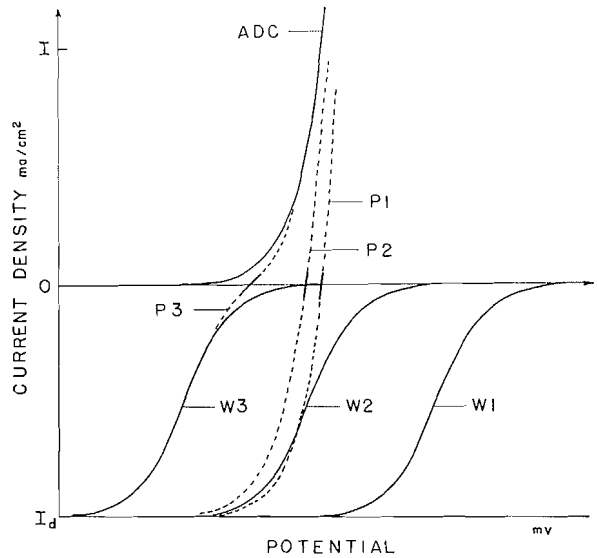


FIG. 1. Polarization curves and their slope combined from partial currents and the respective slopes.

demonstration. Three polarization curves (P1, P2, and P3) are derived from the combination of the anodic dissolution current with the waves. The slope of the diffusion controlled curve P1 is equal to the slope of the anodic dissolution current; the slopes of the curves Pa and P3 are combined from two partial slopes each.

When replacing I_{corr} by

$$\left(-\frac{dW}{dt}\right)\frac{Fn_a}{A\cdot 24\cdot 3600}$$

eq. 10 results in

$$[11] \qquad \frac{dI}{dE} = \left(-\frac{dW}{dt}\right)\frac{F^2 n_a}{RTA\cdot 24\cdot 3600}\left(a_a n_a + a_{ox} n_{ox}\frac{-I_d - I_{corr}}{-I_d}\right)$$

where A = atomic weight, W = weight per unit area, $(-dW/dt)$ = mg(dm)$^{-2}$(day)$^{-1}$ (corrosion rate).

In double logarithmic plotting the values of the corrosion current are located on or between two limiting lines (L1 and L2) which result from eqs. 10 and 11 when $(-I_d)_{ox} = I_{corr}$ (L1) and when $(-I_d)_{ox} \gg I_{corr}$ (L2).

These conditions may be illustrated by a comparison of the relation calculated on the arbitrary assumption $a_a = 1/4$, $n_a = 2$, $a_{ox} = 1/2$, and $n_{ox} = 4$ with the experimental values of Skold and Larson (20). Figure 2 shows that the measured values are close to, or between, the calculated lines. The position of the measured points indicates that the corrosion was controlled by diffusion mainly at high values of the gradients of the polarization curve as expected. The derivation suggests that the empirical relation (Le) is valid only between the calculated lines. For the exact calculation of the limiting lines the coefficients $a_a n_a$ and $a_{ox} n_{ox}$ have to be known.

A final comparison with Stern's equation (21) shows an agreement only of Stern's eq. 8

Can. J. Chem. Downloaded from www.nrcresearchpress.com by 41.223.56.140 on 09/04/12
For personal use only.

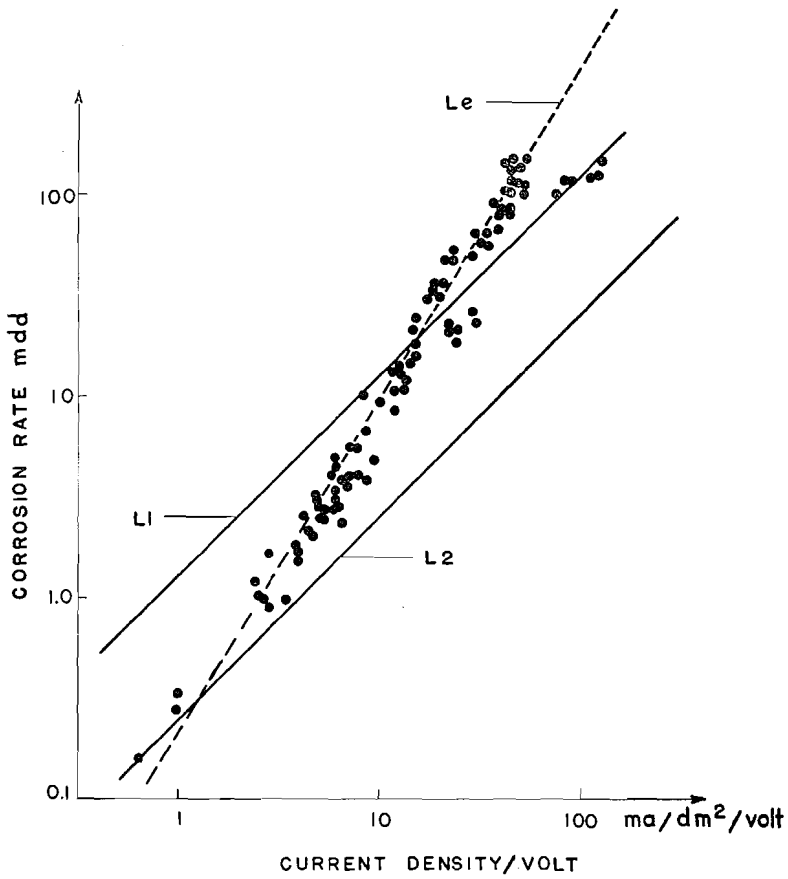


FIG. 2. Skold and Larson's (20) empirical relation between corrosion rate and the slope of the polarization curve (dotted line) in comparison with the calculated limiting condition (extended lines).

with eq. 10 of this paper if the redox reaction is completely controlled by concentration polarization and if Stern's $\beta = RT/a_a n_a F$. This is the well-known case derived from a Tafel reaction according to eq. 4. However, eqs. 10 and 11 are valid at any degree of concentration polarization. In addition to Stern's formulation eqs. 10 and 11 give an explicit relation to the valencies involved in the reaction and the relation to the diffusion current. Equations 10 and 11 reveal to which degree the corrosion under study is diffusion controlled when the "$a.n$" values are known, and they allow a close estimation of corrosion rates from the slope of the polarization curves even if only the metal and the depolarizer are known. The effect of possible reverse reactions such as electrodeposition of the dissolved metal and reducing redox reactions have also been included in these derivations.

The exact validity of the derived equations is limited to polarization curves composed of the partial currents of anodic dissolution of the metal (eq. 2) and of the depolarizing current (eq. 5). If other partial currents, such as listed in the following chapter, contribute to the polarization curve the above equations become inaccurate. Adsorption of anions can also change the basic equations of redox reactions (28).

IV. THE POLARIZATION CURVE COMBINED FROM PARTIAL CURRENTS

The polarization curve of a metal immersed in an electrolyte represents the dependence of the sum of well-defined partial currents on the potential, as follows:

Can. J. Chem. Downloaded from www.nrcresearchpress.com by 41.223.56.140 on 09/04/12
For personal use only.

1. In the active state the anodic dissolution current of the metal which can be characterized by the constants a_a, a_n, I_1, and E_1 (eq. 2). When passivation begins, a characteristic rapid decline of the current density occurs (24, 1, 29).

2. Anodic dissolution current of hydrogen contained in the metal.

3. The partial currents due to redox reactions the products of which are soluble in the oxidized and reduced state. These currents are characterized by n, a_{ox} or a_r, I_d, $E_{\frac{1}{2}}$, and $E°$ (eq. 5)

where a_r = apparent symmetry factor of the reaction of the reducing reagent (25),
$E°$ = standard redox potential.

4. The partial current of deposition of metals also characterized by a, n, I_d, $E_{\frac{1}{2}}$, and $E°$.

5. The partial current due to slow dissolution and rebuilding of the passive film (30), in the passive state.

The various partial currents combined result in the polarization curve. As an example, Fig. 3 shows the schematic construction of the polarization curve of iron in laboratory

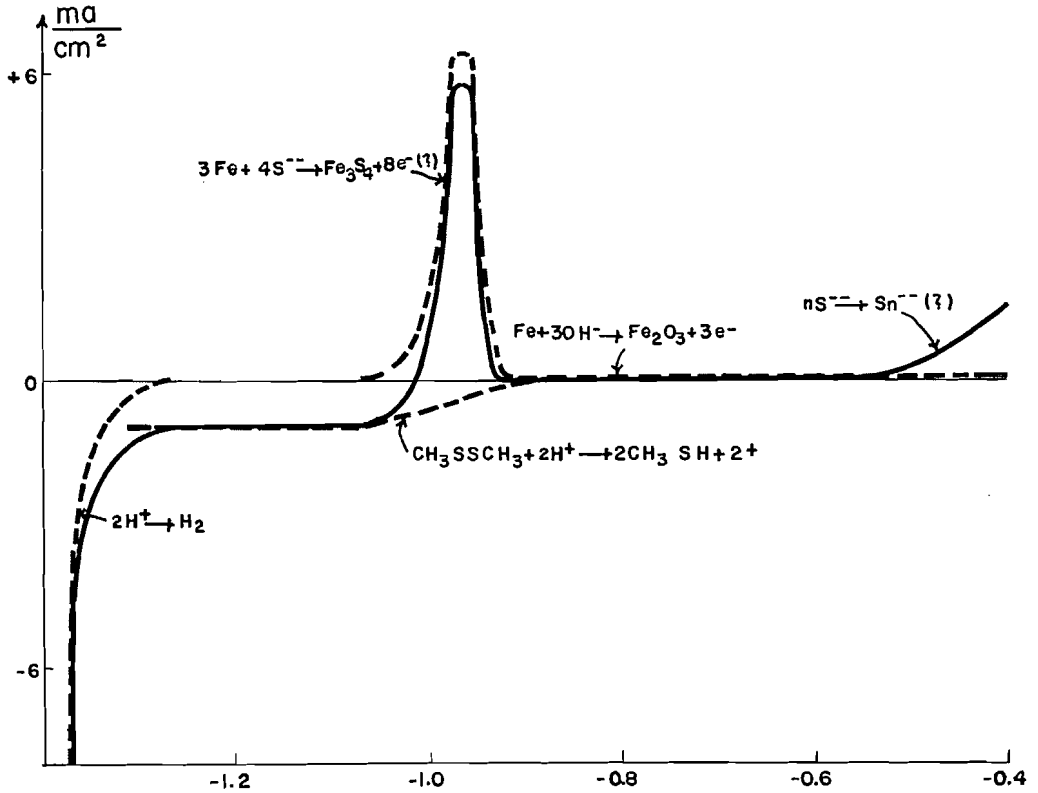


FIG. 3. Construction of the polarization curves of iron in alkaline pulping liquor from the partial currents involved.

white liquor containing 1 g/liter dimethyldisulphide. The partial currents are caused by the development of hydrogen, the redox reaction of dimethyldisulphide, the anodic dissolution current, the slow dissolution and rebuilding process of the passive film, and finally an anodic current probably due to formation of polysulphides from sulphides. The corrosion rate at a certain potential is proportional to the partial current of the anodic dissolution of the metal when in the active state or of the dissolution of the passive film when it is passive.

Can. J. Chem. Downloaded from www.nrcresearchpress.com by 41.223.56.140 on 09/04/12
For personal use only.

When specimens of two different metals, in metallic contact, are immersed in the same electrolyte the respective anodic dissolution currents are different and so are the depolarization currents due to different overpotentials. The same is true with respect to identical specimens in metallic contact when immersed in electrolytes of different composition. The potentials approach one another more closely with improved conductivity of the circuit. The final values of the potentials are located between the potential values of disconnected specimens and they depend on the gradients of the polarization curves and the extent of the exposed areas, as explained before (9, 10).

These conditions can be calculated when currents, rather than current densities, are compared. The potentials E_A and E_C shift to values where

(*a*) the net anodic current of the specimen A equals the net cathodic current of the specimen C;

(*b*) the potential difference $E_A - E_C$ equals the product of the current and the resistance in the cell circuit.

For comparison these conditions are expressed by the diagram of Evans and Hoar (10) in Fig. 4(*a*), and according to Schwarz (16) in Fig. 4(*b*), with reference to two connected

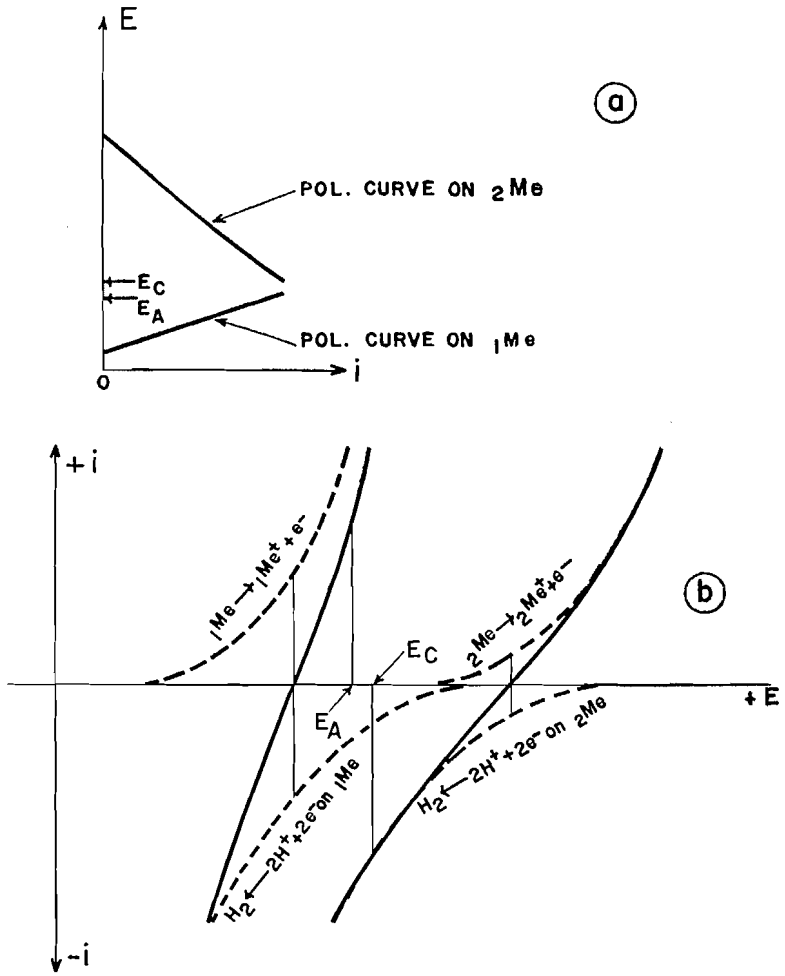


FIG. 4. The electrochemical behavior of a bimetallic system: (*a*) as plotted by Evans, (*b*) as plotted by Schwarz.

Can. J. Chem. Downloaded from www.nrcresearchpress.com by 41.223.56.140 on 09/04/12
For personal use only.

metals immersed in an acidic solution. Anodic and cathodic currents in Fig. 4(*a*) are plotted on the abscissa and the potentials on the ordinate. The corrosion rate is proportional to the current. The figure below (Fig. 4(*b*)) shows the same conditions plotted similarly to the other polarization curves in this paper. The clear distinction between anodic and cathodic currents and the clarification of the sources of these currents are assumed to be advantages of the way of plotting used in Fig. 4(*b*). This advantage becomes evident as soon as at least one of the compared currents results from more than one partial current. Only the method of Fig. 4(*b*) indicates the rate of anodic dissolution, i.e., the corrosion rate, reliably.

V. STABILITY OF THE ACTIVE AND THE PASSIVE STATES AND APPLICABILITY OF ANODIC PROTECTION

The stability of the passive state is of basic importance when it forms the basis of corrosion protection. Two types of stability have to be distinguished with respect to passivity. This paper is not concerned with instability phenomena (31), which cause rhythmic behavior or propagation of activating and passivating waves, nor with the irreversible behavior exhibited by a potential jump which is connected with the change from active to passive states (32). In this paper stability for instance of the passive state means that the passivity is maintained without supply of anodic current. The instability or low degree of stability of the active and passive states of steel in contact with alkaline cooking liquors points to the necessity for clarifying these conditions.

These conditions of stability have been discussed before by Vetter (33) and Edeleanu (24) on the basis of single electrochemical reactions and, in complete agreement with these derivations, by Mueller (1) on the basis of combined polarization curves. The experience gathered during the application of anodic protection of alkaline pulping digesters (34) may justify another discussion, which is mainly concerned with the practical application. Single reactions explain the mechanism of the electrochemical reactions involved. But combined polarization curves are usually measured and they give the information that is practically required, even if none of the single reactions is known; hence they have been chosen for this discussion.

The conditions of electrochemical equilibrium can be expressed by analogy to the definition of a mechanical equilibrium as follows: An equilibrium potential is reached if the potential is constant at zero current density. The equilibrium is stable if the potential, after receiving a small displacement, tends to return to its original values. The criterion of a stable equilibrium (S, Fig. 5) is a positive value of the gradient of the current density versus potential at a zero current density. Stability means that a current which restores the original potential is produced when the potential is changed. The criterion of unstable equilibrium (UE) is a negative gradient of the polarization curve when passing through zero current density. The presence of two stable potentials (Fig. 5(*b*)) requires a positive maximum of the polarization curve in the active state and a negative minimum in the passive state.

If there is no negative minimum of the current density in the passive state (Fig. 5(*a*)) the positive current, which leaves the metal, removes positive charges from the metal thus causing a shift of the potentials to the more negative values in the active state, i.e., the passive state is unstable; and so is the active state (Fig. 5(*c*)) if there is no positive maximum of the current density in the active range. The degree of the stability of the active state is proportional to the value of the positive maximum of current density; and the degree of the stability of the passive state is proportional to the value of the negative

Can. J. Chem. Downloaded from www.nrcresearchpress.com by 41.223.56.140 on 09/04/12
For personal use only.

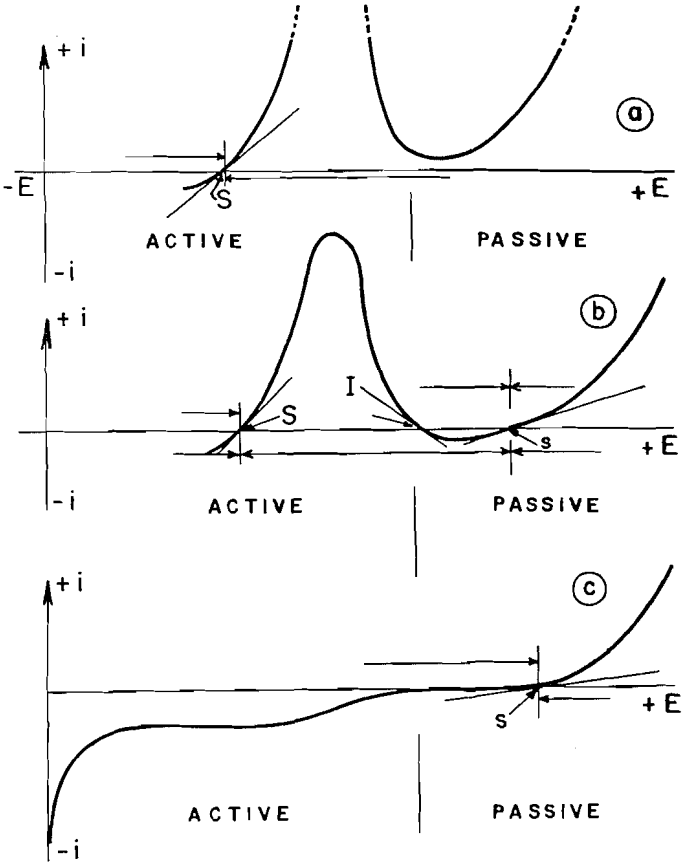


FIG. 5. Stability and instability of the electrochemical equilibrium in the active and passive states: (*a*) only active state stable, (*b*) active and passive states stable, (*c*) only passive state stable.

minimum of the current density. For establishing a stable passivity it is important to know how the partial currents depend on the composition of the electrolyte and on the diffusion conditions.

The three cases of electrochemical stability are demonstrated by potential time curves recorded at alkaline pulping digesters during application of anodic protection (34). The shift of the potential to the active range, when no current is supplied at the beginning of each cook (Fig. 6), shows that only the active state is then stable. Without application of anodic protection the digester remains in the active state for about two hours. However, when applying anodic protection for about one hour the digester apparently has then reached a stable passive state because the potential does not shift back when the current supply is shut off. At the end of the cook only the passive state is stable as the potential shifts to the passive range even without current supply. Thus the three mentioned cases of electrochemical stability are passed in succession during a cook in an alkaline pulping digester. Polarization curves recorded under these conditions corroborated this conclusion.

As another example, this principle gives a new explanation to the result of the study of Brauns and Pier (35) on the intercrystalline corrosion of stainless steel in boiling 5% sulphuric acid. In the case of a properly heat-treated specimen, which is free of intercrystalline corrosion and displays a stable passivity, the minimum of the current density

Can. J. Chem. Downloaded from www.nrcresearchpress.com by 41.223.56.140 on 09/04/12
For personal use only.

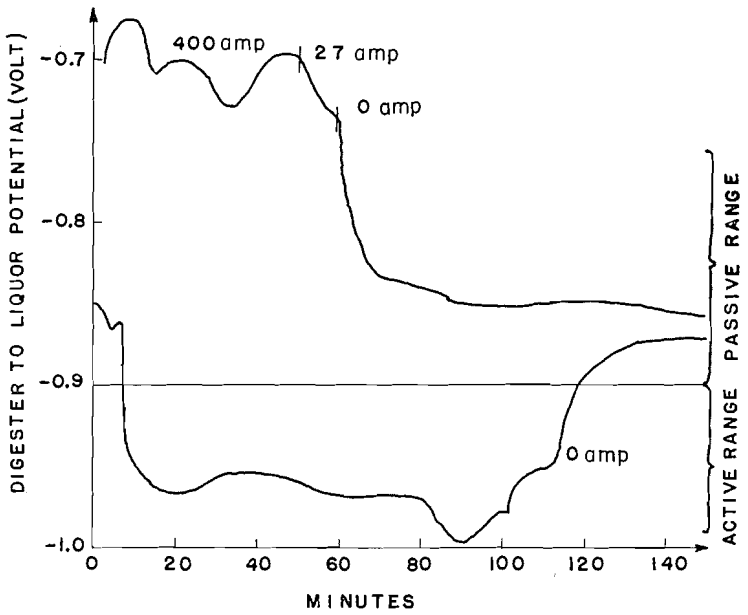


FIG. 6. Potential time curves recorded by varying the current during directly steamed cooks of alkaline pulping digesters.

in the passive state is negative. However, with increasing instability to intercrystalline attack, the minimum shifts to increasingly positive values of the current density.

The known effect of depolarizers, such as oxygen or other oxidizing substances, of stabilizing the passive state consists in the formation of a cathodic partial current which must be sufficiently high to make the minimum current density of the polarization curve in the passive range cathodic. This effect was observed with different concentrations of dimethyl disulphide, which is one of the main depolarizers in oxidized black liquor.

For the passivation of a metal which is in the active state, a high initial current is required to shift the potential past the maximum in the polarization curve in the active state. This current can be reduced by passivating different areas in succession. After reaching stable passivity (stable equilibrium in the passive state) the current can be switched off without causing re-activation. However, if there is no stable equilibrium in the passive state, a current has to be maintained at a level higher than the minimum current indicated by the polarization curve in the passive range. Insufficient supply of current or of depolarizers does not passivate or protect the electrode; on the contrary, it increases the corrosion rate.

The danger of corrosion caused by reaching the transpassive state has also to be taken into consideration for the application of anodic protection. Evidently a shift to extreme anodic potentials may be caused by some changes during long time operation, for instance, when scale is formed on an increasing ratio of the surface. A potential shift to the transpassive range is easily prevented if the polarization curve shows high current densities in the passive range, before reaching transpassivity. If this is not the case potentiostatic control of the applied current is required to prevent a shift of the potential to the transpassive potential range. Figure 3 demonstrates a system in which corrosion by shifting to the transpassive state is not very likely because in the extreme anodic range the anodic

Can. J. Chem. Downloaded from www.nrcresearchpress.com by 41.223.56.140 on 09/04/12
For personal use only.

current density reaches high values when corrosion is still literally zero. Thus the field experiment with the application of anodic protection to alkaline pulping digesters (34) is the first practical application of these theories.

REFERENCES

1. W. A. MUELLER. Can. J. Technol. **34**, 162 (1956).
2. J. N. STEPHENSON. Pulp and paper manufacture. Vol. 1. McGraw-Hill Book Co., New York. 1950.
3. L. RUUS and L. STOCKMAN. Svensk Papperstidn. **56**, 857 (1953); Paper Ind. **35**, 1242 (1954).
4. C. B. CHRISTIANSEN and J. B. LATHROP. Pulp & Paper Mag. Can. **55**, 113 (1954).
5. B. HAEGLUND and B. ROALD. Norsk Skogind. **9**, 351 (1955).
6. W. A. MUELLER. Tappi, **40**, 129 (1957).
7. R. B. KESLER and J. F. BAKKEN. Tappi, **41**, 97–102 (1958).
8. T. W. HASSLER. Tappi, **38**, 265 (1955).
9. U. R. EVANS. Metallic corrosion, passivity and protection. 2nd ed. Edward Arnold & Co., London. (1946).
10. U. R. EVANS. J. Electrochem. Soc. 103, **73** (1956); T. P. HOAR. Proc. Roy. Soc. A, **137**, 359 (1932).
11. H. GRUBITSCH. Chem. Ing. Techn. **27**, 287 (1955); **28**, 9 (1956).
12. E. LANGE and K. NAGEL. Z. Elektrochem. **53**, 21 (1949).
13. G. MASING. Werkstoffe u. Korrosion, **1**, 433 (1950).
14. M. POURBAIX. J. Electrochem. Soc. **101**, 217 C (1954).
15. M. STERN. J. Electrochem. Soc. **102**, 609 (1955); **104**, 56 (1957).
16. W. SCHWARZ. Metall. **10**, 513 (1956); **10**, 921 (1956).
17. N. D. TOMASHOV. Corrosion, **14**, 229 T (1958).
18. W. J. SCHWERDTFEGER and O. N. MCDORMAN. J. Electrochem. Soc. **99**, 407 (1952).
19. E. J. SIMMONS. Corrosion, **11**, 255 (1955).
20. R. V. SKOLD and T. E. LARSON. Corrosion, **13**, 139 (1957).
21. M. STERN. Corrosion, **14**, 440 T (1958).
22. C. WAGNER and W. TRAUD. Z. Electrochem. **44**, 391 (1938).
23. K. F. BONHOEFFER. Z. Elektrochem. **55**, 151 (1951).
24. C. EDELEANU. Nature, **173**, 739 (1954); Metallurgia, **50**, 113 (1954); J. Iron Steel Inst. **185**, 482 (1957); **188**, 122 (1958).
25. W. A. MUELLER. In preparation.
26. J. TAFEL. Z. physik. Chem. **50**, 641 (1905).
27. C. W. TOBIAS, M. EISENBERG, and C. R. WILKE. J. Electrochem. Soc. **99**, 359 C (1952).
28. Y. M. KOLOTYRKIN. Trans. Faraday Soc. **55**, 455 (1959).
29. W. A. MUELLER. J. Electrochem. Soc. In preparation.
30. H. GÖHR and F. LANGE. Z. Elektrochem. **61**, 1291 (1957).
31. U. F. FRANK. Z. Elektrochem. **62**, 649 (1958).
32. H. J. ROCHA. *In* Handbuch der Sonderstahlkunde. Vol. I. E. HOUDREMONT. Springer-Verlag. 1956.
33. K. J. VETTER. *In* Passivierende Filme und Deckschichten. H. FISCHER, K. HAUFFE, and WIEDERHOLT. Springer-Verlag. 1956.
34. W. A. MUELLER. Pulp and Paper Mag. Can. **10**, 3 (1959); Tappi, **42**, 179 (1959).
35. E. BRAUNS and G. PIER. Stahl und Eisen, **75**, 579 (1955).

Can. J. Chem. Downloaded from www.nrcresearchpress.com by 41.223.56.140 on 09/04/12
For personal use only.

Can. J. Chem. Downloaded from www.nrcresearchpress.com by 41.223.56.140 on 09/04/12
For personal use only.

RATES OF ADSORPTION OF HYDROGEN ON PALLADIUM AND ON RHODIUM[1]

MANFRED J. D. LOW

ABSTRACT

A study of the effects of temperature and initial gas pressure on the kinetics of chemisorption of hydrogen on alumina-supported palladium and rhodium catalysts revealed, for both gas–solid systems, that the adsorption proceeded via three distinct and consecutive kinetic stages. Each stage could be described by the Elovich equation. The temporal range of existence of each kinetic stage was temperature- and pressure-sensitive, low initial pressures and high temperatures favoring early appearance of each stage. On increasing the temperatures from 0° to 400° C, the amounts of hydrogen adsorbed on both solids decrease. Over that temperature range the rates of adsorption on Pd decrease, while those on Rh increase, with increasing temperature. The general effect of increasing the initial gas pressure over the range 10–60 mm Hg is to increase both rates and extents of adsorption.

INTRODUCTION

The rates of chemisorption in many gas–solid systems have been shown (1) to obey the Elovich equation,

$$\frac{dq}{dt} = ae^{-\alpha q},$$

where q is the amount of gas taken up at time t, and a and α are constants. The q–t relation can be expressed by an integrated form of the Elovich equation as

$$q = \frac{2.3}{\alpha}\log_{10}(t+k) + \text{constant},$$

where k is a constant, so that a plot of q versus $\log_{10}(t+k)$ is linear. In certain systems isothermal discontinuities (1), or breaks, have been reported, in that abrupt changes in slope occurred in the $q - \log_{10}(t+k)$ plots, and such behavior was ascribed to adsorption on different sites (1). The change in slope corresponded to relatively increased or to decreased rates of adsorption, changes in both directions sometimes occurring within the same gas–solid system (2). Preliminary experiments had shown that such breaks occurred in the system H_2–Pd and H_2–Rh, and suggested more extensive work.

EXPERIMENTAL DETAILS

The uptake of gas by the solids was followed by measuring decreases in pressure with time in systems of constant volume, using previously described techniques (2–6). The adsorbents were: 20.46-g sample of 0.5% Pd supported on the exterior of 3×5 mm γ-Al_2O_3 pellets; 15.85-g sample of 0.5% Pd on exterior of 1×3 mm γ-Al_2O_3 extrudates. The unreduced commercial catalysts were black in color. On heating of the catalysts to 500° C *in vacuo* a copious evolution of gas occurred. A part of the gas was condensible and probably water. After pumping overnight at 500° C a pressure $\leqslant 10^{-6}$ mm Hg was attained, the original black coloration being retained. On exposure to H_2 the catalysts turned gray. A test was made for efficiency of reduction by (*a*) reducing the catalysts at 500° for a specific time with H_2 at 20 l. N.T.P./hour, (*b*) degassing at 500° overnight, (*c*) measuring H_2 uptake on the degassed surface. No significant change in adsorption

[1]*Manuscript received October 13, 1959.*
Contribution from Texas Research Center, Beacon, New York.

occurred on increasing the reduction period from 10 minutes to 48 hours. Identical results were obtained by three alternate steps of exposures to H_2 (at 1 atm for 1 hour at 500°) and degassing at 500° for 30 minutes.

EXPERIMENTS, RESULTS, AND DISCUSSION

The General Nature of the Adsorption

For both gas–solid systems, most plots of q versus log t show the previously described breaks. For all plots k was indistinguishable from zero. Five general types of plots were obtained, shown schematically in Fig. 1. A few linear plots, such as plot 4, were obtained.

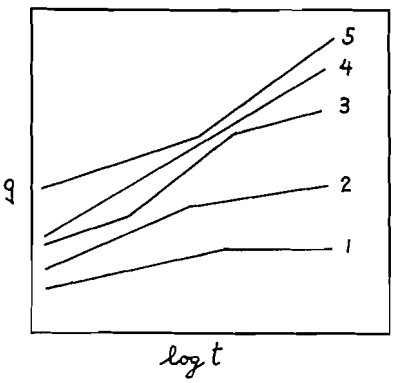


FIG. 1. Types of plots.

For most runs the $q - \log t$ plots were discontinuous, and the rate of adsorption, proportional to the slope of the $q - \log t$ line and hence to the constant $1/\alpha$, became relatively faster (as in plot 5) or relatively slower (as in plot 2).

Inspection of the plots of all data revealed certain consistent features in the occurrence of the various types of plots of Fig. 1. In comparing rate curves of experiments performed at different initial gas pressures and at different temperatures it became apparent that comparisons of kinetic stages, i.e. linear portions of $q - \log t$ plots, on the basis of their temporal order of appearance resulted in misleading correlation and interpretation. If stages were compared on the basis of the relative magnitude of the constant α of the following kinetic stage, using the scheme depicted in Fig. 2, then correlation of the rate

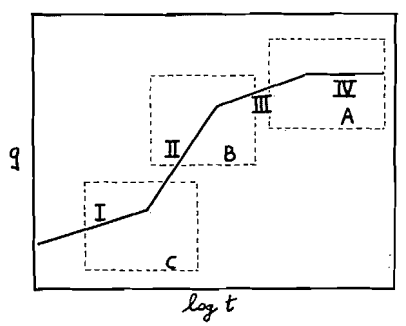


FIG. 2. Composite of multiple kinetic stages.

Can. J. Chem. Downloaded from www.nrcresearchpress.com by 41.223.56.140 on 09/04/12
For personal use only.

parameters of individual stages with temperature and pressure became possible. In Fig. 2 the different kinetic stages are arbitrarily termed I, II, III, and IV, the last representing completion of adsorption.

It is probable that all stages are present in any one run but, because of limitations imposed by the technique and by the experimental variables of temperature and pressure, not all stages necessarily are detected during the course of a single experiment.

Effects of Temperature and Pressure on Kinetic Stages

The plots 1 to 5 of Fig. 1 represent in general fashion the order of appearance of the various types of plots with increasing initial pressure, P_s. For the adsorption of H_2 on Pd and on Rh at pressures of about 10 to 20 cm DBP (dibutylphthalate) several runs were obtained which had the appearance of the schematic plot 1 of Fig. 1. For such runs the $q - \log t$ plots are equivalent to the region A enclosed by dotted lines of Fig. 2. According to the scheme of that figure the segments of the $q - \log t$ plots showing positive slope correspond to stage III, while the portions parallel to the abscissa correspond to stage IV. For such cases the preceding stages I and II are assumed to have appeared before the time of the first measurement.

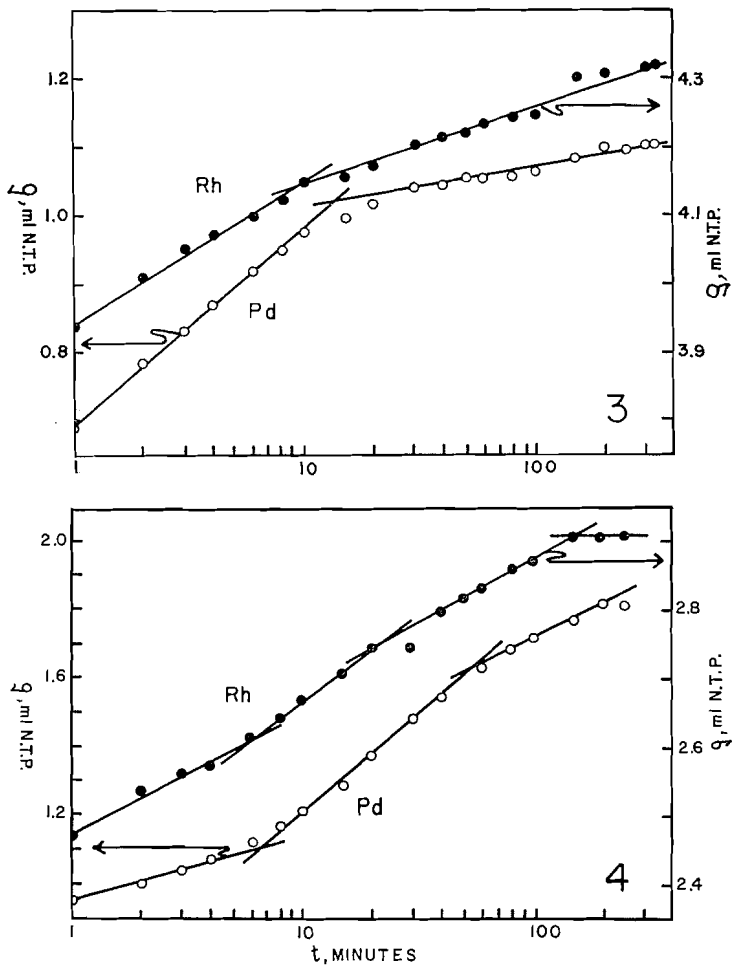


FIG. 3. Typical runs. Rh: run D65, 56° C, 50.5 cm DBP; Pd: run E57, 200° C, 44.2 cm DBP.
FIG. 4. Typical runs. Rh: run D66, 257° C, 51.7 cm DBP; Pd: run E74, 56° C, 50.88 cm DBP.

Can. J. Chem. Downloaded from www.nrcresearchpress.com by 41.223.56.140 on 09/04/12
For personal use only.

At intermediate pressures of about 20 to 50 cm DBP, stages II and III generally appear. The experimental plots have the appearance of the schematic plot 2 of Fig. 1, and correspond to the region B of Fig. 2. Examples of such data are shown by the plots of Fig. 3. For such cases the preceding stage I is assumed to have appeared before the time of the first measurement. Stage IV, the termination of the adsorption, must appear at higher t values.

At intermediate pressures some plots showed the presence of stages I, II, and III, having an appearance like the schematic plot 3 of Fig. 1. This corresponds to a combination of the regions B and C of Fig. 2. Such data is illustrated by the plots of Fig. 4. Such three-stage plots were found frequently with the H_2–Pd system.

Also, at intermediate pressures, several plots were obtained which were linear throughout, like the schematic curve 4 of Fig. 1. Such plots were assigned stage II connotation because the value of the corresponding α corresponds very closely to stage II α values to be expected from a knowledge of α values of stage II of other runs.

At P_s from about 40 to 70 cm DBP, the $q - \log t$ plots had the appearance of the schematic curve 5 of Fig. 1. This implies the appearance of stages I and II. Such plots correspond to the region C of Fig. 2. Examples of such data are shown by the plots of Fig. 5. For these

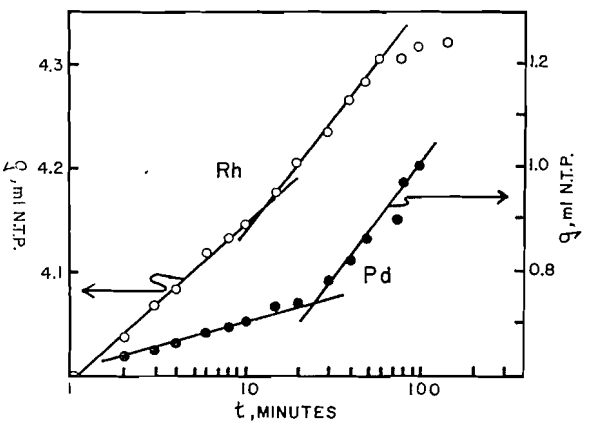


FIG. 5. Typical runs. Rh: run D40, 100° C, 51.3 cm DBP; Pd: run E36, 100° C, 51.7 cm DBP.

cases, stages III and IV would appear if the adsorption could be followed for a sufficiently long period of time. In practice this is frequently not possible because the rate of adsorption at long times becomes so slow that the precision of measurements is poor and hence continuation of the experiment is useless.

The kinetic multiplicity is further complicated by effects of P_s and temperature on the α and a values of individual kinetic stages. Changes in the slopes of the $q - \log t$ plots with changing temperature or pressure are reflected as changes in the co-ordinates of the intersections of two kinetic stages. Such effects are illustrated by the plots of Figs. 6, 7, and 8. In Fig. 6 the q-co-ordinate of the intersection of stages I and II, q_{bI}, is seen to decrease with increasing temperatures. Increase in P_s causes increase in q_{bI} and in q_{bII}, the latter being the co-ordinate of intersection of stages II and III. The corresponding t-co-ordinates, t_{bI} and t_{bII}, decline with increasing P_s, as illustrated by Fig. 8. The t_b-temperature relations are not clear.

The appearance of three consecutive stages in some plots, such as those of Fig. 4, as well as the consistent changes in α values of corresponding stages with changing

Can. J. Chem. Downloaded from www.nrcresearchpress.com by 41.223.56.140 on 09/04/12
For personal use only.

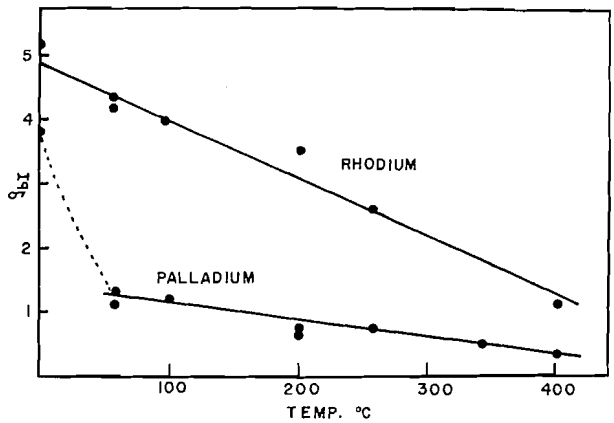


FIG. 6. The influence of temperature on the break.

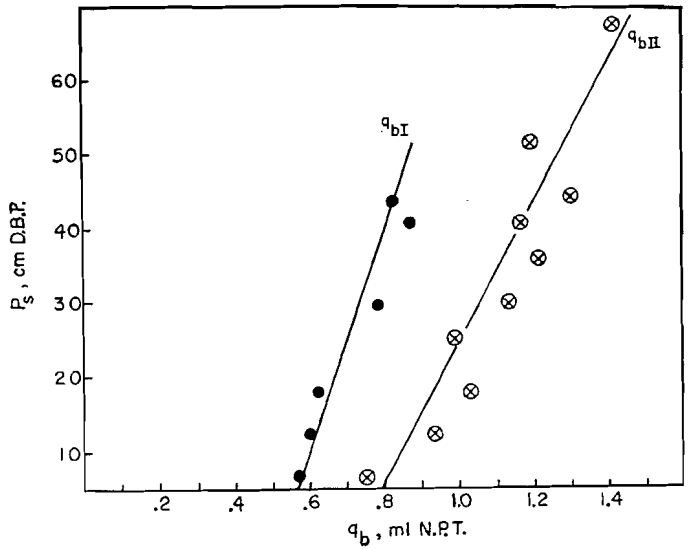


FIG. 7. The influence of P_s on the break. q_{bI} and q_{bII} refer to the q-co-ordinates of the intersection of stages I and II, and stages II and III, respectively. H_2–Pd, 100° C.

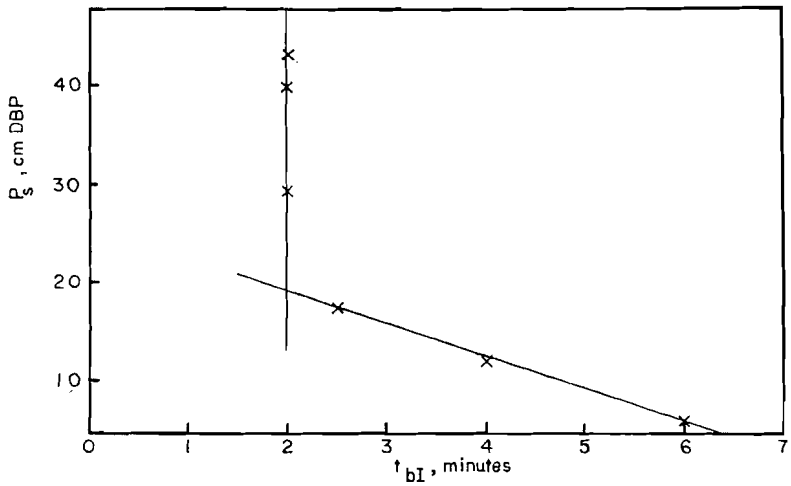


FIG. 8. The influence of P_s on the break. t_{bI} is the t-co-ordinate of the intersection of stages I and II. H_2–Pd, 100° C.

Can. J. Chem. Downloaded from www.nrcresearchpress.com by 41.223.56.140 on 09/04/12
For personal use only.

temperature or pressure, suggest that the composite structure of Fig. 2 is consistent with the data. Similar changes to both relatively faster and slower rates, apparently occurring haphazardly, have been found previously in the system H_2–$ZnO \cdot Cr_2O_3$ (2, 7), and in the system H_2–Ir–Al_2O_3 (4), while in the system H_2–ZnO (8) breaks towards a relatively faster rate were consistently obtained. It appears probable that in those systems a similar succession of kinetic stages exists.

The Effects of P_s and Temperature

At 100°, 200°, and 257° C a series of runs were made at random at different P_s, permitting some observations to be made on the effects of P_s and temperature on the constants a and α. If the scheme of Fig. 2 is adopted then a consistent correlation between values of the parameter a or α for any one stage and P_s and temperature is possible. In this fashion values of α for stage II lines (α_2), for example, are compared with other α_2 values, and the temporal order of appearance of the lines on $q - \log t$ plots is disregarded.

The effects found are less clearcut than those of previous studies because (*a*) different kinetic stages appeared under different conditions of temperature and P_s, in a manner discussed above, so that over some P_s regions not enough data are available for correlation, and (*b*) scatter of parameter values with changing P_s was encountered, this being particularly noticeable in the highly sensitive a values. The correlations between parameters and P_s and temperature were similar to those obtained previously (2–6), roughly linear changes being obtained, so that the following statements, illustrated by the plots of Figs. 9 and 10, suffice to describe the data. (*a*) Multiple kinetic stages exist, as described above. (*b*) For both adsorption systems, an increase in temperature decreases the amounts of gas adsorbed over the range 56°–400° C. This is shown by the plots of Fig. 9, which are

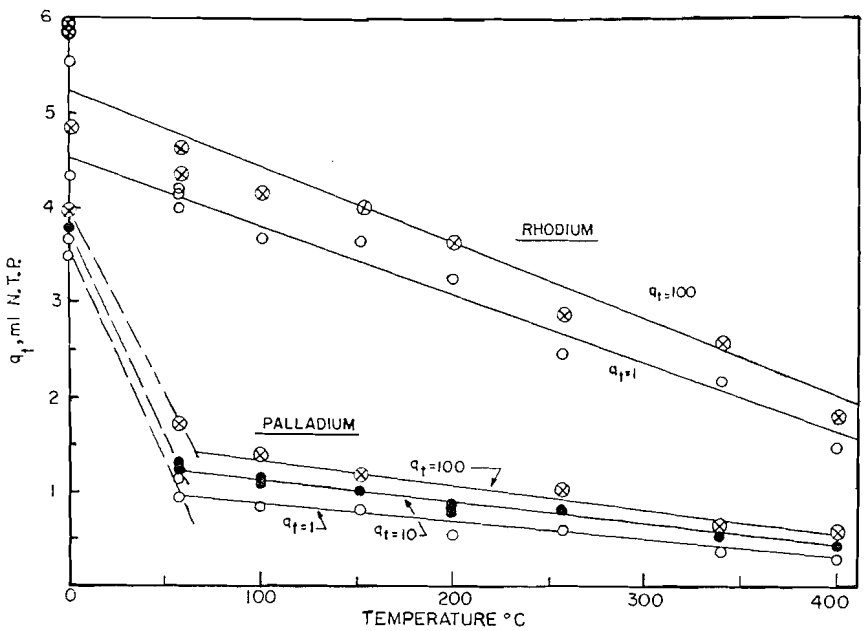


FIG. 9. The effect of temperature on adsorption. q_t is the amount adsorbed after t minutes.

essentially isobars at P_s = 51 cm DBP. (*c*) For the H_2–Rh system, momentary rates of adsorption ($\propto 1/\alpha$) are increased, but values of a are decreased with increasing temperature. (*d*) For the H_2–Pd system, momentary rates of adsorption are decreased with increasing temperatures, and initial rates similarly decrease slightly or remain constant.

Can. J. Chem. Downloaded from www.nrcresearchpress.com by 41.223.56.140 on 09/04/12
For personal use only.

(*e*) For both adsorption systems the general effect of increasing initial gas pressure is to increase adsorption rates, but in discontinuous fashion. At pressures below about 30 cm DBP the effects of increasing P_s on parameter values are larger than those above that pressure. Such discontinuity is illustrated by the α–P_s plots of Fig. 10.

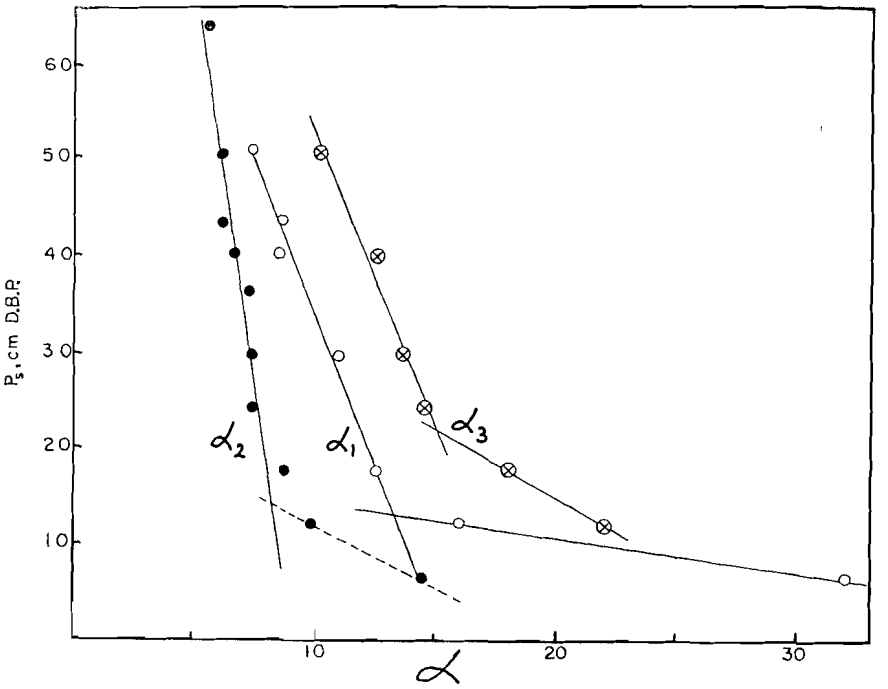


FIG. 10. The effect of P_s on α values. H_2 adsorption on Pd at 100° C.

A complete, physical explanation for the observed multiple stages has not been devised. It is possible that they may result from surface contamination, a suggestion supported by such observations as: originally (3) linear $q - \log t$ plots were found with the system H_2–Ru, while in a later study (5) breaks occurred; with CO adsorption on clean Ru (5) the rate declined monotonically whereas it was discontinuous when H_2 was preadsorbed on the solid; for the H_2–Ni–SiO_2 system (9) on rigorous reduction a fast adsorption was increased in magnitude at the expense of a slow adsorption; under conditions of preadsorption of CO on Ru, two kinetic processes of H_2 adsorption exist (5), the region of discontinuity of rates being approximately linearly dependent on the amount of preadsorbed CO. However, the rigorous reduction conditions, the apparent stability of the adsorbent surfaces, and the dependence of kinetic stages on temperature and pressure suggest that a simple poisoning phenomenon is unlikely to account for the present observations. Rather, some model of a surface is required which changes its character drastically by the very act of adsorption. The present results are reminiscent of the observations of Becker (10) on the change of sticking coefficient with coverage of several molecules on W ribbons, which led to the suggestion that the adsorption properties of a metal surface change rather abruptly when adsorbed species make the first set of valence bonds with every surface metal atom and again when they make second valence bonds. The observed temperature and pressure dependencies of the kinetic stages, however,

Can. J. Chem. Downloaded from www.nrcresearchpress.com by 41.223.56.140 on 09/04/12
For personal use only.

require a different model, such as that suggested by Taylor and Thon (1), according to which the discontinuities would represent change-over of the adsorption process from one kind of site to another before coverage is complete. With homotatic surfaces such as those presented by the probably polycrystalline Ru and Pd adsorbents, such a mechanism is not implausible.

REFERENCES

1. H. A. TAYLOR and N. THON. J. Am. Chem. Soc. **74**, 4169 (1952).
2. M. J. D. LOW and H. A. TAYLOR. J. Electrochem. Soc. **106**, 524 (1959).
3. M. J. D. Low and H. A. TAYLOR. Can. J. Chem. **37**, 544 (1959).
4. M. J. D. Low and H. A. TAYLOR. Can. J. Chem. **37**, 915 (1959).
5. M. J. D. Low and H. A. TAYLOR. J. Electrochem. Soc. **106**, 138 (1959).
6. L. LEIBOWITZ, M. J. D. LOW, and H. A. TAYLOR. J. Phys. Chem. **62**, 471 (1958).
7. J. DECRUE. Ph.D. Thesis, Princeton University, Princeton, New Jersey. 1951.
8. M. J. D. LOW. Can. J. Chem. **37**, 1916 (1959).
9. G. C. A. SCHUIT and N. H. DE BOER. Rec. trav. chim. **70**, 1067 (1957).
10. J. A. BECKER. Solid state physics. Vol. VII. *Edited by* F. Seitz and D. Turnbull. Academic Press Inc., New York. 1958. p. 379.

Can. J. Chem. Downloaded from www.nrcresearchpress.com by 41.223.56.140 on 09/04/12
For personal use only.

Can. J. Chem. Downloaded from www.nrcresearchpress.com by 41.223.56.140 on 09/04/12
For personal use only.

DECOMPOSITION OF ZINC OXIDE[1]

E. A. SECCO

ABSTRACT

Experimental results on the loss in weight of zinc oxide in a closed vessel under varying conditions of temperature, initial zinc pressure, oxygen pressure, and vacuum are reported. The data show more consistency interpreted in terms of dissociation rather than sublimation of the oxide. Plots of $\log_{10} K_p$ versus $1/T$ and $\log_{10} P_{ZnO}$ versus $1/T$ yield slopes corresponding to 24.0±2.0 kcal and 43.0±5.0 kcal, respectively. These results cannot be explained on the basis of available thermodynamic data. Interpretations of these results in terms of an unstable suboxide and non-equilibrium are discussed.

INTRODUCTION

It was observed in 1954 during a study (1) on the exchange between zinc vapor and single crystals of zinc oxide that there occurred appreciable losses from a bucket carrying the oxide in a closed quartz vessel at 1025° C. The oxide losses from the bucket were much greater at low zinc pressures. It was further confirmed that considerable oxide was lost from the bucket in a vacuum, i.e., 5×10^{-4} mm Hg. These observations could not be explained by a decomposition reaction on the basis of the standard free energy for the reaction

$$ZnO_{(c)} = Zn_{(g)} + \tfrac{1}{2}O_{2(g)}$$

that is, $\Delta G^\circ = -114{,}640+51.65\ T$ cal/mole (2). The equilibrium pressures of zinc and oxygen from the above reaction as estimated from the equilibrium constant $K_p = P_{Zn}P_{O_2}^{\frac{1}{2}}$ are many orders of magnitude below the experimental pressures.

A recent study (3) involving zinc oxide at low pressures and lower temperatures has shown a recurrence of appreciable losses of the oxide. This report contains experimental data pertaining to loss in weight of zinc oxide under varying conditions of temperature, initial zinc pressure, oxygen pressure, and vacuum.

EXPERIMENTAL

The polycrystalline ZnO used in this work was the Fisher Certified Reagent Grade with a certified purity of 99.98%. The zinc oxide was stated to be a product of the Dry Process. The oxide powder was dried in an oven at 150° C for at least 10 hours before using. The surface area of the oxide powder was found to be 3.39 m^2/g as determined by krypton adsorption measurements. The particle size is calculated to be ca. 3×10^{-5} cm.

These experiments were carried out in a static system with the use of quartz vessels which has already been described (1). All weighings were done on a single pan, constant load, Gram-atic Balance (E. Mettler, Zürich, Switzerland) and the weights were obtained to 0.05 mg. The weighed bucket bearing the zinc oxide was suspended at the center in the quartz vessel. The vessel was connected to a vacuum system, evacuated for 1 hour at 200° C, sealed, and placed in the furnace. The furnace with its temperature regulation and the timing of the anneal was already described (3). After the anneal the vessel was withdrawn, allowed to cool to room temperature, and opened. The bucket was withdrawn and reweighed. The difference in weighings represented the loss in weight of the oxide.

RESULTS

In Table I are given the losses in weight of zinc oxide at different temperatures while maintaining a constant initial zinc pressure, calculated from the ideal gas equation, i.e.,

[1]*Manuscript received December 23, 1959.*
Contribution from the Chemistry Department, St. Francis Xavier University, Antigonish, Nova Scotia.

TABLE I

Constant initial $P_{Zn} = 0.25$ atm and $s = 0.45$

Run	T °K	Observed loss in weight (mg)	Time (min)	P_{ZnO} (atm)	P_{O_2} (atm)	K_p ($P_{Zn}P_{O_2}^{\frac{1}{2}}$)
1	1073	0.7	70.0	3.2×10^{-3}	1.6×10^{-3}	1.0×10^{-2}
2	1093	1.1	70.1	5.1×10^{-3}	2.5×10^{-3}	1.3×10^{-2}
3	1113	1.3	71.4	6.1×10^{-3}	3.1×10^{-3}	1.4×10^{-2}
4	1133	2.3	70.2	1.1×10^{-2}	5.5×10^{-3}	1.9×10^{-2}
5	1153	3.0	70.2	1.5×10^{-2}	7.5×10^{-3}	2.3×10^{-2}
6	1173	4.5	70.1	2.2×10^{-2}	1.1×10^{-2}	2.8×10^{-2}
7	1193	4.6	75.1	2.3×10^{-2}	1.2×10^{-2}	2.9×10^{-2}
8	1193	2.3	77.2	1.2×10^{-2}	6.0×10^{-3}	2.0×10^{-2}
9	1213	9.0	77.3	4.6×10^{-2}	2.3×10^{-2}	4.5×10^{-2}
10	1233	4.7	76.3	2.4×10^{-2}	1.2×10^{-2}	3.0×10^{-2}
11	1233	4.5	79.1	2.4×10^{-2}	1.2×10^{-2}	3.0×10^{-2}
12	1253	5.7	75.4	3.0×10^{-2}	1.5×10^{-2}	3.4×10^{-2}
13	1253	6.0	77.7	3.2×10^{-2}	1.6×10^{-2}	3.6×10^{-2}
14	1273	13.0	85.0	7.0×10^{-2}	3.5×10^{-2}	6.0×10^{-2}

$PV = nRT$, and constant mole fraction of zinc in the solid oxide, s. The volume of the vessel, V, was 0.24 liter. Included in this table are the observed losses in terms of the pressure of zinc oxide vapor, P_{ZnO}, if the loss was due to evaporation of the oxide and the oxygen pressure, P_{O_2}, if dissociation occurred. The terminal column contains the values of the equilibrium constant, $K_p = P_{Zn}P_{O_2}^{\frac{1}{2}}$, for the dissociation reaction.

Table II contains the loss in weight as a function of initial zinc pressure at constant temperature and constant s. The weight losses are given in terms of P_{ZnO}, P_{O_2}, and K_p as in Table I. The average values of P_{ZnO} and K_p are shown on the bottom of their respective columns. On withdrawal of the vessel from the furnace after the anneal it was invariably observed for experiments involving an initial zinc pressure that the zinc oxide was dark gray or black. The color of the oxide transformed to pale cream within 1 minute after withdrawal, indicating that the adsorbed zinc on the oxide condensed on the cooler walls of the vessel. In experiments 27 and 29 of Table II metallic zinc deposits were observed

TABLE II

Constant $T = 1193°$ K and $s = 0.45$

Run	Observed loss in weight (mg)	Initial P_{Zn} (atm)	Time (min)	P_{ZnO} (atm)	P_{O_2} (atm)	K_p ($P_{Zn}P_{O_2}^{\frac{1}{2}}$)
15	4.0	0.11	81.0	2.0×10^{-2}	1.0×10^{-2}	1.3×10^{-2}
16	3.4	0.16	80.3	1.7×10^{-2}	8.5×10^{-3}	1.6×10^{-2}
17	2.2	0.21	80.5	1.1×10^{-2}	5.5×10^{-3}	1.6×10^{-2}
18	2.9	0.30	80.3	1.5×10^{-2}	7.5×10^{-3}	2.7×10^{-2}
19	2.2	0.41	81.6	1.1×10^{-2}	5.5×10^{-3}	3.1×10^{-2}
20	2.0	0.45	80.5	1.0×10^{-2}	5.0×10^{-3}	3.3×10^{-2}
21	1.6	0.50	80.3	8.1×10^{-3}	4.0×10^{-3}	3.1×10^{-2}
22	2.0	0.57	80.4	1.0×10^{-2}	5.0×10^{-3}	4.1×10^{-2}
23	2.3	0.68	84.1	1.2×10^{-2}	6.0×10^{-3}	5.4×10^{-2}
24	0.9	0.79	80.3	4.5×10^{-3}	2.3×10^{-3}	3.8×10^{-2}
25	1.5	0.82	80.3	7.5×10^{-3}	3.8×10^{-3}	5.1×10^{-2}
26	1.5	0.96	85.5	7.5×10^{-3}	3.8×10^{-3}	5.9×10^{-2}
27	18.6	0	80.2	9.3×10^{-2}	4.7×10^{-2}	2.0×10^{-2}*
28	8.6	0	123.5	4.3×10^{-2}	2.2×10^{-2}	6.4×10^{-3}*
29	53.3	0	82.4	0.27	0.14	1.0×10^{-1}*
Mean values				3.6×10^{-2}		3.6×10^{-2}

*Exchanged radioactive ZnO was used in these experiments.

Can. J. Chem. Downloaded from www.nrcresearchpress.com by 41.223.56.140 on 09/04/12
For personal use only.

on the vessel walls along with a slight yellow zinc oxide deposit which became white on cooling. The zinc deposit in experiment 29 was especially noticeable and was estimated to be ca. 30 mg.

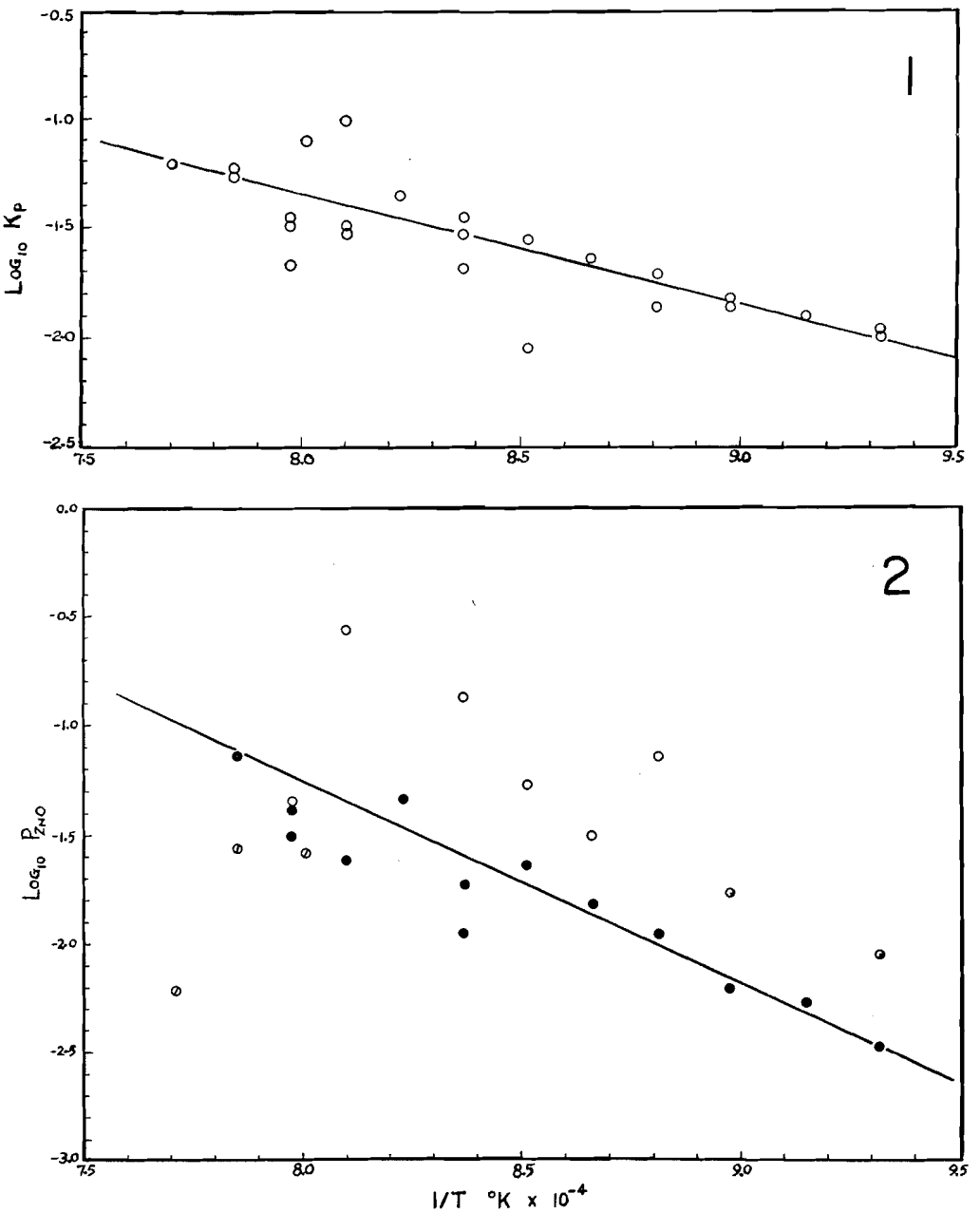


FIG. 1. Plot of $\log_{10} K_p$ against the reciprocal of absolute temperature.
FIG. 2. Plot of $\log_{10} P_{ZnO}$ against the reciprocal of absolute temperature.

● Initial P_{Zn} = 0.25 atm. ⊘ Single crystals ZnO.
◑ Initial P_{Zn} = 0.14 atm. ○ Vacuum, i.e., 5×10^{-4} mm Hg.

Can. J. Chem. Downloaded from www.nrcresearchpress.com by 41.223.56.140 on 09/04/12
For personal use only.

Figure 1 shows a plot of the logarithm of the dissociation constant K_p against the reciprocal of the absolute temperature with the slope of the best straight line yielding an energy term of 24.0±2.0 kcal/mole. In Fig. 2 is given a plot of the logarithm of zinc

TABLE III

Constant T = 1153° K and in vacuum, i.e., 5×10^{-4} mm Hg

Run	Observed loss in weight (mg)	Time (min)	P_{ZnO} (atm)	P_{O_2} (atm)	K_p ($P_{Zn}P_{O_2}^{\frac{1}{2}}$)
30	4.3	30.3	2.1×10^{-2}	1.0×10^{-2}	2.1×10^{-3}*
31	10.1	100.3	4.9×10^{-2}	2.5×10^{-2}	7.7×10^{-3}*
32	2.8	55.3	1.4×10^{-2}	7.0×10^{-3}	1.1×10^{-3}*
33	9.3	76.0	4.5×10^{-2}	2.3×10^{-2}	7.5×10^{-3}*
34	6.2	135.8	3.0×10^{-2}	1.5×10^{-2}	3.7×10^{-3}*
35	4.8	90.3	2.4×10^{-2}	1.2×10^{-2}	2.6×10^{-3}*
Mean values			3.1×10^{-2}		4.5×10^{-3}

*Exchanged radioactive ZnO was used in these experiments.

TABLE IV

Constant T = 1253° K

Run	Observed loss in weight (mg)	Initial P_{Zn} (atm)	Time (min)	P_{ZnO} (atm)	P_{O_2} (atm)	K_p ($P_{Zn}P_{O_2}^{\frac{1}{2}}$)
36	8.1	0	45.1	4.6×10^{-2}	2.3×10^{-2}	7.0×10^{-3}
37	7.9	0	77.3	4.2×10^{-2}	2.1×10^{-2}	6.1×10^{-3}
38	11.8	0.075	62.1	6.3×10^{-2}	3.2×10^{-2}	2.5×10^{-2}
39	7.5	0.075	32.1	4.0×10^{-2}	2.0×10^{-2}	1.6×10^{-2}
40	9.2	0.075	116.2	4.9×10^{-2}	2.5×10^{-2}	2.0×10^{-2}
41	7.6	0.075	73.3	4.0×10^{-2}	2.0×10^{-2}	1.6×10^{-2}
42	12.9	0.075	135.5	6.9×10^{-2}	3.5×10^{-2}	2.7×10^{-2}
43	3.6	0.075	69.4	1.9×10^{-2}	1.0×10^{-2}	9.4×10^{-3}
44	17.2	0.075	327.4	9.1×10^{-2}	4.6×10^{-2}	3.6×10^{-2}
Mean values				5.3×10^{-2}		2.1×10^{-2}

TABLE V

Run	T °K	Observed loss in weight (mg)	Initial P_{Zn} (atm)	Time (min)	P_{ZnO} (atm)	P_{O_2} (atm)	K_p $P_{Zn}P_{O_2}^{\frac{1}{2}}$)
45	1133	14.9	0	70.2	7.1×10^{-2}	3.6×10^{-2}	1.4×10^{-2}
46	1173	10.7	0	70.2	5.3×10^{-2}	2.7×10^{-2}	8.7×10^{-3}
47	1233	52.2	0	61.0	0.27	0.14	1.0×10^{-1}
48	1193	0.0	air (1 atm)	600.0	—	—	—*
49	1073	1.9	0.14	60.0	8.6×10^{-3}	4.3×10^{-3}	1.0×10^{-2}
50	1113	3.5	0.14	60.0	1.7×10^{-2}	8.5×10^{-3}	1.5×10^{-2}
51	1248	0.5	1.12	60.0	2.6×10^{-3}	1.3×10^{-3}	1.3×10^{-2}
52	1298	1.1	1.12	45.0	6.0×10^{-3}	3.0×10^{-3}	6.1×10^{-2}
53	1273	0.0	1.96	60.0	—	—	—
54	1273	2.0	0.20	60.0	—	—	—†
55	1273	10.8	0	150.0	5.8×10^{-2}	2.9×10^{-2}	1.0×10^{-2}*
56	1273	1.2	1.12	60.0	6.4×10^{-3}	3.2×10^{-3}	6.4×10^{-2}
57	1273	27.8	0.22	120.0	1.5×10^{-1}	7.5×10^{-2}	1.0×10^{-1}
Mean values					7.2×10^{-2}		5.8×10^{-2}

*Exchanged radioactive ZnO was used in these experiments.
†Pressure of argon in reaction vessel ca. 1 atm.

Can. J. Chem. Downloaded from www.nrcresearchpress.com by 41.223.56.140 on 09/04/12
For personal use only.

oxide pressure, P_{ZnO}, against the reciprocal of the absolute temperature with the slope of the best straight line corresponding to an energy of 43.0±5 kcal/mole. The values of P_{ZnO} and K_p plotted in Figs. 1 and 2 include all values from all tables; where two or more experiments were carried out at constant temperature, the average values of P_{ZnO} and K_p were plotted. The average values plotted are given on the bottom of their respective columns in each table. It is noteworthy that the K_p values corresponding to the weight losses observed for single crystals, experiments 51, 52, 55–57, are in agreement with the values obtained in this work.

DISCUSSION

The results reported herein defy explanation by simple conventional equilibria, i.e.,

[1] $$ZnO_{(s)} = Zn_{(g)} + \tfrac{1}{2}O_{2(g)}$$

and

[2] $$ZnO_{(s)} = ZnO_{(g)}$$

where the heat of sublimation of [2] is 10.1 kcal/mole (4). Since it has been established (5) that ZnO sublimes only by dissociation into $Zn_{(g)}$ and $O_{2(g)}$, reaction [2] is disregarded in favor of reaction [1] in this discussion. There has been passing reference (6, 7) to the fact that there is an apparent oxygen dissociation pressure of zinc oxide, which is many orders of magnitude greater than that deduced theoretically from the thermodynamic data. More recently Moore and Williams (8) reported some data on dissociation of zinc oxide by zinc vapor. According to their data the rate of evaporation of ZnO in zinc vapor is ca. 10^9 times the equilibrium value as calculated from the standard free energy data. Moore and Williams' data are concordant with our results which indicate that our equilibrium dissociation constant is greater than that calculated from the standard free energy data by a factor of ca. 10^8.

How can ZnO decompose under conditions deemed thermodynamically unfeasible? One *ad hoc* possibility is the existence of an unstable superficial suboxide such as Zn_2O or Zn_4O_3. If the surface of the ZnO becomes covered with an impervious layer of the suboxide so as to isolate the oxide, the dissociation reaction is essentially that of the solid suboxide. This possibility is supported by the observation that the oxide is completely covered with zinc during the anneal. Further evidence for a zinc-rich film on the oxide surface was obtained during sintering studies at 500° C and at oxygen pressure at 10 mm when the oxide became gray and exhibited a positive temperature coefficient of resistance and very high conductivity (7). The formation of the zinc-rich surface on zinc oxide in the latter case has been explained in terms of Schottky disorder where zinc leaves its normal lattice site and takes up normal positions on the surface of the oxide.

Appreciable dissociation of ZnO may be the result of a highly defective surface zone (9) which is without the limits of thermodynamics. Although it is not certain what is defined by this defective surface zone it must be recognized that some surface variable exists which could play an important role in the dissociation reaction. It is of significance that heat treatment and adsorbed gases can affect the activity and hence the defect constitution of the surface. In this regard, experiment 54 shows negligible loss with ca. 1-atm argon as contrasted to experiment 57 without argon. Furthermore, widely divergent weight losses were observed in experiments 27–29 following an identical procedure. In experiment 48, when zinc oxide was exposed to the atmosphere in an open vessel no loss was observed. It is quite reasonable therefore to believe that a non-equilibrium condition exists where

Can. J. Chem. Downloaded from www.nrcresearchpress.com by 41.223.56.140 on 09/04/12
For personal use only.

the decomposition is determined by rate processes, such as diffusion of defects to surfaces and interface reactions. This problem of oxide decomposition at temperatures much lower than those predicted from thermodynamic data is not restricted to ZnO. The decomposition of NiO and alumina have already been reported (10, 11). Very little is known about the detailed mechanisms of such a reaction as decomposition of an oxide at the crystal–gas interface, but the present observations, if extended, may show that such reactions proceed through more complex mechanisms than have been hitherto suspected.

ACKNOWLEDGMENTS

This research was made possible by the generous support of Mr. J. A. Hackett, J. Bradley Streit Company, Ltd., and Mr. Louis Chesler, all of Toronto, Ontario, and of a benefactor who wishes to remain anonymous.

REFERENCES

1. E. A. SECCO and W. J. MOORE. J. Chem. Phys. **26**, 942 (1957). W. J. MOORE and E. A. SECCO. Diffusion and exchange of zinc in crystalline zinc oxide. U.S. Atomic Energy Comm. Rept., Bloomington, Indiana. August, 1955.
2. J. A. KITCHENER and S. IGNATOWICZ. Trans. Faraday Soc. **47**, 1278 (1951).
3. E. A. SECCO. Discussions Faraday Soc. In press. 1959.
4. G. HÜTTIG. Z. anorg. Chem. **207**, 273 (1932).
5. M. POURBAIX. Bull. soc. chim. Belges, **53**, 159 (1944).
6. T. J. GRAY. Discussion during Symposium on Sintering, University of Bristol, England. 1952.
7. T. J. GRAY. J. Am. Ceram. Soc. **37**, 534 (1954).
8. W. J. MOORE and E. L. WILLIAMS. J. Phys. Chem. **63**, 1516 (1959).
9. T. J. GRAY. The defect solid state. Interscience Publishers, Inc., New York. 1957. p. 114.
10. S. J. TEICHNER and J. A. MORRISON. Trans. Faraday Soc. **51**, 961 (1955).
11. S. J. TEICHNER. Discussions Faraday Soc. In press. 1959.

Can. J. Chem. Downloaded from www.nrcresearchpress.com by 41.223.56.140 on 09/04/12
For personal use only.

Can. J. Chem. Downloaded from www.nrcresearchpress.com by 41.223.56.140 on 09/04/12
For personal use only.

THE ACIDITY FUNCTIONS H_0 AND $J_0(H_R)$ FOR THE SYSTEM FORMIC ACID – WATER[1]

ROSS STEWART AND TREVOR MATHEWS

ABSTRACT

The acidity functions H_0 and $J_0(H_R)$ have been measured for the whole range of the formic acid – water system. The large negative J_0 values for the more concentrated solutions fail to correlate with the functions derived by Gold on the basis of certain assumptions regarding the activity coefficients of the species involved. The cause of this deviation is discussed. The term log $[R^+]/[ROH]$ for the ionization of triphenylcarbinols in formic acid has been found to vary linearly with $1/T$.

The Hammett acidity function, H_0, which measures the tendency of a solvent to transfer a proton to a neutral base has found wide application in two important fields, viz. the determination of the strengths of very weak bases and the study of acid-catalyzed reaction mechanisms in strongly acid media. It describes the simple ionization

$$B + H^+ \rightleftharpoons BH^+ \qquad [1]$$

and H_0 values, defined by the equation

$$H_0 \equiv pK_{BH^+} - \log [BH^+]/[B], \qquad [2]$$

have been determined for solutions of several strong acids in water and other solvents (1, 2). The values of pK_{BH^+} for the various indicators used to establish the H_0 scale must be obtained by a stepwise operation starting from a dilute aqueous solution of the acid where the activities of the various species involved in the equilibrium are assumed to be the same as in pure water.

A different acidity function governs the ionization of secondary bases, i.e. those compounds which ionize as follows:

$$ROH + H^+ \rightleftharpoons R^+ + H_2O. \qquad [3]$$

Lowen, Murray, and Williams examined such a system and used the term H_R to describe the acidity function governing the ionization (3). Gold and Hawes (4) soon after used the symbol J_0 for this function which is defined as follows:

$$J_0 \equiv pK_{R^+} - \log [R^+]/[ROH]. \qquad [4]$$

K_{R^+} is the ionization constant which governs reaction 3 and is defined as

$$K_{R^+} = \frac{a_{ROH} \cdot a_{H^+}}{a_{R^+} \cdot a_{H_2O}}. \qquad [5]$$

(Throughout this paper "a" stands for activity, "f" for activity coefficient, [ ] for molar concentration, and $[\ ]_N$ for concentration in units of mole fraction). Here again a stepwise operation is required to find the values of pK_{R^+} for the indicators used to establish the J_0 scale for concentrated acid solutions.

It can be shown that

$$H_0 = -\log (a_{H^+} \cdot f_B/f_{BH^+}) \qquad [6]$$

$$J_0 = -\log \left(a_{H^+} \cdot f_{ROH}/f_{R^+} \cdot \frac{1}{a_{H_2O}} \right) \qquad [7]$$

and Gold and Hawes (4) suggested that $J_0 = H_0 + \log a_{H_2O}$ (equation 7) which is based

[1]*Manuscript received November 2, 1959.*
Contribution from the Department of Chemistry, University of British Columbia, Vancouver, British Columbia.

on the assumption—a reasonable one in view of earlier work—that $f_B/f_{ROH} = f_{BH^+}/f_{R^+}$ (equation 8) where ROH is a secondary base, such as triphenylcarbinol, and where B is a base of the ammonia type used to establish the H_0 scale. Cryoscopic measurements show clearly that triphenylcarbinol is ionized by sulphuric acid as follows (5, 6):

$$(C_6H_5)_3COH + 2H_2SO_4 \rightleftharpoons (C_6H_5)_3C^+ + H_3O^+ + 2HSO_4^- . \quad [8]$$

Gold and Hawes used vapor pressure data to obtain the acitivity of water in sulphuric acid solutions and thus calculated J_0 values for sulphuric acid solutions of from 5% to 95% composition by means of equation 7. Since at that time values of pK_{R^+} had not been established for any secondary bases, the only test of equation 7 and the principles used in its derivation was to plot values of log $[R^+]/[ROH]$ for a secondary base dissolved in sulphuric acid against values of J_0 calculated using equation 7. Equation 4 shows that a straight line of unit slope should result. When data for 4,4′,4″-trinitrotriphenylcarbinol was plotted in this way, a straight line of slope 1.16 was obtained in fairly close agreement with theory.

In 1955 Deno, Jaruzelski, and Schriesheim (7), starting with dilute aqueous solution, used the stepwise technique to determine values of pK_{R^+} for a series of substituted triphenylcarbinols and also values of the acidity function for secondary bases in sulphuric acid from 0–98% concentration. They observed that the acidity function departed very seriously from the values of J_0 obtained from equation 7 and suggested the symbol C_0 for the function defined by equation 4. They showed that this function correlated the change in rate with change in sulphuric acid concentration of several chemical reactions which were believed to proceed via the ionization reactions shown in equation 3.

At about the same time, Gold (8) derived two additional equations similar in form to equation 7 based on certain assumptions regarding the behavior of the various activity coefficients. These functions were designated J_0'' and J_0''' and the function defined by equation 7 as J_0'. Thus the true acidity function for secondary bases defined by equation 4 is referred to by Gold as J_0, and by Deno *et al.* first as C_0 (7) and subsequently as H_R (9). The function defined by equation 7 is now referred to by Gold as J_0' and by Deno *et al.* as J_0. Paul and Long in their review article (1) use J_0 as the symbol for the experimentally determined acidity function for secondary bases. However, since then Deno *et al.* (9) have abandoned C_0 in favor of Williams original symbol, H_R, and it would seem that both J_0 and H_R will continue to appear in the literature for some time. We have accordingly used both symbols throughout this paper to refer to the experimental acidity function and primed J_0 symbols for the derived functions.

Previous work by Stewart (10) and by Evans *et al.* (11) has shown that formic acid reduces the triphenylcarbinol to triphenylmethane probably via hydride transfer from formate ion to the carbonium ion. Formic acid is a medium which facilitates reduction of tertiary carbinols by this mechanism. It is sufficiently acidic to ionize triphenylcarbinols and some olefins to carbonium ions; it has a high dielectric constant (58.5 at 16°) and a high degree of autoprotolysis producing a reasonable concentration of formate ion, the reductant; and its oxidation product, carbon dioxide, is of low energy.

The purpose of this work, then, was to determine the values of the acidity functions, H_0 and $J_0(H_R)$, for formic acid solutions primarily for future use in kinetic studies, but in addition as a test of the validity of Gold's derived functions, J_0', J_0'', and J_0''', as approximations to the experimentally determined function J_0 in a solvent other than sulphuric acid. Bascombe and Bell have recently reported a careful investigation of acidity functions of some aqueous acids but did not list H_0 values for formic acid because of apparent discrepancies between values obtained with different indicators (12).

Can. J. Chem. Downloaded from www.nrcresearchpress.com by 41.223.56.140 on 09/04/12
For personal use only.

Can. J. Chem. Downloaded from www.nrcresearchpress.com by 41.223.56.140 on 09/04/12
For personal use only.

EXPERIMENTAL

Indicators

Triphenylcarbinol and *o*- and *p*-nitroaniline were reagent grade chemicals which were crystallized repeatedly to constant melting point. *p*-Nitrodiphenylamine was prepared from *p*-nitroaniline and bromobenzene by the method of Goldberg and Sissoeff (13). 4-Methoxytriphenylcarbinol was prepared by the Grignard synthesis using phenylmagnesium bromide and ethyl anisate after the method of Brand (14). 4,4′,4″-Trimethoxytriphenylcarbinol was also prepared by this method using 4,4′-dimethoxybenzophenone and *p*-bromoanisole.

Formic Acid

Reagent grade 88–90% formic acid, Baker and Adamson (4 l.), was distilled at reduced pressure and middle cuts of 1600 and 1200 ml were used as stock solutions. Titrations with standard base showed the formic acid content to be 94.5% and 87.4% respectively.

Anhydrous formic acid was prepared by zone freezing, as previously described (10), one liter of formic acid taken from the middle cut of two liters of Baker and Adamson 98–100% formic acid which had been distilled *in vacuo*. After three zone freezings the melting point of the residue (about 400 ml) was found to be 8.4° (15). Titration with standard base gave the formic acid content as 99.9%.

Measurement of H_0

H_0 values were calculated using equation 4 and the revised pK_{BH^+} values of Paul and Long (1). Measurements of the $[BH^+]/[B]$ ratio were made by adding 0.1 ml of a solution of the particular indicator dissolved in acetone to a 1-cm absorption cell fitted with a ground-glass neck and stopper. The acetone was evaporated, 3 ml of formic acid of known composition was added, and the optical density of the resulting solution which was generally of the order of 10^{-4} *M* in indicator was determined at λ_{max} using a Beckman DU spectrophotometer. Then 0.1 ml of the same indicator solution was dissolved in a known volume of water and the light absorption measured as before. The temperature was controlled to $25° \pm 0.5°$ by means of thermospacers. Each of the indicators was colorless in the ionized form but absorbed strongly in the visible or near ultraviolet in the unionized form. It was observed that a slow reaction occurred between the nitroanilines and the formic acid since the spectrum of the solution changed on long standing to resemble that of the corresponding formanilide (16). Extrapolations to zero time were made wherever the reaction was appreciable. Beer's law was checked for each indicator under conditions where $[BH^+]$ is negligible and each indicator was checked to ensure that no shift in λ_{max} occurred in going from water to formic acid solutions. It was observed, however, that values of $[BH^+]/[B]$ were not independent of the concentration of the base. Plots of the ratio against concentration of the base produced approximately straight lines which were extrapolated to zero concentration to determine the ratio used in the calculation.

Measurement of $J_0(H_R)$

$J_0(H_R)$ values were calculated using equation 4 and the pK_{R^+} values of Deno, Jaruzelski, and Schriesheim (7). The method of determining $[R^+]/[ROH]$ was similar to that used in determining $[BH^+]/[B]$ except that ROH was determined by addition of 0.1 ml of the carbinol solution to a known volume of formic acid of such concentration as to completely ionize the carbinol. For these compounds, of course, the colored species is the ion. The solutions were of the order of 10^{-4} to 10^{-5} *M*. The assumption that no change in extinction coefficient occurs with changing formic acid concentration was tested by measuring the optical density of the methoxy-substituted carbinols at λ_{max} for a range of 25% formic

acid above that at which the alcohol was effectively completely ionized to the carbonium ion. In these cases no change in extinction coefficient was observed.

As in the H_0 measurements the values of $[R^+]/[ROH]$ were found to be not independent of the concentration of the carbinol. Deno *et al.* (7) observed this phenomenon in sulphuric acid but found that at extremely low concentrations of carbinol using long path cells the ratio did become independent of concentration. In this work a linear extrapolation was used to find the limiting value of the ratio. This value may be very slightly in error in the light of the work of Deno *et al.*, but, if so, the error is small.

Since reduction of the carbinol can occur (10) in formic acid a plot of optical density against time was made for each carbinol solution in which appreciable fading of the carbonium ion occurred. This plot was extrapolated back to zero time in order to obtain $[R^+]$.

RESULTS AND DISCUSSION

Table I and Fig. 1 show the values of H_0 as a function of formic acid concentration.

TABLE I

H_0 values

o-Nitroaniline

$pK = -0.29$; $\lambda_{max} = 412$ mμ

% formic acid	$[BH^+]/[B]$	H_0
100	79.5	−2.19
99.6	60.0	−2.07
98.8	22.4	−1.65
97.8	13.2	−1.41
96.0	8.90	−1.24
94.4	6.3	−1.08
92.6	4.1	−0.90
89.4	2.9	−0.75
86.5	1.70	−0.52
83.5	1.32	−0.41
80.7	1.08	−0.25
77.5	0.675	−0.12
71.4	.33	+0.19
67.5	.275	+0.27
62.7	.174	+0.47
57.7	.145	+0.55

p-Nitroaniline

$pK = +0.99$; $\lambda_{max} = 380$ mμ

% formic acid	$[BH^+]/[B]$	H_0
86.5	31.0	−0.50
83.5	24.5	−0.40
77.5	13.1	−0.13
71.4	6.3	+0.19
66.5	5.4	+0.26
62.7	3.7	+0.44
57.7	2.7	+0.56
46.5	1.4	+0.85
41.5	1.2	+0.93
35.9	0.93	+1.03
29.5	.676	+1.16
23.9	.540	+1.26
19.2	.431	+1.35
14.7	.355	+1.44
11.2	.324	+1.48
6.1	.268	+1.58
4.4	.230	+1.63
2.0	.173	+1.75
.92	.098	+2.00

Can. J. Chem. Downloaded from www.nrcresearchpress.com by 41.223.56.140 on 09/04/12
For personal use only.

TABLE I *(Concluded)*

H_0 values

p-Nitrodiphenylamine
pK = −2.48; λ_{max} = 404 mμ

% formic acid	[BH$^+$]/[B]	H_0
100	0.55	−2.24

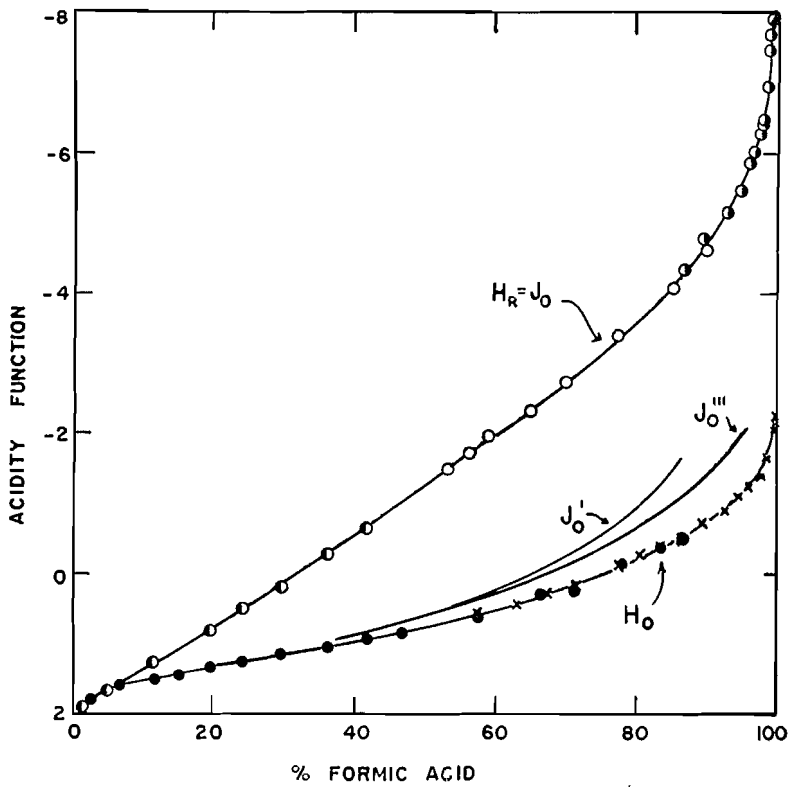


FIG. 1. Variation of acidity functions with formic acid concentration.
◑ Triphenylcarbinol. ○ 4-Methoxytriphenylcarbinol.
◐ 4,4′,4″-Trimethoxytriphenylcarbinol.
× *o*-Nitroaniline. ● *p*-Nitroaniline.

There appears to be satisfactory overlap in H_0 values for the indicators used, indicating that H_0 is independent of the base used for the determination. It should be pointed out, however, that less satisfactory agreement is obtained with our data using the indicator pK values of Bascombe and Bell (12) and that there is a variation in indicator ratio with indicator concentration, as described in the experimental section. This may account for our not observing the discrepancies noted by them. We can only report that for the indicators used in the present work a fair correlation was obtained indicating that H_0 is an approximately valid function in formic acid. In dilute solution the values of H_0 approach pH as required. The pH of 0.22 M formic acid in water should be 2.18; H_0 for this solution is 2.00.

Can. J. Chem. Downloaded from www.nrcresearchpress.com by 41.223.56.140 on 09/04/12
For personal use only.

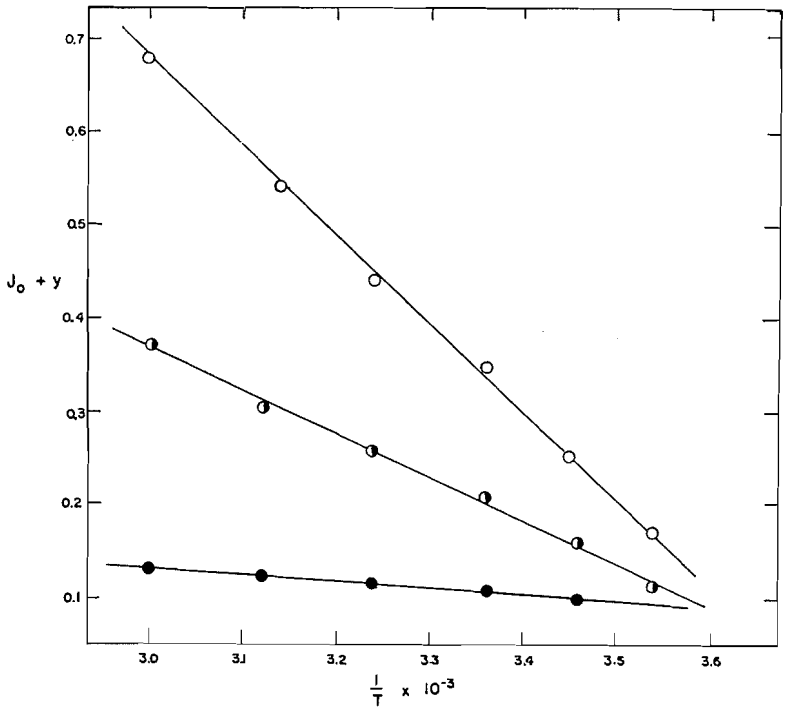


FIG. 2. Variation of apparent $J_0(H_R)$ with absolute temperature.
○ Triphenylcarbinol, $Y = 5.9$. ◑ 4-Methoxytriphenylcarbinol, $Y = 3.8$.
● 4,4′,4″-Trimethoxytriphenylcarbinol, $Y = 1.5$.

Table II and Fig. 1 show $J_0(H_R)$ as a function of formic acid concentration. There is reasonable overlap between triphenylcarbinol and 4-methoxytriphenylcarbinol. Although there is no overlap between 4-methoxytriphenylcarbinol and 4,4′,4″-trimethoxytriphenylcarbinol $dJ_0/d\%$ formic acid is the same for the lower region of the former curve and the upper region of the latter, a sufficient substitute for overlap. The $J_0(H_R)$ function therefore appears to be a valid acidity function in formic acid. As required, the values of $J_0(H_R)$ approach H_0 and pH in dilute formic acid.

Turning to Gold's derived quantities J_0', J_0'', and J_0''' we find them deviating rather widely from the experimental function $J_0(H_R)$. J_0' is defined by equation 9

$$[9] \qquad J_0' = H_0 + \log a_{H_2O}.$$

Values for the activity of water in formic acid solutions were calculated using the vapor pressure data of Takagi (17) and the equation $a_{H_2O} = p_{H_2O}/p^0_{H_2O}$ where $p^0_{H_2O}$ is the vapor pressure of pure water at the same temperature. A slight extrapolation was required to obtain the partial pressures of water at 25° in these solutions but any errors involved in the calculations are small compared with the difference between $J_0(H_R)$ and J_0' as shown in Fig. 1.

J_0'' is defined by equation 10,

$$[10] \qquad J_0'' = 2H_0 + \log [H_3O^+]_N + 1.74.$$

Can. J. Chem. Downloaded from www.nrcresearchpress.com by 41.223.56.140 on 09/04/12
For personal use only.

TABLE II

J_0 values

Triphenylcarbinol

$pK_{R^+} = -6.63$; $\lambda_{max} = 431$ mμ (ion)

% formic acid	$[R^+]/[ROH]$	$J_0(H_R)$
99.5	19.0[a]	−7.91[a]
99.1	11.5[a]	−7.69[a]
98.7	6.7[a]	−7.46[a]
98.3	2.14	−6.96
98.0	0.73	−6.49
97.9	0.667	−6.45
97.5	0.47	−6.30
96.6	0.242	−6.01
96.0	0.184	−5.89
94.5	0.069	−5.47
94.3	0.064	−5.43
92.7	0.036	−5.19
89.4	0.020	−4.81
86.5	0.005	−4.33

4-Methoxytriphenyl carbinol

$pK_{R^+} = -3.40$; $\lambda_{max} = 472$ mμ (ion)

% formic acid	$[R^+]/[ROH]$	$J_0(H_R)$
90.1	16.5	−4.62
85.0	4.5	−4.05
77.7	1.0	−3.40
70.1	0.23	−2.76
64.9	0.084	−2.32
58.8	0.037	−1.97
55.9	0.023	−1.76
53.0	0.0125	−1.50

4,4′,4″-Trimethoxytriphenyl carbinol

$pK_{R^+} = 0.82$; $\lambda_{max} = 483$ mμ (ion)

% formic acid	$[R^+]/[ROH]$	$J_0(H_R)$
41.5	32.0	−0.69
35.9	12.9	−0.29
29.5	4.16	+0.20
23.9	2.08	+0.50
19.2	1.02	+0.81
11.2	0.36	+1.27
4.4	0.14	+1.67

[a] These values must be regarded as approximations only since $[R^+]$ is calculated using the extinction coefficient of the carbonium ion in sulphuric acid.

Information does not appear to be available in the literature for the hydronium ion concentration but it can be shown that, at least for concentrated formic acid solution, rather unlikely values of the hydronium ion concentration would be required to make $J_0(H_R)$ and J_0'' coincide. Thus in 90% to 95% formic acid an hydronium ion concentration of the order of 10^{-4} molar must be assumed decreasing for 99% formic acid to a value closer to 10^{-5} molar. This compares with a known hydronium ion concentration of the order of 10^{-2} molar in 0.1 *M* formic acid and at the other end of the scale a known con-

Can. J. Chem. Downloaded from www.nrcresearchpress.com by 41.223.56.140 on 09/04/12
For personal use only.

centration of $HCO_2H_2^+$ of about 10^{-3} molar in 100% formic acid (6). The H_3O^+ concentration in the 90–99% range must therefore be considerably greater than this.

J_0''' is defined by the equation

$$[11] \qquad J_0''' = H_0 + \log [H_2O]_N.$$

Gold found that for sulphuric acid solutions this was the least satisfactory of the three functions as approximations to $J_0(H_R)$. In agreement with this we find that J_0''' lies between J_0' and H_0 for formic acid solutions. If the data of Gold (8) and Deno *et al.* (7) for sulphuric acid are combined it can be shown that the derived functions all fall between the experimental ones H_0 and $J_0(H_R)$ with J_0'' being the only one of the three which is closer to $J_0(H_R)$ than to H_0.

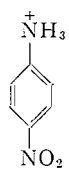
Thus both in sulphuric acid and in formic acid, secondary bases such as triphenylcarbinol ionize to a much greater extent than would be expected from a consideration of equations 9–11. Consider equation 12, which is obtained by the combination of equations 5 and 6; all activity coefficients refer to dilute aqueous solution as the standard state.

$$[12] \qquad J_0(H_R) = H_0 + \log a_{H_2O} + \log \frac{f_B \cdot f_{R^+}}{f_{BH^+} \cdot f_{ROH}}.$$

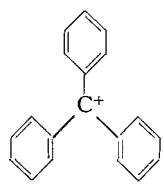
It can be seen from Fig. 1 that the final term in the above equation must make a considerable contribution to $-J_0(H_R)$ and it is worth while speculating on the reason for this since for two bases of the ammonia type, B_1 and B_2, the value of $\log f_{B_1} f_{B_2H^+} / f_{B_1H^+} f_{B_2}$ is effectively zero (1).

Since solvation effects are usually more important for ions than for neutral molecules, we might assume that the principal change in activity due to solvation in going from water to sulphuric or formic acid solution is for the species BH^+ and R^+. In this connection Briegleb (18) has calculated the heat of hydration of typical amines to be 10–12 kcal $mole^{-1}$ while that of the ammonium ions is 83–85 kcal $mole^{-1}$. Cations are solvated best by basic molecules, i.e. those with available pairs of electrons and one would expect water to perform this function better than either sulphuric or formic acid. Thus in going to the latter solutions from water the activity of the cations should increase.

The greatly increased solubility of some weak bases in sulphuric acid of strength below that required to cause appreciable ionization of the base shows that the term f_B can decrease markedly in going from water to sulphuric acid (19, 20). Thus a considerable change in the activity coefficients of the neutral species B and ROH may also occur but it is not obvious why this effect should be greatly different for B than for ROH. A principal difference between the ions BH^+, typified by the nitroanilinium ion (used to determine the H_0 scale), and the carbonium ions (used to determine the $J_0(H_R)$ scale) is the fact that in the former the charge is localized on the nitrogen atom as in I whereas in the carbonium ion (II) the charge is spread by resonance to a very considerable extent into the three rings.



I



II

Can. J. Chem. Downloaded from www.nrcresearchpress.com by 41.223.56.140 on 09/04/12
For personal use only.

Thus solvation is less important to the carbonium ion and when it is transferred to a sulphuric or formic acid solution, the increase in its activity due to the decreased solvation should be less than that for the anilinium ion. This argument is, at least, in qualitative agreement with the experimental fact that the ratio $f_B f_{R^+}/f_{BH^+} f_{ROH}$ does decrease greatly in going from water to sulphuric and formic acid. Deno and Perrizolo (20) have recently determined the ratios of the activity coefficients of several ions in sulphuric acid – water mixtures. Comparing a small unshielded ion like K^+ with a large shielded ion like $(C_4H_9)_4N^+$ they found, in fact, that $d(f_{K^+}/f_{(C_4H_9)_4N^+})/d\%$ H_2SO_4 underwent a 25-fold increase on going from 0% to 70% sulphuric acid. Deno *et al.* found, however, that the concentration of the ion, NO^+, formed by the ionization of HNO_2, follows the acidity function $H_R(J_0)$ in sulphuric acid (9). Since this is a small ion in which extensive charge delocalization is not possible they have suggested that the group of cations which follows this acidity function (carbonium ions and the NO^+ ion) do so because of the presence of an empty available orbital (open sextet) in the ions. They propose that the weak bonding resulting from overlap of the cation's empty orbital and the solvent oxygen's orbitals is a different function of acidity from the usual cation–solvent interaction. It is difficult to reconcile this similarity in behavior of NO^+ and arylcarbonium ions with the charge delocalization concept which we have advanced herein to explain the difference between the experimental acidity function, $J_0(H_R)$, and the calculated values of Gold. Both factors referred to above may be important. It is worth pointing out here that the position of equilibrium between a charge localized ion and its tautomeric delocalized form has been shown in at least two cases (protonated Michler's ketone and Michler's hydrol) to be strongly affected by the nature of the solvent (21).

Variation of $J_0(H_R)$ with Temperature

The effect of a temperature change on $J_0(H_R)$ was determined for three different concentrations of formic acid. Although H_0 is altered only slightly by temperature change, it was found that the ionization of the carbinols studied increased with increasing temperature, the increase being small in dilute formic acid but much larger in concentrated solution. Plots of apparent $J_0(H_R)$, calculated by assuming pK_{R^+} to be constant, against $1/T$ gave straight lines as can be seen in Fig. 2. The significance of this result must await a determination of the effect of temperature on pK_{R^+}. (7).

ACKNOWLEDGMENT

The aid of the President's Research Fund of the University of British Columbia is gratefully acknowledged.

REFERENCES

1. M. A. Paul and F. A. Long. Chem. Rev. **57**, 1 (1957).
2. F. A. Long and M. A. Paul. Chem. Rev. **57**, 935 (1957).
3. A. M. Lowen, M. A. Murray, and G. Williams. J. Chem. Soc. 3321 (1950).
4. V. Gold and B. W. V. Hawes. J. Chem. Soc. 2102 (1951).
5. A. Hantzsch. Z. physik. Chem. **61**, 257 (1908).
6. L. P. Hammett and A. J. Deyrup. J. Am. Chem. Soc. **55**, 1900 (1933).
7. N. C. Deno, J. J. Jaruzelski, and A. Schriesheim. J. Org. Chem. **19**, 155 (1954).
8. V. Gold. J. Chem. Soc. 1263 (1955).
9. N. C. Deno, H. E. Berkheimer, W. L. Evans, and H. J. Peterson. J. Am. Chem. Soc. **81**, 2344 (1959).
10. R. Stewart. Can. J. Chem. **35**, 766 (1957).
11. A. G. Evans. Personal communication.
12. K. N. Bascombe and R. P. Bell. J. Chem. Soc. 1096 (1959).
13. I. Goldberg and C. Sissoeff. Ber. **40**, 4546 (1907).

Can. J. Chem. Downloaded from www.nrcresearchpress.com by 41.223.56.140 on 09/04/12
For personal use only.

14. K. BRAND. J. prakt. Chem. **109**, 14 (1925).
15. J. A. PINFOLD and F. SEBBA. J. Am. Chem. Soc. **78**, 5193 (1956).
16. P. GRAMMATICAKIS. Bull. soc. chim. France, 158 (1950).
17. S. TAKAGI. Bull. Chem. Soc. Japan, **14**, 508 (1939).
18. G. BRIEGLEB. Z. Electrochem. **53**, 350 (1949).
19. L. P. HAMMETT. Physical organic chemistry. McGraw Hill Book Co., Inc., New York. 1940. p. 273.
20. N. C. DENO and C. PERIZZOLO. J. Am. Chem. Soc. **79**, 1345 (1957).
21. R. STEWART and M. MOCEK. Unpublished results.

Can. J. Chem. Downloaded from www.nrcresearchpress.com by 41.223.56.140 on 09/04/12
For personal use only.

Can. J. Chem. Downloaded from www.nrcresearchpress.com by 41.223.56.140 on 09/04/12
For personal use only.

SOLVENT EXTRACTION OF MINERAL ACIDS

PART III. SOLUTE–SOLVENT INTERACTION IN THE SYSTEM HYDROBROMIC ACID – WATER – TRI-*n*-BUTYL PHOSPHATE[1]

A. S. KERTES AND V. KERTES

ABSTRACT

Evidence, based on physical–chemical measurements of the organic layers, has been presented to show that tributyl phosphate extracts hydrobromic acid as its disolvate in medium acid concentrations, and probably as monosolvate in high concentrations. The determination of water in the tributyl phosphate phases indicates that at low and medium acid concentrations the acid is extracted as its tetrahydrate, and at high concentrations as an unhydrated species. From these results, the formation of $[(TBP)_2.HBr.(H_2O)_6]$ and $[TBP.HBr.(H_2O)_3]$ could be deduced.

Compared with the extensive literature on the extraction of inorganic nitrates from aqueous nitric acid solutions by tributyl phosphate, relatively few investigations have dealt with tributyl phosphate extraction of inorganic halides from aqueous solutions of the corresponding hydrohalic acid. The reactions between metal salts or ions and tributyl phosphate can only be correctly understood if the very pronounced tendency of this basic extractant to react with the acid present in such systems is taken into account. It was therefore considered necessary to investigate more thoroughly the solute–solvent interactions involved in the heterogeneous equilibria existing in systems of hydrohalic acid – water – tributyl phosphate. Our earlier research determined the species formed as a result of solute–solvent interaction in the system $HCl–H_2O–TBP$ (1). The second paper in this series dealt with the hydration phenomena of tributyl phosphate – hydrochloric acid complexes existing in the organic layer (2). In the continuation of this research we made a similar investigation of the system $HBr–H_2O–TBP$.

On the experimental side, the present research is an extension of that carried out recently by Baldwin, Higgins, and Soldano (3), in which the distribution coefficient of hydrobromic acid, and its hydration number, were investigated. These authors found that HBr is more effectively extracted than HCl into TBP, and that at low acid concentrations the halogen acids carried water along into the TBP, at the rate of approximately $4H_2O$ per HX. At high acid concentrations it seemed to these authors that water was again forced from the tributyl phosphate. It was also indicated (4) that hydrobromic acid entered the organic phase along with the four water molecules at low acid concentrations. No other studies have been published in the open literature dealing with tributyl phosphate extraction of HBr.

The results reported here reveal the certain existence of a well-defined compound among hydrobromic acid, tributyl phosphate, and water, and indicate the existence of another. The mechanism of extraction of the compounds is suggested.

EXPERIMENTAL

Reagents

B. D. H. Analar grade colorless hydrobromic acid was standardized against standard carbonate-free sodium hydroxide solution. Calculated amounts were taken for 13 stock

[1]*Manuscript received November 16, 1959.*
Contribution from the Department of Inorganic and Analytical Chemistry, The Hebrew University of Jerusalem, Jerusalem, Israel.

solutions of various concentrations as listed in Table I. Tri-*n*-butyl phosphate was treated as reported previously.

Procedure

The procedure for the distribution experiments consisted of equilibrating 5 ml of pure undiluted TBP with 5 ml of initial aqueous acid solution of various concentrations. The changes in volume, the density, viscosity, and conductivity of the organic layers were measured as described in the previous paper (1). The acid and water determinations followed the methods outlined in Part I. All the measurements were performed at room temperature of 20°±1° C and where necessary in a thermostatic water bath at 20°± 0.1° C.

RESULTS AND DISCUSSION

Partition and Ionization of the Acid

Column 2 of Table I shows the molarity of hydrobromic acid in the initial aqueous solutions, and columns 3 and 4 the molarity in the equilibrium aqueous and organic phases respectively. The concentration and mass distribution coefficients, as previously

TABLE I

No. of soln.	Molarity of HBr in: Initial aq. soln.	Equilib. aq. phase	Equilib. org. phase	Volume increase of the organic phase, ml	α	μ	HBr in the organic phase, mmoles	HBr/TBP ratio, mmoles	H_2O in the organic phase, mmoles	H_2O/TBP ratio, mmoles
(1)	(2)	(3)	(4)	(5)	(6)	(7)	(8)	(9)	(10)	(11)
1	0.089	0.090	0.005	0.30	0.052	0.058	0.03		18.9	1.0
2	0.178	0.176	0.011	0.30	0.063	0.071	0.06		19.4	1.1
3	0.446	0.433	0.036	0.30	0.083	0.094	0.19		21.2	1.2
4	0.891	0.811	0.123	0.30	0.151	0.171	0.65	0.04	25.0	1.4
5	1.782	1.576	0.312	0.40	0.199	0.232	1.68	0.09	27.9	1.5
6	2.673	2.275	0.578	0.55	0.254	0.318	3.21	0.18	35.0	1.9
7	3.564	2.986	0.844	0.75	0.283	0.382	4.85	0.27	41.2	2.2
8	4.420	3.783	1.095	0.90	0.290	0.417	6.46	0.35	47.2	2.6
9	5.347	4.578	1.389	1.10	0.303	0.475	8.47	0.46	52.4	2.9
10	6.257	5.347	1.717	1.25	0.321	0.535	10.72	0.59	55.2	3.0
11	7.129	6.304	2.025	1.35	0.322	0.546	12.57	0.69	57.2	3.1
12	8.034	6.968	2.332	1.45	0.334	0.606	15.04	0.82	56.5	3.1
13	8.911	7.774	2.631	1.55	0.339	0.643	17.23	0.95	56.8	3.1

defined (1), are compiled in columns 6 and 7 respectively. Figure 1 represents the graph of the acid molarity in the equilibrium phases. The non-uniform shape of the curve indicates that the species of HBr extracted from aqueous solutions of hydrobromic acid of initial concentrations up to about 1 *M* differ from those extracted from more concentrated solutions. Furthermore, when the TBP phase is equilibrated with aqueous solutions of initial concentrations as above, the decrease in the values of the equivalent conductance (column 5 of Table II, and Fig. 5) suggests that from these dilute aqueous acid solutions the acid passes into the organic phase to a large extent in ionized form. Increase in the acid concentration of the initial aqueous solutions promotes ion-pair formation and causes an increase in the acid content of the organic layer. It should be noted that this interpretation does not agree with the values of the degree of ionization estimated by means of Walden's rule, $\lambda\eta/60$, shown in column 6 of Table II.

Can. J. Chem. Downloaded from www.nrcresearchpress.com by 41.223.56.140 on 09/04/12
For personal use only.

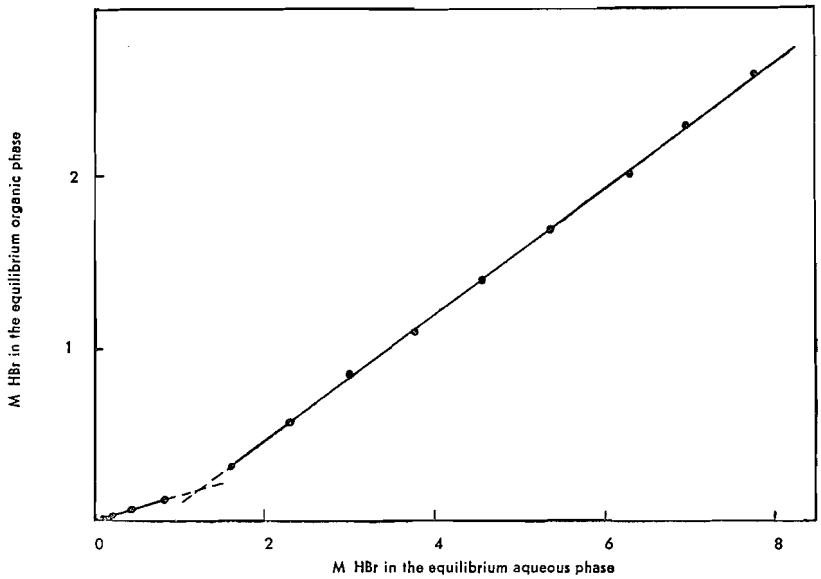


FIG. 1. The plot of HBr molarity in equilibrium organic phases versus its molarity in the equilibrium aqueous phases.

TABLE II

No. of soln.	Density at 20° C, g/cm³	Viscosity at 20° C, Centipoises	Specific conductance at 20° C, mhos 10^3	Equivalent conductance at 20° C	Degree of ionization, %
(1)	(2)	(3)	(4)	(5)	(6)
1	0.977	5.964	0.005	1.086	0.11
2	0.977	5.920	0.011	0.982	0.10
3	0.981	6.172	0.034	0.945	0.10
4	0.986	6.770	0.093	0.760	0.09
5	0.998	8.774	0.515	1.650	0.24
6	1.015	10.97	1.210	2.091	0.38
7	1.029	12.95	1.915	2.269	0.43
8	1.045	15.93	2.583	2.360	0.63
9	1.061	18.16	3.594	2.515	0.77
10	1.079	20.45	4.306	2.508	0.85
11	1.095	21.46	4.483	2.214	0.79
12	1.107	23.59	4.675	2.005	0.79
13	1.123	24.71	4.917	1.870	0.61

Solvation of the Acid

The solvation number of hydrobromic acid in the extractant, i.e. the composition of the compound formed between the acid and the extractant as a result of their interaction, was determined by physical–chemical measurements of the organic layer.

On equilibrating 5 ml of pure TBP (18.35 mmoles) with an equal volume of aqueous acid solution, the volume of the organic phase increases. In Fig. 2 the changes in volume of the organic layer, shown in column 5 of Table I, are plotted against the acid content of this layer. It is clear that there are three different interactions, occurring in low, medium, and high acid concentrations respectively. For acid concentrations up to 1 M, the increase in volume of the organic phase is equal to the increase caused by pure water. For concentrations between 1 M and $\sim$5.5 M there is a greater increase in volume, and

Can. J. Chem. Downloaded from www.nrcresearchpress.com by 41.223.56.140 on 09/04/12
For personal use only.

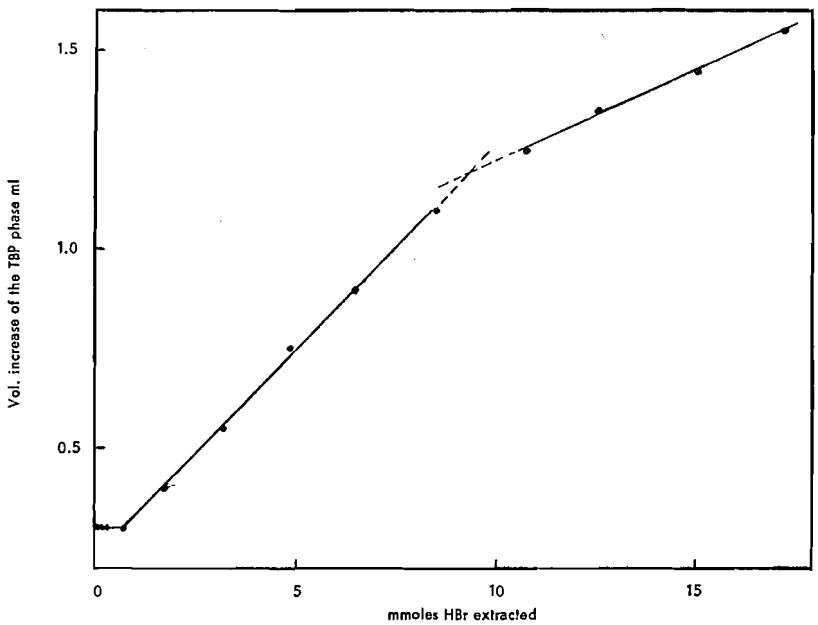


FIG. 2. The plot of the volume increase of the TBP layers after equilibration versus mmoles of HBr extracted.

a break occurs in the curve when the ratio TBP:HBr reaches two. The third type of interaction occurs when the acid concentration exceeds $\sim 5.5\ M$.

When the densities and viscosities (Table II) are plotted against the acid content of the equilibrium organic layers, the curves shown in Figs. 3 and 4 are obtained. When the

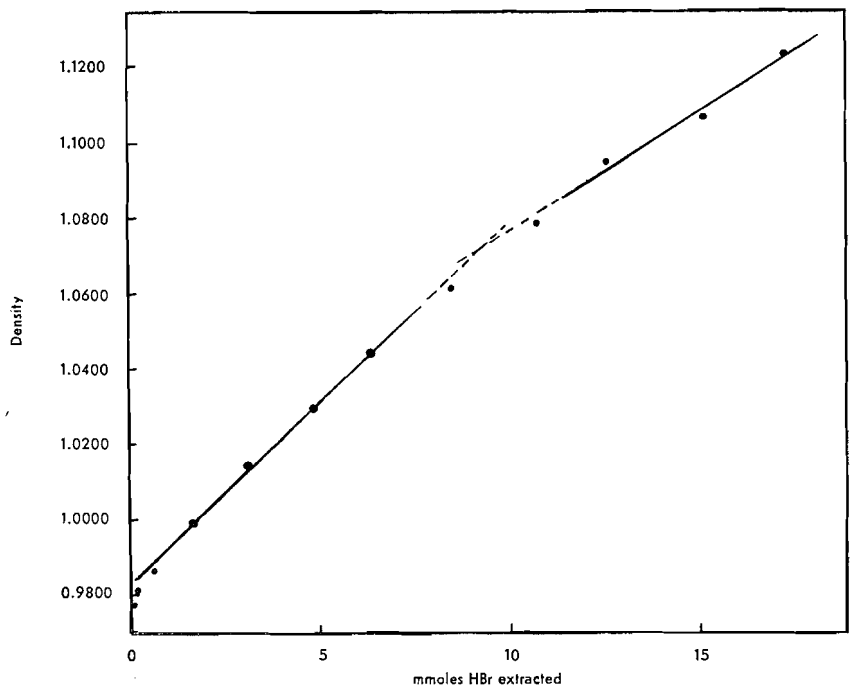


FIG. 3. The plot of density of the equilibrium organic layers versus mmoles of HBr extracted.

Can. J. Chem. Downloaded from www.nrcresearchpress.com by 41.223.56.140 on 09/04/12
For personal use only.

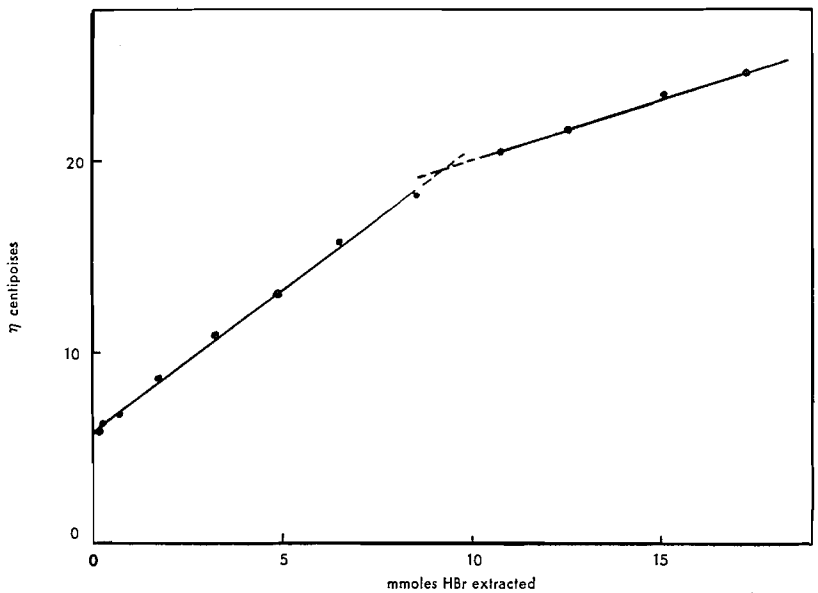


Fig. 4. The plot of viscosity of the equilibrium organic phases versus mmoles of HBr extracted.

TBP phase is equilibrated with aqueous solutions of concentrations up to ~1 *M* HBr, only very slow changes, if any, are observed in these physical data. The interaction in medium acid concentrations is demonstrated by a break in both curves, at a point when the organic layer contains 9.2 mmoles of hydrobromic acid and 18.35 mmoles of tributyl phosphate, i.e. a TBP:HBr ratio of two.

The results of conductivity measurements of the organic phase are given in columns 4 and 5 of Table II. Figure 5 shows the equivalent conductance values, plotted against the

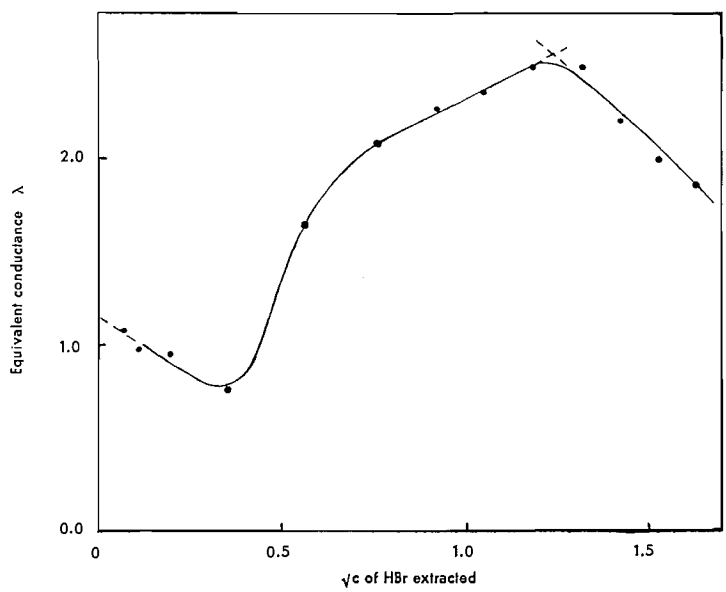


FIG. 5. The plot of equivalent conductance of the equilibrium organic phases versus the square root of the HBr concentration in the organic phase.

Can. J. Chem. Downloaded from www.nrcresearchpress.com by 41.223.56.140 on 09/04/12
For personal use only.

square root of the acid concentration, $\sqrt{c}$. It has already been noted that the appearance of a conductance minimum is very probably associated with the end of an ionization region (maximum concentration of the acid in the organic layers of this region being 0.1 M), and it is characteristic of polar compounds dissolved in media of low dielectric constant. Higher values can be explained by the increased extraction of HBr into the TBP due to ion-pair formation (5, 6). The curve, in addition, shows an interception, on extension over a flat maximum, between the medium and high acid concentration regions. This break corresponds to a TBP:HBr ratio of two, evidence for the formation of $(TBP)_2.HBr$.

The solvation number of inorganic species in organic solvents under conditions of liquid–liquid extraction have so far been deduced from partition data, using undiluted (7) and diluted extractants (8). By the methods employed in this study, the physical–chemical behavior of the tributyl phosphate extractant (in equilibrium with aqueous hydrobromic acid of various concentrations) has revealed that the extracted hydrobromic acid species contains two tributyl phosphate molecules per acid molecule. It was further shown that the solvation number is to a large extent dependent on the acid concentration. In high concentrations the solvation of the extracted acid species is determined by an interaction leading to the formation of a compound which probably contains a TBP:HBr ratio of unity. Although the formulation of this compound cannot be considered as established, the great change in the nature of the organic layers, when using high acid concentrations, seems to indicate results comparable with those of the similar system containing hydrochloric instead of hydrobromic acid (1).

With the exception of our study (1), there seem to be no examples of mineral acids being extracted with two tributyl phosphate molecules. In fact, the solvation numbers of nitric and perchloric acids extracted into TBP appear to be one. This was also found to be true for hydrochloric, and very probably hydrobromic, acids, but only in high acid concentrations. It has now been shown that for medium acid concentrations the main solute–solvent interaction leads to the formation of hydrobromic acid disolvate, analogous to hydrochloric acid disolvate.

Hydration of the Acid

The water content of the organic layer in millimoles, and the corresponding water:extractant ratios, are compiled in the last two columns of Table I. Figure 6 shows the curve obtained by plotting the water content against the acid content of the tributyl phosphate layer. The curve shows the water content of the organic phase in two stages. The points corresponding to tributyl phosphate phases with very low acid content (up to $\sim$0.1 M, that is up to about 0.5 mmole) could not be integrated into these stages, and so at these low acid concentrations nothing could be stated about the hydration mechanism of the acid. For medium acid concentrations (initial acid concentration between $\sim$1 and $\sim$5.5 M), the graph shows a straight line, of slope four, indicating that each acid molecule passing from the aqueous into the organic layer is associated with four water molecules. This relationship holds until the acid content of the tributyl phosphate layer is 9.2 mmoles, when the TBP:HBr ratio is two. After this, the water content no longer changes with increase in the acid content of the organic phase. For these high acid concentrations the H_2O:TBP ratio remains practically constant, and equal to three approximately.

The above results of the acid hydration are completely analogous to those obtained in the system with hydrochloric acid, as is also the stability of hydration (2) of the extracted species.

Can. J. Chem. Downloaded from www.nrcresearchpress.com by 41.223.56.140 on 09/04/12
For personal use only.

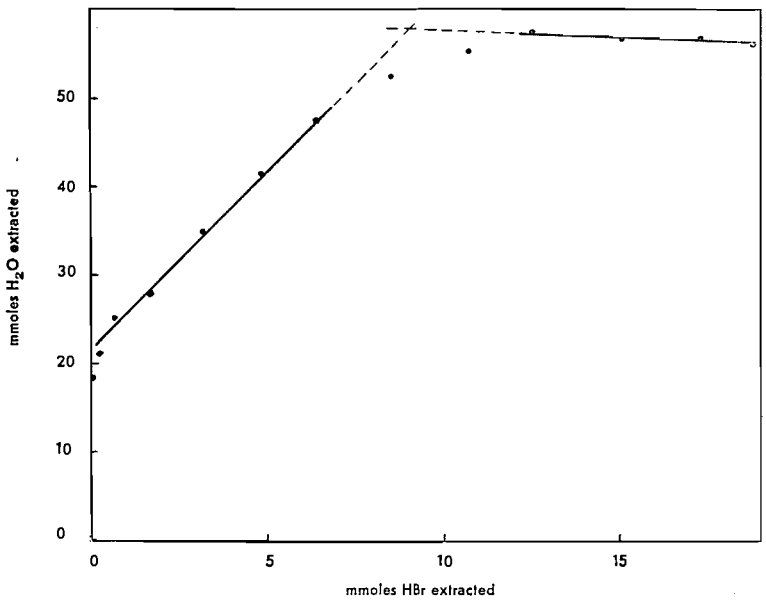


FIG. 6. The plot of mmoles of H_2O versus mmoles of HBr both in the equilibrium organic phases.

CONCLUSIONS

The acid passing into the tributyl phosphate phase from dilute aqueous hydrobromic acid is probably ionized. For these low acid concentrations, the main reaction involved is that between water and the extractant, resulting in the formation of the stable tributyl phosphate monohydrate. For medium acid concentrations, ion-pair formation becomes significant, and each acid molecule is extracted together with four water molecules. The acid–ester interaction leads to the formation of a compound with a TBP:HBr ratio of two, and H_2O:TBP ratio of three. These reactions could be formulated as follows:

$$TBP_{org} + H_2O_{aqu} \rightarrow [TBP.H_2O]_{org}, \quad [1]$$

$$2[TBP.H_2O]_{org} + H^+(H_2O)_{4\,aqu} + Br^-_{aqu} \rightarrow [(TBP)_2.HBr.(H_2O)_6]_{org}. \quad [2]$$

Both these reactions are analogous to those previously found in systems containing hydrochloric acid.

Under the experimental conditions of this investigation, it was found impossible to equilibrate the tributyl phosphate phase so that the acid content corresponded to a TBP:HBr ratio of unity. Therefore for high acid concentrations this system is not completely analogous to that containing HCl. Nevertheless, following the analogy between the two systems, it can be presumed that for high acid concentrations, when the extracted acid is unhydrated, the H_2O:TBP ratio is constant and practically equal to three, and as the TBP:HBr ratio decreases and approaches unity, a further reaction probably takes place. This reaction should be analogous to that in the HCl system at these high acid concentrations, and should be formulated as follows:

$$[(TBP)_2.HBr.(H_2O)_6]_{org} + H^+_{aqu} + Br^-_{aqu} \rightarrow 2[TBP.HBr.(H_2O)_3]_{org}. \quad [3]$$

Can. J. Chem. Downloaded from www.nrcresearchpress.com by 41.223.56.140 on 09/04/12
For personal use only.

REFERENCES

1. A. S. KERTES. J. Inorg. & Nuclear Chem. In press.
2. A. S. KERTES. J. Inorg. & Nuclear Chem. In press.
3. W. H. BALDWIN, C. E. HIGGINS, and B. A. SOLDANO. J. Phys. Chem. **63**, 118 (1959).
4. D. G. TUCK and R. M. DIAMOND. Proc. Chem. Soc. 236 (1958).
5. D. E. CAMPBELL, H. A. CLARK, and W. H. BAUER. J. Phys. Chem. **62**, 506 (1958).
6. H. A. C. MCKAY and A. R. MATHIESON. Trans. Faraday Soc. **47**, 428 (1951).
7. E. GLUECKAUF, H. A. C. MCKAY, and A. R. MATHIESON. Trans. Faraday Soc. **47**, 437 (1951).
8. K. ALCOCK, F. C. BEDFORD, W. H. HARDWICK, and H. A. C. MCKAY. J. Inorg. & Nuclear Chem. **4**, 100 (1957).

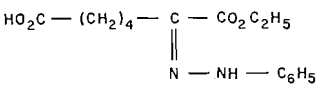
Can. J. Chem. Downloaded from www.nrcresearchpress.com by 41.223.56.140 on 09/04/12
For personal use only.

Can. J. Chem. Downloaded from www.nrcresearchpress.com by 41.223.56.140 on 09/04/12
For personal use only.

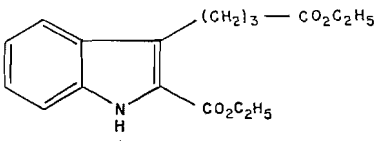
1,6-BIS(γ-CARBETHOXYPROPYL)-2,3,7,8-DIBENZOPYROCOLL. A BY-PRODUCT IN THE PREPARATION OF γ-(3-INDOLYL)BUTYRIC ACID

RICHARD H. MANSKE AND WALTER R. BOOS

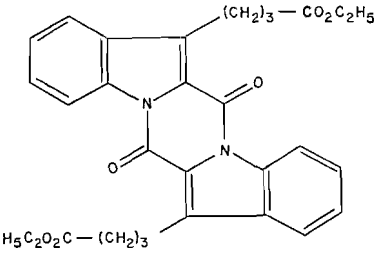
During the preparation of γ-(3-indolyl)butyric acid a by-product was obtained when the phenylhydrazone of the half ester of α-ketopimelic acid (I) was subjected to the Fischer indole synthesis and esterified to ethyl γ-(2-carbethoxy-3-indolyl)butyrate (II). The compound was identified as 1,6-bis(γ-carbethoxypropyl)-2,3,7,8-dibenzopyrocoll (III) by hydrolytic ring fission to γ-(2-carboxy-3-indolyl)butyric acid.



(I)



(II)



(III)

EXPERIMENTAL

1,6-Bis(γ-Carbethoxypropyl)-2,3,7,8-dibenzopyrocoll (III)

A 5-liter round-bottom flask equipped with a reflux condenser was charged with 1052 g of the half ethyl ester of the phenylhydrazone of α-ketopimelic acid (I), 3 liters of 99% ethanol, and 270 ml of sulphuric acid (density = 1.84). The mixture was boiled for 20 hours under reflux on a steam bath. Subsequently the ethanol was distilled off and the remaining liquid was taken up in 1 liter of benzene, washed well with water, then with 5% aqueous sodium bicarbonate solution, and again with water. The benzene was distilled from the extract and an attempt to distill the residue at a pressure of 0.1 mm failed due to partial decomposition. On cooling crystals were obtained, and these were taken

up in 1.5 liters of 99% ethanol. The yellow crystalline material which then separated was removed by filtration; yield was 180 g. (The filtrate was stripped of ethanol and distilled at 0.1 mm and 210° C and yielded 506 g of ethyl γ-(2-carbethoxy-3-indolyl)butyrate (II).) The precipitate was recrystallized twice from benzene and yielded pale yellow plates, m.p. 214.5–215° C. Calc. for $C_{30}H_{30}N_2O_6$: C, 70.02; H, 5.88; N, 5.44; mol. wt., 514. Found: C, 70.06; H, 5.81; N, 5.80; mol. wt., 548 (Rast).

Hydrolytic Degradation of III *to the Diacid of* II

Three grams of the pyrocoll (III) was hydrolyzed by refluxing for 1 hour in 70 ml of propanol together with 5 g of potassium hydroxide. On cooling a colorless precipitate was obtained which was filtered off, washed with propanol, and dissolved in 60 ml of distilled water. Addition of dilute hydrochloric acid yielded a colorless precipitate which was washed with distilled water and recrystallized from 20 ml of a 1:1 mixture of methanol and benzene: yield 2.3 g of colorless plates; m.p. 210° with loss of carbon dioxide. Calc. for $C_{13}H_{13}NO_4$: C, 63.15; H, 5.30. Found: C, 62.82; H, 5.26. Decarboxylation at 220 to 230° in a nitrogen atmosphere readily yielded γ-(3-indolyl)butyric acid melting at 124° either alone or in admixture with an authentic specimen (1).

1. R. W. Jackson and R. H. Manske. J. Am. Chem. Soc. **52**, 5029 (1930).

Received December 18, 1959.
Dominion Rubber Company Research Laboratories,
Guelph, Ontario.

MAGNETIC MOMENT OF Ni^{2+} ION IN $(Ph_3P)_2NiBr_2(PhBr)_2$

Yoshio Matsunaga

Recently Gill, Nyholm, and Pauling (1) have suggested that a regular tetrahedral arrangement of four-covalent spin-free Ni^{2+} complexes is much less probable than a distorted one. If distortion from a regular tetrahedron is small, the magnetic moment of Ni^{2+} ion should be larger than the spin-only value of 2.8 B.M. They have observed the magnetic moment of the Ni^{2+} ion in $(Et_4N)_2(NiCl_4)$ and $(Et_4N)_2(NiBr_4)$ being in the range of 3.8 to 3.9 B.M. Similar high moments have been found in the following cases: the Ni^{2+} ion in the tetrahedral hole of glass, 3.6 B.M. (2), the Ni^{2+} ion in the tetrahedral site of spinel, about 3.6 B.M. (3), and the Ni^{2+} ion in $[(Ph_3PO)_4Ni](ClO_4)_2$, 3.51 B.M. (4). In all of the above-mentioned cases, Ni^{2+} ion is surrounded by four equivalent ions or atoms. Venanzi (5) has found that complexes of the type $(Ph_3P)_2NiX_2$ show the magnetic moments which are only a little higher than the spin-only value and are monomeric in benzene solution. It has been shown by X-ray studies that the Ni^{2+} ion is located at the center of a distorted tetrahedron (6). Here we wish to report the increase of the magnetic moment of the Ni^{2+} ion in $(Ph_3P)_2NiBr_2$ by addition of crystalline solvent.

A number of compounds of the types $(Ph_3P)_2NiX_2Y$ and $(Ph_3P)_2NiX_2Y_2$, where Y is alkyl or phenyl halide, have been described by Reppe and Schweckendiek (7) and by Yamamoto (8). Among them we examined the compounds $(Ph_3P)_2NiBr_2$, $(Ph_3P)_2NiBr_2$ *tert.* BuBr, and $(Ph_3P)_2NiBr_2(PhBr)_2$, which are intense green, green, and grayish blue, respectively. The following values of specific magnetic susceptibility at room temperature and effective magnetic moment of Ni^{2+} ion were obtained: $(Ph_3P)_2NiBr_2$,

Can. J. Chem. Downloaded from www.nrcresearchpress.com by 41.223.56.140 on 09/04/12
For personal use only.

up in 1.5 liters of 99% ethanol. The yellow crystalline material which then separated was removed by filtration; yield was 180 g. (The filtrate was stripped of ethanol and distilled at 0.1 mm and 210° C and yielded 506 g of ethyl γ-(2-carbethoxy-3-indolyl)butyrate (II).) The precipitate was recrystallized twice from benzene and yielded pale yellow plates, m.p. 214.5–215° C. Calc. for $C_{30}H_{30}N_2O_6$: C, 70.02; H, 5.88; N, 5.44; mol. wt., 514. Found: C, 70.06; H, 5.81; N, 5.80; mol. wt., 548 (Rast).

Hydrolytic Degradation of III *to the Diacid of* II

Three grams of the pyrocoll (III) was hydrolyzed by refluxing for 1 hour in 70 ml of propanol together with 5 g of potassium hydroxide. On cooling a colorless precipitate was obtained which was filtered off, washed with propanol, and dissolved in 60 ml of distilled water. Addition of dilute hydrochloric acid yielded a colorless precipitate which was washed with distilled water and recrystallized from 20 ml of a 1:1 mixture of methanol and benzene: yield 2.3 g of colorless plates; m.p. 210° with loss of carbon dioxide. Calc. for $C_{13}H_{13}NO_4$: C, 63.15; H, 5.30. Found: C, 62.82; H, 5.26. Decarboxylation at 220 to 230° in a nitrogen atmosphere readily yielded γ-(3-indolyl)butyric acid melting at 124° either alone or in admixture with an authentic specimen (1).

1. R. W. Jackson and R. H. Manske. J. Am. Chem. Soc. **52**, 5029 (1930).

Received December 18, 1959.
Dominion Rubber Company Research Laboratories,
Guelph, Ontario.

MAGNETIC MOMENT OF Ni^{2+} ION IN $(Ph_3P)_2NiBr_2(PhBr)_2$

Yoshio Matsunaga

Recently Gill, Nyholm, and Pauling (1) have suggested that a regular tetrahedral arrangement of four-covalent spin-free Ni^{2+} complexes is much less probable than a distorted one. If distortion from a regular tetrahedron is small, the magnetic moment of Ni^{2+} ion should be larger than the spin-only value of 2.8 B.M. They have observed the magnetic moment of the Ni^{2+} ion in $(Et_4N)_2(NiCl_4)$ and $(Et_4N)_2(NiBr_4)$ being in the range of 3.8 to 3.9 B.M. Similar high moments have been found in the following cases: the Ni^{2+} ion in the tetrahedral hole of glass, 3.6 B.M. (2), the Ni^{2+} ion in the tetrahedral site of spinel, about 3.6 B.M. (3), and the Ni^{2+} ion in $[(Ph_3PO)_4Ni](ClO_4)_2$, 3.51 B.M. (4). In all of the above-mentioned cases, Ni^{2+} ion is surrounded by four equivalent ions or atoms. Venanzi (5) has found that complexes of the type $(Ph_3P)_2NiX_2$ show the magnetic moments which are only a little higher than the spin-only value and are monomeric in benzene solution. It has been shown by X-ray studies that the Ni^{2+} ion is located at the center of a distorted tetrahedron (6). Here we wish to report the increase of the magnetic moment of the Ni^{2+} ion in $(Ph_3P)_2NiBr_2$ by addition of crystalline solvent.

A number of compounds of the types $(Ph_3P)_2NiX_2Y$ and $(Ph_3P)_2NiX_2Y_2$, where Y is alkyl or phenyl halide, have been described by Reppe and Schweckendiek (7) and by Yamamoto (8). Among them we examined the compounds $(Ph_3P)_2NiBr_2$, $(Ph_3P)_2NiBr_2$ *tert.* BuBr, and $(Ph_3P)_2NiBr_2(PhBr)_2$, which are intense green, green, and grayish blue, respectively. The following values of specific magnetic susceptibility at room temperature and effective magnetic moment of Ni^{2+} ion were obtained: $(Ph_3P)_2NiBr_2$,

Can. J. Chem. Downloaded from www.nrcresearchpress.com by 41.223.56.140 on 09/04/12
For personal use only.

5.64×10^{-6} c.g.s.-e.m.u., 3.2 B.M.; $(Ph_3P)_2NiBr_2$ *tert.* BuBr, 5.37×10^{-6}, 3.4 B.M.; and $(Ph_3P)_2NiBr_2(PhBr)_2$, 5.59×10^{-6}, 3.8 B.M. The high magnetic moment of the Ni^{2+} ion in the latter two suggests that distortion from a regular tetrahedral arrangement can be decreased by the presence of crystalline solvent. The distortion in the compounds $(Ph_3P)_2NiX_2$ (X = Cl, Br, I, and NO_3) seems to be partially due to the steric requirement by the size difference between triphenylphosphine and halide ion. To compensate for such a steric effect in $(Ph_3P)_2NiBr_2$ two molecules of bromobenzene may be more suitable than one molecule of tert.butyl bromide. The appearance of blue tint in many cases of compounds of the types $(Ph_3P)_2NiX_2Y$ and $(Ph_3P)_2NiX_2Y_2$ may have some correlation with rather small distortion from a regular tetrahedral arrangement.

The author wishes to thank Professor H. Akamatu for his interest in this work and also the Mitsui Chemical Industry Company for the gift of the samples studied here.

1. N. S. Gill, R. S. Nyholm, and P. Pauling. Nature, **182**, 168 (1958).
2. P. W. Selwood. Magnetochemistry. Interscience Publishers, Inc., New York. 1956. p. 186.
3. J. T. Richardson and W. O. Milligan. J. Phys. Chem. **60**, 1223 (1956).
4. F. A. Cotton, E. Bannister, R. Barnes, and R. H. Holm. Proc. Chem. Soc. 158 (1959).
5. L. M. Venanzi. J. Chem. Soc. 719 (1958).
6. L. M. Venanzi and H. M. Powell. *Cited in* reference 1.
7. W. Reppe and W. J. Schweckendiek. Ann. **560**, 104 (1948).
8. K. Yamamoto. Bull. Chem. Soc. Japan, **27**, 501 (1954).

Received December 22, 1959.
Department of Chemistry, Faculty of Science,
The University of Tokyo,
Hongo, Tokyo, Japan.

CRYSTALLINE GLYOXYLIC ACID AND ITS SODIUM–CALCIUM SALT

A. A. Eisenbraun* and C. B. Purves

Early researches on the preparation and properties of glyoxylic acid were extensively reviewed by Debus (1) and by Hendricks (2), who noted that the substance occasionally yielded ill-defined rhombic crystals of a monohydrate when stored over a drying agent. In 1925, Hatcher and Holden (3) used the electrochemical method to reduce oxalic acid, isolated barium glyoxylate, decomposed the latter with sulphuric acid, and prepared anhydrous glyoxylic acid for the first time as monoclinic crystals melting at 98°. This result was questioned by Hendricks (2) because oxalic acid monohydrate, a probable impurity, melted at 99° and occurred as monoclinic crystals, and also because his attempts to repeat the crystallization of glyoxylic acid failed. Later workers oxidized tartaric acid or its esters with a glycol-cleaving agent, periodic acid or a periodate (4, 5, 6), lead tetraacetate (7), or sodium perbismuthate (8, 9), but apparently restricted their interest to the preparation of various esters and metallic salts of glyoxylic acid.

In the present work, tartaric acid was oxidized with aqueous periodic acid, by-product iodic acid was removed as the insoluble lead salt, and, after neutralization with barium hydroxide, crystalline barium glyoxylate dihydrate was recovered in high yield. An ion-exchange resin eliminated the cations from an aqueous solution of this salt, and evaporation of the effluent left glyoxylic acid as a clear syrup which eventually crystallized. The melting point was 104–107°, with softening at 94°. The replacement of periodic acid by sodium metaperiodate in the above oxidation, followed by the removal of iodate ion, left

*Holder in 1957–58 of the D. S. and R. H. Gottesman Foundation Scholarship.

Can. J. Chem. Downloaded from www.nrcresearchpress.com by 41.223.56.140 on 09/04/12
For personal use only.

5.64×10^{-6} c.g.s.-e.m.u., 3.2 B.M.; $(Ph_3P)_2NiBr_2$ *tert.* BuBr, 5.37×10^{-6}, 3.4 B.M.; and $(Ph_3P)_2NiBr_2(PhBr)_2$, 5.59×10^{-6}, 3.8 B.M. The high magnetic moment of the Ni^{2+} ion in the latter two suggests that distortion from a regular tetrahedral arrangement can be decreased by the presence of crystalline solvent. The distortion in the compounds $(Ph_3P)_2NiX_2$ (X = Cl, Br, I, and NO_3) seems to be partially due to the steric requirement by the size difference between triphenylphosphine and halide ion. To compensate for such a steric effect in $(Ph_3P)_2NiBr_2$ two molecules of bromobenzene may be more suitable than one molecule of tert.butyl bromide. The appearance of blue tint in many cases of compounds of the types $(Ph_3P)_2NiX_2Y$ and $(Ph_3P)_2NiX_2Y_2$ may have some correlation with rather small distortion from a regular tetrahedral arrangement.

The author wishes to thank Professor H. Akamatu for his interest in this work and also the Mitsui Chemical Industry Company for the gift of the samples studied here.

1. N. S. Gill, R. S. Nyholm, and P. Pauling. Nature, **182**, 168 (1958).
2. P. W. Selwood. Magnetochemistry. Interscience Publishers, Inc., New York. 1956. p. 186.
3. J. T. Richardson and W. O. Milligan. J. Phys. Chem. **60**, 1223 (1956).
4. F. A. Cotton, E. Bannister, R. Barnes, and R. H. Holm. Proc. Chem. Soc. 158 (1959).
5. L. M. Venanzi. J. Chem. Soc. 719 (1958).
6. L. M. Venanzi and H. M. Powell. *Cited in* reference 1.
7. W. Reppe and W. J. Schweckendiek. Ann. **560**, 104 (1948).
8. K. Yamamoto. Bull. Chem. Soc. Japan, **27**, 501 (1954).

Received December 22, 1959.
Department of Chemistry, Faculty of Science,
The University of Tokyo,
Hongo, Tokyo, Japan.

CRYSTALLINE GLYOXYLIC ACID AND ITS SODIUM–CALCIUM SALT

A. A. Eisenbraun* and C. B. Purves

Early researches on the preparation and properties of glyoxylic acid were extensively reviewed by Debus (1) and by Hendricks (2), who noted that the substance occasionally yielded ill-defined rhombic crystals of a monohydrate when stored over a drying agent. In 1925, Hatcher and Holden (3) used the electrochemical method to reduce oxalic acid, isolated barium glyoxylate, decomposed the latter with sulphuric acid, and prepared anhydrous glyoxylic acid for the first time as monoclinic crystals melting at 98°. This result was questioned by Hendricks (2) because oxalic acid monohydrate, a probable impurity, melted at 99° and occurred as monoclinic crystals, and also because his attempts to repeat the crystallization of glyoxylic acid failed. Later workers oxidized tartaric acid or its esters with a glycol-cleaving agent, periodic acid or a periodate (4, 5, 6), lead tetraacetate (7), or sodium perbismuthate (8, 9), but apparently restricted their interest to the preparation of various esters and metallic salts of glyoxylic acid.

In the present work, tartaric acid was oxidized with aqueous periodic acid, by-product iodic acid was removed as the insoluble lead salt, and, after neutralization with barium hydroxide, crystalline barium glyoxylate dihydrate was recovered in high yield. An ion-exchange resin eliminated the cations from an aqueous solution of this salt, and evaporation of the effluent left glyoxylic acid as a clear syrup which eventually crystallized. The melting point was 104–107°, with softening at 94°. The replacement of periodic acid by sodium metaperiodate in the above oxidation, followed by the removal of iodate ion, left

*Holder in 1957–58 of the D. S. and R. H. Gottesman Foundation Scholarship.

Can. J. Chem. Downloaded from www.nrcresearchpress.com by 41.223.56.140 on 09/04/12
For personal use only.

a solution which was mixed with an equimolar amount of aqueous calcium acetate. A white, crystalline, sodium–calcium salt, $CaNa_2(C_2HO_3)_4.4H_2O$, promptly separated. This salt was thought to be new.

EXPERIMENTAL

Glyoxylic Acid

An aqueous solution, 300 ml, containing 15 g (0.1 mole) of L-tartaric acid and 25.1 g (0.11 mole) of paraperiodic acid (H_5IO_6) was kept at 23° in the dark for 10 hours, when a titration by the sodium arsenite – iodine method showed that all of the periodic acid had been reduced. The addition of 110 ml of 0.52 *M* lead acetate (0.114 equivalent) caused the nearly quantitative separation of lead iodate, which was removed by filtration. After residual lead ions were removed as lead sulphide, the clarified liquor was evaporated *in vacuo* to a syrup, by-product acetic and formic acids being incidentally eliminated. The acidity of the syrup was cautiously reduced to pH 8 by the addition of cold 0.3 *N* barium hydroxide, and partial evaporation of the liquor caused the crystallization of 27.8 g (86.8%) of barium glyoxylate dihydrate. Although the solubility of the salt in water was reported (3) as only 0.005% at 18° and 0.08% at 68°, the present sample could be readily recrystallized from hot water. This recrystallization did not significantly change the composition. Calc. for $Ba(C_2HO_3)_2.2H_2O$: Ba, 43.0%. Found: Ba, 42.8, 43.0%. Samples, 0.2580 g and 0.2577 g, reduced 32.5, 32.5 ml, respectively, of 0.104 *N* potassium permanganate (3), the calculated amount being 30.9 ml.

An aqueous solution of 8.0 g of the above salt was freed of barium ions by passage through a column of Amberlite IR-120 cation-exchange resin, and the effluent was evaporated *in vacuo* to a thick syrup. This syrup was dried to nearly constant weight by storage over phosphorus pentoxide in an evacuated desiccator at room temperature. After several months the colorless product, 3.68 g or 99% yield, crystallized solidly. The melting point was 104–107°, with softening at 94°. No solvent suitable for recrystallizing the glyoxylic acid was found.

Sodium – Calcium Glyoxylate Tetrahydrate

Fifteen grams (0.1 mole) of L-tartaric acid dissolved in 300 ml of water was mixed with 200 ml of 0.515 *M* sodium metaperiodate (0.103 mole). The reduction of the latter was complete after the mixture had been kept in the dark and at room temperature for 36 hours. After iodate ion was removed as the lead salt, the filtrate was evaporated *in vacuo* to 50 ml, and was adjusted to pH 8 with 2 *N* sodium hydroxide. A concentrated aqueous solution of 17 g (0.1 mole) of calcium acetate monohydrate was then added, and 19.6 g (87.1%) of the sodium–calcium salt separated as white crystals. Calc. for $Na_2Ca(C_2HO_3)_4.4H_2O$: Na, 10.2; Ca, 8.3%. Found: Na, 9.65, 9.58; Ca, 9.27, 9.21%. Samples, 0.1338 g, 0.2038 g, and 0.1024 g, reduced 24.6 ml, 37.7 ml, and 19.0 ml of 0.101 *N* potassium permanganate (3), the calculated volumes being 23.6 ml, 35.9 ml, and 18.1 ml, respectively.

Two recrystallizations from hot water reduced the over-all yield to about 75% but failed to alter the composition significantly. A 0.0365-g sample of the salt when treated with 2,4-dinitrophenylhydrazine yielded 0.0658 g (79%) of crystalline glyoxylic acid 2,4-dinitrophenylhydrazone with the correct (10) melting point of 191–191.5°.

1. H. DEBUS. J. Chem. Soc. **85**, 1382 (1904).
2. R. H. HENDRICKS. Ph.D. Dissertation, St. Louis University, Missouri, Ill. 1935. Univ. Microfilms (Ann Arbor, Mich.) Pub. No. 183; Chem. Abstr. **35**, 2475 (1941).
3. W. H. HATCHER and G. W. HOLDEN. Trans. Roy. Soc. Canada, Section III (3), **19**, 11 (1925).

Can. J. Chem. Downloaded from www.nrcresearchpress.com by 41.223.56.140 on 09/04/12
For personal use only.

4. P. FLEURY and G. BON-BERNATETS. J. Pharm. Chim. **23**, 85 (1936).
5. A. WEISSBACH and D. B. SPRINSON. J. Biol. Chem. **203**, 1023 (1953).
6. D. E. METZLER, J. OLIVARD, and E. E. SNELL. J. Am. Chem. Soc. **76**, 644 (1954).
7. F. J. WOLFF and J. WEIJLARD. Org. Syntheses, **35**, 18 (1955).
8. W. RIGBY. J. Chem. Soc. 1907 (1950).
9. L. J. HEIDT, E. K. GLADDING, and C. B. PURVES. Paper Trade J. **121** (9), 81 (1945).
10. O. L. BRADY. J. Chem. Soc. 756 (1931).

RECEIVED DECEMBER 31, 1959.
DIVISION OF INDUSTRIAL AND CELLULOSE CHEMISTRY,
McGILL UNIVERSITY AND PULP AND PAPER RESEARCH INSTITUTE OF CANADA,
MONTREAL, QUE.

Can. J. Chem. Downloaded from www.nrcresearchpress.com by 41.223.56.140 on 09/04/12
For personal use only.

DIFFERENTIATION BETWEEN SOME 2,3- AND 2,5-DISUBSTITUTED PYRIDINE DERIVATIVES BY INFRARED SPECTROSCOPY

R. A. ABRAMOVITCH, GIAM CHOO SENG, AND A. D. NOTATION

In connection with studies of the orientation in the nucleophilic addition of phenyllithium to 3-substituted pyridines (1, 2) it became necessary to find a simple method of determining whether the attacking phenyl group had entered into the 2- or the 6-position of the pyridine ring, i.e. of distinguishing between 2- and 6-phenyl-3-substituted pyridines. This could be done by examining the N.M.R. spectrum of the compounds (1, 3) but was limited in that these determinations could not be carried out in our own laboratories. We therefore turned to infrared spectroscopy for such a method.

In theory, it should be quite simple to differentiate between 2,3- and 2,5-disubstituted pyridines by an examination of the aromatic C—H out-of-plane deformation region between 830 and 700 cm^{-1}. Infrared spectra – structure correlations have been found for the alkylbenzenes in the 11–15 μ region which are characteristic of the substitution positions in the benzene ring (4, 5). If one then considers that the pyridine ring corresponds to a monosubstituted benzene as far as the aromatic C—H out-of-plane bendings are concerned then a 2,3-disubstituted pyridine derivative should be equivalent to a 1,2,3-trisubstituted benzene whereas a 2,5-disubstituted pyridine derivative should correspond to a 1,2,4-trisubstituted benzene. The 1,2,3-trisubstituted benzenes show absorption in the 810–750 cm^{-1} range with a second band of medium intensity in the 726–680 cm^{-1} region, whereas 1,2,4-trisubstituted benzenes give rise to a strong band in the range 860–800 cm^{-1} (6). A number of 2,3- and 2,5-disubstituted pyridine derivatives have recently been shown to fall in nicely with this pattern (7, 8, 9). In particular, Podall (7) has studied the problem systematically and shown that 2-methyl-5-alkylpyridines exhibited two bands at 828–813 cm^{-1} and 735–724 cm^{-1}, whereas 2-methyl-3-alkylpyridines (1,2,3-trisubstitution) showed two bands at 813–769 cm^{-1} and 752–725 cm^{-1}.

A number of minor discrepancies in the band pattern in this region were observed in the present work. 2-Phenylnicotine exhibited a band at 805 cm^{-1}, quinoline a band at 805 cm^{-1}, and 5,6,7,8-tetrahydroquinoline a band at 827 cm^{-1} (see also (8)). On the other hand, 2-phenyl-3-alkyl- and 2-phenyl-5-alkyl-pyridines exhibited the expected absorptions though the presence of the monosubstituted phenyl-group obscured the assignment of the higher wavelength band. All that could be said was that most 2-phenyl-5-substituted pyridines exhibited a band of medium intensity between 850 and 800 cm^{-1} whereas most 2-phenyl-3-substituted pyridines did not.

A new and quite useful empirical correlation has now been observed in the C=C and

4. P. FLEURY and G. BON-BERNATETS. J. Pharm. Chim. **23**, 85 (1936).
5. A. WEISSBACH and D. B. SPRINSON. J. Biol. Chem. **203**, 1023 (1953).
6. D. E. METZLER, J. OLIVARD, and E. E. SNELL. J. Am. Chem. Soc. **76**, 644 (1954).
7. F. J. WOLFF and J. WEIJLARD. Org. Syntheses, **35**, 18 (1955).
8. W. RIGBY. J. Chem. Soc. 1907 (1950).
9. L. J. HEIDT, E. K. GLADDING, and C. B. PURVES. Paper Trade J. **121** (9), 81 (1945).
10. O. L. BRADY. J. Chem. Soc. 756 (1931).

RECEIVED DECEMBER 31, 1959.
DIVISION OF INDUSTRIAL AND CELLULOSE CHEMISTRY,
McGILL UNIVERSITY AND PULP AND PAPER RESEARCH INSTITUTE OF CANADA,
MONTREAL, QUE.

Can. J. Chem. Downloaded from www.nrcresearchpress.com by 41.223.56.140 on 09/04/12
For personal use only.

DIFFERENTIATION BETWEEN SOME 2,3- AND 2,5-DISUBSTITUTED PYRIDINE DERIVATIVES BY INFRARED SPECTROSCOPY

R. A. ABRAMOVITCH, GIAM CHOO SENG, AND A. D. NOTATION

In connection with studies of the orientation in the nucleophilic addition of phenyllithium to 3-substituted pyridines (1, 2) it became necessary to find a simple method of determining whether the attacking phenyl group had entered into the 2- or the 6-position of the pyridine ring, i.e. of distinguishing between 2- and 6-phenyl-3-substituted pyridines. This could be done by examining the N.M.R. spectrum of the compounds (1, 3) but was limited in that these determinations could not be carried out in our own laboratories. We therefore turned to infrared spectroscopy for such a method.

In theory, it should be quite simple to differentiate between 2,3- and 2,5-disubstituted pyridines by an examination of the aromatic C—H out-of-plane deformation region between 830 and 700 cm^{-1}. Infrared spectra – structure correlations have been found for the alkylbenzenes in the 11–15 μ region which are characteristic of the substitution positions in the benzene ring (4, 5). If one then considers that the pyridine ring corresponds to a monosubstituted benzene as far as the aromatic C—H out-of-plane bendings are concerned then a 2,3-disubstituted pyridine derivative should be equivalent to a 1,2,3-trisubstituted benzene whereas a 2,5-disubstituted pyridine derivative should correspond to a 1,2,4-trisubstituted benzene. The 1,2,3-trisubstituted benzenes show absorption in the 810–750 cm^{-1} range with a second band of medium intensity in the 726–680 cm^{-1} region, whereas 1,2,4-trisubstituted benzenes give rise to a strong band in the range 860–800 cm^{-1} (6). A number of 2,3- and 2,5-disubstituted pyridine derivatives have recently been shown to fall in nicely with this pattern (7, 8, 9). In particular, Podall (7) has studied the problem systematically and shown that 2-methyl-5-alkylpyridines exhibited two bands at 828–813 cm^{-1} and 735–724 cm^{-1}, whereas 2-methyl-3-alkylpyridines (1,2,3-trisubstitution) showed two bands at 813–769 cm^{-1} and 752–725 cm^{-1}.

A number of minor discrepancies in the band pattern in this region were observed in the present work. 2-Phenylnicotine exhibited a band at 805 cm^{-1}, quinoline a band at 805 cm^{-1}, and 5,6,7,8-tetrahydroquinoline a band at 827 cm^{-1} (see also (8)). On the other hand, 2-phenyl-3-alkyl- and 2-phenyl-5-alkyl-pyridines exhibited the expected absorptions though the presence of the monosubstituted phenyl-group obscured the assignment of the higher wavelength band. All that could be said was that most 2-phenyl-5-substituted pyridines exhibited a band of medium intensity between 850 and 800 cm^{-1} whereas most 2-phenyl-3-substituted pyridines did not.

A new and quite useful empirical correlation has now been observed in the C=C and

C=N stretching vibration region, which seems to apply provided no substituents which absorb in this region (—NH_2, —CO—, —NO_2, etc. . . .) are present. Table I summarizes the results obtained; the compounds are divided into two groups according to whether they are classed as corresponding to 1,2,3-trisubstituted or to 1,2,4-trisubstituted benzenes. 1,2,3-Trisubstituted compounds exhibit a band in the range 1578–1588 cm^{-1} whereas 1,2,4-trisubstituted derivatives give a band in the 1599–1605 cm^{-1} range. A second band at a somewhat higher wavelength is also generally observed but does not seem to be too characteristic. The orientation of the two isomeric phenylnicotines obtained by the action of phenyllithium on nicotine (1) was first assigned on the basis of the infrared bands in this region and later confirmed both by chemical means and also through a comparison of the N.M.R. spectra of the two isomers. The isomeric ethylphenylpyridines were also so oriented and the structure then proved unambiguously by degradative experiments. It is important to emphasize that this new correlation is only useful in determining the orientation of disubstituted pyridines provided one is sure that only these are present. Some trisubstituted pyridines have no bands in this region above 1590 cm^{-1} (e.g. 3,4,5-collidine and 2,3,4-collidine (9)), whereas others have. It is, therefore, not applicable to the possible determination of the number of substitutents present in the pyridine ring as the correlation of the bands due to the aromatic C—H out-of-plane deformation frequencies potentially is.

EXPERIMENTAL

The infrared spectra were measured on a Perkin–Elmer Model 21 recording spectrometer using sodium chloride optics. All the spectra were measured on liquid films and the positions of the bands calibrated by comparison with a polystyrene-film spectrum. All the samples were freshly distilled before use. We wish to express our gratitude to Dr. Hardegger (Zürich) for samples of 3-butyl-4-methylpyridine picrate, 5-butyl-2-

TABLE I

Compound	ν, cm^{-1}	
1,2,4-Trisubstitution		
2,4-Dimethylpyridine	1605	1570
2,5-Dimethylpyridine	1603	1572
3-Butyl-4-methylpyridine	1600	1565
5-Butyl-2-methylpyridine	1603	1572
2-Butyl-5-methylpyridine (10)	1602	1568
5-Ethyl-2-methylpyridine	1605	1570
5-Methyl-2-phenylpyridine	1600	1569
5-Ethyl-2-phenylpyridine	1600	1567
6-Phenylnicotine	1600	1567
3,4-Dimethylpyridine	1600	1564
3-Ethyl-4-methylpyridine	1599	1563
1,2,3-Trisubstitution		
2,6-Dideuteropyridine (11)	1586	1568
2,3-Dimethylpyridine	1580	1540(w)
2,6-Dimethylpyridine	1580	—
3-Butyl-2-methylpyridine	1587	1575
2-Butyl-3-methylpyridine (10)	1588	1576
3-Methyl-2-phenylpyridine	1579	1573
3-Ethyl-2-phenylpyridine	1583	1577
2-Phenylnicotine	1578	1569
3-Hydroxy-2-phenylpyridine*	1578	—
3-Methoxy-2-phenylpyridine	1584	—
5,6,7,8-Tetrahydroquinoline	1588(sh)	1579
5,6,7,8,9-Pentahydrocyclohepta[b]pyridine	1585(sh)	1577

*Nujol mull.

Can. J. Chem. Downloaded from www.nrcresearchpress.com by 41.223.56.140 on 09/04/12
For personal use only.

methylpyridine picrate, and 3-butyl-2-methylpyridine picrate, and to Dr. E. Godar (Chicago) for samples of 5,6,7,8-tetrahydroquinoline and 5,6,7,8,9-pentahydrocyclohepta[b]pyridine. The preparation of the phenylpyridine derivatives will be described in forthcoming papers. The results are summarized in Table I. The hetero-nitrogen atom is considered here as corresponding to a substituted annular carbon atom in benzene.

ACKNOWLEDGMENTS

The authors wish to thank Drs. Hardegger and Godar for the gifts of samples. This work was carried out during the tenure (by A. D. N.) of the Thorvaldson Scholarship, and with the financial support of the National Research Council.

1. R. A. ABRAMOVITCH, A. D. NOTATION, and GIAM CHOO SENG. Tetrahedron Letters, **8**, 1 (1959).
2. R. A. ABRAMOVITCH and GIAM CHOO SENG. Unpublished work.
3. A. D. NOTATION. M.Sc. Thesis, University of Saskatchewan, Saskatoon, Saskatchewan. 1959.
4. N. B. COLTHRUP. J. Opt. Soc. Am. **40**, 397 (1950).
5. R. R. RANDLE and D. H. WHIFFEN. Rept. on Conf. of Molecular Spectroscopy. Paper No. 12. Institute of Petroleum. 1954. p. 111.
6. L. J. BELLAMY. Infrared spectra of complex molecules. Methuen & Co., Ltd., London. 1958. p. 78.
7. H. E. PODALL. Anal. Chem. **29**, 1423 (1957).
8. D. HEINERT and A. E. MARTELL. J. Am. Chem. Soc. **81**, 3933 (1959).
9. H. SHINDO and N. IKEKAWA. Pharm. Bull. (Tokyo), 4, 192 (1596).
10. N. J. LEONARD and B. L. RYDER. J. Org. Chem. **18**, 598 (1953).
11. J. K. WILMSHURST and H. J. BERNSTEIN. Can. J. Chem. **35**, 1183 (1957).

RECEIVED DECEMBER 23, 1959.
DEPARTMENT OF CHEMISTRY,
UNIVERSITY OF SASKATCHEWAN,
SASKATOON, SASKATCHEWAN.

AN N.M.R. STUDY OF ELECTRON RELEASE BY ALKYL AND ALKOXY GROUPS IN VARIOUS SOLVENTS

R. B. MOODIE*, T. M. CONNOR,† AND ROSS STEWART

Recently dipole moment studies (1) and measurements of substrate activity (2) have shown the importance of solvent effect on molecules in their ground state. We have used N.M.R. to measure the chemical shifts of aromatic protons in alkyl and alkoxy benzenes in various solvents. Table I gives the chemical shifts in cycles per second relative to benzene at the same concentration in the same solvent.

TABLE I

Chemical shifts from benzene for the aromatic protons, in cycles/sec

Compound	Solvent			
	C_6H_{12}	$(CH_3)_3N$	CH_3OH	CH_3NO_2
Toluene	5.9	6.2	6.4	6.8
Ethylbenzene	4.4	5.1	5.2	5.3
Isopropylbenzene	3.8	4.1	4.6	4.7
tert-Butylbenzene	1.1*	1.2*	0.9*	1.2*

*These measurements are not to a single peak (see discussion) and are therefore less accurate. Probable error ±0.5 cycle/sec.

**National Research Council Postdoctorate Fellow 1958–60.*
†*Holder of a National Research Council Studentship 1957–59.*

Can. J. Chem. Downloaded from www.nrcresearchpress.com by 41.223.56.140 on 09/04/12
For personal use only.

methylpyridine picrate, and 3-butyl-2-methylpyridine picrate, and to Dr. E. Godar (Chicago) for samples of 5,6,7,8-tetrahydroquinoline and 5,6,7,8,9-pentahydrocyclohepta[b]pyridine. The preparation of the phenylpyridine derivatives will be described in forthcoming papers. The results are summarized in Table I. The hetero-nitrogen atom is considered here as corresponding to a substituted annular carbon atom in benzene.

ACKNOWLEDGMENTS

The authors wish to thank Drs. Hardegger and Godar for the gifts of samples. This work was carried out during the tenure (by A. D. N.) of the Thorvaldson Scholarship, and with the financial support of the National Research Council.

1. R. A. ABRAMOVITCH, A. D. NOTATION, and GIAM CHOO SENG. Tetrahedron Letters, **8**, 1 (1959).
2. R. A. ABRAMOVITCH and GIAM CHOO SENG. Unpublished work.
3. A. D. NOTATION. M.Sc. Thesis, University of Saskatchewan, Saskatoon, Saskatchewan. 1959.
4. N. B. COLTHRUP. J. Opt. Soc. Am. **40**, 397 (1950).
5. R. R. RANDLE and D. H. WHIFFEN. Rept. on Conf. of Molecular Spectroscopy. Paper No. 12. Institute of Petroleum. 1954. p. 111.
6. L. J. BELLAMY. Infrared spectra of complex molecules. Methuen & Co., Ltd., London. 1958. p. 78.
7. H. E. PODALL. Anal. Chem. **29**, 1423 (1957).
8. D. HEINERT and A. E. MARTELL. J. Am. Chem. Soc. **81**, 3933 (1959).
9. H. SHINDO and N. IKEKAWA. Pharm. Bull. (Tokyo), 4, 192 (1596).
10. N. J. LEONARD and B. L. RYDER. J. Org. Chem. **18**, 598 (1953).
11. J. K. WILMSHURST and H. J. BERNSTEIN. Can. J. Chem. **35**, 1183 (1957).

RECEIVED DECEMBER 23, 1959.
DEPARTMENT OF CHEMISTRY,
UNIVERSITY OF SASKATCHEWAN,
SASKATOON, SASKATCHEWAN.

AN N.M.R. STUDY OF ELECTRON RELEASE BY ALKYL AND ALKOXY GROUPS IN VARIOUS SOLVENTS

R. B. MOODIE*, T. M. CONNOR,† AND ROSS STEWART

Recently dipole moment studies (1) and measurements of substrate activity (2) have shown the importance of solvent effect on molecules in their ground state. We have used N.M.R. to measure the chemical shifts of aromatic protons in alkyl and alkoxy benzenes in various solvents. Table I gives the chemical shifts in cycles per second relative to benzene at the same concentration in the same solvent.

TABLE I

Chemical shifts from benzene for the aromatic protons, in cycles/sec

Compound	Solvent			
	C_6H_{12}	$(CH_3)_3N$	CH_3OH	CH_3NO_2
Toluene	5.9	6.2	6.4	6.8
Ethylbenzene	4.4	5.1	5.2	5.3
Isopropylbenzene	3.8	4.1	4.6	4.7
tert-Butylbenzene	1.1*	1.2*	0.9*	1.2*

*These measurements are not to a single peak (see discussion) and are therefore less accurate. Probable error ±0.5 cycle/sec.

**National Research Council Postdoctorate Fellow 1958–60.*
†*Holder of a National Research Council Studentship 1957–59.*

Can. J. Chem. Downloaded from www.nrcresearchpress.com by 41.223.56.140 on 09/04/12
For personal use only.

Shifts were measured on a 40-Mc Model 4300 Varian N.M.R. spectrometer by graphical interpolation between two side bands from the solvent resonances, set as near as possible on either side of the aromatic protons. The side bands were measured with a Hewlett–Packard frequency counter. Samples were 5% solutions sealed *in vacuo*. Six determinations of the cyclohexane–toluene shift by this technique gave a mean-square deviation of ±0.13 cycle/sec. An additional small error may be present in all these measurements

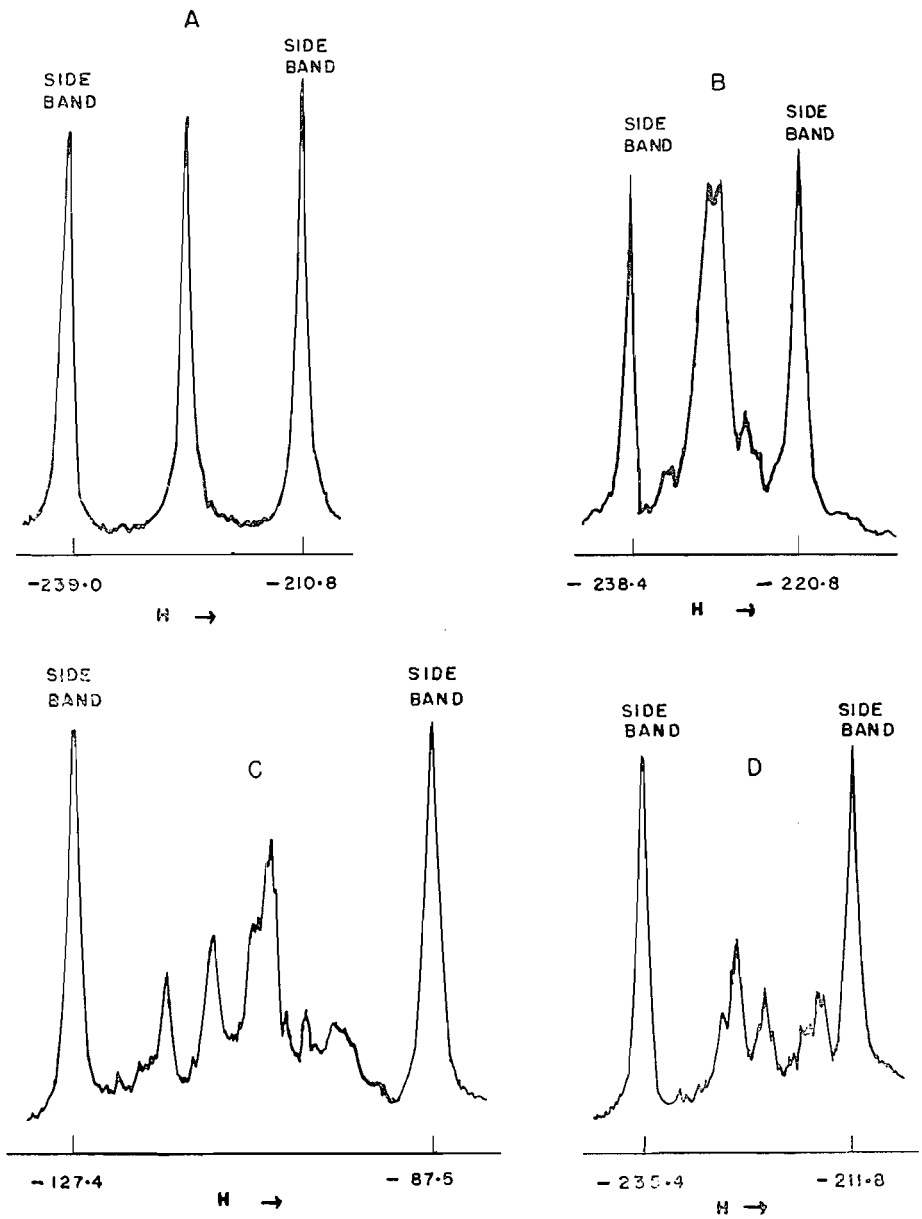


FIG. 1. Spectrum of aromatic protons with side band shifts in cycles per second from the solvent resonance: (A) toluene, (B) *tert*-butylbenzene in cyclohexane, (C) isopropyl phenyl ether in nitromethane, and (D) isopropyl phenyl ether in cyclohexane.

Can. J. Chem. Downloaded from www.nrcresearchpress.com by 41.223.56.140 on 09/04/12
For personal use only.

due to dilution effects, since these figures do not represent extrapolation to infinite dilution (3).

In so far as the shifts reflect the average electron density around the aromatic protons in the substituted compounds, the shifts of the alkylbenzenes indicate that the Baker–Nathan order prevails, even in cyclohexane, in contrast to the evidence of dipole moments (1). Since *tert*-butylbenzene shows a well-resolved fine structure but the other alkylbenzenes do not (Fig. 1), the conclusions for this compound are less valid. (Shifts are for the approximate "center of gravity" of the aromatic proton resonances for this compound.) In the comparison of *p*-bromo-*tert*-butylbenzene and *p*-bromotoluene this objection is removed since measurements on the quartet (which show further fine structure due to cross ring coupling) enable calculations of the chemical shifts of ortho and meta protons (4, 5). These values are given in Table II. (It is assumed that the protons ortho to the alkyl group are responsible for the high field doublet of the quartet.) These show

TABLE II

Ortho coupling constants and chemical shifts from benzene for the aromatic protons in *p*-bromo-alkylbenzenes

	p-Bromotoluene in:		*p*-Bromo-*tert*-butylbenzene in:	
	Solvent C_6H_{12}	Solvent CH_3NO_2	Solvent C_6H_{12}	Solvent CH_3NO_2
Coupling constant in cycles/sec	8.7	8.8	8.6	—[b]
Chemical shift of ortho protons[a]	12.0	10.0	1.5	(−0.4)[b]
Chemical shift of meta protons[a]	−2.0	−0.9	−3.0	(−0.4)[b]

[a]The positions are relative to the alkyl group.

[b]Only a single peak was observed for the aromatic protons of *p*-bromo-*tert*-butylbenzene in nitromethane.

that the ortho and meta protons are more shielded in the methyl than the *tert*-butyl-substituted compound, in agreement with the evidence above. As might be expected, more polar solvents increase the degree of electron release of the alkyl groups in the alkylbenzenes. The benzene–toluene shift in a particular solvent may constitute a useful measure of solvent polarity, if the accuracy of the shift measurements can be improved (by, for example, using a 60-Mc spectrometer and taking the mean of a number of determinations). The solvent effect may be more marked in toluene, ethylbenzene, and isopropyl benzene than in *tert*-butylbenzene (6) but the effect is at present of the same order as the experimental error.

The alkoxy benzenes, anisole, phenetole, isopropyl phenyl ether, and *tert*-butyl phenyl ether, show a more complicated aromatic proton spectrum. Assignment of ortho, meta, and para proton resonances is not possible, and this precludes any precise determination of solvent and substituent effects. Two interesting observations may, however, be made. Firstly, in all four solvents, the aromatic proton resonances of *tert*-butyl phenyl ether are at lower field and show a much less well-defined fine structure than those of the other three ethers. This is due to steric hindrance to conjugation between the oxygen atom and the aromatic π electrons, an effect previously shown to exist from ultraviolet spectral data and from rates of bromination (7). Secondly, there is a sharp contrast between the spectra of anisole, phenetole, and isopropyl phenyl ether in cyclohexane and their spectra

Can. J. Chem. Downloaded from www.nrcresearchpress.com by 41.223.56.140 on 09/04/12
For personal use only.

in the other three solvents. Typical spectra of the two types are shown in Figs. 1C and 1D. This suggests that differential electron release to ortho, meta, and para positions varies with the solvent. A similar effect has been observed in the solvent dependence of the ortho/para ratio in the nitration of phenol (8).

By studying suitably substituted ethers it may be possible to eliminate the uncertainty due to spin–spin splitting of non-equivalent proton resonances.

ACKNOWLEDGMENTS

Two of us (R. B. M. and T. M. C.) would like to thank the National Research Council for the fellowship and studentship.

1. T. L. BROWN. J. Am. Chem. Soc. **81**, 3232 (1959).
2. R. A. CLEMENT and M. R. RICE. J. Am. Chem. Soc. **81**, 326 (1959).
3. J. A. POPLE, W. G. SCHNEIDER, and H. J. BERNSTEIN. High resolution nuclear magnetic resonance. McGraw-Hill Book Co., New York. 1959. p. 424.
4. J. A. POPLE, W. G. SCHNEIDER, and H. J. BERNSTEIN. High resolution nuclear magnetic resonance. McGraw-Hill Book Co., New York. 1959. p. 119.
5. R. B. MOODIE, T. M. CONNOR, and R. STEWART. Can. J. Chem. **37**, 1402 (1959).
6. W. M. SCHUBERT, J. M. CRAVEN, G. MINTON, and R. B. MURPHY. Tetrahedron, **5**, 194 (1959).
7. G. BADDELEY, N. H. P. SMITH, and M. A. VICKARS. J. Chem. Soc. 2455 (1956).
8. J. PODKÓWKA and A. TARNAWSKI. Monatsh. Chem. **90**, 178 (1959).

RECEIVED NOVEMBER 2, 1959.
DEPARTMENT OF CHEMISTRY,
UNIVERSITY OF BRITISH COLUMBIA,
VANCOUVER, BRITISH COLUMBIA.

Can. J. Chem. Downloaded from www.nrcresearchpress.com by 41.223.56.140 on 09/04/12
For personal use only.

Can. J. Chem. Downloaded from www.nrcresearchpress.com by 186.148.149.217 on 09/04/12
For personal use only.

Canadian Journal of Chemistry

Issued by THE NATIONAL RESEARCH COUNCIL OF CANADA

VOLUME 38 MAY 1960 NUMBER 5

THE SEPARATION OF SOME TERPENOID COMPOUNDS BY GAS–LIQUID CHROMATOGRAPHY[1]

E. VON RUDLOFF

ABSTRACT

A study has been made of the degree of separation of mixtures of some terpene hydrocarbons, some of their oxygenated derivatives, two sesquiterpene alcohols, and three monophenols on a variety of columns. Temperature and sample size affected the degree of separation and the solid support Chromosorb W, a calcined diatomaceous earth, was found to combine the advantages of Celite and C-22 firebrick without causing decomposition of the sample at higher temperatures. When Craig polyesters were used as liquid phases, separations equal to those obtained on polyethylene glycol were realized with the added advantage that these produced columns which are stable at 190 to 220° C. Consequently, sesquiterpene alcohols and monophenols were also separated successfully. Another useful liquid phase for both low and high temperatures was found in a meta-linked polyphenyl ether. Squalene was found to be an efficient liquid phase for the separation of terpene hydrocarbons at 130° C and lower. The possible application of the present findings for preparative work is discussed.

INTRODUCTION

A general method for the separation of small amounts of closely related terpene hydrocarbons, some of their oxygenated derivatives as well as some higher boiling sesquiterpene alcohols and monophenols, was required in this laboratory. Such mixtures often have a narrow range of boiling points and separation by fractional distillation not only requires large amounts, but frequently fails to produce pure components. Gas–liquid chromatography (GLC) offers considerable advantages over fractional distillation when quantities of 0.01 to 0.1 g are required, and has in several instances been extended to the gram scale. This technique was, therefore, studied in some detail to find suitable conditions for complete separation of such terpenoid mixtures on a 0.1- to 1-g scale. The experiments were carried out with a Beckman GC-2 chromatograph, using helium as carrier gas, a thermal conductivity cell as detector, and 6-foot columns of 6-mm inner diameter.

Successful separations of terpenoid compounds by GLC have been described in the literature. Bernhard (1) separated five monoterpene hydrocarbons on 20-foot polyethylene glycol and *n*-octyl phthalate columns, but obtained poor results when silicone fluid, Apiezon L, or high vacuum grease was used as liquid phase. Bayer *et al.* (2) used hydrogen as carrier gas and obtained a fair degree of separation for a large variety of terpenoid compounds on columns containing silicone vacuum grease to which alkali capronates had been added. Cvrkal and Janák (3), also using hydrogen, obtained good results for

[1]*Manuscript received December 24, 1959.*
Contribution from the National Research Council of Canada, Prairie Regional Laboratory, Saskatoon, Saskatchewan.
Issued as N.R.C. No. 5605.

terpene hydrocarbons on dimethylsiloxane and proposed glycerol for oxygenated compounds. The use of hydrogen as carrier gas for mixtures containing unsaturated compounds may create difficulties, since activated centers of the solid support could catalyze phases for the separation of many terpene hydrocarbons, but their retention times of 80 minutes and more are rather high. These authors discuss some of the difficulties encountered in the analysis of essential oils and point out the need for polar liquid phases which can be used at 150° C or higher to fractionate oxygenated derivatives. This has been found in the present study in adipate polyethylene glycol, succinate ethylene glycol, and phthalate ethylene glycol polyesters (Craig polyesters) and in a *m*-linked polyphenyl hydrogenation. Liberti and Cartoni (4) used silicone and tricresyl phosphate as liquid ether. Columns with polyethylene glycol were also used by Stanley (5) and Eglington *et al.* (6) and recently Westaway and Williams (7) have separated almost completely α- and β-pinene, α- and γ-terpinene, and limonene on a 6-foot Apiezon M column with nitrogen as carrier gas.

From the data contained in the above communications and in the monograph by Keulemans (8) it was concluded that silicone-type columns could be used for a wide range of compounds at lower and higher temperatures with a fair degree of separation. Far better separation could be expected with polyethylene glycols but the temperature limit of 100 to 130° C (8) would limit its application. These two types of liquid phases were, therefore, used to study the effect of the various physical factors involved and to compare the degree of separation obtained with polyethylene, squalene, Apiezon M, polystyrene, a polyphenyl ether, polyesters of adipic, succinic, and phthalic acids (Craig polyesters), a polyamide, and diglycerol as liquid phases. *d*-Limonene, the mixture of *p*-menthadienes produced by dehydration of α-terpineol with oxalic acid as catalyst (9), and a synthetic mixture containing *d*-limonene, 1,8-cineole, fenchone, citronellal, camphor, α-terpineol, citronellol, and bornyl acetate were used as test compounds. The sesquiterpene alcohols, occidentalol and eudesmol, and the monophenols, anethole, eugenol, and isoeugenol, were used for the chromatographic studies at higher temperatures.

Initial experiments in the present study showed that a number of factors influencing the separation of terpenoid compounds have not been described fully in the literature. Also, most of the liquid phases used to date for this purpose, except the rather inefficient silicone type, cannot be used above 100 to 130° C for any length of time. Furthermore, the above communications are mainly concerned with qualitative determinations and do not give the most favorable conditions for preparative separations. The present investigation was therefore extended to cover the effect of sample size, temperature, flow rate, nature of solid support, and the ratio of solid support to liquid phase, as well as a search for liquid phases which could be used successfully for the wide range required. The results obtained in this study show that sample size, temperature, and, to a lesser degree, the solid support can affect the degree of separation. Some of the liquid phases tested gave poor results when samples of 5 μl or more were used, yet gave excellent separation with 2 μl or less, making these columns useful for analytical work. Two types of liquid phases, Craig polyesters and a polyphenyl ether, could be used equally well at 190–220° C or at lower temperatures. An adipic acid – polyethylene glycol polyester was found to give separations equal to, or better than, those obtained on a polyethylene glycol (Carbowax 400), besides being suitable for high temperature separations, and proved to be the best general purpose column for up to 50 μl of terpenoid compounds investigated thus far.

Can. J. Chem. Downloaded from www.nrcresearchpress.com by 186.148.149.217 on 09/04/12
For personal use only.

Can. J. Chem. Downloaded from www.nrcresearchpress.com by 186.148.149.217 on 09/04/12
For personal use only.

EXPERIMENTAL

Apparatus

A Beckman GC-2 chromatograph equipped with a fraction collector (No. 92730) and a heated inlet (suitable for injection of up to 2 ml) was used in conjunction with a Bristol Dynamaster strip-chart recorder (0.05- to 1.05-mv scale). The chart speed was 0.5 inch per minute and the flow rate of helium carrier gas was measured at the exit by the soap bubble method. Samples were introduced with a Beckman liquid sampler (No. 224000) which allowed the accurate injection of 1.5 to 80 μl quantities. The column exhaust was at atmospheric pressure (710–715 mm Hg) whereas the pressure at the column inlet was varied to give the desired flow rates.

Solid Support and Chemicals

Celite 545 was water-washed to remove the fines, then acid-washed, neutralized with bicarbonate solution, washed with water, and dried. C-22 Firebrick (60–80 mesh) was prepared by wet milling, drying, and sifting of commercial firebrick. Chromosorb W, a flux-calcined diatomaceous earth, produced by Johns–Manville, was obtained commercially. Silicone high vacuum grease (Dow Corning), squalene (90%, Eastman Chemicals), Carbowax 400 (Carbide and Carbon Chem. Co.), the polyphenyl ether *m*-bis(*m*-phenoxyphenoxy)-benzene (Monsanto Corp.), Apiezon M (Metropolitan–Vickers Electrical Co.), and diglycerol (Colgate–Palmolive Co.) were also obtained from commercial sources. The Craig polyesters were kindly supplied by Dr. B. M. Craig and were prepared by reaction of adipic acid with polyethylene glycol (Carbowax 400) and 1% diglycerol as plasticizer and succinic or phthalic acid with ethylene glycol (10). The succinate polyester (SEG) was a solid having m.p. 96–100° C, whereas the adipic (APEG) and phthalate (PEG) polyester were viscous liquids.

Commercial samples of liquid terpenes and oxygenated derivatives were purified by fractional distillation and for critical work by GLC, using the Carbowax 400 or APEG polyester columns. Collection of the samples was carried out with the detector current reduced from 250 ma to 100 ma or completely turned off. The refractive indices of the samples thus obtained are shown in Table I.

TABLE I

Refractive indices of terpenoid compounds

	Boiling point (° C)	n_D^{20}	
		Purified by distillation	Purified by GLC
α-Pinene	155–156	1.4684	1.4671
β-Pinene	—		1.4793
α-Phellandrene	175–176	1.4764	1.4730
α-Terpinene	173.5–174.5	—	1.4780
d-Limonene	176–177	1.4731	1.4722
1,8-Cineole	174.5	1.4583	1.4578
Fenchone	192–193	1.4646	—
Citronellal	205–206	1.4527	—
α-Terpineol	219.8	1.4829	1.4830
Citronellol	222	1.4568	1.4560
Bornyl acetate	223–224	1.4643	—

Eudesmol, m.p. 82–84° C, $[\alpha]_D$ +32°, was obtained by crystallization and sublimation of a commercial sample (Plaimar Ltd., Perth, Australia) which was obtained from

Callitropsis araucarioides Compt. Occidentalol, m.p. 95–96° C, $[\alpha]_D$ +363°, was obtained from the neutral extractives of the heartwood of *Thuja occidentalis* L. as described by Nakatsuka and Hirose (11).

The mixture of *p*-menthadienes obtained by dehydration of α-terpineol (9) was prepared by refluxing oxalic acid (120 g) in water (240 ml) with α-terpineol (40 g) for 6 hours. The mixture was steam-distilled, the distillate extracted with ether, and the ethereal solution was dried over calcium chloride. The mixture of terpene hydrocarbons was used as such after the solvent had been evaporated.

Packing of Columns

The liquid phase (2.5 g) was dissolved in a volume of low-boiling solvent (50 ml chloroform) which is equal to that of the solid support. This solution was placed into a high, narrow beaker or cylinder and the solid support (12.5 g) was added with stirring. Stirring was continued for 3 to 5 minutes after addition and the mixture was spread on a shallow stainless steel tray. After the solvent had evaporated, the residual material was dried *in vacuo* at 60–70° C for about 1 hour. The dried material was poured in small aliquots with tapping into 6-mm inner diameter copper tubing of 6-foot length, taking note of the weight of mixture added. The column was closed on each end with a small glass wool plug and coiled into a 5- to 7-in. diameter coil. It was allowed to equilibrate at the desired temperature and flow rate of helium gas (0.5 to 1.5 hours). Injection of samples was begun when the recorder maintained a steady base line.

When polyethylene (obtained by cutting polyethylene reagent bottles into small pieces) was used as liquid phase, it was dissolved by refluxing in a minimum volume of petrol (b.p. 154–202° C). The solid support was added to the hot solution as above and the drying time was extended to 5 hours.

RESULTS AND DISCUSSION

Initial Experiments

Optimum conditions for each type of column were obtained by trial and error. Columns having Celite 545 as solid support were found to require higher temperatures and inlet pressures than those with C-22 firebrick, but the latter caused decomposition of some compounds at higher temperatures, especially aldehydes and tertiary alcohols. Liberti and Cartoni (4) report that Stermachol, a material similar to C-22 firebrick, is not suitable for terpene alcohols, and used inactivated Celite instead. A more suitable solid support was found in Chromosorb W, which combined the advantages of firebrick without causing decomposition. This support was, therefore, used in all subsequent experiments.

For preparative work a high ratio of liquid phase to solid support is desirable (8, 12), but in the present study the degree of separation deteriorated when 20% or more liquid phase was used. A ratio of 1:6 was found to give consistently good results.

Polyethylene, Apiezon M, polystyrene, and a polyamide (Zytel) gave inferior results and these were not further studied. Solid compounds, such as the SEG polyester (m.p. 96–100° C), gave poor separations below their melting or softening point.

Effect of Physical Factors

The effect of temperature on the degree of separation of the mixture of *p*-menthadienes on the Carbowax column is shown in Fig. 1. Contrary to the report of Bernhard (1), the effect was found to be considerable. Keulemans (8), from theoretical considerations, also considers the effect to be important. The separation at 80° C, the lowest feasible tem-

Can. J. Chem. Downloaded from www.nrcresearchpress.com by 186.148.149.217 on 09/04/12
For personal use only.

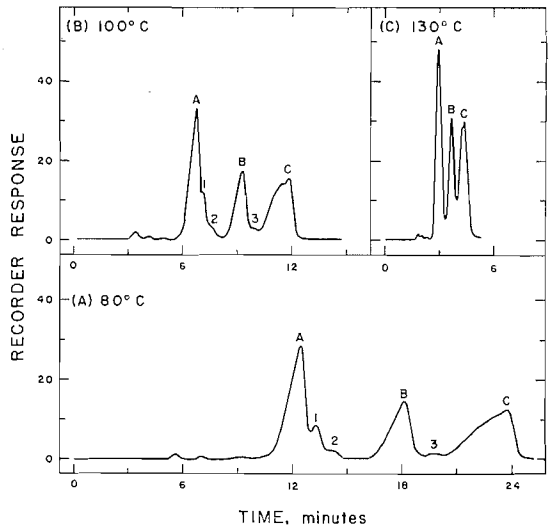


FIG. 1. Separation of the mixture of *p*-menthadienes on the Carbowax column at (A) 80° C and 43.5 ml helium per minute, (B) 100° C and 42.8 ml helium per minute, (C) 130° C and 41.9 ml helium per minute.

perature, was by far the best (Fig. 1(A)), even though the curves are skewed. From a preparative point of view skewing of curves is not detrimental, but is less satisfactory for quantitative calculation. The collection of fractions at the lowest possible temperature has the additional advantage of minimizing the danger of thermal decomposition or rearrangements.

Changes in the flow rate of the carrier gas over the practical range of about 10 to 400 ml (8) did not effect the degree of separation noticeably, which is in agreement with the considerations of Keulemans (8) and the findings of Bernhard (1). Thus, the flow rate was adjusted to give optimum separations at as low a temperature as possible.

The effect of sample size on the retention time of each component was found to be considerable. Table II shows the retention times obtained for *d*-limonene on various columns when samples of 1.5 to 50 μl were injected at optimum temperatures and flow rates. From these results it is evident that an increase in sample size above 1 to 3 μl

TABLE II

Effect of sample size on the retention time (in minutes) of *d*-limonene

Column (liquid phase)	Temp. (°C)	Flow rate (ml He/min)	Sample size (μl) 1.5	3	5	10	20	40	50	Initial emergence of peak (1.5–50 μl)
Silicone (washed)	130	50.5	5.4	5.5	5.6	6.05	6.7*	7.4*	7.8†	4.6–5.0
Silicone (washed)	Duplicate run		5.5	5.6	5.7	6.1	6.8*	7.5*	7.8†	4.7–5.1
Squalene	130	74.2	15.5	15.5	15.6	16.3	17.2*	18.2†	19.0†	14.0–14.3
Carbowax 400	130	46.8	2.85	2.9	2.9	3.0*	3.4*	3.9†	—	2.4–2.5
Polyphenyl ether	130	53.6	6.4	6.55	6.7	6.9*	7.55†	8.1†	—	5.2–5.6
SEG polyester	100	25.0	4.75	4.95	5.35	6.3*	8.2†	—	—	3.6–4.0
APEG polyester	130	41.6	3.95	4.0	4.1	4.3	4.65*	5.25*	5.4†	3.35–3.45
PEG polyester	100	43.5	5.1	5.2	5.5	6.0	6.9*	8.2†	9.0†	3.85–4.25
Diglycerol	80	20.0	2.6	2.75*	3.8†	—	—	—	—	1.2–1.8

*Skewing clearly visible. †Excessive skewing of peak.

Can. J. Chem. Downloaded from www.nrcresearchpress.com by 186.148.149.217 on 09/04/12
For personal use only.

produces considerable delays in the emergence of a peak maximum, and this is accompanied by broadening of the peaks. This is in agreement with the findings of Bens and McBride (13), those obtained by Porter *et al.* (14) with gaseous samples, and those obtained by Bethea and Smutz (15) with aliphatic alcohols on a butyl phthalate column. The latter authors report the optimum sample size for 6-mm diameter columns to be from 4 to 12 μl and detected overloading above 20 μl. Thomas (16) found the optimum for liquid samples to be 30–70 μl. Table II shows that different types of columns have different capacities, silicone and APEG polyester allowing samples of up to 40 μl size, although skewing became noticeable with 10–20 μl samples. Diglycerol has too low a capacity to be attractive for preparative work, but the other liquid phases may be useful since they have a fair capacity and different separation properties.

The fact that larger samples cause a considerable delay of peak maxima has important consequences for both analytical and preparative work. In the former, an unknown peak is often identified by comparing its retention time with those of known compounds run under identical conditions (8). This is only permissible if the sample size of the unknown and known compounds are nearly the same. The technique of adding the known compound to the unknown (8) may be preferred, but actual isolation and comparison of physical constants (e.g., the infrared spectrum) would seem to be a more reliable means of identification. Another alternative is to make use of the fact that the initial emergence time of a peak remains practically constant with different sample sizes up to where the column becomes badly overloaded (14, Table II). However, this can be used only when all peaks are completely separated from one another.

From a preparative point of view the delay of the peak maximum and broadening of the peak caused by a larger sample is not detrimental, provided skewing or broadening does not cause an overlap with neighboring peaks. Even then, an overloaded column may still produce pure fractions if center cuts are collected. The use of columns having larger diameter (12, 17, 18, 19) did not give the same degree of separation as was obtained on the corresponding 6-mm columns when larger samples (50 μl or more) were used. Also, because of the higher flow rates required in larger diameter columns the consumption of helium gas was found to be considerable and it was found more advantageous to carry out repeated runs of 25 to 50 μl on the 6-mm diameter columns. Since most columns required only 15–30 minutes for each run, the collection of 0.1 to 0.5 g of a desired fraction was possible within half a day. When such fractions were collected with a normal detector current of 200 to 250 ma, these were yellowish and on rechromatographing the material, typical decomposition peaks were recorded besides the normal symmetrical peaks for the pure compounds. This difficulty was overcome in most instances by using a detector current of 100 ma, which was sufficient for samples of 20 μl or more. Only in exceptional cases, e.g. α-pinene or tertiary alcohols, was it necessary to carry out preparative runs without the detector, i.e. fractions were collected at times determined previously in a run of the same sample size with the detector current on. A possible means of overcoming the necessity of "blind" runs may be to construct a bypass system, similar to those used with detectors other than the thermal conductivity type.

Separation Obtained with Various Liquid Phases

Terpene hydrocarbons were separated most successfully on columns containing squalene, APEG polyester, and polyphenyl ether, separations being in the same order as those obtained on Carbowax 400 and superior to those obtained on silicone (see Table III). Each column appears to offer slight advantages for one or another compound, a finding which was especially apparent in runs with the complex *p*-menthadiene mixture

Can. J. Chem. Downloaded from www.nrcresearchpress.com by 186.148.149.217 on 09/04/12
For personal use only.

TABLE III

Relative retention times (*d*-limonene = 1) of terpene hydrocarbons

Column (liquid phase)	Silicone	Squalene	Carbowax	Polyphenyl ether	APEG polyester
Temperature (° C)	100	100	100	100	100
Flow rate (ml He/min)	50.5	74.2	42.8	92.4	26.3
d-Limonene (retention time in minutes)	16.75	15.4	8.0	13.2	15.6
α-Pinene	0.57	0.52	0.40	0.39	0.39
β-Pinene	0.72	0.69	0.59	0.59	0.61
α-Phellandrene	0.84	0.83	0.79	0.81	0.82
α-Terpinene	0.92	0.88	0.825	0.88	0.88

(Figs. 1 and 2). The squalene column is unstable at 130° C for prolonged periods of time, and an efficient aliphatic polyunsaturated liquid phase which is stable at 130° C or higher is still lacking.

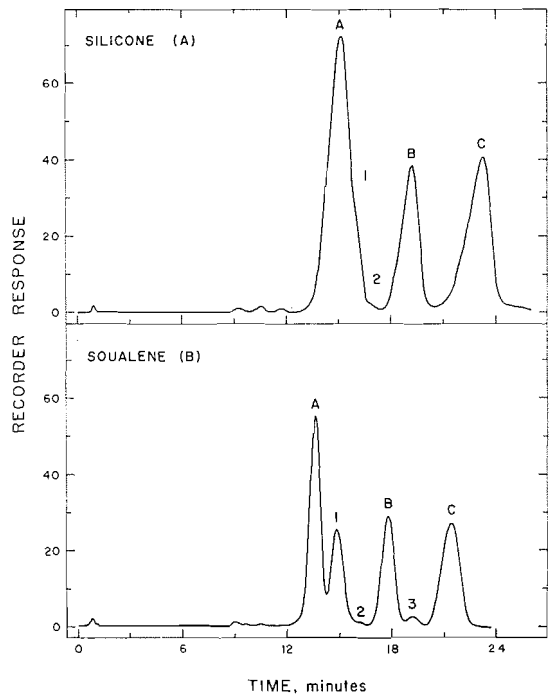


FIG. 2. Separation of the mixture of *p*-menthadienes on (A) silicone (at 100° C and 50.5 ml helium per minute), (B) squalene (at 100° C and 74.2 ml helium per minute).

Resolution of the mixture of *p*-menthadienes on the silicone column (cf. Fig. 2(A)) shows three major peaks A, B, and C, with an indication of further constituents at 1 and 2. The squalene (cf. Fig. 2(B)) and the Carbowax columns (cf. Fig. 1) clearly showed three additional components, 1, 2, and 3, and on the latter column peak C appears to be composed of two compounds in about equal amounts. A very similar separation was obtained with the APEG and SEG polyester columns, whereas the polyphenyl ether column gave the same resolution except that C appeared as a single peak. The best resolution of A, which corresponds to α-terpinene, was obtained on the squalene column, separation from impurity 1 being complete. From these results it follows that the com-

Can. J. Chem. Downloaded from www.nrcresearchpress.com by 186.148.149.217 on 09/04/12
For personal use only.

plex mixture of *p*-menthadienes obtained by dehydration of α-terpineol cannot be resolved by one column alone, but requires successive fractionation on the squalene and polyester columns. For analytical purposes longer columns or the very efficient Golay columns (20, 21) may have to be used. Peak C presents a problem and its composition, as well as the chemical identification of the other components will be the subject of another communication.

TABLE IV

Relative retention times (*d*-limonene = 1) of various monoterpenoid compounds

Column (liquid phase)	Silicone	Squalene	Carbowax	Polyphenyl ether	Polyesters		Diglycerol
					APEG	SEG	
Temperature (° C)	130	130	130	130	130	100	100
Flow rate (ml He/min)	30.0	74.2	42.0	53.6	41.6	26.3	20.0
Inlet pressure (mm Hg)	1531	2029	1531	1531	1531	1531	1014
Retention time of *d*-limonene	8.3	15.5	3.15	6.0	3.8	2.0	1.5
Specific retention volume V_g	19.1	27.2	19.1	23.0	15.9	9.0	8.9
1,8-Cineole (b.p. 174°)	1.1	0.95	1.25	1.2	1.25	1.05	1.5
Fenchone (b.p. 192°)	1.4	—	3.0	2.2	2.9	3.0	3.2
Citronellal (b.p. 205°)	2.0	—	3.8	3.0	3.65	4.2	3.25
Camphor (sublimes)	1.95	—	5.15	3.7	5.1	5.6	6.4
α-Terpineol (b.p. 220°)	2.45	—	11.6	4.7	10.95	11.5	6.6
Citronellol (b.p. 222°)	3.1	—	20.2	4.45	14.6	13.3	6.7
Bornyl acetate (b.p. 223°)	3.85	—	6.2	5.5	5.95	6.2	4.8

Table IV shows the relative retention volumes with respect to *d*-limonene of some oxygenated derivatives. The best degree of separation of these compounds was obtained on the Carbowax and APEG polyester column, and that of the former is compared in Fig. 3 with the separation obtained on silicone (Fig. 3(A)). Since Carbowax cannot be

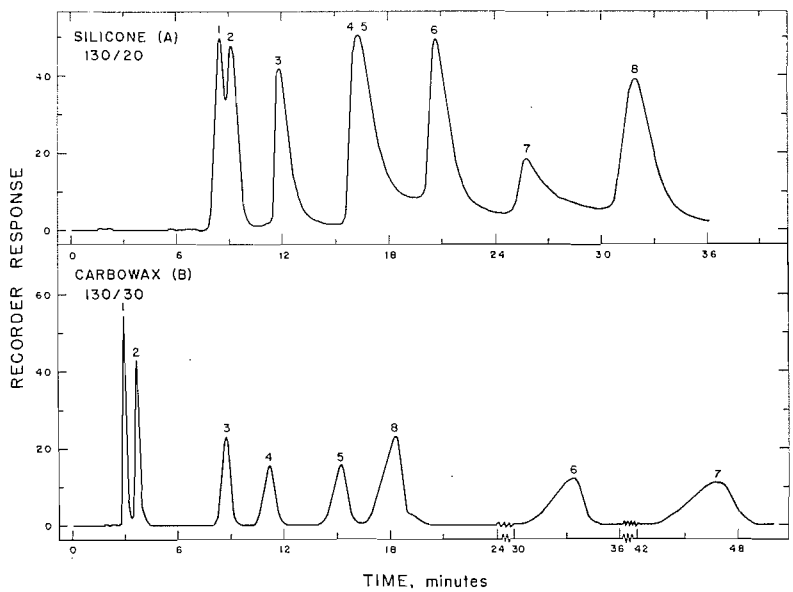


FIG. 3. Separation of terpenoid compounds on (A) silicone (at 130° C and 30.0 ml helium per minute), (B) Carbowax (at 130° C and 42.0 ml helium per minute).
1, limonene; 2, 1,8-cineole; 3, fenchone; 4, citronellal; 5, camphor; 6, α-terpineol; 7, citronellol; 8, bornyl acetate.

Can. J. Chem. Downloaded from www.nrcresearchpress.com by 186.148.149.217 on 09/04/12
For personal use only.

used above 100° to 120° C for long periods (8), the use of APEG polyester is to be preferred, especially so, since the latter has also a higher capacity (cf. Table II) and can be used for high boiling sesquiterpene alcohols and monophenols (see below) as well. All columns, except squalene, eluted *d*-limonene (b.p. 177° C) ahead of 1,8-cineole (b.p. 174° C) and all, except silicone and polyphenyl ether, eluted the higher boiling bornyl acetate ahead of α-terpineol and citronellol. Bornyl acetate was eluted even ahead of camphor on the diglycerol column. Thus the use of different liquid phases can be used to differentiate between different functional groups (22). The sequence of separations on polyphenyl ether as compared with that obtained on the polyesters is noteworthy. From the present findings it is concluded that no single column will satisfy all requirements.

Silicone grease and the Craig polyesters (10) are known to be sufficiently stable at 160 to 220° C to allow the chromatography of compounds with higher boiling points than α-terpineol. In addition, the polyphenyl ether was found to be suitable for runs at higher temperatures, and Table V shows the degree of separation of the closely related

TABLE V

Relative retention times (α-terpineol = 1) of sesquiterpene alcohols

Column (liquid phase)	Silicone	Polyphenyl ether	Polyesters		
			APEG	SEG	PEG
Temperature (° C)	160	160	190	190	190
Flow rate (ml He/min)	99	120	41.6	39.4	62.5
Inlet pressure (mm Hg)	2546	2546	1531	2029	2029
Retention time of α-terpineol	3.1	6.6	5.5	5.8	3.0
Occidentalol	4.9	4.6	3.4	3.0	3.0
Eudesmol a	6.5*	7.0*	5.25	5.1	4.5
Eudesmol b	—	—	5.4	5.3	4.7

*Broad, unresolved peak.

sesquiterpene alcohols, occidentalol ($C_{15}H_{24}O$) and eudesmol ($C_{15}H_{26}O$), as compared with α-terpineol obtained with these columns. Occidentalol differs structurally from eudesmol only by having one more double bond, yet it is completely separated from the latter even on the silicone column. This may, in part at least, be due to steric differences. The superior efficiency of the polyester columns is evident in that eudesmol is resolved partially into the α- and β-isomers.

Since essential oils sometimes contain phenolic compounds, the degree of separation of the monophenols, anethole, eugenol, and isoeugenol, was tested on the APEG polyester and the polyphenyl ether columns. The former, at 190° C and 83.5 ml helium per minute, gave retention times of 5.3, 14.7, and 25.4 minutes, whereas the latter, at 220° C and 70.5 ml helium per minute, gave 4.3, 6.45, and 10.4 minutes respectively. Both columns gave even peaks without any sign of decomposition taking place. The separation of other types of phenols has been described by Janák *et al.* (23, 24).

CONCLUSIONS

1. Monoterpene hydrocarbons are best separated on columns using squalene, Carbowax 400, Craig polyesters, and polyphenyl ether as liquid phase at temperatures of 130° C and lower. At higher temperatures the polyester and polyphenyl ether columns give best results, separating oxygenated terpenes, sesquiterpene alcohols, and monophenols satisfactorily. The adipate polyethylene glycol (APEG) polyester column is most suited for all compounds tested.

Can. J. Chem. Downloaded from www.nrcresearchpress.com by 186.148.149.217 on 09/04/12
For personal use only.

2. The effect of temperature and sample size on the degree of separation is considerable, the lowest possible temperature giving best results from a qualitative and preparative point of view. With 6-mm diameter columns sample sizes above about 3 μl cause considerable delays in the retention time of peak maxima as well as a broadening of peaks. The initial emergence of a peak is practically constant up to sample sizes which cause overloading of the columns. For qualitative work actual isolation of each component and determination of its physical properties is to be preferred over comparison of the retention time (or volume) with those of known compounds.

3. Chromosorb W, a calcined diatomaceous earth, was found to be a better solid support for the separation of terpenoid compounds than either washed Celite 545 or C-22 firebrick.

4. In preparative work with instruments using a thermal conductivity cell as detector, pure samples cannot be obtained with normal detector currents, and collection of thermally labile terpenes must be carried out in "blind" runs.

ACKNOWLEDGMENTS

The author wishes to express his gratitude to Dr. B. M. Craig for helpful advice and for the gift of polyesters, and to Mr. M. Granat for technical assistance.

REFERENCES

1. R. A. BERNHARD. J. Assoc. Offic. Agr. Chemists, **40**, 915 (1957).
2. E. BAYER, G. KUPFER, and K. H. REUTHER. Z. Anal. Chem. **164**, 1 (1958).
3. H. CVRKAL and J. JANÁK. Collection Czechoslov. Chem. Commun. **24**, 1967 (1959).
4. A. LIBERTI and G. P. CARTONI. *In* Gas chromatography. *Edited by* D. H. Desty. Butterworth Scientific Publications, London. 1958. p. 321.
5. R. G. STANLEY. Nature, **182**, 738 (1958).
6. G. EGLINGTON, R. J. HAMILTON, R. HODGES, and R. A. RAPHAEL. Chem. & Ind. 955 (1959).
7. H. WESTAWAY and J. F. WILLIAMS. J. Appl. Chem. **9**, 440 (1959).
8. A. I. M. KEULEMANS. Gas chromatography. Reinhold Publishing Corp., New York. 1957. p. 217.
9. O. WALLACH. Ann. **275**, 103 (1893).
10. B. M. CRAIG and N. L. MURTY. Can. J. Chem. **36**, 1297 (1958).
11. T. NAKATSUKA and Y. HIROSE. Bull. Agr. Chem. Soc. Japan, **20**, 215 (1956).
12. E. BAYER and H. G. WITSCH. Z. Anal. Chem. **170**, 278 (1959).
13. E. M. BENS and W. R. MCBRIDE. Anal. Chem. **31**, 1379 (1959).
14. P. E. PORTER, C. H. DEAL, and F. H. STROSS. J. Am. Chem. Soc. **78**, 2999 (1956).
15. R. M. BETHEA and M. SMUTZ. Anal. Chem. **31**, 1211 (1959).
16. B. W. THOMAS. Ind. Eng. Chem. **47**, 85A (1955).
17. D. E. M. EVANS and J. C. TATLOW. J. Chem. Soc. 1184 (1955).
18. F. CUTHBERTSON and W. K. R. MUSGRAVE. J. Appl. Chem. **7**, 99 (1957).
19. E. HEILBRONNER, E. KOVÁTS, and W. SIMON. Helv. Chim. Acta, **40**, 2410 (1957).
20. M. J. E. GOLAY. *In* Gas chromatography. *Edited by* D. H. Desty. Butterworth Scientific Publications, London. 1958. p. 36.
21. R. D. CONDON. Anal. Chem. **31**, 1717 (1959).
22. E. BAYER. Angew. Chem. **71**, 299 (1959); **69**, 640 (1957).
23. J. JANÁK, R. KOMERS, and J. SIMA. Collection Czechoslov. Chem. Commun. **24**, 1492 (1959).
24. J. JANÁK and R. KOMERS. Collection Czechoslov. Chem. Commun. **24**, 1960 (1959).

Can. J. Chem. Downloaded from www.nrcresearchpress.com by 186.148.149.217 on 09/04/12
For personal use only.

Can. J. Chem. Downloaded from www.nrcresearchpress.com by 186.148.149.217 on 09/04/12
For personal use only.

HYDROGENOLYSIS OF CARBOHYDRATES

VIII. COMPARATIVE STUDIES ON METHYL GLYCOPYRANOSIDES[1]

P. A. J. GORIN

ABSTRACT

Several methyl glycopyranosides have been hydrogenated under pressure at 180° C with copper chromite catalyst in dioxane. Many glycosides underwent hydroxyl group inversion and another reaction observed consisted of hydrogenolytic removal of the methoxyl group coupled with reduction of a hydroxyl group to a methylene group. Other glycosides were stable under these conditions, and these included methyl β- and methyl α-D-glucopyranosides and unexpectedly methyl β-D-mannopyranoside and methyl α-D-talopyranoside. The data indicated that generally β-glycosides are more stable than their α-anomers in the hexopyranoside series and that the methyl hexopyranosides are more stable than the methyl pentopyranosides. Explanations have been made in the theoretical section in order to cover these observations. At 240° C, however, methyl α-D-glucopyranoside is hydrogenolyzed giving 11% of 1,5-anhydro-4-deoxy-hexitols. These polyols have been fractionated and the mixture shown to contain lyxo- and arabo-1,5-anhydro-4-deoxy-D-hexitols.

The earlier findings of von Rudloff, Bauer, and Stuetz (1) showed that the hydrogenolysis of methyl α-D-glucopyranoside yields 1,5-anhydro-4-deoxy-hexitol (11% yield) along with many other products. The hydrogenolytic procedure was vigorous, the experiments being carried out with Adkins' copper chromite catalyst (2) at 240° C using dioxane as solvent under a hydrogen pressure of 170 atmospheres. More recent investigations (3, 4, 5, 6, 7) have indicated that at lower temperatures (180–220° C) some inversion of the asymmetric centers occurs as well as hydrogenolysis. However, methyl α- and methyl β-D-glucopyranosides were found to be virtually unaffected at 180° C. Since the hydroxyl groups on methyl β-L-arabopyranoside are readily inverted by catalytic hydrogenation (3) the behavior of the methyl glucosides seemed anomalous. Therefore, another hexopyranoside methyl α-D-mannopyranoside was hydrogenated at 180° C and was found to yield a mixture of isomeric glycosides.* By fractionation, on a cellulose column (8), methyl α-D-talopyranoside has been isolated from the mixture† together with unchanged methyl α-D-mannopyranoside and a small amount of methyl α-D-glucopyranoside. As the hydroxyl configurations in the substrate appeared to play a role in determining its susceptibility to hydrogenation other methyl α-D-hexopyranosides were examined. Methyl α-D-galacto- and -altro-pyranosides were transformed by hydrogenation to other isomers, mainly methyl α-D-talopyranoside, which is a stable methyl glycoside under the conditions used (Table I). This was confirmed by synthesizing methyl α-D-talopyranoside, hydrogenating it, and isolating the unchanged glycoside.

As well as the α-glycosides, several methyl β-D-hexopyranosides were tested. These included methyl β-D-allo-, -altro-, -galacto-, -gluco-, and -manno-pyranosides (Table I) and as a group these compounds were more stable to hydrogenation than the α-glycosides, a greater percentage of substrate being recovered unchanged. This stability was most pronounced in methyl β-D-gluco- and -manno-pyranosides which were virtually unaffected and were found to be the main end products of hydrogenation of the other β-glycosides.

In contrast to the hexopyranosides the methyl pentopyranosides, as represented by

[1]*Manuscript received January 4, 1960.*
Contribution from the National Research Council of Canada, Prairie Regional Laboratory, Saskatoon, Saskatchewan.
Issued as N.R.C. No. 5604.
The author wishes to thank Dr. A. S. Perlin for this unpublished information.
†*This would appear to be a simple route by which to prepare methyl α-D-talopyranoside.*

TABLE I

Products isolated from hydrogenation of methyl hexopyranosides at 180° C

Substrate	Product (% w/w)
Methyl α-D-glucopyranoside	98% Unchanged material
Methyl α-D-mannopyranoside	Methyl α-D-mannopyranoside (30%) Methyl α-D-talopyranoside (27%) Methyl α-D-glucopyranoside (3%)
Methyl α-D-galactopyranoside	Methyl α-D-glucopyranoside (33%) Methyl α-D-talopyranoside (9%) Polyols (7%) Methyl α-D-galactopyranoside (5%)
Methyl α-D-altropyranoside	Methyl α-D-talopyranoside (20%) Polyols (18%) Methyl α-D-mannopyranoside (11%)
Methyl α-D-talopyranoside	Mainly unchanged material
Methyl β-D-glucopyranoside	Unchanged material
Methyl β-D-mannopyranoside	87% Unchanged material
Methyl β-D-galactopyranoside	Methyl β-D-glucopyranoside (25%) Methyl β-D-galactopyranoside (17.5%) Polyols (16%) Methyl β-D-allopyranoside (3%)
Methyl β-D-altropyranoside	Methyl β-D-altropyranoside (24%) Polyols (16%) Methyl β-D-mannopyranoside (15%)
Methyl β-D-allopyranoside	Polyols (35%) Methyl β-D-allopyranoside } 25% Methyl β-D-glucopyranoside }

methyl α-L-arabo- and -D-lyxo-pyranosides and methyl β-L-arabo- (cf. ref. 3), -D-ribo-, and -D-xylo-pyranosides, were much more prone to hydroxyl group inversion at 180° C (Table II). Acid hydrolysis of the product and detection of the free sugars by paper

TABLE II

Products isolated from hydrogenation of methyl pentopyranosides at 180° C

Substrate	Product (% w/w)
Methyl α-L-arabopyranoside	Polyols (23%) Methyl β-D-ribopyranoside (12%) Methyl α-L-lyxopyranoside (6%) Methyl β-D-xylopyranoside (1%)
Methyl α-D-lyxopyranoside	Polyols (44%) Methyl ribopyranoside (?%) Methyl arabopyranoside } Methyl xylopyranoside } 15% Methyl lyxopyranoside } Methyl α-D-lyxopyranoside (13%)
Methyl β-L-arabopyranoside	Polyols (30%) Methyl β-L-arabopyranoside (10%) Methyl α-D-xylopyranoside (5%)
Methyl β-D-xylopyranoside	Polyols (29%) Methyl β-D-ribopyranoside (17%) Methyl xylopyranoside } 12% Methyl arabopyranoside }
Methyl β-D-ribopyranoside	Polyols (35%) Methyl ribopyranoside (16%) Methyl xylopyranoside } Methyl lyxopyranoside } 7% Methyl arabopyranoside }

Can. J. Chem. Downloaded from www.nrcresearchpress.com by 186.148.149.217 on 09/04/12
For personal use only.

chromatography indicated in each instance easy interconversion since two to four chemically different pentoses were present. Also, the pentopyranosides were hydrogenolyzed with greater ease to dihydroglycals (tetrahydropyrandiols) by reductive elimination of the methoxyl group coupled with reduction of a hydroxyl to a methylene group. The hydrogenation products of the methyl glycopyranosides are summarized in Tables I and II with the percentage of each compound contained in the reaction product as determined on column chromatographic separation.

It appears likely that resistance to catalytic hydroxyl inversion is affected by the shape of the substrate. For example, the 6-hydroxymethyl group seems to exert an influence in limiting hydroxyl group inversion and formation of compounds of the dihydroglycal type. The large substituent on C-5 would render the molecule more bulky and perhaps less flexible so that it could adopt fewer positions suited to reaction on the surface of the catalyst. Unfortunately too little is known about the surface properties of copper chromite to generalize on the probability of individual hydroxyls in the glycosides to invert. If, as has been assumed (7), inversion results from dehydrogenation followed by hydrogenation this ability would be concerned firstly, with the ease of dehydrogenation of the alcohol group to a ketone, and secondly with the specificity of reduction of the ketone to the two possible alcohols (Fig. 1). It has been shown that the rate of dehydrogenation

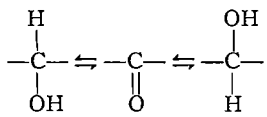


FIG. 1.

of a secondary alcohol with chromic acid in cyclohexane ring systems (9) to a ketone depends on the accessibility of the C-hydrogen atom (10) and not the rate of intermediate ester formation. The dehydrogenation rate was shown to be greater when the C-hydrogen atom was in the less sterically hindered equatorial position (9). However, this is in solution rather than on the surface of a catalyst. In order to explain the surprising observations that methyl β-D-mannopyranoside and methyl α-D-talopyranoside are virtually unaffected under hydrogenation conditions it must be assumed that the catalyst plays a role in limiting dehydrogenation. This may well be because the surface contours of the copper chromite prevent the C-hydrogen atoms, some of which are equatorial (11), from becoming available. On the other hand, methyl α- and β-D-glucopyranosides, which are also stable do not contain equatorial C-hydrogen atoms in their stable C-1 chair forms (11).

Since hydroxyl inversion readily occurs in polyhydroxyl compounds, even at temperatures as low as 180° C, it appeared likely that the syrupy 1,5-anhydro-4-deoxy-D-hexitol formed by hydrogenation of methyl α-D-glucopyranoside at 240° C (1) was a mixture of stereoisomers and accordingly, this product has been examined further. Cellulose column chromatography of the syrupy polyols derived by catalytic deacetylation of the fractionated acetate contained two main components which were distinguishable on paper chromatograms. The fraction which was slower on paper was syrupy but gave a crystalline tris-*p*-nitrobenzoate derivative from which a crystalline polyol (I) of R_{Rh} 1.1* was regenerated. The 1,5-anhydro-4-deoxy-hexitol structure for the substance was indicated by carbon and hydrogen composition and its consumption of 1.0 molar equivalent of sodium periodate. If it is assumed that no inversion at C-5 takes place and that the six-membered ring is not modified in the course of hydrogenolysis the only

**Throughout the text R_{Rh} denotes the distance moved by a spot on a paper chromatogram compared with rhamnose in the n-butanol – ethanol – water (40:11:19) v/v solvent.*

Can. J. Chem. Downloaded from www.nrcresearchpress.com by 186.148.149.217 on 09/04/12
For personal use only.

alternative structure fitting the data is that of a dihydroglycal (IV). However, since periodic acid oxidation of I followed by sodium borohydride reduction gave an optically active triol (III) the dihydroglycal formula is invalidated since it would have given a triol (V) with no asymmetric centers (Fig. 2).

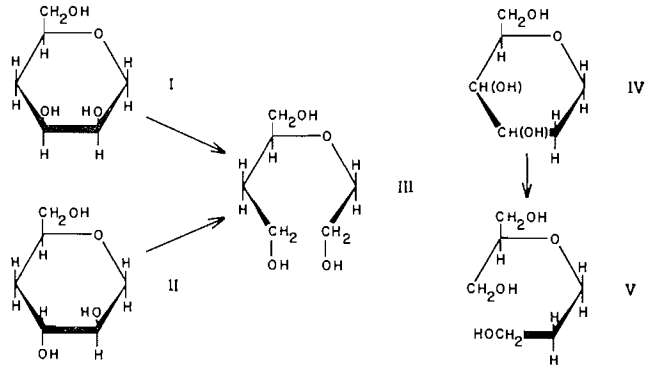


FIG. 2.

The other fraction having R_{Rh} 1.3, from the cellulose column, also gave a crystalline tris-*p*-nitrobenzoate, which on debenzoylation yielded a syrupy polyol (II) which consumed 1.0 molar equivalent of sodium periodate. Periodic acid oxidation and sodium borohydride reduction of the resulting dialdehyde formed the same compound as obtained from I. Their identity was confirmed by comparison of their crystalline tris-*p*-nitrobenzoates.

Comparison of the rates at which I and II consumed lead tetraacetate showed that the former was oxidized 4 times faster in the initial stages. This difference which is appreciable considering that the α-glycol groups are in a six-membered ring (4, 12, 13, 14) is interpreted as evidence that they are *cis* in I and *trans* in II. By consideration of the molecular rotations of various methyl hexopyranosides and 1,5-anhydro-hexitols theoretical values for the specific rotations of the four structural isomers of 1,5-anhydro-4-deoxy-D-hexitol can be calculated by use of Hudson's rules of optical superposition and isorotation (see Table III) (15). Since I has $[\alpha]_D$ $-50°$ it is probably lyxo-1,5-anhydro-4-deoxy-D-hexitol and II ($[\alpha]_D$ $+19°$) corresponds to arabo-1,5-anhydro-4-deoxy-D-hexitol. These compounds are different in hydroxyl configuration from methyl α-D-glucopyranoside and it is likely that the other two possible stereoisomers are present in the hydrogenolysis product, but were not isolated through the limitations of the fractionation procedures. Although the 1,5-anhydro-4-deoxy-hexitols are difficult to distinguish chromatographically from the dihydroglycals of the hexose series, shown to be formed by hydrogenolysis under milder conditions (4), it seems unlikely that they are present, because they are extensively degraded by hydrogenolysis at 220° C (26).

The readiness of methyl glycopyranosides to form polyols on hydrogenolysis parallels their tendency to undergo hydroxyl inversion in the hexose as well as pentose series (except that with the hexoses a higher temperature is generally needed to remove the methoxyl group). For instance, methyl β-D-galactopyranoside is much more reactive at 180° C than methyl α-D-glucopyranoside as far as hydroxyl group inversion is concerned. At 200° C the former is degraded to a mixture of dihydro-D-altral (12%), dihydro-D-glucal (31%), and dihydro-D-galactal (12%). But methyl α-D-glucopyranoside is relatively inert at this temperature and complete hydrogenolysis only takes place at 240° C,

Can. J. Chem. Downloaded from www.nrcresearchpress.com by 186.148.149.217 on 09/04/12
For personal use only.

TABLE III

Calculated specific rotations of 1,5-anhydro-4-deoxy-D-hexitols

Polyols and calculated specific rotations	Reference compounds
ribo-1,5-Anhydro-4-deoxy-D-hexitol +46°	Methyl β-D-allopyranoside ($[M]_D$ −9,510°); Methyl α-D-glucopyranoside (16) ($[M]_D$ +23,210°)
lyxo-1,5-Anhydro-4-deoxy-D-hexitol (I) −31°	Methyl α-D-talopyranoside ($[M]_D$ +4,070°); Methyl β-D-mannopyranoside (17) ($[M]_D$ −13,390°)
−34°	1,5-Anhydro-D-mannitol (18) ($[M]_D$ −8,360°); 1,5-Anhydro-D-talitol (19) ($[M]_D$ −1,800°)
xylo-1,5-Anhydro-4-deoxy-D-hexitol +106°	Methyl α-D-galactopyranoside (20) ($[M]_D$ +38,050°); Methyl β-D-glucopyranoside (21) ($[M]_D$ −6,640°)
+67°	1,5-Anhydro-D-glucitol (22) ($[M]_D$ +7,050°; 1,5-Anhydro-D-galactitol (23) ($[M]_D$ +12,790°)
arabo-1,5-Anhydro-4-deoxy-D-hexitol (II) +20°	Methyl α-D-altropyranoside (24) ($[M]_D$ +24,420°); Methyl β-D-idopyranoside (25) ($[M]_D$ −18,430°)

to form the more stable 1,5-anhydro-4-deoxy-hexitols and degradation products such as ethylene and propylene glycols. Much of these lower molecular weight materials may therefore have been formed through an unstable 1,2-dihydroglycal intermediate rather than 1,5-anhydro-4-deoxy-D-hexitol which does not contain the 1,3-dihydroxy grouping which is susceptible to hydrogenolysis (27).

EXPERIMENTAL

Optical rotations were measured at 25° C. Evaporations were carried out under reduced pressure. The solvent used for paper chromatographic separations was *n*-butanol – ethanol – water (40:11:19 v/v). Reducing sugars were detected with the *p*-anisidine hydrochloride spray (28) and non-reducing sugars with ammoniacal silver nitrate (29). Acid hydrolysis of glycosides was carried out with *N* H_2SO_4 at 100° C for 3 hours, the solutions neutralized with $BaCO_3$, filtered, and evaporated.

A. Preparation of Reference Compounds

Methyl β-D-Allopyranoside

D-Allose (500 mg), kindly supplied by Dr. A. C. Neish, was refluxed in 3% methanolic hydrogen chloride (20 ml) for 5 hours, and the solution neutralized, after it was cooled, with silver oxide which was then filtered off. The filtrate was evaporated to a syrup which crystallized and three recrystallizations from ethanol – ethyl acetate afforded material with m.p. 155–157° C and $[\alpha]_D$ −49° (*c*, 1.0, H_2O), yield 95 mg. Calculated for $C_7H_{14}O_6$: C, 43.3%; H, 7.3%. Found: C, 43.2%; H, 7.3%. The constants of the product agree with those given by Lindberg and Theander (30).

Can. J. Chem. Downloaded from www.nrcresearchpress.com by 186.148.149.217 on 09/04/12
For personal use only.

Methyl α-D-Talopyranoside and Derivative

Syrupy D-talose (1.26 g) was heated for 4 hours in refluxing 3% methanolic hydrogen chloride (40 ml), the acid was neutralized (Ag_2O), the solution filtered and evaporated to a syrup (1.17 g). Examination on a paper chromatogram indicated a main spot having R_{Rh} 1.4 with a minor component of R_{Rh} 1.1. The faster material was isolated by cellulose chromatography using benzene–ethanol–water (500:50:1 v/v) as the mobile phase. The product was a syrup (0.56 g) with $[\alpha]_D$ +105° (*c*, 1.0, H_2O). Calculated for $C_6H_{11}O_5 \cdot OCH_3$: OCH_3, 16.0%. Found: OCH_3, 16.0%. The glycoside was designated the α-configuration because of its strong dextrorotation.

The syrupy product (30 mg) was heated at 100° C for 2 hours in pyridine (0.5 ml) containing triphenylchloromethane (61 mg). After it was cooled, acetic anhydride (0.5 ml) was added and the solution left overnight. Then it was added to aqueous sodium bicarbonate and the insoluble material which formed was isolated and recrystallized twice from aqueous ethanol, then ethanol. The crystals (25 mg) had m.p. 177–178° C and $[\alpha]_D$ +21° (*c*, 1.3, pyridine) and analyzed for 2,3,4-tri-*O*-acetyl-6-*O*-triphenylmethyl methyl α-D-talopyranoside. Calculated for $C_{32}H_{34}O_9$: C, 68.3%; H, 6.1%. Found: C, 68.2%; H, 6.2%.

B. Hydrogenation of Methyl Glycopyranosides at 180° C

In hydrogenation of the following methyl hexopyranosides identical procedures were used. The glycoside was added to one-third its weight of copper chromite in 50 parts of dioxane (v/w). The mixture was shaken at 180° C for 6 hours at a hydrogen pressure of 600 p.s.i. and after it was cooled the solution was filtered and evaporated. An attempt was then made to crystallize any sugars from solution and the resulting syrup was chromatographed on a cellulose column. The solvents for cellulose chromatography were benzene–ethanol–water (500:50:1 v/v) to isolate materials moving faster than rhamnose on a paper chromatogram. For compounds moving slower than rhamnose *n*-butanol one-quarter saturated with water was used.

When methyl pentopyranosides were hydrogenated the procedure was the same as above except for the relative proportion of components in the reaction mixture. In this case the weight of catalyst was 30% that of the methyl pentoside and the solvent used was 45 times that of the pentoside on a volume per unit weight basis.

(*i*) *Methyl α-D-glucopyranoside.*—From the hydrogenation product of the glucoside (2.00 g) mainly unchanged material was recovered by crystallization from ethanol, m.p. and mixed m.p. 165–166° C. Column chromatography yielded only 42 mg of substance that ran at a different rate than methyl glucoside on a paper chromatogram.

(*ii*) *Methyl β-D-glucopyranoside.*—Using the same procedure as with the above α-anomer only 9 mg of material was obtained not corresponding to methyl β-D-glucopyranoside. From ethyl acetate – ethanol the crystals had m.p. and mixed m.p. 115–116° C.

(*iii*) *Methyl α-D-mannopyranoside.*—The mannoside (1.75 g) was hydrogenated and some unchanged glycoside (0.47 g) was recovered from the reaction mixture having m.p. and mixed m.p. 192–195° C. The remainder was fractionated on a cellulose column to give material containing methyl α-D-talopyranoside (0.47 g) with $[\alpha]_D$ +83° (*c*, 3.3, H_2O). Calculated for $C_6H_{11}O_5 \cdot OCH_3$: OCH_3, 16.0%. Found: OCH_3, 16.7%. Acid hydrolysis yielded a sugar which corresponded to talose and ran faster than galactose on a paper chromatogram, and which gave D-lyxohexose phenylosazone on treatment with aqueous phenylhydrazine acetate at 80° for 6 hours. The phenylosazone gave an X-ray diffraction pattern identical with authentic D-lyxohexose phenylosazone and different

Can. J. Chem. Downloaded from www.nrcresearchpress.com by 186.148.149.217 on 09/04/12
For personal use only.

Can. J. Chem. Downloaded from www.nrcresearchpress.com by 186.148.149.217 on 09/04/12
For personal use only.

from D-arabohexose, D-ribohexose, and L-xylohexose phenylosazones. The next fraction contained unchanged methyl α-D-mannopyranoside (63 mg), m.p. and mixed m.p. 192–194° C. A later fraction (46 mg) from the column crystallized and two recrystallizations from ethanol – ethyl acetate yielded methyl α-D-glucopyranoside, m.p. and mixed m.p. 167–168° C. Calculated for $C_7H_{14}O_6$: C, 43.3%; H, 7.3%. Found: C, 43.4%; H, 7.35%.

(*iv*) *Methyl β-D-mannopyranoside.*—Methyl β-D-mannopyranoside (1.16 g) on hydrogenation followed by acid hydrolysis yielded 137 mg of material from a cellulose column that did not correspond to mannose. In another experiment the unchanged glycoside was characterized as its tetraacetate, m.p. and mixed m.p. 161–163° C.

(*v*) *Methyl α-D-galactopyranoside.*—Methyl α-D-galactopyranoside (1.60 g) was hydrogenated and crystals were obtained from an ethanolic ethyl acetate solution of the product. The material (0.36 g) corresponded to methyl α-D-glucopyranoside since it had m.p. and mixed m.p. 163–165° C and $[\alpha]_D$ +161° (*c*, 3.5, H_2O). The mother liquor on cellulose chromatography gave three main fractions. These were a mixture (0.26 g) of polyols and methyl α-D-talopyranoside having OCH_3, 9.3%, and $[\alpha]_D$ +27° (*c*, 1.2, H_2O). The methoxyl content of the mixture corresponded to 58% of glycoside and it was acid hydrolyzed to give free aldose (R_F = talose) which was converted to D-lyxohexose phenylosazone by heating at 80° C for 6 hours with 4 moles of aqueous phenylhydrazine acetate. The identity of the phenylosazone was proved by its X-ray diffraction pattern, which was identical to that of an authentic specimen. The other two fractions which both crystallized from ethyl acetate – ethanol consisted of methyl α-D-glucopyranoside (0.16 g), m.p. and mixed m.p. 165–166° C, and methyl α-D-galactopyranoside (80 mg), m.p. and mixed m.p. 117–118° C.

(*vi*) *Methyl β-D-galactopyranoside.*—Hydrogenation of methyl β-D-galactopyranoside (2.0 g) gave a syrup from which methyl β-D-glucopyranoside (0.34 g), m.p. and mixed m.p. 116–117° C, was isolated. Cellulose chromatography gave as one of the main products a polyol fraction (0.32 g) and another contained glycosides (0.77 g) having R_{Rh} 0.7. The latter was fractionated by crystallization from ethyl acetate – ethanol to give methyl β-D-glucopyranoside (163 mg) as thick prisms with m.p. and mixed m.p. 116–117° C and $[\alpha]_D$ −37° (*c*, 1.0, H_2O) after two further recrystallizations. Calculated for $C_7H_{14}O_6$: C, 43.3%; H, 7.3%. Found: C, 43.2%; H, 7.5%. After the bulky prisms were removed a fluffy solid (62 mg) remained which on two recrystallizations from the same solvent yielded methyl β-D-allopyranoside with m.p. and mixed m.p. 157–158° C and $[\alpha]_D$ −52° (*c*, 1.6, H_2O). Calculated for $C_7H_{14}O_6$: C, 43.3%; H, 7.3%. Found: C, 43.25%; H, 7.4%. The last fraction from the column consisted of unchanged methyl β-D-galactopyranoside (0.35 g) with m.p. and mixed m.p. 179–180° C.

(*vii*) *Methyl α-D-altropyranoside.*—Methyl α-D-altropyranoside (1.80 g) on hydrogenation gave a syrup which yielded crystals (0.19 g) from ethyl acetate – ethanol that corresponded to methyl α-D-mannopyranoside with m.p. and mixed m.p. 191–193° C. Cellulose chromatography afforded three main fractions, the first of which (66 mg) appeared to be a polyol. The next fraction (0.13 g) afforded a sugar with R_{Rh} 1.0 on hydrolysis which was not identified. The last portion of the column eluate gave a mixture (0.61 g) of polyol and methyl α-D-talopyranoside which had OCH_3 9.4% which indicated a glycoside content of 59%. Acid hydrolysis of the mixture afforded an aldose of R_F = talose which, on treatment with 4 moles of aqueous phenylhydrazine acetate at 80° C for 6 hours, gave D-lyxohexose phenylosazone identified by its X-ray diffraction pattern.

(*viii*) *Methyl β-D-altropyranoside.*—Cellulose chromatography of the hydrogenation product of methyl β-D-altropyranoside (1.04 g) afforded three fractions. The first was a

mixture of materials (164 mg) with mobility on a paper chromatogram greater than methyl β-altroside. The following fraction (253 mg) consisted of unchanged glycoside characterized as its tetraacetate, m.p. and mixed m.p. 98–99° C. Calculated for $C_{14}H_{19}O_9 \cdot OCH_3$: OCH_3, 8.35%. Found: OCH_3, 8.6%. The last material from the column was methyl β-D-mannopyranoside (155 mg), characterized as its tetraacetate, m.p. and mixed m.p. 161–163° C. Calculated for $C_{15}H_{22}O_{10}$: C, 49.7%; H, 6.1%. Found: C, 49.8%; H, 6.2%.

(*ix*) *Methyl α-D-talopyranoside.*—Paper chromatography of the product (0.31 g) from hydrogenated methyl talopyranoside (0.34 g) indicated that the material was mainly unchanged taloside with R_{Rh} 1.4. Only a trace of slower-moving material was detected. The product had OCH_3 16.2% indicating that removal of the methoxyl group had not occurred. Acid hydrolysis of the product furnished an aldose, which on treatment with 1 mole of 1-methylphenylhydrazine (31) in refluxing ethanol gave crystals characterized as D-talose 1-methylphenylhydrazone, m.p. and mixed m.p. 150–152° C.

(*x*) *Methyl β-D-allopyranoside.*—Hydrogenation of the glycoside (0.48 g) yielded a syrup (0.36 g) which on cellulose chromatography was found to consist of 0.17 g of materials with $R_{Rh} > 1.0$ on a paper chromatogram and 122 mg of a mixture of methyl β-D-allo- and -gluco-pyranosides. Fractional crystallization from ethyl acetate – ethanol gave 19 mg of the former with m.p. and mixed m.p. 154–156° C and 29 mg of the latter which had m.p. and mixed m.p. 115–116° C.

(*xi*) *Methyl α-L-arabopyranoside.*—The glycoside (2.22 g) was hydrogenated and the resulting mixture chromatographed on cellulose. The first fraction consisted of polyols (0.50 g) and tosylation of the mixture (14) gave a product which was fractionally crystallized to yield ditosyl-*trans*-tetrahydropyrandiol, m.p. and mixed m.p. 157–161° C, and ditosyl-*cis*-tetrahydropyrandiol, m.p. 125–129° C. A second fraction (0.26 g), $[\alpha]_D$ −98° (*c*, 1.0, H_2O), from the column crystallized to give methyl β-D-ribopyranoside from Skelly "F"–ethyl acetate, m.p. and mixed m.p. 83–84° C. The next material eluted (0.13 g) was shown to be methyl α-L-lyxopyranoside, m.p. 109–110° C and $[\alpha]_D$ −57° (*c*, 1.0, H_2O), after two recrystallizations from ethyl acetate – ethanol, which gave an X-ray diffraction pattern identical with that of the D-isomer. Calculated for $C_6H_{12}O_5$: C, 43.9%; H, 7.4%. Found: C, 44.1%; H, 7.4%. The last fraction from the column weighed 0.16 g and from this 16 mg of methyl β-D-xylopyranoside, m.p. and mixed m.p. 159–161° C, was obtained after two recrystallizations from ethanol – ethyl acetate.

(*xii*) *Methyl β-L-arabopyranoside.*—The hydrogenolysis product from methyl β-L-arabopyranoside (2.22 g) was very complex and acid hydrolysis showed that it contained all four chemically different pentosides. On cellulose chromatography a polyol fraction (0.66 g) was obtained corresponding to the two possible tetrahydropyrandiols. Very little further fractionation was obtained although methyl β-L-arabopyranoside (0.22 g), m.p. and mixed m.p. 167–168° C, was crystallized from ethanol and later 109 mg of a syrupy glycoside, with $[\alpha]_D$ +128° (*c*, 2.2, H_2O) which gave xylose on acid hydrolysis, was obtained. Although the latter product did not crystallize it appears that it was methyl α-D-xylopyranoside.

(*xiii*) *Methyl α-D-lyxopyranoside.*—The glycoside (2.22 g) was hydrogenated and on cellulose chromatography three fractions were obtained. A considerable proportion of tetrahydropyrandiols (0.97 g) was shown to be present. In this fraction it appeared that some methyl riboside was present since ribose was obtained on a paper chromatogram by hydrolyzing the syrup with acid. The next fraction (0.29 g) contained methyl α-D-lyxopyranoside, m.p. and mixed m.p. 107–109° C and the last portion (0.33 g) from

Can. J. Chem. Downloaded from www.nrcresearchpress.com by 186.148.149.217 on 09/04/12
For personal use only.

the column was shown to contain xyloside, arabinoside, and lyxoside by acid hydrolysis followed by paper chromatography.

(*xiv*) *Methyl β-D-ribopyranoside.*—When methyl β-D-ribopyranoside (2.20 g) was hydrogenolyzed and the product chromatographed on cellulose a considerable proportion of polyol (1.11 g) was found. The polyol had OCH_3 6.3% and on acid hydrolysis some ribose was formed, which indicates that 31% of the mixture consisted of methyl riboside. The remainder of the column eluate (0.16 g) consisted of a mixture of xyloside, riboside, and arabinoside as shown by paper chromatography of the acid hydrolyzate.

(*xv*) *Methyl β-D-xylopyranoside.*—The xyloside (1.11 g) was hydrogenolyzed and chromatographed on cellulose in the usual way. The initial fraction appeared to be tetrahydropyrandiols (0.32 g) and later portions were obtained which consisted of methyl-β-D-ribopyranoside (m.p. and mixed m.p. 80–81° C; 0.19 g) from ethyl acetate – Skelly F, and a xyloside (0.13 g) which could not be crystallized but which gave xylose on acid hydrolysis.

C. Hydrogenation of Glycosides at Temperatures > 180° C

1,5-Anhydro-4-deoxy-D-hexitols from Hydrogenolysis of Methyl α-D-glucopyranoside at 240° C

The hydrogenolysis of methyl α-D-glucopyranoside at 240° C was described by von Rudloff, Bauer, and Stuetz, who acetylated the product and fractionally distilled the acetates (1). Their still residue contained acetates of the 1,5-anhydro-4-deoxy-D-hexitols and this (7.32 g) was deacetylated with 0.1 mole of sodium methoxide in methanol (150 ml) for 3 hours. The polyols (4.92 g) obtained on evaporation consisted of two main fractions of R_{Rh} 1.1 and 1.3. Cellulose chromatography gave a syrup (1.81 g) consisting of mainly the former and this was heated at 80° C for 1 hour with *p*-nitrobenzoyl chloride (13 g) in pyridine (30 cc). The solution was poured into excess aqueous sodium bicarbonate and after 30 minutes stirring the precipitate was collected, washed with water, and dried. Three recrystallizations from ethyl acetate – Skelly F brought the tris-*p*-nitrobenzoate (4.84 g) to a constant m.p. of 113–115° C; it had $[\alpha]_D$ −83° (*c*, 1.1, $CHCl_3$). Calculated for $C_{27}H_{21}O_{13}N_3$: C, 54.6%; H, 3.6%. Found: C, 54.7%; H, 3.3%. Debenzoylation of the product (4.8 g) with 0.1 mole of sodium for 1 hour in boiling methanol (200 cc), followed by evaporation and deionization yielded crystals which were recrystallized twice from ethyl acetate – methanol. Yield, 0.37 g. The 1,5-anhydro-4-deoxy-D-hexitol corresponded to the fraction having R_{Rh} 1.1 and had m.p. 80–81° C, $[\alpha]_D$ −50° (*c*, 0.8, H_2O) and consumed 1.0 mole of aqueous sodium periodate overnight. Calculated for $C_6H_{12}O_4$: C, 48.6%; H, 8.2%. Found: C, 48.7%; H, 8.2%.

The polyol having R_{Rh} 1.3 was eluted later from the cellulose column and it (1.08 g) gave a tris-*p*-nitrobenzoate having m.p. 115–119° C and $[\alpha]_D$ +59° (*c*, 1.1, $CHCl_3$). Calculated for $C_{27}H_{21}O_{13}N_3$: C, 54.6%; H, 3.6%. Found: C, 54.5%; H, 3.9%. Catalytic debenzoylation furnished a syrupy 1,5-anhydro-4-deoxy-D-hexitol with R_{Rh} 1.3 and $[\alpha]_D$ +19° (*c*, 1.1, H_2O), which consumed 1.0 mole of aqueous sodium periodate in 18 hours.

Structure of the 1,5-Anhydro-4-deoxy-D-hexitols

The anhydro deoxyhexitol of R_{Rh} 1.1 (150 mg) was oxidized with 0.1 *M* periodic acid (1.5 moles) for 18 hours, the solution neutralized ($BaCO_3$) and filtered into an aqueous solution (10 ml) of sodium borohydride (100 mg). After 30 minutes the solution was acidified with acetic acid, treated with Amberlite IR-120, filtered, and evaporated to a

Can. J. Chem. Downloaded from www.nrcresearchpress.com by 186.148.149.217 on 09/04/12
For personal use only.

crust which was repeatedly dissolved in methanol which was then evaporated. The syrupy polyol (132 mg) had $[\alpha]_D$ −20° (*c*, 2.0, H_2O) and 75 mg of it was *p*-nitrobenzoylated in a manner similar to that described above to yield after three recrystallizations from ethyl acetate – pentane a tris-*p*-nitrobenzoate with m.p. 103–104° C and $[\alpha]_D$ −26° (*c*, 2.3, $CHCl_3$). Calculated for $C_{27}H_{23}O_{13}N_3$: C, 54.3%; H, 3.9%. Found: C, 54.3%; H, 3.9%.

Similar treatment of the anhydro deoxyhexitol of R_{Rh} 1.3 (60 mg) with periodic acid and sodium borohydride gave the open chain polyol with $[\alpha]_D$ −16° (*c*, 1.0, H_2O) from which gave an identical tris-*p*-nitrobenzoate, m.p. 98–102° and $[\alpha]_D$ −22° (*c*, 1.4, $CHCl_3$) was prepared. It had an X-ray crystal diagram similar to that of the *p*-nitrobenzoate obtained from the triol of R_{Rh} 1.1. Calculated for $C_{27}H_{23}O_{13}N_3$: C, 54.3%; H, 3.9%. Found: C, 54.5%; H, 3.9%.

Twenty-five milligrams of each 1,5-anhydro-4-deoxy-hexitol was dissolved in water (0.3 ml) and acetic acid (10 ml). A 1% solution of lead tetraacetate in acetic acid (10 ml) was added, the consumption of oxidant followed and the following values obtained:

Time (minutes)	10	35	70	135	205
Material of R_{Rh} 1.1, uptake in moles/mole	0.26	0.62	0.79	0.89	0.88
Material of R_{Rh} 1.3, uptake in moles/mole	0.07	0.16	0.25	0.30	0.34

Hydrogenolysis of Methyl β-D-galactopyranoside at 200° C

Methyl β-D-galactopyranoside (2.00 g) was hydrogenolyzed at 200° C using the proportions described previously. Paper chromatographic examination of the product indicated that all the starting material had been destroyed. In order to decompose any deoxy glycosides that may have been formed in the reaction, the product was heated for 18 hours at 100° C in *N* H_2SO_4. The solution was then neutralized ($BaCO_3$), filtered, and evaporated to a syrup (1.56 g), 0.69 g of which was fractionated on a cellulose column using benzene–ethanol–water (500:50:1 v/v) as solvent. From the column, dihydro-D-altral (80 mg), m.p. 105–106° C, dihydro-D-glucal (213 mg), m.p. 75–76° C, and dihydro-D-galactal (82 mg), m.p. 130–132° C, were obtained. All the above melting points were undepressed on admixture of the crystals with authentic specimens.

ACKNOWLEDGMENTS

The author wishes to thank Dr. A. S. Perlin for helpful discussions during the course of this work, and to Drs. E. von Rudloff, H. F. Bauer, and D. E. Stuetz for the gift of 1,5-anhydro-4-deoxy-hexitol acetates. Thanks are also due to Mr. J. A. Baignée and Mr. M. Mazurek for microanalytical determinations and Miss S. Lubin for technical assistance.

REFERENCES

1. E. von Rudloff, H. F. Bauer, and D. E. Stuetz. Can. J. Chem. **35**, 315 (1957).
2. W. H. Zartman and H. Adkins. J. Am. Chem. Soc. **55**, 4559 (1933).
3. A. S. Perlin, E. von Rudloff, and A. P. Tulloch. Can. J. Chem. **36**, 921 (1958).
4. E. von Rudloff and A. P. Tulloch. Can. J. Chem. **35**, 1504 (1957).
5. P. A. J. Gorin and A. S. Perlin. Can. J. Chem. **36**, 661 (1958).
6. T. Francis and A. S. Perlin. Can. J. Chem. **37**, 1229 (1959).
7. P. A. J. Gorin. J. Org. Chem. **24**, 49 (1959).
8. L. Hough, J. K. N. Jones, and W. H. Wadman. J. Chem. Soc. 2511 (1949).
9. S. Winstein and N. J. Holness. J. Am. Chem. Soc. **77**, 5562 (1955).
10. F. H. Westheimer and N. Nicolaides. J. Am. Chem. Soc. **71**, 25 (1949).
11. R. E. Reeves. *In* Advances in carbohydrate chemistry. Vol. 6. *Edited by* W. W. Pigman and M. L. Wolfrom. Academic Press Inc., New York. 1951. p. 130.
12. R. Criegee, L. Kraft, and B. Rank. Ann. **507**, 159 (1933).
13. A. S. Perlin. J. Am. Chem. Soc. **76**, 5505 (1954).

Can. J. Chem. Downloaded from www.nrcresearchpress.com by 186.148.149.217 on 09/04/12
For personal use only.

14. H. F. BAUER and D. E. STUETZ. J. Am. Chem. Soc. **78**, 4097 (1956).
15. C. S. HUDSON. Rapports sur les hydrates de carbone (glucides). Union Internationale de Chimie, Paris. 1931. pp. 59–78.
16. H. S. ISBELL. J. Research Natl. Bur. Standards, **8**, 1 (1932).
17. E. L. JACKSON and C. S. HUDSON. J. Am. Chem. Soc. **61**, 959 (1939).
18. R. C. HOCKETT and M. CONLEY. J. Am. Chem. Soc. **66**, 464 (1944).
19. D. A. ROSENFELD, N. K. RICHTMYER, and C. S. HUDSON. J. Am. Chem. Soc. **70**, 2201 (1948).
20. C. N. RIIBER, J. MINSAAS, and R. T. LYDE. J. Chem. Soc. 2173 (1929).
21. W. KOENIGS and E. KNORR. Chem. Ber. **34**, 961 (1901).
22. R. K. NESS, H. G. FLETCHER, and C. S. HUDSON. J. Am. Chem. Soc. **72**, 4547 (1950).
23. H. G. FLETCHER and C. S. HUDSON. J. Am. Chem. Soc. **70**, 310 (1948).
24. N. K. RICHTMYER and C. S. HUDSON. J. Am. Chem. Soc. **63**, 1727 (1941).
25. E. SORKIN and R. REICHSTEIN. Helv. Chim. Acta, **28**, 1 (1945).
26. P. A. J. GORIN. Unpublished results.
27. H. ADKINS. Reactions of hydrogen. 4th ed. The University of Wisconsin Press, Madison, Wisconsin. 1946. p. 71.
28. L. HOUGH, J. K. N. JONES, and W. H. WADMAN. J. Chem. Soc. 1702 (1950).
29. S. M. PARTRIDGE. Nature, **158**, 270 (1946).
30. B. LINDBERG and O. THEANDER. Acta Chem. Scand. **8**, 1870 (1954).
31. P. A. LEVENE and R. S. TIPSON. J. Biol. Chem. **93**, 631 (1931).

Can. J. Chem. Downloaded from www.nrcresearchpress.com by 186.148.149.217 on 09/04/12
For personal use only.

Can. J. Chem. Downloaded from www.nrcresearchpress.com by 186.148.149.217 on 09/04/12
For personal use only.

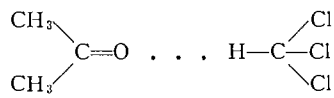
THE ENERGY OF HYDROGEN BONDING IN THE SYSTEM: ACETONE–CHLOROFORM

A. N. Campbell and E. M. Kartzmark[1]

ABSTRACT

It is shown that
(1) acetone and chloroform form a compound stable in the solid state;
(2) acetone and carbon tetrachloride do not form a compound;
(3) the enthalpies of mixing of acetone and chloroform and of acetone and carbon tetrachloride have been determined;
(4) from these figures the energy of hydrogen bonding in the acetone–chloroform system is evaluated as 2.7 kcal ±0.1.

The authors are engaged in a general investigation, including heats of mixing, of the ternary system: acetone–benzene–chloroform. It was pointed out to us, by Dr. W. Schneider of the National Research Council of Canada, that the data obtained would, with slight extension, enable us to determine the energy of formation of the linkage in the compound



The existence of a compound, $(CH_3)_2CO.CHCl_3$, has been long suspected. Indeed, Dolezalek (1) thought that he had proved the existence of this compound by an argument which would not now be considered completely acceptable. Nevertheless, the palpable evolution of heat when acetone and chloroform are mixed indicates, at least, that something of the nature of compound formation is taking place. It was therefore necessary, first, to demonstrate that acetone and chloroform do form a molecular compound and then to determine the enthalpies of mixing of acetone with carbon tetrachloride. Finally, it had to be shown that acetone and carbon tetrachloride do not form a compound as, indeed, from the nature of their formulae, is hardly likely.

EXPERIMENTAL

The existence of a compound was demonstrated by a study of the freezing-point diagram. A copper–constantan thermocouple and a Brown recorder were used; liquid nitrogen was the cooling agent. The mixture was placed in a double-jacketed vessel. The degree of vacuum in the jacket could be varied to produce any desired rate of cooling. All mixtures were stirred vigorously. The reagents were of highest purity and were distilled. The thermocouple was calibrated with acetone, chloroform, and mercury, whose freezing points were taken as −95° C, −63.5° C, and −38.87° C respectively.

The same technique was employed in the investigation of the system acetone – carbon tetrachloride, except that the very small heat of fusion of carbon tetrachloride (4.16 cal per gram) made thermal analysis an insensitive method, for mixtures containing large amounts of carbon tetrachloride. Hence, when dealing with such mixtures, where no appreciable halt or point of inflection could be detected on the cooling curve, the partially

[1]*Manuscript received January 13, 1960.*
Contribution from the Chemistry Department, University of Manitoba, Winnipeg, Manitoba.

frozen mixtures were allowed to heat up slowly, with vigorous stirring and the temperature of disappearance of the last crystals noted. This, admittedly, tends to give high results. Mixtures richer in acetone showed both primary freezing and eutectic halt, without any difficulty.

Heats of mixing were determined by having a weighed amount of one liquid in a magnetically stirred vacuum-walled calorimeter and the second liquid, also weighed, in a second such vessel. One set of junctions of a 20-junction copper–constantan thermopile was in the calorimeter and the other set was in the other vessel, so that the thermopile measured the difference in temperature of the two; allowance was made for any slight original difference in temperature. The thermopile had a sensitivity of about 0.2° C, corresponding to the minimum reading of the recorder chart. A suitable quantity of the second liquid was forced through a coarse capillary into the calorimeter, the amount being obtained by weighing at the end of the experiment. The average rise in temperature was about 7°. The mixing of acetone and carbon tetrachloride is an endothermal process and here the fall in temperature is much less. The usual method of radiation correction was applied and the water equivalent of calorimeter and contents was determined electrically, for each individual experiment. Current through the immersed platinum heating coil was determined from the voltage drop over a standard resistance. By this method, temperatures are not measured as such; the electrical input is multiplied by the ratio of two vertical lines on the recorder graph.

RESULTS

TABLE I

Freezing points of the system: acetone–chloroform

Mole % acetone	F.p. in °C	Eutectic halt
9.8	−72	−108
20.2	−80	−107
20.5	−81	−108
29.8	−93	−107
30.9	−103	−108
34.2	Eutectic	−108.5
34.8	−107	—
40.2	−106.5	−108.5
45.1	−106	−107.5
49.9	−106	—
50.1	−106	—
55.1	−107	—
60.3	−108	—
65.4	−110	—
69.2	−112	—
70.0	−112	—
77.3	−110	−115
90.0	−99	—

When the above results are plotted, a three-branch curve with an extremely flat maximum at 50 mole % composition is obtained. This indicates that the compound $(CH_3)_2CO.CHCl_3$ exists in the solid state but that it is highly dissociated in the molten state. The melting point of the compound is −106° C and the two eutectics lie at −108° (31 mole % acetone) and −115° (74 mole % acetone).

When the above figures are plotted a simple two-branch curve results, with a eutectic

Can. J. Chem. Downloaded from www.nrcresearchpress.com by 186.148.149.217 on 09/04/12
For personal use only.

TABLE II

Freezing points of the system: acetone – carbon tetrachloride

Mole % acetone	F.p. in °C	Eutectic halt
12.7	−39	—
24.6	−51	—
36.0	−55.5	—
41.4	−58	—
46.8	−61.5	—
50.0	−65	—
56.8	−68	—
66.3	−75	—
83.9	−95	−105
92.3	−102	−105

lying at 87.5 mole % acetone and at −105° C. Hence acetone and carbon tetrachloride do not form a compound.

The enthalpies of mixing of acetone and chloroform have been determined by Hirobe (5), by an ingenious and apparently accurate method. Our results are given in Table III.

Wyatt (2), from a study of the freezing-point diagram, finds a 1:1 compound of acetone and chloroform, melting congruently at −99.5° C, the two eutectics lying at −117° (73 mole % acetone) and −114° (38 mole % acetone). Wyatt (3) also claims the existence of a 1:1 compound of acetone and carbon tetrachloride, melting incongruently, with a peritectic at −75.5°, and a eutectic at −101°, and 8.5 mole % carbon tetrachloride. Our figures for the eutectic temperature and composition are in fair agreement with those of Wyatt and our figures do not disprove Wyatt's statement of an allotropic transformation of carbon tetrachloride at −48°. Timmermans (4), however, is unable to find this compound.

On the face of it, the formation of a compound does not seem very likely, since the enthalpy of mixing is positive. For the system, acetone–chloroform, where a compound definitely exists, the enthalpy is strongly negative.

TABLE III

Enthalpies of mixing of acetone and chloroform

Mole % chloroform	ΔH in gram calories per mole mixture	ΔH in gram calories per mole acetone
5.9	−68.3	−72
15.7	−174.2	−206
30.3	−328.1	−471
40.6	−399.7	−673
48.2	−434.1	−838
51.0	−449.7	−918
59.3	−465.9	−1145
70.7	−441.9	−1505
78.2	−362.6	−1664
88.0	−223.3	−1861
93.6	−126.1	−1970

When the above results are plotted along with those of Hirobe, the agreement is seen to be rather close. Our maximum occurs at 59.3 mole % chloroform and $\Delta H = -465.9$, while Hirobe's maximum occurs at 54.8 mole % chloroform and $\Delta H = -471.5$.

Can. J. Chem. Downloaded from www.nrcresearchpress.com by 186.148.149.217 on 09/04/12
For personal use only.

TABLE IV

Enthalpies of mixing of acetone and carbon tetrachloride

Mole % carbon tetrachloride	ΔH in gram calories per mole of mixture	ΔH in gram calories per mole acetone
4.9	6.5	6.8
9.4	5.1	5.6
17.1	11.6	14.0
31.7	16.2	23.7
41.4	30.7	52.0
42.1	30.8	53.2
49.0	40.5	79.4
49.7	45.2	90.0
51.1	50.0	102
62.5	57.0	152
67.6	55.0	170
74.4	55.4	216
74.7	54.8	217
78.9	48.9	232
88.1	41.8	351
92.8	32.9	457

The only reference in the literature to the enthalpy of mixing of acetone and carbon tetrachloride is by Timofeev (6), who gives $Q = -1.7$ kilojoule per mole solute (heat absorbed). The dilution is not stated. The graph of our results exhibits a very flat maximum at about 65 mole % carbon tetrachloride and $\Delta H = 57.0$ cal per mole mixture.

DISCUSSION

Acetone and chloroform form a compound, $(CH_3)_2CO.CHCl_3$, stable in the solid state though highly dissociated in the molten state. In agreement with this, the enthalpy of mixing is negative. Acetone and carbon tetrachloride form no such compound and the enthalpy of mixing is small and positive. This is what would be expected of an ideal mixture (no appreciable interaction other than dilution). Although the compound of acetone and chloroform is highly dissociated in the liquid state, presumably the dissociation will be reduced to zero in the presence of an infinite excess of either chloroform or acetone. It is for this reason that we have evaluated the enthalpies of mixing per mole of acetone. When these values are extrapolated to 100 mole % chloroform (infinite excess per mole of acetone), we obtain, for the acetone–chloroform system, $\Delta H = -2090$ calories, and for the acetone – carbon tetrachloride system, $\Delta H = +625$ calories. We therefore deduce the enthalpy of formation of the compound (energy of hydrogen bonding) to be $-2090-625 = -2715$ calories, say 2.7 ± 0.1 kcal, since the calculation of ΔH for small percentages of acetone involves multiplication by a large factor (say 15) with consequent magnification of experimental error. The form of the graph, however, rules out extreme error, so that the value given for the hydrogen bond is correct to the limits given.

REFERENCES

1. F. Dolezalek. Z. physik. Chem. **64**, 734 (1908).
2. W. F. Wyatt. Trans. Faraday Soc. **25**, 48 (1929).
3. W. F. Wyatt. Trans. Faraday Soc. **24**, 429 (1928).
4. J. Timmermans. Bull. chim. soc. Belg. **37**, 409 (1928).
5. H. Hirobe. J. Fac. Sci. Imp. Univ. Tokyo, Sect. 1, **1** (4), 155 (1926).
6. W. Timofeev. Chem. Zentr. **76** (II), 429 (1905).

Can. J. Chem. Downloaded from www.nrcresearchpress.com by 186.148.149.217 on 09/04/12
For personal use only.

Can. J. Chem. Downloaded from www.nrcresearchpress.com by 186.148.149.217 on 09/04/12
For personal use only.

A CHROMATOGRAPHIC ANALYSIS OF THE PRODUCT FROM THE TRITOSYLATION OF SUCROSE: CRYSTALLINE 6,6′-DI-*O*-TOSYLSUCROSE[1]

R. U. LEMIEUX AND J. P. BARRETTE

ABSTRACT

Chromatographic analysis on silicic acid of the so-called "tri-*O*-tosylsucrose" which is formed in 95% yield on the reaction of 3 moles of *p*-toluenesulphonyl chloride with 1 mole of sucrose in pyridine at 0° has shown the substance to contain penta-, tetra-, tri-, and di-*O*-tosylsucroses in the molar ratios 0.05:0.33:1:1, respectively. Any mono-*O*-tosylsucrose present in the reaction mixture may have been lost in the isolation of the product. The composition of the product was substantially the same when the reaction was performed at −18°. The chromatogram separated the tritosylates into two subfractions. The major subfraction represented 29% by weight of the original "tri-*O*-tosylsucrose" and could be converted to 1′,2:3,6:3′,6′-trianhydrosucrose in 77.4% yield. Therefore, the so-called "tri-*O*-tosylsucrose" can contain only 25–29% of 1′,6,6′-tri-*O*-tosylsucrose. 6,6′-Di-*O*-tosylsucrose crystallized from the di-*O*-tosylsucrose fraction in 10% over-all yield.

Compton (1) obtained evidence that primary hydroxyl groups can undergo tosylation substantially more rapidly than do the secondary positions in a carbohydrate structure. He obtained yields of 41% and 36% of the 6-*O*-tosyl derivatives on monotosylations of the methyl β- and α-D-glucopyranosides, respectively. These results indicate a difference in reactivity between the primary position and the average secondary position in these compounds in the order of 7. On the other hand, Hockett and Downing (2) found that the hydroxyl groups in 1,2:5,6-di-*O*-isopropylidene-α-D-glucose and 1,2:3,4-di-*O*-isopropylidene-α-D-galactose differed in reactivity by a factor of 70. Little is known about the factors responsible for such differences in reactivity. Undoubtedly, non-bonded interactions in the transition state are important and probably mainly responsible for the generally greater reactivity of primary positions (3, 4). It should be noted, for example, that the large difference in reactivity found for the di-*O*-isopropylidene derivatives of glucose and galactose may be mainly due to the fact that the 3-hydroxyl group of the glucose derivative is eclipsed with the 4-position. Lemieux and McInnes (5) have recently shown that intramolecular hydrogen bonding also can strongly influence the rate of reaction. Furthermore, little information is available on the relative rates for the tosylation of the starting material and the first product of tosylation. Experience in related fields has shown (6, 7, 8) that this can be a dominant feature of the esterification of polyhydroxy compounds with hydrophobic reagents. Thus, when it is considered that the reactivities of both the primary and the secondary hydroxyl groups must vary considerably amongst themselves, it seems clear that attempts at preferential tosylations of the primary positions of polyhydroxy compounds can be expected to proceed in widely varying yields.

Hockett and Zief reported the preparation (9) of a substance termed "tritosylsucrose" by treatment of 1 mole of sucrose with 3 moles of tosyl chloride in pyridine at 0°. The product was not well characterized; nevertheless, it was suggested that the compound was probably "almost entirely" substituted at the three primary positions. The product is in fact highly substituted at the 6- and 6′-positions, since reaction with sodium iodide in acetone (10, 11, 12) affords material containing two iodine atoms per tosyl group. Lemieux and Barrette (13) have shown that the 1′-tosyloxy group of 1′,4,6′-tri-*O*-tosyl-

[1]*Manuscript received January 4, 1960.*
Contribution from the Department of Chemistry, University of Ottawa, Ottawa, Ontario. This research is a portion of a thesis presented by J. P. B. in partial fulfillment of the requirements for the Ph.D. degree.

Can. J. Chem. Downloaded from www.nrcresearchpress.com by 186.148.149.217 on 09/04/12
For personal use only.

sucrose pentaacetate is not replaced by iodine when treated with sodium iodide in acetone. Since no information was gained regarding the nature of the third tosyloxy group of the so-called "tri-*O*-tosylsucrose" and since the substance is amorphous, the results shedded no light on either the extent of substitution at the 1′-position or the distribution of the tosyl groups among the sucrose residues. The so-called "tri-*O*-tosylsucrose" was obtained in yields above 95% and analyzed well for a sucrose tritosylate. Consequently, it can be assumed that there is no appreciable tendency for a pile-up of tosyl groups on relatively few sucrose molecules. Bragg and Jones (12) have made a study of the so-called "tri-*O*-tosylsucrose" by methylation, followed by reductive detosylation and hydrolysis, and inspection of the partially methylated D-glucose and D-fructose derivatives thus formed. Inspection of their results reveals no basis for the contention that the substance "consisted mainly therefore of 6,1′,6′-tri-*O*-tosylsucrose". The present authors entertained considerable doubt as to this characterization first of all in view of ordinary kinetic considerations and also in view of the low yield (3.5%) of 1′,2:3,6:3′,6′-trianhydrosucrose which was isolated (13, 14) on alkaline alcoholysis of the substance. It was believed of real interest to obtain a proper characterization of the substance in order the better to orientate our thinking and to justify our suspicions of previous interpretations of experimental results related to this problem. Our approach was to analyze the so-called "tri-*O*-tosylsucrose" by chromatography on silicic acid columns, a procedure which Jeanloz (15) has shown to be of great value for the separation of certain carbohydrate derivatives.

"Tri-*O*-tosylsucrose" was prepared by the method of Hockett and Zief (9) both at 0° and at −18°. The amorphous products were chromatographed on paper impregnated with silicic acid (16), using diisobutyl ketone:acetic acid:water (40:25:5) as solvent. The zones were located by dipping the paper in an aqueous solution of Rhodamine 6G (16). Fluorescent spots were observed under ultraviolet light at R_f values of 0.15, 0.40, 0.65, and 0.90. It was established that these corresponded to zones of di-, tri-, tetra-, and penta-*O*-tosylsucrose, respectively, by the chromatography of the components isolated by *column* chromatography on silicic acid using the same solvent system. This paper chromatographic technique proved extremely useful for a rapid preliminary inspection of a product and the establishment of an appropriate solvent system for the column chromatography.

The column chromatograms allowed the isolation of fractions that require the "tri-*O*-tosylsucrose" prepared at 0° to be, chemically, a highly heterogeneous substance containing penta-, tetra-, tri-, and di-*O*-tosylsucroses in the molar ratios 0.05:0.33:1:1, respectively (see Table I).

TABLE I

Chromatography of "sucrose tritosylates"

	Penta-*O*-tosylsucrose	Tetra-*O*-tosylsucrose	Tri-*O*-tosylsucrose		Di-*O*-tosylsucrose	
			Fraction A	Fraction B	Fraction C*	Fraction D
Color of fluorescence	Red	Pink	Yellow	Pink	Yellow	Yellow
Tube No.	17–22	24–34	39–57	58–62	93–105	86–110
Weight of material (g)	0.18	1.53	2.65	1.17	0.92	2.11
Per cent of mixture (w/w)	2.0	17.0	29.0	13.0	10.0	24.0
Sulphur content (%)						
Found:	13.90	13.40	11.84	11.41	10.12	9.22
Calc.:	14.4	13.38	11.93	11.93	9.85	9.85
$[\alpha]_D$ (chloroform)	+42.3	+35.0	+37.5	+33.0	+54.0	+35.0

NOTE: The material, 9.05 g, was prepared at 0°.
*Crystalline 6,6′-di-*O*-tosylsucrose.

Can. J. Chem. Downloaded from www.nrcresearchpress.com by 186.148.149.217 on 09/04/12
For personal use only.

The tri-*O*-tosylsucrose fraction could be resolved into two subfractions which comprised 29.0% (tri-*O*-tosylsucrose A) and 13.0% (tri-*O*-tosylsucrose B) by weight of the original "tri-*O*-tosylsucrose". Both these fractions have thus far resisted crystallization. Their sulphur contents were in good agreement with that expected for sucrose tritosylates. That the substances were in fact different was obvious from the following properties. Whereas the A fraction gave a yellow fluorescence with Rhodamine 6G, and readily consumed 2.82 moles of periodate per mole, the B fraction produced a pink fluorescence and consumed only 1.75 moles of periodate per mole. Furthermore, the A and B fractions underwent replacement of 1.87 and 1.63 tosyloxy groups when treated with sodium iodide in acetone. These results clearly indicate that both fractions are mixtures of tritosylated sucroses. However, the high periodate consumption by the A fraction shows that it must be mainly (about 78%) 1′,6,6′-tri-*O*-tosylsucrose. This conclusion was substantiated by the formation of 1′,2:3,6:3′,6′-trianhydrosucrose (13) in 77.4% yield on treatment of the A fraction with sodium methoxide in methanol. These results provide unequivocal evidence that the trianhydrosucrose in fact arises from 1′,6,6′-tri-*O*-tosylsucrose (14).

The di-*O*-tosylsucrose fraction deposited a 10% over-all yield (by weight) of crystalline compound (fraction C), m.p. 108–110°, $[\alpha]_D$ +54° in ethanol. The sulphur content corresponded to that expected for di-*O*-tosylsucrose and the compound only reduced Fehling's solution after acid hydrolysis. The compound was acetylated and the acetyl derivative, on treating with sodium iodide in acetone at 100°, produced a substance with the iodine content expected for a diiododideoxysucrose hexaacetate. Also, the nuclear magnetic resonance spectrum of the diiodo compound was devoid of the signals characteristic for the tosyl group. These properties require that the compound be 6,6′-di-*O*-tosylsucrose. The syrup (fraction D) which remained after crystallization of the 6,6′-di-*O*-tosylsucrose had a sulphur content close to that expected for a sucrose ditosylate (see Table I). Treatment of the hexaacetate derivative with sodium iodide in acetone replaced only 1.10 of the tosyloxy groups. This result shows that the 1′-hydroxyl group and perhaps certain secondary groups can compete favorably with the 6- or 6′-hydroxyl groups, or both in the tosylation reaction. It will be seen later on that the competition is undoubtedly mainly from the 1′-position and that, consequently, the di-*O*-tosylsucrose fractions (C and D combined) may be almost entirely composed of not greatly different amounts of the 1′,6-, 1′,6′-, and 6,6′-di-*O*-tosylsucroses.

The substances isolated from the other two bands of the chromatogram possessed sulphur contents in good agreement with those expected for tetra- and penta-*O*-tosylsucroses. The results of the chromatogram are listed in Table I and the course of the tosylation is described in Fig. 1.

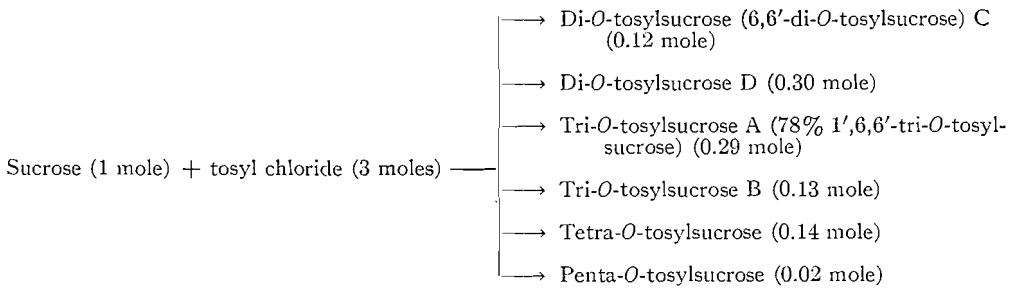


FIG. 1. Distribution of the tosylated sucroses formed in the reaction of 1 mole of sucrose with 3 moles of tosyl chloride in pyridine at 0°.

A consideration of Fig. 1 shows that the so-called "tri-*O*-tosylsucrose" does in fact contain 1′,6,6′-tri-*O*-tosylsucrose as the main component. However, the compound is only present to an extent of about 0.29 mole per mole of sucrose reacted. The fact that the compound was formed in an amount more than twice that of any other tri-*O*-tosylsucrose shows that the 1′-position is substantially more reactive than any secondary hydroxyl group. Consequently, as was discussed above, the uncharacterized di-*O*-tosylsucrose (fraction D) can be expected to consist mainly of 1′,6- and 1′,6′-di-*O*-tosylsucrose. In this respect, it is of interest to note that Hockett and Downing (2) found 2,3:4,6-di-*O*-isopropylidene-L-sorbose to undergo tosylation half as rapidly as 1,2:3,4-di-*O*-isopropylidene-D-galactose. The results clearly render it unlikely that sucrose can be acylated preferentially in high yield at the 6- and 6′-positions only. This conclusion is substantiated by the foregoing results of a ditosylation experiment. The tritylation of sucrose has been shown (17) to yield 1′,6,6′-tri-*O*-tritylsucrose pentaacetate in 45% yield. Table II describes the composition of the product obtained on a tritosylation of sucrose at −18°. It is seen that the course of the reaction was not appreciably affected by the lowering of the reaction temperature.

TABLE II

Chromatography of "sucrose tritosylate"

	Penta- and tetra-*O*-tosylsucrose	Tri-*O*-tosylsucrose		Di-*O*-tosylsucrose	
		Fraction A	Fraction B	Fraction C*	Fraction D
Weight of material (g)	2.0	3.11	1.5	0.75	2.85
Per cent of mixture (w/w)	20.0	31.1	15.0	7.5	28.5
R_f value†	0.9 and 0.65	0.40	0.40	0.15	0.15

NOTE: The material, 10 g, was prepared at −18°.
*Crystalline 6,6′-di-*O*-tosylsucrose.
†On paper impregnated with silicic acid using the solvent system diisobutyl ketone:acetic acid:water (40:25:5).

TABLE III

Chromatography of "sucrose ditosylate"

	Tetra-*O*-tosylsucrose	Tri-*O*-tosylsucrose		Di-*O*-tosylsucrose	
		Fraction A	Fraction B	Fraction C*	Fraction D
Weight of material (g)	1.04	2.79	1.74	1.85	2.60
Per cent of mixture (w/w)	1.04	27.9	17.4	18.5	26.0
Sulphur content (%)					
Found:	12.96	11.82	11.76	10.12	10.11
Calc.:	13.38	11.93	11.93	9.85	9.85

NOTE: The material, 10 g, was prepared at 0°.
*Crystalline 6,6′-di-*O*-tosylsucrose.

The product formed on the ditosylation of sucrose was analyzed chromatographically. The results are presented in Table III and Fig. 2. A comparison of the yields reported in Figs. 1 and 2 shows that the ditosylation produced, as would be expected, a greater yield of 6,6′-di-*O*-tosylsucrose (fraction C). The yield of other sucrose ditosylates (fraction D) was, however, about the same as that obtained in the tritosylation. This result clearly indicates that the 6- and 6′-positions both undergo tosylation somewhat more rapidly than does the 1′-position. The fact that the ditosylation produced nearly as much 1′,6,6′-tri-*O*-tosylsucrose as did the tritosylation clearly reflects the greater reactivity of the three primary positions over the secondary positions of sucrose.

Can. J. Chem. Downloaded from www.nrcresearchpress.com by 186.148.149.217 on 09/04/12
For personal use only.

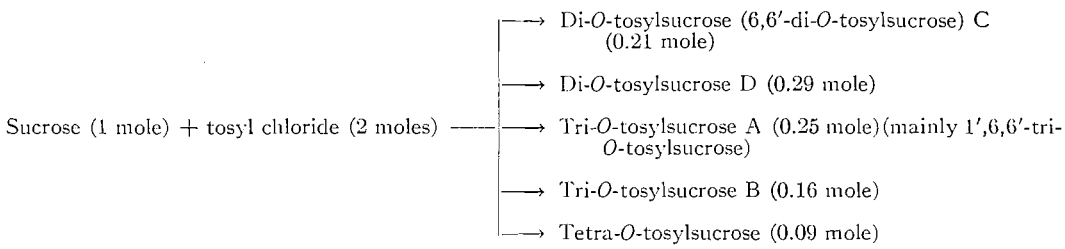


FIG. 2. Distribution of the tosylated sucroses formed in the reaction of 1 mole of sucrose with 2 moles of tosyl chloride in pyridine at 0°.

EXPERIMENTAL

The melting points are uncorrected and were determined on a microheating stage. Mallinckrodt reagent grade (100-mesh, lot 2847) silicic acid was used throughout.

"Tri-O-tosylsucrose"

A preparation was made at 0° in 95% yield using the method described by Hockett and Zief (9) and had a softening point of 65° to 85°, $[\alpha]_D$ +43° (*c*, 2.88 in chloroform). Anal. Calc. for $C_{33}H_{40}O_{17}S_3$: S, 11.93%. Found: S, 11.11%. The composition of this product is described in Table I and in Fig. 1.

A second preparation was made at −18° in a refrigerated bath using the following procedure. Sucrose, 34.2 g (0.1 mole), was dissolved in dry pyridine, 600 ml, by refluxing the mixture for a short time. The solution was then cooled to −18° with vigorous stirring for 2 hours. Tosyl chloride, 57 g (0.3 mole), was dissolved in 150 ml of dry pyridine and the solution was added dropwise to the solution of sucrose over a period of 2 hours. The reaction was left with continuous stirring at −18° for 5 days. The product, isolated in the usual manner, weighed 74.3 g (92.5%) with m.p. 65–85°, $[\alpha]_D$ +42° (*c*, 2.5 in chloroform). Anal. Calc. for $C_{33}H_{40}O_{17}S_3$: S, 11.93%. Found: S, 11.66%. The composition of this product is described in Table II.

Chromatography of "Tri-O-tosylsucrose" on Paper Impregnated with Silicic Acid

The silicic-acid-impregnated paper was prepared by the method of Marinetti, Erbland, and Kochen (16) but using Whatman No. 3 chromatographic paper. The chromatograms were developed by the descending method using the solvent system, diisobutyl ketone: acetic acid:water (40:25:5). The dried paper was immersed in 0.01% aqueous Rhodamine 6G solution (16) and examined under ultraviolet light in a dark room. Both "tri-*O*-tosylsucrose" preparations gave spots of similar intensities having R_f values of 0.15, 0.40, 0.65, and 0.90.

Silicic Acid-Column Chromatography of "Tri-O-tosylsucrose"

The silicic acid, 200 g, was packed as a slurry in chloroform in a 2.5-cm (diameter) column. The "tri-*O*-tosylsucrose", 9–10 g, was dissolved in 20 ml of chloroform and applied to the top of the column. The column was then developed with the solvent system, diisobutyl ketone:acetic acid:water (40:25:5). After the solvent front had displaced all of the chloroform from the column, 3-ml fractions were collected at a rate of 1 tube every 2 minutes. A total of 110 tubes were collected. Further eluant was free of material. The tubes were examined by spotting on paper and applying the Rhodamine 6G color test. Five different zones were apparent in the series of tubes. After the tubes within each zone had been combined, the solvent was removed *in vacuo* and the weights of the residues were determined.

Can. J. Chem. Downloaded from www.nrcresearchpress.com by 186.148.149.217 on 09/04/12
For personal use only.

Can. J. Chem. Downloaded from www.nrcresearchpress.com by 186.148.149.217 on 09/04/12
For personal use only.

The results are given in Tables I and II. Crystals were deposited in the fraction which proved to correspond to the fraction of di-*O*-tosylsucroses. In the case of the "tri-*O*-tosylsucrose" prepared at 0°, the crystalline substance (fraction C) was collected before evaporation of the solvent. The extremely fine needles, 0.92 g, m.p. 101–106°, were extremely soluble in methanol, but sparingly soluble in water, ethanol, or chloroform. After three recrystallizations from water, this compound melted at 108–110°, $[\alpha]_D$ +54° (*c*, 1.66 in ethanol). The compound only reduced Fehling's solution after acid hydrolysis. Anal. Calc. for $C_{26}H_{34}O_{15}S_2$: C, 47.8%; H, 5.22%; S, 9.85%. Found: C, 47.2%; H, 5.29%; S, 10.12%. The experiments described below established the compound to be 6,6′-di-*O*-tosylsucrose.

6,6′-Diiodo-6,6′-dideoxysucrose Hexaacetate

6,6′-Di-*O*-tosylsucrose (fraction C), 0.1 g, was dissolved in 1 ml of dry pyridine, and 2 ml of acetic anhydride and left at 4° for 2 days. The acetate, 126 mg, was isolated in the usual manner. The amorphous solid resisted crystallization. The substance, 76.5 mg, was dissolved in 15 ml of 10% sodium iodide in acetone and the solution was heated at 120° for 16 hours. The sodium tosylate, 36.2 mg, which precipitated represented a replacement of two tosyloxy groups. The syrupy product, 59.2 mg, was isolated in the usual manner. Its nuclear magnetic resonance spectrum was devoid of signals for the aromatic and *C*-methyl hydrogen atoms of the tosyl group. Anal. Calc. for $C_{24}H_{32}O_{15}I_2$: I, 31.4%. Found: I, 29.3%.

Monoiodomonodeoxymono-O-tosylsucrose Hexaacetate

The syrupy di-*O*-tosylsucrose (fraction D), 2.11 g, remaining after the removal of the crystalline 6,6′-*O*-tosylsucrose (see above) was acetylated and the product was subjected to the sodium iodide in acetone treatment. The amount of sodium tosylate recovered represented a replacement of 1.1 tosyloxy groups.

Reaction of Tri-O-tosyl Sucroses A and B with Sodium Iodide

Acetylated samples of tri-*O*-tosylsucrose fractions A, 135 mg, and B, 128 mg, were treated as described above with 10% sodium iodide in acetone. The amounts of sodium tosylate recovered were 49.69 mg and 41.58 mg, respectively. These amounts represent the replacement of 1.87 and 1.63 tosyloxy groups per mole, respectively. Anal. Calc. for $C_{29}H_{36}O_{16}I_2S$: I, 30.7%. Found: I, 28.6% (fraction A) and I, 27.8% (fraction B).

1′,2:3,6:3′,6′-Trianhydrosucrose Diacetate

Tri-*O*-tosylsucrose A, 200 mg, was dissolved in methanol *M* in sodium methoxide and the solution was refluxed for 30 minutes. The reaction mixture was evaporated to dryness and the residue was shaken with boiling pyridine, 50 ml, for 15 minutes. After the mixture was cooled to 0°, 10 ml of acetic anhydride was added. The syrupy product, isolated in the usual manner, crystallized on trituration with methanol. The yield was 71.6 mg (77.4% of theory) of 1′,2:3,6:3′,6′-trianhydrosucrose diacetate, m.p. 179–181°, undepressed when admixed with an authentic specimen.

Periodate Oxidation of the Tri-O-tosylsucroses A and B

To a sample of the tosyl ester, 0.05 millimole, dissolved in 80 ml of glacial acetic acid, 10 ml of 0.25 *N* sodium metaperiodate was added and the solution made up to 100 ml with water. Aliquots, 10 ml, were taken at suitable time intervals and were reacted with potassium iodide and an excess of 0.1 *N* sodium thiosulphate solution (18). The excess thiosulphate was determined by titration to the starch end point with standard

0.005 *N* iodine solution. Periodate was not consumed in the blank determinations. The periodate uptake by fraction A was 0.61, 1.53, 2.02, 2.18, 2.41, 2.78, and 2.82 moles of oxidant per mole of A after 0.5, 1, 10, 18, 32, 85, and 108 hours. The periodate uptake by fraction B was 0.49, 0.51, 0.98, 1.18, 1.59, 1.72, and 1.75 moles of oxidant per mole of B after 0.5, 1, 10, 18, 32, 85, and 108 hours.

Ditosylation of Sucrose

Sucrose, 34.2 g (0.1 mole), was dissolved in 600 ml of dry pyridine and cooled to 0°; tosyl chloride, 38 g (0.2 mole), was added and the reaction mixture was kept at 0° for 5 days. The reaction mixture was then shaken at room temperature with 5 ml water for 30 minutes. The excess pyridine was removed *in vacuo* at 40° to leave a thick syrup. This syrup was dissolved in 1 liter of chloroform and washed with 200 ml of ice-cold 2 *N* sulphuric acid followed by 200 ml of saturated sodium bicarbonate and finally with 200 ml of water. The chloroform solution, after drying over anhydrous sodium sulphate, was evaporated to a dry, amorphous solid, 56 g (86% of theory). Chromatography on silicic-acid-impregnated paper revealed three components, R_f values, 0.13, 0.38, and 0.6. Column chromatography of 10 g of the material allowed the isolation of the fractions described in Table III and in Fig. 2.

ACKNOWLEDGMENTS

The authors wish to thank the Sugar Research Foundation, Inc., New York, for sponsoring this research as their Project 88, and A. G. McInnes for guidance in the chromatographic procedures.

REFERENCES

1. J. Compton. J. Am. Chem. Soc. **60**, 395 (1938).
2. R. C. Hockett and M. L. Downing. J. Am. Chem. Soc. **64**, 2463 (1942).
3. J. M. Sugihara. *In* Advances in carbohydrate chemistry. Vol. 8. Academic Press, Inc., New York.
4. R. S. Tipson. *In* Advances in carbohydrate chemistry. Vol. 8. Academic Press, Inc., New York.
5. R. U. Lemieux and A. G. McInnes. Can. J. Chem. **38**, 136 (1960).
6. I. Belluci. Gazz. chim. ital. **42**, II, 283 (1912).
7. T. P. Hilditch and J. G. Rigg. J. Chem. Soc. 1774 (1935).
8. J. P. Gibbons and R. A. Janke. J. Am. Oil Chemists' Soc. **29**, 467 (1952).
9. R. C. Hockett and M. Zief. J. Am. Chem. Soc. **72**, 1839 (1950).
10. F. Finkelstein. Ber. **43**, 1528 (1910).
11. A. L. Raymond and E. F. Schroeder. U.S. Patent 2, 365, 776 (1944).
12. P. D. Bragg and J. K. N. Jones. Can. J. Chem. **37**, 575 (1959).
13. R. U. Lemieux and J. P. Barrette. J. Am. Chem. Soc. **80**, 2243 (1958).
14. R. U. Lemieux and J. P. Barrette. Can. J. Chem. **37**, 1964 (1959).
15. R. W. Jeanloz. Abstracts of Papers, Am. Chem. Soc. **128**, 2D (1953).
16. G. V. Marinetti, J. Erbland, and J. Kochen. Federation Proc. **16** (3), 837 (1954).
17. G. G. McKeown, R. S. E. Serenius, and L. D. Hayward. Can. J. Chem. **35**, 28 (1957).
18. J. B. Martin. J. Am. Chem. Soc. **75**, 5483 (1953).

Can. J. Chem. Downloaded from www.nrcresearchpress.com by 186.148.149.217 on 09/04/12
For personal use only.

Can. J. Chem. Downloaded from www.nrcresearchpress.com by 186.148.149.217 on 09/04/12
For personal use only.

THE STRUCTURE OF SANDARACOPIMARIC ACID[1]

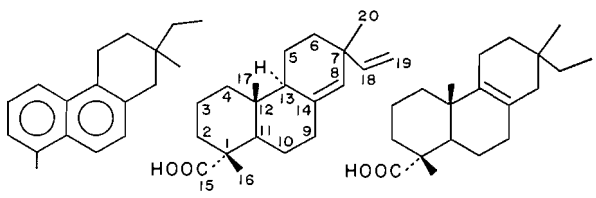
O. E. EDWARDS, A. NICOLSON,[2] AND M. N. RODGER[2]

ABSTRACT

Sandaracopimaric acid has been shown to be 7-epipimara-8(14),18-dienoic acid (II), and Ukita's acid to be 7-epi-13β-pimara-9(14),18-dienoic acid (VI). A hydroxyl-containing acid from Sandarac resin is described.

Sandaracopimaric acid was isolated by Henry (1) and by Tschirch and Wolff (2) from the resin of the N. African sandarac tree (*Callitris quadrivalvis*). Recently an improved isolation procedure was described by Petru and Galik (3), who also demonstrated that the acid belonged to the pimaric group. They claimed (4) that both pimaric acid and sandaracopimaric acid gave the same partial dehydrogenation product I and hence had the same configuration at C-7. Even if this conclusion had been correct their work left the location of the double bond and the stereochemistry at the other asymmetric centers unknown.

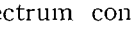
In continuance of our interest in the stereochemistry of the pimaric acids[3] we have examined sandaracopimaric acid, and proved it to be the C-7 epimer (II) of pimaric acid (7-epipimara-8(14),18-dienoic acid).[4]

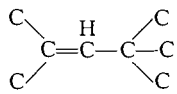


(I) (II) (III)

Using the method of Petru and Galik (3) we obtained an ether-soluble ammonium salt from the resin. This was converted into the sodium salt, which was then precipitated from its aqueous solution by addition of concentrated sodium hydroxide solution. The precipitate did not crystallize readily, so the acids liberated from it were chromatographed on silica gel. In this way a 2.2% yield of sandaracopimaric acid and a 1.3% yield of a higher melting acid were obtained. The latter had m.p. 270° and $[\alpha]_D$ −11° in ethanol. The melting point is close to that of sandaricinolic acid (2), but our analytic figures, which correspond to a hydroxypimaric acid, are widely different from those of Tschirch and Wolff. The infrared spectrum of the high melting acid had rather weak bands which could be ascribed to a vinyl group and a trisubstituted double bond, and a strong hydroxyl band at 3360 cm^{-1}. We hence suggest that it is a hydroxypimaric acid.

[1]*Manuscript received January 12, 1960.*
Contribution from the Division of Pure Chemistry, National Research Council, Ottawa, Canada.
Issued as N.R.C. No. 5627.
[2]*National Research Council of Canada Postdoctorate Fellow.*
[3]*We wish to thank Dr. R. Howe, who first aroused our interest in sandaracopimaric acid.*
[4]*It seems desirable to have a systematic nomenclature for the pimaric acids, in particular to designate transformation products. However, the trivial names for the natural acids provide a convenient shorthand. We suggest that pimaric acid be designated pimara-8(14),18-dienoic acid, from which the other names follow as illustrated in the text. We do not consider the configuration at C-7 in pimaric acid to be settled, hence avoid commitment on this point.*

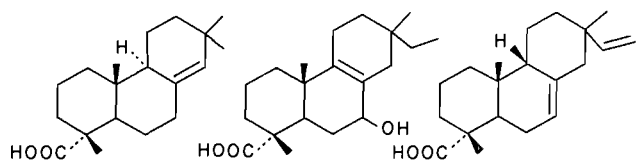
The physical constants for sandaracopimaric acid, m.p. 169°, $[\alpha]_D$ −20° in ethanol, were in good agreement with those reported by the Czech workers. Its rotatory dispersion curve was plain and negative. Its infrared spectrum suggested the presence of a vinyl group (ν_{max} 913 and 994 cm^{-1}) but there was no clear band corresponding to a trisubstituted double bond. The acid was rapidly reduced in the presence of palladium to a dihydro derivative, m.p. 178° (Petru and Galik (3) report m.p. 180°), which now gave a spectrum containing a band at 824 cm^{-1} () but lacking the vinyl absorption. The N.M.R. spectrum of the dihydro compound contained a single signal in the vinyl hydrogen region which was not split by coupling with adjacent hydrogens (band width ca. 4 c.p.s.). This suggests the presence of the system



in the acid.

The presence of the pimaric acid skeleton and the isopimaric configuration at C-7 were next demonstrated by conversion of dihydrosandaracopimaric acid to 7-epipimar-13-enoic (Δ^{13}-dihydroisopimaric) acid (III) using dry hydrogen chloride in chloroform (5). Since a nuclear double-bond location at 8(14) is the only one consistent with the N.M.R. spectrum and formation of III, and since C-13 is the only remaining center at which sandaracopimaric acid can differ from isopimaric acid, it must have structure II.

This conclusion was confirmed in the following way. Sandaracopimaric acid was hydroxylated with osmium tetroxide. The main product was a diol acid, m.p. 255°, in which the vinyl group had been oxidized. The glycol system was rapidly cleaved by periodic acid to an aldehydo acid, m.p. 215°. On Wolff–Kishner reduction this gave 19-norpimar-8(14)enoic acid (IV), identical in all respects with the gem-dimethyl acid prepared earlier from pimaric acid (6). This observation proves the identity of double-bond location and C-13 configuration in pimaric and sandaracopimaric acids, and hence structure II must correctly represent the latter.[5]



(IV) (V) (VI)

This finding removes the last doubt about the structure and stereochemistry of Ukita's acid (5). There was slight possibility that this acid had structure II although no obvious mechanism existed for the transformation of its dihydro derivative to V with selenium dioxide under mild conditions. The rotatory dispersion curve did not exclude II from consideration (7). However, the above results coupled with the rotatory dispersion now require that the acid be 7-epi-13β-pimara-9(14),18-dienoic acid (VI).

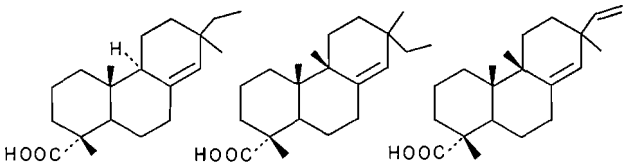
Wenkert has pointed out[6] that the rotatory dispersion curves of dihydropimaric (VII)

The rotatory dispersion observations of Bose and Struck (7) provide an important addition to the body of evidence (6, 8, 9) suggesting that the C-13 hydrogen in pimaric acid is α oriented.

[6]*Personal communication from Professor E. Wenkert.*

Can. J. Chem. Downloaded from www.nrcresearchpress.com by 186.148.149.217 on 09/04/12
For personal use only.

and dihydroisopimaric (VIII) acids (7) are readily interpreted if a small positive contribution from the asymmetric centers in ring A is superimposed on the positive and negative plain curves due to the two mirror image situations in ring C. Extending this



(VII) (VIII) (IX)

argument, since sandaracopimaric acid has a plain negative curve the unknown pimaric acid IX whose ring C is the mirror image of that in II should have a plain positive curve. Hence cryptopimaric acid which has a plain negative curve (7) cannot be this isomer and hence must be a double-bond isomer. Bruun, Ryhage, and Stenhagen (9) concluded that cryptopimaric acid had structure II on the basis of mass spectrometry. This cannot be correct unless the physical constants of cryptopimaric acid are in error. However, their results do suggest the great importance of the C-13 stereochemistry in determining the fragmentation pattern when the nuclear double bond is in the 8(14) position. The uncertainty as to whether this applies to other double bond isomers, and the probable large effect of the vinyl group on the rotatory dispersion curve[7] make it unwise to suggest a structure for cryptopimaric acid at present.

EXPERIMENTAL

Unless otherwise stated, rotations were of ethanol solutions, infrared spectra were of Nujol mulls, and melting points were taken on a Kofler hot stage.

Sandarac Resin Acids

Commercial sandarac resin (900 g) dissolved nearly completely in ether. Ammonia was bubbled through the ether solution until precipitation ceased. The insoluble ammonium salts were removed by filtration and the filtrate extracted with 2% sodium hydroxide solution. The aqueous solution of sodium salts was acidified using 2% acetic acid, the acids collected on a filter, and washed well with water (yield 169 g). The sodium salts of this acid mixture did not crystallize readily, hence the acids were chromatographed on silica gel.

A benzene solution of approximately half the acid (87 g) was added to a column of 100- to 200-mesh silica gel (1.3 kg) and 100 cc eluate fractions collected.

Eluant	Fraction	Weight, g	Remarks
Benzene	1–9	4.5	Amorphous
Benzene–ether 20:1	10–14	6.4	Amorphous
Benzene–ether 10:1	15–20	26.2	8.8 g crystalline material
Benzene–ether 3:1	20–30	9.6	Amorphous
Benzene–ether 1:1	31–44	18.6	5.4 g crystalline material

The remaining fractions did not crystallize.

[7]*Hydrogenation of the vinyl group of sandaracopimaric acid reverses the sign of rotation, hence presumably the sign of the rotatory dispersion curve.*

Can. J. Chem. Downloaded from www.nrcresearchpress.com by 186.148.149.217 on 09/04/12
For personal use only.

Sandaracopimaric Acid

The yield of crude crystals from fractions 15–20 was 8.8 g (2.2% of the resin). The acid was purified by recrystallization from aqueous methanol, recrystallization of its sodium salt, and further recrystallization of the acid. It then had m.p. 169°, $[\alpha]_D$ −20° (*c*, 2.6). Its infrared spectrum had bands at 913 and 994 cm^{-1} (vinyl group), 825 cm^{-1} (very weak) ($>C=C<^{H}$), and at 1692 cm^{-1} (—COOH). Its rotatory dispersion curve was plain and negative, with $[\alpha]_{460}$ −50° and $[\alpha]_{290}$ −250°.

The Hydroxy Acid

The yield of crude crystals from fractions 31–44 was 5.4 g (1.3% of the resin). When recrystallized from aqueous methanol it separated as plates, m.p. 270°, $[\alpha]_D$ −11° (*c*, 0.8). Found: C, 75.59; H, 9.74. Calc. for $C_{20}H_{30}O_3$: C, 75.43; H, 9.50. Its infrared spectrum had rather weak bands at 904 and 987 cm^{-1} (vinyl group) and 822 cm^{-1} ($>C=C<^{H}$), a strong band at 3360 cm^{-1} (hydroxyl group), and a band at 1695 cm^{-1} (—COOH).

Dihydrosandaracopimaric Acid

Sandaracopimaric acid (200 mg) in 15 ml of ethanol was reduced with hydrogen in the presence of 150 mg of presaturated 30% palladium on charcoal. In 5 minutes 16.3 ml of hydrogen was absorbed (calc. for 1 mole, 16.1 ml). The product was recrystallized three times from aqueous methanol giving 128 mg of needles, m.p. 174–178°, $[\alpha]_D$ +21° (*c*, 1.83). Found: C, 78.78; H, 10.54. Calc. for $C_{20}H_{32}O_2$: C, 78.94; H, 10.52. Infrared spectrum: ν_{max} 1692 cm^{-1} (—COOH); 824 cm^{-1} ($>C=C<^{H}$).

Isomerization of Dihydrosandaracopimaric Acid

Dry hydrogen chloride was passed into a solution of 73 mg of dihydrosandaracopimaric acid in dry ethanol-free chloroform at −5° for 4 hours. The solution was then washed free of mineral acid with water, dried, and evaporated. The product (58 mg) crystallized from aqueous acetone as needles, m.p. 109–112°, $[\alpha]_D$ +75° (*c*, 1.0 in chloroform). It did not depress the melting point of Δ^{13}-dihydroisopimaric acid (5) (m.p. 109–112°) and X-ray powder patterns of the two substances were identical.

Hydroxylation of Sandaracopimaric Acid

A solution of 636 mg of sandaracopimaric acid and 530 mg of osmium tetroxide in 10 ml of dry ether was left overnight at 0°. The black precipitate (1.2 g) was collected by filtration. It was then heated for 1 hour on a steam bath in 15 ml of water containing 2.7 g of mannitol and 0.5 g of sodium hydroxide. The resulting solution was acidified with acetic acid and the precipitated acid collected by filtration. This was boiled with methylene chloride to remove more soluble material, and the residue recrystallized three times from methanol. The diol acid separated as needles (410 mg), m.p. 255°, $[\alpha]_D$ +39° (*c*, 0.35). Found: C, 71.58; H, 9.75. Calc. for $C_{20}H_{32}O_4$: C, 71.39; H, 9.59. Infrared spectrum: ν_{max} 825 cm^{-1} ($>C=C<^{H}$), 1685 cm^{-1} (—COOH).

Aldehydo Acid

A solution of 200 mg of the above diol acid in 80 ml of aqueous dioxane (10% water) containing 290 mg of periodic acid was left for 1 hour at room temperature in the dark. The reaction mixture was then concentrated to around 6 ml under reduced pressure,

Can. J. Chem. Downloaded from www.nrcresearchpress.com by 186.148.149.217 on 09/04/12
For personal use only.

water added, and the solution extracted with methylene chloride. The methylene chloride solution was washed with water, dried, and evaporated, leaving 170 mg of crystalline residue. This was absorbed from benzene on 4 g of silica gel. Benzene eluted a small quantity of material. Benzene–ether (50:1, 40 ml fractions) eluted the bulk of the compound. Fractions 2 and 3 had m.p. 200–215° (evacuated capillary). These were combined and recrystallized twice from ether–hexane giving 141 mg, m.p. 215° (evacuated capillary), $[\alpha]_D$ −2° (*c*, 1.3). Found: C, 74.89; H, 9.31. Calc. for $C_{19}H_{28}O_3$: C, 74.96; H, 9.27. Infrared spectrum: ν_{max} 2700, 1727 cm^{-1} (—CHO), 1693 cm^{-1} (—COOH), 823 cm^{-1} ($\rangle C{=}C\langle^{H}$).

19-Norpimar-8(14)-enoic Acid

A solution of the above aldehydo acid (54 mg) in 2 ml of triethylene glycol and 0.5 ml of 95% hydrazine was heated on a steam bath for 30 minutes and at 140° for 30 minutes under an air condenser. Potassium hydroxide (0.64 g) was then added cautiously, the temperature raised to 205°, and maintained at that temperature for 4 hours, while a slow stream of nitrogen was introduced halfway down the condenser. The reaction mixture was then cooled, diluted with water, and extracted with methylene chloride. The methylene chloride was extracted with dilute sodium hydroxide solution, then the combined aqueous layers carefully acidified with 6 *N* sulphuric acid. The acid was again extracted into methylene chloride, the solution washed with water, dried, and distilled. The residual solid was recrystallized from methanol, giving 44 mg of needles, m.p. 238°, $[\alpha]_D$ +18° (*c*, 0.6). This did not depress the melting point of the gem-dimethyl acid from pimaric acid (6), m.p. 238°. Their X-ray powder patterns and infrared spectra were identical.

ACKNOWLEDGMENTS

We wish to thank Professor A. K. Bose for sending his manuscript before publication and for the rotatory dispersion curve of sandaracopimaric acid, Professor E. Wenkert for valuable comments on the rotatory dispersion curves, Professor F. A. L. Anet for the N.M.R. spectrum, Dr. M. Przybylska and Miss C. Philo for the X-ray pattern comparisons, Mr. R. Lauzon for the infrared spectra, and Mr. A. Knoll for technical assistance.

REFERENCES

1. T. A. Henry. J. Chem. Soc. **79**, 1144 (1901).
2. A. Tschirch and M. Wolff. Archiv. Pharm. **244**, 684 (1906).
3. F. Petru and V. Galik. Collection Czech. Chem. Commun. **18**, 717 (1953).
4. V. Galik, F. Petru, and J. Kuthan. Naturwiss. **46**, 322 (1959).
5. O. E. Edwards and R. Howe. Can. J. Chem. **37**, 760 (1959).
6. O. E. Edwards and R. Howe. Chem. & Ind. 537 (1959).
7. A. K. Bose and W. A. Struck. Chem. & Ind. 1628 (1959).
8. B. Green, A. Harris, and W. B. Whalley. J. Chem. Soc. 4715 (1958).
9. H. H. Bruun, R. Ryhage, and E. Stenhagen. Acta Chem. Scand. **12**, 789 (1958).

Can. J. Chem. Downloaded from www.nrcresearchpress.com by 186.148.149.217 on 09/04/12
For personal use only.

Can. J. Chem. Downloaded from www.nrcresearchpress.com by 186.148.149.217 on 09/04/12
For personal use only.

MOLECULAR AREAS OF SOAPS AT THE SURFACE OF LATEX PARTICLES[1]

R. J. Orr and L. Breitman

ABSTRACT

The molecular area (i.e., the area occupied by a molecule of soap adsorbed on a surface) has been determined for a number of anionic, cationic, and non-ionic emulsifiers, adsorbed on latex particles. Measurements were made by surface tension and electron microscopic techniques. The composition of the polymer did not affect the molecular area of either anionic or cationic soaps. When a mixture of non-ionic and anionic soaps was used, interaction between the soaps prevented application of the conventional methods for measuring molecular area. The interaction is manifested by a decrease in the area occupied by an anionic soap molecule which can be explained in terms of reduction in electrostatic repulsive forces between ionic soap molecules. The configuration of the polyethylene oxide chain of the non-ionic on the surface of the latex particle is deduced to be that of caterpillarlike folds.

INTRODUCTION

The emulsion of rubber in water, known to the rubber industry as latex, offers special opportunities for study of physical properties of soaps at the polymer–water interface. This fact was first noted and used by Maron (1), who determined the minimum area which soap molecules in a monolayer occupy at the polymer–water interface. The specific property of the latex on which such studies depend is the ability of the polymer–water interface to adsorb more soap after the synthesis of the latex is complete. The main objectives of the study reported here were

(i) to increase the applicability of titration methods in determining latex particle size and surface areas of adsorbed soaps,

(ii) to learn something about the molecular geometry of the emulsifier at the interface which might be helpful in developing hypotheses concerning the mechanism of stabilization of latex.

THEORETICAL

Soap Titration in One-Component Systems

The area (A) occupied by an adsorbed soap molecule may be obtained from Maron's equation

$$[1] \qquad A = \frac{A_T}{N(S_1+S_a)}$$

where A_T = surface area/g polymer,
S_1 = number of moles of soap adsorbed/g polymer in final latex,
S_a = additional number of moles of soap adsorbed/g polymer, when sufficient soap is added to obtain the critical micelle concentration (c.m.c.) in the aqueous phase,
N = Avogadro's number.

Suppose that two different substrates are dispersed in water, that A_T is the same for both dispersions, and that soap is added to the aqueous phase until the c.m.c. is reached. The substrate with the greater affinity for the soap will adsorb more soap and, from equation [1], it follows that the value of A will be lower for this substrate. Comparison of affinities of soap for polymer by this method is not valid when the c.m.c. is so high

[1]*Manuscript received December 3, 1959.*
Contribution from Polymer Corporation Limited, Research and Development Division, Sarnia, Ontario.

that both substrates adsorb sufficient soap to form a condensed and incompressible monolayer. Since these conditions do not, in general, exist, low values of A may be taken as evidence of high affinity of substrate for soap.

Soap Titration in Two-Component Systems

If two portions of the same latex are titrated to the c.m.c., one with soap A and the other with soap B, then, according to Maron, the following relation holds:

$$S_a^A A^A = S_a^B A^B = A_T - S_1 AN. \quad [2]$$

The superscripts refer to the two soaps, A and B.

Equation [2] enables one to determine areas of soaps which, for practical reasons, cannot be used to prepare the original latex. This equation is valid if the following conditions hold:

(i) no desorption of the original soap occurs during titration with a different soap, and

(ii) at the titration end point, the area per molecule of the initial soap corresponds to its area at its own c.m.c.

As is shown later, these conditions are not always fulfilled.

Determination of A_T by Electron Microscopy

When the latex is not monodisperse, results of electron microscope analysis are readily expressed by the number average particle diameter ($\bar{X}$) and a standard deviation (σ). It may then be shown (see Appendix) that A_T is given by

$$A_T = \frac{6}{\bar{X}d}\left(\frac{\bar{X}^2+\sigma^2}{\bar{X}^2+3\sigma^2}\right) \quad [3]$$

where d is the polymer density.

Use of Surface Tension to Determine Critical Micelle Concentration

The surface tension method was selected for the determination of the c.m.c. of both ionic and non-ionic soaps, since the electrical conductivity method obviously cannot be used for non-ionics. Although the validity of the surface tension method for ionic soaps has been questioned (2), we have found the procedure to be satisfactory (see Results). The theoretical basis for this procedure with non-ionics has been provided by Bury (3). Some insight as to the significance of a surface tension measurement with an ionic soap may be provided by the following argument.

Only one of the ions of a soap is normally capillary-active, but the adsorption of capillary-active ions on the surface sets up an electrical field which tends to attract ions of the capillary-inactive species.

The Gibbs adsorption isotherm for a uni-univalent emulsifier may then be written as

$$-d\gamma/RT = \Gamma_+ d \ln a_+ + \Gamma_- d \ln a_-$$

where a and Γ represent bulk activities and surface excesses respectively of the two ions. At low concentrations of emulsifier, the activities of the ions are equal (4).

The substitution

$$a^+ = a^- \equiv a$$

gives

$$-d\gamma/RT = d \ln a(\Gamma_+ + \Gamma_-).$$

Can. J. Chem. Downloaded from www.nrcresearchpress.com by 186.148.149.217 on 09/04/12
For personal use only.

At high ionic strength, where $\Gamma_+ \rightarrow \Gamma_-$, the above equation reduces to the expression given by Pethica (5) for these conditions.

A plot of γ versus ln c (or ln a) is usually a curve with a more or less sharp change in slope at a concentration which is assumed to be the critical micelle concentration.

CHEMICALS

The various commercial soaps used in this investigation are listed below with trade names, formulae, and suppliers.

Trade name	Formula	Supplier
Agent 180 BK	$(C_9H_{19})_2C_6H_3O(C_2H_4O)_{15}H$	Chemical Developments of Canada
Armac 10	$C_{10}H_{21}NH_2 : CH_3COOH$	Armour Company
Armac 14	$C_{14}H_{31}NH_2 : CH_3COOH$	Armour Company
Brij 30	$C_{12}H_{25}O(C_2H_4O)_4H$	Atlas Powder Co.
Daxad 11	Polymerized sodium salt of alkyl naphthalene sulphonic acid	Dewey and Almy
Dresinate 214	$C_{20}H_{28}O_2K$	Hercules Powder Co.
Igepal CO-880	$C_9H_{19}C_6H_4O(C_2H_4O)_{32}H$	General Aniline Corp.
LOP-100	$C_9H_{19}C_6H_4O(C_2H_4O)_{20}H$	Chemical Developments of Canada
Nacconol	$C_{12}H_{25}C_6H_4SO_3Na$	National Aniline Corp.
Rosin amine D	$C_{19}H_{27}NH_2 : CH_3COOH$	Hercules Powder Co.

EXPERIMENTAL

Impurities in soap may be surface-active or inert. Electrolytes, apart from a slight effect on the critical micelle concentration of the soap, are of no importance. Surface active contamination is serious since small amounts of such impurities have a strong influence on the $\gamma - \ln c$ relation. Miles and Shedlovsky (6) found that minima in the surface tension – concentration relation indicate surface-active impurities. Hutchinson (7) showed that small amounts of octyl alcohol had a pronounced effect on the surface excess of sodium dodecyl sulphate.

The C_{10} and C_{14} *n*-alkyl amines and the rosin amine were purified by steam distillation of the amine regenerated from the commercial emulsifier. The amine was reacidified with C.P. glacial acetic acid. Nacconol, Dresinate 214, and cetyl pyridinium chloride were used without further purification. Other ionic emulsifiers were prepared from C.P. reagents. No sharp minima in the surface tension – concentration relation, characteristic of surface active contamination, were observed with these emulsifiers. A much smaller minimum was observed with Armac 14, the acetate of a C_{14} *n*-alkyl amine, but, since this disappeared when electrolyte was added, it is suggested that this minimum is associated not with impurities, but perhaps with absorption of micelles on the surface, as reported by Judson (8), and Ruyssen and Maebe (9). The Nacconol was 93% pure, having 6% sodium sulphate and 1% volatile (10). The Dresinate 214 and cetyl pyridinium chloride were 100% active. The non-ionic emulsifiers exhibited a distribution of ethylene oxide

Can. J. Chem. Downloaded from www.nrcresearchpress.com by 186.148.149.217 on 09/04/12
For personal use only.

content but were certified as 100% active by the suppliers. Of the non-ionics, only Igepal CO-880 displayed a surface tension minimum (~ 2 dynes/cm).

All surface tension measurements were done with a CENCO du Nuöy ring tensiometer. Readings were corrected for ring diameter and wire thickness by the method of Harkins (11).

Area/gram ratios were calculated from equation [3] with a polymer density of 0.94 for butadiene/styrene and 0.96 for butadiene/acrylonitrile and butadiene/methyl methacrylate copolymers (12).

Preparation of Latices

Latices stabilized with all three types of soap—anionic, non-ionic, and cationic—were prepared by conventional emulsion polymerization techniques. The reaction temperature was 50° C and the source of initiating free radicals was obtained by reaction of a ferrous iron – potassium pyrophosphate complex with diisopropyl benzene hydroperoxide. After 60 to 80% conversion of monomers to polymers, the reaction was stopped and residual monomers were removed by steam distillation. Coagulum formation during polymerization was objectionable since this made estimation of S_1 difficult. It was possible to avoid excessive coagulum formation in all cases, except when cetyl pyridinium chloride was used. Determinations of the area of cetyl pyridinium chloride were made with two coagulum levels in the latex.

Comonomers used with butadiene were styrene, acrylonitrile, and methyl methacrylate. Monomer charge ratios were 70/30 butadiene/styrene and 66/33 butadiene/acrylonitrile, except where otherwise specified.

Electron microscope data on the above latices were determined and are shown in Table I.

TABLE I

Electron microscope data on latices

Emulsifier	Soap in reaction per 100 parts monomer (parts)	Comonomer	Bd in comonomer charge (%)	Average particle diameter (Å)	Standard deviation (σ)
Dodecyl amine acetate	5.0	Styrene	70	915	60
		Styrene	70	1077	104
		Acrylonitrile	80	794	95
		Methyl methacrylate	80	950	146
Cetyl pyridinium chloride	3.0	Styrene	70	1340	10
	4.0			1237	90
	3.0			1028	57
Igepal CO-880, Nacconol	0.5*	Styrene	70	1129	236
	1.0*			1051	208
	1.5*			877	255
Igepal CO-880, K-oleate	0.5*	Styrene	70	1090	247
	1.0*			1026	183
	1.5*			870	187
Dresinate 214, Na fatty acid	—	Styrene	72	570	10
Dresinate 212, Dresinate 214	—	Styrene	50	600	10
Daxad 11, Nacconol	—	Acrylonitrile	67	600	10

*Refers to anionic soap; non-ionic held constant at 5.0 parts.

Can. J. Chem. Downloaded from www.nrcresearchpress.com by 186.148.149.217 on 09/04/12
For personal use only.

Soap Titration

The amount of soap necessary to reach the c.m.c in latex was determined from a plot of log (cc added soap) versus surface tension, as shown in Fig. 1. The soap was added

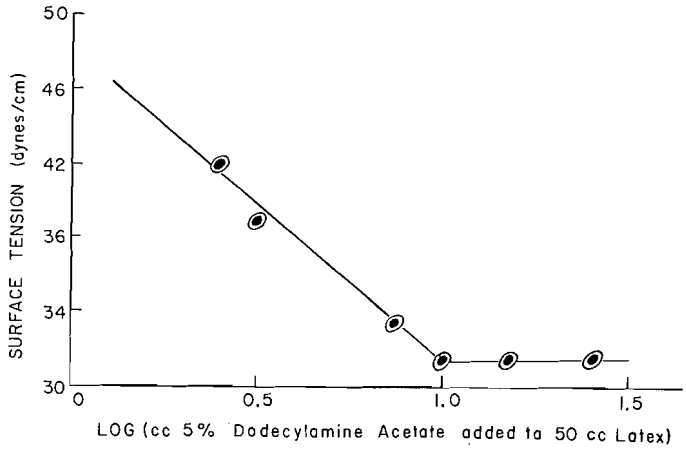


FIG. 1. Variation in surface tension with soap content for 80/20 butadiene-acrylonitrile latex.

to latex which had been adjusted to a solids content of 15%. The pH was maintained at fixed values to prevent hydrolysis of the soap. With cationic lattices, the pH was 4 and with anionic lattices, the pH was 10. Some experiments (where there was a high ratio of non-ionic to anionic) were done at two values of pH, 7 and 10. The temperature was maintained at 26°±1° C.

RESULTS

Surface tension was plotted against logarithm of the concentration for anionic, cationic, and non-ionic soaps. The concentration at which there is a sharp change in the slope of the relation was taken at the c.m.c. Measured values of the c.m.c. were compared, when possible, with those calculated from an empirical equation due to Klevens (13):

$$[4] \qquad \log \text{c.m.c.(mole/liter)} = 2.26 - 0.231\ (\text{length of surface active ion in Å}).$$

TABLE II

Critical micelle concentrations of ionic soaps by the surface tension method (pH = 7)

	Critical micelle concentration (moles/liter)		
	Observed		Calculated from
Soap	% salt	0.1% NaCl	equation [4]
Armac 10	2×10^{-2}	3×10^{-2}	5×10^{-2}
Dodecyl amine acetate	1×10^{-2}	4×10^{-3}	1×10^{-2}
Armac 14	2×10^{-3}	2×10^{-3}	3×10^{-3}
Rosin amine acetate	9×10^{-3}	9×10^{-3}	
Cetyl pyridinium chloride	6×10^{-3}	8×10^{-3}	
Nacconol	1.0×10^{-3}*	7×10^{-4}	
Potassium oleate	9×10^{-4}	1.8×10^{-4}	1×10^{-3}

*2.1×10^{-3} moles per liter Na_2SO_4.

Can. J. Chem. Downloaded from www.nrcresearchpress.com by 186.148.149.217 on 09/04/12
For personal use only.

TABLE III
Critical micelle concentration of non-ionic soaps (pH = 7)

Soap	Hydrophobic group	C_2H_4O, units/molecule soap	Molecular weight	Critical micelle concentration	
				0% salt	0.1% NaCl
Triton X-45	Iso-octyl phenol	5	426	0.6×10^{-4}	0.64×10^{-4}
Brij 30	Lauryl alcohol	4	360	1.25×10^{-5}	4.3×10^{-6}
LOP-100	Nonyl phenol	20	1100	1.8×10^{-4}	—
Brij 35	Lauryl alcohol	23	1200	6.2×10^{-5}	5.0×10^{-5}
Igepal CO-880	Nonyl phenol	32	1628	1.5×10^{-4}	—

Results are listed in Tables II and III. Data in Table III may be compared with results obtained by a similar method by Hsiao, Dunning, and Lorenz (14). The value for LOP-100 agreed closely. The value for Igepal CO-880 was lower, possibly due to the masking effect of the minimum we observed in the surface tension – concentration plot. The good agreement between the calculated and observed values of the c.m.c. confirms the reliability of the surface-tension method.

Area of Cationic Soaps

In calculation of area/soap molecule (A), the values of S_a in equation [1] were determined by subtracting the c.m.c. in water from the amount of soap necessary to reach the c.m.c. (or titration end point) in latex. The change in the c.m.c. in water caused by 0.1% NaCl (see Table II) has negligible effect on the calculated soap area. The areas of dodecyl amine acetate and cetyl pyridinium chloride at titration end point are shown in Table IV. The difficulty in obtaining good reproducibility with cetyl pyridinium chloride

TABLE IV
Molecular areas of cationic soaps at titration end point (equation [1])

Soap	Comonomer	Bd in comonomer charge (%)	Molecular area (Å²)	Average
Dodecyl amine acetate	Styrene	70	22.6	
	Styrene	70	25.0	25.6
	Acrylonitrile	80	27.0	
	Methyl methacrylate	80	26.2	
Cetyl pyridinium chloride	Styrene	70	42.4	46.0
			41.5	
			54.0	

was due, as already mentioned, to the formation of coagulum during polymerization. The areas of dodecyl amine acetate indicate that there is little, if any, difference in the degree of binding of this soap to the different substrates.

Equation [2] was used to determine the areas A^B of cationic soaps which were not used in the polymerization of the latex. Values for A^A were the directly determined ones in Table III. Dodecyl amine acetate or cetyl pyridinium chloride was used as the emulsifier in the polymerization step. The molecular areas so determined are listed in Tables V and VI. The data in these tables indicate that the nature of the polymeric

Can. J. Chem. Downloaded from www.nrcresearchpress.com by 186.148.149.217 on 09/04/12
For personal use only.

TABLE V

Molecular areas of cationic soaps at titration end point by comparative soap adsorption (equation [2])

Soap	Comonomer	Bd in comonomer charge (%)	Area covered by dodecyl amine acetate in original latex (%)*	A^B molecular area (Å²)
Armac 10	Styrene	70	45	19.4
	Acrylonitrile	80	55	19.2
	Methyl methacrylate	80	64	17.2
Armac 14	Styrene	70	45	27.6
	Acrylinotrile	80	55	30.5
Rosin amine D	Styrene	70	45	26.5

*"% area covered" is defined by $NS_iA/A_T \times 100$.

TABLE VI

Molecular areas of cationic soaps at titration end point by comparative soap adsorption (equation [2])

Soap	Comonomer	Bd in comonomer charge (%)	Area covered by cetyl pyridinium chloride in original latex (%)	A^B molecular area (Å²)
Armac 10	Styrene	70	70	20
Armac 14	Styrene	70	70	23

substrate does not significantly affect the molecular area of the cationic soaps at the interface.

The molecular areas of ARMAC 10 and ARMAC 14 may be compared with the value of 26 Å² for lauryl amine hydrochloride at the water–air interface reported by Harkins and co-workers (17).

Areas of Anionic Soaps

Two portions of an anionic latex were titrated, one with potassium oleate (B) and the other with the soap (A) whose area A^A is sought. A^A is calculated from equation [2] in which A^B, the area of the oleate molecule, was taken as 28.2 Å² (1). The results so obtained are shown in Table VII.

TABLE VII

Molecular areas of anionic soaps at titration end point by comparative soap adsorption (equation [2])

Soap	Comonomer	Bd in comonomer charge (%)	Molecular area (Å²)
Sodium dodecyl benzene sulphonate	Styrene	72	32 40
Dresinate 214	Acrylonitrile	66	34 40
	Styrene	50	38 38
Daxad 11*	Acrylonitrile	66	12.8×10^{22} Å²/g soap

*Determined by electron microscopy and titration with oleate.

Can. J. Chem. Downloaded from www.nrcresearchpress.com by 186.148.149.217 on 09/04/12
For personal use only.

It should be noted that there is some question about the accuracy of the area of the oleate molecule assumed here, since values as high as 47 Å² (15) have been reported. For two butadiene/styrene latices the total surface area, as measured by electron microscopy, compared well with that calculated from the values determined from the soap titration data. These results appear to substantiate the low value for the area of oleate.

The area of Daxad 11 (12.8×10^{22} Å²/g) on a butadiene/acrylonitrile latex containing Nacconol compares reasonably well with the value of 11.2×10^{22} Å²/g given by Maron (16) on a butadiene/styrene substrate.

Molecular Areas of Non-ionic Soaps

It was not possible to prepare latices with non-ionic soap alone in which the soap concentration in the aqueous phase was less than c.m.c. It was, therefore, impossible to obtain a titration end point on addition of soap and, accordingly, only a minimum value of the area per molecule could be directly determined. For a nonyl phenyl ethylene oxide condensate (Igepal CO-880) containing 30 moles ethylene oxide per mole nonyl phenol, a minimum value of 120 Å²/molecule was obtained by the procedure described for anionic and cationic soaps with the use of equation [1]. Separate portions of an undercovered anionic latex (i.e. a latex capable of adsorbing more soap at the oil–water interface) were titrated with potassium oleate and the non-ionic soap. Application of equation [2] to the titration data gave the values of molecular area listed in Table VIII.

TABLE VIII

Molecular areas of non-ionic soaps at titration end point by comparative soap adsorption (equation [2])

Comonomer	Bd in comonomer charge (%)	Emulsifier	C_2H_4O, units/molecule soap	Molecular area (Å²)
Styrene	72	Polyoxyethylene Nonyl phenol	30 (Igepal CO-880)	162
			20	125
		Polyoxyethylene Lauryl alcohol	4	40
Styrene	50	Polyoxyethylene Nonyl phenol	20	110
Acrylonitrile	66	Polyoxyethylene Nonyl phenol	30 (Igepal CO-880)	143
		Polyoxyethylene Isopropyl phenol	5	28.1
		Polyoxyethylene Dinonyl phenol	16	73

The correctness of these values, as well as of those in Tables V, VI, and VII, depends upon the validity of the two previously stated assumptions.

Another set of experiments was designed with the object of obtaining undercovered latex particles in which the fraction of surface occupied by the non-ionic could be varied over a wide range. This was accomplished by using varying ratios of non-ionic to ionic soap in the polymerization recipe. It was expected that interactions between the two types of soap in the adsorbed phase would be reflected in the observation that the molecular area at the titration end point is different when a second soap is present.

Separate portions of a given latex with a high ratio of non-ionic to ionic soap were titrated with an anionic soap (A) and a non-ionic soap (B) to obtain values of S_a^A and S_a^B. When the value of A^A was taken to be its characteristic value in the absence of a non-ionic, and the value of A^B was calculated from equation [2], these values of A^A

Can. J. Chem. Downloaded from www.nrcresearchpress.com by 186.148.149.217 on 09/04/12
For personal use only.

and A^B led to a total area of the latex particles which exceeded by about 50% the total area directly determined by electron microscopy. This result demonstrated that equation [2] is inapplicable to systems containing mixtures of ionic and non-ionic soaps, either because of interaction of the two types of soap in the adsorbed phase, or because of displacement of one soap by the other. It was not possible, on the basis of our experiments, to decide between the two alternatives. However, if it is assumed that displacement does not occur, it is then possible to obtain estimates of the changes in molecular areas that resulted from the interaction of the two soap species.

Separate portions of a given latex containing known amounts of anionic soap (S_i^A) and non-ionic soap (S_i^B) may be titrated with an anionic soap (A) and a non-ionic soap (B) to obtain values of S_a^A and S_a^B respectively. The relation between A_T and the concentrations of adsorbed soap is

$$[5] \qquad A_T/N = (S_i^A+S_a^A)A_x^{A*}+S_i^B A_x^{B*} = (S_i^B+S_a^B)A_y^{B*}+S_i^A A_y^{A*}.$$

A_x^{A*} and A_x^{B*} are the molecular areas of anionic and non-ionic soap, respectively, at the titration end point with anionic soap.

A_y^{A*} and A_y^{B*} are molecular areas of anionic and non-ionic soap, respectively, at the titration end point with non-ionic soap.

If it be assumed that the molecular area of a soap in an anionic/non-ionic soap mixture is independent of the relative concentrations of these soaps over the range investigated, one can write

$$[6] \qquad A_x^{A*} = A_y^{A*} \equiv A^{A*}$$

and

$$[7] \qquad A_x^{B*} = A_y^{B*} \equiv A^{B*}.$$

Values of A^{A*} and A^{B*} obtained from solution of equations [5], [6], and [7] are shown in Table IX. The asterisk symbol is used to differentiate molecular area in the mixed soap monolayer from that in a one-component monolayer.

TABLE IX

Molecular areas of anionic soaps and Igepal CO-880 at titration end point (equations [5], [6], and [7])

Anionic emulsifier in polymerization		Area covered by:		Molecular area (Å²)	
Type	Parts	Original anionic	Igepal CO-880	Anionic	Igepal CO-880
Nacconol	0.5	4.1	59.0	18.1	126
Nacconol	1.0	6.5	54.0	19.0	131
Potassium oleate	0.5	4.6	70.0	19.5	130
Potassium oleate	1.0	8.4	60.0	21.0	123

The estimate for the molecular area of Igepal CO-880 in the mixed soap system (Table IX) is about 30 Å² less than the value based on methods that assume no soap interaction. This method of determining areas of the non-ionic soap in the presence of anionic soap was limited to Igepal CO-880 since other non-ionic soaps do not support polymerization. If the area in mixed soap systems is independent of the nature of the non-ionic, then the molecular areas of the non-ionic soaps (Table VIII) determined by equation [2] are all too high. The data in Table VIII were revised on the basis of a

Can. J. Chem. Downloaded from www.nrcresearchpress.com by 186.148.149.217 on 09/04/12
For personal use only.

molecular area for the oleate molecule at 20.2 Å² (Table X) rather than at 28.2 Å² to obtain the values in Table X.

TABLE X

Molecular areas of non-ionic soap at titration end point by comparative soap adsorption (equation [2])

Comonomer	Bd in comonomer charge (%)	Emulsifier	C_2H_4O, units/ molecule soap	Molecular area (Å²)
Styrene	72	Polyoxyethylene Nonyl phenol	30	116
		Polyoxyethylene Lauryl alcohol	20	89
			4	28.6
Styrene	50	Polyoxyethylene Nonyl phenol	20	78
Acrylonitrile	66	Polyoxyethylene Nonyl phenol	30	103
		Polyoxyethylene Isopropyl phenol	5	19.8
		Polyoxyethylene Dinonyl phenol	16	52

The best estimates for the anionic soaps in the mixed soap system are about 8 Å² for oleate, and about 20 Å² for Nacconol, less than those values obtained in systems where there is no soap interaction (Tables V, VI, VII). The decrease in the area of anionic soaps in the presence of non-ionic soaps may be attributed to the absence of electrostatic repulsion forces between anions and neighboring neutral non-ionic soap molecules. A plot of molecular areas (Table X) versus number of C_2H_4O units/soap molecule is shown in Fig. 2. The linearity of the relation indicates that the area per ethylene oxide unit is constant. This constancy is consistent with an orientation of the ethylene

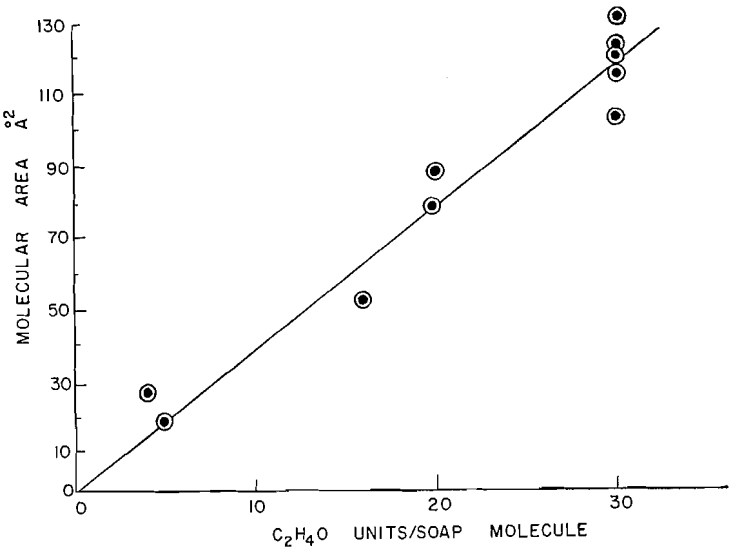


FIG. 2. Variation in area with ethylene oxide content.

Can. J. Chem. Downloaded from www.nrcresearchpress.com by 186.148.149.217 on 09/04/12
For personal use only.

oxide chain which is folded over the surface in a caterpillarlike manner. Such a view is supported by the results of Rosch (18), who suggested that chain contraction in polyethylene oxide chains is caused by the electrostatic attraction of the dipoles formed along the ethylene oxide chain. The actual dimensions of each fold may be determined only if the degree of hydration is known since the height of the fold should increase with increasing hydration. The work of Greenwald and Brown (19), showing a relation between salt content, temperature, and degree of hydration, suggests that measurements of area as a function of salt content would be instructive.

A set of dimensions was calculated for the unhydrated molecule from projections of Fischer–Hirschfelder models and the schematic representation in Fig. 3 was derived in which each fold is 16 Å high and contains 9 ethylene oxide units.

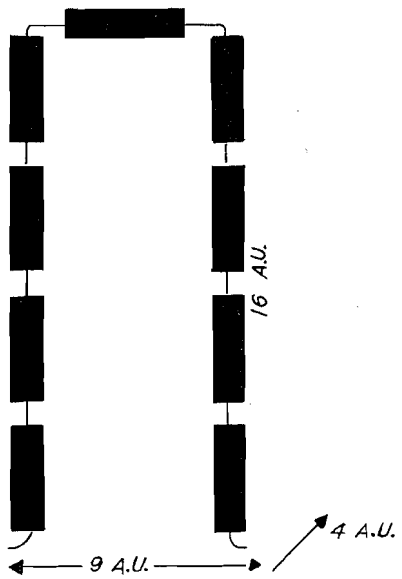


FIG. 3. Diagram of ethylene oxide chain at latex particle surface.

Comparison of Behavior at Air–Water and Polymer–Water Surface

Van Voorst Vader (20) has studied molecular areas of non-ionic and anionic soaps at the air–water interface. Measurements were made of saturation adsorptions, defined by Van Voorst Vader as the area occupied by a soap molecule at soap concentrations, where this area became independent of bulk concentration.

When non-ionic and ionic soaps were mixed, the molecular area of the non-ionic was not changed. The molecular area of the ionic soap was found to increase when non-ionic was added. This was explained by the increased ease of hydration of the ionic soap. When two dissimilar groups are present in the adsorbed soap layer, the water molecules are believed to be oriented to a configuration more suitable for co-ordination with ionic soap. Greater ease of co-ordination should increase the molecular area, since it will tend to decrease the affinity of the soap for the surface. The results we observed at the surface of latex particles, where the molecular area of the ionic soap is found to decrease in the presence of non-ionic, differ from Van Voorst Vader's results. Comparison of the

Can. J. Chem. Downloaded from www.nrcresearchpress.com by 186.148.149.217 on 09/04/12
For personal use only.

molecular areas of non-ionic soaps at the surface of the latex particles with those at the surface of the air–water interphase shows that non-ionic soaps have a greater affinity for the latter interphase. It appears reasonable to attribute the differing behavior of the ionic soap at the two interfaces to the differing affinity of the non-ionic for the surface.

ACKNOWLEDGMENTS

The authors appreciate permission of Polymer Corporation Limited to publish this report. The technical assistance of Mr. W. A. Rupar, electron microscopist, and Mr. V. Smith, chemist assistant, is acknowledged. Helpful discussions were held with Professor W. Heller of Wayne University, Detroit.

REFERENCES

1. S. H. MARON. J. Colloid Chem. **9**, 89 (1954).
2. L. M. KUSHNER and W. D. HUBBARD. J. Phys. Chem. **57**, 898 (1953).
3. C. R. BURY and J. BROWNING. Trans. Faraday Soc. **49**, 209 (1953). C. R. BURY. Phil. Mag. **4**, 980 (1927); C.A. 22:5245.
4. S. GLASSTONE. Textbook of physical chemistry. 2nd ed. D. Van Nostrand Company, Inc., New York. 1956. p. 967. P. DEBYE and E. HUCKEL. Physik. Z. **24**, 305 (1923).
5. B. A. PETHICA. Trans. Faraday Soc. **50**, 413 (1954).
6. G. D. MILES and L. SHEDLOVSKY. J. Phys. Chem. **48**, 57 (1944).
7. E. HUTCHINSON. J. Colloid Sci. **3**, 413 (1948).
8. C. H. JUDSON, A. A. LEREW, J. K. DIXON, and D. J. SALLEY. J. Phys. Chem. **57**, 916 (1953).
9. R. RUYSSEN and J. MAEBE. Ann. Rev. Phys. Chem. p. 400 (1955).
10. NATIONAL ANILINE CO. Private communication.
11. W. D. HARKINS and H. F. JORDAN. J. Am. Chem. Soc. **52**, 1751 (1930).
12. G. S. WHITBY (*Editor-in-Chief*). Synthetic rubber. John Wiley & Sons, Inc., New York. 1954. p. 359.
13. H. B. KLEVENS. J. Am. Oil Chem. Soc. **30**, 75 (1953).
14. L. HSIAO, H. DUNNING, and P. LORENZ. J. Phys. Chem. **60**, 657 (1956).
15. W. D. HARKINS, R. W. MATTOON, and M. L. CORRIN. J. Am. Chem. Soc. **68**, 220 (1946).
16. E. A. WILSON, J. R. MILLER, and E. H. ROWE. J. Phys. and Colloid Chem. **53**, 357 (1949).
17. S. H. MARON and M. E. ELDER. J. Colloid Sci. **9**, 347 (1954).
18. M. ROSCH. Kolloid Z. **150**, 153 (1957).
19. H. L. GREENWALD and G. L. BROWN. J. Phys. Chem. **58**, 825 (1954).
20. F. VAN VOORST VADER. The adsorption of surfactants at the liquid–liquid interphase. Doctoral thesis submitted to University of Utrecht, Utrecht, Holland.
21. COLUMBIAN CARBON CO., RESEARCH LABORATORIES. The particle size and shape of colloidal carbon as revealed by the electron microscope. 1940.

APPENDIX

This treatment is adapted from a similar problem with carbon black (21). The volume of N spherical particles is

$$V = \frac{\pi}{6}\sum_{i=1}^{N} X_i^3 = \frac{\pi}{6}\sum_{i=1}^{N} (\bar{X}-\rho_i)^3 = \frac{\pi}{6}\sum_{i=1}^{N} (\bar{X}^3 - 3\bar{X}^2\rho_i + 3\bar{X}\rho_i^2 - \rho_i^3)$$

where $\bar{X}$ is the average particle diameter.

Now

$$\sum_{i=1}^{N} \rho_i^2 = N\sigma^2,$$

where σ is the standard deviation, and, for symmetrical distribution,

$$\sum_{i=1}^{N} \rho_i = 0 = \sum_{i=1}^{N} \rho_i^3.$$

Can. J. Chem. Downloaded from www.nrcresearchpress.com by 186.148.149.217 on 09/04/12
For personal use only.

Appropriate combination of the three preceding equations gives

$$V = \pi \frac{N}{6} (\bar{X}^3 + 3\bar{X}\sigma^2).$$

In a similar way, it can be shown that the area of N particles is

$$\pi N (\bar{X}^2 + \sigma^2).$$

The area/volume ratio is then

$$\frac{6}{\bar{X}} \frac{(\bar{X}^2 + \sigma^2)}{(\bar{X}^2 + 3\sigma^2)}.$$

The maximum error introduced by the assumption of symmetry was calculated as 3% from the most unsymmetrical distributions obtained.

Can. J. Chem. Downloaded from www.nrcresearchpress.com by 186.148.149.217 on 09/04/12
For personal use only.

Can. J. Chem. Downloaded from www.nrcresearchpress.com by 186.148.149.217 on 09/04/12
For personal use only.

PROTON MAGNETIC RESONANCE MEASUREMENTS OF FORMAMIDE[1]

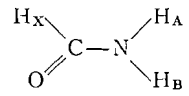
B. SUNNERS,[2] L. H. PIETTE, AND W. G. SCHNEIDER

ABSTRACT

The high-resolution proton resonance spectrum of formamide has been measured and analyzed. Quadrupole broadening of the resonance signals due to the N^{14} nucleus was eliminated by substitution of the isotopic nucleus N^{15}. Twenty-four lines were resolved in the spectrum, which is consistent with restricted rotation about the C—N bond. The non-equivalence of the two protons in the $N^{15}H_2$ group is characterized by a smaller screening constant and a greater spin–spin interaction of the proton which is in the *trans* position relative to the carbonyl group. It is suggested this difference in the spin coupling of the two protons may be associated with different N—H bond lengths. Pronounced changes in the chemical shifts and spin-coupling constants result when formamide is dissolved in dilute solution in water and acetone. In water solution the relative magnitudes of the spin coupling of the two protons in the NH_2 group is reversed from that observed in pure formamide and the coupling of the aldehyde proton to N^{15} varies by nearly 50%. Heating of formamide above room temperature causes rotation of the NH_2 group as well as proton exchange between neighboring molecules. The two effects could be separated. From the observed changes in the proton spectra as a function of temperature the barrier hindering rotation (measured in a 10 mole % solution of formamide in acetone) was found to be 18±3 kcal/mole. The activation energy for proton exchange in pure liquid formamide was found to be 10±3 kcal/mole.

INTRODUCTION

Formamide is generally regarded as an approximately planar molecule. In the absence of free rotation about the C—N bond, the proton resonance spectrum may be expected to be of the type ABX (1) containing a minimum of 12 lines. Assuming the two protons on the nitrogen atom are only slightly non-equivalent the three protons may be labelled as follows:



The observed spectrum of ordinary formamide contains only a broadish doublet partially overlapped by a very broad signal arising from the NH_2 group. The incomplete resolution and the broad nature of the lines derive from the quadrupole coupling of the N^{14} nucleus. This difficulty has been partially overcome by Piette, Ray, and Ogg (2) by use of the double-irradiation technique (3) to decouple the N^{14} nucleus. The resulting spectrum showed six lines of which four could be assigned to the "aldehyde" hydrogen and yielded the coupling constants corresponding to the spin interaction with the two protons in the amide group. The spectrum of the latter could not be completely resolved presumably because of incomplete saturation of the N^{14} nucleus. In the present work an alternative approach has been followed. Quadrupole broadening by N^{14} was eliminated by substitution of the nitrogen isotope N^{15}. Since this has spin $I = \frac{1}{2}$, sharp-line proton signals result, permitting a complete resolution and analysis of the spectrum as well as a study of proton exchange behavior and internal rotation about the C—N bond.

[1]*Manuscript received January 4, 1960.*
Contribution from the Pure Chemistry Division, National Research Council of Canada, Ottawa, and Varian Associates, Palo Alto, California.
Issued as N.R.C. No. 5606.
[2]*National Research Council Postdoctorate Fellow, 1957–59.*

Can. J. Chem. Downloaded from www.nrcresearchpress.com by 186.148.149.217 on 09/04/12
For personal use only.

EXPERIMENTAL

Two isotopically substituted compounds, $HCON^{15}H_2$ and $DCON^{15}H_2$, prepared by Dr. L. Leitch, Pure Chemistry Division, National Research Council, were studied. The formamide-N^{15} was prepared from ethyl formate and ammonia-N^{15}, whereas the deuterated compound was similarly obtained from deuterated ethyl formate. The pure samples (containing at least 95% N^{15}) were vacuum-distilled into 5-mm O.D. glass sample tubes, which were then sealed.

The proton resonance spectra were recorded at 40 Mc/s and at 60 Mc/s with a Varian V-4300 high-resolution spectrometer. Satisfactory resolution of the spectrum of the deuterated compound was obtained at both frequencies. However, the 40-Mc/s spectrum of the undeuterated compound was unsatisfactory for a complete analysis of the spectrum due to extensive overlapping of individual lines. The 60-Mc/s spectrum showed 20 (and in some cases 21) resolved lines out of the possible 24.* Since the spectrum extended over a wide range (~122 cycles/sec), measurement of the more widely separated line spacings tend to be somewhat more inaccurate due to residual drift in the instrument. Where possible, some lines were checked by superposition of sidebands on the oscilloscope screen but most separations were obtained with the aid of sidebands recorded with the spectrum. A further check was provided by superposing a signal from another part of the spectrum on a given signal. This signal was then repeatedly traversed and recorded, the frequency being adjusted to maximize the signal. For well-resolved signals this procedure permits the determination of signal separation to an accuracy of about 0.1 cycle/sec.

RESULTS

The proton resonance spectrum of $DCON^{15}H_2$ recorded at 60 Mc/s is shown reproduced in Fig. 1. If the two protons on the nitrogen atom are non-equivalent, a simple four-line AB-type spectrum is to be expected. Each line of this spectrum would, however, have a large splitting due to spin coupling with N^{15}. It is apparent that the observed spectrum contains additional (triplet) splitting due to the deuterium atom ($I = 1$), but this splitting is observable only on proton H_B, which is in the *trans* position relative to the deuterium atom. The value of the coupling constant, J_{DB}, is 2.1 cycles/sec. From the ratio of the nuclear gyromagnetic ratio of the proton and deuteron, the corresponding proton–proton coupling is calculated to be about 13.7 cycles/sec, in fair agreement with the value reported by Piette, Ray, and Ogg (2). This therefore identifies the signals of proton H_B, which appear at a higher field than those of proton H_A. With this assignment,† a complete analysis of the spectrum yields the chemical shift and spin-coupling constants shown in Table I.

An interesting feature of the above spectrum (cf. Fig. 1) is the noticeably larger separation of the H_A and H_B signals in the low-field half of the spectrum compared with those in the high-field half. The chemical shift, $\nu_0\delta_{AB}$, must of course be identical in both halves of the spectrum. It must be concluded therefore that the spin interaction

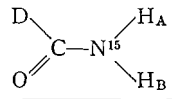
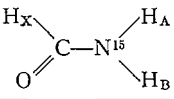
*In a 10 mole % solution of $HCON^{15}H_2$ in acetone all 24 lines of the spectrum could be resolved.

†As in reference 2, the assignment of signals in the spectrum to protons H_A and H_B is made on the assumption that trans coupling constants are much greater than cis coupling constants. This relationship of the coupling constants is well established for olefinic compounds (7, 8) and may be expected to hold also in formamide which is only slightly nonplanar. Moreover, the proton assignment arrived at on the basis of this assumption implies a slightly smaller shielding of the H_A proton compared with that of H_B, which is consistent with the order to be expected from the polar effects of the carbonyl group in the molecule (see below).

of proton H_A with the N^{15} nucleus is greater than that of H_B. The difference in the spin-coupling constants is about 4 cycles/sec.

TABLE I

Proton chemical shifts* and spin-coupling constants of formamide (in cycles/sec)

			8 mole % $HCON^{15}H_2$ in water	10 mole % $HCON^{15}H_2$ in acetone
$\nu_0\delta_{AB}$	12.1	12.0	20.5	12.8
$\nu_0\delta_{AX}$	—	−40.0	−25.3	−64.9
J_{AB}	2.5	2.4	2.3	2.9
J_{AX}	—	2.1	2.1	1.7
J_{BX}	—	12.9	13.6	13.5
J_{DB}	2.1	—	—	—
J_{NA}	91.6	92.0	91.9	91.0
J_{NB}	88.0	88.0	95.4	88.0
J_{NX}	—	19.0	23.3	16.4

*At 60 Mc/s.

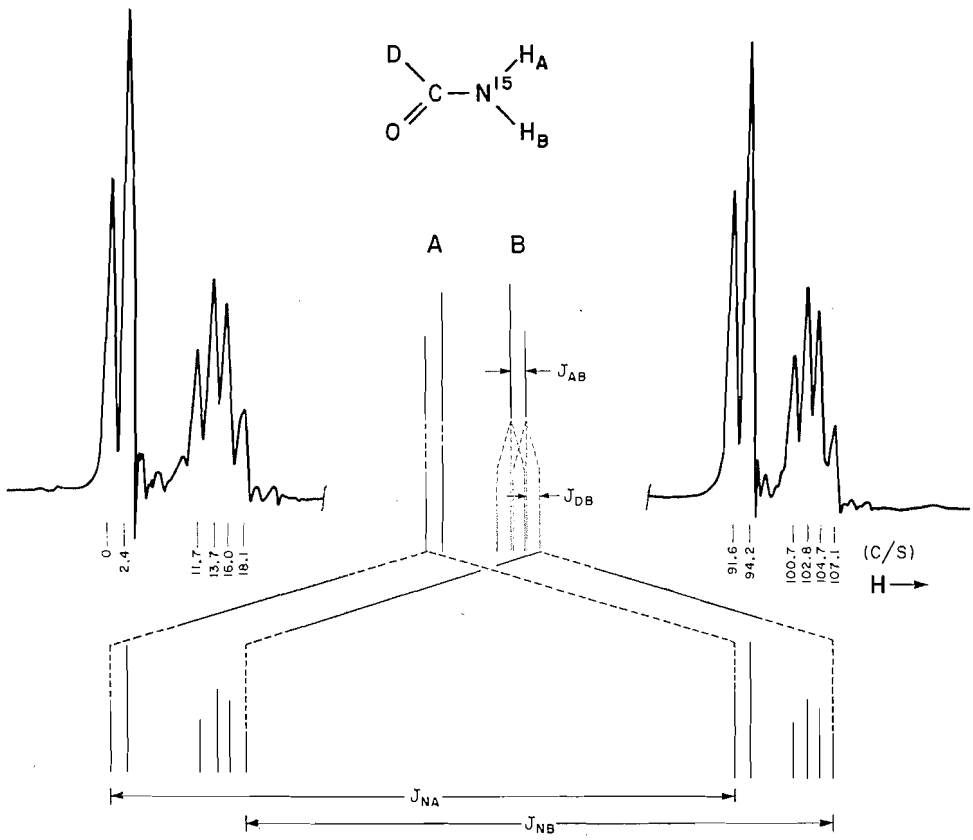


FIG. 1. Proton resonance spectrum of $DCON^{15}H_2$ at 60 Mc/s.

Can. J. Chem. Downloaded from www.nrcresearchpress.com by 186.148.149.217 on 09/04/12
For personal use only.

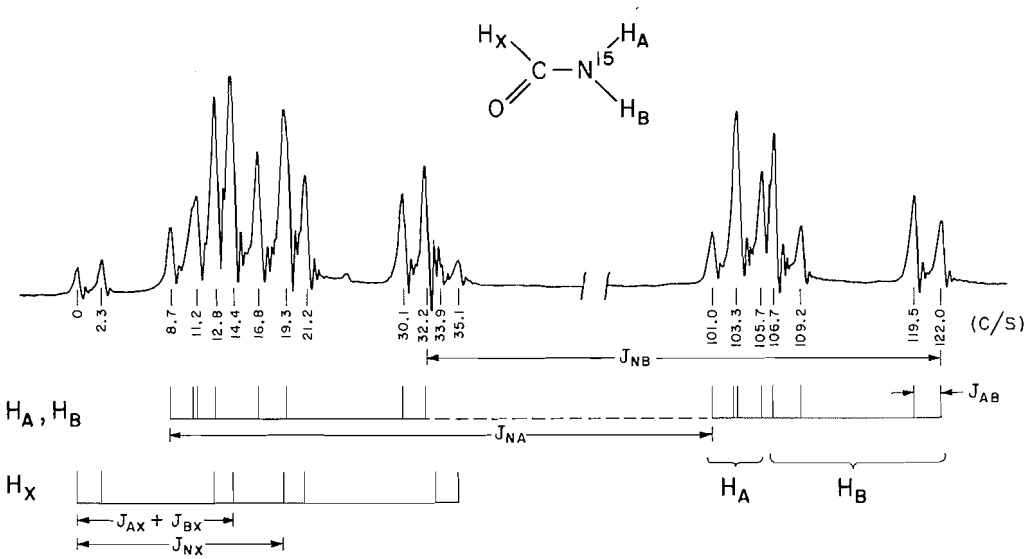


FIG. 2. Proton resonance spectrum of $HCON^{15}H_2$ at 60 Mc/s. The assignment of lines is indicated schematically at the bottom of the spectrum.

Figure 2 shows the complete spectrum of $HCON^{15}H_2$, at 60 Mc/s. If each signal is split by N^{15} the spectrum should contain at least 24 lines. Of these, 20 are clearly resolved. Unfortunately the large splitting of protons H_A and H_B by the N^{15} nucleus causes half of the AB part of the spectrum to be superimposed on the X part of the spectrum (H_X signals). The latter shows a much smaller splitting by the N^{15} nucleus. The assignment of the spectrum is indicated in Fig. 2. The analysis of the spectrum was carried out on the basis of an ABXY system, where Y is the N^{15} nucleus, and assuming the coupling constants J_{AY} and J_{BY} (designated J_{NA} and J_{NB} in Table I) to be unequal. Since J_{AY} and J_{BY} are large, this leads to an effective "chemical shift" of the H_A and H_B nuclei in the low-field and in the high-field spectra of $\nu_0\delta_{AB}+\frac{1}{2}(J_{AY}-J_{BY})$ and $\nu_0\delta_{AB}-\frac{1}{2}(J_{AY}-J_{BY})$ respectively. The X spectrum consists of two sets of four lines. The outer members in each set are separated by $(J_{AX}+J_{BX})$, whereas the separation of the corresponding lines between the two sets is J_{XY} (indicated by J_{NX} in Fig. 2). The separation between the inner lines of the low-field quartet is $2|A_+-A_-|$ and that of the inner lines of the high-field quartet is $2|B_+-B_-|$, where

$$[1] \qquad A_\pm = \tfrac{1}{2}\{[\nu_0\delta_{AB}+\tfrac{1}{2}(J_{AY}-J_{BY})\pm\tfrac{1}{2}(J_{AX}-J_{BX})]^2+J_{AB}^2\}^{1/2},$$

$$[2] \qquad B_\pm = \tfrac{1}{2}\{[\nu_0\delta_{AB}-\tfrac{1}{2}(J_{AY}-J_{BY})\pm\tfrac{1}{2}(J_{AX}-J_{BX})]^2+J_{AB}^2\}^{1/2}.$$

The results of the analysis are given in the third column of Table I. The estimated error in the chemical shifts and spin-coupling parameters is about ± 0.15 cycle/sec. It was not possible to determine relative signs of the spin-coupling constants.

The spin-coupling interaction of the N^{15} nucleus is again found to be greater with proton H_A than with proton H_B. This is a rather unexpected result if the two protons are symmetrically disposed with respect to the C—N bond axis. A very probable interpretation is, however, suggested by a recent structure determination of formamide by Costain and Dowling (4) from the microwave spectrum of the vapor, which showed the molecule to be nonplanar. The NH_2 (amide) group was found to have a pyramidal

Can. J. Chem. Downloaded from www.nrcresearchpress.com by 186.148.149.217 on 09/04/12
For personal use only.

structure with a characteristic inversion frequency. Moreover the two N—H bonds have unequal lengths, that which is *trans* to the carbonyl group having a bond length of 1.000 Å while that of the other is 1.012 Å. This difference in bond lengths would seem to provide a simple explanation for the observed difference in the coupling constants J_{NA} and J_{NB} since it is reasonable to expect a greater spin-coupling interaction in the shorter bond.*

The relative screening constants of protons H_A and H_B may also be expected to be affected by the difference in the N—H bond lengths and bond hybridization and to make the two protons non-equivalent. However, there are undoubtedly other contributing factors to the screening constants. In the first place the results show the proton H_A to be less screened (resonance at lower field) than H_B. This is not the relative order to be expected if the N—H_A bond length is shorter than that of N—H_B. In the liquid state the molecules are strongly hydrogen-bonded which could conceivably alter the degree of planarity of the molecule and the N—H bond lengths from those determined in the gaseous state, thus altering the relative screening constants (and possibly also the spin-coupling constants). The polar effect of the carbonyl group will also contribute to the screening constants of protons H_A and H_B. This contribution will tend to reduce the screening of proton H_A in the isolated molecule (5) and will become further enhanced in the liquid due to the "reaction" field of the surrounding molecules (6).

The present results confirm the large (six-fold) difference between the *cis* and *trans* proton-coupling constants in formamide. The observed values, $J_{AX} = 2.1$ cycles/sec and $J_{BX} = 12.9$ cycles/sec, are in good agreement with those reported by Piette, Ray, and Ogg (2). The relatively small value of J_{AB} (2.4 cycles/sec) is comparable to the small proton–proton coupling constants observed for the gem hydrogens of substituted ethylenes (7).

Solutions of Formamide in Water and Acetone

Proton resonance spectra of an 8 mole % solution of $HCON^{15}H_2$ in water and of a 10 mole % solution in acetone were measured. The results are shown in Table I. Of particular interest are the changes in the chemical shifts and some of the spin-coupling constants compared with those observed in the pure liquid. All three systems are characterized by strong hydrogen-bonding interactions between the molecules and the observed changes in chemical shifts and spin-coupling constants must arise from the different nature of the interaction in the three systems. Changes in hydrogen-bonding interactions are known to produce large changes in proton chemical shifts, but ordinarily proton spin-coupling constants are not appreciably affected by such changes. In the present systems the spin-coupling constants show surprisingly large variations, amounting in one case, J_{NX}, to nearly 50%. Also for the water solution J_{NB} is increased by $\sim$7 cycles/sec and in this instance its magnitude exceeds that of J_{NA}, a reversal of the situation found in the other two systems. Such changes in the coupling constants, which are not well understood at present, may involve in the present example a change in the molecular geometry in addition to changes in molecular charge distributions. There are of course important differences in the nature of the hydrogen-bonding interactions in these systems. Thus in the acetone solution it may be supposed that the protons of the NH_2

This difference in the two coupling constants may also be modified to some extent by small differences in bond hybridization (see, for example, Muller and Pritchard, J. Chem. Phys. **31, 768 (1959) and Karplus and Grant, Proc. Natl. Acad. Sci. **45**, 1269 (1959)). The bond angles ∠ CNH_A and ∠ CNH_B are respectively 120°17′ and 117°11′ with the ∠ H_ANH_B being 119°22′ (ref. 4). Thus if the N—H_A bond has a slightly greater s-character than the N—H_B bond this could contribute to making J_{NA} slightly greater than J_{NB}. We are indebted to a referee for pointing out this possibility.*

Can. J. Chem. Downloaded from www.nrcresearchpress.com by 186.148.149.217 on 09/04/12
For personal use only.

group are strongly bonded to the acetone carbonyl group, leaving the carbonyl group in the formamide molecule itself relatively free. However, in a dilute solution in water the carbonyl group will be monopolized by the water protons, leaving the NH_2 protons to be bonded to the oxygen atoms of neighboring water molecules. The proton resonance spectrum of the water solution at room temperature showed no evidence of proton exchange of the amide protons.

Hindered Internal Rotation and Proton Exchange in Formamide

By analogy with dimethyl formamide, which has a relatively high barrier hindering rotation about the C—N bond (9, 10), an observable hindered rotation of the NH_2 group in formamide may be expected. The onset of the rotation will be characterized by a broadening and ultimate coalescence of lines in the proton spectrum. This does in fact occur when the pure compound is heated above room temperature. It is possible to demonstrate, however, that proton exchange involving the NH_2 groups also sets in and contributes to the observed signal broadening and coalescence. Proton exchange can be satisfactorily eliminated over the required temperature range by working with a dilute solution of formamide in acetone. Under these conditions the formamide molecules are relatively isolated from each other and are hydrogen-bonded to the acetone with which they cannot exchange.

In order to measure the barrier hindering rotation of the NH_2 group the proton spectrum of a 10 mole % solution of formamide in acetone was recorded at intervals of 2 or 3° C as the solution was progressively heated above room temperature. A few illustrative traces are reproduced in Fig. 3. It may be noted that at 25° C all 24 lines of the spectrum are clearly resolved. By far the most striking changes which appear in the spectrum on raising the temperature are those that occur in the H_X spectrum, which consists of eight lines on the extreme left (low-field side) of the spectrum. As mentioned earlier these eight lines result from the N^{15} doubling of the ordinary four-line X spectrum (cf. Fig. 2). For the present purpose we need only consider the quartet at lowest field, i.e. the four lines on the extreme left of the spectrum in Fig. 3. The two outer lines in this quartet have the separation $|J_{AX}+J_{BX}|$ while the two inner lines are separated by $2|A_+-A_-|$, where A_+ and A_- are given by equation [1]. It is apparent from Fig. 3 that as the temperature is raised and internal rotation sets in, the two outer lines remain sharp and unaltered in position whereas the two inner lines broaden and ultimately coalesce. When the rotation of the NH_2 group becomes sufficiently rapid, the quantities $\nu_0\delta_{AB}$, J_{AB}, $(J_{AY}-J_{BY})$, and $(J_{AX}-J_{BX})$ all average to zero, and therefore the quantities A_+ and A_- (see eq. [1]) both become zero and the two inner lines must coalesce. However, the quantity $|J_{AX}+J_{BX}|$ is unaffected and the two outer lines remain unchanged. This sequence of changes converts the quartet to a triplet, the central component being doubly degenerate and separated by $\frac{1}{2}(J_{AX}+J_{BX})$ from the two outer lines. Thus the total formamide spectrum has been changed from one of type ABXY to one of type A_2XY by virtue of rapid rotation of the NH_2 group. This fact suggests that even at 98° proton exchange is still relatively unimportant. If proton exchange were rapid the final spectrum would have consisted of a doublet for the H_X signals, resulting from the N^{15} splitting, and a single line for the NH_2 group. It is apparent, however, that the traces at 75° and 98° in Fig. 3 have broader lines in the X spectrum which may be attributed to the onset of slow proton exchange at these higher temperatures. The progressive shift of the H_A and H_B signals toward higher field with increasing temperature results from increased dissociation of the hydrogen bonds formed by these hydrogens with the acetone solvent.

Can. J. Chem. Downloaded from www.nrcresearchpress.com by 186.148.149.217 on 09/04/12
For personal use only.

Can. J. Chem. Downloaded from www.nrcresearchpress.com by 186.148.149.217 on 09/04/12
For personal use only.

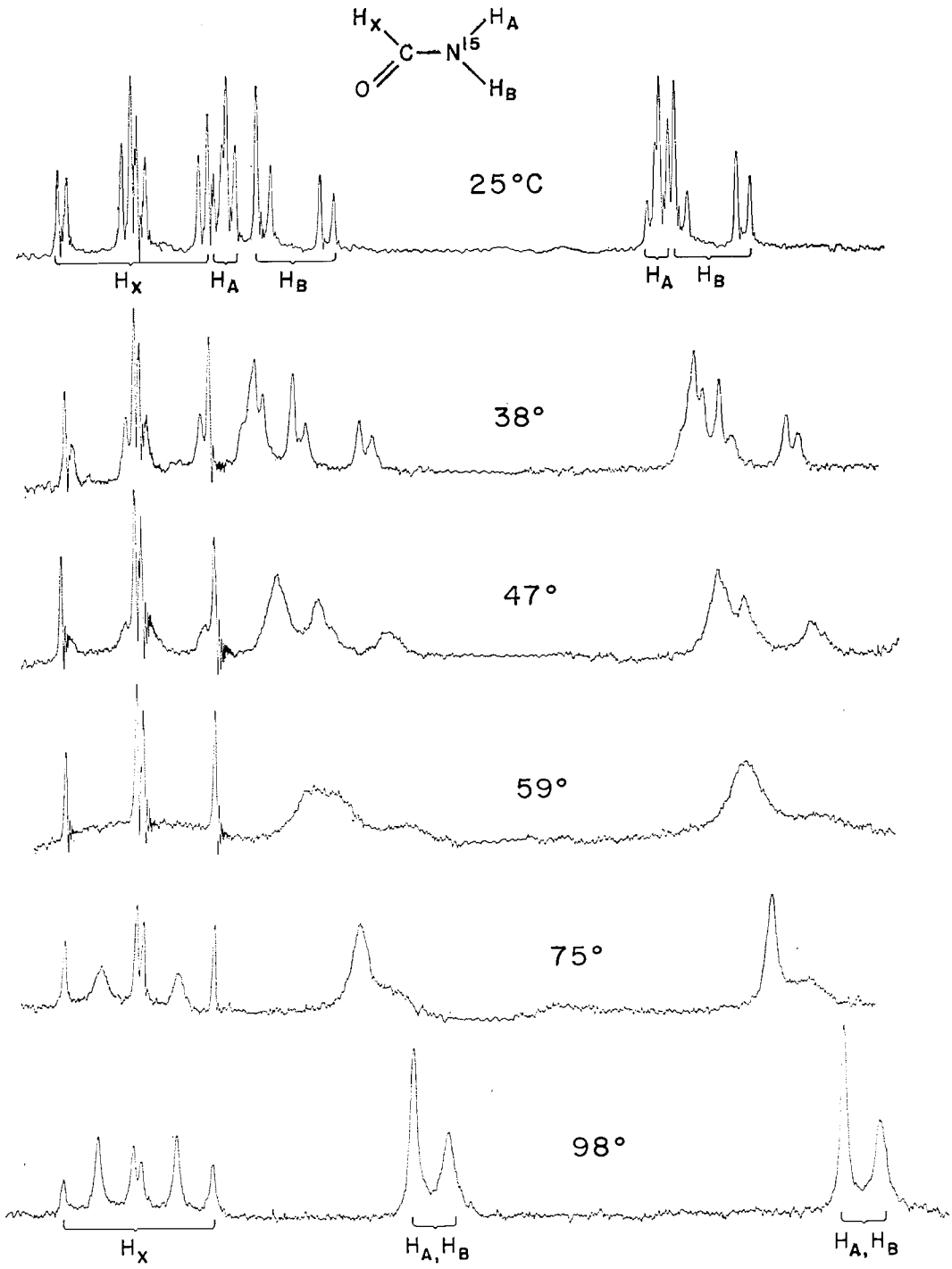


FIG. 3. Proton magnetic resonance spectrum of 10 mole % solution of $HCON^{15}H_2$ in acetone at various temperatures showing signal broadening and coalescence due to hindered rotation of the NH_2 group.

In order to evaluate the potential barrier hindering rotation, the lifetimes, τ, of the protons at positions H_A and H_B were evaluated from the broadening of the lines in the X spectrum from the simple relation

$$[3] \qquad \frac{1}{\tau} = \frac{1}{T_2'} - \frac{1}{T_2}$$

where $1/T_2'$ is taken as the half-band width of the broadened line and $1/T_2$ the effective line width in the absence of rotational broadening. The latter could be conveniently measured from the outer (unbroadened) lines in the X spectrum. To extend the range of observable τ values the additional relation (10)

$$[4] \qquad \tau = \frac{\sqrt{2}}{2\pi\Delta\nu}$$

was employed. Here $\Delta\nu$ (in cycles/sec) is the separation of appropriate spin multiplet peaks in the AB spectrum whose coalescence is observed. The data employed were obtained in the temperature range of 25° to 62° C. From a plot of $\ln \tau$ vs. $1/T$ the mean value of the rotational barrier was found to be 18 ± 3 kcal/mole.

Proton exchange measurements were carried out on samples of pure formamide rather than on the acetone solution. At higher temperatures, where internal rotation is already rapid, a further broadening and signal coalescence results from the onset of rapid proton exchange. Values of τ were evaluated with the aid of the relations given in equations [3] and [4]. A somewhat greater scatter of individual τ values compared with those obtained at lower temperatures was evident. The mean activation energy for proton exchange between formamide molecules was found to be 10 ± 3 kcal/mole.

REFERENCES

1. J. A. POPLE, W. G. SCHNEIDER, and H. J. BERNSTEIN. High resolution nuclear magnetic resonance. McGraw-Hill Book Co., New York. 1959. p. 132.
2. L. H. PIETTE, J. D. RAY, and R. A. OGG. J. Mol. Spectroscopy, **2**, 66 (1958).
3. A. L. BLOOM and J. N. SHOOLERY. Phys. Rev. **97**, 1261 (1955).
4. C. C. COSTAIN and J. M. DOWLING. J. Chem. Phys. In press.
5. A. D. BUCKINGHAM. Can. J. Chem. **38**, 300 (1960).
6. A. D. BUCKINGHAM, T. SCHAEFER, and W. G. SCHNEIDER. J. Chem. Phys. **32**, 158 (1960).
7. H. S. GUTOWSKY, M. KARPLUS, and D. M. GRANT. J. Chem. Phys. **31**, 1279 (1959).
8. M. KARPLUS. J. Chem. Phys. **30**, 11 (1959).
9. W. D. PHILLIPS. J. Chem. Phys. **23**, 1363 (1955).
10. H. S. GUTOWSKY and C. H. HOLM. J. Chem. Phys. **25**, 1228 (1956).

Can. J. Chem. Downloaded from www.nrcresearchpress.com by 186.148.149.217 on 09/04/12
For personal use only.

Can. J. Chem. Downloaded from www.nrcresearchpress.com by 186.148.149.217 on 09/04/12
For personal use only.

ELECTRON SPIN RESONANCE STUDIES OF THE RADIATION-INDUCED ADDITION OF HBr TO C_2H_4 IN THE SOLID STATE[1]

F. W. MITCHELL,[2] B. C. GREEN, AND J. W. T. SPINKS

ABSTRACT

Electron spin resonance measurements at 77° K have been used to study the hydrobromination of ethylene induced by γ irradiation of the solid mixture at liquid nitrogen temperatures. The evidence resulting from these studies has given valuable information regarding the reaction intermediates and has been used in formulating a likely reaction mechanism.

INTRODUCTION

The addition of hydrogen bromide to ethylene under the influence of γ rays has been previously studied by Armstrong and Spinks (1, 2). The reaction is a chain reaction in the gas, liquid, and solid states; for example, with a dose rate of 450 r per minute, an initial G value of about 10^5 was found for additions in the liquid phase. G values in the solid phase were appreciably lower, particularly for long irradiations at liquid nitrogen temperatures.

A free radical chain reaction has been suggested for the reaction. The present work describes additional experiments, emphasizing e.s.r. techniques, bearing on the suggested mechanisms.

EXPERIMENTAL

Purification of Materials

Cylinder HBr and C_2H_4 were passed through a P_2O_5 drying tube and then subjected to a number of bulb-to-bulb distillations under high vacuum at liquid nitrogen temperatures. Both were finally distilled from a bath at −78° C.

Apparatus

A general purpose high vacuum apparatus was used. After measurement the reactants were distilled into a simple reaction vessel constructed of 7-mm Pyrex tubing fitted with stopcock and joint. The volume of solid resulting from the usual amounts of reactants was very close to 0.5 ml.

Irradiations were conducted in a Dewar vessel of liquid nitrogen employing Co^{60} sources of both 90 curies and 1100 curies.

Gas chromatographic studies were made using various columns and introducing the reaction products in the gaseous form. Column temperature control was available.

Electron spin resonance studies were made with a Varian V 4500 spectrometer. A cavity and Dewar were constructed to enable studies to be performed at 77° K. Some quantitative spin measurements were attempted using a range of DPPH solutions in dry benzene as standards.

Hyperfine splittings and line widths were determined by means of a Varian standard supplied by the manufacturers. Ferrous sulphate dosimetry was employed for dose rate estimations.

Results

The normal experimental technique adopted was to mix the reactants after pressure measurements and condense them rapidly into the tip of the reaction vessel. After

[1]*Manuscript received January 21, 1960.*
Contribution from the Department of Chemistry, University of Saskatchewan, Saskatoon, Saskatchewan.
[2]*National Research Council Postdoctorate Fellow, 1958–1960.*

irradiation, the vessel was reattached to the vacuum line and allowed to warm up to room temperature. In agreement with the simple scheme,

$$C_2H_4 + HBr \rightarrow C_2H_5Br,$$

equimolar amounts of reactants undergo a 50% pressure reduction for 100% addition (2). This does not preclude the formation of small amounts of other products, and accordingly the nature of the reaction products was further investigated by gas chromatography.

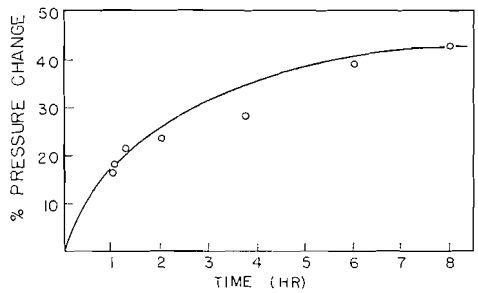


FIG. 1. Pressure change curve.

Figure 1 depicts the percentage pressure change plotted against time for single irradiations of equimolar solid mixtures. It can be seen that a 50% change could not be achieved (though stepwise irradiation of the same mixture with interim melting and cooling results in such a change). A 13-hour single irradiation gave a result slightly lower than that at 8 hours so that the limiting value of percentage of ΔP may be taken as about 42%.

Gas Chromatography

Columns of dinonyl phthalate and silicone Hyvac grease on inert supports were used for the detection of products. Runs in which at least 80% addition had occurred were taken for analysis.

The principal product was clearly ethyl bromide, which had a retention time of 16 minutes at room temperature in a 4-ft DNP column. GLC revealed that attempts to separate mixtures of HBr, C_2H_4, and C_2H_5Br by fractionation at $-120°$ C had been unsatisfactory.

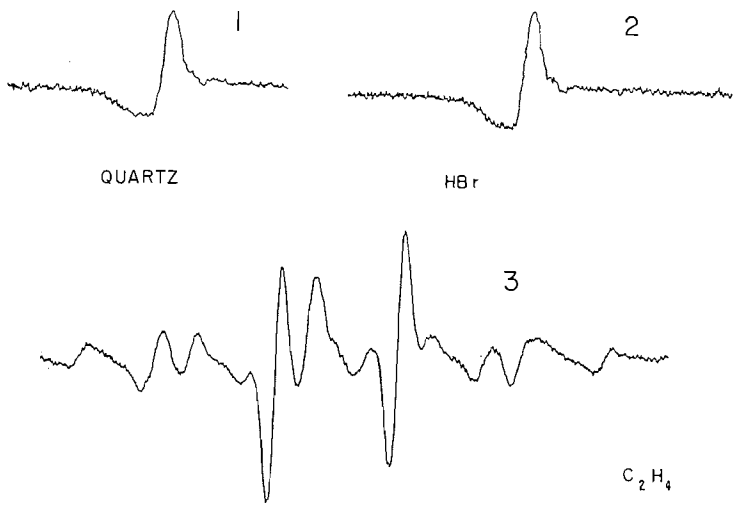
Of interest was the appearance of unknown peaks after 2 minutes at 26° C on the DNP column and 16 minutes at 50° C on the silicone column. Quantitative measurements based on relative peak areas indicated both to be present in a ratio of about 1:4000 compared with the amount of ethyl bromide. A sample of ethylene dibromide was taken and shown to have a retention time identical with that of one of the unknown peaks (16-minute one). The other unknown has a retention time suggesting that it is butene-1.

Electron Spin Resonance Studies

Samples of C_2H_4, HBr, C_2H_5Br, and C_2H_4–HBr mixtures were irradiated at 77° K in a 1100-curie cobalt-60 unit in 5-mm quartz tubing. Previous to irradiation, they were measured and degassed on the vacuum line. The dose rate for all samples was 1545 r per minute, or 8.42×10^{16} ev/g per minute.

The samples which had been irradiated in the dark were then transferred within 1 second to a specially constructed light-tight Dewar vessel, containing liquid nitrogen,

Can. J. Chem. Downloaded from www.nrcresearchpress.com by 186.148.149.217 on 09/04/12
For personal use only.



TRACE 1. Irradiated quartz.
TRACE 2. Irradiated hydrogen bromide.
TRACE 3. Irradiated ethylene.

the tip of which extended into the spectrometer cavity. Some examples of the traces obtained are given.

Trace 1 depicts the thermoluminescence peak arising from an evacuated quartz blank which had been given a dose of 9.26×10^5 r. The entire quartz trace was found to disappear on warming to room temperature. Bleaching with tungsten light at 77° K resulted in an almost complete disappearance of the trace.

Trace 2 arises from 118 cc NTP of HBr at identical spectrometer settings with trace 1 and results from the same dose, i.e., 9.26×10^5 r. No evidence of radical absorption from the sample can be seen. More extensive investigation revealed absorption due to the presence of H atoms but not due to anything else.

Trace 3 was obtained from 118 cc NTP of C_2H_4. On integration and correction for the central thermoluminescence peak (due to the quartz, i.e., trace 1), the corrected absorption curve is as in Fig. 2. The outside line separation was 145.2 gauss and the quartet

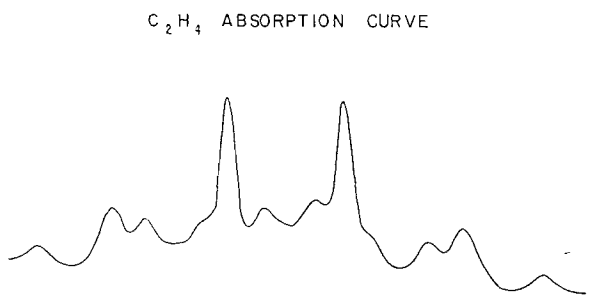


FIG. 2. True ethylene absorption curve (corrected).

separation 87 gauss, the average separation between the quartet peaks being 29 gauss. This appears to correspond well with the quartet of triplets reported by Smaller and Matheson (3), resulting from the γ irradiation of ethane, ethylene, and ethyl chloride (quartet separation 79 gauss).

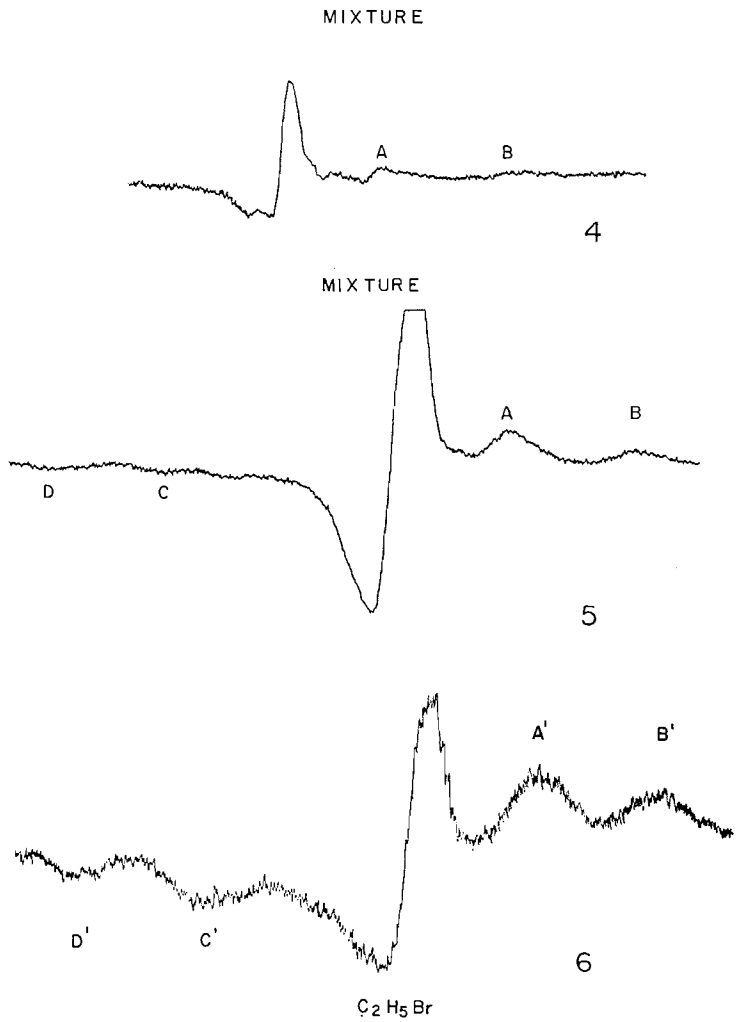
Can. J. Chem. Downloaded from www.nrcresearchpress.com by 186.148.149.217 on 09/04/12
For personal use only.

The number of ethylene molecules present was 3.18×10^{21}. Comparison of trace 3 with a standard DPPH sample in dry benzene indicated that there were 5.4×10^{16} spins present. If the trace arises from ethyl radicals, this indicates their concentration to be about 1 in 5×10^{4} of the ethylene molecules present. The total dose was 9.26×10^{5} r or 0.85×10^{19} ev. Assuming no ethyl radical decay, this gave a G value for their formation of 0.63.

Trace 4 was obtained from a mixture of 59 cc C_2H_4 and 59 cc HBr given a dose of 9.26×10^{5} r. All evidence of ethyl radicals arising in trace 3 was absent. The small 'peaks' at A and B arise from radical structure but are very weak.

Traces 1–4 were made at identical power and spectrometer settings and, as such, are directly comparable.

Trace 5 arises at higher gain settings than trace 4 and brings out the peaks A and B more clearly. An unsuccessful attempt was made to split peak A into hyperfine lines.

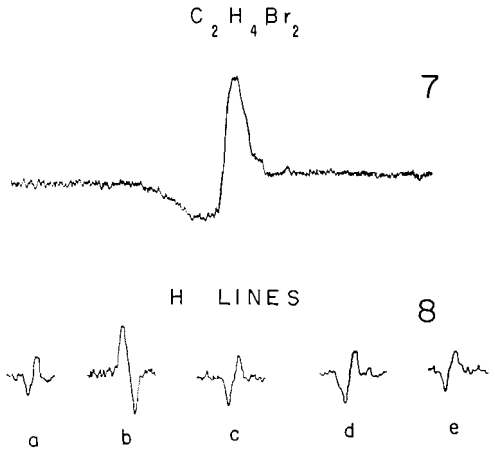


TRACE 4. Irradiated equimolar ethylene – hydrogen bromide mixture.
TRACE 5. As trace 4; higher spectrometer settings.
TRACE 6. Irradiated ethyl bromide.

Can. J. Chem. Downloaded from www.nrcresearchpress.com by 186.148.149.217 on 09/04/12
For personal use only.

Further very weak "peaks" at C and D appear to be present in this trace. The splitting from A to C is 81.6 gauss and from A to B 30.5 gauss.

Trace 6 arises from a sample of ethyl bromide which was degassed, sealed under vacuum, and given a dose of 4.63×10^5 r, i.e., half that of the other samples. The positions of A′, B′, C′, and D′ are identical with those of A, B, C, and D in trace 5. The difference in appearance arises, no doubt, from differing amounts of radicals, but it appears likely that the same radical species is involved in both cases.



TRACE 7. Irradiated 1,2-dibromoethane.
TRACE 8. H lines: (*a*) quartz, (*b*) C_2H_4, (*c*) HBr, (*d*) C_2H_4–HBr, (*e*) $C_2H_4Br_2$.

Trace 7 was obtained from a sample of dibromoethane which had been degassed, sealed under vacuum, and given a dose of 9.26×10^5 r. Surprisingly, no trace of radical structure was observable, and the trace is identical with that arising from quartz treated similarly.

Trace 8 illustrates the high field H lines from (*a*) a quartz blank, (*b*) 118 cc NTP C_2H_4, (*c*) 118 cc NTP HBr, (*d*) 118 cc NTP equimolar C_2H_4–HBr mixture, (*e*) dibromoethane treated as described above. It can be tentatively inferred that the H atom concentration was highest in the ethylene samples, although the unexpected H line resulting from an evacuated quartz blank makes it impossible to ascertain from trace 8 whether H atoms are present in samples other than ethylene. Comparison with a standard sample of DPPH in benzene suggested that the H atom concentration in ethylene was a factor of the order of 10^3 lower than the ethyl radical concentration in the same sample. This is in partial disagreement with Matheson (3), who did not find any H atom doublet for ethylene but did find that at 77° K the hydrogen atom doublet for irradiated ethane was relatively weak compared with the ethyl radical trace.

DISCUSSION

The foregoing work helps to clarify the reaction mechanism suggested by Armstrong and Spinks (1). The presence of small amounts of ethylene dibromide among the end products suggests the reaction:

$$Br + C_2H_4Br \rightarrow C_2H_4Br_2 \qquad [1]$$

as a main termination reaction. The presence of butene-1, if confirmed, would possibly indicate the reaction

$$C_2H_5 + C_2H_3 \rightarrow C_4H_8. \qquad [2]$$

Can. J. Chem. Downloaded from www.nrcresearchpress.com by 186.148.149.217 on 09/04/12
For personal use only.

The main evidence of interest stems from the e.s.r. work which indicates that ethyl radicals result from the irradiation of ethylene and that H atoms result from the irradiation of ethylene. Of great interest is the fact that irradiation of C_2H_4–HBr mixtures shows no measurable trace due to ethyl radicals, indicating that the C_2H_5 radical reacts very rapidly even at liquid nitrogen temperatures. That the radical species present in a C_2H_4–HBr mixture and C_2H_5Br after irradiation should be identical (traces 5 and 6) is also of extreme interest and could possibly be taken to indicate that the chain reaction had already occurred before warming. However, the difficulty of diffusion of large radicals such as C_2H_4Br in the mixture and the energy requirements of the chain propagating steps would make this unlikely at 77° K. A more satisfactory suggestion would be that the radical species involved is C_2H_4Br, which would be the most likely radiation product of C_2H_5Br and which could arise in C_2H_4–HBr mixtures at 77° K in the manner indicated below. Nothing is known of the e.s.r. structure of such a radical at present, but the presence of a bromine isotope with a nuclear spin of 3/2 would undoubtedly make it complex.

As has been mentioned above, an extensive examination of the trace resulting from irradiated HBr revealed no absorption other than that arising from the quartz sample tube. It would also be difficult to state that the hydrogen line arising in trace 8 resulted from any higher concentration of hydrogen atoms than was present in the quartz blank. Bromine atoms, if present, would be paramagnetic and give rise to e.s.r. absorption. It would thus appear likely that neither hydrogen nor bromine atoms produced in the primary radiation processes had escaped recombination. The following series of reactions were proposed by Zubler, Hamill, and Williams (4) to be consistent with their studies on the X radiolysis of HBr.

$$HBr \rightarrow HBr^+ + e \quad [3]$$

$$e + HBr \rightarrow H + Br^- \quad [4]$$

$$Br^- + HBr^+ \rightarrow H + 2Br \quad [5]$$

$$H + HBr \rightarrow H_2 + Br \quad [6]$$

In the solid phase at 77° K the above mechanism is a likely one, and dissociative electron capture by the parent ion will be of increased importance.

$$HBr^+ + e \rightarrow HBr^* \quad [7a]$$

$$HBr^* \rightarrow H + Br \quad [7b]$$

The γ irradiation of pure ethylene might be expected to occur as follows:

$$C_2H_4 \rightarrow C_2H_4^+ + e \quad [8]$$

$$C_2H_4^+ + e \rightarrow C_2H_4^* \quad [9a]$$

$$C_2H_4^* \rightarrow C_2H_3 + H \quad [9b]$$

$$C_2H_4^+ + C_2H_4 \rightarrow C_3H_5^+ + CH_3 \quad [10]$$

Again reaction [9*a*] is a more likely one in the solid phase. The charge transfer reaction [10] which was proposed by Field *et al.* (5) in the electron radiolysis of ethylene can doubtless result in other alternative products.

The e.s.r. studies (traces 3 and 8) strongly suggest that the only radical species present is the ethyl radical and that H atoms are present in the solid phase before warming. Ethyl radicals could arise from the reaction,

$$H + C_2H_4 \rightarrow C_2H_5, \quad [11]$$

Can. J. Chem. Downloaded from www.nrcresearchpress.com by 186.148.149.217 on 09/04/12
For personal use only.

which is likely to have a very low activation energy (6) and which has been shown to occur at liquid air temperatures (7). This mechanism receives strong support from recent work (12, 13) which has indicated that hydrogen atoms readily add to olefins at 77° K to produce alkyl radicals in a manner which is likely to result in their stabilization in the matrix.

If reaction [9*b*] is the chief source of hydrogen atoms, the ethylenyl radical, C_2H_3, presumably disappears by some radical combination reaction such as (2).

In the irradiation of ethylene – hydrogen bromide mixtures energy transfer processes can readily occur.

$$HBr^+ + C_2H_4 \rightarrow HBr + C_2H_4^+ \qquad [12a]$$

$$HBr^* + C_2H_4 \rightarrow HBr + C_2H_4^* \qquad [12b]$$

Ethylene, having a ground state containing a considerable number of states of higher multiplicity than the singlet, is a particularly effective quencher (8).

Traces 4 and 5 indicate that the ethyl radicals arising in the irradiation of pure ethylene are not present in the mixture at 77° K. A simple explanation of their disappearance would be the occurrence of the combination reaction,

$$C_2H_5 + Br \rightarrow C_2H_5Br, \qquad [13a]$$

which is likely to have zero activation energy.

Alternatively, the ethyl radical might disappear by the hydrogen abstraction reaction

$$C_2H_5 + HBr \rightarrow C_2H_6 + Br. \qquad [13b]$$

This has been calculated to have a low activation energy (2 kcal) by Anderson *et al.* (9). The presence of excited HBr molecules would enhance the likelihood of reaction [13*b*].

The identical nature of the radical species present in ethyl bromide and the mixture (traces 5 and 6) might very well be due to the presence of the C_2H_4Br radical, which is the most probable common radiation product of the two systems at 77° K.

Quantitative observations based on DPPH standards suggest that the number of radical spins in the irradiated mixture is very much less than 5.4×10^{16}, which is the calculated value for the ethyl radicals in trace 3.

Vaughan *et al.* (10) proposed a chain mechanism for the photo-addition of hydrogen bromide to ethylene in which the propagating steps were

$$Br + C_2H_4 \rightarrow C_2H_4Br, \qquad [14]$$

$$C_2H_4Br + HBr \rightarrow C_2H_5Br + Br. \qquad [15]$$

It is most probable that the same propagating mechanism is involved in the radiation-induced addition being studied here and the occurrence of reaction [14] at 77° K could obviously account for the presence of C_2H_4Br radicals in the mixture before warming. The activation energy for this reaction has been shown to be zero from studies on the photobromination of ethylene (11).

Evidence exists to show that ethylene and hydrogen bromide form a loose compound ($C_2H_4.HBr$) on condensing the mixture in the solid phase. Thus, the occurrence of the ionization and electron capture reactions [8] and [4], respectively, might well, as a result of proximity, favor the charge neutralization process

$$C_2H_4^+ + Br^- \rightarrow C_2H_4Br \qquad [16]$$

which, therefore, would be an alternative source of C_2H_4Br radicals.

Can. J. Chem. Downloaded from www.nrcresearchpress.com by 186.148.149.217 on 09/04/12
For personal use only.

Termination of the reaction chain can occur in a number of ways as suggested by Armstrong and Spinks in reactions [17] to [20*b*] of their paper (1).

The nature of the radical species present in irradiated ethyl bromide and C_2H_4–HBr mixtures together with other alkyl halides, and the reasons for the somewhat abnormal appearance of their e.s.r. traces are being further investigated. Temperature control above 77° K of samples examined by e.s.r. techniques would obviously be very informative with regard to the warm-up of the irradiated solid mixture.

ACKNOWLEDGMENTS

We are grateful to Dr. J. Bardwell for assistance with the gas chromatography measurements and to the Atomic Energy Control Board for financial assistance. One of us (F. W. M.) is indebted to the National Research Council of Canada for the award of a Postdoctorate Fellowship.

REFERENCES

1. D. A. Armstrong and J. W. T. Spinks. Can. J. Chem. **37**, 1210 (1959).
2. D. A. Armstrong and J. W. T. Spinks. Can. J. Chem. **37**, 1002 (1959).
3. B. Smaller and M. S. Matheson. J. Chem. Phys. **28**, 1169 (1958).
4. E. G. Zubler, W. H. Hamill, and R. R. Williams, Jr. J. Chem. Phys. **23**, 1263 (1955).
5. F. H. Field, J. L. Franklin, and F. W. Lampe. J. Am. Chem. Soc. **79**, 2419 (1959).
6. E. W. R. Steacie. Atomic and free radical reactions. Reinhold Publishing Corp., New York. 1954.
7. K. H. Geib and P. Harteck. Ber. **66**B, 1815 (1933).
8. M. Burton and S. Lipsky. J. Phys. Chem. **61**, 1461 (1957).
9. H. C. Anderson, G. B. Kistiakowsky, and E. R. Van Artsdalen. J. Chem. Phys. **10**, 305 (1942).
10. W. F. Vaughan, F. F. Rust, and T. W. Evans. J. Org. Chem. **7**, 477, 491 (1942).
11. H. Schmitz, H. J. Schumacher, and A. Jager. Z. physik. Chem. B, **51**, 281 (1942).
12. R. Klein and M. D. Scheer. J. Am. Chem. Soc. **80**, 1007 (1958).
13. R. Klein and M. D. Scheer. J. Phys. Chem. **62**, 1011 (1958).

Can. J. Chem. Downloaded from www.nrcresearchpress.com by 186.148.149.217 on 09/04/12
For personal use only.

Can. J. Chem. Downloaded from www.nrcresearchpress.com by 41.223.56.140 on 09/04/12
For personal use only.

POTASSIUM DERIVATIVES OF FLUORENE AS INTERMEDIATES IN THE PREPARATION OF C_9-SUBSTITUTED FLUORENES

I. THE PREPARATION OF 9-FLUORENYL POTASSIUM AND THE INFRARED SPECTRA OF FLUORENE AND SOME C_9-SUBSTITUTED FLUORENES[1]

G. W. H. Scherf and R. K. Brown

ABSTRACT

9-Fluorenylpotassium and 9,9-fluorenyldipotassium have been prepared from the reaction of potassium metal with fluorene in dioxane. These organometallic compounds upon reaction with alkyl and aralkyl halides gave 9-substituted fluorenes.

Six different absorption bands in the spectrum of fluorene could be associated with the methylene group: 2930, 1400, 1298, 952, and 692 cm^{-1}. Evidence for this assignment was obtained from deuteration of the organometallic compounds of fluorene and from 9-substituted fluorenes.

INTRODUCTION

During a study of the reactions of certain substances with fluorene it was found desirable to have at hand direct and relatively simple methods for the preparation of C_9-mono- and C_9-di-substituted fluorenes uncomplicated by contaminating side reactions due to addition of bases (1) usually required to effect reaction at the methylene group. In addition, quite indispensable would be a reliable and rapid method for distinguishing between mono- and di-substitution at C_9, which would thus simplify the assessment of mixtures of 9-mono- and 9-di-substituted fluorenes and permit the investigator to follow more conveniently the separation of such mixtures. It was thought that monovalent metal "salts" of fluorene might lend themselves readily to the attainment of the first goal, while infrared spectroscopy should be most admirably suited to the second. Both the literature evaluation and the experiments described in this report show that this is indeed the case.

9-SUBSTITUTED FLUORENES FROM 9-FLUORENYLSODIUM AND 9,9-FLUORENYLDIPOTASSIUM

Synthesis of C_9-substituted fluorenes has been reviewed by Rieveschl and Ray (2). Generally, alkaline conditions promote the transient formation of the 9-fluorenyl carbanion which then by nucleophilic attack upon compounds of suitable structure produces the desired structure (2, 3). Equimolar proportions of fluorene, base, and substrate are expected to form 9-monosubstituted fluorenes, but there are reports which show that di- rather than mono-substitution has in fact occurred (4).

The formation of 9-fluorenylsodium by direct reactions between fluorene and metallic sodium, although reported in the patent literature, has been found highly unsatisfactory both in this laboratory and by other workers (3). However, Greenhow *et al.* describe the preparation of 9-fluorenylsodium in good yield by the reaction of sodamide with fluorene in boiling decalin (3). Through this organometallic compound the C_9-monosubstituted fluorenes are accessible (3, 5–8). Indirect preparation of 9-fluorenylsodium via interchange with triphenylmethyl sodium (9) and, more conveniently, of 9-fluorenyllithium from alkyllithium compounds (10, 11) provide other routes, though somewhat more complicated, to the preparation of 9-substituted fluorenes. The Grignard reagent, 9-fluorenyl-

[1]*Manuscript received January 4, 1960.*
Contribution from the Department of Chemistry, University of Alberta, Edmonton, Alberta.

magnesium bromide, is reported to lead to monosubstitution at C_9, but reactions leading to dimeric products occur in some of the cases studied (10).

We have repeated the preparation of 9-fluorenylsodium according to Greenhow (3) and although the reported high yields and fine quality of the organometallic compound could not be duplicated, the salt was obtained in reasonable yield and in a state suitable for the synthesis of the 9-monosubstituted fluorenes as described by Greenhow and co-workers (3, 5). The 9-methyl-, 9-allyl-, and 9-benzyl-fluorenes required for this work were made by this method.

The 9,9-disubstituted fluorenes were readily obtained from 9,9-fluorenyldipotassium. Little work appears in the literature concerning the potassium salt of fluorene. Weissgerber (12) reported the preparation of 9-fluorenylpotassium by fusion of solid potassium hydroxide with fluorene at 280° from which was isolated a substance whose analysis indicated the composition $C_{13}H_9K$. This substance he then treated with benzyl chloride to form the 9-benzylfluorene. However, as Thiele and Henle have shown (13), the compound actually obtained was 9,9-dibenzylfluorene. A repetition of Weissgerber's experiment led to the conclusion that this method for the preparation of fluorenylpotassium also was quite unsatisfactory for our purpose.

It was found in this laboratory that potassium metal reacts readily with fluorene in boiling dioxane, protected by an atmosphere of nitrogen, to produce at will either the mono- or di-potassium salt as a reddish-brown precipitate. Hydrogen gas is evolved. This precipitate can be freed of unreacted fluorene by filtration and washing with dry hexane. The monopotassium derivative, obtained by the reaction of equimolar proportions of potassium and fluorene, can be isolated under nitrogen as a solid* quite suitable for further reaction. Usually it is more convenient to leave the solid suspended either in the original dioxane, or in the hexane wash liquid where it can be kept for some time with little decomposition. Exposure to air causes rapid decomposition to a dark mass which is essentially potassium hydroxide, 9-fluorenone, 9-fluorenol, and fluorene, the relative amounts of these depending upon the accessibility to oxygen or water of the air. Attempts to analyze the isolated monopotassium salt gave low values for potassium presumably due to absorption of water and/or oxygen from the air during weighing manipulations. Three analyses gave an average value of 15.3% of potassium. The theoretical value is 19.15%. It was felt that the highly elaborate procedure obviously necessary for a satisfactory potassium analysis was superfluous to our work at this time hence further attempts in this direction were abandoned.

The dipotassium compound, precipitated from the reaction of one equivalent of fluorene with two of potassium, could not be isolated readily as above, and therefore was used in dioxane suspension immediately following its preparation. That we were actually dealing with the dipotassium compound was supported by (*a*) the fact that *two* equivalents of potassium metal were totally consumed by *one* equivalent of fluorene whereas potassium metal itself showed no visible reaction when heated alone with dioxane over a period of 8 hours, (*b*) the infrared spectrum of dideuterated fluorene (described later) obtained from the dipotassium compound, and (*c*) the nuclear magnetic resonance analyses for deuterium† which showed the absence of any peak corresponding to the methylene group of fluorene. On the other hand, the monopotassium compound, when deuterated, showed strong evidence from the infrared spectra that essentially 9-monodeuterofluorene had been obtained, contaminated with a small amount of unreacted

*The presence of particles of unreacted potassium accelerates the decomposition of the organometallic compound hence it is advisable to carry the reaction to completion with respect to the metal.

†The deuterium analyses were made by Dr. W. Schneider of the National Research Council of Canada in Ottawa.

Can. J. Chem. Downloaded from www.nrcresearchpress.com by 41.223.56.140 on 09/04/12
For personal use only.

fluorene and some 9,9-dideuterofluorene. This is supported by the nuclear magnetic resonance spectra which indicate approximately 75% monodeuteration. Rather than postulate that the "9-fluorenylpotassium" contained fluorene *and* 9,9-fluorenyldipotassium (a condition highly unlikely due to the great reactivity of the dipotassium compound) the results can be better explained by assuming that in the presence of KOD and excess D_2O, during the preparation and isolation procedure, a hydrogen–deuterium exchange has occurred, thus producing some C_9-dideuterated fluorene.

The addition of slightly more than two equivalents of alkyl or aralkyl halide to the suspension of the dipotassium compound in dioxane produced 9,9-disubstituted fluorenes in yields of about 65%. No further attempts were made at this time to improve yields since the reactions of the metallated fluorenes will be elaborated in a subsequent publication. In this way 9,9-dimethyl-, 9,9-dibenzyl-, and 9,9-diallyl-fluorene were prepared.

Reaction of the mono- and di-potassium compounds, in dioxane, with excess deuterium oxide gave 9-monodeutero- and 9,9-dideutero-fluorene respectively.

THE INFRARED SPECTRA OF FLUORENE AND SOME OF ITS C_9-MONO- AND C_9-DI-SUBSTITUTED DERIVATIVES

The information concerning the infrared studies of fluorene and its 9-substituted derivatives is meager. Fox and Martin (14) in a study of the absorption in the 3000 cm^{-1} region, due to the methylene group in a number of organic compounds, attributes two frequencies, 2901 cm^{-1} and 2795 cm^{-1}, to the $=CH_2$ of fluorene. In the present work the spectra of fluorene determined in carbon tetrachloride did not reveal absorption at these two frequencies which could be associated with the methylene group in fluorene. Richards and Thomson (15), investigating the spectral changes occurring in liquid–solid state transitions give two frequencies, 1303 cm^{-1} and 1482 cm^{-1}, apparently characteristic of fluorene. Both of these frequencies are found in this work, that in the 1300 cm^{-1} region is definitely associated with the CH_2 group while the 1482 cm^{-1} band appears to be due to some other part of the fluorene structure.

In this paper are reported the infrared spectra of the following compounds: fluorene, 9-mono- and di-deutero-, mono- and di-methyl-, mono- and di-benzyl-, mono- and di-allyl-fluorene as well as 9-benzylidenefluorene. They were found in both carbon disulphide and carbon tetrachloride solution to provide the whole range of absorption from 4000 cm^{-1} to 600 cm^{-1} except for a small region about 1450 cm^{-1} to 1600 cm^{-1} where both solvents show some absorption themselves (16). The instrument available was a Perkin–Elmer double-beam infrared spectrophotometer, equipped with a sodium chloride prism. Six frequencies of medium intensity were found definitely due to the methylene group of fluorene. These are at 2930, 1400, 1298, 1190, 952, and 692 cm^{-1} (Fig. 1). Whether these are all fundamental frequencies or not is not known. There are, no doubt, other frequencies due to the methylene group arising from overtones and combinations, but these were felt to be unnecessary for our work and hence not examined. Two such frequencies of low intensity might be 867 and 853 cm^{-1} (Fig. 1). All six frequencies can be clearly discerned and are of approximately the same intensity in both solvents employed. Since additional frequencies associated with substituting groups appear in the 1400 to 600 cm^{-1} region this area was examined carefully and thus only the spectra for this region, found in carbon disulphide, are reported and shown in Figs. 1 to 13. Each of the six frequencies mentioned is markedly affected by substitution or deuteration at C_9. In all cases, monosubstitution by an alkyl or aralkyl group greatly reduces or eliminates the absorption at these frequencies while disubstitution removes it completely. The removal of some is masked by neighboring frequencies or new frequencies due to the substituting groups but can still

Can. J. Chem. Downloaded from www.nrcresearchpress.com by 41.223.56.140 on 09/04/12
For personal use only.

be readily observed. Mono- and di-deuteration reduces or removes these frequencies similarly but new bands appear for the C—D functions at a lower frequency as expected (Figs. 2 and 3). The relative positions of these new C—D frequencies were estimated beforehand from Fig. 1 by using the suggested factor of 0.73 (16) and thus the new frequencies could be related at least tentatively, if not exactly, to the former C—H frequencies. The experimentally found ratio of the new C—D frequency to the original C—H frequency is approximately 0.7, in agreement with the shift expected by a simple application of Hooke's Law (16). The frequencies for the original C—H group, the new C—D group, the remaining C—H group on monodeuteration, and the ratio of the first two, both calculated and found, are shown in Table I.

TABLE I

Frequencies associated with the methylene group in fluorene and in monodeuterofluorene (cm^{-1})

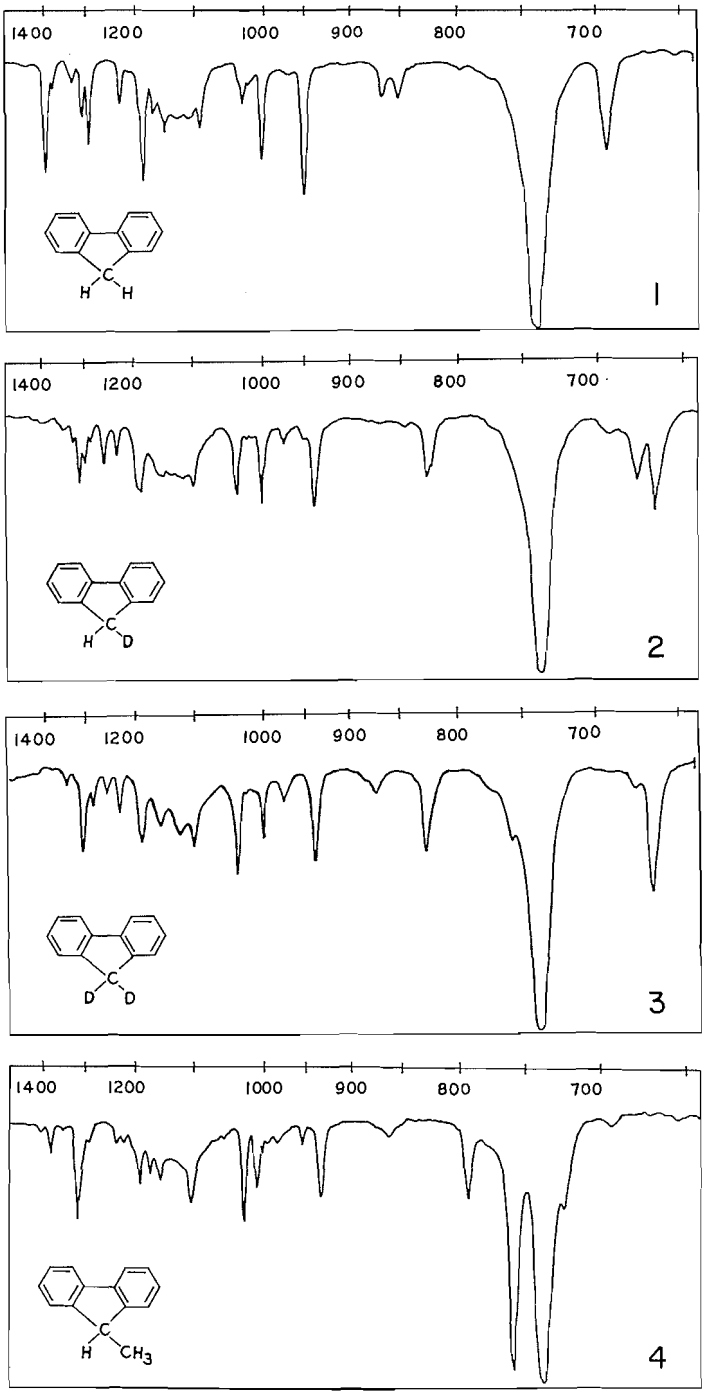
Observed for CH_2	Calculated[a] for HC—D	Observed for HC—D	Observed $\nu C—D / \nu C—H$	Observed for remaining DC—H
692	505	—[b]	—	677
952	694	667	0.70	939
1190	869	827	0.70	—[d]
1298	947	939	0.72	—[d]
1400	1022	974	0.70	—[d]
2930	2050	2150[c]	0.73	—[d]

[a]The product of the observed frequency in column 1, and the factor 0.73 obtained from reference 16.
[b]Beyond the range of the instrument.
[c]This is a very weak absorption and is not certain.
[d]Overlapping and multiplicity of neighboring absorption makes any assignment highly questionable.

The 692 cm^{-1} Band

This band, probably due to methylene rocking vibrations (16), is quite distinct. Monodeuteration (via the monopotassium compound) reduces it markedly (Fig. 2). The residual absorption noticeable at this frequency is most likely due to unreacted fluorene, a contaminant undoubtedly present since the deuterium oxide available at the time of these experiments contained 95% of D_2O. A three- to five-fold excess of deuterium oxide was used to ensure as complete a reaction as possible with the precipitated potassium compound. Purification by separation of deuterated from undeuterated fluorene obviously is extremely difficult. Dideuteration via the dipotassium compound completely eliminates the 692 cm^{-1} band (Fig. 3). The spectrum of the monodeuterated fluorene shows a new band at 677 cm^{-1} which is thought to be associated with the remaining DC—H, shifted from the original frequency of 692 cm^{-1} by the presence of the deuterium atom. This point of view is supported by the fact that dideuteration reduces this 677 cm^{-1} band to a very small value, this residual absorption arising, no doubt, from contaminating monodeuterated fluorene. The frequency corresponding to the new HCD— group, calculated to be in the region of 505 cm^{-1}, is beyond the range studied.

Can. J. Chem. Downloaded from www.nrcresearchpress.com by 41.223.56.140 on 09/04/12
For personal use only.

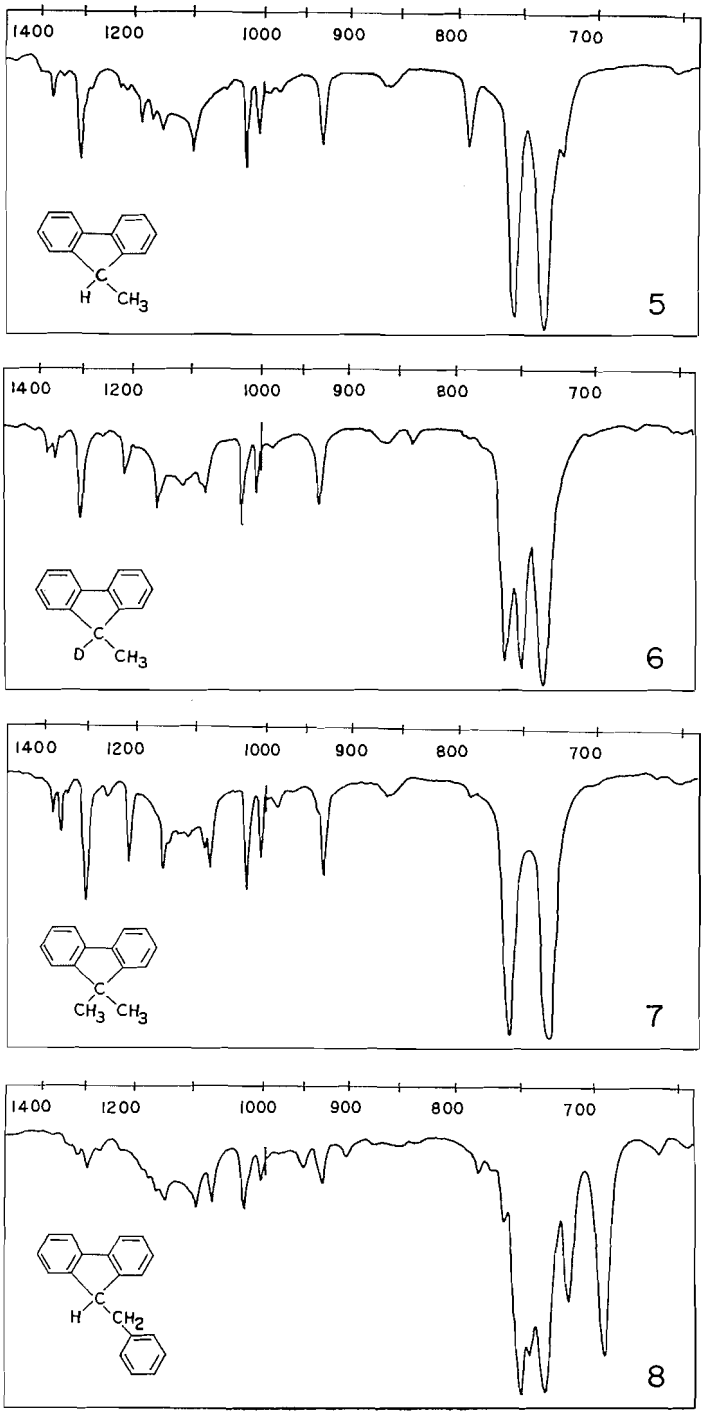


FIGS. 1–4.

Monomethylation reduces the band at 692 cm^{-1} to one of weak absorption at the same frequency (Fig. 4). This was found to be due to contamination by unreacted fluorene since repeated purification by chromatography on activated alumina eliminated the

Can. J. Chem. Downloaded from www.nrcresearchpress.com by 41.223.56.140 on 09/04/12
For personal use only.

absorption at 692 cm^{-1} (Fig. 5). The melting point of the "contaminated" monomethylfluorene is 43–44° C whereas that of the "pure" monomethylfluorene is 45–46° C. Thus, a routine melting point determination of this compound should be carefully done to



FIGS. 5–8.

Can. J. Chem. Downloaded from www.nrcresearchpress.com by 41.223.56.140 on 09/04/12
For personal use only.

differentiate between 100% purity and slight contamination, sufficient to be visible clearly in the infrared spectrum.

The melting point found for 9-methylfluorene is the same as that reported by Greenhow (3). However, other workers give a melting point of 58° (17). This may be another example of two polymorphic forms, a situation already demonstrated in the case of 9,9-dimethylfluorene (18).

The disappearance of the 692 cm^{-1} band on monobenzylation and dibenzylation (Figs. 8 and 9) is masked by the strong absorption at 697 cm^{-1} due to out-of-plane C—H vibrations of monosubstituted benzene (16). Mono- and di-allylation (Figs. 11 and 12) show more clearly the disappearance of the 692 cm^{-1} band.

The expected complete elimination of the 692 cm^{-1} absorption in the 9-benzylidenefluorene (Fig. 13) is obscured by the strong absorption at 697 cm^{-1} due to monosubstituted benzene.

The 952 cm^{-1} Band

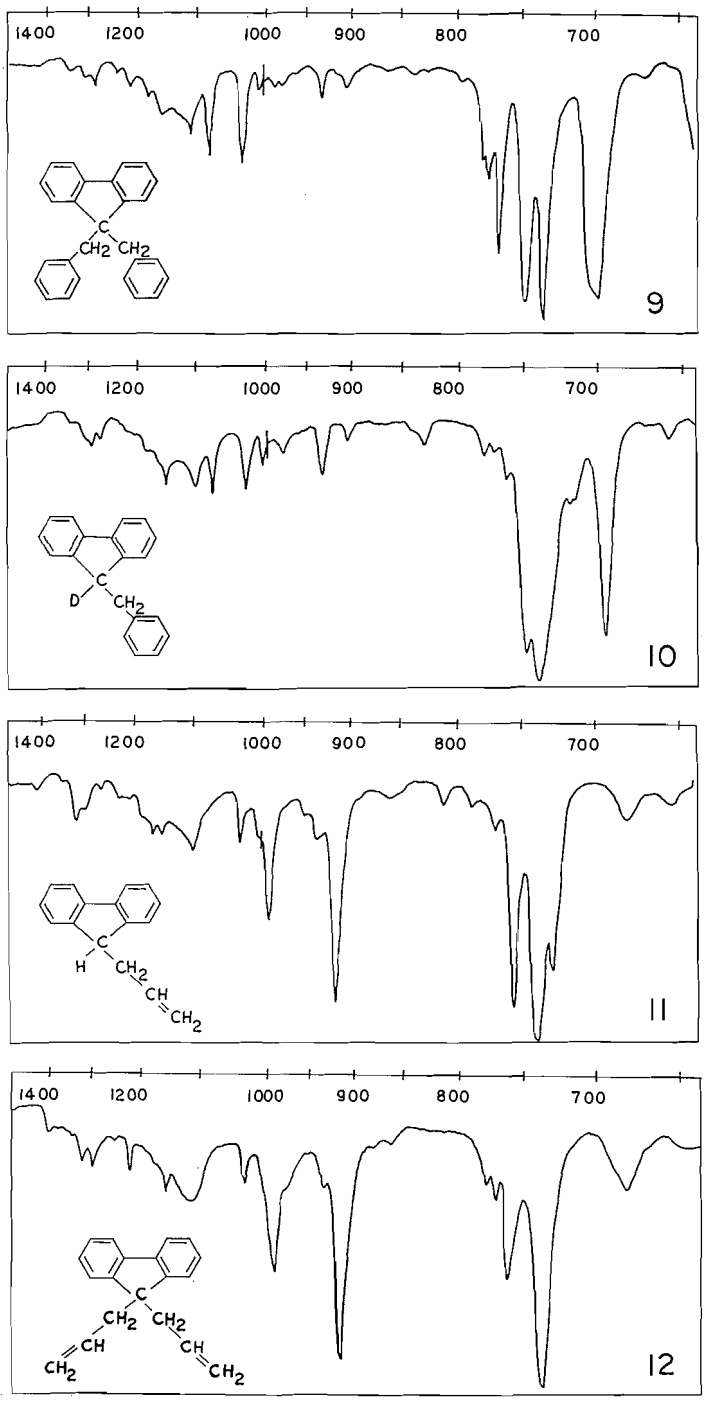
This band whose origin is unknown to us is also quite distinct (Fig. 1). It is nearly eliminated by monodeuteration, the residual absorption most likely being due to contaminating fluorene (Fig. 2). Dideuteration causes complete disappearance of absorption at this frequency. The corresponding HC—D band, calculated to occur in the region of 694 cm^{-1} appears at 667 cm^{-1} and its intensity increases markedly upon dideuteration. The considerably greater intensity of the HC—D band at 667 cm^{-1} as compared to that of the DC—H band at 677 cm^{-1} indicates that in deuteration of the monopotassium compound with excess D_2O, some dideuteration had occurred probably by hydrogen–deuterium exchange.

The band due to the remaining DC—H, if analogous to that of 677 cm^{-1} found for the 692 cm^{-1} band, should occur in the region of 935 cm^{-1}. One actually does appear at 939 cm^{-1} and may contain the DC—H absorption. However, the magnitude of its intensity as well as the fact that dideuteration makes no significant change in its size favors the view that the 939 cm^{-1} band is due in part to the methylene absorption originally at 1298 cm^{-1}, shifted due to formation of the —C—D bond, and in part to absorption from the remaining —C—H bond affected by the deuterium atom.

The monomethyl-, monobenzyl- and monoallyl-fluorene (Figs. 4, 5, 8, 11) all show very strong reduction of intensity or complete elimination of absorption at 952 cm^{-1}, any residual absorption again being due to contamination by unreacted fluorene.

As expected, 9-benzylidenefluorene shows no absorption in the 950–956 cm^{-1} region

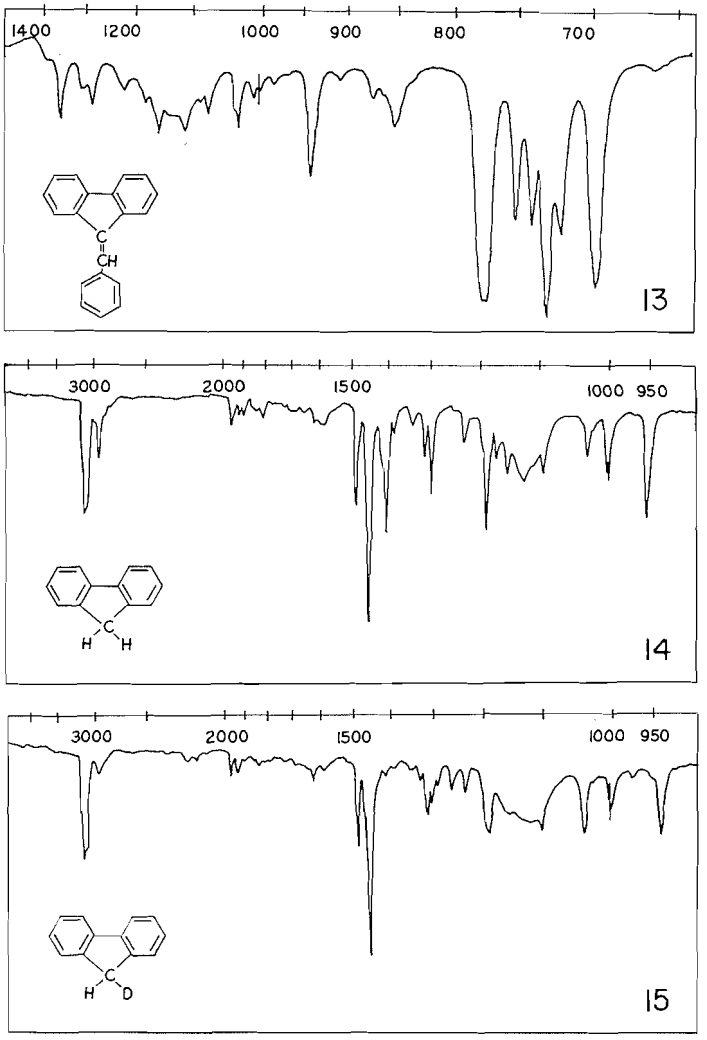
Can. J. Chem. Downloaded from www.nrcresearchpress.com by 41.223.56.140 on 09/04/12
For personal use only.



FIGS. 9–12.

(Fig. 13). A similar result occurs for the other 9,9-disubstituted fluorenes (Figs. 7, 9, 12). The position of the absorption for the remaining C_9—H bond in the monosubstituted fluorenes is determined by deuteration. Comparison of Figs. 5 and 6 show that two bands,

Can. J. Chem. Downloaded from www.nrcresearchpress.com by 41.223.56.140 on 09/04/12
For personal use only.



FIGS. 13–15.

792 cm^{-1} and 722 cm^{-1}, are eliminated on deuteration, hence it is clear that these are due to C_9—H in 9-monomethylfluorene. Whether one of these corresponds to the absorption of the methylene group at 952 cm^{-1} is not known. Similarly, the bands at 787 cm^{-1} (weak) and 719 cm^{-1} (strong) in the spectrum of 9-monobenzylfluorene (Figs. 8 and 10) and those at 789 cm^{-1} (weak) and 727 cm^{-1} (strong) in the 9-monoallylfluorene (Fig. 11) are likewise to be associated with the remaining C_9—H bond, since deuteration or disubstitution eliminates the absorption.

In addition it might be pointed out that the bands at 1100, 1167, and 1185 cm^{-1} are eliminated upon deuteration of the 9-monomethylfluorene (Figs. 5 and 6) hence can be considered as associated with the remaining C_9—H bond.

The 1190 cm^{-1} Band

The cause of absorption at this frequency is not known. It was at first believed to be composed of absorption due to the methylene group *and* to some other structural feature

Can. J. Chem. Downloaded from www.nrcresearchpress.com by 41.223.56.140 on 09/04/12
For personal use only.

since monodeuteration reduces it to about one-half its former intensity while dideuteration produces little further change (Figs. 1–3). However, monosubstitution reduces the band markedly while disubstitution practically removes it, hence the absorption seen at 1190 cm^{-1} in the dideuterated molecule may be due to shifts, or combinations of overtones, stemming from deuteration at C_9.

The frequency of the $\begin{array}{c}|\\ -C-D\\ |\end{array}$ bond is thought to appear at 827 cm^{-1} in agreement with the calculated value.

The position of absorption of the remaining $\begin{array}{c}|\\ -C-H\\ |\end{array}$ bond as affected by the presence of the deuterium atom could not be defined in view of the complexity of the neighboring bands.

The 1298 cm^{-1} Band

This absorption is probably due to methylene wagging vibration (16) and, in agreement with previous observations, is of lower intensity than that from rocking vibration. The band is reduced on monodeuteration or monosubstitution at C_9 while dideuteration or disubstitution largely eliminates it. Neighboring absorption bands mask these effects somewhat with the result that this frequency is less useful than are the others mentioned above.

The $\begin{array}{c}|\\ -C-D\\ |\end{array}$ bond frequency appears at 939 cm^{-1} in the monodeuterated molecule. Since its intensity is practically unchanged upon dideuteration, the view is supported that it is a composite band in the monodeuterated structure, with a contribution from the remaining $\begin{array}{c}|\\ -C-H\\ |\end{array}$ band shifted slightly from 952 cm^{-1}. Dideuteration removes this contribution but adds that from the second C—D bond in dideuterated fluorene (1298 cm^{-1} shifted to 939 cm^{-1}).

The 1400 cm^{-1} Band

This absorption is quite likely derived from scissoring vibration of the methylene group (16) since any type of mono- or di-substitution at C_9 eliminates this band. The absorption attributed to the new —C—D bond obtained on monodeuteration might be that appearing at 974 cm^{-1} and increasing on dideuteration. This agrees quite well with the calculated value (Table I). The band at 1038 cm^{-1} appearing on monodeuteration and increasing in magnitude upon dideuteration agrees roughly with the calculated shift, but examination of the spectra of mono- and di-substituted compounds (Figs. 1–13) shows that *any mono- or di-substitution* at C_9 gives rise to a band, increasing upon disubstitution, at about the same frequency. Hence the absorption at 1038 cm^{-1} certainly cannot be due to the $\begin{array}{c}|\\ -C-D\\ |\end{array}$ bond.

The 2930 cm^{-1} Band

This absorption, arising from C—H stretching frequency, must be due to the methylene

Can. J. Chem. Downloaded from www.nrcresearchpress.com by 41.223.56.140 on 09/04/12
For personal use only.

group since it disappears upon deuteration (Figs. 14 and 15).* No firm assignment could be made for the —C—D band, although weak absorption appears at 2150 cm^{-1} in the deuterated molecule (Table I) in agreement with the calculated shift.

USEFUL BANDS ASSOCIATED WITH PARTICULAR SUBSTITUENTS AT C_9

In all the spectra there is clearly discernible a characteristic strong band at 738 cm^{-1} originating from the two ortho disubstituted benzene nuclei in fluorene (16). Monomethyl-, monoallyl-, and monobenzyl-fluorene and 9-benzylidenefluorene all show weak absorption between 787 and 793 cm^{-1} and strong absorption in the region of 719 to 728 cm^{-1} (overlapping to some extent with the major 738 cm^{-1} band). Only for monomethylfluorene is this latter absorption of weaker intensity, though still quite readily discernible, and the former stronger than in all the other cases examined. Disubstitution at C_9 removed this absorption completely. We have attributed these two bands to the remaining C_9—H bond. The 719–728 cm^{-1} band has been used to differentiate between the mono- and di-substitution and, in particular, to follow the preparation, purification, and identification of 9-monoallylfluorene and 9,9-diallylfluorene whose mixtures with each other and with fluorene itself are separated with difficulty.

Clear distinction of the methylated fluorenes from the allyl or benzyl fluorenes may be made by observation of the strong, isolated band at 758 cm^{-1} in the spectrum of monomethylfluorene, which doubles in intensity upon dimethylation. The monomethyl compound shows another medium-weak, though impressive, band at 793 cm^{-1} which is eliminated upon dimethylation or on deuteration of the remaining C_9—H. Allylfluorenes absorb at 913 cm^{-1}, the intensity of the diallyl being approximately double that found for the monoderivative. This absorption is no doubt that associated with the C—H out-of-plane bending found in olefinic structures (16). The band appearing at 681 cm^{-1} for mono- and di-allylfluorene may also be of analytical value.

The strong absorption at 700 cm^{-1} in 9-monobenzylfluorene (approximately doubled in the dibenzylfluorene) is due to the monosubstituted benzene moiety. Also of some assistance in identifying 9-benzylated fluorenes is the weak band at 905 to 909 cm^{-1}. This appears to be present in 9-benzylidenefluorene. Whether the same absorption is to be found in the allyl fluorenes cannot be shown since the strong 913 cm^{-1} band interferes.

Of some assistance is the strong absorption at 761 to 764 cm^{-1} for *di*allyl- and *di*benzyl-fluorene, whereas for the *mono*allyl- and *mono*benzyl-fluorenes a similar strong absorption occurs at 754 cm^{-1}. Furthermore, a band at 746 to 748 cm^{-1} appears for the mono- and di-benzylfluorene but not for mono- and di-allylfluorene.

The view that the dipotassium compound had been made from two equivalents of potassium and one of fluorene is supported by deuteration experiments. The 9-fluorenylpotassium (also the 9-fluorenylsodium, prepared by Greenhow's method (3)), treated with excess deuterium oxide gave a spectrum (Fig. 2) in which the shifted frequency, due to C_9—H, is thought to be at 677 cm^{-1}. If this assignment is correct, dideuteration should eliminate this band. Such elimination is actually observed in the spectrum of the dideuterated compound obtained from the experiment wherein two equivalents of potassium to one of fluorene were used. No change in extent of deuteration was found when a greater proportion of potassium metal was employed.

**The spectra for Figs. 14 and 15 were obtained in* CCl_4 *solution.*

Can. J. Chem. Downloaded from www.nrcresearchpress.com by 41.223.56.140 on 09/04/12
For personal use only.

Can. J. Chem. Downloaded from www.nrcresearchpress.com by 41.223.56.140 on 09/04/12
For personal use only.

EXPERIMENTAL

The fluorene used in this work was Eastman Kodak 98% practical grade.

Infrared spectra were obtained with the aid of a Perkin–Elmer model 21 double-beam spectrophotometer equipped with a sodium chloride prism. Solutions in carbon tetrachloride and carbon disulphide, containing 20 mg solute per ml of solvent were measured in sodium chloride cells of 0.5-mm thickness.

All melting points are uncorrected.

9-Fluorenylpotassium

Fluorene (8.3 g, 0.05 mole) and potassium metal (1.95 g, 0.05 mole) were heated in refluxing purified dioxane (19) protected by an atmosphere of purified dry nitrogen. In 3 hours all the potassium was consumed. The reaction mixture was cooled to room temperature and the reddish-brown precipitate isolated by filtration under suction and washed with dry hexane to remove unreacted fluorene. Isolation of the monopotassium compound was best carried out in a dry box containing an atmosphere of nitrogen. Samples for analysis were prepared by freeing the fluorenyl potassium from adhering solvent with a stream of nitrogen drawn through the solid product by suction. Analysis was carried out by first treating a weighed portion of the solid with water then titrating the basic solution with standard acid. In three attempts at analyses the "purified" precipitate showed values of 14.9, 15.3, and 15.7% for potassium. The value required for $C_{13}H_9K$ is 19.15%.

9-Deuterofluorene

The 9-fluorenylpotassium was prepared from 1.66 g of fluorene and 0.39 g of potassium in 5 ml of pure dioxane refluxed for 3 hours until all the potassium had reacted. One milliliter of D_2O* (95%) was slowly added and the mixture then stirred for 1 hour. Following the addition of ether, the dioxane and potassium hydroxide were readily removed by extracting the solution of deuterated fluorene with water. When the ethereal solution was dried and the solvent removed there was obtained, upon crystallization of the resulting solid from alcohol, 1.58 g of monodeuterated fluorene.

Analysis for deuterium by N.M.R. show approximately 75% monodeuteration.

9,9-Dideuterofluorene

A mixture of 0.01 mole (1.66 g) of fluorene and 0.02 mole (0.78 g) of potassium was heated for 3.5 hours in 5 ml of refluxing dioxane till all the potassium had been consumed. The addition of 1.5 ml of D_2O and isolation of the product as before gave 1.56 g of dideuterated fluorene.

N.M.R. analysis shows complete absence of absorption at the position attributable to $\diagdown\!\!\diagup CH_2$, indicating complete dideuteration.

9-Methylfluorene

This compound was prepared by the following modification of Greenhow's procedure (3). Fluorene (18 g) and finely powdered sodamide (3.9 g) were heated in a nitrogen atmosphere for 5 hours at 180° C in 50 ml of decahydronaphthalene (dried with sodium and distilled). When the reaction mixture had cooled to room temperature, the solvent was decanted and the remaining black amorphous solid which adhered to the lower portion of the flask was washed several times with hexane (dried with sodium). Methyl iodide (12 ml) in 50 ml of hexane was then added and the magnetically stirred mixture refluxed for 12 hours under nitrogen. After the cautious addition of water to dissolve the

**The D_2O was donated by the National Research Council of Canada.*

potassium iodide, the hexane layer was separated, dried, and the solvent removed. The yellow oil obtained, dissolved in pentane and cooled in a refrigerator, deposited unchanged fluorene. Further purification was accomplished by chromatography of the pentane mother liquor on a 50-cm column of dry, activated alumina (80–200 mesh). The first fraction, obtained by elution with hexane, gave 9-methylfluorene, m.p. 43–44° C. Further purification by repeated chromatography altered the infrared spectrum slightly and changed the melting point of the compound to 45–46° C, lit. 45–47° C (3). (Compare the melting point of 58° reported by Wieland (17).)

9,9-Dimethylfluorene

A solution of 16.6 g of fluorene in 80 ml of dioxane containing 7.8 g of potassium was boiled for 5 hours under an atmosphere of nitrogen. All the potassium was consumed in this time. The slow addition of 20 ml of methyl iodide, to the cooled mixture, produced a vigorous but controllable reaction. Stirring was continued for 1 hour whereupon both ether and water were added to the reaction flask. Several extractions of the ethereal solution with water removed the dioxane. The dried ($CaCl_2$) solution was freed from ether and gave a yellow oil which could not be purified adequately by fractional distillation. However, chromatography with alumina of an hexane solution of this oil separated the unchanged fluorene and monomethyl compound from dimethylfluorene. The first fraction gave the 9,9-dimethylfluorene, m.p. 88–89° C, but when crystallized from methanol melted at 95–96° C, lit. 95–96° C (20). It is interesting that recrystallization from pentane of the 95–96° C melting compound gave a lower and less definite melting point, found in one case to be 78–83° C, which after a second crystallization from pentane gave 81–87° C.

9-Benzylfluorene

The 9-fluorenylsodium was prepared from 18.3 g of fluorene and 3.9 g of sodamide heated in decahydronaphthalene for 4 hours at 180° C under a nitrogen atmosphere (3). The black solid, deposited in the flask, was washed with hexane as in the preparation of 9-methylfluorene and treated with a solution of 40 ml of benzyl chloride in 40 ml of hexane. This mixture was refluxed for 20 hours. To the hexane solution, now diluted with ether, was added water to remove the sodium chloride. Removal of the ether hexane solvent gave a yellow amorphous product which after solution in alcohol deposited 12.5 g of crystalline 9-benzylfluorene melting sharply at 134° C, lit. 135° C (3). Further purification by chromatography on activated alumina raised the melting point to 136° C. Crystallization from alcohol did not change the melting point.

9,9-Dibenzylfluorene

(a) From fluorene.—To the dioxane containing 9,9-fluorenyldipotassium (made from 16.6 g of fluorene and 7.8 g of potassium in 80 ml of dioxane) was added 21 ml of benzyl chloride (an excess). The product of this reaction, only slightly soluble in ether, was isolated quite simply by the addition of water and ether to the dioxane solution whereupon the solid which formed could then be removed by filtration. The 9,9-dibenzylfluorene weighed 11.2 g and melted at 146° C (from alcohol), lit. 147–148° C (13).

(b) From 9-benzylfluorene.—A mixture of 2.6 g of 9-benzylfluorene and 0.39 g of potassium metal (equimolar portions) in 12 ml of dioxane was heated till solution of the metal was complete. Forty minutes of refluxing with 1.2 ml of benzyl chloride gave a solid, isolated as above, with properties and melting point identical with those of 9,9-dibenzylfluorene.

Can. J. Chem. Downloaded from www.nrcresearchpress.com by 41.223.56.140 on 09/04/12
For personal use only.

9-Deutero-9-benzylfluorene

Dioxane (15 ml) containing 2.56 g of *9-benzylfluorene* and 0.39 g of potassium was boiled for 40 minutes, cooled to room temperature, and treated with 0.8 ml (excess) of D_2O. The red precipitate disappeared and the product, isolated as usual by employing ether and water, and crystallized from alcohol, melted at 131° C, yield 0.5 g. Chromatography raised the melting point to 134° C, which crystallization from alcohol did not change.

9-Deutero-9-methylfluorene

This compound was prepared in the same manner as for 9-deutero-9-benzylfluorene and isolated as was 9-methylfluorene, m.p. 45.5° C.

9-Benzylidenefluorene

The procedure was a modified version of that employed by Thiele and Henle (13). The use of potassium ethylate, rather than sodium ethylate, gave the product in 3 days as compared with 14 days reported for Thiele and Henle's method.

To a solution of 2.5 g of potassium in 125 ml of dry ethyl alcohol was added 5 g of fluorene. Freshly distilled benzaldehyde (4.5 g) in 10 ml of alcohol was added and the reaction mixture kept at 45° C for 3 days. The 9-benzylidenefluorene (3.6 g) deposited from the solution was crystallized once from alcohol, m.p. 74°–75° C, lit. 76° C (13).

9-Allylfluorene

This compound was prepared by a modification of Greenhow's method (3).

Sodamide (3.9 g) and fluorene (18 g) were heated in refluxing decalin (40 ml) for 4 hours (nitrogen atmosphere). The decalin was then replaced by pentane (50 ml) and the 9-fluorenylsodium treated with 50 ml of allyl bromide (excess). After 8 hours reflux the product was isolated by removing the sodium chloride with water, then eliminating the solvent as well as the excess allyl bromide. Vacuum distillation gave 11.5 g of a light-yellow liquid boiling at 132–137° C/3 mm. Elution chromatography as described for the methylated fluorenes gave a sample suitable for infrared analysis.

9,9-Diallylfluorene

Fluorene (8.3 g) and potassium metal (3.9 g) were boiled for 4 hours in 100 ml of dioxane (N_2). When the reaction mixture was cooled to room temperature and treated with 8.65 ml of allyl bromide, added dropwise, an exothermic reaction occurred with simultaneous disappearance of the reddish-brown precipitate. After an additional period of stirring for 5 hours the product was isolated as usual by the additon of ether and water. The crude oil (12.1 g) obtained from the ether layer was fractionally distilled under vacuum to yield 7.9 g of light-yellow oil, b.p. 144° C/3 mm, which was submitted to chromatography for additional purification.

ACKNOWLEDGMENTS

The authors are grateful to the National Research Council of Canada for funds which enabled one of us (G. S.) to continue work on this project during the summer months.

Grateful acknowledgment is given to Dr. J. Harrold of the Physics Department of the University of Alberta, Edmonton, and to Dr. P. Krueger of the Chemistry Department of the University of Alberta at Calgary for helpful discussions of the work reported in this paper.

Can. J. Chem. Downloaded from www.nrcresearchpress.com by 41.223.56.140 on 09/04/12
For personal use only.

REFERENCES

1. H. FRANCE, P. MAITLAND, and S. H. TUCKER. J. Chem. Soc. 1739 (1937).
2. G. RIEVESCHL and F. E. FAY. Chem. Rev. **23**, 287 (1938).
3. E. T. GREENHOW, E. N. WHITE, and D. MCNEIL. J. Chem. Soc. 2848 (1951).
4. H. A. BRUSON. J. Am. Chem. Soc. **64**, 2457 (1942).
5. E. J. GREENHOW, D. MCNEIL, and E. N. WHITE. J. Chem. Soc. 986 (1952).
6. G. J. GREENHOW, E. N. WHITE, and D. MCNEIL. J. Chem. Soc. 3099 (1953).
7. E. J. GREENHOW, A. S. HARRIS, and E. N. WHITE. J. Chem. Soc. 3116 (1954).
8. E. J. GREENHOW and D. MCNEIL. J. Chem. Soc. 3204 (1956).
9. W. SCHLENK and E. BERGMANN. Ann. **463**, 188 (1928).
10. H. F. MILLER and G. B. BACHMANN. J. Am. Chem. Soc. **57**, 766 (1935).
11. J. D. DICKINSON and C. EARBORN. J. Chem. Soc. 2337 (1959).
12. R. WEISSGERBER. Ber. **34**, 1659 (1901).
13. J. THIELE and F. HENLE. Ann. **347**, 290 (1906).
14. J. J. FOX and A. E. MARTIN. Proc. Roy. Soc. A, **167**, 257 (1938).
15. R. E. RICHARDS and H. W. THOMPSON. Proc. Roy. Soc. A, **195** (1), (1948–49).
16. A. WEISSBERGER. Chemical applications of spectroscopy. Vol. 9. Interscience Publishers, Inc., New York. 1956.
17. H. WIELAND and E. KRAUSE. Ann. **443**, 133 (1925).
18. M. ANCHELL and A. H. BLATT. J. Am. Chem. Soc. **63**, 1948 (1941).
19. L. F. FIESER. Experiments in organic chemistry. D. C. Heath and Co., Boston. 1957. p. 284.
20. P. LEBEAU and M. PICON. Compt. rend. **173**, 85 (1921).

Can. J. Chem. Downloaded from www.nrcresearchpress.com by 41.223.56.140 on 09/04/12
For personal use only.

Can. J. Chem. Downloaded from www.nrcresearchpress.com by 41.223.56.140 on 09/04/12
For personal use only.

THE PREPARATION OF SOME THIOSEMICARBAZONES AND THEIR COPPER COMPLEXES. PART I[1]

B. A. Gingras, R. W. Hornal, and C. H. Bayley

ABSTRACT

A number of thiosemicarbazones and their 1:1 copper complexes are described and the possible structures of the latter are discussed. Formation of copper complexes from aromatic aldehyde and ketone thiosemicarbazones results in a loss of one H atom as indicated by infrared spectra. In the aliphatic series, no loss of H atom is apparent upon complex formation. It is reasonable to assume that different processes are involved resulting in two possible structures for the aromatic and the aliphatic copper complexes. Some chemical evidence supports this view.

Since the discovery by Domagk (1) of the antitubercular activity of thiosemicarbazones, a number of papers on the pharmacology of this type of compounds have been published (2, 3, 4, 5). Thiosemicarbazones have also been found active in preventing the growth of certain fungi (6, 7). It has been assumed that the microbial activity of thiosemicarbazones is due to their ability to chelate traces of metal (e.g. copper), the metal complexes themselves being the active ingredients (8).

This hypothesis has been substantiated somewhat by the fact that selenosemicarbazones, in which the sulphur atom is replaced by selenium, are more active against fungi than the corresponding thiosemicarbazones, which in turn are more active than semicarbazones. This difference in activity is attributed to the formation of metal complexes which would occur more readily in the case of selenosemicarbazones (9).

There is considerable experimental evidence to support the view that formation of a toxic metal–organo complex is a possible mechanism of fungicidal action. Albert *et al.* (10) have shown that *8*-hydroxyquinoline is relatively non-toxic in triple-distilled water, but that addition of a trace of an iron salt makes it effective. Similarly, Cymerman-Craig *et al.* (11) showed quite conclusively that the high specific activity of isonicotinic hydrazide against *Mycobacterium tuberculosis* is due to formation of a metal complex. The high fungistatic activity of the dithiocarbamates is also believed to be due to their ability to bind metals (12, 13). It is also of interest to note that activity is lost completely when the terminal $-NH_2$ group of *p*-acetamidobenzaldehyde thiosemicarbazone is replaced by $-SCH_3$, the most likely explanation being that the latter group would prevent chelation (14).

In a search for new fungicides and also to test further the hypothesis discussed above, a number of thiosemicarbazones (II) of aliphatic and aromatic aldehydes and ketones and their copper complexes have been prepared, and their activity against two fungi have been examined.

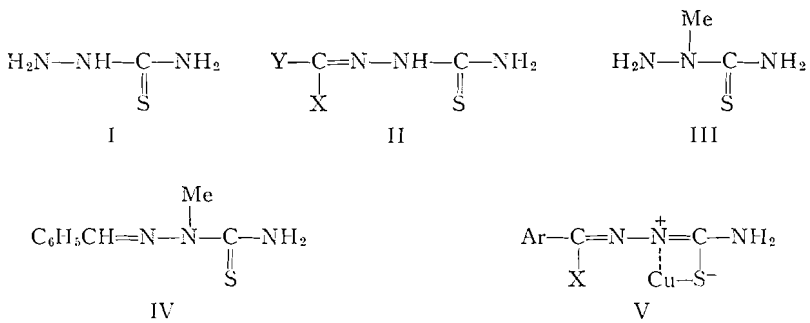
Previous workers have described copper complexes of *p*-substituted benzaldehyde thiosemicarbazones (namely *p*-methoxy- and *p*-acetamido-) and their use in chemotherapy of tuberculosis has been discussed briefly (15). Metallic complexes of a few thiosemicarbazones have also been obtained and their properties discussed mostly in connection with methods of quantitative analysis for cations; the fungicidal activity of the mercury complexes of these compounds has been investigated and they have been found to be inactive (16).

[1]*Manuscript received January 19, 1960.*
Contribution from the Division of Applied Chemistry, National Research Council, Ottawa, Canada. Issued as N.R.C. No. 5618.

Can. J. Chem. Downloaded from www.nrcresearchpress.com by 41.223.56.140 on 09/04/12
For personal use only.

No systematic investigation of the thiosemicarbazones and the possibility of their chelation with metals in relation to their microbiological activity seems to have been made. The purpose of the work described in this paper was to prepare a series of thiosemicarbazones and their copper complexes for use in subsequent studies of their fungicidal properties.

Most of the thiosemicarbazones listed in Table I gave copper complexes. A number of thiosemicarbazones and all of the copper complexes shown are described for the first time. The latter are colored solids of very low solubility in water and organic solvents. The least soluble were the aliphatic ones and consequently, their purification has been particularly tedious and in the case of the C_3, C_4, and C_5 compounds the elementary analysis remains unsatisfactory. However, since they show the expected infrared spectra and copper contents which are in good agreement with the theoretical values, they have been included in the data presented. Some others, viz. acetophenone and *p*-bromoacetophenone, decomposed during the various purification treatments used. The copper complexes are listed in Table II. Most of them underwent no change in color as the result of exposure to daylight and artificial light in the laboratory. In only two, i.e. furfural and *m*-nitrobenzaldehyde, was there any evidence of decomposition.



On the basis of elementary analysis, there can be no doubt that copper and thiosemicarbazones react in a 1:1 ratio. In the aromatic series the infrared spectra of the copper complexes show only two bands in the —NH— stretching region (at about 3450 cm^{-1} and 3350 cm^{-1}, see Table II) whilst the grouping —NH—CS—NH_2 accounts for three bands (at about 3440, 3240, and 3150 cm^{-1}, see Table I) in the case of the free thiosemicarbazones. This indicates that one hydrogen atom is involved in the complex formation.

By a study of the infrared spectra alone, it is difficult to discriminate between those three bands as any of the H atoms in II may take part in bonding, with a resulting shift to lower frequencies (17).

However, in the case of benzaldehyde, when the H atom of the —NH— group in II (Y = C_6H_5, X = H) was replaced by a methyl group, the resulting benzaldehyde methylthiosemicarbazone (IV) did not form a copper complex. Although more experimental evidence is required, this suggests that the H atom of the secondary —NH— group is responsible for the complex formation. A logical structure for the aromatic copper complexes would thus be as in V. It is now possible to speculate that the vibrations of the terminal —NH_2 group are responsible for the two bands at higher frequencies, since these are also present in the spectra of the copper complexes at about the same

TABLE I

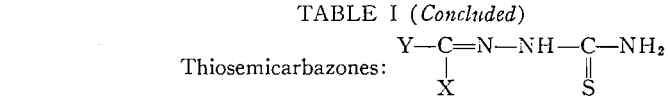
Thiosemicarbazones: $Y-C(X)=N-NH-C(=S)-NH_2$

Y	X	M.p., °C	Lit. m.p., °C	Yield, %	Solvents used in recrystallization	Typical I.R. absorption in the —NH— region, cm^{-1}	Formula	Found, %	Calculated, %
CH_3	CH_3	181	179[c]	75	EtOH–H_2O	3380–3240–3150	$C_4H_9N_3S$		
C_2H_5	H	162	159[c]	55	EtOH–H_2O	3380–3270–3150	$C_4H_9N_3S$		
n-C_3H_7	H	108	108–109[f]	67	EtOH–H_2O	3380–3250–3140	$C_5H_{11}N_3S$		
n-C_4H_9	H	64	65[g]	40	Benzene – *n*-hexane	3400–3260–3160	$C_6H_{13}N_3S$		
iso-C_4H_9	H	58	52–53[g]	75	EtOH–H_2O	3400–3260–3150	$C_6H_{13}N_3S$		
n-C_6H_{13}	H	68		65	EtOH–H_2O	3400–3250–3150	$C_8H_{17}N_3S$	C, 51.24 H, 9.16 N, 22.58 S, 17.54	C, 51.33 H, 9.09 N, 22.45 S, 17.12
n-C_7H_{15}	H	96	94–95[h]	94	EtOH–H_2O	3390–3260–3150	$C_9H_{19}N_3S$		
n-C_8H_{17}	H	77	77[h]	82	EtOH–H_2O	3420–3260–3160	$C_{10}H_{21}N_3S$		
n-C_9H_{19}	H	102	100[h]	80	EtOH	3400–3260–3160	$C_{11}H_{23}N_3S$		
n-$C_{10}H_{21}$	H	86		93	EtOH	3405–3260–3160	$C_{12}H_{25}N_3S$	C, 59.68 H, 10.08 N, 17.05 S, 12.90	C, 59.2 H, 10.28 N, 17.28 S, 13.18
9-$C_{10}H_{19}$	H	72		81	*n*-Hexane	3400–3270–3160	$C_{12}H_{23}N_3S$	C, 59.89 H, 9.55 N, 17.30 S, 13.30	C, 59.7 H, 9.55 N, 17.41 S, 13.28
n-$C_{11}H_{23}$	H	105	100[h]	88	EtOH	3400–3280–3170	$C_{12}H_{27}N_3S$		
n-$C_{11}H_{23}$	CH_3	99		96	EtOH	3400–3240–3140	$C_{14}H_{29}N_3S$	C, 62.54 H, 10.58 N, 15.60 S, 11.80	C, 62.00 H, 10.69 N, 15.49 S, 11.80
n-$C_{15}H_{31}$	CH_3	103		90	EtOH	3400–3240–3140	$C_{16}H_{37}N_3S$	C, 65.95 H, 11.32 N, 12.98 S, 9.65	C, 66.2 H, 11.3 N, 12.85 S, 9.8
CH_3	CO_2H	201		57	EtOH–H_2O	3430–3310–3200	$C_4H_7N_3O_2S$	C, 29.78 H, 4.70 N, 25.80 S, 19.80	C, 29.82 H, 4.35 N, 26.08 S, 19.88
$H_2N-CS-NH-N=CH-$	H	>300	>300[g]	85	Washed with EtOH–acetone	3405–3270–3160	$C_8H_8N_6S_2$		
$CH_2-CH_2-CH_2-$ CH_2-CH_2-		166	165–167[a]	97	EtOH	3370–3200–3130	$C_7H_{13}N_3S$		
$HC=CH-CH=C-$ O	H	160	182–183[a] 148[i]	85	EtOH	3400–3210–3120	$C_6H_7N_3OS$		
C_6H_5	H	162	160[a]	81	EtOH	3420–3240–3140	$C_8H_9N_3S$		
o-OHC_6H_4	H	230	235[a] 231[c]	100	EtOH–acetone	3440–3330–3180	$C_8H_9N_3OS$		
m-OHC_6H_4	H	167	137[a] 174[b]	50	Acetone–ether	3430–3280–3150	$C_8H_9N_3OS$		
p-OHC_6H_4	H	228	236[a] 224[c]	50	EtOH	3460–3410–3310	$C_8H_9N_3OS$		
m-$O_2NC_6H_4$	H	229	239–40[a] 163[c]	78	Acetone	3380–3220–3120	$C_8H_8N_4O_2S$		
o-FC_6H_4	H	185		81	EtOH–H_2O	3420–3240–3140	$C_8H_8FN_3S$	C, 48.83 H, 4.37 N, 21.50 S, 16.35	C, 48.73 H, 4.06 N, 21.32 S, 16.24
m-FC_6H_4	H	192		73	EtOH	3400–3240–3160	$C_8H_8FN_3S$	C, 48.54 H, 4.39 N, 21.20 S, 16.40	C, 48.73 H, 4.06 N, 21.32 S, 16.24

Can. J. Chem. Downloaded from www.nrcresearchpress.com by 41.223.56.140 on 09/04/12
For personal use only.

TABLE I (*Concluded*)

Thiosemicarbazones:



Y	X	M.p., °C	Lit. m.p., °C	Yield, %	Solvents used in recrystallization	Typical I.R. absorption in the —NH— region, cm^{-1}	Formula	Found, %	Calculated, %
p-FC_6H_4	H	193	180[d]	42	EtOH–H_2O	3390-3230-3140	$C_9H_8FN_3S$	N, 21.40 S, 16.25	N, 21.32 S, 16.24
o-ClC_6H_4	H	221	223[a]	97	EtOH	3420-3250-3150	$C_8H_8ClN_3S$		
p-ClC_6H_4	H	219	220[a]	95	EtOH	3420-3280-3150	$C_8H_8ClN_3S$		
2,5-$F(NO_2)C_6H_3$	H	245		63	Acetone–MeOH –hexane	3400-3240-3140	$C_8H_7N_4O_2S$	N, 24.40 S, 14.05	N, 25.1 S, 14.35
p-$(OCH_3)C_6H_4$	H	178	178[a]	81	EtOH	3420-3305-3150	$C_9H_{11}N_3OS$		
2,5-$OH(Cl)C_6H_3$	H	287–290	281–282[a]	72	EtOH–H_2O	3420-3240-3160	$C_8H_8ClN_3OS$		
2,4-$(Cl)_2C_6H_3$	H	238	245[a]	83	EtOH	3440-3250-3140	$C_8H_7Cl_2N_3S$		
2,4-$(OH)_2C_6H_3$	H	236	239–240[a]	76	EtOH	3480-3350-3160	$C_8H_9N_3O_2S$		
C_6H_5	CH_3	122	118–119[a]	96	EtOH–H_2O	3410-3220-3140	$C_9H_{11}N_3S$		
m-$H_2NC_6H_4$	CH_3	148	152–154[a]	37	EtOH	3410-3210-3140	$C_9H_{12}N_4S$		
p-ClC_6H_4	CH_3	202	205–206[a]	96	EtOH	3420-3200-3140	$C_9H_{10}ClN_3S$		
p-BrC_6H_4	CH_3	204	203[a]	98	EtOH–H_2O	3410-3200-3130	$C_9H_{10}BrN_3S$		
$C_6H_5CH(OH)$	C_6H_5	179	176–178[e]	80	EtOH–H_2O	3420-3240-3150	$C_{15}H_{15}N_3OS$		
C_6H_5CO	C_6H_5	96	96[a]	91	EtOH–H_2O	Not well defined	$C_{15}H_{13}N_3OS$		
$C_6H_5NHCOCH_2$	CH_3	158		87	EtOH	3430-3250-3120	$C_{11}H_{14}N_4OS$	C, 52.26 H, 6.06 N, 22.30 S, 12.76	C, 52.8 H, 5.6 N, 22.4 S, 12.8

[a]P. P. T. Sah and T. C. Daniels. Rec. trav. chim. **69**, 1545 (1950).
[b]D. Libermann, M. Moyeux, A. Rouaix, J. Maillard, L. Hengl, and J. Himbert. Bull. soc. chim. 957 (1953).
[c]F. Wild. Characterization of organic compounds. 2nd ed. Cambridge University Press. 1958. pp. 139–141.
[d]Ng. Ph. Buu-Hoi, Ng. D. Xuong, and F. Binon. J. Chem. Soc. 713 (1956).
[e]B. Holmberg. Arkiv Kemi. **9**, 65–80 (1955).
[f]L. K. Evans and A. E. Gillam. J. Chem. Soc. 565 (1943).
[g]C. Neuberg and W. Neimann. Ber. **2**, 2049 (1902).
[h]A. H. Uhl. J. Am. Pharm. Assoc. **24**, 381 (1935).
[i]G. N. Mitra and S. S. Guha-Sircar. J. Indian Chem. Soc. **32** (7), 435 (1955).

frequencies, or, at the most, with only a slight shift to the left. In the thiosemicarbazones the secondary —NH— group would be responsible for the lower frequency band at about 3150 cm^{-1}.

There is no doubt that the nature of Y and X in formula II has a definite effect on the availability of the H atom of the secondary —NH— group to take part in complex formation. When Y is aromatic, both the inductive (−I) and mesomeric effects may alter the electronic density at the nitrogen atom resulting in the weakening of the —N—H bond. When Y is aliphatic, the inductive effect (+I) would affect the —N—H bond in a reverse manner and it is likely that the formation of a copper complex proceeds by another route. Infrared spectra in these cases show consistently three bands in the —NH— stretching region for both free thiosemicarbazones and their copper complexes. On this basis pyruvic acid thiosemicarbazone – copper would be expected to behave like the aromatic compounds, because of the (−I) inductive effect of the carboxyl group. This is indeed the case, as the infrared spectrum of this complex shows two bands, instead of three, in the —NH— region. Similarly, the infrared spectrum of cyclohexanone thiosemicarbazone – copper is similar to that of the aliphatic compounds, whereas furfural thiosemicarbazone – copper gives a spectrum typical of an aromatic compound in the —NH— stretching region.

Can. J. Chem. Downloaded from www.nrcresearchpress.com by 41.223.56.140 on 09/04/12
For personal use only.

TABLE II

Thiosemicarbazone–copper complexes: $\left(\begin{matrix} Y-C=N-NH-C-NH_2 \\ \quad\quad | \quad\quad\quad\quad \| \\ \quad\quad X \quad\quad\quad\quad S \end{matrix}\right)$ Cu

Y	X	M.p., °C	Yield	Methods of purification	Typical I.R. absorptions in the —NH— region, cm^{-1}	Formula	Found, %	Calculated, %
CH_3	CH_3	174	91	*f, d*	3450–3290–3150	$C_4H_9N_3SCu$	C, 24.66 H, 4.01 N, 21.80 S, 16.95 Cu, 32.8	C, 24.8 H, 4.13 N, 21.65 S, 16.52 Cu, 32.8
C_2H_5	H	128	67	*a, b, d, e*	3420–3270–3150	$C_4H_9N_3SCu$	Cu, 31.96	Cu, 32.8
n-C_3H_7	H	168	54	*a, b, d, e*	3440–3360–3100	$C_5H_{11}N_3SCu$	Cu, 31.47	Cu, 30.3
n-C_4H_9	H	175	86	*a, c, g*	3420–3320–3160	$C_6H_{13}N_3SCu$		
n-C_6H_{13}	H	155	96	*a, c, d, e*	3450–3270–3120	$C_8H_{17}N_3SCu$	C, 38.8 H, 6.7 N, 17.2 S, 13.2 Cu, 25.4	C, 38.3 H, 6.4 N, 16.8 S, 12.8 Cu, 25.35
n-C_7H_{15}	H	153	98	*a, c, d*	3440–3270–3100	$C_9H_{19}N_3SCu$	C, 41.11 H, 7.31 N, 15.80 S, 12.40 Cu, 24.3	C, 41.0 H, 6.83 N, 15.92 S, 12.13 Cu, 24.4
n-C_8H_{17}	H	150	91	*a, c, d*	3450–3280–3110	$C_{10}H_{21}N_3SCu$	C, 44.37 H, 7.89 N, 15.10 S, 11.48 Cu, 23.0	C, 43.3 H, 7.22 N, 15.10 S, 11.95 Cu, 22.85
n-C_9H_{19}	H	149	98	*a, c, d*	3420–3270–3100	$C_{11}H_{23}N_3SCu$	N, 13.98 S, 10.63 Cu, 21.42	N, 14.4 S, 10.98 Cu, 21.75
n-$C_{10}H_{21}$	H	148	84	*a, c, d*	3450–3280–3105	$C_{12}H_{25}N_3SCu$	C, 46.97 H, 7.92 N, 14.56 S, 11.08 Cu, 19.9	C. 47.2 H, 7.86 N, 13.72 S, 10.5 Cu, 20.8
n-$C_{11}H_{23}$	H	146	88	*a, c, d*	3440–3280–3100	$C_{13}H_{27}N_3SCu$	C, 49.46 H, 8.07 N, 13.41 S, 10.28 Cu, 19.9	C, 48.8 H, 8.14 N, 13.13 S, 10.10 Cu, 19.86
n-$C_{11}H_{23}$	CH_3	134	88	*a, c, d*	3480–3330–3190	$C_{14}H_{29}N_3SCu$	C, 50.55 H, 8.81 N, 12.20 S, 9.57 Cu, 18.9	C, 50.4 H, 8.4 N, 12.58 S, 9.60 Cu, 19.0
n-$C_{15}H_{31}$	CH_3	127	78	*a, c, d*	3460–3320–3180	$C_{18}H_{37}N_3SCu$	C, 55.64 H, 9.29 N, 10.95 S. 8.33 Cu, 16.4	C, 55.5 H, 9.24 N, 10.8 S, 8.23 Cu, 16.3
$CH_2-CH_2-CH_2-CH_2-CH_2-$		165	83	*a, c, d*	3410–3280–3160	$C_7H_{13}N_3SCu$	C, 34.61 H, 5.43 N, 17.92 S, 13.92 Cu, 26.66	C, 35.8 H, 5.5 N, 17.91 S, 13.64 Cu, 27.0
$CH=CH=CH-C-O-$	H	191	75	*a, c, g*	3460–3350	$C_6H_7N_3OSCu$	C, 31.1 H, 3.0 N, 18.15 S. 13.68 Cu, 26.9	C, 31.1 H, 2.6 N, 18.14 S. 13.82 Cu, 27.0
C_6H_5	H	183	60	*a, c, h, i*	3460–3360	$C_8H_8N_3SCu$	C. 39.88 H, 3.33 N, 17.4 S, 12.80 Cu, 25.6	C. 39.6 H, 3.7 N, 17.3 S. 13.1 Cu, 26.2
o-OHC_6H_4	H	218	71	*a, c, d*	3450–3300	$C_8H_8N_3OSCu$	C, 36.65 H. 3.68 N. 16.40 S, 12.05 Cu, 24.45	C, 37.2 H. 3.1 N. 16.3 S, 12.4 Cu, 24.5

Can. J. Chem. Downloaded from www.nrcresearchpress.com by 41.223.56.140 on 09/04/12
For personal use only.

TABLE II (*Concluded*)

Thiosemicarbazone–copper complexes: $\left(\begin{matrix} Y—C=N—NH—C—NH_2 \\ \quad\quad | \quad\quad\quad\quad\quad\quad \| \\ \quad\quad X \quad\quad\quad\quad\quad\quad S \end{matrix} \right) Cu$

Y	X	M.p., °C	Yield	Methods of purification	Typical I.R. absorptions in the —NH— region, cm^{-1}	Formula	Found, %	Calculated, %
m-OHC_6H_4	H	187	88	*a, c, d, e*	3400–3290	$C_8H_8N_3OSCu$	N, 15.85	N, 16.3
							S, 12.15	S, 12.4
							Cu, 24.43	Cu, 24.5
p-OHC_6H_4	H	>300	60	*a, b, c, d, e*	3460–3340	$C_8H_8N_3OSCu$	N, 16.5	N, 16.3
							S, 12.78	S, 12.4
							Cu, 22.9	Cu, 24.5
m-$O_2NC_6H_4$	H	224	75	*a, c, d, e*	3480–3370	$C_8H_7N_4O_2SCu$	C, 33.15	C, 33.5
							H, 2.53	H, 2.44
							N, 18.50	N, 19.5
							S, 10.7	S, 11.17
							Cu, 22.23	Cu, 22.15
o-FC_6H_4	H	171	88	*a, c, h*	3430–3320	$C_8H_7FN_3SCu$	C, 36.53	C, 37.0
							H, 3.4	H, 2.7
							N, 16.15	N, 16.2
							S, 12.25	S, 12.34
							Cu, 24.5	Cu, 24.5
m-FC_6H_4	H	171	50	*a, c, h*	3440–3330	$C_8H_7FN_3SCu$	C, 37.33	C, 37.0
							H, 3.25	H, 2.7
							N, 15.96	N, 16.2
							S, 12.20	S, 12.34
							Cu, 23.9	Cu, 24.5
p-FC_6H_4*	H	172	50	*a, c, h*	3450–3340	$C_8H_7FN_3SCu$	Cu, 23.0	Cu, 24.5
o-ClC_6H_4	H	195	91	*a, c, g*	3490–3360	$C_8H_7ClN_3SCu$	C, 34.8	C, 34.8
							H, 2.9	H, 2.5
							Cl, 13.2	Cl, 12.9
							N, 15.6	N, 15.2
							S, 12.1	S, 11.6
							Cu, 22.9	Cu, 22.9
p-ClC_6H_4	H	188	86	*a, c, g, j*	3480–3360	$C_8H_7ClN_3SCu$	C, 34.1	C, 34.8
							H, 2.8	H, 2.5
							Cl, 12.4	Cl, 12.9
							N, 15.0	N, 15.2
							S, 11.15	S, 11.6
							Cu, 22.8	Cu, 22.9
p-$(OCH_3)C_6H_4$	H	183	93	*a, c, d*	3460–3330	$C_9H_{10}N_3OSCu$	N, 15.52	N, 15.45
							S, 12.30	S, 11.8
							Cu, 22.5	Cu, 23.4
2,5-$OH(Cl)C_6H_3$	H	>300	89	*a, c, d*	3430–3280	$C_8H_7ClN_3OSCu$	C, 32.16	C, 32.82
							H, 2.97	H, 2.39
							Cl, 12.20	Cl, 12.17
							N, 14.15	N, 14.38
							S, 10.67	S, 10.96
							Cu, 21.3	Cu, 21.75
2,4-$(Cl)_2C_6H_3$	H	204	100	*a, c, d, h*	3480–3360	$C_8H_6Cl_2N_3SCu$	C, 29.9	C, 30.8
							H, 2.00	H, 1.93
							Cl, 22.66	Cl, 22.80
							N, 13.28	N, 13.49
							S, 10.20	S, 10.28
							Cu, 19.9	Cu, 20.4
p-ClC_6H_4	CH_3	165	88	*a, c, g, k*	3410–3260	$C_9H_9ClN_3SCu$	C, 37.20	C, 37.25
							H, 3.97	H, 3.10
							Cl, 14.10	Cl, 12.25
							N, 15.05	N, 14.5
							S, 11.53	S, 11.05
							Cu, 20.8	Cu, 21.8
$C_6H_5CH(OH)$	C_6H_5	216	20	*c*	3460–3260–3140	$C_{15}H_{14}N_3OSCu$	C, 50.7	C, 51.8
							H, 3.7	H, 3.75
							N, 12.3	N, 12.2
							S, 9.3	S, 9.24
							Cu, 18.6	Cu, 18.3

[a]Washed with hydrochloric acid 3%.
[b]Washed with hydrochloric acid 10%.
[c]Washed with boiling methyl alcohol.
[d]Washed with boiling acetone.
[e]Washed with boiling benzene.
[f]Washed with dilute ammonium hydroxide.
[g]Dissolved in acetone and recovered by evaporation of the solvent.
[h]Crystallized from acetone.
[i]Crystallized from aqueous cellosolve.
[j]Crystallized from aqueous dioxan.
[k]Crystallized from aqueous acetone.

*Not enough material for complete analysis.

Can. J. Chem. Downloaded from www.nrcresearchpress.com by 41.223.56.140 on 09/04/12
For personal use only.

In the case of the aromatic hydroxy compounds, it is also possible that the hydroxyl groups are involved in the metal binding process, since their infrared spectra do not show a band in the OH region.

More work is being done at the moment on the structure of those copper complexes.

Although a full discussion of the microbiological data will appear elsewhere (18), it is interesting to note that antifungal activity is restricted to the thiosemicarbazones themselves, most of the copper complexes being found inactive.

EXPERIMENTAL

Carbonyl compounds were obtained from commercial sources except in the case of the four fluorobenzaldehydes which were prepared from the corresponding fluorotoluenes by Etard's reaction (21). Thiosemicarbazones were prepared by the method of Sah and Daniels (19). Copper complexes were made by a method similar to that used by Kuhn and Zilliken (15) using cuprous chloride in ammonium hydroxide. 2-Methylthiosemicarbazide (III) and its benzylidene derivative (IV) were made by the method of Greer and Smith (20). Melting points, yields, solvents used in purification, bonds in the —NH— region of the infrared spectrum, and analyses are reported in Tables I and II. Melting points were taken on a Fisher–John apparatus and are not corrected.

o-Fluorobenzaldehyde Thiosemicarbazone

o-Fluorobenzaldehyde was first prepared using 40 g (0.36 mole) *o*-fluorotoluene (from *o*-toluidine; b.p. 114°, lit. b.p. 114°) (22) in glacial acetic acid (570 ml), acetic anhydride (565 ml), concentrated sulphuric acid (85 ml), and chromium trioxide (100 g). There was obtained *o*-fluorobenzaldiacetate (18 g, 40%, m.p. 25–27°), which was hydrolyzed to the free aldehyde by heating under reflux for $\frac{1}{2}$ hour in a mixture of ethyl alcohol (50 ml), water (25 ml), and sulphuric acid (10 ml). A sample of the resulting solution treated with phenylhydrazine afforded *o*-fluorobenzaldehyde phenylhydrazone (m.p. 89°, lit. m.p. 89.5°) (23).

The rest of the solution was neutralized to litmus and to this was added a solution of thiosemicarbazide (I) (9.1 g, 0.1 mole) in water (150 ml) and acetic acid (10 ml). *o*-Fluorobenzaldehyde thiosemicarbazone (II, Y = *o*-FC_6H_4, X = H) crystallized at once.

m-Fluorobenzaldehyde Thiosemicarbazone

m-Fluorobenzaldehyde was prepared by the same method using *m*-fluorotoluene (31.5 g, 0.28 mole; from *m*-toluidine: b.p. 116°, lit. b.p. 116°) (22). The *m*-fluorobenzaldiacetate obtained had m.p. 37° (18 g, 27%). Anal. calc. for $C_{11}H_{11}FO_4$: mol. wt., 226; C, 58.4; H, 4.9. Found: C, 59.1; H, 5.7.

Hydrolysis of the latter with sulphuric acid (10 ml) in aqueous alcohol gave a solution of *m*-fluorobenzaldehyde. A portion of this solution, reacted with phenylhydrazine to give the expected phenylhydrazone (m.p. 113°, lit. m.p. 114°) (22). After neutralization, the remaining solution was mixed with 300 ml of an aqueous solution of thiosemicarbazide (9.1 g, 0.1 mole) and the thiosemicarbazone crystallized immediately.

p-Fluorobenzaldehyde Thiosemicarbazone

This preparation was carried out as above using *p*-fluorotoluene (11.7 g, 0.1 mole; b.p. 116°, lit. b.p. 117° (22) from *p*-toluidine). The diacetate did not crystallize in this case but was extracted with ether. After evaporation of the solvent, the residual oil was hydrolyzed in the usual manner and its reaction with thiosemicarbazide gave the expected thiosemicarbazone.

Can. J. Chem. Downloaded from www.nrcresearchpress.com by 41.223.56.140 on 09/04/12
For personal use only.

2-Fluoro-5-nitrobenzaldehyde Thiosemicarbazone

This compound was prepared as the previous ones starting with 2-fluoro-5-nitrotoluene (24) (40 g, 0.24 mole). The diacetate was obtained as an uncrystallizable oil (26 g, 38%), which after hydrolysis and reaction with thiosemicarbazide gave the expected thiosemicarbazone.

Preparation of Copper Complexes

The preparation of benzaldehyde thiosemicarbazone – copper complex illustrates the general method used.

To a gently refluxing solution of benzaldehyde thiosemicarbazone (9.8 g, 0.05 mole) in methyl alcohol (200 ml) was added dropwise a solution of cuprous chloride (5 g, 0.05 mole) in ammonium hydroxide (100 ml, sp. gr. 0.9). A yellow precipitate was formed and the mixture was stirred for ½ hour to complete the formation of the complex. After cooling, the solid was collected by filtration and washed with dilute hydrochloric acid, water, and alcohol.

Other purifying procedures are listed, for each compound, in Table II.

ACKNOWLEDGMENTS

Our thanks are due to Mr. E. C. Goodhue and Mr. R. Ironside, both of the Analytical Section, for carrying out the copper analyses and for taking the infrared spectra respectively.

REFERENCES

1. G. Domagk, R. Behnisch, F. Mietzsch, and H. Schmidt. Naturwissenschaften, **33**, 315 (1946).
2. L. Heilmeyer. Deut. med. Wochschr. **74**, 161 (1949).
3. J. P. Jouin and Ng. Ph. Buu-Hoi. Ann. inst. Pasteur, **72**, 580 (1946).
4. E. Hoggarth, A. E. Martin, N. E. Storey, and E. H. P. Young. Brit. J. Pharmacol. **4**, 248 (1949).
5. R. Donovick, F. Pansy, G. Stryker, and J. Bernstein. J. Bacteriol. **59**, 667 (1950).
6. C. W. Johnson, J. W. Joyner, and R. P. Perry. Antibiotics & Chemotherapy, **2**, 636 (1952).
7. H. W. Gausman, C. L. Rhykerd, H. R. Hinderliter, E. S. Scott, and L. F. Audrieth. Botan. Gaz. **114**, 292 (1953).
8. H. Erlenmeyer, J. Baumler, and W. Roth. Helv. Chim. Acta, **36**, 947 (1953).
9. H. G. Mautner, W. D. Kumler, Y. Okano, and R. Pratt. Antibiotics & Chemotherapy, **6**, 51 (1956).
10. A. Albert, C. W. Rees, and A. J. H. Tomlinson. Rec. trav. chim. **75**, 819 (1956).
11. J. Cymerman-Craig, D. Willis, S. D. Rubbo, and J. Edgar. Nature, **176**, 34 (1955).
12. A. Albert. Nature, **182**, 421 (1958).
13. W. O. Foye, I. B. Van de Workeen, Jr., and J. D. Matthes. J. Am. Pharm. Assoc. Sci. Ed. **47**, 8, 556 (1958).
14. D. Hamre, J. Bernstein, and R. Donovick. J. Bacteriol. **59**, 675 (1950).
15. R. Kuhn and F. Zilliken. U.S. Patent No. 2,695,911 (November, 1954).
16. S. S. Guha-Sircar and S. Satpathy. J. Indian Chem. Soc. **31**, 6, 451 (1954). S. S. Guha-Sircar and G. N. Mitra. J. Indian Chem. Soc. **32**, 7, 435 (1955).
17. L. G. Bellamy. The infrared spectra of complex molecules. Methuen & Co. Ltd., London. 1954. p. 175.
18. B. G. Benns, B. A. Gingras, and C. H. Bayley. To be published.
19. P. T. Sah and T. C. Daniels. Rec. trav. chim. **69**, 1545 (1950).
20. A. H. Greer and G. B. L. Smith. J. Am. Chem. Soc. **72**, 874 (1950).
21. Organic syntheses. Vol. II. John Wiley & Sons, Inc., N.Y. 1948. p. 441.
22. Dictionary of organic compounds. Vol. II. *Edited by* Sir Ian Heilbron and H. M. Bunbury. London. 1953. p. 558.
23. J. B. Shoesmith, C. E. Sosson, and R. H. Slater. J. Chem. Soc. 2760 (1926).
24. B. A. Gingras and C. H. Bayley. Can. J. Chem. **37**, 988 (1959).

Can. J. Chem. Downloaded from www.nrcresearchpress.com by 41.223.56.140 on 09/04/12
For personal use only.

Can. J. Chem. Downloaded from www.nrcresearchpress.com by 84.22.46.98 on 09/08/12
For personal use only.

DISTRIBUTION OF SUBSTITUENTS IN A PARTIALLY METHYLATED 4-*O*-METHYLGLUCURONOXYLAN[1]

INGEMAR CROON[2] AND T. E. TIMELL

ABSTRACT

A 4-*O*-methylglucuronoxylan has been partially methylated and the distribution of the substituents has been established. The hydroxyl group at C_3 was less reactive than that at C_2 in both the main xylan chain and in the acid side chains. Caution should be exercised in attributing structural significance to the presence of small amounts of sugars containing C_3 hydroxyl groups in hydrolyzates from methylated xylans.

In a previous investigation (1) the distribution of the substituents in a partly methylated xylan from esparto grass was established. This paper is concerned with the location of the substituents in a partially methylated 4-*O*-methylglucuronoxylan from white birch wood, a type of xylan more frequently encountered than the neutral polymer occurring in esparto.

RESULTS AND DISCUSSION

The polysaccharide was isolated by alkaline extraction of a birch chlorite holocellulose (2). It had previously (3) been found to contain 120 (1 → 4)-linked β-D-xylopyranose residues in a linear chain to which single side chains of 4-*O*-methyl-α-D-glucuronic acid residues were attached through C_2 of every tenth, on the average, of the xylose residues. The xylan was methylated with dimethyl sulphate and alkali until a methoxyl content of 26.6% had been reached. The partly methylated product was subjected to methanolysis and neutral and acidic sugars were separated on a column of anion exchange resin. The acid portion contained as sole component a partly methylated aldobiouronic acid, composed of xylose and glucuronic acid residues. It was esterified, reduced, and hydrolyzed to yield a mixture of reducing sugars. Hydrolysis of the neutral fraction gave a similar sugar mixture.

Both mixtures were separately resolved on a column of charcoal and Celite (4) by gradient elution (5) with aqueous ethanol (6). With one exception, complete resolution was achieved throughout. All sugars were either obtained crystalline or were converted to crystalline derivatives. The results are presented in Table I.

TABLE I

Molar composition in percentage of neutral and acid portions of the 4-*O*-methylglucuronoxylan

Neutral portion		Acid portion	
D-Xylose	10.6	D-Xylose	7.8
2-*O*-Methyl-D-xylose	12.3	3-*O*-Methyl-D-xylose	39.5
3-*O*-Methyl-D-xylose	9.8	4-*O*-Methyl-D-glucose	5.9
2,3-Di-*O*-methyl-D-xylose	67.3	2,4-Di-*O*-methyl-D-glucose	7.0
		3,4-Di-*O*-methyl-D-glucose	3.4
		2,3,4-Tri-*O*-methyl-D-glucose	36.4

[1]*Manuscript received February 9, 1960.*
Contribution from McGill University and the Pulp and Paper Research Institute of Canada, Montreal, Que.
[2]*Harold Hibbert Memorial Fellow, McGill University, 1959.*

In the case of the esparto xylan, a direct comparison between found and statistically calculated distributions (1) showed that the C_2 hydroxyl group was approximately 2.5 times as reactive as the C_3 hydroxyl but that methylation at C_2 doubled the reactivity of the remaining C_3 hydroxyl (7). Such a calculation is less easily applied in the present case. It is evident, however, that in those xylose residues in the main chain which carried no acid side groups, the ratio between the relative reactivities of the C_2 and C_3 hydroxyl groups was lower than the corresponding value for the esparto xylan. The distribution of the C_2 and C_3 methoxyl groups in the acid side chains corresponded to that expected for a partly methylated polysaccharide containing two hydroxyl groups, one of which was two to three times as reactive as the other. Those xylose residues which carried side chains were almost completely substituted.

The results indicate that the C_2 hydroxyl group is more reactive than that at C_3 in both the main xylan chain and in the side chains of a 4-*O*-methylglucuronoxylan. Due to changes in the electron density distribution (1, 7), the reactivity of the C_3 hydroxyl is probably enhanced by substitution at C_2. Complete methylation of polysaccharides is sometimes extremely difficult to achieve. It is clear from the present results that incomplete methylation is likely to cause the presence of mainly 2-*O*-methyl-D-xylose and 2,4-di-*O*-methyl-D-glucuronic acid in the acid hydrolyzate of 4-*O*-methylglucuronoxylans. Caution should be exercised in attributing structural significance to these sugars, even in the absence of the corresponding 3-*O*- and 3,4-di-*O*-substituted derivatives.

EXPERIMENTAL

Specific rotations were equilibrium values and were determined at a temperature of +25° C, at a concentration of 2.0, and with water as solvent. All melting points are corrected. Paper chromatography was carried out with a butan-2-one-water mixture (89:11) and sugars were located by spraying with *o*-aminodiphenyl (8). Paper electrophoresis was carried out with a 0.05 *M* borate buffer at a pH of 9.4.

Methylation of the Hemicellulose

A 4-*O*-methylglucuronoxylan was prepared in 29% yield (based on the wood) from a white birch chlorite holocellulose (2). The hemicellulose gave only xylose and uronic acids on hydrolysis and had a number-average degree of polymerization of 120 (osmometry). 4-*O*-Methylglucuronoxylan (25 g) was dissolved in 24% (w/w) potassium hydroxide (600 ml) in an atmosphere of nitrogen, and dimethyl sulphate (400 ml) was added dropwise at room temperature over a period of 18 hours. The reaction mixture was neutralized with acetic acid and was dialyzed against distilled water for a week. Freeze-drying of the solution gave a white, fluffy material (22 g), OMe, 26.6%.

Methanolysis and Separation of Neutral and Acidic Sugars

The partly methylated hemicellulose (21.5 g) was boiled under reflux for 10 hours with 2% methanolic hydrogen chloride in the presence of Drierite. Neutralization with silver carbonate, filtration through Celite, and evaporation to dryness yielded a pale, yellow sirup (21 g). The mixture of glycosides was dissolved in water (200 ml) and treated with barium hydroxide (10 g) at 70° for 2 hours (9). Excess barium carbonate was removed by addition of solid carbon dioxide, followed by filtration through Celite, after which the solution was treated with Amberlite IR-120 exchange resin and concentrated to 200 ml. The acidic solution was added to the top of a column (5×30 cm) containing Dowex 1-X4 exchange resin (20–50 mesh, acetate cycle). Neutral sugars

Can. J. Chem. Downloaded from www.nrcresearchpress.com by 84.22.46.98 on 09/08/12
For personal use only.

(15.2 g) were eluted with water (5–6 liters), after which an acid fraction (2.5 g) was obtained by elution with 30% aqueous acetic acid (4 liters).

Reduction of the Acid Fraction and Hydrolysis of the Glycosides

The acid fraction was boiled under reflux with 2% methanolic hydrogen chloride and the ester–glucoside mixture was reduced with lithium aluminum hydride (2.5 g) in dry tetrahydrofuran (100 ml). Hydrolysis of the neutral fraction and of the reduced acid fraction yielded two mixtures of reducing sugars (A and B, respectively).

Resolution of Sugar Mixture A

A portion of the mixture of neutral sugars (A) (1.55 g) was added to the top of a Darco G-60 charcoal – Celite column (4) (1:1 w/w, 3.5×55 cm) and the sugars were recovered by gradient elution with aqueous ethanol as described previously (1). Four fractions containing only one compound were obtained, in addition to one which was a mixture of mono-*O*-methylxyloses and which was further resolved by paper electrophoresis. Amount recovered: 1.41 g.

Identification of Sugars

D-*Xylose.*—The first fraction (131 mg) crystallized, m.p. and mixed m.p. 145–146° C, $[\alpha]_D$ +19°.

3-O-Methyl-D-*xylose.*—This sugar (132 mg) also crystallized, m.p. and mixed m.p. 102–103° C, $[\alpha]_D$ +18°.

2-O-Methyl-D-*xylose.*—The crystalline sugar (166 mg) had m.p. and mixed m.p. 133–134° C, $[\alpha]_D$ +36°.

2,3-Di-O-methyl-D-*xylose.*—This sugar which constituted the last fraction (982 mg) had m.p. 101° C after recrystallization from ethyl acetate (10, 11), $[\alpha]_D$ +22°.

Resolution of Sugar Mixture B

Sugar mixture B (2.2 g) was added to the top of the same charcoal–Celite column and successively eluted with the following solvents: water (3 liters) → 10% ethanol (3 liters), 10% ethanol (2 liters) → 20% ethanol (2 liters), 20% ethanol (1 liter) → 50% ethanol (1 liter). The total amount of material recovered was 2.0 g.

Identification of Sugars

D-*Xylose.*—The first fraction (124 mg) crystallized, m.p. and mixed m.p. 145° C, $[\alpha]_D$ +18°.

3-O-Methyl-D-*xylose.*—The crystalline sugar (671 mg) had m.p. and mixed m.p. 102–103° C, $[\alpha]_D$ +18°.

4-O-Methyl-D-*xylose.*—The sirupy sugar (121 mg), $[\alpha]_D$ +61°, was converted to its crystalline osazone, m.p. and mixed m.p. 157–158° C. Its infrared spectrum was identical with that of an authentic specimen.

2,4-Di-O-methyl-D-*glucose.*—This fraction was contaminated with an unknown compound, travelling faster on the paper chromatogram. The mixture (168 mg) was added to the top of a cellulose column (3.8×35 cm) and eluted with butan-2-one saturated with water to yield a pure di-*O*-methylglucose (154 mg). The sirupy sugar, $[\alpha]_D$ +76°, was converted to the crystalline 2,4-di-*O*-methyl-N-*p*-nitrophenyl-D-glucosylamine, m.p. 250–251° C, undepressed on admixture with an authentic sample.

3,4-Di-O-methyl-D-*glucose.*—The crystalline sugar (76 mg) had m.p. and mixed m.p. 113–115° C, $[\alpha]_D$ +95°.

Can. J. Chem. Downloaded from www.nrcresearchpress.com by 84.22.46.98 on 09/08/12
For personal use only.

*2,3,4-Tri-O-methyl-*D*-glucose.*—The sirupy sugar (860 mg), $[\alpha]_D$ +65°, was converted to the crystalline 2,3,4-tri-*O*-methyl-N-phenyl-D-glucosylamine, m.p. and mixed m.p. 144–145° C.

ACKNOWLEDGMENTS

The authors wish to express their gratitude to Dr. C. B. Purves for his kind interest in the present investigation. They are also grateful to Dr. C. T. Bishop and Professor Fred Smith for the gift of several sugar samples. Financial support from the National Research Council is gratefully acknowledged.

REFERENCES

1. I. CROON and T. E. TIMELL. J. Am. Chem. Soc. In press.
2. C. P. J. GLAUDEMANS and T. E. TIMELL. Svensk Papperstidn. **60**, 869 (1957).
3. C. P. J. GLAUDEMANS and T. E. TIMELL. J. Am. Chem. Soc. **80**, 941, 1209 (1958).
4. R. L. WHISTLER and D. F. DURSO. J. Am. Chem. Soc. **72**, 677 (1950).
5. R. S. ALM. Acta Chem. Scand. **6**, 1186 (1952).
6. B. LINDBERG and B. WICKBERG. Acta Chem. Scand. **8**, 569 (1954).
7. I. CROON and B. LINDBERG. Svensk Papperstidn. **60**, 843 (1957).
8. T. E. TIMELL, C. P. J. GLAUDEMANS, and A. L. CURRIE. Anal. Chem. **28**, 1916 (1956).
9. G. G. S. DUTTON and F. SMITH. J. Am. Chem. Soc. **78**, 2505 (1956).
10. J. K. HAMILTON, E. V. PARTLOW, and N. S. THOMPSON. Tappi, **41**, 811 (1958).
11. A. L. CURRIE and T. E. TIMELL. Can. J. Chem. **37**, 922 (1959).

Can. J. Chem. Downloaded from www.nrcresearchpress.com by 84.22.46.98 on 09/08/12
For personal use only.

Can. J. Chem. Downloaded from www.nrcresearchpress.com by 186.148.149.217 on 09/04/12
For personal use only.

ELECTRON SPIN RESONANCE ABSORPTION OF DIPHENYLPICRYLHYDRAZYL – ZINC OXIDE MIXTURES[1]

Y. MATSUNAGA[2] AND C. A. MCDOWELL

ABSTRACT

Electron spin resonance measurements on mixtures of αα-diphenyl-β-picrylhydrazyl (DPPH) and zinc oxide when compared with corresponding determinations on DPPH itself, and with DPPH – potassium chloride mixtures, indicate that there is a transfer of electrons between the DPPH and the zinc oxide. These observations support earlier published views of Harrison and McDowell, who found that the above mixture was able to enhance the catalysis of the ortho–para hydrogen conversion, and the hydrogen–deuterium exchange reaction.

INTRODUCTION

Mixtures of αα-diphenyl-β-picrylhydrazyl (DPPH) and zinc oxide have been found to be more efficient catalysts of the ortho–para hydrogen conversion (1, 2) than either of the two components alone. This led Harrison and McDowell (2) to postulate that the enhancement of the catalysis was caused by an electron transfer process occurring at the DPPH – zinc oxide interface. More recently Eley and Inokuchi (3) have found evidence for partial transfer processes in the systems DPPH–hydrogen, and also in DPPH – hydrogen sulphide. We here report the results of some experiments on the electron spin resonance absorption of mixtures of DPPH and potassium chloride, and DPPH and zinc oxide. These observations, as do also some less complete ones on DPPH – nickel oxide mixtures, confirm the earlier views of Harrison and McDowell (2) that electron transfer processes occur at the DPPH – zinc oxide interface.

EXPERIMENTAL

Pure non-sintered zinc oxide was prepared by treating a slightly acidic solution of zinc sulphate with metallic zinc to remove heavy metal ions. Ferrous iron was oxidized with hydrogen peroxide and removed by coprecipitation with zinc hydroxide by addition of a small quantity of ammonium hydroxide solution. Zinc oxalate was prepared from thus purified solution of zinc sulphate and calcined at 400° C for 6 hours.

αα-Diphenyl-β-picrylhydrazyl (DPPH) was prepared by oxidation of the corresponding hydrazine, supplied by Eastman–Kodak, with lead dioxide and recrystallized from a mixture of benzene and ligroin. Our sample contained crystalline benzene, but the mole ratio is less than one (6). Therefore, there is to be expected an "oxygen effect" as reported by Bennett and Morgan (5).

DPPH and zinc oxide mixtures were prepared, in a ratio of 1:9 by weight, by grinding the compounds in a mortar. The derivative of the electron spin resonance absorption was recorded on our electron spin resonance spectrometer at a frequency of 9000 Mc/sec. For convenience the distance between points of maximum slope ΔH_{ms} and the peak-to-peak intensity I_p on derivative curve will be used in this paper. The area A under the absorption curve can be estimated by the product of the square of ΔH_{ms} and I_p (3). The value of I_p of DPPH in vacuum is taken as unity.

RESULTS AND DISCUSSION

The DPPH used in this experiment had a ΔH_{ms} of 1.4 oersteds *in vacuo*, and a ΔH_{ms} of 1.45 oersteds and an I_p of 0.66 in air. The value of ΔH_{ms} of crystalline solvent-free DPPH

[1]*Manuscript received December 9, 1959.*
Contribution from the Department of Chemistry, University of British Columbia, Vancouver 8, B.C.
[2]*National Research Council Postdoctorate Fellow, 1957–59 (on leave of absence from The Department of Chemistry, University of Tokyo, Tokyo, Japan).*

has been reported to be 0.85 oersted and that with 0.8 mole of crystalline benzene 4.6 oersteds (3). No electron spin resonance absorption was detected in zinc oxide under the conditions of the present experiments.

A preliminary examination of the interaction between DPPH and zinc oxide was carried out in air without considering the oxygen effect. By grinding the compounds for a few minutes the value of I_p decreased to less than 0.4. A further, more rapid, decrease in I_p was caused by prolonged mixing. I_p was also observed to decrease slowly on standing. These results are shown in Fig. 1.

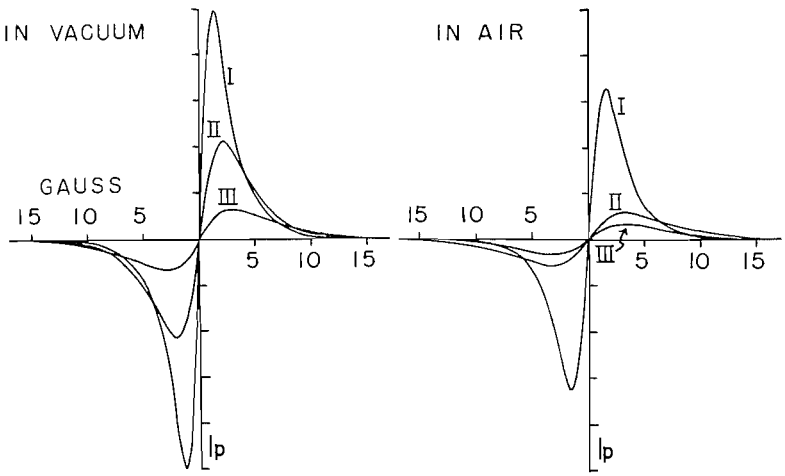


FIG. 1. Electron spin resonance absorption of mixtures of diphenylpicrylhydrazyl and zinc oxide. Curve I refers to DPPH alone; curve II refers to the DPPH–ZnO mixture No. 2 in Table I; curve III refers to the DPPH–ZnO mixture No. 4 in Table I. The value of I_p for DPPH in vacuum is taken as unity.

The variation of I_p with time is shown in Fig. 2. Curves A and B in this figure refer to measurements on the same mixture but at different degrees of mixing. Although the I_p of DPPH shows a marked decrease by grinding with zinc oxide, the area under the

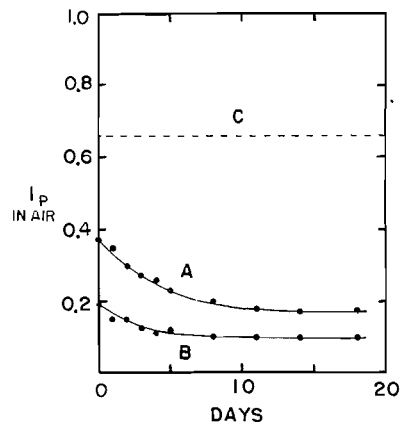


FIG. 2. Variation of the electron spin resonance absorption of mixtures of diphenylpicrylhydrazyl and zinc oxide (1:9) with time. Curves A and B refer to two mixtures with different degrees of admixing (B is the result of prolonged mixing). Curve C refers to a mixture of diphenylpicrylhydrazyl and potassium chloride (1:9); DPPH alone also gives a signal of this magnitude.

Can. J. Chem. Downloaded from www.nrcresearchpress.com by 186.148.149.217 on 09/04/12
For personal use only.

absorption curve, which is proportional to the electron spin concentration, does not change so much because of the increase of ΔH_{ms}. No change of g-value was observed.

The results shown in Figs. 1 and 2 indicate that the values of ΔH_{ms} and I_p mixtures of DPPH and potassium chloride (1:9) do not change with time, nor do these data differ from the values for DPPH alone. Therefore, the observed line broadening in DPPH – zinc oxide mixtures suggests that there is a change of environment of the unpaired electrons by some kind of interaction between the DPPH and the zinc oxide. As this solid–solid interaction proceeds fairly rapidly by grinding, it was found quite difficult to prepare homogeneously mixed samples in different stages of the interaction. A few preparations, which could be considered to be well mixed, were examined *in vacuo* and in air. The results are given in the following table.

TABLE I

Electron spin resonance absorption of DPPH–ZnO mixtures

		In vacuum			In air		
		ΔH_{ms}	I_p	A^*	ΔH_{ms}	I_p	A^*
DPPH–KCl		1.4	1.00	1.0	1.45	0.66	0.7
DPPH–ZnO	(1)	1.85	0.63	1.1	2.5	0.22	0.7
	(2)	2.1	0.43	1.0	3.2	0.12	0.6
	(3)	2.2	0.31	0.8	3.2	0.10	0.5
	(4)	2.85	0.13	0.5	3.5	0.07	0.4

NOTE: The numbers, for example (1), after the DPPH–ZnO refer to different mixtures.
*Estimated error ±0.1.

The data obtained *in vacuo* show that the absorption line is broadened by interaction between DPPH and zinc oxide. The electron spin concentration seems to be constant in the initial stages of mixing, but a permanent decrease is found as time increases. It is not clear whether this apparent loss of spin is due to the real disappearance of unpaired electrons or the fact that some of unpaired electrons are in a different state and show too broad a resonance absorption to be detected. It is, however, apparent that there is some transfer of electrons, though whether this transfer is from the DPPH to the zinc oxide, or vice versa, cannot be deduced from our results.

The decrease of I_p by admission of air is several times larger in DPPH – zinc oxide mixtures than in DPPH alone. This oxygen effect on electron spin resonance absorption is instantaneous and reversible in DPPH (2) and also in DPPH – zinc oxide.

Since zinc oxide is an excess, or n-type, semiconductor, it was of interest to see if the effects observed with mixtures of this compound and DPPH would also occur with a defect, or p-type, semiconductor and DPPH. A few experiments were carried out with DPPH and nickel oxide which is a p-type semiconductor. The nickel oxide was prepared by calcination of the nitrate. The results are shown in Table II.

TABLE II

Electron spin resonance absorption of DPPH–NiO mixtures

		In vacuum			In air		
		ΔH_{ms}	I_p	A^*	ΔH_{ms}	I_p	A^*
DPPH–CCl		1.4	1.00	1.0	1.45	0.66	0.7
DPPH–NiO	(1)	1.7	0.22	0.3	2.0	0.18	0.4
	(2)	2.8	0.045	0.2	3.1	0.036	0.2

Can. J. Chem. Downloaded from www.nrcresearchpress.com by 186.148.149.217 on 09/04/12
For personal use only.

The same trends are observed in the results for the DPPH – nickel oxide mixtures as we found for the DPPH – zinc oxide mixtures. These observations must, therefore, be taken as additional evidence that electron transfer processes do occur at DPPH–oxide interfaces.

ACKNOWLEDGMENTS

We wish to thank the National Research Council of Canada for generous grants-in-aid of this research work.

REFERENCES

1. J. TURKEVICH and P. W. SELWOOD. J. Am. Chem. Soc. **63**, 1077 (1941).
2. L. G. HARRISON and C. A. McDOWELL. Proc. Roy. Soc. A, **228**, 66 (1955).
3. D. D. ELEY and H. INOKUCHI. Z. Elektrochem. **63**, 29 (1959).
4. R. H. POIRIER, E. J. KAHLER, and F. BENINGTON. J. Org. Chem. **17**, 1437 (1952).
5. J. E. BENNETT and E. J. H. MORGAN. Nature, **182**, 199 (1958).
6. J. J. LOTHE and G. EIA. Acta Chem. Scand. **12**, 1535 (1958).

Can. J. Chem. Downloaded from www.nrcresearchpress.com by 186.148.149.217 on 09/04/12
For personal use only.

Can. J. Chem. Downloaded from www.nrcresearchpress.com by 186.148.149.217 on 09/04/12
For personal use only.

THE STUDY OF HYDROGEN BONDING AND RELATED PHENOMENA BY ULTRAVIOLET LIGHT ABSORPTION

PART III. THE STRENGTH OF THE DIMERIC HYDROGEN BOND IN SUBSTITUTED BENZOIC ACIDS AS A MEASURE OF ELECTRONIC AND STERIC INTERACTIONS[1]

W. F. FORBES,[2] A. R. KNIGHT,[3] AND D. L. COFFEN[4]

ABSTRACT

The strength of the intermolecular (dimeric) hydrogen bond in substituted benzoic acids, as estimated from the observed concentration dependence of the ultraviolet absorption spectra, is found to vary with the nature and the position of the substituent. The effects of a number of substituents on the strength of the dimeric hydrogen bond can be rationalized in terms of the usual electronic and steric interactions. The data indicate that *o*-methoxybenzoic acid forms a stronger intramolecular hydrogen bond than *o*-fluorobenzoic acid.

INTRODUCTION

In Part II (1) it was shown that the observed concentration dependences of the main absorption band in the ultraviolet spectra for a number of benzoic acids could be satisfactorily explained by supposing that these changes are caused by the effect of dilution on the benzoic acid monomer–dimer equilibrium. The greatest concentration at which a marked concentration dependence is first observed was taken as an approximate measure of the dimeric bond strength. This "critical" concentration was greater when the intermolecular hydrogen bond was assumed to be weak than if the bond was assumed to be strong. The purpose of the present paper is to summarize the available concentration dependences and to compare these values with other available data.

EXPERIMENTAL

The method of determining the ultraviolet spectra has been described in Part II (1), which also lists some of the relevant concentration dependences. Additional data are listed in Figs. 1, 3, and 4, and Table I lists all the available critical maximal concentrations and the infrared data.

Critical maximal concentrations were used for comparison purposes, rather than to attempt to obtain the dimerization constants, for the following reasons:

(i) It was found impossible to obtain a value of the extinction coefficient which could confidently be associated with the absorption of the monomeric form (see Figs. 1, 3, and 4, which show that no definite flattening out occurs at the left-hand side of the plots). Calculations using the accepted value of K_D ($K_D = [D]/[M]^2$, [D] = concn. of dimer, [M] = concn. of monomer) indicate that the minimal critical concentrations should occur only at ca. 10^{-6} *M*, which lies outside the investigated concentration range. This

[1]*Manuscript received in original form July 20, 1959, and, as revised, January 29, 1960.*
Contribution from the Memorial University of Newfoundland, St. John's, Newfoundland, and the Division of Protein Chemistry, C.S.I.R.O., Melbourne, Victoria, Australia.
[2]*Present address: Division of Protein Chemistry, C.S.I.R.O., 343 Royal Parade, Parkville, N.2 (Melbourne), Victoria, Australia.*
[3]*Present address: Chemistry Department, University of Alberta, Edmonton, Alberta.*
[4]*Present address: Chemistry Department, University of Toronto, Toronto, Ontario.*

confirms the experimental observation that measurements for solutions containing only monomeric species cannot be obtained directly. Moreover, extrapolation to zero concentration of the observed curve to obtain the value corresponding to monomer absorption is considered unreliable since the curve does not obey exactly the relationship suggested by a simple monomer–dimer equilibrium (see below).

(ii) It was found impossible to obtain a reliable value for the absorption of the dimeric form. Although the absorption beyond the critical concentration remains approximately constant, this cannot be assumed to correspond to pure dimer absorption, since the infrared data indicate the presence of monomer even beyond this critical concentration (see Fig. 2). Using the accepted value for K_D of ca. $1.6\times10^{+4}$ for benzoic acid it was found that a theoretical plot of concentration against percentage of dimerized acid afforded a curve approximately but not entirely similar to that shown in Fig. 1, and that at the critical concentration the proportion of monomer would be ca. 82%. Comparison between the calculated and experimentally obtained curve for benzoic acid shows that only in the experimentally obtained curve is a critical maximal concentration dependence obtained. It is difficult to ascribe a reason for this behavior, but we can deduce from this

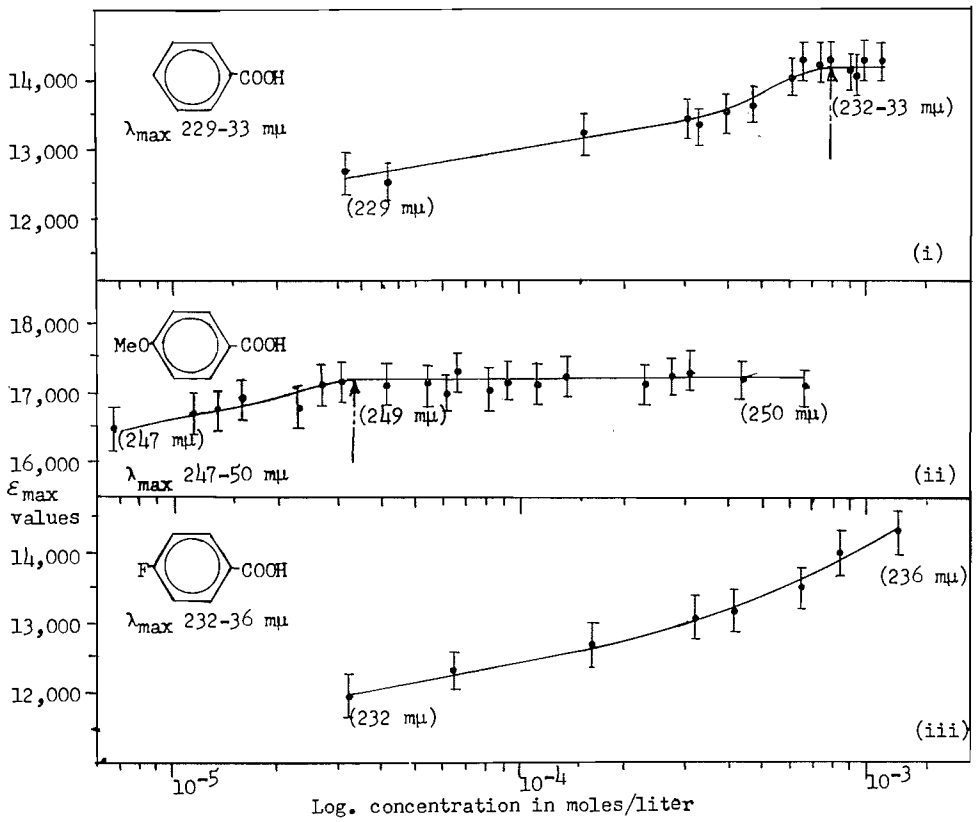


FIG. 1. The variation of ϵ_{max} on changing the solute concentration for (i) benzoic acid in cyclohexane solution, (ii) *p*-anisic acid in cyclohexane solution containing 5% ether,* and (iii) *p*-fluorobenzoic acid in cyclohexane solution.

**It has been shown (1) that the critical maximal concentration is not affected by small quantities of ether in solutions of cyclohexane.*

Can. J. Chem. Downloaded from www.nrcresearchpress.com by 186.148.149.217 on 09/04/12
For personal use only.

that the observed relationship only approximates, but does not correspond exactly to, the simple mass action law relationship. It may also be noted that the infrared carbonyl spectra at concentrations within the solute concentration range 0.5×10^{-2} to 0.5 M—that is above the "critical" level, where the ultraviolet absorption is constant—indicate that the dimer concentration still increases, but the monomer concentration significantly does *not* show a corresponding intensity decrease. This again is taken to indicate that deviations occur from the simple mass action law relationship.

Since the accurate absorption values of both the monomeric and dimeric form are required for the simple mass-law treatment, dimerization constants calculated from the simple mass action law using estimated values were found to afford a wide spread, although the values were approximately of the right order, that is, ranging between $0.5\times10^{+4}$ to $3.5\times10^{+4}$ for the value of K_D.

The infrared spectra at different solute concentrations were determined at 30° C in cyclohexane or carbon tetrachloride on a Unicam SP100 spectrophotometer in 0.5-mm cells, normally using a diffraction grating. Results are listed in Table I and Fig. 2. Figure 2 records the spectra in carbon tetrachloride solution because the lack of solubility of a number of acids in cyclohexane prevented the determination of the spectra in the latter solvent. However, when the acid was soluble in cyclohexane, the spectra were determined in both solvents and were found to be almost identical.

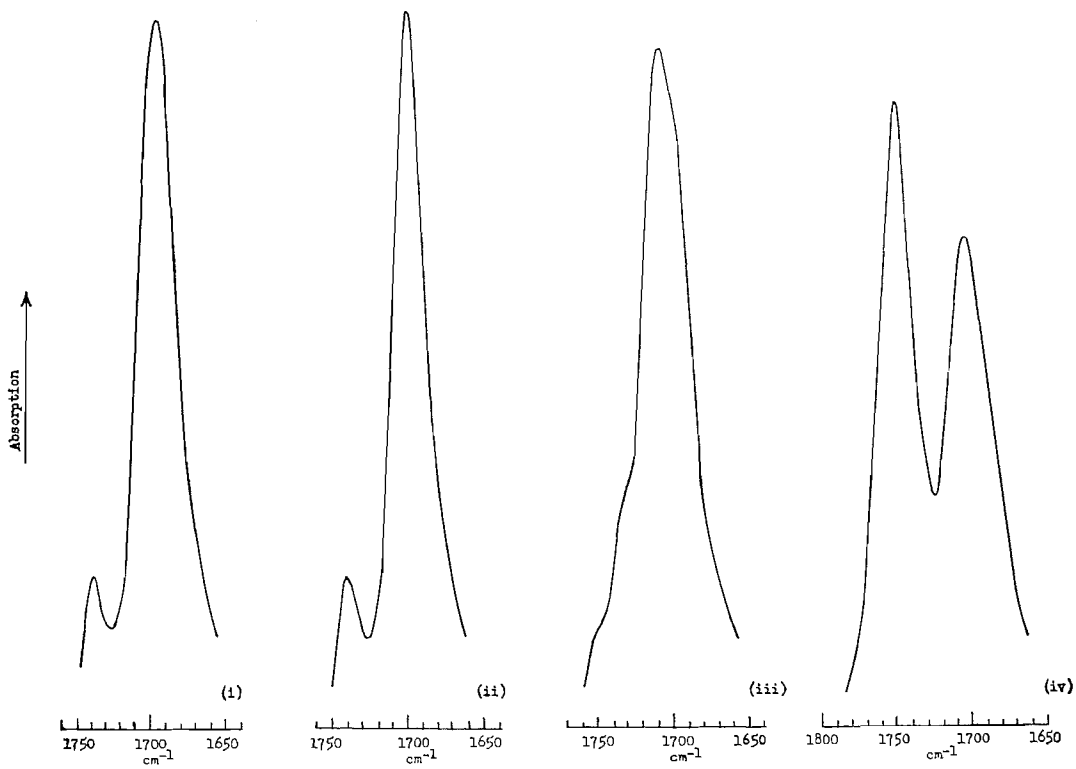


FIG. 2. The infrared carbonyl stretching bands in carbon tetrachloride solution at a concentration of ca. 3.5×10^{-2} moles/liter of (i) benzoic acid, (ii) *p*-fluorobenzoic acid, (iii) *o*-fluorobenzoic acid, and (iv) *o*-methoxybenzoic acid.

Can. J. Chem. Downloaded from www.nrcresearchpress.com by 186.148.149.217 on 09/04/12
For personal use only.

Can. J. Chem. Downloaded from www.nrcresearchpress.com by 186.148.149.217 on 09/04/12
For personal use only.

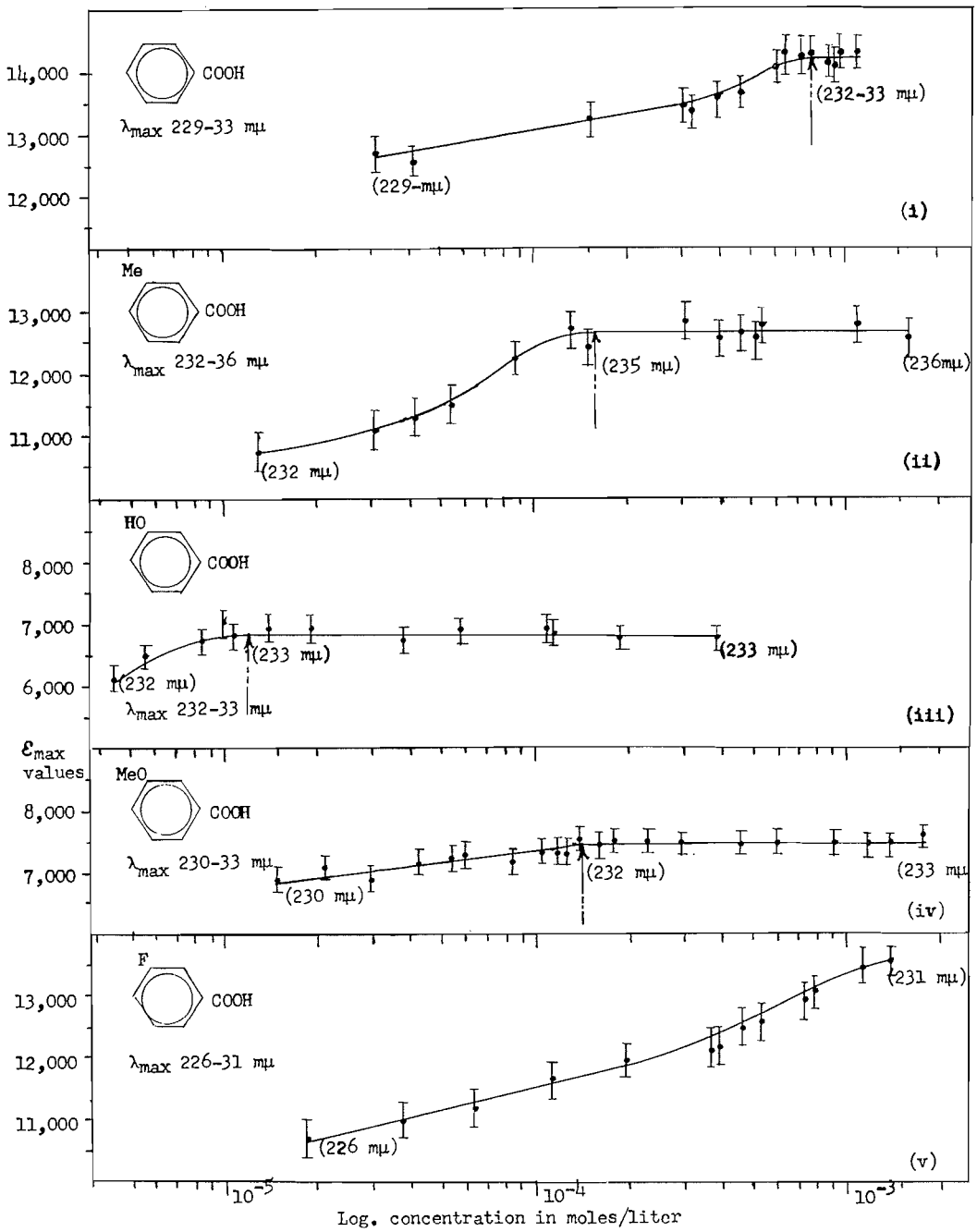


FIG. 3. The variation of ϵ_{max} on changing the solute concentration in cyclohexane solution for (i) benzoic acid, (ii) *m*-toluic acid, (iii) *m*-hydroxybenzoic acid (in cyclohexane solution containing 5% ether), (iv) *m*-methoxybenzoic acid (in cyclohexane solution containing 5% ether), and (v) *m*-fluorobenzoic acid.

Can. J. Chem. Downloaded from www.nrcresearchpress.com by 186.148.149.217 on 09/04/12
For personal use only.

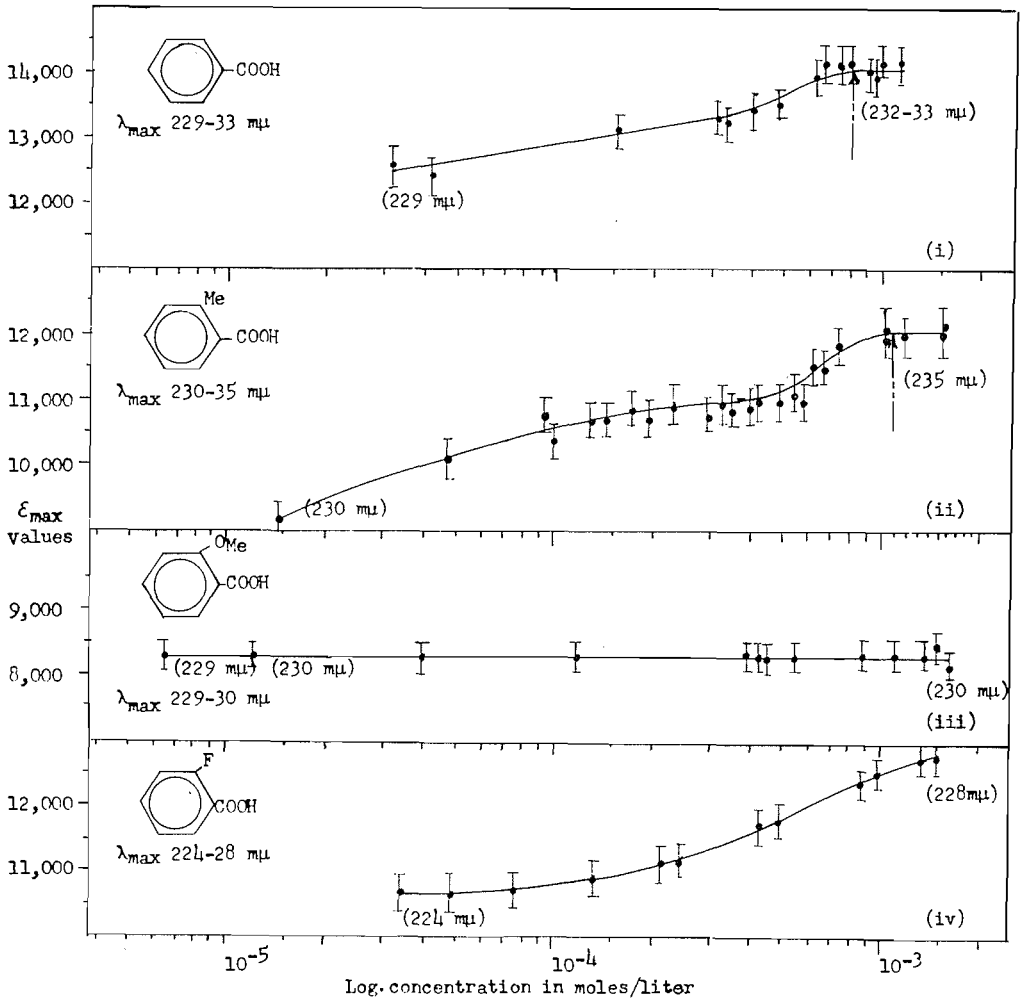


FIG. 4. The variation of ϵ_{max} on changing the solute concentration for (i) benzoic acid, (ii) *o*-toluic acid, (iii) *o*-methoxybenzoic acid, and (iv) *o*-fluorobenzoic acid.

THE STRENGTH OF THE DIMERIC HYDROGEN BOND IN SUBSTITUTED BENZOIC ACIDS

The observed spectral changes for a number of substituted benzoic acids on altering the solute concentration are listed in Figs. 1, 3, and 4 and all the available critical maximal concentrations are listed in Table I.

In the absence of a more quantitative interpretation of the underlying effect, which causes the observed concentration dependences, a detailed analysis of the individual compounds in terms of inductive, mesomeric, and steric effects is perhaps not justified at this stage, but the following observations may be made:

(i) The critical maximal concentrations, which represent a qualitative measure of the strength of the dimeric hydrogen bond in substituted benzoic acids, may be compared with the results obtained from other measurements, for example, with the changes in acid strength on introducing a substituent in benzoic acid, with the wavelength displacements

TABLE I

Critical maximal concentrations (see text) and infrared data for benzoic acids

Substituent	Ultraviolet data, critical maximal concentrations	Infrared data in carbon tetrachloride at a solute concentration of ca. 3.5×10^{-2} moles/l.		
		ν_{max} values of carbonyl bands		Apparent ratio of intensities, $B_{dimer}/B_{monomer}$*
	Solute concentration in moles/liter $\times10^4$	ν_{max} (dimer), cm^{-1}	ν_{max} (monomer), cm^{-1}	
H	8.0†	1696	1744	ca. 10:1
p-CH_3	4.7†	1695	1739	ca. 10:1
p-OH	0.4†		Insufficiently soluble	
p-OCH_3	0.34		Insufficiently soluble	
p-F	‡	1697	1744	ca. 10:1
m-CH_3	1.6	1694	1741	ca. 10:1
m-OCH_3	1.4	1695	1740	ca. 10:1
m-OH	0.12		Insufficiently soluble	
m-F	‡	1701	1746	ca. 10:1
o-CH_3	11	1694	1741	ca. 10:1
o-OH	14†	1657	1691	ca. 5:1
o-OCH_3	‡	1700	1749	ca. 0.9:1
o-F	‡	1704	—	15:1
2,4,6-Tri-*t*-butyl	‡	1696	1750	ca. 10:1

*B is the apparent integrated absorption intensity calculated from $B = 2.93\times\Delta\nu_{\frac{1}{2}}\times\epsilon^a$.
†Value from Part II (1).
‡Not within range.

observed in the ultraviolet region, and with the standard heats of dissociation, ΔH, of different benzoic acids (cf. refs. 2, 3, 4, 5). These comparisons are found to show general similarities since all the data indicate that a *m*-methyl, *p*-methyl, or *p*-hydroxy substituent in benzoic acid strengthens the dimeric hydrogen bond and that an *o*-methyl, *o*-hydroxy, or *o*-methoxy substituent weakens the dimeric hydrogen bond. Most of the data, though not all, agree in indicating that a *p*-methoxy substituent strengthens the intermolecular hydrogen bond in benzoic acid and that a *m*-fluoro substituent weakens the intermolecular hydrogen bond. The disagreements in the latter two benzoic acids require further investigation.

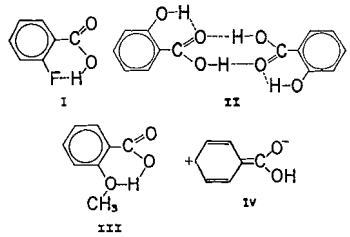
(ii) Conflicting conclusions are suggested by the data for *p*- and *o*-fluorobenzoic acid. Particularly for *o*-fluorobenzoic acid, the almost complete absence of monomer in the infrared carbonyl absorption (see Fig. 2) suggests that the monomer is destabilized by the *o*-fluoro substituent, and this therefore points against any significant contribution of structures of type I. Other data, however, suggest the presence of such an intramolecular hydrogen bond (cf. ref. 5).

Moreover, the present data also suggest that a *m*-methoxy or a *m*-hydroxy substituent strengthens the intramolecular hydrogen bond in benzoic acid (see Table I and Fig. 3). This is of interest since the ordinary inductive effect of these *m*-substituents, on account of the greater electronegativity of the oxygen atom, would be expected to cause an electron withdrawal from the carboxyl group thus leading to an increase in the proportions *both* of the ionized acid and the monomeric species. Moreover, the increased acidity is, in fact, observed (4).

(iii) Steric interactions—that is, the loss of resonance energy because of non-planarity —presumably account for the greater critical maximal concentration in *o*-toluic acid (see Fig. 4). Incidentally, there is no evidence, as judged from the intensities of the infrared

Can. J. Chem. Downloaded from www.nrcresearchpress.com by 186.148.149.217 on 09/04/12
For personal use only.

carbonyl bands, that steric interactions completely prevent dimer formation, since even for 2,4,6-tri-*t*-butylbenzoic acid at a solute concentration of 2.5×10^{-2} moles/liter the apparent ratio of intensities ($B_{\text{dimer}}/B_{\text{monomer}}$) is still ca. 10:1 (cf. Table I).



(iv) An intramolecular hydrogen bond has previously been postulated to weaken the dimeric hydrogen bond in salicylic acid (1). An intramolecular hydrogen bond in *o*-methoxybenzoic acid may likewise account for the absence of concentration dependence within the investigated concentration range for the solutions of *o*-methoxybenzoic acid (see Fig. 4), if it is assumed that the molecule exists in the monomeric form. The difference between the ultraviolet data in Table I (which indicate that salicylic acid forms a weak dimeric hydrogen bond, whereas *o*-methoxybenzoic acid forms no dimeric bond under identical conditions) and the acid dissociation data (which indicate the opposite tendency in the relative strengths of the intramolecular hydrogen bonds (4)) can be related to the observation that while the intramolecularly hydrogen-bonded form of salicylic acid is still able to form a dimeric hydrogen bond as in II, though not necessarily at the same time, this is not readily possible for the intramolecularly hydrogen-bonded form of *o*-methoxybenzoic acid (III).* A different argument, however, applies to the acid dissociation data, where the intramolecular hydrogen bond in structure II may be assumed to decrease the electron density on the carboxyl oxygen atoms and in this way *increase* the acidity of the carboxyl group; for *o*-methoxybenzoic acid, on the other hand, the *only* intramolecularly hydrogen-bonded form possible (III) tends to retain the active hydrogen atom by means of this hydrogen bond and in this way the acidity may not be increased to nearly the same extent as in salicylic acid (see ref. 4). Further evidence for the presence of a fairly strong intramolecular hydrogen bond in *o*-methoxybenzoic acid is provided by the intensity ratios of the infrared carbonyl bands which clearly indicate the relative predominance of the monomer in *o*-methoxybenzoic acid compared with the much smaller proportion of monomer in other substituted benzoic acids (see Fig. 2 and Table I).†

ACKNOWLEDGMENTS

The receipt of research grants from the National Research Council of Canada and from the Research Corporation of New York is gratefully acknowledged.

cf. Reference 5 which also reports considerably more dimeric dissociation for o-methoxybenzoic acid than for salicylic acid and see footnote 19 of that paper for a discussion of the structure of o-methoxybenzoic acid.

†*The similarity of the ultraviolet maxima for benzoic acid (monomer) and o-methoxybenzoic acid at ca. 230 mμ (see Fig. 4) is also of interest since it suggests that the ultraviolet maxima are not appreciably affected by intramolecular hydrogen bonding of type* III, *whereas intramolecular hydrogen bonds as shown in* II *give rise to appreciable bathochromic wavelength displacements (1). This is consistent with the explanation that resonance structures of type* IV *may be considered to be of predominant importance in determining these wavelength displacements in the ultraviolet region.*

Can. J. Chem. Downloaded from www.nrcresearchpress.com by 186.148.149.217 on 09/04/12
For personal use only.

REFERENCES

1. W. F. FORBES and A. R. KNIGHT. Can. J. Chem. **37**, 334 (1959).
2. J. WENOGRAD and R. A. SPURR. J. Am. Chem. Soc. **79**, 5844 (1957).
3. G. ALLEN and E. F. CALDIN. Quart. Revs. **7**, 255 (1953).
4. C. K. INGOLD. Structure and mechanism in organic chemistry. Cornell Univ. Press, Ithaca, N.Y. 1953. pp. 738–750.
5. M. M. DAVIS and H. B. HETZER. J. Research Natl. Bur. Standards, **60**, 569 (1958).

Can. J. Chem. Downloaded from www.nrcresearchpress.com by 186.148.149.217 on 09/04/12
For personal use only.

Can. J. Chem. Downloaded from www.nrcresearchpress.com by 186.148.149.217 on 09/04/12
For personal use only.

A STUDY OF THE DIMER OF ETHYLENE PLATINOUS CHLORIDE BY PROTON MAGNETIC RESONANCE[1]

LEONARD W. REEVES

ABSTRACT

The proton magnetic resonance line of the powdered ethylene platinous chloride dimer complex has a second moment of 13.68 ± 1 gauss^2 at 77° K and an over-all line width of 11.15 ± 0.4 gauss. Measurements at various temperatures between 77° and 329° K show that both second moment and line width decrease slightly with temperature. The mean separation of the doublet observed at 77° K is found to be 4.80 ± 0.3 g.

The results are interpreted in terms of a distorted ethylene molecule whose interproton distances correspond to an intermediate structure between ethylene and an ethane in a cis configuration but with two of the cis protons removed. This is consistent with earlier studies of the Raman spectrum. The π-type bond formed between a metal d orbital and an ethylene π^* orbital is also consistent with the lack of rotation of ethylene at elevated temperatures.

Available results from high-resolution proton resonance studies of ethylene complexed to metal atoms in solutions is discussed.

The bonding of ethylene to the metal in a series of olefin complexes of platinum and palladium II has been treated by Chatt and Duncanson (1). A satisfactory explanation of the infrared and dielectric studies has been achieved in terms of a σ and π bond. The ethylene is co-ordinated to a dsp_2 metal orbital by use of the ethylene π electrons in a σ bond. It has also been suggested that a donation of charge from a metal d orbital into the ethylene π^* orbital forms a π-type bond which also contributes to the stability of the complex.

Further studies of these compounds by X-ray diffraction of the solid have confirmed the suggestions of the earlier workers. Studies of Zeise's salt (2), ethylene palladium chloride dimer (3), and styrene palladium chloride (4) show that the ethylene is at one corner of the square planar complex with the metal at the center. Resolution was adequate to show the scattering from the carbon electrons indicating that the carbon atoms are an equal distance above and below the plane of the complex. In the dimers, such as $[PdCl_2C_2H_4]_2$, there are two chlorine atoms which act as a bridge between the two palladium atoms; the ethylene in the dimer units complexes in the trans positions.

The infrared studies of the C—C stretching mode region indicate the loss of a center of symmetry by the olefin since a weakly allowed infrared absorption occurs in ethylene platinous chloride. The transition moment of this band in the 1500 cm^{-1} region is very low and it is not observed in Zeise's salt. It is thus evident that the symmetry of ethylene is very little changed by co-ordination. Well-defined C—H stretching frequencies at 3068, 3034, and 3010 cm^{-1} can be assigned to the three olefin stretching modes in the spectrum of $K[C_3H_6PtCl_3].H_2O$, a propylene complex.

Since the X-ray studies are unable to detect the proton positions and a certain loss of symmetry of ethylene is suggested by infrared measurements, the present study of proton resonance in the powdered solid ethylene platinous chloride is designed to detect any change in the interproton distances of ethylene on co-ordination and confirm the σ and π bonding proposed (1) by showing the absence of rotation of ethylene about the platinum–platinum axis at elevated temperatures.

[1]*Manuscript received February 4, 1960.*
Contribution from the Department of Chemistry, University of British Columbia, Vancouver 8, British Columbia.

Can. J. Chem. Downloaded from www.nrcresearchpress.com by 186.148.149.217 on 09/04/12
For personal use only.

EXPERIMENTAL

The Varian 40-Mc/s n.m.r. spectrometer V-4250 was used to take spectra at various temperatures from 77° K to 56° C. Spectra at liquid nitrogen temperature were measured using a Dewar which was mounted in a threaded cylinder replacing the Varian high-resolution spinner turbine housing on the induction probe. This was machined inside to fit a standard ground-glass joint. The small half-silvered Dewar was made with a standard taper joint on the outside and during the experiment the Dewar was located in the aluminum cylinder so that the Dewar was just fitted into the 15-mm 40-Mc/s Varian insert and was clear of the bottom of the insert by 1 mm. By careful machining of the locating cylinder actual contact of the insert with the Dewar was avoided so that changes in probe balance due to vibration and movement of the whole probe could be prevented. By thinning out the glass walls of an 8-mm sample tube a favorable proton-packing factor could be achieved. The liquid nitrogen was filtered through glass wool to prevent ice passing into the the Dewar. The Dewar contained enough liquid nitrogen to allow one spectrum to be taken without refilling. Exact reproduction of spectra was obtained. Above −30° C spectra were obtained by use of a second apparatus which will be described in a forthcoming paper by Reid and Connor (7), or with an apparatus described by Bernstein, Schneider, and Pople (7).

The main magnetic field was modulated at 80 c.p.s. and swept across resonance at calibrated rates. Calibration was achieved by observing the signal from liquid water with a modulation width of 30 milligauss and superimposing 5-, 10-, or 20-kilocycle side bands from a Hewlitt–Packard audio oscillator, which was, in turn, calibrated against a Hewlitt–Packard Model 5243 electronic counter. The recorder chart paper could thus be calibrated in gauss per centimeter before and after each series of experiments. No variation in calibration of sweep rates at a given setting was observed throughout the whole series of experiments.

The ethylene platinous chloride showed 98% purity in ethylene content as determined by comparison of the intensity of the high-resolution proton resonance in standard acetonitrite solutions with standard solutions of ethylene gas in the same solvent. The compound was prepared in the laboratory of Professor Orchin at the University of Cincinatti and kindly supplied by courtesy of the Gulf Oil Multiple Fellowship at the Mellon Institute.

RESULTS

Preliminary experiments showed that except at very low r.f. power there was some saturation of the proton resonance. The low power required to avoid signal distortion due to saturation was not practicable for good quantitative measurement of the resonance line parameters. A short irradiation of $\frac{1}{2}$ hour with 50-kv X rays produced sufficient paramagnetic impurity to allow the use of much higher r.f. power giving a signal-to-noise ratio of approximately 30 to 1, with modulation widths of 1 gauss. The paramagnetic impurities persisted at the highest temperature 56° C. There was no systematic difference in line width parameters calculated from the experiments with low r.f. power and those with higher r.f. power with irradiated samples. Thus the impurities introduced by X irradiation did not reach a concentration at which broadening of resonance lines occurs because of large local fields due to the electronic paramagnetism of the impurities (8).

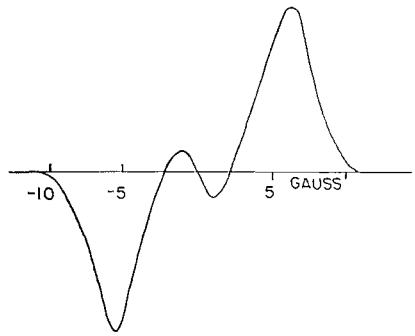


FIG. 1. Proton resonance in powdered ethylene platinous chloride dimer at 77° K.

Figure 1 shows the spectrum of solid ethylene platinous chloride at liquid nitrogen temperature. The curve represents the derivative of the resonance absorption curve obtained by modulating the large magnetic field H_2 and detecting the slope of the absorption curve over the modulation width with a phase-sensitive detector. The curve shown is the average of five spectra with a signal-to-noise ratio of 30 to 1. The derivative curve shows a clear doublet structure for the absorption as would be expected for the ethylene molecule where two closely spaced protons occur (9). The separation of the two peaks in the absorption curve determined from the average of five spectra at 77° K is 4.78 ± 0.3 gauss. The over-all line width determined from the separation of the positions of maximum and minimum slope in the derivative curve is 11.15 ± 0.4 gauss.

A spectrum at $+56°$ C is shown in Fig. 2. Above $-30°$ C the doublet structure of the

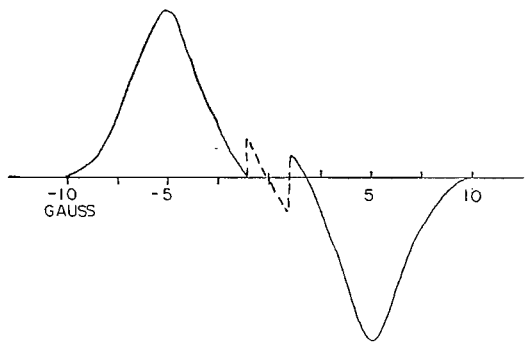


FIG. 2. Proton resonance in powdered ethylene platinous chloride dimer at 329.7° K.

derivative curve is marred by the appearance of a small impurity peak at the resonance center of modulation width preventing an estimation of the doublet separation. It is possible that this impurity may be traces of solvent used in the preparation or a certain amount of free ethylene with considerable motion in the solid lattice at $-30°$ C.

The second moments obtained are quoted in Table I at all temperatures studied. In each case they are the average values taken for at least three curves. They were computed using the formulas given by Andrew (10).

Can. J. Chem. Downloaded from www.nrcresearchpress.com by 186.148.149.217 on 09/04/12
For personal use only.

TABLE I

Line width and second moments of powdered ethylene platinous chloride

Temp., °K	$\Delta(H)_{\frac{1}{2}}$ line width, gauss	$(\Delta H)^2$ second moment, gauss^2
77	11.15±0.4	13.68±1.0
248	10.00	10.6
267	10.10	10.5
301	10.00	10.6
313	10.17	11.1
320	10.33	10.9
329	10.32	11.2

NOTE: Line widths varied for a given temperature up to 0.4 gauss from the mean; second moments deviated up to 1 gauss^2 from the mean.

The narrow component of modulation width shown in Fig. 2 did not grow in intensity with increasing temperature.

DISCUSSION

The Lewis acid–base reaction involving π electrons in olefinic systems and metal ions such as silver, or the halogen molecules, has been studied extensively in optical spectroscopy by observation of the familiar charge transfer bands (11). In the silver–olefin systems an interaction is detected in the Raman spectrum of the olefin by observation of the frequency shift of the C=C stretch (12). This frequency shift in the platinum olefin complexes is about twice that in the silver–olefin association (1).

The chemical shift of the protons from nuclear resonance signals detected in solutions of silver perchlorate in benzene or olefins is almost identical with the proton resonance position in pure benzene or olefin (13). This result is not surprising in view of the fact that π electron density influences the nuclear shielding parameter of a proton directly attached to the olefinic carbon only to a minor extent providing the lifetime of the complex in solution is very short (14). Larger changes in the chemical shift of ring protons in aromatic systems due to complex formation can be ascribed to a specific interaction of a solvent molecule with this proton rather than with π electrons. Large changes in proton chemical shifts (2–5 p.p.m.) in olefins complexed to metal atoms have been observed by Green, Pratt, and Wilkinson (15) and by Lauterbur and Reeves (16). It is expected (15) that such changes in chemical shift in strongly complexed ethylene is due to diamagnetic anisotropy introduced by bonds in the rest of the platinum complex or introduced by σ bond formation using π electrons from the olefin. The bond energy in the platinum–olefin complex is certainly greater than in silver–olefin complexes so that it is possible for chemical exchange effects to minimize chemical shift changes due to diamagnetic anisotropy of an individual complex in the latter case. Further results will be reported in conjunction with Lauterbur at a later date on studies using high-resolution n.m.r.

The suggestions of Chatt and Duncanson (1) are in general confirmed by high resolution studies of proton resonance in solution but these are limited in scope when effects of chemical exchange are not properly taken into account (12). The study of solid complexes using proton resonance will show changes in interproton distances after complex formation (10). The second moment of the resonance absorption line is related to the internuclear distances by the following equation:

Can. J. Chem. Downloaded from www.nrcresearchpress.com by 186.148.149.217 on 09/04/12
For personal use only.

[1] $$S = \frac{6}{5} \cdot I(I+1) g^2 \mu_0^2 N^{-1} \sum_{j>k} r_{jk}^{-6} + \frac{4}{15} \mu_0^2 N^{-1} \sum_{j,f} I_f(I_f+1) \cdot g_f^2 \cdot r_{j,f}^{-6}.$$

S = second moment of absorption line,
I = nuclear spin quantum number of the proton (nucleus under study),
g = nuclear "g" factor for the protons,
μ_0 = nuclear magnetion,
N = number of protons in the system,
r_{jk} = internuclear distance between nuclei j and k in the system,
g_f = nuclear g factor of nuclear species f in the system,
I_f = nuclear spin quantum number of nuclear species f,
r_{jf} = internuclear distance between proton j and a nucleus f of the f system.

The second moment of an isolated ethylene molecule is calculated to be 11.05 gauss^2. A theoretical second moment for an undistorted ethylene molecule, complexed in the platinum ethylene chloride dimer, can be estimated using the crystal structure of the ethylene palladium chloride dimer since the atomic radius of palladium is very little different from platinum (3). The proton nuclear moment system gives rise to a second moment contribution almost equal to that in the isolated ethylene molecule. The closest approach of a proton outside the ethylene molecule in the crystal is 4.67 Å. The contribution of protons in the crystal outside the ethylene molecule can be obtained by replacing the first summation in equation 1 by an integral between 4.67 Å and infinity (18). The volume of unit cell is 1038 Å and this contains four dimers or 16 protons or 1.54×10^{-2} protons per cubic Å

[2] $$S_{\text{Inter}} = \frac{4 \cdot \pi \cdot 357 \cdot 8 \cdot \rho}{3} \left(\frac{1}{r^3}\right)_{\infty}^{4.47}.$$

The first summation replaced by an integral is given by equation 2, where 357.8 corresponds to the presummation term evaluated for r expressed in Å, ρ is the density of protons per cubic Å. Sinter (evaluated between 4.67 Å and ∞) gives a value 0.22 gauss^2. There will be small contributions from the 33.7% Pt^{195} and Cl^{35} and Cl^{37}; these will only be effective within the same dimer. The platinum nuclear moment contributes only 5×10^{-3} gauss^2 and this has been neglected. The chlorine contributions are approximately 1×10^{-2} gauss^2 and can also be neglected in the second moment.

The theoretical second moment for the proton resonance line in ethylene platinous chloride is therefore 11.3 gauss^2. This is considerably less than the measured value and the discrepancy can only be due to a modification of the interproton distances in the ethylene molecule.

The modification of distances is expected to involve a lengthening of the C—C bond due to lowering of bond order since some π electron density is located between the C—C axis and the platinum atom in the σ bond. The C—H bond distances would not be expected to change greatly but the complexing will cause this —C—H bond to lean back from the direction of the platinum atom. In fact the general structure of the ethylene in the complex will approach that of ethane with one hydrogen missing on each carbon.

The second moment calculated from such a hypothetical arrangement in the crystal of ethylene platinous chloride would be 14.75 gauss^2. The experimental second moment of 13.68 gauss^2 has an intermediate value between the undistorted ethylene and ethane structures. Since the lowering of bond order in the C—C bond tends to lower the

Can. J. Chem. Downloaded from www.nrcresearchpress.com by 186.148.149.217 on 09/04/12
For personal use only.

theoretical moment and the leaning back of the C—H bonds tends to raise it, then it is possible to fit the experimental second moment with a wide range of C—C distances and H—C—H angles. It is evident, however, that the distortion of ethylene suggested by Chatt and Duncanson (1) is consistent with the present study.

The n.m.r. spectrum of a rigid closely spaced proton pair in a polycrystalline material is a doublet provided all other interacting protons are sufficiently distant. The separation of the doublet is related to the proton separation in the pair by (10)

$$[3] \qquad \frac{3\mu}{r^3} \cong \Delta H_{\text{doublet}}.$$

This separation is a minimum value of the splitting since the system consists of nuclei outside the closely interacting and this causes broadening of the doublet and a reduction of the splitting. Equation 3 gives a value of $r = 2.08$ Å in this case. The separation of 1.1 protons in pure ethylene is 1.85 Å and in ethane 1.78 Å. The precision of the present result is particularly limited since the distance between cis protons in ethylene is 2.42 Å. The cis proton–proton distance invalidates the 'interacting pair' assumption and causes the observed doublet structure to correspond to proton separations between 1.85 and 2.42 Å. The second moments observed and calculated in this work are consistent with the results obtained previously from Raman spectra of this compound in solution (1).

If the ethylene were not located by π^* bonds it is likely that rotation about an axis perpendicular to the C—C axis would occur. This is not observed. The small decrease in second moment between 77° K and 329° K can be accounted for on the basis of rocking motions perpendicular to platinum–ethylene bond and on wagging about the C—C axis. This is a good evidence therefore for the additional π^* attachment suggested.

This work was supported by the National Research Council of Canada and the Research Corporation.

REFERENCES

1. J. Chatt and L. A. Duncanson. J. Chem. Soc. 2939 (1953).
2. D. P. Mellor and J. A. Wunderlich. Acta Cryst. **7**, 130 (1954); **8**, 59 (1955).
3. J. N. Dempsey and N. C. Baenziger. J. Am. Chem. Soc. **77**, 4984 (1955).
4. J. R. Holden and N. C. Baenziger. J. Am. Chem. Soc. **77**, 4987 (1955).
5. J. J. Fox and A. E. Martin. Proc. Roy. Soc. A, **167**, 257 (1938); A, **175**, 208 (1940).
6. A. Pozefsky and N. D. Coggeshall. Anal. Chem. **23**, 1611 (1951).
7. C. Reid and T. M. Connor. To be published.
   H. J. Bernstein, W. G. Schneider, and J. A. Pople. Proc. Roy. Soc. A, **236**, 515 (1956).
8. N. Bloembergen. Physica, **15**, 386 (1949).
9. H. S. Gutowsky, G. B. Kistiakowsky, G. B. Pake, and E. M. Purcell. J. Chem. Phys. **17**, 972 (1949).
10. E. R. Andrew. Nuclear magnetic resonance. Cambridge University Press. 1955. p. 163.
11. R. S. Mulliken. J. Am. Chem. Soc. **72**, 600 (1950).
12. H. J. Taufen, M. J. Murray, and F. F. Cleveland. J. Am. Chem. Soc. **63**, 3500 (1941).
13. L. W. Reeves. Unpublished work.
14. T. Schaeffer and W. G. Schneider. Private communication.
15. M. H. L. Green, L. Pratt, and G. Wilkinson. Private communication; J. Chem. Soc. 3753 (1959).
16. L. W. Reeves and P. C. Lauterbur. To be published.
17. H. S. Gutowsky and A. Saika. J. Chem. Phys. **21**, 1688 (1953).
18. H. S. Gutowsky and C. H. Holm. J. Chem. Phys. **25**, 1228 (1956).

Can. J. Chem. Downloaded from www.nrcresearchpress.com by 186.148.149.217 on 09/04/12
For personal use only.

Can. J. Chem. Downloaded from www.nrcresearchpress.com by 186.148.149.217 on 09/04/12
For personal use only.

HEAT OF MIXING OF CARBON TETRACHLORIDE WITH FURFURAL

S. K. Jeun and Benjamin C.-Y. Lu

In the course of investigations of various thermodynamic properties of solutions, the heat of mixing of carbon tetrachloride and furfural over the complete concentration range was determined at 27° and 40° C in a Dewar calorimeter of a type similar to that used by Tsao and Smith (1) and Murti and van Winkle (2). Heating and cooling curves were taken before and after mixing for each determination and were used to eliminate the possible errors due to radiation, vaporization, and condensation, following a procedure which modified that proposed by Williams (3) for determining specific heats of liquids.

The heat-of-mixing data are expressed in terms of the amount of heat absorbed per mole of mixture when the pure components are mixed at constant temperature and pressure. The results are listed in Table I and are represented in functions of the mole

TABLE I
Experimental data

System carbon tetrachloride – furfural at 27° C		System carbon tetrachloride – furfural at 40° C	
Mole fraction furfural	Heat of mixing, cal/mole mixture	Mole fraction furfural	Heat of mixing, cal/mole mixture
0.041	68.1	0.021	37.5
0.120	157.2	0.048	76.3
0.231	216.6	0.064	97.2
0.355	241.0	0.094	134.6
0.453	234.3	0.108	146.2
0.563	210.7	0.171	206.3
0.684	167.1	0.265	260.7
0.792	117.2	0.307	289.8
0.903	58.0	0.437	298.1
		0.547	281.2
		0.658	244.9
		0.746	182.2
		0.778	166.3
		0.816	135.3
		0.820	141.0
		0.865	102.4
		0.875	95.4
		0.917	65.4
		0.923	56.8
		0.951	38.2
		0.967	25.0

fraction of furfural by Fig. 1. The maximum error resulting from vaporization and condensation effects and in the measurement of experimental data was estimated to be 2%. Repeated runs at fixed condition indicated that the data were reproducible with a discrepancy of less than 1%. It is believed that the results presented have an accuracy of 2% or better.

It is observed that the heat of mixing data are positive over the temperature range investigated. The temperature effect on heat of mixing in the diluted furfural solutions seems to be negligible, while in the concentrate furfural solutions the heat of mixing is increased by increasing the temperature. It may be concluded that over the temperature range investigated the logarithm of the activity coefficient of furfural at infinite dilution

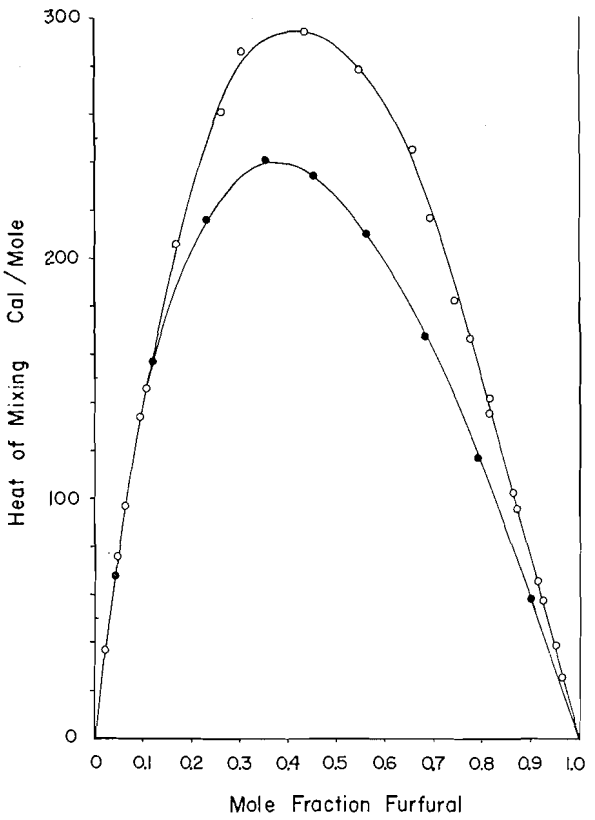


FIG. 1. Heat of mixing data for system carbon tetrachloride – furfural. ● 27° C, ○ 40° C.

varies linearly with the reciprocal of the absolute temperature and that the temperature effect on the activity coefficient of carbon tetrachloride at infinite dilution is more complex.

We are grateful to the National Research Council of Canada for a grant-in-aid of this research.

1. C. C. TSAO and J. M. SMITH. Chem. Eng. Progr. Symposium Ser. No. 7, **49**, 107 (1953).
2. P. S. MURTI and M. VAN WINKLE. Chem. & Eng. Data Ser. **3**, 65 (1958).
3. G. C. WILLIAMS. Ind. Eng. Chem. **40**, 340 (1948).

RECEIVED DECEMBER 29, 1959.
DEPARTMENT OF CHEMICAL ENGINEERING,
UNIVERSITY OF OTTAWA,
OTTAWA, ONTARIO.

A POSSIBLE MECHANISM FOR THE PRODUCTION OF $O_2^*(^3\Sigma_u^-)$ IN FLAMES

ROBERT J. FALLON, IRWIN TOBIAS, JOSEPH T. VANDERSLICE, AND WILLIAM G. MAISCH

The emission spectra of a number of flames containing oxygen show the Schumann–Runge (1–6) bands which are associated with the transition $B^3\Sigma_u^- \rightarrow X^3\Sigma_g^-$ in O_2. The mechanism for the production of $O_2^*(^3\Sigma_u^-)$ in flames has been a matter of concern for some time (4–6). Originally, it was suggested that it might be produced through a chemical reaction (7), and both Laidler (7) and Shuler (8) have suggested possible reactions which might account for the presence of these bands in various flames. It is now felt, however,

Can. J. Chem. Downloaded from www.nrcresearchpress.com by 186.148.149.217 on 09/04/12
For personal use only.

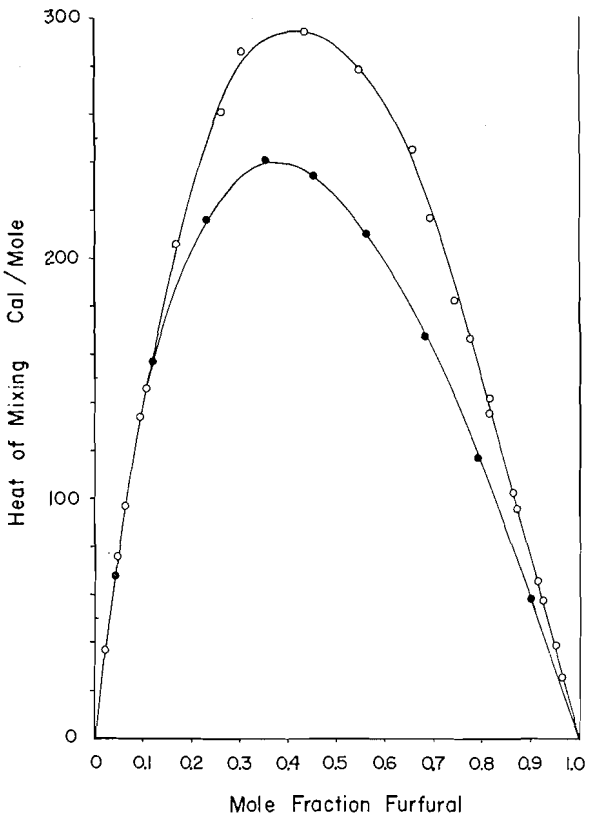


FIG. 1. Heat of mixing data for system carbon tetrachloride – furfural. ● 27° C, ○ 40° C.

varies linearly with the reciprocal of the absolute temperature and that the temperature effect on the activity coefficient of carbon tetrachloride at infinite dilution is more complex.

We are grateful to the National Research Council of Canada for a grant-in-aid of this research.

1. C. C. TSAO and J. M. SMITH. Chem. Eng. Progr. Symposium Ser. No. 7, **49**, 107 (1953).
2. P. S. MURTI and M. VAN WINKLE. Chem. & Eng. Data Ser. **3**, 65 (1958).
3. G. C. WILLIAMS. Ind. Eng. Chem. **40**, 340 (1948).

RECEIVED DECEMBER 29, 1959.
DEPARTMENT OF CHEMICAL ENGINEERING,
UNIVERSITY OF OTTAWA,
OTTAWA, ONTARIO.

A POSSIBLE MECHANISM FOR THE PRODUCTION OF $O_2^*(^3\Sigma_u^-)$ IN FLAMES

ROBERT J. FALLON, IRWIN TOBIAS, JOSEPH T. VANDERSLICE, AND WILLIAM G. MAISCH

The emission spectra of a number of flames containing oxygen show the Schumann–Runge (1–6) bands which are associated with the transition $B^3\Sigma_u^- \rightarrow X^3\Sigma_g^-$ in O_2. The mechanism for the production of $O_2^*(^3\Sigma_u^-)$ in flames has been a matter of concern for some time (4–6). Originally, it was suggested that it might be produced through a chemical reaction (7), and both Laidler (7) and Shuler (8) have suggested possible reactions which might account for the presence of these bands in various flames. It is now felt, however,

Can. J. Chem. Downloaded from www.nrcresearchpress.com by 41.223.56.140 on 09/04/12
For personal use only.

that the $O_2^*(^3\Sigma_u^-)$ is formed thermally and not as a result of any chemical process (5, 9).

Laidler (4) has pointed out that, although the mode of formation of $O_2^*(^3\Sigma_u^-)$ might be specific for each flame, the fact that this species occurs in so many different flames would seem to indicate that the reactions leading to the production of $O_2^*(^3\Sigma_u^-)$ are common to all flames and thus independent of the nature of the fuel. He has suggested, therefore, that the reaction initially proposed by Feast (10) to explain the production in a high pressure arc

$$O(^3P) + O(^1D) + M \rightarrow O_2(^3\Sigma_u^-) + M \qquad [1]$$

must be considered as a possible source of the excited O_2 molecule since atomic oxygen is definitely present in H_2/O_2 and CO/O_2 flames (11). The $O(^1D)$ may be produced thermally since its excitation energy is only 1.97 ev or it may be produced by the thermal dissociation of one of the reaction intermediates.

There are several difficulties in considering reaction [1]. No evidence for excited atomic oxygen has been found in the CO/O_2 flame (1). Also, if reaction [1] were responsible for the production of the Schumann–Runge bands, one might expect that transitions involving some of the higher vibrational levels of the $B^3\Sigma_u^-$ state would be observed. However, only the lower vibrational levels ($v' = 0, 1, 2$) have been seen in the CO/O_2 and H_2/O_2 flames (1, 6).

The purpose of this note is to suggest a mechanism for the production of thermally excited $O_2^*(^3\Sigma_u^-)$ in flames on the basis of some recently determined potential curves of O_2 (12). The methods of obtaining these curves are discussed in reference (12) and those of importance in the present discussion are shown in Fig. 1. It is found that the $^3\Pi_u$ and

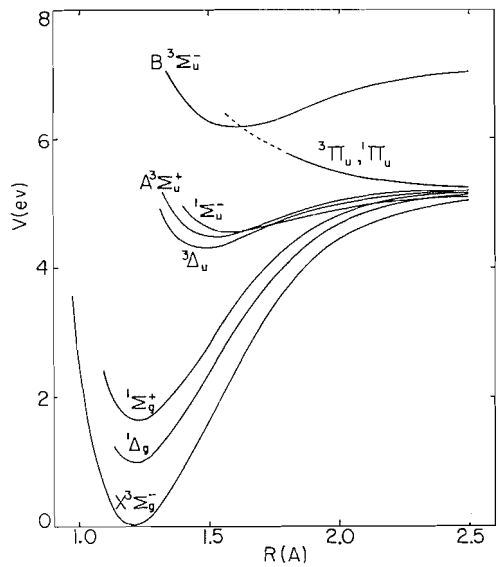


FIG. 1. Potential energy curves for O_2.

the $^1\Pi_u$ have approximately the same energy of interaction and seem to cross the curve for the $B^3\Sigma_u^-$ state around the minimum. Of all the repulsive states which arise from the interaction of two ground-state atoms, only the $^3\Pi_u$ can predissociate the $B^3\Sigma_u^-$ state strongly according to Kronig's rules (13). An oxygen molecule in the $^3\Pi_u$ state can, there-

Can. J. Chem. Downloaded from www.nrcresearchpress.com by 41.223.56.140 on 09/04/12
For personal use only.

fore, make a non-radiative transition to the B state. This process can be represented as

$$O(^3P) + O(^3P) \rightarrow O_2(^3\Pi_u) \rightarrow O_2^*(^3\Sigma_u^-) \quad [2]$$

and requires an energy of only about 1 ev. An excitation process like [2] would explain why the observed Schumann–Runge bands originate only from the lower vibrational levels of the B state. One might also expect that the rate of reaction [2] is much greater than that of [1] since the latter is a three-body collision.

If the above mechanism is correct, then it would be of interest to speculate on possible processes that might contribute to the continuum that has been noticed in some flames (14). In the H_2/O_2 and NH_3/O_2 flat diffusion flames, a continuum has been observed that lies roughly in the same region as the Schumann–Runge emission. Since this is near the oxygen side of the flame, Gaydon (14) suggests atomic oxygen as one of the reactants. Radiative transitions from the $^3\Pi_u$ or $^1\Pi_u$ state to some of the lower attractive states would result in a continuum. One would expect this continuum to arise from the same region of the flame as the Schumann–Runge bands in agreement with the observations. There are other transitions that could contribute to the continuum, for example, a transition from the repulsive side of the $A^3\Sigma_u^+$ state to the ground state. One might expect, however, that these would not be strong since they are not permitted by the selection rules although the latter might well be relaxed at these pressures.

A continuum has also been observed in flames containing carbon monoxide (15). This has been studied recently by Kaskan (16), who concludes that the production reaction involves an oxygen atom and a carbon monoxide molecule. However, since the Schumann–Runge bands are observed in these flames (15) there is a possibility that a small amount of the continuum might be due to the interaction of two oxygen atoms as suggested by Hoare and Walsh (17) and Hornbeck (18).

In conclusion, we would like to suggest that the $O_2^*(^3\Sigma_u^-)$ found in flames burning with O_2 is formed by the thermal collision of two $O(^3P)$ atoms interacting along the $^3\Pi_u$ repulsive curve which undergoes a radiationless transition to the $^3\Sigma_u^-$ state. Also, part of the continuum observed in these flames might arise from transitions from the repulsive branches of the $A^3\Sigma_u^+$, $^3\Delta_u$, or $^1\Sigma_u^-$ states down to one of the lower attractive states.

The financial support of the National Aeronautics and Space Administration is gratefully acknowledged.

1. G. A. Hornbeck and H. S. Hopfield. J. Chem. Phys. **17**, 982 (1949).
2. A. G. Gaydon. Nature, **164**, 22 (1949).
3. K. J. Laidler and K. E. Shuler. Chem. Revs. **48**, 153 (1951).
4. K. J. Laidler. The chemical kinetics of excited states. Oxford University Press, London. 1954. p. 75.
5. A. G. Gaydon and F. Guedeney. Trans. Faraday Soc. **51**, 894 (1955).
6. A. G. Gaydon. The spectroscopy of flames. John Wiley and Sons, Inc., New York. 1957. p. 77.
7. K. J. Laidler. J. Chem. Phys. **17**, 221 (1949).
8. K. E. Shuler. J. Chem. Phys. **19**, 888 (1951).
9. H. G. Wolfhard and W. G. Parker. Proc. Phys. Soc. A, **62**, 722 (1949); A, **65**, 2 (1952).
10. M. W. Feast. Proc. Phys. Soc. A, **63**, 772 (1950).
11. A. G. Gaydon. Proc. Phys. Soc. A, **183**, 111 (1944); Trans. Faraday Soc. **42**, 292 (1946).
12. J. T. Vanderslice, E. A. Mason, and W. G. Maisch. J. Chem. Phys. 32 (1960).
13. G. Herzberg. Spectra of diatomic molecules. D. Van Nostrand Co., Inc., New York. 1950. p. 416.
14. A. G. Gaydon. The spectroscopy of flames. John Wiley and Sons, Inc., New York. 1957. pp. 78, 214.
15. A. G. Gaydon. The spectroscopy of flames. John Wiley and Sons, Inc., New York. 1957. Chap. 6.
16. W. E. Kaskan. Combustion and Flame, **3**, 39 (1959).
17. D. E. Hoare and A. D. Walsh. Trans. Faraday Soc. **50**, 37 (1954).
18. G. A. Hornbeck. Symposium on Combustion, Flame and Explosion Phenomena. 3rd Symposium, Madison, Wis., 1948 (Pub. 1949). p. 501.

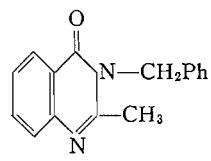
Received January 14, 1960.
Institute for Molecular Physics,
University of Maryland,
College Park, Maryland.

Can. J. Chem. Downloaded from www.nrcresearchpress.com by 41.223.56.140 on 09/04/12
For personal use only.

3-BENZYL-2-METHYL-3,4-DIHYDRO-4-KETOQUINAZOLINE

RAGINI ANET* AND S. SOMASEKHARA

As a part of investigations (1) on fused heterocyclic systems incorporating the quinazoline nucleus, 3-benzyl-2-methyl-3,4-dihydro-4-ketoquinazoline (I) was required. A preparation of this base was reported by Bogert and Beal (2) from acetylanthranil and benzylamine. However, these workers analyzed their compound, m.p. 123°, for nitrogen only, and did not prepare any derivatives. A hydrochloride, m.p. 232°–234°, of the required base was prepared by Grimmel, Guenther, and Morgan (3) from acetylanthranilic acid and benzylamine in presence of phosphorus trichloride. Once again, the compound was poorly characterized, no analysis figures were reported, nor was the free base or any derivatives prepared. As 2-methyl-4-hydroxy-quinazoline (II) was readily available, we studied its alkylation with benzyl chloride.



I

Treatment of the potassium salt of II with benzyl chloride in acetone gave a product whose analysis and infrared spectrum (4) were consistent with structure I. The melting point (74°) was different from that reported by Bogert and Beal, although that of the hydrochloride of our base was in agreement with that reported by Grimmel *et al.* The alkylation of 4-hydroxyquinazolines with alkyl halides in presence of alkali normally gives the 3-alkyl derivatives but in view of the reported ethylation of the sodium salt of 4-hydroxyquinazoline with ethyl iodide in alcohol to give largely the 4-ethoxy derivatives (5), an alternate synthesis of I was carried out from *o*-nitrobenzoyl chloride via N-benzyl-*o*-nitrobenzamide, N-benzyl-*o*-aminobenzamide, and N-benzyl-*o*-acetylaminobenzamide (III). The quinazoline derivative obtained by the cyclization of III with aqueous benzylamine was identical (mixed melting points and infrared spectra) with our benzylation product.

Having established that the product obtained on benzylation of II was indeed the required base I, it was of interest to find out the nature of Bogert and Beal's compound. Repetition of their work gave at first a product identical with our benzylation product. However, if slightly less than the calculated amount of benzylamine was used, a compound, m.p. 118°, could be obtained. Its infrared spectrum showed all the bands present in the spectrum of I but in addition showed bands in the —NH or —OH stretching region similar to those shown by the spectrum of N-benzyl-*o*-acetylaminobenzamide III. In fact, the compound was an equimolecular complex of I and III. This was shown by its elementary analysis and by its separation with cold benzene into the two components. Oxidation of I with selenium dioxide in aqueous dioxan gave the 2-aldehyde, which was characterized as its 2,4-dinitrophenylhydrazone.

It is of interest to note that the hydrochloride of I underwent debenzylation at its melting point.

**Present address: Department of Chemistry, University of Ottawa, Ottawa, Ontario.*

Can. J. Chem. Downloaded from www.nrcresearchpress.com by 186.148.149.217 on 09/04/12
For personal use only.

Can. J. Chem. Downloaded from www.nrcresearchpress.com by 186.148.149.217 on 09/04/12
For personal use only.

EXPERIMENTAL

3-Benzyl-2-methyl-3,4-dihydro-4-ketoquinazoline (I)

2-Methyl-3,4-dihydro-4-ketoquinazoline (8.5 g), benzyl chloride (7 g), and powdered potassium hydroxide (12 g) were refluxed in 500 ml of acetone for 6 hours. After removal of the solvent, the residue was extracted with chloroform and the chloroform evaporated. The oil thus obtained was treated with cold dilute hydrochloric acid to give a crystalline hydrochloride. Liberation of the base in the usual manner gave 5 g of the 3-benzyl derivative (I), which was crystallized from benzene – petrol ether (30°–60° b.p.) in plates, m.p. 74°. Found: C, 76.6; H, 5.5; N, 11.0%. Calc. for $C_{16}H_{14}NO_2$: C, 76.8; H, 5.6; N, 11.2%.

The hydrochloride, prepared by cooling a hot solution of the base in hydrochloric acid, formed needles, m.p. 233° (lit. (2), m.p. 232°–234°). Found: N, 9.2%. Calc. for $C_{16}H_{15}N_2OCl.H_2O$: N, 9.2%.

Acetylanthranil (0.9 g) and benzylamine (0.6 g) were heated together at 150° for 30 minutes. On cooling, the melt solidified and was treated with aqueous sodium bicarbonate to give 0.9 g of a white solid. After several crystallizations from ethanol it melted at 118°. (Bogert and Beal (2) give m.p. 123°.) Found: C, 74.0; H, 5.9; N, 10.8%. Calc. for $C_{16}H_{14}N_2O.C_{16}H_{16}N_2O_2$: C, 74.1; H, 5.8; N, 10.8%.

The compound was soluble in hot benzene, alcohol, and chloroform. Treatment with a small quantity of cold benzene gave a benzene-soluble compound, m.p. 74°, identical with I and a residue, m.p. 129°–137°, which after crystallization from aqueous alcohol melted at 147° to 148°, identical with N-benzyl-*o*-acetylaminobenzamide (IV) described below.

Repetition of the above experiment with a slight excess of benzylamine gave I exclusively.

3-Benzyl-3,4-dihydro-4-ketoquinazoline-2-aldehyde

Freshly prepared selenium dioxide (0.42 g) was added to 1 g of I in 25 ml dioxan and the mixture was refluxed for 1 hour. The precipitated selenium was filtered off and the filtrate passed through a 3-in. column of alumina to remove colloidal selenium. The dioxan solution was concentrated and the residue treated with petrol ether to give 1 g of the aldehyde, which crystallized from benzene in needles, m.p. 143°–144°. Found: C, 72.4; H, 4.6; N, 10.7%. Calc. for $C_{16}H_{12}O_2N_2$: C, 72.7; H, 4.5; N, 10.6%.

The 2,4-dinitrophenylhydrazone prepared in the usual manner gave needles, m.p. 275°–277°. Found: N, 19.1%. Calc. for $C_{22}H_{16}N_6O_5$: N, 18.9%.

N-*Benzyl-o-nitrobenzamide*

o-Nitrobenzoic acid (1 g) and thionyl chloride (3 ml) were refluxed in 5 ml of dry benzene for 1 hour. The solution was concentrated under reduced pressure and the residue was dissolved in 2 ml of dry benzene. To a cold solution of the acid chloride, a solution of 1 ml benzylamine in 3 ml benzene was added, followed by 10 ml of petrol ether. The crude benzamide (1.1 g), m.p. 122°–123°, separated out and was crystallized from benzene. Found: N, 10.9%. Calc. for $C_{14}H_{12}O_3N_2$: N, 10.9%.

N-*Benzyl-o-aminobenzamide*

A 1-g quantity of the *o*-nitrobenzamide was gently refluxed with 3 g of zinc dust in 100 ml of 5% acetic acid for 2 hours, and filtered hot. The filtrate, on cooling, gave the *o*-amino derivative, m.p. 123°. It was crystallized from aqueous alcohol in needles, m.p. 124°. Found: N, 12.6%. Calc. for $C_{14}H_{14}ON_2$: N, 12.4%.

N-*Benzyl-o-acetylaminobenzamide* (III)

One hundred milligrams of the *o*-amino derivative was heated with 3 ml of acetic anhydride at 100° for 10 minutes. The reaction mixture was cooled and poured into water to give 100 mg of the acetyl derivative. It was crystallized from aqueous alcohol in needles, m.p. 147°–148°. Found: C, 71.4; H, 5.9; N, 10.5%. Calc. for $C_{16}H_{16}N_2O_2$: C, 71.6; H, 6.0; N, 10.5%.

Cyclization of the N-*Benzyl-o-acetylaminobenzamide*

Fifty milligrams of the acetylamino derivative was added to 3 ml of water containing two drops of benzylamine. The mixture was boiled for 2 to 3 minutes and cooled. Dilute hydrochloric acid precipitated the hydrochloride (40 mg), which was converted to the base with potassium hydroxide. Chloroform extraction gave an oil which crystallized from benzene – petrol ether in plates, m.p. 73°–74° (mixed m.p. with I, 73°–74°).

Debenzylation of the Hydrochloride of I

The hydrochloride of I (0.8 g) was maintained at 235° for 30 minutes. The product was washed with a 5% sodium carbonate solution. Crystallization of the solid from dilute ethanol (charcoal) gave 0.15 g of 2-methyl-4-hydroxyquinazoline (II), m.p. 234° (5). Mixed melting point with an authentic sample was undepressed.

ACKNOWLEDGMENT

We wish to thank the Government of India for a Research Studentship to one of us (S. S.).

1. R. Anet and S. Somasekhara. Unpublished work. Cf. S. Somasekhara, D. Phil. Thesis, Mysore University. 1957.
2. M. T. Bogert and G. D. Beal. J. Am. Chem. Soc. **34**, 516 (1912).
3. H. W. Grimmel, A. Guenther, and J. F. Morgan. J. Am. Chem. Soc. **68**, 542 (1946).
4. H. Culbertson, J. C. Decius, and B. E. Christensen. J. Am. Chem. Soc. **74**, 4834 (1952).
5. M. T. Bogert and H. A. Seil. J. Am. Chem. Soc. **29**, 517 (1907).

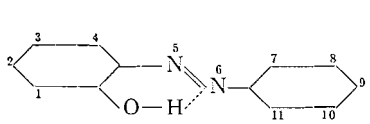
Received January 26, 1960.
Department of Chemistry,
Indian Institute of Science,
Bangalore 3, India.

NUCLEAR SHIELDING PARAMETERS FOR PROTONS IN STRONG HYDROGEN BONDS I. ORTHOHYDROXY AZO COMPOUNDS

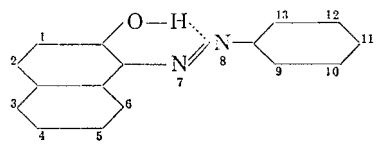
Leonard W. Reeves*

INTRODUCTION

In connection with studies of nuclear shielding parameters in strong hydrogen bonds (1, 2) measurements have been made on a series of compounds of the basic skeleton shown below:



I



II

*Department of Chemistry, University of British Columbia, Vancouver, British Columbia.

Can. J. Chem. Downloaded from www.nrcresearchpress.com by 186.148.149.217 on 09/04/12
For personal use only.

N-*Benzyl-o-acetylaminobenzamide* (III)

One hundred milligrams of the *o*-amino derivative was heated with 3 ml of acetic anhydride at 100° for 10 minutes. The reaction mixture was cooled and poured into water to give 100 mg of the acetyl derivative. It was crystallized from aqueous alcohol in needles, m.p. 147°–148°. Found: C, 71.4; H, 5.9; N, 10.5%. Calc. for $C_{16}H_{16}N_2O_2$: C, 71.6; H, 6.0; N, 10.5%.

Cyclization of the N-*Benzyl-o-acetylaminobenzamide*

Fifty milligrams of the acetylamino derivative was added to 3 ml of water containing two drops of benzylamine. The mixture was boiled for 2 to 3 minutes and cooled. Dilute hydrochloric acid precipitated the hydrochloride (40 mg), which was converted to the base with potassium hydroxide. Chloroform extraction gave an oil which crystallized from benzene – petrol ether in plates, m.p. 73°–74° (mixed m.p. with I, 73°–74°).

Debenzylation of the Hydrochloride of I

The hydrochloride of I (0.8 g) was maintained at 235° for 30 minutes. The product was washed with a 5% sodium carbonate solution. Crystallization of the solid from dilute ethanol (charcoal) gave 0.15 g of 2-methyl-4-hydroxyquinazoline (II), m.p. 234° (5). Mixed melting point with an authentic sample was undepressed.

ACKNOWLEDGMENT

We wish to thank the Government of India for a Research Studentship to one of us (S. S.).

1. R. Anet and S. Somasekhara. Unpublished work. Cf. S. Somasekhara, D. Phil. Thesis, Mysore University. 1957.
2. M. T. Bogert and G. D. Beal. J. Am. Chem. Soc. **34**, 516 (1912).
3. H. W. Grimmel, A. Guenther, and J. F. Morgan. J. Am. Chem. Soc. **68**, 542 (1946).
4. H. Culbertson, J. C. Decius, and B. E. Christensen. J. Am. Chem. Soc. **74**, 4834 (1952).
5. M. T. Bogert and H. A. Seil. J. Am. Chem. Soc. **29**, 517 (1907).

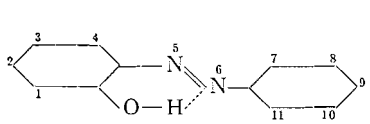
Received January 26, 1960.
Department of Chemistry,
Indian Institute of Science,
Bangalore 3, India.

NUCLEAR SHIELDING PARAMETERS FOR PROTONS IN STRONG HYDROGEN BONDS I. ORTHOHYDROXY AZO COMPOUNDS

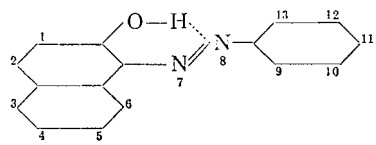
Leonard W. Reeves*

INTRODUCTION

In connection with studies of nuclear shielding parameters in strong hydrogen bonds (1, 2) measurements have been made on a series of compounds of the basic skeleton shown below:



I



II

*Department of Chemistry, University of British Columbia, Vancouver, British Columbia.

Can. J. Chem. Downloaded from www.nrcresearchpress.com by 186.148.149.217 on 09/04/12
For personal use only.

Can. J. Chem. Downloaded from www.nrcresearchpress.com by 186.148.149.217 on 09/04/12
For personal use only.

The substituents introduced into the aromatic ring systems will be identified by skeleton type I or II and substitution position related to above numbering system. The correlation of hydrogen bonding strength with nuclear shielding parameter ($\sigma_{reference} - \sigma_{OH}$) is now well established (3) although quantitative comparison of ($\sigma_{ref} - \sigma_{OH}$) and heat of formation directly is rarely possible. Spectral shifts in the infrared are more often used as the correlative parameter (3, 4). There is an advantage in measuring the shielding parameter in intramolecular hydrogen bonds since in dilute solution the entropy term due to dilution is not dominant in causing dissociation of the bond. This is shown clearly in many dilution shift studies (5, 9, 10) where intramolecular hydrogen bonds exist. If the intramolecular hydrogen bond is fairly weak as in O-chloro phenol, competition with stronger intermolecular hydrogen bonds in concentrated solutions causes dilution chemical shifts in this region. However, even in this case isolation of the hydrogen-bonding species in an inert solvent such as CCl_4 enables a nuclear shielding parameter for an undissociated intramolecular hydrogen bond to be obtained (5). Charges in nuclear shielding due to hydrogen bonding has been treated theoretically by Marshall and Pople (11).

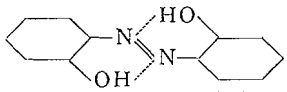
EXPERIMENTAL

Measurements were made using a solvent 99.5 mole % CCl_4 and 0.5 mole % cyclohexane in which the compounds were soluble up to 1 mole %, except for nitro derivatives. A 40-Mc/s Varian spectrometer V4300 with field stabilizer VK3506 was used and samples were made up in 5-mm O.D. tubes. The 0.5% cyclohexane served as an internal reference. Chemical shifts were measured by the usual side band technique with an audio oscillator calibrated by using 'lissajoux' figures at multiples of the 60 c.p.s. mains frequency.

RESULTS AND DISCUSSION

Column 2 of the Table I shows the value of ($\sigma_{cyclohexane} - \sigma_{OH}$) measured directly in the manner described. In an attempt to correct for the difference in shielding effect at the proton under study due to the additional diamagnetic anisotropy introduced by the naphthalene rings, a correction has been made to all compounds for the low field shift

TABLE I

Compound	($\sigma_{C_6H_{12}} - \sigma_{OH}$) p.p.m.	($\sigma_{C_6H_{12}} - \sigma_{OH}$) p.p.m. corrected	Compound
I 	−11.03	−9.98	1
	−10.52	−9.48	2
I 3,9-Dimethyl	−11.00	−9.95	3
I 3-Methyl	−10.95	−9.90	4
I 5 —CH= replaces —N=	−11.40	−10.37	5
II	−14.26	−13.06	6
II 9-Methyl	−14.62	−13.42	7
II 11-Methyl	−14.12	−13.92	8
II 9-Chloro	−14.25	−13.05	9
II 11-Chloro	−13.97	−12.77	10

due to currents in all aromatic rings. The correction to high field is slightly larger for the naphthalene compounds. The free electron model of Pople was used (6) and the interatomic distances were those for trans azo benzene (7). In addition the C—O—H bond, lengths and angles were taken to be the same as those in a phenol. The molecule is probably

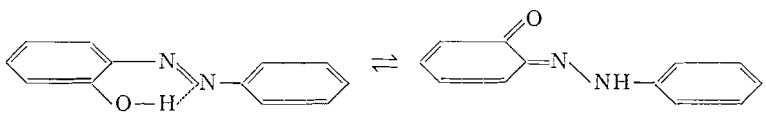
very nearly planar and was taken to be so in the calculation. Column 3 in the table contains shielding parameters corrected in this manner. These values are more correct when comparing with shielding parameters of strong hydrogen bonds in systems without large magnetically anisotropic centers.

The main feature of the results is the large shift of ~3 p.p.m. to low field in the naphthalene derivatives indicating a much stronger hydrogen bond. A good measure of the decreased shielding is shown in compounds 1 and 6 which differ by 3.08 p.p.m. It is clear that the electron-withdrawing action of the larger resonance system in naphthalene makes the hydroxyl group a much stronger acceptor. A parallel can be drawn in the greater acidity of the β hydroxy naphthalene over that of phenol (8).

Among the trans azo benzene derivatives the dihydroxy compound 2 has greatest shielding and is thus the weakest hydrogen bond of this series. It is expected that the donor properties of one nitrogen will be affected to a small degree by the use of the other in a hydrogen bond. Methyl substitution is not effective in changing the hydrogen bond strength; however the replacement of one nitrogen by a —CH= group leads to decreased shielding of the hydrogen-bonding proton. The difference in electronegativity of nitrogen and the —CH= group will increase the donor property of the nitrogen and thus to a small degree the hydrogen bond formed will be stronger.

In the β OH naphthalene derivatives substitution on the benzene ring only was studied. Chlorine substitution has very little effect on chemical shift but the inductive effect of methyl substitution appears to increase donor properties of the conjugated nitrogen considerably, resulting in a stronger hydrogen bond.

Some of these compounds were studied in the melt at higher temperature. In all cases the OH peak showed broadening indicative of proton exchange. The signals in 1% CCl_4 solution were quite sharp. As the temperature was further raised some OH peaks broadened below noise level (over 40 c.p.s. half width). This proton transfer process may be intermolecular or involve transfer across the intramolecular hydrogen bond. In the latter case the imino form of these compounds would appear in equilibrium with the azo form.



It is of some interest that the imino form has been shown to exist in the solid state in these compounds (12, 13) and the existence in solution is also suggested. Other workers (14) have shown, however, that the azo form of *o*-azophenols is the only stable species in solution. Since it is unlikely that proton transfer to the imino form occurs in dilute CCl_4 solution at room temperature where the proton resonance of the —OH proton is sharp, then the nuclear shielding parameters are attributed to pure azo form. Measurements of the intensity of the methyl resonance in methyl derivatives compared with the intensity of the —OH peak showed that no appreciable amount of material is in the imino form. It is presumed that protons transferred to the imino form will not show resonance peaks because of quadrupole relaxation. Intensity measurements in dilute solution cannot be better than $\pm 5\%$ in this experiment.

Previous studies of tautomerism (1) have shown that the proton transfer process is quite slow at room temperature and that the lifetime in individual environments is greater than a millisecond. In this case also, the nuclear shielding parameters measured

Can. J. Chem. Downloaded from www.nrcresearchpress.com by 186.148.149.217 on 09/04/12
For personal use only.

here would correspond to the azo form only since quadrupole relaxation will prevent detection of a small amount of imino form.

The author wishes to thank the National Research Council of Canada and the Research Corporation for financial aid in this research. The chemicals were obtained from Dr. Y. Matsunaga, Department of Analytical Chemistry, University of Tokyo. I am grateful for the gift of these compounds.

1. L. W. REEVES. Trans. Faraday Soc. **55**, 1684 (1959).
2. L. W. REEVES. Can. J. Chem. **35**, 1351 (1957).
3. W. G. SCHNEIDER, H. J. BERNSTEIN, and J. A. POPLE. J. Chem. Phys. **28**, 601 (1958).
4. G. KORINEK and W. G. SCHNEIDER. Can. J. Chem. **35**, 1157 (1957).
5. C. M. HUGGINS, G. C. PIMENTEL, and J. N. SHOOLERY. J. Chem. Phys. **60**, 1311 (1955).
6. J. A. POPLE. J. Chem. Phys. **24**, 1111 (1956).
7. INTERATOMIC DISTANCES. Chemical Society of London. (1958).
8. L. N. FERGUSON. Electron structures of organic molecules. Prentice Hall. 1952.
9. S. FÖRSEN. J. Chem. Phys. **31**, 852 (1959).
10. S. FÖRSEN and M. NILSSEN. Acta Chem. Scand. **13**, 1383 (1959).
11. T. W. MARSHALL and J. A. POPLE. Mol. Phys. **7**, 199 (1958).
12. D. HADZI. J. Chem. Soc. 2143 (1956).
13. A. BURAVOY, A. G. SALEM, and A. R. THOMPSON. J. Chem. Soc. 4793 (1952).
14. R. KUHR and F. BAR. Ann. **516**, 143 (1935).

RECEIVED FEBRUARY 4, 1960.
DEPARTMENT OF CHEMISTRY,
UNIVERSITY OF BRITISH COLUMBIA,
VANCOUVER, BRITISH COLUMBIA.

Can. J. Chem. Downloaded from www.nrcresearchpress.com by 186.148.149.217 on 09/04/12
For personal use only.

Can. J. Chem. Downloaded from www.nrcresearchpress.com by 186.148.149.217 on 09/04/12
For personal use only.

Canadian Journal of Chemistry

Issued by THE NATIONAL RESEARCH COUNCIL OF CANADA

VOLUME 38 JUNE 1960 NUMBER 6

SYNTHESIS OF SUGARS FROM SMALLER FRAGMENTS

PART XII. SYNTHESIS OF D-GLYCERO-D-ALTRO-, L-GLYCERO-L-GALACTO-, D-GLYCERO-L-GLUCO-, AND D-GLYCERO-L-GALACTO-OCTULOSE[1]

J. K. N. JONES AND H. H. SEPHTON[2]

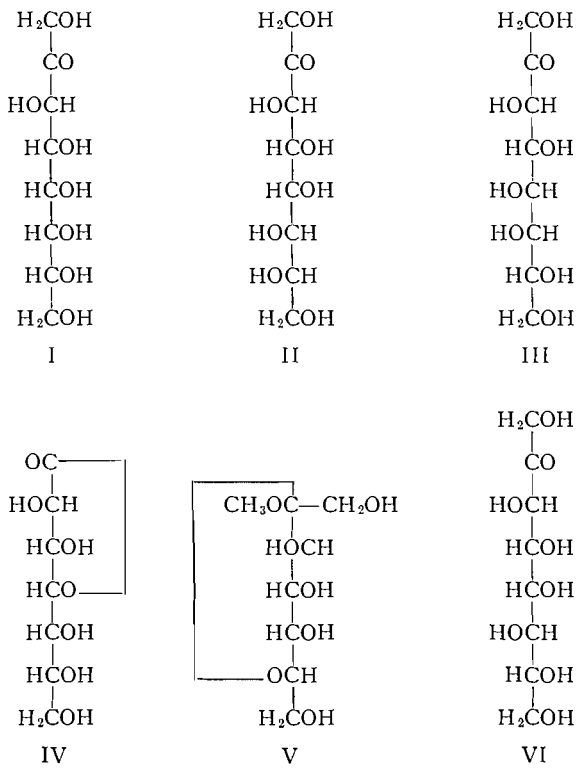
ABSTRACT

1,3-Dihydroxy-2-propanone phosphate condenses with D-ribose, L-arabinose, D-lyxose, and D-xylose in the presence of rabbit muscle aldolase to yield octulose phosphates from which the octuloses named in the title were prepared.

Previous publications (1, 2, 3) have demonstrated that 1,3-dihydroxy-2-propanone phosphate (dihydroxyacetone phosphate) will combine with aldehydes, in the presence of the enzyme aldolase, to yield 2-keto-sugars in which the hydroxyl groups on C_3 and C_4 have the D-threo-configuration. Thus, with glycolaldehyde a D-threo-pentulose is produced, L-lactaldehyde yields 6-deoxy-L-sorbose, and D-erythrose gives rise to D-altro-heptulose. It was of interest to see whether aldolase would cause dihydroxyacetone phosphate to condense with pentoses and thus form octuloses. At about the time that we had obtained paper chromatographic evidence that such a reaction was taking place, albeit in very small yield, Dr. N. K. Richtmyer informed us that he and Dr. A. J. Charlson had isolated an octulose from the avocado (4). This octulose was the first found in nature and was shown to have the D-glycero-D-manno-configuration. It has subsequently also been isolated from a species of the *Sedum* plant (5). We have prepared four octuloses by the aldolase-catalyzed condensation of dihydroxyacetone phosphate with D-ribose, L-arabinose, D-lyxose, and D-xylose. The first three products have been shown to be D-glycero-D-altro- (I), L-glycero-L-galacto- (II), and D-glycero-L-gluco-octulose (III) respectively. These octuloses are syrups (glasses) and were characterized as their crystalline 2,5-dichlorophenylhydrazones (from I and II) and as the phenylosazones (from II and III). The fourth product (from D-xylose) appears to be D-glycero-L-galacto-octulose (VI). All these sugars possess the D-threo-configuration of hydroxyl groups on C_3 and C_4. They give a characteristic color reaction on paper chromatograms when sprayed with the orcinol spray reagent for ketoses (6) and heated at 110°, viz. crimson that fades to grey. D-Glycero-L-gluco-octulose has also previously been obtained from the corresponding heptonyl chloride by Wolfrom and Cooper by diazomethane synthesis (7).

The products were identified in the following manner: D-glycero-D-altro-octulose (I) was oxidized with oxygen in alkaline solution (8) and yielded the known crystalline D-glycero-D-altro-heptono-γ-lactone (IV); its configuration was thus proved. L-Glycero-L-galacto-octulose (II) was identified with its known enantiomorph (9) by optical rotation

[1]*Manuscript received January 6, 1960.*
Contribution from the Department of Chemistry, Queen's University, Kingston, Ontario. A summary of this work was given at the Atlantic City Meeting of the American Chemical Society, September, 1959.
[2]*Present address: Laboratory of Chemistry, NIAMD, National Institutes of Health, Bethesda 14, Maryland, U.S.A.*



data and by infrared absorption and melting point data on the 2,5-dichlorophenylhydrazone derivatives of the enantiomorphs. The methyl glycoside of the second octulose (II) was oxidized with 1 mole of periodate and the product reduced with sodium borohydride. The resulting heptuloside (V) was hydrolyzed and found to behave like L-galacto-heptulose on a paper chromatogram (orcinol spray test). This observation is in accord with the expected high susceptibility to periodate attack of the C_7—C_8 bond of the octuloside in the pyranose form. The third octulose (III) when heated in aqueous solution with phenylhydrazine acetate yielded D-glycero-L-gluco-octose phenylosazone, which was found to be identical with a phenylosazone prepared from a specimen of the known synthetic D-glycero-L-gluco-octulose (7). The small quantity of the fourth octulose (VI) obtained precluded its positive identification. It was oxidized with oxygen in alkaline medium (8) and the lactone produced was found to behave like D-glycero-L-galacto-heptonic lactone (10) on a paper chromatogram. The methyl glycoside of this octulose (VI) was oxidized with 1 mole of periodate and the product reduced with potassium borohydride and hydrolyzed. The reducing compound thus obtained moved at the same rate as L-galacto-heptulose on a paper chromatogram.

When L-arabinose-1C^{14} was used as a substrate, a radioactive octulose 1-phosphate was produced. This on hydrolysis with acid gave an octulose which was indistinguishable chromatographically from L-glycero-L-galacto-octulose. The radiogram also indicated that a faster-moving material, probably an anhydro octulose (orcinol spray test), had also been formed. A similar product was also readily obtained upon acid hydrolysis of either the 1-phosphate or the methyl glycoside of D-glycero-D-altro-octulose. To avoid as far as possible the formation of anhydro octulose derivatives, phosphate groups were

Can. J. Chem. Downloaded from www.nrcresearchpress.com by 186.148.149.217 on 09/04/12
For personal use only.

removed from the octulose phosphate preparations by means of the enzyme phosphatase. All condensations were carried out at pH 6.7 to avoid non-enzymic-type condensation. The aldolase was prepared from rabbit muscle and was twice recrystallized. Two other enzymic syntheses of an octulose have been recorded: an octulose 8-phosphate was prepared from the action of transaldolase on a mixture of D-ribose 5-phosphate and D-fructose 6-phosphate (11), and in a footnote to this publication reference is made to the preparation of an octulose 1,8-diphosphate, which was prepared by Dische from ribose 5-phosphate, dihydroxyacetone phosphate, and muscle aldolase. These products were not characterized and their probable configurations (D-glycero-D-altro-octulose) were not discussed.

The stereospecificity of the aldolase condensation as illustrated above precludes it as the mechanism by which D-glycero-D-manno-octulose (4) is formed in nature unless the latter arises from D-glycero-D-altro-octulose phosphate by the action of an epimerase on C_4.

EXPERIMENTAL

General Methods

Distilled aqueous 1-butanol was used to elute cellulose column chromatograms. Materials to be chromatographed were dissolved in methanol, cellulose powder was added, and the solvent subsequently removed under vacuum from the suspension to precipitate the material onto the cellulose powder. The latter was resuspended in 1-butanol and allowed to settle under gravity in the form of a horizontal band on top of the packed cellulose column before elution was begun. Individual fractions from the columns were examined by paper chromatography using 1-butanol – ethanol – water (3:1:1) by the descending method. Sugars were detected by the silver nitrate spray in acetone followed by the ethanolic sodium hydroxide spray reagent (12) and ketoses by the orcinol and trichloroacetic acid in tertiary butanol spray reagent (6). Octuloses and anhydro octuloses were found to give a characteristic color reaction upon heating at 110° with the latter reagent, viz. a bright crimson which upon further heating fades to a more or less stable grey. Individual fractions were reduced to small volume by evaporation under vacuum in a rotary evaporator with a bath temperature of less than 50°.

Rabbit Muscle Aldolase

One fully grown female rabbit was anesthetized by intravenous injection of Nembutal and most of the blood drained through one of the jugular veins. The carcass was rapidly skinned and the main skeletal muscles cut out. Subsequent operations were carried out at 4° following the procedure described by Taylor (13). The microcrystalline enzyme obtained was kept as a suspension in 50% ammonium sulphate solution (1500 ml) at 4°. Under these conditions no appreciable loss in enzyme activity was observed after 5 months' storage.

Preparation of Substrates

Barium D-fructose 1,6-diphosphate (Nutritional Biochemicals Corp.), a biochemical source of dihydroxyacetone phosphate, was purified by reprecipitation and washing according to the method detailed by Dounce and Beyer (14). Substrates were prepared by stirring the barium salt in a small volume of distilled water to which Amberlite IR-120 resin was added as required to effect solution. Decationization was completed (negative test for barium) by passing the solution through a column of this resin. The pH of the fructose diphosphate solution obtained was adjusted to 6.7 by the addition of 2 *N* sodium hydroxide.

Can. J. Chem. Downloaded from www.nrcresearchpress.com by 186.148.149.217 on 09/04/12
For personal use only.

Can. J. Chem. Downloaded from www.nrcresearchpress.com by 186.148.149.217 on 09/04/12
For personal use only.

Preparation of D-*Glycero*-D-*altro-octulose* (I)

A substrate (pH 6.6) of disodium fructose diphosphate was prepared from purified barium fructose diphosphate (7 g) and D-ribose (4.5 g) was added. Rabbit muscle aldolase was collected from the ammonium sulphate suspension preparation (200 ml) by filtration and washed through the filter paper into the substrate with distilled water. The pH of the medium (500 ml) was readjusted to 6.7 and toluene (2 drops) was added. The flask was covered with aluminum foil and placed in an incubator at 32° for 4 days, during which time the pH of the medium dropped to 6.4. The enzyme protein was coagulated by heating the reaction mixture to 80° on the boiling-water bath and removed by filtration. Amberlite IR-120 resin was cautiously added to the cooled filtrate to adjust the pH to 4.3 and immediately removed by filtration. Acid phosphatase (Nutritional Biochemicals Corp.) (0.3 g) was added to the filtrate; the flask was covered and left in the incubator at 32° for 2 days. The protein was coagulated by heating the substrate to 80° on the boiling-water bath and the solids were removed by filtration. The cooled filtrate was completely deionized by passage through columns of Amberlite IR-120 and Duolite A-4 resins respectively and evaporated to a syrup (4.37 g). Paper chromatograms indicated the presence of D-ribose (R_f, 0.26), D-fructose (R_f, 0.18), and an octulose (R_f, 0.10) (orcinol spray). The syrup was separated by chromatography on a column of packed cellulose powder (4.5×25 cm) and eluted with aqueous 1-butanol. Three distinct fractions were obtained but the octulose (third) fraction (0.120 g) was slightly contaminated with D-ribose as a result of relative overloading of the column with respect to the latter constituent. The contaminating D-ribose was removed by rechromatographing the octulose fraction on a cellulose column (2.5×25 cm). The product (86 mg) had $[\alpha]_D^{22}$ +7.9° (*c*, 3.3 in methanol). Two additional batches of the octulose were prepared by similar procedures.* One had $[\alpha]_D^{26}$ +8.0° (*c*, 2.5 in methanol) with $[\alpha]_D^{26}$ +2.9° (*c*, 1.4 in water, inaccurate) and the other $[\alpha]_D^{27}$ +8.4° (*c*, 5.5 in methanol) (no mutarotation observed). These products were obtained (in 3.1%, 2.1%, and 1.1% yields respectively, based on fructose diphosphate, FDP) as hygroscopic amorphous solid foams upon removal of solvents under vacuum. When acid hydrolysis (pH 1 at 50° for 6 hours) was employed in another experiment to split the phosphate esters, an octulose, chromatographically identical with the above products, was obtained. In addition, the presence of an anhydro octulose in the acid hydrolyzate was indicated by paper chromatography (R_f, 0.28; orcinol spray reagent). This product was also readily formed upon acid hydrolysis of the pure octulose methyl glycoside.

D-*Glycero*-D-*altro-octulose 2,5-Dichlorophenylhydrazone*

The octulose (0.070 g) was treated with an equal weight of 2,5-dichlorophenylhydrazine in dry methanol (2.5 ml) under reflux for 2 hours. The solvent was removed under vacuum, the solid residue washed with ether by decantation to remove excess reagent, and the product recrystallized from a small volume of methanol, m.p. 169.5–170.5° (decomp.) (Kofler microstage, corrected). $C_{14}H_{20}Cl_2N_2O_7$ requires: C, 42.2; H, 5.0; Cl, 17.8; N, 7.0. Found: C, 42.3; H, 5.2; Cl, 18.0; N, 6.9.

Oxidative Degradation of D-*Glycero*-D-*altro-octulose to* D-*Glycero*-D-*altro-heptono*-γ-*lactone*

The octulose (0.049 g) was shaken with *N* potassium hydroxide (1.5 ml) in a small flask filled with oxygen and connected to an oxygen burette, at room temperature (28.5°) and atmospheric pressure. The volume of oxygen absorbed was measured after

**The conditions used were not necessarily the optimum conditions nor were the yields obtained necessarily the opitmum yields.*

suitable time intervals (4.0 ml; 4 hours) until it remained constant (7.5 ml; overnight). The alkaline solution was decationized with Amberlite IR-120 resin, filtered, and the volatile acidic products removed by evaporating the aqueous solution to dryness several times. The syrupy product (0.030 g) was examined by paper chromatography. The presence of at least six reducing components was revealed by alkaline silver nitrate spray reagent; the main component (R_f, 0.23) moved with the same speed as authentic D-glycero-D-altro-heptono-γ-lactone (kindly provided by Dr. N. K. Richtmyer). This component was isolated on Whatman No. 3 mm paper and obtained as a clear syrup (0.010 g) which crystallized upon nucleating with authentic D-glycero-D-altro-heptono-γ-lactone. The syrup had $[\alpha]_D^{30}$ +22.2° (*c*, 0.9 in water) (no mutarotation observed). The crystals, washed with methanol, had m.p. 122–123.5°, undepressed by mixing with authentic D-glycero-D-altro-heptono-γ-lactone.

Preparation of L-*Glycero*-L-*galacto-octulose* (II)

A substrate was prepared as described above from purified barium fructose 1,6-diphosphate (16 g) and adjusted to pH 6.7 (450 ml). Muscle aldolase was collected from the enzyme preparation (280 ml) by filtration and washed through the filter into the substrate with distilled water (150 ml). The pH of the preparation was readjusted to 6.7 and L-arabinose (12 g) added, followed by toluene (2 drops). The preparation was incubated at 32° for 4 days. The protein in the solution (pH 6.4) was coagulated by heating it to 80° on a boiling-water bath and the precipitate removed by filtration. The filtrate was adjusted to pH 4.3 by careful addition of Amberlite IR-120 resin and filtration. Acid phosphatase (1.0 g) was added to the filtrate and the solution was left in the incubator (32°) for 2 days. The enzyme was denatured by heating the solution to 75° on the boiling-water bath and removed by filtration. The filtrate was deionized by passage through columns of Amberlite IR-120 and Duolite A-4 and concentrated to a syrup. The octulose (0.318 g) was obtained from the syrup after chromatographing twice on cellulose columns as described for the previous octulose preparation (yield: 5.1% based on FDP). The product was obtained as a clear amorphous hygroscopic glassy foam after removal of all solvents under vacuum; $[\alpha]_D^{25}$ −62° (*c*, 0.105 in water) (no mutarotation observed). A second reducing product was eluted from the cellulose column following closely on the octulose. This material did not give the typical octulose color reaction. It was rechromatographed and a homogeneous product (0.085 g) obtained having $[\alpha]_D^{25}$ −20° (*c*, 0.8 in methanol). This material was not investigated.

L-*Glycero*-L-*galacto-octulose Phenylosazone*

The octulose (0.0095 g) was heated in a 10-ml test tube with water (0.5 ml), phenylhydrazine (0.05 ml, redistilled), and acetic acid (0.05 ml) for 7 minutes in a steam bath. The osazone started to crystallize at this stage and the solution was allowed to cool slowly to room temperature. The crystalline phenylosazone was collected by filtration on a small Büchner funnel, washed with water and methanol, and dried in vacuum over P_2O_5. The product (0.005 g) had m.p. 202–206° (decomp.). $C_{20}H_{26}N_4O_6$ requires: N, 13.4. Found: N, 13.0.

L-*Glycero*-L-*galacto-octulose 2,5-Dichlorophenylhydrazone*

The octulose (0.040 g) was heated with an equal weight of 2,5-dichlorophenylhydrazine in methanol (3 ml) under reflux for 2 hours. The solvent was removed under vacuum and the solid residue washed with ether by decantation. The residue was recrystallized from a small volume of methanol. Thrice-recrystallized material (12 mg) had m.p.

Can. J. Chem. Downloaded from www.nrcresearchpress.com by 186.148.149.217 on 09/04/12
For personal use only.

194–195° (decomp. corrected). $C_{14}H_{20}Cl_2N_2O_7$ requires: C, 42.2; H, 5.0; Cl, 17.8; N, 7.0. Found: C, 41.9; H, 5.3; Cl, 16.5; N, 6.8. The 2,5-dichlorophenylhydrazone prepared as above from D-glycero-D-galacto-octulose (0.018 g) (kindly provided by Professor M. L. Wolfrom) had m.p. 196–197° (decomp. corrected). $C_{14}H_{20}Cl_2N_2O_7$ requires: C, 42.2; H, 5.0; Cl, 17.8; N, 7.0. Found: C, 42.5; H, 5.3; Cl, 16.5; N, 6.6. The mixed melting points of these two substances lay between those of the individual constituents. The infrared spectra of these materials (0.8% in KBr) were recorded and were found to have closely corresponding absorption peaks throughout.

Periodate Oxidation of Methyl L-*Glycero*-L-*galacto-octuloside*

The octulose (0.004 g) was treated with 2% methanolic hydrogen chloride (3 ml) under reflux for 3 hours. The solution was neutralized to pH 7.8 (dilute sodium hydroxide) and the methanol removed under vacuum. The remaining aqueous solution (10 ml) was filtered and a 25% aliquot (2.5 ml) used for the oxidation. Sodium metaperiodate (0.46 ml 0.01 *N*) (1 mole) was added and the solution left at room temperature (27°) for 12 minutes. Excess sodium borohydride was added and the solution was left at room temperature for 3 hours. The solution was rendered acidic by the addition of Amberlite IR-120 resin and filtered. The methyl glycosides were hydrolyzed by heating the solution on the boiling-water bath for 1 hour. The solution was evaporated to dryness under vacuum and this was repeated several times after addition of methanol (5 ml) to remove methyl borate. The residue was taken up in water and deionized on Duolite A-4 resin. The neutral solution was evaporated to a syrup and chromatographed on Whatman No. 1 filter paper. The orcinol – trichloroacetic acid spray reagent indicated the presence of a heptulose (intense blue spot) which had an R_f value similar to that of L-galacto-heptulose.

Preparation of D-*Glycero*-L-*gluco-octulose* (III)

The substrate was prepared as detailed above using barium fructose 1,6-diphosphate (12 g) and D-lyxose (10 g) in water (500 ml) at pH 6.7 with muscle aldolase from the above enzyme preparation (190 ml). The mixture was incubated at 32° for 5 days and worked up as in the previous case, using acid phosphatase (0.3 g) to hydrolyze the phosphate esters. After removal of the protein the deionized solution was evaporated to a syrup, dissolved in methanol (10 ml), and nucleated with D-lyxose. Crystalline D-lyxose (7 g) was removed by filtration and the octulose isolated from the mother liquors by chromatography on a cellulose column. The product (0.186 g) was obtained as a hygroscopic solid glassy foam (yield 4.0% based on FDP); $[\alpha]_D^{27}$ −46.9° (*c*, 2.73 in water) (no mutarotation observed).

The phenylosazone, prepared from the octulose (0.0098 g) as described above, had m.p. 199–202° (decomp. corrected). A similar osazone, prepared from D-glycero-L-gluco-octulose obtained from Professor Wolfrom (7) had m.p. 199–204° (decomp.). The mixed melting point of these two derivatives was 199–202° (decomp.). The infrared spectra of these two osazones were obtained (0.6% in KBr) and were found to be closely similar.

Preparation of D-*Glycero*-L-*galacto-octulose* (VI)

The substrate was prepared as previously described using disodium fructose 1,6-diphosphate (0.4 g) and D-xylose (1 g) in water (50 ml) at pH 6.7 and muscle aldolase from the enzyme preparation (20 ml) was added. After incubation at 32° for 108 hours the enzyme was precipitated by heating the solution on the water bath to 80° and was removed by filtration. The filtrate was rendered acidic (pH 1–2) by decationizing with

Can. J. Chem. Downloaded from www.nrcresearchpress.com by 186.148.149.217 on 09/04/12
For personal use only.

Amberlite IR-120 and warmed overnight at 55° to hydrolyze the phosphate esters. The cooled solution was deacidified (Duolite A-4) and evaporated to a syrup. The octulose (0.006 g) was isolated from the syrup by chromatography on thick filter paper and by exhaustively extracting the appropriate area with methanol; $[\alpha]_D^{28}$ −43.4° → −13.4° (3 hours, *c*, 0.6 in water).

Degradation of D-*Glycero*-L-*galacto-octulose*

Spengler–Pfannenstiel Oxidation

The octulose (3 mg) was oxidized overnight in *N* potassium hydroxide (0.5 ml) under an oxygen atmosphere as described previously. The solution was diluted with water and decationized on Amberlite IR-120 resin. The effluent was repeatedly concentrated to a syrup after addition of water (3 ml) to remove the volatile acids. The residue was examined on paper chromatograms sprayed with the silver oxide (12) and with the lactone spray reagents (15). Both results indicated that the lactone produced was chromatographically indistinguishable from authentic D-glycero-L-galacto-heptonic lactone (10) provided by Dr. N. K. Richtmyer.

Periodate Oxidation

The octulose (1.5 mg) was treated under reflux with methanolic hydrogen chloride for 4 hours. The solution was neutralized to pH 7.8 with 0.1 *N* aqueous sodium hydroxide and the methanol removed under vacuum. Sodium metaperiodate (1.3 mg) was added and the solution left at room temperature for 12 minutes. Excess potassium borohydride was now added and the solution left at room temperature for 6 hours. The solution was rendered acidic by decationizing (IR-120 resin) and the methyl esters hydrolyzed by heating under reflux for 1 hour. The solution was evaporated several times with methanol (5 ml) to remove methyl borate. The residue was deionized and examined by paper chromatography. Three components were indicated; the main component moved at the same rate as authentic L-galacto-heptulose (silver oxide spray reagent).

Preparation of Isotopically Labelled L-*Glycero*-L-*galacto-octulose*

The substrate was prepared as previously described using barium fructose 1,6-diphosphate (0.6 g) and L-arabinose (0.14 g) to which was added L-arabinose-1C^{14} (1.42 mg containing 5 μc activity) in water (50 ml) at pH 6.7. Muscle aldolase from the preparation (20 ml) was added and the solution incubated at 32° for 108 hours. The enzyme was precipitated by warming the solution to 80° and removed by filtration. The cooled solution was decationized with Amberlite IR-120 resin and the acidic solution (pH 1–2) warmed overnight at 55° to hydrolyze phosphate esters. The cooled solution was deacidified (Duolite A-4) and evaporated to a syrup. The syrup was dissolved in methanol (5 ml) and nucleated with L-arabinose. The crystalline L-arabinose was removed by filtration and the mother liquors concentrated to a syrup and chromatographed on thick filter paper. A radiogram was obtained (14 days exposure) on X-ray film showing the presence of radioactive octulose and anhydro octulose (by crimson color reactions with orcinol spray reagent on the paper chromatogram).

ACKNOWLEDGMENTS

The authors thank the National Research Council of Canada for financial assistance. This work was carried out during the tenure of a Postdoctoral Fellowship (awarded to H. H. S.).

Can. J. Chem. Downloaded from www.nrcresearchpress.com by 186.148.149.217 on 09/04/12
For personal use only.

REFERENCES

1. L. HOUGH and J. K. N. JONES. J. Chem. Soc. 4047 (1952).
2. L. HOUGH and J. K. N. JONES. J. Chem. Soc. 4052 (1952).
3. L. HOUGH and J. K. N. JONES. J. Chem. Soc. 342 (1953).
4. A. J. CHARLSON and N. K. RICHTMYER. J. Am. Chem. Soc. **81**, 1512 (1959).
5. A. J. CHARLSON and N. K. RICHTMYER. J. Am. Chem. Soc. In press.
6. R. KLEVSTRAND and A. NORDAL. Acta Chem. Scand. 4, 1320 (1950).
7. M. L. WOLFROM and P. W. COOPER. J. Am. Chem. Soc. **71**, 2668 (1949).
8. O. SPENGLER and A. PFANNENSTIEL. Z. Wirtschaftsgruppe Zuckerind. **85**, Tech. Tl. 547 (1935).
9. M. L. WOLFROM and P. W. COOPER. J. Am. Chem. Soc. **72**, 1345 (1950).
10. A. T. MERRILL, W. T. HASKINS, R. M. HANN, and C. S. HUDSON. J. Am. Chem. Soc. **69**, 70 (1947).
11. E. RACKER and E. SCHROEDER. Arch. Biochem. Biophys. **66**, 241 (1957).
12. W. E. TREVELYAN, D. P. PROCTOR, and J. S. HARRISON. Nature, **166**, 444 (1950).
13. J. F. TAYLOR. Biochem. Preparations, **5**, 12 (1957).
14. A. L. DOUNCE and G. T. BEYER. J. Biol. Chem. **173**, 159 (1948).
15. M. ABDEL-AKHER and F. SMITH. J. Am. Chem. Soc. **73**, 5859 (1951).

Can. J. Chem. Downloaded from www.nrcresearchpress.com by 186.148.149.217 on 09/04/12
For personal use only.

Can. J. Chem. Downloaded from www.nrcresearchpress.com by 186.148.149.217 on 09/04/12
For personal use only.

ARYLPYRIDINES

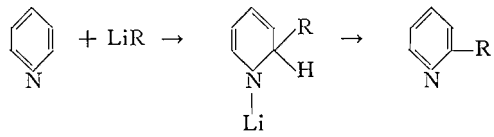
PART I. ORIENTATION IN THE REACTION OF PHENYLLITHIUM WITH SOME 3-SUBSTITUTED PYRIDINES[1]

R. A. Abramovitch, Giam Choo Seng, and A. D. Notation

ABSTRACT

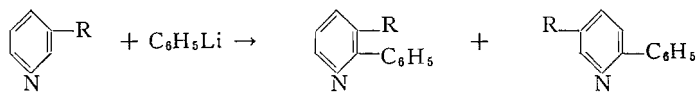
The orientation of the entering phenyl substituent in the addition of phenyllithium to 3-picoline and nicotine has been studied. In the first case the main product was 3-methyl-2-phenylpyridine together with a small amount of 5-methyl-2-phenylpyridine, the ratio of the isomers being 19:1. The structure of the isomers was established by oxidation to the corresponding phenylnicotinic acids, by infrared and n.m.r. spectroscopy. Quantitative analysis of the crude mixture of isomers was effected by vapor phase chromatography. Phenylation of nicotine gave 2-phenyl- and 6-phenyl-nicotine in the ratio of 1:1. Separation of the isomers was effected by preparative vapor phase chromatography and their orientation established as above. Evidence that the 3-substituent exerts an appreciable steric effect in the end product of the addition is presented. The results are taken to mean that addition of phenyllithium, and probably of other nucleophilic reagents, to 3-substituted pyridines occurs preferentially at the 2-position but the 3-substituent, if sufficiently bulky, may exert a steric effect resulting in appreciable addition at the 6-position also.

The reaction of lithium alkyls and aryls with dry pyridine is well known (1, 2). An intermediate (I) is probably first formed and this on heating loses lithium hydride to give the 2-substituted pyridine.



I

The formation of a 4-substituted pyridine has not been reported in such reactions. It is clear, therefore, that the addition of 1 mole of phenyllithium to a 2- or a 4-substituted pyridine can only lead to the formation of one compound. On the other hand, addition to a 3-substituted pyridine may lead to one, or a mixture, of two isomers. Very little is known about the directive effect of such a 3-substituent upon the entering phenyl group.



II III IV

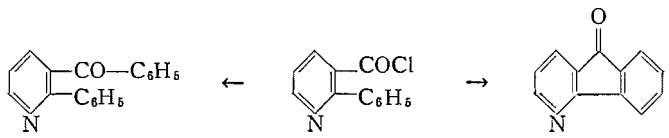
Miller, Osuch, Goldberg, and Levine (3) claimed that the reaction of 3-picoline (II, R = CH_3) with phenyllithium gave 5-methyl-2-phenylpyridine (IV, R = CH_3) exclusively. Similarly, Wiley, Jarboe, Callahan, and Nielsen (4) reported that the reaction of 3-phenylpyridine (II, R = C_6H_5) with phenyllithium gave 2,5-diphenylpyridine (IV, R = C_6H_5) as the only isomer isolated. On the other hand, the reaction of 3-substituted pyridines with other nucleophilic reagents has yielded different results. Plazek, Marcinikow, and Stammer (5), for example, established the preferential formation of 2-amino-3-methylpyridine in the reaction of 3-picoline with sodamide while Seide reported the

[1]*Manuscript received January 14, 1960.*
Contribution from the Department of Chemistry, University of Saskatchewan, Saskatoon, Saskatchewan.

exclusive formation of this isomer when potassium amide was used (6). Hardegger and Nikles studied the amination of 3-*n*-butylpyridine (II, R = *n*-Bu) with sodamide; the product, obtained in 50% yield, was a mixture containing 80% of the 2,3-isomer and 20% of the 2,5-isomer (7). Similarly, Leonard and Ryder found that the reaction of butyllithium with 3-picoline produced predominantly 2-butyl-3-methylpyridine (8).

The various observations recorded above appear to be contradictory. It was therefore of interest to establish conclusively the orientation in the addition of phenyllithium to 3-substituted pyridines and to this end it was proposed to study in the first instance the reaction with 3-picoline. This reaction was carried out in the usual way, the addition of the picoline to phenyllithium being carried out in ether solution and the temperature eventually raised to ca. 110° by the replacement of the ether by toluene. The product (42.4% yield) consisted mainly of a mixture of the two phenylated 3-picolines. Preliminary attempts at separating the mixture by vapor phase chromatography were unsuccessful. The isomers were eventually separated by fractional distillation using a spinning band column, and were obtained in the ratio of 8:1 by weight. The major product was characterized as 3-methyl-2-phenylpyridine (III, R = CH_3) as follows:

(i) Oxidation with neutral aqueous potassium permanganate gave 2-phenylpyridine-3-carboxylic acid (III, R = CO_2H), m.p. 167–169°. Ishiguro, Morita, and Ikushima (9) report m.p. 168–169° for this acid whereas Benary and Psille (10) give m.p. 229° for 2-phenylpyridine-5-carboxylic acid. The acid (III, R = CO_2H) was converted into its acid chloride which was then treated with aluminum chloride in benzene, when it failed to undergo the expected intramolecular acylation but gave instead a product $C_{18}H_{13}ON$ exhibiting a strong band at 1663 cm^{-1} characteristic of an aromatic ketone and two strong bands at 742 and 690 cm^{-1} characteristic of a monosubstituted phenyl group, thus showing the product to be 3-benzoyl-2-phenylpyridine (V). The intramolecular acylation was achieved by carrying out the reaction in light petroleum as the solvent instead of benzene. 4-Azafluorenone (VI), m.p. 139.5–141.5°, was thus obtained, identical with the



V VI

product described by Skraup and Cobenzl (11) (infrared bands at 1725 and 745 cm^{-1}).

(ii) The n.m.r. spectrum was measured through the courtesy of Mr. LeRoy Johnson of Varian Associates, who interpreted the following data as being only compatible with the 2,3-isomer, and not with a 2,5-disubstituted pyridine. This is in agreement with the findings of Schneider, Bernstein, and Pople (11*a*) for pyridine, and of Bernstein and Schneider (11*b*) and Anet and Eves (11*c*) for substituted pyridines. The signal at 506 c.p.s. is due to the α-proton which must be adjacent to a β-proton as indicated by the magnitude of the ortho-coupling constant $J_{5,6}$ = 5 c.p.s. (for pyridine $J_{2,3}$ = 5.5 and $J_{2,4}$ = 1.9 c.p.s. (11*a*)). This supports the 2,3- and not the 2,5-orientation for this disubstituted pyridine.

(iii) The infrared spectrum of the major product exhibited a band at 1579 cm^{-1} characteristic of a 2,3-disubstituted pyridine derivative (12). No band was observed above this one in the 6 μ region. The minor product had a band at 1604 cm^{-1} characteristic of 2,5-disubstituted pyridines (12).

Can. J. Chem. Downloaded from www.nrcresearchpress.com by 186.148.149.217 on 09/04/12
For personal use only.

TABLE I

N.m.r. spectrum of 3-methyl-2-phenylpyridine in carbon tetrachloride solution with tetramethylsilane as an internal reference standard

Ring position	C.p.s. from $SiMe_4$ (approximately)	Spin–spin coupling observed
4	438–447	$J_{4,5}$ = ca. 7 c.p.s.; $J_{4,6}$ = 1 c.p.s.
5	416–431	$J_{4,5}$ = 7 c.p.s.; $J_{5,6}$ = 5 c.p.s.
6	495–513	$J_{5,6}$ = 5 c.p.s.; $J_{4,6}$ = 1 c.p.s.

NOTE: Frequency 60 Mc/sec.

(iv) While this work was in progress Ishiguro, Morita, and Ikushima reported an unambiguous synthesis of 3-methyl-2-phenylpyridine involving the condensation of allyl alcohol and 1-phenyl-1-propanone with ammonia over a high-temperature catalytic bed (9). Dr. Ishiguro kindly supplied us with an authentic sample of this base and of its picrate. Comparison of the infrared absorption spectra of the bases and their picrates as well as a mixed melting point of the picrates established the identity of the major product obtained from the phenyllithium reaction with 3-methyl-2-phenylpyridine.

The minor fraction from the distillation proved to be somewhat impure 5-methyl-2-phenylpyridine (IV, R = CH_3). This was shown by oxidation of the base with neutral permanganate to 2-phenylpyridine-5-carboxylic acid, m.p. 232° (molecular formula $C_{12}H_9O_2N$), and by its infrared spectrum, which exhibited a band at 1600 cm^{-1} characteristic of 2,5-disubstituted pyridines (12).

It was subsequently found that the mixture of phenylpicolines could be resolved quite easily by vapor phase chromatography using an Apiezon "N" column, the retention time of the 2,5-isomer being appreciably greater than that of the 2,3-isomer under the conditions used. This permitted a much more accurate quantitative measurement of the isomer ratio, the determination being carried out on the crude mixture of bases. In this way it was found that the ratio 2,3/2,5 was 95:5, and not 8:1 as previously estimated by fractional distillation.

In view of this result the procedure described by Miller *et al.* (3) for the obtention of 5-methyl-2-phenylpyridine was reinvestigated. This method involved adding 3-picoline to an ethereal solution of phenyllithium, the total addition time being 10 minutes; the ether solution was then boiled under reflux (temperature below 50°) for $\frac{1}{2}$ hour and the mixture was then hydrolyzed with water. None of the phenylpicolines were obtained under these conditions; instead, an oil, b.p. 120–215°/0.32 mm, was obtained whose infrared spectrum did not show any bands characteristic of a pyridine ring in the 800 cm^{-1} region. The conditions of the reaction appear to be too mild to lead to the elimination of lithium hydride. After hydrolysis the dihydro derivative may have been obtained, which might account for the absence of the characteristic pyridine bands in the infrared. It may be possible to oxidize this to the required phenylpyridine but this was not investigated.

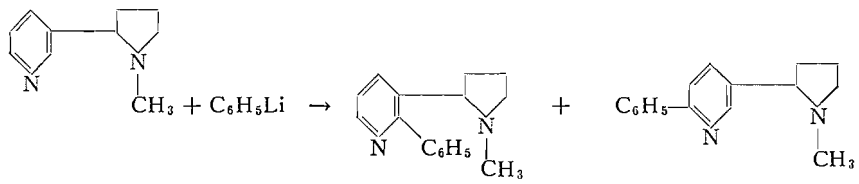
In one of the runs during the preparation of the phenylpicolines a small amount of high boiling material was obtained. This appeared to be a mixture since several peaks appeared in a gas chromatographic analysis using a silicone-on-celite column at 220°. A pure picrate, m.p. 204–206°, could be obtained from this material and the analytical figures for this derivative fitted those of a dipicrate of a base $C_{12}H_{12}N_2$, which corresponds to the molecular formula of a dimethyldipyridyl. There was insufficient material for a molecular weight determination so that as a working hypothesis the by-product was assumed to be

Can. J. Chem. Downloaded from www.nrcresearchpress.com by 186.148.149.217 on 09/04/12
For personal use only.

a dipicolyl. Stoehr and Wagner (13) obtained 3,3′-dimethyl-4,4′-dipyridyl by the action of metallic sodium on 3-picoline, and a product presumed to be 6,6′-di-*tert*-butyl-2,2′-dipyridyl has been obtained by the action of methyllithium on 2-*tert*-butylpyridine (14).

The picrate of the base obtained above depressed the melting point of 3,3′-dimethyl-4,4′-dipyridyl picrate (m.p. 231°) prepared from 3-picoline and sodium (13). 3,3′-Dimethyl-2,2′-dipyridyl was prepared from 2-amino-3-picoline via 2-bromo-3-picoline using Case's procedure (15) but again its dipicrate, m.p. 191–192°, proved different from that of the unknown base. A similar method was used to synthesize 5,5′-dimethyl-2,2′-dipyridyl from 2-amino-5-methylpyridine. This base formed a monopicrate, m.p. 175.5–176.5°, which was clearly different from that of the unknown base. No further work was done at this stage to attempt to identify this compound.

In view of the results of Wiley *et al.* (4) the possible steric effect of the 3-substituent upon the orientation of the entering phenyl group was investigated. Nicotine (VII) was chosen because of its ready availability and the fact that the 2-*N*-methylpyrrolidyl group is appreciably larger than the methyl group. The reaction was carried out as for 3-picoline



VII VIII IX

to give a 34% yield of product, b.p. 120–200°/0.1 mm. This was shown by vapor phase chromatography on a silicone-on-firebrick (1:4) column to be a mixture of two compounds, assumed to be 2-phenylnicotine (VIII) and 6-phenylnicotine (IX) in the ratio of 1:1 by weight. These findings are qualitatively similar to those of Tschitschibabin and Kirssanow (16), who obtained a mixture of 2- and 6-substituted nicotines on treatment of nicotine with sodamide in xylene at 140°. The isomers were then separated by preparative vapor phase chromatography using a 1/2-in. preparative column packed with silicone-on-celite to give one base, b.p. 145°/0.75 mm, and the other with a longer retention time, b.p. 165°/0.6 mm. Each of these gave analytical results compatible with the molecular formula $C_{16}H_{18}N_2$, confirming the assumption that they were the isomeric phenylnicotines.

The base eluted first had a band at 1588 cm^{-1} in the infrared and was, therefore, tentatively assigned the 2,3-orientation (12) whereas the second one had a band at 1600 cm^{-1} and was assumed to be the 2,5-isomer (IX). This latter assignment (and therefore the former as well) could be confirmed by oxidation of the more slowly eluted base with potassium permanganate to give 2-phenylpyridine-5-carboxylic acid identical with that obtained from 5-methyl-2-phenylpyridine.

Further confirmatory evidence for the structures assigned to these isomers was obtained from their n.m.r. spectra which were measured by Varian Associates through the courtesy of Mr. L. Johnson. Mr. Johnson also kindly interpreted the spectra and his report reads as follows: "The NMR spectrum for the first sample fits the structure of 2-phenylnicotine. The signal from the proton on the carbon in ring position 6 appears 506 c.p.s. from the tetramethylsilane and shows five cycle ortho coupling to the proton on C5 and two cycle meta coupling to the proton on C4. Likewise the signal around 478 from the proton on C4

Can. J. Chem. Downloaded from www.nrcresearchpress.com by 186.148.149.217 on 09/04/12
For personal use only.

exhibits an eight cycle coupling to the proton on C5 and again a two cycle coupling to the proton on C6. Finally, the proton on C5 at 432 shows the five and eight cycle coupling to the other two protons on this ring. The benzene ring protons are all very nearly equivalent and produce a single sharp line at 440.

The NMR spectrum of the second sample is quite different in that the protons on the benzene ring are separated into two groups; one from two of the protons in the benzene ring at 478, the other group from the three remaining protons centered around 440. This case is similar to that of acetophenone . . . . The proton α- to the nitrogen produces a signal at 506 and in this case is a close-spaced triplet due to spin coupling to the protons at C4 and C5. Coincidentally the signals from the protons on C4 and C5 appear at exactly the same field position, 460 c.p.s from tetramethylsilane, and show the spin coupling to the C2 proton of about 1.5 c.p.s. In an attempt to shift the C4 and C5 proton signals we dissolved the sample in dioxane; however, this unfortunately did not shift these signals relative to each other . . . . This is convincing evidence for assigning the 6-phenylnicotine structure to the second sample." Once again the signal at 506 c.p.s. in the case of the first compound is at the expected field position for an α-proton and consists essentially of a quartet as required for ortho- and meta-coupling. The $J_{5,6}$ and $J_{4,6}$ values are of the correct order of magnitude confirming the assignment of the 2,3-disubstituted orientation for this compound. In the case of the second sample the magnitude of the spin–spin coupling constants for the α-proton at 506 c.p.s. is small as would be expected for meta- and para-coupling (11*a*), but not for ortho-coupling.

The isomer ratio in the phenylation of nicotine as compared with 3-picoline clearly shows the presence of a steric effect of the 3-substituent upon the orientation of the product obtained. This effect is being studied in greater detail and the results obtained on changing the size of the 3-substituent systematically will be reported soon. It was of interest, however, to try and see whether even a small group such as methyl did exert any appreciable steric interference. To this end the ultraviolet absorption spectra of 2-phenylpyridine, 3-methyl-2-phenylpyridine, 5-methyl-2-phenylpyridine, 2-phenylnicotine, and 6-phenylnicotine in ethanol were compared. The results are shown in Fig. 1 where it can be seen that the spectra of 2-phenylpyridine, 5-methyl-2-phenylpyridine, and 6-phenylnicotine are very similar and only show slight intensity variations. On the other hand, the spectra of 3-methyl-2-phenylpyridine and 2-phenylnicotine formed a separate group. The maxima exhibited a hypsochromic shift and a decrease in intensity compared with the first three curves. This indicated that in these latter two compounds the 3-substituent was exerting an appreciable steric effect resulting in the non-coplanarity of the two rings. It should be pointed out, however, that such a steric effect as is evidenced here was observed in the *final product*; this does not necessarily mean that the same effect is in operation *in the transition state* also, though there can be little reason to doubt that such an effect, though smaller, would also be exerted in this instance. No such steric effect should be present in the phenylation at the 6-position so that the latter mode of reaction would be the more probable one if steric considerations were the sole factors involved.

The above results seem to indicate that in spite of a moderate steric effect nucleophilic addition takes place preferentially at the 2-position though the 3-substituent, if sufficiently bulky, may direct appreciable addition to the 6-position also. The exclusive formation of 2,5-diphenylpyridine (4) might be attributed to steric inhibition of coplanarity in the transition state (e.g. X) in the formation of the 2,3-isomer, whereas no such inhibition exists in the transition state for the 2,5-isomer (e.g. XI). Other factors may

Can. J. Chem. Downloaded from www.nrcresearchpress.com by 186.148.149.217 on 09/04/12
For personal use only.

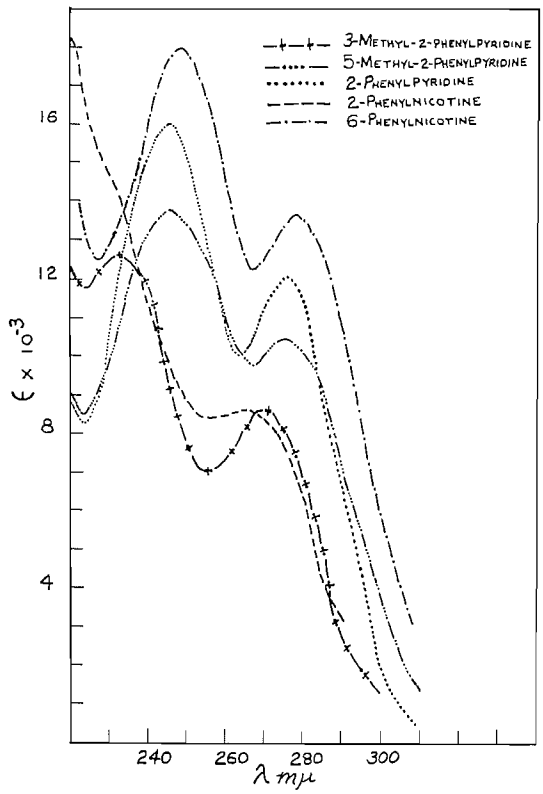
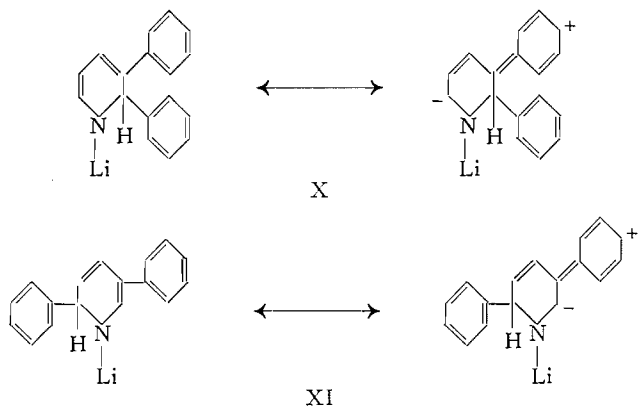


FIG. 1.

very well be involved also. Similar results concerning the preferential formation of the 2,3-isomer have been obtained by Professor H. C. Brown from a study of the addition of methyllithium to 3-substituted pyridines (14).



EXPERIMENTAL

Melting points are uncorrected. Infrared spectra were measured using a Perkin–Elmer Model 21 instrument using sodium chloride optics. Ultraviolet absorption spectra were

Can. J. Chem. Downloaded from www.nrcresearchpress.com by 186.148.149.217 on 09/04/12
For personal use only.

measured on a Beckman DK-2 recording spectrophotometer. The vapor phase chromatographic work was carried out using a Beckman GC-2 unit with helium as the carrier gas.

Reaction of Phenyllithium with 3-Picoline

(i) Phenyllithium was prepared from lithium (14 g) and bromobenzene (156 g) in anhydrous ether under dry nitrogen. 3-Picoline (110 ml) in anhydrous ether (110 ml) was added dropwise with stirring at such a rate as to maintain gentle boiling under reflux. When the addition was complete the ether was distilled off and simultaneously replaced by dry toluene (210 ml) in order that the temperature of the solution might be raised to ca. 110°. The reaction mixture was stirred under dry nitrogen and boiled under reflux for $7\frac{1}{2}$ hours. Water was then cautiously added to the cooled solution with stirring, the toluene layer separated, and the aqueous layer ether extracted repeatedly. The combined ether and toluene layers were dried (KOH pellets), filtered, and distilled up to 130° at atmospheric pressure. The residue was distilled under vacuum using a Podbielniak Mini-Cal spinning band fractional distillation column (Series 3400). Fractions, b.p. 107–119°/0.3 mm, consisted of slightly impure 3-methyl-2-phenylpyridine; those boiling at 119–133°/0.3 mm consisted of impure 5-methyl-2-phenylpyridine. The over-all yield based on bromobenzene was 42.4%. The isomers were obtained in the ratio of 8:1 by weight respectively. After three fractional distillations pure 3-methyl-2-phenylpyridine had b.p. 159–160°/31 mm. Calc. for $C_{12}H_{11}N$: C, 85.17; H, 6.55. Found: C, 84.94; H, 6.99. I.R. spectrum (liquid film) (main peaks only): 1589 (s), 1573 (s), 800 (s), 788 (s), 750 (s), 703 cm^{-1} (s). λ_{max} 232, 272 mμ, $\epsilon \times 10^{-3}$ 12.56, 8.67 (in ethanol). The picrate, on recrystallization from ethanol, had m.p. 164–166°, undepressed on admixture with an authentic sample. Ishiguro, Morita, and Ikushima (9) report m.p. 163.5–165.5° for this picrate. Calc. for $C_{12}H_{11}N,C_6H_3O_7N_3$: C, 54.27; H, 3.54. Found: C, 54.62; H, 3.49.

Several fractional distillations of 5-methyl-2-phenylpyridine, b.p. 164–166°/16 mm, failed to give a completely pure analytical sample. Vapor phase chromatography indicated the presence of some contaminant. A pure sample was obtained by vapor phase chromatography using the conditions described below and the eluted fraction collected in a dry ice – acetone trap. One further distillation under vacuum gave the required pure isomer. Found: C, 84.65; H, 6.49. I.R. spectrum (liquid film) (main peaks only): 1604 (m), 1566 (m), 835 (m), 775 (s), 736 (s), 693 cm^{-1} (s). λ_{max} 245, 275 mμ. $\epsilon \times 10^{-3}$ 13.8, 10.59 (in ethanol). After several recrystallizations from ethanol the picrate had m.p. 182–183°. Found: C, 54.10; H, 3.76.

In a previous run, a fraction, b.p. 155–180°/9 mm, was forced over. Gas chromatographic analysis of a sample of this material on a 2-ft silicone-on-celite (1:4) column with an inlet pressure of helium of 30 p.s.i. and operated at 220° gave rise to several poorly resolved peaks, indicating that this fraction was a mixture of compounds. A picrate could be prepared which, on recrystallization from ethanol, had m.p. 204–206° (decomp.). Calc. for $C_{12}H_{12}N_2,2C_6H_3O_7N_3$: C, 44.87; H, 2.82. Found: C, 44.68; H, 2.91. On subsequent similar reactions this product could not be isolated again.

Quantitative Analysis.—This was effected by vapor phase chromatography using the following conditions: $5\frac{1}{2}$ ft × $\frac{1}{4}$ in. copper tubing column packed with Apiezon "N" on "Embacel" Kieselguhr (May and Baker) (1:4 by weight); column temperature 220°; inlet temperature 235°; helium inlet pressure 30 p.s.i. Under these conditions the retention time was found to vary with the sample volume; the 'emergence time' (i.e. the time at which the compound began to emerge from the column, or the foot of the peak) was constant, however, and independent of sample size. The 'emergence time' for 3-methyl-2-

Can. J. Chem. Downloaded from www.nrcresearchpress.com by 186.148.149.217 on 09/04/12
For personal use only.

Can. J. Chem. Downloaded from www.nrcresearchpress.com by 186.148.149.217 on 09/04/12
For personal use only.

phenylpyridine was 11 minutes whereas that of 5-methyl-2-phenylpyridine was 16 minutes 20 seconds. In both cases the area under the curve was proportional to the sample size. For the analysis the reaction was carried out as described above but the combined ether and toluene layers were extracted with dilute hydrochloric acid (leaving any diphenyl behind in the organic phase). The acid extract was shaken several times with small quantities of ether, made strongly alkaline, and extracted continuously with ether. The ether extract of the bases was dried (KOH pellets), the solvent evaporated, and the residue used directly for the quantitative estimation. The ratio of 2,3/2,5 isomers was thus found to be 95:5 or 19:1.

(ii) The reaction was repeated using the procedure of Miller, Asuch, Goldberg, and Levine (3). To a solution of phenyllithium (from 2.8 g of lithium and 21 ml of bromobenzene) in dry ether (250 ml) was added 3-picoline (18.6 ml) with stirring under nitrogen over 10 minutes. The mixture was then boiled under reflux for 30 minutes, water (75 ml) added carefully, and the mixture then poured onto ice (500 g) and 6 *N* hydrochloric acid (100 ml). The ether layer was separated and extracted several times with 6 *N* hydrochloric acid. The combined acid extracts were treated with 20% aqueous sodium hydroxide until the mixture was only slightly acid. Solid sodium carbonate was then added to make the mixture slightly basic. The suspension was repeatedly extracted with ether leaving behind a copious amount of light orange resinous material. The combined ether extracts were dried ($MgSO_4$), filtered, and evaporated on a water bath. The residue was distilled under vacuum giving a fraction with a boiling point up to 190°/0.32 mm (2.5 g) and then one having a boiling point 190–215°/0.32 mm (1.5 g). A pure picrate could not be isolated from any of the fractions. I.R. spectrum of the second fraction (liquid film) (main peaks only): 2870 (s) (broad), 1600 (w), 1577 (w), 1560 (w), 865 (m), 745 (s) (broad), 698 cm^{-1} (s). Miller *et al.* (3) reported a yield of 30.8% of a product, b.p. 241–245°/2 mm, to which they assigned the structure of 5-methyl-2-phenylpyridine.

2-Phenylpyridine-3-carboxylic Acid

3-Methyl-2-phenylpyridine (6 g) was boiled under reflux with a solution of potassium permanganate (11.2 g) in water (400 ml) until the solution was decolorized; more solid potassium permanganate was then added in small portions and heating continued, the process being repeated until no more oily material appeared in the reflux condenser. The excess permanganate was destroyed by adding a few drops of methanol and heating, the hot mixture was filtered, the solid residue washed three times with hot water, and the combined filtrates evaporated down to ca. 40 ml. The solution was made just acid by adding a slight excess of acetic acid, and a saturated solution of copper acetate (70 ml) was stirred into the mixture, which was warmed for a few minutes and then allowed to stand while precipitation of the copper salt occurred. This was filtered, washed with cold water, slurried in water, and decomposed with hydrogen sulphide. The mixture was boiled to remove the excess hydrogen sulphide, filtered hot, the black sulphide precipitate washed with hot water, and the combined filtrates evaporated to give 2-phenylpyridine-3-carboxylic acid (2.85 g), m.p. 167–169°. Ishiguro, Morita, and Ikushima (9) report m.p. 168–169° for this acid.

2-Phenylpyridine-5-carboxylic Acid

5-Methyl-2-phenylpyridine was oxidized as described above for the 3-isomer to give the carboxylic acid, which, after recrystallization from aqueous ethanol, had m.p. 232°. Benary and Psille (10) report a melting point of 229° for this acid. Calc. for $C_{12}H_9O_2N$:

C, 72.51; H, 4.44. Found: C, 72.55; H, 4.55. I.R. spectrum (Nujol mull) (main peaks only): 1678 (s) (broad), 1602 (s), 749 (s), 720 (w), 678 cm^{-1} (m).

2-Phenylpyridine

This compound was prepared according to the procedure of Evans and Allen (2). It had λ_{max} 223, 245, 275 mμ. $\epsilon \times 10^{-3}$ 8.27, 16.08, 12.12 (in ethanol).

3,3′-Dimethyl-2,2′-dipyridyl

This was prepared from 2-bromo-3-methylpyridine by Case's method (15). The dipicrate (from ethanol) had m.p. 191–192.5°, depressed on admixture with the unknown dipyridyl dipicrate. Case reports a melting point of 188–189° for this dipicrate.

5,5′-Dimethyl-2,2′-dipyridyl

2-Bromo-5-methylpyridine (2 g) and copper powder (3.2 g) were mixed and heated to 220°; the temperature was gradually increased to 240° over a period of $\frac{3}{4}$ hour. When the mixture had cooled it was extracted with dilute hydrochloric acid, the combined extracts basified, extracted with ether, and the ether extracts dried (Na_2SO_4). Evaporation of the solvent gave 5,5′-dimethyl-2,2′-dipyridyl which was converted directly to the picrate. A monopicrate was formed which, on recrystallization from ethanol, had m.p. 175.5–176.5°. Calc. for $C_{12}H_{12}N_2,C_6H_3O_7N_3$: C, 52.30; H, 3.66. Found: C, 52.10; H, 3.66.

3,3′-Dimethyl-4,4′-dipyridyl

This compound was obtained in 20% yield from 3-picoline and sodium according to the procedure of Stoehr and Wagner (13). The base, b.p. 300°/720 mm, gave a picrate, m.p. 231°, depressed to 190° (decomp.) on admixture with the unidentified picrate. Stoehr and Wagner report a boiling point of 300° for the free base and melting point of 231° for its picrate. I.R. spectrum of the free base (liquid film) (main peaks only): 1587 (s), 853 (w), 806 (m), 800 (w), 710 cm^{-1} (m).

3-Benzoyl-2-phenylpyridine

2-Phenylpyridine-3-carboxylic acid (1 g) was allowed to stand with thionyl chloride (10 ml) at room temperature for $1\frac{1}{2}$ hours. The excess thionyl chloride was removed under vacuum and the residue treated with dry benzene. The benzene was evaporated to dryness and the process repeated. The residue was taken up in anhydrous benzene (30 ml) and stirred while anhydrous aluminum chloride (2 g) was slowly added. A dark-colored complex formed which, after $\frac{3}{4}$ hour, turned a dark greenish-grey. The complex was decomposed with ice, the mixture basified with aqueous sodium hydroxide, the benzene layer separated, and the aqueous layer extracted with ether. The extracts (which exhibited a slight green fluorescence) were combined, dried (Na_2SO_4), and evaporated. Distillation of the residue (1.03 g) gave 3-benzoyl-2-phenylpyridine, b.p. 167°/0.45 mm. Calc. for $C_{18}H_{13}ON$: C, 83.37; H, 5.05. Found: C, 82.26; H, 5.20. I.R. spectrum (liquid film) (main peaks only): 1663 (s), 1598 (w), 1579 (m), 1556 (w), 923 (s), 790 (w), 742 (s), 690 cm^{-1} (s). In view of the poor value for the carbon analysis the compound was further characterized as its picrate which, after recrystallization from alcohol, had m.p. 137.5–138.5° (after sintering at 135.5°). Calc. for $C_{18}H_{13}ON,C_6H_3O_7N_3$: C, 59.02; H, 3.30. Found: C, 58.98; H, 3.26.

4-Azafluorenone

2-Phenylpyridine-3-carboxylic acid (0.1 g) was allowed to stand with an excess of thionyl chloride (2 ml) and worked up as described above. The acid chloride was stirred in dry light petroleum (b.p. 40–60°) (20 ml) and an excess of anhydrous aluminum

Can. J. Chem. Downloaded from www.nrcresearchpress.com by 186.148.149.217 on 09/04/12
For personal use only.

chloride (0.5 g) slowly added. Stirring was continued for 2 hours when a red complex had formed on the sides of the flask. Ice was added to decompose the complex, the mixture was made alkaline with aqueous sodium hydroxide, the petroleum ether layer separated, and the aqueous layer extracted with ether. The combined extracts were dried (Na_2SO_4) and evaporated to yield a solid residue which, on recrystallization from ethanol, gave 4-azafluorenone (0.086 g), m.p. 139.5–141.5°. Skraup and Cobenzl (11) reported m.p. 141° for this compound. Calc. for $C_{12}H_7ON$: C, 79.55; H, 3.98. Found: C, 79.58; H, 3.91. I.R. spectrum (Nujol mull) (main peaks only): 1725 (s) (broad), 1615 (w), 1600 (m), 1569 (w), 918 (m), 742 cm^{-1} (s).

Reaction of Phenyllithium with Nicotine

Nicotine (12 g) in anhydrous ether (30 ml) was added dropwise to a solution of phenyllithium (prepared from lithium (1.0 g) and bromobenzene (12 ml) in dry ether (130 ml) under nitrogen) at such a rate as to maintain gentle boiling of the ether. The ether was then evaporated and simultaneously replaced by dry toluene (50 ml) and the temperature raised to ca. 110°. Stirring and heating under nitrogen was then continued for 8 hours. The reaction mixture was cooled, carefully treated with water, and the toluene layer separated. The aqueous layer was extracted with ether and the organic phases combined and extracted with 10% hydrochloric acid. The aqueous acid extracts were made alkaline and extracted with ether, the ether extracts combined, dried (KOH pellets), and evaporated. Vacuum distillation of the residue gave the following fractions:

(i) up to 120°/0.09 mm	1.1 g pale yellow liquid;
(ii) 120–200°/0.09 mm	5.5 g deep yellow liquid;
(iii) 200°/0.15 mm–326°/0.67 mm	4.3 g deep red resin.

Fraction (ii) was found to consist of a mixture of 2- and 6-phenylnicotine (48% yield).

The ratio of the two isomers was found to be close to 1:1. The analysis was performed by vapor phase chromatography of the crude reaction product before distillation. A 1 ft × $\frac{1}{4}$ in. copper tubing column packed with silicone-on-firebrick (1:4) was used. The samples were run in ether solution. At 220° and with a helium inlet pressure of 30 p.s.i. the retention time for 2-phenylnicotine was $6\frac{3}{4}$ minutes and that for 6-phenylnicotine was $12\frac{2}{3}$ minutes, whereas at 190° these were $16\frac{1}{3}$ minutes and 38 minutes respectively. The areas under the peaks were found to be proportional to the concentration of each isomer. The results were as follows:

2-phenylnicotine	49.4%	6-phenylnicotine	50.6%
	49.8%		50.2%

Separation of the two isomers was effected by preparative vapor phase chromatography using an injection cell preheater and a fraction collector. Fraction (ii) from the distillation was used. The column was a 2-ft preparative column ($\frac{1}{2}$-in. diameter) packed with Embacel (May and Baker, 60–100 mesh) and silicone oil (4:1), and was operated at 190° with a helium inlet pressure of 30 p.s.i. The first fraction collected proved to be 2-phenylnicotine which, after redistillation, had b.p. 145°/0.5 mm. Calc. for $C_{16}H_{18}N_2$: C, 80.63; H, 7.61. Found: C, 80.05; H, 7.67. I.R. spectrum (liquid film) (main peaks only): 1578, 1569, 805, 791, 750, and 696 cm^{-1}. λ_{max} 264 mμ; λ_{infl} 225, 255 mμ. $\epsilon \times 10^{-3}$ 8.57, 15.76, 8.45. 2-Phenylnicotine dipicrate was recrystallized from alcohol and had m.p. 211–213°. Calc. for $C_{16}H_{18}N_2,2C_6H_3O_7N_3$: C, 48.28; H, 3.74. Found: C, 48.62; H, 3.98. The second fraction proved to be 6-phenylnicotine, which was redistilled and had a boiling point of 165°/0.6 mm. Found: C, 80.33; H, 7.20. I.R. spectrum (liquid film) (main

Can. J. Chem. Downloaded from www.nrcresearchpress.com by 186.148.149.217 on 09/04/12
For personal use only.

peaks only): 1600, 1567, 841, 779, 740, 691 cm^{-1}. λ_{max} 249, 279 mμ. $\epsilon \times 10^{-3}$ 17.97, 13.66. The picrate had m.p. 166–167°.

Oxidation of 6-Phenylnicotine to 2-Phenylpyridine-5-carboxylic Acid

6-Phenylnicotine (0.2 g) was boiled under reflux in water (50 ml) while small amounts of potassium permanganate were added as long as the solution was decolorized and oily material appeared in the reflux condenser. The mixture was then decolorized by the addition of a few drops of methanol to the hot solution and the carboxylic acid isolated as described for 2-phenylpyridine-3-carboxylic acid. The crude 2-phenylpyridine-5-carboxylic acid (20 mg) was recrystallized from water to give colorless crystals, m.p. 230–233° (decomp.), undepressed on admixture with an authentic sample.

ACKNOWLEDGMENTS

The authors are grateful to Dr. L. Vining for the use of a recording ultraviolet spectrophotometer and to Mr. LeRoy Johnson of the Applications Laboratory of Varian Associates for kindly determining and interpreting the n.m.r. spectra reported in this paper. They would also like to thank Dr. Ishiguro for a sample of 3-methyl-2-phenylpyridine and its picrate, Dr. H. C. Brown for communicating to us some of his results before publication, and the University of Saskatchewan for the award of the Thorvaldson Scholarship to one of us (A. D. N.). This work was supported by a grant from the National Research Council.

REFERENCES

1. K. Ziegler and H. Zeiser. Ber. **63**, 1847 (1930).
2. J. C. W. Evans and C. F. H. Allen. Org. Syntheses, Collective Vol. II, 517 (1943).
3. A. D. Miller, C. Osuch, N. N. Goldberg, and R. Levine. J. Am. Chem. Soc. **78**, 674 (1956).
4. R. H. Wiley, C. H. Jarboe, P. X. Callahan, and N. J. Nielsen. J. Org. Chem. **23**, 780 (1958).
5. E. Plazek, A. Marcinikow, and Ch. Stammer. Roczniki Chem. **15**, 505 (1935); Chem. Abstr. **30**, 1377 (1936).
6. O. Seide. Ber. **57**, 1802 (1924).
7. E. Hardegger and E. Nikles. Helv. Chim. Acta, **39**, 505 (1956).
8. N. J. Leonard and B. L. Ryder. J. Org. Chem. **18**, 598 (1953).
9. T. Ishiguro, Y. Morita, and K. Ikushima. Yakugaku Zasshi, **78**, 220 (1958); Chem. Abstr. **52**, 11846g (1958).
10. E. Benary and H. Psille. Ber. **57**, 828 (1924).
11. Z. Skraup and A. Cobenzl. Monatsh. **4**, 436 (1883).
11. (*a*) W. G. Schneider, H. J. Bernstein, and J. A. Pople. Ann. N.Y. Acad. Sci. **70**, 806 (1958).
11. (*b*) H. J. Bernstein and W. G. Schneider. J. Chem. Phys. **24**, 499 (1956); H. J. Bernstein, J. A. Pople, and W. G. Schneider. Can. J. Chem. **35**, 65 (1957).
11. (*c*) F. A. L. Anet and C. R. Eves. Can. J. Chem. **36**, 902 (1958).
12. R. A. Abramovitch, Giam Choo Seng, and A. D. Notation. Can. J. Chem. **38**, 624 (1960).
13. C. Stoehr and M. Wagner. J. prakt. Chem. **48**, 1 (1893).
14. H. C. Brown. Personal communication.
15. F. H. Case. J. Am. Chem. Soc. **78**, 2574 (1946).
16. A. E. Tschitschibabin and A. W. Kirssanow. Ber. **57**, 1163 (1924).

Can. J. Chem. Downloaded from www.nrcresearchpress.com by 186.148.149.217 on 09/04/12
For personal use only.

Can. J. Chem. Downloaded from www.nrcresearchpress.com by 186.148.149.217 on 09/04/12
For personal use only.

THE INFRARED SPECTRA OF SOME URANYL COMPOUNDS[1]

G. L. CALDOW,[2] A. B. VAN CLEAVE, AND R. L. EAGER

ABSTRACT

The infrared spectra for the di- and hexa-hydrates of uranyl nitrate, for anhydrous uranyl acetate, and for sodium zinc uranyl acetate hexahydrate have been obtained using the potassium bromide pressed disk technique. Where possible, samples were prepared by freeze-drying aqueous solutions of the appropriate compound and potassium bromide. The uranyl nitrate hydrates gave spectra with peaks characteristic of both nitrate and nitrato groups. For uranyl acetate the type of spectra obtained depended upon the ratio of uranyl acetate to potassium bromide in the freeze-dried mixture. It is postulated that, for relatively large ratios of uranyl acetate to potassium bromide, the carbonyl oxygen atoms of the acetate groups are chelated to the uranium atom. The spectrum of sodium zinc uranyl acetate hexahydrate is quite similar to that reported by Jones for sodium uranyl acetate. Using the 933 cm^{-1} peak, the Beer–Lambert law was obeyed for samples prepared by freeze-drying solutions containing uranyl nitrate and potassium bromide.

INTRODUCTION

The authors have been interested in the infrared spectra of uranyl compounds and in the possible application to a quantitative determination of uranium by infrared spectrophotometry. Various investigations have been made of the infrared spectra of uranium compounds (1, 2, 3, 4, 5, 6, 7). The repeated occurrence in the infrared spectra of uranyl compounds of a strong absorption band at 10.87 μ (920 cm^{-1}) led to the suggestion by Lecompte and Freymann (2) that this band could be used for the identification of uranyl ions. For water-soluble substances the potassium bromide disk technique (8, 9), combined with the freeze-drying of aqueous solutions containing both the substance whose spectrum is being investigated and potassium bromide, gives good quantitative results (10).

EXPERIMENTAL

Apparatus and Reagents

The spectra were recorded with a Perkin–Elmer model 21 double-beam infrared spectrophotometer equipped with a sodium chloride prism.

The sample chamber of the freeze-drying apparatus was a 250-mm vacuum desiccator from which the ground-glass sleeve had been removed. The desiccator was connected to a 1-liter trap by means of a 55/40 standard taper ground-glass joint and 40-mm I.D. glass tubing. A length of rubber tubing and a 18/7 ball and socket joint were used to connect the trap to a high vacuum system. A freezing mixture of dry ice – acetone was used to cool the trap.

The die used to prepare the potassium bromide disks was of the type described by Bauer, Epp, and Lemieux (11). The disk holder is removable and fits into an adapter which can be inserted into the standard sample slide on the spectrophotometer. A 20-ton hydraulic press was used to apply pressure to the die.

Reagent grade chemicals were used. Sodium zinc uranyl acetate was prepared from zinc uranyl acetate and sodium chloride solutions using the method of Barber and Kolthoff (12).

Sample Preparation

The freeze-dried mixtures were prepared by mixing together, in Erlenmeyer flasks,

[1]*Manuscript received January 7, 1960.*
Contribution from the Department of Chemistry, University of Saskatchewan, Saskatoon, Saskatchewan, with financial assistance from the National Research Council of Canada. Presented in part at the 40th Annual Conference of the Chemical Institute of Canada, Vancouver, B.C., June 3–5, 1957.
[2]*Present address: Oxford University, Oxford, England.*

appropriate quantities of aqueous solutions of the substance whose spectrum was being determined and potassium bromide. The mixtures were frozen rapidly by immersing the Erlenmeyer flasks in a dry ice – acetone mixture and swirling their contents. The Erlenmeyer flasks of a given run were left in the dry ice – acetone mixture until all the samples were prepared, after which they were placed in the sample chamber of the freeze-drying apparatus. The apparatus was immediately evacuated, and the samples left for approximately 24 hours. The product was a very fine fluffy powder (10).

Some of the uranyl salt – potassium bromide mixtures were prepared by mixing the dry solids in a small plastic vial attached to a vibrating tool. Freeze-dried potassium bromide was used in all of these preparations in order to ensure small particle size (10). Freeze-dried uranyl salts were used except in the case of uranyl nitrate hexahydrate, which was ground in a mortar until the crystals would pass through a 200-mesh screen.

Approximately 0.5 g of the uranyl salt – potassium bromide mixture was placed in the partly assembled die, care being taken to distribute the sample evenly in the disk holder. The powder was tamped down using the flattened end of a glass rod. The assembled die was then placed in the hydraulic press and evacuated, by means of a mechanical oil vacuum pump, for 1 minute. While still evacuated the die was subjected to a pressure of 99,000 pounds per square inch for 1 minute. After the pressure had been released, air was allowed to leak slowly into the die. The resulting transparent window was cleaned of loose powder.

Recording the Spectra

For a qualitative survey of the infrared spectra of uranyl compounds the spectrophotometer was operated essentially as recommended by the manufacturer using slit schedule 4 (13). It was found that the noise level was lowered if a gain of 5.5 was used, instead of the recommended 6.5–7, and if zero suppression was used, instead of the recommended 2. For quantitative work the recommended slit schedule 2 was used. It was found that better results were obtained in the quantitative work when a potassium bromide blank was used in the reference beam. However, a blank was not necessary in order to obtain good qualitative spectra.

RESULTS AND DISCUSSION

Preparation of Lower Hydrates of Uranyl Compounds by Freeze-Drying

Uranyl nitrate hexahydrate and uranyl acetate dihydrate were used to prepare the mixtures for freeze-drying. Since other hydrates of these salts can exist, it was of interest to determine the degree of hydration of the products when aqueous solutions of either uranyl nitrate or of uranyl acetate were freeze-dried. The freeze-dried samples were analyzed for their uranium content by the method of Kolthoff and Lingane (14). The results shown in Table I indicate the formation of anhydrous uranyl acetate and of

TABLE I

Analysis of freeze-dried uranyl compounds

Sample	Uranium, %	Deviation from theoretical value
Freeze-dried uranyl acetate	61.26	0.07
Theoretical for $UO_2(C_2H_3O_2)_2$	61.33	
Freeze-dried uranyl nitrate	55.14	0.21
	55.28*	0.07
Theoretical for $UO_2(NO_3)_2.2H_2O$	55.35	

*The trap was cooled with liquid nitrogen in this experiment.

Can. J. Chem. Downloaded from www.nrcresearchpress.com by 186.148.149.217 on 09/04/12
For personal use only.

uranyl nitrate dihydrate. It was assumed in the subsequent work that the same compounds would be formed whether or not potassium bromide was present during the freeze-drying process. The fact that uranyl nitrate dihydrate was formed, and not the monohydrate or the anhydrous salt, is interesting since all of the many attempts to prepare these salts have been unsuccessful (15, 16).

The results indicate that the freeze-drying technique may be a convenient and relatively simple method for preparing the lower hydrates for substances which form more than one hydrate. The method eliminates the use of elevated temperatures which have been used in the preparation of many hydrates, and which often results in undesired decomposition reactions.

It should be noted that the product obtained from freeze-drying a solution of uranyl nitrate and potassium bromide will not necessarily be only a mixture of these two compounds. It is quite possible that uranyl bromide and potassium nitrate will also be present, perhaps even in relatively large quantities, since bromide ions and potassium ions were originally present in large excess. However, when a solution prepared by dissolving uranyl acetate and potassium bromide in water is freeze-dried, it is likely that the product will be largely uranyl acetate and potassium bromide. This follows from the fact that there is good evidence (17, 18, 19) that in aqueous solution, the tendency for covalent bond formation between acetate and uranyl ions is large.

Spectra

In general, all the spectra could be interpreted as consisting of the spectra of the anion present and of the uranyl ion. The spectra of all samples show strong absorption in the 930 cm^{-1} region, which has been assigned to the antisymmetrical normal vibration, ν_3, of the uranyl ion (1). In a few of the samples of uranyl nitrate dihydrate, prepared by freeze-drying an aqueous solution of uranyl nitrate and potassium bromide, there is a definite, but quite weak, absorption at 856 cm^{-1}. This absorption at 856 cm^{-1} could be the 860 cm^{-1} band, which has been assigned to the symmetrical normal vibration, ν_1, of the uranyl ion (1) and which, for the free gaseous ion, would be infrared inactive.

(*a*) *Uranyl Nitrate Hydrates*

The spectra of uranyl nitrate hexahydrate mixed with potassium bromide by the vibration technique, of freeze-dried uranyl nitrate dihyrate mixed with potassium bromide by the vibration technique, and of uranyl nitrate dihydrate mixed with potassium bromide by the freeze-drying technique are shown in Figs. 1, 2, and 3 respectively. The frequencies of the observed maxima are given in Table II. The close similarity of the spectra of the dihydrate and of the hexahydrate is contrary to the results of Sevchenko and Stepanov (3), of Tridot (6), and of Gatehouse and Comyns (7). The above authors used the solid hydrate samples, which were either pressed between fluorite plates (3), suspended in carbon tetrachloride (6), or mulled with Nujol (7). These authors found, for example, that a peak at 1390 cm^{-1} was present in the spectra of the hexahydrate but was not in the spectra of the dihydrate, whereas peaks present in the 1300 cm^{-1} and 1550 cm^{-1} regions of the spectra of the dihydrate were not present in the spectra of the hexahydrate. In contrast, all three peaks were observed in the spectra of both the hexahydrate and the dihydrate in the present work. Gatehouse and Comyns (7) have made the most detailed assignment of the bands in the infrared spectrum of the uranyl nitrate hydrates by the use of compounds enriched in N^{15}. They reached the conclusion that co-ordinated nitrato groups are present in the dihydrate (and also in the trihydrate), whereas ionic nitrate

Can. J. Chem. Downloaded from www.nrcresearchpress.com by 186.148.149.217 on 09/04/12
For personal use only.

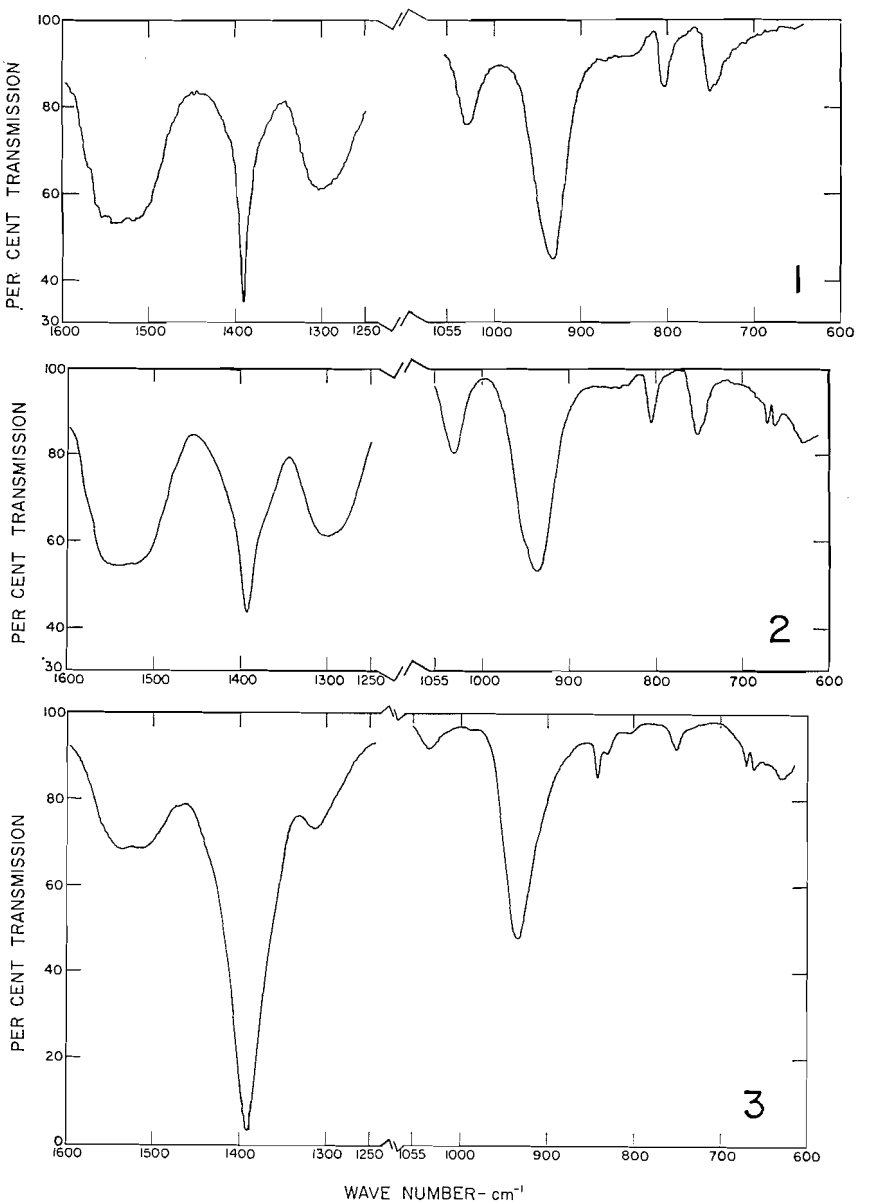


FIG. 1. Infrared spectrum of uranyl nitrate hexahydrate mixed with potassium bromide by vibration.
FIG. 2. Infrared spectrum of uranyl nitrate dihydrate mixed with potassium bromide by vibration.
FIG. 3. Infrared spectrum of uranyl nitrate dihydrate mixed with potassium bromide by freeze-drying.

groups are present in the hexahydrate. Their results for the dihydrate and for the hexahydrate, both containing natural nitrogen, are also given in Table II. The symbols of the nitrate vibrations are designated by an asterisk in Table II.

The symmetry of the nitrate ion is D_{3h} whereas that for the co-ordinated nitrato group is C_{2v}, hence for the nitrato group the doubly degenerate vibrations, ν_3 and ν_4, of the

Can. J. Chem. Downloaded from www.nrcresearchpress.com by 186.148.149.217 on 09/04/12
For personal use only.

TABLE II

Infrared spectra of uranyl nitrate hydrates (frequencies in cm^{-1})

	Dihydrate			Hexahydrate	
Assignments	Vib. mixed with KBr	Freeze-dried with KBr	Gatehouse and Comyns (7)	Vib. mixed with KBr	Gatehouse and Comyns (7)
ν_5[a]	662 670	662 670	706		
ν_3[a]	745 (vw, sh) 752	752	743 748 (sh)		
ν_4*				745 (vw, sh) 752	748
ν_2*				804	803 835
ν_6	805	805 (vw)	801		
ν_2* (KNO_3)		830 842	811[b] 826		
ν_3 (UO_2^{++})	937	933	951	933	941
ν_1*				1032	1030
ν_2	1032	1035	1026 1044		
ν_1	1298 (bd)	1312	1280 1311	1300	
ν_3*	1392	1392		1392	1366
ν_4	1520 1535	1515 1537	1515 1547	1515 1531	
Unassigned	630	630			

[a]The assignment of the lower frequency to ν_5 and of the higher frequency to ν_3 is arbitrary (7).
[b]These results are from Decius (22).
*Denotes vibrations of the nitrate ion.

nitrate ion are both split (20). The conventions for numbering the vibrations of the nitrate ion (21) differ from those used for the co-ordinated nitrato group (20). To avoid confusion in the following discussion a summary of the relations between these two conventions is given in Table III (7). It was observed by Gatehouse and Comyns (7) that

TABLE III

Summary of designation of vibrations for the nitrate ion and the nitrato group (7)

	ν_1	ν_2	ν_3		ν_4	
NO_3^-	NO stretch	Out of plane	NO_2 stretch		NO_2 bend	
O_2NO	ν_2 NO stretch	ν_6 Out of plane	ν_1 NO_2 stretch sym	ν_4 NO_2 stretch antisym	ν_3 NO_2 bend sym	ν_5 NO_2 bend antisym

some of the vibrations for both the nitrate and the nitrato group were split. It was concluded that this splitting was the result of the in-phase and the out-of-phase vibrations of adjacent nitrate, or nitrato, groups having slightly different frequencies.

Considering first the spectra of the dihydrates, it is seen from Figs. 2 and 3 and Table II that the spectra obtained in the present work are similar in most respects to the spectra obtained by Gatehouse and Comyns. Hence it appears that nitrato groups, co-ordinated to the uranyl ion, are present in these samples. However, the intense peak at 1392 cm^{-1} is

Can. J. Chem. Downloaded from www.nrcresearchpress.com by 186.148.149.217 on 09/04/12
For personal use only.

Can. J. Chem. Downloaded from www.nrcresearchpress.com by 186.148.149.217 on 09/04/12
For personal use only.

undoubtedly due to the normal vibration ν_3 of the nitrate ion, which was not observed by Gatehouse and Comyns for the dihydrate. For the sample prepared by freeze-drying an aqueous solution of uranyl nitrate and potassium bromide this peak is extremely intense, as shown in Fig. 3. It seems likely, as suggested earlier, that in the freeze-drying step, some potassium nitrate was formed. By comparing Figs. 2 and 3 it is seen that the intensities of the peaks assigned to the nitrato group are weaker in Fig. 3 than in Fig. 2, indicating that in the sample prepared entirely by freeze-drying, an appreciable amount of the original nitrate appeared as such in the final product. The presence of nitrate in the sample mixed by vibration, Fig. 2, can be explained by the observation (20) that some compounds with co-ordinated nitrato groups react with sodium chloride windows and that the products give the spectrum of the nitrate ion. Possibly a similiar reaction could occur with potassium bromide. The presence of potassium nitrate in the sample mixed with potassium bromide by freeze-drying would also explain a feature of the spectrum of this sample which differs from that for the sample mixed with potassium bromide by vibration. In the spectrum, Fig. 2, of the latter sample there is a peak at 805 cm^{-1} which has been assigned by Gatehouse and Comyns (7) to the out-of-plane vibration of the nitrato group. This peak is only faintly evident in the spectrum, Fig. 3, of the sample mixed with potassium bromide by freeze-drying. There is, however, in the spectrum of the latter a weak peak at 830 cm^{-1} and a relatively stronger one at 842 cm^{-1}. Decius (22) observed that in potassium nitrate, the out-of-plane vibration of the nitrate ion, ν_2, is split to give a weak peak at 811 cm^{-1} and a strong one at 826 cm^{-1}. The splitting observed by him is 15 cm^{-1} while that shown in Fig. 3 is 12 cm^{-1}.

The remainder of the spectrum for both dihydrate samples is quite similar to that observed by Gatehouse and Comyns (7) except for the splitting of some of the peaks. A splitting of 8 cm^{-1} was observed in the present work for ν_5 whereas Gatehouse and Comyns (7) observed only a single peak. A splitting of 5 cm^{-1} (708 and 713 cm^{-1}) was observed by Dieke and Duncan (23) for a sample of $CsUO_2(NO_3)_3$. No shoulder is evident on the low frequency side of the 752 cm^{-1} peak for the freeze-dried sample, indicating that the frequency ν_3 was not split. However, the intensity of this peak is low and it would be difficult to observe a shoulder. Neither ν_2 nor ν_1 shows splitting in the present work, although in the sample mixed by vibration the 1298 cm^{-1} peak is broad and some splitting may be present. Gatehouse and Comyns (7) observed a splitting for both of these vibrations. No assignment is offered for the weak 630 cm^{-1} peak observed in the spectra of both of the dihydrate samples.

The spectrum of the hexahydrate, Fig. 1, shows more resemblance to those of the dihydrates, Figs. 2 and 3, than it does to the one obtained by Gatehouse and Comyns for the hexahydrate (7). It is particularly similar to the spectrum obtained for the dihydrate sample mixed with potassium bromide by vibration, Fig. 2. The only difference is in the 600 to 700 cm^{-1} region. In this region the hexahydrate has negligible absorption whereas the dihydrate has moderate absorption with peaks at 662, 670, and 630 cm^{-1}. The spectrum does have the strong peak at 1392 cm^{-1}, characteristic of nitrates, but it also has strong peaks in the 1300 and 1500 cm^{-1} regions which were not observed for the hexahydrate by Gatehouse and Comyns (7). The presence of these latter peaks suggests that the symmetry of the nitrate ion has been lowered from that of D_{3h} and consequently the ν_3 vibration of the nitrate ion has been split.

Why the symmetry of the nitrate ion should change is not immediately obvious. It is conceivable that a deformation of the crystal structure occurred as a result of subjecting the sample to the high pressures used in forming the disk. This deformation might cause

a lowering of the symmetry of the nitrate ion. Another possibility is that at the high pressures used, and in the presence of a large excess of potassium bromide, the hexahydrate was partially dehydrated. With the loss of water molecules the uranyl ion would then perhaps react with nitrate ions to form co-ordinated nitrato groups.

(*b*) *Uranyl Acetate*

In earlier work (1, 2, 3) the samples used appear to have been hydrates of uranyl acetate, although this is not always definitely stated. In the present work freeze-dried uranyl acetate was used, hence, as indicated by the results shown in Table I, the samples contained anhydrous uranyl acetate. Preliminary experiments, using samples obtained by freeze-drying aqueous solutions of uranyl acetate and potassium bromide, indicated that the type of spectra obtained depended upon the ratio of uranyl acetate to potassium bromide. To investigate this effect further a series of solutions containing uranyl acetate and potassium bromide in varying porportions were freeze-dried. The freeze-dried mixtures were next mixed by vibration with additional freeze-dried potassium bromide to give sufficient material for pressing into disks. There was always approximately the same amount of uranyl ion present in each disk. In Figs. 4 and 5 are shown portions of the

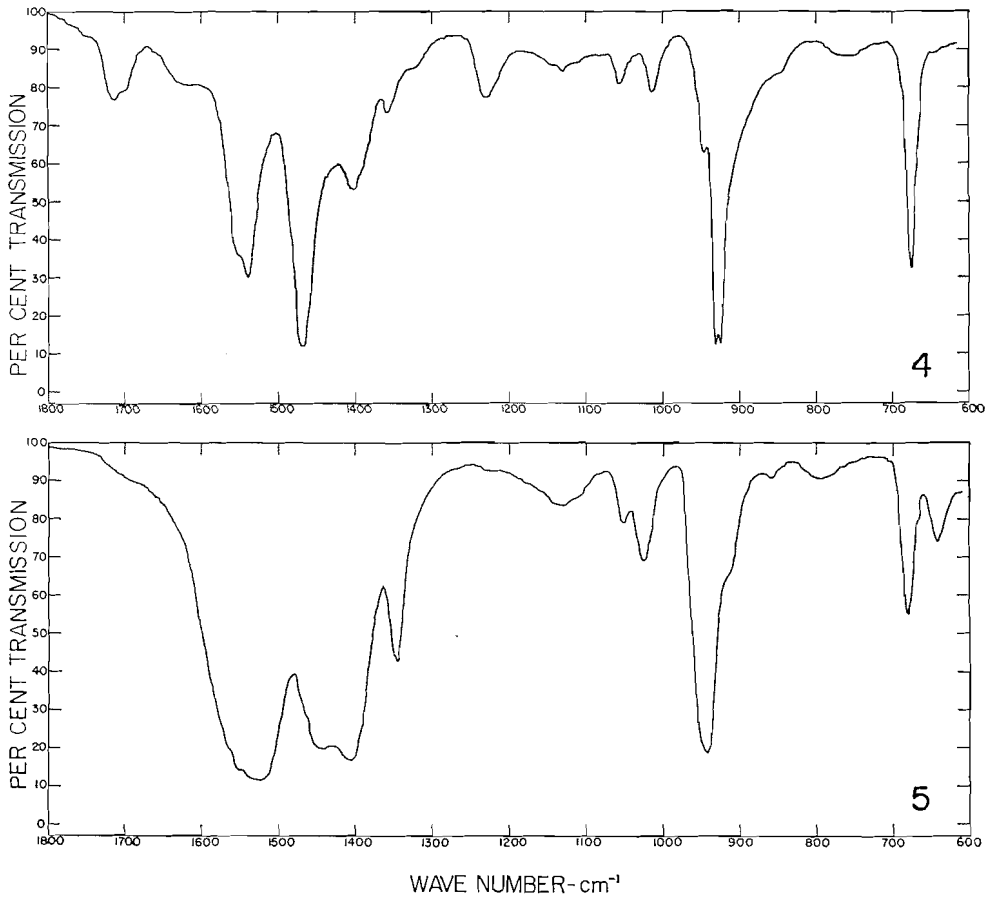


FIG. 4. Infrared spectrum of uranyl acetate mixed with potassium bromide by freeze-drying. Molar ratio of uranyl acetate to potassium bromide 0.1 to 1.

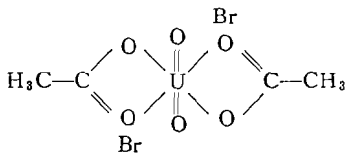
FIG. 5. Infrared spectrum of uranyl acetate mixed with potassium bromide by freeze-drying. Molar ratio of uranyl acetate to potassium bromide 1000 to 1.

Can. J. Chem. Downloaded from www.nrcresearchpress.com by 186.148.149.217 on 09/04/12
For personal use only.

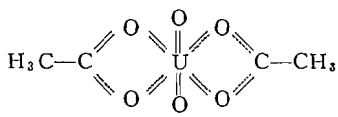
spectra of samples in which the molar ratio of uranyl acetate to potassium bromide during the freeze-drying process was 0.1 to 1 and 1000 to 1 respectively. The type of spectra obtained showed a smooth transition from that shown in Fig. 4 to that shown in Fig. 5 as the molar ratio was varied between the above limits. In the following discussion spectra of the type shown in Fig. 4, i.e. from samples where a small molar ratio of uranyl acetate to potassium bromide was present during freeze-drying, will be designated as type I spectra, whereas spectra of the type shown in Fig. 5, i.e. from samples where a large molar ratio of uranyl acetate to potassium bromide was present during freeze-drying, will be designated as type II spectra.

The strong peak in the neighborhood of 930 cm^{-1} is undoubtedly due to the asymmetric normal vibration, ν_3, of the uranyl ion. In type I spectra there is a strong double peak at 924 and 930 cm^{-1} together with a shoulder at 945 cm^{-1}. In type II spectra the intense peak is at 942 cm^{-1} with a shoulder on the low wave number side.

The strong absorption at 676 cm^{-1} may arise as the result of the acetate groups being attached to the uranyl group by covalent bonds. There is considerable evidence (17, 18, 19) which indicates that in aqueous solution the tendency for covalent bond formation between the acetate group and the uranyl group is large. Hence it seems reasonable to expect that in solid uranyl acetate the acetate groups are attached, as indicated in formula I, by covalent bonds. The force constants for C=O, C=C, C=N, and N=O



I



II

bonds are approximately double those of the corresponding C—O, C—C, C—N, and N—O bonds (24). If the assumption is made that this relationship also holds for U=O and U—O bonds then a peak due to the U—O bond might be expected in the region 927 $cm^{-1}/\sqrt{2}$ = 655 cm^{-1}. This calculation assumes the vibration to be harmonic, which is probably not true for the solid state. Thus, considering also the approximation made concerning the bond strength, the agreement with the observed peak at 676 cm^{-1} is as good as could be expected. A peak at 678 cm^{-1} has been reported for $NaUO_2(C_2H_3O_2)_3$ (5). This peak was assigned (5) to a CO_2 deformation vibration by comparison with the similar assignment of a peak at 645 cm^{-1} observed for sodium acetate (25). However, there is good evidence that in $NaUO_2(C_2H_3O_2)_3$ the uranyl and acetate ions are present as the complex anion $UO_2(C_2H_3O_2)_3^-$ (27). Considering the large tendency for covalent bond formation between the acetate and uranyl groups (17, 18, 19), it is unlikely that any appreciable amount of free acetate ions is present. Hence a CO_2 deformation vibration is not very likely and the assignment of the 676 cm^{-1} peak to a C—O bond appears to be reasonable.

The peaks at 1713 and 1230 cm^{-1}, which are present in type I spectra but which are absent in type II spectra, are probably due to the C=O and C—O stretching vibrations of the acetate group (24, 26). It would ordinarily be expected that the intensities of these peaks, especially the 1713 cm^{-1} peak (24) would be greater than those observed in type I spectra.

In type II spectra a peak is present at 642 cm^{-1} which is absent in type I spectra. The intensity of this peak progressively increases as the ratio of uranyl acetate to potassium bromide is increased.

Can. J. Chem. Downloaded from www.nrcresearchpress.com by 186.148.149.217 on 09/04/12
For personal use only.

Can. J. Chem. Downloaded from www.nrcresearchpress.com by 186.148.149.217 on 09/04/12
For personal use only.

A tentative explanation for the change in the spectra from type I to type II as the ratio of uranyl acetate to potassium bromide is increased is that the uranium atom of the uranyl group becomes chelated to the carbonyl oxygen atom of the acetate groups instead of being bonded to bromide ions. There is strong evidence that the uranium atom in the uranyl ion has a tendency for a co-ordination number greater than six (17, 18). Hence it is possible that besides the co-ordinate covalent bonds formed with the oxygen atoms of the two C—O groups, the uranium atom will show a tendency to form co-ordinate covalent bonds with other atoms, such as possibly bromide ions or the oxygen atoms of water molecules. Thus in uranyl acetate dihydrate the water molecules are perhaps attached to the uranium atom by co-ordinate covalent bonds. When uranyl acetate is freeze-dried, water molecules are no longer available and if a relatively large excess of potassium bromide is present it is possible that two, or perhaps more, bromide ions are bound to the uranium atom by co-ordinate covalent bonds, giving the compound represented by formula I. In the presence of a relatively small amount of potassium bromide, however, it is possible that the tendency of the uranium atom to form additional co-ordinate covalent bonds may be satisfied by chelation with the carbonyl oxygen atoms of the acetate groups giving a compound represented by formula II. In the resulting compound it is likely that the two oxygen atoms of each of the acetate groups will be equivalent.

Chelation of the carbonyl group often results in a considerable lowering in frequency of the band in the 1700 cm^{-1} region (26) and this effect could account for the disappearance of the 1713 cm^{-1} peak together with the increase in intensity and the broadening of the bands in the 1500 cm^{-1} region. The disappearance of the 1230 cm^{-1} band would also be expected. The shift of the asymmetrical normal vibration, ν_3, of the uranyl group from the 927 cm^{-1} region, type I spectra, to 942 cm^{-1}, type II spectra, could be the result of the changes which have occurred in the neighborhood of the uranium atom.

The 642 cm^{-1} peak which is present in type II spectra may be due to some vibration of the  group. This would account for the appearance of this peak as the ratio of uranyl acetate to potassium bromide increases. The low intensity, mentioned earlier, of the 1713 and 1230 cm^{-1} bands of the carbonyl group in type I spectra suggests that some chelation with the carbonyl oxygen atoms of the acetate groups has already occurred, even at a low uranyl acetate to potassium bromide ratio. Hence type I spectra probably results from the presence in the sample of a mixture of compounds I and II rather than from the presence of compound I alone.

In the above discussion intermolecular chelation has been postulated. It is conceivable that intramolecular chelation is either partially, or wholly, responsible for the changes observed in the spectrum as the uranyl acetate to potassium bromide ratio is varied.

(*c*) *Sodium Zinc Uranyl Acetate,* $NaZn(UO_2)_3(C_2H_3O_2)_9.6H_2O$

The spectrum was obtained from a sample prepared by mixing the compound with freeze-dried potassium bromide by vibration. The spectrum is very similar to that obtained by Jones (5) for $NaUO_2(C_2H_3O_2)_3$. A peak of moderate intensity which was not observed for $NaUO_2(C_2H_3O_2)_3$ was found in the present work at 1355 cm^{-1}. A very broad peak was observed at 3380 cm^{-1}. This region was not investigated by Jones (5). It is possible that this latter peak is due to the water of crystallization. As mentioned earlier for $NaUO_2(C_2H_3O_2)_3$, there is good evidence (27) that in $NaZn(UO_2)_3(C_2H_3O_2)_9.6H_2O$ the uranyl and acetate ions are present as the complex anion $UO_2(C_2H_3O_2)_3^-$. Hence it is not surprising that the infrared spectrum of these two compounds are quite similar. For

the same reasons as presented earlier in the discussion of the spectrum of uranyl acetate, it is believed that the intense peak observed at 680 cm^{-1} for $NaZn(UO_2)_3(C_2H_3O_2)_9.6H_2O$ is due to a C—O bond vibration rather than to a CO_2 deformation vibration as postulated by Jones for $NaUO_2(C_2H_3O_2)_3$ (5).

Infrared Spectrophotometric Determination of Uranyl Ion

An examination of the spectra of samples prepared by freeze-drying aqueous solutions of uranyl salts and potassium bromide indicated that the 923 cm^{-1} peak of uranyl nitrate might be suitable for the infrared spectrophotometric determination of the uranyl ion. This peak is relatively intense and sharp, and there is little interference from neighboring bands.

Solutions of known compositions were prepared by adding various volumes of a standard uranyl nitrate solution to known volumes of a standard potassium solution. The amount of potassium bromide used for each sample was 0.2 g. After freeze-drying, the samples were pressed into disks and their spectra recorded. The weight of the disk, which could not be removed from the die, was found by taking the difference between the weight of the die plus the disk after the excess material had been removed and the weight of the clean die. From a knowledge of the proportion of uranyl nitrate to potassium bromide used, the weight of uranyl ion present in the disk could be calculated. If the Beer–Lambert law is obeyed a plot of the optical density against the weight of uranyl ion present in the disk should give a straight line. The baseline optical density method of Heigl, Bell, and White (28) was used to determined the optical density. A potassium bromide blank was used in the reference beam. In Fig. 6 the optical density is plotted against the weight, in milli-

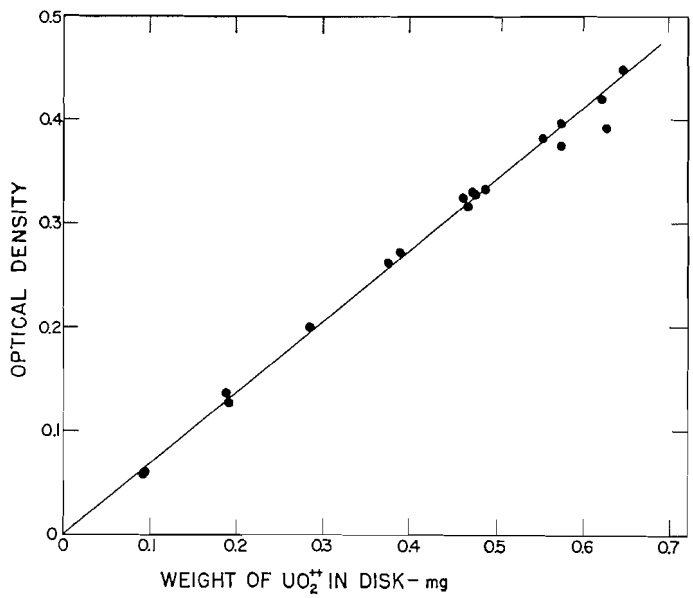


FIG. 6. Beer–Lambert's law plot for uranyl ion. Uranyl nitrate and potassium bromide mixed by freeze-drying. Wave number, 923 cm^{-1}.

grams, of uranyl ion present in the disk. The results indicate that with samples of uranyl nitrate prepared by the above technique and for the concentration range used, the Beer–Lambert law is obeyed.

Can. J. Chem. Downloaded from www.nrcresearchpress.com by 186.148.149.217 on 09/04/12
For personal use only.

ACKNOWLEDGMENTS

In the interpretation of the spectra of the uranyl acetate samples we wish to acknowledge the helpful suggestions made by Dr. R. A. Abramovitch. We are indebted to Mr. E. C. Bailey for the preparation of the sodium zinc uranyl acetate. One of us (G. L. C.) wishes to thank the National Research Council of Canada for financial assistance in the form of a Bursary and a Studentship.

REFERENCES

1. G. K. T. Conn and C. K. Wu. Trans. Faraday Soc. **34**, 1483 (1938).
2. J. Lecompte and R. Freymann. Bull. soc. chim. **8**, 622 (1941).
3. A. N. Sevchenko and B. I. Stepanov. Zhur. Eksp. i Teoret. Fiz. **19**, 1113 (1949).
4. L. H. Jones and R. A. Penneman. J. Chem. Phys. **21**, 542 (1953).
5. L. H. Jones. J. Chem. Phys. **23**, 2105 (1955).
6. G. Tridot. Ann. chim. (Paris), **10**, 225 (1955).
7. B. M. Gatehouse and A. E. Comyns. J. Chem. Soc. 3965 (1958).
8. N. M. Stimson and M. J. O'Donnell. J. Am. Chem. Soc. **74**, 1805 (1952).
9. U. Schiedt and H. Reinwein. Z. Naturforsch. **7**(*b*), 270 (1952).
10. U. Schiedt, as reported by H. Hausdorff. Appl. Spectroscopy, **7**, 75 (1953).
11. H. F. Bauer, A. Epp, and R. U. Lemieux. The mounting of samples in potassium bromide for infrared spectroscopy. Prairie Regional Laboratory, National Research Council of Canada, Saskatoon, Sask.
12. H. H. Barber and I. M. Kolthoff. J. Am. Chem. Soc. **50**, 1625 (1928).
13. Instruction Manual, Volume 3B. Model 21 infrared spectrophotometer operating and maintenance instructions. The Perkin-Elmer Corp., Norwalk, Connecticut. 1952.
14. I. M. Kolthoff and J. J. Lingane. J. Am. Chem. Soc. **55**, 1871 (1933).
15. J. J. Katz and G. T. Seaborg. The chemistry of the actinide elements. Methuen and Co., Ltd., London. 1957. p. 193.
16. H. R. Hoekstra and J. J. Katz. *In* The actinide elements. National Nuclear Energy Series. Vol. IV-14A. *Edited by* G. T. Seaborg and J. J. Katz. McGraw-Hill Book Co., Inc., New York. 1954. p. 146.
17. L. Sacconi and G. Giannoni. J. Chem. Soc. 2368 (1954).
18. L. Sacconi and G. Giannoni. J. Chem. Soc. 2751 (1954).
19. G. H. Tishkoff. *In* Pharmacology and toxicology of uranium compounds. National Nuclear Energy Series. Vol. VI-1. *Edited by* C. Voegtlin and H. C. Hodge. McGraw-Hill Book Co., Inc., New York. 1949. Chap. 1, Appendix B. pp. 125–146.
20. B. M. Gatehouse, S. E. Livingstone, and R. S. Nyholn. J. Chem. Soc. 4222 (1957).
21. G. Herzberg. Infrared and raman spectra of polyatomic molecules. Van Nostrand, New York. 1945. p. 178.
22. J. C. Decius. J. Chem. Phys. **23**, 1290 (1955).
23. G. H. Dieke and A. B. F. Duncan. Spectroscopic properties of uranium compounds. McGraw-Hill Book Co., Inc., New York. 1949.
24. R. N. Jones and C. Sandorfy. *In* Technique of organic chemistry. Vol. IX. *Edited by* A. Weissberger. Interscience Publishers, Inc., New York. 1956. pp. 334, 443, 453, 476.
25. H. L. Jones and E. McLaren. J. Chem. Phys. **22**, 1796 (1954).
26. L. J. Bellamy. The infra-red spectra of complex molecules. John Wiley and Sons, Inc., New York. 1954. pp. 123, 153.
27. H. Brintzinger *et al.* As reported in reference (16). p. 169.
28. J. J. Heigl, M. F. Bell, and J. U. White. Ind. Eng. Chem. Anal. Ed. **19**, 293 (1947).

Can. J. Chem. Downloaded from www.nrcresearchpress.com by 186.148.149.217 on 09/04/12
For personal use only.

EFFECT OF MEAN PORE SIZE ON THE LOW-TEMPERATURE ADSORPTION OF NITROGEN ON ALUMINA[1]

J. L. BLUMENTHAL, S. SOURIRAJAN, AND KEN NOBE

ABSTRACT

The effect of mean pore size on the low-temperature adsorption of nitrogen on two samples of alumina has been studied. The mean pore radius of one sample of alumina was 37 Å, and that of the other was 3100 Å. The two adsorption isotherms at −195.8° C have been plotted in terms of the volume of gas adsorbed per square meter of surface area vs. relative pressure ratio. The data have been found to fall into three distinct regions. In the first region extending up to the relative pressure ratio of 0.3, the two isotherms are nearly identical. In the second region extending from the relative pressure ratio of 0.3 to 0.75, the isotherm for the small mean pore size alumina lies above that for the large mean pore size sample. In the third region extending from the relative pressure ratio of 0.75 up to saturation, the isotherm for the small mean pore size sample tends to level off whereas that for the large mean pore size sample rises rapidly with increase in the relative pressure ratio. The above experimental observations have been explained on the basis of capillary condensation.

INTRODUCTION

The object of this investigation was to determine experimentally the effect of the mean pore size on the nitrogen adsorption isotherms of two samples of porous solids having the same chemical composition. This paper reports the results of a study of the low-temperature adsorption of nitrogen gas on two samples of alumina having widely different surface areas and mean pore radii.

EXPERIMENTAL

The apparatus used in this study for the determination of the gas adsorption isotherms and the total pore volume of the alumina samples was similar to the one described by Joyner (1). Pure dry nitrogen gas was used for adsorption, and helium gas was used to determine the dead space volumes. The sample bulb was immersed in a constant-temperature liquid nitrogen bath at −195.8° C during the experiment. Adsorption measurements were taken from relative pressures of 0.02 up to the saturation pressure. The surface area of the alumina samples were determined by the B.E.T. method (2). The total pore volumes of the samples were determined by the helium–mercury method by measuring the difference between the helium dead space and mercury dead space in a bulb containing the alumina sample (3). The mean radius of the pores in each of the samples was then calculated from the known surface area and pore volume data assuming the pores to be cylindrical.

RESULTS AND DISCUSSION

Alumina sample I had a surface area of 272 sq. meters per gram, and a mean pore radius of 37 Å. Alumina sample II had a surface area of 1.3 sq. meters per gram, and a mean pore radius of 3100 Å. The experimental adsorption data of nitrogen gas on the above alumina samples are given in Tables I and II respectively. In order to compare the two adsorption isotherms on a common basis, the data are plotted in Fig. 1 in terms of the volume of gas adsorbed per unit (sq. meter) of surface area vs. relative pressure ratio.

[1]*Manuscript received February 12, 1960.*
Contribution from the Department of Engineering, University of California, Los Angeles 24, California.

Can. J. Chem. Downloaded from www.nrcresearchpress.com by 186.148.149.217 on 09/04/12
For personal use only.

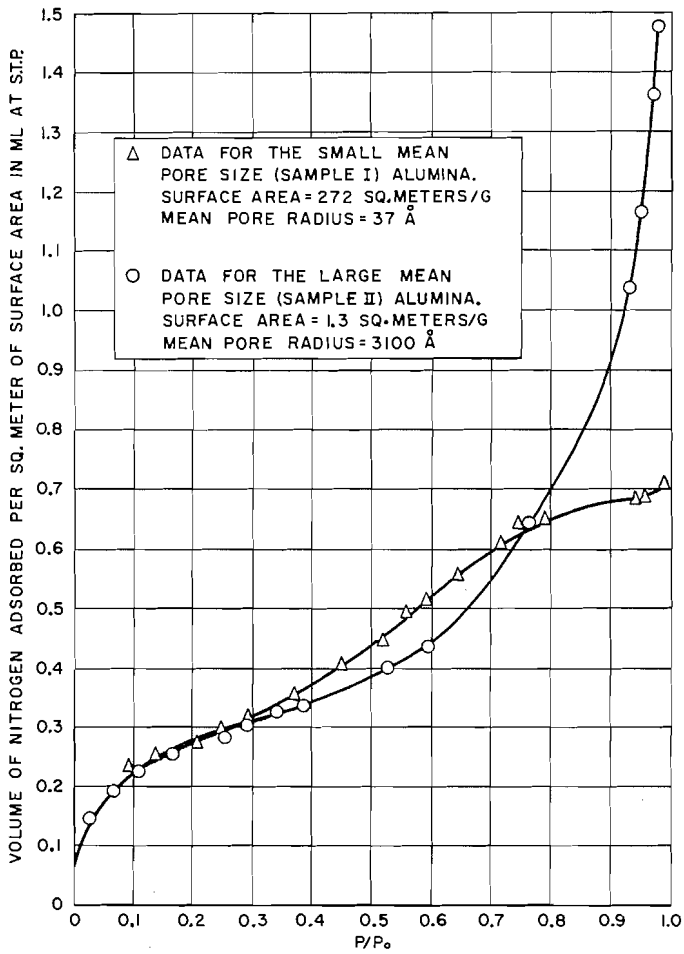


FIG. 1. Adsorption isotherms for the small mean pore size and the large mean pore size alumina samples.

From Fig. 1, it is seen that the data fall into three distinct regions. In the first region, which extends up to a relative pressure ratio of 0.3, the curves for both the small mean pore size (high surface area) alumina, and the large mean pore size (low surface area) alumina are nearly identical. This is the part of the isotherm which is useful for the B.E.T. plot. In the second region, which extends from the relative pressure ratio of 0.3 up to 0.75, the adsorption isotherm for the small mean pore size alumina lies above that for the large mean pore size sample. In the third region, which extends from the relative pressure ratio of 0.75 up to saturation, the isotherm for the small mean pore size sample almost levels off, whereas that for the large mean pore size sample rises very rapidly with increase in the relative pressure ratio. The above experimental observations can be explained as being due to the predominant effect of capillary condensation of nitrogen in the pores of the samples in the second and third regions. According to the well-known Kelvin equation (4), the relative pressure at which capillary condensation can take place increases exponentially with increase in pore size. Hence, a given amount of capillary condensation can take place at a lower relative pressure in the case of the

Can. J. Chem. Downloaded from www.nrcresearchpress.com by 186.148.149.217 on 09/04/12
For personal use only.

TABLE I

Nitrogen gas adsorption data for sample I alumina

Volume of gas adsorbed at S.T.P. in ml	Relative pressure ratio, P/P_0	Volume of gas adsorbed at S.T.P. per sq. meter of surface area, in ml
15.5	0.091	0.237
16.7	0.137	0.255
18.3	0.205	0.279
20.3	0.247	0.310
21.0	0.290	0.321
23.5	0.363	0.359
26.7	0.443	0.407
29.4	0.515	0.448
32.6	0.552	0.497
33.6	0.588	0.513
36.2	0.647	0.553
39.9	0.715	0.610
42.2	0.742	0.643
42.8	0.790	0.650
44.8	0.938	0.683
45.1	0.953	0.687
47.0	0.985	0.717

NOTE: Weight of sample: 0.2401 gram.
Surface area: 272 sq. meters/gram.
Total pore volume: 0.51 ml/gram.
Mean pore radius: 37 Å.
Adsorption temperature: −195.8° C.
P = adsorption pressure.
P_0 = vapor pressure of nitrogen at its normal boiling point.

TABLE II

Nitrogen gas adsorption data for sample II alumina

Volume of gas adsorbed at S.T.P. in ml	Relative pressure ratio, P/P_0	Volume of gas adsorbed at S.T.P. per sq. meter of surface area, in ml
2.11	0.022	0.134
3.09	0.062	0.195
3.52	0.108	0.223
3.97	0.165	0.252
4.49	0.251	0.284
4.74	0.292	0.300
5.27	0.384	0.334
6.31	0.522	0.400
6.93	0.591	0.438
10.2	0.760	0.645
16.4	0.930	1.04
18.5	0.948	1.17
21.7	0.970	1.37
23.4	0.978	1.48

NOTE: Weight of sample: 12.20 grams.
Surface area: 1.3 sq. meters/gram.
Total pore volume: 0.21 ml/gram.
Mean pore radius: 3100 Å.
Adsorption temperature: −195.8° C.

small mean pore size alumina than in the case of the large mean pore size sample. This explains the relative positions of the adsorption isotherms in the region 2. At the close of the region 2, it is reasonable to assume that most of the pores in the small mean pore size sample are already filled, whereas most of the pores in the large mean pore size

Can. J. Chem. Downloaded from www.nrcresearchpress.com by 186.148.149.217 on 09/04/12
For personal use only.

sample are yet to be filled. Hence in the region 3, at relative pressures above 0.75, the adsorption isotherm for the small mean pore size alumina tends to level off, whereas that for the large mean pore size sample rises rapidly with increase in the relative pressure ratio.

ACKNOWLEDGMENTS

This investigation forms part of the catalysis studies in the Air Pollution Research program of the Department of Engineering, University of California at Los Angeles. The authors are grateful to Professor L. M. K. Boelter and Professor W. C. Hurty for their support and encouragement of this work.

REFERENCES

1. L. G. JOYNER. Gas adsorption apparatus for measuring surface areas. *In* Scientific and industrial glass blowing and laboratory techniques. W. E. Barr and Victor J. Anhorn. Instruments Publishing Co., Pittsburg. 1949. p. 257.
2. S. BRUNAUER, P. H. EMMETT, and E. TELLER. J. Am. Chem. Soc. **60**, 309 (1938).
3. P. H. EMMETT. Catalysis. Vol. II. Reinhold Publ. Corp., New York. 1955. Chap. 2.
4. P. H. EMMETT. Catalysis. Vol. I. Reinhold Publ. Corp., New York. 1954. Chap. 1.

Can. J. Chem. Downloaded from www.nrcresearchpress.com by 186.148.149.217 on 09/04/12
For personal use only.

Can. J. Chem. Downloaded from www.nrcresearchpress.com by 186.148.149.217 on 09/04/12
For personal use only.

REARRANGEMENT STUDIES WITH C^{14}

IX. THE FORMOLYSIS OF METHYL-C^{14}-ISOPROPYLCARBINYL *p*-TOLUENESULPHONATE

A. J. FINLAYSON[2] AND C. C. LEE

ABSTRACT

Formolysis of methyl-C^{14}-isopropylcarbinyl *p*-toluenesulphonate (I) at reflux temperature gave a mixture of 2-methyl-2-butene (II), 2-methyl-1-butene (III), and 3-methyl-1-butene (IV). The relative amounts of olefins II, III, IV were measured by gas–liquid chromatography to be 88%, 11%, and 1%, respectively. When the formolysis was carried out at 50° C, besides olefins II, III, and IV, some *t*-amyl formate was obtained indicating a substitution reaction with neighboring hydrogen participation. Degradation of the mixture of olefins from formolysis gave, among other compounds, radioactive acetone, indicating an isotope position rearrangement in the chief product, 2-methyl-2-butene (II). This rearrangement may be attributed to a 1,2-methyl shift in one of the processes that gave rise to olefin II. A comparison of the data from the acetolysis and the formolysis of I showed that in the E_1 reactions, neighboring hydrogen participation is predominant in either solvent. For a change of solvent from acetic acid to the more ionizing formic acid, it was demonstrated that there is a greater degree of neighboring methyl participation while the process involving no neighboring group participation assumes less importance.

The acetolysis of methyl-C^{14}-isopropylcarbinyl *p*-toluenesulphonate (I) at reflux temperature gave only olefinic products while at 50° C, a small amount of *t*-amyl acetate was obtained besides the olefins (1). The elimination reactions were found to involve processes with no neighboring group participation, and with neighboring hydrogen and neighboring methyl participation, the hydrogen participation being predominant (1). In kinetic studies, a change of solvent from acetic to formic acid may help to disclose driving force due to participation by allowing neighboring group participation to displace nucleophilic assistance by solvent and by making the rate of solvolysis of a reference substance less assisted by nucleophilic driving force (2). Thus Winstein and Marshall (2) have studied the formolysis rates of a series of secondary alkyl *p*-bromobenzenesulphonates and have concluded that there is some assistance to ionization from neighboring hydrogen and/or carbon during solvolysis of methylisopropylcarbinyl derivatives. In the present work, solvolysis of methyl-C^{14}-isopropylcarbinyl *p*-toluenesulphonate (I) was carried out in formic acid and the results compared with those reported for the acetolysis of I (1).

RESULTS AND DISCUSSIONS

As in the acetolysis, the formolysis of I at reflux temperature gave a mixture of 2-methyl-2-butene (II), 2-methyl-1-butene (III), and 3-methyl-1-butene (IV) with no isolatable amount of substitution product. At 50° C, a yield of about 10% crude *t*-amyl formate and 42% of the mixture of olefins II, III, and IV were obtained. The relative amounts of II, III, and IV, as measured by gas–liquid chromatography, are tabulated in Table I. For comparison, the olefin composition in the products of acetolysis is also given in Table I.

Degradation of the mixture of olefins II, III, and IV by treatment with performic acid followed by cleavage with sodium metaperiodate yielded a mixture of formaldehyde, acetaldehyde, isobutyraldehyde, acetone, and methyl ethyl ketone. Separation of these carbonyl compounds as their 2,4-dinitrophenylhydrazones was effected by adsorption

[1]*Manuscript received January 4, 1960.*
Contribution from the Department of Chemistry, University of Saskatchewan, Saskatoon, Sask. For paper VIII, see Lee, C. C., Tkachuk, R., and Slater, G. P. Tetrahedron, 7, 206 (1959).
[2]*Present address: Prairie Regional Laboratory, National Research Council, Saskatoon, Saskatchewan.*

TABLE I

Relative amounts of olefins from solvolyses of methyl-C^{14}-isopropylcarbinyl *p*-toluenesulphonate

Reaction temperature	Olefin	% composition in formolysis products			% composition in acetolysis products[a]
		Analyzed by gas chromatography	Analyzed by radioactivity		Analyzed by gas chromatography
			Run 1	Run 2	
Reflux	2-Methyl-2-butene	88	83	84	80
	2-Methyl-1-butene	11			18
	3-Methyl-1-butene	1			2
50° C	2-Methyl-2-butene	91	88	93	83
	2-Methyl-1-butene	9			16
	3-Methyl-1-butene	trace			1

[a]Data from reference 1.

chromatography in a silicic acid – celite column as described previously (1). The 2,4-dinitrophenylhydrazones of acetaldehyde and acetone, which were derived from degradation of the chief product, 2-methyl-2-butene (II), were recovered and their radioactivity

TABLE II

Radioactivity data from formolyses of methyl-C^{14}-isopropylcarbinyl *p*-toluenesulphonate

Reaction temperature	Compound assayed	Specific activity (c.p.m. on a molar basis)		% of total activity		% rearrangement in 2-methyl-2-butene		% rearrangement in 2-methyl-2-butene from acetolysis[c]	
		Run 1	Run 2	Run 1	Run 2	Run 1	Run 2	Run 1	Run 2
Reflux	Glycol mixture from olefins II, III, and IV	20500	13020	100	100				
	CH_3CHO[a]	16100	10250	78.6	78.8				
	CH_3COCH_3[a]	885	646	4.3	5.0	5.2	5.8	2.6	2.4
	CBr_4[b]	1065	835	5.2	6.4				
50° C	Glycol mixture from olefins II, III, and IV	17000	15750	100	100				
	CH_3CHO[a]	14660	14300	86.3	90.8				
	CH_3COCH_3[a]	312	329	1.8	2.2	2.1	2.3	0.9	0.9
	CBr_4[b]	334	330	1.9	2.2				

[a]As the 2,4-dinitrophenylhydrazone.
[b]From reaction of ketonic degradation products with bromine and sodium hydroxide.
[c]Data from reference 1.

determined. The results are given in Table II. The sum of the activities of acetaldehyde and acetone is a measure of the amount of olefin II in the mixture of II, III, and IV. This serves as a check on the gas chromatographic analysis of II given in Table I.

The presence of C^{14} activity in the acetone indicated that there was some isotope position rearrangement in the chief olefinic product, 2-methyl-2-butene (II). For the formolysis at reflux temperature run No. 1, this rearrangement amounted to

$$\{885/(16100+885)\} \times 100 = 5.2\%.$$

Such rearrangement data are included in Table II. For comparison, the degrees of

Can. J. Chem. Downloaded from www.nrcresearchpress.com by 186.148.149.217 on 09/04/12
For personal use only.

isotope position rearrangement in 2-methyl-2-butene obtained from acetolysis are also presented in Table II.

The interpretations of the results summarized in Tables I and II may be made in a way exactly analogous to the interpretations of the results from acetolysis of I (1). The *t*-amyl formate obtained from formolysis at 50° C indicates that the substitution reaction involves neighboring hydrogen participation resulting in a 1,2-hydrogen shift. The elimination reactions may be discussed in terms of reaction sequences 1, 2, and 3, representing processes without neighboring group participation, with neighboring hydrogen participation, and with neighboring methyl participation, respectively.

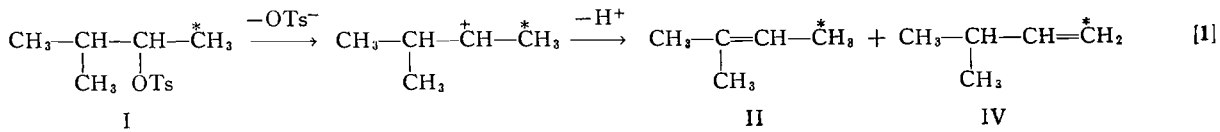
According to Saytzeff's rule, each of these three processes is expected to give a greater amount of the chief product, 2-methyl-2-butene (II or II_r). The presence of only very small amounts of 3-methyl-1-butene (IV or IV_r), as shown in Table I, indicates that reaction sequence 1 makes a relatively minor contribution to the over-all elimination reactions. It is even possible that all or a large part of the 3-methyl-1-butene detected by gas chromatography may have been due to reaction sequence 3, which results in the production of some isotopically rearranged olefin IV_r. By analogy with findings from acetolysis studies (1, 3) and from the presence of fairly large quantities of 2-methyl-1-butene (III) in the olefinic products of formolysis, it is reasonable to conclude that reaction sequence 2 depicts the predominant elimination process. The participation of neighboring methyl group (reaction sequence 3) results in the formation of isotopically rearranged 2-methyl-2-butene (II_r), the degradation of which gave radioactive acetone. The degree of this isotope position rearrangement in the 2-methyl-2-butene from formolysis is greater than the corresponding rearrangement after acetolysis by a factor of about 2 (Table II). This indicates a greater extent of neighboring methyl participation in formolysis than in acetolysis.

The location of C^{14} in the methyl group, and not in the carbonyl group, of acetone is required by reaction sequence 3. This was shown to be the case in the following way. After degradation of the mixed olefins II, III, and IV, the carbonyl compounds obtained were treated with neutral potassium permanganate to destroy all aldehydes (4). The remaining acetone and methyl ethyl ketone, recovered as an aqueous solution by distillation, were treated with bromine and sodium hydroxide to give carbon tetrabromide. If much of the C^{14} activity were present in the carbonyl group of acetone, the activity of the carbon tetrabromide would be lower than that of acetone and this was not observed (Table II). Actually, in the formolysis at 50° C, the C^{14} activity of acetone and of carbon tetrabromide was about equal. For the formolysis at reflux temperature, the carbon tetrabromide activity was even somewhat higher than the activity of acetone. Possibly, this difference may be due to some C^{14} located in the methyl group of methyl ethyl ketone. Results similar to this were noted in the acetolysis of I and it was suggested that the location of C^{14} in the methyl group of methyl ethyl ketone may be explained by a process involving first a 1,2-methyl shift followed by a 1,2-hydrogen shift before the formation of olefins (1).

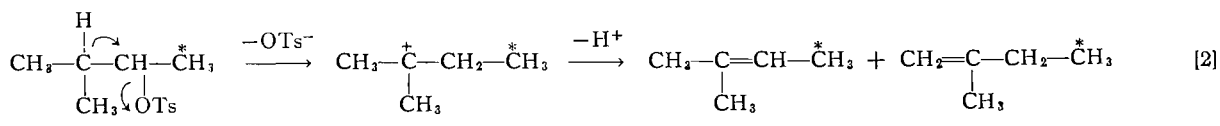
In conclusion, it is evident that the formolysis of I involves processes similar to those operating in the acetolysis of I. The isolated substitution product results only from neighboring hydrogen participation. In the E_1 reactions, hydrogen participation also predominates. Comparing the data from formolysis and acetolysis, the greater degrees of isotope position rearrangement in 2-methyl-2-butene, coupled with the smaller amount of 3-methyl-1-butene in the over-all olefinic products, indicate a greater extent of

Can. J. Chem. Downloaded from www.nrcresearchpress.com by 186.148.149.217 on 09/04/12
For personal use only.

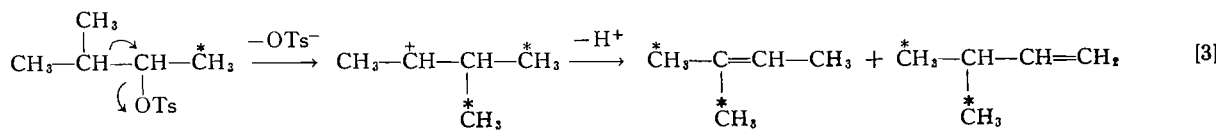
Can. J. Chem. Downloaded from www.nrcresearchpress.com by 186.148.149.217 on 09/04/12
For personal use only.



I II IV [1]



I II III [2]



I II_r IV_r [3]

neighboring group participation and a lesser importance of the process without participation for the formolysis. This is in agreement with expectation that a change of solvent from acetic acid to the more ionizing formic acid would enhance the degree of participation by neighboring groups in E_1 as well as S_N1 reactions.

EXPERIMENTAL

Procedures for the synthesis of methyl-C^{14}-isopropylcarbinyl *p*-toluenesulphonate (I), and for the analysis and degradation of the products of solvolyses, have been described previously (1).

Formolysis at Reflux Temperature

A solution of I (5.80 g, 0.024 mole) in 45 ml of anhydrous formic acid, m.p. 8.2–8.3° C (lit. (5) m.p. 8.4° C), containing 2.3 g (0.027 mole) of anhydrous potassium formate was gently refluxed for 2.5 hours. During the reflux period, the olefins formed were swept out by a stream of dry nitrogen and collected in a dry-ice-cooled trap.

After the refluxing, the reaction mixture was cooled, poured into 200 ml of ice and water containing 50 g of dissolved sodium chloride, and then repeatedly extracted with a 1:3 solution of ether – petroleum ether. The extracts were washed free of acid by a 5% solution of sodium carbonate and dried over anhydrous magnesium sulphate. Removal of the solvent, however, left no residue, indicating no recoverable quantity of substitution product.

The mixture of olefins collected in the dry-ice-cooled trap weighed 1.25 g (75%). It was distilled once, b.p. 35–38° C, before being used for degradation and gas chromatographic analysis.

Formolysis at 50° C

Methyl-C^{14}-isopropylcarbinyl *p*-toluenesulphonate (I) (10.0 g, 0.041 mole) was dissolved in 70 ml of anhydrous formic acid containing 3.7 g (0.044 mole) of anhydrous potassium formate. The solution was stirred mechanically in a bath maintained at 50±1° C for 3 hours. During the heating period, the olefins formed were swept out by dry nitrogen and collected in a dry-ice-cooled trap.

The reaction mixture was poured into 300 ml of ice and water containing 60 g of dissolved sodium chloride and then worked up as described under formolysis at reflux temperature. The removal of the ether – petroleum ether solvent left a colorless residue from which 0.5 g of material, b.p. 110–112° C, distilled and 1.0 g of unreacted I was recovered. The liquid product was redistilled at 112–113° C (lit. (6) b.p. of *t*-amyl formate, 113° C). Infrared and gas chromatographic analysis indicated that it was *t*-amyl formate contaminated with a small amount of *t*-amyl alcohol. The yield of this crude *t*-amyl formate was about 10% based on the 9.0 g of I used up in the reaction.

The mixture of olefins collected in the dry-ice-cooled trap weighed 1.10 g (42% based on 9.0 g of I). It was distilled once and then utilized for degradation and analysis.

ACKNOWLEDGMENTS

Sincere thanks are extended to Dr. J. Bardwell for the use of his apparatus for gas–liquid chromatography and to the National Research Council of Canada for generous financial support.

Can. J. Chem. Downloaded from www.nrcresearchpress.com by 186.148.149.217 on 09/04/12
For personal use only.

REFERENCES

1. A. J. FINLAYSON and C. C. LEE. Can. J. Chem. **37**, 940 (1959).
2. S. WINSTEIN and H. MARSHALL. J. Am. Chem. Soc. **74**, 1120 (1952).
3. S. WINSTEIN and J. TAKAHASHI. Tetrahedron, **2**, 316 (1958).
4. J. D. ROBERTS, R. E. MCMAHON, and J. S. HINE. J. Am. Chem. Soc. **72**, 4237 (1950).
5. L. C. BATEMAN and E. D. HUGHES. J. Chem. Soc. 1187 (1937).
6. BEILSTEIN'S HANDBUCH DER ORGANISCHEN CHEMIE. Vol. II. 4th ed. Julius Springer, Berlin. 1920. p. 22.

Can. J. Chem. Downloaded from www.nrcresearchpress.com by 186.148.149.217 on 09/04/12
For personal use only.

Can. J. Chem. Downloaded from www.nrcresearchpress.com by 186.148.149.217 on 09/04/12
For personal use only.

CONSTITUTION OF A GLUCOMANNAN FROM JACK PINE (PINUS BANKSIANA, LAMB)[1]

C. T. BISHOP AND F. P. COOPER

ABSTRACT

A hemicellulose fraction from jack pine wood has been shown to contain D-mannose, D-glucose, and D-galactose in a molar ratio of 49:17:2. The glucomannan was electrophoretically homogeneous and showed a degree of polymerization of 18–21 by three different methods of end group analysis. Methylation and hydrolysis yielded the following *O*-methyl ethers: 2,3,4,6-tetra-*O*-methyl-D-glucose (2.8 moles); 2,3,4,6-tetra-*O*-methyl-D-galactose (1 mole); 2,3,6-tri-*O*-methyl-D-mannose (52 moles); 2,3,6-tri-*O*-methyl-D-glucose (15.3 moles); di-*O*-methyl-D-glucose (1 mole); di-*O*-methyl-D-galactose (2 moles). Lack of survival of any monosaccharides in the periodate-oxidized glucomannan showed that there was no branching through C_2 or C_3 of any of the units. Gas–liquid partition chromatography was used to analyze products from methylation and hydrolysis and from periodate oxidation and reduction of the polysaccharides. The results showed that the glucomannan from jack pine was composed of $1 \rightarrow 4$ linked β-D-mannose and β-D-glucose residues with D-galactose residues present as non-reducing terminal units. Branching, if any, must occur through C_6 of units making up the polysaccharide. This structure is compared with those of glucomannans found in other soft woods.

It has been known for a long time that a large percentage of the non-cellulosic polysaccharides in soft woods give rise to D-mannose on hydrolysis (1, 2, 3). However, reports on the isolation of mannose-containing polysaccharides and studies of the mode of linkage of the mannose residues are of much more recent date (4–19). It was apparent from the earliest of these reports (4, 5) that at least some of the mannose residues in slash pine α-cellulose were joined to glucose units. Subsequent publications described the isolation of glucomannans from western hemlock (6), white spruce (7, 8), loblolly pine (9), Norwegian spruce (10), and a Mitscherlich pulp (11) and showed with reasonable certainty, by fractionation and fragmentation analysis, that these polysaccharides were true glucomannans and not mixtures of mannans, glucans, and glucomannans. These results have been supported by recent structural studies on glucomannans from loblolly pine (12, 13), Sitka spruce (14, 15), Norwegian spruce (16), western hemlock (17), western red cedar (18), and Scots pine (19). All of these glucomannans possessed the main structural feature of a linear chain of $1 \rightarrow 4$ linked residues of β-D-mannose and β-D-glucose. However, there were smaller but significant differences which involved the question of branching in the polysaccharide and the presence or absence of D-galactose units as an integral part of the molecule.

This paper reports the isolation and structural study of a glucomannan from jack pine (*Pinus banksiana*, Lamb) and forms a further contribution to the general chemistry of this class of polysaccharides. A previous report (20) described a water-soluble arabogalactan isolated from the same wood and therefore the present work also provides further information about the carbohydrates in a single biological species.

The isolation of polysaccharides from jack pine wood is shown schematically in Fig. 1. The sugars listed are those which were released by acid hydrolysis of the various polysaccharide fractions and detected chromatographically. Polysaccharides containing glucose, mannose, and galactose could be obtained from the first two alkaline extracts by repeated complexing with copper but yields were low, presumably because of interference

[1]*Manuscript received February 5, 1960.*
Contribution from the Division of Applied Biology, National Research Council of Canada, Ottawa, Canada. Presented at the 136th meeting of the American Chemical Society, Atlantic City, N.J., September, 1959.
Issued as N.R.C. No. 5644.

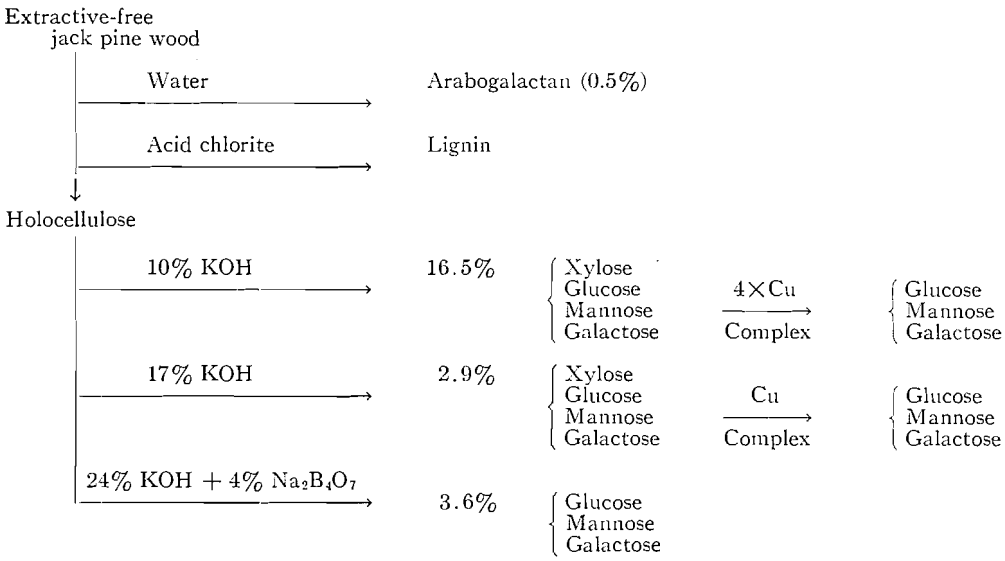


FIG. 1. Isolation of polysaccharides from jack pine wood.

by the large amounts of xylan present in these extracts. Structural studies were therefore carried out on the polysaccharide which were extracted by alkali and borate (21) and which yielded on hydrolysis glucose, mannose, and galactose as the only products detectable by paper chromatography. The monosaccharide composition of this material (mannose:glucose:galactose, 49:17:2, molar ratio) was unchanged by repeated complexing with copper. The significance of the persistent galactose component will be referred to later in comparing the structure of the present polysaccharide with those of other glucomannans.

The glucomannan isolated from the alkaline borate extraction showed a single sharp peak on electrophoresis (Fig. 2; the first, non-mobile, peak has been shown to be a false

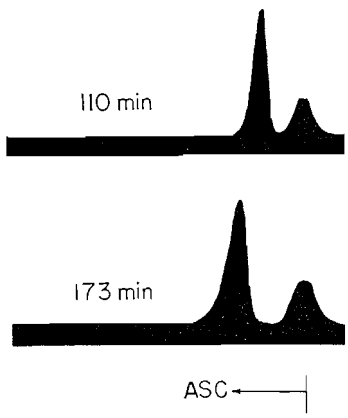


FIG. 2. Electrophoresis of glucomannan from jack pine.

boundary, see experimental) and had a specific rotation of $-26°$ indicative of β-glycosidic linkages. The observation that the polysaccharide was not hydrolyzed in hot dilute oxalic

Can. J. Chem. Downloaded from www.nrcresearchpress.com by 186.148.149.217 on 09/04/12
For personal use only.

acid showed that no terminal furanoside ring forms were present. On periodate oxidation the polysaccharide consumed 1.11 moles of oxidant per mole anhydrohexose with production of 0.10 mole of formic acid per mole anhydrohexose. The oxidized polysaccharide was examined by the procedure developed by Smith and his co-workers (22) with an innovation that utilized the unique analytical powers of gas–liquid partition chromatography (23, 24). The sequence of reactions is outlined in Fig. 3 and consisted of oxidation,

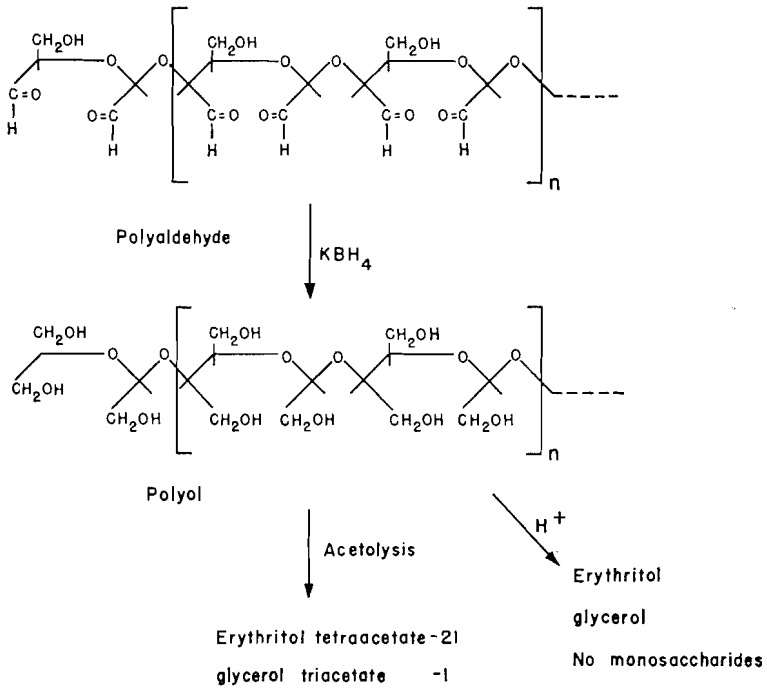


FIG. 3. Smith degradation of 1 → 4 linked hexosan.

reduction, and hydrolysis of the polysaccharide to yield erythritol and glycerol as the only products detectable by paper chromatography. The polyol was also subjected to acetolysis and the products were analyzed by gas–liquid partition chromatography (Fig. 4) giving a ratio of erythritol to glycerol of 20.8:1.0. This procedure also permitted the unequivocal identification of erythritol as its crystalline tetraacetate. The erythritol and glycerol found by this sequence of reactions must have arisen from 1 → 4 linked units and non-reducing terminal residues respectively and the ratio between them is a measure of degree of polymerization for a linear polysaccharide (22). The amount of formic acid produced in periodate oxidation of a linear polysaccharide can also be used as a measure of degree of polymerization. Under the conditions of periodate oxidation (pH 4.37) and formic acid estimation (release of iodine from potassium iodide in the presence of iodate) used here it is likely that C_1 of the reducing unit would remain attached as a formyl ester and hence would not be detected in the estimation. The polysaccharide would therefore liberate only 2 moles of formic acid and the amount found (0.10 mole per mole anhydrohexose) would give a degree of polymerization of 20, in good agreement with the value of 21 found by the erythritol:glycerol ratio. A linear chain of twenty 1 → 4 linked residues would consume 22 moles of periodate or 1.10 moles per mole anhydrohexose, a

Can. J. Chem. Downloaded from www.nrcresearchpress.com by 186.148.149.217 on 09/04/12
For personal use only.

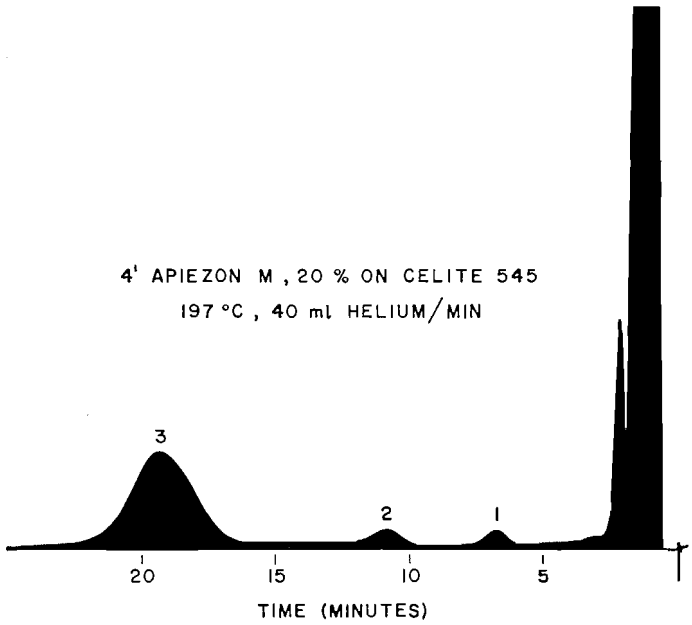


FIG. 4. Gas–liquid partition chromatogram of acetolysate from oxidized, reduced glucomannan. (1) Glycerol triacetate. (2) Not identified, possibly acetate of glycolic aldehyde. (3) Erythritol tetraacetate.

value which agrees with the periodate consumption (1.11 moles per mole anhydrohexose) determined experimentally. In a $1 \rightarrow 4$ linked polysaccharide any branching through C_2 or C_3 results in the unit forming the branch point being resistant to periodate oxidation because of a lack of vicinal hydroxyl groups. The absence of any monosaccharides in the hydrolyzate of the oxidized, reduced glucomannan showed that there was no branching through C_2 or C_3 of any of the monosaccharide units in the chain. Branching, if any, must have been through C_6.

The glucomannan was methylated and the hydrolysis products were separated, as their methyl glycosides, by gas–liquid partition chromatography (23, 24). The separations are shown in Figs. 5 and 6 and the quantitative data, obtained from measurements of areas under these peaks, is given in Table I. Component 6, Table I, was clearly evident

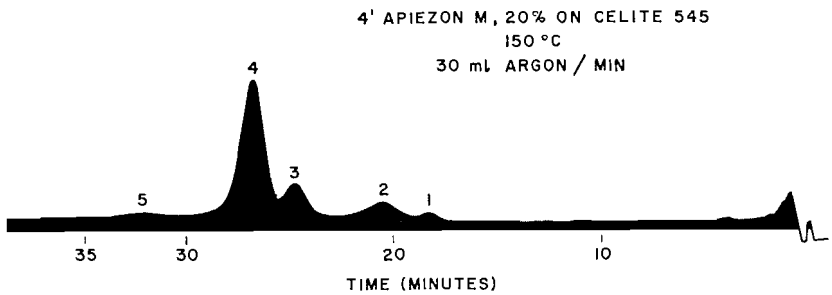


FIG. 5. Gas–liquid partition chromatogram of methanolysis products from methylated glucomannan. (1) Methyl 2,3,4,6-tetra-*O*-methyl α- and β-D-glucopyranoside. (2) Methyl 2,3,4,6-tetra-*O*-methyl α- and β-D-galactopyranoside and methyl 2,3,6-tri-*O*-methyl-β-D-glucopyranoside. (3) Methyl 2,3,6-tri-*O*-methyl-α-D-glucopyranoside. (4) Methyl 2,3,6-tri-*O*-methyl-α-D-mannopyranoside. (5) Methyl-di-*O*-methyl (α,β?)-D-galactoside.

Can. J. Chem. Downloaded from www.nrcresearchpress.com by 186.148.149.217 on 09/04/12
For personal use only.

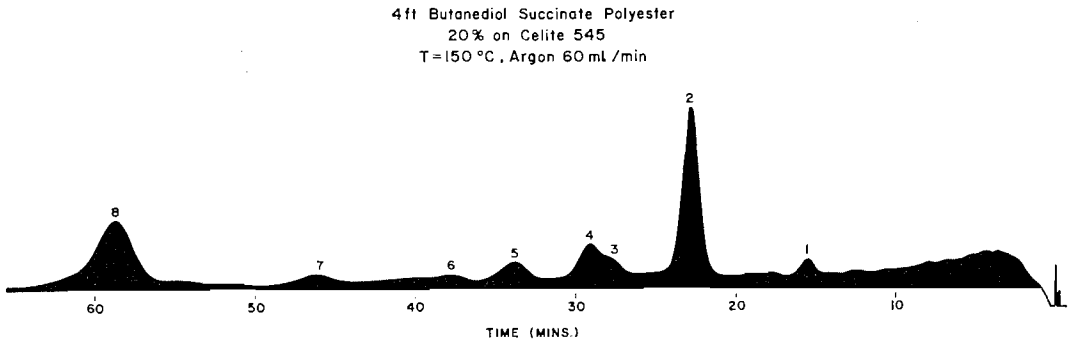


FIG. 6. Gas–liquid partition chromatogram of peaks 1 and 2, Fig. 5. (1) Methyl 2,3,4,6-tetra-*O*-methyl-β-D-glucopyranoside. (2) Methyl 2,3,4,6-tetra-*O*-methyl-α-D-glucopyranoside. (3) Methyl 2,3,4,6-tetra-*O*-methyl-β-D-galactopyranoside. (4) Methyl 2,3,4,6-tetra-*O*-methyl-α-D-galactopyranoside. (5, 6, 7) Not identified; probably methyl-di-*O*-methyl pentosides. (8) Methyl 2,3,6-tri-*O*-methyl-β-D-glucopyranoside.

TABLE I

Hydrolysis products from methylated glucomannan

	Molar ratio
(1) 2,3,4,6-Tetra-*O*-methyl-D-glucose	2.8
(2) 2,3,4,6-Tetra-*O*-methyl-D-galactose	1
(3) 2,3,6-Tri-*O*-methyl-D-mannose	52
(4) 2,3,6-Tri-*O*-methyl-D-glucose	15.3
(5) Di-*O*-methyl galactose	2
(6) Di-*O*-methyl glucose	1

in the gas–liquid partition chromatograms but had such a large retention volume that space did not permit its inclusion in Fig. 5. The peaks in Figs. 5 and 6 were identified by comparison with authentic samples on the gas–liquid partition chromatogram. These identities were confirmed by collection of samples from the effluent gas stream of a semi-preparative apparatus and isolation of crystalline derivatives. There were not sufficient amounts of components 5 and 6, Table I, to permit complete identification; it was only possible to establish the parent sugar by demethylation and chromatography. In Table I components 1 and 2 represent the non-reducing terminal units and components 3 and 4 must have originated from a series of 1 → 4 linked D-mannose and D-glucose units. The structural significance of components 5 and 6 is rather more difficult to assess. Hydrolysis products of the periodate-oxidized, reduced glucomannan showed that any branch points in the polysaccharide must be through C_6 and therefore, to be structurally significant, these di-*O*-methyl hexoses must be the 2,3-di-*O*-methyl isomers. Unfortunately it was not possible to make positive identifications which would decide this point. It is possible, of course, that the di-*O*-methyl hexoses were products of incomplete methylation or of demethylation during hydrolysis. However, it was noteworthy that none of the major monosaccharide component (D-mannose) in the polysaccharide showed up as a di-*O*-methyl derivative. It may be that different monosaccharides are methylated or demethylated to different extents depending perhaps on their position in the polysaccharide and on the spatial disposition (conformation) of their hydroxyl groups. These are points which seem worthy of investigation and until they are clarified the authors are reluctant to assign a branch point to the polysaccharide. It is worth mentioning that the di-*O*-methyl hexoses were barely detectable by paper chromatography and almost certainly would

Can. J. Chem. Downloaded from www.nrcresearchpress.com by 186.148.149.217 on 09/04/12
For personal use only.

have been dismissed as trace amounts in any quantitative estimation by that technique. The more accurate data available from gas–liquid partition chromatography would appear to necessitate a reassessment of the methylation technique for studying polysaccharides. The ratio of tetra- to tri-*O*-methyl ethers from the methylated glucomannan was 1:17.7, a value in reasonable agreement with the degrees of polymerization of 20 and 21 found respectively by formic acid production during periodate oxidation and by the erythritol:glycerol ratio in the hydrolyzate of the oxidized, reduced polysaccharide. Because of this agreement a linear structure is favored for the polysaccharide. The observations that the polysaccharide was electrophoretically homogeneous, that D-galactose persisted as a component sugar through repeated copper complexing, and that 50% of the D-galactose showed up in the methylated polysaccharide as non-reducing terminal units showed that D-galactose was an integral part of the polysaccharide and was not present in a contaminant.

Two structures are possible for the glucomannan from jack pine: (*a*) linear chains of $1 \rightarrow 4$ linked β-D-glucose and β-D-mannose units some of which are terminated by glucose and others by galactose units, (*b*) the same linear chains but with a proportion of the molecules (approximately 1 in 2.8) containing D-galactose units attached as single unit side chains. It is not possible to decide between these alternatives from the evidence available at the present time. The presence of D-galactose in glucomannans has been observed before but it has not always been considered to be an integral part of the polysaccharide. Loblolly pine contains a polysaccharide made up of D-glucose, D-mannose, and D-galactose residues (12, 13). In the first investigation (12) of this material all of the D-galactose was found as non-reducing terminal units and was considered to have arisen from a galactomannan present in admixture with the glucomannan. In a later investigation (13) of the same hemicelluloses, D-galactose was present as non-reducing terminal unit and there were two such units (one of mannose and one of galactose) per chain of 27–33 residues. Hamilton and Partlow (18) found di-*O*-methyl- and 2,3,4,6-tetra-*O*-methyl-D-galactose in the methylated glucomannan from western red cedar and attributed these results to the presence of a contaminating galactoglucomannan. Dutton and Hunt (15) found D-galactose as a non-reducing terminal unit in one fraction of a glucomannan from Sitka spruce. They concluded that it was part of a low molecular weight polysaccharide because dialysis of another fraction of the same material yielded a product which contained no D-galactose. Glucomannan fractions from Scots pine (19) contained D-galactose and D-xylose but both of these sugars were removed by further delignification of the polysaccharides. From this result it was postulated that several polysaccharides might be joined to the same lignin molecule and their separation prevented thereby. D-Galactose was not found as a constituent sugar in glucomannans from western hemlock (17), Norwegian spruce (16), and in another investigation of Sitka spruce (14).

Other differences between glucomannans from various sources are in the non-reducing terminal units, other than D-galactose, and in the results of periodate oxidation. In the present work D-glucose formed the only non-reducing terminal units other than D-galactose. It is certain that no 2,3,4,6-tetra-*O*-methyl-D-mannose was present because it would have been separated from 2,3,4,6-tetra-*O*-methyl glucose by gas–liquid partition chromatography and would have emerged before peak 1, Fig. 5. Similar results have been obtained from the glucomannan of western red cedar (18) but those of western hemlock (17) and Scots pine (19) contained non-reducing terminal units of both D-glucose and D-mannose. On the other hand glucomannans from loblolly pine (12, 13), Sitka spruce (14, 15), and Norwegian spruce (16) had non-reducing terminal units of D-mannose and

Can. J. Chem. Downloaded from www.nrcresearchpress.com by 186.148.149.217 on 09/04/12
For personal use only.

none of D-glucose. It is possible that some of these differences have been caused by the difficulty in separating the 2,3,4,6-tetra-*O*-methyl ethers of D-glucose and D-mannose from each other (14).

Only the glucomannans of western hemlock (6), Norwegian spruce (16), and Scots pine (19) have been examined by the Smith degradation (22). All of these yielded D-glucose plus a trace of D-mannose in hydrolyzates of the periodate-oxidized, reduced polysaccharides and the results were interpreted as indicative of branching through C_2 or C_3 of the glucose units. No D-glucose or D-mannose was found in the present work after the same sequence of reactions had been applied to the glucomannan from jack pine. This difference may have been caused by the different times allowed for oxidation. The glucomannans from western hemlock (6), Norwegian spruce (16), and Scots pine (19) were oxidized for 432, 350, and 174 hours respectively while that from jack pine was oxidized for 552 hours. It has been shown (25) that sugar units are resistant to oxidation by periodate if the hydroxyls on C_2 and C_3 are in *trans* position in a rigid conformation. Although little is known about the conformation of sugar units in polysaccharides it is possible that the above conditions could obtain for a chain of $1 \rightarrow 4$ linked D-glucose units. This would account for the presence in the periodate-oxidized glucomannans of more D-glucose than D-mannose which has its C_2 and C_3 hydroxyls in *cis* orientation. Hamilton and Smith (26) have stressed the importance of prolonged oxidation if this technique is to be used to detect branch points.

Clearly, further work is necessary to ascertain the structural significance of the D-galactose residues in glucomannans, and to decide whether branch points are present or absent. One possible approach to these questions, fragmentation analysis by enzyme hydrolysis, is now in progress in this laboratory.

EXPERIMENTAL

Paper chromatograms were run by the descending method using the following solvent systems (v/v):

(A) butan-1-ol:pyridine:water, 6:4:3;
(B) ethyl acetate:acetic acid:water, 4:1:4;
(C) butan-1-ol:ethanol:water, 3:1:1.

Reducing sugars were detected on paper chromatograms by the *p*-anisidine hydrochloride spray reagent (27); non-reducing components were detected by silver nitrate and sodium hydroxide sprays (28). Evaporations were carried out in a rotary film evaporator under diminished pressure at 35° C or less. Melting points are corrected and rotations are equilibrium values unless otherwise stated.

Isolation of Glucomannan

The sequence of extractions is shown in Fig. 1. Extractive-free jack pine wood was extracted with water which removed an arabogalactan (0.5%) (20). The residue from this extraction was delignified by acid chlorite (29) and then extracted successively with 10% and 17% potassium hydroxide and finally with 24% potassium hydroxide containing 4% of sodium tetraborate (21). Three extractions, each of 24-hour duration, were made at each alkali concentration. Each extract was neutralized with acetic acid, dialyzed to remove inorganic salts, and the non-dialyzables were freeze-dried to yield the crude polysaccharides.

Figure 1 shows the order of the above extractions and the component sugars in the polysaccharides as detected by paper chromatography (solvents A and B) after hydrolysis

Can. J. Chem. Downloaded from www.nrcresearchpress.com by 186.148.149.217 on 09/04/12
For personal use only.

Can. J. Chem. Downloaded from www.nrcresearchpress.com by 186.148.149.217 on 09/04/12
For personal use only.

for 12 hours at 97° C by *N* hydrochloric acid. Yields of polysaccharides in the alkaline extractions were based on holocellulose. The 10% potassium hydroxide removed mainly xylan as shown by the predominance of xylose in the hydrolyzate from this polysaccharide mixture. The 17% potassium hydroxide extraction yielded roughly equal quantities of pentosan and hexosan; the final extraction with 24% potassium hydroxide and 4% sodium tetraborate yielded a polysaccharide which contained only glucose, mannose, and galactose. The polysaccharides in the 10% and 17% potassium hydroxide extracts were precipitated as their copper complexes. The precipitates were washed thoroughly with water, dissolved in cold *N* hydrochloric acid, and poured into 4 volumes of ethanol to reprecipitate the polysaccharides which were then examined by hydrolysis and chromatography as described above. Four precipitations of the copper complex were required to yield a glucomannan from the polysaccharides extracted by 10% potassium hydroxide. One such treatment sufficed to give the same result with the polysaccharides extracted by 17% potassium hydroxide. However, yields of glucomannan from these fractions were low (ca. 1% of the fraction) and the remainder of the work was carried out on the polysaccharide extracted by 24% potassium hydroxide and 4% sodium tetraborate.

The polysaccharide showed a single sharp peak (Fig. 2) ($\mu = 9.86 \times 10^{-5}$ cm^2, volts^{-1}, sec^{-1}) on moving boundary electrophoresis in 0.05 *M* borate buffer carried out in a Spinco Model H Tiselius-type apparatus. Electrophoretic patterns at two time intervals are included in Fig. 2 to show that the first peak did not migrate and is in fact a false boundary. This has been proved by Adams (30), who has isolated material responsible for this peak, which always occurs in electrophoresis in borate, and showed that it yielded no sugars on hydrolysis. The monosaccharide composition, mannose:glucose:galactose, 49:17:2, determined by the phenol–sulphuric acid method (31), was unchanged by repeated fractionation of the polysaccharide as its copper complex. The glucomannan had $[\alpha]_D^{27} = -26°$ (*c*, 1% in *N* sodium hydroxide) and did not yield any sugars detectable by paper chromatography when heated at 97° C with 0.025 *N* oxalic acid for 3 hours.

Periodate Oxidation of Glucomannan

Sodium metaperiodate (6.47 g) was dissolved in water (150 ml) and *N* sodium hydroxide was added to adjust the solution to pH 4.37. This reagent (30 ml) was added to duplicate samples (121 mg) of the polysaccharide suspended in water (120 ml). Reagent blanks were also prepared and the oxidations were allowed to proceed in the absence of light and with continuous shaking. At the intervals noted below samples were removed for estimation of periodate consumption and formic acid production.

For estimation of formic acid, 2,3-butanediol (6 drops) was added to the sample (20 ml), which was then kept in the dark for 30 minutes. A few crystals of potassium iodide were then added and the liberated iodine was titrated to a starch end point with 0.01 *N* sodium thiosulphate.

Periodate was estimated by the excess arsenite method of Fleury and Lange (32, 33). Results of these two estimations in moles per mole anhydrohexose at various time intervals were as follows:

Time (hours)	21	45	47	69	71	93	95	167	170	552
Formic acid	0.067	0.077	—	0.086	—	0.088	—	0.098	—	0.106
Periodate	—	—	0.087	—	0.85	—	0.85	—	0.88	1.11

In a separate experiment (Fig. 3) (22) the glucomannan (1.0 g) was oxidized by 0.4 *M* sodium metaperiodate (50 ml) at 21° C for 23 days. Iodate and excess periodate were

precipitated by addition of 0.5 *M* barium acetate and the precipitate was filtered. The filtrate was deionized by Amberlite ion exchange resins IR-45 and IR-120 and potassium borohydride (1.0 g) was then added. After 48 hours the solution was neutralized with acetic acid and deionized by Amberlite IR-45 and IR-120. The solution was then evaporated to dryness and last traces of borate were removed from the residue by repeated evaporation with methanol. The residue was dissolved in water (50 ml) and an aliquot (1 ml) was hydrolyzed by *N* hydrochloric acid (1 ml) at 97° C for 6 hours. Paper chromatograms (solvents A and B) showed the presence of two components that were identical with authentic samples of erythritol and glycerol run on the same paper strips. No component corresponding to a monosaccharide could be found, even on heavily loaded chromatograms. Another aliquot of the polyol solution (5 ml) was evaporated to dryness and the residue, dried *in vacuo*, was heated at 80° C for 20 hours in a solution (20 ml) of acetic anhydride containing 2% of sulphuric acid. The acetolysate was examined directly by gas–liquid partition chromatography (23, 24) and the separation curve is shown in Fig. 4. Authentic samples of glycerol triacetate and erythritol tetraacetate gave the same retention volumes as peaks 1 and 3, Fig. 4, respectively, either when run separately or when added to the unknown mixture. The compound giving peak 3 was collected from the effluent gas stream and the product crystallized spontaneously. Recrystallization from ether: petroleum ether (30–60° C) gave a compound with a melting point of 84–85° C. A mixed melting point with authentic erythritol tetraacetate was 84–86° C. The compound giving peak 1 was also collected but glycerol triacetate is liquid at room temperature and there was not sufficient material to permit deacetylation and formation of another derivative.

The ratio of erythritol to glycerol was 20.8:1 as determined from the relative areas under peaks 3 and 1 (24).

Methylation of Glucomannan

The glucomannan (1.5 g) was acetylated with acetic anhydride (30 ml) in pyridine (45 ml). The mixture was poured into water and the precipitated polysaccharide acetate was centrifuged, washed with water, and dried *in vacuo*; yield, 1.3 g. This product was dissolved in tetrahydrofuran (25 ml), sodium hydroxide (17 g) was added, and the mixture was stirred during dropwise addition of dimethyl sulphate (20 ml) (34). A second addition of reagents was made and the mixture was then refluxed for 1 hour. A further 10 additions of the same quantities of sodium hydroxide and dimethyl sulphate were made over a period of 4 days with continuous stirring and occasional addition of tetrahydrofuran to maintain fluidity. The solution was refluxed for 1 hour, cooled, and filtered. The filtrate and the residual solids (dissolved in water) were extracted continuously with chloroform for 24 hours. The aqueous phases from the two extractions were evaporated to dryness and the residues were extracted with chloroform and methanol. All extracts were combined, dried, and evaporated to yield a product (1.12 g) with a methoxyl content of 38.0%. This product was methylated six times with Purdie's reagents using the same amounts of methyl iodide (25 ml) and silver oxide (5 g) for each methylation. The product (0.76 g) from these methylations had a methoxyl content of 42.2% and showed no hydroxyl absorption in the infrared.

Hydrolysis of Methylated Glucomannan

The methylated glucomannan (0.72 g) was hydrolyzed by formic acid according to the procedure of Jones and Wilkie (35). The hydrolyzate was examined by paper chromatography (solvent C) and showed a major component which corresponded to 2,3,6-tri-*O*-

Can. J. Chem. Downloaded from www.nrcresearchpress.com by 186.148.149.217 on 09/04/12
For personal use only.

methyl-D-mannose; minor components were chromatographically identical with 2,3,4,6-tetra-*O*-methyl-D-glucose; 2,3,4,6-tetra-*O*-methyl-D-galactose; and 2,3,6-tri-*O*-methyl-D-glucose. Trace amounts of two di-*O*-methyl hexoses were also present.

The mixture of sugars was refluxed with 5% methanolic hydrogen chloride and the resulting mixture of glycosides was analyzed by gas–liquid partition chromatography (23, 24). Figure 5 shows the separation of the total mixture on a liquid phase of Apiezon M. In addition to the components shown there was another di-*O*-methyl hexose, present in half the quantity of peak 5, Fig. 5, which had a much larger retention volume and could not be included in the diagram. Identities of the peaks were established by comparison with authentic samples of the compounds listed and were confirmed by isolation of crystalline derivatives as described below. Because it was known that several methylated sugars had the same retention volumes of peaks 1 and 2, Fig. 5, under the conditions used, the compounds giving these two peaks were collected as one fraction from the effluent gas stream and were re-run using butanediol succinate polyester as the liquid phase. The separation, shown in Fig. 6, illustrated clearly that the major component of peak 2, Fig. 5, was the β-methyl glycoside of 2,3,6-tri-*O*-methyl-D-glucose. Figure 6 also shows that no tetra-*O*-methyl-D-mannose was present because it would have appeared between the anomeric methyl glycosides of 2,3,4,6-tetra-*O*-methyl-D-glucose. Peaks 5, 6, and 7, Fig. 6, were not identified conclusively but were probably di-*O*-methyl pentoses arising from a small amount of pentosan present as impurity in the glucomannan. The detection of these components serves to illustrate the sensitivity of gas–liquid partition chromatography because no pentoses could be detected by paper chromatography in hydrolyzates of the polysaccharide or of its methyl ether.

The quantitative data given in Table I were obtained directly from the curves shown in Figs. 5 and 6 by measurement of the areas under the peaks. Areas of peaks representing anomeric glycosides of the same sugar were, of course, added together.

Identification of O-Methyl Ethers

Semipreparative gas–liquid partition chromatography of the mixture of methyl glycosides was carried out at 180° C on an 8-ft column (6-mm I.D.) containing 20% Apiezon M on Celite 545. The apparatus used (23) permitted collection of 1–15 mg of each component.

2,3,4,6-Tetra-O-methyl-D-glucose

This component was collected from the effluent gas stream as its liquid α-methyl glycoside. The glycoside (1 mg) was hydrolyzed at 97° C in *N* hydrochloric acid (0.5 ml) for 6 hours and the hydrolyzate was evaporated to dryness. Ethanol (0.2 ml) and freshly distilled aniline (1 drop) were added, the solution was refluxed for 20 minutes, and then cooled at 5° C for 20 hours. The fine, white needles that separated had a melting point of 115–120° C. Recrystallization from ethanol:water gave a product with a melting point of 134–135° C, and a mixed melting point with an authentic sample of *N*-phenyl 2,3,4,6-tetra-*O*-methyl-D-glucosylamine was 134–136° C. Reported (36): m.p. 135° C.

2,3,4,6-Tetra-O-methyl-D-galactose

This component was collected from the effluent gas stream as a mixture of its anomeric methyl glycosides. These were hydrolyzed and anilide formation was carried out as just described. The crystalline product had a melting point of 192° C, undepressed by admixture with an authentic sample of *N*-phenyl-2,3,4,6-tetra-*O*-methyl-D-galactosylamine. Reported (37): m.p. 192° C.

Can. J. Chem. Downloaded from www.nrcresearchpress.com by 186.148.149.217 on 09/04/12
For personal use only.

*2,3,6-Tri-O-methyl-*D*-glucose*

The anomeric methyl glycosides of this component were widely separated by gas–liquid partition chromatography and were collected separately. Methyl 2,3,6-tri-*O*-methyl-β-D-glucopyranoside crystallized in the collection tube and was recrystallized from ether: petroleum ether (30–60° C), m.p. 59° C and mixed m.p. 59–60° C with an authentic sample of methyl-2,3,6-tri-*O*-methyl-β-D-glucopyranoside. Reported (38): m.p. 58–60° C.

The α-methyl glycoside was hydrolyzed with *N* hydrochloric acid at 97° C for 6 hours. The hydrolyzate was neutralized with Amberlite IR-45 ion exchange resin and evaporated to dryness in a desiccator. The residue crystallized, m.p. 115–120° C, and was recrystallized from ether to yield a product with m.p. 121–122° C, undepressed by admixture with authentic 2,3,6-tri-*O*-methyl-D-glucose. Reported (39): m.p. 121–123° C.

*2,3,6-Tri-O-methyl-*D*-mannose*

This component was collected as its sirupy α-methyl glycoside (15 mg) which was then hydrolyzed by *N* hydrochloric acid at 97° C for 6 hours. The hydrolyzate was evaporated to dryness and anilide formation was carried out as described for 2,3,4,6-tetra-*O*-methyl-D-glucose. The product was recrystallized from ether:petroleum ether (30–60° C) to m.p. 128° C, undepressed by admixture with an authentic sample of *N* phenyl-2,3,6-tri-*O*-methyl-D-mannosylamine. Reported (40): m.p. 127–128° C.

Di-O-methyl Hexoses

Peak 5, Fig. 5, and the other di-*O*-methyl-hexose which had too large a retention volume to be included in Fig. 5 were collected separately and were hydrolyzed and demethylated simultaneously by 48% hydrobromic acid at 97° C in a sealed tube for 20 minutes. The solutions were neutralized (silver carbonate), concentrated, and the total samples were examined by paper chromatography (solvent A). Galactose was obtained from peak 5, Fig. 5, by this procedure while the other di-*O*-methyl hexose yielded glucose.

ACKNOWLEDGMENTS

The authors wish to thank Dr. T. E. Timell, who generously donated samples of 2,3,6-tri-*O*-methyl ethers of D-glucose and D-mannose. Analyses were done by Mr. A. E. Castagne.

REFERENCES

1. G. Bertrand. Compt. rend. **129**, 1025 (1899).
2. K. Hess and M. Ludtke. Ann. **466**, 18 (1928).
3. E. Husemann. J. prakt. chem. **155**, 13 (1940).
4. J. G. Leech. Tappi, **35**, 249 (1952).
5. A. Anthis. Tappi, **39**, 401 (1956).
6. J. K. Hamilton, H. W. Kircher, and N. S. Thompson. J. Am. Chem. Soc. **78**, 2508 (1956).
7. T. E. Timell and A. Tyminski. Tappi, **40**, 519 (1957).
8. G. A. Adams. Tappi, **40**, 721 (1957).
9. J. K. N. Jones and T. J. Painter. J. Chem. Soc. 669 (1957).
10. B. Lindberg and H. Meier. Svensk. Papperstidn. **60**, 785 (1957).
11. E. Merler and L. E. Wise. Tappi, **41**, 80 (1958).
12. D. H. Ball, J. K. N. Jones, W. H. Nicholson, and T. J. Painter. Tappi, **39**, 438 (1956).
13. J. K. N. Jones and T. J. Painter. J. Chem. Soc. 573 (1959).
14. G. O. Aspinall, R. A. Laidlaw, and R. B. Rashbrook. J. Chem. Soc. 4444 (1957).
15. G. G. S. Dutton and K. Hunt. J. Am. Chem. Soc. **80**, 5697 (1958).
16. I. Croon and B. Lindberg. Acta Chem. Scand. **12**, 453 (1958).
17. J. K. Hamilton and H. W. Kircher. J. Am. Chem. Soc. **80**, 4703 (1958).
18. J. K. Hamilton and E. V. Partlow. J. Am. Chem. Soc. **80**, 4880 (1958).
19. I. Croon, B. Lindberg, and H. Meier. Acta Chem. Scand. **13**, 1299 (1959).
20. C. T. Bishop. Can. J. Chem. **35**, 1010 (1957).
21. J. K. N. Jones, L. E. Wise, and J. P. Jappe. Tappi, **39**, 139 (1956).
22. M. Abdel-Akher, J. K. Hamilton, R. Montgomery, and F. Smith. J. Am. Chem. Soc. **74**, 4970 (1952).

Can. J. Chem. Downloaded from www.nrcresearchpress.com by 186.148.149.217 on 09/04/12
For personal use only.

23. A. G. McINNES, D. H. BALL, F. P. COOPER, and C. T. BISHOP. J. Chromato. **1**, 556 (1958).
24. C. T. BISHOP and F. P. COOPER. Can. J. Chem. **38**, 388 (1960).
25. B. H. ALEXANDER, R. J. DIMLER, and C. L. MEHLTRETTER. J. Am. Chem. Soc. **73**, 4658 (1951).
26. J. K. HAMILTON and F. SMITH. J. Am. Chem. Soc. **78**, 5910 (1956).
27. L. HOUGH, J. K. N. JONES, and W. H. WADMAN. J. Chem. Soc. 1702 (1950).
28. W. E. TREVELYAN, D. P. PROCTER, and J. S. HARRISON. Nature, **166**, 444 (1950).
29. L. E. WISE, M. MURPHY, and A. A. D'ADDIECO. Paper Trade J. **122**, 35 (1946).
30. G. A. ADAMS. Unpublished results.
31. M. DUBOIS, K. A. GILLES, J. K. HAMILTON, P. A. REBERS, and F. SMITH. Anal. Chem. **28**, 350 (1956).
32. P. P. FLEURY and J. LANGE. J. pharm. chim. **17**, 107 (1933).
33. D. H. GRANGAARD, E. K. GLADDING, and C. B. PURVES. Paper Trade J. **115**, 41 (1942).
34. E. L. FALCONER and G. A. ADAMS. Can. J. Chem. **34**, 338 (1956).
35. J. K. N. JONES and K. C. B. WILKIE. Can. J. Biochem. and Physiol. **37**, 377 (1959).
36. J. C. IRVINE and A. M. MOODIE. J. Chem. Soc. 93, 95 (1908).
37. J. C. IRVINE and D. MCNICOLL. J. Chem. Soc. 97, 1449 (1910).
38. J. C. IRVINE and I. M. A. BLACK. J. Chem. Soc. 862 (1926).
39. J. C. IRVINE and E. L. HIRST. J. Chem. Soc. 121, 1213 (1922).
40. W. N. HAWORTH, E. L. HIRST, and H. R. L. STREIGHT. J. Chem. Soc. 1349 (1931).

Can. J. Chem. Downloaded from www.nrcresearchpress.com by 186.148.149.217 on 09/04/12
For personal use only.

Can. J. Chem. Downloaded from www.nrcresearchpress.com by 186.148.149.217 on 09/04/12
For personal use only.

11-OCTADECENOIC ACID AND OTHER FATTY ACIDS OF ASCLEPIAS SYRIACA SEED OIL[1]

MARY J. CHISHOLM AND C. Y. HOPKINS

ABSTRACT

The seed oil of *Asclepias syriaca* L., family Asclepidaceae, was examined by gas chromatography and distillation of the methyl esters. The fatty acids were found to include a considerable proportion of *cis*-11-octadecenoic acid, which has not been observed previously in seed oils. It was obtained as a concentrate ($\simeq$ 80%) by low-temperature crystallization of the C18 acids and identified as 11,12-dihydroxystearic acid. The amount of 11-octadecenoic acid in the oil was determined by oxidative splitting of the total fatty acids and estimation of the resulting azelaic and undecanedioic acids by gas chromatography.

The C16 acids included 9,12-hexadecadienoic acid, which is rare in seed oils, and an unusually large proportion of 9-hexadecenoic acid. The percentage composition of the fatty acids was estimated from the data as follows: palmitic 4,9-hexadecenoic 10, 9,12-hexadecadienoic 2, stearic <1, oleic 15, 11-octadecenoic 15, linoleic 53, linolenic <1. The unsaturated acids have the *cis* configuration.

INTRODUCTION

In preparation for a study of the development of oil in a maturing seed, it was desired to know the normal composition of the seed oil of *Asclepias syriaca* L. (common milkweed), family Asclepidaceae. The oil of this species has been examined by a number of workers in the past and the fatty acids have been reported for the most part as consisting of the ordinary oleic, linoleic, and saturated acids (1, 2, 3). However, there are some indications in these reports of the presence of less common constituents.

In the present work, the seed oil of *Asclepias syriaca* L. was examined by distillation of the methyl esters, followed by low-temperature crystallization and gas chromatography of the fractions. The identity of the individual acids was determined with certainty by orthodox procedures.

The results show that the oil has by no means a simple palmitic–oleic–linoleic composition. A novel constituent is 11-octadecenoic acid, reported here for the first time in a seed oil. The amount is substantial and is estimated to be 15% of the total fatty acids. Ordinary oleic acid is present also.

The composition of the C16 acids is distinctly different from that of the common seed oils. The major C16 acid is 9-hexadecenoic and the ratio of 9-hexadecenoic acid to palmitic acid is 2:1 or greater. There is an appreciable amount of 9,12-hexadecadienoic acid, which is known in only one other seed oil (4).

The presence of an isomer of oleic acid (other than the well-known petroselinic acid) in seed oils has been suspected from time to time. As early as 1927, Hilditch, Riley, and Vidyarthi reviewed the claims for the existence of such an isomer in rapeseed oil and examined a number of Cruciferae oils (5). They found strong evidence of a possible 1 or 2% of isomers of oleic acid in rapeseed and mustard-seed oils but did not succeed in identifying them. Millican and Brown noticed similar indications of an isomer or isomers in rapeseed and soybean oils (6).

The present investigation establishes the occurrence of *cis*-11-octadecenoic acid* in the glycerides of *Asclepias syriaca* seed oil. No evidence was found of any other octadecenoic acid except the ordinary oleic acid.

[1]*Manuscript received February 15, 1960.*
Contribution from the Division of Pure Chemistry, National Research Council, Ottawa, Canada. Presented at the meeting of the American Chemical Society, Cleveland, Ohio, April, 1960.
Issued as N.R.C. No. 5646.
**If a trivial name is desired, it is suggested that cis-11-octadecenoic acid be called "asclepic acid".*

Can. J. Chem. Downloaded from www.nrcresearchpress.com by 186.148.149.217 on 09/04/12
For personal use only.

EXPERIMENTAL

Seed pods of *Asclepias syriaca* L. were collected in late September, 1959, from a stand of wild plants near Ottawa. The seed was removed from the pods by hand, dried, ground, and extracted with petroleum ether. The following data were recorded: moisture in seeds as harvested, 39.6%; mean weight of seeds (moisture-free) per pod, 0.82 g; weight of 100 seeds (moisture-free), 0.57 g; oil content of seeds (moisture-free basis), 19.4%. Constants of the oil are shown in Table I.

TABLE I

Properties of the oil

Iodine value	127.2	Acetyl value	0
Acid value	1.5	Refractive index, 25°	1.4748
Unsaponifiable matter, %	2.2	Equiv. wt. of mixed fatty acids	279.0

Separation of the Fatty Acids

The oil was converted to methyl esters by methanolysis with dry hydrogen chloride catalyst and the esters were examined by gas–liquid chromatography, using a polyester liquid phase. The detector was a thermistor type of thermal conductivity cell. Column length was 1 meter, temperature 190°, and helium flow rate 95 ml/minute, at an inlet pressure of 12.5 p.s.i. The chromatogram is shown in Fig. 1.

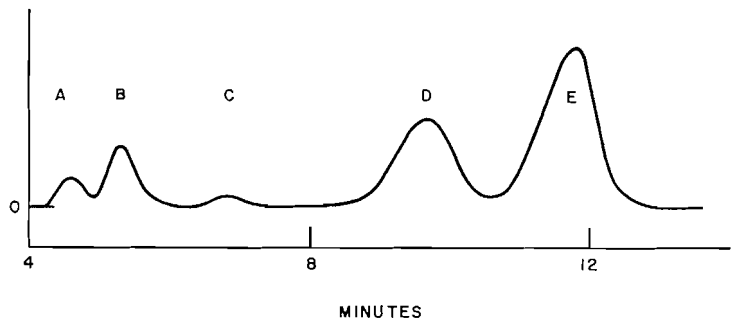


FIG. 1. Main portion of the gas chromatogram of the methyl esters. The peaks represent esters of the following acids: A, palmitic; B, hexadecenoic; C, hexadecadienoic; D, octadecenoic; E, linoleic. A small peak at 15.4 minutes (not shown) is assigned to linolenic acid.

Tentative identification of peaks A, D, and E was made by comparing emergence times with those of authentic samples. The identity of all of the main components was established after distillation of the esters as described below. The chromatogram also indicated the presence of traces of stearic and linolenic acids (less than 1% of each) but no C20 acids.

The main portion of the methyl esters was distilled through a spinning band column at 0.5 mm pressure in order to collect the C16 acids. Distillation data are given in Table II.

Examination of the distilled portions by gas chromatography showed that fraction 1 consisted of three acids in the C16 range, presumably palmitic, hexadecenoic, and hexadecadienoic. The intermediate fraction 2 contained these in lesser amounts along with octadecenoic and octadecadienoic acids. Fraction 3 consisted almost entirely of C18 acids.

TABLE II

Distillation of methyl esters

Fraction	Temp., °C (0.5 mm)	Weight, g	Predominant chain length	Iodine value	Refractive index, 25°
1	120–122	9.1	C16	76.9	1.4472
2	122–131	0.9	—	104.4	1.4517
3	131–133	9.8	C18	145.1	1.4571
R	Residue				

THE C16 ACIDS

Fraction 1 was estimated by gas chromatography to contain 14% of hexadecadienoate. Ultraviolet absorption analysis after alkali isomerization (45 minutes at 180° in glycerol–air) gave a value of 16.3% for dienoic ester, calculated as hexadecadienoate. A portion of fraction 1 (8 g) was subjected to fractional crystallization from acetone at low temperature (Table III). When examined by gas chromatography, the portion recovered from the final filtrate was found to consist of equal parts of hexadecenoate and hexadecadienoate.

TABLE III

Fractional crystallization of C16 methyl esters

Fraction	Crystallizing temp., °C	Yield, g	Refractive index, $n_D^{25°}$
1	−12	1.55	Solid at 25°
2	−60	0.80	Solid at 25°
3	−65*	3.05	1.4493
4	Filtrate	1.78	1.4548

*Crystallizing temperature after removing half of the solvent.

Palmitic Acid

Fraction 1 (Table III) was methyl palmitate. On saponification it gave pure palmitic acid directly, m.p. 62–62.5° alone and mixed with an authentic sample.

9-Hexadecenoic Acid

Fraction 3 (Table III) was almost entirely methyl hexadecenoate. It was identified by hydroxylation with alkaline permanganate (7). The product, when recrystallized from ethyl acetate, melted at 125–126° and did not lower the melting point of a known sample of erythro-9,10-dihydroxy-palmitic acid. The original acid was therefore *cis*-9-hexadecenoic acid.

9,12-Hexadecadienoic Acid

Fraction 4 (Table III) was hydroxylated in the same way and the dihydroxy acid was removed from the product by leaching with warm ethyl acetate. The remaining tetrahydroxy acid was recrystallized from a large volume of ethyl acetate. It melted at 163–164°. Calculated for tetrahydroxypalmitic acid, $C_{16}H_{32}O_6$: C, 59.98; H, 10.07. Found: C, 59.79; H, 9.92. This substance has not been reported hitherto.

In order to determine the position of the original double bonds, a portion of fraction 4 was subjected to oxidative splitting by periodate–permanganate (8). At the end of the reaction, the excess of reagents was destroyed by sodium bisulphite and the products

Can. J. Chem. Downloaded from www.nrcresearchpress.com by 186.148.149.217 on 09/04/12
For personal use only.

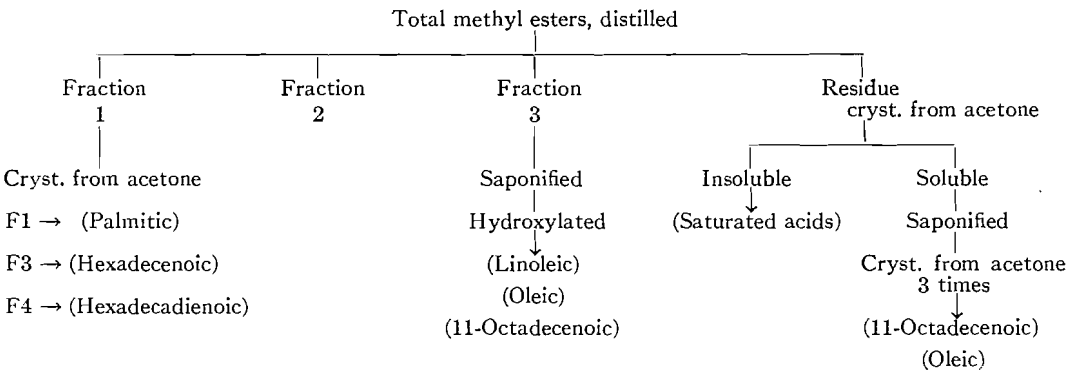
were extracted with ether. The ether solution was made alkaline to prevent loss of volatile acids and it was taken to dryness. *n*-Butanol containing an excess of dry hydrogen chloride was added and the mixture was refluxed to convert all of the acids to butyl esters. The excess butanol was allowed to remain and the mixture was examined by gas chromatography at a column temperature of 80°.

Since fraction 4 contained both monoenoic and dienoic acids, the products of splitting would include heptanoic and azelaic acids arising from 9-hexadecenoic acid, as well as those from the dienoic acid. The chromatogram showed peaks corresponding to two monobasic acids, butyric and heptanoic, in approximately equal amounts (as butyl esters). It is apparent that the heptanoic acid came from oxidation of the hexadecenoic acid since it has already been shown that its double bond is Δ^9. The butyric acid must have come from the dienoic acid. Thus, one double bond in the dienoic acid is situated between the fourth and fifth carbon atoms, counting from the methyl end of the chain. The chromatogram also showed traces of pentanoic and hexanoic acids, which may have arisen from minor proportions of isomeric monoene or diene acids.

The mixture of butyl esters was then chromatographed at a column temperature of 190°. Azelaic acid was the only dibasic acid detected. Thus both the monoenoic and dienoic acids gave azelaic acid. The corresponding double bond of the diene acid is therefore in the 9,10 position, counting from the carboxyl end of the chain and the acid is 9,12-hexadecadienoic acid. The tetrahydroxy acid (described above) must be erythro, erythro-9,10,12,13-tetrahydroxypalmitic acid, since permanganate oxidation of *cis* double bonds gives the erythro structure. The infrared spectrum of the C16 methyl esters (fraction 1, Table II) showed no *trans* absorption (965 cm^{-1}), hence both the monoene and diene acids are considered to have *cis* unsaturation.

THE C18 ACIDS

Examination of the esters of C16 and C18 acids is summarized in the following diagram, which shows in parentheses the acids identified in the various fractions from the ester distillation (Table II). The separation of the C18 acids is described below.



Linoleic Acid

A portion of fraction 3 of the distilled methyl esters (Table II) was saponified and the acids were hydroxylated by alkaline permanganate (7). Upon fractional crystallization from ethyl acetate, the most insoluble part of the product melted sharply at 171–172° and was identified by mixed melting point as erythro, erythro-tetrahydroxystearic acid, from ordinary linoleic acid.

Can. J. Chem. Downloaded from www.nrcresearchpress.com by 186.148.149.217 on 09/04/12
For personal use only.

Can. J. Chem. Downloaded from www.nrcresearchpress.com by 186.148.149.217 on 09/04/12
For personal use only.

Octadecenoic Acids

The more soluble portion, presumably dihydroxystearic acid, melted at 114–115°, unchanged on further recrystallization. It was evidently not the ordinary erythro-9,10-dihydroxystearic acid which melts when pure at 132°. The equivalent weight of the substance was 318.1 (dihydroxystearic acid 316.5).

It was subjected to splitting by permanganate–periodate (8). At the end of the reaction the acidic products were extracted with ether and the ether solution was made alkaline and evaporated to dryness. Methanol containing excess hydrogen chloride was added and refluxed gently. The mixture was poured into water and the methyl esters were extracted with cyclohexane, washed with a little aqueous sodium bicarbonate and water, and dried. The cyclohexane solution was submitted to gas chromatography at 80° and 130°. Monobasic acids were represented by two major peaks, corresponding in emergence times to heptanoate and nonoate, with a very small peak corresponding to hexanoate. There was no indication of octanoate or decanoate. It was concluded that the substance with a melting point of 114–115° must be a mixture of 9,10- and 11,12-dihydroxystearic acids, formed from oleic acid and 11-octadecenoic acid. The ratio of nonoate (from oleic) to heptanoate (from 11-octadecenoic), determined from the area of the peaks, was 5:4.

The hexanoate was probably formed from a little tetrahydroxystearic acid (from linoleic acid) present in the dihydroxy acid mixture. It amounted to 6% of the total of the C6–C9 acids by peak area measurement.

When the mixture of methyl esters was chromatographed at 170°, peaks corresponding to azelate and undecanedioate appeared. There was no evidence of sebacate. This confirms the presence of 9,10- and 11,12-dihydroxystearic acids in the original mixture. The undecanedioate could not have arisen from eicosenoic acid since the chromatogram of the total esters of the oil showed that no C20 acids were present. The ratio of azelate to undecanedioate was 5:4.

Identification of 11-Octadecenoic Acid

Confirmatory evidence of the presence of 11-octadecenoic acid was sought. The residue from the distillation of methyl esters (Table II) (46.0 g) was crystallized from 400 ml of acetone at −30°. The crystals (4.1 g) were saponified and recrystallized twice from ethanol, giving 1.1 g of solid acid(s) melting at 66–68°. It depressed the melting point of pure stearic acid and is judged to contain some higher saturated acid(s).

The filtrate from the crystallization of the esters was evaporated, the esters saponified, the unsaponifiable matter removed, and the acids recovered (38.0 g). These acids (largely linoleic acid) were crystallized successively from 380 ml of acetone at −45° and from 50 ml of acetone at −35°, giving 4.3 g of acids of refractive index $\alpha_D^{25°}$ 1.4595 (oleic acid, 1.4581). This product was crystallized fractionally from 40 ml of acetone as follows:

Fraction	Temp. of crystallization, °C	Yield, g	Iodine value	$\alpha_D^{25°}$
1	−22	1.3	78.3	Semisolid
2	−40	1.3	89.6	1.4591
3	Filtrate	1.3		1.4645

Fraction 1 probably contained a little stearic acid and fraction 3 some linoleic acid. The fraction of iodine value 78.3 was hydroxylated by alkaline permanganate for 15 minutes at 10°, yielding a dihydroxystearic acid, m.p. 128–128.5° after three crystallizations from

ethyl acetate, and washing with petroleum ether (yield 0.62 g). The equivalent weight was 315.8 (calculated for dihydroxystearic acid, 316.5). On mixing with erythro-9,10-dihydroxystearic acid (from oleic acid), it melted at 116–122°.

It was identified as erythro-11,12-dihydroxystearic acid by comparison with an authentic sample, kindly furnished by Dr. F. D. Gunstone. There was no depression of melting point in admixture with this sample. The melting point of erythro-11,12-dihydroxystearic acid from synthetic 11-octadecenoic acid is given by Ahmad (9) as 127–128° and by Huber (10) as 129–130°. Thus fraction 1 (iodine value 78.3) was mainly 11-octadecenoic acid.

To confirm the identification, the dihydroxy acid with a melting point of 128–128.5° was subjected to oxidative splitting by permanganate–periodate. The reaction mixture, when acidified, gave a precipitate with a melting point of 107–108°, raised to 109–110° by one crystallization from ethyl acetate. This proved to be undecanedioic acid. The equivalent weight was 109.2 (calc. 108.1). Its melting point was unchanged in admixture with an authentic sample prepared by oxidative splitting of 11,12-dihydroxyarachidic acid made from jojoba oil.

The filtrate from the oxidation was treated as before to convert the monobasic acids to methyl esters without loss. The mixture of esters was chromatographed at 80° and 130°. It gave only one peak in the region of medium chain length and that had the correct emergence time for methyl heptanoate, by comparison with an authentic sample. There was no evidence of monobasic acids of chain length C8–C12. The hydroxylated acid is therefore erythro-11,12-dihydroxystearic acid and the original acid in the oil is *cis*-11-octadecenoic acid.

The second fraction of the octadecenoic acids (I.V. 89.6) was submitted to oxidative splitting and the fragments were esterified and chromatographed at 80° and 170°. Peaks corresponding in emergence time to nonoate and azelate (from oleic acid) and to heptanoate and undecanedioate (from 11-octadecenoic acid) were recorded. There were no peaks in the regions corresponding to hexanoate, octanoate, suberate, and sebacate. The ratio of oleic acid to 11-octadecenoic acid in this fraction was estimated from the area of the peaks to be 28:72.

Total Composition

The fatty acid composition of the oil was estimated from the entire data, including the measurement of the peak areas in the gas chromatography of the methyl esters, the results of examination of the distilled ester fractions, and analysis of certain fractions by ultraviolet absorption. Calculated in this manner, the content of octadecenoic acids is 30% of the total fatty acids of the oil and the percentages of the other acids are as shown in Table IV.

TABLE IV

Estimated fatty acid composition (% of total fatty acids)

Acid	%	Acid	%
Palmitic	4	Stearic*	<1
9-Hexadecenoic	10	Oleic	15
9,12-Hexadecadienoic	2	11-Octadecenoic	15
		Linoleic	53
		Linolenic*	<1

*Identified by its emergence time under gas chromatography.

Can. J. Chem. Downloaded from www.nrcresearchpress.com by 186.148.149.217 on 09/04/12
For personal use only.

The content of 11-octadecenoic acid was determined by treating a sample of the total fatty acids of the oil with permanganate–periodate and determining the ratio of the resulting dibasic acids by gas chromatography at 170° (as methyl esters). In this reaction 11-octadecenoic acid yields undecanedioic acid while each of the other unsaturated acids of this oil gives azelaic acid. The ratio of undecanedioic acid to azelaic acid (w/w) was 16.5:83.5 (mean ratio of peak areas from triplicate samples). Allowing for the approximately 5% of saturated acids and taking into account the stoichiometric yield of the two dibasic acids from the various original unsaturated acids, the content of 11-octadecenoic acid is calculated to be 15% of the total fatty acids. Since the total octadecenoic acids are estimated at 30%, the content of oleic acid, by difference, is also 15% of the total fatty acids. The fatty acid composition is summarized in Table IV.

Other Samples

Samples of seed harvested in 1952 and 1958 were also examined. The oil content of these was 21.5% and 22.7% respectively (moisture free basis). The 1958 oil had iodine value 127.5, acid value 1.1, unsaponifiable matter 1.8%, and equivalent weight of the fatty acids 279.4. The oil from both lots was analyzed by gas chromatography and the 1952 sample was also treated by fractional distillation of its methyl esters and examination of the fractions. However, the ratio of oleic to 11-octadecenoic acid was not determined. The estimated percentages of fatty acids in the 1952 and 1958 oils were respectively: palmitic 5, 5; hexadecenoic 11, 12; hexadecadienoic 1.3, 1.7; octadecenoic acids 30, 33; linoleic acid 52, 47.

DISCUSSION

The oil is unusual in respect to the composition of both the C16 and C18 acids. One other seed oil of the family Asclepidaceae has been studied, viz. *Cryptostegia grandiflora* R. Br. (11). It was reported to be composed of the ordinary oleic, linoleic, and saturated fatty acids.

The occurrence of 11-octadecenoic acid in *Asclepias* oil was unexpected. An isomer of oleic acid was indicated when the erythro-dihydroxystearic acid was found to melt at 114–115° instead of the usual 132°. Apparently an equilibrium mixture was formed with the ordinary 9,10-dihydroxystearic acid which was not separable by ordinary crystallization from solvents. A similar anomalous melting point was observed by Watson and Levitin (12) when the oil of the *pods* of *Asclepias syriaca* was examined. Their dihydroxystearic acid melted at 116° but was not investigated further. Hilditch and co-workers obtained repeatedly a dihydroxy acid or mixture of acids, melting at 117–118°, from the C18 fractions of rapeseed and mustard-seed oils (5). A similar product was obtained by one of us (13) from the seed oil of *Conringia orientalis* L. (Cruciferae). On the basis of the present results, it seems likely that all of these consisted of mixtures of two or more position isomers of dihydroxystearic acid.

The possibility that 11-octadecenoic acid was formed by isomerization of oleic acid or ester during treatment is considered very unlikely. Similar treatment of many oils in this laboratory did not give evidence of such isomerization. The temperature reached in the distillation of the methyl esters in the present instance was lower than usual because only one-third of the esters was distilled off. It is also considered very unlikely that isomerization (shift of the double bond) occurred during the hydroxylation by alkaline permanganate or during the oxidative splitting by permanganate–periodate. Simple olefinic acids do not undergo a double-bond shift in these reactions to our knowledge.

Can. J. Chem. Downloaded from www.nrcresearchpress.com by 186.148.149.217 on 09/04/12
For personal use only.

11-Octadecenoic acid has been observed previously in the fat of bacteria, fish, and animals (14). The *trans* form is most common in animal fats and is thought to originate by bacterial action in the digestive process. Thus 11-octadecenoic acid may be to some extent characteristic of the lower forms of living matter. If so, its occurrence in *Asclepias*, along with the unusually large amount of unsaturated C16 acids, may give an indication of the place of this genus in the scale of evolution of plants.

11-Octadecenoic acid differs from most natural unsaturated fatty acids in having the double bond at the seventh carbon atom from the methyl end of the chain. In this respect, it is the same as 9-hexadecenoic acid which accompanies it in similar amount in this oil.

The unusually high content of 9-hexadecenoic acid and an appreciable content of 9,12-hexadecadienoic acid are noteworthy. The amount of hexadecenoic acid is exceeded in one other seed oil, viz. *Macadamia ternifolia* (Proteaceae) (15). Hexadecadienoic acid has been found in one other seed oil, viz. *Acacia giraffae* (Leguminosae) (4). The estimated amounts of C16 acids in these oils are as follows:

	C16 acids in total fatty acids, wt.%		
Species	Palmitic	Hexadecenoic	Hexadecadienoic
Asclepias syriaca	4	10	2
Macadamia ternifolia (15)	8	20	0 (16)
Acacia giraffae (4)	13	7	1

ACKNOWLEDGMENTS

The authors are grateful to Dr. R. W. Watson and Dr. H. A. Senn for assistance in procuring seed and to Mr. R. Lauzon for determination of infrared spectra.

REFERENCES

1. E. W. Eckey and L. P. Miller. Vegetable fats and oils. Reinhold Publishing Corp., New York. 1954. p. 727.
2. H. J. Lanson, D. Habib, and P. E. Spoerri. Ind. Eng. Chem. **37**, 179 (1945).
3. I. K. Matzurevich. J. Appl. Chem. (U.S.S.R.), **9**, 509 (1936); Chem. Abstr. **30**, 7887 (1936).
4. G. S. Harrison and F. Hawke. J. S. African Chem. Inst. **5**, 1, 23 (1952).
5. T. P. Hilditch, T. Riley, and N. L. Vidyarthi. J. Soc. Chem. Ind. (London), **46**, 462 T (1927).
6. R. C. Millican and J. B. Brown. J. Biol. Chem. **154**, 437 (1944).
7. A. Lapworth and E. N. Mottram. J. Chem. Soc. **127**, 1628 (1925).
8. R. U. Lemieux and E. von Rudloff. Can. J. Chem. **33**, 1701 (1955).
9. K. Ahmad, F. M. Bumpus, and F. M. Strong. J. Am. Chem. Soc. **70**, 3391 (1948).
10. W. F. Huber. J. Am. Chem. Soc. **73**, 2730 (1951).
11. R. H. Siddiqui and S. A. Warsi. Indian J. Pharm. **7**, 75, 88 (1945).
12. R. W. Watson and N. Levitin. Can. J. Research, F, **24**, 95 (1946).
13. C. Y. Hopkins. Can. J. Research, B, **24**, 211 (1946).
14. T. P. Hilditch. Chemical constitution of natural fats. 3rd ed. Chapman & Hall Ltd., London. 1956. p. 524.
15. R. E. Bridge and T. P. Hilditch. J. Chem. Soc. 2396 (1950).
16. C. Y. Hopkins. To be published.

Can. J. Chem. Downloaded from www.nrcresearchpress.com by 186.148.149.217 on 09/04/12
For personal use only.

EQUILIBRIUM DECOMPOSITION PRESSURES OF K_2TiCl_6[1]

S. N. Flengas and T. R. Ingraham

ABSTRACT

The equilibrium decomposition pressures of K_2TiCl_6 were measured at temperatures between 370° and 530° C, using a glass-bellows mercury manometer.

The pressure–temperature relationship was found to obey the equation

$$\log_{10} P(\text{cm of Hg}) = -\{(5.774\times10^3)/T\} + 9.120$$

and the heat of the reaction

$$K_2TiCl_{6(s)} \rightleftharpoons 2KCl_{(s)} + TiCl_{4(g)}$$

was found to be

$$\Delta H = +26.4\pm1.3 \text{ kcal/mole.}$$

INTRODUCTION

Because of its relatively high degree of stability at room temperature, the compound K_2TiCl_6 offers interesting possibilities as a source of $TiCl_4$ for the electrolytic preparation of titanium in fused salt baths. Indeed, K_2TiCl_6 may be an intermediate in the chain of chemical reactions proceeding in electrolytic cells which are supplied with gaseous $TiCl_4$ and contain KCl as a constituent of the bath.

K_2TiCl_6 has been prepared by wet chemical methods involving the dissolution of the mineral ilmenite ($FeO.TiO_2$) in aqueous sulphuric acid, and the salting out of K_2TiCl_6 by HCl in the presence of KCl (1) at 0° C. Unsuccessful attempts have been made to prepare the compound in an autoclave at about 300° C, by the direct reaction of KCl with $TiCl_4$ (2).

At higher temperatures, the direct reaction of KCl with $TiCl_4$ has been used successfully in these laboratories to prepare K_2TiCl_6 for use in studies of the potentials of the various titanium ions in molten salt solutions. In this preparation, which was reported in a previous paper (3), the experiments were done at temperatures from 230° to 500° C. It was observed that the rate of reaction was relatively slow at temperatures up to about 300° C, and attained a maximum rate at about 410° C. At temperatures substantially above 400° C, at which the rate of reaction might have been expected to increase, the rate of reaction decreased. It seemed probable that the compound K_2TiCl_6 was becoming increasingly unstable as the temperature was increased.

To confirm these implications, and to establish some of the thermodynamic properties of K_2TiCl_6 which might be of interest in evaluating it as a possible source of titanium tetrachloride for electrowinning cells, it was decided to study the equilibrium decomposition pressures of titanium tetrachloride over the compound.

Since our previous experience in preparing the compound had suggested that this solid–gas state reaction was relatively slow to establish equilibrium, a static method, rather than a dynamic method, of measuring the decomposition pressure was selected.

EXPERIMENTAL

The compound K_2TiCl_6 was prepared in a 1-in. diameter tube, bent in a right angle, and sealed at one end. Purified titanium tetrachloride was introduced into the closed vertical arm and was frozen with liquid air. A silica boat containing potassium chloride

[1]*Manuscript received February 10, 1960.*
Contribution from the Extraction Metallurgy Division, Mines Branch, Department of Mines and Technical Surveys, Ottawa, Ontario.

Can. J. Chem. Downloaded from www.nrcresearchpress.com by 186.148.149.217 on 09/04/12
For personal use only.

powder of a particle size less than 325 mesh was then placed in the horizontal arm and the tube was evacuated and sealed. By heating the titanium tetrachloride to a temperature between 130 and 134° C, and the potassium chloride to a temperature of about 400° C, for 12 hours, K_2TiCl_6 was formed quantitatively. When prepared by this method, the compound contained a small excess of adsorbed titanium tetrachloride. To prevent attack by moisture, the samples were transferred in a dry box to airtight glass containers.

The equilibrium decomposition pressures were measured in the apparatus shown diagrammatically in Fig. 1. The most important feature of the apparatus is the glass-

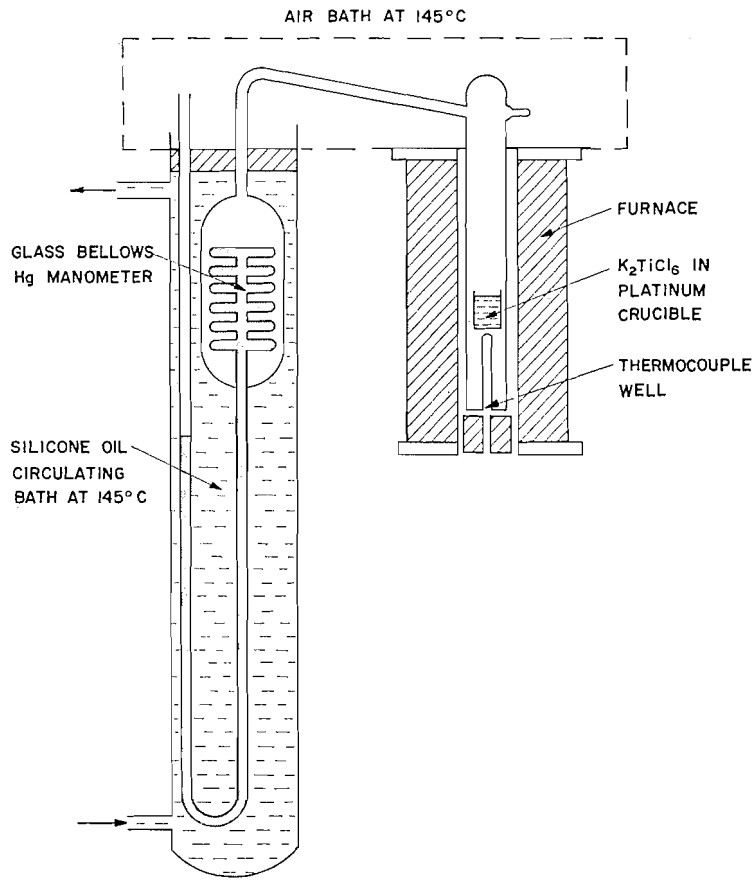


FIG. 1. Pressure measuring apparatus.

bellows mercury manometer, originally designed by Spence (4). It was modified for use in these experiments. This type of manometer is well suited to studies of equilibrium pressures in systems in which the decomposition product is a highly corrosive gas, which would be likely to attack conventional manometric liquids.

The manometer was calibrated at various pressures, and the relationship between the height of the mercury column of the manometer and the pressure was found to be linear over the pressure range between 1.2 and 76 cm. A deflection of 1.000 cm Hg was equivalent to a 1.540 cm of Hg pressure change. Pressure changes were observed with a cathetometer and were corrected for barometric fluctuations.

The reaction cell was constructed from Pyrex and Vycor. The Vycor section extended

Can. J. Chem. Downloaded from www.nrcresearchpress.com by 186.148.149.217 on 09/04/12
For personal use only.

out of the hot zone of the furnace, where it was joined, through a graded seal, to the Pyrex part of the apparatus. To avoid the condensation of titanium tetrachloride (b.p. 136.4° C), the bellows manometer was thermostatically controlled at a temperature of 145.0±0.1° C, using silicone oil (Dow Corning 550 fluid) as the heat transfer medium in a circulating bath. The connecting tube between the reaction cell and the manometer was also maintained at a temperature of 145.0±0.5° C by means of a thermostatically controlled air bath.

The reaction cell was heated in a tubular furnace, the temperature of which was kept constant, within ±1° C, by a thermocouple set in a well just below the sample and connected with a Kelwyn–Hughes phototransistor proportional temperature controller, type MIK IV.

To begin an experiment, about 10 grams of K_2TiCl_6 was transferred to a platinum crucible and the crucible was placed just above the thermocouple well. The open end of the reaction tube was then sealed and the apparatus was evacuated through a side arm for about 20 hours to remove excess titanium tetrachloride adsorbed on the K_2TiCl_6 powder. After evacuation was complete, the apparatus was sealed under vacuum and the furnace was heated to a predetermined temperature. Readings of the pressure were made at 2-hour intervals and equilibrium was considered to have been established when the pressure remained unchanged for a period of 12 hours. In the initial runs, it was observed that, at low temperatures, the same equilibrium pressure was not obtained readily when the temperature was approached from above and below. It was found that in spite of the 20-hour evacuation period, a small excess of $TiCl_4$ remained adsorbed on the sample. The $TiCl_4$ was removable by evacuation at higher temperatures, but it was found more convenient to mix excess KCl with the K_2TiCl_6 before beginning the run. When this was done, the same equilibrium pressures could be established readily on either an increasing or a decreasing temperature cycle.

RESULTS

The results obtained in three typical runs are shown in Table I.

TABLE I

Equilibrium decomposition pressures of K_2TiCl_6

Temperature (°C)	P (cm of Hg)		
	Run 1, using K_2TiCl_6	Run 2, using K_2TiCl_6	Run 3, using K_2TiCl_6 + KCl
On heating			
373	—	—	1.89
432	—	—	8.44
456	—	21.52	—
469	22.33	—	—
485	—	—	29.33
489	—	36.77	—
494	—	39.16	—
506	—	48.47	48.75
515	—	—	55.65
518	—	65.32	—
525	52.84	—	—
529	66.44	—	72.67
On cooling			
512	—	53.40	—
509	—	51.86	—
432	—	—	8.58
374	—	—	1.83

Can. J. Chem. Downloaded from www.nrcresearchpress.com by 186.148.149.217 on 09/04/12
For personal use only.

From Table I it may be seen that the decomposition of K_2TiCl_6 begins at a temperature of about 350° C, and that the decomposition pressure of $TiCl_4$ at about 530° C is 1 atm.

The equilibrium constant for the decomposition of K_2TiCl_6,

$$K_2TiCl_{6(s)} \rightleftharpoons 2KCl_{(s)} + TiCl_{4(g)},$$

is given by the equation

$$K_p = P_{TiCl_4}.$$

The results shown in Table I were used to calculate log K_p and $1/T$, and when these were plotted, the straight-line relationship shown in Fig. 2 was obtained by applying the least-squares method. It is evident from Fig. 2 that the linear relationship holds

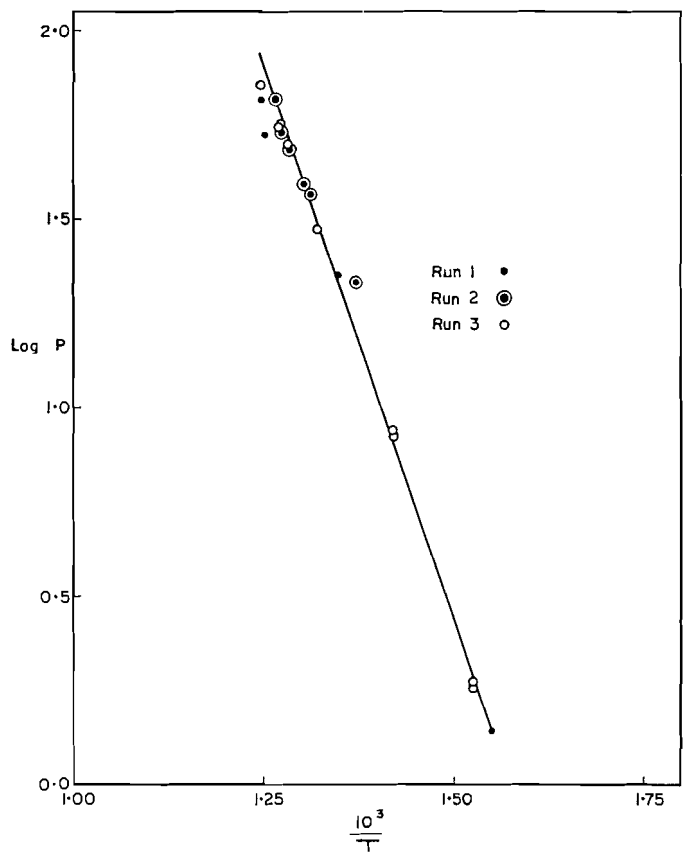


FIG. 2. The variation of log P with the reciprocal of the absolute temperature.

reasonably well for pressures between 2 and 76 cm. From Fig. 2, the variation of pressure with temperature corresponds with the equation

$$\log_{10} P(\text{cm of Hg}) = -\{(5.774\times10^3)/T\} + 9.120.$$

The average error, a, of a single observation, as calculated by the least-squares method, is

$$\log a = \pm 0.045.$$

Can. J. Chem. Downloaded from www.nrcresearchpress.com by 186.148.149.217 on 09/04/12
For personal use only.

The heat of reaction was calculated from the slope of the straight line in Fig. 2 in accordance with the van't Hoff equation

$$\Delta H = +26.4 \pm 1.3 \text{ kcal/mole.}$$

This is in good agreement with +27 kcal/mole obtained by Ehrlich and Framm (2) from their experiments using the isoteniscope method.

Free energy and entropy changes for the decomposition were calculated at selected temperatures. The results are shown in Table II.

TABLE II

Thermodynamic functions for the reaction
$K_2TiCl_{6(s)} \rightleftharpoons 2KCl_{(s)} + TiCl_{4(g)}$

Temp. (°C)	K_p (atm)	ΔH (kcal/mole)	ΔF (kcal/mole)	ΔS (e.u.)
350	9.36×10^{-3}	+26.40	+5.77	33.6
400	4.56×10^{-2}	+26.40	+3.88	33.4
450	1.79×10^{-1}	+26.40	+2.52	33.0
500	5.88×10^{-1}	+26.40	+0.81	33.1

CONCLUSIONS

Since the reaction

$$K_2TiCl_{6(s)} \rightleftharpoons 2KCl_{(s)} + TiCl_{4(g)}$$

is endothermic, the formation of the compound is promoted at lower temperatures. However, from kinetic considerations (3) it appears that the rate of reaction at temperatures below 300° C is slow; this would explain the inability of Ehrlich and Framm (2) to prepare K_2TiCl_6 in an autoclave at 300° C.

Furthermore, the thermal stability of K_2TiCl_6 in the temperature range of 300–400° C indicates that the compound might be used as a constituent of a low-melting-point fused salt bath, e.g. KCl + LiCl, for the production of titanium metal by electrolysis. Indeed, it appears that the accepted practice of using fused salt baths at high temperatures, e.g. KCl + NaCl at 700° C, would hinder the introduction of gaseous titanium tetrachloride into the melt, under circumstances where the introduction depended upon the formation of K_2TiCl_6.

ACKNOWLEDGMENT

The authors wish to thank Mr. George Ensell, National Research Council of Canada glass blower, for constructing the glass-bellows mercury manometer.

REFERENCES

1. F. V. SCHOSSBERGER. Ind. Eng. Chem. **51** (5), 669 (1959).
2. B. EHRLICH and E. FRAMM. Z. Naturforsch. **9b**, 326 (1954).
3. S. N. FLENGAS. Solubilities of titanium tetrachloride in mixtures of potassium and sodium chlorides, and the electrode potentials of the titanium chlorides in 1/1 mole KCl + NaCl solutions. Paper presented at the New York Academy of Science, April, 1959.
4. R. SPENCE. Trans. Faraday Soc. **36**, 417 (1940).

Can. J. Chem. Downloaded from www.nrcresearchpress.com by 186.148.149.217 on 09/04/12
For personal use only.

Can. J. Chem. Downloaded from www.nrcresearchpress.com by 186.148.149.217 on 09/04/12
For personal use only.

ELECTRON CORRELATION AND MOLECULAR SHAPE[1]

R. J. GILLESPIE

ABSTRACT

It is proposed that the arrangements of the electron pairs in the valency shell of a central atom of a polyatomic molecule can be predicted by considering the equilibrium arrangements of similar particles on the surface of a sphere with an appropriate law of force between the particles. The arrangements resulting from an inverse square law of force, corresponding to electrostatic repulsions, and a force which is proportional to $1/r^n$ where n is large, corresponding to Pauli forces, are considered specifically. It is shown that the arrangements predicted agree with those found experimentally for molecules containing only non-transitional elements. The possible arrangements for seven, eight, and nine pairs of electrons in a valency shell are discussed in detail. A method is suggested for predicting the arrangements of electron pairs in valency shells containing lone pairs which can occupy alternative non-equivalent positions. The effect of the interactions of electron pairs on bond lengths in certain molecules is discussed. The extension of the same principles to molecules containing transitional elements is briefly outlined.

It was shown recently by Gillespie and Nyholm (1) that the shapes of a wide range of molecules can be correctly predicted by means of the simple rule that the electron pairs, including both shared (i.e. bonding) pairs and unshared (i.e. lone) pairs, of the valency shell of a central atom of a polyatomic molecule adopt certain definite arrangements which depend only on their total number as shown in Table I.

TABLE I

Predicted arrangements of electron pairs in valency shells (1)

Number of electron pairs	Arrangement
2	Linear
3	Equilateral triangle
4	Tetrahedron
5	Trigonal bipyramid
6	Octahedron

These arrangements are a consequence of the mutual interactions of the valency shell electrons due to

(i) electrostatic repulsions, and to

(ii) the operation of the Pauli exclusion principle, as a consequence of which electrons of the same spin tend to keep as far apart as possible while electrons of opposite spin tend to be drawn together (2).

The interaction arising from the Pauli exclusion principle is in general more important than that arising from electrostatic repulsions and the arrangements of electron pairs given in Table I can be deduced from a consideration of this interaction alone ignoring electrostatic repulsions. It has been shown by several authors (2–10) that, by assigning the electrons to appropriate s, p, and d atomic orbitals, writing the complete antisym-

[1]*Manuscript received January 22, 1960.*
Contribution from the Department of Chemistry, McMaster University, Hamilton, Ontario.

metric wave function for these electrons, thereby taking account of the Pauli exclusion principle, and then calculating the most probable distribution of the electrons, the arrangements of electron pairs that are obtained are identical with those given in Table I. The same results can be obtained in a simple qualitative manner as follows. As a consequence of its kinetic energy, an electron will tend to occupy as much as possible of the space in which it is confined and as a consequence of the Pauli exclusion principle will tend to keep all other electrons having the same spin out of this space. Thus one electron in the central force field of a single nucleus will spread out to occupy a spherical region of space around the nucleus; it is said to occupy an *s* orbital. A second electron of opposite spin can also independently occupy the same region of space, i.e. the same orbital, but a second electron of the same spin will tend to keep as far as possible from the first electron and they will share the available spherical volume; each electron thus effectively occupies a hemispherical region on either side of the nucleus (digonal *sp* orbitals). The most probable distribution of these two electrons will be that in which the angle between the two electrons and the nucleus has a value of 180°. For a total of four electrons, two of one spin and two of opposite spin, the tendency of electrons of opposite spin to keep apart and for electrons of the same spin to come together causes the most probable arrangement of the electrons to be that in which there are two pairs making an angle of 180° with the nucleus, or in other words a pair of opposite spin in each of two equivalent digonal orbitals. Three electrons of the same spin or three pairs of opposite spin will each tend to occupy one-third of the available spherical space and their most probable distribution will be at the corners of an equilateral triangle making angles of 120° with the nucleus. We say that the electrons occupy a set of three equivalent trigonal sp^2 orbitals. For four electrons of the same spin or four pairs of opposite spin the most probable arrangement, i.e. that which maximizes their distance apart or gives them equivalent segments of the available spherical space, is the tetrahedral arrangement (8). Four electrons of the same spin or four pairs of opposite spin may be regarded as occupying four equivalent tetrahedrally directed segments of the available spherical volume, i.e. a set of four equivalent tetrahedral sp^3 orbitals. The same result may be obtained by constructing a set of equivalent hybrid orbitals from the available atomic orbitals. Because such hybrid orbitals are so constructed that they overlap only slightly, the electron distribution that would be obtained if these orbitals were independently occupied by electron pairs differs only slightly from that obtained from the complete antisymmetrical wave function and in particular the positions of maximum probability for the electron pairs coincides with the directions of the maxima of the hybrid orbitals (1, 3, 6, 11).

The most probable arrangements for five or more single electrons of the same spin or pairs of opposite spin is not, perhaps, immediately obvious. If these cases are treated by assigning the electrons to appropriate atomic orbitals and then calculating the most probable distribution of the electrons from the antisymmetrized wave function, a problem arises because of the non-equivalence of the various *d* orbitals that may be used. Some examples are given in Table II where it may be seen that different combinations of one *s* and three *p* orbitals with the various *d* orbitals give different most probable arrangements of electron pairs. It is therefore not possible to unambiguously predict by this method the shapes of molecules whose central atom has a valency shell containing five or more electron pairs. One can only find which shapes are possible, i.e. are compatible with the available atomic orbitals, but one cannot decide which of the possible shapes will be adopted in any particular case.

Can. J. Chem. Downloaded from www.nrcresearchpress.com by 186.148.149.217 on 09/04/12
For personal use only.

TABLE II

Most probable arrangements of electron pairs for various orbital combinations*

Number of electron pairs	Occupied orbitals	Arrangement	References
2	sp	Linear	1, 6
3	sp^2	Equilateral triangle	1, 6
4	sp^3	Tetrahedron	6, 7, 8
5	$sp^3d_{x^2-y^2}$	Square prism	10
	$sp^3d_{z^2}$	Trigonal bipyramid	10, 12
6	$sp^3d_{x^2-y^2}d_{z^2}$	Octahedron	10
	$sp^3d_{xz}d_{yz}$	Trigonal prism	10, 13
7	$sp^3d_{x^2-y^2}d_{z^2}d_{xy}$	Pentagonal bipyramid	14
	$sp^3d_{xy}d_{xz}d_{yz}$	†	15
8	$sp^3d_{x^2-y^2}d_{xy}d_{xz}d_{yz}$	Square antiprism	16
	$sp^3d_{z^2}d_{xy}d_{xz}d_{yz}$	Dodecahedron	10, 16
9	sp^3d^5	"Tripyramid"‡	15

*This table is not intended to be complete but only to illustrate some of the probable arrangements of electron pairs that correspond to the occupation of different combinations of atomic orbitals. It does not, for example, include any arrangements based on the partial use of two or more d orbitals, or any arrangement based on the use of d orbitals in preference to p orbitals.
†This polyhedron is obtained by adding one extra point over the center of one rectangular face of a trigonal prism.
‡This polyhedron is obtained by adding an extra point over the center of each of the rectangular faces of a trigonal prism.

Arrangements of Similar Particles on a Spherical Surface

One method of determining which of the possible arrangements of a given number of electron pairs is the most probable is to consider the possible arrangements of similar particles on the surface of a sphere under the action of some appropriate force law. If we assume that the electron pairs in a valency shell are all at the same average distance from the nucleus, which will in fact be the case for two, three, four, and six electron pairs bonding the central atom to a set of identical atoms and will almost certainly be a reasonably good approximation in other cases, then the problem of determining the most probable arrangement of these electron pairs is the same as that of determining the arrangement of a set of particles on the surface of a sphere under the action of an appropriate force law. Since the Pauli exclusion principle causes electrons of the same spin to avoid one another they behave as if there was a force between them. This force has been called a Pauli force or an exchange force (18). The magnitude of this force increases rapidly with the increasing overlap of the orbitals of two electrons with the same spin and therefore can be represented by an inverse function of some large power of the interelectron distance. The arrangement of particles on the surface of a sphere under such a force law is the same as that which is obtained by maximizing the least distance between any two particles (19) and this problem has been treated by Shutte and van der Waerden (20), who obtained the results given in Fig. 1. The arrangement of particles on the surface of a sphere under the action of an inverse square law of force, which would be appropriate if the arrangement of electrons were determined only by electrostatic forces, has been studied by Foppl (21), whose results are given in Table III. In all cases except that of seven particles the two force laws lead to the same arrangements and it seems reasonable to conclude that these will also therefore be the arrangements of these numbers of equivalent pairs of electrons in the valency shell of a central atom. The case of seven electron pairs is further discussed below. For any number of electron pairs up to six these are also the arrangements given by Gillespie and Nyholm (1) which, they point out, lead, without exception, to the correct prediction of the shapes of molecules

Can. J. Chem. Downloaded from www.nrcresearchpress.com by 186.148.149.217 on 09/04/12
For personal use only.

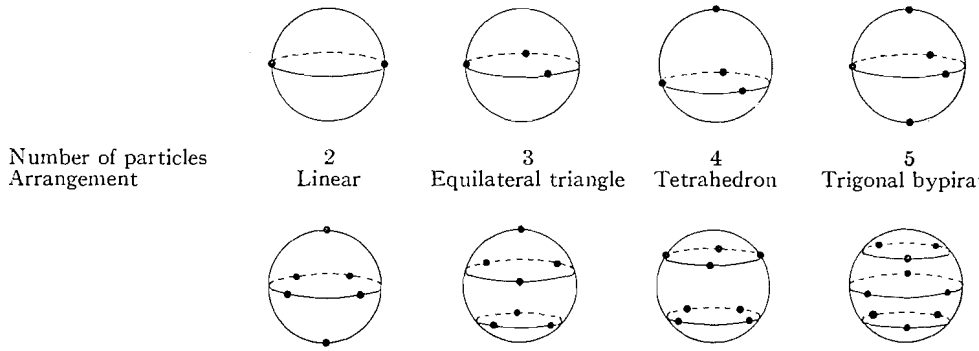


FIG. 1. Arrangements of similar particles on the surface of a sphere obtained by maximizing the least distance between any two particles.

TABLE III

Equilibrium arrangements of similar particles on the surface of a sphere under the action of an inverse square law of force

Number of particles	Arrangement
2	Linear
3	Equilateral triangle
4	Tetrahedron
5	Trigonal bipyramid
6	Octahedron
7	Pentagonal bipyramid
8	Square antiprism

containing only non-transitional elements even if not all the electron pairs are equivalent because they are forming bonds to different atoms or are lone pairs. Although Gillespie and Nyholm (1) discussed the shapes of some molecules involving seven, eight, and nine electron pairs in the valency shell of the central atom, they were not able to satisfactorily extend their rules to cover these cases which will therefore be discussed in more detail now.

Seven Electron Pairs

Figure 2 shows that for an interparticle force that is proportional to $1/r^n$, where n is large, the arrangement of seven particles is at the corners of an irregular octahedron

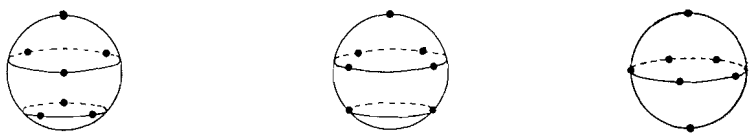


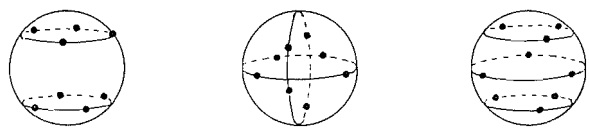
FIG. 2. Arrangements of seven particles on the surface of a sphere.

Can. J. Chem. Downloaded from www.nrcresearchpress.com by 186.148.149.217 on 09/04/12
For personal use only.

with an additional particle opposite the middle of one of its faces, i.e. a "1:3:3" arrangement (I), while for an inverse square law the equilibrium arrangement of seven particles is the pentagonal bipyramid, i.e. a "1:5:1" arrangement (III). It seems reasonable to suppose that as the exponent n is decreased the equilibrium arrangement will pass from I to III through the intermediate II, which is an irregular trigonal prism with an additional particle opposite one of its rectangular faces, i.e. a "1:4:2" arrangement. Iodine heptafluoride IF_7(22–25), the ions UF_7^{3-} and $UO_2F_5^{3-}$ (25), and probably ZrF_7^{3-} (26) have the pentagonal bipyramid structure III* while the ions TaF_7^{2-}, NbF_7^{2-}, and $NbOF_6^{2-}$ have the distorted trigonal prism structure II (25). In the A-modification oxides of the X_2O_3 of La, Ce, Pr, and Nd the metal atom is seven-co-ordinated and the oxygen atoms have the arrangement I (27). The antimony atom in the ion $SbBr_6^{2-}$ has a valency shell containing seven electron pairs, one of which is a lone pair. This ion has been reported to have an octahedral structure (25): if this is in fact a not quite regular octahedral structure it would indicate that the arrangement of the seven electron pairs is as in I with the lone pair at one pole, i.e. opposite one face of the distorted octahedron. Since lone pairs exert greater repulsions than bond pairs (1) the arrangement of seven electron pairs including one lone pair is likely to be that in which the lone pair has a minimum number of nearest neighbors and this is structure III. The three structures I, II, and III probably have rather similar energies, and which structure is adopted in any particular case presumably depends on factors such as the size of the central atom, the electronegativities of the ligands, and the non-equivalence of one or more of the electron pairs.

Eight Electron Pairs

For a valency shell containing eight equivalent electron pairs the predicted arrangement is the square antiprism IV and this is indeed the structure that has been found for TaF_8^{3-} (25) and for thorium acetylacetonate $Th(C_5H_7O_2)_4$ (28). The only other arrangement of eight bonds around a central atom that has been observed is the dodecahedral arrangement V (Fig. 3) found in the complex $Mo(CN)_8^{4-}$ ion of the transition metal



	(IV)	(V)	(VI)
Number of particles	8	8	9
Arrangement	Square antiprism	Dodecahedron $Mo(CN)_8^{4-}$	"Tripyramid"

FIG. 3. Arrangements of eight and nine particles on the surface of a sphere.

molybdenum. There are, however, actually nine electron pairs in the valency shell of the molybdenum atom in this ion, one of which is a lone pair. In transition metal complexes unshared pairs do not necessarily have such an important stereochemical effect as in compounds of non-transition elements (see below) and it is difficult to predict the effect of the single lone pair in this case although it may be said with certainty that if it does have any effect the arrangement of the eight bonds will not be the antiprism. The cube has been suggested (29) as a possible structure for eight-co-ordinated atoms but it is evident that for eight particles (e.g. electron pairs) that repel each other with a force that is proportional to any inverse power of their distance apart the cubic arrangement will always be less stable than the antiprism.

**It is possible that in the crystal the molecule of IF_7 has a slightly distorted pentagonal bipyramid structure (23, 24).*

Can. J. Chem. Downloaded from www.nrcresearchpress.com by 186.148.149.217 on 09/04/12
For personal use only.

Nine Electron Pairs

For nine electron pairs the predicted arrangement is the trigonal prism arrangement of six pairs with an additional electron pair opposite each rectangular faces, i.e. a "tripyramid" (Fig. 1), and this is indeed the arrangement of the nine bonds around a central atom found in a number of crystalline compounds such as UCl_3, $LaCl_3$, NH_4CdCl_3, $Nd(BrO_3)_39H_2O$, and $SrCl_26H_2O$ (26). Although the degree of covalent character of the bonds concerned here is uncertain it is interesting that they all do have the predicted arrangement and that this is in fact the only arrangement that has been observed for nine co-ordination.

We may summarize by saying that the predicted arrangements of two, three, four, five, and six electron pairs in a valency shell are as given in Table I. These are found experimentally for all molecules of non-transitional elements even when some of the electron pairs are not equivalent either because they bond different ligands or because one or more are lone pairs. The preferred arrangement for eight equivalent pairs is the antiprism. For nine equivalent pairs the most probable arrangement is the "tripyramid" (Fig. 1). For seven equivalent pairs the three different arrangements I, II, and III seem to be possible.

Valency Shells Containing Lone Pairs

In order to be able to decide between possible alternative locations of lone pairs in valency shells it is necessary to take account of the fact that repulsions exerted by lone pairs are greater than those exerted by bond pairs (1). The orbital associated with a bonding electron pair which is under the influence of two nuclei is smaller, or more localized, than the orbital of a lone pair which, being under the influence of only one nucleus, is able to spread out more and take up more of the available space than the bond pairs (9, 30). Thus bond pairs can approach more closely to each other than lone pairs before appreciable overlap of their orbitals occurs. This is equivalent to saying that bond pairs repel each other less than lone pairs. Alternatively one can say that lone pairs which are under the influence of a single nucleus will be at a slightly smaller average distance from the central nucleus than will the bond pairs which are also under the influence of the ligand nucleus, hence, if all the electron pairs had a symmetrical angular arrangement, the lone pairs would be closer together than the bond pairs and therefore they would repel each other more than the bond pairs. Hence bond pair – bond pair (b–b) repulsions are smaller than bond pair – lone pair (b–l) repulsions which are in turn smaller than lone pair – lone pair (l–l) repulsions. The reality of these differences in the repulsions between lone pairs and bond pairs is borne out by the bond angles in a series of molecules such as CH_4, NH_3, and H_2O. The introduction of one lone pair in NH_3 causes a decrease in the bond angle to 106.6° from the tetrahedral angle in CH_4 and the introduction of a second lone pair in H_2O causes a further reduction in the bond angle to 104.5° (25).

Since Pauli forces play the dominant role in the electron interactions that we have been considering and since these fall off rapidly with distance it seems reasonable to consider only the interactions between a given electron pair and its nearest neighbors in predicting the shapes of molecules with one or more lone pairs in the valency shell of a central atom. Thus in structures based on the trigonal bipyramid we need only consider interactions between electron pairs that make angles of 90° at the nucleus; interactions between electron pairs that make angles of 120° and 180° at the nucleus will be much smaller and can be ignored at least to a first approximation. Thus for ClF_3, BrF_3, and $C_6H_5ICl_2$, which each have three bonding pairs and two lone pairs in the valency shell of the central

Can. J. Chem. Downloaded from www.nrcresearchpress.com by 186.148.149.217 on 09/04/12
For personal use only.

atom and may be described as AX_3L_2 molecules where X stands for a ligand atom and L for a lone pair of electrons, the three structures VII, VIII, and IX (Fig. 4) are possible.

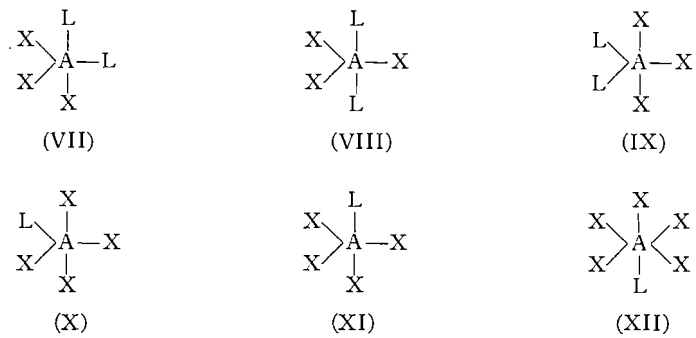


FIG. 4. Possible structures of AX_3L_2, AX_4L, and AX_5L molecules.

Considering only interactions of electron pairs making angles of 90° with the nucleus, VII has one l–l repulsion, three b–l repulsions, and two b–b repulsions, VIII has six b–l repulsions, while IX has four b–l and two b–b repulsions; thus IX will be more stable than either VII or VIII in agreement with the results of experimental determinations of the structures of these molecules (25, 31). For SeF_4, $TeCl_4$, $(CH_3.C_6H_4)_2SeCl_2$, and $(CH_3.C_6H_4)_2SeBr_2$, which may be described as AX_4L molecules, the structures X and XI (Fig. 4) are possible. In X there are two b–l and four b–b repulsions while in XI there are three b–l and three b–b repulsions; evidently X will be the more stable. This is consistent with the experimentally determined structures of these molecules (25). It is interesting to note that the bond angles in ClF_3 are only 87.5° (25), and in BrF_3 only 86.2° (31); this can be attributed to the strong repulsions exerted by the two equatorial lone pairs. Similar small bond angles of less than 90° have been found in BrF_5 (32) and this can be attributed to the strong repulsions exerted by a lone pair in an octahedral arrangement of six pairs (XII).

Bond Lengths

In the tetrahedral and octahedral arrangements of four and six electron pairs respectively, all the pairs have equivalent positions with respect to each other but in the trigonal bipyramidal arrangement of five electron pairs this is not the case; thus the pairs at the poles each have three nearest neighbors with which they make angles of 90° at the nucleus while the equatorial pairs have only two nearest neighbors at 90° and two more further away at 120°. Thus if all the electron pairs are at the same distance from the nucleus the repulsions between the polar electrons and those at the equator will be greater than the repulsions between the equatorial electrons. It may therefore be expected that the distances of the electron pairs from the nucleus will adjust themselves slightly so as to attempt to equalize these repulsions; this will lead to the polar electron pairs being at a slightly greater distance from the nucleus than the equatorial pairs and hence the axial bonds will be slightly longer than the equatorial bonds. The equatorial and axial bond lengths are respectively 2.04 Å and 2.19 Å in PCl_5, 2.31 Å and 2.43 Å in $SbCl_5$, 1.598 Å and 1.698 Å in ClF_3, and 1.721 Å and 1.810 Å in BrF_3 (25, 31). It is therefore not necessary to postulate that the bond to the equatorial fluorine atom has a double-bond character in order to account for the bond lengths in ClF_3 and BrF_3 (33). Similar effects can occur in octahedral arrangements of six electron pairs including one lone

Can. J. Chem. Downloaded from www.nrcresearchpress.com by 186.148.149.217 on 09/04/12
For personal use only.

pair which gives rise to square pyramidal molecules such as BrF_5 and IF_5 and ions such as SbF_5^{--} and $SbCl_5^{--}$ (XII). The four electron pairs at the base of the pyramid are not equivalent to the pair at the apex and as a consequence the corresponding bonds might be expected to differ in length. It seems difficult to predict which bonds would be the longest. The equatorial and axial bonds respectively have lengths of 1.68 Å and 1.79 Å in BrF_5 (30) and 2.02 Å and 2.08 Å in SbF_5^{--} (25), i.e. the equatorial bonds are shorter than the apical bond, but in $SbCl_5^{--}$ the reverse is the case (equatorial 2.62 Å, apical 2.36 Å) (25). The reason for this difference is not clear. Similarly in IF_7 the bond lengths would be expected to differ: experimentally it has been found that the equatorial bonds have a length of 1.83 Å while the axial bonds have a length of 1.94 Å although the accuracy of these values seems uncertain (23, 24).

Transitional Elements

In the preceding discussion it has been assumed that all the electron pairs occupy localized (i.e. hybrid) orbitals. This will necessarily be the case for bonding pairs but not for unshared or lone pairs of electrons. For the non-transitional elements for which all the valency electrons *s*, *p*, and *d* belong to the same quantum shell there appear to be no exceptions to the rule that the unshared pairs occupy localized orbitals and have an equally important effect in determining the stereochemistry of an atom as do the bonding pairs (1). However, for the transitional elements in which the valency electrons are in general associated with two quantum shells, electron interactions may lead to most probable configurations in which some or all of the non-bonding electrons occupy non-localized (i.e. atomic or "unhybridized") *d* orbitals and are at a somewhat smaller average distance from the nucleus than the bonding electrons. Such non-localized non-bonding electrons may have only a relatively small influence on the arrangement of the bonding electrons and therefore on the stereochemistry. Thus six-co-ordinated complex ions of the transitional metals are in general octahedral irrespective of whether or not they have additional unshared electrons in the valency shell (1). The six bonding pairs of electrons have the same octahedral arrangement that they would have if no non-bonding electrons were present and they may be conveniently described as occupying octahedral d^2sp^3 or sp^3d^2 equivalent hybrid orbitals. Up to six non-bonding electrons can occupy one or more of the set of equivalent $d_{xy}d_{xz}d_{yz}$ orbitals which each have four maxima between the directions of the octahedral orbitals and in which they have a somewhat smaller average distance from the nucleus than the bonding electrons. Electrons in these orbitals will have little or no effect on the octahedral arrangement of the six bonding pairs of electrons. Thus, for example, TiF_6^{3-}, VF_6^{3-}, $Cr(NH_3)_6^{3+}$, $Fe(CN)_6^{3-}$, and $Co(CN)_6^{3-}$ have one, two, three, five, and six non-bonding *d* electrons respectively and they all have regular octahedral structures. However, if there are more than six non-bonding *d* electrons these must go into the d_{z^2} and $d_{x^2-y^2}$ orbitals, which have their maxima along the octahedral directions of the bonding pairs, and they may therefore exert repulsions on these bonding pairs that are sufficient to distort the shape of the octahedron. The configurations d_{z^2}, $d_{z^2}^2$, and $d_{z^2}^2d_{x^2-y^2}$ may by virtue of the repulsions that they exert on the bonding pairs cause two trans bonds to be longer than the other four. If the repulsions are sufficiently strong they may cause two trans ligands to be lost completely leaving a square planar complex. Thus depending on the strength of the interaction between the bonding electron pairs and the non-bonding *d* electrons the structure of a six-co-ordinated transition metal complex molecule or ion may be an octahedron, or a distorted octahedron with two long bonds, and in some cases as a

Can. J. Chem. Downloaded from www.nrcresearchpress.com by 186.148.149.217 on 09/04/12
For personal use only.

result of strong repulsions two trans ligands may be lost giving a four-co-ordinated square planar complex. For example, the ions $Co(NH_3)_6^{3+}$ and $Ni(NH_3)_6^{3+}$ with seven and eight non-bonding d electrons respectively have regular octahedral structures but Pd(diarsine)$_2$ I_2 with eight non-bonding d electrons has a distorted octahedral structure with two unusually long Pd—I bonds (11). The complex compounds of Cu(II), which has nine non-bonding d electrons, are generally square planar, e.g. $Cu(H_2O)_4^{2+}$ and $Cu(NH_3)_4^{2+}$, but in the crystal these ions often attach two further ligands at longer distances to form irregular octahedral complexes (26). When there are 10 d electrons the d shell is complete and symmetrical and the arrangement of six bonding pairs will again be that of a regular octahedron.

Four pairs of electrons in the absence of any non-bonding electrons are arranged tetrahedrally. In a transitional metal complex up to four non-bonding d electrons can be accommodated in the d_{z^2} and $d_{x^2-y^2}$ orbitals, whose maxima lie between the direction of the tetrahedral orbitals occupied by the bonding pairs. Further d electrons must go into the $d_{xy}d_{yz}d_{xz}$ orbitals in which they may exert considerable repulsions on the bonding pairs and may cause the tetrahedral arrangement to be less stable than the square planar arrangement. Thus, for example, VCl_4 with one d electron and $FeCl_4^-$ with five d electrons are tetrahedral but $PtCl_4^-$ and $Cu(NH_3)_4^{2+}$ with eight and nine non-bonding d electrons respectively are square planar.

ACKNOWLEDGMENT

The author is indebted to Dr. J. Leech for helpful correspondence.

REFERENCES

1. R. J. Gillespie and R. S. Nyholm. Quart. Revs. **9**, 339 (1957).
2. P. G. Dickens and J. W. Linnett. Quart. Revs. **9**, 291 (1957).
3. Sir John Lennard-Jones. Proc. Roy. Soc. A, **198**, 14 (1949).
4. Sir John Lennard-Jones. J. Chem. Phys. **20**, 1024 (1952).
5. Sir John Lennard-Jones. Advance of Sci. **51**, 136 (1954).
6. Sir John Lennard-Jones and J. A. Pople. Proc. Roy. Soc. A, **202**, 166 (1950).
7. A. Brickstock and J. A. Pople. Phil. Mag. **43**, 581, 1090 (1953); **44**, 697, 705 (1954).
8. H. K. Zimmerman and P. Van Rysselberghe. J. Chem. Phys. **17**, 598 (1949).
9. J. W. Linnett and A. J. Poe. Trans. Faraday Soc. **47**, 1033 (1951).
10. J. W. Linnett and C. E. Mellish. Trans. Faraday Soc. **50**, 657 (1954).
11. R. J. Gillespie and R. S. Nyholm. Progress in stereochemistry. Academic Press, New York. 1958. p. 261.
12. G. H. Duffey. J. Chem. Phys. **17**, 196 (1949).
13. G. H. Duffey. J. Chem. Phys. **17**, 1328 (1949).
14. G. H. Duffey. J. Chem. Phys. **18**, 943 (1950).
15. G. H. Duffey. J. Chem. Phys. **19**, 553 (1951).
16. G. H. Duffey. J. Chem. Phys. **18**, 746 (1950).
17. G. H. Duffey. J. Chem. Phys. **18**, 1444 (1950).
18. W. Kauzmann. Quantum chemistry. Academic Press, New York. 1957. p. 319.
19. J. Leech. Math. Gazette, **41**, 81 (1957).
20. K. Shutte and B. L. van der Waerden. Math. Ann. **123**, 96 (1951). See also L. L. Whyte. American Math. Monthly, **59**, 606 (1952).
21. L. Foppl. J. reine angew. Math. **141**, 251 (1912).
22. R. D. Burbank and F. N. Bensey. J. Chem. Phys. **27**, 981 (1957).
23. J. Donohue. J. Chem. Phys. **30**, 1618 (1959).
24. R. D. Burbank. J. Chem. Phys. **30**, 1619 (1959).
25. Interatomic Distances. Chem. Soc. Special Publication. No. 11. 1958.
26. W. H. Zachariasen. Acta Cryst. **7**, 792 (1954).
27. A. F. Wells. Structural inorganic chemistry. Oxford University Press. 1950.
28. D. Grdenic and B. Matokovic. Nature, **182**, 465 (1958).
29. L. E. Marchi, W. C. Fernelius, and J. P. McReynolds. J. Am. Chem. Soc. **65**, 329 (1943).
30. A. W. Searcy. J. Chem. Phys. **31**, 1 (1959).
31. D. W. Magnusson. J. Chem. Phys. **27**, 223 (1957).
32. R. D. Burbank and F. N. Bensey. J. Chem. Phys. **27**, 982 (1957).
33. R. D. Burbank and F. N. Bensey. J. Chem. Phys. **21**, 642 (1953).

Can. J. Chem. Downloaded from www.nrcresearchpress.com by 186.148.149.217 on 09/04/12
For personal use only.

Can. J. Chem. Downloaded from www.nrcresearchpress.com by 186.148.149.217 on 09/04/12
For personal use only.

THE PYROLYSIS OF DIALLYL (1,5-HEXADIENE)[1]

D. J. Ruzicka and W. A. Bryce

ABSTRACT

The mechanism of decomposition of diallyl has been studied in a static system in the temperature range 460–520° C. The principal gaseous products (room temperature) were propylene, methane, ethylene, and 1-butene, and the liquid products were cyclopentene, cyclopentadiene, 1-hexene, and benzene. The over-all activation energy of decomposition was 31.3±1.0 kcal/mole for an A factor of 10^7 sec^{-1}. A mechanism of decomposition based on hydrogen abstraction by allyl and the addition of allyl to olefinic double bonds is proposed. Some decomposition by a non-radical mechanism may also occur.

INTRODUCTION

A recent study of the pyrolysis of 1-butene (1) has provided evidence that allyl radicals play an important part in the mechanism. The primary step in the decomposition is, almost certainly,

$$CH_3—CH_2—CH=CH_2 \rightarrow CH_3 + CH_2—CH=CH_2.$$

Propylene, one of the major decomposition products, is presumably formed by hydrogen abstraction by allyl from unreacted 1-butene. Bryce and Kebarle (1) postulated also that the formation of substantial amounts of various cyclic unsaturated hydrocarbons occurred through the addition of allyl to the double bond of 1-butene and propylene.

The amount of information in the literature on the reactivity of the allyl radical is very limited. The inhibiting power of propylene in certain hydrocarbon decompositions has been said to be due to the formation of allyl radicals by abstraction of hydrogen from propylene. The resonance-stabilized allyl radical has been assumed to be relatively unreactive and not capable of acting as a chain carrier (2). In a recent review of relative radical reactivities Semenov (3) calculates a value of −21.5 kcal/mole for the heat of reaction of the allyl radical in a series of reactions for which the reactivities of the vinyl, methyl, and benzyl radicals are +9.4, 0, and −17.4 kcal/mole respectively. The low reactivity of allyl is presumably a reflection of the electron delocalization that occurs on formation of the radical. The resonance or delocalization energy of allyl has been estimated by Coulson (4) to be 15.4 kcal/mole and by Bolland and Gee (5) to be 18.7 kcal/mole.

The formation of the allyl radical has been proposed (6) for the primary step in the pyrolysis of propylene studied with a flow system in the temperature range 680–870° C.

$$CH_2=CH—CH_3 \rightarrow CH_2=CH—CH_2 + H$$

The formation of allene as a major pyrolysis product led to the conclusion that allyl disappeared principally by the reaction

$$CH_2=CH—CH_2 \rightarrow CH_2=C=CH_2 + H.$$

No allene was detected, however, among the products in the pyrolysis of 1-butene in a static system at temperatures near 500° C (1).

Abstraction of hydrogen atoms by allyl has been proposed as a reaction in the pyrolysis of isobutene (7). McNesby and Gordon (8) have shown recently that very little abstraction by allyl occurs at 381° C in the pyrolysis of cyclopentane–acetone mixtures. Most of the

[1]*Manuscript received in original form July 3, 1959, and, as revised, March 3, 1960.*
Contribution from the Department of Chemistry, University of British Columbia, Vancouver 8, B.C. From a thesis presented by D. J. R. in partial fulfillment of the requirements for the degree of Master of Science.

allyl formed combines with methyl to form 1-butene. At 453° C 1-butene is still formed but hydrogen abstraction occurs from both cyclopentane and acetone. Allyl appears to abstract hydrogen extensively at temperatures above 500° C, a result supported by the conclusions of Bryce and Kebarle.

Lossing and his co-workers (9) found allyl to be the main radical product of the pyrolysis of 1,5-hexadiene (diallyl) in a flow reactor attached to a mass spectrometer for the temperature range 690–890° C. It seems reasonable to assume therefore that the pyrolysis of diallyl in a static system at lower temperatures should involve the production of allyl in the primary step

$$CH_2{=}CH{-}CH_2{-}CH_2{-}CH{=}CH_2 \rightarrow 2CH_2{=}CH{-}CH_2. \qquad [1]$$

The present study of the decomposition of diallyl was undertaken in the hope that it would reveal something of the properties of the allyl radical. This compound has also been used as a source of allyl in studying reactions between allyl and other hydrocarbons (10) with a view to gaining additional information about the mechanism of decomposition of olefins, and about the role of propylene as an inhibitor in hydrocarbon decompositions.

EXPERIMENTAL

The diallyl used was a standard sample (99.9% pure) obtained from the American Petroleum Institute, Pittsburgh. The pyrolyses were done in a quartz vessel of 300-ml capacity attached to a conventional static vacuum system. Rapid admission to the reaction vessel of the sample to be pyrolysed was achieved through the use of a calibrated pre-expansion volume. Samples for gas chromatographic analysis were obtained by expansion of the reaction products through a heated sampling line into evacuated pipettes equipped with metal–teflon taps. Standard gas chromatographic techniques were used for the qualitative and quantitative determination of the decomposition products. Individual compounds were identified, when necessary, by trapping them as they emerged from the column and introducing the sample into a mass spectrometer.

Decomposition Products

The principal products formed in the pyrolysis of 70 mm of diallyl at 521° C are shown in the chromatogram presented in Fig. 1. This separation was achieved on a 6-ft alumina column using the technique of increasing the column temperature progressively

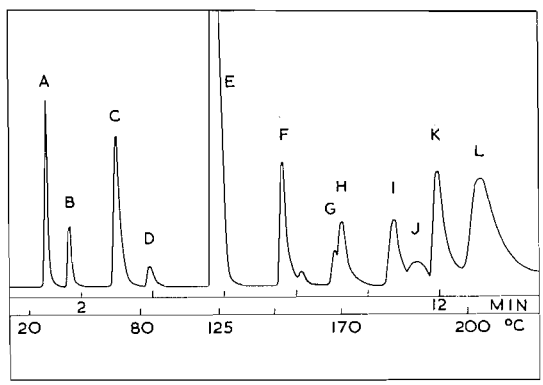


FIG. 1. Chromatogram showing principal products of decomposition of diallyl: A, methane; B, ethane; C, ethylene; D, propane; E, propylene; F, 1-butene; G, cyclopentene; H, cyclopentadiene; I, 1-hexene; J, cyclohexene plus methylcyclopentene; K, diallyl; L, benzene.

Can. J. Chem. Downloaded from www.nrcresearchpress.com by 186.148.149.217 on 09/04/12
For personal use only.

to speed up the elution of the less volatile sample constituents. The diallyl was approximately 90% decomposed in this particular analysis but essentially the same products were found in samples in which the decomposition was only approximately 5%. No definite evidence as to the extent of formation of C_6 cyclic products was obtained since at this low conversion the large peak of the undecomposed diallyl covered the region of the chromatogram presumably occupied by these compounds.

The sensitivity of the apparatus to the components of the reaction mixture was determined by calibration with a synthetic mixture of methane, ethane, propylene, 1-butene, cyclopentene, 1,5-hexadiene, and benzene in proportions corresponding approximately to those found in the reaction mixture under standard conditions. The sensitivities of compounds for which no internal standards were available were assumed to be equal to those of the available standards with the closest retention volumes under comparable conditions. Peak areas were taken as the measure of amount of compound.

Analytical Results

Analytical results for the products of pyrolysis of 70 mm of diallyl in the temperature range 460–521° C are given in Table I. The values shown are expressed as mole% of the

TABLE I

Products of 1,5-hexadiene pyrolysis at various temperatures

	Temp., ° C							
	460	470.5	480	490	501	506	510	521
Products	Concentrations expressed as mole%							
Hydrogen	1.0	2.0	3.3	4.5	6.3	6.5	7.0	7.8
Methane	1.4	1.5	2.6	4.6	4.1	6.3	5.4	7.7
Ethane	0.9	0.8	1.5	2.2	2.0	3.4	2.3	2.7
Ethylene	4.7	4.2	6.7	9.2	9.2	9.2	8.4	10.3
Propane	0.11	0.17	0.28	0.8	0.6	1.3	1.1	1.3
Propylene	18.2	16.6	26.8	35.3	35.6	36.7	31.0	35.3
1-Butene	3.2	2.9	4.4	5.7	5.3	5.3	4.5	5.1
Cyclopentene	1.7	1.3	1.3	2.3	0.9	0.8	0.85	1.0
Cyclopentadiene	3.2	2.6	4.5	5.4	3.9	3.1	2.6	2.5
1-Hexene	1.7	1.5	2.4	2.7	2.2	1.6	1.9	2.2
Cyclohexene and methylcyclopentene	1.4	1.4	1.6	2.1	0.7	1.0	0.6	0.7
1,5-Hexadiene	43.5	36.2	16.8	11.2	5.3	4.2	3.2	3.2
Benzene	2.4	2.9	4.6	7.7	6.4	8.7	6.9	8.8
Total mole%	75.4	74.1	76.8	93.7	82.5	89.1	75.8	88.6

NOTE: Reaction time, 5 minutes; P_{init} = 70 mm.

sample withdrawn. It can be seen that the analysis has accounted for an average of 85% of the volatile reaction products. The failure to achieve a complete mass balance may be a consequence of the irreversible adsorption on the chromatographic column of the reaction products with molecular weights greater than benzene. Furthermore, reliable sensitivities were known for only half the reaction products. It can be seen that higher recoveries of products were attained at higher temperatures. Polymerization reactions leading to less volatile products are thus apparently more important at lower temperatures. The supposition that such polymeric products are formed in the present system, in which the concentrations of large relatively stable radicals may be fairly high, is supported by the observation that in subsequent work the reactions of allyl with ethylene and propylene (10) identical analytical techniques were used and complete mass balances were obtained.

Can. J. Chem. Downloaded from www.nrcresearchpress.com by 186.148.149.217 on 09/04/12
For personal use only.

Kinetic Results

The decomposition was found to be first order for low conversions at a given temperature but the order rose to higher values as more extensive reaction occurred. An Arrhenius plot (Fig. 2) of first-order rate constants based on gas chromatographic analysis for diallyl

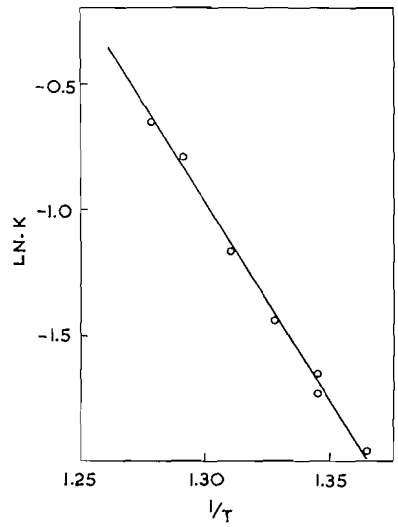


FIG. 2. Arrhenius plot for diallyl decomposition.

consumed gave a value of 31.3 ± 1.0 kcal/mole for the over-all activation energy. The corresponding A factor was 10^7 sec^{-1}.

The variation with time in the concentrations of the light hydrocarbon products for the pyrolysis of 70 mm of diallyl at 501° C is given in Fig. 3. The concentrations of the

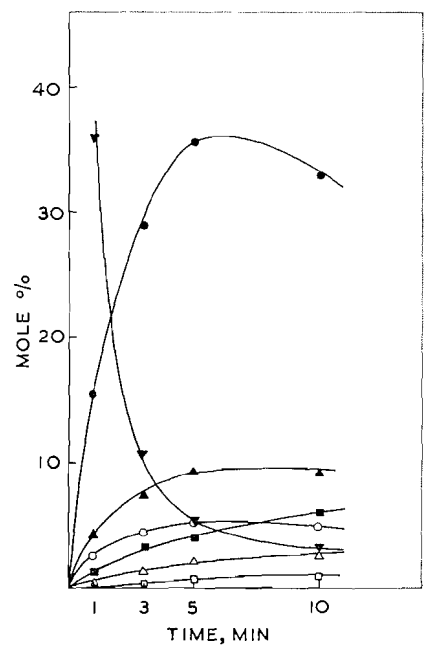


FIG. 3. Variation with time of light hydrocarbon products at 501° C: ●, propylene; ▲, ethylene; ■, methane; ○, 1-butene; ▼, 1,5-hexadiene; △, ethane; □, propane.

Can. J. Chem. Downloaded from www.nrcresearchpress.com by 186.148.149.217 on 09/04/12
For personal use only.

unsaturated products (propylene, ethylene, and 1-butene) level off as the hexadiene disappears from the system. The concentrations of the saturated products (methane, ethane, propane) show a progressive increase with time. The concentrations of the higher hydrocarbon products (Fig. 4), largely unsaturated cyclic compounds, go through maxima

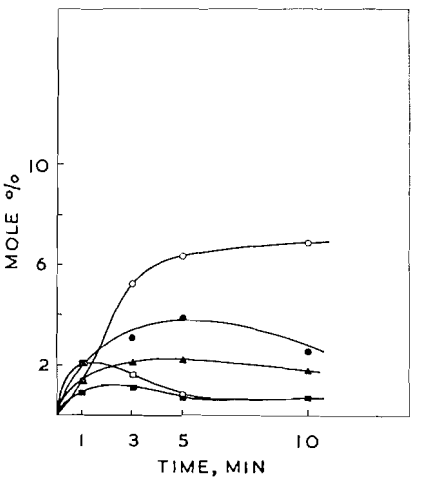


FIG. 4. Variation with time of cyclic products at 501° C. ○, benzene; ●, cyclopentadiene; ▲, 1-hexene; ■, cyclopentene; □, cyclohexene, methylcyclopentene.

as the reaction proceeds, with the exception of benzene. Results very similar to those shown in Fig. 4 are obtained if concentration is plotted against temperature for constant reaction time, i.e. the relative concentrations of saturated hydrocarbons and hydrogen increase with temperature while the concentrations of unsaturated hydrocarbons, excepting benzene, go through maxima.

DISCUSSION

The change from first to higher orders with extent of reaction indicates the increasing complexity of the mechanism as secondary reactions become important. The value of 31.3 ± 1.0 kcal/mole obtained for the over-all activation energy is significantly less than the estimate of 42 kcal/mole which has been made for the dissociation energy of the allyl–allyl bond (6). The apparent activation energy for a reaction involving chain propagation is given (11) by the expression

$$E_A = E_P + (1/w)(E_i - E_t)$$

where E_p, E_i, and E_t are the activation energies for propagation, initiation, and termination respectively, and w is the order of the chain-terminating step. Hence the apparent activation energy, E_A, may well be smaller than E_i either because of a non-zero value for E_t or because of a second-order chain-breaking process. The activation energy for recombination of two allyl radicals or for the disappearance of allyl by some other radical capture process may be greater than zero. Unfortunately no data are available from which this energy, nor E_p, the activation energy for propagation by allyl, can be calculated with any certainty.

Mechanism of the Reaction

The wide variety of products produced in the pyrolysis of diallyl suggest very strongly the operation of a complex free radical mechanism. The observation (9) that at a high

Can. J. Chem. Downloaded from www.nrcresearchpress.com by 186.148.149.217 on 09/04/12
For personal use only.

temperature (690–890° C) the molecule decomposes in the primary step by splitting the central bond provides evidence that initiation of the reaction at the temperatures used in the present study occurs in the same way. No evidence has been obtained in the present study as to whether this initiation is homogeneous or heterogeneous. It has also been shown (10) that diallyl present in 5 mole% concentration can serve to initiate the decomposition of hydrocarbons such as 1-butene, propylene, ethylene, and *n*-butane, and that the rate of initiation is linearly related to the square root of the diallyl concentration. Such a dependence is consistent with a primary dissociation of diallyl into two radicals, each capable of initiating further decomposition of the substrate molecules. The present results will therefore be interpreted principally in terms of a free radical mechanism, although the possibility exists that a significant portion of the decomposition occurs by a molecular, non-radical, mechanism. Such a mechanism could account for the occurrence of appreciable amounts of ethylene in the decomposition products

$$CH_2{=}CH{-}CH_2{-}CH_2{-}CH{=}CH_2 \rightarrow CH_2{=}CH_2 + CH_2{=}CH{-}CH{=}CH_2.$$

The butadiene that would be formed simultaneously in a molecular decomposition of this type was not found in the gas chromatographic analysis. Its concentration could have been kept low, however, by rapid reaction with various radicals formed in the system.

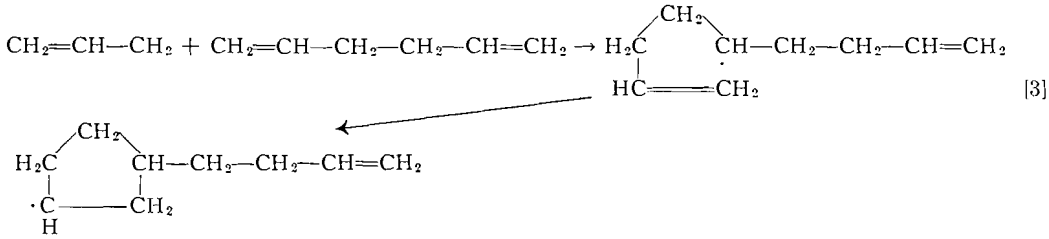
Reactions of the Allyl Radical

The allyl radical produced in the primary decomposition would be expected to be relatively stable at low temperatures because of its high delocalization energy. The observation that propylene is a major pyrolysis product of both 1-butene and diallyl at temperatures around 500° C provides direct evidence that hydrogen abstraction by allyl occurs readily under these conditions, an observation which confirms the work of other investigators. The most probable reaction would be

$$CH_2{=}CH{-}CH_2 + CH_2{=}CH{-}CH_2{-}CH_2{-}CH{=}CH_2 \rightarrow CH_2{=}CH{-}CH_3 + CH_2{=}CH{-}CH{-}CH_2{-}CH{=}CH_2. \quad [2]$$

Hydrogen abstraction by allyl from products formed in the decomposition of the hexadienyl radical would occur in later stages of the reaction as the concentrations of these products became appreciable. The observation that the concentrations of a number of these products go through maxima with both time and temperature suggest that they undergo secondary reactions with radicals such as allyl.

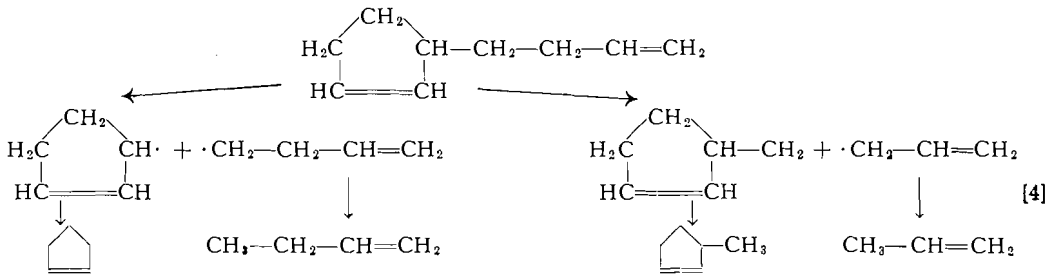
The formation of cyclopentene, cyclopentadiene, and methylcyclopentene can best be explained on the basis of the addition of allyl to the double bonds of the parent molecule followed by intramolecular addition:



[3]

The product radical would most probably split off its side group and undergo an H-atom shift to form cyclopentene. It could undergo a further hydrogen abstraction from the ring to produce a 1-butenyl-substituted cyclopentene which could react in a variety of ways to produce some of the observed reaction products:

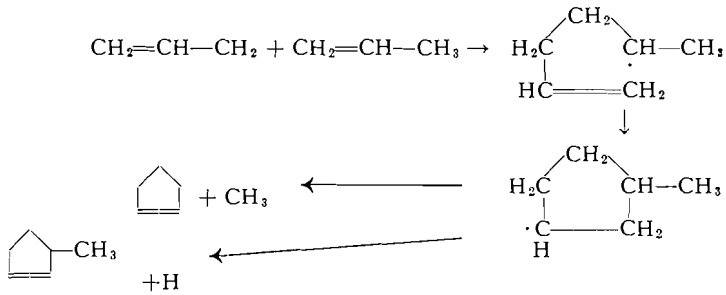
Can. J. Chem. Downloaded from www.nrcresearchpress.com by 186.148.149.217 on 09/04/12
For personal use only.



[4]

The radical formed by the addition to the non-terminal carbon of the double bond would either be identical with that produced in reaction [3], or would lead to the formation of a substituted six-membered ring, depending on the mode of ring closure.

Addition of allyl to the double bond of propylene, the major decomposition product, could proceed as follows:



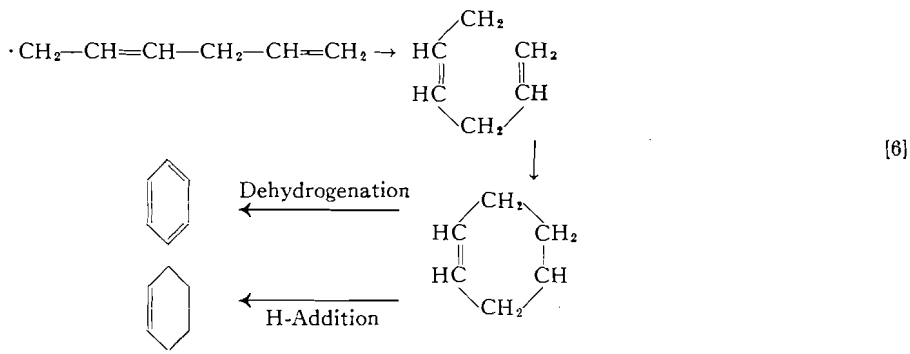
[5]

Cyclopentadiene is assumed to be formed by further dehydrogenation of the cyclopentene formed in reactions [4] and [5].

The occurrence of ethylene as a substantial product cannot involve the pyrolyses of the allyl radical to vinyl and methylene because of the high endothermicity (120–130 kcal) of this reaction. Its formation may occur as a result of a molecular decomposition of diallyl as has been mentioned earlier.

The Fate of the 1,5-Hexadienyl Radical

The concentration of the hexadienyl radical in the early stages of the reaction is presumably fairly high because of its formation by hydrogen abstraction. It can be considered to disappear from the system by rearrangement to the alternate canonical form followed by intramolecular addition:



[6]

Can. J. Chem. Downloaded from www.nrcresearchpress.com by 186.148.149.217 on 09/04/12
For personal use only.

The failure to observe cyclohexadiene as an intermediate in the dehydrogenation process may be a consequence of the high degree of resonance stabilization which the radical formed by hydrogen abstraction from the diene would have. The conversion of cyclohexadiene to benzene would, of course, be favored because of the over-all enthalpy decrease accompanying the reaction.

Decomposition of the radical with the formation of allyl and allene may occur. The failure to observe allene among the pyrolysis products of diallyl may be because of the slowness of the pyrolysis of the stabilized radical or because of the high reactivity which allene would exhibit towards all radicals present in the system. The 1,5-hexadienyl radicals would also be expected to disappear by combination with other radicals producing compounds adsorbed irreversibly on the gas chromatographic column. Since the steady-state concentration of this radical is presumably quite high the amounts of such addition products may have been appreciable. These compounds may be responsible for the failure to achieve a complete mass balance in the gas chromatographic analysis.

Other Radical Reactions

In the above discussion mechanisms for the formation of the following reaction products were suggested: propylene, ethylene, 1-butene, cyclopentene, cyclopentadiene, cyclohexene, methylcyclopentene, benzene. The formation of the remaining reaction products is assumed to proceed largely by the following reactions:

Methane: $CH_3 + RH \rightarrow CH_4 + R$

Ethane: $CH_3 + CH_3 \rightarrow C_2H_6$

$CH_2{=}CH_2 + H \rightarrow C_2H_5$

$C_2H_5 + RH \rightarrow C_2H_6 + R$

Propane: $CH_2{=}CH{-}CH_3 + H \rightarrow CH_2{-}CH_2{-}CH_3$

$CH_2{-}CH_2{-}CH_3 + RH \rightarrow C_3H_8 + R$

1-Hexene: $CH_2{=}CH{-}CH_2{-}CH_2{-}CH{=}CH_2 + H \rightarrow C_6H_{11}$

$C_6H_{11} + RH \rightarrow C_6H_{12} + R$

Hydrogen: $H + RH \rightarrow H_2 + R$

The activation energies of all these reactions are sufficiently low to permit them to occur rapidly at the temperatures used in the present work.

ACKNOWLEDGMENTS

We are indebted to Dr. S. A. Ryce for advice in connection with the gas chromatographic analysis and to Mr. E. C. W. Clarke for the mass spectrometric identification. This investigation was supported by the Defence Research Board (DRB44-50-01-10), to whom we express our thanks. One of us (D. J. R.) is indebted to the B. C. Sugar Refining Company for a scholarship.

REFERENCES

1. W. A. Bryce and P. Kebarle. Trans. Faraday Soc. **54**, 1660 (1958).
2. E. W. R. Steacie. Atomic and free radical reactions. Reinhold Publishing Corp., New York. 1954. p. 125.
3. N. N. Semenov. Some problems of chemical kinetics and reactivity. Vol. I. Pergamon Press, London. 1958. p. 37.
4. C. A. Coulson. Proc. Roy. Soc. A, **164**, 383 (1938).
5. J. L. Bolland and G. Gee. Trans. Faraday Soc. **42**, 244 (1946).
6. M. Szwarc. J. Chem. Phys. **17**, 284 (1949).
7. M. J. Molera and J. F. Stubbs. J. Chem. Soc. 381 (1952).
8. J. R. McNesby and A. S. Gordon. J. Am. Chem. Soc. **79**, 4593 (1957).
9. F. P. Lossing, K. U. Ingold, and I. H. S. Henderson. J. Chem. Phys. **22**, 621 (1954).
10. W. A. Bryce and D. J. Ruzicka. This issue.
11. A. A. Frost and R. G. Pearson. Kinetics and mechanism. John Wiley & Sons, Inc., New York. 1953. p. 232.

Can. J. Chem. Downloaded from www.nrcresearchpress.com by 186.148.149.217 on 09/04/12
For personal use only.

Can. J. Chem. Downloaded from www.nrcresearchpress.com by 186.148.149.217 on 09/04/12
For personal use only.

REACTIONS OF ALLYL RADICALS WITH OLEFINS[1]

W. A. Bryce and D. J. Ruzicka

ABSTRACT

A study has been made of the mechanisms of the reactions of allyl radicals, produced thermally from diallyl, with various hydrocarbons in the temperature range 460–506° C. The allyl radical is capable of abstracting hydrogen from certain hydrocarbons and of adding to olefinic double bonds at these temperatures. The rates of formation of the principal products in the reactions between allyl and 1-butene, propylene, and ethylene are linearly related to the square root of the diallyl concentration. Mechanisms are proposed to account for the reaction products formed. In addition to reacting readily with olefins the allyl radical is observed to sensitize the decomposition of *n*-butane at 506° C. The implications of the present results with respect to inhibition in pyrolysis of hydrocarbons are discussed briefly.

INTRODUCTION

The information available in the literature on the reactivity of the allyl radical has been reviewed briefly in an earlier paper (1). The formation of allyl has been proposed as the primary step in the pyrolysis of diallyl (1), propylene (2), allyl bromide (3, 4), isobutene (5), and 1-butene (6). The action of propylene as an inhibitor for certain organic decompositions has been commonly ascribed to the formation of allyl by hydrogen abstraction from the propylene by active radicals like methyl and ethyl. It has been fairly generally assumed that in the temperature range in which pyrolyses in static systems normally occur the allyl radical has sufficient resonance stabilization to render it incapable of propagating reaction chains (7, p. 126). The resonance stabilization energy has been estimated by Coulson (8) to be 15.4 kcal/mole and by Bolland and Gee (9) to be 18.7 kcal/mole. Semenov (10) ascribes to the allyl radical a reactivity less than that of benzyl and a delocalization energy of 23 kcal/mole.

The formation of allyl has been observed directly in the pyrolysis of allyl iodide and of diallyl using a mass spectrometer with a flow system at temperatures between 690 and 890° C (11). The mechanism of decomposition of this latter compound in a static system at temperatures between 460 and 520° C can best be understood (1) on the assumption that the primary step involves a split into two allyl radicals which can subsequently abstract hydrogen to form propylene or add to olefinic double bonds to form the cyclic unsaturated products which are formed in substantial amounts. The conclusion that allyl abstracts hydrogen readily under these conditions is in agreement with recent results of McNesby and Gordon (12).

The present study was undertaken to demonstrate more clearly the nature of allyl reactivity and to gain further insight into the mechanism of its reaction with unsaturated hydrocarbons. Reactions with 1-butene were of particular interest because of work done previously in this laboratory on the pyrolysis of this compound (6), the results of which provided strong evidence for reactions between it and the allyl radical.

EXPERIMENTAL

The substance used as a thermal source of allyl radicals was diallyl (1,5-hexadiene) obtained from the American Petroleum Institute, Pittsburgh (99.9 mole% pure). Other hydrocarbons used were all Research Grade (Philips Petroleum Co., Bartlesville, Okla.).

The experimental techniques used were similar to those described earlier (1). Diallyl

[1]*Manuscript received in original form July 3, 1959, and, as revised, March 3, 1960.*
Contribution from the Department of Chemistry, University of British Columbia, Vancouver 8, B.C. From a thesis presented by D. J. R. in partial fulfillment of the requirements for the degree of Master of Science.

and the substrate hydrocarbon were premixed and then admitted rapidly to the reaction vessel. Extensive decomposition of diallyl occurred in nearly all cases at temperatures well below those at which decomposition of the substrate hydrocarbon normally occurred. Analyses were done by gas chromatography supplemented by mass spectrometry where necessary.

RESULTS AND DISCUSSION

The Decomposition of 1-Butene – Diallyl Mixtures

The pyrolysis of 1-butene by itself and of 1-butene containing 5% by volume of diallyl was studied at 506° C with a total pressure of 200 mm Hg. The variation in pressure with time (Fig. 1) provides a measure of the effect of diallyl on the rate of decomposition

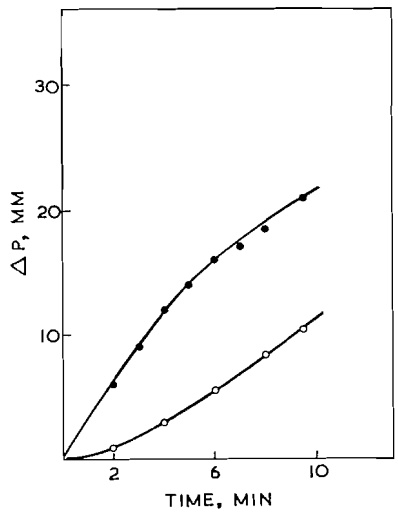


FIG. 1. Pressure–time curves showing effect of 5% diallyl on the rate of decomposition of 1-butene. Open circles, butene alone.

of 1-butene. A value of 6.5 was obtained for the relative rates of pyrolysis of 1-butene with and without diallyl for a reaction time of 1 minute.

The dissociation of diallyl, R_2, would yield allyl radicals, R, which could undergo reaction with the substrate olefin, M, leading to the formation of the products observed. If termination of the chains occurs by bimolecular radical recombination processes of the types

$$2R \rightarrow R_2$$

$$RM. + R \rightarrow RMR$$

and if the rate constant for the decomposition of diallyl is very much less than the propagation and termination rate constants, the rate of the over-all reaction will be given by

$$-d[M]/dt = k[R_2]^{\frac{1}{2}}[M].$$

The concentration of products resulting from the reaction between allyl and olefin ought therefore to be linearly related to the square root of the diallyl concentration for a constant reaction time.

The effect of varying the initial diallyl concentration on the rates of formation of

Can. J. Chem. Downloaded from www.nrcresearchpress.com by 186.148.149.217 on 09/04/12
For personal use only.

reaction products was studied with diallyl concentrations ranging from 0 to 11.4% for a total pressure of 200 mm Hg. The reaction time was 5 minutes at 506° C. Earlier experiments (1) had shown that decomposition of the diallyl under these conditions would be 95% complete. The concentrations of the principal decomposition products of 1-butene are plotted against the square root of the diallyl concentration in Fig. 2. An approximately

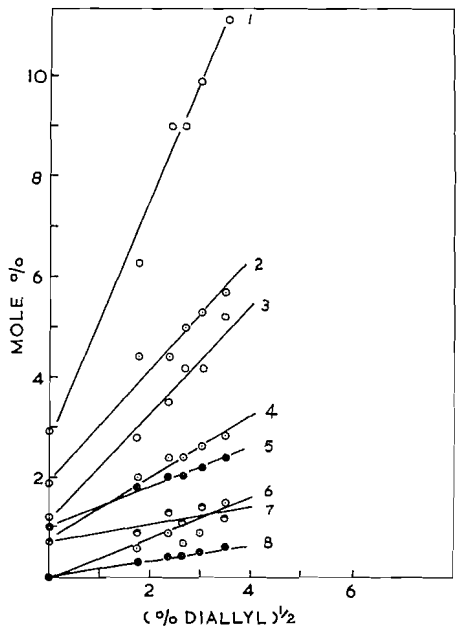


FIG. 2. Concentrations of principal decomposition products of 1-butene versus square root of diallyl concentration; 1, propylene; 2, methane; 3, ethylene; 4, ethane; 5, cyclopentadiene; 6, benzene; 7, cyclopentene; 8, cyclohexene plus methylcyclohexene.

linear dependence is obtained for each product. The decomposition of 1-butene by itself at this temperature could contribute to each product an amount given by the ordinate at zero diallyl concentration. A significant amount of the increased yield of propylene with increasing diallyl concentration would result of course from the increase in diallyl itself. However, it is not possible to account for the increase in propylene by assuming that the diallyl and 1-butene decompose independently, i.e. the increase in propylene is very much greater than can be accounted for by the diallyl present. The possible contribution of diallyl to the concentrations of all other products is at most a few per cent of the amount of diallyl present and hence can be neglected. The three compounds whose concentrations are most affected by increasing the diallyl concentration (propylene, methane, and ethylene) are the chief products formed in the decomposition of 1-butene.

The allyl radical can react with 1-butene in two ways: by abstraction of hydrogen to form propylene and the butenyl radical, or by addition to the double bond. The reaction sequences proposed for these two processes are given below.

Hydrogen Abstraction

$$CH_2{=}CH{-}CH_2\cdot + CH_2{=}CH{-}CH_2{-}CH_3 \rightarrow CH_2{=}CH{-}CH_3 + CH_2{=}CH{-}\dot{C}H{-}CH_3$$

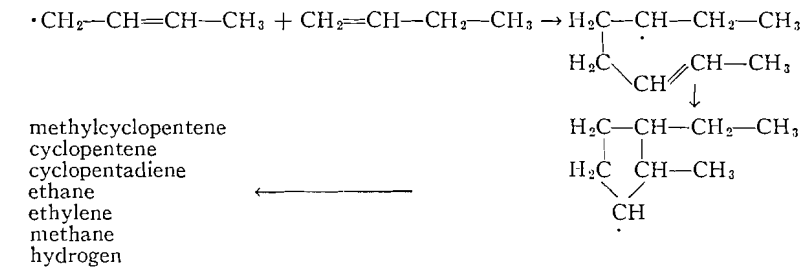
Kinetic evidence (6) favors the abstraction of the allylic hydrogen from 1-butene but

Can. J. Chem. Downloaded from www.nrcresearchpress.com by 186.148.149.217 on 09/04/12
For personal use only.

the butenyl radical thus formed can be represented as existing in two alternative canonical forms,

$$CH_2{=}CH{-}\dot{C}H{-}CH_3 \leftrightarrow \cdot CH_2{-}CH{=}CH{-}CH_3.$$

The extensive isomerization of 1-butene to 2-butene that occurs in the temperature range 450–520° C if methyl radicals are added to 1-butene (13) provides convincing evidence that the butenyl radical can be considered to react in the 2-butenyl form to a substantial degree. This radical may be removed by hydrogen abstraction or by addition to the double bond of 1-butene followed by intramolecular addition to form various cyclic unsaturated products:



An H-atom shift is required for the formation of cyclopentene in the dissociation of the cyclic radical shown.

The formation of both methane and ethylene is markedly increased by the addition of allyl radicals to the system. The increase is considerably greater than that for the cyclic compounds and hence ethylene and methane cannot be assumed to be formed primarily from the cyclization reaction given above although the ethyl and methyl radicals eliminated in the formation of the cyclic compounds could lead to ethane, ethylene, and methane as follows:

$$C_2H_5 \rightarrow C_2H_4 + H,$$
$$C_2H_5 + C_2H_5 \rightarrow C_2H_4 + C_2H_6,$$
$$CH_3 + RH \rightarrow CH_4 + R.$$

The increased formation of ethylene and methane must be a consequence of pyrolysis of higher radicals. Their formation as a result of the decomposition of the butenyl radical,

$$CH_2{=}CH{-}\dot{C}H{-}CH_3 \rightarrow CH_2{=}CH{-}\dot{C}H\cdot + CH_3,$$
$$CH_2{=}CH{-}\dot{C}H{-}CH_3 \rightarrow CH_2{=}\dot{C}H + CH_2{=}CH_2,$$

seems improbable because of the relatively high endothermicities of these reactions. Butenyl might be expected to stabilize itself under the present conditions by hydrogen loss,

$$CH_2{=}CH{-}CH{-}CH_3 \rightarrow CH_2{=}CH{-}CH{=}CH_2 + H,$$

or by disproportionation with allyl,

$$CH_2{=}CH{-}CH_2 + CH_2{=}CH{-}CH{-}CH_3 \rightarrow CH_2{=}CH{-}CH_3 + CH_2{=}CH{-}CH{=}CH_2.$$

Butadiene was not observed in the reaction products although the gas chromatographic column used may have retained it because of its high degree of unsaturation. Similarly any allene formed by allyl decomposition,

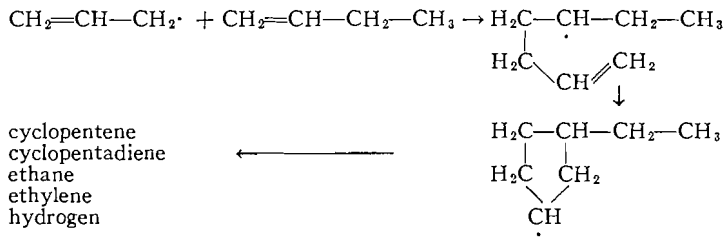
$$CH_2{=}CH{-}CH_2 \rightarrow CH_2{=}C{=}CH_2 + H,$$

Can. J. Chem. Downloaded from www.nrcresearchpress.com by 186.148.149.217 on 09/04/12
For personal use only.

would also tend to be retained in the chromatographic column. Furthermore both compounds would most probably disappear from the system rapidly through reaction with the variety of radicals present. It is not possible to decide, therefore, whether or not such reactions are important in the present study.

Addition to the Double Bond

The mechanism proposed for this reaction is similar to that suggested for the decomposition of diallyl (1):



Ethane and ethylene could be formed from the elimination of the ethyl group and hydrogen from the conversion of the cyclopentene to cyclopentadiene. The results for the pyrolysis of 1-butene (6) provide evidence that such radical elimination reactions are an effective method of dehydrogenation of the cyclic addition products.

The Decomposition of Ethylene–Diallyl Mixtures

A series of experiments was done in which diallyl in proportions ranging from 0 to 10.1% by volume was mixed with ethylene and decomposed for 5 minutes at a temperature of 506° C. The total initial pressure in each case was again 200 mm Hg. No reaction of the ethylene occurred in the absence of diallyl but reaction was observed to occur when diallyl was present. The pressure change in the system was negative indicating that products of molecular weight greater than ethylene were being formed. The analytical results, given in Table I, show that a satisfactory mass balance was obtained in all cases.

TABLE I

Analytical results for pyrolysis of ethylene–diallyl mixtures for 5 minutes at 506° C

	Mole % diallyl				
	2.9	5.2	6.7	8.9	10.1
Product	Mole %				
Hydrogen	0.22	0.35	0.47	0.65	0.71
Methane	0.06	0.35	0.50	0.47	0.67
Ethane	0.51	1.1	1.3	1.4	1.6
Ethylene	92	93	89	88	86.5
Propylene	2.2	2.8	3.7	4.4	4.6
1-Butene	0.40	0.65	1.0	1.1	1.1
Cyclopentene + 1,4-pentadiene	1.8	2.7	3.8	4.3	4.7
Diallyl	0	0.06	0.07	0.31	0.40
Total	97.2	100.0	99.8	100.6	100.3

Propylene is again a major product, formed by the hydrogen abstraction reactions of allyl. The variation of the amount of propylene with the square root of the diallyl concentration is linear (Fig. 3). The abstraction of hydrogen by allyl from ethylene

Can. J. Chem. Downloaded from www.nrcresearchpress.com by 186.148.149.217 on 09/04/12
For personal use only.

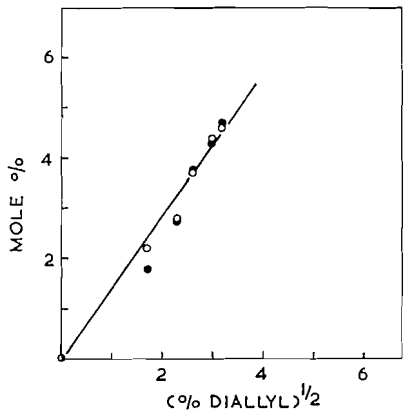


FIG. 3. Variation of propylene (open circles) and of cyclopentene plus 1,4-pentadiene with diallyl concentration in the reaction with ethylene.

would be endothermic by some 30 kcal and therefore seems unlikely. The most probable reaction between allyl and ethylene is addition to form the pentenyl radical

$$CH_2{=}CH{-}CH_2 + CH_2{=}CH_2 \rightarrow H_2C(\cdot){-}CH_2{-}CH_2{-}CH{=}CH_2, \qquad [1]$$

which could undergo intramolecular addition to form the cyclopentyl radical

$$H_2C(\cdot){-}CH_2{-}CH_2{-}CH{=}CH_2 \rightarrow H_2C(\cdot){-}CH_2{-}CH_2{-}CH{-}CH_2 \qquad [2]$$

In view of the high allyl concentration the following reactions are probable:

$$CH_2{=}CH{-}CH_2 + H_2C(\cdot){-}CH_2{-}CH_2{-}CH{=}CH_2 \rightarrow HC{\equiv}CH_2{-}CH_2{-}CH{=}CH_2 + CH_2{=}CH{-}CH_3 \qquad [3]$$

$$CH_2{=}CH{-}CH_2 + H_2C(\cdot){-}CH_2{-}CH_2{-}CH{=}CH_2 \rightarrow CH_2{=}CH{-}CH_3 + H_2C{-}CH_2{-}CH{-}CH \qquad [4]$$

Cyclopentene and 1,4-pentadiene are formed as significant products of the reaction between allyl and ethylene. Cyclopentene is formed in only trace amounts in the decomposition of diallyl and 1,4-pentadiene is not formed at all (1). They thus provide a direct measure of the extent of the allyl–ethylene reaction. They were not separated from each other in the analyses given in Table I but their identification was achieved by mass spectrometry.

The results presented in Fig. 3 show that the rate of formation of 1,4-pentadiene plus cyclopentene is numerically equal to the rate formation of propylene, an observation which is explained by reactions [3] and [4] above. A quantitative separation was achieved in the analysis of the reaction mixture for a single experiment, using a squalane–pelletex column at 0° C. The initial diallyl concentration in this experiment was 6.7%. The analytical result obtained gave the ratio

$$\text{1,4-pentadiene/cyclopentene} = 11/20.$$

Can. J. Chem. Downloaded from www.nrcresearchpress.com by 186.148.149.217 on 09/04/12
For personal use only.

This ratio is presumably a measure of the relative rates of reactions [3] and [4].

Other reactions which presumably occur in this system include

$$\cdot CH_2{-}CH{=}CH_2 + CH_3 \rightarrow CH_3{-}CH_2{-}CH{=}CH_2,$$
$$CH_2{=}CH{-}CH_2{-}CH_3 \rightarrow CH_2{=}CH{-}CH_2\cdot + CH_3,$$
$$CH_3 + RH \rightarrow CH_4 + R,$$
$$CH_3 + CH_3 \rightarrow CH_3CH_3,$$
$$H + RH \rightarrow H_2 + R.$$

The Decomposition of a Propylene–Diallyl Mixture

Propylene containing 5.3% diallyl was decomposed for 5 minutes at 506° C and an initial total pressure of 200 mm Hg. At this temperature propylene by itself is quite stable. A slight pressure increase occurred. The composition of the reaction mixture is given in Table II.

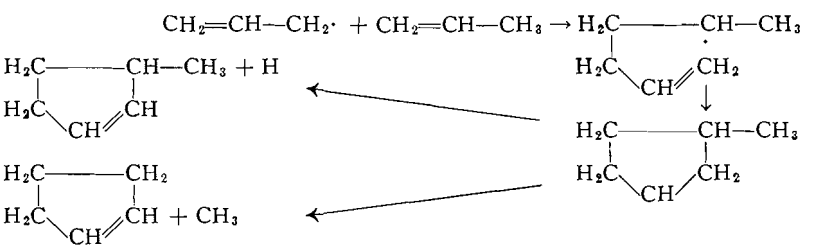
TABLE II

Analytical results for pyrolysis of 5.3% diallyl in propylene for 5 minutes at 506° C

Hydrogen	0.37 mole%
Methane	1.17
Ethane	0.16
Ethylene	2.29
Propane	0.73
Propylene	92.0
1-Butene	1.11
Cyclopentene	0.94
1-Hexene	0.94
Methylcyclopentene	0.28
Diallyl	0.50
Total	100.2

The range of products formed is very similar to that obtained in the pyrolysis of diallyl itself but the amounts formed in nearly all cases are very much greater than can be accounted for by decomposition of the diallyl only. For example the pyrolysis of diallyl at 506° C yields 9.2% ethylene (1). Hence the maximum possible contribution of diallyl to the ethylene yield given in Table II, assuming an independent decomposition, would be 0.5%. Thus most, if not all, of the ethylene formed in the diallyl–propylene system is produced by the decomposition of propylene initiated by the added allyl radicals.

The only primary reaction of allyl with propylene that is of interest is addition to the double bond; the hydrogen abstraction reaction is trivial. The mechanism proposed for the addition reaction is as follows:



Can. J. Chem. Downloaded from www.nrcresearchpress.com by 186.148.149.217 on 09/04/12
For personal use only.

The only two cyclic products are thus accounted for by two alternative modes of reaction of the addition product. The analytical results indicate that the decomposition to cyclopentene and the methyl radical has approximately the same probability as the dehydrogenation to methylcyclopentene. Two isomeric methylcyclopentenes appear to be formed.

The 1-butene may be formed by the combination of allyl and methyl

$$CH_2{=}CH{-}CH_2\cdot + CH_3 \rightarrow CH_2{=}CH{-}CH_2{-}CH_3.$$

The high yield of ethylene indicates again that decomposition of a higher radical must occur readily at these temperatures. One possibility is the pyrolysis of allyl,

$$CH_2{=}CH{-}CH_2\cdot \rightarrow CH_2{=}CH\cdot + \cdot CH_2.$$

However, the relatively high endothermicity of this process makes it rather improbable under the present conditions. Propane is presumably formed by the addition of hydrogen atoms to propylene.

$$H + CH_2{=}CH{-}CH_3 \rightarrow C_3H_7$$
$$C_3H_7 + RH \rightarrow C_3H_8$$

The Decomposition of an n-Butane – Diallyl Mixture

In order to compare the reactivity of allyl with olefins and paraffins the pyrolysis of a *n*-butane – diallyl mixture was studied in one experiment. The results for a system containing 5% diallyl at 506° C (200 mm total pressure) are given in Table III.

TABLE III

Analytical results for the pyrolysis of 5% diallyl in *n*-butane for 5 minutes at 506° C

	Non-sensitized mole%	Sensitized mole%	Sensitized / Non-sensitized
Methane	2.0	4.9	2.5
Ethane	0.9	2.0	2.2
Ethylene	0.9	3.4	3.8
Propylene			3.5
1-Butene	Negligible	1.7	
1-Pentene	—	0.85	
Benzene	—	Negligible	

The principal products from the pyrolysis of *n*-butane alone are propylene methane, ethane, and ethylene. Since the yield of each of the latter three compounds in the complete pyrolysis of diallyl by itself is less than 10% of the diallyl decomposed it is apparent that the allyl radicals have initiated the decomposition of *n*-butane to a significant extent. The concentration ratios for these three products in the sensitized and non-sensitized experiments provides a measure of the accelerating effect of the allyl radicals. The analytical results for propylene were inconclusive because of the difficulty in separating propylene and *n*-butane completely on the alumina column used for these analyses.

Substantial amounts of both 1-butene and 1-pentene were formed in the allyl-sensitized reaction, presumably by the following processes:

$$CH_2{=}CH{-}CH_2\cdot + CH_3 \rightarrow CH_2{=}CH{-}CH_2{-}CH_3,$$
$$CH_2{=}CH{-}CH_2\cdot + \cdot CH_2{-}CH_3 \rightarrow CH_2{=}CH{-}CH_2{-}CH_2{-}CH_3.$$

Can. J. Chem. Downloaded from www.nrcresearchpress.com by 186.148.149.217 on 09/04/12
For personal use only.

The formation of both methyl and ethyl radicals has been proposed as primary steps in the pyrolysis of *n*-butane (7, p. 153). Both of these radicals could, of course, come from the pyrolysis of the butyl radical formed in the primary reaction between *n*-butane and allyl.

$$CH_2{=}CH{-}CH_2\cdot + CH_3CH_2CH_2CH_3 \rightarrow CH_2{=}CH{-}CH_3 + CH_3CH_2\dot{C}HCH_3$$

$$CH_3CH_2\dot{C}HCH_3 \rightarrow CH_3 + CH_2{=}CH{-}CH_3$$

$$\rightarrow CH_3CH_2 + CH_2{=}CH_2$$

Inhibition in Decomposition Reactions

The results obtained in the present study have shown that in the temperature region around 500° C allyl radicals can not only add to olefinic double bonds but are sufficiently reactive to abstract hydrogen from a variety of positions in hydrocarbons. This reactivity makes it difficult to assume that the residual reaction in hydrocarbon decomposition inhibited by the addition of propylene does not involve free radical mechanisms, as it is apparent that the allyl radicals formed under the present conditions are capable of propagating radical chains. The residual reactions in hydrocarbon decomposition fully inhibited by propylene may therefore be processes in which chains are propagated by less effective radicals like allyl, the concentration of the highly reactive alkyl radicals being kept at very low values by reaction with propylene. This idea is in accordance with suggestions made many years ago (16) that thermal decomposition of certain organic compounds may involve more than one type of chain mechanism, not all of which are suppressed by the addition of an inhibitor.

Chain propagation by stabilized radicals has been proposed for the decomposition of 1-butene (6), a system believed to be fully self-inhibited. The reaction of such radicals with substrate hydrocarbon in the propylene-inhibited pyrolysis of paraffins could maintain the propagation process and would result in the formation of products from the decomposition of the paraffinic radicals not greatly different from those obtained in normal pyrolyses.

In the inhibition of hydrocarbon pyrolysis by nitric oxide a similar mechanism may operate. The efficiency of nitric oxide as an inhibitor, roughly 12 times that of propylene (17), is very much less than might be expected assuming that both inhibitors operate by the removal of radicals like methyl from the system. The rate of reaction of methyl with nitric oxide is 400 times the rate of its reaction with propylene (18). However, nitric oxide may be capable only of removing active propagators like methyl and ethyl by converting them fairly rapidly into stable products. The reaction between nitric oxide and electronically stabilized radicals like allyl may be ineffective because of the weakness of the bond formed. Hence the residual reaction in nitric-oxide-inhibited pyrolyses of paraffins may be, to a considerable extent at least, a short-chain process propagated by stabilized radicals formed by H-abstraction from decomposition products like propylene and butene. Propylene may have an inhibition efficiency relative to nitric oxide greater than that expected from their relative rates of reaction with methyl because it can remove radicals by addition reactions as well as by serving as a source of hydrogen for abstractions.

The position of nitric oxide as an inhibitor is confused by the observation that in some systems it is unable to inhibit processes which seem fairly clearly to involve methyl radicals while in other systems it appears to function as a chain initiator (18). A more definitive study of the role played by both nitric oxide and propylene in various reaction

Can. J. Chem. Downloaded from www.nrcresearchpress.com by 186.148.149.217 on 09/04/12
For personal use only.

systems, based on a study of the rate at which they are removed and on the nature of the products formed, would be valuable in endeavoring to understand their function as inhibitors.

ACKNOWLEDGMENTS

We are indebted to Dr. S. A. Ryce for advice in connection with the gas chromatographic analyses and to Mr. E. C. W. Clarke for the mass spectrometric identifications. This work was supported by the Defence Research Board (DRB44-50-01-10), to whom we express our thanks. One of us (D. J. R.) is indebted to the B. C. Sugar Refining Company for a scholarship.

REFERENCES

1. D. J. Ruzicka and W. A. Bryce. Can. J. Chem. This issue.
2. M. Szwarc. J. Chem. Phys. **17**, 284 (1949).
3. M. Szwarc, B. N. Ghosh, and A. H. Sehon. J. Chem. Phys. **18**, 1142 (1950).
4. A. Maccoll. J. Chem. Phys. **17**, 1350 (1949).
5. M. J. Molera and J. F. Stubbs. J. Chem. Soc. 381 (1952).
6. W. A. Bryce and P. Kebarle. Trans. Faraday Soc. **54**, 1660 (1958).
7. E. W. R. Steacie. Atomic and free radical reactions. Reinhold Publishing Corp., New York. 1954.
8. C. A. Coulson. Proc. Roy. Soc. A, **164**, 383 (1938).
9. J. L. Bolland and G. Gee. Trans. Faraday Soc. **42**, 244 (1946).
10. N. N. Semenov. Some problems of chemical kinetics and reactivity. Vol. I. Pergamon Press, London. 1958.
11. F. P. Lossing, K. N. Ingold, and I. H. S. Henderson. J. Chem. Phys. **22**, 621 (1954).
12. J. R. McNesby and A. S. Gordon. J. Am. Chem. Soc. **79**, 4593 (1957).
13. W. A. Bryce and S. A. Ryce. To be published.
14. M. Szwarc. Chem. Rev. **47**, 75 (1950).
15. J. S. Roberts and H. A. Skinner. Trans. Faraday Soc. **45**, 339 (1945).
16. C. N. Hinshelwood. Kinetics of chemical change. Oxford. 1940.
17. F. J. Stubbs and C. N. Hinshelwood. Proc. Roy. Soc. (London), A, **200**, 458 (1950).
18. A. F. Trotman-Dickenson. Gas kinetics. Butterworths, London. 1955. p. 156.

Can. J. Chem. Downloaded from www.nrcresearchpress.com by 186.148.149.217 on 09/04/12
For personal use only.

Can. J. Chem. Downloaded from www.nrcresearchpress.com by 186.148.149.217 on 09/04/12
For personal use only.

THE AQUEOUS BENZOATE SYSTEM AS A SENSITIVE DOSIMETER FOR IONIZING RADIATIONS[1]

W. A. Armstrong and D. W. Grant

ABSTRACT

The aqueous benzoate system, as typified by $6\times10^{-4}M$ calcium benzoate, meets many of the requirements for a sensitive chemical dosimeter. The concentration of salicylic acid, determined spectrophotofluorometrically, increases linearly with radiation dose in the range 5 to 5000 rads and is independent of temperature from 15 to 45° C, of energy from 160 kev to 3 Mev, and of dose rate from 4 to about 1000 rads/minute. The decrease in sensitivity with increasing dose rate from 1000 to 85,000 rads/minute is reported.

INTRODUCTION

The ideal chemical dosimeter should be easy to prepare and stable indefinitely under ordinary storage conditions. The concentration of radiolytic product should be proportional to radiation dose, and independent of radiation intensity (dose rate), radiation energy, and temperature. There should be no postirradiation change in the concentration of that radiolytic product. The method of analysis for the product should be simple, accurate, and precise throughout the range of product concentrations corresponding to the dose range of the dosimeter.

For radiobiological work, a number of additional characteristics are desirable. In particular the system should be tissue-equivalent. This means that the radiation dose absorbed in the dosimeter system should be the same as that absorbed in an identical volume of tissue exposed under identical conditions. This condition is approximately satisfied if the system is water-based. In addition, the system should be sensitive to radiation doses in the range 1 rad (100 ergs/g) to a few thousand rads and be able to discriminate between neutrons and electromagnetic radiation.

Although many radiation-induced chemical reactions have been studied, no system has been developed which meets all of the above requirements. All proposed water-based systems have responses which depend to varying degrees on the radiation energy and at present it seems likely that more than one type of system will have to be exposed simultaneously for dosimetry of mixed neutron–gamma fields.

The two main factors which determine the lowest dose measurable by a given dosimeter are the yield (the amount of product P formed per unit of radiation dose, usually designated as G_P = number of molecules of P formed per 100 ev of energy absorbed) and the sensitivity of the analytical method for P. In general, a G_P greater than 20 indicates that the radiation-induced reaction involves some chain mechanism and, therefore, a dosimeter based on such a system will be dose rate dependent (1). If G_P is small an extremely sensitive analytical method is required. For example, if $G_P = 1$ a dose of 100 rads will produce approximately 10^{-7} moles of P per liter, a concentration barely detectable by even the most sensitive colorimetric methods. A dosimeter based on the oxidation of a leuco base to a dye by the radiolysis products of water and having a G_{dye} approximately equal to 1 has been developed (2, 3). However, it is not sufficiently sensitive for accurate use in the very low dose range.

The simplest analytical method capable of accurate measurements at such high dilutions is spectrophotofluorometry. Thus an extremely sensitive dosimeter might be based on the radiation-induced formation of a fluorescent species from a non-fluorescent

[1]*Manuscript received February 11, 1960.*
Contribution from Defence Research Board, Defence Research Chemical Laboratories, Ottawa, Ontario. Issued as D.R.C.L. Report No. 306.

precursor. Such a system is the benzoate ion in aqueous solution, which on irradiation undergoes partial conversion to the salicylate ion (4). In a preliminary communication (5), the authors have shown that doses down to 5 rads produce accurately measurable amounts of salicylate ion in aqueous calcium benzoate solutions. The present paper describes the results of the experiments undertaken to determine how well a benzoate system meets the requirements for a chemical dosimeter.

EXPERIMENTAL

Materials

Water from a Barnsted still was redistilled from alkaline $KMnO_4$ in an all Pyrex apparatus which incorporated a splash column. Calcium benzoate as the monohydrate (judged by weight loss on heating) was prepared by mixing solutions of reagent grade calcium chloride and benzoic acid dissolved in dilute sodium hydroxide, followed by repeated recrystallizations of the calcium benzoate from aqueous solution. The salicylic acid was reagent grade material recrystallized from aqueous solution and dried. All other materials were reagent grade and were used without further purification.

All glass equipment was vigorously cleaned with fresh chromic acid followed by repeated washings with redistilled water. Steam from boiling dilute alkaline permanganate was then passed through the Pyrex irradiation vessels and the flasks used for storing solutions.

Radiations

The following radiations were used: γ-rays from 2 curies of Cs^{137} and 200 curies of Co^{60}; X rays from a 3-Mev Van de Graaff generator. All dose rates were determined using the Fricke dosimeter (6), assuming $G_{Fe(III)}$ to be 15.5 for all radiations employed. The usual corrections were made for the decreased energy absorption in water.

The 2-curie Cs^{137} source has been described previously (3). The 200-curie Co^{60} source is housed in a facility similar to the one described by Schwarz and Allen (7). The cobalt is located in a pipe 1 in. by 4 in. welded to the center of the bottom of a cylindrical tank 7 ft high and 1 ft in diameter. The tank is sunk about 6 feet in the ground and filled with water. The earth and water provide adequate shielding. Samples were irradiated at dose rates of 70 to 1500 rads/minute in a jig designed to fit over the source.

The 3-Mev Van de Graaff generator, a High-Voltage Corp. horizontal model, was used for high dose rate studies. Samples were dropped through a lucite tube into the X-ray beam for a period of time controlled by an interval timer. With this arrangement, it was possible to irradiate samples with doses of a few thousand rads at dose rates up to 85,000 rads/minute.

Analysis

Fluorescence measurements were made with a Bowman–Aminco spectrophotofluorometer normally using 1-cm quartz cells, although microcells requiring as little as 0.1 ml have been used successfully. The salicylic acid formed on irradiation was determined by comparing the fluorescence of the irradiated sample at 400 mμ when activated with light of 295 mμ, with that of a standard salicylic acid solution. As fluorescent measurements may be affected by the presence of non-fluorescent species, all standards were prepared by adding the desired amount of salicylic acid to a solution of the same composition as the solution to be irradiated. In the concentration range investigated ($<10^{-5}$ M) and with the pH between 4 and 8, neither quenching effects nor interference from other products were encountered.

Can. J. Chem. Downloaded from www.nrcresearchpress.com by 186.148.149.217 on 09/04/12
For personal use only.

RESULTS

1. *Dose*

From Fig. 1 it is seen that for a benzoate ion concentration of 1.2×10^{-3} M, the amount

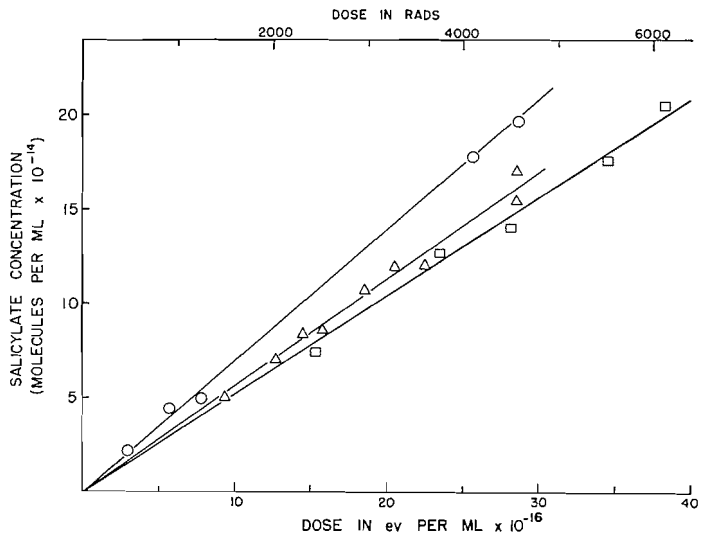


Fig. 1. Effect of dose rate on the formation of salicylic acid in aqueous solutions $1.2\times10^{-3}M$ in benzoate ion: ○ 4 rads/minute (Cs^{137} γ-rays), △ 18,000 rads/minute (3-Mev X rays), □ 85,000 rads/minute (3-Mev X rays).

of salicylic acid produced is a linear function of dose up to about 5000 rads. As the system was studied primarily for the measurement of doses of radiobiological interest (0–1000 rads), few measurements were taken at higher doses. However, there is an indication (not shown) that at high dose rates (18,000 rads/minute), the yield of salicylic acid tends to fall off slightly above 6000 rads even with benzoate ion concentrations as high as 1.2×10^{-2} M. At low benzoate ion concentrations (2.4×10^{-4} M) the product yield appears to decrease when the dose exceeds 1500 rads.

2. *Concentration of Benzoate Ion*

As shown in Fig. 2, the yield of salicylic acid, G_{Sal} (the number of molecules of

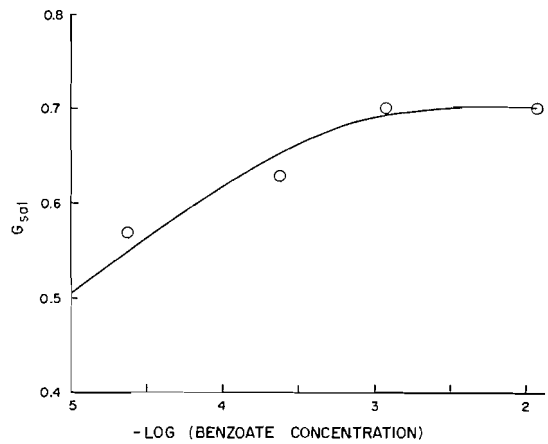


FIG. 2. Effect of benzoate ion concentration on G_{Sal}. Calcium benzoate solutions were irradiated with Cs^{137} γ-rays at 4 rads/minute.

Can. J. Chem. Downloaded from www.nrcresearchpress.com by 186.148.149.217 on 09/04/12
For personal use only.

salicylic acid formed per 100 ev of energy absorbed), increases with increasing benzoate ion concentration from 0.57 for 2.4×10^{-5} M to a limiting value of 0.70 at about 10^{-3} M benzoate ion.

3. Radiation Energy

It has been reported previously (5) that G_{Sal} is independent of radiation energy over the range 1.25 Mev to 0.16 Mev but is 20% lower at an energy of 0.05 Mev.

4. Dose Rate

G_{Sal} decreases with increasing dose rate. The results of irradiations of 6×10^{-4} M calcium benzoate solutions at three dose rates, plotted in Fig. 1, give $G_{Sal} = 0.70$ at 4 rads/minute, 0.59 at 18,000 rads/minute, and 0.53 at 85,000 rads/minute. Intermediate values were obtained using dose rates of 70, 3000, 5000, and 10,000 rads/minute. These are not listed as they lie within the experimental error ($\pm5\%$) of those values obtained for either 4 rads/minute or 18,000 rads/minute.

5. Temperature

Samples of 1.2×10^{-4} M calcium benzoate, thermostatted to within 0.5° C as previously described (3), were irradiated at a rate of 4 rads/minute with Cs^{137} γ-rays. Changes in temperature over the range 15–45° C were found to have no detectable effect on the radiation-induced reaction.

6. pH

The effect of pH on the fluorescence of salicylic acid and *m*-hydroxybenzoic acid has been described by Thommes and Leininger (8). The fluorescence of salicylic acid is due to the salicylate ion and is independent of pH in the range 4–13. However, *m*-hydroxybenzoic acid, which has been identified as a primary product of the radiolysis of benzoate solutions (9), exhibits fluorescence in solutions of pH greater than 8. Thus salicylic acid can best be determined fluorometrically in solutions of pH 4 to 8.

Unbuffered 6×10^{-4} M calcium benzoate solutions having a pH of about 6.3 were used almost exclusively in the radiation studies. Unbuffered 10^{-3} M benzoic acid solutions having a pH of about 3.6 were used successfully with irradiations at low dose rates by comparing the fluorescence of irradiated samples with that of standard salicylic solutions made up in 10^{-3} M benzoic acid. However, such a procedure is not recommended as small changes in pH produce large changes in fluorescence.

The results of the irradiation of alkaline benzoate solutions (pH 11.8) are shown in Fig. 3. The amount of salicylic acid plotted is not the true amount as it was calculated by comparing the total fluorescence due to the salicylic acid and the *m*-hydroxybenzoic acid in irradiated samples with that of a salicylic acid standard. From Fig. 3 the apparent $G_{Sal} = 1.08$ for Co^{60} γ-rays at 70 rads/minute and 0.87 for 3-Mev X rays at 18,000 rads/minute. This decrease in sensitivity with increasing dose rate is similar to that found in neutral solutions. As the sensitivity of neutral solutions is considered adequate, alkaline solutions were not further investigated.

7. Other Effects

Although benzoate solutions decarboxylate to some extent on prolonged standing, no effect attributable to this was found during any irradiation. No salicylate was detected in solutions which had been stored for many weeks in Pyrex flasks.

No detectable postirradiation effect was observed over a period of 24 hours. This was noted for samples receiving doses of about 100 rads at a dose rate of 4 rads/minute and also for samples receiving doses of about 2000 rads at a dose rate of 18,000 rads/minute.

Can. J. Chem. Downloaded from www.nrcresearchpress.com by 186.148.149.217 on 09/04/12
For personal use only.

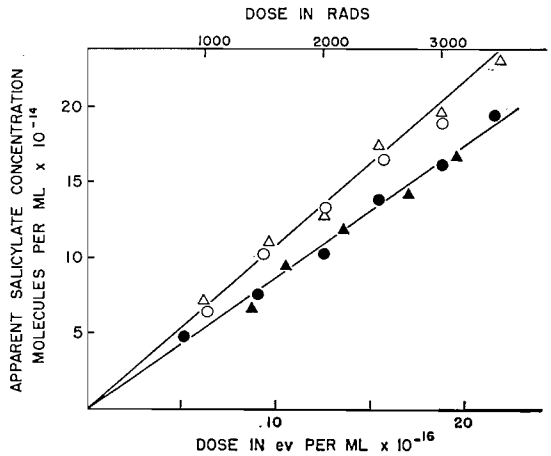


FIG. 3. Results of the irradiation of benzoate solutions 0.01 M in sodium hydroxide: ○ 6×10^{-4} M calcium benzoate, △ 10^{-3} M benzoic acid. Open symbols indicate irradiation with Co^{60} γ-rays at 70 rads/minute, darkened symbols irradiation with 3-Mev X rays at 18,000 rads/minute.

Calcium benzoate was used almost exclusively in this investigation primarily because it can be easily purified by repeated crystallizations from water. Samples of sodium and potassium benzoate as well as benzoic acid available at the outset of the investigation contained traces of salicylic acid and other impurities. The traces of salicylic acid caused high blank fluorescences and made the solutions unsuitable for the measurement of low doses. The other impurities caused some postirradiation changes. At a later date pure potassium benzoate was obtained and shown to give results identical with those obtained with calcium benzoate. Zone-refined PVS benzoic acid was also investigated briefly. As has been mentioned, millimolar benzoic acid solutions are too acidic for the accurate measurement of salicylate fluorescence. However, as shown in Fig. 3, the irradiation of alkaline benzoic acid and alkaline calcium benzoate gave similar results.

DISCUSSION

The results indicate that the aqueous benzoate system, as typified by 6×10^{-4} M calcium benzoate, meets many of the requirements for a sensitive chemical dosimeter. It is stable, easy to prepare, and exhibits no postirradiation change. The concentration of salicylic acid increases linearly with radiation dose in the range 5 to 5000 rads and is independent (within the estimated experimental error of $\pm5\%$) of temperature from 15 to 45° C, of energy from 160 kev to 3 Mev, and of dose rate from 4 to about 1000 rads/minute. With radiation energies lower than 160 kev, the response decreases with decreasing photon energy and at 50 kev is 17% lower (5). The indicated dose, on the basis of $G_{Sal} = 0.70$, will be lower than the actual dose by 5 to 15% with dose rates of 1000 to 18,000 rads/minute and by 16 to 24% with dose rates of 18,000 to 85,000 rads/minute.

It must be stressed that the sensitivity of this system as a dosimeter depends on the method of analysis. The ultimate sensitivity of any dosimeter which is based on fluorescence measurements is dependent on the ratio of the intensities of fluorescent and scattered light at a given wavelength λ, $(I_f/I_s)_\lambda$. In the Bowman–Aminco instrument, a high I_f is obtained by the use of a high intensity light source while I_s is kept to a minimum by the use of diffraction grating monochromators and excellent optical design.

Can. J. Chem. Downloaded from www.nrcresearchpress.com by 186.148.149.217 on 09/04/12
For personal use only.

However, it should be possible to adapt for accurate salicylate analysis any fluorometer which is equipped with an ultraviolet light source by the use of appropriate optical filters.

A discussion of the results reported here in terms of a mechanism for the radiation-induced reactions in aqueous benzoate solutions is beyond the scope of this paper. A report describing the formation of products other than salicylic acid and discussing the theoretical aspects of the benzoate system will be published soon.

ACKNOWLEDGMENTS

The authors wish to thank Mr. F. A. Bury for his assistance with the experiments which required the use of the Van de Graaff generator.

REFERENCES

1. G. J. HINE and G. L. BROWNELL. Radiation dosimetry. Academic Press Inc. 1956. Chap. 8.
2. W. A. ARMSTRONG and G. A. GRANT. Radiation Research, **8**, 375 (1958).
3. W. A. ARMSTRONG and G. A. GRANT. Can. J. Chem. **36**, 1398 (1958).
4. M. J. DAY and G. STEIN. Nature, **164**, 671 (1949).
5. W. A. ARMSTRONG and D. W. GRANT. Nature, **182**, 747 (1958).
6. J. WEISS, A. O. ALLEN, and H. A. SCHWARZ. Proceedings of the International Conference on the Peaceful Uses of Atomic Energy, Geneva, **14**, 179 (1955).
7. H. A. SCHWARZ and A. O. ALLEN. Nucleonics, **12** (2), 58 (1954).
8. G. A. THOMMES and E. LEININGER. Anal. Chem. **30**, 1361 (1958).
9. H. LOEBL, G. STEIN, and J. WEISS. J. Chem. Soc. 405 (1951).

Can. J. Chem. Downloaded from www.nrcresearchpress.com by 186.148.149.217 on 09/04/12
For personal use only.

Can. J. Chem. Downloaded from www.nrcresearchpress.com by 186.148.149.217 on 09/04/12
For personal use only.

RADIATION CHEMISTRY OF CYCLOHEXANE

II. DOSE RATE EFFECTS ON THE FORMATION AND DESTRUCTION OF CYCLOHEXENE[1]

P. J. Dyne and J. W. Fletcher

ABSTRACT

Prolonged radiolysis of cyclohexane leads to a steady-state concentration of cyclohexene where G(cyclohexene) = 0. At concentrations greater than this steady concentration, cyclohexene is destroyed. It is shown that this steady-state concentration is a function of dose rate, varying approximately as the fourth root of the radiation intensity. A discussion of these and other observations indicates that dose rate and L.E.T. effects are observed in cyclohexane only if radical scavengers are present and that cyclohexene, a product of radiolysis, acts as a radical scavenger in irradiated cyclohexane.

INTRODUCTION

Cyclohexene and bicyclohexyl are the two major high molecular weight products formed in the radiolysis of cyclohexane. Dewhurst and Schuler (1) have shown that the initial G values (molecules formed/100 ev absorbed) for cyclohexene and bicyclohexyl are independent of the L.E.T. (Linear Energy Transfer)* of the irradiation. Dewhurst (2) showed that G(cyclohexene) decreases with dose (i.e. with increasing cyclohexene concentration) and, further, that in concentrated solution (5×10^{-4} moles/g), cyclohexene is destroyed. It follows that prolonged irradiation of cyclohexane or of solutions of cyclohexene in cyclohexane leads to a "steady-state" concentration of cyclohexene where G(cyclohexene) = 0. Dewhurst and Schuler (1) found some evidence that G(cyclohexene) fell off more rapidly with cyclohexene concentration at low dose rates, using a Co^{60} γ-ray source, than at the higher dose rates obtained with electron and particle beams.

We have studied the formation and destruction of cyclohexene as a function of the dose rate, using Co^{60} γ-rays and have shown that the "steady-state" concentration increases slowly with the dose rate. The dependence is less than a proportionality to the square root of radiation intensity and approximates to a fourth root dependence.

EXPERIMENTAL

Samples of cyclohexane (spectroscopic grade from various manufacturers) were irradiated in sealed glass vessels. The liquids were degassed by freezing, pumping, and thawing five times. Two Co^{60} sources were used (3) having dose rates of 1.4×10^{19} ev/g hr and 9.6×10^{17} ev/g hr. These dose rates were established using the Fricke dosimeter, $G(Fe^{3+})$ = 15.5 ions/100 ev. Analysis for cyclohexene was done by infrared spectrophotometry of the 640 cm^{-1} band of cyclohexene using a Perkin–Elmer, model 21, spectrometer. Path lengths of 0.2–4.0 mm were used with compensating cells containing pure cyclohexane for the thicker cells. The irradiations were made over an extended period of time (irradiations of up to 1400 hours at the low dose rate). The solutions were stored after irradiation and were all analyzed at one time together with a series of standard solutions of known concentration. The concentrations were determined by graphical interpolation from the measurements of the standard spectra. At the low

[1]*Manuscript received February 2, 1960.*
Contribution from the Research Chemistry Branch, Atomic Energy of Canada Limited, Chalk River, Ontario.
Issued as A.E.C.L. No. 1005.
**Equivalent to the ionization density along the track.*

dose rates the range of the experiments was increased by irradiating solutions that already contained cyclohexene. These results fitted smoothly into the curves obtained in the irradiation of pure cyclohexane.

RESULTS

Most of the experimental results for the high and low dose rates are shown in Figs. 1 and 2 respectively. It should first be noted that at the lower dose rate cyclohexene is

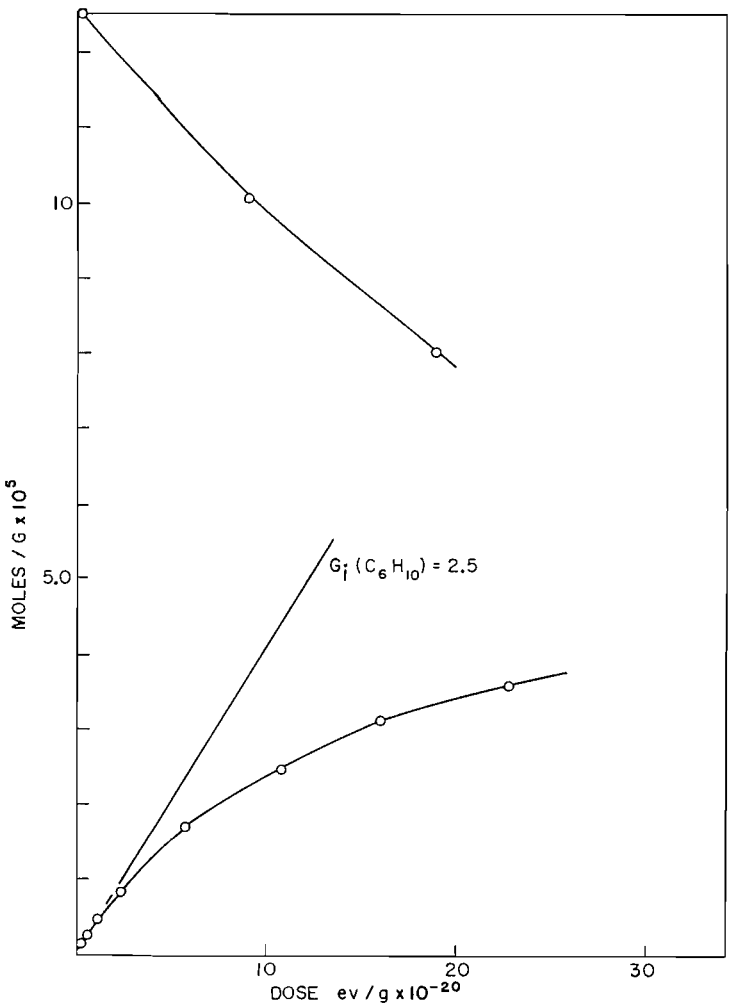


FIG. 1. Formation and destruction of cyclohexene at a dose rate of 1.4×10^{19} ev/g hr.

destroyed at concentrations such as 3.0×10^{-5} moles/g where it is still being formed at the higher dose rate. A similar comparison can be made between our high dose rate results, where decomposition occurs at concentrations greater than 4.5×10^{-5} moles/g, and Dewhurst's results with an electron beam (1), where net decomposition is observed only at concentrations greater than 4.0×10^{-4} moles/g.

We have drawn an initial slope, equivalent to $G(C_6H_{10}) = 2.5$, equal to Dewhurst's

Can. J. Chem. Downloaded from www.nrcresearchpress.com by 186.148.149.217 on 09/04/12
For personal use only.

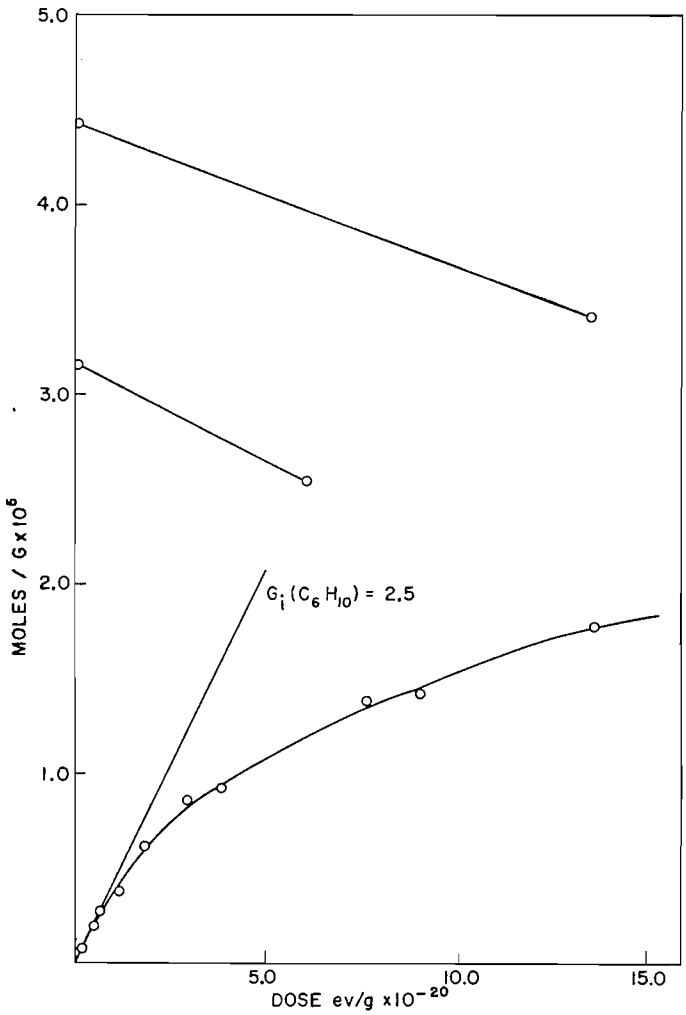


FIG. 2. Formation and destruction of cyclohexene at a dose rate of 9.6×10^{17} ev/g hr.

value, on both Figs. 1 and 2. It can be seen that there is no significant change in the initial *G*-value with dose rate. The *G*-value indicated by the first point (at the lowest cyclohexene concentration) in Fig. 1 and in Dewhurst's Fig. 1 are between 3.0 and 3.2. The value of 2.5 must be regarded as a minimum value; it is possible that the true limiting *G*-value is 3.0 or higher.

We have calculated *G*-values for each successive pair of experimental points in Figs. 1 and 2 and for Dewhurst's experimental results. In Fig. 3 the *G*-values are plotted against the concentration of the first point, i.e. the one with lower concentration where *G*-cyclohexene is positive and the one with the higher concentration when *G*-cyclohexene is negative. This procedure is, we feel, preferable to drawing a smooth curve through the experimental points and measuring graphically the slopes of a series of tangents. Due to the fairly steep curvature of the plots of $G(C_6H_{10})$ vs. cyclohexene concentration this is a plot of minimum *G*-values ($G(C_6H_{10})$ and $G(-C_6H_{10})$ both having positive signs). The high initial points, $G = 3.0$–3.2 mentioned in the previous paragraph, are seen on the

Can. J. Chem. Downloaded from www.nrcresearchpress.com by 186.148.149.217 on 09/04/12
For personal use only.

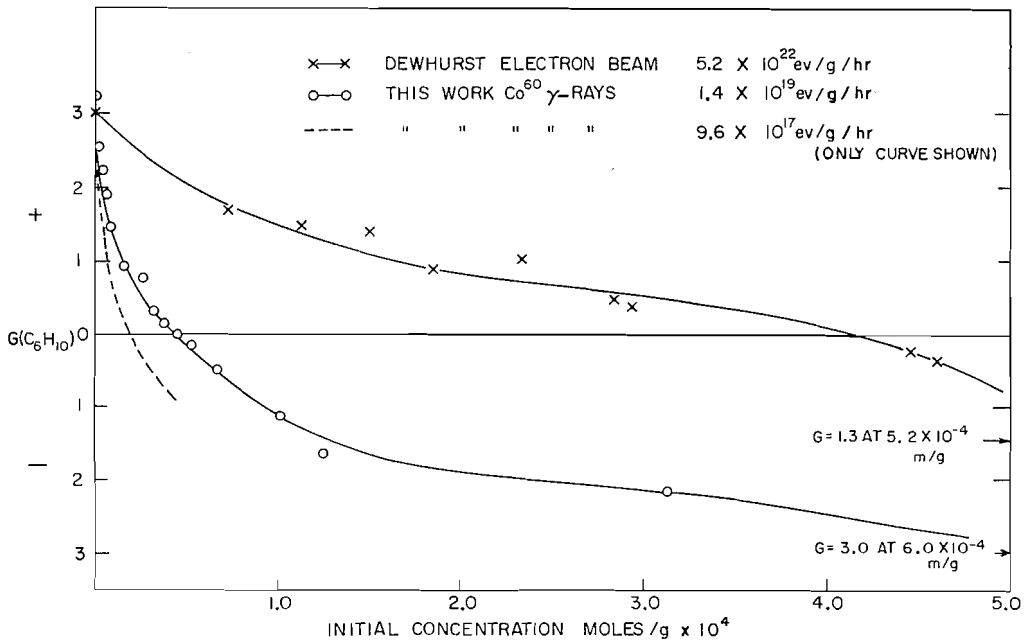


FIG. 3. *G*-values for formation and destruction of cyclohexene as a function of cyclohexene concentration. See text for method of calculation.

graph. The locus of $G(C_6H_{10})$ vs. C_6H_{10} for the lower dose rate (9.6×10^{17} ev/g hr) experiments is also shown in Fig. 3. At this low dose rate $G(C_6H_{10}) = 0$ at a cyclohexene concentration of 2×10^{-5} moles/g and the largest observed value of $G(-C_6H_{10})$ is 1.6 at 6.1×10^{-4} moles/g. The largest observed value of $G(-C_6H_{10})$ at our higher dose rate of 1.4×10^{19} ev/g hr was 3.0 at 6.0×10^{-4} moles/g. Dewhurst reports a value of $G(-C_6H_{10}) = 2.3$ at 5.2×10^{-4} moles/g at the high dose rate obtained with the electron beam. This value is greater than that shown in Fig. 3 as it was derived from the initial slope of a smoothed curve.

The steady-state concentrations determined from Fig. 3 are given in Table I, which includes the relative concentrations and dose rates and shows that the steady-state concentration varies approximately as the fourth root of the dose rate. The term steady state is, perhaps, somewhat unfortunate as it implies that this concentration will never change. With very long irradiations, 10 or more times the highest doses used here, further reactions must be expected. The term refers only to the dose range of the present experiments.

TABLE I

Variation of steady-state concentration with dose rate

Dose rate, ev/g hr	Steady-state concn., moles/g	Relative dose rate	Relative concn.	(Relative dose rate)$^{1/2}$	(Relative dose rate)$^{1/4}$
9.6×10^{17}	2.0×10^{-5}	1.0	1.0	1.0	1.0
1.4×10^{19}	4.5×10^{-5}	14.5	2.25	3.80	1.94
5.2×10^{22}	4.2×10^{-4}	5.4×10^{4}	21.0	2.32×10^{2}	15.2

Can. J. Chem. Downloaded from www.nrcresearchpress.com by 186.148.149.217 on 09/04/12
For personal use only.

Irradiation of cyclohexane in a spent fuel-element γ-ray source, reported by Nixon and Thorpe (4), gave a concentration of 2.7×10^{-5} moles/g cyclohexene at a dose of 4.8×10^{21} ev/g, equivalent to G(cyclohexene) = 0.34. When compared with the initial G(cyclohexene) = 2.5 this low G-value indicates that the system was approaching a steady state. The steady-state concentration at their dose rate ($\sim4\times10^{19}$ ev/g hr or perhaps somewhat less) (5) is, by interpolation from the data in Table I, $\sim6\times10^{-5}$ moles/g.

DISCUSSION

Two different, but closely related, effects have to be explained; the invariance of initial yields with L.E.T. and with dose rate, and the variation of yields with dose rate in the presence of cyclohexene. It is well known that both L.E.T. and dose rate effects are generally due to a competition between reactions R + R $\rightarrow$ products, P_1 involving two precursors (free radicals) and reactions R + S $\rightarrow$ products, P_2 involving one precursor and a stable molecule S present in macro quantities. The products P_1 and P_2 may consist of more than one species. Variations in yield with L.E.T. occur because the balance of the competition is largely determined by the initial distribution of the precursor R. The chief features of the radiation chemistry of water are explicable in these terms.

Variations of yields with dose rate occur, in general, because the steady-state concentration of precursors is determined by functions involving the dose rate and the square root of the dose rate: the square root arising from the bimolecular removal of precursors in a reaction R + R $\rightarrow P_1$. This situation occurs if the precursors are reacting homogeneously, track effects being absent (as in photochemistry).

The chief experimental observations to be correlated and explained are:

1. The initial yield of hydrogen from cyclohexane is independent of L.E.T. and dose rate. This was demonstrated by Schuler and Allen (6).

2. The initial yield of cyclohexene is also independent of dose rate and L.E.T. This may be stated, using E for cyclohexene, as $(dE/dt)\ (E \rightarrow 0) = k_1 I$, where I is the dose rate. This also expresses the fact that dose rate and/or L.E.T. effects are observed only in the presence of cyclohexene.

3. The yield of cyclohexene from unimolecular processes $C_6H_{12} \rightarrow C_6H_{10} + H_2$ has a G-value less than 1.0; the major fraction of the yield ($\sim2/3$) is produced by bimolecular processes, probably the disproportionation of cyclohexyl radicals, $2C_6H_{11} \rightarrow C_6H_{10} + C_6H_{12}$. This conclusion was reached by Dewhurst (2) from studies of the yield of cyclohexene in the presence of oxygen (1) and is in agreement with the measurements made by Dyne and Jenkinson (7) of the yield of deuterium produced in unimolecular processes from C_6D_{12}.

4. The steady-state concentration of cyclohexene varies slowly with radiation intensity, approximately as the fourth root of I, i.e. $E_s \simeq k_2 I^{1/4}$.

5. The yield of cyclohexene drops very sharply with cyclohexene concentration at the lower dose rates. Cyclohexene inhibits its own formation very effectively, more effectively than it reduces the yield of molecular hydrogen.

The invariance of the hydrogen yield with L.E.T. can be simply explained. Hydrogen is presumably formed by $H + C_6H_{12} \rightarrow H_2 + C_6H_{11}$; this is essentially the scavenging reaction R + S $\rightarrow$ products, where S is present at a very high concentration—so high that the probability of the recombination reaction $H + H \rightarrow H_2$ is very small. It should also be noted that the scavenging reaction gives one molecule H_2 for one hydrogen atom

Can. J. Chem. Downloaded from www.nrcresearchpress.com by 186.148.149.217 on 09/04/12
For personal use only.

Can. J. Chem. Downloaded from www.nrcresearchpress.com by 186.148.149.217 on 09/04/12
For personal use only.

while the recombination reaction gives one molecule H_2 for two hydrogen atoms. If the two reactions rates were comparable then the hydrogen yield would *decrease* with increasing L.E.T. as the probability of bimolecular recombination would increase.

The invariance of the initial yield of cyclohexene with L.E.T. may arise from the opposite circumstance; all the precursors of cyclohexene react $R + R \rightarrow$ products (e.g. cyclohexene) and the scavenging reaction is non-existent. Scavengers (cyclohexene itself, for instance) may be formed during the radiolysis. Changes in yield with L.E.T. would then be observed in solutions containing cyclohexene but not in pure cyclohexane. This is in agreement with experiment. The variation in yield of bicyclohexyl with dose rate, which is similar to the behavior of cyclohexene observed by Dewhurst and Schuler (1), would be explained similarly.

With reference to the steady-state concentration, it is not possible to distinguish properly between L.E.T. and dose rate effects. The dose rate variation has been observed with Co^{60} γ-rays. No α-particle or proton beam experiments have been reported in which the total dose rate was varied or in which the irradiation was carried to a sufficiently high dose rate for the observation of the radiation steady state.

Dose rate effects in γ-ray irradiations can occur only when radicals (or precursors) have an appreciable probability of escaping from the spur in which they were formed and of reacting with radicals produced in other spurs. Homogeneous kinetics, as in photochemistry, are then applicable. A competition between $R + R \rightarrow P_1$ reactions (second order in R) and $R + S \rightarrow P_2$ reactions (first order in R) will give rise to dose rate dependence of the yields of P_1 and P_2 and of the disappearance of S. The present evidence suggests that cyclohexene is the scavenger S as its presence generates the dose rate effects. The effectiveness of cyclohexene in the inhibition of its own formation suggests, also, that in the $R + R \rightarrow P_1$ reactions, P_1 includes cyclohexene. Cyclohexene is destroyed in the scavenging reactions and in some of these same reactions it destroys its own precursors. As G(cyclohexene) falls more rapidly than $G(H_2)$ with cyclohexene concentration (i.e. the reduction in $G(H_2)$ is not equivalent to the reduction in G(cyclohexene)), cyclohexene must presumably be reacting with other precursors as well as with hydrogen atoms.*

Schuler (8), using a variety of ionizing radiations, measured the disappearance of iodine in cyclohexane solutions and equated this yield with the total radical yield. The radical yield obtained with 33-Mev helium ions is about 30% less than that found in electron beam irradiations. Compared with the effects in water this is a small change in yield with L.E.T. Under the particular experimental conditions used (dose rate, scavenger concentration, etc.) the scavenging reaction is dominating the recombination reaction over the whole L.E.T. range. Detailed studies of scavenging, similar to those done by Charlesby and Lloyd (9) on anthracene are needed to put this and other observations (such as those presented in this paper on cyclohexene) on a quantitative basis.

The relations $dE/dt.(E \rightarrow 0) = k_1 I$ and $E_s \simeq k_2 I^{1/4}$ are reduced, approximate forms of the general rate equation $dE/dt = F - D$ where F is the rate function for all processes forming cyclohexene and D the rate function for all processes destroying cyclohexene. Both these rates F and D are likely to be functions of E and I. We may speculate on the form of F and D, as follows. The $I^{1/4}$ function is probably derived from the $I^{1/2}$ dependence found in many radical chain mechanisms. The relation $E_s \simeq k_2 I^{1/4}$ is possibly

**This conclusion is contrary to the argument given by Dewhurst, who equates the change in hydrogen yield with the value of $G(-C_6H_{10})$ at a concentration of 5.2×10^{-4} moles/g. The correct value for the comparison is $[G_{\text{initial}}(C_6H_{10}) + G(-C_6H_{10})]$ and this is greater than the reduction in hydrogen yield.*

a simplification of $E_s^2 \simeq k_2^2 I^{1/2}$. This equation is a reduced form of the relation $D = F$ when $E = E_s$. Now F, the processes of formation, are likely to be proportional to I; they are certainly so when $E = 0$. The process of destruction is likely to be a reaction of cyclohexene with a reactive intermediate with a rate governed by $k.E.R$ where R is the steady-state concentration of this intermediate. If this is the intensity-dependent process, it may have the form $k''EI^{1/2}$. The relation $E_s^2 \simeq k_2^2 I^{1/2}$ can be rearranged to $E_s I^{1/2} \simeq k_2^2 I/E_s$ which we identify with $D = F$. Now F cannot be inversely proportional to E as $E \to 0$—it must have a form of the type: $k_2^2 I/(k_3+E)$, in which k_3 is sufficiently small that E quickly becomes the dominating term in the denominator.

The true rate equations must be more complex than this. We know that there are two processes, one unimolecular, the other bimolecular, forming cyclohexene, i.e. $F = F_1+F_2$, each presumably having a different dependence on E and I. There may again be more than one process destroying cyclohexene. The sum of all destruction $\Sigma_1 D_1$ and formation processes are related by $\Sigma_1 D_1 = F_1+F_2$ at the steady state. The relation $E_s I^{1/2} \simeq k_2^2 I/(k_3+E)$ is a simplification of this relation which is observed over a possibly limited range of values of E and I.

In summary, the chief conclusion of this study is that, in liquid cyclohexane, scavengers must be present before dose rate and L.E.T. effects are observed and that a major product of the radiolysis, cyclohexene, acts as a scavenger.

ACKNOWLEDGMENTS

It is a pleasure to acknowledge the helpful and critical interest Dr. R. H. Betts has shown in this work.

REFERENCES

1. H. A. DEWHURST and R. H. SCHULER. J. Am. Chem. Soc. **81**, 3210 (1959).
2. H. A. DEWHURST. J. Phys. Chem. **63**, 813 (1959).
3. P. B. AITKEN, P. J. DYNE, and E. C. TRAPP. Nucleonics, **15**, 100 (1957).
4. A. C. NIXON and R. E. THORPE. J. Chem. Phys. **28**, 1004 (1958).
5. A. C. NIXON. Private communication.
6. R. H. SCHULER and A. O. ALLEN. J. Am. Chem. Soc. **77**, 507 (1955).
7. P. J. DYNE and W. M. JENKINSON. Can. J. Chem. **38**, 539 (1960).
8. R. H. SCHULER. J. Phys. Chem. **63**, 925 (1959).
9. A. CHARLESBY and D. G. LLOYD. Proc. Roy. Soc. A, **249**, 51 (1958).

Can. J. Chem. Downloaded from www.nrcresearchpress.com by 186.148.149.217 on 09/04/12
For personal use only.

Can. J. Chem. Downloaded from www.nrcresearchpress.com by 186.148.149.217 on 09/04/12
For personal use only.

THE DECOMPOSITION OF METHANE BY LOW-ENERGY ELECTRONS[1]

J. E. MANTON[2] AND A. W. TICKNER

ABSTRACT

The decomposition of methane by a beam of electrons having energies between 15 and 100 ev has been studied using methane pressures between 10^{-2} and 10^{-3} mm of mercury. The products were frozen out on a surface cooled to about $-220°$ C and situated approximately 5 millimeters from the electron beam.

Ethane, ethylene, and acetylene were found to be the main products along with smaller amounts of saturated and unsaturated higher hydrocarbons. The results provide some evidence that under these experimental conditions ions do not play a major part in the decomposition and a free radical mechanism has been proposed to explain the formation of the main products.

INTRODUCTION

Recently the authors have become interested in the study of chemical reactions in the electric discharge. For many years, the interpretation of the results of such studies was based largely on the reactions of free radicals, ionic reactions not being considered of importance. During the last few years, however, it has been observed, initially by Stevenson (1), that ions frequently have enhanced cross sections for reaction. This has led to a reappraisal of the role played by ions in radiation and discharge chemistry.

As an aid to understanding the decomposition of methane in a discharge, the experimental conditions have been simplified in such a way that many of the experimental parameters could be separately controlled. In addition, an effort has been made to reduce the extent to which secondary reactions occur by providing for the rapid removal of the products from the reaction zone. In this way, it was hoped to obtain some information concerning the primary products of the discharge reaction.

EXPERIMENTAL

A conventional vacuum system, capable of maintaining a background pressure of less than 10^{-6} mm Hg, was used. The essential details of the apparatus are shown in Figs. 1 and 2.

An electrically heated (a-c.) tungsten ribbon filament was the source of electrons, the filament being enclosed in a housing with its own pumping for the removal of pyrolysis products. The beam of electrons was defined by apertures 1.5 mm in diameter in a series of Chromel A plates. Further alignment and collimation of the beam were obtained by the use of a permanent magnet which provided a uniform field strength of 870 gauss over an area about 4 centimeters in diameter at the center of the gap. Onto the final collimator (collimator 2) was soldered a hollow brass cone, A, which fitted into the glass tube surrounding the reaction zone. This arrangement caused the major pressure drop to be across the defining aperture in the center of the collimator. The collector served to monitor the electron beam. The collector grid, about 1 mm in front of it, consisted of 90% transparent tungsten mesh and was maintained at the same potential as the final collimator, thus creating a field free reaction zone 4.5 centimeters in length.

The various potentials were obtained from a regulated d-c. supply and were chosen to give the maximum beam current consistent with stability and reasonable filament

[1]*Manuscript received January 27, 1960.*
Contribution from the Division of Applied Chemistry, National Research Council, Ottawa, Canada. Presented in part at the Annual Conference of the Chemical Institute of Canada, May, 1959.
Issued as N.R.C. No. 5668.
[2]*N.R.C. Postdoctorate Fellow. Present address: Royal Military College, Kingston, Ontario, Canada.*

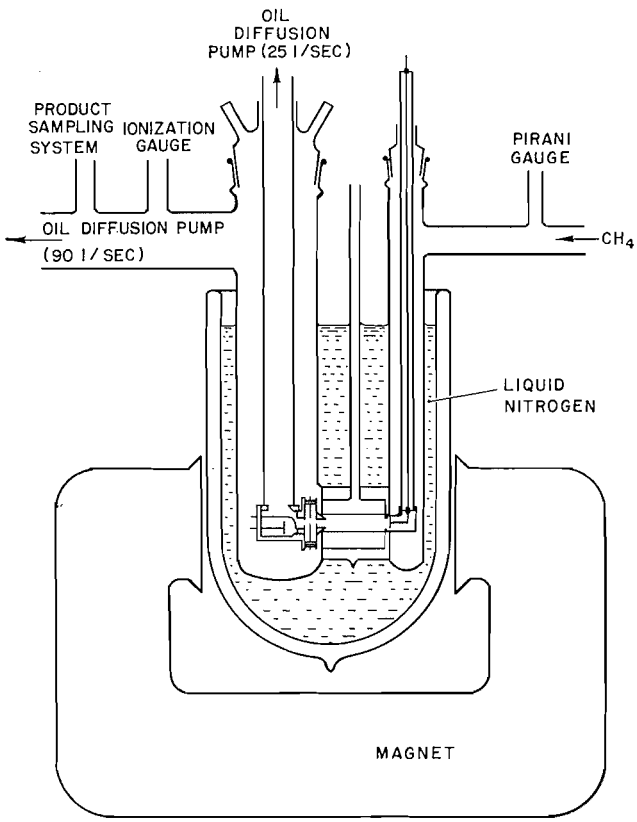


FIG. 1. Apparatus.

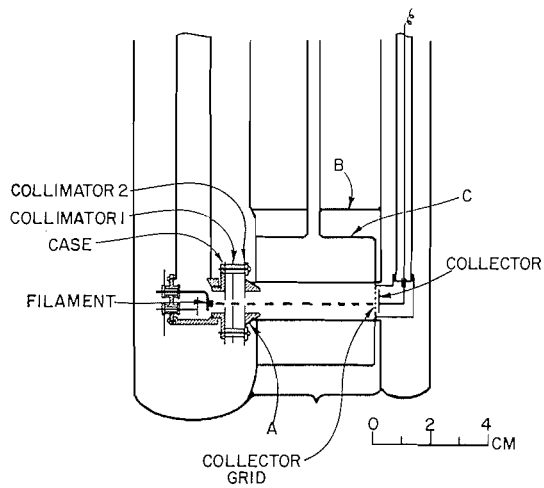


FIG. 2. Details of electron beam tube.

life. The filament housing was maintained at +25 v and collimator 1 at +10 v to +15 v, all potentials being established with respect to the center of the filament. Collimator 2 and the collector grid were set at the electron energy required for the experiment and

Can. J. Chem. Downloaded from www.nrcresearchpress.com by 186.148.149.217 on 09/04/12
For personal use only.

the collector was maintained about 25 volts more positive. The electron beam current was controlled manually by adjusting the filament current.

The path of the electron beam through the methane could be observed, in a darkened room, as a faint bluish column, approximately the diameter of the defining apertures and extending the whole length of the reaction zone. After the initial experiments, the inside surface of the glass tube surrounding the reaction zone was gold-coated by evaporation in order to prevent charge accumulation on the walls. A spring contact connected the gold layer electrically to the collector grid.

The reaction products were expected to be mixtures of the lower hydrocarbons similar to those obtained in the decomposition of methane in the d-c. glow discharge at low temperatures (2, 3). The estimated rates of formation, based on the low-temperature discharge work, together with values of the vapor pressures of the C_2 hydrocarbons, obtained by extrapolation of the data of Tickner and Lossing (4), indicated that a temperature of about $-215°$ C would be necessary to freeze out the reaction products quantitatively. The refrigerant used was solid nitrogen, obtained by reducing the pressure above liquid nitrogen. The solid nitrogen was in chamber C in Fig. 2, this being surrounded by the evacuated chamber B, and the whole immersed in liquid nitrogen. In this way, the walls of the tube surrounding the reaction zone could be cooled to slightly below $-220°$ C, as indicated by the vapor pressure of methane.

The methane used was Matheson C.P. grade and was purified by fractional distillation before admission to the storage reservoir. From this reservoir, the methane was admitted to the reaction system via a needle valve, which controlled the flow rate, and a trap maintained at the freezing point of nitrogen, $-210°$ C for final purification. The methane pressure was measured with a Pirani gauge, which had been calibrated, *in situ*, against a standard McLeod gauge.

In carrying out an experiment, a steady flow of methane was established and the electron beam turned on for the required time. The length of a run, about 20 minutes, was chosen in order to obtain the maximum quantity of products consistent with maintaining sufficient solid nitrogen in the jacket for efficient trapping. At the end of an experiment, the methane was turned off and the system pumped briefly to a low pressure and then isolated. After the reaction system had warmed up, the products were quantitatively transferred to a gas burette by means of a Toepler pump and the volume measured. A sample was then taken and analyzed on the mass spectrometer.

EXPERIMENTAL RESULTS

In order to determine the contributions of materials formed by pyrolysis on the filament, blank runs at 5×10^{-3} mm and 10×10^{-3} mm pressure of methane were performed. The experimental conditions, including the filament current, were the same as those used in the other runs except that no d-c. potentials were applied to the system. Small amounts of the C_2 hydrocarbons were found, which did not exceed 2% of the amounts formed during any of the experiments. In addition, propylene was found in amounts up to 5% and butene in amounts up to 25% of the quantities obtained as products in subsequent runs. The quantity of pentene found in the blank corresponded to between 25% and 50% of the amounts recovered in subsequent experiments. Since in almost every case, the corrections would be small compared with the other uncertainties involved, no corrections have been made for the presence of pyrolysis products among the reaction products.

The variation of the reaction products with electron energy is shown in Fig. 3. The

Can. J. Chem. Downloaded from www.nrcresearchpress.com by 186.148.149.217 on 09/04/12
For personal use only.

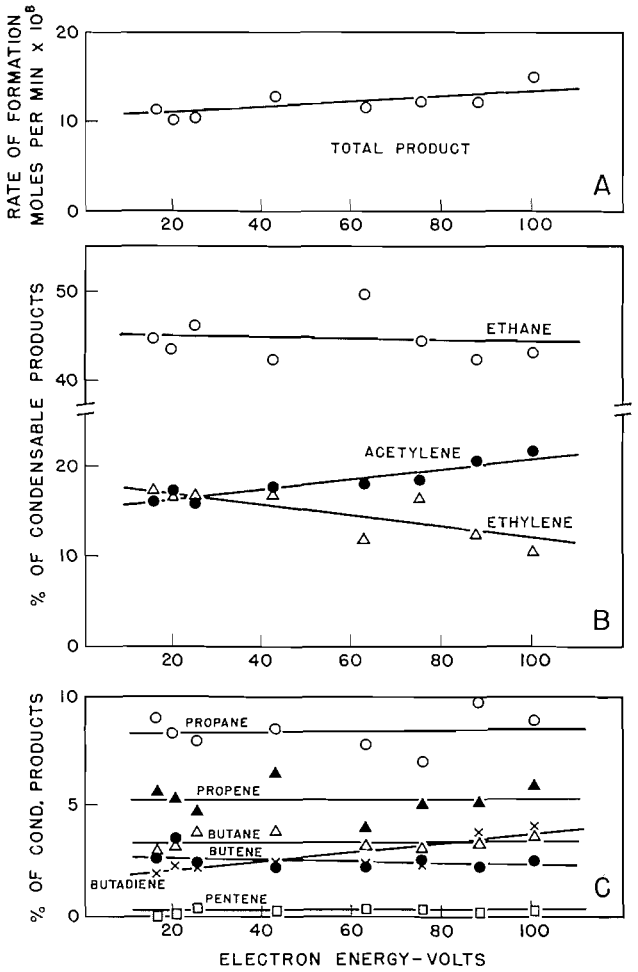


FIG. 3. Variation of products with electron energy.

values were obtained at a pressure of 5.2×10^{-3} mm of methane and collector currents of $250(\pm5)$ μa. It was not found possible to extend the measurements to lower voltages because the electron beam became unstable below about 15 volts. At 50 ev the extent of decomposition was about 3% and in all cases the contact time was estimated to be about 0.02 second.

The effect of pressure on the reaction products is shown in Fig. 4. These experiments were carried out with collector currents of $230(\pm10)$ μa and at an electron energy of 50 ev. At the temperature used to trap the products ($-220°$ C) the maximum pressure of methane which could be used is the vapor pressure (about 10^{-2} mm). The lower limit to the pressure range was set by the fact that the rate of formation of products decreased as the pressure was lowered. Consequently, the more volatile products could not be recovered quantitatively below about 2×10^{-3} millimeters.

Figure 5 shows the effect of collector current on the products, using 50-v electrons and a pressure of 5.2×10^{-3} mm of methane. The lower limit of 100 μa was again

Can. J. Chem. Downloaded from www.nrcresearchpress.com by 186.148.149.217 on 09/04/12
For personal use only.

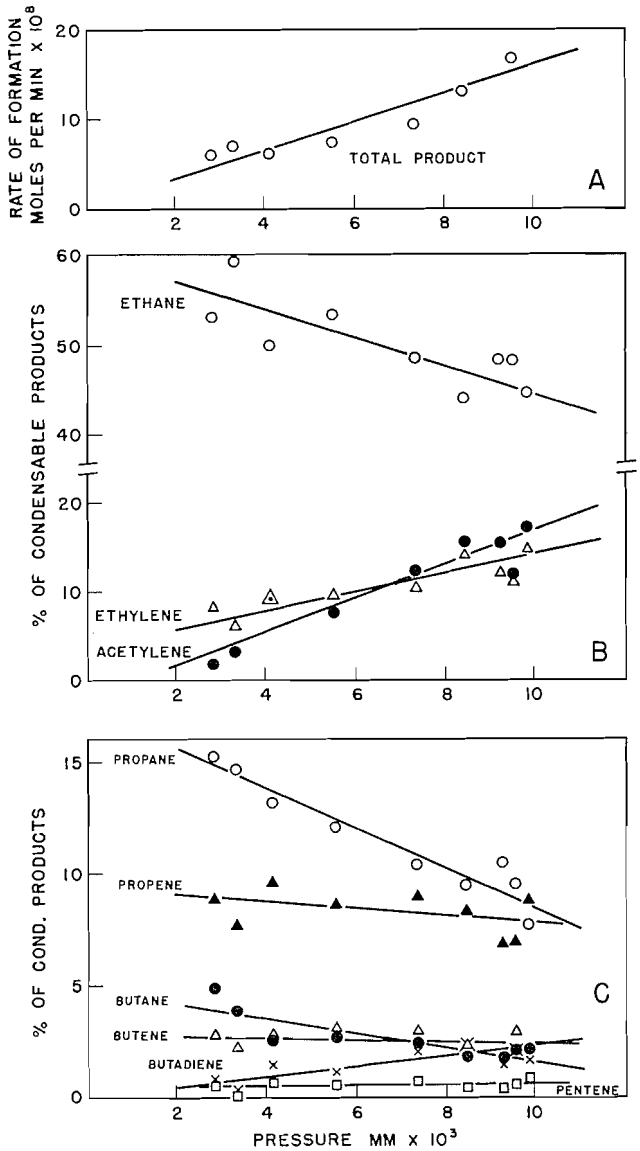


FIG. 4. Variation of products with pressure.

determined by the vapor pressures of the products and the efficiency with which they could be trapped.

No analyses were made for the hydrogen which was presumably formed in the decomposition. Such an analysis would have been difficult to perform accurately since the concentration of hydrogen in the reacted gas would have been less than 3% and the total gas pressure downstream from the reaction zone was less than 10^{-4} mm of mercury. A study of the decomposition of methane in the negative glow of a d-c. discharge (3) has shown that under comparable conditions the products are very similar to those reported here. In the discharge experiments, which could be carried to higher con-

Can. J. Chem. Downloaded from www.nrcresearchpress.com by 186.148.149.217 on 09/04/12
For personal use only.

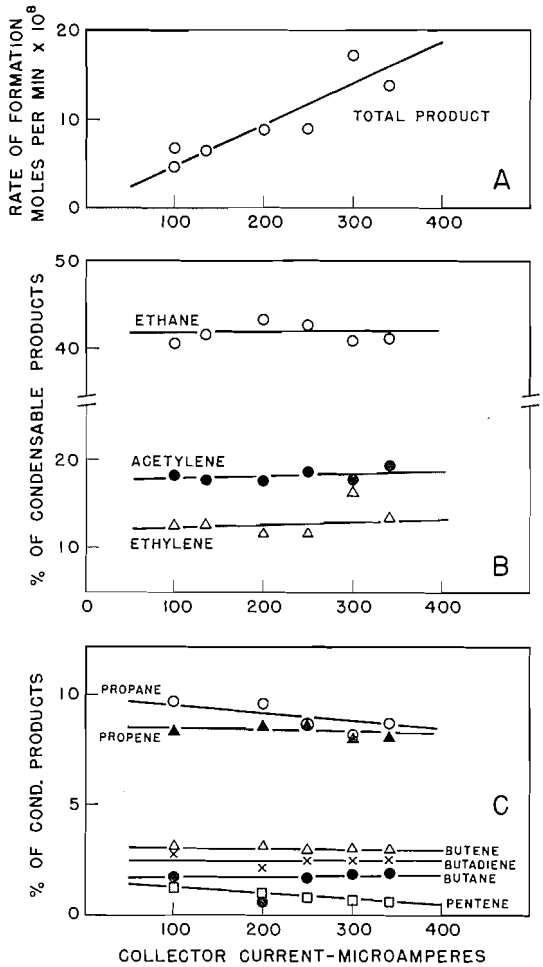


FIG. 5. Variation of products with collector current.

versions and in which the gas could be sampled at much higher pressures, analysis of the reacted gas showed that the theoretical amount of hydrogen was in fact produced.

The experimental conditions made it difficult to study the effect of the reaction products on the over-all reaction, except for hydrogen. Experiments with up to 10% hydrogen in the methane showed no significant change in either the percentage composition or the rate of formation of the products. Similarly, in an experiment with 2% of deuterium in the methane, no deuteration of the products was detected.

The values of the methane pressure given throughout this report are those measured on the calibrated Pirani gauge. The true pressures in the reaction zone were undoubtedly somewhat lower than the measured values due to the existence of a small pressure gradient. In addition, it was difficult to fit the brass cone on the final collimator reproducibly into the end of the glass tube surrounding the reaction zone. Since it was necessary to disturb the alignment of the cone each time the filament was replaced (about once in 10 runs), each filament had associated with it a different pressure gradient and hence a different relationship between the measured value of the pressure and the true value.

Can. J. Chem. Downloaded from www.nrcresearchpress.com by 186.148.149.217 on 09/04/12
For personal use only.

The experimental points in each figure were obtained using a single setting of the collimator but the values of the pressure given in different figures are not directly comparable. From a comparison of the results obtained with a number of different collimator settings we believe that all of the values of the pressure given agree with the true value within a factor of 2.

In general the results show a considerable amount of scatter due to the small amount of product formed and the uncertainties involved in working out the composition from the mass spectrum of such a complex mixture. Straight lines have been drawn through the points in all cases for the purpose of indicating trends.

In two cases there is some ambiguity in the identification of the products. The mass spectra provide some evidence that the substance appearing at $m/e = 42$ may consist of cyclopropane as well as propene. Because of the overlapping of the spectra and the small amounts involved it was not possible to distinguish quantitatively between these two compounds and in reporting the experimental results this product has simply been called propene. Similarly, the product appearing at $m/e = 54$ could, on the basis of the mass spectra, be either butadiene or butyne. Because propyne, for which there was qualitative evidence but which could not be determined accurately, was present only in smaller amounts, this compound has been designated butadiene.

DISCUSSION

The results in Fig. 3A indicate that the rate of formation of products varies only slightly with electron energy from 100 v to within a few volts of the ionization potential of methane. If the products were formed mainly by a process depending on the formation of ions, it would be expected that the rate of formation would fall off rapidly below about 50 ev in accordance with Tozer's values (5) for the ionization cross section of methane. Thus, although ions are undoubtedly formed, there seems to be no evidence that they play an important role in the formation of the products.

This conclusion is in agreement with that of Williams (6), who has studied the decomposition of methane using photoelectrons which are accelerated through the gas. Although the work he reports was carried out at much higher pressures and in the presence of an electric field, the products he obtained are similar to those obtained in this work. The absence of unsaturated hydrocarbons among his reaction products seems reasonable since his experiments were carried out in a static system for relatively long periods at room temperature. Thus, the more reactive unsaturated hydrocarbons which might have formed initially could have reacted to form saturated hydrocarbons or polymers. Since in this work the products were trapped within a few mean free paths of the reaction zone it is evident that they were removed from the reaction at a much earlier stage.

Although their work is not entirely comparable it is interesting to note that recently Yang and Manno (7), using nitric oxide as an inhibitor, have determined the free radical contribution to the various products formed in the γ-radiolysis of methane. They estimated the free radical contribution to the formation of ethane, propane, butane, and pentene, which together make up nearly all of their hydrocarbon products and which constitute most of ours, to be 85% or greater.

Figure 4A shows that the quantity of product increases linearly with methane pressure. Although the composition of the product changes as the pressure is raised the changes, to a large extent, offset the effect of one another on the carbon balance. Thus, the amount of methane decomposed is approximately proportional to the pressure over the range studied.

Can. J. Chem. Downloaded from www.nrcresearchpress.com by 186.148.149.217 on 09/04/12
For personal use only.

The experiments recorded in Fig. 5A indicate that the amount of product formed is directly proportional to the electron current. Since the composition of the product changes little over the range of currents studied, the products apparently arise in each case as the result of a single collision of an electron with a methane molecule. Secondary collisions between the product molecules and other electrons do not appear to play an important part.

If the electron efficiency is defined as the number of molecules of methane decomposed per electronic charge passed through the system, then our results yield a value of 1.8 for 50 ev electrons and a methane pressure of 5×10^{-3} mm. This assumes that all of the methane decomposed is recovered as volatile hydrocarbon products; if additional involatile products are formed, the electron efficiency would be correspondingly greater. Experiments utilizing the negative glow of a d-c. discharge under comparable conditions have led to electron efficiencies of about 10 (2, 3). The difference in the values seems reasonable since the discharge experiments were carried out at higher pressures and our results show that the electron efficiency increases with pressure. In addition, the electron multiplication and recombination which occur in a discharge would tend to increase the value of the electron efficiency as calculated on the above basis. Williams (6) has reported values of the electron efficiency which vary with pressure and with the voltage gradient and which lie within the range 0 to 10.

Because the products do not appear to depend to any large extent on ions for their formation, the discussion of mechanism will be limited to a consideration of the manner in which the products might be formed by free radical processes. A further restriction upon the possible reactions to be considered is imposed by the low temperature at which the experiments were carried out. This restricts the reactions to those having very low activation energies or those involving excited species.

The chemical effects of the high-energy irradiation of methane have been attributed largely to the action of secondary electrons having energies of the same order as the electrons used in this work (8). Thus it seems reasonable to expect that free radicals which have been detected in the radiolysis of methane may also play a part in the decomposition of methane under the conditions of our experiments. Gevantman and Williams (9), using iodine as a free radical scavenger, concluded that methyl, methylene, and ethyl radicals were important in the decomposition of methane by high-energy X rays and electrons. More recently, Meisels, Hamill, and Williams (10) studied the irradiation of methane in mixtures with argon and krypton and concluded that methyl and ethyl radicals and ethylene were significant intermediates. Because no ketene was formed in the radiolysis of mixtures of argon, methane, and carbon monoxide, they concluded that CH_2 was not formed.

There is also a great similarity between the results reported here for the decomposition of methane in a beam of electrons and the decomposition of methane in an electric discharge. This is especially true for the negative glow of a d-c. discharge when small currents are used and the discharge tube is cooled to low temperatures. Under these conditions the products are almost identical with those reported here (2, 3). Jen, Foner, Cochran, and Bowers (11), using electron spin resonance, have detected methyl radicals in the products of a low-power discharge in methane when the products were frozen out rapidly at 4.2° K. Under conditions of high-power input and high conversion, as used by Wiener and Burton (12), the main hydrocarbon product of the discharge decomposition of methane is acetylene. In their work they consider that both methyl and methylene radicals contribute to the over-all reaction.

Can. J. Chem. Downloaded from www.nrcresearchpress.com by 186.148.149.217 on 09/04/12
For personal use only.

In view of the above evidence and our experimental results it seems reasonable to assume that in our experiments methane decomposes according to reaction 1. The main product, ethane, would then be formed by reaction 2 which may occur to a large extent on the wall.

$$CH_4 \xrightarrow{e} CH_3 + H \quad [1]$$

$$2CH_3 \longrightarrow C_2H_6 \quad [2]$$

It would be difficult, however, to account for the complex product obtained solely on the basis of the reactions of methyl radicals, even allowing for the possible subsequent formation of other saturated radicals. During the last few years a considerable amount of chemical evidence has been obtained for the existence of excited methylene radicals (13) and recently the existence of the methylene radical in an excited state has been confirmed spectroscopically (14). Burton and Magee (15) have suggested that excited methylene radicals play an important part in the discharge decomposition of methane.

The data in Figs. 4A and 5A indicate that the rate of decomposition of methane increases linearly with both current and pressure, presumably due to the increase in the number of collisions between electrons and methane molecules. However, the amounts of ethylene and acetylene formed increase more rapidly with pressure than that of ethane, whereas the relative amounts of these products do not change with increasing current. This can be accounted for by assuming that, in addition to reaction 1, methane can decompose to yield another species which is capable of reacting with methane at the low temperature of the experiment. Thus, a reaction such as reaction 3 is indicated, where * designates an excited species. This would then be followed by reactions such as 4, 5, 6, and 7. Reaction 6 may occur to a large extent on the wall.

$$CH_4 \xrightarrow{e} CH_2^* + H_2 \quad [3]$$

$$CH_2^* + CH_4 \longrightarrow [C_2H_6]^* \quad [4]$$

$$[C_2H_6]^* \longrightarrow C_2H_4^* + H_2 \quad [5]$$

$$C_2H_4^* \xrightarrow{M} C_2H_4 \quad [6]$$

$$C_2H_4^* \longrightarrow C_2H_2 + H_2 \quad [7]$$

It has been reported (16) that energy-rich ethylene molecules may stabilize by deactivation as in reaction 6 or by decomposition as in reaction 7. If the excited state of ethylene involved in this work is different from that encountered in the mercury-photosensitized decomposition, it is possible that reactions 5 and 7 may involve as intermediates ethyl and vinyl radicals, with the resulting formation of hydrogen atoms. From the fact that the experiments with methane containing up to 10% hydrogen showed no appreciable change in the products, it seems probable that hydrogen atoms do not play a major part in the over-all reaction scheme.

Assuming that most of the methyl radicals combine to form ethane as in reaction 2, it follows that the rate of formation of ethane should increase linearly with both pressure and current, which is approximately the case. The rates of formation of ethylene and acetylene should increase linearly with current but, because of the dependence of reaction 4 on methane concentration, should increase more rapidly than that of ethane as the methane pressure is increased.

The increase in the rate of formation of acetylene, at the apparent expense of ethylene, with increasing electron energy (Fig. 3B) might be explained on the basis of the inter-

Can. J. Chem. Downloaded from www.nrcresearchpress.com by 186.148.149.217 on 09/04/12
For personal use only.

dependence of reactions 6 and 7. If the energy imparted to the methylene radical increases as the electron energy is increased this might result in an ethylene molecule possessing increasing amounts of energy and therefore in an increase in the rate of its decomposition (reaction 7) at the expense of deactivation (reaction 6).

Although the over-all extent of methane decomposition is small, most of the decomposition occurs within the electron beam giving locally a relatively high concentration of radicals and product molecules. As a result, radical–radical and radical–product reactions might be expected to occur. There is thus the possibility of forming other radicals by reactions such as 8 and 9.

$$CH_2^* + CH_3 \longrightarrow C_2H_5^* \quad [8]$$

$$C_2H_5^* \longrightarrow C_2H_3 + H_2 \quad [9]$$

The formation of the hydrocarbons of higher molecular weight may be accounted for in a general way as being due to further reactions of the free radicals present. Some of them may arise by simple radical combination reactions such as 10 and 11.

$$CH_3 + C_2H_5 \longrightarrow C_3H_8 \quad [10]$$

$$2C_2H_5 \longrightarrow C_4H_{10} \quad [11]$$

Others may be formed by reactions between radicals and product molecules. Vanpee and Grard (17) have suggested that higher hydrocarbons can be formed stepwise by reactions like 12 and 13.

$$CH_2 + C_2H_4 \longrightarrow C_3H_6 \quad [12]$$

$$CH_2 + C_2H_6 \longrightarrow C_3H_8 \quad [13]$$

Their suggestion has been confirmed by much recent work (13, 18). In addition, Gordon and McNesby (19) have shown that the polymerization of ethylene by methyl radicals results in the formation of many of the higher hydrocarbons found here.

One of the higher products, butadiene, seems to deserve individual consideration. The curves giving the variation in the percentage of this compound are not consistent with those of the other C_4 hydrocarbons but instead parallel those of acetylene. There is thus evidence that butadiene is formed by some species associated with the formation of acetylene. One possibility is given by reaction 14.

$$2C_2H_3 \longrightarrow C_4H_6 \quad [14]$$

The narrow limits within which the experiments could be carried out and the large amount of scatter in the experimental points make it difficult to arrive at a definite mechanism for the formation of most of the C_3 and C_4 products. The reactions occurring may involve highly excited species and therefore may not be comparable with the work referred to in the preceding paragraphs. Nevertheless, it seems to follow from Fig. 4 that the slopes of the lines representing the saturated hydrocarbon products are similar to one another, and that the olefins behave as another group. It is tempting to relate this to a stepwise process for the formation of the higher hydrocarbons as suggested by Vanpee and Grard (17).

ACKNOWLEDGMENTS

The authors wish to express their appreciation to Dr. R. J. Cvetanović for several helpful discussions, to Mr. S. Tong for assistance with the experimental work, and to Mr. R. Sander, who carried out the mass spectrometer analyses.

Can. J. Chem. Downloaded from www.nrcresearchpress.com by 186.148.149.217 on 09/04/12
For personal use only.

REFERENCES

1. D. P. STEVENSON and D. O. SCHISSLER. J. Chem. Phys. **23**, 1353 (1955).
2. L. M. YEDDANAPALLI. J. Chem. Phys. **10**, 249 (1942).
3. A. W. TICKNER. To be published.
4. A. W. TICKNER and F. P. LOSSING. J. Phys. Chem. **55**, 733 (1951).
5. B. A. TOZER. J. Electronics and Control, **4**, 149 (1958).
6. R. R. WILLIAMS. J. Phys. Chem. **63**, 776 (1959).
7. K. YANG and P. J. MANNO. J. Am. Chem. Soc. **81**, 3507 (1959).
8. RADIATION BIOLOGY. Vol. I. High energy radiation. *Edited by* A. Hollaender. McGraw-Hill Book Co. Inc., New York. 1954.
9. L. H. GEVANTMAN and R. R. WILLIAMS. J. Phys. Chem. **56**, 569 (1952).
10. G. G. MEISELS, W. H. HAMILL, and R. R. WILLIAMS. J. Phys. Chem. **61**, 1456 (1957).
11. C. K. JEN, S. N. FONER, E. L. COCHRAN, and V. A. BOWERS. Phys. Rev. **112**, 1169 (1958).
12. H. WIENER and M. BURTON. J. Am. Chem. Soc. **75**, 5815 (1953).
13. H. M. FREY and G. B. KISTIAKOWSKY. J. Am. Chem. Soc. **79**, 6373 (1957).
H. M. FREY. Proc. Roy. Soc. A, **250**, 409 (1959); A, **251**, 575 (1959).
14. G. HERZBERG and J. SHOOSMITH. Nature, **183**, 1801 (1959).
15. M. BURTON and J. L. MAGEE. J. Chem. Phys. **23**, 2195 (1955).
16. D. J. LEROY and E. W. R. STEACIE. J. Chem. Phys. **9**, 829 (1941).
A. B. CALLEAR and R. J. CVETANOVIĆ. J. Chem. Phys. **24**, 873 (1956).
17. M. VANPEE and F. GRARD. Ann. mines Belg. **49**, 701 (1950).
18. W. VON E. DOERING and H. PRINZBACH. Tetrahedron, **6**, 24 (1959).
19. A. S. GORDON and J. R. MCNESBY. J. Chem. Phys. **31**, 853 (1959).

Can. J. Chem. Downloaded from www.nrcresearchpress.com by 186.148.149.217 on 09/04/12
For personal use only.

Can. J. Chem. Downloaded from www.nrcresearchpress.com by 186.148.149.217 on 09/04/12
For personal use only.

THE CELL WALL POLYSACCHARIDES OF CANDIDA ALBICANS: GLUCAN, MANNAN, AND CHITIN[1]

C. T. BISHOP, F. BLANK,[2] AND P. E. GARDNER[3]

ABSTRACT

Cells of *Candida albicans*, a pathogenic yeast, have been shown to contain, in addition to chitin, a glucan ($[\alpha]_D$ −30°) and a mannan ($[\alpha]_D$ +78°) in the approximate ratio of 1.00:0.64. The two polysaccharides were easily distinguishable by moving boundary electrophoresis in borate buffer and were separated from each other by fractionation of their copper complexes. Methylation and hydrolysis of the glucan yielded the following *O*-methyl ethers of D-glucose: 2,3,4,6-tetra-*O*-methyl (7 moles); 2,3,4-tri-*O*-methyl (13 moles); 2,4,6-tri-*O*-methyl (trace); 2,4-di-*O*-methyl (6 moles); and 2-*O*-methyl (1 mole). It was concluded that the glucan was a highly branched polysaccharide containing $\beta\,1 \rightarrow 6$ and $\beta\,1 \rightarrow 3$ linked residues. Periodate oxidation of the glucan supported this conclusion.

Methylation and hydrolysis of the mannan yielded the following *O*-methyl ethers of D-mannose: 2,3,4,6-tetra-*O*-methyl (1.65 moles); 3,4,6-tri-*O*-methyl (1.00 mole); 2,3,6-tri-*O*-methyl (0.18 mole); 3,4-di-*O*-methyl (1.90 moles). The mannan was therefore a highly branched polysaccharide with short chains of $\alpha\,1 \rightarrow 2$ linked mannose residues joined together by $\alpha\,1 \rightarrow 6$ linkages. Results of periodate oxidation agreed with this structure.

The differences between these two polysaccharides and glucans and mannans found in other yeasts are discussed.

Structural investigations of polysaccharide components of yeasts have been limited, with only one exception, to those in bakers' yeast (*Saccharomyces cerevisiae*) and there are a number of reports dealing with the glucan (1–4) and mannan (5–7) that occur in this species. The only report dealing with structures of polysaccharides from other yeast species appears to be that by Gorin and Perlin (8) which described a mannan produced by *Saccharomyces rouxii*. There have been other publications on the composition of cell walls of yeasts (9–18) and some of these (13–18) have dealt with species other than *Saccharomyces cerevisiae*. However, these papers were concerned primarily with examination of fractions of yeast cell walls by X-ray diffraction, electrophoresis, and chromatography of hydrolyzates; structures of polysaccharides were not investigated and constituent sugars were identified only by paper chromatography. The identification of D-arabinose as a constituent of polysaccharides found in *Nocardia asteroides* (19) and *Mycobacterium tuberculosis* (20) has shown that sugars can occur in unusual configurations in microorganisms. For this reason the distinction of enantiomorphic forms of naturally occurring sugars is of considerable significance and such distinction cannot be made by paper chromatography. It was therefore of interest to examine the polysaccharides of another species of yeast, *C. albicans*, to see if they differed in structure or constituent sugars from the polysaccharides of bakers' yeast. In addition to this a report that the polysaccharides of *C. albicans*, a pathogenic yeast, are serologically active (21) indicated that elucidation of their structures could be of immunological significance.

Isolation of Glucan and Mannan from C. albicans

Crude polysaccharides were isolated from powdered cells of *C. albicans* by the procedure given in the Experimental section. The product contained no nitrogen and hence was free from any proteinaceous material. Examination of this crude preparation by moving

[1]*Manuscript received January 29, 1960.*
Contribution from the Division of Applied Biology, National Research Council, Ottawa, and the Department of Bacteriology and Immunology, McGill University, Montreal, Que. Presented in part at the Annual Conference of the Chemical Institute of Canada, Halifax, June 1959.
Issued as N.R.C. No. 5662.
[2]*Department of Bacteriology and Immunology, McGill University, Montreal, Que.*
[3]*National Research Council Postdoctorate Fellow 1957–1959.*

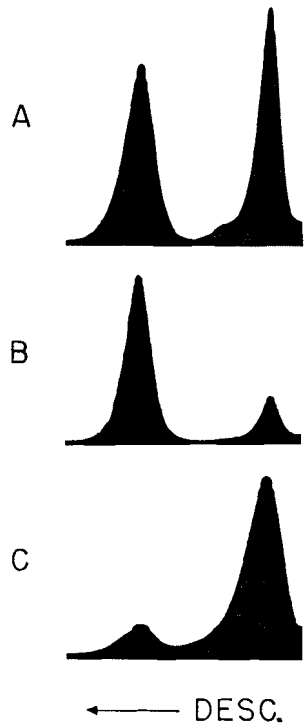


FIG. 1. Moving boundary electrophoresis of (A) crude polysaccharides, (B) mannan + trace of glucan, (C) glucan + trace of mannan.

boundary electrophoresis in borate buffer gave the separation pattern shown in Fig. 1A. The result clearly indicated two components; these were present in an approximate ratio of 0.61–0.67:1.00. Hydrolysis and chromatography of the crude polysaccharide preparation revealed the presence of mannose and glucose in a molar ratio of 0.50:1.00. The reasonable agreement between this ratio and the ratio of the two components found by electrophoresis indicated that these two components were a glucan and a mannan. This conclusion was confirmed by the isolation of a glucan and a mannan by fractionation with Fehling's solution. Fractions in which each polysaccharide still contained traces of the other were used to identify the two peaks in the electrophoretic separation. Figure 1B is the electrophoretic pattern given by the mannan-rich fraction and Fig. 1C is that given by the glucan-rich fraction. All three separations shown in Fig. 1 were photographed after the same time interval; the results show clearly that the component of greater mobility was the mannan, and the one with lower mobility the glucan. Electrophoretic mobilities of the two components were the same after fractionation as before, an indication that the separation procedure had not altered the polysaccharides.

Isolation of a glucan and a mannan from *C. albicans* has not been reported before. Jonsen *et al.* (15) isolated a polysaccharide preparation from the same organism and identified glucose and mannose by paper chromatography after hydrolysis. However, these authors obtained a single peak on electrophoresis of the polysaccharide in acetate buffer and accepted this as indicative of homogeneity. Polysaccharides, unless they contain acidic groups, would be expected to have very similar mass:charge ratios and hence would not be separable by electrophoresis in acetate buffer. The electrophoretic

Can. J. Chem. Downloaded from www.nrcresearchpress.com by 186.148.149.217 on 09/04/12
For personal use only.

separations reported in the present communication depended on the polysaccharides being complexed to different extents with borate (22) thereby acquiring different mass: charge ratios which permitted their separation. More recently Kessler and Nickerson (18) have reported the isolation of glucomannan–protein and glucan–protein complexes from three strains of *C. albicans*. However, the fractionation procedure used, alkali extraction and ammonium sulphate precipitation, was not designed to separate the polysaccharides nor was any criterion of homogeneity of the fractions reported. It is very likely, in view of the present work, that the glucomannans reported (15, 18) in *C. albicans* were mixtures of a glucan and mannan.

The glucan and mannan found in *Saccharomyces cerevisiae* have been established as components of the cell wall (9); this is also thought to be true for the glucan and mannan from *C. albicans* because an isolated cell wall preparation yielded glucose and mannose on hydrolysis.

A small amount of chitin was isolated from the cell wall of *C. albicans* and identified by X-ray diffraction. These results agree with those of other workers (12, 13, 14) who have reported the presence of chitin in small and variable amounts in the cell walls of a number of yeast species, including *C. albicans*.

Glucan from C. albicans

The glucan gave a number average degree of polymerization of 30 ± 2. On acid hydrolysis it yielded D-glucose, characterized as the *p*-nitroanilide and by specific rotation, as the only detectable sugar. Its negative rotation ($[\alpha]_D$ $-30°$) indicated that a high proportion of β-glycosidic bonds were present and its stability to hot dilute oxalic acid showed that furanose ring forms were absent.

When oxidized by periodate the glucan consumed 1.60 moles of oxidant and yielded 0.72 mole of formic acid per mole anhydroglucose. The latter value indicated that about 70% of the D-glucose units were non-reducing terminal units or were joined to adjacent units by $1 \rightarrow 6$ linkages. The very small amount of oxidant not accounted for by formic acid production indicated that most, if not all, of the remaining 28% of glucose units were substituted so that they were resistant to oxidation by periodate. This conclusion was confirmed by reduction and hydrolysis of the periodate-oxidized polysaccharide (23) which yielded glycerol and glucose as the only products detectable by paper chromatography. The glycerol arose from C_4, C_5, and C_6 of those glucose units which were terminal or 1,6-disubstituted and the glucose represented those units in the glucan that were not oxidized. No erythritol could be found in the hydrolyzate of the oxidized, reduced polysaccharide and therefore no $1 \rightarrow 4$ linkages were present in the glucan (23). The above results showed that in the glucan 72% of the glucose units were non-reducing terminal units or were joined by $1 \rightarrow 6$ linkages, the remainder being $1 \rightarrow 3$ linked or highly substituted in a branched structure.

The glucan was methylated and hydrolyzed to give the methyl ethers listed in Table I.

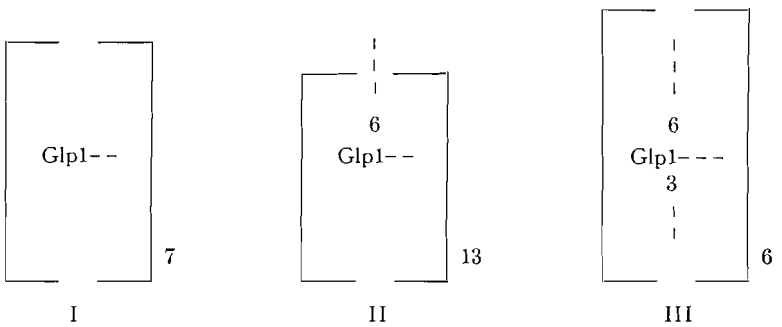
TABLE I

Hydrolysis products of methylated glucan

2,3,4,6-Tetra-*O*-methyl-D-glucose	(7 moles)
2,3,4-Tri-*O*-methyl-D-glucose	(13 moles)
2,4,6-Tri-*O*-methyl-D-glucose	(Trace)
2,4-Di-*O*-methyl-D-glucose	(6 moles)
2-*O*-Methyl-D-glucose	(1 mole)

Can. J. Chem. Downloaded from www.nrcresearchpress.com by 186.148.149.217 on 09/04/12
For personal use only.

The main products shown here must have arisen from the following structural units in the polysaccharide:



Thus 2,3,4,6-tetra-*O*-methyl-D-glucose represented non-reducing terminal units substituted only in position 1 (I); 2,3,4-tri-*O*-methyl-D-glucose came from units that were joined through positions 1 and 6 (II); 2,4-di-*O*-methyl-D-glucose arose from units that were linked through positions 1, 3, and 6 (III). The significance of the 2,4,6-tri-*O*-methyl-D-glucose and the 2-*O*-methyl-D-glucose is difficult to assess because of the small amounts found and because the methylated glucan, methylated to constant methoxyl and showing no hydroxyl absorption in the infrared, still contained only 40.5% methoxyl (calc. 45.6%). It is possible that the polysaccharide contained an impurity other than protein (e.g. lipid) which caused this low methoxyl. A glucan, containing the above three structural units in the amounts indicated, would consume 1.54 moles of periodate per mole anhydroglucose with production of 0.77 mole of formic acid per mole anhydroglucose. These are in good agreement with the values of 1.60 and 0.72 that were found for periodate consumption and formic acid production respectively in the purified glucan. If there was an impurity in the glucan which caused the low methoxyl then it must have consumed periodate, otherwise these values would be lower than theoretical. The results of the methylation study therefore confirmed the conclusions based on periodate oxidation and showed clearly that the glucan from *C. albicans* was a highly branched polysaccharide formed from β 1 $\rightarrow$ 6 and β 1 $\rightarrow$ 3 linked glucose residues. This structure is quite different from those proposed by various workers (1, 2, 3, 4) for the glucan from *Saccharomyces cerevisiae*. Hassid *et al.* (1) found 2,4,6-tri-*O*-methyl-D-glucose as the only product from methylation and hydrolysis of that glucan and therefore proposed a straight chain, β 1 $\rightarrow$ 3 linked structure. On the other hand, Bell and Northcote (2) reported similar experiments in which the products from methylation and hydrolysis showed that the glucan was branched with chains of β 1 $\rightarrow$ 3 linked units being joined by 1 $\rightarrow$ 2 interchain links. Peat *et al.* (3) have shown by fragmentation analysis that the glucan from *Saccharomyces cerevisiae* was a linear polysaccharide formed by β 1 $\rightarrow$ 3 and β 1 $\rightarrow$ 6 glycosidic linkages. A succeeding report (4) showed that some 10–20% of the linkages were β 1 $\rightarrow$ 6. The glucan from *C. albicans* differs from these three structures reported for the glucan from *Saccharomyces cerevisiae* in being much more highly branched and having a preponderance (73%) of β 1 $\rightarrow$ 6 linkages.

Mannan from C. albicans

The mannan showed a number average degree of polymerization of 41$\pm$2 and had a

Can. J. Chem. Downloaded from www.nrcresearchpress.com by 186.148.149.217 on 09/04/12
For personal use only.

specific rotation of $+78°\pm2°$. Mannose was the only sugar detectable by paper chromatography and electrophoresis after acid hydrolysis and it was proved to be D-mannose by the specific rotation ($+13°\pm2°$) and by isolation of its crystalline phenylhydrazone. The decrease in rotation after hydrolysis indicated that α-glycosidic bonds were predominant. The mannan was stable to hot, dilute oxalic acid showing that no furanose ring forms were present.

On methylation and hydrolysis the mannan yielded the components shown in Fig. 2.

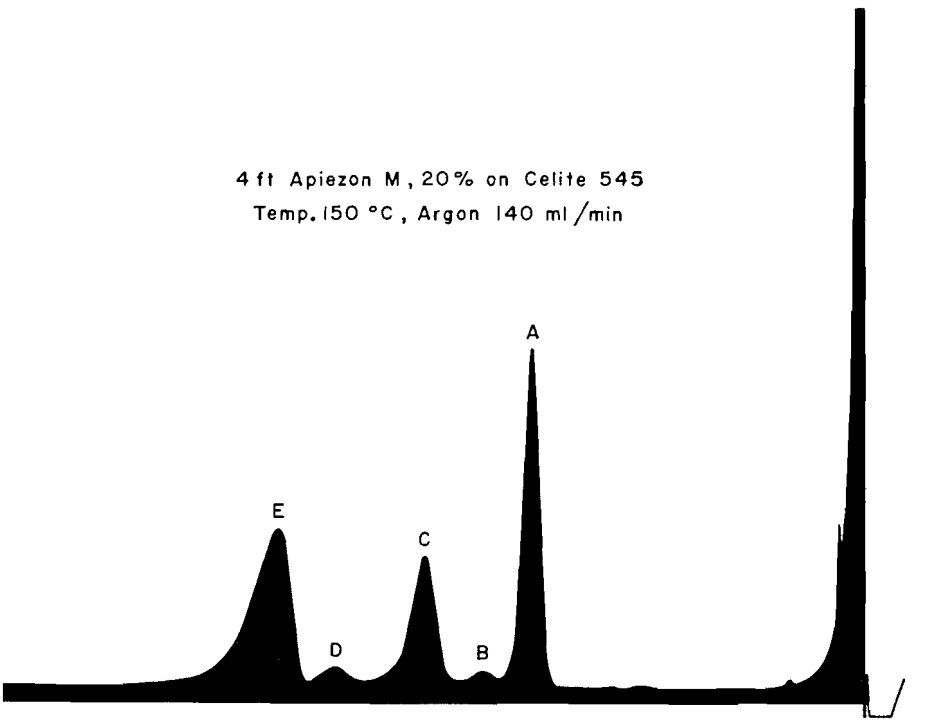
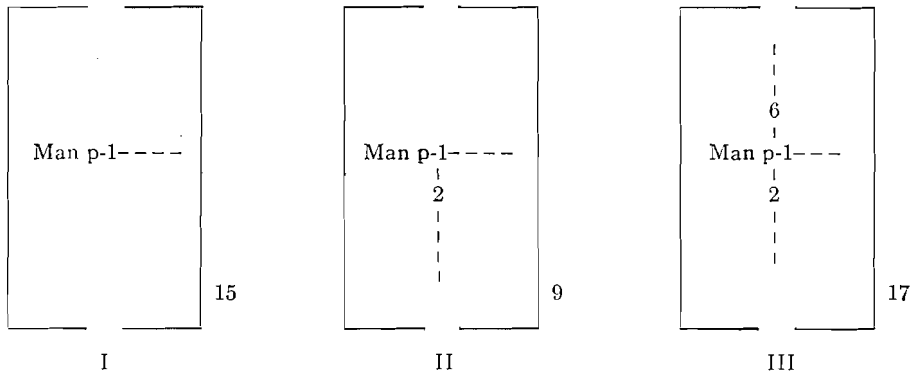


FIG. 2. Separation of methanolysis products from methylated mannan by gas–liquid partition chromatography.

		Molar ratio
(A)	Methyl-2,3,4,6-tetra-*O*-methyl-α-D-mannopyranoside	1.65
(B)	Unknown	0.13
(C)	Methyl-3,4,6-tri-*O*-methyl-α-D-mannopyranoside	1.00
(D)	Methyl-2,3,6-tri-*O*-methyl-α-D-mannopyranoside	0.18
(E)	Methyl-3,4-di-*O*-methyl-α-D-mannopyranoside	1.90

This is a reproduction of the separation curve from gas–liquid partition chromatography of the methanolysis products from the methylated mannan. This technique was developed only recently (24, 25) and was not available for use when the glucan from *C. albicans* was being investigated. Components A, C, and E were identified by isolation of crystalline derivatives and represented the main structural units of the mannan. The quantities of components B and D were too small to permit unequivocal identifications but component D was identical on gas–liquid partition chromatograms with an authentic sample of methyl-2,3,6-tri-*O*-methyl-α-D-mannopyranoside. The main structural features of the mannan could therefore be represented by the following units.

Can. J. Chem. Downloaded from www.nrcresearchpress.com by 186.148.149.217 on 09/04/12
For personal use only.



Thus components A, C, and E in Fig. 2 represented structural units I, II, and III respectively. The significance of components B and D in Fig. 4 is uncertain because of the possibility that they were products of incomplete methylation or of demethylation on hydrolysis. The amount of non-reducing terminal end groups (I) is slightly less than required to account for the branch points (III). A loss of 13% of the 2,3,4,6-tetra-*O*-methyl-D-mannose during evaporations of the formic acid hydrolyzate could account for this. It is possible that such discrepancies have not been detected previously because of the lack of accurate quantitative data as supplied by gas–liquid partition chromatography. A polysaccharide composed of structural units I, II, and III should consume 1.37 moles of periodate per mole anhydromannose with production of 0.37 mole of formic acid per mole anhydromannose. The values actually found, 1.13 and 0.27 moles per mole anhydromannose, respectively, were slightly lower and could have been caused by an impurity present in the mannan during periodate oxidation but removed during methylation, or again could be a result of greater accuracy of the gas–liquid partition chromatography data as compared with the periodate oxidation data. After periodate oxidation the resulting polyaldehyde was reduced and hydrolyzed (23). Glycerol was the only polyol detectable in the hydrolyzate, in agreement with the finding from methylation that only $1 \rightarrow 2$ and $1 \rightarrow 6$ bonds were present. It was clear from the foregoing data that the mannan possessed a highly branched structure in which relatively short chains of $\alpha\, 1 \rightarrow 2$ linked mannose units were joined together by $\alpha\, 1 \rightarrow 6$ linkages. The mannan from *C. albicans* is therefore somewhat different from the mannan isolated from bakers' yeast (*Saccharomyces cerevisiae*) (5, 6, 7) and more closely resembles that found in *Saccharomyces rouxii* (8). All of these mannans exhibited high positive specific rotations, which indicated the presence of α-glycosidic linkages, and this has been confirmed unequivocally (8) for the $1 \rightarrow 2$ linkage in the mannan from *Saccharomyces rouxii*. The difference lies in the tri-*O*-methyl-D-mannoses found after hydrolysis of the methylated mannans. The methylated mannans from bakers' yeast (5, 6, 7) yielded equimolar amounts of 2,4,6- and 3,4,6-tri-*O*-methyl-D-mannose indicative of an equal number of $1 \rightarrow 3$ and $1 \rightarrow 2$ linkages in the unbranched portion of the polysaccharide. On the other hand, the methylated mannan from *Saccharomyces rouxii* (8) yielded 2,4,6- and 3,4,6-tri-*O*-methyl-D-mannose in a ratio of 2:7 indicating that $1 \rightarrow 2$ linkages predominated over $1 \rightarrow 3$. The mannan from *C. albicans* yielded no 2,4,6-tri-*O*-methyl-D-mannose after methylation and hydrolysis and therefore could not have contained any $1 \rightarrow 3$ linkages. This conclusion was substantiated by the absence of mannose in the hydrolyzate of the periodate-oxidized mannan because any $1 \rightarrow 3$ linked mannose residues would have survived the oxidation. This

Can. J. Chem. Downloaded from www.nrcresearchpress.com by 186.148.149.217 on 09/04/12
For personal use only.

absence of 1 → 3 linkages and the high degree of branching constitute the main differences between the mannan from *C. albicans* and those so far examined from other yeasts.

EXPERIMENTAL

Paper chromatograms were run by the descending method using the following solvent systems (v/v ratio):

(A) butan-1-ol:pyridine:water, 6:4:3;
(B) butan-1-ol:ethanol:water, 9:3:3;
(C) 2-butanone:water, azeotrope.

Paper electrophoreses were done on Whatman 3 MM paper in 0.1 *M* borate buffer (22) using a potential gradient of 25 v/cm for 1 hour. Sugars were detected on chromatograms and electrophorograms by the *p*-anisidine hydrochloride spray reagent (26). Non-reducing compounds were detected on chromatograms by silver nitrate : sodium hydroxide sprays (27). Moving boundary electrophoreses were carried out in 0.05 *M* borate buffer in a Tiselius-type, Spinco Model H apparatus. Evaporations were carried out under diminished pressure at 35° C or less on a rotary film evaporator. Melting points are corrected and specific rotations are equilibrium values unless stated otherwise.

Isolation of Crude Polysaccharides

C. albicans was cultured in a liquid medium containing the following nutrients: 4% cerelose (crude glucose), 2% neopeptone "Difco", 0.05% yeast extract, 0.001% thiamin, 0.005% inositol. After incubation at 37° C for 5–12 days the cultures were autoclaved at 121° C for 20 minutes; cells were then separated in a continuous centrifuge, freeze-dried, and ground in a ball mill for 16 hours. Extraction with petroleum ether (30–60° C) removed lipid, and digestion with trypsin destroyed protein. The residue from these two treatments was then extracted with boiling 3% aqueous sodium hydroxide to solubilize the polysaccharides, which were freed from low molecular weight impurities by dialysis and precipitation with ethanol. The polysaccharide preparation thus obtained (6.3% of the dried, powdered cells) was a light tan powder which contained no nitrogen as shown by microanalysis. A sample of this material was hydrolyzed by *N* hydrochloric acid at 97° C in a sealed tube for 16 hours. Paper chromatography (solvent A) and paper electrophoresis of the hydrolyzate showed two components which were identical with samples of glucose and mannose run on the same paper strips. Another sample (150 mg) of the polysaccharide preparation was dissolved in 0.05 *M* sodium tetraborate, equilibrated with the buffer by dialysis, and examined by moving boundary electrophoresis. Figure 1A shows the complete separation of two components that was obtained by this procedure. The electrophoretic mobilities (μ) of these two components were respectively 4.38 and 9.34×10^{-5} cm^2 v^{-1} sec^{-1}. Areas under the two peaks were measured from diagrams obtained at two different times and gave ratios of the two components of 0.61:1.00 and 0.67:1.00. The molar ratio of mannose to glucose in the hydrolyzate of the polysaccharide mixture was 0.50:1.00 as determined by the densitometer method of Martin (28).

Separation of Glucan and Mannan

The crude polysaccharides (8.0 g) were stirred vigorously in water (1200 ml) for 3 hours. Insoluble material was removed by centrifugation and dried by solvent exchange with ethanol and ether (yield, 0.9 g). Paper electrophoresis of a hydrolyzate of a sample from this fraction showed that glucose was the only component sugar present. Hydrolysis and paper electrophoresis of the material in solution showed the presence of both glucose and mannose. An attempt was made to separate the mixture of polysaccharides in aqueous

Can. J. Chem. Downloaded from www.nrcresearchpress.com by 186.148.149.217 on 09/04/12
For personal use only.

Can. J. Chem. Downloaded from www.nrcresearchpress.com by 186.148.149.217 on 09/04/12
For personal use only.

solution by fractional precipitation with ethanol (29) but the fractions obtained showed no variation in glucose and mannose composition. These fractions were therefore combined, redissolved in water, and the polysaccharides were precipitated as copper complexes by addition of Fehling's solution. This method was used successfully by Haworth *et al.* (5) to isolate a mannan from bakers' yeast. The precipitated copper complex was washed repeatedly with water and at the sixth washing the precipitate dissolved. This solution was poured into 5 volumes of 10% methanolic hydrogen chloride to precipitate the polysaccharide which was dried by solvent exchange with ethanol and ether (yield, 2.13 g). Paper electrophoresis of a hydrolyzate of a sample from this fraction showed that mannose was the only component sugar present. The washings from the precipitated copper complex were combined and the polysaccharides were recovered by precipitation with acidified ethanol. This material was then recomplexed with copper and washed with water in the same way as before. Four repetitions of this procedure yielded two more polysaccharide fractions, one yielding mainly mannose but with a trace of glucose on hydrolysis and the other yielding mainly glucose with a trace of mannose. To preserve the chemically pure glucan and mannan for structural studies these impure fractions were used to determine the identities of the two peaks found in electrophoresis. The electrophoretic diagram shown in Fig. 1B is that given by the fraction yielding mainly mannose on hydrolysis but with a trace of glucose. Figure 1C shows the electrophoretic pattern given by the fraction yielding glucose on hydrolysis with only a trace of mannose. Fractionation in the same way of another 6.0 g of crude polysaccharides provided further quantities of pure glucan (0.60 g) and mannan (1.5 g).

Properties of Purified Glucan and Mannan

Glucan

This polysaccharide had $[\alpha]_D^{26} = -30° \pm 2°$ (*c*, 1.0% in *N* sodium hydroxide) changing to $[\alpha]_D^{26} = +53° \pm 2°$ (*c*, 2.0% in *N* hydrochloric acid) after hydrolysis in *N* hydrochloric acid at 97° C for 16 hours. The hydrolyzate was neutralized (Amberlite IR-45 ion exchange resin), evaporated to dryness, and the residue was heated with *p*-nitroaniline in methanol solution for 40 minutes. The solution was cooled and the crystals which separated were recrystallized from methanol to yield *N*-*p*-nitrophenyl-D-glucopyranosylamine dihydrate (30), m.p. 183–184° C, $[\alpha]_D^{25} = -199° \pm 1°$ (*c*, 1.0% in pyridine). Attempted partial hydrolysis of the glucan by 0.025 *N* oxalic acid at 97° C for 3 hours released no cleavage products detectable by paper chromatography. The degree of polymerization of the glucan was 30 ± 2 as determined by hypoiodite oxidation of the reducing end group in phosphate buffer (31).

Mannan

This polysaccharide had $[\alpha]_D^{26} = +78 \pm 2°$ (*c*, 1.1% in water) changing to $[\alpha]_D^{26} = +13° \pm 2°$ (*c*, 2.0% in *N* hydrochloric acid) after hydrolysis in *N* hydrochloric acid at 97° C for 16 hours. The hydrolyzate was neutralized (Amberlite IR-45 ion exchange resin), mixed with an equal volume of an aqueous solution of phenylhydrazine acetate, and allowed to stand at 25° C for 20 hours. The crystals which formed were recrystallized twice from water:ethanol to yield mannose phenylhydrazone (32), m.p. 198–199° C (d), $[\alpha]_D^{24} = +25° \pm 2°$ (*c*, 1.0% in pyridine). Like the glucan, the mannan showed no evidence of partial hydrolysis when heated with 0.025 *N* oxalic acid at 97° C for 3 hours. The degree of polymerization of the mannan, estimated in the same way as for the glucan, was 41 ± 2.

Periodate Oxidations

The glucan (111.2 mg, 0.66 mmole) and mannan (122.3 mg, 0.75 mmole) were dissolved separately in water (125 ml) and 0.25 *M* sodium periodate (25 ml) was added to each. Reagent blanks were also prepared and oxidations were carried out at 25° C in the absence of light. At the intervals noted below samples were removed for estimation of formic acid and periodate. For estimation of formic acid the excess periodate in a 10-ml aliquot was destroyed by 2,3-butanediol, a few crystals of potassium iodide were added and the liberated iodine was titrated to a starch end point with 0.01 *N* thiosulphate. For periodate estimations (33, 34) sodium bicarbonate (1.7 g), 0.1 *N* sodium arsenite (5 ml), and a few crystals of potassium iodide were added to 10-ml aliquots from the oxidations. The solutions were stored in the dark for 30 minutes and were then titrated with 0.022 *N* iodine solution to a starch end point. The results, given in moles per anhydrohexose unit were as follows:

Time, hours	Glucan		Mannan	
	Formic	Periodate	Formic	Periodate
24	0.68	1.60	0.21	1.10
44	0.71	1.58	0.26	1.10
70	0.72	1.61	0.27	1.13

After the oxidations were complete excess periodate was destroyed by 2,3-butanediol and salts and acetaldehyde were removed by dialysis. The oxidized polysaccharides were then reduced by potassium borohydride, hydrolyzed by *N* hydrochloric acid at 97° C for 3 hours and the hydrolyzates were examined by paper chromatography (solvent B, silver nitrate : sodium hydroxide sprays) (23). By this sequence of reactions the glucan yielded glycerol and glucose while the mannan gave only glycerol. Erythritol was not found in either hydrolyzate.

Methylation of Glucan and Mannan

Glucan

The glucan (893 mg) was methylated five times for 24 hours in 30% sodium hydroxide (20 ml) and dimethyl sulphate (10 ml). The product was isolated by extraction into chloroform and was treated for 24 hours in that solvent (10 ml) with methyl iodide (6 ml) and silver oxide (3.0 g). After three further methylations with methyl iodide and silver oxide, the methylated polysaccharide was precipitated as a white powder (1.0 g, methoxyl = 40.5%) from chloroform solution by addition of petroleum ether (30–60° C). The methoxyl content of this product was not increased by another methylation and an infrared spectrum showed only a trace of hydroxyl absorption. The powdery product was extracted with petroleum ether and then successively with petroleum ether containing increasing amounts of chloroform. All fractions showed identical hydrolysis products on paper chromatograms and the main portion of the product dissolved in petroleum ether : chloroform mixtures of 6:4, 5:5, and 4:6. These three fractions were combined and reprecipitated to give a white powder (660 mg, methoxyl 40.5%) showing no hydroxyl absorption in the infrared.

Mannan

The mannan (2.14 g) was methylated five times with 30% sodium hydroxide

Can. J. Chem. Downloaded from www.nrcresearchpress.com by 186.148.149.217 on 09/04/12
For personal use only.

(5×100 ml) and dimethyl sulphate (5×50 ml) in the same way as described for the glucan. The product (2.29 g) showed distinct hydroxyl absorption in the infrared so it was methylated again, this time in tetrahydrofuran (30 ml) with sodium hydroxide (10 g) and dimethyl sulphate (15.5 ml) (35). The product still showed hydroxyl absorption in the infrared and had methoxyl equal to 39.7% so it was methylated again in tetrahydrofuran as before. This methylation gave a product (2.20 g) having no hydroxyl absorption in the infrared and with methoxyl equal to 40.4%, unchanged by another methylation. The methylated polysaccharide was extracted with boiling petroleum ether (30–60° C). The extract was removed by decantation and evaporated to yield an oily product (methoxyl = 29%) which was discarded. The residue from this extraction was stirred in ether and the insoluble portion was removed by centrifugation. The ethereal supernatant was evaporated to yield the methylated mannan (1.56 g, methoxyl = 43.2%), which showed no hydroxyl absorption in the infrared.

Hydrolysis Products from Methylated Glucan

The methylated glucan (650 mg) was hydrolyzed by formic acid according to the procedure described by Jones and Wilkie (36). Qualitative and quantitative (37) paper chromatography gave approximate molar ratios of the methyl ethers of glucose shown in Table I.

The mixture of methylated sugars (645 mg) was resolved on a cellulose column (2.3×28 cm) using solvent C to give four fractions. *Fraction 1* (73.5 mg) contained only 2,3,4,6-tetra-*O*-methyl-D-glucose; *fraction 2* (126.4 mg) contained 2,3,4,6-tetra-*O*-methyl-D-glucose and 2,3,4-tri-*O*-methyl-D-glucose; *fraction 3* (236.8 mg) contained 2,3,4-tri-*O*-methyl-D-glucose and a trace of 2,4,6-tri-*O*-methyl-D-glucose; *fraction 4* (126.7 mg) contained 2,4-di-*O*-methyl-D-glucose with a trace of 2-*O*-methyl-D-glucose (recovery = 563.4 mg, 87.4%). Those fractions which were mixtures were resolved further by preparative paper chromatography on Whatman 3 MM paper using solvent C, and individual components were identified as described below.

2,3,4,6-Tetra-O-methyl-D-glucose

The unknown showed the same chromatographic mobility in solvents A, B, and C as an authentic sample of 2,3,4,6-tetra-*O*-methyl-D-glucose. The product crystallized from petroleum ether (30–60° C) and was recrystallized from *N*-hexane to give a compound with a melting point of 88–89° C and $[\alpha]_D^{24} = +82° \pm 2°$ (*c*, 0.16% in water). The melting point was unchanged by admixture with an authentic sample of 2,3,4,6-tetra-*O*-methyl-D-glucose.

2,3,4-Tri-O-methyl-D-glucose

The sirupy unknown had R_g values of 0.90 and 0.75 in solvents B and C respectively. Authentic samples of tri-*O*-methyl-D-glucoses showed the following R_g values in the same solvents: 2,3,4—0.90, 0.75; 2,4,6—0.85, 0.62; 2,3,6—0.88, 0.70. The unknown (97.3 mg) was refluxed for $1\frac{1}{2}$ hours with aniline (41.0 mg) in ethanol (2 ml). The solvent was evaporated and the crystalline residue was recrystallized from ether to give a product having a melting point of 144.5–145.5° C and $[\alpha]_D^{26} = +70° \pm 1°$ (*c*, 0.83% in ethanol). Peat *et al.* (38) report a melting point of 145–146° C for *N*-phenyl-2,3,4-tri-*O*-methyl-D-glucosylamine. Mother liquors from the above crystallization yielded a product having a melting point of 137–138° C unchanged by repeated recrystallization. The analysis and infrared spectrum of this material were identical with those of the product melting at 144.5–145.5° C and it appeared to be another crystalline form of the same compound. Analysis: Calc. for $C_{15}H_{23}O_5N$: C, 60.59%; H, 7.74%. Found: C, 60.61%, H, 7.42%.

Can. J. Chem. Downloaded from www.nrcresearchpress.com by 186.148.149.217 on 09/04/12
For personal use only.

*2,4,6-Tri-O-methyl-*D*-glucose*

Only a trace of this compound was present. It gave the same color reaction with *p*-anisidine hydrochloride on paper chromatograms and had the same R_g values (0.85, 0.62) in solvents B and C as an authentic sample of 2,4,6-tri-*O*-methyl-D-glucose.

*2,4-Di-O-methyl-*D*-glucose*

The unknown sample gave the same color reaction with *p*-anisidine hydrochloride on paper chromatograms as 2,4-di-*O*-methyl-D-glucose. In solvents A, B, and C it had R_g values of 0.81, 0.67, and 0.31 respectively. Authentic samples of di-*O*-methyl-D-glucoses had the following R_g values in the same solvents: 2,4—0.81, 0.67, 0.31; 2,3—0.83, 0.72, 0.36; 3,6—0.79, 0.66, 0.28. The unknown product (96.6 mg) was dissolved in ethanol (3 ml) to which *p*-nitroaniline (80 mg) and glacial acetic acid (2 drops) were added. The solution was kept at 25° C for $1\frac{1}{2}$ hours, heated on a steam bath for 2 hours and stored at room temperature overnight. A brown precipitate was filtered and washed with ethanol and ethyl acetate which removed much of the color. It was found that the light tan residue, consisting of microcrystals, could be purified by sublimation at 0.01 mm pressure at 200° C (bath temperature) to give *N*-*p*-nitrophenyl-2,4-di-*O*-methyl-D-glucosylamine, m.p. 250–251° C (*d*) (39).

*2-O-Methyl-*D*-glucose*

The unknown sample had the same R_g value (0.55) in solvent A as 2-*O*-methyl-D-glucose and gave the same color reaction with *p*-anisidine. R_g values of mono-*O*-methyl glucoses in solvent A were as follows: 2-*O*-methyl-, 0.55; 3-*O*-methyl-, 0.57; 4-*O*-methyl-, 0.51; 6-*O*-methyl-, 0.49. Attempts to isolate the compound in crystalline form or to prepare a crystalline derivative were unsuccessful because of insufficient material.

Hydrolysis Products from Methylated Mannan

The methylated mannan (1.54 g) was hydrolyzed by the formic acid procedure of Jones and Wilkie (36). A portion (100 mg) of the hydrolyzate was refluxed with 4% methanolic hydrogen chloride for 16 hours. The resulting mixture of methyl glycosides was resolved by gas–liquid partition chromatography (24, 25), which gave the separation and quantitative data shown in Fig. 2. To identify the constituents of the mixture the remainder (1.44 g) of the hydrolyzate was fractionated on a cellulose column using solvent C to give five fractions:

Fraction 1, tetra-*O*-methyl-D-mannose (0.150 g).
Fraction 2, tetra- and tri-*O*-methyl-D-mannoses (0.692 g).
Fraction 3, tri-*O*-methyl-D-mannose (0.065 g).
Fraction 4, tri- and di-*O*-methyl-D-mannoses (0.241 g).
Fraction 5, di-*O*-methyl-D-mannose (0.207 g).
Recovery = 1.355 (94.1%).

The major components in these fractions were identified as follows:

*2,3,4,6-Tetra-O-methyl-*D*-mannose*

On paper chromatograms fraction 1 showed only one component having R_g values of 0.99 and 0.98 in solvents B and C respectively. The specific rotation was $[\alpha]_D^{28} = +30° \pm 1°$ (*c*, 3.0% in methanol) and the product yielded a crystalline anilide, m.p. 144–145° C, $[\alpha]_D^{26} = +42° \rightarrow 8°$ (*c*, 0.72% in methanol). These values are in agreement with those reported for 2,3,4,6-tetra-*O*-methyl-D-mannose (40) and its anilide (41). After methanolysis fraction 1 showed one peak, corresponding to peak A, Fig. 2, on gas–liquid partition chromatography.

Can. J. Chem. Downloaded from www.nrcresearchpress.com by 186.148.149.217 on 09/04/12
For personal use only.

*3,4,6-Tri-O-methyl-*D*-mannose*

On paper chromatograms fraction 3 was identical with 3,4,6-tri-*O*-methyl-D-mannose and had R_g values of 0.90 and 0.76 in solvents B and C respectively. The product crystallized when nucleated with an authentic sample of 3,4,6-tri-*O*-methyl-D-mannose. Recrystallization from ether:hexane yielded a product with a melting point of 102–104° C and $[\alpha]_D^{28} = +33° \pm 3°$ (*c*, 3.2% in methanol), which are in agreement with the reported values (42). This compound showed only one peak, corresponding to peak C, Fig. 2, on gas–liquid partition chromatography after methanolysis.

*3,4-Di-O-methyl-*D*-mannose*

R_g values of fraction 5 on paper chromatograms were 0.74 and 0.44 in solvents B and C respectively, identical with those given by authentic 3,4-di-*O*-methyl-D-mannose. The product crystallized when nucleated with an authentic sample and recrystallization from ethyl acetate yielded a product with a melting point of 70–73° C (8, 43), and $[\alpha]_D^{28} = +32 \pm 1°$ (*c*, 2.0% in methanol) (6). This compound was methanolyzed and the methyl glycoside gave one peak, corresponding to peak E, Fig. 2, on gas–liquid partition chromatography.

Isolation of Chitin from C. albicans

Chitin was isolated from dried *C. albicans* cells (9.0 g) by the procedure of Scholl (44), which involved exhaustive extraction with boiling 10% potassium hydroxide, oxidation with 1% aqueous potassium permanganate, and removal of manganese dioxide by dilute (0.8%) hydrochloric acid. The residue from these reactions was dried with ethanol and ether to yield a product (545 mg, 6.05%) which was shown by X-ray diffraction to contain chitin and traces of corundum.

Isolation and Hydrolysis of Cell Walls from C. albicans

Cells of *C. albicans* were extracted with petroleum ether to remove lipid, incubated with trypsin to destroy protein, and suspended in water at a concentration of 1%. This suspension was shaken with fine glass beads for 45 minutes in a Mickle disintegrator (45). The glass beads were then removed by filtration on sintered glass and the turbid filtrate was centrifuged for 1 minute at 1000 r.p.m. Microscopic examination of the precipitate revealed the presence of many whole cells but further centrifugation of 1 minute at 1000 r.p.m. yielded a precipitate in which no intact cells could be detected. Hydrolysis and paper chromatography of this precipitate revealed the presence of glucose and mannose. The supernatant liquid from the second precipitate was centrifuged for 15 minutes at 15,000 r.p.m. to yield a creamy precipitate which yielded neither glucose nor mannose after hydrolysis.

ACKNOWLEDGMENTS

The authors gratefully acknowledge the careful technical assistance of Mr. F. P. Cooper (National Research Council) and Mr. A. A. Strachan (Department of Bacteriology and Immunology, McGill University). Authentic samples of *O*-methyl ethers of D-glucose were kindly donated by Dr. T. E. Timell, Division of Cellulose Chemistry, McGill University; authentic samples of *O*-methyl ethers of mannose were obtained from Dr. G. A. Adams, Division of Applied Biology, National Research Council. Analyses were done by Mr. A. E. Castagne and the X-ray diffraction diagram was done by the Eidgenossische Materialprufungs-und Versuchsanstalt, Zürich, Switzerland.

Can. J. Chem. Downloaded from www.nrcresearchpress.com by 186.148.149.217 on 09/04/12
For personal use only.

Can. J. Chem. Downloaded from www.nrcresearchpress.com by 186.148.149.217 on 09/04/12
For personal use only.

REFERENCES

1. W. Z. Hassid, M. A. Joslyn, and R. M. McCready. J. Am. Chem. Soc. **63**, 295 (1941).
2. D. J. Bell and D. H. Northcote. J. Chem. Soc. 1944 (1950).
3. S. Peat, W. J. Whelan, and T. E. Edwards. J. Chem. Soc. 3862 (1958).
4. S. Peat, J. R. Turvey, and J. M. Evans. J. Chem. Soc. 3868 (1958).
5. W. N. Haworth, E. L. Hirst, and F. A. Isherwood. J. Chem. Soc. 784 (1937).
6. W. N. Haworth, R. L. Heath, and S. Peat. J. Chem. Soc. 833 (1941).
7. J. A. Cifonelli and F. Smith. J. Am. Chem. Soc. **77**, 5682 (1955).
8. P. A. J. Gorin and A. S. Perlin. Can. J. Chem. **34**, 1796 (1956).
9. D. H. Northcote and R. W. Horne. Biochem. J. **51**, 232 (1952).
10. W. E. Trevelyan and J. S. Harrison. Biochem. J. **50**, 298 (1952).
11. P. A. Roelofsen. Biochim. et Biophys. Acta, **10**, 477 (1953).
12. A. L. Houwink and D. R. Kreger. Antonie van Leeuwenhoek. J. Microbiol. Serol. **19**, 1 (1953).
13. P. A. Roelofsen and I. Hoette. Antonie van Leeuwenhoek. J. Microbiol. Serol. **17**, 297 (1951).
14. D. R. Kreger. Biochim. et Biophys. Acta, **13**, 1 (1954).
15. J. Jonsen, S. Rasch, and A. Strand. Acta Pathol. Microbiol. Scand. **37**, 449 (1955).
16. M. W. Miller and H. J. Phaff. Antonie van Leeuwenhoek. J. Microbiol. Serol. **24**, 225 (1958).
17. M. Shifrine and H. J. Phaff. Antonie van Leeuwenhoek. J. Microbiol. Serol. **24**, 274 (1958).
18. G. Kessler and W. J. Nickerson. J. Biol. Chem. **234**, 2281 (1959).
19. C. T. Bishop and F. Blank. Can. J. Microbiol. **4**, 35 (1958).
20. N. Haworth, P. W. Kent, and M. Stacey. J. Chem. Soc. 1211 (1948).
21. J. Jonsen, S. Rasch, and A. Strand. Acta Pathol. Microbiol. Scand. **37**, 449 (1955).
22. A. B. Foster. Advances in Carbohydrate Chem. **12**, 81 (1957).
23. M. Abdel-Akher, J. K. Hamilton, R. Montgomery, and F. Smith. J. Am. Chem. Soc. **74**, 4970 (1952).
24. A. G. McInnes, D. H. Ball, F. P. Cooper, and C. T. Bishop. J. Chromatog. **1**, 556 (1958).
25. C. T. Bishop and F. P. Cooper. Can. J. Chem. **38**, 388 (1960).
26. L. Hough, J. K. N. Jones, and W. H. Wadman. J. Chem Soc. 1702 (1950).
27. W. E. Trevelyan, D. P. Procter, and J. S. Harrison. Nature, **166**, 444 (1950).
28. S. M. Martin. Chem. & Ind. (London), 823 (1957).
29. R. L. Whistler and J. N. BeMiller. J. Am. Chem. Soc. **78**, 1163 (1956).
30. S. A. Barker, A. B. Foster, I. R. Siddiqui, and M. Stacey. J. Chem. Soc. 2358 (1958).
31. S. K. Chanda, E. L. Hirst, J. K. N. Jones, and E. G. V. Percival. J. Chem. Soc. 1289 (1950).
32. E. Fischer. Ber. **20**, 821 (1887).
33. P. P. Fleury and J. Lange. J. pharm. chim. **17**, 107 (1933).
34. D. H. Grangaard, E. K. Gladding, and C. B. Purves. Paper Trade J. **115**, 41 (1942)
35. E. L. Falconer and G. A. Adams. Can. J. Chem. **34**, 338 (1956).
36. J. K. N. Jones and K. C. B. Wilkie. Can. J. Biochem. and Physiol. **37**, 377 (1959).
37. H. D. Fowler. Nature, **168**, 1123 (1951).
38. S. Peat, E. Schlüchterer, and M. Stacey. J. Chem. Soc. 581 (1939).
39. J. W. Van Cleve and W. C. Schaefer. J. Am. Chem. Soc. **77**, 5341 (1955).
40. R. D. Greene and W. L. Lewis. Science, **64**, 206 (1926).
41. J. C. Irvine and D. McNicoll. J. Chem. Soc. **97**, 1449 (1910).
42. H. G. Bott, W. N. Haworth, and E. L. Hirst. J. Chem. Soc. 1395 (1930).
43. D. H. Ball and G. A. Adams. Can. J. Chem. **37**, 1012 (1959).
44. E. Scholl. Monatsh. Chem. **29**, 1023 (1908).
45. M. R. J. Salton and R. W. Horne. Biochim. et Biophys. Acta, **7**, 177 (1951).

Can. J. Chem. Downloaded from www.nrcresearchpress.com by 186.148.149.217 on 09/04/12
For personal use only.

ALIPHATIC CHEMISTRY OF FLUORENE

PART II. AN UNUSUAL GRIGNARD REACTION[1]

P. M. G. BAVIN[2]

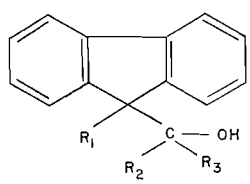
ABSTRACT

The reaction between methyl 9-methylfluorene-9-carboxylate and phenyl magnesium iodide gave 9,9′-dimethyl-9,9′-difluorenyl in almost quantitative yield. Evidence is presented which shows that 9-methylfluorene anion is an intermediate. The probable intervention of elemental iodine is discussed.

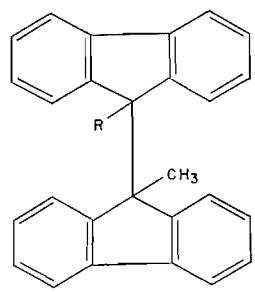
9-Methyl-9,9′-difluorenyl and 9,9′-dimethyl-9,9′-difluorenyl have been synthesized. A convenient preparation of 9,9′-difluorenylidene is described.

Some years ago we were interested in the reaction between phosphorus pentoxide and tertiary alcohols having structure I, where R is not hydrogen (1). We succeeded in preparing only two alcohols of the desired structure (I, $R_1 = R_2 = R_3$ = methyl or ethyl) by the reaction between methyl 9-methyl or ethylfluorene-9-carboxylate and the corresponding alkyl magnesium halide. The similar reaction between methyl 9-methylfluorene-9-carboxylate and phenyl magnesium bromide gave an easily crystallized hydrocarbon of melting point 209–210°, which has now been identified as 9,9′-dimethyl-9,9′-difluorenyl (II*b*). Although this hydrocarbon has been reported previously (2, 3, 4) identity has been established by the following unambiguous syntheses.

9-Bromofluorene reacted rapidly with methyl fluorene-9-carboxylate anion to give methyl 9-(9′-fluorenyl)-fluorene-9-carboxylate (the ethyl ester has been prepared previously from 9,9′-difluorenyl (5)), which was saponified and decarboxylated to 9,9′-difluorenyl. Methylation with methyl lithium and methyl iodide gave finally 9,9′-dimethyl-9,9′-difluorenyl (II*b*).

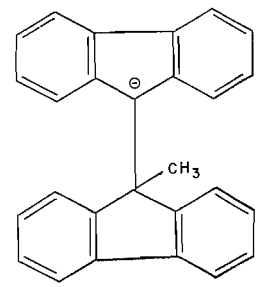


(I)



(II)

(a) R = H
(b) R = CH_3



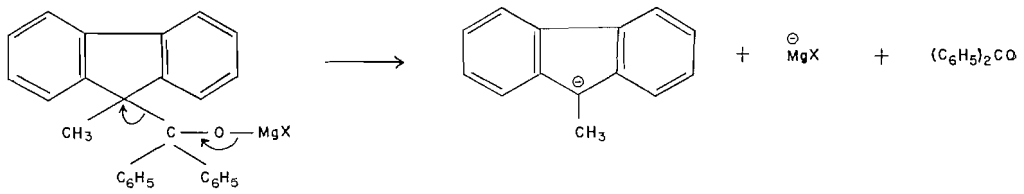
(III)

In the second synthesis, the anion (III) was prepared by the addition of methyl lithium to 9,9′-difluorenylidene. The further reaction with methyl iodide gave 9,9′-dimethyl-9,9′-difluorenyl. The preparation of 9-methyl-9,9′-difluorenyl (II*a*) by hydrolysis of the anion (III) with water proved unexpectedly difficult, residual methyl iodide giving

[1]*Manuscript received December 1, 1959.*
Contribution from the Chemistry Department, the University, Hull, East Yorkshire, England.
[2]*I.C.I. Fellow.*

instead dimethyldifluorenyl (II*b*). After removing the last traces of methyl iodide with magnesium, 9-methyl-9,9′-difluorenyl was obtained in 80–90% yield.

The yield of the hydrocarbon (II*b*) in the Grignard reaction was almost quantitative when phenyl magnesium iodide was used, from which it was inferred that the tertiary alkoxide (IV) was formed in the usual way. By analogy with certain tertiary aliphatic alkoxides recently investigated by Zook (6), decomposition should lead to 9-methylfluorene anion (V) and benzophenone, as shown in the annexed scheme (Fig. 1). The



(IV) (V)

FIG. 1.

necessary driving force for the decomposition is supplied by the mesomeric nature of the ion (V) (cf. the facile base-induced cleavage of 9-methyl-9-benzoylfluorene (7)), which accounts for the unusually low reaction temperature (cf. (6)).*

The use of organic iodides in the preparation of Grignard reagents, or of a crystal of iodine to initiate their formation, may often result in the presence of traces of free iodine in such reactions, probably owing their formation to aerial oxidation. It is well known that iodine brings about the dimerization of many esters in the presence of strong base (e.g. phenylacetic ester (8)) and, by analogy, it might be expected to bring about dimerization of the anion (V) to dimethyldifluorenyl (II*b*).

Evidence is presented below which supports the postulated decomposition of the tertiary alkoxide (IV) and the participation of iodine in the formation of the hydrocarbon (II*b*).

Evidence for the Formation of the 9-Methylfluorene Anion (V)

The most convincing evidence for the formation of the anion (V) came from a study of the reactions of 9-methyl-9-benzoylfluorene, which has recently been prepared for the first time (7). The ketone reacted with ethereal methyl or phenyl lithium and with ethereal phenyl magnesium bromide to produce a deep red color, which was fully developed in a few minutes. In order to demonstrate the presence of the anion (V), methyl iodide was added. 9,9-Dimethylfluorene could then be isolated from amongst the products. Triphenylmethanol could be isolated from the products of reaction with phenyl lithium or the corresponding Grignard reagent, thereby accounting for the benzophenone formed in the decomposition of the tertiary alkoxide (IV). Prolonged reaction times favored formation of the hydrocarbon (II*b*). Other experiments showed that methyl 9-methylfluorene-9-carboxylate gave the same products under the same conditions.

It is probable that the formation of the anion (V) from the ketone proceeds by way of the tertiary alkoxide (IV), but it may equally well involve base-induced cleavage of the non-enolizable ketone (7), with methyl or phenyl anion acting as base. Similar

**Zook (6) has emphasized that the decompositions are the reversal of addition of an organometallic reagent to a ketone.*

Can. J. Chem. Downloaded from www.nrcresearchpress.com by 186.148.149.217 on 09/04/12
For personal use only.

mechanisms can account for the formation of acetophenone and triphenylmethane from the reaction between benzopinacolin and methyl magnesium bromide (reference 3 quoted in 6). In both cases the direction of cleavage is controlled by formation of the mesomeric ions (V) and the triphenylmethyl anion. Differentiation between the decomposition and cleavage mechanisms might be possible by kinetic studies.

The Role of Iodine

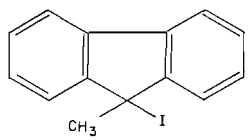
The importance of iodine may be judged from the following experimental results.

(i) The yield of the hydrocarbon (II*b*) from methyl 9-methyl-fluorene-9-carboxylate was almost quantitative when phenyl magnesium iodide was used, but was considerably less with phenyl magnesium bromide.

(ii) The anion (V), generated from 9-methylfluorene with phenyl lithium, reacted rapidly with iodine to give a good yield of the hydrocarbon (II*b*). Under similar conditions fluorene gave 9,9′-difluorenyl.

(iii) The reaction between 9-methylfluorene, ethyl lithium, and ethyl iodide produced 10% of the hydrocarbon (II*b*). The similar reaction using ethyl bromide and ethyl lithium prepared from ethyl bromide gave only 9-ethyl-9-methylfluorene.

Since many Grignard reagents react with iodine to give good yields of iodides (9, pp. 1332–1335) the tertiary iodide (VI) has to be considered as a possible intermediate in the formation of the hydrocarbon (II*b*) by reaction with the anion (V). Evidence for the formation of a reactive iodo compound in the dimerization of phenylacetic ester has already been reported (8, footnote on page 446; see also 10), and it has now been observed that traces of unstable iodo compounds are present in the products of the dimerization of fluorene or 9-methylfluorene with iodine and phenyl lithium.



(VI)

Tertiary halides do not as a general rule give C-alkylation products with organic anions. However, methyl fluorene-9-carboxylate anion has been shown to be exceptional in this respect (11, 12). It has now been found that methyl 9-bromofluorene-9-carboxylate reacts rapidly with methyl fluorene-9-carboxylate anion to give dimethyl 9,9′-difluorenyl-9,9′-dicarboxylate, at a rate comparable with that observed for the iodine-induced dimerization of the anion. These results suggest the feasibility of the anion (V) reacting with the iodide (VI) to give II*b*.

Comparable experiments with 9-bromo-9-methylfluorene and methyl fluorene-9-carboxylate anion have been unsuccessful. Crude preparations of the bromide, difficult to obtain pure (30), gave a low yield of what is probably methyl 9-(9′-fluorenylmethyl)-fluorene-9-carboxylate as the product of Michael addition of methyl fluorene-9-carboxylate anion to 9-methylenefluorene. Experiments with the corresponding chloride, which has not been obtained pure (13, 30), gave similar results.

Alternative mechanisms for the formation of the hydrocarbon (II*b*) obviously cannot be ruled out. For example, oxidation of the anion (V) by iodine might give the radical,

Can. J. Chem. Downloaded from www.nrcresearchpress.com by 186.148.149.217 on 09/04/12
For personal use only.

leading by dimerization to II*b*. In addition, trace amounts of certain metals are known to bring about oxidative coupling of organic anions (9).

Summing up the available evidence, it is clear that formation of dimethyldifluorenyl (II*b*) in the reaction between methyl 9-methylfluorene-9-carboxylate and a phenyl Grignard reagent proceeds through 9-methylfluorene anion (V), formed either by decomposition of the tertiary alkoxide (IV) or by basic cleavage of 9-methyl-9-benzoylfluorene. Iodine seems to play an essential part but its exact role is uncertain.

The formation of 9,9′-difluorenyl by the reaction between Grignard reagents and 9-chlorofluorene (14) may very well be related to its formation from fluorene, phenyl lithium, and iodine, mentioned above. The annexed scheme (Fig. 2) shows the reactions

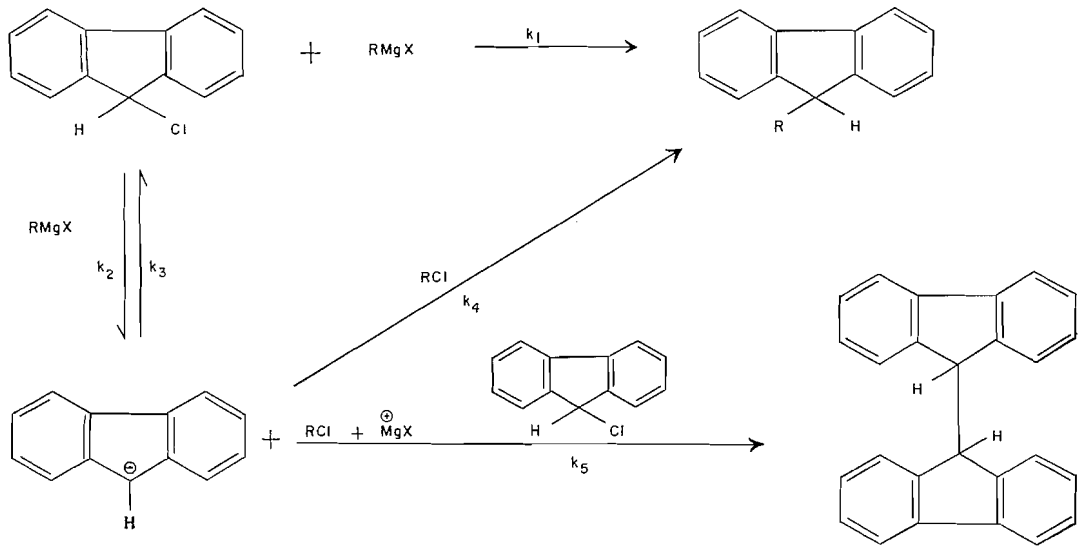


FIG. 2.

likely to be involved. It will be seen that an essential postulated reaction is a Grignard exchange having forward rate k_2. The existence of at least two such reactions has been convincingly demonstrated (15, 16) but it has been claimed that 9-chlorofluorene does not exchange with methyl magnesium bromide (17) because fluorene-9-carboxylic acid was not isolated from amongst the products of carbonation. These workers seem to have been unaware of the earlier paper by Bachmann (14); neglect to report on the neutral products obviously invalidates their work. The reaction between 9-bromofluorene and methyl magnesium iodide has been found to give 9,9′-difluorenyl in more than 90% yield, even in the presence of added methyl iodide. This observation confirms Bachmann's results (14).

Bachmann's efforts to explain his results (14), particularly the infrequent formation of 9-alkylfluorenes, in terms of the structure of the Grignard reagent are almost certainly invalid in view of recent studies with the ^{28}Mg isotope (18). The alternative scheme shown in Fig. 2 may provide a complete explanation. The rate k_1 is likely to be small compared with k_2 so that *the products formed will depend on the reactivities of 9-chlorofluorene and the halide RCl towards fluorene anion*, the reactivities being measured by k_5 and k_4.

An outstanding property of fluorene anions is the speed with which they react with a very wide range of alkyl halides (7, 11, 12). It has now been demonstrated that the anions from fluorene, 9-methylfluorene, and 9-phenylfluorene react almost instantaneously

Can. J. Chem. Downloaded from www.nrcresearchpress.com by 186.148.149.217 on 09/04/12
For personal use only.

with methyl iodide, providing convenient preparations of 9,9-dimethylfluorene and 9-methyl-9-phenylfluorene. The relative reactivities of various alkyl halides to methyl fluorene-9-carboxylate anion are being measured by competition and will be reported later. The formation of difluorenyl from the reaction between 9-bromofluorene and methyl Grignard in the presence of methyl iodide suggests that the fluorene halide is the more reactive.

The reaction between 9-bromofluorene and sodium *t*-butoxide has been found to give 9,9′-difluorenylidene in 85% yield, representing a considerable improvement in both yield and convenience over published preparations (20, 21).

The existence (19) has been confirmed of two polymorphic forms of 9,9-dimethylfluorene.

EXPERIMENTAL

9,9′-Dimethyl-9,9′-difluorenyl (II*b*)

(i) Methyl 9-methylfluorene-9-carboxylate (2.24 g, 0.01 mole) was boiled under reflux for 4 hours with ethereal phenyl magnesium iodide (from iodobenzene, 12 g, 0.06 mole). The complex was decomposed with ice and ammonium chloride and the product crystallized from heptane to give pale yellow prisms, m.p. 186–190° (1.76 g, almost quantitative yield). Two further crystallizations yielded colorless well-defined rhombs (1.6 g), m.p. 209–210°. Found for two samples: C, 93.71, 93.97; H, 6.29, 6.19%. Calculated for $C_{28}H_{22}$: C, 93.81; H, 6.19% (lit. m.p.: 209° corr. (2), 209–210° (3), 205° (4)).

Phenyl magnesium bromide was used in earlier experiments, formation of the Grignard reagent being assisted by the addition of a crystal of iodine. The hydrocarbon (II*b*) was obtained in 45% yield only after 24 hours. In the absence of iodine the hydrocarbon was not formed.

(ii) 9-Bromofluorene (22), prepared by Bolton, reacted rapidly at 30–35° with one equivalent of methanolic methyl fluorene-9-carboxylate anion. *Methyl 9-(9′-fluorenyl)-fluorene-9-carboxylate*, isolated in the usual way, formed well-defined rhombs (76%) from benzene–hexane, m.p. 215–216°. Found: C, 86.11; H, 5.18%. Calculated for $C_{28}H_{20}O_2$: C, 86.57; H, 5.19%.

The ester was boiled under reflux for 2 hours with twice its weight of potassium hydroxide in ethylene glycol. Cooling and diluting with water precipitated 9,9′-difluorenyl, which crystallized as slender colorless needles (94%) from benzene–hexane, m.p. 248–249°.

9,9′-Difluorenyl (2 g) in benzene (200 ml) was added to ethereal phenyl lithium (from bromobenzene, 20 g) to give a deep red solution, the color of which was almost instantly discharged on addition of methyl iodide (8 g). The *hydrocarbon* crystallized as rhombs (1.4 g) from benzene–hexane, m.p. 209–210°. Identity with the product from (i) was established by mixed melting point determination and comparison of infrared spectra.

(iii) 9-Methylfluorene (1 g) was added to ethereal phenyl lithium (from bromobenzene, 5 g) followed by crystals of iodine until the color of the latter persisted. The product (0.8 g) had a melting point of 207–209° and was identical with that obtained from (i).

Under similar conditions fluorene (1 g) gave 9,9′-difluorenyl (0.7 g), m.p. and mixed m.p. 245–246°.

The crude products from both preparations were washed with a solution of sodium metabisulphite to remove iodine, but traces of the latter were always formed during crystallization.

(iv) 9,9′-Difluorenylidene (1 g) was boiled under reflux for 30 minutes with ethereal methyl lithium (from methyl iodide, 10 g) and methyl iodide (10 g). The product crystal-

Can. J. Chem. Downloaded from www.nrcresearchpress.com by 186.148.149.217 on 09/04/12
For personal use only.

lized from heptane as small colorless prisms (0.9 g), m.p. 208–210°, and was identical with the product from (i).

9,9′-Difluorenylidene

A hot solution of sodium *t*-butoxide (from sodium, 7 g) in *t*-butanol (500 ml) was added to 9-bromofluorene (25 g) and the mixture boiled under reflux for 15 minutes. Most of the solvent was recovered by distillation and the residue poured into dilute hydrochloric acid (500 ml). The reddish-orange solid was collected, washed with water, dried, and crystallized from carbon tetrachloride – ethanol, which was the best solvent system found. Difluorenylidene was obtained as beautiful red needles (14.2 g, 85%, in two crops), m.p. 187–189° (lit. m.p. 185–187° (20, 21)).

9-Methyl-9,9′-difluorenyl

Ethereal methyl lithium was prepared from methyl iodide (28 g) and lithium (3 g). When the reaction was apparently complete, magnesium (5 g) was added and the mixture boiled gently under reflux for 30 minutes. Residual solids were removed by decantation through a plug of glass wool to give a solution of methyl lithium in ether free from methyl iodide.

Difluorenylidene (1 g) was warmed for 15 minutes with an excess of the above methyl lithium reagent. The ether layer was washed with water, dried, and evaporated, leaving the product as a yellow solid. The product was purified by passing a hexane solution through a column of activated alumina, crystallization of the eluted material from heptane yielding small colorless prisms (0.85 g), m.p. 169–170° (lit. m.p. 172° (4)). Found: C, 94.25; H, 5.89%. Calculated for $C_{27}H_{20}$: C, 94.15; H, 5.85%.

A mixed melting point determination with dimethyldifluorenyl was 151–179°.

9-Ethyl-9-methylfluorene

(i) 9-Methylfluorene (1 g) was added to ethereal ethyl lithium (from ethyl bromide, 4 g), followed by ethyl bromide (4 g). The product crystallized readily from methanol as white needles (0.8 g), m.p. 59–60.5° (lit. m.p. 61–62° (23)).

(ii) Ethyl iodide replaced ethyl bromide in (i). Crystallization of the product from heptane gave small colorless prisms (0.1 g), m.p. 204–207°, identified as 9,9′-dimethyl-9,9′-difluorenyl. The mother liquors contained impure ethylmethylfluorene.

9,9-Dimethylfluorene

(i) Fluorene (16.6 g, 0.1 mole) was added to ethereal methyl lithium (from methyl iodide, 43 g, 0.3 mole). Methyl iodide was added dropwise until the solution became colorless. The product crystallized from methanol as colorless prismatic needles (17.3 g, 89%), m.p. 90–93°, raised to 95–96° by a further crystallization.

Phenyl lithium gave less satisfactory yields unless the product was distilled at 1 to 2 mm prior to crystallization.

(ii) Methylation of 9-methylfluorene with methyl lithium – methyl iodide gave, in the same way, 9,9-dimethylfluorene in 92%.

Two melting points have been recorded for 9,9-dimethylfluorene: 71° (19) and 69–70° (24), 95–96° (19, 25) and 96° (23). Through the kindness of Dr. C. C. Barker, his original sample (24) has been examined after a lapse of several years and found to have a melting point of 81–92°, raised to 95–96° by one crystallization from methanol. Attempts by Emmerson (24) to obtain the higher melting form had been unsuccessful but the present author has been unable to obtain the lower melting form. The existence of the two crystalline forms reported earlier (19) is thus confirmed.

Can. J. Chem. Downloaded from www.nrcresearchpress.com by 186.148.149.217 on 09/04/12
For personal use only.

9-Methyl-9-phenylfluorene

Methylation of 9-phenylfluorene as described for fluorene gave methylphenylfluorene in 87% yield, crystallizing as colorless lustrous plates from methanol, m.p. 86–86.5° (lit. m.p. 84–85° (26), 86–87° (27)). Found: C, 93.97; H, 6.19%. Calculated for $C_{20}H_{16}$: C, 93.71; H, 6.29%.

Experiments with 9-Methyl-9-benzoylfluorene

(i) 9-Methyl-9-benzoylfluorene (2 g) in dry ether (100 ml) was added to ethereal phenyl lithium (from bromobenzene, 5 g). The solution immediately assumed a deep red color, similar to that produced by adding 9-methylfluorene to phenyl lithium. The color was rapidly discharged by the addition of methyl iodide (2 g). The product crystallized from methanol as colorless prismatic needles (0.9 g), m.p. 94–96°, identified as 9,9-dimethylfluorene. Found: C, 92.46; H, 7.04%. Calculated for $C_{15}H_{14}$: C, 92.74; H, 7.26%.

(ii) The experiment was performed as in (i) but without the addition of methyl iodide. The product crystallized as long needles (0.17 g) from methanol, m.p. 163–164°, after several crystallizations. Found: C, 87.43; H, 6.13%. Calculated for $C_{19}H_{16}O$: C, 87.66; H, 6.20%. Identity with triphenylmethanol was established by mixed melting point determination and comparison of infrared spectra. The oily residues were not examined.

In other experiments, methyl 9-methylfluorene-9-carboxylate satisfactorily replaced the ketone, and methyl lithium replaced phenyl lithium, although attempts were not made to isolate methyldiphenylmethanol.

9,9′-Difluorenyl

Ethereal methyl magnesium iodide (from methyl iodide, 4 g) was decanted from magnesium and added dropwise to a solution of 9-bromofluorene (2.4 g) and methyl iodide (2 g) in ether. After 10 minutes, the complex was decomposed with ice and ammonium chloride. The product was crystallized from heptane to give, in two crops, difluorenyl (1.5 g), m.p. and mixed m.p. 244–246°.

Dimethyl 9,9′-difluorenyl-9,9′-dicarboxylate

Methyl 9-bromofluorene-9-carboxylate (1.3 g) was added to a solution of methyl fluorene-9-carboxylate (1 g) in methanol containing sodium methoxide (from sodium, 0.2 g) and the suspension was warmed for 10 minutes. The product crystallized as small prisms (1.1 g) from benzene–hexane, m.p. 238–240°, identical with a sample prepared by the reaction between methyl fluorene-9-carboxylate anion and iodine (cf. 29) (lit. m.p. 237° (28)).

Methyl 9-(9′-fluorenylmethyl)-fluorene-9-carboxylate (?)

9-Methyl-9-fluorenol (1 g) was warmed for a few minutes with dry ether (30 ml) and acetyl bromide (1 ml). The solvent was evaporated below 30° and to the residual oil was added a solution of methyl fluorene-9-carboxylate (1.1 g) in methanol (30 ml) containing sodium methoxide (from sodium, 0.2 g). Polymeric material was removed by filtration, after which the clear yellow filtrate was warmed for 30 minutes. Careful dilution with water and scratching induced crystallization. After two crystallizations from heptane the colorless prisms (0.2 g) had a melting point of 173–174°. Found: C, 85.97; H, 6.16%. Calculated for $C_{29}H_{22}O_2$: C, 86.54; H, 5.51%.

Saponification in ethylene glycol was incomplete after 2 hours and yielded an unresolved mixture from which 9-methyl-9,9′-difluorenyl was not obtained by seeding, although a careful comparison of infrared spectra suggested its presence.

Can. J. Chem. Downloaded from www.nrcresearchpress.com by 186.148.149.217 on 09/04/12
For personal use only.

ACKNOWLEDGMENTS

The author is indebted to Professor N. B. Chapman for his interest and encouragement, to Doctors K. Clarke and J. Parrick for commenting on the manuscript, and to Dr. G. W. Gray and Miss A. Stephenson for the infrared spectra. Mr. R. Bolton kindly provided details of unpublished work on the 9-halo-9-methylfluorenes.

REFERENCES

1. F. A. L. ANET and P. M. G. BAVIN. Can. J. Chem. **36**, 763 (1958).
2. A. WANSCHIEDT and B. MOLDAVSKII. Ber. **64**, 917 (1931).
3. E. J. GREENHOW, E. N. WHITE, and D. MCNEIL. J. Chem. Soc. 3099 (1953).
4. O. EXNER. Chem. listy, **47**, 869 (1953).
5. S. WAWZONEK and E. DUFEK. J. Am. Chem. Soc. **78**, 3530 (1956).
6. H. D. ZOOK, J. MARCH, and D. F. SMITH. J. Am. Chem. Soc. **81**, 1617 (1959).
7. P. M. G. BAVIN. Can. J. Chem. **37**, 2023 (1959).
8. H. WREN and C. J. STILL. J. Chem. Soc. **107**, 444 (1915).
9. M. S. KHARASCH and O. REINMUTH. Grignard reactions of non-metallic substances. Prentice-Hall, Inc., New York. 1954.
10. A. MCKENZIE, H. D. K. DREW, and G. H. MARTIN. J. Chem. Soc. **107**, 26 (1915).
11. F. A. L. ANET and P. M. G. BAVIN. Can. J. Chem. **34**, 991 (1956).
12. P. M. G. BAVIN. Anal. Chem. In press.
13. BEILSTEIN'S HANDBUCH DER ORGANISCHEN CHEMIE. Vol. V, 2nd Suppl. p. 551.
14. H. F. MILLER and G. B. BACHMANN. J. Am. Chem. Soc. **57**, 766 (1935).
15. M. S. KHARASCH, F. L. LAMBERT, and W. H. URRY. J. Org. Chem. **10**, 298 (1945).
16. C. D. HURD and K. WILKINSON. J. Am. Chem. Soc. **70**, 739 (1948).
17. M. S. KHARASCH and C. F. FUCHS. J. Org. Chem. **10**, 292 (1945).
18. R. E. DESSY, G. S. HANDLER, J. H. WOTIZ, and C. A. HOLLINGSWORTH. J. Am. Chem. Soc. **79**, 3476 (1957).
19. M. ANCHELL and A. H. BLATT. J. Am. Chem. Soc. **63**, 1948 (1941).
20. J. R. SAMPEY and E. E. READ. J. Am. Chem. Soc. **69**, 234 (1947).
21. C. R. HAUSER *et al.* J. Am. Chem. Soc. **78**, 1653 (1956).
22. N. BUU-HOI and J. LECOCQ. Compt. rend. **226**, 87 (1948).
23. E. J. GREENHOW and D. MCNEIL. J. Chem. Soc. 3204 (1956).
24. R. G. EMMERSON. Thesis. London. 1955.
25. P. LEBEAU and M. PICON. Compt. rend. **173**, 84 (1921).
26. E. BERGMANN and A. BONDI. Ber. **64**, 1455 (1931).
27. J. R. DICE, T. E. WATKINS, and H. L. SCHUMAN. J. Am. Chem. Soc. **72**, 1738 (1950).
28. R. STOLLÉ and F. WOLF. Ber. **46**, 2251 (1913).
29. W. WISLICENUS and W. MOCKER. Ber. **46**, 2778 (1913).
30. R. BOLTON. Unpublished experiments.

Can. J. Chem. Downloaded from www.nrcresearchpress.com by 186.148.149.217 on 09/04/12
For personal use only.

Can. J. Chem. Downloaded from www.nrcresearchpress.com by 186.148.149.217 on 09/04/12
For personal use only.

SOME OPEN-CHAIN DERIVATIVES OF GLUCOSE AND MANNOSE[1]

E. J. C. CURTIS AND J. K. N. JONES

ABSTRACT

The dimethyl thioacetals of D-glucose and D-mannose have been condensed with acetone. Mannose dimethyl thioacetal forms a crystalline 3,4:5,6-di-*O*-isopropylidene derivative while glucose forms a mixture of the crystalline 3,4:5,6-di-*O*-isopropylidene and syrupy 2,3:5,6-di-*O*-isopropylidene isomers. These three di-*O*-isopropylidene dimethyl thioacetals have been converted via crystalline intermediates into the corresponding di-*O*-isopropylidene dimethyl acetals. These derivatives are suitable open-chain compounds for use in Koenigs–Knorr syntheses and provide (*a*) mannose with the C_2 hydroxyl free, (*b*) glucose with the C_2 hydroxyl free, and (*c*) glucose with the C_4 hydroxyl free.

INTRODUCTION

It has already been shown (1) that in Koenigs–Knorr syntheses of disaccharides much greater yields may be obtained by the use of an open-chain hydroxyl reactant rather than the more generally used ring-form derivatives. This is presumably because there is less steric hindrance to reaction in the case of the open-chain compound. In the synthesis of lactose, however (1), the hydroxyl reactant used (syrupy 2,3:5,6-di-*O*-isopropylidene-D-glucose dimethyl acetal) contained small amounts of other di-*O*-isopropylidene isomers due to the method of synthesis. This, of course, resulted in an impure product from the Koenigs–Knorr reaction, there being small amounts of other disaccharides present in addition to lactose. In the present work syntheses are described of open-chain derivatives of (*a*) mannose with the C_2 hydroxyl group free, (*b*) glucose with the C_2 hydroxyl group free, and (*c*) glucose with the C_4 hydroxyl group free. All of these have been made via pure crystalline intermediates and should prove very useful in Koenigs–Knorr syntheses.

Schinle (2) condensed D-glucose dibenzyl thioacetal with acetone in the presence of anhydrous copper sulphate and obtained a syrupy mixture of mono- and di-*O*-isopropylidene derivatives. There was at first some doubt as to the structure of the di-*O*-isopropylidene material but Munro and Percival (3) later showed this to be a mixture of 2,3:5,6- and 3,4:5,6-di-*O*-isopropylidene isomers of D-glucose dibenzyl thioacetal. Condensation of D-glucose diethyl thioacetal with acetone (1) gives a syrupy mixture which consists largely of the 2,3:5,6-di-*O*-isopropylidene derivative.

Pacsu and Trister (4) condensed D-mannose dibenzyl thioacetal with acetone and obtained a syrupy di-*O*-isopropylidene derivative which was shown to be mainly the 3,4:5,6 isomer. Condensation of D-mannose diethyl thioacetal with acetone yields a syrupy product which has been shown to be largely the 3,4:5,6-di-*O*-isopropylidene derivative (5).

In the present work condensation of D-mannose dimethyl thioacetal with acetone in the normal way resulted in a crystalline di-*O*-isopropylidene derivative in high yield. This compound was shown by methylation experiments to be 3,4:5,6-di-*O*-isopropylidene-D-mannose dimethyl thioacetal. The compound formed a crystalline benzoate which then was converted into 2-*O*-benzoyl-3,4:5,6-di-*O*-isopropylidene-D-mannose dimethyl acetal using a modification of the method of Wolfrom (6). Debenzoylation yielded 3,4:5,6-di-*O*-isopropylidene-D-mannose dimethyl acetal.

Condensation of D-glucose dimethyl thioacetal with acetone resulted in a syrupy product which partially crystallized on standing. The crystalline portion (19% yield)

[1]*Manuscript received February 18, 1960.*
Contribution from the Department of Chemistry, Queen's University, Kingston, Ontario.

was shown by methylation experiments to be 3,4:5,6-di-*O*-isopropylidene-D-glucose dimethyl thioacetal, while methylation of the syrupy portion (76% yield) showed this to be mainly the 2,3:5,6-di-*O*-isopropylidene isomer. Both isomers formed benzoates. 2-*O*-Benzoyl-3,4:5,6-di-*O*-isopropylidene-D-glucose dimethyl thioacetal was converted into the dimethyl acetal, which on debenzoylation yielded 3,4:5,6-di-*O*-iso-propylidene-D-glucose dimethyl acetal. By a similar route, 2,3:5,6-di-*O*-isopropylidene-D-glucose dimethyl acetal was also formed. 3,4:5,6-Di-*O*-isopropylidene-D-glucose dimethyl acetal formed a crystalline toluene-*p*-sulphonyl derivative.

EXPERIMENTAL

Optical rotations were measured in water at 21°±2° C unless otherwise stated. Solutions were concentrated under reduced pressure at 40° C. The following solvent systems (v/v) were used to separate sugars on paper chromatograms: (A) ethyl acetate:acetic acid:water, 9:2:2; (B) *n*-butanol:ethanol:water, 3:1:1. Sugars were detected using the *p*-anisidine hydrochloride spray (7). Infrared absorptions were measured as solutions in chloroform or as a powder suspended in a potassium bromide pellet on a Perkin–Elmer Model 21 spectrophotometer.

Preparation of Di-O-isopropylidene-D-mannose Dimethyl Thioacetal

Mannose dimethyl thioacetal (22 g) was added to a mixture of dry acetone (400 ml), anhydrous copper sulphate (12 g), and concentrated sulphuric acid (2 ml), and the resulting mixture was shaken at room temperature for 24 hours. The solution was neutralized with concentrated ammonium hydroxide solution and filtered. The precipitate was washed with acetone and filtrate and washings were evaporated to a colorless syrup. This was diluted with chloroform (200 ml) and extracted once with water. The chloroform solution was dried ($MgSO_4$), filtered, and evaporated to a syrup (23 g) which crystallized completely on standing. After recrystallization from light petroleum the material weighed 21.8 g (76% yield) and had a melting point of 58–59° C and $[\alpha]_D$ +5.0° (*c*, 7.6, chloroform). Anal. Calc. for $C_{14}H_{26}O_5S_2$: C, 49.70; H, 7.69; S, 18.94. Found: C, 49.87; H, 7.78; S, 18.99.

Methylation of Di-O-isopropylidene-D-mannose Dimethyl Thioacetal

Di-*O*-isopropylidene-D-mannose dimethyl thioacetal (2 g) was dissolved in methyl iodide (20 ml). Silver oxide (3.6 g) plus Drierite (2 g) were added to the solution which was then shaken in the dark at room temperature for 24 hours. Filtration and subsequent evaporation yielded a brown syrup (1.5 g). Isopropylidene and thioacetal groupings were removed by refluxing for 5 hours with aqueous ethanol (20%) containing hydrochloric acid (5%). The solution was neutralized by passage through a column of Duolite A-4 resin (OH form) and concentrated to a syrup (0.9 g). Chromatographic examination of this (solvent A) showed mainly a spot at R_{mannose} 2.15, with smaller spots corresponding to mannose and arabinose. Part of this syrup (200 mg) was separated by chromatography on sheets of Whatman No. 1 filter paper using solvent B as eluent. Guide strips were cut and sprayed and the fraction R_{mannose} 2.15 was cut out and eluted with acetone. The acetone solution was evaporated to dryness. The residue was diluted with a little ethanol, warmed with charcoal, and filtered. Evaporation of the filtrate yielded a syrup (77 mg) which crystallized on dilution with a little ethanol.

After recrystallization from methanol/ether the material had a melting point of 134–136° C and $[\alpha]_D$ +5.2° (constant) (*c*, 1.2). It formed a phenylhydrazone which had a melting point of 161–163° C and $[\alpha]$ −60.5° (constant) (*c*, 0.38, pyridine). Authentic

Can. J. Chem. Downloaded from www.nrcresearchpress.com by 186.148.149.217 on 09/04/12
For personal use only.

2-*O*-methyl-α-D-mannose has a melting point of 136–137° C and $[\alpha]_D$ +7.0° → +4.5° (constant) and forms a phenylhydrazone with a melting point of 163° C and $[\alpha]_D$ −49.1° → −60.7° (pyridine, constant) (4).

*2-O-Benzoyl-di-O-isopropylidene-*D*-mannose Dimethyl Thioacetal*

Di-*O*-isopropylidene-D-mannose dimethyl thioacetal (17.2 g) was dissolved in dry pyridine (180 ml). The solution was stirred mechanically and cooled externally. The temperature was kept at −5° C while a solution of benzoyl chloride (18 g) in pyridine (30 ml) was added dropwise. Cooling was continued at −5° C (30 minutes) and then at 0° C (7 hours), and the solution was finally stored at room temperature (14 hours). The product was precipitated by slowly pouring the solution into ice plus water (700 ml). After 30 minutes at room temperature, the crude crystalline material was filtered and washed with water. It was recrystallized from methanol and weighed 19.3 g (86% yield). It had a melting point of 83–84° C and $[\alpha]_D$ +7.8° (*c*, 1.0, methanol). Anal. Calc. for $C_{21}H_{30}O_6S_2$: S, 14.48. Found: S, 14.68.

*2-O-Benzoyl-di-O-isopropylidene-*D*-mannose Dimethyl Acetal* (ref. 6)

2-*O*-Benzoyl-di-*O*-isopropylidene-D-mannose dimethyl thioacetal (10 g) was dissolved in dry methanol (300 ml). Cadmium carbonate (87 g) was added to the solution and a solution of mercuric chloride (87 g) in methanol (100 ml) was then added portionwise with vigorous stirring at room temperature. After completion of the addition (5 hours), stirring was continued for a further 15 hours at room temperature, and the solution was then boiled under reflux for 15 minutes. The cooled solution was filtered through a Celite pad and the precipitate was washed with methanol. Filtrate and washings were concentrated to ca. 150 ml and this solution was poured into 200 ml each of chloroform and water. The chloroform layer was extracted with water until chloride-free, dried ($MgSO_4$), filtered, and evaporated to a syrup (7.5 g) which crystallized on standing overnight. Recrystallization from methanol yielded 6.5 g of product (70%). After further recrystallizations from methanol and from light petroleum the material had a melting point of 73.5–74° C and $[\alpha]_D$ −1.6° (*c*, 3.5, chloroform). Anal. Calc. for $C_{21}H_{30}O_8$: C, 61.43; H, 7.37. Found: C, 61.35; H, 7.53.

*3,4:5,6-Di-O-isopropylidene-*D*-mannose Dimethyl Acetal*

2-*O*-Benzoyl-di-*O*-isopropylidene-D-mannose dimethyl acetal (0.67 g) was dissolved in 50% aqueous ethanol (30 ml) containing potassium hydroxide (0.12 g) and the solution was warmed at 70° C (4 hours). The solution was concentrated to a small volume to remove ethanol and then extracted with chloroform. The chloroform solution was extracted three times with water, dried ($MgSO_4$), filtered, and evaporated to a syrup (0.49 g, 98%). Infrared analysis showed no absorption for carbonyl group (1700–1750 cm^{-1}). The material had $[\alpha]_D$ −1.3° (*c*, 1.6, methanol).

*Preparation of a Mixture of Di-O-isopropylidene-*D*-glucose Dimethyl Thioacetals*

Glucose dimethyl thioacetal (20 g) was added to a mixture of dry acetone (400 ml), anhydrous copper sulphate (12 g), and concentrated sulphuric acid (2 ml) and the resulting solution was shaken at room temperature for 24 hours. The solution was neutralized with concentrated ammonium hydroxide solution, filtered, and the precipitate was washed with acetone. Filtrate and washings were evaporated to a syrup which was diluted with chloroform (150 ml) and extracted once with water. The chloroform solution was dried ($MgSO_4$), filtered, and evaporated to a syrup (26 g). This partially crystallized on standing. The mixture of crystals and syrup was diluted with light

Can. J. Chem. Downloaded from www.nrcresearchpress.com by 186.148.149.217 on 09/04/12
For personal use only.

petroleum and refrigerated. Subsequent filtration yielded 3.1 g crystalline material. Concentration of the filtrate followed by seeding produced a further 2.0 g crystals; total yield of crystalline product 5.1 g (19%). This was recrystallized from light petroleum and had a melting point of 92–94° C and $[\alpha]_D$ −1.0° (*c*, 9.8, chloroform). Anal. Calc. for $C_{14}H_{26}O_5S_2$: C, 49.70; H, 7.69; S, 18.94. Found: C, 49.64; H, 7.52; S, 18.86.

When all the above crystalline material had been removed from the reaction product there remained 20.6 g (76%) syrup which could not be crystallized. It had $[\alpha]_D$ −92.4° (*c*, 1.2, chloroform). Anal. Calc. for $C_{14}H_{26}O_5S_2$: S, 18.94. Found: S, 18.72, 18.64.

*Methylation of Crystalline Di-O-isopropylidene-*D*-glucose Dimethyl Thioacetal*

Crystalline di-*O*-isopropylidene-D-glucose dimethyl thioacetal (0.93 g) was dissolved in dry tetrahydrofuran (20 ml). Small pieces of clean sodium were then added to the solution until no further reaction took place. Methyl iodide (0.5 ml) was added to the solution which was stored in a darkened, stoppered flask at room temperature for 24 hours, further small quantities of sodium and methyl iodide being added at intervals. The solution was filtered and the precipitate was washed with tetrahydrofuran. Filtrate and washings were evaporated to dryness and the residue was dissolved in chloroform and washed with water until free from iodide. The solution was dried (Na_2SO_4), filtered, and evaporated to a syrup (0.91 g). Infrared examination of this indicated only a very small amount of free hydroxyl group present. Thioacetal groupings were removed by the method of Wolfrom (8), using mercuric chloride in the presence of cadmium carbonate in aqueous ethanol and isopropylidene groupings were subsequently hydrolyzed by warming the product in sulphuric acid (0.5 *N*) solution. The solution was deionized by passage through a column of Amberlite IR-120 (H form) and Duolite A-4 (OH form) resins in series and the neutral eluate was concentrated to a syrup (0.50 g). Chromatography of this (solvent A) showed mainly a spot at $R_{glucose}$ 2.61, with much smaller spots at $R_{glucose}$ 1.01, 3.92, and 7.30, these latter two being presumably due to unhydrolyzed isopropylidene derivatives.

The syrup was stored in a stoppered flask at room temperature and after 6 weeks it was found that a crystal nucleus had developed. When this was mixed with the syrup the mass crystallized. Part of the crude material (200 mg) was transferred to a porous tile and the crystals were cleaned by rapidly washing them with methanol. This material (110 mg) was recrystallized from methanol/ether. Chromatography in solvent A showed a single spot at $R_{glucose}$ 2.61. It had a melting point of 156–158° C and $[\alpha]_D$ +26.3° → +67.8° (constant) (*c*, 2.3). It formed a tetrabenzoate which had a melting point of 167°–168° C and $[\alpha]_D$ −8.4° (*c*, 0.6, chloroform). 2-*O*-Methyl-β-D-glucose has a melting point of 157–159° C and $[\alpha]_D$ +12.0 → +66.0 (constant) (9) and forms a tetrabenzoate with a melting point of 169°–170° C and $[\alpha]_D$ −6.2° (10). Under drastic conditions the material formed an osazone whose infrared spectrum was identical with that of authentic D-glucosazone.

*Methylation of Syrupy Di-O-isopropylidene-*D*-glucose Dimethyl Thioacetal*

Syrupy di-*O*-isopropylidene-D-glucose dimethyl thioacetal (5 g) was methylated using silver oxide and methyl iodide in the same way as described for di-*O*-isopropylidene-D-mannose dimethyl thioacetal. After removal of thioacetal and isopropylidene groupings and deionization, a clear syrup (1.9 g) was obtained. Chromatography of this (solvent A) showed spots at $R_{glucose}$ 1.00 and 2.56 with much smaller spots at 2.65, 3.40, and 4.45. The spot at $R_{glucose}$ 2.65 was presumably due to 2-*O*-methyl-D-glucose, formed from traces of the 3,4:5,6-di-*O*-isopropylidene isomer not removed by crystallization.

Can. J. Chem. Downloaded from www.nrcresearchpress.com by 186.148.149.217 on 09/04/12
For personal use only.

The spots at 3.40 and 4.45 were due either to unhydrolyzed isopropylidene residues or to methylation of mono-isopropylidene materials. Part of the syrup (1.4 g) was separated by chromatography on a column of powdered cellulose using solvent A as eluent. A fraction (0.73 g) was collected which showed a single spot at $R_{glucose}$ 2.56 in solvent A. The material had $[\alpha]_D$ +52.1° (*c*, 2.4). It did not crystallize. Authentic 4-*O*-methyl-D-glucose has $[\alpha]_D$ +53° (3). It formed an osazone which had a melting point of 157–159° C and $[\alpha]_D$ −17.4° (constant) (*c*, 0.6, pyridine). Anal. Calc. for $C_{19}H_{24}O_4N_4$: OMe, 8.35. Found: OMe, 8.15. 4-*O*-Methyl-D-glucose phenylosazone has a melting point of 158–160° C and $[\alpha]_D$ −32.6° → −15.5° (constant) (3).

Part of the syrup was converted into 4-*O*-methyl-D-glucose methyl glucoside by refluxing it for 3 hours with hydrochloric acid in methanol (2%). The solution was neutralized (Ag_2CO_3) and filtered, and the filtrate was evaporated to a clear syrup. This crystallized after it was diluted with a drop of ethyl acetate and nucleated with authentic 4-*O*-methyl-D-glucose methyl-α-D-glucoside. The material was washed on a porous tile with ethyl acetate and dried. It showed an infrared spectrum identical with that of 4-*O*-methyl-D-glucose methyl-α-D-glucoside.

2-O-Benzoyl-di-O-isopropylidene-D-glucose Dimethyl Thioacetal

3,4:5,6-Di-*O*-isopropylidene-D-glucose dimethyl thioacetal (3.1 g) was dissolved in dry pyridine (30 ml). The solution was stirred mechanically and cooled to −5° C while a solution of benzoyl chloride (2 g) in pyridine (10 ml) was added dropwise, after which the temperature was kept at −5° C (30 minutes) and then at 0° C (4 hours). The solution was finally stored at room temperature (20 hours). It was poured slowly into ice plus water (200 ml) when the product separated as an oil which did not crystallize on standing. The solution was extracted with chloroform (4×40 ml) and the combined extracts were washed successively with solutions of dilute sulphuric acid, sodium bicarbonate, and water. The solution was dried ($MgSO_4$), filtered, and evaporated to a syrup (3.9 g). This proved difficult to crystallize. However, seed crystals were obtained by dissolving part of the syrup in methanol and cooling this in an acetone/Dry Ice bath, and at the same time scratching the side of the vessel with a glass rod. The syrup crystallized completely on subsequent seeding. Recrystallization from methanol yielded 3.8 g (93%). The material had a melting point of 85–86° C and $[\alpha]_D$ −15.5° (*c*, 1.0, methanol). Anal. Calc. for $C_{21}H_{30}O_6S_2$: S, 14.48. Found: S, 14.66.

2-O-Benzoyl-di-O-isopropylidene-D-glucose Dimethyl Acetal

2-*O*-Benzoyl-di-*O*-isopropylidene-D-glucose dimethyl thioacetal (3 g) was converted to the acetal using the method described above for the preparation of 2-*O*-benzoyl-di-*O*-isopropylidene-D-mannose dimethyl acetal. A syrup (2.7 g) was obtained which crystallized on standing. Recrystallization from aqueous methanol yielded 2.5 g material (90%). After further recrystallizations from methanol and from light petroleum it had a melting point of 71–72.5° C and $[\alpha]_D$ −40.8° (*c*, 2.0, chloroform). Anal. Calc. for $C_{21}H_{30}O_8$: C, 61.43; H, 7.37. Found: C, 61.39; H, 7.34.

3,4:5,6-Di-O-isopropylidene-D-glucose Dimethyl Acetal

2-*O*-Benzoyl-di-*O*-isopropylidene-D-glucose dimethyl acetal (1.11 g) was dissolved in 50% aqueous ethanol (40 ml) containing potassium hydroxide (0.17 g) and the solution was warmed at 70° C (5 hours). The product was worked up as described above for the corresponding mannose derivative. A syrup (0.77 g, 93%) was obtained which crystallized on standing in a vacuum desiccator. After recrystallization from light petroleum it had

Can. J. Chem. Downloaded from www.nrcresearchpress.com by 186.148.149.217 on 09/04/12
For personal use only.

a melting point of 88–89° C and $[\alpha]_D$ −9.0° (*c*, 4.2, methanol). Infrared analysis showed no absorption for the carbonyl group (1700–1750 cm^{-1}).

*2-O-Tosyl-di-O-isopropylidene-*D*-glucose Dimethyl Acetal*

3,4:5,6-Di-*O*-isopropylidene-D-glucose dimethyl acetal (0.113 g) was dissolved in dry pyridine (1 ml) and toluene *p*-sulphonyl chloride (0.098 g) was added to the solution. Moisture was excluded from the solution, which was kept at room temperature (18 hours) and then warmed to 70° C on a water bath (30 minutes). The product was isolated in the usual way, a syrup (0.116 g, 68%) being obtained which crystallized immediately. After recrystallization from light petroleum the material had a melting point of 109–111° C and $[\alpha]_D$ +10.4° (*c*, 2.5, chloroform). Anal. Calc. for $C_{21}H_{32}O_9S$: S, 6.96. Found: S, 6.82.

*Benzoylation of Syrupy Di-O-isopropylidene-*D*-glucose Dimethyl Thioacetal*

Syrupy di-*O*-isopropylidene-D-glucose dimethyl thioacetal (14.3 g) was benzoylated as described above. A clear syrup (21 g) was obtained which showed no absorption for hydroxyl group (3500–3600 cm^{-1}) on infrared analysis. It had $[\alpha]_D$ +34.0° (*c*, 1.05, methanol).

*4-O-Benzoyl-di-O-isopropylidene-*D*-glucose Dimethyl Acetal*

Syrupy 4-*O*-benzoyl-di-*O*-isopropylidene-D-glucose dimethyl thioacetal (9.3 g) was converted to the dimethyl acetal in the usual way. A syrup (7.7 g) was obtained which crystallized on standing. Recrystallization from methanol yielded 4.9 g (56%). After further recrystallization from light petroleum the material had a melting point of 101.5–102° C and $[\alpha]_D$ −5.8° (*c*, 1.85, chloroform). Anal. Calc. for $C_{21}H_{30}O_8$: C, 61.43; H, 7.35. Found: C, 61.47; H, 7.38.

*2,3:5,6-Di-O-isopropylidene-*D*-glucose Dimethyl Acetal*

4-*O*-Benzoyl-di-*O*-isopropylidene-D-glucose dimethyl acetal (2.73 g) was dissolved in 50% aqueous methanol (100 ml) containing sodium hydroxide (0.27 g) and the solution was warmed at 70° C (4 hours). Following the usual method of isolation a syrup (1.92 g, 95%) was obtained. This had $[\alpha]_D$ −15.9° (*c*, 3.5, methanol). Infrared analysis showed no absorption for carbonyl peak.

The authors wish to thank the National Research Council for grants which made this work possible.

REFERENCES

1. E. J. C. Curtis and J. K. N. Jones. Can. J. Chem. **37**, 358 (1959).
2. R. Schinle. Ber. **65** B, 315 (1932).
3. J. Munro and E. G. V. Percival. J. Chem. Soc. 873 (1935).
4. E. Pacsu and S. M. Trister. J. Am. Chem. Soc. **63**, 925 (1941).
5. Unpublished results.
6. M. L. Wolfrom, L. T. Tanghe, R. W. George, and S. W. Waisbrot. J. Am. Chem. Soc. **60**, 1932 (1938).
7. L. Hough, J. K. N. Jones, and W. H. Wadman. J. Chem. Soc. 1702 (1950).
8. M. L. Wolfrom. J. Am. Chem. Soc. **51**, 2188 (1929).
9. J. W. H. Oldham and J. K. Rutherford. J. Am. Chem. Soc. **54**, 1086 (1932).
10. J. W. H. Oldham. J. Am. Chem. Soc. **56**, 1360 (1934).

Can. J. Chem. Downloaded from www.nrcresearchpress.com by 186.148.149.217 on 09/04/12
For personal use only.

Can. J. Chem. Downloaded from www.nrcresearchpress.com by 186.148.149.217 on 09/04/12
For personal use only.

THE STUDY OF HYDROGEN BONDING AND RELATED PHENOMENA BY ULTRAVIOLET LIGHT ABSORPTION

PART IV. INTERMOLECULAR HYDROGEN BONDING IN ANILINES AND PHENOLS[1]

J. C. DEARDEN[2] AND W. F. FORBES[3]

ABSTRACT

Intermolecular hydrogen bonding in anilines and phenols can be subdivided into bonding involving solute molecules only, and into bonding involving both solute and solvent molecules. Interactions which do not involve hydrogen bonding are also possible between solute and solvent molecules. Spectral effects which may be associated with each of these interactions are described and discussed for anilines and phenols. By noting the effects of substituents on the various interactions, tentative conclusions can be deduced concerning the nature of these interactions.

INTRODUCTION

Intermolecular hydrogen bonding is a well-known phenomenon in a number of phenols and anilines, since the changes caused by the bonding can be detected by the changes in a number of physical properties such as melting points, solubilities, dipole moments, spectral effects, and other properties. The spectral changes caused by intermolecular hydrogen bonding in substituted benzoic acids have been discussed in previous parts of this series (1). The purpose of the present paper is to extend this investigation to anilines and phenols.

HYDROGEN BONDING BETWEEN SOLUTE MOLECULES ONLY

Von Keussler (2) has shown that an increase of the solute concentration beyond the more readily accessible concentration range (i.e. solute concentration greater than ca. 10^{-2} moles/liter) causes a concentration dependence in the *C*-band of the ultraviolet spectrum for solutions of phenol in cyclohexane. (For band nomenclature used, see previous parts of this series.) We have verified von Keussler's results and have also investigated the corresponding spectral changes in both the *B*-band and the *C*-band for a number of phenols, and for anisole. The relevant data are listed in Table I. Table I and also Ito's recently obtained values for the *C*-bands of phenol and anisole (3) show that only phenol and certain alkyl-substituted phenols give rise to appreciable spectral changes in the *C*-band and this suggests that the spectral changes are caused by intermolecular hydrogen bonding between phenol molecules. The relevant spectral curves are shown in Fig. 1. The ultraviolet data in this way confirm the well-known fact that phenol forms an intermolecular hydrogen bond with other phenol molecules, and incidentally that this bond is weaker than the intermolecular hydrogen bond between benzoic acid molecules since greater solute concentrations are required for the phenol solutions before a concentration dependence is observed. This conclusion has frequently been deduced from other spectral data which indicate that phenol molecules associate by means of hydrogen bonding to form dimers, trimers, and even polymers with the degree of association

[1]*Manuscript received February 16, 1960.*
Contribution from the Memorial University of Newfoundland, St. John's, Newfoundland, and from the Division of Protein Chemistry, C.S.I.R.O., Melbourne, Australia. Presented in part at the meetings of the Chemical Institute of Canada, Halifax, Nova Scotia, May, 1959.
[2]*Present address: "Shell" Research Limited, P.O. Box 1, Chester, England.*
[3]*Present address: Division of Protein Chemistry, C.S.I.R.O., 343 Royal Parade, Parkville, N.2, Melbourne, Victoria, Australia. (All correspondence should be addressed to this author.)*

TABLE I

Concentration dependence data in cyclohexane solution for phenol, aniline, and related compounds*

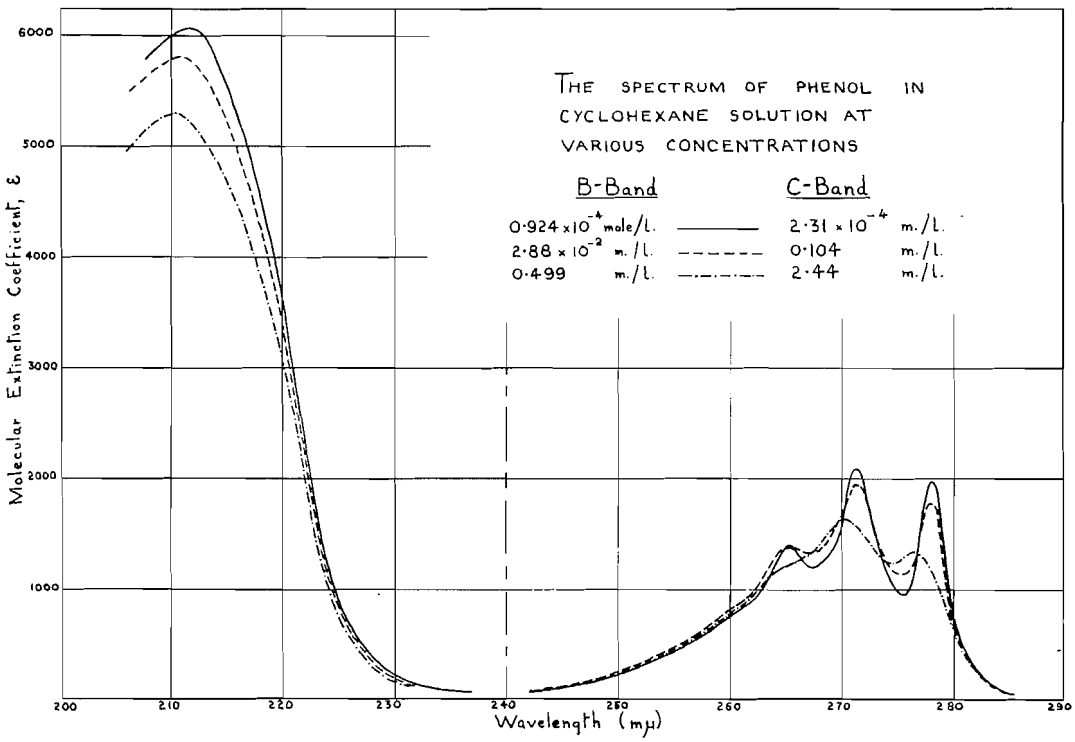
	B-Band			*C*-Band		
	Concn. (molar)	λ_{max}	ϵ_{max}	Concn. (molar)	λ_{max}	ϵ_{max}
Phenol	2.88×10^{-2}	211	5,800	0.104	265 271 278	1,400 1,940 1,770
	0.499	210	5,300	2.44	ca. *265* 270 276	*1,230* 1,600 1,320
Anisole	3.14×10^{-2}	219	7,850	0.137	266 272 278	1,480 2,150 2,120
	0.470	219	6,250	1.46	266 272 278	1,290 1,830 1,680
o-Cresol	3.52×10^{-2}	212–213	7,170	0.146	272 278	1,860 1,720
	0.374	212	7,500	1.16	271 277	1,400 1,230
m-Cresol	5.33×10^{-2}	214	6,580	0.107	273 279	1,600 1,640
	0.580	214–215	5,800	0.958	272–273 278	1,500 1,500
p-Cresol	4.83×10^{-2}	220	6,080	9.65×10^{-2}	271 274	1,420 1,620
					277 279 285.5	1,860 1,950 1,730
	0.437	220	5,150	0.873	277–278 283	1,680 1,390
2,6(t.Bu)$_2$-phenol	3.49×10^{-2}	213	8,050	6.98×10^{-2}	270–271 277–278	1,920 1,950
	0.175	214	7,070	0.349	270–271 277–278	1,770 1,750
Aniline	4.25×10^{-2}	233	8,850	0.127	281 284–285 287–288 ca. *291*	1,700 1,850 1,880 *1,720*
	0.319	233	8,500	1.28	287	1,430
N,N-Dimethylaniline	1.61×10^{-2} 0.250	251 251	15,800 13,700	8.06×10^{-2} 1.25	297–298 297	2,380 2,300

NOTE: Wavelengths are corrected in this and subsequent tables. Values in italics represent inflections.
*Two cell thicknesses were used throughout. 25.1 μ for concentrations ca. 10^{-2}–10^{-1} molar, and 2.91 μ for concentrations ca. 0.1–2 molar.

apparently being proportional to concentration, and also that appreciable hydrogen bonding does *not* occur below a solute concentration of about 0.01 mole/liter (see refs. 4, 5 and compare also, for example, refs. 6, 7, 8, which suggest that the related alcohols also do not associate appreciably below a solute concentration of ca. 0.005 mole/liter).*

**Neither the ultraviolet spectrum of aniline within the concentration range 1.00×10^{-2} to 3.36×10^{-4} moles/liter in cyclohexane solution (9), nor the ultraviolet spectrum of phenol within the concentration range 2.88×10^{-2} to 0.92×10^{-4} moles/liter in cyclohexane solution (this paper) shows any appreciable concentration dependence. Since under these conditions the benzoic acid spectrum shows a concentration dependence which has been ascribed to intermolecular hydrogen bonding (1), this again supports the hypothesis that within this same concentration range aniline and phenol do not associate appreciably.*

Can. J. Chem. Downloaded from www.nrcresearchpress.com by 186.148.149.217 on 09/04/12
For personal use only.



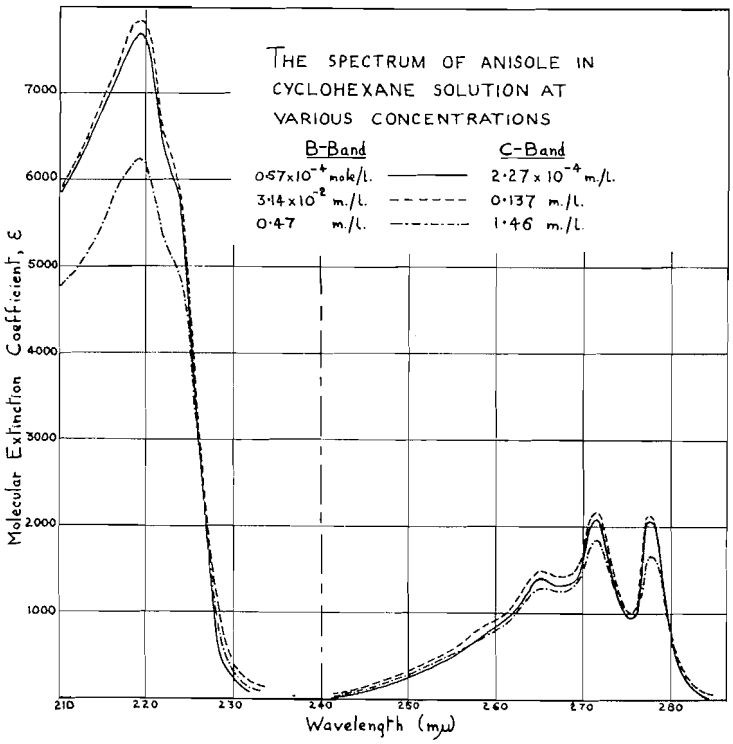


FIG. 1. The spectra of (A) phenol and (B) anisole in cyclohexane solution.

Can. J. Chem. Downloaded from www.nrcresearchpress.com by 186.148.149.217 on 09/04/12
For personal use only.

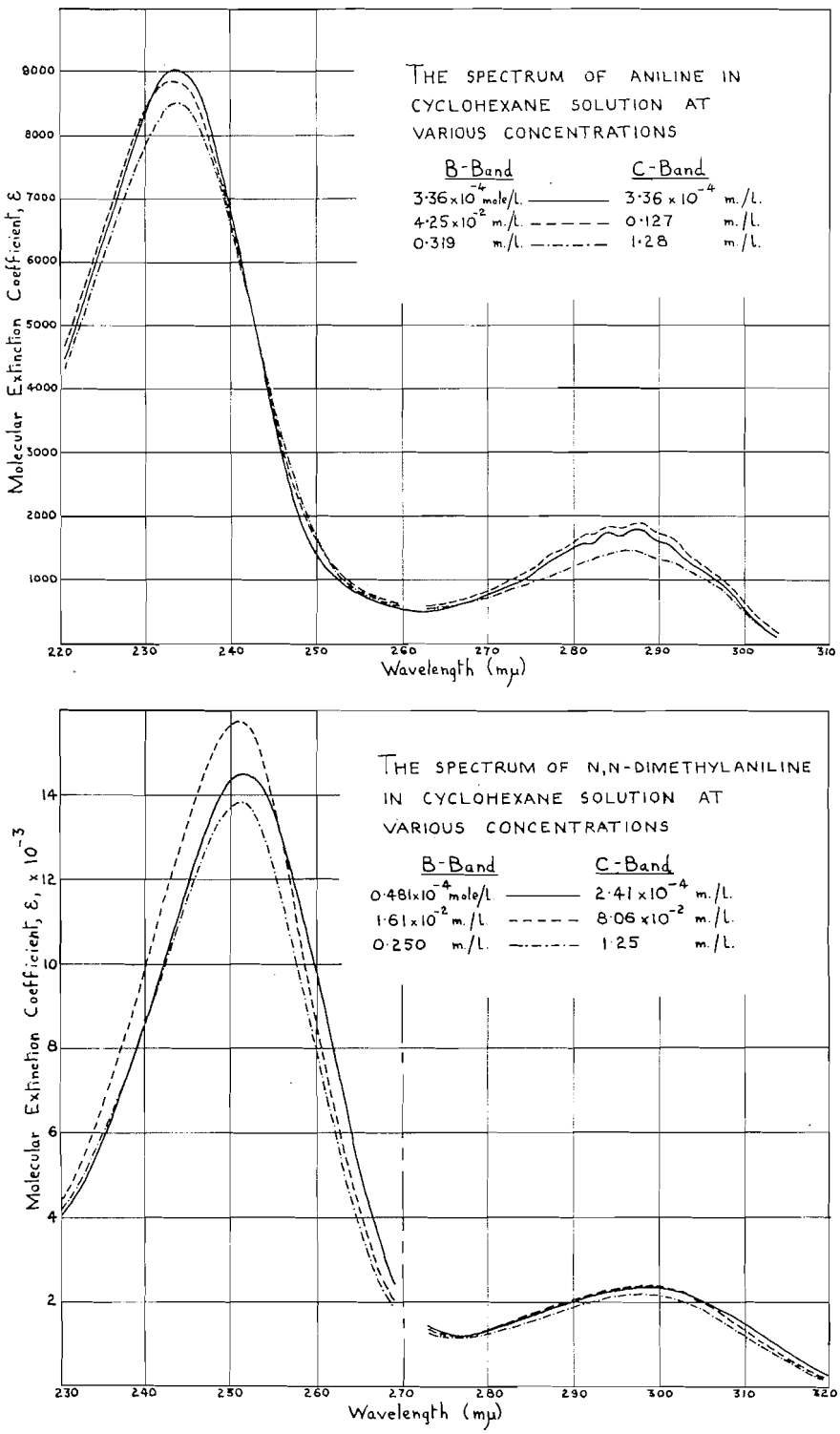


FIG. 2. The spectra of (A) aniline and (B) N,N-dimethylaniline in cyclohexane solution.

Can. J. Chem. Downloaded from www.nrcresearchpress.com by 186.148.149.217 on 09/04/12
For personal use only.

Can. J. Chem. Downloaded from www.nrcresearchpress.com by 186.148.149.217 on 09/04/12
For personal use only.

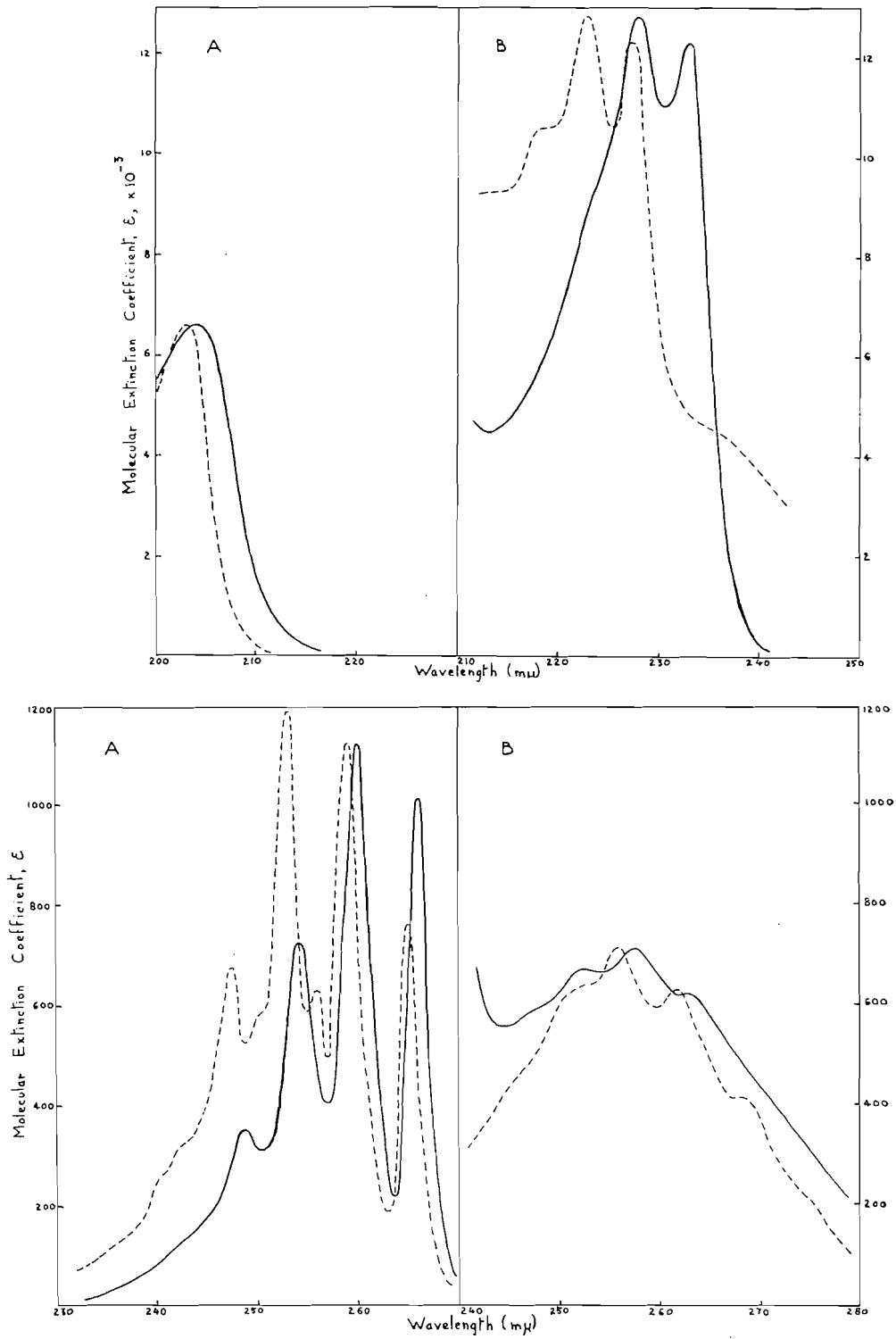


FIG. 3. The *B*-bands (above) and the *C*-bands (below) of (A) fluorobenzene and (B) iodobenzene in the vapor phase (– – –) and in cyclohexane solution (——). (ε values in the vapor phase are arbitrarily chosen.)

Our own data for the infrared hydroxyl band of phenol solutions in cyclohexane are as follows: at a solute concentration of 1.0 mole/liter, ν_{max} = 3613 cm^{-1} for what is assumed to be the unassociated hydroxyl band, the absorption being weak compared with the absorption ascribed to associated hydroxyl bands; at a solute concentration of 0.1 mole/liter, ν_{max} = 3622 cm^{-1}, and this band associated with free hydroxyl absorption is now considerably more intense than the other hydroxyl absorption.

The observed concentration dependences for the ultraviolet spectra of aniline and N,N-dimethylaniline are shown in Fig. 2. As might be anticipated from the *C*-band spectral changes observed for phenol and for the methyl-substituted analogue anisole, the *C*-band of aniline shows a decreased fine structure with increase of solute concentration. N,N-Dimethylaniline shows no fine structure even at the lowest concentrations.

From theoretical considerations it might be expected that an O—H...O hydrogen bond is energetically more favorable than an N—H . . . N hydrogen bond for the molecules under consideration, and this indication is again supported by the infrared data (see ref. 5 and cf. also refs. 10, 11). Our own data for the infrared N—H stretching bands of aniline solutions in cyclohexane are as follows: at a solute concentration of 1.00 mole/liter, ν_{max} = 3358 and 3449 cm^{-1} whereas at a solute concentration of 0.20 mole/liter, ν_{max} = 3366 and 3456 cm^{-1}. It is also noteworthy that these bands are still intense in a solution of aniline in cyclohexane containing 4% ether.

SOLUTE–SOLVENT INTERACTIONS INVOLVING ONLY SOLUTE AND INERT SOLVENT

If the ultraviolet absorption spectra of phenol or aniline are determined in the vapor phase and in an inert solvent it is found that a wavelength displacement occurs for each compound. This displacement cannot be caused exclusively by intermolecular X—H . . . Y hydrogen bonding because similar wavelength displacements are observed for anisole, and comparable wavelength displacements are also observed for a number of other compounds in which intermolecular hydrogen bonding is unlikely to occur to any marked extent. These observations are illustrated in Table II and the spectral curves for fluorobenzene and iodobenzene are also recorded in Fig. 3.

The data in Table II show that the main absorption bands of a number of aromatic conjugated compounds tend to be bathochromically displaced on passing from the vapor phase spectrum to the spectrum in cyclohexane solution, an observation which has previously been noted by Bayliss and McRae (15). Also, the observed fine structure appears to decrease in cyclohexane solution (see Fig. 3). The displacement appears to be qualitatively related to the dipole moment of the solute, since it is generally larger for compounds possessing an appreciable dipole moment such as nitrobenzene, and larger still for compounds like *p*-iodonitrobenzene (see Table II). Further, altering the temperature does not appreciably affect the wavelength of maximal absorption of some of the compounds in the vapor phase (14), and the spectra of some of these compounds are, moreover, similar in hexane and cyclohexane solution (see "Experimental").

It may further be noted that this somewhat unexpected solvent effect is not confined to the ultraviolet spectra since a "general" solvent effect is also observed in the infrared spectra; for example, the locations of the maximal frequencies of the two infrared NH absorptions for aniline and related compounds are appreciably displaced to lower frequency, i.e. to longer wavelength, in carbon tetrachloride solution, compared with the vapor phase spectrum (see ref. 16, and cf. also refs. 7, 17, 18). The most probable explanation is to associate this solvent effect with oriented solvent molecules which, by virtue of an induced dipole, facilitate the absorption.

Can. J. Chem. Downloaded from www.nrcresearchpress.com by 186.148.149.217 on 09/04/12
For personal use only.

TABLE II

Wavelength displacements between vapor phase spectra and spectra in cyclohexane solution

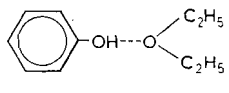
Absorption band		λ_{max}(mμ) (vapor)	λ_{max}(mμ)* (in cyclohexane)	Wavelength displacement (mμ)	Source
Aniline	*B*-band	230	234.5	4.5	Ref. 9
Aniline	*C*-band	ca. 283	289	6	Ref. 9
Phenol	*B*-band	205	210	5	Ref. 12
Phenol	*C*-band	264 267 269.5 ca. *273* 276	266 272 279	ca. 2	Ref. 12
Anisole	*B*-band	214.5	220	5.5	Ref. 13
Anisole	*C*-band	ca. *256* ca. *262* 264 269 270 275.5	ca. *268* 273 279	ca. 7	Ref. 13
Fluorobenzene	*B*-band	203	204	1	*
Fluorobenzene	*C*-band	249.5 255 258 261 267	251 256 262 268	ca. 1	*
Iodobenzene	*B*-band	ca. *219* 224 228	ca. *225* 229 234	ca. 6	*
Iodobenzene	*C*-band	ca. *254* 258 264	255 259.5 265	ca. 1	*
Nitrobenzene	*B*-band	239.1	253	13.9	Ref. 14
p-Fluoronitrobenzene	*B*-band	245.1	256	10.9	Ref. 14
p-Chloronitrobenzene	*B*-band	251.3	264.7	13.4	Ref. 14
p-Bromonitrobenzene	*B*-band	254.6	269	14.4	Ref. 14
p-Iodonitrobenzene	*B*-band	264.1	287.6	23.5	Ref. 14

*This paper.

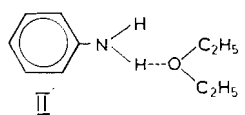
SOLUTE–SOLVENT INTERACTIONS INVOLVING HYDROGEN BONDING IN SOLUTIONS OF ANILINES AND PHENOLS

Apart from the general solvent effect discussed in the previous section we can discern spectral effects which are ascribed to intermolecular hydrogen bonding between solute and solvent. For example, ether frequently causes a bathochromic wavelength displacement in the *B*-band which is ascribed to intermolecular hydrogen bonding of type I or II, because replacement of the relevant hydrogen atom by a methyl group tends to destroy this effect (see Fig. 4 and cf. ref. 19), and also because parallel effects may be deduced from *C*-band and dipole moment data (20, cf. also 21).

Figure 4 shows that the spectral change ascribed to hydrogen bonding is greater for



I



II

Can. J. Chem. Downloaded from www.nrcresearchpress.com by 186.148.149.217 on 09/04/12
For personal use only.

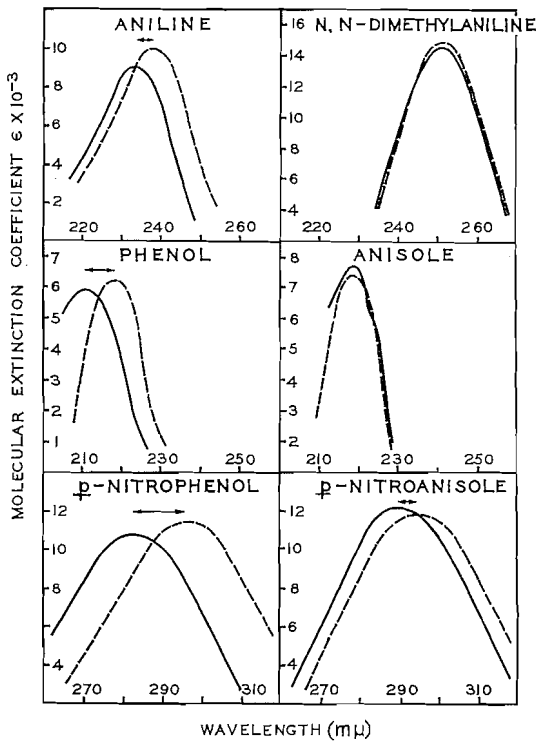
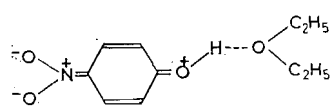


FIG. 4. *B*-Bands of anilines, phenol, and *p*-nitrophenol, and methyl-substituted analogues in cyclohexane (full lines) and in ether (dotted lines).

phenol than for aniline, which supports the previously noted hypothesis that an O—H ... X hydrogen bond is energetically more favored than an N—H ... X hydrogen bond for the molecules under consideration. A fuller list of spectra of phenols, aromatic amines, and their O- and N-methyl derivatives in cyclohexane and ether solutions is provided in Table III.

Table III indicates that for a number of *p*- or *m*-substituted compounds, where the relevant spectra are available, the observed wavelength displacements are similar to those in the parent compounds, phenol or aniline. That is, the bathochromic wavelength displacement, ascribed to the intermolecular hydrogen bond, is comparable for compounds like *p*-nitrophenol and for phenol, remembering that part of the observed wavelength displacement also occurs in *p*-nitroanisole or nitrobenzene and is therefore not caused by the same intermolecular hydrogen bonding involving the phenol group (see Fig. 4 and Table III). Moreover, since the total displacement, if expressed in wave numbers, for *p*-nitrophenol is only slightly smaller than the sum of the effects in phenol and nitrobenzene, this suggests that interactions which can be represented by resonance structures of type III do not appreciably affect the intermolecular hydrogen bond.



III

Can. J. Chem. Downloaded from www.nrcresearchpress.com by 186.148.149.217 on 09/04/12
For personal use only.

TABLE III

Bathochromic wavelength displacements ($\Delta\lambda$ in mμ and $\Delta\nu$ in cm^{-1}) between *B*-bands in cyclohexane (non-bonded species) and ether (hydrogen-bonded species) solutions

Solute	λ_{max}(mμ) (in cyclohexane)	ϵ_{max}	λ_{max}(mμ) (in ether)	ϵ_{max}	$\Delta\lambda$ (in mμ)	$\Delta\nu$ (in cm^{-1})
Aniline	234.5	9,000	238	10,000	3.5	600
N,N-Dimethylaniline	251	14,500	251.5	14,800	(0.5)	100
Phenol	210	6,000	218	6,400	8	1,700
Anisole	220	7,500	219	7,400	(−1)	−200
p-Nitrophenol	286	10,800	299	11,400	13	1,500
p-Nitroanisole	294	12,100	298	11,800	(4)	450
Nitrobenzene	253	9,000	256	8,500	(3)	500
p-Fluorophenol	210–211	4,200	217	4,000	6.5	1,400
p-Fluoroanisole	217	5,400	217.5	5,200	(0.5)	100
p-Chlorophenol	225	8,800	228	10,000	3	600
p-Chloroanisole	228	11,700	228	12,400	(0)	0
p-Bromophenol	225	10,250	226	11,300	1	200
p-Bromoanisole	227	12,500	227	13,000	(0)	0
p-Aminoanisole	237	9,100	239	9,500	(2)	400
p-Cresol	221	5,900	223	6,600	2	400
p-Methoxyphenol	225	7,000	225	7,250	0	0
p-Methoxyanisole	227	9,700	226	9,500	(−1)	−200
m-Nitrophenol	222	10,200	226	10,000	4	800
m-Nitroanisole	224	13,000	225	11,500	(1)	200
m-Cresol	214	6,100	221	5,600	7	1,450
m-Nitroaniline	234 ca. *263–264*	15,500 *4,000*	234 ca. *274*	18,500 *4,000*	0 ca. *10.5*	0
m-Hydroxyacetophenone	242.5 *248*	8,650 *7,250*	247 ca. *253*	9,300 *7,250*	4.5	750
m-Hydroxybenzaldehyde	245 251	10,000 9,500	250 *255*	9,800 *9,200*	5	800
o-Hydroxyacetophenone	248.5 255	9,000 8,700	249 ca. *253*	9,000 *8,500*	(−0.5)	−100
o-Hydroxybenzaldehyde	251 258	11,000 11,700	ca. *251* 255.5	*10,400* 10,700	(−1)	−150
o-Nitrophenol	269	7,350	268–269	6,900	−0.5	−100
o-Nitroanisole	248–249	3,400	250–251	3,050	(2)	300
o-Fluorophenol	212	5,800	216	5,500	4	900
o-Fluoroanisole	218	7,100	219	7,000	(1)	200
o-Chlorophenol	212	6,450	217	6,200	5	1,100
o-Chloroanisole	219 223	7,500 7,400	219 222	7,500 7,500	(0)	0
o-Bromophenol	212	8,700	219	7,000	7	1,550
o-Bromoanisole	ca. *219*	*8,300*	219	8,800	(0)	0
o-Cresol	213	7,500	218	5,350	5	1,100
o-Methoxyphenol	216	6,200	220	6,200	4	800
o-Aminoanisole	237	8,500	239	9,000	2	350

Other *p*-substituents, such as —Cl, —CH_3, etc., appear to have a similar effect and also tend to weaken slightly the intermolecular hydrogen bond as judged by the observed frequency displacements (see Table III). A *m*-substituent again sometimes appears to reduce the strength of the hydrogen bond, as indicated by the reduced frequency displacements (see Table III). A possible explanation is that a *m*- or *p*-substituent tends to interact with the π-electrons of the benzene ring, and that this interaction is competitive in as much as it reduces the benzene ring—OH group interaction which facilitates intermolecular hydrogen bonding.

o-Substituted compounds are evidently less satisfactory for comparison purposes since steric interactions *and* intramolecular hydrogen bonding would be expected to interfere with the conformations of the molecule and with the solvent–solute interactions. However, it may be noted as shown in Fig. 5 that the spectra of some intramolecularly bonded molecules such as *o*-hydroxyacetophenone are almost identical in ether and cyclohexane

Can. J. Chem. Downloaded from www.nrcresearchpress.com by 186.148.149.217 on 09/04/12
For personal use only.

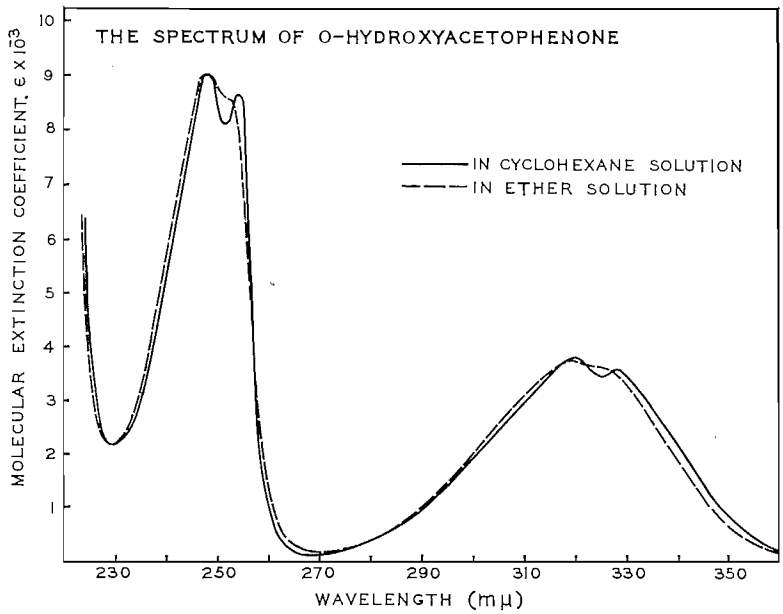


FIG. 5. The ultraviolet spectrum of *o*-hydroxyacetophenone in cyclohexane (full line) and ether (dotted line) solution.

solution (see also Table III for the *B*-bands of *o*-hydroxyacetophenone and *o*-hydroxybenzaldehyde and relevant reference compounds), and this is assumed to show that an intramolecular hydrogen bond prevents the formation of an intermolecular hydrogen bond, since intermolecular hydrogen bonding normally gives rise to spectral changes. *o*-Fluorophenol, however, does give rise to an appreciable wavelength displacement (cf. ref. 1 for the spectrum of *o*-fluorobenzoic acid, which also indicates the absence of a strong intramolecular hydrogen bond for the latter *o*-fluoro compound).

The data in Figs. 6 and 7 for phenol and *p*-nitrophenol in cyclohexane–ether solvent mixtures show that only small amounts of ether are necessary to cause the appearance of the absorption characteristic of the hydrogen-bonded structures. Support for this hypothesis is also received from the infrared spectrum of phenol. This shows that at a concentration of 0.1 mole/liter, i.e. at a concentration at which in cyclohexane solution the free hydroxyl band at 3622 cm^{-1} predominates, addition of 1% of ether to the solution considerably decreases the intensity of this band at the expense of a band at 3331 cm^{-1}, which is ascribed to associated hydroxyl absorption. In cyclohexane solution containing 2% ether the band at 3622 cm^{-1} occurs at 3618 cm^{-1} with yet further decreased absorption intensity and the hydroxyl absorption associated with hydrogen-bonded structures of type I at 3331 cm^{-1} accounts almost completely for the observed hydroxyl absorption. This again suggests that a relatively strong hydrogen bond is formed between the phenolic OH group and the ether molecules, a bond which may be regarded almost as a stoichiometric linkage (cf. also ref. 20 for the effect of small quantities of dioxane on the ultraviolet *C*-band of phenol). Previously determined data, on the other hand, indicated that small amounts of ether do *not* appreciably alter the typical aniline spectrum (see Table I in ref. 9), and this must be taken as evidence against the formation of a "stable stoichiometric" hydrogen bond between aniline and ether molecules under the conditions of the experiment. That is, the data again suggest that the N—H...X bond is weaker than the O—H...X hydrogen bond.

Can. J. Chem. Downloaded from www.nrcresearchpress.com by 186.148.149.217 on 09/04/12
For personal use only.

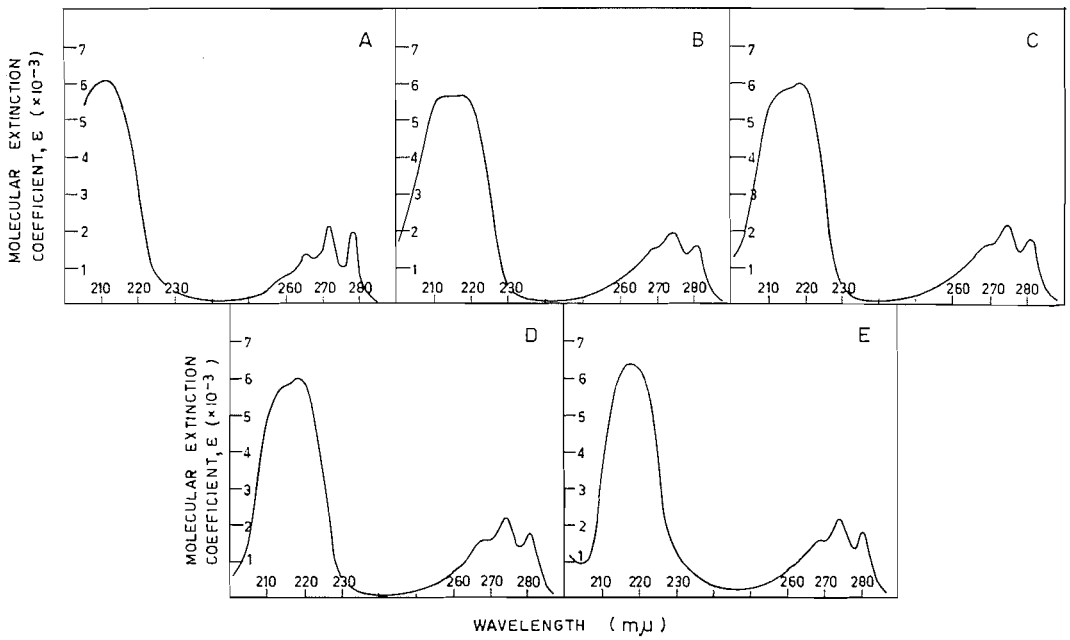


FIG. 6. The spectrum of phenol in (A) cyclohexane; (B) cyclohexane containing ca. 2% ether; (C) ether, cyclohexane volume ratio 1:9; (D) ether, cyclohexane volume ratio 1:3; and (E) ether.

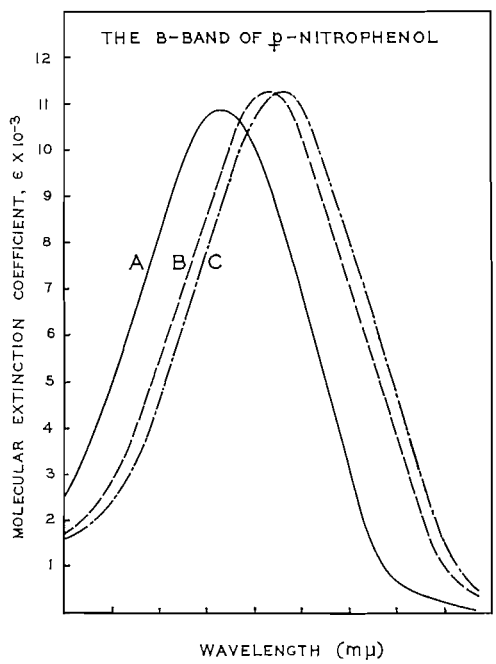


FIG. 7. The spectrum of *p*-nitrophenol in (A) cyclohexane solution (——); (B) cyclohexane solution containing ca. 1% ether (– – –); and (C) ether solution (— – — –).

Can. J. Chem. Downloaded from www.nrcresearchpress.com by 186.148.149.217 on 09/04/12
For personal use only.

Can. J. Chem. Downloaded from www.nrcresearchpress.com by 186.148.149.217 on 09/04/12
For personal use only.

SOLUTE-SOLVENT INTERACTIONS INVOLVING THE OXYGEN OR NITROGEN ATOMS OF PHENOLS AND ANILINES

Another spectral effect which may be caused by intermolecular hydrogen bonding is the observed hypsochromic wavelength displacement in the *B*-bands of aniline, N,N-dimethylaniline, phenol, and anisole on changing the solvent from cyclohexane or ethanol to water. A selection of the relevant data is listed in Table IV.

TABLE IV

Wavelength displacements ($\Delta\lambda$ in mμ) between *B*-bands in cyclohexane (non-bonded species) and ethanol or aqueous solutions

Solute	λ_{max}(mμ) (in cyclohexane)	ϵ_{max}	λ_{max}(mμ) (in ethanol)	ϵ_{max}	$\Delta\lambda$ relative to cyclohexane	λ_{max}(mμ) (in water)	ϵ_{max}	$\Delta\lambda$ relative to cyclohexane	Source
Aniline	234.5	9,000	235.5	8,000	1	231	8,000	−3.5	Ref. 9
N,N-Dimethylaniline	251	14,500	251	12,900	0	244	8,700	−7	Ref. 22
Phenol	210*	6,000	219	6,000	—	210	6,000	−9⊕	Ref. 12
Anisole	220	7,500	219.5	7,000	−0.5	217.5	4,300	2.5	Ref. 13
p-Aminoacetophenone	284	19,500§	319	20,000	35	311–312	16,500	27.5	Ref. 9
p-Hydroxyacetophone	258	12,600§	278	15,300	20	278	11,000	20	Ref. 23, †
p-Methoxyacetophenone	264	18,000	272	16,400‡	8				Ref. 13, †
p-Nitroaniline	322	14,600	371	15,500	49	380	13,000	58	Refs. 9, 25
p-Nitrophenol	286	10,800	314	13,000	28	317	9,300	31	Refs. 12, 24
p-Nitroanisole	294	12,100	305	13,000	11	316	10,500	22	Refs. 13, 24
p-Aminoanisole	237	9,100	234	9,000	−3				Ref. 13, †
p-Fluorophenol	210–211	4,200	216	3,800	5.5	207	4,500	−3.5	Ref. 12, †
p-Fluoroanisole	217	5,400	217	5,100	0	213	3,600	−4	Ref. 13, †
p-Chlorophenol	225	8,800	228	9,400	3	225	8,600	0	Ref. 12, †
p-Chloroanisole	228	11,700	228	11,200	0	226	9,000	−2	Ref. 13, †
p-Bromophenol	225	10,250	227	10,600	2	224	9,300	−1	Ref. 12, †
o-Bromoanisole	ca. *219* ca. *224*	*8,300* *7,400*	ca. *213.5* ca. *218* ca. *221*	*8,200* *7,900* *7,200*	ca. −2	ca. *213* ca. *219*	*7,500* *6,500*	ca. −5	Ref. 13, †

*This value is believed to be caused preferentially by transitions involving locally excited states and hence the absorption is considered anomalous (see ref. 12).

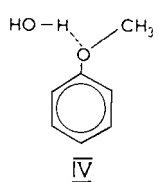
⊕Relative to ethanol.

†This paper.

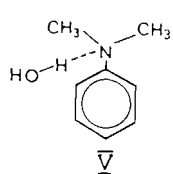
‡W. G. Douben and J. W. Collette (J. Am. Chem. Soc. **81**, 967 (1959)) report an ϵ_{max} value of 6600 for this compound, but this ϵ value is almost certainly too low.

§Values in *n*-heptane (see ref. 23).

Table IV shows that definite wavelength displacements now occur also for the methyl analogues, anisole, and N,N-dimethylaniline, and hence the wavelength displacements cannot be caused exclusively by hydrogen-bonded structures of type I or II. The wavelength displacements in Table IV can, however, be associated—at least partly—with hydrogen-bonded structures of type IV and V, since structures of this type can be imagined to decrease the electronic interaction between the nitrogen or oxygen atoms and the benzene ring, and so cause the *hypsochromic* wavelength displacement (cf. 19,



IV



V

20, 22), and incidentally the frequently observed decreased absorption intensity in the ultraviolet region for spectra of this type in aqueous media.*

However, while the above is probably a contributing factor it is evidently not the sole contributing factor, since, for example, the previously mentioned interactions will also contribute to the observed spectral changes. Therefore, a variety of spectral changes would be expected and are, in fact, observed. For example, in the spectra of compounds like *p*-nitroanisole or *p*-nitrophenol, water or ethanol molecules can attach themselves to the nitro group and this presumably accounts partly for the observed *bathochromic* wavelength displacement between cyclohexane, ethanol, and aqueous solutions (see Table IV). Moreover, dipole–dipole interactions would also be expected to cause *bathochromic* wavelength displacements, which may again hide any *hypsochromic* wavelength displacement caused by the solute–solvent interaction under discussion, and hydrogen bonding involving the hydrogen atoms of a phenolic OH group would be expected to have a similar effect. Hence wavelength displacements appear to be of doubtful diagnostic value. It is, however, significant that for a number of compounds of this type a characteristic intensity decrease is observed if the spectra are determined in aqueous solution (see Table IV).

Next, the solvent changes in the spectra of phenol for solutions containing various ethanol–water solvent mixtures are shown in Fig. 8. Figure 8 indicates a gradual change

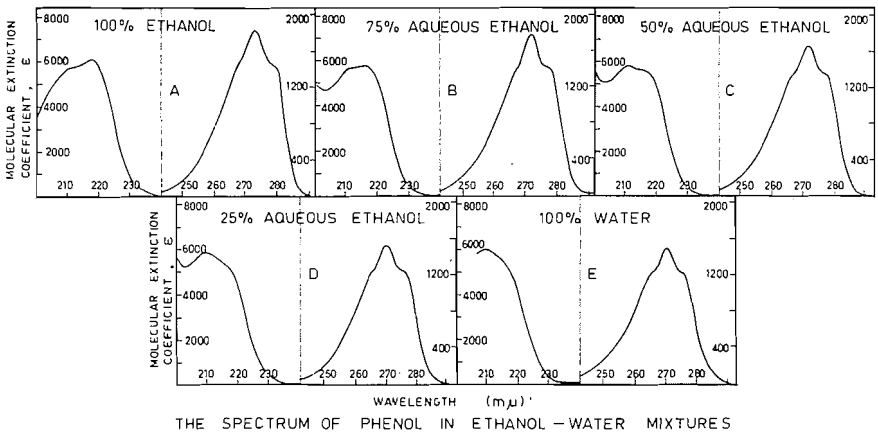


FIG. 8. The spectrum of phenol in (A) ethanol; (B) 75% aqueous ethanol; (C) 50% aqueous ethanol; (D) 25% aqueous ethanol; and (E) water.

in the spectrum of phenol on replacing ethanol by water as the solvent, and this suggests the absence of a stable predominating hydrogen bond between phenol and water. This follows because the spectral changes shown in Figs. 6 and 8 are different, and consequently the hydrogen bond between phenol and ether molecules probably differs from the solute–

**More precisely, this decreased interaction between the π-electrons of the benzene ring and the p-electrons of the nitrogen or oxygen atom may be caused in two ways; either the hydrogen bond directly removes electrons from the nitrogen or oxygen atoms, or because the hydrogen-bonded structure increases the effective size of the oxygen- or nitrogen-substituted group and a consequent twisting of the group out of the plane of the benzene ring may cause the observed hypsochromic wavelength displacement. There is, in fact, some evidence for the operation of steric factors because steric interactions have previously been noted to be able to prevent the formation of intermolecular hydrogen bonding (cf. the discussion of the spectra of o-substituted phenols in ref. 12). Moreover, the postulate of steric interactions can be used to rationalize the greater effectiveness of the water molecule in forming this type of hydrogen bond, since a larger solvent molecule such as ethanol might be expected to have greater difficulty in approaching the oxygen or nitrogen atoms (see, for example, the spectra of N, N-dimethylaniline and anisole in Table IV).*

Can. J. Chem. Downloaded from www.nrcresearchpress.com by 186.148.149.217 on 09/04/12
For personal use only.

solvent interaction involving the oxygen or nitrogen atoms in solutions of phenols or anilines. If phenol were to form a considerably stronger hydrogen bond with water than with ethanol it would be expected that only small quantities of water were necessary to produce a spectrum similar to the spectrum of phenol in water. A probable explanation of the above spectral changes is that *both* water and ethanol are continually forming and reforming hydrogen bonds with the phenol molecules (cf. ref. 1). According to this view the difference between the spectral changes in Fig. 6 and Fig. 8 can be explained because for solutions of phenol in cyclohexane–ether mixtures any hydrogen bonds competing with phenol–ether hydrogen bonds are likely to be insignificant, while for solutions of phenol in ethanol–water mixtures hydrogen bonds competing with phenol–water hydrogen bonds are probably important.

Apart from the wavelength displacements observed in Fig. 8 it may be noted that the change to the more polar solvent (water) decreases the fine structure of the phenolic *B*-band. A decreased fine structure in the *C*-band of phenol and anisole has previously (12, 13) been associated with hydrogen bonding or other solvent–solute interactions, and this view also receives support from the *B*-band of benzaldehydes (26) and of other compounds (27) where the characteristic fine structure is markedly decreased in the presence of ethanol or ether.

EXPERIMENTAL

The ultraviolet absorption spectra were determined by standard methods using a Unicam SP500 spectrophotometer. For each compound at least two independent sets of observations were made. The accuracy of λ_{max} values is estimated to be ± 1 mμ, and the precision of ϵ_{max} values $\pm 5\%$ or better. Values were reproducible in most cases to $\pm 2\%$. Vapor spectra were obtained by allowing specially designed 1-cm cells (Research and Industrial Instruments Co., Brixton, London, S.W.9, England) to remain in an atmosphere of the relevant compound until the optical density was within the permissible limits, and the cells were then sealed (see also footnote of Table I).

Some of the spectra have previously been described by other workers but whenever convenient the spectra were redetermined to ensure identical conditions for all the recorded spectra. The spectrum of *m*-iodobenzaldehyde was determined in both hexane and cyclohexane solution, and the determinations were found to be identical within experimental error.

The infrared spectra were determined on a Unicam SP100 instrument, using a NaCl prism.

The compounds under investigation were mostly commercial materials, purified by distillation or recrystallization until their boiling points and refractive indices or melting points showed them to be sufficiently pure. The solvents used were spectroanalyzed cyclohexane (Fisher), *n*-hexane specially prepared for spectroscopy (BDH), ethyl ether (Spectro Grade, Eastman), commercially available absolute ethanol suitable for spectroscopy, and freshly distilled water.

ACKNOWLEDGMENTS

The authors are greatly indebted to Miss N. Joan Smith for very competent technical assistance in the spectral determination of some of the compounds, and thanks are due to Mr. D. L. Coffen for determining the infrared spectra.

They also wish to thank the Fisheries Research Board of Canada for financial support, since part of this work was carried out under a contract between the Fisheries Research

Can. J. Chem. Downloaded from www.nrcresearchpress.com by 186.148.149.217 on 09/04/12
For personal use only.

Board of Canada and the Memorial University of Newfoundland. The authors further gratefully acknowledge the general assistance of the National Research Council in support of these studies.

REFERENCES

1. W. F. FORBES, A. R. KNIGHT, and D. L. COFFEN. Can. J. Chem. **38**, 728 (1960); W. F. Forbes and A. R. Knight. **37**, 334 (1959).
2. V. VON KEUSSLER. Z. Elektrochem. **58**, 136 (1954).
3. M. ITO. J. Mol. Spectroscopy, **4**, 125 (1960).
4. C. M. HUGGINS, G. C. PIMENTEL, and J. N. SHOOLERY. J. Phys. Chem. **60**, 1311 (1956).
5. N. FUSON, M-L. JOSIEN, R. L. POWELL, and E. UTTERBACK. J. Chem. Phys. **20**, 145 (1952).
6. M. SAUNDERS and J. B. HYNE. J. Chem. Phys. **29**, 1319 (1958).
7. U. LIDDEL and E. D. BECKER. Spectrochim. Acta, **10**, 70 (1957).
8. W. C. COBURN JR. and E. GRUNWALD. J. Am. Chem. Soc. **80**, 1318 (1958).
9. W. F. FORBES and I. R. LECKIE. Can. J. Chem. **36**, 1371 (1958).
10. H. RICHTERING. Z. Phys. Chem. **9**, 393 (1956).
11. L. J. BELLAMY and R. L. WILLIAMS. Spectrochim. Acta, **9**, 341 (1957).
12. J. C. DEARDEN and W. F. FORBES. Can. J. Chem. **37**, 1294 (1959).
13. J. C. DEARDEN and W. F. FORBES. Can. J. Chem. **37**, 1305 (1959).
14. W. M. SCHUBERT, J. M. CRAVEN, and H. STEADLY. J. Am. Chem. Soc. **81**, 2696 (1959).
15. N. S. BAYLISS and E. G. MCRAE. J. Phys. Chem. **58**, 1002 (1954).
16. W. J. ORVILLE-THOMAS, A. E. PARSONS, and C. P. OGDEN. J. Chem. Soc. 1047 (1958).
17. C. G. CANNON. Spectrochim. Acta, **10**, 341 (1958).
18. U. LIDDEL and E. D. BECKER. J. Chem. Phys. **25**, 173 (1956).
19. T. MASAMUNE. J. Am. Chem. Soc. **79**, 4418 (1957).
20. S. NAGAKURA and H. BABA. J. Am. Chem. Soc. **74**, 5693 (1952).
21. J. W. SMITH and S. M. WALSHAW. J. Chem. Soc. 3217 (1957).
22. H. E. UNGNADE. J. Am. Chem. Soc. **75**, 432 (1953).
23. J. TANAKA, S. NAGAKURA, and M. KOBAYASHI. J. Chem. Phys. **24**, 311 (1956).
24. A. BURAWOY and J. T. CHAMBERLAIN. J. Chem. Soc. 2310 (1952).
25. C. J. TIMMONS. J. Chem. Soc. 2613 (1957).
26. J. C. DEARDEN and W. F. FORBES. Can. J. Chem. **36**, 1362 (1958).
27. J. DERKOSCH and W. KALTENEGGER. Monatsh. **88**, 778 (1957).

Can. J. Chem. Downloaded from www.nrcresearchpress.com by 186.148.149.217 on 09/04/12
For personal use only.

Can. J. Chem. Downloaded from www.nrcresearchpress.com by 186.148.149.217 on 09/04/12
For personal use only.

ALIPHATIC CHEMISTRY OF FLUORENE

PART III. SOME DERIVATIVES OF FLUORENE AND PHENANTHRENE[1]

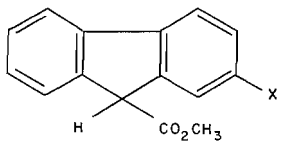
P. M. G. Bavin

ABSTRACT

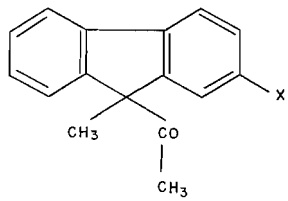
Methyl fluorene-9-carboxylate and 9-methyl-9-acetylfluorene have been nitrated and the products converted to 2-nitrophenanthrene and 2-nitro-9,10-dimethylphenanthrene, respectively.

Acetylation of 9,10-dimethylphenanthrene has given only one ketone, probably the 3-isomer. 4-Nitrofluorenone has been synthesized by a convenient route.

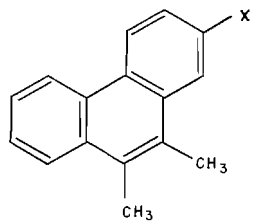
All five mononitrophenanthrenes have been synthesized (1) but only the 2-isomer is readily accessible (1, 2). Another closely related route to 2-nitrophenanthrene has now been found. Methyl 2-nitrofluorene-9-carboxylate (II), prepared by nitrating the ester (I), was reduced with lithium borohydride and the crude carbinol heated with polyphosphoric acid to give 2-nitrophenanthrene in 45% yield. In a similar way, 2-nitro-9,10-dimethylphenanthrene (VI) was prepared from 9-methyl-9-acetylfluorene (III) via the nitro-ketone (IV).



I, X = H
II, X = NO_2

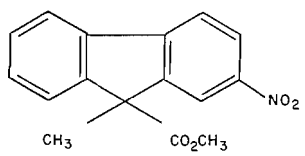


III, X = H
IV, X = NO_2

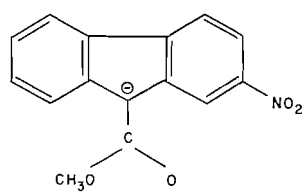


V, X = H
VI, X = NO_2
VII, X = NH_2
VIII, X = $NH \cdot CO \cdot CH_3$

During the isolation of the nitro-ester (II), it was noted that washing a chloroform solution of the nitration products with 2% sodium hydroxide solution resulted in the formation of a deep purple color, most easily observed by dissolving the pure nitro-ester in methanol containing sodium methoxide. Under the latter conditions, the color was rapidly discharged by methyl iodide with formation of what is considered to be the C-methyl derivative (IX) (cf. the alkylation of I (3)). The deep purple color was attributed to the anion (X) (cf. methyl fluorene-9-carboxylate anion (3)). These observations led directly to investigations of several aspects of the chemistry of fluorene (3, 4, 5) which are still in progress.



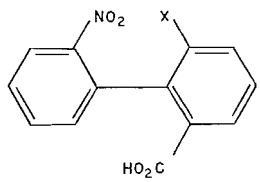
IX



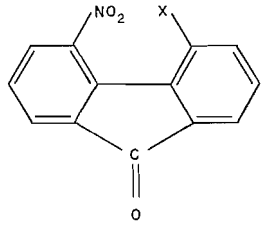
X

[1]*Manuscript received February 5, 1960.*
Contribution from the Chemistry Department, the University, Hull, East Yorkshire, England.

4-Nitrofluorenone (XIV) has been synthesized by the cyclization of the nitro-acid (XI) (cf. the acids XII and XIII which gave XV and XVI (6, 7)), but its conversion to 4-nitrofluorene, a desirable intermediate for the synthesis of the very inaccessible 4-nitrophenanthrene, was not achieved.



XI, X = H
XII, X = NO_2
XIII, X = CO_2H



XIV, X = H
XV, X = NO_2
XVI, X = CO_2H

The use of methyl fluorene-9-carboxylate as a synthetic tool has made several otherwise inaccessible hydrocarbons readily available (3, 8). One of these, 9,10-dimethylphenanthrene, has now been acetylated. Under homogeneous conditions in nitrobenzene at room temperature, only one ketone was isolated in 75–85% yield after reaction times of either 12 hours or 14 days. Prolonged efforts to degrade the ketone to the amine or carboxylic acid have failed. Attempts to synthesize reference compounds other than the amine (VII) have been unsuccessful but are reported in the Experimental section. The orientation of the *x*-acetyl-9,10-dimethylphenanthrene remains unestablished, but it is probably the 3-isomer by analogy with the acetylation of phenanthrene (9, 10 but see also Gore (11)).

9,10-Dimethylphenanthrene has been oxidized by aqueous sodium dichromate at 250° to phenanthrene-9,10-dicarboxylic acid (94%), 2-methyltriphenylene yielding the corresponding acid in 98% yield.* This technique should prove of great value in the preparation of derivatives of polycyclic hydrocarbons.

EXPERIMENTAL

2-Nitrophenanthrene

Methyl fluorene-9-carboxylate (2 g) was nitrated as described for 9-fluorenylmethyl acetate (1). *Methyl 2-nitrofluorene-9-carboxylate* crystallized from xylene–pentane as pale yellow needles (0.8 g), m.p. 178–179°. Found: C, 67.0; H, 4.31; N, 5.21%. Calc. for $C_{15}H_{11}NO_4$: C, 66.91; H, 4.12; N, 5.20%. Less satisfactorily, 2-nitrofluorene-9-carboxylic acid (13) was esterified with methanolic hydrogen chloride.

The nitro-ester dissolved in methanol containing sodium methoxide to give a black solution, purple at high dilution. The color was rapidly discharged by methyl iodide with formation of *methyl 9-methyl-2-nitrofluorene-9-carboxylate*, pale yellow prisms from heptane, m.p. 122–123°. Found: C, 67.73; H, 4.19%. Calc. for $C_{16}H_{13}NO_4$: C, 67.84; H, 4.63%.

The nitro-ester (II) was reduced with lithium borohydride in tetrahydrofuran (14, 15) to give an orange resin. A part of the resin was acetylated with isopropenyl acetate (1) and the product purified by passing a hexane solution of it through a column of activated

**The author is indebted to Dr. D. Fishel of the State University of South Dakota for these experiments (12, p. 22P).*

Can. J. Chem. Downloaded from www.nrcresearchpress.com by 186.148.149.217 on 09/04/12
For personal use only.

alumina. The eluted material crystallized as pale yellow prisms (22%) from hexane, m.p. 123–125°, not depressed by authentic 2-nitro-9-fluorenylmethyl acetate (1).

The other part of the resin was heated with polyphosphoric acid as described for 9-fluorenylmethyl acetate (1) to give 2-nitrophenanthrene as yellow needles from heptane (45%), m.p. 118–119°, not depressed by an authentic sample (1). Oxidation with periodic acid in boiling acetic acid gave 2-nitrophenanthraquinone, orange plates from acetic acid, m.p. 270–272°, not depressed by an authentic specimen (16). Found: C, 65.79; H, 2.60%. Calc. for $C_{14}H_7NO_4$: C, 66.41; H, 2.79%.

2-Nitro-9,10-dimethylphenanthrene

Pure 9-methyl-9-acetylfluorene (8) was nitrated as described for 9-fluorenylmethyl acetate (1). *2-Nitro-9-methyl-9-acetylfluorene* (70%) formed pale yellow prisms from methanol, m.p. 136–138°, raised to 138–139° by two further crystallizations. Found: C, 71.99; H, 5.19%. Calc. for $C_{16}H_{13}NO_3$: C, 71.90; H, 4.90%.

The *carbinol*, obtained as an oil by reducing the nitro-ketone with methanolic sodium borohydride, was esterified with *p*-toluenesulphonyl chloride in pyridine (3). The crude *tosylate* was boiled under reflux for 12 hours with 94% formic acid, *2-nitro-9,10-dimethylphenanthrene* crystallizing on cooling. Purification by passing a hexane solution of it through a column of activated alumina and concentration of the eluant gave bright yellow needles (74% based on nitro-ketone), m.p. 163–164°. Found: C, 76.75; H, 5.31%. Calc. for $C_{16}H_{13}NO_2$: C, 76.47; H, 5.57%.

2-Amino-9,10-dimethylphenanthrene, prepared by reducing the nitro compound with hydrazine and palladized charcoal (17), crystallized as white needles from ethanol, m.p. 141–142°. The *N-acetyl* derivative crystallized from toluene as small white needles, m.p. 256–257°. A sample was sublimed at 220°/10^{-3} mm for analysis. Found: C, 82.16; H, 6.86%. Calc. for $C_{18}H_{17}NO$: C, 82.10; H, 6.51%.

4-Nitrofluorenone

2′-Nitrodiphenyl-2-carboxylic acid (18) (1.2 g) was maintained for 20 minutes at 115° with concentrated sulphuric acid (40 ml). Pouring onto ice precipitated a yellow solid, which crystallized from methanol (Norite) as long yellow needles (0.98 g), m.p. 173–174° (lit. m.p. 173–174° (19)).

9,10-Dimethylphenanthrene

Crude 9-acetylfluorene (20) (1 mole) was methylated with methyl iodide (2.1 moles) in methanol containing sodium methoxide (2 moles), the reaction being complete after 6 hours at room temperature. The crude ketone (96%, m.p. 82–84°) (lit. m.p. 85–86° (8)) was reduced with ethereal lithium aluminum hydride to 1′-(9-methyl-9-fluorenyl)-ethanol (98%, m.p. 77–80°) (lit. m.p. 81° (8)). The *tosylate*, prepared in the usual way (3), formed colorless prisms from chloroform–hexane, m.p. 88–90° with decomposition to 9,10-dimethylphenanthrene. Found: S, 8.62%. Calc. for $C_{23}H_{22}O_3S$: S, 8.47%.

9,10-Dimethylphenanthrene was prepared either by boiling the crude tosylate with 94% formic acid, or by boiling the carbinol with its own weight of phosphorus pentoxide in xylene for 2 hours. It formed long white needles (85–91%) from toluene–hexane, m.p. 143–144° (lit. m.p. 143–144° (8)).

Phenanthrene-9,10-dicarboxylic acid

9,10-Dimethylphenanthrene was oxidized by aqueous sodium dichromate solution at 250° (12), giving crude phenanthrene-9,10-dicarboxylic acid in 94% yield. The anhydride

Can. J. Chem. Downloaded from www.nrcresearchpress.com by 186.148.149.217 on 09/04/12
For personal use only.

crystallized from acetic anhydride as pale yellow needles, m.p. 322–324°, not depressed by an authentic specimen (21).* The dimethyl ester formed pale yellow needles from benzene, m.p. 132–133° (lit. m.p. 131° (21)).

Triphenylene-2-carboxylic Acid

2-Methyltriphenylene (22), oxidized as above, gave triphenylene-2-carboxylic acid in 98% yield. The methyl ester crystallized as colorless needles from toluene, m.p. 129–130°. Found: C, 83.81, 84.01; H, 5.26, 5.34%. Calc. for $C_{20}H_{14}O_2$; C, 83.90; H, 4.93% (lit. m.p. 122–124° (23)).

x-Acetyl-9,10-dimethylphenanthrene

Anhydrous aluminum chloride (43 g, 2.2 moles) was dissolved in dry nitrobenzene (150 ml) and the solution cooled to 0°. 9,10-Dimethylphenanthrene (29.8 g, 1 mole) was added, followed by freshly distilled acetyl chloride (16 g, 1.4 moles). The mixture was left at room temperature for 14 days with exclusion of moisture. The complex was decomposed with ice and hydrochloric acid and the nitrobenzene removed by distillation with steam. Distillation of the residue at 1–2 mm gave the ketone as an almost colorless oil, which soon crystallized. One crystallization from acetone–methanol gave very pale yellow prisms (26 g, 73%), m.p. 108–110°. Fractional crystallization gave a further 4.5 g of ketone of the same melting point. A second ketone was not found.

The first crop of ketone was recrystallized once from methanol–acetone and twice from toluene–heptane to give colorless prisms (20 g, 56%), m.p. 111.5–112°. This melting point was not raised by further crystallizations. Found: C, 86.94; H, 6.55%. Calc. for $C_{18}H_{16}O$: C, 87.06; H, 6.50%.

The *oxime*, prepared in pyridine–ethanol, crystallized as white needles from toluene–heptane, m.p. 209–210°. OH stretching band (CS_2 solution) 3586 cm^{-1}. Found: C, 82.13; H, 6.65%. Calc. for $C_{18}H_{17}NO$: C, 82.11; H, 6.51%.

The *azine*, prepared by warming the ketone with hydrazine in ethanol, separated from xylene as golden-yellow plates, m.p. 280–281°. Found: C, 87.82; H, 6.41; N, 5.80%. Calc. for $C_{36}H_{32}N_2$: C, 87.77; H, 6.55; N, 5.69%.

x-Ethyl-9,10-dimethylphenanthrene was prepared by boiling the ketone (1 g) under reflux for 6 hours with hydrazine hydrate (10 ml) and diethylene glycol (100 ml). The purified hydrocarbon, obtained by passing a hexane solution of it through a column of activated alumina, crystallized from methanol as long white needles, m.p. 45.5–46°. Found: C, 92.32; H, 5.72%. Calc. for $C_{18}H_{18}$: C, 92.26; H, 5.74%. The 1,3,5-trinitrobenzene complex crystallized from methanol as bright yellow needles, m.p. 164–166°.

Numerous attempts to oxidize the ketone using aqueous sodium hypochlorite and pyridine or dioxane as diluent gave tars and only traces of acidic material. Reaction with sodium azide in acetic acid (24) also failed to yield useful products.

Reaction between the pure oxime and phosphorus pentachloride – benzene, hydrogen chloride – acetic acid or polyphosphoric acid gave uniformly low yields of mixtures, from which traces of an amine were obtained by hydrolysis with ethanolic hydrogen chloride. The amine rapidly turned red in air, behavior similar to that of 3-aminophenanthrene, and had an infrared spectrum markedly different from that of 2-amino-9,10-dimethylphenanthrene.

3-Ethylphenanthrene-9-carboxylic acid

3-Acetyl-9-bromophenanthrene (55 g, m.p. 151–153°) (lit. m.p. 150–151° (25)) was

*The author is indebted to I. Ungar of the Battelle Memorial Institute for this sample.

Can. J. Chem. Downloaded from www.nrcresearchpress.com by 186.148.149.217 on 09/04/12
For personal use only.

Can. J. Chem. Downloaded from www.nrcresearchpress.com by 186.148.149.217 on 09/04/12
For personal use only.

boiled under reflux for 4 hours with cuprous cyanide (20 g) and dimethylformamide (150 ml) containing 2 drops of pyridine. After cooling, the mixture was poured into concentrated aqueous ammonia and the precipitated solid crystallized from toluene, 3-acetyl-9-cyanophenanthrene (50 g) separating as yellow needles, m.p. 226–227° (lit. m.p. 220–221° (25)).

The nitrile (49 g) was boiled under reflux with hydrazine hydrate (40 ml) and diethylene glycol (300 ml). After 1 hour a solution of potassium hydroxide (40 g) in water (60 ml) was added dropwise. The mixture was distilled until a distillate temperature of 195° was reached. After a further 4 hours, the mixture was cooled and poured into excess dilute hydrochloric acid. The *acid* was collected, washed, and dissolved in 5% aqueous potassium carbonate solution and the solution filtered into dilute hydrochloric acid. The purified acid was dried and converted to the methyl ester by successive reactions with thionyl chloride and methanol. After distillation at 200–210° and 1–2 mm, the colorless ester was saponified, giving the acid as an oil which crystallized during several days. The yield was 20 g. Two crystallizations from methanol–acetone gave almost colorless needles, m.p. 180–182°, with previous sintering. Found: C, 82.30, 82.20; H, 5.57, 5.68%. Calc. for $C_{17}H_{14}O_2$: C, 81.58; H, 5.64%.

3-Ethyl-9,10-phenanthraquinone

3-Acetylphenanthrene (9) was reduced to 3-ethylphenanthrene using hydrazine and diethylene glycol. The hydrocarbon, which has not been obtained crystalline (26), was distilled and purified through the picrate, which crystallized from methanol as orange needles, m.p. 120–121°. Oxidation with chromic oxide in acetic acid gave 3-ethylphenanthraquinone, slender orange needles from ethanol, m.p. 173–174° (lit. m.p. 168–170° (26)). Heating the quinone with potassium hydroxide in water or aqueous alcohol gave tars and only traces of acidic material.

3-Methylfluorene

Benzyl *p*-tolyl ketone (218 g, 55%) was prepared from phenylacetyl chloride (2 moles) and toluene, as described for benzyl phenyl ketone (27, p. 156). It formed plates from methanol, m.p. 109–110° (lit. m.p. 110–110.5° (28)). Found: C, 85.57; H, 6.88%. Calc. for $C_{15}H_{14}O$: C, 85.68; H, 6.71%. The *2,4-dinitrophenylhydrazone* formed irregular red prisms from benzene, m.p. 213–214°. Found: C, 64.45; H, 4.47%. Calc. for $C_{21}H_{18}N_4O_4$: C, 64.60; H, 4.65%.

The preceding desoxybenzoin was converted to 4-methylbenzoin* by a general procedure (29, p. 296) involving successively photobromination, reaction with sodium ethoxide, and hydrolysis with dilute hydrochloric acid. It crystallized from aqueous ethanol as long colorless needles (65%), m.p. 112–113° (lit. m.p. 110° (30)). Found: C, 79.81; H, 6.39%. Calc. for $C_{15}H_{14}O_2$: C, 79.62; H, 6.24%.

Oxidation of the benzoin with cupric sulphate and pyridine (31, p. 715) gave 4-methylbenzil as a yellow oil, which largely crystallized after distillation (lit. m.p. 31° (32)). Conversion to 4-methylbenzilic acid proceeded in high yield (31, p. 715), but the acid proved remarkably difficult to crystallize. The yield of white needles from chloroform–hexane, m.p. 132–134°, was only 41% (lit. m.p. 132° (32)).

Cyclization of the benzilic acid has already been reported (34) but proceeds in higher yield by a more recent procedure (33). The crude dried 3-methylfluorene-9-carboxylic acid was decarboxylated by distillation at 1 mm, giving 3-methylfluorene in 43% yield

**Primes (') are used for substituents on the ring adjacent to the carbinol group.*

based on the benzilic acid. It crystallized from methanol as colorless plates, m.p. 87–88° (lit. m.p. 88° (34)).

Prepared similarly, *benzyl p-ethylphenyl ketone* (71%) crystallized as lustrous colorless plates from methanol, m.p. 62–64°. Found: C, 85.41; H, 7.02%. Calc. for $C_{16}H_{16}O$: C, 85.67; H, 7.19%. The *2,4-dinitrophenylhydrazone* formed iridescent vermilion scales from benzene, m.p. 186–187°. Found: C, 65.10; H, 5.48%. Calc. for $C_{22}H_{20}N_4O_4$: C, 65.01; H, 5.48%.

4-Ethylbenzoin formed clusters of needles from heptane, m.p. 89–90°. Found: C, 79.91; H, 6.44%. Calc. for $C_{16}H_{16}O_2$: C, 79.97; H, 6.71%. 4-Ethylbenzil and 4-ethylbenzilic acid have failed to crystallize and have not been characterized.

ACKNOWLEDGMENTS

This work has been carried out during the tenure of a National Research Council of Canada Postdoctoral Fellowship (University of Ottawa, 1954–1956) and an I.C.I. Fellowship (the University, Hull, 1958–1960).

REFERENCES

1. P. M. G. Bavin and M. J. S. Dewar. J. Chem. Soc. 4477 (1955).
2. J. D. Loudon, A. D. B. Sloan, and L. A. Summers. J. Chem. Soc. 3814 (1957).
3. F. A. L. Anet and P. M. G. Bavin. Can. J. Chem. **34**, 991 (1956).
4. F. A. L. Anet and P. M. G. Bavin. Can. J. Chem. **36**, 763 (1958).
5. P. M. G. Bavin. Can. J. Chem. **37**, 2023 (1959).
6. F. E. Ray and W. C. Francis. J. Org. Chem. **8**, 52 (1943).
7. C. Angelini. Ann. chim. (Rome), **43**, 247 (1953).
8. E. J. Greenhow, D. McNeil, and E. N. White. J. Chem. Soc. 986 (1952).
9. E. Mosettig and J. van de Kamp. J. Am. Chem. Soc. **52**, 3704 (1930).
10. P. M. G. Bavin and M. J. S. Dewar. J. Chem. Soc. 164 (1956).
11. P. H. Gore. Chem. Revs. **55**, 229 (1955).
12. H. Shechter, D. Fishel, and L. Friedman. Abstracts of Papers, 136th Meeting of the American Chemical Society, Atlantic City, N.J. September, 1959.
13. F. L. Rose. J. Chem. Soc. 2360 (1932).
14. R. Paul and N. Joseph. Bull. soc. chim. France, 758 (1953).
15. J. Kollonitsch, O. Fuchs, and V. Gábor. Nature, **173**, 125 (1954).
16. A. J. Nunn, K. Schofield, and R. S. Theobald. J. Chem. Soc. 2797 (1952).
17. P. M. G. Bavin. Can. J. Chem. **36**, 238 (1958).
18. R. G. Shuttleworth, W. S. Rapson, and E. T. Stewart. J. Chem. Soc. **72** (1944).
19. C. Courtot. Ann. chim. (Paris), **14**, (10), 5 (1930).
20. J. Von and E. C. Wagner. J. Org. Chem. **9**, 162 (1944).
21. A. Jeannes and R. Adams. J. Am. Chem. Soc. **59**, 2608 (1937).
22. W. S. Rapson. J. Chem. Soc. 15 (1941).
23. J. W. Cook and C. L. Hewett. J. Chem. Soc. 401 (1933).
24. J. R. Dice and P. A. S. Smith. J. Org. Chem. **14**, 181 (1949).
25. J. Schultz, M. A. Goldberg, E. P. Ordas, and G. Carsch. J. Org. Chem. **11**, 309 (1946).
26. R. A. Barnes and R. T. Gottesman. J. Am. Chem. Soc. **74**, 35 (1952).
27. C. F. H. Allen and W. E. Barker. *In* Organic syntheses. Collective Vol. II. John Wiley and Sons, New York. 1943. p. 156.
28. K. Isimura. Bull. Chem. Soc. Japan, **16**, 196 (1941).
29. W. S. Ide and J. S. Buck. Organic reactions. Vol. IV. John Wiley and Sons, New York. 1948. p. 296.
30. R. T. Arnold and R. C. Fuson. J. Am. Chem. Soc. **58**, 1295 (1936).
31. A. I. Vogel. A text-book of practical organic chemistry. Longmans, Green and Co., London. 1957. p. 715.
32. H. H. Hatt, A. Pilgrim, and W. J. Hurran. J. Chem. Soc. 93 (1936).
33. H. J. Richter. Org. Syntheses, **33**, 37 (1953).
34. D. Vörlander and C. Pritzsche. Ber. **46**, 1793 (1913).

Can. J. Chem. Downloaded from www.nrcresearchpress.com by 186.148.149.217 on 09/04/12
For personal use only.

Can. J. Chem. Downloaded from www.nrcresearchpress.com by 186.148.149.217 on 09/04/12
For personal use only.

ALIPHATIC CHEMISTRY OF FLUORENE

PART IV. PREPARATION AND ALKYLATION OF SOME SULPHIDES AND SULPHONES[1]

P. M. G. BAVIN[2]

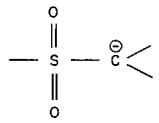
ABSTRACT

The preparations are described of some 9-fluorenyl sulphides which have been oxidized with peracetic acid to the corresponding sulphones.

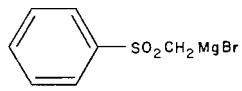
9-Fluorenyl *p*-tolyl sulphone has been alkylated with a range of alkyl halides; other sulphones, including 2-nitro-9-fluorenyl *p*-tolyl sulphone, have been methylated.

Methyl fluorene-9-carboxylate anion was reduced by *p*-toluenesulphonyl chloride to dimethyl 9,9′-difluorenyl-9,9′-dicarboxylate.

The acidity of methylene hydrogen activated by the sulphone group has been known for some time, but opinions have been divided on the reasons. Recent studies by Doering and his co-workers (1, 2, 3) have established that anions of type I are resonance stabilized by overlap between carbon $2p$ and sulphur $3d$ orbitals. The spectroscopic studies of Fehnel and Carmack (4) lend strong support to these conclusions. The latter workers found no evidence for the formation of anions from methylene activated only by a sulphone group, but Grignard derivatives of dialkyl sulphones (5, 6) and aralkyl sulphones (7, where references are given to prior publications) are well known. Field, Holsten, and Clark (7) have recently examined some reactions of phenylsulphonylmethyl magnesium bromide (II) and shown that it was alkylated in modest yield by benzyl chloride and



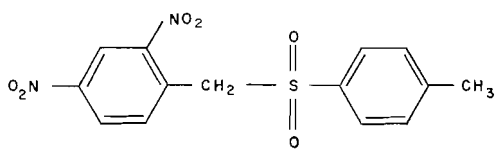
I



II

hexyl *p*-toluenesulphonate, in low yield by benzhydryl chloride, and not at all by *t*-butyl chloride and hexyl iodide, results which prompted its formulation as a weakly nucleophilic Grignard reagent rather than as a carbanion salt.

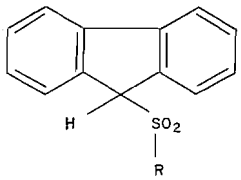
Nitrobenzyl sulphones are more acidic than the unsubstituted sulphones, and 2,4-dinitrobenzyl *p*-tolyl sulphone (III) has been methylated (8) using potassium ethoxide as base. The only simple sulphone to have been alkylated under comparable conditions is ethyl 9-fluorenyl sulphone (IV) (9).



III

The remarkable facility with which methyl fluorene-9-carboxylate anion reacts with a wide range of alkyl halides (10, 11, 12) has prompted an examination of other 9-substituted fluorenes. Some experiments with 9-benzoylfluorene have already been reported (13). The present paper describes the alkylation of 9-fluorenyl *p*-tolyl sulphone (VII),

[1]*Manuscript received February 5, 1960.*
Contribution from the Chemistry Department, the University, Hull, East Yorkshire, England.
[2]*I.C.I. Fellow.*

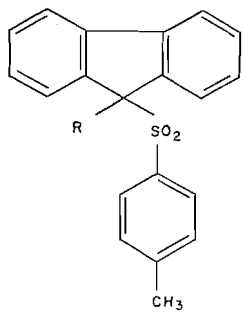


IV, R = CH_3CH_2 VI, R = C_6H_5

V, R = CH_3 VII, R = p-$CH_3 \cdot C_6H_4$

prompted by the work on ethyl 9-fluorenyl sulphone mentioned above (9), together with miscellaneous experiments on related systems.

9-Fluorenyl *p*-tolyl sulphone dissolved in warm ethanol containing sodium ethoxide with formation of a yellow solution. Under similar conditions 2-nitro-9-fluorenyl *p*-tolyl sulphone gave a purple-brown solution, similar to those reported for methyl 2-nitrofluorene-9-carboxylate (14) and 2,4-dinitrobenzyl *p*-tolyl sulphone (8). These solutions undoubtedly contained the organic anions and, in confirmation of this, 9-methyl-, -ethyl-, -isopropyl-, -allyl-, -benzyl-, and -cyclohexyl-9-fluorenyl *p*-tolyl sulphones (VIII,



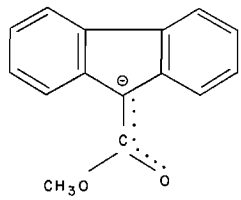
VIII

R = alkyl) were prepared by reaction with appropriate alkyl halides. In a similar manner were prepared 9-methyl-2-nitro-9-fluorenyl *p*-tolyl sulphone, 9-methyl-9-fluorenyl phenyl sulphone, and the methyl and isopropyl derivatives of 9-fluorenyl methyl sulphone. Comparison of these results with those reported for phenylsulphonylmethyl magnesium bromide (7) shows that anions of the type X are powerful nucleophiles which behave as true anion metal salts.

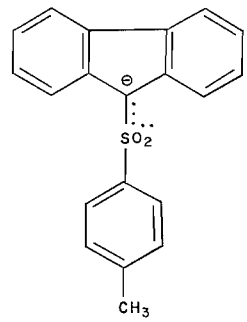
Fluorene has not been alkylated using ethanolic sodium ethoxide as base, so the reactions described above establish that fluorene anion is stabilized by a sulphone group. Although the anions derived from 9-fluorenyl *p*-tolyl sulphone, methyl fluorene-9-carboxylate, and 9-benzoylfluorene show many similar reactions, there are important differences. The sulphone (VII) was recovered unchanged after attempted bromination in acetic acid in the presence of sodium acetate, conditions which gave good yields of methyl 9-bromofluorene-9-carboxylate (11). From the reaction between *t*-butyl chloride and the anion of VII, only unreacted sulphone (30%) was isolated in a pure state. However, examination of the infrared spectrum of the crude product showed the presence of one or more additional compounds, with bands in the positions reported (15) for the *t*-butyl group (cf. methyl 9-*t*-butylfluorene-9-carboxylate (11)). Prolonged reaction times

Can. J. Chem. Downloaded from www.nrcresearchpress.com by 186.148.149.217 on 09/04/12
For personal use only.

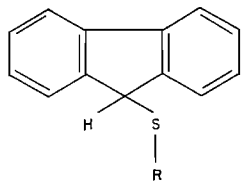
led to the formation of fluorenone, probably by anionic oxidation (16). It follows that the ester anion (IX) is more nucleophilic than the sulphone anion (X), differences in their behavior towards *t*-butyl chloride being of degree rather than kind.



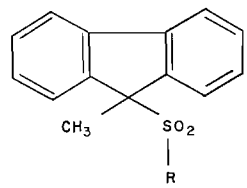
IX



X



XI, R = CH_3
XII, R = C_6H_5
XIII, R = *p*-$CH_3C_6H_4$



XIV, R = CH_3
XV, R = C_6H_5
XVI, R = *p*-$CH_3C_6H_4$

The sulphides (XI, XII, and XIII) have been prepared, the first from 9-fluorenylmercaptan and the others from thiophenol and thio-*p*-cresol, respectively. Methylation with ethereal methyl lithium – methyl iodide (cf. fluorene (17)) gave the tertiary sulphides (XIV, XV, and XVI), the mild conditions employed precluding the rearrangement observed for some 9-fluorenyl ethers (18). All six sulphides were oxidized with peracetic acid to the corresponding sulphones, confirming the structures of the methylation products of sulphones (V, VI, and VII). Attempts were made to oxidize 9-fluorenyl *p*-tolyl sulphide to the sulphoxide but mixtures were always obtained, consisting of the desired sulphoxide together with the sulphone and fluorenone, as shown by infrared spectra.

9-Methyl-9-fluorenyl *p*-tolyl sulphone was not cleaved by sodium piperidide (19, 20), although 9-methylfluorene was slowly formed by reaction with caustic soda in boiling diethylene glycol (cf. 21).

Characteristic sulphone bands have been recorded for the compounds reported in this paper but, being more complex than those reported for other sulphones (15), are being discussed elsewhere (22).

Although keto-esters have been prepared from fluorene-ester anion with acetyl (10) and benzoyl (28) chlorides, the similar reaction with *p*-toluenesulphonyl chloride gave dimethyl 9,9′-difluorenyl-9,9′-dicarboxylate by reductive dimerization of the anion.

Can. J. Chem. Downloaded from www.nrcresearchpress.com by 186.148.149.217 on 09/04/12
For personal use only.

Can. J. Chem. Downloaded from www.nrcresearchpress.com by 186.148.149.217 on 09/04/12
For personal use only.

EXPERIMENTAL

Sulphides

9-Fluorenylmercaptan (9) was prepared from 9-bromofluorene (23) via the thiouronium salt. Methylation with methyl iodide – methanolic sodium methoxide gave *9-fluorenyl methyl sulphide*, which crystallized from methanol as large colorless blades (77%), m.p. 47–48°. Found: C, 79.42; H, 5.92%. Calc. for $C_{14}H_{12}S$: C, 79.20; H, 5.65%.

9-Fluorenyl phenyl sulphide was prepared by warming 9-bromofluorene (1 mole) and thiophenol (1.1 moles) with methanol containing sodium methoxide (1 mole).* The reaction was complete in 10 minutes. The product crystallized as blades (69%) from methanol, m.p. 48–49°. Found: C, 83.10; H, 4.97%. Calc. for $C_{19}H_{14}S$: C, 83.17; H, 5.14%.

Prepared in a similar way, *9-fluorenyl p-tolyl sulphide* formed laths or dense prisms from ethanol (88%), m.p. 85–86°. Found: C, 83.20; H, 5.43%. Calc. for $C_{20}H_{16}S$: C, 83.29; H, 5.59%.

The foregoing sulphides were methylated with ethereal methyl lithium – methyl iodide, as described for fluorene (17), giving the following:

Methyl 9-methyl-9-fluorenyl sulphide crystallized as rhombohedral plates from methanol (71%), m.p. 63–65°. Found: C, 79.47; H, 6.19%. Calc. for $C_{15}H_{14}S$: C, 79.60; H, 6.23%.

9-Methyl-9-fluorenyl phenyl sulphide formed colorless needles from ethanol after cooling to and keeping at 0° (65%), m.p. 39.5–41.5°. Found: C, 83.30; H, 5.49%. Calc. for $C_{20}H_{16}S$: C, 83.26; H, 5.59%.

9-Methyl-9-fluorenyl p-tolyl sulphide formed well-defined prisms from acetone–methanol, m.p. 72–73° (82%). Found: C, 83.08; H, 5.83%. Calc. for $C_{21}H_{18}S$: C, 83.40; H, 5.60%.

Sulphones

The six sulphides described in the preceding section were oxidized with 50% hydrogen peroxide (1 volume) in acetic acid (3 volumes). The reactions, which were exothermic, were complete in a few minutes at 50°. Yields varied from 72 to 88% (24, 25).

9-Fluorenyl methyl sulphone formed long white needles from methanol or acetic acid, m.p. 188–189°. Found: C, 68.76; H, 5.09%. Calc. for $C_{14}H_{12}O_2S$: C, 68.87; H, 4.95%.

Methyl 9-methyl-9-fluorenyl sulphone crystallized from hexane as colorless prisms or needles, m.p. 136–137°. Found: C, 69.85; H, 5.77%. Calc. for $C_{15}H_{14}O_2S$: C, 69.74; H, 5.46%.

9-Fluorenyl phenyl sulphone formed colorless prisms from acetone–heptane, m.p. 182–183°. Found: C, 74.34; H, 4.45%. Calc. for $C_{19}H_{14}O_2S$: C, 74.48; H, 4.61%.

9-Methyl-9-fluorenyl phenyl sulphone crystallized as plates from ethanol, m.p. 165–167°. Found: C, 74.30; H, 4.94%. Calc. for $C_{20}H_{16}O_2S$: C, 74.97; H, 5.03%.

9-Fluorenyl p-tolyl sulphone crystallized as plates from benzene, m.p. 226–228°, identical with an authentic sample (21).

9-Methyl-9-fluorenyl p-tolyl sulphone formed colorless prisms from benzene–heptane, m.p. 151–152°. Found: C, 75.34; H, 5.26%. Calc. for $C_{21}H_{18}O_2S$: C, 75.42; H, 5.42%.

Attempts to oxidize 9-fluorenyl *p*-tolyl sulphide to the sulphoxide by standard techniques (25, 26) gave mixtures, not resolved by chromatography.

9-Fluorenyl *p*-tolyl sulphone, used in the alkylation experiments described below, was obtained from the reaction between 9-bromofluorene and sodium *p*-toluenesulphinate (21, 29). Prepared similarly, *2-nitro-9-fluorenyl p-tolyl sulphone* (from 9-bromo-2-nitrofluorene (27)) formed almost colorless plates from benzene, m.p. 217–219° with de-

**It is important to have present a slight excess of thiophenol over alkoxide to prevent formation of difluorenylidene.*

composition. The first crystallization required judicious separation from traces of dinitrodifluorenylidenes. Found: C, 65.70; H, 4.16%. Calc. for $C_{20}H_{15}NO_4S$: C, 65.74; H, 4.14%.

9-Fluorenyl *p*-tolyl sulphone (1 g) was dissolved in ethanol (200 ml) containing sodium ethoxide (from sodium, 0.5 g). The alkyl halide (2–3 g) was added and the mixture was left at room temperature overnight.

9-Methyl-9-fluorenyl p-tolyl sulphone, prepared in this way (81%), crystallized as prisms from hexane, m.p. 150–151°, identical with the sample described above.

9-Ethyl-9-fluorenyl p-tolyl sulphone (76%) formed clusters of long blades from methanol, m.p. 168–169°. Found: C, 75.73; H, 5.81%. Calc. for $C_{22}H_{20}O_2S$: C, 75.83; H, 5.79%.

9-isoPropyl-9-fluorenyl p-tolyl sulphone (75%) crystallized as needles from heptane, m.p. 181–182°. Found: C, 76.27; H, 6.04%. Calc. for $C_{23}H_{22}O_2S$: C, 76.21; H, 6.12%.

9-Allyl-9-fluorenyl p-tolyl sulphone (89%) formed prisms from heptane, m.p. 175–176°. Found: C, 76.78; H, 5.54%. Calc. for $C_{23}H_{20}O_2S$: C, 76.63; H, 5.59%.

9-Benzyl-9-fluorenyl p-tolyl sulphone (86%) formed well-defined prisms from heptane, m.p. 201–202°. Found: C, 78.99; H, 5.51%. Calc. for $C_{27}H_{22}O_2S$: C, 78.99; H, 5.40%.

9-cycloHexyl-9-fluorenyl p-tolyl sulphone (77%) crystallized as small colorless prisms from heptane, m.p. 209–210°. Found: C, 77.87; H, 6.82%. Calc. for $C_{26}H_{26}O_2S$: C, **77.57**; H, 6.51%.

The following were also prepared:

9-Methyl-2-nitro-9-fluorenyl p-tolyl sulphone (81%) formed pale yellow prisms from benzene–hexane, m.p. 187–188°. Found: C, 66.28; H, 4.46%. Calc. for $C_{21}H_{17}NO_4S$: C, 66.47; H, 4.52%. (The solution of the starting sulphone in ethanolic sodium ethoxide was filtered to remove traces of dinitrodifluorenylidenes.)

9-Methyl-9-fluorenyl phenyl sulphone (76%) crystallized as plates from ethanol, m.p. 164–166°, identical with the sample described above.

Methyl 9-methyl-9-fluorenyl sulphone (69%) formed colorless prisms from hexane, m.p. 134–136°, identical with the sample described above.

Methyl 9-isopropyl-9-fluorenyl sulphone (72%) crystallized as almost colorless prisms from hexane, m.p. 122–124°. Found: C, 71.24; H, 6.10%. Calc. for $C_{17}H_{18}O_2S$: C, 71.30; H, 6.33%.

Dimethyl 9,9′-Difluorenyl-9,9′-dicarboxylate

Methyl fluorene-9-carboxylate (2.3 g) was dissolved in methanol (50 ml) containing sodium methoxide (from sodium, 0.5 g). Addition of *p*-toluenesulphonyl chloride (3.5 g) resulted in the rapid separation of a microcrystalline solid. Recrystallization from chloroform–hexane gave small needles (1.7 g), m.p. 240–242°, identical with an authentic specimen of the above-named ester (10, 17). Found: C, 79.92; H, 4.81%. Calc. for $C_{30}H_{22}O_4$: C, 80.70; H, 4.97%.

REFERENCES

1. W. von E. Doering and L. K. Levy. J. Am. Chem. Soc. **77**, 509 (1955).
2. W. von E. Doering and K. C. Schreiber. J. Am. Chem. Soc. **77**, 514 (1955).
3. W. von E. Doering and A. K. Hoffmann. J. Am. Chem. Soc. **77**, 521 (1955).
4. E. A. Fehnel and M. Carmack. J. Am. Chem. Soc. **71**, 231 (1949).
5. W. E. Truce and K. R. Buser. J. Am. Chem. Soc. **76**, 3577 (1954).
6. L. Field and J. W. McFarland. J. Am. Chem. Soc. **75**, 5583 (1953).
7. L. Field, J. R. Holsten, and R. D. Clark. J. Am. Chem. Soc. **81**, 2572 (1959).
8. R. L. Shriner and S. O. Greenlee. J. Org. Chem. **4**, 242 (1939).
9. M. M. Klenk, C. M. Suter, and S. Archer. J. Am. Chem. Soc. **70**, 3846 (1948).
10. W. Wislicenus and W. Mocker. Ber. **46**, 2778 (1913).
11. F. A. L. Anet and P. M. G. Bavin. Can. J. Chem. **34**, 991 (1956).

Can. J. Chem. Downloaded from www.nrcresearchpress.com by 186.148.149.217 on 09/04/12
For personal use only.

12. P. M. G. BAVIN. Unpublished data.
13. P. M. G. BAVIN. Can. J. Chem. **37**, 2023 (1959).
14. P. M. G. BAVIN. Can. J. Chem. This issue.
15. L. J. BELLAMY. The infrared spectra of complex molecules. Methuen and Co. Ltd., London. 1954.
16. Y. SPRINZAK. J. Am. Chem. Soc. **80**, 5449 (1958).
17. P. M. G. BAVIN. Can. J. Chem. This issue.
18. G. WITTIG, H. DOSER, and I. LORENZ. Ann. **562**, 192 (1949).
19. W. BRADLEY. J. Chem. Soc. 1091 (1937).
20. W. BRADLEY. J. Chem. Soc. 458 (1938).
21. G. W. FENTON, C. K. INGOLD and J. A. JESSOP. J. Chem. Soc. 705, 708 (1930).
22. P. M. G. BAVIN, G. W. GRAY, and A. STEPHENSON. In preparation.
23. N. BUU-HOI and J. LECOCQ. Compt. rend. **226**, 87 (1948).
24. S. HUNIG and O. BOES. Ann. **579**, 23 (1953).
25. M. GAZDAR and S. SMILES. J. Chem. Soc. **93**, 1834 (1908).
26. R. KNOLL. J. prakt. Chem. **113**, 40 (1926).
27. E. D. HUGHES and S. V. ANANTAKRISHNAN. J. Chem. Soc. 1607 (1935).
28. W. SCHLENK, H. HILLEMANN, and I. RODLOFF. Ann. **487**, 135 (1931).
29. F. ADICKES. J. prakt. Chem. **145**, 235 (1936).

Can. J. Chem. Downloaded from www.nrcresearchpress.com by 186.148.149.217 on 09/04/12
For personal use only.

Can. J. Chem. Downloaded from www.nrcresearchpress.com by 186.148.149.217 on 09/04/12
For personal use only.

CARBON-13 KINETIC ISOTOPE EFFECTS IN THE SOLVOLYSIS OF 1-BROMO-1-PHENYLETHANE[1]

J. B. STOTHERS[2] AND A. N. BOURNS

ABSTRACT

Carbon-13 kinetic isotope effects have been measured for the solvolysis in methanol and ethanol of 1-bromo-1-phenylethane of natural isotopic abundance. Methanolysis of the bromide at 25° C gave a kinetic isotope effect (k^{12}/k^{13}) of 1.0065±0.0006, and ethanolysis at 45° C gave 1.0064±0.0010. These surprisingly low effects for a bond-rupture process have been interpreted in terms of a model for the transition state in which the bonding of the isotopic carbon is strengthened by conjugation of the electron deficient center with the ring. The results are considered to provide support for the mass fragment model for evaluation of the effective mass term of the Bigeleisen expression for the theoretical calculation of kinetic isotope effects.

INTRODUCTION

It has been known for many years that molecules differing only in the isotopic mass of a component atom may react at different rates (1, 2, 3). These kinetic isotope effects are largest when some bond associated with the isotopic atom is undergoing rupture in the rate-determining step of the process. Consequently, isotope effect studies have played an important role in the elucidation of reaction mechanisms (1, 4).

Following the discovery (5, 6, 7) of carbon kinetic isotope effects of considerable magnitude, Bigeleisen (8, 9) proposed equations for the theoretical evaluation of kinetic isotope effects using spectroscopic data. In applying these equations to the rather complex molecular systems for which kinetic isotope effects had been studied experimentally, it was usually found necessary to make the simplifying assumption that the vibrational frequencies of all bonds other than the bond undergoing rupture remain unaltered in the transition state (3, 9). Notwithstanding this and other approximations, surprisingly good agreement has been obtained between calculated and experimental isotope effects in a number of reactions.

Since, in principle, kinetic isotope effects provide information concerning the nature of the transition state, it was decided to undertake a carbon isotope effect study of the reaction of nucleophilic substitution at a saturated carbon atom, a reaction which is one of the most important in organic chemistry and which has been the subject of detailed mechanistic study for over 25 years. At the outset of the investigation it was thought that kinetic isotope effects might provide a useful criterion of mechanism since, on the basis of a simplified theoretical treatment, one might expect that reaction by the unimolecular, or S_N1, mechanism, in which the main covalency change in the rate-determining step is the rupture of a bond associated with the isotopic atom, would give rise to a larger effect than reaction by the bimolecular, or S_N2, mechanism, in which bond formation and bond rupture are synchronous. It was hoped, also, that the investigation might serve as a test for the theoretical equations and, in particular, might help in deciding between the Slater and mass fragment methods for evaluation of the temperature-independent term of these equations.

While this work was in progress two papers by Bender appeared (10, 11) reporting

[1]*Manuscript received February 5, 1960.*
Contribution from the Charles E. Burke Laboratories, Department of Chemistry, Hamilton College, McMaster University, Hamilton, Ontario.
[2]*Graduate student and a recipient of National Research Council Studentships (1954–57). Present address: Department of Chemistry, University of Western Ontario, London, Ontario.*

the results of a carbon-14 isotope effect study of the displacement reactions of methyl iodide and *tert*-butyl chloride. In the S_N2 reaction of methyl iodide with hydroxide ion and with several tertiary amines k^{12}/k^{14} ratios ranging from 1.09 to 1.14 were observed. Solvolysis of methyl iodide in aqueous ethanol in the presence of silver ion, which was considered to be a borderline case between a S_N2 and S_N1 reaction, gave an isotope effect which was essentially no different from effects found in the pure S_N2 processes. These large effects are of the same magnitude as many effects observed in reactions involving only bond rupture and agree with the predictions of the Bigeleisen equation based on a model for the transition state in which only the bond undergoing fission is considered to have changed in the activation process. Hydrolysis of *tert*-butyl chloride in aqueous dioxane, somewhat surprisingly, gave rise to a smaller effect, $k^{12}/k^{14} = 1.03$, than did the reactions proceeding by the bimolecular mechanism. From these results, Bender concluded that kinetic isotope effect studies are of very limited value in differentiating between S_N1 and S_N2 reactions.

The present paper is concerned with a carbon-13 study of the solvolysis of 1-bromo-1-phenylethane in methanol and ethanol. Carbon-13 was chosen as the heavier isotope rather than carbon-14 since, using mass spectrometry, a higher order of precision in evaluation of the isotope effect is possible (± 0.001 in this study, compared with ± 0.005 to ± 0.015 in Bender's work), contamination of samples is less likely to give rise to spurious effects, and isotopic labelling is unnecessary. The choice of 1-bromo-1-phenylethane as the reactant was dictated by two considerations. First, depending upon the conditions, the compound may be made to undergo reaction either exclusively by the S_N1 or by the S_N2 mechanism (12, 13); under solvolytic conditions in solvents of high ionizing power the reaction exhibits characteristics of a unimolecular process, while pure second-order kinetics are observed for reaction in ethanol using ethoxide concentrations of 1.5 *M* or higher. Secondly, the compound and its reaction products, 1-methoxy- and 1-ethoxy-1-phenylethane, may be degraded so as to furnish, in good yield for mass spectrometer analysis, carbon dioxide derived exclusively from the carbon at the seat of displacement.

EXPERIMENTAL

Materials

Absolute methanol and ethanol were prepared from commercial "absolute" products using magnesium, followed by distillation through a 20-in. Vigreux column.

1-Bromo-1-phenylethane was prepared by passing dry hydrogen bromide into 1-phenylethanol maintained at 0° C (14). The product, purified by fractional distillation, was obtained in 85–93% yields (b.p. 83–84° C (10 mm), n_D^{25} 1.5592).

1-Methoxy-1-phenylethane and 1-ethoxy-1-phenylethane, products of the solvolysis reactions, were required for testing the degradation procedures. These were prepared in approximately 75% yield by heating a solution of 1-bromo-1-phenylethane in the anhydrous alcohol for 24 hours at reflux temperatures. The physical constants of the ethers were: 1-methoxy-1-phenylethane, b.p. 55–56° C (10 mm), n_D^{25} 1.4900; 1-ethoxy-1-phenylethane, b.p. 65–66° C (11 mm), n_D^{25} 1.4821.

To test for possible isotopic exchange between the ether product and 1-bromo-1-phenylethane it was necessary to prepare 1-ethoxy-1-phenylethane-1-C^{13}. Acetophenone-carbonyl-C^{13} (8.6 g, 0.072 mole), prepared from sodium acetate-1-C^{13} by the method of Shantz and Rittenberg (15), was reduced to the carbinol using lithium aluminum hydride

Can. J. Chem. Downloaded from www.nrcresearchpress.com by 186.148.149.217 on 09/04/12
For personal use only.

(2.0 g, 0.053 mole) in anhydrous ether (50 ml). The complex was decomposed with 20% sulphuric acid and the product isolated by ether extraction. The crude carbinol was dissolved in carbon tetrachloride (25 ml) and treated with anhydrous hydrogen bromide until there was no further absorption of gaseous halide. The reaction mixture was poured into water and extracted with carbon tetrachloride. The combined extracts were dried, concentrated, and taken up in absolute ethanol (100 ml). This solution was heated under reflux for 24 hours while small amounts of a solution of sodium ethoxide in ethanol were added periodically to neutralize the hydrogen bromide formed. At the end of this period the solution was poured into cold water and extracted with ether. Fractional distillation gave 1-ethoxy-1-phenylethane-1-C^{13} (b.p. 64–65° C (10 mm), n_D^{25} 1.4821) in 65% yield, based on the acetophenone.

Kinetic Measurements

The rates of solvolysis of 1-bromo-1-phenylethane in absolute methanol and ethanol were followed by acid–base titration of the product, hydrogen bromide. Reaction temperatures were chosen such that there was approximately 5% reaction in 15 minutes. This was a convenient rate for the partial reactions in the subsequent isotope effect experiments. A solution of the bromide in the alcohol was maintained to within ±0.02° C of the desired temperature and at appropriate time intervals accurately measured aliquots were removed and quickly placed in a cold mixture of benzene and water. The resulting mixture was immediately titrated with standard sodium hydroxide using phenolphthalein as indicator. The rate constants were obtained from a least-squares plot of reaction time versus log[RBr].

Isotope Effect Experiments

In the determination of the carbon-13 isotope effect, 1-bromo-1-phenylethane of normal isotopic abundance was solvolyzed to some small known extent of reaction, the ether product separated from unreacted bromide and degraded so as to furnish carbon dioxide derived exclusively from the alkoxy-bearing carbon. The isotopic ratio for this carbon dioxide and that of the carbon dioxide formed from the original reactant by a similar degradation procedure were measured mass spectrometrically. The rate constant ratios, k^{12}/k^{13}, were calculated from the isotopic ratios using an expression derived by Stevens and Attree (16), which takes into account the extent of reaction.

The detailed procedure was as follows. One liter of the appropriate alcohol was equilibrated to the desired reaction temperature and a weighed sample of 1-bromo-1-phenylethane was added. The resulting solution, approximately 0.5 *M* in organic bromide, was allowed to stand in the constant-temperature bath for an accurately measured time corresponding to approximately 5% reaction, and then was quickly poured into a mixture of 3–4 liters of cold water and 600 ml of benzene. The quenched reaction mixture was vigorously shaken, the layers separated, and the aqueous layer extracted with three 300-ml portions of fresh benzene. The combined extracts were thoroughly washed with water and dried over calcium chloride, and the benzene then removed by distillation under reduced pressure. The small amount of product was separated from the large amount of unreacted bromide by careful fractional distillation under reduced pressure using a 50-cm tantalum-wire column described by Cason and Rapoport (17). One such distillation was sufficient to separate the methyl ether; a second distillation was required for 1-ethoxy-1-phenylethane. Trial experiments on synthetic mixtures of 1-ethoxy-1-phenylethane and the organic bromide showed that ether of 93–95% purity could be separated with

Can. J. Chem. Downloaded from www.nrcresearchpress.com by 186.148.149.217 on 09/04/12
For personal use only.

better than 90% recovery. The impurity, which was mainly bromide, would not be expected to affect significantly the isotopic ratios subsequently determined.

Under the normal solvolytic conditions, hydrogen bromide concentration builds up as the reaction proceeds and, as a result, there might be some tendency for ether cleavage with the regeneration of starting bromide. If this were to happen, the measured isotopic fractionation would not be that resulting from a strictly unidirectional process but rather from a process tending toward equilibrium. Since, in all experiments, the reaction was stopped before more than 10% of organic halide had been consumed, the back reaction, if it occurred at all, would be expected to make only a very minor contribution to the measured effect. Nevertheless, to establish this point, two isotope effect experiments in methanol were carried out in which sodium methoxide was present in a concentration which was sufficient to neutralize the hydrogen bromide formed in the partial reaction but not sufficient to induce any significant amount of bimolecular reaction (12, 13). The isotope effects obtained in the presence and in the absence of methoxide ion differed only very slightly, if at all.

It was also necessary to establish that no isotopic exchange occurred during the separation of the ether product from the large amount of unreacted organic bromide. This was accomplished by subjecting a mixture of 1-ethoxy-1-phenylethane-1-C^{13} and unlabelled 1-bromo-1-phenylethane to the usual separation procedure and determining the loss of label in the recovered ether. It was found that an upper limit for the exchange, if it occurred at all, was 5%. This would have no measurable effect on the results.

Degradation Method

Since the isotopic ratio for the carbon atom at the center of displacement must be determined for the reactant and for the product of partial reaction, it was necessary to develop a degradation procedure whereby this atom could be removed from the rest of the molecule and converted in high yield to carbon dioxide for mass spectrometric analysis. The method consisted of oxidation of the bromide and ether to benzoic acid followed by decarboxylation using the Schmidt reaction.

Oxidation to Benzoic Acid

Best over-all yields of benzoic acid were obtained by a two-stage oxidation procedure. In the first stage, the compounds were oxidized with alkaline permanganate in a pyridine–water solvent to give a mixture of benzoic acid and benzoylformic acid. This acid mixture was then further oxidized with hydrogen peroxide whereby the benzoylformic acid was quantitatively converted to benzoic acid.

1-Bromo-1-phenylethane (1.65 g, 0.0089 mole) was placed in pyridine (50 ml) and water (100 ml) and potassium hydroxide (5 g, 0.089 mole) was added. The mixture was heated under reflux for 15 minutes with vigorous stirring. Solid potassium permanganate (8 g, 0.051 mole) was then added slowly at reflux temperature to the stirred solution over a period of 15 minutes and the reaction mixture heated for an additional 30 minutes with vigorous stirring. The mixture was cooled to about 50° C and excess potassium permanganate destroyed by the addition of ethanol. The inorganic solids were removed by filtration and washed thoroughly with hot water. The filtrate was cooled, acidified with concentrated hydrochloric acid, and extracted four times with ether. Ether was removed and the residue stirred vigorously for 2 to 3 hours with 5% hydrogen peroxide (30 ml). The reaction mixture was allowed to stand overnight and then heated under reflux to destroy excess peroxide, additional water being added to

Can. J. Chem. Downloaded from www.nrcresearchpress.com by 186.148.149.217 on 09/04/12
For personal use only.

effect complete solution of the benzoic acid. The solution was allowed to cool and the benzoic acid collected. Additional acid was recovered by ether extraction of the filtrate. Total yield of pure acid was 0.909 g (84%), m.p. 121.5°–121.8° C (corr.).

A similar procedure using, however, 50% more oxidizing agent was followed for the two ether products. Yields of benzoic acid were generally slightly higher than those obtained from the bromide.

Decarboxylation of Benzoic Acid

An apparatus similar to that described by Phares (18) was used. A solution containing approximately 1 millimole of benzoic acid in 3–4 ml of concentrated sulphuric acid was placed in the reaction flask and cooled to 0° C. Approximately 80 mg of sodium azide was added and the flask connected to the absorption traps. The reaction mixture was maintained at about 40° C for 2 hours while the carbon dioxide was swept by means of a slow stream of purified nitrogen into 0.2 *M* carbonate-free sodium hydroxide. The trapped gas was precipitated as barium carbonate (19). Great care was taken in all operations to avoid contamination with atmospheric carbon dioxide. Yields of barium carbonate were in the range 91–93%.

Tests for Rearrangement and Isotopic Fractionation in the Degradation Reactions

There is a possibility, albeit an unlikely one, that rearrangement might occur during the two-stage oxidation of bromide and ether to benzoic acid, with the result that the carbon atom in the carboxyl group of the acid would not be the atom originally joined to the benzene ring. To test for this, some labelled ether, 1-ethoxy-1-phenylethane-1-C^{13}, was subjected to the usual alkaline oxidation while another sample was oxidized by chromic anhydride to acetophenone, which was then converted to benzoic acid by means of the haloform reaction. Carbon dioxide samples were prepared in the usual way from each benzoic acid sample and analyzed mass spectrometrically. The isotopic ratios obtained for the two samples were identical within the precision limits of the measurements and they corresponded closely to the ratio expected on the basis of the carbon-13 content of the barium carbonate used in the synthesis of the labelled ether. From this result it may be concluded that no rearrangement occurred during the degradation.

Although the yields in each of the degradation steps were good, the possibility remained that isotopic fractionation during the conversion of bromide or ether to carbon dioxide might affect, to a measurable extent, the isotopic abundance of this gas. To test for this possibility the following interconversions were carried out: (1) 1-phenylethanol of normal isotopic abundance to 1-bromo-1-phenylethane using dry hydrogen bromide; (2) a sample of this bromide to 1-methoxy-1-phenylethane by methanolysis; and, (3) a further sample of the 1-phenylethanol to 1-methoxy-1-phenylethane using methyl sulphate. Since conversion (3) involved no change in the bonding of the carbon atom alpha to the ring, the isotopic abundance for this carbon should be identical in the alcohol and the ether product. Furthermore, since conversion (1) proceeded in better than 90% yield the isotopic ratio of the bromide should correspond very closely to that of the alcohol. One or more samples of the alcohol, ether, and bromide were oxidized in the usual way to benzoic acid, samples of which were then converted in duplicate or triplicate to carbon dioxide for mass spectrometric analysis. The fourteen carbon dioxide samples prepared in this way gave C^{12}/C^{13} ratios which were the same within the limits of the mass spectrometric analysis. These results definitely establish that either there was no isotopic fractionation in the degradation reactions or that any small fractionation

Can. J. Chem. Downloaded from www.nrcresearchpress.com by 186.148.149.217 on 09/04/12
For personal use only.

that did occur was the same for the ether and the bromide. In either case, the degradations were entirely suitable for the isotope effect studies in which an intercomparison of isotopic ratios was being made.

Preparation of Carbon Dioxide Samples for Mass Spectrometric Analysis

Carbon dioxide was liberated from the barium carbonate samples by means of concentrated sulphuric acid using standard high vacuum techniques. The gas was trapped at liquid nitrogen temperatures, distilled at −78° C through an "anhydrone" drying tube, and condensed into a standard mass spectrometer sample tube.

Mass Spectrometry

All carbon dioxide samples were analyzed in a 180° direction-focussing mass spectrometer. The C^{12}/C^{13} ratios were obtained from the mass 44 / mass 45 ion current ratio after applying a suitable correction for the contribution to mass 45 of the molecule species $C^{12}O^{16}O^{17}$. Each carbon dioxide sample in a given series of experiments was analyzed relative to a standard, the standard being one of the samples of carbon dioxide prepared from the reactant used in that series. An arbitrary value of 85.00 for the mass 44/45 ratio was assigned to these standards. The procedure was to analyze the standard, the unknown, and the standard again all in the shortest possible time. A single analysis consisted of a series of at least six double spectrograms, each double spectrogram being obtained from a scan of the masses in the order 44, 45, 45, 44. A single analysis was considered satisfactory if the mean deviation of the 44/45 ratios was less than 0.1%, and the mean for the unknown was accepted if the mean for the standard, before and after analysis of unknown, differed by no more than this value.

RESULTS

The results of the kinetic measurements for the solvolysis of 1-bromo-1-phenylethane in absolute methanol and in absolute ethanol are summarized in Table I.

TABLE I

Kinetic results for solvolyses of 1-bromo-1-phenylethane

Solvent	Temp., °C	Concn. of RBr, *M*	$k_1 \times 10^5$ sec^{-1}
Methanol	25.0	0.112	5.70
		0.114	5.72
		0.303	5.57
			Average 5.67
Ethanol	45.0	0.486	5.87
		0.525	6.07
		0.512	6.07
			Average 6.00

The results of the isotope effect experiments on the methanolysis and the ethanolysis of 1-bromo-1-phenylethane are given in Tables II and III, respectively. Each individual experiment consisted of a partial reaction of bromide to ether followed by parallel degradations to carbon dioxide of a sample of the original reactant and of the product. The rate constant ratios, k^{12}/k^{13}, were calculated from the C^{12}/C^{13} ratios and the percentage of reaction (16).

Can. J. Chem. Downloaded from www.nrcresearchpress.com by 186.148.149.217 on 09/04/12
For personal use only.

TABLE II

C^{12}/C^{13} ratios and kinetic isotope effects in the methanolysis of 1-bromo-1-phenylethane at 25° C

Expt. No.	Compound degraded	Reaction, %	C^{12}/C^{13} ratios	k^{12}/k^{13}
1	RBr		91.16	1.0063
	$ROCH_3$	5.1	91.72	
2	RBr		91.13	1.0070
	$ROCH_3$	5.1	91.75	
3	RBr		90.95	1.0061
	$ROCH_3$	4.7	91.49	
4	RBr		91.00	1.0068
	$ROCH_3$	4.8	91.60	
5	RBr		90.94	1.0070
	$ROCH_3$	4.8	91.56	
6	RBr		90.87	1.0076
	$ROCH_3$	4.7	91.54	
7[a]	RBr		91.07	1.0054
	$ROCH_3$	5.0	91.54	
8[a]	RBr		90.99	1.0060
	$ROCH_3$	5.0	91.52	
		Mean value of isotope effect		1.0065[b]

[a]Experiments carried out in the presence of ~0.03 *M* $NaOCH_3$.
[b]Standard deviation 0.0007; 95% confidence limit 0.0006.

TABLE III

C^{12}/C^{13} ratios and kinetic isotope effects in the ethanolysis of 1-bromo-1-phenylethane at 45° C

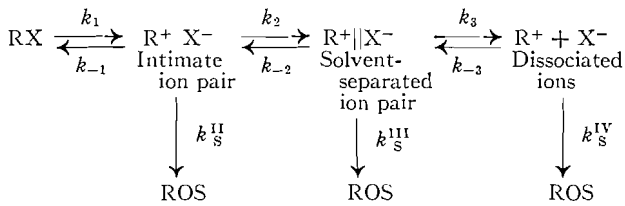
Expt. No.	Compound degraded	Reaction, %	C^{12}/C^{13} ratios	k^{12}/k^{13}
1	RBr		90.86	1.0067
	ROC_2H_5	4.9	91.45	
2	RBr		90.88	1.0054
	ROC_2H_5	4.9	91.35	
3	RBr		90.97	1.0070
	ROC_2H_5	5.8	91.59	
4	RBr		91.02	1.0065
	ROC_2H_5	5.6	91.59	
		Mean value of isotope effect		1.0064[a]

[a]Standard deviation 0.0007; 95% confidence limit 0.0011.

DISCUSSION

It seems reasonable to assume on the basis of the results of extensive kinetic and stereochemical studies (12, 13, 20, 21) that the solvolysis of 1-phenylethyl halides in good ionizing solvents, including methanol and ethanol, proceeds by a S_N1 mechanism in the sense that some type of carbonium ion intermediate is involved. Winstein and co-workers (22, 23) have recently proposed that the ionization process for a compound RX can involve two discrete ion pair intermediates, as well as dissociated carbonium ions, and that one or all of these ion types may interact with solvent to form product.

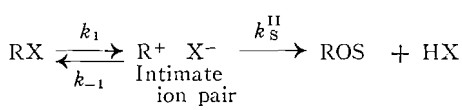
Can. J. Chem. Downloaded from www.nrcresearchpress.com by 186.148.149.217 on 09/04/12
For personal use only.



Grunwald and co-workers (24) have presented cogent arguments in support of the idea that for 1-phenylethyl compounds the ratio k_2/k_S^{II} is small and, therefore, that substitution occurs mainly at the intimate ion pair stage. This seems reasonable since the 1-phenylethyl carbonium ion should be very reactive, particularly in the moderately nucleophilic solvents, methanol and ethanol, used in the present investigation.

There remains the question of the relative rates of reaction of the intimate ion pair with solvent and its collapse to re-form RX (internal return). Winstein (25) has reported that in the acetolysis of 1-bromo-1-phenylethane the true ionization rate is about seven times greater than the titrimetric solvolysis rate. Assuming that product is formed mainly by interaction of solvent with the intimate ion pair, the ratio k_{-1}/k_S^{II} in acetolysis is therefore 6. In methanol and ethanol, which are more nucleophilic solvents (26), there should be a smaller tendency for internal return. One cannot assume, however, that the alcoholysis rates will be determined solely by the ionization step.

On the basis of these considerations the mechanism of solvolysis of 1-phenylethyl bromide may be formulated as follows:



For a theoretical evaluation of the carbon isotope effect in this reaction, it is useful to examine two limiting cases, one in which the ionization step is rate determining ($k_S^{II} \gg k_{-1}$), and the other in which the intimate ion pair is in equilibrium with the organic halide ($k_S^{II} \ll k_{-1}$). In the former case, the observed isotope effect will be the kinetic isotope effect associated with the ionization process. In the latter case, the observed effect will be the result of two fractionation processes, that associated with the equilibrium between substrate and intimate ion pair and that associated with the interaction of intimate ion pair with solvent. It may be readily shown in this case that the over-all isotope effect is given by the expression

$$k/k' = K_{exch} \cdot \frac{k_S^{II}}{k_S^{II'}} \qquad [1]$$

where k and k' are the specific reaction rate constants for solvolysis of the light and heavy isotopic organic halides, RX and R′X, respectively, k_S^{II} and $k_S^{II'}$ are the corresponding rate constants for interaction of the intimate ion pairs, R^+X^- and $R^{+\prime}X^-$, with solvent, and K_{exch} is the equilibrium constant for the isotopic exchange process

$$RX + R^{+\prime}X^- \rightleftarrows R'X + R^+X^-.$$

Bigeleisen and Mayer (27) have shown that the equilibrium constant for an isotopic exchange process can be expressed as the ratio of the so-called isotopic partition functions ratios, f, for the reacting species. For the exchange process given above,

Can. J. Chem. Downloaded from www.nrcresearchpress.com by 186.148.149.217 on 09/04/12
For personal use only.

[2] $$K_{exch} = \frac{f_{RX}}{f_{R^+X^-}}$$

where f_{RX} is the isotopic partition function ratio for organic halide and $f_{R^+X^-}$ the ratio for the intimate ion pair. For a rate process, the ratio of the rate constants for the isotopic molecules is given by an expression developed by Bigeleisen (8), which, for the present case of the interaction of solvent molecules with the intimate ion pair, takes the form

[3] $$\frac{k_s^{II}}{k_s^{II'}} = \frac{K}{K'} \cdot \left[\frac{m_{ROS}^{\ddagger'}}{m_{ROS}^{\ddagger}}\right]^{\frac{1}{2}} \cdot \frac{f_{R^+X^-}}{f_{ROS}^{\ddagger}}$$

where the K's are transmission coefficients, the ratio of which may be taken as unity, $m_{ROS}^{\ddagger}$ and $m_{ROS}^{\ddagger'}$ are, respectively, the effective masses of the light and heavy transition states in the direction of the reaction co-ordinate, and $f_{ROS}^{\ddagger}$ is the isotopic partition function ratio for these states.

The over-all isotope effect for solvolysis proceeding through an intimate ion pair in equilibrium with undissociated organic halide is, therefore,

[4] $$\frac{k}{k'} = K_{exch} \cdot \frac{k_s^{II}}{k_s^{II'}} = \left[\frac{m_{ROS}^{\ddagger'}}{m_{ROS}^{\ddagger}}\right]^{\frac{1}{2}} \cdot \frac{f_{RX}}{f_{ROS}^{\ddagger}}.$$

If, on the other hand, there is little or no internal return, the rate of solvolysis will be equal to the rate of ionization and, therefore, the istope effect will be given by

[5] $$\frac{k}{k'} = \left[\frac{m_{RX}^{\ddagger'}}{m_{RX}^{\ddagger}}\right]^{\frac{1}{2}} \cdot \frac{f_{RX}}{f_{RX}^{\ddagger}}$$

where the m's and $f_{RX}^{\ddagger}$ refer to the isotopic transition states for the ionization step.

The f functions appearing in these equations depend upon molecular vibrations only (27) and are of the form

[6] $$f = 1 + \sum_{1}^{3n-6} G(u_1)\Delta u_1$$

where

$$G(u_1) = \frac{1}{2} - \frac{1}{u_1} - \frac{1}{e^{u_1}-1}$$

$$u_1 = h\nu/kT$$

$$\Delta u_1 = h/kT(\nu_1 - \nu_1').$$

The ν and ν' quantities are fundamental vibrations of the light and heavy isotopic species, respectively.

The rate constant ratio, k/k', for the solvolysis reaction proceeding through an intimate ion pair in equilibrium with RX now becomes

[7] $$k/k' = \left[\frac{m_{ROS}^{\ddagger'}}{m_{ROS}^{\ddagger}}\right]^{\frac{1}{2}} \left[1 + \sum_{1}^{3n-6} G(u_{RX_1})\Delta u_{RX_1} - \sum_{1}^{3n-6} G(u_{ROS_1}^{\ddagger})\Delta u_{ROS_1}^{\ddagger}\right]$$

Can. J. Chem. Downloaded from www.nrcresearchpress.com by 186.148.149.217 on 09/04/12
For personal use only.

whereas this rate ratio for solvolysis in which the ionization step is rate determining takes the form

$$[8] \qquad k/k' = \left[\frac{m^{\ddagger'}_{RX}}{m^{\ddagger}_{RX}}\right]^{\frac{1}{2}}\left[1+\sum_{1}^{3n-6} G(u_{RX_1})\Delta u_{RX_1} - \sum_{1}^{3n-6} G(u^{\ddagger}_{RX_1})\Delta u^{\ddagger}_{RX_1}\right].$$

It can be seen that equations [7] and [8] differ in the effective mass term and in the second summation of the free energy term. In equation [7] these quantities refer to the transition state for covalent bond formation between carbonium ion and solvent; in equation [8] they refer instead to the transition state of the ionization process. It is, therefore, important to compare the nature of these transition states.

Since the intimate ion pair formed from 1-bromo-1-phenylethane is a high-energy intermediate, the energy of activation both for its reaction with solvent and for internal return to organic halide will be very small. Both transition states, therefore, will resemble the intimate ion pair (28). In other words, the carbon–bromine bond of the halide should be almost completely broken in the transition state for the first step and the carbon–oxygen bond should be only starting to form in the transition state of the second step. As a result, the change in vibrational energy resulting from the substitution of carbon-13 for carbon-12 will be much the same for the two transition states and will correspond closely to the change in energy resulting from isotopic substitution in the intermediate itself. The only significant difference then in the magnitude of the isotope effect for reaction in which the intimate ion pair is in equilibrium with RX and for reaction in which it is not, should arise from a difference in the effective mass factor.*

For calculation of the effective mass term Bigeleisen (8) originally applied a theorem of Slater (29) which in effect considers the reaction to be simply the formation or dissociation of a hypothetical diatomic molecule consisting of the two atoms between which the bond change is taking place. Each value of $m^{\ddagger}$ is then the reduced mass, μ, of the corresponding diatomic molecule and the effective mass term is the square root of the ratio of the reduced masses of the two isotopic molecules,

$$[9] \qquad \left[\frac{m^{\ddagger'}}{m^{\ddagger}}\right]^{\frac{1}{2}} = \left[\frac{\mu'}{\mu}\right]^{\frac{1}{2}} = \left[\left(\frac{1}{m_A}+\frac{1}{m_B}\right)\Big/\left(\frac{1}{m'_A}+\frac{1}{m_B}\right)\right]^{\frac{1}{2}}.$$

For rupture of a C—Br bond $m_A = 12$, $m'_A = 13$, and $m_B = 80$; for formation of a C—O bond $m_A = 12$, $m'_A = 13$, and $m_B = 16$.

Recently Bigeleisen (9) has suggested that since the reaction path for a polyatomic molecule involves not merely motion of individual atoms A and B, but rather motion of whole reacting fragments α and β, a more reasonable formulation of the mass term is

$$[10] \qquad \left[\frac{m^{\ddagger'}}{m^{\ddagger}}\right]^{\frac{1}{2}} = \left[\left(\frac{1}{M_\alpha}+\frac{1}{M_\beta}\right)\Big/\left(\frac{1}{M'_\alpha}+\frac{1}{M_\beta}\right)\right]^{\frac{1}{2}}.$$

For ionization of 1-bromo-1-phenylethane $M_\alpha = 105$, $M'_\alpha = 106$, and $M_\beta = 80$; for bond formation between 1-phenylethyl carbonium ion and methanol $M_\alpha = 105$, $M'_\alpha = 106$, and $M_\beta = 32$. In ethanol, M_β equals 46.

The effective mass terms for each transition state of the solvolytic reaction, calculated both from the Slater and the mass fragment models, are given in Table IV. It is of interest

**Since the vibrational stretching frequency of a carbon–oxygen bond is higher than that of a carbon–bromine bond, the summation for the transition state for covalent bond formation might be slightly higher than that for ionization.*

Can. J. Chem. Downloaded from www.nrcresearchpress.com by 186.148.149.217 on 09/04/12
For personal use only.

TABLE IV

Effective mass and free energy values for the transition states of 1-bromo-1-phenylethane solvolysis

Reaction[a]	Effective mass term		$(k^{12}/k^{13})_{expt}{}^{b}/(m^{\mp 13}/m^{\mp 12})^{\frac{1}{2}}$	
	Slater	Mass fragment	Slater	Mass fragment
R—Br → R^+Br^-	1.0352	1.0021	0.972	1.004
R^+Br^- → $ROCH_3$	1.0227	1.0011	0.984	1.005
R^+Br^- → ROC_2H_5	1.0227	1.0014	0.984	1.005

[a] R = $C_6H_5\dot{C}HCH_3$. [b] $(k^{12}/k^{13})_{expt}$ taken as 1.006.

to calculate from these mass terms the values of the free energy terms,

$$\left[1+\sum_{1}^{3n-6} G(u_1)\Delta u_1 - \sum_{1}^{3n-6} G(u_1^{\mp})\Delta u_1^{\mp}\right],$$

which would be required to produce the experimentally observed isotope effect of 1.006. These are shown in the last two columns of the Table IV.

The values of less than unity for the free energy term, which are obtained by dividing the experimental isotope effect by mass terms calculated from the Slater model, require that the difference in the vibrational energies for the isotopic transition states be greater than the corresponding difference for the isotopic RX molecules,

$$\sum_{1}^{3n-6} G(u_1^{\mp})\Delta u_1^{\mp} > \sum_{1}^{3n-6} G(u_1)\Delta u_1.$$

This could only come about if the isotopic atom were considerably more "tightly bound" in the transition state than in the initial state (8), a situation which would seem most unlikely in the present reaction system in which the transition state in both the ionization step and the bond formation step closely resembles the carbonium ion intermediate.

The low isotope effect observed in the solvolysis of 1-bromo-1-phenylethane, therefore, lends support to the mass fragment method of evaluating the effective mass term.

A common procedure in calculating from vibrational frequency data the free energy term of the Bigeleisen equation is to assume a model for the transition state in which the force constant for the bond being broken is equal to zero and the vibrational frequencies of all other bonds are the same as those for the initial state (3). The summations for the transition state in equations [7] and [8] then become zero and the initial state term can be readily calculated from the vibrational stretching frequency of the isotopic bond which is undergoing rupture in the reaction. To the extent that the bond in question is less than completely broken in the transition state, or other bonds associated with the isotopic atom are formed or strengthened, the over-all free energy term, calculated on the assumption of a zero value for the transition state summation, will be too high.

Using this very approximate method, one obtains a theoretical value of 1.018 for the free energy term in equations [7] and [8] at 25° C.* Comparison with the values given in the last two columns of Table IV shows that this value is much too high to account for the observed isotope effect. Even when combined with the low mass term given by the mass fragment theory it leads to an isotope effect of about 2%, and when combined with a mass term calculated on the basis of the Slater theorem it gives an effect of over 4%.

An even larger value is given by a more recent equation which makes use of the theorem of the trace (9).

Can. J. Chem. Downloaded from www.nrcresearchpress.com by 186.148.149.217 on 09/04/12
For personal use only.

It is suggested that the origin of this discrepancy arises mainly from the complete neglect of the transition state term.

Of the two simplifying assumptions upon which neglect of this term was based, that involving the assignment of a zero force constant to the carbon–bromine bond in the transition state of the ionization step and to the carbon–oxygen bond in the transition state of the second step would seem justified since, for reasons already given, the two transition states must closely resemble the intimate ion pair intermediate. What undoubtedly is not justified is the assumption that the vibrational frequencies of all other bonds associated with the isotopic carbon will remain unchanged in the transition state. Indeed, the bonding of this carbon to the benzene ring will be considerably strengthened as a result of overlap of its fairly well-developed vacant p orbital with the π orbitals of the benzene ring. Added to this, but of lesser importance, will be hyperconjugative interaction with the attached methyl group. The low isotope effect observed in the reaction would suggest that this conjugation in the transition state compensates to a considerable degree for the loss of the carbon–bromine vibration.

Some support for this interpretation of the low isotope effect is found in a recent study by Magee and Daniels (30) of the carbon-13 isotope effect in the unimolecular decomposition of substituted ureas, the results of which are summarized in Table V. Given also in

TABLE V

Unimolecular decomposition of substituted ureas

Reactant	$(k^{12}/k^{13})_{expt}$	$(k^{12}/k^{13})_{expt}/(m^{\mp 13}/m^{\mp 12})^{\frac{1}{2}}$
sym-Dimethylurea	1.027	1.024
Phenylurea	1.016	1.015
sym-Diphenylurea	1.008	1.006
3,3′-Dimethylcarbanilide	1.007	1.005

this table are the $(k^{12}/k^{13})_{expt}/(m^{\mp 13}/m^{\mp 12})^{\frac{1}{2}}$ values calculated using the mass fragment model for evaluation of the effective mass term. These authors attribute the effect of phenyl substitution on the magnitude of the isotope effect to resonance stabilization of the transition state resulting in a strengthening of a bond associated with isotopic carbon. This would tend to increase the $G(u_1^{\mp})\Delta u_1^{\mp}$ term and result in a lowering of the over-all free energy term.

It may be noted also that the carbon-14 isotope effect observed by Bender and Buist (11) in the hydrolysis of *tert*-butyl chloride is lower than would be predicted on the assumption of a zero transition state term. Using a mass term calculated from the mass fragment hypothesis one obtains a value for $(k^{12}/k^{14})_{expt}/(m^{\mp 14}/m^{\mp 12})^{\frac{1}{2}}$ of 1.014 ± 0.015, whereas the free energy term calculated on the assumption of complete carbon–chlorine bond rupture and no change in other vibrational frequencies is 1.045. It has been suggested that the low effect may be due in part to the electron-releasing effect of the three methyl groups which would tend to loosen the carbon–chlorine bond in the initial state resulting in a lower free-energy term. Another possibility is that hyperconjugative interaction of the three methyl groups with the isotopic carbon tends to strengthen the bonding of this atom in the transition state, hence increasing the free energy term for this state.

ACKNOWLEDGMENTS

The authors are indebted to Dr. J. Bigeleisen for a helpful discussion and to the National Research Council of Canada for financial assistance.

Can. J. Chem. Downloaded from www.nrcresearchpress.com by 186.148.149.217 on 09/04/12
For personal use only.

REFERENCES

1. K. B. WIBERG. Chem. Revs. **55**, 713 (1955).
2. J. G. LINDSAY, A. N. BOURNS, and H. G. THODE. Can. J. Chem. **29**, 192 (1951).
3. J. BIGELEISEN. J. Phys. Chem. **56**, 823 (1952).
4. E. GROVENSTEIN, JR. and G. A. ROPP. J. Am. Chem. Soc. **78**, 2560 (1956).
5. O. BEECK, J. W. OTVOS, D. P. STEVENSON, and C. D. WAGNER. J. Chem. Phys. **16**, 255 (1948).
6. P. E. YANKWICH and M. CALVIN. J. Chem. Phys. **17**, 109 (1949).
7. J. G. LINDSAY, D. E. MCELCHERAN, and H. G. THODE. J. Chem. Phys. **17**, 589 (1949).
8. J. BIGELEISEN. J. Chem. Phys. **17**, 675 (1949).
9. J. BIGELEISEN and M. WOLFSBERG. Advances in Chem. Phys. **1**, 15 (1958).
10. M. L. BENDER and D. F. HOEG. J. Am. Chem. Soc. **79**, 5649 (1957).
11. M. L. BENDER and G. J. BUIST. J. Am. Chem. Soc. **80**, 4304 (1958).
12. E. D. HUGHES, C. K. INGOLD, and A. D. SCOTT. J. Chem. Soc. 1201 (1937).
13. E. D. HUGHES, C. K. INGOLD, S. MASTERMAN, and B. J. MCNULTY. J. Chem. Soc. 899 (1940).
14. J. B. CONANT and A. H. BLATT. J. Am. Chem. Soc. **50**, 554 (1928).
15. E. M. SHANTZ and D. RITTENBERG. J. Am. Chem. Soc. **68**, 2109 (1946).
16. W. H. STEVENS and R. W. ATTREE. Can. J. Research, B, **27**, 807 (1949).
17. J. CASON and H. RAPOPORT. Laboratory text in organic chemistry. Prentice-Hall, New York. 1954.
18. E. F. PHARES. Arch. Biochem. Biophys. **33**, 173 (1951).
19. M. CALVIN, C. HEIDELBERGER, J. C. REID, B. M. TOLBERT, and P. E. YANKWICH. Isotopic carbon. J. Wiley and Sons, New York. 1949.
20. L. WILPUTTE-STEINERT and P. J. C. FIERENS. Bull. soc. chim. Belges, **64**, 287 (1955).
21. A. H. FAINBERG and S. WINSTEIN. J. Am. Chem. Soc. **79**, 1602 (1957).
22. S. WINSTEIN, E. CLIPPINGER, A. H. FAINBERG, R. HECK, and G. C. ROBINSON. J. Am. Chem. Soc. **78**, 328 (1956).
23. S. WINSTEIN and G. C. ROBINSON. J. Am. Chem. Soc. **80**, 169 (1958).
24. E. GRUNWALD, A. HELLER, and F. S. KLEIN. J. Chem. Soc. 2604 (1957).
25. S. WINSTEIN, A. H. FAINBERG, and E. GRUNWALD. J. Am. Chem. Soc. **79**, 4146 (1957).
26. H. L. GOERING, T. D. NEVITT, and E. F. SILVERSMITH. J. Am. Chem. Soc. **77**, 5026 (1955).
27. J. BIGELEISEN and M. G. MAYER. J. Chem. Phys. **15**, 261 (1947).
28. G. S. HAMMOND. J. Am. Chem. Soc. **77**, 334 (1955).
29. N. B. SLATER. Proc. Roy. Soc., A, **194**, 112 (1948).
30. E. M. MAGEE and F. DANIELS. J. Am. Chem. Soc. **79**, 829 (1957).

Can. J. Chem. Downloaded from www.nrcresearchpress.com by 186.148.149.217 on 09/04/12
For personal use only.

Can. J. Chem. Downloaded from www.nrcresearchpress.com by 186.148.149.217 on 09/04/12
For personal use only.

THE DIFFERENTIAL THERMAL ANALYSIS OF NATURAL AND SYNTHETIC HYDRATES OF CALCIUM SULPHATE[1]

W. E. P. Fleck, M. H. Jones, R. A. Kuntze, and H. G. McAdie

ABSTRACT

A variety of naturally occurring forms of calcium sulphate dihydrate produce substantially identical differential thermograms under conditions of uniform heating rate and particle size. These thermograms closely resemble those for synthetic dihydrate and β-hemihydrate, showing four endothermic effects and one exothermic effect below 500° C. Two of these endothermic effects, at about 170° and 300° C, respectively, which have not been reported previously, were found to be easily masked by changes in heating rate or sample concentration. Resolution of the several effects was improved by using different heating rates at different stages of the thermogram. Thermograms of the α-hemihydrate were similar, except that the endothermic effect at 300° C was not evident and the exothermic effect occurred at a much lower temperature than for the dihydrate. No conspicuous differences were found in the temperatures corresponding to the various endothermic and exothermic effects which might be correlated with the general dehydration behavior of the particular material. The endothermic effect at about 170° C appears to be associated with part of the hemihydrate to soluble anhydrite transition, possibly arising during the removal of the last traces of water.

In the differential thermograms reported for many natural and synthetic gypsums of widely different origin (1–7), two large endothermic effects occurring below 200° C have been attributed to the formation of the hemihydrate and its subsequent decomposition to soluble anhydrite. The exact temperatures at which these effects appear depend on a variety of experimental conditions, the resolution of the two endotherms being improved at slow rates of heating (2). In the region of 400° C an exothermic effect, not found when natural anhydrite is heated from room temperature, has been attributed to the conversion of β-soluble anhydrite to insoluble or natural anhydrite (3). A contradiction exists in the literature regarding the presence (8) or absence (4, 5) of a similar exothermic effect in the case of the α-soluble anhydrite. No further thermal effects have been reported below about 1200° C where a high-temperature modification of anhydrite is formed (1, 6, 7).

It has been recorded that the above exothermic effect appears at different temperatures, depending upon the origin of the gypsum sample (2, 3), and in the gypsum industry it is known that natural gypsums of different origin produce hemihydrates of widely differing properties. Hence an examination of several natural gypsums, as well as the pure hydrates of calcium sulphate, was undertaken by differential thermal analysis to investigate the possibility that some correlation might exist between both the endothermic and exothermic effect temperatures and the dehydration behavior of the particular gypsum. The natural gypsums selected represented several mineralogical forms and attention was focused on thermal effects appearing below 500° C.

EXPERIMENTAL

The instrument used contained a horizontal furnace, wound with 15-gauge Kanthal A wire, having a maximum operating temperature of 1300° C. No attempt was made to control the atmosphere within this furnace except in cases where a sample was cooled in a stream of dry nitrogen, after determination of a thermogram, prior to determination of a second thermogram on the same sample.

[1]*Manuscript received February 23, 1960.*
Contribution from the Department of Chemistry, Ontario Research Foundation, 43 Queen's Park Crescent, Toronto 5, Ontario. This paper was presented at the 137th Meeting of The American Chemical Society, Cleveland, April 5–14, 1960. Published with the permission of The American Chemical Society.

Can. J. Chem. Downloaded from www.nrcresearchpress.com by 186.148.149.217 on 09/04/12
For personal use only.

For measurement of temperature above 200° C, and control of heating rate over the entire temperature range, a Leeds and Northrup Model S Speedomax G indicating and recording temperature-program controller was used. Heating rates up to 20° C min^{-1} were possible, and above 200° C the sample temperature could be read to 1–2° C. Below 200° C another recorder, calibrated for 0–200° C with an iron–constantan thermocouple, was used to measure sample temperature to within 0.5° C. The differential temperature of a pair of Pt–Pt/13% Rh thermocouples was measured with a Speedomax G millivolt recorder fed from a stabilized microvolt amplifier. Differential temperatures of the order of 0.2 μv, corresponding to 0.03° C and about 2-mm deflection on the recorder chart, could be detected.

Below 200° C a heating rate of 3° C min^{-1} was found to give the best combination of peak definition and resolution. Smaller peaks occurring above 200° C were found to be better defined at higher heating rates, so that above this temperature the heating rate was increased to 12° C min^{-1}. The sample was contained in a palladium block having separate cavities for sample and reference material. At 3° C min^{-1} the difference between block and bulk sample temperature was found to be 2–4° C, while at 12° C min^{-1} this difference was 10–12° C. Since the temperature-measuring thermocouples were always in contact with the block, the peak temperatures to be reported are those of the sample block at the particular maximum differential temperature.

Ignited reagent grade α-alumina, having an average particle diameter, by the Fisher Sub-Sieve Sizer, of about 12 μ, was used as reference material and as diluent for the sample. With this material in both cavities of the palladium block, no significant differential temperature could be measured over the temperature range of interest.

A preliminary study of the effect of particle size on peak temperature showed that lower and more reproducible peak temperatures were obtained as the particle size of the sample was decreased. Some variation in relative peak heights with particle size was also noted. The most satisfactory results were obtained with a −325-mesh sample diluted to 20% concentration in ignited alumina.

The materials investigated are listed in Tables III and IV. The synthetic materials were prepared as follows. Calcium sulphate dihydrate was precipitated from 0.5 *M* solutions of calcium nitrate and sulphuric acid at room temperature, thoroughly washed and air-dried. The α-hemihydrate was precipitated from a boiling 50% nitric acid solution of the dihydrate. The β-hemihydrate was obtained by dehydrating dihydrate at 100° C in a stream of nitrogen containing water vapor until the theoretical hemihydrate composition was reached. These two hemihydrates were identified by measuring their heats of solution in 2 *N* hydrochloric acid (9), and their analyses, together with that of the synthetic dihydrate, are given in Table I. The agreement of experimental heats of solution with accepted values (9) provides sufficient identification of the hemihydrates.

TABLE I

Analysis of synthetic calcium sulphates

Material	% Ca		% H_2O		ΔH soln. (298° K) (cal $mole^{-1}$)	
	Exptl.	Theor.	Exptl.	Theor.	Exptl.	Accepted (9)
$CaSO_4 \cdot 2H_2O$	23.31	23.28	20.88	20.93	—	—
$CaSO_4 \cdot \frac{1}{2}H_2O(\alpha)$	27.59	27.61	6.24	6.21	+1580	+1600
$CaSO_4 \cdot \frac{1}{2}H_2O(\beta)$	27.57	27.61	6.25	6.21	+1085	+1100

Can. J. Chem. Downloaded from www.nrcresearchpress.com by 186.148.149.217 on 09/04/12
For personal use only.

RESULTS

For convenience, the peaks corresponding to the various endothermic and exothermic effects are numbered from the low-temperature end of the differential thermogram. Thus, peak No. 1 corresponds to the endothermic transition from dihydrate to hemihydrate, peak No. 2 to the endothermic transition from hemihydrate to soluble anhydrite, peaks Nos. 3 and 4 to further endothermic transitions to be discussed below, and peak No. 5 to the exothermic transition to insoluble anhydrite.

Natural Gypsums

The results shown in Table II are typical of the various samples studied. These data show that the reproducibility of peak temperatures at constant concentration and heating rate was satisfactory, and that peak temperatures were displaced upwards when sample concentration, heating rate, or particle size was increased.

TABLE II

Peak temperatures in the differential thermograms of selenite (Windsor, N.S.)

Particle size	Concn. (%)	Heating rate (°C min^{-1})	Final temp. (°C)	Endotherm peak temperature (°C)				Exotherm peak temperature (°C)
				No. 1	No. 2	No. 3	No. 4	No. 5
60–80 mesh	20	3	190	147	161	170	—	—
−325 mesh	10	3	180	124	140	155	—	—
−325 mesh	20	3	177	135	157	170	—	—
−325 mesh	20	3	197	137	158	169	—	—
−325 mesh	20	12	500	157	189	202	300	410
−325 mesh	100	3	215	144	191	202	—	—

Representative results for the various natural forms of calcium sulphate studied are given in Table III and some typical differential thermograms are shown in Fig. 1. Small

TABLE III

Peak temperatures in the differential thermograms of natural forms of calcium sulphate dihydrate

Sample	Concn. (%)	Heating rate (°C min^{-1})	Final temp. (°C)	Endotherm peak temp. (°C)				Exotherm peak temp. (°C)
				No. 1	No. 2	No. 3	No. 4	No. 5
Alabaster Hillsborough, N.B.	20	3, 12	500	130	149	162	300	395
Alabaster Pomaia, Italy	20	3, 12	500	129	154	169	300	410
Massive gypsum Caledonia, Ont.	20	3, 12	500	131	151	166	310	400
Massive gypsum Grand Rapids, Mich.	20	3, 12	500	129	156	169	300	410
Massive gypsum Halifax County, N.S.	20	3, 12	500	132	151	166	310	390
Massive gypsum Hillsborough, N.B.	20	3, 12	505	126	149	163	300	430
Massive gypsum Nappan, N.S.	20	3, 12	500	126	149	163	310	400
Satinspar Amarillo, Texas	20	3, 12	500	132	155	169	300	410
Satinspar Windsor, N.S.	20	3, 12	500	133	151	165	300	395
Selenite Penfield, N.S.	20	3, 12	500	134	154	169	310	400
Selenite Windsor, N.S.	20	3, 12	500	137	158	169	300	410

differences in the size and shape of peaks may be due to packing of the sample within the block as well as to differences in its dihydrate content. In all cases the samples were heated to about 200° C at 3° C min^{-1}, and at 12° C min^{-1} thereafter to give better definition to the smaller high-temperature peaks. The broken lines in Fig. 1 indicate the region in which the heating rate, and hence the base line, was changing. Independent experiments at both 3° C and 12° C min^{-1} showed no thermal effects occurring in the 200° to 300° C region.

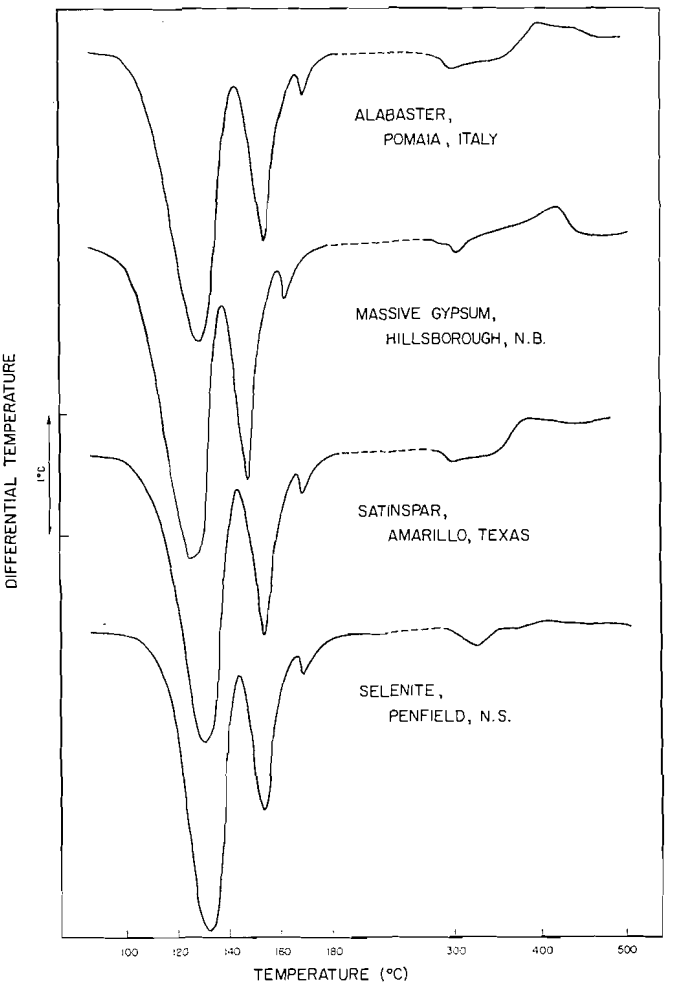


FIG. 1. Differential thermograms of natural calcium sulphate dihydrate.

In addition to the two endothermic peaks below 200° C (Nos. 1 and 2), another endothermic peak (No. 3) was consistently found associated with the dehydration of the hemihydrate (peak No. 2). Although peak No. 3 was observed under all conditions, there was a tendency for it to be masked by the larger peak No. 2 at both higher heating rates and sample concentrations. The occurrence of peak No. 3 was found to be independent of the particle size of the sample, the type or origin of the gypsum (natural or synthetic), the ambient humidity, and the diluent used. The fact that it was found when either

Can. J. Chem. Downloaded from www.nrcresearchpress.com by 186.148.149.217 on 09/04/12
For personal use only.

Can. J. Chem. Downloaded from www.nrcresearchpress.com by 186.148.149.217 on 09/04/12
For personal use only.

ignited alumina or powdered nickel metal was used as diluent and reference indicates that it is unlikely to be due to any sample–diluent interaction.

When a sample was heated at 12° C min^{-1} a further small endothermic peak (No. 4) was indicated in the vicinity of 300° C, appearing often as a doublet. This effect appeared to be independent of the origin of the sample and the diluent used, and was too small to be detected in samples heated to 500° C at 3° C min^{-1}. It was not possible to isolate this effect further at present.

The exothermic peak (No. 5) was moderately well defined at heating rates of 12° C min^{-1}. Throughout the variety of natural dihydrates studied, it was not possible to obtain large differences in the temperature at which this exothermic effect occurred (2, 3), although the shape of the peak varied between samples.

To ascertain if peak No. 3 could be associated with the transition to insoluble anhydrite, a series of experiments were carried out on samples of a massive gypsum whose differential thermograms had previously been obtained up to 250°, 300°, 350°, and 440° C. Since it is possible to hydrate a soluble anhydrite to the corresponding hemihydrate by moistening it with 80% ethanol and evaporating off the residual liquid (10), whereas if pure water is used the hydration will proceed completely to the dihydrate, these samples were each treated with 80% ethanol, the residual liquid evaporated off at 46° C until a uniform base line was again obtained on the thermogram, and the differential thermogram redetermined. The samples heated initially to 250°, 300°, and 350° C all produced second differential thermograms comparable to their initial ones, except for the absence of peak No. 1, indicating that no dihydrate was formed under the conditions of rehydration. The areas under peaks Nos. 2 and 3 were somewhat reduced and the temperatures corresponding to these peaks were slightly lower than in the initial thermograms, possibly due to changes in particle size and sample porosity resulting from the technique. The sample heated initially to 440° C lacked any peaks in the second differential thermogram, as did a sample heated to 500° C and cooled in a stream of dry nitrogen before the differential thermogram was redetermined. These results support the suggestion that the exothermic peak in the vicinity of 400° C is associated with the soluble to insoluble anhydrite transition (2, 3, 8), so that peak No. 3 occurs well below this temperature and does not appear to be associated with this particular transition.

Synthetic Hydrates

Table IV gives representative results of the differential thermal analysis of synthetic calcium sulphates, the thermograms appearing in Fig. 2. No significant differences between the thermograms of natural and synthetic varieties of calcium sulphate dihydrate were found.

TABLE IV

Peak temperatures in the differential thermograms of synthetic forms of calcium sulphate

Sample	Concn. (%)	Heating rate (°C min^{-1})	Final temp. (°C)	Endotherm peak temp. (°C)				Exotherm peak temp. (°C)
				No. 1	No. 2	No. 3	No. 4	No. 5
$CaSO_4 \cdot 2H_2O$	20	3, 12	500	134	154	169	305	390
$CaSO_4 \cdot \frac{1}{2}H_2O$ (α)	20	3, 12	500	—	156	172	—	177
$CaSO_4 \cdot \frac{1}{2}H_2O$ (β)	20	3, 12	500	—	154	172	310	400

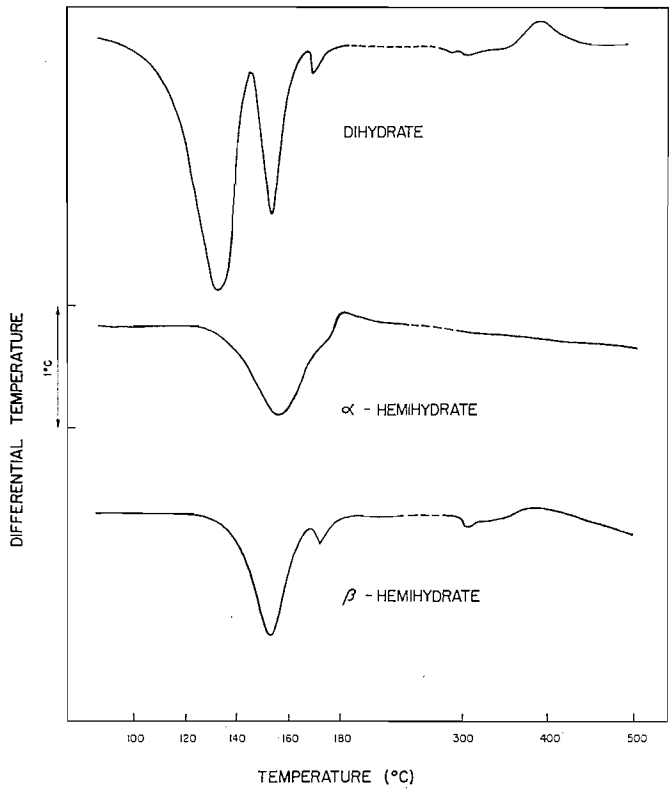


FIG. 2. Differential thermograms of synthetic hydrates of calcium sulphate.

With the α-hemihydrate, endothermic peak No. 3 was found, associated again with peak No. 2, at about the same temperature as in the case of the dihydrate. However, it was very much smaller than for the dihydrate or the β-hemihydrate (Fig. 2), appearing only as a shoulder on the high-temperature side of peak No. 2. An effort to resolve these peaks further at heating rates of the order of 1° C min^{-1} was unsuccessful. There was some indication that endothermic peak No. 4 might be present in the thermograms of α-hemihydrate, but its magnitude approached the sensitivity of the instrument.

The exothermic peak (No. 5) appeared at a considerably lower temperature with the α-hemihydrate than with the dihydrate or the β-hemihydrate, and was smaller and relatively sharper. Samples of α-hemihydrate, heated to 250°, 300°, and 350° C initially, were treated with 80% ethanol as described earlier and second differential thermograms were obtained. The sample initially heated to 250° C showed a small but definite peak No. 2 (transition of hemihydrate to soluble anhydrite) but no evidence of other peaks. The relative magnitudes of peak No. 2 in the first and second thermograms in this case indicated that any other peaks in the second thermogram would be beyond the sensitivity of the instrument. Samples heated initially to 300° and 350° C gave no clear indication of any peaks in the second thermogram. Such behavior would be expected if the α-soluble anhydrite is not completely converted to insoluble anhydrite at the exothermic peak temperature, as reported by Powell (8). Contrary to some reports (4, 5) there seems to be no doubt that this exothermic effect also exists in the case of the α-hemihydrate.

Can. J. Chem. Downloaded from www.nrcresearchpress.com by 186.148.149.217 on 09/04/12
For personal use only.

The differential thermogram of the β-hemihydrate closely resembled those of the various dihydrates, both natural and synthetic, indicating that the dehydration of these materials proceeded via the β-series of products as expected (9).

In an effort to identify peak No. 3 more fully, synthetic dihydrate was heated to 190° C, peak No. 3 being recorded at 169° C in this case, and slowly cooled to room temperature in a stream of dry nitrogen. The differential thermogram obtained on reheating this sample gave no indication of any peaks below 200° C suggesting that peak No. 3 is not due to some reversible, temperature-dependent phase change within the dehydrated sample, but rather appears to be associated directly with the loss of water during the dehydration of the hemihydrate.

COMMENT

Peaks Nos. 1 and 2 agree with those already reported in the literature for the dehydration of calcium sulphate dihydrate to hemihydrate and thence to soluble anhydrite at moderate heating rates, and need not be commented on further. Exothermic peak No. 5 has been confirmed as arising from the transition of soluble to insoluble anhydrite, and this process occurs when either α- or β-soluble anhydrite is heated, a much lower temperature being observed in the case of the α-soluble anhydrite.

Of the two further endothermic effects found, peak No. 4 in the vicinity of 300° C appears to be a reality when β-hemihydrate is heated, and not due to instrumentation, although it has not been possible to isolate this effect further. It is uncertain whether the same effect exists when α-hemihydrate is heated, and an instrument of higher sensitivity might resolve this point.

It has been found that the remaining endothermic effect (peak No. 3) cannot be ascribed to some interaction between sample and diluent, and that it is present only under conditions where the hemihydrate and corresponding soluble anhydrite can be interconverted. The transition of the sample to insoluble anhydrite erases both peaks Nos. 2 and 3. Heating of a sample to just above the conclusion of peak No. 3, cooling under anhydrous conditions, and reheating results in the absence of all of the first three endothermic peaks in the second thermogram, independent of the length of the initial heating. It is therefore reasonable to suggest that peak No. 3 is not due to some reversible temperature-dependent phase change occurring in the absence of water vapor within the calcium sulphate lattice.

An attempt has been made to estimate the enthalpy change associated with peak No. 3 by comparison with peak No. 2. The enthalpy change associated with this latter peak was calculated from the data of Kelley *et al.* (9), who consider the first reaction taking place on the dehydration of β-hemihydrate to be

$$CaSO_4 \cdot \tfrac{1}{2}H_2O(\beta)_s = CaSO_4(\beta)^*_s + \tfrac{1}{2}H_2O_g.$$

The product $CaSO_4(\beta)^*$ may contain up to 0.07 mole H_2O, which appear to be considerably more difficult to remove than the remainder of the 0.5 mole H_2O originally present. The corrected enthalpy equation for the above process (9) gives $\Delta H_{427°K} = +7.4$ kcal mole^{-1}. Comparison of areas under peaks Nos. 2 and 3, by means of a compensating planimeter, indicates that on this basis the enthalpy change associated with peak No. 3 is $\Delta H_{445°K} = +0.7$ kcal mole^{-1} $CaSO_4(\beta)^*$, equivalent to about 10 kcal mole^{-1} of residual H_2O.

In the case of the α-hemihydrate, dehydration produces a virtually water-free soluble

Can. J. Chem. Downloaded from www.nrcresearchpress.com by 186.148.149.217 on 09/04/12
For personal use only.

anhydrite containing perhaps 0.002 to 0.004 mole H_2O (9). The enthalpy change for the process

$$CaSO_4 \cdot \tfrac{1}{2}H_2O(\alpha)_s = CaSO_4(\alpha)_s + \tfrac{1}{2}H_2O_g$$

is $\Delta H_{427°K} = +6.9$ kcal mole^{-1}. As seen from Fig. 2, the area under peak No. 3 in this case, although too small to estimate with any degree of accuracy, may be roughly an order of magnitude less than in the case of the β-hemihydrate. Since the residual H_2O in the α-soluble anhydrite is also roughly an order of magnitude less than in the $CaSO_4(\beta)$*, it is possible that the enthalpy change associated with peak No. 3, per mole of residual H_2O, is about the same as that in the case of the β-hemihydrate. Thus, it may be speculated that the beginning of release of these last traces of water gives rise to the observed small endothermic effect, and that just as the conversion of soluble to insoluble anhydrite is not completed until temperatures above the end of the exothermic peak associated with this change, so these last traces of water continue to be removed over a wide temperature range as reported by Powell (8).

Another possible explanation for the presence of peak No. 3 might be as a "false peak" similar to those reported by Borchardt and Daniels (11) in the dehydration of several salt hydrates, and due to the vaporization of liquid water released from a previous dehydration reaction. Under this interpretation, peak No. 3 would be due to vaporization of liquid water produced from the dehydration of the hemihydrate (peak No. 2). However, in the cases reported (11) these "false peaks" were of a magnitude comparable to the peak associated with the original dehydration process producing the liquid water and the magnitudes of peaks Nos. 2 and 3 are sufficiently different as to suggest another explanation must be sought for the appearance of peak No. 3.

ACKNOWLEDGMENTS

The authors wish to express their gratitude to Mr. L. J. Chapman, Department of Physiography, Ontario Research Foundation, for placing the required instrumentation at their disposal. Two of them (R. A. K., H. G. M.) also thank Gypsum, Lime and Alabastine, Canada, Ltd., for permission to devote some of their time to the direction of this work.

REFERENCES

1. R. M. GRUVER. J. Am. Ceram. Soc. **34**, 353 (1951).
2. J. A. SCHEDLING and J. WEIN. Österr. Akd. Wiss. Math. naturw. Kl. Sitzber. Abt. II. **164**, 175 (1955).
3. J. A. SCHEDLING and J. WEIN. Acta Phys. Austriaca, **10**, 247 (1956).
4. L. G. BERG and V. N. SVESHNIKOVA. Izvest. Akad. Nauk S.S.S.R., Otdel. Khim. Nauk, 19 (1946).
5. P. P. BUDNIKOV and Z. S. KOSYREVA. Voprosy Petrog. i. Mineral. Akad. Nauk S.S.S.R. **2**, 342 (1953).
6. E. S. NEWMAN. J. Research Natl. Bur. Standards, **22**, 191 (1941).
7. W. GRAHMANN. Z. anorg. Chem. **81**, 257 (1913).
8. D. A. POWELL. Nature, **182**, 792 (1958).
9. K. K. KELLEY, J. C. SOUTHARD, and C. T. ANDERSON. U.S. Bureau of Mines, Tech. Paper No. 625, 1941.
10. National Gypsum Co., Buffalo, N.Y. Private communication.
11. H. J. BORCHARDT and F. DANIELS. J. Phys. Chem. **61**, 917 (1957).

Can. J. Chem. Downloaded from www.nrcresearchpress.com by 186.148.149.217 on 09/04/12
For personal use only.

Can. J. Chem. Downloaded from www.nrcresearchpress.com by 186.148.149.217 on 09/04/12
For personal use only.

THE SYNTHESIS OF 2-*O*-β-D-GLUCOPYRANOSYL-D-XYLOSE[1]

J. K. N. Jones and P. E. Reid

ABSTRACT

A synthesis of the disaccharide named in the title is described. Some aspects of the periodate oxidation of this sugar and of analogous sugar derivatives have been examined.

INTRODUCTION

Aldobiouronic acids containing D-glucuronic acid or 4-*O*-methyl-D-glucuronic acid and D-xylose have been isolated from a number of xylans. We are attempting the synthesis of oligosaccharides which may occur in nature and as part of this program we have synthesized 2-*O*-β-D-glucopyranosyl-D-xylose. This compound provides a possible route to the aldobiouronic acid 2-*O*-β-D-glucuronosidyl-D-xylose and its 4-*O*-methyl-D-glucuronosidyl isomer, which have recently been synthesized by Timell and Bowering (1).

3,5-*O*-Isopropylidene-α + β-methyl-D-xylofuranosides were condensed with acetobromglucose (2,3,4,6-tetra-*O*-acetyl-α-D-glucopyranosyl bromide) under standard Koenigs–Knorr conditions (2). After removal of the blocking groups the mixture of monosaccharides and oligosaccharides was fractionated by chromatography on a charcoal column and yielded a white crystalline disaccharide fraction in small yield. The use of argentic oxide (3) instead of the more usual argentous oxide in the Koenigs–Knorr condensation apparently made very little difference to the course of the reaction.

Hydrolysis and paper chromatography of the hydrolyzate showed that the compound contained glucose and xylose only. The theoretical results to be expected from the periodate oxidation of the possible reducing disaccharides containing glucose and xylose where (*a*) xylose is the reducing group and (*b*) the xylose residue has been reduced to a pentitol are shown in Tables I and II. In Table I the assumption is made that the rate-determining steps in the oxidation of the reducing disaccharide are, first, the rate of hydrolysis of the hemiacetal group, which is present in the product of oxidation of the 1,2-linked disaccharide, and, second, the rate of hydrolysis of any formyl esters produced.

TABLE I

Oxidation at acid pH – unbuffered conditions

Linkage	Moles of periodate taken up per mole of disaccharide	Moles of formic acid (as free acid) released per mole of disaccharide	Moles of formic acid per mole disaccharide as formyl ester	Overoxidation expected
1 → 2	3	1	—	Yes
1 → 3	3	1	1	Yes (see ref. 7)
1 → 4	4	2	1	No
1 → 5	4	2	1	No

Periodate oxidation of the disaccharide at 4° C proceeded rapidly and at 20 hours the periodate consumption was 5.4 moles and the formic acid released 4.1 moles. When the results obtained were plotted graphically and the flattened portion of the curve extrapolated to zero time the results obtained were 3.07±.13 moles of sodium metaperiodate consumed and 1.09±.11 moles of formic acid released per mole of disaccharide.

[1]*Manuscript received December 1, 1959.*
Contribution from the Department of Chemistry, Queen's University, Kingston, Ontario.

TABLE II

Oxidation at acid pH – unbuffered conditions

Linkage	Moles of periodate consumed per mole of disaccharide	Moles of formic acid released per mole disaccharide	Overoxidation expected
1 → 2	4	2	No
1 → 3	4	1	Yes
1 → 4	4	2	No
1 → 5	5	3	No

When the oxidation was carried out at 23°±2° C the oxidation was extremely rapid in the initial stages. After 3 hours 5 moles of periodate was consumed and 2.85 moles of formic acid was released, while after 20 hours the totals were 7.15 moles periodate consumed and 5.35 moles of formic acid released. It was evident that in both these cases extensive overoxidation had occurred. Overoxidation is known to occur with 1 → 2 linked disaccharides (4, 5). For example, periodate oxidation of 2-*O*-α-D-glucopyranosyl-D-glucose (5) resulted in a periodate uptake of 6.1 moles of periodate and a formic acid yield of 3.1 moles per mole after 22 hours at room temperature.

From Table I it will be seen that a 1 → 2 linked disaccharide should take up 3 moles of periodate and produce 1 mole of formic acid providing the first assumption is correct. To test this the periodate oxidation of 2-*O*-methyl-D-xylose and 2-*O*-β-D-glucopyranosyl-D-glucose* as models for 2-*O*-β-D-glucopyranosyl-D-xylose was examined.

Schwarz and MacDougall (6) have investigated the periodate oxidation of 2-*O*-benzyl-D-arabinose at 15–18° C. They found that the oxidation proceeded in three stages. One mole of periodate was consumed rapidly (ca. 5 minutes) and after 14 hours the uptake was 4 moles of periodate, oxidation then proceeded slowly. The fact that they were able to isolate benzyloxymalondialdehyde from the reaction mixture after 5 minutes suggests that the hydrolysis of the intermediary hemiacetal must be rapid. Mitchell (6*a*) has examined the periodate oxidation of 2-*O*-methyl-D-arabinose at 5° C and has isolated after a short time interval of oxidation the bisphenyl hydrazone of methoxymalondialdehyde. Methyl glyoxylate and glycollic aldehyde were also detected as products of oxidation. This work indicates that the hydrolysis of the hemiacetal is rapid and that overoxidation of methoxymalondialdehyde then occurs, as would be expected from the results of Schwarz and MacDougall (6).

Periodate oxidation of 2-*O*-methyl-D-xylose at 4° C was initially rapid and then became slow: 1.28 moles per mole (25 minutes); 3.1 moles (12 hours). The release of formic acid was relatively slow, 0.23 mole per mole (25 minutes); 1.1 moles (12 hours). These results are explicable on the basis of rapid hydrolysis of the hemiacetal linkage followed by oxidation of the glycollic aldehyde and methoxymalondialdehyde so formed (7, 8).

When the oxidation was carried out at 23°±2° C there was a rapid initial uptake of periodate and release of formic acid followed by a slower oxidation. (Periodate uptake: 0.9 mole (5 minutes); 3.4 moles (25.5 hours). Formic acid released: 0.22 mole (5 minutes); 2.02 moles (25.5 hours).) The high apparent yield of formic acid is not readily explicable on the basis of the above mechanism. If the rate of hydrolysis of the hemiacetal is a rate-limiting step it might be expected that a break in the rate curve would occur such that extrapolation to zero time would, in the case of 2-*O*-methyl-D-xylose, give a consumption of 1 mole of periodate and a release of no formic acid. When the figures obtained

**The authors thank Professors A. Thompson and M. L. Wolfrom for a gift of this material.*

Can. J. Chem. Downloaded from www.nrcresearchpress.com by 186.148.149.217 on 09/04/12
For personal use only.

Can. J. Chem. Downloaded from www.nrcresearchpress.com by 186.148.149.217 on 09/04/12
For personal use only.

were plotted graphically no such results were obtained. Similarly 2-*O*-β-D-glucopyranosyl-D-glucose would be expected to take up 3 moles of periodate and release 1 mole of formic acid. However, this result was not obtained when the experimental results were plotted graphically. In agreement with previous results (4, 5) extensive overoxidation was observed.

These results indicate that the rate of the hydrolysis of the hemiacetal is rapid and that the satisfactory results obtained from the extrapolation to zero time in the case of the oxidation of the disaccharide must be viewed with caution and indeed are probably fortuitous, particularly as the apparent final quantity of formic acid produced is higher than would be expected from the apparent periodate consumption (6). A substituted malondialdehyde would be expected to neutralize 1 mole of alkali.

Nevertheless the results of the periodate oxidations follow the same pattern as those expected of a synthetic 2-*O*-β-D-glucopyranosyl-D-xylose.

Table I shows that the disaccharides expected to overoxidize are those containing $1 \rightarrow 2$ and $1 \rightarrow 3$ linkages. The absence of a $1 \rightarrow 3$ type linkage in the synthetic disaccharide is indicated because 3-*O*-β-D-glucopyranosyl-D-xylose has been synthesized (7) and the physical constants differ from those of the synthetic disaccharide reported here.

Table II shows that a reduced $1 \rightarrow 2$ linked disaccharide on reduction followed by periodate oxidation would be expected to take up 4 moles of periodate and to release 2 moles of formic acid. The results actually obtained (periodate consumption: 4.05 moles; formic acid released: 2.15 moles) are in good agreement with those expected from theoretical considerations. Observed overoxidation was very low.

Periodate oxidation of 2-*O*-methyl-D-xylitol as a model for the oxidation of the reduced disaccharide resulted in the consumption of 1.97 moles of periodate and the release of 0.92 mole of formic acid. No overoxidation was observed. This result is in good agreement with theoretical predictions (periodate consumption: 2 moles; formic acid released: 1 mole).

Table II indicates that a $1 \rightarrow 4$ linked disaccharide would be expected to give the same result as a $1 \rightarrow 2$ linked compound, but since the $1 \rightarrow 4$ linked compound does not overoxidize when in a non-reduced form it is distinguished from a $1 \rightarrow 2$ linked compound.

EXPERIMENTAL

Optical rotations were measured in water at 23°±2° C and in water unless otherwise indicated. Solutions were concentrated at reduced pressure below 50° C. The following solvent systems were used to separate sugars on paper chromatograms: (*a*) ethyl acetate, acetic acid, formic acid, water (18:3:1:4); (*b*) butan-1-ol, ethanol, water (3:1:1); and (*c*) butan-1-ol, pyridine, water (10:3:3) (all volume/volume).

Reducing sugars were detected with the *p*-anisidine spray (9) and non-reducing sugars were detected by the alkaline silver nitrate spray (10). Rates of movement of sugars on paper chromatograms are quoted relative to the rate of movement of D-galactose (R_{gal}).

Acetobrom-glucose (2,3,4,6-Tetra-O-acetyl-α-D-glucopyranosyl Bromide)

This was prepared by the method of Barczai-Martos and Korosy (11). 3,4-*O*-Isopropylidene methyl-α + β-D-xylosides were prepared by the methods of Baker, Schaub, and Williams (12).

Can. J. Chem. Downloaded from www.nrcresearchpress.com by 186.148.149.217 on 09/04/12
For personal use only.

Condensation of Acetobrom-glucose and 3,5-O-Isopropylidene-methyl-α + β-D-xyloside

3,4-*O*-Isopropylidene methyl-α + β-D-xylosides (11.1 g) in pure dry chloroform (170 ml) was shaken for 30 minutes with Drierite (67.5 g), glass beads (51 g), argentic oxide (33.75 g), and iodine (3.38 g). Acetobrom-glucose (48 g) in pure dry chloroform (142 ml) was then added and the mixture shaken until a test for ionizable bromine was negative. The mixture was shaken for a further 2 days and filtered, and the filtrate concentrated to a syrup. The syrup was boiled under reflux with methanolic sodium hydroxide (400 ml) (4% w/v) for 3 hours and the cations removed by passage down a bed of Amberlite IR-120 (H-form) ion exchange resin. The resulting acidic solution was heated at 70–80° C for 5 hours, cooled, deionized by passage down a bed of Duolite A4 (OH-form) ion exchange resin, and concentrated to a syrup (14 g). Chromatography (solvent (*a*)) indicated the presence of glucose, xylose, a red spot R_{gal} 0.55, and a trace of yellow spot, R_{gal} 0.142. The syrup was dissolved in water and fractionated on a column of charcoal (Darco-G-60). Elution with water (2 l.) removed all the monosaccharides and the disaccharide was recovered by elution with varying concentrations of alcohol up to 50%. The solution was concentrated to a syrup (2 g). Attempts to prepare a crystalline acetate were unsuccessful. The syrup (1.4 g) was set aside when it crystallized in part. The crystalline material was recrystallized from a mixture of methanol and butan-1-ol and ran as a single discrete spot in solvents (*a*), (*b*), and (*c*). Microanalysis of this compound indicated the presence of ash (5%) and the results of the periodate oxidations carried out on this sample have been adjusted accordingly. The material was dissolved in water, the solution deionized by use of IR 120 (H-form) and IR-45 (OH-form) Amberlite ion exchange resins, concentrated, and the residue dissolved in boiling ethanol. The crystalline material so obtained had a melting point of 200°–202° C, $[\alpha]_D$ ±0° (equil.). Calc. for $C_{11}H_{20}O_{10}$: C, 42.3%; H, 6.4%. Found: C, 42.51%; H, 6.56%. The infrared spectrum was determined in potassium bromide at 0.4% concentration. The spectrum showed the following absorption maxima recorded as frequency cm^{-1}: 3340 (s), 2900 (m), 2860 (m), 1410 (m), 1385 (m), 1360 (m), 1345 (m), 1300 (w), 1280 (m), 1260 (m), 1230 (m), 1163 (m), 1143 (m), 1105 (s), 1078 (s), 1030 (s), 930 (w), 915 (m), 900 (m), 800 (m), 755 (w), 715 (w), 650 (w). (Intensity: s = strong, m = medium, w = weak.)

Hydrolysis of Disaccharide

The disaccharide (10 mg) was hydrolyzed with sulphuric acid (*N*) in a sealed tube for 11 hours at 100°. The hydrolyzate was neutralized with barium carbonate, filtered, and passed down a small bed of IR 120 (OH-form) ion exchange resin, and then concentrated to a syrup. Chromatographic examination in solvent (*a*) indicated the presence of glucose and xylose only.

Preparation of the Reduced Disaccharide

The disaccharide (18.2 mg) was dissolved in water (10 ml) and sodium borohydride (37 mg) was added. After 24 hours the solution was acidified with glacial acetic acid passed through a bed of IR 120 (H-form) Amberlite ion exchange resin and concentrated to a syrup. Boric acid was removed as methyl borate by codistillation with methanol (×20) and the residual syrup was dried over phosphorus pentoxide under reduced pressure (yield, 17.5 mg). Chromatographic examination in solvent (2) indicated the absence of reducing sugar (no reaction was observed with the *p*-anisidine hydrochloride spray). When the chromatogram was sprayed with alkaline silver nitrate a positive reaction resulted indicating the disaccharide had been reduced to the D-xylitol derivative.

Preparation of 2-O-Methyl-D-xylitol

2-*O*-Methyl-D-xylitol was prepared by the reduction of 2-*O*-methyl-D-xylose by the same procedure as described above.

Periodate Oxidations

The periodate oxidations of 2-*O*-methyl-D-xylose and 2-*O*-β-D-glucopyranosyl-D-glucose were carried out on accurately weighed samples (ca. 10 mg) with 0.3 *M* sodium metaperiodate (2 ml) made up to 25 ml with distilled water. The reactions were carried out in the dark at room temperature or at 4° C. Aliquots (1 ml) were used for analysis. The periodate was estimated by the method of Neumüller and Vasseur (13). The formic acid by that of Andrews *et al.* (14).

Oxidation of 2-O-Methyl-D-xylose

Moles of periodate consumed and moles of formic acid produced per mole at stated time intervals *at 4° C*: 0.67, 0.045 (10 minutes); 1.28, 0.23 (25 minutes); 2.25, 0.27 (1 hour); 2.47, 0.36 (2 hours); 2.67, 0.43 (4 hours); 2.92, 0.82 (6 hours, 10 minutes); 3.1, 1.1 (12 hours).

At room temperature (ca. 20° C): 0.84, 0.072 (5 minutes); 1.24, 0.072 (10 minutes); 1.75, 0.192 (20 minutes); 1.75, 0.51 (40 minutes); 2.39, 1.20 (2 hours); 2.69, 1.75 (3 hours); 3.02, 1.99 (7.5 hours); 3.1, 1.99 (15 hours); 3.22, 2.03 (28 hours).

Oxidation of 2-O-β-D-Glucopyranosyl-D-glucose

Moles of periodate consumed and formic acid produced at the time intervals stated at 4° C: 0.26, 0.07 (15 minutes); 0.75, 0.2 (30 minutes); 1.72, 0.46 (1 hour); 2.14, 0.57 (3 hours); 2.32, 0.62 (5 hours); 2.75, 1.02 (8 hours); 3.16, 1.08 (10 hours); 4.2, 1.92 (24 hours); 4.9, 2.04 (27 hours).

Oxidation of 2-O-β-D-Glucopyranosyl-D-xylose

Oxidations were carried on accurately weighed samples (ca. 10 mg) with 0.3 *M* sodium metaperiodate (1 ml made up to 10 ml with distilled water). Moles of periodate consumed and moles of formic acid released at stated time intervals *at room temperature*: 3.38, 0.75 (30 minutes); 3.82, 1.54 (1.5 hours); 5.07, 2.88 (3 hours); 6.35, 4.7 (7 hours); 7.15, 5.35 (20 hours).

At 4° C: 1.35, 0.75 (30 minutes); 2.4, 1.0 (1 hour); 2.7, — (2 hours); 3.0, 1.6 (3 hours); 3.25, 1.6 (4 hours); 3.7, 1.6 (5 hours); 3.95, — (3.95 hours); 5.4, — (21 hours); and 4.1, — (20 hours).

The periodate oxidations of the reduced disaccharide and of 2-*O*-methyl-D-xylose were carried out on weighed samples (ca. 10 mg) as described above.

Reduced Disaccharide

Moles of periodate consumed and moles of formic acid produced at the time intervals stated: 2.38, 1.15 (20 minutes); 2.7, — (40 minutes); 2.7, 1.15 (1 hour); 3.18, 1.6 (2 hours, 10 minutes); 3.82, 1.6 (3 hours, 10 minutes); 3.93, 1.6 (4 hours, 10 minutes); 4.27, 2.3 (5 hours); 4.45, 2.6 (21 hours).

2-O-Methyl-D-xylitol

Periodate consumption and moles of formic acid produced at the time intervals stated: 1.83, 0.78 (10 minutes); 2.02, 0.82 (30 minutes); 2.01, 0.92 (60 minutes); 2.02, 0.88 (165 minutes); 2.02, 0.92 (540 minutes).

Can. J. Chem. Downloaded from www.nrcresearchpress.com by 186.148.149.217 on 09/04/12
For personal use only.

ACKNOWLEDGMENTS

The authors thank the National Research Council of Canada and the Ontario Research Foundation for financial assistance.

REFERENCES

1. T. E. TIMELL and W. D. S. BOWERING. Am. Chem. Soc. 136th Meeting, Atlantic City, September, 1959.
2. W. KOENIGS and E. KNORR. Ber. **34**, 957 (1901).
3. INORG. SYNTHESES, **4**, 12 (1953).
4. A. J. CHARLSON and A. S. PERLIN. Can. J. Chem. **34**, 1805 (1956).
5. R. W. BAILEY, S. A. BARKER, E. Y. BOURNE, P. M. GRANT, and M. STACEY. J. Chem. Soc. 1895 (1958).
6. J. C. P. SCHWARZ and M. MACDOUGALL. J. Chem. Soc. 3065 (1956).
6*a*. P. W. D. MITCHELL. Proc. Roy. Irish Acad. B, **59**, 43 (1958).
7. A. R. ARCHIBALD, D. J. MANNERS, and J. L. THOMPSON. Biochem. J. **73**, 295 (1959).
8. J. C. P. SCHWARZ. Chem. & Ind. (London), 1000 (1954).
9. L. HOUGH, J. K. N. JONES, and W. H. WADMAN. J. Chem. Soc. 1702 (1950).
10. W. E. TREVELYAN, D. D. PROCTOR, and J. S. HARRISON. Nature, **166**, 444 (1950).
11. M. BÁRCZAI-MARTOS and F. KŐRÖSY. Nature, **165**, 369 (1950).
12. B. R. BAKER, R. E. SCHAUB, and J. H. WILLIAMS. J. Am. Chem. Soc. **77**, 9 (1955).
13. G. NEUMÜLLER and E. VASSEUR. Arkiv Kemi, **2**, 235 (1953).
14. P. ANDREWS, L. HOUGH, and J. K. N. JONES. J. Chem. Soc. 806 (1959).

Can. J. Chem. Downloaded from www.nrcresearchpress.com by 186.148.149.217 on 09/04/12
For personal use only.

Can. J. Chem. Downloaded from www.nrcresearchpress.com by 186.148.149.217 on 09/04/12
For personal use only.

GRISEOVIRIDIN: THE C_6 FRAGMENT[1]

P. DE MAYO[2] AND A. STOESSL

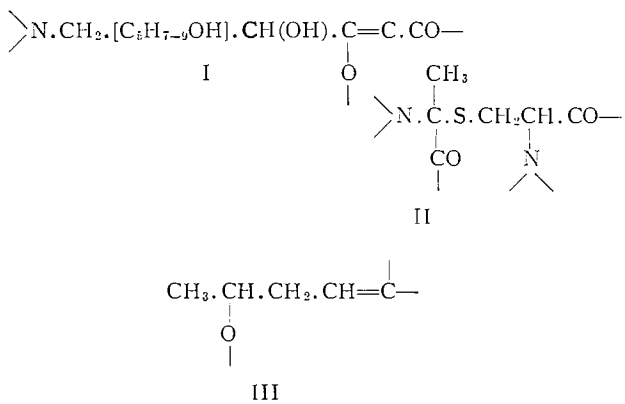
ABSTRACT

The structure of a hydrolytic degradation product from griseoviridin, isolated as the 2,4-dinitrophenylhydrazone, has been shown, by synthesis, to be IV. A by-product of the synthesis was the stereoisomeric 2,4-dinitrophenylhydrazone. This establishes IX as a part structure of griseoviridin. Evidence is provided that the previously proposed structural environment of the sulphur atom is incorrect, and that the sulphur may, in fact, be attached to the C_6 fragment.

The antibiotic griseoviridin, isolated from cultures of a strain of *Streptomyces griseus* (1) has been studied by Ames, Bowman, and their collaborators (2, 3, 4), who were able to establish the empirical formula $C_{22}H_{29\pm2}O_7N_3S$. In their extended investigations they provided evidence for the presence, in this molecule, of three moieties.

First, the existence of a C_{10} fragment was established by the isolation, after reduction and hydrolysis, of ω-amino-decanoic acid. For this portion of the molecule the part structure I was tentatively proposed (4). Secondly, they showed by hydrolysis the presence of two alanine residues (4) in octahydrodesthiogriseoviridin diacetate, a reduced substance from which the sulphur had been removed by Raney nickel. Griseoviridin itself, on the other hand, gave no alanine on hydrolysis, but yielded cystine and some serine together with 1 mole ammonia. From this and other evidence, they deduced the part structure II, the sulphur being part of a ring since removal of the sulphur did not cause the disruption of the molecule. Finally some indication of the disposition of the remaining carbon atoms was obtained from the following experiments (3).

Ozonolysis of griseoviridin (or its diacetate) followed by decomposition of the ozonide and mild treatment with acid or base and steam distillation gave crotonaldehyde, characterized as its 2,4-dinitrophenylhydrazone. The hydrochloride,[3] obtained from griseoviridin by the action of concentrated hydrochloric acid, in contrast, gave crotonaldehyde *directly* after ozonolysis, whilst hexahydrogriseoviridin diacetate gave no aldehyde at all. The facts were construed to indicate the part structure III.



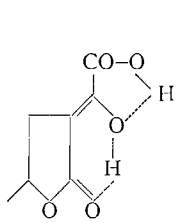
I II III

[1]*Manuscript received February 9, 1960.*
Contribution from the Departments of Chemistry, Imperial College, London, S.W.7, England, and the University, Glasgow, Scotland.
[2]*Present address: Department of Chemistry, University of Western Ontario, London, Ontario.*
[3]*The hydrochloride was reported to have an anomalous analysis. Satisfactory analyses for it, and derivatives, are reported in the Experimental section.*

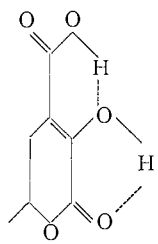
Can. J. Chem. Downloaded from www.nrcresearchpress.com by 186.148.149.217 on 09/04/12
For personal use only.

Such formulations accounted for all but one of the 22 carbon atoms in griseoviridin, and since some evidence, derived from infrared spectra, was adduced for the presence of a diacylimide the remaining carbon atom was conjecturally attached to the fragment represented by III. The present communication is mainly concerned with this fragment.

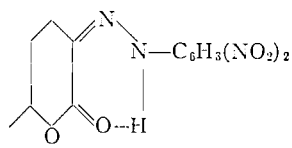
Although griseoviridin itself does not yield a 2,4-dinitrophenylhydrazone, Ames and Bowman (3) reported that after acid hydrolysis such a derivative, $C_{14}H_{14}O_7N_4$, was obtained, corresponding to a fragment $C_8H_{10}O_3$. Re-examination of this substance, purified by chromatography on bentonite–celite, showed that it had, in fact, the formula $C_{12}H_{12}O_6N_4$, corresponding to a derivative of a compound $C_6H_8O_3$. The material was optically active and so contained at least one asymmetric carbon, whilst Kuhn–Roth oxidation indicated the presence of one C-methyl group. The ultraviolet spectrum (λ_{max} 365 mμ) suggested the derivative of a saturated ketone and precluded the presence of any other high intensity chromophore in the molecule. The infrared spectrum, however, showed a band at 1680 cm^{-1} to be attributed to a remaining carbonyl function. Since the empirical formula required the presence, in the original substance, of three double-bond equivalents, and, since the remaining oxygen was not a hydroxyl group, a cyclic structure seemed inevitable. Bearing in mind the implications of the part structure III the formulation IV appeared attractive. Such a structure with the appropriate geometry would, by hydrogen bonding and conjugation, be expected to lower the normal δ-lactone frequency to that actually found. Furthermore, a band at 3154 cm^{-1}, to be attributed to the N—H stretch, was lower, as would be expected for hydrogen bonding, than is usual for such bonds in these derivatives: the accepted region is in the vicinity of 3300 cm^{-1}. Since the amounts of material available did not allow of chemical degradation the racemate of IV was, accordingly, synthesized by the following steps.



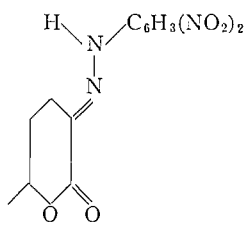
V



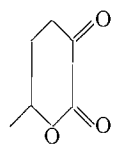
VI



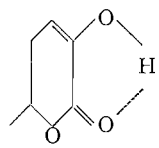
IV



VIII



VII*a*



VII*b*

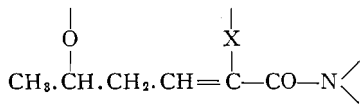
γ-Valerolactone was condensed with ethyl oxalate to give, after hydrolysis, an acid, $C_7H_8O_5$, corresponding to one or more of the tautomers of V or VI. It liberated carbon dioxide from sodium hydrogen carbonate, titrated as a monobasic acid, and gave an intense purple color with ferric chloride.

The acid was decarboxylated (with the evolution of one molecule of carbon dioxide) to give VII*a*, $C_6H_8O_3$, which appeared to exist largely as the enol (VII*b*). This substance also titrated sharply as a monobasic acid, and although it could be obtained pure by recrystallization after sublimation it rapidly decomposed on exposure to air, as do the corresponding γ-lactones (5).

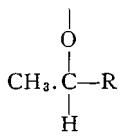
The preparation of the 2,4-dinitrophenylhydrazone was accomplished in the usual way, the acidic material isolated then being cyclized to the lactone by refluxing in chloroform. Chromatography on bentonite–celite then afforded racemic IV, m.p. 230–231°. The ultraviolet spectrum, and the infrared spectra, both in chloroform and methylene dichloride solution, were superposable on that of IV from hydrolytic degradation.

Concomitant with the formation of IV, a second, isomeric, 2,4-dinitrophenylhydrazone was isolated. This absorbed at somewhat shorter wavelength in the ultraviolet, and, in the infrared spectrum showed bands at 3300 (free N—H) and 1724 cm^{-1}. This substance is accordingly attributed the structure VIII. Such pairs of isomers have been previously separated and our interpretation has ample analogy (6).

The structural identification of IV indicated the presence, in griseoviridin, of the six-carbon fragment (IX) which, with I and II, or their equivalents, accounts for all the carbon atoms. The formulation (IX) is supported by the fact that whilst both griseoviridin and hexahydrodeoxygriseoviridin (obtained by hydrogenation of the hydrochloride) give iodoform (35 and 48% respectively) when treated with iodine and base, griseoviridin gives acetaldehyde merely on refluxing with 4 *N* sodium hydroxide. This process, presumably involving a dealdolization, occurs also in the hydrochloride but not in the reduced hydrochloride where one of the requisite structural features, the double bond, is no longer present as is shown by the non-formation of crotonaldehyde on ozonolysis. Formic and acetic acids are formed, in addition to acetaldehyde, in the hydrolysis of griseoviridin.



IX

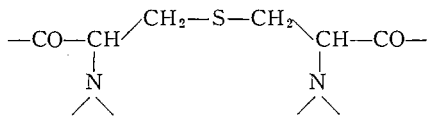


X

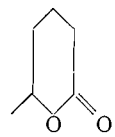
The atom (X) in IX may be oxygen, or, less probably, nitrogen. Evidence is available that, in fact, sulphur cannot be excluded and that the part structure II is incorrect. First, Kuhn–Roth oxidation of griseoviridin suggests (2) the presence of 1 C—Me group which is surely that present in IX. Secondly, the n.m.r. spectrum in deuterochloroform of griseoviridin diacetate and several other derivatives showed a doublet at 8.55 p.p.m. (relative to tetramethylsilane as 10) ($J \sim 7$ c.p.s.) attributable to the system X: no other bands (other than acetate) attributable to C—Me could be detected. We are much indebted to Dr. L. M. Jackman for the determination of these spectra.

Finally although modification of II to XI would circumvent these difficulties, evidence is available that the situation is more subtle. Thus, griseoviridin reacts with perbenzoic acid (2) to give an "oxide" which does not show sulphone bands in the infrared (7) and which gives cystine and traces of serine on acid hydrolysis, as does griseoviridin itself.

Can. J. Chem. Downloaded from www.nrcresearchpress.com by 186.148.149.217 on 09/04/12
For personal use only.



XI



XII

Since sulphides are, in general, rapidly oxidized by peracids this observation appears incompatible with II or XI. But, by contrast, hexahydrodeoxygriseoviridin rapidly gives a sulphone further characterized by a number of derivatives. The implication is, therefore, that reduction or hydrogenolysis in the vicinity of the sulphur atom renders it open to oxidation, a fact not readily interpretable in terms of II and XI. If the sulphur is not assigned to the two alanine molecules it then becomes available for inclusion in part formula IX. Consistent with this is the fact that basic hydrolysis of octahydrodethiogriseoviridin diacetate readily affords δ-caprolactone (XII) whereas hexahydrodeoxygriseoviridin, in which the sulphur link remains, does not. In this case some second hydrogenolysable function is required to mask the second potential alanine moiety.

EXPERIMENTAL

Melting points were taken on the Kofler Hot Stage. Rotations were determined in chloroform and ultraviolet spectra in 95% ethanol. Except where otherwise indicated the phrase 'petroleum ether' refers to the fraction of boiling range 60–80°; unless otherwise stated infrared spectra were determined as Nujol mulls.

Preparation of the 2,4-Dinitrophenylhydrazone (IV)

Griseoviridin (200 mg) was hydrolyzed with 6 *N* hydrochloric acid and the crude 2,4-dinitrophenylhydrazone was prepared as described by Ames and Bowman (3). The crude, dried product (40 mg) was dissolved in chloroform and applied to a short column of bentonite–celite (1:1 by volume). Elution with ethanol–chloroform (1:6) gave, after evaporation and crystallization from ethanol–chloroform, the almost pure 2,4-dinitrophenylhydrazone (7.6 mg), m.p. 223–226° (Ames and Bowman record 220–222°), $[\alpha]_D$ +84 (*c*, 0.20); λ_{max} 258, 365 mμ and log ε 3.91 and 4.35 respectively. The compound has maxima in the infrared at 3154, 3090, 1680, and 1615 cm^{-1}. Found: C, 46.78%; H, 4.12%; N, 18.09%; C—Me, 4.38%. $C_{12}H_{12}N_4O_6$ requires: C, 46.75%; H, 3.92%; N, 18.18%; C—Me, (1), 4.88%.

2-Oxalyl-γ-valerolactone

A mixture of diethyl oxalate (100 ml) and γ-valerolactone (10 g) was added to a solution of sodium (2.3 g) in absolute ethanol (40 ml) and the mixture heated under reduced pressure (10 cm Hg) at 55° for 1 hour, the pressure lowered (2 cm Hg), and heating continued for a further 2 hours. After the mixture was cooled the precipitated solid was collected, washed with ether, and just acidified with *N* hydrochloric acid. Extraction with ether and evaporation under reduced pressure then gave the crude required, 2-oxalyl-γ-valerolactone (16.2 g).

The crude ester (8.0 g) was dissolved in sodium hydroxide solution (125 ml, 1.1 *N* NaOH) and set aside overnight. Acidification followed by repeated extraction with ether gave the crude lactone (5.9 g). Crystallization from ether, extraction with benzene to remove small amounts of oxalic acid, and recrystallization from carbon tetrachloride gave the γ-lactone, m.p. 93–102° (variable, dependent on rate of heating and solvent).

Can. J. Chem. Downloaded from www.nrcresearchpress.com by 186.148.149.217 on 09/04/12
For personal use only.

Found: C, 48.7%; H, 4.80%; equiv. 90. $C_7H_8O_5$ requires: C, 48.85%; H, 4.69%; equiv. 86. The substance had λ_{max} 276 mμ (log ϵ 3.54) and bands in the infrared at 3546, 3460, 3300, 1718, 1698, 1669, and 1631 cm^{-1}.

2-Oxo-δ-caprolactone

The γ-lactone (840 mg) was refluxed in water for 2 hours. The solution was then cooled and evaporated under reduced pressure at 40° to give a yellow oil (760 mg) which crystallized after sublimation. The crystals liquefied after brief exposure to the atmosphere, but could be purified by crystallization from petroleum ether to give the δ-lactone, m.p. 56–59°. Found: C, 56.18%; H, 6.33%; equiv. 130. $C_6H_8O_3$ requires: C, 56.24%; H, 6.29%; equiv. 128. The substance had λ_{max} 256 mμ (log ϵ 3.70) (neutral) and λ_{max} 246 (log ϵ 3.64) (.001 *N* NaOH), and bands in the infrared spectrum at 3068, 1675 (broad), and 1613 cm^{-1}.

The 2,4-Dinitrophenylhydrazones of (±)-2-Oxo-1,5-hexanolide

The δ-lactone (400 mg) in water (25 ml) was added to 2,4-dinitrophenylhydrazone (1.2 g) in sulphuric acid (10 ml) and water (75 ml). After 24 hours the precipitate formed was extracted into chloroform containing 10% ethanol, and the acidic material isolated, in the usual manner, by extraction with a saturated solution of sodium hydrogen carbonate (100 ml), followed by acidification and re-extraction with chloroform. Evaporation gave the crude acid (733 mg) which was cyclized by refluxing in chloroform and partial removal of solvent by distillation. After removal of acidic contaminants with sodium hydrogen carbonate solution the remaining neutral material (305 mg) was crystallized from benzene to give fraction A (90 mg). This was retained. The mother liquors were added to a bentonite (10 g) – celite column (equal volumes). Elution with ethyl acetate – benzene (1:9) gave fraction B, whilst ethanol – ethyl acetate (1:9) gave material identical with fraction A.

(*a*) The trans (±)-2,4-dinitrophenylhydrazone was obtained by crystallization of fraction A from benzene. It melted unsharply at 200–210°, but the ultraviolet spectrum and melting point were unchanged on repeated crystallization. Found: C, 47.01%; H, 4.15%; N, 17.96%. $C_{12}H_{12}N_4O_6$ requires: C, 46.75%; H, 3.92%; N, 18.18%. The compound had λ_{max} 255, 350 mμ; log ϵ 4.38 and 3.90 respectively.

(*b*) The cis (±)-2,4-dinitrophenylhydrazone was obtained by crystallization of fraction B from ethanol–chloroform and from benzene, m.p. 230–231°. Found: C, 46.96%; H, 4.08%; N, 18.36%. The infrared spectrum in chloroform and methylene dichloride were superposable on that of the active material.

The Hydrolysis of Griseoviridin

(*a*) A solution of griseoviridin (505 mg) in aqueous sodium hydroxide (4 *N*, 50 ml) was distilled at constant volume in a nitrogen atmosphere, the distillate being collected in an aqueous sulphuric acid solution of 2,4-dinitrophenylhydrazone. The precipitate was collected (176 mg) and the absorption curve in the ultraviolet accurately paralleled that of the acetaldehyde derivative, indicating the absence of any crotonaldehyde. Chromatography of the crude product or alumina (Brockman Grade III, 20 g) gave, on elution with benzene – petroleum ether (1:5) followed by crystallization from methanol–chloroform, acetaldehyde 2,4-dinitrophenylhydrazone, melting point and melting point on admixture with an authentic specimen of the same melting point, 163–166°.

(*b*) The alkaline hydrolyzate was acidified with 6 *N* sulphuric acid, the gummy precipitate removed by filtration, and the volatile acids isolated by distillation at constant

Can. J. Chem. Downloaded from www.nrcresearchpress.com by 186.148.149.217 on 09/04/12
For personal use only.

Can. J. Chem. Downloaded from www.nrcresearchpress.com by 186.148.149.217 on 09/04/12
For personal use only.

volume under nitrogen. Qualitative paper chromatography showed the presence of both acetic and formic acids. Treatment after concentration to 20 ml of an aliquot (150 ml of a total of 250) at room temperature with sodium hydrogen carbonate (1 g) and a few drops of bromine (8) destroyed the formic acid and after removal of the excess bromine in a stream of air the aqueous acid was distilled. Titration showed the presence of 0.4 mole of acid. Paper chromatography confirmed the presence of acetic acid only and identity was confirmed by the infrared spectrum of the residue of sodium acetate on evaporation, and by conversion to *p*-phenyl – phenacyl acetate identical in every respect with an authentic specimen.

In another aliquot (100 ml) the carbon dioxide evolved by oxidation of the formic acid with orange mercuric oxide (250 mg) (9) was collected in barium hydroxide. Titration of the barium carbonate produced indicated the presence in the original solution of 0.9 mol. formic acid. The identity of the acid was confirmed by extraction of the salts (138 mg) from the hydrolysis of griseoviridin (1 g) with 95% ethanol and crystallization from absolute ethanol. The sodium formate so obtained had a melting point of 251–256°; its infrared spectrum could be superimposed on that of an authentic specimen. Found: Na, 34.08%; Calc. for CHO_2Na: Na, 33.81%.

Alkaline Hydrolysis of Octahydrodethiogriseoviridin Diacetate

The diacetate (213 mg) was refluxed in solution in aqueous sodium hydroxide (4 *N*, 20 ml) under nitrogen for 30 minutes. No precipitate was obtained by distillation into 2,4-dinitrophenylhydrazine solution. The hydrolyzate was acidified and distilled at constant volume until the titer was negligible. Addition of excess alkali and backtitration indicated the presence of 0.8 mol. lactone. Repeated extraction of the acidified solution with ether gave, after evaporation, an oil (12 mg) which was distilled at 100°/3 mm to give (+)-δ-caprolactone (5.4 mg), m.p. ca. 15°, $[\alpha]_D$ +39 (*c*, 0.54). The infrared spectrum in chloroform was superposable on that of synthetic (±)-δ-caprolactone, and the two substances behaved in the same way on partition chromatography in a propanol–ammonia system (10).

In another experiment the crude alkaline titration solution was mixed with a solution of chromic acid in 2 *N* sulphuric acid (0.4 *N*, 4 ml) and set aside for 16 hours. The excess oxidant was then destroyed (sulphur dioxide) and the mixture treated with Brady's reagent. The resultant precipitate, after collection, was chromatographed on bentonite–celite (1:1 by volume) the fraction eluted with ethanol–chloroform (1:4) then being crystallized from benzene to give 5-oxocaproic acid 2,4-dinitrophenylhydrazone, m.p. 137–139°, unchanged on admixture with an authentic specimen (11) of the same melting point. The infrared spectra in Nujol mull were superposable.

Hexahydrodeoxygriseoviridin

Griseoviridin hydrochloride was prepared as described by Ames and Bowman. Crystallized from ether–methanol it had $[\alpha]_D$ −177° (*c*, 0.53 in MeOH). Found: C, 50.87%; H, 5.86%; Cl, 7.07%. $C_{22}H_{29}O_7N_3S.HCl$ requires: C, 51.20%; H, 5.86%; Cl, 6.87%.

The hydrochloride (3 g) was hydrogenated in ethanol solution in the presence of palladized charcoal (9 g). The filtered solution was evaporated and the glassy residue was crystallized from ethanol. The product had a melting point of 246–248°, $[\alpha]_D$ −55°. Found: C, 56.62%; H, 6.93%; O, 20.75%; N, 8.92%; S, 6.85%. $C_{22}H_{33}O_6N_3S$ requires: C, 56.49%; H, 7.11%; O, 20.53%; N, 8.99%; S. 6.85%. The substance had λ_{max} 212 mμ (log ε 4.29) in neutral solution. In ethanol containing .01 *N* sodium hydroxide it had λ_{max} 255 mμ (log ε 3.89). No crotonaldehyde was obtained by ozonolysis and distillation.

Hydrolysis with 6 *N* hydrochloric acid and distillation of the residue from citrate buffer and ninhydrin (4) gave no volatile carbonyl compounds. No acetaldehyde was formed on alkaline hydrolysis.

Acetylation (pyridine – acetic anhydride at room temperature) gave the monoacetate which, after crystallization from ethanol, had a melting point of 226–228°. Found: C, 56.92%; H, 7.02%; N, 8.34%; S, 6.11%; $C_{24}H_{35}O_7N_3S$ requires: C, 56.54%; H, 6.92%; N, 8.25%; S, 6.28%. The compound has $[\alpha]_D$ −53° (*c*, 1.89).

Benzoylation (pyridine–benzoyl chloride at room temperature for 4.5 hours) afforded the monobenzoate which, after crystallization from ethanol, had a melting point of 193–196°. Found: C, 61.22%; H, 6.38%; N, 7.25%. $C_{29}H_{37}O_7N_3S$ requires: C, 60.92%; H, 6.52%; N, 7.35%. The compound had λ_{max} 227 mμ (log ε 4.14).

Hexahydrodeoxygriseoviridin Sulphone

The deoxy compound (70 mg) in chloroform (10 ml) was added to a solution of perbenzoic acid in benzene (2 ml, 0.4 *N*) and the mixture was left overnight. The solution was then diluted with chloroform and washed with sodium hydrogen carbonate solution and water, and the solution concentrated to give the sulphone, m.p. 205–220° (dec.) unchanged by repeated crystallization from chloroform–ethanol. Found: C, 52.91%; H, 6.74%; O, 25.32%; N, 8.31%. $C_{22}H_{33}O_8N_3S$ requires: C, 52.87%; H, 6.60%; O, 25.63%; N, 8.41%. In neutral solution it showed λ_{max} 212 mμ (log ε 4.21) λ_{Inf} 258 mμ (log ε 3.85). The infrared spectrum showed bands at 1295 and 1126 cm^{-1}. A similar, but quantitative, experiment showed that the uptake of oxidant ceased at 2 moles perbenzoic acid.

Similar oxidation of the monoacetate gave the corresponding sulphone, m.p. 220–230° (from ethanol–chloroform). Found: C, 53.33%; H, 6.59%; O, 26.37%; N, 7.78%. $C_{24}H_{35}O_9N_3S$ requires: C, 53.21%; H, 6.51%; O, 26.59%; N, 7.76%. It had bands in the infrared spectrum at 1290 and 1124 cm^{-1}. This compound was also prepared by acetylation of the sulphone (acetic anhydride – pyridine at room temperature). Oxidation of the benzoate gave the corresponding sulphone, m.p. ca. 200° (from ethanol–chloroform). Found: C, 57.81%; H, 6.38%; N, 6.41%. $C_{29}H_{37}O_9S$ requires: C, 57.70%; H, 6.18%; N, 6.96%. The compound had $[\alpha]_D$ +25 (*c*, 2.0) and showed bands in the infrared at 1294 and 1121 cm^{-1}.

Dehydrohexahydrodeoxygriseoviridin Sulphone

Hexahydrodeoxygriseoviridin sulphone (50 mg) was dissolved in acetic acid (glacial, 5 ml) and a solution of chromic acid in acetic acid (1.05 ml, 0.2 *N*) was added. The mixture was set aside for 5 hours, after which the product was isolated with chloroform. Crystallized from methanol–chloroform the substance had a melting point of approximately 230° (with previous sintering), unchanged by further crystallization. Found: C, 53.37%; H, 6.34%; N, 8.85%. $C_{22}H_{31}O_8N_3S$ requires: C, 53.09%; H, 6.28%; N, 8.44%. The substance in neutral solution had λ_{max} 220 mμ (log ε 4.17) and in .01 *N* ethanolic hydroxide λ_{max} 299 mμ (log ε 4.30). The compound had $[\alpha]_D$ −4° (*c*, 0.85) and showed bands in the infrared at 1709, 1282, and 1119 cm^{-1}.

Iodoform Reaction

Griseoviridin (26 mg) in aqueous potassium hydroxide (10%, 0.5 ml) was warmed until dissolved, cooled to 60°, and iodine – potassium iodide solution added. Iodoform (melting point and mixed melting point with an authentic specimen 119°) (7.2 mg) was isolated equivalent to 0.35 mole per molecule of griseoviridin. A similar experiment on the hexahydrodeoxygriseoviridin gave 0.48 mole iodoform.

Can. J. Chem. Downloaded from www.nrcresearchpress.com by 186.148.149.217 on 09/04/12
For personal use only.

ACKNOWLEDGMENTS

We wish to thank Mr. J. M. L. Cameron (Glasgow) and Miss J. Cuckney (Imperial College) and their associates for the microanalyses. We are also very grateful to Dr. R. E. Bowman (Parke, Davis, England) and to Dr. L. M. Long (Parke, Davis, Detroit) for making the material available to us.

REFERENCES

1. Q. R. Bartz *et al.* Second Annual Symposium on Antibiotics, Washington. 1954.
2. D. E. Ames, R. E. Bowman, J. F. Cavalla, and D. D. Evans. J. Chem. Soc. 4260 (1955).
3. D. E. Ames and R. E. Bowman. J. Chem. Soc. 4264 (1955).
4. D. E. Ames and R. E. Bowman. J. Chem. Soc. 2925 (1956).
5. H. Schinz and M. Hinder. Helv. Chim. Acta, **30**, 1349 (1947).
6. F. A. Isherwood and R. L. Jones. Nature, **175**, 419 (1955).
7. K. C. Schreiber. Anal. Chem. **21**, 1168 (1949).
8. I. M. Kolthoff and R. Belcher. Volumetric analysis. Vol. III. Interscience, N.Y. 1957. p. 567.
9. W. L. Evans and H. B. Hass. J. Am. Chem. Soc. **48**, 2703 (1926).
10. F. A. Isherwood and C. S. Hanes. Biochem. J. **55**, 824 (1953).
11. A. Eschenmoser and A. Frey. Helv. Chim. Acta, **35**, 1660 (1952).

Can. J. Chem. Downloaded from www.nrcresearchpress.com by 186.148.149.217 on 09/04/12
For personal use only.

Can. J. Chem. Downloaded from www.nrcresearchpress.com by 186.148.149.217 on 09/04/12
For personal use only.

THE FREEZING OF WATER AND BENZENE IN POROUS VYCOR GLASS[1]

C. HODGSON[2] AND R. MCINTOSH

ABSTRACT

Freezing has been detected in the adsorbed water and benzene of porous Vycor glass at temperatures below that at which the bulk phases freeze. The evidence presented by equilibrium pressure measurements and dimensional changes of the systems is considered in terms of theories of capillary condensation and freezing in cements and soil. Although not all the results can be explained, it is concluded that the freezing process is a gradual one for both adsorbate–adsorbent systems. The evidence further suggests that hysteresis is absent in isotherms if the solid phase has formed.

INTRODUCTION

In a note from this laboratory (1) the detection of the freezing of water in porous Vycor glass was reported. The method of detection was the observation of the change of linear dimension of the adsorbate–adsorbent system using an extensometer of a type previously described (2). At approximately −22° C a large expansion of the system occurred, in striking contrast with the gradual contraction found as the temperature was lowered in a range above −22° C.

A qualitative explanation of the finding was suggested as either or both of the following possibilities. As in the case for the bulk phases, the solid adsorbate may have a larger molar volume than the liquid adsorbate. Or, since the contractive force due to concave menisci has been demonstrated (3), it is possible that the destruction of concave menisci by the formation of solid adsorbate might also allow a large expansion. To try to distinguish between these possibilities and to establish a broader basis for discussion of the phenomena associated with adsorption hysteresis in general, experiments using benzene as the adsorbate were undertaken. Differences in the behavior of the two adsorbates are marked, and some of the differences are undoubtedly due to the unusual molar volume change in the transition of water. However, insufficient understanding of all the phenomena has been achieved, and it is necessary to compare the results for the two systems in detail. It is also pertinent to analyze the theories so far advanced to rationalize the known transition phenomena and to comment upon claims made by Puri, Singh, and Myer (4) of excellent agreement between the predictions of capillary condensation theory and observation.

One advantage of the experimental method employed in this investigation is that it reveals that the freezing phenomenon does not occur at a single temperature as may be seen from Figs. 1A, 2A. The observation of a sudden change in the rate at which the equilibrium pressure changes with temperature need not mean a sharp phase transition, but it has apparently been interpreted in this way, and a transition temperature, rather than a transition range, has been discussed by many authors. Other evidence against the occurrence of sharp transitions is contained in the work of Jones and Gortner (5), and Patrick and Kemper (6). The evidence obtained using benzene also points to a gradual freezing. The behavior of the two substances differs,

[1]*Manuscript received November 30, 1959.*
Contribution from the Department of Chemistry, University of Toronto. Based upon a thesis by Hodgson submitted in partial fulfillment of the requirements for the degree of Ph.D.
[2]*Holder of the Union Carbide Fellowship (1957–58) and National Research Council Studentship (1958–59). Present address: Canadian Industries Limited, Textiles Fibres Division, Kingston, Ontario.*

however, in that water begins to freeze at a temperature which is insensitive to the quantity adsorbed, while the initial freezing temperature of benzene varies in a readily discernible manner with quantity adsorbed. In the case of benzene, since the higher equilibrium pressures were more readily measured, it was possible to show that there is no hysteresis in that part of the isotherm where solid benzene may exist. This fact supports the suggestion made earlier (1) that meniscus effects of the liquid phase may be the fundamental cause of hysteresis.

Because of the very large amount of data involved, most of the information will be presented in graphical form.

EXPERIMENTAL

As the extensometer and system for temperature control have been described previously (2), only the form of pressure gauge and the minor modification made to the injector for the adsorbates will be discussed. The pressure gauge was a form suggested by Pearson (7) and in this case butylphthalate was used rather than mercury, so that a magnification of 179 relative to readings of a U-tube type of mercury manometer was obtained. In practice the manometer was not free from error. Difficulty was experienced in measuring the low pressures of water because of degassing of the butylphthalate.

The injector holding the adsorbate was arranged with a heating wire around connecting metal valves and tubing, so that after allowing adsorbate to distill from the capillary to the adsorbent chamber, the slow drift in the level of adsorbate in the capillary tube of the injector due to adsorption on metal valves and walls was eliminated. This difficulty has been noted by Amberg (8), but had not been corrected.

The temperature was varied by increments usually less than 10 degrees. Before length and pressure measurements were taken at a new temperature, the system was allowed to come to apparent equilibrium, a process which took between 8 and 12 hours.

RESULTS

1. Water. Length Changes and Equilibrium Pressures

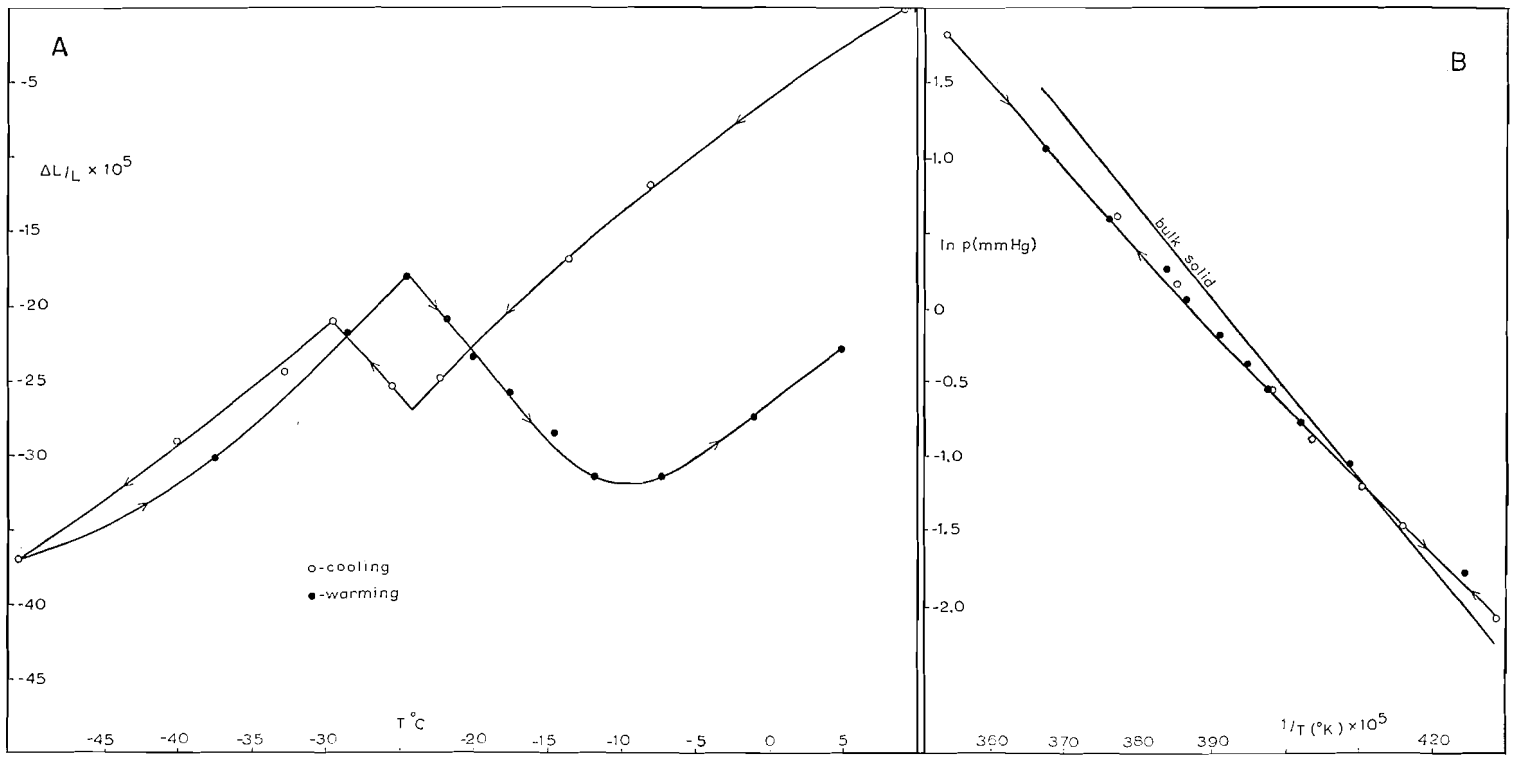
The results of a typical cooling and heating experiment for water at an initial content of 0.175 g/g, established as an adsorption point at 9° C, is given in Fig. 1A. It should be noted that the temperature range over which the expansion (i.e. freezing) occurs on the cooling curve differs from the temperature range over which contraction (i.e. melting) occurs on the heating curve. An important displacement of the two curves is evident, showing a difference of the absolute lengths of the rod. Repeated cycles did not eliminate this behavior. By contrast, it is seen that the equilibrium pressure values of Fig. 1B lie on the same curve for both heating and cooling.

2. Benzene. Length Changes and Equilibrium Pressures

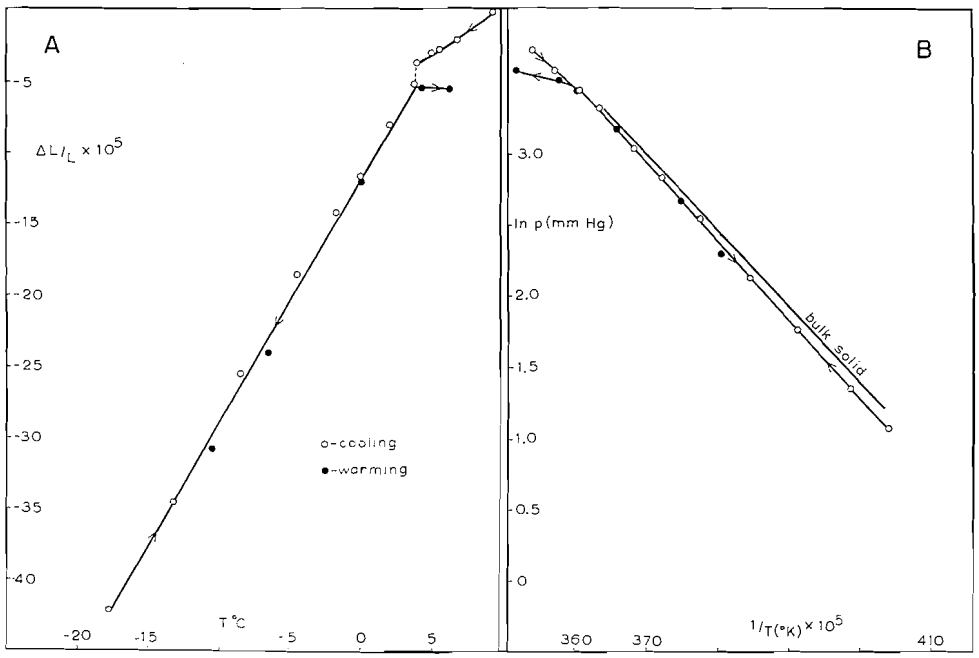
Two typical sets of curves showing length changes as a function of temperature for both heating and cooling and the corresponding equilibrium pressure data are given in Figs. 2, 3, and 4. The contents of benzene are respectively 0.233 g/g, 0.162 g/g, and 0.170 g/g. The reason for giving these figures is that comparison shows the shift of the temperature at which freezing begins with quantity adsorbed. It should also be noted that the sudden change of slope of the equilibrium pressure curves occurs at the same temperature as the change of slope of the length versus temperature plots. Table I contains a further comparison.

Can. J. Chem. Downloaded from www.nrcresearchpress.com by 186.148.149.217 on 09/04/12
For personal use only.

Can. J. Chem. Downloaded from www.nrcresearchpress.com by 186.148.149.217 on 09/04/12
For personal use only.



FIGS. 1A, 1B. Typical plots of length variation and equilibrium pressure as functions of temperature for the system water – Vycor glass. Amount of water adsorbed 0.175 g/g.



FIGS. 2A, 2B. Length variation and equilibrium pressure as functions of temperature for the system benzene – Vycor glass. Amount of benzene adsorbed 0.233 g/g.

TABLE I

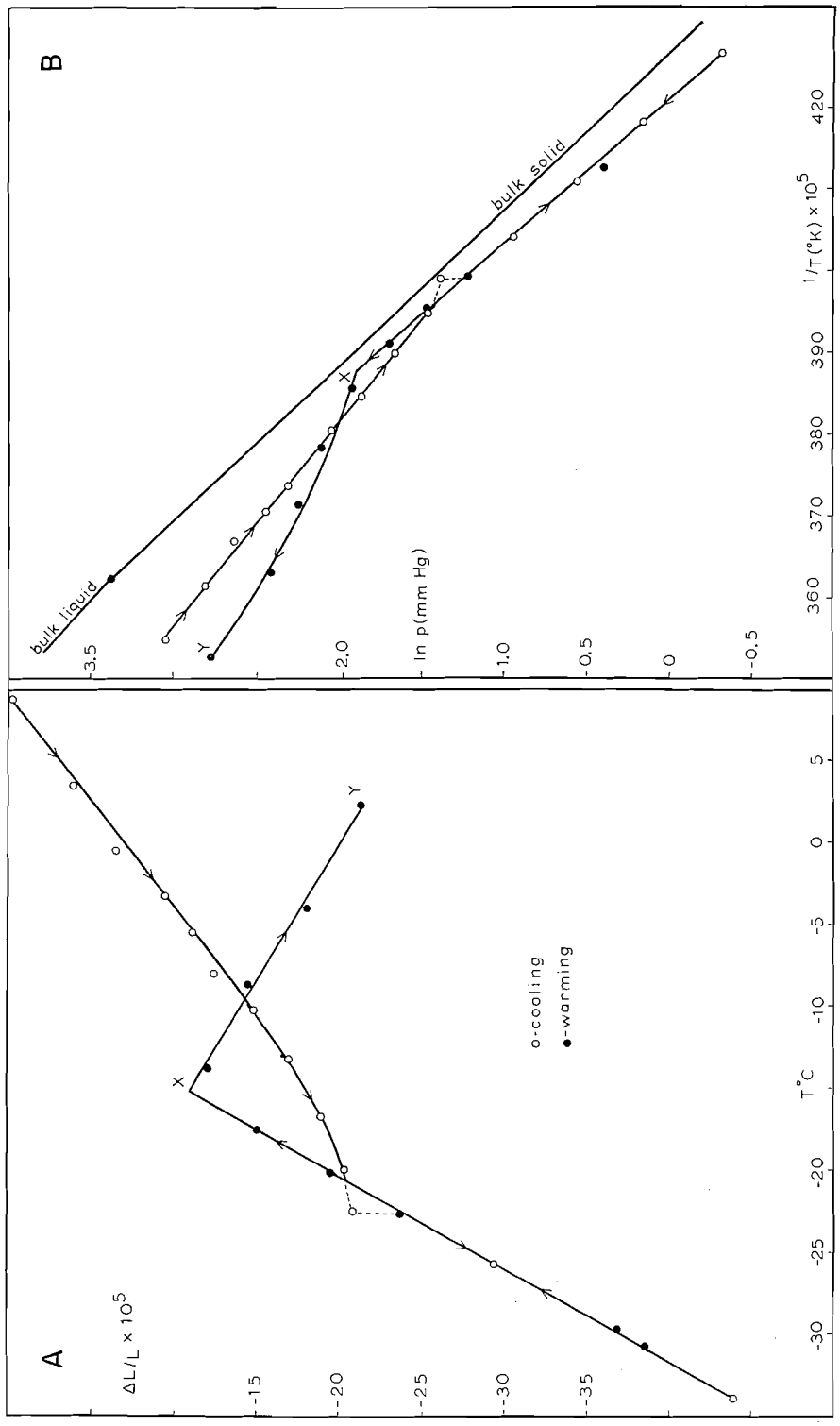
The freezing and melting point depressions of benzene–Vycor systems

Benzene content, g/g	Depression of freezing point from pressure data	Depression of freezing point from length data
0.233	1.6° (f.p.)	1.6°
0.210	4.1 (f.p.)	4.1
0.179	11.5 (f.p.)	11.1
0.170	25.6 (f.p.)	27.3 (f.p.)
	19.4 (m.p.)	19.1 (m.p.)
0.162	28.1 (f.p.)	28.2 (f.p.)
	20.4 (m.p.)	20.8 (m.p.)

There are many points of difference between the behavior of benzene, as exhibited in these graphs, and of water, the behavior of which was depicted earlier. First, no sudden expansion occurs at the start of the transition, which fact therefore supports the view that the increase of the molar volume of the adsorbate rather than a meniscus effect is of primary importance in causing expansion. Second, the gradual transition of benzene is revealed by the persistence of the changed rate of contraction, rather than by the range of temperature over which an expansion occurs. Third, in the case of benzene, the length as a function of temperature does not show hysteresis below the temperature at which transition begins on the initial cooling. Fourth, the equilibrium pressure of benzene for a heating run follows the same curve as for a cooling run below the temperature at which the transition begins, and the rate of variation persists for some degrees above this temperature on heating. This persistence suggests that melting is incomplete,

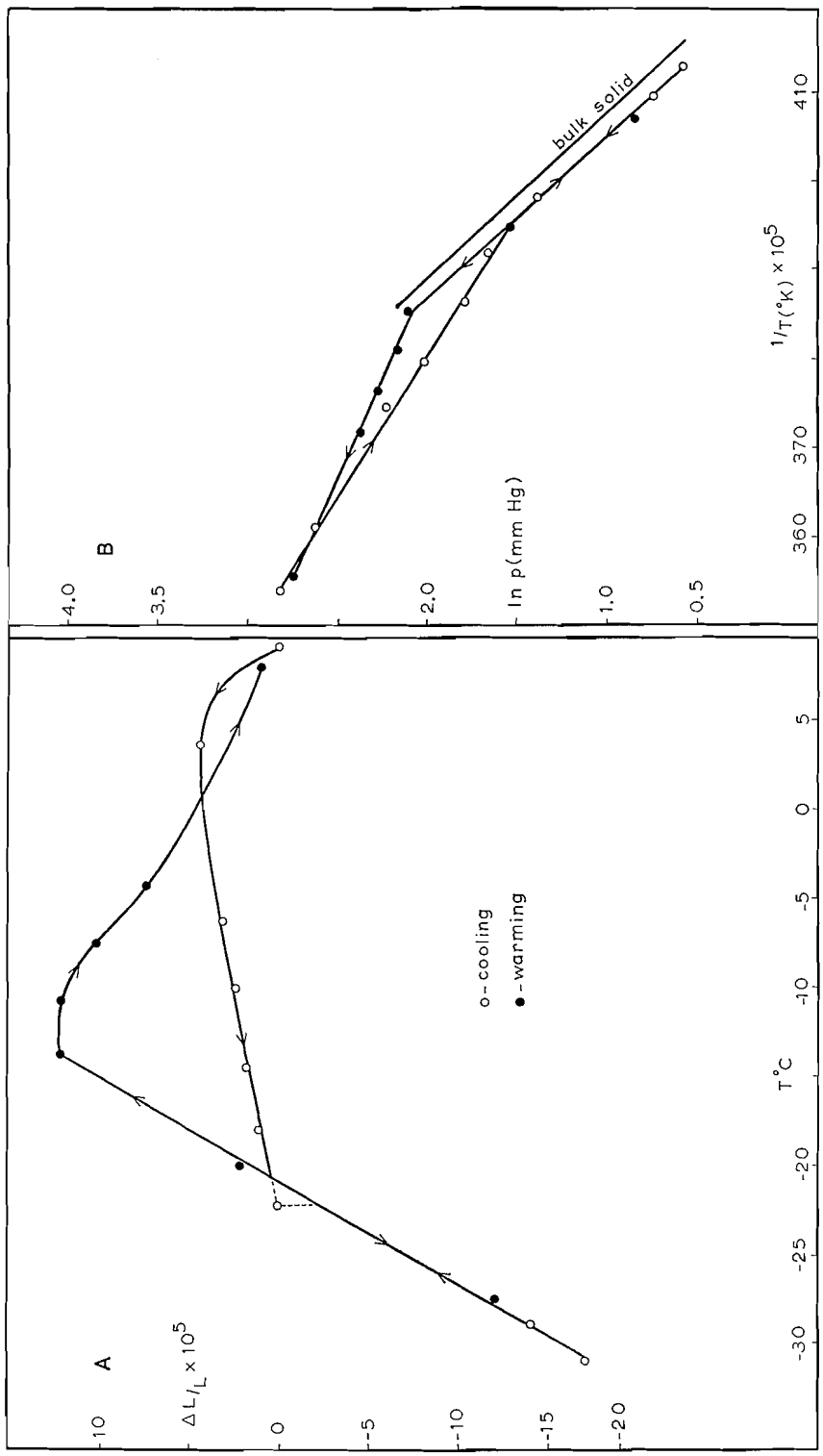
Can. J. Chem. Downloaded from www.nrcresearchpress.com by 186.148.149.217 on 09/04/12
For personal use only.

Can. J. Chem. Downloaded from www.nrcresearchpress.com by 186.148.149.217 on 09/04/12
For personal use only.



FIGS. 3A, 3B. Length variation and equilibrium pressure as functions of temperature for the system benzene – Vycor glass. Amount of benzene adsorbed 0.162 g/g.

Can. J. Chem. Downloaded from www.nrcresearchpress.com by 186.148.149.217 on 09/04/12
For personal use only.



FIGS. 4A, 4B. Length variation and equilibrium pressure as functions of temperature for the benzene – Vycor glass system. Amount of benzene adsorbed 0.170 g/g.

and that heating and cooling would show a common reversible curve in this region. The separation of the curves at the point at which melting is complete is believed to be due to transfer of adsorbate in the gas phase, and consequent change in the curvature of the menisci. Fifth, the equilibrium pressure of the solid adsorbate is lower than for bulk benzene at the same temperature, whereas the (less reliable) data for water suggest a reversal of this at the lower temperatures.

There are, however, two important points of similarity in the behavior of water and benzene: (*a*) both adsorbates show a gradual transition to the solid form; (*b*) both adsorbates complete their melting processes at higher temperatures than those for the inception of freezing.

Finally, it should be stated that throughout the upper temperature range for many conditions using benzene, complicating effects existed due to the adsorption from the gas phase. For example, in cooling a system with 0.170 g/g of adsorbed benzene (see Fig. 4) an initial expansion occurred and this was followed by the normal type of contraction. Such complications emphasize the desirability of restricting the volume of the gaseous phase and maintaining isosteric conditions when possible.

3. Isotherms for Benzene

In Fig. 5 are shown isotherms of benzene and the concomitant length changes. Only one isotherm has been investigated fully, that at +9° C. It is similar in shape to those for water, ethyl chloride, ammonia, and butane on the same adsorbent (2, 3). The closure of the hysteresis loop occurs, however, at an appreciably lower pressure. The length variations are noteworthy for two observations: (*a*) a contraction below the initial length occurs; (*b*) the first approximately horizontal region of the length change versus weight adsorbed plot ceases to be horizontal as temperature is lowered. Observation (*a*) has not previously been made for Vycor systems although Haines and McIntosh (9) observed this for the charcoal–water system. Presumably it occurs because the contraction due to the concave menisci exceeds the spreading force in the adsorbed layers due to interaction with the solid.

In these graphs it is clearly shown that the relative pressure approaches a value of 1.0 asymptotically when p_s^0 is employed as the reference value for those temperatures below the normal freezing point of benzene. Because of the experimental arrangement, the pressure cannot exceed p_s^0. Nevertheless, it is suggestive of freezing of the benzene that the approach to this value is asymptotic. If, for example, the adsorbed phase consisted of a physical arrangement resembling bulk liquid, the equilibrium pressure should approach p_1^0 at the temperature of the isotherm as the amount adsorbed is increased. Experimentally it cannot approach more closely than the value p_s^0. In this event the experimental curve would tend to the ordinate at the value p_s^0 at a finite angle rather than asymptotically. But since the approach is asymptotic it is deduced that solid adsorbate has formed by a condition represented as point *B*. It is to be noted that the region *BC* begins at values of relative pressure progressively farther removed from the value 1.0 as the temperature is lowered.

A second observation which may support the view that freezing has occurred at the situation designated by point *B* is the following. Point *B* for isotherms above the bulk transition temperature has been interpreted as marking the condition that all pores are filled and menisci exist of the curvature appropriate to the relative pressure. Since it is known from the dimensional variation of the adsorbent alone that pore volume does not change appreciably with temperature, and since one would normally expect the

Can. J. Chem. Downloaded from www.nrcresearchpress.com by 186.148.149.217 on 09/04/12
For personal use only.

Can. J. Chem. Downloaded from www.nrcresearchpress.com by 186.148.149.217 on 09/04/12
For personal use only.

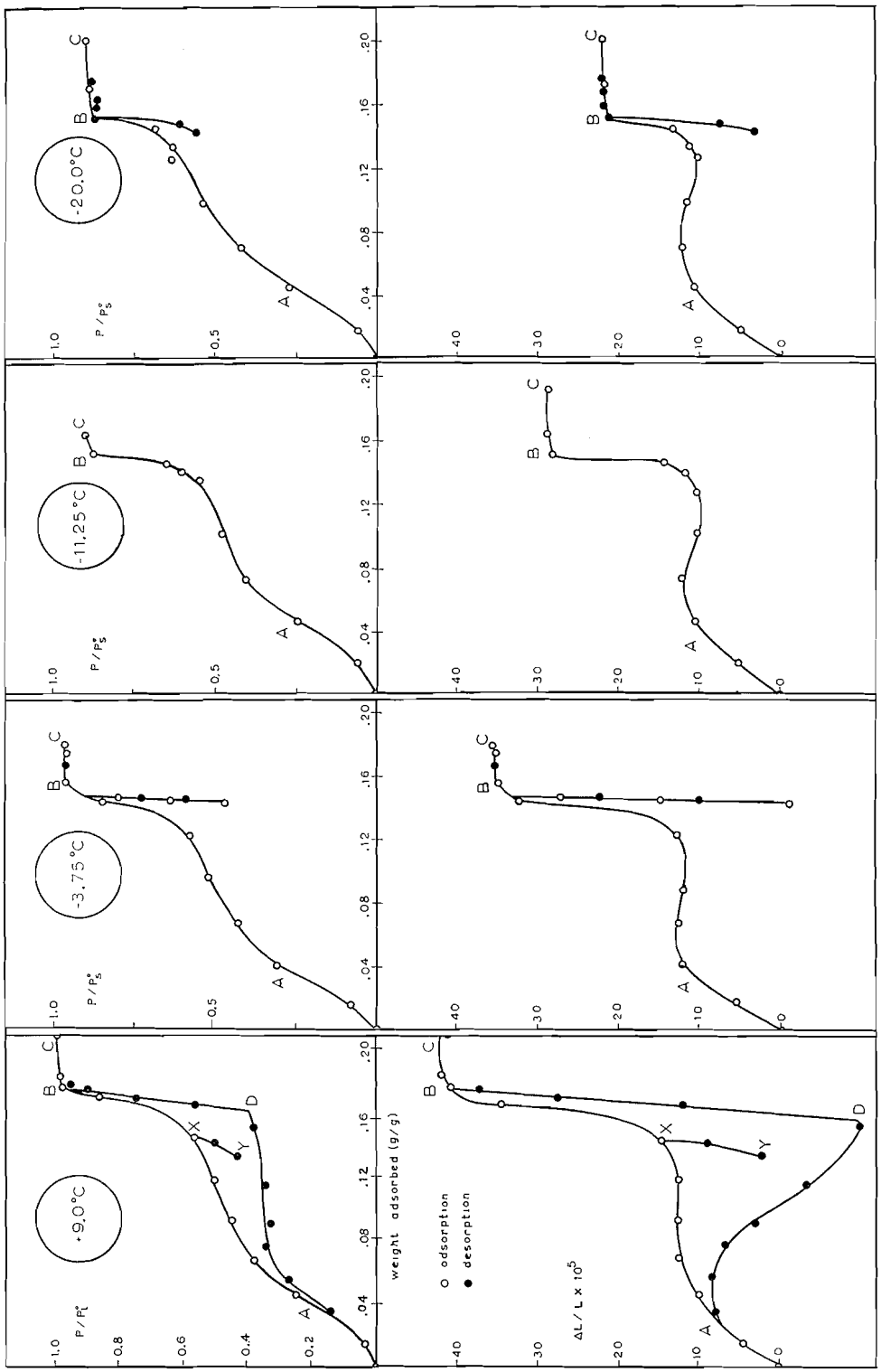


FIG. 5. Isotherms of benzene on Vycor glass at various temperatures.

density of the adsorbate to increase as temperature is reduced, one would expect the amount adsorbed at the condition of filled pores to increase with decreasing temperature. The experimental fact is the opposite of this. It is concluded, therefore, that point B has a different significance below the bulk transition temperature, namely, that solid has formed, and that this is the reason that hysteresis is not observed for adsorptions greater than point B. For temperatures above the transition temperature the filling of pores would end the region of hysteresis, but as argued above, the situation does not conform with expectation on this basis alone, and another cause for the reversible isotherm above point B is required. The best evidence that hysteresis is absent above point B is obtained from cooling and heating curves, such as those represented in Fig. 3A. Once solid phase has disappeared from the system, further increase of temperature brings about more desorption, and presumably because all menisci are now liquid, irreversible phenomena are observed (see region XY of Fig. 3A).

For the present it is sufficient to state that the behavior of the benzene–Vycor system at constant temperature is consistent with its behavior when temperature is changed. Further, it is noteworthy that even some 25 degrees below the normal triple point, hysteresis still persists in the isotherms. If the suggestion of the cause of hysteresis, namely the existence of liquid-like menisci and no solid present, is valid, then such conditions may persist to relatively low temperatures.

DISCUSSION

1. *Capillary Condensation Theory Applied to the Prediction of a Transition Temperature*

Most theoretical discussions are based upon the concept of condensed liquid in capillaries, with the liquid existing under concave menisci of the appropriate radius of curvature, and thus under negative hydrostatic pressure. On this basis the free energy per mole of the liquid adsorbate may be predicted as a function of temperature, and always lies below that for bulk liquid. If concave menisci exist for the solid adsorbate, a similar evaluation is possible provided that the surface free energy of the solid vapor interface is known. Stated first in terms of relative pressures of the solid and liquid adsorbates, the relation becomes

$$RT' \ln \frac{p_l^0 p_s}{p_s^0 p_l} = \frac{(T'-T_t)\overline{\Delta H}_{l,s}}{T_t} - T' \int_{T_t}^{T'} \frac{\Delta C}{T}\, dT + \int_{T_t}^{T'} \Delta C\, dT$$

where T' is the temperature of the transition; p_l^0, p_s^0 refer to the vapor pressures over bulk phases; p_s and p_l over the adsorbate; T_t the normal freezing point of bulk; $\overline{\Delta H}_{l,s}$ the molar heat of fusion for the bulk phases; and ΔC is the difference of specific heats of the solid and liquid bulk materials. The two integrals are normally ignored, and the relative pressures of the left-hand side calculated by employment of the Kelvin equation in the form $RT \ln p^0/p = 2\sigma \bar{V}/r$ for the appropriate interface, so that one obtains $\Delta T = 2T_t(\sigma_{lv}\bar{V}_l - \sigma_{sv}\bar{V}_s)/r\Delta H_{ls}$, where $\Delta T = T_t - T'$. Some authors, e.g. Puri, Myer, and Singh (4), assume that $p_s/p_s^0 = 1.0$ although from their published graph this situation is not exhibited, in agreement with our data for benzene shown earlier. Had Puri, Myer, and Singh actually employed the equilibrium pressure data for the solid adsorbate, agreement between theory and experiment would not have been good. However, they used the Kelvin relation and data obtained well above the transition range and extrapolated to obtain the value of p_l/p_l^0 at the initial temperature of the transition, a procedure which results in too high values and reduces the predicted value of ΔT and brings it into closer agreement with experiment (10).

Can. J. Chem. Downloaded from www.nrcresearchpress.com by 186.148.149.217 on 09/04/12
For personal use only.

Can. J. Chem. Downloaded from www.nrcresearchpress.com by 186.148.149.217 on 09/04/12
For personal use only.

If freezing is, indeed, a process occurring over a range of temperature, this is a fact which is in disagreement with the use of the Kelvin concepts. At a given relative pressure, all menisci must have the same value of the radius of curvature, and a sharp transition should be observed. Appeal to equilibrium pressure data might appear to support a sharp transition, as a sudden change in the slope of pressure–temperature curves is found. In itself, however, this means nothing, since the situation is akin to the freezing of a macroscopic two-component system. Deposition of solid will begin at some temperature dependent upon the composition, and more solid will be deposited as the temperature is lowered. Over this range of temperature the equilibrium partial pressure of the component which has formed the solid phase must be identical with that of the solid. Similarly, if a solid adsorbate phase forms, since equality of chemical potential must exist for the two phases, the equilibrium pressure as a function of temperature must be that for the solid phase.

This realization is useful in connection with other observations. It was noted earlier that no hysteresis is observed for vapor pressure data until melting is complete. Evidence was also presented which showed that for temperatures, and over ranges of pressure, where there appears to be solid benzene, no hysteresis loop is discerned in the isotherms. If one presumes, therefore, that adsorbed solid benzene does not form menisci, and if meniscus effects are the basic cause of hysteresis, none will be observed when solid benzene is present. This argument should be of general application to all adsorbates.

One concludes, therefore, that appeal to capillary condensation theory will not suffice to explain observation. The points of disagreement are (*a*) the freezing of both water and benzene occurs over a range of temperature; (*b*) the inception of freezing for benzene is a function of amount adsorbed, but that for water is not; (*c*) hysteresis between cooling and heating curves is observed for both adsorbates.

2. Prediction of the Freezing Point by the Theory of Liquid-like Layers due to Frenkel (11), Halsey (12), and Hill (13)

As pointed out by Hill (14), one of the major criticisms which may be levelled at the B.E.T. multilayer theory is the fact that ϕ, the spreading force of the film, does not remain finite for the infinite adsorption permitted at $p/p^0 = 1.0$. The thick layer theory, giving an isotherm of the form $\ln p/p^0 = -a/\Gamma^3$ does not suffer from this disadvantage, and moreover agrees quite well with experimental isotherms on certain non-porous adsorbents in the region of high relative pressure. Due to the model upon which the theory is based, it is possible to calculate explicitly values of $\ln p/p^0$ for both liquid- and solid-adsorbed layers. In the case of the systems studied here, the form of the isotherm does not agree with experiment, and it is not very meaningful to attempt its use. This fact also forbids the evaluation of "a" from the experimental isotherm and therefore the empirical determination of the parameters e_1, r_1, e, and r^* in the equation

$$a = \frac{\pi\rho^3}{6kT}(\rho_1 e_1 r_1^6 - \rho e r^{*6}).$$

Here ρ and ρ_1 are the densities of the adsorbate and adsorbent in molecules per cubic centimeter, e and e_1 the depths of the potential wells for the pure liquid and the liquid–adsorbent interaction, and r_1 and r^* the distances of closest approach of the liquid–adsorbent and bulk liquid molecules, respectively. Estimates of these parameters were therefore made. From the value of the heat of adsorption of water at zero coverage obtained from the data of Amberg and McIntosh (3), a value of 20,000 cal mole^{-1} was

obtained. Assuming a value of r_1 of 1 Å, it was possible to obtain $\rho_1 e_1 r_1^6$ from the equation

$$\frac{q_0 - RT}{N} = -\frac{\pi \rho_1 e_1 r_1^3}{6}$$

which gives the interaction energy between the liquid layer and the underlying adsorbent. Similarly $\rho e r^6$ was evaluated from the equation

$$\frac{\lambda - RT}{N} = -\frac{2}{3}\frac{\pi \rho e r^{*3}}{}.$$

The bulk density was assigned to the adsorbed water, and a cubic packing arrangement in evaluating r^*. Similar calculations were made for ice using parameters for bulk ice where that is appropriate and assuming that $\rho_1 e_1 r_1^6$ remains the same for adsorbate in the temperature range where bulk solid would be stable. By evaluating $\mu_{ads} - \mu_{bulk\ liq}$ at +20 and +10° C, and $\mu_{ads} - \mu_{bulk\ sol}$ for −10 and −20° C, a freezing point lowering of about 1.5° was predicted for an adsorbate content of 0.20 g/g of water. This procedure cannot be accurate since the expression was found to be very sensitive to values of r_1, but would be more useful if "a" could be obtained from experimental data. Our object here has been to show that the theory does not predict a depression of transition temperature of the magnitude found, and to suggest that transition temperatures, if known, may form another basis for testing the validity of an explicit adsorption theory.

3. Theory of Jackson and Chalmers

In dealing with the concave meniscus theory, interfaces between liquid and vapor or solid and vapor were considered to form. Jackson and Chalmers (15) have considered the conditions in a capillary pore in which liquid has a zero wetting angle with the wall and a stable interface of solid and liquid is presumed to form in the capillary pore. As the meniscus is concave to the liquid and convex to the solid, the liquid is under a negative pressure and the solid under a positive pressure. At some temperature these two phases may be in equilibrium, and this must be at a temperature below the normal transition temperature. The temperature of coexistence will vary with the radius of the tube and become less for smaller tubes, thus explaining a gradual transition. The quantitative relation for fluids of zero wetting angle (e.g. benzene and glass, Richards and Carver (16)) is approximately $\Delta T = -\sigma_{l,s} T_t / \overline{\Delta H}_{l,s} r$. It should be noted particularly that at the transition temperature, the molar free energy of liquid adsorbate is below that of the bulk liquid but that the molar free energy of solid is above that of bulk solid. Such would appear to be the case according to the supposed equilibrium pressure values for water in Fig. 1B, but is certainly not the case for benzene. That such a situation might obtain in impermeable soils or cements may be possible, but that it could obtain for equilibrium conditions in the porous Vycor glass system, where distillation into and out of the adsorbent is relatively easy, does not appear possible. Bulk solid would form on the walls by condensation from the vapor phase and transfer from adsorbent to the walls of the cell would proceed. The theory therefore does not seem applicable to the systems investigated and the apparent confirmation from the data for water could merely reflect the inaccuracy of the data.

Actually, this theory and the theory due to Powers (17) need not be dismissed, provided that equilibrium conditions do not exist in the systems under study. Before amplifying this statement the theory due to Powers will be briefly outlined.

Can. J. Chem. Downloaded from www.nrcresearchpress.com by 186.148.149.217 on 09/04/12
For personal use only.

4. Theory of Freezing due to Powers

In a porous material, such as cement, Powers assumes the existence of (*a*) large voids, (*b*) cavity spaces of narrower dimensions, and (*c*) a matrix of cement which is porous and thus permeable to water, but which is of very fine porosity and through which adsorbed water would diffuse as molecules. On lowering temperature water can freeze as bulk water in the large voids if these are present. At lower temperatures (because of the influence of the force field from the solid) nucleation may next occur in cavities. When nucleation occurs in these regions, there is expansion of adsorbate in a confined space and large hydrostatic stresses are established. Water will then begin to diffuse from regions where its chemical potential is greater than that of bulk solid at that temperature to the regions where bulk solid may exist. After appreciable freezing has occurred and some period of time has elapsed, the location of the adsorbed water throughout the mass will have altered. If, during this period of time, a measurement of pressure of the water vapor could be made, the pressure would presumably be greater than that of bulk ice at the same temperature. It should be noted that this theory, in common with that given by Jackson and Chalmers (15), predicts this situation which is anomalous if equilibrium conditions are assumed. It should also be recalled that this situation is observed for water if the pressure data are accurate. As pressure data within this same temperature range were obtained for lower water contents which were below the value at which freezing was observed, and these data did not reveal values greater than those for bulk solid, there is some reason to suppose that these data are meaningful. In conjunction with this observation, the form of the warming curve for water should be recalled, which reveals that the melting range persists to higher temperatures than the inception of freezing. On Powers' theory this can be explained by some of the water having migrated to regions where stress was less and freezing point higher. In fact, as already pointed out, distillation could occur to the wall of the cell where bulk solid would be formed and the water content of the rod thus be diminished. In this event the rod should be shorter (see Fig. 1A) than when cooling was begun, unless sufficient time is allowed for the system to return to its original state. It is possible that the system might not be restored in any event, since the presence of a hysteresis loop in the isotherm implies that the previous history of the starting system may have to be repeated.

In the case of benzene, as contraction rather than expansion is to be expected when adsorbed solid forms, large hydrostatic stresses are presumably not established. Thus the condition for equilibrium pressure greater than that for the bulk solid would not obtain. It could arise from the mechanism visualized in the Jackson and Chalmers' theory, but according to experimental observation, it does not occur. The data for water thus support Powers' theory while the data for benzene contradict the Jackson and Chalmers theory.

Two important facts remain unexplained. Melting of benzene is not complete until temperatures are reached which are higher than those at which freezing began. No explanation of this superheating has become evident, nor would the rate of cooling employed in the experiments suggest any marked departure from equilibrium conditions.

The second observation is that the initial freezing temperature for water is independent of the water content of the adsorbent over the range investigated. Until these observations are accounted for, any understanding of the transition phenomena must be considered as very incomplete.

Can. J. Chem. Downloaded from www.nrcresearchpress.com by 186.148.149.217 on 09/04/12
For personal use only.

APPENDIX

As shown in Fig. 6, the apparent temperature coefficient for the water–Vycor system diminishes in a regular way with increasing water content up to water contents at

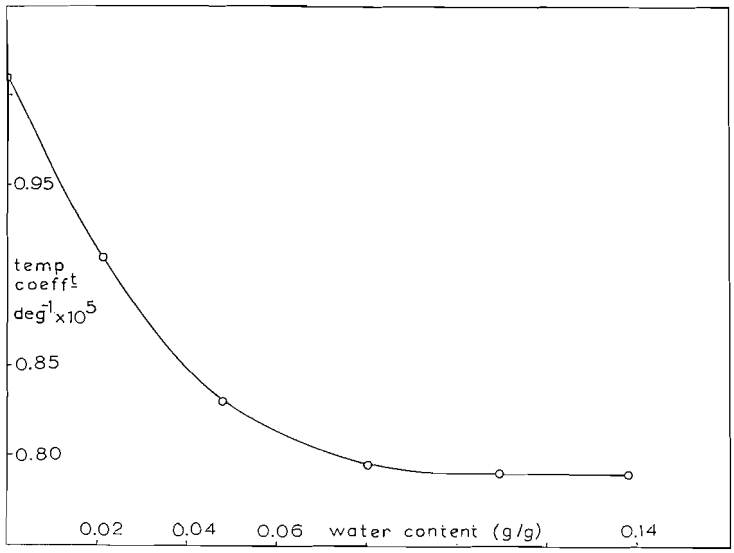


FIG. 6. The temperature coefficient of Vycor glass as a function of initial water content.

which complications due to freezing or adsorption from the vapor phase prevent further observation. The same fact has been established in the case of benzene. A straightforward analysis of the situation has been given by Hermans (18) and is set out below.

As the reasonable assumption of isotropic structure of the rod may be made, a length change may be interpreted as directly proportional to a volume change. The experimental fact is, therefore, that

$$\frac{\partial}{\partial n_T}\left(\frac{\partial V}{\partial T}\right)_{ex} < 0.$$

The subscript "ex" signifies experimental conditions. As pressure varies little in the experiments, the result is for constant hydrostatic pressure, and this restriction is to be understood throughout. Since, however, condensation from the gas phase may be important, it should be emphasized that n, the quantity of adsorbate is not constant.

The treatment assumes, in addition to the assumption that the properties are single-valued in n and T, that the sign of the volume changes, resulting from variations of adsorbate content and temperature, is revealed by the experimental measurements. The true magnitudes are doubtful because of the fact that the actual volume of the solid–adsorbate system is never measured for the porous system.

We have

$$\left(\frac{\partial V}{\partial T}\right)_{ex} = \left(\frac{\partial V}{\partial T}\right)_{n} + \left(\frac{\partial V}{\partial n}\right)_{T}\left(\frac{\partial n}{\partial T}\right)_{ex}$$

$$0 > \frac{\partial}{\partial n_T}\left(\frac{\partial V}{\partial T}\right)_{ex} = \left(\frac{\partial \bar{V}}{\partial T}\right)_{n} + \left(\frac{\partial \bar{V}}{\partial n}\right)_{T}\left(\frac{\partial n}{\partial T}\right)_{ex} + \bar{V}\frac{\partial}{\partial n_T}\left(\frac{\partial n}{\partial T}\right)_{ex}$$

Can. J. Chem. Downloaded from www.nrcresearchpress.com by 186.148.149.217 on 09/04/12
For personal use only.

where $\bar{V}$ is the partial molal volume of adsorbate. Of the terms on the right-hand side of the equation $(\partial \bar{V}/\partial T)_n$ is positive, and $(\partial \bar{V}/\partial n)_T$ is negative because the length plotted against n is concave towards the n axis in the appropriate range of n. Obviously $(\partial n/\partial T)_{ex}$ is negative. It follows that $\bar{V}(\partial/\partial n_T)(\partial n/\partial T)_{ex}$ must be negative. This conclusion has been confirmed by means of the data from three runs, and at 0° C $(\partial/\partial n_T)(\partial n/\partial T)_{ex}$ has a value of -6×10^{-4} deg^{-1} for water. Qualitatively the finding merely states that the effect of temperature on the population of a surface is greater if the surface concentration is high than if it is low. Thus the experimental observation is simply explained.

ACKNOWLEDGMENT

Grateful acknowledgment is hereby made to the National Research Council of Canada for financial support of this investigation.

REFERENCES

1. C. HODGSON and R. MCINTOSH. Can. J. Chem. **37**, 1278 (1959).
2. H. W. QUINN and R. MCINTOSH. Proc. Intern. Conf. of Surface Activity. 2nd Conf. Butterworth Scientific Publications, London. 1957.
3. C. H. AMBERG and R. MCINTOSH. Can. J. Chem. **30**, 1012 (1952).
4. B. R. PURI, Y. P. MYER, and D. D. SINGH. Trans. Faraday Soc. **53**, 530 (1957).
5. I. D. JONES and R. A. GORTNER. J. Phys. Chem. **36**, 387 (1932).
6. W. A. PATRICK and W. A. KEMPER. J. Phys. Chem. **42**, 369 (1938).
7. T. G. PEARSON. Z. physik. Chem. (Leipzig), A, **156**, 86 (1931).
8. C. H. AMBERG. Ph.D. thesis, University of Toronto, Toronto, Ont. 1952.
9. R. HAINES and R. MCINTOSH. J. Chem. Phys. **15**, 28 (1947).
10. M. H. PANCKHURST. Private communication.
11. Y. I. FRENKEL. Kinetic theory of liquids. Oxford University Press, London. 1946. p. 407.
12. G. D. HALSEY. J. Chem. Phys. **16**, 931 (1948).
13. T. L. HILL. J. Chem. Phys. **17**, 590 (1949).
14. T. L. HILL. Advances in catalysis. Vol. IV. Academic Press Inc., New York. 1952. p. 230.
15. K. A. JACKSON and B. CHALMERS. J. Appl. Phys. **29**, 1178 (1958).
16. T. W. RICHARDS and E. K. CARVER. J. Am. Chem. Soc. **43**, 827 (1921).
17. T. C. POWERS. J. Am. Concrete Inst. **16**, 245 (1944).
18. J. J. HERMANS. State University of Forestry, Syracuse, N.Y. Private communication.

Can. J. Chem. Downloaded from www.nrcresearchpress.com by 186.148.149.217 on 09/04/12
For personal use only.

Can. J. Chem. Downloaded from www.nrcresearchpress.com by 186.148.149.217 on 09/04/12
For personal use only.

STEROIDS

PART I. THE SYNTHESIS OF SOME HETEROCYCLIC STEROID DERIVATIVES[1]

BARBARA G. KETCHESON[2] AND ALFRED TAURINS

ABSTRACT

Cyanoacetamide reacted with 3β-hydroxy-16-hydroxymethylene-5-androsten-17-one to form 1-cyano-2-hydroxy-2(16′-3′β-hydroxy-17′-oxo-5′-androstenyl) propionamide or 3-cyano-4,5-dehydro-6-hydroxy-5,6(16′,17′-3′β-hydroxy-5′-androstenyl)-2-piperidone depending on whether a catalytic or a molecular amount of piperidine was used as the basic condensing agent. Carboxamidoacetamidine, and acetamidine hydrochlorides, were condensed with the sodium salt of 3β-hydroxy-16-hydroxymethylene-5-androsten-17-one, and 3β-chloro-16-chloromethylene-5-androsten-17-one yielding 2-amino-3-carboxamido-5,6(16′,17′-3′β-hydroxy-5′-androstenyl) pyridine and 2-methyl-5,6(16′,17′-3′β-chloro-5′-androstenyl) pyrimidine respectively.

DISCUSSION

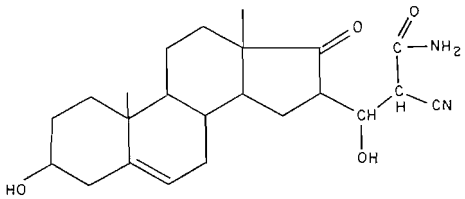
The elucidation of the structure of a number of steroidal alkaloids (1), combined with their well-established physiological activity, has stimulated efforts to synthesize a variety of nitrogen-containing steroids. In many instances, the synthetic products have not displayed the anticipated physiological properties, but in several cases, the nitrogen derivatives of steroids have exhibited pharmacological properties of the same type and order of magnitude as some of the steroidal alkaloids (2, 3, 4).

With this in mind, the present investigation, concerned with the attachment of six-membered nitrogen-containing rings to the 16,17-positions of the steroid nucleus, was undertaken. As a first approach to the problem, the piperidine-catalyzed Knoevenagel condensation of 3β-hydroxy-16-hydroxymethylene-5-androsten-17-one (I) (5) with cyanoacetamide was considered. In the cyclopentane (6), cyclohexane (7), and tetrahydrophenanthrene (8) series, the reaction of hydroxymethylene ketones with cyanoacetamide had given rise to pyridine, quinoline, and azachrysene derivatives respectively.

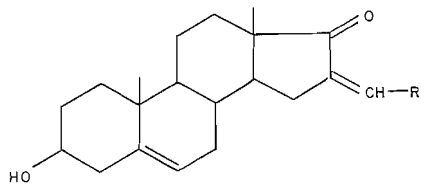
In the preliminary attempt to accomplish the condensation, cyanoacetamide and I were allowed to stand in ethanolic solution in the presence of a catalytic amount of piperidine for 8 days at 40°. Only starting materials were obtained under these conditions. However, when an identical reaction mixture was heated at the reflux temperature for 2 days, two products were obtained. The major product proved to be the aldol addition product 1-cyano-2-hydroxy-2(16′-3′β-hydroxy-17′-oxo-5′-androstenyl) propionamide (II). On heating II with a 10% potassium hydroxide solution in methanol, ammonia was given off. The infrared spectrum of the alkaline hydrolysis product confirmed the presence of a carboxylic group in the molecule. The isolation of II from the reaction was surprising, since generally in the Knoevenagel condensation of cyanoacetamide with hydroxymethylene ketones, the initially formed aldol addition products readily lose a molecule of water, and ring closure to dehydropiperidone structure occurs (9, 10, 11). However, instances have been reported (12, 13) in which the aldol addition products analogous to II have been isolated.

[1]*Manuscript received February 8, 1960.*
Contribution from the Department of Chemistry, McGill University, Montreal, Que., with financial assistance from the National Research Council, Ottawa, Canada. Presented in part before the Division of Organic Chemistry, Chemical Institute of Canada, Toronto, Ontario, May 26, 1958. Abstracted from a portion of the thesis submitted by Barbara G. Ketcheson to the Department of Chemistry, McGill University, Montreal, Que., August 1958, in partial fulfilment of the requirements for the Ph.D. degree.
[2]*Holder of a National Research Council Studentship, 1956–57, and of Canadian Industries (1954) Limited Fellowships, 1955–56 and 1957–58.*

The second product obtained from the reaction was a condensation product of piperidine and I and, in agreement with the well-established reactivity of hydroxymethylene ketones with secondary amines, was formulated as 3β-hydroxy-16-piperidinomethylene-5-androsten-17-one (III*a*). An identical product was obtained quantitatively by refluxing an ethanolic solution of the hydroxymethylene ketone (I) and piperidine for several hours. On warming III*a* with aqueous acetic acid, 3β-acetoxy-5-androsten-17-one was obtained. The formation of the piperidinomethylene ketone (III*a*) during the reaction of cyanoacetamide and 3β-hydroxy-16-hydroxymethylene-5-androsten-17-one (I) was unexpected, and no previous instance of the formation of an analogous piperidinomethylene derivative from the corresponding hydroxymethylene compound during a Knoevenagel



(II)



(I), R = OH

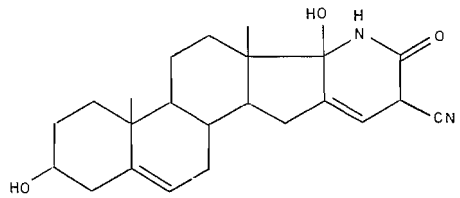
(IIIa), R = N

(IIIb), R = N O

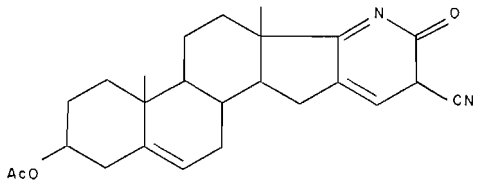
(IIIc), R = $N(C_2H_5)_2$

(IIId), R = $NHCH_3$

(IIIe), R = NH



(IV)



(V)

reaction could be found. However, Dev (14) had reported that when the Knoevenagel condensation of ethyl cyanoacetate with ethyl 2(2′-1′-oxo-cyclopentano)-*n*-butyrate was carried out using ammonium acetate or benzylamine as catalysts, condensation of the catalyst with the keto-ester occurred.

Subsequently it was found that morpholine, diethylamine, methylamine, and aniline also condensed readily with the hydroxymethylene ketone (I) to form the corresponding aminomethylene ketones (III$_{b-e}$) in high yields.

Can. J. Chem. Downloaded from www.nrcresearchpress.com by 186.148.149.217 on 09/04/12
For personal use only.

In a later attempt to effect the condensation of cyanoacetamide with I, an ethanolic solution of the reactants was refluxed in the presence of an equimolecular amount of piperidine for 3 days. Two products were isolated. They were identified as 3β-hydroxy-16-piperidinomethylene-5-androsten-17-one (III*a*), and 3-cyano-4,5-dehydro-6-hydroxy-5,6(16′,17′-3′β-hydroxy-5′-androstenyl)-2-piperidone (IV). As expected, treatment of IV with excess acetic anhydride in pyridine at room temperature led to the elimination of a molecule of water and formation of a monoacetate, 3-cyano-5,6(16′,17′-3′β-acetoxy-5′-androstenyl)-2-pyridone (V).

It appeared, from a consideration of the experimental results obtained, that this Knoevenagel reaction proceeded by different paths depending on whether a catalytic or molecular proportion of piperidine was used as the condensing agent. The formation of the piperidinomethylene ketone (III*a*) in the reactions indicated that two simultaneously proceeding reactions were occurring, or that III*a* was being formed as an intermediate product. To investigate the latter possibility, an ethanolic solution of III*a* and cyanoacetamide was refluxed for 3 days. A 20% yield of the dehydropiperidone (IV) was obtained. This result provided evidence that when the condensation of the hydroxymethylene ketone (I) and cyanoacetamide was carried out in the presence of a molecular proportion of piperidine, reaction proceeded via the formation of the stable intermediate 3β-hydroxy-16-piperidinomethylene-5-androsten-17-one (III*a*). When the reaction was performed using a catalytic amount of piperidine, apparently two separate processes occurred with the formation of the aldol addition product (II) and the piperidinomethylene compound (III*a*).

To account for the reaction occurring in the presence of a molecular amount of piperidine a mechanism is proposed in Fig. 1.

Initially there is a nucleophilic attack by the piperidine at the hydroxymethylene carbon atom. The addition product thus formed loses a molecule of water and the piperidinomethylene compound is produced. Then the carbanion of cyanoacetamide attacks at the piperidinomethylene atom forming an addition product from which the piperidine moiety is expelled. Ring closure to the dehydropiperidone structure is the final step.

Other investigators had found that the Michael reaction of cyanoacetamide and hydroxymethylene ketones led to the production of condensation products identical with those obtained by the Knoevenagel procedure (7, 9). However, when attempts were made to condense cyanoacetamide with the hydroxymethylene ketone (I) using sodium ethylate as the basic condensing agent, the product isolated was 3β-hydroxy-5-androsten-17-one (VI). On one occasion, a very small quantity of a substance whose infrared spectrum was identical with that of the aldol addition product (II) was obtained. The formation of VI in this reaction was believed to occur by a base-catalyzed reverse aldol reaction which brought about the loss of an anion from the initial aldol addition product of cyanoacetamide and I.

As another approach to accomplishing the synthesis of steroids with a nitrogen-containing ring attached to the 16,17-positions of the molecule, an effort was made to condense carboxamidoacetamidine hydrochloride (15, 16) with the sodium salt of 3β-hydroxy-16-hydroxymethylene-5-androsten-17-one (I). Dornow and Neuse (17, 18) had reported that condensation of certain hydroxymethylene ketones with carboxamidoacetamidine hydrochloride resulted in the formation of nicotinamide derivatives. In the present case, two products were obtained. One of these had a molecular formula $C_{23}H_{31}O_2N_3$, and was formulated as 2-amino-3-carboxamido-5,6(16′,17′-3′β-hydroxy-5′-androstenyl) pyridine (VII). The infrared absorption spectrum affirmed the presence of

Can. J. Chem. Downloaded from www.nrcresearchpress.com by 186.148.149.217 on 09/04/12
For personal use only.

Can. J. Chem. Downloaded from www.nrcresearchpress.com by 186.148.149.217 on 09/04/12
For personal use only.

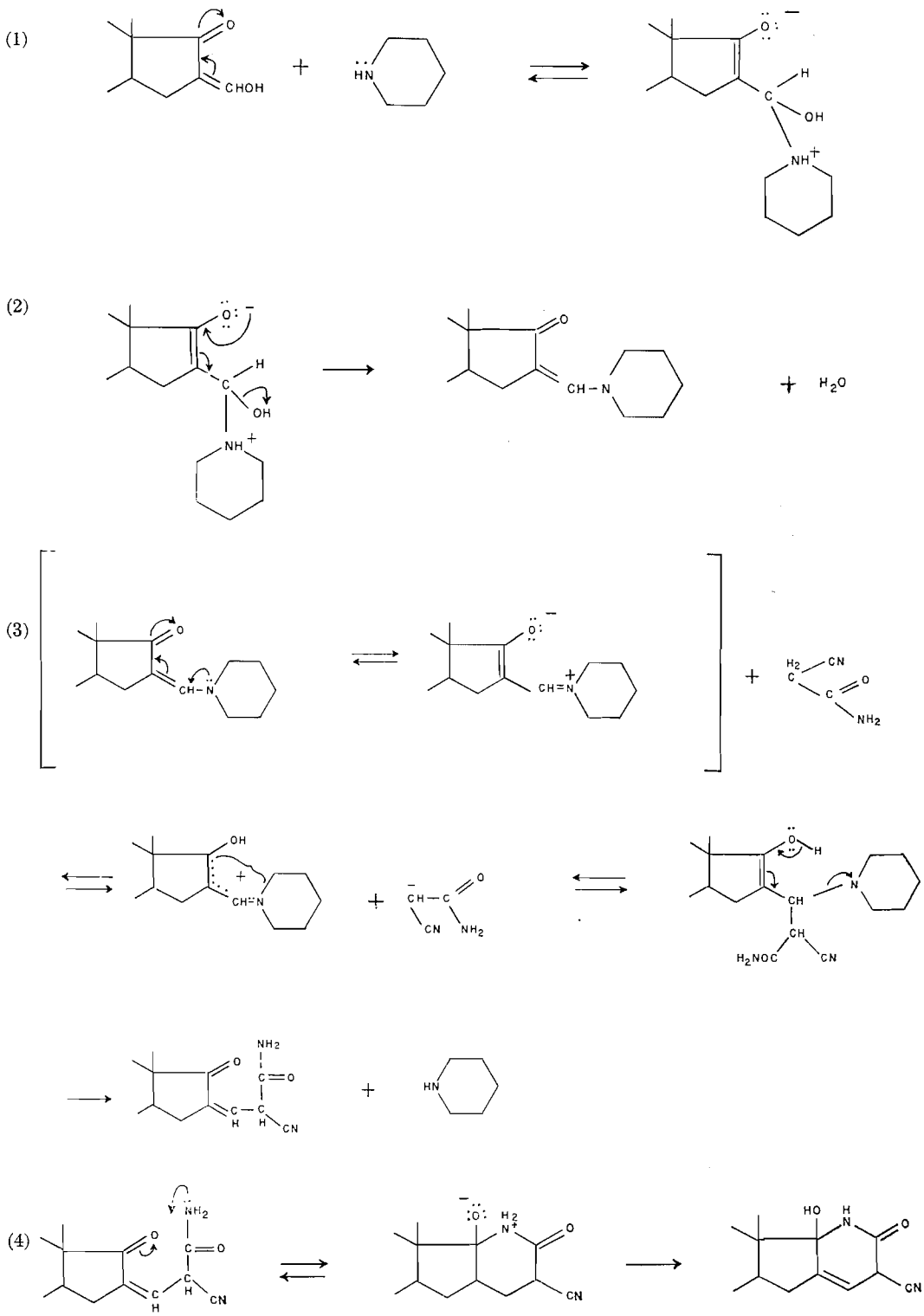
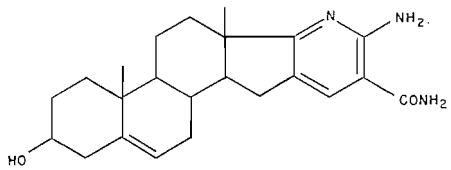


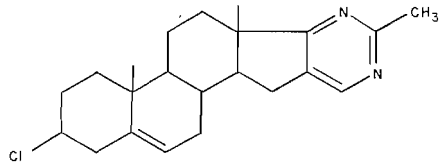
FIG. 1

a primary amide group, a primary amine function, and a pyridine ring in the molecule. The second product proved to be identical with the hydroxy ketone (VI). A reverse aldol condensation was considered responsible for the formation of VI in the reaction.

In another endeavor to achieve the synthesis of heterocyclic steroids, an attempt was made to attach a pyrimidine ring to the 16-, 17-positions of the nucleus. Since in the tetrahydrophenanthrene series, acetamidine hydrochloride had condensed with a chloromethylene ketone to form a pyrimidine derivative (8), the hydroxymethylene ketone (I) was converted to 3β-chloro-16-chloromethylene-5-androsten-17-one (VIII) by means of thionyl chloride, and allowed to react with acetamidine hydrochloride in absolute ethanol in the presence of sodium. The only product which could be isolated from the reaction mixture, melted at 145–148°, had the formula $C_{22}H_{29}ClN_2$, and in the infrared displayed absorption bands characteristic of a pyrimidine ring, and of the C—Cl stretching frequency. The product was formulated as 2-methyl-5,6(16′,17′-3′β-chloro-5′-androstenyl) pyrimidine (IX).



(VII)



(IX)

The investigation of these and related compounds is continuing, and it is hoped that a report on their physiological activity can be issued shortly.

EXPERIMENTAL

The analyses were carried out in the W. Manser Laboratory, Zurich, Switzerland. Infrared spectra were determined in potassium bromide, unless otherwise stated, on a Perkin–Elmer Model 21 double-beam instrument equipped with a sodium chloride prism.

Reaction of Cyanoacetamide with 3β-Hydroxy-16-hydroxymethylene-5-androsten-17-one (I) *in the Presence of a Catalytic Amount of Piperidine*

A mixture of I (2.0 g) and cyanoacetamide (680 mg) in ethanol (70 ml) was refluxed in the presence of piperidine (0.1 ml) for 2 days. A yellow solid material (930 mg) which was formed during the reaction was filtered and dried. Recrystallization from dimethylformamide–water provided 1-cyano-2-hydroxy-2(16′-3′β-hydroxy-17′-oxo-5′-androstenyl) propionamide (II), m.p. 221–223°. ν_{max}^{Nujol} 3420, 3330 (sh), 3220, 1718, 1700, 1665, 1648 (sh), 1623, 1040 cm^{-1}. Anal. Calc. for $C_{23}H_{32}O_4N_2.H_2O$: C, 66.01; H, 8.19; N, 6.70. Found: C, 66.28; H, 8.04; N, 6.67%.

The filtrate was concentrated and chromatographed on alumina (80–200 mesh). Elution with methanol–ether (1:9) yielded a crystalline product (320 mg) which, after recrystallization from dimethylformamide–water, afforded 3β-hydroxy-16-piperidino-

Can. J. Chem. Downloaded from www.nrcresearchpress.com by 186.148.149.217 on 09/04/12
For personal use only.

methylene-5-androsten-17-one (III*a*), m.p. 218–224°. ν_{max} 3360, 1683, 1580 cm^{-1}. Anal. Calc. for $C_{25}H_{37}O_2N$: C, 78.25; H, 9.72; N, 3.65. Found: C, 78.12; H, 9.69; N, 3.67%. Acetyl derivative, m.p. 221–222° (from methanol). ν_{max} 1735, 1685, 1585, 1250, 1030 cm^{-1}. Anal. Calc. for $C_{27}H_{39}O_3N$: C, 76.19; H, 9.24; N, 3.29. Found: C, 76.15; H, 9.28; N, 3.26%.

Condensation of Amines with 3β-Hydroxy-16-hydroxymethylene-5-androsten-17-one (I)

A solution of I (300 mg) and a slight excess of amine in ethanol was refluxed for several hours. Dilution with water precipitated the aminomethylene steroid. The solid product was isolated by filtration and purified (refer to Table I).

Reaction of Cyanoacetamide and 3β-Hydroxy-16-hydroxymethylene-5-androsten-17-one (I) *in the Presence of a Molecular Amount of Piperidine*

A mixture of I (2.0 g), cyanoacetamide (680 mg), and piperidine (0.6 ml) was refluxed in ethanol for 3 days. On cooling, crystalline material (300 mg) precipitated out of solution. Recrystallization of the material from acetic acid gave 3-cyano-4,5-dehydro-6-hydroxy-5,6(16′,17′-3′β-hydroxy-5′-androstenyl)-2-piperidone (IV), m.p. 348–352° (dec.). ν_{max} 3480, 3150, 3040 (sh), 2230, 1660, 1580 cm^{-1}. Anal. Calc. for $C_{23}H_{30}O_3N_2$: C, 72.22; H, 7.91; N, 7.32. Found: C, 72.79; H, 7.83; N, 7.26%.

The filtrate was concentrated and a solid material precipitated. The product (1.79 g), purified by recrystallization from dimethylformamide–water, was identified by its infrared absorption spectrum, and a mixed melting point determination with the authentic sample, as 3β-hydroxy-16-piperidinomethylene-5-androsten-17-one (III*a*).

3-Cyano-5,6(16′,17′-3′β-hydroxy-5′-androstenyl)-2-pyridone (V)

A solution of 3-cyano-4,5-dehydro-6-hydroxy-5,6(16′,17′-3′β-hydroxy-5′-androstenyl)-2-piperidone (IV) (100 mg) in pyridine – acetic anhydride (1:1, 10 ml) was allowed to stand overnight at room temperature. It was then poured into water (150 ml) and solid material (100 mg) settled. Recrystallization of the product from dioxane provided 3-cyano-5,6(16′,17′-3′β-hydroxy-5′-androstenyl)-2-pyridone (V), m.p. 351–353° (dec.). ν_{max} 2230, 1730, 1665, 1580, 1245 cm^{-1}. Anal. Calc. for $C_{25}H_{30}O_3N_2$: C, 73.87; H, 7.44; N, 6.90. Found: C, 73.90; H, 7.39; N, 6.79%.

3-Cyano-4,5-dehydro-6-hydroxy-5,6(16′,17′-3′β-hydroxy-5′-androstenyl)-2-piperidone (IV)

An ethanolic solution of 3β-hydroxy-16-piperidinomethylene-5-androsten-17-one (III*a*) (1.0 g) and cyanoacetamide (340 mg) was refluxed for 3 days. The crystalline material (200 mg) which formed on cooling was identified by its infrared spectrum, and by a mixed melting point determination with an authentic sample, as 3-cyano-4,5-dehydro-6-hydroxy-5,6(16′,17′-3′β-hydroxy-5′-androstenyl)-2-piperidone (IV).

Attempted Condensation of 3β-Hydroxy-16-hydroxymethylene-5-androsten-17-one (I) *with Cyanoacetamide Using Sodium Ethylate as the Condensing Agent*

A solution of sodium (75 mg) in absolute ethanol (20 ml) was prepared in a nitrogen atmosphere. A slurry of I (300 mg) and cyanoacetamide (100 mg) in absolute ethanol (10 ml) was added, and the reaction mixture was refluxed for 17 hours in a nitrogen atmosphere. The solvent was evaporated under reduced pressure and the residue was chromatographed on alumina (80–200 mesh). Elution with petroleum ether (30–60°) afforded a product (160 mg) which was identified by its infrared absorption spectrum, and a mixed melting point determination with an authentic sample as 3β-hydroxy-5-androsten-17-one (VI). In one instance, a very small amount of a solid material, m.p.

Can. J. Chem. Downloaded from www.nrcresearchpress.com by 186.148.149.217 on 09/04/12
For personal use only.

Can. J. Chem. Downloaded from www.nrcresearchpress.com by 186.148.149.217 on 09/04/12
For personal use only.

TABLE I

Reaction of amines with 3β-hydroxy-16-hydroxymethylene-5-androsten-17-one

No.	3β-Hydroxy-5-androsten-17-one	Reflux time (hours)	Method of purification	Yield %	Melting point	Empirical formula	Analyses						Infra-red ν_{max} in cm^{-1}
							Calculated (%)			Found (%)			
							C	H	N	C	H	N	
III*a*	16-Piperidino-methylene	22	Recrystn. from dimethylformamide–water	99	215–220°	$C_{25}H_{37}O_2N$	78.25	9.72	3.65	78.12	9.69	3.67	3360 1683 1580
III*b*	16-Morpholino-methylene	24	Recrystn. from acetone	91.6	239–242°	$C_{24}H_{35}O_3N$	74.77	9.15	3.63	74.85	9.14	3.68	3460 1680 1580
III*c*	16-Diethyl-aminomethylene	24	Recrystn. from acetone	90.8	167–169°	$C_{24}H_{37}O_2N$	77.58	10.03	3.77	77.49	10.13	3.76	3400 1678 1575
III*d*	16-Methylamino-methylene	48	Recrystn. from dimethylformamide–water	90.2	204–206°	$C_{21}H_{31}O_2N.H_2O$			4.03			4.10	3360 1680 1607–1525
III*e*	16-Anilinomethylene	48	Elution with benzene–petroleum ether (30–60°) (1:9) from alumina; recrystn. from methanol–water	90.5	127–129°	$C_{26}H_{33}O_2N$			3.58			3.56	3400 3320 3040 1692 1622 1602 1585 1500 1267 750 690

227–232°, was isolated from the reaction mixture. The infrared spectrum of this product coincided in all respects with that of 1-cyano-2-hydroxy-2(16′-3′β-hydroxy-17′-oxo-5′-androstenyl)propionamide (II).

Reaction of 3β-Hydroxy-16-hydroxymethylene-5-androsten-17-one, Sodium Salt, with Carboxamidoacetamidine Hydrochloride

A solution of the sodium salt of 3β-hydroxy-16-hydroxymethylene-5-androsten-17-one (1.0 g) and carboxamidoacetamidine hydrochloride (420 mg) in absolute ethanol was refluxed in a nitrogen atmosphere for 17 hours. The solvent was evaporated under reduced pressure, and the residue was chromatographed on alumina (80–200 mesh). Elution with petroleum–ether (30–60°) provided crystalline material (170 mg), m.p. 142–144°. A mixed melting point determination with an authentic sample of 3β-hydroxy-5-androsten-17-one (VI) showed no depression. Further elution with methanol–ether (1:5) yielded another crystalline product (480 mg). Recrystallization of this material from methanol–benzene gave 2-amino-3-carboxamido-5,6(16′,17′-3′β-hydroxy-5′-androstenyl)pyridine (VII), m.p. 281–284° (dec.). ν_{max} 3400, 3330, 3200, 1650, 1615, 1597, 1538 cm^{-1}. Anal. Calc. for $C_{23}H_{31}O_2N_3$: C, 72.41; H, 8.19; N, 10.98. Found: C, 72.27; H, 8.35; N, 10.88%.

3β-Chloro-16-chloromethylene-5-androsten-17-one (VIII)

Thionyl chloride (3 ml) was added to 3β-hydroxy-16-hydroxymethylene-5-androsten-17-one (I) (1.0 g). A vigorous effervescence ensued, and the reaction mixture changed to a dark red liquid. The reaction was allowed to continue for 1 hour, then the liquid was poured into ice-cold 2 *N* sodium hydroxide solution (200 ml), and allowed to stand for 2 hours. The solid material (1.05 g), m.p. 199–207°, which formed, on recrystallization from benzene–methanol afforded 3β-chloro-16-chloromethylene-5-androsten-17-one (VIII), m.p. 204–210° (dec.). ν_{max} 1725, 1630, 890–666 cm^{-1}. Anal. Calc. for $C_{20}H_{26}OCl_2$: C, 67.98; H, 7.42. Found: C, 68.21; H, 7.47%.

2-Methyl-5,6(16′,17′-3′β-chloro-5′-androstenyl)pyrimidine (IX)

To a solution of sodium (235 mg) in absolute ethanol (50 ml) was added, in a nitrogen atmosphere, a slurry of 3β-chloro-16-chloromethylene-5-androsten-17-one (VIII) (1.0 g) and acetamidine hydrochloride (245 mg) in absolute ethanol (10 ml). The reaction mixture was refluxed for 1.5 hours, then was allowed to stand overnight at room temperature in a nitrogen atmosphere. The mixture was filtered, and the filtrate concentrated *in vacuo*. The residue was chromatographed on alumina (80–200 mesh). Elution with ether gave a crystalline product (200 mg). Recrystallization of the product from dioxane–water furnished 2-methyl-5,6(16′,17′-3′β-chloro-5′-androstenyl)pyrimidine (IX), m.p. 145–148°. ν_{max} 1598, 1560, 763 cm^{-1}. Anal. Calc. for $C_{22}H_{29}ClN_2$: C, 74.05; H, 8.19; N, 7.85. Found: C, 73.87; H, 8.08; N, 7.86.

REFERENCES

1. L. F. Fieser and M. Fieser. Steroids. Reinhold. 1959. p. 847.
2. F. C. Uhle. J. Am. Chem. Soc. **73**, 883 (1951).
3. D. Gould, E. L. Shapiro, and E. B. Hershberg. J. Am. Chem. Soc. **76**, 5567 (1954).
4. D. Gould, E. L. Shapiro, L. E. Finckenor, F. Gruen, and E. L. Hershberg. J. Am. Chem. Soc. **78**, 3158 (1956).
5. L. Ruzicka, V. Prelog, and J. Battegay. Helv. Chim. Acta, **31**, 1296 (1948).
6. W. C. Thompson. J. Am. Chem. Soc. **53**, 3160 (1931).
7. H. K. Sen-Gupta. J. Chem. Soc. **107**, 1347 (1915).

Can. J. Chem. Downloaded from www.nrcresearchpress.com by 186.148.149.217 on 09/04/12
For personal use only.

8. J. W. COOK and W. H. S. THOMSON. J. Chem. Soc. 395 (1945).
9. U. BASU. J. Indian Chem. Soc. **7**, 481 (1930).
10. C. BARAT. J. Indian Chem. Soc. **8**, 801 (1931).
11. H. HENECKA. Ber. **82**, 36 (1949).
12. C. BARAT. J. Indian Chem. Soc. **7**, 321 (1930).
13. E. P. KOHLER and B. L. SOUTHER. J. Am. Chem. Soc. **44**, 2903 (1922).
14. S. DEV. J. Indian Chem. Soc. **30**, 443 (1953).
15. S. M. MCELVAIN and J. W. NELSON. J. Am. Chem. Soc. **64**, 1825 (1942).
16. S. M. MCELVAIN and B. E. TATE. J. Am. Chem. Soc. **73**, 2760 (1951).
17. A. DORNOW and E. NEUSE. Arch. Pharm. **287**, 361 (1954).
18. A. DORNOW and E. NEUSE. Ber. **84**, 296 (1951).

Can. J. Chem. Downloaded from www.nrcresearchpress.com by 186.148.149.217 on 09/04/12
For personal use only.

Can. J. Chem. Downloaded from www.nrcresearchpress.com by 186.148.149.217 on 09/04/12
For personal use only.

STEROIDS

PART II. 6-AMINO STEROIDS[1]

BARBARA G. KETCHESON[2] AND ALFRED TAURINS

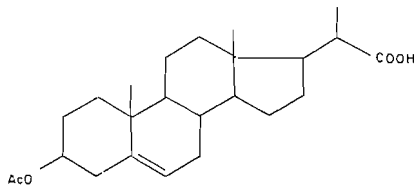
ABSTRACT

Reduction of methyl 3β-acetoxy-6-oximinodinorcholanate using sodium in *n*-propyl alcohol, and acetylation, gave 6α-acetamido-3β-acetoxydinorcholanic acid; treatment with lithium aluminum hydride in tetrahydrofuran provided 3β,22ξ-dihydroxydinorcholan-6-one. High-pressure hydrogenation of methyl 3β-acetoxy-6-nitro-5-dinorcholenate, using palladium black as catalyst in acetic acid medium, afforded methyl 6ξ-acetamido-3β-acetoxy-5α-dinorcholanate. Under identical conditions, catalytic hydrogenation of 3β-acetoxy-6-nitro-5-cholestene resulted in the formation of 6β-acetamido-3β-acetoxy-5α-cholestane and 6ξ-acetamido-3β-acetoxy-5β-cholestane.

DISCUSSION

A variety of amino steroids have been synthesized and tested for biological activity (1–10). In view of the fact that 6-aminocholestan-3β-ol (1), and several amino derivatives of 3β-acetoxy-5-dinorcholenic acid (5), had been found to possess appreciable antibacterial properties, the present investigation dealing with the preparation of 6-amino steroids of the dinorcholenic acid and cholestane series was undertaken.

When 3β-acetoxy-5-dinorcholenic acid (I) was nitrated by the procedure of Anagnostopoulos and Fieser (11), an oil was obtained which crystallized only after standing at room temperature for several weeks. However, conversion of I to its methyl ester (II) (12, 13), and treatment of the latter with fuming nitric acid resulted in the formation of



(I)

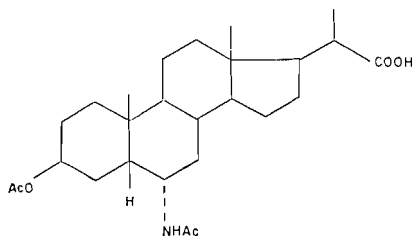
a crystalline nitration product. The product was formulated as methyl 3β-acetoxy-6-nitro-5-dinorcholenate (III), since it is well-established that nitration of a Δ^5-steroid leads to the production of the corresponding 6-nitro-Δ^5 compound (14).

When 6-nitro-Δ^5-steroids are treated with zinc dust and acetic acid, the corresponding saturated 6-oxosteroids are formed (14). However, when methyl 3β-acetoxy-6-oxodinorcholanate (IV) was prepared by this method, a very low yield was obtained. An alternative procedure was developed which involved refluxing a methanolic solution of the nitro compound (III) for several hours with iron filings in the presence of a small amount of hydrochloric acid. In this way, a 58% yield of IV was obtained.

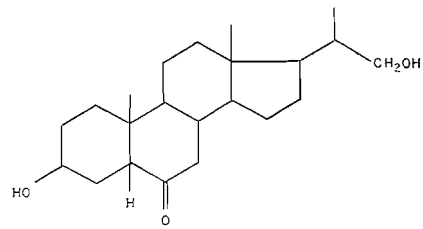
[1]*Manuscript received March 9, 1960.*
Contribution from the Department of Chemistry, McGill University, Montreal, Que., with financial assistance from the National Research Council, Ottawa, Canada. Abstracted from a portion of the thesis submitted by Barbara G. Ketcheson to the Department of Chemistry, McGill University, Montreal, Que., August 1958, in partial fulfilment of the requirements for the Ph.D. degree.
[2]*Holder of a National Research Council Studentship, 1956–57, and of Canadian Industries (1954) Limited Fellowships, 1955–56 and 1957–58.*

Methyl 3β-acetoxy-6-oximinodinorcholanate (V) was prepared, and reduced with sodium in *n*-propyl alcohol. Although Vanghelovici (15) had reported that similar reductions of the ethyl esters of 3,7,12-trihydroxycholanic, 3,12-dihydroxycholanic, and cholenic acids had brought about the transformation of the ester group to a primary alcoholic function, James *et al.* (2) had not observed the Bouveault–Blanc effect in the reduction of ethyl 3,12-dihydroxy-7-oximinocholanate. Since the 22 position of the steroid molecule is definitely hindered, sodium–alcohol treatment of V was not expected to bring about the reduction of the ester group. The infrared spectrum provided confirmatory evidence that the reduction product was in fact 6α-amino-3β-hydroxydinorcholanic acid (VI). Acetylation of VI with acetic anhydride – pyridine at room temperature provided 6α-acetamido-3β-acetoxydinorcholanic acid (VII). The α-configuration was assigned to the amino group on the basis of mode of preparation (16, 17).

The oxime (V) also was reduced by means of lithium aluminum hydride in tetrahydrofuran. A ratio of 1:10 of V to the reducing agent was used. From the reaction, a single product was isolated in 86% yield. It contained no nitrogen, and had a molecular formula $C_{22}H_{36}O_3$. In the infrared spectrum there was a strong broad band at 3300 cm^{-1}



(VII)



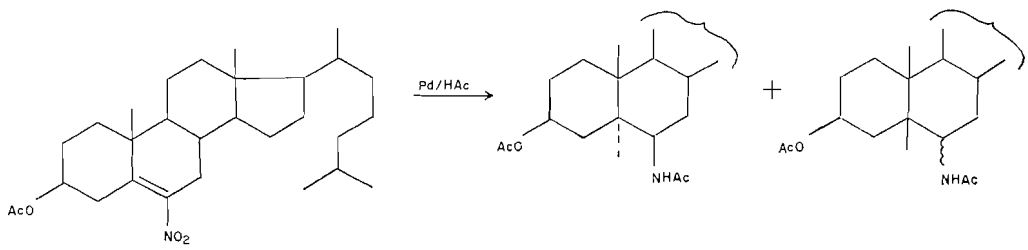
(VIII)

indicating the presence of an associated hydroxyl group or groups. A single narrow peak at 1712 cm^{-1} could be attributed to absorption by a 6-ketone of the normal series (18). The product was postulated as 3β,22ξ-dihydroxydinorcholan-6-one (VIII). In order to substantiate the formulation of VIII, the compound was acetylated, and the oxime derivative was prepared. The infrared spectrum of the oxime derivative demonstrated the presence of associated hydroxyl groups and an oxime group, but there was no indication of any carbonyl absorption. Analysis and the infrared spectrum were in agreement with the product of acetylation being 3β, 22ξ-diacetoxydinorcholan-6-one (IX). The formation of VIII by the lithium aluminum hydride reduction of the oximinoester (V) was unexpected. It was felt that the oxime group was converted to the ketone under the alkaline hydrolytic conditions of the reaction mixture when wet solvent was added to destroy the unreacted excess lithium aluminum hydride.

Catalytic hydrogenation of 3β-substituted-Δ^5-steroids is known to provide mainly saturated steroids of the A/B trans series. In some cases, the principal product may be accompanied by small quantities of saturated steroids of the A/B cis series (19).

3β-Acetoxy-6-nitro-5-cholestene (X) (11) was hydrogenated using palladium black as the catalyst in an acetic acid medium at 53 atmospheres pressure and 150° for 6 hours. Previously, X had been catalytically hydrogenated at 40 atmospheres pressure and a temperature of 100–180°, and a saturated amine $C_{29}H_{51}O_2N$, m.p. 122°, or its acetyl derivative had been obtained as the product (20). However, in the present investigation, two products were isolated, the main one in the form of dense rhombic crystals, and the

Can. J. Chem. Downloaded from www.nrcresearchpress.com by 186.148.149.217 on 09/04/12
For personal use only.

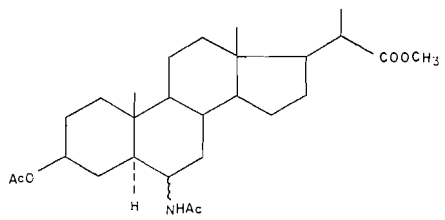


(X) (XI) (XII)

other as slender needles. Both compounds had a molecular formula $C_{31}H_{53}O_3N$. The main product melted at 167°, and the other substance at 94–96°. The compounds were postulated as 6-acetamido-3β-acetoxycholestane (XI) and 6-acetamido-3β-acetoxy-5β-cholestane (XII). A comparison of the infrared spectra of XI and 6β-acetamido-3β-acetoxycholestane (16), m.p. 166–168°, revealed that the two were identical in all respects. A mixed melting point determination of these substances showed no depression. On the basis of mode of preparation, it would be expected that the acetamido group in XII would be β-oriented.

In connection with the preparation of 6β-aminocholestan-3β-ol (XIII) from 3β-acetoxy-6-oximinocholestane (XIV) by reduction using lithium aluminum hydride, it was noted that Shoppee *et al.* (16) encountered considerable difficulty with the analysis of the hydroxy amine XIII, m.p. 128–130° (methanol). He attributed the unsatisfactory analytical values obtained to the rapid absorption of water and (or) carbon dioxide. No yield of product was reported for the reaction. In the present case, the reduction was carried out in tetrahydrofuran rather than ether, and the product was isolated in a 57% yield. No difficulty was experienced in obtaining entirely satisfactory analytical results for 6β-aminocholestan-3β-ol (XIII), m.p. 129–132° (dimethylformamide–water).

It was thought that the main product resulting from the high-pressure hydrogenation of methyl 3β-acetoxy-6-nitro-5-dinorcholenate (III) would be methyl 6-acetamido-3β-acetoxy-5α-dinorcholanate (XV). The hydrogenation was carried out under the same conditions as had been used in the α series. A single substance was isolated from the



(XV)

reaction in a 67% yield. On the basis of its infrared spectrum and analysis, the product was designated as methyl 6ξ-acetamido-3β-acetoxy-5α-dinorcholanate (XV). No configuration was assigned to the acetamido group, although on the basis of mode of preparation it would be expected that the group would have the axial conformation and thus be β-oriented.

Can. J. Chem. Downloaded from www.nrcresearchpress.com by 186.148.149.217 on 09/04/12
For personal use only.

Can. J. Chem. Downloaded from www.nrcresearchpress.com by 186.148.149.217 on 09/04/12
For personal use only.

EXPERIMENTAL

The melting points were determined in a Thiele–Dennis melting point tube containing Dow Corning silicone fluid No. D.C. 550. All melting points are uncorrected. Microanalyses were carried out in the W. Manser Laboratory, Zurich, Switzerland, and in the Schwarzkopf microanalytical laboratory, Woodside, N.Y., U.S.A. The infrared absorption spectra were determined in potassium bromide by means of a Perkin–Elmer Model 21 double-beam spectrophotometer equipped with a sodium chloride prism.

Methyl 3β-Acetoxy-6-nitro-5-dinorcholenate (III)

A solution of methyl 3β-acetoxy-5-dinorcholenate (II) (25.0 g) in absolute ether (300 ml) was cooled to −20°. Fuming nitric acid (150 ml) was added, with stirring, at such a rate that the temperature did not rise above −10°. When the addition had been completed, the reaction mixture was stirred for 1½ hours, while the temperature slowly rose to 0–5°. The ethereal solution was neutralized by washing with a 2.5% sodium hydroxide solution (600 ml), and with a saturated solution of sodium chloride. The ether was removed *in vacuo* and a solid crystalline residue remained. After recrystallization from methanol, the material (22.9 g) melted at 145–147°. Further purification from methanol provided methyl 3β-acetoxy-6-nitro-5-dinorcholenate (III), m.p. 147–149°. ν_{max} 1735, 1527, 1240 cm^{-1}. Anal. Calc. for $C_{25}H_{37}O_6N$: C, 67.08; H, 8.33; N, 3.13. Found: C, 67.10; H, 8.31; N, 3.21%.

Methyl 3β-Acetoxy-6-oxodinorcholanate (IV)

To a mixture of iron filings (40 mesh, 20.0 g) and methyl 3β-acetoxy-6-nitro-5-dinorcholenate (III) (10.0 g) were added methanol (300 ml) and concentrated hydrochloric acid (3 ml). The reaction mixture was refluxed with stirring for 17 hours, then filtered hot. The residue on the filter was washed thoroughly with hot methanol. The methanolic filtrate and washings were concentrated and set aside for crystallization. The crystalline product (5.42 g) obtained melted at 160–162°. Purification by recrystallization from methanol afforded methyl 3β-acetoxy-6-oxodinorcholanate, m.p. 164.5–166.5°. ν_{max} 1745, 1730 (sh), 1718, 1280 (sh), 1263, 1248 cm^{-1}. Anal. Calc. for $C_{25}H_{38}O_5$: C, 71.72; H, 9.50. Found: C, 71.78; H, 9.31%.

Methyl 3β-Acetoxy-6-oximinodinorcholanate (V)

An ethanolic solution of methyl 3β-acetoxy-6-oxodinorcholanate IV (0.4 g), sodium acetate (0.5 g), and hydroxylamine hydrochloride (0.4 g) was refluxed for 24 hours. Water was added to the solution until a slight permanent cloudiness was observed. On standing, crystalline material (0.34 g) was deposited and isolated. It melted at 202–205°. Recrystallization from ethanol provided methyl 3β-acetoxy-6-oximinodinorcholanate (V), m.p. 207–209°. ν_{max} 3300, 1735, 1720, 1655, 1245 cm^{-1}. Anal. Calc. for $C_{25}H_{39}O_5N$: C, 69.25; H, 9.06; N, 3.23. Found: C, 69.73; H, 9.02; N, 3.29%.

6α-Acetamido-3β-acetoxydinorcholanic Acid (VII)

In a nitrogen atmosphere, small pieces of sodium (2.0 g) were added over a period of 1½ hours to a solution of methyl 3β-acetoxy-6-oximinodinorcholanate (V) (500 mg) in dry *n*-propyl alcohol (35 ml) at 70°. When the sodium had been added, the solution was refluxed for 9 hours. Then it was poured into distilled water (500 ml), and allowed to stand at room temperature for several days. Solid material precipitated out of solution and was isolated. Recrystallization of the product afforded 6α-amino-3β-hydroxydinorcholanic acid (VI), m.p. 176–178°. ν_{max} 3420,1640, 1568 cm^{-1}.

A solution of VI (100 mg) in acetic anhydride (5 ml) and pyridine (5 ml) was allowed to stand at room temperature overnight. The solution was poured into water (200 ml). The solid material (90 mg) which formed on standing was isolated and melted at 161–165°. Recrystallization from ethanol–water gave 6α-acetamido-3β-acetoxydinorcholanic acid (VII), m.p. 158–159°. ν_{max} 3340, 1735, 1663, 1540, 1245 cm^{-1}. Anal. Calc. for $C_{26}H_{41}O_5N$: N, 2.86. Found: N, 2.75%.

3β,22ξ-Dihydroxydinorcholan-6-one (VIII)

In a nitrogen atmosphere was added, dropwise, and with stirring, a solution of methyl 3β-acetoxy-6-oximinodinorcholanate (V) (1.0 g) in dry tetrahydrofuran, to a refluxing suspension of lithium aluminum hydride (1.0 g) in anhydrous tetrahydrofuran (20 ml). The resulting reaction mixture was refluxed under these conditions for 18 hours. After cooling to room temperature, wet tetrahydrofuran was carefully added to the mixture with vigorous stirring. The suspension was filtered with suction, and the filter cake was washed thoroughly with ether. The filtrate was evaporated *in vacuo* leaving a solid product (690 mg). Recrystallization from dioxane–water yielded 3β,22ξ-dihydroxydinorcholan-6-one (VIII), m.p. 190–194°. ν_{max} 3300, 1712, 1062 cm^{-1}. Anal. Calc. for $C_{22}H_{36}O_3$: C, 75.80; H, 10.41. Found: C, 75.52; H, 10.39%.

3β,22ξ-Diacetoxydinorcholan-6-one (IX)

A solution of 3β,22ξ-dihydroxydinorcholan-6-one (VIII) (140 mg) in acetic anhydride (5 ml) and pyridine (5 ml) was allowed to stand at room temperature overnight. Then it was poured into water (200 ml). Solid material (90 mg) separated from solution was isolated, and on recrystallization from dimethylformamide–water gave 3β,22ξ-diacetoxydinorcholan-6-one (IX), m.p. 115–117°. ν_{max} 1737, 1255 cm^{-1}. Anal. Calc. for $C_{26}H_{40}O_5$: C, 72.19; H, 9.32. Found: C, 72.25; H, 9.25%.

High-pressure Hydrogenation of 3β-Acetoxy-6-nitro-5-cholestene (X)

A solution of X (2.0 g) in glacial acetic acid (30 ml) was hydrogenated in a Parr high-pressure hydrogenation apparatus for 6 hours at 150° and 53 atmospheres pressure using 10% palladium on charcoal (1.0 g) as catalyst. The reaction mixture was filtered, and the residue on the filter was washed thoroughly with acetic acid. The solvent was removed *in vacuo*, and the residue was taken up in ethanol. On standing, small rhombic crystals were formed. The product (1.15 g) was purified by recrystallization from dioxane–water yielding 6β-acetamido-3β-acetoxycholestane (XI), m.p. 167°. ν_{max} 3375, 3320, 1733, 1645, 1550, 1250 cm^{-1}. Anal. Calc. for $C_{31}H_{53}O_3N$: C, 76.33; H, 10.95; N, 2.87. Found: C, 76.33; H, 10.91; N, 2.85%.

On standing, crystalline material in the form of slender needles separated from the filtrate. This product (200 mg) melted at 80–84°. Recrystallization from methanol–water gave 6ξ-acetamido-3β-acetoxy-5β-cholestane (XII), m.p. 94–96°. ν_{max} 3380, 1737, 1655, 1243 cm^{-1}. Anal. Calc. for $C_{31}H_{53}O_3N$: C, 76.33; H, 10.95. Found: C, 76.59; H, 10.93%.

6β-Aminocholestan-3β-ol (XIII)

In a nitrogen atmosphere, and with stirring, a solution of 3β-acetoxy-6-oximinocholestane (XIV) (500 mg) in anhydrous tetrahydrofuran (25 ml) was added dropwise to a refluxing suspension of lithium aluminum hydride (500 mg) in dry tetrahydrofuran (20 ml). The reaction was allowed to continue under these conditions for 18 hours. Wet tetrahydrofuran was added dropwise with vigorous stirring, then the mixture was filtered, and the filter cake was washed thoroughly with wet tetrahydrofuran. The filtrate was concentrated under reduced pressure, and the solid material which precipitated out of

Can. J. Chem. Downloaded from www.nrcresearchpress.com by 186.148.149.217 on 09/04/12
For personal use only.

solution was isolated. A yield of 250 mg of product melting at 123–129° was obtained. Further purification by recrystallization from dimethylformamide–water yielded 6β-aminocholestan-3β-ol (XIII), platelets, m.p. 129–132°. ν_{max} 3400 (sh), 3300 (sh), 3200, 1600 cm^{-1}. Anal. Calc. for $C_{27}H_{49}ON$: C, 80.33; H, 12.24; N, 3.47. Found: C, 80.21; H, 12.19; N, 3.44%.

6β-Acetamido-3β-acetoxycholestane (XI)

A solution of 6β-aminocholestan-3β-ol (XIII) (100 mg) in acetic anhydride (5 ml) and pyridine (5 ml) was allowed to stand overnight at room temperature. The reaction mixture was poured into water (150 ml), and the solid material (80 mg) which formed on standing was isolated. Recrystallization from ethyl acetate furnished 6β-acetamido-3β-acetoxycholestane (XI), m.p. 166–168°. ν_{max} 3375, 3320, 1733, 1645, 1550, 1250 cm^{-1}. Anal. Calc. for $C_{31}H_{53}O_3N$: N, 2.87. Found: N, 2.71%.

Methyl 6ξ-Acetamido-3β-acetoxy-5α-dinorcholanate (XV)

Methyl 3β-acetoxy-6-nitro-5-dinorcholenate (III) (2.0 g) in glacial acetic acid (30 ml) was hydrogenated in a Parr high-pressure hydrogenation apparatus using a 10% palladium on charcoal catalyst (1.0 g). The hydrogenation was carried out for 6 hours at 150° and 53 atmospheres pressure. The mixture was filtered, and the filter cake was washed thoroughly with acetic acid. The solvent was removed *in vacuo* and the residue taken up in ethanol. The ethanolic solution was heated to boiling and water was added until a faint cloudiness persisted. On cooling, a solid (1.41 g) separated from solution and was isolated. Recrystallization from benzene – petroleum ether (30–60°) yielded methyl 6ξ-acetamido-3β-acetoxy-5α-dinorcholanate (XV), m.p. 236–238° (dec.). ν_{max} 3290, 3070, 1737, 1655, 1558, 1242 cm^{-1}. Anal. Calc. for $C_{27}H_{43}O_5N$: N, 3.05. Found: N, 3.06%.

ACKNOWLEDGMENTS

The authors wish to thank Frank W. Horner Ltd. of Montreal for the use of their high-pressure hydrogenation equipment, and Dr. G. Frangatos for his valuable technical assistance.

REFERENCES

1. J. Barnett, B. Ryman, and F. Smith. J. Chem. Soc. 524, 526, 528 (1946).
2. S. P. James, F. Smith, M. Stacey, and M. Webb. J. Chem. Soc. 665 (1946).
3. A. S. Jones, M. Webb, and F. Smith. J. Chem. Soc. 2164 (1949).
4. R. A. Micheli and C. K. Bradsher. J. Am. Chem. Soc. **77**, 4788 (1955).
5. H. L. Herzog, C. C. Payne, and E. B. Hershberg. J. Am. Chem. Soc. **77**, 5324 (1955).
6. D. Gould, E. L. Shapiro, L. E. Finckenor, F. Gruen, and E. B. Hershberg. J. Am. Chem. Soc. **78**, 3158 (1956).
7. D. P. Dodgson and R. D. Haworth. J. Chem. Soc. 67 (1952).
8. F. C. Uhle. J. Am. Chem. Soc. **73**, 883 (1951).
9. L. F. Fieser and W. Huang. J. Am. Chem. Soc. **75**, 6306 (1953).
10. D. Gould, E. L. Shapiro, and E. B. Hershberg. J. Am. Chem. Soc. **76**, 5567 (1954).
11. C. E. Anagnostopoulos and L. F. Fieser. J. Am. Chem. Soc. **76**, 532 (1954).
12. E. Fernholz. Ann. **507**, 128 (1933).
13. A. Butenandt and G. Fleischer. Ber. **70**B, 96 (1937).
14. L. F. Fieser and M. Fieser. Steroids. Reinhold. 1959. p. 43.
15. M. Vanghelovici. Bul. soc. chim. România, **18**, 103 (1936); Chem. Zentr. II, 2533 (1937).
16. C. W. Shoppee, D. E. Evans, and G. H. R. Summers. J. Chem. Soc. 97 (1957).
17. C. W. Shoppee, R. J. W. Cremlyn, D. E. Evans, and G. H. R. Summers. J. Chem. Soc. 4364 (1957).
18. R. N. Jones and F. Herling. J. Org. Chem. **19**, 1252 (1954).
19. J. R. Lewis and C. W. Shoppee. J. Chem. Soc. 1365 (1955).
20. I. G. Farbenindustrie. Fr. Patent No. 885,439 (1943); Chem. Zentr. II, 563 (1944).

Can. J. Chem. Downloaded from www.nrcresearchpress.com by 186.148.149.217 on 09/04/12
For personal use only.

Can. J. Chem. Downloaded from www.nrcresearchpress.com by 186.148.149.217 on 09/04/12
For personal use only.

STEROIDS

PART III. REDUCTION OF OXIMINOCHOLANIC ACIDS[1]

TED H. WAID[2] AND ALFRED TAURINS

ABSTRACT

The reduction of 12-oximino-, 3,12-dioximino-, and 7,12-dioximino-cholanic acids using sodium in alcohol resulted in the formation of 12β-amino-, 3α,12β-diamino-, and 7β,12β-diamino-cholanic acids respectively. The reaction of 3,12-dioximinocholanic acid with lithium aluminum hydride provided cholane-3ξ,12ξ,24-triol, while similar treatment of 7,12-dioximinocholanic acid afforded 7ξ-amino-12-oximinocholan-24-ol.

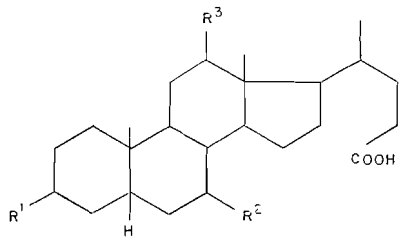
DISCUSSION

Basic derivatives of bile acids and esters, having amino functions located in positions 3 (1, 2), 6 (3), 7 (2, 4, 5), 11 (6), and 12 (2, 5, 7) of the steroidal nucleus, have been described. Their synthesis has been accomplished for the most part by reduction of the corresponding oximes with sodium in alcohol, and has been prompted primarily by the possibility of such compounds being physiologically active.

In the present investigation, a study has been made of the reduction of 12-oximino- (I) (8), 3,12-dioximino- (II) (9), and 7,12-dioximino-cholanic acids (III) (10), using sodium in alcohol and lithium aluminum hydride. In the reductions using sodium, *n*-propyl and *n*-butyl alcohols gave the best yields of purest products. The color of reaction mixtures in isoamyl alcohol was darker, and the crude products contained appreciable amounts of tarry impurities. Since reductions of oximes with alkali metals and proton donors are known to give predominantly the equatorial conformation (11, 12), the conformation of amino groups in the steroidal amino acids synthesized by reductions with sodium in alcohol were assigned on the basis of mode of preparation. Preliminary experiments of oxime reductions using lithium aluminum hydride in tetrahydrofuran showed that two- to five-fold molar excesses of lithium aluminum hydride led to the formation of mixtures of products. When a 10-fold excess of the reagent was used, definite reaction products could be isolated in all cases.

12-Oximinocholanic acid (I) was prepared from 3α,12α-dihydroxycholanic acid (IV) by oxidation of IV to 3,12-dioxocholanic acid (V) (13), Clemmensen reduction of V to 12-oxocholanic acid (VI) (14, 15, 16), and preparation of the oxime (I). The oxidation of the dihydroxy acid (IV) to the dioxo derivative (V) was carried out using the procedure described by Heilbron (17) for the oxidation of acetylenic carbinols. This method gave consistent yields of over 90% of pure product as compared with the 70% yield obtained by Wieland's method (13) of oxidation in acetic acid. As expected, the reduction of the oximino acid (I) with sodium in alcohol provided 12β-aminocholanic acid (VII) in good yield. That VII existed as a dipole ion was confirmed by the infrared spectrum which showed bands characteristic of the carboxylate ion at 1550 cm^{-1} and of the NH_3^+ group at 1625 cm^{-1}. Several treatments of VII with concentrated hydrochloric acid resulted in the formation of the corresponding hydrochloride. The infrared spectrum of the latter showed suppression of the band due to the carboxylate ion and release of the carboxyl

[1]*Manuscript received March 9, 1960.*
Contribution from the Department of Chemistry, McGill University, Montreal, Que., wtih financial assistance from the National Research Council, Ottawa, Canada. Abstracted from a portion of the thesis submitted by Waid to the Department of Chemistry, McGill University, Montreal, Que., April 1957, in partial fulfilment of the requirements for the Ph.D. degree.
[2]*Holder of a National Research Council Studentship 1955–56. Present address: Monsanto Canada Ltd., Montreal, Que.*



(VII) $R^1 = R^2 = H$; $R^3 = NH_2$

(VIII) $R^2 = H$; $R^1 = R^3 = NH_2$

(XII) $R^1 = H$; $R^2 = R^3 = NH_2$

band at 1705 cm^{-1}. Treatment of the oximino acid (I) with 3% sodium amalgam resulted in the transformation of the oxime group to the keto group. The keto acid (VI) was identified by a mixed melting point determination with an authentic sample.

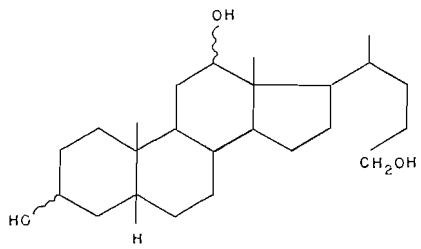
3,12-Dioximinocholanic acid (II) was prepared from 3α,12α-dihydroxycholanic acid (IV) by oxidation of IV to 3,12-dioxocholanic acid (V) and oximation of V to the dioxime (II). The reduction of II with sodium in alcohol resulted in the formation of 3α,12β-diaminocholanic acid (VIII) in good yield. Possessing one carboxyl and two amino groups, this diaminocarboxylic acid behaved as a base and formed a dihydrochloride. The infrared spectrum confirmed the presence of the NH_2 group (1660 cm^{-1}), the NH_3^+ ion (1623 cm^{-1}), and the carboxylate ion (1575 cm^{-1}).

A product containing no nitrogen and insoluble in both acids and bases was formed in the reaction of the oximino acid (II) with lithium aluminum hydride. The infrared spectrum had a very strong band at 3340 cm^{-1}, which was attributed to absorption by associated OH groups, and a series of high intensity bands in the region 1075–1011 cm^{-1}. The latter could be assigned to C—O stretching vibrations in a steroid alcohol. On the basis of the infrared spectrum and the analytical results, the compound was formulated as cholane-3ξ,12ξ,24-triol (IX). The steric course of reductions with lithium aluminum hydride being uncertain, the conformations of the hydroxyl groups at 3- and 12-positions were not assigned.

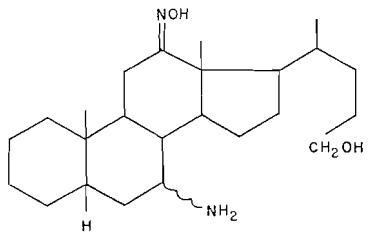
The formation of IX was quite unexpected, although a somewhat similar result had been obtained by Redel and his co-workers (2) in their attempts to reduce methyl 3α,12α-diformoxy-7-oximinocholanate in ethanolic solution by catalytic hydrogenation under pressure using Raney nickel. Mignonac (18, 19) and Paul (20) also had observed the formation of secondary alcohols on reductions of oximes. It was considered that the reaction of the oximino acid (II) with lithium aluminum hydride proceeded via an unstable imine, which, under hydrolytic conditions, was transformed into the corresponding ketone. The latter was, in turn, reduced to the secondary alcohol (IX) by the lithium aluminum hydride still present in the reaction mixture.

Clemmensen reduction of 3,7,12-trioxocholanic acid (X) to 7,12-dioxocholanic acid (XI) and oximation provided 7,12-dioximinocholanic acid (III). The reduction of III with sodium in *n*-propyl or *n*-butyl alcohol produced 7β,12β-diaminocholanic acid (XII) in high yields, as anticipated. When the reduction of III was carried out under similar conditions to those used for the reduction of the dioximino acid (II) with lithium

Can. J. Chem. Downloaded from www.nrcresearchpress.com by 186.148.149.217 on 09/04/12
For personal use only.



(X)



(XIII)

aluminum hydride, a nitrogen-containing product was obtained. In the infrared spectrum there was no carbonyl absorption, but the band at 3300 cm^{-1} indicated the presence of an alcoholic function. The medium intensity band at 1660 cm^{-1} could be due to absorption by an amine, an oxime, or both. Acidic hydrolysis of the reaction product gave a material which contained nitrogen, and in the infrared exhibited a carboxyl band at 1700 cm^{-1}, and bands at 3300 cm^{-1} and 1655 cm^{-1}. The hypothesis of an amino, oximino carbinol fully agreed with the analytical results. Since the 12-position is more sterically hindered than the 7-position, the reaction product was postulated as 7ξ-amino-12-oximinocholan-24-ol (XIII) and its hydrolysis product as 7ξ-amino-24-hydroxycholan-12-one (XIV).

EXPERIMENTAL

The melting points were determined in a Thiele–Dennis melting point tube containing Dow Corning silicone fluid No. D.C. 550, and are uncorrected. The analyses were carried out in the W. Manser laboratory, Zurich, Switzerland. Infrared spectra were determined in potassium bromide on a Perkin–Elmer Model 21 double-beam instrument equipped with a sodium chloride prism.

3,12-Dioxocholanic Acid (V)

To a solution of chromium trioxide (13.35 g) in water (20 ml) concentrated sulphuric acid (11.5 ml) was added dropwise, with stirring so as to avoid the formation of any precipitate. The cold solution was diluted to 50 ml. 3α,12α-Dihydroxycholanic acid (IV) (30 g) was dissolved in acetone (2.2 l.), and the resulting solution was cooled to 20° in an ice-water bath. The oxidizing solution was then added dropwise from a microburette until an orange-brown color persisted (about 45 ml of reagent was required). The solution

Can. J. Chem. Downloaded from www.nrcresearchpress.com by 186.148.149.217 on 09/04/12
For personal use only.

Can. J. Chem. Downloaded from www.nrcresearchpress.com by 186.148.149.217 on 09/04/12
For personal use only.

was decanted from the inorganic residue, and was diluted with water to a volume of 6 l. The product (23.4 g) precipitated immediately, and was isolated. A second crop (5.35 g) was obtained by diluting the filtrate with another 2 l. of water. The 3,12-dioxocholanic acid (V) melted at 184–185°.

12β-Aminocholanic Acid (VII)

In a nitrogen atmosphere, sodium (2.5 g), in small pieces, was added over a period of 3.5 hours to a refluxing solution of 12-oximinocholanic acid (I) (0.5 g) in dry *n*-propyl alcohol (58 ml) with stirring. Then the reaction mixture was cooled in an ice-water bath, and made slightly acidic with 4% sulphuric acid. The propyl alcohol was distilled off *in vacuo* in a nitrogen atmosphere, and some precipitation occurred. The precipitation was made complete by adjusting the pH to 5.6–5.8 with 1% sulphuric acid. The yellow solid (0.48 g) was isolated. It melted at 122–126° to an opaque viscous liquid which cleared at 138–140°. The product was dissolved in hot acetone (20 ml), and the yellow solution filtered with suction through celite and carbon Nuchar C190-N. The colorless filtrate was concentrated under reduced pressure to a 10-ml volume, and heated to boiling. Hot water was added dropwise until the solution became slightly turbid. Upon cooling to room temperature, needles were deposited from solution. Recrystallization from acetone–water provided 12β-aminocholanic acid (VII) melting at 115–116° to a liquid which became transparent at 120°. ν_{max} 3440 (O—H), 3040 (sh) ($\overset{+}{N}H_3$), 1625 ($\overset{+}{N}H_3$), 1550 cm^{-1} (COO^-). Anal. Calc. for $C_{24}H_{41}O_2N \cdot 3H_2O$: C, 67.13; H, 10.95; N, 3.24. Found: C, 67.20; H, 10.88; N, 3.53%. Hydrochloride: Addition of concentrated hydrochloric acid (0.5 ml) to VII (0.4 g) and evaporation to dryness under reduced pressure was repeated 5 times. The white residue obtained, on recrystallization from methanol–water, gave the hydrochloride as a white powder, m.p. 257–258°. ν_{max} 1705 (C=O), 1610 cm^{-1} ($\overset{+}{N}H_3$).

Attempted Reduction of 12-Oximinocholanic Acid (I) *with Sodium Amalgam in Absolute Ethanol*

Sodium amalgam (3%, 26.6 g) was added in a nitrogen atmosphere to a refluxing solution of I (0.2 g) in absolute ethanol (20 ml), and the mixture was stirred for 6 hours. The major part of the amalgam seemed to have reacted. The supernatant solution was decanted, allowed to cool, diluted with water to 50 ml, and neutralized with 4% sulphuric acid. A white product (0.18 g) which precipitated was isolated. It melted at 178–179° to a milky liquid which cleared completely at 198–201°. Recrystallization from ethanol provided platelets, m.p. 180–182°, which were identified as 12-oxocholanic acid (VI) by a mixed melting point determination (183–184°) with an authentic sample of the keto acid. An oxime derivative of the reaction product was prepared, and a mixed melting point determination with an authentic sample of I showed no depression.

3α,12β-Diaminocholanic Acid (VIII)

To a refluxing solution of 3,12-dioximinocholanic acid (II) (0.4 g) in dry *n*-propyl alcohol (60 ml) were added, with stirring in a nitrogen atmosphere, small pieces of sodium (4.0 g) over a period of 4 hours. The reaction mixture was cooled in an ice-water bath, and treated with 4% sulphuric acid until pH 9 was reached. The propyl alcohol was evaporated under reduced pressure and the pH of the aqueous solution was further adjusted with 1% sulphuric acid to 8.6–8.8. A yellow product (0.25 g) precipitated and was isolated. Recrystallization from methanol–water gave 3α,12β-diaminocholanic acid

(VIII), m.p. 244–245°. ν_{max} 3380 (O—H, NH_2), 1660 (sh) (NH_2), 1623 ($\overset{+}{N}H_3$), 1575 cm^{-1} (COO^-). Anal. Calc. for $C_{24}H_{42}O_2N_2 \cdot H_2O$: C, 70.58; H, 10.78; N, 6.86. Found: C, 70.35; H, 10.63; N, 6.59%.

Reduction of 3,12-Dioximocholanic Acid (II) *with Lithium Aluminum Hydride in Tetrahydrofuran*

To a refluxing suspension of lithium aluminum hydride (0.37 g) in dry tetrahydrofuran (20 ml) in a nitrogen atmosphere was added dropwise, and with stirring, a solution of II (0.3 g) in dry tetrahydrofuran (30 ml). The resulting mixture was stirred and refluxed for a further period of 2 hours, then was cooled to room temperature. A saturated solution (50 ml) of sodium potassium tartrate was added dropwise with stirring. The tetrahydrofuran was removed by evaporation under reduced pressure, and a semisolid material separated in the aqueous phase. It was extracted with three 40-ml portions of *n*-butyl alcohol. The alcoholic extract was washed with 1% sulphuric acid, and with water, then was dried over anhydrous magnesium sulphate. After filtration, the solvent was removed *in vacuo* leaving an amorphous residue (0.23 g), which contained no nitrogen. The product was dissolved in 2 ml of boiling ethanol, and hot water was added dropwise until a slight cloudiness was observed. The solution was seeded with crystals obtained by cooling a few drops of the solution in a dry ice – acetone mixture for 2–3 minutes, and keeping the resulting solid in a refrigerator overnight, and long needles were obtained. Recrystallization from acetone–water yielded cholane-3ξ,12ξ,24-triol (IX), m.p. 166–169°. ν_{max} 3340 cm^{-1} (H—O), 1075, 1055, 1042, 1011 cm^{-1} (C—O). Anal. Calc. for $C_{24}H_{42}O_3$: C, 76.19; H, 11.11. Found: C, 75.86; H, 11.45%.

7β,12β-Diaminocholanic Acid (XII)

In a nitrogen atmosphere, sodium (2.0 g) was added in small pieces, with stirring, to a refluxing solution of 7,12-dioximinocholanic acid (III) (0.2 g) in dry *n*-propyl alcohol (40 ml) over a period of 3 hours. The reaction mixture was cooled in an ice-water bath, and adjusted to pH 9 with 4% then 2% sulphuric acid. The propyl alcohol was removed under reduced pressure, and 1% sulphuric acid was added until precipitation occurred at pH 8.3–8.6. The crude product (0.16 g) was dissolved in 8 ml of ethanol, and the yellow solution was filtered through celite and carbon Nuchar C190-N. The filtrate was concentrated to 4 ml and, when it was left to stand at room temperature, needles were deposited and isolated. Recrystallization from acetone–water afforded 7β,12β-diaminocholanic acid (XII), m.p. 128–130°. ν_{max} 3400 cm^{-1} (O—H), 1635, 1560, 1630 cm^{-1} (NH_2, $\overset{+}{N}H_3$), 1550 cm^{-1} (COO^-). Anal. Calc. for $C_{24}H_{42}N_2O_2 \cdot 1.5H_2O$: C, 69.06; H, 10.31; N, 6.71. Found: C, 68.52; H, 10.32; N, 6.57%.

7ξ-Amino-12-oximinocholan-24-ol (XIII)

A solution of 7,12-dioximinocholanic acid (III) (0.60 g) in dry tetrahydrofuran (80 ml) was added in a nitrogen atmosphere to a refluxing suspension of lithium aluminum hydride (0.73 g) in dry tetrahydrofuran (50 ml), with stirring, over a period of 40 minutes. The reaction mixture was stirred under reflux for a further 2.5 hours. When the suspension had cooled to room temperature, it was hydrolyzed by the dropwise addition of 100 ml of a saturated sodium potassium tartrate (Rochelle salt) solution. The tetrahydrofuran was removed under reduced pressure, and a white precipitate separated from the aqueous solution. The product was extracted with four 50-ml portions of *n*-butanol, and the extract was washed once with 1% sulphuric acid, twice with water, and then was dried over anhydrous magnesium sulphate. The solution was filtered, and the butanol was removed

Can. J. Chem. Downloaded from www.nrcresearchpress.com by 186.148.149.217 on 09/04/12
For personal use only.

under reduced pressure leaving a crystalline residue (0.45 g) which melted at 203–209° and became transparent at 215°. Recrystallization from ethanol gave 7ξ-amino-12-oximinocholan-24-ol (XIII) in shiny plates, m.p. 234–236°. ν_{max} 3300 cm^{-1} (O—H), 1660 cm^{-1} (C=N, NH_2). Anal. Calc. for $C_{24}H_{38}O_2N_2$: C, 71.79; H, 9.74; N, 7.17. Found: C, 71.15%; H, 10.17; N, 7.15%.

7ξ-Amino-12-oxocholan-24-ol (XIV)

7ξ-Amino-12-oximinocholan-24-ol (XIII) (15 mg) was dissolved in ethanol (3 ml), and one drop of 4% hydrochloric acid was added to the solution. The reaction mixture was refluxed for 20 minutes, then was concentrated to a volume of 1 ml *in vacuo*, and the needles which separated when the mixture was left to stand at room temperature were isolated; the needles melted at 180–183°. Recrystallization from ethanol–water provided 7ξ-amino-12-oxocholan-24-ol (XIV) in the form of needles, m.p. 183–184°. ν_{max} 3300 cm^{-1} (O—H); 1700 cm^{-1} (C=O); 1655 cm^{-1} (NH_2). Anal. Calc. for $C_{24}H_{37}ON \cdot 1.5H_2O$: C, 71.39; H, 9.95. Found: C, 70.83; H, 9.98%.

REFERENCES

1. A. S. Jones, M. Webb, and F. Smith. J. Chem. Soc. 2164 (1949).
2. J. Redel, A. Bouteville, B. Gauthier, and Nguyen Hun Quy. Bull. soc. chim. France, (5) **16**, 877 (1949).
3. B. G. Ketcheson and A. Taurins. Can. J. Chem. This issue.
4. S. P. James, F. Smith, M. Stacey, and M. Webb. J. Chem. Soc. 665 (1946).
5. J. Hadacek and B. Duchoslav. Publs. fac. sci. Univ. Masaryk, **357**, 251 (1954); Chem. Abstr. **49**, 14015 (1954).
6. J. Barnett and T. Reichstein. Helv. Chim. Acta, **22**, 75 (1939).
7. H. B. MacPhillamy and C. R. Scholz. J. Org. Chem. **14**, 643 (1949).
8. M. Schenck and H. Kirchhof. Z. physiol. Chem. **163**, 120 (1927).
9. M. Schenck and H. Kirchhof. Z. physiol. Chem. **180**, 115 (1929).
10. M. Schenck and H. Kirchhof. Z. physiol. Chem. **180**, 107 (1929).
11. D. H. R. Barton and C. H. Robinson. J. Chem. Soc. 3045 (1954).
12. D. H. R. Barton. J. Chem. Soc. 1029 (footnote 23) (1953).
13. H. Wieland. Z. physiol. Chem. **194**, 257 (1931).
14. H. Wieland and O. Schlicting. Z. physiol. Chem. **150**, 267 (1925).
15. H. Wieland and E. Boersche. Z. physiol. Chem. **106**, 190 (1919).
16. H. Wieland and E. Dane. Z. physiol. Chem. **210**, 281 (1932).
17. I. Heilbron, E. R. H. Jones, and G. F. Woods. J. Chem. Soc. 461 (1953).
18. G. Mignonac. Bull. soc. chim. France, (4) **27**, 387 (1921).
19. G. Mignonac. Ann. chim. (Paris), **2**, 255 (1934).
20. R. Paul. Bull. soc. chim. France, (5) **4**, 1121 (1937).

Can. J. Chem. Downloaded from www.nrcresearchpress.com by 186.148.149.217 on 09/04/12
For personal use only.

Can. J. Chem. Downloaded from www.nrcresearchpress.com by 186.148.149.217 on 09/04/12
For personal use only.

THEORETICAL STUDIES ON SOLVATION

PART II. NEW THEORY FOR EVALUATION OF IONIC SOLVATION NUMBER FOR DIVALENT IONS AT 25° C[1]

A. M. AZZAM

ABSTRACT

The concepts of ionic solvation are discussed and the definition of four types are suggested. Utilizing Webb's theory, values of the dielectric constant of water in terms of distance from a divalent ion are evaluated. The statistical mechanics of the distribution of solvent molecules round a divalent ion in aqueous solution has been worked out.

The present theory shows that all divalent ions with radius less than 1.6 Å can have a saturated envelope of eight water molecules in excess of the Goldschmidt co-ordination number have to be accounted for as inner primary solvation number. The concept of catonium is suggested for such a stable aquo-complex entity. The catonium entity is further hydrated electrostatically in the normal way by primary and secondary solvation types. The conditions governing all types of solvation and their possible termination boundaries are discussed and evaluated.

The theoretically calculated values of the ionic solvation numbers are in good agreement with the experimental results.

1. INTRODUCTION

Solvation plays an extremely important part in most solution phenomena (1, 2, 4). Most investigations have dealt with aqueous solutions and several experimental methods (1, 4) have been used to find out the degree of hydration of ions but they give widely divergent results as shown in Table I.

TABLE I

Values of the hydration number of alkaline earth metal ions in dilute solution at room temperature by various experimental methods

Method	Reference	Be^{++}	Mg^{++}	Ca^{++}	Sr^{++}	Ba^{++}
Mobility (Ulich)	(16)		10.5–13	7.5–10.5		5–9
Entropy (Ulich)	(1)		13	10		8
Compressibility (Passynski)	(1)	8	16	16		
Cryoscopic (Bourin *et al.*)	(1)		22.3	21.6	21.3	20.1
Cryoscopic (Van Ruynen)	(11)	30	15	10.5	10	9
Dialysis (Brintzinger)	(1)		37.5	33.4	29.1	25.1
Partial molar volume (Darmoir)	(1)		6.6	5.2		4
Solubility of gases (Manchot)	(1)		13	14.6		16.8

The most outstanding problem connected with solvation lies in the need of theoretical calculations to supply definite quantitative knowledge of the nature of the solvation sheath and the structure of the solvated ion. Such information may also throw light on the general problem of the interionic attraction theory of electrolytes (7, 8, 9) which has reached a quasi-static position. No further essential advances in the field of more concentrated solution appears possible without the concept of ion–solvent interaction (5, 6, 7, 8, 9, 11).

In a previous paper (3), the present author worked out the basis of a statistical mechanical method for the calculation of solvation number of ions and the following equation was developed:

$$[1] \qquad ds = 4\,\pi\,n_0\,e^{-(w/kt)}\,r^2\,dr$$

[1]*Manuscript received January 28, 1960.*
Contribution from the Department of Chemistry, Faculty of Science, A'in Shams University, Cairo, Egypt.

where ds = the number of solvent molecules associated with the ion in the spherical shell between r and $r+dr$ from the center of the ion;
n_0 = the number of solvent molecules per cubic centimeter in the bulk of the solution;
w = net potential energy of a solvent molecule in the solvation sheath. This energy is the algebraic sum of energies of ion–dipole and dipole–dipole interactions;
k = Boltzman's constant;
t = temperature.

The theoretically calculated values of primary solvation number (for definition see Discussion) for alkali metal and halide ions are in good agreement with those obtained by four mutually self-consistent experimental methods (3).

The purpose of the present paper is to verify the above-mentioned theory by applying it to the calculation of solvation number for alkaline earth metal and divalent transition metal ions.

2. CONCEPTS OF IONIC SOLVATION

In spite of much experimental work (1), the significance of the term solvation has remained somewhat vague. Considering the former concepts of ionic solvation (13, 14, 15, 16, 17), together with conclusions derived from the present author's theory (3), a possible classification and definition of the different types of solvation can be given as follows:

(a) Permanent Solvation (Chemical Bonds)

This term refers to solvent molecules which are firmly associated with the ion through the formation of chemical bonds. These forces between ions and solvent molecules are so strong that an ion can retain this type in crystals. In other words, this type of solvation persists in the solid as well as in its solutions (e.g. co-ordinated water of crystallization).

(b) Primary Solvation (Physical Forces)

This term refers to solvent molecules which are firmly associated with the ion by electrostatic attraction. They have lost their translational degree of freedom and move as one entity with the ion during its Brownian motion. In other words, they cannot be dislodged by thermal motion.

(c) Secondary Solvation (Physical Forces)

This term refers to solvent molecules which undergo electrostatic attraction with the primary solvated ions. These molecules are much more weakly held but the electrostatic attraction predominates over the separating action of thermal motion sufficiently to affect solvation-dependent quantities, e.g. salting out.

(d) Hydrodynamical Solvation (Streaming Effect)

This term refers to solvent molecules which could be transferred hydrodynamically as the hydrated ion moves *under* the influence of an applied electrostatic field. This effect is mainly due to change in momentum between the solvated ion and the solvent molecules.

These different types of solvation play parts of different order or degree in the various experimental phenomena depending on specific factors (2, 3, 4, 18).

However, the number of solvent molecules in both the permanent and the primary solvation sheaths have definite values, moving with the ion as a single entity without exchange with bulk solvent. On the other hand, the number of solvent molecules in the secondary solvation sheath have variable values dependent on the phenomena observed. Ions continuously exchange these solvent molecules as they wander about in solution.

Can. J. Chem. Downloaded from www.nrcresearchpress.com by 186.148.149.217 on 09/04/12
For personal use only.

Hydrodynamical solvation is relevant only in dynamic experiments such as in measurements of transport number. This explains the fact that hydrodynamical methods for the determination of solvation number give much too high values (2, 3, 4, 18).

This scheme of classification gives a clear understanding of the reason for the large discrepancy between the results obtained by various experimental methods (1, 2, 3, 4, 18).

3. PROPOSED STRUCTURE OF HYDRATED DIVALENT IONS

Divalent metals such as Be, Mg, Ca, Sr, Ba, Zn, Cd, Fe, Co, Ni, Cu, . . . form a very large number of hydrated salts of definite constitution in the solid state (19, 20, 21, 24, 28, 29, 32, 33, 34). X-Ray crystallography has confirmed that definite hydrated cation complexes such as $[Be(H_2O)4]^{2+}$, $[Cu(H_2O)_4]^{2+}$, $[Mg(H_2O)_6]^{2+}$, $[Ni(H_2O)_6]^{2+}$ . . . are components of the corresponding polar lattices. $[M(H_2O)_n]^{2+}$ is the general formulation of such a stable hydrated entity in the solid state. These entities thus persist in the solid as well as in aqueous solution and have as much right (18, 34) to be considered complex ions as $[PtCl_4]^{2-}$ and $[Fe(CN)_6]^{4-}$.

The conclusion which follows is that divalent cations, which are hydrated in the solid state $[M(H_2O)_n]^{2+}$, never exist in very dilute aqueous solution as the bare ion M^{2+} but as a stable hydrated form. It is not known whether the number of water molecules in the nearest layer around the ion in dilute aqueous solution will remain "n" (as in the solid state) or whether and to what extent primary solvation will contribute in this first layer. To overcome this difficulty, it will be assumed that "x" (where $x \geqslant n$) is the number of water molecules in the first layer around the ion in very dilute aqueous solution.* Accordingly the formulation of the stable hydrated entity in dilute aqueous solution is $[M(H_2O)_x]^{2+}$ or more generally $\left[M\begin{matrix}(H_2O)_n \\ (H_2O)_{x-n}\end{matrix} \right]^{2+}$. It is suggested that this entity be called "*a catonium*".

This terminology is the more correct form and should be more often used, but for simplicity the symbol M^{2+} may be accepted.†

The catonium entity is further hydrated in the normal way (see section on concept of ionic solvation) by purely electrostatic forces depending on the field strength at the surface of the catonium. The new situation arising on the dissolution of a hydrated salt with a co-ordinated hydrated cation is depicted as follows:

$$[M(H_2O)_n]^{2+} \underset{\text{crystallization}}{\overset{\text{dissolution}}{\rightleftharpoons}} \left[M\begin{matrix}(H_2O)_n \\ (H_2O)_{x-n}\end{matrix} \right]^{2+} \cdot (H_2O)_p(H_2O)_s(H_2O)_h \qquad [2]$$

(hydrated cation in crystal) — (hydrated catonium in very dilute aqueous solution)

where x represents the permanent solvation number,

$(x - n)$ represents the inner primary solvation number,

$[M(H_2O)_n]^{2+}$ represents the hydrated cation in crystal,

$\left[M\begin{matrix}(H_2O)_n \\ (H_2O)_{x-n}\end{matrix} \right]^{2+}$ represents the catonium entity in solution,

p represents the primary solvation number of the catonium or outer primary solvation,

s represents the secondary solvation number of the catonium,

h represents the hydrodynamical solvation number of the catonium.

This proposed structure is diagrammatically shown in Fig. 1.

Some authors (18) seem to be of the opinion that n and x are the same, but there is no evidence for such a statement.

†*In analogy with the use of* (H^+) *for the hydroxonium ion* $(H_3O)^+$.

Can. J. Chem. Downloaded from www.nrcresearchpress.com by 186.148.149.217 on 09/04/12
For personal use only.

Can. J. Chem. Downloaded from www.nrcresearchpress.com by 186.148.149.217 on 09/04/12
For personal use only.

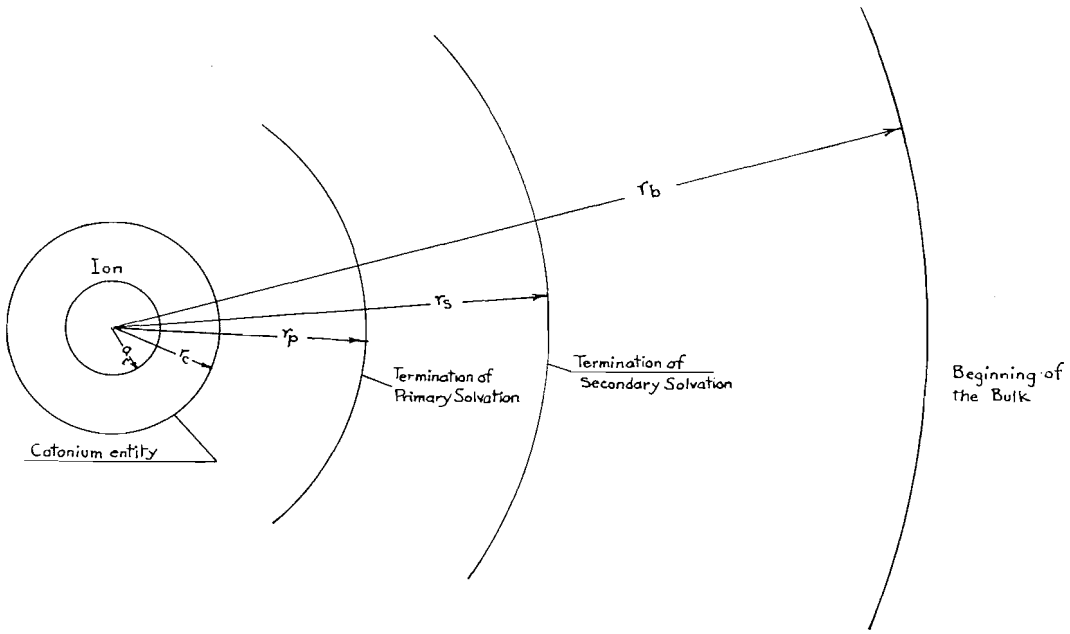


FIG. 1. The proposed structure of a solvated divalent ion in dilute aqueous solution.

4. METHOD OF CALCULATION

A serious difficulty, which occurs generally in the evaluation of ion–dipole interaction, is the lack of knowledge of the values of the dielectric constant near an ion. The only values reported in the literature (10, 12) are those near a monovalent ion. Utilizing Webb's theory (10), values of the dielectric constant of water in terms of distance from a divalent ion could be evaluated (see Fig. 2). Knowing this relation, the solvation number

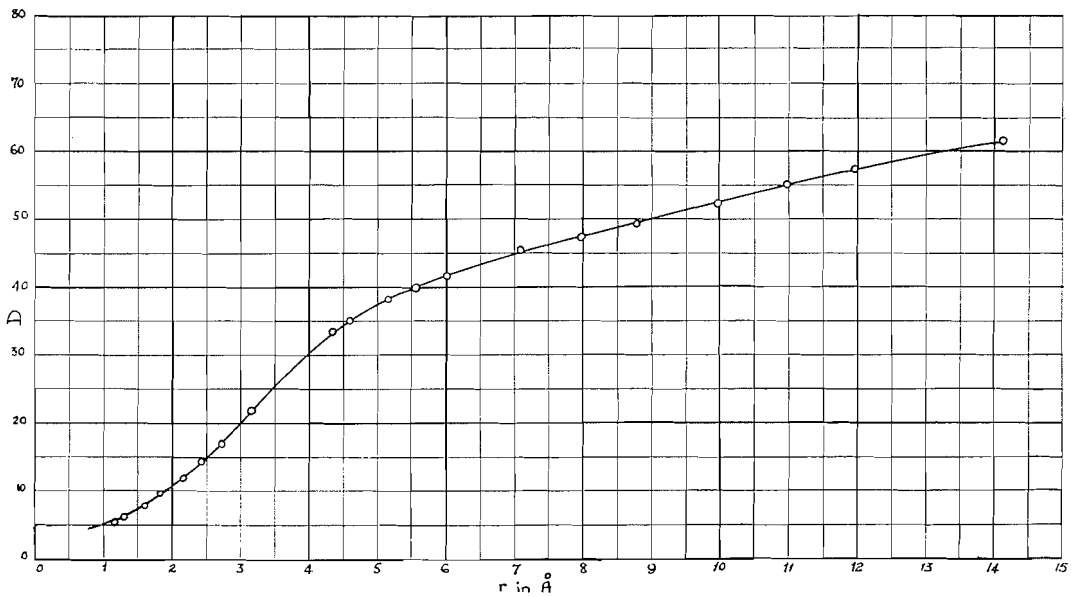


FIG. 2. Variation of the dielectric constant of water D in the vicinity of a divalent ion.

of divalent ions can be calculated by following the method of calculation previously given for monovalent ions (3). All data which are needed in the present calculation are recorded in Table II. The corresponding relation $[e^{-(w/kt)}r^2 - r]$, which is required for the graphical evaluation of solvation numbers (3), is shown plotted in Fig. 3. The curve is of

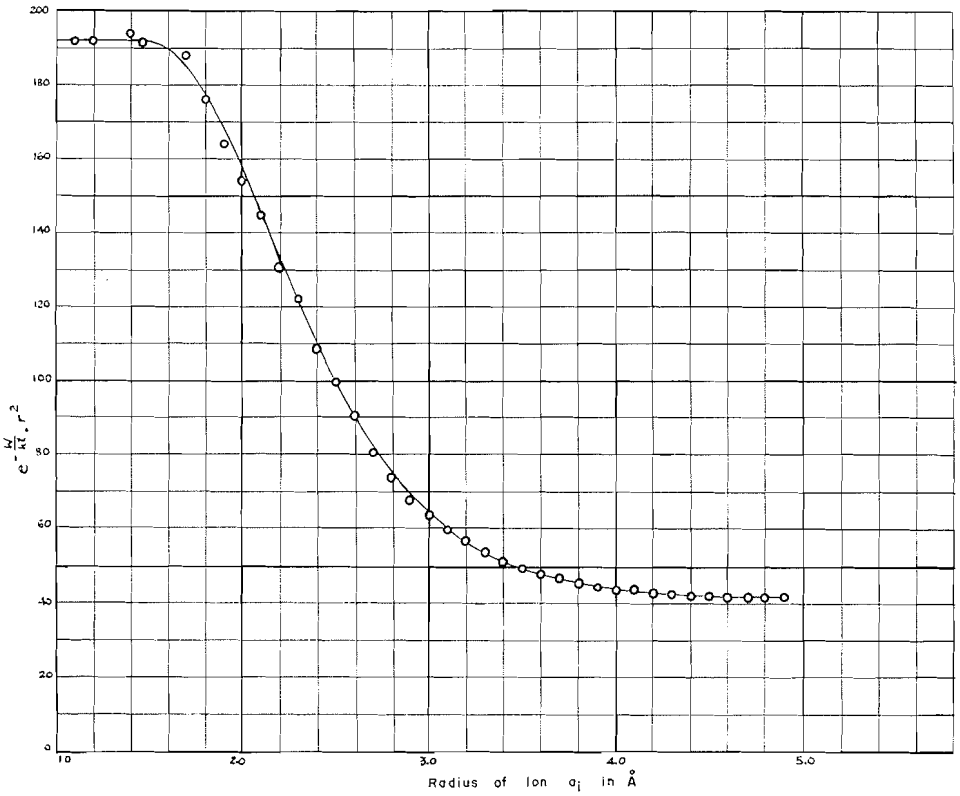


FIG. 3. Relation between $e^{-w/kt}$. r^2 and radius of ions.

the sigmoid type. It shows a horizontal portion at first extending to a distance $r = 1.6$ Å (from the center of the ion), followed by a rapid decrease which extends up to a distance $r = 3.2$ Å and finally a steady insignificant decrease.

5. DISCUSSION

Permanent and primary solvations are the only types involving definite solvent molecules in association with the ion (see section on concepts of ionic solvation). Each experiment measures the above-mentioned types plus some contribution from the other types of solvation depending on the phenomenon observed. Accordingly, Part I of this discussion is devoted to permanent and primary solvation types. Possible termination boundaries of the different types of solvation are given in Part II. In Part III, values of the ionic radii are discussed.

(I) Permanent and Primary Solvation Numbers

Examination of the present analysis (see Table II and Fig. 3) shows that the statistical possible number of water molecules which could be accommodated in the first layer

Can. J. Chem. Downloaded from www.nrcresearchpress.com by 186.148.149.217 on 09/04/12
For personal use only.

TABLE II

Data needed for the present statistical analysis

a_i	U_1	U_2	U_3	$(U_1-U_2-U_3)$	w/kt	$e^{-(w/kt)r^2}$	
1.0	0.4189	0.0213	0.2488	0.1487	3.3751	194.5	
1.1	0.3767	0.0196	0.2122	0.145	3.284	191.5	
1.2	0.3474	0.018	0.1796	0.142	3.212	191.7	
1.3	0.312	0.0169	0.1560	0.1391	3.142	192.0	Approximately constant value
1.4	0.278	0.0168	0.1244	0.1369	3.087	193.9	
1.5	0.2567	0.0152	0.1080	0.1335	3.004	191.4	
1.6	0.2325	0.015	0.0870	0.1305	2.932	189.8	
1.7	0.2123	0.014	0.0708	0.1275	2.859	187.7	
1.8	0.1928	0.0135	0.0571	0.1225	2.736	176.3	
1.9	0.1755	0.0131	0.0456	0.1169	2.6	163.0	
2.0	0.1603	0.0127	0.0352	0.1122	2.486	154.0	
2.1	0.1468	0.0124	0.0271	0.1073	2.367	144.5	
2.2	0.1334	0.0121	0.0203	0.1009	2.212	130.5	
2.3	0.1228	0.0119	0.0150	0.0958	2.089	121.9	
2.4	0.1124	0.0117	0.0113	0.0894	1.931	109.3	
2.5	0.1037	0.0115	0.0088	0.0835	1.788	99.6	
2.6	0.0958	0.0113	0.0069	0.0776	1.646	90.6	
2.7	0.0875	0.0111	0.0054	0.0709	1.483	80.7	
2.8	0.0809	0.0109	0.0046	0.0655	1.35	74.0	
2.9	0.0748	0.0108	0.0038	0.0603	1.223	68.2	
3.0	0.0698	0.0106	0.0032	0.0559	1.118	64.1	
3.1	0.0649	0.0105	0.0028	0.0515	1.01	60.1	A possible boundary of primary solvation
3.2	0.0631	0.0104	0.0024	0.0475	0.913	57.0	
3.3	0.0562	0.0103	0.0021	0.0438	0.823	54.2	
3.4	0.0521	0.0102	0.0018	0.0401	0.732	51.6	
3.5	0.0487	0.0101	0.0016	0.0370	0.657	49.8	
3.6	0.0453	0.0100	0.0014	0.0339	0.58	47.9	
3.7	0.0425	0.0099	0.0012	0.0313	0.518	46.8	
3.8	0.0396	0.0098	0.0011	0.0287	0.454	45.6	
3.9	0.0370	0.0097	0.0010	0.0262	0.395	44.6	
4.0	0.0347	0.0096	0.0009	0.0230	0.316	43.0	
4.1	0.0325	0.0095	0.0008	0.0222	0.318	44.0	
4.2	0.0305	0.0095	0.0008	0.0202	0.248	42.8	
4.3	0.0287	0.0094	0.0007	0.0185	0.207	42.5	
4.4	0.0270	0.0093	0.0007	0.0169	0.169	42.3	A possible boundary of secondary solvation
4.5	0.0255	0.0093	0.0007	0.0155	0.133	42.3	
4.6	0.0239	0.0092	0.0006	0.0140	0.098	42.3	
4.7	0.0225	0.0092	0.0006	0.0127	0.066	42.1	Approximately constant value
4.8	0.0212	0.0091	0.0006	0.0116	0.039	42.3	
4.9	0.020	0.0091	0.0005	0.0104	0.010	42.6	
5.0	0.0188	0.0090	0.0005	0.0092			

around a divalent ion is 8.06 water molecules. This could be considered as a possible value of "x" provided that the mode of association is purely electrostatic. On the other hand, several lines of evidence (18, 19, 21, 24, 32, 33, 34) combine to show that the value of "n", which is a measure of the tendency of an ion to co-ordinate in the solid state, is given by the Goldschmidt co-ordination number. According to Sidgwick (21), the value of "n" for an element depends upon its position in the periodic classification, but the co-ordination number can only assume these values (2, 4, 6, or 8). The values 4 and 6 are the most usual. Following these lines of discussion, it could be concluded that in very dilute aqueous solution, the number of water molecules in the first shell around an ion is 8 irrespective of the mode of association. It seems very probable that when the binding capacity of a cation (as given by the value of n) appears exhausted, it can link up with other water molecules by physical forces and build up a more complex structure to an upper limit which is given by the average value 8.06 water molecules. In other words, the 8.06 water molecules in the first layer around an ion constitute a mixture of both permanent and primary solvation types.

The values of these two types are given by "n" and "$8.06-n$" respectively. As this

Can. J. Chem. Downloaded from www.nrcresearchpress.com by 186.148.149.217 on 09/04/12
For personal use only.

primary solvation number of the ion $(8.06-n)$ is within the catonium entity, it is better to refer to this number as the "*inner primary solvation number*".

The catonium entity as stated before is further hydrated in the normal way (primary, secondary) by electrostatic forces depending on the field strength at the surface of the catonium (see equation 2 and Fig. 1). The most important fact which results from the present theory is that primary solvation of the catonium entity exists for only one layer of water molecules. This result follows from the application of the concept of screening effect (3, 30). The calculated values of "p" are shown in Table IV. This number of water molecules attached to the catonium can be called the "*outer primary solvation number*".

(II) The Termination Boundaries of the Different Types of Solvation of the Catonium Entity

It could be postulated that for primary solvation, as qualitatively defined above, the interaction of the catonium with dipole is such that the net interaction energy in the solvation sheath minus the solvent–solvent interactions in the bulk is greater than the kinetic thermal energy. The possible termination of primary solvation can thus be regarded as the point at which $w/kt \geqslant 1$. This condition is reached at $r \simeq 3.1$ Å (see Table II and see Fig. 1). This indicates that all catoniums of radius less than 3.1 Å are primary hydrated.

After the termination of primary solvation, the ion and dipoles from the bulk of the solution compete and where the energy of the catonium–dipole interaction is equal and opposite to that of dipole–dipole interaction, $w = 0$, so that the secondary solvation may be regarded as terminated. This condition is reached at r about 4.4 Å. It is also characterized by an approximately constant value of ds as shown in Table II. This indicates that all *primary solvated catoniums* of radius less than 4.4 Å are secondary hydrated.

The beginning of the bulk can be recognized as the critical radius inside which no water molecule has the normal dielectric properties. This is reached for r about 22 Å (see Fig. 2).

(III) Crystal Radii and Univalent Radii

With regard to ionic radii, in general, no unique radius can be ascribed to the ion. Comprehensive assignment of fixed radii to ions has frequently been attempted, notably by Lande (23), Wasestjerna (23), Goldschmidt (24), and Pauling (22). Most of the ionic radii values adopted by these authors are different (see Table III). The difference is mainly due to the arbitrary nature of the allotment of fixed extension to ions. However, Pauling formulated a semi-empirical set of ionic radii. These radii are known as univalent radii of the ions and are shown in Table III. These radii are the radii the multivalent ions would possess if they were to retain their electron distributions and enter into coulomb interaction as if they were univalent. It seems very probable that these univalent radii are in harmony and more suitable for use than the crystal radii. The following simple arguments can be given in support of this:

1. The univalent radii are very accurate to about 1% and form a complete set under comparable conditions.

2. These radii represent correctly the relative sizes of the outer electron shells of the ions compared with those for the alkali and halogen ions.

3. They have absolute values such as to cause their sums to be equal to the equilibrium interionic distance in standard crystals.

4. In ionic crystals, the crystal radii sums decrease about 10% for the change from *a crystal* M^+X^- to its *isoelectronic* $M^{++}X^{--}$. This decrease is not due to lack of compensation of the charges in the electron distribution but results rather from the effect of doubling

Can. J. Chem. Downloaded from www.nrcresearchpress.com by 186.148.149.217 on 09/04/12
For personal use only.

the electric charges on the ions. On the other hand, the univalent radius sums remain nearly constant.

5. If both univalent radii and crystal radii are represented graphically as functions of the atomic number, it will be seen that there is great regularity in the univalent radii sequences (22).

TABLE III

Crystal ionic radii and univalent crystal radii

Ion	Crystal ionic radii					Univalent crystal radii (Pauling (22))
	Pauling (22)	Wasestjerna (23)	Wyckoff (29)	Zachariasen (31)	Goldschmidt (24)	
Be^{++}	0.31		0.3	0.55	0.34	0.44
Mg^{++}	0.65	0.75	0.75	0.89	0.78	0.82
Ca^{++}	0.99	1.02	1.06	1.17	1.06	1.18
Sr^{++}	1.13	1.2	1.18	1.34	1.27	1.32
Ba^{++}	1.35	1.4	1.38	1.49	1.43	1.53
Zn^{++}	0.74		0.83		0.83	0.88
Cd^{++}	0.97		0.99		1.03	1.14
Hg^{++}	1.10		0.66		1.12	1.25
Mn^{++}			0.83		0.91	
Fe^{++}			0.80		0.87	
Co^{++}			0.78		0.82	
Ni^{++}			0.74		0.78	
Sn^{++}						
Pb^{++}			1.18		1.32	
Ti^{++}					0.76	
Cu^{++}					0.80	
Pt^{++}					0.52	
Pd^{++}					0.50	

The list of univalent radii, however, is incomplete while a complete list of crystal radii is available (see Table III).

For this reason, and for testing the significance of this new concept, the primary solva-

TABLE IV

Permanent and primary solvation numbers $(x+p)$

Ion	Outer primary solvation number (p)		Permanent and inner primary solvation number (x)	$(x+p)$
	Using Pauling univalent crystal radii	Using Goldschmidt crystal ionic radii		
Be^{++}	7.2	7.56	8.06	15.62
Mg^{++}	5.3	5.5	8.06	13.56
Ca^{++}	3.78	4.26	8.06	12.32
Sr^{++}	3.25	3.4	8.06	11.46
Ba^{++}	2.79	3.02	8.06	11.08
Zn^{++}	5.04	5.27	8.06	13.33
Cd^{++}	3.9	4.37	8.06	12.43
Hg^{++}	3.4	3.99	8.06	12.05
Mn^{++}		4.89	8.06	12.95
Fe^{++}		5.08	8.06	13.14
Co^{++}		5.3	8.06	13.36
Ni^{++}		5.5	8.06	13.56
Sn^{++}		4.85	8.06	12.91
Pb^{++}		3.25	8.06	11.31
Ti^{++}		5.65	8.06	13.71
Cu^{++}		5.38	8.06	13.44
Pt^{++}		6.66	8.06	14.72
Pd^{++}		6.91	8.06	14.97

NOTE: (*a*) Goldschmidt's values of crystal ionic radii are used in the present calculation of $(x+p)$.

(*b*) Pauling's value of univalent crystal radii are not complete and have been used to demonstrate the effect of this new concept on solvation number.

Can. J. Chem. Downloaded from www.nrcresearchpress.com by 186.148.149.217 on 09/04/12
For personal use only.

tion number "p" was calculated using Pauling's univalent radii and the Goldschmidt crystal ionic radii. As can be seen from Table IV, the difference between the two cases is less than 0.5, and this is insignificant.

CONCLUSIONS

1. Concepts of ionic solvation are discussed and the definition of the following four types is suggested: "permanent, primary, secondary, and hydrodynamic".

2. The variation of the dielectric constant of water in the vicinity of divalent ion is evaluated.

3. The dissolution process of a co-ordinated cation is depicted as

$$[M(H_2O)_n]^{2+} \underset{\text{crystallization}}{\overset{\text{dissolution}}{\rightleftharpoons}} \left[M\begin{matrix}(H_2O)_n\\(H_2O)_{x-n}\end{matrix}\right]^{2+} . (H_2O)_p . (H_2O)_s .$$

4. The permanent solvation type "n", which persists in solid state and in solution, is given by Goldschmit co-ordination number (4 or 6) and its mode of association has been assumed not to be purely physical.

5. Divalent cations in solution are not simply cations corresponding to the symbol M^{2+} but rather catonium entities $\left[M\begin{matrix}(H_2O)_n\\(H_2O)_{x-n}\end{matrix}\right]^{2+}$.

6. All divalent ions with radius less than 1.6 Å can have an envelope of 8.06 water molecules ($x = 8.06$). This is a mixture of both permanent solvation type "n" and inner primary solvation type $(x-n)$.

7. All catonium ions with radius less than 3.1 Å are primary solvated "p". This is called the outer primary solvation number.

8. The outer primary solvation number exists for only one layer of water molecules around the catonium entity. This result follows from the application of the concept of screening effect.

9. The following critical radii have been calculated:

(*a*) Inner primary solvation types exist inside the critical radii 1.6 Å.

(*b*) Outer primary solvation types exist inside the critical radii 3.1 Å.

(*c*) Secondary solvation types exist inside the critical radii 4.7 Å.

(*d*) Water does not have the normal dielectric properties inside the critical radius of about 22 Å.

10. The present theory demonstrates

(*a*) Azzam's theory of ionic solvation which was previously given in Part I,

(*b*) Fuoss's theory of the screening effect,

(*c*) Webb's theory of the variation of the dielectric constant of water near an ion,

(*d*) Pauling univalent radii concept.

11. The theoretically calculated values of ionic solvation of divalent ions are in good agreement with those obtained by mutually self-consistent experimental methods.

TABLE V

Comparison between the theoretically calculated values and values of the self-consistent experimental methods

Method	Be^{++}	Mg^{++}	Ca^{++}	Sr^{++}	Ba^{++}	Zn^{++}	Cd^{++}	Hg^{++}	Mn^{++}	Fe^{++}	Co^{++}	Ni^{++}	Sn^{++}	Pb^{++}	Ti^{++}	Cu^{++}	Pt^{++}	Pd^{++}
The present method	15.6	13.5	12.3	11.4	11	13.3	12.4	12	13	13.1	13.3	13.5	12.9	11.3	13.7	13.4	14.7	15
Average of: Mobility (16), Entropy (1), Compressibility (1)		14	12.2		9	12.2	12			12.2						12.2		

Can. J. Chem. Downloaded from www.nrcresearchpress.com by 186.148.149.217 on 09/04/12
For personal use only.

Can. J. Chem. Downloaded from www.nrcresearchpress.com by 186.148.149.217 on 09/04/12
For personal use only.

REFERENCES

1. J. Baborovsky. Rec. trav. chim. **42**, 229 (1923); Collection Czechoslov. Chem. Commun. **11**, 542 (1938).
   H. Brintzinger. Z. anorg. u. allgem. Chem. **223**, 101 (1935).
   E. H. Riesenfeld. Z. physik. Chem. **66**, 672 (1909).
   H. Remy. Z. physik. Chem. **126**, 161 (1927).
   N. Bjerrum. Z. anorg. u. allgem. Chem. **109**, 275 (1920).
   H. Ulich. Z. Elektrochem. **36**, 497 (1930).
   A. Passynski. Acta Physicochim. U.R.S.S. **8**, 385 (1938).
   E. Darmoir. J. phys. radium, **2**, 2 (1941).
   F. Bourin and E. Rouyer. Compt. rend. **204**, 1420 (1937).
   M. Cordier. J. chim. phys. **43**, 345 (1946).
   H. Freunlich and A. Schnell. Z. physik. Chem. **133**, 151 (1928).
   W. Manchot *et al.* Z. anorg. Chem. **141**, 38 (1924).
2. A. M. Azzam. Ph.D. Thesis. University of London, London, 1949.
3. A. M. Azzam. Part I. Z. Elektrochem. **58**, 889 (1954).
4. J. O'M. Bockris. Quart. Rev. **3**, 173 (1949).
5. N. Bjerrum. Z. anorg. u. allgem. Chem. **109**, 275 (1920).
6. G. Scatchord. J. Am. Chem. Soc. **17**, 2098 (1925).
7. H. S. F. Frank. J. Am. Chem. Soc. **63**, 1789 (1941).
8. R. Stoke and R. Robinson. J. Am. Chem. Soc. **70**, 1870 (1948).
9. O. Halpern and P. Gress. J. Chem. Phys. **2**, 136 (1934).
10. T. J. Webb. J. Am. Chem. Soc. **48**, 2589 (1926).
11. B. H. Van Puynen. Chem. Weekblad. **53**, 461 (1957).
12. P. Debye. Marx handbuch der radiologie. Leipzig. 1925. Vol. VI, pp. 618, 680.
    C. H. Collie, J. B. Hasted, and D. M. Ritson. J. Chem. Phys. **16**, 1 (1948).
    G. Schwartzenback. Z. physik. Chem. **176**, A, 133 (1936).
13. S. Aschkanasi. Z. Elektrochem. **36**, 504 (1930).
14. K. Fajans. Verb. Dtsch. Physik Ges. **21**, 709 (1919).
    K. Fajans. Z. Elektrochem. **34**, 502 (1928).
15. M. Born. Z. Physik, **1**, 45 (1920).
16. H. Ulich. Hand-u. Jahrb. Chem. Physik, **6**, 186 (1933).
    H. Ulich. Z. physik. Chem. **168**, 141 (1934).
    H. Ulich. Trans. Faraday Soc. **23**, 392 (1927).
17. R. Lindeman. Z. physik. Chem. **23**, 387 (1927).
18. J. Bernal and R. Fowler. J. Chem. Phys. **1**, 515 (1933).
19. R. Fricks and H. Schitzdellor. Z. anorg. chem. **131**, 132 (1923).
    R. Schurtz *et al.* Z. anorg. Chem. **226**, 33 (1935).
    H. J. Emeléus and J. S. Anderson. Modern aspects of inorganic chemistry. London. 1943.
20. J. Langmiur. J. Am. Chem. Soc. **41**, 868 (1919).
    L. Cambi, A. Cagnasso *et al.* Gazz. chim. ital. **64**, 758 (1938).
21. N. V. Sidgwick. Ann. Rept. Chem. Soc. **30**, 110 (1933); Electronic theory of valency. Oxford. 1927.
22. L. Pauling. J. Am. Chem. Soc. **49**, 765 (1927); Proc. Roy. Soc. A, **114**, 181 (1927).
23. H. Brück. Z. Physik, **51**, 707 (1928).
    W. E. Bleich *et al.* J. Chem. Phys. **2**, 252 (1934).
    J. A. Wasestjerna. Soc. Sci. Fennica Commentationes Phys. Math. **6**, 22 (1932).
    B. O. Gronblow. Soc. Sci. Fennica Commentationes Phys. Math. **8**, 13 (1935).
    A. Landé. Z. Physik, **1**, 191 (1920).
24. V. M. Goldschmidt. Trans. Faraday Soc. **25**, 253 (1929); Geochemische verteilungsgestze der element. Oslo. 1926; Ber. **60**, 1263 (1927).
25. M. Volmer. Ann. **200**, 440 (1924).
26. A. E. Van Arkel *et al.* Chemical binding. Leipzig. 1931.
27. E. J. W. Verwey. Rec. trav. chim. **61**, 127 (1942).
28. G. T. Morgan. J. Chem. Soc. **117**, 1639 (1920).
29. R. W. G. Wyckoff. The structure of crystals. 2nd ed. Chemical Catalogue Co., New York. 1931.
30. R. M. Fuoss. Trans. Faraday Soc. **30**, 970 (1934).
    R. H. Fowler. Statistical mechanics. The University Press, Cambridge, Eng. 1936.
31. W. Zachariasen. Z. Krist. **80**, 137 (1931).
32. H. J. Emeléus and J. S. Anderson. Modern aspects of inorganic chemistry. London. 1943.
33. A. Werner. Komplexverbindungen. 1924.
    O. Schmitz and Dumont. Z. anorg. Chem. **226**, 33 (1935).
    A. Werner. Ber. **41**, 345 (1908).
34. G. Wagner. Z. anorg. Chem. **124**, 289 (1922).
    F. J. Garrick. Phil. Mag. VII, **9**, 131 (1930).

Can. J. Chem. Downloaded from www.nrcresearchpress.com by 84.22.46.98 on 09/08/12
For personal use only.

ACID ACTIVATION OF MONTMORILLONITE[1]

R. D. Heyding, R. Ironside, A. R. Norris,[2] and R. Y. Prysiazniuk[3]

ABSTRACT

A Pembina montmorillonite clay has been activated with sulphuric acid at various dosages by the conventional wet process and by the new "dry" process. The products are compared with respect to the fractions of the metal ion components remaining after leaching, the hydrated silica content, the bleaching capacity, and the B.E.T. nitrogen and water surface areas which they exhibit. Surface areas were also determined after calcining the products *in vacuo*. The surface areas are discussed with reference to the removal of metal ions occupying octahedral lattice sites in a model clay particle.

INTRODUCTION

Montmorillonite clays are employed extensively as bleaching agents for mineral and vegetable oils, and as cracking catalysts in the petroleum industry. Often the capacity of a particular montmorillonite with respect to either of these functions is enhanced by "activation", that is, by the removal of basic constituents in the clay lattice by leaching with acid. In the conventional activation procedure the clay is refluxed with relatively dilute sulphuric (or hydrochloric) acid, filtered, and washed. The acid concentration is limited by the consistency of the clay/water/acid system, while the temperature attainable in open vats is limited by atmospheric pressure. A new procedure developed by Puddington and Farnand (1) permits higher concentrations of acid for a given dosage (acid-to-clay ratio) since only sufficient water is used to produce a reasonably free-flowing crumb on mixing, and this may be heated to about 200° C to promote rapid reaction. Subsequent treatment is similar to the conventional process. It is convenient to describe these two methods as the "wet" process and the "dry" process, respectively.

The dry process embodies obvious technical advantages as far as production of activated clay is concerned. The present study was designed to evaluate the products of dry activation by comparison of some of their physical characteristics with those of wet activated clays. The physical properties were chosen on the assumption that their variation would indicate the nature of the degradation of the clay lattice on activation.

The montmorillonite lamina or pseudo unit cell consists of partially hydrated silica/alumina/silica layers in which some of the octahedral aluminum sites are occupied by trivalent iron or divalent magnesium. The substitution of trivalent ions by divalent metal ions implies an electrostatic inequality within each lamina which is cancelled by the inclusion of hydrogen, alkali metal, or alkaline earth ions (the exchangeable ions) between adjacent laminae in the lattice. In the presence of water vapor, water is included in the interlaminar space resulting in an expansion of lattice along the c axis. It is not certain whether the water is adsorbed or chemisorbed by hydration of the interlaminar ions, or by hydration of the silica forming the faces of the interlaminar area. The last possibility is the basis of the montmorillonite model proposed by Edelman and Favejee (2), in which the tetrahedral silica units point into the interlaminar space. This model is not as generally accepted as the Hoffman–Endell–Wilm–Marshall–Hendricks model (3) in which the silica units point into the lattice and away from the interlaminar region.

[1]*Manuscript received December 4, 1959.*
Contribution from the Division of Applied Chemistry, National Research Council, Ottawa, Canada. Issued as N.R.C. No. 5663.
[2]*N.R.C. Summer Student, 1958. Present address: Graduate School, University of Chicago, Chicago, Illinois.*
[3]*N.R.C. Summer Student, 1959. Present address: Graduate School, Iowa State College, Ames, Iowa.*

Although these models differ considerably in detail, the existence of silica/alumina/silica structural layers separated by exchangeable ions is not disputed. In what follows, either model will serve as the basis for the argument, and the data do not serve to distinguish between them.

According to Bradley and his co-workers (3), water is adsorbed in monomolecular layers between the silicate laminae as are many polar but otherwise neutral molecules. This water is accommodated reversibly regardless of heat treatment below ca. 300° C; above 500° C water of hydration is removed, and the laminae are bound together irreversibly. After calcination at 600° C, that is, after the conversion of the clay to a silica/alumina catalyst, no water is adsorbed in the interlaminar areas. Nitrogen, on the other hand, is not adsorbed in the interlaminar region even in non-calcined montmorillonite. These phenomena have been exploited by Mooney, Keenan, and Wood (4), who have reasoned that while B.E.T. nitrogen surface areas can represent external particle area only, B.E.T. water surface areas must indicate the interlaminar area as well. The interlaminar area obtained by difference in the two B.E.T. areas is quite consistent with the crystal model.

On leaching with acid, the metal ions in the middle layer of the silicate lamina are dissolved, according to Mills *et al.* (5), in essentially the same proportions in which they were present in the original clay. With the removal of these ions, the surface area can be expected to increase, and there is ample proof of this in the literature (5, 6, 7, 8, 9, 10). Usually intercorrelation of data obtained by various workers is difficult, as a result of differences in the raw clays and in the many variables associated with the activation and the subsequent treatment of the product. It is apparent, however, that the ability of a clay to decolorize mineral and vegetable oils is directly proportional to the B.E.T. nitrogen surface area of the clay, other factors, such as heat treatment, water content, and exchangeable ion, remaining constant. On the other hand, no direct relation between area and catalytic activity is observed (5); clays with similar activation and calcination histories and similar nitrogen areas need not necessarily exhibit similar catalytic properties.

The quantitative comparison of B.E.T. nitrogen and water surface areas as applied to natural montmorillonites by Mooney and his co-workers is a convenient means of studying the clay lattice before and after acid activation. We have activated a montmorillonite by both wet and dry processes at several acid dosages, and have measured the B.E.T. nitrogen and water surface areas of the products. These data, together with the total analyses of the clays, permit a self-consistent interpretation of the activation process. Redetermination of these surface areas after calcining the clays indicates in turn the extent of the modification of the lattice on irreversible dehydration. The decolorizing characteristics of the clays were measured, but no attempt was made to evaluate the calcined clays as catalysts.

EXPERIMENTAL PROCEDURE

The montmorillonite was supplied by Pembina Mountain Clays, Ltd., Manitoba. X-ray diffraction patterns showed no crystalline impurities in measurable amounts. The raw clay was ground to 80% −200 mesh and stored in airtight glass containers until used. Separate batches were used in the wet and dry activation experiments. The water content of the raw clay was determined by drying specimens at 110° C, and allowance was made for this adsorbed water in calculating the quantities of water and acid required by the activation procedure.

Can. J. Chem. Downloaded from www.nrcresearchpress.com by 84.22.46.98 on 09/08/12
For personal use only.

To activate by the wet method, 100 g (110° C dry basis) of clay was mixed with weighed amounts of 98% reagent grade sulphuric acid corresponding to 0 to 50% of the clay by weight, and sufficient water, including the water adsorbed by the clay, to bring the total liquid content to 400 g. This mixture was refluxed at 100° C for 6 hours with mechanical stirring. The product was filtered and washed to a pH of 3.0–3.5, at which point the washings were in all instances free of sulphate ion. The liquor and washings were recovered for analysis. The filter cake was dried overnight at 90° C and reground to −80 mesh. The fraction with particle sizes in the −80 to 100 mesh range was retained for surface area determinations.

The clay designated by the number 7A was subjected to two 50% acid leaches each of 6-hour duration, while clay 7B was leached three times in a similar manner.

To activate by the dry method, 454 g of clay (110° C dry basis) was mixed in a small muller for 30 minutes with 0–50% acid based on the dry clay and sufficient water to bring the total liquid content to 454 ml. After mixing, a 100- to 200-g portion was heated for 4 hours at 150° C in a drying oven, mixed with water while hot, filtered, and washed to a pH of 3.0–3.2. Subsequent treatment was identical with that of the wet activated clays. Since there was no means of determining weight changes during the mulling operation, the washings were not recovered for analysis.

The bleaching power of the activated clays was determined by adding 1 g of clay (−200 mesh material equilibrated overnight in a moisture cabinet) to 33 g of a semi-finished test oil kindly supplied by Imperial Oil Limited. The mixture was stirred mechanically while the temperature was increased in 5 to 7 minutes to 142° C. After cooling in air to 100° C, the oil was filtered and the percentage of transmittance measured in a Lumetron colorimeter equipped with red (6500 Å), green (5300 Å), and blue (4200 Å) filters. All transmissions were determined relative to Stanolax, a water-white medicinal oil produced by Standard Oil of Indiana.

Conventional procedures were used in analyzing the clays.* An estimate of "hydrated silica" was included in the analysis, although the precise significance of the determination is problematical. The difference in solubility of crystalline and amorphous silica in weak sodium carbonate solution, established by Lunge and Millberg (15), has been made the basis of several procedures for estimating the degree of chemical decomposition of clay minerals (9, 16). The fraction of the silica in the clay which dissolves in a sodium carbonate solution under certain conditions is defined as "hydrated silica" and presumably represents the amorphous silica contained in the mineral. Since the conditions are essentially empirical, the details of the method used in these analyses are given below.†

The activated clays were calcined *in vacuo* at 600°±5° C. Approximately 30 minutes

**The major components, viz.* SiO_2, Al_2O_3, MgO, *and* CaO, *were determined by the conventional gravimetric and volumetric procedures appropriate to samples of this nature (11, 12).* Na_2O *and* K_2O *were determined by flame photometry using methods adapted from well-established techniques for siliceous materials (13). The determination of sulphate ion was complicated by the presence in these samples of silicon and iron. The determination was made, finally, by a method based on the chromatographic separation of the sulphate ion from perchloric acid solution according to Nydahl (14).*

†To estimate "hydrated silica" content, 1.000±0.001 g of clay and 2.00 g Na_2CO_3 *were weighed into a stainless steel beaker. 100 ml of water was added and the solution heated to boiling within 6 minutes. Boiling was continued for 10 minutes, and the steel beaker was then removed from the heat. After settling for 4 minutes, the clear liquid was decanted into a filter of paper pulp supported on a perforated steel filter plate. The filter was sucked dry. 25 ml of 2% w/v hot solution of* Na_2CO_3 *was added and the liquid boiled for 2 minutes. After settling for 4 minutes, the clear liquid was again decanted into the filter funnel which was again sucked dry. This was repeated once more with a further 25-ml portion of* Na_2CO_3 *solution. 25 ml of hot 2% w/v* NaCl *solution was then added to the residue in the steel beaker, and the suspension poured into the filter funnel. Another 25 ml of hot* NaCl *solution was used to rinse the beaker and this too was added to the filter funnel when it had sucked dry. The filtrate was made up to 500 ml and a 5-ml aliquot taken for the determination of silica by the usual colorimetric method using ammonium molybdate and reading the yellow color developed on a filter photometer.*

Can. J. Chem. Downloaded from www.nrcresearchpress.com by 84.22.46.98 on 09/08/12
For personal use only.

were required to bring the sample to temperature if "boiling" was to be avoided, and the total heating time was 2.5 hours. The volatile products were collected in a liquid nitrogen cooled trap. Loss in weight was determined, and the volatile products examined qualitatively.

Nitrogen sorption isotherms were determined in a volumetric system in the usual manner. Water adsorption isotherms to 94% of saturation at 25° C were determined gravimetrically using Worden quartz springs of 2 g maximum capacity and 100 mg/cm sensitivity. The water vapor pressure in the system was controlled by a liquid water reservoir maintained at constant temperatures between −19° and 25° C. The clay samples were brought to constant weight in the system by repeated sorption/evacuation cycles before determination of the isotherm was begun.

RESULTS AND DISCUSSION

1. *Analyses*

For convenience, the activated clays have been designated W-1, W-2, . . . , W-6, the wet activated series, with 0%, 10%, . . . , 50% acid, and D-1, D-2, . . . , D-6, the dry activated series, with comparable acid concentrations. Clays W-1 and D-1 constitute "blanks", and represent the products obtained by the leaching process in the absence of sulphuric acid. As mentioned earlier, clays D-7A and D-7B were the products of two and three consecutive 50% acid leaches, respectively.

TABLE I

Analysis of activated clays

Basis, clay dried at 105° C; ignition temperature, 950° C. Series W, wet activated; series D, dry activated

Clay No.	% H_2SO_4 in activation	Ignition loss, %	$SO_4^=$, %	H_2O, %	SiO_2, %	Fe_2O_3, %	Al_2O_3, %	MgO, %	CaO, %	Na_2O, %	K_2O, %	Hydrated silica, %
Raw clay	—	8.86	3.66	5.81	61.30	3.82	19.59	4.36	0.97	0.16	0.15	0.58
W-1	0	9.46	2.07	7.74	60.85	3.53	20.31	4.62	1.02	0.40	0.14	0.60
W-2	10	8.90	1.11	7.98	63.21	3.02	20.24	4.22	—	—	—	0.82
W-3	20	8.52	0.64	7.99	64.08	2.66	20.00	4.66	0.38	0.26	0.07	1.66
W-4	30	8.15	0.35	7.86	66.40	1.85	19.44	4.89	—	—	—	3.16
W-5	40	7.85	0.12	7.75	68.08	1.42	18.40	4.76	0.36	0.02	0.04	4.98
W-6	50	7.92	0.50	7.49	70.62	1.25	16.75	3.38	—	—	—	8.35
W-7A	2×50	6.76	1.46	5.54	80.93	0.82	9.53	1.67	—	—	—	22.1
W-7B	3×50	5.56	1.07	4.67	88.18	0.48	4.53	0.56	—	—	—	28.8
D-1	0	7.94	2.69	5.70	64.21	3.58	18.92	4.36	0.97	0.61	0.16	0.81
D-2	10	7.92	1.14	6.98	65.82	2.94	18.89	4.07	—	—	—	1.84
D-3	20	7.20	1.41	6.03	69.57	1.88	17.48	3.79	0.16	0.04	0.09	5.05
D-4	30	6.64	1.45	5.43	71.27	1.47	17.73	3.30	—	—	—	9.98
D-5	40	6.30	0.55	5.85	75.02	1.30	14.02	2.82	0.20	0.05	0.05	15.0
D-6	50	6.27	0.68	5.71	77.81	1.26	11.80	2.23	0.22	0.04	0.06	16.0

The analyses of the activated clays are given in Table I, and the analyses of the wet activation leach liquors in Table II. To be comparative, these quantities must be reduced with reference to some invariant component to a common basis. It will be seen in Table II that the dissolution of silica during the wet activation process is less than 0.7% of the total silica, and can be regarded as negligible. Similarly, semiquantitative estimates of the silica removed from the clay by the dry activation process were of the same order of magnitude. The assumption can be made, therefore, that the silica content of the clays is a constant for each series, and the analyses can be expressed in terms of the "blanks", W-1 and D-1. The residual compositions calculated on this basis are recorded in Table III.

Can. J. Chem. Downloaded from www.nrcresearchpress.com by 84.22.46.98 on 09/08/12
For personal use only.

TABLE II

Analysis of wet activation liquor
Basis: clay as activated, 110° C dry

Clay No.	SiO_2, %	Fe_2O_3, %	Al_2O_3, %	MgO, %	CaO, %
W-1	0.07	0.03	0.10	0.11	0.22
W-2	0.38	0.50	1.23	0.41	0.68
W-3	0.31	1.03	2.15	0.53	0.76
W-4	0.37	1.79	3.36	0.78	0.84
W-5	0.25	1.70	5.28	1.05	0.84
W-6	0.34	2.12	7.21	1.46	0.86
W-7A	0.34	2.33	13.85	2.71	0.94
W-7B	0.43	2.52	17.55	3.45	0.96

TABLE III

Residual composition of activated clays
Assumption: No silica removed by activation process

Clay No.	(1) $SO_4^=$, g	(2) H_2O, g	(3) Fe_2O_3 g	(3) Fe_2O_3 % rem.*	(4) Al_2O_3 g	(4) Al_2O_3 % rem.*	(5) MgO g	(5) MgO % rem.*	(6) $M^{2+, 3+}$, % rem.†	(7) Hydrated SiO_2, g
				Wet activated clays						
				Basis, 100 g clay W-1; SiO_2 content, 60.85 g						
W-1	2.07	7.74	3.53		20.31		4.62			0.60
W-2	1.07	7.68	2.91	(82.6)	19.49	(96.0)	4.06	(87.9)	(93.2)	0.79
W-3	0.61	7.58	2.53	(71.8)	18.99	(93.5)	4.43	(95.9)	(92.2)	1.57
W-4	0.32	7.20	1.70	(48.3)	17.81	(87.7)	4.48	(97.0)	(86.4)	2.90
W-5	0.11	6.93	1.27	(36.1)	16.44	(81.0)	4.25	(92.0)	(79.6)	4.45
W-6	0.43	6.45	1.08	(30.7)	14.43	(71.1)	2.91	(63.0)	(66.3)	7.20
W-7A	1.10	4.17	0.62	(17.6)	7.17	(35.3)	1.26	(27.3)	(32.4)	16.6
W-7B	0.74	3.22	0.33	(9.4)	3.13	(15.4)	0.39	(8.4)	(13.4)	19.9
				Dry activated clays						
				Basis, 100 g clay D-1; SiO_2 content, 64.21 g						
D-1	2.69	5.70	3.58		18.92		4.36			0.81
D-2	1.11	6.81	2.87	(80.2)	18.43	(97.4)	3.97	(91.1)	(94.7)	1.79
D-3	1.30	5.57	1.74	(48.6)	16.13	(85.2)	3.50	(80.3)	(81.1)	4.66
D-4	1.31	4.89	1.32	(36.9)	15.97	(84.4)	2.97	(68.1)	(77.3)	8.99
D-5	0.47	5.00	1.11	(31.0)	11.20	(59.2)	2.41	(55.2)	(56.1)	12.8
D-6	0.56	4.71	1.04	(29.0)	9.74	(51.5)	1.84	(42.2)	(47.8)	13.2

*Percentage of component remaining in the clay.
†Percentage of metal ions remaining in the clay.

Summations of the quantities of the various components found in the leach liquor and the clay residues are consistent within the limits of uncertainty in analysis and homogeneity of the clay samples.

The sulphate contents (Table III, column 2), particularly of the blanks and the dry activated clays, are abnormally large. Indeed, during the calcining of these clays, SO_2 as well as water was recovered in the gaseous products. In the montmorillonite deposit from which the raw clay was obtained, the clay strata are bounded by sulphide bearing deposits. It is generally accepted that the sulphates produced by natural oxidation of the sulphides and carried in solution into the clay deposits dissolve metal ions and produce, *in situ*, a semiactivated clay. Consequently an appreciable sulphate content in the raw clay is to be expected. The refluxing and washing operations which produced clays W-1 and D-1 might be expected to remove essentially all of the metal sulphates which might

Can. J. Chem. Downloaded from www.nrcresearchpress.com by 84.22.46.98 on 09/08/12
For personal use only.

be present with the exception of $CaSO_4$. Now if most of the sulphur in these clays is present as $CaSO_4$, appreciable quantities of SO_2 would not be produced on heating *in vacuo* at 600° C. It appears logical to propose that some sulphate ions are associated with the montmorillonite lattice itself, and this suggestion is substantiated by the relatively high sulphate content of clays W-7A and W-7B.

The natural leaching of these clays is responsible for the variation in composition from batch to batch. The difference in composition of clays W-1 and D-1 is unfortunate, but not significant in what follows.

Metal ions are removed by the activation process, but in these clays the fractions dissolved are not in proportion to the quantities present in the unactivated clays. Iron is removed to a much greater extent than aluminum or magnesium, while aluminum is the least removed of the three. It may be that the concentration of iron (and, to a lesser extent, magnesium) in the octahedral sites is greater near the surfaces of the particles than in the bulk of the crystal.

For a given acid dosage, the metal ions are removed to a greater extent by dry activation than by wet activation (Table III, column 6). However, a more notable variation in the two series is the greater "hydrated silica" content of the dry activated clays (Table III, column 7), even though the constitutional water content is consistently less than that of the wet activated clays. In view of the rather arbitrary nature of the quantity, it is rather doubtful that any structural argument explaining the difference could be supported.

The decolorizing capacities of the activated clays are recorded in Table IV. The results

TABLE IV

Decolorizing characteristics of activated montmorillonite
Transmissions relative to Stanolax. Red, 6500 Å;
green, 5300 Å; blue, 4200 Å

Wet activated				Dry activated			
Clay No.	% transmission			Clay No.	% transmission		
	Red	Green	Blue		Red	Green	Blue
W-1	91.5	67.3	25.8	D-1	90.5	65.5	25.0
W-2	95.0	75.0	32.0	D-2	95.0	78.3	36.3
W-3	98.0	87.0	46.0	D-3	99.0	92.0	54.5
W-4	99.7	91.8	52.5	D-4	99.5	94.0	58.5
W-5	100	95.8	61.0	D-5	99.0	94.0	58.0
W-6	100	96.5	61.4	D-6	99.0	93.3	55.3
W-7A	100	97.5	65.0				
W-7B	99.0	89.0	45.3				
S*	100	94.0	55.5	S*	99.0	92.5	54.0

*Control using the commercial decolorizing agent Superfiltrol.

are consistent with the conclusions drawn by Farnand and Peterson (17) based on the examination of a great number of activated clays obtained under a wide variety of experimental conditions: Dry activated clays produced with 0 to 35% acid are more efficient bleaching agents than are wet activated clays obtained with comparable acid dosages. Above 40% acid dosages, the capacity of the dry activated clays decreases and in the 35–50% region dry activated clays are inferior to wet activated clays. The maximum in decolorizing capacity of wet activated clays occurs at acid dosages in excess of 50%; nevertheless, a dry activated clay obtained with 20% acid is equivalent in capacity to a wet activated clay obtained with 30% acid.

Can. J. Chem. Downloaded from www.nrcresearchpress.com by 84.22.46.98 on 09/08/12
For personal use only.

2. Sorption Isotherms

Typical nitrogen sorption isotherms are reproduced in Fig. 1, and typical water sorption isotherms in Figs. 2 and 3.

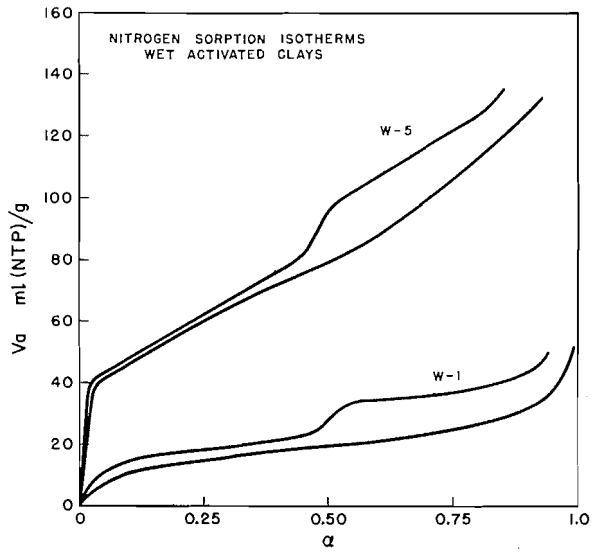


FIG. 1. Typical nitrogen sorption isotherms, wet activated clays.

The water isotherms are of characteristic form, although we could detect no inflections normally attributed to the completion of one and two water layers in the interlaminar region of the lattice. The curves were reproducible, although it should be reiterated that these isotherms were determined only after constant clay weight had been obtained by adsorption/evacuation cycles. The D-1 and W-1 isotherms are essentially identical. For strict comparison, the isotherms of the activated clays W-6 and D-6 should lie some 10% closer to the abscissa since the experimental data are expressed in terms of the product rather than the unactivated clay; nevertheless the decreased adsorption at low relative pressures and increased adsorption near saturation is quite evident. On the other hand, the adsorption capacity of the clay with respect to nitrogen is increased at all relative pressures by activation.

The hysteresis exhibited in the nitrogen isotherms is not uncommon among montmorillonites, but is not always observed. The "break" in the desorption loop was observed at relative pressures between 0.43 and 0.53 in all of the clays for which complete isotherms were obtained.

On calcining the clays at 600° C, the water isotherms are altered as shown in Fig. 4, and become quite similar in form to the nitrogen isotherms of the uncalcined clays. Since the calcined clays can no longer sorb water in the interlaminar regions, adsorption can occur only on surfaces which are also available for nitrogen adsorption, and the similarity in isotherms is to be expected. Presumably these isotherms are inherent in the water isotherms of the uncalcined clays, but are masked by the greater volumes adsorbed in the interlaminar spaces.

Can. J. Chem. Downloaded from www.nrcresearchpress.com by 84.22.46.98 on 09/08/12
For personal use only.

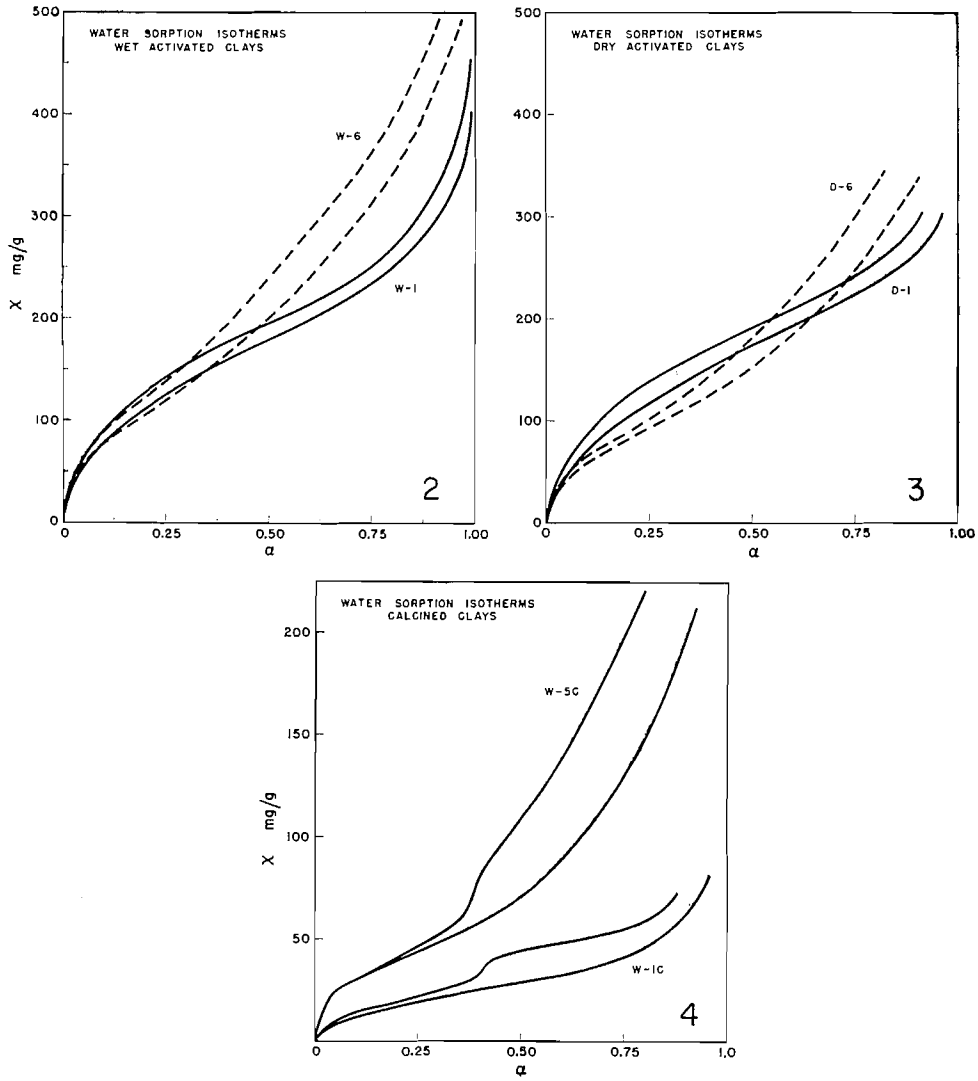


FIG. 2. Typical water sorption isotherms, wet activated clays.
FIG. 3. Typical water sorption isotherms, dry activated clays.
FIG. 4. Typical water sorption isotherms, calcined clays.

3. *B.E.T. Surface Areas*

The classical B.E.T. function has been applied to the desorption arms of the nitrogen and water isotherms as indicated in Fig. 5. The results are compiled in Tables V and VI. Again these data have been expressed in terms of the common denominators W-1 and D-1 on the assumption that the loss of SiO_2 from the lattice has been negligible.

A comparison of surface areas as a function of acid dosage is given in Fig. 6. Water surface areas decrease with increasing acid dosage more rapidly for the dry activated clays. The initial increase in nitrogen area is greater for the dry activated clays, but the

Can. J. Chem. Downloaded from www.nrcresearchpress.com by 84.22.46.98 on 09/08/12
For personal use only.

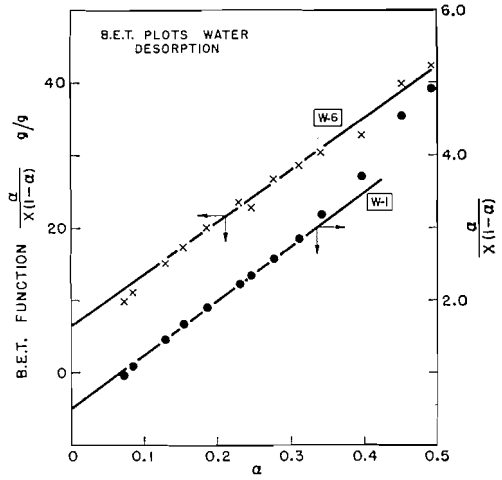


FIG. 5. Typical B.E.T. plots obtained from desorption isotherms.

TABLE V

B.E.T. nitrogen and water surface areas, wet and dry activated clays

Clay No.	N_2, m^2/g	H_2O, m^2/g	Area relative to W-1: N_2, m^2/g W-1	Area relative to W-1: H_2O, m^2/g W-1
W-1	60	454	60	454
W-2	94	—	90	—
W-3	138	444	132	426
W-4	205	492	188	451
W-5	225	—	201	—
W-6	269	467	231	402
W-7A	367	296	276	223
W-7B	366	238	253	164

Clay No.	N_2, m^2/g	H_2O, m^2/g	Area relative to D-1: N_2, m^2/g D-1	Area relative to D-1: H_2O, m^2/g D-1
D-1	61	444	61	444
D-2	110	425	107	415
D-3	185	393	171	363
D-4	215	391	193	352
D-5	229	—	196	—
D-6	239	352	197	290

areas of the wet activated clays are greater at high acid dosage. Maximum areas are attained at 33% and >50% acid for the dry and wet procedures, respectively.

The decolorizing capacity of each series as a function of nitrogen area is illustrated in Fig. 7. For areas below 220 m^2/g the bleaching capacity appears to be a function of area alone; however, above this point the capacity of the dry activated clays decreases. The corresponding decrease in wet activated clay capacity occurs at ca. 360 m^2/g.

Can. J. Chem. Downloaded from www.nrcresearchpress.com by 84.22.46.98 on 09/08/12
For personal use only.

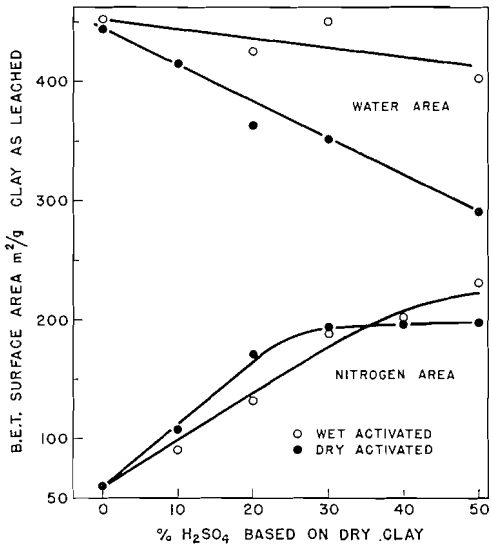


FIG. 6. B.E.T. water and nitrogen surface areas of wet and dry activated clays as a function of acid dosage.

TABLE VI

B.E.T. nitrogen and water surface areas, calcined clays

Clay No.	Weight loss, %	N_2, m^2/g	H_2O, m^2/g	Areas relative to W-1 and D-1	
				N_2, m^2/g	H_2O, m^2/g
W-1C	8.7	46	76	50	83
W-3C	7.7	97	98	100	101
W-5C	7.5	181	150	175	145
W-6C	—	240	—	—	—
W-7AC	—	367	—	—	—
W-7BC	4.6	360	—	259	—
D-1C	9.3	56	78	62	86
D-3C	7.3	154	124	153	123
D-5C	6.3	203	160	179	141

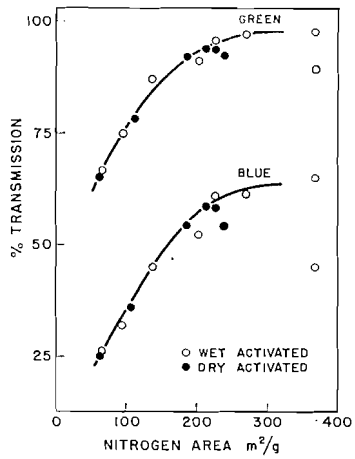


FIG. 7. Bleaching capacity of wet and dry activated clays as a function of nitrogen surface area.

Can. J. Chem. Downloaded from www.nrcresearchpress.com by 84.22.46.98 on 09/08/12
For personal use only.

It has been observed (17) that decolorizing capacity is a function of adsorbed water content. In general, the capacity increases with increasing water content, with the upper limit dictated by the degree of frothing of the oil/clay mixture which can be tolerated during bleaching. One might reasonably assume that adsorption of color bodies occurs on the interlaminar faces of the clay, and that water is required to expand the lattice and facilitate penetration by the color groups. However, since the capacity is a function of the nitrogen surface area rather than the water surface area, the interlaminar areas appear to be relatively unimportant. It may be that the adsorbed water is responsible for a modification in the silicate surface which facilitates the chemisorption of the color groups in the oil.

The reduction in nitrogen surface areas on calcining is less than 30%, but water surface areas decrease from ca. 400 m^2/g to values equal to or less than the nitrogen areas. Insofar as comparison of the two activation processes are concerned, the calcined dry activated clays exhibit higher surface areas, particularly at intermediate acid dosages.

4. Surface Areas and Structure

On the basis of the analysis, the quasi-unit cell of clay W-1 contains

$$Si_8{}^{IV}(Al_{3.2}Fe_{0.3}Mg_{0.9})^{VI}O_{20}(OH)_4(SO_4)_{0.2}\,.$$

Assuming the dimensions of this cell are $5\times10\times10$ Å, the interlaminar area is approximately 410 m^2/g. The observed water surface area is 454 m^2/g, and the nitrogen area 60 m^2/g. According to Mooney, Keenan, and Wood, the interlaminar area is the difference in these two values, i.e. 393 m^2/g. In this argument it is implied that the external surface is indifferent to both nitrogen and water vapor, and the B.E.T. external surface areas are identical for both adsorbates.

The disintegration of the montmorillonite lattice on leaching can be considered in the following way. For the model clay particle illustrated in Fig. 8, we shall assume p silicate

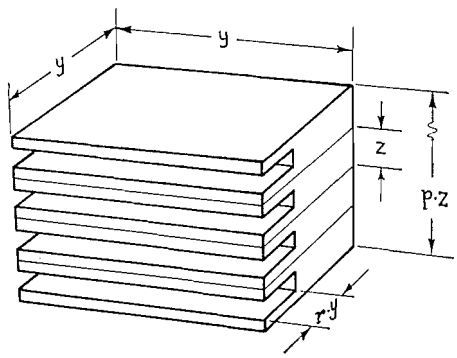


FIG. 8. Model activated montmorillonite particle.

laminae z Å thick, and y Å in length and width. If n is the number of such particles per gram of clay, the density, ρ, in grams per cubic angstrom, is given by

$$\rho = 1/npzy^2. \qquad [1]$$

When the lattice is attacked by acid, metal ions in the intralaminar octahedral sites are removed. This can be represented in an idealized manner as indicated in Fig. 8; the increase in nitrogen area per gram, ΔA_N, is given by

$$\Delta A_N = nmpry^2 \qquad [2]$$

Can. J. Chem. Downloaded from www.nrcresearchpress.com by 84.22.46.98 on 09/08/12
For personal use only.

in which r is the fraction of metal ions removed from the lattice, and m is the number of layers of nitrogen which can be accommodated in the intralaminar pores, and can have the values $1 \leqslant m \leqslant 2$.

Substituting for n in eq. 2 in terms of eq. 1,

$$\Delta A_N = mr/\rho z (\text{Å}^2/\text{g}). \quad [3]$$

Assuming a lattice dimension z of 10 Å, and a density of 2.5 g/cc,

$$\Delta A_N = 400mr \ (\text{m}^2/\text{g}). \quad [4]$$

This expression can be obtained simply by extension of the interlaminar water area argument given earlier, but the development from the model shows that the increase in nitrogen area is quite independent of particle size and shape. Unfortunately it is not likely that m will be independent of r. For low values of r, that is, when the lattice is not seriously attacked, the intralaminar pores will likely admit only one layer of nitrogen which will be adsorbed by both upper and lower silica surfaces. For intermediate values of r, the silica layers may be distorted to such an extent that almost two layers can be admitted. For higher values of r, the silica lattice may be expected to collapse on itself, and m will decrease. When the metal ions have been removed to such an extent that the montmorillonite lattice can not be considered to exist, the model and the equation will not apply.

There is reason to suspect that clays W-1 and D-1 have already been subjected to natural leaching processes, because of their high sulphate content and high nitrogen surface areas. Most natural montmorillonites exhibit nitrogen areas of 10 to 30 m²/g, although some hydrogen montmorillonites may have areas of 40 m²/g. Assuming that clays W-1 and D-1 would exhibit areas of 30 m²/g had natural leaching not occurred, and assuming m is unity, then by eq. 4, r equals 0.075, and 0.925 of metal ions are still retained in the lattice. The fraction of metal ions remaining in the artificially activated clays can then be obtained directly using the analyses in Table III, column 6, and the increase in area to be expected calculated using eq. 4. The results are given in Table VII.

TABLE VII

Observed and calculated nitrogen area increments equation 4
(areas in m²/g)
Assumption: r for W-1, D-1 = 0.075

Clay No.	$1-r$	r	$\Delta A_{N\ calc}$	$\Delta A_{N\ obs}$	Clay No.	$1-r$	r	$\Delta A_{N\ calc}$	$\Delta A_{N\ obs}$
W-1	0.925	0.075	30	30	D-1	0.925	0.075	30	30
W-2	0.86	0.14	56	60	D-2	0.875	0.125	50	67
W-3	0.85	0.15	60	102	D-3	0.75	0.25	100	141
W-4	0.80	0.20	80	158	D-4	0.715	0.285	114	163
W-5	0.74	0.26	104	170	D-5	0.52	0.48	192	166
W-6	0.61	0.39	156	200	D-6	0.44	0.56	224	167
W-7A	0.30	0.70	280	246					
W-7B	0.12	0.88	350	223					

In spite of the simplicity of the model, the agreement in observed and calculated nitrogen area increments is satisfactory. In no instance is ΔA_N observed greater than twice ΔA_N calculated, and consequently the discrepancies are within the limits of m. For the wet activated clays, m attains a maximum value of 1.98 at W-4 (30% acid, 20% ion

Can. J. Chem. Downloaded from www.nrcresearchpress.com by 84.22.46.98 on 09/08/12
For personal use only.

removal); beyond this point the silicate layers appear to collapse reducing the value of m. For clays W-7A and W-7B the clay lattice is destroyed to the extent that the equation is no longer tenable. In the dry activated series, the maximum value of m is only 1.4, and the collapse of the lattice begins at slightly lower acid concentrations. For clay D-6 (50% acid) the model is not valid.

As metal ions are removed, the water sorbed in the interlaminar spaces will decrease, particularly if they are associated with the exchangeable ions in the formation of hydrates. The interlaminar area can then be estimated by multiplying the idealized interlaminar area, 410 m²/g, by the factor $(1-r)$. The total water surface area should then be the sum of this area plus the nitrogen surface area of the sample. The results of the approximation are given in Table VIII.

TABLE VIII

Observed and calculated water areas
(areas in m²/g)

Clay No.	$410(1-r)$	A_{N_2}	$A_{H_2O\ calc}$	$A_{H_2O\ obs}$	Clay No.	$410(1-r)$	A_{N_2}	$A_{H_2O\ calc}$	$A_{H_2O\ obs}$
W-1	380	60	440	454	D-1	380	61	441	444
W-2	352	90	442	—	D-2	358	107	465	415
W-3	349	132	481	426	D-3	307	171	478	363
W-4	328	188	516	451	D-4	293	193	486	352
W-5	304	201	505	—	D-5	213	196	409	—
W-6	250	231	481	402	D-6	180	197	377	290
W-7A	123	276	399	223					
W-7B	48	253	301	164					

With the exception of W-1 and D-1, the agreement is poor, particularly for heavily leached samples. The major source of error may lie in the equation of water and nitrogen external surface areas. For clays W-7A, W-7B, and the calcined clays W-5C, D-3C, and D-5C, the observed total water areas are less than the observed nitrogen areas. In all of these samples the interlaminar adsorption will be negligible; hence it appears that the external water areas are less than the nitrogen areas by a factor of 0.67 to 0.80. For clays with relatively low nitrogen areas the correction is small; but the subtraction of nitrogen areas from total water areas as a measure of the interlaminar area of activated clays is not generally valid unless some correction factor is introduced.

5. Summary

1. In this particular montmorillonite, metal ions in octahedral sites are not removed by acid activation in the proportions in which they are originally present. On both wet and dry activation, the rates of removal are in the order Fe > Mg > Al.

2. At any given acid dosage, the extent of removal of metal ions, the formation of "hydrated silica", and the general degradation of the lattice is greater by the dry process than by the wet process.

3. The bleaching capacity with respect to mineral oil is a function of nitrogen surface area up to 220 m²/g for dry activated clays, and 360 m²/g for wet activated clays.

4. The nitrogen areas and the bleaching capacities of clays activated with 30% acid by the dry process are superior to the analogous wet activated clays.

5. On calcining, water isotherms become similar in form to nitrogen isotherms. Nitrogen areas are decreased slightly, water surface areas, drastically. At comparable acid dosages

Can. J. Chem. Downloaded from www.nrcresearchpress.com by 84.22.46.98 on 09/08/12
For personal use only.

surface areas of calcined dry activated clays are larger than the areas of calcined wet activated clays.

6. External silicate surfaces do not appear to give equivalent B.E.T. nitrogen and water surface areas.

7. According to the model presented, the montmorillonite lattice is essentially intact even after removal of 25% of the metal ions. With greater removal the residual silica layers collapse, and above 50% removal, the product no longer behaves as montmorillonite towards the adsorption of nitrogen and water vapor.

ACKNOWLEDGMENTS

We are indebted to Mr. A. E. McIlhinney and Mr. L. Pageau for assistance in the preparation of the dry activated clays, and for the determination of bleaching capacities.

REFERENCES

1. I. E. PUDDINGTON and J. R. FARNAND. Can. Patent No. 583,497 (1959).
2. C. H. EDELMAN and J. CH. L. FAVEJEE. Z. Krist. **100**, 417 (1940).
3. G. W. BRINDLEY. The X-ray identification and crystal structures of clay minerals. The Mineralogical Soc., London. 1951.
4. R. W. MOONEY, A. G. KEENAN, and L. A. WOOD. J. Am. Chem. Soc. **74**, 1367 (1952).
5. G. A. MILLS, J. HOLMES, and E. B. CORNELIUS. J. Phys. & Colloid Chem. **54**, 1170 (1950).
6. J. ESCARD. J. chim. phys. **51**, 638 (1954).
7. S. TEICHNER. Compt. rend. **227**, 392, 427 (1948).
8. W. T. GRANQUIST and G. G. SUMNER. Proceedings of the Sixth National Conference on Clays and Clay Minerals. Pergamon Press. 1959. p. 292.
9. J. DE D. LOPEZ-GONZALEZ and V. R. DEITZ. J. Research Natl. Bur. Standards, **48**, 325 (1952).
10. K. YAMAMOTO and Y. MORITA. J. Chem. Soc. Japan, Ind. Chem. Sect. **55**, 745 (1952).
11. Am. Soc. Testing Materials. Chemical analysis of refractory materials, Method C18–52. Book of Standards, Part 3. 1955.
12. W. F. HILDEBRAND, G. E. F. LUNDELL, H. A. BRIGHT, and J. I. HOFFMAN. Applied inorganic analysis. 2nd ed. John Wiley. 1953.
13. Am. Soc. Testing Materials. Spec. Tech. Publ. No. 116. 1952.
14. F. NYDAHL. Anal. Chem. **26**, 580 (1954).
15. G. LUNGE and C. MILLBERG. Z. angew. Chem. **393**, 425 (1897).
16. U.S.A. Dept. of the Interior, Geological Survey Professional Paper 205-B. Minerals of the montmorillonite group. Washington. 1945. p. 36.
17. J. R. FARNAND and W. S. PETERSON. National Research Council, Canada. Private communication.

Can. J. Chem. Downloaded from www.nrcresearchpress.com by 84.22.46.98 on 09/08/12
For personal use only.

Can. J. Chem. Downloaded from www.nrcresearchpress.com by 186.148.149.217 on 09/04/12
For personal use only.

NOTES

MOLECULAR COMPLEXES DERIVED FROM 1,3,6,8-TETRANITROPYRENE

P. M. G. BAVIN*

The low solubility and particularly the ready availability of 1,3,6,8-tetranitropyrene (I) (1) suggested its use as a complexing agent for the isolation of traces of polycyclic hydrocarbons. Molecular complexes are indeed formed (Table I) but are valueless for

TABLE I

Hydrocarbon	Complex	Solvent	Formula	Calculated (%) C	Calculated (%) H	Found (%) C	Found (%) H
Naphthalene	Crimson needles[d]	[a, b]	$C_{36}H_{22}N_4O_8$	67.71	3.47	67.77	3.84
Indole	Purple needles[d]	[a]	$C_{32}H_{20}N_6O_8$	62.34	3.27	63.91	2.92
Fluorene	Bright red needles[d]	[a]	$C_{29}H_{16}N_4O_8$	63.50	2.94	65.79	3.46
Carbazole	Dark blue needles	[a]	$C_{28}H_{15}N_5O_8$	61.20	2.75	61.36	2.84
Phenanthrene	Brick red needles[c, e]	[a]	$C_{30}H_{16}N_4O_8$	64.29	2.88	66.61	3.49
Anthracene	Very dark green needles	[a, b]	$C_{30}H_{16}N_4O_8$	64.29	2.88	64.96	2.98
9,10-Dimethylphenanthrene	Purple needles[d, e]	[a, b]	$C_{32}H_{20}N_4O_8$	65.30	3.43	63.73	3.66
Benz[a]anthracene	Olive-green needles	[a]	$C_{34}H_{18}H_4O_8$	66.88	2.97	67.54	3.05
Pyrene	Very dark green needles	[a, b]	$C_{32}H_{16}N_4O_8$	65.75	2.76	65.61	2.61
Benzidine	Black needles	[a]	$C_{28}H_{18}N_6O_8$	59.36	3.20	59.44	3.07
4,4″-Diamino-*p*-terphenyl	Black needles	[a]	$C_{34}H_{22}N_6O_8$	63.55	3.45	63.91	3.12

[a]Xylene. [b]Acetic acid. [c]M.p. 222–224° (decomp.), rapid heating in sealed capillary. [d]M.p. 262–264° (decomp.), rapid heating in sealed capillary. [e]Crystals decomposed by washing with fresh solvent.

purposes of characterization or isolation (except, perhaps, in the cases of benzidine and 4,4″-diamino-*p*-terphenyl), as their isolation in a crystalline state requires the presence of a large excess of the hydrocarbon. This may be due to the very low solubility of the tetranitropyrene which, in solution, is in equilibrium with hydrocarbon and complex:

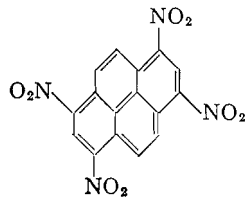
$$\text{tetranitropyrene} + \text{hydrocarbon} \rightleftharpoons \text{complex}.$$

Whether complex or tetranitropyrene crystallizes from a given system depends on their relative solubilities and the position of the equilibrium.

Some of the crystalline complexes are decomposed by washing with fresh solvent. All of them can be recrystallized only in the presence of added hydrocarbon so that the microanalyses in Table I refer to crude preparations. Only naphthalene and indole form 2:1 complexes, the others being 1:1.

The complexes decompose when heated, only those of phenanthrene and 9,10-dimethylphenanthrene melting reasonably sharply. Indole and naphthalene sublime from their complexes below 100°; those of pyrene, anthracene, and benz[a]anthracene decompose above 320°.

**I.C.I. Fellow.*



I

EXPERIMENTAL

Microanalyses are by Drs. Weiler and Strauss of Oxford.

Reagent

1,3,6,8-Tetranitropyrene was prepared as described in the literature (1). The hydrocarbons, etc. were mostly available samples but the author is indebted to I. Ungar for a very pure sample of carbazole and to Dr. D. Lewis for the 4,4″-diamino-*p*-terphenyl.

Preparation of the Complexes

Approximately 0.1 g tetranitropyrene was dissolved in the minimum of boiling xylene (occasionally acetic acid was used) and the volume increased by one-fourth to prevent crystallization. The hydrocarbon was added and the solution decanted from any impurities. The complexes slowly separated on cooling and were collected before crystallization of tetranitropyrene occurred. The crystals were sucked free of mother liquor, washed with fresh solvent (unless this decomposed them), and dried at 100° and 1–2 mm (40° in the cases of naphthalene and indole).

Some idea of the difficulties encountered in obtaining pure crystalline complexes may be gathered from the fact that almost 20 g naphthalene was necessary to obtain 0.1 g complex whereas little more than the theoretical amount of benzidine gave a good yield of complex.

Complex formation is largely dependent on the electron acceptor properties of the tetranitropyrene and the donor properties of the hydrocarbons. Consequently benzidine, which is a much stronger base than naphthalene, will form complexes more readily than the latter and should be more stable. The solubilities of the complexes will be determined primarily by their ionic character. Complexes with the amines would have more ionic character than those with polycyclic hydrocarbons and would therefore be less soluble in solvents such as xylene.

1. H. Vollmann, H. Becker, M. Corell, and H. Streeck. Ann. **531**, 1 (1937).

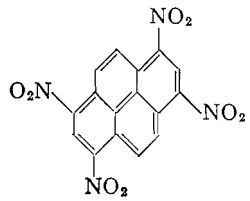
Received December 1, 1959.
Chemistry Department,
The University,
Hull, East Yorkshire, England.

Can. J. Chem. Downloaded from www.nrcresearchpress.com by 186.148.149.217 on 09/04/12
For personal use only.

O—H STRETCHING FREQUENCIES FOR SOME PHENOLS AND THEIR RELATIONSHIPS TO THE THERMODYNAMICS OF IONIZATION

William J. Canady

The O—H stretching frequencies of a large number of phenols have been studied by Ingraham, Corse, Bailey, and Stitt (1). The results were correlated with the Hammett



I

EXPERIMENTAL

Microanalyses are by Drs. Weiler and Strauss of Oxford.

Reagent

1,3,6,8-Tetranitropyrene was prepared as described in the literature (1). The hydrocarbons, etc. were mostly available samples but the author is indebted to I. Ungar for a very pure sample of carbazole and to Dr. D. Lewis for the 4,4″-diamino-*p*-terphenyl.

Preparation of the Complexes

Approximately 0.1 g tetranitropyrene was dissolved in the minimum of boiling xylene (occasionally acetic acid was used) and the volume increased by one-fourth to prevent crystallization. The hydrocarbon was added and the solution decanted from any impurities. The complexes slowly separated on cooling and were collected before crystallization of tetranitropyrene occurred. The crystals were sucked free of mother liquor, washed with fresh solvent (unless this decomposed them), and dried at 100° and 1–2 mm (40° in the cases of naphthalene and indole).

Some idea of the difficulties encountered in obtaining pure crystalline complexes may be gathered from the fact that almost 20 g naphthalene was necessary to obtain 0.1 g complex whereas little more than the theoretical amount of benzidine gave a good yield of complex.

Complex formation is largely dependent on the electron acceptor properties of the tetranitropyrene and the donor properties of the hydrocarbons. Consequently benzidine, which is a much stronger base than naphthalene, will form complexes more readily than the latter and should be more stable. The solubilities of the complexes will be determined primarily by their ionic character. Complexes with the amines would have more ionic character than those with polycyclic hydrocarbons and would therefore be less soluble in solvents such as xylene.

1. H. Vollmann, H. Becker, M. Corell, and H. Streeck. Ann. **531**, 1 (1937).

Received December 1, 1959.
Chemistry Department,
The University,
Hull, East Yorkshire, England.

Can. J. Chem. Downloaded from www.nrcresearchpress.com by 186.148.149.217 on 09/04/12
For personal use only.

O—H STRETCHING FREQUENCIES FOR SOME PHENOLS AND THEIR RELATIONSHIPS TO THE THERMODYNAMICS OF IONIZATION

William J. Canady

The O—H stretching frequencies of a large number of phenols have been studied by Ingraham, Corse, Bailey, and Stitt (1). The results were correlated with the Hammett

sigma values for these compounds. Some phenols were also studied by Stone and Thompson (2), Flett (3), and Brown (4).

Goulden (5) studied the O—H stretching frequencies of a large number of acid substances and found that they could be correlated with the pK values of the compounds in aqueous solution. The results showed that separate plots were obtained, depending upon the type of acid under consideration.

Bavin and Canady (6) demonstrated the same type of behavior with a number of phenols. It was shown that the failure to obtain a single plot with a number of substituted benzoic acids could not be ascribed to variations in electrostatic contributions, but was probably due to structural factors. No correlation was attempted with ortho constituents which could bring about appreciable hydrogen bonding.

Since the pK of an acid, and hence the free energy of ionization, may be related to the O—H stretching frequency, the question arises as to whether any similar relationships may exist for the changes in heat content and entropy of ionization.

At the time of the last-mentioned work, insufficient precise data were available to test this possibility. Recently, however, precise measurements of ΔH and ΔS for all of the mono- and dimethyl-substituted phenols have become available (7).

Table I shows the values for ΔF, ΔH, and ΔS as well as the O—H stretching frequencies for this series of phenols.

TABLE I

	Compound	ΔF (kcal)	ΔH (kcal)	ΔS cal/mole deg	Stretching frequency, cm^{-1}
1	Phenol	13.63	5.60	−27.0	3600
2	*d*-Cresol	14.03	7.13	−23.2	3606
3	*m*-Cresol	13.76	4.90	−30.7	3605
4	*p*-Cresol	14.00	4.23	−32.8	3604
5	2,3-Xylenol	14.14	6.61	−25.3	3608
6	2,4-Xylenol	14.29	7.68	−22.1	3610
7	2,5-Xylenol	13.90	6.22	−25.7	3606
8	2,6-Xylenol	14.46	4.95	−31.9	3618
9	3,4-Xylenol	13.86	8.24	−18.9	3605
10	3,5-Xylenol	13.67	7.51	−20.7	3602

The O—H stretching frequencies for the phenols are those of Bavin and Canady (6) and were measured in carbon disulphide. The instrument used was a Beckman DK-2. Since the frequencies measured are close to the cutoff point of the prism, resolution is very good.

The thermodynamical quantities are taken from the work of Papeé, Canady, Zawidzki, and Laidler (7).

The plot of stretching frequency vs. ΔF of ionization for phenol and methyl-substituted phenols can be seen in Fig. 1A. It may be noted that reasonably linear results are obtained.

Figures 1B and 1C show the O—H stretching frequencies plotted against ΔH and ΔS respectively for the phenols.

Figures 1B and 1C indicate that no particular relationship between stretching frequency and the heat and entropy of ionization can be demonstrated.

These findings tend to support the contention of Laidler (8), who has suggested that while the free energies of ionization of a particular series may be related to the vibrational frequencies involved, the effects on ΔH and ΔS are masked by solute–solvent interactions.

Can. J. Chem. Downloaded from www.nrcresearchpress.com by 186.148.149.217 on 09/04/12
For personal use only.

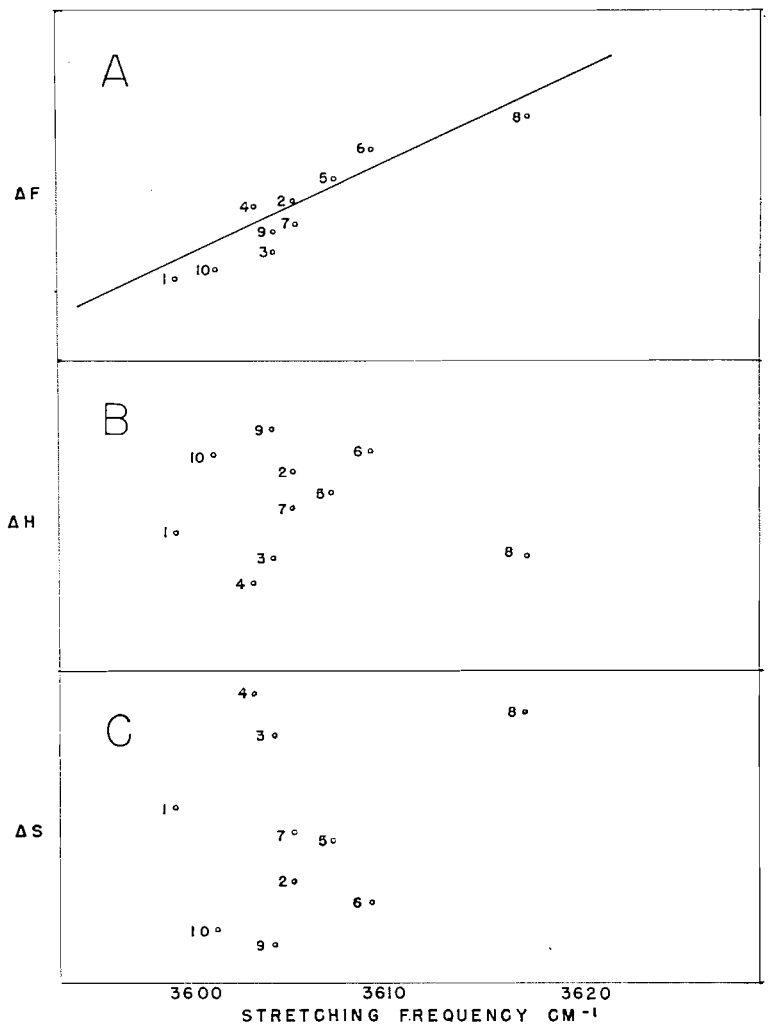


FIG. 1.

1. L. L. INGRAHAM, J. CORSE, G. F. BAILEY, and F. STITT. J. Am. Chem. Soc. **74**, 2297 (1952).
2. P. J. STONE and H. W. THOMPSON. Spectrochim. Acta, **10**, 17 (1957).
3. M. StC. FLETT. Spectrochim. Acta, **10**, 21 (1957).
4. T. L. BROWN. J. Phys. Chem. **61**, 820 (1957).
5. J. D. S. GOULDEN. Spectrochim. Acta, **6**, 129 (1953–54).
6. P. M. G. BAVIN and W. J. CANADY. Can. J. Chem. **35**, 1555 (1957).
7. H. M. PAPEÉ, W. J. CANADY, T. W. ZAWIDZKI, and K. J. LAIDLER. Trans. Faraday Soc. **55**, 1734 (1959).
8. K. J. LAIDLER. Trans. Faraday Soc. **55**, 1725 (1959).

RECEIVED FEBRUARY 29, 1960.
DEPARTMENT OF BIOCHEMISTRY,
WEST VIRGINIA UNIVERSITY SCHOOL OF MEDICINE,
MORGANTOWN, WEST VIRGINIA,
U.S.A.

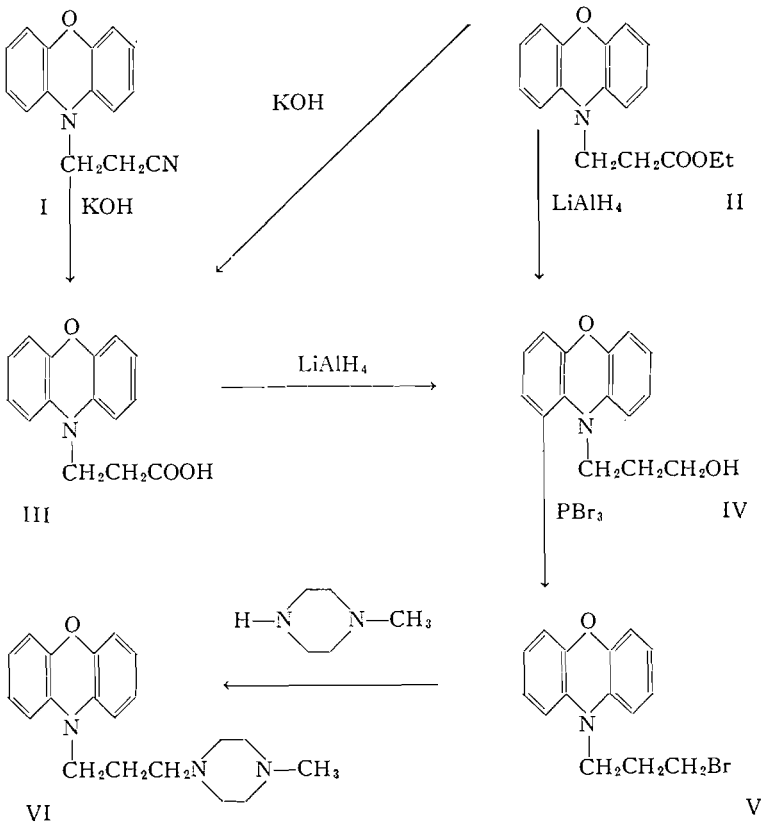
Can. J. Chem. Downloaded from www.nrcresearchpress.com by 186.148.149.217 on 09/04/12
For personal use only.

THE SYNTHESIS OF 10-SUBSTITUTED PHENOXAZINES

GERASSIMOS FRANGATOS, GEZA KOHAN, AND FRANCIS L. CHUBB

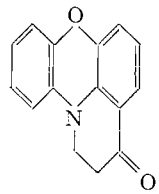
The recent publication by Muller, Buu Hoi, and Rips (1) describing the cyanoethylation of phenoxazine, and the issuing of a Belgian patent (2) describing the preparation of a series of 10-dialkylaminoalkyl phenoxazines, prompt us to report some work on the chemistry of phenoxazine, which has been in progress in these laboratories for some time. Dialkylaminoalkyl chlorides reacted with phenoxazine in the presence of freshly prepared sodamide to yield a series of 10-dialkylaminoalkyl phenoxazines which are listed in Table I. Some differences in the physical constants of these compounds from those reported by the Belgian workers are noted.

The addition of phenoxazine to acrylonitrile (1) and ethyl acrylate yielded 3-(10-phenoxazinyl)propionitrile (I) and ethyl 3-(10-phenoxazinyl)propionate (II) respectively and they were both hydrolyzed to 3-(10-phenoxazinyl)propionic acid (III). Lithium aluminum hydride reduction of II and III yielded 10-(3-hydroxypropyl)phenoxazine (IV). Attempts to prepare the corresponding chloride by treatment of IV with either thionyl chloride or phosphorus pentachloride only resulted in extensive polymerization. However, IV reacted smoothly with phosphorus tribromide to yield 10-(3-bromopropyl)phenoxazine (V). When V was allowed to react with 1-methylpiperazine, 10-(3-(3-methyl-1-piperazinyl)propyl)phenoxazine (VI) was formed.



Can. J. Chem. Downloaded from www.nrcresearchpress.com by 84.22.46.98 on 09/08/12
For personal use only.

3-(10-Phenoxazinyl)propionic acid (III) underwent cyclization with phosphorus pentoxide to give a yellow ketone, assumed to be 2,3-dihydro-1H-pyrido(3,2,1-*kl*) phenoxazine-3-one (VII), m.p. 104–105°. Muller, Buu Hoi, and Rips have reported a melting point of 144° for this compound.



VII

EXPERIMENTAL

10-(3-Dimethylaminopropyl)phenoxazine

The procedure for the synthesis of 10-(3-dimethylaminopropyl)phenoxazine is a general one and has been followed for the synthesis of all 10-dialkylaminoalkyl phenoxazines listed in Table I.

A suspension of sodamide in 100 ml of xylene was prepared from 100 ml of liquid ammonia and 3.04 g of sodium according to the procedure of Hauser, Swamer, and Adams (3). To this stirred and refluxing mixture a solution of 22 g of phenoxazine in 150 ml of xylene was slowly added. During the addition the reaction mixture turned a greenish color. It was stirred and refluxed for another hour. To this mixture a solution of dimethylaminopropyl chloride (obtained from 19 g of the corresponding hydrochloride treated with 18 g of sodium hydroxide in 66 ml of H_2O and extracted with 75 ml of xylene and dried over sodium sulphate) was added. The reaction mixture thus obtained was stirred and refluxed for 6 hours. After this mixture was cooled and filtered, the xylene was distilled under reduced pressure. The oily residue was distilled *in vacuo*. Twenty-six grams (80.5%) of a yellow oil was obtained distilling at 178°/2 mm.

Addition of Phenoxazine to Ethyl Acrylate or Acrylonitrile

To a stirred and ice-cooled mixture of 20 g phenoxazine and 33 ml ethyl acrylate (or 50 ml acrylonitrile), 2 ml of 35% methanolic benzyltrimethylammonium hydroxide was added dropwise. After the addition was completed the reaction was heated overnight (or 1 hour) on the steam bath. The excess of ethyl acrylate (or acrylonitrile) was distilled under reduced pressure. The residual ethyl 3-(10-phenoxazinyl)propionate (II) was distilled *in vacuo* to yield 20.6 g (66.5%), b.p. 187°/1 mm.

The residual 3-(10-phenoxazinyl)propionitrile was recrystallized from aqueous ethanol to yield 19.5 g (72.9%), m.p. 121–122°.

3-(10-Phenoxazinyl)propionic Acid (III)

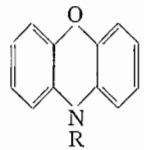
(*a*) A mixture of 4 g of 3-(10-phenoxazinyl)propionitrile, 4 g sodium hydroxide, 12 ml of water, and 40 ml of methanol was refluxed for 15 hours. The hydrolysis product was poured into ice water, acidified with dilute hydrochloric acid, filtered, and recrystallized from aqueous ethanol. 2.3 g of III was obtained, m.p. 136–138°.

(*b*) Ethyl-3-(10-phenoxazinyl)propionate (14.15 g, 0.05 mole) was dissolved in 300 ml of 10% ethanolic potassium hydroxide and refluxed for 2 hours. To this mixture after being cooled, 300 ml of water was added. The alcohol (300 ml) was distilled and the

Can. J. Chem. Downloaded from www.nrcresearchpress.com by 84.22.46.98 on 09/08/12
For personal use only.

Can. J. Chem. Downloaded from www.nrcresearchpress.com by 84.22.46.98 on 09/08/12
For personal use only.

TABLE I

10-Substituted phenoxazines 

No.	R	Yield %	B.p.	M.p.	Carbon		Hydrogen		Nitrogen	
					Calc.	Found	Calc.	Found	Calc.	Found
1	$(H_3C)_2NCH_2CH_2$	60.2	168°/2.5 mm[a]		75.54	75.75	7.08	7.01	11.02	11.11
2	$(H_3C)_2NCH_2CH_2CH_2$	80.5	178°/2 mm		76.07	75.80	7.46	7.75	10.44	10.59
3	$(H_5C_2)_2NCH_2CH_2$ hydrochloride	54.8		241–242°[b]	67.79	67.72	7.24	6.88	8.81	8.88
4	$(H_3C)_2NCHCH_2$ $\quad\quad\quad

remaining mixture was acidified with 6 *N* hydrochloric acid. 3-(10-Phenoxazinyl)propionic acid (III) precipitated and was recrystallized from aqueous ethanol; 7.3 g (57%) of the acid (III) was obtained melting at 137–138°.

10-(3-Hydroxypropyl)phenoxazine (IV)

A solution of 14 g of ethyl 3-(10-phenoxazinyl)propionate in 100 ml of ether was added slowly to a mixture of lithium aluminum hydride (2 g) in 100 ml of ether at such a rate as to maintain gentle refluxing. The reaction mixture was stirred and refluxed for 45 minutes. The excess hydride was destroyed with 2 ml of water. The reaction mixture was poured into ice water, acidified cautiously with 2 *N* sulphuric acid, and the ether layer was separated. The aqueous layer was saturated with ammonium sulphate and further extracted with ether. The combined ether extracts were washed with water and dried over sodium sulphate. The solvent was distilled and the residue recrystallized from a mixture of benzene ligroin. Eight grams (65.5%) of IV was obtained, m.p. 68°. 10-(3-Hydroxypropyl)phenoxazine was also obtained in a similar yield when 3-(10-phenoxazinyl)propionic acid (III) was reduced by lithium aluminum hydride in ether according to the procedure of Dahlbom (4) for the phenothiazine analogue.

10-(3-Bromopropyl)phenoxazine (V)

Freshly redistilled phosphorus tribromide (4.2 ml) was added to 15 g of 10-(3-hydroxypropyl)phenoxazine with cooling. The reaction mixture was heated on the steam bath for 1 hour and then poured onto crushed ice. The bromide (V) separated as an oil which solidified on standing overnight. It was filtered, washed with water on the filter, and after recrystallization from ethanol melted at 55–56°. The yield was 9 g (48%).

10-(3-(4-Methyl-1-piperazinyl)propyl)phenoxazine (VI)

A mixture of 9 g of 10-(3-bromopropyl)phenoxazine and 18 ml of 1-methylpiperazine was heated on the steam bath for 4 hours. Eighty milliliters of 10% sodium hydroxide solution was added to the reaction mixture which was then thoroughly extracted with ether. The ether extracts were combined and dried over Na_2SO_4. The ether was distilled and the residue was recrystallized from ligroin. Seven grams (73.6%) of VI was obtained, m.p. 89–91°.

2,3-Dihydro-1H-pyrido(3,2,1-kl)phenoxazine-3-one

The procedure of Smith (5) and Buu Hoi (6) for the phenothiazine and phenoselenazine analogue was followed in principle.

Fifty grams of phosphorus pentoxide was suspended in 200 ml of benzene and 10 g of 3-(10-phenoxazinyl)propionic acid was added to the stirred and heated reaction mixture. The mixture was stirred and refluxed for 1 hour and then left at room temperature overnight. It was filtered and the material remaining on the filter was washed thoroughly with an additional quantity (100 ml) of benzene. The benzene was removed from the filtrate by distillation and the residue was recrystallized from a minimum amount of ethanol; 4.5 g (48.4%) of a yellow ketone was obtained, m.p. 104°. Anal. for $C_{15}H_{11}NO_2$. Calc.: C, 75.95; H, 4.64; N, 5.91%. Found: C, 75.50; H, 4.68; N, 5.90%.

The corresponding semicarbazone was prepared and melted at 232°. Anal. for $C_{16}H_{14}N_4O_2$. Calc.: C, 65.3; H, 4.76%. Found: C, 65.13; H; 4.92%.

1. P. Muller, N. P. Buu Hoi, and R. Rips. J. Org. Chem. **24**, 1699 (1959).
2. Belg. Patent No. 569,697 (January, 1959): Chem. Abstr. **54**, 586 (1960).

Can. J. Chem. Downloaded from www.nrcresearchpress.com by 84.22.46.98 on 09/08/12
For personal use only.

3. C. R. HAUSER, F. W. SWAMER, and J. T. ADAMS. *In* Organic reactions. Vol. VIII. R. Adams. John Wiley & Sons Inc., New York. 1954. p. 122.
4. R. DAHLBOM. Acta Chem. Scand. **6**, 310 (1952).
5. N. L. SMITH. J. Org. Chem. **15**, 1125 (1950).
6. P. MULLER, N. P. BUU HOI, and R. RIPS. J. Org. Chem. **24**, 37 (1959).
7. U.S. PATENT No. 2,687,414 (August, 1954): Chem. Abstr. **50**, 1092 (1956).

RECEIVED FEBRUARY 8, 1960.
RESEARCH LABORATORIES,
FRANK W. HORNER LIMITED,
MONTREAL, QUE.

Can. J. Chem. Downloaded from www.nrcresearchpress.com by 84.22.46.98 on 09/08/12
For personal use only.

Can. J. Chem. Downloaded from www.nrcresearchpress.com by 186.148.149.217 on 09/04/12
For personal use only.

Canadian Journal of Chemistry

Issued by THE NATIONAL RESEARCH COUNCIL OF CANADA

VOLUME 38 JULY 1960 NUMBER 7

FREE RADICAL MECHANISMS FOR INHIBITED ORGANIC DECOMPOSITIONS[1]

B. W. WOJCIECHOWSKI AND K. J. LAIDLER

ABSTRACT

It is suggested that organic decompositions that are fully inhibited by substances such as nitric oxide and propylene proceed not by molecular mechanisms, but by special types of free radical mechanisms in which the inhibitor is involved in both initiation and termination. In the case of nitric oxide inhibition, initiation is considered to be by the abstraction of a hydrogen atom by NO, while termination involves reaction between the most plentiful chain carrier and either HNO or NO, depending upon whether or not H is a chain carrier. Specific mechanisms are proposed for the decompositions of paraffins, ethers, and aldehydes, when inhibited by nitric oxide, and the resulting rate equations are shown to be consistent with the behavior observed experimentally. It is shown for the ethane decomposition that the same limiting rate is obtained for any inhibitor that can become involved in the same type of mechanism.

INTRODUCTION

In spite of the very considerable amount of work that has been done on the inhibition, by substances such as nitric oxide and propylene, of gaseous organic decompositions, the nature of the mechanisms still remains something of a problem. Certain of the evidence,* such as that, in many cases, the inhibition leads to constant limiting rates and that the same limiting rates are given by different inhibitors, appears to point to the conclusion that the reactions are molecular in nature. This position has in fact been taken by Hinshelwood and his co-workers, and Stubbs and Hinshelwood (2, 3) have reviewed the evidence leading to this conclusion. On the other hand, there are certain characteristics of the fully inhibited reactions that seem to be incompatible with the view that a purely molecular mechanism is involved. These are in brief as follows:

(1) It has been found by Voevodsky and Poltorak (4) and by Rice and co-workers (5, 6) that hydrogen–deuterium mixing reactions take place as rapidly (relative to the decomposition rates) in certain fully inhibited reactions as they do in the uninhibited reactions.

(2) The fully inhibited reactions frequently exhibit a well-defined induction period, during which the pressure–time curves are S-shaped (7).

(3) The rates of the fully inhibited reactions are sometimes *decreased* by increasing the surface:volume ratio (8).

It would seem to be quite impossible to reconcile these facts with the hypothesis of a simple molecular mechanism, and it is therefore necessary to develop mechanisms of the free radical type that will give rise to limiting rates at high inhibitor concentrations, and will explain the fact that different inhibitors give the same limiting rates.

A suggestion to avoid these difficulties has recently been put forward by Voevodsky

[1]*Manuscript received February 25, 1960.*
Contribution from the Department of Chemistry, University of Ottawa, Ottawa, Canada.
**The main experimental results referred to in this paper are reviewed in Steacie's book (1).*

(9), who has interpreted the fully inhibited decompositions of paraffin hydrocarbons in terms of the idea that initiation and termination both take place on the surface of the vessel. It is proposed by Voevodsky that the initiation reactions are caused by irreversible and reversible surface processes, of which the former can be suppressed by the inhibitors. Full inhibition corresponds to complete coverage of the active centers on the wall. Voevodsky proposes no specific mechanisms, and his suggestion is subject to one serious difficulty: the amount of nitric oxide required to give complete inhibition should depend on the surface:volume ratio, and this is certainly not the case. Also, the S-shaped pressure–time curves, implying abnormally small initial rates, seem inconsistent with Voevodsky's suggestion.

The object of the present paper is to propose specific free radical mechanisms, involving the participation of inhibitor molecules, that appear to be consistent with all of the facts. The essence of our proposals is that in the presence of inhibitors the main initiating processes are hydrogen-abstraction reactions such as

$$C_2H_6 + NO \rightarrow C_2H_5 + HNO.$$

Chain termination is suggested as sometimes involving reactions such as

$$C_2H_5 + HNO \rightarrow C_2H_6 + NO,$$

but when hydrogen atoms are not the chain carriers chain termination is regarded as involving NO rather than HNO. Specific reaction mechanisms will be proposed for various types of reactions, including hydrocarbon decompositions and the decompositions of aldehydes and ethers. Additional experimental support for our proposals is being obtained, and the details will be published later.

THE DECOMPOSITION OF ETHANE

The thermal decomposition of ethane is a typical example of the decomposition of a paraffin hydrocarbon; the mechanism proposed for this case can readily be modified for the higher paraffins.

The mechanism proposed is

$$C_2H_6 + NO \xrightarrow{k_1} C_2H_5 + HNO,$$

$$C_2H_5 \xrightarrow{k_2} C_2H_4 + H,$$

$$H + C_2H_6 \xrightarrow{k_3} C_2H_5 + H_2,$$

$$H + NO \underset{k_{-4}}{\overset{k_4}{\rightleftharpoons}} HNO,$$

$$C_2H_5 + HNO \xrightarrow{k_{-1}} C_2H_6 + NO.$$

This scheme leads to the following expression for the rate

$$[1] \qquad v = (k_1k_2k_3k_{-4}/k_{-1}k_4)^{1/2}[C_2H_6].$$

The mechanism is seen to lead to first-order kinetics, as found experimentally (7, 10, 11, 12, 13).

Several comments may be made about this mechanism. Our estimate of the dissociation energy of HNO into H + NO is 44 kcal and this leads to an activation energy of 56 kcal for the initial reaction. The over-all activation energy is then found to be approximately

Can. J. Chem. Downloaded from www.nrcresearchpress.com by 186.148.149.217 on 09/04/12
For personal use only.

[2] $$E = \tfrac{1}{2}(E_1+E_2+E_3+E_{-4}-E_{-1}-E_4),$$

[3] $$= \tfrac{1}{2}(56+40+10+44-0-0) = 75 \text{ kcal},$$

which is close to the experimental value (74–77 kcal). Using these values it is found that with about 10% of nitric oxide the rate of the initiation reaction is appreciably greater than that of the splitting of ethane into two methyl radicals, so that in the presence of excess nitric oxide the latter reaction may be neglected. The fully inhibited reaction therefore occurs largely by the mechanism proposed above, and the rate is seen to be independent of the nitric oxide concentration. At lower concentrations of nitric oxide the two mechanisms occur at comparable rates and inhibition is only partial. The steady-state equation then involves the solution of a cubic equation, and a simple expression for the rate of the partially inhibited reaction cannot be obtained.

As will be discussed in more detail in a separate paper (13), the NO-inhibited decomposition of ethane has an S-shaped pressure–time curve. The initial rates are found to exhibit 3/2-order kinetics, and this can be explained by taking the chain-ending step to be

$$H + HNO \xrightarrow{k_6} H_2 + NO.$$

The rate equation is now

[4] $$v = k_3(k_1k_{-4}/k_4k_6)^{1/2}[C_2H_6]^{3/2}.$$

In general, termination involving reaction between HNO and a μ radical (one undergoing first-order reactions) leads to first-order kinetics, while the reaction of HNO with a β radical (one undergoing second-order reactions) leads to kinetics of order 3/2. At the very beginning of the inhibited reaction H atoms are more plentiful than C_2H_5 radicals, but as small amounts of ethylene accumulate this situation is reversed as a result of the reaction

$$C_2H_4 + H \rightarrow C_2H_5;$$

the main chain-ending step, therefore, changes in the manner indicated.

When the ethane decomposition is partially inhibited by nitric oxide the degree of inhibition is found to be less at higher ethane concentrations (10, 11). This effect is attributed to the fact that nitric oxide competes with ethane for hydrogen atoms. It is significant that this effect is not found with the ethers for which, as discussed below, chain termination is believed to involve NO and not HNO.

The fact that propylene and other inhibitors inhibit to exactly the same limiting extent as NO is readily explained in terms of equation [1]. It is postulated that in propylene inhibition the allyl radicals (produced in the decomposition of propylene) play the same role as NO and initiate chains according to the reaction

$$C_2H_6 + C_3H_5 \rightarrow C_2H_5 + C_3H_6.$$

Propylene itself plays the same role as HNO, and terminates by the reaction

$$C_2H_5 + C_3H_6 \rightarrow C_2H_6 + C_3H_5.$$

In equation [1] the rate constants involving the inhibitor are k_1, k_{-1}, k_4, and k_{-4}, and they appear in the ratio

$$k_1/k_{-1} \cdot k_{-4}/k_4.$$

This ratio is the equilibrium constant for the reaction

$$C_2H_6 \rightleftharpoons C_2H_5 + H$$

Can. J. Chem. Downloaded from www.nrcresearchpress.com by 186.148.149.217 on 09/04/12
For personal use only.

and since this reaction does not involve the inhibitor the limiting rate will be the same for all inhibitors capable of inhibiting by this type of mechanism. The result that more propylene is required to give the same inhibition as produced by NO is attributed to the fact that NO is more plentiful than allyl radicals.

THE DECOMPOSITION OF METHANE

The decomposition of methane offers an interesting contrast to that of ethane, since both of the chain-propagating reactions are of the second order. The chain carriers are H and CH_3, and one obtains 3/2-order kinetics whether one assumes the chain termination to involve $CH_3 + HNO$ or $H + HNO$. The former is preferred since the methyl radical concentration is probably usually higher than the concentration of hydrogen atoms. The mechanism to which we are therefore led is as follows:

$$CH_4 + NO \xrightarrow{k_1} CH_3 + HNO$$

$$CH_3 + CH_4 \xrightarrow{k_2} C_2H_6 + H$$

$$H + CH_4 \xrightarrow{k_3} CH_3 + H_2$$

$$H + NO \underset{k_{-4}}{\overset{k_4}{\rightleftharpoons}} HNO$$

$$CH_3 + HNO \xrightarrow{k_{-1}} CH_4 + NO$$

The expression for the limiting rate is

$$v = (k_1k_2k_3k_{-4}/k_{-1}k_4)^{1/2}[CH_4]^{3/2}. \quad [5]$$

The conclusion that the order is 3/2 is consistent with the experimental results (11).

THE DECOMPOSITION OF ETHERS

In the reactions discussed above hydrogen atoms were involved in chain-propagating steps. In ether decompositions, on the other hand, this is not the case; the chain-propagating reactions in the case of dimethyl ether are probably

$$CH_3OCH_2 \rightarrow CH_3 + CH_2O$$

and

$$CH_3 + CH_3OCH_3 \rightarrow CH_4 + CH_3OCH_2.$$

In view of this the concentration of HNO is very small, and the participation of HNO in chain termination is therefore unlikely. Our suggestion is that in these reactions chain termination involves nitric oxide itself, reacting with whichever radical is present in greater concentration; in the ether decomposition these are the μ radicals. The mechanism to which we are led is therefore as follows:

$$CH_3OCH_3 + NO \xrightarrow{k_1} CH_3OCH_2 + HNO$$

$$CH_3OCH_2 \xrightarrow{k_2} CH_3 + CH_2O$$

$$CH_3 + CH_3OCH_3 \xrightarrow{k_3} CH_4 + CH_2OCH_3$$

$$HNO \xrightarrow{k_4} H + NO$$

Can. J. Chem. Downloaded from www.nrcresearchpress.com by 186.148.149.217 on 09/04/12
For personal use only.

$$H + CH_3OCH_3 \xrightarrow{k_5} H_2 + CH_3OCH_2$$

$$CH_3OCH_2 + NO \xrightarrow{k_6} CH_3OCH_2NO$$

Application of the steady-state treatment gives rise to the rate equation

$$v = (2k_1k_2/k_6)[CH_3OCH_3]. \quad [6]$$

The result that the reaction is of the first order is in general agreement with experiment, although some complications certainly exist (14, 15).

The proposed mechanism for the diethyl ether decomposition is similar, as follows:

$$C_2H_5OC_2H_5 + NO \xrightarrow{k_1} C_2H_5OC_2H_4 + HNO$$

$$C_2H_5OC_2H_4 \xrightarrow{k_2} C_2H_5O + C_2H_4$$

$$C_2H_5O \xrightarrow{k_3} CH_3 + CH_2O$$

$$CH_3 + C_2H_5OC_2H_5 \xrightarrow{k_4} CH_4 + C_2H_5OC_2H_4$$

$$HNO \xrightarrow{k_5} H + NO$$

$$H + C_2H_5OC_2H_5 \xrightarrow{k_6} H_2 + C_2H_5OC_2H_4$$

$$C_2H_5OC_2H_4 + NO \xrightarrow{k_7} C_2H_5OC_2H_4NO$$

The rate equation is now

$$v = (2k_1k_2/k_7)[C_2H_5OC_2H_5] \quad [7]$$

and the order is again the first, as found experimentally (16).

It is significant that in these ether decompositions the nitric oxide is in no way in competition with the ether molecules themselves. The nitric oxide reacts with a μ radical, and the situation is to be contrasted with that in the case of ethane where nitric oxide competes with C_2H_6 for reaction with hydrogen atoms. In the ether decompositions the degree of inhibition produced by a given nitric oxide concentration is thus independent of the amount of ether, a prediction that is consistent with experiment.

In contrast to the situation with methane and ethane (and by analogy with the higher paraffins), the mechanism proposed for the ethers does not lead to the general conclusion that the fully inhibited rate should be the same for all inhibitors. Smith and Hinshelwood (16) and Freeman (15) have obtained results that tend to show that the same rates are obtained with both nitric oxide and propylene and this being so it must be assumed, if our mechanisms are correct, that the agreement of rates is fortuitous. It should, however, be pointed out that in the case of the ether decompositions there does remain a possibility that the fully inhibited reactions are molecular processes, since no isotopic exchange experiments have been carried out on these reactions.

THE DECOMPOSITION OF ACETALDEHYDE

The acetaldehyde decomposition differs from the hydrocarbon decompositions, and is similar to the ether decompositions in that hydrogen atoms are not chain carriers. Chain termination will therefore involve NO rather than HNO. The chain carriers are CH_3 and CH_3CO, of which the former are in excess; it is therefore postulated that the chain-ending step is reaction between CH_3 (a β radical) and NO.

Can. J. Chem. Downloaded from www.nrcresearchpress.com by 186.148.149.217 on 09/04/12
For personal use only.

The mechanism to which we are led is therefore:

$$CH_3CHO + NO \xrightarrow{k_1} CH_3CO + HNO,$$

$$CH_3CO \xrightarrow{k_2} CH_3 + CO,$$

$$CH_3 + CH_3CHO \xrightarrow{k_3} CH_4 + CH_3CO,$$

$$HNO \xrightarrow{k_4} H + NO,$$

$$H + CH_3CHO \xrightarrow{k_5} H_2 + CH_3CO,$$

$$CH_3 + NO \xrightarrow{k_6} CH_3NO.$$

The rate corresponding to this mechanism is

$$[8] \qquad v = (2k_1k_3/k_6)[CH_3CHO]^2 + 2k_1[CH_3CHO]\,[NO].$$

This rate expression, as in previous cases, corresponds to the rate when there is a sufficient excess of nitric oxide: much more complicated expressions result if the uninhibited initiation step is included also. The mechanism in this case leads to initial inhibition, with acceleration at higher nitric oxide concentrations as the second term in the rate equation becomes predominant. This is in fact the behavior observed experimentally (16). At moderate concentrations of nitric oxide the first term will predominate, and the kinetics should therefore be of the second order, as is found experimentally (16).

THE DECOMPOSITION OF ACETONE

The nitric oxide inhibited decomposition of acetone is very similar to that of acetaldehyde (there is again catalysis at high concentrations) and a similar mechanism is therefore probably involved.

$$CH_3COCH_3 + NO \xrightarrow{k_1} CH_3COCH_2 + HNO$$

$$CH_3COCH_2 \xrightarrow{k_2} CH_3 + CH_2CO$$

$$CH_3 + CH_3COCH_3 \xrightarrow{k_3} CH_4 + CH_3COCH_2$$

$$HNO \xrightarrow{k_4} H + NO$$

$$H + CH_3COCH_3 \xrightarrow{k_5} H_2 + CH_3COCH_2$$

$$CH_3 + NO \xrightarrow{k_6} CH_3NO$$

The resulting rate expression is

$$[9] \qquad v = (2k_1k_3/k_6)[CH_3COCH_3]^2 + 2k_1[CH_3COCH_3]\,[NO],$$

which is consistent with experiment (17).

The fact that the proposed mechanisms for these last two examples lead to the conclusion that there is catalysis at high nitric oxide concentrations, as observed experimentally, provides valuable support for the general scheme of reactions proposed in this paper.

Can. J. Chem. Downloaded from www.nrcresearchpress.com by 186.148.149.217 on 09/04/12
For personal use only.

Can. J. Chem. Downloaded from www.nrcresearchpress.com by 186.148.149.217 on 09/04/12
For personal use only.

GENERAL DISCUSSION

The suggestion that the initiating processes in reactions fully inhibited by nitric oxide involve a hydrogen atom abstraction by NO is not new; it was first made by Rice and Polly (18) and was discussed by Goldanskii (19). However, the postulation of reactions between radicals and HNO as chain-terminating steps appears to be new,* and seems to be required in order to account for the observed kinetics, and more particularly to explain the cases of limiting rates at high nitric oxide concentrations. Our view is that in the paraffin decompositions, where rather high temperatures are involved, reactions such as

$$C_2H_5 + NO \rightleftharpoons C_2H_5NO$$

merely proceed to equilibrium and do not disturb the steady-state concentrations of radicals; they therefore need not be included in the reaction schemes. In reactions at lower temperatures, however, such reactions are important chain-ending steps.

The idea that the radical HNO plays an important role in reaction mechanisms is reasonable in view of the fact that this substance has been prepared and its spectrum analyzed (21). Since the molecule is isoelectronic with O_2 it may be expected to be quite stable with respect to H + NO.

The reaction mechanisms discussed above may be seen to fall into four main classes, and Table I summarizes the main features and gives examples of each type.

TABLE I

Summary of reaction types for inhibition by nitric oxide

Case	H as chain carrier	Chain-ending step	Order of reaction	Examples	Chain carriers (most abundant given first)	Chain-ending step
I	Yes	μ + HNO	1	C_2H_6	C_2H_5, H	C_2H_5 + HNO
II	Yes	β + HNO	3/2	C_2H_6 (initial rates)	H, C_2H_5	H + HNO
				CH_4	CH_3, H	CH_3 + HNO
III	No	μ + NO	1	CH_3OCH_3	CH_3OCH_2, CH_3	CH_3OCH_2 + NO
				$C_2H_5OC_2H_5$	$C_2H_5OC_2H_4$, CH_3	$C_2H_5OC_2H_4$ + NO
IV	No	β + NO	2	CH_3CHO	CH_3, CH_3CO	CH_3 + NO
				CH_3COCH_3	CH_3, CH_3COCH_2	CH_3 + NO

ACKNOWLEDGMENTS

The authors thank Drs. E. W. R. Steacie and K. O. Kutschke for helpful discussions. One of us (B. W. W.) is grateful to the Consolidated Mining and Smelting Company of Canada for a Fellowship.

REFERENCES

1. E. W. R. Steacie. Atomic and free radical reactions. Reinhold Publishing Corp., New York. 1954.
2. F. J. Stubbs and C. N. Hinshelwood. Discussions Faraday Soc. **10**, 129 (1951).
3. C. N. Hinshelwood. Chem. Soc. (London), Spec. Publ. No. 9, 49 (1957).
4. V. V. Voevodsky and V. A. Poltorak. Doklady Akad. Nauk S.S.S.R. **91**, 585 (1953).
5. F. O. Rice and R. E. Varnerin. J. Am. Chem. Soc. **76**, 324 (1954).
6. R. E. Varnerin and J. S. Dooling. J. Am. Chem. Soc. **78**, 2042 (1956).
7. F. J. Stubbs and C. N. Hinshelwood. Proc. Roy. Soc. A, **200**, 458 (1950).
8. K. U. Ingold, F. J. Stubbs, and C. N. Hinshelwood. Proc. Roy. Soc. A, **203**, 486 (1950).
9. V. V. Voevodsky. Trans. Faraday Soc. **55**, 65 (1959).

*Except for the rather special case of the nitrite decompositions for which Levy (20) includes RO + HNO → ROH + NO as a minor chain-ending step which does not affect the over-all rate expression.

10. L. A. K. STAVELEY. Proc. Roy. Soc. A, **162**, 557 (1937).
11. J. E. HOBBS and C. N. HINSHELWOOD. Proc. Roy. Soc. A, **167**, 447 (1938).
12. E. W. R. STEACIE and G. SHANE. Can. J. Research, B, **18**, 351 (1940).
13. B. W. WOJCIECHOWSKI and K. J. LAIDLER. To be published.
14. G. R. FREEMAN, C. J. DANBY, and C. N. HINSHELWOOD. Proc. Roy. Soc. A, **245**, 28 (1958).
15. G. R. FREEMAN. Proc. Roy. Soc. A, **245**, 49 (1958).
16. J. R. E. SMITH and C. N. HINSHELWOOD. Proc. Roy. Soc. A, **180**, 237 (1942).
17. J. R. E. SMITH and C. N. HINSHELWOOD. Proc. Roy. Soc. A, **183**, 33 (1944).
18. F. O. RICE and O. L. POLLY. J. Chem. Phys. **6**, 273 (1938).
19. V. E. GOLDANSKII. Uspekhi Khim. **16**, 140 (1947).
20. J. B. LEVY. J. Am. Chem. Soc. **76**, 3790 (1954); **78**, 1780 (1956). Ind. Eng. Chem. **48**, 762 (1956).
21. F. W. DALBY. Can. J. Phys. **36**, 1336 (1958).

Can. J. Chem. Downloaded from www.nrcresearchpress.com by 186.148.149.217 on 09/04/12
For personal use only.

Can. J. Chem. Downloaded from www.nrcresearchpress.com by 186.148.149.217 on 09/04/12
For personal use only.

THE STRUCTURE AND STEREOISOMERISM OF THREE MITRAGYNA ALKALOIDS[1]

J. C. Seaton,[2] M. D. Nair,[2] O. E. Edwards, and Léo Marion

ABSTRACT

Isorhyncophylline, the isomer into which rhyncophylline is convertible, has been found to occur in nature. Both bases are interconvertible. Isorhyncophylline on hydrolysis with dilute hydrochloric acid is converted to an aldehyde reducible to isorhyncophyllol. When the aldehyde is reduced in the Wolff–Kishner reaction, it is also isomerized and the product is isorhyncophyllane. This reduction product is oxidized by mercuric acetate to a neutral dilactam which still contains the oxindole carbonyl and further contains a new lactam carbonyl present in a six-membered ring. Reduction of the dilactam with lithium aluminum hydride gave a product having the spectroscopic properties of an indole. This confirms the assumption previously made that in rhyncophylline, ring C is five-membered. The isomerization of rhyncophylline, mitraphylline, and formosanine is described. Formosanine has been shown to be identical with uncarine-B and thus uncarine-A is the iso base derivable from formosanine.

It has been reported first by Kondo, Fukuda, and Tomita (1) that rhyncophylline in acetic acid isomerizes to isorhyncophylline. It has now been possible to isolate isorhyncophylline from *Adina rubrostipulata* K. Schuman. It separated from the mother liquors that had already yielded rhyncophylline and mitraphylline. It was isolated as the perchlorate from which the crystalline base was liberated. Its ultraviolet spectrum was identical with that of rhyncophylline, and the infrared spectra of the two bases were very similar so that the isomerization did not seem to involve the chromophoric groups. When either rhyncophylline or its isomer was refluxed in pyridine it was converted to a mixture consisting of 30% rhyncophylline – 70% isorhyncophylline.

Whereas on catalytic hydrogenation rhyncophylline is converted to hexahydrorhyncophylline, in which the enol-ether double bond has survived, the similar hydrogenation of isorhyncophylline converts it to octahydroisorhyncophylline. The ultraviolet spectrum of this product showed only end absorption while the infrared spectrum contained absorption bands due to an unconjugated ester group (1743 cm^{-1}) and an oxindole carbonyl (1700 cm^{-1}) although it contained no absorption attributable to a benzene ring or an enol ether.

Hydrolysis of isorhyncophylline with dilute hydrochloric acid yielded a product having the properties of an aldehyde (a precipitate with Brady's reagent and restoration of color to Schiff's reagent), but it was not possible to induce the base or a salt to crystallize. The base appeared to polymerize on standing for a short time.

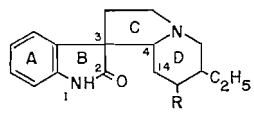
Reduction of the crude product, however, with sodium borohydride gave a base isomeric with rhyncophyllol (2), i.e., isorhyncophyllol ($C_{19}H_{26}O_2N_2$), the picrate of which crystallized. The regenerated base was a glass and its infrared spectrum in chloroform showed bands at 3610 cm^{-1} (hydroxyl), 3425 cm^{-1} (imino group), 1717 cm^{-1} (oxindole carbonyl), and 1628 cm^{-1} (benzene ring).

The amorphous aldehydic product of the hydrolysis of isorhyncophylline (i.e. isorhyncophyllal) when subjected to the Wolff–Kishner reaction suffered reduction of its aldehyde group. The product (73% yield) was identical with rhyncophyllane ($C_{19}H_{26}ON_2$) obtained previously (2) from rhyncophylline by the same reactions. In view of the fact that the thermal rearrangement of rhyncophylline and of rhyncophyllol gives mixtures in which

[1]*Manuscript received January 28, 1960.*
Contribution from the Division of Pure Chemistry, National Research Council, Ottawa, Canada.
Issued as N.R.C. No. 5676.
[2]*National Research Council of Canada Postdoctorate Fellow.*

the isobase always predominates, it is more likely that this common product is isorhyncophyllane. Consequently, rhyncophyllane would have been more correctly named isorhyncophyllane, and we propose to adopt the latter designation.

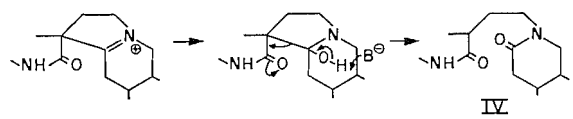
The structure of rhyncophylline represented by formula I has been suggested previously (2). From the foregoing results isorhyncophylline must also be represented by formula I



I, R = $CH_3OOC—C=CH.OCH_3$
II, R = $—CH_2.CH_2OH$
III, R = $.CH_2CH_3$

although the stereochemistry of the bases is different while isorhyncophyllol must be II and isorhyncophyllane III. Methylation with sodium methoxide converted isorhyncophyllane to N-methylisorhyncophyllane, which was crystallized as its picrate, m.p. 182–184°.

The final evidence needed to complete the proof that rhyncophylline (2) and its stereoisomer isorhyncophylline have structure I was the point of linkage of C-3 to ring D, and this has now been provided. Isorhyncophyllane reacted quickly with 1 mole of mercuric acetate giving rise to a neutral dilactam which in the infrared showed bands at 1715 cm^{-1} (oxindole carbonyl) and at 1625 cm^{-1} (six-membered lactam). This dilactam could not be crystallized, nor could it be purified completely because of partial decomposition when it was dissolved in a hot solvent. Lithium aluminum hydride in refluxing dioxane reduced the dilactam to a sensitive base which could not be purified without decomposition, but had an infrared spectrum showing no carbonyl absorption and an ultraviolet spectrum similar to an indole spectrum. The indication of indole formation on reduction, although not rigorous, does show, if taken in conjunction with the formation of a lactam in the reaction with mercuric acetate, the location of the new carbonyl. Thus the evidence is consistent with structure IV for the dilactam which must have been produced via the immonium ion and



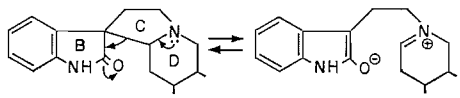
carbinolamine as shown. It further establishes the five-membered nature of ring C.

Perhaps the most intriguing feature of rhyncophylline chemistry is the isomerization to isorhyncophylline. That the enol–ether system was not involved was shown by the fact that rhyncophyllol isomerizes in identical manner. Nozoye (3, 4) has suggested that the isomerism involves the configuration at C-4. A more plausible explanation of this phenomenon seemed to us to be the following thermal (possibly also acid-catalyzed) fission-recoupling process,[3] which involves the two asymmetric centers C-3 and C-4.

The pair of structures which represent rhyncophylline and its isomer must satisfy the requirements that the equilibrium between the two lies 70% on the side of the iso series,

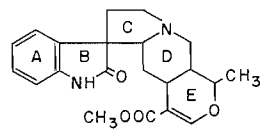
[3]*This mechanism was recently independently suggested by Wenkert, Udelhofen, and Bhattacharyya (5).*

Can. J. Chem. Downloaded from www.nrcresearchpress.com by 186.148.149.217 on 09/04/12
For personal use only.



that rhyncophylline and derivatives are inert to mercuric acetate while the iso series react rapidly, and that the rhyncophylline series are stronger bases than the iso series. A rigorous assignment of stereochemical structures is not yet possible.[4]

An equilibrium mixture of 20% mitraphylline and 80% isomitraphylline is formed when either base is refluxed in pyridine overnight. It has not been possible to obtain isomitraphylline crystalline, but its picrate was a well-defined compound and the analytical figures obtained for this salt corresponded to $C_{21}H_{24}O_4N_2$ for the base. The ultraviolet spectrum of isomitraphylline was almost identical with that of mitraphylline (6) and the infrared spectra of the two bases showed no significant shift in the frequencies of the bands corresponding to the functional groups. Isomitraphylline when oxidized with mercuric acetate gave an amorphous product which on hydrogenation over Adams' catalyst produced a mixture of isomitraphylline and mitraphylline. The isomerism parallels that of rhyncophylline. Mitraphylline has been shown (6) to possess structure V, which must also represent isomitraphylline.



V

The alkaloid formosanine was isolated from *Orouparia formosana* Mats by Raymond-Hamet (7). It has the formula $C_{21}H_{24}O_4N_2$ and contains one methoxyl group. It has been suggested by Loudon (8) and by Raymond-Hamet (9) that uncarine-B isolated by Kondo (10) from *Uncaria kawakamii* Hayata was identical with formosanine because their melting points, rotations, and ultraviolet spectra were almost identical. We have now been able to make a direct comparison of formosanine[5] with a sample of uncarine-B kindly supplied by Professor H. Kondo. The melting point of the mixture of the bases showed no depression and their X-ray powder diagrams were identical while their infrared absorption spectra were virtually identical. This confirms the claim of Raymond-Hamet (9) that formosanine and uncarine-B are identical.

The pair of alkaloids uncarine-A–uncarine-B (formosanine) have been assigned structure V (3), which is also that of mitraphylline (6). When boiled with pyridine, formosanine is equilibrated to a mixture of about 20% formosanine and 80% isoformosanine. Formosanine is isomeric with mitraphylline, but not identical with it. Whereas mitraphylline was hydrogenated catalytically to hexahydromitraphylline in which the

[4]*An analysis of the stereochemistry is possible, and leads to a conclusion respecting the structures of the two isomers. This speculation, however, is based on rather arbitrary assumptions which will require further experimental confirmation.*

[5]*Dr. Raymond-Hamet kindly gave us a generous sample of formosanine and we acknowledge our indebtedness and gratitude.*

Can. J. Chem. Downloaded from www.nrcresearchpress.com by 186.148.149.217 on 09/04/12
For personal use only.

isolated double bond was still present, catalytic hydrogenation converted formosanine to octahydroformosanine.

The three alkaloids rhyncophylline, mitraphylline, and formosanine have a very low solubility in ether, and crystallize readily, while the bases of the iso series are very soluble in ether and either crystallize with difficulty or not at all. The bases equilibrate under the same conditions and in the mixtures produced, the iso base always predominates. Furthermore, the normal series are stronger bases than the iso series. It is therefore most probable that the isomerization in each case is of the same type.

It has been shown (3) that formosanine (uncarine-B) possesses the same structure V as mitraphylline, and also that uncarine-A (isoformosanine) is different from isomitraphylline or its isomer. Hence mitraphylline and formosanine must differ by an isomerism other than that differentiating mitraphylline from isomitraphylline.

The infrared spectra were measured on a Perkin–Elmer double-beam spectrophotometer model 21. Unless otherwise mentioned the spectra were taken in Nujol mulls, and the absorption bands are reported in wave numbers sometimes followed by a numeral in parentheses indicating the percentage absorption.

EXPERIMENTAL

Isolation of Isorhyncophylline

Both rhyncophylline and mitraphylline have already been reported as occurring in *Adina rubrostipulata* K. Schuman. The mother liquors from which the two bases had separated still contained basic material which was precipitated with picric acid. A sample of the crude picrate was suspended in methanol and shaken with Amberlite IRA 400 (basic form) and the mixture poured on a column of Amberlite IRA 400. Elution with methanol gave a solution of bases which was evaporated to dryness under diminished pressure. The basic residue was dissolved in the minimum volume of methanol and the solution made just acid to Congo red with perchloric acid. About half the solvent was evaporated and water added to incipient turbidity. After cooling and scratching a salt crystallized which was recrystallized from methanol from which it separated as colorless needles, m.p. 158–160°. It did not depress the melting point of an authentic sample of isorhyncophylline perchlorate prepared from rhyncophylline by isomerization. Found: C, 52.84; H, 6.19; N, 5.45. Calc. for $C_{22}H_{28}O_4N_2.HClO_4.H_2O$: C, 52.53; H, 6.21; N, 5.57%.

To liberate the base, the perchlorate was suspended in aqueous ammonia and the mixture extracted repeatedly with ether. The extract was washed with water, evaporated to dryness, and the residue dissolved in ether–hexane from which it crystallized as colorless fine needles, m.p. 150°. The infrared spectrum of the free base, 3420 cm^{-1} (HN), 1730 cm^{-1} (ester carbonyl), 1705 cm^{-1} (oxindole carbonyl), 1645 cm^{-1} (enol-ether), 1625 and 755 cm^{-1} (benzene ring), was identical with that of isorhyncophylline, and so were the ultraviolet spectra, $[\alpha]_D^{28}$ +5.9 (*c*, 3.95 in ethanol). Found: C, 68.89; H, 7.40; N, 7.21. Calc. for $C_{22}H_{28}O_4N_2$: C, 68.72; H, 7.34; N, 7.29%.

Octahydroisorhyncophylline

Isorhyncophylline (100 mg) was hydrogenated in glacial acetic acid (10 ml) over Adams' catalyst (100 mg) at 27° and a pressure of 755 mm of mercury. The absorption of hydrogen amounted to 26.7 ml and the volume calculated for four double bonds was 25.8 ml. After removal of the catalyst and solvent the residue was alkalized with sodium carbonate and the mixture extracted with ether. The extract was dried, the solvent

Can. J. Chem. Downloaded from www.nrcresearchpress.com by 186.148.149.217 on 09/04/12
For personal use only.

evaporated, and the residue crystallized in ether from which it separated as colorless prisms, m.p. 169–172°, $[\alpha]_D^{24}$ +46.9° (*c*, 0.49 in ethanol). Found: C, 67.33; H, 9.14. Calc. for $C_{22}H_{36}O_4N_2$: C, 67.31; H, 9.24%. Infrared spectrum: 1745, 1700, and 1110 cm^{-1}. Ultraviolet spectrum: end absorption.

Isomerization of Isorhyncophylline

Isorhyncophylline (280 mg) was refluxed with acetic anhydride (6 ml) for 3 hours. The solvent was removed under diminished pressure, the residue dissolved in benzene and chromatographed on alumina. Elution with benzene–ether gave a fraction (200 mg) which failed to crystallize, but formed a perchlorate which, after crystallization from methanol–ether, melted at 219–220° identical with isorhyncophylline perchlorate by mixed melting point and comparison of infrared spectra. Further elution with chloroform yielded rhyncophylline, m.p. 209–211° identical with an authentic specimen.

Equilibration of Rhyncophylline and Isorhyncophylline

Rhyncophylline (342 mg) was refluxed overnight in pyridine (7 ml). The solvent was evaporated off, the residue dissolved in ether, and the solution seeded with rhyncophylline. The crystalline base (96 mg) identified with rhyncophylline by melting point, mixed melting point, and infrared spectrum was filtered and the filtrate made just acid with perchloric acid. The crystalline salt (330 mg) was identical with isorhyncophylline perchlorate. Hence the equilibrium mixture contains approximately 30% rhyncophylline and 70% isorhyncophylline.

Isorhyncophyllol

It has been shown earlier (2) that rhyncophylline is converted to rhyncophyllal by the action of dilute hydrochloric acid. In an attempt to prepare isorhyncophyllal, isorhyncophylline (1.65 g) was refluxed similarly with 8% hydrochloric acid (200 ml) for 3.5 hours. The cooled solution was neutralized with sodium bicarbonate and extracted with ether. The extract was dried over sodium sulphate and evaporated to dryness. The residual gum was soluble in ether, acetone, benzene, methanol, and ethanol, but much less in hexane. After a short time it became only partially soluble in ether. The product could not be crystallized nor could its picrate and perchlorate. It behaved as an aldehyde in that it gave a precipitate with Brady's reagent and restored the color to Schiff's reagent.

The gummy product of the above reaction (100 mg) was dissolved in 80% methanol (15 ml) and sodium borohydride (1.0 g) was added to the solution. After 2 hours the methanol was evaporated and a little water added to the residue which was extracted with ether. The extract was dried over sodium sulphate and the solvent distilled off. There was left a gum which was converted to a picrate that crystallized from methanol as large yellow prisms (0.8 g), m.p. 168–170°. Found: C, 55.39; H, 5.31. Calc. for $C_{19}H_{26}O_2N_2.C_6H_3O_7N_3$: C, 55.24; H, 5.38%. The base was regenerated from a solution of the picrate in methanol on a basic resin (Amberlite IRA 400). It consisted of a colorless glass which could not be crystallized, $[\alpha]_D^{22}$ +41.9° (*c*, 0.99 in ethanol). Found: C, 72.73; H, 8.34; N, 8.81. Calc. for $C_{19}H_{26}O_2N_2$: C, 72.58; H, 8.34; N, 8.91%.

Isomerization of Rhyncophyllol

A sample (2) of crystalline rhyncophyllol (100 mg) was refluxed in pyridine (25 ml) overnight. The solvent was then evaporated leaving a gum which failed to crystallize. It was dissolved in methanol and converted to the picrate which separated in yellow prisms (135 mg), m.p. 168–169°, undepressed in admixture with the picrate of isorhyncophyllol obtained by reduction of isorhyncophyllal.

Can. J. Chem. Downloaded from www.nrcresearchpress.com by 186.148.149.217 on 09/04/12
For personal use only.

Can. J. Chem. Downloaded from www.nrcresearchpress.com by 186.148.149.217 on 09/04/12
For personal use only.

Wolff–Kishner Reduction of Isorhyncophyllal

Amorphous isorhyncophyllal (400 mg) was reduced by the Huang–Minlon modification of the Wolff–Kishner reaction. The reaction mixture, after being cooled, was acidified with *N* hydrochloric acid and extracted with ether. The aqueous layer was alkalized with sodium carbonate and extracted repeatedly with ether. The extract from the basic solution was washed with water, dried over sodium sulphate, and evaporated to dryness. The residual stiff gum (205 mg) was distilled at 200° under 6.3 mm and obtained as a colorless glass which formed a picrate that crystallized from ethanol, m.p. 226–227°, either alone or in admixture with rhyncophyllane picrate (2). Found: C, 56.95; H, 5.26. Calc. for $C_{19}H_{26}ON_2.C_6H_3O_7N_3$: C, 56.92; H, 5.54%. The base, liberated on Amberlite IRA 400, had $[\alpha]_D^{24}$ +26.2° (*c*, 2.1 in ethanol) and its infrared absorption spectrum was identical with that of rhyncophyllane. As explained above, this compound should be renamed isorhyncophyllane.

N-Methylisorhyncophyllane

To a solution of isorhyncophyllane (60 mg) in methanol (5 ml) was added a methanolic solution of sodium methoxide (sodium, 50 mg, in methanol, 5 ml) and methyl iodide (1 ml). The mixture was refluxed on the water bath for 3 hours and then evaporated to dryness. The residue was extracted with ether, the extract washed with water, dried over sodium sulphate, and evaporated. A gummy residue was thus obtained which was dissolved in ethanol and converted to the picrate which separated as yellow prisms (50 mg), m.p. 182–184°. Found: C, 58.12; H, 5.86. Calc. for $C_{20}H_{28}ON_2.C_6H_3O_7N_3$: C, 57.66; H, 5.77%. The base liberated on Amberlite IRA 400 did not show any absorption bands in the NH—OH region of the infrared.

Mercuric Acetate Oxidation of Isorhyncophyllane

To a solution of isorhyncophyllane (400 mg) in 5% aqueous acetic acid (5 ml) was added mercuric acetate (2.4 g) dissolved in 5% aqueous acetic acid (10 ml) and the mixture heated on the steam bath. A precipitate of mercurous acetate started to appear after 15 minutes. The mixture was heated for 4 hours, cooled, and filtered. The dried mercurous acetate weighed 687 mg. The filtrate was boiled and treated with hydrogen sulphide until precipitation was complete. The mercuric sulphide was filtered off through supercel and the filtrate alkalized with excess sodium carbonate and extracted three times with chloroform. The extract was washed first with several portions of dilute hydrochloric acid then with water, dried over sodium sulphate, and evaporated. It left a neutral residue (180 mg) which could not be induced to crystallize and could not be distilled without some decomposition. The infrared spectrum of the product showed in addition to the oxindole carbonyl at 1705 cm^{-1} a strong band at 1625 cm^{-1} indicative of a six-membered lactam. Found: C, 70.99; H, 8.20. Calc. for $C_{19}H_{26}O_2N_2$: C, 72.58; H, 8.34%.

Reduction of Oxidation Product

Reduction of the oxidation product with lithium aluminum hydride in ether, in tetrahydrofuran, and in dioxane was attempted under the usual experimental conditions. Although the six-membered lactam carbonyl was reduced readily, the oxindole carbonyl could not be completely reduced. To a solution of lithium aluminum hydride (150 mg) in dry ether was added a solution of the oxidation product (98 mg) in dioxane (10 ml). The ether was evaporated off and the resulting slurry boiled under reflux for 24 hours under dry nitrogen. After the reaction mixture was cooled, the excess lithium aluminum hydride

was decomposed with water and the solution extracted with chloroform. The extract was washed with water and then with *N* sulphuric acid. The acid solution turned violet. It was made basic with aqueous sodium carbonate and extracted with chloroform. The extract yielded a gum (29 mg) which could not be crystallized and from which no crystalline salt could be obtained. The infrared spectrum of the product still contained a weak oxindole carbonyl band, but the lactam carbonyl absorption had completely disappeared.

Isomitraphylline

Mitraphylline (325 mg) was refluxed in pyridine (25 ml) overnight. The solvent was evaporated and the residue dissolved in a small volume of ether. After cooling for several hours, mitraphylline, m.p. 265 (66 mg), had crystallized. The residue recovered from the mother liquor was converted into a picrate which crystallized from methanol as yellow prisms, m.p. 223° (dec.) (377 mg). Found: C, 54.31; H, 4.38. Calc. for $C_{21}H_{24}O_4N_2.C_6H_3O_7N_3$: C, 54.36; H, 4.56%. The base, regenerated from the picrate on Amberlite IRA 400 was soluble in ether. It could not be induced to crystallize. Found: C, 68.03; H, 6.60; N, 7.42. Calc. for $C_{21}H_{24}O_4N_2$: C, 68.46; H, 6.57; N, 7.60%. Infrared spectrum in chloroform: 3440, 1720(87), 1626(72), 1118(63), 1098(62) cm^{-1}.

Dehydrogenation of Isomitraphylline and Mitraphylline

(*a*) Isomitraphylline (110 mg) and mercuric acetate (400 mg) in 5% acetic acid (4 ml) was kept at 40–50°. Precipitation of mercurous acetate started after 2 minutes. After 7 hours the reaction mixture was worked up as described for isorhyncophylline, and the product was converted to perchlorate. Reduction of the perchlorate in 80% methanol with sodium borohydride produced a mixture which was separated into mitraphylline (2 mg) and isomitraphylline isolated as the picrate (20 mg), m.p. 223–227°, undepressed by admixture with an authentic sample.

(*b*) When mitraphylline (100 mg) and mercuric acetate in 5% acetic acid were kept at 40–50° for 7 hours, only a trace of mercurous acetate had precipitated.

Octahydroformosanine

Formosanine (25 mg) was hydrogenated in glacial acetic (10 ml) over Adams' catalyst (50 mg) at 27° and 756 mm. The hydrogen absorbed was 8.1 ml (calculated for four double bonds, 7.2 ml). The catalyst and solvent were removed and the residue alkalized with sodium carbonate solution and extracted with ether. The extract was dried over sodium sulphate, evaporated to dryness, and the residue crystallized from ether from which it separated as colorless cubes (12.5 mg), m.p. 110–120°. Found: C, 66.74; H, 8.59. Calc. for $C_{21}H_{32}O_4N_2$: C, 66.99; H, 8.57%. Infrared spectrum: 1745(80), 1707(92), 1100(81) cm^{-1}.

Equilibration of Formosanine

Formosanine (45 mg) was refluxed in pyridine overnight. The solvent was evaporated and the residue dissolved in a small volume of ether from which crystals of formosanine, m.p. 218° (8 mg), were deposited. The fraction more readily soluble in ether did not crystallize (uncarine-A) and was dissolved in carbon disulphide for determination of its infrared spectrum.

ACKNOWLEDGMENTS

We acknowledge with thanks the courtesy of Professor H. Kondo for the sample he sent us and Dr. Raymond-Hamet for his generous gift of formosanine. We are also grateful to Mr. R. Lauzon for taking the infrared spectra and to Mr. J. R. H. Seguin for the microanalyses.

Can. J. Chem. Downloaded from www.nrcresearchpress.com by 186.148.149.217 on 09/04/12
For personal use only.

REFERENCES

1. H. KONDO, T. FUKUDA, and M. TOMITA. J. Pharm. Soc. Japan, **48**, 54 (1928).
2. J. C. SEATON and L. MARION. Can. J. Chem. **35**, 1102 (1957).
3. T. NOZOYE. Pharm. Bull. (Tokyo), **6**, 300 (1958).
4. T. NOZOYE. Pharm. Bull. (Tokyo), **6**, 309 (1958).
5. E. WENKERT, J. H. UDELHOFEN, and N. K. BHATTACHARYYA. J. Am. Chem. Soc. **81**, 3763 (1959).
6. J. C. SEATON, R. TONDEUR, and L. MARION. Can. J. Chem. **36**, 1031 (1958).
7. RAYMOND-HAMET. Compt. rend. **203**, 1383 (1936).
8. J. D. LOUDON. Symposium on naturally occurring nitrogen heterocyclic compounds. The Chemical Society, London. 1955.
9. RAYMOND-HAMET. Compt. rend. **245**, 1460 (1957).
10. H. KONDO and T. IKEDA. J. Pharm. Soc. Japan, **61**, 130 (1941).

Can. J. Chem. Downloaded from www.nrcresearchpress.com by 186.148.149.217 on 09/04/12
For personal use only.

Can. J. Chem. Downloaded from www.nrcresearchpress.com by 186.148.149.217 on 09/04/12
For personal use only.

THE RADIOLYSIS OF CYCLOHEXANE

II. CYCLOHEXANE–CYCLOHEXENE SOLUTIONS AND PURE CYCLOHEXENE[1]

G. R. FREEMAN

ABSTRACT

The γ-radiolysis of cyclohexane–cyclohexene solutions and of pure cyclohexene has been investigated. The previously determined yields of the two activated species in irradiated cyclohexane have been confirmed. $G(c\text{-}C_6H_{12}'') = 3.0\pm0.3$ and $G(c\text{-}C_6H_{12}') = 2.4\mp0.3$.

The yields of the main products of cyclohexene radiolysis are $G(H_2) = 1.2$, $G(c\text{-}C_6H_{12}) = 1.0$, $G[(c\text{-}C_6H_9)_2] = 1.4$, and $G(c\text{-}C_6H_{10} \rightarrow \text{higher polymer}) \approx 4$. There were smaller amounts of ethylene, acetylene, a C_4 hydrocarbon (probably butadiene), cyclohexylcyclohexene, and dicyclohexyl.

For the reactions

$$2c\text{-}C_6H_9 \rightarrow (c\text{-}C_6H_9)_2, \qquad [6a]$$

$$c\text{-}C_6H_9 + c\text{-}C_6H_{11} \rightarrow c\text{-}C_6H_9\text{–}C_6H_{11}, \qquad [7a]$$

and

$$2c\text{-}C_6H_{11} \rightarrow (c\text{-}C_6H_{11})_2 \qquad [8a]$$

the value $k_{7a}/(k_{8a}k_{6a})^{\frac{1}{2}} = 0.45\pm0.08$ was determined.

The reaction mechanism that occurs during the radiolysis of cyclohexane–cyclohexene solutions is similar to that which occurs during the radiolysis of cyclohexane–benzene solutions (Part I of this series) with the additional consideration that cyclohexene itself is considerably decomposed during the radiolysis.

INTRODUCTION

Two distinct reactive species appear to be important in the γ-radiolysis of cyclohexane (1). One reactive species, $c\text{-}C_6H_{12}''$, is subject to energy transfer "protection" by benzene and the other, $c\text{-}C_6H_{12}'$, is not. It also appears that $c\text{-}C_6H_{12}'$ decomposes to produce "cold" hydrogen atoms that can be scavenged by benzene,

$$c\text{-}C_6H_{12}' \rightarrow c\text{-}C_6H_{11} + \text{cold H},$$

whereas $c\text{-}C_6H_{12}''$ decomposes to produce "hot" hydrogen atoms that cannot be scavenged by benzene,

$$c\text{-}C_6H_{12}'' \rightarrow c\text{-}C_6H_{11} + \text{hot H}.$$

The possibility that $c\text{-}C_6H_{12}''$ decomposes to produce molecular hydrogen has not been eliminated, however.

The purpose of the present study was to determine the effect of cyclohexene on the cyclohexane radiolytic system.

EXPERIMENTAL

Materials

Eastman spectro-grade cyclohexane was used.

Cyclohexene was obtained from Matheson, Coleman, and Bell and from Eastman. The results obtained with the cyclohexene from the two sources were the same within experimental error.

Cyclohexylcyclohexene was prepared by dehydrating 2-cyclohexylcyclohexanol with phosphorus pentoxide and distilling the olefin from the reaction mixture.

[1]*Manuscript received January 25, 1960.*
Contribution from the Department of Chemistry, University of Alberta, Edmonton, Alberta.

Preparation of the Samples

One- and two-milliliter samples were irradiated in sealed pyrex cells of approximately 2- and 4-ml capacity, respectively.

The cells were filled by conventional vacuum techniques. Briefly, the liquids were measured by pipette and were thoroughly degassed before being distilled into the irradiation cells.

Irradiation of the Samples

The samples were irradiated with Co^{60} γ-rays. Dose rates were determined with the Fricke dosimeter, using $G(Fe^{+++}) = 15.6$ and $\epsilon(Fe^{+++}$ in 0.8 N H_2SO_4, 25° C, 304 mμ) $= 2225$. The dose rates varied from 5.9×10^{17} to 10.4×10^{17} ev/ml hr for the Fricke dosimeter at 25° C. The amount of energy absorbed per milliliter per hour in the organic liquids was calculated by multiplying the energy absorbed per milliliter per hour in the Fricke dosimeter by the ratio of the electron densities at the appropriate temperatures. The electron densities, at 24° C, of the Fricke dosimeter, cyclohexane, and cyclohexene were 0.566, 0.442, and 0.452 e^- moles/ml, respectively. Temperature corrections were applied when necessary.

Analyses

Gas fractions were separated by distillation at −195° C and −112° C. Each fraction was collected and measured in a combination Toepler pump – McLeod gauge and then analyzed by gas chromatography. The remaining liquid was also analyzed by gas chromatography.

RESULTS

The dose received by the samples was $2.7\pm0.5\times10^{20}$ ev/ml, 24° C. Since the slight decrease in most product yields with increasing dose in the pure cyclohexane system is probably due to the accumulation of an inhibitor, the G values used in this paper for pure cyclohexane will be those obtained by extrapolation to zero dose (1), unless otherwise mentioned.

Cyclohexane–Cyclohexene Solutions

Products Volatile at −195° C

This fraction consisted of hydrogen and methane. The amounts of methane were too small to measure accurately. For pure cyclohexane $G(CH_4) = 0.02$ and the value decreased to less than 0.01 when the electron fraction of cyclohexene, ϵ_e, in the solution was greater than about 0.04.

[i] $$\epsilon_e = \frac{46n_e}{46n_e+48n_c}$$

where n_e and n_c are the respective numbers of moles of cyclohexene and of cyclohexane in the solution, and 46 and 48 are the numbers of electrons in a cyclohexene molecule and a cyclohexane molecule respectively.

The hydrogen yield, $G(H_2)$, decreased rapidly as ϵ_e was increased from 0 to 0.05 and decreased slowly as ϵ_e was increased further (see Fig. 1A).

Products Volatile at −112° C

This fraction consisted of about 70% ethylene with small amounts of ethane, acetylene, and propylene and traces of propane and butene.

Can. J. Chem. Downloaded from www.nrcresearchpress.com by 186.148.149.217 on 09/04/12
For personal use only.

The total yield of the fraction, $G(-112°\ C)$, varied only slightly with ϵ_e (see Fig. 1B). For pure cyclohexane, the value of $G(-112°\ C)$ decreased very markedly with increasing dose (1), so the value plotted in Fig. 1B is the one that was obtained at a dose of 2.5×10^{20} ev/ml (about the same dose as was received by the solutions). Thus the increase in $G(-112°\ C)$ between $\epsilon_e = 0$ and $\epsilon_e = 0.026$ may not have much significance.

These results will not be discussed further until they have been investigated more fully.

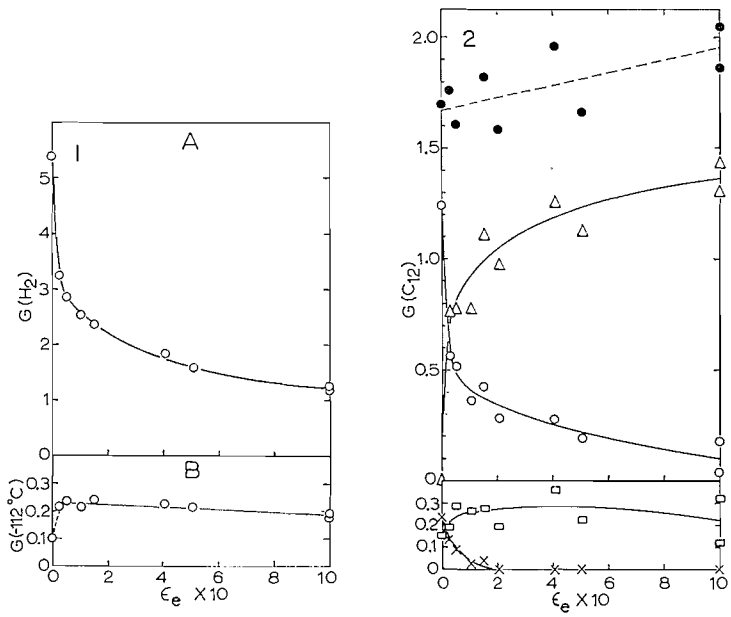


FIG. 1. (A) Variation of hydrogen yield with composition of solution. (B) Variation of yield of $-112°$ C gas fraction with composition of solution. ϵ_e = electron fraction of cyclohexene in the solution.

FIG. 2. Variation of C_{12} hydrocarbon yields with electron fraction of cyclohexene, ϵ_e, of solution. ○ dicyclohexyl; △ dicyclohexenyl; ● total C_{12}, measured on Apiezon L column; □ cyclohexylcyclohexene; × cyclohexylhexene.

Liquid Products

The measured liquid products were dicyclohexyl, cyclohexylcyclohexene, dicyclohexenyl, cyclohexylhexene, and total C_{12} hydrocarbons (see Fig. 2). There were no detectable products with carbon numbers between C_6 and C_{12}. Cyclohexane was a product in the pure cyclohexene system and cyclohexene was produced from pure cyclohexane, but these substances could obviously not be measured as products in the irradiated solutions. The maximum amount of decomposition that occurred in any irradiated sample corresponded to about 0.2% of the initial cyclohexane plus cyclohexene.

The dicyclohexyl yield decreased rapidly with increasing cyclohexene concentration at low concentrations ($0 < \epsilon_e < 0.05$) and decreased slowly as the cyclohexene concentration was increased further.

The dicyclohexenyl yield increased rapidly with increasing cyclohexene concentration at low concentrations ($0 < \epsilon_e < 0.05$) and increased slowly as the concentration was increased further.

The cyclohexylcyclohexene yield varied only to a small extent in the region $0 \leqslant \epsilon_e \leqslant 1$.

Can. J. Chem. Downloaded from www.nrcresearchpress.com by 186.148.149.217 on 09/04/12
For personal use only.

The cyclohexylhexene yield decreased from 0.23 to zero in the region $0 \leqslant \epsilon_e \leqslant 0.2$.

The total yield of C_{12} hydrocarbons, measured on the Apiezon L chromatographic column, increased slightly as ϵ_e was increased from 0 to 1. The Apiezon L column did not resolve the dicyclic C_{12} hydrocarbons but did separate them from isomers containing an open chain.

The total polymer yield was determined for a solution with $\epsilon_e = 0.405$ by evaporating 1 ml of irradiated solution and 1 ml of unirradiated solution under identical conditions. The weight of each sample was determined as a function of time and the weight vs. time curves were compared. A weight vs. time curve was determined for dicyclohexyl under the same conditions. It was found that $G(C_6$ units $\rightarrow$ polymer$) = 4.5$. This compares with the value 3.9 obtained by gas-chromatographic analysis ($2 \times G$(total C_{12})). A similar determination of total polymer in irradiated cyclohexene gave G(cyclohexene $\rightarrow$ polymer) ≈ 8. Only about four of these units were accounted for by the C_{12} hydrocarbon analysis. The remaining four units of "other polymer" were probably of higher molecular weight. Manion and Burton (2) determined the polymer yield in irradiated cyclohexene by evaporation and weighing and reported that G(cyclohexene $\rightarrow$ polymer) $= 12.4$, but that it was difficult to decide when solvent evaporation was complete. It would seem, from the present experiments, that this difficulty was caused by small amounts of intermediate compounds that were present in the original cyclohexene.

The present results are in general agreement with those of Dewhurst (3), who found that, in the presence of 5.2×10^{-4} mole cyclohexene/g solution ($\epsilon_e = 0.040$), $G(H_2) = 2.9$, $\Delta G(H_2) = -2.4$, $G(c\text{-}C_6H_{10}) = -2.3$, and that the dicyclohexyl yield was unchanged. However, the present results confirm the previous suspicion (1) that Dewhurst's "dicyclohexyl" was not pure dicyclohexyl but probably was a measure of the total C_{12} hydrocarbons. At $\epsilon_e = 0.040$ only one third of the C_{12} hydrocarbons is dicyclohexyl (see Fig. 2).

Pure Cyclohexene

The detected products and their yields were as follows:

Product	G	Product	G
Hydrogen	1.2	Dicyclohexenyl	1.36
Ethylene	0.16	Cyclohexylcyclohexene	0.22
Acetylene	0.022	Dicyclohexyl	0.11
C_4 hydrocarbon	0.10	Total C_{12} hydrocarbons	1.96
Cyclohexane	1.0	Total polymer	8 cyclohexene units

The cyclohexene from Matheson, Coleman, and Bell contained 0.6 mole % cyclohexane and that from Eastman contained 0.04 mole % cyclohexane. Corresponding corrections were applied before calculating G(cyclohexane).

The total C_{12} hydrocarbons were measured on the Apiezon L column. The total polymer was determined by weighing.

DISCUSSION

Pure Cyclohexene

If the radiolysis of cyclohexene is considered as

$$c\text{-}C_6H_{10} \rightarrow H_2 + X,$$

then the total hydrogen deficiency in the yields of the products X should be equal to $G(H_2) = 1.2$. It is evident from Table I that the hydrogen equivalent of about one

Can. J. Chem. Downloaded from www.nrcresearchpress.com by 186.148.149.217 on 09/04/12
For personal use only.

TABLE I

Material balance of products from irradiation of cyclohexene

Product	G	H_2 equivalent
$C_2 + C_4$ hydrocarbons	0.28	0.0
Cyclohexane	1.0	−1.0
Dicyclohexenyl	1.36	1.36
Cyclohexylcyclohexene	0.22	0.0
Dicyclohexyl	0.11	−0.11
Other polymer	4.6 C_6 units	?
Total		0.25+?
H_2	1.2	1.2

NOTE: The hydrogen equivalent of a product corresponds to the amount of hydrogen that was produced when that product was formed from cyclohexene.

G unit of hydrogen-deficient hydrocarbon products have remained unidentified. These products might not be entirely included in the "other polymer" because some possible products, such as cyclohexadiene, might have been missed under the present analytical conditions.

The formation of the major identified products can be explained by the following mechanism.

$$c\text{-}C_6H_{10} \xrightarrow{I^*} c\text{-}C_6H_{10}^* \qquad [1^*]$$

$$\xrightarrow{I^{**}} c\text{-}C_6H_{10}^{**} \qquad [1^{**}]$$

$$c\text{-}C_6H_{10}^* \rightarrow c\text{-}C_6H_9 + \text{cold H} \qquad [2^*]$$

$$c\text{-}C_6H_{10}^{**} \rightarrow c\text{-}C_6H_9 + \text{hot H} \qquad [2^{**}]$$

$$\text{hot H} + c\text{-}C_6H_{10} \rightarrow H_2 + c\text{-}C_6H_9 \qquad [3]$$

$$\text{cold H} + c\text{-}C_6H_{10} \rightarrow c\text{-}C_6H_{11} \qquad [4]$$

$$c\text{-}C_6H_{11} + c\text{-}C_6H_{10} \rightarrow c\text{-}C_6H_{12} + c\text{-}C_6H_9 \qquad [5]$$

$$2c\text{-}C_6H_9 \rightarrow (c\text{-}C_6H_9)_2 \text{ (dicyclohexenyl)} \qquad [6a]$$

$$\rightarrow c\text{-}C_6H_{10} + c\text{-}C_6H_8 \qquad [6b]$$

$$c\text{-}C_6H_9 + c\text{-}C_6H_{11} \rightarrow c\text{-}C_6H_9\text{-}C_6H_{11} \text{ (cyclohexylcyclohexene)} \qquad [7a]$$

$$\rightarrow c\text{-}C_6H_8 + c\text{-}C_6H_{12} \qquad [7b]$$

$$\rightarrow 2c\text{-}C_6H_{10} \qquad [7c]$$

$$2c\text{-}C_6H_{11} \rightarrow (c\text{-}C_6H_{11})_2 \text{ (dicyclohexyl)} \qquad [8a]$$

$$\rightarrow c\text{-}C_6H_{10} + c\text{-}C_6H_{12} \qquad [8b]$$

By analogy with the cyclohexane system (1) it is postulated that there are at least two distinct activated species of cyclohexene. One activated species, $c\text{-}C_6H_{10}^*$, decomposes to produce "cold" hydrogen atoms (reaction [2*]), while the other activated species, $c\text{-}C_6H_{10}^{**}$, decomposes to produce "hot" hydrogen atoms (reaction [2**]). It is further postulated that the hot hydrogen atoms abstract from cyclohexene according to reaction [3] and that most of the cold hydrogen atoms add to cyclohexene according to reaction [4]. The possibility that $c\text{-}C_6H_{12}''$ generates molecular hydrogen directly cannot be eliminated by the present experiments, and future work may require the inclusion of such a reaction, perhaps in place of reactions [2**] and [3]. The reaction

$$\text{cold H} + c\text{-}C_6H_{10} \rightarrow H_2 + c\text{-}C_6H_9$$

Can. J. Chem. Downloaded from www.nrcresearchpress.com by 186.148.149.217 on 09/04/12
For personal use only.

may be neglected by comparison with reaction [4]. This will be discussed further in the next section.

The large yield of cyclohexane, $G(c\text{-}C_6H_{12}) = 1.0$, seems to indicate that reaction [5] occurs. Reaction [5] will be mentioned again in the next section.

Although reactions [6*b*], [7*b*], [7*c*], and [8*b*] probably occur to an appreciable extent their products were not observed. Cyclohexadiene could not be detected by the present analytical technique, cyclohexane appeared to be produced more copiously by reaction [5], and cyclohexene was the starting material.

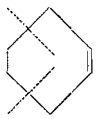
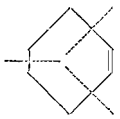
The products of ring fission can be accounted for by the following reactions, if the C_4 hydrocarbon product is butadiene:

$$c\text{-}C_6H_{10} \rightarrow C_2H_4 + C_4H_6, \qquad [9]$$

and

$$c\text{-}C_6H_{10} \rightarrow 2C_2H_4 + C_2H_2. \qquad [10]$$

Thus $G(C_4) + 2G(C_2H_2) = 0.144$ agrees fairly well with $G(C_2H_4) = 0.16$. This involves two types of ring fission

I  and II  .

In the liquid phase radiolysis by γ-rays, type I appears to occur four to five times as frequently as type II. Of the cyclohexene molecules that reacted under the present conditions, less than 3% reacted by ring fission.

The "other polymer" might have been produced by ion–molecule reactions. Thus far there seems to be no evidence that ion–molecule reactions are important in the radiolysis of liquid saturated hydrocarbons, but there is evidence that they are important in the radiolysis of liquid olefins, especially in polymer formation (4–6). The possibility that some or all of the identified products were formed by ion–molecule reactions cannot be ruled out by the present results, but their formation can be explained by free radical reactions (see preceding mechanism).

Cyclohexane–Cyclohexene Solutions

It has been assumed that, if there were no interaction between the different components of the solution, the cyclohexane product yields would be directly proportional to the electron fraction of cyclohexane, ϵ_e, in the solution, and that the cyclohexene product yields would be proportional to ϵ_e. This is probably not strictly correct but electron fraction has been used for lack of a better function.

In the cyclohexane–benzene solutions, when the electron fraction of benzene, ϵ_b, was increased from zero to 0.027, $G(H_2)$ decreased from 5.37 to 3.16 (1). At least 20%, and perhaps all of this decrease, appeared to be due to the scavenging of "cold" hydrogen atoms by benzene. In the cyclohexane–cyclohexene solutions, at $\epsilon_e = 0.026$, $G(H_2) = 3.22$. Thus, at this low concentration of solute, the same amount of decrease is produced in the hydrogen yield from cyclohexane by both benzene and cyclohexene. It is unlikely that the ratio of rate constants, k_{11}/k_{12}, has the same value when the unsaturate, RH,

$$H + RH \rightarrow RH_2 \qquad [11]$$

$$\rightarrow H_2 + R \qquad [12]$$

is benzene as when it is cyclohexene. It may therefore be concluded that reaction [12] occurs to a negligible extent with the cold hydrogen atoms generated by $c\text{-}C_6H_{12}'$. Reaction [12] can, however, occur with the hot hydrogen atoms generated by $c\text{-}C_6H_{12}''$.

Can. J. Chem. Downloaded from www.nrcresearchpress.com by 186.148.149.217 on 09/04/12
For personal use only.

The experimental results were tested against several different mechanisms. The mechanism that appeared to best fit the results included all the reactions [1] to [8] in the pure cyclohexene mechanism plus the reactions

$$c\text{-}C_6H_{12} \xrightarrow{I'} c\text{-}C_6H_{12}' \qquad [13']$$

$$\xrightarrow{I''} c\text{-}C_6H_{12}'' \qquad [13'']$$

$$c\text{-}C_6H_{12}' \rightarrow c\text{-}C_6H_{11} + \text{cold H} \qquad [14']$$

$$c\text{-}C_6H_{12}'' \rightarrow c\text{-}C_6H_{11} + \text{hot H} \qquad [14'']$$

$$\text{hot H} + c\text{-}C_6H_{12} \rightarrow H_2 + c\text{-}C_6H_{11} \qquad [15a]$$

$$\text{cold H} + c\text{-}C_6H_{12} \rightarrow H_2 + c\text{-}C_6H_{11} \qquad [15b]$$

$$c\text{-}C_6H_{12}'' + c\text{-}C_6H_{10} \rightarrow c\text{-}C_6H_{12} + c\text{-}C_6H_{10}^{***} \qquad [16]$$

$$c\text{-}C_6H_{10}^{***} \rightarrow c\text{-}C_6H_9 + x \text{ hot H} + (1-x) \text{ cold H}, \quad 0 \leqslant x \leqslant 1. \qquad [2^{***}]$$

This is essentially the same mechanism as that postulated for the cyclohexane–benzene system (1) except that cyclohexene itself undergoes several reactions that benzene does not (e.g., the benzene counterparts of reactions [2*], [2***], [5], [6*a*, 6*b*], and [7*a*, 7*b*, 7*c*] were not observed). In reaction [2***] the x represents the fraction of the $c\text{-}C_6H_{10}^{***}$ that decomposes to form hot hydrogen atoms, and hence molecular hydrogen. The value of x was determined by kinetic analysis (see later). Reaction [15*b*] could occur in the pure cyclohexane system because the only competing reactions involving the cold hydrogen atoms would be radical combination, and the radical concentrations are very small. The counterpart of reaction [15*b*] probably occurs to a certain extent in the cyclohexene system, but, as mentioned earlier, it appears to be negligible (within the accuracy of the present experiments) by comparison with reaction [4].

Since the over-all mechanism is complex, the kinetic analysis will be simplified by treating one product at a time. It will be assumed that I' and I'' are each directly proportional to the electron fraction of cyclohexane, ϵ_c, and that I^* and I^{**} are each directly proportional to ϵ_e.

Hydrogen

By analogy with the cyclohexane–benzene system (1), the rapid decrease in hydrogen yield at low cyclohexene concentrations ($\epsilon_e < 0.05$) is largely due to scavenging of the cold hydrogen atoms generated by $c\text{-}C_6H_{12}'$. The slower decrease at higher cyclohexene concentrations is mainly due to energy transfer "protection" of the species $c\text{-}C_6H_{12}''$. These effects may be separated and measured by kinetic analysis. It was found in the cyclohexane–benzene system that $I'' = (3.0 \pm 0.4)\epsilon_c$ and $I' = (2.4 \mp 0.4)\epsilon_c$.

The production of hydrogen involves reactions [1**], [2**], [2***], [3], [4], [13'], [13''], [14'], [14''], [15*a*], [15*b*], and [16]. Reactions [13'] and [14'] are important mainly at low cyclohexene concentrations. Reactions [1*] and [2*] do not contribute appreciably to hydrogen production because, when the cyclohexene concentration is high enough that these reactions occur to an appreciable extent, reaction [4] occurs with great efficiency.

The only reactions involved to an appreciable extent in the production of molecular hydrogen from cold hydrogen atoms are reactions [13'], [14'], [15*b*], and [4]. The hydrogen yield from this source will be represented as $G(H_2)'$ because it is generated by $c\text{-}C_6H_{12}'$. This hydrogen can be scavenged by cyclohexene. Steady-state treatment of the above reactions gives

$$[ii] \qquad G(H_2)' = \frac{I'}{1 + k_4(c\text{-}C_6H_{10})/k_{15b}(c\text{-}C_6H_{12})}.$$

Can. J. Chem. Downloaded from www.nrcresearchpress.com by 186.148.149.217 on 09/04/12
For personal use only.

For pure cyclohexane the yield of hydrogen is given approximately by the equation

[iii] $$G(H_2) = 5.37 - 0.08 \times \text{dose}(10^{20}\ \text{ev/ml cyclohexane, } 24^\circ\ \text{C})$$

over the dose range 0 to 2.5×10^{20} ev/ml (1). Assuming that this decrease in hydrogen yield with increasing dose is due to the accumulation of cyclohexene in the system, the value of the ratio k_4/k_{15b} can be determined from equations [ii] and [iii], using $I' = 2.4\epsilon_c$ and the average value of $(c\text{-}C_6H_{10})/(c\text{-}C_6H_{12})$ over the dose range considered. Over the range 0 to 2.5×10^{20} ev/ml, $\Delta G(H_2) = 0.20$ and the average $(c\text{-}C_6H_{10})/(c\text{-}C_6H_{12}) = 4.6 \times 10^{-4}$. Therefore $k_4/k_{15b} = 200$. Guentner, Hardwick, and Nejak (7) concluded, from a comparison of their pure cyclohexane results with the cyclohexane–cyclohexene solution results of Manion and Burton (2), that the accumulated cyclohexene alone was not sufficient to explain the observed decrease in hydrogen yield with increasing dose. Their conclusion may be incorrect, however, because at the concentrations of cyclohexene used by Manion and Burton both energy transfer protection and hydrogen atom scavenging were probably occurring.

Thus the amount of unscavenged hydrogen, $G(H_2)'$, can be calculated from equation [ii] for the various cyclohexene solutions studied, and can be subtracted from the observed hydrogen yield, $G(H_2)_{obs}$.

In pure cyclohexene $G(H_2) = 1.2$ and the only reactions that enter into the production of hydrogen in this system are reactions [1**], [2**], and [3]. It may therefore be assumed that the amount of hydrogen resulting from the direct excitation of cyclohexene, $G(H_2)^{**}$, is given by

[iv] $$G(H_2)^{**} = I^{**} = 1.2\epsilon_e.$$

The amount of hydrogen that results from the initial formation of $c\text{-}C_6H_{12}''$, $G(H_2)''$, can then be determined from

[v] $$G(H_2)'' = G(H_2)_{obs} - G(H_2)' - G(H_2)^{**}.$$

This hydrogen cannot be scavenged by cyclohexene but $G(H_2)''$ may be decreased by energy transfer from $c\text{-}C_6H_{12}''$ to cyclohexene, provided that all the excited cyclohexene molecules, $c\text{-}C_6H_{10}^{***}$, so formed do not decompose to produce hot hydrogen atoms and hence molecular hydrogen. Only reactions [13''], [14''], [15*a*], [16], [2***], and [3] enter into the production of hydrogen from this source. Steady-state treatment of these reactions gives

[vi] $$G(H_2)'' = I''\left[\frac{k_{14}'' + x k_{16}(c\text{-}C_6H_{10})}{k_{14}'' + k_{16}(c\text{-}C_6H_{10})}\right],$$

which may be rearranged to

[vii] $$[1 + y(c\text{-}C_6H_{10})]I''/G(H_2)'' = 1 + k_{16}(c\text{-}C_6H_{10})/k_{14}'', \\ = R'',$$

where $y = x\ k_{16}/k_{14}''$, x = fraction of $c\text{-}C_6H_{10}^{***}$ that decomposes to form hot hydrogen atoms and hence molecular hydrogen, and R'' represents the left-hand side of equation [vii]. Various sets of R'' were calculated, using $I'' = 3.0\epsilon_c$ and various values of y, and each set of R'' values was plotted against cyclohexene concentration (moles/l.). The best straight line was obtained with $y = 0.3$ (see Fig. 3). The slope of the line gives $k_{16}/k_{14}'' = 0.54$ l./mole. Therefore $x = 0.56$.

Can. J. Chem. Downloaded from www.nrcresearchpress.com by 186.148.149.217 on 09/04/12
For personal use only.

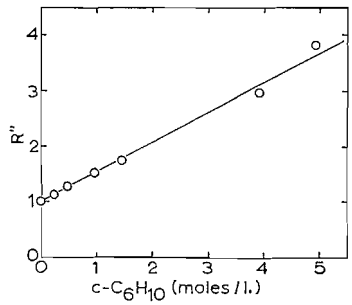


FIG. 3. Variation of R'' with cyclohexene concentration.
$R'' = [1+y(c\text{-}C_6H_{10})]I''/G(H_2)''$.

Since the cyclohexane–benzene system would allow I'' to have a value in the range $(3.0\pm0.4)\epsilon_c$, the best value being $3.0\epsilon_c$, the above kinetic analysis was repeated for the cyclohexane–cyclohexene system using various sets of values of I'' and $I' = (5.4-I'')\epsilon_c$. The corresponding value of k_4/k_{15b} was calculated for each set and the numerical and graphical analysis was done as described above. It was found that the present system would allow $I'' = (3.0\pm0.3)\epsilon_c$. Therefore $I' = (2.4\mp0.3)\epsilon_c$, $k_4/k_{15b} = 200\pm30$, and $x = 0.56\pm0.10$, but $k_{16}/k_{14}'' = 0.54\pm0.4$ l./mole. The experimental value of k_{16}/k_{14}'' is much more flexible than are the other experimentally determined constants. The ratio k_{16}/k_{14}'' in the present system corresponds to the previously reported k_3''/k_4'' in the cyclohexane–benzene system (1). Similar analysis of the latter system gave $k_3''/k_4'' = 0.78\pm0.11$ l./mole, which is relatively clearly defined. The main reason for the difference in precision of determination of the value of this ratio of rate constants in the two systems seems to be the presence of the extra adjustable parameter, x, in the cyclohexene system, together with a slightly lower precision in the measured hydrogen yields in this system.

Dicyclohexyl, Cyclohexylcyclohexene, and Dicyclohexenyl

Since cyclohexyl radicals are produced when the cold hydrogen atoms are scavenged by cyclohexene, the observed sharp decrease in dicyclohexyl yield in the region $\epsilon_e = 0$ to 0.026 was probably caused by the reaction of cyclohexyl radicals with cyclohexene (reaction [5]). This would also explain the sharp increase in dicyclohexenyl yield in this region.

The rates of formation of these three products are given by

[viii] $$d(\text{dicyclohexyl})/dt = k_{8a}(c\text{-}C_6H_{11})^2,$$

[ix] $$d(\text{cyclohexylcyclohexene})/dt = k_{7a}(c\text{-}C_6H_{11})(c\text{-}C_6H_9),$$

and

[x] $$d(\text{dicyclohexenyl})/dt = k_{6a}(c\text{-}C_6H_9)^2.$$

Since the rates of formation of the products are related to their G values by the same proportionality constant,

[xi] $$\frac{k_{7a}}{(k_{8a}k_{6a})^{\frac{1}{2}}} = \frac{G(\text{cyclohexylcyclohexene})}{[G(\text{dicyclohexyl})\,G(\text{dicyclohexenyl})]^{\frac{1}{2}}}.$$

Can. J. Chem. Downloaded from www.nrcresearchpress.com by 186.148.149.217 on 09/04/12
For personal use only.

The values of this ratio, calculated from equation [xi], at the various cyclohexene concentrations, are

ϵ_e	0.026	0.051	0.102	0.153	0.204	0.405	0.506	1.00
$k_{7a}/(k_{8a}k_{6a})^{\frac{1}{2}}$	0.30	0.44	0.49	0.40	0.37	0.59	0.48	0.56

The average value is 0.45 ± 0.08.

Cyclohexylhexene

The cyclohexylhexene yield varied with cyclohexene concentration (Fig. 2) in the same way it did with benzene concentration (reference 1). The previously postulated reactions which affect the yield of this product appear to apply equally well when cyclohexene is substituted for benzene.

Total C_{12} Hydrocarbons

The variation of the total C_{12} hydrocarbon yield with cyclohexene concentration is the main evidence that the protection of cyclohexane by cyclohexene is sacrificial, i.e. that a cyclohexene molecule decomposes for each cyclohexane molecule that is "protected".

ACKNOWLEDGMENTS

The author would like to express his gratitude to the National Research Council of Canada and to the TransMountain Oil Pipeline Co. for financial support.

The author would also like to thank Dr. S. Usiskin for aid with the irradiations, and the Government of Alberta Cancer Clinic for permission to use the Co^{60} therapy unit.

REFERENCES

1. G. R. FREEMAN. J. Chem. Phys. In press.
2. J. P. MANION and M. BURTON. J. Phys. Chem. **56**, 560 (1952).
3. H. A. DEWHURST. J. Phys. Chem. **63**, 813 (1959).
4. W. H. T. DAVISON, S. H. PINNER, and R. WORRAL. Proc. Roy. Soc. A, **252**, 187 (1959).
5. P. C. CHANG, N. C. YANG, and C. D. WAGNER. J. Am. Chem. Soc. **81**, 2060 (1959).
6. F. W. LAMPE. J. Phys. Chem. **63**, 1986 (1959).
7. W. S. GUENTNER, T. J. HARDWICK, and R. P. NEJAK. J. Chem. Phys. **30**, 601 (1959).

Can. J. Chem. Downloaded from www.nrcresearchpress.com by 186.148.149.217 on 09/04/12
For personal use only.

Can. J. Chem. Downloaded from www.nrcresearchpress.com by 186.148.149.217 on 09/04/12
For personal use only.

RELATIVE RATES OF REACTION OF OZONE WITH OLEFINS IN THE VAPOR PHASE[1]

T. VRBASKI[2] AND R. J. CVETANOVIĆ

ABSTRACT

Relative rates of reaction of ozone with a number of olefins in the vapor phase have been determined by the use of the competitive method and GLC analysis of the reaction products. The results indicate a basic electrophilic trend onto which is superimposed a trend due to a partially inhibiting effect of the substituent groups, in particular of those on the more substituted carbon atom of the olefinic double bond. The results are discussed particularly in terms of a two-step addition process, involving an initial formation of an ozone–olefin π-complex and a slower rearrangement of the π-complex into the cyclic "initial ozonide".

INTRODUCTION

A study of the relative rates of reactions of oxygen atoms with olefins in the vapor phase has been recently carried out in this laboratory (1), and some aspects of these reactions are still under investigation. This study uncovered simple correlations of the logarithms of the rate constants with some physical properties of the olefins and established experimentally the electrophilic character of oxygen atoms in their reactions with olefins. The results of this vapor phase investigation were compared with some other series of electrophilic reactions in solution and with the very few literature values available at the time for the vapor phase reactions of ozone with olefins. On this basis, nothing could be said with certainty about the reagent character which ozone exhibited in its reactions with olefins, although qualitatively an electrophilic trend was known from the work of Wibaut and his co-workers (2) for ozone in reactions with some aromatic compounds.

In view of the potentially useful information which comparative studies of this kind may provide, it was thought of interest to attempt to obtain the relative rates of ozone reactions with a number of representative olefins. In the course of this investigation, some information was obtained on the products formed in these reactions under the particular experimental conditions employed, and, this part of the work has already been described (3) (referred to in the following as Part I). In the present communication the relative rate constants obtained for these reactions are reported and their trends with olefin structure discussed.

EXPERIMENTAL

The reaction system, the method of analysis, and apart from some additional detail, the general experimental procedures used in this work have been already described in Part I. In present case pairs of olefins in various concentration ratios were introduced into the 188-cc spherical reaction vessel. Their total amount was in most experiments 400 μmoles to which was subsequently added the equivalent of 25 μmoles of ozone. This was done by admitting slowly the required pressure of ozonized oxygen (2.6 to 3.2% by volume of ozone) into the mixture of olefin vapors at $25\pm2°$. The total pressure was therefore 110 to 135 mm. In some experiments, especially in the case of *cis*-2-butene, *trans*-2-butene, and tetramethyl ethylene, the total amount of the two olefins was reduced

[1]*Manuscript received March 2, 1960.*
Contribution from the Division of Applied Chemistry, National Research Council, Ottawa, Canada. Issued as N.R.C. No. 5689.
[2]*National Research Council Postdoctorate Fellow, 1957–59.*

to 200 μmoles, to which then only the equivalent of 10 μmoles of ozone was added and the total pressure was 50 to 60 mm. These smaller amounts were used in order to decrease the excess quantities of the original olefins remaining at the end of the reaction and thus to make easier the subsequent analysis of the products by gas–liquid chromatography (GLC).

The olefins used were of the highest available grade and were freed of any peroxides present and thoroughly degassed and bulb-to-bulb distilled *in vacuo*. A mercury gauge was used to measure the pressures; this was separated from the rest of the reaction system by two ice traps in order to minimize the concentration of mercury vapor. As described in Part I, no noticeable decrease in ozone concentration resulted from the small amount of mercury vapor present. Silicone grease was used for the stopcocks in the parts of the system exposed to ozone–oxygen mixtures.

The products were frozen out in two liquid nitrogen traps in series while excess oxygen and any noncondensable products were pumped off slowly through a capillary constriction. The condensable products were then transferred to GLC. In some instances excess olefins were removed beforehand on a Le Roy still (4). The details of the GLC arrangements used have been given in Part I.

RESULTS

The method of competing reactions has been used to determine the relative rates of the reactions of ozone with various olefins. This has been done by comparing the GLC peak areas of the major carbonyl compounds formed from two olefins (ΔP_1 and ΔP_2, respectively) at different ratios of their initial concentrations ($[A_2]_1/[A_1]_1$). If the two competing reactions are

$$A_1 + O_3 \rightarrow \alpha_1 P_1 + \text{other products} \qquad [1]$$

and

$$A_2 + O_3 \rightarrow \alpha_2 P_2 + \text{other products} \qquad [2]$$

and if the initial concentrations of the two olefins are sufficiently high so that they remain essentially unaltered in the course of the reaction, then the ratio of the rate constants may be derived from the expression

$$\frac{\Delta P_1}{\Delta P_2} = \frac{k_1}{k_2}\frac{\alpha_1}{\alpha_2}\frac{[A_1]_1}{[A_2]_1}. \qquad [3]$$

A plot of $\Delta P_1/\Delta P_2$ vs. $[A_1]_1/[A_2]_1$ should be linear with zero intercept and the slope is then (k_1/k_2) (α_1/α_2). To get the ratio of the rate constants, the ratio α_1/α_2 has to be known. This is determined from the amounts of products formed (ΔP^*) when each of the two olefins is taken singly, i.e. $\alpha = \Delta P^*/\Delta O_3$ and $\alpha_1/\alpha_2 = \Delta P_1^*/\Delta P_2^*$ provided the same amount of ozone is used in the two "single" runs and ozone is consumed exclusively in reactions [1] and [2]. This last requirement is presumably met when relatively large concentrations of olefins are used.

Under similar conditions also $\Delta P_1/\alpha_1 + \Delta P_2/\alpha_2 = \Delta P_1^*/\alpha_1$, so that

$$\frac{\Delta P_1}{\Delta P_1^* - \Delta P_1} = \frac{k_1}{k_2}\frac{[A_1]_1}{[A_2]_1} \qquad [4]$$

an alternative expression which can be used when ΔP_2 cannot be measured.

In most of the present work use was made of eq. [3]. Fairly good linear plots through the origin were obtained as shown in Figs. 1, 2, and 3, and the slopes divided by the corresponding α_1/α_2 values gave the relative rate constants k_1/k_2 summarized in Table I.

Can. J. Chem. Downloaded from www.nrcresearchpress.com by 186.148.149.217 on 09/04/12
For personal use only.

Can. J. Chem. Downloaded from www.nrcresearchpress.com by 186.148.149.217 on 09/04/12
For personal use only.

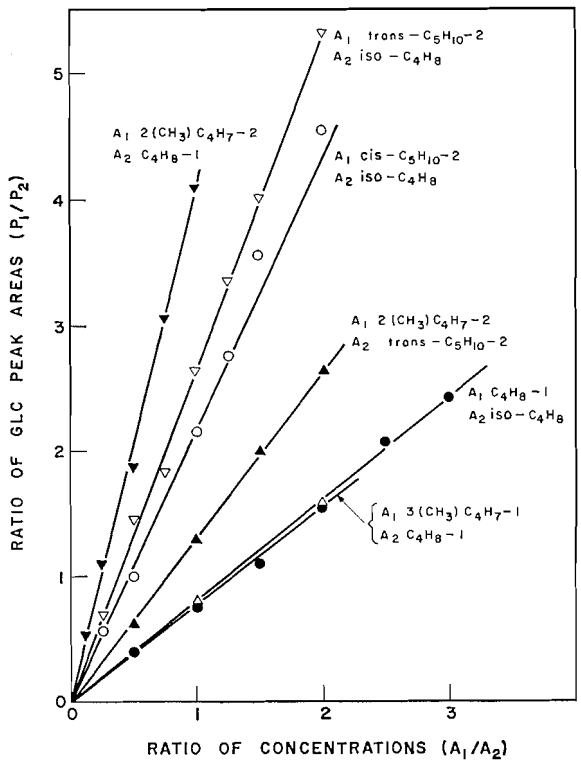


FIG. 1. Determination of the ratios of rate constants for 2-methyl-2-butene and 1-butene, *trans*-2-pentene and isobutene, *cis*-2-pentene and isobutene, 2-methyl-2-butene and *trans*-2-pentene, 1-butene and isobutene, 3-methyl-1-butene and 1-butene.

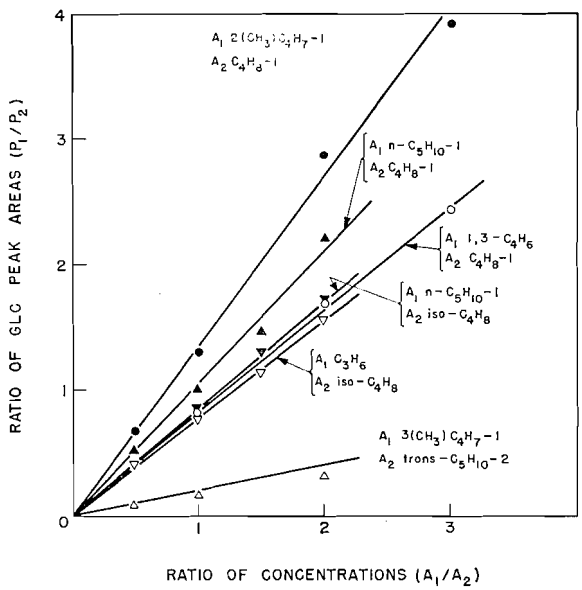


FIG. 2. Determination of the ratios of rate constants for 2-methyl-1-butene and 1-butene, *n*-1-pentene and 1-butene, *n*-1-pentene and isobutene, 1,3-butadiene and 1-butene, propylene and isobutene, 3-methyl-1-butene and *trans*-2-pentene.

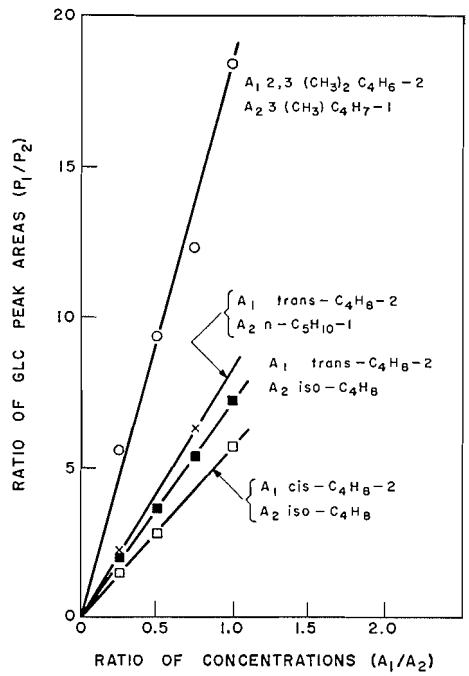


FIG. 3. Determination of the ratios of the rate constants for 2,3-dimethyl-2-butene and 3-methyl-1-butene, *trans*-2-butene and *n*-1-pentene, *trans*-2-butene and isobutene, *cis*-2-butene and isobutene.

TABLE I

The mean values of the ratios of the rate constants

	Reactant olefins		Products used for rate determinations				
	A_1	A_2	P_1	P_2	α_1/α_2	Mean, k_1/k_2	Equation used
1	C_2H_4	iso-C_4H_8	—	Acetone	—	0.51	4, 4*a*
2	C_3H_6	iso-C_4H_8	Acetaldehyde	Acetone	0.551	1.41	3
3	C_4H_8-1	iso-C_4H_8	Propanal	Acetone	0.749	1.07	3
4	*cis*-C_4H_8-2	iso-C_4H_8	Acetaldehyde	Acetone	1.53	3.69	3, 3*a*
5	*trans*-C_4H_8-2	iso-C_4H_8	Acetaldehyde	Acetone	1.58	4.56	3, 3*a*
6*	*trans*-C_4H_8-2	*n*-C_5H_{10}-1	Acetaldehyde	*n*-Butanal	1.94	4.24	3, 3*a*
7	1,3-C_4H_6	*n*-C_4H_8-1	Acroleine	Propanal	0.726	1.07	3
8	*n*-C_5H_{10}-1	*n*-C_4H_8-1	*n*-Butanal	Propanal	1.05	1.00	3
9*	*n*-C_5H_{10}-1	iso-C_4H_8	*n*-Butanal	Acetone	0.789	1.06	3
10	*cis*-C_5H_{10}-2	iso-C_4H_8	Propanal	Acetone	0.763	2.84	3, 3*a*
11	*trans*-C_5H_{10}-2	iso-C_4H_8	Propanal	Acetone	0.756	3.50	3, 3*a*
12	2-$(CH_3)C_4H_7$-1	*n*-C_4H_8-1	$CH_3.CO.C_2H_5$	Propanal	1.28	1.03	3
13*	3-$(CH_3)C_4H_7$-1	*n*-C_4H_8-1	Isobutanal	Propanal	0.985	0.79	3
14	3-$(CH_3)C_4H_7$-1	*trans*-C_5H_{10}-2	Isobutanal	Propanal	0.928	0.22	3
15*	2-$(CH_3)C_4H_7$-2	*n*-C_4H_8-1	Acetone	Propanal	1.35	3.02	3, 3*a*
16	2-$(CH_3)C_4H_7$-2	*trans*-C_5H_{10}-2	Acetone	Propanal	1.31	0.99	3
17	2,3-$(CH_3)_2C_4H_6$-2	3-$(CH_3)C_4H_7$-1	Acetone	Isobutanal	4.06	4.50	3, 3*a*
18	*n*-C_6H_{12}-1	iso-C_4H_8	—	Acetone	—	1.28	4
19	Cyclohexene	iso-C_4H_8	—	Acetone	—	3.74	4, 4*a*

*Asterisks indicate the experiments for the cross-checking of the values of k_1/k_2.

Can. J. Chem. Downloaded from www.nrcresearchpress.com by 186.148.149.217 on 09/04/12
For personal use only.

The reaction products P_1 and P_2 and the values obtained for α_1/α_2 are shown and the equation used indicated.

For the pairs of olefins ethylene and isobutene, *n*-1-hexene and isobutene, and cyclohexene and isobutene, the relative rate constants were determined from measurements of the GLC peak areas of acetone (formed from isobutene) using eq. [4]. Fairly good linear plots through the origin are again obtained, as shown in Fig. 4, and the values of k_1/k_2 evaluated from the slopes are shown in Table I.

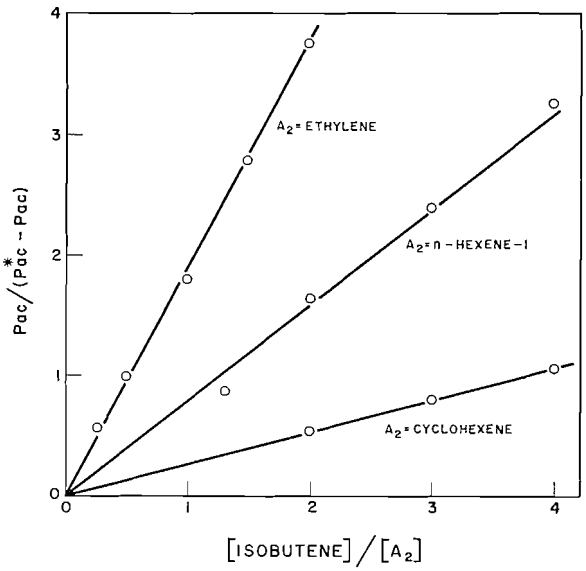


FIG. 4. Determination of the ratios of the rate constants based on eq. [4] for ethylene and isobutene, *n*-1-hexene and isobutene, cyclohexene and isobutene.

In some instances there was appreciable deviation from the assumed constancy of the concentrations of the olefins and the more complex logarithmic expressions (1) instead of eqs. [3] and [4] (referred in Table I as eqs. [3*a*] and [4*a*], respectively) were then used to calculate the ratios of the rate constants. However, this led only to relatively small corrections.

There is a satisfactory mutual consistency of the k_1/k_2 values in the cases where cross determinations (marked in Table I with asterisks) have been made. For example, the value for *trans*-2-butene and *n*-1-pentene from run 6 is 4.2 and it is 4.4 when calculated from runs 5, 8, and 3; the value for *n*-1-pentene and isobutene in run 9 is 1.06 and it is 1.07 when calculated from runs 8 and 3; for 3-methyl-1-butene and 1-butene the value is 0.79 in run 13 and 0.70 calculated from runs 14, 11, and 3; for 2-methyl-2-butene and 1-butene it is 3.02 from run 15 and 3.23 calculated from runs 16, 11, and 3.

In Table II are listed the relative rate constants obtained in the present work taking the value for ethylene as unity. The absolute rate constants are then calculated by adopting the value of Cadle and Schadt (5) for ethylene (1.8×10^3 l. mole^{-1} sec^{-1}) and these are compared with the determinations of Cadle and Schadt (5), of Hanst *et al.* (6), and of Saltzman (7).

Can. J. Chem. Downloaded from www.nrcresearchpress.com by 186.148.149.217 on 09/04/12
For personal use only.

TABLE II

The relative rate constants of the ozone–olefin reactions and comparison with the literature values of the absolute rate constants at room temperature

Olefin	Relative rate constants (ethylene = 1)	Absolute rate constants (l. mole^{-1} sec^{-1} $\times 10^{-3}$)	
		Present work[a]	Literature
Ethylene	1.00	1.8	1.8,[b] 0.8[c]
Propylene	2.78	5.1	3.8,[b] 4.9[c]
1-Butene	2.12	3.9	
n-1-Pentene	2.11	3.9	3.2,[b] 4.5[c]
n-1-Hexene	2.52	4.6	6.1,[b] 6.1,[c] 5.5[d]
3-Methyl-1-butene	1.65	3.0	
Isobutene	1.97	3.6	3.7[c]
2-Methyl-1-butene	2.19	4.0	
cis-2-Butene	7.26	13	29[c]
trans-2-Butene	8.98	17	
cis-2-Pentene	5.59	10	98[c,e]
trans-2-Pentene	6.90	13	
Cyclohexene	7.37	14	35[b]
Trimethyl ethylene	6.39	12	
Tetramethyl ethylene	7.49	14	
Butadiene	2.26	4.2	4.9[c]

[a]Calculated from the relative values in column 1 by adopting for ethylene the value of Cadle and Schadt (1.8×10^3 l. mole^{-1} sec^{-1}, reference 5).
[b]Cadle and Schadt, reference 5.
[c]Hanst *et al.*, reference 6.
[d]Saltzman, reference 7.
[e]Mixture of *cis*- and *trans*-2-pentene.

DISCUSSION

The trend in the rate constants of ozone reactions with olefins obtained in the present work agrees for several olefins quite well with the corresponding literature values, as is seen in Table II. At the same time, the literature values for cyclohexene, *cis*-2-butene, and 2-pentene are considerably larger, in particular so the much larger value for 2-pentene. The reasons for these discrepancies are not clear, although some of the potential difficulties inherent in experimental studies of these complex reactions have been briefly discussed in Part I. Further experimental work will be necessary to clarify this point, and in the meantime parts of the following discussion of the relative rate constants obtained in the present work must be regarded as of a tentative character.

The question to which a study of the trends in the rate constants with the olefin structure is hoped to answer is whether in its reactions with alkenes ozone behaves as an electrophilic, nucleophilic, or radical reagent. For aromatic compounds Wibaut and his co-workers (2) have already shown that the qualitative trend is such as expected for an electrophilic reagent. This has been recently further confirmed by a study of the trend in the rates in polyalkyl benzenes, although a concurrent screening effect by the bulkier substituent groups has also been indicated (8).

A qualitative inspection of the relative values in Table II shows that in its reactions with olefins in the vapor phase ozone appears also to behave as an electrophilic reagent. A radical reagent would be expected to react much more rapidly with butadiene, and a nucleophilic reagent would exhibit a trend in the rates opposite to that observed as the number of substituents in the ethylene molecule is increased. However, there are also some irregularities in the trends: for electrophilic reagents the rates of α,α-disubstituted ethylenes such as isobutene should be approximately equal to those of the α,β-disubstituted derivatives (such as 2-butene) and here they are appreciably smaller. Also the rates of trimethyl and tetramethyl ethylene should be greater than those of the α,β-disubstituted ethylenes while the observed values are about equal.

Can. J. Chem. Downloaded from www.nrcresearchpress.com by 186.148.149.217 on 09/04/12
For personal use only.

As reported in a previous publication (1) mutual linear log k – log k (free energy) plots can be constructed for the reactions of some electrophilic reagents with olefins. A similar plot for ozone reactions (Fig. 5) shows appreciable scatter and in particular the points

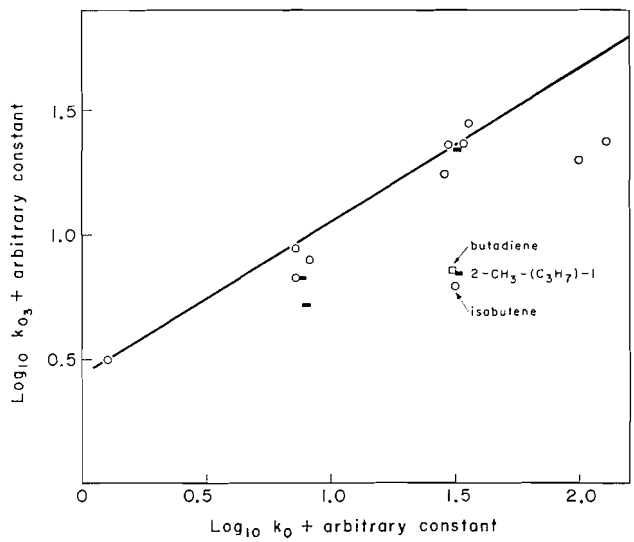


FIG. 5. The "free energy" plot (log k vs. log k) for the reactions of ozone and oxygen atoms with olefins. k_{O_3} are the relative rate constants of the reactions of ozone with olefins and k_O are the relative rate constants of the corresponding oxygen atom reactions. Filled rectangles represent values for k_O not known experimentally but estimated approximately from the general trends established for such reactions (reference 1).

for butadiene, isobutene, and 2-methyl-1-butene deviate very strongly. (In this plot some values for log k_O, i.e. for the corresponding oxygen atom reactions, are not known and have been approximately estimated—they are indicated in Fig. 5 by filled rectangles.)

Intuitively a correlation may be anticipated between the rates of reactions of electrophilic reagents with olefins and the ionization potentials of the latter. The existence of an approximate linear dependence of the log k values for some electrophilic reagents on the ionization potentials of the olefins has been pointed out before (1). This is illustrated again in Fig. 6, which also incorporates some additional experimental values and the data of Doering and Henderson (9) for CCl_2 and CBr_2, the latter instead of those of Skell and Garner (10) because of the potentially more accurate analytical procedure used in the more recent work. The values for the ozone reactions have also been plotted and there is evidently a large scatter of points, although the general trend appears to be of an electrophilic reagent.

The apparent irregularities and scatter of points for the ozone plot in Fig. 6 can be qualitatively explained by a superposition on a general electrophilic trend of a partly inhibiting effect by the substituent groups. This inhibiting effect could be due to a screening by the substituent groups (steric hindrance) as has been suggested for the reactions of ozone with some aromatics (8) (polyalkyl benzenes). In this case the deviations in Fig. 6 from the values such as indicated for example by the interrupted line may be qualitatively explainable: on the whole the deviations tend to become progressively greater as a screening effect might be expected to become greater. The case of butadiene would be somewhat difficult to explain on that basis, but it is doubtful whether this fact alone could be taken to invalidate a general explanation of this kind.

Can. J. Chem. Downloaded from www.nrcresearchpress.com by 186.148.149.217 on 09/04/12
For personal use only.

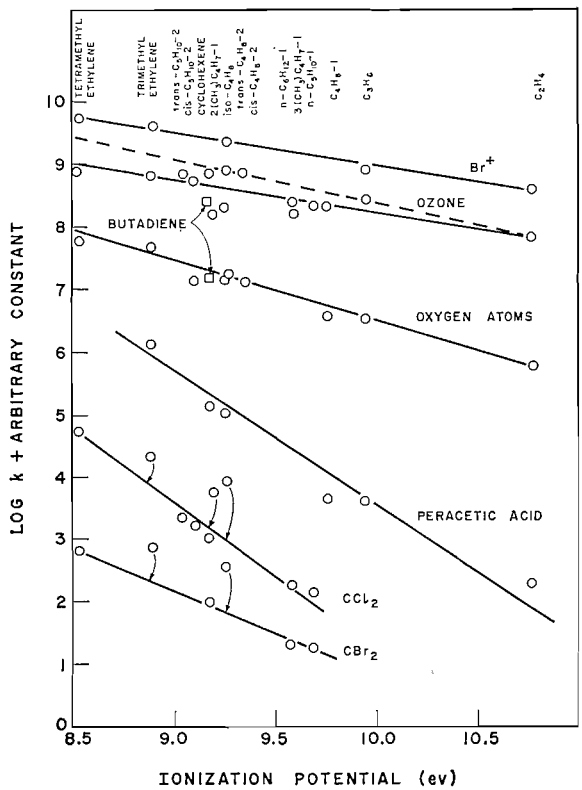


FIG. 6. Plots of log k for several series of electrophilic reactions with olefins against the ionization potentials of the olefins.

The sources of data are: ionization potentials: Collin and Lossing, J. Am. Chem. Soc. **81**, 2064 (1959), and, for 1-hexene, Honig, J. Chem. Phys. **16**, 105 (1948); bromination reactions: Anantakrishnan and Ingold, J. Chem. Soc. 984, 1396 (1935); ozone reactions: present work; oxygen atom reactions: Cvetanović, reference 1 and some unpublished data; peracetic acid reactions: Böeseken and Stuurman, Rec. trav. chim. **56**, 1034 (1937), Böeseken and Hanegraff, Rev. trav. chim. **61**, 69 (1942), Swern, J. Am. Chem. Soc. **69**, 1692 (1947); CCl_2 and CBr_2: Doering and Henderson, reference 9.

A superposition of an additional structural effect on an electrophilic trend could be caused by such a direct screening of the double bond by the substituent groups and the consequent decreased efficiency of a single step attack. Also, it may be due to a more complex addition process, represented for example by the following two-step reaction sequence:

$$\text{olefin} + O_3 \underset{k_{-5}}{\overset{k_5}{\rightleftharpoons}} [\text{olefin}, O_3] \qquad [5]$$

$$[\text{olefin}, O_3] \xrightarrow{k_6} \text{initial addition product} \qquad [6]$$

Under such conditions the observed rate constant k_{O_3} is a composite quantity

$$k_{O_3} = k_5/(1+k_{-5}/k_6) \qquad [7]$$

and when k_6 is small relative to k_{-5},

$$k_{O_3} = \frac{k_5}{k_{-5}} k_6 = Kk_6 \qquad [8]$$

Can. J. Chem. Downloaded from www.nrcresearchpress.com by 186.148.149.217 on 09/04/12
For personal use only.

Can. J. Chem. Downloaded from www.nrcresearchpress.com by 186.148.149.217 on 09/04/12
For personal use only.

where K is the equilibrium constant of reaction [5] and is therefore a measure of stability of the postulated olefin–ozone complex formed in the primary step. This complex would have to be of the nature of a "π-complex" since no isomerization of *cis*-2-butene to the *trans* isomer was found under the reaction conditions, as reported in Part I. The electrophilic character of ozone is then readily explained by the dependence of k_{O_3} on K, i.e. on the basicity of the olefins.

The retarding effect of the substituents on reaction [6], i.e. on the rearrangement of the π-complex into the initial addition product (the "initial ozonide"), may again be predominantly due to steric inhibition. Alternatively, the inductive effects of the substituents on the more substituted carbon atom of the double bond, the most probable position of the nucleophilic ring closure necessary for the formation of the "initial ozonide", may play a contributing and perhaps a decisive role in determining the rate of reaction [6]. This last possibility has some distinctly attractive features. It can readily explain the exceptionally low values of the rate constants of the reactions of ozone with such compounds as butadiene and isobutene, and, in contrast to this, the fast reactions with α,β-disubstituted olefins.

In view of eq. [8], a trend in log k_{O_3} for various olefins is a superposition of the trend in log K, which parallels the basicity of the olefins, and of log k_6, which incorporates an inhibiting effect. If it is assumed that (*a*) this inhibiting effect is absent in ethylene, (*b*) that it is four times* as large for tetramethyl ethylene, i.e. when the more substituted carbon carries two methyl groups, as for propylene, in which it carries only one methyl group, and (*c*) that log K is a linear function of the ionization potentials of the olefins, it is then possible to calculate the corresponding values of the inhibiting effects for the other olefins. These represent the additive corrections in $\log_{10}$ units (Δ) which have to be made in order to obtain a linear plot of (log $k_{O_3}+\Delta$) against the ionization potentials. A fair consistency is obtained under such conditions for the olefins which have only methyl radicals as the substituents, with Δ of about 0.23 when one methyl radical is present and about four times as much when two methyl radicals are present on the more substituted carbon. On the same basis the values of Δ for some other radicals (when present singly on the more substituted carbon) were about 0.55 for C_2H_5, n-C_3H_7, and n-C_4H_9; 0.75 for *sec*-C_3H_7; 0.42 for cyclohexene; and 0.93 for C_2H_3 in butadiene.

While the present results appear to be most logically explainable in terms of the two-step mechanism defined by reactions [5] and [6] and an emphasis is placed on this interpretation, they do not represent a definite proof of validity of such a mechanism. Experimentally, it seems to be difficult to discriminate with certainty between a two-step and a one-step addition mechanism. The conflicting views have been recently reviewed and discussed in some detail by Bailey (11). The two-step mechanism discussed in the present work incorporates the features of the π-complex mechanism outlined by Bailey (12) and, in addition, it specifies the kinetics of the process. However, it does not attempt to differentiate between a five-membered ring structure for the "initial ozonide" and the four-membered ring ("molozonide") favored by Bailey (12).

Of the six series of reactions plotted in Fig. 6 only those of oxygen atoms and of ozone are gas phase reactions. The other reactions, all carried out in solution, are in principle subject to complexities resulting from solvent effects. For bromination and peracetic acid reactions there appear to be no pronounced irregularities which could be ascribed to such effects although it would be desirable to have the values of the rate constants for a greater variety of olefins. The reaction series for CCl_2 and CBr_2 additions to olefins

**The over-all consistency requires this value to be about 4 to 4.5.*

appear at first sight to show no correlation with the ionization potentials, as was stressed by Doering and Henderson (9) at the time when the relative rate constants for these two reaction series were reported by these authors. At the same time, there appears to be a significant similarity in the pattern of the plots for these two species in Fig. 6. The meaning of deviations from the lines arbitrarily drawn in Fig. 6 through the experimental points so as to connect most of the points is not clear. The same compounds "deviate" (are too fast relative to the arbitrarily drawn lines) in both series and it is of interest that at least two of these, isobutene and 2-methyl-1-butene, both α,α-disubstituted ethylenes, strongly deviate in the case of ozone reactions as well (perhaps best shown in Fig. 5) but in the opposite direction, being too slow in comparison with the α,β-disubstituted ethylenes. It is not possible to say at present how far-reaching these analogies and contrasts are until experimental information on the rates of reaction of such reagents with a greater number of olefins becomes available.

REFERENCES

1. R. J. CVETANOVIĆ. Can. J. Chem. **36**, 623 (1958); J. Chem. Phys. **30**, 19 (1959).
2. J. P. WIBAUT, F. L. J. SIXMA, L. W. F. KAMPSCHMIDT, and H. BOER. Rec. trav. chim. **69**, 1355 (1950); J. P. WIBAUT and F. L. J. SIXMA. Rec. trav. chim. **71**, 761 (1952).
3. T. VRBASKI and R. J. CVETANOVIĆ. Can. J. Chem. This issue.
4. D. J. LE ROY. Can. J. Research, B, **28**, 492 (1950).
5. R. D. CADLE and C. SCHADT. Taken from P. A. Leighton and W. A. Perkins *in* Photochemical secondary reactions in urban air. Rept. No. 24, Air Pollution Foundation, San Marino, Calif. August, 1958. p. 72.
6. P. L. HANST, E. R. STEPHENS, W. E. SCOTT, and R. C. DOERR. Div. Petrol. Chem. Am. Chem. Soc., Gen. Papers, **4** (4), A-7. Atlantic City, N.J. September, 1959.
7. B. E. SALTZMAN. Ind. Eng. Chem. **51**, 1415 (1959).
8. L. J. ANDREWS, T. W. NAKAGAWA, and R. M. KEEFER. Abstracts of Papers, 136th Meeting, Am. Chem. Soc., Atlantic City, N.J. September, 1959. p. 77 P.
9. W. VON E. DOERING and W. A. HENDERSON, JR. J. Am. Chem. Soc. **80**, 5274 (1958).
10. P. S. SKELL and A. Y. GARNER. J. Am. Chem. Soc. **78**, 5430 (1956).
11. P. S. BAILEY. Chem. Revs. **58**, 925 (1958).
12. P. S. BAILEY. *In* Ozone chemistry and technology. Advances in Chemistry No. 21. Am. Chem. Soc., Washington, 1959. p. 133.

Can. J. Chem. Downloaded from www.nrcresearchpress.com by 186.148.149.217 on 09/04/12
For personal use only.

Can. J. Chem. Downloaded from www.nrcresearchpress.com by 186.148.149.217 on 09/04/12
For personal use only.

A STUDY OF THE PRODUCTS OF THE REACTIONS OF OZONE WITH OLEFINS IN THE VAPOR PHASE AS DETERMINED BY GAS–LIQUID CHROMATOGRAPHY[1]

T. VRBASKI[2] AND R. J. CVETANOVIĆ

ABSTRACT

A broad comparative survey has been made of the products of the vapor phase reactions of ozone with ethylene, propylene, 1-butene, 1-pentene, 1-hexene, 3-methyl-1-butene, isobutene, 2-methyl-1-butene, *cis*-2-butene, *trans*-2-butene, *cis*-2-pentene, *trans*-2-pentene, trimethyl ethylene, tetramethyl ethylene, cyclohexene, and 1,3-butadiene as determined by gas–liquid chromatography and, to a smaller extent, by other analytical methods.

INTRODUCTION

Ozonization of olefinic compounds in the liquid phase has been the subject of numerous investigations. This extensive field has been adequately reviewed, in particular recently by Bailey (1). The corresponding reactions in the vapor phase are of greater complexity and have received considerably less attention. The recent recognition of their importance in the photochemically induced processes in polluted atmosphere leading to "smog" formation has been largely responsible for the renewed interest in these reactions (2–6).

In connection with current studies of the correlation of the rates of the olefin–oxygen atom reactions with the molecular structure of the olefins (7), it was thought of interest to attempt to obtain the relative rates of the corresponding olefin–ozone reactions. In the course of this study a certain amount of information has been accumulated on the products of a number of olefin–ozone reactions in the vapor phase. A brief report of these results is given in the present paper.

EXPERIMENTAL

The reactions were carried out at room temperature in a spherical reaction vessel 188 cc in volume, incorporated in a conventional high vacuum apparatus. A batch procedure was employed. The olefin was first transferred into the reaction vessel by freezing in liquid nitrogen and was subsequently vaporized by warming up to room temperature. The required amount of oxygen, containing 2.6 to 3.2% by volume of ozone, was then allowed to stream slowly into the reaction vessel. It was found that at least in some cases, especially when ozone concentration exceeded 3.2%, too rapid introduction of ozone–oxygen mixture could initiate virtually complete combustion of the reacted olefin to carbon dioxide and water accompanied by substantial warming of the reaction vessel and occasional light emission.

Ozone was freshly produced for each run in a standard Towers ozone apparatus by silent electric discharge at 7500 volts and 15 milliamperes. Cylinder oxygen dried over phosphorous pentoxide was used. The ozone concentration was determined iodometrically in the stream of oxygen as it leaves the ozonizer and also immediately prior to the reaction vessel. The two values agreed within the experimental error. The olefins used were of the highest available grade and were thoroughly degassed and bulb-to-bulb distilled *in vacuo* before use.

[1]*Manuscript received March 2, 1960.*
Contribution from the Division of Applied Chemistry, National Research Council, Ottawa, Canada.
Issued as N.R.C. No. 5694.
[2]*National Research Council Postdoctorate Fellow, 1957–59.*

The initial amounts of olefins and ozone were 400 and 100 μmoles and in some cases these quantities were reduced to facilitate the analysis of the products to 200 and 25 μmoles, respectively. The total pressure in the reaction vessel was, therefore, 360 to 440 mm in the former and 100 to 130 mm in the latter case. A mercury gauge was used to measure the pressures of the reactants, but attempt was made to bring ozone in contact with mercury as little as possible and the slight consumption of ozone in the reaction with some mercury vapor present did not decrease its concentration noticeably.

The condensable reaction products were retained by pumping off the non-condensable gas slowly, using a capillary constriction, through two liquid nitrogen traps in series. No attempt was made to analyze the non-condensable gas which contained the huge excess of oxygen. The analysis of most of the condensable products was done by gas–liquid chromatography (GLC). A Le Roy still (8) was occasionally used to separate the products from excess initial olefin. The hydrocarbon gases formed and carbon dioxide were analyzed mass spectrometrically after preliminary separation by GLC. Formic acid was determined qualitatively from infrared spectra of the products (using a gas cell 10 cm long) after removal of more volatile compounds on the Le Roy still and quantitatively by titrating with $N/50$ NaOH using phenolphthalein indicator. No quantitative determinations of formaldehyde were attempted because of its tendency to polymerize and consequently its difficult quantitative recovery from the reaction apparatus. In the case of some terminal olefins its presence was shown qualitatively by reaction with chromotropic acid and by the infrared spectra of the condensable products. On the whole, in most cases not too important quantities of formaldehyde appeared to be recovered.

The products eluted by GLC were collected in liquid nitrogen traps and their identity was confirmed by infrared and mass spectroscopy. The GLC arrangement was essentially as described previously (9) but with an internal capillary regulating the outlet pressure instead of an external leak. Two 1/4-in. I.D. columns were alternatively used: (1) a 40-ft tricresyl phosphate (TCP) on firebrick column (40 wt.% TCP) operated at 125° C, and (2) an 8-ft dinonylphthalate (DNP) on glass beads column (4 wt.% DNP) operated at room temperature. Helium was used as the carrier gas in both cases. Some separations of lighter gases (CO_2, ethane, ethylene) were kindly made by Dr. N. F. Foster on a 40-ft dimethyl sulpholane (DMS) on firebrick column (40 wt.% DMS) operated at room temperature.

For comparison with the data obtained in the vapor phase the liquid-phase ozonization of ethylene, isobutene, and 1-butene was carried out at −78° C in ethylchloride solution in a separate series of experiments.

RESULTS

The products of the reactions of ozone with a number of olefins in the vapor phase, as observed by the analytical procedures used in the present work, are shown in Table I. The quantities are expressed as molecules of products formed per molecule of ozone consumed.

It should be stressed that the quantities of the carbonyl compounds shown in Table I are based on GLC peak areas and are, therefore, the products observed *after* the condensables are passed through the GLC column and include any products of decomposition of the original compounds in the course of the analysis. This is, in particular, true of the initially present peroxides (shown qualitatively by a positive KI test, for example in the liquid products of isobutene, 1-butene, *cis*-2-pentene, and *trans*-2-pentene) which appear to be reduced to the corresponding carbonyl compounds. Thus in the case of isobutene

Can. J. Chem. Downloaded from www.nrcresearchpress.com by 186.148.149.217 on 09/04/12
For personal use only.

Can. J. Chem. Downloaded from www.nrcresearchpress.com by 186.148.149.217 on 09/04/12
For personal use only.

TABLE I

Number of moles of products formed per 1 mole of ozone consumed

Olefin	CO_2	C_2H_4	C_2H_6	C_3H_6	C_3H_8	C_4H_8	C_4H_{10}	HCOOH	CH_3OH	Acetone	MEK[a]	Aldehydes: Ac[b]	Pr[c]	*n*-Bu[d]	iso-Bu[e]	*n*-Val[f]	Acrolein	MF[g]
C_2H_4	n.d.	n.d.	n.d.	n.d.	n.d.	n.d.	n.d.	.25	—	—	—	.019	—	—	—	—	—	—
C_3H_6	.32	n.d.	n.d.	n.d.	n.d.	n.d.	n.d.	.34	.033	.008	—	**.38**	.003	—	—	—	—	.003
C_4H_8-1	.40	.031	.056	.002	—	n.d.	n.d.	.24	.014	—	—	.133	**.48**	.006	—	—	—	tr.
n-C_5H_{10}-1	.29	—	—	.046	.129	—	—	.20	—	—	—	.061	.161	**.32**	—	—	—	—
n-C_6H_{12}-1	.23	—	.005	tr.	—	.027	.076	.24	—	.015	—	.005	—	.056	—	**.118**	—	—
3$(CH_3)C_4H_7$-1	.29	—	—	.081	.132	—	—	.25	.015	.074	—	.032	—	—	**.30**	—	—	.001
iso-C_4H_8[h]	.37	—	—	.005	.009	—	—	.66	.013	**.53**	—	—	—	—	.005	—	—	.005
2$(CH_3)C_4H_7$-1	.54	—	—	—	—	—	tr.	.33	.113	—	**.42**	.130	—	—	—	—	—	—
cis-C_4H_8-2	.42	—	—	.023	—	—	tr.	.20	.152	—	—	**1.02**	—	—	—	—	—	—
trans-C_4H_8-2	.35	—	—	.014	tr.	—	—	.23	pr.	—	—	**1.06**	—	—	—	—	—	—
cis-C_5H_{10}-2	.30	—	.014	—	—	—	—	.20	.013	—	.001	**.56**	**.56**	.0003	—	—	—	—
trans-C_5H_{10}-2	.36	.018	.096	.003	—	—	—	.16	.012	—	n.d.	**.56**	**.56**	n.d.	—	—	—	—
$C(CH_3)_2$:$C(CH_3)H$	.29	—	—	tr.	tr.	.026	—	.24	.058	**.43**	—	**pr.**	—	—	—	—	—	—
$C(CH_3)_2$:$C(CH_3)_2$	.40	—	—	tr.	—	—	—	.22	pr.	**1.49**	—	.010	—	—	—	—	—	.007
Cyclohexene	.59	.118	—	—	—	—	—	.29	—	—	—	.014	—	—	—	—	—	—
Butadiene-1,3	.24	.114	—	.014	—	.004	.004	.18	—	—	—	.026	—	—	—	—	**.43**	.001

NOTE: n.d. = not determined; tr. = perhaps a trace present; pr. = qualitatively identified but not measured quantitatively. The meaning of the singly and doubly underlined figures and the figures in boldface type is explained in the text.

[a]MEK = methyl ethyl ketone. [b]Ac = CH_3CHO. [c]Pr = C_2H_5CHO. [d]*n*-Bu = *n*-C_3H_7CHO. [e]iso-Bu = iso-C_3H_7CHO. [f]*n*-Val = *n*-C_4H_9CHO. [g]MF = methyl formate.

[h]Isobutene produced also methyl acetate (.005) and *tert.*-butanol (.009).

only a fraction (about 13%) of the total acetone was recovered from the liquid products on the Le Roy still at −75°, at which temperature-free acetone should be recovered readily. Some other olefins seemed to show similar behavior but the amounts of the "free" and the "bound" carbonyl compounds were not determined separately.

Since in the present experiments large excess of the olefins was always used, it was not feasible in some cases to analyze for the reaction products of volatilities or GLC elution times similar to those of the olefins; thus the information obtained for the reaction with ethylene is very incomplete. In the case of 2-methyl-2-butene acetaldehyde could not be evaluated quantitatively by GLC analysis, although it was evidently formed in significant amounts as anticipated. Also, any compounds of very low volatility and long GLC elution times would not be readily detected. This is very probably responsible for the limited information on the products of the reaction of cyclohexene.

In order to test whether some double-bond isomerization may occur in the course of these reactions, the butene recovered from the reaction of excess *cis*-2-butene with ozone was analyzed by GLC and found not to have undergone any isomerization.

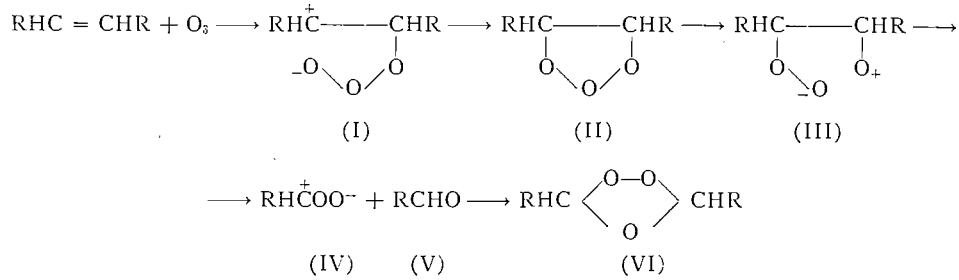
Liquid-phase ozonization of ethylene, isobutene, and 1-butene produced the expected ozonides in addition to minor amounts of degradation products (carbon dioxide, formaldehyde, formic acid). However, in the case of both isobutene and 1-butene small amounts of ethylene ozonide (about 10% of the main ozonide in each case) were also recovered by GLC analysis and its identity was confirmed by infrared spectroscopy (10). In addition, the GLC analysis showed about 20% of acetone in the case of isobutene and about 10% of propanal in the case of 1-butene, both apparently formed by degradation of the ozonide. In the case of isobutene, a fair amount of non-explosive crystals (melting point of the crude crystals 91–95°) of peroxidic character (giving positive KI test) were isolated on leaving the reaction product stand overnight at room temperature.

DISCUSSION

Most of the previous investigations of the products of the reactions of ozone with olefins in the vapor phase have been recently reviewed by Leighton and Perkins (11). The present work agrees in its main outlines with the previous observations although there are also some differences between the results obtained by various workers. However, in comparing and assessing the results of such studies there are in particular two features of these processes which have to be kept in mind: (1) Appreciable quantities of relatively unstable intermediate peroxidic compounds are initially formed (12, 13) and the final stable products observed will depend on the conditions under which the degradation takes place. The particular analytical procedure used may therefore strongly affect the amounts and the type of the stable products observed. (2) The reactions are highly exothermic and the liberated heat is as a rule likely to affect their course, at least to some extent and sometimes very drastically, especially in the presence of large excess of molecular oxygen as is usually the case. Under conditions of the present experiments too rapid introduction of ozonized oxygen into the olefin vapor led, at least in some cases, to strong warming of the reaction vessel and GLC analysis then showed essentially only large amounts of CO_2 and water in the products, indicating complete combustion. With slow introduction of the ozone–oxygen mixture no significant warming of the reaction vessel occurred and no water peak was observed by GLC although some CO_2 was always formed, as shown in Table I and as observed in most of the previous work. Evidently, it is difficult to eliminate altogether quantitative uncertainties about the possible effect of "hot" products in these reactions.

Can. J. Chem. Downloaded from www.nrcresearchpress.com by 186.148.149.217 on 09/04/12
For personal use only.

Substantial fractions of the products formed under the particular experimental conditions employed in the present work have been isolated in most cases and can be discussed briefly in terms of the generally accepted mechanism of ozone interaction with olefinic compounds. With some vagueness as to the exact detail, this mechanism can be written down as follows:



(I) (II) (III) (IV) (V) (VI)

The initial addition may be a two-step process, as indicated above, in which case I could equally well be visualized as a π-complex (14). On the other hand, a one-step addition would lead directly to the "initial ozonide" (II), which is extremely unstable. Criegee has recently obtained evidence that the initial ozonide is formed at least under some conditions (15). He and his co-workers have also been responsible for the identification of IV as a relatively stable and long-lived zwitterion which can enter into reactions such as addition to an aldehyde (V) to form an ozonide (VI). At low temperatures in solution this last reaction is, no doubt, assisted by the solvent cage effect and usually predominates. At higher temperatures and in the vapor phase other competing reactions of the zwitterion (IV) become important and the process is then characterized by considerable complexity. The types of reactions which the zwitterion (IV) can undergo are of particular importance. These include dimerization and polymerization, with or without participation of water, into peroxidic substances; reactions with any reactive compounds present in sufficient concentration; rearrangement; and decomposition.

The presence of peroxidic intermediates in the products obtained in the present work was shown qualitatively. In the course of GLC analysis these appeared to decompose with the release of the "bound" carbonyl compounds. Some years ago Briner and co-workers isolated and at least partially characterized some of the peroxidic substances formed in the vapor phase olefin–ozone reactions (12, 13). Hydrolysis of these compounds led to the release of the "bound" carbonyl compounds and acids. In the case of 2-butenes and propylene, in addition to the predominant amounts of formic acid, they also observed after hydrolysis smaller quantities of acetic acid. Since, in our case, acids could not be observed directly by GLC analysis, infrared spectra were taken of the products before GLC analysis and in all cases only formic acid was found to be present. The values in Table I given as formic acid, however, have been obtained by titration and may also include any higher acids liberated on hydrolysis. Ozonides were not observed, although some of the more volatile ozonides (ethylene-, isobutene-, and 1-butene-ozonide) produced by low temperature ozonization in solution could be analyzed readily by GLC in spite of their relative instability. This is in agreement with the results of Hanst *et al.* (4), although these authors observed by the use of long path infrared spectroscopy the ozonide formation from some heavier olefins (1-pentene, 1-hexene, 3-heptene). However, less volatile ozonides would not be readily observed under conditions of our GLC analysis and no attempt was made to explore this analytical possibility further.

Can. J. Chem. Downloaded from www.nrcresearchpress.com by 186.148.149.217 on 09/04/12
For personal use only.

Decomposition of the zwitterion (IV) has been postulated to explain the formation of various light compounds in the ozonization products (3, 4), thus

$$HCHO_2 \rightarrow H_2O + CO \quad [1]$$

$$CH_3CHO_2 \rightarrow CH_3OH + CO \quad [2]$$

$$CH_3CHO_2 \rightarrow CH_4 + CO_2 \quad [3]$$

$$CH_3CHO_2 \rightarrow H_2O + CH_2{=}C{=}O \quad [4]$$

Reaction [3] and its homologues can readily explain the major amounts of paraffins as well as of ethylene in the case of butadiene (shown doubly underlined in Table I), and of the substantial amount of carbon dioxide formed in our experiments. Together with these paraffins, olefins containing the same number of carbon atoms (shown singly underlined in Table I) are also formed, although in somewhat smaller amounts. The formation of these olefins could perhaps be visualized as resulting from rearrangement through hydrogen migration of the zwitterion (IV) followed by decomposition, for example,

$$CH_3CH_2 \cdot CHO_2 \rightarrow (CH_3CH \cdot CH_2O_2) \rightarrow C_2H_4 + CH_2O_2 \quad [5]$$
(VII)

where CH_2O_2 may again be a zwitterion (IV) and undergo further reactions. Equally well, the olefin formation may be a consequence of a "peroxide-formate" rearrangement (16) followed by decomposition in a particular way. This type of rearrangement is known to occur under some conditions and has been frequently invoked to explain the "abnormal" products of ozonization of olefins, such as formic acid, methanol, etc.

The major carbonyl compounds are the "normal" products (shown in Table I in boldface type). Small amounts of aldehydes containing the same number of carbon atoms as the original olefins (acetaldehyde from C_2H_4, propanal from C_3H_6, *n*-butanal from 1-C_4H_8, isobutyraldehyde from iso-C_4H_8) are occasionally formed, suggesting that perhaps some molecular oxygen splits off from the intermediate (III) and the remainder then rearranges to an aldehyde. However, the quantities of these compounds formed are very small. Much more important amounts are formed of the carbonyl compounds one and, to a lesser extent, two carbon atoms shorter than the "normal" carbonyl compounds. They are underlined in Table I and include, for example, acetaldehyde in the case of 1-butene (besides the "normal" carbonyl compound propanal), acetone in the case of 3-methyl-1-butene (besides the "normal" isobutyraldehyde), etc. This degradation could again be visualized as being induced by "peroxide-formate" rearrangement although other mechanisms could be postulated as well, such as for example secondary oxidation or cyclization followed by decomposition of the rearranged intermediate (VII).

In view of the uncertainties mentioned at the beginning of this discussion and because of the analytical limitations, in particular lack of information on the exact nature of the intermediate peroxidic substances, a subject currently receiving considerable attention (17), and on the amounts of formaldehyde and non-condensable products (CO, H_2, CH_4) formed, the present results evidently provide only a limited picture of these complex vapor phase reactions. However, a preliminary broad survey has been made for a number of olefins under comparable conditions and it is hoped that the information obtained may supplement the observations of other workers made with the use of different analytical techniques and, in particular, help in the planning of more extensive future studies of selected individual reactions.

The products obtained in the low temperature ozonization in solution agree with the results of previous workers. However, it is of interest that in the case of 1-butene and

Can. J. Chem. Downloaded from www.nrcresearchpress.com by 186.148.149.217 on 09/04/12
For personal use only.

isobutene appreciable amounts of ethylene ozonide were isolated by GLC in addition to the expected ozonides of these two olefins. The formation of ethylene ozonide, in spite of some hindrance because of the solvent cage effect and the statistical probability favoring the formation of the unsymmetrical ozonides, seems to indicate that in the initial ozonides (II) of these two olefins the ring opening is not exclusively one way.

ACKNOWLEDGMENTS

The authors are grateful to the analytical section of this division for infrared analyses and to Dr. A. W. Tickner for mass spectrometric analyses.

REFERENCES

1. P. S. BAILEY. Chem. Revs. **58**, 925 (1958).
2. P. L. HANST, E. R. STEPHENS, and W. E. SCOTT. Proc. Am. Petrol. Inst. (III), **35**, 175 (1955); J. Air Pollution Control Assoc. **5**, 219 (1956).
3. W. E. SCOTT, E. R. STEPHENS, P. L. HANST, and R. C. DOERR. Proc. Am. Petrol. Inst. (III), **37**, 171 (1957).
4. P. L. HANST, E. R. STEPHENS, W. E. SCOTT, and R. C. DOERR. Am. Chem. Soc., Div. Petrol. Chem., Gen. Papers, 4, (4), A-7. Atlantic City, N.J. September, 1959.
5. E. A. SCHUCK and G. J. DOYLE. Photo-oxidation of hydrocarbons in mixtures containing oxides of nitrogen and sulphur dioxide. Rept. No. 29, Air Pollution Foundation, San Marino, Calif. October, 1959.
6. B. E. SALTZMAN and N. GILBERT. Ind. Eng. Chem. **51**, 1415 (1959).
7. R. J. CVETANOVIĆ. J. Chem. Phys. **30**, 19 (1959); S. SATO and R. J. CVETANOVIĆ. J. Am. Chem. Soc. **81**, 3223 (1959).
8. D. J. LE ROY. Can. J. Research, B, **28**, 492 (1950).
9. A. B. CALLEAR and R. J. CVETANOVIĆ. Can. J. Chem. **33**, 1256 (1955).
10. D. GARVIN and C. SCHUBERT. J. Phys. Chem. **60**, 807 (1956).
11. P. A. LEIGHTON and W. A. PERKINS. Photochemical secondary reactions in urban air. Rept. No. 24, Air Pollution Foundation, San Marino, Calif. August, 1958.
12. E. BRINER and P. SCHNORF. Helv. Chim. Acta, **12**, 154, 181 (1929).
13. E. BRINER and R. MEIER. Helv. Chim. Acta, **12**, 529 (1929).
14. P. S. BAILEY. Chem. Revs. **58**, 940 (1958).
15. R. CRIEGEE. Abstracts of Papers, 136th Meeting Am. Chem. Soc., Atlantic City, N.J. September, 1959. p. 87 P.
16. P. S. BAILEY. Chem. Revs. **58**, 947 (1958).
17. N. A. MILAS and I. BELIC. Abstracts of Papers, 136th Meeting Am. Chem. Soc., Atlantic City, N.J. September, 1959. p. 78 P.

Can. J. Chem. Downloaded from www.nrcresearchpress.com by 186.148.149.217 on 09/04/12
For personal use only.

Can. J. Chem. Downloaded from www.nrcresearchpress.com by 186.148.149.217 on 09/04/12
For personal use only.

CIS AND TRANS 1-ACETOXY-1,3-BUTADIENE: PHYSICAL AND CHEMICAL PROPERTIES, INFRARED AND ULTRAVIOLET SPECTRA[1]

K. K. Georgieff and A. Dupré

ABSTRACT

1-Acetoxy-1,3-butadiene was prepared by the reaction of crotonaldehyde with acetic anhydride in the presence of potassium or sodium acetate. The product was found to consist of two forms which, from their physical properties and infrared spectra, appear to be cis and trans. Mass and ultraviolet spectra, and methods of analysis are also reported. The cis form was found to be a substantially stronger inhibitor than the trans in the bulk polymerization of vinyl acetate using benzoyl peroxide as catalyst.

INTRODUCTION

In a recent investigation on the inhibitory effect of various compounds on the rate of polymerization of vinyl acetate (which will be reported elsewhere), some unexpected results were obtained. 1-Acetoxy-1,3-butadiene was prepared from crotonaldehyde and acetic anhydride using potassium or sodium acetate as catalyst (1, 2). On distillation, a series of fractions were obtained with gradually changing boiling points, freezing points, refractive indices, specific gravity, and inhibitory effect on the bulk polymerization of vinyl acetate. To try to establish the reason for these differences, mass, infrared, and ultraviolet spectra were obtained.

EXPERIMENTAL

Preparation of 1-Acetoxy-1,3-butadiene

A modification of the method of Wacker (1) was used. A 240-g quantity of potassium acetate (Mallinckrodt analytical reagent) was charged into a 3-liter round-bottom flask fitted with a Tru-Bore stirrer, a feeding funnel, and a reflux condenser. The apparatus was evacuated and filled with nitrogen. Acetic anhydride (Shawinigan Chemicals Ltd., commercial grade) (440 g) was added and the mixture refluxed. Crotonaldehyde (Shawinigan Chemicals Ltd., redistilled) (240 g) was added drop-wise over a period of 3 hours and the mixture refluxed for an additional 20 minutes. The reaction mixture was cooled and shaken with 1200 cc of water. The organic layer was extracted first with just enough 10% sodium carbonate solution to neutralize the acetic acid, then with 1 liter of 40% sodium bisulphite solution, and finally with 200–300 cc of 10% sodium carbonate solution. After each extraction, the spent aqueous layer was extracted with 100–200 cc of ether and the ether layer added to the crude product. The crude product was dried with anhydrous sodium sulphate, stabilized with 2 g of para-tertiary butylcatechol and 2.5 g of copper resinate, and distilled in a copper column (3 ft long and 1 in. I.D.) packed with $\frac{1}{4}$-in. copper rings. The ether was distilled at atmospheric pressure and the product at 30 mm Hg absolute. Yield based on croton was about 60% and the conversion 50%.

The product was analyzed by saponification, reaction with dodecyl mercaptan (3), and bromination (4). Saponification was carried out in the presence of an excess of aqueous $N/10$ sodium hydroxide solution for 2 hours at room temperature. Results were 101–104% of theory. Analysis by the dodecyl mercaptan method using a reaction time of 2 minutes gave values from 95 to 99.9% based on the reaction with both double

[1]*Manuscript received February 26, 1960.*
Contribution from the Research Laboratories, Shawinigan Chemicals Ltd., Shawinigan Falls, Que.

bonds. Bromination with an aqueous mixture of bromine, sodium bromide, hydrochloric acid, and methanol for 30–60 minutes gave results of about 99%, based on the reaction with one double bond.

The inhibitory effect of 1-acetoxy-1,3-butadiene on the rate of the bulk polymerization of vinyl acetate was determined by a modification of a method previously used (5). The open flame heating was replaced by a Glas-Col mantle in order to increase reproducibility. Inhibition factors, which have been arbitrarily defined as the number of seconds by which pure vinyl acetate is made less active by 1 p.p.m. of inhibitor, were determined. Further details on this phase will be reported elsewhere.

Ultraviolet spectra were obtained with a Beckman DK-2 instrument using 1-cm cells. Infrared spectra were obtained with a Perkin–Elmer 12-C single-beam spectrometer having a sodium chloride prism and the mass spectra with a 60° Nier type instrument using 50 electron volts.

RESULTS

The product was distilled into three fractions and each fraction redistilled into three or four fractions using a 6-ft column, 1 in. in diameter, packed with $\frac{1}{4}$-in. Berl saddles. In Table I will be found the data for that series of final fractions which was most completely studied.

TABLE I

Properties of a series of fractions of 1-acetoxy-1,3-butadiene

Fr. No.	B.p. (uncorr.) at 32 mm abs.	d_4^{20}	n_D^{20}	M.p.	Analysis: By sapn., %	Analysis: By merc., %	Inhibition of vinyl acetate, sec/p.p.m.	Ultraviolet spectrum: λ_{max}, mμ	Ultraviolet spectrum: ϵ_{max}
1*	53.2–54.2	0.949		Below −78°	101.3	96.0	2.00	233.8	26,000
2	54.2–54.6	0.948	1.4647	Below −78°	104.0	99.9	1.98	233.8	26,100
3	54.6–55.0	0.947		Below −78°	102.9	99.1	1.88	233.4	26,500
4*	55.0–55.3	0.948	1.4703	∼−55 to −60°	102.0	95.3	1.68	233.2	26,000

*Contained trace of water.

To try to establish the reason for the differences between fractions as given in Table I, mass spectra were first obtained. There was no indication of the presence of substantial amounts of impurities. The parent peak had a mass of 112 and the base peak 43. All the major peaks could be justified on the basis of the 1-acetoxy-1,3-butadiene structure. Further confirmation of the molecular weight (i.e. 112) was obtained from the analyses (i.e. saponification, reaction with dodecyl mercaptan, and bromination).

The reaction of both double bonds in 1-acetoxy-1,3-butadiene with dodecyl mercaptan did not always go to 100% completion. Doubling the amount of potassium hydroxide catalyst and the duration of reaction made no difference to the results in the one fraction studied. However, the values were sufficiently high to establish clearly the presence of two double bonds. On the other hand, only one double bond brominated in aqueous medium but the reaction was very close to quantitative and can be used as a method of analysis.

Further evidence of the structure was obtained from the ultraviolet spectrum (cf. Fig. 1 and Table I). Both the wave length and the molar extinction coefficient were

Can. J. Chem. Downloaded from www.nrcresearchpress.com by 186.148.149.217 on 09/04/12
For personal use only.

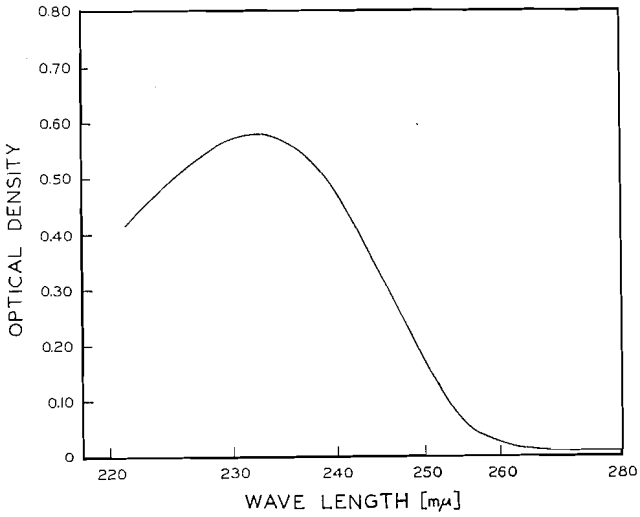
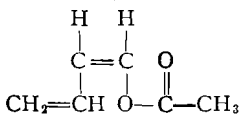


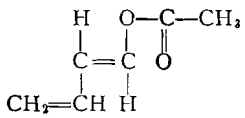
FIG. 1. Ultraviolet absorption spectrum of cis and trans 1-acetoxy-1,3-butadiene.

close to the values expected for the 1,3-butadiene structure. A 1,2- or 2,3-butadiene, on the other hand, would have been expected to absorb at lower wave lengths and have a much lower extinction coefficient.

A study of the data in Table I suggested the presence of at least two forms of 1-acetoxy-1,3-butadiene and therefore one attempt was made to make a separation by gas chromatography. This was unsuccessful although a shoulder on the main band was obtained. This is in direct contrast to the ease with which 1-acetoxy-1,3-butadiene was separated from 2-acetoxy-1,3-butadiene. It was thus apparent that the two or more forms present were more closely related than position isomers and hence cis–trans isomerism was suspected. In most, if not all, compounds the cis form melts at a lower temperature than



Cis



Trans

the trans. It was, therefore, surmised that the lowest boiling fraction (fraction No. 1) was predominately cis while the highest boiling (fraction No. 4) was chiefly trans. This was confirmed by the infrared spectra which are given in Fig. 2. Wave lengths of the bands are given in Table II.

In compounds of the form $R_1CO.OCH{=}CHR_2$ the expected position of the carbonyl band in the infrared is at about 1770 cm^{-1} (6, 7, 8, 9, 10). In all of our fractions the band was at 1763 cm^{-1}. The possibility of having a compound of the form $R_1CH{=}CH.COOR_2$ which has a carbonyl absorption at about 1720 cm^{-1} was clearly eliminated (6, 7, 8, 11). The C—O stretching vibrations of carboxylic esters of the form $CH_3.CO.OCH{=}CHR$ give strong bands between 1218 and 1204 cm^{-1} and between 1159 and 1096 cm^{-1} (6, 12, 13). These bands are usually accompanied by weak bands between 1300 and 1000 cm^{-1}. An examination of our spectra shows definitely these characteristic bands. The terminal methylene group undoubtedly gives rise to the band at 1375 cm^{-1} while

Can. J. Chem. Downloaded from www.nrcresearchpress.com by 186.148.149.217 on 09/04/12
For personal use only.

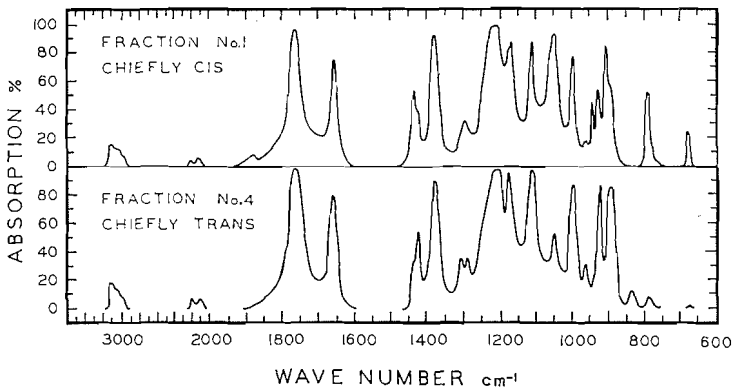


FIG. 2. Infrared absorption spectra of cis and trans 1-acetoxy-1,3-butadiene 5% solution in CCl_4 or CS_2, 0.121-mm cell.

TABLE II

Infrared bands of trans and cis 1-acetoxy-1,3-butadiene

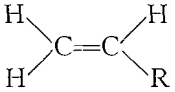
Fr. IV, trans	Fr. I, cis	Remarks
3102W	3102W	
3052VW	3042VW	Shift
3008VW	3000VW	Shift
2210VW	2210VW	
2100VW	2115VW	Shift
	1878VW	
1763S	1763S	Stronger in trans than in cis
1659M	1656M	Shift
1423M	1432M	Shift
1375S	1375S	
1307W		
1289W	1291W	Shift
1209VS	1213VS	
1178S	1172M	Shift and stronger in trans
1111S		Characteristic
	1049S	Characteristic
998S	998S	Stronger in trans than in cis
959W		Characteristic
	941M	Characteristic
924S		Characteristic
	907S	Characteristic
893S		Characteristic
835W		Characteristic
	788M	Characteristic
	675W	Characteristic

NOTE: The bands that are believed to be due to mutual contamination have been omitted.

the terminal methyl gives a band at 1432 cm^{-1} in fraction No. 1 and at 1423 in fraction No. 4. The infrared spectrum would, therefore, appear to be consistent with a 1-acetoxy-1,3-butadiene structure.

The following infrared data confirm the previous indication of cis–trans isomerism. The intensity of the carbonyl band in esters has been found by Allan, Meakins, and Whiting (14) to vary with the nature of the unsaturated bond but is stronger in the trans compound than in the cis. In our product, the carbonyl band in fraction No. 4 was stronger than that in fraction No. 1. Therefore, fraction No. 4 would be expected to be predominantly trans and fraction No. 1 chiefly cis. Furthermore, conversion of

Can. J. Chem. Downloaded from www.nrcresearchpress.com by 186.148.149.217 on 09/04/12
For personal use only.

the α,β-ethylenic bond from trans to cis has been found by the same authors (14) to cause a shift of the C=C stretching bond to lower frequency. The bands in our fraction No. 4 were found to be at higher frequencies than those in fraction No. 1. The terminal C=C of the form  is expected to give rise to two unsaturation bands at about 990 and about 910 cm^{-1}, the latter being three times the intensity of the former (6). In our fraction No. 4 (trans), two bands at 998 and 893 cm^{-1} are observed, the relative intensities being as previously stated. In the case of fraction No. 1 (cis), bands are observed at 998 and 907 cm^{-1} although the intensity of the latter is about the same order of magnitude as the former. However, this irregularity is often observed in the cis form. It has been noted that the spectrum of the cis is usually weaker than the trans. The α,β-ethylenic group, which gives rise to the cis–trans isomerism, is expected to give bands between 990 and 910 cm^{-1}. In fraction No. 4 (trans), the bands at 924 and 959 cm^{-1} are undoubtedly due to this group. In fraction No. 1 (cis), the band at 941 and possibly the ones at 788 and 675 cm^{-1} can be attributed to this unsaturation. The bands due to cis isomerism have not been rigorously established in the literature.

Only one band was observed due to C=C stretching, i.e. at 1659 cm^{-1} (trans) and 1656 cm^{-1} (cis). Another one at about 1640 cm^{-1} was expected. This suggests that the two C=C groups are not in the same plane (15).

Further confirmation of the cis and trans assignments was made from the nuclear magnetic resonance spectra (16) by Bernstein (National Research Council, Ottawa). Agreement with the infrared data was near quantitative for mixtures of the two forms.

From the data in Table I, it is obvious that the cis form (fraction No. 1) is a stronger inhibitor than the trans (fraction No. 4) for the bulk polymerization of vinyl acetate using benzoyl peroxide as catalyst. In all the distillation fractions studied, the highest inhibition factor obtained was 2.02 seconds per p.p.m. (cis) and the lowest 1.55 (trans). Inhibition factors for the total product were found to vary somewhat from run to run, e.g. with sodium acetate as catalyst 1.79 and 1.87 and with potassium acetate 1.87. However, sufficient work was not done to establish which factors influenced the proportion of the two forms produced.

ACKNOWLEDGMENTS

The authors wish to express their thanks to Shawinigan Chemicals Ltd. for permission to publish this paper, to Dr. C. Sandorfy for his valuable discussion on the infrared spectra, to Dr. H. J. Bernstein for obtaining the NMR spectra, to Mrs. Y. Richard for the mass spectra, and to Mr. E. Blais for the other spectra.

REFERENCES

1. Alexander Wacker Gesellschaft für Elektrochemische Industrie, G. m. b. h. Brit. Patent No. 493,196 (1938).
2. O. Wichterle and M. Hudlický. Collection Czechoslov. Chem. Communs. **12**, 564 (1947).
3. American Cyanamid Company. The chemistry of acrylonitrile. Beacon Press, Inc., New York. 1951. p. 69.
4. Carbide and Carbon Chemicals Company. Tech. Bull. on "Acrolein", F-7389 B. p. 24.
5. K. K. Georgieff. J. Polymer Sci. **14**, 589 (1954).
6. W. West, A. B. F. Duncan, W. Gordy, R. N. Jones, F. A. Matsen, and C. Sandorfy. Chemical applications of spectroscopy. Technique of organic chemistry. Vol. IX. Interscience Publishers, Inc., New York. 1956. pp. 378, 379, 453, 503, and 576.
7. G. M. Barrow. J. Phys. Chem. **21**, 2008 (1953).
8. J. F. Grove and H. A. Willis. J. Chem. Soc. 877 (1951).
9. E. J. Hartwell, R. E. Richards, and H. W. Thompson. J. Chem. Soc. 1436 (1948).

Can. J. Chem. Downloaded from www.nrcresearchpress.com by 186.148.149.217 on 09/04/12
For personal use only.

10. R. S. RASMUSSEN, D. D. TUNNICLIFF, and R. R. BRATTAIN. J. Am. Chem. Soc. **71**, 1068 (1949).
11. R. S. RASMUSSEN and R. R. BRATTAIN. J. Am. Chem. Soc. **71**, 1073 (1949).
12. R. N. JONES and F. HERLING. J. Org. Chem. **19**, 1252 (1954).
13. H. W. THOMPSON and P. TORKINGTON. J. Chem. Soc. 640 (1945).
14. J. L. H. ALLAN, G. D. MEAKINS, and M. C. WHITING. J. Chem. Soc. 1874 (1955).
15. C. SANDORFY. Verbal communication.
16. H. J. BERNSTEIN. Private communication.

Can. J. Chem. Downloaded from www.nrcresearchpress.com by 186.148.149.217 on 09/04/12
For personal use only.

Can. J. Chem. Downloaded from www.nrcresearchpress.com by 186.148.149.217 on 09/04/12
For personal use only.

THE THERMAL DECOMPOSITION OF PHENYL METHYL SULPHIDE[1]

MARGARET H. BACK[2] AND A. H. SEHON

ABSTRACT

The thermal decomposition of phenyl methyl sulphide was investigated in a flow system in an excess of toluene. The main products were methane, thiophenol, and dibenzyl. The primary mode of decomposition was ascribed to the reaction

$$C_6H_5SCH_3 \rightarrow C_6H_5S + CH_3.$$

The rate constant for this process was given by the expression

$$k = 3\times10^{14}.\ e^{-60{,}000/RT}\ \text{sec}^{-1}.$$

INTRODUCTION

The benzyl radical has long been known to be fairly stable thermally and relatively unreactive (1, 2). These properties have been attributed to its conjugated structure which allows the free electron to be largely delocalized (3, 4). Radicals with structures similar to that of the benzyl radical might also be expected to be stabilized by resonance and hence to form relatively weak bonds with other radicals. It was anticipated that the phenylsulphide radical, C_6H_5S, satisfies these conditions. To test this hypothesis the kinetics of the thermal decomposition of phenyl methyl sulphide in a stream of toluene was studied.

EXPERIMENTAL

Materials

Phenyl methyl sulphide was kindly supplied by Dr. W. L. Hawkins of Bell Telephone Laboratories, N.J., and was further purified by distillation at low pressure. Toluene was generously supplied by Gulf Oil Corporation, Pittsburgh, Pa., and was purified by distillation through an efficient column. The fraction boiling at 110.5° C was used in this study.

Apparatus

The pyrolysis was studied in a conventional vacuum flow system similar to those employed in previous investigations using the toluene carrier technique (5). The toluene pressure was varied between 5.7 and 10.1 mm Hg. Weighed amounts of the sulphide were admitted from a small detachable vial through a short capillary which led into the toluene stream. The vapor pressure of the sulphide could be changed by heating the vial to different temperatures with a removable bath containing dibutylphthalate. The temperature of the bath was varied between 80° C and 96° C, giving a partial pressure of sulphide from 0.5% to 2% of the toluene pressure. The decomposition was studied over the temperature range 550° C to 706° C.

Analysis

The products were condensed in a series of three traps maintained at −5° C, −78° C, and −188° C. The material collected in the first trap was weighed and analyzed for disulphide according to the procedure outlined by Kolthoff (6). The contents of the trap maintained at −78° C were titrated for mercaptan with 0.1 *N* silver nitrate solution,

[1]*Manuscript received March 7, 1960.*
Contribution from the Department of Chemistry, McGill University, Montreal, Que.
[2]*Submitted in partial fulfillment of the requirements for the degree of Ph.D. Present address: Division of Applied Chemistry, National Research Laboratories, Ottawa, Ontario.*

using a rotating platinum electrode and a microammeter (7). The method was calibrated with thiophenol solution of known concentrations. Some titrations were also done potentiometrically with a silver wire electrode (8). The two methods of titration gave identical results and the former method was generally used. Non-condensable gases were pumped into calibrated bulbs with the aid of two diffusion pumps connected in series and were analyzed by combustion on copper oxide at 300° C.

RESULTS AND DISCUSSION

Products

The main products of the decomposition, shown in Table I, were methane and a mercaptan, which was considered to be thiophenol. The ratio of mercaptan to methane varied from 1.1 to 1.6, increasing with increasing temperature. Methane accounted for 90 to 96% of the non-condensable gases and the remainder was hydrogen.

TABLE I

Products of the decomposition of phenyl methyl sulphide

Expt. No.	T, °A	t, sec	Toluene pressure, mm Hg	P_s/P_t*	Non-cond. gases, mmoles	CH_4, %	H_2, %	CH_4, mmoles	SH^-, mmoles	Dibenzyl, mmoles	$\frac{SH^-}{CH_4}$	$\frac{\text{Dibenzyl}}{CH_4}$	% decomp.	k, sec^{-1}	k', sec^{-1}
33	823	.56	12.15		.0435	93.4	6.6	.0387							.025
8	842	.79	10.9	.014	.0682	94.1	5.9	.0616	.078	.033	1.27	.54	5.2	.068	.053
9	842	.79	12.3	.005	.0624	91.8	8.2	.0538	.068		1.26		5.2	.066	.051
7	852.5	.66	10.9	.015	.0699	94.5	5.5	.0635		.043		.68			.084
27	857	.32	10.5	.0064	.0598	92.8	7.2	.0527	.060	.023	1.14	.44	3.8	.121	.106
28	858	.34	10.3	.013	.0696	94.5	5.6	.0632		.046		.73			.098
30	870	.44	5.1	.009	.1053	95.6	4.3	.0978		.084		.86			.159
31	870	.34	11.4	.010	.0853	95.0	5.0	.0782							.168
26	880.5	.32	9.9	.0085	.1046	94.6	5.4	.0953	.125	.061	1.31	.64	9.9	.326	.246
10	882.5	.66	10.5	.015	.218	95.5	4.6	.201	.273	.167	1.36	.83	20.2	.348	.248
2	883	.61	9.9	.032	.1478	94.5	5.5	.134	.184	.129	1.37	.96	16.0	.283	.200
3	883	.62	10.1	.005	.188	94.5	5.5	.171	.207	.114	1.21	.61	18.3	.328	.266
32	891.5	.38	11.6	.012	.1560	95.2	4.8	.1437							.351
25	904	.32	10.15	.0073	.220	95.4	4.7	.203	.28	.180	1.38	.89	24.8	.891	.621
29	905	.31	10.1	.0075	.225	95.5	4.5	.208	.300	.18	1.44	.87	25.0	.916	.629
6	906	.61	10.0	.023	.292	92.8	7.2	.258	.370	.240	1.43	.93	36.4	.740	.480
12	907	.78	5.8	.015	.370	94.8	5.2	.337	.512	.31	1.52	.92	47.6	.821	.478
4	922	.58	10.1	.018	.470	92.0	8.0	.407	.591	.374	1.45	.92	58.2	1.49	.877
5	923	.60	10.2	.0068	.597	95.2	4.8	.549	.767	.517	1.40	.94	67.5	1.86	1.09
14	923	.76	5.7	.0145	.514	93.5	6.5	.458	.723		1.58	.79	67.2	1.47	.730
24	934.5	.32	10.4	.007	.455	94.6	5.4	.414	.580	.360	1.40	.87	55.9	2.53	1.57
23	951	.29	10.1	.008	.519	93.9	6.1	.466		.41		.88			2.12
21	979	.28	10.2	.0074	.418	90.4	9.6	.351	.560	.32	1.60	.91	89.9	8.29	3.11
22	979	.27	10.4	.007	.444	90.1	9.8	.371	.542	.33	1.46	.89	82.2	6.31	3.09

*P_s and P_t refer to the partial pressures of phenyl methyl sulphide and toluene, respectively.

No disulphide was detected in the trap maintained at −5° C. The product collected in this trap was shown to be dibenzyl. Neither ethane nor methyl mercaptan were detected among the products.

Mechanism of Decomposition

The results suggested that the primary step in the pyrolysis of phenyl methyl sulphide involved the dissociation of the C—S bond,

$$C_6H_5SCH_3 \rightarrow C_6H_5S + CH_3, \qquad [1]$$

Can. J. Chem. Downloaded from www.nrcresearchpress.com by 186.148.149.217 on 09/04/12
For personal use only.

and that the phenylsulphide and methyl radicals formed reacted further with toluene to form thiophenol and methane,

$$C_6H_5S + C_6H_5CH_3 \rightarrow C_6H_5SH + C_6H_5CH_2 \quad [2]$$

$$CH_3 + C_6H_5CH_3 \rightarrow CH_4 + C_6H_5CH_2. \quad [3]$$

In addition, the benzyl radicals formed in reactions [2] and [3] recombined, at least in part, to give dibenzyl.

According to this mechanism thiophenol, methane, and dibenzyl would be formed in equimolar amounts. However, the yield of methane was always less than that of the mercaptan, this discrepancy becoming more pronounced with increasing temperature. Furthermore, the amount of dibenzyl formed was found to be slightly less than the yield of methane. Therefore, reactions [1], [2], [3], and the dimerization of benzyl radicals do not fully represent the mechanism of the decomposition.

These findings may be explained by postulating that methyl radicals may not react sufficiently rapidly with toluene in the temperature range of the decomposition, 550° C to 706° C, to be quantitatively converted to methane. Similar conclusions were reached by Szwarc and Taylor (9), who showed that at 780° C about 25% of the methyl radicals produced in the thermal decomposition of acetone in a stream of toluene were removed by recombination with benzyl radicals,

$$CH_3 + C_6H_5CH_2 \rightarrow C_6H_5CH_2CH_3, \quad [4]$$

and about 1 to 2% by dimerization,

$$CH_3 + CH_3 \rightarrow C_2H_6, \quad [5]$$

rather than by reaction with toluene. In the present study no ethane was detected among the products; however, its rate of production would be expected to be much less than that of ethylbenzene, because the steady-state concentration of benzyl radicals is probably much greater than that of methyl radicals.

With increase in temperature, the rate of reaction [4] would be expected to increase more rapidly than the rate of reaction [3]. This trend was indeed observed as evidenced by the increase in the ratio of thiophenol to methane with increasing temperature.

If reactions [1] to [4] occurred, the yield of dibenzyl should equal that of methane. The ratio of dibenzyl to methane was usually between 0.70 and 0.95, and it is suggested that losses of the dibenzyl due to inefficient trapping could account for the deviation of these values from unity (10).

The first-order rate constants for the decomposition of phenyl methyl sulphide were calculated from the rates of formation of methane and thiophenol, and are given in Table I. The rate constant for the production of methane, k', was always less than that for the production of thiophenol, k. The plots of log k and log k' against $1/T$ are shown in Fig. 1. Both curves deviate from linearity at high temperatures, but the drop in k' is more pronounced than that in k. The effect of changes in contact time, partial pressures of phenyl methyl sulphide and toluene are shown in Tables II, III, and IV, respectively. These results suggest that the decomposition of phenyl methyl sulphide may be considered to be a first-order process.

The extent of reaction [3] may, with certain assumptions, be calculated. The concentration of benzyl radicals may be estimated if it is assumed that there is little recombination in the hot zone. As a first approximation, the total production of benzyl radicals will then be equal to the sum of the thiophenol and methane produced less the amount

Can. J. Chem. Downloaded from www.nrcresearchpress.com by 186.148.149.217 on 09/04/12
For personal use only.

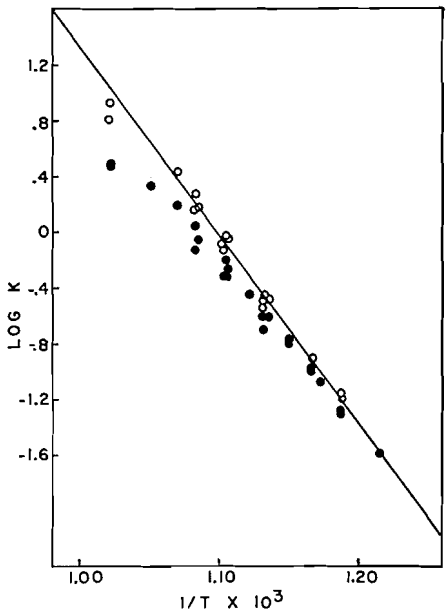


FIG. 1. Plot of log k against $1/T$ for the thermal decomposition of phenyl methyl sulphide. ○ calculated from the production of thiophenol (k). ● calculated from the production of methane (k').

TABLE II

Effect of reaction time on k

Expt. No	T, °A	t, sec	k, sec^{-1}
26	880.5	.31	.326
3	883	.62	.328
29	905	.31	.916
12	907	.78	.821

TABLE III

Effect of pressure of phenyl methyl sulphide on k

Expt. No.	T, °A	Phenyl methyl sulphide, mm Hg	k, sec^{-1}
9	842	.06	.066
8	842	.15	.068
3	883	.05	.328
10	882.5	.17	.348
2	883	.32	.283

removed by recombination with methyl radicals. The latter quantity may be taken as the difference between the thiophenol and methane formed. Thus, the total production of benzyl radicals is equal to twice the production of methane, and its average yield may be considered as one half of this quantity. Assuming that the concentration of methyl

Can. J. Chem. Downloaded from www.nrcresearchpress.com by 186.148.149.217 on 09/04/12
For personal use only.

TABLE IV

Effect of toluene pressure on k

Expt. No.	T, °A	Toluene pressure, mm Hg	k, sec^{-1}
12	907	5.8	.821
6	906	10.0	.740
14	923	.57	1.47
4	922	1.01	1.49

radicals is stationary, the rate of production of methane is given by the following equation:

$$\frac{d(CH_4)}{dt} = \frac{k_1k_3(C_6H_5SCH_3)(C_6H_6CH_3)}{k_3(C_6H_5CH_3)+k_4(C_6H_5CH_2)}.$$

The rate constant for the reaction of methyl radicals with toluene, k_3, has been measured by Trotman-Dickenson and Steacie (11), who found $k_3 = 1.4\times10^{11}.e^{-8300/RT}$ $mole^{-1}$ cc sec^{-1}. The rate of production of thiophenol was taken as a measure of the rate of reaction [1], i.e., k_1 was taken equal to k. The production of methane for any particular experiment may then be calculated if a value is assumed for the rate constant, k_4, for the recombination of benzyl and methyl radicals. In a similar calculation Szwarc and Taylor (9) took this rate constant to be 10^{12} $mole^{-1}$ cc sec^{-1}, which is slightly less than the value for the recombination of methyl radicals. With these values the yield of methane was calculated for eight experiments, and the results were compared with the observed yields of methane (Table V).

TABLE V

Calculated and observed yields of methane

Expt. No.	T, °A	Yield CH_4, mmoles	
		Calc.	Obs.
9	842	.055	.054
27	857	.050	.053
26	880.5	.088	.095
25	904	.164	.203
29	905	.179	.208
4	922	.156	.407
5	923	.375	.549
24	934.5	.308	.414

The agreement between the observed and calculated values is better than could be expected in view of the approximations made and the uncertainty in the values k_3 and k_4, and suggests that under the conditions of the experiments methyl radicals were not completely scavenged by toluene and that some reacted with benzyl radicals to give ethylbenzene. However, at the higher temperatures some of the ethylbenzene would be decomposed to give methyl radicals* and, therefore, one would expect, as actually

**The activation energy and the frequency factor for the decomposition of ethylbenzene are 3 kcal/mole greater than and 10 times less than the corresponding parameters for the decomposition of phenyl methyl sulphide. Therefore, the rate constant for the decomposition of ethylbenzene is considerably less than that for phenyl methyl sulphide and was neglected in the calculation of the concentration of methyl radicals.*

Can. J. Chem. Downloaded from www.nrcresearchpress.com by 186.148.149.217 on 09/04/12
For personal use only.

observed, an increase in the production of methane at the higher temperatures relative to the calculated values.

If recombination reactions of the phenylsulphide radical occurred, the rate constant for the production of thiophenol, k, would be expected to fall as the temperature was increased. The Arrhenius plot exhibited in fact some deviation from linearity, but only at the highest temperature attained. Thus, it would appear that phenylsulphide radicals, unlike methyl radicals, were efficiently scavenged by toluene. This seems plausible because the possible recombination products of the phenyl sulphide radical, i.e. diphenyldisulphide or phenylbenzyl sulphide, would probably not be sufficiently stable and would, therefore, not be formed in the hot reaction zone. In consequence one may consider the phenyl radicals to be removed only in reaction [2] with toluene and one may conclude that, in the region where the plot of log k vs. $1/T$ is linear, the rate of production of thiophenol is to a good approximation a measure of the rate of decomposition of phenyl methyl sulphide into phenylsulphide and methyl radicals. The activation energy and frequency factor calculated from the linear portion of the plot were 60 kcal/mole and 3×10^{14} sec^{-1}, respectively.

The effect of the surface of the reaction vessel on the decomposition was not investigated and, therefore, the activation energy of 60 kcal/mole may be only tentatively identified with the dissociation energy of the $C_6H_5S—CH_3$ bond. A value of 73 kcal/mole was suggested by Franklin and Lumpkin (12) for $D(CH_3S—CH_3)$ on the basis of their results obtained with the electron impact method. The difference between $D(CH_3S—CH_3)$ and $D(C_6H_5S—CH_3)$, which may amount to 13 kcal/mole, represents then the difference in resonance energies of the methylsulphide and the phenylsulphide radicals. Hence, the actual value of the resonance energy of the phenylsulphide radical would be at least 13 kcal/mole.

ACKNOWLEDGMENTS

This work was supported in part by a grant from the Petroleum Research Fund administered by the American Chemical Society. Grateful acknowledgment is hereby made to the donors of said fund. The authors wish to thank also the National Research Council of Canada for continued financial assistance.

REFERENCES

1. M. Szwarc. J. Chem. Phys. **16**, 128 (1948).
2. M. Szwarc. J. Chem. Phys. **17**, 431 (1949).
3. C. A. Coulson. Discussions Faraday Soc. **2**, 9 (1947).
4. A. Pullman. Discussions Faraday Soc. **2**, 26 (1947).
5. M. Szwarc, B. N. Ghosh, and A. H. Sehon. J. Chem. Phys. **18**, 1142 (1950).
6. I. M. Kolthoff, D. R. May, P. Morgan, H. A. Laitinen, and A. S. O'Brien. Ind. Eng. Chem., Anal. Ed. **18**, 442 (1946).
7. I. M. Kolthoff and W. E. Harris. Ind. Eng. Chem., Anal. Ed. **18**, 161 (1946).
8. M. W. Tamele and L. B. Ryland. Ind. Eng. Chem., Anal. Ed. **8**, 16 (1936).
9. M. Szwarc and J. W. Taylor. J. Chem. Phys. **23**, 2310 (1955).
10. E. H. Braye, A. H. Sehon, and B. de B. Darwent. J. Am. Chem. Soc. **77**, 5282 (1955).
11. A. F. Trotman-Dickenson and E. W. R. Steacie. J. Chem. Phys. **19**, 329 (1951).
12. J. L. Franklin and H. W. Lumpkin. J. Am. Chem. Soc. **74**, 1023 (1952).

Can. J. Chem. Downloaded from www.nrcresearchpress.com by 186.148.149.217 on 09/04/12
For personal use only.

Can. J. Chem. Downloaded from www.nrcresearchpress.com by 186.148.149.217 on 09/04/12
For personal use only.

THE SYNTHESIS OF SOME BASIC ESTERS OF 3,4,5-TRIMETHOXYBENZOIC ACID[1]

GERASSIMOS FRANGATOS, GEZA KOHAN, AND FRANCIS L. CHUBB

ABSTRACT

A series of basic esters of 3,4,5-trimethoxybenzoic acid was obtained from the reaction of 2-chloroethyl and 3-chloropropyl 3,4,5-trimethoxybenzoate with secondary amines including 1,2,3,4-tetrahydro-β-carboline. The latter compound was prepared by the lithium aluminum hydride reduction of 1,2,3,4-tetrahydro-1-oxo-β-carboline.

The remarkable effect of reserpine on the central nervous system has resulted in a wide application of this alkaloid primarily in states of hypertension and anxiety. However, the serious side effects of the drug and its high cost made it desirable to explore synthetic routes for the preparation of moieties which would retain the desirable pharmacodynamic properties with lesser or no interference from adverse side reactions. Miller and Weinberg (1), in view of the fact that the presence of the 3,4,5-trimethoxybenzoyl group in the reserpine molecule was necessary for its activity, prepared a number of basic esters of 3,4,5-trimethoxybenzoic acid. They reported reserpine-like activity for some of these compounds, especially those which contain three carbon atoms between the nitrogen and the ester group. This observation stimulated the synthesis and pharmacological testing of compounds of this type. Vejděl̆k (2), Supniewski (3), Sastry and Lasslo (4), Shapiro (5), Latuis and Combes (6), and Solov'ev (7) have synthesized a number of basic esters by bringing about the esterification of an aminoalcohol with 3,4,5-trimethoxybenzoyl chloride.

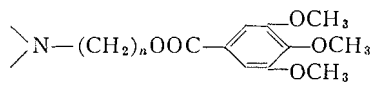
This communication reports some of the work done in these laboratories in which another route to the synthesis of basic esters was followed. The esters of halogenated alcohols with 3,4,5-trimethoxybenzoic acid were prepared and subsequently used as the alkylating agents in a series of secondary amines including 1,2,3,4-tetrahydro-β-carboline. This method is especially advantageous in cases where the aminoalcohol is not readily available. The reaction was carried out with or without solvent usually in the presence of an acid acceptor such as K_2CO_3. In this case 2-chloroethyl 3,4,5-trimethoxybenzoate (I) and 3-chloropropyl 3,4,5-trimethoxybenzoate (II), prepared from 3,4,5-trimethoxybenzoyl chloride and the corresponding alcohol, were used as alkylating agents. The basic esters (III) prepared are listed in Table I. The reaction sequence is shown below.

1,2,3,4-Tetrahydro-β-carboline (IV) was prepared from 1,2,3,4-tetrahydro-1-oxo-β-carboline (V). The latter compound was prepared by applying a modification (8) of the procedure of Abramovitch and Shapiro (9). These authors have cyclized 2,3-dioxopiperidine-3-phenylhydrazone (VI) to V by using polyphosphoric acid or formic acid as acidic catalyst. This method had its limitations for it could not be used for relatively large scale operations due to the extensive polymerization and tar formation which occurred. However, when a mixture of concentrated hydrochloric acid and acetic acid was used the cyclization of VI to V proceeded in a satisfactory manner.

[1]*Manuscript received March 14, 1960.*
Contribution from the Research Laboratories, Frank W. Horner Limited, Montreal, Que.

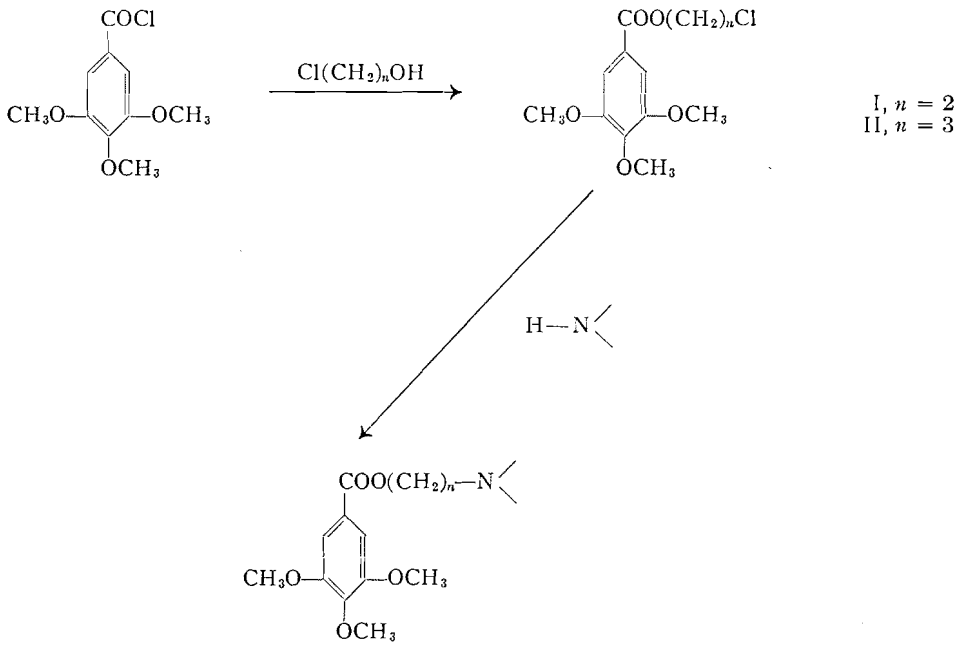
TABLE I

Basic esters of 3,4,5-trimethoxybenzoic acid



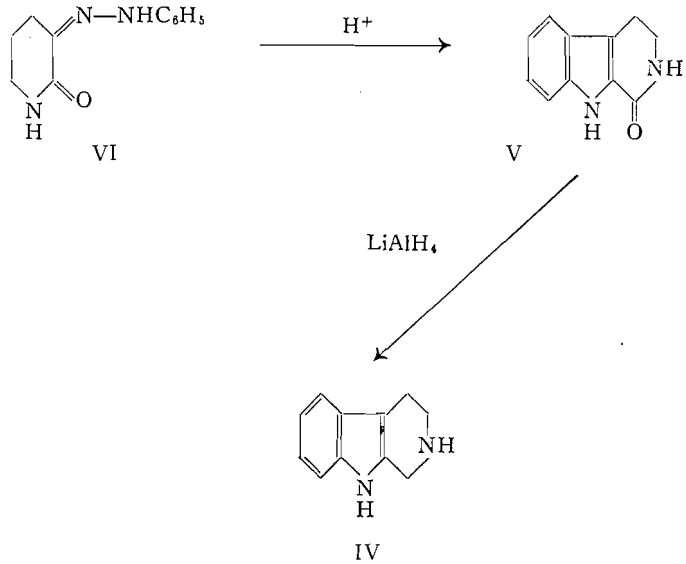
No.	N	n	Yield, %	Derivative	M.p.	Formula	Analyses: Calculated, % C	H	N	Found, % C	H	N
1[a]	Morpholine	2	69.2	Hydrochloride	213°	$C_{16}H_{24}ClNO_6$	53.11	6.63	3.87	52.98	6.62	4.00
				Picrate	178°	$C_{22}H_{26}N_4O_{13}$	47.65	4.69	10.10	47.95	4.89	9.85
2	Morpholine	3	61.2	Hydrochloride	174°	$C_{17}H_{26}ClNO_6$	54.32	6.92	3.43	54.07	7.08	3.79
3	Piperidine	2	72.3	Hydrochloride	210°	$C_{17}H_{26}ClNO_5$	56.75	7.23	3.89	56.92	7.48	4.07
				Picrate	165°	$C_{23}H_{28}N_4O_{12}$	50.00	5.07	10.14	49.91	5.22	10.51
4	Piperidine	3	68.3	Hydrochloride	168°	$C_{18}H_{28}ClNO_5$	57.83	7.49	3.74	57.24	7.56	3.72
5	Pyrrolidine	2	53.6	Hydrochloride	182°	$C_{16}H_{24}ClNO_5$	55.57	6.94	4.05	55.31	6.96	4.57
				Picrate	163°	$C_{22}H_{26}N_4O_{12}$	49.07	4.85	10.41	48.93	4.80	10.88
6	Pyrrolidine	3	55.6	Hydrochloride	154°	$C_{17}H_{26}ClNO_5$	56.74	7.23	3.89	56.47	7.24	3.93
7[b]	Diethylamine	2	54.8	Hydrochloride	159°	$C_{16}H_{26}ClNO_5$	55.25	7.48	4.02	54.95	7.52	4.32
				Picrate	140°	$C_{22}H_{28}N_4O_{12}$	48.89	5.18	10.37	48.41	5.18	10.54
8[c]	Diethylamine	3	47.0	Hydrochloride	174°	$C_{17}H_{28}ClNO_5$	56.43	7.74	3.87	56.45	7.87	3.84
9	1,2,3,4-Tetrahydro-β-carboline	2	58.0	Free base	151°	$C_{23}H_{26}N_2O_5$	67.31	6.34	6.82	67.33	6.46	6.64
10	1,2,3,4-Tetrahydro-β-carboline	3	54.3	Hydrochloride Monohydrate	199°	$C_{24}H_{29}ClN_2O_5H_2O$	60.19	6.48	5.85	59.99	6.52	5.75

[a]Reported (7) no yield melting point of the hydrochloride 199–200.5°.
[b]Reported (7) no yield melting point of the hydrochloride 156.5–157.5°.
[c]Reported (1, 7) low yield melting point of the hydrochloride 168°.



III

Can. J. Chem. Downloaded from www.nrcresearchpress.com by 186.148.149.217 on 09/04/12
For personal use only.



Lithium aluminum hydride reduction of V to IV had been attempted previously but without success (9). However, lithium aluminum hydride in boiling dioxane reduced V to IV in better than 90% yield. The reaction of IV with 2-chloroethyl 3,4,5-trimethoxybenzoate (I) and 3-chloropropyl 3,4,5-trimethoxybenzoate (II) was carried out in dimethylformamide solution using anhydrous potassium carbonate as the acid acceptor.

EXPERIMENTAL

Melting points are uncorrected. Microanalyses were carried out at the Microanalytical Laboratory of E. Thommen, Thannerstrasse 45, Basel, Switzerland.

3,4,5-Trimethoxybenzoyl Chloride

The procedure of Lasslo and Jordan (10) was followed except that the crude product was further purified by distillation *in vacuo*, b.p. 110–112°/0.5 mm.

2-Chloroethyl 3,4,5-Trimethoxybenzoate (I)

A mixture of 23.05 g of 3,4,5-trimethoxybenzoyl chloride, 8.05 g of 2-chloroethanol, and 10 g of anhydrous potassium carbonate in 200 ml of dry benzene was stirred and refluxed for 4 hours. At the end of the reaction period the evolution of carbon dioxide ceased. The inorganic salts were separated by filtration. The benzene was distilled from the filtrate under reduced pressure and the remaining liquid was distilled *in vacuo*. The fraction boiling at 155–158°/1 mm was collected and further purified by recrystallization from aqueous alcohol. A yield of 18.1 g (66.1%), m.p. 72°, was obtained. Anal. Calc. for $C_{17}H_{15}ClO_5$: C, 52.46; H, 5.46; Cl, 12.91. Found: C, 52.33; H, 5.40; Cl, 13.15.

3-Chloropropyl 3,4,5-Trimethoxybenzoate (II)

The same procedure as in the case of 2-chloroethyl 3,4,5-trimethoxybenzoate was used. A yield of 68.3%, b.p. 162–164° (1 mm) and m.p. 58° (aqueous ethanol), was obtained. Anal. Calc. for $C_{13}H_{17}ClO_5$: C, 54.08; H, 5.89; Cl, 12.28. Found: C, 54.31; H, 6.01; Cl, 12.00.

Can. J. Chem. Downloaded from www.nrcresearchpress.com by 186.148.149.217 on 09/04/12
For personal use only.

2-Piperidinoethyl 3,4,5-Trimethoxybenzoate

2-Chloroethyl 3,4,5-trimethoxybenzoate (5.49 g, 0.02 mole) was dissolved in 20 ml of freshly distilled piperidine. The reaction mixture was refluxed for 3 hours while a semi-solid material separated. The mixture was cooled and then treated with 25% aqueous sodium hydroxide and extracted thoroughly three times with chloroform. The chloroform layer was washed with water and dried over sodium sulphate. Distillation of the chloroform and the excess of piperidine under reduced pressure left an oily residue which did not crystallize. It was dissolved in chloroform and a slow stream of dry hydrogen chloride was passed through the solution for 15 minutes. Addition of ether precipitated the hydrochloride which was recrystallized from a mixture of isoamyl alcohol and ethyl acetate; 5.2 g (72.3%) of 2-piperidinoethyl 3,4,5-trimethoxybenzoate hydrochloride was obtained melting at 209–210°. Anal. Calc. for $C_{17}H_{26}ClNO_5$: C, 56.75; H, 7.23; Cl, 9.86; N, 13.89. Found: C, 56.92; H, 7.48; Cl, 10.07; N, 4.07. The picrate, m.p. 165–166°, was recrystallized from alcohol. Anal. Calc. for $C_{23}H_{28}N_4O_{12}$: C, 50.00; H, 5.07; N, 10.14. Found: C, 49.91; H, 5.22; N, 10.51. The remaining compounds in the series were prepared as above, and are listed in Table I.

Piperid-2,3-dione-3-phenylhydrazone

Piperid-2,3-dione-3-phenylhydrazone was prepared from 3-carbethoxy-2-piperidone according to the procedure of Abramovitch and Shapiro (9).

1,2,3,4-Tetrahydro-1-oxo-β-carboline

Fifty-eight grams of piperid-2,3-dione-3-phenylhydrazone (m.p. 244–245°) was added to a mixture of 135 ml of concentrated hydrochloric acid and 270 ml of glacial acetic acid. The reaction mixture was stirred and refluxed for 3 hours. The dark solution obtained was treated with charcoal and filtered. The filtrate was distilled under reduced pressure. The remaining dark material was treated with 75 ml of ice-cold acetone. The acetone was decanted and the residue was recrystallized from boiling acetone. The crystalline material obtained was recrystallized from aqueous alcohol and melted at 183–185°. Repeated crystallization from aqueous alcohol raised the melting point to 188°. Reported 183–184° (9), 189° (11). A yield of 26 g (49%) was obtained.

1,2,3,4-Tetrahydro-β-carboline

A sample of 1,2,3,4-tetrahydro-1-oxo-β-carboline (9.5 g) was dried *in vacuo* over phosphorous pentoxide and subsequently dissolved in 125 ml of boiling dry dioxane. This solution was added dropwise to a stirred and refluxing suspension of 9.5 g powdered lithium aluminum hydride in 200 ml of dioxane. During the addition the dioxane refluxed smoothly without external heating. The reaction mixture was stirred and refluxed in a nitrogen atmosphere for 4 hours and then was cooled. The excess of lithium aluminum hydride was destroyed with wet dioxane.

The mixture was brought to boiling and filtered hot. The dioxane was evaporated under reduced pressure and the solid residue was recrystallized from aqueous alcohol; 8.4 g (95.7%) of 1,2,3,4-tetrahydro-β-carboline, m.p. 208° (reported 200–202° (9), 204° (12)), was obtained. It gave a picrate melting at 253° with decomposition (reported 253° dec. (9, 11)).

2-(1,2,3,4-Tetrahydro-β-carbolinyl-2)ethyl 3,4,5-Trimethoxybenzoate

A mixture of 1.72 g (0.01 mole) of 1,2,3,4-tetrahydro-β-carboline, 2.74 g (0.01 mole) of 2-chloroethyl 3,4,5-trimethoxybenzoate, and 4 g of anhydrous potassium carbonate in

Can. J. Chem. Downloaded from www.nrcresearchpress.com by 186.148.149.217 on 09/04/12
For personal use only.

10 ml of dimethylformamide was stirred and refluxed for 4 hours. The reaction mixture was cooled and then filtered. The inorganic salts remaining on the filter were washed with dimethylformamide. The combined filtrates were distilled under reduced pressure until all the dimethylformamide was removed. The residue was dissolved in 100 ml of chloroform and passed through an alumina column which was eluted with an additional 150 ml of chloroform. The chloroform was removed from the combined eluates by distillation and the residual oil crystallized on trituration with a few drops of methanol. It was recrystallized from methanol and melted at 151°. Yield of 2.38 g (58%) was obtained. Anal. Calc. for $C_{23}H_{26}N_2O_5$: C, 67.31; H, 6.34; N, 6.82. Found: C, 67.33; H, 6.46; N, 6.64.

3-(1,2,3,4-Tetrahydro-β-carbolinyl-2)propyl 3,4,5-Trimethoxybenzoate

This compound was prepared as above, except that it was isolated as the hydrochloride hydrate. The eluate from the alumina column was treated with dry hydrogen chloride. Upon addition of ether an oil was deposited which crystallized on trituration. It was recrystallized from isoamyl alcohol to yield 2.6 g (54.3%), m.p. 199–200°. Anal. Calc. for $C_{24}H_{29}ClN_2O_5.H_2O$: C, 60.19; H, 6.48; N, 5.85. Found: C, 59.99; H, 6.52; N, 5.75.

REFERENCES

1. F. M. Miller and M. S. Weinberg. Chem. Eng. News, **34**, 4760 (1956).
2. Z. J. Vejděleк and V. Tříka. Chem. listy, **52**, 1622 (1958); Chem. Abstr. **53**, 1325 (1959).
   Z. J. Vejděleк and K. Macek. Chem. listy, **52**, 2140 (1958); Chem. Abstr. **53**, 3255 (1959).
   Z. J. Vejděleк and V. Tříka. Collection Czechoslov. Chem. Communs. **24**, 1860 (1959).
3. J. Supniewski, K. Bednarz, and J. Krupinska. Dissertationes Pharm. **10**, 191 (1958); Chem. Abstr. **53**, 7435 (1959).
4. B. V. Rama Sastry and A. Lasslo. J. Org. Chem. **23**, 1577 (1958).
5. S. L. Shapiro, H. Soloway, H. J. Shapiro, and L. Freedman. J. Am. Chem. Soc. **81**, 3993 (1959).
6. R. Ratouis and G. Combes. Bull. soc. chim. France, 576 (1959).
7. V. M. Solov'ev, A. P. Arendaruk, and A. P. Skoldinov. Zhur. Obscheĭ Khim. **29**, 613 (1959); Chem. Abstr. **54**, 388 (1960).
8. Z. Pelchovicz and E. D. Bergmann. J. Chem. Soc. 847 (1959).
9. R. A. Abramovitch and D. Shapiro. J. Chem. Soc. 4589 (1956).
10. A. Lasslo and W. D. Jordan. J. Org. Chem. **21**, 805 (1956).
11. S. Keimatsu, S. Sugasawa, and G. Kasuya. J. Pharm. Soc. Japan, **48**, 762 (1928); Chem. Abstr. **23**, 834 (1929).

Can. J. Chem. Downloaded from www.nrcresearchpress.com by 186.148.149.217 on 09/04/12
For personal use only.

Can. J. Chem. Downloaded from www.nrcresearchpress.com by 186.148.149.217 on 09/04/12
For personal use only.

HEATS OF MIXING OF POLYISOBUTYLENE WITH SOME ORGANIC SOLVENTS[1]

CLAUDE WATTERS,[2] HUBERT DAOUST, AND MARCEL RINFRET

ABSTRACT

The heats of mixing of four fractions of polyisobutylene with five organic solvents have been measured at 25° C with the use of a Tian–Calvet microcalorimeter. The maximum concentrations attained were of the order of 3% in polymer. It has been found that the enthalpy parameter κ_0 is independent of the molecular weight of the polymer sample in the investigated molecular weight range. All the values for κ_0 calculated from the Van Laar – Scatchard equation for the different polymer–solvent pairs are different from the values estimated from the partial molal quantities. This is explained with the use of new theories on the thermodynamics of high polymer solutions by Orofino and Flory and by Huggins.

INTRODUCTION

The physical state of a pure polymer at rest is ill-defined. For many types of high polymers, their state presents some degree of crystallinity or molecular orientation but most polymers are amorphous except under special conditions. Polyisobutylene is an amorphous polymer but below −70° C, its molecules are frozen in the so-called glassy state (1) and the transition from that state to the "liquid" state takes place over a rather wide temperature range. However, at room temperature, the dissolution of pure polyisobutylene in a liquid solvent will probably not involve any heat of transition. This investigation has been carried out to check that hypothesis and to show the importance of the data on heats of mixing for the study of high polymer solutions.

EXPERIMENTAL PART

Materials

Four fractions of polyisobutylene have been used in this investigation. The fractions PD-5 ($\bar{M}_v$ = 392,000) and PD-6 ($\bar{M}_v$ = 252,000) have been obtained from a fractionation of commercial Vistanex L-100 having a viscosity average molecular weight of about 1,360,000. The fractions PIJ-1-2 ($\bar{M}_v$ = 108,000) and PIJ-4 ($\bar{M}_v$ = 63,000) have been obtained from a fractionation of commercial Vistanex MH having a viscosity average molecular weight of about 68,000. Both commercial polymer samples have been obtained through the courtesy of Enjay Co., Inc. The fractionations have been carried out in accordance with previous procedures (2) and the molecular weights determined by the usual viscosity treatment of cyclohexane solutions. The reagent-grade solvents were purified in a high efficiency distilling column and stored over sodium wire.

Apparatus

The calorimetric measurements of the heats of mixing have been carried out using a Tian–Calvet microcalorimeter, a differential isothermal type which has been described elsewhere (3, 4). In our installation, a photopen recorder follows the spot of light reflected from the galvanometer mirror. The apparatus is calibrated electrically, and the measurement of the area under the curve gives the heat developed during the course of the reaction. This microcalorimeter is sensitive to a heat effect of 0.001 calorie per hour and is especially designed to follow a reaction over a long period of time.

[1]*Manuscript received January 15, 1960.*
Contribution from the Department of Chemistry, Université de Montréal, Montreal, Que. This paper has been presented in part at the Eighth Canadian High Polymer Forum at McDonald College, Ste Anne de Bellevue, Que., May 12–14, 1958.
[2]*Present address: Montreal Cancer Institute, Notre-Dame Hospital, Montreal, Que.*

The dissolution of the polymer was realized in a very simple way (5). A given quantity of polymer was weighed in a stainless steel mesh cage which was attached to a stainless steel wire and immersed under a quantity of mercury in a stainless steel cell. A weighed amount of solvent was added and the cell tightly stoppered. After thermal equilibrium was attained, the cage was then raised into the solvent and the thermal phenomenon measured.

RESULTS

The data obtained in this investigation are given in Table I. In this table, m is the weight of polymer used in each experiment; V_M, the total volume of the mixture; ϕ, the volume fraction of the polymer; and ΔH_M, the integral heat of mixing. The quantity B_0 represents the characteristic interaction constant for a given polymer–solvent pair and is calculated from the Van Laar – Scatchard equation, supposing that there is no volume change upon mixing,

$$\Delta H_M = B_0 V_M \phi (1-\phi). \quad [1]$$

DISCUSSION

Within the experimental errors, the values of B_0 for fractions PIJ-4 and PD-6 with chlorobenzene are practically the same. So, there is no significant variation of B_0 with molecular weight, at least in the range we have investigated. A résumé of the data is given in Table II and one sees that there is a direct relation between the Flory temperature θ and the enthalpy parameter κ_0 as predicted by theory. The parameter κ_0 is related to B_0 by the following equation

$$\kappa_0 = B_0 V_1/RT \quad [2]$$

where V_1 is the molar volume of the solvent.

However, the calculated values for κ_0 are all different from those given for κ_1. The parameter κ_1 is calculated from the partial molal quantities obtained by direct measurement of the heat of dilution or by indirect methods as viscosimetry, osmometry, and vapor pressure measurements. The large differences between the two sets of values for the enthalpy parameters may be due to three factors: (*a*) there may be an important volume change upon mixing, (*b*) there may be an important transition in the polymer state upon mixing, and (*c*) there may be a real difference between κ_0 and κ_1. The first factor is readily rejected since the volume changes are rather slight in the concentration range we have investigated. For example, the specific volume of pure polyisobutylene is 1.094 cc/g at 25° C (7); in dilute benzene solutions, the partial specific volume of the polymer increases to a constant value of 1.105 cc/g (8). The value of κ_0 would be increased to 0.70 because of this volume change upon mixing and the discrepancy with κ_1 would be still greater.

The possibility of the existence of a heat of transition will now be considered. If we assume that the difference between the values of the heats of dissolution of polyisobutylene in benzene as measured in this investigation and those calculated with $\kappa_1 = 0.21$ is due to some heat of transition, we come to the conclusion that the value for this heat is approximately 185 calories per monomer unit, a value which is not too high when compared with those obtained for other polymers. But this value should be independent of the nature of the solvent, and in athermal or slightly exothermic solvents as cyclohexane and *n*-heptane (see Table II), this endothermic heat of transition should have shown up.

Can. J. Chem. Downloaded from www.nrcresearchpress.com by 186.148.149.217 on 09/04/12
For personal use only.

TABLE I

Heats of mixing of polyisobutylene with some organic solvents at 25° C

m, g	V_m, ml	ϕ	ΔH_M, cal	B_0, cal/ml
		Fraction PIJ-4 in benzene		
0.046_0	7.052	0.00714	0.218	4.35
0.073_5	5.787	0.0139	0.352	4.44
0.082_2	5.311	0.0169	0.391	4.42
0.086_8	4.979	0.0191	0.413	4.44
0.080_7	3.836	0.0230	0.376	4.36
0.077_6	3.404	0.0249	0.360	4.35
0.088_6	3.477	0.0279	0.423	4.48
0.094_7	3.622	0.0286	0.438	4.35
0.126_0	3.973	0.0347	0.579	4.35
0.143_4	4.274	0.0367	0.657	4.35
0.090_3	2.618	0.0377	0.425	4.46
0.284_7	5.244	0.0593	1.304	4.45
		Fraction PIJ-4 in chlorobenzene		
0.033_8	6.555	0.00559	0.101	2.77
0.050_4	6.035	0.00914	0.155	2.83
0.059_4	6.014	0.0108	0.184	2.86
0.066_2	6.008	0.0121	0.209	2.91
0.083_5	6.069	0.0151	0.255	2.83
0.089_2	6.079	0.0161	0.282	2.94
0.137_5	8.443	0.0178	0.433	2.93
0.122_5	6.144	0.0218	0.385	2.93
0.127_7	6.135	0.0226	0.380	2.81
0.155_4	6.121	0.0278	0.483	2.92
0.160_5	6.138	0.0286	0.508	3.00
0.215_6	6.217	0.0379	0.665	2.92
		Fraction PD-6 in chlorobenzene		
0.023_6	6.137	0.00420	0.071	2.77
0.037_6	6.928	0.00594	0.122	2.99
0.039_0	6.350	0.00671	0.125	2.95
0.041_0	5.983	0.00749	0.125	2.81
0.047_9	6.033	0.00869	0.150	2.86
0.051_9	6.192	0.00917	0.161	2.86
0.066_3	6.286	0.0115	0.218	3.03
0.076_6	6.133	0.0137	0.239	2.89
0.083_1	6.071	0.0152	0.266	2.93
0.085_6	6.023	0.0155	0.267	2.90
0.118_6	6.191	0.0210	0.384	3.02
0.116_3	6.068	0.0210	0.381	3.14
		Fraction PD-6 in ethylbenzene		
0.038_2	6.072	0.00688	0.082	1.98
0.046_0	6.231	0.00807	0.097	1.93
0.060_9	6.489	0.0103	0.126	1.91
0.070_3	6.338	0.0121	0.152	2.00
0.083_3	6.423	0.0142	0.174	1.94
0.084_1	6.316	0.0146	0.173	1.91
0.085_9	6.378	0.0147	0.176	1.90
0.089_8	6.304	0.0156	0.200	2.06
0.100_8	6.244	0.0177	0.211	1.95
0.101_7	6.172	0.0180	0.206	1.88
0.121_1	6.407	0.0207	0.259	2.00
0.189_6	6.289	0.0330	0.363	1.81
		Fraction PIJ-4 in cyclohexane		
0.194_9	6.642	0.0321	−0.027	−0.13
0.194_0	6.551	0.0324	−0.043	−0.21
		Fraction PD-6 in *n*-heptane		
0.059_7	6.266	0.0104	−0.029	−0.45
0.085_5	6.138	0.0152	−0.037	−0.40
0.243_2	6.240	0.0426	−0.097	−0.38

Can. J. Chem. Downloaded from www.nrcresearchpress.com by 186.148.149.217 on 09/04/12
For personal use only.

TABLE II

Résumé of data on heat parameters for polyisobutylene in some organic solvents at 25° C

Solvent	θ, °K	κ_0	κ_1
Benzene	297.7[a]	0.66	0.21 (cal.)[c]
Chlorobenzene	262[b]	0.50	0.15 (vis.)[b]
Ethylbenzene	251[a]	0.40	0.117 (vis.)[a]
Cyclohexane	126[a]	−0.03	0.059 (vis.)[a]
			0.07 (osm.)[d]
n-Heptane	0[a]	−0.10	0 (vis.)[a]

NOTE: cal.: calorimetry; vis.: viscosimetry; osm.: osmometry.
[a]See reference 1.
[b]M. Senez. M.Sc. Thesis, Université de Montréal, Montreal, Que., 1958.
[c]See reference 6.
[d]P. J. Flory and H. Daoust. J. Polymer Sci. **25**, 429 (1957).

Although we do not discard the possibility of the existence of some heat of transition, we believe that the data can be discussed in regard to a new approach to the theory of the heat of mixing. Recently, Orofino and Flory (9) and Huggins (10, 11) have published new theories on the thermodynamics of high polymer solutions. The new semiempirical equation proposed by Orofino and Flory for the free energy of mixing is given by

$$[3] \qquad \Delta F_M = RT\{n_1 \ln(1-\phi)+n_2 \ln \phi+xn_2[\chi_0-\sum_{i=1}(\chi_i/i)\phi^i]\}$$

where n_1 and n_2 are the number of moles of the solvent and the polymer in the mixture and x is the ratio of the molar volumes of the polymer and the solvent, V_2/V_1. This equation has been derived to account for the polymer–solvent pairs for which a single interaction parameter cannot be used. The physical meaning of the parameters χ_0, χ_1, is not given but each of them is assumed to be independent of the concentration of the solution. From the equation [3], through the use of standard thermodynamic equations, the heat of mixing may be shown to be given by

$$[4] \qquad \Delta H_M = -T^2[\partial(\Delta F_M/T)/\partial T]_p = RT\kappa_0 n_2 x - RT\kappa_1 n_2 x\phi - RT\kappa_2 n_2 x\phi^2 - \ldots$$

where $\kappa_1 = -T(\partial\chi_1/\partial T) = B_1V_1/RT$. Equation [4] may be reduced to equation [1] when $\kappa_0 = \kappa_1$ and κ_2 and higher parameters vanish.

The new equation proposed by Huggins for the heat of mixing of "liquid" polymers with liquid solvents is given by

$$[5] \qquad \Delta H_M = N\Delta H_2^* n_2 - aN\Delta H_2^* n_2\phi - bN\Delta H_2^* n_2\phi^2 - \ldots$$

where N is the Avogadro number and a, b, etc. are fractional quantities. The quantity ΔH_2^* is defined by Huggins as the increase of heat content when a single molecule of polymer is transferred from pure polymer to pure solvent. The sign and the magnitude of ΔH_2^* are functions of the molecular structure of polymer and solvent and of the intermolecular forces involved in 1–1, 2–2, and 1–2 contacts.

The partial molal quantities derived from equations [3], [4], or [5] will not contain any interaction parameter with the subzero index and the results obtained from measurements of the integral heat of mixing and the results obtained from measurements of the heat of dilution may give different values for the heat parameter at infinite dilution. Even if there is a real difference between κ_0 and κ_1 as predicted by Huggins' treatment, this

Can. J. Chem. Downloaded from www.nrcresearchpress.com by 186.148.149.217 on 09/04/12
For personal use only.

difference should not be very large for mixtures of monomers since the molecular configuration changes are minor in that case. But in the case of a mixture of a polymeric solute in a monomeric solvent, $RT\kappa_0 n_2 x$ or $\Delta H_2^* N n_2$, which represents the energy change when Nn_2 macromolecules are transferred from their pure state to their solute state, depends on the degree of self-coiling of the chains which in turn depends on the polymer–solvent specific interactions. The sudden change in the configuration of the polymer chains upon mixing in a poor solvent will then be responsible for the large difference between the mixing parameter κ_0 and the infinite dilution parameter, κ_1.

The process of mixing may be considered as a series of dilutions starting with $\phi = 1$ and according to the results shown in Table II, the dilution of a very concentrated polymer solution would produce a higher apparent heat parameter than the dilution of a less concentrated solution. This observation has been confirmed by calorimetric measurements (6) and indirect measurements (12) of the heats of dilution of the polyisobutylene–benzene system for which the apparent heat parameter increases from 0.21 at high dilution to approximately 0.6 at very high polymer concentration. The major part of the enthalpy of mixing for that system would thus come from the first neighbor interaction between polymer and solvent molecules and from the molecular configuration changes of the polymeric chains due to this interaction at the beginning of the mixing process.

ACKNOWLEDGMENTS

We wish to thank the National Research Council of Canada for the generous financial assistance in this investigation. We also thank the Scientific Research Bureau of the Province of Quebec for the award of a bursary to C.W. while doing this research.

REFERENCES

1. P. J. Flory. Principles of polymer chemistry. Cornell Univ. Press, Ithaca, N.Y. 1953.
2. P. J. Flory. J. Am. Chem. Soc. **65**, 372 (1943).
3. E. Calvet. *In* Experimental thermochemistry. *Edited by* F. D. Rossini. Interscience Publishers, Inc., New York. 1956. Chap. 12.
4. E. Calvet et H. Prat. Microcalorimétrie: applications physico-chimiques et biologiques. Masson et Cie, Paris. 1956.
5. H. Daoust and M. Rinfret. Can. J. Chem. **32**, 492 (1954).
6. M. A. Kabayama and H. Daoust. J. Phys. Chem. **62**, 1127 (1958).
7. T. G. Fox and P. J. Flory. J. Phys. & Colloid. Chem. **55**, 221 (1951).
8. A. Horth, D. Patterson, and M. Rinfret. J. Polymer Sci. **39**, 189 (1959).
9. T. A. Orofino and P. J. Flory. J. Chem. Phys. **26**, 1067 (1957).
10. M. L. Huggins. J. Polymer Sci. **16**, 209 (1955).
11. M. L. Huggins. Physical chemistry of high polymers. John Wiley & Sons, Inc., New York. 1958.
12. C. E. H. Bawn and R. D. Patel. Trans. Faraday Soc. **52**, 1664 (1956).

Can. J. Chem. Downloaded from www.nrcresearchpress.com by 186.148.149.217 on 09/04/12
For personal use only.

Can. J. Chem. Downloaded from www.nrcresearchpress.com by 186.148.149.217 on 09/04/12
For personal use only.

THE INFRARED FREQUENCIES AND INTENSITIES OF THE HYDROXYL GROUP IN 2,6-DI-*tert*-BUTYL-4-SUBSTITUTED PHENOLS[1]

K. U. INGOLD

ABSTRACT

The infrared frequencies, intensities, and apparent half band widths of the O—H stretching band of a series of 2,6-di-*tert*-butyl-4-substituted phenols have been measured in carbon tetrachloride solution and compared with the corresponding 4-substituted phenols. The frequencies of the former are 36 cm^{-1} higher than the latter and the intensities are also slightly higher. Both the frequency and intensity follow a Hammett $\rho\sigma$ relation. It is shown that the O—H bond lies in the plane of the benzene ring, the increase in frequency and intensity being ascribed to a steric repulsion of the phenolic hydrogen by the adjacent *tert*-butyl group.

INTRODUCTION

Previous work on the frequencies and intensities of the hydroxyl group of substituted phenols has dealt mainly with meta- and para-monosubstitution (1, 2, 3, 4), although some work has been done on the effects of orthosubstituents (5) and the frequencies of a few 2,6-di-*tert*-butyl phenols have been measured, but not with high precision (6, 7).

The present work was devoted mainly to the changes in frequency, intensity, and half band width produced by various 4-substituents on the O—H band in 2,6-di-*tert*-butyl phenols. The corresponding monosubstituted phenols were also examined.

EXPERIMENTAL

A Beckman I.R.4 spectrophotometer with lithium fluoride optics was used to measure the O—H bands, the frequencies being calibrated by the standard absorption lines of water vapor. The effective slit width was about 4 cm^{-1}. Band areas were obtained by graphical integration. Solution concentrations in the range 0.01–0.005 molar were employed and the cell thickness was 1.0 mm. At this concentration even the sterically non-hindered phenols show no evidence of hydrogen bonding in carbon tetrachloride.

The preparation of most of the compounds employed has been described previously (8)* but the preparation of 2,6-di-*tert*-butyl-4-methoxyphenol deserves some discussion as the present data in the literature are somewhat misleading. First attempts to prepare this compound by the butylation of *p*-methoxyphenol in petroleum ether with isobutylene and sulphuric acid at 50° C (9) gave, after recrystallization from *n*-hexane, a 60% yield of a product, m.p. 103.5–104.5° C. Analysis: Found: C, 76.5; H, 10.1; CH_3O, 13.4. Calculated for $C_{15}H_{24}O_2$: C, 76.22; H, 10.24; CH_3O, 13.13. The melting point agrees with a previously reported value (6), but both the frequency and intensity of the O—H band were much lower than expected. The required phenol has also been reported by Müller and Ley (7), who prepared it from 4-methoxy-2,4,6-tri-*tert*-butyl-2,5-cyclohexadiene-1-one. Their product melted at 106–107° and they also obtained an identical compound by the butylation of *p*-methoxyphenol in 84% yield, but with recrystallization from methanol.

An examination of the spectrum of the raw product obtained by butylating *p*-methoxyphenol showed two bands, the larger corresponding to the product already separated (m.p. 103.5–104.5) and the smaller having the frequency expected for 2,6-di-*tert*-butyl-

[1]*Manuscript received March 14, 1960.*
Contribution from the Division of Applied Chemistry, National Research Council, Ottawa, Canada. Issued as N.R.C. No. 5698.
**References to the original preparations are given in reference 8.*

Can. J. Chem. Downloaded from www.nrcresearchpress.com by 186.148.149.217 on 09/04/12
For personal use only.

4-methoxyphenol. The two components were readily separated by an initial recrystallization from *n*-hexane to remove a large amount of the compound previously obtained, followed by recrystallization twice from methyl alcohol to yield the second component, m.p. 106–107° C. Analysis: Found: C, 76.2; H, 10.1; CH_3O, 15.0.

The lower melting compound must be 2,5-di-*tert*-butyl-4-methoxy phenol and the higher the 2,6-compound. The structural assignments were made on the basis of O—H frequency (see Discussion) since the 1600–2000 cm^{-1} region is too complicated to give unequivocal results. The assignments were confirmed by gas phase chromatography through a polar column (polyester succinate), the 2,6-compound having a retention time of about one third of the 2,5-compound, which is in agreement with similar hindered and non-hindered phenols. Adsorption chromatography on alumina of the raw butylated product showed that the ratio of 2,6 to 2,5 is 3:7. The high yield previously reported (7) must be because the reported yields are based on raw product, not on the purified material.

RESULTS

The frequency of the band maximum ν_m, intensity A, and apparent half band widths $\Delta\nu_{\frac{1}{2}}^{A}$ for the phenols examined are given in Table I. The intensities have been corrected for wing absorption (10) and are given in units of 1×10^4 $mole^{-1}$ liter cm^{-2} using $\log_{10}(I_0/I)$. The frequencies are probably correct to within about 1 cm^{-1}. The results obtained with monosubstituted phenols in carbon tetrachloride are in good agreement with previous work. The solvent 1,2-dichloroethane was used in order to get the hydroxy and nitro derivatives of phenol into solution in 0.01 molar concentration for intensity measurements. Since this solvent had such a pronounced effect on the O—H band, the other monosubstituted phenols were also examined in this solvent for comparative purposes.

TABLE I

Frequencies, intensities, and apparent half band widths of the O—H stretching band in substituted phenols

Substituent	$\Sigma\sigma$ (12)	$\nu_m(cm^{-1})$			1×10^4 A $mole^{-1}$ liter cm^{-2}			$\Delta\nu_{\frac{1}{2}}^{A}(cm^{-1})$		
		a	*b*	*c*	*a*	*b*	*c*	*a*	*b*	*c*
4-NO_2	1.270	3592	3538	3626.5	0.82	1.49	0.84	25	71	15.5
4-CHO	1.126	3595.5	3541.5	3630	0.83	1.49	0.80	24.5	67	16
4-CN	1.000	3595.5		3631	0.75		0.79	24		14.5
3-NO_2	0.710	3600	3549		0.70	1.30		22	64	
3-Cl	0.373	3604	3557.5		0.63	1.14		21	62	
4-Cl	0.227	3607.5	3561	3643.5	0.62	1.12	0.60	20	59	15
—	0.000	3609.5	3566	3645.5	0.55	1.04	0.57	18	53	16.5
4-$(CH_3)_2NCH_2$				3646			0.62			17
3-CH_3	−0.069	3610			0.55			18.5		
4-$C_6H_5(CH_3)_2C$		3610.5		3647	0.58		0.58	17.5		18
4-$C_2H_5(CH_3)CH$	−0.123	3612.5		3648	0.53		0.54	16		17
4-CH_3	−0.170	3612	3569.5	3648	0.50	0.98	0.53	16	51	18.5
4-$C_2H_5(CH_3)_2C$	−0.190	3612		3647	0.57		0.53	16.5		18
4-$(CH_3)_3C$	−0.197	3611	3569	3647.5	0.51	0.98	0.55	16.5	48	18.5
4-CH_3O	−0.268	3615	3574	3649	0.50	0.95	0.51	17.5	50	20.5
4-OH	−0.357	3614.5	3574.5	3649		0.96	0.49	15.5	49	20
4-CH_3O-3-$C(CH_3)_3$	−0.388	3615			0.50			18		
4-OH-3,5-di-$C(CH_3)_3$	−0.597	3615			0.51			18		
4-NH_2	−0.660	3616	3576	3650.5			0.45	15	46	22

NOTE: (*a*) Phenols in CCl_4; (*b*) phenols in $(CH_2Cl)_2$; (*c*) 2,6-di-*tert*-butyl phenols.

The results given in Table I can be correlated by a Hammett $\rho\sigma$ relation (1–5) as is shown in Figs. 1, 2, and 3. In Fig. 2 the intensities relative to phenol and to 2,6-di-*tert*-

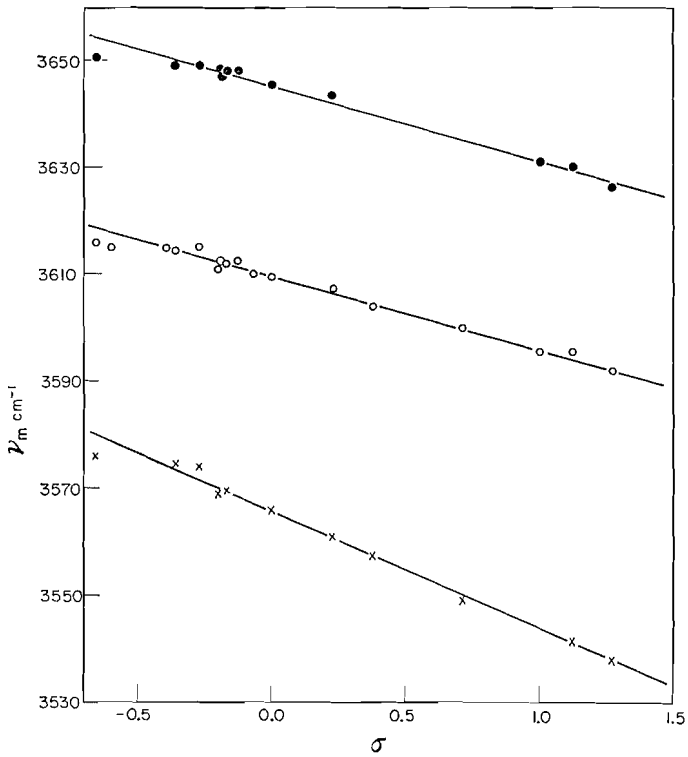


FIG. 1. Wavelength of O—H band against σ. ○ = Phenols in CCl_4; × = phenols in $(CH_2Cl)_2$; ● = 2,6-di-*tert*-butyl phenols in CCl_4.

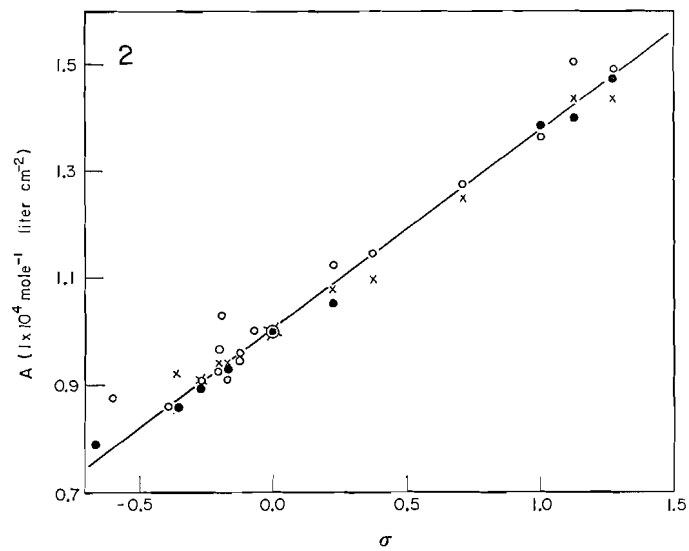


FIG. 2. Intensity of O—H band against σ. ○ = Phenols in CCl_4; × = phenols in $(CH_2Cl)_2$; ● = 2,6-di-*tert*-butyl phenols in CCl_4.

Can. J. Chem. Downloaded from www.nrcresearchpress.com by 186.148.149.217 on 09/04/12
For personal use only.

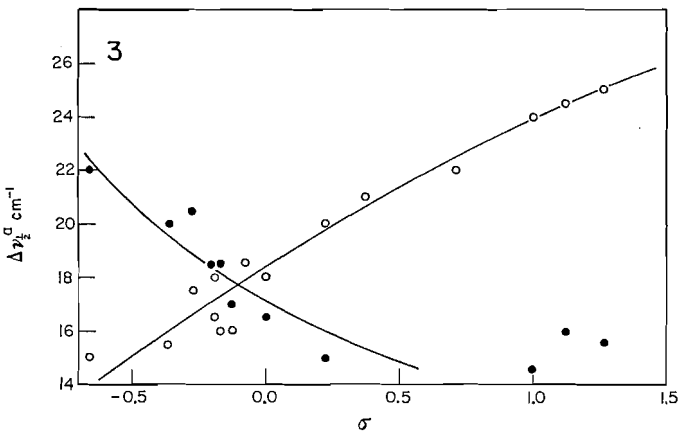


FIG. 3. Apparent half band width of O—H band against σ. ○ = Phenols in CCl_4; ● = 2,6-di-*tert*-butyl phenols in CCl_4.

butyl phenol have been plotted against σ. It is obvious that a good straight line can be obtained without the necessity of plotting log A against σ (4, 11). With regards to the determination of band intensities, Ramsay (10) has suggested a simple formula for computing the true intensity in terms of the observed peak absorbance and apparent half band width. Values calculated by means of this formula were found to be higher than the directly measured intensities by between 10 and 20% (4).

DISCUSSION

The increase in frequency observed with the 2,6-di-*tert*-butyl-4-substituted phenols compared with the corresponding unhindered phenols is too large (36 cm^{-1}) to be accounted for by the resonance and inductive contribution of the two *tert*-butyl groups. σ Values for orthosubstituents have recently been derived by Taft (13) and are generally close to the σ_{para} values for the same substituent. At first sight the increase might therefore be attributed to the twisting of the O—H bond out of the plane of the benzene ring which would decrease the resonance interaction and increase the bond order and therefore the frequency. However, it can be seen from Fig. 1 that the lines through the phenols and the 2,6-di-*tert*-butyl phenols in CCl_4 are parallel. Both types of phenols must, therefore, have a similar structure since, if the O—H bond were twisted out of the plane of the ring, resonance interaction between the O—H and the strongly electron-attracting groups would be decreased. For example, σ para-NO_2 has a value of 1.27 for phenols (and for anilines) but for other compounds its σ_{para} value is 0.78. If the O—H bond were at right angles to the benzene plane, the latter σ value for NO_2 should be observed and, if it lies between 0 and 90°, an intermediate value. It must, therefore, be concluded that the O—H bond is in the plane, further verification being the use of the larger σ_{para} values (to be used with phenols and anilines) for the CN and CHO group.

This conclusion has been verified by examining the characteristic group frequencies of certain of the *p*-substituents. The results are given in Table II. It has been shown that the frequencies of all these groups follow a Hammett $\rho\sigma$ plot (5, 14, 15, 16). Therefore, if the OH bond is twisted out of the plane by the *tert*-butyl groups, the effective σ will be less than the sum of the σ for O—H para (−0.36) plus two *tert*-butyl groups (meta) (2 × −0.12), i.e. less than −0.60 (17) and, therefore, the frequency shifts ($\Delta\nu_m$) given in

Can. J. Chem. Downloaded from www.nrcresearchpress.com by 186.148.149.217 on 09/04/12
For personal use only.

Table II will not be in the ratio 3:5; but, if the OH bond is in the plane, the frequency shifts will be in proportion to $\Sigma\sigma$, i.e. 3:5. If the O—H is tilted up from plane, the angle can be calculated from the measured ratio of the frequency shifts (17). It is apparent that with the strongly electron-attracting groups CHO and CN in the para position the O—H bond lies in the plane. The results for the OH and NH_2 group are more ambiguous. It seems improbable that the structure changes as drastically as the results might suggest (i.e. angle to the plane $\backsim$ 35° in OH case). It seems more probable that we are dealing here with a saturation of the electronic effects produced by the four electron-releasing groups on the ring because, if the hindered O—H was tilted to the plane, its frequency would be expected to increase whereas with the parasubstituents NH_2 and OH the frequency is slightly below the expected value. This saturation effect is also observed with the ordinary phenols (where there is no steric force tending to push the O—H out of the plane) when $\sigma > -0.4$.

TABLE II

Influence of a hindered hydroxyl group on the bond properties of parasubstituents

								X = NH_2				
		X = CHO		X = CN		X = OH		Antisymmetric		Symmetric		A_{anti}
Compound	$\Sigma\sigma$ (12)	ν_m	$\Delta\nu_m$	ν_m	$\Delta\nu_m$	ν_m	$\Delta\nu_m$	ν_m	$\Delta\nu_m$	ν_m	$\Delta\nu_m$	A_{sym}
C_6H_5X	0.00	1710	0	2230.0	0	3609.5	0	3481	0	3396	0	0.93
$4HOC_6H_4X$	−0.36	1701	−9	2228.4	−1.6	3614.5	5	3456	25	3380	16	3.0
3,5-di-$C(CH_3)_3$-$4HOC_6H_2X$	−0.60	1695	−15	2227.2	−2.8	3615.0	5.5	3455	26	3379	17	1.5

Absolute intensities of the bands of the groups in Table II were not measured (with the exception of (OH)), but the ratio of the intensities of the two N—H bands was measured. The ratio for aniline is in fair agreement with the value reported previously (16) and for 2,6-di-*tert*-butyl-4-amino phenol is within the expected range for $\Sigma\sigma = -0.60$; the large ratio for *p*-hydroxy aniline is quite unexpected. It is also surprising that the half band width of the CN group of 2,6-di-*tert*-butyl-4-cyano phenol is twice as great as for the other two cyano compounds (15).

A stereochemical configuration with the hindered O—H in the benzene plane can be seen to be quite plausible by the use of molecular models and we have checked this by calculating the position of the phenolic hydrogen relative to the adjacent *tert*-butyl group placed in the most favorable configuration. Using Pauling's (18) values for the van der Waal's radii of the atoms, the interpenetration of the phenolic hydrogen with each of four equivalent hydrogens is 0.25 Å and is about the same with the two equivalent carbons. This suggests a total compression energy of the order of 0.1–0.2 kcal/mole (19), which is very much smaller than the resonance energy gained by keeping the O—H bond in the plane ($\backsim$ 7.0 kcal/mole (18)). Furthermore, these "rigid model" compressions are a maximum, a little flexibility in the bonds would reduce the compression energy even further.

The increase in frequency of the 2,6-di-*tert*-butyl phenols, over and above that due to the electropositivity of the two *tert*-butyl groups, must be due to the snug fitting of the phenolic hydrogen into the adjacent *tert*-butyl group. The repulsion of the latter will build up as the O—H bond stretches and will therefore narrow the potential energy curve, increase its asymmetry, and thereby raise the frequency and intensity. That is, since the repulsion is due to interpenetration of the electron clouds it is exerted primarily

Can. J. Chem. Downloaded from www.nrcresearchpress.com by 186.148.149.217 on 09/04/12
For personal use only.

Can. J. Chem. Downloaded from www.nrcresearchpress.com by 186.148.149.217 on 09/04/12
For personal use only.

on the electrons of the phenolic hydrogen, and only through them on the proton itself. Thus, the interpenetration process will tend to keep back the electrons more than the proton. This will increase the dipole moment of the bond (μ) and the more the O—H bond stretches the more the dipole moment will be increased; and so $\partial\mu/\partial r$ will be increased and hence the intensity. This can be seen in Table I where, instead of the expected decrease in intensity (owing to the electropositivity of the two *tert*-butyl groups) of 0.05×10^4 mole^{-1} liter cm^{-2} on going from phenol to 2,6-di-*tert*-butyl phenol, an increase of 0.02×10^4 is instead observed. The similarity in the relative intensities of the two sets of phenols shown in Fig. 2 is to be expected if they have similar configurations.

The results given in Table III are arranged to show the effect of a single alkyl substituent ortho to the hydroxyl group. The σ constants given in the second column are derived from Jaffe (12) and Taft ortho factors (13) with certain exceptions. The σ values derived for ortho-*tert*-butyl and ortho-*tert*-amyl were obtained from ν_m but it should be pointed out that these values probably only apply to this system. The σ values for the three multiple substituted phenols are derived from the ortho-*tert*-butyl value and regular σ values. They can be used to calculate the expected frequencies. For instance, the calculated value for 2,5-di-*tert*-butyl-4-methoxyphenol is 3611.3 cm^{-1}, thus confirming the structure assigned to this compound. The predicted frequency for the corresponding 4-hydroxy phenol is 3612.5 cm^{-1}. 2-*tert*-Butyl-4-hydroxyphenol should have two bands at 3610.9 and 3616.4; these are not resolved but the measured value of ν_m is in close agreement with their average.

TABLE III

Influence of a single orthosubstituent on phenols in CCl_4

Substituent	$\Sigma\sigma$ (12)	ν_m, cm^{-1}	1×10^4 A mole^{-1} liter cm^{-2}	$\Delta\nu_{\frac{1}{2}}^a$, cm^{-1}
—	0.000	3609.5	0.55	18
2-CH_3	−0.17 (13)	3612	0.54	19
2-C_2H_5	−0.151	3611	0.49	18.5
2-n-C_3H_7	−0.126	3611	0.53	18
2-$C(CH_3)_3$	0.26*	3606	0.47	16.5
2-iso-C_5H_{11}	−0.225	3612	0.46	16
2-*tert*-C_5C_{11}	0.15*	3607.5	0.53	19.5
4-CH_3O-2,5-di-$C(CH_3)_3$	−0.128	3610.5	0.42	16
4-OH-2,5-di-$C(CH_3)_3$	−0.217	3610.5		14
4-OH-2-$C(CH_3)_3$	−0.477 and −0.097	3612.5	0.46	18

*See text.

The quite large positive value of σ for the *o-t*-butyl group in this system is rather surprising. A possible explanation is that the *tert*-butyl group effectively raises the barrier to rotation of the O—H group around the phenyl–oxygen bond. It can be seen with molecular models that interaction between the two groups can occur when the O—H bond is at right angles to the benzene plane. Although there is certainly a minimum in the potential energy curve when the O—H bond points directly toward the *tert*-butyl group, it is presumably not as deep as when it points away from it. This increased barrier to rotation means that the O—H is held more rigidly in the plane of the ring; increased resonance with the ring therefore occurs and the frequency drops. The results with the two ortho-amyl phenols confirms that this frequency decrease is caused by steric factors.

The solvent 1,2-dichloroethane was used for those phenols which were only very slightly soluble in carbon tetrachloride before it was realized that very thick cells ($\backsim$ 5 cm)

could be used with the latter solvent. It can be seen from Fig. 1 that the frequency is decreased and that the difference increases as the substituents become more electron-attracting. This kind of an effect can readily be explained as being due to hydrogen bonding involving the structure ϕ—O—H . . . $(CH_2Cl)_2$. Such interaction will obviously increase as the acidity of the phenol increases. Effects of this nature may help to explain the failure of the Bauer and Magat equation to interpret frequency shifts in different solvents (20). In this connection it is interesting to note that although the intensities in dichloroethane are roughly twice as great as in carbon tetrachloride, the relative intensities in the two solvents are unaffected by the nature of the parasubstituent (15) (see Fig. 2).

The results given in Fig. 3 (in which the apparent half band widths are plotted against σ) show one of the most striking differences between the hindered and unhindered phenols. No complete explanation can be advanced to account for the differences in the sign of the slopes of the lines. The values for the hindered phenols with strongly electronegative groups are undoubtedly somewhat larger than their true values owing to the effect of finite slit width (10). In the hindered phenols the O—H group cannot be solvated at the hydrogen end but only at the oxygen, and this must reduce the influence of the solvent on the band. The generally lower values of $\Delta\nu_{\frac{1}{2}}^{0}$ for the hindered phenols compared with the unhindered may also be partly due to the effect of the *tert*-butyl groups in increasing the moments of inertia of the molecule. It is interesting to note that in all previous cases where frequencies and half band widths of benzene derivatives have been shown to obey a Hammett $\rho\sigma$ relation, the slopes of these two functions have opposite sign (20) whereas with hindered phenols they have the same sign.

REFERENCES

1. L. L. INGRAM *et al.* J. Am. Chem. Soc. **74**, 2297 (1952).
2. J. D. S. GOULDEN. Spectrochim. Acta, **6**, 129 (1954).
3. T. L. BROWN. J. Phys. Chem. **61**, 820 (1957).
4. P. J. STONE and H. W. THOMPSON. Spectrochim. Acta, **10**, 17 (1957).
5. P. J. KRUEGER and H. W. THOMPSON. Proc. Roy. Soc. A, **250**, 22 (1959).
6. W. C. SEARS and L. J. KITCHEN. J. Am. Chem. Soc. **71**, 4110 (1949).
7. E. MÜLLER and K. LEY. Ber. **88**, 601 (1955).
8. K. U. INGOLD and I. E. PUDDINGTON. J. Phys. Chem. In press.
9. G. H. STILLSON, D. W. SAWYER, and C. K. HUNT. J. Am. Chem. Soc. **67**, 303 (1945).
10. D. A. RAMSAY. J. Am. Chem. Soc. **74**, 72 (1952).
11. T. L. BROWN. Chem. Revs. **58**, 581 (1958).
12. H. H. JAFFE. Chem. Revs. **53**, 191 (1953).
13. R. W. TAFT. Steric effects in organic chemistry. J. Wiley & Sons, Inc., New York. 1956. Chap. 13.
14. H. W. THOMPSON, R. W. NEEDHAM, and D. JAMESON. Spectrochim. Acta, **9**, 208 (1957).
15. M. R. MANDER and H. W. THOMPSON. Trans. Faraday Soc. **53**, 1402 (1957).
16. P. J. KRUEGER and H. W. THOMPSON. Proc. Roy. Soc. A, **243**, 143 (1957).
17. R. W. TAFT and H. D. EVANS. J. Chem. Phys. **27**, 1427 (1957).
18. L. PAULING. Nature of the chemical bond. Cornell Press, New York. 1940.
19. I. DOSTROVSKY, E. D. HUGHES, and C. K. INGOLD. J. Chem. Soc. 173 (1946).
20. H. W. THOMPSON. Spectrochim. Acta, **14**, 165 (1958).

Can. J. Chem. Downloaded from www.nrcresearchpress.com by 186.148.149.217 on 09/04/12
For personal use only.

Can. J. Chem. Downloaded from www.nrcresearchpress.com by 186.148.149.217 on 09/04/12
For personal use only.

ALIPHATIC CHEMISTRY OF FLUORENE

PART V. SPIRO-KETONES[1]

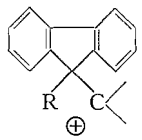
P. M. G. BAVIN[2]

ABSTRACT

A novel synthesis is described of 1,2;3,4-dibenzophenanthrene, based on the spiro-ketone (III*b*), which was cleaved by strong base to the acid (VII*b*).

An example is described of acylation of aliphatic carbon.

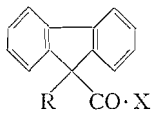
The ease with which methyl fluorene-9-carboxylate anion reacts with a wide range of alkyl halides (1, 2, 3) together with the formation of phenanthrene derivatives from carbonium ions (I) prompted the investigations described in this paper.

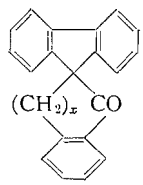


I

It has been reported (4) that 9-benzylfluorene-9-carboxylic acid chloride (II*a*) was cyclized by aluminum chloride to the spiro-ketone (III*a*), which may be converted via the alcohol (IV*a*) to 1,2;3,4-dibenzofluorene. This synthesis has been repeated and some yields improved. In particular, phosphorus pentoxide under boiling xylene rather than fused zinc chloride is the reagent of choice for dehydrating the alcohol (IV*a*).

The synthesis has been extended by the preparation and cyclization of 9-(2′-phenylethyl)-fluorene-9-carboxylic acid (II*c*), cyclization being effected by hydrogen fluoride. The homologous acid (II*b*) was unaffected by this reagent, in accord with the known





II*a*, R = $C_6H_5 \cdot CH_2$; X = Cl

II*b*, R = $C_6H_5 \cdot CH_2$; X = OH

II*c*, R = $C_6H_5 \cdot CH_2CH_2$; X = OH

II*d*, R = $C_6H_5 \cdot CH_2CH_2CH_2$; X = OH

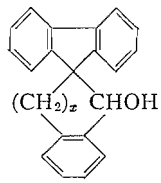
III*a*, x = 1

III*b*, x = 2

(5, p. 116) easier formation of six-membered ketones. All attempts to cyclize 9-(3′-phenylpropyl)-fluorene-9-carboxylic acid (II*d*) or its chloride have failed.

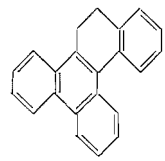
The formation of cyclic ketones from the tertiary acids is surprising since Lewis acids would have been expected to bring about decarbonylation. This exceptional behavior may be attributed to instability of the fluorene cation, which would be formed in the decarbonylation process (6).

[1]*Manuscript received March 8, 1960.*
Contribution from the Chemistry Department, the University, Hull, East Yorkshire, England.
[2]*I.C.I. Fellow.*



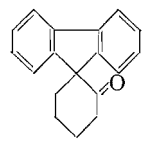
IV*a*, $x = 1$

IV*b*, $x = 2$



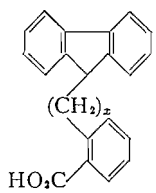
V

The ketone (III*b*) was converted via the alcohol (IV*b*) to 1,2;3,4-dibenzo-9,10-dihydrophenanthrene (V). In agreement with earlier workers (7) the hydrocarbon could not be obtained crystalline but was dehydrogenated in good yield to 1,2;3,4-dibenzophenanthrene, completing a novel synthesis of this ring system. It was intended that this work should be extended to more complex ring systems, but lack of time has curtailed the work. Some 9-aralkyl derivatives of methyl fluorene-9-carboxylate, prepared as desirable starting compounds, are described in the Experimental section. In addition, methyl 9-(4′-cyanobutyl)-fluorene-9-carboxylate has been prepared, as a possible precursor of VI. During its preparation, dimethyl butane-1,4-di-9′-fluorenyldi-9′-carboxylate was isolated as a by-product and identified by synthesis.



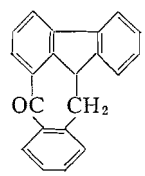
VI

The spiro-ketones (III*a* and III*b*) were cleaved by strong base, as expected for non-enolizeable ketones, giving the acids (VII*a* and VII*b*), isomeric with (II*a* and II*c*). The direction of cleavage is controlled by formation of the more stable anion, as previously noted for 9-methyl-9-benzoylfluorene (8).

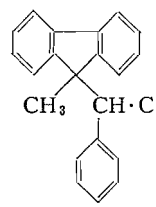


VII*a*, $x = 1$

VII*b*, $x = 2$



VIII



IX

The chloride of the acid (VII*a*) reacted with aluminum chloride to reform the spiro-ketone (III*a*) and not, as had been hoped, the isomeric ketone (VIII). A few similar examples of acylation of aliphatic carbon are known, e.g. the acetylation and benzoylation of 9,10-dihydroanthracene (9).

The chloride prepared from the alcohol (IV*a*) closely resembled IX (8), decomposing at its melting point or in boiling formic acid with formation of 1,2;3,4-dibenzofluorene. Silver acetate in acetic acid gave unrearranged acetate. A similar stabilization of neopentyl-type carbonium ions by phenyl has been reported (10, and references quoted therein).

Can. J. Chem. Downloaded from www.nrcresearchpress.com by 186.148.149.217 on 09/04/12
For personal use only.

Other examples of non-rearrangement of neopentyl carbonium ions probably involve neighboring group participation (11). In agreement with this, the reaction between 9-methyl-9-fluorenylmethyl chloride and silver acetate gave 9-methylphenanthrene.

EXPERIMENTAL

Methyl fluorene-9-carboxylate anion was alkylated in the usual way (2) to give the following:

9-Benzylfluorene-9-carboxylic acid, prepared by saponification of the methyl ester (2), formed well-defined prisms from benzene–hexane, m.p. 204–205° (4). Found: C, 84.25; H, 5.24%. Calc. for $C_{21}H_{16}O_2$: C, 83.97; H, 5.37%.

Methyl 9-(2′-phenylethyl)-fluorene-9-carboxylate crystallized as long white needles (74%) from methanol, m.p. 67–68°. Found: C, 83.81; H, 5.99%. Calc. for $C_{23}H_{20}O_2$: C, 84.12; H, 6.14%. The *acid* (81%) crystallized as colorless rhombic plates from benzene–hexane, m.p. 143–144°. Found: C, 83.76; H, 5.66%. Calc. for $C_{22}H_{18}O_2$: C, 84.05; H, 5.77%.

9-(3′-Phenylpropyl)-fluorene-9-carboxylic acid, obtained by saponifying the oily methyl ester, formed large pale yellow prisms (76%) from benzene–hexane, m.p. 125–127°. Found: C, 84.11; H, 6.13%. Calc. for $C_{23}H_{20}O_2$: C, 84.12; H, 6.14%.

Methyl 9-(2′-thienylmethyl)-fluorene-9-carboxylate crystallized as small white needles (71%) from hexane, m.p. 104–105°. Found: C, 75.13; H, 5.17%. Calc. for $C_{20}H_{16}O_2S$: C, 74.99; H, 5.03%.

Methyl 9-(3′-thienylmethyl)-fluorene-9-carboxylate formed clusters of white prisms (76%) from hexane, m.p. 119.5–120.5°. Found: C, 74.99; H, 5.22%. Calc. for $C_{20}H_{16}O_2S$: C, 74.99; H, 5.03%.

*Methyl 9-(1′-naphthylmethyl)-fluorene-9-carboxylate** crystallized as small prisms (73%) from benzene–hexane, m.p. 154–156°. Found: C, 85.36; H, 5.48%. Calc. for $C_{26}H_{20}O_2$: C, 85.69; H, 5.53%.

*Methyl 9-(2′-naphthylmethyl)-fluorene-9-carboxylate** formed small needles (79%) from benzene–hexane, m.p. 189–191°. Found: C, 85.82; H, 5.71%. Calc. for $C_{26}H_{20}O_2$: C, 85.69; H, 5.53%.

Methyl 9-(4′-cyanobutyl)-fluorene-9-carboxylate

1,4-Dibromobutane, b.p. 63–65° at 5 mm, n_D^{21} 1.5163, was prepared from tetrahydrofuran in 68% yield.

1,4-Dibromobutane (209 g, 0.84 mole) was stirred and boiled under reflux for 6 hours with potassium cyanide (55 g, 0.8 mole), water (65 ml), and ethanol (220 ml). After being diluted with water, the products were isolated with ether and separated by precise fractionation, giving δ-bromovaleronitrile (86 g), b.p. 102–103° at 8 mm, n_D^{23} 1.4776.

Prepared in the usual way, *methyl 9-(4′-cyanobutyl)-fluorene-9-carboxylate* crystallized as long white needles (93%) from methanol, m.p. 89–90°. The analytical sample was obtained after two further crystallizations and had a melting point of 90.5–91.0°. Found: C, 79.05; H, 6.74; N, 4.59%. Calc. for $C_{20}H_{19}NO_2$: C, 78.66; H, 6.27; N, 4.59%. C≡N stretching band, 2220 cm^{-1}; C=O stretching band, 1740 cm^{-1}.

Commercial δ-bromovaleronitrile (Sapon Laboratories) gave 63% of the cyano-ester and 31% of a substance insoluble in hot methanol. The latter crystallized from toluene as small colorless needles, m.p. 221.0–221.5°, after three crystallizations. Found: C, 80.64; H, 5.57%. Calc. for $C_{34}H_{30}O_4$: C, 81.25; H, 6.02%. It was identified as *dimethyl butane-1,4-di-9′-fluorenyldi-9′-carboxylate* by synthesis from 1,4-dibromobutane (0.56 g, 0.5 mole) and a solution of methyl fluorene-9-carboxylate (1.23 g, 2.2 moles) in methanol

*Prepared by Mr. R. C. Wilson.

Can. J. Chem. Downloaded from www.nrcresearchpress.com by 186.148.149.217 on 09/04/12
For personal use only.

containing sodium methoxide (from sodium, 0.23 g, 2.1 atoms), identity being established by mixed melting point determination and comparison of infrared spectra.

Saponification of the diester in ethylene glycol gave *1,4-(di-9'-fluorenyl)-butane*, which crystallized from acetone–methanol as small white needles, m.p. 161.0–161.5°. Found: C, 93.52; H, 6.49%. Calc. for $C_{30}H_{26}$: C, 93.22; H, 6.78%.

Spiro-compounds

Indan-1-one-2-spiro-9'-fluorene (III*a*) was prepared as described in the literature (4) in a maximum yield of 67%. Reduction with ethereal lithium aluminum hydride gave indan-1-ol-2-spiro-9'-fluorene (IV*a*) in almost quantitative yield. It formed prisms from cyclohexane, m.p. 159–160° (lit. m.p. 160° and 168° (dimorphic) (4)). Found: C, 88.27; H, 5.48%. Calc. for $C_{21}H_{16}O$: C, 88.74; H, 5.67%.

1-Chloroindane-2-spiro-9'-fluorene, prepared by the reaction between the alcohol and thionyl chloride, crystallized from heptane as elongated prisms (77%), m.p. 172–173° with decomposition to 1,2;3,4-dibenzofluorene. The chloride decomposed similarly in boiling 94% formic acid. Found: C, 83.20; H, 4.89%. Calc. for $C_{21}H_{15}Cl$: C, 83.30; H, 4.99%.

1-Acetoxyindane-2-spiro-9'-fluorene, prepared either by acetylating the alcohol or by the reaction between the chloride and silver acetate in acetic acid, formed colorless prisms from benzene–hexane, m.p. 132–133°. Found: C, 84.66; H, 5.62%. Calc. for $C_{23}H_{18}O_2$: C, 84.64; H, 5.56%.

Heating the alcohol (IV*a*) with twice its weight of phosphorus pentoxide under boiling xylene gave, after 1 hour, 1,2;3,4-dibenzofluorene (94%) which crystallized from heptane as slender white needles, m.p. 162–163°. Oxidation gave 1,2;3,4-dibenzofluorenone, identical with an authentic sample (8).

1,2,3,4-Tetrahydronaphthalene-1-one-2-spiro-9'-fluorene (III*b*) was prepared by cyclizing the acid (II*c*) (3 g) in dry ether (50 ml) with hydrogen fluoride (150 ml). During 2 days at room temperature most of the solvents evaporated. The neutral product crystallized from cyclohexane as white needles (2.3 g), m.p. 201–202°. Found: C, 89.71; H, 5.32%. Calc. for $C_{22}H_{16}O$: C, 89.16; H, 5.44%.

1-Hydroxy-1,2,3,4-tetrahydronaphthalene-2-spiro-9'-fluorene (IV*b*), prepared by reducing the ketone with ethereal lithium aluminum hydride, crystallized from cyclohexane as small colorless blades (91%), m.p. 197.0–197.5°, depressed to 175–180° by the ketone. Found: C, 88.68; H, 6.11%. Calc. for $C_{22}H_{18}O$: C, 88.56; H, 6.08%.

1,2,3,4-Dibenzo-9,10-dihydrophenanthrene (V). Dehydration of the alcohol (IV*b*) (2 g) with phosphorus pentoxide under boiling xylene followed by purification over alumina gave a colorless oil (1.5 g) which has failed to crystallize. The *1,3,5-trinitrobenzene adduct* separated from methanol as vermilion rods, m.p. 161–162°. Found: C, 67.98; H, 3.72%. Calc. for $C_{28}H_{19}N_3O_6$: C, 68.15; H, 3.88%.

Oxidation with chromic acid in acetic acid gave a trace of 1,2;3,4-dibenzophenanthrene-9,10-quinone.

1,2,3,4-Dibenzophenanthrene was prepared as follows. Dehydrogenation of the dihydro compound over 10% palladium-on-charcoal at 300° gave an almost quantitative yield of dibenzophenanthrene, which crystallized as white needles from heptane, m.p. 115–116°. Identity was established by comparison with two authentic samples (12,* 13) and by preparation of the quinone and picrate. The *1,3,5-trinitrobenzene adduct* crystallized as slender orange needles from methanol, m.p. 165–166°. Found: C, 68.30; H, 3.64%.

**Provided by Dr. C. C. Barker.*

Can. J. Chem. Downloaded from www.nrcresearchpress.com by 186.148.149.217 on 09/04/12
For personal use only.

Calc. for $C_{28}H_{17}N_3O_6$: C, 68.43; H, 3.49%. (This derivative has been reported as forming bright yellow needles from benzene, m.p. 167° (13).)

Cleavage of the Spiro-ketones

The ketone (1 g) was warmed for 30 minutes with a solution of potassium hydroxide (1 g) in industrial alcohol (50 ml) and the acidic product isolated.

2-(9'-Fluorenylmethyl)-benzoic acid (VII*a*) crystallized as slender needles (85%) from cyclohexane, m.p. 188–189°. Found: C, 83.72; H, 5.61%. Calc. for $C_{21}H_{16}O_2$: C, 83.97; H, 5.37% (lit. m.p. 185–186° (14)). The acid chloride ($SOCl_2$) in benzene at 10° reacted with aluminum chloride to reform the spiro-ketone (57%), identified by mixed melting point determination and comparison of infrared spectra.

2-(2'-(9''-Fluorenyl)-ethyl)-benzoic acid (VII*b*) crystallized from benzene–hexane as colorless blades (81%), m.p. 163–164°. Found: C, 84.21; H, 6.03%. Calc. for $C_{22}H_{18}O_2$: C, 84.05; H, 5.77%.

9-Methylphenanthrene

The reaction between 9-methyl-9-fluorenylmethanol (2) and thionyl chloride gave a semisolid product which would not form a crystalline picrate from ethanol. The reaction with silver acetate in acetic acid was rapid, silver acetate separating. 9-Methylphenanthrene was isolated as its orange picrate (61%, from ethanol), identical with an authentic specimen (2).

ACKNOWLEDGMENTS

Some preliminary experiments were carried out at the University of Ottawa during the tenure of a National Research Council of Canada Postdoctorate Fellowship at the University of Ottawa (1954–56), and the author is indebted to Dr. F. A. L. Anet for his interest and helpful suggestions.

REFERENCES

1. W. Wislicenus and W. Mocker. Ber. **46**, 2772 (1913).
2. F. A. L. Anet and P. M. G. Bavin. Can. J. Chem. **34**, 991 (1956).
3. P. M. G. Bavin. Anal. Chem. In press.
4. M. Vaillant. Compt. rend. **234**, 534 (1952).
5. W. S. Johnson. Organic reactions. Vol. II. John Wiley & Sons, Inc., New York. 1949.
6. M. E. Grundy, Wei-Hwa Hsü, and E. Rothstein. J. Chem. Soc. 581 (1958).
7. C. K. Bradsher and H. Rapoport. J. Am. Chem. Soc. **66**, 1281 (1944).
8. P. M. G. Bavin. Can. J. Chem. **37**, 2023 (1959).
9. C. D. Nenitzescu, I. Gavat, and D. Cocora. Ber. **72**, 819 (1939).
10. P. Skell and C. R. Hauser. J. Am. Chem. Soc. **64**, 2633 (1942).
11. W. von E. Doering and L. K. Levy. J. Am. Chem. Soc. **77**, 509 (1955).
12. C. C. Barker, R. G. Emmerson, and J. D. Periam. J. Chem. Soc. 1077 (1958).
13. P. M. G. Bavin and M. J. S. Dewar. J. Chem. Soc. 4479 (1955).
14. W. Wislicenus and P. Neber. Ann. **418**, 274 (1918).

Can. J. Chem. Downloaded from www.nrcresearchpress.com by 186.148.149.217 on 09/04/12
For personal use only.

Can. J. Chem. Downloaded from www.nrcresearchpress.com by 186.148.149.217 on 09/04/12
For personal use only.

LIGHT ABSORPTION STUDIES

PART XVII. THE ULTRAVIOLET ABSORPTION SPECTRA OF CHLOROBENZENES[1]

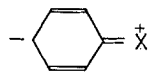
W. F. FORBES[2]

ABSTRACT

The ultraviolet absorption spectra of a series of chlorobenzenes are determined. The spectral data suggest that the apparent mesomeric effect of the chlorine atom is greater than that of the fluorine atom, that solvent–solute interactions are generally less important in chlorobenzenes than in fluorobenzenes, and that, as expected, the effective interference radius of the chlorine atom is large. Moreover, spectral changes in *o*-substituted chlorobenzenes are consistent with the assumption that maximum electronic interaction requires the chlorine atom to be in the same plane as the benzene ring. The conformations of *o*-chloroacetophenone and *o*-chlorophenol are briefly discussed.

INTRODUCTION

In previous parts of these studies (1), it was found that changes in the location of the so-called *B*-band (for nomenclature employed see refs. 1 and 2) in the ultraviolet spectrum provide a measure of mesomeric interactions;* that is, spectral changes in the *B*-band could usually be related with changes in the appropriate extended dipolar resonance form of the molecule. For example, the *B*-band of a halogen-substituted benzene can be imagined to owe its existence to the resonance form I, and if this resonance



I

form is favored, as it is by a number of electron-attracting *p*-substituents, the absorption occurs at longer wavelength and with increased absorption intensity. Other interactions which do not directly affect the resonance form, for example the interactions caused by a *m*-substituent, were found to be only of secondary importance. The *B*-band spectral changes in this way afford a readily available semiquantitative measure of mesomeric interactions as defined above, and generally the information obtained concerning these mesomeric interactions is much as would be expected from simple resonance considerations. One somewhat surprising exception is that for the halogen-substituted benzenes the bathochromic wavelength displacements compared with benzene are in the order iodobenzene > bromobenzene > chlorobenzene > fluorobenzene, and this implies an order of apparent mesomeric interaction I > Br > Cl > F. This is contrary to the order usually accepted (cf. refs. 1(*a*), 1(*b*)).

The *B*-band spectra of the chlorobenzenes are hence of interest and it is the purpose of the present paper to examine, or to re-examine, these spectra assuming that the chlorine atom possesses a greater mesomeric effect, or at least a greater apparent mesomeric effect, than the fluorine atom.

[1]*Manuscript received January 25, 1960.*
Contribution from the Memorial University of Newfoundland, St. John's, Newfoundland, and the Division of Protein Chemistry, C.S.I.R.O. Wool Research Laboratories, Parkville N.2 (Melbourne), Victoria, Australia.
[2]*Present address: Division of Protein Chemistry, C.S.I.R.O., Victoria, Australia.*
**Mesomeric interactions have been defined, for the purpose of this series of papers, as interactions associated with electron mobility acting along systems of conjugated bonds. These mesomeric interactions were found in some instances to be different from the mesomeric interactions as deduced from chemical equilibria (cf. 1(a), 1(b)).*

Can. J. Chem. Downloaded from www.nrcresearchpress.com by 186.148.149.217 on 09/04/12
For personal use only.

THE SPECTRUM OF CHLOROBENZENE

The spectra of chlorobenzene in different solvents are listed in Table I.

TABLE I

Main ultraviolet absorption maxima of chlorobenzene in various solvents

Solvent	*B*-Band		*C*-Band	
	λ_{max} (mμ)	ϵ_{max}	λ_{max} (mμ)	ϵ_{max}
Vapor phase	211 215 ca. *219*	*	243 250 256 259 262 267 269	*
Cyclohexane	211 215 ca. *219*	7500 7500 *6000*	245 251 257 261 264 271	70 120 180 170 250 190
Ether	211 214 ca. *218*	7000 7000 *6000*	244 250 257 264 271	65 105 160 210 155
Ethanol	211 214 ca. *218*	7000 7000 *5500*	245 250 257 264 271	65 110 160 200 140
Water	210 214	5000 4500	244 250 256 263 270	65 100 135 165 115

NOTE: Values in italics represent inflections in this and the following table.
*Intensities not determined.

The similarity of the spectra of fluorobenzene and benzene has been noted in the previous paper (1(*a*)). This similarity is no longer present between the spectra of chlorobenzene and benzene since the *B*-bands of chlorobenzene, and to a lesser extent the *C*-bands also, are displaced to longer wavelength (see Table I and cf. ref. 1(*a*)). This spectral change in the *B*-band is related to the increased contributions of resonance forms of type I. That is, it is assumed that at least in the electronic excited state, the chlorine atom is more readily able to interact with the benzene ring than is the fluorine atom.

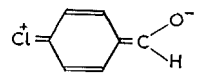
The spectral changes of the chlorobenzene bands with change of solvent are smaller than for fluorobenzene (see Table I and ref. 1(*a*)). In fact, the only experimentally significant spectral change in the *B*-band is a decreased absorption intensity for the spectrum of chlorobenzene in aqueous solution, which is generally observed for compounds of this type. Particularly interesting is the virtual absence of a wavelength displacement for the *B*-band on determining the spectrum in the vapor phase and in cyclohexane solution ($\Delta\lambda$ less than 1 mμ, see Table I), since a number of other compounds examined (3) afford a wavelength displacement appreciably greater than 1 mμ

under these conditions. These observations then suggest that general solvent effects, solvent orientation effects, as well as other solvent–solute interactions such as intermolecular hydrogen bonding, are not important in determining the *B*-band absorption of chlorobenzene.

The *C*-band of chlorobenzene in all solvents is found to be considerably less intense than the *C*-band of fluorobenzene (cf. ref. (1*a*)).

THE SPECTRA OF PARASUBSTITUTED CHLOROBENZENES

Using the simplified concept illustrated by resonance structures of type I, the spectra of *p*-substituted chlorobenzenes can be divided into two groups. (*a*) First, the group of compounds in which the *p*-substituent is electron-donating, when the *B*-band resembles the *B*-band of the monosubstituted benzene derivative. Of the two substituents, the substituent with the greater electron-donating power will predominantly determine the wavelength and intensity of the monosubstituted benzene *B*-band while the other substituent will exert only a "secondary" effect on the *B*-band. (*b*) The second group



II

represents compounds in which the *p*-substituent is electron-withdrawing and resonance interaction is enhanced because of appreciable contributions of resonance forms of type II. These generalizations are illustrated by the data in Table II.

Examination of the data in Table II and of suitable reference compounds shows that generally the *B*-bands of *p*-substituted chlorobenzenes can be identified without undue difficulty. For example, as expected, only one *B*-band, the monochlorobenzene *B*-band, is observed for *p*-dichlorobenzene; somewhat surprisingly, the chlorobenzene *B*-band has been displaced to longer wavelength by about 10 mμ on account of the second chlorine substituent (see Tables I and II). This indicates that the secondary effect of the chlorine atom is such as to favor the transition, and consideration of resonance form I suggests that the second chlorine atom may donate electrons in the electronic excited state and in this way facilitate the transition. Next, the ultraviolet absorption of 1-chloro-4-fluorobenzene has previously been ascribed to chlorobenzene absorption (1(*a*)), and this again suggests that at least in this compound the chlorine atom possesses the greater mesomeric effect. The only other *B*-band which is associated with chlorobenzene absorption is the band at 221 mμ in *p*-chlorotoluene; this assignment is made because the methyl substituent, like the chloro substituent, would be expected to cause absorption at longer wavelength and because the *C*-band indicates the characteristic chlorobenzene fine structure (see Tables I and II). The *B*-band of the remaining *p*-substituted chlorobenzenes, in which the *p*-substituent is electron-donating, i.e. Br, I, OH, OCH_3, or NH_2, is similar to the *B*-band of the corresponding monosubstituted benzene derivative, that is, it is similar to the *B*-band of bromobenzene, iodobenzene, etc.* Again generally, the *p*-chloro substituent appears to facilitate the absorption since normally the *p*-substituted compound tends to absorb at slightly longer wavelength and with increased

**It may be noted that p-chlorophenol is tentatively assumed to absorb as phenol rather than as chlorobenzene although chlorobenzene absorbs at longer wavelength, that is, the transition involves less energy. However, this apparent anomaly can be explained by the previously made suggestion (1(c)) that the p-electrons of the* OH*-group in phenol are not in the most favorable position for electronic excitation and that because of this, phenol absorbs at unusually short wavelength. It is possible that in p-chlorophenol the* OH*-group tends to twist towards an energetically more favorable position for transition and that consequently the phenol B-band absorption is favored.*

Can. J. Chem. Downloaded from www.nrcresearchpress.com by 186.148.149.217 on 09/04/12
For personal use only.

Can. J. Chem. Downloaded from www.nrcresearchpress.com by 186.148.149.217 on 09/04/12
For personal use only.

TABLE II—Main ultraviolet absorption maxima of substituted chlorobenzenes in cyclohexane solution

	Para isomer				Meta isomer						Ortho isomer					
	B-Band		*C*-Band		*B*-Band		2nd *B*-Band		*C*-Band		*B*-Band		2nd *B*-Band		*C*-Band	
Substituent	λ_{max} (mμ)	ϵ_{max}	λ_{max} (mμ)	ϵ_{max}	λ_{max} (mμ)	ϵ_{max}	λ_{max} (mμ)	ϵ_{max}	λ_{max} (mμ)	ϵ_{max}	λ_{max} (mμ)	ϵ_{max}	λ_{max} (mμ)	ϵ_{max}	λ_{max} (mμ)	ϵ_{max}
—Cl	225	13,500	ca. *253*	*130*	217	8,500	—	—	250	70	216	8,500	—	—	249	75
			260	225	221	8,000			256	150	219	8,300			ca. *255*	*125*
	ca. *229*	*10,500*	265	350					263	250	ca. *224*	*5,500*			261	250
			ca. *268*	*310*	ca. *225*	*4,300*			270	375					ca. *265*	*200*
			273	500					277	315					270	350
			281	450											277	325
—Br	224	13,500	ca. *260*	*250*			ca. *212*	*12,000**	251	120						
			267	340			ca. *218*	*10,500*	257	165						
	ca. *230*	*10,000*	274	415			ca. *224*	*7,000*	264	300						
			282	335			ca. *228*	*5,500*	271	400						
									278	325						
—I	234	18,000	258	1,100	224	9,000*	231	12,000	252	650	222	7,000*	231	10,500	252	575
			264	1,000					258	720					258	620
	239	17,500	274	750	*227*	*10,000*	236	11,000	266	730	*228*	*9,000*	237	11,000	264	660
			ca. *286*	*375*					274	650					269	585
									281	480					273	610
															280	450
—CH_3	221	9,000	*244*	*100*	214	8,000			254	140	212	8,500			ca. *253*	*130*
			ca. *251*	*160*					261	215					258	200
			256	240					267	320					ca. *262*	*230*
			263	370					ca. *271*	*175*					266	300
			269	500					274	270					273	280
			277	520												
—OH	224	8,800	ca. *275*	*1,400*			216	6,500	268	1,300			212	6,450*	ca. *268*	*1,550*
			281	1,850					274	2,050					274	2,350
			289	1,700					281	2,000					281	2,450
—OCH_3	228	11,700	ca. *276*	*1,400*			219	7,300	ca. *269*	*1,350*			219	7,500*	ca. *270*	*1,600*
			282	1,900					275	2,150					275.5	2,400
			290	1,850					282	2,150			223	7,400	283	2,450
—NH_2	243	12,500	ca. *291*	*1,650*			238	8,500	289	2,100			236	8,700	291	2,900
			297	1,900												
			ca. *306*	*1,300*												
—$COCH_3$	249	17,000	272	900			239	10,000	286	1,100			235	5,700	280	650
			284	500					295	900						
—CHO	253	19,000	276	1,500			241–242	11,500	288	1,400			246	11,000	292	1,750
	259	*15,500*	286	1,000			248	10,000	298	1,200			252	8,500	300	1,400
															302	1,400
—NO_2	214	10,700*	ca. *290*	*3,000*	213	19,000*	254	7,800	ca. *286*	*1,250*	210	16,000*	244	4,000	286	1,300
	ca. *219*	*9,000**							290	1,350	216	14,000				
	265	12,000			ca. *218*	*14,000*			299	1,300	ca. *223*	*9,000*			ca. *295*	*1,100*
	ca. *273*	*11,000*							ca. *309*	*800*						

**B*-Band assignment doubtful.

absorption intensity compared with the non-chlorosubstituted parent compound. For example, in cyclohexane solution, anisole absorbs maximally at 220 mμ, $\epsilon = 7500$ (1(*d*)), whereas *p*-chloroanisole absorbs maximally at 228 mμ, $\epsilon = 11{,}700$ (see Table II).

Although the *p*-chloro substituent, in the examples listed in the last paragraph, gives rise to an appreciable intensity increase, for example, in the anisole *B*-band of chloroanisole, this intensity increase is generally less than if the non-chloro substituent is electron-withdrawing. This is shown by the observed high absorption intensities of the *p*-substituted chlorobenzenes listed towards the end of Table II. This increased transition probability, as well as the generally more pronounced bathochromic wavelength displacement compared with chlorobenzene or compared with the non-chloro-monosubstituted benzene derivatives, suggests resonance structures of type II, since the contribution of resonance forms of type II would be expected, on the basis of our general hypothesis relating resonance interaction and *B*-band absorption, to cause intensified *B*-band absorption occurring at longer wavelength. In this way, the *B*-bands of these *p*-substituted chlorobenzenes are associated, at least partly, with resonance structures involving the *entire* molecule, whereas the *B*-bands of the previously mentioned *p*-substituted chlorobenzenes are associated with resonance structures involving, as a first approximation, only *part* of the molecule; that is, they are associated with transitions involving predominantly so-called locally excited states.

THE SPECTRA OF METASUBSTITUTED CHLOROBENZENES

The frequent occurrence of two *B*-bands in the spectra of *m*-disubstituted benzene derivatives has previously been noted and may be rationalized in terms of simple resonance theory. That is, resonance forms of type I will not normally be greatly affected by a *m*-substituent and thus the *B*-band of the *m*-disubstituted compound will resemble the *B*-band of one of the monosubstituted parent compounds. Moreover, if electrons are highly localized in both substituent groups, two *B*-bands corresponding to both monosubstituted parent compounds can apparently sometimes be identified (see refs. 1(*c*), 1(*d*), 1(*e*)).

For *m*-substituted chlorobenzenes therefore the chlorobenzene *B*-band would be expected to occur near 215 mμ (see Table I), that is, at a location at which it cannot always be identified with certainty since *A*-band absorption (cf. ref. 2) also frequently occurs near this wavelength. However, in compounds like *m*-dichlorobenzene, the band near 220 mμ evidently represents the chlorobenzene *B*-band, and the bands near 225 mμ in *m*-chloroiodobenzene and near 215 mμ in *m*-chlorotoluene are also tentatively ascribed to chlorobenzene *B*-band absorption (see Table II). In all these examples the second substituent, if electron-donating, facilitates the chlorobenzene *B*-band absorption, apparently in a less pronounced, though presumably similar, manner as has been postulated for the corresponding *p*-isomers. If the second substituent is electron-withdrawing, as for example in *m*-chloronitrobenzene, the reverse effect is tentatively assumed to occur since the chlorobenzene *B*-band appears to be displaced to *shorter* wavelength and probably occurs near 210 mμ. This, unfortunately, is at a wavelength at which it can no longer be identified with certainty because of possible *A*-band absorption (see Table II).

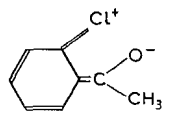
The effect of the *m*-chloro substituent on the *B*-band, associated with the non-chloro-monosubstituted benzene derivative, appears generally to be small and is certainly smaller than the effect of the *p*-chloro substituent. Usually, a small bathochromic

Can. J. Chem. Downloaded from www.nrcresearchpress.com by 186.148.149.217 on 09/04/12
For personal use only.

wavelength displacement is observed on account of the *m*-chloro substituent, but sometimes the *B*-band absorption maxima are almost identical. For example, anisole in cyclohexane solution absorbs maximally at 220 mμ, ε = 7500 (1(*d*)) whereas *m*-chloroanisole under identical conditions absorbs maximally at 219 mμ, ε = 7300 (see Table II). Or, benzaldehyde in hexane solution absorbs maximally at 241 mμ, ε = 14,000 whereas *m*-chlorobenzaldehyde under similar conditions absorbs maximally at 241–242 mμ, ε = 11,500 (1(*e*)). It may be noted that a related effect has also been reported for some of the infrared data. For example, the location of the hydroxyl band in phenol at 3608 cm^{-1} is reported close to the hydroxyl band in *m*-chlorophenol (3607 cm^{-1}; $A = 6.7\times10^{-7}$); the band is, however, slightly enhanced compared with the intensity of the corresponding phenol band ($A = 5.8\times10^{-7}$) (4).

THE SPECTRA OF ORTHOSUBSTITUTED CHLOROBENZENES

The *B*-bands of *o*-substituted chlorobenzenes generally resemble the *B*-bands of the corresponding meta isomers. In terms of canonical resonance forms this suggests that dipolar excited states of type III are not important in determining the *B*-band. This may



III

be because of steric considerations, that is, because the two substituents are not sufficiently coplanar for effective resonance interaction to occur, or it may be because the molecule inherently absorbs by means of transitions involving predominantly locally excited states. For example, if the non-chloro substituent is electron-donating, as in *o*-chlorophenol, *o*-chloroaniline, etc., dipolar resonance forms of type III may be neglected and *B*-bands associated with locally excited states, that is phenol and aniline *B*-bands would be expected and are in fact observed (see Table II).* For *o*-substituted chlorobenzenes, however, in which the non-chloro substituent is electron-withdrawing, the steric hypothesis is favored since if the non-chloro substituent is relatively small, as in *o*-chlorobenzaldehyde, there is observed a slight bathochromic wavelength displacement relative to the *B*-band in the meta isomer, indicative of resonance interaction of type III; in *o*-chloroacetophenone and *o*-chloronitrobenzene on the other hand, no such bathochromic wavelength displacement is observed and this therefore suggests that only in *o*-chlorobenzaldehyde are the two *o*-substituents in the same plane.

Since the benzaldehyde, nitrobenzene, and acetophenone absorption is still readily discerned (see Table II) in the spectra of the *o*-chlorosubstituted compounds and since, moreover, there is quite generally a similarity between the spectra of ortho and meta isomers in compounds of this type, this suggests that non-planarity is caused, at least partly, at the expense of the chlorine atom. Hence it may tentatively be assumed that not only are the formyl, acetyl, or nitro groups twisted out of the plane of the benzene ring but also that the chlorine atom is bent away from the plane of the benzene ring,

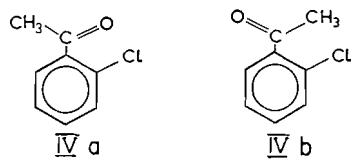
**In some o-substituted chlorobenzenes, such as o-chloroanisole, it is possible that the observed B-band corresponds, at least partly, to chlorobenzene B-band absorption. However, the present spectral evidence, for example, the spectral changes observed on altering the solvent for o-chloroanisole which closely resemble the solvent changes observed for anisole (3) do not favor this possibility, nor do the infrared data (see Experimental).*

Can. J. Chem. Downloaded from www.nrcresearchpress.com by 186.148.149.217 on 09/04/12
For personal use only.

and it may be because of this bending away that the chlorine atom is frequently no longer able to interact effectively with the benzene ring in the manner required to give rise to resonance interaction as shown in structure III.

Although the precise relation between steric interactions and spectral effects in *o*-substituted chlorobenzenes is evidently not entirely clear, some form of steric interaction in a number of *o*-substituted chlorobenzenes is indicated by the pronounced intensity decreases in the *B*-bands of compounds like *o*-chloroacetophenone and *o*-chloronitrobenzene compared with the intensities for the corresponding meta isomers or compared with the *B*-band intensities of the corresponding non-chloromonosubstituted benzene derivatives (see Table II and ref. 1). The intensity decrease in these *o*-substituted chlorobenzenes is greater than in the corresponding methylacetophenones (1(*f*)) or methylnitrobenzenes (1(*g*)), and this suggests that the effective interference radius of the chlorine atom is greater than that of the methyl group. On the other hand, the reported spectra of the *o*-chloro- and *o*-methyl-acetanilides (5), for example, suggest an opposite order. However, even then the observed intensity decrease in the *B*-band of the *o*-chloro compound is appreciable, and this then at least confirms the belief that the effective interference radius of the chlorine atom is large. The present data, as well as other related data, hence clearly indicate the presence of appreciable steric interactions caused by an *o*-chloro substituent (6, 7, 8). (Indications that the chlorine atom, when attached to a benzene ring, causes appreciable steric interactions are also provided by the postulated puckered nature of the benzene ring in hexachlorobenzene (9).)

Concerning the actual conformation of a compound like *o*-chloroacetophenone, the infrared carbonyl band shows a doublet which has been assumed to indicate that *o*-chloroacetophenone exists in two *s-cis, s-trans* conformations IV*a* and IV*b*, with IV*b*



IV a IV b

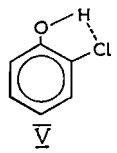
representing the slightly more stable conformation (10).* Because of electrostatic and steric considerations, it seems unlikely that either of these conformations should be entirely coplanar, and this observation relates well with the low intensity of the *B*-band in the ultraviolet region, which indicates non-planarity of the molecule. On the other hand, the acetyl group must be, at least partly, coplanar with the benzene ring because the characteristic acetophenone maximal absorption near 235 mμ is still evident in *o*-chloroacetophenone (see Table I). The most probable explanation consistent with all the above-mentioned observations seems to be that *o*-chloroacetophenone exists in at least two conformations, most of them not entirely coplanar, with the preferred angle between the plane of the nitro group and that of the C—Cl bond being very approximately 30°.

The spectral data discussed above suggest the operation of steric interactions in a number of *o*-substituted chlorobenzenes. On the other hand, neither *B*-band nor *C*-band

**Two s-cis, s-trans conformations have also been postulated for o-chloroanisole (11) on the basis of a doublet in the ultraviolet region. However, doublets are frequently observed in the ultraviolet region, even if no s-cis, s-trans isomerism is possible (cf., for example, the observed doublet in the ultraviolet spectrum of benzaldehyde (1(e)). Further, no evidence for two conformations, in the form of doublets, has been obtained for the infrared spectrum of o-chloroanisole (see Experimental), and Banerjee's hypothesis is therefore not favored.*

Can. J. Chem. Downloaded from www.nrcresearchpress.com by 186.148.149.217 on 09/04/12
For personal use only.

data provide any convincing evidence for the existence of an intramolecular hydrogen bond as has frequently been postulated for compounds like *o*-chlorophenol (V). (For



V

recent discussions concerning this type of intramolecular hydrogen bonding see refs. 12, 13, 14, 15, 16.) That is, comparing the spectra of *o*- and *m*-chlorophenol, no bathochromic wavelength displacements are observed in the *B*- and *C*-bands of the *o*-isomer, the ϵ_{max} value of the *B*-band in the *o*-isomer is not greater than the corresponding ϵ_{max} value in the *m*-isomer, and the ϵ_{max} value of the *C*-band in the *o*-isomer, although slightly larger than for the *m*-isomer, is not large as for *o*-chloroanisole and, moreover, the increase in ϵ_{max} values between ortho and meta isomers are comparable for chlorophenols and chloroanisoles (see Table II). Further, *o*-chlorophenol in ethanolic solution absorbs as follows: λ_{max} 216 mμ, ϵ = 6400; λ_{max} 276.5 mμ, ϵ = 2350; and λ_{infl} ca. 280 mμ, ϵ = 2000; and in ether solution *o*-chlorophenol absorbs as follows: λ_{max} 217 mμ, ϵ = 6200; λ_{max} 275 mμ, ϵ = 2400; and λ_{infl} ca. 281 mμ, ϵ = 2000; these spectra are appreciably different from the absorption spectrum of *o*-chlorophenol in cyclohexane solution (see Table II). Since an intramolecular hydrogen bond in *o*-chlorophenol would be expected to cause bathochromic wavelength displacements in both *B*- and *C*-bands accompanied by intensity increases, and since, further, the spectrum of an intramolecular hydrogen-bonded compound would not be unduly affected by solvent changes, the ultraviolet data point against the presence of structures of type V for solutions of *o*-chlorophenol in ethanol or ether solutions and to a lesser extent to the absence of such structures also in cyclohexane solution.

EXPERIMENTAL

The ultraviolet absorption spectra were determined by standard methods in 1-cm cells using a Unicam SP500 spectrophotometer calibrated against a didymium filter. For each compound at least two independent sets of observations were made. The accuracy of λ_{max} values is estimated to be $\pm$2 mμ, and the precision of ϵ_{max} values $\pm$5% or better. Values of ϵ_{max} were reproducible in most cases to $\pm$2%. The ultraviolet data are listed in Tables I and II and in the discussion of *o*-chlorophenol. Some of the spectra have previously been described in this series and elsewhere. Whenever possible, the chlorobenzene spectra were determined under conditions identical with those under which previous spectra in this series had been determined. Frequently, but not always, the data were in good agreement with recent values reported by other workers (cf. for example, ref. 17).

The infrared spectra were determined on a Unicam SP100 instrument, using a NaCl prism and a diffraction grating.

The infrared spectrum of *o*-chloroanisole was determined in the liquid phase in the region 650–2000 cm^{-1} and was found to be more like the infrared spectrum of anisole than the infrared spectrum of chlorobenzene under identical conditions. No evidence in the way of doublet formation, for two different conformations, could be detected for the infrared spectrum of *o*-chloroanisole within this region.

Can. J. Chem. Downloaded from www.nrcresearchpress.com by 186.148.149.217 on 09/04/12
For personal use only.

The chlorobenzenes were mostly commercial materials, purified by distillation or recrystallization until their boiling points and refractive indices or melting points showed them to be sufficiently pure. The solvents used were spectroanalyzed cyclohexane (Fisher) or other commercially available spectroanalyzed solvents.

ACKNOWLEDGMENTS

The author is greatly indebted to Miss Florence Jackman for the careful determination of the ultraviolet spectral data and to Mr. D. L. Coffen for the infrared data. Some of the spectra have also been determined by Mr. J. C. Dearden in preparation for his Ph.D. thesis and the author is indebted to Mr. Dearden for making these data available.

Grateful acknowledgment for financial assistance in support of these studies is made to the National Research Council of Canada.

REFERENCES

1. (*a*) W. F. FORBES. Can. J. Chem. **37**, 1977 (1959).
   (*b*) W. F. FORBES and W. A. MUELLER. Can. J. Chem. **35**, 488 (1957).
   (*c*) J. C. DEARDEN and W. F. FORBES. Can. J. Chem. **37**, 1294 (1959).
   (*d*) J. C. DEARDEN and W. F. FORBES. Can. J. Chem. **37**, 1305 (1959).
   (*e*) J. C. DEARDEN and W. F. FORBES. Can. J. Chem. **36**, 1362 (1958).
   (*f*) W. F. FORBES, W. A. MUELLER, A. S. RALPH, and J. F. TEMPLETON. Can. J. Chem. **35**, 1049 (1957).
   (*g*) W. F. FORBES. Can. J. Chem. **36**, 1350 (1958).
2. W. F. FORBES and R. SHILTON. ASTM Bull. Symposium on Spectroscopy. In press. 1960.
3. J. C. DEARDEN and W. F. FORBES. Can. J. Chem. **38**, 896 (1960).
4. P. J. STONE and H. W. THOMPSON. Spectrochim. Acta, **10**, 17 (1957).
5. H. E. UNGNADE. J. Am. Chem. Soc. **76**, 5133 (1954).
6. R. J. FRANCEL. J. Am. Chem. Soc. **74**, 1265 (1952).
7. R. D. KROSS, V. A. FASSEL, and M. MARGOSHES. J. Am. Chem. Soc. **78**, 1332 (1956).
8. S. D. ROSS. J. Am. Chem. Soc. **70**, 4039 (1948).
9. O. SCHNEPP and R. KOPELMAN. J. Chem. Phys. **30**, 868 (1959).
10. R. N. JONES, W. F. FORBES, and W. A. MUELLER. Can. J. Chem. **35**, 504 (1957).
11. S. B. BANERJEE. Indian J. Phys. **31**, 135 (1957).
12. A. W. BAKER. J. Am. Chem. Soc. **80**, 3598 (1958).
13. S. B. ROY. Indian J. Phys. **32**, 525 (1958).
14. S. C. SIRKAR, A. R. DEB, and S. B. BANNERJEE. Indian J. Phys. **32**, 345 (1958).
15. S. NAGAKURA. J. Chem. Soc. Japan, Pure Chem. Sect. **75**, 734 (1954); Chem. Abstr. **48**, 10434*d* (1954).
16. D. K. GHOSH. Indian J. Phys. **29**, 450 (1955).
17. A. BURAWOY and A. R. THOMPSON. J. Chem. Soc. 4314 (1956).

Can. J. Chem. Downloaded from www.nrcresearchpress.com by 186.148.149.217 on 09/04/12
For personal use only.

Can. J. Chem. Downloaded from www.nrcresearchpress.com by 186.148.149.217 on 09/04/12
For personal use only.

DISINTEGRATION-RATE DETERMINATION BY 4π-COUNTING

PART V. FURTHER STUDIES ON ABSORPTION AND SCATTERING OF β-RADIATION[1]

L. YAFFE AND J. B. FISHMAN[2, 3]

ABSTRACT

The work of Pate and Yaffe on the study of absorption and scattering of β-radiation in a 4π-counter has been extended to greater source-mount thickness. As the thickness is increased, the backscattering curves assume the juxtaposition obtained in $<2\pi$ geometrical systems. The saturation backscattering value S is attained at a mass approximately one-fifth that of the range of the β-radiation. The relationship $S = 0.070 \log_{10} E_{max} + 0.142$, where E_{max} is the maximum energy of the β-radiation, is obeyed over the range studied. The phenomenon of coincident discharges, while adequately explained by Pate and Yaffe as caused by wall- and gas-scattering if thin film source mounts are used, cannot completely account for the results with thicker films. Other phenomena, such as bremsstrahlung and secondary electron production, begin to play a role.

INTRODUCTION

Previous publications in this series (1, 2, 3, 4, 5) have described experimental work aimed at improving the accuracy of determination of disintegration rates using a 4π β-proportional counter. In one of these papers (4) Pate and Yaffe studied some of the scattering and absorption processes involved in a 4π steradian geometrical arrangement.

Normally, when the disintegration rate is to be determined, a sample is evaporated on a thin film and placed between two half-counters, the anodes of which are connected in parallel. It has been found by some workers that 'coincident' discharges occur in such an arrangement, i.e. both halves of the counter are discharged within the resolving time of the apparatus by a single disintegration. Pate and Yaffe attempted to fix the cause of these coincidences, in addition to studying the absorption and scattering of the radiation by the source-mounting film.

They have shown that if one uses thin films, of the order of a few hundred micrograms per square centimeter or less, these coincidences are due to backscattering of the radiation from the counter gas and counter walls. The frequency of occurrence of these discharges (as high as 20% of the disintegration rates of pure β-emitters even with very thin source mounts) allowed them to eliminate many other suggested causes of this phenomenon. Of those eliminated, only the possible production of secondary electrons, resulting from interaction between the incident β-radiation and the source-mounting film, will be enhanced by the thicker films used in this later study. For simplicity this is omitted in the ensuing treatment.

Following Pate and Yaffe (4) one can set up a simple model for the absorption and scattering processes which occur in a 4π-counter.

If both half-counter anodes are connected in parallel, then

$$[1] \qquad N_t = N_a + N_b - N_c$$

where N_t is the total counting rate, N_a and N_b are the half-counter rates, and N_c the coincidence rate.

[1]*Manuscript received March 7, 1960.*
Contribution from the Radiochemistry Laboratory, Department of Chemistry, McGill University, Montreal, Que., with financial assistance from the National Research Council of Canada.
[2]*Holder of a National Research Council Studentship.*
[3]*Present address: U.S. Nuclear, Burbank, California.*

Pate and Yaffe showed that the following relationship held:

$$N_a = \tfrac{1}{2}N_0[(1+P_2)+P_1P_5P_6] \quad [2]$$

$$N_b = \tfrac{1}{2}N_0[(1-P_2)P_1+P_5P_6] \quad [3]$$

$$N_c = \tfrac{1}{2}N_0(P_5P_6+P_1P_5P_6) \quad [4]$$

where N_0 = disintegration rate of the active sample,

P_1 = transmission of the film to incident β-radiation from the source,

P_2 = the probability that β-radiation originally emitted in the direction of one of the counter halves will be scattered by the film so as to enter the opposite counter half,

P_5 = the transmission of the film to backscattered radiation arising from wall and gas backscattering, and

P_6 = the probability that the β-radiation incident into either hemisphere is backscattered by the counter gas and/or counter walls so as to enter the other hemisphere ($= P_3+P_4$ as defined by Pate and Yaffe).

Values of P_6 were determined by Pate and Yaffe from experiments in which the coincidence rate between the two half-counters was measured with different counter gases and varying aperture sizes. They also obtained values of N_a, N_b, and N_c for a range of values of E, the maximum energy of the β-radiation, and d, the superficial density of the source mount. This enabled them to solve equations [2], [3], and [4] simultaneously and thus determine P_1, P_2, and P_5. Their results are being extended in this paper to greater source-mount superficial densities.

EXPERIMENTAL AND RESULTS

The β^--emitters used were Ni^{63}, S^{35}, Tl^{204}, and P^{32}. This gave a range of maximum energies of the β-radiation from 0.067 to 1.70 Mev. These nuclides were available in solutions which were either 'carrier-free' or of such a high specific activity that evaporation of a suitable aliquot produced a weightless point source on a thin gold-coated VYNS film (1) of superficial density 5–10 $\mu g/cm^2$, mounted on an aluminum ring of 2.5 cm diameter. The source mount was built up by laminating calibrated VYNS films on to the original source mount on the side opposite to that on which the active nuclide had been deposited. This was repeated until the total superficial density was of the order of 1 mg/cm^2.

Since the thickest film conveniently produced by the method previously described is only about 20 $\mu g/cm^2$, a different procedure was adopted for producing thicker films. The VYNS resin was dissolved in acetone and the solution poured into plane-bottom dishes floating on mercury. The acetone was allowed to evaporate slowly, the resultant film was peeled off and mounted on a ring. In this way uniform films of superficial densities up to 60 mg/cm^2 were obtained. The thicker films were rendered conducting by coating them with an evaporated film of gold. They were then placed temporarily in direct contact with the underside of the source-mount films to give a range of film thicknesses above the 1 mg/cm^2 region.

The 4π β-proportional gas counter was identical with that described previously. Each anode was operated as a separate unit so that individual half-counter rates and coincidence rates could be determined. Performance of each unit was carefully matched using the threshold of the plateau obtained with Ni^{63} as a criterion. Corrections were made for random coincidences as described in the previous paper.

Can. J. Chem. Downloaded from www.nrcresearchpress.com by 186.148.149.217 on 09/04/12
For personal use only.

N_a, N_b, and N_c were determined for the series of β^--emitters over a range of source-mount superficial densities. The total counting rate N_t, obtained from equation [1], was checked periodically against the counting rate obtained with both anodes connected in parallel.

The results obtained by plotting N_a, N_b, N_c, and N_t against the superficial density of the source mount are shown in Figs. 1–4 inclusive. The values of P_1 and P_5, obtained for the various nuclides, are shown in Figs. 5 and 6. The former shows data obtained with superficial densities up to 1 mg/cm², while the latter gives data to over 200 mg/cm².

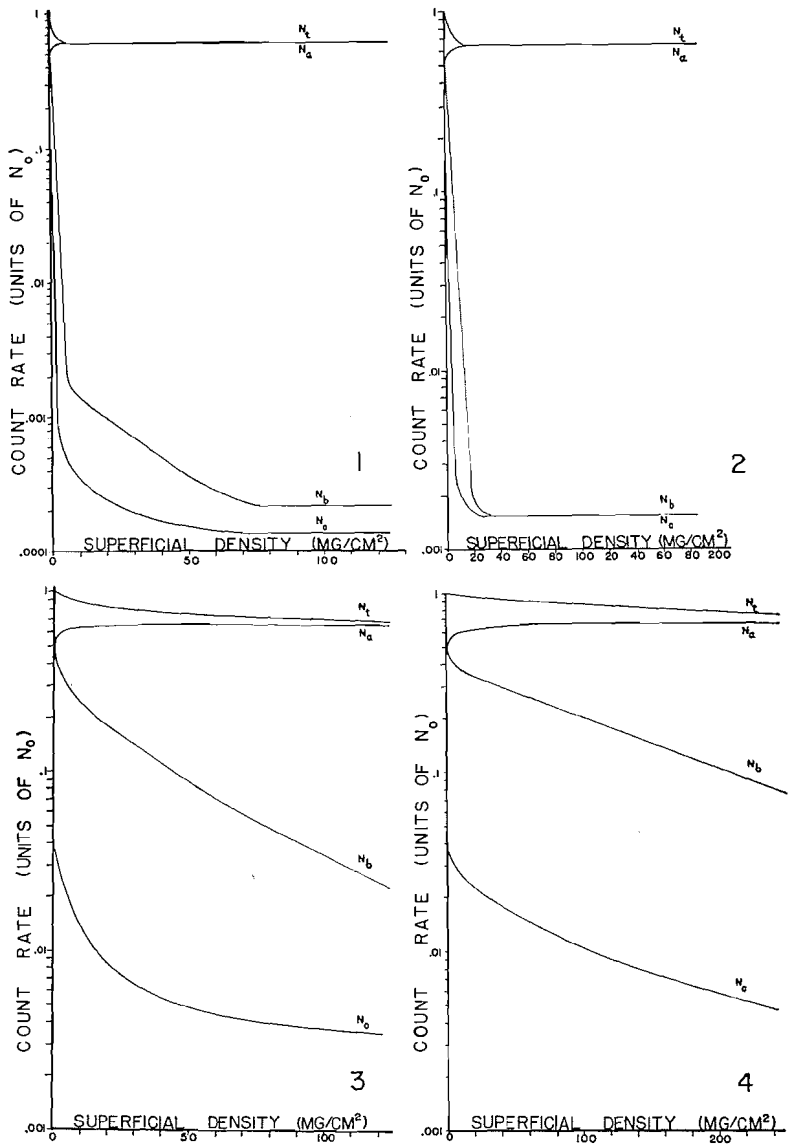


FIG. 1. Variation of N_A, N_B, N_C, and N_T with increase in superficial density of source mount for Ni^{63}.
FIG. 2. Variation of N_A, N_B, N_C, and N_T with increase in superficial density of source mount for S^{35}.
FIG. 3. Variation of N_A, N_B, N_C, and N_T with increase in superficial density of source mount for Tl^{204}.
FIG. 4. Variation of N_A, N_B, N_C, and N_T with increase in superficial density of source mount for P^{32}.

Can. J. Chem. Downloaded from www.nrcresearchpress.com by 186.148.149.217 on 09/04/12
For personal use only.

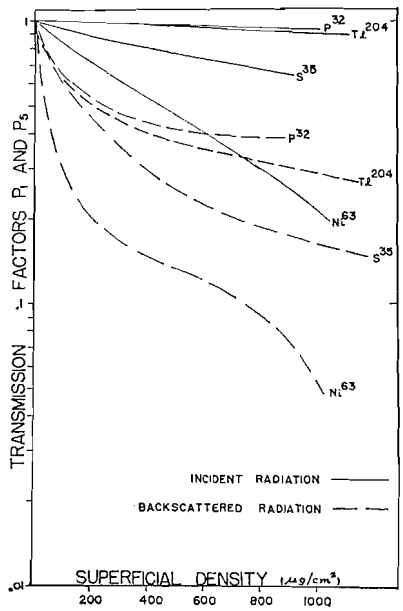


FIG. 5. Variation of transmission factors P_1 and P_5 with increasing superficial density of source mount (to 1 mg/cm²).

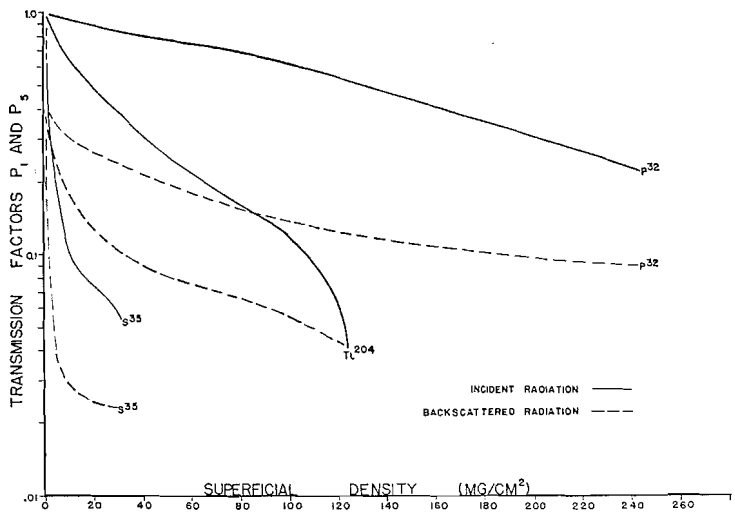


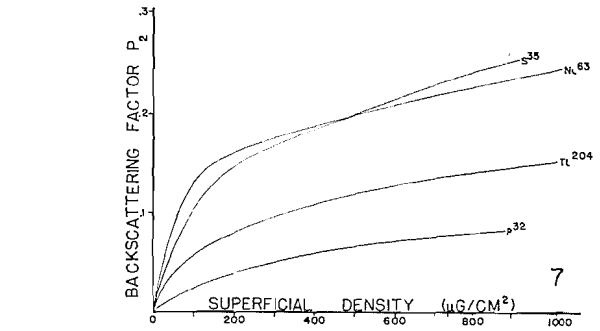
FIG. 6. Variation of transmission factors P_1 and P_5 with increasing superficial density of source mount (to 60 mg/cm²).

DISCUSSION

For small film thicknesses, less that 600 μg/cm², the backscattering data are essentially similar to those of Pate and Yaffe (4), and are shown in Fig. 7. However, the backscattering coefficients are somewhat lower, due possibly to the smaller amount of gold coating on the VYNS films in this series of experiments. As the film thickness increases above the range employed by Pate and Yaffe, as shown in Fig. 8, the curves assume the

Can. J. Chem. Downloaded from www.nrcresearchpress.com by 186.148.149.217 on 09/04/12
For personal use only.

juxtaposition similar to those obtained in $<2\pi$ geometrical arrangements (6, 7, 8), i.e. that nuclide with β-radiation of greatest maximum energy has the greatest backscattering factor.



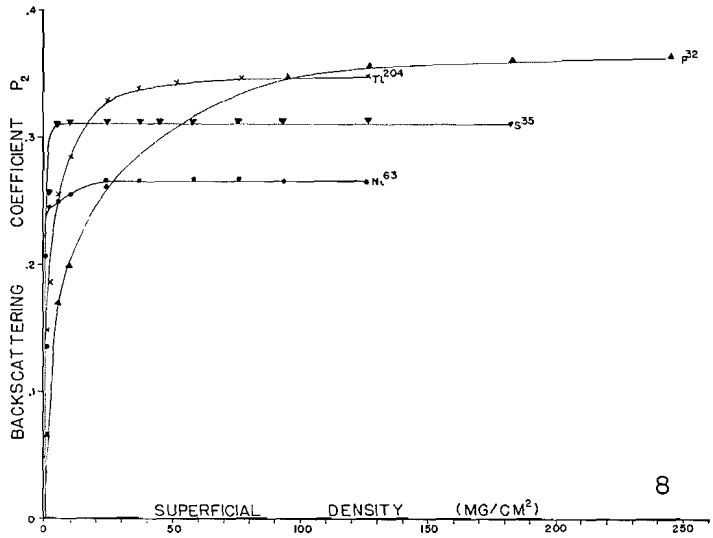


FIG. 7. Variation of the backscattering factor P_2 with increasing superficial density of source mount (to 1 mg/cm²).

FIG. 8. Variation of the backscattering factor P_2 with increasing superficial density of source mount (to 250 mg/cm²).

In Fig. 9 is shown the entire range on a logarithmic plot. The range of the β-radiation is indicated and, as in the case of $<2\pi$ geometrical systems, saturation backscattering is obtained with approximately that amount of material corresponding to about one-fifth the range of the β-radiation.

One can clearly note the transition from the single scattering events, observed with thin films, to the region of multiple scattering. The single scattering events involve electrons incident at small angles to the film and will be greatest for small electron energies as shown in Fig. 7. The behavior of this type of scattering has been described by McKinley and Feshbach (9) amongst others. As the film thickness increases the intermediate region of 'plural' scattering is encountered. The effect of β end-point energy is very pronounced in this region. With Ni^{63}, for example, the backscattering coefficient rises very rapidly and then attains a maximum value characteristic of the electron diffusion

Can. J. Chem. Downloaded from www.nrcresearchpress.com by 186.148.149.217 on 09/04/12
For personal use only.

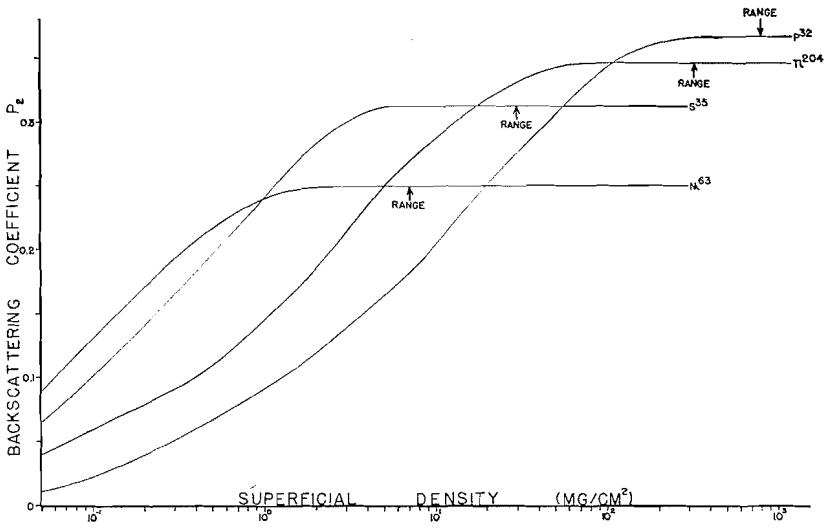


FIG. 9. Variation of the backscattering factor P_2 with the logarithm of the superficial density of the source mount.

type characterized as 'multiple' scattering. For P^{32}, however, the rise is gradual and the rate of change of slope to the maximum backscattering value is very much less than for Ni^{63}. The greater the β end-point energy, the greater is the region of 'plural' scattering.

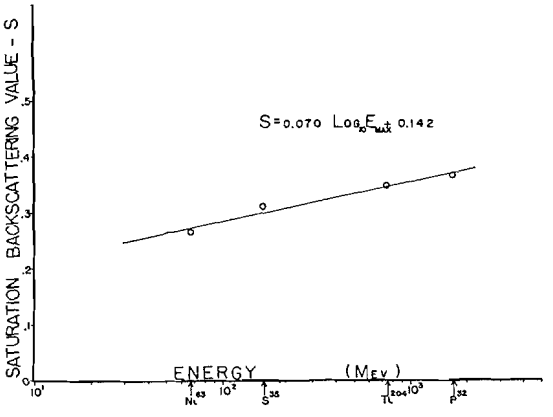


FIG. 10. Variation of the saturation backscattering value with the logarithm of the maximum energy of the β-emitter.

In Fig. 10 is shown the saturation backscattering value S plotted against the logarithm of the maximum energy of the β-radiation. This is essentially linear and follows the empirical equation

$$S = 0.070 \log_{10} E_{max} + 0.142.$$

The saturation backscattering factors found were much larger than those obtained in arrangements with much smaller geometrical efficiency. These are shown in Fig. 11,

Can. J. Chem. Downloaded from www.nrcresearchpress.com by 186.148.149.217 on 09/04/12
For personal use only.

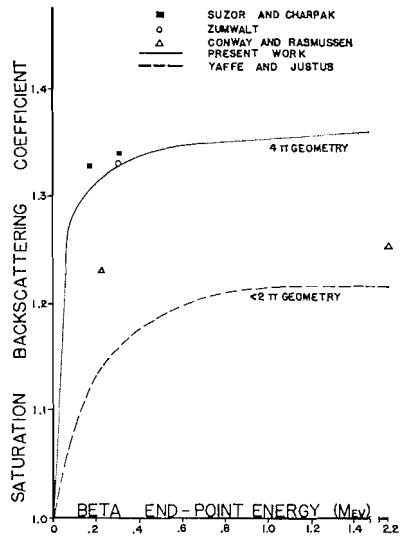


FIG. 11. Variation of saturation backscattering coefficient with β^- end-point energy.

together with extrapolated data for systems of $<2\pi$ geometrical efficiency of Yaffe and Justus (7) and Burtt (10) for saturation backscattering with backing material of mean atomic number $\bar{Z} = 11.2$, the mean atomic number of the VYNS film employed, where

$$\bar{Z} = (\sum_i n_i Z_i^2)/(\sum_i n_i Z_i).$$

Cooper and Yaffe (11) have shown that the above formulation gives the effective mean $\bar{Z}$ for backscattering by a compound where n_i refers to the number of atoms of an element of atomic number Z_i in the compound. The results in Fig. 11 agree with those of other workers who found that the backscattering effect is greater, the greater the geometrical efficiency of the detection system (6, 12, 13, 14).

The increased backscattering coefficient is undoubtedly due to the detection in windowless 2π- or 4π-counters of backscattered radiation degraded too much in energy to pass through the window of a Geiger tube. The extent of energy degradation is evident from Figs. 5 and 6, from the previous work by Pate and Yaffe (4), and the observation by Balfour (15) of a large portion of low-energy rays in the spectrum of backscattered radiation. Another reason why some of these low-energy backscattered particles miss detection in small geometry systems is the fact, ascertained by Brownell (16), that the average energy for backscattered radiation varies with the angle of scattering, with a greater amount of particles having a lower average energy at low scattering angles.

Published data dealing with saturation backscattering coefficients in windowless counters of geometrical systems of 2π or greater are very sparse, so that comparison with present results is very difficult. Suzor and Charpak (17) obtained saturation backscattering coefficients for S^{35} and Co^{60} with aluminum in a 4π-counter. However, since they used the 'sandwich' technique for determining the absolute disintegration rates, their results are slightly in error (4). Their values are shown in Fig. 11 for comparison. Zumwalt's (6) values for Co^{60} in a 2π-counter, extrapolated to $\bar{Z} = 11.2$, are also shown for comparison. Conway and Rasmussen's (14) values for Pm^{147} and Sr^{90}–Y^{90}, determined in a 2π-counter, included in the same diagram, are much lower than ours or those of Zumwalt.

Can. J. Chem. Downloaded from www.nrcresearchpress.com by 186.148.149.217 on 09/04/12
For personal use only.

Christian *et al.* (18) determined backscattering coefficients for Ni^{63}, Co^{60}, P^{32}, and S^{35} in a 2π-counter. Their value for Ni^{63} corresponds well with ours. However, their other points seem too erratic and unsystematic to be very useful.

If one examines equations [2], [3], and [4], it is apparent that, as d, the thickness of film, increases beyond the range of the backscattered and incident β^--radiation, then P_5 and P_1 approach zero. This would mean that N_b and N_c would approach zero. Examination of Figs. 1–4 shows that the curves do not reach zero, but level off (as is shown markedly in the case of the weaker β^--emitters). It seems obvious then that the assumptions made in the derivation of the above equations, i.e. that the only processes causing coincidences are counter wall- and gas-scattering, are only approximate. As the film thickness is increased other phenomena, such as bremsstrahlung or secondary electron production, begin to play a role.

It has been shown by Bolgiano *et al.* (19) that the probability of inner bremsstrahlung production is in the order of 10^{-4}. Thus, coupled with the low probability for detection of photons in the 4π-counter, this process will contribute very little.

The radiation from external bremsstrahlungen has a maximum photon energy equal to the energy of the β-radiation and an intensity proportional to the mean atomic number of the absorbing material. It has been shown (20) that the fraction of the β-energy, which appears as external bremsstrahlung, is given approximately by $\bar{Z}E_{max}/3000$. For VYNS and P^{32} this amounts to about 0.5%. As before, this low probability and the low probability of photon detection would only contribute a small amount to the coincidences taking place.

This then leaves secondary electron production. Their liberation by the photoelectric effect may again be ignored owing to the low probability, of the order of 10^{-4}. However, if an electron of initial energy E produces by collision two electrons of energy W and $E-W$, then Mott (21) has shown that the number of secondary electrons, I, produced in a distance dx, in the energy range W to $W-dW$ is

$$I = \bar{Z}N\,dx\,d\phi\,(E, W) \qquad [5]$$

where $\bar{Z}$ is the mean atomic number of the stopping material and N the number of atoms per square centimeter of the stopping material.

The differential scattering cross section $d\phi\,(E, W)$ has been determined by Page (22). He found that, for β^--radiation between 0.6 and 1.7 Mev, the value of $d\phi\,(E, W)$ in collodion was of the order of 10^{-24} cm^2. If this value is substituted into equation [5], taking $\bar{Z} = 11.2$, $N \approx 10^{23}$, and $dx \approx 0.1$ cm, then $I = 0.10$. This is now a reasonably high probability, so that this process can no longer be ignored since every electron produced will be detected.

This, of course, cannot account for the 'coincident discharge' with films of thickness greater than the range of the original β-radiation, e.g. in the case of Ni^{63}. In these instances, the discharges must be due to a combination of causes which could include bremsstrahlungen from the counter gas and walls, the bremsstrahlungen discussed above, and perhaps a small contribution from a hard cosmic ray component which would trigger both counters contributing to the coincidences.

Pate and Yaffe (3) have determined the absorption parameter (N_T/N_0) as a function of β end-point energy for a series of film thicknesses. This is shown in Fig. 3 in their paper. These data have been extended, as shown in Fig. 12 of this paper, to lower energies with the inclusion of results obtained by the study of H^3 (E_{max} = .018 Mev). The added data fall into place in very satisfactory fashion.

Can. J. Chem. Downloaded from www.nrcresearchpress.com by 186.148.149.217 on 09/04/12
For personal use only.

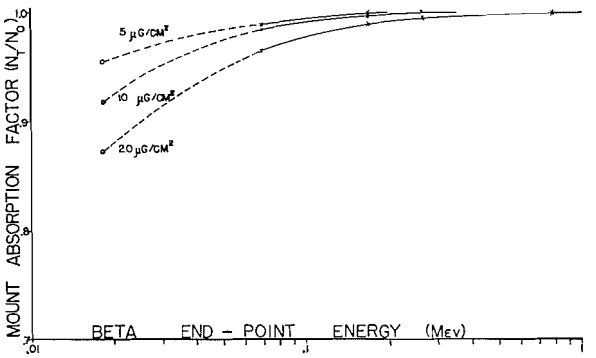


FIG. 12. Absorption parameter (N_T/N_0) as a function of β end-point energy. The data of Pate and Yaffe (3) are extended to lower end-point energies.

ACKNOWLEDGMENTS

The authors are indebted to Dr. R. E. Bell and Dr. B. D. Pate for valuable discussions during the preparation of this manuscript.

REFERENCES

1. B. D. PATE and L. YAFFE. Can. J. Chem. **33**, 15 (1955).
2. B. D. PATE and L. YAFFE. Can. J. Chem. **33**, 610 (1955).
3. B. D. PATE and L. YAFFE. Can. J. Chem. **33**, 929 (1955).
4. B. D. PATE and L. YAFFE. Can. J. Chem. **33**, 1656 (1955).
5. B. D. PATE and L. YAFFE. Can. J. Chem. **34**, 265 (1956).
6. L. R. ZUMWALT. U.S. Atomic Energy Comm., Rept. MDDC 1346 (1949).
7. L. YAFFE and K. M. JUSTUS. J. Chem. Soc. Suppl. S341 (1949).
8. B. P. BURTT. Nucleonics, **5**, 28 (1949).
9. W. A. MCKINLEY, JR. and H. FESHBACH. Phys. Rev. **74**, 1759 (1948).
10. B. P. BURTT. Preliminary Report No. 8, Nuclear Science Ser., N.R.C., Washington, D.C. (1950).
11. M. COOPER and L. YAFFE. To be published.
12. C. J. BORKOWSKI. Preliminary Report No. 8, Nuclear Science Ser., N.R.C., Washington, D.C. (1950).
13. L. MEYER-SCHÜTZMEISTER and D. H. VINCENT. Z. Physik, **134**, 9 (1952).
14. D. CONWAY and J. RASMUSSEN. U.S. Atomic Energy Comm., Rept., UCRL-2075 (1953).
15. J. BALFOUR. J. Sci. Instr. **31**, 395 (1954).
16. G. J. BROWNELL. Nucleonics, **10** (6), 41 (1952).
17. F. SUZOR and G. CHARPAK. J. phys. radium, **13**, 1 (1952).
18. D. CHRISTIAN, W. W. DUNNING, and D. S. MARTIN. Nucleonics, **10** (5), 41 (1952).
19. P. BOLGIANO, L. MADANSKY, and F. RASETTI. Phys. Rev. **89**, 679 (1953).
20. R. D. EVANS. The atomic nucleus. McGraw-Hill Book Co., New York. 1955. p. 619.
21. N. F. MOTT. Proc. Roy. Soc. A, **126**, 259 (1930).
22. L. A. PAGE. Phys. Rev. **81**, 1062 (1951).

Can. J. Chem. Downloaded from www.nrcresearchpress.com by 186.148.149.217 on 09/04/12
For personal use only.

Can. J. Chem. Downloaded from www.nrcresearchpress.com by 186.148.149.217 on 09/04/12
For personal use only.

THE REACTION OF SULPHURYL CHLORIDE WITH GLYCOSIDES AND SUGAR ALCOHOLS. PART II[1]

J. K. N. Jones, M. B. Perry, and J. C. Turner

ABSTRACT

The structures of methyl 4,6-dichloro-4,6-dideoxy-α-D-hexoside and methyl "4-chloro-4-deoxy-β-pentoside" (I) have been investigated. The desulphation reaction leading to the formation of the latter compound is described. Replacement of the hydroxyl group at $C_{(4)}$ by a chlorine atom in both compounds is shown to have occurred with inversion of configuration.

INTRODUCTION

In Part I (1) the product of the reaction of sulphuryl chloride with methyl α-D-glucopyranoside was shown to be probably methyl 4,6-dichloro-4,6-dideoxy-α-D-hexoside 2,3-sulphate which on desulphation gave methyl 4,6-dichloro-4,6-dideoxy-α-D-hexoside (I). It was possible that the replacement of the hydroxyl group at $C_{(4)}$ by the chlorine atom had occurred with inversion of configuration to give the galactose configuration.

This problem was investigated using a synthetic route to a methyl 4,6-dichloro-4,6-dideoxy-α-D-hexoside of known configuration. Methyl 4-chloro-4-deoxy-α-D-glucopyranoside was synthesized by the method of Buchanan (2). Reaction with sulphuryl chloride and subsequent desulphation gave a complex mixture from which was isolated methyl 4,6-dichloro-4,6-dideoxy-α-D-glucopyranoside (II) which was found to be different from that obtained from the reaction of sulphuryl chloride with methyl α-D-glucopyranoside (I). It was found that II consumed periodate extremely slowly (1.04 moles, 167 hours) and this bore some resemblance to the parent methyl 4-chloro-4-deoxy-α-D-glucopyranoside which was oxidized under somewhat similar conditions (1.03 moles, 170 hours) (3, 3*a*). Accordingly the chlorine atom at $C_{(4)}$ of I was placed in the galactose configuration since this was the only position in which I and II differed.

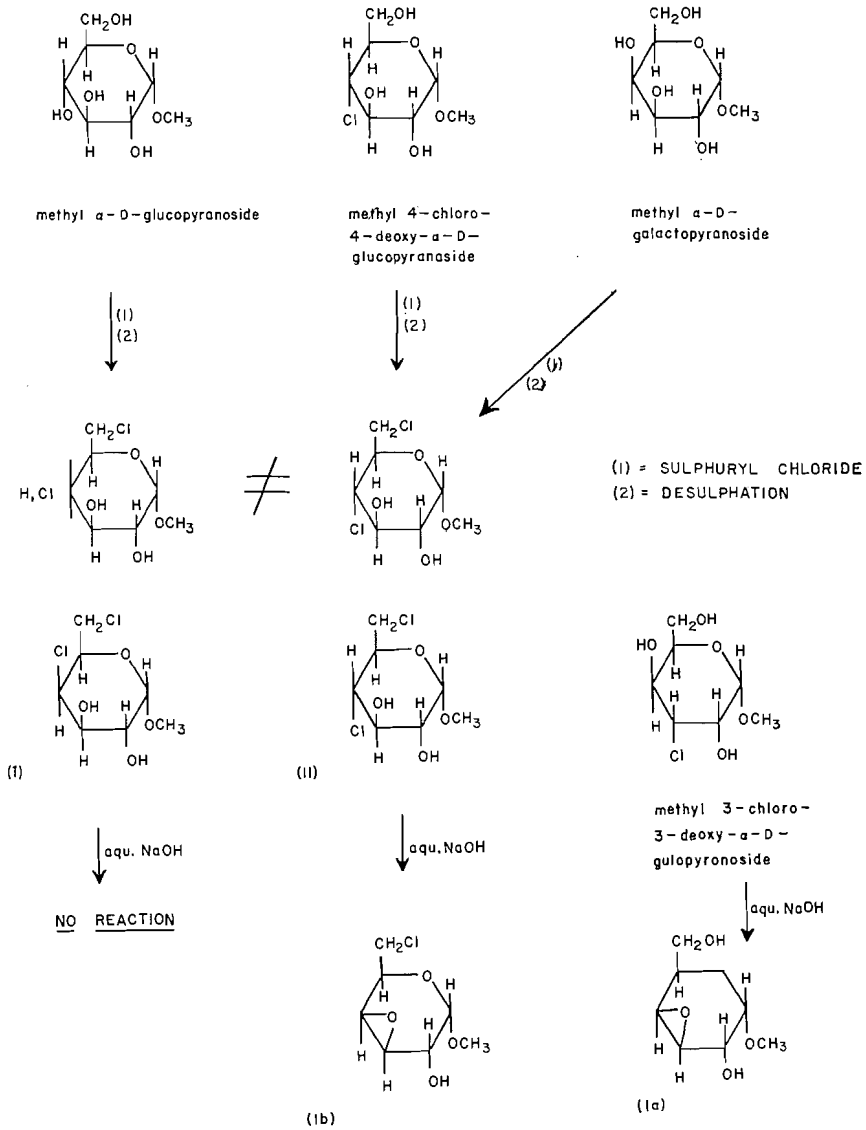
Further evidence as to the configuration at $C_{(4)}$ of I was obtained when the reaction of sulphuryl chloride with methyl α-D-galactopyranoside was examined. Desulphation of the fully substituted product gave a complex mixture from which was isolated a methyl dichloro-dideoxy-α-D-hexoside identical with II.

Compound I did not react with sodium hydroxide, whereas II lost approximately 1 equivalent of chlorine under the same conditions probably to give I*b*. It was found that methyl 3-chloro-3-deoxy-α-D-gulopyranoside, with sodium hydroxide, lost chlorine to give methyl 3,4-anhydro-α-D-galactopyranoside (I*a*) in good yield. These findings were related to the configurations of the chlorine atom at $C_{(4)}$ and the hydroxyl group at $C_{(3)}$ in I and II, and it was concluded that a trans configuration was necessary for the elimination of chlorine from $C_{(4)}$ to take place.

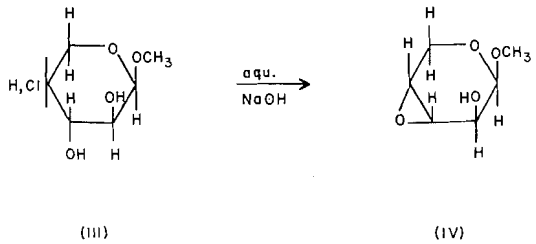
Since the threo configuration was retained in I at $C_{(2)}$ and $C_{(3)}$ during desulphation (1) and the $C_{(3)}$ and $C_{(4)}$ hydroxyl group and chlorine atom were cis disposed it was concluded that I possessed the galactose configuration and that elimination of hydroxyl at $C_{(4)}$ by chlorine had occurred with inversion of configuration.

Accordingly I would be methyl 4,6-dichloro-4,6-dideoxy-α-D-galactopyranoside, and the fully substituted compound from which it was obtained by desulphation would be methyl 4,6-dichloro-4,6-dideoxy-α-D-galactopyranoside 2,3-sulphate.

[1]*Manuscript received February 29, 1960.*
Contribution from the Chemistry Department, Queen's University, Kingston, Ontario.

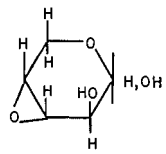


The monochloro monodeoxy pentoside (III) from methyl β-D-arabinopyranoside possessed the chlorine atom at $C_{(4)}$ (1). On treatment of III with sodium hydroxide, chlorine was eliminated, presumably with the formation of the anhydro pentoside (IV).

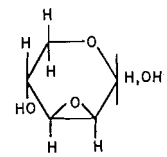


Can. J. Chem. Downloaded from www.nrcresearchpress.com by 186.148.149.217 on 09/04/12
For personal use only.

On hydrolysis IV gave two pentoses, D-lyxose and xylose. (The latter was not completely characterized as only a small amount was produced.) The structure of IV was therefore very probably as written, namely, methyl 3,4-anhydro-β-D-arabinopyranoside. As shown previously, elimination of chlorine under the influence of sodium hydroxide occurred when the chlorine atom and hydroxyl group involved were trans to one another. Since the configuration of the hydroxyl groups on $C_{(2)}$ and $C_{(3)}$ did not change on desulphation (1) and $C_{(3)}$ and $C_{(4)}$ groups were trans, III possessed the L-xylose configuration and was therefore methyl 4-chloro-4-deoxy-α-L-xylopyranoside. The fully substituted compound from which III was obtained by desulphation also possessed the L-xylose configuration and was methyl 4-chloro-4-deoxy-α-L-xylopyranoside 2,3-sulphate. The desulphation of the latter compound was investigated more fully. In addition to methyl 4-chloro-4-deoxy-α-L-xylopyranoside and 4-chloro-4-deoxy-L-xylose, five other compounds were isolated in small amount from the desulphated mixture. They were: two anhydro pentoses, D-lyxose, xylose, and D-arabinose. One anhydro pentose (V) gave on hydrolysis xylose and lyxose, while the other (VI) gave xylose and arabinose which were identified chromatographically because the pentoses were present in too small an amount to be completely characterized in this instance.



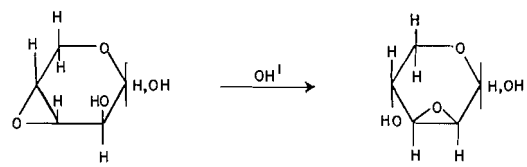
V(3,4-anhydro-D-arabinose)



VI(2,3-anhydro-D-lyxose)

Very probably V and VI gave rise to D-lyxose, xylose, and D-arabinose during the second stage of desulphation (treatment with 2 *N* sulphuric acid). The mechanism of formation of VI is less certain but a possible explanation is outlined below.

An apparently anomalous reaction is proposed in the conversion of methyl 3,4-anhydro-β-D-arabinopyranoside 2-sulphate (a postulated reaction intermediate) to methyl 2,3-anhydro-β-D-lyxopyranoside by 2 *N* sulphuric acid. Reactions of the type V $\rightarrow$ VI are



(V) (VI)

known to occur, under the influence of alkali (4), but not in an acid medium. However, no free ionic sulphate could be detected after the first stage of desulphation (treatment with methanolic ammonia) and the sulphate residue remaining on $C_{(2)}$ would presumably prevent migration of the epoxide ring from $C_{(3)}$–$C_{(4)}$ to $C_{(2)}$–$C_{(3)}$. Therefore the migration was presumed to occur in the second stage in which the sulphate residue was removed (treatment with 2 *N* sulphuric acid).

The initial reaction in the desulphation, the cleavage of the cyclic sulphate ring with

Can. J. Chem. Downloaded from www.nrcresearchpress.com by 186.148.149.217 on 09/04/12
For personal use only.

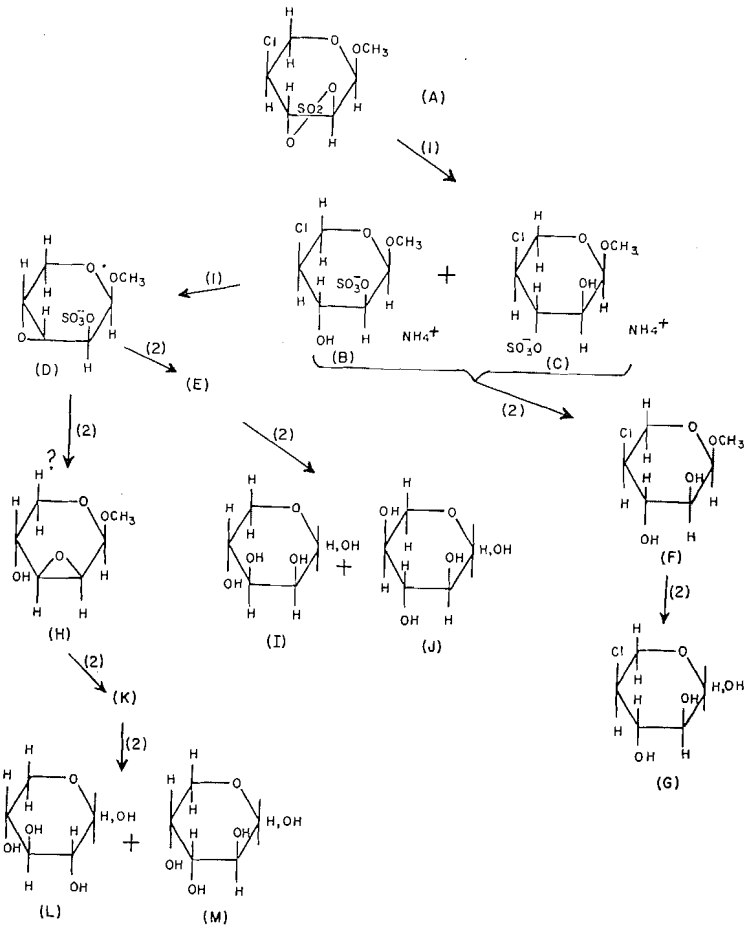


FIG. 1. The desulphation of methyl 4-chloro-4-deoxy-α-L-xyloside 2,3-sulphate (A).
LEGEND: First stage of desulphation ($MeOH/NH_3$) (1).
Second stage of desulphation (2 *N* H_2SO_4) (2).
(B) and (C) Ammonium salts of opened sulphate ring. (D) 3,4-Anhydro-β-D-arabinose 2-sulphate. (E) 3,4-Anhydro-D-arabinose. (F) Methyl 4-chloro-4-deoxy-L-xylose. (G) 4-Chloro-4-deoxy-L-xylose. (H) 2,3-Anhydro-β-D-lyxoside. (I) D-Lyxose. (J) L-Xylose. (K) 2,3-Anhydro-D-lyxose. (L) D-Xylose. (M) D-Arabinose.

ammonia, very probably gave two compounds ((B) and (C) in diagram). The ratio of (B) to (C) was not known, but it was unlikely that a very high proportion of (B) was present, as chlorine would then have been eliminated by the methanolic ammonia due to the trans configuration of the chlorine atom on $C_{(4)}$ and the hydroxyl group on $C_{(3)}$.

An analogous sequence of reactions leading to the formation of complex mixtures would be expected to occur with all those fully substituted derivatives containing a chlorine atom trans to an adjacent potential secondary hydroxyl group, and this was found to be the case (see above) with methyl 4,6-dichloro-4,6-dideoxy-α-D-glucopyranoside 2,3-sulphate. The corresponding derivative from methyl α-D-glucopyranoside, possessing the galactose configuration, gave only methyl 4,6-dichloro-4,6-dideoxy-α-D-galactopyranoside (I) and 4,6-dichloro-4,6-dideoxy-D-galactose on desulphation.

Can. J. Chem. Downloaded from www.nrcresearchpress.com by 186.148.149.217 on 09/04/12
For personal use only.

Can. J. Chem. Downloaded from www.nrcresearchpress.com by 186.148.149.217 on 09/04/12
For personal use only.

EXPERIMENTAL

Melting points are uncorrected and were determined on a Kofler microheating stage. All evaporations were carried out under reduced pressure. Optical rotations were measured in water at 21±3° C unless otherwise stated. Paper chromatograms were run using a descending flow (5) and Whatman No. 1 paper in the following solvent systems:

(*a*) butan-1-ol:ethanol:water (3:1:1),
(*b*) butan-1-ol:pyridine:water (10:3:3),
(*c*) ethyl acetate:acetic acid:formic acid:water (18:3:1:4).

Reaction of Sulphuryl Chloride with Methyl 4-Chloro-4-deoxy-α-D-glucopyranoside

The chloro sugar was obtained as a syrup contaminated with a small amount of methyl 3-chloro-3-deoxy-α-D-gulopyranoside, by the method of Buchanan (2). The syrup (0.5 g) gave with sulphuryl chloride a pale yellow syrup (0.388 g) containing sulphur and chlorine. On desulphation first with methanolic ammonia and then with 2 *N* sulphuric acid in the usual manner (1) a complex mixture was obtained (0.180 g) which consisted of seven components of R_f values 0.19, 0.21, 0.40, 0.48, 0.73, 0.78, 0.81, in solvent (*a*). Alkaline silver nitrate spray (6) was used to detect the sugars. An aqueous solution of the mixture was continuously extracted with chloroform for 24 hours. The chloroform extract on evaporation gave a syrup (43 mg) which crystallized. The syrup contained the three components R_f 0.73, R_f 0.78, R_f 0.81, of which the component R_f 0.78 was the major one. The syrupy crystals were recrystallized twice from chloroform/light petroleum (60°–80° C) to give white needles of melting point 119–121° C and $[\alpha]_D$ +121° (*c*, 1.8). Analysis: Calc. $C_7H_{12}O_4Cl_2$: C, 36.4%; H, 5.2%. Found: C, 37.0%; H, 5.3%.

Periodate Oxidation of the Methyl Dichloro-dideoxy-α-D-hexoside Prepared from Methyl 4-Chloro-4-deoxy-α-D-glucopyranoside

The oxidation was carried out at 25° C, using a small sample (8.5 mg) of the compound in distilled water (25 ml) containing 0.3 *M* sodium metaperiodate (1 ml). The results are shown below and are compared with those of Buchanan (3) for methyl 4-chloro-4-deoxy-α-D-glucopyranoside.

TABLE I

Substance	Time of oxidation (hours)	Consumption of periodate (mole/molecule)	Acid production (mole/molecule)
Methyl dichloro-dideoxy-α-D-hexoside	3.8	0.195	
	10	0.310	
	24.5	0.415	
	167	1.04	
	243	1.07	0.00
Methyl 4-chloro-4-deoxy-α-D-glucopyranoside	20	0.42	
	40	0.58	Not reported
	170	1.03	
	212	1.06	

Reaction of Sulphuryl Chloride with Methyl α-D-Galactopyranoside

Methyl α-D-galactopyranoside was prepared by the method of Dale and Hudson (7), purified by recrystallization from hot absolute ethanol, and dried *in vacuo* at 40° C. With sulphuryl chloride, methyl α-D-galactopyranoside (5 g) gave a brown syrup (3.7 g)

which contained chlorine and sulphur (sodium fusion). The syrup could not be obtained crystalline.

Desulphation of the syrup with methanolic ammonia and 2 *N* sulphuric acid gave a mixture (0.73 g) containing four components of R_f values 0.12, 0.22, 0.42 (major component), 0.71 (solvent (*a*); alkaline silver nitrate and anisidine hydrochloride (8) sprays). An aqueous solution of the mixture was continuously extracted with chloroform for 24 hours. The chloroform extract on evaporation gave a colorless syrup (0.3 g). On nucleation with the methyl dichloro-dideoxy-α-D-hexoside which had been prepared from methyl 4-chloro-4-deoxy-α-D-glucopyranoside (see above) rapid crystallization occurred.

When recrystallized from chloroform/light petroleum (60°–80° C) the crystals had a melting point of 119–121° C, mixed melting point with the above compound 119–121° C, $[\alpha]_D$ +122° (*c*, 1.9) and were therefore identical with that compound. Analysis: Calc. for $C_7H_{12}O_4Cl_2$: Cl, 30.7%. Found (Schöniger combustion method (9)): Cl, 30.4%.

The Reaction of Chloro Sugars with Sodium Hydroxide

The Methyl 4,6-Dichloro-4,6-dideoxy-α-D-hexoside from Methyl α-D-Glucopyranoside (1)

The hexoside (150 mg) was dissolved in water (25 ml) and phenolphthalein was added. The solution was then titrated with 0.232 *N* sodium hydroxide solution. No sodium hydroxide was neutralized even after 4 hours at 40° C. The solution was deionized with resin and the eluate concentrated to a crystalline mass (151 mg). The crystals had a melting point of 156–158° C and mixed melting point with the starting material, 156–158° C. Analysis: Calc. for $C_7H_{12}O_4Cl_2$: Cl, 30.7%. Found: starting material, 31.0%; product, 31.4%.

The Methyl Dichloro-dideoxy-α-D-hexoside from Methyl α-D-Galactopyranoside

The hexoside (m.p. 119–121° C, 0.875 mg) was dissolved in distilled water (1 ml) and sodium hydroxide solution (1 ml of 0.01 *N*) was added. The solution was allowed to stand for 6 hours at room temperature, then neutralized exactly with 0.01 *N* sulphuric acid, using screened methyl red – methylene blue indicator. To the neutralized solution was added neutralized mercuric oxycyanide solution (5 ml of 2% solution) and the resultant alkaline solution titrated to exact neutrality with 0.01 *N* sulphuric acid. The titer was 0.330 ml, which corresponded to the elimination of 0.88 mole chlorine per molecule of hexoside. The titration mixture was deionized with resin and examined on paper chromatograms. Three components were observed of R_f values 0.04 (faint), 0.38 (major component), 0.71 (faint co-chromatographing with starting material) (solvent (*a*), alkaline silver nitrate spray).

The Methyl 3-Chloro-3-deoxy-α-D-gulopyranoside (2)

The gulopyranoside (164 mg) was dissolved in water (25 ml) and titrated with sodium hydroxide (0.232 *N*) as described above. The solution took up 1 equivalent (3.31 ml) of sodium hydroxide over a period of 72 hours at 40° C and was then evaporated to dryness. The residue was extracted three times with 100-ml portions of boiling ether. The combined ether extracts on evaporation gave a syrup (101 mg, 74%) which rapidly crystallized. The crystals had a melting point of 117–118° C undepressed on admixture with an authentic specimen of methyl 3,4-anhydro-α-D-galactopyranoside (m.p. 117.5–118.5° C).

The Methyl 4-Chloro-4-deoxy-β-pentoside from Methyl β-D-Arabinopyranoside (1)

The pentoside (67 mg) was dissolved in water (3.0 ml) and sodium hydroxide solution

Can. J. Chem. Downloaded from www.nrcresearchpress.com by 186.148.149.217 on 09/04/12
For personal use only.

(0.45 ml of 0.232 *N*) was added. The change in optical rotation was followed at intervals up to 5 hours.

TABLE II

Time of reaction (hours)	$[\alpha]_D$
0	+108°
0.25	+82°
0.50	+73°
1.0	+72°
1.75	+63°
4.0	+61°
5.0	+59°

The slight excess of sodium hydroxide remaining after 8 hours was neutralized with nitric acid, the solution evaporated to dryness, and the residue extracted with ether. The extract on evaporation gave a colorless syrup (47 mg), while the residue gave a positive test for ionic chloride. The syrup gave one main spot, R_f 0.53 (solvent (*a*)), on paper chromatograms. The syrup was heated with 2 *N* sulphuric acid at 100° C for 14 hours, neutralized with barium carbonate, filtered, and deionized with resin. The eluate was concentrated to a colorless syrup (30 mg) which consisted of xylose and lyxose as shown by paper chromatograms, and paper electrophoresis in pH 9.5 borate buffer at 2500 volts for 40 minutes. An attempted separation of the pentoses using phenol saturated with water as the chromatographic solvent (10) with a descending flow on Whatman 3MM paper was unsuccessful. The pentoses were separated by paper electrophoresis under the conditions mentioned above. The lyxose (10 mg) $[\alpha]_D$ −18° (*c*, 1) was characterized by its rate of movement on chromatograms and as its phenyl osazone, m.p. 158–161° C, unchanged on admixture with authentic D-lyxose (xylose) phenylosazone (11). The xylose could not be satisfactorily characterized due to its small amount (ca. 2 mg).

The Desulphation of Methyl 4-Chloro-4-deoxy-β-pentoside 2,3-Sulphate (1)

The desulphated mixture (0.9 g) was separated on a cellulose column using butan-1-ol: water (19:1). Besides methyl 4-chloro-4-deoxy-β-pentoside and 4-chloro-4-deoxy pentose, four other fractions were isolated: Fraction I, a syrup (53 mg) with R_f 0.44 (in solvent (*a*)) was obtained. On hydrolysis with sulphuric acid it gave xylose and lyxose, identified by paper chromatography and paper electrophoresis: Fraction II was a syrup (15 mg) with R_f 0.39 (solvent (*a*)). On hydrolysis it gave xylose and arabinose, identified by paper chromatography and paper electrophoresis. Fraction III was a syrup (78 mg) with R_f 0.24 (solvent (*a*)). This fraction consisted of xylose and lyxose as shown by paper chromatograms and paper electrophoresis. A partial separation was achieved on a column of Dowex 50W sulphuric acid resin (86×2.2 cm, 8% cross-linked with divinyl benzene, 200–400 mesh, barium salt form). The lyxose was obtained pure, and characterized as its *p*-toluene sulphonhydrazone (12), m.p. 152–153° C, which did not depress the melting point of authentic D-lyxose *p*-toluene sulphonhydrazone (141° C). The xylose could not be completely characterized. Fraction IV, syrupy crystals (51 mg), R_f 0.214 (solvent (*a*)), consisted of D-arabinose as shown by paper chromatograms. It was contaminated with some water-insoluble material and had $[\alpha]_D$ −74° (5 minutes) → −66° (8 hours) (*c*, 0.4 in methanol). It was characterized as the benzoyl hydrazone, m.p. 190–195° C, undepressed on admixture with authentic D-arabinose benzoyl hydrazone, m.p. 190–195° C (13).

Can. J. Chem. Downloaded from www.nrcresearchpress.com by 186.148.149.217 on 09/04/12
For personal use only.

ACKNOWLEDGMENTS

One of the authors (J. C. T.) wishes to express his thanks to Dr. R. Wall for practical aid with the Dowex 50W resin column, to Dr. P. D. Bragg for helpful advice and to the National Research Council for a grant.

REFERENCES

1. P. D. BRAGG, J. K. N. JONES, and J. C. TURNER. Can. J. Chem. **37**, 1412 (1959).
2. J. G. BUCHANAN. J. Chem. Soc. 2511 (1958).
3. J. G. BUCHANAN. J. Chem. Soc. 995 (1958).
3*a*. J. G. BUCHANAN. Personal communication.
4. W. M. G. LAKE and S. PEAT. J. Chem. Soc. 1069 (1939).
5. S. H. PARTRIDGE. Biochem. J. **42**, 238 (1948).
6. W. E. TREVELYAN, D. D. PROCTOR, and J. S. HARRISON. Nature, **166**, 444 (1950).
7. J. K. DALE and C. S. HUDSON. J. Am. Chem. Soc. **52**, 2534 (1930).
8. L. HOUGH, J. K. N. JONES, and W. H. WADMAN. J. Chem. Soc. 1702 (1950).
9. W. SCHONIGER. Mikrochim. Acta, 123 (1955).
10. L. HOUGH and J. K. N. JONES. J. Chem. Soc. 1122 (1951).
11. H. I. WHEELER and B. TOLLENS. Ber. **22**, 1046 (1889).
12. D. G. EASTERBY, L. HOUGH, and J. K. N. JONES. J. Chem. Soc. 3416 (1951).
13. E. L. HIRST, J. K. N. JONES, and E. A. WOODS. J. Chem. Soc. 1048 (1947).

Can. J. Chem. Downloaded from www.nrcresearchpress.com by 186.148.149.217 on 09/04/12
For personal use only.

Can. J. Chem. Downloaded from www.nrcresearchpress.com by 186.148.149.217 on 09/04/12
For personal use only.

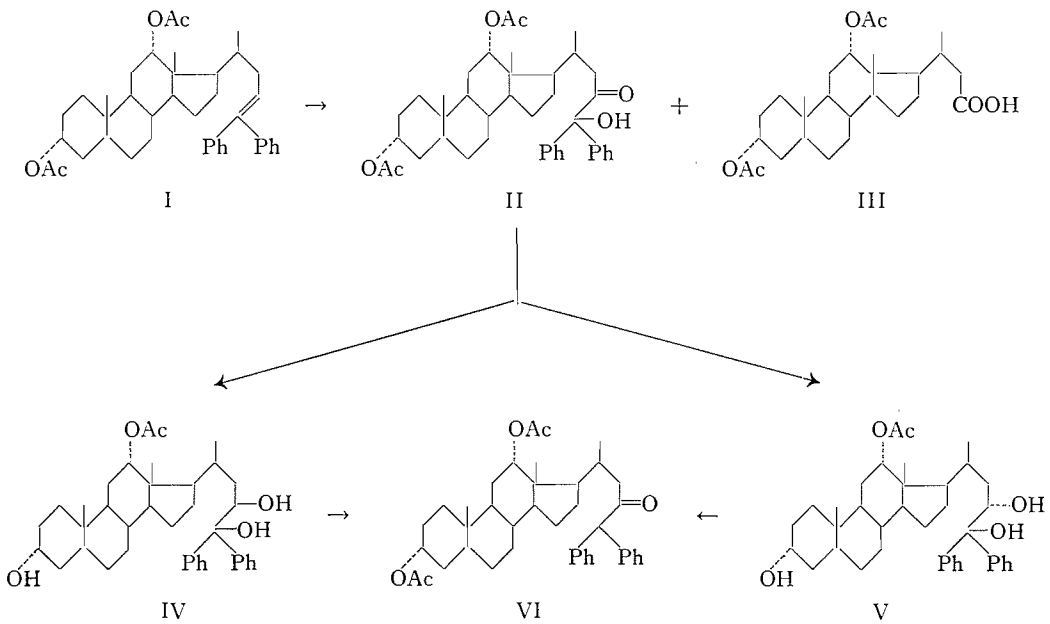
BILE ACID DERIVATIVES[1]

A. A. Amos and P. Ziegler

ABSTRACT

The potassium permanganate oxidation of 3α,12α-diacetoxy-24,24-diphenyl-Δ^{23}-cholene yielded a new compound which was identified as 3α,12α-diacetoxy-23-keto-24-hydroxy-24,24-diphenylcholane. The latter steroid, on reduction with sodium borohydride, produced two isomeric glycols which were subsequently dehydrated to provide the corresponding 23-keto-24,24-diphenyl derivative.

Desoxycholic acid is used extensively as a starting material for the preparation of steroidal hormones. One important phase of this conversion consists of the partial degradation of the bile acid side chain which is attached to C-17 of the steroid nucleus. This degradation can be accomplished by the classical Barbier–Wieland procedure, or preferably by the Miescher–Wettstein (1) scheme. Both methods produce the acetylated diphenylethylene derivative I as an intermediary product. According to the directions of Miescher and Wettstein, I is brominated in the allylic position, then dehydrobrominated to the corresponding diene, which in turn is oxidized to the 20-ketone. It has been found in our laboratories that the dienes thus produced are often contaminated with the ethylene derivative I; this impurity can be detected by its absorption at 252 mμ. When the crude diene was then treated with potassium permanganate, a useful (2) oxidizing agent for such compounds, the isolation of 3α,12α-diacetoxypregnan-20-one proved to be difficult; in fact, it was found that the yields of 20-ketone increased markedly with increasing purity of diene. This observation indicated that I or its oxidation products interfered with the normal course of the permanganate oxidation of the diene, or with the subsequent isolation of the 20-ketone. It was therefore decided to investigate the products derived from I by this oxidation.



[1]*Manuscript received March 9, 1960.*
Contribution from the Research and Development Laboratories of Canada Packers Limited, Toronto, Ontario.

Can. J. Chem. Downloaded from www.nrcresearchpress.com by 186.148.149.217 on 09/04/12
For personal use only.

The oxidation was carried out in refluxing aqueous acetone, containing potassium dihydrogen phosphate as a buffer, which provided the desired neutral pH. The reaction products were then separated to give 30% of acidic material which was identified as nordesoxycholic acid diacetate (III). The neutral fraction, after crystallization, afforded 45% of a compound (II) which in turn was converted to III by oxidation with chromic acid. Compound II failed to react with the Malaprade reagent or with acetic anhydride and pyridine at 20°, and on the basis of this evidence a 23,24-glycol structure was eliminated. The presence of a ketone group in II was indicated clearly by its ultraviolet and infrared absorption, though the compound did not form a 2,4-dinitrophenylhydrazone or an oxime. This result is attributed to steric effects which are known (3) to be operative in similar cases. The ultraviolet spectrum of the ketol II showed bands at 260 mμ (ϵ = 440) and at 297 mμ (ϵ = 360). The absorption at the lower wavelength is undoubtedly due to the two unconjugated phenyl groups (4, 5) in the molecule; the band at the higher wavelength results from the interaction of the ketone function with the phenyl groups. In studies of α,α-diphenylketones, it has previously been shown (4, 6, 7) that the carbonyl absorption peak in the ultraviolet region is more intense and is shifted towards longer wavelength than that of most ketones. The above data as well as the results of elemental analyses for II and its hydrolysis product provided the evidence for the ketol structure in these compounds.

When the ketol II was reduced with sodium borohydride and the reaction products were hydrolyzed, two isomeric glycols (IV and V) were isolated. Both compounds gave positive Malaprade tests, and the predominant isomer (IV) formed a well-defined acetonide; since V was obtained in only small yield, its reactivity towards acetone could not be determined. The two isomers showed the ultraviolet absorption bands at 260 mμ due to the phenyl groups, but the ketone peak was absent; in the infrared region there appeared the characteristic absorption of associated hydroxyl groups. On treatment with acidic reagents, both glycols yielded 3α,12α-diacetoxy-23-keto-24,24-diphenylcholane (VI). The latter compound again showed the ketone band at 293 mμ, and in the infrared the hydroxyl peak was absent. These findings, in conjunction with the results of elemental analyses, established the structures for IV, V, and VI.

The oxidation of 3α,12α-diacetoxy-24,24-diphenyl-Δ^{23}-cholene (I) by chromic acid has been reported (8, 9) to yield 60–70% of the noracid III; ozonization (10) of the diphenylethylene derived from cholic acid afforded the corresponding noracid in lower yield. Invariably, these oxidations produced relatively large amounts of neutral, unidentified fractions which may well contain the related ketols. The good yield of II obtained from the permanganate oxidation is not surprising in view of some recent reports. In the steroid field, this oxidizing agent has been employed to produce ketols from the corresponding $\Delta^{5,6}$-unsaturated compounds (11) as well as from $\Delta^{17,20}$-analogues (12, 13). The mild permanganate treatment (14) of oleic acid similarly provided high yields (70–75%) of ketohydroxystearic acid.

EXPERIMENTAL[2,3]

The Permanganate Oxidation of 3α,12α-Diacetoxy-24,24-diphenyl-Δ^{23}-cholene (I)

Compound I (20 g) and potassium dihydrogen phosphate (2 g) were suspended in acetone (195 ml) and water (5 ml). The mixture was stirred and there was then added, in

[2]*The microanalyses were kindly performed by Mr. E. Thommen, Basel, Switzerland.*
[3]*The infrared absorption data were obtained through the courtesy of Dr. G. D. Laubach of Chas. Pfizer & Co., Brooklyn, N.Y.*

four equal portions, at intervals of 30 minutes, potassium permanganate (32 g). On addition of each batch of oxidizing agent, vigorous refluxing began and gradually subsided after several minutes. After all the permanganate had been added, the reaction was continued under reflux conditions for an additional $2\frac{1}{2}$ hours. The excess oxidizing agent was destroyed by charcoal (5 g) and, after 1 hour's stirring, the solids were filtered off. The filtrate was evaporated to dryness, the residue (16 g) was dissolved in ethyl acetate and extracted with 2.5% sodium carbonate solution. After being washed with water, the solvent extract was evaporated, the residual gum was taken up in ether to provide, on cooling, 9.45 g (45%) of II, m.p. 169–171° C. Recrystallization from acetone gave material, m.p. 175–175.5° C, and $[\alpha]_D^{25}$ +81.3° (*c*, 0.994, dioxane). This compound failed to react with a solution of bromine in carbon tetrachloride, with 2,4-dinitrophenylhydrazine, trichloroacetic acid, the Zimmermann reagent, and was negative in the Malaprade test. Its ultraviolet spectrum showed weak bands at 260 mμ (ϵ = 440) and at 297 mμ (ϵ = 360). Analysis: Calculated for $C_{40}H_{52}O_6$: C, 76.39; H, 8.34; O, 15.27. Found: C, 76.37, 76.48; H, 8.56, 8.47; O, 15.37, 15.41.

The carbonate extract as well as the water washings from the cake of solids (manganese salts, etc.) were acidified and extracted with ether. The solvent phase was washed, dried, and evaporated; crystallization of the residue from ether–hexane afforded 4.5 g (29%) of crude 3α,12α-diacetoxy-norcholanic acid (III), m.p. 180–190° C. This material was recrystallized from hexane–ether to give a melting point of 203–205° C.

3α,12α-Diacetoxy-norcholanic Acid (III) *from* II

Compound II (1 g) was suspended in acetic acid (15 ml) and there was then added dropwise, over a period of $\frac{1}{2}$ hour, a solution of chromic acid (1 g) in acetic acid (24 ml) and water (1 ml). The mixture was kept at 20° C for 2 hours and an equal period of time at 35° C with occasional shaking. The excess oxidizing agent was decomposed by sodium bisulphite; water was added, and the products were extracted with ether. The solvent phase, after having been washed, dried, and evaporated, yielded a residue (1.12 g) which crystallized readily from acetone. The noracid III (472 mg), m.p. 203–205° C, thus obtained, was recrystallized from ether–hexane to give pure III, m.p. 211–213° C.

3α,24-Dihydroxy-12α-acetoxy-23-keto-24,24-diphenylcholane

The diacetoxy-ketol II (0.5 g) was dissolved by warming in methanol (24 ml) and water (1 ml), containing potassium hydroxide (0.2 g). The solution was kept at room temperature for 66 hours, after which time most of the methanol was removed *in vacuo*. The residue was taken up in ether and dilute mineral acid, the ether phase was washed to neutrality, dried, and evaporated to give a residue (0.46 g) which crystallized from ether–hexane to yield 367 mg of material, m.p. 188–190° C. Two further recrystallizations from ether–hexane provided needles, m.p. 190–191.5° C and $[\alpha]_D^{24}$ +68.9° (*c*, 0.779, dioxane). Analysis: Calculated for $C_{38}H_{50}O_5$: C, 77.78; H, 8.59; O, 13.63. Found: C, 77.83, 77.91; H, 8.75, 8.75; O, 13.63.

Sodium Borohydride Reduction of the Ketol II

Compound II (1 g) was partially dissolved in ether (50 ml) and sodium borohydride (0.5 g) was added. The mixture was kept at 20° C for 15 hours, and was subsequently refluxed for $3\frac{1}{2}$ hours. The excess reducing agent was destroyed by addition of acetic acid, the mixture was diluted with water and extracted exhaustively with ether. The combined solvent extracts were washed, dried, and evaporated to provide a residue (1 g), which

Can. J. Chem. Downloaded from www.nrcresearchpress.com by 186.148.149.217 on 09/04/12
For personal use only.

Can. J. Chem. Downloaded from www.nrcresearchpress.com by 186.148.149.217 on 09/04/12
For personal use only.

was saponified at room temperature for 15 hours with 2.5% methanolic potassium hydroxide. Dilution with water, extraction with ether, and working up in the usual fashion gave the residue (0.98 g) which crystallized from ether–hexane to provide, in two crops, 451 mg of material; these crystals melted at 127–135° C, the melt resolidified at 145–150° C and finally melted at 215–218° C. Two recrystallizations from ethyl acetate yielded pure IV, m.p. 216.5–219° C and $[\alpha]_D^{25}$ +121.2° (*c*, 0.366, dioxane). This substance gave a positive Malaprade test; in the ultraviolet region, it exhibited a weak band at 260 mμ (ϵ = 380). Analysis: Calculated for $C_{38}H_{52}O_5$: C, 77.51; H, 8.90; O, 13.59. Found: C, 77.66, 77.55; H, 9.07, 8.99; O, 13.65, 13.74.

The filtrate from IV was reduced in volume and, on refrigeration, three more crops of crystals were isolated. These weighed 295 mg and had a melting point of 177–185° C. Several recrystallizations from ether–hexane provided a small, pure sample of V, m.p. 193–194° C and $[\alpha]_D^{23}$ +16.9° (*c*, 0.655, dioxane). This compound, on admixture with IV, had a melting point of 178–183° C; V, like IV, gave a positive Malaprade test. Analysis: Calculated for $C_{38}H_{52}O_5$: C, 77.51; H, 8.90; O, 13.59. Found: C, 77.78; H, 9.15; O, 13.24.

The Acetonide of IV

Compound IV (250 mg) was dissolved in dry acetone (20 ml), *p*-toluenesulphonic acid (50 mg) was added, and the solution was kept at 25° C for 16 hours. The solution was neutralized with solid sodium bicarbonate, diluted with water, and extracted with ether. The solvent extract was washed, dried, and evaporated to a white solid (270 mg) which crystallized from ether–hexane to give 220 mg of material, m.p. 227–228° C. Three recrystallizations from the same solvent system yielded the acetonide of IV, m.p. 228–230° C and $[\alpha]_D^{25}$ +158.3° (*c*, 0.647, dioxane). Analysis: Calculated for $C_{41}H_{56}O_5$: C, 78.30; H, 8.98; O, 12.72. Found: C, 78.42, 78.34; H, 9.17, 9.22; O, 12.79, 12.68.

3α,12α-Diacetoxy-23-keto-24,24-diphenylcholane (VI)

(a) From IV

Compound IV (120 mg) was refluxed gently for 2 hours with acetic acid (8 ml) and concentrated hydrochloric acid (0.8 ml); an additional 0.8 ml of hydrochloric acid was added then, and refluxing was continued for 2 more hours. The reaction mixture was poured into water, extracted with ether, and the solvent phase worked up in the customary manner. Crystallization of the residue from hexane–ether yielded 70 mg of substance which melted at 127–129° C, partially recrystallized, and finally melted at 155–158° C. Three recrystallizations from hexane–ether provided a pure sample of VI, having a double melting point 133–136° and 167–170° C. When VI is crushed to a very fine powder, it melts at 167–168° C; $[\alpha]_D^{23}$ +67.5° (*c*, 0.591, dioxane). This compound absorbs in the ultraviolet at 260 mμ (ϵ = 515) and at 293 mμ (ϵ = 270). Analysis: Calculated for $C_{40}H_{52}O_5$: C, 78.39; H, 8.55; O, 13.05. Found: C, 78.54, 78.77; H, 8.88, 8.53; O, 13.14, 13.05.

(b) From V

Compound V (80 mg) and *p*-toluenesulphonic acid (300 mg) were refluxed for 3 hours in acetic acid (8 ml). The solution was diluted with water and then extracted with ether; washing, drying, and evaporating the solvent phase provided a residue (86 mg) which crystallized from hexane–ether to give 27 mg of crude VI, m.p. 160–164° C. Recrystallization from ethanol gave pure VI, showing the double melting point, 132–135° C and 165.5–167° C. This material gave no melting point depression on admixture with a sample of VI obtained by dehydration of IV.

REFERENCES

1. CH. MEYSTRE, L. EHMANN, R. NEHER, and K. MIESCHER. Helv. Chim. Acta, **28**, 1252 (1945).
2. K. R. BHARUCHA. J. Chem. Soc. 2555 (1956).
3. W. COLE and P. L. JULIAN. J. Am. Chem. Soc. **67**, 1369 (1945).
4. E. L. ALPEN, W. D. KUMLER, and L. A. STRAIT. J. Am. Chem. Soc. **72**, 4558 (1950).
5. A. R. GILLAM and E. S. STERN. Electronic absorption spectroscopy. Edward Arnold (Publishers) Ltd., London. 1955. p. 121.
6. W. B. BENNET and A. BURGER. J. Am. Chem. Soc. **75**, 84 (1953).
7. W. D. KUMLER, L. A. STRAIT, and E. L. ALPEN. J. Am. Chem. Soc. **72**, 1463 (1950).
8. W. M. HOEHN and H. L. MASON. J. Am. Chem. Soc. **60**, 1493 (1938).
9. B. RIEGEL, R. B. MOFFETT, and A. V. MCINTOSH. Org. Syntheses, **24**, 38 (1944).
10. H. MORSMAN, M. STEIGER, and T. REICHSTEIN. Helv. Chim. Acta, **20**, 3 (1937).
11. R. E. MARKER and E. ROHRMANN. J. Am. Chem. Soc. **62**, 516 (1940).
12. J. HEER and K. MIESCHER. Helv. Chim. Acta, **34**, 359 (1951).
13. R. TULL, R. E. JONES, S. A. ROBINSON, and M. TISHLER. J. Am. Chem. Soc. **77**, 196 (1955).
14. J. E. COLEMAN, C. RICCIUTI, and D. SWERN. J. Am. Chem. Soc. **78**, 5342 (1956).

Can. J. Chem. Downloaded from www.nrcresearchpress.com by 186.148.149.217 on 09/04/12
For personal use only.

Can. J. Chem. Downloaded from www.nrcresearchpress.com by 186.148.149.217 on 09/04/12
For personal use only.

N-DICHLOROACETYL DERIVATIVES OF SERINE AND THREONINE AND OF THEIR ESTERS AND SODIUM SALTS[1]

I. LEVI, A. E. KOLLER, G. LAFLAMME, AND J. W. R. WEED

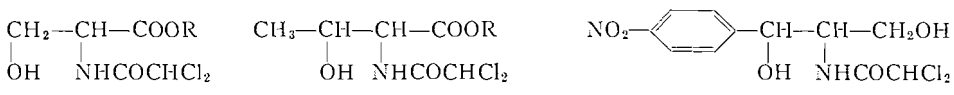
ABSTRACT

The N-dichloroacetyl derivatives of DL-serine and DL-threonine were prepared by the Schotten–Baumann reaction from the amino acids and dichloroacetyl chloride. Negative ninhydrin tests coupled with elementary analyses indicated that only the amino group was acylated. The ester derivatives of these compounds were prepared either by esterification of the N-dichloroacetyl-DL-amino acid with diazomethane or by the reaction of the amino acid ester with dichloroacetyl chloride in the presence of triethylamine. The sodium salts and the esters were tested for antitumor activity against sarcoma 37 in mice and Walker carcinoma 256 in rats. In both cases regression of the tumors was obtained.

The original studies of Cornman (1) and of Stock, Sugiura, and Rhoads (2) demonstrated that certain antibiotics obtained from the culture filtrates of bacteria and molds inhibited the growth of transplanted tumors in animals. Many other workers have since reported on the antitumor activity of a variety of antibiotic substances (3–16). Two of these antibiotics, azaserine (O-diazoacetyl-L-serine) (15) and DON (6-diazo-5-oxo-L-norleucine) (16), which were isolated from the culture filtrates of two species of *Streptomyces*, and which retarded the growth of sarcoma 180 in the mouse, are diazo amino acids. This is noteworthy because a search for amino acid derivatives which might serve as antagonists in the metabolism of tumor cells, first suggested by Greenberg and Schulman (17), has been going on for many years.

In view of the above, it was reasoned that if some of the common amino acids were modified to contain an essential portion of a natural antibiotic, antimetabolites useful for cancer chemotheraphy might result. Since it is generally believed that chloramphenicol is a specific inhibitor of protein synthesis (18), and since the N-dichloroacetyl group is essential for its maximum antibiotic activity (19), it seemed logical to modify the structure of amino acids with the N-dichloroacetyl radical in an attempt to achieve this aim.

A number of N-dichloroacetyl amino acids were therefore prepared and investigated for their pharmacological activities particularly with respect to their antitumor and antibiotic effects. In this paper only serine and its homologue, threonine, are considered because there is a close structural relationship between their N-dichloroacetyl derivatives (I*a* and II*a* respectively) and chloramphenicol (III), and also because of the unique biological position serine occupies in the metabolism of normal cells (20–27) and of neoplastic cells (28–31).



I

II

III

I*a*, R = H
I*b*, R = Na
I*c*, R = CH_3
I*d*, R = C_2H_5

II*a*, R = H
II*b*, R = Na
II*c*, R = CH_3
II*d*, R = C_2H_5

DL-Serine was acylated with N-dichloroacetyl chloride in the presence of aqueous sodium hydroxide solution according to the usual Schotten–Baumann procedure. Due to

[1]*Manuscript received April 4, 1960.*
Contribution from the Research Laboratories, Charles E. Frosst & Co., Montreal, Que.

the low solubility of its sodium salt (I*b*) it was possible to recover the major portion of the product in this form from the cold aqueous reaction mixture. However, if the free acid (I*a*) was desired, the reaction mixture was acidified and worked up in the usual manner.

The free acid (I*a*) prepared from the sodium salt (I*b*) by treatment with hydrochloric acid, and the sodium salt prepared from the free acid with sodium hydroxide, were identical in each case with the corresponding products isolated directly from the acylation reaction. Both of these compounds gave a negative ninhydrin test indicating the acylation of the amino group.

The hitherto unreported methyl ester of N-dichloroacetyl-DL-serine (I*c*) was prepared by two methods. The first consisted in esterifying N-dichloroacetyl-DL-serine with diazomethane, the second in reacting a chloroform solution of DL-serine methyl ester with dichloroacetyl chloride in the presence of triethylamine. The latter method was also employed for the synthesis of the N-dichloroacetyl derivative of DL-serine ethyl ester (I*d*), previously prepared (32) by a modification of this reaction.

DL-Serine methyl ester was prepared as the hydrochloride from DL-serine and hydrogen chloride in anhydrous methanol using a modification of the Fischer esterification technique. Fischer and Suzuki (33) first prepared this ester in 1905 and reported the melting point as 114°. This was confirmed by Mattocks and Hartung (34). Fischer's value was questioned, however, by King (35), who prepared the ester hydrochloride from three different samples of DL-serine and in each case obtained a product which melted at 134°. Chambers and Carpenter (36) confirmed King's melting point as 133–134° and indeed, in our own work, we repeatedly obtained a pure product which melted at 134°.

Similar reactions, applied to DL-threonine, yielded the methyl ester hydrochloride and the hitherto undescribed N-dichloroacetyl-DL-threonine (II*a*), its sodium salt (II*b*), and methyl ester (II*c*). Several attempts to prepare the ethyl ester of N-dichloroacetyl-DL-threonine (II*d*) were unsuccessful, chiefly due to the initial insolubility of DL-threonine ethyl ester (and its hydrochloride) in the solvents such as chloroform, benzene, and ether, normally used in the acylation experiments involving triethylamine. The sodium salt of N-dichloroacetyl-DL-threonine (II*b*) has a far greater solubility in water than has the sodium salt of N-dichloroacetyl-DL-serine (I*b*) and therefore could not be isolated directly from the acylation reaction. Although DL-threonine methyl ester hydrochloride can be prepared by the Fischer esterification procedure, the use of thionyl chloride gave a much better yield of product in this case.

The sodium salt of N-dichloroacetyl-DL-serine (I*b*) has been investigated the most extensively in our laboratories for antitumor activity. It depresses the growth of sarcoma 37 in mice, causing, in some animals, complete regressions of the tumor. The compound is non-toxic to mice in doses up to 4 grams per kilo of body weight. A preliminary report of these results has been published (37).

EXPERIMENTAL

The melting points were obtained with a Fisher–Johns apparatus and are uncorrected. Infrared spectra were determined with a Beckman IR-5 spectrophotometer equipped with a sodium chloride prism, using potassium bromide pellets. All melting points and temperature readings are in degrees Centigrade.

Dichloroacylation of DL-*Serine*

(a) N-*Dichloroacetyl*-DL-*serine Isolated as Sodium Salt* (I*b*)

DL-Serine (36 g, 0.34 mole) was dissolved in 4 *N* sodium hydroxide solution (85.6 ml,

Can. J. Chem. Downloaded from www.nrcresearchpress.com by 186.148.149.217 on 09/04/12
For personal use only.

Can. J. Chem. Downloaded from www.nrcresearchpress.com by 186.148.149.217 on 09/04/12
For personal use only.

0.34 mole) in a 1 liter, four-necked, round-bottomed flask fitted with a thermometer, motor-driven stirrer, and two dropping funnels. The clear colorless solution of the sodium salt of DL-serine was cooled in an ice–salt mixture to −5°. Dichloroacetyl chloride (63.2 g, 0.42 mole) and 4 *N* sodium hydroxide solution (107 ml, 0.42 mole) were then added dropwise and simultaneously from the two dropping funnels to the stirred, cooled solution at such a rate that the reaction mixture remained on the basic side throughout the additions and the temperature of the reaction mixture remained at 0°±4°.* During these additions, which required about one hour, the product settled out as a fine white crystalline precipitate. When the additions were completed the reaction mixture was stirred in the cold for an additional 30 minutes. The product, 38.6 g (47.3% yield), was removed by filtration, washed with a little ice-cold water, and dried at 50° in a vacuum oven, m.p. 172–176°. After recrystallization from water, the sodium salt of N-dichloroacetyl-DL-serine melted at 178–179°. It has a solubility in water of 11% at 27°, is slightly soluble in cold ethanol, and insoluble in most other organic solvents. Heating at 105° for 1 hour did not change its physical appearance, melting point, or infrared absorption curve. When recrystallized from water it retains approximately 15% by weight of the water, which is not substantially removed by air-drying. The anhydrous product is obtained by drying under a pressure of less than 1 mm for a period of 6 hours at 60°. Anal. Calc. for $C_5H_6Cl_2NO_4Na$: C, 25.23; H, 2.54; N, 5.89. Found: C, 25.09; H, 2.42; N, 5.75.

The filtrate from the crude product of (*a*) was acidified and worked up as described below in (*b*) to yield 4.0 g (5.4%) of N-dichloroacetyl-DL-serine (I*a*), m.p. 118–119°.

(b) N-*Dichloroacetyl*-DL-*serine Isolated as the Acid* (I*a*)

The acylation of DL-serine (21 g, 0.2 mole) was carried out as for the sodium salt derivative described above, which in this case was not isolated. Instead, the total reaction mixture was acidified with dilute hydrochloric acid (7.3 g concentrated hydrochloric acid in 192 ml water) and the clear, colorless solution was concentrated to dryness under vacuum, using a water bath at 60 to 70°. The residue, which consisted of pale yellow viscous syrup mixed with crystalline sodium chloride, was extracted with hot ethyl acetate (4×100 ml). The combined extracts were dried over anhydrous magnesium sulphate, filtered, and the filtrate again evaporated to dryness as above. The resulting residual light yellow clear oil was shaken with petroleum ether (30–60°) (2×50 ml) to remove any dichloroacetic acid present, and crystallized from ethyl acetate – petroleum ether (30–60°) to give 16.4 g (38%) I*a*, m.p. 116–118°. (Other experiments gave yields up to 55.9%.)

An analytical sample recrystallized from ethyl acetate consisted of a fine crystalline powder which melted at 119–121°. It is soluble in ethanol, acetone, diethyl ether, dioxane, and ethyl acetate, is insoluble in ethylene dichloride, N-hexane, benzene, and petroleum ether. It has a solubility in water of 41% by weight at 27°. Anal. Calc. for $C_5H_7Cl_2NO_4$: C, 27.80; H, 3.26; N, 6.48. Found: C, 27.69; H, 3.22; N, 6.60.

This product (2 g) was dissolved in 10% sodium hydroxide solution (3.6 ml) and the solution evaporated to dryness. The partially solidified colorless residue was recrystallized from ethanol yielding crystals of I*b*, m.p. 176–178°, the infrared absorption curve of which was identical with that of I*b* described above in (*a*).

N-*Dichloroacetyl*-DL-*serine from the Sodium Salt*

The sodium salt of N-dichloroacetyl-DL-serine (I*b*) (5.0 g) was dissolved in dilute

**Subsequent experiments indicated that this low temperature range is not critical, since the same yield of product was obtained when the acylation was carried out between 15° and 20°.*

hydrochloric acid solution (25 ml water containing 2.1 ml concentrated hydrochloric acid). The clear solution was evaporated to dryness under vacuum at 50–60°. The residue was extracted with hot ethyl acetate (4×15 ml). The combined extracts were dried over anhydrous magnesium sulphate, filtered, and concentrated to yield an oil, which solidified to a mass of white crystals (3.3 g). Recrystallization from ethyl acetate – petroleum ether yielded N-dichloroacetyl-DL-serine (I*a*), m.p. 118–119°, the infrared absorption curve of which was identical with that of I*a* described above. The melting point of a mixture of the two was not depressed.

DL-*Serine Methyl Ester Hydrochloride*

A rapid stream of dry hydrogen chloride gas was passed into a suspension of 1 mole of serine (105 g) in anhydrous methanol (500 ml) until the serine dissolved and the clear solution reached its boiling point. The alcohol was then distilled off under reduced pressure. The oily residue was redissolved in fresh anhydrous methanol (500 ml), the solution cooled in an ice bath, and again saturated with a stream of hydrogen chloride gas, during a 1-hour period. The product resulting from the removal of the methanol after this second treatment with hydrogen chloride gas was washed with anhydrous ether (3×50 ml) and dissolved in anhydrous methanol (100 ml) to which a few milliliters of anhydrous ether was added. The ester hydrochloride began to crystallize almost at once. Weight 135 g (87% yield), m.p. 134° (35, 36). Anal. Calc. for $C_4H_{10}ClNO_3$: C, 30.87; H, 6.47; N, 9.00. Found: C, 30.67; H, 6.30; N, 9.01.

DL-*Serine Ethyl Ester Hydrochloride*

This compound was prepared from serine (105 g, 1.0 mole) and anhydrous ethanol according to the procedure described above for the methyl ester hydrochloride. The product (144.1 g, 85% yield) was obtained as white crystals which, after recrystallization from ethanol–ether, melted at 98°. The melting point for this ester hydrochloride has been reported as 94–97° (38) and 100–102° (39). Anal. Calc. for $C_5H_{11}ClNO_3$: N, 8.26. Found: N, 8.31.

N-*Dichloroacetyl*-DL-*serine Methyl Ester* (I*c*)

(a) By Esterification of N-*Dichloroacetyl*-DL-*serine with Diazomethane*

N-Dichloroacetyl-DL-serine (I*a*) (12.0 g) was covered with ether (100 ml) in a 1-liter round-bottomed flask. An ether solution containing diazomethane (approximately 4.7 to 5.0 g) prepared from N-nitroso-N-methyl urea (17.7 g) was added cautiously and with stirring to this partially dissolved mixture. When the evolution of nitrogen subsided the clear yellow solution was allowed to stand in a fume hood overnight. It was then filtered from a small amount of extraneous material and glacial acetic acid (2 ml) was added to destroy residual diazomethane. The residue obtained on removal of the ether yielded long white needles of I*c* (7.2 g, 56.7%), and an additional 3.2 g (25.2%) of crystalline product was recovered from the mother liquors. An analytical sample was recrystallized from ether – petroleum ether and dried over P_2O_5 at 60° for 8 hours, m.p. 82–83.5°. It is soluble in water (20% at 27°) and in most common organic solvents. Anal. Calc. for $C_6H_9Cl_2NO_4$: C, 31.32; H, 3.94; N, 6.09. Found: C, 31.36; H, 3.85; N, 6.28. The infrared absorption curve of this product was identical with that of the same product synthesized by route (*b*) below.

(b) By N-*Dichloroacylation of* DL-*Serine Methyl Ester*

Triethylamine (101 g, 1.0 mole) was added to DL-serine methyl ester hydrochloride (155.6 g, 1.0 mole) suspended in chloroform (1000 ml). The liberated ester base and the

Can. J. Chem. Downloaded from www.nrcresearchpress.com by 186.148.149.217 on 09/04/12
For personal use only.

Can. J. Chem. Downloaded from www.nrcresearchpress.com by 186.148.149.217 on 09/04/12
For personal use only.

triethylamine hydrochloride dissolved in the chloroform. The clear solution was cooled in a salt–ice bath to −5°. Dichloroacetyl chloride (147.5 g, 1.0 mole) and a second portion of triethylamine (101.0 g, 1.0 mole) were then added simultaneously and dropwise over a period of 1½ hours so that the temperature in the reaction flask did not rise above 10°. When the additions were completed the solution was stirred at room temperature for an additional half hour. It was then filtered from some extraneous material and the chloroform removed with vacuum from a water bath at 40–50°. The residual oily solid was extracted with boiling anhydrous ether (4×100 ml) whereby the product was separated from ether-insoluble triethylamine hydrochloride. The hot ether solution was filtered and on cooling deposited a voluminous mass of white feathery crystals (132.5 g, 57% yield), m.p. 82–83°. Anal. Calc. for $C_6H_9Cl_2NO_4$: C, 31.32; H, 3.94; N, 6.09. Found: C, 31.34; H, 3.98; N, 6.37.

N-*Dichloroacetyl*-DL-*serine Ethyl Ester* (I*d*)

This compound was prepared from DL-serine ethyl ester hydrochloride (84.8 g, 0.5 mole), triethylamine (101.0 g, 1.0 mole), and dichloroacetyl chloride (73.7 g, 0.5 mole) in chloroform solution following the procedure described above for the preparation of I*c*. The colorless compound (65.7 g, 53% theory) was recrystallized from diethyl ether, m.p. 75–76° (literature value for m.p. 76°) (32). Anal. Calc. for $C_7H_{11}Cl_2NO_4$: C, 34.44; H, 4.54; N, 5.73. Found: C, 34.41; H, 4.38; N, 5.75.

N-*Dichloroacetyl*-DL-*threonine* (II*a*)

This compound was prepared from DL-threonine (238 g, 2.0 mole) and dichloroacetyl chloride (368.8 g, 2.5 mole) in the presence of 6 *N* sodium hydroxide solution (750 ml) according to the above described procedure for serine. Yield, 218.9 g (47%), colorless crystals, m.p. 138–140°. An analytical sample recrystallized from ethyl acetate melted at 140–141°. Anal. Calc. for $C_6H_9Cl_2NO_4$: C, 31.32; H, 3.94; N, 6.08. Found: C, 31.14; H, 3.99; N, 6.17.

Sodium Salt of N-*Dichloroacetyl*-DL-*threonine* (II*b*)

N-Dichloroacetyl-DL-threonine was treated with sodium hydroxide according to the procedure described above for the preparation of I*b*. The crystalline product, after three recrystallizations from methanol – diethyl ether melted at 176–178°. The sodium salt was very soluble in water, soluble in ethanol, and insoluble in the common organic solvents. Anal. Calc. for $C_6H_8Cl_2NO_4Na$: C, 28.59; H, 3.20; N, 5.56. Found: C, 28.60; H, 3.00; N, 5.56.

DL-*Threonine Methyl Ester Hydrochloride*

Thionyl chloride (14.9 ml, 0.2 mole) was added carefully to methanol (100 ml) and maintained at −10° by cooling in a salt–ice bath. To this solution was then added 23.8 g (0.2 mole) of DL-threonine and allowed to stand 2 hours at room temperature and then refluxed for 20 minutes. The solution was concentrated to dryness under reduced pressure and the residual oil crystallized from anhydrous methanol – diethyl ether. The product was obtained as colorless needles. Weight 19.9 g (58.7%), m.p. 124–125° (lit. m.p. 125°) (40). A second crop, 5.3 g (15.6%), of less pure material (m.p. 118–120°) was recovered from the filtrate. An analytical sample was obtained by recrystallization from methanol – ethyl ether, m.p. 125°. Anal. Calc. for $C_5H_{12}ClNO_3$: C, 35.40; H, 7.13; N, 8.26. Found: C, 35.18; H, 6.98; N, 8.26.

N-*Dichloroacetyl*-DL-*threonine Methyl Ester* (II*c*)

DL-Threonine methyl ester hydrochloride (8.48 g, 0.05 mole), triethylamine (10.1 g,

0.10 mole), and dichloroacetyl chloride (7.37 g, 0.05 mole) were reacted in 75 ml chloroform following the procedure described above for Ic. The white crystalline compound (10.7 g, 87% yield) melted at 105–106°. An analytical sample was prepared by recrystallization from diethyl ether, m.p. 106°. In contrast to the high solubility in water of the corresponding serine derivative (Ic) this compound had a solubility of 5.9% at 27°. Anal. Calc. for $C_7H_{11}Cl_2NO_4$: C, 34.44; H, 4.05; N, 5.74. Found: C, 34.31; H, 4.27; N, 5.76.

ACKNOWLEDGMENT

The authors wish to thank Mrs. G. Shimizu for the analyses.

REFERENCES

1. I. Cornman. J. Gen. Physiol. **28**, 113 (1944).
2. C. C. Stock, K. Sugiura, and C. P. Rhoads. Acta Unio Internat. contra Cancrum, **6**, 550 (1948).
3. H. C. Reilly. Cancer Research, **13**, 821 (1953).
4. H. W. Dion *et al.* J. Am. Chem. Soc. **78**, 3075 (1956).
5. J. H. Burchenal *et al.* Proc. Soc. Exptl. Biol. Med. **86**, 891 (1954).
6. D. A. Clarke, H. C. Reilly, and C. C. Stock. Antibiotics & Chemotherapy, **7**, 653 (1957).
7. S. Farber, C. Maddock, and M. Swaffield. Proc. Am. Assoc. Cancer Research, **2**, 104 (1956).
8. G. B. Magill *et al.* Cancer Research, **16**, 960 (1956).
9. H. C. Reilly *et al.* Cancer Research, **13**, 684 (1953).
10. B. Sokoloff and W. H. Eddy. Cancer Research, **11**, 282 (1951).
11. C. C. Stock. Am. J. Med. **8**, 658 (1950).
12. C. C. Stock *et al.* Nature, **173**, 71 (1954).
13. K. Sugiura and C. C. Stock. Proc. Soc. Exptl. Biol. Med. **88**, 127 (1955).
14. K. Sugiura *et al.* Cancer Research, **18**, 66 (1958).
15. J. Ehrlich *et al.* Nature, **173**, 72 (1954).
16. J. Ehrlich *et al.* Antibiotics & Chemotherapy, **6**, 487 (1956).
17. D. M. Greenberg and M. P. Schulman. Science, **106**, 271 (1947).
18. E. F. Gale. Ciba Foundation Symposium. Amino Acids and Peptides with Antimetabolic Activity. J. & A. Churchill Ltd., London. 1958. p. 19.
19. F. E. Hahn *et al.* Antibiotics & Chemotherapy, **6**, 531 (1956).
20. S. Kit and A. C. Griffin. Cancer Research, **18**, 621 (1958).
21. M. R. Heinrich and D. W. Wilson. J. Biol. Chem. **186**, 447 (1950).
22. D. Elwyn and D. B. Sprinson. J. Biol. Chem. **184**, 465 (1950).
23. P. Siekevitz and D. M. Greenberg. J. Biol. Chem. **180**, 845 (1949).
24. S. Weinhouse and B. Friedmann. J. Biol. Chem. **197**, 733 (1952).
25. M. Brenner. Ciba Foundation Symposium. Amino Acids and Peptides with Antimetabolic Activity. J. & A. Churchill Ltd., London. 1958. pp. 157–170.
26. G. H. Dixon, D. L. Kauffman, and H. Neurath. J. Biol. Chem. **233**, 1373 (1958).
27. R. E. Neuman and A. A. Tytell. Proc. Soc. Exptl. Biol. Med. **103**, 71 (1960).
28. S. Kit and O. L. Graham. Cancer Research, **16**, 937 (1956).
29. S. Kit and O. L. Graham. Cancer Research, **16**, 117 (1956).
30. T. A. McCoy and R. E. Neuman. J. Natl. Cancer Inst. **16**, 1221 (1956).
31. R. Z. Lockart, Jr. and H. Eagle. Science, **129**, 252 (1959).
32. H. Bretschneider and G. Piekarski. Monatsh. Chem. **85**, 1112 (1954).
33. E. Fischer and U. Suzuki. Ber. **38**, 4193 (1905).
34. A. M. Mattocks and W. H. Hartung. J. Biol. Chem. **165**, 501 (1946).
35. J. A. King. J. Am. Chem. Soc. **69**, 2738 (1947).
36. R. W. Chambers and F. H. Carpenter. J. Am. Chem. Soc. **77**, 1522 (1955).
37. I. Levi, H. Blondal, and E. Loziński. Science, **131**, 666 (1960).
38. F. W. Holly and C. H. Stammer. U.S. Patent No. 2,772,281. November 27, 1956.
39. D. F. Elliott. J. Chem. Soc. 589 (1949).
40. M. Kinoshita and S. Umezawa. J. Chem. Soc. Japan, **72**, 382 (1951); Chem. Abstr. **46**, 3005h (1952).

Can. J. Chem. Downloaded from www.nrcresearchpress.com by 186.148.149.217 on 09/04/12
For personal use only.

Can. J. Chem. Downloaded from www.nrcresearchpress.com by 186.148.149.217 on 09/04/12
For personal use only.

ANODIC OXIDE FILMS ON NIOBIUM: THICKNESS, DIELECTRIC CONSTANT, DISPERSION, REFLECTION MINIMA, FORMATION FIELD STRENGTH, AND SURFACE AREA[1]

L. YOUNG

ABSTRACT

The wavelengths of minimum specular reflectivity (at 11° incidence) due to interference were determined using a spectrophotometer for a series of films formed on chemically polished niobium. With a value of the refractive index $n = 2.46 \pm 1\%$ at 4358 Å wavelength by the Abelès method (reported elsewhere), the spectrophotometric data give the refractive index as a function of the wavelength λ, $n = 2.26 + 0.398/(\lambda/10^3\ \text{Å} - 2.56)^{1\cdot2}$. To analyze the spectrophotometric results, an auxiliary measure of thickness was required (though, with the chart given below, the thickness of a film may be determined directly from spectrophotometric measurements alone). A combination of measurements of the a-c. capacity and of the charge required to form the films gives a suitable measure of thickness (in terms of ρ/ϵ, where ϵ = dielectric constant and ρ = density) which is not dependent on a knowledge of the true surface area. The spectrophotometric data provide a calibration of this measure of thickness and thus give ϵ/ρ. With $\rho = 4.36$ g cm^{-3} (reported for the bulk amorphous oxide) this gives ϵ about 41 (compared with about 27.6 for Ta_2O_5). The effective surface area of the chemically polished metal was then found to be about 7% greater than the apparent area. At the ionic current density used to form the films (10 ma cm^{-2}), the field strength in the oxide was estimated as 4.96×10^6 v cm^{-1} within a few per cent uncertainty. Because the field to produce a given ionic current is lower than with Ta_2O_5 films, the capacity of films formed to a given voltage at a given current density and temperature is not so much greater for niobium than for tantalum as the dielectric constants might lead one to expect. It is suggested that there may be a correlation between dielectric constant and ionic conductivity. The Nb_2O_5 films recrystallize like Ta_2O_5 films under an applied field but more readily, at least with the purity of metal now available.

INTRODUCTION

As might be expected from their close chemical similarity, niobium and tantalum behave very similarly when anodically polarized. The present investigation of some of the properties of the film material followed the same method as was applied recently to tantalum (1). The aim was to obtain further data towards the comparative study of the various metals (Al, Nb, Ta, Ti, Zr, W, etc.) which show similar anodic film forming properties. Niobium is of particular interest because of its possible future use as an electrolytic capacitor anode. The kinetics of formation and some other topics have been discussed elsewhere (2, 3, 4).

EXPERIMENTAL METHODS

The electrodes (2×0.5 cm with a tab) were cut (using a die to obtain a reproducible size) from Fansteel Metallurgical Corporation 0.005-in. sheet of greater than 99.9% purity. They were stopped off and chemically polished as previously described (2). To obtain uniformity in the surface finish they were prepared in batches. After being stored dry, they were dipped in a dichromate–sulphuric acid cleaning mixture before use.

The solution was 0.2 N H_2SO_4 in demineralized water. The cell was immersed in a water thermostat at 25.8° C. The oxide films were formed at a constant current density of about 10 ma cm^{-2}. This high current density was chosen to obtain the maximum current efficiency. An electronic, automatic control device was used which records the times to traverse intervals of potential (about 4 seconds for 10 volts at the current density used) and terminates formation at a preset potential with respect to a reference electrode. At

[1]*Manuscript received March 11, 1960.*
Contribution from the British Columbia Research Council, University of British Columbia, Vancouver 8, British Columbia.

this current density, it is necessary to circulate the solution rapidly to eliminate heating effects (5).

A Cary double-beam recording spectrophotometer was used to locate the minima in the specular reflectivity at an angle of incidence of 11°. A simple device was specially made to hold the specimens and two front aluminized mirrors which reflected the light beam on to the specimens and back into its original path. A specimen which had been chemically polished but not anodized was used in the reference beam.

The capacity measurements were made at 1 kc/sec with a small a-c. signal.

RESULTS

The specimens were first formed to 10 v and the capacity was measured. The formation was then continued to the final potential. A procedure of this sort is necessary because of the pre-existing film. The charge to form to 10 v depends on the thickness of the film already present—and its measurement could be used to determine the thickness of this film and might prove a better method than anodic polarization measurements at low current densities (6, 7) where leakage current tends to interfere—but the charge to form from 10 to (say) 100 v can reasonably be assumed to be independent of the thickness of the pre-existing film. Similar considerations apply to the reciprocal capacity.

The increase in the reciprocal of the series equivalent capacity C which occurs when the thickness of the film is increased by an amount x is assumed to be given by

$$\Delta(1/C) = 4\pi x/\epsilon A \qquad [1]$$

where ϵ = dielectric constant and A = effective area. The amount of charge which must flow through the film to produce the increment of thickness is assumed to be

$$Q = Ax\rho 10F/M \qquad [2]$$

where ρ = density, F = the Faraday, and M = molecular weight of Nb_2O_5. It is assumed that the film is Nb_2O_5 and that it does not contain appreciable amounts of water or anions. From [1] and [2]

$$\{Q\Delta(1/C)\}^{1/2} = x(4\pi\rho\, 10F/\epsilon M)^{1/2}. \qquad [3]$$

The expression on the left-hand side gives a measure of thickness (in terms of the ratio, ρ/ϵ) which is independent of the area of the surface. The above expressions are not exact if A changes with thickness but [3] is a good approximation if A only changes slightly.

The wavelengths of the minima in the specular reflectivity are plotted against the above measure of thickness in Fig. 1. Since the frequency of "leaky" and otherwise abnormal specimens is of interest, the results obtained from all the specimens are plotted though only those for films of less than about 2200 Å thickness have been used in the calculations. Two types of non-ideal behavior occurred as the thickness increased: (*a*) decreased dV/dt (V = potential, t = time) due to leakage paths developing in the oxide giving oxygen evolution and (*b*) steadily increasing dV/dt, previously associated (with tantalum) with surface roughness (8, 9). At lower current densities, recrystallization has time to occur. Less pure niobium showed much worse behavior, and was also less easy to polish chemically to a satisfactory finish.

The minima* in the reflectivity are caused by destructive interference. This occurs when

$$2n\cos\theta\,(D+X) = \{(2r-1)/2\}\lambda \qquad [4]$$

**The maxima could be used but less satisfactorily since they are less sharp.*

Can. J. Chem. Downloaded from www.nrcresearchpress.com by 186.148.149.217 on 09/04/12
For personal use only.

where D = film thickness, n = refractive index; θ = angle of refraction; X = a constant at a given wavelength which allows for the difference between the phase changes during reflection at the oxide/air and metal/oxide interfaces respectively; r = 1,2,3 . . .; and λ = wavelength. Consequently, the vertical separation between the curves in Fig. 1 corresponds to an increase in thickness ($\lambda/2n \cos\theta$).

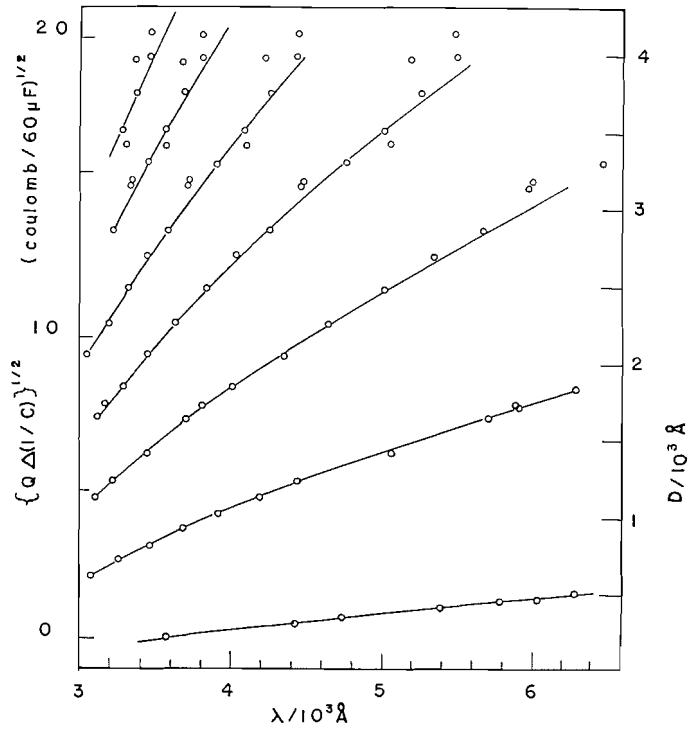


FIG. 1. Wavelengths at which destructive interference occurred plotted against $\{Q\Delta(1/C)\}^{\frac{1}{2}}$. A scale in angstrom units is given at the right.

A value of n at one wavelength is required to obtain a calibration of the thickness. Durbin, Wagner, and Harman (10) have recently determined n for the two axes of the high temperature crystalline modification of Nb_2O_5 as 2.27 and 2.31 in sodium light. Holtzberg, Reisman, Berry, and Berkenblit (11) have determined the densities at 25° C of some of the various forms. These are: amorphous, 4.36 g cm^{-3}; γ, 5.17 g cm^{-3}; and α, 4.55 g cm^{-3}. Assuming that $(n-1)/\rho$ = constant, we obtain n = 2.24 for the amorphous oxide.

The Becke immersion method (1) was not applied to the films because it was found to be difficult to strip sufficient oxide. Orme and Young (unpublished) have used the Brewster angle method of Abelès (12). They found that the reflectivity of the oxide coated metal for light of wavelength 4358 Å polarized in the plane of incidence was independent of the thickness of oxide at an angle of incidence 67° 51′. This shows that the index of the outer layers of oxide is constant at a value tan 67° 51′ = 2.46. The uncertainty is about $\pm 1\%$. With the present evidence that capacity, Faraday's laws, and spectrophotometric data are consistent with a uniform film (apart from the pre-existing film), the above index is assumed to be that of the whole film.

With this value for n at 4358 Å, and with the value of $\rho/n^2\epsilon$ from the data of Fig. 1,

Can. J. Chem. Downloaded from www.nrcresearchpress.com by 186.148.149.217 on 09/04/12
For personal use only.

we obtain ϵ about 41.4. The dependence on assumed constants may be expressed by writing $\epsilon = 41.4\ (\rho/4.36\ \text{g cm}^{-3})\{2.46/n(4358\ \text{Å})\}^2$. Apart from the uncertainty due to the uncertainty in ρ and n, this value is believed to be accurate to within 2 or 3% for the experimental conditions stated. With the refractive index known at one wavelength, the values of the thickness increments $\lambda/2n \cos\theta$ at other wavelengths give the refractive index at these wavelengths (Fig. 2). The smooth curve is the Hartmann equation, $n = 2.26+0.398(\lambda/10^3\ \text{Å}-2.56)^{-1.2}$. The value of λ_0 in $n = a+b(\lambda-\lambda_0)^{-1.2}$ is greater than the value for Ta_2O_5 films (1), and although the Hartmann equation is empirical, this difference does in fact correspond to a greater long wavelength limit of the intrinsic absorption. This had the effect that the measurements could only be taken to about 3000 Å. With tantalum the limit was about 2700 Å. As with Ta_2O_5 films, the minima became very flat beyond 6000 Å wavelength.

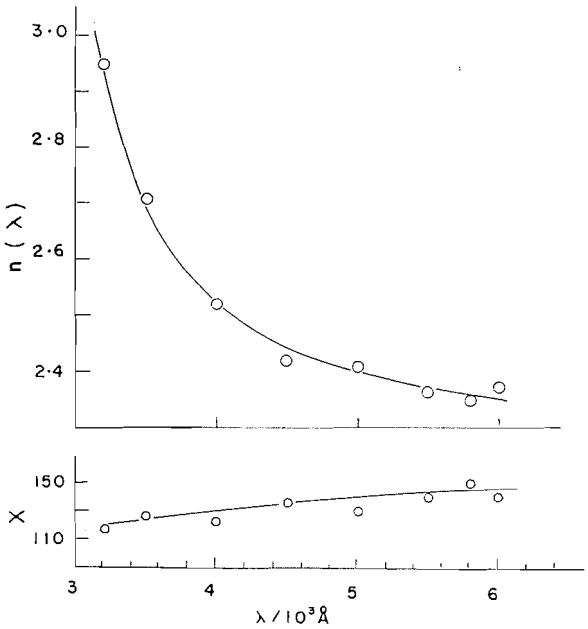


FIG. 2. Refractive index of films, and X (equation 4) as function of wavelength.

The ratio of increments of potential to increments of thickness is one measure of the field strength in the oxide. (Strictly, the field strength, like absolute metal/solution potential differences, is not an experimental observable, but it can be approximated if suitable assumptions are made.) The values obtained are shown in Fig. 3 as a function of voltage and thickness. The mean below 120 volts is $E = 4.96\times10^6$ v cm^{-1}, with an uncertainty of 1% due to the uncertainty in n, and a further 2 or 3% due to other sources of error.

Estimates of the field are also given in Fig. 3 with the thickness obtained from the charge passed using Faraday's laws with the "apparent" area. These estimates differ systematically from the above values because the effective area is greater than the apparent area.

With the dielectric constant now determined, the combination of capacity and Faraday's

Can. J. Chem. Downloaded from www.nrcresearchpress.com by 186.148.149.217 on 09/04/12
For personal use only.

law data give an estimate of the ratio of the effective to the apparent area. From [1] and [2]

$$A/a = (1/a)(M4\pi/10\rho F\epsilon)^{1/2}\{Q/\Delta(1/C)\}^{1/2}.$$

The values obtained are plotted in Fig. 3. They indicate a slight decrease in area with increasing thickness of oxide. This would not be unexpected since it would occur if there were surface irregularities on the scale of the thickness of the oxide film, but it could also be due to a deviation from the ideal behavior assumed in [1] and [2].

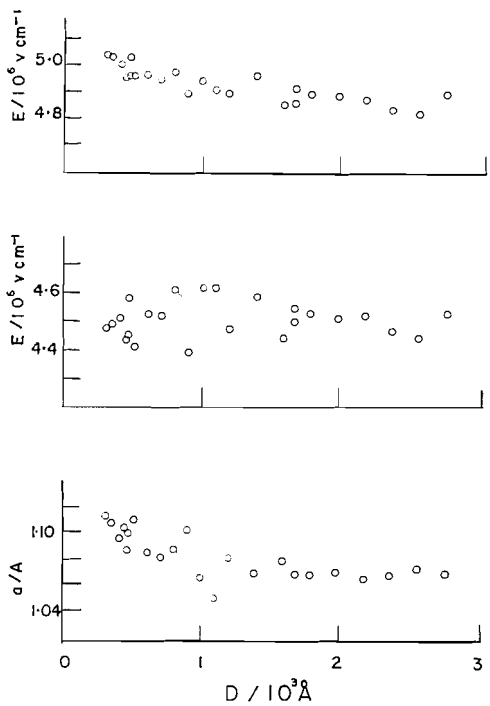


FIG. 3. (*Top*) Field strength $(V/\{Q\Delta(1/C)\}^{\frac{1}{2}})$. One point per specimen.
(*Middle*) Apparent field strength using thickness calculated from charge passed assuming $a = A$, and $\rho = 4.36$ g cm^{-3}.
(*Bottom*) A/a = ratio of effective to apparent area.

The above procedures establish the thickness of the films only with reference to an arbitrary zero, namely the thickness of films formed to 10 volts (sat. cal.) under the conditions stated. The optical method does not give an absolute measure of thickness because the optical constants of the metal are not known with sufficient accuracy. Instead, having shown that $\Delta V/\Delta D$ is constant (Fig. 3), we assume that, if $V - V_0$ is the overpotential for the production of oxide, $(V - V_0)/D = \Delta V/\Delta D$. This gives the zero of the scale of thickness to the right of Fig. 1 and the values of X (equation 4) shown in Fig. 2.

The films recrystallize under the influence of an applied field in very much the same manner as do those on tantalum (Vermilyea (13)). However, with our samples of metal, the crystalline nuclei appeared much more quickly than with tantalum. In contrast with tantalum, the kinetics were not very sensitive to the surface preparation (chemically polished, etched in HF, mechanically polished) though the shape of the crystalline areas

Can. J. Chem. Downloaded from www.nrcresearchpress.com by 186.148.149.217 on 09/04/12
For personal use only.

varied (e.g. mechanically polished surfaces gave epicycloid-shaped areas). Sectors like those which are seen with crossed nicols in Ta_2O_5 crystalline areas were not apparent.

DISCUSSION

The thickness of a given film can be obtained within a few per cent by the use of Fig. 1 in conjunction with a simple spectrophotometric measurement. The curves in Fig. 1 for films thicker than about 2000 Å are based on the results for the thinner films (using [4]).

In an earlier paper (3), the thickness was calculated from the charge passed (using [2]) taking $a = A$ and assuming $\rho = 5$ cm^{-3} (which was about in the middle of the range of the values of ρ reported at that time). The corrections for conversion to $\rho = 4.36$ g cm^{-3}, and $A = (1.07a)$ cancel. The experimental results are, therefore, in good agreement (the ratio A/a may have been slightly different). In the earlier work, the field strength was determined only at lower current densities but extrapolation gives a value of about 4.4×10^6 v cm^{-1}, which is again in satisfactory agreement with present values calculated in the same way from [2] with $a = A$ (Fig. 3).

The large difference between the dielectric constants for Nb_2O_5 and Ta_2O_5 (27.6) is notable. It could be due either to an extra contribution to $(\epsilon - n^2)$ of the infrared lattice vibrations in Nb_2O_5,* or to a larger contribution from ionic relaxation processes associated with interstitial ions.

The ratio of the a-c. capacities per unit area of niobium and tantalum electrodes formed to the same potential at the same current density and temperature is given by

$$(E_{Nb_2O_5}\epsilon_{Nb_2O_5})/(E_{Ta_2O_5}\epsilon_{Ta_2O_5})$$

where E = field strength in the oxide. At 10 ma cm^{-2} this ratio is between 1.1 and 1.2. The lower field strength required in Nb_2O_5 to give a particular ionic current thus means that the high dielectric constant does not give much advantage in using niobium in place of tantalum in electrolytic capacitors, the chief advantages to be obtained being the more plentiful reserves of the metal and its lower density.

The above results are applicable only to films formed in dilute solution.

The fact that with Al_2O_3 films the dielectric constant is again lower (about 10), and the fields higher, suggests that there is a correlation between the dielectric properties of the oxide and its ionic conductivity.

ACKNOWLEDGMENTS

This work was supported by the Defence Research Board of Canada and is published with their permission. I thank Dr. G. M. Shrum and Dr. R. H. Wright of the British Columbia Research Council for their encouragement. The electronic control apparatus was designed and built by Mr. R. Cuthbert and Mr. F. J. Curzon.

REFERENCES

1. L. YOUNG. Proc. Roy. Soc. A, **244**, 41 (1958).
2. L. YOUNG. Trans. Faraday Soc. **51**, 1250 (1955).
3. L. YOUNG. Trans. Faraday Soc. **52**, 502 (1956).
4. L. YOUNG. Trans. Faraday Soc. **52**, 516 (1956).
5. L. YOUNG. Trans. Faraday Soc. **53**, 279 (1957).
6. R. K. HART. Proc. Roy. Soc. A, **236**, 68 (1956).
7. S. HUNTER and P. FOWLE. J. Electrochem. Soc. **101**, 481 (1954).
8. D. A. VERMILYEA. Acta Met. **2**, 476 (1954).

*$\epsilon - n^2 = 4\{(n^2+2)/3\}^2 (e^2N/m\, w_t^2)$ *where* e = *effective charge on ions,* N = *number of unit cells per unit volume,* m = *reduced mass of ions,* w_t = *traverse vibration frequency (14). If* w_t *were assumed to be about the same, the observed difference could be ascribed to* m.

Can. J. Chem. Downloaded from www.nrcresearchpress.com by 186.148.149.217 on 09/04/12
For personal use only.

9. L. YOUNG. Acta Met. **5**, 711 (1957).
10. E. A. DURBIN, A. E. WAGNER, and C. G. HARMAN. Batelle Memorial Institute Repts., B.M.I. 792 (1952).
11. F. HOLTZBERG, A. REISMAN, M. BERRY, and M. BERKENBLIT. J. Am. Chem. Soc. **79**, 2039 (1957).
12. F. ABELÈS. Compt. rend. **228**, 553 (1949).
13. D. A. VERMILYEA. J. Electrochem. Soc. **102**, 207 (1955).
14. H. FRÖHLICH. Theory of dielectrics. Oxford. 1949.

Can. J. Chem. Downloaded from www.nrcresearchpress.com by 186.148.149.217 on 09/04/12
For personal use only.

Can. J. Chem. Downloaded from www.nrcresearchpress.com by 186.148.149.217 on 09/04/12
For personal use only.

ALIPHATIC CHEMISTRY OF FLUORENE

PART VI. 3,4-BENZOFLUORENE-9-SPIRO-CYCLOHEXANE[1]

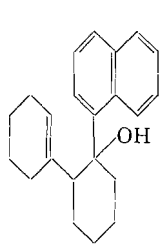
P. M. G. BAVIN[2]

ABSTRACT

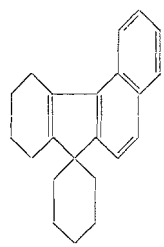
The quinoxaline (VI) has been prepared from 3,4-benzofluorene, establishing the structure of the cyclization product of I as 3,4-benzo-5,6,7,8-tetrahydrofluorene-9-spiro-cyclohexane. 3,4-Benzo-9,9-dimethylfluorene has been prepared and oxidized to the quinone (VIII) which formed the quinoxaline (IX), structurally related to VI.

1,2:7,8-Dibenzo-9-methylfluorene has been synthesized from 1,2:7,8-dibenzofluorenone which, contrary to an earlier report (13), forms an oxime.

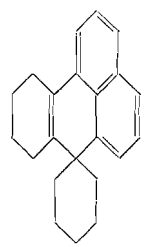
Cyclization of the tertiary alcohol (I)* by aluminum chloride was shown to give a hydrocarbon A, for which two structures have been proposed (II (1, 2), III (3)). Dehydrogenation of A gave a new hydrocarbon B, by loss of four atoms of hydrogen. Oxidation of B gave a crimson quinone which, contrary to an earlier report (3), has now been shown to condense with *o*-phenylenediamine with formation of a quinoxaline. The structures of the hydrocarbons A and B have been established by preparing the quinoxaline from 3,4-benzofluorene.



I



II

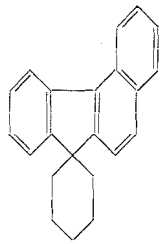


III

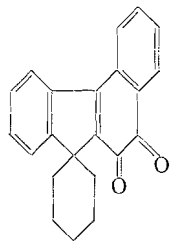
The reaction between 3,4-benzofluorene, phenyl lithium, and 1,5-dibromopentane gave a semisolid hydrocarbon mixture which was purified through its picrate and then oxidized with chromic oxide. Condensation of the crude quinone with *o*-phenylenediamine gave a quinoxaline in 7% over-all yield, which was shown to be identical with the quinoxaline derived from A. This preparation unambiguously establishes the structures of A and B as being II and IV, respectively. Structure V for the quinone is based on the very reasonable assumption that oxidation of IV occurred in the substituted naphthalene ring, as it does in electrophilic substitution reactions of 1,2-dimethylnaphthalene (6, 7, 8). It follows that the quinoxaline has structure VI.

The structures ascribed to B were based on a comparison of its ultraviolet spectrum with those of 3,4-benzofluorene (2) and benzanthrene (3). Although the spectra of the latter two hydrocarbons are quite similar (9, spectra numbers 430 and 436), the difference is sufficient to justify Jones' original assignment (2) of structure IV to B. Before attempting the synthesis of the quinoxaline (VI), 3,4-benzo-9,9-dimethylfluorene (VII) was prepared as a more suitable model. Oxidation gave a quinone which formed a quinoxaline.

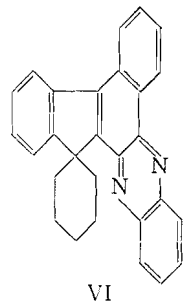
[1]*Manuscript received March 8, 1960.*
Contribution from the Chemistry Department, the University, Hull, East Yorkshire, England.
[2]*I.C.I. Fellow.*
**The isomeric cyclohexylidene structure has been used (4) but is incorrect since it has been shown (5) that the starting material is 2-cyclohex-1'-enylcyclohexanone.*



IV

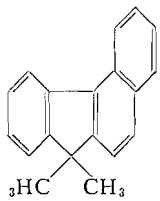


V

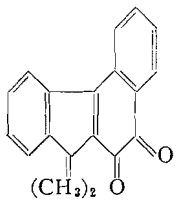


VI

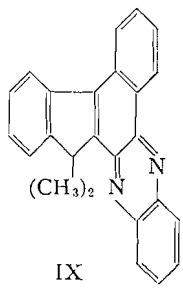
For reasons outlined above, these are given structures VIII and IX, respectively. The ultraviolet spectra of the pairs IV–VII, V–VIII, and IV–IX were almost superposable and the infrared spectra were remarkably similar, even in the fingerprint region.



VII



VIII



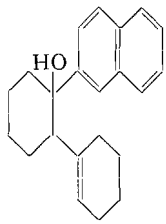
IX

Bergmann and Eschinazi (1) were unable to prepare either A (II) or B (IV) crystalline, and the picrate of A was accompanied by a second, unidentified, picrate. Our original procedure (3) has been repeated but only one picrate (of A) could be isolated. Both A and B are readily obtained crystalline after purification of their picrates. The sample of B examined by Jones (2) was impure since its ultraviolet spectrum showed low intensity bands at wavelengths greater than 340 mμ in contradistinction to our crystallized sample. Data presented in the section dealing with spectra (see Experimental) suggests strongly that the impurity was perylene. This could have been formed under the vigorous conditions used for the cyclization by oxidative dimerization (10) of naphthalene present as impurity in the tertiary alcohol (I). It is significant that the sample of B was described (2) as 'yellow'.

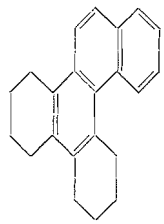
The cyclization described above is of particular interest since a five-membered ring is formed by substitution at a β-naphthyl position although α-substitution to give a six-membered ring seemed feasible. Similar cyclizations have been reported (11, 12) and it is agreed (4, 11, 12) that they proceed by way of mesomeric carbonium ions, but plausible reasons for the preferred direction of cyclization have not been advanced. The tertiary alcohol (X), isomeric with I, was cyclized to (XI) (3), showing that six-membered rings may be formed by α-substitution.

Under the influence of stannic chloride, 1,1-diphenylethylene is well known to dimerize, the initial product undergoing further reactions. Wolf (11) has reported that the same reagent cyclizes 1,1-(di-α,β-naphthyl)-ethylene to 1,2:5,6-dibenzo-9-methylfluorene, and 1,1-(di-α,α-naphthyl)-ethylene to 1,2:7,8-dibenzo-9-methylfluorene (XII). Under comparable conditions 1,1-(di-β,β-naphthyl)-ethylene was dimerized. It has now been found

Can. J. Chem. Downloaded from www.nrcresearchpress.com by 186.148.149.217 on 09/04/12
For personal use only.



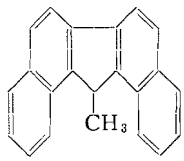
X



XI

that 1-(α-naphthyl)-1-phenylethylene is recovered unchanged after being heated on the steam bath with stannic chloride, for periods up to 48 hours. A reasonable interpretation of these facts is not available.

The structure of Wolf's hydrocarbon (XII) has been confirmed by synthesis from 1,2:7,8-dibenzofluorenone which, contrary to an earlier report (13), forms an oxime.*



XII

EXPERIMENTAL

3,4-Benzo-5,6,7,8-tetrahydrofluorene-9-spiro-cyclohexane (A, II)

2-Cyclohex-1′-enyl-1-α-naphthyl-cyclohexanol (I) was prepared as described previously (3). A sample slowly crystallized, recrystallization from hexane giving small prisms, m.p. 102–104° (lit. m.p. 104.0–104.5° (15)). Cyclization with aluminum chloride, using carbon disulphide as solvent, followed by distillation at 1 mm gave a pale yellow gum, which was converted to the dark red picrate, m.p. 163–164° (1, 3). Regeneration of the hydrocarbon by passing a solution of the picrate in benzene through a column of activated alumina gave an easily crystallized product which formed prisms from methanol, m.p. 96–98° (3).

3,4-Benzofluorene-9-spiro-cyclohexane (B, IV)

Dehydrogenation of a crystallized sample of the preceding hydrocarbon at 300°, using 10% palladium on charcoal as catalyst, gave an oil which was converted to the bright red picrate, m.p. 142–143° (1, 3). Regeneration of the hydrocarbon gave an oil which crystallized after it was cooled with liquid air. Recrystallization from acetone–methanol gave colorless prisms, m.p. 88–90° (3). The yield based on I was 38%.

Oxidation with CrO_3 in acetic acid gave 3,4-benzofluorene-1,2-quinone-9-spiro-cyclohexane (V), which crystallized as lustrous crimson plates from acetic acid, m.p. 224–225° (1, 3).

14H-Benz[a]indeno[1,2-c]phenazine-14-spiro-cyclohexane (VI)

The crude quinone (1 g) was boiled for 30 minutes with a solution of *o*-phenylenediamine (3 g) in acetic acid (70 ml). After pouring into dilute hydrochloric acid (500 ml)

**9-Benzoylanthracene has also been reported not to form an oxime (14) but should do so under the conditions described in the Experimental.*

Can. J. Chem. Downloaded from www.nrcresearchpress.com by 186.148.149.217 on 09/04/12
For personal use only.

the product was extracted with chloroform. Evaporation left a brown solid which was dissolved in hexane and the solution passed through a column of activated alumina. A bright yellow highly fluorescent band was eluted with benzene–hexane (1:2) and the eluant evaporated. Crystallization from heptane gave bright yellow prisms (0.6 g), m.p. 235–236°. Found: C, 87.15; H, 5.71; N, 7.14. Calc. for $C_{28}H_{22}N_2$: C, 87.01; H, 5.74; N, 7.25%.

1,5-Dibromopentane (2 g) was added to a solution of 3,4-benzofluorene (2 g) in ether containing phenyl lithium (from bromobenzene, 10 g). The color of the fluorene anion had disappeared after 8 minutes. Inorganic salts were removed by washing with water and the ether was evaporated to leave an oily hydrocarbon. After purification through the bright red picrate, m.p. 122–136°, the hydrocarbon mixture partly crystallized when seeded with IV. Oxidation with CrO_3 (5 g) in acetic acid followed by condensation with *o*-phenylenediamine gave a quinoxaline, which was purified as described above. Crystallization from heptane gave bright yellow prisms (0.25 g, 7% based on 3,4-benzofluorene), m.p. 232–234°, not depressed by the quinoxaline from B. Found: C, 86.91; H, 5.82. Comparison of infrared spectra confirmed the identity.

3,4-Benzo-9,9-dimethylfluorene (VII)

3,4-Benzofluorene (5 g) was methylated as described for fluorene (16). The oily product was converted to the *picrate*, which crystallized from ethanol as beautiful dark red needles, m.p. 147–149°. Found: C, 63.59; H, 4.14. Calc. for $C_{25}H_{19}N_3O_7$: C, 63.42; H, 4.05%.

Decomposition of the picrate on alumina gave an easily crystallized product which formed colorless prisms from acetone–methanol, m.p. 82–83°. Many of the crystals showed extensive twinning. Found: C, 93.65; H, 6.61%. Calc. for $C_{19}H_{16}$: C, 93.40; H, 6.60%.

Oxidation with CrO_3 in acetic acid was complete after a few minutes on the steam bath. *3,4-Benzo-9,9-dimethylfluorene-1,2-quinone* (VIII) crystallized as lustrous crimson plates from acetic acid, m.p. 216–217.5°. Found: C, 83.03; H, 5.13. Calc. for $C_{19}H_{14}O_2$: C, 83.19; H, 5.14%.

14,14-Dimethyl-14H-benz[a]indeno[1,2-c]phenazine (IX)

Prepared and purified as described for VI, the quinoxaline formed bright yellow blades from heptane, m.p. 193–194°. Found: C, 86.70; H, 5.26. Calc. for $C_{25}H_{18}N_2$: C, 86.67; H, 5.24%.

1,2:7,8-Dibenzo-9-methylfluorene (XII)

The reaction between ethereal methyl lithium and 1,2:7,8-dibenzofluorenone (17) gave an almost quantitative yield of 1,2:7,8-dibenzo-9-methyl-9-fluorenol, which crystallized from toluene as colorless plates, m.p. 216–218° (not analyzed). The fluorenol (1 g) was reduced by warming with acetic acid (200 ml) and zinc dust (20 g), a few drops of concentrated hydrochloric acid being added every 5 minutes during 30 minutes. The product crystallized from heptane as colorless lustrous plates (0.7 g), m.p. 173–174°, not depressed by an authentic sample of Wolf's hydrocarbon (11). During the preparation of the latter it was noted that stannic chloride from a new bottle did not react with the dinaphthylethylene, but addition of a drop of water initiated the reaction observed by Wolf (11). This experiment was carried out in Ottawa during a prolonged cold spell (−20° F) when the relative humidity was very low.

Can. J. Chem. Downloaded from www.nrcresearchpress.com by 186.148.149.217 on 09/04/12
For personal use only.

1,2:7,8-Dibenzofluorenone Oxime

The ketone (0.1 g), hydroxylamine hydrochloride (1 g) and dry pyridine (10 ml) were boiled under reflux for 2 hours. The mixture was poured onto ice and hydrochloric acid and the precipitate crystallized from toluene–heptane to give slender orange needles (0.08 g), m.p. 211–212° with decomposition. Found: N, 4.63. Calc. for $C_{21}H_{13}NO$: N, 4.74%.

The known oximes of fluorenone and 3,4:5,6-dibenzofluorenone were prepared similarly in excellent yields.

1,1-Diphenylethylene (10 g, f.p. 7–8°) and stannic chloride (25 g) were warmed on the steam bath for 10 minutes. Pouring onto ice and hydrochloric acid precipitated a white solid which crystallized from acetone–methanol as white prisms (5.5 g), m.p. 112–113°, completely identified as 1,1,3,3-tetraphenylbut-1-ene (lit. m.p. 113–114 (18)) by oxidation with CrO_3 to benzophenone (2,4-dinitrophenylhydrazone) and α,α-diphenylpropionic acid, identical with an authentic sample (19).

1-α-Naphthyl-1-phenylethylene (20) was recovered unchanged in more than 90% yield after it was heated on the steam bath with stannic chloride for periods up to 48 hours.

SPECTRA

Infrared spectra were obtained using a Unicam SP-100 spectrophotometer with samples prepared as solutions in chloroform and as potassium bromide disks.

Ultraviolet spectra were obtained using a Beckmann DK-2 recording spectrophotometer with ethanol as solvent. The data is collected in *Table I*, for the hydrocarbons and quinones. The quinoxalines showed peaks at 432, 415, 320, 307, 278, 255, and 229 mμ (log ϵ values not recorded).

TABLE I

Compound										
				Hydrocarbons						
VII				339 4.17	324 4.07	314 4.13	303 4.01	247* 4.34	240* 4.5	231‡ 4.68
IV (3, 21)†				340 4.19	325 4.04	316 4.05	305* 3.93	250* 4.29		234‡ 4.61
(2)	436 1.69	410.5 1.61	384.5 1.38	339.5 4.55	325 4.43	315 4.45		Not recorded		
Perylene (22)	434‡ 4.6	406‡ 4.45	387‡ 4.1							
				Quinones						
VIII	453‡ 3.43	329‡ 3.89	265‡ 4.28		246‡ 4.25					
V (3, 21)†	439 3.41	308 3.80	264 4.30	255* 4.28	249 4.26					
(2)	460 3.49	333 3.94	268 4.32		247 4.28					

NOTE: The data is presented as $\lambda(m\mu)/\log \epsilon$.
*Shoulder or inflection. †Solvent: cyclohexane. ‡Broad peak.

ACKNOWLEDGMENTS

The author is indebted to Dr. G. W. Gray and Miss A. Stephenson for the infrared spectra, and to Dr. C. Daglish (Reckitt and Sons, Ltd.) for the ultraviolet spectra. Dr. K. Clarke kindly read the manuscript.

Can. J. Chem. Downloaded from www.nrcresearchpress.com by 186.148.149.217 on 09/04/12
For personal use only.

REFERENCES

1. F. BERGMANN and H. E. ESCHINAZI. J. Am. Chem. Soc. **66**, 183 (1944).
2. R. N. JONES. J. Am. Chem. Soc. **66**, 185 (1944).
3. P. M. G. BAVIN and M. J. S. DEWAR. J. Chem. Soc. 4479 (1955).
4. F. BERGMANN and S. ISRAELASHWILI. J. Am. Chem. Soc. **68**, 1 (1946).
5. J. REESE. Ber. **75**, 384 (1942).
6. C. L. HEWETT. J. Chem. Soc. 293 (1940).
7. P. A. PLATTNER and A. RONEO. Helv. Chim. Acta, **27**, 400 (1944).
8. R. T. ARNOLD *et al.* J. Am. Chem. Soc. **69**, 2322 (1947).
9. R. A. FRIEDAL and M. ORCHIN. Ultra-violet spectra of aromatic compounds. John Wiley & Sons, Inc., New York. 1951.
10. R. SCHOLL, C. SEER, and R. WEITZENBÖCK. Ber. **43**, 2202 (1910).
11. G. WOLF. J. Am. Chem. Soc. **75**, 2673 (1953).
12. E. BERLINER. J. Am. Chem. Soc. **64**, 2894 (1942).
13. A. WANSCHEIDT. J. Russ. Phys. Chem. Soc. **58**, 55 (1926); Chem. Abstr. **21**, 581 (1927).
14. W. E. BACHMANN and M. X. BARTON. J. Org. Chem. **3**, 303 (1939).
15. C. C. BARKER, R. G. EMMERSON, and J. D. PERIAM. J. Chem. Soc. 1077 (1958).
16. P. M. G. BAVIN. Can. J. Chem. **38**, 882 (1960).
17. A. WANSCHEIDT. Ber. **59**, 2092 (1926).
18. W. SCHMIDT-NICKELS. Ber. **62**, 917 (1929).
19. F. A. L. ANET and P. M. G. BAVIN. Can. J. Chem. **35**, 1084 (1957).
20. C. D. HURD and C. N. WEBB. J. Am. Chem. Soc. **49**, 546 (1927).
21. P. M. G. BAVIN. Thesis, London. 1954.
22. E. CLAR. Spectrochim. Acta, **4**, 119 (1950).

Can. J. Chem. Downloaded from www.nrcresearchpress.com by 186.148.149.217 on 09/04/12
For personal use only.

Can. J. Chem. Downloaded from www.nrcresearchpress.com by 186.148.149.217 on 09/04/12
For personal use only.

THE REACTION OF 2-CYANO-2-PROPYL FREE RADICALS WITH OXYGEN

2-CYANO-2-PROPYL HYDROPEROXIDE[1]

M. TALÂT-ERBEN[2] AND NEVZAT ÖNOL

ABSTRACT

The reaction with oxygen of cyanisopropyl free radicals generated by the polymerization catalyst 2,2′-azobisisobutyronitrile has been investigated. In xylene, or benzene, as solvent at 55° the products identified are: (1) a new compound, 2-cyano-2-propyl hydroperoxide; (2) acetone cyanohydrin; (3) hydrogen cyanide; (4) cyanogen; (5) acetone; (6) *p*-methyl benzaldehyde (in xylene only); and (7) tetramethylsuccinodinitrile. The hydroperoxide is surprisingly stable; its physical constants are: b.p. 37° C at 1 mm Hg; m.p. −9 to −8°; n_D^{20} 1.4138; d_{20} 1.013 g/ml. In benzene under the same experimental conditions, only a very small amount of the hydroperoxide is obtained, the principal product being acetone cyanohydrin. A free-radical mechanism is proposed. The induced decomposition of the hydroperoxide, which is important in benzene, is almost completely inhibited in the presence of xylene. The new hydroperoxide can be used as a polymerization catalyst at moderately elevated temperatures.

INTRODUCTION

The thermal decomposition of 2,2′-azobisisobutyronitrile (Porofor N) has been studied extensively in the absence of oxygen (1, 2). Ziegler *et al.* (3) state that during decomposition in the presence of air, the total pressure of the gas phase does not change, owing to the fact that the increase of pressure due to the nitrogen evolved, is compensated by the equimolecular amount of oxygen taken up simultaneously by the cyanisopropyl radicals produced. These authors postulated the formation of di-(2-cyano-2-propyl) peroxide,

$$2(NC)\dot{C}(CH_3)_2 + O_2 \rightarrow (NC)(CH_3)_2C—O—O—C(CN)(CH_3)_2.$$

Van Hook and Tobolsky (4), on the other hand, observed that when the azo compound is decomposed in the presence of air, the optical density of the solution becomes higher than in the case in which the decomposition is carried out in an oxygen-free atmosphere, indicating that some peroxides are formed which absorb light in the ultraviolet region. However, neither Ziegler and co-workers nor Van Hook and Tobolsky attempted to isolate these products. Therefore, it would be of interest to investigate this reaction.

EXPERIMENTAL

The azo compound was recrystallized from benzene, m.p. 101° C with decomposition. The reaction was carried out at 55°, benzene (E. Merck) or xylene (E. Merck) being used as solvent. The solvent was dried with anhydrous sodium sulphate. A continuous stream of tiny bubbles of oxygen was passed at the rate of about 3 liters per hour, through the solution containing 30 g of the azo compound in 300 ml of solvent. The tiny bubbles were produced by forcing the gas to pass through a sintered-glass filter surface, placed at the bottom of the reaction vessel. The oxygen was purified by passage through towers containing soda lime and calcium chloride. The gas leaving the reaction vessel was passed through a reflux condenser to trap the solvent as well as other liquid products that it probably carried with it, then bubbled through a solution of potassium hydroxide to absorb the hydrogen cyanide and cyanogen, which were found to be reaction products (see below). After about 100 hours the reaction was stopped, and the excess of solvent

[1]*Manuscript received March 22, 1960.*
Contribution from the Faculty of Mining Engineering, Technical University of Istanbul, Istanbul, Turkey.
[2]*Present address: Research and Analytical Section, Eurochemic, Mol-Donk, Belgium.*

Can. J. Chem. Downloaded from www.nrcresearchpress.com by 186.148.149.217 on 09/04/12
For personal use only.

was removed by distillation under reduced pressure. The residual solution was extracted 15 to 20 times with 50 ml of distilled water. The combined aqueous solutions were extracted with ether. The ethereal solution was dried with anhydrous sodium sulphate, then evaporated at 60°, until all the ether was removed. The residue from the ether extract, which consisted of a yellowish liquid, was fractionated by vacuum distillation in an all-glass apparatus with a Claisen head, and two fractions were obtained. Fraction A, collected between 60 to 65° at 15 mm Hg, proved to be acetone cyanohydrin, whereas the subsequent fraction B has been identified as 2-cyano-2-propyl hydroperoxide, $(NC)(CH_3)_2C—O—O—H$.

Identification of Acetone Cyanohydrin

A sample of fraction A, further purified by fractional distillation, b.p. 62°/15 mm Hg, n_D^{20} 1.3990, boiled at about 110° at atmospheric pressure, and decomposed while boiling. Two products of decomposition were detected: a liquid, trapped by means of a reflux condenser, and a gas absorbed in potassium hydroxide. The liquid, b.p. 51°/76 cm Hg, n_D^{20} 1.3550, formed with 2,4-dinitrophenylhydrazine a crystalline precipitate with a melting point of 126° C. This liquid must, therefore, be acetone. In the potassium hydroxide solution, cyanide was detected (Berlin blue). It follows that fraction A is acetone cyanohydrin. Nitrogen content found (Kjeldahl): 16.07%. Calculated for C_4H_7ON: 16.46%. Yield: 85 (mole)% in benzene, 20 (mole)% in xylene, based on the azo compound decomposed.

Identification of 2-Cyano-2-propyl Hydroperoxide

Fraction B is a peroxide. Its high solubility in water suggests that it is a hydroperoxide, rather than a di-(cyano-alkyl) peroxide. This has been confirmed by the following observations. The product from vacuum distillation was further purified by fractional crystallization. On cooling to −10°, colorless crystals were obtained. By use of the analytical procedure of Vaughan and co-workers (5) a molecular weight of 105 was found, assuming that only one —O—O— group is contained in the molecule. A cryoscopic molecular weight determination in benzene gave a value of 95. The two results compare well with the theoretical molecular weight of 101, corresponding to the structure $(NC)(CH_3)_2C—O—O—H$, and they are incompatible with the structure $(NC)(CH_3)_2C—O—O—C(CH_3)_2(CN)$. Nitrogen content found (Kjeldahl): 13.52%. Calculated for $C_4H_7O_2N$: 13.86%. This product must, therefore, be isobutyronitrile hydroperoxide of at least 96% purity. Its physical constants are: b.p. 37°/1 mm Hg, m.p. −9 to −8°, n_D^{20} 1.4138, d_{20} 1.013 g/ml.

This hydroperoxide is surprisingly stable. The pure material decomposes only above 120°. Yield in xylene: 46 (mole)% with respect to the azo compound; in benzene the yield is negligible (2 (mole)%).

Polymerization Experiment

About 0.3 gram of hydroperoxide was added to 15 ml of methacrylonitrile in a test tube, and heated at 80°. Approximately 20% of the monomer polymerized in 3 hours. This indicates that the hydroperoxide can be used as a polymerization catalyst.

Detection of Hydrogen Cyanide, Cyanogen, and Acetone

The alkaline solution, through which the oxygen was bubbled after it had left the reaction vessel, was analyzed, and both cyanide and cyanate were found. The former was characterized by the formation of Berlin blue, and the latter by the pyridine test (6). The amount (in moles) of cyanide formed is higher than that of cyanate, indicating

that not only $(CN)_2$ but HCN also is a reaction product. The excess of solvent, which was removed immediately before extraction with ether, was found to contain an appreciable amount of acetone (color test with salicylaldehyde).

Tetramethylsuccinodinitrile

The residue from water extraction was left standing overnight at −20°. A large amount of tetramethylsuccinodinitrile crystals were obtained, m.p. 168° C.

Isolation of p-Methylbenzaldehyde

After tetramethylsuccinodinitrile (TMSDN) crystals were separated, the residual solution was vacuum-distilled to remove the solvent; the brown, viscous residue was left standing at −20° overnight, and more TMSDN crystals precipitated. The viscous phase was subjected to a vacuum distillation at 40° (bath temperature), the products being collected in a flask immersed in a dry ice and acetone mixture. At first, more solvent (xylene) and water were collected. The next fraction was refluxed with 30% sulphuric acid in order to hydrolize and dissolve the nitriles (if any). Then, the dark oily residue was purified by steam distillation, and a light yellowish liquid was obtained. This had a strong odor of bitter almond, and a refractive index of 1.548. It proved to be an aldehyde (mirror test). The refractive index is very close to that of *p*-methylbenzaldehyde. Therefore, it is reasonable to assume that this is an oxidation product of the solvent (xylene) sensitized by the free radicals. In fact, it is known that if, under ultraviolet illumination, oxygen is bubbled through toluene for a long time some benzaldehyde is obtained (8). This identification is further supported by the fact that this product was not found in the residues from the runs in which benzene was used as solvent.

DISCUSSION

The nature and diversity of the reaction products which have been identified in this work show that the reaction of cyanisopropyl radicals with oxygen is a very complicated one. Di-(2-cyano-2-propyl) peroxide, the formation of which was postulated by Ziegler *et al.* (3), has not been found in the present work. This could mean that this peroxide is thermally unstable at the operating temperature, or it is very sensitive to the radical-induced decomposition caused by the free radicals which are present at relatively high concentrations during the entire course of the reaction. Undoubtedly, this peroxide must be much more unstable than its unsubstituted analogue, di-tertiary butyl peroxide, owing to the electron-attracting character of the two nitrile groups in the molecule. Its main decomposition products would be acetone and .CN free radicals. The former has actually been detected as shown in the experimental part; the recombination product of the latter, cyanogen, has also been identified. The fact that the hydroperoxide is not obtained when benzene is used as solvent could be explained by the greater stability of the benzene molecule with respect to hydrogen abstraction by the $(NC)(CH_3)_2C—O—O.$ radicals. Consequently, these radicals would have a longer mean life in benzene; this would favor their combination with other radicals. Therefore, a transient formation of di-cyanisopropylperoxide is more probable in benzene than in xylene. This conclusion could be correlated with the observation that in some runs with benzene, in which the reaction was stopped at an early stage owing to an experimental difficulty of some kind, an explosive reaction took place during the vacuum distillation of the reaction mixture. Another possible explanation is that the hydroperoxide does actually form in benzene by hydrogen abstraction from other sources (molecules or free radicals available), but in the reaction medium which contains a high concentration of free radicals, it undergoes

Can. J. Chem. Downloaded from www.nrcresearchpress.com by 186.148.149.217 on 09/04/12
For personal use only.

a fast-induced decomposition in this particular solvent. In fact, we found that the hydroperoxide which, when pure is very stable up to 120° C, decomposes with a measurable rate in benzene at temperatures as low as 75° C, in the presence of the azo compound. On the other hand, we found that the decomposition of the hydroperoxide in the presence of the azo compound is negligible at the same temperature when xylene is used instead of benzene.

The experimental evidence available does not seem to permit a final conclusion concerning the two alternatives. However, it can be concluded that the nature of the reaction products identified in this work indicates that there must be a complete analogy between the mechanisms of the thermal decomposition of the cyano-alkyl peroxides and that of the corresponding alkyl peroxides. In other words, a reaction scheme similar to that proposed by Vaughan *et al.* (7), for the liquid phase decomposition of *t*-butylhydroperoxide, can be used to account for the decomposition of cyanisopropyl hydroperoxide, if it is assumed that dismutation of cyanisopropoxy radicals, $(NC)(CH_3)_2C—O.$, produced by cleavage of the O—O bond, gives .CN free radicals. A similar mechanism would be applicable to the more unstable di-(cyanisopropyl) peroxide.

An experimental investigation of the kinetics of the thermal decomposition of cyanisopropylhydroperoxide, and its properties as a polymerization catalyst, is under way in these laboratories, and will be the subject of a subsequent publication.

ACKNOWLEDGMENTS

The authors wish to thank Dr. S. Bywater of the National Research Council of Canada, for a gift of azobisisobutyronitrile, without which the present work could not be carried out. Another gift of Porofor N by Bayer Aktiengesellschaft, Leverkusen, Germany, is also gratefully acknowledged.

REFERENCES

1. A. F. Bickel and W. A. Waters. Rec. trav. chim. **69**, 1940 (1950).
2. M. Talât-Erben and S. Bywater. J. Am. Chem. Soc. **77**, 3710 (1955).
3. K. Ziegler, W. Parade, and W. Meye. Ann. 567 (1950).
4. J. P. Van Hook and A. V. Tobolsky. J. Am. Chem. Soc. **80**, 779 (1958).
5. F. H. Dickey, J. H. Raley, F. F. Rust, R. S. Tresede, and W. E. Vaughan. Ind. Eng. Chem. **41**, 1673 (1949); R. Mesrobian and A. V. Tobolsky. Organic peroxides. John Wiley & Sons, Inc., New York. 1954.
6. W. W. Scott. Standard methods of chemical analysis. 5th ed. Van Nostrand and Co., Inc., New York. 1947. p. 2363.
7. E. R. Bell, J. H. Raley, F. F. Rust, F. H. Seubold, and W. E. Vaughan. Discussions Faraday Soc. **10**, 246 (1951).
8. V. Grignard (*Editor*). Traité de chimie organic. Vol. VII. Paris. 1950. p. 334.

Can. J. Chem. Downloaded from www.nrcresearchpress.com by 186.148.149.217 on 09/04/12
For personal use only.

Can. J. Chem. Downloaded from www.nrcresearchpress.com by 186.148.149.217 on 09/04/12
For personal use only.

THE ELECTRON SPIN RESONANCE ABSORPTION SPECTRA OF SEMIQUINONE IONS

PART I. THE HYPERFINE SPLITTING DUE TO ALKOXY GROUPS[1]

Y. MATSUNAGA[2] AND C. A. MCDOWELL

ABSTRACT

The electron spin resonance absorption spectra of semiquinone ions with alkoxy groups have been examined and compared with those with substituted alkyl groups. The splitting constant for the alkoxy protons has been found to be about one-half that of alkyl protons in the corresponding free radical. Hyperfine splittings due to methoxy, ethoxy, and isopropoxy protons have been demonstrated using the semiquinone ions formed by oxidation of alkyl gallates. The available evidence suggests that, in accounting for the hyperfine splitting due to alkyl protons, spin polarization is as important as electron delocalization.

INTRODUCTION

The electron spin resonance (e.s.r.) absorption spectra of semiquinone ions have been examined extensively by many workers. The rather simple structure of the free radicals of this kind makes possible the analysis of the hyperfine structure of the observed resonance absorption spectra. It has been shown by the studies of the methyl-substituted benzo- and naphtho-semiquinone ions (1, 2) that both the ring and the methyl protons contribute to the hyperfine splitting in comparable magnitude. The cause of the methyl proton splitting has been ascribed to hyperconjugation, and the details have been accounted by the molecular orbital and the valence bond theories of hyperconjugation (3, 4). Proton hyperfine splitting for more complicated substituents has been described in some cases. Hyperfine splitting due to *tert.*-butyl protons in benzosemiquinone ions has been observed by Hoskins (5) and by Fraenkel (6). The three triplets found in the spectrum of the semiquinone ion formed by the oxidation of *n*-propyl gallate may be assigned (7) to two ring protons and two *n*-propyl protons.

Here we wish to present the results of a study of the contribution of alkoxy protons to the hyperfine structure of the e.s.r. absorption spectra of some semiquinone ions. With the view to ascertaining the effect of the oxygen atoms we examined the spectra of the 2,5-dimethoxy- and 2,5-diethoxy-*p*-benzosemiquinone ions, and also the 3,3′,5,5′-tetramethyl-*p*-biphenosemiquinone ion, and compared these with those of the 2,5-dimethylbenzo- and 3,3′,5,5′-tetramethyl-*p*-bipheno-semiquinone ions. Secondly, to demonstrate the contribution of methoxy, ethoxy, and isopropoxy protons, we examined the semiquinone ions formed by the oxidation of various alkyl gallates.

The hyperfine splitting observed in the e.s.r. spectra of free radicals is caused by the interaction between nuclei with a magnetic moment, and an unpaired electron, through direct dipole–dipole forces, and also through the isotopic Fermi interaction between the nuclear magnetic moment and the electron–spin magnetic moment. Free radicals in solution can show only hyperfine splitting due to the latter interaction, because the rapid tumbling of the molecule averages out the anisotropic dipolar interaction (8). The magnitude of the splitting due to the Fermi interaction is proportional to the spin density at the nucleus. If we adopt a single configurational molecular orbital description, the spin density will be replaced by the unpaired electron density. It has been shown that

[1]*Manuscript received March 7, 1960.*
Contribution from the Department of Chemistry, University of British Columbia, Vancouver 8, British Columbia.
[2]*National Research Council Postdoctorate Fellow 1957–59.*

the magnitude of ring proton splitting is approximately proportional to the density of the unpaired π-electron in the aromatic carbon atom (9), and a similar relation holds for the methyl protons (4).

The spin Hamiltonian for an organic free radical of the semiquinone type may be written as

$$[1] \qquad H = g\beta \mathbf{H} \cdot \mathbf{S} + \sum_i A_i (\mathbf{S} \cdot \mathbf{I}_i)$$

which has eigen values

$$[2] \qquad E = g\beta H M_S + \sum_i A_i M_S M_I .$$

For the transitions $(M_S \rightarrow M_S' \pm 1)(M_I \rightarrow M_I)$ this yields, for the strong field case, the frequencies

$$[3] \qquad \nu = \frac{1}{h}\left\{ g\beta M + \sum_i A_i M_{I_i} \right\}.$$

The subscript i refers to the nucleus which is coupled to the electron spin. The summation is taken over all such nuclei in the radical. The nuclear magnetic quantum number M_I takes on the values, I_i, $I_i+1, \ldots, -I_i$. There are $2I+1$ such values. If the coupling constants for all the nuclei are equal (i.e. $A_1 = A_2 \ldots = A_i$) the hyperfine splitting constant for each line will be $AM/g\beta$ where M is the total magnetic quantum number. In the case of protons, the spin is $\frac{1}{2}(h/2\pi)$; therefore the absorption spectrum for a free radical with N equivalent proton consists of $N+1$ hyperfine components with the relative intensities given by the binomial distribution $1:N:N(N-1)/2:\ldots N!/k!(N-k)!:\ldots:N:1$.

EXPERIMENTAL

2,5-Dimethoxy- and 2,5-diethoxy-*p*-benzoquinones were prepared by the reaction of the corresponding alcohols with benzoquinone, using anhydrous zinc chloride as a catalyst (10). The compounds were purified by vacuum sublimation. By reduction with sodium dithionite, these two quinones, on dissolving in a mixture of pyridine and 2 *M* KOH (1:1 by volume), give fairly stable free radicals. It was hoped to stabilize the monomeric form of the semiquinone ions by the use of pyridine (11). 3,3′,5,5′-Tetramethyl- and 3,3′,5,5′-tetramethoxy-*p*-biphenols were prepared from the quinones starting from 2,6-dimethylphenol and 2,6-dimethoxyphenol, respectively (12, 13). These biphenols were purified by recrystallization from ethanol and finally by sublimation in vacuum. The semiquinone ions were obtained by air oxidation of the biphenols dissolved in the above-mentioned mixed solvent. The esters of gallic acid were prepared by the standard methods of esterification using sulphuric acid or hydrogen chloride gas as a catalyst (14, 15). The compounds were finally sublimed in a vacuum. The semiquinone ions were obtained by air oxidation of the esters dissolved in a mixture of ethanol and 2 *M* KOH (1:1 by volume). These free radicals could not be found when the parent compound was dissolved in a mixture of pyridine and 2 *M* KOH. The choice of ester is of great advantage in the preparation of the samples with the desired alkoxy groups. However, the hydrolysis during the course of the measurements could not be prevented (see the following section).

An e.s.r. spectrometer with a transmission cavity was used at room temperature, as described previously (16). The spectra shown in this paper are the first derivative of the

Can. J. Chem. Downloaded from www.nrcresearchpress.com by 186.148.149.217 on 09/04/12
For personal use only.

actual absorption lines. The estimated error for the splitting constants is about 0.02 gauss provided the lines are sharp enough. The intensity of the magnetic field increases from left to right in all the figures.

RESULTS AND DISCUSSION

2,5-Dimethoxy- and 2,5-Diethoxy-p-benzosemiquinone Ions

2,5-Dimethoxy-*p*-benzosemiquinone ion (I*a*) shows seven main lines with a hyperfine splitting of 1.05 oersteds (Fig. 1). Although the asymmetric pattern suggests the overlap of the spectra due to other free radicals from impurities or reaction products, further splitting of each line into a triplet could be observed except for the outermost lines (Fig. 2). The 2,5-diethoxy-*p*-benzosemiquinone ion (I*b*) gives a five-line spectrum with a spacing of 1.17 oersteds (Fig. 3). Apparently the major splitting can be attributed to

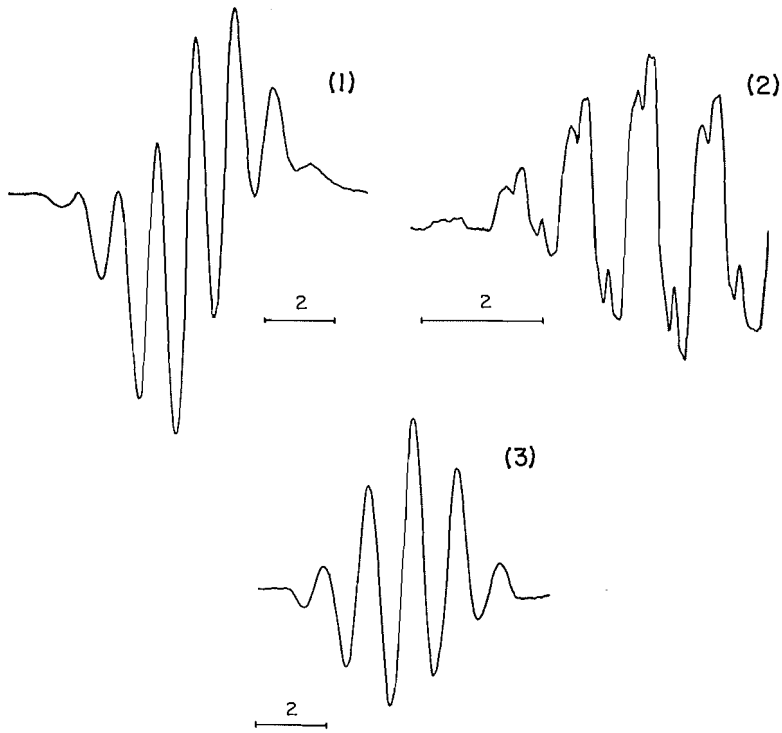
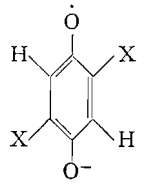


FIG. 1. First derivative of e.s.r. absorption spectrum of the 2,5-dimethoxy-*p*-benzosemiquinone ion (I*a*).
FIG. 2. First derivative of a part of e.s.r. absorption spectrum of semiquinone ion (I*a*) under higher resolution.
FIG. 3. First derivative of e.s.r. absorption spectrum of the 2,5-diethoxy-*p*-benzosemiquinone ion (I*b*).

hyperfine coupling with the alkoxy protons and the minor one of 0.30 oersted found in the methoxy derivative can be ascribed to coupling with the ring protons. In the case of the 2,5-dimethyl-*p*-benzosemiquinone ion examined by Venkataraman and Fraenkel (1), the splitting constant for the ring protons was reported to be 1.83 oersteds and that for the methyl protons 2.26 oersteds. The considerable decrease of the splitting constant of the ring protons resulting from the change of the substituent from alkyl to alkoxy suggests the possible preferential localization of the unpaired electron on the oxygen atoms in the alkoxy groups. Nevertheless, the splitting constant of the alkoxy protons is also less than that of the alkyl protons.

Can. J. Chem. Downloaded from www.nrcresearchpress.com by 186.148.149.217 on 09/04/12
For personal use only.



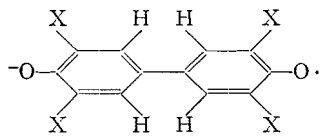
(*a*) X = CH_3O

(*b*) X = CH_3CH_2O

I

3,3′,5,5′-Tetramethyl- and 3,3′,5,5′-Tetramethoxy-p-biphenosemiquinone Ions

The 3,3′,5,5′-tetramethyl-*p*-biphenosemiquinone ion (II*a*) has four ring protons and 12 methyl protons; therefore, if the two benzene nuclei are equivalent five sets of 13 lines are to be expected. Only 21 lines with equidistant spacings were detected because of overlap and small intensity of some of the lines (Fig. 4). The values of the splitting constants, 2.34 oersteds for the ring protons, and 0.78 oersted for the methyl protons, seem to give the pattern which is most consistent with the experimental one. The following intensity ratio is predicted: 1:12:66:224:543:1056:1810:2844:4059:5240:6252:7008:7306:7008:6252:5240:4059:2844:1810:1056:543:224:66:12:1. Among these 25 lines the two at each end of the spectrum are too weak to be detected.



(*a*) X = CH_3

(*b*) X = CH_3O

II

The 3,3′,5,5′-tetramethoxy-*p*-biphenosemiquinone ion (II*b*) has the same number of ring and methyl protons as the tetramethyl derivative. However, the total spread of the spectrum was found to be less than one third of that of the tetramethyl derivative. The observed 13-line spectrum (Fig. 5) can be explained with a splitting constant of 0.49

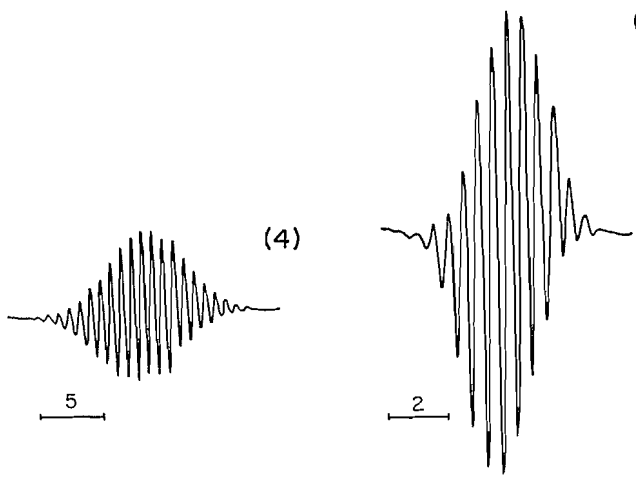


FIG. 4. First derivative of e.s.r. absorption spectrum of the 3,3′,5,5′-tetramethyl-*p*-biphenosemiquinone ion (II*a*).

FIG. 5. First derivative of e.s.r. absorption spectrum of the 3,3′,5,5′-tetramethoxy-*p*-biphenosemiquinone ion (II*b*).

Can. J. Chem. Downloaded from www.nrcresearchpress.com by 186.148.149.217 on 09/04/12
For personal use only.

oersted for both the ring and the methoxy protons. The predicted intensity ratio is 1:16:120:560:1820:4368:8008:11440:12870:11440:8008:4368:1820:560:120:16:1. Again the two lines at each end are expected to be too low in intensity to be detectable. The decrease of the splitting constant of the ring protons is again observed on changing the substituent from methyl to methoxy.

TABLE I

Proton splitting constants in alkyl and alkoxy derivatives of *p*-benzo- and *p*-bipheno-semiquinone ions

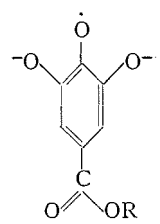
Semiquinone ion	Proton splitting constant in oersteds	
	a (ring)	*a* (alkyl or alkoxy)
I with X = H	2.37*	—
I with X = CH_3	1.83†	2.26†
I*a*	0.30	1.05
I*b*	?	1.17
II*a*	2.34	0.78
II*b*	0.49	0.49

*See references 1 and 7.
†See references 1 and 3.

Later work (see Part III of this series) has, however, indicated that in *p*-biphenosemiquinone salts the unpaired electron density given by the simple LCAO–MO method for carbon atom *a* (adjacent to the C—O bond) is 1.5, or more, times larger than that on carbon atom *b*, regardless of the magnitude of the coulomb integral for the oxygen atoms in the range of $\alpha_O = \alpha_C$ to $\alpha_C + \beta_{CC}$. This permits an alternative assignment of 0.78 oersted for the ring protons and 1.56 oersteds for the methyl protons. The following intensity ratios result and the 21 lines could be those which are not enclosed in parentheses: (1, 4, 18, 52) 139, 312, 628, 1144, 1881, 2860, 3982, 5148, 6171, 6864, 7128, 6864, 6171, 5148, 3982, 2860, 1881, 1144, 628, 312, 139 (52, 18, 4, 1).

Semiquinone Ions from Gallic Acid and Alkyl Gallates

The spectrum of the semiquinone ion (III*a*) formed by oxidation of gallic acid has been reported by Adams, Blois, and Sands (7). The two ring protons give a triplet with a splitting of 1.07 oersteds and a *g*-value of 2.00489.



III

(*a*) R = e^-
(*b*) R = CH_3
(*c*) R = CH_3CH_2
(*d*) R = $(CH_3)_2CH$

The semiquinone ion (III*b*) from methyl gallate gives 10 lines (Fig. 6). The center lines of the expected 12-line spectrum overlap to give a theoretical pattern with an intensity ratio 1:3:3:4:9:9:4:3:3:1. In Fig. 6, the third, the sixth, and the ninth lines from left to right do not follow the above-mentioned ratio. The intensity of these three

Can. J. Chem. Downloaded from www.nrcresearchpress.com by 186.148.149.217 on 09/04/12
For personal use only.

lines, compared with the others, increases on standing and this anomaly can be attributed to the presence of a triplet of slightly lower g-value from gallic acid formed by hydrolysis. The splitting constants for the ring and the methyl protons are estimated as 1.14 and 0.38 oersteds, respectively.

The semiquinone ion (III*c*) from ethyl gallate shows three triplets as expected (Fig. 7). The predicted intensity ratio is 1:2:1:2:4:2:1:2:1. The deviation from the theoretical pattern again suggests the presence of the semiquinone ion from the free acid. Although the third line of the triplet due to gallic acid overlaps nearly perfectly with the eighth line due to the ethyl ester, the resolution of the other two lines becomes better on standing for $\frac{1}{2}$ hour. As we can see in Fig. 8, the ester has a slightly higher g-value than the acid.

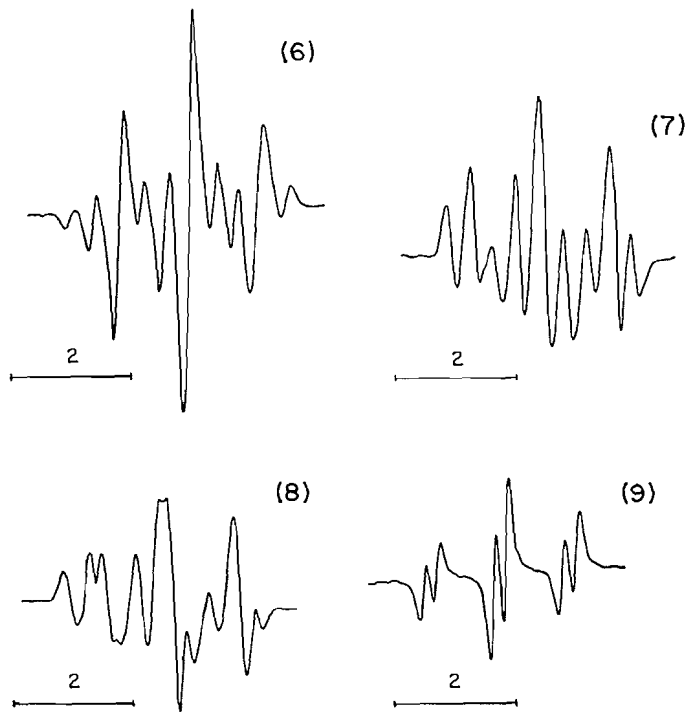


FIG. 6. First derivative of e.s.r. absorption spectrum of the semiquinone ion (III*b*) from methyl gallate.
FIG. 7. First derivative of e.s.r. absorption spectrum of the semiquinone ion (III*c*) from ethyl gallate.
FIG. 8. First derivative of e.s.r. absorption spectrum of the semiquinone ions from hydrolyzed ethyl gallate.
FIG. 9. First derivative of e.s.r. absorption spectrum of the semiquinone ion (III*d*) from isopropyl gallate.

The splitting constants are 1.12 oersteds for the ring protons and 0.36 oersted for two of the ethyl protons. The hyperfine splitting due to the other three protons in the ethyl group is too small to be resolved. *n*-Propyl gallate on oxidation gives essentially the same pattern as the ethyl ester. Adams, Blois, and Sands (7) reported two splitting constants, 1.13 and 0.38 oersteds, and a g-value of 2.00490. Our values for the ethyl ester are in good agreement with those for the *n*-propyl ester within the limit of the experimental errors.

The semiquinone ion (III*d*) from isopropyl gallate shows three doublets (Fig. 9). This

Can. J. Chem. Downloaded from www.nrcresearchpress.com by 186.148.149.217 on 09/04/12
For personal use only.

ester is fairly stable in an alkaline medium and the sample, from which unreacted acid was carefully removed by sublimation in vacuum, does not show the signals due to gallic acid. The splitting constants are estimated as 1.13 oersteds for the ring protons and 0.24 oersted for one proton in the isopropyl group.

TABLE II

Proton splitting constants in semiquinone ions from gallic acid and alkyl gallate

Semiquinone ion	Proton splitting constant in oersteds	
	a (ring)	*a* (alkyl)
III*a*	1.07*	—
III*b*	1.14	0.38
III*c*	1.12	0.36
III with R = *n*-propyl	1.13*	0.38*
III*d*	1.13	0.24

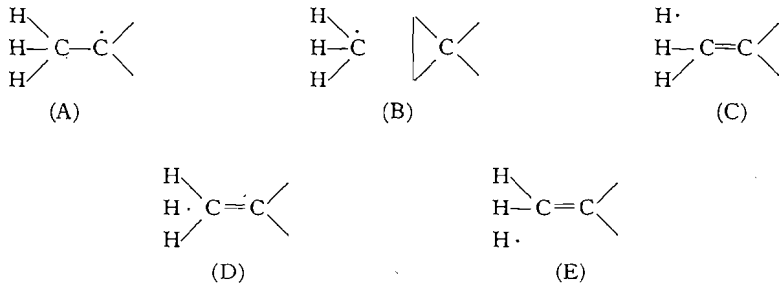
*See reference 7.

The magnitude of the ring proton splitting in these four esters seems to be constant regardless of the kind of alkyl group; however, it must be noted that the splitting due to the isopropyl proton is found to be about two thirds of those of the methyl and the ethyl protons. The semiquinone ion can be considered as the gallate ion with one positive hole. The small increase of the ring proton splitting by esterification shows that the ability of the negatively charged carbonyl group to attract the positive hole is higher, but only slightly, than that of the neutral carboalkoxy group.

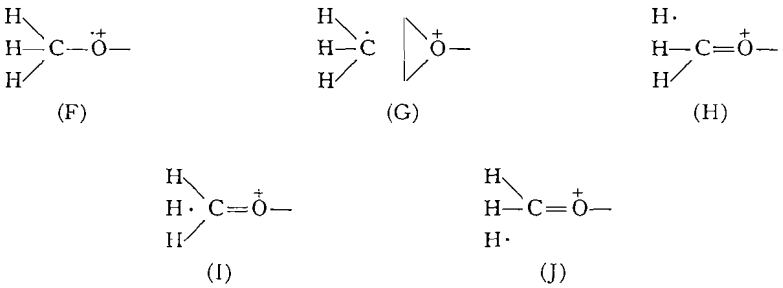
Recently Müller and his collaborators (17) have compared the hyperfine splitting due to the methoxy, the ethoxy, and the isopropoxy protons observed for the alkoxy-2,6-di-*tert.*-butyl-phenoxyl radicals. The splitting constants have been found to be 1.6 oersteds for the methoxy and the ethoxy protons and 1 oersted for the isopropoxy proton. The relative magnitude of the splitting constants of these protons is in very good agreement with the present results.

Based on the above experimental results, we can conclude that there is no essential difference between alkyl and alkoxy protons as to their contribution to hyperfine splitting and the effect of alkoxy protons can be ascribed to hyperconjugation. In the molecular orbital theory of hyperconjugation, the π-character of the orbitals in methyl and methylene groups can be found by the use of hydrogen group orbitals (18, 19). The spin densities on the methyl protons have been calculated by Bersohn (3) by taking into account the delocalization of the unpaired electron onto the methyl group. He found general agreement between the calculated and the observed splitting constants in a number of methyl-substituted benzosemiquinone ions; however, the orbital of isopropyl hydrogen has no π-character in this sense. This delocalization of unpaired electron means there is a charge transfer to methyl group, as the unpaired electron in the semiquinone ions is accompanied by a positive hole. In the valence bond theory, hyperconjugation can be understood to mean the introduction of unconventional pairing schemes or spin polarization of the bonds in a methyl group without any accompanying transfer of charge. McLachlan (4) has explained the hyperfine splitting due to methyl protons by considering the following resonance structures and concluded that spin polarization mechanism may be at least as important as electron delocalization in accounting for the hyperfine splitting due to methyl protons.

Can. J. Chem. Downloaded from www.nrcresearchpress.com by 186.148.149.217 on 09/04/12
For personal use only.



The application of the valence bond theory can be extended to methoxy group by considering analogous resonance structures. In the methoxy group the oxygen atom with a positive hole takes the place of a trigonal carbon atom in a methyl group. Therefore, the resonance structures H, I, J are probably less important than the structures C, D, E. We may expect that the electronic interaction between the alkyl protons and the oxygen



atom in the alkoxy group is less than that between the alkyl protons and the carbon atom to which the alkyl group is attached. The behavior of two ethyl protons and one isopropyl proton can be explained similarly. We may attribute the difference between the proton splitting constants for methyl and isopropyl groups to the presence of electron delocalization in the former group. In the case of the isopropyl derivative there is the additional possibility that steric hindrance may cause part of the change observed.

ACKNOWLEDGMENT

We wish to thank the National Research Council of Canada for generous grants-in-aid of this research.

REFERENCES

1. B. VENKATARAMAN and G. K. FRAENKEL. J. Chem. Phys. **23**, 588 (1955).
2. J. E. WERTZ and J. L. VIVO. J. Chem. Phys. **24**, 479 (1956).
3. R. BERSOHN. J. Chem. Phys. **24**, 1066 (1956).
4. A. D. MCLACHLAN. Mol. Phys. **1**, 234 (1958).
5. R. H. HOSKINS. J. Chem. Phys. **23**, 1975 (1955).
6. G. K. FRAENKEL. Ann. N. Y. Acad. Sci. **67**, 546 (1957).
7. M. ADAMS, M. S. BLOIS, JR., and R. H. SANDS. J. Chem. Phys. **28**, 774 (1958).
8. S. I. WEISSMAN. J. Chem. Phys. **22**, 1378 (1954).
9. H. M. MCCONNELL. J. Chem. Phys. **24**, 764 (1956).
10. E. KNOEVENAGEL and C. BÜCKEL. Ber. **34**, 3993 (1901).
11. L. MICHAELIS and S. GRANICK. J. Am. Chem. Soc. **70**, 624 (1948).
12. K. AUWERS and T. V. MARKOVITS. Ber. **38**, 226 (1905).

Can. J. Chem. Downloaded from www.nrcresearchpress.com by 186.148.149.217 on 09/04/12
For personal use only.

13. A. W. HOFMANN. Ber. **11**, 329 (1878).
14. J. CLARKE, R. ROBINSON, and J. C. SMITH. J. Chem. Soc. 2647 (1927).
15. W. G. CHRISTIANSEN. J. Am. Chem. Soc. **48**, 1358 (1926).
16. W. CORFIELD, J. B. FARMER, A. HORSFIELD, and C. A. MCDOWELL. To be published.
17. E. MÜLLER, K. LEY, K. SCHEFFLER, and R. MAYER. Chem. Ber. **91**, 2682 (1958).
18. R. S. MULLIKEN, C. A. RIEKE, and W. G. BROWN. J. Am. Chem. Soc. **63**, 41 (1941).
19. C. A. COULSON. Valence. Oxford University Press, London. 1952. p. 310.

Can. J. Chem. Downloaded from www.nrcresearchpress.com by 186.148.149.217 on 09/04/12
For personal use only.

Can. J. Chem. Downloaded from www.nrcresearchpress.com by 186.148.149.217 on 09/04/12
For personal use only.

THE ELECTRON SPIN RESONANCE ABSORPTION SPECTRA OF SEMIQUINONE IONS

PART II. THE HYPERFINE SPLITTING DUE TO AMINO GROUPS[1]

Y. MATSUNAGA[2] AND C. A. MCDOWELL

ABSTRACT

The electron spin resonance absorption spectra of amino-substituted *p*-benzosemiquinone ions have been examined. The hyperfine splittings due to the amino protons and the amino nitrogen atom have been demonstrated. It has been found that the magnitude of the hyperfine splitting constants due to these two kinds of nuclei depends very much on the nature of the free radical.

INTRODUCTION

Though the hyperfine splitting due to a nitrogen atom has been reported in the electron spin resonance (e.s.r.) of a number of organic-free radicals, the hyperfine splitting of the amino nitrogen atom and protons is not yet clear. The nuclear moment of N^{14} is one, so we can expect one N^{14} nucleus to cause a splitting of the resonance absorption into a triplet. 1,1-Diphenyl-2-picrylhydrazyl and its analogues (1), di-*p*-anisyl-nitrogen oxide (2), and cyano-di-*tert.*-butyl-phenoxyl (3) are the examples of the neutral free radicals which show the N^{14} splitting. Hyperfine splittings for both the N^{14} in, and out of, the aromatic ring in positively charged free radicals have been demonstrated in the cases of the phenazine semiquinone ion (4), and triarylaminium ions (5). Nitrobenzene anion (6), and the semiquinone ion from 3-nitrophthalic anhydride (7), show the hyperfine splitting due to N^{14} in the nitro group. Wurster's blue ions are the only kinds of free radicals with amino groups already studied (8, 9). Unlike those in the above-mentioned free radicals (10) the nitrogen atoms in these positively charged free radicals do not contribute to the hyperfine structure. Therefore, it seemed of interest to examine the hyperfine splitting due to the amino group in the other kind of free radicals. For this purpose, the negatively charged semiquinone ions formed by reduction of 2-amino-5-hydroxy-3,6-dichloro-*p*-benzoquinone; 2,5-diamino-3,6-dichloro-*p*-benzoquinone; 2,5-dianilino-3,6-dichloro-*p*-benzoquinone; and 2,5-di(N-piperidyl)-3,6-dichloro-*p*-benzoquinone have been chosen because of the lack of other substituents, which can contribute to hyperfine splitting. Although chlorine has a nuclear moment of spin, this splitting is known too small to be resolved (11).

EXPERIMENTAL

The parent quinones were prepared starting from chloranil by the methods described in the references. 2-Amino-5-hydroxy-3,6-dichloro-*p*-benzoquinone was prepared by reaction with ammonia in water (12). 2,5-Diamino-3,6-dichloro-*p*-benzoquinone was prepared by the reaction with ammonia in absolute ethanol (13). 2,5-Dianilino-3,6-dichloro-*p*-benzoquinone and 2,5-di(N-piperidyl)-3,6-dichloro-*p*-benzoquinone were obtained by the reaction with aniline and piperidine in ethanol, respectively (13, 14). By reduction with sodium dithionite, these quinones on dissolving in a mixture of pyridine, ethylene glycol, and 2 *M* KOH (1:2:1 by volume) give fairly stable free radicals. Pyridine was used with the hope of improving the solvating power and of stabilizing the mono-

[1]*Manuscript received March 7, 1960.*
Contribution from the Department of Chemistry, University of British Columbia, Vancouver 8, British Columbia.
[2]*National Research Council Postdoctorate Fellow 1957–59.*

meric form of semiquinone ion (15). The use of ethylene glycol or glycerol has been recommended by Hausser (16). The high viscosity of these compounds contributes to the resolution of the spectra. The solubility of 2,5-di(N-piperidyl)-3,6-dichloro-*p*-benzoquinone in the above-mentioned mixed solvent was found too small; therefore, the concentrated pyridine solution of the quinone was diluted with the mixed solvent containing the reducing reagent.

The e.s.r. absorption of these semiquinone ions was examined at room temperature at a frequency of 9 kMc/s as described previously (17).

RESULTS AND DISCUSSION

The semiquinone ion (I) from 2-amino-5-hydroxy-3,6-dichloro-*p*-benzoquinone gives three triplets as expected from the presence of one amino nitrogen and two protons (Fig. 1). The intensity ratios are 1:2:1:1:2:1:1:2:1; therefore, we can confidently assign the major splitting to the amino nitrogen and the minor one to the amino protons. The former splitting constant is estimated as 2.5 oersteds and the latter as 0.6 oersted. It must be noted that the magnitude of the amino proton splitting is only about one fourth of that of the amino nitrogen splitting.

The semiquinone ion (II) from 2,5-diamino-3,6-dichloro-*p*-benzoquinone shows a 13-line spectrum (Fig. 2). If the splitting constant of the amino nitrogen is nearly twice,

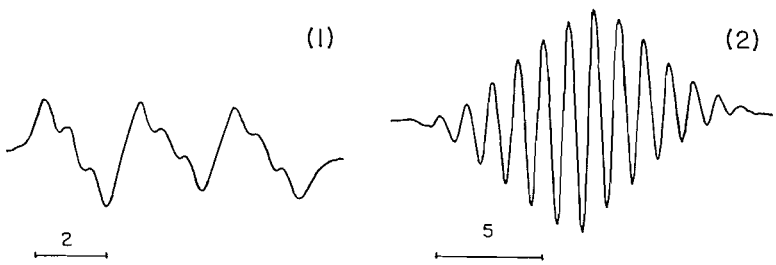
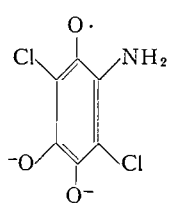
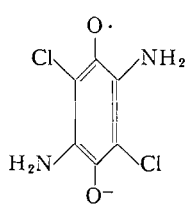


FIG. 1. First derivative of e.s.r. absorption spectrum of the semiquinone ion (I) from 2-amino-5-hydroxy-3,6-dichloro-*p*-benzoquinone.
FIG. 2. First derivative of e.s.r. absorption spectrum of the semiquinone ion (II) from 2,5-diamino-3,6-*p*-benzoquinone.

or one half of that of the amino protons, we can expect 13 lines with the relative intensities 1:4:8:12:16:20:22:20:16:12:8:4:1 or 1:2:7:10:19:20:26:20:19:10:7:2:1. The observed pattern seems to be in agreement with the former. The splitting constants of the nitrogen and the protons are 2.3 oersteds and 1.15 oersteds, respectively. In this case, the nitrogen splitting is a little smaller than that of the semiquinone ion (I) and the proton splitting is increased by a factor of two.



I



II

Can. J. Chem. Downloaded from www.nrcresearchpress.com by 186.148.149.217 on 09/04/12
For personal use only.

Can. J. Chem. Downloaded from www.nrcresearchpress.com by 186.148.149.217 on 09/04/12
For personal use only.

The semiquinone ion (III) from 2,5-dianilino-3,6-dichloro-*p*-benzoquinone has two amino nitrogen atoms and two amino protons. The contribution from two phenyl groups is not expected to be resolvable. As shown in Fig. 3, seven lines with a spacing of 1.1 oersteds are detected. If these seven lines are the whole of the spectrum, the splitting constants of the amino nitrogens and the amino protons must be of the same magnitude (1.1 oersteds) and the intensity ratio must be 1:4:8:10:8:4:1. The resolution of this spectrum is not good, because of the weak concentration of the free radical, and the use of high modulation of the magnetic field. Therefore, we may have missed the outermost weak line at each side. In such a case, the predicted intensity ratio is 1:2:5:6:8:6:5:2:1. The magnitude of the amino proton splitting becomes 2.2 oersteds, namely twice that of the amino nitrogen splitting. The latter values are probably more reasonable.

The semiquinone ion (IV) from 2,5-di(N-piperidyl)-3,6-dichloro-*p*-benzoquinone gives nine lines with an equidistant spacing of 1.2 oersteds (Fig. 4). The eight protons attached

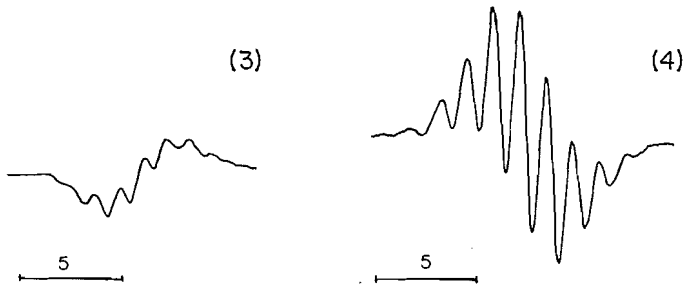
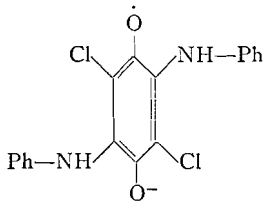
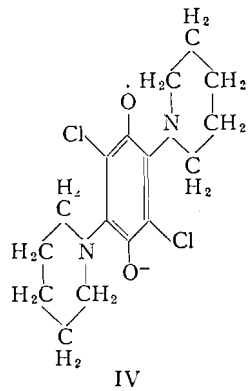


FIG. 3. First derivative of e.s.r. absorption spectrum of the semiquinone ion (III) from 2,5-dianilino-3,6-dichloro-*p*-benzoquinone.
FIG. 4. First derivative of e.s.r. absorption spectrum of the semiquinone ion (IV) from 2,5-di(N-piperidyl)-3,6-dichloro-*p*-benzoquinone.

to the carbon atoms adjacent to the nitrogen atoms in two piperidyl rings can be expected to contribute by hyperconjugation to hyperfine splitting with the intensity ratio 1:8:28:56:70:56:28:8:1. Therefore, the observed nine lines can be assigned to these eight protons and the contribution from two piperidyl nitrogen atoms must be too small to be resolved. The magnitude of the proton splitting in the present semiquinone ion must be, at least, several times larger than that of the nitrogen splitting.



III



IV

TABLE I

Splitting constants of nitrogen and proton in amino derivatives of 3,6-dichloro-*p*-benzosemiquinone ion

Semiquinone ion	Splitting constants in oersteds		
	a_N	a_H	a_N/a_H
I	2.5	0.6	4
II	2.3	1.15	2
III	1.1	2.2 (or 1.1)	1/2 (or 1)
IV	?	1/2	?

The present results show clearly that the amino nitrogen can contribute to hyperfine splitting. The assumption made by McLachlan (10) that the nitrogen atoms contribute no structure as N^{14} has a quadrupole moment which links its spin orientation to the molecular rotation cannot be considered as general for amino group in organic-free radicals. However, as summarized in Table I, the ratios of the splitting constants of the amino (probably and the alkylamino) protons to those of the amino nitrogen depend considerably on the nature of the molecule. Although the number of the radicals examined is quite small, the increase of the amino proton splitting constant seems to be accompanied by a decrease in the amino nitrogen splitting. This suggestion is consistent with the observation on Wurster's blue ions. For example, in the free radical from tetramethyl-*p*-phenylenediamine, the dimethylamino proton splitting has been reported as large as 7.4 oersteds and no nitrogen splitting has been detected (9).

According to theory, the hyperfine splitting is proportional to the Fermi contact term and the magnitude of this Fermi interaction is proportional to the spin density at the nucleus. The unpaired electron in our semiquinone ions is supposed to be in a π-orbital which has a node in the plane of the molecule. The unpaired electron must have some probability of interacting with the *s*-orbitals of hydrogen and nitrogen. It has been shown that $\sigma-\pi$ interaction is responsible for the hyperfine splitting due to ring protons. The magnitude of the hyperfine splitting is approximately proportional to the spin density in the π-orbital of the neighboring aromatic carbon atom (18). This relation has been supported by a number of experiments (19). The geometrical configuration of the CH group can be considered to be nearly same in every hydrocarbon. Nevertheless, this proportionality constant has been found to depend on the size of aromatic molecule and also on the sign of the charge by the experiments on hydrocarbon negative and positive ions. Therefore, we may expect that the magnitude of hyperfine splitting depends strongly on the nature of the electronic configuration of the group concerned.

The complete planarity of the amino group with the aromatic nucleus favors resonance stabilization. On the other hand, some energy will be required to change the hybridization at the nitrogen atom from the tetrahedral character in aliphatic amines to the trigonal type. We must consider also steric effects in some cases. By compromise between these factors, it seems probable that the geometrical and the electronic configurations of the amino group can be modified by a small change in the nature of the molecule. Consequently, a considerable change in the magnitude of the splitting constants of amino proton and nitrogen can be expected.

In connection with these results, it may be interesting to mention the spectrum of the semiquinone ion with a betaine-like structure. The e.s.r. absorption of the semiquinone ion (V), formed by reduction of the compound $C_{11}H_5O_3NCl_2$, which can be prepared by the

Can. J. Chem. Downloaded from www.nrcresearchpress.com by 186.148.149.217 on 09/04/12
For personal use only.

condensation between chloranil and pyridine (20), has been examined. Unlike the naphthoquinone analogue (VI) (21) the structure of this product seems to be not yet well defined. The position of the substituents given in V are the most probable. The semiquinone ion shows only one absorption line and there is no structure due to the positively charged and trigonal-type nitrogen atom (Fig. 5).

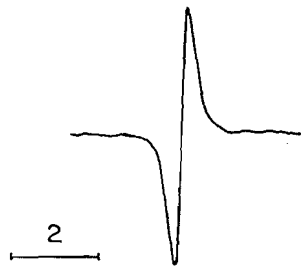
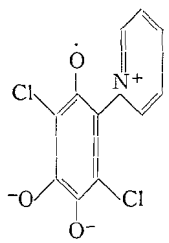
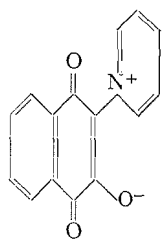


FIG. 5. First derivative of e.s.r. absorption spectrum of the semiquinone ion (V).



V



VI

ACKNOWLEDGMENTS

We wish to thank the National Research Council of Canada for generous grants-in-aid of this work.

REFERENCES

1. H. S. JARRETT. J. Chem. Phys. **21**, 761 (1953).
2. D. BIJL and A. ROSE-INNES. Phil. Mag. (7) **44**, 1187 (1953).
3. E. MULLER, K. LEY, K. SCHEFFLER, and R. MAYER. Chem. Ber. **91**, 2682 (1958).
4. Y. FELLION and J. UEBERSFELD. Arch. sci. (Geneve), **10** (special Vol.), 95 (1957).
5. O. R. GILLIAM, R. I. WALTER, and V. W. COHEN. J. Chem. Phys. **23**, 1540 (1955).
6. R. L. WARD and M. P. KEIN. J. Chem. Phys. **28**, 518 (1958).
7. M. ADAMS, M. S. BLOIS, JR., and R. H. SANDS. J. Chem. Phys. **28**, 774 (1958).
8. S. I. WEISSMAN. J. Chem. Phys. **22**, 1135 (1954).
9. T. R. TUTTLE, JR. J. Chem. Phys. **30**, 331 (1959).
10. A. D. McLACHLAN. Mol. Phys. **1**, 234 (1958).
11. J. E. WERTZ and J. L. VIVO. J. Chem. Phys. **23**, 2441 (1955).
12. O. L. ERDMANN. Ann. **37**, 341 (1941).
13. H. v. KNAPP and G. SCHULTZ. Ann. **210**, 164 (1881).
14. N. P. BUU-HOI, R. ROYER, and B. ECKERT. Rec. trav. chim. **71**, 1059 (1952).
15. L. MICHAELIS and S. GRANICK. J. Am. Chem. Soc. **70**, 624 (1948).
16. K. H. HAUSSER. Naturwissenschaften, **45**, 158 (1958).
17. W. CORFIELD, J. B FARMER, A. HORSFIELD, and C. A. McDOWELL. To be published.
18. H. M. McCONNELL. J. Chem. Phys. **24**, 764 (1956).
19. E. DE BOER and S. I. WEISSMAN. J. Am. Chem. Soc. **80**, 4549 (1958).
20. H. IMBERT. Compt. rend. **133**, 162 (1901).
21. F. ULLMANN and M. ETTISCH. Ber. **54**, 259 (1921).

Can. J. Chem. Downloaded from www.nrcresearchpress.com by 186.148.149.217 on 09/04/12
For personal use only.

Can. J. Chem. Downloaded from www.nrcresearchpress.com by 186.148.149.217 on 09/04/12
For personal use only.

THE ELECTRON SPIN RESONANCE ABSORPTION SPECTRA OF SEMIQUINONE IONS

PART III. FREE RADICAL SALTS OF QUINHYDRONES[1]

YOSHIO MATSUNAGA[2]

ABSTRACT

Electron spin resonance absorption was observed in alkali salts of tetrachloro-*p*-benzoquinhydrone, *p*-biphenoquinhydrone, and its tetrachloro and tetrabromo derivatives. The magnitude of *g*-value was found to be in the order of unsubstituted < chloro derivative < bromo derivative, and benzoquinhydrone salt < the corresponding *p*-biphenoquinhydrone salt. The frequency of C—O stretching vibration was observed in the range 1525 to 1550 cm^{-1}. Based on these frequencies the estimation of the parameters which are necessary for the molecular orbital treatment of semiquinone ions was attempted. A set of $\alpha_O = \alpha + (1/3-1/2)\beta$ and $\beta_{CO} = \beta$ were derived. Independently values of $\alpha_O = \alpha + 2/3\beta$ and $\beta_{CO} = \beta$ were estimated using the hyperfine structure of the electron spin resonance spectrum of the α-naphthosemiquinone ion.

INTRODUCTION

A number of unstable salts of quinhydrones have been described by organic chemists (1). It is well known that quinhydrones, which have no unpaired electron, dissociate into free radical ions in alkaline solution. Therefore, it seemed to be of interest to study the electronic structure of alkali salts of quinhydrones in the solid state. Electron spin resonance (e.s.r.) absorption has been detected in the quinhydrones adsorbed on barium hydroxide octahydrate (2). The highly colored reaction products of tetrahalogeno-*p*-benzoquinones with alkali iodides have been examined by the magnetic resonance method and found to be free radical salts (3). Here we wish to present the results of the e.s.r. and the infrared absorption measurements on sodium salts of *p*-biphenoquinhydrone and its halogeno derivatives.

EXPERIMENTAL

Materials.—Potassium salt of tetrachloro-*p*-benzoquinhydrone was prepared by the method of Torrey and Hunter (4). Chloranil was dissolved in cold, dry acetone and treated with crystals of potassium iodide. The grass green precipitate was filtered and washed with ether. According to Torrey and Hunter, the composition of the product is $C_6Cl_4O_2 . C_6Cl_4(ONa)_2$. The sodium salt was also prepared by a similar method. Oxidation of biphenol with ferricyanide in alkaline medium gave sodium salt of biphenoquinhydrone as described by Willstätter and Kalb (5). Biphenol was used in excess to avoid overoxidation. The blue product was quickly filtered and dried without washing. This salt decomposes quickly in contact with water. Tetrachloro-*p*-biphenol, which was obtained by chlorination of biphenol suspended in acetic acid (6), was dissolved in aqueous solution of sodium hydroxide and oxidized to sodium salt of quinhydrone using ferricyanide. The precipitate changes its color from violet to blue by washing with water. This free radical salt is so stable as to be prepared in the presence of a large excess of the oxidizing reagent. The dark blue salt of tetrabromo-*p*-biphenoquinhydrone was prepared similarly (7). Bromination of biphenol was carried out as described by Magatti (6).

Magnetic measurements.—Electron spin resonance absorption was measured at room temperature at a frequency of 9 kMc/s. The *g*-value was estimated by comparison with

[1]*Manuscript received March 7, 1960.*
Contribution from Department of Chemistry, University of British Columbia, Vancouver 8, British Columbia, and Department of Chemistry, Faculty of Science, University of Tokyo, Hongo, Tokyo, Japan.
[2]*National Research Council Postdoctorate Fellow 1957–59.*

diphenylpicrylhydrazyl (DPPH). The line width was taken as the distance in oersteds between the points of maximum slope.

Optical measurements.—Infrared spectrum was recorded using a Perkin–Elmer spectrometer model 21. The sample was examined in a potassium bromide disk.

RESULTS AND DISCUSSION

All of our specimens showed e.s.r. absorption and we could conclude that alkali salts of quinhydrones consists of negatively charged semiquinone ions and alkali cations. The spin concentration in our specimens was found to be in the order of 10^{21} to 10^{23} spins per mole. The *g*-value, line width of e.s.r. absorption, and the frequency of C—O stretching vibration are presented in Table I. Our *g*-values for tetrachloro-*p*-benzoquinhydrone salts are in agreement with 2.0044 ± 0.0008 for the sodium salt reported by Kainer, Bijl, and Rose-Innes (3). The infrared spectra of a number of ionic molecular compounds between quinones and aromatic diamines have been examined by Kainer and Otting (8). They have assigned the strong absorption band found in the region of 6.5 (ca. 1540 cm^{-1}) to the C—O stretching vibration in tetrahalogeno-*p*-benzosemiquinone ions. Our results on much simpler compounds support their assignment.

TABLE I

g-Value and line width of e.s.r. absorption and frequency of C—O stretching vibration in alkali salts of quinhydrones

	E.s.r. absorption		
	g-Value	Line width in oersteds	C—O vibration in cm^{-1}
Na tetrachloro-*p*-benzoquinhydrone	2.0051 ± 0.0003	6.7	1530 ± 10
K tetrachloro-*p*-benzoquinhydrone	2.0048 ± 0.0003	7	1525 ± 5
Na *p*-biphenoquinhydrone	2.0044 ± 0.0003	5	1550 ± 5
Na tetrachloro-*p*-biphenoquinhydrone	2.0064 ± 0.0003	2.2	1540 ± 5
Na tetrabromo-*p*-biphenoquinhydrone	2.012 ± 0.001	1.5	1530 ± 5

The magnitude of *g*-values of biphenoquinhydrone salts was found to be in the following order:

unsubstituted < chloro derivatives < bromo derivatives.

The *g*-value for sodium salt of tetrabromo-*p*-benzoquinhydrone has been reported to be 2.0068 ± 0.001 (3); therefore, the above order seems to be followed also by the series of benzoquinhydrone salts. The same tendency is found in the series of substituted DPPH and of substituted triarylaminium perchlorates (9). Consequently, we may conclude that substituted bromine atoms are more effective in enhancing spin-orbital coupling and in increasing the magnitude of *g*-value than substituted chlorine atoms regardless of the sign of charge on free radical molecules. However, it must be noted that the magnitude of *g*-value depends also on the size of semiquinone ions. Biphenoquinhydrone salts give higher *g*-value than the corresponding benzoquinhydrone salts. These tendencies seem to be in sharp contrast to the results on aromatic hydrocarbon–iodine complexes (10). In the latter case, their *g*-values have been found to be close to that for free electron (2.0023) and the magnitude decreased with the increasing of the size of hydrocarbon molecule. In connection with the different behavior between these two kinds of halogens, it may be interesting to cite Wahler and Thon's observation that the magnitude of

Can. J. Chem. Downloaded from www.nrcresearchpress.com by 186.148.149.217 on 09/04/12
For personal use only.

Can. J. Chem. Downloaded from www.nrcresearchpress.com by 186.148.149.217 on 09/04/12
For personal use only.

g-value of diarylnitrogen oxide in solution shows a marked decrease by addition of complex-forming agent, *m*-dinitrobenzene and *s*-trinitrobenzene (11).

The hyperfine structure of the e.s.r. spectra of semiquinone ions in the dissolved state arises from the interaction between the magnetic moment of the unpaired electron and the magnetic moments of the protons in the molecule. Based on the spectra of *o*- and *p*-benzosemiquinone ions McConnell has suggested that the magnitude of ring proton splitting is approximately proportional to the density of the unpaired π-electron on the adjacent carbon atom (12). This approximation has been applied successfully to the case of aromatic hydrocarbon monopositive and mononegative ions (13, 14) and even to the case of DPPH (15). McConnell has used in his molecular orbital treatment of benzosemiquinone ions the following parameters without considering the effect of negative charge on the magnitude of coulomb integral for the oxygen atoms, $\alpha_O = \alpha+\beta$ and $\beta_{CO} = \beta$ which were originally estimated for the oxygen atoms in neutral quinone molecules. It seems desirable to find a correct set of parameters for the application of this approximation to semiquinone ions with more complicated molecular structure. Therefore, we examined the C—O stretching vibration in the above-mentioned salts of quinhydrones and attempted to estimate the required parameters based on it.

Bonino and Scrocco (16) have suggested the use of the following relation between the mobile bond order (p_{CO}) and the force constant of C=O bond (k) for the estimation of stretching vibration frequency,

$$k = \xi p_{CO} + \sigma(1-p_{CO}), \qquad [1]$$

where ξ is the force constant for the "imaginary" double bond with $p_{CO} = 1$, and σ is that for C—O single bond. Although Berthier, Pullman, and Pontis (17) have presented a more refined equation considering the autopolarizability of the bond, we may use the above approximation ignoring the minor correction term. The values for the C=O bond in the formaldehyde molecule are used to estimate the magnitude of ξ, i.e. $k = 13.45\times10^5$ dyne/cm (18) and $p_{CO} = 0.958$ (17, 19), and we assume $\sigma = 5\times10^5$ dyne/cm. The relation between the vibration frequency (ν) and the force constant estimated by equation [1] can be approximated by

$$\nu = 1744\ (k/13.45\times10^5)^{\frac{1}{2}}\ \text{cm}^{-1} \qquad [2]$$

where 1744 cm^{-1} is the observed frequency for the C=O bond of the formaldehyde molecule (18).

TABLE II

Calculated mobile bond orders, force constants, and stretching frequencies for the C—O bond in semiquinone ions

	α_O	Mobile bond order, p_{CO}	Force constant $k\times10^{-5}$ by eq. [1]	Frequency in cm^{-1} by eq. [2]
p-Benzosemiquinone ion	α	0.655	10.77	1561
	$\alpha+1/2\beta$	0.609	10.36	1531
	$\alpha+\beta$	0.561	9.94	1499
p-Biphenosemiquinone ion	α	0.672	10.91	1571
	$\alpha+1/2\beta$	0.608	10.35	1530
	$\alpha+\beta$	0.537	9.73	1483

The calculated mobile bond order, force constant, and vibration frequency for benzo- and bipheno-semiquinone ions are summarized in Table II. These results were obtained assuming $\alpha_O = \alpha+\beta_{CO} = \beta$. The relation between the parameter and the vibration frequency ν for the C—O bond in *p*-benzosemiquinone ion can be approximated by $\nu = 1561-61\delta$ in cm^{-1}. The observed frequencies given in Table I suggest that the value of δ in the present case is about one half. If we assume a similar linear relationship in the case of *p*-biphenosemiquinone ion, the value of δ will be estimated as one-third to one-half. These two estimations are in good agreement with each other.

The magnitude of parameters δ can be estimated based on the hyperfine structure of e.s.r. spectrum. α-Naphthosemiquinone ion (Fig. 1) gives a spectrum of three quintets; therefore the density of unpaired electron on the aromatic carbon atoms 5 and 5′ is practically equal to that on the carbon atoms 6 and 6′ (see structural formula). If the square of the coefficient of $2p$ function at the carbon atoms 5 and 6 are supposed to be equal to each other in the singly occupied molecular orbital, we obtain $\delta = 2/3$ and the following densities of unpaired π-electron by the secular equations assuming $\alpha_O = \alpha+\beta$ and $\beta_{CO} = \beta$; 0.225 on the oxygen atoms 1 and 1′, 0.100 on the carbon atoms 2, 2′, 3, and 3′, and 0.025 on the carbon atoms 4, 4′, 5, 5′, 6, and 6′. If we apply the relation $a_j = 34\rho_j$ given by McConnell for benzosemiquinone ions, where a_j is the ring proton splitting constant and ρ_j is the density of the unpaired π-electron on the adjacent carbon atom j, we may expect the splitting constants of 3.40 oersteds for the ring protons 2 and 2′, and 0.85 oersted for the ring protons 5, 5′, 6, and 6′. Although we cannot reproduce the observed pattern of spectrum using these constants, the estimated values are in good agreement with 3.22 ± 0.03 oersteds and 0.57 ± 0.03 oersteds given by Adams, Blois, and Sands (20).

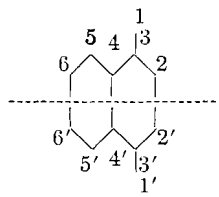


FIG. 1.

ACKNOWLEDGMENTS

The author wishes to thank Professor C. A. McDowell for his interest and guidance in this work, which was supported by grants from the National Research Council of Canada.

REFERENCES

1. S. GOLDSCHMIDT and F. CHRISTMANN. Ber. **57**, 711 (1924) and references cited therein.
2. D. BIJL, H. KAINER, and A. C. ROSE-INNES. Nature, **174**, 830 (1954).
3. H. KAINER, D. BIJL, and A. C. ROSE-INNES. Nature, **178**, 1462 (1956).
4. H. A. TORREY and W. H. HUNTER. J. Am. Chem. Soc. **34**, 702 (1912).
5. R. WILLSTÄTTER and L. KALB. Ber. **38**, 1232 (1905).
6. G. MAGATTI. Ber. **13**, 224 (1880).
7. J. MOIR. S. African J. Sci. **9**, 322 (1912).
8. H. KAINER and W. OTTING. Chem. Ber. **88**, 1921 (1955).
9. R. I. WALTER, R. S. CODRINGTON, A. F. D'ADAMO, and H. C. TORREY. J. Chem. Phys. **25**, 319 (1956).
10. Y. MATSUNAGA. J. Chem. Phys. **30**, 855 (1959).
11. B. E. WAHLER and H. G. THON. Arch. sci. (Geneva), **11**, 165 (1958).
12. H. M. MCCONNELL. J. Chem. Phys. **24**, 632 (1956).

Can. J. Chem. Downloaded from www.nrcresearchpress.com by 186.148.149.217 on 09/04/12
For personal use only.

13. E. DE BOER and S. I. WEISSMAN. J. Am. Chem. Soc. **80**, 4549 (1958).
14. A. CARRINGTON, F. DRAVNIEKS, and M. C. R. SYMONS. J. Chem. Soc. 947 (1959).
15. R. BERSOHN. Arch. sci. (Geneva), **11**, 177 (1958).
16. G. B. BONINO and E. SCROCCO. Atti accad. naz. Lincei. Rend. Classe sci. fis. mat. e nat. (8) **6**, 421 (1949).
17. G. BERTHIER, B. PULLMAN, and J. PONTIS. J. chim. phys. **49**, 367 (1952).
18. G. B. B. M. SUTHERLAND and D. M. DENNISON. Proc. Roy. Soc. (London), A, **148**, 259 (1935).
19. E. SCROCCO and P. CHIORBOLI. Atti accad. naz. Lincei. Rend. Classe sci. fis. mat. e nat. (8) **8**, 248 (1950).
20. M. ADAMS, M. S. BLOIS, JR., and R. H. SANDS. J. Chem. Phys. **28**, 774 (1958).

Can. J. Chem. Downloaded from www.nrcresearchpress.com by 186.148.149.217 on 09/04/12
For personal use only.

THE ELECTRIC MOMENTS OF SUPPOSEDLY SYMMETRICAL CYCLIC SUBSTANCES[1]

C. C. Meredith and George F Wright

ABSTRACT

The distortion polarizations of polysubstituted benzenes and cyclobutanes which have been examined by the randomly oriented solid pellet technique seem to be lower but never higher than the electronic polarization values derived from bond refractions, and are considered to be more reliable than the latter. In almost all of the supposedly symmetrical substances which have been examined the total solute polarization always exceeds the measured distortion polarization and usually exceeds the calculated MR_D. These substances must then be polarized, although the moments which have been determined are not numerically reliable because of solvent effects. Whenever possible the temperature coefficients of these apparent moments have been determined and are usually but not always positive. From these temperature coefficients it is presumed that some substances, like naphthalene, are rigidly dipolar whereas others, like hexachlorobenzene, have activation states which are unsymmetrical and therefore contributory to the moment which actually is measured.

The graphic formula of a single molecule is patently a cursory description of a chemical substance, useful chiefly for illustrative and bibliotechnical communication. Nevertheless there seems to be a tendency to ascribe to the graphic formula a verity which it does not deserve. Especially is this the case when molecular symmetry is concerned. Indeed the simple diagram may become an unexcited state of reference in analysis of "loss" determinations such as those of absorption spectroscopy, or it may be used as the basis for trial stuctures during diffraction studies. There is some danger that the inadequate graphic formula thus becomes "built into" the physical interpretation.

Although a reactance determination, of which dielectric constant is an example, has the obvious disadvantage of an integrated, non-detailed result in which the entire system participates it does not require the same degree of preconception that is common to some other physical methods. No irreversible energy transfer occurs, so that the measurement is that of the actual system if sufficiently weak electromagnetic fields are applied. If environmental influences can be evaluated, say by variation of solvent, temperature, and concentration, the modulated value of electrical polarization sets a definition to which the molecular construct of the substance must conform.

This definition is especially applicable to substances for which the graphic formula would predict, for reasons of symmetry, a zero dipole moment. Several examples in which the inadequacy of the ordinary graphical construct becomes apparent, have recently been reported (1–4).

In the present report this list has been extended to include aromatic hydrocarbons with aliphatic and halogeno substituents. These substances would not be expected to display any orientation polarization if the frequently quoted symmetries and the graphic formulae specifying them were valid.

In some instances zero moments have been assigned heretofore to substances showing low total polarizations, P_T, because the intuitive decision from the graphic formula was at least as meaningful as the ostensible orientation polarization remaining after subtraction from P_T of a questionably calculated distortion polarization (P_{e+a}). Little accuracy can be claimed for the usual (2–5% of P_E) assignment of atom polarization. However, now we are aided in this respect by the actual determination of the entire distortion

[1]*Manuscript received October 19, 1959.*
Contribution from the Department of Chemistry, University of Toronto, Toronto, Ontario.

Can. J. Chem. Downloaded from www.nrcresearchpress.com by 186.148.149.217 on 09/04/12
For personal use only.

TABLE I

Distortion polarizations and molecular refractions

Substance	Density	Dielectric constant	P_{e+a}, cc	Vogel C_{ar}—C_{ar}	Vogel C=C+ C—C, cc	Eisenlohr, cc
Naphthalene	1.156	2.729	40.5	43.0	42.0	41.6
Anthracene	1.243	3.022	57.7	59.7	57.6	57.0
Phenanthrene	1.176	2.852	57.8	59.7	57.6	57.0
Chrysene	1.284	3.045	72.0	76.6	72.6	72.3
Pyrene	1.280	2.921	61.6	67.8	64.4	61.6
Hexahelicene	1.249	2.850	100.2	110.2	104.3	103.0
Coronene	1.378	3.192	91.2	100.8	93.5	92.0
Fluorene	1.209	2.821	51.9	52.9	53.4	52.8
Durene	1.036	2.340	39.9	44.8	45.0	44.8
Hexamethylbenzene	1.043	2.366	48.6	54.1	54.3	54.0
Acenaphthene	1.204	2.738	46.9	50.2	47.3	48.7
o-Diphenylbenzene	1.173	2.660	69.8	74.4	75.2	74.5
p-Diphenylbenzene	1.231	2.888	72.2	74.4	75.2	74.5
1,4-Di-*tert*-butylbenzene	0.950	2.281	59.8	63.4	63.6	63.2
Azulene	1.275	3.078	41.1	43.0	42.0	41.6
Ferrocene	1.537	2.844	46.2	43.6[a]	41.2[a]	41.1[a]
1,2,3,4-Tetraphenyl-cyclobutane, m.p. 163°	1.162	2.626	109.0	121.3[b]	116.2[b]	114.8
Same, m.p. 149.7°	1.159	2.623	109.2	121.3	116.2	114.8
Hexachlorobenzene	2.045	2.833	53.0	55.2	55.5	55.5
1,2,4,5-Tetrachlorobenzene	1.732	2.586	43.1	45.5	45.8	45.8
1,4-Dimethyl-2,3,5,6-tetrachlorobenzene	1.703	2.738	50.9	54.8	55.1	55.0
Azobenzene	1.205	2.743	55.5	55.3	55.8	
trans-Stilbene	1.144	2.7307	59.1	59.6	60.3	59.2
1,4-Diphenylbutadiene	1.121	2.850	70.2	67.1	67.8	67.3
1,6-Diphenylhexatriene	1.075	2.695	78.0	74.6	75.4	76.6
2,5-Diphenyldithiene	1.363	3.038	79.6	80.4	81.0	81.1
Methyleneanthrone	1.331	3.120	64.1	61.7	62.2	61.6
Beta-carotene	1.141	2.940	184.8		174.7	177.4
1,2-Diiodotetrafluorobenzene	2.966	2.719	49.4	50.7	50.9	49.8
1,2,4,5-Tetrachlorobenzene	1.732	2.586	43.1	45.5	45.7	45.8
1,4-bis-Chloromethylbenzene	1.432	2.915	47.6	45.2	45.4	45.3
1,4-bis-Trichloro-methylbenzene	1.743	2.649	63.6	64.5	64.8	64.8
Tetraphenylethylene	1.148	2.466	95.7	107.3	108.4	107.3

[a]The calculated refractions do not include iron II for which a value of 5.0 cc may be estimated.

[b]If Vogel's value for the cyclobutane C—C bond refraction had been used (1.37 cc) instead of the usual C—C value (1.29 cc) these additive refractions would be higher than is recorded.

[c]Kindly furnished by H. J. Matsuguma, Picatinny Arsenal, Dover, N.J., m.p. 50.5–51.8°. Prepared by W. J. Pummer, R. E. Florin, and L. A. Wall. J. Research Natl. Bur. Standards, **62**, 113 (1959).

polarization from the dielectric constant of the randomly oriented, highly compressed solid in which no orientation polarization should be detectable (1). In general the results have conformed with expectations. However in some instances apparent abnormal atom polarizations, previously assigned in order to conciliate an observed total polarization with an intuitively defined zero moment, have been found to be non-existent (1, 3, 4). On the other hand some hitherto unsuspected atom polarizations have been discovered (2).

Although the measured distortion polarization ought to be and customarily is higher than the molecular refraction (because the latter does not include atom polarization) we have earlier encountered an exception in diphenylmercury (4). Since we have suspected that this behavior is due to the phenyl groups, and our present candidates are aromatic, we have examined a series of this type of hydrocarbon in respect of distortion polarization measured in pellets at 23°. The results are shown in Table I together with molecular refractions calculated in three ways.

Can. J. Chem. Downloaded from www.nrcresearchpress.com by 186.148.149.217 on 09/04/12
For personal use only.

In the column "Vogel C_{ar}—C_{ar}" (5) the value of 2.69 cc has been used for aromatic ring bonds. In the following column "Vogel C=C+C—C," 4.17 cc and 1.30 cc respectively are used for aromatic rings. Finally in the last column are the additions of atom refractions according to Eisenlohr (6), all being values for the Na_D frequency.

The three additive refraction calculations are not interconsistent. Of present interest is the comparison of these calculated molecular refractions with our measured distortion polarizations (P_{e+a}). First it may be seen that P_{e+a} for simple aromatic hydrocarbons is consistently lower than MR_D from Vogel's C_{ar}—C_{ar} bond value (perhaps because he derived the value from the most aromatic of all hydrocarbons, benzene) and to a lesser extent lower than MR_D from Vogel's C=C+C—C values. On the other hand MR_D from Eisenlohr's values agrees with our measured P_{e+a}. But this latter agreement must be fortuitous because all MR_D values are larger than measured P_{e+a} when substituents (either alkyl, halogen, or even phenyl) are considered.

In several instances there is good agreement between MR_D calculated and P_{e+a} observed, for example, azobenzene and stilbene. The case of stilbene is especially propitious because the refractive indices of the crystals have already been measured carefully at a series of wavelengths (7) in the visible region. If the mean of the indices along the three principal axes $(\eta_\alpha+\eta_\beta+\eta_\gamma)/3$, is calculated for each wavelength the linear distribution of these mean values with respect to wavelength justifies the application of the Cauchy dispersion equation (8) for calculation of the refractive index at infinite wavelength,

$$n_\infty = \frac{(3650)^2\cdot 10^6(1.931) - (6908)^2\cdot 10^6(1.739)}{10^6\cdot(3650)^2 - (6908)^2\cdot 10^6} = 1.664,$$

whence the MR_∞ may be calculated

$$\frac{(1.664)^2-1}{(1.664)^2+2}\cdot\frac{180}{1.144} = P_e = 58.5 \text{ cc.}$$

This electronic polarization is about 1% lower than our measured P_{e+a}, as might be expected for a normal contribution of atom polarization. On the other hand MR_D calculated according to Vogel is 1–3% higher than our measured P_{e+a}. It would seem that Vogel's bond refractions derived at short wavelength thus are not closely applicable to distortion polarizations in the radiofrequency range.

Even the Eisenlohr value of 59.2 cc for MR_D of stilbene may be too high, despite apparent agreement with P_{e+a}, if an exaltation not calculated into MR_D actually is included in the distortion polarization which we have measured. The existence of this exaltation is not improbable if one considers the measured distortion polarizations of *trans–trans*-1,4-diphenylbutadiene and *trans–trans–trans*-diphenylhexatriene, which are appreciably higher than the MR_D values for which no exaltation has been included (Table I). These observations of exaltation in the radiofrequency range seem to be reliable since other substances like β-carotene and, perhaps, methyleneanthrone also give exalted values (Table I). On the other hand the measurement P_{e+a} for the highly degenerate tetraphenylethylene is quite low.

Further examinations of the polarizations shown in Table I disclose many discrepancies between observed and calculated values. The measured distortion polarizations of the polynuclear hydrocarbon are in reasonable agreement with Eisenlohr calculations of MR_D, but both are markedly lower (particularly note coronene) than Vogel's calculated MR_D, especially when Vogel's C_{ar}—C_{ar} value is used. On the other hand the Eisenlohr MR_D

Can. J. Chem. Downloaded from www.nrcresearchpress.com by 186.148.149.217 on 09/04/12
For personal use only.

seems to be at least as much higher (and sometimes more so) than the measured P_{e+a} as is the Vogel value when the aromatic nucleus is substituted by methyl, chloro, or phenyl groups. If experimental errors (such as preferential orientation or dimensional non-uniformity of the compressed wafer) are avoided the measured distortion polarization ought to be the most reliable value. Likewise the lowest value ought to be the most realistic because errors due to electrical conduction or dielectric loss tend to raise the apparent dielectric constant. Therefore one may fairly question the calculated electronic polarization for substances in which aromatic linkages exist.

In point of fact the vagaries of calculated distortion polarization have been significant in the consideration of total polarizations when a certain orthodoxy would decree zero moment for the substance under examination. The polarization of naphthalene is a typical instance. The concept of resonance, supported by careful X-ray diffraction studies of crystalline naphthalene (9), and despite some minor discrepancies (10), seems to have firmly established the planar symmetry of this substance. However, in benzene at 20° the total solute polarization (P_T) was found to be 45.1 cc (11). In heptane at 20° the P_T must have been found to be 45.4 cc (12) because a tentative moment of 0.34 Debye (D) was calculated. But this value was abandoned in favor of $\mu = 0$ by deduction of 10 to 15% as atom polarization. The lowest total polarization reported in the literature is 43.3 cc but the author (13) was trying to avoid a previous error. Perhaps he overcorrected.

In all of these instances there seems to have been an effort to force the dipole moment of naphthalene to zero. This tendency is understandable in view of the orthodox expectancy from X-ray diffraction studies versus a distrust of the electrical measurement. This distrust is not unreasonable when low orientation polarizations are involved because a consistent error (say residual cell capacitance and/or inductance in leads) can easily lead to a spurious value of polarization.

Of course techniques have improved during the past 25 years. Among these improvements are those in our own apparatus in which inductance and capacitance errors have been avoided in large part by rigid location of the test capacitance as close as possible to the principal parts of the resonant circuit. We are accustomed to test the effectiveness of this and other precautions by polarization measurements of carbon tetrachloride in benzene and of benzene in carbon tetrachloride. Examples of such tests are shown in Table II.

It may be seen that neither benzene nor carbon tetrachloride shows an appreciable orientation polarization.

TABLE II
Electrical polarizations of carbon tetrachloride, benzene, and naphthalene

Solute	Solvent	Temp., °C	Dielectric constant of solvent: Determined	Dielectric constant of solvent: Extrapolated	Spec. vol. of solvent: Determined	Spec. vol. of solvent: Extrapolated	$\delta\epsilon/\delta\omega$	$\delta V/\delta\omega$	P_T, cc	MR_D, cc	P_θ, cc	μ, D
C_6H_6	Dioxane	20	2.2179	2.2175	0.96743	0.96740	0.04	0.168	26.1	26.2	−0.1	0
C_6H_6	CCl_4	20	2.2409	2.2410	0.62707	0.62705	0.07	0.500	26.1	26.2	−0.1	0
CCl_4	C_6H_6	20	2.2846	2.2846	1.13769	1.13770	−0.09	0.500	26.9	26.2	0.7	0.05
$C_{10}H_8$	C_6H_6	20	2.2846	2.2845	1.1377	1.13790	0.43	0.195	46.6	40.5[a] or 41.6	5.0–6.1	0.49–0.55
$C_{10}H_8$	C_6H_6	40	2.2405	2.2412	1.1673	1.16750	0.31	0.130	46.4		4.8–5.9	0.49–0.54
$C_{10}H_8$	CCl_4	20	2.2378	2.2373	0.6270	0.6270	−0.35	0.129	43.1		1.5–2.6	0.3
$C_{10}H_8$	C_6H_{12}	20	2.0243	2.0245	1.2787	1.2787	0.28	0.158	43.2		1.6–2.7	0.3

[a]Directly determined distortion polarization.

Can. J. Chem. Downloaded from www.nrcresearchpress.com by 186.148.149.217 on 09/04/12
For personal use only.

On the other hand this table shows that for naphthalene in benzene a significant orientation polarization (40.5 cc) or of the Eisenlohr MR_D (41.6 cc) from the observed total polarization. The latter value (46.5 cc) is quite comparable with those obtained by Parts and by Briegleb, but unlike the latter worker we choose to assign a moment of 0.49–0.54 D to naphthalene in benzene. The apparent moments in carbon tetrachloride and cyclohexane are lower but still significant.

Although this assignment may seem to be anomalous in view of X-ray diffraction studies it is not unexpected on the basis of chemical evidence. Since both rings cannot be complemented by pi sextets some other charge distribution must be prevalent. The behavior of naphthalene upon ozonization and addition of halogen strongly indicates (14) that the electronic distribution tends toward 6:4. That is to say, one ring tends to be fully aromatic and the other to be conjugated aliphatic in behavior. The substance may then be classified as mesoionic in its degeneracy and this resonance state is justified by the independence of dipole moment with respect to temperature (Table II). The mesoionic concept seems not to be contradicted by the normal distortion polarization of naphthalene because azulene, which is certainly mesoionic, does not exhibit any abnormality in the measured P_{e+a}.

The examples which are elaborated above provide some justification for the use of measured distortion polarizations in moment studies, but there are many unexplained differences between P_{e+a} and MR_D to be found in Table I. In the search for error there are several possibilities. In the experimental determination low values are to be expected if the compressed wafer which we measure is not at maximum density. However, this error may be detected either by nonlinearity of the plot of thickness versus apparent dielectric constant, or else by comparison of the density of individual crystal fragments with the density of the wafers. Another error, that of preferred orientation of crystal fragments (say, of plate-like crystals), may be avoided simply by our practice of reforming ground wafers.

Turning from the practical to the theoretical aspects, the application of polarizations determined in the crystalline state to systems in which lattice forces are not present might be thought to introduce a damping error. But in measurements of dielectric constant which have been made in the vicinity of the melting point (15, p. 134) there seems to be no evidence of a significant lattice restriction on distortion polarization. Moreover, the concept that atom polarization is a reactive compensation of electronic charge deformation would imply for a restriction of atom polarization in crystals a corresponding difference in refractive index between liquids and solids. In general such differences are not observed (16). In particular the comparison of molar refractions calculated from $(\eta_\alpha+\eta_\beta+\eta_\gamma)/3$ (which is essentially the same as when calculated from $\sqrt[3]{\eta_\alpha \cdot \eta_\beta \cdot \eta_\gamma}$) with the MR_D calculated from group refractions for stilbene in the present publication and for N,N′-dinitropiperazine in an earlier one (17) show that the electronic polarization is not altered appreciably by change of state. Therefore from both the practical and theoretical aspects the direct measurements of distortion polarization would seem to be reliable.

On the other hand errors in molecular refraction are less easy to define. When solids are involved the calculation is usually indirect, involving generalized atom or bond refractions. The summation of additive refractions has been shown in Table I to be capricious. Moreover, the extrapolation from optical to radio frequencies is unreliable unless the electromagnetic losses (spectral absorption or loss tangent) are known. Unfortunately instruments are not yet available to cover this entire spectral range. Even if these faults of evaluation could be overcome, the actual atom polarization would only be estimated

Can. J. Chem. Downloaded from www.nrcresearchpress.com by 186.148.149.217 on 09/04/12
For personal use only.

as an arbitrary increment to equate electronic to the entire distortion polarization. Indeed the only reliable method (except for the direct measurement of pelletted solids) is the measurement of total polarization for a substance the dipole moment of which is zero. In this instance total and distortion polarization are equal. However, it is shown below that substances of zero dipole moment are uncommon.

POLARIZATIONS OF SUBSTANCES TO WHICH CENTROSYMMETRY OFTEN IS ASCRIBED

Some of the substances described in Table III have been studied because considerations of the graphic formulae (sometimes fortified by X-ray diffraction) would indicate absence of electric moment. Of course these graphic formulae depict unperturbed molecules isolated in space, a circumstance never realized during ordinary chemical reactions. Nevertheless if the activated states and the effects of environment were grossly symmetrical the moments ought to be zero. It may be seen in Table III that this expectation is not realized.

In the case of hexamethylbenzene the answer is dependent on the choice of a distortion polarization value. The calculated electronic polarization happens to be about the same according to either Vogel or Eisenlohr. We suspect by perusal of Table I that this agreement involves a compensation of error. However, the value is so close to that of the total polarization at 20° or 40° that the moment might be specified as zero. On the other hand the measured distortion polarization is sufficiently lower than P_T that a moment of 0.52 D may be assigned. This apparent moment is not sufficiently augmented (0.56 D) at 40° to justify an assignment more definite than 0 to 0.5 D for hexamethylbenzene, depending upon whether measured P_{e+a} or calculated MR_D is used in the calculation.

The situation is somewhat clearer for 1,4-di-*tert*-butylbenzene because both the calculated (P_e) and observed (P_{e+a}) distortion polarizations are less than the total polarization. Since P_{e+a} is lower than MR_D (calculated) there is no justification for inclusion of an abnormal atom polarization with the latter value. The calculated moment of 0.58 D (or 0.4 D in respect of MR_D) in benzene at 20° is augmented to 0.64 D at 40°. This difference (which is beyond our estimated error of ±0.01 D) would indicate that the *tert*-butyl groups comprise an opposed quadrupole in absence of thermal agitation. Therefore at some temperature much below those which must be chosen if benzene is the solvent a zero moment should be observed.

Similarly the orientation polarization of 1,4-diphenylbenzene may be attributed to thermal agitation. The measured P_{e+a} and calculated MR_D differ by about 3%, but they are both lower than P_T in benzene at 20° so a moment of 0.60 to 0.51 D may be calculated, which is 0.73–0.64 D at 40°.

It is evident that substances like these of ostensible zero moment cannot be used for standardization of electrical polarization equipment if they display orientation polarizations. In this connection it is pertinent to review the polarization studies of 1,4-dichlorobenzene which is sometimes considered to be such a standard substance. Thus Briegleb (12) must have observed a total polarization at 20° in heptane of 40.4 cc and an electronic polarization of 36.1 cc, yet he discards the predicted moment of 0.45 D, preferring a hypothetical atom polarization to contradiction of an intuitive expectation of static symmetry. Unfortunately for purposes of clarification we cannot contradict Briegleb by measurement of the dielectric constant of 1,4-dichlorobenzene because its low melting point prevents the preparation of satisfactory pellets. However, we obtain polarization values in benzene and in dioxane from which moments of 0.43 D and 0.33 D, respectively,

Can. J. Chem. Downloaded from www.nrcresearchpress.com by 186.148.149.217 on 09/04/12
For personal use only.

TABLE III

Dipole moments of hydrocarbons and their halogenated derivatives

Substance	Solvent	Temp., °C	$\delta\epsilon/\delta\omega$	$\delta V/\delta\omega$	P_T	P_{e+a}	R_D calc.	μ from P_{e+a}	μ from R_D	Comments
Hexamethylbenzene	Benzene	20	0.060	0.057	54.3	48.6	54.1	0.52	0	
		40	0.051	0.044	54.8			0.56		
1,4-Di-*tert*-butylbenzene	Benzene	20	0.030	0.025	67.3	60.2	63.4	0.58	0.4	
		40	0.017	0.099	68.3			0.64		
1,4-Diphenylbenzene	Benzene	20	0.43	0.247	79.8	72.2	74.6	0.60	0.51	
		40	0.51	0.280	82.5			0.73	0.64	
Hexahelicene	Benzene	20	0.56	0.363	110.4	100.2	105	0.70	0.4	
1-↓-2-↓-3↑-4↑-Tetraphenylcyclobutane, m.p. 163°	Benzene	20			113			0.44	0[a]	[a]Latter values actually calculated as if R_D was 113 cc
	Benzene	40			126			0.93	0.82	
	Dioxane	20			126	109	116	0.90	0.80	
	Dioxane	40			151			1.46	1.38	
1-↓-2,3,4-↑-Tetraphenylcyclobutane, m.p. 149°	Benzene	20			119.4			0.69	0.55[a]	
	Benzene	40			147.6			1.41	1.32	
	Dioxane	20			142.6	109	116	1.27	1.16	
	Dioxane	40			182.0			1.92	1.87	
α-Methylstyrene	Benzene	20	0.80	0.055	55.9		39.4		0.89	
trans-Propenylbenzene	Benzene	20	0.52	0.034	50.5		40.7		0.68	
cis-Propenylbenzene	Benzene	20	0.57	0.048	51.1				0.70	
		40	0.57	0.088	51.4		40.8		0.69	
2-Methyl-1-phenyl-1-propene	Benzene	20	0.63	0.050	63.8		49.4		0.83	
1,4-Dichlorobenzene	Dioxane	20	0.23	0.195	38.4		36.0		0.33	[b]n_D^{30} gives R_D of 36.7
							36.7[b]		0.28	
	Benzene	20	0.18	0.353	39.5		36.0		0.41	
	Benzene	30	0.14	0.336	39.4		36.0		0.41	
Hexachlorobenzene		20	0.23	0.58	59.8	53.0	55.5	0.54		[c]Determinations made with temperature-variant apparatus
		30	0.33	0.60	64.3			0.72		
	Benzene	30[c]	0.35	0.599	65.7			0.76		
		35	0.37	0.58	68.8			0.80		
		40[c]	0.34	0.600	68.4			0.86		
		60[c]	0.38	0.600	70.3			0.95		
	CCl_4	20	0.28	0.071	54.7			0.21		
		30	0.45	0.092	58.7			0.50		
Hexafluorobenzene	Cyclohexane	20	0.09	0.605	36.2		26.5		0.67	
		30	0.10	0.49	38.9		26.5		0.81	n_D^{20} = 1.3760
	Benzene	40	0.10	0.49	40.2				0.83	
		60	0.10	0.49	40.9				0.88	d_4^{20} = 1.612
1,2-Diiodotetrafluorobenzene	Benzene	20	1.16	0.768	131.4				1.96	
		30	1.065	0.794	123.6	49.4	50.4		1.89	
		40	0.96	0.802	119.2				1.86	
1,4-Dimethyl-2,3,5,6-tetrachlorobenzene	Benzene	20	0.16	0.370	63.4	50.9	55.0	0.77	0.63	
		30	0.40	0.476	67.5			0.90	0.78	
		40	0.52					1.04	0.95	
1,2,4,5-Tetrachlorobenzene	Benzene	20	0.35	0.51	54.2	43.1	45.5	0.72	0.64	
		30	0.34	0.52	54.2			0.73	0.65	
		40	0.33	0.53	54.0			0.74	0.66	
1,4-Diiodotetrafluorobenzene	Benzene	30	0.12	0.80	50.8	49.4	50.4	0.14	0	
1,2,3,4-Tetrafluorobenzene	Benzene	20	0.412	0.36	150.0		25.1		2.43	
		30	0.392	0.39	145.6				2.41	
Tetraphenylethylene	Benzene	40	0.392	0.248	114.7	95.1	107.3	0.99	0.61	
	Benzene	20	0.03	0.179	97.3	95.1	107.3	0.33	−0.69	Absurd
	Dioxane	20	0.462	0.101	107.5	95.1	107.3	0.77	0	

may be calculated after substraction of Briegleb's distortion polarization value. This solvent effect would not have been observed if an electrical dipole were absent. Therefore we see no reason to attribute a zero moment to *p*-dichlorobenzene at ordinary temperature nor to consider it as a reference standard, especially since in Table I analogous substances do not show abnormal distortion polarizations. Despite expectations from other studies

Can. J. Chem. Downloaded from www.nrcresearchpress.com by 186.148.149.217 on 09/04/12
For personal use only.

(18) the four polyhalogenobenzenes listed in the table all have P_{e+a} values which are about 4% lower than the calculated MR_D values.

The high group moments which may be anticipated in these halogenobenzenes makes them of especial interest with respect to studies of molecular symmetry. Among these substances hexachlorobenzene has been examined most completely by other physical methods. Single crystal X-ray diffraction studies show it to be planar (19) although a modern study might alter this opinion, especially in respect of the carbon atoms. Actually it is somewhat surprising that a centrosymmetrical molecule should exist in the polymorphic forms (20) that have been reported for this substance. At any rate when hexachlorobenzene is freed from its crystal lattice the chlorine atoms no longer remain coplanar. A displacement from planarity of about 25° is claimed on the basis of quadrupole moment (21). Indeed displacement is not even symmetrically disposed according to electron diffraction studies (22) which attribute this asymmetry to out-of-phase bending of the carbon–chlorine linkages.

Not only is this asymmetry indicated by our electrical polarization studies, but also the data of Table III show that the moment of hexachlorobenzene in benzene increases from 0.54 D to 0.95 D when the temperature is raised from 20° to 60°. Of course the absolute values of moment are in doubt. Quantitative assignments are precluded because of the disparity between calculated and observed distortion polarizations. Also (Table III) the solvent seems to be involved in the polarization because the apparent moment is smaller (0.2 D) in carbon tetrachloride at 20° than it is in benzene. Nevertheless the moment in carbon tetrachloride seems to be real, because it is augmented to 0.5 D at 30°. But also it cannot be an absolute value if it is temperature-dependent.

Although the lesser moment in carbon tetrachloride may be expected in view of the lesser polarizability of this medium, still one is not justified to specify the observed moment value as absolute. It is true that a substance like iodine displays no orientation in cyclohexane (23), and probably would not do so in carbon tetrachloride. In benzene, on the other hand, a moment is observed which must be due to mutual polarization of solvent and solute (iodine) either of which alone has no dipole moment. But when a solute (like hexachlorobenzene) is polar, at least in activated states, it may be expected to distort and therefore polarize substances like carbon tetrachloride which bound the solvent cavity in which it exists. In this sense the absolute polarity of a substance cannot be defined if it has neighbors. *But the existence of polarity can be defined.* Perhaps solvents like benzene and dioxane should be considered to be useful in enhancement of otherwise meager moments, at least until the time that more precise methods than now are known become available for measurement of electrical polarization.

Despite this limitation on the quantitative significance of the polarization of hexachlorobenzene it seems to be undeniable that this polarization shows it to be a nonplanar substance, the asymmetry of which increases with rising temperature. In order to understand this situation other halogenobenzenes have been examined. The first of these, 1,2,4,5-tetrachlorobenzene, apparently has a moment in benzene at 20° which is larger (Table II) than that of hexachlorobenzene. However, the augmentation of this moment with rising temperature is so slight that it is almost within experimental error. By contrast when methyl groups occupy the hydrogen positions in the tetrachlorobenzene, as in 1,4-dimethyl-2,3,5,6-tetrachlorobenzene, the moment in benzene at 20° is only slightly higher than in absence of these methyl groups. However, this moment is markedly augmented by increasing temperature (see Table III). It would seem that while steric obstruction (minimal in 1,2,4,5-tetrachlorobenzene) is not significantly responsible for

Can. J. Chem. Downloaded from www.nrcresearchpress.com by 186.148.149.217 on 09/04/12
For personal use only.

the inherent moments, it is largely responsible for the temperature-induced polarizability.

Polysubstitution of fluorine instead of chlorine on the benzene ring ought to reduce the steric obstruction, and indeed this expectation is borne out in the polarizability of the hexafluorobenzene kindly supplied to us by Dr. Wall of N. B. S. (24).

As was observed for hexachlorobenzene the apparent moment of the fluoro analogue is lower in cyclohexane than it is in benzene which is ostensibly more polarizable. However, the apparent moments for hexafluorobenzene in either solvent at 20° are higher (Table II) than the comparable values for the hexachloro analogue. This result would not be expected, if the moments were due to static nonplanarity, in view of the evidence (15, p. 253) that the group moment (1.46 D) for C—F is lower than that of C—Cl (1.58). On the other hand the result could be due to a dynamic nonplanarity in activated states. The difference in apparent moment is not great; indeed if one were to choose the admittedly improbable state of activation involving all six halogen atoms on one side of an assumed planar hexagon of carbon atoms the apparent moment would be accounted for by an angular deviation of 3° for the chlorine atoms and 5° for the fluorine atoms. Among the complexity of possible conformations of activation it is possible for the resultant moment of hexafluorobenzene to exceed that of hexachlorobenzene, especially since the lower force constant of the C—F bond would allow greater amplitude of deformation.

Of interest in relation to this concept of moment contributions from such a dynamic "structure" is the observation that the apparent moment of hexafluorobenzene increases by only 0.07 D over a temperature range of 40°. By contrast the apparent moment of hexachlorobenzene (although it is lower than that of hexafluorobenzene at 20° in benzene) increases by 0.41 D over the same range of temperature. This difference might be ascribed to a higher activation energy for hexachlorobenzene (due largely to steric obstruction) which is observed as a greater temperature coefficient for the dipole moment.

This interpretation is based upon the assumption that the activated states are appreciably unsymmetrical and that this asymmetry is accentuated when the activated state tends to be more sterically hindered than the base state. It is of interest to examine the behavior of a substance which undoubtedly is hindered in the base state. This condition prevails in the 1,2-diiodotetrafluorobenzene (25), which we have obtained by courtesy of Dr. Matsuguma at Picatinny Arsenal.

If this substance were entirely coplanar one would expect the moment to be the arithmetic difference between the moments of 1,2-difluorobenzene (2.38 D in benzene at 22°) (26) and of 1,2-diiodobenzene (1.70 D in benzene at 23°) (27). Instead of the expected 0.68 D the apparent moment of 1,2-diiodotetrafluorobenzene in benzene at 20° has been found to be 1.96 D.

Of course an abnormality for this compound is not entirely unexpected since the observed moment for 1,2-diiodobenzene is somewhat lower than the calculated (ref. 15, p. 332) value, 2.25 D. Presumably this diminution may be attributed to steric repulsion of the iodine atoms so that they are spread apart in a planar structure, or else oppositely forced above and below a plane.

It is evident that these deformations are not applicable to the structure of 1,2-diiodotetrafluorobenzene. The high moment would indicate the presence of contributing conformations where fluorine as well as iodine is forced asymmetrically from the plane of carbon atoms assumed to exist in these substituted benzenes. Of course the assumption of ring planarity is arbitrary, but it allows a simple description of conformation in which fluorine–carbon moments are supporting rather than detracting from iodine carbon moments.

Can. J. Chem. Downloaded from www.nrcresearchpress.com by 186.148.149.217 on 09/04/12
For personal use only.

By contrast the observed moment of 1,4-diiodotetrafluorobenzene, in which obstruction may be expected to be minimal, is very low (0.14 D in benzene at 30°), indicating cancellation of opposing group moments. In like manner the 1,4-fluorine atoms in 1,2,3,4-tetrafluorobenzene must be compensatory because the observed moment of this substance (2.43 D) is very close to that of 1,2-difluorobenzene. The absence of obstruction which is indicated by this agreement is further supported by the virtual invariance of moment in benzene at 20° and 30° (2.43 vs. 2.41 D, Table III).

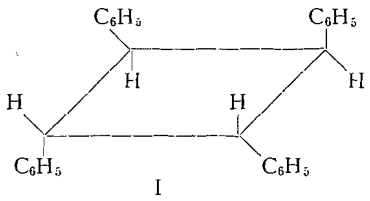
It may be seen from these examples that the effect of iodine atoms vicinally located on a benzene ring in which fluorine atoms prevent lateral spacing is profound. This is the circumstance in 1,2-diiodotetrafluorobenzene with its abnormally high apparent moment. It might be expected that when obstruction is sufficiently great it cannot become greater but must necessarily be less in activated states.

It may then be significant that the apparent moment of 1,2-diiodotetrafluorobenzene, alone among the moments of substances under consideration in this report, decreases slightly but significantly (1.96 to 1.84 D from 20° to 40°) with increasing temperature. The behavior is remindful of certain sterically hindered diastereomers, the moments of which have been studied recently with respect to temperature (28).

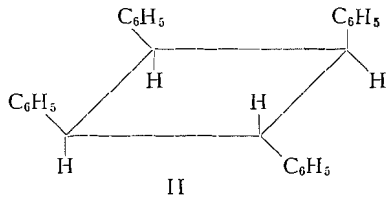
THE TETRAPHENYLCYCLOBUTANES

Several of the diastereomers of tetraphenylcyclobutane will now be discussed separately from the foregoing items of Table III because of the rigidity imposed by the cyclobutane ring.

The isomers are 1-↓-2-↓-3-↑-4-↑-tetraphenylcyclobutane, I, and 1-↓-2,3,4-↑-tetraphenylcyclobutane according to Morton, Bright, and Flood, who kindly loaned them to us. They specified these structures on the basis of nuclear magnetic resonance studies (29).



I



II

These workers obtained II (m.p. 149.7°) together with stilbene from the reaction of benzyl chloride with potassium amide in liquid ammonia. The preparation of I (m.p. 163°) had been accomplished by Fulton (30) when he irradiated stilbene and/or stilbamidine with ultraviolet light. Fulton also obtained in trace amounts an isomer melting at 149°. However, this isomer is not identical with II, at least according to comparison of the X-ray pattern of II with that of a sample of Fulton's isomer, kindly furnished to us by Professor Dunitz, University of Zürich. Insufficient material was in hand to determine whether the difference was due to diastereoisomerism or polymorphism. Our studies have been made with the proved isomers I and II.

Actually the configuration of I was demonstrated by Professor Dunitz by a thorough single crystal X-ray study (31). However, he found that the isomer I was not conformationally symmetrical. Not only were abnormalities of bond shortening at C–phenyl observed, but also it appeared that the phenyl rings were not axially disposed with respect to these bonds; deviations up to 7° were suggested.

Can. J. Chem. Downloaded from www.nrcresearchpress.com by 186.148.149.217 on 09/04/12
For personal use only.

Can. J. Chem. Downloaded from www.nrcresearchpress.com by 186.148.149.217 on 09/04/12
For personal use only.

In this X-ray diffraction study Dunitz did not suggest any nonplanarity of the cyclobutane ring although he did report that the bond lengths differed. Later he and others presented evidence from studies of various cyclobutanes (including electron diffraction and infrared absorption) which indicate a dihedral angle in the cyclobutane ring, which may be as low as 162°. It is of interest that a calculation of the dipole moment of tetramethylcyclobutanedione-1,3, assuming that carbonyl moments of 2.5 D are inclined axially at 162°, gives the same resultant (0.8 D) which was obtained from the measured electrical polarization (3). It is against this background that we have studied the electrical polarizations of the tetraphenylcyclobutanes, I and II.

This study has brought forth several apparent anomalies. Firstly a measurement of the dielectric constant of the randomly oriented compressed solid isomers I and II gives distortion polarization (P_{e+a}) values (109 cc, Table I) which are somewhat below the electronic polarization calculated from Vogel's and Eisenlohr's generalized bond refractions (32, 33) (121.3–114.8 cc). The measured value of 109 cc also is lower than that which may be calculated indirectly (116.5 cc) from the molecular refraction of cyclobutanecarboxylic ester (34).

In Table III it may be seen that the total polarization of isomer I in benzene at 20° is 113 cc. Since all of the values for MR_D are higher than 113 cc a moment calculation from the known refraction values would be absurd.* Therefore we have assumed arbitrarily that the orientation polarization of isomer I is zero, i.e. that the distortion polarization is 113 cc. The moments in other solvents and at other temperatures have been calculated in this way to give "μ from R_D" in Table III. The moments calculated from the measured distortion polarization are shown as "μ from P_{e+a}".

By either calculation it may be seen in Table III that the orientation polarization increases as the temperature is raised. Moreover, it is evident from the profound solvent effect that the moment values are only apparent ones. Nevertheless it seems reasonable to seek an explanation for an average moment of about 0.4 D at room temperature.

An adequate and authenticated explanation has not been found. But since we suspect from Dunitz' X-ray analysis that isomer I is inadequately described by a simple rigid centrosymmetrical structure we have chosen a model in which the cyclobutane ring is symmetrical and planar while the phenyl groups are randomly rotating, their planes at an angle (α) from linearity with the C–phenyl bond. This dynamic model will account for a dipole moment in isomer I.

The magnitude of this moment will depend on the group moment to be assigned to phenyl—C—hydrogen. The group moment for phenylalkyl seems to be 0.3–0.7 D depending upon the alkyl group (15). In consideration of cyclic substances a moment of 0.49 D has been reported for phenylcyclopropane in benzene at 25° (35) while the phenyl–carbon moment of the four methyl-substituted styrenes (36) would appear to be about 0.5 D.

The resultant moment may be calculated according to the relationship

$$\mu = 2(m) \sin \alpha$$

where m is the C–phenyl moment, α is the angular deviation from linearity of the C–phenyl bond and the phenyl plane, and where all phenyl groups are rotating randomly.

*It is of interest that tetraphenylethylene, which resembles tetraphenylcyclobutane in structural character, also would give an absurd value (Table III, −0.69 D) for moment of 20° in benzene if the calculated value of molecular refraction were used. On the other hand the use of the measured distortion polarization (Table II) leads to a real and reasonable value of apparent moment in benzene which is augmented by measurement at 40°.

If m is taken as 0.5 then moments of 0.15 D, 0.30 D, and 0.50 D would require α values of 10, 20, and 30° respectively. It is doubtful that the phenyl groups are inclined at even the smallest of these angles. Either the solvent effect is much greater than would be expected by the usual comparisons of the moments of vapors with those of solutions or else the model which we have assumed for tetraphenylbutane is incorrect. We suggest, as have others mentioned above, that the cyclobutane ring is not rigidly planar.

We have not been able to make a satisfactory calculation for the expected moment if the cyclobutane ring of isomer I is normally bent at a dihedral angle of 160°. However, our attempts do show us that a lesser deviation from C–phenyl linearity would be required than if the cyclobutane ring were planar in order to account for moment magnitudes of 0.1–0.4 D. It would seem that at the present time the experimental results can best be explained by non-planarity of the cyclobutane ring.

It may be seen in Table III that the apparent moments for isomer II are higher than those of isomer I. We have been unsuccessful in attempts to correlate mathematically the two sets of moments. This failure is not unexpected because entirely different sets of activated state conformations would maintain for the two isomers. However, the higher moment values of the ostensibly less symmetrical isomer II, over those of isomer I, show that both isomers are to some extent polar.

The authors wish to thank Mr. G. K. White for aid in the calculations and Dr. Dunitz for submission of samples used for X-ray diffraction studies. The chlorinated benzenes were kindly supplied by Dr. A. L. Rocklin of the Dow Chemical Company and by The Diamond Alkali Company. Funds for technical aid and for equipment have been furnished by the National Research Council to whom we are grateful. The generous co-operation of Dr. M. S. Newman and Dr. L. A. Wall are greatly appreciated.

EXPERIMENTAL

Materials

All of the substances listed in Tables I and III have been purified to constant melting point and in the case of liquids to constant refractive index. The hexachlorobenzene received from Dr. Rocklin was better than 99.5% pure; its Nujol mull absorbed at 3000 (S), 2850 (M shoulder), 1460 (W), 1378 (VW), 1340 (VS), 1297 (S), 930 (VW), 718 (VW), and 694 (S). The substituted styrenes have been purified according to a previous description (37). The tetraphenyl cyclobutanes were pure as received from Dr. Flood but were crystallized from methanol. The 1-↓-2↓-3-↑-4↑-isomer showed a diffraction pattern (CuK_α radiation, Ni filtered) in Angstroms at relative intensities $[I/I_1]$ as follows: [10]-5.34, 4.07[7]3.32[4]5.01[3]3.77[2]9.93, 8.50, 4.79[1]4.25, 3.90, 3.44, 3.16. The 1-↓-2,3,4-↑-isomer gave a pattern of [10]4.73[9]3.88[8]5.06, 3.78[6]5.77[4]9.06[3]3.19[2]10.84, 5.02[1]-3.56, 2.61 in contrast to the isomer of the same melting point (149°) isolated by Fulton (30) and sent to us by Dr. Dunitz. This sample showed [10]4.28[8]5.52[7]4.74[6]4.50[5]-5.86[4]6.96[2]10.35, 9.45, 2.76[1]4.92, 4.15, 4.00, 3.93, 3.56, 3.31.

Dielectric Constant Determinations

The dielectric constants of solids were determined according to methods described previously (2, 3). It has been found that when a binder is necessary for preparation of satisfactory pellets polyethylene wax (10–30 microns diameter) is at least as satisfactory as koroseal. However, a change of crystal habit, effected by recrystallization, usually renders the use of a binder unnecessary. Oftentimes good pellets are obtained by grinding unsatisfactory ones prior to repelletting. By this technique one is assured of random

Can. J. Chem. Downloaded from www.nrcresearchpress.com by 186.148.149.217 on 09/04/12
For personal use only.

orientation of the substance.

The dielectric constants of solutions were determined in the apparatus described previously (38) and also in a modification designed for determination of dielectric constant at a series of temperatures for each solution in order to reduce the time required for determination of temperature coefficients. The test cell was constructed from Corning No. 7740 glass. At the top of the inner concentric electrode was sealed through a Kovar metal rod to which connection could be made internally. On the outside of this electrode was burned in a gold paint (E.I. Du Pont No. 5732) compatible with the pyrex at 550° C. This metal coating which also covered the protruding Kovar rod as a resistance-free conductor was burnished and then polished with rouge (in turpentine) and then talc. The outside concentric electrode (0.7 mm clearance to give 60-pf capacitance when it was 23 mm I.D. by 85 mm long) was equipped at the top with an 8-mm diameter Kovar tube and was coated inside with gold as was described above so that a resistance-free connection could be made to ground from the outside of this metal tube. To the top of this Kovar tube was scaled a "burette" comprised of six 100-mm lengths of capillary tubing (0.8 mm I.D. graduated in millimeters) which were connected together by bulbs of 0.25-ml capacity. The two electrodes were ring-sealed together with an inlet tube at the bottom which terminated into a Kovar tube 0.9 mm O.D. of length sufficient to reach to the bottom of the pear-shaped flask (16–19 mm capacity) used previously for preparation and reference specific volume (at 25° C) of the test solution. A dry ice bath applied to the tapered bottom of this flask served to freeze and thus retain the solution within the test capacitor after it had been forced in by air pressure. If this apparatus were to be constructed again we would use Corning 7052 glass for the electrodes.

The solvent must be frozen and outgassed before use in this apparatus and the solution must finally be heated *in situ* at 5° above the highest temperature of the determination until no more bubbles appear; since at this time the level is slightly below the bottom of the burette the addition of a little more of the non-heated solution is necessary after cooling, but this amount does not supersaturate the test-cell content at the highest temperature of the determination. The temperature is maintained $\pm 0.02°$ by a surrounding jacket (also around the burette) containing refluxing carbon tetrachloride under a standard system for regulating pressure from 760 mm to 10 mm. The reflux system must be surmounted by a dry ice cooled condenser following a water condenser which follows an air condenser. The latter ensures that the refluxing carbon tetrachloride which pours down the jacket surrounding the burette is not too cold. The burette is best read by means of a cathetometer. It is recommended that the apparatus be calibrated by means of a non-aqueous solvent (benzene) since water tends to weaken the gold-glass bond.

Connection between the inner electrode and the resonance circuit of the variable frequency oscillator is made by a vertical threaded rod which meets the Kovar rod inside the electrode end-to-end inside of a close-fitting glass sleeve. The screw feed which advances the threaded rod to make contact is calibrated so as to reproduce inductance and capacitance in this switch and thus to maintain the precision of measurement to ± 0.001 pf.

REFERENCES

1. C. C. MEREDITH, L. WESTLAND, and G. F WRIGHT. J. Am. Chem. Soc. **79**, 2385 (1957).
2. M. V. GEORGE and G. F WRIGHT. Can. J. Chem. **36**, 189 (1958).
3. P. PODELESCHKA, L. WESTLAND, and G. F WRIGHT. Can. J. Chem. **36**, 574 (1958).
4. H. SAWATZKY and G. F WRIGHT. Can. J. Chem. **36**, 1555 (1958).
5. A. I. VOGEL, W. T. CRESSWELL, G. H. JEFFREY, and J. LEICESTER. J. Chem. Soc. 514 (1952).
6. F. EISENLOHR. Z. physik. Chem. **75**, 585 (1910); **79**, 129 (1912).

Can. J. Chem. Downloaded from www.nrcresearchpress.com by 186.148.149.217 on 09/04/12
For personal use only.

7. W. M. D. BRYANT. J. Am. Chem. Soc. **65**, 96 (1943).
8. C. J. F. BOETTCHER. Theory of electrical polarization. Elsevier Publishing Co., New York. 1952. p. 255.
9. S. C. ABRAHAMS, J. M. ROBERTSON, and J. G. WHITE. Acta Cryst. **2**, 233 (1949).
10. F. R. AHMED and D. J. W. CRUICKSHANK. Acta Cryst. **5**, 852 (1952).
11. A. PARTS. Z. physik. Chem. B, **10**, 264 (1930).
12. G. BRIEGLEB. Z. physik. Chem. B, **16**, 276 (1932).
13. J. W. WILLIAMS. J. Am. Chem. Soc. **52**, 2096 (1931).
14. Y. S. MUSABEKOV. Izest. Azerbaidzhan Sel'skokhoz Inst. No. 6,21-3 (1940); Chem. Abstr. **38**, 735 (1944).
15. C. P. SMYTH. Dielectric behavior and structure. McGraw-Hill Book Co. Inc., New York. 1955.
16. PHYSICAL METHODS of organic chemistry. Interscience Publishers, Inc., New York. 1945. p. 669.
17. M. V. GEORGE and G. F WRIGHT. J. Am. Chem. Soc. **80**, 1200 (1958).
18. A. TULINSKY and J. G. WHITE. Acta Cryst. **11**, 7 (1958).
19. R. KAISER. Z. physik. Chem. **36**, 92 (1935).
20. K. SCHAUM, K. SCHAELING, and F. KLAUSING. Ann. **411**, 161 (1916).
21. J. DUCHESNE and A. MONFILS. J. Chem. Phys. **22**, 562 (1954).
22. E. HARNICK, F. H. HERBSTEIN, G. M. J. SCHMIDT, and F. L. HIRSCHFELD. J. Chem. Soc. 3288 (1954).
23. F. FAIRBROTHER. J. Chem. Soc. 1051 (1948).
24. M. HELLMAN, E. PETERS, W. J. PUMMER, and L. A. WALL. J. Am. Chem. Soc. **79**, 5654 (1957).
25. W. J. PUMMER, R. E. FLORIN, and L. A. WALL. J. Research Natl. Bur. Standards, **62**, 113 (1959).
26. E. BERGMANN, L. ENGEL, and S. SANDOR. Z. physik. Chem. B, **10**, 106 (1930).
27. L. TIGANIK. Z. physik. Chem. B, **13**, 425 (1931).
28. H. SAWATZKY, G. K. WHITE, and G. F WRIGHT. Can. J. Chem. **37**, 1132 (1959).
29. J. M. MORTON, E. A. FLOOD, and F. H. BRIGHT. Can. J. Chem. **35**, 1097 (1957).
30. J. D. FULTON. Brit. J. Pharmacol. **3**, 75 (1948).
31. J. D. DUNITZ. Acta Cryst. **2**, 1 (1949).
32. A. I. VOGEL. J. Chem. Soc. 134 (1946).
33. A. I. VOGEL. J. Chem. Soc. 654 (1948).
34. INTERNATIONAL CRITICAL TABLES. VII. p. 37.
35. M. T. ROGERS. J. Am. Chem. Soc. **69**, 2544 (1947).
36. E. BRINER, K. RYFFEL, and E. PERRETTOT. Helv. Chim. Acta, **22**, 927 (1939).
37. W. R. R. PARK and G. F WRIGHT. J. Org. Chem. **19**, 1435 (1954).
38. C. C. MEREDITH and G. F WRIGHT. Can. J. Technol. **33**, 182 (1954).

Can. J. Chem. Downloaded from www.nrcresearchpress.com by 186.148.149.217 on 09/04/12
For personal use only.

Can. J. Chem. Downloaded from www.nrcresearchpress.com by 186.148.149.217 on 09/04/12
For personal use only.

ISOLATION AND CHARACTERIZATION OF A CELLULOSE FROM THE INNER BARK OF WHITE BIRCH (*BETULA PAPYRIFERA*)[1]

A. Jabbar Mian and T. E. Timell

ABSTRACT

A pectic acid, a 4-*O*-methylglucuronoxylan, and a cellulose have been isolated from the inner bark of white birch (*Betula papyrifera*), in addition to minor amounts of other polysaccharides. The cellulose, which comprised 28% of the bark, yielded only D-glucose on hydrolysis, had a number-average degree of polymerization of 315 and, on methylation and hydrolysis, gave 2,3,6-tri-*O*-methyl-D-glucose and 2,3,4,6-tetra-*O*-methyl-D-glucose in a mole ratio of 59:1. The *O*-methylcellulose had a degree of polymerization of 125, thus suggesting the possibility of branching. Direct nitration of the bark gave a nitrate in a yield corresponding to 28% cellulose in the bark. Light-scattering measurements on this derivative indicated a weight-average degree of polymerization of 7500. While the low intrinsic viscosity of this nitrate did not exclude the possibility of branching, further evidence is needed to establish the linear or non-linear nature of birch bark cellulose.

Although it has been assumed for some time that cellulose is probably present in the inner bark of trees (1, 2), it was only recently that a pure, albeit degraded, cellulose was isolated from spruce bark (3). Since cellulose constitutes the most valuable part of a tree, it was considered to be of a certain interest to establish to what extent it is present in a hardwood bark and whether it is similar to the cellulose present in the wood. In a series of previous investigations (4–6), the isolation and properties of a cellulose from the wood of white birch (*Betula papyrifera* Marsh.) were studied. The present paper is concerned with the constitution and molecular properties of a cellulose from the inner bark (secondary phloem) of the same species.

RESULTS AND DISCUSSION

The inner bark, which had been completely freed from cortex, cambium, and secondary xylem, was exhaustively extracted with organic solvents after which it was treated with hot water and subsequently with aqueous ammonium oxalate for removal of pectic material. Treatment with acid chlorite removed 25% of the extractive-free product. Subsequent extraction with aqueous potassium hydroxide resulted in isolation of a pure xylan (7). Alkaline borate removed a polysaccharide mixture and left a residue which could not be further fractionated and which corresponded to 28% of the bark. The yield and relative composition of the various fractions are given in Table I.

TABLE I

Yield* and carbohydrate composition† of bark fractions

Component	Yield	Galacturonic acid	Galactose	Glucose	Mannose	Arabinose	Xylose
Water extract	1.5	5	8	25	16	11	35
Pectic material	4.2	90	Trace	Nil	Nil	10	Nil
Glucuronoxylan	26.6	Trace	Nil	Trace	Nil	Nil	87‡
Alkali–borate extract	3.8	26	13	16	Nil	45	Nil
Cellulose	28.4	Nil	Nil	100	Nil	Nil	Trace

*Percentage of original, extractive-free bark.
†Percentage of total reducing sugar content of each fraction.
‡In addition to 13% of 4-*O*-methylglucuronic acid.

[1]*Manuscript received March 22, 1960.*
Contribution from the Pulp and Paper Research Institute of Canada and the Department of Chemistry, McGill University, Montreal, Que.

The predominant hemicellulose was a linear, (1 → 4)-β-linked 4-*O*-methylglucuronoxylan, containing on the average one (1 → 2)-α-linked acid side chain per 10 xylose residues. Its number- and weight-average degrees of polymerization were 230 and 470, respectively (7). Water extracted a mixture of polysaccharides. The subsequent fraction consisted of a (1 → 4)-α-linked pectic acid which could not be obtained free from arabinose residues. Alkaline borate removed a polysaccharide mixture, almost half of which consisted of arabinose residues.

The absolute composition of the bark in terms of sugar residues was computed from the total content of reducing sugar (54%) and the various amounts of polysaccharide residues present. The result is given in Table II. The carbohydrate content is considerably higher than that previously reported (8) for the entire bark of the same species, but the relative composition is approximately the same. The directly determined values were also compared with those which could be calculated from the percentage and composition of the various fractions. Except for the galacturonic acid and galactose residues, the agreement is good, thus indicating that the entire polysaccharide portion of the bark had been accounted for in the fractions isolated.

TABLE II

Carbohydrate composition of the extractive-free bark*

Component	Galacturonic acid	Galactose	Glucose	Mannose	Arabinose	Xylose
Found†	2.2	1.1	28	Trace	2.7	21
Calculated‡	5.6	0.6	29	0.2	2.3	23

*Percentage of oven-dry material.
†Found by direct analysis of the bark.
‡Calculated from yield and composition of the fractions.

The residual material, a white powder, was insoluble in aqueous alkali, yielded only D-glucose on hydrolysis, and consumed 1 mole of periodate per glucose residue. Its X-ray powder diagram and infrared spectrum were identical to those of cellulose II. The polysaccharide was methylated to completion and hydrolyzed. The resulting sugar mixture was resolved on a charcoal–Celite column by gradient elution with aqueous ethanol to yield 2,3,6-tri-*O*-methyl-D-glucose (59 parts) and 2,3,4,6-tetra-*O*-methyl-D-glucose (1 part), both of which were obtained crystalline. The number-average degree of polymerization ($\bar{P}_n$) of the *O*-methylcellulose, as determined by osmometry, was 125, thus suggesting the presence of 2.1 non-reducing end groups per average molecule.

The cellulose was converted to its nitrate derivative with an acid mixture known to cause little or no depolymerization of polysaccharides (9, 10). Osmotic pressure measurements on the nitrate indicated a $\bar{P}_n$ value of 315. It is well known that cellulose suffers degradation under the action of both acid chlorite (4) and alkali (11). It was evident therefore that the $\bar{P}_n$ value obtained could hardly represent the molecular weight of the cellulose as it originally occurred in the bark. Direct nitration of wood with the above acid mixture has been shown (12) to result in the isolation of cellulose nitrates in almost quantitative yield, while nitrated pectic acid and hemicelluloses are largely removed. When the extractive-free bark was subjected to a similar treatment, both before and after removal of pectic material, cellulose nitrates were obtained in yields corresponding to 25–28% cellulose in the bark. Denitration, followed by hydrolysis, indicated the presence of glucose and traces of xylose residues. The intrinsic viscosities

Can. J. Chem. Downloaded from www.nrcresearchpress.com by 186.148.149.217 on 09/04/12
For personal use only.

of the nitrates showed that they possessed molecular weights much higher than that of the material remaining after complete extraction of the bark.

The nitrate from the pectin-free bark was subjected to light-scattering measurements in acetone solution, essentially as reported previously (13). The results were evaluated according to Zimm (14) and gave a weight-average molecular weight of 2.17×10^6, corresponding to a degree of polymerization ($\bar{P}_w$) of 7500, and a root-mean-square *Z*-average radius of gyration of 1730 Å. The corresponding values for the cellulose present in the wood of the same species were 2.73×10^6, 9400, and 1770 Å, respectively (13).

It is evident from the isolation of D-glucose and 2,3,6-tri-*O*-methyl-D-glucose that the polysaccharide was a (1 → 4)-linked glucoglycan, and that the 2,3,4,6-tetra-*O*-methyl-D-glucose originated from the non-reducing end groups. Since the polysaccharide did not give any color with iodine, starch was absent. The infrared spectrum suggested the presence of β-pyranosidic bonds (15). The polysaccharide was therefore probably cellulose. This conclusion was corroborated by the fact that its X-ray diffraction pattern coincided with that of cellulose II. Birch bark cellulose apparently has a molecular weight somewhat lower than that of the cellulose in the wood of the same species. The range involved, 7500–9500, is that typical of most native celluloses from various natural sources (16, 17). The yields on nitration agreed excellently with the amount obtained after complete removal of non-cellulosic polysaccharides and also compared well with the known glucose content of the bark. It is probable therefore that the bark contained approximately 28% cellulose. Bark from white spruce has previously (3) been reported to contain at least 16% cellulose.

In a previous study (17), a relationship was developed between the intrinsic viscosity and weight-average degree of polymerization of cellulose nitrates as determined by light scattering. According to this equation, the intrinsic viscosity of the present nitrate (33.0 dl/g at trisubstitution) should correspond to a degree of polymerization of only 4300, much lower than the directly determined value of 7500. This fact suggests the presence of a branched polysaccharide, since a branched macromolecule exhibits an intrinsic viscosity lower than that of a linear polymer of the same molecular weight (18–20). That branching might be involved is also suggested by the fact that the degraded *O*-methylcellulose contained 2.1 non-reducing end groups, corresponding to 1.1 branch points per average molecule.

If branching had occurred, however, the ratio of the root-mean-square radius of gyration to the *Z*-average molecular weight would have been expected to be lower than the value computed (0.90) (18, 21). The evidence is accordingly equivocal and more information is necessary before any statement can be made as to the linear or branched nature of birch bark cellulose. All other native celluloses so far studied have been found to be linear.

EXPERIMENTAL

All specific rotations are equilibrium values and were determined at 20° C unless otherwise stated. Melting points are corrected. Evaporations were carried out *in vacuo* at 40–50° C.

Paper Chromatography

Solvents (v/v) used for separating sugars were (A) ethyl acetate:acetic acid:water (9:2:2), (B) butan-1-ol:pyridine:water (10:3:3), and (C) butanone:water (89:11). Separations were carried out by the descending technique on Whatman No. 1 filter paper and with *o*-aminodiphenyl as the spray reagent (22).

Can. J. Chem. Downloaded from www.nrcresearchpress.com by 186.148.149.217 on 09/04/12
For personal use only.

Can. J. Chem. Downloaded from www.nrcresearchpress.com by 186.148.149.217 on 09/04/12
For personal use only.

Analytical Methods

The bark was analyzed by standard methods developed for wood (23). A portion of the bark was hydrolyzed to completion (24) and the reducing sugar content of the hydrolyzate was determined by the *o*-aminodiphenyl method (22). Corrections were applied for the different rates of hydrolysis of the sugars (24) and the polysaccharide content was calculated from the relative amounts of the various sugar residues present. The ratios between the sugars present were estimated after quantitative separation by paper chromatography (solvents A and B) (22).

Isolation of the Bark

An autumn-felled specimen of a healthy white birch was immediately immersed in aqueous ethanol for several days after which the outer bark was easily removed. The brown, inner bark was separated manually from the cambium and the wood, was treated with boiling methanol, and was dried in the air. The tree contained 3.8% outer and 10.4% inner bark, based on the oven-dry weight of the trunk. The bark was converted to sawdust and the 20- to 80-mesh fraction was collected. Anal. Klason "lignin", 28.6; pentosan, 26.7; ash, 5.2; uronic anhydride, 6.9; and polysaccharides, 54%. Successive extractions with ethanol–benzene (1:2 v/v), methanol, and acetone removed 3.2, 0.8, and 0.7%, respectively. Water extracted 6.0% of material.

Isolation of Polysaccharides

A detailed description of this isolation has been given elsewhere (7). Treatment of the bark with hot water removed a mixture of polysaccharides corresponding to 1.5% of the extractive-free bark. Further extraction with hot, aqueous 0.5% ammonium oxalate gave 4.5% of a pectic material composed of galacturonic acid together with minor quantities of arabinose. At this point, the residual bark was digested with acid chlorite which removed 25.0% of material, mostly of non-carbohydrate nature. Subsequent extraction with 24% aqueous potassium hydroxide resulted in the isolation of a pure 4-*O*-methylglucuronoxylan (7) in a yield of 26.6%. When the remaining material was extracted with 17.5% sodium hydroxide containing 4.0% boric acid (25, 26), a mixture of polysaccharides was obtained (3.8%). After exhaustive washing with alkali and water, the remaining portion was acidified with dilute acetic acid and was washed until neutral with water and then with ethanol and petroleum ether (b.p. 30–60° C). Drying *in vacuo* over potassium hydroxide yielded a white powder, corresponding to 28.4% of the extractive-free bark. The yield and composition of each fraction are given in Table I.

Characterization of the Cellulose

The infrared spectrum of the cellulose showed a maximum at 886 cm^{-1}, indicative of the presence of β-pyranosidic bonds (15).

A portion of the cellulose (1.0 g) was hydrolyzed to yield a sirup (0.9 g). Paper chromatography (solvents A and B) indicated the presence of glucose and a faint trace of xylose. On standing, the sirup crystallized, $[\alpha]_D$ +53° (*c*, 5.3 in water), m.p. and mixed m.p. 144–145° C. The *p*-nitroaniline derivative had a melting point of 182° C (27).

The X-ray powder diagram was determined with a Seifert X-ray unit. The radiation used was nickel-filtered Cu K_α. The following interplanar lattice spacings (Å) were obtained: 4.2 (s), 3.0 (w), 2.5 (w), and 2.3 (w). An authentic sample of cellulose II had the following distances: 4.1 (s), 3.1 (w), 2.6 (w), and 2.2 (w). Both diagrams were in accord with published data (28).

Periodate Oxidation of the Cellulose

Dry cellulose (150 mg) was dispersed in 0.05 *M* sodium metaperiodate (50.0 ml) and shaken in the dark at +30° C for various lengths of time. The consumption of periodate was determined by the excess arsenite method. The following moles of oxidant were consumed per glucose residue (days): 0.79–2, 0.89–3, 1.02–5, 1.04–7, 1.05–8, 1.06–9, 1.07–10. Extrapolation of the later part of the conversion–time curve to zero time gave the consumption of periodate, 1.00±0.02 moles per glucose residue.

Methylation of the Cellulose

Cellulose (20 g) was dispersed in 40% (w/w) aqueous sodium hydroxide (400 ml) in an atmosphere of nitrogen, and dimethyl sulphate (250 ml) was added dropwise over a period of 20 hours. This process was repeated three times. Solid sodium hydroxide (200 g) was added, followed by dimethyl sulphate (dropwise, 250 ml). This treatment was repeated nine times, water being added whenever necessary for efficient stirring. The mixture was neutralized with concentrated sulphuric acid to pH 4, diluted, and heated to 90° C. The precipitated, partly methylated cellulose was recovered by filtration, washed with hot water, and dried *in vacuo* to give a hard powder (17.5 g).

The product was dissolved in dry dimethyl formamide (250 ml) and treated with methyl iodide (50 ml) and silver oxide (50 g) at room temperature for 24 hours (29). This process was repeated three times. The solid residue was exhaustively extracted with chloroform and the resulting suspension was centrifuged. The chloroform solution was then washed with 5% aqueous potassium cyanide (29) and water. After drying over anhydrous sodium sulphate, the solution was concentrated to 200 ml and added slowly to petroleum ether (1.5 liters). The precipitate formed was recovered by filtration, washed with petroleum ether, and dried to yield a white powder (10.2 g). Anal. Calc. for a fully methylated cellulose: $[C_6H_7O_2(OCH_3)_3]_n$: OCH_3, 45.6%. Found: OCH_3, 44.5%.

Three further methylations according to Purdie (30) failed to increase the methoxyl content of the product (31). Its infrared diagram suggested the presence of hardly any hydroxyl groups.

Methanolysis and Hydrolysis of the Methylated Cellulose

A portion of the methylated cellulose (3.0 g) was boiled under reflux with 0.7 *N* methanolic hydrogen chloride (75 ml) for 7 hours. The methanol was partly evaporated and the residue was boiled under reflux with *N* hydrochloric acid (75 ml) for 7 hours. After neutralization with silver carbonate, filtration through Celite, treatment with hydrogen sulphide, and filtration, evaporation gave a sirup (2.8 g). Paper chromatography (solvent C) suggested the presence of a trace of a di-*O*-methylhexose, a tri-*O*-methylhexose, and a small amount of a tetra-*O*-methylhexose.

Separation of the Methylated Glucoses

A portion of the methylated sugar mixture (0.90 g) was added to the top of a Darco G-60 charcoal–Celite (1:1 w/w) column (3.5×55 cm) (32) and resolved by gradient elution (33, 34) with 3 liters each of 5% aqueous ethanol → 25% ethanol and 25% ethanol → 40% ethanol. Fractions, 25 ml each, were collected at a rate of 50 ml/hr. Every third fraction was examined by paper chromatography (solvent C). Only two main fractions were obtained, a tri-*O*-methylglucose (790 mg) and a tetra-*O*-methylglucose (14.7 mg).

*Identification of 2,3,6-Tri-O-methyl-*D*-glucose*

This fraction, the first to be eluted from the column, crystallized spontaneously. After

Can. J. Chem. Downloaded from www.nrcresearchpress.com by 186.148.149.217 on 09/04/12
For personal use only.

recrystallization from ethyl ether, the melting point was 119–120° C, undepressed on admixture with an authentic sample of 2,3,6-tri-*O*-methyl-D-glucose, $[\alpha]_D$ +68° (*c*, 2.0 in water) (35).

Identification of 2,3,4,6-Tetra-O-methyl-D-glucose

On recrystallization from petroleum ether, this fraction had a melting point of 54–55° C (36), $[\alpha]_D$ +25° → +82° (equilibrium, *c*, 1.0 in water).

Nitration of the Cellulose

Dry cellulose (31.0 g) was added in small portions and with vigorous stirring to a mixture of nitric acid, phosphoric acid, and phosphorous pentoxide (64:26:10, w/w) (11) cooled to −5° C. The reaction was allowed to proceed in the dark at +17° C for 1.5 hours (12). After removal of most of the acid mixture by filtration through fritted glass, the nitrated product was washed with ice water until neutral and then with methanol. Drying *in vacuo* gave a white powder (46.5 g, 88%) with a nitrogen content (37) of 13.10%, corresponding to a degree of substitution of 2.61.

Determination of the Number-Average Molecular Weight of the Methylated and Nitrated Celluloses

Osmotic pressure measurements were carried out at +30° C as described previously (38) with modified (39) Zimm–Myerson (40) osmometers and gel cellophane membranes. The solvent for the methylated cellulose was a 9:1 mixture (v/v) of chloroform and ethanol and for the nitrate, *n*-butyl acetate. The results are summarized in Table III.

TABLE III

Osmometry data

O-Methylcellulose			Cellulose nitrate		
*w**	*h*†	*h/w*	*w*	*h*	*h/w*
2.416	2.680	1.109	5.373	1.645	0.306
1.967	1.998	1.016	4.301	1.120	0.260
1.817	1.921	1.057	3.220	0.990	0.307
1.312	1.362	1.038	2.155	0.629	0.292
1.134	1.202	1.060	1.146	0.362	0.316
0.646	0.656	1.015	1.063	0.315	0.296
0	—	1.01	0	—	0.29

*Concentration in grams/kilograms solution.
†Osmotic height in centimeter solution.

Isolation of Cellulose by Direct Nitration of the Bark

Dry birch bark (20.0 g), previously extracted with hot water and aqueous ammonium oxalate, was treated with the nitrating mixture referred to above (400 g) at +17° for 5 hours. Most of the acid mixture was removed by filtration and the solid residue was washed immediately with a 1:1 mixture of acetic acid and water cooled to −16° C (4 liters). The product was washed successively with water, with saturated sodium bicarbonate, with 10% aqueous acetic acid, and finally with water until the filtrate was neutral. A part of the nitrated, non-carbohydrate material was removed by extraction with methanol. The residue was dissolved in acetone (2 liters) and solid material was removed on the centrifuge. The clear solution was poured into water and the precipitate was washed with water and methanol and dried *in vacuo* at room temperature to give a white, fibrous material (A, 9.3 g, 25.0%). Nitrogen content: 13.73%, corresponding to a degree of substitution of 2.84.

Can. J. Chem. Downloaded from www.nrcresearchpress.com by 186.148.149.217 on 09/04/12
For personal use only.

A similar treatment of the extractive-free bark before removal of pectic material (20.0 g) gave a similar cellulose nitrate (B, 8.8 g, 26.0%). Nitrogen content: 13.72%. Nitration of the same product for 24 hours gave a nitrate in a yield of 28.1%.

A portion of nitrate A was treated with 20% ammonium hydrosulphide at room temperature for 7 hours (41). The denitrated product was hydrolyzed and examined by paper chromatography (solvents A and B). Only glucose and traces of xylose residues were present.

Determination of the Intrinsic Viscosity of the Cellulose Nitrates

The instrument used was a Craig–Henderson viscometer (42). The temperature was +30° C and the solvent was *n*-butyl acetate. Measurements were carried out as described previously (17). No corrections were applied for shear dependence. The logarithm of the relative viscosities, when plotted against concentrations, gave linear relationships which were extrapolated to zero concentration to yield the intrinsic viscosities. The values obtained were 28.5 and 24.6 dl/g (nitrates A and B), corresponding to 33.0 and 28.1 dl/g at trisubstitution (43).

Determination of the Weight-Average Molecular Weight of Cellulose Nitrate A

Light-scattering measurements were carried out essentially as described previously (13). The solvent was freshly redistilled acetone, b.p. 56.3–56.8° C. After ultracentrifugation at 140,000 *g* for 3 hours, the polymer solution (0.1%) was transferred to a light-scattering cell especially designed for eliminating both floating and sedimenting debris (44). The cell was subjected to ultracentrifugation at 35,000 *g* for 1 hour and then transferred directly to the photometer, a Brice–Phoenix instrument which had been considerably modified (46). Scattering intensities were measured at angles from 35° to 135° relative to the incident beam and at different concentrations. The refractive index increment had previously been estimated as 0.105 ml/g (21). Concentrations were determined by precipitating several aliquots of the original solution into water. The fibrous precipitate was washed with water and methanol and dried *in vacuo* at +60° C for 3 hours.

Zimm plots (14) were obtained in the usual way by plotting Kc/R_θ versus $\sin^2\theta/2 + 2000c$ where $K = 2\pi^2 n_0^2 (dn/dc)^2 N\lambda^4$ and the symbols have their usual significance (21). The weight-average molecular weight, $\bar{M}_w$, was obtained from the relationship

$$\bar{M}_w = 1/(Kc/R_\theta)_{c,\theta=0}.$$

The corresponding degree of polymerization, $\bar{P}_w$, was calculated from the relationship $\bar{P}_w = \bar{M}_w/M_r$ where M_r was the molecular weight of the nitrated glucose residue (290). The root-mean-square *Z*-average radius of gyration, $\sqrt{\bar{s}_z^2}$, was computed from the initial slope of the $c = 0$ line in the Zimm plot according to the relationship (21)

$$\frac{\text{initial slope}}{\text{intercept}} = (16\pi^2/3).\ \bar{s}_z^2(n_0/\lambda)^2.$$

ACKNOWLEDGMENTS

The authors wish to express their gratitude to Dr. D. A. I. Goring and Dr. R. St. J. Manley for valuable help. They are also thankful to Mr. W. L. Steyn, who carried out the light-scattering measurements. Financial support from the National Research Council of Canada is gratefully acknowledged.

Can. J. Chem. Downloaded from www.nrcresearchpress.com by 186.148.149.217 on 09/04/12
For personal use only.

Can. J. Chem. Downloaded from www.nrcresearchpress.com by 186.148.149.217 on 09/04/12
For personal use only.

REFERENCES

1. G. H. SEGALL and C. B. PURVES. Pulp Paper Mag. Can. **47**, No. 3, 149 (1946).
2. E. F. KURTH. Chem. Revs. **40**, 33 (1947).
3. P. E. GARDNER. Ph.D. Thesis, McGill University, Montreal, Que. 1957.
4. T. E. TIMELL and E. C. JAHN. Svensk Papperstidn. **54**, 831 (1951).
5. T. E. TIMELL. Svensk Papperstidn. **59**, 1 (1956).
6. T. E. TIMELL, C. P. J. GLAUDEMANS, and J. K. GILLHAM. Pulp Paper Mag. Can. **59**, No. **10**, 242 (1958); Tappi, **42**, 623 (1959).
7. A. JABBAR MIAN and T. E. TIMELL. In press.
8. YING-PE CHANG and R. L. MITCHELL. Tappi, **38**, 315 (1955).
9. W. J. ALEXANDER and R. L. MITCHELL. Anal. Chem. **21**, 1497 (1949).
10. C. F. BENNETT and T. E. TIMELL. Svensk Papperstidn. **58**, 281 (1955).
11. R. L. WHISTLER and J. N. BEMILLER. Advances in Carbohydrate Chem. **13**, 289 (1958).
12. T. E. TIMELL. Tappi, **40**, 25, 30 (1957).
13. D. A. I. GORING and T. E. TIMELL. Svensk Papperstidn. In press.
14. B. H. ZIMM. J. Chem. Phys. **16**, 1093, 1099 (1948).
15. S. A. BARKER, E. J. BOURNE, R. STEPHENS, and D. H. WHIFFEN. J. Chem. Soc. 3468 (1954).
16. G. V. SCHULZ and M. MARX. Makromol. Chem. **14**, 52 (1954).
17. T. E. TIMELL. Svensk Papperstidn. **60**, 836 (1957).
18. B. H. ZIMM and W. H. STOCKMAYER. J. Chem. Phys. **17**, 1309 (1949).
19. R. W. KILB. J. Polymer Sci. **38**, 403 (1959).
20. B. H. ZIMM and R. W. KILB. J. Polymer Sci. **37**, 19 (1959).
21. M. M. HUQUE, D. A. I. GORING, and S. G. MASON. Can. J. Chem. **36**, 952 (1958).
22. T. E. TIMELL, C. P. J. GLAUDEMANS, and A. L. CURRIE. Anal. Chem. **28**, 1916 (1956).
23. TESTING METHODS of the technical association of the pulp and paper industry. New York, N.Y.
24. F. J. SAEMAN, W. E. MOORE, R. L. MITCHELL, and M. A. MILLETT. Tappi, **37**, 336 (1954).
25. J. K. N. JONES, L. E. WISE, and J. P. JAPPE. Tappi, **39**, 139 (1956).
26. J. K. HAMILTON and G. R. QUIMBY. Tappi, **40**, 781 (1957).
27. F. WEYGAND, W. PERKOW, and P. KUHNER. Ber. **84**, 596 (1951).
28. K. R. ANDRESS. Z. physik. Chem. (Leipzig), B, **4**, 190 (1929).
29. R. KUHN, H. TRISCHMANN, and I. LÖW. Angew. Chem. **67**, 32 (1955).
30. T. PURDIE and J. C. IRVINE. J. Chem. Soc. **83**, 1021 (1903).
31. P. KARRER and E. ESCHER. Helv. Chim. Acta, **19**, 1192 (1936).
32. R. L. WHISTLER and D. F. DURSO. J. Am. Chem. Soc. **72**, 677 (1950).
33. R. S. ALM. Acta Chem. Scand. **6**, 1186 (1952).
34. B. LINDBERG and B. WICKBERG. Acta Chem. Scand. **8**, 569 (1954).
35. J. C. IRVINE and E. L. HIRST. J. Chem. Soc. **121**, 1213 (1922).
36. T. PURDIE and J. C. IRVINE. J. Chem. Soc. **85**, 1049 (1904).
37. T. E. TIMELL and C. B. PURVES. Svensk Papperstidn. **54**, 303 (1951).
38. D. A. I. GORING and T. E. TIMELL. To be published.
39. J. V. STABIN and E. H. IMMERGUT. J. Polymer Sci. **14**, 209 (1954).
40. B. H. ZIMM and I. MYERSON. J. Am. Chem. Soc. **68**, 911 (1946).
41. T. E. TIMELL. Pulp Paper Mag. Can. **56**, No. 2, 107 (1955).
42. A. W. CRAIG and D. A. HENDERSON. J. Polymer Sci. **19**, 215 (1956).
43. C. H. LINDSLEY and M. B. FRANK. Ind. Eng. Chem. **45**, 2491 (1953).
44. M. M. HUQUE, J. JAWORZYN, and D. A. I. GORING. J. Polymer Sci. **39**, 9 (1959).

Can. J. Chem. Downloaded from www.nrcresearchpress.com by 186.148.149.217 on 09/04/12
For personal use only.

STEROIDS AND RELATED PRODUCTS

XIV. THE SYNTHESIS OF 17α-HALOGENATED 20,21-KETOLS OF THE CORTICOID TYPE[1, 2]

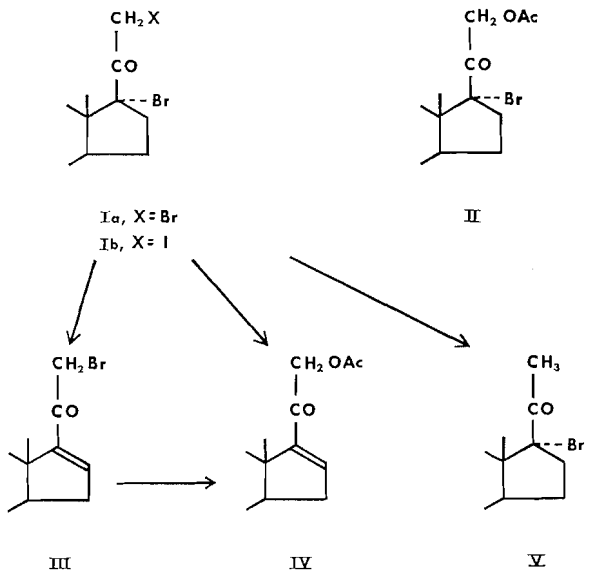
CH. R. ENGEL, R.-M. HOEGERLE,[3] AND R. DEGHENGHI

ABSTRACT

In continuation of previous work, the hindering effect of 17α-substituents on replacement reactions in position 21 of the steroid molecule was further studied. It is shown that the impossibility of replacing a 21-halogen substituent by an acetoxy group in the presence of a bromine atom in position 17α is due both to a steric effect of the bulky 17-substituent and to its facile elimination. It is further shown that the replacement reaction in 21 may be carried out in the presence of the smaller and less readily eliminated 17α-chlorine substituent. In connection with these investigations, 17α-chloro-11-dehydrocorticosterone, the 17-chloro analogue of cortisone, was synthesized. The introduction of a chlorine atom into position 17 lowers the glucocorticoid activity.

In a recent publication of this series (2) we reported the synthesis of 17α-bromo-11-dehydrocorticosterone, the first 17-halogenated glucocorticoid. In that synthesis, the halogen substituent was introduced subsequent to the elaboration of the ketol side chain.

At first sight it would have appeared attractive to transform a readily available 17,21-dihalogenated 20-ketone (compare partial formula I) to a 17-bromo-21-acetoxy ketone (compare II) by the classical reaction with an alkali acetate. However, it was known from earlier work by Plattner, Heusser, and Angliker (3) that treatment of a 17,21-dibromo-20-ketone (I*a*), with potassium acetate in acetic acid, led predominately



to elimination of hydrogen bromide in positions 16–17, without replacement of the 21-bromine atom (compare III). The elimination of hydrogen bromide from a tertiary

[1]*Manuscript received March 21, 1960.*
Contribution from the Department of Chemistry, Laval University, Quebec, Que. Some of the results reported in this paper were included in a communication presented before the 4th International Congress of Biochemistry, Vienna, September, 1958; other results were in a paper presented before the 17th Congress of the French-Canadian Association for the Advancement of Science, Montreal, October, 1959.
[2]*For paper* XIII *of this series see reference 1.*
[3]*N.R.C. Postdoctorate Fellow, 1958–59.*

bromide, in conjugation with a carbonyl group, is of course easily understood. On the other hand, it seems plausible to assume that in the presence of as bulky a 17-substituent as a bromine atom, the replacement of the halogen group in 21, by acetate, should present considerable difficulties, since it is known that a 17-methyl group seriously hinders reactions in this position (4–8). Plattner and co-workers (3) showed that an unsaturated bromide of type III can be converted to the 21-acetate by treatment with potassium acetate in acetic acid, in the presence of acetic anhydride, and that a 17,21-dibromide (compare I*a*) can be transformed, under analogous conditions, directly but in low yield to the same unsaturated ketol acetate (compare IV). It seems reasonable to assume that in this reaction the unsaturated bromide (compare III) is an intermediate and, hence, that the dehydrobromination precedes the substitution in 21.[4]

In the course of the present study, we investigated the reaction of an iodo bromide of type I*b* [17α-bromo-21-iodo-3α-acetoxy-11,20-dioxopregnane (I*c*, see Experimental)] with potassium acetate in boiling acetone. After 1 hour, the starting material was recovered practically unchanged, which seems in accord with the assumption that the bulky 17-bromine substituent hinders the replacement reaction in 21. After prolonged treatment, reduction of the 21-iodine substituent occurred, leading to the 17α-bromo-21-methyl-20-ketone (compare V), as well as partial elimination of hydrogen bromide, evidenced by the Δ^{16}-20-ketone chromophore detected in the mother liquors of the reaction product. Absolutely no replacement of the halogen in 21 by an acetoxy group had taken place.

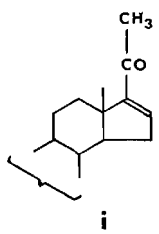
In summary, the 21-halogen atom of a 21-halo-20-ketone cannot be replaced by an acetoxy group in the presence of a 17α-bromine substituent (with preservation of the latter), because of both the steric effect of the bulky 17-bromine substituent and competing reactions.

We considered that the situation would be different in the case of a 17α-chlorine substituent. Indeed, the smaller chlorine atom should exert a smaller steric effect and should not lend itself with the same ease to an elimination reaction as a bromine substituent.

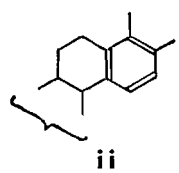
In order to prove this assumption, we subjected 21-bromo-17α-chloro-3α-hydroxy-11,20-dioxopregnane (XI) to the action of potassium acetate in the presence of potassium iodide; as we had expected, the 21-acetoxy-17-chloro-20-ketone IX was formed without difficulty. We thus established further evidence of the fact that a bulky group in position 17 hinders reactions in position 21.[5]

The 21-bromo-17-chloro-20-ketone XI employed in this reaction was readily obtained from 3α-acetoxy-11,20-dioxopregnane (VI).[6] Whereas the 17α-chloride VIII can be

[4]*When a 17-bromo-21-iodo ketone (compare Ib) is treated with silver acetate in pyridine, in the presence of acetic anhydride—conditions which allow the replacement of a 21-iodine substituent by an acetoxy group in the presence of a 17-methyl group (compare 7 and 8)—reduction in position 21 occurs, the reaction leading to a mixture composed of a Δ^{16}-20-ketone (compare i) and an aromatic rearrangement product of type ii (6).*



i



ii

[5]*It should be pointed out that even in the presence of a relatively small hydroxy substituent in position 17, the substitution in 21 proceeds less readily than in the case of a 17-unsubstituted product (compare for instance 9).*

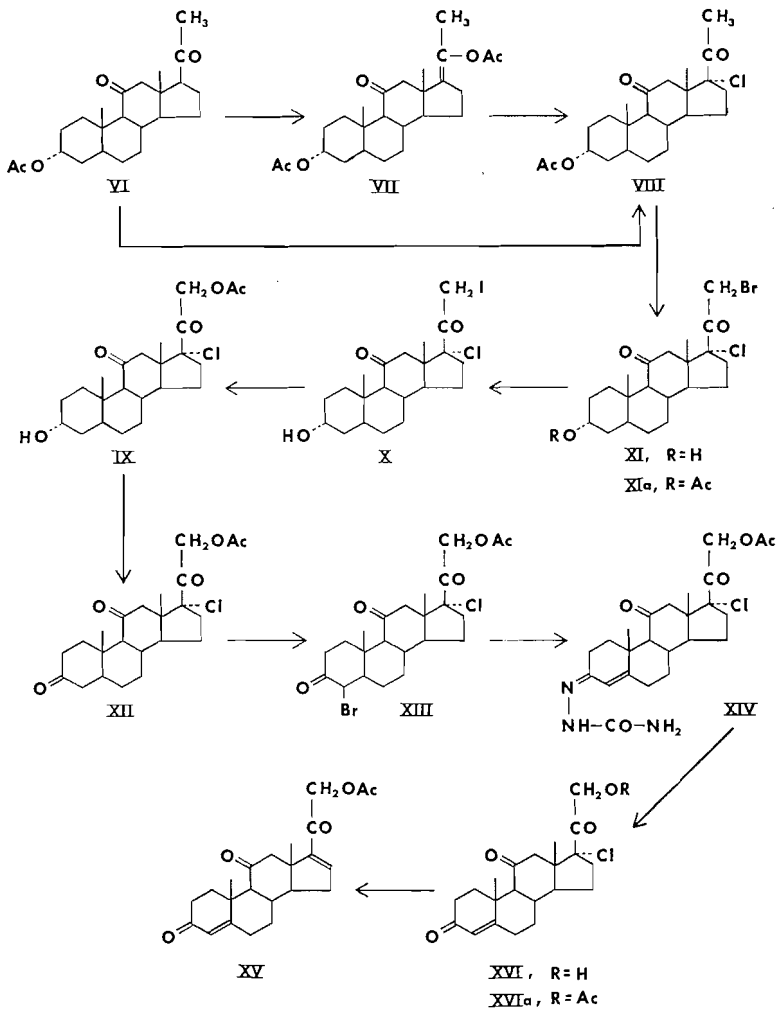
[6]*We are indebted to the Schering Corporation, Bloomfield, New Jersey, for the generous gift of this starting material.*

Can. J. Chem. Downloaded from www.nrcresearchpress.com by 186.148.149.217 on 09/04/12
For personal use only.

produced by direct chlorination of VI, a much better product was obtained by chlorination of the monoenol acetate VII. We synthesized the latter product, previously described by Anderson *et al.* (10), either by reaction of VI with isopropenyl acetate and sulphuric acid followed by chromatography, or, even more conveniently, by Barton's method (11) with acetic anhydride and perchloric acid. Using the latter procedure both geometric isomers of VII were isolated.[7]

The 17-chloro-20-ketone VIII was readily brominated in 21 (XI*a*), with molecular bromine in acetic acid, at 60°.[8] Hydrolysis of the acetate with perchloric acid in methanol (12 and 13) gave the 3-hydroxy chloro bromide XI, which, as stated above, can be transformed in good yield to the corresponding 21-acetate IX.

Since our group has been interested for some time in the influence of the chemical nature of the 17α-substituent on hormonal activities (compare, for instance, 1, 2, 7, 13, 14, 15, 16, 17, 18), we considered it attractive to convert the 17α-chloro-21-acetoxy-20-ketone IX to the 17-chloro analogue of cortisone (XVI). The synthesis followed classical



[7]*In our hands the method of Anderson et al. (10) for the preparation of* VII *from* VI, *using acetic anhydride and an acid catalyst in toluene, gave unsatisfactory results.*

[8]*We established in preliminary experiments that bromination in chloroform was not satisfactory.*

Can. J. Chem. Downloaded from www.nrcresearchpress.com by 186.148.149.217 on 09/04/12
For personal use only.

lines. Oxidization of IX with chromic acid and sulphuric acid (19, 20) gave the triketone XII which was transformed via the 4-bromide XIII and the semicarbazone XIV (compare 21) to the 4-unsaturated acetate XVI*a*, readily hydrolized with perchloric acid in methanol (12, 13) to 17α-chloro-11-dehydrocorticosterone (XVI). The free alcohol XVI was easily reacetylated to XVI*a* and the position of the chlorine substituent was proved by conversion of the latter, with dimethylformamide and potassium iodide, to 17-anhydrocortisone acetate (XV) (22).[9] The α-configuration of the 17-substituent was assumed in analogy with the proved configuration of the corresponding bromides (compare 23).

It is of interest to note that 17α-chlorination of a 20-ketone causes a marked levorotatory shift, which is, however, not quite as pronounced as the one brought about by 17-bromination (1, 2, 13, 24). In Table I we have computed representative molecular rotational differences produced by various substitutions of 20-ketones in position 17; values for hydroxy, methyl, chlorine, and bromine derivatives are given. It can be seen that all these substitutions lead to a levorotatory shift and that the strength of the effect increases in the order in which the substituents are mentioned above.

TABLE I

Molecular rotational differences of 17α-substituted 20-keto steroids[a]

Product	$[M]_D$	$[M]_D^{17\alpha\text{-der.}} - [M]_D^{17\alpha\text{-H}}$
3α-Acetoxy-11,20-dioxopregnane	495°[b]	
	455° (acetone)[c]	
17α-Hydroxy-	330° (acetone)[d]	−125° (acetone)
17α-Chloro-	85°[e]	−410°
17α-Bromo-	5°[f]	−490°
3α-Hydroxy-21-acetoxy-11,20-dioxopregnane	425° (acetone)[g]	
17α-Hydroxy-	320° (acetone)[h]	−105°
17α-Chloro-	50°[e]	−375°[p]
17α-Bromo-	20°[f]	−405°[p]
21-Acetoxy-3,11,20-trioxopregnane	425°[h]	
	405° (acetone)[i]	
17α-Hydroxy-	335° (acetone)[j]	−70° (acetone)
17α-Methyl-	185°[k]	−240°
17α-Chloro-	65°[e]	−360°
17α-Bromo-	0°[f]	−425°
Δ^4-21-Acetoxy-3,11,20-trioxopregnene	925°[l]	
17α-Hydroxy-	860°[m]	−65°
17α-Methyl-	680°[k]	−245°
17α-Chloro-	440°[e]	−485°
17α-Bromo-	435°[f]	−490°
Δ^4-21-Hydroxy-3,11,20-trioxopregnene	890° (EtOH)[n]	
17α-Hydroxy-	760° (EtOH)[o]	−130°
17α-Methyl-	625°[k]	−265°[p]
17α-Chloro-	535°[e]	−355°[p]
17α-Bromo-	360°[f]	−530°[p]

[a]The molecular rotations were calculated to the nearest 5°. When not otherwise specified, rotations were taken in $CHCl_3$. [b]Means of values reported in references 25 and 26. [c]Reference 27. [d]Reference 28. [e]Experimental. [f]Reference 2. [g]Reference 29. [h]Reference 30. [i]Reference 31. [j]Means of values given in references 28 and 32. [k]Reference 15. [l]Reference 33. [m]Reference 34. [n]Reference 35. [o]Means of values given in references 34 and 36. [p]The values can only be considered as indicative because comparisons were made between rotations in different solvents.

Dr. P. Perlman and Dr. S. Tolksdorf of Bloomfield, New Jersey, kindly tested the new hormone analogue XVI and its acetate XVI*a* in their eosinophil assay and found that the products had the same order of activity as their bromo analogues (2). A detailed account of the biological investigations is to be published elsewhere. The preliminary

[9]*We wish to thank sincerely Dr. S. Bernstein for kindly providing us with an authentic sample for comparison.*

Can. J. Chem. Downloaded from www.nrcresearchpress.com by 186.148.149.217 on 09/04/12
For personal use only.

results confirm that the electronegativity of the 17α-substituent is not, at least to an appreciable extent, an enhancing factor of glucocorticoid and related corticoid activities (compare 2).[10]

EXPERIMENTAL[11, 12, 13]

Reaction of 17α-Bromo-21-iodo-3α-acetoxy-11,20-dioxopregnane (Ic) *with Potassium Acetate in Acetone*

(*a*) A quantity of 1.5 g of 17α,21-dibromo-3α-acetoxy-11,20-dioxopregnane was transformed in the usual fashion to 17α-bromo-21-iodo-3α-acetoxy-11,20-dioxopregnane (Ic) (compare the procedure described in reference 3), by treatment with 0.5 g of sodium iodide in 150 cc of boiling acetone. To the cooled solution was added potassium acetate, freshly prepared from 6 g of potassium bicarbonate and 3.5 cc of acetic acid, and the mixture was refluxed under nitrogen for 1 hour. The volume of the solution was reduced *in vacuo* and the organic product was precipitated in water. The mixture was extracted with dichloromethane, the organic solution was washed with water and was dried over sodium sulphate. Removal of the solvent gave 1.6 g of almost colorless crystals, m.p. 163–170° decomp.; the melting point was not depressed upon admixture of iodide Ic. The product gave a positive iodine test and the infrared spectrum corroborated the identity of the product with iodide Ic.

(*b*) A quantity of 1.485 g of 17α,21-dibromo-3α-acetoxy-11,20-dioxopregnane was transformed with 1.5 g of sodium iodide in 250 cc of acetone to the bromo iodide Ic. To this solution, potassium acetate, freshly prepared from 12 g of potassium bicarbonate and 7 cc of acetic acid, was added and the mixture was refluxed for 24 hours. The colorless solution (which had been yellow at the beginning of the reaction) was cooled and poured into cold water. The precipitate was extracted with dichloromethane, the organic layer was washed with water and dried over sodium sulphate. Removal of the solvent gave 1.4 g of an oil which, upon crystallization from dichloromethane–ether–hexane, gave 350 mg of colorless crystals, m.p. 150–155° decomp. Recrystallization from ether raised the melting point to 156–158° decomp. The infrared spectrum of the product was identical with that of authentic 17α-bromo-3α-acetoxy-11,20-dioxopregnane (15) and the mixed melting point showed no depression upon admixture of authentic material.

The mother liquors of the crystallized product showed in the infrared the typical absorption of a Δ^{16}-20-ketone ($\nu_{max}^{CHCl_3}$ 1592 and 1665 cm^{-1}) and no absorption band attributable to a 21-acetoxy group.

$\Delta^{17(20)}$-3α,20-Diacetoxy-11-oxopregnene (VII)

(*a*) A solution of 1.5 g of 3α-acetoxy-11,20-dioxopregnane (VI) in 5 cc of isopropenyl acetate was refluxed for 2 hours with 0.1 cc of concentrated sulphuric acid. The mixture was cooled and extracted with ether; the ethereal solution was washed with sodium bicarbonate solution and with water and was dried over sodium sulphate. The solvent was removed and the product (1.6 g) was chromatographed on 50 g of aluminum oxide

[10]*Drs. H. L. Herzog, M. Jevnik Gentles, H. M. Marshall, and E. B. Hershberg informed us of their independent synthesis of 17α-chloro-11-dehydrocorticosterone acetate* (XVIa) *by a different route. It was agreed that their article should appear in the Journal of the American Chemical Society simultaneously with the present one in this journal.*

[11]*The melting points were taken in the evacuated capillaries and the temperatures were corrected.*

[12]*The microanalyses were performed by Dr. O. Schwarzkopf, New York, N.Y., and by Dr. Alfred Bernhardt, Mülheim (Ruhr). We wish to express to them and their associates our sincere appreciation.*

[13]*For chromatography we used Davison's silica gel No. 923, Woelm's aluminum oxide, activity* II–III, *and Merck's aluminum oxide treated as described under footnote 31 of reference 7. We wish to thank Merck and Co., Montreal, for a generous gift of this material.*

Can. J. Chem. Downloaded from www.nrcresearchpress.com by 186.148.149.217 on 09/04/12
For personal use only.

(pH 6.5). Petroleum ether – benzene mixtures eluted 500 mg of the enol diacetate VII, m.p. 99–110°. Benzene eluted 600 mg of starting material (VI), m.p. 124–126°, not depressed upon admixture of authentic VI; the product was further identified by comparison of the infrared spectra. Considering the recovery of the starting material, the yield of VII from VI was 55%.

A portion of the enol diacetate VII was recrystallized four times from acetone–hexane for analysis: silky needles, m.p. 127.5–129.5°, $[\alpha]_D^{26}$ +56° (*c*, 1.0 in $CHCl_3$), ν_{max}^{KBr} 1220, 1245 cm^{-1} (acetates), 1695 cm^{-1} (11-ketone), 1722 and 1730 cm^{-1} (shoulder) (acetates); positive tetranitromethane reaction. Anal. Calc. for $C_{25}H_{36}O_5$: C, 72.08; H, 8.71. Found: C, 71.99; H, 8.68.

(*b*) To a solution of 2 g of 3α-acetoxy-11,20-dioxopregnane (VI) in 30 cc of carbon tetrachloride were added 10 cc of acetic anhydride and 0.4 cc of 50% perchloric acid. The mixture was stirred for 1.5 hours at room temperature and the resulting solution was diluted with dichloromethane and was washed with cold sodium bicarbonate solution and with water. After drying, the solvent was removed and the resulting amorphous product (2.605 g) was chromatographed on 75 g of aluminum oxide (pH 6–6.5). Petroleum ether – benzene (1:1) eluted 1 g of crystalline VII, m.p. 125–126°, identical with the product described under (*a*). The following fractions (150 mg) were amorphous. Petroleum ether – benzene (1:4) eluted 300 mg of a second crystalline substance, m.p. 126–130°, depressed upon admixture of both VI and VII; $\nu_{max}^{CHCl_3}$ 1258 cm^{-1} (acetate), 1715 cm^{-1} (11-ketone), 1730 and 1735 cm^{-1} (3α- and 20-acetates). The crude crystalline product which gave a positive tetranitromethane reaction was analyzed for its acetyl contents. Anal. Calc. for $C_{25}H_{36}O_5$: CH_3CO, 20.67. Found: CH_3CO, 17.87. We considered this product to be the geometric isomer of VII and proved its structure by the following reaction. To a solution of 277 mg of this substance in 10 cc of carbon tetrachloride was added 90 mg of N-bromosuccinimide and the mixture was refluxed over a photoflood lamp for 10 minutes. The usual working up afforded 271 mg of a yellow oil which gave, upon filtration through 10 g of silica gel, 200 mg of crystalline *Δ¹⁶-3α-acetoxy-11,20-dioxopregnene*, m.p. 149–152°, not depressed upon admixture of an authentic sample; the infrared spectrum of the product was identical with that of an authentic sample. The formation of the Δ¹⁶-20-ketone in the reaction confirms that the second crystalline product isolated from the enol acetylation reaction was the geometric isomer of VII.[14]

The benzene–ether–methanol fractions of the original chromatogram consisted of 420 mg of starting material VI. Considering the recovery of starting material, the yield of the enol acetates was 83%.

17α-Chloro-3α-acetoxy-11,20-dioxopregnane (VIII)

(a) From the 11,20-Diketone VI

To a solution of 2 g of 3α-acetoxy-11,20-dioxopregnane (VI) in 20 cc of acetic acid was added, dropwise and with stirring, 52.2 cc of a 0.205 *N* solution of chlorine in acetic acid. The mixture was stirred for another 10 minutes and poured into ice water. The precipitate was filtered, washed to neutral, and dried. The colorless solid (2.05 g), m.p. 80–95°, was recrystallized from ether and thus gave 60 mg of a chlorinated product, m.p. 152–160°, $[\alpha]_D^{26}$ +72.6° (*c*, 1.0 in $CHCl_3$), representing probably the 17,21-dichloride.

The mother liquors of this crystallization were chromatographed on 60 g of aluminum oxide (pH 7). Petroleum ether – benzene (1:1) eluted 450 mg (20%) of monochloride VIII, m.p. 130–142°. After one recrystallization from ether, the product melted at 141–144°,

[14]*Compare reference 37.*

Can. J. Chem. Downloaded from www.nrcresearchpress.com by 186.148.149.217 on 09/04/12
For personal use only.

$[\alpha]_D^{26}$ +25.4° (*c*, 1.1 in $CHCl_3$). The melting point was not depressed upon admixture with authentic VIII (see below); the infrared spectra of the two samples were identical.

Benzene–ether (4:1) eluted 320 mg of crude crystalline Δ^{16}-3α-acetoxy-11,20-dioxopregnene, identified by its infrared spectrum and mixed melting point with an authentic sample. The ethyl acetate fractions gave 270 mg of crystalline Δ^{16}-3α-hydroxy-11,20-dioxopregnene, m.p. 180–195°, identified by infrared comparison and mixed melting point with an authentic sample.

(b) From the Enol Diacetate VIII

To a solution of 1.45 g of $\Delta^{17(20)}$-3α,20-diacetoxy-11-oxopregnene (VII), m.p. 102–117°, in 60 cc of acetic acid was added, at room temperature, dropwise and with stirring, 38.5 cc of a 0.183 *N* solution of chlorine in acetic acid. The colorless mixture was poured into ice water, and the precipitate was filtered, washed to neutral, and dried. The product (1.401 g) was recrystallized from ether and gave 1.2 g of monochloride VIII, m.p. 137–140° (84% yield). The melting point was raised upon one recrystallization to 147–149°. A sample was recrystallized once for analysis: needles, m.p. 150–151°, $[\alpha]_D^{25}$ +20.5° (*c*, 1.02 in $CHCl_3$), ν_{max}^{KBr} 1245 cm^{-1} (acetate), 1708 cm^{-1} (11-ketone), 1735 cm^{-1} (broad band) (acetate and 20-ketone). Anal. Calc. for $C_{23}H_{33}O_4Cl$: C, 67.55; H, 8.13; Cl, 8.67. Found: C, 67.22; H, 8.00; Cl, 8.59.

21-Bromo-17α-chloro-3α-acetoxy-11,20-dioxopregnane (XI*a*)

A solution of 650 mg of 17α-chloro-3α-acetoxy-11,20-dioxopregnane (VIII), m.p. 147–149°, in 10 cc of acetic acid, containing 2 cc of a 20% hydrogen bromide solution in acetic acid, was heated to 60°. To this mixture, a solution of 255 mg of bromine in 16 cc of acetic acid was added, dropwise and with stirring, in the course of 15 minutes. Subsequently, the almost colorless solution was poured into ice water, the precipitate was filtered, washed to neutral, and dried. The resulting colorless product (822 mg) was recrystallized from ether to give 490 mg (63% yield) of bromide XI*a*, m.p. 170–174°. A sample was recrystallized three times for analysis: needles, m.p. 183–184°, $[\alpha]_D^{26}$ +35° (*c*, 0.411 in $CHCl_3$), ν_{max}^{KBr} 1260 cm^{-1} (acetate), 1700 cm^{-1} (11-ketone), 1718 cm^{-1} (broad band) (21-bromo-20-ketone and acetate). Anal. Calc. for $C_{23}H_{32}O_4BrCl$: C, 56.62; H, 6.61; Br, 16.38; Cl, 7.27. Found: C, 56.62; H, 6.84; Br, 16.28; Cl, 7.26.

21-Bromo-17α-chloro-3α-hydroxy-11,20-dioxopregnane (XI)

A quantity of 460 mg of 21-bromo-17α-chloro-3α-acetoxy-11,20-dioxopregnane (XI*a*), m.p. 170–174°, was suspended in a solution of 1 cc of 70% perchloric acid in 39 cc of methanol. The mixture was shaken for 22 hours at room temperature. During that time the product dissolved gradually. Subsequently, the solution was poured into an ice-cold sodium bicarbonate solution and the precipitate was extracted with dichloromethane. The organic solution was washed with water and dried over sodium sulphate. The solvent was removed *in vacuo* and the colorless residue (420 mg) was crystallized from ether. There was obtained 285 mg of small prisms, m.p. 160–162°. A sample was recrystallized twice from ether–acetone–hexane for analysis: m.p. 167–169°, $[\alpha]_D^{26}$ +20.4° (*c*, 0.756 in $CHCl_3$), ν_{max}^{KBr} 1698 cm^{-1} (11-ketone), 1721 cm^{-1} (21-bromo-20-ketone), 3450 cm^{-1} (hydroxy). Anal. Calc. for $C_{21}H_{30}O_3BrCl$: C, 56.57; H, 6.78; Br, 17.92; Cl, 7.95. Found: C, 56.80; H, 6.56; Br, 17.88; Cl, 7.65.

17α-Chloro-21-acetoxy-3α-hydroxy-11,20-dioxopregnane (IX)

A mixture of 3.683 g of 21-bromo-17α-chloro-3α-hydroxy-11,20-dioxopregnane (XI), m.p. 150–152°, 100 mg of potassium iodide, and 7.4 g of freshly fused potassium acetate

Can. J. Chem. Downloaded from www.nrcresearchpress.com by 186.148.149.217 on 09/04/12
For personal use only.

Can. J. Chem. Downloaded from www.nrcresearchpress.com by 186.148.149.217 on 09/04/12
For personal use only.

was refluxed in 200 cc of absolute acetone and 10 cc of acetic acid for 22 hours in a nitrogen atmosphere. The product was diluted with methylene chloride, and the organic solution was washed with cold sodium bicarbonate solution and with water and was dried over sodium sulphate. Removal of the solvent afforded 3.616 g of a foamish material which crystallized from ether. One recrystallization gave 1.08 g of slightly yellowish prisms, m.p. 160–170° decomp. A sample was recrystallized twice from ethyl acetate – ether for analysis: m.p. 188° decomp., $[\alpha]_D^{26}$ +12° (*c*, 1.0 in $CHCl_3$), ν_{max}^{KBr} 1230 cm^{-1} (acetate), 1705 cm^{-1} (11-ketone), 1725 and 1750 cm^{-1} (21-acetoxy-20-keto doublet), 3400 cm^{-1} (hydroxy). Anal. Calc. for $C_{23}H_{33}O_5Cl$: C, 65.00; H, 7.83; Cl, 8.35. Found: C, 65.02; H, 8.05; Cl, 8.35.

The mother liquors of the first crystallization were chromatographed on 200 g of silica gel. Benzene – ethyl acetate (87:13) eluted 687 mg of IX, m.p. 177–179° decomp. (total yield 50%).

17α-Chloro-21-acetoxy-3,11,20-trioxopregnane (XII)

To a stirred solution of 982 mg of 17α-chloro-21-acetoxy-3α-hydroxy-11,20-dioxopregnane (IX), m.p. 177–179° decomp., in 50 cc of absolute acetone was added, dropwise, at 0–5°, 1.6 cc of an oxidizing solution prepared by dissolving 267 mg of chromic acid in 230 cc of concentrated sulphuric acid and 770 cc of water. After 2.5 minutes the solution was poured into water and the precipitate was filtered, washed, and dried. The product (977 mg) was recrystallized from ether to give 888 mg (90% yield) of colorless needles, m.p. 184–185° decomp. A sample was recrystallized twice from acetone–hexane for analysis: m.p. 203.5–205.5° decomp., $[\alpha]_D^{26}$ +15° (*c*, 1.01 in $CHCl_3$), ν_{max}^{KBr} 1708 cm^{-1} (double band of 3- and 11-ketones), 1740 cm^{-1} (shoulder) (21-acetoxy-20-ketone), 1765 cm^{-1} (20-keto-21-acetate).

Δ⁴-17α-Chloro-21-acetoxy-3,11,20-trioxopregnene (XVI*a*)

To a solution of 439 mg of 17α-chloro-21-acetoxy-3,11,20-trioxopregnane (XII), m.p. 201–202° decomp., in 25 cc of acetic acid were added, dropwise and with stirring, 0.1 cc of a 15% hydrogen bromide solution in acetic acid and subsequently 2.18 cc of a 0.96 *N* bromine solution in acetic acid. Some of the reaction product crystallized from the mixture towards the end of the addition. The mixture was poured into ice water and the precipitate was filtered, washed, and dried. The resulting crude bromide (522 mg) gave, upon one recrystallization from methylene chloride – hexane, 334 mg of pure *4β-bromo-17α-chloro-21-acetoxy-3,11,20-trioxopregnane* (XIII), m.p. 190–191° decomp. The mother liquors yielded a second crop of 83 mg of the same substance of lesser purity, m.p. 180–182° decomp. (total yield 80%), ν_{max}^{KBr} 1240 cm^{-1} (acetate), 1708 cm^{-1} (double band of 3- and 11-ketones), 1735 and 1762 cm^{-1} (21-acetoxy-20-keto doublet).

A portion of the pure bromo chloride (XIII) (322 mg, m.p. 190–192° decomp.) was dissolved in 60 cc of dichloromethane and 40 cc of *t*-butyl alcohol and treated in the usual manner (26), during 120 minutes, with 96 mg of semicarbazide base in a carbon dioxide atmosphere. The product was taken to dryness *in vacuo* and further dried by azeotropic distillation with benzene. The residue was slurried with a small amount of aqueous ethanol and the mixture was poured into 500 cc of water. The precipitate was filtered, washed, and dried. There was obtained 283 mg (83% yield from XIII) of colorless *Δ⁴-17α-chloro-21-acetoxy-3,11,20-trioxopregnene-3-semicarbazone*, (XIV), m.p. 210° decomp., λ_{max}^{EtOH} 270 mμ (log ε 4.3).

A quantity of 280 mg of semicarbazone (XIV) was dissolved in 14 cc of acetic acid and 4 cc of water. The solution was flushed with carbon dioxide and 0.72 cc of a 1.62 *N*

pyruvic acid solution was added. The mixture was stirred and kept for 18 hours at room temperature under carbon dioxide. The usual working up gave 274 mg of crude crystalline *Δ^4-17α-chloro-21-acetoxy-3,11,20-trioxopregnene* (XVI*a*). One crystallization from ether gave 183 mg (74% yield from XIV) of pure 17α-chloro-11-dehydrocorticosterone acetate (XVI*a*), m.p. 131–132°. A sample was recrystallized twice from ether for analysis: colorless needles, m.p. 137–138°, $[\alpha]_D^{26}$ +105° (*c*, 0.75 in $CHCl_3$), λ_{max}^{EtOH} 238 mμ (log ε 4.2), ν_{max}^{KBr} 1238 cm^{-1} (acetate), 1625 and 1680 cm^{-1} (Δ^4-3-keto doublet), 1709 cm^{-1} (11-ketone), 1738 and 1762 cm^{-1} (21-acetoxy-20-keto doublet). Anal. Calc. for $C_{23}H_{29}O_5Cl$: C, 65.63; H, 6.95; Cl, 8.42. Found: C, 65.58; H, 7.25; Cl, 8.40.

Δ^4-17α-Chloro-21-hydroxy-3,11,20-trioxopregnene (XVI)

A quantity of 150 mg of 17α-chloro-11-dehydrocorticosterone acetate (XVI*a*), m.p. 133–135°, was dissolved in a mixture of 9.8 cc of methanol and 0.25 cc of 70% perchloric acid. The solution was stored in a carbon dioxide atmosphere for 22 hours. Subsequently, the product was taken up in dichloromethane and the solution was washed with cold sodium bicarbonate solution and with water and was dried over sodium sulphate. Removal of the solvent *in vacuo* gave 148 mg of an amorphous product which crystallized from acetone–hexane. One crystallization afforded 120 mg of 17α-chloro-11-dehydrocorticosterone (XVI), m.p. 104° decomp. A sample was recrystallized twice from acetone–hexane for analysis: fine needles, m.p. 107° decomp., $[\alpha]_D^{26}$ +141° (*c*, 0.733 in $CHCl_3$), λ_{max}^{EtOH} 238 mμ (log ε 4.1), ν_{max}^{KBr} 1620 and 1675 cm^{-1} (Δ^4-3-keto doublet), 1708 cm^{-1} (double band of 11- and 20-ketones), 3450 cm^{-1} (21-hydroxy). Anal. Calc. for $C_{21}H_{27}O_4Cl$: C, 66.57; H, 7.18; Cl, 9.36. Found: C, 66.68; H, 7.43; Cl, 9.42.

Acetylation

To a solution of 95 mg of ketol XVI, m.p. 90–100° decomp., in 4 cc of pyridine, 0.5 cc of acetic anhydride was added. The mixture was kept overnight at room temperature and worked up in the usual fashion. There was obtained 96 mg of a colorless foam which crystallized upon trituration with ether, m.p. 131–132°. The melting point was not depressed upon admixture with authentic acetate XVI*a* and the infrared spectrum of the product was identical with that of an authentic sample prepared as described above.

$\Delta^{4,16}$-21-Acetoxy-3,11,20-trioxopregnadiene (XV)

To a solution of 91 mg of 17α-chloro-11-dehydrocorticosterone acetate (XVI*a*), m.p. 132–133°, in 5 cc of dimethylformamide, was added 10 mg of potassium iodide and the mixture was refluxed for 2 hours in a nitrogen atmosphere. After cooling, 0.5 cc of acetic anhydride was added and the reaction mixture was stored at room temperature for 20 hours. The usual working up gave 89 mg of a brown oil which was chromatographed on 3 g of aluminum oxide. Benzene eluted 17 mg of starting material, m.p. 135–136°, and benzene–ether mixtures eluted 10 mg of the diene XV, identified by mixed melting point and by infrared comparison with an authentic sample (compare reference 22 and footnote 9).

ACKNOWLEDGMENTS

We extend sincere thanks to Mrs. J. Capitaine, Mr. D. Capitaine, and Miss R. McLean for their expert assistance in these experiments and to Dr. S. Tolksdorf and Dr. P. Perlman, Bloomfield, New Jersey, for carrying out preliminary biological tests. We acknowledge with gratitude financial support from the National Research Council of Canada, the Schering Corporation, Bloomfield, New Jersey, and the Schering Corporation Ltd., Montreal.

Can. J. Chem. Downloaded from www.nrcresearchpress.com by 186.148.149.217 on 09/04/12
For personal use only.

Can. J. Chem. Downloaded from www.nrcresearchpress.com by 186.148.149.217 on 09/04/12
For personal use only.

REFERENCES

1. CH. R. ENGEL and R. DEGHENGHI. Can. J. Chem. **38**, 452 (1960).
2. R. DEGHENGHI and CH. R. ENGEL. J. Am. Chem. Soc. **82** (1960).
3. PL. A. PLATTNER, H. HEUSSER, and E. ANGLIKER. Helv. Chim. Acta, **29**, 468 (1946).
4. PL. A. PLATTNER, H. HEUSSER, and P. TH. HERZIG. Helv. Chim. Acta, **32**, 270 (1949).
5. H. HEUSSER, P. TH. HERZIG, and CH. R. ENGEL. Unpublished results. Swiss Federal Institute of Technology, Zurich.
6. CH. R. ENGEL. D.Sc. thesis, Swiss Federal Institute of Technology, Zurich. 1951.
7. CH. R. ENGEL and G. JUST. J. Am. Chem. Soc. **76**, 4909 (1954); and subsequent papers of this series.
8. H. HEUSSER, E. BERIGER, and CH. R. ENGEL. Helv. Chim. Acta, **37**, 2166 (1954).
9. G. ROSENKRANTZ, J. PATAKI, ST. KAUFMANN, J. BERLIN, and C. DJERASSI. J. Am. Chem. Soc. **72**, 4081 (1950).
10. H. V. ANDERSON, E. R. GARRETT, F. H. LINCOLN, JR., A. H. NATHAN, and J. A. HOGG. J. Am. Chem. Soc. **76**, 743 (1954).
11. D. H. R. BARTON, R. M. EVANS, J. C. HAMLET, P. G. JONES, and T. WALKER. J. Chem. Soc. 747 (1954).
12. J. FRIED and E. F. SABO. J. Am. Chem. Soc. **79**, 1130 (1957).
13. CH. R. ENGEL and H. JAHNKE. Can. J. Biochem. and Physiol. **35**, 1047 (1957).
14. CH. R. ENGEL and R. L. NOBLE. J. Endocrinol. **14**, 16 (1956).
15. CH. R. ENGEL. J. Am. Chem. Soc. **78**, 4727 (1956).
16. CH. R. ENGEL, K. F. JENNINGS, and G. JUST. J. Am. Chem. Soc. **78**, 6153 (1956).
17. CH. R. ENGEL. Can. J. Chem. **35**, 131 (1957).
18. CH. R. ENGEL and R. L. NOBLE. Endocrinology, **61**, 318 (1957).
19. K. BOWDEN, I. M. HEILBRON, E. R. H. JONES, and B. C. L. WEEDON. J. Chem. Soc. 39 (1946).
20. C. DJERASSI, R. R. ENGLE, and A. BOWERS. J. Org. Chem. **21**, 1547 (1956).
21. W. F. MCGUCKIN and E. C. KENDALL. J. Am. Chem. Soc. **74**, 5811 (1952).
22. W. S. ALLEN and S. BERNSTEIN. J. Am. Chem. Soc. **77**, 1028 (1955).
23. N. L. WENDLER, R. P. GRABER, and G. G. HAZEN. Tetrahedron, **3**, 144 (1958).
24. H. HEUSSER, CH. R. ENGEL, P. TH. HERZIG, and PL. A. PLATTNER. Helv. Chim. Acta, **33**, 2229 (1950).
25. O. MANCERA, A. ZAFFARONI, B. A. RUBIN, F. SONDHEIMER, G. ROSENKRANTZ, and C. DJERASSI. J. Am. Chem. Soc. **74**, 3711 (1952).
26. R. B. TURNER, V. R. MATTOX, W. F. MCGUCKIN, and E. C. KENDALL. J. Am. Chem. Soc. **74**, 5814 (1952).
27. J. VON EUW, A. LARDON, and T. REICHSTEIN. Helv. Chim. Acta, **27**, 821 (1944).
28. L. H. SARETT. J. Am. Chem. Soc. **70**, 1454 (1948).
29. J. VON EUW, A. LARDON, and T. REICHSTEIN. Helv. Chim. Acta, **27**, 1287 (1944).
30. A. LARDON and T. REICHSTEIN. Pharm. Acta Helv. **27**, 287 (1952).
31. A. LARDON and T. REICHSTEIN. Helv. Chim. Acta, **26**, 747 (1943).
32. F. B. COLTON, W. R. NES, D. A. VAN DORP, H. L. MASON, E. C. KENDALL, and A. J. LAVINE. J. Biol. Chem. **194**, 235 (1952).
33. J. FRIED, R. W. THOMA, J. R. GERKE, J. E. HERZ, M. N. DONIN, and P. PERLMAN. J. Am. Chem. Soc. **74**, 3962 (1952).
34. V. R. MATTOX and E. C. KENDALL. J. Biol. Chem. **188**, 287 (1951).
35. M. H. KUIZENGA and G. F. CARTLAND. Endocrinology, **24**, 526 (1939).
36. O. WINTERSTEINER and J. J. PFIFFNER. J. Biol. Chem. **116**, 291 (1936).
37. C. DJERASSI and C. R. SCHOLZ. J. Org. Chem. **14**, 660 (1949).

Can. J. Chem. Downloaded from www.nrcresearchpress.com by 186.148.149.217 on 09/04/12
For personal use only.

SOLID–LIQUID REACTIONS

PART I. THE DETERMINATION OF SOLID–LIQUID REACTION MECHANISMS[1]

ROGER KELLY[2]

ABSTRACT

A tracer method has been described by Graham, Spinks, and Thorvaldson for investigating the mechanisms of solid–liquid reactions. The present work represents an attempt to develop the theory of this method in detail and thereby allow for a greater variety of experimental conditions. Thus, no restrictions are placed on the compositions of the reacting and product solids, nor on the initial location of the tracer. The effect of exchange between the liquid and both solids is taken into account. Furthermore, two different *systems* of mechanisms are considered. In the one, which is shown to be the more realistic when rapid, multidirectional "external" exchange is present, mechanisms are classified according to whether or not the reaction proceeds at the surfaces of the solids; in the other, applicable in the absence of "external" exchange or when the exchange is slow, mechanisms are classified according to the degree of mixing with the liquid of successively reacting portions of the reacting solid.

INTRODUCTION

A solid–liquid reaction may be defined as one in which a solid of low solubility (the reacting solid) reacts with a liquid to form a second solid of even lower solubility (the product solid), the term liquid being here intended to include both solvent and solute indiscriminately. Reactions of this kind are of particular interest in cement chemistry, since they are responsible for both the setting and deterioration of cementitious substances (2). Specific examples include the hydrations of the calcium silicates (1), $CaSO_4.\frac{1}{2}H_2O$ (3), and CaO (4); the conversion of insoluble sulphates to carbonates (5, p. 585); and the reactions described in reference 6.

Innumerable variations in the details of solid–liquid reaction mechanisms are undoubtedly possible; however, the mechanisms will tend to fall into general classes or *systems* which represent to first approximation the limits of experimental distinguishability. One such system, much used in past work (1, 3, 4), considers the *degree of mixing* with the liquid of successively reacting portions of the reacting solid (Fig. 1A). Thus, in a "through-solution" mechanism the reacting solid passes into solution before precipitating as product solid (7). In a "direct" mechanism, on the other hand, the reacting solid is converted to the product solid without an intermediate mixing with the body of the liquid; the liquid is, however, assumed to receive or supply material as required by the balanced reaction equation (3, 4). Depending on the relative ease of the "through-solution" and "direct" routes, mixed mechanisms might also occur.

A possible alternative to the above system of mechanisms considers whether or not the reaction proceeds at the surfaces of the solids (Fig. 1B). In a "surface" mechanism material is transferred from the surface of the reacting solid to that of the product solid, with or without mixing with the body of the liquid. In an "internal" mechanism reaction proceeds as a result of liquid diffusing, or otherwise penetrating, into the interior of the reacting solid. The reaction thus occurs *without* mixing, and the product solid is

[1]*Manuscript received December 16, 1959.*
Contribution from the Department of Chemistry, University of Saskatchewan, Saskatoon, Saskatchewan, with financial assistance from the National Research Council of Canada.
[2]*Holder of a National Research Council Bursary 1955–56. Present address: Atomic Energy of Canada Limited, Chalk River, Ontario.*

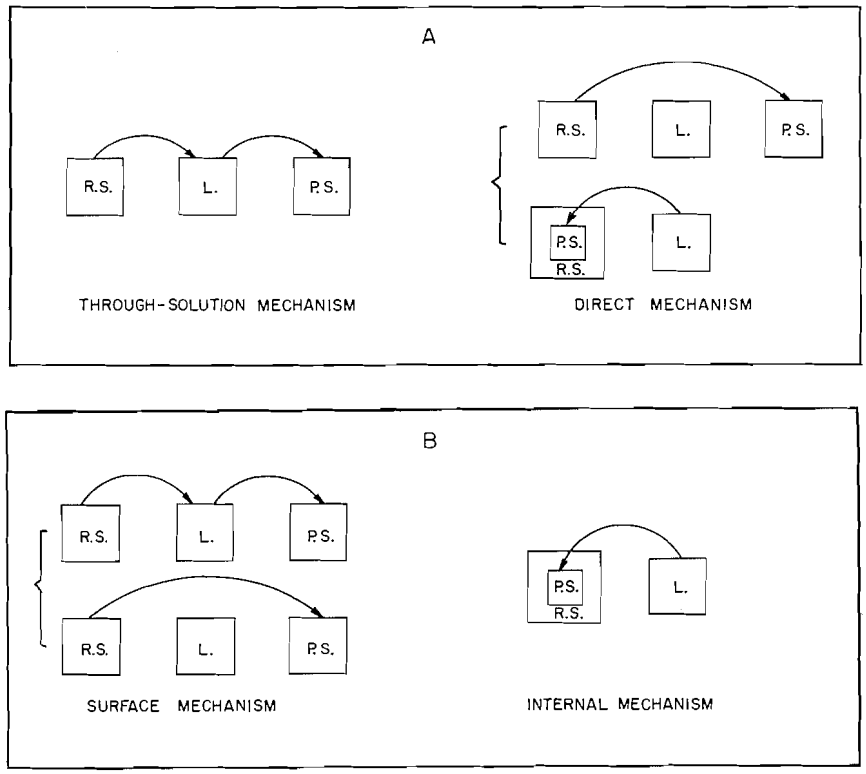


FIG. 1. (A) Schematic representation of solid–liquid reaction mechanisms as classified according to the degree of mixing with the liquid of successively reacting portions of the reacting solid. The following abbreviations are used: R.S. = reacting solid, L. = liquid, P.S. = product solid. The arrows may in general be interpreted as the routes taken by material from the reacting solid and liquid during the course of the reaction; however, it has been necessary to leave out certain steps in which differences in composition between the reacting and product solids are made up by the liquid, since the details of these steps depend on the actual compositions of the solids.

(B) Schematic representation of solid–liquid reaction mechanisms as classified according to whether or not the reaction proceeds at the surfaces of the solids. Abbreviations and use of arrows are as in (A).

deposited within the reacting solid, out of contact with the liquid (cf. the hydration of soft-burnt CaO (4)). Mixed mechanisms would again be possible.

Perhaps the most powerful method for investigating solid–liquid reaction mechanisms within either system is the tracer method of Graham, Spinks, and Thorvaldson (1). A suitable label, which will be assumed here to be a radioactive nuclide, is introduced into the liquid or reacting solid or both. The reaction is then allowed to proceed under conditions of vigorous agitation, and concurrent measurements of radioactivity and composition are made on the *filtered* liquid at suitable time intervals. A different relation between these measured quantities exists for each mechanism within a given system, *provided the system is applicable.*

The remainder of the present work will be concerned with a detailed treatment, in the light of the two systems of mechanisms just described, of the problem of correlating the activity and composition of the liquid during labeled solid–liquid reactions. This will lead to a precise definition of the conditions under which a given system of mechanisms is physically realistic, and will also provide a set of general equations with which to interpret

Can. J. Chem. Downloaded from www.nrcresearchpress.com by 186.148.149.217 on 09/04/12
For personal use only.

experimental results.[3] *It will be assumed, in all cases, that the reaction mixture is subjected to sufficient agitation to maintain a uniform composition in the liquid.*

SOLID–LIQUID REACTIONS ACCOMPANIED BY EXTERNAL EXCHANGE

In any attempt to correlate the activity and composition of the liquid in labeled solid–liquid reactions, close attention must be given to the effect of exchange between the liquid and both solids. Such exchange has been recognized to be of three extreme types (8, p. 37): surface exchange, self-diffusion, and recrystallization. Closely related to recrystallization is the formation of solid intermediates. For the present purposes, however, a slightly different systematization will be used:

(i) "external" exchange: exchange which occurs between a liquid and ions located in the *outer* layers of a solid, and which proceeds irrespective of crystallographic differences between the ions of the solid. Surface exchange and recrystallization are probably always of this sort.

(ii) "internal" exchange: exchange occurring between a liquid and a crystallographically determined fraction of a solid and thence, when rapid, occurring throughout the entire relevant portion of the crystal lattice. Self-diffusion may be of this sort in particular cases, for example compounds with a defect structure (9, 10).

Consider first a reaction accompanied by rapid, multidirectional external exchange *in one or both* solids, with or without a component of similar internal exchange in addition. (By rapid is meant having a rate greater than the rate of reaction, while multidirectional is the opposite of unidirectional (cf. 8, p. 35).) The result of such exchange is that the surfaces of the affected solids tend to have the same specific activity as the liquid. Accordingly, if the reaction proceeds at the surfaces, the material undergoing reaction is always in radioactive equilibrium with the liquid *whatever the degree of mixing*. Mechanisms based on the degree of mixing are therefore not experimentally significant, and the reaction is more readily described in terms of "surface" and "internal" mechanisms (cf. Fig. 1B).

(a) Surface Mechanism

Let a be the amount of labeled species with specific activity $f(0)$ initially present in the liquid. Let b be the amount of labeled species with specific activity g initially present in the reacting solid, x being the portion of b which has reacted. For $x > 0$ the specific activity of the liquid is then $f(x)$. Let m_1 and m_2 be the numbers of moles of labeled species in the formulae of, respectively, the reacting and product solids as derived from *the balanced reaction equation*.[4] Let n_1 and n_2 be such portions of, respectively, m_1 and m_2 that the total amount of rapidly and multidirectionally exchanging material, whether external or internal, in a given solid can be represented as a fraction n_i/m_i of the total *amount* of solid. This material has specific activity $f(x)$. (In a more rigorous treatment, the amount of *externally* exchanging material would be put proportional to the surface area of the solid, i.e. to $(amount)^{2/3}$.)

In accordance with this nomenclature, a "surface" mechanism can be envisaged as involving the reaction of successive elements of material, Δx, from the surface of the reacting solid, together with corresponding changes in activity. The latter are as follows: $\Delta x f(x)$ leaves the reacting solid, $(1-n_1/m_1)\Delta x g$ becomes exchangeable beneath the

[3] *Equations applicable in certain specific cases have already been given by Thorvaldson et al. (1, 3).*

[4] *For example, in the reaction* $2(3CaO.SiO_2)+(n+3)H_2O \rightarrow 3CaO.2SiO_2.nH_2O+3Ca^{++}+6\ OH^-$, $m_1 = 6$ *and* $m_2 = 3$ *if calcium is labeled (cf. 1).*

Can. J. Chem. Downloaded from www.nrcresearchpress.com by 186.148.149.217 on 09/04/12
For personal use only.

surface of the reacting solid,[5] $(m_2/m_1)\Delta x f(x)$ deposits on the product solid, $(1-n_2/m_2)(m_2/m_1)\Delta x f(x)$ ceases to be exchangeable beneath the surface of the product solid,[5] and the liquid gains $(1-m_2/m_1)\Delta x f(x)$. The specific activity of the liquid and the exchanging portions of the solids therefore changes from $f(x)$ to

$$f(x+\Delta x) = \text{(total mobile activity)/(total mobile amount)}$$

$$= \frac{\left[a+\left(1-\frac{m_2}{m_1}\right)(x+\Delta x)\right]f(x)+\left[\frac{n_1}{m_1}(b-x)f(x)-\Delta x f(x)+\left(1-\frac{n_1}{m_1}\right)\Delta x g\right]+\left[\frac{n_2}{m_1}x+\frac{m_2}{m_1}\Delta x-\left(1-\frac{n_2}{m_2}\right)\frac{m_2}{m_1}\Delta x\right]f(x)}{\left[a+\left(1-\frac{m_2}{m_1}\right)(x+\Delta x)\right]+\left[\frac{n_1}{m_1}(b-x)-\Delta x+\left(1-\frac{n_1}{m_1}\right)\Delta x\right]+\left[\frac{n_2}{m_1}x+\frac{m_2}{m_1}\Delta x-\left(1-\frac{n_2}{m_2}\right)\frac{m_2}{m_1}\Delta x\right]}.$$

If $[f(x+\Delta x)-f(x)]/\Delta x$ is now formed, $df(x)/dx$ can be obtained in the limit as $\Delta x \to 0$. Integrating the latter expression under the condition that

$$f(x) = \frac{af(0)+n_1bg/m_1}{a+n_1b/m_1}$$

when $x = 0$, i.e. allowing for the initial "burst" of exchange, the result is

[1] $$f(x) = g+\frac{f(0)-g}{1+n_1b/m_1a}\left(1+\frac{m_1-m_2-n_1+n_2}{m_1a+n_1b}x\right)^{(-m_1+n_1)/(m_1-m_2-n_1+n_2)}.$$

The activity of the liquid as a function of x follows directly from equation [1]:

[2] $$\text{activity} = (a+x-m_2x/m_1)f(x) \equiv Af(x),$$

or, in units of fraction of total activity present,

[3] $$\text{fractional activity} = \frac{Af(x)}{af(0)+bg}.$$

The term

[4] $$A \equiv a+x-m_2x/m_1$$

represents the measured amount of labeled species present in the liquid at any stage of reaction; that is, it is simply the "composition" of the liquid.

In those cases where the activity is confined initially to either the liquid or solid, and $n_1 = n_2 \to 0$, equations [1] to [3] simplify considerably, the last designated giving

[5] $$\begin{cases} g = 0, & m_1 \neq m_2 \\ g = 0, & m_1 = m_2 \end{cases} \qquad \begin{aligned} \text{fractional activity} &= (A/a)^{m_2/(m_2-m_1)} \\ &= e^{-x/a} \end{aligned}$$

[5] *The origin of the factors $(1-n_1/m_1)$ and $(1-n_2/m_2)$ is as follows. Let n_i' and n_i'' correspond, respectively, to externally and internally exchanging material. Then the removal or deposition in the course of reaction of Δx units of material at the outside of the surface layer described by n_i' will cause an amount on the inner side of this layer to become, or cease to be, exchangeable which is given by* Δx times *a factor $(1-n_i'/m_i)$ to take into account the reduced amount of material inside the layer,* times *a factor $(1-n_i''/m_i)$ since only part of the new material is not already exchanging. Noting that $n_i = n_i'+n_i''-n_i'n_i''/m_i$, it follows that the total amount of material becoming, or ceasing to be, exchangeable is $(1-n_i/m_i)\Delta x$.*

Can. J. Chem. Downloaded from www.nrcresearchpress.com by 186.148.149.217 on 09/04/12
For personal use only.

[6] $\begin{cases} f(0) = 0, & m_1 \neq m_2 \quad \text{fractional activity} = A/b - \dfrac{a}{b}(A/a)^{m_2/(m_2-m_1)} \\ f(0) = 0, & m_1 = m_2 \quad = \dfrac{a}{b}(1-e^{-x/a}). \end{cases}$

If the reacting solid suffers total exchangeability, i.e. $n_1 \rightarrow m_1$, the reductions of equations [1] and [3] are, respectively,

[7] $$f(x) = \frac{af(0)+bg}{a+b} \quad \text{and} \quad \text{fractional activity} = \frac{A}{a+b}.$$

These expressions are seen to describe radioactive equilibrium. The case $n_2 \rightarrow m_2$ is equivalent to the occurrence of extensive recrystallization in the product solid, which is discussed later. If the exchange is slow or unidirectional, though such that the outer surfaces of at least one solid maintain radioactive equilibrium with the liquid, the activity will be bounded by that obtained with full values of n_1 and n_2, and that obtained with $n_1 = n_2 \rightarrow 0$.

An equation somewhat different from [1] is obtained when m_2 is not a constant but a function of A: see Appendix.

(b) Internal or Mixed Mechanism

The derivation of an equation analogous to [1] for cases in which either a purely "internal" mechanism, or a mixture of "surface" and "internal" mechanisms, occurs is complicated by the fact that the product solid, either completely or in part, is now lodged inaccessibly within the reacting solid and contributes to the exchangeability of the system only as the reacting solid is depleted.[6] It will therefore be assumed for the present that $n_2 \rightarrow 0$, the case $n_2 \rightarrow m_2$ being covered in the subsequent discussion of recrystallization. The elemental activity changes occurring as a result of the reaction of Δx units of material from the reacting solid, $k\Delta x$ of which is from a surface and $(1-k)\Delta x$ from the interior, are then as follows: $k\Delta x f(x)$ leaves the surface of the reacting solid, $k(1-n_1/m_1)\Delta x g$ becomes exchangeable beneath the surface of the reacting solid,[5] and the liquid gains

$$\left(1-\frac{m_2}{m_1}\right)\Delta x f(x) \qquad \text{if } m_1 < m_2,$$

$$k\left(1-\frac{m_2}{m_1}\right)\Delta x f(x) + (1-k)\left(1-\frac{m_2}{m_1}\right)\Delta x\left(\frac{n_1}{m_1}f(x) + \left(1-\frac{n_1}{m_1}\right)g\right) \qquad \text{if } m_1 > m_2.$$

In the latter expression, the term beginning with $(1-k)$ is strictly valid only if soluble reaction products formed in the interior of the reacting solid as a result of the "internal" component of the reaction are able to diffuse out rapidly. Following through the derivation, two expressions for $f(x)$ are finally obtained:

[8] $m_1 < m_2$ $$f(x) = g + \frac{f(0)-g}{1+n_1b/m_1a}\left(1+\frac{m_1-m_2-n_1}{m_1a+n_1b}x\right)^{-k(m_1-n_1)/(m_1-m_2-n_1)}$$

[9] $m_1 > m_2$ $$f(x) = g + \frac{f(0)-g}{1+n_1b/m_1a}\left(\cdots\right)^{\left[-k(m_1-n_1)(1-k)\left(1-\frac{m_2}{m_1}\right)(m_1-n_1)\right]/(m_1-m_2-n_1)}$$

[6] *It has been assumed, both here and in the initial description of the "internal" mechanism (see Introduction), that that portion of the product solid laid down within the reacting solid remains inaccessible to the liquid until the covering layer of reacting solid has disappeared. Actually, it is conceivable that in some cases the liquid might have continuous access to the internal product solid. The reaction would then show an "internal" mechanism only if the external exchange exhibited by the product solid were slow or non-existent; otherwise the reaction would follow a "surface" mechanism.*

Can. J. Chem. Downloaded from www.nrcresearchpress.com by 186.148.149.217 on 09/04/12
For personal use only.

Hence, if $n_1 \rightarrow 0$,

$$[10] \quad \begin{cases} g = 0, & m_1 < m_2 \quad \text{fractional activity} = (A/a)^{[m_2-(1-k)m_1]/(m_2-m_1)} \\ g = 0, & m_1 = m_2 \quad = e^{-kx/a} \\ g = 0, & m_1 > m_2 \quad = (A/a)^{-km_2/(m_1-m_2)} \end{cases}$$

[11] $f(0) = 0$ like equations [6] but with exponents as above.

SOLID–LIQUID REACTIONS ACCOMPANIED BY INTERNAL OR NO EXCHANGE

If the external exchange is either slow or non-existent in both solids, though without restriction to the internal exchange, a distinction between "surface" and "internal" mechanisms is no longer experimentally convenient. Different *degrees of mixing* (cf. Fig. 1A) are, however, readily distinguished. It can be shown that, since the "through-solution" mechanism results in a complete mixing with the liquid of successively reacting portions of the reacting solid, the relation between the activity and composition of the liquid for this mechanism is identical with that for a "surface" mechanism: see equations [1], [5], [6], and [16], the last designated applying when m_2 is a function of A. Similarly, for a "direct" or mixed mechanism the activity is given by equations [8] to [11].

Previously studied solid–liquid reactions were described as following mechanisms based on the degree of mixing (1, 3, 4). There is reason to believe, however, that the product solids in at least two of the reactions (the hydrations of $CaSO_4.\frac{1}{2}H_2O$ (3) and CaO (4)) exhibit rapid, multidirectional external exchange.[7] The reactions in question are therefore perhaps better represented in terms of "surface" or "internal" mechanisms; passage through solution may still have occurred, but was not rigorously demonstrated.

RECRYSTALLIZATION AND INTERMEDIATE FORMATION

The possibility that extensive recrystallization will take place in the freshly formed product solid, or that solid–intermediate formation will occur, is always a problem in studying a solid–liquid reaction, since neither effect can be predicted from the behavior of the product solid in isolation.

Consider first recrystallization. Assume limiting conditions, i.e. (i) that the recrystallization is rapid, complete, and multidirectional, and (ii) that no product solid is lodged inaccessibly within the reacting solid as might occur with an "internal" or "direct" mechanism, a condition which should be well met as the reaction enters its later stages and the amount of unconverted reacting solid diminishes. Then, *regardless of the reaction mechanism*,

$$f(x) = (\text{total mobile activity})/(\text{total mobile amount})$$

$$[12] \quad = \frac{af(0)+xg+n_1(b-x)g/m_1}{a+x+n_1(b-x)/m_1}.$$

Forms for fractional activity follow readily using equation [3]; in particular, if $g = 0$ and either $n_1 \rightarrow 0$ or $x \rightarrow b$,

[7]*That is, the product solids in these reactions both exhibit rapid* surface *exchange, a mode of exchange which may in general be expected to be multidirectional and external. For* $Ca(OH)_2$, *see reference 4; for* $CaSO_4.2H_2O$, *compare reference 11, where surface exchange is shown to occur with* $SrSO_4$.

Can. J. Chem. Downloaded from www.nrcresearchpress.com by 186.148.149.217 on 09/04/12
For personal use only.

$$[13] \qquad \text{fractional activity} = \frac{A}{a+x} = \frac{(A/a)(1-m_2/m_1)}{A/a-m_2/m_1}.$$

Similar equations can be obtained by letting $n_2 \rightarrow m_2$ in equation [1]. If the recrystallization is slow, incomplete, or unidirectional, or a portion of the product solid is inaccessible (i.e. if in effect $n_2 < m_2$), the specific activity of the liquid will lie between that given by equation [12] and that for the unperturbed reactions (either equation [1] (with $n_2 = 0$), [8], or [9]).

Solid–intermediate formation will be largely equivalent to recrystallization in the product solid in such cases as (i) "surface" or "through-solution" mechanisms occur, and (ii) the intermediates are reasonably long-lived, i.e. not transient.

Note that equations [12] and [13] were derived without regard to the reaction mechanism; in other words, recrystallization and intermediate formation tend to mask the differences between mechanisms.

RELATIVE VALUES OF THE SPECIFIC ACTIVITIES

By way of conclusion, it is interesting to consider the relative values of the specific activities of the liquid to be expected under the various mechanisms after a given extent of reaction, i.e. for a given value of x or A (equations [1], [8], and [9]). Exchange will be assumed to be slight, hence $n_1 = n_2 \rightarrow 0$; and mixed mechanisms will be assumed not to occur, hence $k = 1$ or $k = 0$. These specific activities will be compared with the values occurring initially ($f(0)$), at radioactive equilibrium (equations [7]), and when limiting recrystallization or intermediate formation occur (equation [12]). Representing a given specific activity by the appropriate name, one obtains, for $f(0) > g$,

$$[14] \qquad \left.\begin{matrix}\text{(surface or through-solution)} \\ \text{(equilibrium)}\end{matrix}\right\} < \text{(recrystallization)} < \text{(internal or direct)} < \text{(initial)};$$

except that, for $m_1 \leqslant m_2$, (internal or direct) = (initial), while when the reaction is complete, i.e. $x \rightarrow b$, (equilibrium) = (recrystallization). For $f(0) < g$ the inequalities in equation [14] are reversed. Relative values similar to those in equation [14] also hold for *total* activities, except that the position of the initial activity cannot be predicted simply. The various relationships are further illustrated in Figs. 2A and 2B, where the progress of the specific activity of the liquid is plotted as a function of x for two particular sets of conditions.

It is seen that only with a "surface" or "through-solution" mechanism does the specific activity of the liquid proceed from its initial value *across* the limiting recrystallization value (or, when $x \rightarrow b$, the equilibrium value). Stated differently, the limiting recrystallization and equilibrium activities, whether specific or total, define a boundary between the activities attainable under the different mechanisms of a given system.

An interesting example of the "crossing phenomenon" in a field outside of formal solid–liquid reactions was found by Kolthoff and Eggertsen (12). When fresh $PbCrO_4$ was allowed to recrystallize in a solution containing Pb^{212}, a transient activity *beyond* the usually encountered equilibrium value was observed. Noting that unidirectional recrystallization is in all respects equivalent to a solid–liquid reaction with $m_1 = m_2$ which follows a "surface" or "through-solution" mechanism, this observation indicates that the recrystallization was partially unidirectional. A similar conclusion was reached by the authors.

Can. J. Chem. Downloaded from www.nrcresearchpress.com by 186.148.149.217 on 09/04/12
For personal use only.

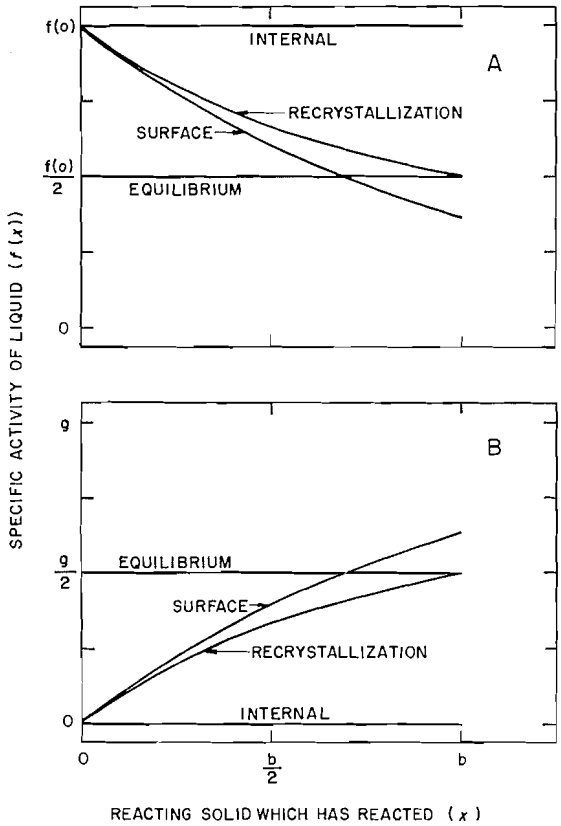


FIG. 2. (A) The progress of the specific activity of the liquid ($f(x)$) during a labeled solid–liquid reaction in which the tracer is confined initially to the liquid ($g = 0$), the numbers of moles of labeled species in the formulae of the reacting and product solids are the same ($m_1 = m_2$; cf. footnote 4), exchange is slight ($n_1 = n_2 \rightarrow 0$), and equal amounts of the labeled species are present initially in the liquid and solid phases ($a = b$). Since $m_1 = m_2$, the specific activity is proportional to the total activity. The reaction necessarily terminates when the amount of labeled species from the reacting solid which has reacted (x) equals the total amount originally present (b).

(B) The progress of the specific activity of the liquid during a labeled solid–liquid reaction under the same conditions as in Fig. 2A except that the tracer is confined initially to the solid ($f(0) = 0$).

ACKNOWLEDGMENT

The work described here is largely an outgrowth of a project (6) carried out under the direction of Dr. T. Thorvaldson of this department. Dr. Thorvaldson's assistance is gratefully acknowledged.

REFERENCES

1. W. A. G. GRAHAM, J. W. T. SPINKS, and T. THORVALDSON. Can. J. Chem. **32**, 129 (1954).
2. R. H. BOGUE. The chemistry of portland cement. Reinhold Publishing Corp., New York. 1955.
3. F. W. BIRSS and T. THORVALDSON. Can. J. Chem. **33**, 870 (1955).
4. F. W. BIRSS and T. THORVALDSON. Can. J. Chem. **33**, 881 (1955).
5. G. CHARLOT and D. BEZIER. Quantitative inorganic analysis. John Wiley & Sons, Inc., New York. 1957.
6. R. KELLY. Can. J. Chem. **38**, 1218 (1960).
7. H. LE CHATELIER. Experimental researches on the constitution of hydraulic mortars. *Translated by* J. L. Mack. McGraw Pub. Co., New York. 1905.
8. O. E. MYERS and R. J. PRESTWOOD. *In* Radioactivity applied to chemistry. *Edited by* A. C. Wahl and N. A. Bonner. John Wiley & Sons, Inc., New York. 1951.
9. W. BUSER. Helv. Chim. Acta, **37**, 2334 (1954).
10. W. BUSER and U. IMOBERSTEG. Helv. Chim. Acta, **37**, 2345 (1954).
11. R. SINGLETON and J. W. T. SPINKS. Can. J. Research, B, **27**, 238 (1949).
12. I. M. KOLTHOFF and F. T. EGGERTSEN. J. Am. Chem. Soc. **63**, 1412 (1941).

Can. J. Chem. Downloaded from www.nrcresearchpress.com by 186.148.149.217 on 09/04/12
For personal use only.

Can. J. Chem. Downloaded from www.nrcresearchpress.com by 186.148.149.217 on 09/04/12
For personal use only.

APPENDIX

SOLID–LIQUID REACTIONS WHERE THE COMPOSITION OF THE PRODUCT SOLID VARIES

Suppose, as in the hydration of $3CaO.SiO_2$ (1), that the composition of the product solid depended on the concentration of the liquid. The quantity m_2 could then be expressed as a function of A,

$$m_2(A) = c_0 + c_1A + c_2A^2 \ldots \approx c_0 + c_1A,$$

where c_0, c_1, and c_2 are constants. Now, in such a case, there is a possibility that that portion of the product solid characterized by c_1A would not remain inert once precipitated, but (in particular near a surface) would tend to maintain composition equilibrium *and thence* radioactive equilibrium with the liquid. An external equilibrating shell would therefore occur which, to first approximation, could be envisaged as containing a mole fraction h of the total variable portion of the product solid, and thence hc_1Ax/m_1 units of material.[8]

Assuming that the reaction follows a "surface" or "through-solution" mechanism, though with $n_1 = n_2 \rightarrow 0$, the relation between the activity and composition of the liquid when m_2 is a variable is readily derived. Let x units of reacting solid already have reacted and another Δx react. The specific activity of the liquid and the equilibrating portion of the product solid therefore changes from $f(x)$ to

$$(x+\Delta x) = \frac{Af(x) + \Delta xg + (hc_1Ax/m_1)f(x)}{A + \Delta x + hc_1Ax/m_1},$$

where

$$[15] \qquad A = a + x - (c_0 + hc_1A)x/m_1 - \int_0^x (1-h)(c_1A/m_1)dx'.$$

Proceeding as before, an expression for $df(x)/dx$ is obtained. The term dx can be eliminated by differentiating equation [15], and $f(x)$ then found by integration. The result, with $m_2(A)$ substituted for $(c_0 + c_1A)$, is

$$[16] \qquad f(x) = g + [f(0) - g]\left\{\frac{[m_1 - m_2(A)]a}{[m_1 - m_2(a)]A}\right\}^{m_1/[m_1 - m_2(0)]}.$$

The activity in the liquid as a function of A can now be derived as indicated by equations [2] and [3]. Equation [16] is *not* valid if $m_1 = m_2(0)$ or $m_2(a)$, or if m_1 lies within the path of $m_2(A)$.

An important property of equation [16] is that, provided it is expressed in terms of A and not x, it does not require knowledge of the value of h, i.e. of the division of product solid into equilibrating and nonequilibrating portions. It can be shown from a more general derivation, in which c_1A is replaced by $m_2(A)$ and h by the generalized form $h(A)$, and c_0 is dropped from equation [15], that this result is contingent on the following relation:

$$\frac{dh(A)m_2(A)}{dA} = \frac{h(A)m_2(A)}{A};$$

hence $h(A)m_2(A) = \text{constant} \cdot A = hc_1A$. In other words, independence of h occurs *accidentally* when certain specific conditions are met.

Equation [16] should be of use in determining values of $m_2(A)$ in cases where the reaction mechanism is not in doubt.

[8] *Ideally, the amount of product solid capable of equilibration would be put proportional to the surface area of the product solid; this would, however, introduce an unwieldy two-thirds power.*

Can. J. Chem. Downloaded from www.nrcresearchpress.com by 186.148.149.217 on 09/04/12
For personal use only.

SOLID–LIQUID REACTIONS

PART II. SOLID–LIQUID REACTIONS AMONGST THE CALCIUM ALUMINATES AND SULPHOALUMINATES[1]

ROGER KELLY[2]

ABSTRACT

When $3CaO.Al_2O_3.6H_2O$ (i.e. C_3AH_6) was placed in contact with a solution of $Ca(OH)_2$ labeled with Ca^{45} and maintained at 25° C, there was very little change in either the activity or composition of the liquid. These observations, when taken together, indicate that the compound is *probably* stable in the system used. On the other hand, when either C_3AH_6 or $3CaO.Al_2O_3.CaSO_4.12H_2O$ (i.e. $C_3A\Sigma H_{12}$) was added to a mixed $Ca(OH)_2$–$CaSO_4$ solution, the composition of the liquid varied in a manner consistent with the formation of $3CaO.Al_2O_3.3CaSO_4.31H_2O$ (i.e. $C_3A\Sigma_3H_{31}$). The activity also changed markedly, and a detailed consideration of the relations between activity and composition enabled the reaction mechanisms to be determined. In further experiments, the reactions of C_3AH_6 and $C_3A\Sigma H_{12}$ to form $C_3A\Sigma_3H_{31}$ were shown to proceed also at 70° and 90° C. The consistently greater *ultimate* stability of $C_3A\Sigma_3H_{31}$ over $C_3A\Sigma H_{12}$ between 25° and 90° C is to be contrasted with the fact, observed in the course of preparing the $C_3A\Sigma H_{12}$, that when solutions of $Al_2(SO_4)_3$, $CaSO_4$, and $Ca(OH)_2$ are mixed the *immediate* precipitate is $C_3A\Sigma_3H_{31}$ at room temperature, but $C_3A\Sigma H_{12}$ at boiling temperature.

An abbreviated chemical symbolism, similar to the one used by Bogue (1), will be employed in what follows: $A \equiv Al_2O_3$, $C \equiv CaO$, $H \equiv H_2O$, $\Sigma \equiv CaSO_4$. *Thus* $3CaO.Al_2O_3.CaSO_4.12H_2O$ *will be represented by* $C_3A\Sigma H_{12}$.

Calcium forms four well-defined anhydrous aluminates (CA, C_3A, C_3A_5, and C_5A_3 (2)) together with perhaps 10 hydrated forms. The most well-known of the latter are C_3AH_6 (cubic), C_2AH_8, C_3AH_{12}, and C_4AH_{12} (all platy hexagonal) (1, p. 552), though there is general agreement that the cubic C_3AH_6 is the only stable aluminate in the system C—A—H between room temperature and 215° C (3, 4). Representing a further stage of chemical complexity are two long series of insoluble compounds with general formulae C_3AXH_{12} (platy hexagonal) and $C_3AX_3H_{31}$ (acicular hexagonal), where X may be essentially any calcium salt (5). For X = $CaSO_4$ only the acicular form is apparently stable in aqueous systems (6).

These compounds are of importance principally in their relation to portland cement. Thus C_3A is a constituent of the cement powder (it lowers the preparation temperature), while hydrated forms arising from the C_3A are present in set cement. When set cement, as in mortar or concrete, is exposed to sulphate, the hydrated aluminates are converted to the bulky sulphoaluminate $C_3A\Sigma_3H_{31}$ with resultant disintegration of the material.

The present work represents a study of three of the many possible aluminate reactions that might occur in cement: that of C_3AH_6 with $Ca(OH)_2$ solutions, that of C_3AH_6 with mixed $Ca(OH)_2$–$CaSO_4$ solutions, and that of $C_3A\Sigma H_{12}$ with mixed $Ca(OH)_2$–$CaSO_4$ solutions. Since these reactions fall into the category of *solid–liquid* reactions (7), they will be considered in terms of the tracer method of Graham, Spinks, and Thorvaldson (8) as extended by Kelly (7).

[1]*Manuscript received December 16, 1959.*
Contribution from the Department of Chemistry, University of Saskatchewan, Saskatoon, Saskatchewan, with financial assistance from the National Research Council of Canada.
[2]*Holder of a National Research Council Bursary 1955–56. Present address: Atomic Energy of Canada Limited, Chalk River, Ontario.*

Can. J. Chem. Downloaded from www.nrcresearchpress.com by 186.148.149.217 on 09/04/12
For personal use only.

EXPERIMENTAL

Solutions

Solutions saturated in $Ca(OH)_2$ or $CaSO_4$ or both were prepared by shaking for several weeks an excess of the appropriate solid (CaO or $CaSO_4.2H_2O$) with redistilled water in glass containers. Less concentrated solutions were made up by dilution. It was attempted at all times to minimize carbonation.

C_3AH_6

Since wet preparations generally lead to the metastable hexagonal aluminates, a hydrothermal technique due to Thorvaldson and Grace (9) was used to prepare C_3AH_6. Starting with a 3:1 mixture of CaO and Al_2O_3, C_3A was formed by alternately igniting at 1400° C and grinding to 325 mesh. The C_3A was then converted to C_3AH_6 by exposure to the equilibrium vapor pressure of water at 150° C for 8 days.

$C_3A\Sigma H_{12}$

The only methods for preparing $C_3A\Sigma H_{12}$ apparently recorded involve precipitations *at room temperature* from solutions of carefully controlled composition (see, for example, 10). There are, however, isolated examples in which a hexagonal phase resembling $C_3A\Sigma H_{12}$ has been obtained at elevated temperatures (5). Following the lead of the latter, 150-cc portions of a solution containing 3.06 g $Al_2(SO_4)_3.18H_2O$ in 1 liter of saturated $CaSO_4$ (i.e. $Al_2O_3:SO_3::1:6$) were mixed with 600-cc portions of a $Ca(OH)_2$ solution containing about 0.55 g CaO per liter, *both solutions being at boiling temperature.* In every instance an immediate precipitate with a striking silky luster and platy hexagonal form was observed (Fig. 1A). Ten minutes at boiling temperature were allowed for crystal growth, if any, before the precipitate was separated. The samples analyzed variously as $C_3A\Sigma_{0.44}H_{9.7}$, $C_3A\Sigma_{0.86}H_{9.7}$, $C_3A(\Sigma_{0.62}C_{0.46})H_{10.0}$, etc., indicating that the desired substance had been obtained, though as a member of a solid–solution series (cf. the series C_3AH_{12}–$C_3A\Sigma H_{12}$–C_4AH_{12} proposed by Kalousek (11)). The deficient water contents probably represent equilibrium compositions at the temperature used.

It was not found possible to prepare *pure* $C_3A\Sigma H_{12}$ at temperatures below boiling temperature. Thus, when the $Al_2(SO_4)_3$–$CaSO_4$ solution described above was mixed with twice the volume of a $Ca(OH)_2$ solution containing about 1.1 g CaO per liter, mixtures of $C_3A\Sigma H_{12}$ and $C_3A\Sigma_3H_{31}$ were obtained between 50° and 75° C, and $C_3A\Sigma_3H_{31}$ alone at room temperature (Figs. 1B and 1C). Over the same temperature range, but when the concentration of the $Ca(OH)_2$ in the *combined* solutions was lower, there was either no immediate precipitate, or else hydrated Al_2O_3 formed (cf. 10, p. 721).

The implication in the experiments just described that there may be a change in the relative stabilities of the two sulphoaluminates as the temperature is increased will be considered later.

Method of Conducting Experiments

Following Graham *et al.* (8), calcium-45[3] was first introduced into the liquid. About 0.05 g of solid and exactly 50 cc of liquid were next sealed in cylindrical steel tubes of 110-cc capacity which were lined with gold or silver (cf. 8). In order that the reaction mixtures might be kept continuously agitated, the tubes were attached to a slowly revolving wheel.

After periods of reaction of several days, the tubes were opened and the liquid separated either by filtration through a "fine" sintered-glass filter or by centrifugation. Using 25 cc

[3]*Obtained from Atomic Energy of Canada Limited, Chalk River, Ontario.*

of liquid, calcium was determined as the oxalate, and sulphate as $BaSO_4$; alternatively, the sum of a sulphate measurement plus a titration with HCl was used to estimate calcium. Four 1/2-cc portions of liquid were also pipetted onto aluminum dishes. The calcium was then precipitated with ammonium oxalate, acetone was added to disperse the precipitate, and, when the samples were dry, the Ca^{45} activity was measured with a simple end-window Geiger–Mueller tube. The relation between the activity and composition of the liquid determined whether a reaction had occurred and the mechanism of the reaction.

Unless otherwise specified, the reactions took place at a temperature of $25\pm0.5°$ C.

THEORY

Define "external" exchange as exchange which occurs between a liquid and ions located in the *outer* layers of a solid, and which proceeds irrespective of crystallographic differences between the ions of the solid; define "internal" exchange as exchange occurring between a liquid and a crystallographically determined fraction of a solid (7). Then, according to reference 7, the mechanisms of solid–liquid reactions may be classified in at least two ways. When rapid, multidirectional *external* exchange occurs in either the reacting or product solid, with or without a component of internal exchange in addition, it is convenient to consider mechanisms based on whether the reaction proceeds at the surfaces of the solids or in the interior, and thence to distinguish "surface" and "internal" mechanisms and mixtures thereof. When the external exchange is either slow or non-existent in both solids, though without restriction to the *internal* exchange, the degree of mixing with the liquid of successively reacting portions of the reacting solid is more important, and one then recognizes the alternatives of complete mixing ("through-solution" mechanism) and no mixing ("direct" mechanism), as well as intermediate situations. General equations giving the relations between the activity and composition of the liquid for these mechanisms are developed in reference 7, and it is shown that when, as in the present work, the reacting solid is initially inactive and the extent of *all* rapid, multidirectional exchange is slight, these equations reduce to

[1] "surface" or "through-solution" mechanism fractional activity $= (A/a)^{m_2/(m_2-m_1)}$,

[2] "internal" or "direct" mechanism, $m_1<m_2$ fractional activity $= (A/a)$,

where "fractional activity" refers to the activity of the liquid in units of fraction of the initial value, a is the amount of labeled species (i.e. calcium) initially present in the liquid, A is the variable amount of labeled species in the liquid at any time, and m_1 and m_2 are the numbers of moles of labeled species in the formulae of, respectively, the reacting and product solids. Mixed mechanisms would give intermediate activities.

An important property of the "surface" and "through-solution" mechanisms is that they alone cause the specific activity of the liquid to progress from its initial value to a point *beyond* the equilibrium value as the reaction goes to completion (cf. Figs. 2A and 2B of reference 7).

When pure exchange rather than a reaction occurs, then analogous to equations [1] and [2] one has

$$[3] \qquad \text{fractional activity} = a/(a+nb/m),$$

where m is the number of moles of labeled species in the formula of the solid, n is the *apparent* portion of m which is exchangeable, and b is the amount of labeled species

Can. J. Chem. Downloaded from www.nrcresearchpress.com by 186.148.149.217 on 09/04/12
For personal use only.

present in the solid. Equation [3] with the substitution $n = m$ describes radioactive equilibrium.

RESULTS

Reaction and Exchange of C_3AH_6 *with* $Ca(OH)_2$ *Solutions*

Though it is reasonably well-established that C_3AH_6 is a stable phase in the system C—A—H at room temperature, it is interesting to demonstrate this stability in an indirect manner by determining if a solid–liquid reaction occurs when inactive C_3AH_6 is placed in contact with a solution of $Ca(OH)_2$ labeled with Ca^{45}. Results are given in Table I. Some word is perhaps required about those experiments in which a finite time is

TABLE I

Activity changes when inactive C_3AH_6 is added to solutions of $Ca(OH)_2$ labeled with Ca^{45}

Calcium in solid, *b* (mole×10^4)	Calcium in initial solution, *a* (mole×10^4 per 50 cc)*	Duration of experiment in days: (*a*) Before labeling	Duration of experiment in days: (*b*) After labeling	Observed activity (fraction of initial value)	Activity to be expected at radioactive equilibrium (eq. [3])	Extent of exchange, *n* (moles calcium per mole C_3AH_6) (eq. [3])
5.47	3.57	0	8	.83	.40	.40
3.71	3.41	0	25	.91	.48	.27
4.67	3.41	0	81	.85	.42	.38
3.19	3.20	1	7	.93	.50	.23
3.27	3.20	5	7	.81	.49	.69
3.75	3.20	8	7	.83	.46	.52
4.03	3.20	55	7	.78	.44	.67
7.92	8.71	2.5	1/24†	.92	.52	.29
			15/24	.93	.52	.25
			1	.90	.52	.37
			4	.86	.52	.54
						Mean = 0.42±0.1

*One mole×10^4 per 50 cc corresponds to 0.112 g CaO per liter. The final calcium contents of the solutions, *A*, were very close to the initial calcium contents.
†Four successive samplings were made in the final experiment.

indicated *before* labeling. In these experiments, in contrast to all others, the activity was added as concentrate to the centrifuged mixtures at the times indicated. "Initial" values for the activity were then derived by shaking the mixtures for 1 minute, centrifuging again, and sampling.

A decision as to whether C_3AH_6 is stable is not possible simply on the basis of the observed lack of change in the composition of the liquid (Table I, footnote *); thus, no change in composition would accompany such processes as solvation or crystal transformation. However, consider the activity changes. It was stated in Theory that the "surface" and "through-solution" mechanisms both cause the *specific* activity of the liquid to cross the equilibrium value as the reaction goes to completion. Noting that, in cases such as the present where the composition of the liquid remains essentially unchanged, *specific* activity is proportional to *total* activity, it is clear that such a relation is not observed (Table I, columns 5 and 6). C_3AH_6 is therefore stable with respect to any reactions following the stated mechanisms. The significance of this is that, as will be shown in the Discussion, these mechanisms may be expected with high probability.

The observed activity changes can evidently be attributed to exchange. Since knowledge of the exchange behavior of C_3AH_6 is required in the following section, values of the quantity n as defined by equation [3] have been included in Table I (final column). It

Can. J. Chem. Downloaded from www.nrcresearchpress.com by 186.148.149.217 on 09/04/12
For personal use only.

will be noted that a low, though rather fluctuant, limiting value of n was reached within an hour and that this value persisted even when the solid had been kept in contact with the liquid for up to two months prior to labeling. The exchange is thus slight in extent, rapid, and multidirectional. These are the characteristics, of course, of either surface exchange or multidirectional recrystallization, both of which will in general fall within the broader category of "external" exchange, as defined earlier.

Reaction of C_3AH_6 *with Mixed* $Ca(OH)_2$–$CaSO_4$ *Solutions*

When C_3AH_6 was added, not to a solution of $Ca(OH)_2$ as in the preceding section, but to a mixed $Ca(OH)_2$–$CaSO_4$ solution, both the composition and activity of the solution changed markedly (see Table II). The changes in composition, as plotted in Fig. 2,

TABLE II

Reaction of inactive C_3AH_6 with mixed $Ca(OH)_2$–$CaSO_4$ solutions labeled with Ca^{45}

Calcium in solid, b (mole×10^4)	Initial composition of solution (mole×10^4 per 50 cc)		Loss from solution (moles per mole C_3AH_6)*			Calcium in final solution, A (mole×10^4 per 50 cc)	Duration of experiment (days)	Observed activity (fraction of initial value)
	(*a*) Calcium, a	(*b*) Sulphate	(*a*) $Ca(OH)_2$	(*b*) $CaSO_4$	(*c*) Total CaO			
3.61	14.81	5.43	0	0.11	0.11	14.68	1/2	.99
"	"	"	0.13	0.40	0.53	14.16	1	.93
"	"	"	0	1.38	1.38	13.15	3	.77
"	"	"	0.27	2.60	2.87	11.35	6	.61
"	"	"	0.20	2.68	2.88	11.34	14	.62
3.97	14.36	5.22	0.21	1.47	1.68	12.13	3	—†
3.61	14.47	5.24	0	2.44	2.44	11.54	5	—
"	"	"	0.42	2.67	3.09	10.76	12	—
"	"	"	0.49	2.90	3.39	10.39	23	—
4.05	14.64	5.68	0.14	1.44	1.58	12.51	3	.75
4.07	"	"	0.20	2.78	2.98	10.59	7	.53
3.97	"	"	0.10	2.88	2.98	10.71	14	.55
4.04	8.17	7.08	0.06	0	0.06	8.09	3	.98
4.22	"	"	0.16	2.90	3.06	3.86	7	.25
3.86	"	"	0.20	2.89	3.09	4.19	14	.28
4.72	"	"	0.17	2.88	3.05	3.38	70	.19

*To convert to mole×10^4, multiply by (calcium in solid)/3. Then (total CaO) = $a - A$.

†No activity was present in the sixth to ninth experiments. In a further experiment similar to these, activity was added as concentrate on the 10th day. The *total* resulting exchange was as follows: n = 0.1, 0.6, 0.8, and 0.9 in, respectively, 1/24, 1, 5, and 12 days. The exchange is thus *rapid* relative to the rate of reaction, though may be only partially *multidirectional*.

indicate that the sulphoaluminate $C_3A\Sigma_3H_{31}$ has formed, the reaction time being about six days. The presence of this compound was confirmed by microscopic examination (Fig. 1B).

The interrelations between activity and composition enable the reaction mechanism to be determined. Note in this regard that the extent of *all* rapid, multidirectional exchange between the liquid and both solids was slight; thus for C_3AH_6, $n/m = 0.42/3$ (Table I), while for $C_3A\Sigma_3H_{31}$, $n/m \leqslant 0.6/6$ (Table II, footnote †). Hence equations [1] and [2] are valid, with the former assuming the form $(A/a)^2$ for $m_1 = 3, m_2 = 6$. The theoretical activities according to equations [1] and [2], and the observed values as given in Table II, are compared in Fig. 3 (outer curves only). The indication is that the reaction follows a pure "surface" or "through-solution" mechanism, of which the former is more realistic since the exchange observed with C_3AH_6 probably fell within the definition of "external".

Can. J. Chem. Downloaded from www.nrcresearchpress.com by 186.148.149.217 on 09/04/12
For personal use only.

Can. J. Chem. Downloaded from www.nrcresearchpress.com by 186.148.149.217 on 09/04/12
For personal use only.

PLATE I

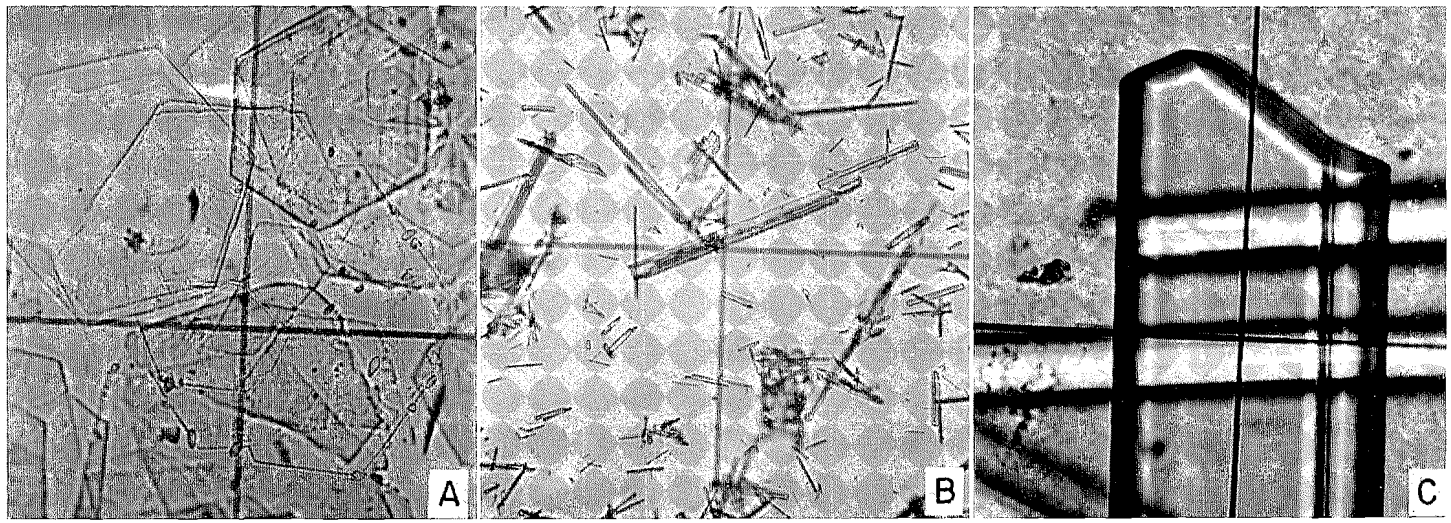


FIG 1. Photomicrographs without nicols, ×360. (A) Plates of $C_3A\Sigma H_{12}$ prepared by mixing *boiling* solutions of $Al_2(SO_4)_3$, $CaSO_4$, and $Ca(OH)_2$. (B) $C_3A\Sigma_3H_{31}$ needles prepared by mixing *unheated* solutions of $Al_2(SO_4)_3$, $CaSO_4$, and $Ca(OH)_2$. (C) Giant crystals of $C_3A\Sigma_3H_{31}$ obtained as before but with the mother liquor allowed to partially evaporate.

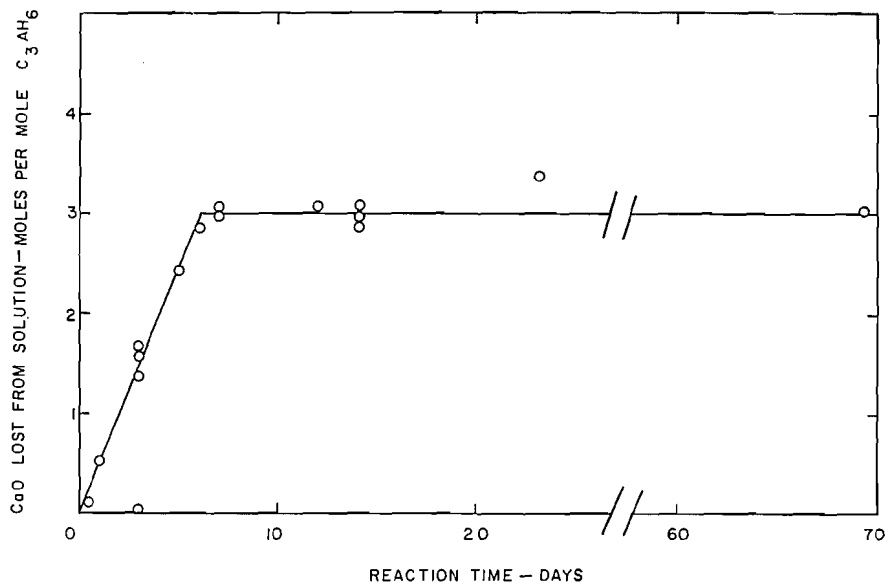


FIG. 2. Rate curve for the conversion of C_3AH_6 to $C_3A\Sigma_3H_{31}$ in mixed $Ca(OH)_2$–$CaSO_4$ solutions.

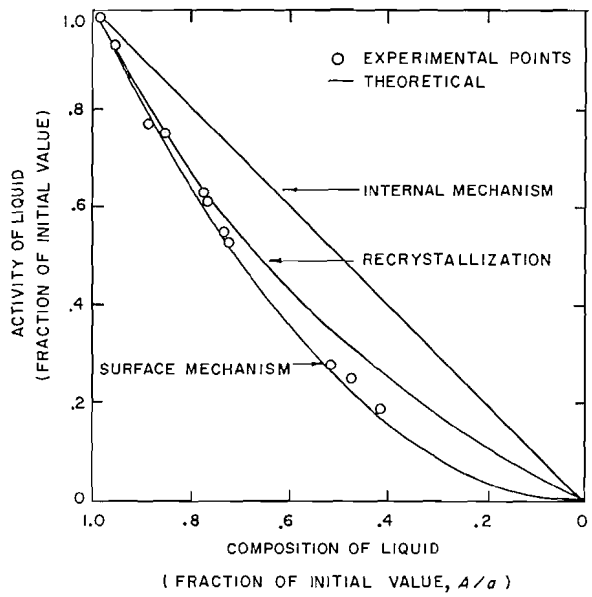


FIG. 3. Conversion of C_3AH_6 to $C_3A\Sigma_3H_{31}$ in mixed $Ca(OH)_2$–$CaSO_4$ solutions labeled with Ca^{45}: comparison of the observed activity of the liquid (in units of fraction of the initial value) with various predictions as functions of the composition of the liquid (again in units of fraction of the initial value, i.e. A/a).

Reaction of $C_3A\Sigma H_{12}$ *with Mixed* $Ca(OH)_2$–$CaSO_4$ *Solutions*

The reaction of $C_3A\Sigma H_{12}$ with mixed $Ca(OH)_2$–$CaSO_4$ solutions is of general interest, since it not only demonstrates the relative stabilities of the two sulphoaluminates in the solutions used, but may be considered representative of the behavior of the entire solid–solution series C_3AH_{12}–$C_3A\Sigma H_{12}$–C_4AH_{12}. The results are given in Table III, from which

Can. J. Chem. Downloaded from www.nrcresearchpress.com by 186.148.149.217 on 09/04/12
For personal use only.

TABLE III

Reaction of inactive $C_3A\Sigma H_{12}$ with mixed $Ca(OH)_2$–$CaSO_4$ solutions labeled with Ca^{45}

Calcium in solid, b (mole$\times10^4$)*	Loss from solution (moles calcium per mole $C_3A\Sigma H_{12}$)†	Duration of experiment (days)	Observed activity (fraction of initial value)	Predicted activities		
				(a) Surface or through-solution	(b) Internal or direct	(c) Recrystallization‡
6.43	2.08	3	.45	.43	.76	.51
6.63	1.97	4	.42	.42	.75	.50
6.68	(Lost)	9	.46	.42	.75	.50
6.88	2.14	15	.42	.40	.74	.49

*Samples of $C_3A\Sigma H_{12}$ having analyses near $C_3A\Sigma H_{10}$ (formula weight = 586.5) were used.
†The original solutions contained, per 50 cc, 13.13×10^{-4} mole calcium (a) and 8.8×10^{-4} mole sulphate.
‡Using the relation, fractional activity = $(a-b/2)/(a+b)$, as obtained from equation [13] of reference 7.

it can be seen that the loss of calcium from solution always corresponds to the complete conversion of the $C_3A\Sigma H_{12}$ to $C_3A\Sigma_3H_{31}$. In agreement with this, the large flat hexagons of $C_3A\Sigma H_{12}$ (Fig. 1A) were always found to be replaced by fine needles (Fig. 1B), even in the 3-day experiment.

Again equations [1] and [2] may be used to correlate the activity and composition of the liquid for the various possible mechanisms. However, since the reaction was complete, it is convenient to replace the variable A with b (the amount of labeled species initially present in the reacting solid). Noting that b is given by $A = a+b-m_2b/m_1$ (cf. equation [4] of reference 7), where $m_1 = 4$ and $m_2 = 6$, the result is

"surface" or "through-solution" mechanism — fractional activity $= (1-b/2a)^3$,

"internal" or "direct" mechanism — fractional activity $= (1-b/2a)$.

The theoretical and observed activities are compared in Table III (columns 4 to 6). A pure "surface" or "through-solution" mechanism is indicated, though a decision between these mechanisms cannot be made from the limited exchange data available.

Reactions at Elevated Temperatures

It will be recalled that the method used for preparing $C_3A\Sigma H_{12}$ involved mixing *boiling* solutions of $Al_2(SO_4)_3$, $CaSO_4$, and $Ca(OH)_2$ (see Experimental). A final group of experiments was therefore undertaken to determine if $C_3A\Sigma H_{12}$ could also be obtained as a product of a solid–liquid reaction. Samples of C_3AH_6 and $C_3A\Sigma H_{12}$ weighing about 0.05 g were added to 50-cc portions of a mixed $Ca(OH)_2$–$CaSO_4$ solution such that each portion contained 13.32×10^{-4} mole calcium and 6.45×10^{-4} mole sulphate, and were shaken inside an oven for periods of up to 7 days. For temperatures of 70° and 90° C the reaction products were consistently acicular, and solution analyses confirmed that $C_3A\Sigma_3H_{31}$ had formed. $C_3A\Sigma H_{12}$ can therefore *not* be obtained as a product of a solid–liquid reaction under the conditions of the experiments.

Though the solutions were labeled, the rapid attainment of radioactive equilibrium made it impossible to distinguish different reaction mechanisms.

DISCUSSION

Stabilities

Little need be said about the observed stability of C_3AH_6 in $Ca(OH)_2$ solutions at 25° C. On the other hand, it is significant that at 25°, 70°, and 90° C the compounds C_3AH_6 and $C_3A\Sigma H_{12}$ consistently reacted with mixed $Ca(OH)_2$–$CaSO_4$ solutions to form

Can. J. Chem. Downloaded from www.nrcresearchpress.com by 186.148.149.217 on 09/04/12
For personal use only.

$C_3A\Sigma_3H_{31}$. $C_3A\Sigma_3H_{31}$ thus appears to be the stabler sulphoaluminate over the entire temperature range 25° to 90° C, so that the ready formation of $C_3A\Sigma H_{12}$ by mixing hot solutions, as described earlier, must have been associated with a greater *crystallizability*, as distinct from *stability*, for this compound at elevated temperatures.

Mechanisms

From the observed relations between the activity and composition of the liquid, the C_3AH_6–$C_3A\Sigma_3H_{31}$ reaction was concluded to proceed with a "surface" mechanism, and the $C_3A\Sigma H_{12}$–$C_3A\Sigma_3H_{31}$ reaction with either a "surface" or "through-solution" mechanism. Now, in making the various calculations to determine mechanisms, the extent of *all* rapid, multidirectional exchange between the liquid and both solids was assumed to be slight; or, what is equivalent, n_1 and n_2 (the portions of m_1 and m_2 undergoing rapid, multidirectional exchange, whether external or internal) were approximated as approaching zero. It is interesting to consider what the activity predictions would have been for the C_3AH_6–$C_3A\Sigma_3H_{31}$ reaction had the actual values of n_1 and n_2 been taken into account. Introducing $n_1 = 0.42$ (Table I) and $n_2 \sim 0.6$ (Table II, footnote †) into equation [1] of reference 7, substituting the latter into equation [3] of reference 7, and assuming the reaction to be complete, one obtains

$$[4] \qquad \text{fractional activity} = \frac{1-b/a}{1+0.42b/3a}\left\{1-\frac{2.82b}{3a+0.42b}\right\}^{0.915}.$$

For the case $a = 4b$ (as in the first experiments of Table II), equation [4] yields 0.572, to be compared with 0.563 from equation [1]. Similarly for $a = 2b$ (as in the last experiments of Table II) one obtains, respectively, 0.276 and 0.250 from the full and abbreviated expressions. The differences in the activity predictions are thus not great, though the predictions using equation [4] lie in such a direction as to bring about a slightly better fit between experiment and theory (cf. Fig. 3).

A more serious difficulty than the presence of various *known* exchange processes in determining solid–liquid reaction mechanisms is the possibility that the freshly formed product solid may have been subject to unexpectedly extensive recrystallization, or else that long-lived (i.e. non-transient) solid intermediates may have occurred. As pointed out in reference 7, these effects tend to make the activity the same for all mechanisms in the later stages of reaction. Thus for the C_3AH_6–$C_3A\Sigma_3H_{31}$ reaction, assuming $n_1 \to 0$, the activity would always be close to (from equation [13] of reference 7)

$$[5] \qquad \text{fractional activity} = \frac{A/a}{2-A/a}.$$

Equation [5] is plotted in Fig. 3, where it is seen that, while the experimental data for high values of A/a are equally consistent with either equations [1] or [5] and therefore quite ambiguous (cf. 8, p. 141–142), the three experiments with low A/a still point to a simple "surface" mechanism. The originally proposed mechanisms also appear to be adequate for the $C_3A\Sigma H_{12}$–$C_3A\Sigma_3H_{31}$ reaction (see Table III, columns 4, 5, and 7).

No substantial objection to assigning "surface" or "through-solution" mechanisms to the reactions studied appears to exist. Four other reactions have also been shown to follow one or the other of these mechanisms:[4] the hydrations of $3CaO.SiO_2$, $2CaO.SiO_2$

[4]*In the original work these reactions are* all *described as following a "through-solution" mechanism. However, as pointed out in reference 7, there is reason to believe that the hydrations of* $CaSO_4.\frac{1}{2}H_2O$ *and dead-burnt* CaO, *in particular, are actually more nearly consistent with a "surface" mechanism.*

Can. J. Chem. Downloaded from www.nrcresearchpress.com by 186.148.149.217 on 09/04/12
For personal use only.

(8), $CaSO_4.\frac{1}{2}H_2O$ (12), and dead-burnt CaO (13). In only one case has a different mechanism been observed: the hydration of soft-burnt (i.e. porous) CaO (13), which proceeds with a mixture of "surface" and "internal" mechanisms (cf. footnote 4). It therefore seems likely that, except with porous substances, a "surface" or "through-solution" mechanism occurs *invariably*. Which of these two mechanisms will prevail in individual cases depends, of course, on the presence or absence of rapid, multidirectional *external* exchange; however, *surface* exchange is probably always multidirectional and external, and is usually also rapid (14), so that the "surface" mechanism may be expected to be generally applicable.

ACKNOWLEDGMENTS

The work described here was carried out under the direction of Dr. T. Thorvaldson of this department. Dr. Thorvaldson's assistance is gratefully acknowledged.

REFERENCES

1. R. H. BOGUE. The chemistry of portland cement. Reinhold Publishing Corp., New York. 1955.
2. G. A. RANKIN and F. E. WRIGHT. Am. J. Sci. **39**, 1 (1915).
3. R. B. PEPPLER and L. S. WELLS. J. Research Natl. Bur. Standards, **52**, 75 (1954).
4. E. T. CARLSON. J. Research Natl. Bur. Standards, **61**, 1 (1958).
5. F. E. JONES. Symposium on the chemistry of cements. Ingeniörsvetenskapsakademien, Stockholm. 1939. p. 231.
6. F. E. JONES. Trans. Faraday Soc. **35**, 1484 (1939).
7. R. KELLY. Can. J. Chem. **38**, 1209 (1960).
8. W. A. G. GRAHAM, J. W. T. SPINKS, and T. THORVALDSON. Can. J. Chem. **32**, 129 (1954).
9. T. THORVALDSON and N. S. GRACE. Can. J. Research, **1**, 36 (1929).
10. W. LERCH, F. W. ASHTON, and R. H. BOGUE. J. Research Natl. Bur. Standards, **2**, 715 (1929).
11. G. L. KALOUSEK. Thesis, University of Maryland. 1941. *Reviewed by* H. H. Steinour *in* Aqueous cementitious systems containing lime and alumina. Portland Cement Assoc., Chicago. 1951.
12. F. W. BIRSS and T. THORVALDSON. Can. J. Chem. **33**, 870 (1955).
13. F. W. BIRSS and T. THORVALDSON. Can. J. Chem. **33**, 881 (1955).
14. J. H. WANG. *In* Radioactivity applied to chemistry. *Edited by* A. C. Wahl and N. A. Bonner. John Wiley & Sons, Inc., New York. 1951.

Can. J. Chem. Downloaded from www.nrcresearchpress.com by 186.148.149.217 on 09/04/12
For personal use only.

Can. J. Chem. Downloaded from www.nrcresearchpress.com by 186.148.149.217 on 09/04/12
For personal use only.

NOTES

A NOTE ON THE CYCLIZATION OF 3-(2′-NAPHTHYL)-BUTYRIC ACID

P. M. G. Bavin

In reporting the ultraviolet spectra of some polyalkylphenanthrenes prepared by Haworth and his co-workers, Askew (1) noted that three of them showed additional peaks at wavelengths longer than those expected for phenanthrene derivatives. The anomalous peaks are collected in Table I for comparison with the longest wavelength

TABLE I

	Anomalous peaks (mμ)		
1,7-Dimethylphenanthrene	381	371	359
2,3-Dimethylphenanthrene	379		358
1,6,7-Trimethylphenanthrene	380		360
Anthracene (5, p. 175)	374.5		354.5

peaks of anthracene. There can be little doubt that the polyalkylphenanthrenes contained at least traces of the corresponding alkylanthracenes since the observed spectral shifts are of the order expected for two or three methyl substituents, if it is assumed that the shifts are additive. This assumption is widely accepted (2) and is supported by published spectra of polyalkylphenanthrenes (1, 3) and polyalkylnaphthalenes (2). (For the spectrum of 9-methylanthracene see ref. 4 and ref. 5 (p. 63) and for the spectrum of 1-methylanthracene see ref. 6. The spectrum of 2-methylanthracene has not been published but the effect of the methyl group has been obtained by difference (2).)

The cyclization of 3-(2′-naphthyl)-butyric acid by hydrogen fluoride has now been examined. The crude neutral product was successively reduced and dehydrogenated to give phenanthrene containing 2% anthracene, as determined spectroscopically.

These results emphasize the difficulty of obtaining pure compounds by routes involving cyclization, and show that, like most substitution reactions of naphthalene, both α and β products are to be expected. Cyclizations occurring predominantly at a β-position may be attributed to steric hindrance (7, 8, and references therein).

1-Aza-anthracene could not be detected among the products of the Skraup reaction on 2-aminonaphthalene, possibly because of the ease with which it is oxidized (9).

EXPERIMENTAL

Pure 3-(2′-naphthyl)-butyric acid (2.7 g), prepared from naphthalene, was dissolved in hydrogen fluoride (150 ml) and the solution left at room temperature for 48 hours. The neutral product was reduced (Clemmenson–Martin) and the crude hydrocarbon dehydrogenated (10% palladium on charcoal at 300°). The crude aromatic hydrocarbons dissolved in hexane were passed through a short (1×1 in.) column of activated alumina to remove traces of tar, elution being continued with benzene–hexane (1:5) to recover all the product. The eluted material was dissolved in ethanol and the ultraviolet spectrum recorded, using a Beckmann DK-2 recording spectrophotometer. Comparison with

standard mixtures* showed the phenanthrene to contain 2% anthracene. For the analysis, anthracene peaks at 376 and 357 mμ (cf. 5, p. 175) and phenanthrene peaks at 339, 330, and 323 mμ (cf. 5, p. 142) were used.

A separate experiment established that phenanthrene was not isomerized on the palladium catalyst.

The products from the Skraup reaction on 2-aminonaphthalene (11) were dissolved in hot heptane and passed through a column of alumina to remove tar, elution being continued with benzene–hexane (1:5) to recover all of the products. The eluted material was fractionally crystallized from ethanol to show that at least 95% was 1-aza-phenanthrene. The residues were chromatographed (hexane–alumina) and the ultraviolet spectra recorded for successive fractions. Those fractions showing peaks at wavelengths longer than 360 mμ were examined further,† by descending chromatography on buffered paper (12) at pH's 3 and 6, using *n*-butanol saturated with water as solvent. Spots located under an ultraviolet lamp were eluted with ethanol and the spectra of the solutions recorded. A trace of an unidentified compound was detected, having characteristic absorption peaks at 396, 386, and 375 mμ. (1-Aza-anthracene has peaks at 384, 366.5, 356.5, and 340 mμ (13) and these values were confirmed by preparing and examining an authentic specimen (14).)

ACKNOWLEDGMENT

This work was carried out at the University of Ottawa during the tenure of a National Research Council Postdoctorate Fellowship (1954–56).

1. F. A. Askew. J. Chem. Soc. 509 (1935).
2. D. Peters. J. Chem. Soc. 646 (1951).
3. E. Mosettig and W. R. Nes. J. Org. Chem. **20**, 897 (1955).
4. R. N. Jones. Chem. Revs. **41**, 366 (1947).
5. E. Clar. Aromatisches Kohlenwasserstoffe. Verlag von Julius Springer, Berlin. 1952.
6. W. L. Mosby. J. Org. Chem. **18**, 965 (1953).
7. H. Bendas and C. Djerassi. J. Am. Chem. Soc. **78**, 2474 (1956).
8. C. Djerassi and G. R. Pettit. J. Org. Chem. **2**, 393 (1957).
9. A. Etiennes. Compt. rend. **218**, 841 (1944).
10. P. M. G. Bavin and M. J. S. Dewar. J. Chem. Soc. 164 (1956).
11. W. J. Clem and C. S. Hamilton. J. Am. Chem. Soc. **62**, 2349 (1940).
12. H. Brindle, J. E. Carless, and H. B. Woodhead. J. Pharm. and Pharmacol. **3**, 793 (1951).
13. A. Etienne and M. Legrand. Bull. soc. chim. France, 108 (1953).
14. A. Etienne. Ann. chim. (Paris), **1**, 5 (1946).

Received February 25, 1960.
Chemistry Department,
The University,
Hull, East Yorkshire, England.

Pure and puriss grades of phenanthrene from several sources contained 1–2% anthracene, removed by reaction with maleic anhydride (10).

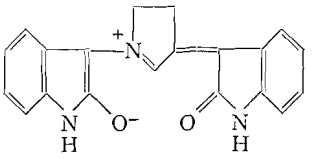
†*The author is indebted to Dr. C. R. Eves, R.C.M.P., for these experiments.*

Can. J. Chem. Downloaded from www.nrcresearchpress.com by 186.148.149.217 on 09/04/12
For personal use only.

A COLOR TEST FOR CERTAIN PIPERIDINE AND PYRROLIDINE ALKALOIDS*

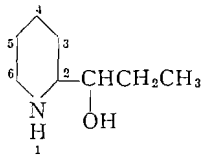
D. J. McCaldin†

The blue color formed from isatin and proline has frequently been used as a method for detecting this imino acid after paper chromatography (1). On the basis of recent work (2) the structure of this pigment has been revised (I), and it is now possible to extend the use of the reaction for the detection of similar compounds in alkaloidal extracts.

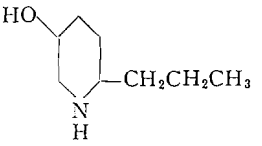


I

The test described is specific for alkaloids with a single six- (or five-) membered ring containing the sequence —NH—CH_2—CH_2—. Thus conhydrine (II) gives a positive reaction whereas ψ-conhydrine (III) does not, owing to the presence of substituents in both the 2 and the 5 positions.

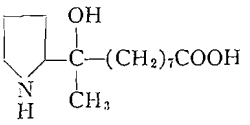


II

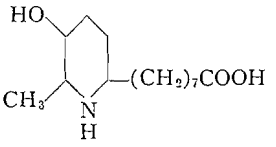


III

Previous workers (3) suggested that the sequence required for pigment formation was —CH_2—NH—CH_2—, and the earlier structure proposed for carpamic acid (IV) was based on its negative reaction with isatin (4). In fact, a compound with this structure would be expected to react, whereas the revised structure (V) would not (5).



IV



V

Certain α-imino acids, such as 4-hydroxyproline, do not appear to contain the arrangement of atoms necessary for color development. However, the carboxyl group is lost in each case during the reaction and the conditions for pigment formation are thus fulfilled. The negative results obtained from hygrine, stachydrine, hygric acid, and N-methylpipecolic acid can be explained by the absence of the —NH— group. Azetidine 2-carboxylic acid (6) and hexamethyleneimine did not react normally, showing that ring

Issued as N.R.C. No. 5688.

†*National Research Council Postdoctorate Fellow.*

Can. J. Chem. Downloaded from www.nrcresearchpress.com by 186.148.149.217 on 09/04/12
For personal use only.

size is a critical factor. An imino acid extracted from apples (11) also yields a positive result in this test, and is tentatively regarded as 4-hydroxymethylproline.

This method of detecting certain alkaloids after paper chromatography can be used in conjunction with other techniques. The individual components of a mixture of such compounds may be detected in the following manner. The chromatogram is sprayed

TABLE I

Color obtained with isatin reagent

Alkaloid	Color	Alkaloid	Color
Azetidine 2-carboxylic acid	—	4-Hydroxypipecolic acid (9)	Brown
Proline	Blue	5-Hydroxypipecolic acid (10)	Blue
4-Hydroxyproline	Blue	Piperazine	Blue
3-Methylproline	Blue	Conhydrine	Blue-green
4-Methylproline (7)	Blue	ψ-Conhydrine	—
norHygrine (8)	Blue	Coniine	Blue
Stachydrine	—	isoPelletierine (8)	Blue
3-Hydroxypipecolic acid (9)	Blue	Anabasine	—
		Hexamethyleneimine	—

with isatin, baked, and subsequently treated with Dragendorff's reagent (12). Hygric acid and N-methylpipecolic acid are shown to be present when the paper is first treated with potassium permanganate (to remove the N-methyl group). Other N-methylated compounds, such as methyl hygrate, are not converted to the corresponding secondary imines.

EXPERIMENTAL

General Method

A descending one-dimensional paper chromatographic technique was used to separate and detect a typical mixture of proline and coniine. The mixture and reference compounds were placed on a paper strip (Whatman No. 1) and developed with the upper phase of a butan-1-ol – acetic acid – water (4:1:5 by volume) mixture as solvent. The detecting agent was a 0.1% (w/v) solution of isatin in aqueous acetic acid (5%). Since coniine is rather volatile, the developed chromatogram was only partially dried (15 minutes at room temperature) before it was sprayed with the isatin solution. The colors developed after baking in the oven at 130° for 5 minutes; the proline spot had $R_F = 0.39$, and the coniine spot $R_F = 0.81$ at 25°.

Detection of Hygric Acid or N-*Methylpipecolic Acid*

Two paper strips were prepared and developed as described above. The chromatograms were dried and a cold, saturated solution of potassium permanganate in a mixture of acetone and pyridine (95:5) was sprayed onto one paper. The positions of the chromatographed materials were apparent from the appearance of yellow spots on the purple background. The corresponding areas on the second chromatogram were then sprayed with the oxidant and the paper dried at room temperature. It was then treated in the normal manner as previously described.

ACKNOWLEDGMENTS

The author wishes to thank Dr. R. K. Hill of Princeton University for the gift of a sample of conhydrine and Dr. L. Marion for samples of ψ-conhydrine and anabasine.

Can. J. Chem. Downloaded from www.nrcresearchpress.com by 186.148.149.217 on 09/04/12
For personal use only.

1. R. ACHER, C. FROMAGEOT, and M. JUTISZ. Biochim. et Biophys. Acta, **5**, 81 (1950).
2. A. W. JOHNSON and D. J. MCCALDIN. J. Chem. Soc. 3470 (1957).
3. W. GRASSMANN and K. VON ARNIM. Ann. **519**, 192 (1935).
4. G. BARGER, R. ROBINSON, and T. S. WORK. J. Chem. Soc. 711 (1937).
5. H. RAPOPORT, H. BALDRIDGE, and E. J. VOLCHECK. J. Am. Chem. Soc. **75**, 5290 (1953).
6. L. FOWDEN. Biochem. J. **64**, 323 (1956).
7. A. C. HULME and W. ARTHINGTON. Nature, **173**, 588 (1954).
8. A. J. CLARKE and P. J. MANN. Biochem. J. **71**, 596 (1959).
9. L. FOWDEN. Private communication.
10. A. VIRTANEN and S. KARI. Acta Chem. Scand. **8**, 1290 (1954).
11. G. URBACH. Nature, **175**, 170 (1955).
12. R. MUNIER and M. MACHEBOEUF. Bull. soc. chim. biol. **33**, 846 (1951).

RECEIVED JANUARY 15, 1960.
DIVISION OF PURE CHEMISTRY,
NATIONAL RESEARCH COUNCIL,
OTTAWA, CANADA.

SOME NEW BENZILIC ACID DERIVATIVES

FRANCIS L. CHUBB, GERASSIMOS FRANGATOS, AND JACQUELINE NISSENBAUM

Morrison, Konigstein, and Cohen (1) have synthesized a series of esters of benzilic acid (I) related in structure to benadryl and trasentin. Klosa (2) has also reported that 2-dimethylaminoethyl esters of alkoxydiphenylacetic acid (II) possess strong analgesic and sedative action. In this communication we wish to describe the synthesis of some new benzilic acid derivatives similar in structure to both I and II. These compounds (III–VI) are listed in Table I. The intermediates required for their preparation are listed in Table II.

TABLE I

$$(C_6H_5)_2\overset{\displaystyle O-CH_2CH_2R}{\overset{|}{C}}-COOCH_2CH_2R_1$$

Compound	R	R_1	Yield, %	M.p. or b.p.	Formula	Analysis* Calculated C	H	N	Found C	H	N
III	Cl	$-N(CH_3)_2$.HCl	51	145–148°	$C_{20}H_{25}NO_3Cl_2$	60.32	6.33	3.52	61.3	6.61	3.72
IV	H	$-N$(pyrrolidine).HCl	64	166–168°	$C_{22}H_{28}NO_3Cl$	67.76	7.21	3.59	67.72	7.24	3.59
V	H	N(morpholine).HCl	80	172–174°	$C_{22}H_{28}NO_4Cl$	65.08	6.95	3.45	64.82	7.06	3.45
VI	$-N$(pyrrolidine)	$N(C_2H_5)_2$	74	195–197/1 mm	$C_{26}H_{36}N_2O_3$	73.55	8.55	6.60	73.11	8.44	6.75

*Calc.: for III Cl, 17.80. Found: Cl, 17.92.

When an attempt was made to prepare dimethylaminoethyl diphenyl(2-hydroxyethoxy) acetate hydrochloride (VII) by the reaction of ethylene glycol with dimethylaminoethyl chlorodiphenylacetate hydrochloride, ring closure to form the cyclic lactone VIII occurred. Alkaline hydrolysis converted VIII to the corresponding acid IX.

Can. J. Chem. Downloaded from www.nrcresearchpress.com by 186.148.149.217 on 09/04/12
For personal use only.

1. R. ACHER, C. FROMAGEOT, and M. JUTISZ. Biochim. et Biophys. Acta, **5**, 81 (1950).
2. A. W. JOHNSON and D. J. MCCALDIN. J. Chem. Soc. 3470 (1957).
3. W. GRASSMANN and K. VON ARNIM. Ann. **519**, 192 (1935).
4. G. BARGER, R. ROBINSON, and T. S. WORK. J. Chem. Soc. 711 (1937).
5. H. RAPOPORT, H. BALDRIDGE, and E. J. VOLCHECK. J. Am. Chem. Soc. **75**, 5290 (1953).
6. L. FOWDEN. Biochem. J. **64**, 323 (1956).
7. A. C. HULME and W. ARTHINGTON. Nature, **173**, 588 (1954).
8. A. J. CLARKE and P. J. MANN. Biochem. J. **71**, 596 (1959).
9. L. FOWDEN. Private communication.
10. A. VIRTANEN and S. KARI. Acta Chem. Scand. **8**, 1290 (1954).
11. G. URBACH. Nature, **175**, 170 (1955).
12. R. MUNIER and M. MACHEBOEUF. Bull. soc. chim. biol. **33**, 846 (1951).

RECEIVED JANUARY 15, 1960.
DIVISION OF PURE CHEMISTRY,
NATIONAL RESEARCH COUNCIL,
OTTAWA, CANADA.

SOME NEW BENZILIC ACID DERIVATIVES

FRANCIS L. CHUBB, GERASSIMOS FRANGATOS, AND JACQUELINE NISSENBAUM

Morrison, Konigstein, and Cohen (1) have synthesized a series of esters of benzilic acid (I) related in structure to benadryl and trasentin. Klosa (2) has also reported that 2-dimethylaminoethyl esters of alkoxydiphenylacetic acid (II) possess strong analgesic and sedative action. In this communication we wish to describe the synthesis of some new benzilic acid derivatives similar in structure to both I and II. These compounds (III–VI) are listed in Table I. The intermediates required for their preparation are listed in Table II.

TABLE I

$$(C_6H_5)_2\overset{\displaystyle O-CH_2CH_2R}{\overset{|}{C}}-COOCH_2CH_2R_1$$

Compound	R	R_1	Yield, %	M.p. or b.p.	Formula	Analysis* Calculated C	H	N	Found C	H	N
III	Cl	$-N(CH_3)_2$.HCl	51	145–148°	$C_{20}H_{25}NO_3Cl_2$	60.32	6.33	3.52	61.3	6.61	3.72
IV	H	$-N$(pyrrolidine).HCl	64	166–168°	$C_{22}H_{28}NO_3Cl$	67.76	7.21	3.59	67.72	7.24	3.59
V	H	N(morpholine).HCl	80	172–174°	$C_{22}H_{28}NO_4Cl$	65.08	6.95	3.45	64.82	7.06	3.45
VI	$-N$(pyrrolidine)	$N(C_2H_5)_2$	74	195–197/1 mm	$C_{26}H_{36}N_2O_3$	73.55	8.55	6.60	73.11	8.44	6.75

*Calc.: for III Cl, 17.80. Found: Cl, 17.92.

When an attempt was made to prepare dimethylaminoethyl diphenyl(2-hydroxyethoxy) acetate hydrochloride (VII) by the reaction of ethylene glycol with dimethylaminoethyl chlorodiphenylacetate hydrochloride, ring closure to form the cyclic lactone VIII occurred. Alkaline hydrolysis converted VIII to the corresponding acid IX.

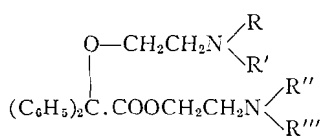
Can. J. Chem. Downloaded from www.nrcresearchpress.com by 186.148.149.217 on 09/04/12
For personal use only.

TABLE II

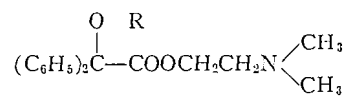
Intermediates $(C_6H_5)_2C(R)—COOR'$

R	R'	M.p. or b.p.	Yield, %	Formula	Analysis: Calculated C	Calculated H	Calculated N	Found C	Found H	Found N
OH	$CH_2CH_2N(CH_3)_2$ HCl	150–160°[a]	57							
OH	CH_2CH_2N(pyrrolidine) .HCl	174–175°[b]	78							
OH	CH_2CH_2N(morpholine) .HCl	178–180°[c]	61							
Cl	$CH_2CH_2N(CH_3)_2$ .HCl	184–186°[d]	83							
Cl	CH_2CH_2N(pyrrolidine) .HCl	165–167°	88	$C_{20}H_{23}NO_2Cl_2$	63.17	6.10	3.68	63.13	6.12	3.75
Cl	CH_2CH_2N(morpholine) .HCl	139–140°[e]	81							
OCH_2CH_2N(pyrrolidine)	C_2H_5	195–197°/1 mm	58	$C_{22}H_{25}NO_3$	74.54	7.96	3.95	74.74	7.72	4.34
OCH_2CH_2N(pyrrolidine)	Na	291–292°	81	$C_{20}H_{23}NO_3Na$	68.95	6.65	4.02	69.24	6.51	4.13

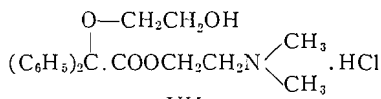
[a]Lit. value 184–186° (5). [b]Lit. value 173–173.5° (6). [c]Lit. value 181.5–182.5° (6). [d]Lit. value 183–185° (4). [e]Lit. value 151.5–152° (7).



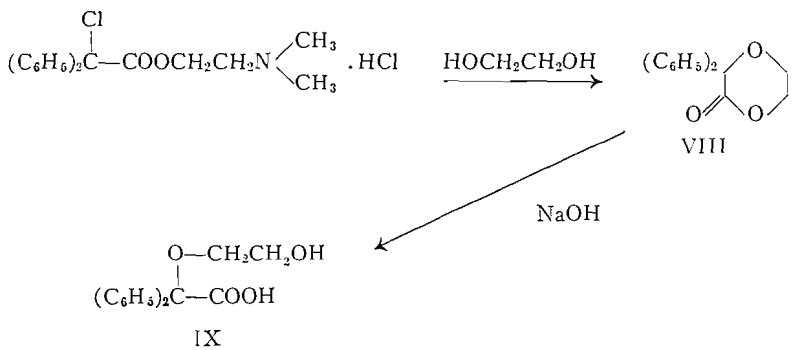
I



II



VII



VIII

IX

Can. J. Chem. Downloaded from www.nrcresearchpress.com by 186.148.149.217 on 09/04/12
For personal use only.

Can. J. Chem. Downloaded from www.nrcresearchpress.com by 186.148.149.217 on 09/04/12
For personal use only.

EXPERIMENTAL

Dialkylaminoethyl Benzilate Hydrochlorides (Table II)

These compounds were prepared from benzilic acid and the required 2-chloroethyldialkylamine according to the general method of Horenstein and Pahlicke (3).

Dialkylaminoethyl Alkoxydiphenylacetate Hydrochlorides (Table I)

Compounds III, IV, and V were prepared from the dialkylaminoethyl benzilate hydrochlorides by way of the corresponding chlorodiphenylacetate hydrochlorides as described by Klosa (4). Details of the preparation of dimethylaminoethyl 2-chloroethoxydiphenylacetate (III) are given below, since Klosa's procedure was modified in this case.

A mixture of 15 g of dimethylaminoethyl chlorodiphenylacetate hydrochloride, 3 g of calcium carbonate, and 76 ml of freshly distilled 2-chloroethanol was refluxed for 24 hours with mechanical stirring. The hot reaction mixture was filtered and then allowed to cool. The solvent was distilled under reduced pressure and the residue extracted with acetone and filtered. After distillation of the acetone the residue was treated with 200 ml of 10% sodium hydroxide and extracted with ether. The dried ether layer (calcium chloride) was then saturated with hydrogen chloride at 3 to 4°. The hydrochloride precipitated as a crystalline product, 8.5 g (51%), m.p. 145–151°.

The material was purified by dissolving it in isoamyl alcohol and slowly pouring the resulting solution into anhydrous ether containing some seed crystals, m.p. 145–148°. The mixture was not stirred but kept overnight at 5°. Filtration yielded crystals melting at 145–148°.

Diethylaminoethyl 2-(1-Pyrrolidyl)ethoxydiphenylacetate (VI)

This compound was prepared from ethyl benzilate according to the method of Morrison, Konigstein, and Cohen (1).

2,2-Diphenyl-3-keto-1,4-dioxane (VIII)

A mixture of 20 g of dimethylaminoethyl chlorodiphenylacetate hydrochloride, 4.5 g of calcium carbonate, and 100 ml of ethylene glycol was heated for 24 hours at 90–100°. After the solution was filtered it was made basic with sodium hydroxide. The resulting solid was filtered and washed with dilute hydrochloric acid. After recrystallization from alcohol–water a yield of 8.5 g (59%), m.p. 95–97°, was obtained. A second recrystallization raised the melting point to 98–99°. Anal. Calc. for $C_{16}H_{14}O_3$: C, 75.59; H, 5.51. Found: C, 75.11; H, 5.62.

Diphenyl(2-hydroxyethoxy)acetic Acid (IX)

2,2-Diphenyl-3-keto-1,4-dioxane (1 g) was refluxed with 10 ml 10% sodium hydroxide for 2 hours. After dilution and acidification of the solution, the product, m.p. 122–123°, after recrystallization from alcohol–water, was obtained. Anal. Calc. for $C_{16}H_{16}O_4$: C, 70.6; H, 5.88. Found: C, 70.64; H, 6.06. Neut. eq. Calc.: 272. Found: 272.

1. A. L. Morrison, M. Konigstein, and A. Cohen. J. Chem. Soc. 2887 (1950).
2. J. Klosa. Arch. Pharm. **287**, 321 (1954).
3. H. Horenstein and H. Pahlicke. Ber. **71**, 1644 (1938).
4. J. Klosa. Arch. Pharm. **288**, 42 (1955).
5. J. Klosa. Deut. med. Wochschr. **75**, 870 (1950).
6. R. B. Moffett, J. L. White, B. D. Aspergren, and F. E. Visscher. J. Am. Chem. Soc. **77**, 1565 (1955).
7. L. C. Cheney and W. G. Bywater. J. Am. Chem. Soc. **64**, 970 (1942).

Received March 23, 1960.
Research Laboratories,
Frank W. Horner, Ltd.,
Montreal, Que.

EFFECT OF NITRIC OXIDE IN THE γ-RADIOLYSIS OF ETHANE AT VERY LOW CONVERSIONS

KANG YANG

Back and Miller (1) investigated the radiolysis of gaseous saturated hydrocarbons at very low conversions. They found an important fact: The $G(H_2)$ values corresponding to initial rates are approximately twice the values estimated at the higher conversions.

We investigated the formation of hydrogen in ethane and ethane – nitric oxide systems. Our results very closely agree with the results of Back and Miller and also with inhibition data of Back (2) using ethylene as a radical scavenger.

In this note we summarize our results. This probably strengthens the contribution of Back and Miller. In addition a new conclusion is drawn: nitric oxide scavenges hydrogen atoms with negligible effect on the nonradical processes leading to the molecular hydrogen in the ethane radiolysis.

EXPERIMENTAL

Phillips' research grade ethane is carefully degassed by repeated evacuations at liquid nitrogen temperature and then subjected to four-stage bulb-to-bulb distillation each time retaining only the middle third. Purified ethane is introduced in Pyrex vessels (156 cc). The gamma source was four spent fuel elements from the Engineering Test Reactor, Arco, Idaho. Energy input rate was 7.9×10^{-4} electron volts per hour per molecule of ethane. This was estimated assuming that $G(H_2)$ in methane radiolysis is 5.7 molecules per 100 electron volts (3).

Hydrogen in irradiated samples was analyzed by gas adsorption chromatography (silica gel column, argon carrier, room temperature).

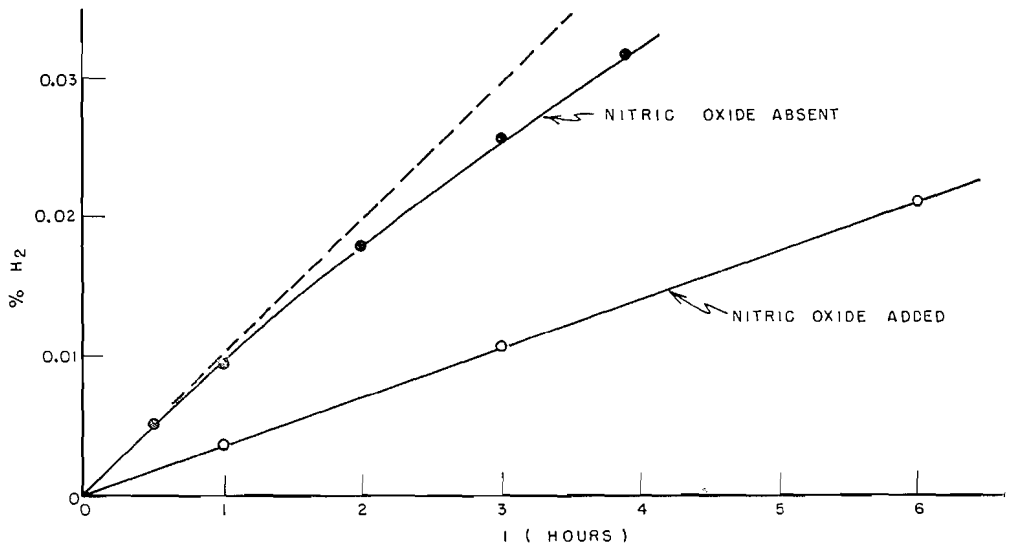


FIG. 1. Formation of hydrogen in ethane radiolysis in the presence and absence of nitric oxide.

Can. J. Chem. Downloaded from www.nrcresearchpress.com by 186.148.149.217 on 09/04/12
For personal use only.

Can. J. Chem. Downloaded from www.nrcresearchpress.com by 186.148.149.217 on 09/04/12
For personal use only.

RESULTS AND DISCUSSION

In Fig. 1 the rate of formation of hydrogen is shown as a function of irradiation time. In the absence of nitric oxide, the rate decreases with increasing conversion. Initial rate estimated from Fig. 1 is 1.93 times the rate at 0.68% conversion of ethane.

In the presence of nitric oxide, the rate is constant. Estimated percentage of radical contribution to the hydrogen formation at the initial period of the reaction was 64% (4).* The value is in close agreement with Back's result of 63% obtained using ethylene as a scavenger (2).

We have seen that both ethylene and nitric oxide give the same yield for the molecular hydrogen. This can best be explained by assuming that high enough concentrations of nitric oxide and ethylene to scavenge most of the hydrogen atoms had no measurable effect on the nonradical processes yielding molecular hydrogen, an important condition that a satisfactory radical scavenger in the radiolysis reactions should satisfy.

From Fig. 1 it is also clear that only $G(H_2)$ due to radical reactions decreases with increasing conversion. This supports Back's explanation that decrease in $G(H_2)$ at high conversion is due to the formation of unsaturated radiolysis products.

1. R. A. Back and N. Miller. Trans. Faraday Soc. **55**, 911 (1959).
2. R. A. Back. J. Phys. Chem. **64**, 124 (1960).
3. F. W. Lampe. J. Am. Chem. Soc. 1055 (1957).
4. K. Yang and P. J. Manno. J. Am. Chem. Soc. **81**, 3507 (1959); L. M. Dorfman. J. Phys. Chem. **62**, 29 (1958).

Received April 6, 1960.
Radiation Laboratory,
Continental Oil Company,
Ponca City, Oklahoma.

This is much higher than the values estimated at the higher conversion.

A MECHANISM FOR THE INDUCTIVE EFFECT

Henry A. Bent

To the author's knowledge, no detailed mechanism has yet been given to explain the *modus operandi* of the inductive effect. It is the purpose of this note to propose a mechanism for the inductive effect and to show that this effect must be coupled in a predictable manner to certain differential changes in molecular geometry. The language chosen for the present discussion is the familiar language of valence-bond theory and hybrid atomic orbitals; although it may be noted that well-known, but for present purposes less convenient, alternatives do exist (1–5).

Discussion of the experimental evidence that has been marshalled in support of the present argument may be separated into two related parts: (1) the effect of electronegative groups on atom hybridization and (2) the effect of atom hybridization on electronegativity.

(1) The Effect of Electronegative Groups on Atom Hybridization

The XOY bond angles in CH_3OCH_3, CH_3OH, HOH, and FOF are, respectively, 111° (6), 109° (7), 105° (8), and 101° 30′ (5). In CH_3SH and HSH the bond angles are, respectively, 100° (9) and 92° (5). The same consistent decreases in interbond angle

Can. J. Chem. Downloaded from www.nrcresearchpress.com by 186.148.149.217 on 09/04/12
For personal use only.

RESULTS AND DISCUSSION

In Fig. 1 the rate of formation of hydrogen is shown as a function of irradiation time. In the absence of nitric oxide, the rate decreases with increasing conversion. Initial rate estimated from Fig. 1 is 1.93 times the rate at 0.68% conversion of ethane.

In the presence of nitric oxide, the rate is constant. Estimated percentage of radical contribution to the hydrogen formation at the initial period of the reaction was 64% (4).* The value is in close agreement with Back's result of 63% obtained using ethylene as a scavenger (2).

We have seen that both ethylene and nitric oxide give the same yield for the molecular hydrogen. This can best be explained by assuming that high enough concentrations of nitric oxide and ethylene to scavenge most of the hydrogen atoms had no measurable effect on the nonradical processes yielding molecular hydrogen, an important condition that a satisfactory radical scavenger in the radiolysis reactions should satisfy.

From Fig. 1 it is also clear that only $G(H_2)$ due to radical reactions decreases with increasing conversion. This supports Back's explanation that decrease in $G(H_2)$ at high conversion is due to the formation of unsaturated radiolysis products.

1. R. A. Back and N. Miller. Trans. Faraday Soc. **55**, 911 (1959).
2. R. A. Back. J. Phys. Chem. **64**, 124 (1960).
3. F. W. Lampe. J. Am. Chem. Soc. 1055 (1957).
4. K. Yang and P. J. Manno. J. Am. Chem. Soc. **81**, 3507 (1959); L. M. Dorfman. J. Phys. Chem. **62**, 29 (1958).

Received April 6, 1960.
Radiation Laboratory,
Continental Oil Company,
Ponca City, Oklahoma.

This is much higher than the values estimated at the higher conversion.

A MECHANISM FOR THE INDUCTIVE EFFECT

Henry A. Bent

To the author's knowledge, no detailed mechanism has yet been given to explain the *modus operandi* of the inductive effect. It is the purpose of this note to propose a mechanism for the inductive effect and to show that this effect must be coupled in a predictable manner to certain differential changes in molecular geometry. The language chosen for the present discussion is the familiar language of valence-bond theory and hybrid atomic orbitals; although it may be noted that well-known, but for present purposes less convenient, alternatives do exist (1–5).

Discussion of the experimental evidence that has been marshalled in support of the present argument may be separated into two related parts: (1) the effect of electronegative groups on atom hybridization and (2) the effect of atom hybridization on electronegativity.

(1) The Effect of Electronegative Groups on Atom Hybridization

The XOY bond angles in CH_3OCH_3, CH_3OH, HOH, and FOF are, respectively, 111° (6), 109° (7), 105° (8), and 101° 30′ (5). In CH_3SH and HSH the bond angles are, respectively, 100° (9) and 92° (5). The same consistent decreases in interbond angle

with increasing electronegativity of the substituent group occurs in phosphorus and arsenic compounds (10) and in the series $N(CH_3)_3$, NH_3, and NF_3, where the XNX interbond angles are, respectively, 109° (10), 106° 46′ (10), and 102° 30′ (5). Additional examples are cited by Mellish and Linnett (5). As noted by these authors, it is an interesting fact that changes in interbond angles are often in the reverse direction from what one would expect if repulsions between nonbonded atoms were the most important effect operating. In every case, it would appear that replacement of an atom or group of atoms by a group of greater electronegativity causes the atom on which substitution occurred to rehybridize in such a manner that some of its *s*-character is withdrawn from the orbital where substitution occurred. Further evidence of this may be obtained from a study of interatomic distances.

Currently there is increasing recognition of the suggestion that atom hybridization has an appreciable effect not only on bond angles, as is well known, but on bond lengths as well. Data bearing on this issue has been summarized recently by Brown (11). If the view that atom hybridization may have a pronounced effect on bond lengths is adopted, the conclusion is quickly reached that bond lengths decrease noticeably as the *s*-character in the bond increases. Typically, the carbon–carbon single-bond distance appears to decrease by about 0.04 Å each time one of the participating carbon atoms changes hybridization from sp^3 to sp^2 or from sp^2 to sp. For carbon–halogen bonds, the effect appears to be even more pronounced. While it is not our purpose here to offer a detailed explanation of these effects in terms of an hybridization-ratio-dependent covalent radius, we may note that preliminary considerations do suggest that such an explanation may be possible. Adoption of this hypothesis conjointly with the data on bond angles cited above leads to the supposition that bond lengths should vary with the electronegativity of adjacent substituents. Indeed, the noticeable foreshortening of bond lengths that occurs when fluorine atoms are introduced into molecules has been commented upon (12). For example, the C–F distance is 1.391 Å in CH_3F, whereas it is only 1.323 Å in CF_4. Numerous other examples exist in the current literature that illustrate the foreshortening that occurs in bond lengths when an atom of relatively low electronegativity, such as hydrogen, is replaced by an atom of greater electronegativity, such as fluorine, or one of the other halogens. It is interesting to note that the change in molecular parameters is again often in the reverse direction from what one would expect if repulsions between nonbonded atoms were the important effect operating.

If unshared pairs are regarded as electrons in a bond to an atom of zero electronegativity, the evidence cited above concerning the effect of electronegative groups on molecular geometry may be summarized in the statement: *The s-character of an atom tends to concentrate in orbitals that are directed toward electropositive groups.*

(2) The Effect of Atom Hybridization on Electronegativity

Inductive constants for a carbon atom in an sp^3 valency, sp^2 valency, and an sp valency have been given by Taft (13). He finds $H_3C- = -0.100$, $CH_3\overset{\overset{O}{\|}}{C}- = +0.60$, and $NC- = +1.300$. On this scale the inductive constant for chlorine is +1.10. More recently, Petro has calculated from dipole moment data and infrared dispersion data these carbon–carbon bond moments: $(sp^3)^+-(sp^2)^- = 0.68D$, $(sp^2)^+-(sp)^- = 1.15D$, and $(sp^3)^+-(sp)^- = 1.48D$ (14). He finds, also, that chlorine constitutes the positive end

Can. J. Chem. Downloaded from www.nrcresearchpress.com by 186.148.149.217 on 09/04/12
For personal use only.

of the C—Cl bond moment in HC≡CCl. These results provide strong confirmation of the statement by Mulliken (15) and Walsh (16) that *the more s-character in an atomic valency, the more electronegative is the atom in that valency.*

Combining these two attributes of the *s*-character of an atom, one obtains the following picture of the inductive effect. Consider the array A—X—B, and suppose that the electronegativity of the group at B increases. This change will cause X to rehybridize slightly, so as to shift some of its *s*-character from the bond B to the bond to A, where the low potential energy space characteristic of an *s*-orbital will be used to greater advantage. In effect, the electronegativity of X toward A becomes greater. In turn, by an identical, but smaller, operation of the same mechanism, the electronegativity of A toward attached groups (other than X) becomes greater.

1. J. E. Lennard-Jones. Proc. Roy. Soc. **198**, 1, 14 (1949); J. A. Pople. Quart. Rev. **11**, 273 (1957).
2. J. W. Linnett and A. J. Poe. Trans. Faraday Soc. **47**, 1033 (1951).
3. J. W. Linnett. J. Chem. Soc. 275 (1956).
4. P. G. Dickens and J. W. Linnett. Quart. Rev. **11**, 291 (1957).
5. C. E. Mellish and J. W. Linnett. Trans. Faraday Soc. **50**, 657 (1954).
6. R. S. Mulliken. J. Am. Chem. Soc. **77**, 887 (1955).
7. P. Venkakswarlu and W. Gordy. J. Chem. Phys. **23**, 1200 (1955).
8. G. H. Herzberg. Infrared and Raman spectra of polyatomic molecules. D. van Nostrand & Co., New York. 1945. p. 489.
9. N. Solimene and B. P. Dailey. J. Chem. Phys. **23**, 124 (1955).
10. R. E. Weston, Jr. J. Am. Chem. Soc. **76**, 2645 (1954).
11. M. G. Brown. Trans. Faraday Soc. **55**, 694 (1959); C. C. Costain and B. P. Stoicheff. J. Chem. Phys. **30**, 777 (1959).
12. L. S. Bartell and L. O. Brockway. J. Chem. Phys. **23**, 1860 (1955).
13. R. W. Taft, Jr. *In* Steric effects in organic chemistry. *Edited by* M. S. Newman. John Wiley & Sons, Inc., New York. 1956. Chap. 13.
14. A. J. Petro. J. Am. Chem. Soc. **80**, 4230 (1958).
15. R. S. Mulliken. J. Phys. Chem. **41**, 318 (1937).
16. A. D. Walsh. Disc. Faraday Soc. **2**, 18 (1947).

Received March 21, 1960.
School of Chemistry,
Institute of Technology,
University of Minnesota,
Minneapolis, Minnesota.

THIAZOLES. IV. PROTON MAGNETIC RESONANCE SPECTRA OF THIAZOLE AND ITS METHYL DERIVATIVES*,†

A. Taurins and W. G. Schneider

The proton resonance spectra of five-membered cyclic unsaturated compounds are of considerable interest not only from the standpoint of structure determination in complex organic molecules, but also in connection with the rather unusual proton spin-coupling interactions in these systems (1, 2, 3). In this connection the high-resolution proton resonance measurements of thiazole, which contains two heteroatoms in the five-membered ring, are of some interest. Figure 1 shows a reproduction of the proton

*Issued as N.R.C. No. 5699.
†Thiazoles. III. A. Taurins, J. G. E. Fenyes, and R. N. Jones. Can. J. Chem. **35**, 423 (1957).

Can. J. Chem. Downloaded from www.nrcresearchpress.com by 186.148.149.217 on 09/04/12
For personal use only.

of the C—Cl bond moment in HC≡CCl. These results provide strong confirmation of the statement by Mulliken (15) and Walsh (16) that *the more s-character in an atomic valency, the more electronegative is the atom in that valency.*

Combining these two attributes of the *s*-character of an atom, one obtains the following picture of the inductive effect. Consider the array A—X—B, and suppose that the electronegativity of the group at B increases. This change will cause X to rehybridize slightly, so as to shift some of its *s*-character from the bond B to the bond to A, where the low potential energy space characteristic of an *s*-orbital will be used to greater advantage. In effect, the electronegativity of X toward A becomes greater. In turn, by an identical, but smaller, operation of the same mechanism, the electronegativity of A toward attached groups (other than X) becomes greater.

1. J. E. Lennard-Jones. Proc. Roy. Soc. **198**, 1, 14 (1949); J. A. Pople. Quart. Rev. **11**, 273 (1957).
2. J. W. Linnett and A. J. Poe. Trans. Faraday Soc. **47**, 1033 (1951).
3. J. W. Linnett. J. Chem. Soc. 275 (1956).
4. P. G. Dickens and J. W. Linnett. Quart. Rev. **11**, 291 (1957).
5. C. E. Mellish and J. W. Linnett. Trans. Faraday Soc. **50**, 657 (1954).
6. R. S. Mulliken. J. Am. Chem. Soc. **77**, 887 (1955).
7. P. Venkakswarlu and W. Gordy. J. Chem. Phys. **23**, 1200 (1955).
8. G. H. Herzberg. Infrared and Raman spectra of polyatomic molecules. D. van Nostrand & Co., New York. 1945. p. 489.
9. N. Solimene and B. P. Dailey. J. Chem. Phys. **23**, 124 (1955).
10. R. E. Weston, Jr. J. Am. Chem. Soc. **76**, 2645 (1954).
11. M. G. Brown. Trans. Faraday Soc. **55**, 694 (1959); C. C. Costain and B. P. Stoicheff. J. Chem. Phys. **30**, 777 (1959).
12. L. S. Bartell and L. O. Brockway. J. Chem. Phys. **23**, 1860 (1955).
13. R. W. Taft, Jr. *In* Steric effects in organic chemistry. *Edited by* M. S. Newman. John Wiley & Sons, Inc., New York. 1956. Chap. 13.
14. A. J. Petro. J. Am. Chem. Soc. **80**, 4230 (1958).
15. R. S. Mulliken. J. Phys. Chem. **41**, 318 (1937).
16. A. D. Walsh. Disc. Faraday Soc. **2**, 18 (1947).

Received March 21, 1960.
School of Chemistry,
Institute of Technology,
University of Minnesota,
Minneapolis, Minnesota.

THIAZOLES. IV. PROTON MAGNETIC RESONANCE SPECTRA OF THIAZOLE AND ITS METHYL DERIVATIVES*,†

A. Taurins and W. G. Schneider

The proton resonance spectra of five-membered cyclic unsaturated compounds are of considerable interest not only from the standpoint of structure determination in complex organic molecules, but also in connection with the rather unusual proton spin-coupling interactions in these systems (1, 2, 3). In this connection the high-resolution proton resonance measurements of thiazole, which contains two heteroatoms in the five-membered ring, are of some interest. Figure 1 shows a reproduction of the proton

*Issued as N.R.C. No. 5699.
†Thiazoles. III. A. Taurins, J. G. E. Fenyes, and R. N. Jones. Can. J. Chem. **35**, 423 (1957).

Can. J. Chem. Downloaded from www.nrcresearchpress.com by 186.148.149.217 on 09/04/12
For personal use only.

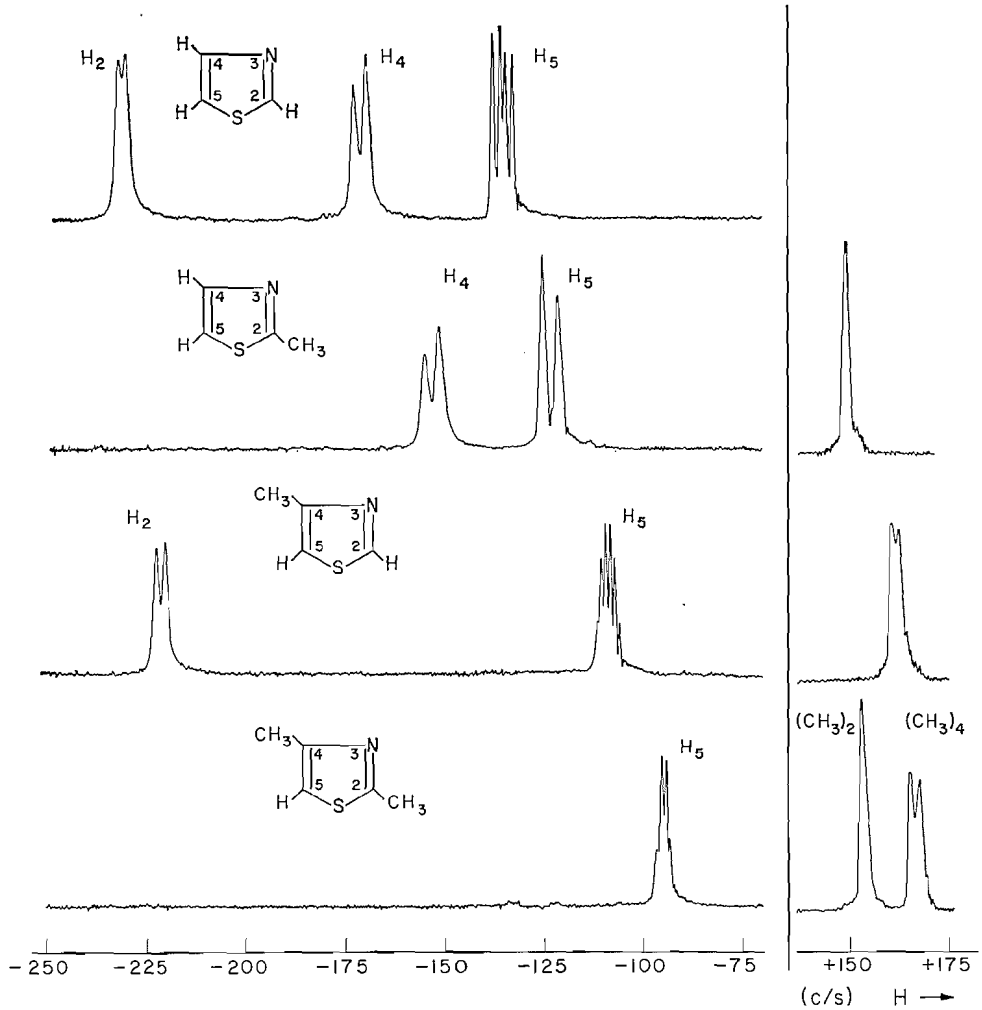


FIG. 1. Proton magnetic resonance spectra of thiazole and its methyl derivatives at 60 Mc/s. Samples were measured as the pure liquids. Frequency scale is relative to an external water reference. The signals of the methyl group protons were recorded at a lower gain than those of the protons bonded to the thiazole ring.

resonance spectrum at 60 Mc/s for thiazole and for three methyl derivatives. With the aid of the spectra of the latter compounds an unambiguous assignment can be made for the parent compound, as shown in Fig. 1. The measured chemical shifts and spin-coupling constants for the protons bonded to the ring are summarized in Table I. The additional signals arising from the methyl substituents, which appear on the high field side of the reference water signal, are also shown in Fig. 1. A splitting of about 1 cycle/second between proton 5 and a methyl group in the 4 position is observed.

The most striking features of the above spectra are the relatively broad signals arising from the protons at positions 2 and 4, and in contrast, the sharp signal arising from the proton at position 5. (In the compound 2-methylthiazole the H_5 signal appears somewhat broader due to an unresolved coupling arising from the methyl group at position 2.) Protons H_2 and H_4 are both two bonds removed from the nitrogen atom whereas H_5 is

Can. J. Chem. Downloaded from www.nrcresearchpress.com by 186.148.149.217 on 09/04/12
For personal use only.

TABLE I

Proton chemical shifts and spin-coupling constants for thiazole and methylthiazoles

Compound	Chemical shifts* (cycles/sec)			Spin-coupling constants (cycles/sec)		
	H_2	H_4	H_5	J_{24}	J_{45}	J_{25}
Thiazole	−231	−170	−135	0	3.1	1.8
2-Methylthiazole	—	−152	−125	—	3.6	—
4-Methylthiazole	−220	—	−107	—	—	2.0
2,4-Dimethylthiazole	—	—	−94	—	—	—

*Measured at 60 Mc/s, in cycles per second relative to proton resonance of water (external reference).

three bonds removed. It is evident that the H_2 and H_4 signals are broadened by the nitrogen quadrupole relaxation and that this perturbation becomes sufficiently attenuated at proton H_5 to give rise to more nearly normal proton line widths. A similar behavior is observable in the proton resonance spectrum of pyridine, the proton signals of the α-hydrogens being noticeably broader than those of the β-hydrogens. In both thiazole and pyridine the electronic charge distribution about the nitrogen atom can be concluded to be highly asymmetric.

The electronegativity of C and S atoms is generally considered to be comparable and significantly less than that of the N atom (4). Thus the signals of H_2 and H_4 may be expected to appear at lower field than that of H_5, but the reason for the large difference in chemical shift between H_2 and H_4 is not readily apparent. The signal of proton H_2, which is in the α-position with respect to both S and N atoms, appears at considerably lower field than that of H_4, which is in the α-position with respect to C and N atoms. It may be noted further that methyl substitution in all cases shifts the ring proton signals to higher field, suggesting a high degree of "aromaticity" in the ring.

A further anomaly is to be found in the spin-coupling constants. Thus the proton pairs H_2 and H_4 and H_2 and H_5 are separated by an equal number of bonds between them, but while J_{25} is of the order of 2.0 cycles/sec, J_{24} could not be resolved. The possibility that the spin coupling between H_2 and H_4, which must go via the N atom, is perturbed by the nitrogen quadrupole relaxation must be considered. Since the coupling between H_2 and H_5 is via the S atom, which is a non-magnetic nucleus, this coupling is unperturbed. The coupling between H_2 and H_4 can of course also proceed via the S atom, but since this path involves an additional bond the coupling will be significantly less.

The authors wish to thank Mr. J. Nicholson for technical assistance.

1. P. L. Corio and I. Weinberg. J. Chem. Phys. **31**, 569 (1959).
2. S. Gronowitz and R. A. Hoffman. Arkiv Kemi, **13**, 279 (1958).
3. R. J. Abraham and H. J. Bernstein. Can. J. Chem. **37**, 1056, 2095 (1959).
4. L. Pauling. Nature of the chemical bond. Cornell Univ. Press, Ithaca, N.Y. 1942. p. 60.

Received March 30, 1960.
Chemistry Department,
McGill University,
Montreal, Que.
and
Pure Chemistry Division,
National Research Council,
Ottawa, Canada.

Can. J. Chem. Downloaded from www.nrcresearchpress.com by 186.148.149.217 on 09/04/12
For personal use only.

Can. J. Chem. Downloaded from www.nrcresearchpress.com by 186.148.149.217 on 09/04/12
For personal use only.

Canadian Journal of Chemistry

Issued by THE NATIONAL RESEARCH COUNCIL OF CANADA

VOLUME 38 AUGUST 1960 NUMBER 8

STUDIES OF RATES OF CONVERSION AND POPULATIONS OF VARIOUS CONFORMATIONS OF SATURATED RING COMPOUNDS BY N.M.R.

I. CHLOROCYCLOHEXANE AND BROMOCYCLOHEXANE[1]

L. W. REEVES AND K. O. STRØMME[2]

ABSTRACT

The populations of equatorial and axial halogen forms of chloro- and bromo-cyclohexane have been studied by proton magnetic resonance between 25° and −104° C in carbon disulphide solution. From the equilibrium constants obtained the free energy change between the two conformations is obtained. The bromo compound has 82% of the equatorial halogen form and the chloro compound 77%. Estimates of the populations are also available for room temperature from the chemical shift measurements. The energy barrier for conversion between the two forms is approximately 10,850 calories. A simple Lennard-Jones potential with the available estimates of van der Waals radii is used to calculate the differences in energy of the two forms.

The difference in nuclear shielding between the axial and equatorial protons in acetylated sugars was first detected by Lemieux, Kullnig, Bernstein, and Schneider (1). This has become a very useful method of determining the conformation of sugars and has been followed up by studies of trioxanes (2) and the isomeric hexachlorocyclohexanes (3). In almost all these compounds the conformations are locked by large groups so that in most cases distinct isomers can be isolated. In the case of the hexachlorocyclohexanes the theoretically possible isomers are reduced to just a few known compounds by the fact that steric hindrance renders almost all of these conformations unfavorable (4).

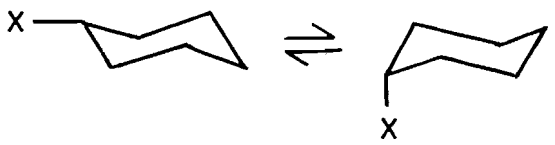
In contrast to the highly substituted derivatives, the simpler cyclohexanes do not show proton resonance spectra with distinct signals for axial and equatorial protons (5). The lack of large substituted groups allows the rapid interconversion of the various conformations and only the averaged shielding parameter is effective (6). The proton resonance technique has proved a useful method of measuring the lifetime of nuclei in distinct chemical environments (7, 8, 9, 10) and the present and future studies of these systems will be aimed at measuring the rates of interconversion between conformations and the population of the conformers in equilibrium at temperatures where distinct proton resonances can be obtained for the individual species.

Such studies will give enthalpy differences and energy barriers for the internal conversion over series of related compounds.

[1]*Manuscript received April 19, 1960.*
Contribution from the Department of Chemistry, University of British Columbia, Vancouver 8, British Columbia.
[2]*Permanent address: Chemistry Department, University of Oslo, Blindern, Norway.*

3094?2

In this present paper two compounds of the type



are studied. The equilibrium populations are obtained in one solvent at various temperatures. An estimated rate is obtained at one temperature but the study of variation of solvent will be left for later work. The influence of solvent on such isomeric equilibria in solution has been dealt with by Bernstein and Powling (11) and Reeves (12, 10).

EXPERIMENTAL

Analytical grade chlorocyclohexane and bromocyclohexane were used without further purification. The solutions were prepared with redistilled carbon disulphide, which is the most suitable solvent for low-temperature work and has the advantage of no external dipole moment and no proton resonance. It is intended to vary polarity of solvent in later work.

The solutions prepared had the following composition:
(A) mole% $C_6H_{11}Cl$ = 54.5, mole% CS_2 = 37.4, mole% tetramethyl silane = 8.1;
(B) mole% $C_6H_{11}Br$ = 55.4, mole% CS_2 = 41.2, mole% tetramethyl silane = 3.4.

A 40 Mc/sec Varian V4300 high-resolution spectrometer was used for the work. The low-temperature arrangement used was a modification of an apparatus described by Schneider, Bernstein, and Pople (13). The arrangement will be described more completely later. The samples are contained in 3-mm I.D. tubes which are sealed off in vacuum and have two bearings: the upper one, a tungsten wire, sealed into glass, and the lower one, a glass tit bearing, which lowers into a drilled teflon plate. The sealing and accurate alignment of bearings is achieved by use of a microglass lathe to be described by one of us (L. W. R.).

The tube is contained in a Dewar arrangement previously described (13). A 15-mm Varian insert is used and there is Dewar insulation between the insert coil and the cooled sample. The small air space between the Dewar and the insert wall is circulated with dry nitrogen at room temperature so that no cooling or condensation can occur even on the outside of the transparent Dewar. Spurious water peaks are thus avoided.

Cooling is achieved by a heater placed in a 25-liter metal Dewar of liquid nitrogen with exit tube and blowoff valve. In cases where it is necessary to heat the sample at any time, a small heating coil in the nitrogen stream is used. The cooled nitrogen stream spins the sample from tangential holes striking the shaped glass rod top of the sample tube. Since a more or less constant spinning rate is desirable the faster streams of nitrogen obtained at low temperatures are bled off in a side tube and only part of the stream is used for spinning and cooling.

A previous study of methyl nitrite at low temperatures demonstrates the reproducibility of the apparatus (12(*b*)). Providing the viscosity of materials is favorable, high-resolution spectra comparable to those taken at room temperature can be obtained down to $-180°$ C and in this work spectra were measured in the region as low as $-120°$ C. The temperature control as indicated by a copper constantan thermocouple in the exit stream near the sample is approximately $\pm 1°$ C down to $-80°$ C and $\pm 1.5°$ C below this, over 15-minute periods.

Can. J. Chem. Downloaded from www.nrcresearchpress.com by 186.148.149.217 on 09/04/12
For personal use only.

Can. J. Chem. Downloaded from www.nrcresearchpress.com by 186.148.149.217 on 09/04/12
For personal use only.

RESULTS

Spectra of solution A and solution B at 28° C are shown in Fig. 1. Spectrum (*a*) corresponds to bromocyclohexane in CS_2 and spectrum (*b*) corresponds to chlorocyclohexane in CS_2. Peak II is the proton resonance in the —CHX— proton and peak I in the $—C_5H_{10}—$ protons. The internal standard tetramethyl silane is shown to high field as peak 0. The spectrum is calibrated by 50, 100, 150, and 200 c.p.s. side bands in some

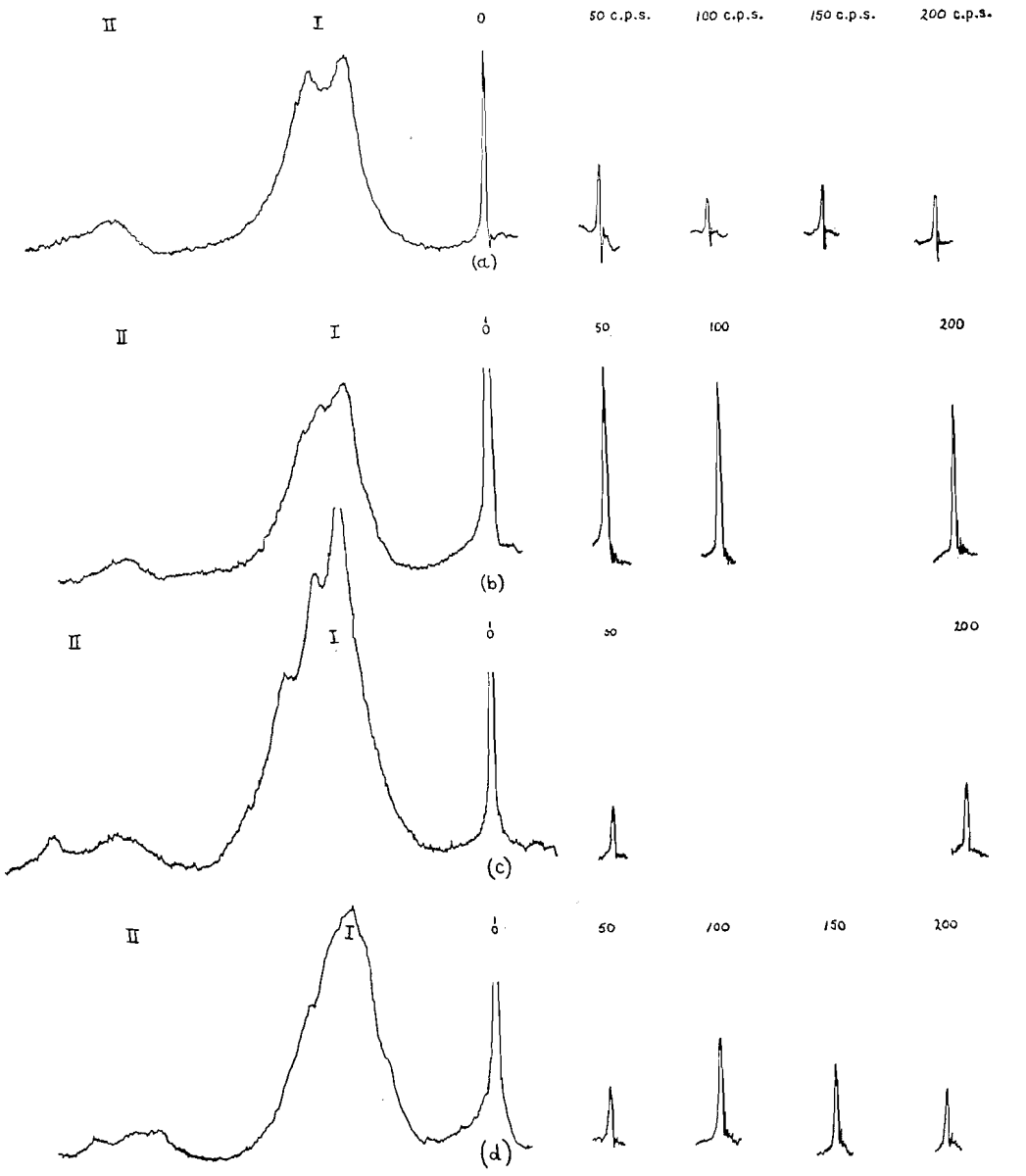


FIG. 1. (*a*) Spectrum of bromocyclohexane at 40 Mc/sec in CS_2 with $Si(Me)_4$ standard signal. Solution B 28° C. (*b*) Spectrum of chlorocyclohexane solution in CS_2 at 28° C. (*c*) Spectrum of bromocyclohexane at −104.5° C. (*d*) Spectrum of chlorocyclohexane at −91° C.

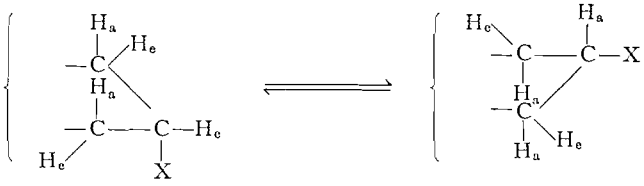
cases, as shown in Fig. 1. The irregular base line which occurs during the seep between side bands due to the process of switching off the audio oscillator and resetting at a new value is caused by side bands of the $-C_5H_{10}-$ peaks. The base line has therefore been removed in most cases. The lack of ringing off the first tetramethyl silane peak is due to a prompt addition of 50 c.p.s. side bands after passing through this signal. The instrumental resolution is better seen from the audio side band peaks.

The —CHX— signal is seen to be a broad band approximately 12 c.p.s. in half width. This arises from a number of similar coupling constants with nuclei which are considerably chemically shifted ($-C_5H_{10}-$) and is characteristic of similar situations which arise in substituted hydrocarbon chains (3, p. 235–238). The fine structure of this peak can to a certain extent be resolved with higher gains and slower passage through resonance but this has not been relevant to the present study. The signal I in spectrum (*a*) for bromocyclohexane consists of two main broad peaks. The low-field peak is due to the $-CH_2-$ groups on each side of the —CHX— grouping and the high-field part of this group of lines is due to the remote $-(CH_2)_3-$ protons from the —CHX— grouping.

The main features of the chlorocyclohexane spectrum are similar, except that signal I is not so well resolved into the methylene groups adjacent to —CHX— and the remote methylene peaks.

The lack of two main components for the low-field signal in each case at 28° C shows a rapid equilibrium between the two chair forms. The —CHX— proton is rapidly converted between axial and equatorial position. On the cooling of both solutions, a distinct broadening of the low-field signal is observed at −40° C and single broad signal occurs at −55° C. Below this temperature two signals are resolved which do not change in appearance appreciably between −70° C and the solidification point (∼−95° C for the chlorocyclohexane solution and ∼−110° C for the bromocyclohexane solution). Marked changes in the general shape of the high-field signal can be detected as high as −25° C. The bromocyclohexane spectrum at high field shows the appearance of an additional low field peak, but the lack of resolvable structure in chlorocyclohexane makes it difficult to classify the changes which occur here.

The chemical shifts of all signals in these spectra are shown in Table I. The highest field component of signal II in both compounds does not show large variation with temperature. The assignment of spectra at low temperature is based on the previous experience with locked conformations where it is found that the low field signal is due to equatorial protons in the cyclohexane ring (3, p. 390 ff.). In the hexachlorocyclohexanes the downfield shift is approximately 0.2–0.6 p.p.m. in agreement with the measured value for chlorocyclohexane at −70° C and −90° C of 0.65 and 0.58 p.p.m.* The corresponding chemical shift separation for the axial and equatorial —CHBr— polar is 0.68 p.p.m. The peak for the equatorial position is narrower than that for the axial position. This finds a ready explanation in terms of the coupling constants involved. The two environments of the —CHX— proton are set out below.



**The center of the roughly gaussian line shape is used for the chemical shift measurement. In view of the overlapping splitting due to J coupling which is symmetrical about the proton concerned, this is a reasonable assumption.*

Can. J. Chem. Downloaded from www.nrcresearchpress.com by 186.148.149.217 on 09/04/12
For personal use only.

TABLE I

Chemical shifts of signals in the spectra of chloro- and bromo-cyclohexane at various temperatures with respect to tetramethylsilane

	Chemical shifts (p.p.m.) from $Si(Me)_4$ signal			
	Chlorocyclohexane			
	I		II	
Temp., °C	Weighted average for equatorial and axial		(i)	(ii)
28	−3.935		−2.31 −2.11	−1.54
−26	−3.890		−1.79	−1.55
	(i)	(ii)		
−70	−4.34	−3.76		−1.58
−91	−4.44	−3.79	−2.09	−1.58
	Equatorial proton	Axial proton	(i) Shoulders appearing due to $-CH_2-$ protons adjacent to —CHX— group	(ii) Remote $-(CH_2)_4-$ group
	Bromocyclohexane			
	(i) and (ii)		(i)	(ii)
28	−4.16		−1.95	−1.55
−29	−4.16		−1.95	−1.55
−75	−4.64,	−3.97	−2.12, −1.84	−1.55
−95	−4.65,	−3.97	−2.16, −1.84	−1.55
−104.5	−4.65,	−3.98	−2.17, −1.84	−1.59
	Equatorial proton	Axial proton	$-(CH_2)-$ protons adjacent to —CHX—	Remote $-(CH_2)_3-$ group

If the —CHX— proton is equatorial then coupling constants to the adjacent $-CH_2-$ groups involve ee and ea protons. If the —CHX— proton is axial, aa and ae coupling constants are involved. A comparison of typical coupling constants in some acetylated sugars (3, p. 397) shows that e–e coupling is generally less than 3 c.p.s. and e–a coupling is about 2–5 c.p.s. while a–a coupling is 6–12 c.p.s. The much broader signal for the axial proton is consistent with a larger a–a coupling constant and resolution of some structure is possible within the broad peak (Figs. 2*a* and 2*b*). The spectra at low field

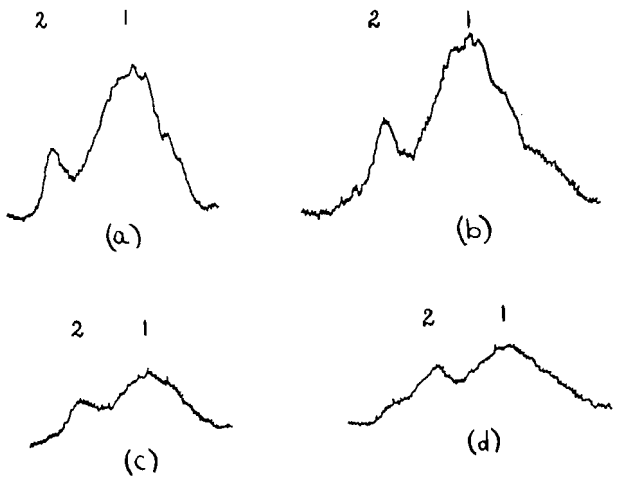


FIG. 2. Spectra of low-field —CHX— proton resonance signal at two temperatures. (*a*) Bromocyclohexane −88° C. (*b*) Bromocyclohexane −97° C. (*c*) Chlorocyclohexane −80° C. (*d*) Chlorocyclohexane −92.5° C.

Can. J. Chem. Downloaded from www.nrcresearchpress.com by 186.148.149.217 on 09/04/12
For personal use only.

consist of the 'X' part of an A_2B_2X spectrum in the terminology of Bernstein, Schneider, and Pople (14).

Populations of the equatorial and axial —CHX— proton in equilibrium are given in Table II at various temperatures. The populations were obtained by weighing the peaks after they were traced on to thick graph paper. At each temperature four independent spectra were selected and each traced five times. The total weight of five tracings of each spectrum was then obtained. The smaller peak was then cut off and the remaining axial peak weighed.

TABLE II

Measured populations of equatorial halogens in two cyclohexane derivatives at various temperatures between −80° C and −104° C

Monobromocyclohexane, 55.4 mole% in CS_2		Monochlorocyclohexane, 54.5 mole% in CS_2	
Temp.,°C	Equatorial Br, mole%	Temp.,°C	Equatorial Cl, mole%
−86	78.2	−80	77.0
−87	79.0	−82	79.9
−89	85.4	−91	71.3
−89	73.2	−92	79.5
−89	81.6	−92	80.9
−89	75.6	−93	72.0
−97	84.8	−93	79.8
−97	81.0		
−97	82.7		
−98	83.4		
−98	83.7		
−98	86.6		
−99	82.9		
−103	80.4		
−103	79.0		
−103	76.4		
−103	79.6		
−103	81.4		
−104	79.3		
−104	83.2		
−104	84.1		

NOTE: Mean values of populations: equatorial bromine = 82.0%; equatorial chlorine = 77.2%.

DISCUSSION

The results in Table II show no significant changes in population of the equatorial halogen form over an ~25° temperature range near −100° C. The energy content of the two equilibrium forms is almost the same. We may calculate a 'ΔF' free energy change from the equation $\Delta F = -RT \log_e K$. The values of the ΔF function are

$$[1] \qquad \Delta F_{ea} = -RT \log_e \frac{[\text{equatorial } 'X']}{[\text{axial } 'X']},$$

$$\Delta F_{ea} = -511 \text{ cal/mole for } C_6H_{11}Br,$$

$$\Delta F_{ea} = -406 \text{ cal/mole for } C_6H_{11}Cl.$$

We may assume $\Delta S_{ea} = 0$. Thus the Gibbs free energy function becomes equal to the enthalpy change ΔH_{ea}, which in turn is almost identical with the energy content function at constant volume ΔE_{ea}. Thus the free energy obtained from experiments can

Can. J. Chem. Downloaded from www.nrcresearchpress.com by 186.148.149.217 on 09/04/12
For personal use only.

be equated to changes in the energy in going from one conformation to the other. It is to be noted that such small changes, in energy content observed, give negligible changes in population over a 30° C range so that experimental measurement does not detect them.

The populations of the axial chloro and bromo conformers can be obtained at room temperature by using the weighted average of the chemical shifts for axial and equatorial —CHX— form

$$\delta_M = x_a\delta_a + x_e\delta_e. \quad [2]$$

x_a and x_e are mole fractions of chlorocyclohexane in axial and equatorial form. δ_M is the measured chemical shift. δ_a and δ_e are the chemical shifts of axial and equatorial —CHX— proton available from low-temperature measurements.

The mole% equatorial halogen is computed to be 73.2% in bromocyclohexane and 77.4% in chlorocyclohexane. Since the chemical shift measurements of broad peaks are much less accurate than the intensity measurement at low temperature these estimates are subject to large errors.

The measurement of rates of interconversion between conformers using the standard techniques of n.m.r. (8, 9, 10) is not possible in this case because of complex spectra; the line width parameter T_2 cannot be measured. At the coalescence temperature (10) for axial and equatorial —CHX— protons the fine structure is averaged and it is legitimate to calculate an average lifetime τ_c. We have the equation

$$\tau_c \text{ (sec)} = \frac{1}{\sqrt{2}.\ \pi.\ \Delta\nu} \quad [3]$$

where $\Delta\nu$, frequency separation of resolved signals at low temperature (c.p.s.), is equal to 8.9×10^{-3} sec for bromocyclohexane. The coalescence temperature observed was ~218° K in both cases. If we assume a normal frequency factor of $kT/h \simeq \nu_0$ for the conversion process we may calculate an activation energy from

$$\frac{1}{2\tau_c} = 4.36\times10^{12}\exp\left(\frac{\Delta E}{436}\right). \quad [4]$$

The activation energy for the conversion is found to be 10,850 calories, a value subject to large error. Studies are at present being made on substituted cyclohexane having protons which are not coupled to the methylene protons in the ring and more reliable energy barriers will be available.

Although no accurate calculations are available, the small population of the axial halogen form is considered to be due mainly to van der Waals repulsive forces with the 3.5 axial hydrogen atoms (4, 15). Such a calculation is made here in an attempt to estimate the potential energy difference between the axial and equatorial form based on the Lennard-Jones equation (16).

The values ϵ/k = 277° K and 295° K (17) for the bromine–hydrogen and chlorine–hydrogen interactions are used; k is the Boltzmann constant.

Let $$\sigma = \frac{r \text{ van der Waals}}{2^{1/6}} = 2.55 \text{ Å and } 2.42 \text{ Å}$$

for the bromo and chloro compounds respectively. The calculation considers two repulsion terms of the halogen with a hydrogen atom and the van der Waals interaction of this

Can. J. Chem. Downloaded from www.nrcresearchpress.com by 186.148.149.217 on 09/04/12
For personal use only.

halogen in the equatorial position with atoms within the van der Waals interaction sphere.

Interatomic distances in the two conformations are obtained from the work of Hassel and co-workers (18). The calculation neglects distortion of halogen or hydrogens from true axial direction in the axial form. Values of 338.5 calories and 50.5 calories are obtained for bromocyclohexane and chlorocyclohexane respectively. The former represents fair agreement for a crude calculation but the latter, although in the correct order of the measured ΔE_{ea}'s, is only of the correct order of magnitude.

ACKNOWLEDGMENT

This research was supported by grants (to L. W. Reeves) from the National Research Council of Canada and the Research Corporation.

REFERENCES

1. R. M. Lemieux, R. K. Kulling, H. J. Bernstein, and W. G. Schneider. J. Am. Chem. Soc. **80**, 6008 (1958).
2. A. Novak and E. Whalley. Can. J. Chem. **36**, 1116 (1958).
3. J. A. Pople, H. J. Bernstein, and W. G. Schneider. High resolution nuclear magnetic resonance. McGraw-Hill Book Co., Inc., New York. 1959. p. 390.
4. O. Hassel. Quart. Revs. (London), **7**, 221 (1953).
5. E. L. Eliel. Chem. & Ind. (London), 568 (1959).
6. H. S. Gutowsky and A. Saika. J. Chem. Phys. **21**, 1688 (1953).
7. H. S. Gutowsky and C. H. Holm. J. Chem. Phys. **25**, 1228 (1956).
8. H. M. McConnell. J. Chem. Phys. **28**, 430 (1958).
9. S. Meiboom, Z. Luz, and D. Gill. J. Chem. Phys. **27**, 1411 (1957).
10. P. Gray and L. W. Reeves. J. Chem. Phys. In press.
11. H. J. Bernstein and J. Powling. J. Am. Chem. Soc. **73**, 1815 (1951).
12. L. W. Reeves. (*a*) Can. J. Chem. **35**, 1351 (1957); (*b*) J. Chem. Phys. In press.
13. W. G. Schneider, H. J. Bernstein, and J. A. Pople. J. Chem. Phys. **28**, 601 (1958).
14. H. J. Bernstein, J. A. Pople, and W. G. Schneider. Can. J. Chem. **35**, 65 (1957).
15. D. H. R. Barton and R. C. Cookson. Quart. Revs. (London), **10**, 44 (1956).
16. J. E. Lennard-Jones. Proc. Roy. Soc. (London), A, **112**, 214 (1926).
17. J. O. Hirschfelder, C. F. Curtis, and R. B. Bird. Molecular theory of gases and liquids. J. Wiley & Sons, New York. 1954.
18. Interatomic Distances. Chem. Soc. (London), Spec. Publ. No. 11 (1958).

Can. J. Chem. Downloaded from www.nrcresearchpress.com by 186.148.149.217 on 09/04/12
For personal use only.

Can. J. Chem. Downloaded from www.nrcresearchpress.com by 186.148.149.217 on 09/04/12
For personal use only.

NUCLEAR SHIELDING PARAMETERS FOR PROTONS IN HYDROGEN BONDS

II. CORRELATION OF CHEMICAL SHIFTS IN INTRAMOLECULAR HYDROGEN BONDS WITH INFRARED STRETCHING FREQUENCIES[1]

L. W. Reeves, E. A. Allan, and K. O. Strømme

ABSTRACT

Nuclear shielding parameters have been obtained for 24 intramolecularly hydrogen-bonded phenols and naphthols. The shielding parameters are corrected for large diamagnetic anisotropies and a value $\Delta\sigma_{OH}$ obtained which represents the change in shielding parameter in parts per million with reference to the infinite dilution chemical shift of phenol, α-naphthol, or β-naphthol. These values of $\Delta\sigma_{OH}$ are approximately proportional to the change $\Delta\nu_{OH}$ in the OH stretching frequency on formation of the hydrogen bond.

The present study follows from a recent publication on nuclear shielding parameters for the strongly hydrogen-bonded proton (1) in orthohydroxy azo compounds. It was shown that the corrected chemical shift correlated well with the known acidity of phenol and β-naphthol and hence with the hydrogen-bonding strength, in a series of compounds of quite similar structure. A recognition of the fact that strong intramolecular hydrogen bonds are very little dissociated in dilute solution enables chemical shifts for a completely formed hydrogen bond to be quoted (2, 3). The study of strong dimer bonds (carboxylic acids) and intramolecular hydrogen bonds, both strong and weak, is extended in this present work in an attempt to make a broad and cross correlation with the shift of the infrared —OH stretching frequency. Many of the compounds studied might be expected to deviate from such a correlation (4) and deviations will be examined in detail in future work. Correlations between the frequency shift of the A—H stretch and heat of formation of the hydrogen bond, internuclear distances X—H- -Y across the bond in series of compounds where X and Y are the same atoms, half width of the A—H stretch in the hydrogen bond, and the intensity change ΔB on formation of a hydrogen bond are now well established (4). It is important therefore to obtain a link between infrared and n.m.r. methods so that hydrogen bond strengths might be indicated by either technique. Such a link has been suggested by earlier work (5, 6) where, however, the consideration of a completely formed hydrogen bond is in doubt since intermolecular hydrogen bonds were studied. There has also been a limited amount of study on chelated enolic hydrogen bonds by Försen and Nilsson (7).

EXPERIMENTAL

Some 26 commercially available substances known to contain intramolecular hydrogen bonds of the type —O—H- -Y were purified by fractional distillation or recrystallization from solvents such as cyclohexane, chloroform, ether, alcohol, or acetone depending on which solvent was the most suitable for the particular compound.

Chemical shifts for the intramolecularly hydrogen-bonded proton were measured. The solvent system used was redistilled carbon tetrachloride stored over P_2O_5 to which was added $\frac{1}{2}$ mole% cyclohexane. The cyclohexane served as an internal reference signal and its concentration was accounted for in the calculation of the mole fraction. When the substances under study were liquid, the concentration was made accurately to

[1]*Manuscript received April 11, 1960.*
Contribution from the Chemistry Department, University of British Columbia, Vancouver 8, British Columbia.

2.0±0.2 mole%. Many of the solid substances were not sufficiently soluble to achieve this concentration and were therefore studied at a concentration of 1±0.2 mole%. A smaller number of substances were not even soluble to 1 mole%; in some of these it was possible to heat the 1% mixture in the sealed evacuated 5-mm sample tubes in hot water and achieve a supersaturated solution of 1 mole% on cooling. In a few compounds the —OH proton resonance was detected in solutions in contact with solid material with a concentration approaching the limit for detection (approximately 0.3 mole%).

A Varian V4300 n.m.r. spectrometer detecting proton resonance at a frequency of 40 Mc/sec was used for this work. The chemical shifts were measured with respect to the signal of cyclohexane using the side band technique. Each chemical shift measurement was counted with a Hewlitt Packard electronic counter model 524B. Chemical shifts of the order of 200–500 c.p.s. were reproducible to ±1.5 c.p.s. using independently prepared solutions. When less than 200 c.p.s. was measured, the chemical shifts had a maximum deviation ±0.75 c.p.s. and did not vary over the concentration range 1 to 2 mole% for a given compound.

Some compounds were examined on a Perkin–Elmer model 21 infrared spectrometer to determine the frequency shift from free to hydrogen-bonded —O—H '$\Delta\nu_{OH}$'. The wave number calibration of the infrared spectrometer was assured by measurements of atmospheric water vapor in the region under study, with single-beam operation. In many cases literature values were available for $\Delta\nu_{OH}$ and agreement with the present measurements was satisfactory. The most precise measurements come from the work of Baker and co-workers (8, 9). These authors used a differential method for detecting frequency shifts in some compounds which gives values of $\Delta\nu_{OH}$ approaching an estimated error of ±1 cm^{-1}. The method of direct reading of the calibrated chart paper can only be accurate to ±3 cm^{-1}, which was the limit of error in the present study. Measurements taken from the literature are acknowledged and compared where they overlap with our results in Table I.

RESULTS AND DISCUSSION

Correlations with Infrared Measurements

The compounds studied contain at least one benzene ring and are of the phenolic —O—H type. The measured chemical shifts have been corrected, in order to reduce their shielding parameters to a common basis. These corrections are for the low-field shift due to the diamagnetic anisotropy of the π electron system (10). The bond distances and angles, where available, were taken from the literature (11), and in cases where the actual distances in the compound under study were not available, a reasonably precise molecular structure could be constructed by considering known structures of related molecules. The correction for the large anisotropy is not precise enough to require the position of the proton in the molecule more accurately than can be estimated in this way. The corrections for the present series of compounds are almost the same in all cases.

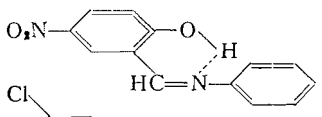
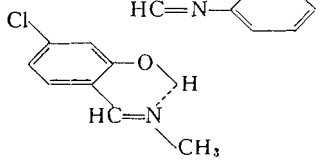
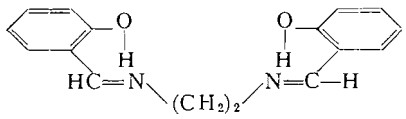
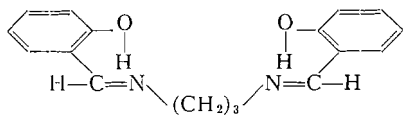
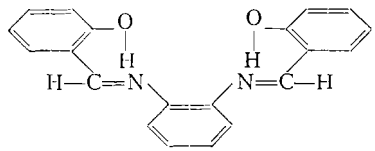
The position of the phenol —O—H peak is −2.80 p.p.m. (−112 c.p.s.) with respect to cyclohexane at infinite dilution, a figure in agreement with the previously reported value (12). Corresponding figures obtained in this study for α- and β-naphthols are −3.78 p.p.m. (−151 c.p.s.) and −3.49 p.p.m. (−139.5 c.p.s.).

On the basis of differences in magnetic anisotropy the difference in chemical shift

Can. J. Chem. Downloaded from www.nrcresearchpress.com by 186.148.149.217 on 09/04/12
For personal use only.

Can. J. Chem. Downloaded from www.nrcresearchpress.com by 186.148.149.217 on 09/04/12
For personal use only.

TABLE I

Compound	$(\sigma_{c C_6H_{12}} - \sigma_{O-H})$, p.p.m.	$(\sigma_{c C_6H_{12}} - \sigma_{OH})$ corrected, p.p.m.‡	$\Delta\sigma_{OH}$ corrected, p.p.m.‡	$\Delta\nu_{OH}$, cm^{-1}
1. Salicylaldehyde	−9.51	−8.83	6.71	471*
2. 5-Nitrosalicylaldehyde	−10.05	−9.37	8.70	500*
3. 5-Bromosalicylaldehyde	−9.38	−8.70	6.58	454*
4. *o*-Nitrophenol	−9.14	−8.46	6.34	346§, 364*
5. 2,4-Dinitrophenol	−9.64	−8.96	6.84	388§
6. Methylsalicylate	−9.12	−8.44	6.32	395*
7. *o*-Bromobenzoic acid	−11.25	−10.70	8.58	570*, 96†
8. *o*-Chlorophenol	−3.97	−3.27	1.17	61§
9. 2,4-Dichlorophenol	−3.99	−3.31	1.19	63§
10. 2,4,6-Trichlorophenol	−4.20	−3.52	1.40	75§
11. *o*-Bromophenol	−3.95	−3.27	1.15	92*
12. 2,4-Dibromophenol	−3.98	−3.30	1.18	83§
13. *o*-Iodophenol	−4.13	−3.45	1.33	105§
14. *o*-Methoxyphenol	−3.98	−3.30	1.18	60§
15. 2,6-Dimethoxyphenol	−3.82	−3.14	1.02	56§
16. *o*-Allylphenol	−3.87	−3.19	1.07	63§
17. *o*-Cresol	−3.12	−2.44	0.32	−8*
18. 	−12.49	−11.54	9.42	Overlaps —C—H stretch <3000 cm^{-1}
19. 	−11.27	−10.59	8.47	
20. 	−11.13	−10.45	8.33	544*
21. 	−11.36	−10.68	8.56	532*
22. 	−11.03	−10.08	7.96	531*
23. 1-Nitro-2-naphthol	−10.53	−9.70	7.04	538*
24. 2,4-Dinitro-1-naphthol	−11.20	−10.28	7.42	543*

NOTE: Reference for benzene derivatives is OH proton signal in phenol, while for naphthalene derivatives it is OH in 1- and 2-naphthol respectively.
*Measured in this work. †Infrared frequency of small monomer peak. ‡Corrected for ring currents. §cf. reference 8.

between the isolated phenol and β-naphthol molecules should be 0.2 p.p.m. (10). Table II shows the measured chemical shifts of isolated phenol, α-naphthol, and β-naphthol

TABLE II

Infrared stretching frequencies of monomers and isolation chemical shifts in phenol and in 1- and 2-naphthol

Compound (referred to infinite dilution in CCl_4)	$(\sigma_c C_6H_{12} - \sigma_{OH\infty dil})$, p.p.m.	$(\sigma_c C_6H_{12} - \sigma_{OH\infty dil})$ corrected, p.p.m.	ν_{OH}, cm^{-1}
Phenol	2.80	3.12	3604†
2-Naphthol	3.49	2.66	3601*
1-Naphthol	3.78	2.86	3594*

*Measured in this work. †cf. reference 8.

in column 2. Column 3 shows the corrected isolation chemical shifts for these molecules assuming the —O—H atoms lie in the plane of the molecule in one of two positions (4). It is assumed in the case of β-naphthol that these positions are equally populated. In α-naphthol the cis position to the second aromatic ring is seriously hindered by the α-hydrogen in the second ring so 100% population of the trans position is assumed in the correction.

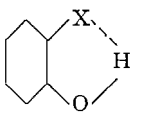
It is interesting to note that the difference in isolation chemical shift of these three molecules after correction is in the same order as the —O—H stretching frequencies. Differences in the corrected chemical shifts are due to changes in the polarity of the —O—H bond and thus reflect the charge density at the proton. It is probable that the acidity increases in the order phenol, β-naphthol, α-naphthol. The wave number measurements of the free —O—H stretch frequency were not accurate enough to indicate the precise correlation between isolation chemical shift and frequency shift.

Figure 1 shows the differences in shielding parameter between the free —O—H signal and the hydrogen-bonded proton plotted against the infrared frequency shift of the —OH stretch on formation of the intramolecular hydrogen bond. The plot shows an approximate linear relationship from the weakest hydrogen bond 2,6-dimethoxyphenol to the strong hydrogen bond in some orthohydroxy Schiff's bases.

In intermolecular hydrogen bonds the heat of formation correlates well with the frequency shift $\Delta\nu_{OH}$ (4). The intensification of the —OH stretch vibrational transition can also be used to indicate the heat of formation and the intensification is more sensitive detection of hydrogen bond formation. In the formation of intramolecular hydrogen bonds, however, only the frequency shift $\Delta\nu_{OH}$ shows normal behavior in correlating with the heat of formation of the bond (4).

Unpublished work of Pimentel and Brown (4) shows that the original linear correlation of Badger and Bauer (14) does not hold but that low-frequency shifts $\Delta\nu_{OH}$ correspond to disproportionately high heats of formation compared with the large values of $\Delta\nu_{OH}$. The systems studied were phenol in a series of bases and therefore relevant to the present study of intramolecularly hydrogen-bonded phenols.

Weak Intramolecular Hydrogen Bonds



In compounds of the type shown above where a weak hydrogen bond is formed as in

Can. J. Chem. Downloaded from www.nrcresearchpress.com by 186.148.149.217 on 09/04/12
For personal use only.

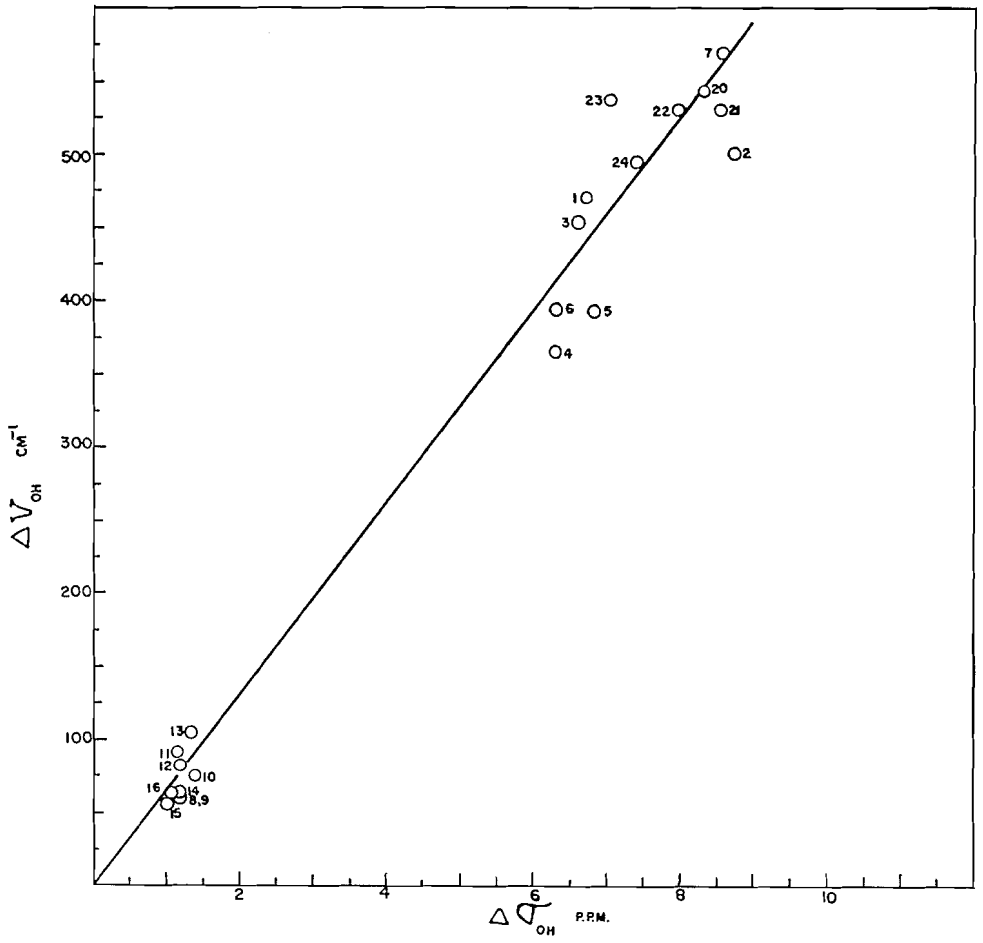


FIG. 1. Plot of $\Delta\nu_{OH}$ versus $\Delta\sigma_{OH}$ for intramolecular hydrogen bonds in phenols and naphthols. Numbered points refer to compounds in Table I.

the case of the halogens or orthomethoxy phenols, the population of the trans position must be taken into account, in order to justify a measurement of the change in shielding parameter on hydrogen bond formation. The careful infrared studies of Baker and co-workers (8, 9, 13) show that the free phenolic —OH stretch is observed as well as the band due to a hydrogen-bonded proton (15). After careful purification of the *o*-halophenols Baker concluded that the cis/trans ratios in *o*-chloro-, *o*-bromo-, and *o*-iodo-phenol were 1/56, 1/38, and 1/13.5 respectively. If we assume the chemical shifts in these compounds to be characteristic of the average environment then there is less than a 10% error in considering the most unfavorable case *o*-iodophenol as a completely cis configuration.

The chemical shift changes on formation of the hydrogen bond are roughly proportional to $\Delta\nu_{OH}$. Baker has shown, however, that hydrogen bond strengths are in the order Cl > Br > F > I (9). In these molecules the O—H- -O angle is distorted at least 85° from a straight line and interorbital repulsion plays a part in the anomalous order of $\Delta\nu_{OH}$ (9).

There are reasons why anomalies should occur in the chemical shift measurement. In

Can. J. Chem. Downloaded from www.nrcresearchpress.com by 186.148.149.217 on 09/04/12
For personal use only.

addition to steric factors which favor the order suggested by Baker there is the increasing diamagnetic anisotropy of the C—X bond as X changes from fluorine to iodine. The ratio $\Delta\nu_{OH}/\Delta\sigma_{OH}$ shows that in going from chlorine to iodine we have the values 50.2, 67.8, and 78.8 cm^{-1}/p.p.m., indicating a term which lowers $\Delta\sigma_{OH}$ as we go from chlorine to iodine.

In the weak intramolecular hydrogen bonds there are several exceptions to the correlation of $\Delta\sigma_{OH}$ and $\Delta\nu_{OH}$ with ΔH_f the heat of formation of the bond (9). It must be remembered, however, that this region of the correlation represents a small portion of the total range ($\sim$2.5–3.5 kcal = ΔH_f) of hydrogen bond energies studied (0–8 kcal/mole = ΔH_f).

Further detailed studies of this restricted region are in progress to extract the artifacts peculiar to magnetic properties of these molecules.

ACKNOWLEDGMENT

This work was supported by research grants to L. W. Reeves from the National Research Council of Canada and the Research Corporation.

REFERENCES

1. L. W. Reeves. Can. J. Chem. **38**, 736 (1960).
2. L. W. Reeves. Trans. Faraday Soc. **55**, 1684 (1959).
3. L. W. Reeves. Can. J. Chem. **35**, 1351 (1957).
4. G. C. Pimentel and A. L. McLellan. The hydrogen bond. W. M. Freeman, San Francisco. 1960.
5. G. Korinek and W. G. Schneider. Can. J. Chem. **35**, 1157 (1957).
6. W. G. Schneider, H. J. Bernstein, and J. A. Pople. J. Chem. Phys. **28**, 601 (1958).
7. S. Försen and M. Nilsson. Acta Chem. Scand. **13**, 1383 (1959).
8. A. W. Baker and A. T. Shulgin. J. Am. Chem. Soc. **80**, 5358 (1958).
9. A. W. Baker and W. W. Kaeding. J. Am. Chem. Soc. **81**, 5904 (1959).
10. J. A. Pople. J. Chem. Phys. **24**, 1111 (1956).
11. Interatomic distances. Chem. Soc. (London), Spec. Publ. No. 11 (1958).
12. C. M. Huggins, G. C. Pimentel, and J. N. Shoolery. J. Chem. Phys. **23**, 311 (1956).
13. J. W. Baker. J. Phys. Chem. **62**, 744 (1958).
14. R. M. Badger and S. M. Bauer. J. Chem. Phys. **5**, 839 (1937).
15. A. W. Baker. J. Am. Chem. Soc. **80**, 3598 (1958).

Can. J. Chem. Downloaded from www.nrcresearchpress.com by 186.148.149.217 on 09/04/12
For personal use only.

Can. J. Chem. Downloaded from www.nrcresearchpress.com by 186.148.149.217 on 09/04/12
For personal use only.

OROTIC ACID AND ITS ANALOGUES

PART II. ON THE ALKALINE REARRANGEMENT OF 5-CARBOXYMETHYLIDENEHYDANTOIN[1, 2]

R. Deghenghi and G. Daneault

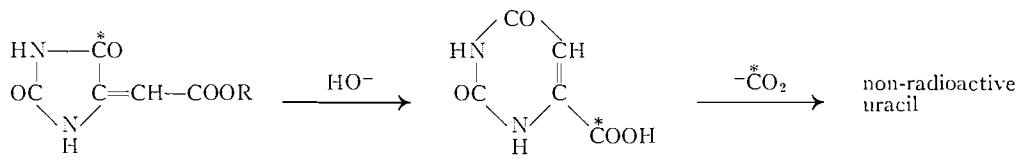
ABSTRACT

The in vitro conversion of 5-carboxymethylidenehydantoin to orotic acid is not likely to occur in vivo since the two substances have antagonistic effects (2). A sulphur analogue of the above hydantoin has been prepared and shown not to undergo alkaline rearrangement to the corresponding metathiazine structure. The mechanism of orotic acid formation is discussed.

Since its discovery in 1905 by Biscaro and Belloni (3), orotic acid (II) has aroused an enormous interest among biochemists (see in particular (4) and (5)) for its importance as a pyrimidine precursor of nucleic acids. A large amount of synthetic work has been done on orotic acid itself (6) and on its analogues (7), but comparatively little attention has been given to the mechanisms of its formation, from a purely chemical point of view.

At first orotic acid was believed to be a seven-membered ring compound (3), but it was soon shown to be uracil-6-carboxylic acid (8, 9). Its synthesis from ethyl oxaloacetate and urea was erroneously believed to give directly ethyl orotate (10); later the ester was proved to be in fact 5-carbethoxymethylidenehydantoin (11). A similar error was made by Biltz and Kramer (12), who studied the alkaline decomposition of a diazoacetate derivative of alloxan to give again the hydantoin and not the six-membered ring ester.

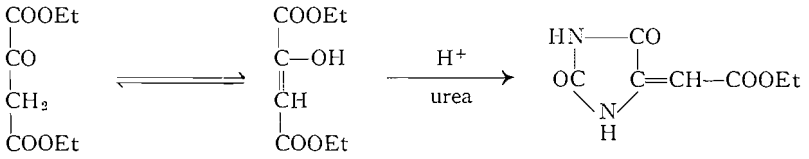
All these facts prompted us to reinvestigate the mechanism of the formation of orotic acid and we chose at first the reaction of ethyl oxaloacetate and urea (III → I), as described by Müller (13) and discussed by Nyc and Mitchell (14). The latter authors postulated a mechanism which involves opening of the hydantoin ring between positions three and four to give the hydantoic acid which closes again to give the pyrimidine. The reaction was followed spectrophotometrically in alkaline solution and it was found that orotic acid is formed previous to acidification. The hydantoic acid was not isolated, though in other unsaturated hydantoins evidence of the open-chain compound has been obtained (14). That an open-chain-ring tautomerism exists in the hydantoin conversion to orotic acid was clearly demonstrated by Langley (15), who was able to show that a C^{14} carbon atom in position four in the hydantoin ring is present as a carboxyl in the orotic acid; this was confirmed by the quantitative recovery of the radioactivity in the CO_2 following decarboxylation (the remaining uracil being inactive). We were interested



(I) (II)

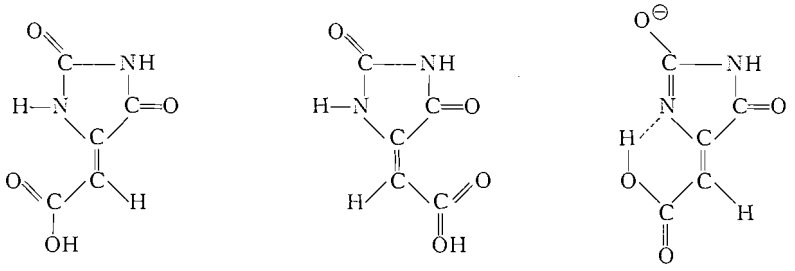
[1]*Manuscript received April 13, 1960.*
Contribution from the Department of Chemistry, Laval University, Quebec, Que. Taken from the thesis submitted by G. Daneault for the degree of Bachelor of Science.
[2]*Part I: See reference 1.*

to investigate (*a*) why the hydantoin is the first intermediate when urea condenses with oxaloacetic ester, (*b*) whether the same kind of ring enlargements were possible with other five-membered ring substances, and (*c*) the isolation of possible intermediates of the above rearrangement (I → II).



(III) (IV) (I)

Oxaloacetic acid and its esters (III) are present in the pure state or in non-polar solvents (16, 17) as the enol form (IV) which may exist in the *trans* (hydroxy-fumaric) or *cis* (hydroxy-maleic) form. It is formally the latter which, after condensation with urea, gives the five-membered ring hydantoin. In fact, one could reasonably expect ethyl orotate only from the *trans* (fumaric) form of the intermediate hydantoic ester (ureidofumaric acid). For the same reason one could expect a cis–trans isomerization to occur previous to or during the alkaline conversion of the hydantoin to orotic acid. We were able to isolate two isomeric forms of the hydantoin (V, VI), one of which has not been described previously, by eluting the potassium salt of I through a column of cation-exchange resin (cf. Experimental). Proof of the structure was obtained by ultraviolet spectra, which showed two peaks at 235 mμ and 294 mμ characteristic of hydantoin structure (cf. 14), by infrared spectra, by the facile conversion of one isomer to the other, and by the fact that both substances gave, upon reduction with sodium amalgam, the same hydantoin-5-acetic acid. Furthermore, we were led to attribute tentatively structure V to the lower melting isomer, on the basis that the increase of the infrared frequency of the carbonyl in position four and the decrease of the C=O frequency in position two, together with the shift of the OH frequency due to hydrogen bonding, are better explained by structures of the type VII. Therefore the complete mechanism



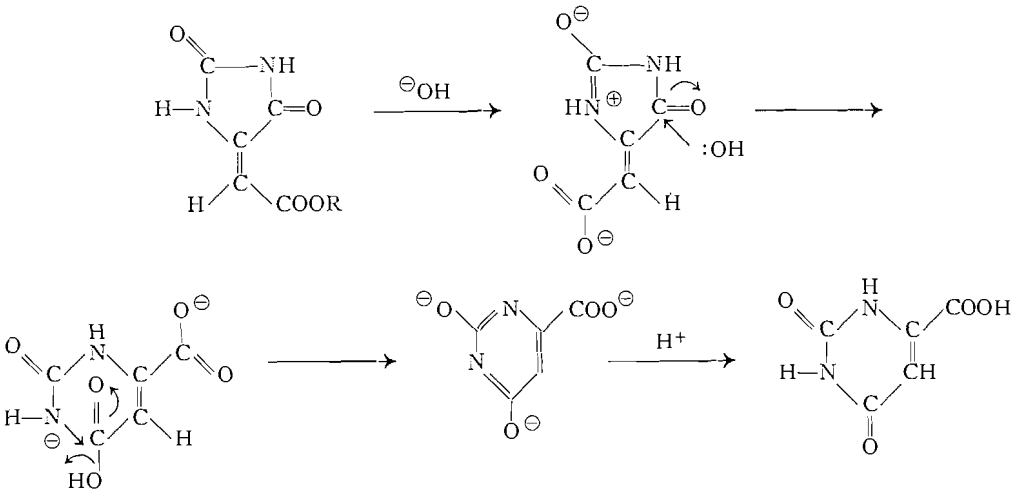
(V) (VI) (VII)

for the alkaline conversion of I to orotic acid may reasonably assume the following form going through the steps: (*a*) cis–trans isomerization,[3] (*b*) alkaline cleavage, and (*c*) aromatization to the more stable pyrimidine structure.[4]

[3]*The reversible addition of the elements of water to the double bond (cf. 19) is a possible mechanism for this isomerization.*

[4]*Orotic acid is essentially a hydroxy pyrimidine in alkaline medium (cf. 18).*

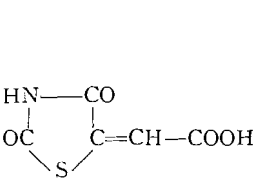
Can. J. Chem. Downloaded from www.nrcresearchpress.com by 186.148.149.217 on 09/04/12
For personal use only.



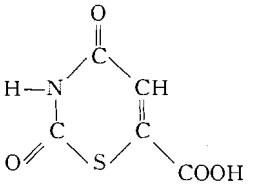
For a parallel experiment with a parent compound, we chose the corresponding pseudo-thio-hydantoin (VIII) which we synthesized in good yields from thiourea and maleic anhydride through the saturated thiazolidinedione-5-acetic acid. The ultraviolet spectrum of the new substance VIII in ethanol resembles closely that of 5-carboxymethylidene-hydantoin (cyclic, five-membered structure) and the infrared spectrum of the corresponding methyl or ethyl esters shows the four expected bands at 1772 cm^{-1} (4-CO), 1735 cm^{-1} (2-CO), 1690 cm^{-1}, and 1620 cm^{-1} (α,β-unsaturated ester). The free acid had a similar spectrum but with two more bands (KBr) at 1785 and 1700 cm^{-1} which could possibly arise from dimerization[5] (20). The free acid has a remarkable stability; it was recovered unchanged after being refluxed with an aqueous solution of $HClO_4$ and, when subjected to the same conditions for the orotic acid alkaline rearrangement, the starting material or its monopotassium salt were recovered again in high yield (cf. Experimental).

The potassium salt[6] by elution through a cationic exchange resin gave, like the above hydantoin, an isomer whose cyclic structure was evidenced by ultraviolet absorption, and which could be converted to the other form by crystallization from boiling water. Both isomers were reduced to the same saturated acid by the action of sodium amalgam.

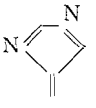
The fact that in the case of the five-membered ring sulphur compound a ring enlargement to the corresponding metathiazine structure (IX) was not achieved, in spite of



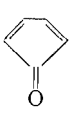
(VIII)



(IX)



(X)



(XI)

[5]*For a discussion about carbonyl band splitting, cf. (26).*
[6]*Cf. (9) for the remarkable stability of potassium orotate.*

Can. J. Chem. Downloaded from www.nrcresearchpress.com by 186.148.149.217 on 09/04/12
For personal use only.

the isomerization, may be explained by considering the stability of structures of the type X which could arise from the enolic form of the hydantoin (21). The polarity of the exocyclic double bond (conjugated with the acid) would be strongly opposed in the structure X as it is in the case of 1,2-cyclopentenediones (enol form XI) (22) which, accordingly, exist only in the keto form. With the sulphur compound evidently no enol structure of the type XI (in alkaline solution) would be possible, thus explaining the observed stability of the five-membered thiazolidine ring.

It may be mentioned here that the in vitro conversion of 5-carboxymethylidene-hydantoin to orotic acid is not likely to occur in vivo, since the two substances show antagonistic effects following subcutaneous administration in the rat (2). An account of the biological activity of the sulphur analogue of the above hydantoin will be reported elsewhere.

EXPERIMENTAL[7]

2-Imino-4-oxo-5-thiazolidineacetic Acid

This compound was prepared in 72% yield from thiourea, according to the method of Andreasch (23) reported by Flett and Gardner (24), m.p. 252–253° dec. (reported to decompose above 220°). ν_{max}^{KBr} 3300, 3150 cm^{-1} (OH, NH); 2400 cm^{-1} (broad); 1690, 1645 cm^{-1} (C=N and C=O). Calc. for $C_5H_6N_2O_3S$: C, 34.48%; H, 3.47%; N, 16.09%; S, 18.40%. Found: C, 34.62%; H, 3.71%; N, 16.34%; S, 18.28%.

2,4-Dioxothiazolidine-5-acetic Acid

A solution of 63.237 g of 2-imino-4-oxo-5-thiazolidineacetic acid was refluxed for 2 hours with 630 ml of 20% sulphuric acid. Upon cooling, 42.6 g of 2,4-dioxothiazolidine-5-acetic acid crystallized out, m.p. 168° (lit. 168–169° (25)).

Extraction of the mother liquors with ethyl acetate and evaporation of the solvent *in vacuo* gave another 19.9 g of less pure product, m.p. 163–168°. Total yield 98%. ν_{max}^{KBr} 3200, 3080 cm^{-1} (OH, NH); 1760, 1740 cm^{-1} (4 and 2 C=O); 1700 cm^{-1} (acid C=O).

5-Carboxymethylidene-2,4-dioxothiazolidine (VIII)

A mixture of 26.25 g of 2,4-dioxothiazolidine-5-acetic acid in 90 ml of acetic acid containing 8.2 ml of bromine was refluxed for 2 hours. Hydrogen bromide was evolved and from the clear solution, upon cooling, the product crystallized out in 60% yield. The crystals were collected on a filter, washed with a little acetic acid and water, m.p. 248° dec. A sample was recrystallized from water three times for analysis; needles, m.p. 252–253° dec. Calc. for $C_5H_3NO_4S$: C, 34.68%; H, 1.75%; N, 8.09%; S, 18.51%. Found: C, 34.80%; H, 1.92%; N, 7.98%; S, 18.30%. λ_{max}^{EtOH} 236 mμ (ε 4360), 302 mμ (ε 6320). ν_{max}^{KBr} 3240, 3080, 2950 (OH, NH); 1775, 1758 cm^{-1} and 1725, 1700 cm^{-1} (split carbonyls); 1670 and 1622 cm^{-1} (α,β-unsaturated acid).

The *methyl ester* was prepared by refluxing the acid (0.5 g) in 10 ml of methanol and 0.5 ml of sulphuric acid for 1 hour. Dilution with water gave 5-carbomethoxymethylidene-2,4-dioxothiazolidine, m.p. 160–162°, in 80% yield. The product was recrystallized from water for analysis, m.p. 163–164°. Calc. for $C_6H_5O_4NS$: C, 38.49%; H, 2.69%; N, 7.48%; S, 17.13%. Found: C, 38.24%; H, 2.89%; N, 7.66%; S, 17.21%. ν_{max}^{KBr} 3250 cm^{-1} (NH); 1770 and 1732 cm^{-1} (4 and 2 C=O); 1690 and 1618 cm^{-1} (α,β-unsaturated CO).

The *ethyl ester* was prepared in an analogous manner, m.p. 128–130°, λ_{max}^{EtOH} 240 mμ

[7]*Melting points, taken in evacuated capillaries, are corrected. Analyses by Schwarzkopf Microanalytical Laboratories, Woodside, N.Y. The infrared spectra were taken with a Beckman IR-4 spectrophotometer* (NaCl *optics).*

Can. J. Chem. Downloaded from www.nrcresearchpress.com by 186.148.149.217 on 09/04/12
For personal use only.

Can. J. Chem. Downloaded from www.nrcresearchpress.com by 186.148.149.217 on 09/04/12
For personal use only.

(ϵ 3940), 305 mμ (ϵ 6000). ν_{max}^{KBr} 3300 (NH); 1770 and 1720 cm^{-1} (4- and 2- CO); 1690 and 1630 cm^{-1} (α,β-unsaturated CO).

Stability of 5-Carboxymethylidene-2,4-dioxothiazolidine in Acidic Conditions

To a solution of VIII, 0.449 g in 20 ml of water, was added 2 ml of 72% perchloric acid and the whole was refluxed for 30 minutes. Upon cooling, 0.3 g of the starting material (VIII), m.p. 248° dec., crystallized out. The product was identified by infrared spectra and mixed melting point with authentic material.

Stability of 5-Carboxymethylidene-2,4-dioxothiazolidine in Alkaline Conditions

A solution of VIII, 0.693 g in 15 ml of 1 *N* KOH, was kept 30 minutes at 100°. After cooling, 8 ml of 1 *N* HCl was added. The monopotassium salt of VIII crystallized out; needles, m.p. 270° dec. (with previous browning). Calc. for $C_5H_2NO_4SK$: C, 28.43%; H, 0.95%; N, 6.63%. Found: C, 28.55%; H, 1.02%; N, 6.69%. λ_{max}^{EtOH} 235 mμ (ϵ 1330), 298 mμ (ϵ 2600). ν_{max}^{KBr} 2550 (broad); 1730, 1690, 1630, 1580 cm^{-1} (4- and 2-CO, α,β-unsaturated ionized acid). The same salt (infrared and mixed melting point comparison) was obtained when the unsaturated acid (VIII) was neutralized with 1 *N* KOH in the cold, followed by concentration of the solution *in vacuo*.

Lower Melting 5-Carboxymethylidene-2,4-dioxothiazolidine

A solution of 0.782 of the potassium salt of VIII in water was passed through a column of cation exchange resin Amberlite I.R.-120 (H). The aqueous fractions were extracted with ethyl acetate and the organic solvent was evaporated *in vacuo* to give a crystalline residue (0.7 g), m.p. 200–205° dec. ν_{max}^{KBr} 3400, 3220, 3080 (OH, NH); 1768 and 1722 (4 and 2 C=O); 1690 (shoulder); 1670 and 1615 cm^{-1} (α,β-unsaturated CO). λ_{max}^{EtOH} 240 mμ (ϵ 3840), 303 mμ (ϵ 4000). When this substance was crystallized from water, the original higher melting isomer was obtained, and identified by infrared and mixed melting-point determinations.

Reduction of 5-Carboxymethylidene-2,4-dioxothiazolidine

To a suspension of 0.759 g of VIII in 25 ml of water, stirred in an ice-water bath in a CO_2 atmosphere, 25 g of 2% sodium amalgam was added piecemeal.

After 2 hours the clear solution was decanted from the mercury, acidified with 20% sulphuric acid, and extracted with ethyl acetate. Evaporation of the solvent gave 217 mg of 2,4-dioxothiazolidine-5-acetic acid, identified by mixed melting point and infrared determination with authentic material.

When the *lower melting isomer* was reduced in a similar way, the same product, 2,4-dioxothiazolidine-5-acetic acid, was obtained in similar yield.

5-Carbethoxymethylidenehydantoin (I, R = Et)

This substance was prepared according to the method of Müller (13) from ethyl-oxaloacetate and urea. The yields were in the 10–20% range, m.p. 184–186° (reported 188°). λ_{max}^{EtOH} 235 mμ (ϵ 7920), 300 mμ (ϵ 7500), ν_{max}^{KBr} 3250 (NH); 1800, 1760 (4- and 2-CO); 1695 (C=N), 1680, 1640 cm^{-1} (shoulder) (α,β-unsaturated CO).

5-Carboxymethylidenehydantoin (I, R = H)

This acid was prepared by careful hydrolysis of the corresponding ester (I, R = Et), 184 mg, dissolved in 2.3 ml of ethanol, by addition of 0.1 g KOH in 0.4 ml water. The yellow solid formed was dissolved in 5.6 ml of water. Acidification with concentrated HCl precipitated the product, m.p. above 300° with gradual decomposition. λ_{max}^{EtOH} 237 mμ

(ϵ 7800), 300 mμ (13000). ν_{max}^{KBr} 3550, 3300, 3100 cm^{-1} (OH, NH); 1790 and 1745 cm^{-1} (4 and 2 C=O); 1680 (broad); 1638 cm^{-1} (shoulder) (α,β-unsaturated C=O). A lower melting isomer was obtained by dissolving the above acid in 1 *N* KOH and by eluting the slightly alkaline solution through a column of Amberlite I.R.-120 (H) (cation exchange resin).

The aqueous fractions combined were extracted with ethyl acetate, the solvent removed *in vacuo* to give an acid, m.p. 250° dec. ν_{max}^{KBr} 3250 (broad); 2995 (bonded OH, NH); 1800 cm^{-1} (4-CO in β,γ-unsaturated ring), 1725 (2 CO or C=N), 1690 cm^{-1} (acid CO). λ_{max}^{EtOH} 235 mμ (ϵ 5150), 294 mμ (ϵ 8850). When this substance was recrystallized from water, the higher melting isomer was obtained (infrared spectra identical). Both isomers gave, upon reduction with Na/Hg (compare the above described procedure), the same 5-hydantoin acetic acid, m.p. 212° dec. (lit. 214° (14)).

Orotic Acid

This substance was obtained by the alkaline rearrangement of 5-carboxymethylidenehydantoin according to Nyc and Mitchell (14), m.p. 320° dec. ν_{max}^{KBr} 3580, 3150, 3050 cm^{-1} (OH, NH); 1740 (shoulder); 1715 and 1680 cm^{-1} (broad) (C=N, C=O). The infrared spectrum was identical with that of an authentic sample.

ACKNOWLEDGMENTS

The present work was supported by a grant of the National Research Council. We are grateful to Professor Ch. R. Engel for his kind interest and encouragement and for making the facilities of his laboratory available to us.

REFERENCES

1. R. Deghenghi. Chem. Ber. **90**, 255 (1957).
2. C. Mentzer. Compt. rend. soc. biol. **150**, 1360 (1956).
3. G. Biscaro and E. Belloni. Ann. Soc. Chim. Milano, **XI**, fasc. I and II (1905).
4. P. Reichard. The function and biosynthesis of orotic acid. *In* The nucleic acids. Vol. II. *Edited by* E. Chargaff and J. W. Davidson. Academic Press Inc., New York. 1955. p. 299.
5. Symposium on Pyrimidines. cf. C. A. Rossi *et al.* Acta Vitaminol. **12**, 195 (1958).
6. V. Grignard. Traité de chimie organique. Vol. XX, 1953. p. 1340.
7. J. E. Stone and V. R. Potter. Cancer Research, **16**, 1033 (1956).
8. M. Bachstez. Chem. Ber. **63**, 1000 (1930).
9. T. B. Johnson and W. T. Caldwell. J. Am. Chem. Soc. **51**, 873 (1929).
10. H. L. Wheeler. Am. Chem. J. **37**, 392 (1907).
11. H. K. Mitchell and J. F. Nyc. J. Am. Chem. Soc. **69**, 674 (1947).
12. H. Biltz and E. Kramer. Ann. **436**, 165 (1924).
13. R. Müller. J. prakt. Chem. **56**, 488 (1897).
14. J. F. Nyc and H. K. Mitchell. J. Am. Chem. Soc. **69**, 1382 (1947).
15. B. W. Langley. Yale J. Biol. and Med. **27**, 135 (1954).
16. K. H. Meyer. Chem. Ber. **45**, 2843 (1912).
17. A. Hantzsch. Chem. Ber. **48**, 1407 (1915).
18. C. Cooper. J. Biol. Chem. **216**, 37 (1955).
19. D. Shugar and K. L. Wierzchowski. Biochim. et Biophys. Acta, **23**, 657 (1957).
20. M. M. Davies and G. B. B. M. Sutherland. J. Chem. Phys. **6**, 755 (1938).
21. E. Ware. Chem. Revs. **46**, 403 (1950).
22. G. S. Hammond. *In* Steric effects in organic chemistry. *Edited by* M. S. Newman. John Wiley. 1956. p. 451.
23. R. Andreasch. Monatsh. **18**, 56 (1897).
24. L. H. Flett and W. H. Gardner. Maleic anhydride derivatives. John Wiley. 1952. p. 234.
25. R. Tambach. Ann. **280**, 233 (1894).
26. R. N. Jones, C. L. Angell, T. Ito, and R. J. D. Smith. Can. J. Chem. **37**, 2007 (1959).

Can. J. Chem. Downloaded from www.nrcresearchpress.com by 186.148.149.217 on 09/04/12
For personal use only.

Can. J. Chem. Downloaded from www.nrcresearchpress.com by 186.148.149.217 on 09/04/12
For personal use only.

THE THERMAL DECOMPOSITION OF PHENYLACETIC ACID[1]

MARGARET H. BACK[2] AND A. H. SEHON

ABSTRACT

The thermal decomposition of phenylacetic acid was investigated by the toluene-carrier technique over the temperature range 587 to 722° C. The products of the pyrolysis were carbon dioxide, carbon monoxide, hydrogen, methane, dibenzyl, and phenylketene. From the kinetics of the decomposition it was concluded that the reaction

$$C_6H_5CH_2COOH \rightarrow C_6H_5CH_2 + COOH$$

was a homogeneous, first-order process and that the rate constant of this dissociation step was represented by the expression $k = 8\times10^{12}.e^{-55,000/RT}$ sec^{-1}. The activation energy of this reaction may be identified with $D(C_6H_5CH_2—COOH)$. The possible reactions of carboxyl radicals are discussed.

INTRODUCTION

Due to the resonance stabilization of the benzyl radical, the dissociation energies of the bonds $C_6H_5CH_2—R$ are smaller than the corresponding bond dissociation energies in related compounds of the type $CH_3—R$, where R is a radical or atom (1, 2). Therefore, compounds of the type $C_6H_5CH_2—R$ have proved particularly suitable for determination of these dissociation energies and of the heats of formation of radicals R using the toluene-carrier technique (3, 4, 5).

In the present study the thermal decomposition of phenylacetic acid in a stream of toluene was investigated for the purpose of producing carboxyl radicals by the rupture of the $C_6H_5.CH_2—COOH$ bond and for studying their subsequent reactions. Furthermore, it was anticipated that from the kinetics of the pyrolysis one might be able to derive the dissociation energy of this bond.

EXPERIMENTAL

Materials

Phenylacetic acid (m.p. 77° C) was obtained from Eastman Kodak Co. and used without further purification. The toluene was generously supplied by Gulf Oil Corporation, Pittsburgh, Pa. It was stirred for 24 hours with dilute sodium hydroxide, dried, and distilled through an efficient column. The fraction boiling at 110.5° C was used in this study.

Apparatus and Procedure

The pyrolysis was studied in a vacuum flow system similar to those used in previous investigations employing the toluene-carrier technique (6). The reaction vessel was 26 mm in diameter and 20 cm long, with a volume of about 200 cc. It was provided with a central thermocouple well to enable one to measure the temperature along the length of the whole reaction vessel. The gradient along this length was not more than 4 degrees and fell sharply on either side. Adequate preheating was ensured by allowing the gas to pass through a length of tubing intermediate in size between that of the reaction vessel and the inlet lead. The temperature of the furnace surrounding the reaction vessel was regulated within ±2° with a Thermo Electric regulator.

The surface dependence of the reaction was examined by using a similar reaction vessel

[1]*Manuscript received April 11, 1960.*
Contribution from the Department of Chemistry, McGill University, Montreal, Que. The results of this study were presented at the 135th Meeting of the American Chemical Society, Boston, April, 1959.
[2]*Submitted in partial fulfillment of the requirements for the degree of Ph.D. Present address: Division of Applied Chemistry, National Research Council, Ottawa, Ontario.*

packed with silica wool, supplied by Microchemical Specialties, Berkeley, Calif. The average diameter of the silica fibers was 3×10^{-3} cm and the average length was 15 cm. The surface-to-volume ratio of this vessel was about 27 times that of the unpacked vessel. The decomposition of phenylacetic acid was studied over the temperature range 587 to 772° C.

Known weights of the acids were introduced into a U-tube in the form of pellets. This method proved convenient and accurate and avoided errors due to handling losses of the solid powder. One arm of the U-tube was connected with the toluene reservoir and the other led directly to the furnace. The U-tube was heated by a removable bath containing dibutyl phthalate for the lower temperatures and Fisher bath wax for the higher temperatures. The temperature of the bath was maintained constant with a Fenwall thermoregulator.

The tubes leading to and from the furnace were heated electrically with Nichrome wire to prevent condensation of the acid and products. The pressure of toluene and reactant during an experiment was maintained constant with a manostat and measured with a mercury manometer, read with a cathetometer to an accuracy of ±0.01 mm. Variations in pressure caused the mercury in the sloping arm of the manostat to make and break contact with a platinum wire connected to a suitable relay, which in turn controlled the heater of the water bath surrounding the toluene.

The products were fractionated through a series of three traps maintained at $-5°$ C, $-78°$ C, and $-188°$ C. The non-condensable gases were removed by two diffusion pumps connected in series and collected into calibrated bulbs. The undecomposed acid and dibenzyl were trapped together at $-5°$ C and weighed. The recovered acid was titrated and the yield of dibenzyl was calculated by difference. The dibenzyl collected from a few experiments was purified by recrystallization and mixed with a pure sample; its mixed melting point was 52° C. Carbon dioxide was measured in a gas burette and identified by its vapor pressure – temperature curve. Samples of the non-condensable gases were analyzed by combustion over copper oxide at 300° C.

RESULTS

The main product of the decomposition was carbon dioxide, with much smaller amounts of carbon monoxide. Hydrogen and methane were formed in amounts varying between 20 and 60% of the carbon dioxide, and the ratio of hydrogen to methane varied from 2.0 to 3.5. The yield of dibenzyl approached that of the non-condensable gases. Table I shows the main products and the amounts of acid decomposed under different experimental conditions. The experiments marked with letter P refer to those done in the packed vessel.

The carbon dioxide and carbon monoxide did not account for all the acid decomposed. It was found that the decomposition also yielded phenylketene,* a yellow compound which was trapped with the toluene. The ketene reacted with water to give phenylacetic acid which was titrated with sodium hydroxide. However, the amounts of phenylketene recovered in this way did not account completely for the acid deficit. Phenylketene has been reported to be a very reactive compound which rapidly dimerizes (8) and this might have prevented its quantitative conversion to the acid. The production of phenylketene was considerably increased in the packed reaction vessel, and this mode of decomposition

Reaction of this compound with aniline gave the anilide of phenylacetic acid, which was identified by a mixed melting point determination with a pure sample prepared according to the method described by Shriner and Fuson (7). The melting point of the mixed sample was 114 to 115° C.

Can. J. Chem. Downloaded from www.nrcresearchpress.com by 186.148.149.217 on 09/04/12
For personal use only.

TABLE I

Products of the decomposition of phenylacetic acid

Expt. No.	T, °A	Total pressure, mm Hg	P_a/P_t*	t, sec	Acid decomp., mmoles	% decomp.	CO_2, mmoles	Non-condensable gases, mmoles	% CH_4	% CO	% H_2	Dibenzyl / (H_2+CH_4+CO)	H_2 / CH_4	k (sec^{-1})	k_1 (sec^{-1})
123	860	12.45	.038	1.03	.57	19.6	.191	.038	27.4	12.3	60.2	.87	2.2	.21	.07
124	870.5	12.8	.036	.98	.57	21.0	.234	.059	28.9	9.1	62.0	.73	2.1	.24	.10
119	876	10.8	.027	.35	.375	11.4	.1415	.020	27.8	8.8	63.4		2.3	.35	.13
136P	876	11.5	.010	.42	2.26	73.0	.128	.0265	12.6	52.5	34.9		2.8	2.98	.18
118	877	11.3	.030	.41	.36	12.0	.147	.024	28.0	8.9	63.2	.75	2.3	.31	.12
98	879	6.3	.016	.37	.40	19.2	.119	.021	28.8	13.3	57.9	.71	2.0	.58	.17
120	881	12.0	.024	.36	.32	12.8	.131	.021	28.3	7.3	64.4		2.3	.38	.15
96	881	12.1	.017	.49	.43	21.5	.139	.028	30.6	11.2	58.2	.61	1.9	.49	.16
97	881	5.5	.033	.85	.61	30.6	.232	.068	27.2	11.1	61.7	.84	2.3	.43	.17
131P	881.5	12.2	.013	.345	1.38	57.0	.123	.018	15.7	45.0	39.3		2.5	2.45	.22
125	882.5	13.1	.033	.95	.67	24.5	.340	.1075	29.1	7.7	63.2	.81	2.2	.30	.15
115	891.5	4.7	.029	.42	.38	16.9	.1915	.043	27.1	8.3	64.6	.67	2.4	.44	.22
116	892	12.7	.019	.39	.43	17.6	.201	.201	29.5	6.2	64.4	.80	2.2	.50	.23
135P	892	12.2	.010	.39	1.67	77.5	.123	.031	14.2	51.4	34.4		2.4	3.88	.31
126	904	11.6	.013	.975	.87	47.5	.417	.208	28.1	10.2	61.7	.84	2.2	.66	.34
109	904	11.4	.012	.31	.31	18.1	.175	.041	30.9	5.6	63.7	1.00	2.1	.65	.36
111	904	11.25	.013	.29	.32	16.1	.213	.041	31.4	4.6	64.0	.66	2.0	.60	.40
110	904.5	11.4	.016	.41	.34	19.8	.230	.067	30.8	4.3	64.9	.79	2.1	.54	.36
82	914	11.2	.015	.345	.39	25.5	.224	.0765	30.2	9.6	60.2	.82	2.0	.85	.50
134P	920	11.5	.0083	.33	.31	20.6	.139	.061	15.5	50.5	33.9		2.2	6.18	.78
94	926	12.9	.0094	.30	.69	44.1	.253	.090	29.4	9.2	61.4	.76	2.1	1.58	.69
95	926	5.3	.031	.47	.60	47.6	.312	.142	22.4	12.5	65.1	.89	2.9	1.36	.74
127	928	10.2	.022	1.05	1.07	69.8	.569	.4115	24.1	12.9	63.0	.81	2.6	1.13	.65
117	931.5	10.6	.038	.33	.69	32.3	.4605	.193	25.1	5.8	69.1	.88	2.8	1.20	.81
100	938	10.3	.011	.27	.73	43.7	.316	.143	27.8	10.8	61.4	.74	2.2	2.12	.95
101	938.5	10.9	.018	.56	.96	67.0	.477	.307	25.6	13.4	61.0	.79	2.4	1.96	1.05
102	939	11.0	.031	.30	.45	30.4	.388	.159	25.8	2.3	71.9	.54	2.8	1.20	1.03
103	939.5	10.7	.013	.35	.55	34.6	.454	.218	28.6	2.7	68.6	.86	2.4	1.22	1.00
133P	940	11.75	.0081	.30	.48	29.3	.211	.129	16.3	48.4	35.3		2.2	7.83	1.42
83	947	11.3	.011	.28	.72	46.5	.459	.241	26.8	9.1	64.1	.76	2.4	2.24	1.47
84	950	10.0	.038	.34	.93	55.6	.601	.305	20.8	10.8	68.4	.95	3.3	2.44	1.64
112	956	4.7	.023	.40	.87	60.9	.629	.356	20.2	10.1	69.8	.89	3.5	2.37	1.80
113	957	11.1	.020	.35	.73	55.5	.554	.3195	24.0	6.6	69.4	.86	2.9	2.32	1.81
114	957	11.4	.016	.28	.67	50.0	.453	.256	25.4	5.9	68.6	.80	2.7	2.33	1.69
93	960.5	11.1	.015	.31	.80	64.4	.517	.315	23.5	11.9	64.6	.80	2.7	3.36	2.28
106	968	4.9	.031	.39	.61	69.1	.515	.286	18.3	7.4	74.4	.91	4.1	2.94	2.60
108	968	11.0	.010	.28	.54	57.4	.4155	.264	25.4	5.9	68.6	.82	2.7	3.05	2.41
107	968.5	10.9	.012	.35	.55	65.2	.461	.295	24.1	6.1	69.8	.83	2.9	3.00	2.64
105	980	10.7	.011	.27	.53	65.7	.462	.303	24.0	5.2	70.7	.80	2.9	4.00	3.55
104	980.5	11.1	.012	.31	.63	70.6	.610	.3725	23.7	4.3	71.9	.83	3.0	4.07	3.91
99	986	6.8	.022	.35	.74	87.8	.507	.371	16.7	20.4	63.0	.77	3.8	5.90	4.63
92	990	6.6	.028	.35	.74	88.7	.581	.388	15.1	19.1	65.8	.77	4.4	6.32	5.52
91	991	11.0	.015	.29	.685	85.9	.501	.383	20.3	17.3	62.3	.72	3.1	6.88	5.61
121	995.5	11.1	.014	.285	.91	85.2	.709	.542	19.8	13.1	67.1	.79	3.4	6.77	5.74
122	995.5	11.1	.012	.26	.86	85.6	.660	.496	20.7	12.4	67.0		3.2	6.60	5.49

*P_a and P_t refer to partial pressures of phenylacetic acid and toluene, respectively.

may be partly heterogeneous. The percentage carbon monoxide in the non-condensable gases also increased to about 50% although the total production of non-condensable gases was only very slightly increased (Table II).

In one experiment the contents of the dry ice – acetone trap were tested for the presence of phenol by following the pH change of an acid–base titration. Comparison of this curve with a curve obtained from titration of a synthetic mixture containing an amount of phenol corresponding to about 1% of the initial concentration of phenylacetic acid used in the experiment showed that negligible, if any, amounts of phenol were produced in the decomposition.

Can. J. Chem. Downloaded from www.nrcresearchpress.com by 186.148.149.217 on 09/04/12
For personal use only.

TABLE II

Effect of packed reaction vessel on % decomposition of phenylacetic acid, % CO, k, and k_1

Expt. No.	T, °A	Total % decomp.	% CO	k (sec^{-1})	k_1 (sec^{-1})
119	876	11.4	8.8	.35	.13
136P	876	71.5	52.5	2.98	.18
97	881	30.4	11.1	.43	.17
131P	881.5	57.0	45.0	2.45	.22
116	892	17.7	6.2	.50	.23
135P	892	77.6	1.4	3.88	.31
94	920	37.9	9.2	1.58	.70
134P	920	87.1	50.5	6.18	.78
103	939.5	34.7	2.7	1.22	1.00
133P	940	90.5	48.4	7.83	1.42

Attempts were made to detect formic acid in the reaction products but the large excess of toluene and the presence of other reaction products made the analysis extremely difficult and positive identification was not made.

From two experiments in the packed vessel the contents of the trap maintained at −5° C were titrated by following the pH change, and the presence of a small amount of a strong acid was evident. Although positive identification was not made, this acid was suspected to be oxalic. No evidence for the formation of oxalic acid was observed in the unpacked vessel.

DISCUSSION

Mechanism of Decomposition

The results suggested that the decomposition might occur by two simultaneous processes,

$$C_6H_5CH_2COOH \xrightarrow{k_1} C_6H_5CH_2. + .COOH, \quad [1]$$

$$C_6H_5CH_2COOH \xrightarrow{k_2} C_6H_5CHCO + H_2O, \quad [2]$$

reaction [1] being predominant. If each carboxyl radical is assumed to yield subsequently one molecule of either carbon dioxide or carbon monoxide, the rate of production of (CO_2 + CO) would be a measure of the rate of reaction [1]. To calculate the rate constant of this step, it was assumed that both processes [1] and [2] were first-order with respect to the acid concentration. The rate of decomposition of acid, A, may then be written

$$-\frac{dA}{dt} = (k_1+k_2)A = kA$$

where k is the over-all rate constant for the disappearance of acid. The rate of production of carbon dioxide plus carbon monoxide is then given by

$$\frac{d(CO_2+CO)}{dt} = k_1A = k_1(A_0e^{-kt})$$

and on integration it follows that

$$[CO_2+CO] = \frac{k_1}{k}A_0(1-e^{-kt}) = \frac{k_1}{k}(A_0-A).$$

Can. J. Chem. Downloaded from www.nrcresearchpress.com by 186.148.149.217 on 09/04/12
For personal use only.

The rate constant k was calculated in terms of the amount of acid decomposed and rate constant k_1 could then be evaluated from the measured yield of $(CO_2 + CO)$. It ought to be pointed out that this calculation is not sensitive to the order of reaction [2], especially at low conversions, and also does not depend on an analysis for phenylketene. The rate constant k_2 represents the difference between k and k_1. Because of the large error necessarily involved in determining a small difference between two rate constants, no attempt was made to calculate an activation energy for reaction [2].

The first-order rate constants, k and k_1, measured for a variety of experimental conditions are listed in Table I. The rate constant k_1 remained almost unaffected, within the experimental accuracy, when the reaction time was varied by a factor of 4, the partial pressure of acid by a factor of 3, and the total pressure of toluene by a factor of 3. These results are shown in Tables IV, V, and VI. The small increase of about 30% in k_1

TABLE III

Effect of variation of toluene pressure on composition of non-condensable gases

Expt. No.	T, °A	Toluene pressure, mm	% CH_4	% CO	% H_2
98	879	6.3	28.8	13.3	57.9
96	881	12.1	30.6	11.2	58.2
112	956	4.7	20.2	10.1	69.8
113	957	11.1	24.0	6.6	69.4
106	968	4.9	18.3	7.4	74.4
107	968.5	10.0	24.1	6.1	69.8
92	990	6.6	15.1	19.1	65.8
91	991	10.9	20.3	17.3	62.3

in the packed reaction vessel is not considered significant because the surface-to-volume ratio had been increased by a factor of about 27. Therefore, the rate of reaction [1], as measured by the rate of production of carbon dioxide plus carbon monoxide, is considered to be a homogeneous, first-order dissociation process. The plot of log k_1 vs. $1/T$ was represented by a straight line over the range of temperature studied and is shown in Fig. 1. From this line the activation energy of reaction [1] was calculated as 55 kcal/mole and the frequency factor as 8×10^{12} sec^{-1}.

The largest source of error in the measurements was considered to be the uncertainty in the temperature of the reaction vessel during an experiment, due both to fluctuations in the temperature of the furnace as a whole and to variation in temperature along the length of the reaction vessel. The error in the rate constant k_1 resulting from these fluctuations was estimated to be about 8%. This would give an uncertainty of not more than 1 kcal/mole to the activation energy for reaction [1] calculated from the slope of the plot of log k_1 against $1/T$. However, in kinetic studies such as this there is an uncertainty, inherent in the assumption of a reaction mechanism, which prevents the unequivocal identification of the measured rate with the rate of the postulated processes. Part of this uncertainty arises from side reactions which may affect the products by which the rate of the primary step is measured. Thus, an activation energy assigned to a specific reaction probably contains errors larger than those estimated solely from the measurements involved. Unfortunately, the magnitude of such errors is very difficult to assess.

Can. J. Chem. Downloaded from www.nrcresearchpress.com by 186.148.149.217 on 09/04/12
For personal use only.

Can. J. Chem. Downloaded from www.nrcresearchpress.com by 186.148.149.217 on 09/04/12
For personal use only.

TABLE IV

Effect of reaction time on first-order rate constant k_1

Expt. No.	T, °A	Time of contact, sec	k_1 (sec^{-1})
120	881	.36	.15
98	879	.37	.17
96	881	.49	.16
97	881	.85	.17
125	882.5	.95	.15
111	904	.29	.40
109	904	.31	.36
110	904	.41	.36
126	904	.975	.34
94	926	.30	.69
95	926	.47	.74
127	928	1.05	.65

TABLE V

Effect of partial pressure of acid on first-order rate constant k_1

Expt. No.	T, °A	Acid pressure, mm Hg	k_1 (sec^{-1})
98	879	0.10	0.17
97	881	0.18	0.17
96	881	0.21	0.16
120	881	0.29	0.15
100	938	0.11	.95
101	938.5	0.20	1.05
102	939	0.34	1.03
83	947	0.12	1.47
84	950	0.38	1.64

TABLE VI

Effect of toluene pressure on first-order rate constant k_1

Expt. No.	T, °A	Toluene pressure, mm Hg	k_1 (sec^{-1})
96	881	12.1	.16
98	879	6.3	.17
116	892	12.7	.23
115	892	4.7	.22
94	926	12.9	.69
95	926	5.3	.74
113	957	11.1	1.81
112	956	4.7	1.80
107	968.5	10.9	2.64
106	968	4.9	2.60
91	991	11.0	5.61
92	990	6.6	5.52

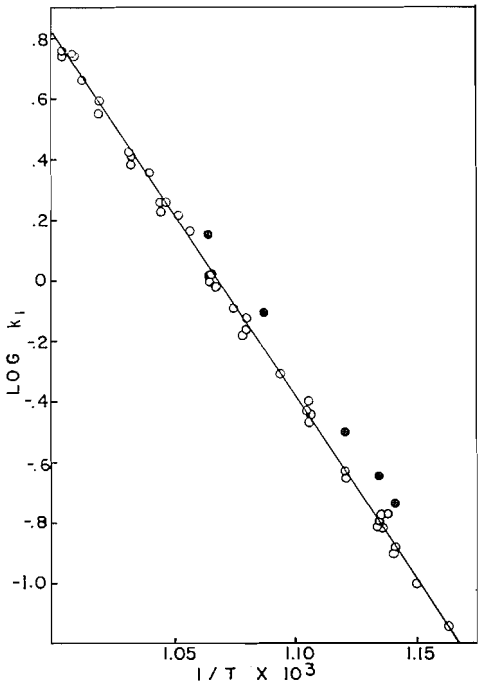


FIG. 1. Plot of log k_1 against $1/T$ for the thermal decomposition of phenylacetic acid.
○Experiments done in the unpacked reaction vessel.
●Experiments done in the packed reaction vessel.

Fate of the Carboxyl Radical

The carboxyl radical may decompose thermally in the following ways:

$$COOH \rightarrow CO_2 + H \quad [3]$$

$$COOH \rightarrow CO + OH \quad [4]$$

According to this scheme each carbon dioxide molecule is accompanied by a hydrogen atom, and each carbon monoxide molecule by a hydroxyl radical. On the basis of previous results (9) it was expected that the hydrogen atoms would react with toluene to give hydrogen and methane in the ratio 3:2.

$$H + C_6H_5CH_3 \rightarrow C_6H_5CH_2 + H_2 \quad [5a]$$

$$H + C_6H_5CH_3 \rightarrow C_6H_6 + CH_3 \quad [5b]$$

$$H + C_6H_5CH_3 \rightarrow C_6H_5 + CH_4 \quad [5c]$$

The most probable reaction of hydroxyl radicals with toluene was thought to be abstraction of a hydrogen atom to form water.

$$OH + C_6H_5CH_3 \rightarrow C_6H_5CH_2 + H_2O \quad [6a]$$

However, the displacement reactions, similar to reactions [5*b*] and [5*c*],

$$OH + C_6H_5CH_3 \rightarrow C_6H_5OH + CH_3 \quad [6b]$$

$$OH + C_6H_5CH_3 \rightarrow C_6H_6 + CH_3OH \quad [6c]$$

might also participate. Failure to detect phenol showed that reaction [6*b*] did not occur.

Can. J. Chem. Downloaded from www.nrcresearchpress.com by 186.148.149.217 on 09/04/12
For personal use only.

It was therefore assumed that hydroxyl radicals reacted with toluene to give products trapped at −78° C.

If all the benzyl radicals dimerized to give dibenzyl,

$$2C_6H_5CH_2 \rightarrow (C_6H_5CH_2)_2, \qquad [7]$$

the following stoichiometry should have been observed:

$$CO_2 = H_2 + CH_4$$
$$(C_6H_5CH_2)_2 = CO_2 + CO = H_2 + CH_4 + CO$$
$$H_2/CH_4 = 1.5$$

None of these conditions was in fact observed. As mentioned previously, the carbon dioxide was always greater than the sum of the hydrogen and methane, and the ratio of hydrogen to methane varied from 2.0 to 3.5. The first-order rate constant calculated from the amount of $(H_2 + CH_4 + CO)$ produced was always lower than that calculated from the yield of $(CO_2 + CO)$ and varied with reaction time. Moreover, the Arrhenius plot of the former rate constant was not rectilinear over the whole temperature range studied. The yield of dibenzyl was always much less than that of the carbon dioxide plus carbon monoxide, but was usually between 75 and 90% of the non-condensable gases (Table I).

Reactions [3] to [6] are therefore insufficient to account for the products formed. If carboxyl radicals do not all decompose rapidly by reactions [3] and [4], they may react with each other according to reactions [8] or [9].

$$2COOH \rightarrow 2CO_2 + H_2 \qquad [8]$$
$$2COOH \rightarrow CO_2 + CO + H_2O \qquad [9]$$

Either of these reactions produces one molecule of carbon dioxide or carbon monoxide for each carboxyl radical, and the formation of $(CO_2 + CO)$ is still a measure of the extent of reaction [1]. However, only one molecule of non-condensable gas is produced for every two carboxyl radicals, and the total amount of non-condensable gases will be less than the sum of the carbon dioxide and carbon monoxide. Reaction [8] also produces molecular hydrogen unaccompanied by methane and will result in a ratio of hydrogen to methane greater than that observed from the reaction of hydrogen atoms with toluene. The indication that under certain conditions oxalic acid may have been a product of the decomposition in the packed reaction vessel suggests that carboxyl radicals have a sufficiently long lifetime under the conditions of the present experiments to react with each other.

If carboxyl radicals react with each other, then reaction between carboxyl and benzyl radicals may be considered at least as probable. If the radicals recombined to reform phenylacetic acid, the rate constant k_1 would not appear to be first-order over the temperature range studied and under the different conditions of decomposition. Therefore, the recombination between benzyl and carboxyl radicals is not considered significant. An alternative and possibly more probable reaction for benzyl and carboxyl radicals would be the disproportionation reaction

$$C_6H_5CH_2 + COOH \rightarrow C_6H_5CH_3 + CO_2, \qquad [10]$$

which is exothermic to the extent of about 63 kcal/mole. This value represents the difference between $D(C_6H_5CH_2—H) = 83$ kcal/mole (11) and $D(COO—H) = 20$ kcal/mole. The latter value is deduced in the last paragraph of this paper.

Reactions [8], [9], and [10] lead to an excess of carbon dioxide relative to dibenzyl or

Can. J. Chem. Downloaded from www.nrcresearchpress.com by 186.148.149.217 on 09/04/12
For personal use only.

hydrogen plus methane, but the total amount of non-condensable gases should equal the amount of dibenzyl.

$$CO_2 + CO > (C_6H_5CH_2)_2 = H_2 + CH_4 + CO$$

The latter condition was indeed found to hold within the experimental accuracy for the recovery of dibenzyl. The ratio of dibenzyl to non-condensable gases varied between 0.75 and unity (Table I). In previous studies it was shown that dibenzyl was not trapped quantitatively at about $-5°$ C from a stream of toluene, and the recoveries were of the order of 80–90% of the expected amount (10). It was considered, therefore, that the yield of dibenzyl was probably equal to the yield of non-condensable gases ($H_2 + CH_4 + CO$).

Reaction of the carboxyl radical with toluene may also occur, probably to produce carbon dioxide and hydrogen, or carbon monoxide and water.

$$COOH + C_6H_5CH_3 \rightarrow C_6H_5CH_2 + (HCOOH) \begin{cases} \nearrow CO_2 + H_2 & [11a] \\ \searrow CO + H_2O & [11b] \end{cases}$$

These reactions yield one molecule of carbon dioxide or carbon monoxide for each carboxyl radical, but they also produce a molecule of dibenzyl for each carbon dioxide or carbon monoxide formed. If formic acid were the product of the reaction, the yield of dibenzyl relative to that of ($CO_2 + CO$) would be even greater than if carbon dioxide or carbon monoxide were formed only by reactions [3] and [4].

Moreover, if reaction [11*a*] or [11*b*] occurred, each would be favored by an increase in toluene pressure and more hydrogen or carbon monoxide would be expected to be produced at the expense of methane under these conditions. However, as shown in Table III, this trend was not observed.

In previous studies with the toluene-carrier technique the production of dibenzyl was taken as a measure of the extent of the decomposition of the reactant into free radicals. The small amounts of dibenzyl formed relative to carbon dioxide may be interpreted, therefore, as an indication of an alternate mode of decomposition of phenylacetic acid by a molecular rearrangement into carbon dioxide and toluene.

$$C_6H_5CH_2COOH \rightarrow CO_2 + C_6H_5CH_3 \qquad [12]$$

If reaction [12] occurred simultaneously with reaction [1] the plot of log k_1 vs. $1/T$ would be expected to be a composite curve representing the sum of the rate constants of two processes which would probably require different activation energies. Because the plot of log k_1 vs. $1/T$ was represented by a straight line it would appear that if the molecular decomposition occurred it must have the same activation energy and the same frequency factor as reaction [1]. Therefore, although the occurrence of reaction [12] cannot be ruled out unequivocally,* its participation would not affect the conclusions derived for reaction [1], which is represented by the homogeneous, unimolecular dissociation process,

$$C_6H_5CH_2COOH \rightarrow C_6H_5CH_2 + COOH.$$

The activation energy of this step was calculated as 55 kcal/mole and the frequency factor as 8×10^{12} sec^{-1}. With the usual assumption that the recombination of radicals requires no activation energy, the value of 55 kcal/mole may be identified with the dissociation energy of the $C_6H_5CH_2$—COOH bond.

**It is possible to visualize that if reaction [12] occurred to a small extent, the linearity of the Arrhenius plot may not be seriously affected though the activation energy calculated from it may be erroneous.*

Can. J. Chem. Downloaded from www.nrcresearchpress.com by 186.148.149.217 on 09/04/12
For personal use only.

The heat of formation of carboxyl radical can be calculated using the thermochemical relation

$$\Delta H_f(\text{COOH}) = \Delta H_f(\text{C}_6\text{H}_5\text{CH}_2\text{COOH}) + D(\text{C}_6\text{H}_5\text{CH}_2\text{—COOH}) - \Delta H_f(\text{C}_6\text{H}_5\text{CH}_2).$$

Although the value for the heat of formation of benzyl radical is somewhat uncertain, a reasonable estimate for it seems to be 42 kcal/mole (11). No recent determination of the heat of formation of phenylacetic acid in its monomeric form in the gaseous phase is available. However, a value of -75 kcal/mole for $\Delta H_f(\text{C}_6\text{H}_5\text{CH}_2\text{COOH})$ may be computed from relevant thermochemical data.* In this calculation, the present authors have assumed that the heat of vaporization determined by Stull (12) corresponds to the heat of vaporization of phenylacetic acid into monomers. Taking for $D(\text{C}_6\text{H}_5\text{CH}_2\text{—COOH})$ the value of 55 kcal/mole derived in this study, it follows that $\Delta H_f(\text{COOH}) \simeq -62$ kcal/mole. In turn this value leads to the following dissociation energies $D(\text{COO—H}) = 20$ kcal/mole and $D(\text{CO—OH}) = 45$ kcal/mole.

ACKNOWLEDGMENTS

This work was supported in part by a grant from the Petroleum Research Fund administered by the American Chemical Society. Grateful acknowledgment is hereby made to the donors of said fund. The authors wish to thank also the National Research Council of Canada for continued financial assistance. We should also like to express our appreciation to the Eastman Kodak Co. for the award of a fellowship to one of us (M. H. B.).

REFERENCES

1. M. Szwarc. Chem. Revs. **47**, 75 (1950).
2. C. A. Coulson. Discussions Faraday Soc. **2**, 9 (1947).
3. M. Szwarc, B. N. Ghosh, and A. H. Sehon. J. Chem. Phys. **18**, 1142 (1950).
4. M. Szwarc. J. Chem. Phys. **17**, 505 (1949).
5. A. H. Sehon and B. de B. Darwent. J. Am. Chem. Soc. **76**, 4806 (1954).
6. C. H. Leigh, A. H. Sehon, and M. Szwarc. Proc. Roy. Soc. A, **209**, 97 (1951).
7. R. L. Shriner and R. C. Fuson. The systematic identification of organic compounds. J. Wiley & Sons. 1948. p. 158.
8. H. Staudinger. Ber. 44, 533 (1911).
9. M. Szwarc. J. Chem. Phys. **16**, 128 (1948).
10. E. H. Braye, A. H. Sehon, and B. de B. Darwent. J. Am. Chem. Soc. **77**, 5282 (1955).
11. A. H. Sehon and M. Szwarc. Ann. Rev. Phys. Chem. **8**, 439 (1957).
12. D. R. Stull. Ind. Eng. Chem. **39**, 517 (1947).
13. M. S. Kharasch. J. Research Natl. Bur. Standards, **2**, 359 (1929).
14. Handbook of chemistry and physics. 39th ed. Chemical Rubber Pub. Co. 1957–58.
15. Selected values of chemical thermodynamic properties. Natl. Bur. Standards (U.S.), Circ. 500, **48**, 206 (1952).
16. R. F. Barrow. Arkiv Fysik, **11**, 281 (1956).

*$\Delta H_{\text{combustion}}(\text{C}_6\text{H}_5\text{CH}_2\text{COOH})_s = 930.2$ *kcal/mole (13),* $\Delta H_{\text{fusion}}(\text{C}_6\text{H}_5\text{CH}_2\text{COOH}) = 30$ *cal/g (14),* $\Delta H_{\text{vaporization}}(\text{C}_6\text{H}_5\text{CH}_2\text{COOH}) = 16.4$ *kcal/mole (12),* $\Delta H_f(\text{CO}_2)_g = -94.05$ *kcal/mole (15),* $\Delta H_f(\text{H}_2\text{O})_l = -68.32$ *(15). From these data it follows that the heats of formation of phenylacetic acid in the solid, liquid, and gaseous forms are* -95.48, -91.4, *and* -75 *kcal/mole, respectively. For the calculation of* $D(\text{CO}_2\text{—H})$ *and* $D(\text{CO—OH})$ *the following heats of formation were used:* $\Delta H_f(\text{CO})_g = -26.4$ *kcal/mole (15),* $\Delta H_f(\text{H}) = 52.1$ *kcal/mole (15), and* $\Delta H_f(\text{OH}) = 9.5$ *kcal/mole based on the value of 101.3 kcal/mole (16) for* $D(\text{O—H})$.

Can. J. Chem. Downloaded from www.nrcresearchpress.com by 186.148.149.217 on 09/04/12
For personal use only.

Can. J. Chem. Downloaded from www.nrcresearchpress.com by 186.148.149.217 on 09/04/12
For personal use only.

THE THERMAL DECOMPOSITION OF DIPHENYLACETIC ACID[1]

MARGARET H. BACK[2] AND A. H. SEHON

ABSTRACT

The pyrolysis of diphenylacetic acid was investigated over the temperature range 515–636° C using the toluene-carrier technique. The main products of this system were similar to those formed in the thermal decomposition of phenylacetic acid. The rate constant for the reaction

$$(C_6H_5)_2CH.COOH \xrightarrow{k_1} (C_6H_5)_2CH + COOH$$

was calculated as $k_1 = 8\times10^{12}.\exp(-52{,}000/RT)$ sec^{-1}.

The over-all decomposition reaction was found to be partly heterogeneous and, therefore, the activation energy for reaction [1] may be only tentatively identified with $D[(C_6H_5)_2CH—COOH]$.

The investigation described in the foregoing paper (1) was extended to the thermal decomposition of diphenylacetic acid in a stream of toluene for the purpose of producing carboxyl radicals from another source and for studying their reactions further. On theoretical grounds the diphenylmethyl radical ought to be stabilized by resonance to a larger extent than the benzyl radical. Therefore, it was expected that the bond $(C_6H_5)_2CH—COOH$ would be weaker than the bond $C_6H_5CH_2—COOH$, and that diphenylacetic acid would decompose more readily than phenylacetic acid.

EXPERIMENTAL

The apparatus and procedure used were identical with those employed for the thermal decomposition of phenylacetic acid (1).

Diphenylacetic acid (m.p. 140° C) was obtained from Eastman Kodak Co. and used without further purification. The toluene was generously supplied by Gulf Oil Corporation, Pittsburgh, Pa. It was purified by treatment with dilute sodium hydroxide for 24 hours, dried, and distilled through an efficient column. The fraction boiling at 110.5° C was used in this study.

RESULTS

The products from the decomposition of diphenylacetic acid were similar to those from phenylacetic acid and are shown in Table I. Carbon dioxide was again the major product and carbon monoxide a minor product only. The sum of the hydrogen and methane produced amounted to 20–50% of the carbon dioxide, and the ratio of hydrogen to methane varied from 1.9 to 4.5, both trends increasing with increasing temperature. Carbon monoxide accounted for 30–40% of the non-condensable gases, compared with about 10% in the pyrolysis of phenylacetic acid.

The sum of the carbon dioxide and carbon monoxide produced and the undecomposed acid recovered accounted for 94–98% of the initial amount of acid. Therefore, analysis was not attempted, as with phenylacetic acid (1), for other possible products. However, small amounts of a brilliant yellow compound, suspected to be diphenylketene, were observed in the trap maintained at −5° C. The contents of this trap were dissolved in alcohol, since the latter is known to react rapidly with diphenylketene to form the ester

[1]*Manuscript received April 11, 1960.*
Contribution from the Department of Chemistry, McGill University, Montreal, Que.
[2]*Submitted in partial fulfillment of the requirements for the degree of Ph.D. Present address: Division of Applied Chemistry, National Research Council, Ottawa, Ontario.*

TABLE I

Products and rate constants of the decomposition of diphenylacetic acid

Expt. No.	T, °A	t. sec	Total pressure, mm Hg	Pressure acid, mm Hg	% decomp.	CO_2, mmoles	Non-condensable gases, mmoles	% CH_4	% CO	% H_2	H_2/CH_4	k, sec^{-1}	k_1, sec^{-1}
3P	788	.57	11.1	0.09	30.2	.037	.011	4.9	82.4	17.6	3.6	.63	.08
14	804	.695	5.55	0.1	9.3	.044	.009	13.5	51.6	34.9	2.6	.14	.06
16	805	.56	11.5	0.07	9.0	.040	.010	13.3	42.8	43.9	3.3	.17	.06
39	806	.87	10.6	0.12	8.9	.068	.012	21.2	38.3	40.5	1.9	.11	.07
35	807	1.75	10.8	0.18		.128	.029	14.0	47.4	38.6	2.8		.08
38	813	.82	10.2	0.13	11.6	.087	.015	20.5	36.9	42.5	2.1	.15	.10
29	821	.48	10.5	0.14	11.0	.057	.013	17.5	35.0	47.5	2.7	.24	.12
42	824.5	.87	10.2	0.30	15.4	.133	.027	18.4	30.3	51.3	2.8	.19	.13
41	826	.89	10.3	0.12	16.0	.125	.028	22.1	29.4	48.5	2.2	.20	.14
28	835	.46	4.05	0.13	15.6	.0885	.023	16.9	34.9	48.2	2.85	.37	.21
40	836.5	.87	10.4	0.11	22.0	.183	.044	21.2	30.3	48.5	2.3	.28	.25
2P	844	.47	10.5	0.08	61.1	.167	.0785	5.3	81.0	13.6	2.6	2.0	.71
30	849.5	.72	5.4	0.11	26.3	.192	.063	15.6	32.7	51.6	3.3	.42	.33
18	850	.49	11.9	0.15	23.0	.172	.051					.53	.37
17	851	.475	11.9	0.06	23.8	.142	.045	19.5	34.8	46.2	2.4	.57	.40
5P	852	.67	5.5	0.14	73.2	.207	.142	3.2	85.2	11.6	3.6	2.0	.81
31	866	.44	11.0	0.19	28.8	.219	.074	18.0	27.2	54.8	3.0	.77	.61
4P	867.5	.45	10.3	0.08	84.4	.203	.181	4.3	83.8	11.9	2.8	4.17	1.99
25	868.5	.555	5.1	0.08	35.1	.240	.099	15.6	33.6	50.8	3.3	.78	
26	869	.66	5.7	0.08	39.3	.334	.140	14.6	32.2	53.2	3.6	.76	.68
27	870.5	.51	11.7	0.10	35.4	.304	.108	18.3	29.4	52.4	2.9	.85	.81
32	877	.72	5.3	0.09	50.5	.409	.183	12.4	33.0	54.6	4.4	.98	.90
33	877	.51	12.9	0.15	40.0	.344	.131	17.4	23.2	59.4	3.4	1.00	.90
19	880.5	.45	11.15	0.05	44.2	.351	.163	19.7	28.8	51.4	2.6	1.29	1.10
20	880.5	.46	10.4	0.18	42.6	.366	.133	14.1	28.6	57.3	4.1	1.21	1.10
1P	897	.41	10.6	0.07	86.6	.324	.433	5.6	78.1	16.4	2.9	4.87	3.87
24	897	.43	10.7	0.14	55.7	.496	.225	14.6	27.5	57.9	4.0	1.90	1.80
23	897.5	.42	11.1	0.13	57.5	.619	.235	14.7	25.2	60.2	4.1	2.04	
21	903	.43	10.7	0.14	66.6	.610	.287	13.1	27.6	59.4	4.5	2.57	2.50
34	904	.42	10.7	0.13	62.6	.568	.278	14.3	24.3	61.4	4.3	2.32	2.19
22	909	.43	10.95	0.13	71.2	.629	.312	13.2	26.8	60.0	4.55	2.93	2.82

(2). In consequence, the ketene was not expected to interfere with the titration for the undecomposed acid. The weight of diphenylketene was obtained by assuming that this compound accounted for the difference between the acid decomposed and the (CO_2 + CO) recovered.

The recombination of benzyl and diphenylmethyl radicals may produce three possible products: dibenzyl, 1,1,2,2-tetraphenylethane, and 1,1,2-triphenylethane. A white solid, insoluble in alcohol, was deposited in the trap at −5° C, and it is suggested that this might be 1,1,2,2-tetraphenylethane, since the other recombination products are soluble in alcohol. The weight of the recombination products was estimated by subtracting the weights of undecomposed acid and of diphenylketene from the total weight of products trapped at −5° C. The moles of recombination products were obtained by assuming that benzyl and diphenylmethyl radicals were formed in equal amounts. Although the errors were necessarily large, the quantities obtained were consistently lower than the (CO_2 + CO) but slightly higher than the total amount of non-condensable gases. This will be discussed later.

No acid was found in the trap kept at −78° C, and it was concluded that formic acid was not a product of the reaction. This lends support to the conclusion that formic acid was also not a product of the decomposition of phenylacetic acid, which was previously deduced by indirect evidence in the thermal decomposition of phenylacetic acid.

Can. J. Chem. Downloaded from www.nrcresearchpress.com by 186.148.149.217 on 09/04/12
For personal use only.

Can. J. Chem. Downloaded from www.nrcresearchpress.com by 186.148.149.217 on 09/04/12
For personal use only.

DISCUSSION

These results suggest that the two modes of decomposition postulated for phenylacetic acid also occurred in the decomposition of diphenylacetic acid, but that in this case reaction [2] was of much less importance.

$$(C_6H_5)_2CHCOOH \xrightarrow{k_1} (C_6H_5)_2CH + COOH$$

$$(C_6H_5)_2CHCOOH \xrightarrow{k_2} (C_6H_5)_2C{=}C{=}O + H_2O$$

Since the general pattern of the decomposition of diphenylacetic acid was essentially similar to that of phenylacetic acid, it appeared that carboxyl radicals formed from the decomposition of diphenylacetic acid disappeared by the same reactions postulated in the decomposition of phenylacetic acid (1). Decomposition of the carboxyl radical into carbon dioxide is energetically more favorable than decomposition into carbon monoxide, and it is unlikely that the activation energy for the homogeneous reaction to give carbon dioxide would be greater than for the reaction producing carbon monoxide. However, carbon monoxide formed a larger fraction of the non-condensable gases from diphenylacetic acid than from phenylacetic acid. Furthermore, the ratio of carbon monoxide to carbon dioxide, although it was always less than one, was greater at the lower temperatures used for the decomposition of diphenylacetic acid. It would seem, therefore, that at least one of the reactions giving carbon monoxide has a lower activation energy than those giving carbon dioxide. With both acids the production of carbon monoxide was increased in the packed vessel (Table II) and was also favored at low toluene pressures

TABLE II

Effect of packed reaction vessel on % decomposition of diphenylacetic acid, % CO, k,* and k_1

Expt. No.	T, °A	Total % decomp.	% CO	k, sec^{-1}	k_1, sec^{-1}
30	849.5	26.3	32.7	.42	.42
2P	844	61.1	81.0	2.04	1.33
17	851	23.8	34.8	.57	.40
5P	852	73.2	85.2	1.97	1.15
31	866	28.8	27.2	.77	.61
4P	867.5	84.4	83.8	4.17	1.86
24	897	55.7	27.5	1.90	1.80
1P	897	86.6	78.1	4.87	2.86

*k refers to the first-order rate constant for the over-all reaction calculated in terms of the acid decomposed.

(Table III). Consequently, it is suggested that carboxyl radicals decomposed primarily heterogeneously to yield carbon monoxide and a hydroxyl radical. The activation energy for such a reaction might be fairly low.

The interaction of carboxyl radicals by reactions [8] and [9] of the scheme postulated in the previous paper (1) leaves an excess of diphenylmethyl radicals over benzyl radicals. Thus the weight of product condensed at 0° C would be greater than it would be if diphenylmethyl radicals and benzyl radicals were formed in equal molar ratios. This would make the estimation of the moles of recombination product, based on a 1:1 molar ratio of diphenylmethyl and benzyl radicals, too high. This might explain why the calculated

TABLE III

Effect of variation of toluene pressure on composition of non-condensable gases of diphenylacetic acid

Expt. No.	T, °A	Toluene pressure, mm Hg	% CH_4	% CO	% H_2
32	877	5.3	12.4	33.0	54.6
33	877	12.9	17.4	23.2	59.4
25	868.5	5.1	15.6	33.6	50.8
31	866	11.0	18.0	27.2	54.8
14	804	5.6	13.5	51.6	34.9
39	806	10.6	21.2	38.3	40.5

amounts of recombination products were greater than the amounts of non-condensable gases, although the results are not sufficiently accurate to permit a quantitative estimate of the effect.

The rate constant k_1 was calculated from the rate of production of carbon dioxide plus carbon monoxide, assuming both reactions [1] and [2] to be first-order. The results are shown in Table I. This rate constant was practically unaffected by varying the partial pressure of acid by a factor of 3 (Table IV), the reaction time by a factor of 2

TABLE IV

Variation of k_1 with partial pressure of acid

Expt. No.	T, °A	Acid pressure, mm Hg	k_1, sec^{-1}
16	805	0.07	.08
39	806	0.12	.07
35	807	0.18	.08
41	826	0.12	.14
42	824.5	0.30	.13
17	851	0.06	.40
18	850	0.15	.37
19	880.5	0.04	1.10
20	880.5	0.17	1.10

(Table V), and the total pressure of toluene by a factor of 2 (Table VI). The plot of log k_1 against $1/T$ was represented by a straight line over the range of temperatures studied and

TABLE V

Variation of k_1 with reaction time

Expt. No.	T, °A	t, sec	k_1, sec^{-1}
16	805	.56	.06
39	806	.87	.07
29	821	.48	.12
41	826	.89	.14
28	835	.46	.21
40	836.5	.87	.23

TABLE VI

Variation of k_1 with toluene pressure

Expt. No.	T, °A	Toluene pressure, mm Hg	k_1, sec^{-1}
14	804	5.55	.06
16	805	11.5	.06
26	869	5.6	.68
27	870.5	11.7	.81
32	877	5.3	.90
33	877	12.9	.90

Can. J. Chem. Downloaded from www.nrcresearchpress.com by 186.148.149.217 on 09/04/12
For personal use only.

is shown in Fig. 1. From the slope of this line an activation energy of 52 kcal/mole and a frequency factor of 8×10^{12} sec^{-1} were calculated.

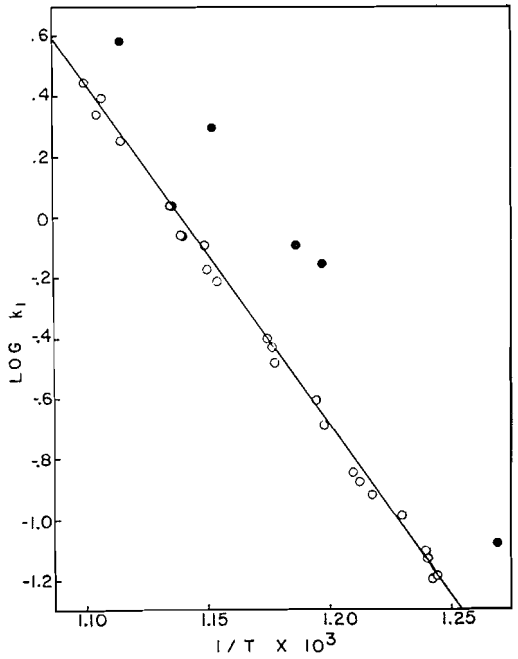


FIG. 1. Plot of log k_1 against $1/T$ for the thermal decomposition of diphenylacetic acid.

○ Experiments done in the unpacked reaction vessel.

● Experiments done in the packed reaction vessel.

The pyrolysis of diphenylacetic acid appeared to be more affected by the surface conditions than that of phenylacetic acid. In the packed reaction vessel the over-all decomposition was greatly increased and much larger quantities of the yellow compound, suspected to be diphenylketene, were observed. The rate constant calculated from the amount of (CO_2 + CO) produced was increased by a factor of almost three as compared with the values obtained with the unpacked reaction vessel (Table II). However, the slope of the plot of log k_1 against $1/T$ was similar to that obtained with the values calculated for the unpacked reaction vessel. Since in the packed reaction vessel the surface to volume ratio was increased by a factor of about 27, an increase in k_1 by a factor of 3 may be interpreted as an indication that only about 11% of the free radical decomposition occurred on the surface of the vessel. Therefore, the pyrolysis of diphenylacetic acid may be considered to be primarily a homogeneous reaction.

Because of the uncertainty of the role of the surface in this decomposition, the identification of the activation energy with the bond dissociation energy, $D[(C_6H_5)_2CH—COOH]$, is somewhat tentative. However, the frequency factor is close to that expected for a unimolecular dissociation and, remarkably, it is identical with that for the decomposition of phenylacetic acid. Moreover, the value of 52 kcal/mole is reasonable considering that the bond dissociation energy assigned to the corresponding bond in phenylacetic acid was estimated at 55 kcal/mole. The difference between these two bond dissociation

Can. J. Chem. Downloaded from www.nrcresearchpress.com by 186.148.149.217 on 09/04/12
For personal use only.

energies is supported by the results obtained from the studies of the thermal decompositions of benzyl and diphenylmethyl bromides (3). In the latter studies the diphenylmethyl radical was found to be slightly more stabilized by resonance than the benzyl radical.

ACKNOWLEDGMENTS

This work was supported in part by a grant from the Petroleum Research Fund administered by the American Chemical Society. Grateful acknowledgment is hereby made to the donors of said fund. The authors wish to thank also the National Research Council of Canada for continued financial assistance. We should also like to express our appreciation to the Eastman Kodak Co. for the award of a fellowship to one of us (M. H. B.).

REFERENCES

1 M. H. BACK and A. H. SEHON. Can. J. Chem. **38**, 1261 (1960).
2. H. STAUDINGER. Ber. **38**, 1735 (1905).
3. J. J. THROSSELL. Ph.D. Thesis, College of Forestry, State University of New York, Syracuse, N.Y. 1955.

Can. J. Chem. Downloaded from www.nrcresearchpress.com by 186.148.149.217 on 09/04/12
For personal use only.

Can. J. Chem. Downloaded from www.nrcresearchpress.com by 186.148.149.217 on 09/04/12
For personal use only.

CLAM POISON

I. THE PAPER CHROMATOGRAPHIC PURIFICATION OF CLAM POISON DIHYDROCHLORIDE[1]

A. A. Casselman, R. Greenhalgh, H. H. Brownell, and R. A. B. Bannard

ABSTRACT

A semimicro (10–25 mg) paper chromatographic method for purification of clam poison has been developed. This procedure when applied to a partially purified (toxicity 4150 MU/mg) sample of the toxin gave a 74% recovery of clam poison dihydrochloride of purity identical with that of the best material obtained by Schantz *et al.* (2) via the alumina chromatographic method. The upper limit of purity of toxin resulting from paper chromatography is estimated to be 98% because of traces of impurity introduced by the paper. The paper chromatographic procedure has been found capable of enriching low-grade toxic residues (35%) from the alumina process to a purity of 75% with an over-all recovery of 70%.

INTRODUCTION

Mold and co-workers (1) recently described the criteria for purity of clam poison dihydrochloride, the paralytic poison which can be isolated from the siphon of the toxic Alaska butter clam *Saxidomus giganteus* (2). Among other properties, the paper chromatography of clam poison dihydrochloride was examined in several solvent systems and it was observed (1) that the compound gave only one typical pink spot with Weber reagent (3) (R_F 0.30) when phenol–water (4:1) or *t*-butanol – acetic acid – water (2:1:1) was used as developer. The above-mentioned workers kindly provided us with 300 mg of partially purified (toxicity 4150 MU*/mg) clam poison which we wished to use for structural investigation. Paper chromatograms revealed, however, that the sample contained at least five components and it became evident to us that further purification was necessary. Because of the small quantity at our disposal, the method of purification used by Schantz *et al.* (2), involving as its final step chromatography on acid-washed alumina, was considered likely to be too wasteful due to the relatively low recovery of material of high toxicity (25–45%). Furthermore, prior to commencing degradative studies it was considered necessary to develop a semimicro method applicable to reaction mixtures from clam poison which would make feasible both the isolation of products and recovery in a high state of purity of any unreacted toxin. In addition, it was desired to examine the feasibility of paper chromatography as a means for purification of the clam poison residues of low toxicity (hereinafter designated as clam poison tailings) which on reworking by a variety of chromatographic methods (4) had failed to produce material with an enhanced toxicity. The work now to be outlined describes the development of the paper chromatographic method of purification and its application to (*a*) recovery and further investigation of the components contained in the partially purified sample of toxin furnished by Schantz *et al.* (2), and (*b*) enrichment of clam poison tailings.

RESULTS AND DISCUSSION

Chromatography of the partially purified clam poison dihydrochloride sample on *unwashed* Whatman No. 1 paper, using *t*-butanol – acetic acid – water (2:1:1)† as

[1]*Manuscript received March 7, 1960.*
Contribution from Defence Research Chemical Laboratories, Ottawa, Canada. Presented in part at the 41st Annual Conference of the Chemical Institute of Canada, Toronto, Ontario, May 26–28, 1958.
Issued as D.R.C.L. Report No. 283.
*MU = *mouse unit.*
†*All chromatograms were developed in this solvent system unless otherwise specified.*

developer gave three pink spots, R_F 0.19, 0.32, and 0.53, on spraying with Weber (3) reagent. These components could also be detected as blue spots by spraying with bromcresol green, or as fluorescent spots on exposure to ultraviolet light. Ultraviolet light also revealed the presence of another component, R_F 0.0. When the chromatograms were sprayed with Sakaguchi (5, 6) reagent, which is specific for monoalkylguanidines (7), a typical red spot appeared at R_F 0.70, indicating the presence of a fifth component. Component 3 (see Table I) appeared as an atypical greenish yellow spot with Sakaguchi reagent and as an atypical yellow spot with ninhydrin. Resolution of the clam poison sample into five components was also observed when other solvent systems were used, as shown in Table I. From these results, and those of Mold *et al.* (1), it seemed probable that component 3 is clam poison and that the other components present in the sample are impurities either present initially or formed by partial decomposition during storage in aqueous solution at pH 5.

TABLE I

Paper chromatography of clam poison dihydrochloride

	R_F in solvent system				
Component	*t*-Butanol – acetic acid – water (2:1:1)	Phenol–water (4:1)	*t*-Butanol – 1% hydrochloric acid (3:1)	*n*-butanol – acetic acid – water (25:6:25)	*n*-Butanol – 1% hydrochloric acid (5:6)
1*	0.00	0.03	0.00	0.02	0.00
2*†‡	0.19	0.20	0.05	0.07	0.05
3*†‡	0.32	0.30	0.17	0.23	0.08
4*†‡	0.53	0.40	0.42	0.39	0.24
5§	0.70	0.91	0.64	0.55	0.24

*UV fluorescent. †Weber positive. ‡Bromcresol green positive. §Sakaguchi positive.

Application of paper chromatographic techniques to purification and recovery of the components present in the sample of partially purified clam poison dihydrochloride revealed that impurities were being introduced during the process, since greater than theoretical recoveries were at first obtained. The most probable source of such error is the presence of extractable impurities in the paper, or debris produced during chromatography by partial degradation of cellulose by the solvent system. Other workers (8, 9, 10, 11) have found that extensive purification or pretreatment of the paper is essential if reproducible results in quantitative paper chromatography are to be obtained where acidic or basic solvent systems are employed. Accordingly, several procedures for pretreatment of Whatman No. 1 paper were examined with the object of eliminating or minimizing extractable materials. After pretreatment according to the procedures given in Table II, blank runs were performed using only the pretreated paper and the developing solvent. After drying, strips corresponding in location and area to the five components previously found to be present in the sample were cut from the "chromatograms", eluted with water, and the eluates concentrated, lyophilized, and weighed. The amount of residue thus obtained should correspond to the amount of impurity introduced into a given component during actual purification. The results presented in Table III make it evident that procedure 2 (see Table II) yields eluates containing the smallest amounts of impurities, and this method was adopted for all subsequent quantitative work.

In Table III, three sets of results are given under procedure 2. The first column represents minimum quantities of impurities introduced by the method. The next two

Can. J. Chem. Downloaded from www.nrcresearchpress.com by 186.148.149.217 on 09/04/12
For personal use only.

TABLE II

Washing procedures for Whatman No. 1 paper

Procedure 1		Procedure 2		Procedure 3		Procedure 4	
Solution	Duration (days)	Solution	Duration (days)	Solution	Duration (days)	Solution	Duration (days)
0.01 *N* HCl	3	1 *N* Na_2CO_3	4.5	2 *N* HOAc	2.5	0.01 *N* HCl	3
H_2O	4	H_2O	2.5	H_2O	2	H_2O	4
		2 *N* HOAc	2	0.5 *N* LiOH	9	Phenol–water (4:1)	4
		H_2O	2	H_2O	5	H_2O	4
		0.1 *N* $Ca(OAc)_2$	2	1.5% 8-hydroxyquinoline (in 95% EtOH)	2.5		
		H_2O	2	95% EtOH	2.5		
		1.5% 8-hydroxyquinoline (in 95% EtOH)	2.5	Solvent system*	4		
		95% EtOH	4	H_2O	4		
		Solvent system*	4				
		H_2O	4				

*t-BuOH – HOAc – H_2O (2:1:1).

TABLE III

Impurity introduced during chromatographic purification of toxin components

		Weight of impurity (mg) for pretreatment					
Component No.	R_F	Procedure 1*	2*			3*	4†
1	0.00	0.24	0.17	0.19	0.22	0.46	0.31
2	0.19	0.29	0.14	0.25	0.21	0.40	0.36
3	0.32	0.59	0.19	0.26	0.23	0.37	0.49
4	0.53	0.56	0.25	0.51	0.50	0.52	0.37
5	0.70	1.05	0.26	0.41	0.37	0.81	0.37

*Solvent system *t*-butanol – acetic acid – water (2:1:1). †Solvent system phenol–water (4:1).

columns represent duplicate assays on another batch of paper pretreated in the same manner and are the maximum amounts of impurities encountered by the method. Thus, the quantity of impurity introduced per component is consistent for sheets within a given batch of paper, but some variation is to be expected from batch to batch. For actual purification of clam poison, therefore, blank runs were performed on two sheets from the batch of pretreated paper to be used in the purification. The arithmetic mean of the values thus obtained in the two runs for a given component was taken as the correction factor to be subtracted from the weight of that component recovered in actual chromatograms.

In procedure 2 the sodium carbonate treatment is used to open up the fiber structure of the paper and to remove hemicellulose (12), polypeptides (9), and acidic impurities. Treatment with acetic acid removes basic impurities and the alkaline earth metal ions Ca^{++} and Mg^{++} which can lead to ghost spots (8). Bad streaking effects have been observed, however, in the chromatography of amino acids and peptides (11) and the calcium acetate wash is used to overcome this disadvantage by replacement of some of the calcium ion removed in the preceding step. In acidic solvent systems, traces of heavy metal ions have been found responsible for the appearance of diffuse spots presumably due to formation of chelated complexes (8) and treatment with 8-hydroxyquinoline is used to remove these impurities. Finally, prolonged elution with the developing solvent

Can. J. Chem. Downloaded from www.nrcresearchpress.com by 186.148.149.217 on 09/04/12
For personal use only.

system is intended to minimize further degradation of the paper by the solvent during subsequent chromatography.

Further examination of the washing procedure revealed that no significant difference in quantities of extractables was caused by the use of the ascending rather than the descending technique. This result was somewhat unexpected since it was anticipated that the much longer development time required by the former method (40 hours vs. 16 hours) would lead to greater degradation of the paper and thus yield larger quantities of impurities. The fact that such did not occur attests to the effectiveness of the pretreatment process. Quantities of extractables were also not significantly affected by treating eluates with Amberlite IRA-400 (Cl) resin prior to lyophilization. The latter step is required during actual recovery of the toxin to ensure that it is completely converted to the dihydrochloride.

No difference in resolution of the components was observed by use of the two techniques referred to in the preceding paragraph and the descending method was adopted in all subsequent work because of the shorter development time required.

An effort was made by means of ultraviolet, fluorescence, and infrared spectral measurements to determine the nature of the impurities eluted from the pretreated paper in locations corresponding to components 1 to 5 in Table I. In the ultraviolet region, all the fractions showed weak absorption ($E^{1\%}_{1\,cm}$ = 8–28) at 255–260 mμ. Each fraction also exhibited a strong to medium intensity fluorescence at 350 mμ. The infrared spectra (KBr pellet) of all the fractions were very similar, but the bands (at 1000–1100 cm^{-1}; 1380–1410 cm^{-1}; 1570–1630 cm^{-1}; and 3100–3500 cm^{-1}) were broad rather than sharp. It was therefore not possible to draw any definite conclusion regarding the chemical structure of the impurities except that all the fractions, as expected, are of very similar if not identical composition.

For quantitative purification, 12–17 mg of partially purified clam poison dihydrochloride (toxicity 4150 MU/mg) was applied to specially pretreated Whatman No. 1 paper, chromatographed, and the components recovered and bio-assayed as described in the Experimental section. The results for a typical experiment, shown in Table IV, indicate that 96% of the material applied to the paper has been recovered, and that component 3, the only fraction which possesses significant toxicity, accounts for 74% of the sample. In other experiments performed in the same manner, 94–97% of the sample was accounted for with product distributions similar to that given in Table IV. The toxicity of component 3 by the mouse unit (MU) assay method (13) compares favorably with the value 5500±500 MU/mg reported by Schantz (2) and co-workers. In an LD_{50} assay, agreement was even better, the value found being 9.5 γ/kg (IP mice) vs. 10±1 γ/kg reported (14). In addition, the specific rotation ($[\alpha]^{25}_{D}$ +128°) was within the limits +130±5° given by Schantz *et al.* (2) and the substance gave an infrared spectrum identical with that reported (15, see Fig. 3). It is therefore evident that component 3 and the best material obtained by Schantz *et al.* by the alumina chromatographic method are of identical purity. The purity of component 3 was estimated on the basis of impurity known to be introduced from the paper to be 98% and in view of the supporting data given above this figure seems to be a realistic appraisal. Clam poison dihydrochloride, as recovered from the paper, was frequently obtained as a colorless to pale yellow glass. On two occasions, however, it was obtained as a mixture of glass and crystals with the latter predominating. The latter were very hygroscopic and did not melt but sintered above 200°.

Components 1, 2, 4, and 5 were not obtained in as high a degree of purity as clam poison because of the smaller quantities which were present and the relatively larger amount of

Can. J. Chem. Downloaded from www.nrcresearchpress.com by 186.148.149.217 on 09/04/12
For personal use only.

TABLE IV

Paper chromatographic purification of clam poison dihydrochloride

Component No.	R_F	Weight recovered (mg)	Corrected* weight (mg)	% recovery	Estimated % purity	Toxicity (MU/mg)	Dosage (mg/kg)
1	0.0	0.63	0.46	3.6	73	Nil	0.8
2	0.19	1.62	1.48	11.5	91	Nil	0.4
3	0.32	9.63	9.44	73.6	98	4800	0.018
4	0.53	0.84	0.59	4.6	70	Nil	1.0
5	0.70	0.65	0.40	3.1	61	Nil	1.4
			12.37†	96.4			

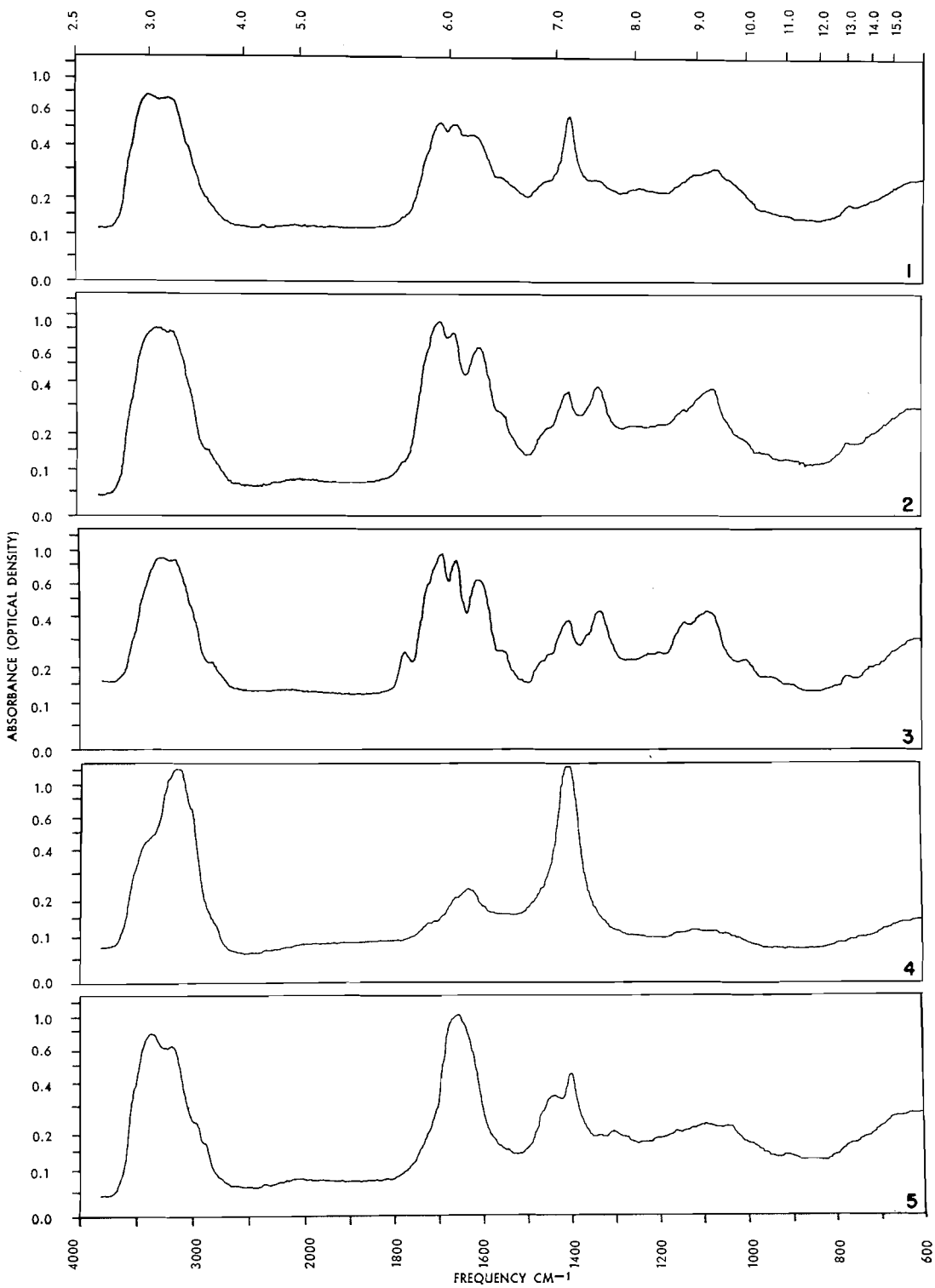
*Weight recovered — blank. †Theoretical recovery 12.83 mg.

impurity consequently introduced into each fraction by the paper chromatographic method. However, each of these substances was further purified by paper chromatography after a sufficient number of identical fractions from several chromatograms had been accumulated to ensure that a significant improvement in purity could be achieved. Ultimately, each fraction was obtained in purity exceeding 90% and the infrared spectrum was measured (KBr pellet). The spectra of the five components are given in Figs. 1–5 from which it is evident that components 1, 4, and 5 differ markedly from clam poison. Component 2, however, has a spectrum identical with that of clam poison dihydrochloride except that a weak band present in the toxin at 1770 cm^{-1} is absent from component 2. It is concluded, therefore, that the two substances are very similar in structure. The infrared spectrum of clam poison dihydrochloride is not very helpful from the viewpoint of identification of structural features of the molecule. Schantz and co-workers (15) have pointed out that the spectrum suggests the presence of OH or NH groups (3100–3300 cm^{-1}); C=O or C=N linkages (1600–1750 cm^{-1}) with a good possibility of the presence of an amide structure; and C—O or C—N bonds (1100 cm^{-1}). Also, the absence of a lactone, ester, anhydride, or aromatic structure seems assured. The only addition which we can make to this evaluation is the suggestion that the bands in the 1680–1770 cm^{-1} region could owe their origin to the presence of a cyclic imide, cyclic urea, or hydantoin-type structure (16, 17, 18).

Components 1, 2, and 5 when chromatographed again under the same conditions by which they were first isolated, each gave only one spot of R_F identical with that originally found. These substances were concluded to be impurities in the original sample, since a purer reference specimen of clam poison dihydrochloride furnished later by the U.S. Army Chemical Warfare Laboratories did not contain any of these materials.

Chromatography of pure clam poison dihydrochloride (component 3) on Whatman No. 1 paper which had been pretreated according to procedure 1 or 2 (Table II) gave only one Weber-positive spot, R_F 0.32, but the use of *unwashed* Whatman No. 1 paper under otherwise identical conditions led to two Weber-positive spots, R_F 0.32 and 0.53. Repeated recovery and rechromatography of the substance of R_F 0.32 on *unwashed* paper consistently gave the same result. Two spots of identical R_F were also obtained when clam poison was chromatographed on pretreated or *unwashed* paper after basification with ammonia. Component 4 when rechromatographed on *unwashed* or pretreated Whatman No. 1 paper gave two Weber-positive spots, R_F 0.32 and 0.53, with the latter predominating unless the material was acidified with hydrochloric acid prior to chromatography, when only one Weber-positive spot, R_F 0.32, was obtained. Multiple spots have

Can. J. Chem. Downloaded from www.nrcresearchpress.com by 186.148.149.217 on 09/04/12
For personal use only.



FIGS. 1–5. Infrared spectra of clam poison components 1–5.

Can. J. Chem. Downloaded from www.nrcresearchpress.com by 186.148.149.217 on 09/04/12
For personal use only.

frequently been observed during chromatography of pure substances and a review of the causes has been given by Pollard *et al.* (19). Where polyfunctional basic compounds are chromatographed in acidic solvent systems, the explanation most frequently invoked is the generation of more than one ionic species of the base by reaction of the substance with the mobile phase (20, 21), but the formation of tautomers has also been postulated (22). Since clam poison has two basic centers and Mold *et al.* (1) obtained some evidence from countercurrent distribution studies at pH 8 that clam poison consists of two tautomers of differing toxicity, either of the explanations mentioned above was a possibility.

Owing to the marked similarity in chromatographic behavior of the various materials of R_F 0.32 and 0.53 described in the foregoing paragraph it was initially assumed that all the substances of identical R_F were identical and that the substance of R_F 0.32 was an ionic species of the toxin corresponding to a diacid salt whereas the substance of R_F 0.53 was an ionic species corresponding to a monoacid salt. Such behavior is exhibited by certain alkaloids of the lupin group where stable monoacid and diacid salts have been obtained (23, 24). Some support for this view was obtained by the behavior of clam poison acetate on paper chromatography which is now to be described. The acetate was prepared from the dihydrochloride by ion exchange on Amberlite IRA-400 resin and gave an infrared spectrum (Fig. 6) which differed from that of the dihydrochloride only in those

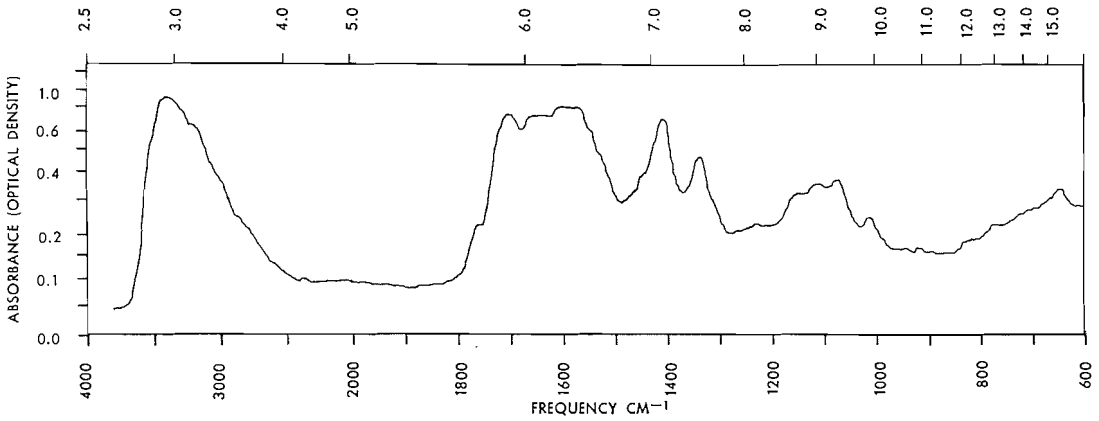


FIG. 6. Infrared spectrum of clam poison acetate.

regions where the ionized carboxyl group would be expected to modify it. Paper chromatography of the acetate on *unwashed* Whatman No. 1 paper gave only one Weber-positive spot, R_F 0.53, but on paper pretreated according to procedure 1 or 2 (Table II) a faint spot at R_F 0.32 was observed in addition to the strong one at 0.53. Reconversion of the acetate to the hydrochloride via ion exchange on Amberlite IRA-400 resin gave a substance with infrared spectrum identical with that of the original dihydrochloride and which showed no abnormality in paper chromatographic behavior (i.e. one spot on pretreated paper, R_F 0.32, two spots on *unwashed* paper, R_F 0.32 and 0.53). These results, coupled with the observation that the major component of clam poison and chloride ion have identical R_F's on *unwashed* paper suggested that the components of R_F 0.32 were the dihydrochloride, whereas the components of R_F 0.53 were the acetate possibly in the mono form. Unfortunately, however, this unifying theory had to be rejected in the light of the work now to be described.

If the substances of R_F 0.32 and 0.53 were different ionic species of the same base in

Can. J. Chem. Downloaded from www.nrcresearchpress.com by 186.148.149.217 on 09/04/12
For personal use only.

Can. J. Chem. Downloaded from www.nrcresearchpress.com by 186.148.149.217 on 09/04/12
For personal use only.

equilibrium, then it should be possible to convert one to the other by a suitable adjustment of pH, and the same situation could obtain in the event that the two substances were tautomers in equilibrium. Judging from the chromatographic behavior described above, high pH's favor the faster-moving species and low pH's favor the slower-moving species. Even if there were a marked difference in toxicity between the two, it should be possible to regenerate the toxicity of pure clam poison by acidification to pH 3, which is the pH of maximum stability of clam poison and therefore the pH at which the bio-assay is performed (13). The complete lack of toxicity of component 4 (see Table IV) gave an indication that the simple ionic species theory is inadequate and furnished definite evidence that component 4 is not the minor tautomeric constituent B isolated by Mold *et al.* (1). The latter substance possessed significant toxicity but less than that exhibited by the major constituent A. It was observed furthermore (1) that if constituent B was acidified and allowed to stand for 16–24 hours the toxicity finally observed was identical with that of constituent A. Freshly prepared solutions of component 4 in hydrochloric acid of pH 3.0 showed no toxicity at a dosage of 1 mg/kg and no toxicity developed if such solutions were kept for periods of up to 5 days at pH 3.0 or 1.3. Chromatography of these solutions on pretreated Whatman No. 1 paper gave one Weber-positive substance, R_F 0.30, quantitative recovery and bio-assay of which confirmed that it was not clam poison dihydrochloride, since it was non-toxic. It was therefore concluded that component 4 is an impurity in, or a decomposition product from, the original clam poison sample, rather than another ionic species of the toxin or the tautomeric constituent B isolated by Mold *et al.* (1). Furthermore, the Weber-positive substance of R_F 0.30 generated by the action of aqueous hydrochloric acid on component 4 is not clam poison.

Attention was then turned to the substance of R_F 0.53 obtained by chromatography of pure clam poison on *unwashed* Whatman No. 1 paper, which is hereinafter referred to as substance X. An attempt was made to establish that substance X was identical with clam poison acetate. The substance X obtained by chromatography of the pure dihydrochloride on *unwashed* paper was impure because of the relatively large quantity of extractable impurity present in Whatman No. 1 paper. Rechromatography on specially pretreated (procedure 2) paper effected only a partial purification so that positive identification via the infrared spectrum was prevented. The substance possessed sufficient toxicity, however (525 MU/mg), to rule out the possibility that it is identical with component 4 from the original toxin sample. The substance was converted to the chloride salt by ion exchange in the usual manner, in the expectation that, after further purification by chromatography, a specimen of clam poison dihydrochloride would be obtained which could be identified by its infrared spectrum. A Weber-positive substance, R_F 0.35, was obtained which had a toxicity of 2150 MU/mg, but the infrared spectrum (Fig. 7) was quite different from that of clam poison dihydrochloride. It is therefore concluded that component 4, substance X, and clam poison acetate are non-identical and that the first two of these are not merely different ionic species of clam poison. It is also no longer considered that the substance of R_F 0.53 generated by the action of ammonia on clam poison is identical with component 4, substance X, or clam poison acetate. The nature of substance X and its relation to clam poison is still obscure but it seems likely that it is most probably a degradation product. If such is the case, it is of considerable interest because of the mild conditions of its formation and its intrinsic toxicity. A more detailed investigation of this substance must await more effective means for its purification. Clam poison acetate was shown to be a diacid rather than a monoacid salt by a pK determination, which revealed the presence of two basic groups pK_1 8.1 and pK_2 11.1 and a molecular weight in agreement with that reported by Schantz *et al.* (2) for the dihydrochloride.

To summarize the results of the multiple spots observed during chromatography of the samples of clam poison dihydrochloride and acetate available to us it has been concluded that component 4 from the original sample is a non-toxic impurity which is not reconverted to clam poison by treatment with acid. It is not identical with clam poison acetate or substance X, which is formed as a minor Weber-positive component from clam poison dihydrochloride during chromatography on *unwashed* Whatman No. 1 paper. Substance X is a toxic unidentified substance which is possibly a degradation product of clam poison. It also does not regenerate clam poison on treatment with acid but does produce another toxic Weber-positive substance of R_F 0.35. Clam poison acetate is a diacid salt like the hydrochloride and is convertible to the latter by ion exchange. The substance of R_F 0.53 formed during chromatography of clam poison dihydrochloride after basification with ammonia is not considered to be identical with component 4, substance X, or clam poison acetate.

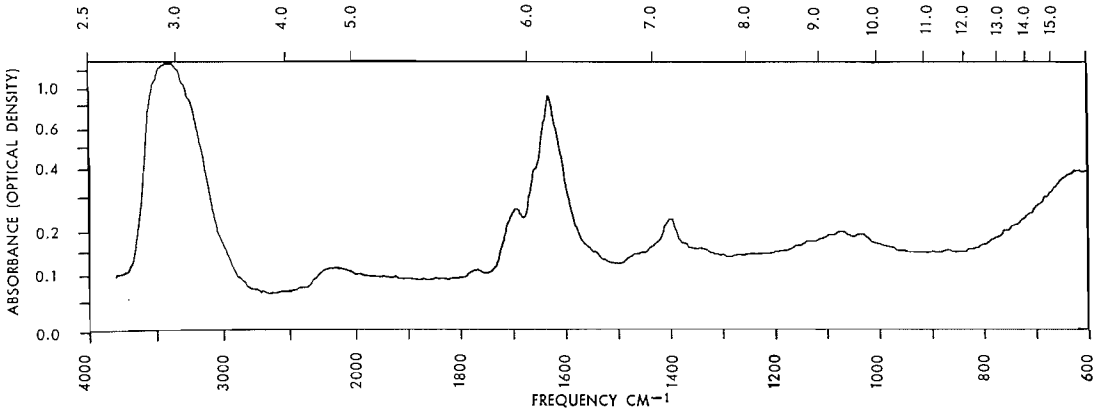


FIG. 7. Infrared spectrum of substance X in the chloride form.

The usefulness of the paper chromatographic method for purification of clam poison tailings has been studied. Preliminary chromatograms with the acetate revealed the presence of three ultraviolet-fluorescent spots, R_F 0.51, 0.53, and 0.62, the last two of which were Weber-positive. As expected, the major component had R_F 0.53. The chloride form, on the other hand, gave on chromatography five ultraviolet-fluorescent spots, R_F 0.20, 0.25, 0.30, 0.36, and 0.58, the last three of which were Weber-positive. The major component had R_F 0.30. It was therefore evident that better resolution of the Weber-positive components and therefore a better purification of the tailings was to be expected by the use of the chloride salt.

A sample of clam poison tailings (11.7 mg, 2000 MU/mg) was purified by quantitative chromatography on an $18\frac{1}{4}\times22\frac{1}{4}$-in. sheet of specially pretreated (procedure 2) Whatman No. 1 paper. The results given in Table V show that the percentage recovery on a weight basis was 95.5% and on a mouse unit assay basis was 81.5%. As expected, most of the toxicity (76%) was contained in the Weber-positive fraction of R_F 0.30, and a substantial improvement in the purity of the toxin was achieved judging by the enhanced toxicity. A portion of the recovered toxin (5.30 mg) was repurified by the same method, yielding 3.26 mg of clam poison dihydrochloride with toxicity 4150 MU/mg. Thus, 13,500 MU of a possible 14,500 MU (93%) was recovered in the second treatment. The total recovery for two purifications was 70.5% and the purity was increased from ca. 36% to ca. 75% (assuming the toxicity of the pure hydrochloride to be 5500 MU/mg). The infrared

Can. J. Chem. Downloaded from www.nrcresearchpress.com by 186.148.149.217 on 09/04/12
For personal use only.

spectrum of the final product was identical with that of clam poison dihydrochloride. These results clearly establish the usefulness of the paper chromatographic technique as a method for enrichment of clam poison tailings on a small scale. In contrast to this, paper or cellulose column chromatography using 95% ethanol, triethylamine (1:1) as developer, chromatography on Amberlite XE-64 resin, and chromatography in absolute ethanol on Woelm's acidic alumina was found to be incapable of improving the purity of clam poison tailings (4). Paper chromatographic purification of the tailings in the acetate form was also briefly examined. The toxic component was located, as expected, at R_F 0.53. The enrichment was not quite as great as in the case of the hydrochloride, the toxicity on one purification being increased to 2200 MU/mg from 1600 MU/mg.

TABLE V

Purification of clam poison dihydrochloride tailings

Fraction No.	R_F	Corrected weight (mg)	Toxicity (MU/mg)	Total MU
UV_1	0.20	0.37	400	148
UV_2	0.25	1.81	400	725
W_1	0.30	5.78	2900	16800
W_2	0.36	0.98	167	163
W_3	0.58	1.62	93	151
		10.56*		17987*

*Theoretical recovery = 11.05 mg or 22,100 MU.

EXPERIMENTAL

Paper Chromatography of Clam Poison Dihydrochloride

For paper chromatography, 20 microliters of a 1.2% aqueous solution (pH 5) (240 γ) of the clam poison dihydrochloride sample received from Schantz *et al.* (2) was applied to *unwashed* Whatman No. 1 paper and developed overnight in a glass chromatographic tank by the descending technique. The air-dried chromatograms were sprayed with Weber reagent (3), Sakaguchi reagent (5), or bromcresol green indicator, or examined under an ultraviolet lamp for location of the components. Results are given in Table I for several solvent systems.

Procedure for Pretreatment of Papers

All papers used were Whatman No. 1, $18\frac{1}{4}\times22\frac{1}{4}$ in. on which $\frac{1}{2}$-in. serrations were cut along the bottom edge to assure even dripping during washing. The papers were washed chromatographically in a Model A 300 Chromatocab (Research Equipment Corp., Oakland, California) by the descending technique. Between each washing step, the papers were air-dried at room temperature. The washing procedures examined are shown in Table II.

Blank Runs on Pretreated Papers

The pretreated paper was developed overnight by the descending method until the solvent front was ca. 1 to $1\frac{1}{2}$ inch from the serrated edge (16 hours). The "chromatogram" was air-dried at room temperature and a vertical strip $1\frac{3}{8}$ in. wide (corresponding to the reference strip removed for exact location of the Weber-positive spots in actual chromatograms) was removed. Rectangular strips were then cut from the remainder of the chromatogram at R_F's corresponding to those of the clam poison components. Since the

Can. J. Chem. Downloaded from www.nrcresearchpress.com by 186.148.149.217 on 09/04/12
For personal use only.

widths of the bands formed in actual chromatograms were found to vary, the widths of strips removed for extraction in the control runs were not identical for all components and were as follows: components 1, 2, and 4, 1 in.; component 3, $1\frac{1}{8}$ in.; component 5, $\frac{3}{4}$ in. The strips were eluted with water (1.5–2.0 ml) and the eluates transferred to small tared flasks with ground caps which had been previously weighed on a microbalance. The solutions were frozen, lyophilized, and the residues were weighed again. The quantities of residues obtained corresponding to the various components of the clam poison sample from papers pretreated according to the methods given in Table II are shown in Table III.

Purification of Clam Poison Dihydrochloride

A sample of the partially purified clam poison dihydrochloride solution (1.2% aqueous) containing 13–17 mg total solids was applied to a sheet of Whatman No. 1 paper ($18\frac{1}{4} \times 22\frac{1}{4}$ in. pretreated according to procedure 2) as 18 spots located on a start line 3 inches from the top of the paper. The two outside spots were placed $\frac{3}{4}$ inch from the edge of the paper and all others were spaced approximately 15/16 inch apart. To keep the area of the applied spots small, 5λ aliquots of the solution were applied at each location, and all spots were allowed to dry prior to subsequent application. The paper was developed exactly as described for the control runs. The air-dried chromatogram was examined under ultraviolet light to determine the straightness of the bands, and the width of component 1. A vertical strip $1\frac{1}{8}$ in. wide was cut from the chromatogram and sprayed with Weber and Sakaguchi reagent to determine the exact widths of the bands due to components 2, 3, 4, and 5. The bands were cut from the chromatograms and eluted with water (1.5–2.0 ml). Each eluate was passed through IRA-400 (Cl) resin (1 ml) to reconvert the basic components to the chloride form. A fresh sample of resin was used for each component and each column was eluted with a further 2 ml of water to ensure complete recovery. The resin used in these experiments was washed prior to use for 1 week with water after conversion to the chloride form, and it was ascertained in independent experiments that similar treatment of eluates from blank runs introduced no significant amounts of impurities. The solutions were transferred to tared flasks, and the components recovered and weighed as described for the blank runs. The areas of the strips of paper from which the components were eluted were measured by means of a planimeter, and the weight of impurity introduced during elution of each strip calculated after the data in Table III was converted to milligrams of impurity per square inch of paper extracted. The weights of impurities thus calculated were deducted from the weights of components recovered by the procedure given above, to give the actual weight recovered. The weight of material lost by spraying the reference strip was deducted from the original sample weight to give the actual weight of sample used. Results for a typical assay by this method are shown in Table IV. Clam poison dihydrochloride (component 3) was obtained as a colorless to pale yellow mixture of glass and crystals which did not melt but sintered above 220°, $[\alpha]_D^{25}$ +128° (1% aqueous solution). The other components of the sample were obtained as colorless to pale yellow glasses. Bio-assays were performed by the mouse unit (MU) assay method of Schantz *et al.* (13) and infrared spectra were measured as potassium bromide pellets (0.5 mg of sample + 300 mg of KBr) on a Perkin–Elmer model 21 spectrometer.

Attempted Reconversion of Component 4 to Clam Poison Dihydrochloride

Component 4 recovered from the purification of clam poison dihydrochloride was dissolved in hydrochloric acid at pH 3.00 at 20°, producing a solution containing exactly 200 γ/ml. Aliquots of this solution were removed and solutions containing 1, 5, 10, and

Can. J. Chem. Downloaded from www.nrcresearchpress.com by 186.148.149.217 on 09/04/12
For personal use only.

20 γ/ml were prepared using the dilute hydrochloric acid mentioned above. Bio-assays of these solutions by the MU assay method revealed that none of these solutions was toxic at dosage levels of 50–1000 γ/kg when freshly prepared, nor did toxicity develop in such solutions on standing for periods of up to 5 days at room temperature. The experiment was repeated using hydrochloric acid of pH 1.30 for preparation of the solutions but the increased acidity did not change the results in any respect. Chromatograms performed on the residual solutions from the experiments described above, using pretreated (procedure 1) Whatman No. 1 paper gave one Weber-positive spot, R_F 0.30. Quantitative isolation of the latter material from a separate chromatogram followed by bio-assay confirmed its non-toxic nature.

Isolation of Substance X *and Attempted Reconversion to Clam Poison Dihydrochloride*

A sample of clam poison dihydrochloride (24.2 mg) was chromatographed quantitatively using the procedure described previously for the purification of the toxin, except that two sheets of *unwashed* Whatman No. 1 paper were used. Two control chromatograms were run simultaneously to determine the quantities of extractables recovered at R_F's corresponding to the two Weber-positive substances formed. In this manner 21.2 mg of clam poison dihydrochloride (R_F 0.32) containing 2.8 mg of impurity and 15.1 mg of substance X (R_F 0.53) containing 11.8 mg of impurity were obtained. Substance X was thus only ca. 20% pure and was rechromatographed quantitatively on pretreated (procedure 2) Whatman No. 1 paper. After two such treatments, the purity of substance X had been increased to only 33%. An infrared spectrum on a portion of this material therefore gave an inconclusive result (i.e. identity or non-identity of substance X with the Weber-positive material of R_F 0.53 obtained during the paper chromatography of clam poison acetate was not established) but bio-assay revealed that substance X, even in its impure condition, had a toxicity of 525 MU/mg. The substance X remaining (6.50 mg, containing 2.24 mg of pure substance X) was passed through an Amberlite IRA-400 (Cl) resin column and the resultant material was purified by quantitative paper chromatography on pretreated (procedure 2) Whatman No. 1 paper, yielding 1.32 mg of Weber-positive substance, R_F 0.35, of estimated purity 75%. This substance had an infrared spectrum (Fig. 7) quite different from that of clam poison dihydrochloride and had a toxicity of 2150 MU/mg. Clam poison dihydrochloride of the same purity (recovered from tailings) had a toxicity of 4150 MU/mg and an infrared spectrum identical with that of a pure specimen of the dihydrochloride.

Purification of Clam Poison Tailings

A solution of clam poison tailings in the acetate form (220 ml, 1.16 mg/ml total solids, toxicity 1600 MU/mg) from the column chromatographic purification method of Schantz *et al.* (2) was found to be too dilute for paper chromatographic work and was lyophilized, yielding 255 mg of residue. The residue was dissolved in water to give a solution containing 25.5 mg/ml of total solids. Exactly 5 ml of the solution was converted to the chloride form by elution through Amberlite IRA-400 (Cl) resin, the eluate was lyophilized, and the residue (108 mg) made up to exactly 5 ml in water. A bio-assay on the two solutions revealed the acetate to have toxicity 1600 MU/mg and the chloride 2000 MU/mg.

Clam poison tailings chloride (11.7 mg) was purified on an $18\frac{1}{4}\times22\frac{1}{4}$-in. sheet of pretreated (procedure 2) Whatman No. 1 paper in the same manner as described for the original clam poison sample, after a control chromatogram had been performed to determine the weight of impurity which would be introduced into each fraction. A bio-assay

Can. J. Chem. Downloaded from www.nrcresearchpress.com by 186.148.149.217 on 09/04/12
For personal use only.

was performed on each fraction and results are given in Table V. Fraction W_1, R_F 0.30, accounted for 76% of the toxicity of the original sample and exhibited enhanced toxicity (2900 MU/mg). A portion of fraction W_1 (5.30 mg) was repurified by the same method, using, however, a $12 \times 18\frac{1}{4}$-in. sheet of pretreated paper, and gave 3.26 mg (93%) of clam poison with toxicity 4150 MU/mg. The infrared spectrum of the final product was identical with that of clam poison dihydrochloride.

Chromatographic Behavior of Clam Poison Acetate

Clam poison acetate was prepared from the dihydrochloride by ion exchange using Amberlite IRA-400 resin. The infrared spectrum of the acetate was measured and is shown in Fig. 6. Reconversion of a sample of the acetate to the dihydrochloride by ion exchange produced material with an infrared spectrum identical with that of the original dihydrochloride.

Paper chromatograms with the acetate on *unwashed* Whatman No. 1 paper in the usual manner gave only one Weber-positive spot, R_F 0.53, but on paper pretreated according to procedures 1 or 2 (Table II) a faint spot at R_F 0.30 was observed in addition to the strong one at 0.53.

Potentiometric Titration of Clam Poison Acetate

For potentiometric titration ca. 5-mg samples of clam poison acetate were dissolved in CO_2-free water in a nitrogen-swept microflask equipped with a Beckmann Probe Assembly 290-32 glass electrode and 270-32 reference electrode (attached to a Beckmann Model GS pH meter) and Gilmont ultramicroburet, and titrated vs. 0.1 *N* barium hydroxide. Found: pK_1 8.1, pK_2 11.1, molecular weight 455. Calc. for $C_{10}H_{17}N_7O_4 . 2\ CH_3COOH$, molecular weight 419.

ACKNOWLEDGMENTS

We wish to thank Dr. E. J. Schantz, of the U.S. Army Biological Warfare Laboratories, Fort Detrick, Frederick, Maryland, for 300 mg of clam poison dihydrochloride and the U.S. Army Chemical Warfare Laboratories, Army Chemical Center, Maryland, for samples of pure clam poison dihydrochloride and clam poison tailings.

We are greatly indebted to Dr. N. R. Stephenson and Dr. G. S. Wiberg, Food and Drug Laboratory, Department of National Health and Welfare, Ottawa, for their excellent co-operation in performing the bio-assays. Thanks are also extended to Dr. R. N. Jones and Mr. R. Lauzon, Division of Pure Chemistry, National Research Council, Ottawa, for measurement of the infrared spectra.

REFERENCES

1. J. D. Mold, J. P. Bowden, D. W. Stanger, J. E. Maurer, J. M. Lynch, R. S. Wyler, E. J. Schantz, and B. Riegel. J. Am. Chem. Soc. **79**, 5235 (1957).
2. E. J. Schantz, J. D. Mold, D. W. Stanger, J. Shavel, J. Riel, J. P. Bowden, J. M. Lynch, R. S. Wyler, B. Riegel, and H. Sommer. J. Am. Chem. Soc. **79**, 5230 (1957).
3. C. J. Weber. J. Biol. Chem. **78**, 465 (1948).
4. E. A. Metcalf. Private communication.
5. S. Sakaguchi. J. Biochem. (Tokyo), **5**, 13, 25 (1925).
6. A. A. Albanese and J. E. Frankston. J. Biol. Chem. **159**, 185 (1945).
7. J. D. Mold, J. M. Ladino, and E. J. Schantz. J. Am. Chem. Soc. **75**, 6321 (1953).
8. C. S. Hanes and F. A. Isherwood. Nature, **164**, 1107 (1949).
9. C. S. Hanes, F. J. R. Hird, and F. A. Isherwood. Biochem. J. **51**, 25 (1952).
10. F. A. Isherwood and C. S. Hanes. Biochem. J. **55**, 824 (1953).
11. G. E. Connell, G. H. Dixon, and C. S Hanes Can. J. Biochem. and Physiol. **33**, 416 (1955).
12. G. W. Huffman, P. A. Rebers, D. R. Sprietstersbach, and F. Smith Nature, **175**, 990 (1955).
13. E. J. Schantz, E. F. McFarren, M. L. Schafer, and K. H. Lewis. J. Assoc. Offic. Agr. Chemists, **41**, 160 (1958).
14. E. J. Schantz. Private communication.

Can. J. Chem. Downloaded from www.nrcresearchpress.com by 186.148.149.217 on 09/04/12
For personal use only.

15. E. J. SCHANTZ *et al.* To be published.
16. L. J. BELLAMY. The infrared spectra of complex molecules. Methuen & Co. Ltd., London. 1954. p. 180.
17. J. KEBRLE, K. SCHMID, K. HOFFMANN, J. P. VUILLEUMIER, and K. BERNHARD. Helv. Chim. Acta, **42**, 417 (1959).
18. H. M. RANDALL, R. G. FOWLER, N. FUSON, and J. R. DANGL. Infrared determination of organic structures. D. Van Nostrand Co. Inc., New York. 1949. pp. 171–176
19. F. H. POLLARD, J. F. W. MCOMIE, J. V. MARTIN, and J. C. HARDY. J. Chem. Soc. 4332 (1955).
20. A. J. LANDUA, R. FUERST, and J. AWAPARA. Anal. Chem. **23**, 162 (1951).
21. S. ARONOFF. Science, **110**, 590 (1949).
22. D. H. PETERSON and L. M. REINECKE. J. Am. Chem. Soc. **72**, 3598 (1950).
23. J. F. COUCH. J. Am. Chem. Soc. **59**, 1469 (1937).
24. C. MOUREU and A. VALEUR. Bull. soc. chim. France, **29**, 1135 (1903).

Can. J. Chem. Downloaded from www.nrcresearchpress.com by 186.148.149.217 on 09/04/12
For personal use only.

Can. J. Chem. Downloaded from www.nrcresearchpress.com by 186.148.149.217 on 09/04/12
For personal use only.

COMPLEX MANGANESE PERIODATES[1]

M. W. Lister and Y. Yoshino

ABSTRACT

The preparation of complex periodatomanganates, from manganous salts reacting with sodium (or potassium) hypochlorite and periodate, is described. The products were $Na_7H_4Mn(IO_6)_3.17H_2O$ and $K_7H_4Mn(IO_6)_3.8H_2O$. The manganese was shown to be tetravalent from its redox equivalent in its reaction with iodide and with ferrous ions, and from its magnetic moment, which was 3.87 Bohr magnetons, corresponding to three unpaired electron spins. The ion has an absorption maximum at 483 mμ. Rather complicated pH curves were found for this compound in acid–base titrations. The complex ion decomposes slowly to permanganate and iodate; the kinetics of this reaction have been measured, and a possible mechanism has been suggested. The reaction proceeds in several steps by way of simpler complex ions. The same applies to the reaction between iodide ions and the complex ions when the pH is about 9.

In a recent paper (1) the present writers reported on the preparation and properties of complex cobalt periodates. Similar copper compounds have been prepared and examined (2, 3), as have somewhat similar nickel compounds (4). The ability of periodate ions to oxidize manganese to permanganate suggested that manganese would not give a similar compound; but, on making the experiment, it was found that complex salts of tetravalent manganese could in fact be prepared. The object of the present paper is to describe the preparation and properties of these compounds.

1. *Preparation of Compounds*

(a) Sodium Periodatomanganate (IV)

After various preliminary attempts, the method used in a typical preparation was as follows. Twenty grams of sodium periodate, $Na_2H_3IO_6$, was dissolved in a mixture of 200 ml of water and 25 ml of 6 *M* nitric acid. To this was added 5 g of manganous chloride tetrahydrate dissolved in 20 ml of water, and then, before any precipitation could occur, a mixture of 100 ml of 1.5 *M* sodium hypochlorite and 15 g of sodium hydroxide dissolved in 20 ml of water. Some brown precipitate formed (presumably manganese dioxide), and after centrifuging this off, a red solution was obtained. Alcohol was added till the solution was 40% alcohol by volume, when a red sticky material precipitated. This was dissolved in 100 ml of dilute sodium hydroxide, filtered on sintered glass, and reprecipitated with alcohol, when a dark red precipitate was obtained. This purification process was repeated twice, and the precipitate was finally dissolved in water, which was allowed to evaporate slowly. Red crystals were obtained, filtered off, washed with a little cold water, and dried. The yield was somewhat variable, but was between 4.5 and 10 g on various occasions.

To analyze the solid, it was dissolved in water and sulphur dioxide was passed into the solution; complete reduction occurred. Excess sulphur dioxide was boiled out, and silver nitrate was added. Silver iodide was filtered off, washed, dried, and weighed. The silver in the filtrate was removed as silver chloride, and the solution was run through a column of Dowex 50W-X8 cation exchange resin in its hydrogen form. The sodium and manganese ions were adsorbed, and the sodium was then eluted with 0.4 *M* HCl, which leaves the manganese on the column. The sodium solution was evaporated and the sodium chloride was weighed; the purity of the sodium chloride was then checked

[1]*Manuscript received March 31, 1960.*
Contribution from the Department of Chemistry, University of Toronto, Toronto, Ontario.

by silver nitrate titration. The column was then further eluted with 2.0 *M* HCl, which removes manganese. Sulphuric acid was added to the manganese solution, which was evaporated, and the manganese was weighed as $MnSO_4$. The water content of the crystals was determined from the weight loss at 150° C.

The results were Na 13.3%, Mn 4.60%, I 31.6%, water 25.3%. Calculated for $Na_7H_4Mn(IO_6)_3.17H_2O$ are Na 13.4$_5$%, Mn 4.60%, I 31.8$_5$%, water 25.6%. This analysis is the mean of two closely agreeing analyses.

A confirmation of this formula was obtained by passing a solution of a known weight of sodium periodatomanganate (IV) through an anion exchange resin (Dowex 1-X4) in its chloride form. The displaced chloride was titrated with silver nitrate. It was found that 1.415×10^{-3} g-molecules of chloride was displaced by 0.2016×10^{-3} g-molecules of the sodium salt, a ratio of 7 to 1. If R is the resin, the reaction is

$$7RCl + Na_7H_4Mn(IO_6)_3 \rightarrow R_7H_4Mn(IO_6)_3 + 7NaCl.$$

(b) Potassium Periodatomanganate (IV)

This compound was prepared in a similar fashion to the sodium salt, but with potassium periodate, KIO_4, and potassium hypochlorite as starting materials. It proved to be much less easy to crystallize than the sodium salt, as it is evidently more soluble in water, and readily gives a rather sticky precipitate with alcohol. An alternative preparation by running a solution of the sodium salt through a cation exchange resin, in its potassium form, gave a similar product. Slow evaporation over calcium chloride gave a dark red-brown solid.

Similar analysis as for the sodium salt gave K 23.3%, Mn 4.72%, I 32.4%, and H_2O 11.9%. Calculated for $K_7H_4Mn(IO_6)_3.8H_2O$ are K 23.9%, Mn 4.79%, I 33.2%, H_2O 12.6%.

(c) Barium Periodatomanganate (IV)

A solution of the sodium complex salt was mixed with barium hydroxide, when a brown precipitate formed. Its composition was approximately $Ba_5HMn(IO_6)_3.10H_2O$, but was somewhat variable, and no method was found to recrystallize the product, as it was insoluble in water and decomposed by acids. Its observed oxidation equivalent (see below) with potassium iodide and acid was 63.2 (calculated 61.2). It is probably the above salt contaminated by impurities such as barium carbonate, or barium periodate.

2. Valency of Manganese

The analyses above do not, of course, give any indication of the valency of the manganese. This was determined by various titrations, and by magnetic measurements, which are now described.

(a) Iodometric Titration

A weighed amount of the sodium salt was added to acidified potassium iodide. The liberated iodine was titrated with thiosulphate. The observed equivalent weight varied from 45.66 to 45.75 in three analyses, with a mean of 45.72. The calculated equivalents are Mn (III) 47.84, Mn (IV) 45.95, Mn (V) 44.22; these assume that the periodate is reduced to iodine and the manganese to Mn^{++}. The results agree with the presence of manganese (IV) in the compound.

(b) Potentiometric Titration with Ferrous Ammonium Sulphate

It was found that sodium periodatomanganate, like the corresponding cobalt salt, could be titrated against ferrous ions in acid solution. A weighed amount of the salt

Can. J. Chem. Downloaded from www.nrcresearchpress.com by 186.148.149.217 on 09/04/12
For personal use only.

was dissolved in 1 N sulphuric acid and titrated against approximately 0.1 M ferrous ammonium sulphate. The titration was followed potentiometrically with the cell: $Pt/Na_7H_4Mn(IO_6)_3/Hg_2Cl_2$ in saturated KCl/Hg. The platinum was the positive pole, and a typical titration of 0.0037 M complex salt against 0.0995 M Fe^{++} at 25° C gave:

ratio										
0	1.97	3.94	5.90	7.38	7.87	7.92	7.97	8.06	8.36	8.86
e.m.f. (volts)										
1.102	1.098	1.090	1.089	1.082	1.045	0.750	0.711	0.653	0.578	0.542

Here "ratio" means the number of gram-molecules of ferrous ions divided by the gram-molecules of complex salt. In this titration the inflection comes at 7.90; in another titration this was at 7.99; it is evident that 1 g-molecule of the complex salt reacts with 8 of ferrous sulphate.

$$2Na_7H_4Mn(IO_6)_3 + 16FeSO_4 + 17H_2SO_4 \rightarrow 7Na_2SO_4 + 2MnSO_4 + 8Fe_2(SO_4)_3 + 6HIO_3 + 18H_2O.$$

This also supports a formula with tetravalent manganese. With the corresponding cobalt compound, and with sodium periodate itself, there is reason to believe that the cell is not giving the true equilibrium voltage (see reference 1); this probably applies to the sodium periodatomanganate also. However, the evidence that this is tetravalent manganese is quite definite.

(c) Reduction with Sulphur Dioxide

An aqueous solution of the sodium periodatomanganate is reduced by sulphur dioxide, and after the excess sulphur dioxide was boiled off, the sulphuric acid produced in the oxidation can be titrated with sodium hydroxide. One gram equivalent of sulphuric acid was produced by 60.1 g of the compound; calculated are Mn (III) 62.9, Mn (IV) 59.7, Mn (V) 56.8. Thus this result also supports a formula with Mn (IV). The reaction is

$$Na_7H_4Mn(IO_6)_3 + 13SO_2 + 8H_2O \rightarrow 3NaI + 2Na_2SO_4 + MnSO_4 + 10H_2SO_4.$$

(d) Magnetic Properties

Magnetic measurements were made on the solid compound, using a Goüy apparatus of the conventional type. The compound was suspended in a tube surrounded by a jacket in which water at various temperatures could be circulated. The tube was calibrated with sucrose, whose susceptibility was taken to be -0.566×10^{-6}/g (5). The observed susceptibilities are given below; as is to be expected the compound is paramagnetic, and the magnetic moment was calculated after allowing for the diamagnetic susceptibility of the various atoms by means of Angus's method (6).

Temp., °C	3.0	25.6	39.7
χ_g	4.695	4.323	4.154×10^{-6}
$\chi_{g\text{-molecule}}$	5611	5166	4964×10^{-6}
Corr. for diamagnetism	6141	5696	5494×10^{-6}

These results fit a Curie–Weiss equation, $\chi = C/(T+\theta)$, where $\theta = 21°$ and $C = 1.826$. This makes the magnetic moment 3.84 Bohr magnetons. The calculated value for a "spin-only" atom with three unpaired electron spins is 3.87. Hence these results strongly support a formula with Mn (IV).

3. Absorption Spectrum

Solutions of sodium periodatomanganate (IV) are red in color. The absorption spectrum

Can. J. Chem. Downloaded from www.nrcresearchpress.com by 186.148.149.217 on 09/04/12
For personal use only.

measured on a Beckmann DU spectrophotometer was as follows for a 1.04×10^{-3} M solution containing 0.100 M sodium hydroxide:

wavelength (mμ)									
800	750	700	650	600	580	560	540	520	500
490	480	470	460	450	440	430	420	410	400
extinction coefficient									
3	4	7	13	54	98	169	266	354	409
423	428	417	398	378	369	393	453	602	870

There is thus a single maximum at 483 mμ. In acid solution the complex is stable enough to be measured; the general shape of the curve is the same but the maximum is less well marked. In 0.106 M perchloric acid, the spectrum in the neighborhood of the maximum (at 479 mμ) was:

wavelength	500	490	480	470	460	450
extinction coefficient	397	406	416	408	418	438

If the free acid was made by passing a solution of the sodium salt through an ion exchange resin in its hydrogen form, a somewhat different spectrum was obtained, with a shoulder at 480 mμ instead of a maximum. When the solution was allowed to stand for 2–3 days the spectrum of the permanganate ion appeared, but this was not visible at first. If the free acid was made alkaline with sodium hydroxide (0.05 M), a modified spectrum was obtained, again with a shoulder instead of a maximum at 480 mμ, though the general shape and size of extinction coefficients (412 at 480 mμ) were much the same. The nature of the change in the complex is not entirely clear, but related observations will be given below. If the adsorption maximum at 483 mμ is due to a $t_g \rightarrow e_g$ transition for one 3d electron, as seems possible, this corresponds to a splitting of 59 kcal between these levels. Sodium periodatocobaltate (III), which is diamagnetic, has a similar spectrum (1) with a maximum at 625 mμ.

4. pH Measurements

Since sodium periodatomanganate (IV) was fairly stable in acid solutions, its behavior in acid–base titrations was examined. The pH in these titrations was followed by a Beckmann pH meter with glass and saturated calomel electrodes. When 2.53×10^{-3} M sodium periodatomanganate (IV) was titrated against 0.1009 M perchloric acid, only one inflection was observed in the curve of pH plotted against the ratio of acid to sodium periodatomanganate (IV). This was after addition of two equivalents of acid, and corresponds to $Na_5H_6Mn(IO_6)_3$; the pH was then 7.48. These results are plotted in Fig. 1. If the acidified solution was allowed to stand briefly, and then titrated in the

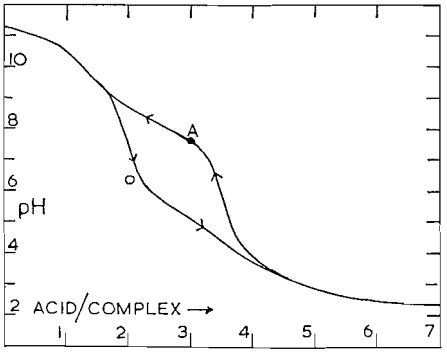


FIG. 1.

Can. J. Chem. Downloaded from www.nrcresearchpress.com by 186.148.149.217 on 09/04/12
For personal use only.

reverse direction with sodium hydroxide, a different curve resulted with an inflection at 4NaOH to one molecule of $H_{11}Mn(IO_6)_3$, that is, at $Na_4H_7Mn(IO_6)_3$. Thus the shape of the pH curves is like a hysteresis loop. Very nearly the same curve was obtained if the sodium periodatomanganate solution was run through a cation exchange resin in its acid form, and the resulting solution was titrated with NaOH; again the inflection was at $Na_4H_7Mn(IO_6)_3$. However, if the acid solution was allowed to stand for 24 hours before titration, the inflection shifted somewhat to about $3\frac{1}{2}$NaOH per molecule of the complex acid.

When 4NaOH was rapidly added per molecule of freshly prepared complex acid, the pH was 7.50 (A in Fig. 1); this is on the top branch of the loop. When a solution of $Na_7H_4Mn(IO_6)_3$ was prepared and $2HClO_4$ was rapidly added per molecule of complex, the pH was 6.32 on the lower branch of the loop; the same solution on standing for 24 hours had a pH of 7.68. If the free acid was made alkaline, its pH behavior was then the same as that of the original salt, so no permanent change was produced by acidification.

In another run the free complex acid was titrated against barium hydroxide. The pH was generally lower than in titrations with sodium hydroxide, but a precipitate formed. The first inflection on the pH curve was at $Ba_2H_7Mn(IO_6)_3$ (pH = 4.7), followed by a less well-defined rise between Ba_3 and Ba_4.

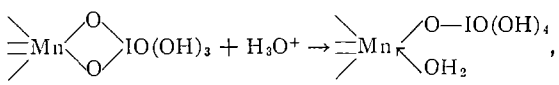
If the free acid was prepared by passing through a cation exchange resin in its acid form, and the free acid was immediately allowed to run through an anion exchange resin in its chloride form, three chlorides were displaced by one molecule of the complex acid, i.e.,

$$H_{11}Mn(IO_6)_3 + 3RCl \rightarrow R_3H_8Mn(IO_6)_3 + 3HCl.$$

However, the anion exchange resin acquired the brown color of finely divided manganese dioxide, and it is possible that all this experiment proves is that the sodium periodatomanganate (IV) contains three periodates per manganese. Each periodic acid displaced one chloride from the resin, as would be expected from its ionization constants, which are $pK_1 = 1.6$, $pK_2 = 7$ (7).

The pH of 2.5×10^{-3} M solutions of the free complex acid was found to be close to 2.30. This corresponds to two ionized hydrogens per molecule.

The explanation of all these observations is not too clear. Starting at the alkaline end, the main drop in pH was at $Na_5H_6Mn(IO_6)_3$ or $Na_5Mn(H_2IO_6)_3$. This is a formula with all periodates equally ionized. In the free acid two hydrogens are ionized, presumably as $(H_3O^+)_2[Mn(H_3IO_6)_3]^{--}$. The loop in the pH curve must be due to some rearrangement in the periodatomanganate ion on acidification, and this rearrangement, and its reverse on making alkaline again, must be slow. The nature of the process might be the replacement of a manganese–periodate bond by a band to water,



or dissociation to a lower complex (see later), but this is speculative. It is possible on this basis to write fairly plausible symmetrical formulae for the complex acid and its ions, but the evidence is not sufficient to establish them.

One other quantity can be calculated from these measurements. The pH of 0.00253 M sodium periodatomanganate was 10.87. Assuming that this is due to the hydrolysis of the $H_4Mn(IO_6)_3^{-7}$ ion, the hydrolysis constant can be calculated to be 3×10^{-4}.

Can. J. Chem. Downloaded from www.nrcresearchpress.com by 186.148.149.217 on 09/04/12
For personal use only.

5. Decomposition of Sodium Periodatomanganate (IV)

It was found that solutions of sodium periodatomanganate (IV) spontaneously changed on standing to a solution of sodium permanganate. The over-all reaction is

$$2Na_7H_4Mn(IO_6)_3 + 2H_2O \rightarrow 2NaMnO_4 + 3NaIO_3 + 3Na_2H_3IO_6 + 3NaOH.$$

Experiments were made on the rate of this reaction under various conditions. Solutions were kept immersed in a water thermostat, regulated to better than 0.1° C, and the change was followed by light adsorption measurements with a Beckmann DU spectrophotometer.

In the first experiments the pH was controlled by means of a sodium phosphate buffer, but when the rates were compared with those obtained in sodium hydroxide solution, it became evident that the buffer did not influence the rate solely through its control of pH. Presumably the phosphate altered the rate by combining with one of the reacting species. Hence the runs that will be considered below will be ones in which the reacting solution was made up solely from sodium hydroxide, sodium periodate, sodium periodatomanganate, and water. The optical density was mostly measured at 550 mμ, where the extinction coefficients are: $Na_7H_4Mn(IO_6)_3$ 217, Na_2MnO_4 768, $NaMnO_4$ 2190; this is an adsorption maximum for sodium permanganate. The results are given in Table I.

If the color density is assumed to be due solely to the complex and to permanganate, then we can calculate the complex concentration at different times. Runs 1, 2, and 3 show that the rate is proportional to the complex concentration, when other factors are kept the same. A plot of log (complex) against time is nearly linear for all three runs, with a slope of 2.80×10^{-3}. Runs 3, 8, 9, 10 give the effect of sodium hydroxide concentration. If $d\log(\text{complex})/dt$ is taken from a plot for each run the results are:

$d\log X/dt$	0.06	0.54	2.73	8.32×10^{-4}: X = [complex]
$[OH^-]$	0.05	0.02	0.01	0.005 *M*

This is roughly, though not precisely, proportional to $[OH^-]^{-2}$; other powers of $[OH^-]$ give a much worse agreement with experiment. Finally runs 3, 4, 5, 6, and 7 give the effect of periodate concentration:

$d\log X/dt$	6.84	5.46	4.03	2.70	1.93×10^{-3}
[periodate]	2.46	3.27	4.91	7.37	9.82×10^{-4} *M*

The rate is inversely proportional to the added periodate concentration, though there is some drift from this simple relationship at low concentrations. It is readily calculated that the extra hydroxide ions, contributed by the hydrolysis of the complex ion, should not alter the rate by more than ½% for any of these runs.

The temperature variation of the rate (runs 5, 11, 12) makes the apparent activation energy about 46 kcal. This is so high that it is evident it is not a genuine activation energy, but must contain other factors; these will be discussed below.

One other set of results deserves comment: these are runs 13, 14, and 15, all with no added periodate. Here again a plot of log (complex) against time is linear at first, though levelling off towards the end of the run. The slopes of the linear parts are not very different.

It is not possible to be sure of the detailed mechanism of the reaction from these rate measurements, although it must be somewhat as follows. The complex must presumably be in equilibrium with a simpler complex, which is the reactive species, and the inverse relationship to periodate and hydroxide concentrations shows the nature of this equilibrium. The products of decomposition of the reactive species are not so certain, but it

Can. J. Chem. Downloaded from www.nrcresearchpress.com by 186.148.149.217 on 09/04/12
For personal use only.

Can. J. Chem. Downloaded from www.nrcresearchpress.com by 186.148.149.217 on 09/04/12
For personal use only.

TABLE I

Decomposition of sodium periodatomanganate (IV)

Run 1 Temp. 35° C		Run 2 Temp. 35° C		Run 3 Temp. 35° C		Run 4 Temp. 35° C		Run 5 Temp. 35° C		Run 6 Temp. 35° C	
[Periodate] 7.37×10^{-4}	[OH^-] 0.01 *M*	[Periodate] 7.37×10^{-4}	[OH^-] 0.01	[Periodate] 7.37×10^{-4}	[OH^-] 0.01	[Periodate] 9.82×10^{-4}	[OH^-] 0.01	[Periodate] 4.91×10^{-4}	[OH^-] 0.01	[Periodate] 3.27×10^{-4}	[OH^-] 0.01
Time (min)	[Complex]	Time	[Complex]	Time	[Complex]	Time (min)	[Complex]	Time	[Complex]	Time	[Complex]
0	4.01×10^{-4} *M*	0	2.97×10^{-4}	0	2.16×10^{-4}	0	2.18×10^{-4}	0	2.22×10^{-4}	0	2.13×10^{-4}
7	3.91	9	2.87	10	2.09	10	2.15	9	2.11	5	2.07
14	3.78	17	2.77	20	1.97	20	2.08	19	1.95	10	1.95
24	3.54	26	2.61	35	1.80	30	1.98	30	1.74	18	1.77
34	3.28	42	2.35	55	1.55	55	1.79	45	1.50	27	1.57
45	3.05	56	2.14	85	1.27	82	1.59	67	1.20	37	1.38
60	2.77	75	1.90			116	1.35	94	0.96	55	1.10
92	2.27					150	1.16	100	0.92		
								134	0.71		

Run 7 Temp. 35° C		Run 8 Temp. 35° C		Run 9 Temp. 35° C		Run 10 Temp. 35° C		Run 11 Temp. 40° C		Run 12 Temp. 30° C	
[Periodate] 2.46×10^{-4}	[OH^-] 0.01	[Periodate] 7.37×10^{-4}	[OH^-] 0.05	[Periodate] 7.37×10^{-4}	[OH^-] 0.02	[Periodate] 7.37×10^{-4}	[OH^-] 0.005	[Periodate] 4.91×10^{-4}	[OH^-] 0.01	[Periodate] 4.91×10^{-4}	[OH^-] 0.01
Time (min)	[Complex]	Time	[Complex]	Time	[Complex]	Time (min)	[Complex]	Time	[Complex]	Time	[Complex]
0	2.05×10^{-4}	0	2.100×10^{-4}	0	2.04×10^{-4}	0	2.05×10^{-4}	0	2.06×10^{-4}	0	2.08×10^{-4}
5	1.90	11	2.095	10	2.03	6	1.87	8	1.64	12	2.05
12	1.73	27	2.084	32	1.99	12	1.67	16	1.27	38	1.96
20	1.50	74	2.079	93	1.86	23	1.34	24	0.99	63	1.84
26	1.36	135	2.059	132	1.76	30	1.16	35	0.73	103	1.64
35	1.16					33	1.08	48	0.55	145	1.44
50	0.93					43	0.90	72	0.34		
76	0.68					55	0.72	98	0.25		

Run 13 Temp. 35° C		Run 14 Temp. 35° C		Run 15 Temp. 35° C	
[Periodate] 0	[OH^-] 0.01	[Periodate] 0	[OH^-] 0.01	[Periodate] 0	[OH^-] 0.01
Time (min)	[Complex]	Time	[Complex]	Time	[Complex]
0	2.81×10^{-4}	0	1.97×10^{-4}	0	1.56×10^{-4}
4	2.55	5	1.68	5	1.33
9	2.18	10	1.44	6	1.30
15	1.85	15	1.23	10	1.13
23	1.51	20	1.06	16	0.98
35	1.16	25	0.93	26	0.79
		35	0.73	47	0.575
		55	0.49		

was observed that in partially reacted mixtures a weak adsorption band appeared in the neighborhood of $\lambda = 610$ to 620 mμ. This is probably due to manganate ions which have an adsorption maximum at 610 mμ. Manganate ions can be oxidized to permanganate by periodate, and some measurements have been made on this reaction which will be reported separately. In general two reaction schemes would fit the facts.

(A)

$$H_4Mn(IO_6)_3^{-7} + 2H_2O \rightleftharpoons H_3Mn(IO_6)_2^{-3} + H_3IO_6^{-2} + 2OH^- \quad [i]$$

$$H_3Mn(IO_6)_2^{-3} \rightarrow Mn(OH)_3IO_6^{-2} + IO_3^- \quad [ii]$$

$$Mn(OH)_3IO_6^{-2} + 2OH^- \rightarrow MnO_4^{--} + H_3IO_6^{--} + H_2O \quad [iii]$$

$$2MnO_4^{--} + H_3IO_6^{--} \rightarrow 2MnO_4^- + IO_3^- + 3OH^- \quad [iv]$$

Reaction [i] is a rapidly established equilibrium, and reaction [ii] is the slow stage. Reactions [iii] and [iv] would be at least fairly fast; reaction [iv] is not meant to be necessarily a simple single-stage reaction.

An alternative is:

(B)

$$H_4Mn(IO_6)_3^{-7} + 2H_2O \rightleftharpoons MnIO_6^- + 2H_3IO_6^{--} + 2OH^- \quad [i]$$

$$MnIO_6^- + H_3IO_6^{--} \rightarrow Mn(OH)_2IO_6^- + IO_3^- + H_2O \quad [ii]$$

$$Mn(OH)_2IO_6^- + 3OH^- \rightarrow MnO_4^{--} + H_3IO_6^{--} \quad [iii]$$

$$2MnO_4^{--} + H_3IO_6^{--} \rightarrow 2MnO_4^- + IO_3^- + 3OH^- \quad [iv]$$

As before, reaction [i] is a rapid equilibrium, and reaction [ii] is slow; reactions [iii] and [iv] are fairly fast. It will be recognized that for both schemes A and B the products of reaction [ii] might differ in detail, though the manganese must be hexavalent.

Applying ordinary kinetic considerations to scheme A, and assuming that the added periodate is not too low, we get the equation

$$\frac{2K.K_e}{3C_0[OH^-]^2} \cdot t = -\left(1+\frac{2u_0}{3C_0}\right) \ln \alpha - (1-\alpha)$$

where K_e is the equilibrium constant of reaction [i],
K is the rate constant of reaction [ii],
C_0 and u_0 are respectively the initial concentrations of complex and of added periodate,
and α is the fraction of complex left undecomposed.

If u_0 is not too small, then

$$\frac{d \ln (\text{complex})}{dt} = -\frac{2K.K_e}{[OH^-]^2\{2u_0+3C_0(1-\alpha)\}},$$

which will be reasonably constant at first. If an apparent rate constant, K^*, is defined by

$$\frac{d \ln (\text{complex})}{dt} = -\frac{K^*}{[OH^-]^2 u_0}$$

then $K^* = K.K_e/\{1+(3C_0/2u_0)(1-\alpha)\} = K.K_e$ initially. The observed values of K^* show a drift, with C_0/u_0, of the size predicted by the above equation, if the average value of α is taken as 0.8, which was in fact approximately correct. This makes $K^* = 2.1 \times 10^{-10}$ (g-molecules/l.)^3 min^{-1} at 35° C. The observed apparent activation

Can. J. Chem. Downloaded from www.nrcresearchpress.com by 186.148.149.217 on 09/04/12
For personal use only.

energy (46 kcal) will be the sum of the heat of reaction of reaction [i] and the activation energy of reaction [ii]; it is, of course, impossible to divide it between the two. It still seems to be rather high considering the nature of these two reactions.

The reactions of scheme B will give an identical equation relating α and t, if the same approximations are made. Hence the same remarks apply to scheme B.

Finally we must consider the observation that in the absence of added periodate a low, but fairly constant, value is obtained for $d\ln(\text{complex})/dt$. This could be explained for scheme A on the assumption that, under these conditions, the equilibrium of reaction [i] is fairly largely to the right. Then, at least initially, $d\ln(\text{complex})/dt = K\beta$, where β is the fraction dissociated. Runs 13, 14, and 15 make $K\beta$ about 3×10^{-2}. Allowing for the fact that $[OH^-] = 10^{-2}$ throughout, consistent results are obtained if we take $K_e = 2\times10^{-9}$ and $K = 0.11$. These numbers make the complex between 23 and 29% dissociated in these runs, and lead to a drift of the initial values $d\ln(\text{complex})/dt$ of about what is found. Thus although the results cannot give very accurate constants, they agree quite well with this explanation. Scheme B does not lead to a roughly constant value of $d\ln(\text{complex})/dt$ for different C_0 values, for the conditions of these runs, and hence scheme A is to be preferred.

It is also evident that the same dependence on hydroxide ion concentration cannot hold in acid solution, as, otherwise, acidified solutions would decompose much faster than they do. However, the pH titration curves gave evidence of rearrangement of the ion at moderate pH values, and this presumably also changes the rate of decomposition to permanganate.

One other set of experiments was made in the hope of throwing some light on the mechanism of decomposition. It was observed that when iodide was added to a solution of the complex, iodine was slowly liberated. It seemed possible that this might measure the rate of breaking up of the complex to a simpler ion and a periodate ion, which then rapidly oxidized iodide. If this were so, the rate should not depend on the iodide concentration. However, on making the experiment it was found that the rate at 25° C actually followed an equation

$$\text{rate} = -\frac{x}{x_0}\{0.9+3.0[I^-]\}10^{-6}$$

where x is the concentration of the complex at any time, and x_0 is its initial concentration; the time is measured in minutes. This is evidently a complex reaction, and the hope that it goes at a rate determined by the breaking up of the complex is not fulfilled. The inverse relation of rate to initial concentration of complex does presumably indicate an initial breaking up reaction, but it is not possible to suggest a detailed mechanism.

REFERENCES

1. M. W. LISTER and Y. YOSHINO. Can. J. Chem. **38**, 45 (1960).
2. L. MALATESTA. Gazz. chim. ital. **71**, 467, 580 (1941).
3. M. W. LISTER. Can. J. Chem. **31**, 638 (1953).
4. P. RAY and B. SARMA. J. Indian Chem. Soc. **25**, 205 (1948).
5. P. W. SELWOOD. Magnetochemistry. 2nd ed. Interscience Publishers. p. 26.
6. W. R. ANGUS. Proc. Roy. Soc. A, **136**, 569 (1932).
7. N. RAE. J. Chem. Soc. 876 (1931).

Can. J. Chem. Downloaded from www.nrcresearchpress.com by 186.148.149.217 on 09/04/12
For personal use only.

Can. J. Chem. Downloaded from www.nrcresearchpress.com by 186.148.149.217 on 09/04/12
For personal use only.

SOME OBSERVATIONS ON THE THEORY OF π-BONDING IN INORGANIC COMPOUNDS[1]

A. D. WESTLAND

ABSTRACT

Evidence for the existence of multiple bonding due to *d*-electron donation by non-inert gas type ions is discussed briefly. A quantitative relation between the heats of formation of binary halides and chalcides containing non-inert gas type cations, on the one hand, and inert gas type cations, on the other, reveals an enhanced lattice energy in the former class of compounds. It is shown that this may be accounted for in the case of iron group elements without recourse to the postulate of participation of *d*-electrons in the bonding, as satisfactory estimates of the lattice energies of halides and sulphides may be made on the basis of values for group II*a* compounds.

The bond between the metal atom and carbon in carbonyl compounds is described as consisting of a dative σ-bond and a π-bond, the latter resulting from the overlap of an occupied *d*-orbital of the metal atom and a vacant orbital of the ligand (1). Such bonding is called upon to explain the observations of Carleson and Irving (2) and Ahrland and Chatt (3) that throughout a certain group of metals designated as "*b*-class" elements the stabilities of halo complexes increase in the order F < Cl < Br < I, whereas the order for most elements is I < Br < Cl $\ll$ F. Chatt and co-workers have extended the argument to complexes containing sulphur, phosphorus, etc., which elements they conceive as π-acceptor ligands (4), and they have proposed that the trans-directing influence of certain ligands in substitution reactions may be likewise ascribed to *d*-orbital participation (5).

The postulate of double bonding to the carbonyl group seems unavoidable if an implausibly large accumulation of negative charge at the metal atom is to be avoided. Apart from this rule of "small formal charge", evidence hitherto cited in support of π-bonding has been of an equivocal character. Thus Keller and Parry argue that certain cyano complexes such as $Cr(CN)_6^{3-}$ can hardly owe their great stability to π-bonding because they lack sufficient *d*-electron pairs (6). A recent argument (7) purporting to demonstrate π-bonding through a quantitative relation between absorption band frequencies and complex stability has been refuted by Williams, who maintained that these results and also the relative stabilities of halide complexes of *b*-class elements may be explained satisfactorily as a consequence of polarization of the ligands by the central atom (8). The *b*-class elements are just those which, as cations, have unusually large polarizing power due to inefficient shielding of the nuclear charge by their outer *d*-electrons. It may thus be argued that π-bonding is not required to explain many of the effects which have recently been attributed to it.

Williams' conclusions appear to be based upon a somewhat unsatisfactory argument, however. His measure of polarizing power, R = [ionization potential/$(100Z^2/r)$], is apparently meaningless for ions of inert gas configuration for it increases with increasing atomic number in a given periodic group. There is, however, little doubt that his relations correctly emphasize the fact that polarization may be used to explain many of the phenomena attributed to *d*-electron bonding. It seems that a thermochemical comparison of complexes containing central ions of inert gas and of non-inert gas configurations

[1]*Manuscript received April 22, 1960.*
Contribution from the Department of Chemistry, University of Ottawa, Ottawa, Ontario.

respectively is desirable but this is not yet possible because of the lack of sufficient data for the former. Among binary compounds, however, it is possible to make such comparison and in what follows it is demonstrated that Williams' conclusions are borne out by the thermochemistry of transition metal halides and chalcides.

It has been shown in a previous publication (9) that it is possible to relate the heats of formation of various series of compounds with good precision by means of the quantity

$$-\Delta H^{**} = (-\Delta H_f + S + I)/\text{equivalents per mole},$$

in which ΔH_f is the heat of formation of the compound formed from the elements in their standard states, S is the sublimation energy of the metal, and I is its ionization potential. The $-\Delta H^{**}$ functions for various series of compounds of a given set of cations (or anions) yield straight lines if plotted one against the other providing certain conditions of crystal structure are met. It follows that if we were to attempt to relate the $-\Delta H^{**}$ values of a series of compounds, of which some members possess π-bonds, to those of a series in which no such additional bonding is possible, the singular cases would be revealed. Compounds of third period elements may be thus compared with the corresponding compounds of group II*a* elements, for example. In Fig. 1 the $-\Delta H^{**}$ values for third period halides are plotted against $-\Delta H^{**}$ for the corresponding oxides. Figure 2 illustrates similar relations

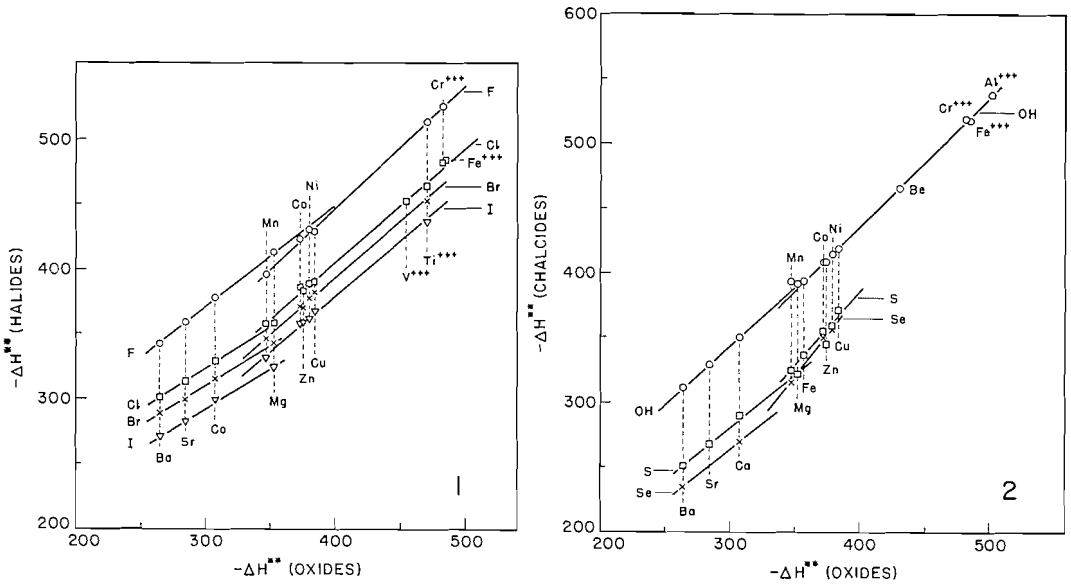


FIG. 1. Plot of $-\Delta H^{**}$ for halides against $-\Delta H^{**}$ for corresponding oxides.
FIG. 2. Plot of $-\Delta H^{**}$ for hydroxides and chalcides against $-\Delta H^{**}$ for oxides.

among the chalcides. The values for these plots are expressed in kilocalories/gram equivalent and were calculated from heats of formation published by the National Bureau of Standards, Washington (10).

An immediate conclusion which may be drawn is that there is no marked difference between the plots for fluorides and hydroxides, for which π-bonding is not possible, and the plots for anions containing vacant *d*-orbitals. The values for transition metals fall on lines which, however, are not extensions of the group II*a* plots. It must now be shown

Can. J. Chem. Downloaded from www.nrcresearchpress.com by 186.148.149.217 on 09/04/12
For personal use only.

that the deviations can be explained on the basis of a model simply involving polarization of the anion.

The value of $-\Delta H^{**}$ for nickel oxide is greater than that for magnesium oxide. This, like the higher ionization potential of nickel, may be interpreted as the result of a greater effective nuclear charge. This means that ions containing outer *d*-electrons possess a greater polarizing power than inert gas type ions of the same charge and radius. It is here assumed that the energy of polarization per gram equivalent in the halides and hydroxides is $N\alpha(Z+z)^2/r^4$, where N is the number of ion–dipole interactions per gram equivalent, α is the polarizability of the anion, Z is the charge on the cation, z is the additional effective nuclear charge due to the presence of outer *d*-electrons, and r is the sum of the cation and anion radii. This expression may be written

$$P = N\alpha[Z^2\{1+(z/Z)\}^2]/r^4. \qquad [1]$$

If z be assumed small with respect to Z, the increase in energy of polarization due to the additional effective nuclear charge is approximated by

$$\Delta P = N\alpha z^2/r^4. \qquad [2]$$

Let us now consider the compounds of cobalt, for example, and assume that the radius of the bivalent ion is 0.82 Å. The contribution to $-\Delta H^{**}$ for the oxide due to the additional polarization is $\Delta P_{CoO} = -\Delta H^{**}-(-\Delta H_h^{**})$, where $-\Delta H_h^{**}$ is the energy value for an hypothetical oxide of an inert gas type cation of radius 0.82 Å. This may be obtained from a plot of $-\Delta H^{**}$ for the group II*a* oxides against ionic radii. This procedure gives $\Delta P_{CoO} = 30.5$ kcal/equivalent. Substituting this value in the expression

$$\Delta P_{oxide} = N\alpha z^2/2r^4, \qquad [3]$$

we obtain $z = 2.46\times10^{-10}$ e.s.u. (The numeral 2 appears in the denominator of [3] because there are only half as many anions per equivalent in the oxide as in the halides.) Upon substituting this value and the appropriate values of α and r obtained from the literature (11, 12) in [2] we may calculate ΔP values for the other cobalt compounds.

Values of $-\Delta H_h^{**}$ for hypothetical halides of an inert gas type cation of radius 0.82 Å are read from plots of the values for group II*a* halides against ionic radii. When the polarization energies calculated as described above are added to these $-\Delta H_h^{**}$ values, calculated values of $-\Delta H^{**}$ are obtained. These are shown in Table I along with the

TABLE I

Comparison of calculated and experimental values (in kilocalories/gram equivalent) of $-\Delta H^{**}$ for third period elements

	Cation									
	Mn^{++}		Co^{++}		Ni^{++}		Cr^{++}		Fe^{+++}	
Anion	Calc.	Exptl.	Calc.	Exptl.	Calc.	Exptl.	Calc.	Exptl.	Calc.	Exptl.
F	406	395	428	423	433	430	524±5	525	—	—
Cl	363	358	387	385	387	388	483	482	487	484
Br	349	346	375	372	375	377	—	—	—	—
I	335	330	362	356	361	361	—	—	—	—
S	327	325	355	353	355	359	—	—	—	—

Can. J. Chem. Downloaded from www.nrcresearchpress.com by 186.148.149.217 on 09/04/12
For personal use only.

experimental values. The agreement is very good for a calculation of this type. However, it was not possible to account for the large lattice energies of selenides.*

Points for the second and third long period elements fall above the lines of Figs. 1 and 2 in those cases where π-bonding is a possibility. The heights of the points above the curves are given in Table II. In keeping with expectation for π-bonding, the energy differences

TABLE II

Experimental values of $-\Delta H^{**}$ minus the graphical interpolation values in kilocalories/gram equivalent

	Sn (II)	Pb (II)	Pd (II)	Cd	Hg (II)	In	Tl
F	—	4	—	4	—	6	—
Cl	−4	3	4	5	7	3	8
Br	−4	5	4	7	10	4	10
I	−2	8	—	10	19	5	—
OH	0	−1	0	0	—	−1	—
S	11	13	—	10	13	—	—

are greatest for third long period elements in iodides and sulphides and further, the hydroxides exhibit no enhancement of lattice energies in contrast to the sulphides. The differences for PbF_2 and CdF_2 are anomalous if we assume the origin of the effects to be in π-bonding but it should be noted that there is more uncertainty about the position of the best fluoride plot than there is about any of the others. Moreover, the differences in the case of these two compounds are equally anomalous even if a polarization argument is adduced to explain these effects.

Although it is here suggested that the plots of $-\Delta H^{**}$ provide some argument for π-bonding, it is recognized that polarization or other causes may well be responsible. It is evident, at least, that the participation of the *d*-electrons is very slight at most in these compounds.

We should expect *d*-electron donation to be more favorable when the metal atom possesses a smaller formal charge. Thermochemical data for compounds of zero-valent elements and, next best, for monovalent ones would be very welcome in this regard. At present we may make comparisons between compounds of silver and those of the alkali elements. Proceeding in this case as described above for bivalent ions, the data in Table III were obtained.

TABLE III

Comparison of calculated and experimental values of $-\Delta H^{**}$ for compounds of silver

Anion	Calc.	Exptl.
Cl	266	268.5
Br	259	269
I	248	260
S	255	253

The large discrepancies for the heavier halides favor the principle of π-bonding although this is not so for the sulphide. The explanation based upon polarization is less

*There is some evidence of participation in the bonding on the part of the d-electrons in these compounds with the NiAs structure since the magnetic moments indicate extensive superexchange among unpaired spins.

Can. J. Chem. Downloaded from www.nrcresearchpress.com by 186.148.149.217 on 09/04/12
For personal use only.

satisfactory here because the differences between calculated and experimental values are equally as great as, or greater than, those in the compounds of the neighboring ions Pd^{++} and Cd^{++}. Such a large polarizing power would be surprising in an ion which has a greater radius and is only singly charged.

We conclude that there is little or no π-bonding in the binary halides and sulphides of third period elements but there is a possible indication of such in the case of heavier elements. It is probable that extensive π-bonding occurs only in more covalent compounds in which the formal charge on the metal atom is zero or negative as is the case in the metal carbonyls.

REFERENCES

1. L. PAULING. The nature of the chemical bond. Cornell Univ. Press, Ithaca, N.Y. 1949. p. 250.
2. B. G. F. CARLESON and H. IRVING. J. Chem. Soc. 4390 (1954).
3. S. AHRLAND and R. LARSSON. Acta Chem. Scand. **8**, 354 (1954).
4. J. CHATT. J. Chem. Soc. 652 (1951); J. CHATT and L. M. VENANZI. J. Chem. Soc. 2787 (1955); S. AHRLAND, J. CHATT, N. R. DAVIES, and A. A. WILLIAMS. J. Chem. Soc. 264, 267 (1958).
5. J. CHATT, L. A. DUNCANSON, and L. N. VENANZI. J. Chem. Soc. 4456 (1955).
6. R. N. KELLER and R. W. PARRY. *In* Chemistry of co-ordination compounds. *Edited by* J. C. Bailar. Reinhold, New York. 1956. p. 190.
7. H. IRVING and J. J. COX. Proc. Chem. Soc. 324 (1959).
8. R. J. P. WILLIAMS. Proc. Chem. Soc. 20 (1960).
9. A. D. WESTLAND. Can. J. Chem. **37**, 1451 (1959).
10. NATL. BUR. STANDARDS Circ. 500, Washington (1952).
11. B. E. CONWAY. Electrochemical data. Elsevier, Amsterdam. 1952.
12. V. M. GOLDSCHMIDT. Geochem. Verteilungsgezetze der Elemente, **8**, 69 (1926).

Can. J. Chem. Downloaded from www.nrcresearchpress.com by 186.148.149.217 on 09/04/12
For personal use only.

Can. J. Chem. Downloaded from www.nrcresearchpress.com by 186.148.149.217 on 09/04/12
For personal use only.

THE SYNTHESIS OF 3-*O*-β-D-XYLOPYRANOSYL-D-XYLOSE AND THE RECHARACTERIZATION OF SOME BENZYLIDENE DERIVATIVES OF D-XYLOSE[1]

E. J. C. CURTIS AND J. K. N. JONES

ABSTRACT

The benzylidene groups of the di-*O*,*O*-benzylidene derivative of D-xylose diethyl dithioacetal have been located at the 2,4:3,5 positions, and *not* at the 2,3:4,5 positions suggested by Zinner, Rembarz, Linke, Ulbricht. Partial hydrolysis yielded the 2,4-*O*-benzylidene compound, from which 3-*O*-β-D-xylopyranosyl-D-xylose (rhodymenabiose) was prepared.

INTRODUCTION

An attempt was made to synthesize 4-*O*-β-D-xylopyranosyl-D-xylose by condensing tri-*O*-acetyl-α-D-xylopyranosyl bromide under standard Koenigs–Knorr conditions with a D-xylose derivative which had all the hydroxyl groups substituted with the exception of that at C_4. It was also desired that this substance be in the open-chain form since experiments have indicated (2) that such reactants give greater yields than those in a ring form due to a lessening of steric hindrance in the Koenigs–Knorr reaction. It was decided that such a derivative might be synthesized using as starting material the mono-*O*,*O*-benzylidene-D-xylose diethyl dithioacetal prepared by Zinner *et al.* (1). This was obtained in low yield by the partial hydrolysis of a di-*O*,*O*-benzylidene-D-xylose diethyl dithioacetal formed by condensing D-xylose diethyl dithioacetal with benzaldehyde in the presence of hydrochloric acid. The above workers (1) assigned the 2,3-linkage to the mono-*O*,*O*-benzylidene compound and gave the 2,3:4,5-linkage to the di-*O*,*O*-benzylidene compound.

Accordingly, the crystalline *O*-benzylidene derivative was prepared and was acetylated to yield a crystalline di-*O*-acetyl-mono-*O*,*O*-benzylidene-D-xylose diethyl dithioacetal, which was then demercaptalated with mercuric chloride and cadmium carbonate in dry methanol, yielding a crystalline di-*O*-acetyl-mono-*O*,*O*-benzylidene-D-xylose dimethyl acetal. Deacetylation of the latter compound produced a crystalline mono-*O*,*O*-benzylidene-D-xylose dimethyl acetal, which was then partially benzoylated using one equivalent of benzoyl chloride in pyridine at low temperature. This reaction yielded a crystalline *O*-benzoyl-*O*,*O*-benzylidene-D-xylose dimethyl acetal. From the reaction sequence, this compound should be 5-*O*-benzoyl-2,3-*O*-benzylidene-D-xylose dimethyl acetal, which has all its hydroxyl groups substituted except that at C_4, a position which is sterically unhindered owing to the absence of a hemiacetal ring. Hence, it was a suitable intermediate for the desired synthesis of 4-*O*-β-D-xylopyranosyl-D-xylose.

O-Benzoyl-*O*,*O*-benzylidene-D-xylose dimethyl acetal was therefore condensed with tri-*O*-acetyl-α-D-xylopyranosyl bromide under standard Koenigs–Knorr conditions (3). The reaction product was deacetylated and debenzoylated by warming it with sodium hydroxide solution, and benzylidene and acetal groups were subsequently removed by hydrolysis with warm dilute sulphuric acid. There resulted a syrup which, from chromatographic examination, consisted mainly of xylose and a disaccharide with an unexpectedly high mobility on chromatograms. The mixture was separated by chromatography on a cellulose column, and the disaccharide component was isolated as a syrup which crystallized. The disaccharide showed on chromatograms a single spot with an unexpectedly

[1]*Manuscript received March 25, 1960.*
Contribution from the Department of Chemistry, Queen's University, Kingston, Ontario.

high mobility (R_{xylose} 0.53, solvent A; 0.64, solvent B), whereas the mobility of the expected 4-*O*-β-D-xylopyranosyl-D-xylose* was much lower (R_{xylose} 0.20, solvent A; 0.38, solvent B). The disaccharide was, in fact, shown to be 3-*O*-D-xylopyranosyl-D-xylose, from its oxidation with sodium periodate and the formation of an osazone. The specific rotation ($-35° \rightarrow -22°$ (constant)) showed the compound to be 3-*O*-β-D-xylopyranosyl-D-xylose. 3-*O*-α-D-Xylopyranosyl-D-xylose has a specific rotation of $+106° \rightarrow +118°$ (constant) (5).

Howard (6) has obtained a xylose-containing disaccharide by partial hydrolysis of a xylan produced by *Rhodymenia palmata*. This disaccharide, "rhodymenabiose", has the same physical constants as the synthetic xylobiose, which is now identified as 3-*O*-β-D-xylopyranosyl-D-xylose. The structure of "rhodymenabiose" was tentatively suggested to be 3-*O*-β-D-xylopyranosyl-D-xylose but no attempts were made to characterize it (6).

As the disaccharide obtained in the Koenigs–Knorr synthesis was not that expected, it was decided to re-examine the structure of the *O*-benzoyl-*O*,*O*-benzylidene-D-xylose dimethyl acetal (VII) used in the condensation. Compound VII was methylated using silver oxide and methyl iodide. The compound proved difficult to methylate, but, after three repetitions of the methylation procedure, a crystalline monomethyl ether was isolated. Debenzoylation yielded a crystalline mono-*O*,*O*-benzylidene-*O*-methyl-D-xylose dimethyl acetal which, on acid hydrolysis, was converted into crystalline 3-*O*-methyl-D-xylose (7).

Compounds VI and VII were then treated with toluene-*p*-sulphonyl chloride, and mono-*O*,*O*-benzylidene-di-*O*-tosyl-D-xylose dimethyl acetal and *O*-benzoyl-*O*,*O*-benzylidene-*O*-tosyl-D-xylose dimethyl acetal were formed, respectively. Reaction of the first of these two tosyl derivatives with sodium iodide under standard conditions (8) showed the presence of one primary hydroxyl group, while, under the same conditions, the second compound showed primary hydroxyl groups to be absent.

These data, together with the formation of 3-*O*-methyl-D-xylose, characterize VI as 2,4-*O*-benzylidene-D-xylose dimethyl acetal and VII as 5-*O*-benzoyl-2,4-*O*,*O*-benzylidene-D-xylose dimethyl acetal. Compound VI was not oxidized by sodium metaperiodate under standard conditions (9) and this is consistent with the benzylidene group in the 2,4 position, there being no free hydroxyl groups on adjacent carbon atoms in 2,4-*O*-benzylidene-D-xylose dimethyl acetal. If the benzylidene group were attached in the 2,3 position a consumption of one equivalent of periodate would be expected. Reaction of VII with tri-*O*-acetyl-α-D-xylopyranosyl bromide would therefore be expected to yield a (1 → 3)-linked xylopyranosyl–xylose and not the (1 → 4)-linked disaccharide originally expected in the condensation.

3-*O*-β-D-Xylopyranosyl-D-xylose was obtained in 11% yield, which is less than might be expected from a condensation involving an open-chain sugar (2). However, although the sugar was in the open-chain form, the hydroxyl group involved in the reaction—that at C_3—was part of a ring system which involved the benzylidene group, and, thus, reaction was sterically hindered to some extent. That the hydroxyl group at C_3 was not very reactive was shown by the difficulties encountered in methylating and tosylating this group.

In order to determine if the mono-*O*,*O*-benzylidene derivatives III, IV, and V had the benzylidene group in the 2,4 position or if the group had wandered during one of the interconversions, the structure of mono-*O*,*O*-benzylidene-D-xylose diethyl dithioacetal

**Prepared by partial hydrolysis of a hemicellulose from aspen (Populus tremuloides) (4).*

Can. J. Chem. Downloaded from www.nrcresearchpress.com by 186.148.149.217 on 09/04/12
For personal use only.

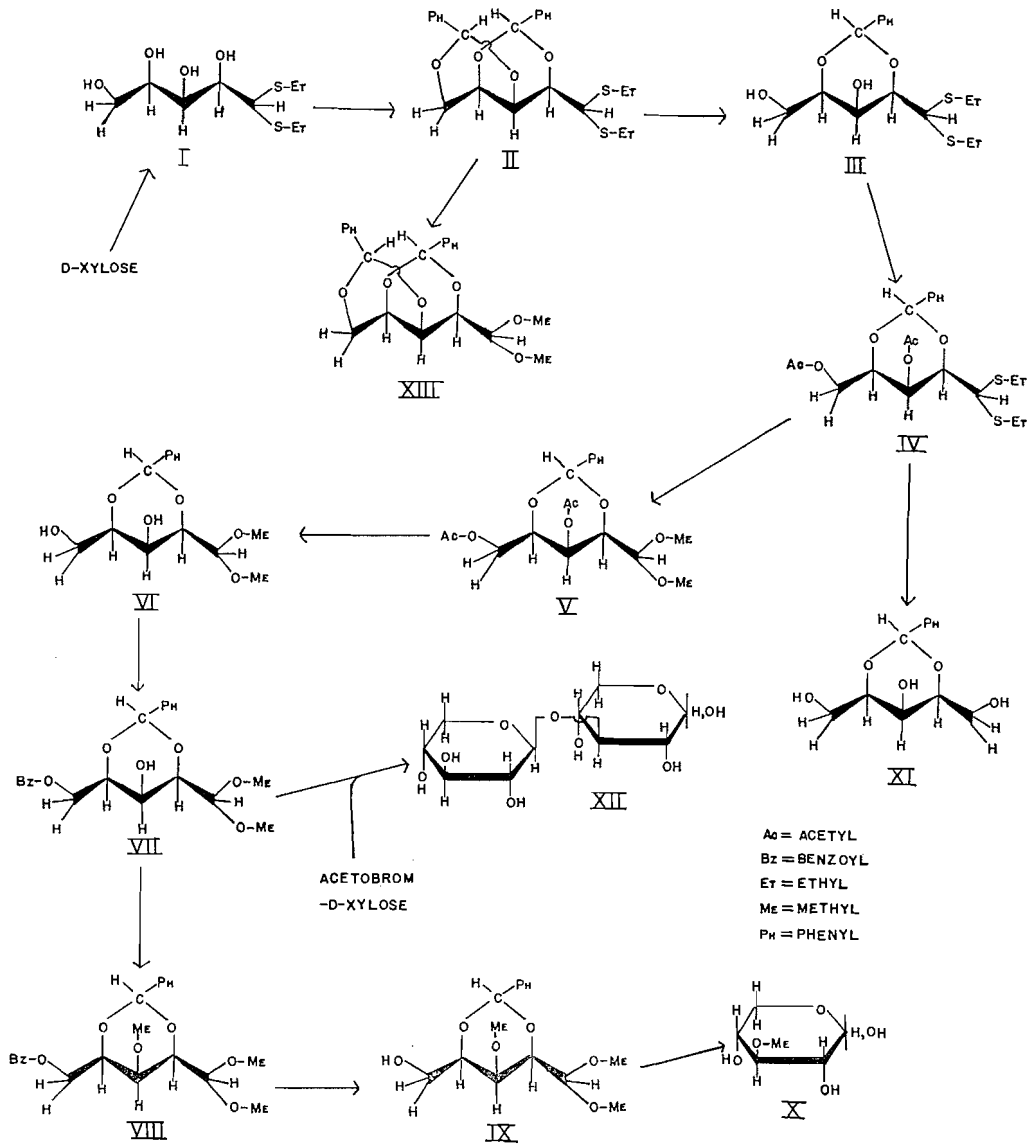
Can. J. Chem. Downloaded from www.nrcresearchpress.com by 186.148.149.217 on 09/04/12
For personal use only.

(III) was examined. The formulation of this as the 2,3-*O*-benzylidene isomer (Zinner *et al.* (1)) rests upon its oxidation with lead tetraacetate, when one equivalent of the oxidizing agent was consumed and formaldehyde (amount not stated) was liberated. This consumption of oxidant was interpreted to mean that the compound contained hydroxyl groups on adjacent carbon atoms. It is known, however (10, 11), that lead tetraacetate oxidation of thioacetals is an unreliable guide to the presence of hydroxyl groups on adjacent carbon atoms, due to the oxidation of the dithioacetal grouping. In particular, Huebner *et al.* (10) have examined the lead tetraacetate oxidation of the analogous mono-*O,O*-benzylidene derivatives of L-arabinose diethyl dithioacetal. With the fully substituted di-*O*-benzylidene-L-arabinose diethyl dithioacetal, one equivalent of oxidant was consumed rapidly (5 minutes) and a further one equivalent was consumed slowly (2 hours). This consumption they assumed to be due to oxidation of the dithioacetal group—a rapid oxidation of one sulphur atom followed by a slower oxidation of the second. With mono-*O,O*-benzylidene-L-arabinose diethyl dithioacetal, a consumption of two equivalents (rapid) plus two equivalents (slow) of lead tetraacetate per mole was observed, which, it was assumed, was due partially to oxidation of the thioacetal groups (one fast plus one slow) and partially to oxidation of hydroxyl groups on adjacent carbon atoms (also, one fast plus one slow). It would, therefore, seem from these observations that the data reported (1) for the lead tetraacetate oxidation of mono-*O,O*-benzylidene-D-xylose diethyl dithioacetal would support the view that this compound does *not* possess hydroxyl groups on adjacent carbon atoms, rather than the reverse.

By demercaptalation of II, Zinner *et al.* (1) obtained a 2,3,4,5-di-*O*-benzylidene-*aldehydo*-D-xylose which, by heating with methanol, they converted into a crystalline 2,3,4,5-di-*O*-benzylidene-D-xylose methyl hemiacetal. They point out that the physical constants (melting point and specific rotation) of this compound are very similar to those of a 2,3,4,5-di-*O*-benzylidene-L-xylose methyl hemiacetal, which was prepared by lead tetraacetate oxidation of a 1,2,3,4-di-*O*-benzylidene-D-glucitol and subsequent treatment with methanol (Wolfe, Hann, and Hudson (12)). However, although the structures of these L-xylose and D-glucitol derivatives were at first in doubt, di-*O,O*-benzylidene-D-glucitol was later shown by Angyal and Lawler (13) to have the benzylidene groups spanning the 1,3 and 2,4 hydroxyl groups. These workers isolated, by partial hydrolysis, 2,4-*O*-benzylidene-D-glucitol, the structure of which was previously known. It therefore follows that the 2,3,4,5-di-*O*-benzylidene-L-xylose methyl hemiacetal must, in fact, have the 2,4:3,5 structure, and the identity of physical constants of this and di-*O,O*-benzylidene-D-xylose methyl hemiacetal would indicate that the latter compound *too* has the 2,4:3,5 structure.

Finally, to characterize compounds II, III, and IV, di-*O*-acetyl-*O,O*-benzylidene-D-xylose diethyl dithioacetal (IV) was demercaptalated, using mercuric chloride and cadmium carbonate in aqueous acetone (14), to yield di-*O*-acetyl-*O,O*-benzylidene-*aldehydo*-D-xylose. This compound was reduced with sodium borohydride in aqueous methanol, and the resulting alkaline solution was heated on a water bath to complete removal of the acetyl groups. The solution was deionized and evaporated to a crystalline residue which was shown to be the well-characterized, symmetrical 2,4-*O*-benzylidene-xylitol (XI) (15, 16). Compound IV is, therefore, 3,5-di-*O*-acetyl-2,4-*O*-benzylidene-D-xylose diethyl dithioacetal, whereas compounds II and III must be 2,4:3,5-di-*O*-benzylidene-D-xylose diethyl dithioacetal and 2,4-*O*-benzylidene-D-xylose diethyl dithioacetal, respectively.

The real sequence of reactions in the synthesis of the disaccharide was therefore:



Demercaptalation of 2,4:3,5-di-*O*-benzylidene-D-xylose diethyl dithioacetal (II), using mercuric chloride and cadmium carbonate in dry methanol, yielded crystalline 2,4:3,5-di-*O*-benzylidene-D-xylose dimethyl acetal (XIII). This was shown to be identical with the di-*O*,*O*-benzylidene-D-xylose dimethyl acetal prepared by Breddy and Jones (17) by condensing D-xylose with benzaldehyde and methanol in the presence of hydrochloric acid, and used by them for the estimation of xylose. The structure of this compound was not previously known.

Zinner *et al.* (1), in addition to preparing the mono-*O*,*O*-benzylidene (III) and di-*O*,*O*-benzylidene (II) derivatives of D-xylose diethyl dithioacetal, also prepared, in the same

Can. J. Chem. Downloaded from www.nrcresearchpress.com by 186.148.149.217 on 09/04/12
For personal use only.

way, a mono-*O,O*-benzylidene-D-xylose dipropyl dithioacetal, and di-*O,O*-benzylidene derivatives of the methyl, propyl, *n*-butyl, isobutyl, and benzyl dithioacetals of D-xylose. These, like II and III, were assigned the 2,3-linkage (in the case of the mono-*O,O*-benzylidene-D-xylose dipropyl dithioacetal) and the 2,3:4,5-linkage (in the case of the di-*O,O*-benzylidene derivatives of the various D-xylose dithioacetals). No attempt has been made to investigate the structures of these derivatives, but it would seem likely that they, like II and III, have the di-*O,O*-benzylidene groups in the 2,4:3,5 positions and the mono-*O,O*-benzylidene group in the 2,4 position.

EXPERIMENTAL

Optical rotations were measured at 21° ± 2° C and in water unless otherwise stated. Solutions were concentrated under reduced pressure at 40° C. The following solvent systems (v/v) were used to separate sugars on paper chromatograms: (A) 1-butanol:ethanol:water, 3:1:1; (B) ethyl acetate:acetic acid:water, 9:2:2. Sugars were detected with the *p*-anisidine hydrochloride spray (18). Infrared absorptions were measured either as solutions in chloroform or as a powder (mulled in a potassium bromide pellet) on a Perkin–Elmer Model 21 spectrophotometer.

D-*Xylose Diethyl Dithioacetal* (I)

D-Xylose (100 g), ice-cold ethanethiol (100 g), and ice-cold hydrochloric acid (100 ml) were shaken together in a stoppered flask and the resulting mixture was left overnight at room temperature. The solution was diluted with water (200 ml) and then deionized by passage through Amberlite IR 400 (OH) resin. The eluate was concentrated to a syrup which was diluted with ether (200 ml) and refrigerated. The product crystallized and was filtered and washed with ether. Yield: 140 g (82%), m.p. 63–64° C.

2,4:3,5-Di-O-benzylidene-D-*xylose Diethyl Dithioacetal* (II)

D-Xylose diethyl dithioacetal (50 g) was dissolved in redistilled benzaldehyde (500 ml) with warming and after being cooled to 5° C in ice, dry hydrogen chloride was bubbled through the solution. After 5 minutes a semisolid mass was formed which was diluted with ethanol (400 ml), shaken, and filtered under suction. The crude crystalline product was dried *in vacuo* and recrystallized from boiling ethanol. Yield: 40.6 g (48%), m.p. 181–182° C, $[\alpha]_D$ −36° (*c*, 4.95, chloroform). Literature (1) gives a melting point of 181–182° C and $[\alpha]_D$ −36.7° (*c*, 2.53, chloroform).

2,4-O-Benzylidene-D-*xylose Diethyl Dithioacetal* (III)

The conditions given by Zinner *et al.* (1) (hydrolysis with ethanol (3 parts) plus 80% acetic acid (4 parts) for 1 hour) were found to produce only a small yield of mono-*O,O*-benzylidene compound. After various hydrolyzing mixtures were tried, the following conditions were found to be most satisfactory. A mixture of di-*O,O*-benzylidene-D-xylose diethyl dithioacetal (80 g), acetone (1800 ml), and 80% acetic acid (1200 ml) was refluxed for 3 hours. The resulting solution was cooled to 10° C in ice water, and unhydrolyzed di-*O*-benzylidene material was removed by filtration. The filtrate was concentrated to a small volume and the acid was neutralized with cold potassium hydroxide solution followed by sodium bicarbonate solution. The aqueous solution was extracted with chloroform (3×100 ml) and the combined extracts were washed once with water, dried ($MgSO_4$), and filtered. Evaporation of the filtrate yielded a crystalline residue which was extracted with boiling water. The aqueous extract was cooled and mono-*O,O*-benzylidene-D-xylose diethyl dithioacetal was removed by filtration. Yield: 5.5 g (43% after recovery

Can. J. Chem. Downloaded from www.nrcresearchpress.com by 186.148.149.217 on 09/04/12
For personal use only.

of unchanged di-*O*-benzylidene compound). After recrystallization from water and from ether it had a melting point of 146–147° C and $[\alpha]_D$ −22° (*c*, 2.0, methanol). Literature (1) gives a melting point of 147° C and $[\alpha]_D$ −23.3° (*c*, 2.76, methanol).

3,5-Di-O-acetyl-2,4-O-benzylidene-D-*xylose Diethyl Dithioacetal* (IV)

2,4-*O*-Benzylidene-D-xylose diethyl dithioacetal (29.4 g) was dissolved in dry pyridine (300 ml), and acetic anhydride (250 ml) was added dropwise to the solution while this was cooled and stirred mechanically. After the addition (1 hour) stirring was continued for 1 hour more and the solution was then left at room temperature (16 hours), after which it was poured with stirring into ice water (1200 ml). The product precipitated from solution and was collected, washed with water, and air-dried. After recrystallization from methanol it weighed 35 g (96%) and had a melting point of 92.5–93° C and $[\alpha]_D$ −2° (*c*, 4.35, chloroform). Anal. Calc. for $C_{20}H_{28}O_6S_2$: S, 14.95. Found: S, 14.96.

3,5-Di-O-acetyl-2,4-O-benzylidene-D-*xylose Dimethyl Acetal* (V)

3,5-Di-*O*-acetyl-2,4-*O*-benzylidene-D-xylose diethyl dithioacetal (10 g) was dissolved in dry methanol (300 ml). Cadmium carbonate (90 g) was added to the solution, which was stirred vigorously, and a solution of mercuric chloride (90 g) in dry methanol (100 ml) was added portionwise at room temperature. After the addition (1 hour) stirring was continued for a further 15 hours at room temperature and the mixture was then refluxed (40 minutes). The solution was filtered through a Celite pad and the precipitate was washed with methanol. Filtrate and washings were concentrated to ca. 200 ml and this solution was poured into 500 ml each of chloroform and water. The chloroform layer was extracted with water until chloride-free, dried ($MgSO_4$), filtered, and evaporated to a syrup (9.6 g). This crystallized when allowed to stand in the desiccator. The crude product was recrystallized from methanol. Yield: 6.5 g (76%), m.p. 82.5–83.5° C, $[\alpha]_D$ +34° (*c*, 4.3, chloroform). Anal. Calc. for $C_{18}H_{24}O_8$: C, 58.71; H, 6.52; S, nil. Found: C, 58.94; H, 6.34; S, 0.07.

2,4-O-Benzylidene-D-*xylose Dimethyl Acetal* (VI)

3,5-Di-*O*-acetyl-2,4-*O*-benzylidene-D-xylose dimethyl acetal (1.45 g) was dissolved in dry methanol (30 ml) and the resulting solution was cooled to 5° C. Methanolic sodium methoxide (0.88 *N*, 1 ml) was added and the solution was then stored at 7° C (22 hours) in a stoppered flask. The solution was neutralized (glacial acetic acid and then sodium bicarbonate solution) and then evaporated to dryness, to yield a white crystalline residue. This was recrystallized from ether. Yield: 0.90 g (81%), m.p. 142–143° C, $[\alpha]_D$ +32° (*c*, 1, methanol). Infrared examination showed no absorption for carbonyl group (1700–1750 cm^{-1}). Anal. Calc. for $C_{14}H_{20}O_6$: C, 59.16; H, 7.04. Found: C, 59.41; H, 7.15.

5-O-Benzoyl-2,4-O-benzylidene-D-*xylose Dimethyl Acetal* (VII)

The method used was similar to that described by Zinner *et al.* (19). 2,4-*O*-Benzylidene-D-xylose dimethyl acetal (4.8 g) was dissolved in dry pyridine and the solution was cooled to −15° C and stirred mechanically. A solution of redistilled benzoyl chloride (2.5 g) in dry pyridine (10 ml) was then added dropwise while the temperature was kept below −10° C (40 minutes). The solution was stored at −5° C (4 hours), then at 0° C (16 hours), and finally at room temperature (2 hours), after which the product was precipitated by pouring the solution into ice water (700 ml). The mixture was left at room temperature (2 hours) to complete hydrolysis of excess benzoyl chloride and was then filtered. The precipitate was washed with water and after drying *in vacuo* it weighed 4.5 g (69%). The material was recrystallized from methanol and then had a melting point of 120–121° C

Can. J. Chem. Downloaded from www.nrcresearchpress.com by 186.148.149.217 on 09/04/12
For personal use only.

and $[\alpha]_D$ +44° (*c*, 4.06, chloroform). Anal. Calc. for $C_{21}H_{24}O_7$: C, 64.94; H, 6.19. Found: C, 65.21; H, 6.40.

*Condensation of 5-O-Benzoyl-2,4-O-benzylidene-*D*-xylose Dimethyl Acetal with Tri-O-acetyl-α-*D*-xylopyranosyl Bromide*

5-*O*-Benzoyl-2,4-*O*-benzylidene-D-xylose dimethyl acetal (8 g) was dissolved in dry, alcohol-free chloroform (80 ml) and to the solution were added Drierite (10 g) and silver oxide (10 g). The solution was shaken in the dark to dry the reagents. After 1 hour tri-*O*-acetyl-α-D-xylopyranosyl bromide (20) (14.4 g) in dry, alcohol-free chloroform (50 ml) and a few crystals of iodine were added and the shaking was continued at room temperature. After 48 hours a test for ionizable bromine was negative. After a further 48 hours the solution was filtered through a Celite pad, and evaporated to a syrup which was dissolved in a solution of water (4 parts) plus methanol (1 part) (200 ml) containing sodium hydroxide (8 g). The solution was warmed on a water bath at 70° C (4 hours), after which it was cooled and deionized by passage through columns of Amberlite IR 400 (OH) and IRC 50 (H) resins in series; the former resin also removed the bulk of the free xylose. The neutral eluate was concentrated to a syrup (5.4 g) which was dissolved in aqueous *N*/100 sulphuric acid, and the resulting solution was warmed at 70° C (5 hours). The solution was cooled and deionized by passage through Duolite A-4 (OH) resin. Concentration of the eluate yielded a syrup which was shown by paper chromatography (solvent B) to consist, in addition to xylose, of a main component with R_{xylose} 0.64 and smaller components with R_{xylose} 1.23 and 0.38.

The syrup was partially fractionated by chromatography on a column of Dowex 50W resin (94×3.3 cm) (21) and fractionation and concentration of the eluate yielded a syrup (2.3 g) which was enriched with the chromatographically slower-moving components. Part of this (0.9 g) was fractionated by chromatography on a cellulose column (40×3 cm) (22) using as eluent 1-butanol half saturated with water.

Fraction 1: A syrup (0.62 g) which chromatographic examination showed to consist mainly of xylose, plus a much smaller component with R_{xylose} 1.23 (solvent B). This latter was presumed to be a partially unhydrolyzed xylose acetal or ester.

Fraction 2: A syrup (0.255 g) which crystallized on standing. Chromatography showed a single spot with R_{xylose} 0.53 (solvent A) and 0.64 (solvent B).

Fraction 3: A syrup (0.04 g) which chromatographic examination showed to consist of a major component with R_{xylose} 0.26 (solvent A) and 0.38 (solvent B) and a minor component with R_{xylose} 0.53 (solvent A) and 0.64 (solvent B). This fraction was not examined further.

Fraction 2 was recrystallized from methanol and then had a melting point of 192–193° C and $[\alpha]_D$ −35° (4 minutes) → −22° (constant) (*c*, 2.5).

Acid hydrolysis (*N* sulphuric acid at 80° C for 12 hours) showed only xylose to be present. Anal. Calc. for $C_{10}H_{18}O_9$: C, 42.53; H, 6.43. Found: C, 42.71; H, 6.56.

Periodate Oxidation of Fraction 2 (XII)

Portions (ca. 10 mg) of fraction 2 were oxidized with aqueous sodium metaperiodate using standard procedures, (*a*) in acid pH unbuffered conditions, and (*b*) in solution buffered at pH 8. The periodate uptake was estimated by the method of Neumüller and Vasseur (9) and the formic acid liberation by that of Andrews *et al.* (23).

The molar periodate consumptions per mole of disaccharide were as follows: (*a*) in unbuffered solution, 1.38 (after 14 minutes), 1.75 (39 minutes), 2.36 (1.2 hours), 2.41 (2 hours), 2.78 (4 hours), 2.97 (7.5 hours), and 3.04 (21 hours); (*b*) in solution buffered at

Can. J. Chem. Downloaded from www.nrcresearchpress.com by 186.148.149.217 on 09/04/12
For personal use only.

pH 8, 1.48 (after 13 minutes), 2.88 (38 minutes), 7.11 (4 hours), and 8.73 (21 hours). The molar production of formic acid in unbuffered solution was 0.47 (after 39 minutes), 0.58 (1.2 hours), 0.82 (2 hours), 0.99 (4 hours), 1.20 (7.5 hours), and 1.33 (21 hours). Extrapolation of the flat part of the curve to zero time gave values for the experiment in unbuffered solution: uptake of metaperiodate, 2.95 moles per mole of sugar; formic acid production, 1.05 moles per mole of sugar.

The theoretical results for oxidation of a xylobiose in acid pH unbuffered conditions are: for (1 → 2) and (1 → 3)-linked disaccharides, 3 moles of periodate consumed per mole of sugar and 1 mole of formic acid liberated per mole of sugar, and for (1 → 4)- and (1 → 5)-linked disaccharides, 4 moles of periodate per mole and 2 moles of formic acid per mole assuming hydrolysis of formyl ester is slow. The extrapolated values obtained therefore indicated that the glycosidic linkage was either (1 → 2) or (1 → 3), and the overoxidation values showed that it was in fact the latter. There was very little overoxidation in unbuffered solution (only 3.05 moles of periodate were consumed after 21 hours) and this is typical of (1 → 3)-linked disaccharides where initial oxidation produces a formyl ester-containing residue which is stable under the acid pH which results in unbuffered conditions. With (1 → 3)-linked sugars overoxidation is rapid in alkaline solution as the formyl ester is unstable under these conditions, and fraction 2 showed a rapid overoxidation in solution buffered at pH 8. It is known (25) that with (1 → 2)-linked disaccharides overoxidation is rapid even in acid conditions because the residue resulting from initial oxidation does not contain a formyl ester and hence is unstable.

*3-O-β-*D*-Xylopyranosyl-*D*-xylose Phenyl Osazone*

The sugar (50 mg) was dissolved in water (0.5 ml) and acetic acid (0.2 ml) plus phenyl hydrazine (0.15 ml) were added. The solution was warmed at 70° C (1.5 hours) and then cooled and diluted with water (3 ml). An oil separated which crystallized on standing. This was recrystallized from hot water and then had a melting point of 194–196° C and $[\alpha]_D$ +47° (*c*, 1.25, pyridine). Anal. Calc. for $C_{22}H_{28}O_7N_4$: N, 12.18. Found: N, 12.28.

*5-O-Benzoyl-2,4-O-benzylidene-3-O-methyl-*D*-xylose Dimethyl Acetal* (VIII)

5-*O*-Benzoyl-2,4-*O*-benzylidene-D-xylose dimethyl acetal (1.19 g) was dissolved in methyl iodide (25 ml). Silver oxide (2 g), Drierite (2 g), and a few crystals of iodine were added to the solution, which was then shaken in the dark (21 hours) and finally boiled under reflux (5 hours) with exclusion of moisture. The solution was filtered and the residue was washed with acetone. Filtrate and washings were evaporated to dryness, yielding a partially crystalline residue which was finally dried *in vacuo*. It then weighed 1.17 g and, on infrared analysis, showed appreciable amounts of hydroxyl group to be still present. The above methylation procedure was repeated twice (the materials were boiled under reflux for a total time of 70 hours), after which a crystalline product (1.17 g, total yield i.e. recovery, 96%) was obtained which, when subjected to infrared analysis, showed only a small peak corresponding to free hydroxyl group. The product was dissolved in warm ethanol and cooling the resulting solution induced partial crystallization. The crystalline material was filtered, washed with ethanol, and dried. It weighed 0.37 g and had a melting point of 137–138° C. Further cooling of the solution produced a second crop of crystals (0.16 g, m.p. 137–138° C), after which a third crop was obtained which had a melting point of 90–98° C and was presumably a mixture of methylated and nonmethylated materials. The material with a melting point of 137–138° C was combined (0.53 g, 43%) and recrystallized from ethanol. It then had a melting point of 138–139° C and $[\alpha]_D$ +40° (*c*, 2.5, chloroform). Infrared examination showed there to be no peak for

Can. J. Chem. Downloaded from www.nrcresearchpress.com by 186.148.149.217 on 09/04/12
For personal use only.

free hydroxyl group present. Anal. Calc. for $C_{22}H_{26}O_7$: OMe, 23.14. Found: OMe, 23.32.

*2,4-O-Benzylidene-3-O-methyl-*D*-xylose Dimethyl Acetal* (IX)

5-*O*-Benzoyl-2,4-*O*-benzylidene-3-*O*-methyl-D-xylose dimethyl acetal (0.34 g) was dissolved in a solution of ethanol (10 ml) plus aqueous *N*/10 sodium hydroxide solution (10 ml) and the materials were then warmed on a water bath at 70° C (2 hours). The solution was cooled and concentrated to dryness and yielded a residue which was dissolved in chloroform (20 ml). The resulting solution was washed twice with water, dried ($MgSO_4$), filtered, and evaporated to dryness. A crystalline residue was obtained (0.22 g, 88%) which after recrystallization from ether had a melting point of 134–135° C and $[\alpha]_D$ +9° (*c*, 1.55, methanol). Anal. Calc. for $C_{15}H_{22}O_6$: OMe, 31.2. Found: OMe, 31.0.

*3-O-Methyl-*D*-xylose* (X)

2,4-*O*-Benzylidene-3-*O*-methyl-D-xylose dimethyl acetal (0.22 g) was added to aqueous *N*/60 sulphuric acid (10 ml) and sufficient methanol was then added to dissolve the material. The solution was warmed at 70° C (5 hours), cooled, and deionized by passage through Duolite A-4 resin (OH form). Concentration of the eluate yielded a colorless syrup (0.12 g 95%), which crystallized completely after nucleation with authentic 3-*O*-methyl-D-xylose. After recrystallization from acetone the material had a melting point of 96° C and mixed melting point with authentic 3-*O*-methyl-D-xylose 95–96° C, $[\alpha]_D$ +57° (4 minutes) → +19° (constant) (*c*, 1.6). Literature gives a melting point of 103–104° C and $[\alpha]_D$ +52.2° → +14.8° (constant) (7), m.p. 95° C, and $[\alpha]_D$ +45° → +19° (constant) (26). The infrared spectra of this material and of authentic 3-*O*-methyl-D-xylose were identical.

*2,4-O-Benzylidene-3,5-di-O-tosyl-*D*-xylose Dimethyl Acetal*

2,4-*O*-Benzylidene-D-xylose dimethyl acetal (1.07 g) was dissolved in dry pyridine (4 ml) and the solution was cooled to 10° C. A solution of toluene-*p*-sulphonyl chloride (1.6 g) in pyridine (3 ml) was then added and the material was left in a stoppered flask at room temperature (2 hours). Excess tosyl chloride was hydrolyzed by the slow dropwise addition of water, and the mixture was then poured into an excess (100 ml) of water. The resulting solution was extracted with chloroform and the combined chloroform extracts were washed successively with solutions of dilute sulphuric acid and sodium bicarbonate, and finally with water. The solution was dried, filtered, and evaporated to a hard glass (1.97 g). Infrared examination of this showed a slight peak for free hydroxyl group so the tosylation procedure was repeated; a colorless glass (1.93 g, 86%) was thus obtained. This showed no peak corresponding to free hydroxyl group on infrared examination, $[\alpha]_D$ +14° (*c*, 3.4, chloroform). Anal. Calc. for $C_{28}H_{32}O_{10}S_2$: S, 10.77. Found: S, 10.80.

*Reaction of 2,4-O-Benzylidene-3,5-di-O-tosyl-*D*-xylose Dimethyl Acetal with Sodium Iodide*

The conditions used were those recommended by Tipson (8). 2,4-*O*-Benzylidene-3,5-di-*O*-tosyl-D-xylose dimethyl acetal (0.23 g) plus a 10% solution of sodium iodide in acetone (2.3 ml) were sealed in a glass tube, which was then placed in a boiling water bath (2 hours). After being cooled to room temperature the materials were filtered and the precipitated sodium toluene-*p*-sulphonate was washed with acetone. Yield: 0.03 g, which, allowing for the solubility of sodium toluene-*p*-sulphonate in acetone (8), represents 44% reaction from one tosyl group.

*5-O-Benzoyl-2,4-O-benzylidene-3-O-tosyl-*D*-xylose Dimethyl Acetal*

5-*O*-Benzoyl-2,4-*O*-benzylidene-D-xylose dimethyl acetal (0.30 g) was treated with

Can. J. Chem. Downloaded from www.nrcresearchpress.com by 186.148.149.217 on 09/04/12
For personal use only.

tosyl chloride using the procedure described above. After three repetitions of the tosylation process a colorless glass (0.41 g, 97%) was obtained which showed no peak corresponding to free hydroxyl group on infrared examination. It had $[\alpha]_D$ +4° (*c*, 4.62, chloroform). Anal. Calc. for $C_{28}H_{30}O_9S$: S, 5.90. Found: S, 5.88.

The material was heated with sodium iodide in acetone as described for 2,4-*O*-benzylidene-di-*O*-tosyl-D-xylose dimethyl acetal. After 2 hours in the boiling water bath no sodium toluene-*p*-sulphonate was produced.

2,4-O-Benzylidene-xylitol (XI)

3,5-Di-*O*-acetyl-2,4-*O*-benzylidene-D-xylose diethyl dithioacetal (IV) (5.15 g) was dissolved in a solution of acetone (4 parts) plus water (1 part) (80 ml). Cadmium carbonate (12 g) was added to the solution, which was stirred vigorously while a solution of mercuric chloride (12.3 g) in acetone (40 ml) was added portionwise at room temperature. After the addition (3 hours) stirring was continued for a further 15 hours at room temperature and the mixture was then boiled under reflux (40 minutes). The product was worked up as described for 2,4-*O*-benzylidene-3,5-di-*O*-acetyl-D-xylose dimethyl acetal, a clear syrup (3.7 g) being obtained.

The above crude 3,5-di-*O*-acetyl-2,4-*O*-benzylidene-aldehydo-D-xylose (3.0 g) was dissolved in 50% aqueous methanol (100 ml) and to the cooled solution was added an excess (2.2 g) of sodium borohydride. The solution was left at room temperature (3 hours) after which excess sodium borohydride was destroyed with glacial acetic acid. The solution was deionized by passage through a column of Amberlite IR-400 (OH) resin and the acidic eluate was shaken with Amberlite IR-120 (H) resin in the cold. The neutral solution was evaporated to dryness and boric acid was removed as methyl borate by codistillation with methanol (4×40 ml). A residue remained (1.05 g, 46% over-all yield) which crystallized on standing and was recrystallized from water. It had a melting point of 142–143° C and showed no optical rotation. Literature (16) gives a melting point of 143–144° C. The material formed a crystalline triacetate which had a melting point of 94–95° C and showed no optical rotation. Literature (16) gives a melting point of 94–95° C.

2,4:3,5-Di-O-benzylidene-D-xylose Dimethyl Acetal (XIII)

2,4:3,5-Di-*O*-benzylidene-D-xylose diethyl dithioacetal (5 g) was demercaptalated using mercuric chloride and cadmium carbonate in dry methanol as described for 3,5-di-*O*-acetyl-2,4-*O*-benzylidene-D-xylose diethyl dithioacetal (IV). The product was extracted in the same way yielding a white crystalline residue (3.1 g, 72%) which was recrystallized from chloroform/light petroleum. It had a melting point of 210–211° C and $[\alpha]_D$ −9° (*c*, 2.2, chloroform).

Di-*O*-benzylidene-D-xylose dimethyl acetal was also prepared as described by Breddy and Jones (17) by allowing D-xylose to react with methanol and benzaldehyde in the presence of hydrochloric acid. The white crystalline product was recrystallized from chloroform/light petroleum and had a melting point of 210–211° C undepressed by admixture with 2,4:3,5-di-*O*-benzylidene-D-xylose dimethyl acetal and $[\alpha]_D$ −9° (*c*, 2.25, chloroform). Literature (17) gives a melting point of 211° C and $[\alpha]_D$ −9° (*c*, 1.2, chloroform). The infrared spectrum of this material and that of 2,4:3,5-di-*O*-benzylidene-D-xylose dimethyl acetal were identical.

ACKNOWLEDGMENTS

The authors wish to thank the National Research Council for grants which made this work possible.

Can. J. Chem. Downloaded from www.nrcresearchpress.com by 186.148.149.217 on 09/04/12
For personal use only.

REFERENCES

1. H. ZINNER, G. REMBARZ, H. LINKE, and G. ULBRICHT. Ber. **90**, 1761 (1957).
2. E. J. C. CURTIS and J. K. N. JONES. Can. J. Chem. **37**, 358 (1959).
3. W. L. EVANS, D. D. REYNOLDS, and E. A. TALLEY. Advances in carbohydrate chemistry. Vol. 6. Academic Press, Inc., New York. 1951. p. 27.
4. J. K. N. JONES and L. E. WISE. J. Chem. Soc. 2750 (1952).
5. D. H. BALL and J. K. N. JONES. J. Chem. Soc. 33 (1958).
6. B. H. HOWARD. Biochem. J. **67**, 643 (1957).
7. P. A. LEVENE and A. L. RAYMOND. J. Biol. Chem. **102**, 331 (1933).
8. R. S. TIPSON. Advances in carbohydrate chemistry. Vol. 8. Academic Press, Inc., New York. 1953. p. 190.
9. G. NEUMÜLLER and E. VASSEUR. Arkiv Kemi, **2**, 235 (1953).
10. C. F. HUEBNER, R. A. PANKRATZ, and K. P. LINK. J. Am. Chem. Soc. **72**, 4811 (1950).
11. H. ZINNER, W. BOCK, and H. P. KLÖCKING. Ber. **92**, 1307 (1959).
12. J. K. WOLFE, R. M. HANN, and C. S. HUDSON. J. Am. Chem. Soc. **64**, 1493 (1942).
13. S. J. ANGYAL and J. V. LAWLER. J. Am. Chem. Soc. **66**, 837 (1944).
14. M. L. WOLFROM. J. Am. Chem. Soc. **51**, 2188 (1929).
15. P. J. VAN DER LAAN and L. P. VAN DER M. DEKKER. Rec. trav. chim. **62**, 824 (1943).
16. R. M. HANN, A. T. NESS, and C. S. HUDSON. J. Am. Chem. Soc. **68**, 1769 (1946).
17. L. J. BREDDY and J. K. N. JONES. J. Chem. Soc. 738 (1945).
18. L. HOUGH, J. K. N. JONES, and W. H. WADMAN. J. Chem. Soc. 1702 (1950).
19. H. ZINNER, K. WESSELY, W. BOCK, K. RIECKHOFF, F. STRANDT, and W. NIMMICH. Ber. **90**, 500 (1957).
20. M. BÁRCZAI-MARTOS and N. KŐRÖSY. Nature, **165**, 369 (1950).
21. J. K. N. JONES, R. A. WALL, and (*in part*) A. O. PITTET. Chem. & Ind. 1196 (1959).
22. L. HOUGH, J. K. N. JONES, and W. H. WADMAN. J. Chem. Soc. 2511 (1949).
23. P. ANDREWS, L. HOUGH, and J. K. N. JONES. J. Chem. Soc. 806 (1954).
24. W. A. D. DUNCAN, D. J. MANNERS, and J. L. THOMPSON. Biochem. J. **73**, 295 (1959).
25. P. E. REID and J. K. N. JONES. Can. J. Chem. **38**, 944 (1960).
26. R. A. LAIDLAW and E. G. V. PERCIVAL. J. Chem. Soc. 528 (1950).

Can. J. Chem. Downloaded from www.nrcresearchpress.com by 186.148.149.217 on 09/04/12
For personal use only.

Can. J. Chem. Downloaded from www.nrcresearchpress.com by 186.148.149.217 on 09/04/12
For personal use only.

STEREOCHEMICAL STUDIES

I. CONFIGURATIONS OF SOME 4-AZACHOLESTANES[1]

J. T. Edward and Peter F. Morand[2]

ABSTRACT

The Beckmann rearrangement of the oxime of A-nor-5β-cholestan-3-one gave 4-aza-5β-cholestan-3-one; the isomeric lactam obtained by the reduction of the oxime of 5-oxo-3,5-seco-A-norcholestan-3-oic acid with sodium in alcohol must consequently be 4-aza-5α-cholestan-3-one. Other methods of reducing the oximino acid afforded hydroxamic acids. 4-Aza-5α- and 4-aza-5β-cholestane were obtained by reduction of the appropriate lactam or hydroxamic acid.

For stereochemical studies we required 4-aza-5α-cholestane (VIII, R = H) and 4-aza-5β-cholestane (III, R = H), and hence the 5α- (VII) and 5β-lactam (II).

Bolt (1) obtained a lactam of this structure, but of undetermined configuration at the 5-position, by reduction of the oxime (V) of Windaus' keto acid (IV) (2) with sodium in ethanol. We have repeated Bolt's work and have obtained a lactam having properties agreeing closely with those reported. This lactam would be expected, from previous experience of reductions by sodium in alcohol (3, 4), to have a trans fusion of rings A and B, as shown in the structure VII. This stereochemistry is also suggested by the direct preparation of the lactam from the keto acid (IV) by the Leuckart reaction, which is known to be sensitive to steric effects (5, 6) and which with 5α-cholestan-3-one gives β-amino derivatives (7).

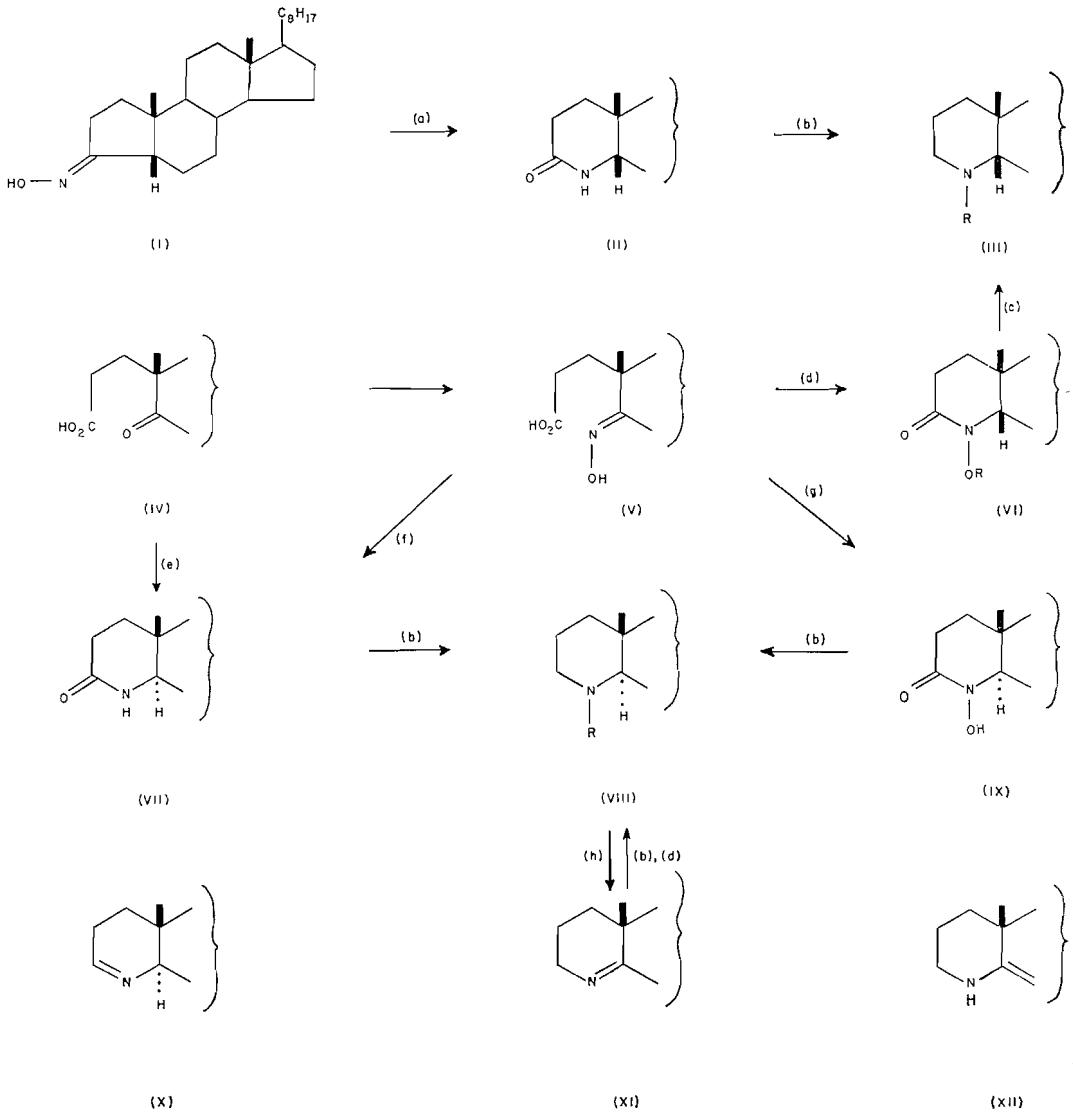
The structure (VII) for Bolt's lactam has now been proved by preparing the isomeric cis-fused lactam (II) by the Beckmann rearrangement of the oxime (I) of Windaus' norketone (8, 9). The configuration of the migrating center is known to be retained in the Beckmann rearrangement (10), and the migration of the 5- rather than 3-carbon atom would be expected from analogy with a similar reaction in the cholanic acid series (11). Evidence confirming this expectation is given below.

The lactams (VII and II) afforded 4-aza-5α- (VIII, R = H) and 4-aza-5β-cholestane (III, R = H) respectively on reduction with lithium aluminum hydride. The latter azasteroid could be obtained only as an oil but gave a crystalline perchlorate.

Bolt (12) claimed that hydrogenation over platinum of the oximino acid (V) gave the same lactam (VII) as did reduction with sodium in ethanol (1), together with a smaller amount of an amino acid. In our hands catalytic reduction has given as sole product a hydroxamic acid, shown to have the cis-fused structure (VI, R = H) by its further reduction with tin in hydrochloric acid to 4-aza-5β-cholestane (III, R = H). This reaction establishes also the 4-aza structure for the lactam (II) obtained by the Beckmann rearrangement. The isomeric trans-fused hydroxamic acid (IX, R = H) was obtained by reduction of the oximino acid (V) with zinc in acetic acid; its structure was established by its conversion to 4-aza-5α-cholestane (VIII, R = H) with lithium aluminum hydride. The differing stereochemical effects of the reducing agents in giving the isomeric hydroxamic acids are as expected (3).

While the infrared absorption frequencies of the carbonyl group in hydroxamic acids (13, 14) are generally lower than in the corresponding amides, the differences are considerably greater for the six-membered (VI, R = H, and IX) than for five-membered

[1]*Manuscript received March 8, 1960.*
Contribution from the Department of Chemistry, McGill University, Montreal, Que.
[2]*Holder of N.R.C. Studentships, 1957–59.*



REAGENTS: (*a*) *p*-Acetamidobenzenesulphonyl chloride, (*b*) $LiAlH_4$, (*c*) Sn in HCl, (*d*) H_2/Pt, (*e*) HCO_2NH_4, (*f*) Na in ethanol, (*g*) Zn in AcOH, (*h*) $Hg(OAc)_2$.

cyclic compounds (15). The very low values for the former compounds (1623 and 1630 cm^{-1}) may be due to the more effective intramolecular hydrogen bonding possible between the carbonyl and hydroxyl groups. Some support for this view comes from the higher frequencies of the derivatives (VI, R = PhCO (1677 cm^{-1}) and VI, R = Me, (1658 cm^{-1})).

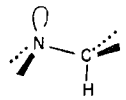
Oxidation of 4-aza-5α-cholestane (VIII, R = H) with mercuric acetate afforded 4-azacholest-4-ene (XI). The alternative structures X and XII, considered less likely from the course of oxidation of analogous compounds (16), were eliminated by the absence of absorption bands in the regions 3030–3040 cm^{-1} and 800–970 cm^{-1}, characteristic of =C—H stretching vibrations and out-of-plane deformation vibrations (17),

Can. J. Chem. Downloaded from www.nrcresearchpress.com by 186.148.149.217 on 09/04/12
For personal use only.

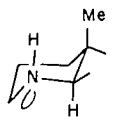
and by the absence of an absorption maximum which could be assigned to an N—H stretching vibration.

Reduction of 4-azacholest-4-ene with lithium aluminum hydride gave back 4-aza-5α-cholestane. The same product was obtained by catalytic hydrogenation which might, by analogy with the hydrogenation of cholest-4-ene in neutral solution (8), have been expected to give the 5β compound.

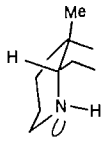
From a study of the infrared spectra of about 50 nitrogenous bases, Bohlmann (18) has suggested that the structural unit XIII, in which the tertiary hydrogen and the orbital containing the unshared electrons of the nitrogen are coplanar and trans, gives rise to an absorption band in the frequency region 2700–2800 cm^{-1}. The absence of absorption in this region by 4-aza-5α- and 4-aza-5β-cholestane may be interpreted as evidence for the conformations XIV and XV of these compounds. Such conformations



(XIII)



(XIV)



(XV)

for piperidines have been postulated by Barton and Cookson (19), who consider the space-filling requirements of the orbital containing the unshared electron pair to be greater than those of the hydrogen atom; and recently these conformations have been supported by measurements of molar Kerr constants (20). On these grounds one would expect the stable conformations of the N-methyl compounds (III and VIII, R = Me) to contain the structural unit XIII, since the space-filling characteristics of the methyl group will certainly be greater than those of the pair of unshared electrons. N-Methyl-4-aza-5α-cholestane (VIII, R = Me) and N-methyl-4-aza-5β-cholestane (III, R = Me) were prepared by heating the secondary amines (VIII and III, R = H) with formaldehyde and formic acid, and each showed an absorption band of medium intensity at 2775 cm^{-1} which disappeared when the perchlorate was formed. However, N-methyl amines generally show a peak in this region of the spectrum (21) which disappears on salt formation (22). Recently McKenna and Tulley (J. Chem. Soc. 945 (1960)) have described the preparation of the compounds III, R = Me, and VIII, R = Me, the former by a route differing from ours. On the basis of the products given by the Hofmann degradation of these compounds, they assign them the configurations assigned on other grounds in this paper.

EXPERIMENTAL

Where not otherwise specified, Merck acid-washed alumina was used for chromatography. Infrared spectra were obtained on a Perkin–Elmer Model 21 spectrophotometer; in listing the frequencies of absorption bands, the intensities are designated w (weak), m (medium), s (strong), sh (shoulder). Microanalyses were carried out by W. Manser (Zurich) and A. Bernhardt (Mülheim, Germany).

A-Nor-5-β-cholestan-3-one

3,4-Seco-5β-cholestane-3,4-dioic acid (2.60 g) (23), covered with 12 ml of acetic anhydride, was gradually heated, over a period of 30 minutes, to remove most of the

Can. J. Chem. Downloaded from www.nrcresearchpress.com by 186.148.149.217 on 09/04/12
For personal use only.

Can. J. Chem. Downloaded from www.nrcresearchpress.com by 186.148.149.217 on 09/04/12
For personal use only.

acetic anhydride by distillation at atmospheric pressure. The temperature was then raised and the fraction distilling at 260°–274° C/4 mm was collected as a pale yellow oil. An ether solution of the oil was washed with alkali and then water, dried (sodium sulphate), and concentrated. The residue dissolved partially in warm methanol, from which crystals (0.57 g), m.p. 72°–73° C, separated on cooling. The residue from the mother liquors was taken up in pentane and chromatographed on alumina. Elution with pentane containing increasing amounts of benzene gave, on concentration, a further crop (1.00 g), m.p. 72°–73° C. Recrystallization of the combined crops from methanol afforded 1.35 g (60% yield) of A-nor-5β-cholestan-3-one, m.p. 73°–74° C, $[\alpha]_D^{24}$ +122° (*c*, 1.995 in chloroform) (lit. m.p. 73°–74° C (8), $[\alpha]_D$ +105° (chloroform) (24)).

A-Nor-5β-cholestan-3-one Oxime (I)

A mixture of A-nor-5β-cholestan-3-one (0.60 g), hydroxylamine hydrochloride (0.5 g), and anhydrous sodium acetate (0.6 g) in 75% aqueous ethanol (50 ml) was refluxed for 4 hours. The precipitate obtained on dilution with water was crystallized from methanol to give rosettes of the *oxime* (0.55 g), m.p. 123°–124° C, $[\alpha]_D^{24}$ +81.7° (*c*, 0.416 in chloroform), $\nu_{max}^{CCl_4}$ in cm^{-1}: 3630 m, 3290 m, 3170 sh, 2940 s, 2860 sh, 1617 w, 1465 s, 1440 m, 1425 sh, 1377 m, 1364 w, 1342 w, 1319 w, 1304 w, 949 m, 919 m, 888 m. Calc. for $C_{22}H_{45}ON$: C, 80.55; H, 11.71; N, 3.62%. Found: C, 80.57; H, 11.80; N, 3.62%.

4-Aza-5β-cholestan-3-one (II)

A solution of A-nor-5β-cholestan-3-one oxime (0.50 g) and *p*-acetylaminobenzenesulphonyl chloride (0.25 g) in absolute pyridine (13 ml) was allowed to stand for 2 days (cf. 25). The solution was then diluted with water and acidified with dilute sulphuric acid. The pale brown solid (0.49 g) thus obtained contained lactam (strong infrared band at 1660 cm^{-1}) and oxime (bands at 949, 919, and 888 cm^{-1}), and melted at 119–135° C. After several recrystallizations from methanol, the material (258 mg) was chromatographed on alumina (6 g, activity I). Elution with ether–acetone and acetone removed starting material (173 mg). Further elution with ethanol:acetone (1:2, 100 ml) afforded impure 4-aza-5β-cholestan-3-one (59 mg), purified by repeated recrystallization from methanol to give the lactam (19 mg), m.p. 151–155° with decomposition (bath preheated to 140° C), $[\alpha]_D^{24}$ +68.2° (*c*, 0.909 in chloroform), $\nu_{max}^{CCl_4}$ in cm^{-1}: 3410 w, 3205 w, 3080 w, 2940 s, 2870 sh, 1660 s, 1460 m, 1443 m, 1408 w, 1377 m, 1355 w, 1303 m, 920 w. Calc. for $C_{26}H_{45}ON$: C, 80.55; H, 11.71; N, 3.62%. Found: C, 80.40; H, 11.57; N, 3.58%.

N-*Hydroxy-4-aza-5β-cholestan-3-one* (VI, R = H)

The oxime of 5-oxo-3,5-A-norcholestan-3-oic acid (2.20 g), prepared according to Windaus (2), was dissolved in acetic acid (125 ml) and hydrogenated in a Parr apparatus for 4.5 hours in the presence of platinum oxide (0.50 g). After removal of the platinum, the solution was concentrated at reduced pressure to give a brownish residue. Recrystallization of this material from methanol gave a first crop (1.30 g) of white crystals of N-hydroxy-4-aza-5β-cholestan-3-one; a second crop (0.35 g) was obtained from the mother liquors. After two more crystallizations, the melting point was 122°–124° C, $[\alpha]_D^{24}$ +31.8° (*c*, 1.949 in chloroform), $\nu_{max}^{CCl_4}$ in cm^{-1}: 3240 w, 2940 s, 2870 sh, 1623 s, 1465 m, 1443 sh, 1430 sh, 1388 m, 1360 sh, 1328 w, 1314 sh, 1299 m, 1165 w, 1140 w, 1095 w. With chloroform as solvent, the carbonyl absorption occurred at 1607 cm^{-1}. In both carbon tetrachloride and chloroform the carbonyl frequency was not changed by dilution of the solution. The compound gave a reddish-purple color in alcoholic ferric chloride

solution. When the compound was dried at 65°/0.1 mm, it analyzed as a monohydrate. Calc. for $C_{26}H_{47}O_2N$: C, 74.07; H, 11.23; N, 3.32%. Found: C, 74.25, 74.14; H, 11.13, 11.14; N, 3.33%. When dried at 110°/0.1 mm for 4 hours the water of crystallization was lost. Calc. for $C_{26}H_{45}ON$: C, 77.40; H, 11.24; N, 3.47%. Found: C, 77.33; H, 11.28; N, 3.55, 3.48%.

N-*Benzoyloxy-4-aza-5β-cholestan-3-one* (VI, R = PhCO)

A solution of N-hydroxy-4-aza-5β-cholestan-3-one (200 mg) and benzoyl chloride (1.5 ml) in absolute pyridine (3.0 ml) was refluxed for 1 hour. After the reaction mixture was cooled, it was diluted with ether and washed with aqueous sodium bicarbonate and then with water. After it had been dried (magnesium sulphate) and concentrated the ether produced a yellow oil which was chromatographed on alumina (5 g, Woelm, activity II–III). Elution with benzene–ether (1:1, 50 ml; 1:3, 50 ml) gave 40 mg of crystalline material, which, after one recrystallization from ligroin–benzene, had a melting point of 209°–212° C, $[\alpha]_D^{24}$ −6.4° (*c*, 0.621 in chloroform), $\nu_{max}^{CCl_4}$ in cm^{-1}: 3420 w, 3220 w, 3080 w, 2940 s, 2870 sh, 1720 s, 1677 s, 1565 m, 1450 m, 1443 sh, 1425 sh, 1377 m, 1357 w, 1330 w, 1312 m, 1265 s, 1174 m, 1110 s, 1093 sh, 1065 m, 1025 m, 902 w. Calc. for $C_{33}H_{49}O_3N$: C, 78.06; H, 9.73; N, 2.76%. Found: C, 77.55; H, 9.66; N, 3.10%.

N-*Methoxy-4-aza-5β-cholestan-3-one* (VI, R = Me)

A mixture of N-hydroxy-4-aza-5β-cholestan-3-one (475 mg), methyl iodide (0.35 ml), and 7% aqueous potassium hydroxide (2.0 ml) in ethanol (10 ml) was refluxed for 4.5 hours. The alcohol was removed under reduced pressure, the mixture was diluted with aqueous 10% potassium hydroxide, and extracted several times with ether. The ether extract, worked up in the usual way, gave a white solid (278 mg). Part of the substance (95 mg) was chromatographed over alumina (3.0 g, Woelm, activity II). Elution with benzene–hexane (4:1, 20 ml) and benzene (80 ml) gave crystalline material (70 mg), m.p. 106°–108° C. One recrystallization from aqueous methanol gave plates, m.p. 114°–115° C, $\nu_{max}^{CCl_4}$ in cm^{-1}: 2945 s, 2870 sh, 1688 sh, 1658 s, 1470 m, 1445 m, 1385 m, 1333 w, 1295 m, 1245 w, 1220 w, 1097 w, 1051 m, 955 w, 955 w, 909 w, 892 w, 850 w. Calc. for $C_{27}H_{48}O_2N$: C, 77.46; H, 11.55; N, 3.35%. Found: C, 77.69; H, 11.43; N, 3.40%.

4-Aza-5β-cholestane (III, R = H)

(a) By the Reduction of 4-Aza-5β-cholestan-3-one

A mixture of lithium aluminum hydride (0.30 g) and 4-aza-5β-cholestan-3-one (309 mg) in dioxane (35 ml) was refluxed for 40 hours. The mixture was then treated with water, and extracted four times with chloroform. The extracts were dried over magnesium sulphate and evaporated to give 4-aza-5β-cholestane as an uncrystallizable oil, $[\alpha]_D^{33}$ +22.1° (*c*, 1.808 in chloroform), ν_{max}^{film} in cm^{-1}: 3305 w, 2940 s, 2870 sh, 2800 sh, 2730 sh, 2620 sh, 1467 s, 1445 s, 1382 s, 1337 w, 1312 m, 1254 w, 1234 w, 1214 w, 1169 w, 1128 m, 1108 sh, 1067 w, 1030 w, 988 w, 968 w, 931 w, 884 w, 860 w, 837 w, 806 w, 777 w, 724 w. The *perchlorate* was precipitated by adding a few drops of 70% perchloric acid to 4-aza-5β-cholestane (50 mg) in methanol (5 ml). Crystallized from methanol, it had a melting point of 203–206° C, $[\alpha]_D^{33}$ +21.4° (*c*, 2.049 in chloroform), $\nu_{max}^{CCl_4}$ in cm^{-1}: 3190 sh, 3100 m, 2950 s, 2870 sh, 1590 w, 1467 m, 1455 sh, 1430 w, 1407 w, 1381 m, 1366 sh, 1336 w, 1309 w, 1287 w, 1125 s, 1090 s, 918 w, 903 sh, 856 w. Calc. for $C_{26}H_{48}O_4NCl$: C, 65.85; H, 10.20; N, 2.95%. Found: C, 65.70; H, 10.29; N, 2.99%.

(b) By the Reduction of N-*Hydroxy-4-aza-5β-cholestan-3-one*

A mixture of granulated tin (3.0 g) and N-hydroxy-4-aza-5β-cholestan-3-one (307 mg)

Can. J. Chem. Downloaded from www.nrcresearchpress.com by 186.148.149.217 on 09/04/12
For personal use only.

Can. J. Chem. Downloaded from www.nrcresearchpress.com by 186.148.149.217 on 09/04/12
For personal use only.

in ethanol (9 ml) and concentrated hydrochloric acid (3 ml) was refluxed on the steam bath for 7 hours. Every hour a further 1 ml of hydrochloric acid was added, as well as enough ethanol to keep the organic material in solution. The solution was decanted from tin and diluted with water, giving 4-aza-5β-cholestane hydrochloride (295 mg), obtained after two recrystallizations from acetone as short needles which darkened at 237° and melted at 256°–265° C (bath preheated to 230° C). Calc. for $C_{26}H_{48}NCl$: C, 76.14; H, 11.80%. Found: C, 75.92; H, 11.76%.

The free base, obtained in the usual way as an uncrystallizable oil, $[\alpha]_D^{33}$ +24.2 (*c*, 0.910 in chloroform), was converted by treatment with 70% perchloric acid to a crystalline perchlorate, which, after one recrystallization from methanol, had a melting point of 201°–205° C, $[\alpha]_D^{33}$ +19.7° (*c*, 1.521 in chloroform). This compound was shown by mixed melting point and by its infrared spectrum to be identical with the perchlorate obtained by reduction of 4-aza-5β-cholestan-3-one.

N-*Methyl-4-aza-5β-cholestane* (III, R = Me)

A mixture of 4-aza-5β-cholestane (97 mg), 40% formaldehyde solution (1.0 ml), and 99% formic acid (1.0 ml) was heated on the steam bath for 3 hours. After the mixture was cooled, it was diluted with water and made basic with ammonium hydroxide. Extraction with ether and working up in the usual way gave a colorless uncrystallizable syrup (90 mg), $\nu_{max}^{CCl_4}$ in cm^{-1}: 2940 s, 2870 sh, 2775 m, 2715 sh, 2620 w, 1465 s, 1445 s, 1376 s, 1263 w, 1236 w, 1215 w, 1200 w, 1187 w, 1173 w, 1143 w, 1112 w, 1090 w, 1073 w, 1025 sh, 1014 m, 978 w, 960 w, 930 w, 877 w, 833 w. The *perchlorate* had a melting point of 246°–251° C; in its infrared spectrum the absorption band at 2775 cm^{-1} had disappeared and bands at 1100 and 1052 cm^{-1} (perchlorate anion) had appeared. Calc. for $C_{27}H_{50}O_4NCl$: C, 66.40; H, 10.32; N, 2.87%. Found: C, 66.60; H, 10.39; N, 3.04%.

4-Aza-5α-cholestan-3-one (VII)

Ammonium formate (2.5 g) was distilled from a 25-ml conical flask until a temperature of 165° C was reached in the flask. 5-Oxo-3,5-seco-A-norcholestan-3-oic acid (1.70 g) suspended in nitrobenzene (10 ml) was introduced into the flask and the temperature of the resulting mixture was kept at 180°–200° C for 24 hours (cf. 26). After the reaction mixture was cooled, it was washed with water. The water-insoluble liquid was refluxed for 2 hours in 6 *N* hydrochloric acid (8 ml) and ethanol (7 ml). After the removal of nitrobenzene and ethanol by steam distillation, the aqueous solution was extracted with ether. The ether solution was washed with dilute sodium carbonate and with water, dried over sodium sulphate, and evaporated to dryness. The residue, after one recrystallization from methanol, weighed 1.27 g, m.p. 240°–251° C. Several recrystallizations from methanol raised the melting point to 250°–252° C with decomposition (bath preheated to 240° C), $[\alpha]_D^{22}$ +45° (*c*, 1.585 in chloroform), (lit. m.p. 252°–253° C, $[\alpha]_D$ +44 (in pyridine) (1)). The melting point and infrared spectrum of this compound were identical with those of authentic 4-aza-5α-cholestan-3-one obtained by the reduction of the oxime of 5-oxo-3,5-seco-A-norcholestan-3-oic acid (V) with sodium and alcohol (1); $\nu_{max}^{CCl_4}$ in cm^{-1}: 3422 w, 3210 w, 3070 w, 2940 s, 2870 sh, 1662 s, 1467 s, 1444 sh, 1404 m, 1383 m, 1358 m, 1306 m, 1223 w, 1162 w, 1132 w. Calc. for $C_{26}H_{45}ON$: N, 3.62%. Found: N, 3.70%.

N-*Hydroxy-4-aza-5α-cholestan-3-one* (IX)

The oxime of 5-oxo-3,5-seco-A-norcholestan-3-oic acid (0.64 g) and zinc dust (1.09 g) in acetic acid (20 ml) were heated to 90–95° C for 1 hour. The zinc was then removed

by filtration, and the filtrate diluted with water to yield N-hydroxy-4-aza-5α-cholestan-3-one as a fluffy white solid (0.59 g, m.p. 140°–153° C). Repeated recrystallizations from ethyl acetate and then from methanol raised the melting point to 185°–187° C with decomposition (bath preheated to 150° C), $[\alpha]_D^{28}$ −49.5° (*c*, 1.98 in chloroform), $\nu_{max}^{CCl_4}$ in cm^{-1}: 3260 w, 2940 s, 2870 sh, 1677 sh, 1630 s, 1487 s, 1461 s, 1448 sh, 1428 w, 1395 s, 1380 s, 1328 w, 1315 w, 1306 m, 1267 w, 1223 s, 1187 w, 1138 w, 1072 w, 940 m, 925 w, 887 w, 860 w. Calc. for $C_{26}H_{45}O_2N$: C, 77.40; H, 11.24; N, 3.47%. Found: C, 77.23; H, 10.99; N, 3.39%. In methanolic ferric chloride the compound gave a reddish-purple color.

4-Aza-5α-cholestane (VIII, R = H)

(a) By the Reduction of 4-Aza-5α-cholestan-3-one

A mixture of 4-aza-5α-cholestan-3-one (509 mg) and lithium aluminum hydride (0.50 g) in dioxane (75 ml) was refluxed for 40 hours. Isolation of the product in the usual way gave a solid, melting at 114°–115° C, after two recrystallizations from acetone (lit. m.p. 116°–117° C (1)), $[\alpha]_D$ +36° (chloroform), ν_{max}^{KBr} in cm^{-1}: 3270 w, 2940 s, 2870 sh, 1470 s, 1445 s, 1384 s, 1368 sh, 1210 w, 1173 w, 1128 m, 1116 sh, 1077 w, 946 w, 933 m, 905 w, 889 w, 867 w, 858 w, 840 w. Calc. for $C_{26}H_{47}N$: C, 83.56; H, 12.68; N, 3.75%. Found: C, 83.44; H, 12.69; N, 3.71%.

The *perchlorate*, crystallized from methanol, had a melting point of 224°–225° C, $[\alpha]_D^{33}$ +21.1 (*c*, 2.36 in chloroform), $\nu_{max}^{CCl_4}$ in cm^{-1}: 3190 sh, 3100 m, 2950 s, 2870 sh, 1590 w, 1467 m, 1450 m, 1392 sh, 1383 w, 1377 sh, 1366 sh, 1330 w, 1307 w, 1125 s, 1090 s, 918 w. Calc. for $C_{26}H_{48}O_4NCl$: C, 65.85; H, 10.20; N, 2.95%. Found: C, 65.67; H, 10.14; N, 2.72%.

(b) By the Reduction of N-Hydroxy-4-aza-5α-cholestan-3-one

A mixture of N-hydroxy-4-aza-5α-cholestan-3-one (121 mg) and lithium aluminum hydride (0.30 g) in dry ether (50 ml) was refluxed for 12 hours. Then water (0.60 ml) and 10% aqueous sodium hydroxide (0.48 ml) were added, and the mixture stirred for 10 minutes. The inorganic salts were removed by filtration, and the filtrate was evaporated to dryness. The brown syrupy residue (93 mg) had an infrared spectrum which showed no carbonyl peak. When treated with 70% perchloric acid it gave a salt, m.p. 222°–224° C, which was shown by its infrared spectrum and by a mixed melting point to be identical with the perchlorate of 4-aza-5α-cholestane obtained from 4-aza-5α-cholestan-3-one.

N-*Methyl-4-aza-5α-cholestane* (VIII, R = Me)

4-Aza-5α-cholestane (95 mg) was treated with 99% formic acid (1.0 ml) and 40% formaldehyde solution (1.0 ml) under the conditions described for preparing N-methyl-4-aza-5β-cholestane. The product (77 mg) after two crystallizations from methanol had a melting point of 63°–64° C (lit. m.p. 61°–62° C (12)), $\nu_{max}^{CCl_4}$ in cm^{-1}: 2950 s, 2870 sh, 2775 m, 2715 sh, 2620 w, 1465 s, 1445 s, 1378 m, 1365 sh, 1328 w, 1179 m, 1160 m, 1107 m, 1068 w, 1022 m, 1000 sh, 970 sh. Calc. for $C_{27}H_{49}N$: C, 83.64; H, 12.74%. Found: C, 83.82; H, 12.97%.

The *perchlorate* melted at 231°–235° C, and had no absorption band at 2775 cm^{-1}. Calc. for $C_{27}H_{50}O_4NCl$: C, 66.40; H, 10.32; N, 2.87%. Found: C, 66.18; H, 10.24; N, 2.93%.

N-*p-Nitrobenzoyl-4-aza-5α-cholestane*

A solution of 4-aza-5α-cholestane (330 mg) and *p*-nitrobenzoyl chloride (0.25 g) in dry benzene (15 ml) was refluxed for 1.5 hours. After the solution was cooled, it was

Can. J. Chem. Downloaded from www.nrcresearchpress.com by 186.148.149.217 on 09/04/12
For personal use only.

washed with dilute sodium carbonate, dilute hydrochloric acid, and water, dried over sodium sulphate, and evaporated to dryness. Crystallization of the residue from methanol gave 180 mg of substance melting at 232°–238° C; after several recrystallizations the melting point rose to 243°–245° C (decomp.), $\nu_{max}^{CCl_4}$ in cm^{-1}: 2940 s, 2865 sh, 1647 s, 1600 m, 1520 w, 1465 m, 1434 s, 1382 sh, 1363 sh, 1346 s, 1308 m, 1287 m, 1175 w, 1140 w, 1117 w, 1103 w, 1010 w, 945 w, 927 w, 856 w, 848 w. Calc. for $C_{33}H_{51}O_3N_2$: C, 75.67; H, 9.82; N, 5.32%. Found: C, 75.55; H, 9.72; N, 5.32%.

4-Azacholest-4-ene (XI)

A solution of 4-aza-5α-cholestane (0.51 g) and mercuric acetate (1.78 g) in 5% aqueous acetic acid (10 ml) was heated on the steam bath for 2 hours. After the solution was cooled, mercurous acetate was removed by filtration. The filtrate was saturated with hydrogen sulphide, centrifuged, and the supernatant liquid made strongly basic with aqueous 40% sodium hydroxide solution. The solid which precipitated was taken up in ether and the ether solution washed with water and dried (magnesium sulphate). Evaporation of the ether left a semisolid residue (0.33 g) which was dissolved in methanol (5 ml) and treated with a few drops of 70% perchloric acid. The *perchlorate* precipitated, and after one recrystallization from methanol had a melting point of 212°–213° C, ν_{max}^{KBr} in cm^{-1}: 3240 w, 3120 w, 2950 s, 2870 sh, 1680 s, 1468 s, 1455 sh, 1382 m, 1367 sh, 1335 w, 1283 w, 1213 w, 1105 s, 1080 s, 927 w. In carbon tetrachloride the C=N absorption occurred at 1677 cm^{-1}. Calc. for $C_{26}H_{26}O_4NCl$: C, 66.15; H, 9.82; N, 2.97; Cl, 7.51%. Found: C, 65.93; H, 9.68; N, 2.97; Cl, 7.34%.

The *free base* obtained from the perchlorate had a melting point of 101°–102° C after two crystallizations from acetone, $\nu_{max}^{CCl_4}$ in cm^{-1}: 2945 s, 2870 sh, 2800 sh, 2720 sh, 1649 s, 1467 s, 1445 s, 1383 m, 1377 sh, 1366 m, 1328 w, 1320 w, 1305 w, 1166 w, 1127 m, 1075 w, 1054 w, 1027 w, 954 w, 928 w, 854 w. In potassium bromide pellet also, no absorption occurred in the region 3100–3450 cm^{-1}. Calc. for $C_{26}H_{45}N$: C, 84.04; H, 12.21; N, 3.77%. Found: C, 83.78; H, 12.18; N, 3.79%.

Reduction of 4-Aza-cholest-4-ene Perchlorate

(a) With Lithium Aluminum Hydride

A slurry of 4-azacholest-4-ene perchlorate (30 mg) and lithium aluminum hydride (0.10 g) in anhydrous ether (8 ml) was refluxed with stirring for 4.5 hours, after which the excess of lithium aluminum hydride was destroyed with 30% aqueous sodium hydroxide. The aqueous solution was extracted three times with ether, and the combined ether extracts dried and concentrated to give a brownish solid (21 mg). The perchlorate of this material melted at 222°–224° C and was shown by mixed melting point and infrared spectrum to be identical with 4-aza-5α-cholestane perchlorate.

(b) By Catalytic Hydrogenation

A solution of 4-azacholest-4-ene perchlorate (92 mg) in ethanol was hydrogenated at atmospheric pressure in the presence of platinum oxide (35 mg). The calculated amount of hydrogen was taken up in 8 minutes. Removal of the catalyst by filtration, and basification and concentration of the filtrate gave a white solid, crystallizing from acetone as needles, m.p. 113°–114° C. The compound was shown by mixed melting point and infrared spectrum to be 4-aza-5α-cholestane.

ACKNOWLEDGMENTS

The authors are grateful to Dr. A. Taurins for help in obtaining infrared spectra and to the National Research Council for generous financial support.

Can. J. Chem. Downloaded from www.nrcresearchpress.com by 186.148.149.217 on 09/04/12
For personal use only.

REFERENCES

1. C. C. BOLT. Rec. trav. chim. **57**, 905 (1938).
2. A. WINDAUS. Ber. **39**, 2008 (1906).
3. D. H. R. BARTON. J. Chem. Soc. 1027 (1953).
4. D. E. EVANS, C. W. SHOPPEE, and G. H. R SUMMERS. Chem. & Ind. (London), 1535 (1954).
5. D. S. NOYCE and F. W. BATCHELOR. J. Am. Chem. Soc. **74**, 4577 (1952).
6. M. MOUSSERON, R. JACQUIER, and R. ZAGDOUN. Bull. soc. chim. France, 974 (1953).
7. R. R. SAUERS. J. Am. Chem. Soc. **80**, 4721 (1958).
8. A. WINDAUS. Ber. **52**, 170 (1919).
9. L. F. FIESER and M. FIESER. Steroids. Reinhold Publishing Corp., New York. 1959. p. 80.
10. J. KENYON and D. P. YOUNG. J. Chem. Soc. 263 (1941). A. CAMPBELL and J. KENYON. J. Chem. Soc. 25 (1946).
11. S. HARA. Pharm. Bull. (Tokyo), **3**, 209, 297 (1955); Chem. Abstr. **50**, 10117, 13061 (1956).
12. C. C. BOLT. U.S. Patent No. 2,227,876 (1941); Chem. Abstr. **35**, 2681 (1941).
13. M. F. MATHIS. Compt. rend. **232**, 505 (1951).
14. D. HADZI and D. PREVORSEK. Spectrochim. Acta, **10**, 38 (1958).
15. R. BONNET, R. F. C. BROWN, V. M. CLARK, I. O. SUTHERLAND, and A. TODD. J. Chem. Soc. 2094 (1959).
16. B. WITKOP. J. Am. Chem. Soc. **78**, 2873 (1956).
17. R. N. JONES, P. HUMPHRIES, E. PACKHARD, and K. DOBRINER. J. Am. Chem. Soc. **72**, 86 (1950).
18. F. BOHLMANN. Angew. Chem. **69**, 641 (1957).
19. D. H. R. BARTON and R. C. COOKSON. Quart. Revs. (London), **10**, 73 (1956).
20. M. ARONEY and R. J. W. LEFEVRE. Proc. Chem. Soc. 82 (1958).
21. R. D. HILL and G. D. MEAKINS. J. Chem. Soc. 760 (1958).
22. J. T. BRAUNHOLTZ, E. A. V. EBSWORTH, F. G. MANN, and N. SHEPPARD. J. Chem. Soc. 2780 (1958).
23. R. LANGER. Z. physiol. Chem. **216**, 191 (1933).
24. B. B. SMITH and H. R. NACE. J. Am. Chem. Soc. **76**, 6119 (1954).
25. R. ANLIKER, M. MÜLLER, J. WOHLFAHRT, and H. HEUSSER. Helv. Chim. Acta, **38**, 1404 (1955).
26. A. W. INGERSOLL, S. H. BROWN, C. K. KIM, W. D. BEAUCHAMP, and G. JENNINGS. J. Am. Chem. Soc. **58**, 1808 (1936).

Can. J. Chem. Downloaded from www.nrcresearchpress.com by 186.148.149.217 on 09/04/12
For personal use only.

Can. J. Chem. Downloaded from www.nrcresearchpress.com by 186.148.149.217 on 09/04/12
For personal use only.

STEREOCHEMICAL STUDIES

II. CONFIGURATIONS OF SOME 4-OXACHOLESTANES[1]

J. T. EDWARD AND PETER F. MORAND[2]

ABSTRACT

The oxidation of A-nor-5β-cholestan-3-one with peracids gave 4-oxa-5β-cholestan-3-one. This was identical with one of the two lactones produced by the reduction of Windaus' keto acid; the other lactone must be 4-oxa-5α-cholestan-3-one. The two lactones were reduced by lithium aluminum hydride to diols, which were cyclized to 4-oxa-5α- and -5β-cholestane.

Turner (1) obtained by catalytic reduction of Windaus' keto acid (I) (2) two lactones, m.p. 109.5°–110° C and 116°–116.5° C, the former in larger amount. He tentatively assigned to these compounds the structures V and VI, respectively, because of their optical rotations and because hydrogenation of 4-oxacholest-5-en-3-one, which should be expected to give VI, gave the higher melting isomer.

Further evidence for these structures comes from a consideration of their molecular rotations (3) including the differences between the molecular rotations of the lactones and of the amides (II or III, R = NH_2) or hydrazides (II or III, R = $NHNH_2$), which are, as shown in Table I, in the directions predicted by the Klyne–Hudson "lactone rule"

TABLE I

Molecular rotation $[M]_D$ values

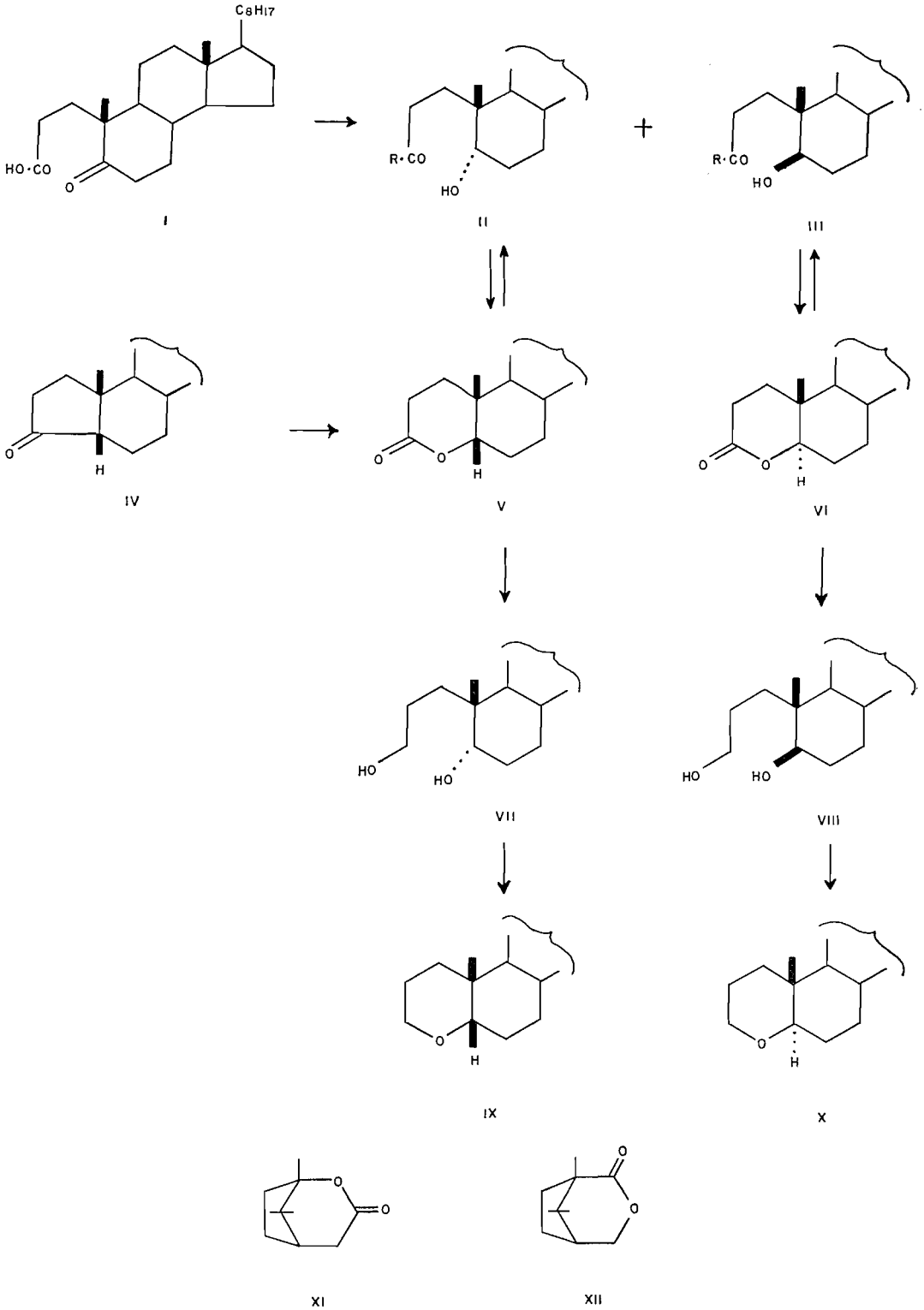
Lactones	Amides	Δ	Hydrazides	Δ
V	II, R = NH_2		II, R = $NHNH_2$	
+80°,[a] +70°[b]	+92°[a]	−12°[a]	+93°[b]	−23°[b]
VI	III, R = NH_2		III, R = $NHNH_2$	
+325°,[a] +311°[b]	+124°[a]	+201°[a]	+161°[b]	+150°[b]

[a]In 95% ethanol. [b]In chloroform.

(3). Finally, unequivocal proof comes from the Baeyer–Villiger oxidation of Windaus norketone (IV), which is known to have the cis ring juncture shown (4). With peracetic acid this affords the lactone with the lower melting point. The Baeyer–Villiger reaction proceeds with retention of configuration of migrating optically active groups (5, 6) and almost always, as in the present case, involves the migration of the more alkylated of the two carbon atoms flanking the carbonyl group (7, 8).

A notable exception to the latter generalization is afforded by the oxidation of camphor, carried out by Baeyer and Villiger themselves (9). In reinvestigating this reaction, Sauers (10) found that in acetic acid camphor is oxidized by peracetic acid to the expected lactone (XI) (82% yield) but in the presence of concentrated sulphuric acid is oxidized to campholide (XII) (30% yield), although some of the isomeric lactone (XI) also may be formed but destroyed in the strongly acidic solution. Sauers explained the formation of campholide by a mechanism involving a protonated form of the Criegee intermediate (11, 12). In the destruction of this intermediate the electronic effects which favor the migration of the more heavily alkylated carbon atom become less important than they are in the destruction of the neutral Criegee intermediate. Conformational and

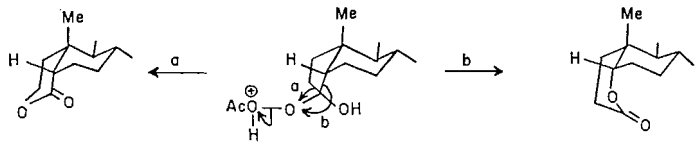
[1]*Manuscript received March 8, 1960.*
Contribution from the Department of Chemistry, McGill University, Montreal, Que.
[2]*Holder of N.R.C. Studentships, 1957–59.*



Can. J. Chem. Downloaded from www.nrcresearchpress.com by 186.148.149.217 on 09/04/12
For personal use only.

other effects may then become relatively more important. It had already been argued by Murray *et al.* (13) that conformational effects favor the formation of campholide since the transition state leading to it has a chair conformation, while the transition state leading to the lactone (XI) has a boat conformation.

Serious doubt is cast on this argument by the fact that A-nor-5β-cholestan-3-one (IV) even in the presence of sulphuric acid is oxidized to 4-oxa-5β-cholestan-3-one (V = XV). The line of reasoning developed by Murray *et al.* (13) would indicate that in this reaction the protonated form of the Criegee intermediate (XIV) would have a greater tendency to rearrange to give 3-oxa-5β-cholestan-4-one (XIII): indeed, the conformational effects favoring XIII over XV would appear to be greater than those favoring XII over XI.



XIII XIV XV (=V)

We have found the most convenient method of preparing the trans lactone (VI) to be the reduction of Windaus' keto acid (I) with sodium borohydride, but the yield of pure product (35%) is not great. Bolt (14) obtained this lactone by carrying out the reduction with sodium in alcohol, but his reported yield of 75% is based on the crude product; we obtained a satisfactory product, m.p. 115°–116° C, in only 34% yield. Reduction with sodium in isopropanol (15) gave a slightly higher yield (41%). Reduction with aluminum isopropoxide in isopropanol gave an oily product shown by infrared spectroscopy to contain both cis and trans lactones.

Reduction of the lactones (V and VI) with lithium aluminum hydride gave the diols (VII and VIII), from which the 4-oxacholestanes (IX and X) were obtained by treatment with benzenesulphonyl chloride and pyridine or lutidine (16). As expected, the 4-oxacholestane having the trans fusion of rings A and B had a higher melting point than the cis compound; however, the trans 4-oxa- and 4-aza-cholestanes had higher molecular rotations than the cis compounds, unlike their carbocyclic analogue (Table II). Replacing the carbon atom at position 4 by oxygen had a much greater effect on optical rotation than replacing it by nitrogen; this may be due to the greater alteration in molecular shape caused by substitution by the smaller oxygen atom, since the polarizabilities of the two atoms are not greatly different (17).

TABLE II

Physical properties of cholestanes and 4-heterocholestanes

	5α-Compounds		5β-Compounds	
4-Group	m.p. (°C)	$[M]_D$	m.p. (°C)	$[M]_D$
—CH_2—	80 (18)	+91° (3)	70 (18)	+97° (3)
—NH—	115 (19)	+134° (19)	(Oil) (19)	+82° (19)
—O—	90	+158°	52	+14°

Can. J. Chem. Downloaded from www.nrcresearchpress.com by 186.148.149.217 on 09/04/12
For personal use only.

Can. J. Chem. Downloaded from www.nrcresearchpress.com by 186.148.149.217 on 09/04/12
For personal use only.

EXPERIMENTAL

4-Oxa-5β-cholestan-3-one (V)

A solution of peracetic acid (20) in glacial acetic acid (4.0 ml containing 0.46 g of peracetic acid) (21) and *p*-toluenesulphonic acid (0.02g) were added to A-nor-5β-cholestan-3-one (0.20 g) dissolved in 2.0 ml of glacial acetic acid. The solution was left in the dark for 24 hours at 35° C. Dilution with water precipitated a product which, after one recrystallization from dilute methanol, yielded 0.17 g (90% of the theoretical) of transparent plates, m.p. 90°–99° C. Repeated recrystallizations from dilute methanol raised the melting point to 107°–107.5° C, $[\alpha]_D^{24}$ +18.6° (*c*, 6.129 in chloroform) (lit., m.p. 109.5°–110° C, $[\alpha]_D$ +18.3° (1)). The infrared spectrum of this compound was identical with that of an authentic sample of 4-oxa-5β-cholestan-3-one obtained by catalytic hydrogenation of 5-oxo-3,5-seco-A-norcholestan-3-oic acid (1), $\nu_{max}^{CCl_4}$ in cm^{-1}: 2940 (s), 2870 (sh), 1738 (s), 1470 (s), 1432 (sh), 1425 (sh), 1384 (m), 1367 (m), 1345 (m), 1325 (sh), 1235 (w), 1198 (m), 1173 (w), 1156 (m), 1113 (w), 1095 (w), 1075 (w), 1040 (s), 1016 (sh) (s = strong; m = medium; w = weak band; sh = shoulder). Calc. for $C_{26}H_{44}O_2$: C, 80.38; H, 11.41%. Found: C, 80.24; H, 11.24%.

In another experiment, a solution of the norketone (205 mg) in glacial acetic acid (2 ml) and concentrated sulphuric acid (0.75 ml) was treated with a solution of peracetic acid in glacial acetic acid (0.75 ml 40%). The solution was left in the dark at 27° for 5 days, and then worked up as before. The product crystallized once from aqueous ethanol gave plates (55 mg), m.p. 85°–95°; after several recrystallizations the melting point was raised to 107°–108° C, and the product was shown by mixed melting point and infrared spectrum to be 4-oxa-5β-cholestan-3-one. No other crystalline product could be isolated from the mother liquors.

4-Oxa-5α-cholestan-3-one (VI)

5-Oxo-3,5-seco-A-norcholestan-3-oic acid (2.5 g) (1) was dissolved in 30 ml of 0.8 *N* sodium hydroxide and 7.5 ml of ethanol. Sodium borohydride (0.29 g) was added over a period of 10 minutes and the mixture was heated under reflux for 1.5 hours. The excess sodium borohydride was destroyed with acetic acid and the acidified reaction mixture was refluxed for 10 minutes longer to bring about complete lactonization of the hydroxy acid. After the precipitated product was filtered, several recrystallizations from petroleum ether (b.p. 66°–75° C) yielded 0.90 g of 4-oxa-5α-cholestan-3-one, m.p. 114°–115° C, $[\alpha]_D^{24}$ +80.0° (*c*, 1.526 in chloroform) (lit., m.p. 116°–116.5° C, $[\alpha]_D$ +80.5° (1)), $\nu_{max}^{CCl_4}$ in cm^{-1}: 2940 (s), 2870 (sh), 1740 (s), 1467 (m), 1448 (sh), 1392 (sh), 1383 (w), 1372 (sh), 1342 (w), 1186 (m), 1130 (w), 1077 (m), 1047 (s). The residue from the mother liquors (0.96 g) was dissolved in benzene and chromatographed on alumina (24 g). Elution with benzene (90 ml) and benzene–acetone (19:1, 175 ml) gave 0.46 g of material with melting range 78°–106° C. Several recrystallizations from dilute methanol yielded 4-oxa-5β-cholestan-3-one (0.11 g), m.p. 107°–107.5° C, $[\alpha]_D^{24}$ +18.1°.

5β-Hydroxy-3,5-seco-A-norcholestan-3-amide (III, R = NH_2)

A solution of 4-oxa-5α-cholestan-3-one (VI) (0.13 g) in methanol saturated with ammonia deposited plates (0.12 g) of 5β-hydroxy-3,5-seco-A-norcholestan-3-amide, which after recrystallizing from methanol had a melting point of 149°–155° C (in a bath preheated to 135° C), $[\alpha]_D^{23}$ +30.5° (*c*, 0.918 in 95% ethanol). Calc. for $C_{26}H_{47}O_2N$: C, 76.98; H, 11.68; N, 3.45%. Found: C, 76.41; H, 11.33; N, 3.10%. The compound decomposed at its melting point (which was unsharp and dependent on the rate of heating) to regenerate the lactone (VI), identified by melting point, mixed melting point, and infrared spectrum.

5α-Hydroxy-3,5-seco-A-norcholestan-3-amide (II, R = NH_2)

Prepared in the same manner from the cis lactone (V), the amide melted at 153°–159° C (bath preheated to 135° C), $[\alpha]_D^{23}$ +22.6° (*c*, 1.06 in 95% ethanol). Calc. for $C_{26}H_{47}O_2N$: N, 3.45%. Found: N, 3.21%.

5β-Hydroxy-3,5-seco-A-norcholestan-3-hydrazide (III, R = $NHNH_2$)

A solution of 4-oxa-5α-cholestan-3-one (0.25 g) and 95% hydrazine (0.25 ml) in methanol (5 ml) after 15 hours deposited needles of the hydrazide, m.p. 168°–170° C (bath preheated to 160° C), $[\alpha]_D^{24}$ +38.4° (*c*, 2.70 in chloroform). Calc. for $C_{26}H_{48}O_2N_2$: C, 74.25; H, 11.50; N, 6.66%. Found: C, 74.27; H, 11.56; N, 6.75%.

5α-Hydroxy-3,5-seco-A-norcholestan-3-hydrazide (III, R = $NHNH_2$)

Prepared in the same way from the cis lactone (V), the hydrazide melted at 178°–181° C (bath preheated to 160° C), $[\alpha]_D^{24}$ +22.0° (*c*, 0.910 in chloroform). Calc. for $C_{26}H_{48}O_2N_2$: C, 74.25; H, 11.50; N, 6.66%. Found: C, 74.02; H, 11.56; N, 6.63%.

3,5-Seco-A-norcholestan-3,5α-diol (VII)

A solution of 4-oxa-5β-cholestan-3-one (454 mg) in ether (10 ml) was added to a solution of lithium aluminum hydride (376 mg) in ether (25 ml) in 10 minutes with stirring. The mixture was refluxed for 2.5 hours, and then water (1.0 ml) and 10% aqueous sodium hydroxide (0.8 ml) were added dropwise with continued stirring. The precipitated inorganic salts were removed by filtration. Concentration of the ether filtrate and washings gave white flakes (396 mg), m.p. 121°–127° C, raised by several recrystallizations from aqueous methanol to a melting point of 130°–131° C, $[\alpha]_D^{28}$ +45.7 (*c*, 0.656 in chloroform), $\nu_{max}^{CCl_4}$ in cm^{-1}: 3655 (w), 3360 (m), 2940 (s), 2870 (sh), 1468 (m), 1445 (m), 1380 (m), 1368 (sh), 1112 (w), 1053 (m), 1032 (sh), 995 (w), 960 (w), 929 (w), 917 (w). Calc. for $C_{26}H_{48}O_2$: C, 79.50; H, 12.32%. Found: C, 79.20; H, 12.14%.

4-Oxa-5β-cholestane (IX)

Benzene sulphonyl chloride (0.09 ml) was added over a period of 5 minutes to a refluxing solution of 3,5-seco-A-norcholestan-3,5α-diol (232 mg) in 2,6-lutidine (0.21 ml). The mixture was cooled, diluted with water (15 ml), and extracted with ether. Removal of the ether left a brownish semisolid residue (210 mg), which in petroleum ether (b.p. 35–60°, 100 ml) was passed through an alumina column (5.0 g, Woelm, activity III) to give waxy crystals (107 mg), m.p. 39–46°. Rechromatography on alumina (3.5 g, Woelm, activity I), followed by crystallization from methanol gave rosettes of white needles, m.p. 51°–52° C, $[\alpha]_D^{27}$ +3.8° (*c*, 2.10 in chloroform), $\nu_{max}^{CCl_4}$ in cm^{-1}: 2940 (s), 2860 (sh), 2720 (w), 1466 (s), 1443 (s), 1377 (s), 1365 (sh), 1356 (sh), 1340 (w), 1328 (w), 1250 (w), 1204 (w), 1193 (w), 1165 (w), 1155 (w), 1113 (sh), 1098 (s), 1086 (s), 1067 (sh), 1026 (m), 982 (w), 958 (w), 937 (sh), 932 (w), 905 (w), 880 (m), 857 (w). Calc. for $C_{26}H_{46}O$: C, 83.36; H, 12.37%. Found: C, 83.23; H, 12.25%.

3,5-Seco-A-norcholestan-3,5β-diol (VIII)

A mixture of 4-oxa-5α-cholestan-3-one (0.50 g) and lithium aluminum hydride (0.06 g) in tetrahydrofuran (50 ml) was stirred for 4 hours at room temperature, and then treated with water (50 ml) and 1 *N* sulphuric acid (5.0 ml). Extraction with ether followed by removal of the ether gave a gelatinous material (0.39 g), m.p. 128°–131° C. One recrystallization from methanol raised the melting point to 134°–135° C, $[\alpha]_D^{18}$ +25.3° (*c*, 1.61 in chloroform), $\nu_{max}^{CCl_4}$ in cm^{-1}: 3655 (w), 3395 (m), 2940 (s), 2870 (sh), 1467 (m), 1446 (m), 1383 (m), 1366 (sh), 1338 (w), 1082 (w), 1051 (m), 1025 (m), 1000 (sh), 950 (w), 925 (w), 905 (w). Calc. for $C_{26}H_{48}O_2$: C, 79.50; H, 12.32%. Found: C, 79.38; H, 12.62%.

Can. J. Chem. Downloaded from www.nrcresearchpress.com by 186.148.149.217 on 09/04/12
For personal use only.

4-Oxa-5α-cholestane (X)

Benzene sulphonyl chloride (0.19 ml) was added over 5 minutes to a refluxing solution of 3,5-seco-A-norcholestan-3,5β-diol (0.51 g) in absolute pyridine (0.45 ml). The solution was refluxed for another 5 minutes, cooled, diluted with water (50 ml), and extracted with ether. The ether extracts were washed with dilute sulphuric acid and then with water, dried (Na_2SO_4), and concentrated to give a crude brownish product (0.33 g). After several recrystallizations from methanol this had a melting point of 89°–90° C, $[\alpha]_D^{23}$ +42.3° (*c*, 1.33 in chloroform), $\nu_{max}^{CCl_4}$ in cm^{-1}: 2940 (s), 2860 (sh), 2720 (w), 1465 (s), 1445 (s), 1383 (s), 1377 (sh), 1367 (sh), 1267 (w), 1193 (w), 1169 (w), 1154 (w), 1122 (m), 1101 (s), 1086 (s), 1040 (m), 1027 (w), 978 (w), 954 (w), 928 (m), 909 (w), 876 (w), 854 (w). Calc. for $C_{26}H_{48}O$: C, 83.36; H, 12.37%. Found: C, 82.96; H, 12.29%.

ACKNOWLEDGMENTS

We are grateful to Miss I. S. Kaseno and Miss M. M. M. Bilevicius for technical assistance, to W. C. Hardesty Co. for a gift of peracetic acid, and to the National Research Council for financial support.

REFERENCES

1. R. B. TURNER. J. Am. Chem. Soc. **72**, 579 (1950).
2. A. WINDAUS. Ber. **39**, 2008 (1906).
3. W. KLYNE. Chem. & Ind. 1198 (1954).
4. A. WINDAUS. Ber. **52**, 170 (1919); L. F. FIESER and M. FIESER. Steroids. Reinhold, New York. 1959. p. 80.
5. R. B. TURNER. J. Am. Chem. Soc. **72**, 879 (1950).
6. K. MISLOW and J. BRENNER. J. Am. Chem. Soc. **75**, 2319 (1953).
7. W. E. DOERING and L. SPEERS. J. Am. Chem. Soc. **72**, 5515 (1950).
8. S. L. FRIESS and N. FARNHAM. J. Am. Chem. Soc. **72**, 5518 (1950).
9. A. BAEYER and V. VILLIGER. Ber. **32**, 3625 (1899).
10. R. R. SAUERS. J. Am. Chem. Soc. **81**, 925 (1959).
11. R. CRIEGEE. Ann. **560**, 127 (1948).
12. M. F. HAWTHORNE, W. D. EMMONS, and K. S. MCCALLUM. J. Am. Chem. Soc. **80**, 6393 (1958).
13. M. F. MURRAY, B. A. JOHNSON, R. L. PEDERSON, and A. C. OTT. J. Am. Chem. Soc. **78**, 981 (1956).
14. C. C. BOLT. Rec. trav. chim. **70**, 940 (1951).
15. K. TSUDA, K. TANABE, I. IWAI, and K. FUNAKOSHI. J. Am. Chem. Soc. **79**, 5721 (1957).
16. D. D. REYNOLDS and W. O. KENYON. J. Am. Chem. Soc. **72**, 1953 (1950).
17. J. H. BREWSTER. J. Am. Chem. Soc. **81**, 5475 (1959).
18. J. MAUTHNER. Monatsh. **30**, 635 (1909).
19. J. T. EDWARD and P. MORAND. Can. J. Chem. This issue.
20. J. BOESEKEN and J. GREUP. Rec. trav. chim. **58**, 528 (1939).
21. D. SWERN. Organic reactions. Vol. VII. Wiley, New York. 1953. p. 392.

Can. J. Chem. Downloaded from www.nrcresearchpress.com by 186.148.149.217 on 09/04/12
For personal use only.

Can. J. Chem. Downloaded from www.nrcresearchpress.com by 186.148.149.217 on 09/04/12
For personal use only.

CO-ORDINATION COMPLEXES OF TITANIUM (IV) HALIDES

1. PREPARATION AND INFRARED SPECTRA OF THE COMPLEXES OF TITANIUM (IV) HALIDES WITH N,N-DIMETHYL AND N,N-DIPHENYL FORMAMIDE[1]

JACQUES ARCHAMBAULT[2] AND ROLAND RIVEST

ABSTRACT

Co-ordination complexes of titanium (IV) halides with N,N-dimethyl formamide and N,N-diphenyl formamide have been prepared and their infrared spectra have been measured. In all these complexes, there is a metal-to-oxygen bond as evidenced in the infrared spectra by a negative shift of the carbonyl stretching frequency and a positive shift of the CN stretching frequency. The relative values of these shifts and the ease of decomposition observed for these complexes indicate that their stability decreases with decreasing the electronegativity of the halide bonded to titanium (IV).

In the complexes of N,N-diphenyl formamide, the effect of the conjugated phenyl groups has been observed. In these complexes the decrease of double-bond character of the carbonyl group and the increase of double-bond character of the CN group, resulting from the metal-to-oxygen co-ordination bond, are quite larger than in the complexes of N,N-dimethyl formamide.

INTRODUCTION

When a Lewis acid, as an example MX_4, is a covalent molecule, its behavior is analogous to that of a metallic ion M^{+4} of which the co-ordination sphere is partially filled. The acidity of the molecule depends upon the tendency of the ion to complete its co-ordination sphere. The nature of the negative ion X^- affects the acidity of the central metallic ion. If X^- increases in size and decreases in electronegativity, it will be more polarized by the central ion and will decrease the affinity of this ion for an additional electron pair.

In the case of the halides of titanium (IV), the equation of Hannay and Smith (1) and the electronegativity scale of Pauling (2) indicate a bonding predominantly ionic for titanium tetrafluoride and predominantly covalent for the other three halides. The acidity of these covalent halides decreases from the chloride to the iodide, the partial ionic character of the latter being less than 20%.

In a previous paper (3) the formation of complexes of titanium tetrachloride with formamide and N,N-dimethyl formamide was explained by a co-ordination through the oxygen of the amide. In order to see how the difference in covalent character between the tetrahalides of titanium would influence the co-ordination of amides to titanium (IV), we have extended our investigation to titanium tetrabromide and titanium tetraiodide.

If a donor molecule contains some electrons related to the donor atom by a conjugated system, some type of interactions between these electrons and the donor atom should be noticeable when the latter is used in co-ordination. We have then prepared the complexes of N,N-diphenyl formamide and we have observed that the electrons of the phenyl groups have a strong influence on the co-ordination bond.

EXPERIMENTAL

Materials and Manipulations

Reagent grade titanium tetrachloride was purified by the method of Gilchrist (4), redistilled, and the medium fraction was used for our experiments. Titanium tetrabromide, supplied by E. D. Mackay, New York, has been distilled under reduced pressure.

[1]*Manuscript received March 28, 1960.*
Contribution from the Department of Chemistry, University of Montreal, Montreal, Que.
[2]*Fellow of the Office Provincial des Recherches Scientifiques de la Province de Québec. Present address: Department of Chemistry, University of Florida, Gainesville, Florida.*

The medium fraction, distilling at 100° C under 10 mm Hg, had the following composition: Ti, 13.04%; Br, 85.80%. The calculated values for pure $TiBr_4$ are: Ti, 13.03%; Br, 86.97%.

Titanium tetraiodide of E. D. Mackay Co., New York, was contaminated by free iodine. The material was first heated at 100° C under vacuum to sublimate the iodine. It was then distilled at 170–175° C under 2 mm Hg. The medium fraction had the following composition: Ti, 8.71%; I, 90.1%. The calculated value for pure TiI_4 are Ti, 8.62%; I, 91.38%.

Reagent grade of N,N-dimethyl formamide has been redistilled and the medium fraction used for our experiments was kept over dry sodium sulphate.

Reagent grade of N,N-diphenyl formamide was dried under vacuum and kept in a desiccator containing phosphorus pentoxide.

The solvents used for our experiments were anhydrous. Their water content, checked by the Karl Fischer method, was only a few parts per million.

The water-sensitive complexes were prepared and handled in a dry box continuously flushed with dry nitrogen. The dry box was provided with electricity and vacuum so that all the operations could be performed in an atmosphere of very low humidity content. Under these experimental conditions, there is always a certain amount of hydrolysis of the halide, as the results of elementary analyses indicate.

The methods of analysis for chlorine, titanium, carbon, and hydrogen were described previously (3). Bromine and iodine determinations were made by the volumetric method of Volhard. Nitrogen was determined by the Kjeldahl method or by the micro-Dumas method as specified by a "k" or a "d" in each case.

The setup used for the preparation of complexes from solutions of the reactants was identical with the one used in previous experiments (3). For the preparation of the iodide complex, solid TiI_4 was added to the amide solution.

The spectroscopic measurements were carried out on a Perkin–Elmer infrared spectrophotometer, model 21, using a sodium chloride prism. The spectra of the complexes were determined in solutions of suitable solvents.

The System $TiCl_4$, $2HCON(C_6H_5)_2$

Twenty-five milliliters of an 8.5% solution of titanium tetrachloride in carbon tetrachloride was added dropwise to 45 ml of a 13% solution of N,N-diphenyl formamide in the same solvent. There was no precipitation at the beginning, but precipitation occurred when 80% of the titanium tetrachloride was added, leading to an orange-yellow powder, melting at 119–121° C. The powder was washed many times with pure carbon tetrachloride on a fritted glass filter, and then dried *in vacuo*. This powder is very slightly soluble in carbon tetrachloride, but is soluble in aromatic hydrocarbons and in halogen derivatives of aliphatic hydrocarbons. The analysis of this adduct led to the following results.

	% Ti	% Cl	% N	% C	% H	Ti/Cl
Calc. for $TiCl_4 . 2HCON—(C_6H_5)_2$	8.20	24.28	4.8	53.45	3.80	1/4.00
Found	8.05	22.39	4.7d	54.74	3.73	1/3.76

The System $TiBr_4$—$HCON(C_6H_5)_2$

Fifteen milliliters of a 13% solution of diphenyl formamide in carbon tetrachloride was added dropwise to 20 ml of a 10% solution of titanium tetrabromide in the same

Can. J. Chem. Downloaded from www.nrcresearchpress.com by 186.148.149.217 on 09/04/12
For personal use only.

solvent. The adduct obtained was a red oil. By evaporation of the solvent the compound became a solid of resinous appearance. It was washed many times with normal hexane and dried *in vacuo*. The final compound was a red powder which decomposed at 60–65° C. The elementary analysis gave the following results.

	% Ti	% Br	% N	% C	% H	Ti/Br
Calc. for $TiBr_4.2HCON(C_6H_5)_2$	6.29	41.95	3.67	40.97	2.91	1/4.00
Found	6.91	40.40	3.3d	36.21	3.02	1/3.50

The System $TiBr_4.2HCON(CH_3)_2$

Thirty milliliters of a 20% solution of $TiBr_4$ in carbon tetrachloride was added dropwise to 30 ml of a 10% solution of the amide. A red oil was obtained at the beginning of the reaction and after agitation for many hours a red solid precipitated. Its melting point was 178–181° C. The elementary analyses led to the following results.

	% Ti	% Br	% N	% C	% H	Ti/Br
Calc. for $TiBr_4.2HCON(CH_3)_2$	9.32	62.22	5.45	14.03	2.75	1/4.00
Found	9.32	60.3	5.04k 5.73d	14.03	3.76	1/3.87

The System TiI_4—HCON—$(CH_3)_2$

Powdered titanium tetraiodide was added by small quantities to a solution of the amide in carbon tetrachloride. A deep brown solution was first observed and precipitation occurred. The brown powder so obtained was washed with carbon tetrachloride to remove the excess of amide. The powder was extremely unstable even in the absence of moisture. It melted at room temperature, becoming like a paste after a few days.

Two series of experiments were performed between the iodide and the solutions of the amide where the ratio of titanium tetraiodide to the amide was 1 to 3 and 1 to 4,2 respectively. In a third experiment, the iodide was added to a 10-fold excess of the pure amide, without solvent. In each experiment, the appearance of the compound obtained was the same but the analytical results were quite different.

	% Ti	% I^-	% T_2	Ti/I total
Expt. 1, found	5.76	56.8±0.5	1.5	1/3.9
Expt. 2, found	5.28	59.9±0.5	2.1	1/4.2
Calc. for $TiI_4.4HCON(CH_3)_2$	5.65	59.7	0	1/4.00
Expt. 3, found	4.21	42.	2.5	1/4
Calc. for $TiI_4.8HCON(CH_3)_2$	4.2	44.5	0	1/4

These analytical data are not necessarily indicating a higher co-ordination number for Ti(IV) but might be the result of a solvation effect of the complex $TiI_4.2HCON(CH_3)_2$ with the pure amide.

In a previous paper (5), we have demonstrated the existence of a compound of the following composition $TiCl_3OC_4H_9.6C_4H_9OH$. Fowles (6) also reported the formation of complexes of titanium halides with ammonia where the molecular formula was $TiX_4.8NH_3$. As explained by this author, it is very unlikely that the co-ordination number of titanium (IV) is higher than six but it is more probable that the extra molecules of

Can. J. Chem. Downloaded from www.nrcresearchpress.com by 186.148.149.217 on 09/04/12
For personal use only.

ligands are held in a secondary sphere of influence rather like the ammoniates formed by cobaltammine-type ion (7). The presence of free iodine in these compounds could be related to the formation of trivalent titanium. Fowles (8) has proposed that mechanism to explain the formation of iodine in the thermal decomposition of $TiI_4.6NH_3$.

Infrared Spectra and Structure Discussion

The Complexes of N,N-*Dimethyl Formamide*

The absorption maxima observed for the complexes of the titanium halides with N,N-dimethyl formamide are listed in Table I and illustrated in Fig. 1. The carbonyl

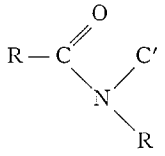
TABLE I

Frequencies of N,N-dimethyl formamide complexes

$HCON(CH_3)_2$		$TiCl.2HCON(CH_3)_2$	$TiBr_4.2HCON(CH_3)_2$		$TiI_4.nHCON(CH_3)_2$	Assignment
Soln. CH_2Cl_2	Pure liquid	Soln. CH_2Cl_2	Soln. CH_2Cl_2	Nujol mulls	Soln. CH_2Cl_2	
1730 sh	1725 sh	1657 sh	1655 sh	1662 sh	1665 sh 1680 m	—
1681 vs	1675 vs	1643 vs	1647 vs	1642 vs	1653 vs	ν(C=O)
1442 w		1428 w	1425 m	1412 m	1430 m	
1413						
1393 s	1393 s	1362 m	1362 m	1340 s	1367 s	
1093 m	1094 m	1118 w		1127 w	1123 w 1096	Possible ν(CN)
1064	1065 w			1053 w	1060 w	

ABBREVIATIONS: vs, very strong; m, medium; w, weak; sh, shoulder.

stretching frequency is shown to be lowered by 37, 34, and 27 cm^{-1} in the spectra of the chloride, of the bromide, and of the iodide complex respectively. Another band tentatively assigned to the C—N stretching vibration is shifted to higher frequencies by about the same value. As it was explained in a previous paper (3), no data are available concerning the assignment of the infrared absorption bands of N,N-dimethyl formamide. According to the following skeleton,



some authors consider the C—N vibrations in disubstitute amides as being confused with the C=O stretching band at about 1650 cm^{-1}. Mizushima and others (9) assigned the absorption bands at 1160 and 1040 cm^{-1} of N-methyl acetamide to the C—N and C′—N vibrations respectively. More recently, De Graff and Sutherland (10) proposed that a band at 956 cm^{-1} of N-methyl acetamide be assigned to C′—N stretching vibration. It seemed reasonable to us that a positive frequency shift of the band located at 1093 cm^{-1} when the amide co-ordinates to Ti(IV) was an argument in favor of its assignment to the C—N stretching vibration. The frequency shifts of the carbonyl band and of the C—N band are an indication of co-ordination through the oxygen atom. The shifts observed seem to decrease from the chloride complex to the iodide complex. If the magnitude of the shift can be related to the stability of the co-ordinated bond, the observed trend is in good agreement with the temperature of decomposition, which are 220–225° C for the chloride complex, 178–181° C for the bromide complex, and room

Can. J. Chem. Downloaded from www.nrcresearchpress.com by 186.148.149.217 on 09/04/12
For personal use only.

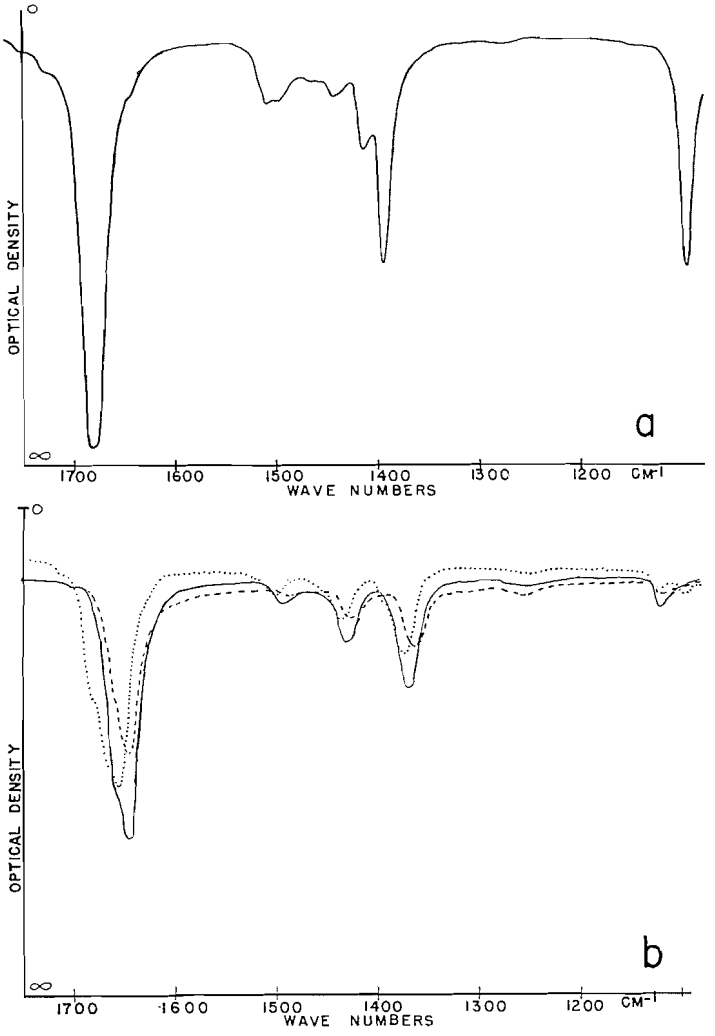


FIG. 1. Infrared spectra in methylene chloride solutions.
(*a*) ——— N,N-dimethyl formamide.
(*b*) ——— $TiCl_4.2HCON(CH_3)_2$; --- $TiBr_4.2HCON(CH_3)_2$; . . . $TiI_4.2HCON(CH_3)_2$.

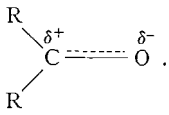
temperature for the iodide complex. This behavior is also in agreement with the decreasing electronegativities and increasing steric hindrance of the halogens from chlorine to iodine.

It is noticeable that the infrared spectrum of the iodide complex showed the carbonyl frequency and the CN frequency of the free amide. This is an indication of the presence of some unco-ordinated amide associated with the complex.

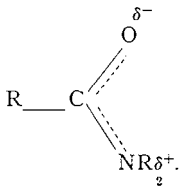
The shifts of the carbonyl frequencies in the spectra of these complexes are quite smaller than those observed for other similar complexes. We prepared the complex $TiCl_4.2CH_3COCH_3$ and observed a shift of 47 cm^{-1} when the spectrum was measured in methylene chloride solution. The small shifts observed with amide complexes can be explained by the fact that, in amides, one is dealing with a conjugated system.

Can. J. Chem. Downloaded from www.nrcresearchpress.com by 186.148.149.217 on 09/04/12
For personal use only.

In a carbonyl compound like acetone the electronic pull of a Lewis acid is confined to the carbonyl group



In amides, where the carbonyl group is part of a conjugated system, three atoms are involved in the electronic rearrangement caused by co-ordination.



The Complexes of N,N-*Diphenyl Formamide*

The infrared spectra of the complexes of titanium tetrachloride and titanium tetrabromide with N,N-diphenyl formamide are listed in Table II and illustrated in Fig. 2.

TABLE II

Frequencies of N,N-diphenyl complexes (solutions in methylene chloride)

$HCON(C_6H_5)_2$	$TiCl_4.2HCON(C_6H_5)_2$	$TiBr_4.2HCON(C_6H_5)_2$	Assignment
1715 sh			
	1685 w		
1689 vs	1623 vs	1623 vs	ν(C═O)
1602 s	1580 vs	1582 vs	Aromatic ring vibrations
1501 s	1501 s	1501 s	
1456 w	1461 w	1462 w	
1344 m			
1305 w	1373 s	1373 s	CN vibrations
1304 w			
1137 w			

A carbonyl frequency shift of 66 cm^{-1} was measured in the spectra of the halide complexes. Furthermore, a very broad band with four maxima at 1344, 1305, 1304, and 1260 cm^{-1}, which is in the region usually assigned to the CN stretching vibrations, is replaced in the complexes by a narrow band at 1373 cm^{-1}. If one takes 1310 cm^{-1} as the center of the broad band, a positive shift of about 60 cm^{-1} is calculated for the CN vibrations. These shifts are twice as large as those observed in the spectra of similar complexes of N,N-dimethyl formamide. The proximity of the phenyl groups on the nitrogen of the amide seems to increase the basic character of the carbonyl. This is evidenced not only by the increase of the shifts but also by the perturbations of the aromatic ring vibrations.

Susz (11) has mentioned that, for the complexes of benzophenone and acetophenone with Lewis acids, coupling of the carbonyl and phenyl vibrations appears to be appreciable, the phenyl band at 1580 cm^{-1} being considerably enhanced. An increased resonance involving electrons of the carbonyl and the phenyl groups would likely account for this behavior. The electronic pull of a Lewis acid has the same effect as the presence on the

Can. J. Chem. Downloaded from www.nrcresearchpress.com by 186.148.149.217 on 09/04/12
For personal use only.

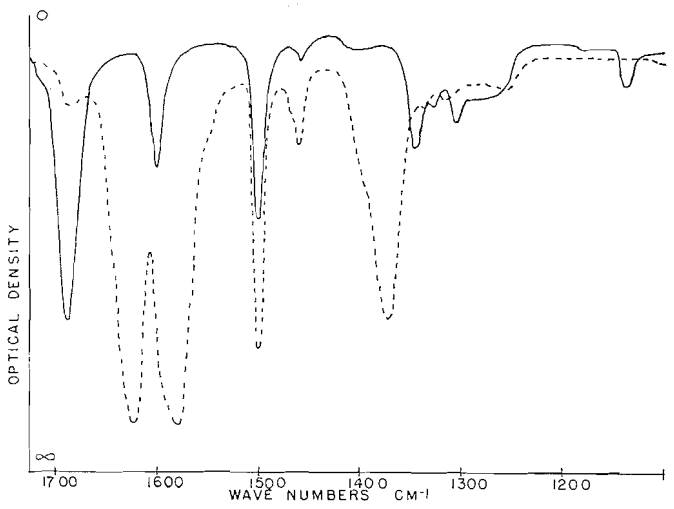


FIG. 2. Infrared spectra in methylene chloride solutions.
——— N,N-diphenyl formamide; – – – $TiCl_4.2HCON(C_6H_5)_2$.

aromatic ring of a nucleophilic parasubstituent. The spectra of N,N-diphenyl formamide complexes exhibit a similar coupling of the carbonyl band with a reinforced phenyl band, appearing at 1580–1582 cm^{-1} instead of 1602 cm^{-1} in the pure amide. In this case, the aromatic ring is not adjacent to the carbonyl, but the electron delocalization induced by the Lewis acid is likely to be transmitted through the conjugated N—C—O skeleton. This statement is further supported by Randall (12) and Bellamy (13), who consider the appearance of a band at 1580 cm^{-1} as an indication of a conjugated phenyl.

ACKNOWLEDGMENTS

The authors are indebted to the National Research Council of Canada for its financial assistance (R. R.) and to l'Office de Recherches Scientifiques de la Province de Québec, for a fellowship to one of us (J. A.). They are also grateful to Prof. Camille Sandorfy for very useful discussions on the infrared spectra measured.

RÉSUMÉ

On a préparé des complexes de coordination des halogénures de titane (IV) avec la N,N-diméthyl formamide et la N,N-diphenyl formamide. Les spectres infrarouges comparés des amides pures et des complexes nous ont permis de prouver que l'effet bathochrome de la fréquence carbonyle est fonction de l'halogène lié au titane (IV) et aussi de la nature des substituants sur l'azote de la molécule de l'amide. Tous les composés préparés sont expliqués en supposant que la coordination au titane se fait par l'oxygène de l'amide.

REFERENCES

1. N. B. HANNAY and C. P. SMITH. J. Am. Chem. Soc. **68**, 171 (1946).
2. L. PAULING. The nature of the chemical bond. 2nd ed. Cornell University Press, Ithaca, N.Y. 1940. pp. 58–69.
3. J. ARCHAMBAULT and R. RIVEST. Can. J. Chem. **36**, 1461 (1958).
4. W. S. CLABAUGH, R. T. LESLIE, and R. GILCHRIST. J. Research, Natl. Bur. Standards, **55**, 261 (1955).

Can. J. Chem. Downloaded from www.nrcresearchpress.com by 186.148.149.217 on 09/04/12
For personal use only.

5. J. ARCHAMBAULT and R. RIVEST. Can. J. Chem. **35**, 879 (1957).
6. G. W. A. FOWLES and D. NICHOLS. J. Chem. Soc. 990 (1959).
7. G. SPACU and P. VOICHESCU. Z. anorg. u. allgem. Chem. **243**, 288 (1940).
8. G. W. A. FOWLES and F. U. POLLARD. J. Chem. Soc. 4128 (1953).
9. S. MIZUSHIMA, T. SIMANOUTI, *et al.* J. Am. Chem. Soc. **72**, 3490 (1950).
10. D. E. DE GRAFF and G. B. B. M. SUTHERLAND. J. Chem. Phys. **26**, 716 (1957).
11. B. P. SUZS and P. CHALANDON. Helv. Chim. Acta, **41**, 1332 (1958).
12. H. M. RANDALL, R. G. FOWLER, V. FUSON, and J. R. DANGL. Infrared determination of organic structures. D. Van Nostrand Co., Inc., New York. 1949.
13. L. J. BELLAMY. The infrared spectra of complex molecules. John Wiley & Sons, Inc., New York. pp. 60–63.

Can. J. Chem. Downloaded from www.nrcresearchpress.com by 186.148.149.217 on 09/04/12
For personal use only.

Can. J. Chem. Downloaded from www.nrcresearchpress.com by 186.148.149.217 on 09/04/12
For personal use only.

THE ABSTRACTION OF HYDROGEN ATOMS FROM AMINES AND RELATED COMPOUNDS[1]

R. K. BRINTON

ABSTRACT

The reaction of methyl radicals with a group of amines and amine-like compounds has been investigated in the temperature range 125° to 157° C. The abstraction activation energies of hydrogen atoms from these compounds, the corresponding pre-exponential factors, and the actual reaction rates indicate that the N—H hydrogen atoms are more labile than the C—H atoms in these compounds.

INTRODUCTION

The abstraction of hydrogen atoms by methyl radicals from various compounds has been studied in detail by Trotman-Dickenson and Steacie (1). In the case of those compounds with hydrogen atoms attached only to the carbon atom skeleton, they were able to correlate the abstraction activation energies, pre-exponential factors, and actual rates of reaction with the structure of the molecules. Compounds such as amines and alcohols having hydrogen atoms attached to nitrogen or oxygen as well as carbon atoms were found more difficult to evaluate, and they made no attempt to assess the effect of structural factors or the relative importance of the N—H and O—H hydrogen as compared with the C—H hydrogen in the over-all contribution to methane formation.

A little more information on this problem was furnished by the work of Brinton and Volman (2), who reported the activation energy for the methyl radical abstraction of hydrogen from ethylenimine to be 4.8 kcal/mole, a value much lower than any C—H type abstraction found by Trotman-Dickenson and Steacie. Brinton and Volman felt that these data indicated a greater lability of N—H hydrogen than C—H hydrogen in this compound. However, their tacit assumption that the N—H hydrogen was the active species in the abstraction was not founded on any experimental evidence.

Recently Kozak and Gesser (3) investigated the photolysis of triethylamine. In the course of the study they determined the activation energies of methane formation in the reaction of methyl radicals with trimethylamine, triethylamine, and diethylamine by a technique similar to that of Trotman-Dickenson and Steacie. The values obtained, 8.0, 5.3, and 5.7 kcal/mole respectively, led them to conclude that the hydrogen attached to carbon was being abstracted in all of these compounds, and that this was probably the case for ethylenimine also.

Confirmation of Kozak and Gesser's mechanism is to be found in the course of a number of condensations between the α-carbon of an amine and a 1-olefin occurring in the liquid phase (4). These reactions are induced by peroxides or light so a radical process may be inferred, and it is probable that an abstraction similar to that postulated by Kozak and Gesser is responsible for the type of products found.

The present study was initiated in an attempt to clarify the kinetics of the reaction of methyl radicals with amines. It was hoped that if a clear difference between the ease of hydrogen abstraction from carbon and nitrogen atoms does indeed exist, sufficient data could be obtained so predictions could be unequivocally made concerning the course of the abstraction reactions for amine-type compounds.

[1]*Manuscript received April 4, 1960.*
Contribution from the Department of Chemistry, University of California, Davis, California.

Can. J. Chem. Downloaded from www.nrcresearchpress.com by 186.148.149.217 on 09/04/12
For personal use only.

EXPERIMENTAL

The apparatus and experimental technique have been described previously (5). In the present study the methane and ethane fractions were separated at −215° (solid nitrogen) and −185° (liquid oxygen). Mass spectrometric analyses were made of both fractions. The −185° fraction was in all cases more than 99% ethane. The −215° fraction was 70–99% methane, depending on the sample size. Very small samples (<1 μ mole) contained appreciable amounts of nitrogen produced from the residual air left in the rather large (3 liters) reaction system.

Di-*t*-butyl peroxide was kindly supplied by the Shell Development Co.; it was purified by bulb-to-bulb distillation *in vacuo*. A center fraction was used in the pyrolysis experiments.

Methylamine and ethylamine were generated from the hydrochloride salts with saturated KOH solution. The amines were dried over KOH pellets, degassed, and distilled *in vacuo*.

Dimethylamine, diethylamine, and diisopropylamine were Eastman White Label products. They were used without further purification except for the degassing procedure.

t-Butyl ethylenimine was supplied by Dr. Albert Bottini (6).

t-Butyl acetaldimine was prepared according to the method of Hurwitz (7) from *t*-butylamine and acetaldehyde. The fraction of boiling range 78.0–78.1° (uncorr.) from a 20-plate helice column was collected for the pyrolyses.

The acetaldazine sample used was that employed in previously described work from this laboratory (8).

The pyrolyses were carried out at two temperatures: 156.73° C at which a 4-minute reaction period was used, and 124.82° where 2 to 4 hours were required for sufficient reaction. The DTBP concentration was about the same in all experiments, 4.6×10^{-7} mole cm^{-3} (ca. 11 mm). The pressure of the added compound was adjusted, insofar as it was possible, to produce comparable and significant amounts of methane and ethane so that the analyses of these gases were of good precision. Approximately 3.5% of the DTBP was decomposed at 156.73° and from 2 to 4% at 124.82°. In most trials the percentage of the added compound reacting was from 0.3 to 2%. In two experiments (dimethylamine and diethylamine at 124.82°) the percentage reacted was about 6%. The average concentration of the added compound was used in all calculations.

RESULTS AND DISCUSSION

The pyrolysis of DTBP has been frequently used as a source of methyl radicals in this laboratory (2, 5, 9, 10, 11). The important reactions are:

$$(CH_3)_3COOC(CH_3)_3 \xrightarrow{k_1} 2(CH_3)_3CO \qquad [1]$$

$$(CH_3)_3CO \xrightarrow{k_2} CH_3COCH_3 + CH_3 \qquad [2]$$

$$2CH_3 \xrightarrow{k_3} C_2H_6 \qquad [3]$$

$$CH_3 + (CH_3)_3COOC(CH_3)_3 \xrightarrow{k_4} CH_4 + (CH_3)_3COO(CH_3)_2CH_2 \qquad [4]$$

If another hydrogen-containing source, RH, is present additional methane is formed by the process

$$CH_3 + RH \xrightarrow{k_5} CH_4 + R. \qquad [5]$$

In the present study the total rate of CH_4 production, $R_{CH_4}^{total}$, the summation of [5] and [4], was corrected for the CH_4 formed by [4] in order to evaluate the rate of CH_4 formed in process [5] only, R_{CH_4}. This correction was made by the following formula:

$$R_{CH_4} = R_{CH_4}^{total} - R_{CH_4}^{DTBP}[R_{C_2H_6}/R_{C_2H_6}^{DTBP}]^{1/2}.$$

Here $R_{CH_4}^{DTBP}$ and $R_{C_2H_6}^{DTBP}$ are the rates of CH_4 and C_2H_6 production in a pyrolysis containing only DTBP. The quantity $R_{C_2H_6}$ is the rate of C_2H_6 production in a pyrolysis containing RH as an additive. As the concentration of DTBP was about identical in all trials, the ratio of rates of methane formation by process [4] of any two pyrolyses would be expected to be equal to the half power of the ratio of the corresponding rates of ethane formation in the same two experiments. In most of the experiments the correction calculated from $R_{CH_4}^{DTBP}$ was relatively small, 3–15% of the $R_{total}^{CH_4}$. However, the *t*-butyl acetaldimine reacted so slowly that the corrections in these pyrolyses were approximately equal to the methane formed by the hydrogen abstraction from acetaldimine itself.

The values of $R_{CH_4}/R_{C_2H_6}^{1/2}$ [M] = $k_5/k_3^{1/2}$ have been calculated for the listed concentration, [M], of various amine and amine-like additives. These quantities as well as the activation energies, E_5, and the log A_5 are listed in Table I. Gomer and Kistiakowsky's (12) values of $E_3 = 0$ and $A_3 = 4.5\times10^{13}$ for the combination of methyl radicals were used to calculate the individual E_5 and log A_5 in the table. For most compounds, determinations were made at two temperatures only. The previous studies with ethylenimine (2) showed the Arrhenius plot to be a straight line at least over the rather limited temperature range imposed by the use of DTBP as a methyl radical source. Pyrolyses using dimethylamine and diethylamine were made at 138.6° C as well as for the two temperatures shown in Table I. The values of $k_5/k_3^{1/2}$, 12.05 and 15.31 respectively, gave good straight lines in the Arrhenius plots of these two compounds.

The data of Table I give strong indication that the N—H hydrogen is active in the formation of methane in the methyl radical abstraction process rather than the hydrogen on the carbon alpha to the nitrogen. This evidence is most easily demonstrated by considering certain groups of Table I separately.

TABLE I

The reaction of methyl radicals with amines and related compounds

	124.8° C		156.73° C			
Reactant (M)	[M]×10⁷	$R_{CH_4}/R_{C_2H_6}^{1/2}$[M]	[M]×10⁷	$R_{CH_4}/R_{C_2H_6}^{1/2}$[M]	E_5, kcal	log A_5
Methylamine	2.73	0.944	2.73	1.92	7.6	10.9
Ethylamine	1.02	2.81	1.90	5.45	7.1	11.2
Dimethylamine	0.982	8.77	1.68	17.30	7.2	11.7
Diethylamine	0.97	11.34	1.89	22.20	7.2	11.8
Diisopropylamine	1.00	8.70	0.755	18.02	7.8	12.0
Ethylenimine	3.0	16.6[a]	—	—	4.8	10.7
t-Butyl ethylenimine	8.38	0.14	10.78	0.26	6.6[b]	9.6[b]
t-Butyl acetaldimine	8.62	1.09	10.66	2.26	7.8	11.1
Acetaldazine	5.89	2.26	5.33	3.99	6.1	10.5

NOTE: All rates and concentrations are expressed in units of moles, cm³, and sec.

[a]Data on ethylenimine are from ref. 2.

[b]These calculated values are of low accuracy because of the very low R_{CH_4} and the relatively large correction, $R_{CH_4}^{DTBP}$, used in the R_{CH_4} calculation.

1. Dimethylamine (DMA), *Diethylamine* (DEA), *and Diisopropylamine* (DIA)

These compounds, all secondary amines, have quite different structures of the two

Can. J. Chem. Downloaded from www.nrcresearchpress.com by 186.148.149.217 on 09/04/12
For personal use only.

aliphatic side chains. All six of the aliphatic group hydrogens of DMA are on primary carbons, four of the 10 hydrogens of DEA are on secondary carbons, and two of the 14 hydrogens of DIA are on tertiary carbons. Table I indicates that all three of these compounds have very similar abstraction activation energies, E_5, and pre-exponential factors A_5. Trotman-Dickenson and Steacie (1) and Trotman-Dickenson (13) found the analogous reactions in hydrocarbon systems to be quite sensitive to the type of carbon containing the abstractable hydrogen. If the side-chain hydrogens were being abstracted from the amines, it would be expected that the three amines being considered would show a similar trend, say to the analogous series ethane, *n*-butane, and 2,3-dimethyl butane, which have respectively the abstraction energies 10.4, 8.3, and 6.9 kcal/mole (1). In addition, if DMA is assumed to have six abstractable hydrogen atoms (primary), DEA four (secondary), and DIA two (tertiary) the actual values of $R_{CH_4}/R_{C_2H_6}$ [M] at 124.8° per "active" hydrogen are in the ratios of 1:1.9:3.0. The corresponding ratios for ethane, *n*-butane, and 2,3-dimethyl butane found by Trotman-Dickenson and Steacie (1) are 1:7.5:51.7 at 182° C. Thus neither the abstraction activation energies nor the rates of abstraction indicate that the side-chain hydrogens of the amines are participating in the abstraction process. It must be inferred rather that the amine hydrogen is active in the reaction and the similarity of activation energy, pre-exponential factors, and the actual rates of abstraction may be attributed to their being secondary amines.

2. Ethylenimine and t-Butyl Ethylenimine

The abstraction activation energy for ethylenimine given previously (2) is considerably lower than others reported for H-atom abstraction by methyl radical from organic compounds. In this former investigation it was assumed that the N—H bond was the active participant in the reaction. It is proposed in the present study to test the validity of such a mechanism by reacting the methyl radicals with *t*-butyl ethylenimine wherein the N—H hydrogen has been replaced by the *t*-butyl group. Table I shows the rate of abstraction from the *t*-butyl ethylenimine to be less than 10% of the analogous reaction from ethylenimine itself at 124.8°. Inasmuch as the ring hydrogens are available to an equal degree from both these compounds, a strong argument can be made to eliminate these H atoms as sources of methane production and to establish the N—H hydrogen as the principal reactant with the methyl radicals. The activation energy and pre-exponential factor for *t*-butyl ethylenimine are shown bracketed in Table I. The very low rate of methane production for this compound at both experimental temperatures introduces considerable error into these calculated quantities. They should be considered as approximations only and no significance can be attributed to their values relative to the values of the corresponding constants for ethylenimine.

3. t-Butyl Acetaldimine and Acetaldazine

t-Butyl acetaldimine $(CH_3)_3C—N{=}CH—CH_3$ and acetaldazine $CH_3CH{=}N—N{=}CHCH_3$ have been included to show the behavior of compounds which do not have N—H hydrogens available. Again it is not certain which hydrogen is entering into reaction, those of the terminal CH_3 group or the H atoms on the carbon of N=C bond. However, it is quite significant that the rate at 124.8° for the acetaldazine abstraction is almost exactly twice that for *t*-butyl acetaldimine. Two hydrogens on the C=N carbon and six hydrogens on CH_3 groups are available in acetaldazine, and one hydrogen on C=N carbon and 12 hydrogens on CH_3 groups are contained on the *t*-butyl acetaldimine. Thus the

Can. J. Chem. Downloaded from www.nrcresearchpress.com by 186.148.149.217 on 09/04/12
For personal use only.

abstraction rates of the two compounds are compatible with the interpretation that the C═N carbon atom furnishes the hydrogen for the abstraction although the evidence is not extensive enough to justify a definite conclusion.

4. Methylamine and Ethylamine

The data in Table I for these two compounds do not furnish further confirmation for the thesis that the N—H hydrogen is active in the abstraction process. On the other hand the evidence is not necessarily contradictory. The similarity in the abstraction activation energies does tend to support the idea of N—H hydrogen abstraction but it is not clear why the abstraction rate at 124.8° for ethylamine is about three times that of methylamine.

The conclusions reached in the preceding discussion as well as some of the experimentally determined data differ markedly from those of Kozak and Gesser's study (3). Their conclusion that low and similar abstraction energies for triethylamine and diethylamine probably indicate a labile C—H rather than N—H hydrogen is reasonable on basis of this evidence alone. However, their value for the abstraction constant of diethylamine ($\log A = 10.9$,* $E = 5.7$) is somewhat different from that shown in Table I ($\log A = 11.8$, $E = 7.2$). Reasons for this difference are speculative as the experimental methods used in both investigations have proved to be reliable in a large number of previously tested cases. It should be pointed out that the data of Trotman-Dickenson (13) for methylamine ($\log A = 11.3$, $E = 8.4$) and dimethylamine ($\log A = 11.3$, $E = 7.2$) are in good agreement with the corresponding quantities shown in Table I, and in addition their value for trimethylamine ($\log A = 11.8$, $E = 8.8$) agrees reasonably well with Kozak and Gesser's result ($\log A = 12.6$, $E = 8.0$) for this same compound. Thus all three studies show conformity between at least some compounds that were mutually tested.

A possible clue to the wide difference in abstraction activation energies for diethylamine between the present study and Kozak and Gesser's work may be seen in their Arrhenius plots for diethylamine and triethylamine. In both curves there is a pronounced falling off in the values of $k_{abs}/k_{comb}^{1/2}$ at the higher temperature. Their explanation for this curvature, the growing importance of the reaction,

$$CH_3 + (C_2H_5)_2NH \rightarrow C_2H_5NHCH_2 + C_2H_6, \qquad [6]$$

as temperature is increased is compatible with the experimental evidence. However, their assumption that the straight lines drawn through the limited low-temperature points truly represent the behavior of reaction [5] only is open to considerable doubt. It seems reasonable that the effect of reaction [6] is active to a degree, at least, over the whole temperature range and that the slopes of the Arrhenius lines should be somewhat steeper, thereby yielding higher activation energies for triethylamine and diethylamine. Whether both curves would be affected in a similar fashion is not predictable, but it is not unlikely that the relative magnitude of the two activation energies might shift so that different conclusions could be drawn concerning the role of the various hydrogens in the abstraction process.

The argument in the previous paragraph would apply equally as well to the present study if reaction [6] were taking place even to a limited extent in the lower temperature range. As the total rate of ethane production would then be the sum of processes [3] and

*The values calculated by Kozak and Gesser for this corresponding quantity for diethylamine, $A_{19}/A_8^{1/2} = 9\times10^{-5}$ is in error. The value should be 1.4×10^{-8} molecule$^{-1/2}$ cm$^{3/2}$ sec$^{-1/2}$. Similarly their value of $A_{11}/A_8^{1/2}$ for triethylamine shown as 3×10^{-5} should be 6.8×10^{-9}.

Can. J. Chem. Downloaded from www.nrcresearchpress.com by 186.148.149.217 on 09/04/12
For personal use only.

[6], the error made by using the total $R_{C_2H_6}$ in place of $R_{C_2H_6}$ by [3] would depend on the relative rates of the two ethane-producing reactions. It can be shown that

$$\frac{R_{CH_4}}{R_{C_2H_6}^{1/2}[M]} = \frac{k_5}{k_3^{1/2}}\left[1+\frac{k_6[M]}{k_3[CH_3]}\right]^{-1/2}.$$

Thus the effect of process [6] on the value determined for $k_5/k_3^{1/2}$ will be minimized by low concentrations of additive, [M], as well as high methyl radical concentrations, $[CH_3]$.

It is significant that there is appreciable difference between the magnitude of both these variables in the two studies under comparison. The diethylamine concentrations used by Kozak and Gesser in their photolyses (12.4×10^{-7} to 16.9×10^{-7} mole cm^{-3}) were about 10 times those used in the DTBP pyrolyses. Clearly in this case the effect of the additive term in the above expression will be only about 1/10th as great for this study as for Kozak and Gesser's work.

The consequence of using an appreciably higher methyl radical steady-state concentration at 156.7° in the peroxide work than in the photolyses is not so easily evaluated. In the present work on diethylamine $R_{C_2H_6}$ is approximately 3.0×10^{-12} and 115×10^{-12} mole cm^{-3} sec^{-1} at 124.8° and 156.7° respectively. The lower temperature rate is about comparable to that of Kozak and Gesser's 123° experiment (2.5×10^{-12}), but the higher temperature rate is about 50 times the rate of their 155° photolysis (2.1×10^{-12}). From the above expression it may be seen that for a constant [M] the activation energy measured by the change in $R_{CH_4}/R_{C_2H_6}^{1/2}$ [M] as a function of temperature will be exactly that of E_5 if $k_6/[CH_3]$ is maintained constant over the range of temperature variation. Kozak and Gesser's Arrhenius curves for diethylamine and triethylamine indicate that E_6 is considerably higher than E_5, perhaps of the order of 15 kcal/mole, and therefore $k_6(156.7°)/k_6(124.8°) \cong 4$. In order for $k_6/[CH_3]$ to maintain its constancy the ratio $R_{C_2H_6}(156.7°)/R_{C_2H_6}(124.8°)$ must be of the order of 16. If this estimate of E_6 is valid and if $R_{C_2H_6}^{1/2}$ may be taken as being proportional to $[CH_3]$, the experimental technique of Kozak and Gesser in which $[CH_3]$ was about constant would yield a value somewhat too small for E_5 while that of the present work would give too large an activation energy. The magnitude of the error of course depends on the size of the additive term within the bracketed expression of the above formula. Determination of the absolute magnitude of the effect of [6] on ethane formation and thus on the value of E_5 is perhaps possible by a detailed study of diethylamine variation at constant temperature in the case of the DTBP pyrolyses. In a like manner investigation of the effect of intensity and diethylamine variation at constant temperature for the photolyses of Kozak and Gesser should produce similar information.

ACKNOWLEDGMENTS

The author wishes to thank the National Science Foundation for financial assistance in carrying out this study. He is also indebted to Dr. Amos Newton and Mr. Aldo Sciamanna of the Lawrence Radiation Laboratory, University of California, Berkeley, California, for some of the mass spectrometric analyses.

REFERENCES

1. A. F. Trotman-Dickenson and E. W. R. Steacie. J. Chem. Phys. **19**, 329 (1951).
2. R. K. Brinton and D. H. Volman. J. Chem. Phys. **20**, 25 (1952).
3. P. J. Kozak and H. Gesser. J. Chem. Soc. 448 (1960).
4. W. H. Urry, O. O. Juveland, and F. W. Stacey. J. Am. Chem. Soc. **74**, 6155 (1952).

Can. J. Chem. Downloaded from www.nrcresearchpress.com by 186.148.149.217 on 09/04/12
For personal use only.

5. D. H. VOLMAN. J. Chem. Phys. **19**, 668 (1951).
6. A. T. BOTTINI and J. D. ROBERTS. J. Am. Chem. Soc. **80**, 5203 (1958).
7. M. O. HURWITZ. U.S. Patent No. 2,582,128 (1952).
8. R. K. BRINTON. J. Am. Chem. Soc. **77**, 842 (1955).
9. D. H. VOLMAN and R. K. BRINTON. J. Chem. Phys. **20**, 1764 (1952).
10. D. H. VOLMAN and R. K. BRINTON. J. Chem. Phys. **22**, 929 (1954).
11. R. K. BRINTON. J. Chem. Phys. **29**, 781 (1958).
12. R. GOMER and G. B. KISTIAKOWSKY. J. Chem. Phys. **19**, 84 (1951).
13. A. F. TROTMAN-DICKENSON. Gas kinetics. Butterworth Scientific Publications, London. 1955.

Can. J. Chem. Downloaded from www.nrcresearchpress.com by 186.148.149.217 on 09/04/12
For personal use only.

Can. J. Chem. Downloaded from www.nrcresearchpress.com by 186.148.149.217 on 09/04/12
For personal use only.

INTERACTION OF TWO PARALLEL PLATES IN A BINARY ASYMMETRICAL ELECTROLYTE

I. UNIVALENT COAGULATING ION[1]

S. LEVINE[2] AND G. M. BELL[3]

ABSTRACT

The interaction of two charged plate-like parallel colloidal particles immersed in a binary asymmetrical electrolyte of valency type $1-m$, where the coagulating ion is univalent, is considered. Applying the Derjaguin–Verwey–Overbeek theory of colloid stability, it is assumed that the plate surface potential is independent of the plate separation. The Stern modification in the absence of specific adsorption of the coagulating ion is also considered. It is demonstrated that as the valency m of the non-coagulating ion increases, the concentration of the coagulating ion at flocculation increases somewhat, but not to the extent predicted by Ostwald's activity coefficient rule. Application of the Stern theory reduces this trend and may even produce a decrease, with increasing m, in the coagulating ion concentration, particularly for a 1–2 electrolyte.

1. INTRODUCTION

According to the Schulze–Hardy rule, the concentration of a binary electrolyte required to flocculate a hydrophobic sol depends mainly on the valency of the ion whose charge is opposite in sign to that on the particles and only slightly on the valency of the ion with a charge of the same sign as that on the particles. The stability theory of Derjaguin and Landau (1) and Verwey and Overbeek (2) reproduces approximately the experimental dependence of the limiting concentration for coagulation on the valency of the flocculating (oppositely charged) ion. However, no systematic theoretical investigation of the corresponding (secondary) dependence on the valency of the like-charged ion has been made and it is the purpose of this paper to determine the relationship which is derived from the above theory for the case of a univalent flocculating ion. According to Ostwald and his collaborators (3), the coagulation concentrations for a number of hydrophobic sols are described approximately by Ostwald's empirical rule, which states that the electrolyte in the dispersion medium flocculates at the same value for the coefficient of activity of the dominating (coagulating) counter-ion. If the Debye–Huckel theory of strong electrolytes at dilute concentrations is applied to a binary electrolyte whose ion types 1 and 2 have densities n_1^0 and n_2^0 and valencies z_1 and z_2 respectively, then Ostwald's rule states that for a given colloidal system, the activity coefficient f_1 of the coagulating ion (which is assumed to be of type 1) is given by

$$[1.1] \qquad \frac{1}{\sqrt{m}} \log f_1 = -z_1^2 \left[\frac{\pi e^6}{(\epsilon k T)^3} \frac{(n_1^0 z_1^2 + n_2^0 z_2^2)}{m} \right]^{\frac{1}{2}} = \text{constant},$$

where e is the electronic charge, ϵ the dielectric constant of the electrolyte medium, k Boltzmann's constant, T the absolute temperature, and m the number of ions of type 1 in a molecule. For a univalent coagulating ion

$$[1.2] \qquad m = -(z_2/z_1) = n_1^0/n_2^0,$$

[1]*Manuscript received April 12, 1960.*
Contribution from the Division of Applied Chemistry, National Research Council, Ottawa, Canada; the Department of Mathematics, University of Manchester, England; and the Department of Mathematics, Manchester College of Science & Technology, England.
Issued as N.R.C. No. 5766.
[2]*Visiting scientist, Division of Applied Chemistry, National Research Council, Ottawa. On leave of absence from the Department of Mathematics, University of Manchester, England.*
[3]*Department of Mathematics, Manchester College of Science & Technology, England.*

making use of the condition of electrical neutrality

$$n_1^0 z_1 + n_2^0 z_2 = 0. \qquad [1.3]$$

The factor $1/\sqrt{m}$ in [1.1] does not occur in the theory of electrolytes so that Ostwald does not employ the usual definition of activity coefficient. The introduction of this factor in colloids emphasizes the significance of the coagulating ion concentration. It follows from Ostwald's rule that for an electrolyte series of valency types $z_1 - z_2$ where $z_1 = 1$ and z_2 takes the values $-1, -2, -3, \ldots$, the quantity $n_1^0(1+m)/m$ should be a constant at the flocculating electrolyte concentration. Various objections, however, have been made to Ostwald's activity coefficient rule. Weiser (4) has commented on the wide spread in the experimental results over which Ostwald averaged and Weiser and Milligan (5) have demonstrated its limited applicability. Tezak and his school (6, 7) maintain that most of the activity coefficients compiled by Ostwald refer to concentrated sols, whereas a physical meaning to the activity coefficient of the flocculating ion can only be given for small sol concentrations. In view of the different premises on which the current theory of colloid stability is based, the Ostwald rule is inadequate theoretically and should be regarded as an empirical result.

In this paper, the interaction of two parallel plate-like particles immersed in a large volume of a binary electrolyte will be examined. It is assumed that the plates are negatively charged, the coagulating cation is univalent ($z_1 = 1$), and the valency z_2 of the anion may have the values $-1, -2, -3, -4$, or $-\infty$. Following Verwey and Overbeek (2), the charge on the plates is supposed to be due to potential-determining ions whose concentration in the dispersion medium is negligible and the binary flocculating electrolyte is indifferent, i.e. there is no specific adsorption of the cation on the plate surface. This means that the potential at the plates is constant, independent of plate separation and of both the nature and concentration of the coagulating electrolyte. Extensive work on the interaction of two parallel plates in a binary symmetrical electrolyte have been carried out by a number of authors (1, 2, 8). The corresponding problem in a 1–2 electrolyte has been treated by Levine and Suddaby (9) and related work on the solution of the Poisson–Boltzmann equation in electrolyte mixtures containing ions of valencies 1 to 4 has been published by Wood and Robinson (10, 11, 12). Electrolyte mixtures of univalent and divalent ions have also been investigated by Glazman and his collaborators (13, 14). Provided the electrolyte in the dispersion medium contains only univalent and divalent ions, it is possible to express the interaction energy of the electric double layers of the plates in terms of elliptic integrals which are tabulated. However, with electrolytes containing higher valency ions, this interaction is obtained in terms of hyperelliptic integrals which are not tabulated. We shall avoid the use of such integrals by expanding the expression for the interaction energy in the form of a series which converges rapidly provided the plate separation is not too large and the surface potential not too small. This will permit the determination of the conditions for flocculation. The investigations of the various authors mentioned above are all based on the Gouy–Chapman theory, in which the diffuse layer is assumed to extend right up to the plate walls. However, we shall also consider the modification (due to Stern) which corrects for the finite size of the ions in the absence of specific adsorption.

By an obvious change in the sign of the surface potential the formulae derived in this paper can be applied to a $m-1$ valency electrolyte, in which the coagulating ion has the valency m. This will be considered in a later paper.

Can. J. Chem. Downloaded from www.nrcresearchpress.com by 186.148.149.217 on 09/04/12
For personal use only.

Can. J. Chem. Downloaded from www.nrcresearchpress.com by 186.148.149.217 on 09/04/12
For personal use only.

2. GENERAL EXPRESSION FOR INTERACTION ENERGY

Let $2h$ be the separation of the plates and x the distance measured from the median plane. If the linear dimensions of the plates are large compared with both h and the so-called thickness of the diffuse layers, then the electrostatic potential ψ at any position x will be a function of x only. It is assumed that the potential $\psi = \psi(x)$ satisfies the classical Poisson–Boltzmann equation throughout the range $-h < x < h$ of the overlapping diffuse layers in the region between the plates. This equation reads

$$[2.1] \qquad \frac{d^2\psi}{dx^2} = -\frac{4\pi e}{\epsilon}[n_1^0 z_1 \exp(-\beta z_1 e\psi) + n_2^0 z_2 \exp(-\beta z_2 e\psi)],$$

where $\beta = 1/kT$. The potential at the median plane will be $\psi_m = \psi(0) < 0$ and that at each plate $\psi_0 = \psi(h) < \psi_m$, the potential zero being taken in the interior of the electrolyte dispersion medium. The classical electrostatic energy per unit area of the two plates is given by

$$[2.2] \qquad E_e(h) = \frac{\epsilon}{4\pi}\int_0^h \left(\frac{d\psi}{dx}\right)^2 dx.$$

The ideal (osmotic) pressure due to the thermal motion of the ions at any x in the diffuse layers where the local ion densities are n_1 and n_2 and the corresponding pressure in the electrolyte interior are respectively,

$$[2.3] \qquad \Pi = kT(n_1 + n_2) \quad \text{and} \quad \Pi_0 = kT(n_1^0 + n_2^0).$$

Also the surface charge density on each plate is

$$[2.4] \qquad \sigma = \frac{\epsilon}{4\pi}\left(\frac{d\psi}{dx}\right)_{x=h}.$$

There are a number of completely equivalent expressions for the free energy to be associated with the electric double layers of the two plates. Thus, per unit area of plates, this energy can be written as

$$[2.5] \qquad F(h) = -2\int_0^{\psi_0} \sigma d\Psi = -E_e(h) - 2\int_0^h (\Pi - \Pi_0)dx.$$

These forms include the so-called electrical and chemical contributions to the free energy and were first used by Verwey and Overbeek (2); a general derivation has been given by Levine (15). In the first integral in [2.5] it is imagined that the surface charge density σ varies from 0 to its full (actual) value σ_0 and the surface potential is Ψ which is a function $\Psi(\sigma)$ of σ; thus $\psi_0 = \Psi(\sigma_0)$. The corresponding double layer force of repulsion per unit area (the electric double layer pressure) can be expressed in the forms

$$[2.6] \qquad p_e(h) = -\frac{1}{2}\left(\frac{\partial F}{\partial h}\right)_{\psi_0} = kT(n_1^{(m)} + n_2^{(m)} - n_1^{(0)} - n_2^{(0)}),$$

where the derivative with respect to h is taken at constant plate potential ψ_0 and $n_1^{(m)}$ and $n_2^{(m)}$ are the ion densities at the median plane $x = 0$. The first form was derived by Verwey and Overbeek (2) and the second independently by Frumkin and Gorodetskaja (16) and by Langmuir (17). A first integral of the Poisson–Boltzmann equation [2.1] is

$$[2.7] \qquad \frac{d\psi}{dx} = -\left[\left(\frac{8\pi kT}{\epsilon}\right)\sum_{i=1}^{2} n_i^0 \{\exp(-\beta z_i e\psi) - \exp(-\beta z_i e\psi_m)\}\right]^{\frac{1}{2}}$$

for $x > 0$, remembering that the above derivative is negative when the plates are negatively charged. This may also be expressed as

$$\Pi - \Pi_0 - \frac{\epsilon}{8\pi}\left(\frac{d\psi}{dx}\right)^2 = p_e(h), \qquad [2.8]$$

where the left-hand side refers to any point x in the diffuse layers. It follows from [2.5] and [2.8] that

$$F(h) = -2E_e(h) - 2hp_e(h). \qquad [2.9]$$

In addition to the double layer repulsion the van der Waals attraction between the plates must be considered. If the thickness of the plates is large compared with h, the energy of attraction per unit area takes the particularly simple form (1, 2)

$$W(h) = -A/48\pi h^2, \qquad [2.10]$$

where the constant A depends upon the material of the plates and of the dispersion medium in which the plates are immersed. The resultant interaction energy per unit area of the two plates is

$$U(h) = F(h) + W(h) - F(\infty). \qquad [2.11]$$

Following Derjaguin and Landau (1) and Verwey and Overbeek (2) we shall use the following conditions to define the transition from the stable to unstable sol (i.e. the critical flocculating relations)

$$U(h) = 0, \qquad [\partial U(h)/\partial h]_{\psi_0} = 0. \qquad [2.12]$$

The second condition in [2.12] may be expressed as

$$p_e(h) = A/48\pi h^3. \qquad [2.13]$$

Making use of [2.10] and [2.13], the first relation in [2.12] can be put in the form

$$2E_e(h) + 3hp_e(h) + F(\infty) = 0. \qquad [2.14]$$

3. GENERAL FORM OF COAGULATION CONDITIONS

It is convenient to introduce a Debye–Huckel parameter K for the positive ions only, defined by

$$K^2 = 8\pi n_1^0 z_1^2 e^2/\epsilon kT, \qquad [3.1]$$

and also the quantities

$$\xi = \exp(\beta z_1 e\psi_m) < 1, \qquad u = \xi \exp(-\beta z_1 e\psi) > 1 \qquad [3.2]$$

and

$$f(u, \xi, m) = \left[\exp(-\beta z_1 e\psi) - \exp(-\beta z_1 e\psi_m) + \frac{1}{m}\left\{\exp(-\beta z_2 e\psi) - \exp(-\beta z_2 e\psi_m)\right\}\right]^{\frac{1}{2}} = \xi^{-\frac{1}{2}}\left[u - 1 + \frac{1}{m}\xi^{m+1}(u^{-m} - 1)\right]^{\frac{1}{2}}. \qquad [3.3]$$

Then [2.7] becomes

$$\frac{d\psi}{dx} = -\left(\frac{8\pi n_1^0 kT}{\epsilon}\right)^{\frac{1}{2}} f(u, \xi, m), \qquad [3.4]$$

Can. J. Chem. Downloaded from www.nrcresearchpress.com by 186.148.149.217 on 09/04/12
For personal use only.

so that the formula [2.2] for the electrostatic energy reads

$$[3.5] \qquad E_e(h) = \frac{\epsilon}{4\pi}\int_{\psi_m}^{\psi_0}\frac{d\psi}{dx}d\psi = \frac{2n_1^0kT}{K}\int_1^{u_0}\frac{f(u,\xi,m)}{u}du,$$

where $u_0 = \xi\exp(-\beta z_1 e\psi_0)$. Also the double layer pressure [2.6] is

$$[3.6] \qquad p_e(h) = n_1^0kT\left(\frac{1}{m}\xi^m+\xi^{-1}-\frac{m+1}{m}\right),$$

and from [3.4]

$$[3.7] \qquad Kh = K\int_{\psi_m}^{\psi_0}\frac{dx}{d\psi}d\psi = \int_1^{u_0}\frac{du}{uf(u,\xi,m)},$$

which, indeed, becomes the solution of the Poisson–Boltzmann equation if h and u_0 are replaced by x and u respectively.

When $h = \infty$, $\psi_m = 0$ and therefore $\xi = 1$. To calculate $F(\infty)$ we apply the first relation in [2.5] to unit area of both sides of a single plate immersed in an infinite volume of the electrolyte. The surface charge density at a single plate surface, whose potential is Ψ, is given by

$$[3.8] \qquad \sigma(\infty) = \frac{\epsilon}{4\pi}\lim_{h\to\infty}\frac{d\psi}{dx} = -\left(\frac{n_1^0kT\epsilon}{2\pi}\right)^{\frac{1}{2}}f(v,1,m),$$

where $v = \exp(-\beta z_1 e\Psi)$. Noting that the surface potential ψ_0 is independent of h, it follows that

$$[3.9] \qquad F(\infty) = -2\int_0^{\psi_0}\sigma(\infty)d\Psi = -\frac{8n_1^0kT}{K}J(\psi_0,m),$$

$$[3.10] \qquad J(\psi_0,m) = -\frac{1}{2}\frac{z_1e}{kT}\int_0^{\psi_0}f(v,1,m)d\psi = \frac{1}{2}\int_1^{v_0}\frac{f(v,1,m)}{v}dv,$$

where $v_0 = \exp(-\beta z_1 e\psi_0)$.

Substituting [3.5], [3.6], [3.7], and [3.9] into the coagulation criterion [2.14] and dividing through by $8n_1^0kT/K$ this criterion appears in the form

$$[3.11] \qquad \frac{1}{2}\int_1^{u_0}\frac{f(u,\xi,m)}{u}du+\frac{3}{8}\left(\frac{1}{m}\xi^m+\xi^{-1}-\frac{m+1}{m}\right)\int_1^{u_0}\frac{du}{uf(u,\xi,m)}-J(\psi_0,m) = 0,$$

which, indeed, applies to any binary electrolyte. It is immediately obvious that the electrolyte concentration variable has been eliminated from [3.11] and that for given ψ_0 and m the value of ξ at which coagulation occurs is obtained. Once [3.11] has been solved for ξ, equation [3.7] then gives Kh and the critical value of K can be obtained from [2.13] and [3.6], from which we derive

$$[3.12] \qquad K = \frac{6\epsilon}{A}\left(\frac{kT}{z_1e}\right)^2(Kh)^3\left[\frac{1}{m}\xi^m+\xi^{-1}-\frac{m+1}{m}\right].$$

Certain points about the behavior of the left-hand side of [3.11], as a function of ξ, appear on considering the left-hand side of [2.14], which is the same expression multiplied by $8n_1^0kT/K$. As a preliminary we observe that if $\xi = 1$ (which means $h = \infty$), the integral in [3.5] becomes identical with $2J(\psi_0,m)$. This shows that $F(\infty) = -2E_e(\infty)$

Can. J. Chem. Downloaded from www.nrcresearchpress.com by 186.148.149.217 on 09/04/12
For personal use only.

and also, using [2.9], that $\lim_{h\to\infty} hp_e(h) = 0$. Hence, the right-hand side of [2.14] vanishes at $h = \infty$ and so $\xi = 1$ is a solution of [3.11]. Now

$$[3.13] \quad 2E_e(h)+3hp_e(h)+F(\infty) = hp_e(h)-F(h)+F(\infty) = hp_e(h)-2\int_h^\infty p_e(h)dh,$$

making use of [2.9] and the first relation in [2.6]. For large h this quantity is positive since it can be shown (see Levine and Suddaby (8)) that $p_e(h)$ diminishes exponentially with h as h increases. At $h = 0$, it is equal to $F(\infty)$ since both $F(h)$ and $hp_e(h)$ vanish. (The charge density σ vanishes at $h = 0$ if the surface potential ψ_0 is constant.) But $F(\infty)$ is negative and so the expression [3.13] must have a second zero for some finite h. As h increases from 0 to ∞, ξ increases from u_0^{-1} to 1. It follows that there is (at least) one root of [3.11] where $\xi < 1$ (see Fig. 1). This is the required solution of [3.12].

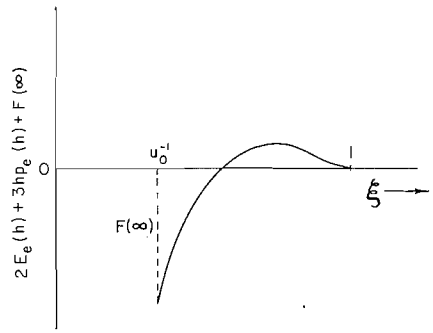


FIG. 1.

4. DETERMINATION OF $F(\infty)$

The expression [3.10] for $J(\psi_0, m)$ can be obtained in closed form for $m = 1, 2, 3, 4$, and ∞. It is helpful to take out a factor $(v-1)v^{-m/2}$ from $f(v, 1, m)$ and then [3.10] becomes

$$[4.1] \quad J(\psi_0, m) = \frac{1}{2}\int_1^{v_0} \frac{(v-1)}{v^{m/2+1}}\left\{v^{m-1}+\frac{(m-1)}{m}v^{m-2}+\ \ldots\ +\frac{2v}{m}+\frac{1}{m}\right\}^{\frac{1}{2}} dv,$$

which is integrated as follows for the above values of m.

(i) $m = 1$

$$[4.2] \quad J(\psi_0, 1) = \frac{1}{2}\int_1^{v_0} \frac{(v-1)}{v^{3/2}}dv = v_0^{\frac{1}{2}}+v_0^{-\frac{1}{2}}-2.$$

(ii) $m = 2$

$$[4.3] \quad J(\psi_0, 2) = \frac{1}{2}\int_1^{v_0} \frac{(v-1)}{v^{\frac{3}{2}}}(v+\tfrac{1}{2})^{\frac{1}{2}}dv = \frac{1}{2\sqrt{2}}\left\{\frac{(2v_0+1)^{3/2}}{v_0}-3\sqrt{3}\right\}.$$

(iii) $m = 3$

$$[4.4] \quad J(\psi_0, 3) = \frac{1}{2}\int_1^{v_0} \frac{(v-1)}{v^3}(v^3+\tfrac{2}{3}v^2+\tfrac{1}{3}v)^{\frac{1}{2}}dv$$

$$= \frac{1}{3}\left\{\frac{(v_0^3+\frac{2}{3}v_0^2+\frac{1}{3}v_0)^{\frac{1}{2}}}{v_0^{\frac{2}{3}}}-\sqrt{2}\right\}+\frac{1}{2}\int_1^{v_0}\frac{(v+\frac{1}{9}v^{-1})dv}{(v^3+\frac{2}{3}v^2+\frac{1}{3}v^3)^{\frac{1}{2}}}.$$

Can. J. Chem. Downloaded from www.nrcresearchpress.com by 186.148.149.217 on 09/04/12
For personal use only.

The integrand contains the square root of a cubic in the denominator and so the integral can be expressed in terms of elliptic integrals. By making the substitution

$$cn(t, k) = \frac{v\sqrt{3}-1}{v\sqrt{3}-1}, \qquad k^2 = \frac{\sqrt{3}-1}{2\sqrt{3}},$$

where k is the parameter of the Jacobian elliptic function $cn(t, k)$ (see Byrd and Friedman (18)), integration can be performed. If we put

$$\cos\phi_0 = \frac{v_0\sqrt{3}-1}{v_0\sqrt{3}+1}, \qquad \cos\phi_1 = \frac{\sqrt{3}-1}{\sqrt{3}+1},$$

then it follows that

$$[4.5] \qquad \frac{1}{2}\int_1^{v_0} \frac{(v+\frac{1}{9}v^{-1})dv}{(v^3+\frac{2}{3}v^2+\frac{1}{3}v)^{\frac{1}{2}}} = \frac{2}{3^{5/4}}\left[2E(\phi, k)-F(\phi, k)+\frac{(1+2\cos\phi)(1-k^2\sin^2\phi)^{\frac{1}{2}}}{\sin\phi}\right]_{\phi_1}^{\phi_0}.$$

Here $F(\phi, k)$ and $E(\phi, k)$ are elliptic integrals of the first and second kinds respectively. Substitution of [4.5] into [4.4] gives the required value of $J(\psi_0, 3)$.

(iv) $m = 4$

$$[4.6] \qquad J(\psi_0, 4) = \frac{1}{2}\int_1^{v_0}\frac{(v-1)}{v^3}(v^3+\tfrac{3}{4}v^2+\tfrac{1}{2}v+\tfrac{1}{4})^{\frac{1}{2}}dv$$

$$= -\frac{1}{4}\left[\left\{\frac{(v_0-1)}{v_0^2}(v_0^3+\tfrac{3}{4}v_0^2+\tfrac{1}{2}v_0+\tfrac{1}{4})^{\frac{1}{2}}\right\}+\frac{5}{8}\int_1^{v_0}\frac{vdv}{(v^3+\frac{3}{4}v^2+\frac{1}{2}v+\frac{1}{4})^{\frac{1}{2}}}\right].$$

The integration may be performed by elliptic substitution as in the case $m = 3$. If the elliptic parameter k equals 0.905943 while

$$\cos\phi_0 = \frac{v_0-0.226242}{v_0+1.437902}, \qquad \cos\phi_1 = \frac{1-0.226242}{1+1.437902} = 0.317387,$$

it turns out that

$$[4.7] \qquad \frac{5}{8}\int_1^{v_0}\frac{vdv}{(v^3+\frac{3}{4}v^2+\frac{1}{2}v+\frac{1}{4})^{\frac{1}{2}}} = 1.140225\left[E(\phi, k)-0.135951F(\phi, k)+\frac{(1+\cos\phi)(1-k^2\sin^2\phi)^{\frac{1}{2}}}{\sin\phi}\right]_{\phi_1}^{\phi_0}.$$

Substitution of [4.7] into [4.6] yields $J(\psi_0, 4)$.

For higher values of m the integrals will be of the hyperelliptic type, which in general are not tabulated. For $m = 5$ and $m = 6$, for instance, the integrands will involve the square root of a quintic. It is possible to express $J(\psi_0, m)$ as a series, which will be indicated in the following section, but no calculations for $m = 5$ or 6 will be made in this paper.

(v) $m = \infty$

$$[4.8] \qquad J(\psi_0, \infty) = \frac{1}{2}\int_1^{v_0}\frac{(v-1)^{\frac{1}{2}}}{v}dv = (v_0-1)^{\frac{1}{2}}-\tan^{-1}(v_0-1)^{\frac{1}{2}}.$$

In Table I, values of $J(\psi_0, m)$ are given for the two values $\beta z_1 e\psi_0 = -2$ and -4, corresponding to $\psi_0 = 50$ and -100 mv respectively at room temperature, when $z_1 = 1$.

Can. J. Chem. Downloaded from www.nrcresearchpress.com by 186.148.149.217 on 09/04/12
For personal use only.

TABLE I
Values of $J(\psi_0, m)$

ψ_0	m	1	2	3	4	∞
−50 mv	Exact	1.086	1.162	1.203	1.228	1.333
	Equation [5.19]			1.216	1.238	1.333
−100 mv	Exact	5.524	5.654	5.714	5.75	5.886
	Equation [5.19]			5.729	5.76	5.886

5. CALCULATION OF COAGULATION VALUES OF ELECTROLYTE

In order to determine the critical value of ξ it is necessary to evaluate the two integrals in [3.11] which come from the equations [3.5] and [3.7] for $E_e(h)$ and Kh respectively. If the substitution $u = 1+y^2$ is made, then

$$[5.1] \qquad \frac{1}{2}\int_1^{u_0}\frac{f(u,\xi,m)}{u}du = \xi^{-\frac{1}{2}}\int_0^{y_0}\frac{y^2}{(1+y^2)}\left[1-\frac{1}{m}\xi^{m+1}\frac{[1-(1+y^2)^{-m}]}{y^2}\right]^{\frac{1}{2}}dy$$

where $u_0 = 1+y_0^2$. Now it is seen from [3.2] that provided the potential at the median plane ψ_m is appreciable, then ξ will be significantly smaller than unity particularly if h is not too large and the surface potential ψ_0 large enough. Since

$$\frac{\xi^{m+1}}{m}\cdot\frac{(1-u^{-m})}{(u-1)} = \frac{\xi^{m+1}}{m}u^{-m}(1+u+\ldots+u^{m-1}) < \xi^{m+1},$$

this suggests that if $\xi < 1$ the integrand in [5.1] be expanded in powers of ξ^{m+1}. The series for the symmetrical case $m = 1$ will be the most slowly converging and we shall retain four terms in this case, namely,

$$[5.2] \qquad \frac{1}{2}\int_1^{u_0}\frac{f(u,\xi,1)}{u}du = \xi^{-\frac{1}{2}}[\tan\theta-\theta-\tfrac{1}{2}\xi^2(\theta-I_2)-\tfrac{1}{8}\xi^4(I_2-I_4)-\tfrac{1}{16}\xi^6(I_4-I_6)+\ldots],$$

where it is convenient to introduce

$$[5.3] \qquad y_0 = \tan\theta, \qquad \xi = u_0/v_0 = \sec^2\theta/v_0,$$

and

$$[5.4] \qquad I_n = \int_0^{y_0}\frac{dy}{(1+y^2)^{n/2+1}} = \int_0^{\theta}\cos^n\alpha d\alpha.$$

This is readily evaluated from the relations

$$[5.5] \qquad I_2 = \tfrac{1}{2}(\theta+\sin\theta\cos\theta), \qquad I_n = \frac{(n-1)}{n}I_{n-2}+\frac{1}{n}\sin\theta\cos^{(n-1)}\theta.$$

Retaining three terms for $m = 2$,

$$[5.6] \qquad \frac{1}{2}\int_1^{u_0}\frac{f(u,\xi,2)}{u}du = \xi^{-\frac{1}{2}}[\tan\theta-\theta-\tfrac{1}{4}\xi^3(\theta-I_4)-\tfrac{1}{32}\xi^6(I_2+I_4-I_6-I_8)+\ldots].$$

For $m \geqslant 3$, it is sufficient to retain only two terms, i.e.

$$[5.7] \qquad \frac{1}{2}\int_1^{u_0}\frac{f(u,\xi,m)}{u}du = \xi^{-\frac{1}{2}}\left[\tan\theta-\theta-\frac{1}{2m}\xi^{m+1}(\theta-I_{2m})+\ldots\right].$$

Can. J. Chem. Downloaded from www.nrcresearchpress.com by 186.148.149.217 on 09/04/12
For personal use only.

The integral in [3.7] may be similarly approximated. Thus

$$[5.8]\qquad \int_1^{u_0}\frac{du}{uf(u,\xi,m)} = 2\xi^{\frac{1}{2}}\int_0^{y_0}\frac{1}{(1+y^2)}\left[1-\frac{1}{m}\xi^{m+1}\frac{[1-(1+y^2)^{-m}]}{y^2}\right]^{-\frac{1}{2}}dy,$$

and expanding again, in powers of ξ^{m+1},

$$[5.9]\qquad \int_1^{u_0}\frac{du}{uf(u,\xi,1)} = 2\xi^{\frac{1}{2}}(\theta+\tfrac{1}{2}\xi^2 I_2+\tfrac{3}{8}\xi^4 I_4+\tfrac{5}{16}\xi^6 I_6+\ldots),$$

$$[5.10]\qquad \int_1^{u_0}\frac{du}{uf(u,\xi,2)} = 2\xi^{\frac{1}{2}}\{\theta+\tfrac{1}{4}\xi^3(I_2+I_4)+\tfrac{3}{32}\xi^6(I_4+2I_6+I_8)+\ldots\},$$

and for $m \geqslant 3$

$$[5.11]\qquad \int_1^{u_0}\frac{du}{uf(u,\xi,m)} = 2\xi^{\frac{1}{2}}\left\{\theta+\frac{1}{2m}\xi^{m+1}(I_2+I_4+\ldots+I_{2m})+\ldots\right\}.$$

If the first two terms are retained in the expansions of [5.1] and [5.8] in powers of ξ^{m+1}, it follows that [3.11] simplifies to

$$[5.12]\quad \xi^{-\frac{1}{2}}\left[\tan\theta-\theta\left\{\frac{1}{4}+\frac{3}{4}\left(1+\frac{1}{m}\right)\xi\right\}\right]$$
$$+\frac{1}{2m}\xi^{m+\frac{1}{2}}\left[\frac{\theta}{2}+I_{2m}+\frac{3}{4}\left\{1-\left(1+\frac{1}{m}\right)\xi+\frac{1}{m}\xi^{m+1}\right\}(I_2+I_4+\ldots+I_{2m})\right]+\ldots = J(\psi_0,m),$$

where ξ is defined in [5.3], and we may also write

$$1-\left(1+\frac{1}{m}\right)\xi+\frac{1}{m}\xi^{m+1} = (1-\xi)^2\left[1+\frac{(m-1)}{m}\xi+\frac{(m-2)}{m}\xi^2+\ldots+\frac{1}{m}\xi^{m-1}\right].$$

The higher terms in the expansion, required for $m = 1$ and $m = 2$, are readily obtained from the relevant equations above. It is convenient to solve for θ rather than for ξ.

The cases $m \gg 1$ and $\xi \ll 1$ are of particular interest. The equation [5.12] becomes, very nearly,

$$[5.13]\qquad \xi^{-\frac{1}{2}}\left[\tan\theta-\theta\left\{\frac{1}{4}+\frac{3}{4}\left(1+\frac{1}{m}\right)\xi\right\}\right] = J(\psi_0,m)$$

and also [3.7] simplifies to

$$[5.14]\qquad Kh = 2\xi^{\frac{1}{2}}\theta = 2\xi^{\frac{1}{2}}\tan^{-1}[\xi\exp(-\beta z_1 e\psi_0)-1]^{\frac{1}{2}},$$

which can also be written in the form

$$[5.15]\qquad \psi_0-\psi_m = \frac{2kT}{z_1 e}\log\cos\left(\tfrac{1}{2}Kh\xi^{-\frac{1}{2}}\right).$$

This result was first given by Langmuir (17) and represents the limiting case where the potential ψ is very large at all positions in the diffuse layers of the two plates. The concentration of anions is so small compared with that of the cations that we may omit the term in n_2^0 in the Poisson–Boltzmann equation [2.1], which consequently has as solution equation [5.15]. This omission of the term in n_2^0 implies that either $m \gg 1$ or $\xi \ll 1$. If $-\psi_0$ is put equal to infinity, then it follows from [5.15] that

$$[5.16]\qquad \cos\left(\tfrac{1}{2}Kh\xi^{-\frac{1}{2}}\right) = 0 \quad \text{or} \quad \xi = (hK/\pi)^2$$

Can. J. Chem. Downloaded from www.nrcresearchpress.com by 186.148.149.217 on 09/04/12
For personal use only.

and so the pressure between the plates becomes

$$[5.17] \qquad p_e(h) = kTn_1^0\left(\frac{1}{\xi}-1\right) \approx \frac{\pi\epsilon}{8}\left(\frac{kT}{z_1e}\right)^2\frac{1}{h^2}$$

if $\xi \ll 1$. Since [5.14] can also be written as

$$[5.18] \qquad \xi\cos^2(\tfrac{1}{2}hK\xi^{-\frac{1}{2}}) = \exp(\beta z_1e\psi_0),$$

we see that to this approximation (applicable when h is small and ψ_0 is large), at a specified separation $2h$ the electrical force is expressed as a function of the surface potential ψ_0 and concentration n_1^0 of coagulation counter-ions only. This is the "zero-order" theory, which states that if ψ_0 is assumed independent of h, then the flocculating concentration depends only on the concentration of the ions oppositely charged to the plates and is independent of the concentration or nature of the ions carrying a charge of the same sign as the plates.

The equation [5.12] for θ, and therefore for ξ, has been solved numerically for $m = 1$, 2, 3, 4, and ∞. Substitution into [3.7] then yields Kh and hence, from [3.12], the quantity $(AK/6\epsilon)(z_1e/kT)^2$ can be determined. This provides a measure of the concentration n_1^0 of the coagulating univalent ions. The results are given in Table II.

TABLE II

	$\psi_0 = -50$ mv					$\psi_0 = -100$ mv				
m	1	2	3	4	∞	1	2	3	4	∞
θ	0.885	0.872	0.865	0.864	0.880	1.23	1.23	1.23	1.24	1.26
ξ	0.338	0.327	0.322	0.321	0.334	0.168	0.166	0.168	0.170	0.190
Kh	1.08	1.01	0.98	0.98	1.02	1.02	1.01	1.01	1.02	1.09
$(KA/6\epsilon)\ (z_1e/kT)^2$	1.62	1.66	1.71	1.76	2.10	4.21	4.61	4.77	4.90	5.58
$(K_m/K_1)^2$	1	1.05	1.10	1.17	1.67	1	1.20	1.28	1.35	1.76
$2m/(1+m)$	1	1.33	1.50	1.60	2	1	1.33	1.50	1.60	2

According to the Derjaguin–Verwey–Overbeek theory, in which the Gouy–Chapman theory of the diffuse layer is applied for all distances from the particle wall and the surface potential ψ_0 is assumed independent of separation, the critical coagulating value of K and therefore of n_1^0 increases with the valency m of the non-flocculating ion. Denoting the value of K for the electrolyte type $1-m$ by K_m, the ratio $(K_m/K_1)^2$, which equals the corresponding ratio of the flocculating ion concentrations, is given in Table II. Ostwald's rule states that for a given sol $n_1^0(1+m)/m$ is a constant and therefore K is proportional to $\{m/(1+m)\}^{\frac{1}{2}}$; this yields $(K_m/K_1)^2 = 2m/(1+m)$, which is also given in the table. It is seen that Ostwald's rule is not verified by the Derjaguin–Verwey–Overbeek theory in the particular case of a $1-m$ binary electrolyte in which the flocculating ion is univalent, although the difference is not large.

It is possible to obtain a good approximation to the free energy $F(\infty)$ for a single plate when m is large ($\geqslant 4$ say) by employing the expansion [5.7]. Thus $F(\infty)$ is given by [3.9] where, from [3.10] and [5.7],

$$[5.19] \qquad J(\psi_0, m) = \tan\theta_0 - \theta_0 - \frac{1}{2m}\{\theta_0 - I_{2m}(\theta_0)\} + \ldots,$$

where $\sec^2\theta_0 = v_0 = \exp(-\beta z_1e\psi_0)$. The two terms on the right are calculated for $m = 3$ and 4 and $\psi_0 = -50$ and -100 mv in Table I. The first term on the right is identical with [4.8] and gives the exact result for $m = \infty$.

Can. J. Chem. Downloaded from www.nrcresearchpress.com by 186.148.149.217 on 09/04/12
For personal use only.

Can. J. Chem. Downloaded from www.nrcresearchpress.com by 186.148.149.217 on 09/04/12
For personal use only.

6. APPLICATION OF STERN MODEL IN THE ABSENCE OF SPECIFIC ADSORPTION

Only one of the two modifications which Stern introduced in the Gouy–Chapman theory will be considered here, namely, the effect of the finite ion size, which is sufficient when specific adsorption of ions on the plate surface is absent. It is assumed that there is a layer of water molecules at the wall which is free of ions, the thickness d, say, of this layer being the minimum distance of approach of the ions of the coagulating electrolyte. Experimental evidence (19, 20, 21) indicates that the water in this inner region of thickness d is partially oriented even in the absence of any charge on the surface and as a result of this partial dielectric saturation, the effective dielectric constant of this inner region, which will be denoted by ϵ_1, is found to be much less than that of bulk water. If $\Psi = \Psi(\sigma)$ is the potential at the colloidal wall, $x = h$ when the plate charge density is σ, and $\Psi_d = \Psi_d(\sigma)$ that at the other boundary, $x = h-d$ of the inner region (Fig. 2) then we may assume the relation

$$\Psi - \Psi_d = \frac{4\pi d\sigma}{\epsilon_1} + \chi_d, \qquad [6.1]$$

where χ_d is the potential drop due to the dipole orientation in the absence of surface charge σ; this contributes to the so-called Lange χ-potential. It will be shown in a later paper that ϵ_1 should be interpreted as a differential rather than an integral dielectric constant. The limit of the diffuse layer is now assumed to be situated at $x = h-d$ instead of $x = h$, as in the Gouy–Chapman theory.

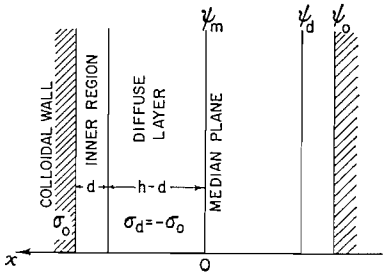


FIG. 2.

To determine the free energy for the above model of the electric double layers, it is necessary to discuss the origin of the first equation in [2.5]. The free energy consists of two terms, an 'electrical' part $F_e(h)$ given by

$$F_e(h) = 2\int_0^{\sigma_0} \Psi d\sigma \qquad [6.2]$$

and a chemical part F_c, which takes the form

$$F_c = 2C\sigma_0, \qquad [6.3]$$

where C is a constant, when the potential-determining ions responsible for the surface charge form part of the particle lattice. Since $F(h)$ must be a minimum with respect to transfer of potential-determining ions from the electrolyte dispersion medium to the plates,

$$\frac{dF(h)}{d\sigma_0} = \frac{d}{d\sigma_0}\Big[F_e(h) + F_c\Big] = 0, \qquad [6.4]$$

Can. J. Chem. Downloaded from www.nrcresearchpress.com by 186.148.149.217 on 09/04/12
For personal use only.

or, since $\psi_0 = \Psi(\sigma_0)$,

$$\psi_0 + C = 0. \qquad [6.5]$$

Integrating by parts

$$F(h) = F_e(h) + F_c = 2(\psi_0 + C)\sigma_0 - 2\int_0^{\psi_0} \sigma d\Psi = -2\int_0^{\psi_0} \sigma d\Psi. \qquad [6.6]$$

Substituting [6.1] we obtain

$$F(h) = -2\int_0^{\psi_d} \sigma d\Psi_d - \frac{4\pi d\sigma_0^2}{\epsilon_1}, \qquad [6.7]$$

where $\psi_d = \Psi_d(\sigma_0)$ is the potential at the limit of the diffuse layer $x = h - d$ when the plate is fully charged. The last result was given by Mackor (22). Levine (23) considered the more general case where the inner region contains an adsorbed layer of counter-ions and his formula reduces to [6.6] in the case of no specific adsorption.

The charge density σ is equal in magnitude and opposite in sign to the charge σ_d, say, contained in a column of the diffuse layer of unit cross section and situated between the planes $x = 0$ and $x = h - d$. It follows that, apart from the constant factor d/ϵ_1, the energy expression [6.7] depends solely on the charge distribution in the diffuse layer, and this is also true of the formula in [2.5]. Furthermore, the double layer repulsion per unit area can be written as

$$p_e(h') = -\frac{1}{2}\left[\frac{\partial F_e(h)}{\partial h}\right]_{\sigma_0} = \left[-\frac{\partial}{\partial h}\int_0^{\sigma_0} \Psi_d d\sigma\right]_{\sigma_0}, \qquad [6.8]$$

where $h' = h - d$, and [6.1] is substituted into [6.2]. The proof of the first relation in [6.8] has been given by Verwey and Overbeek (2), Levine (24), and Bell and Levine (25). Since $\sigma = -\sigma_d$, this means that the force per unit area also depends on the charge distribution in the diffuse layer only and thus is given by the last expression in [2.6]. Indeed it has already been stressed (26, 27) that the latter force formula, which is expressed in terms of the ion densities at the median plane, is always valid, being independent of the particular conditions at the particle surface, *provided* the median plane is embedded in the diffuse layers and the Gouy–Chapman equations can be applied to the diffuse layer. It follows that the first term on the right of [6.7] may be equated to the expression [2.9] if h is replaced by $h' = h - d$ and ψ_0 by ψ_d, and so

$$F(h) = -2E_e(h') - 2h'p_e(h') - \frac{4\pi d\sigma_0^2}{\epsilon_1}. \qquad [6.9]$$

The van der Waals attraction will take a different form from [2.10] since the inner region of water not only has a different dielectric constant but is probably in a state of considerable electrostriction. It is convenient to write the van der Waals energy in the form

$$W(h') = -\frac{A}{48\pi h'^2} + A'F_w(h'), \qquad [6.10]$$

where the second term is the correction due to the difference between the materials of the inner region and the colloidal plates. Certainly for large separations the first term on the right will be the dominant one and in view of the mathematical complexities

it seems sufficient for the present purposes to neglect the second term. In this case, the two stability conditions [2.12] become

$$[6.11] \qquad p_e(h') = \frac{A}{48\pi h'^3}, \qquad 2E_e(h')+3h'p_e(h')+F'(\infty)+\frac{4\pi d\sigma_0^2}{\epsilon_1} = 0,$$

where $F'(\infty)$ is the free energy per unit area of a single plate.

It is convenient to introduce

$$[6.12] \qquad v_d = \exp(-\beta z_1 e\psi_d), \qquad u_d = \xi v_d, \qquad v_d(\infty) = \exp\{-\beta z_1 e\psi_d(\infty)\},$$

where ξ is already defined in [3.2], and noting that ψ_d varies with separation $2h$, its value at infinite separation is denoted by $\psi_d(\infty)$. Then $E_e(h')$ is given by [3.5] and similarly Kh' by [3.7], provided the upper limit of integration u_0 on the right-hand side of both equations is replaced by u_d. Also $p_e(h')$ is again given by [3.6]. If σ_0 has the value $\sigma_0(\infty)$ at infinite separation and $J(\psi_d(\infty), m)$ is defined by [3.10], when the upper limit of integration is replaced by $v_d(\infty)$, then

$$[6.13] \qquad F'(\infty) = -8n_1^0kTJ(\psi_d(\infty), m)-\frac{4\pi d\sigma_0^2(\infty)}{\epsilon_1}.$$

By [3.4] the charge density σ_0 can be written as

$$[6.14] \qquad \sigma_0 = -\left(\frac{n_1^0kT\epsilon}{2\pi}\right)^{\frac{1}{2}} f(u_d, \xi, m)$$

and the corresponding form for $\sigma_0(\infty)$ is obtained by replacing u_d by $v_d(\infty)$ and ξ by 1. Thus the second condition in [6.11] reads

$$[6.15] \qquad \frac{1}{2}\int_1^{u_d}\frac{f(u, \xi, m)}{u}du+\frac{3}{8}\left(\frac{1}{m}\xi^m+\xi^{-1}-\frac{(m+1)}{m}\right)\int_1^{u_d}\frac{du}{uf(u, \xi, m)}-J(\psi_d(\infty), m)$$
$$= \frac{Kd\epsilon}{4\epsilon_1}[f^2(v_d(\infty), 1, m)-f^2(u_d, \xi, m)]$$

after dividing through by $8n_1^0kT/K$. This relation becomes identical with [3.11] when the thickness d of the inner region tends to zero. For non-vanishing d, however, it differs from [3.11] in that the electrolyte concentration variable has not been eliminated and it is no longer possible to solve for ξ in terms of u_d without introducing the other stability condition in [6.11].

It is convenient to express the condition [6.1] as

$$[6.16] \qquad -\beta z_1 e\psi_d = \log v_d = \Phi_0-\frac{Kd\epsilon}{\epsilon_1}f(u_d, \xi, m),$$

where $\Phi_0 = \beta z_1 e(\chi_d-\psi_0)$, which is constant independent of d. If use is made of [3.3], then at $h = \infty$ (when $\xi = 1$) this relation can be put in the form

$$[6.17] \qquad \log v_d(\infty)+\frac{Kd\epsilon}{\epsilon_1}[v_d^{\frac{1}{2}}(\infty)-v_d^{-\frac{1}{2}}(\infty)]H^{\frac{1}{2}}(v_d(\infty), m) = \Phi_0$$

where

$$[6.18] \qquad H(s, m) = 1+\frac{(m-1)}{m}\cdot\frac{1}{s}+\frac{(m-2)}{m}\cdot\frac{1}{s^2}+\ldots+\frac{1}{ms^{m-1}}.$$

Can. J. Chem. Downloaded from www.nrcresearchpress.com by 186.148.149.217 on 09/04/12
For personal use only.

Can. J. Chem. Downloaded from www.nrcresearchpress.com by 186.148.149.217 on 09/04/12
For personal use only.

Thus

$$H(s,1) = 1, \qquad H(s,2) = 1+\frac{1}{2s}, \qquad H(s,3) = 1+\frac{2}{3s}+\frac{1}{3s^2},$$

$$H(s,4) = 1+\frac{3}{4s}+\frac{1}{2s^2}+\frac{1}{4s^3}, \qquad H(s,\infty) = \frac{s}{(s-1)}.$$

The equation [6.17] yields $v_d(\infty)$ (or $\psi_d(\infty)$) as a function of K. Now χ_d measures a residual potential drop in the absence of surface charge and will be assumed independent of electrolyte type (i.e. of m). Since ψ_0 also does not depend on valency type we may presume Φ_0 to be independent of m. The thickness d of the Stern layer is some mean of the two distances of nearest approach to the colloidal wall of the cation and anion, which we denote by d_I and d_{II} respectively. For simplicity, let $d_I = d_{II}$ for the 1–1 electrolyte and noting that the radius of the hydrated anion will in general increase with its hydration number let d_{II} increase with its valency m. Then it is likely that for small $m > 1$, $d > d_I$ but the following considerations suggest that as m increases d diminishes again, tending to d_I. If the hydration number is assumed proportional to m then the ratio d_{II}/d_I will be roughly proportional to $m^{1/3}$ whereas the ratio of the concentration of anions to cations at a distance $x = d_{II}$, where the potential is $\psi_{II}(<0)$ say, will be $(1/m)\exp[\beta e(m+1)\psi_{II}]$, which rapidly tends to zero with increasing m. This means that the number of anions that would be present in the region $d_I < x < d_{II}$ if they were not excluded through steric hindrance, would be so small for $m \geqslant 3$, say, that the distance d is determined by the cations only and is therefore equal to d_I. This behavior of d as a function of m will be borne in mind below.

To examine the relation [6.16] for general h we introduce $u_d = \sec^2\alpha$ and therefore $v_d = \sec^2\alpha/\xi$. Then, making use of [3.3], [6.16] can be written as

$$[6.19] \quad \log\left(\frac{\sec^2\alpha}{\xi}\right)+\frac{Kd\epsilon}{\epsilon_1}\xi^{-\frac{1}{2}}\tan\alpha\left[1-\frac{1}{m}\xi^{m+1}\cos^{2m}\alpha\{1+\sec^2\alpha+\ldots+\sec^{2(m-1)}\alpha\}\right]^{\frac{1}{2}} = \Phi_0.$$

Similarly, equation [6.15] reads:

$$[6.20] \quad \xi^{-\frac{1}{2}}\left[\tan\alpha-\alpha\left\{\frac{1}{4}+\frac{3}{4}\left(1+\frac{1}{m}\right)\xi\right\}\right]$$
$$+\frac{1}{2m}\xi^{m+\frac{1}{2}}\left[\frac{\alpha}{2}+I_{2m}+\frac{3}{4}\left\{1-\left(1+\frac{1}{m}\right)\xi+\frac{1}{m}\xi^{m+1}\right\}(I_2+I_4+\ldots+I_{2m})\right]$$
$$+\ldots-J(\psi_d(\infty),m) = \frac{Kd\epsilon}{4\epsilon_1}\left[\frac{(v_d(\infty)-1)^2}{v_d(\infty)}H(v_d(\infty),m)\right.$$
$$\left.-\xi^{-1}\tan^2\alpha\left\{1-\frac{1}{m}\xi^{m+1}\cos^{2m}\alpha(1+\sec^2\alpha+\ldots+\sec^{2(m-1)}\alpha)\right\}\right],$$

where, as in [5.12] only two terms in the expansion in powers of ξ^{m+1} have been retained on the left-hand side. In the three equations [6.17], [6.19], and [6.20], there are four unknowns α, ξ, K, and $\psi_d(\infty)$ (or $v_d(\infty)$) so that one more equation is required; this is provided by the first stability condition in [6.11]. Making use of [3.7] and [5.11], this condition is equivalent to [3.12] provided h, u_0, and θ are replaced by h', u_d, and α. The required fourth relation is therefore

$$[6.21] \quad M = C\xi^{\frac{1}{2}}\left\{1-\left(1+\frac{1}{m}\right)\xi+\frac{1}{m}\xi^{m+1}\right\}\left[\alpha+\frac{1}{2m}\xi^{2m+1}(I_2+I_4+\ldots+I_{2m})+\ldots\right]^3,$$

where

$$[6.22] \qquad M = \frac{Kd\epsilon}{\epsilon_1}, \qquad C = \frac{48d\epsilon^2}{A\epsilon_1}\left(\frac{kT}{z_1e}\right)^2,$$

and the I_n are functions of α in [6.20] and [6.21].

The simplest case is $m = \infty$. Attaching a suffix ∞ to the quantities M and C and introducing $\phi = -\beta z_1 e\psi_d(\infty) > 0$ the four equations are readily obtained, namely

$$[6.23] \qquad M_\infty = \frac{\Phi_0-\phi}{(e^\phi-1)^{\frac{1}{2}}} = \frac{\Phi_0-\log(\sec^2\alpha/\xi)}{\xi^{-\frac{1}{2}}\tan\alpha} = C_\infty\xi^{\frac{1}{2}}\alpha^3(1-\xi),$$

$$\xi^{-\frac{1}{2}}\left[\tan\alpha-\frac{\alpha}{4}(1+3\xi)\right]-J(\psi_d(\infty),\infty) = \frac{M_\infty}{4}\left[e^\phi-1-\xi^{-1}\tan^2\alpha\right].$$

For $m = 1$, attaching the suffix 1 to the quantities M and C, the corresponding equations are

$$[6.24] \qquad M_1 = \frac{\Phi_0-\phi}{2\sinh\phi/2} = \frac{\Phi_0-\log(\sec^2\alpha/\xi)}{\xi^{-\frac{1}{2}}\tan\alpha(1-\xi^3\cos^2\alpha)^{\frac{1}{2}}}$$

$$= C_1\xi^{\frac{1}{2}}(1-\xi)^2\left[\alpha+\frac{1}{2}\xi^2I_2+\frac{3}{8}\xi^4I_4+\ldots\right]^3$$

and

$$[6.25] \qquad \xi^{-\frac{1}{2}}\left[\tan\alpha-\frac{\alpha}{4}(1+6\xi)\right]+\frac{1}{2}\xi^{3/2}\left[\frac{\alpha}{2}+I_2+\frac{3}{4}(1-\xi)^2I_2\right]$$

$$+\frac{1}{8}\xi^{7/2}\left[I_4-I_2+\frac{9}{4}(1-\xi)^2I_4\right]+\ldots-J(\psi_d(\infty),1)$$

$$= \frac{M_1}{4}\left[4\sinh^2\frac{\phi}{2}-\xi^{-1}\tan^2\alpha(1-\xi^2\cos^2\alpha)\right],$$

where three terms in the expansion in the powers of $\xi^{m+1} = \xi^{3/2}$ on the left-hand side of [6.20] have been retained. For $m = 2$ we obtain

$$[6.26] \qquad M_2 = \frac{\Phi_0-\phi}{2\,(1+\frac{1}{2}e^{-\phi})^{\frac{1}{2}}\sinh\phi/2} = \frac{\Phi_0-\log(\sec^2\alpha/\xi)}{\xi^{-\frac{1}{2}}\tan\alpha[1-\frac{1}{2}\xi^3(\cos^2\alpha+\cos^4\alpha)]^{\frac{1}{2}}}$$

$$= C_2\xi^{\frac{1}{2}}(1-\xi)^2\left(1+\frac{1}{2}\xi\right)\left[\alpha+\frac{1}{4}\xi^3(I_2+I_4)+\ldots\right]^3$$

and

$$[6.27] \qquad \xi^{-\frac{1}{2}}\left[\tan\alpha-\frac{\alpha}{8}(2+9\xi)\right]+\frac{1}{4}\xi^{5/2}\left[\frac{\alpha}{2}+I_4+\frac{3}{8}(1-\xi)^2(2+\xi)(I_2+I_4)\right]+\ldots$$

$$-J(\psi_d(\infty),2) = \frac{M_2}{4}\left[4\sinh^2\frac{\phi}{2}\,(1+\tfrac{1}{2}e^{-\phi})-\xi^{-1}\tan^2\alpha\{1-\tfrac{1}{2}\xi^3(\cos^2\alpha+\cos^4\alpha)\}\right].$$

Some numerical solutions of the above equations are given in Table III for $\Phi_0 = 10$ ($|\psi_0-\chi_d| = 250$ mv). An examination of [6.17] shows that for specified Φ_0 and Kd the magnitude of the potential $\psi_d(\infty)$ diminishes with increasing m. This suggests that if

Can. J. Chem. Downloaded from www.nrcresearchpress.com by 186.148.149.217 on 09/04/12
For personal use only.

the value $\phi = 2$ ($\psi_d(\infty) = -50$ mv), for example, is chosen for $m = 1$ then $\phi < 2$ for $m > 1$. The subscripts 1, 2, or ∞ have been assigned to various quantities to designate that $m = 1$, 2, or ∞ respectively. Values of ϕ have been chosen to provide a range of values for the ratio d_m/d_1, of the thicknesses of the inner region in 1–1 and 1–m electrolytes. From the definition of C in [6.22], $d_m/d_1 = C_m/C_1$ and the corresponding ratio of the coagulating ion concentrations is $(K_m/K_1)^2 = (M_m d_1/M_1 d_m)^2$. It is seen that

TABLE III

m		1	2		∞	
ϕ		2	2	1.9	1.96	1.8	1.75
M_m		3.40	3.29	3.55	3.40	3.65	3.78
α		0.917	0.920	0.870		0.864	0.857
ξ		0.310	0.305	0.285		0.293	0.302
C_m		14.9	13.4	16.9	14.9	14.8	15.7
d_m/d_1			0.90	1.14	1	0.99	1.06
$\left(\frac{K_m}{K_1}\right)^2$	Stern		1.16	0.84	1.00	1.17	1.11
	Gouy–Chapman		1.05			1.67	($\phi = 2$)
	Ostwald (any ϕ)			1.33		2	

if $d_m \geqslant d_1$ then the Stern theory yields a greater divergence from Ostwald's rule than the Gouy–Chapman theory. In view of the variation with sol concentration of the coagulating ion activity coefficient, as stressed by Weiser and Tezak, at best the Ostwald rule seems to be an empirical approximation. On the other hand, it is probable that for asymmetrical electrolytes where $m \geqslant 3$, the Poisson–Boltzmann equation, which is the basis of the Gouy–Chapman–Stern theory of the diffuse layer, is also inadequate because of the neglect, for example, of the fluctuation or self-atmosphere effect. It is well known that the limitations of the classical Debye–Huckel theory for electrolytes containing ions of high valency are largely attributed to this fluctuation term. Since the theory developed in this paper applies to very dilute sols whereas Ostwald's rule apparently holds for concentrated sols, the measure of agreement between the Gouy–Chapman–Stern theory and experiment for the valency type 1–m is not easily determined.

ACKNOWLEDGMENTS

The authors are indebted to Mr. D. F. Ferguson, University of Manchester, for assisting with the numerical computations in the tables and to Dr. I. E. Puddington, Division of Applied Chemistry, National Research Council, Ottawa, for his helpful suggestions.

REFERENCES

1. B. V. Derjaguin and L. Landau. Acta Physicochim. U.R.S.S. **14**, 633 (1941).
2. E. J. W. Verwey and J. Th. G. Overbeek. Theory of the stability of lyophobic colloids. Elsevier Press Inc., New York. 1948.
3. W. Ostwald. (*a*) J. Phys. Chem. **42**, 981 (1938); (*b*) Kolloid-Z. **88**, 1 (1939).
4. H. B. Weiser. Inorganic colloid chemistry. Vol. III. John Wiley & Sons Inc., New York. 1938. p. 190.
5. H. B. Weiser and W. O. Milligan. J. Am. Chem. Soc. **62**, 1942 (1940).
6. B. Tezak. Arkiv. kem. **22**, 26 (1950).
7. E. Matijevic and B. Tezak. Kolloid-Z. **125**, 1 (1952).
8. S. Levine and A. Suddaby. (*a*) Proc. Phys. Soc. A, **64**, 287 (1951); (*b*) Proc. Phys. Soc. A, **64**, 431 (1951).
9. S. Levine and A. Suddaby. Proc. Phys. Soc. A, **65**, 405 (1952).
10. L. A. Wood. J. Chem. Phys. **13**, 429 (1945).
11. L. A. Wood and L. B. Robinson. J. Chem. Phys. **14**, 258 (1946).
12. L. B. Robinson. J. Chem. Phys. **16**, 734 (1948).

Can. J. Chem. Downloaded from www.nrcresearchpress.com by 186.148.149.217 on 09/04/12
For personal use only.

13. Y. M. GLAZMAN and I. M. DYKMAN. (*a*) Proc. Acad. Sci. U.S.S.R. **100**, 299 (1955); (*b*) Colloid J. (U.S.S.R.), **18**, 13 (1956).
14. Y. M. GLAZMAN, I. M. DYKMAN, and E. A. STRELTSOVA. Proc. Acad. Sci. U.S.S.R. **117**, 829 (1957).
15. S. LEVINE. Proc. Phys. Soc. A, **64**, 781 (1951).
16. A. FRUMKIN and A. GORODETSKAJA. Acta Physicochim. U.R.S.S. **9**, 327 (1938).
17. I. LANGMUIR. J. Chem. Phys. **6**, 893 (1938).
18. P. F. BYRD and M. D. FRIEDMAN. Handbook of elliptic integrals of engineers and physicists. Springer, Berlin. 1954. p. 88.
19. J. TH. G. OVERBEEK and E. L. MACKOR. Compt. rend. 3ième. Reunion, CITCE, 1951. p. 346. C. Manfredi, Milan. 1952.
20. J. LIJKLEMA. Thesis, University of Utrecht, Utrecht, Netherlands. 1957.
21. J. TH. G. OVERBEEK and J. LIJKLEMA. *In* Electrophoresis. *Edited by* M. Bier. Academic Press Inc., New York. 1959. Chap. 1.
22. E. L. MACKOR. Rec. trav. chim. **70**, 841 (1951).
23. S. LEVINE. Colloid Sci. **6**, 1 (1951).
24. S. LEVINE. Trans. Faraday. Soc. **42** B, 102 (1946).
25. G. M. BELL and S. LEVINE. Trans. Faraday Soc. **54**, 785 (1958).
26. Y. IKEDA. J. Phys. Soc. Japan, **8**, 49 (1953).
27. N. E. HOSKIN and S. LEVINE. Phil. Trans. Roy. Soc. London, **248**, 449 (1956).

Can. J. Chem. Downloaded from www.nrcresearchpress.com by 186.148.149.217 on 09/04/12
For personal use only.

Can. J. Chem. Downloaded from www.nrcresearchpress.com by 186.148.149.217 on 09/04/12
For personal use only.

THE SULPHURIC ACID SOLVENT SYSTEM

PART I. ACID–BASE REACTIONS[1]

R. H. Flowers, R. J. Gillespie, and E. A. Robinson

ABSTRACT

Acid–base reactions in the solvent sulphuric acid are discussed. Such reactions are conveniently studied by electrical conductivity measurements. A relation between the composition at which the conductivity has a minimum value and the strengths of the acid and base is derived. Values of the dissociation constants of acids and bases obtained in this way are shown to be in good agreement with values obtained by other methods.

INTRODUCTION

Sulphuric acid is an amphoteric solvent that undergoes fairly extensive autoprotolysis (1, 2).

$$2H_2SO_4 = H_3SO_4^+ + HSO_4^-$$

An acid of the sulphuric acid system may be defined as any substance that gives rise to the sulphuric acidium ion $H_3SO_4^+$. A simple monoprotic acid would ionize according to the equation

$$HA + H_2SO_4 = H_3SO_4^+ + A^-.$$

A base may be defined as any substance that gives rise to the hydrogen sulphate ion HSO_4^-. A simple monoprotic base would ionize according to the equation

$$B + H_2SO_4 = BH^+ + HSO_4^-.$$

Reaction between an acid and a base occurs according to the equation

$$H_3SO_4^+ + HSO_4^- = 2H_2SO_4,$$

which is, of course, just the reverse of the autoprotolysis reaction.

Because of the abnormally high mobilities of the $H_3SO_4^+$ and HSO_4^- ions the electrical conductivity of any solutions can be regarded, to a reasonably good approximation, as being due to these ions alone (1, 2). In acid–base reactions in which, for example, a base is added to a solution of an acid, the concentration of $H_3SO_4^+$ decreases and the concentration of HSO_4^- increases, causing the conductivity to decrease initially, pass through a minimum, and increase again. The position of minimum conductivity depends on the strengths of the acid and base and on their modes of ionization. By following the change in conductivity accompanying an acid–base reaction, information on the nature of the reaction and on the strength of the acid and base may be obtained. This paper gives a general treatment of the variation of the electrical conductivity during an acid–base reaction and some examples of the determination of acid and base strengths by this method are discussed.

THEORY

The detailed treatment of acid–base reactions is somewhat complicated by the existence of another form of self-dissociation of the solvent in addition to autoprotolysis, namely self-dehydration (1, 2), which may be summarized by the equations

$$2H_2SO_4 = H_2S_2O_7 + H_2O,$$
$$H_2S_2O_7 + H_2SO_4 = H_3SO_4^+ + HS_2O_7^-,$$
$$H_2O + H_2SO_4 = H_3O^+ + HSO_4^-.$$

[1]*Manuscript received April 6, 1960.*
Contribution from the Department of Chemistry, University College, London, W.C.1, England, and the Department of Chemistry, McMaster University, Hamilton, Ontario.

The concentrations of all the species in a solution containing an acid HA and a base B are related by the following expressions: the four equilibrium constants describing the self-dissociation of the solvent, whose values are given in Table I (3, 4),

$$K_{ap} = [H_3SO_4^+][HSO_4^-]^* \quad [1]$$

$$K_{id} = [H_3O^+][HS_2O_7^-] \quad [2]$$

$$K_{H_2S_2O_7} = [H_3SO_4^+][HS_2O_7^-]/[H_2S_2O_7] \quad [3]$$

$$K_{H_2O} = [H_3O^+][HSO_4^-]/[H_2O], \quad [4]$$

the dissociation constants of the acid and the base,

$$K_a = [H_3SO_4^+][A^-]/[HA] \quad [5]$$

$$K_b = [BH^+][HSO_4^-]/[B], \quad [6]$$

the condition for electrical neutrality,

$$[BH^+] + [H_3O^+] + [H_3SO_4^+] = [A^-] + [HS_2O_7^-] + [HSO_4^-], \quad [7]$$

and the condition that the composition of the solvent is H_2SO_4,

$$[H_3O^+] + [H_2O] = [HS_2O_7^-] + [H_2S_2O_7]. \quad [8]$$

TABLE I

Equilibrium constants for the self-dissociation reactions of sulphuric acid

	10° C	25° C
$K_{ap} = [H_3SO_4^+][HSO_4^-]$	1.7×10^{-4}	2.4×10^{-4}
$K_{id} = [H_3O^+][H_2S_2O_7^-]$	3.0×10^{-5}	4.2×10^{-5}
$K_{H_2S_2O_7} = [H_3SO_4^+][HS_2O_7^-]/[H_2S_2O_7]$	1.4×10^{-2}	1.4×10^{-2}
$K_{H_2O} = [H_3O^+][HSO_4^-]/[H_2O]$	1	1

For the special case where $H_2S_2O_7$ is the acid equation [5] is not needed and equations [7] and [8] are replaced by

$$[BH^+] + [H_3O^+] + [H_3SO_4^+] = [HS_2O_7^-] + [HSO_4^-] \quad [9]$$

and

$$m^s_{H_2S_2O_7} = [HS_2O_7^-] + [H_2S_2O_7] - [H_3O^+] - [H_2O] \quad [10]$$

where $m^s_{H_2S_2O_7}$ is the stoichiometric molal concentration of $H_2S_2O_7$.

For the special case where water is the base being neutralized equation [6] is not needed and [7] and [8] are replaced by

$$[H_3O^+] + [H_3SO_4^+] = [A^-] + [HS_2O_7^-] + [HSO_4^-] \quad [11]$$

and

$$m^s_{H_2O} = [H_3O^+] + [H_2O] - [H_2S_2O_7] - [HS_2O_7^-] \quad [12]$$

where $m^s_{H_2O}$ is the stoichiometric molal concentration of water. The concentrations of all the species for any concentrations of acid and base in an acid–base reaction may be calculated from these equations by the method that has been previously described (3).

The acids of the sulphuric acid system, e.g. tetra(hydrogensulphato) boric acid, $HB(HSO_4)_4$ (5), and disulphuric acid, $H_2S_2O_7$, are either known only in solution in sulphuric acid, or are only easily handled in solution, whereas the common bases, e.g.

**All concentrations in this paper are in molal units and* [A] *and* m_A *are both used to denote the molal concentration of the species A.*

Can. J. Chem. Downloaded from www.nrcresearchpress.com by 186.148.149.217 on 09/04/12
For personal use only.

potassium sulphate, benzoic acid, and nitrobenzene, are easily obtained in the pure state and they are easily handled as such. Thus it is convenient to carry out acid–base reactions by adding the pure base to a solution of the acid. The position of minimum conductivity is then most conveniently expressed in terms of the ratio $r = n_b/n^1_a$ of the number of moles of added base, n_b, to the initial number of moles of acid n^1_a. Figures 1 and 2 show

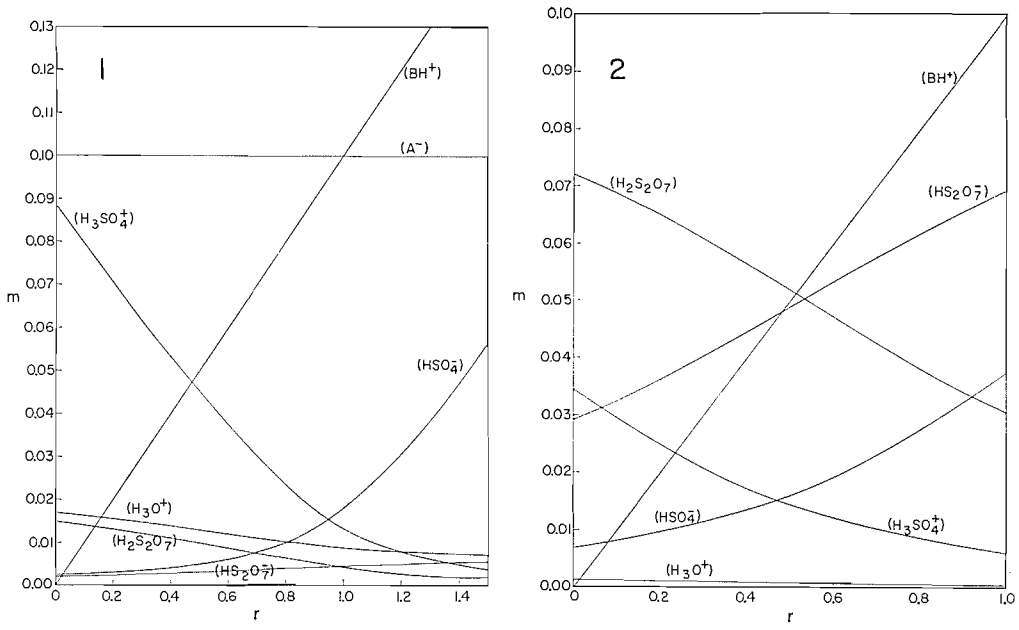


FIG. 1. Concentrations of species in a strong acid – strong base reaction at 25° ($m^i_{HA} = 0.1$).
FIG. 2. Concentrations of species in a disulphuric acid – strong base reaction at 25° ($m^i_{H_2S_2O_7} = 0.1$).

how the concentrations of all the species in reactions of the acids HA and $H_2S_2O_7$ with a strong base B vary with r for an initial concentration of acid $m^1_{H_2S_2O_7}$ or $m^1_{HA} = 0.1$.

The conductivity of the solution at any point in such a reaction is given by

$$\kappa = 10^{-3}\rho([H_3SO_4^+]\lambda_{H_3SO_4^+} + [HSO_4^-]\lambda_{HSO_4^-} + [H_3O^+]\lambda_{H_3O^+} + [HS_2O_7^-]\lambda_{HS_2O_7^-} + [BH^+]\lambda_{BH^+} + [A^-]\lambda_{A^-}) \quad [13]$$

where the λ's represent ion mobilities (molar conductances) and where it has been assumed that molar concentrations c may be replaced by $m\rho$ where m is the molal concentration and ρ the density of the solution. In view of the very small conductivities of all normally conducting ions (2) it is a reasonably good approximation to neglect their contribution to the conductivity of the solution in comparison with the relatively large contribution made by the highly conducting $H_3SO_4^+$ and HSO_4^- ions; hence we may write

$$\kappa = 10^{-3}\rho\ (\lambda_+ m_+ + \lambda_- m_-) \quad [14]$$

where λ_+ and λ_- are the mobilities, and m_+ and m_- are the molal concentrations of $H_3SO_4^+$ and HSO_4^- respectively. The mobilities of $H_3SO_4^+$ and HSO_4^- decrease with increasing concentration but at total ion concentrations of the order of $0.2m$, such as occur in the experiments described later, the variation of these mobilities with concentration is small (6) and is unlikely to be sufficiently large to appreciably affect the position of the

Can. J. Chem. Downloaded from www.nrcresearchpress.com by 186.148.149.217 on 09/04/12
For personal use only.

conductivity minimum. The ratio $\mu = \lambda_+/\lambda_-$ is, at least approximately, independent of concentration and has the value 1.45 (4). Hence we may write

$$\kappa = 10^{-3}\,\lambda_-(m_+\mu + K_{ap}/m_+). \qquad [15]$$

Since μ is constant and assuming that λ_- is also constant we have

$$\frac{\partial \kappa}{\partial m_+} = 10^{-3}\rho\lambda_-(\mu - K_{ap}/m_+^{\,2}) \qquad [16]$$

At the composition of minimum conductivity $\partial\kappa/\partial m_+ = 0$ and therefore

$$\mu - K_{ap}/(m_+)^2_{min} = 0,$$

or

$$(m_+)_{min} = \sqrt{K_{ap}/\mu}, \qquad (m_-)_{min} = \sqrt{K_{ap}\mu}. \qquad [17]$$

Substituting the values of K_{ap} given in Table I and $\mu = 1.45$ we find

$$(m_+)_{min} = 0.0132 \text{ at } 25° \quad \text{and} \quad 0.0108 \text{ at } 10°$$

$$(m_-)_{min} = 0.0182 \text{ at } 25° \quad \text{and} \quad 0.0157 \text{ at } 10°$$

Base–HA *Reactions*

Using the relation

$$[HS_2O_7^-] = \left(\frac{K_{id}\cdot K_{H_2S_2O_7}}{[H_3SO_4^+] + K_{H_2S_2O_7}}\right)^{1/2} \qquad [18]$$

which can be derived from equations [1] to [3] we obtain

$$[HS_2O_7^-]_{min} = 0.0045 \text{ at } 25° \text{ and } 0.0041 \text{ at } 10°$$

and from equation [2]

$$[H_3O^+]_{min} = 0.0088 \text{ at } 25° \text{ and } 0.0075 \text{ at } 10°.$$

Since

$$[BH^+] = m_b/(1 + [HSO_4^-]/K_b)$$

where m_b is the molality of added base B

and

$$[A^-] = m^i_a/(1 + [H_3SO_4^+]/K_a)$$

where m^i_a is the initial molality of the acid HA and if we write

$$y = [BH^+] - [A^-] = [HSO_4^-] + [HS_2O_7^-] - [H_3SO_4^+] - [H_3O^+]$$

we have

$$r_{min} = (m_b)_{min}/m^i_a = (1 + [HSO_4^-]_{min}/K_b)\{(1 + [H_3SO_4^+]_{min}/K_a)^{-1} + y/a\} \qquad [19]$$

where $a = m^i_a$.

Substituting the values given above for 25° we have

$$r_{min} = (1 + 0.018/K_b)\,\{(1 + 0.013/K_a)^{-1} + 0.0007/a\}. \qquad [20]$$

Values of r_{min} for various values of K_a and K_b are given in Table II for $a = 0.1m$.

Can. J. Chem. Downloaded from www.nrcresearchpress.com by 186.148.149.217 on 09/04/12
For personal use only.

TABLE II

Calculated values of r_{min} ("end points") for acid–base reactions

		Strong acid ($K_a = \infty$)			
K_b	∞	1.0	10^{-1}	10^{-2}	10^{-3}
r_{min}	1.01	1.02	1.19	2.82	19.1
		Strong base ($K_b = \infty$)			
K_a	∞	1.0	10^{-1}	10^{-2}	10^{-3}
r_{min}	1.01	0.98	0.89	0.44	0.08
		Disulphuric acid			
K_b	∞	1.0	10^{-1}	10^{-2}	10^{-3}
r_{min}	0.56	0.57	0.66	1.58	11.3
		Water			
K_a	∞	1.0	0.3	10^{-1}	10^{-2}
r_{min}	1.00	1.00	1.00	0.93	0.42

Base–$H_2S_2O_7$ Reactions

For reactions of $H_2S_2O_7$, $[HS_2O_7^-]_{min}$ can be calculated from the expression

$$[HS_2O_7^-] = \frac{a + \{a^2 + 4K_{id}(1 + [H_3SO_4^+]/K_{H_2S_2O_7})\}^{1/2}}{2(1 + [H_3SO_4^+]/K_{H_2S_2O_7})} \quad [21]$$

where $a = m^1_{H_2S_2O_7}$ and which can be derived from equations [2], [3], and [10]. Then $[H_3O^+]_{min}$ can be obtained from equation [2] and $[BH^+]_{min}$ from equation [9]. For $a = 0.1$, for example, we thus obtain

$$[H_3O^+]_{min} = 0.0008, \quad [HS_2O_7^-]_{min} = 0.0519, \quad \text{and } [BH^+]_{min} = 0.0561.$$

Now we have

$$r_{min} = \frac{[BH^+]_{min}}{a}\{1 + [HSO_4^-]_{min}/K_b\}. \quad [22]$$

Hence for $a = 0.1$ at 25°

$$r_{min} = 0.56\ (1+0.018/K_b). \quad [23]$$

Table II gives values of r_{min} for various illustrative values of K_b.

H_2O–*Acid Reactions*

For reactions of H_2O and an acid HA, $[H_3O^+]_{min}$ can be calculated from the expression

$$[H_3O^+]_{min} = [([A^-] + 0.0050) + \{([A^-] + 0.0050)^2 + 4K_{id}\}^{\frac{1}{2}}]/2, \quad [24]$$

which can be derived from equations [2] and [11] and the values of $[H_3SO_4^+]_{min}$ and $[HSO_4^-]_{min}$ given above, and where

$$[A^-] = a \Big/ \left(\frac{[H_3SO_4^+]_{min}}{K_a} + 1\right). \quad [25]$$

Then $[HS_2O_7^-]_{min}$ can be obtained from equation [2], $[H_2S_2O_7]$ from equation [3], and $m^s_{H_2O}$ from equation [12]. Thus, for example, for $HB(HSO_4)_4$ ($K_a = 0.3$) and $a = 0.1$ we have $[H_3O^+]_{min} = 0.1012$ and $[HSO_7^-]_{min} = [H_2S_2O_7]_{min} = 0.0004$. Hence $(m^s_{H_2O})_{min} = 0.1004$ and $r_{min} = (m^s_{H_2O})_{min}/a = 1.004$. Values of r_{min} for various values of K_a are given in Table II.

Can. J. Chem. Downloaded from www.nrcresearchpress.com by 186.148.149.217 on 09/04/12
For personal use only.

The conductivity minimum in the special case of the H_2O–$H_2S_2O_7$ reaction has been discussed in detail in an earlier paper (4).

RESULTS

$H_2S_2O_7$ – *Strong Base Reactions*

The variation in the conductivity during the reactions of the strong bases $KHSO_4$ and benzoic acid with disulphuric acid solutions of various concentrations is shown in Fig. 3.

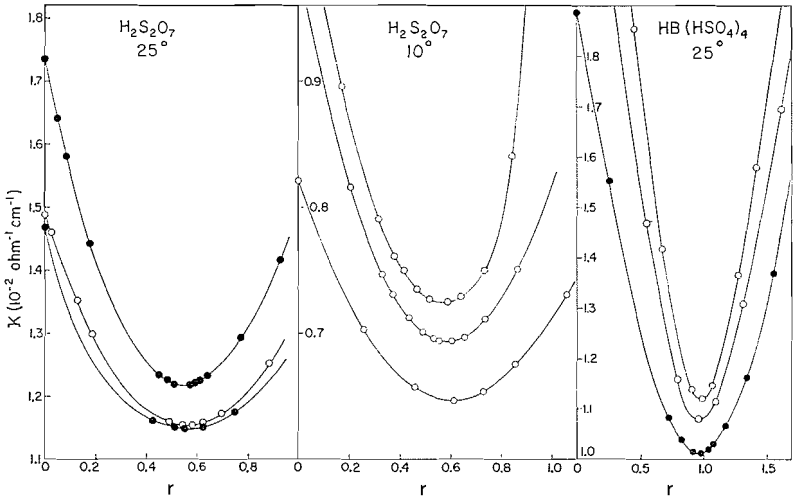


FIG. 3. Conductimetric titrations of strong bases with the acids $H_2S_2O_7$ and $HB(HSO_4)_4$. ○ $KHSO_4$, ● benzoic acid.

These experiments may be regarded as conductimetric acid–base "titrations" although the purpose of these titrations is not, as is usual, to estimate the concentration of either the solution of the acid or the base but rather to determine the dissociation constant of the acid or the base. In the present case the strengths of both the acid and the base are known so we may test the theory given above by comparing the predicted value of the "end point", i.e. the position of minimum conductivity, r_{min}, calculated from equation [23] with the observed value as is done in Table III. The agreement between observed and calculated values is excellent at 25° and good at 10°. The somewhat poorer agreement at 10° is probably due to the relatively greater contribution of the normally conducting ions to the conductivity at this temperature. This good agreement between the calculated and observed positions of the end point, r_{min}, provides support for the approximations made in the above theory and enables the equations to be used with confidence for the estimation of the strengths of weak acids and bases.

$HB(HSO_4)_4$ – *Strong Base Reactions*

The variation in the conductivity during the reactions of the strong bases $KHSO_4$ and benzoic acid with solutions of $HB(HSO_4)_4$ of various concentrations is shown in Fig. 3. The observed "end points", i.e. values of r_{min}, are given in Table III together with values for K_a calculated by means of equation [20]. The mean value, $K_a = 0.3$, is in good agreement with the value obtained from the conductivities of $HB(HSO_4)_4$ solutions (7) and

Can. J. Chem. Downloaded from www.nrcresearchpress.com by 186.148.149.217 on 09/04/12
For personal use only.

TABLE III

Disulphuric acid – strong base reactions					$HB(HSO_4)_4$ – weak base reactions (25° C)			
Base	a	r_{min}^{obs}	r_{min}^{calc}	T	Base	a	r_{min}	K_b
Benzoic acid	0.095	0.56	0.56	25°	*p*-Nitrotoluene	0.107	1.15	0.095
$KHSO_4$	0.099	0.56	0.56	25°	*o*-Nitrotoluene	0.050	1.22	0.071
Benzoic acid	0.154	0.55	0.55	25°	*m*-Nitrotoluene	0.118	2.00	0.017
$KHSO_4$	0.060	0.61	0.63	10°	*m*-Nitrotoluene	0.225	2.00	0.017
$KHSO_4$	0.112	0.59	0.61	10°	Nitrobenzene	0.116	2.90	0.009
$KHSO_4$	0.148	0.58	0.60	10°				
$HB(HSO_4)_4$ – strong base reactions (25° C)					$H_2S_2O_7$ – weak base reactions (25° C)			
Base	a	r_{min}	K_a		Base	a	r_{min}	K_a
Benzoic acid	0.079	0.97	0.3		*m*-Nitrotoluene	0.102	0.94	0.023
$KHSO_4$	0.114	0.97	0.3			0.153	0.94	0.023
$KHSO_4$	0.143	0.97	0.4		Nitrobenzene	0.102	1.20	0.014
						0.151	1.20	0.014

TABLE IV

Dissociation constants (K_b) of weak bases obtained by different methods

Base	Titration		Conductivity, ref. 9	Cryoscopy, ref. 10	Spectroscopy	
	$H_2S_2O_7$	$HB(HSO_4)_4$			Ref. 7	Ref. 11
p-Nitrotoluene	—	0.095	0.095	0.094	0.100	0.077
o-Nitrotoluene	—	0.071	0.067	0.062	—	—
m-Nitrotoluene	0.023	0.017	0.023	0.020	0.019	0.024
Nitrobenzene	0.013	0.009	0.010	0.011	0.010	0.009

shows that $HB(HSO_4)_4$ is a moderately strong acid but is not completely ionized as had been concluded previously (5) from freezing point and conductivity measurements on solutions of boric acid in sulphuric acid which contain the electrolyte $H_3O.B(HSO_4)_4$. However, the degree of solvolysis of this electrolyte implied by $K_a = 0.3$ is too small to have been detected in these measurements.

$HB(HSO_4)_4$, $H_2S_2O_7$ – *Weak Base Reactions*

Acid – weak base reactions were studied using the acids $H_2S_2O_7$ and $HB(HSO_4)_4$ and the weak bases *o*-, *m*-, and *p*-nitrotoluenes and nitrobenzene. Of these four bases only *m*-nitrotoluene and nitrobenzene could be successfully titrated with $H_2S_2O_7$ as the other two sulphonated at an appreciable rate. All four bases were quite stable in $HB(HSO_4)_4$ solutions. This would, incidentally, seem to confirm the suggestion (8) that sulphur trioxide which is present in appreciable concentration in $H_2S_2O_7$, but not in $HB(HSO_4)_4$ solutions, is the sulphonating agent rather than $H_3SO_4^+$, which is present in both solutions in appreciable concentration. The results of some of the conductivity measurements are shown in Fig. 4 and the observed end points, i.e. values of r_{min}, are given in Table III together with the values of K_b calculated by means of equations [20] and [22]. These values of K_b are in good agreement with those obtained by other methods, which are given in Table IV for comparison. This agreement confirms the reliability of this "conductimetric titration" method of determining the strengths of weak bases in the sulphuric acid solvent system.

Can. J. Chem. Downloaded from www.nrcresearchpress.com by 186.148.149.217 on 09/04/12
For personal use only.

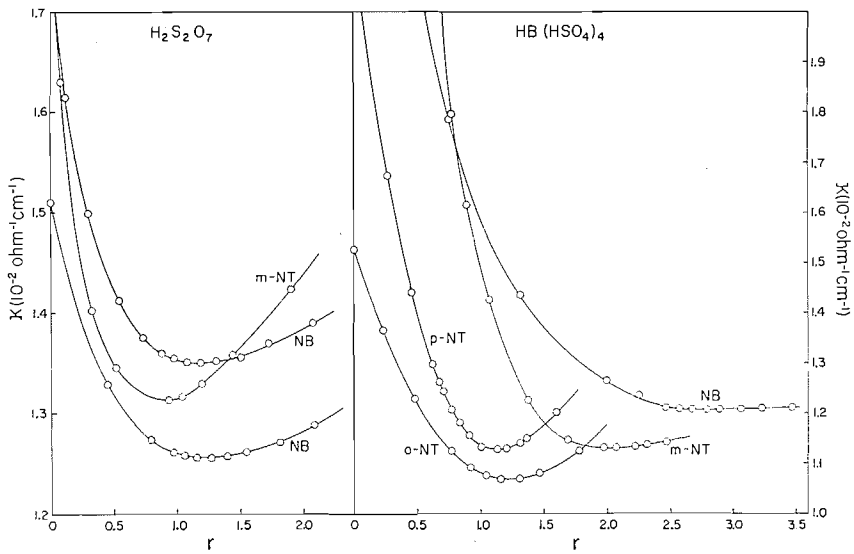


FIG. 4. Conductimetric titrations of weak bases with the acids $H_2S_2O_7$ and $HB(HSO_4)_4$. NB, nitrobenzene; *o*-NT, *o*-nitrotoluene; *m*-NT, *m*-nitrotoluene; *p*-NT, *p*-nitrotoluene.

EXPERIMENTAL

The apparatus and general procedure for making the electrical conductivity measurements have been described elsewhere (12).

Sulphuric acid was prepared as previously described (12) and the composition was adjusted until it had the conductivity corresponding to the composition 100% H_2SO_4 ($\kappa = 0.010439$ ohm^{-1} cm^{-1}) (12). Solutions of disulphuric acid were prepared by distilling sulphur trioxide from fuming sulphuric acid into "AnalaR" sulphuric acid. Solutions of $HB(HSO_4)_4$ were prepared by adding boric acid to an oleum, whose composition was known from its conductivity, in accordance with the stoichiometric equation

$$H_3BO_3 + 3H_2S_2O_7 = HB(HSO_4)_4 + 2H_2SO_4.$$

"AnalaR" grade potassium sulphate was dried at 120°. Benzoic acid, m.p. 121 to 122° C, was recrystallized from water and dried at 100°. *p*-Nitrotoluene, recrystallized from alcohol, had a melting point of 54°. Liquid solutes were dried and redistilled: nitrobenzene, b.p. 209°, $n_D^{25} = 1.550$; *o*-nitrotoluene, b.p. 218°, $n_D^{25} = 1.543$; *m*-nitrotoluene, b.p. 228°, $n_D^{25} = 1.544$.

REFERENCES

1. R. J. GILLESPIE and E. A. ROBINSON. Advances in Inorg. Chem. Radiochem. 1, 386 (1959).
2. R. J. GILLESPIE. Rev. Pure and Appl. Chem. **9**, 1 (1959).
3. S. J. BASS, R. J. GILLESPIE, and E. A. ROBINSON. J. Chem. Soc. 821 (1960).
4. R. J. GILLESPIE, E. A. ROBINSON, and C. SOLOMONS. J. Chem. Soc. In press. 1960.
5. R. H. FLOWERS, R. J. GILLESPIE, and J. V. OUBRIDGE. J. Chem. Soc. 1925 (1956).
6. R. H. FLOWERS, R. J. GILLESPIE, E. A. ROBINSON, and C. SOLOMONS. J. Chem. Soc. In press. 1960.
7. R. J. GILLESPIE and E. A. ROBINSON. Unpublished measurements.
8. C. K. INGOLD. Structure and mechanism in organic chemistry. Cornell University Press. 1953. p. 299.
9. R. J. GILLESPIE and C. SOLOMONS. J. Chem. Soc. 1796 (1957).
10. R. J. GILLESPIE and E. A. ROBINSON. J. Chem. Soc. 4233 (1957).
11. J. C. D. BRAND, W. C. HORNING, and M. B. THORNLEY. J. Chem. Soc. 1374 (1952).
12. R. J. GILLESPIE, J. V. OUBRIDGE, and C. SOLOMONS. J. Chem. Soc. 1804 (1957).

Can. J. Chem. Downloaded from www.nrcresearchpress.com by 186.148.149.217 on 09/04/12
For personal use only.

Can. J. Chem. Downloaded from www.nrcresearchpress.com by 186.148.149.217 on 09/04/12
For personal use only.

PROTON MAGNETIC RESONANCE SHIFTS FOR THE H_2O–SO_3 SYSTEM AND SOME ELECTROLYTE SOLUTIONS IN SULPHURIC ACID[1]

R. J. GILLESPIE[2] AND R. F. M. WHITE

ABSTRACT

Proton magnetic resonance shifts have been measured for the H_2O–SO_3 system. The results have been used to calculate the degree of ionization of water in solutions containing excess sulphuric acid. The shifts produced by a number of electrolytes in sulphuric acid have also been measured. The results are interpreted in terms of solute–solvent interactions, particularly polarization and hydrogen bonding, and are compared with the results of similar previous measurements on aqueous solutions.

INTRODUCTION

There have been two previous studies of the shift of the proton nuclear magnetic resonance in the H_2O–SO_3 system (1, 2). The present measurements on this system were undertaken as a preliminary to a more general study of the effects of both electrolytes and non-electrolytes on the proton resonance of sulphuric acid. Some differences were found between our results for the H_2O–SO_3 system and those of the earlier workers and so these results are given and discussed in some detail.

It has been found that electrolytes cause appreciable shifts in the proton resonance of water and this has been attributed to polarization and structure-breaking effects (3). Both cations and anions polarize water in such a manner that the electron density in the region of the protons is reduced and therefore resonance occurs at lower applied fields. The solvation of ions in general causes some structure-breaking in the solvent since the orientation of solvent molecules around ions is in general not the same as that in the bulk solvent and consequently a number of hydrogen bonds between the molecules in the solvation layer and those in the bulk of the solvent are broken. It has been established that generally the result of breaking hydrogen bonds is to shield the proton more effectively from the external field, thus shifting the resonance to higher applied fields (4). As ion–solvent interaction in sulphuric acid has been fairly extensively studied (5) it was of interest to see if proton shifts in sulphuric acid could be interpreted in a similar manner.

EXPERIMENTAL

The proton resonance shifts relative to pure water, $\delta = 10^6(H - H_{H_2O})/H_{H_2O}$, were measured with a Varian V4300B high-resolution spectrometer, operating at 40 Mc. Spectra were calibrated by the side-band technique using a Muirhead–Wigan L. F. Decade Oscillator. In preliminary experiments samples were sealed in 3-mm O. D. pyrex tubes, which were inserted into 5-mm O. D. tubes (2). The narrow annular space between the tubes contained distilled water which provided the reference signal. The results obtained using this type of sample tube showed a small scatter, probably due to tube imperfections. In order to reduce these effects the measurements were repeated using a different type of sample container. A small ground glass cone and socket joint was sealed to the end of a 5-mm O. D. sample tube. A reference capillary of water was sealed to the cone so that when it was inserted in the socket the capillary was centrally located in the sample tube. Scratch marks on the sample and reference tube ensured that they could

[1]*Manuscript received April 25, 1960.*
Contribution from the Department of Chemistry, University College, London, England.
[2]*Present address: Department of Chemistry, McMaster University, Hamilton, Ontario.*

always be put together in the same relative orientation. Although this technique does not completely eliminate effects due to tube imperfections any such effects will be almost constant in magnitude for all samples. Only results obtained using the second type of sample tube are reported; the results obtained from the first experiments agree with the reported results except for a somewhat greater scatter.

The diamagnetic susceptibilities of the solutions were measured by means of a Gouy balance (6). The apparatus available was designed for measurements on paramagnetic solids, and when used for diamagnetic solutions the accuracy obtainable was not better than 1%, mainly due to the small size of the sample. The measured susceptibilities and values calculated from Pascal's constants and the Wiedmann mixture law (6) indicate that the susceptibility correction (7)

$$g = (2\pi/3)\,(-0.721\times10^{-6}-\chi)\times10^{6},$$

where χ is the volume susceptibility of the solution, is almost negligible. As we give a largely qualitative interpretation of the observed shifts, susceptibility corrections have not in general been made except where stated. Sulphuric acid was prepared as previously described (8). Solutions containing small amounts of excess SO_3 or H_2O were analyzed by direct determination of their electrical conductivities (8) while those containing larger amounts of SO_3 or H_2O were analyzed by adding a known weight of the solution to a weighed amount of acid of known conductivity and measuring the change in conductivity.

RESULTS AND DISCUSSION

The Water – Sulphur Trioxide System

The results of our measurements on the H_2O–SO_3 system are given in Table I and Fig. 1.

TABLE I

Proton chemical shifts in the H_2O–SO_3 system

Solutions of composition between H_2O and H_2SO_4				Solutions of composition between H_2SO_4 and SO_3	
Mole fraction H_2O	δ (p.p.m.)	Mole fraction H_2O	δ (p.p.m.)	Mole fraction SO_3	δ (p.p.m.)
1.00	0.00	0.164	−6.39	0.0076	−5.95
0.913	−2.10	0.151	−6.36	0.013	−5.95
0.840	−3.40	0.149	−6.36	0.015	−5.95
0.685	−5.24	0.141	−6.34	0.022	−5.97
0.626	−5.78	0.091	−6.25	0.134	−5.98
0.510	−6.38	0.071	−6.19	0.207	−5.97
0.358	−6.57	0.045	−6.12	0.298	−5.96
0.323	−6.57	0.028	−6.03	0.411	−5.87
0.236	−6.48	0.015	−5.97	0.481	−5.79
0.197	−6.42	0.014	−5.98	0.509	−5.73
0.193	−6.43	0.006	−5.95	0.578	−5.62
		0.000	−5.95	0.723	−5.38

They agree well with Hood and Reilly's uncorrected results (2) up to about $x_{H_2SO_4} = 0.7$ but deviate from theirs at higher sulphuric acid concentrations. Although Gutowsky and Saika (1) only gave their results in graphical form they also appear to agree quite well with ours except at the highest sulphuric acid concentrations. Thus Hood and Reilly give $\delta_{H_2SO_4}$ (corrected) = −6.15 and $\delta_{H_2SO_4}$ (uncorrected) = −6.40, Gutowsky and Saika give $\delta_{H_2SO_4}$ (uncorrected) = −6.1, while we find $\delta_{H_2SO_4}$ (corrected) = −5.90 and $\delta_{H_2SO_4}$ (uncorrected) = −5.95. The earlier workers used reagent grade sulphuric acid for the

Can. J. Chem. Downloaded from www.nrcresearchpress.com by 186.148.149.217 on 09/04/12
For personal use only.

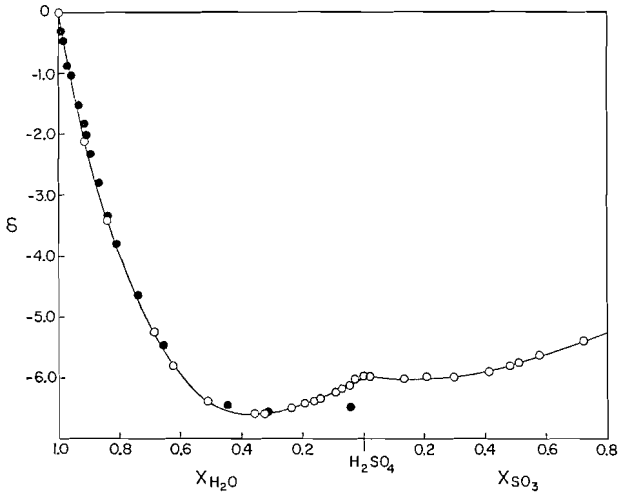


FIG. 1. Proton chemical shifts in the H_2O-SO_3 system.
○ This work; ● Hood and Reilly (2).

preparation of their solutions and determined their compositions by chemical analysis, while we have determined the composition of all our solutions by accurate conductivity measurements. It is likely that the differences in the uncorrected values of $\delta_{H_2SO_4}$ are merely a reflection of the fact that the composition of the more concentrated sulphuric acid solutions used by the earlier workers was not known with sufficient accuracy. Measurements for only two concentrations of oleum have been reported previously (1) and the same shift as for sulphuric acid was found in both cases. Our measurements on oleum solutions extend and essentially confirm these observations, showing that there is actually a very slight decrease in the shift in dilute oleum followed by a very flat minimum and a slight increase as the SO_3 concentration is increased up to and beyond the composition $H_2S_2O_7$.

Detailed analysis of the results is difficult because of the number of different species present in these solutions. We consider only the shifts in the region $x_{H_2SO_4} = 0.5$ to 1.0. Addition of water to sulphuric acid causes a shift in the proton resonance, which varies linearly with mole fraction up to approximately $x_{H_2SO_4} = 0.9$ (Figs. 1 and 3).

If we assume that the reaction that occurs when water is added to sulphuric acid can be represented simply by the equation

$$H_2O + H_2SO_4 = H_3O^+.HSO_4^-$$

then if x is the stoichiometric mole fraction of the water and α is the degree of ionization of the water the mole fractions of the species actually present in the solution are

$$N_{H_2O} = \frac{(1-\alpha)x}{1-\alpha x}, \qquad N_{H_2SO_4} = \frac{1-(1+\alpha)x}{1-\alpha x}, \qquad N_{H_3O.HSO_4} = \frac{\alpha x}{1-\alpha x}.$$

The corresponding proton fractions (i.e. the fractions of the total number of protons that are associated with any one species) are

$$p_{H_2O} = (1-\alpha)x, \qquad p_{H_2SO_4} = 1-(1+\alpha)x, \qquad p_{H_3O.HSO_4} = 2\alpha x.$$

Consequently the observed shift is given by

$$\delta = \delta_{H_2SO_4} - (1+\alpha)x\,\delta_{H_2SO_4} + 2\alpha x\,\delta_{H_3O.HSO_4}.$$

Can. J. Chem. Downloaded from www.nrcresearchpress.com by 186.148.149.217 on 09/04/12
For personal use only.

If the ionization of water is complete and $\alpha = 1$ then

$$\delta = \delta_{H_2SO_4} - 2x(\delta_{H_3O.HSO_4} - \delta_{H_2SO_4})$$

and we see that δ is a linear function of the mole fraction x. Experimentally this is found to be the case from $x = 0$ up to approximately $x = 0.10$. This indicates therefore that water is fully ionized over this range and by extrapolating this linear portion of the plot of δ against x to $x = 0.5$ we find $\delta_{H_3O.HSO_4} = -7.4$. At concentrations of water greater than $x = 0.10$ the curvature of the plot indicates that water is incompletely ionized. The degree of ionization α is given by

$$\alpha = \frac{\delta - \delta_{H_2SO_4}(1-x)}{x(2\delta_{H_3O.HSO_4} - \delta_{H_2SO_4})}.$$

Values of α obtained in this way are given in Table II and in Fig. 2 they are compared

TABLE II

Degree of ionization of water in H_2SO_4

Mole fraction H_2O	δ	α
0.5	−6.40	0.77
0.4	−6.56	0.84
0.3	−6.55	0.89
0.2	−6.46	0.96
0.1	−6.27	1.00

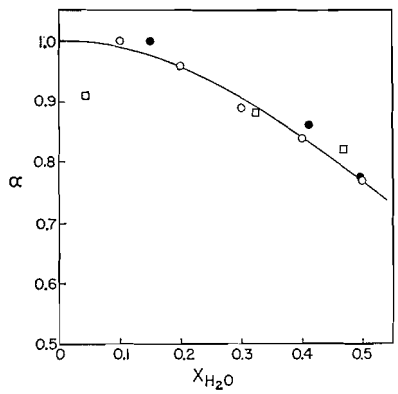


FIG. 2. Degree of ionization of water in sulphuric acid. ○ This work; ● Young, Maranville, and Smith (9); □ Hood and Reilly (2).

with values calculated from Hood and Reilly's results (1) and with values calculated from the Raman spectral data of Young *et al.* (9). In view of the assumptions involved in both methods the agreement between our results and those of Young *et al.* seems reasonable. The agreement with Hood and Reilly's results is also satisfactory, except at their lowest water concentration.

It is difficult to separate $\delta_{H_3O.HSO_4}$ into individual values for H_3O^+ and HSO_4^- on the basis of the results for the H_2O–SO_3 system alone. Hood and Reilly attempted to do this in the following way; they obtained expressions for two quantities symbolized as s_4 and

Can. J. Chem. Downloaded from www.nrcresearchpress.com by 186.148.149.217 on 09/04/12
For personal use only.

s_5, which are functions of the shifts $\delta_{H_3O.HSO_4}$ and $\delta_{H_2SO_4}$. The quantity s_4 was determined from the measured shifts in the region $x = 0$ to 0.2 while s_5 was estimated from the measured shifts in the region $x = 0.5$ to 1.0 using the second dissociation constant of sulphuric acid obtained from e.m.f. and conductivity data and the Raman spectral measurements of Young *et al.* (9) for this region. From these values of s_4 and s_5 they obtained $\delta_{H_3O^+} = -13.1$ and hence from their results it may be calculated that $\delta_{HSO_4^-} = 10.8$. Their calculations assume that the chemical shifts of the various species in the solution are independent of the composition of the solution over the whole range from water to sulphuric acid. We believe that this assumption is not justified. Considerable difficulties arise in interpreting the shifts of metal hydrogen sulphate solutions if the value $\delta_{HSO_4^-} = 10.8$ is accepted; as is shown in the following section, a negative value is more probable. Our calculations assume that the shifts produced by H_3O^+ and HSO_4^- are constant over the composition range $x = 0$ to 0.5, which is somewhat better than Hood and Reilly's assumption but is still only an approximation.

Metal Hydrogen Sulphate Solutions

The results of the measurements of the shifts produced by a number of metal hydrogen sulphates in sulphuric acid are given in Table III and Fig. 3. If x is the stoichiometric mole fraction of the metal hydrogen sulphate the proton fraction for a univalent metal hydrogen sulphate is $p_{MHSO_4} = x/(2-x)$ and for a divalent metal hydrogen sulphate it is

TABLE III

Proton chemical shifts of hydrogen sulphates in sulphuric acid

$H_3O.HSO_4$			$NaHSO_4$			$KHSO_4$		
x	p	δ	x	p	δ	x	p	δ
0.006	0.012	−5.95	0.0388	0.0198	−5.98	0.0505	0.026	−6.04
0.014	0.028	−5.98	0.1211	0.0645	−6.18	0.1128	0.0598	−6.22
0.015	0.030	−5.97	0.1740	0.0951	−6.31	0.1661	0.0907	−6.41
0.028	0.056	−6.03	0.2026	0.1125	−6.39	0.2464	0.1405	−6.67
0.045	0.090	−6.12						
0.071	0.142	−6.19						
0.091	0.182	−6.25						

$TlHSO_4$			NH_4HSO_4			
x	p	δ	x	p	δ (H_2SO_4 protons)	δ (NH_4^+ protons)
0.01644	0.00828	−6.04	0.0410	0.0209	−6.02	—
0.06309	0.0325	−6.21	0.1084	0.0573	−6.21	−1.13
0.08498	0.0444	−6.34	0.1232	0.0655	−6.25	−1.14
0.1440	0.0775	−6.57	0.1413	0.0760	−6.31	−1.15
			0.2331	0.1317	−6.62	−1.23
			0.2986	0.1758	−6.82	−1.28

$Ba(HSO_4)_2$		Acetone $(CH_3)_2COH.HSO_4$		
$x = p$	δ	$x = p$	δ (H_2SO_4 protons)	δ (CH_3 protons)
0.0134	−6.01	0.1753	−6.79	1.86
0.0239	−6.09	0.2439	−7.21	1.91
0.0314	−6.14	0.2616	−7.25	2.00
0.0386	−6.20			
0.0509	−6.34			

Can. J. Chem. Downloaded from www.nrcresearchpress.com by 186.148.149.217 on 09/04/12
For personal use only.

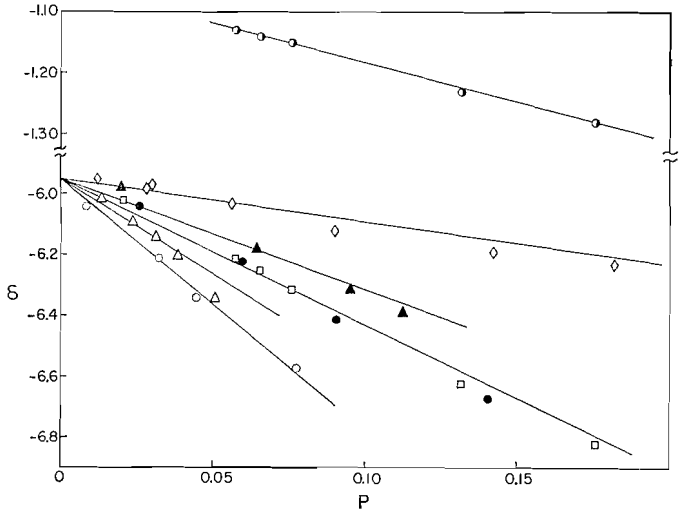


FIG. 3. Proton chemical shifts for hydrogen sulphates in sulphuric acid.
◑ HN_4; ◇ $H_3O.HSO_4$; ▲ $NaHSO_4$; ● $KHSO_4$;
□ $NH_4.HSO_4$; △ $Ba(HSO_4)_2$; ○ $TlHSO_4$.

$p_{M(HSO_4)_2} = x$. The proton shift would be expected to be the same linear function of the proton fraction p for all metal hydrogen sulphates:

$$\delta = \delta_{H_2SO_4} + p(\delta_{HSO_4^-} - \delta_{H_2SO_4}).$$

Figure 3 shows that the various metal hydrogen sulphates give linear, but nevertheless different, plots. It must be concluded that the metal ion also causes a shift in the proton resonance of the solvent in addition to that produced by the hydrogen sulphate ion. It has been found that electrolytes, even if they do not themselves contain any protons, cause appreciable shifts in the proton resonance of water (3); this has been attributed to polarization of the solvent molecules and breaking-up of the hydrogen-bonded structure of the solvent by the ions of the electrolyte. It has been shown that in aqueous solutions the polarizing effect of a cation is smaller than that of an anion of comparable size (3). This difference arises from the fact that a water molecule is oriented by a cation so that its hydrogen atoms are screened from the polarizing field by the oxygen atom. This screening effect would be considerably greater in sulphuric acid solutions because of the greater size of the sulphuric acid molecule compared with a water molecule. In sulphuric acid solutions the polarization effect of cations is therefore likely to be relatively small and the effect of cations on the proton resonance can most probably be attributed mainly to their structure-breaking effect on the solvent. The greater the extent of solvation of an ion the greater will be the number of hydrogen bonds broken and the more the resonance will shift to higher fields. Other measurements (5) have shown the extent of solvation of cations in sulphuric acid to be in the order

$$Na > NH_4 \sim K > Tl$$

and this is indeed the order of the shift of the proton resonance to high field (compared with Tl) in solutions of their hydrogen sulphates. Although the barium ion is more highly solvated than any of the univalent metal ions we have mentioned, solutions of barium di(hydrogen sulphate) give a smaller shift to high field (compared with Tl)

Can. J. Chem. Downloaded from www.nrcresearchpress.com by 186.148.149.217 on 09/04/12
For personal use only.

Can. J. Chem. Downloaded from www.nrcresearchpress.com by 186.148.149.217 on 09/04/12
For personal use only.

than solutions of sodium hydrogen sulphate. This can be attributed to the fact that at a given value of p the concentration of barium ion is only half that of a univalent metal ion and also to the fact that the dipositive charge of the barium ion will give rise to a much larger polarization effect, which may cause a significant shift of the proton resonance to low field.

Since the extent of solvation of the thallium ion is probably very small (5) it is reasonable to assume that its effect on the proton resonance is also small. An approximate value for the hydrogen sulphate ion shift may therefore be obtained by assuming that the shift produced by the thallium ion is in fact zero and that the whole of the shift observed for $TlHSO_4$ is due to the HSO_4^- ion. Hence we find $\delta_{HSO_4^-} = -13.9$. The positive value for $\delta_{HSO_4^-}$ obtained from the equations used by Hood and Reilly seems much less likely since in order to account for the observed shifts of metal hydrogen sulphates it would be necessary to attribute large low-field shifts to all metal ions, which in turn would suggest that all such metal ions produce very large polarization effects and this is rather unlikely. Moreover, if polarization of the solvent were the most important effect of the cations in these solutions it would be expected that the smallest ions would produce the greatest effects and consequently the order of the shifts of the proton resonance by different cations would be the reverse of that observed.

The large shift to low field produced by HSO_4^- is of interest. The electron density around the proton in an isolated HSO_4^- ion must be greater than that around the two protons in a sulphuric acid molecule and such an isolated HSO_4^- ion would be expected to have a proton resonance at a higher field than H_2SO_4. The shift to low field that is observed must be due to strong interaction with the solvent. Although the charge on HSO_4^- is rather dispersed it may nevertheless polarize the OH bonds of nearby sulphuric acid molecules since the hydrogen atoms will be oriented towards the HSO_4^- ion. This will cause a shift in the proton resonance of the solution to low field. The sulphuric acid molecules surrounding an HSO_4^- ion will be bound to it by hydrogen bonds and since the ion fits easily into the structure of sulphuric acid it may well cause no over-all bond-breaking but might well cause some increase in the total extent of hydrogen bonding in the solution, which would also cause a shift in the proton resonance to low field.

The shift produced by $H_3O.HSO_4$ is smaller than that of the metal hydrogen sulphates investigated and this may be attributed to the shift of H_3O^+ being smaller than that of H_2SO_4. We have that

$$\delta_{H_3O.HSO_4} = \delta_{HSO_4^-}/4 + 3\delta_{H_3O^+}/4$$

and using the values $\delta_{HSO_4^-} = -13.9$ and $\delta_{H_3O.HSO_4} = -7.4$ we find $\delta_{H_3O^+} = -5.2$. These values differ very considerably from those deduced by Hood and Reilly and they are probably only significant in systems containing excess H_2SO_4. It seems probable that the shifts produced by ions such as H_3O^+ and HSO_4^- which can hydrogen bond with the solvent change appreciably with the composition of the solvent. In order to account for the shift in the proton resonance caused by the addition of KNO_3 to HNO_3, Happe and Whittaker (10) have postulated the existence of the definite solvated species $NO_3^-.2HNO_3$ and $NO_3^-.HNO_3$ each producing its own shift and the latter gradually replacing the former with increase in the concentration of KNO_3. Similarly in predominately aqueous solutions of sulphuric acid it is very probable that the H_3O^+ ion exists in a solvated form such as $H_3O^+(H_2O)_3$ and as the concentration of acid is increased this is replaced by less hydrated complexes such as $H_3O^+(H_2O)_2$ and $H_3O^+(H_2O)$ and in strongly acid media by species such as $(H_3O^+)(H_2SO_4)_2$ (5, 11). It seems likely that the relatively

strong hydrogen-bonding in these complexes will cause each of them to have their own characteristic proton shifts. Unfortunately, if this is the case it makes any detailed analysis of this aqueous portion of the H_2O–SO_3 system almost impossible at the present time.

TABLE IV
Proton chemical shifts in HX–MX systems

Reference	HX–MX	Concn.	δ (ref. HX)
This work	H_2SO_4–$KHSO_4$	$p = 0.1$	−0.50
Gutowsky and Saika (1)	H_2O–KOH	$p = 0.1$	−1.00
Happe and Whittaker(10)	HNO_3–KNO_3	$x = 0.1$	−1.28
Unpublished (12)	HSO_3F–KSO_3F	$x = 0.1$	−1.38

Table IV shows the shifts in the proton resonance produced in different systems of the type HX–MX. All the shifts are negative, that is towards low fields, and they are all of the same magnitude. It seems reasonable to conclude that in each case X^- dissolved in HX produces a shift in the proton resonance to low field for the same reasons as given above for the HSO_4^-–H_2SO_4 system. The shifts are smallest in the cases of H_2O and H_2SO_4, which is consistent with the fact that in addition to the effects of interaction between the anions and the solvent the anions OH^- and HSO_4^- have their own intrinsic shifts, which must be to high field thus causing the over-all shift to low field to be smaller than the shift due to the anion–solvent interactions alone.

The Ammonium Ion

The proton resonance of the ammonium ion was observed as a separate peak indicating that these protons do not undergo rapid exchange with those of the solvent. The peak is a triplet due to spin–spin coupling with the nitrogen nucleus and shifts were measured from the center of this triplet which occurs on the low-field side of water and shifts to lower fields with increasing concentration (Table III and Fig. 3). This shift with increasing concentration can be plausibly attributed to an increased strength of the hydrogen bonds between the ammonium ion and the solvent as a consequence of the increasing basicity of the solvent with increasing concentration of HSO_4^-.

Acetone

Acetone produces a shift in the sulphuric acid resonance towards low field which varies linearly with mole fraction and which is of comparable magnitude to that produced by the metal hydrogen sulphates (Table III). Acetone is fully ionized (13) according to the equation

$$(CH_3)_2CO + H_2SO_4 = (CH_3)_2COH^+ + HSO_4^-$$

and if x is the mole fraction of $(CH_3)_2COH.HSO_4$ and the proton fraction is p then $p = x$. No detailed interpretation is possible at present because we cannot separate the intrinsic shift of $(CH_3)_2COH^+$ from the effect of its interaction with the solvent.

It is interesting that there is an appreciable shift in the CH_3 proton resonance to high field with increasing concentration of acetone. This could be due to a direct interaction of the CH_3 protons with the solvent, i.e. hydrogen-bonding or polarization of the C—H bond electrons by the negatively charged oxygen atoms of neighboring sulphuric acid molecules. Both these effects would lead to a shift in the proton resonance to low field with increasing concentration of hydrogen sulphate ion produced by the ionization of

Can. J. Chem. Downloaded from www.nrcresearchpress.com by 186.148.149.217 on 09/04/12
For personal use only.

the acetone. The observed shift is, however, to high field; the direct interaction of the CH_3 group with the solvent must therefore be small and the observed shift must be attributed to an indirect effect of the interaction of some other part of the molecule with the solvent. The protonated carbonyl group will be hydrogen-bonded to the solvent to an extent that will increase with the concentration of hydrogen sulphate ion and the positive charge on the oxygen atom will diminish correspondingly. This positively charged oxygen atom will polarize the C—H bond electrons of the CH_3 group and this polarization will therefore diminish with increasing concentration of hydrogen sulphate ion produced by the ionization of the acetone causing a shift in the resonance of these protons to high field.

The Fluorosulphuric Acid – Sulphuric Acid System

If the stoichiometric mole fraction of fluorosulphuric acid is x the corresponding proton fraction is $p_{HSO_3F} = x/(2-x)$. A plot of the shift of the proton resonance (Table V) against p_{HSO_3F} is linear (Fig. 4) as would be expected if there were no ionization or other interaction between the fluorosulphuric acid and the sulphuric acid. It has been found that HSO_3F is very slightly ionized in H_2SO_4 (14) but no effect of this is seen in the proton shifts.

The Chlorosulphuric Acid – Sulphuric Acid System

The proton resonance is independent of the composition of the system (Fig. 4 and Table V) and is the same as that for sulphuric acid itself. Presumably there is no ionization nor any appreciable change in hydrogen-bond strengths.

TABLE V

Proton chemical shifts in acid – sulphuric acid systems

Electrolyte	x	p	δ
$HB(HSO_4)_4$	0.037	0.122	−6.11
	0.118	0.311	−6.47
	0.264	0.662	−6.84
	0.420	0.901	−7.09
$HFSO_3$	0.182	0.100	−5.88
	0.287	0.168	−5.86
	0.311	0.184	−5.86
	0.639	0.470	−5.65
	0.767	0.624	−5.54
	1.000	1.000	−5.24
$HClSO_3$	0.216	0.121	−5.95
	0.417	0.263	−5.95
	0.735	0.581	−5.95
	1.000	1.000	−5.95

The Tetra(hydrogensulphato) Boric Acid – Sulphuric Acid System

Tetra(hydrogensulphato) boric acid, $HB(HSO_4)_4$, has been shown to ionize in sulphuric acid solvent as a moderately strong acid (14, 15, 16).

$$HB(HSO_4)_4 + H_2SO_4 = H_3SO_4^+ + B(HSO_4)_4^-$$

If the stoichiometric mole fraction of $HB(HSO_4)_4$ is x then the mole fractions of the species actually present in solution are

$$N_{H_3SO_4.B(HSO_4)_4} = x/(1-x) \text{ and } N_{H_2SO_4} = (1-2x)/(1-x)$$

Can. J. Chem. Downloaded from www.nrcresearchpress.com by 186.148.149.217 on 09/04/12
For personal use only.

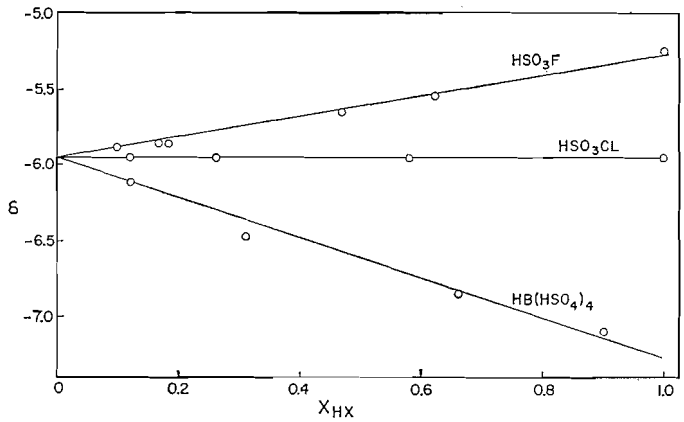


FIG. 4. Proton chemical shifts in HX – sulphuric acid systems.

and the corresponding proton fractions are

$$p_{H_3SO_4.B(HSO_4)_4} = 7x/(2+3x), \quad p_{H_2SO_4} = (2-4x)/(2+3x)$$

and the proton shift would be expected to be a linear function of $p_{H_3SO_4.B(HSO_4)_4}$:

$$\delta = \delta_{H_2SO_4} + p_{H_3SO_4.B(HSO_4)_4}\{\delta_{H_3SO_4.B(HSO_4)_4} - \delta_{H_2SO_4}\}.$$

The observed shift (Fig. 4 and Table V) is in fact a linear function of $p_{H_3SO_4.B(HSO_4)_4}$ and is smaller than that due to the metal hydrogen sulphates. There is not sufficient information on this system available at present to enable a detailed analysis of the observed shifts to be made.

REFERENCES

1. H. S. GUTOWSKY and A. SAIKA. J. Chem. Phys. **21**, 1688 (1953).
2. G. C. HOOD and C. A. REILLY. J. Chem. Phys. **27**, 1126 (1957).
3. J. N. SHOOLERY and B. J. ALDER. J. Chem. Phys. **23**, 805 (1955).
4. J. A. POPLE, W. G. SCHNEIDER, and H. J. BERNSTEIN. High resolution nuclear magnetic resonance. McGraw-Hill, New York. 1959. p. 400.
5. R. J. GILLESPIE. Rev. Pure and Appl. Chem. **9**, 1 (1959).
6. P. W. SELWOOD. Magnetochemistry. Interscience, New York. 1956.
7. J. A. POPLE, W. G. SCHNEIDER, and H. J. BERNSTEIN. High resolution nuclear magnetic resonance. McGraw-Hill, New York. 1959. p. 80.
8. R. J. GILLESPIE, J. V. OUBRIDGE, and C. SOLOMONS. J. Chem. Soc. 1804 (1957).
9. T. F. YOUNG, L. F. MARANVILLE, and H. M. SMITH. *In* The structure of electrolytic solutions. *Edited by* W. J. Hamer. Wiley, New York. 1959. p. 35.
10. J. A. HAPPE and A. G. WHITTAKER. J. Chem. Phys. **30**, 417 (1959).
11. R. P. BELL. The proton in chemistry. Cornell University Press. 1960. p. 83.
12. R. J. GILLESPIE and R. F. M. WHITE. Unpublished measurements.
13. R. J. GILLESPIE and J. A. LEISTEN. Quart. Revs. (London), **8**, 40 (1954).
14. R. J. GILLESPIE and E. A. ROBINSON. Advances in Inorg. Chem. and Radiochem. **1**, 385 (1959).
15. R. H. FLOWERS, R. J. GILLESPIE, and J. V. OUBRIDGE. J. Chem. Soc. 1925 (1956).
16. R. H. FLOWERS, R. J. GILLESPIE, and E. A. ROBINSON. Can. J. Chem. **38**, 1363 (1960).

Can. J. Chem. Downloaded from www.nrcresearchpress.com by 186.148.149.217 on 09/04/12
For personal use only.

Can. J. Chem. Downloaded from www.nrcresearchpress.com by 186.148.149.217 on 09/04/12
For personal use only.

THE PRESENCE OF MONOTHIOCARBONATE SUBSTITUENTS IN CELLULOSE XANTHATES[1]

D. A. ANDREWS,[2] F. G. HURTUBISE, AND H. KRÄSSIG

ABSTRACT

The presence of monothiocarbonate substituents in viscose has been demonstrated by the infrared spectra of the gases evolved during the acid hydrolysis of cellulose xanthate salts and viscose. A comparison of the results of various methods of sulphur determination and the results obtained by ultraviolet spectroscopy has been made. The results of investigations on sodium cellulose monothiocarbonate preparations support the concept of monothiocarbonate substitution.

INTRODUCTION

Sodium cellulose xanthate as normally prepared commercially from alkali cellulose and carbon disulphide is accompanied by numerous by-products. The composition of this mixture and of its solution in aqueous sodium hydroxide (viscose) changes as a result of complex hydrolytic and oxidative reactions. It is well established that the proportion of trithiocarbonate, the main by-product, increases as a result of the hydrolysis of sodium cellulose xanthate and that hydrolysis and oxidation of the trithiocarbonate lead to sulphide, perthiocarbonate, and thiosulphate (1, 2, 3, 4). The presence of other components, often suggested to account for the complex reactions, is less clearly established. Mono- and dithio-carbonate ions (5, 6) have been invoked as intermediate stages in the xanthation and side reactions, and cellulose monothiocarbonate ions can be postulated as a reaction product of monothiocarbonate ions and cellulose and as a hydrolysis product of sodium cellulose xanthate. Monothiocarbonates yield carbonyl sulphide on acid hydrolysis and the presence of this substance among the gaseous products of acidified viscose would provide substantial evidence for the existence of such derivatives.

RESULTS AND DISCUSSION

Infrared Spectra of Gases Evolved from Acidified Viscose

The presence of carbonyl sulphide in gaseous mixtures containing carbon disulphide, carbon dioxide, and hydrogen sulphide can be demonstrated by the infrared spectrum, and considerably less than 5% can be readily detected by the most sensitive band at 2030 cm^{-1} (Fig. 1).

The gaseous products of acidified viscose undoubtedly contained carbonyl sulphide (Fig. 2, Table I), and essentially the same relative proportion of carbonyl sulphide was obtained from impure viscose and from a solution of sodium cellulose xanthate purified from small anions by passage through an anion exchange column (7). This observation strongly suggests that much of the carbonyl sulphide was chemically linked to the cellulose, a conclusion supported by the observation that the viscose impurities formed from alkali and carbon disulphide gave a much smaller proportion of carbonyl sulphide than freshly prepared viscose. The relative proportion of carbonyl sulphide was smaller for a "ripened" viscose, an observation in agreement with the known fact that cellulose monothiocarbonate hydrolyzes more rapidly than cellulose xanthate (8).

These results are in agreement with those recently reported by Philipp (9), who

[1]*Manuscript received April 4, 1960.*
Contribution from the Basic Research Division of Industrial Cellulose Research Limited, Hawkesbury, Ontario.
[2]*Present address: Ciba Limited, Toms River, New Jersey.*

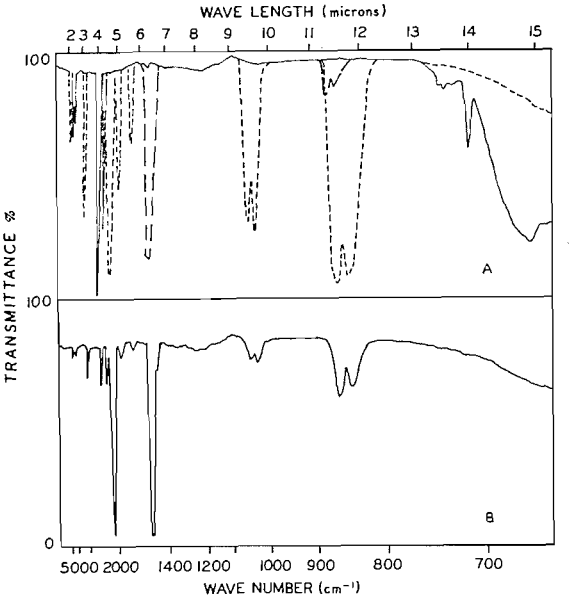


FIG. 1. Infrared spectra: (A) CO_2 ———, COS – – – –, CS_2 — — —; (B) mixture (76 ml), H_2S 88%, COS 4%, CS_2 8%.

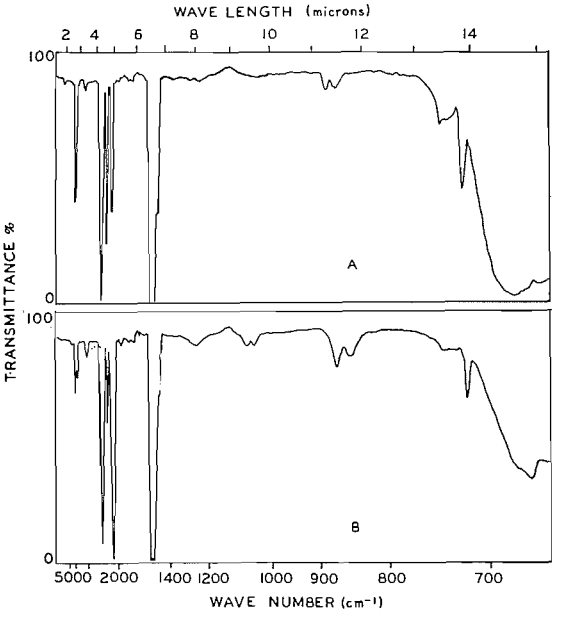


FIG. 2. Infrared spectra: gases from (A) purified "ripened" viscose (150 ml), (B) freshly prepared sodium cellulose xanthate (61 ml).

estimated the carbonyl sulphide evolved from viscose polarographically as ammonium monothiocarbamate. Very little reliance, however, can be placed on the quantitative data reported in this paper. Carbon disulphide, absorbed as ammonium dithiocarbamate, was found to seriously interfere in the polarographic estimations, and, under the conditions

Can. J. Chem. Downloaded from www.nrcresearchpress.com by 186.148.149.217 on 09/04/12
For personal use only.

TABLE I

Proportional band intensities of COS and CS_2 obtained on gases generated by hydrolysis

Hydrolysis gases from:	$\frac{(\log T_0/T \text{ (COS at 2030 cm}^{-1})}{(\log T_0/T \text{ (CS}_2 \text{ at 2179 cm}^{-1})}$
(1) Sodium cellulose xanthate	
(*a*) Freshly prepared	8.56
(*b*) Viscose (solution of (*a*) in 7% sodium hydroxide; 7% cellulose concentration)	3.23
(*c*) (*b*) Anion-exchanged concentrated	4.42
(*d*) (*b*) Anion-exchanged dilute	2.55
(*e*) After 2 days ripening at 8° C	0.78
(*f*) (*e*) Anion-exchanged concentrated	0.85
(*g*) (*e*) Anion-exchanged dilute	0.66
(2) Potassium cellulose xanthate Dissolved in 5% potassium hydroxide; approx. 7% cellulose concentration; anion-exchanged dilute	12.10
(3) NaOH + CS_2 (viscose by-products)	1.18

used to minimize its absorption, only a portion of the total carbonyl sulphide was absorbed. The necessary large corrections render the method inaccurate. In addition, cadmium acetate was used to remove hydrogen sulphide from gaseous mixtures, a reagent which we found to react to some extent with carbonyl sulphide. In contrast to our observation, Herrent and Inoff (10) concluded from indirect analytical methods of somewhat doubtful validity that the proportion of monothiocarbonate increased as viscose ripened.

A quantitative assessment of the proportion of carbonyl sulphide has not been attempted. The gaseous hydrolytic products of viscose could be completely freed from the precipitated cellulose only by prolonged boiling which, in presence of acid, is said to decompose carbonyl sulphide (9). Quantitative removal of the gases in a stream of nitrogen at room temperature and subsequent absorption in alcoholic potassium hydroxide or ammonia solutions was attempted, but a quantitative recovery of the carbonyl sulphide was not possible since these reagents gave by-products, sulphide and carbonate, in addition to monothiocarbonate and monothiocarbamate, respectively.

Comparison of Results of Various Sulphur Determination Methods

Xanthates in solution are commonly estimated by oxidation to sulphate and by iodometric titration (11). Both methods are said to be quantitative for sulphides and monothiocarbonates, but we have not been able to confirm a quantitative reaction, according to equation 1, of iodine and potassium ethyl monothiocarbonate.

$$2RO{-}COS^- + I_2 \rightarrow 2I^- + RO{-}CO{-}S{-}S{-}CO{-}OR \qquad [1]$$

The presence of these substances in mixtures with xanthate, however, should be revealed by application of both methods: the assumption that sulphur is present only as xanthate would lead to higher calculated amounts of sulphur from the iodine method. In many sets of careful analyses of a variety of commercially prepared viscose samples, of which two typical examples are given (Table II, (*a*) and (*b*)), the amounts of sulphur estimated iodometrically in samples purified by ion exchange were not systematically different from those estimated as sulphate. Purified samples of potassium cellulose xanthates, however,

Can. J. Chem. Downloaded from www.nrcresearchpress.com by 186.148.149.217 on 09/04/12
For personal use only.

TABLE II

Comparison of results of various sulphur determination methods on sodium and potassium cellulose xanthates

		Not ion-exchanged			Ion-exchanged				
					Concentrated	Dilute			
		% Sulphur				% Sulphur			
						Total by:		By hydrolysis	
No.	Ripening time (days)	Total (by $BaSO_4$)	As CS_3^{2-}	Salt index	% Sulphur total (by $BaSO_4$)	$BaSO_4$	Iodine	H_2S	CS_2
		(*a*) Commercial viscose (sodium cellulose xanthate dissolved in 6% NaOH)							
1	—	2.31	0.36	—	—	1.82	1.82	0.02	1.75
2	—	1.90	0.22	11.2	—	1.48	1.46	—	—
3	—	1.73	1.36	—	—	1.45	1.45	—	—
4	—	2.06	0.32	9.7	—	1.44	1.57	0.05	1.45
5	—	1.78	0.30	11.5	—	1.42	1.43	—	—
6	—	1.86	0.60	4.0	—	1.27	1.20	0.03	1.15
		(*b*) Commercial viscose (series ripened at 8° C)							
1	—	1.83	0.29	10.5	1.39	1.44	1.39	—	—
2	1	1.85	0.34	9.7	1.35	1.36	1.29	—	—
3	2	1.82	0.39	8.9	1.31	1.36	1.30	0.03	1.30
4	3	1.81	0.42	8.1	1.29	1.30	1.29	—	—
5	4	1.80	0.45	7.4	1.25	1.25	1.23	0.02	1.27
6	7	1.79	0.56	5.6	1.16	1.13	1.12	0.01	1.19
7	8	1.81	0.57	5.1	1.09	1.12	1.11	0.01	1.06
8	9	1.79	0.63	4.7	1.03	1.09	1.09	—	1.02
9	10	1.79	0.64	4.0	—	1.02	1.03	—	—
		(*c*) Potassium cellulose xanthate (dissolved in 5% KOH)							
1	—	2.20	0.90	—	—	1.34	3.51	—	—
2	—	4.13	—	—	—	2.13	2.84	—	—
3	—	5.05	3.25	—	—	1.98	2.33	—	—
4	—	6.04	3.53	—	—	2.71	3.09	—	—
5	—	5.13	2.31	—	—	2.90	3.40	—	—
6	—	7.38	4.17	—	—	2.97	3.04	—	—
7	—	6.27	4.93	—	—	1.73	2.75	—	—
8	—	6.44	3.46	—	—	2.67	2.88	—	—

NOTE: All analytical data given are mean values from triplicate determinations.

showed large differences (Table II (*c*)). These samples, of higher degree of substitution, gave a much larger proportion of carbonyl sulphide on hydrolysis (Table I), and it is evident that the proportion of monothiocarbonate in commercial viscose is not sufficiently large to produce significant differences in the two analytical methods.

Ultraviolet Spectra of Various Cellulose Xanthates

In solution, absorption bands are shown by sodium cellulose xanthate at 382 and 302 mμ and by potassium ethyl xanthate at 380 and 300 mμ (12, 13). The extinction coefficients (Table III) are similar and appear to increase slightly with concentration.

The mean values for the molecular extinction coefficients of potassium ethyl xanthate and sodium cellulose xanthate in the 300–302 mμ region are 19,130 and 16,710 liters $mole^{-1}$ cm^{-1} respectively. Since monothiocarbonate does not absorb at 300 mμ, the extinction coefficient at 300 mμ of 1 mole of pure xanthate is therefore 19,130. Assuming that the lower extinction coefficient of sodium cellulose xanthate is due to the presence of monothiocarbonate, then the ratio of monothiocarbonate to xanthate groups in sodium cellulose xanthate would be

$$(19{,}130 - 16{,}710)/19{,}130 = 0.127.$$

Can. J. Chem. Downloaded from www.nrcresearchpress.com by 186.148.149.217 on 09/04/12
For personal use only.

TABLE III

Extinction coefficients of potassium ethyl xanthate and sodium cellulose xanthate in aqueous NaOH (pH 11.3)

	380 mμ		382 mμ			300 mμ		302 mμ	
	Sample					Sample			
	Et—O—CS_2—K		Cell—O—CS_2—Na			Et—O—CS_2—K		Cell—O—CS_2—Na	
Slit width, mm	c, moles/l. $\times 10^3$	ϵ, l./mole	c, moles/l. $\times 10^3$	ϵ, l./mole	Slit width, mm	c, moles/l. $\times 10^5$	ϵ, l./mole $\times 10^{-4}$	c, moles/l. $\times 10^5$	ϵ, l./mole $\times 10^{-4}$
0.125	1.951	60.48	3.152	58.07	0.087	0.975	1.754	1.051	1.625
					0.145		1.764		1.694
0.026	3.902	58.94	5.253	56.36	0.310				1.713
0.032		58.13		56.73					
0.060		58.18		57.11	0.087	1.951	1.835	2.101	1.594
					0.145		1.871		1.613
0.025	7.804	56.13	6.303	57.91	0.310		1.896		1.623
0.032		56.38		57.91					
0.040		56.51		58.22	0.087	3.902	1.881	3.152	1.618
0.060		56.66		58.54	0.145		1.907		1.644
0.112		57.02		58.54	0.310		1.922		1.648
0.026	11.710	56.64	8.404	57.12	0.093	5.853	1.865	4.202	1.618
0.038		56.72		57.71	0.145		1.931		1.642
0.115		56.06		57.82	0.310		1.961		1.654
0.025	15.610	56.00	10.510	57.69	0.087	7.804	1.961	5.253	1.618
0.038		56.51		58.07	0.142		1.986		1.647
0.115		56.64		58.26	0.310		2.063		1.656
0.025	19.510	56.30	12.600	57.35	0.087			6.303	1.623
0.038		56.36		57.59	0.145	0.981	1.856		1.653
0.112		56.38		58.29	0.310				1.662
0.025			14.710	58.47	0.087			8.404	1.648
0.038				59.02	0.145	1.961	1.882		1.725
0.112				59.84	0.310				1.731
0.025			16.810	56.40	0.087			10.510	1.713
0.038				57.18	0.145	2.941	1.904		1.866
0.112				57.71	0.310				1.884
0.025			18.910	57.00	0.310	3.921	1.887		
0.038				58.17	0.310	5.888	1.917		
0.112				58.49	0.310	7.844	2.014		
0.025			21.010	58.21					
0.038				59.02					
0.112				59.49					

If this value is now applied to the comparison of the percentage of sulphur estimated iodometrically and as barium sulphate the percentage of sulphur values calculated from the iodometric results should be considerably larger than those actually found (Table II). It is therefore not possible to consider the ultraviolet spectral data as conclusive evidence for the presence of monothiocarbonate substituents in the sodium cellulose xanthates investigated.

A comparison of the molecular extinction coefficients of sodium and potassium cellulose xanthate (Table IV) shows an even larger difference (e.g. 16,710 vs. 11,860). The fact that the percentage of sulphur values of potassium cellulose xanthate preparations calculated as xanthate from the iodometric method are consistently larger than those obtained by the barium sulphate method as well as the observed presence of large amounts

Can. J. Chem. Downloaded from www.nrcresearchpress.com by 186.148.149.217 on 09/04/12
For personal use only.

TABLE IV
Extinction coefficients of sodium cellulose xanthates and potassium cellulose xanthates

λ = 302 mμ, sodium cellulose xanthates				λ = 303 mμ, potassium cellulose xanthate		
Sample No.*	*c*,† moles/l. ×10⁵	At pH 10 ε, l./mole ×10⁻⁴	At pH 6 ε, l./mole ×10⁻⁴	Sample No.‡	*c*,‡ moles/l. ×10⁵	At pH 10 ε, l./mole ×10⁻⁴
(*b*)/1	2.52	1.49	1.49	(*c*)/1	2.10	1.03
	3.50	1.52	1.49		4.19	1.01
	6.76	1.54	1.52		6.29	1.04
2	2.13	1.49	1.51	2	3.32	1.14
	4.25	1.53	1.52		6.64	1.15
	6.38	1.54	1.56		9.97	1.24
3	2.13	1.41	1.45	3	2.69	1.45
	4.26	1.46	1.51		6.17	1.17
	6.39	1.50	1.52		9.26	1.22
4	2.09	1.41	1.44	4	4.23	1.04
	4.17	1.44	1.46		8.47	1.06
	6.26	1.48	1.48		12.70	1.10
5	1.95	1.39	1.44	5	4.52	1.39
	3.90	1.48	1.48		9.02	1.49
	5.85	1.52	1.50		13.55	1.34
6	1.78	1.58	1.59	6	4.63	1.17
	3.56	1.59	1.60		9.26	1.18
	5.34	1.62	1.61		13.46	1.27
7	1.74	1.54	1.57	7	3.45	1.17
	3.48	1.60	1.60		5.17	1.16
	5.23	1.61	1.63		10.08	0.98
8	1.71	1.47	1.47	8	4.20	1.20
	3.42	1.51	1.54		8.37	1.23
	5.14	1.58	1.55		12.59	1.23
9	1.59	1.45	1.59			
	3.19	1.49	1.50			
	4.80	1.54	1.55			

*Samples are from the sodium cellulose xanthate series mentioned in Table I, Section (*b*).
†Determined from sulphur as $BaSO_4$ (mean values).
‡Samples are from the potassium cellulose xanthates mentioned in Table I, Section (*c*).

of carbonyl sulphide in the gases generated from the hydrolysis are indicative of the presence of monothiocarbonate substituents.

The formation of the colored by-products in purified cellulose xanthate solutions may readily be detected by a shoulder at 325 mμ; higher concentrations increase the extinction coefficient at 382 mμ and eventually produce a slight shift to longer wavelengths. These criteria are more sensitive than the detection of the trithiocarbonate absorption band at 500 mμ. The band at 382 mμ, but not that at 302 mμ, is immediately altered at a pH of between 4 and 6. The maximum is first shifted to 390 mμ and then the absorbance rapidly decreases. This observation supports previous statements (15) that the bands at 302 and 382 mμ are a result of the excitation of the C=S bond and the complete xanthate group, respectively.

Investigations on Sodium Cellulose Monothiocarbonate

Sodium cellulose monothiocarbonate was prepared at a low temperature from alkali cellulose and carbonyl sulphide, which had been carefully purified until carbon disulphide could not be detected spectroscopically. The freshly prepared white products were

Can. J. Chem. Downloaded from www.nrcresearchpress.com by 186.148.149.217 on 09/04/12
For personal use only.

partially soluble in sodium hydroxide solution (7%), but one experiment gave a completely soluble product. About two thirds of the sulphur present was not retained by an anion exchange resin (Table V), and some carbonyl sulphide was regenerated on acid hydrolysis.

TABLE V
Comparison of results of various sulphur determination methods on sodium cellulose monothiocarbonate

	Not ion-exchanged				Ion-exchanged			
		% Sulphur				% Sulphur		
			By hydrolysis					
Sample No.	% Cell.	Total (by $BaSO_4$)	H_2S	COS	% Cell.	Total (by $BaSO_4$)	By iodine as monothiocarbonate	D.S.
1	16.44	5.29	—	—	12.10	1.81	2.85	0.19*
2	25.58	2.78	1.54	0.67	25.10	1.99	3.25	0.10*
3	12.15	3.00	—	—	10.90	2.00	2.44	0.23*
4	10.56	2.24	—	—	15.32	2.41	3.15	0.20†

*White, from pure COS.
†Prepared from COS containing CS_2; green.

In contrast to the results obtained using sodium cellulose xanthate, the iodometrically derived sulphur values, assuming pure monothiocarbonate, are higher than those derived from barium sulphate estimations, indicating appreciable decomposition to sulphide under the conditions of the purification and estimation.

The cellulose monothiocarbonate solutions showed no spectroscopic absorption bands in the visible and ultraviolet regions at 385 and 302 mμ and cellulose xanthate was therefore absent. Only one preparation of cellulose monothiocarbonate, obtained from impure carbonyl sulphide, contained any xanthate as shown by its spectrum (cf. Fig. 3). Potassium ethyl monothiocarbonate, however, similarly prepared from carbonyl sulphide

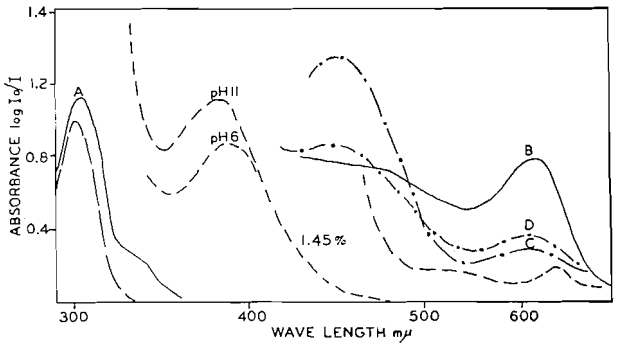


FIG. 3. Ultraviolet and visible absorption spectra of solutions of purified viscose (– – –); sodium cellulose monothiocarbonate (impure) (———): (A) in alkali, (B) acetone extract; aqueous sodium sulphide, carbon disulphide, and acetone (— · —): (C) 20 hours, (D) 26 hours.

(spectroscopically free of carbon disulphide) and potassium hydroxide in ethanol, was accompanied by detectable amounts of potassium ethyl xanthate.

In previous descriptions (14) of the reaction between alkali cellulose and carbonyl sulphide, it is stated that the product is not completely alkali soluble, but aside from some qualitative X-ray data, no analytical details are given. Philipp (8) describes the product

Can. J. Chem. Downloaded from www.nrcresearchpress.com by 186.148.149.217 on 09/04/12
For personal use only.

as a green solid. Our products were green only when the carbonyl sulphide contained carbon disulphide. Acetone produced a more intense green or blue color, which soon faded in air, and sulphur precipitated. Such behavior is reminiscent of the oxidation of hydrosulphides, said to produce disulphides responsible for the intense color (15). Similar colors are sometimes to be seen in the mother liquors from viscose precipitated with acetone, in reaction mixtures of sodium sulphide, carbon disulphide, and acetone, and in freshly prepared viscose samples as they emerge from a column of anion exchange resin. In all cases an absorption band at about 650 mμ was observed (Fig. 3).

Infrared Spectra of Solid Samples

The infrared spectra of impure and 96% pure potassium ethyl monothiocarbonate are shown in Figs. 4A and 4C. The spectrum of the fraction containing the impurities is shown in Fig. 4B. Monothiocarbonate is characterized by important absorption bands in

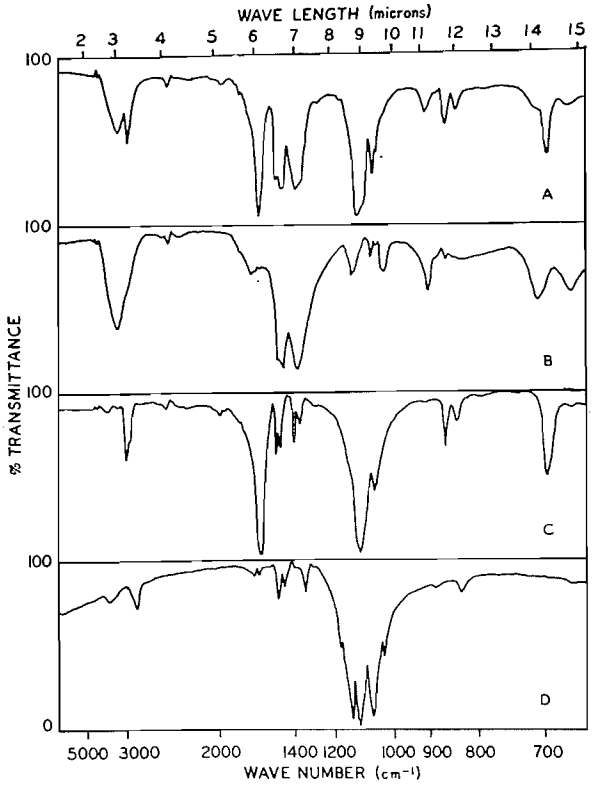


FIG. 4. Infrared spectra of potassium ethyl monothiocarbonate: (A) impure product, (B) insoluble fraction, (C) second recrystallization (96% pure). Infrared spectra of potassium ethyl xanthate (D).

the 1000–1200 cm^{-1} region, and at 1650 cm^{-1}. A less intense band occurs at 690 cm^{-1} and this is probably due to the C—S vibration. Comparison of the spectrum of potassium ethyl monothiocarbonate with that of potassium ethyl xanthate (Fig. 4D) shows that only the 1650 cm^{-1} band and to some extent the 690 cm^{-1} band can be used to detect monothiocarbonate groups in the presence of xanthate groups.

In the spectra of xanthates, intense absorption is always found in the 1060–1040 cm^{-1} region. At least two additional bands are usually found in the 1200–1100 cm^{-1} region. The

Can. J. Chem. Downloaded from www.nrcresearchpress.com by 186.148.149.217 on 09/04/12
For personal use only.

bands in the 1200–1000 cm^{-1} region are thought to be due to vibrations of the R—O—C part of the molecule.

The infrared absorption spectra of cellulose and alkali cellulose are shown in Figs. 5A and 5B. The nature of the bands in the cellulose spectrum have previously been discussed (16). The differences between the alkali cellulose spectrum and that of cellulose are mainly due to the presence of carbonate bands and to a general lowering of the cellulose bands due to changes in fine structure.

The infrared absorption spectrum of dried samples of sodium cellulose monothiocarbonate (Figs. 5C and 5D) revealed only the bands of cellulose and carbonate. Freshly

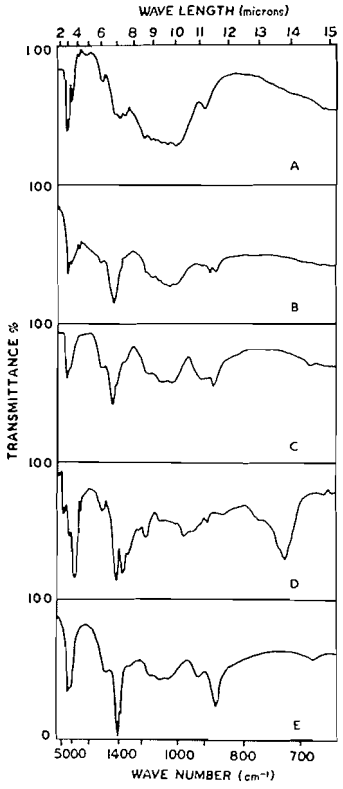


FIG. 5. Infrared spectra of cellulose (A), alkali cellulose (B), dried sodium cellulose monothiocarbonate (C, D), and freshly prepared wet sodium cellulose monothiocarbonate (E).

prepared wet samples were made into potassium bromide pellets with much difficulty (Fig. 5E). The main bands shown by this sample are those due to carbonate.

In an attempt to provide positive evidence for the presence of cellulose monothiocarbonate, the infrared spectra of potassium bromide pellets of samples of sodium cellulose xanthate precipitated from various viscose preparations (Fig. 6A) were examined as well as the corresponding S-methyl (Fig. 6B) and diethylacetamido (Fig. 6C) derivatives.

No bands analogous to those which can be ascribed to the monothiocarbonate are to be observed (Fig. 4). The degree of substitution of the cellulose monothiocarbonate samples was low, the bands are not pronounced and, as the amounts of monothiocarbonate were much less, it is not surprising that it escaped detection.

Can. J. Chem. Downloaded from www.nrcresearchpress.com by 186.148.149.217 on 09/04/12
For personal use only.

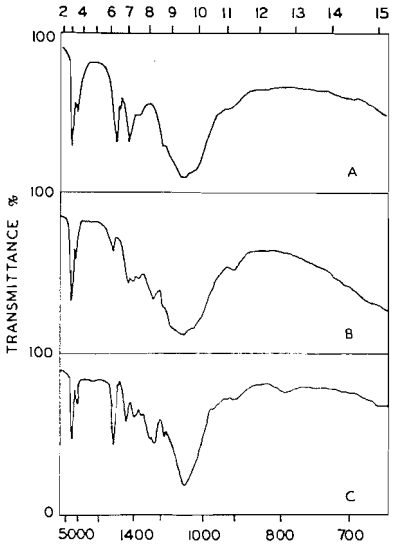


FIG. 6. Infrared spectra of cellulose xanthate precipitated from viscose (A), its S-methyl derivative (B), and its diethylacetamido derivative (C).

The precipitation of the cellulose xanthate salts by acetone or methanol at 0–5° C (17) and of the diethylacetamido derivative (18) from viscose by described methods was found to be accompanied by some loss of xanthate groups. The previous work showed no such loss. The two pronounced bands found for the sodium cellulose xanthate samples at 1563 and 1428 cm^{-1} were probably the result of impurities. Similar bands were found for some samples of the S-methyl derivative and these disappeared after successive extractions with water, acetone, and ether.

EXPERIMENTAL

Materials and Analytical Methods

Commercial samples of hydrogen sulphide (19), carbon disulphide, and carbon dioxide (20) were purified by established methods. Carbonyl sulphide was passed through sodium hydroxide solution (33%) and concentrated sulphuric acid and then liquefied by cooling with solid carbon dioxide and acetone. Two distillations through an externally cooled (−35° C) Vigreux column at a reflux ratio of about 3:1 were necessary to obtain carbonyl sulphide free of carbon disulphide. Triethylphosphine in nitrobenzene (1:10) also absorbed carbon disulphide from the impure mixture (21, 22), but some could still be detected in the infrared spectrum of the carbonyl sulphide.

Generation of Gases

One arm of a long U-tube (1 m × 2 cm diameter), separated from the other arm by a stopcock and containing the viscose (20 g), sodium cellulose xanthate or monothiocarbonate (5–10 g), was evacuated and phosphoric acid (50%) was admitted from the other arm. The heat necessary to free the gases from the cellulose was supplied externally. The reaction product of sodium hydroxide (8%, 160 ml) and carbon disulphide (25 ml) at room temperature (18 hours) was hydrolyzed similarly.

All gases were dried with phosphorus pentoxide and stored over mercury. Measured volumes in a 10-cm cell were examined in a Perkin–Elmer model 13 infrared spectrophotometer.

Can. J. Chem. Downloaded from www.nrcresearchpress.com by 186.148.149.217 on 09/04/12
For personal use only.

Preparation of Viscose

Viscose was prepared by standard commercial methods (23). All samples and solutions were kept at −5° to 0° C to minimize hydrolytic decomposition, and analyses were performed immediately after purification. Samples of viscose were allowed to "ripen" in a constant temperature bath at 8° C.

The total sulphur in viscose (10 g) diluted in sodium hydroxide solution (8%) at −5° C to 100 ml was estimated in aliquots (20 ml) by analytical method No. 2 below. The trithiocarbonate was estimated approximately from the extinction at 500 mμ of samples in 1-cm silica cells. (An extinction coefficient of 449 liters $mole^{-1}$ cm^{-1} was found using sodium trithiocarbonate solutions (16) prepared under nitrogen and estimating the trithiocarbonate content by method 1.)

Purification of Viscose

Amberlite anion exchange resin IRA 400 (8, 24) was used for purifying the viscose.

1. Viscose (100 g) was forced through the resin (200 g) by air pressure (30 lb in^{-2}) in an apparatus similar to that described by Dux (24).

2. Viscose (25 g) at 0° C was diluted with sodium hydroxide solution (8%, 250 ml) and passed through an externally cooled (−5° C) resin column (100 g, 2 cm diameter) and eluted to 1 liter. Dilution and elution with water instead of sodium hydroxide solution was found to cause a remarkable increase in elution time, particularly for cellulose xanthate of high xanthate substitution (D.S. = 0.7). The viscosity of cellulose xanthate solutions decreases with increasing alkali concentration (25).

Analytical Methods

1. Aliquots of purified viscose solution (100 ml) were oxidized by hydrogen peroxide (30%, 20 ml). After 10 minutes at room temperature, the solutions were diluted (100 ml), boiled to decompose the excess peroxide (20 minutes), cooled, made up accurately to 250 ml, and filtered. The sulphate in an aliquot (150 ml) was estimated gravimetrically as barium sulphate (26).

2. Similar aliquots were added to cooled mixtures of acetic acid (50%, 50 ml) and iodine (0.04 *M*) in potassium iodide solution (0.1 *M*, 50 ml), and excess iodine was titrated against standardized sodium thiosulphate solution (0.05 *N*) after 5 minutes.

3. The gases evolved from similar aliquots (using 150 ml of 50% phosphoric acid) were removed by a stream of nitrogen and passed through a solution of cadmium chloride (0.1 *M*) and sodium acetate (0.1 *M*) at pH = 6.8 to absorb hydrogen sulphide and subsequently through methanolic potassium hydroxide to absorb carbon disulphide (13). The sulphur was estimated either by the barium sulphate method (method 1) or by the iodometric method (method 2). Carbonyl sulphide was found to precipitate cadmium sulphide from solutions buffered at pH 4–7 with acetic acid and sodium acetate (26), and its presence invalidates the method.

4. The cellulose in aliquots (40 ml) was estimated by oxidation (27) with potassium dichromate (1 *N*) and sulphuric acid (70% in reacting solutions). Excess dichromate was titrated against ferrous ammonium sulphate using platinum and calomel electrodes.

Measurement of Ultraviolet Spectra

Aliquots were accurately diluted in sodium hydroxide solution (8%) to give a suitable range of concentrations, and the extinction for maxima at about 380 and 300 mμ was measured using 1-cm silica cells in a Beckman D.K. 2 spectrophotometer. The calculated extinction coefficient evidently depended upon the slit width which adjusts automatically at a given sensitivity.

Can. J. Chem. Downloaded from www.nrcresearchpress.com by 186.148.149.217 on 09/04/12
For personal use only.

Potassium Cellulose Xanthate

Samples of dissolving pulp (25 g) were steeped in potassium hydroxide solution (40%) at 5° C for 3 hours, filtered, and subjected to an air current for 3 hours. The alkali cellulose (35 g) and potassium hydroxide solution (100–400 ml, 40%) were stirred with carbon disulphide (400 ml) for 16–40 hours. Excess carbon disulphide was removed under vacuum (15 mm), and samples were examined as described for viscose.

Sodium Cellulose Xanthate

Viscose (50 g; S, 1.45; cellulose, 6.78%; D.S., 0.51), diluted with ice water (250 ml), was titrated with cold acetic acid (6 *M*) to pH 6–7 using glass and calomel electrodes. Cold acetone (750 ml), run in over about 10 minutes, gave a precipitate which was either centrifuged or filtered off and ground successively in a mortar with cold acetone (3×50 ml), acetone–ether mixtures (40:10, 30:20, 20:30, 10:40), and finally with anhydrous cold ether (3×50 ml). Samples for analysis (methods 1 and 4) and spectroscopic examination were dried at 20° C (0.5 mm Hg over phosphorus pentoxide). The use of methanol in place of acetone gave a more gelatinous precipitate, which was more difficult to filter or centrifuge, and which resulted in extensive xanthation of the methanol (λ_{max} = 380, 300 mμ). Dissolution of these products in cold sodium hydroxide solution formed more trithiocarbonate (λ_{max} 500 mμ; shoulder 325 mμ). Sample A, Fig. 4, found: S, 9.27; cellulose, 62.6%; D.S., 0.38.

S-*Methyl Cellulose Xanthate*

S-Methyl cellulose xanthate (cell—O—CS—SCH_3) was prepared from the precipitated sodium cellulose xanthate sample (D.S., 0.38) and methyl iodide, essentially as recently described (17). The product was washed successively with acetone, water, acetone, and solvent exchanged into ether. Sulphur in samples dried to constant weight at 20° C (0.5 mm Hg) was determined by use of a Parr bomb (28). All samples were insoluble in pyridine and lost sulphur in this solvent at 100° C (29). Sample B, Fig. 6B, found: C, 39.05; H, 5.57; S, 9.01. Calculated for D.S. of 0.26: C, 42.19; H, 5.71; S, 9.01%.

Diethylacetamido Cellulose Xanthate

Diethylacetamido cellulose xanthate (cell—O—CS—S—CH_2—$CONEt_2$) was precipitated from the same sample (D.S., 0.51) of diluted viscose neutralized to pH 6.5 as described (13), and dried to constant weight at 20° C (0.1 mm Hg). Sulphur (28) and nitrogen (30) were estimated by standard methods. This substance lost sulphur in pyridine at 100° C. Sample C, Fig. 4, found: S, 11.94; N, 2.36%; D.S., 0.47; 0.40 respectively. After reprecipitation from dimethyl sulphoxide by ether, found: S, 10.2%; D.S. 0.40.

Cellulose Dixanthate

Cellulose dixanthate (cell—O—CS—S—)$_2$, obtained in iodometric titration (method 2) of the same viscose sample, was filtered, washed with solvents (as for cellulose xanthate), and dried at 80° C (0.5 mm Hg). Sulphur (28) determinations showed loss of xanthate. Found: C, 40.73; H, 5.81; S, 9.93. Calculated for D.S. of 0.29: C, 40.64; H, 5.33; S, 9.93%.

Potassium Ethyl Xanthate

Potassium ethyl xanthate was recrystallized from acetone and dried at 80° C (0.1 mm Hg). Sulphur, determined by methods 1, 2, and 3, gave 39.3, 39.13, and 39.01% respectively (purity 98%).

Can. J. Chem. Downloaded from www.nrcresearchpress.com by 186.148.149.217 on 09/04/12
For personal use only.

Potassium Ethyl Monothiocarbonate

Potassium hydroxide (6.6 g) in pure ethanol (30 ml) at −15° C absorbed less (5½ liters) than the calculated amount of pure carbonyl sulphide (11 liters) and precipitated a white solid A (10 g), which was filtered off and rapidly extracted with ethanol (50 ml) at 50° C, leaving a hygroscopic powder B (5.3 g, S 2.39%) containing much carbonate. The ethanol extract, cooled to 5° C, gave white needles C (2.6 g, S 18.54%), which on similar extraction left an insoluble powder (10 mg); cooling to 0° C gave white needles D (1 g). Found S: 21.34% C_2H_5COS; K requires S, 22.22%, purity 96%. The infrared spectra (Fig. 4) of these samples showed bicarbonate as an impurity which was not completely removed. The mother liquor showed absorption maxima at 380 and 300 mμ, which are characteristic of the ethyl xanthate.

Four similar preparations and the use of sodium hydroxide, sodium ethoxide in toluene, and potassium hydrosulphide with ethylchloroformate in ethanol gave similar mixtures. Extraction with ethanol at lower temperatures (−5 to −10° C) gave small amounts of impure products. Previous accounts of this preparation (e.g. 31) apparently resulted in a purer product. Samples of our crude reaction product A, analyzed by methods 1, 2, and 4, evidently contained sulphide as indicated by the higher iodometric results. The fact that carbonyl sulphide reacted with the cadmium reagent invalidated the gas analytical method (sulphur in sample A: by Ba_2SO_4, 10.87%; by iodometry, 11.9%; as COS^-, 9.91%; as $S^=$, 0.96%; from gas analysis: absorbed by $Cd(OAc)_2$, 1.44%; absorbed by KOH/CH_3OH = 9.12%).

Sodium Cellulose Monothiocarbonate

Alkali cellulose from cotton linters and sodium hydroxide solution was treated with liquid carbonyl sulphide at −70° C and the temperature was allowed to rise to −5° C over 18 hours. Weighed samples of the white solid were analyzed and partial solutions in 8% purified sodium hydroxide were prepared as described for viscose. Solutions in aqueous sodium hydroxide showed no absorption maxima at 382 and 302 mμ, indicating the absence of xanthate. Samples prepared by passing carbonyl sulphide gas over alkali cellulose at −15° C were green in color only when carbon disulphide was present in the carbonyl sulphide. The green color was extracted into acetone at −15° C under nitrogen, and the spectrum (Fig. 3) was examined in 1-cm silica cells; in air the color faded, and sulphur precipitated.

Diethylacetamido Cellulose Monothiocarbonate, Attempted Preparation

Sodium cellulose monothiocarbonate (10 g) in cold sodium hydroxide solution (100 ml) and N,N-diethylchloroacetamide (5 ml) were mixed and the solution was neutralized to pH 7 with cold acetic acid (6 *N*) using glass and calomel electrodes. After 2 hours, the gelatinous precipitate (3.9 g) was filtered, washed with water and solvents (13), and dried at 28° C over phosphorus pentoxide (0.1 mm Hg). The product contained neither sulphur nor nitrogen. Found: C, 40.25, 42.43; H, 6.63, 6.41. Calculated for $(C_6H_{10}O_5)_n$: C, 44.4; H, 6.22%.

Infrared Examination

Solid samples (1.5 mg) were dried at 20° C under 0.1 mm Hg pressure over phosphorus pentoxide, finely divided and made into pellets with potassium bromide (300 mg) (33). Freshly prepared cellulose monothiocarbonate samples containing appreciable quantities of water were examined as pellets and as Nujol mulls. All spectra were measured with a Perkin–Elmer model 13 infrared spectrophotometer equipped with NaCl optics and operated in double-beam mode.

Can. J. Chem. Downloaded from www.nrcresearchpress.com by 186.148.149.217 on 09/04/12
For personal use only.

REFERENCES

1. H. KOBAYASHI and I. KAGAWA. J. Chem. Soc. Japan, **53**, 289 (1950).
2. S. N. DANILOV. Trans. Conf. on High Mol. Compds. (U.S.S.R.), 4th Conf., 1948. 64–80; cf. Chem. Abstr. **47**, 7207h (1953).
3. S. N. DANILOV, N. M. GRAD, and E. T. GEINE. Zhur. Obshcheĭ Khim. **19**, 826 (1949).
4. S. N. DANILOV, N. M. GRAD, and A. F. VOROB'EVA. Zhur. Obshcheĭ Khim. **19**, 1257 (1949).
5. H. GROTJAHN. Z. Elektrochem. **57**, 305 (1953).
6. I. KAGAWA and H. KOBAYASHI. J. Polymer Sci. **7**, 421 (1951).
7. O. SAMUELSON and F. GÄRTNER. Acta Chem. Scand. **5**, 596 (1951).
8. M. A. TYUGANOVA and Z. A. ROGOVIN. Izvest. Vysshykh Ucheb. Zavedeniĭ, Khim. i. Khim. Tekhnol. 153 (1958); cf. Chem. Abstr. **53**, 2613d (1959).
9. B. PHILIPP. Faserforsch. u. Textiltech. **6**, 13 (1955).
10. P. HERRENT and E. INOFF. J. Polymer Sci. **5**, 727 (1950); **3**, 487, 834 (1948).
11. J. MITCHELL, JR., I. M. KOLTHOFF, E. S. PROSKAUER, and A. WEISSBERGER. Organic analyses. Vol. I. Interscience Publishers, Inc., New York. 1953. pp. 368–369.
12. E. TREIBER, W. LANG, and F. MADER. Holzforschung, **8**, 97 (1954).
13. K. ATSUKI and T. TAKATA. J. Soc. Chem. Ind. Japan, 43, 394 (1940).
14. K. HESS and H. GROTJAHN. Z. Electrochem. **56**, 58 (1952).
15. G. INGRAM and B. A. TOMS. J. Chem. Soc. 4328 (1957).
16. F. G. HURTUBISE and H. KRÄSSIG. Anal. Chem. **32**, 177 (1960).
17. E. G. ADAMEK and C. B. PURVES. Can. J. Chem. **35**, 967 (1957).
18. E. TREIBER, J. GIERER, J. REHNSTRÖM, and J. SCHURZ. Holzforschung, **10**, 36 (1956).
19. L. F. AUDRIETH. Inorganic synthesis. Vol. III. McGraw-Hill Book Co. Ltd., New York. 1950. pp. 14–15.
20. A. I. VOGEL. Textbook of practical organic chemistry. Longmans, Green & Co., Inc., London. 1948. p. 173.
21. W. HEMPEL. Z. angew. Chem. (2) **14**, 865 (1901).
22. H. HIBBERT. Ber. **39**, 161 (1906).
23. E. OTT, H. M. SPURLIN, and M. W. GRAEFFLIN. Cellulose and cellulose derivatives. Pt. II. Interscience Publishers Inc., New York. 1954. p. 962.
24. J. R. DUX and L. H. PHIFER. Anal. Chem. **29**, 1842 (1957).
25. L. OLDSBERG and O. SAMUELSON. Svensk Papperstidn. **60**, 745 (1957).
26. A. I. VOGEL. Textbook of quantitative inorganic analysis. Longmans, Green & Co., Inc., London. 1945. p. 808.
27. E. GEIGER and B. J. WEISS. Helv. Chim. Acta, **36**, 2009 (1953).
28. MANUAL No. 121, Parr Instrument Co., Moline, Ill.
29. L. ALEKSANDRU and Z. ROGOVIN. Zhur. Obshcheĭ Khim. **23**, 1203 (1953).
30. J. GRANT. Quantitative organic microanalysis. (Based on F. Pregl.) Churchill Ltd., London. 1951. p. 95.
31. C. BENDER. Liebigs Ann. Chem. **148**, 137 (1868).
32. E. OTT, H. M. SPURLIN, and M. W. GRAEFFLIN. Cellulose and cellulose derivatives. Pt. II. Interscience Publishers Inc., New York. 1954. p. 1000.
33. R. T. O'CONNOR, E. F. DUPRE, and E. R. MCCALL. Anal. Chem. **29**, 998 (1957).

Can. J. Chem. Downloaded from www.nrcresearchpress.com by 186.148.149.217 on 09/04/12
For personal use only.

Can. J. Chem. Downloaded from www.nrcresearchpress.com by 186.148.149.217 on 09/04/12
For personal use only.

NOTES

THE IDENTITY OF BAYERITE-*a* AND BAYERITE-*b*

G. YAMAGUCHI AND K. SAKAMOTO

In 1928 Fricke (1) reported the existence of two types of bayerite, $Al_2O_3.3H_2O$, which he called *a* and *b*. Both give almost identical X-ray diffraction powder patterns except that the relative intensities of some of the lines are not the same in both patterns. The most striking example is the 00.1 line, which is one of the strongest in the pattern of type *b* and is a little stronger than the 10.0 line, while in type *a* it is conspicuously weaker than the latter. Nishimura (2) has recently obtained the less common type *a* while preparing Raney nickel from a Ni–Al alloy. He has confirmed the very weak intensity of the 00.1 line and has found that it varies in relative intensity according to the conditions under which the bayerite is formed. We have repeated the preparation of type *a* by Nishimura's method and have obtained type *b* by a procedure reported elsewhere (3). Both types have now been examined by the X-ray diffraction powder method (Fig. 1), by electron microscopy (Fig. 2), and by electron microdiffraction techniques (Fig. 3). The observed *d* spacings, derived from the diffractometer charts reproduced in Fig. 1, are listed in Table I,

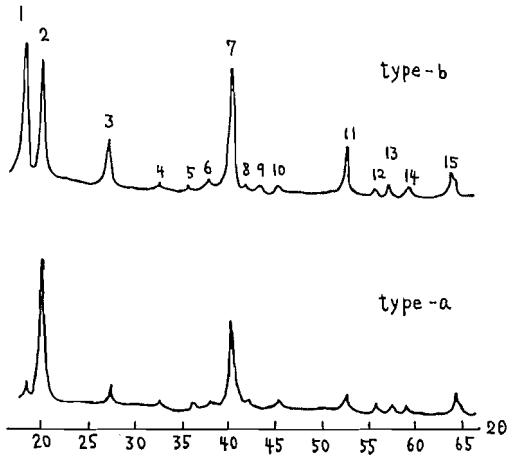


FIG. 1. X-Ray diffraction patterns of bayerite-*a* and bayerite-*b* (Cu $k\alpha_1$, filtered; Norelco-type diffractometer).

where it will be seen that, except for relative intensities, the powder patterns of type *a* and type *b* are identical. The electron micrographs (Fig. 2) show that type *a* crystallizes with a needle-like, or lath-like, habit and a tendency towards parallel growth along the direction of the needle axis, while type *b* crystallizes in thin, hexagonal plates. The structural periodicity shown in the electron microdiffraction photograph of a single crystal of type *a* (Fig. 3) was found to be 4.71 Å by comparison with an electron diffraction photograph of gold foil; this value is in good agreement with the length of the *c* axis of type *b* (a = 5.047 Å, c = 4.730 Å; S.G., $P\bar{3}1m$) reported elsewhere (4). These results indicate that bayerite-*a* and bayerite-*b* are structurally identical, that the crystals of type *a* are elongated in the direction of the *c* axis, and that the observed differences between types *a*

TABLE I

X-Ray diffraction powder data for bayerite-*a* and bayerite-*b*

	Bayerite-*a*		Bayerite-*b*			
Line	d_{obs}	I/I_1	d_{obs}	I/I_1	d_{calc}*	*hk.l*
1	4.745	7	4.745	100	4.730	00.1
2	4.381	100	4.385	90	4.371	10.0
3	3.209	9	3.210	34	3.210	10.1
4	2.706	2	2.705	2	—	—
—	—	—	—	—	2.523	11.0
5	2.468	4	2.468	2	—	—
6	2.365	1	2.368	7	2.365	00.2
7	2.222	62	2.227	90	2.226	11.1
—	—	—	—	—	2.185	20.0
8	2.176	3	2.171	2	—	—
9	—	—	2.079	3	2.080	10.2
10	1.989	4	1.987	4	1.984	20.1
11	1.722	11	1.725	45	1.726	11.2
12	1.647	4	1.653	3	1.652	12.0
13	1.605	4	1.604	10	1.605	20.2
—	—	—	—	—	1.577	00.3
14	1.558	5	1.560	15	1.560	12.1
—	—	—	—	—	1.483	10.3
15	1.458	6	1.460	25	1.457	30.0

*d_{calc} from $a = 5.047$ Å, $c = 4.730$ Å for bayerite-*b* (4).

and *b* in the relative intensities of some of the X-ray diffraction powder lines, particularly the abnormally weak 00.1 line of type *a*, are the result of preferred orientation of the crystals of type *a* parallel to their length.

Grateful acknowledgment is made to Dr. S. Nishimura for helpful advice regarding the preparation of bayerite-*a*.

1. R. Fricke. Z. anorg. allg. Chem. **175**, 249 (1928).
2. S. Nishimura. Bull. Chem. Soc. Japan, **32**, 61 (1959).
3. G. Yamaguchi and K. Sakamoto. J. Chem. Soc. Japan, Ind. Eng. Ed. **61**, 307 (1958).
4. G. Yamaguchi and K. Sakamoto. Bull. Chem. Soc. Japan, **31**, 140 (1958).
5. X-Ray powder data file. American Society for Testing Materials, Philadelphia, Pa., U.S.A. 1959.

Received February 5, 1960.
Department of Applied Chemistry,
Faculty of Engineering,
University of Tokyo,
Tokyo, Japan.

DIPHENYLCYANAMIDE DERIVATIVES. IV. 1,1-bis(4-CHLOROPHENYL)-UREA*

J. R. Robinson

The synthesis of 1,1-bis(4-chlorophenyl)-urea was reported as resulting from the aqueous alkaline hydrolysis of 4,4′-dichlorodiphenylcyanamide; it was described as a white solid, m.p. 220°–222° (1). Subsequent investigation has shown this material to be a complex mixture containing 1,1-bis(4-chlorophenyl)-urea, some 4,4′-dichlorodiphenylamine, and a polymeric compound containing silicon leached from the Pyrex flask. (No

*Issued as contribution No. 169.

Can. J. Chem. Downloaded from www.nrcresearchpress.com by 186.148.149.217 on 09/04/12
For personal use only.

TABLE I

X-Ray diffraction powder data for bayerite-*a* and bayerite-*b*

	Bayerite-*a*		Bayerite-*b*			
Line	d_{obs}	I/I_1	d_{obs}	I/I_1	d_{calc}*	*hk.l*
1	4.745	7	4.745	100	4.730	00.1
2	4.381	100	4.385	90	4.371	10.0
3	3.209	9	3.210	34	3.210	10.1
4	2.706	2	2.705	2	—	—
—	—	—	—	—	2.523	11.0
5	2.468	4	2.468	2	—	—
6	2.365	1	2.368	7	2.365	00.2
7	2.222	62	2.227	90	2.226	11.1
—	—	—	—	—	2.185	20.0
8	2.176	3	2.171	2	—	—
9	—	—	2.079	3	2.080	10.2
10	1.989	4	1.987	4	1.984	20.1
11	1.722	11	1.725	45	1.726	11.2
12	1.647	4	1.653	3	1.652	12.0
13	1.605	4	1.604	10	1.605	20.2
—	—	—	—	—	1.577	00.3
14	1.558	5	1.560	15	1.560	12.1
—	—	—	—	—	1.483	10.3
15	1.458	6	1.460	25	1.457	30.0

*d_{calc} from $a = 5.047$ Å, $c = 4.730$ Å for bayerite-*b* (4).

and *b* in the relative intensities of some of the X-ray diffraction powder lines, particularly the abnormally weak 00.1 line of type *a*, are the result of preferred orientation of the crystals of type *a* parallel to their length.

Grateful acknowledgment is made to Dr. S. Nishimura for helpful advice regarding the preparation of bayerite-*a*.

1. R. Fricke. Z. anorg. allg. Chem. **175**, 249 (1928).
2. S. Nishimura. Bull. Chem. Soc. Japan, **32**, 61 (1959).
3. G. Yamaguchi and K. Sakamoto. J. Chem. Soc. Japan, Ind. Eng. Ed. **61**, 307 (1958).
4. G. Yamaguchi and K. Sakamoto. Bull. Chem. Soc. Japan, **31**, 140 (1958).
5. X-Ray powder data file. American Society for Testing Materials, Philadelphia, Pa., U.S.A. 1959.

Received February 5, 1960.
Department of Applied Chemistry,
Faculty of Engineering,
University of Tokyo,
Tokyo, Japan.

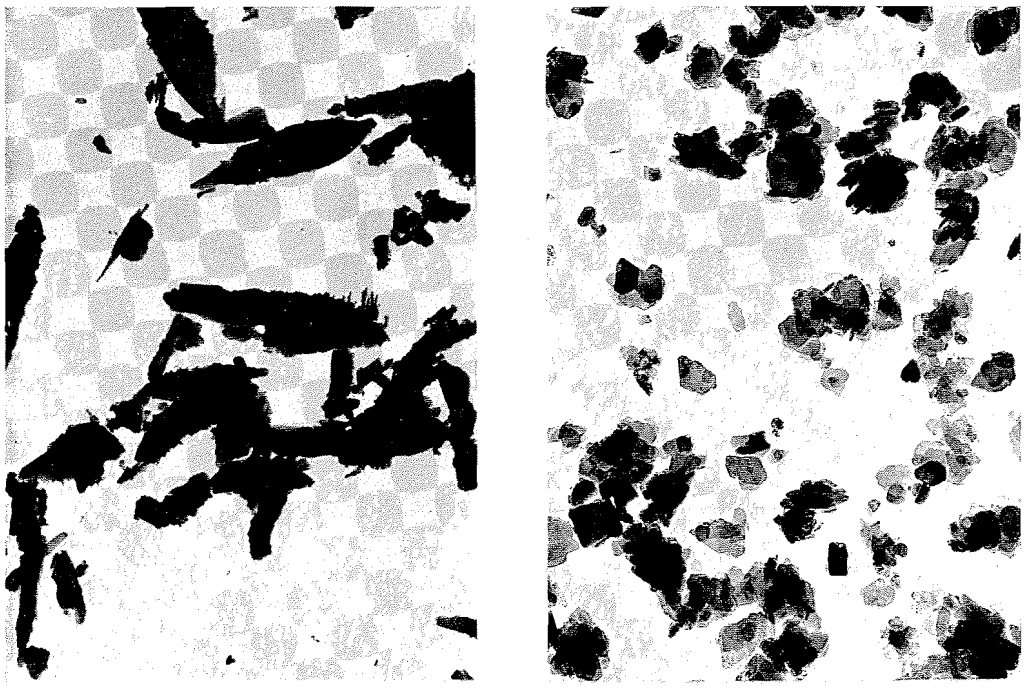
DIPHENYLCYANAMIDE DERIVATIVES. IV. 1,1-bis(4-CHLOROPHENYL)-UREA*

J. R. Robinson

The synthesis of 1,1-bis(4-chlorophenyl)-urea was reported as resulting from the aqueous alkaline hydrolysis of 4,4′-dichlorodiphenylcyanamide; it was described as a white solid, m.p. 220°–222° (1). Subsequent investigation has shown this material to be a complex mixture containing 1,1-bis(4-chlorophenyl)-urea, some 4,4′-dichlorodiphenylamine, and a polymeric compound containing silicon leached from the Pyrex flask. (No

*Issued as contribution No. 169.

Can. J. Chem. Downloaded from www.nrcresearchpress.com by 186.148.149.217 on 09/04/12
For personal use only.



2



3

FIG. 2 Electron micrographs of bayerite-*a* and bayerite-*b* (×27,000).
FIG. 3. Electon microdiffraction pattern of bayerite-*a* (acceleration voltage 100 kv).

Can. J. Chem. Downloaded from www.nrcresearchpress.com by 186.148.149.217 on 09/04/12
For personal use only.

silicone grease was used.) The purpose of this note is to record a corrected description of 1,1-bis(4-chlorophenyl)-urea in the pure state.

This unsymmetrically substituted urea has now been obtained by a different method and characterized through conversion to known derivatives by the well-established reactions illustrated in Fig. 1.

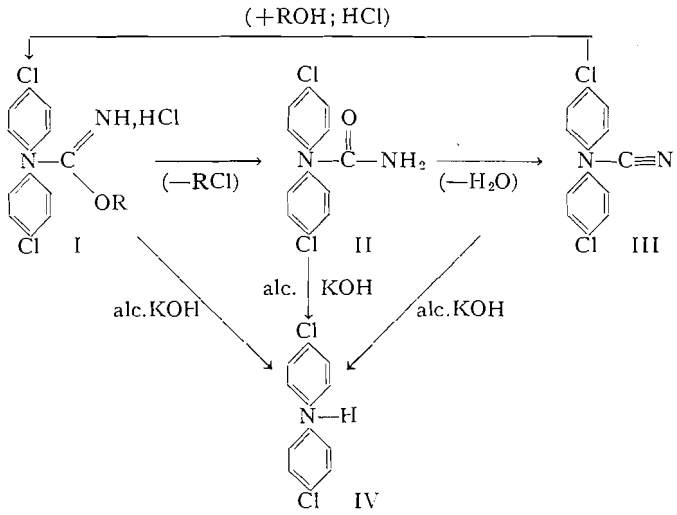


FIG. 1. The synthesis and hydrolysis of 1,1-bis(4-chlorophenyl)-urea.

Although the 3,3-diphenyl-2-alkylpseudoureas are known to undergo rearrangement and cleavage on heating to form diphenylamine and the corresponding alkyl isocyanate (2), their hydrochloride salts, when heated, retain the urea skeleton resulting in the formation of unsymmetrical diphenylurea and the corresponding alkyl chloride (3). Similar behavior of the 3,3-dialkyl-2-alkylpseudoureas was reported by McKee (4). This property has provided a convenient method for synthesis of 1,1-bis(4-chlorophenyl)-urea (II, Fig. 1). The reaction of water with the pseudourea salts, at room temperature, is observed to produce the same material, though slowly.

Evidence for the structure of II is provided by its ready dehydration to 4,4′-dichlorodiphenylcyanamide (III) using Kurzer's technique (5), as well as by its hydrolysis to 4,4′-dichlorodiphenylamine (IV) in alcoholic potassium hydroxide. Further, the infrared spectrum* of the material in the region 3600–3200 cm^{-1} is identical with that of 1,1-diphenylurea and 1,1-bis(4-methoxyphenyl)-urea, each having absorption peaks characteristic of $—NH_2$ at 3540 and 3430 cm^{-1}, as well as a strong peak at 1675 cm^{-1} typical of an amide carbonyl; a peak at 830 cm^{-1} is further indication of the paradisubstituted phenyl groups in this material.

The degradation of the 3,3-bis(4-chlorophenyl)-2-alkylpseudourea salts (I) to 4,4′-dichlorodiphenylamine may also be accomplished directly in boiling alcoholic potassium hydroxide; 4,4′-dichlorodiphenylcyanamide undergoes similar conversion (1).

*Acknowledgment is made to Mr. R. W. White of this laboratory for recording and interpreting the infrared spectra of these materials.

Can. J. Chem. Downloaded from www.nrcresearchpress.com by 186.148.149.217 on 09/04/12
For personal use only.

Can. J. Chem. Downloaded from www.nrcresearchpress.com by 186.148.149.217 on 09/04/12
For personal use only.

EXPERIMENTAL*

3,3'-Bis(4-chlorophenyl)-2-alkylpseudoureas

3,3-Bis(4-chlorophenyl)-2-alkylpseudoureas (Fig. 1, I where R = C_1 to C_{12} alkyl groups) were prepared by the alkoxide catalyzed addition of alcohols to 4,4'-dichlorodiphenylcyanamide (1, 3).

1,1-Bis(4-chlorophenyl)-urea

(a) By Thermal Decomposition of 3,3-Bis(4-chlorophenyl)-2-n-heptylpseudourea Hydrochloride

The pseudourea salt (2.0 g, 4.8 mmoles) was spread thinly over a watch glass and kept in a 90° oven until odorless and no longer water-soluble (5 days). The residue was recrystallized from methanol–water, ethanol–water, then dried *in vacuo* over calcium chloride. The yield of purified material (fine, colorless needles) was 1.0 g (75%); it gave a positive test for organic halogen, a negative test for halide, and melted at 187°–188° C. Its infrared absorption characteristics are described above. Anal. Calc. for $C_{13}H_{10}N_2OCl_2$: C, 55.53; H, 3.58%. Found: C, 55.75; H, 3.57%.

(b) By Thermal Decomposition of 3,3-Bis(4-chlorophenyl)-2-n-butylpseudourea Hydrochloride

The salt (1.17 g, 3.18 mmoles) was kept at the melting point, under vacuum (0.2 mm of mercury), on a manifold to which a cold trap was attached. After 90 minutes the crude residue weighed 0.87 g (97%) and repeated recrystallization from ethanol–water gave fine, colorless needles, m.p. 187°–188°.

The distillate in the cold trap weighed 0.265 g (90%) and had the boiling point (77°–78°) and refractive index (1.4014) of *n*-butylchloride.

(c) By the Action of Water on 3,3-Bis(4-chlorophenyl)-2-methylpseudourea Hydrochloride

An aqueous solution of the salt (0.5 g, 1.5 mmoles in 100 ml of water) was left standing in the dark at room temperature. After several days, long needle-like crystals began to grow. After 7 months the material was filtered off and recrystallized from methanol–water and ethanol–water, giving colorless needles, m.p. 187°–188°.

The three products (*a*, *b*, and *c*) were identical in chemical and physical properties.

4,4'-Dichlorodiphenylcyanamide

A solution of 0.84 g (2.98 mmoles) of 1,1-bis(4-chlorophenyl)-urea (above) in 25 ml of pyridine was treated with 1.77 g (10 mmoles) of benzenesulphonyl chloride and left standing at room temperature for 12 hours. The reaction product, after precipitation with water, filtration, and washing, was recrystallized from methanol yielding 0.58 g (73%) of long colorless needles of 4,4'-dichlorodiphenylcyanamide, m.p. 114°–115°. The material was confirmed by a mixed melting point with an authentic sample (1).

4,4'-Dichlorodiphenylamine

A 5-ml methanolic potassium hydroxide solution of 1,1-bis(4-chlorophenyl)-urea (0.12 g, 0.42 mmole) was boiled under reflux for 24 hours; some ammonia was evolved. After crystals of potassium carbonate were filtered off, the product was precipitated by adding water and recrystallized from 110° petroleum ether yielding 0.085 g (85%) of 4,4'-dichlorodiphenylamine, colorless needles, m.p. 77°–78°.

The identical product was obtained in 80–90% yield, by the same technique, starting with any of the 3,3-bis(4-chlorophenyl)-2-alkylpseudourea hydrochlorides.

**Melting points were obtained using a Fisher–Johns block and are uncorrected. Carbon and hydrogen analyses were by J. F. Alicino, Metuchen, N.J.*

1. J. R. ROBINSON and W. H. BROWN. Can. J. Chem. **29**, 1069 (1951).
2. J. R. ROBINSON. Can. J. Chem. **32**, 557 (1954).
3. J. R. ROBINSON. Diphenylcyanamide derivatives. Ph.D. Thesis, The University of Western Ontario, London, Ontario. 1953.
4. R. H. MCKEE. Am. Chem. J. **42**, 1 (1909).
5. F. KURZER. J. Chem. Soc. 3035 (1949).

RECEIVED APRIL 14, 1960.
PESTICIDE RESEARCH INSTITUTE,
CANADA DEPARTMENT OF AGRICULTURE,
UNIVERSITY SUB POST OFFICE,
LONDON, ONTARIO.

Can. J. Chem. Downloaded from www.nrcresearchpress.com by 186.148.149.217 on 09/04/12
For personal use only.

Can. J. Chem. Downloaded from www.nrcresearchpress.com by 91.191.171.90 on 09/05/12
For personal use only.

Canadian Journal of Chemistry

Issued by THE NATIONAL RESEARCH COUNCIL OF CANADA

VOLUME 38 SEPTEMBER 1960 NUMBER 9

THE HYDROGEN ISOTOPE EFFECT IN THE PYROLYSIS OF ETHYL-1,1,2,2-d_4 ACETATE[1]

ARTHUR T. BLADES AND P. W. GILDERSON

ABSTRACT

The hydrogen isotope effect in the pyrolysis of ethyl-1,1,2,2-d_4 acetate has been measured in the temperature range 442–650° C. Making allowance for symmetry numbers in the formation of the ethylene products C_2D_4 and C_2D_3H, the isotope effect may be expressed as

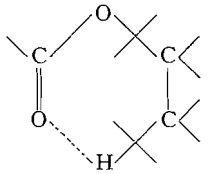
$$k_H/k_D = 0.99e^{1145/RT}.$$

The data are interpreted as indicating a reaction co-ordinate in which a C—H bond is breaking, but contributions to the isotope effect from residual C—H and (or) incipient O—H vibrations, and from bending vibrations, must be included to explain the results satisfactorily.

INTRODUCTION

Recent studies in the pyrolysis of alkyl esters by Bailey *et al.* (1) as a preparative method for olefins have revived interest in the mechanism of this reaction. Bailey's results were characterized by the almost exclusive production of that olefin which might be described as the least-substituted ethylene, i.e. where competitive reactions were possible, the reaction followed the Hoffmann rule. This selectivity has since been shown (2) not to exist in the homogeneous reaction, the major factor influencing the ratio of products being purely statistical.

The accepted transition state for the reaction is a six-membered ring with the



β-hydrogen of the alkyl group bonded to the acyl oxygen. De Puy and Leary (3) have suggested that the reaction co-ordinate involves the simultaneous breaking of both the C—H and the C—O bonds and the development of double-bond character in the carbon–carbon bond. The alternate possibility of breaking of the C—O bond followed by the C—H bond, which they liken to an E_1 elimination, is ruled out on the basis of relative rates of pyrolysis of substituted benzyl acetates.

More recently, Maccoll (4) has suggested that this reaction may be considered to be "quasi-heterolytic", and likens the elimination to an E_2 type where the rate is primarily determined by the forming O—H bond, rather than by the breaking C—O bond. This

[1]*Manuscript received April 22, 1960.*
Contribution No. 114 from the Research Council of Alberta, Edmonton, Alberta.

suggestion has been disputed by De Puy, King, and Froemsdorf (5), who find no evidence of C—O heterolytic bond breaking, and observe a considerable hydrogen isotope effect in the pyrolysis of 1-methyl cyclohexyl-2,2,6,6-d_4 acetate, indicating the importance of the C—H bond breaking in the reaction co-ordinate. Quantitatively, this hydrogen isotope effect, 1.7 at 500° C, and 1.9 at 400° C, is interesting in that it is less than the "theoretical maxima" of 2.1 and 2.3, respectively, which they suggest is due to simultaneous O—H bond formation.

The present study of the intramolecular isotope effect in the pyrolysis of ethyl-1,1,2,2-d_4 acetate allows a more careful appraisal of the effect in a simpler compound.

EXPERIMENTAL

All pyrolyses were carried out in a conventional toluene carrier gas system as has been described previously (6). To extend the temperature range in this pyrolysis, an aluminum furnace with a glass reaction cell of about 10 times the normal volume was used for runs at 443 and 497° C. All runs were carried out at approximately two centimeters of mercury pressure where the ethyl acetate decomposition is known to be first order.

The ethylene products (C_2D_3H and C_2D_4) were separated from the reaction mixture at −80° C, and were freed from traces of toluene and ethyl acetate by passage through a trap at −160° C. The parent peaks in the mass spectrum (masses 31 and 32) were used to determine the ratio of these ethylenes. No allowance was made for sensitivity differences (7), or for possible discrimination in the source of the mass spectrometer, since these would be expected to be small and would affect only the relative frequency factors for the two modes of decomposition.

The ethyl-d_4 acetate was supplied by Merck & Co., and was 99% deuterated as indicated. Since this implies 4% of improperly deuterated ethyl acetate, the assumption was made that this consisted of 2% ethyl-1,1,2-d_3 acetate and 2% ethyl-1,2,2-d_3 acetate; a correction was applied for the production of C_2D_3H from these two impurities.

RESULTS

The relative rate data for the production of C_2D_4 and C_2D_3H are presented in Table I, and an Arrhenius plot of the data is shown in Fig. 1. The relative rate constant expression, omitting experiment 2, is

$$k_H/k_D = 0.99\, e^{1145\pm 15/RT}$$

TABLE I

Relative rate data for ethyl-1,1,2,2-d_4 acetate

Expt. No.	Temp., °K	Conversion, %	C_2D_4:C_2D_3H	$k_H/2k_D$
1	866.4	50	.891	.922
2	866.7	52	.883	.913
3	922.6	82	.862	.888
4	922.8	90	.860	.886
5	799.4	14	.938	.974
6	799.6	14	.939	.975
7	715.6	11	1.022	1.063
8	715.6	11	1.020	1.061
9	769.2	59	.967	1.002
10	772.2	59	.966	1.001

Can. J. Chem. Downloaded from www.nrcresearchpress.com by 91.191.171.90 on 09/05/12
For personal use only.

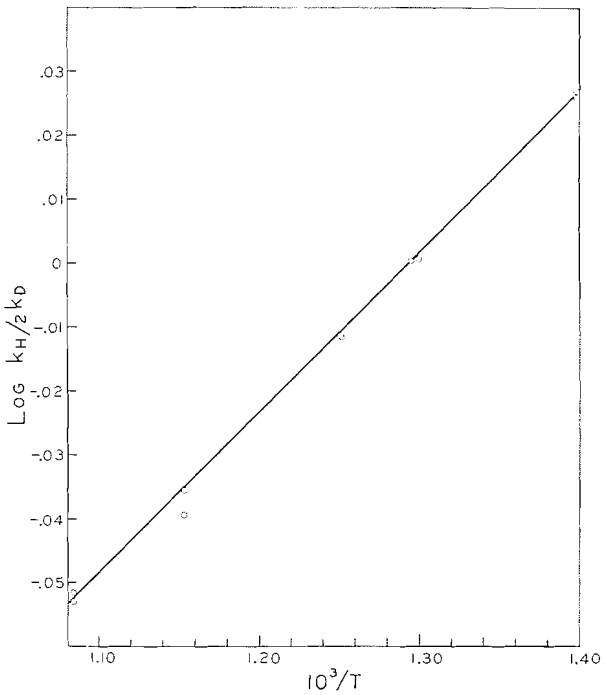


FIG. 1. Arrhenius plot for the production of C_2D_4 and C_2D_3H.

where allowance has been made for the symmetry number of two in the formation of C_2D_3H, i.e.

$$k_H/k_D = 2\,[C_2D_4/C_2D_3H]_{\text{corrected}}.$$

The correction introduced in the activation energy difference by the impurity correction was about 50 cal/mole. In view of the uncertainty in the amount and nature of the impurity, a more realistic uncertainty in the energy term would be ± 50 cal/mole.

DISCUSSION

To interpret the experimental isotope effect in terms of the mechanism of the reaction, the theoretical equation due to Bigeleisen (8) will be used,

$$k_H/k_D = \left(\frac{\mu^*_D}{\mu^*_H}\right)^{1/2} \frac{f}{f^{\ddagger}}.$$

μ^*_H, μ^*_D are the reduced masses in the reaction co-ordinate, and f and $f^{\ddagger}$ are the ratios of the partition functions of the isotopic species for the normal and activated states of the molecule. The function f is defined by the equation

$$f = \frac{s_H}{s_D} \prod_{i=1}^{3n-6} \left(\frac{\nu_D}{\nu_H}\right)_i e^{[h(\nu_H-\nu_D)_i]/2kT} \left(\frac{1-e^{-h\nu_H/kT}}{1-e^{-h\nu_D/kT}}\right)_i,$$

where s_H and s_D are symmetry numbers indicating the number of equivalent atoms

Can. J. Chem. Downloaded from www.nrcresearchpress.com by 91.191.171.90 on 09/05/12
For personal use only.

involved in reaction and contribute nothing to the isotope effect,

ν_H and ν_D are the vibrational frequencies of the $3n - 6$ vibrational modes,

h is Planck's constant,

k is Boltzmann's constant, and

T is the absolute temperature.

$f^{\ddagger}$ is a similar function, the product being taken over the $3n - 7$ vibrational degrees of freedom in the activated complex, excluding the mode associated with the reaction co-ordinate.

For an intramolecular isotope effect, as is being considered here, $f = s_H/s_D$. The isotope effect must then arise in the reduced mass term and in the function $f^{\ddagger}$.

It has become conventional to compare experimental hydrogen isotope effects with so-called "maximum" values, obtained by assuming that the only mode making a significant contribution is the stretching mode in the breaking bond, and that residual bonding is lacking in the activated complex. The major contributions to $f^{\ddagger}$ from C—H and C—D stretching vibrations in the present molecule are from those hydrogens not directly involved in the reaction, i.e. for C—H bond break, there remain two C—D modes, and for C—D bond break, there is one C—D and one C—H mode. The net contribution to $f^{\ddagger}$ is that from one such vibrational mode; the "Arrhenius" plot for this maximum vibrational contribution, times the reduced mass term ($\sim$1.4) is shown as curve A in Fig. 2. Curve B is a best fit straight line drawn through curve A over the experimental

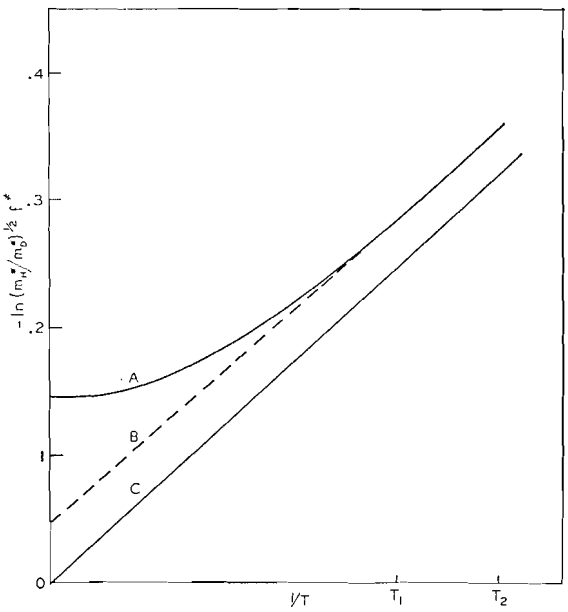


FIG. 2. Arrhenius plots: A, maximum isotope effect from reduced mass term and C—H stretching vibration; B, best fit straight line over the range T_1 to T_2; C, experimental plot extrapolated to $1/T = 0$.

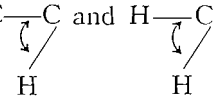
temperature range, T_1 (925° K) to T_2 (715° K). This indicates that if just this one mode is contributing to activation, then the experimental isotope effect equation should have a frequency factor ratio greater than one, and an activation energy difference of about 100 cal/mole less than the zero-point energy difference between a C—H and a C—D bond. Curve C shows the experimental equation extrapolated to $1/T = 0$. The lack of

Can. J. Chem. Downloaded from www.nrcresearchpress.com by 91.191.171.90 on 09/05/12
For personal use only.

coincidence between curves B and C indicates that this model is not adequate to explain the experimental results.

The contribution to the isotope effect of the function $f^{\ddagger}$ due to residual carbon–hydrogen, or to incipient hydrogen–oxygen bonding, where the reacting hydrogen is considered, is shown in Fig. 3, curves A and B being as previously defined except that the reduced mass ratio is not included. Inclusion of these terms in the isotope effect equation has the effect of further increasing the discrepancy between the model and experiment.

Terms in $f^{\ddagger}$ arising from C—C and H—C bending modes give rise to the curves



A and A′ in Fig. 4, the curve A representing the effect of vibrations of the hydrogen atom involved in the reaction, and the curve A′ representing only those hydrogen atoms more or less uninfluenced by the reaction. Since vibrations involving the reacting hydrogen will have the smaller force constants, the total contribution from bending vibrations will be some curve such as A″, and over the experimental temperature range, the Arrhenius line B. Adding these terms to those derived from stretching vibrations will have a tendency to bring the theoretical isotope effect curve more into agreement with the experimental. It must be pointed out that, in view of the appreciable and opposite curvature of the plots in Figs. 3 and 4 in the experimental temperature range, it is necessary to include both of these effects to explain the remarkable linearity of the experimental Arrhenius plot.

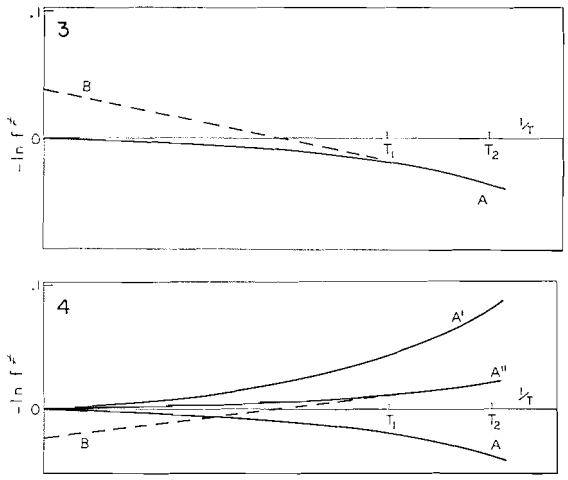


FIG. 3. Arrhenius plots: A, isotope effect from residual C—H stretching; B, best fit straight line over the range T_1 to T_2.

FIG. 4. Arrhenius plots: A, isotope effect from residual bending, A′, from other bending, A″, resultant from all bending; B, best fit straight line over the range T_1 to T_2.

These isotope effect data are then consistent with a cyclic transition state for the decomposition of alkyl esters, in which the β-hydrogen of the alkyl group is only loosely bound to either the original carbon atom, or the acyl oxygen atom, or both.

This conclusion is in complete accord with the observations of De Puy *et al.* (5) from the decomposition of 1-methyl cyclohexyl-2,2,6,6-d_4 acetate. Their conclusions are based on isotope effects being considerably below "maximum" values, i.e. 2.1 at 500° C and 2.3

Can. J. Chem. Downloaded from www.nrcresearchpress.com by 91.191.171.90 on 09/05/12
For personal use only.

at 400° C. Since the present study indicated exactly these values for the isotope effect, it would seem that some appreciable difference in the reaction co-ordinate must exist between cyclohexyl and ethyl esters.

Some support for this view is evident in the pyrolysis of 1-methyl cyclohexyl acetate, where attention is focused on the relative rates of production of the "exo" and "endo" products, methylene cyclohexane and 1-methyl cyclohexene. The expected 60:40 ratio of these products based on the relative number of available hydrogens (which is the major determining factor with straight chain alkyl esters) is quite different from the experimental ratio of 27:73. This, and the low isotope effect, would seem to be consistent with an activated complex for the endo elimination where O—H bond formation is quite important, as suggested by De Puy *et al.*, and where the activation energy would be appreciably lower than for the exo elimination. The invariance of the product ratio over 100° C in this pyrolysis is, however, not compatible with this interpretation.

ACKNOWLEDGMENTS

The authors wish to thank Drs. M. G. H. Wallbridge and H. W. Habgood for valuable discussions.

REFERENCES

1. W. J. Bailey and H. R. Golden. J. Am. Chem. Soc. **75**, 4780 (1953); W. J. Bailey and D. King. J. Am. Chem. Soc. **77**, 75 (1955).
2. D. H. Froemsdorf, C. H. Collins, G. S. Hammond, and C. H. De Puy. J. Am. Chem. Soc. **81**, 643 (1959).
3. C. H. De Puy and R. E. Leary. J. Am. Chem. Soc. **79**, 3705 (1957).
4. A. Maccoll. J. Chem. Soc. 3398 (1958).
5. C. H. De Puy, R. W. King, and D. H. Froemsdorf. Tetrahedron, **7**, 123 (1959).
6. A. T. Blades and G. W. Murphy. J. Am. Chem. Soc. **74**, 6219 (1952).
7. V. H. Dibeler, F. L. Mohler, and M. de Hemptinne. J. Research, Natl. Bur. Standards, **53**, 107 (1954).
8. J. Bigeleisen. J. Chem. Phys. **17**, 675 (1949).

Can. J. Chem. Downloaded from www.nrcresearchpress.com by 91.191.171.90 on 09/05/12
For personal use only.

THE SECONDARY HYDROGEN ISOTOPE EFFECTS IN THE PYROLYSIS OF ETHYL-d_5 ACETATE AND ETHYL ACETATE-d_3[1]

ARTHUR T. BLADES AND P. W. GILDERSON

ABSTRACT

Rate constant expressions have been obtained for ethyl acetate and ethyl-d_5 acetate in the temperature ranges 500–603° C and 501–614° C.

$$k_{(\text{ethyl acetate})} = 3.86\times10^{12} \exp -(48{,}000\pm400/RT) \text{ sec}^{-1}$$

$$k_{(\text{ethyl-}d_5\text{ acetate})} = 4.84\times10^{12} \exp -(49{,}500\pm300/RT) \text{ sec}^{-1}$$

By measuring the relative rate of production of C_2H_4 and C_2D_4 from identical mixtures of the two esters at the temperatures 387 and 490° C, it has been possible to determine the temperature coefficient of the relative rate constant more accurately. This, coupled with the relative rate constants at 500° C derived from the above equations, gives the relative rate constant expression

$$k_H/k_D = 0.8\, e^{1515\pm35/RT}.$$

These data are compared with the intramolecular isotope effect in the decomposition of ethyl-1,1,2,2-d_4 acetate, and the differences attributed to secondary isotope effects.

The rate of decomposition of ethyl acetate-d_3 was found to be identical within experimental error with that of the normal acetate.

INTRODUCTION

In the preceding paper (1) it was shown that it was necessary to include bending vibrations and residual and (or) incipient bonding in the activated complex to explain the kinetic isotope effect data on the pyrolysis of ethyl-1,1,2,2-d_4 acetate. In that compound there is relatively little chance for contributions from secondary isotope effects. The comparison of the relative rates of pyrolysis of ethyl and ethyl-d_5 acetates provides an opportunity of evaluating the importance of these effects.

Since this is an intermolecular isotope effect rather than intramolecular as in ethyl-1,1,2,2-d_4 acetate, this pyrolysis serves as a better comparison with the previous isotope effect study on 1-methyl cyclohexyl acetate by De Puy *et al.* (2). This is especially desirable due to their finding of smaller isotope effects than in the d_4 acetate, since in the latter, the occurrence of an isotope effect does not establish that there is an isotope effect in the rate-controlling step.

It has been reported (3) that the pyrolysis of esters of different fatty acids proceed at roughly equivalent rates. It has been found, however, that although ethyl formate and acetate decompose at roughly the same rate, the acetate requires about 4 kcal/mole greater activation energy (4). Believing this to be significant information on the mechanism, an attempt has been made to study the effect of deuteration on the rate of pyrolysis of ethyl acetate-d_3.

EXPERIMENTAL

All pyrolyses were carried out using the toluene carrier gas technique as has been described previously (5). Since in both rate studies the data had relevance only when compared with normal ethyl acetate, a parallel study was carried out on this compound also. In the ethyl – ethyl-d_5 comparison, alternate runs were carried out under essentially identical conditions with each compound at various temperatures between 500–614° C.

[1]*Manuscript received April 22, 1960.*
Contribution No. 115 from the Research Council of Alberta, Edmonton, Alberta.

Can. J. Chem. Downloaded from www.nrcresearchpress.com by 210.87.254.5 on 09/05/12
For personal use only.

Experiments were carried out on the ethyl acetate-d_3 at the two extremes of temperature, 502 and 592° C. The percentage decomposition in each case was determined by titration of the acetic acid produced.

Since the isotope effect studies on the ethyl-d_5 acetate gave an unsatisfactorily large error in the activation energy difference, a procedure was developed whereby this could be measured directly, although isotope effects were not measured. The procedure adopted was to mix the ethyl acetate and the ethyl-d_5 acetate as liquids, and then introduce the mixture into the toluene stream for pyrolysis. This provides a mixture of acetates whose composition over a number of experiments, if not constant, is at least changing slowly. This mixture is then decomposed by a small but known amount.

Then, if X^0_H, X^0_D are the original number of moles of the normal and deuterated compounds, and k_H and k_D are the corresponding rate constants,

$$\frac{C_2H_4}{C_2D_4} = \frac{X^0_H(1-e^{-k_H t})}{X^0_D(1-e^{-k_D t})} \approx \frac{k_H t X^0_H(1-k_H t/2)}{k_D t X^0_D(1-k_D t/2)}.$$

The approximation is adequate up to about 10% conversion, which must be known to ±.5%, i.e. 10±.5%; this accuracy is readily achieved.

Since it was unknown how constant the ratio X^0_H/X^0_D would remain over a series of runs, the system was further complicated by dividing the reactant stream such that one portion was pyrolyzed at high temperature in a small reactor to about 6% conversion, and the other at lower temperature in a 10 times larger reactor to about 1% conversion. Separate product handling systems were provided such that each experiment provided two mixtures of ethylenes.

Then

$$\frac{\left.\frac{C_2H_4}{C_2D_4}\right|_{T_1}}{\left.\frac{C_2H_4}{C_2D_4}\right|_{T_2}} \approx \frac{\left.\frac{k_H}{k_D}\right|_{T_1}}{\left.\frac{k_H}{k_D}\right|_{T_2}} \cdot \frac{(1-k_H t/2)_{T_1}}{(1-k_D t/2)_{T_1}},$$

which to a sufficient approximation may be written

$$\frac{\left.\frac{C_2H_4}{C_2D_4}\right|_{T_1}}{\left.\frac{C_2H_4}{C_2D_4}\right|_{T_2}} \approx \frac{\left.\frac{k_H}{k_D}\right|_{T_1}}{\left.\frac{k_H}{k_D}\right|_{T_2}} \left[1-\frac{(\alpha_H-\alpha_D)_{T_1}-(\alpha_H-\alpha_D)_{T_2}}{2}\right],$$

where α_H, etc. are the fractional conversions at T_1, T_2 for the H and D compounds. The temperature coefficient of the isotope effect can then be obtained by an analysis of the two ethylene mixtures and measurements of temperature and approximate conversions in the two furnaces, since

$$\frac{k_H/k_D|_{T_1}}{k_H/k_D|_{T_2}} = e^{\frac{-(E_H-E_D)}{R}\left(\frac{1}{T_1}-\frac{1}{T_2}\right)}$$

where E_H and E_D are the activation energies for the H and D compounds.

The two reactor volumes used were about 30 and 300 cc, the relative contact times being about 1:20. The ethylene ratios were determined mass spectrometrically, masses 27 and 32 being used as representative of C_2H_4 and C_2D_4 respectively. In practice, the C_2D_4 made a small contribution at mass 27; this was subtracted from mass 27 for C_2H_4 estimation. Two sets of analyses were made on each ethylene mixture at fixed sample

Can. J. Chem. Downloaded from www.nrcresearchpress.com by 210.87.254.5 on 09/05/12
For personal use only.

pressures as it was found that the ratio of $C_2H_3^+$ to $C_2D_4^+$ varied slightly with sample pressure.

The deuterated ethyl acetates were supplied by Merck & Co., Montreal, and were 99% deuterated as indicated. A correction was applied for 3% of the impurity $CH_3COOCD_2CD_2H$ in the ethyl-d_5 acetate simultaneous pyrolysis experiments. No further purification was attempted on the deuterated compounds.

Rate constant expressions were determined by a least-squares treatment of the rate data, and errors in activation energies were obtained from the average deviation of rate constants from the least-squares line.

RESULTS

The rate data for ethyl and ethyl-d_5 acetates gave the rate constant expressions:

$$k_{(\text{ethyl acetate})} = 3.86\times10^{12}\exp(-48{,}000\pm400/RT)\ \text{sec}^{-1}, \qquad T = 500\text{–}603^\circ\text{ C}$$

and

$$k_{(\text{ethyl-}d_5\text{ acetate})} = 4.84\times10^{12}\exp(-49{,}500\pm300/RT)\ \text{sec}^{-1}, \qquad T = 501\text{–}614^\circ\text{ C}$$

the average error in k being $\pm1.5\%$ and $\pm1\%$ respectively. A plot of these data is shown in Fig. 1, along with a single rate determination for ethyl-1,1,2,2-d_4 acetate.

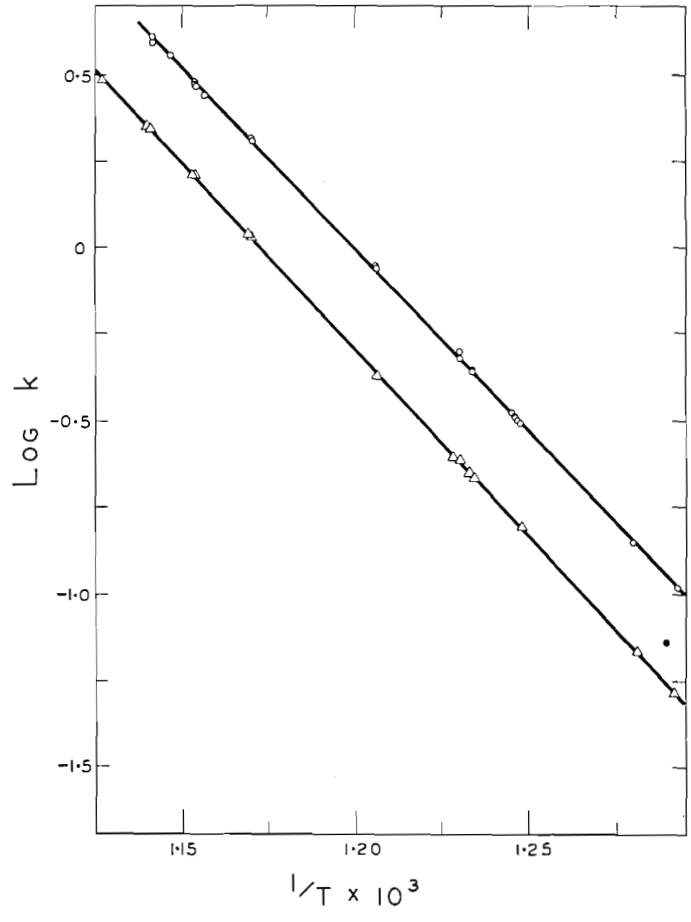


FIG. 1. Arrhenius plot for ethyl, ○, ethyl-d_5, △, and ethyl-1,1,2,2-d_4, ●, acetates.

Can. J. Chem. Downloaded from www.nrcresearchpress.com by 210.87.254.5 on 09/05/12
For personal use only.

The results from the direct comparison study are shown in Table I. The average value of "ΔE" is very close to that observed in the separate pyrolysis study, the error being

TABLE I

Data for the copyrolysis of ethyl and ethyl-d_5 acetates
(The duplicate ethylene ratios were determined at different mass spectrometer sample pressures)

Expt. No.	T_1, °K	T_2, °K	$C_2H_3^+:C_2D_4^+$ at T_1	$C_2H_3^+:C_2D_4^+$ at T_2	ΔE
8	656.8	763.7	2.371	1.971	1590
			—	—	—
9	660.5	761.6	2.368	2.010	1480
			2.300	1.954	1480
10	661.8	763.6	2.377	2.007	1540
			2.303	1.950	1510
11	660.6	763.2	2.377	2.011	1490
			2.310	1.961	1460
14	659.9	762.4	2.449	2.060	1550
			2.381	2.006	1530
					Av. 1515±35

reduced from ±700 to ±35 cal/mole. The relative rate equation $k_H/k_D = 0.8\ e^{1515\pm35/RT}$, T = 387–490° C, may then be derived, the isotope effect at 500° C being used to fix the pre-exponential factor.

Several rate constant determinations were made on the ethyl acetate-d_3 at 502 and 592° C; no isotope effect in the rate of decomposition could be observed in this temperature range within ±2%.

DISCUSSION

In the previous paper on the pyrolysis of ethyl-1,1,2,2-d_4 acetate, the isotope effect was explained on the basis of the reduced mass term and differences in the value of $f^{\ddagger}$, the value of f being determined solely by symmetry numbers. For the intermolecular isotope effect between ethyl and ethyl-d_5 acetates, the major isotope effect arises in the reduced mass term and f, terms in $f^{\ddagger}$ serving only to reduce the contributions of individual modes of vibration to f. It is therefore convenient to consider only the function f, it being understood that maximum values only are implied.

Since the activated complexes have identical structures in the ethyl-d_4, and the ethyl and the ethyl-d_5 acetate decompositions, it must be assumed that all of the modes contributing to the primary effect in the former must remain operative in the latter. The major interest in the latter centers then on the decreased frequency factor ratio (0.99 to 0.80) and on the increased activation energy difference (1145 to 1515 cal/mole). All primary effects have been accounted for in the d_4 isotope effect, so these changed constants must be a result of secondary effects.

The most obvious source of these secondary effects is in the bending vibrations at the β-carbon atom, some of which have already been considered in the d_4 compound analysis; the justification for their reconsideration is that their contribution has been increased, e.g., the $C\begin{smallmatrix}H\\ \\D\end{smallmatrix}$: $C\begin{smallmatrix}D\\ \\D\end{smallmatrix}$ comparison has become $C\begin{smallmatrix}H\\ \\H\end{smallmatrix}$: $C\begin{smallmatrix}D\\ \\D\end{smallmatrix}$.

Can. J. Chem. Downloaded from www.nrcresearchpress.com by 210.87.254.5 on 09/05/12
For personal use only.

An additional, and probably important, source of secondary isotope effects could arise at the α-carbon atom if the C—O bond is breaking in the reaction co-ordinate. Both the



bending and further contributions from bending at the β-carbon atom would have the effect of reducing the frequency factor ratio, and increasing the activation energy difference over the d_4 compound, where these effects could not exist. The coincidence of this model with the observed facts instills considerable confidence not only in the present rationalization, but also in the previous analysis of the ethyl-d_4 acetate data. The suggestion of secondary isotope effects at the α-carbon atom has further interesting implications with respect to the activated complex, suggesting a concerted mechanism, wherein the β-hydrogen transfers to the acyl–oxygen atom simultaneously with the C—O bond break.

A direct comparison can be made between this intermolecular isotope effect and a similar isotope effect in the decomposition of 1-methyl cyclohexyl 2,2,6,6-d_4 acetate (2). For that molecule, De Puy *et al.* found an isotope effect of 1.7 at 500° C and 1.9 at 400° C, whereas in this study our isotope effects at the same two temperatures are 2.1 and 2.4 respectively, slightly higher, in fact, than the intramolecular effect shown by ethyl-d_4 acetate as reported in the previous paper. The inconsistency between the two intermolecular effects supports the view that the reaction co-ordinates of cyclohexyl and ethyl esters are appreciably different.

The failure to observe an isotope effect in the decomposition of ethyl acetate-d_3 lends no support to the suggestion that this methyl influences the rate through an inductive effect. Recently, however, it has been shown by Weston (6) that such an isotope effect, being due to the failure of isotopic molecules to have exactly the same potential energy surfaces, would be immeasurably small for organic reactions. The present results will serve as experimental justification of this theory, if independent evidence for this supposed inductive effect can be found.

ACKNOWLEDGMENTS

The authors are indebted to Dr. M. G. H. Wallbridge and to Dr. R. M. Elofson for many fruitful discussions.

REFERENCES

1. A. T. Blades and P. W. Gilderson. Can. J. Chem. **38**, 1401 (1960).
2. C. H. De Puy, R. W. King, and D. H. Froemsdorf. Tetrahedron, **7**, 123 (1959).
3. W. J. Bailey and J. J. Hewitt. J. Org. Chem. **21**, 543 (1956).
4. A. T. Blades. Can. J. Chem. **32**, 366 (1954).
5. A. T. Blades and G. W. Murphy. J. Am. Chem. Soc. **74**, 6219 (1952).
6. R. E. Weston. Tetrahedron, **6**, 31 (1959).

Can. J. Chem. Downloaded from www.nrcresearchpress.com by 210.87.254.5 on 09/05/12
For personal use only.

KINETICS OF THE THERMAL DECOMPOSITION OF ETHYL PROPIONATE[1]

ARTHUR T. BLADES AND P. W. GILDERSON

ABSTRACT

The pyrolysis of ethyl propionate has been studied in the temperature range 505–602° C, yielding the Arrhenius equation

$$k = 5.2\times10^{12} \exp(-48{,}500\pm350/RT) \text{ sec}^{-1}.$$

By the copyrolysis of this compound with ethyl-d_5 acetate at 384 and 488° C, and comparison of this temperature coefficient with that for the isotopic ethyl acetates, an activation energy difference between ethyl acetate and propionate of 20±65 cal/mole was found, rather than 500 cal/mole as indicated in the individual studies. Since other evidence exists for an inductive effect in the decomposition due to the acid alkyl group, the lack of difference in activation energies is attributed to the change in effect being small and obscured by other effects.

INTRODUCTION

Studies of the kinetics of the pyrolysis of alkyl esters have indicated that the acid group forming the ester has little influence on the rate. Thus Gordon, Price, and Trotman-Dickenson (1), Rudy and Fugassi (2), and Warwick and Fugassi (3) observe about equal rates in the pyrolysis of *t*-butyl formate, acetate, and propionate; similar observations have been made in the pyrolysis of ethyl and isopropyl formates and acetates (4). More recently, Bailey and Hewitt (5) have compared a number of esters of fatty acids, chloro-acetic acid, and substituted benzoic acid, and found a correlation of rate with dissociation constant of the acid. Smith and Wetzel (6) have made other correlations, and De Puy, Bishop, and Golders (7) have noted the variability of rate between *sec*-butyl acetate and formate, and monochloro-, dichloro-, and trifluoro-acetate.

Despite the similarity of the rates for formates and acetates, a considerable difference in energy of activation has been observed between ethyl formate (44.1 kcal/mole) (4) and ethyl acetate (48.0 kcal/mole) (8). The view that this difference is the result of the inductive effect of the methyl group on the breaking of the carbon–oxygen bond gains considerable support from the above-mentioned rate data for halo-substituted acetates, where the rate is enhanced by substitution.

The present study of the decomposition of ethyl propionate was undertaken to evaluate the effect of further methyl substitution.

EXPERIMENTAL

The pyrolyses of the ethyl propionate were carried out in a conventional toluene carrier gas system as has been described previously (9), the identical apparatus being used as for the ethyl acetate pyrolysis. Rate constants were determined by titration of the propionic acid produced with 0.1 *N* sodium hydroxide solution.

In the copyrolysis of ethyl propionate and ethyl-d_5 acetate, the same technique of pyrolyzing parts of the reaction mixture simultaneously at the two temperature extremes was used as for the ethyl and ethyl-d_5 acetates (8), except that the two reactants were introduced into the toluene stream through separate capillaries; hence their proportion was not reproducible for consecutive experiments. The same procedure was adopted for mass spectrometer analysis of the ethylene, and for the correction of the data for isotopic impurities and degree of conversion.

[1]*Manuscript received April 22, 1960.*
Contribution No. 116 from the Research Council of Alberta, Edmonton, Alberta.

Can. J. Chem. Downloaded from www.nrcresearchpress.com by 91.191.171.90 on 09/05/12
For personal use only.

The ethyl-d_5 acetate (Merck & Co.) was the same sample as used in the previous acetate comparison (8). The ethyl propionate was fractionally distilled and degassed before use.

RESULTS

In the separate pyrolysis of ethyl propionate, variations in contact times from 0.26 to 1.56 sec and pressures from 1.5–2.0 cm Hg showed no effect on rate constants. The Arrhenius rate equation, derived from 15 consecutive runs over the temperature range 505.2–602.4° C is

$$k = 5.2\times10^{12}\exp(-48{,}500\pm350/RT)\ \text{sec}^{-1},$$

the average error in k being $\pm1.3\%$. A plot of these data is shown in Fig. 1.

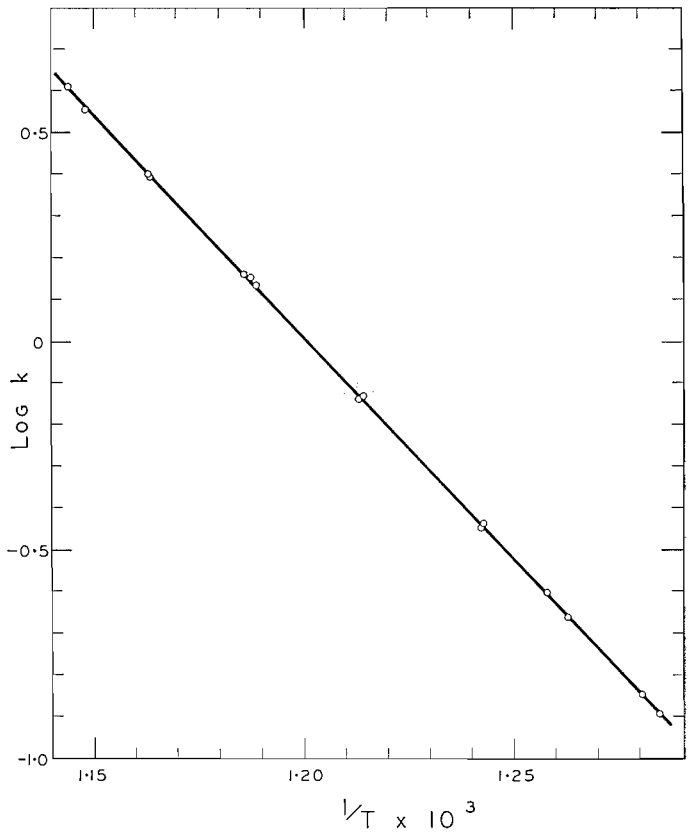


FIG. 1. Arrhenius plot for ethyl propionate.

This Arrhenius equation is to be compared with that for ethyl acetate obtained on the same apparatus,

$$k = 3.86\times10^{12}\exp(-48{,}000\pm400/RT)\ \text{sec}^{-1}.$$

In the copyrolysis experiments, only four satisfactory experiments were performed; the data for these are presented in Table I. The average value of the difference in activation energy (1495±30 cal/mole) is to be compared with the corresponding value for the

Can. J. Chem. Downloaded from www.nrcresearchpress.com by 91.191.171.90 on 09/05/12
For personal use only.

TABLE I

Relative rate data for ethyl propionate and ethyl-d_5 acetate

Expt. No.	Temperature, °K	Ion ratio, $C_2H_3^+$:$C_2D_4^+$	Δ log ion ratio (corr.)*	ΔE, cal/mole
2	659.4	2.55	.0671	1490
	762.8	2.16		
3	657.0	.218	.0685	1500
	761.1	.184		
4	658.2	.210	.0693	1550
	760.7	.1775		
5	657.8	.328	.0646	1440
	760.7	.280		

*This "Δ log ion ratio" has been corrected for degree of conversion and for the production of C_2D_4 from improperly deuterated ethyl-d_5 acetate; it is equivalent to "Δ log k" over the temperature range.

ethyl – ethyl-d_5 acetate difference (1515±35 cal/mole) (8). The indicated activation energy difference between ethyl acetate and propionate is then 20 cal/mole within limits of less than ±100 cal/mole.

DISCUSSION

The purpose of this investigation was to obtain further evidence on a supposed inductive effect of the acid alkyl group on the activation energy for the decomposition of alkyl esters. Although the individual rate constant expression determinations indicated a difference of 500 cal/mole between ethyl propionate and acetate, this was not substantiated by the comparison through the copyrolysis technique.

There is other evidence that an inductive effect is operative in these pyrolyses in that chloro- and fluoro-acetates show much greater rates of decomposition (7) and presumably lower activation energies than acetates. This is in agreement with the opposite electron-sharing character of the methyl and halo-methyl groups as is indicated in the acidity constants of the acids in Table II (10). The relatively large difference in these constants

TABLE II

Acidity constants × 10^5

Formic acid	17.7
Acetic acid	1.8
α-Chloroacetic acid	155
Propionic acid	1.3
n-Butyric acid	1.5

between formic and acetic acids dwarfs the difference between acetic and propionic; nevertheless, if a similar effect is operative in the ester decompositions and acid dissociations, the activation energy difference being sought here could have been expected to be several hundred calories.

A possible explanation of the negligible difference found is indicated in the increased acidity constant of *n*-butyric over propionic acid, for which there is no satisfactory

Can. J. Chem. Downloaded from www.nrcresearchpress.com by 91.191.171.90 on 09/05/12
For personal use only.

explanation. As suggested by Ingold (10), hyperconjugation may reduce the difference in acidity constants of acetic and propionic acids; such an effect may also be operative in the pyrolyses.

The use of the copyrolysis technique for the determination of differences in activation energy would seem to have wide applicability especially for molecular reactions where there is an interest in a homologous series. The major requirements for reactions to be successfully compared are that they shall proceed at roughly the same rate and that neither products nor reactants shall interfere with the normal course of reaction. A fairly accurate analytical method must be available for one product in each reaction, mass spectrometry seeming to be the most widely applicable, with vapor phase chromatography a possibility.

REFERENCES

1. E. GORDON, S. J. W. PRICE, and A. F. TROTMAN-DICKENSON. J. Chem. Soc. 2813 (1957).
2. C. E. RUDY and P. FUGASSI. J. Phys. Chem. **52**, 357 (1948).
3. E. WARWICK and P. FUGASSI. J. Phys. Chem. **52**, 1314 (1948).
4. A. T. BLADES. Can. J. Chem. **32**, 366 (1954).
5. W. J. BAILEY and J. J. HEWITT. J. Org. Chem. **21**, 543 (1956).
6. G. G. SMITH and W. H. WETZEL. J. Am. Chem. Soc. **79**, 875 (1957).
7. C. H. DE PUY, C. A. BISHOP, and C. GOLDERS. Unpublished work referred to by C. H. DE PUY and R. W. KING. Chem. Revs. In press. 1960.
8. A. T. BLADES and P. W. GILDERSON. Can. J. Chem. **38**, 1407 (1960).
9. A. T. BLADES and G. W. MURPHY. J. Am. Chem. Soc. **74**, 6219 (1952).
10. C. K. INGOLD. Structure and mechanism in organic chemistry. Cornell University Press. 1953. pp. 734–737.

Can. J. Chem. Downloaded from www.nrcresearchpress.com by 91.191.171.90 on 09/05/12
For personal use only.

Can. J. Chem. Downloaded from www.nrcresearchpress.com by 91.191.171.90 on 09/05/12
For personal use only.

THE SYNTHESIS OF HIGHLY RADIOACTIVE ISOPROPYL METHYLPHOSPHONOFLUORIDATE (SARIN) CONTAINING P^{32} AS TRACER ELEMENT[1]

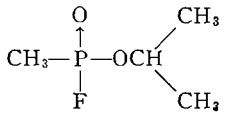
J. B. Reesor, B. J. Perry, and E. Sherlock[2]

ABSTRACT

Procedures are described for the safe processing of multicurie quantities of irradiated red phosphorus into isopropyl methylphosphonofluoridate (sarin) having a specific activity of 250 to 300 millicuries per gram. The use of costly remote-handling equipment is avoided by suitable choice of synthetic route and apparatus design.

INTRODUCTION

Several years ago, a requirement arose for radioactively tagged (P^{32}) isopropyl methylphosphonofluoridate (sarin) I, in order to study the biological effects and mode



I

of action of the so-called "nerve gases". The degree of dilution likely to be encountered in such biological studies indicated that quantities of the order of 50 grams with a specific activity of 250–300 mc/g would be required. Safe handling of multicurie sources of radiation is ordinarily achieved by placing operators behind shields and manipulating apparatus with various remote-handling devices. Such devices are complex and costly. Since the hazard depends not only upon the intensity of radiation but the duration of exposure to it, it was visualized that the greater speed of direct handling might give less actual radiation dosage than the much longer exposures to lower levels of radiation attendant on the usual remote-handling operations. The greater surety against accidents provided by direct handling was a further consideration in the synthesis of a highly toxic compound.

Accordingly a careful study of synthetic methods was carried out with a view to elimination of operations requiring long periods of attention. A time study was made of the known alternative routes of synthesis to assess the approximate radiation hazard associated with each procedure. These routes are illustrated diagrammatically in Fig. 1. The results clearly indicated that the route involving the direct conversion of phosphorus trichloride via the APC complex to methylphosphonic dichloride, followed by fluorination to methylphosphonic difluoride and preparation of sarin from the equimolecular mixture of dichloride and difluoride, was the safest practical method to use. The very high yield and purity of the agent produced by this method was a further advantage.

Investigations of this chosen route led to modifications in the chemistry and in the synthetic apparatus used which further simplified the reactions and reduced the hazards considerably. Principally, improvement was obtained in the preparation of methylphosphonic dichloride by an anhydrous procedure (1), which eliminated a filtration, and

[1]*Manuscript received May 16, 1960.*
Contribution from the Chemistry Section, Defence Research Board of Canada, Suffield Experimental Station, Ralston, Alberta, as Suffield Technical Paper No. 169. D.R.B. project No. D52-20-20-20.
[2]*Present address: Imperial Chemical Industries, Wokingham, Berks, England.*

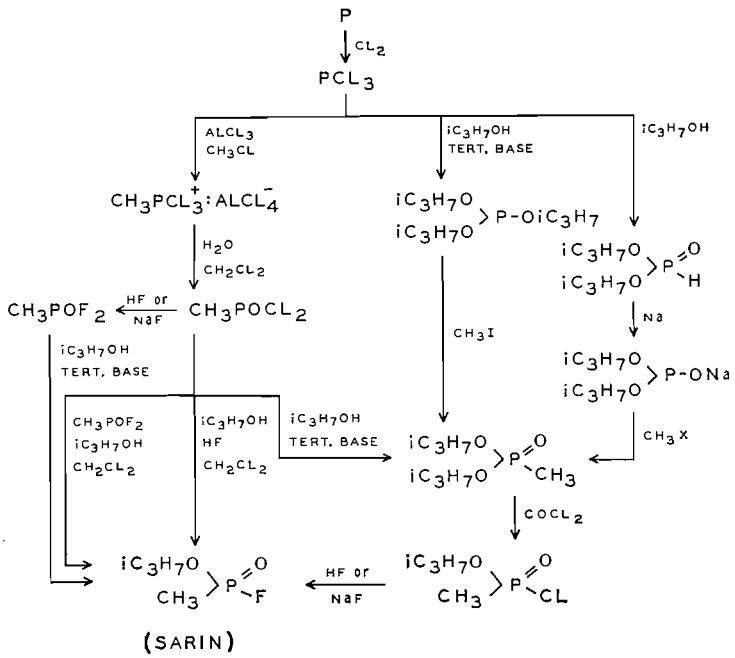


FIG. 1. Synthetic routes to sarin.

the direct conversion of methylphosphonic dichloride to sarin by the use of anhydrous hydrofluoric acid isopropyl alcohol, which eliminated a reaction and a filtration.

Our method is illustrated schematically in Fig. 2.

$$P \xrightarrow{Cl_2} PCl_3 + PCl_5 \xrightarrow{Sb} PCl_3$$

$$PCl_3 \xrightarrow[CH_3Cl]{AlCl_3} CH_3PCl_3^+.AlCl_4^-$$

$$CH_3PCl_3^+.AlCl_4^- \underset{(DEP)}{\overset{\text{diethyl phthalate}}{\rightleftharpoons}} CH_3PCl_4 + DEP.AlCl_3$$

$$CH_3PCl_4 \xrightarrow{SO_2} CH_3POCl_2 + SOCl_2$$

$$CH_3POCl_2 \xrightarrow[HF]{iC_3H_7OH} \underset{(sarin)}{CH_3PO(F)(iC_3H_7O)} + 2HCl$$

FIG. 2. Chosen synthetic route.

Over a period of approximately 5 years, 12 complete syntheses of sarin (I) containing P^{32} as tracer element have been successfully carried out. The product (I), at the desired specific activity of 250–300 mc/g, was obtained in quantity from 20 to 30 g red phosphorus of specific activity of approximately 2.2 curies/gram.

Can. J. Chem. Downloaded from www.nrcresearchpress.com by 91.191.171.90 on 09/05/12
For personal use only.

Can. J. Chem. Downloaded from www.nrcresearchpress.com by 91.191.171.90 on 09/05/12
For personal use only.

EXPERIMENTAL

Purification of Red Phosphorus

The phosphorus to be irradiated is purified in our laboratory by treatment of reagent grade material with concentrated hydrochloric acid at reflux temperature for approximately 1 hour, followed by washing with copious quantities of boiling distilled water. Repeated water washing, and decanting from the phosphorus to remove most of the "fines", give a product which is more easily handled since the inclusion of the very fine phosphorus particles sometimes results in a sintered irradiated sample. Finally the phosphorus is filtered, washed with alcohol, ether, and dried in a vacuum desiccator.

When the irradiation was carried out at Idaho Falls, Idaho, the purified red phosphorus was charged into clean, pure (Sl grade) aluminum capsules, 15 g of phosphorus per capsule, and sealed in an atmosphere of dry helium. Atomic Energy of Canada at Chalk River do their own packing, and bulk lots of purified phosphorus were sent to them in polyethylene bottles.

Transfer of Irradiated Phosphorus to the Phosphorus Trichloride Apparatus

The transfer of the irradiated phosphorus to the tared PCl_3 reaction flask is accomplished by normal "hot" radiological dry box technique under an atmosphere of dry nitrogen.

Preparation of Phosphorus Trichloride

Phosphorus trichloride is synthesized in the apparatus illustrated in Fig. 3.

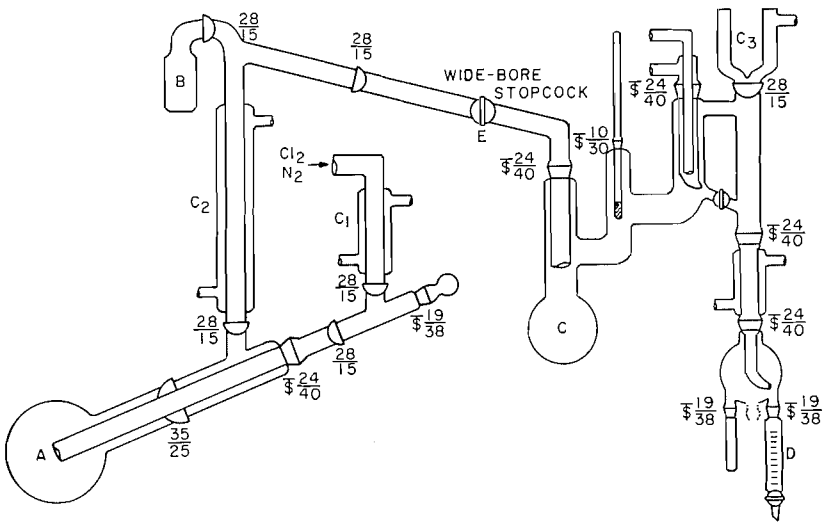


FIG. 3. PCl_3 apparatus.

Approximately 40 grams of dry boiling chips are placed in the reaction flask A, which is then evacuated and heated to dispel as much air as possible from the boiling chips. Dry nitrogen is let into the evacuated flask and the process of heating, evacuation, and admission of dry nitrogen is repeated so as to ensure that all oxygen (which would cause oxidation of the trichloride to oxychloride) is removed. The flask is then stoppered, weighed, and placed in the dry box ready for receipt of the irradiated phosphorus.

The stoppered flask is removed from the dry box after the addition of the irradiated

Can. J. Chem. Downloaded from www.nrcresearchpress.com by 91.191.171.90 on 09/05/12
For personal use only.

phosphorus, is weighed to determine weight of phosphorus (approximately 30 grams), and coupled up to the apparatus as shown in Fig. 3.

A slow stream of dry nitrogen is passed into the apparatus through the gas inlet tube to sweep out residual traces of oxygen, and the reaction flask is heated to 110°–120° C. At this stage the slow stream of nitrogen is replaced by a metered stream (6 to 7 liters per hour) of dry chlorine gas and at the same time a jet of cool air is directed on the upper, unheated surface of the reaction flask. Reaction occurs and the phosphorus pentachloride sublimes to the cool upper surface of the flask as it is formed. After 3/4 hour, when a fairly thick crust of phosphorus pentachloride has sublimed to the cool upper surface, chlorination is stopped and a very slow stream of nitrogen (sufficient to maintain a positive pressure only) is substituted for the chlorine. The reaction flask is then rotated through 180° on its ball joint so that the phosphorus pentachloride is covered with unreacted red phosphorus. Heating, without chlorination, is continued for about 15 minutes, by which time the phosphorus pentachloride is largely reduced by the unreacted red phosphorus to phosphorus trichloride. Chlorination is recommenced and the whole procedure repeated until a 20% excess of chlorine has been introduced. Heating is continued for 1 hour or until the residual phosphorus has disappeared.

This stage is fairly easy to observe and is facilitated by the use of boiling chips. Initially glass chips were used to keep the phosphorus mobile, but it was found that they become stained a dark brown by the intense radiation which tends to obscure the end point. The white boiling chips are hardly affected by the radiation and so provide a background against which the unreacted phosphorus is readily discerned.

The mixture in the flask now consists of phosphorus trichloride and phosphorus pentachloride. The mixture is allowed to cool to room temperature. Pure granular antimony (100 g) is then added to the mixture by tipping the antimony container B, which is built onto the apparatus. Powdered antimony reacts very vigorously with phosphorus pentachloride but results in a somewhat inferior product due to the surface film of antimony oxide normally present on the surface of the antimony, giving phosphorus oxychloride as a by-product. Granular antimony reacts more slowly, and a larger excess is required: the product, however, is purer. It is found that $-20+80$ mesh antimony is most suited to the reaction as a compromise between speed and purity.

Flask C is surrounded by a dry ice – acetone mixture and the nitrogen stream increased to approximately 2 liters per hour to help sweep out the trace amounts of phosphorus pentachloride sublimed into the gas inlet tube and also to prevent phosphorus trichloride distilling too far up the inlet tube in the subsequent operations.

The reaction mixture is then slowly heated. At approximately 75° C a strongly exothermic reaction sets in and phosphorus pentachloride is reduced to phosphorus trichloride by the antimony, antimony trichloride being formed at the same time. When the initial reaction has moderated, it is normal to obtain a yellowish-brown solid precipitate in the reaction mix. Reaction is regarded as complete when the liquid layer in the reaction flask is homogeneous and it has been found that this can only be attained quickly by strongly heating the reaction mixture. The heating mantle temperature is thus slowly raised to 280°–300° C and the elevated temperature is maintained until the liquid layer becomes homogeneous. During this period of heating, the rapidly refluxing phosphorus trichloride washes the last traces of sublimed phosphorus pentachloride into the reaction flask for reduction to trichloride. At the same time some 7–9% of the trichloride, entrained by the slow stream of nitrogen, condenses out in C_3 and is collected in the receiver.

Should there still be yellow solid material in the reaction mix after heating to

280°–300° C for 1 hour, the mixture may be cooled and a further quantity of the antimony added. The initial amount added, however, is a large excess and the further addition of antimony has been required only in those cases where the phosphorus was overchlorinated to give a large quantity of the pentachloride.

When the liquid layer becomes homogeneous the heating mantle temperature is reduced to 230° C, the water removed from the condenser C_2, and the product of phosphorus trichloride distilled in a slow stream of dry nitrogen while maintaining the charge of dry ice – acetone around receiver C. Distillation is continued until white fumes of antimony trichloride are observed in the reaction flask A.

Stopcock E is closed and the crude PCl_3 redistilled from a few grams of antimony to reduce any PCl_5 which might have been sublimed from the reaction flask during the reaction. The receiver is calibrated volumetrically so that the weight of product synthesized may be calculated directly without recourse to weighing and handling the "hot" product.

Yields of pure phosphorus trichloride, based on the phosphorus used, have varied from 92–99%.

Preparation of the Aluminum Chloride:Phosphorus Trichloride:Methyl Chloride (APC) *Complex*

The apparatus devised for this synthesis is illustrated in Fig. 4. The radioactive phos-

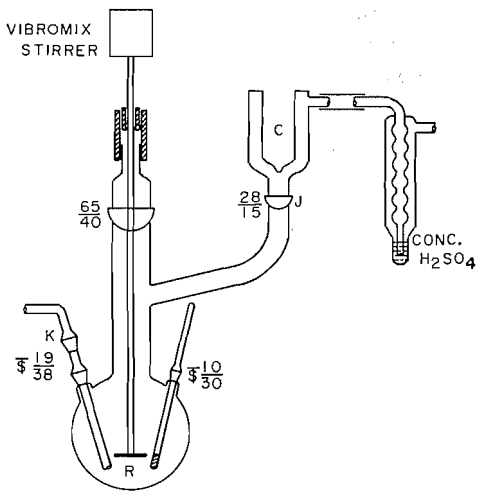


FIG. 4. APC complex apparatus.

phorus trichloride is run into the reaction flask R, which contains 1.5 molar proportions of very finely powdered anhydrous aluminum chloride. The very thick mixture is heated to 70°–75° C and agitated with a "vibrator"-type stirrer of fixed period but variable amplitude. The condenser C is charged with a dry ice – acetone mixture and a slow stream (1 to 1½ liters per hour) of dry methyl chloride is passed into the mixture as close to the point of stirring as possible. In the early stages reaction is slow, but after approximately 1 hour the mixture becomes fluid and the rate of absorption of methyl chloride increases markedly. When the mixture becomes fluid the efficiency of stirring is increased and the rate of addition of methyl chloride stepped up. On an approximate molar scale, absorption of methyl chloride is fairly rapid for approximately 2½ to 3 hours, when the mixture

Can. J. Chem. Downloaded from www.nrcresearchpress.com by 91.191.171.90 on 09/05/12
For personal use only.

becomes more viscous and crystals begin to separate on the walls of the flask. At this stage the rate of addition of methyl chloride is reduced to a very slow stream (approximately 1/2 to 1 liter per hour) while heating and stirring are continued. After a further 2 hours the mixture is a semisolid mush of crystals and the reaction is virtually complete. Methyl chloride addition is stopped and heating and stirring are continued for a further hour to ensure completion of the reaction. Heating and stirring are then stopped, the dry ice – acetone is removed from the condenser, and the excess methyl chloride is allowed to boil off. Throughout the whole of the reaction the rate of methyl chloride addition must be carefully controlled so that too great a reflux return to R is not obtained, as otherwise the reaction mixture is cooled below the temperature at which the formation of complex proceeds rapidly. During the period of rapid absorption, the maximum rate of addition of methyl chloride is always used commensurate with maintaining the reaction temperature of 70°–75° C.

Preparation of Methylphosphonic Dichloride from the APC *Complex*

The apparatus used in the radioactive synthesis is illustrated in Fig. 5.

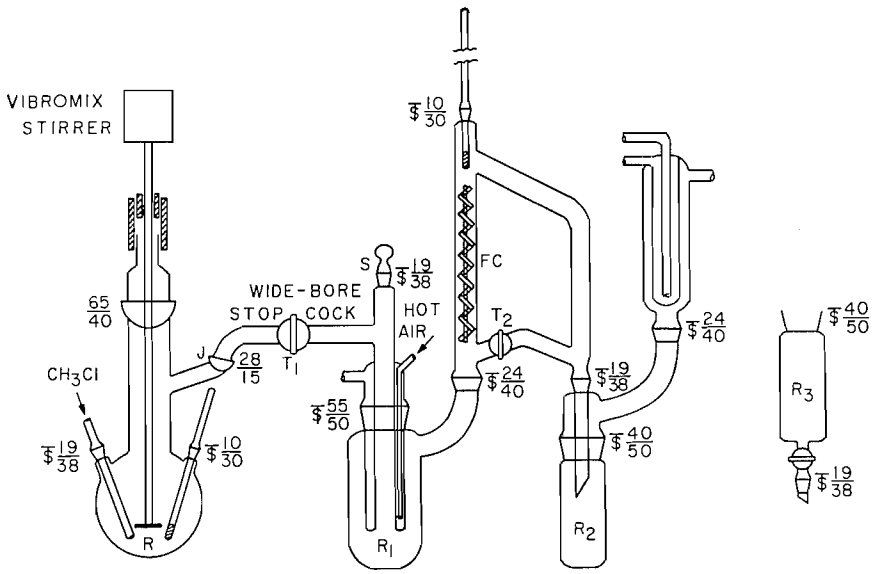


FIG. 5. Methylphosphonodichloridate apparatus.

The reaction flask in which the APC complex is prepared is also used for the breakdown of the complex and as the distillation flask for the recovery of the crude methylphosphonic dichloride. On completing the preparation of the APC complex the ball joint J (Fig. 4) is opened and 3 moles/mole complex of dry diethyl phthalate is added to the complex. The joint J is remade and stirring is begun to dissolve the complex as far as possible in the diethyl phthalate. Solution is accompanied by a pronounced rise in temperature and external water cooling should be used to prevent "hot spots" in the early stages until the solid breaks up. At this point a stream (10–12 liters/hour) of dry sulphur dioxide is passed through the stirred mixture via the inlet tube used for methyl chloride. An exothermic reaction occurs and the temperature of the reaction mixture normally rises to a maximum of approximately 50° C, and after approximately 2 hours begins to fall.

Can. J. Chem. Downloaded from www.nrcresearchpress.com by 91.191.171.90 on 09/05/12
For personal use only.

Sulphur dioxide is passed into the stirred mixture for a further 30 minutes and the mixture is then allowed to stand for a further 1 hour to ensure completion of reaction. During the passage of the sulphur dioxide the small amount of undissolved but dispersed complex rapidly dissolves and a very fine precipitate of the diethyl phthalate : aluminum chloride complex appears.

On completion of the reaction, the joint J is opened, and the whole reaction flask and contents are transferred to the distillation unit shown in Fig. 5 and joined up via the ball joint J (Fig. 5), the reaction flask then becoming the distillation flask R of Fig. 5. The inlet joint K at the upper end of the gas inlet tube is disconnected and replaced with a capillary air bleed coupled to an air-drying train. The reaction mixture is then thoroughly degassed under water pump vacuum.

The receivers R_1 and R_2 are immersed in dry ice – acetone cooling mixture and the apparatus evacuated by a high-capacity high-vacuum pump to approximately 0.1–0.5 mm Hg. The distillation flask is then heated to 85° to 90° C, when the residual thionyl chloride and methylphosphonic dichloride distill from the diethyl phthalate into receiver R_1. During the radioactive synthesis 6 hours is allowed, after which time the distillation is considered to be complete. This crude distillation is carried out with the tap T_2 in the open position to avoid a pressure drop which might be caused by the fractionating column FC and to ensure as high a pumping speed as possible at the distillation flask. The taps T_1 and T_2 are then closed, heating is discontinued, the dry ice – acetone cooling mixtures are removed, and dry air is let into the main receiver part of the apparatus.

The receiver R_1 is then heated by a heating mantle and the thionyl chloride is fractionally distilled from the recovered mixture at atmospheric pressure via the column FC. Heating is continued until the temperature at the top of the column is approximately 150°–155° C, which indicated that methylphosphonic dichloride is about to distill. Heating is then stopped and the apparatus allowed to cool to room temperature. The stopper S is replaced by a fine capillary bleed and the receiver R_2 is removed and replaced by the receiver R_3 for methylphosphonic dichloride. The apparatus is evacuated to approximately 60 mm Hg using a water pump and R_1 is again heated to recover pure methylphosphonic dichloride by fractional distillation.

During the evacuation of the apparatus to 60 mm Hg the last traces of thionyl chloride are removed from the upper part of the column and condenser surfaces. At 60 mm Hg the methylphosphonic dichloride distills at 84°–85° C and is distilled at a sufficiently rapid rate to prevent crystallization in the cool parts of the receiver. The product receiver is weighed before and after to determine the yield.

Yields of 88–89%, based on the phosphorus trichloride, are obtained.

Preparation of Radioactive Sarin

The apparatus used in the synthesis is illustrated in Fig. 6.

The dropping funnel which forms the receiver R_3 for the collection of methylphosphonic dichloride in the previous synthesis is transferred to one neck of the three-necked reaction flask and its molten contents are run in. The funnel is washed through into the flask with 100 ml of dry methylene chloride, and the mixture, stirred by means of a magnetic stirrer, is brought to reflux. During this stage of the reaction, water is led through the jacket of the beryl-saddle-packed fractionating column F, so that it acts as a reflux condenser.

A mole/mole solution of anhydrous hydrofluoric acid in anhydrous isopropanol is then prepared. A 5% excess over the theoretical weight of this solution required to react with the methylphosphonic dichloride previously synthesized is introduced into the copper

Can. J. Chem. Downloaded from www.nrcresearchpress.com by 91.191.171.90 on 09/05/12
For personal use only.

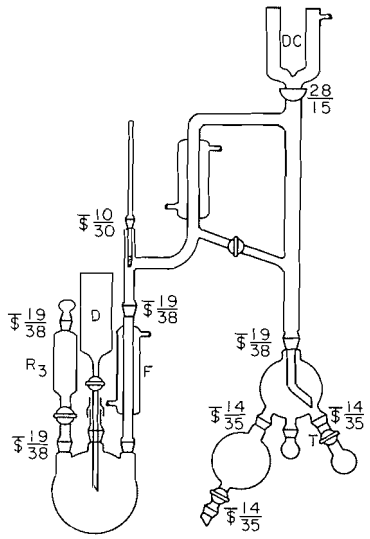


FIG. 6. Sarin apparatus.

dropping funnel D and from there run dropwise into the methylphosphonic dichloride solution at such a rate as to maintain gentle reflux without application of external heat. When addition is complete, the mixture is refluxed for 15 minutes, the water is drained from around the column F, and methylene chloride is distilled off for 15 minutes at atmospheric pressure, by which time evolution of HCl is virtually complete. The remaining methylene chloride is taken off and degassing is completed under water pump vacuum.

At this stage 10 ml of diethylaniline is added, the copper dropping funnel is replaced by a capillary bleed, and fractionation is begun at a pressure of about 10 millimeters. The condenser DC is charged with dry ice – acetone to prevent the loss of sarin which has been found to occur when distilling at this pressure. The forerun is collected in a receiver which may be shut off from the system by means of a tap T when collection is complete, thus preventing its contents from distilling back into the main fraction as distillation proceeds. This measure has been found to increase the purity of the sarin produced from 96–97% up to 99% or better. The main fraction is collected in a dropping-funnel-type receiver to facilitate subsequent dispensing of the product.

Using this method, yields of between 82 and 87% of sarin are obtained. The purity of this material has been found to be consistently better than 99%.

DISCUSSION

Safety

P^{32} is a pure β emitter and these particles are readily stopped by light weight lucite sheets. The bremsstrahlung X rays from such a source as we were handling, however, require thick, heavy metal sheets for complete protection. No laboratory with remote-handling equipment was available at Suffield but after careful consideration of the problem it was decided that the synthetic program could be undertaken using the facilities of our tracer laboratory. The laboratory consists of a main laboratory with seven in-line fumehoods each 5 ft wide and 2 ft 6 in. deep, and auxiliary observation, storage, and changing rooms. The fumehoods are of modern streamline design with all

Can. J. Chem. Downloaded from www.nrcresearchpress.com by 91.191.171.90 on 09/05/12
For personal use only.

service outlets inside and to the front whereas all service controls are outside. The hoods can be used singly or jointly as the size of apparatus dictates.

The bases of the fumehoods are of concrete cast in the form of a shallow sink and are lead lined; they are sufficiently robust to allow the heavy screening of local hot spots, such as reaction flasks, with lead bricks or thick sheet lead. The heavy screening of the whole apparatus was found to be impracticable and, in fact, undesirable during general distillation procedures. For general screening work, mobile screens of 1/2-in. thick Lucite (polymethyl methacrylate) faced each side with 1/16-in. steel were found to be ideal. These screens are 15 in. wide and extend the full height of the fumehood face. They run on ball races on permanent tracks along the front of the hoods, and are quickly and very easily moved to the desired screening position. Windows cut in the steel allow observations at the required height and the width of the screen allows an operator to work with his body shielded while using both hands for required manipulations in the fumehood. The steel-lined Lucite screens completely stop all β rays and reduce the bremsstrahlung X rays to approximately 15% of the unscreened value. The main face window of each hood is a vertically rising sheet of 1/2-in. Lucite and is coupled to a damper in the ventilation duct of the hood so that the draft is increased or decreased as the main window is raised or lowered respectively. With the main window completely closed each hood is positively ventilated at a low speed.

The bank of fumehoods is ventilated by a communal system powered by an 8000 cu. ft/min (at $1\frac{1}{2}$ in. static water pressure) exhaust fan. This flow is ample to allow work to proceed safely at three or four fumehoods simultaneously. Inlet air is filtered, thermostatically heated, and enters via the auxiliary rooms into the main laboratory and so to the fumehoods. This system ensures that at all times the operators work in a positive flow of clean air from the clean to the dirty parts of the laboratory.

The concept of dividing the laboratory into "clean" and "dirty" areas was vigorously enforced and easily removed coveralls and boots were worn, as were respirators at all times of transfers in order to eliminate ingestion hazards.

Monitoring of the personnel engaged in the syntheses has been carried out in three ways:

(i) by plotting the low energy X-ray dosage fields and observing the time spent by each operator at any position,

(ii) by wearing $\beta\gamma$ film badges, and

(iii) by wearing pocket dosimeters.

Probably the most important point pertaining to safety is the particular care which must be paid to the design of apparatus and choice of reaction conditions which enable the syntheses to be carried out with a minimum of handling and infrequent observation.

The five-stage synthesis is carried out in 5 days—a total of approximately 60 working hours—by three of the personnel. By dividing the hazardous tasks between the three (monitoring was continuously carried out to facilitate this), each worker receives less than 300 μr per person, the radiation dosage recommended at that time as the limit for those working continuously with radioactive materials. Since a decay period of at least 3 months is allowed to elapse between syntheses, our experience to date has indicated that complex organic syntheses involving high level sources can be carried out safely without remote handling provided adequate attention is paid to process flow and apparatus design.

Purification of Red Phosphorus

Our first irradiation of commercial red phosphorus graphically illustrated the need for

Can. J. Chem. Downloaded from www.nrcresearchpress.com by 91.191.171.90 on 09/05/12
For personal use only.

a preliminary purification of this material. Trace quantities of sodium ion must be eliminated in order to prevent the inclusion of a high-intensity γ source in the starting material.

Preparation of Phosphorus Trichloride

$$2P + 3Cl_2 \rightarrow 2PCl_3$$
$$PCl_3 + Cl_2 \rightarrow PCl_5$$
$$2Sb + 3PCl_5 \rightarrow 3PCl_3 + 2SbCl_3$$

The method (2) of chlorinating red phosphorus to phosphorus trichloride on a large scale, although a straightforward reaction, suffers the disadvantage that an excess of phosphorus must be used to prevent the appearance of the pentachloride in the product. Saunders and Worthy (3) have developed a method for the complete conversion of small (1 g) amounts of phosphorus to the trichloride. Such a method proved impractical on the scale required at Suffield since it required careful standardization of procedures and constant supervision. To avoid waste of the active phosphorus the method of chlorination was modified and advantage was taken of the reducing properties of pure antimony to convert phosphorus pentachloride to the trichloride. The purity of the phosphorus trichloride, checked by infrared spectroscopy, is excellent. The absorption spectrum (Fig. 7) shows a very small percentage of P=O, much less than by reagent grade commercial product triply distilled in dry nitrogen.

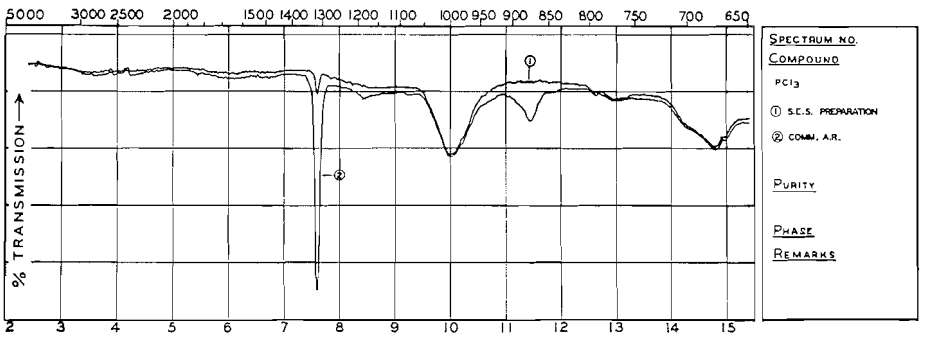


FIG. 7. Spectrum of PCl_3. (1) Synthetic product; (2) commercial product, AR grade.

Preparation of the Aluminum Chloride:Phosphorus Trichloride:Methyl Chloride (APC) *Complex*

The formation of the 1:1:1 molar aluminum chloride:phosphorus trichloride:methyl chloride (APC) complex proceeds very smoothly in pressure-type apparatus to give yields which are virtually quantitative. When the method is applied to the synthesis of radioactive APC complex, however, it has one marked disadvantage in that the solid has to be transferred from the pressure-type reaction apparatus to the reactor in which the subsequent breakdown of the complex is to be carried out. This introduces a severe radiological hazard since, of necessity, it results in external contamination of the apparatus with consequent risk of ingestion in subsequent operations. The use of the high-boiling electron-donating solvent (used in the breakdown of the APC complex) to dissolve the complex from the pressure reactor reduced, but did not eliminate, this hazard.

Fortunately, it was discovered that the formation of the APC complex at atmospheric pressure proceeds very smoothly at the temperature of refluxing phosphorus trichloride,

Can. J. Chem. Downloaded from www.nrcresearchpress.com by 91.191.171.90 on 09/05/12
For personal use only.

and yields are very good provided that loss of the trichloride by the purging action of the methyl chloride passing through the reaction mixture is prevented, and that the reactants are vigorously agitated. The 1:1:1 molar complex can not be made satisfactorily by this method due to the high melting point of this complex, and accordingly an excess of aluminum chloride is used to give a mixture of the 1:1:1 and 2:1:1 aluminum chloride: phosphorus trichloride:methyl chloride complexes, which remain sufficiently fluid for adequate mixing at a temperature of 70°–75° C until absorption of methyl chloride is complete.

Preparation of Methylphosphonic Dichloride

The successful preparation of alkylphosphonic dichlorides was first reported by Kinnear *et al.* (4) and by Clay (5). Their method involved the hydrolysis of a refrigerated solution of the complex in methylene chloride by means of water according to the following reaction:

$$CH_3PCl_3^+.AlCl_4^- + 10H_2O \rightarrow CH_3POCl_2 + AlCl_3.9H_2O + 2HCl.$$

The temperature limits for the hydrolysis (−20° C to −30° C) are critical, and it is essential to filter off immediately the precipitate of the non-anhydrate from this very cold mixture on completion of the reaction. In the laboratory, the high cooling rate could be maintained only by the continuous addition of dry ice. Constant supervision was also required to determine the end point of the hydrolysis.

The breakdown of the complex by this method would prove to be a most difficult and radiologically dangerous part of the synthesis.

An investigation of the breakdown process was made, therefore, and resulted in a novel method, which eliminated almost entirely the excessive hazards intrinsic in the old water hydrolysis reaction scheme. The details of this process, which is completely anhydrous in its function, are reported elsewhere (1). For clarity, however, the following brief account is made.

It was found initially that a high-boiling polyether, dimethoxytetraglycol, not only exhibits excellent solvent properties but also, by complexing with the aluminum chloride itself, frees the phosphorus-containing moiety of the APC complex. The methylphosphonic tetrachloride so liberated reacts smoothly with sulphur dioxide to give thionyl chloride and methylphosphonic dichloride.

$$CH_3PCl_3^+.AlCl_4 + CH_3O(CH_2CH_2O)_4CH_3 \rightleftharpoons CH_3O(CH_2CH_2O)_4CH_3{:}AlCl_3 + CH_3PCl_4$$

$$CH_3PCl_4 + SO_2 \rightarrow CH_3POCl_2 + SOCl_2.$$

The original discovery of the role of dimethoxytetraglycol has been extended to diethyl phthalate, a more stable electron donor.

The methylphosphonic dichloride is readily recovered in excellent yields (80–85% of pure redistilled product) by vacuum distillation.

It can be seen, by comparison with the original aqueous procedure, that the new method has eliminated most of the hazardous procedures; all contaminated residues are left in the flask, no filtration is required, no refrigeration is required, no contaminated volatile gases are evolved, and observation and control are easily effected from a distance.

Preparation of Radioactive Sarin

The two-stage synthesis (reactions 3 and 4) of sarin from methylphosphonic dichloride is relatively simple to carry out and gives good yields of very pure product. The main disadvantage is the radiological hazard which results from the numerous handling

Can. J. Chem. Downloaded from www.nrcresearchpress.com by 91.191.171.90 on 09/05/12
For personal use only.

procedures involved in preparing the equimolar di–di (methylphosphonic dichloride and methylphosphonic difluoride) mixture required for the esterification stage.

The mechanism of the di–di reaction (6) clearly indicated that it should be possible to produce sarin from methylphosphonic dichloride by direct esterification and fluorination in one stage provided that the half esterification of the dichloride is carried out in the presence of free hydrofluoric acid. The reaction was investigated using non-radioactive dichloride and was found to proceed smoothly in methylene chloride as a diluent using reaction conditions very similar to those employed in the normal di–di reaction. Distillation of the product from diethylaniline removes last traces of free acid, and the trace amount that codistills with the pure sarin stabilizes the final product. Yields of pure sarin obtained by this method are virtually the same as those by the normal di–di reaction, viz. 82–87%.

The synthesis of sarin by this one-stage process from the dichloride has the following advantages:

(*a*) The elimination of one stage decreases the time of synthesis and the radiological exposure of the operators.

(*b*) The handling procedures required in making the equimolar di–di mixture are eliminated.

(*c*) The over-all yield of sarin from dichloride is increased since the fluorination stage, which gave a 90–92% yield of difluoride, is eliminated as are small losses which were inevitable in making up the accurate equimolar di–di mixture.

The purity of the sarin prepared by the one-stage process, like that of the normal di–di reaction, is better than 99% (7) with careful fractionation.

ACKNOWLEDGMENTS

The authors wish to acknowledge their indebtedness to Drs. D. G. Coe and J. L. Ferron for their professional assistance, to Mr. W. C. Carpenter for technical assistance, to Mr. D. O'Connor for his fabrication of the glass apparatus, and to Misses B. Melanson and L. Norton for drafting.

REFERENCES

1. J. B. Reesor, B. J. Perry, and E. Sherlock. In preparation.
2. W. C. Fernelius (*Editor*). Inorganic syntheses. Vol. II. McGraw-Hill Book Co., Inc., New York. 1946. p. 145.
3. B. C. Saunders and T. S. Worthy. J. Chem. Soc. 1320 (1950).
4. A. M. Kinnear and E. A. Perren. J. Chem. Soc. 3437 (1952).
5. J. P. Clay. J. Org. Chem. **16**, 892 (1951).
6. Ministry of Supply, U.K. Unpublished report.
7. B. Gehauf, J. Epstein, G. B. Wilson, B. Witten, S. Sass, V. E. Bauer, and W. H. C. Rueggeberg. Anal. Chem. **29**, 278 (1957).

Can. J. Chem. Downloaded from www.nrcresearchpress.com by 91.191.171.90 on 09/05/12
For personal use only.

Can. J. Chem. Downloaded from www.nrcresearchpress.com by 186.148.149.217 on 09/04/12
For personal use only.

ORGANO ARSENIC COMPOUNDS

I. N,N-DIALKYL AMIDODICHLOROARSENITES AND N-ALKYL IMIDOCHLOROARSENITES[1]

G. A. Olah and A. A. Oswald[2]

N,N-Dialkyl amidodichloroarsenites were prepared by the reaction of arsenic trichloride with aliphatic secondary amines. Arsenic trichloride and primary amines react similarly, but the N-alkyl amidodichloroarsenites formed usually lose HCl and give N-alkyl imidoarsenites on distillation.

The reaction of aromatic amines with arsenic trichloride has been studied earlier (1–6). These studies were concerned with both the addition reaction and the formation of N-aryl amidohaloarsenites. The main aim of the work reported was to ascertain the mechanism of phenarsazin syntheses.

There are two N,N-dialkyl amidodichloroarsenites described in the literature. In 1896 Michaelis and Luxembourg (7) published the synthesis of "diisobutylamino-dichloro-arsin" by adding diisobutylamine to arsenic trichloride. This method is analogous to that used for the corresponding phosphorus compounds. In 1935 Doak (8) synthesized "diethylamino dichloro arsenamide" by adding arsenic trichloride to a solution of diethylamine in *n*-heptane. When piperidine was used in the place of diethylamine, 20.95% crystalline arsenous acid tripiperidide trihydrochloride and a yellow oil (b.p. 98° C at 1 mm), supposedly piperidinodichloroarsenite, were obtained. No yields were reported for any of these compounds.

In this work the reaction of arsenic trichloride with some aliphatic secondary amines was examined.

$$AsCl_3 + 2R_2NH \rightarrow R_2NAsCl_2 + R_2NH.HCl$$

By adding 2 moles of secondary amine (dimethylamine, diethylamine, piperidine, morpholine) to every mole of arsenic trichloride (both in benzene solution), the corresponding amidodichloroarsenites were obtained in good yields as is shown in the following table:

TABLE I

N,N′-Dialkyl amidodichloroarsenites

R,R_2NAsCl_2

R	R_2	Boiling point, °C/mm	Refractive index, n_D^{20}	Molecular weight Calc.	Molecular weight Found (in benzene*)	Chlorine, % Calc.	Chlorine, % Found	Nitrogen, % Calc.	Nitrogen, % Found	Yield, %
Methyl	Methyl	50–51/10	1.5564	189.9	201	37.34	37.5	7.37	7.41	81
Ethyl	Ethyl	70–71/9†	1.5345	218	235	32.53	32.5	6.42	6.65	78.5
Piperidyl		91/10‡	1.5675	230	248	30.87	31.2	6.09	6.27	75
Morphonyl		125–7/13§	—	231.9	—‖	30.57	30.8	6.03	6.21	76

*Literature references 12, 14, 15 for method of determination.
†Doak (8) found a boiling point of 107° C at 38 mm.
‡Doak's compound (8), which boils at 90° C at 1 mm, is different from the piperididodichloroarsenite obtained by this method.
§M.p. 87.
‖The compound is only slightly soluble in benzene.

[1]*Manuscript received April 19, 1960.*
Contribution No. 14 from the Exploratory Research Laboratory of Dow Chemical of Canada, Limited, Sarnia, Ontario.
[2]*Present address: Research Department, Imperial Oil Ltd., Sarnia, Ontario.*

Can. J. Chem. Downloaded from www.nrcresearchpress.com by 186.148.149.217 on 09/04/12
For personal use only.

The dimethylamido-, diethylamido-, and piperidino-dichloroarsenites are colorless liquids. The morpholidodichloroarsenite is a white, crystalline compound. All of the amidodichloroarsenites which we have prepared are decomposed by water in a violent, exothermic reaction. As a consequence of their sensitivity towards hydrolysis, the liquid compounds "fume" in contact with wet air. They cause an immediate, burning pain and later, blisters appear on contact with the skin.

No literature data were found on the reaction of monoalkyl amines with arsenic trichloride. We have studied the reaction of arsenic trichloride with some simple primary aliphatic amines under the conditions used with the secondary amines. The reaction of *tert*-butyl amine and arsenic trichloride gave a white crystalline compound, also sensitive towards hydrolysis. The analysis of the compound did not correspond to an amidodichloroarsenite, but to an imidochloroarsenite, namely N-*tert*-butyl-imidochloroarsenite. This new type of compound was formed presumably through HCl elimination from the primary amidodichloroarsenite.

$$AsCl_3 + 2\,tert\text{-}C_4H_9NH_2 \longrightarrow \begin{matrix} Cl \\ Cl \end{matrix}\!\!\diagdown\!\!\diagup As{-}NH{-}t\text{-}C_4H_9 + t\text{-}C_4H_9NH_2.HCl$$

$$\downarrow -HCl$$

$$Cl{-}As{=}N{-}t\text{-}C_4H_9$$

Michaelis and Schroeter (10) obtained a phosphorus compound with similar structure (N-phenyl imidochlorophosphite) by heating aniline hydrochloride with phosphorus trichloride. They called it benzolphosphazochloride. Arsenimides, which contain an N=As (arsazo) bond on the basis of their monomeric structural formula, were obtained by reacting aliphatic or aromatic dichloroarsines with ammonia or primary amines (12, 13). These compounds, like all compounds containing a double-bonded arsenic atom, have multiple molecular weights (12). On the basis of the freezing point depressions of their benzene solutions their molecular weights are 4 times greater than that calculated from the monomeric formula (14). In this work a twofold double molecular weight was found for the N-*t*-butyl imidochloroarsenite, which seems therefore to be present in the dimeric form. The synthesis of N-alkyl imidochloroarsenites was also effected with ethylamine and isopropylamine. However, the derivatives obtained in these cases were less stable and they decomposed slightly on vacuum distillation.

TABLE II

Imidochloroarsenites

Cl—As=N—R

R	Boiling point, °C/mm Hg	Refractive index, n_D^{20}	Molecular weight: Calc. (monomeric)	Molecular weight: Found (in benzene)	Chlorine, % Calc.	Chlorine, % Found	Nitrogen, % Calc.	Nitrogen, % Found	Yield, %
C_2H_5	155/10 mm dec., m.p. 90–95° C		153.5	505	23.10	25.2	9.12	8.89	71
i-C_3H_7	152–153/10 dec.	1.5964	167.5	527	21.17	21.7	8.36	7.96	65
t-C_4H_9	114–115/10		181.5	375	19.53	19.9	7.72	7.80	66.5

The raw product obtained from the reaction of cyclohexylamine and arsenic trichloride showed good analytical agreement for cyclohexyl amidodichloroarsenite, but decomposed on attempted distillation. The latter fact suggests that the imidochloroarsenites are formed from amidodichloroarsenite intermediates by losing hydrogen chloride.

Can. J. Chem. Downloaded from www.nrcresearchpress.com by 186.148.149.217 on 09/04/12
For personal use only.

EXPERIMENTAL

Owing to the sensitivity of the products towards hydrolysis, all the work was carried out with the exclusion of moisture.

N,N-*Dialkyl Amidodichloroarsenites*

To a benzene solution (200 ml) of 18.1 g (0.1 mole) arsenic trichloride a solution of 0.21 mole aliphatic secondary amine in benzene (50 ml) was added slowly while the mixture was stirred and cooled with ice. Right at the start of the addition the precipitation of amine hydrochloride began. After the addition was completed the mixture was stirred for another 10 minutes and during this time cooling was also maintained to control the exothermic reaction. To complete the reaction cooling was discontinued, but stirring was continued for another half an hour at room temperature. The reaction mixture was then filtered by suction and the precipitate washed with benzene. From the filtrate the solvent was removed by distillation at 100 mm Hg and the raw products were purified by vacuum fractionation at about 10 mm Hg to obtain the corresponding dialkyl amidodichloroarsenites, usually as colorless liquids. Some data on the compounds prepared are shown in Table I.

N-*Alkyl Imidochloroarsenites*

Arsenic trichloride (18.1 g (0.1 mole)) was reacted with 0.21 mole of the corresponding primary aliphatic amine (ethyl-, *i*-propyl-, *t*-butyl-) as described for the preparation of alkyl amidodichloroarsenites. After the reaction was completed, the solvent was removed by distillation and the remaining raw product was fractioned in vacuum. The alkyl imidochloroarsenites are colorless; if slightly decomposed they are yellow compounds. The *t*-butyl and ethyl compound solidifies after distillation. Yields, physical data, and analytical data are summarized in Table II.

N-*Cyclohexyl Amidodichloroarsenites*

The reaction between 18.1 g (0.1 mole) arsenic trichloride and 20.9 g (0.21 mole) cyclohexylamine was carried out as described. After volatile components were removed from the filtrate of the reaction mixture at 100° C/10 mm, 17.5 g pale yellow, transparent liquid was obtained. This is a 72.8% yield calculated for N-cyclohexyl amidodichloroarsenite. An attempt to distill it at 5 mm resulted in decomposition. $C_6H_{12}NAsCl_2$: molecular weight calculated, 244; found, 508. N%: calculated, 6.71; found, 6.82. Cl%: calculated, 29.06; found, 29.8.

REFERENCES

1. H. SCHIFF. Compt. rend. **56**, 1095 (1863).
2. R. ANSCHUTZ and H. WEYER. Ann. **261**, 279 (1890).
3. G. T. MORGAN and F. M. G. MICKLETHWAIT. J. Chem. Soc. **45**, 1473 (1909).
4. H. WIELAND and W. RHEINHEIMER. Ann. **423**, 1 (1921).
5. J. M. SCHMIDT. J. Am. Chem. Soc. **43**, 2449 (1921).
6. C. S. GIBSON, J. D. A. JOHSON, and D. C. VINING. Rec. trav. chim. **49**, 1006 (1930).
7. A. MICHAELIS and K. LUXEMBOURG. Ber. **29**, 710 (1896).
8. G. O. DOAK. J. Am. Pharm. Assoc. **24**, 453 (1935).
9. C. S. LEONARD. J. Am. Chem. Soc. **43**, 2618 (1921).
10. A. MICHAELIS and G. SCHROETER. Ber. **27**, 490 (1894).
11. A. MICHAELIS. Ann. **320**, 271 (1902).
12. V. IPATIIEW, G. RASUWAJEV, and V. STROMSKI. Ber. **62**, 598 (1929).
13. C. K. BANKS, J. F. MORGAN, R. L. CLARK, E. B. HATLEID, F. H. KEHLER, H. W. PAXTON, E. J. GRAGOE, R. J. ANDRES, B. ELPERN, R. F. COLES, J. LAWHEAD, and C. S. HAMILTON. J. Am. Chem. Soc. **69**, 927 (1947).
14. F. F. BLICKE and F. D. SMITH. J. Am. Chem. Soc. **52**, 2946 (1930).
15. A. R. MORGAN and S. T. BOWDEN. Trans. Faraday Soc. **36**, 394 (1940).

Can. J. Chem. Downloaded from www.nrcresearchpress.com by 210.87.254.105 on 09/05/12
For personal use only.

ORGANO ARSENIC COMPOUNDS

II. N,N-DIALKYL AMIDODIFLUOROARSENITES AND N-ALKYL IMIDOFLUOROARSENITES[1]

GEORGE A. OLAH AND ALEXIS A. OSWALD[2]

ABSTRACT

The reaction of arsenic fluoride with aliphatic amines was studied. Secondary amines gave N,N-dialkyl amidodifluoroarsenites. Primary amines while reacting similarly lose HF subsequently and yield N-alkyl imidofluoroarsenites.

The reaction of aliphatic primary and secondary amines with arsenic trichloride was examined in the first part of this work (1). We report now the behavior of these amines towards arsenic trifluoride. On reacting gaseous ammonia and arsenic trifluoride, Besson (2) obtained a solid addition product, $2AsF_3.5NH_3$. Woolf and Greenwood (3) examined the complex formation of arsenic trifluoride. They found that arsenic trifluoride gives less stable complexes than boron trifluoride or antimony pentafluoride.

By adding 2 moles of a secondary amine to 1 mole of arsenic trichloride in benzene solution, N,N-dimethylamido-, N,N-diethylamido-, and piperidino-difluoroarsenites were synthesized according to the following equation:

$$AsF_3 + 2R_2NH \rightarrow R_2NAsF_2 + R_2NH.HF.$$

After the amine hydrofluoride was filtered off, the amidodifluoroarsenites were purified by vacuum distillation and obtained as colorless liquids. All these compounds have characteristic odors and are sensitive to hydrolysis.

TABLE I

Amidodifluoroarsenites
$R'R''NAsF_2$

R′	R″	Boiling point, °C/mm	Refractive index, n_D^{20}	Nitrogen, % Calc.	Nitrogen, % Found	Fluorine, % Calc.	Fluorine, % Found	Yield, %	Molecular weight Calc.	Molecular weight Found
Methyl	Methyl	43–44/40	1.4461	8.92	8.89	24.20	24.3	59	157	182
Ethyl	Ethyl	39–40/20	1.4857	7.57	7.59	20.53	20.8	75	185	204
Piperidyl		44–45/10	1.4920	7.10	7.09	19.28	19.5	69	197	206
Cyclohexyl	H	94/9*	—	6.63	6.75	18.00	18.3	67	211	218

*M.p. 65–66.

Some aliphatic primary amines were also reacted with arsenic trifluoride under the same conditions which were used with the secondary amines. Ethyl-, *i*-propyl-, and *t*-butyl-amines gave the corresponding N-alkyl imidofluoroarsenites.

$$AsF_3 + 2RNH_2 \rightarrow RNHAsF_2 + RNH_2.HF$$
$$\downarrow -HF$$
$$R{-}N{=}As{-}F$$

The latter compounds can be all distilled in vacuum without decomposition. However,

[1]*Manuscript received April 19, 1960.*
Contribution No. 15 from the Exploratory Research Laboratory of Dow Chemical of Canada, Limited, Sarnia, Ontario.
[2]*Present address: Research Department, Imperial Oil Ltd., Sarnia, Ontario.*

they are sensitive towards hydrolysis. Their molecular weights are 2 to 4 times greater on the basis of the freezing point depressions of benzene solutions than the calculated values for the monomeric formula shown in the above equation. Consequently they are similar to the arsenimides of other type (4) and may be characterized as low molecular weight polymers.

The reaction of arsenic trifluoride with cyclohexylamine under similar conditions did not give N-cyclohexyl imidofluoroarsenite, but instead yielded N-cyclohexyl amidodifluoroarsenite. In this case the primary amine derivative did not lose hydrogen fluoride to form the corresponding imidofluoroarsenite.

TABLE II
Imidofluoroarsenites
$(RNAsF)_n$

R	Boiling point, °C/mm Hg	Refractive index, n_D^{20}	Nitrogen, % Calc.	Nitrogen, % Found	Fluorine, % Calc.	Fluorine, % Found	Yield, %	Molecular weight Calc. (monomeric)	Molecular weight Found
Ethyl	180–182/12	1.5752	10.23	10.61	13.90	13.4	60	137	560
i-Propyl	150–155/9	1.5492	9.27	9.22	12.58	12.6	63	151	775
t-Butyl	91–92/8*	—	8.48	8.52	11.51	11.7	67	175	360

*M.p. 90–91.

EXPERIMENTAL

Arsenic trifluoride was prepared according to Russel, Rundle, and Yost (5), distilled twice, and stored in a polyethylene flask. Absolute benzene and available purest anhydrous amines were used. The work was carried out with the strictest exclusion of air and moisture. The use of arsenic trifluoride (6) and the fluoroarsenite products require careful work since these arsenic compounds have both the properties of arsenic and hydrogen fluoride regarding vapor and contact effect. For molecular weight determination, the freezing point depression of benzene solutions was used.

N,N-*Dialkyl Amidodifluoroarsenites*

A solution of 0.2 mole of the secondary amine in 50 ml toluene (or benzene) was added slowly to a mixture of 13.2 g (0.1 mole) arsenic trifluoride and 150 ml toluene (or benzene) between 0 and 10° C under cooling and effective stirring. The amine hydrofluoride started to precipitate as soon as the amine addition began. After the addition of the amine was completed, the reaction mixture was kept for an additional 15 minutes below 0° C and then was allowed to come to room temperature. The stirring was continued at room temperature for about 1 hour. Then the amine hydrofluoride was filtered by suction and washed carefully with a small amount of toluene (benzene). From the clear filtrate so obtained the solvent was removed by distillation between 50 and 100 mm. This left the raw products behind as a yellow liquid. It was purified by fractionation in vacuum. In this manner the N,N-dimethylamido-, N,N-diethylamido-, and piperidino-difluoroarsenites were obtained as colorless liquids with an unpleasant smell. Yields, physical data, and analytical data of the compounds are shown in Table I.

N-*Alkyl Amidodifluoroarsenites*

Starting from 0.2 mole of the corresponding primary amine (ethyl-, *i*-propyl-, or *t*-butyl-amine) and 13.2 g (0.1 mole) arsenic trifluoride, the preparations were carried out in the same manner as that described for N,N-dialkyl amidodifluoroarsenites. After

Can. J. Chem. Downloaded from www.nrcresearchpress.com by 210.87.254.105 on 09/05/12
For personal use only.

the solvent was removed by distillation, the raw product remaining was fractionated in vacuum. The N-ethyl- and N-*i*-propyl-imidofluoroarsenites were obtained as almost colorless and odorless liquids. The N-*t*-butyl imidofluoroarsenite solidified to white crystals. Physical and analytical data and the yields of the compounds prepared are shown in Table II.

N-*Cyclohexyl Amidodifluoroarsenites*

Benzene solutions of 19.8 g (0.2 mole) cyclohexylamine and 13.2 g (0.1 mole) arsenic trifluoride were reacted in the manner used with previous examples. After being filtered by suction, the cyclohexylamine hydrofluoride was washed with benzene. The filtrate containing the main product was distilled. At first benzene was distilled over and then at 95° C/9 mm N-cyclohexyl amidodifluoroarsenite, which solidified to white crystals melting at 65–66° C. Further data are shown in Table I.

REFERENCES

1. G. A. OLAH and A. A. OSWALD. Can. J. Chem. This issue.
2. M. BESSON. Compt. rend. **110**, 1258 (1890).
3. A. A. WOOLF and N. N. GREENWOOD. J. Chem. Soc. 2200 (1950).
4. F. F. BLICKE and F. D. SMITH. J. Am. Chem. Soc. **52**, 2946 (1930).
5. H. RUSSEL, JR., R. E. RUNDLE, and D. N. YOST. J. Am. Chem. Soc. **63**, 2825 (1941).
6. J. B. A. DUMAS. Ann. chim. et phys. (2) **31**, 433 (1826).

Can. J. Chem. Downloaded from www.nrcresearchpress.com by 210.87.254.105 on 09/05/12
For personal use only.

Can. J. Chem. Downloaded from www.nrcresearchpress.com by 210.87.254.105 on 09/05/12
For personal use only.

THE SYNTHESIS OF SOME INDOLYLALKYLAMINOALCOHOLS[1]

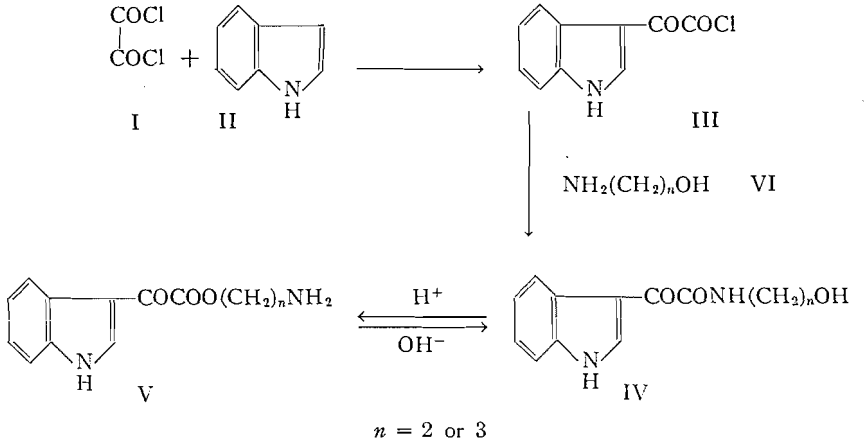
GERASSIMOS FRANGATOS, GEZA KOHAN, AND FRANCIS L. CHUBB

ABSTRACT

A series of 3-indolylalkylaminoalcohols have been obtained from the lithium aluminum hydride reduction of the amides prepared by the reaction of 3-indoleglyoxylyl chloride and 2-methyl-3-indoleglyoxylyl chloride with primary aminoalcohols. When acetone was used as solvent in the reaction of 3-indoleglyoxylyl chloride and either 2-aminoethanol or 3-aminopropanol, the solvent participated in the reaction resulting in the formation of 2,2-dimethyl-3-(3-indoleglyoxyl)oxazolidine and 2,2-dimethyl-3-(3-indoleglyoxyl)tetrahydro-1,3-oxazine respectively. When the latter two compounds were reduced by lithium aluminum hydride, both carbonyl groups were completely reduced and reductive cleavage of the oxazolidine and tetrahydro-1,3-oxazine rings occurred to form the corresponding open-chain alcohols.

It has been shown (1) that oxalyl chloride (I) reacts readily with indole (II) to form 3-indoleglyoxylyl chloride (III), which in turn reacts with amines to give the corresponding amide. Lithium aluminum hydride reduction of these amides resulted in the synthesis of a variety of substituted or unsubstituted tryptamines, except in a few cases (2, 3), where hydroxyamines were isolated from the reaction mixture, because of partial reduction of the carbonyl group to a carbinol instead of to a methylene group.

As part of a program leading to the synthesis of basic esters (4) related in structure to reserpine, the reaction of III with 2-aminoethanol and 3-aminopropanol was investigated. When III was added to a dioxane solution of a slight excess of the aminoalcohol, the corresponding amide IV was obtained in excellent yield. An excess of the aminoalcohol was necessary to prevent the rearrangement (5) of the amide to the isomeric ester V or even simultaneous formation of V. Thus when the aminoalcohols VI were added to III, the amides IV were obtained but apparently were contaminated by the isomeric esters. Lithium aluminum hydride reduction of the amides, carried out in boiling dioxane with a large excess of lithium aluminum hydride, gave the corresponding indolylalkylamines as distillable oils, listed in Table I.



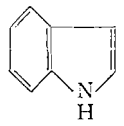
[1]*Manuscript received May 9, 1960.*
Contribution from the Research Laboratories, Frank W. Horner Limited, Montreal, Que.

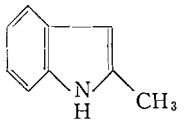
Can. J. Chem. Vol. 38 (1960)

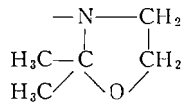
Can. J. Chem. Downloaded from www.nrcresearchpress.com by 210.87.254.105 on 09/05/12
For personal use only.

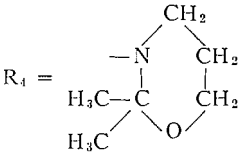
TABLE I

Indoleglyoxylamides and indolylalkylaminoalcohols

R_1 = 

R_2 = 

R_3 = 

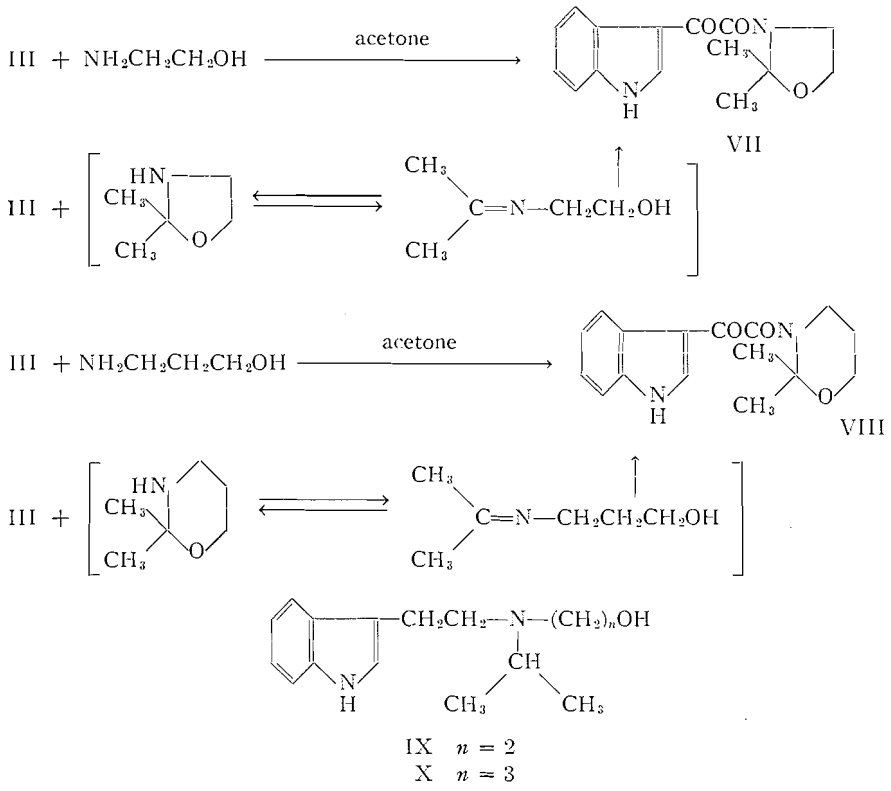
R_4 = 

No.	Structure	Yield, %	Derivative	M.p., °C	B.p., °C	Molecular formula	Analyses					
							Calculated, %			Found, %		
							C	H	N	C	H	N
(1)	$R_1COCONHCH_2CH_2OH$	79.0		213		$C_{12}H_{12}N_2O_3$	62.06	5.21	12.07	61.77	5.29	12.02
(2)	$R_1COCONHCH_2CH_2CH_2OH$	68.3		212		$C_{13}H_{14}N_2O_3$	63.40	5.72	11.38	63.03	5.86	11.40
(3)	R_1COCOR_3	74.5		208		$C_{16}H_{16}N_2O_3$	66.16	5.92	10.29	65.84	6.12	10.06
(4)	R_1COCOR_4	68.6		216		$C_{16}H_{18}N_2O_3$	67.11	6.33	9.79	67.32	6.38	9.94
(5)	$R_1CH_2CH_2N(CH(CH_3)_2)—CH_2CH_2OH$	56.0	Hydrochloride	182		$C_{15}H_{23}ClN_2O$	63.70	8.20	9.91	63.74	8.16	9.62
			Picrate	146		$C_{21}H_{25}N_5O_8$	53.05	5.30	14.73	53.52	5.44	14.84
(6)	$R_1CH_2CH_2NHCH_2CH_2CH_2OH$	72.0			210/1 mm	$C_{13}H_{18}N_2O$			12.84			12.86
			Hydrochloride	122		$C_{13}H_{19}ClN_2O$	61.30	7.46	11.02	61.11	7.41	11.15
			Picrate	163		$C_{19}H_{21}N_5O_8$	51.00	4.73	15.65	51.00	4.92	16.06
(7)	$R_1CH_2CH_2NHCH_2CH_2OH$	64.5	Hydrochloride	148		$C_{12}H_{17}ClN_2O$	59.86	7.12	11.64	60.06	7.07	11.53
(8)	$R_1CH_2CH_2N(CH(CH_3)_2)CH_2CH_2CH_2OH$	48.8		128		$C_{16}H_{24}N_2O$	73.80	9.29	10.76	73.44	9.35	10.80
(9)	$R_2C(=O)—C(=O)—NHCH_2CH_2OH$	71.0		168		$C_{13}H_{14}N_2O_3$	63.40	5.72	11.38	63.34	5.81	11.20
(10)	$R_2C(=O)—C(=O)—NHCH_2CH_2CH_2OH$	69.2	Monohydrate	104		$C_{14}H_{16}N_2O_3 . H_2O$	60.42	6.52	10.07	60.57	6.38	10.42
(11)	$R_2CH_2CH_2NHCH_2CH_2OH$	58.0		121	205/0.5 mm	$C_{13}H_{18}N_2O$	71.52	8.31	12.84	71.29	8.33	13.10
			Picrate	172		$C_{19}H_{21}N_5O_8$	51.00	4.73	15.65	51.13	4.83	15.70
(12)	$R_2CH_2CH_2NHCH_2CH_2CH_2OH$	53.7	Hydrochloride	176		$C_{14}H_{21}ClN_2O$	62.55	7.88	10.42	62.63	7.88	10.45
			Picrate	181		$C_{20}H_{23}N_5O_8$	52.06	5.02	15.18	52.37	5.25	14.60

Can. J. Chem. Downloaded from www.nrcresearchpress.com by 210.87.254.105 on 09/05/12
For personal use only.

When acetone was used as a solvent in the reaction of III with 2-aminoethanol and 3-aminopropanol it was found that the amides obtained were different from those obtained when dioxane was used as the solvent. Analysis and infrared spectra showed that acetone had participated in the reaction to furnish a substituted oxazolidine VII and tetrahydro-1,3-oxazine VIII respectively. The infrared spectrum of these compounds exhibited a triplet of bands in the 1020–1210 cm^{-1} region, characteristic of the oxazolidine (6) and 1,3-tetrahydrooxazine (7) rings while hydroxy group absorption was absent. Additional supporting evidence was provided by the fact that both compounds VII and VIII were obtained from the reaction of III with the preformed condensation products of acetone and either 2-aminoethanol or 3-aminopropanol. It has been shown (8, 9) that the reaction product of 2- or 3-primary aminoalcohols and aliphatic ketones is a mixture of either oxazolidine or tetrahydro-1,3-oxazine and the corresponding Schiff base in a state of mobile equilibrium. However, when a substituent other than hydrogen is attached to the nitrogen, this state of equilibrium no longer exists because the Schiff base cannot form and only the oxazolidine or tetrahydro-1,3-oxazine structure remains.

When VII and VIII were subjected to lithium aluminum hydride reduction in boiling dioxane, both carbonyl groups were completely reduced and reductive cleavage of the oxazolidine and tetrahydro-1,3-oxazine rings occurred to give the open-chain alcohols IX and X, respectively. This reductive cleavage was in agreement with earlier reports (10) on the cleavage of oxazolidines.



2-Methyl-3-indoleglyoxylyl chloride (XI) reacted with 2-aminoethanol and 3-aminopropanol in dioxane to give the corresponding amides. The latter compounds were

reduced by lithium aluminum hydride to the corresponding 2-methyl-3-indolylethyl-aminoalcohols (see Table I).

An attempt to effect the reaction of XI with 2-aminoethanol and 3-aminopropanol in acetone solution or with the preformed condensation products of acetone and 2-amino-ethanol or 3-aminopropanol only resulted in the formation of tars. Molecular models (Stuart) of the expected compounds showed that the hindrance was not purely steric.

EXPERIMENTAL*

3-Indoleglyoxylyl Chloride

The procedure of Nogradi (11) was followed for the preparation of this compound. 2-Methyl-3-indoleglyoxylyl chloride was similarly prepared.

2-(3-Indoleglyoxyl)amidoethanol

Freshly prepared 3-indoleglyoxylyl chloride (29.5 g) was suspended in 125 ml of dioxane and cooled to 15°. This suspension was added slowly with stirring to a solution of 25 ml of 2-aminoethanol in 100 ml of dioxane. During the addition and for another half hour, the reaction was kept at 12–15°. Most of the dioxane (175 ml) was distilled under reduced pressure and 150 ml of water was added to the mixture. A yellowish coarse powder precipitated, which was filtered and air-dried. Recrystallization from ethanol yielded 26 g (79%), m.p. 213°.

2-(3-Indolylethyl)aminoethanol

Nine grams of 2-(3-indoleglyoxyl)amidoethanol was dissolved in 350 ml of dry dioxane. This solution was added with mechanical stirring and under an atmosphere of dry nitrogen to a suspension of 12.5 g of pulverized lithium aluminum hydride in 230 ml of boiling dioxane. The solution was added at such a rate as to maintain refluxing of the reaction mixture without external heating. After the addition was over the heating was resumed. Great care had to be exercised during the first hour of refluxing because the reaction mixture occasionally started to foam badly. At this point heating and stirring were discontinued for a short time. After the foaming ceased the mixture was refluxed for 6 hours and cooled. The excess lithium aluminum hydride was destroyed cautiously with wet dioxane. The reaction mixture was again brought to the boiling point and filtered hot. The filter cake was washed with 50 ml of hot dioxane. The combined clear filtrates were distilled under reduced pressure and the residual oil was distilled *in vacuo*. 2-(3-Indolylethyl)aminoethanol (5.2 g, 64.5%) was obtained distilling at 205°/0.2 mm. A chloroform solution of this compound was treated with dry hydrogen chloride and the corresponding hydrochloride precipitated. It was recrystallized from a minimum amount of methanol and melted at 148°.

The amides and aminoalcohols listed in Table I (Nos. 2, 6, 9, 10, 11, 12) were prepared in the same way as 2-(3-indoleglyoxyl)amidoethanol and 2-(3-indolylethyl)aminoethanol.

2,2-Dimethyl-3-(3-indoleglyoxyl)oxazolidine

(A) Fifty grams of 2-aminoethanol was dissolved in 500 ml of acetone at 0°. To this solution a suspension of 50 g of 3-indoleglyoxylyl chloride was added slowly with stirring. The reaction mixture was cooled and stirred for an additional half hour. The yellow color of the suspension gradually faded and an oily layer separated at the bottom of the flask. The acetone was distilled under reduced pressure. The viscous residue was dissolved in

**Melting points are uncorrected. Analyses were determined by E. Thommen, Basel, Switzerland. Infrared spectra were obtained in a Perkin–Elmer 21 double-beam spectrophotometer using sodium chloride optics in potassium bromide disks.*

Can. J. Chem. Downloaded from www.nrcresearchpress.com by 210.87.254.105 on 09/05/12
For personal use only.

100 ml of boiling ethanol, treated with charcoal, and precipitated upon addition of water. 2,2-Dimethyl-3-(3-indoleglyoxyl)oxazolidine (36.5 g, 62.3%) was obtained, m.p. 208°. It exhibited a triplet absorption band in the infrared at 1104, 1131, and 1171 cm^{-1}.

(B) "2,2-Dimethyloxazolidine" was prepared according to the directions of Bergmann (9). Thirty-seven grams of freshly prepared "2,2-dimethyloxazolidine" was dissolved in 500 ml of absolute ether. To this mixture a suspension of 32 g of 3-indoleglyoxylyl chloride in 250 ml of ether was added at room temperature with stirring. After the addition was completed the reaction mixture was stirred and refluxed gently for 20 minutes. It was cooled and filtered. The crude product was washed on the filter with water and recrystallized from aqueous ethanol. Twenty-eight grams (74.5%) of 2,2-dimethyl-3-(3-indoleglyoxyl)oxazolidine was obtained melting at 208° and showing no depression of melting point upon mixing with a sample obtained according to procedure A.

2-(3-Indolylethyl)isopropylaminoethanol

The reduction of 2,2-dimethyl-3-(3-indoleglyoxyl)oxazolidine was effected by lithium aluminum hydride in boiling dioxane. The procedure already described for the synthesis of 2-(3-indolylethyl)aminoethanol was followed. It exhibited infrared absorption bands at 3538 (OH) and 3252 cm^{-1} (NH) (12).

2,2-Dimethyl-3-(3-indoleglyoxyl)tetrahydro-1,3-oxazine

This compound was obtained from the reaction of 3-indoleglyoxylyl chloride with either 3-aminopropanol in acetone solution or "2,2-dimethyltetrahydro-1,3-oxazine" (7). Similar experimental conditions to those used for the synthesis of 2,2-dimethyl-3-(3-indoleglyoxyl)oxazolidine (procedures A and B). It exhibited a triplet absorption band in the infrared at 1067, 1105, and 1148 cm^{-1}.

3-(3-Indolylethyl)isopropylaminopropanol

The lithium aluminum hydride reduction of 2,2-dimethyl-3-(3-indoleglyoxyl)tetrahydro-1,3-oxazine to 3-(3-indolylethyl)isopropylaminopropanol was effected by a procedure similar to that used for the reduction of 2-(3-indoleglyoxyl)aminoethanol.

REFERENCES

1. M. E. Speeter and W. C. Anthony. J. Am. Chem. Soc. **76**, 6208 (1954).
2. F. V. Brutcher, Jr. and W. D. Vanderwerff. J. Org. Chem. **23**, 147 (1958).
3. A. F. Ames, D. E. Ames, C. R. Coyne, T. F. Grey, I. M. Lockhart, and R. S. Ralph. J. Chem. Soc. 3388 (1959).
4. G. Frangatos, G. Kohan, and F. L. Chubb. Can. J. Chem. In press.
5. A. P. Phillips and R. Baltzly. J. Am. Chem. Soc. **69**, 200 (1947).
6. E. D. Bergmann, E. Zimkin, and S. Pinchas. Rec. trav. chim. **71**, 168 (1952).
7. E. D. Bergmann and A. Kaluszyner. Rec. trav. chim. **78**, 315 (1959).
8. G. E. McCasland and E. C. Horswill. J. Am. Chem. Soc. **73**, 3923 (1951).
9. E. D. Bergmann, E. Gil-Av, and S. Pinchas. J. Am. Chem. Soc. **75**, 358 (1953).
10. E. D. Bergmann, D. Lavie, and S. Pinchas. J. Am. Chem. Soc. **73**, 5662 (1951).
11. Th. Nogradi. Monatsh. **88**, 768 (1957).
12. E. Millich and E. I. Becker. J. Org. Chem. **23**, 1096 (1958).

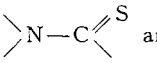
Can. J. Chem. Downloaded from www.nrcresearchpress.com by 210.87.254.105 on 09/05/12
For personal use only.

Can. J. Chem. Downloaded from www.nrcresearchpress.com by 210.87.254.40 on 09/05/12
For personal use only.

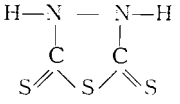
ABSORPTION SPECTRA OF 2,5-DIMERCAPTO-1,3,4-THIADIAZOLE AND ITS METHYL DERIVATIVES[1]

G. D. THORN

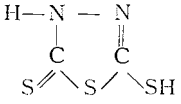
ABSTRACT

The absorption spectra of the three tautomeric forms of 2,5-dimercapto-1,3,4-thiadiazole have been determined by using the N- and S-methyl derivatives. In the ultraviolet region, a hypsochromic shift in absorption maxima is shown in the change from the dithionic to the thionic–thiolic and to the dithiolic forms. Strong bands in the infrared at 1508–1475 cm^{-1} and 1435–1415 cm^{-1} have been assigned to  and , respectively.

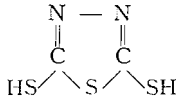
Theoretically the title compound can exist in any of three tautomeric forms (IA, IB, or IC) and thus the name 2,5-dimercapto-1,3,4-thiadiazole may be too rigid. An analogy exists in maleic hydrazide, for which the structure II has been assigned (1), and from which the various N- and (or) O-methyl derivatives have been obtained by alkylation under varied conditions. Zahradník (2) has obtained the ultraviolet absorption spectrum of dimercaptothiadiazole, and has designated the structure as being that of form IA. Sheinker *et al.* (3) believe the compound to have a mixed thionic–thiolic structure (IB).



IA

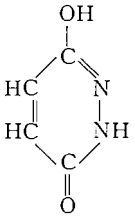


IB

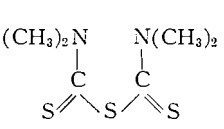


IC

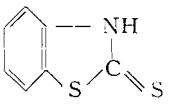
Substitution of alkyl groups for SH or NH hydrogen in 2,5-dimercapto-1,3,4-thiadiazole forces the molecule into one of the tautomeric forms IA, IB, or IC. An investigation of the ultraviolet and infrared spectra of the various alkyl-substituted derivatives was made therefore with a view to assigning specific molecular structures to the various absorption bands of the parent compound.



II



III



IV

The dithiocarbamate grouping, as in esters of dithiocarbamic acids, or in tetramethylthiuram monosulphide (III), shows strong ultraviolet absorption bands in the regions 275–290 mμ and 245–260 mμ (both with log ϵ about 4), and weaker absorption in the region 325–360 mμ (log ϵ about 1.8) (see, for example, Janssen (4)). Zahradník (2)

[1]*Manuscript received April 25, 1960.*
Contribution No. 174, Pesticide Research Institute, Canada Department of Agriculture, University Sub P.O., London, Ontario.

observed that dimercaptothiadiazole did not follow this pattern, but instead showed strong absorption at 332 mμ (log ε 4.2, in ethanol) and a weaker absorption band at 265 mμ. This "anomalous" behavior was also seen in the spectrum of mercaptobenzothiazole (IV), and was explained on the basis of the —S—C(=S)— groups giving the ring a pseudoaromatic character. With tetramethylthiuram monosulphide (III), where the nitrogens are not joined to form a heterocyclic ring, the expected absorption maximum at 280 mμ is observed.

EXPERIMENTAL

2,5-Dimercapto- and *2-mercapto-5-methylmercapto-1,3,4-thiadiazole* (I and IV, respectively) were prepared according to Thorn and Ludwig (5).

2,5-Dimethylmercapto-1,3,4-thiadiazole (VI) was prepared by the reaction of the dimercaptothiadiazole in aqueous ethanol with stoichiometric amounts of methyl iodide and potassium hydroxide, according to Busch and Ziegele (6). Fractional distillation of the water-insoluble product gave a colorless liquid, b.p. 87–88° at 0.05 mm; $n_{23.5}^{D}$ 1.6530. Calc. for $C_4H_6N_2S_3$: S, 54.0%. Found: S, 54.1%. Busch and Ziegele (6) record a melting point of 136°, but in this laboratory a solid product was not obtained in any of several preparations.

2-Mercapto-4-methyl-1,3,4-thiadiazoline-5-thione (VII) was obtained from methylhydrazine and CS_2 according to the method of Busch and Ziegele (7). The product melted at 65–66° after crystallization from diethyl ether. Busch and Ziegele (7) record a melting point of 69°. Calc. for $C_3H_4N_2S_3$: S, 58.6%. Found: S, 58.6%.

2-Methylmercapto-4-methyl-1,3,4-thiadiazoline-5-thione (VIII) was prepared from VII according to Busch and Ziegele (7) and melted at 81–82° after crystallization from 95% ethanol. Lit. (7) gives a melting point of 88°. Calc. for $C_4H_6N_2S_3$: S, 54.0%. Found: S, 53.8%.

3,4-Dimethyl-1,3,4-thiadiazolidine-2,5-dithione (IX) was prepared by heating under reflux for 9 hours an alcohol solution of stoichiometric amounts of dimethylhydrazine dihydrochloride, potassium hydroxide, and carbon disulphide. The product was precipitated from the reaction mixture by the addition of water; yield, 50%. The melting point was 168–169°, after crystallization from 95% ethanol. Calc. for $C_4H_6N_2S_3$: S, 54.0%. Found: S, 53.7%.

Ultraviolet absorption spectra were measured in ethanol solution with the Beckman DK-1 spectrophotometer. Infrared spectra were recorded with the Perkin–Elmer Model 21 instrument with NaCl prism, in chloroform solution or KBr disk.

DISCUSSION

The various tautomeric structures for the dimercaptothiadiazole derivatives studied are given in Fig. 1, together with the ultraviolet absorption bands of these compounds. Nearly identical spectra (λ_{max} 327–335 and 260–268 mμ) are shown by compounds I, VII, and IX. This absorption thus establishes the thione structure for these compounds, as in IX the possibility of enethiolization does not exist. Forcing one of the thiocarbamoyl groups into the enethiol form as in V and VIII results in a hypsochromic shift of both absorption bands. The similarity in spectra for these latter two compounds suggests that in V the second thiocarbamoyl group is in the thione form. The fixing of both thiocarbamoyl groups into the enethiol arrangement results in a further hypsochromic shift

Can. J. Chem. Downloaded from www.nrcresearchpress.com by 210.87.254.40 on 09/05/12
For personal use only.

Can. J. Chem. Downloaded from www.nrcresearchpress.com by 210.87.254.40 on 09/05/12
For personal use only.

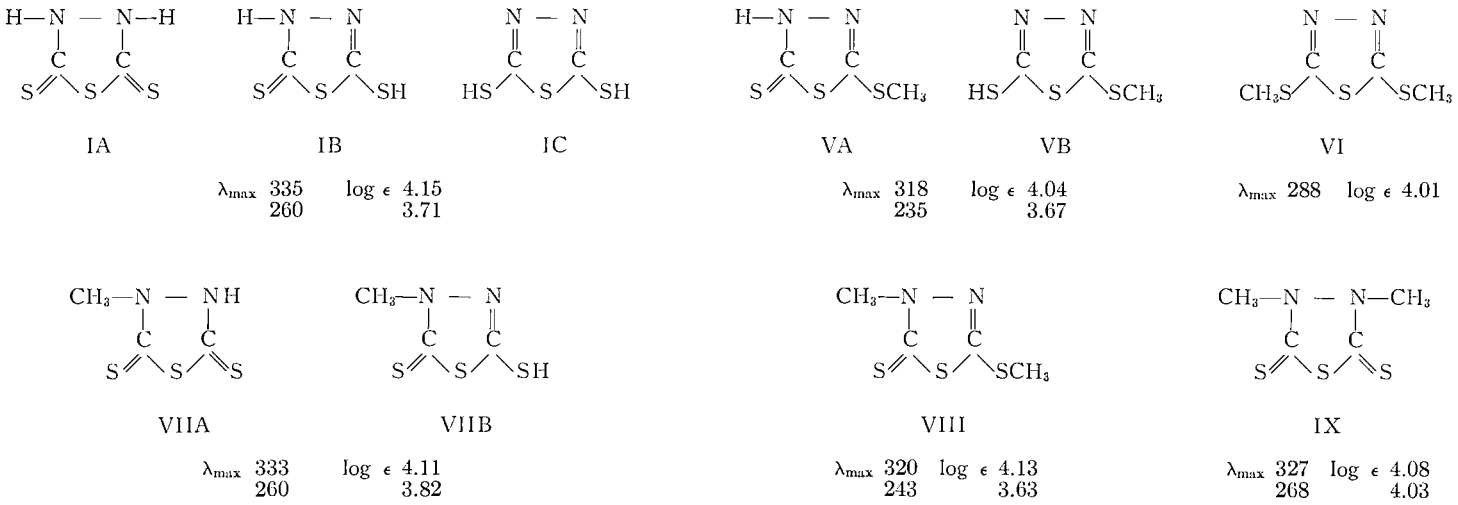
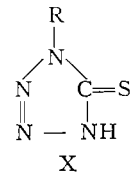


FIG. 1. Possible tautomeric forms for 2,5-dimercapto-1,3,4-thiadiazole and its methyl derivatives, and their ultraviolet absorption maxima (ethanol solution).

of the band of longer wavelength, with loss, in the region studied, of the shorter wavelength band.

Thus, on a consideration of ultraviolet absorption spectra alone, definite assignments of structure can be made. A study of the infrared absorption spectra, however, suggests that these assignments are not as categorical as given above.

The strong band in the region 1610–1470 cm^{-1} appearing in the spectra of compounds containing the $>N-C(=S)<$ group has been assigned by Randall *et al.* (8) to a ν_{CN} frequency strengthened by the ionic form $>N-\overset{+}{C}(-S^-)<$, and was termed by these authors as a "thioureide ion" band. Chatt *et al.* (9), however, have assigned this band to the contribution by the canonical form $>N^+=C(S^-)<$, in the case of dithiocarbamate esters and heavy metal complex salts, and have restricted the "thioureide ion" band to the region 1542–1480 cm^{-1}. Other workers (10, 11, 12) have concluded that this thioureide band is due to a δ_{NH} frequency. An appraisal has been made by Elmore (13) of the nature of the thioureide band. Elmore has suggested that since this band occurs with compounds having no NH group, it cannot be entirely due to a δ_{NH} vibration, although he postulated that coupling between δ_{NH} and ν_{CN} modes may occur in some instances. Lieber *et al.* (14) on the basis of the spectra of a number of 1-substituted tetrazolinethiones and 4-substituted semicarbazides have made a frequency assignment of 1555–1474 cm^{-1} for the $>N-C(=S)-$ grouping and 1395–1338 cm^{-1} for the $>C=S$ linkage. Lieber *et al.* (14) used the occurrence of these bands in 1-substituted tetrazolines (X) together with the absence of the SH band in the region 2600–2550 cm^{-1} (15) to support the thione rather than the thiol structure for these compounds.



X

Table I summarizes the important bands observed for the dimercaptothiadiazoles. In all but two of the compounds, two strong bands, at 1435–1415 cm^{-1} and 1508–1475 cm^{-1} (chloroform solution), are observed. The former is not given by compound IX, the latter not by compound VI. The above results lead us to the view that the 1508–1475 cm^{-1} is indeed assignable to the $>N-C(=S)<$ grouping, perhaps modified by resonance as suggested by Chatt *et al.* (9), and that the band at 1435–1415 cm^{-1} is associated with the $-N=C(S-)<$ grouping.

Lieber *et al.* have made a frequency assignment of 1395–1338 cm^{-1} for the C=S linkage. Mecke and Mecke (16) and Mecke *et al.* (12) had previously assigned a band of strong intensity in the region 1200–1050 cm^{-1} to the C=S grouping, and a band in the 1350–1300 cm^{-1} region to CN vibration. In the dimercaptothiadiazoles, a strong band

Can. J. Chem. Downloaded from www.nrcresearchpress.com by 210.87.254.40 on 09/05/12
For personal use only.

Can. J. Chem. Downloaded from www.nrcresearchpress.com by 210.87.254.40 on 09/05/12
For personal use only.

TABLE 1

Principal infrared bands of 2,5-dimercapto-1,3,4-thiadiazole and its methyl derivatives

Compound	Position of methyl(s)	Solvent system	Absorption bands, cm^{-1}												
I	—	Sat. $CHCl_3$	3430	3100	2590w	1508	1420	1345		1165	1127	1070			
V	S	1% $CHCl_3$	3370	3060		1487	1415	1370			1120	1055		975	
VI	S,S′	10% $CHCl_3$					1435	1395	1320	1230w	1135m	1048		973m	
VII	N	10% $CHCl_3$			2555	1485	1425	1350	1265	1230w	1130		1013m	945m	905
VIII	N,S	10% $CHCl_3$				1475	1428	1357	1265		1125	1065m	1012m	975m	907
IX	N,N′	1% $CHCl_3$				1480		1375	1285m			1097		935m	875m

is given by chloroform solution of all the compounds studied, including the S,S′-dimethyl ether (V), in the 1395–1338 cm^{-1} region assigned by Lieber *et al.* to C=S. An exception is that dimercaptothiadiazole itself does not show absorption in this region in the KBr disk. Strong bands are given also by all these compounds in Mecke's 1050–1200 cm^{-1} region. It may be mentioned that for the methyl and ethyl esters of N,N-dimethyl- and N-methyl-dithiocarbamic acid and of dithiocarbamic acid itself, a strong band is seen (17) in the region 1385–1345 cm^{-1}, but that strong absorption is shown in the 1200–1050 cm^{-1} region only by those dithiocarbamates substituted in the nitrogen, and not by ethyl or methyl dithiocarbamate. On the basis of the above, the author tends to the assignment of Lieber *et al.* of 1395–1338 cm^{-1} for C=S when forming part of the thioureide grouping, made tentative, however, by the two anomalies mentioned in the dimercaptothiadiazole compounds. The thiocarbonyl stretching frequency has been assigned recently to the region 1220–1080 cm^{-1} by Spinner (18), on the basis of unambiguous identity in such compounds as thioformaldehyde and thiocarbonyl chloride. Haszeldine and Kidd (19) previously had given the $\nu_{C=S}$ vibration as 1078 cm^{-1} for ethylene trithiocarbonate. Thus, as is pointed out by Jones *et al.* (20), the frequency for C=S is dependent on the structural environment and falls within the wide range 1400–1000 cm^{-1}.

Mention was made in the discussion on the ultraviolet absorption spectra of the dimercaptothiadiazole derivatives that the assignment of structure made was perhaps too rigorous. The infrared spectra of compounds I and VII in chloroform solution made it apparent that these compounds possess an SH group (absorption in the 2600–2550 cm^{-1} region (15)). The postulate may be advanced that in concentrated chloroform solution these two compounds are primarily in the form of structures IB and VIIB, whereas in dilute alcohol solution the dithione structures IA and VIIA are the predominant forms. For structural systems of this type it has been found that a change in medium may alter the tautomeric equilibrium position (see Spinner (20) and references quoted by him).

ACKNOWLEDGMENTS

The author is grateful for the discussions with Robert W. White on the infrared absorption spectra and expresses his thanks to Dorle Bongart for microanalyses and to Marilyn Coleman for technical assistance.

REFERENCES

1. D. M. Miller and R. W. White. Can. J. Chem. **34**, 1510 (1956).
2. R. Zahradník. Collection Czechoslov. Chem. Communs. **24**, 3193 (1959).
3. Yu. N. Sheinker, I. Ya. Postovskiĭ, and N. M. Voronina. Zhur. Fiz. Khim. **33**, 302 (1959).
4. M. J. Janssen. The electronic structure of organic thion compounds. Doctoral dissertation, Utrecht, Netherlands. 1959.
5. G. D. Thorn and R. A. Ludwig. Can. J. Botany, **36**, 389 (1958).
6. M. Busch and E. Ziegele. J. prakt. Chem. **60**, 40 (1899).
7. M. Busch and E. Ziegele. J. prakt. Chem. **60**, 51 (1899).
8. H. M. Randall, R. G. Fowler, N. Fuson, and J. R. Dangl. Infrared determination of organic structure. D. Van Nostrand Co. Inc., New York. 1949.
9. J. Chatt, L. A. Duncanson, and L. M. Venanzi. Suomen Kemistilehti, **29**B, 75 (1956).
10. L. K. Ramachandran, A. Epp, and W. B. McConnell. Anal. Chem. **27**, 1734 (1955).
11. D. Hadži. J. Chem. Soc. 847 (1957).
12. R. Mecke, R. Mecke, and A. Lüttringhaus. Chem. Ber. **90**, 975 (1957).
13. D. T. Elmore. J. Chem. Soc. 3489 (1958).
14. E. Lieber, C. N. R. Rao, C. N. Pillai, J. Ramachandran, and R. D. Hites. Can. J. Chem. **36**, 801 (1958).
15. L. F. Bellamy. The infrared spectra of complex molecules. Methuen & Co., Ltd., London. 1954.
16. R. Mecke, Jr. and R. Mecke, Sr. Chem. Ber. **89**, 343 (1956).
17. G. D. Thorn. Unpublished results.
18. E. Spinner. J. Chem. Soc. 1237 (1960).
19. R. N. Haszeldine and J. M. Kidd. J. Chem. Soc. 3871 (1955).
20. J. I. Jones, W. Kynaston, and J. L. Hales. J. Chem. Soc. 614 (1957).

Can. J. Chem. Downloaded from www.nrcresearchpress.com by 210.87.254.40 on 09/05/12
For personal use only.

Can. J. Chem. Downloaded from www.nrcresearchpress.com by 210.87.254.5 on 09/05/12
For personal use only.

ARYLPYRIDINES

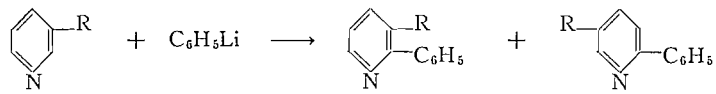
PART II. REACTION OF PHENYLLITHIUM WITH 3-METHOXY- AND 3-AMINO-PYRIDINE[1,2]

R. A. Abramovitch and A. D. Notation

ABSTRACT

Phenyllithium has been shown to react with 3-methoxy- and 3-amino-pyridine to give exclusively 3-methoxy-2-phenylpyridine and 3-amino-2-phenylpyridine respectively. The orientation of the products has been established unambiguously. None of the 2,5-isomer was detected in either case. An explanation for this unique orientation is suggested.

In Part I of this series (1) the orientation of the entering phenyl substituent in the addition of phenyllithium to 3-picoline and to nicotine was studied. In the first case the main product was 3-methyl-2-phenylpyridine (II; R = CH_3) together with a small amount of 5-methyl-2-phenylpyridine (III; R = CH_3), the ratio of the isomers being 19:1. On the other hand phenylation of nicotine gave 2-phenyl- (II; R = -α-$C_4H_7NCH_3$) and 6-phenyl-nicotine (III; R = -α-$C_4H_7NCH_3$) in a 1:1 ratio. Evidence that the 3-substituent exerts an appreciable steric effect in the end product of the addition was



I II III

also presented. The results were interpreted to mean that addition of phenyllithium to 3-substituted pyridines occurs preferentially at the 2-position but that the 3-substituent, if sufficiently bulky, could exert a steric effect resulting in appreciable addition at the 6-position also.

The present paper gives an account of the extension of this study to 3-amino- and 3-methoxy-pyridines both of which are readily available and the products from which could serve as valuable intermediates in synthetic work. Molecular models indicate that the steric effect of a methoxyl group would be expected to be less than that of a methyl group whereas that of a primary amino group, particularly as its lithium salt, should be comparable with that of a methyl group. 3-Methoxypyridine was prepared by methylation of 3-hydroxypyridine according to Prins's procedure (2).

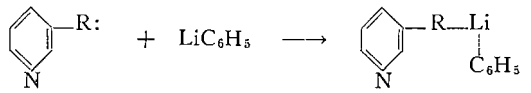
3-Aminopyridine (I; R = NH_2) was treated with a 3-molar excess of phenyllithium to give a 24.5% yield of product. That probably only a single isomer was present was indicated by vapor phase and by column chromatography, and that this isomer was 3-amino-2-phenylpyridine (II; R = NH_2) was shown by comparison of the base and of its picrate with authentic specimens prepared unambiguously from 3-methyl-2-phenylpyridine (3). No evidence for the presence of any 5-amino-2-phenylpyridine in the mixture could be obtained.

In a similar manner, 3-methoxypyridine reacted with phenyllithium to give a 21.2% yield of product $C_{12}H_{11}ON$. Once again this was shown chromatographically to consist

[1]*Manuscript received March 10, 1960.*
Contribution from the Department of Chemistry, University of Saskatchewan, Saskatoon, Saskatchewan.
[2]*Part I: Can. J. Chem.* **38**, *761 (1960).*

of a single isomer which proved to be 3-methoxy-2-phenylpyridine. This could be established quite readily by demethylation to 3-hydroxy-2-phenylpyridine, an authentic specimen of which was obtained from the above 3-amino-2-phenylpyridine. The physical properties of the phenol corresponded also to those reported for 3-hydroxy-2-phenylpyridine (II; R = OH) by Leditschke (4). The infrared spectrum of 3-methoxy-2-phenylpyridine exhibited a band at 1584 cm^{-1} which has been shown to be characteristic of such 2,3-disubstituted pyridine derivatives (5). Once again no 5-hydroxy-2-phenylpyridine was detected in the crude reaction product.

It would seem, therefore, that in the present instance the entering phenyl group is directed *exclusively* to the 2-position. A possible explanation of this observation is that in both the examples studied here the 3-substituent has a pair of electrons which can co-ordinate with the lithium atom to form a complex such as IV in which the phenyl group would be suitably oriented for attack at the 2-position. This, together with the already established tendency for preferential addition to the 2-position (1), would account for the fact that no 6-substitution was observed. Stereospecificity in the addi-



IV

tion of phenyllithium to α-hydroxyketones has been similarly attributed to the formation of a lithium complex as an intermediate (6).

EXPERIMENTAL

Melting points are uncorrected. Infrared spectra were measured using a Perkin–Elmer Model 21 instrument and the vapor phase chromatographic work was carried out using a Beckman GC-2 unit with helium as the carrier gas.

Reaction of Phenyllithium with 3-Aminopyridine

Lithium (1.65 g) was finely cut and suspended in anhydrous ether (50 ml) under dry nitrogen. Bromobenzene (11.4 ml; 17 g) in anhydrous ether (20 ml) was added dropwise at such a rate as to maintain gentle reflux. When the formation of phenyllithium was complete 3-aminopyridine (4 g) in anhydrous ether (80 ml) was added over a period of 20 minutes during which time a brilliant yellow suspension was formed. The ether was distilled off and simultaneously replaced by dry toluene (100 ml) and the temperature was raised to the boiling point. The mixture was boiled under reflux with stirring for $7\frac{1}{2}$ hours during which time the color turned a dark brown. Water was carefully added to the cold suspension, the toluene layer separated, and the aqueous layer extracted repeatedly with ether. The combined ether and toluene layers were extracted with dilute hydrochloric acid, the acid extract made strongly basic with sodium hydroxide, and the product extracted with ether. The ether layer was dried (Na_2SO_4), evaporated, and the residue distilled under vacuum to give crude 3-amino-2-phenylpyridine (1.5 g). This was redistilled and obtained as a pale yellow oil, b.p. 119–121°/0.35 mm, which solidified on cooling and was recrystallized from benzene – light petroleum (b.p. 40–60°) giving colorless crystals, m.p. 62–64°. Calc. for $C_{11}H_{10}N_2$: C, 77.62; H, 5.92. Found: C, 77.90; H, 5.78. Infrared spectrum (Nujol mull) (main peaks only): 3350 (m) (br), 3220 (m) (br), 1620 (s) (br), 1585 (s), 798 (s), 743 (s), 730 (w), 695 cm^{-1} (w).

Can. J. Chem. Downloaded from www.nrcresearchpress.com by 210.87.254.5 on 09/05/12
For personal use only.

The monopicrate, on recrystallization from ethanol, had a melting point of 204–206°. Calc. for $C_{11}H_{10}N_2$, $C_6H_3O_7N_3$: C, 51.13; H, 3.28. Found: C, 51.18; H, 3.17.

A sample of crude reaction product (0.1193 g) was chromatographed on a narrow column of alumina (5 g). Elution was carried out using the following sequence of solvents: light petroleum (b.p. 40–60°), benzene – light petroleum, benzene, benzene–ether, ether, ether–methanol, and finally methanol. Only a single colorless band, exhibiting blue fluorescence under ultraviolet light was eluted, and this with benzene–ether. Different portions of the benzene–ether eluate were converted to the picrate. In each case, only 3-amino-2-phenylpyridine picrate, m.p. 204–206°, was obtained. Also, the individual fractions had identical infrared spectra. The total recovery from the column was 0.1018 g. The mixed melting point of the picrate with that of an authentic sample (3) was undepressed. Also, the infrared spectrum of the free base was identical with that of the authentic sample. Only one peak was observed on vapor phase chromatography of the crude free base under a variety of conditions.

Reaction of Phenyllithium with 3-Methoxypyridine

Phenyllithium was prepared from lithium (0.5 g) and bromobenzene (5.7 g) in anhydrous ether. 3-Methoxypyridine (4 g) in anhydrous ether (30 ml) was added dropwise over a period of 20 minutes, after which the ether was distilled off and simultaneously replaced by dry toluene (40 ml). The reaction mixture was stirred and boiled under reflux under an atmosphere of nitrogen for 7 hours, water was carefully added to the cooled suspension, and the toluene layer separated. The aqueous layer was extracted with ether, the combined ether and toluene extracts washed with dilute hydrochloric acid, and the acid solution basified and extracted with ether. The dried (Na_2SO_4) ether extract was evaporated and the residue distilled under vacuum, the fraction (1.4 g), b.p. 120–160°/0.34 mm, being collected. Redistillation gave pure 3-methoxy-2-phenylpyridine, b.p. 110–112°/0.34 mm. Calc. for $C_{12}H_{11}ON$: C, 77.81; H, 5.99. Found: C, 78.13; H, 6.43. Infrared spectrum (liquid film) (main peaks only): 1575 (s), 1265 (s) (br), 1195 (s), 1125 (s), 1015 (s), 795 (s), 735 (s), 692 cm^{-1} (s).

The picrate was recrystallized from ethanol and had a melting point of 153.5–155°. Calc. for $C_{12}H_{11}ON$, $C_6H_3O_7N_3$: C, 52.18; H, 3.41. Found: C, 52.53; H, 3.86.

The crude base was shown to consist of a single compound by column and vapor phase chromatography as described for 3-amino-2-phenylpyridine.

3-Hydroxy-2-phenylpyridine

(i) From 3-Methoxy-2-phenylpyridine

3-Methoxy-2-phenylpyridine (0.2 g) was boiled under reflux for 4 hours with 47% hydrobromic acid (3 ml). The excess hydrobromic acid was then evaporated off and the residue neutralized with 10% sodium carbonate solution and ether extracted. The dried (Na_2SO_4) ether extract was evaporated and the residue of 3-hydroxy-2-phenylpyridine recrystallized from ethanol to give colorless crystals, m.p. 206–207.5°. Leditschke (4) reported a melting point of 205° for this compound. The infrared spectrum of this product was identical with that of an authentic specimen prepared as described under (ii) below. Also, its melting point was undepressed on admixture with the authentic specimen.

(ii) From 3-Amino-2-phenylpyridine

3-Amino-2-phenylpyridine (0.4 g) was dissolved in a mixture of concentrated sulphuric acid (0.8 ml) and water (2 ml). The solution was cooled to 0–5° and diazotized with sodium nitrite (0.3 g) in water (1 ml) and after ½ hour at 0–5° the excess nitrous acid

Can. J. Chem. Downloaded from www.nrcresearchpress.com by 210.87.254.5 on 09/05/12
For personal use only.

was decomposed with urea. The solution was then boiled under reflux for 1 hour after which time it gave a negative alkaline β-naphthol test. The reaction mixture was treated with solid sodium carbonate and ether extracted repeatedly. The combined ether extracts were dried (K_2CO_3) and evaporated giving crude 3-hydroxy-2-phenylpyridine (0.35 g) contaminated with some orange impurity. Recrystallization from ethanol gave the pure phenol, m.p. 206–207.5°. Infrared spectrum (Nujol mull) (main peaks only): 1573 (m), 1280 (s) (br), 1182 (s), 1115 (m), 802 (m), 735 (s), 693 cm^{-1} (m).

ACKNOWLEDGMENTS

This work was carried out during the tenure (by A. D. N.) of the Thorvaldson Scholarship. Financial assistance from the National Research Council is gratefully acknowledged.

REFERENCES

1. R. A. Abramovitch, Giam Choo Seng, and A. D. Notation. Can. J. Chem. **38**, 761 (1960).
2. D. A. Prins. Rec. trav. chim. Pays-Bas, **76**, 58 (1957).
3. R. A. Abramovitch, K. A. H. Adams, and A. D. Notation. To be published.
4. H. Leditschke. Ber. **85**, 202 (1952).
5. R. A. Abramovitch, Giam Choo Seng, and A. D. Notation. Can. J. Chem. **38**, 624 (1960).
6. D. J. Cram and K. R. Kopecky. J. Am. Chem. Soc. **81**, 2748 (1959).

Can. J. Chem. Downloaded from www.nrcresearchpress.com by 210.87.254.5 on 09/05/12
For personal use only.

THE ATTACK OF CHROMITE BY SULPHURIC ACID[1]

W. J. Biermann and Menno Heinrichs

ABSTRACT

A study was made of the attack of a "low grade" chromite concentrate by sulphuric acid of various concentrations with a view toward formulating a more adequate description, or mechanism, of the process. Consideration of available evidence eliminates the possibility of hydrolysis playing an important role in the process. A qualitative mechanism consistent with the available facts is based on an initial protonic attack, followed by formation of various sulphate complexes of chromium.

INTRODUCTION

The utilization of chromites which are currently classed as "low grade", due, in great measure, to the large amount of contained iron, has been the subject of numerous investigations. These have been comprehensively collected by Udy (1) and an earlier review by Downes and Morgan (2) gives an excellent critical recount of efforts directed toward development of the North American deposits. Methods based on sulphuric acid leaching figure prominently in these reviews.

The present work started as a simple attempt to establish conditions required for the complete conversion of chromite concentrate to a soluble product by sulphuric acid digestion, preparatory to other studies. After a few experiments it became obvious that the attack of chromite by sulphuric acid was not a simple process, and the series of experiments described herein was undertaken to give some clarification to the process involved. It is, in a sense, an extension of the leaching experiments at the Mines Branch laboratories, described by Downes and Morgan. Their objective was the establishment of optimum conditions for the removal of iron by treating the chromite with insufficient acid for complete destruction of the chromite lattice. Their conclusion was that only a fixed portion of iron could be removed by leaching, and a mechanism involving hydrolysis of dissolved cations was postulated to explain this limit of beneficiation.

EXPERIMENTAL METHODS

For the rate of attack of chromite by sulphuric acid to be conveniently rapid, it is necessary that the sulphuric acid be somewhat diluted and that the temperature be maintained above the normal boiling point of the solution. A simple steel pressure vessel, sealed by a Teflon "O" ring, was found to be more convenient than the customary sealed glass tubes for containing the reactants. The reactants themselves were placed in an open glass tube, whose upper end was loosely closed by a wisp of glass wool to prevent mechanical spraying of sulphuric acid onto the inner walls of the steel container. A pressure gauge gave a rough measure of the rate of reaction; as sulphuric acid is used up the vapor pressure increases, leveling off to a constant value as the rate of reaction decreases. Experimentally, a known weight of chromite and a weighed amount of sulphuric acid of known concentration were placed in the glass vessel and digested until the constancy of the pressure reading showed that the rate of reaction had slowed down to a negligible value. The contents of the glass tube were then removed and analyzed.

After a digestion of chromite concentrate with sulphuric acid the reaction vessel contained solution, unattacked chromite, and a finely divided insoluble substance; this latter, for lack of a more definitive designation, we have called "altered chromite".

[1]*Manuscript received March 11, 1960.*
Contribution from the Department of Chemistry, University of Manitoba, Winnipeg, Manitoba.

Can. J. Chem. Downloaded from www.nrcresearchpress.com by 210.87.254.6 on 09/05/12
For personal use only.

The total amount of solid residue was determined by washing with either hot water or dilute sulphuric acid, the amount of residue generally being greater when an acid was used and, under similar washing conditions, reproducible to within a few per cent. Resolution of the total solid into unattacked and altered chromite was hampered by the slow reactivity of the altered chromite. After some experimentation it was found that boiling with two molar sodium hydroxide solutions converted the altered chromite to a readily acid-soluble, gelatinous substance, permitting the isolation of the unattacked chromite by filtration. The weight of altered chromite is the difference between the total residue weight and the excess chromite. Composition of the altered chromite was obtained by analysis of the filtrate from the chromite separation.

The determination of chromium and iron was done with a standard redox titration. Sulphate was determined by precipitation and weighing as barium sulphate. Acetylacetone was added to prevent loss of sulphate by complexation with chromium (III) ions. Aluminum was determined spectrophotometrically by using alizarin red-S in the presence of calcium (3). Shapiro and Brannock (4) have shown that no interferences will result from substances present in these samples. Magnesium was titrated with standard ethylenediamminetetraacetic acid. The amounts of calcium, manganese, and titanium present were too small to have any significant effect on the conclusions reached here and hence were generally ignored.

The chromite used in these experiments was a concentrate prepared from material taken from the Bird River chromite complex and supplied through the courtesy of the Research Department of the Hudson Bay Mining and Smelting Co. This concentrate assayed 41.8% Cr_2O_3, had a chromium–iron ratio of 1.36 to 1, and the particle size was about 80 mesh.

EXPERIMENTAL RESULTS

Table I shows the weights of the three materials obtained by digestions under a variety of conditions. The amount of sulphuric acid is described in terms of "percentages of equivalence", an equivalent of sulphuric acid being calculated as the amount of sulphuric acid required to convert the concentrate completely to a mixture of normal sulphates. Concentration of sulphuric acid is described by a conventional volume ratio of concentrated sulphuric acid to water.

The data suggest that the amount of chromite unattacked by sulphuric acid is determined primarily by the amount of acid present. When the acid used is about 50% of equivalence, the unattacked chromite is generally quite close to the amount anticipated from stoichiometry, provided sufficient time is allowed for equilibrium to be established. Some silica is dissolved by the sodium hydroxide, accounting for the small apparent excess of attack. In no case was the excess attack great enough to indicate significant regeneration of sulphuric acid by hydrolysis. Figure 1 shows a relationship between the amount of unattacked chromite and the sulphuric acid concentration, most effective attack occurring in the region of equal volumes of sulphuric acid and water. A diminished rate of attack at lower concentration is anticipated in a presumably protonic attack on the chromite lattice; the falling off of rate at higher concentrations is most readily rationalized on a purely mechanical basis because, as shown in Fig. 2, the amount of "altered chromite" begins to increase rapidly at sulphuric acid concentrations higher than 1 to 1.

Selection of data for inclusion in Figs. 1 and 2 was necessary in order to compare runs which differed only in the experimental variables plotted. Examination of runs not

Can. J. Chem. Downloaded from www.nrcresearchpress.com by 210.87.254.6 on 09/05/12
For personal use only.

TABLE I

Products formed on sulphuric acid digestion of chromite

Run No.†	Conc. H_2SO_4:H_2O, ml/ml	% equivalence	Temp., °C	Time, hours	Unattacked chromite, g/g*	"Altered chromite", g/g*
1w	1:1	200	250	24	.256	1.76
2w	2:1	200	250	24	.386	1.06
3w	2:1	200	210	21	.105	.193
4w	1:1	200	210	21	.009	.057
5w	1:1.5	200	210	21	.380	.004
6w	1:2	200	210	21	.588	.013
7w	1:1.5	200	200	7.5	.406	.000
8w	1:2	200	200	7.5	.708	.000
9	1:1	100	250	24	.258	
10a	1:2	100	250	19	.362	.228
11w	1:2	100	250	19	.362	.310
12a	2:1	52.5	250	7.5	.477	.320
13w	2:1	52.5	250	7.5	.499	.158
14a	1.5:1	53.1	250	7	.484	.339
15w	1.5:1	53.1	250	7	.508	.189
16a	1:1	53.1	250	6	.424	.454
17w	1:1	53.1	250	6	.433	.458
18a	1:1	53.1	250	7	.424	.522
19a	1:1.5	40.6	250	7.5	.600	.324
20w	1:1.5	40.6	250	7.5	.619	.211
21a	1:1.5	52.5	250	19.5	.452	.419

*The weights of products are grams per gram of chromite in the digestion charge.
†The symbol (w) after the number means that soluble products were removed with hot water; the symbol (a) means that dilute sulphuric acid was used.

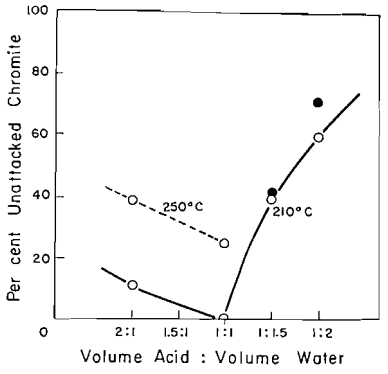


FIG. 1. Degree of attack of chromite as a function of acid concentration. The amount of acid present is 200% of equivalence and the time is 21 hours, except for blackened points which are 7.5 hours and 200° C.

included in these plots discloses no behavior contrary to the conclusions drawn from the data selected.

The dotted portion of Fig. 1 shows that the rate of attack at higher acid concentrations drops as the temperature is increased to 250° C. Comparing runs numbers 1, 2, 3, and 4 in Table I shows how this increase in temperature simultaneously brings about a marked increase in the amount of "altered chromite".

The insoluble material, which we have designated "altered chromite", is formed whenever the acid concentration is high enough to give a reasonable rate of attack on chromite. This, presumably, is the same material which the Mines Branch workers consider to be

Can. J. Chem. Downloaded from www.nrcresearchpress.com by 210.87.254.6 on 09/05/12
For personal use only.

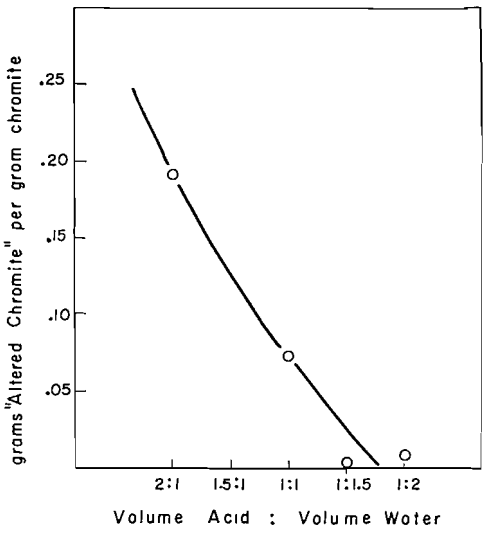


FIG. 2. Formation of "altered chromite" as a function of acid concentration. Acid is 200% of equivalence, time is 21 hours, and the temperature is 200° C.

hydrolysis products of the trivalent ions, but which assumption is not consistent with their observation, substantiated in this work, that the amount of this material increases with sulphuric acid concentration. The physical and chemical properties (finely divided, grey-green, and acid-insoluble) are also suggestive that an alternate explanation is required. Chemical analyses of two representative samples of the "altered chromite" are presented in Table II, and the cation:anion ratio seems to indicate conclusively that

TABLE II

Analysis of typical "altered chromites"

From digestion No.	% Cr	Fe	Al	Mg	SO_4	Ratio equivalents, cations:anion
18a	7.25	9.56	4.39	1.82	60.0	1.12
2	10.37	6.43	2.42	1.55	68.2	.88

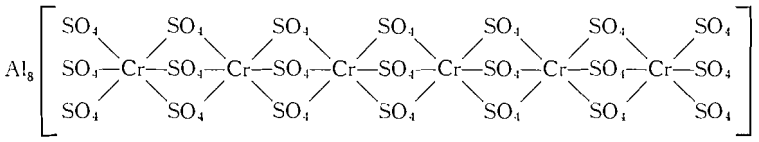
hydrolysis cannot be a significant factor in the formation of the insoluble material. Complete analysis of the products was not generally made, partial analysis of the products showing that the results were quite constant within a given region of acid excess. The slight excess of cation over sulphate was typical of the runs using 50% equivalence of acid. This is ascribed to hydrolysis of the product during the manipulations subsequent to digestion; during extraction of the soluble products the precipitate tended to develop a gelatinous nature, suggestive of an hydroxylation process.

The available facts are better explained on the postulate that the "altered chromite" is a mixture of the hydrogen, aluminum, magnesium, and iron (II) salts of sulphato-polychromate (III) anions. Recoura's work (5), in general confirmed by Whitney (6), substantiates the probability of this explanation, since he reports the preparation of a series of "chromium polysulphuric acids" under conditions similar to the digestion conditions, and observed most of their salts were insoluble and closely resembled the "altered chromite" in appearance. The formation and composition of such polynuclear

Can. J. Chem. Downloaded from www.nrcresearchpress.com by 210.87.254.6 on 09/05/12
For personal use only.

complexes will be a function of ligand concentration, central ion concentration (7), and of the relative concentrations of protons and other metals which can function as cations. This is completely consistent with the observation that high sulphate concentrations favor formation of the insoluble compounds, that the percentage of sulphate in these compounds is observed to increase when excess sulphuric acid is used, and that the removal of iron and chromium (III) is lowest with concentrated sulphuric acid, which is also the most favorable condition for formation of these complexes.

To further strengthen this explanation, typical compounds of the type postulated were prepared under similar conditions. By digesting chromium (III) sulphate with sulphuric acid, in a molar ratio of 1 to 4, a water and acid-insoluble substance, whose analysis corresponded closely to $H_2[Cr_2(SO_4)_4]$, separated. On baking until sulphur trioxide fumes ceased to appear, the analysis of the solid corresponds to $H_2[Cr_4(SO_4)_7]$, agreeing in properties and chemical analysis with the product Recoura designated the "isomeric form". Digestion of an equimolar mixture of aluminum and chromium (III) sulphates with excess sulphuric acid gave precipitation of a substance corresponding in analysis to $Al_8[Cr_2(SO_4)_7]_3$. Improbable though this compound first looks, it can be assigned a provisional structure of



This is consistent with the known co-ordination chemistry of chromium (8).

DISCUSSION

The Mines Branch mechanism for the attack of chromite by sulphuric acid would seem to profit by modification to the following scheme. The initial step is a protonic attack of the chromite lattice, bringing the metallic constituents into solution in the same ratio as they occur in the lattice. Precipitation takes place in a second step. Sulphato complexes of chromium (III) are formed and, under conditions of sufficiently high concentration of chromium (III) ions and sulphate ions, these will include various anionic polynuclear species whose hydrogen or other salts are insoluble. Increasing temperature also favors formation of these polynuclear products. Attack of the chromite may become very slow after accumulation of these insoluble salts, hence the failure to complete the decomposition of the chromite in a reasonable time when excess of sulphuric acid is used.

The more obvious weaknesses of the hydrolysis theory are: first, the precipitated iron is almost completely in the form of iron (II) which is not easily hydrolyzable; second, precipitation takes place when large amounts of unused acid are present; and, third, hydrolysis cannot account for the fact that the percentage of insoluble products increases as the concentration of sulphuric acid increases.

A quantitative description of the over-all process requires considerably more knowledge of the sulphato polychromium (III) complexes, particularly equilibrium constant information, than is now available. Such information we hope will be forthcoming in part, as a result of continued work on the chemistry of chromite in this laboratory.

Metallurgically, this work makes a somewhat negative contribution to substantiating the observation that there is a limit to the amount of iron removal possible from untreated chromite by sulphuric acid leaching. A second fact, that the percentage of chromium

Can. J. Chem. Downloaded from www.nrcresearchpress.com by 210.87.254.6 on 09/05/12
For personal use only.

convertible from chromite to insoluble polynuclear forms can be varied over a wide range by altering the concentration and temperature of the leaching acid, is an observation whose metallurgical significance cannot be assigned until the chemistry of these compounds is further explored.

ACKNOWLEDGMENTS

One of us (M. H.) gratefully acknowledges the encouragement given by Canadian Industries, Ltd., in the form of a Research Assistantship. We also acknowledge the financial assistance given by the National Research Council.

REFERENCES

1. M. J. UDY. *In* Chromium: recovery of chromium from its ores. *Edited by* M. J. Udy, Reinhold Publishing Co., New York. 1956.
2. K. W. DOWNES and D. W. MORGAN. Utilization of low grade domestic chromite. Canada Department of Mines and Technical Surveys, Mines Branch. 1951. (Reprint 1958.)
3. G. A. PARKER and A. P. GODDARD. Anal. Chim. Acta, **4**, 517 (1950).
4. L. SHAPIRO and W. W. BRANNOCK. U.S. Geological Survey Bull. 1036-C. 1956.
5. A. RECOURA. Bull soc. chim. Belges, **7**, 200 (1892); **9**, 586 (1893); **15**, 315 (1896).
6. W. R. WHITNEY. J. Am. Chem. Soc. **21**, 1075 (1899); Z. physik. Chem. **20**, 40 (1896).
7. A. RINGBOM. *In* Treatise on analytical chemistry: complexation reactions. *Edited by* I. M. KOLTHOF and P. J. ELVING. Interscience Publishers, Inc., New York. 1959.
8. H. ERDMANN. Angew. Chem. **64**, 500 (1952).

Can. J. Chem. Downloaded from www.nrcresearchpress.com by 210.87.254.6 on 09/05/12
For personal use only.

Can. J. Chem. Downloaded from www.nrcresearchpress.com by 210.87.254.42 on 09/05/12
For personal use only.

QUANTITATIVE ANALYSIS OF COMBUSTION PRODUCTS BY GAS CHROMATOGRAPHY

THE OXIDATION OF A RICH *n*-PENTANE–AIR MIXTURE IN A FLOW SYSTEM[1]

S. SANDLER[2] AND J. A. BEECH[3]

ABSTRACT

A description is given of an apparatus suitable for investigations of the oxidation and decomposition reactions of volatile hydrocarbon vapors in a flow system. Most of the reaction products are analyzed quantitatively by gas chromatography in a single-stage process involving a simple column-temperature programming technique. The products of the oxidation of a rich mixture of *n*-pentane and air in an annular reactor of Vycor over a wide temperature range are shown in detailed analysis. The products, as identified by several techniques including time-of-flight mass spectrometry and infrared spectrophotometry, include C_2—C_5 mono-olefins, two di-olefins, C_1—C_4 saturated aldehydes, an unsaturated aldehyde, and 2-methyl tetrahydrofuran in addition to those usually associated with the complete oxidation of *n*-pentane.

INTRODUCTION

Earlier studies in this laboratory of the low-temperature oxidation of *n*-pentane (1, 2) indicated the need for an efficient means of analyzing the complex mixture of products so obtained. It was possible to determine the effect of certain variables on the total concentration of any particular class of components, but this information was insufficient for the determination of a reaction mechanism. The analytical difficulty is largely responsible for the lack of quantitative information concerning the effect of temperature and other variables on the mechanism of the oxidation of hydrocarbons.

One of the first attempts at a detailed analysis was that of Ubbelohde (3), who identified some of the liquid oxidation products of pentane after fractional distillation, using ultraviolet spectroscopy and chemical methods. With the development of liquid partition chromatography and polarography more of the products could be analyzed, as demonstrated by Malmberg and others (4, 5), but the experimental method was complicated and the results were of limited quantitative value.

Detailed analyses of complex mixtures of combustion products can now be effected by using the newly developed gas chromatographic techniques. Thus Yokley and Ferguson (6) were able to investigate qualitatively some of the products of the cool flame combustion of propane; Kyryacos, Menapace, and Boord (7) determined the identity of many of the components of the cool flame combustion products of *n*-hexane, and Hughes, Hurn, and Edwards (8) separated and identified oxygenated hydrocarbons in automotive engine combustion products using a three-stage unit.

Gas chromatography was used in earlier work by the authors to separate liquid oxidation products, in conjunction with Orsat analysis of the normally gaseous products. The liquid products were collected in traps surrounded by dry ice – acetone and ice–water mixtures and the condensates had to be transferred by micrometer syringe to the chromatographic column. This procedure entailed large sources of error in the handling of the samples and volatilization of some of the components. In addition, calculation of selectivities (i.e. moles of product formed/mole of fuel consumed) was tedious because it was necessary to combine the analyses of the two condensates. In addition, the calculations

[1]*Manuscript received March 9, 1960.*
Contribution from the Combustion Research Laboratory, University of Toronto, Department of Mechanical Engineering, Toronto, Ontario. Part XXXV *of an investigation of the mechanism of the oxidation, decomposition, ignition, and detonation of fuel vapors and gases.*
[2]*Department of Chemical Engineering, University of Toronto, Toronto, Ontario.*
[3]*Present address: Department of Pharmacology, University of Maryland, Maryland, U.S.A.*

involved the assumptions of uniformity of the flow rate and the furnace temperature, which were shown to be variable over the long period required for sampling.

The present development of a reproducible sampling method allowed this technique to be extended to a more detailed study of the influence of temperature on the oxidation of an *n*-pentane – air mixture.

APPARATUS

General Description

The apparatus is shown diagrammatically in Fig. 1. The required mixture of carbon-

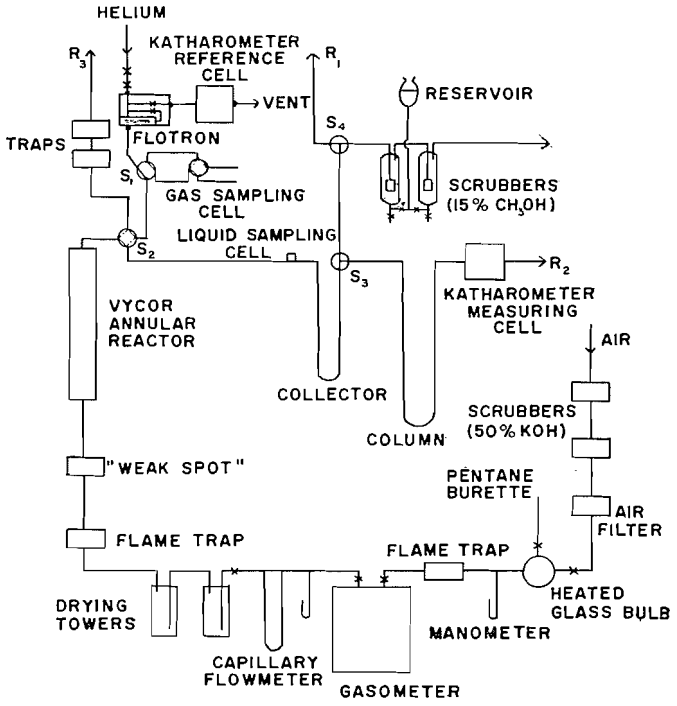


FIG. 1. Schematic diagram of apparatus.

dioxide-free air and *n*-pentane was prepared and stored in the gasometer. From this vessel it was passed at a known rate of flow through the reactor, which, for this study, was constructed of Vycor glass and was annular in form. The reactor dimensions and its positioning in a tubular furnace have already been described (2).

Until steady-state conditions were fully established so that a sample could be taken for analysis, the oxidized mixture was allowed to flow from the reactor through ice–water and dry ice – acetone cooled condenser traps to vent at the rotameter, R_3.

During this period, the eluent gas (helium) was passed through reducing valves to the Burrell "Flotron". This is a device for maintaining a reproducible volume flow and splitting the eluent stream to allow a small flow through the katharometer reference cell of the modified Burrell K1 Kromotog which was used for the analysis of the condensable oxidation products. The eluent was allowed to bypass the gas sampling cell at S_1 and pass through the collector, the column, and the katharometer measuring cell to vent at the rotameter, R_2.

Sampling for Chromatographic Analysis

In taking a condensable product sample for chromatographic analysis the flow streams

Can. J. Chem. Downloaded from www.nrcresearchpress.com by 210.87.254.42 on 09/05/12
For personal use only.

were redirected so that helium passed through S_2 and the traps to vent at R_3 while the reactor effluent was passed during a measured time interval (usually 5 minutes) through the liquid-air-cooled collector and three-way stopcocks S_3 and S_4 to vent at rotameter R_1. The collector was a U tube with a side-arm joined to it by a three-way stopcock. It was wound with resistance tape and contained glass wool and a small amount of crushed firebrick to prevent minute crystals of condensate from being blown through it.

To complete the sampling, four-way stopcock S_2 was turned to allow eluent gas to sweep the sample remaining in the lines into the collector. Then stopcock S_3 was turned so that eluent flowed through the column. Finally, the liquid-air bath was removed and the sample in the collector was volatilized into the helium stream proceeding to the column by heating the collector for 4 minutes at about 150° C.

The uncondensed gases emerging at R_1 during the early stages of the above sampling procedure were sampled by microsyringe from the exit line leading to R_1. This sample was transferred to a homemade chromatographic unit with a Veco thermistor detector cell for analysis on an adsorption column.

The Column Material and Analysis Technique

The separation of the compounds condensed from the reactor effluent was effected on an 8-ft column packed with 25% w/w bis[2-(2-methoxyethoxy)ethyl] ether (MEEE) on 30–60 mesh C-22 firebrick. This substrate was selected as a result of a series of comparison tests using 11 different stationary phases. The operating details for these tests and a comparison of the effectiveness of these substrates for various separations are given in Table I. Subsequently it was observed that the same choice of optimum stationary phase had been made by Yokley and Ferguson (6). Chromatograms of the separations

TABLE I

Comparison of various stationary phases

Stationary phase 25% w/w on 30–60 mesh C-22 firebrick	Maximum usable temp., °C	Ethylene and carbon dioxide separation	*cis* and *trans* 2-Pentene separation	Hydrocarbon peaks	Aldehyde peaks	Water peak	Remarks
β,β′-Oxydipropionitrile	100	P	P	P	E	F	Unusual order of elution
Acetonyl acetone	20	E	F	E	F	P	Baseline unstable
Dimethyl sulpholane	40	F	P	E	E	E	Unstable at higher temp. otherwise good
Triethanolamine	40	P	P	P	F	P	No peaks beyond acetaldehyde
Acetoacetic ester	40	E	F	F	P	P	Water strongly held
Ethylene glycol monoethyl ether	40	P	P	F	P	P	No peaks beyond pentenes
Triacetin	80	P	P	F	E	E	Good for higher temp. separations
Bis(2-methoxyethyl) phthalate	100	P	P	E	E	E	Good for higher temp. separations
Bis[2-(2-methoxyethoxy)ethyl] ether	70	E	F	E	E	E	Best stationary phase tested
Dinonyl phthalate	130	P	P	F	F	F	Unusual order of elution
Carbowax 20M	225	P	P	E	E	E	Tested at 60° C; ineffective at 40° C

NOTE: E = excellent, F = fair, P = poor or not observable. Column details: eluent, helium at 50 cc/minute; sample, oxidation products of 54 μl of *n*-pentane. Column temperature, 40° C.

Can. J. Chem. Downloaded from www.nrcresearchpress.com by 210.87.254.42 on 09/05/12
For personal use only.

effected by two of the poorer substrates are shown in Fig. 2. Compounds corresponding to the various peak numbers are listed in Table II. These chromatograms afford yet

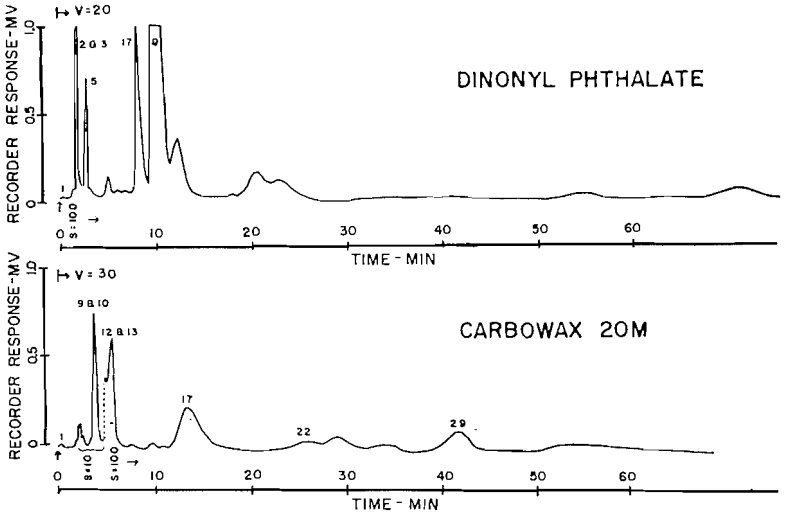


FIG. 2. Comparison of the separations on different substrates.

TABLE II

Identification of products shown in chromatograms

Peak No.	Compound	R.R.T. standards	R.R.T. products	Method of identification		
				M	I	R.R.T.
1	Air	0.00	0.00			x
2	Ethylene	0.06	0.06	x		x
3	Carbon dioxide	0.10	0.10	x		x
4	Unknown		0.18			
5	Propylene	0.18	0.19	x		x
5A	Unknown		0.34			
6	1-Butene	0.46	0.49	x_p		x
7	*trans*-2-Butene	0.58	0.61	x_p		x
8	*cis*-2-Butene	0.70	0.72	x_p		x
8A	Unknown		0.95			
9	*n*-Pentane	1.00	1.00	x	x	x
10	1-Pentene	1.30	1.29	x		x
12	*trans*-2-Pentene		1.57	x_p		x
13	*cis*-2-Pentene		1.60	x_p		x
16	Cyclopentane	2.3	2.4	x		x
17	Acetaldehyde	2.7	2.6	x	x	x
18	1,3-Pentadiene		2.9	x_p		
19	1,4-Pentadiene		3.1	x_p		
20, 21	Unknown		3.4			
22	Propionaldehyde	4.3	4.2	x	x	x
23	Acetone	4.7	4.6	x	x	x
24	Acrolein		5.0	x		
25, 26	Methyl alcohol		5.3	x	x	
27	Unknown		5.5			
28	Unknown		5.9			
29	2-Methyl tetrahydrofuran	6.6	6.4	x	x	x
30	*n*-Butyraldehyde	6.5(?)	7.0	x		x_p
31	Unknown		7.4			
31A	Unknown		8.0			
32, 33	Water	8.8	9.0			x

NOTE: R.R.T. = Relative retention time, *n*-pentane = 1.00 on 25% w/w bis[2-(2-methoxyethoxy)ethyl] ether and 30–60 mesh C-22 firebrick column at 25° C.
M = Mass spectrometry.
I = Infrared spectroscopy.
x = Identified, x_p = tentatively identified.

Can. J. Chem. Downloaded from www.nrcresearchpress.com by 210.87.254.42 on 09/05/12
For personal use only.

another example of the remarkable versatility of the gas–liquid chromatographic technique. Thus, the order of elution of the polar compound, acetaldehyde (peak 17), relative to the non-polar *n*-pentane (peak 9), can be radically altered, as shown, by suitable choice of stationary phase polarity.

The following very simple but quite effective system of column-temperature programming was used to obtain a reasonably efficient separation of the condensed sample in a single operation. The column temperature at the beginning and for the first 10 minutes of each analysis was 25° C. At the end of this period an electric current at a potential of 30 volts was passed through the resistance wire wound on the column. The rate of increase of temperature was such that a temperature of 60° C was attained in another 15 minutes. A fixed eluent flow rate of 100 ml per minute (25° C and 760 mm Hg), as measured at the downstream end of the chromatograph, was always maintained by the "Flotron". Hence there was little or no change in the base line due to the temperature change.

With the MEEE substrate a low initial temperature was ideal for the separation of carbon dioxide and the lower olefins. On the other hand, the gradually increasing temperatures in the following period prevented excessive peak broadening of the higher boiling components without seriously impairing their separation. The temperature finally attained allowed the analyses to be completed in less than 1 hour. A representative chromatogram obtained in this manner from a 5-minute sample of the reactor effluent taken when the maximum wall temperature was 509° C is given in Fig. 3. The excellent

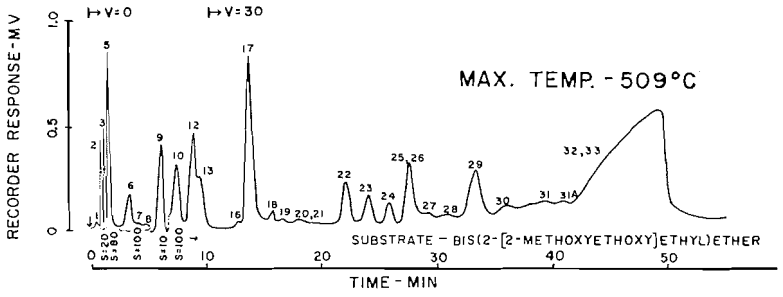


FIG. 3. Representative oxidation product chromatogram.

separation of most of the constituents and the stability of the base line despite the relatively large change in column temperature are readily apparent.

A further temperature increase to 90° C would have permitted the analysis of part of the organic acid content of the sample. However, a noticeable "bleeding" of the substrate occurs at this temperature. Hence, the analysis for the acid content was performed on a separate sample by a titration method.

The uncondensed gases were separated on a 15-ft column of 30–60 mesh 5A Linde molecular sieves. This material was dried for 6 hours in a nitrogen stream at a temperature of 300° C prior to packing. Hydrogen, oxygen, nitrogen, methane, and carbon monoxide were readily separated and all but the hydrogen were quantitatively determined on this column at a temperature of 100° C with helium flowing at 50 ml per minute. With this eluent, the sensitivity for hydrogen was about 1/20th of that for the other gases due to the similarity of its thermal conductivity to that of helium. Hence quantitative results for this gas were not obtained unless its concentration exceeded about 1% by volume of the uncondensables.

Can. J. Chem. Downloaded from www.nrcresearchpress.com by 210.87.254.42 on 09/05/12
For personal use only.

Formaldehyde Analysis

Initially, it was hoped to measure formaldehyde by gas chromatography. However, a number of experiments showed that polymerization of formaldehyde at low temperatures would require the use of a column temperature exceeding 100° C and controlled within fine limits. At these elevated temperatures a formaldehyde peak was observed. However, other oxidation products which could not be resolved interfered and a quantitative determination could not be made. In addition the substrate "bleeding" mentioned earlier became appreciable at temperatures above 100° C and the useful life of the column was thereby excessively reduced. Work on a gas chromatographic separation of formaldehyde is continuing.

The polarographic methods for formaldehyde could not be applied because of the mixture complexity and especially because of the presence of acrolein, which interferes. Hence, a chemical method of analysis was indicated. Since a large number of analyses was projected the specific reaction with chromotropic acid as recommended by West and Sen (9) was adopted rather than the precipitation and separation of derivatives.

The sample was collected prior to the one for gas chromatographic analysis by a precisely similar technique. This was transferred to and absorbed in scrubbers containing 15% methyl alcohol. An aliquot of this solution was treated with chromotropic acid in sulphuric acid solution. After the mixture was heated in a boiling water bath for 5 minutes to develop the color, the color maximum at 560 mμ was read and compared with that of a similarly treated standard formaldehyde solution.

Acid Analysis

The sampling technique was modified by (*a*) condensing the sample in a dry ice – acetone cooled collector and (*b*) absorbing this sample in a scrubber containing 0.01 *N* sodium hydroxide. An aliquot of this solution was backtitrated with 0.01 *N* hydrochloric acid solution to the phenolphthalein end point. The results were calculated as formic acid.

Peroxide Analysis

Liquid air was again used for condensation and the sample was run into a scrubber containing isopropyl alcohol. An aliquot of this solution was analyzed by iodometric titration. Since the peroxide content of the effluent in the conditions of these experiments proved to be negligible, the more sensitive test of Widmaier and Mauss (10) was also applied. Again, results indicated the absence of peroxides.

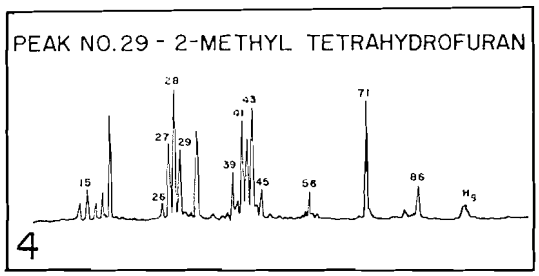
PRODUCT IDENTIFICATION

The qualitative analysis of the oxidation products was effected using several techniques and is still not quite complete. The Bendix time-of-flight mass spectrometer, applied as described by Gohlke (11), successfully identified several compounds. At 100 intervals during the running of the chromatograms the column effluent was leaked into the mass spectrometer and a full mass spectrum of the compound was obtained by a very sensitive amplification and rapid-scan method. A representative spectrum which was identified as that due to 2-methyl tetrahydrofuran is shown in Fig. 4.

Our experience in the interpretation of spectra from the time-of-flight mass spectrometer leads to the following conclusions:

(*a*) Several compounds may be scanned at the same time if the chromatographic column does not have sufficient resolving power. However, by comparing scans taken at the beginning and end of a peak elution this can be detected more easily than by conventional mass spectrometer.

Can. J. Chem. Downloaded from www.nrcresearchpress.com by 210.87.254.42 on 09/05/12
For personal use only.



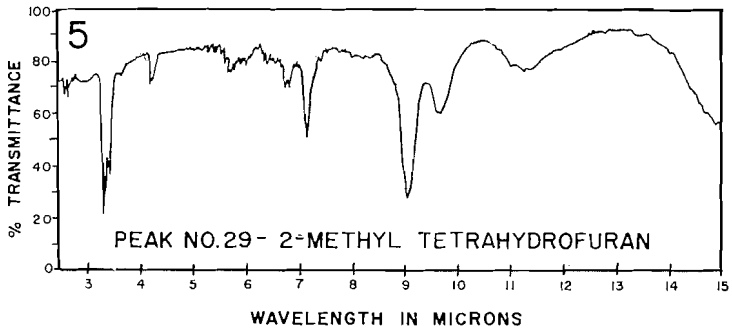


FIG. 4. Representative time-of-flight mass spectrum.
FIG. 5. Representative micro-gas-cell infrared spectrum.

(*b*) The accelerating chamber or the spectrometer lead-in is not completely swept between samples. As a result, there is a doubt as to whether any given peak is retained from a previous scan.

(*c*) With the mass scale used in our analyses, the numerical value of mass numbers greater than 80 was uncertain. We have, however, been informed that wider mass scales are now available.

(*d*) The background peaks gradually change in height when a number of scans is taken. There is therefore no way of knowing which contribution of a given mass is due to background and which to the component. This fault is also to be found, to a lesser extent, with conventional mass spectrometers.

Despite the above comments, the time-of-flight mass spectrometer has great potentialities for use in this field. The identity of most of the peaks analyzed by this means was confirmed by trapping the compound as it left the column and analyzing it by conventional mass spectrometer. For small peaks adjacent to large ones, however, the time-of-flight machine had a decided advantage.

In addition to the above analyses, the identity of seven of the peaks was confirmed by using a combination of gas chromatography and infrared spectrophotometry. Samples of the effluent from the chromatographic column were passed directly into a 600-mm path-length infrared micro-gas-cell designed by White (12). These were analyzed in a Beckman IR 4 infrared spectrophotometer equipped with a micro-optical system.

The spectrum of a representative reaction product peak, 2-methyl tetrahydrofuran, is shown in Fig. 5. It should be emphasized that the procedure described above was purposely adopted for convenience of sampling, i.e. to eliminate the troublesome sample freeze-out and transfer steps usually required. To do this, optimum spectrophotometric operating conditions were abandoned. Thus, for example, sample pressure was one atmosphere (mostly helium) rather than 50–100 mm Hg as usually recommended.

Can. J. Chem. Downloaded from www.nrcresearchpress.com by 210.87.254.42 on 09/05/12
For personal use only.

The infrared spectra thus obtained were correspondingly poorer than they might have been. Better resolution is obtained by trapping the samples in a liquid-air-cooled vessel, which may subsequently be evacuated while cool to remove helium and from which the sample may be flashed into the evacuated micro-gas-cell to the optimum pressure.

Further confirmation of the identity of any suspected component was obtained, whenever a sample of the pure compound was available, by comparison of their retention times relative to that of *n*-pentane. The compounds listed in Table II were identified by one or more of the above techniques. The relative retention times (*n*-pentane = 1) for these compounds are included in Table II. These values are the averages of from 5 to 15 determinations each, with deviations, generally, of less than $\pm 5\%$.

QUANTITATIVE EVALUATION OF RESULTS

To convert component peak areas to component concentrations, known volumes of pure compounds were analyzed under conditions similar to those used for the oxidation product mixture and calibration factors were then calculated. With eluent gas flowing through the column and the collector in a liquid-air bath, the standards were injected on to the heated connecting tube through a silicone seal in the liquid sampling cell and the eluent carried them into the collector where they were condensed. They were then transferred to the column by the technique already described. When the actual compound to be measured was not available in the pure state a similar type of compound was used as a standard. Where the peak was not positively identified the figures used for molecular weight and density in the calculation of selectivity were estimated on the basis of the suspected values. The concentrations were calculated by weight ratio. Generally areas were estimated as the product of peak height and peak width at half height. Where the base line undulated, the areas were measured by planimeter. For the water peak a piece of paper equal to the peak in area was weighed and for the earlier peaks, peak height was more convenient to measure than area.

RESULTS AND DISCUSSION

The state of the surface of the reactor is known to affect the initial rate at which oxidation occurs. The material of the reactor, together with the interrelated shape, mixture residence time, and flow configuration also affects the course of the reaction. When the reactor was first used it was found to give erratic results. Stability of the surface was rapidly obtained, however, when a little nitric acid was introduced at about 500° C and the temperature was slowly raised to 1000° C. After cooling the reactor to 500° C, a of stream helium was passed through until no chromatographic peak due to the nitric acid was obtained from a sample of the effluent.

On establishing that a fairly stable and reproducible surface could be prepared in this way, at least for the reaction of rich mixtures of pentane and air, a preliminary program was outlined for demonstrating the effectiveness of the gas chromatographic method and for obtaining new information regarding the effect of temperature on the product distribution from the reaction of one particular mixture of *n*-pentane and air. This program consisted of a series of runs at certain temperatures between 375 and 800° C with a 1.3 stoichiometric *n*-pentane – air mixture supplied to the reactor at the rate of 100 ml/minute as measured at 25° C and 1 atmosphere pressure. Product analyses were carried out on samples of the effluent from each run as outlined previously using both gas chromatographic and chemical methods.

A representative chromatogram of the oxidation products of *n*-pentane obtained from

Can. J. Chem. Downloaded from www.nrcresearchpress.com by 210.87.254.42 on 09/05/12
For personal use only.

a run at a maximum reactor wall temperature of 509° C has been given in Fig. 3. By reference to Table II, which gives the key to the peak numbers, an idea of the mixture complexity and of the particular value of this method of analysis may readily be obtained. The results of calculations made from a series of such chromatograms in conjunction with those obtained from the chemical analyses are presented in Table III and Figs. 6–9.

TABLE III

Carbon balances
(carbon selectivity, %)

Temperature, °C	450	500	550	600	650	700	750	800
Oxides of carbon	22.5	15.4	12.0	9.8	8.7	16.0	55.2	71.6
Aldehydes and ketones	24.2	24.9	23.4	20.1	15.8	9.7	2.6	0.1
Methyl alcohol	8.4	5.4	2.2	0.4	—	—	—	—
2-Methyl tetrahydrofuran	17.8	20.0	18.6	14.2	9.0	3.5	—	—
Methane	—	—	—	—	1.2	4.0	4.9	4.5
Acids	4.6	4.4	2.6	0.3	—	—	—	—
Olefins	15.4	21.2	28.2	35.5	43.2	33.2	13.3	9.1
Deficiency	7.1	8.7	13.0	19.7	22.1	33.6	24.0	14.7

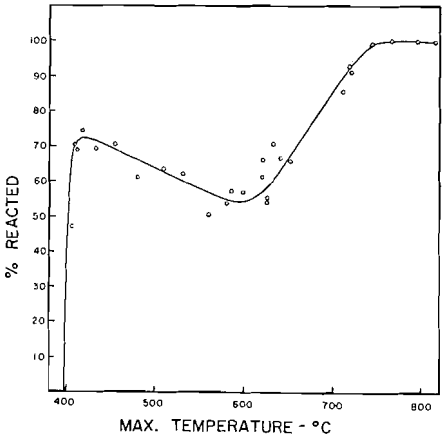


FIG. 6. The effect of temperature on the percentage of *n*-pentane reacted.

In Fig. 6 the percentage of pentane reacted is plotted against maximum reactor wall temperature. The curve for *n*-pentane reacted rises sharply to a maximum at 410° C and then falls off slowly as the temperature increases to 625° C demonstrating again the now familiar negative temperature coefficient of the reaction in these conditions. From this point the percentage of pentane reacted rises sharply to 100%. The second sharp rise in the curve occurs when the mechanism of the over-all process changes so that carbon monoxide, carbon dioxide, and water become the major oxidation products.

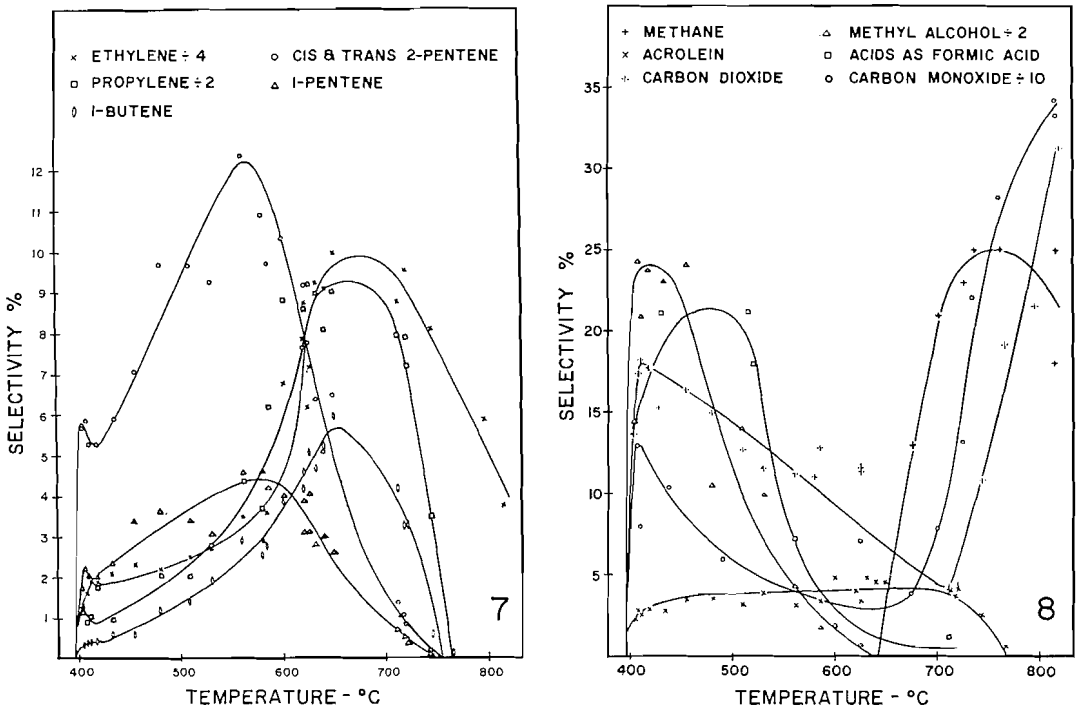
The variations in product distribution with reactor temperature are indicated in Figs. 7–9. Several facets of the results deserve comment.

1. The absence of peroxides is significant in view of the proved sensitivity of the methods of detection employed. However, on the basis of former studies with a reactor of high surface-to-volume ratio (2), this result was not unexpected.

2. The surprisingly high concentration of 2-methyl tetrahydrofuran in the products, which accounts for as much as 20% of the carbon content of the *n*-pentane reacted, Table III, should be noted. The conditions of high surface-to-volume ratio and nitric acid pretreatment of the surface seem to favor the formation of this product.

Can. J. Chem. Downloaded from www.nrcresearchpress.com by 210.87.254.42 on 09/05/12
For personal use only.

Can. J. Chem. Downloaded from www.nrcresearchpress.com by 210.87.254.42 on 09/05/12
For personal use only.



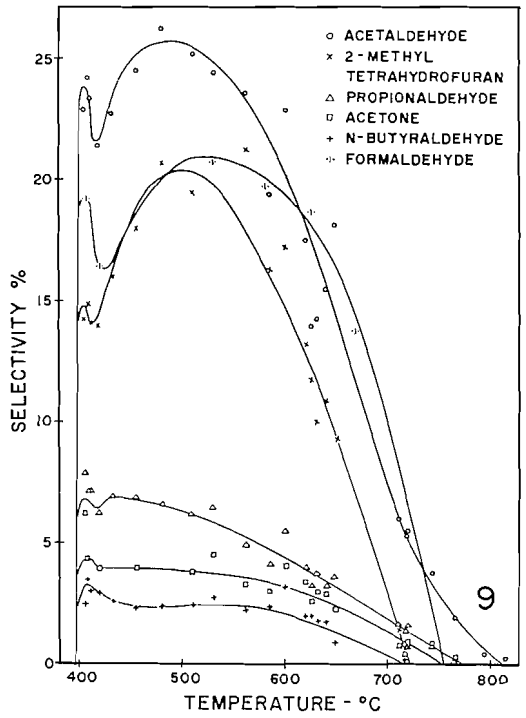


FIG. 7. The effect of reactor wall temperature on olefin selectivity.
FIG. 8. The effect of reactor wall temperature on product selectivity.
FIG. 9. The effect of reactor wall temperature on product selectivity.

Can. J. Chem. Downloaded from www.nrcresearchpress.com by 210.87.254.42 on 09/05/12
For personal use only.

3. A small but quite distinct dip in the product selectivities (Figs. 7 and 9) for the olefins and oxygenated compounds other than the acids, methanol, and oxides of carbon occurs at about 420° C. This is followed by a rapid increase in product concentration to a maximum and finally by a more gradual decrease.

4. A two-stage reaction mechanism, at least, is indicated. Methane is a product of the high-temperature reaction. Its formation is not evident below about 650° C (Fig. 8). On the other hand, the rate of formation of methanol and organic acids becomes negligible at this temperature. It is interesting that the high methane concentration in the high-temperature region is not accompanied by a correspondingly high hydrogen content (the hydrogen concentration was not detectable). This is further confirmation of the view that the lower olefins are formed via an oxidation mechanism and not by simple pyrolysis of the hydrocarbon in this temperature range.

5. The rate of formation of the simple olefins, ethylene, propylene, and butylene, becomes a maximum at about 700° C and the mechanism at higher temperatures appears to involve the further oxidation of these olefins. Ethylene is the most stable in this regard. The higher olefins attain their maximum concentrations at lower temperatures (550°–600°). When the concentration of the simpler olefins has reached a maximum that of the higher olefins has become negligible.

6. Epoxides, such as ethylene and propylene oxides, which were postulated by Boord (13) and observed by Kyryacos, Menapace, and Boord (7), were not found in the present study but may have escaped detection since they come off near the large acetaldehyde peak.

7. The relatively constant acrolein concentration (Fig. 8) over the wide range of temperature between 400 and 700° C is remarkable. An explanation for this observation is not available at this time.

8. The relative preponderance of carbon monoxide over carbon dioxide in the products (Fig. 8) is consistent with the results expected from the oxidation of a rich mixture.

9. Carbon balances on the identified products of the reaction for selected temperatures from the product selectivity – temperature graphs are given in Table III. A useful and rapid means of obtaining these carbon balances has been employed here. This is the concept of a carbon selectivity of a particular product, which may be defined as the product of component percentage selectivity and the ratio of the number of carbon atoms per mole of component and reactant respectively. Considering the omission from this tabulation of the carbon in the minor and the unidentified components and in those compounds less volatile than water, these balances indicate that this method of analysis can be used to provide the detailed information required to study the kinetics and mechanism of complex reactions.

CONCLUSION

1. The purpose of this preliminary work was to develop an integrated apparatus for the investigation of an oxidation or decomposition reaction with the principal aid of the gas chromatographic technique. In this respect a method of sampling has been described which will obviate many of the difficulties associated with the transfer of gaseous or liquid samples from the reactor to the gas chromatographic apparatus and will also allow samples to be taken for the more usual chemical or physical methods of analysis. Most of the condensable products may be analyzed in a single-stage process by a simple column-temperature programming technique.

2. The use of several qualitative microanalytical methods including time-of-flight

mass spectrometry and infrared spectrophotometry for identifying the products separated by the gas chromatographic method has been described and critically evaluated.

3. Although a mechanism for the reaction studied here will not be presented until further studies involving the effects on product distribution of varying the mixture strength, residence time, and condition of the surfaces have been completed, some of the interesting features of the results have been discussed. Thus, a method of obtaining a reproducible surface has been described, variations in product distribution with temperature have been noted, and the presence of certain suspected and some unsuspected compounds in the reaction product mixture has been confirmed or determined.

ACKNOWLEDGMENTS

The research was carried out with the co-operation of Dr. R. R. McLaughlin, Dean of of the Faculty of Applied Science and Engineering, University of Toronto, and Dr. G. R. Lord, Head of the Department of Mechanical Engineering. The work was supported by the Defence Research Board of Canada in accordance with the terms of Defence Production Contract No. CD 800102. The authors are indebted to Mr. R. O. King, Director of the Combustion Research Section, for his constant advice and encouragement and to Mrs. K. Kjaer and Mrs. M. Spencer of this laboratory for their painstaking laboratory, calculation, and typing assistance. Sincere thanks are also extended to the Bendix Corporation for the time-of-flight mass spectra, to Beckman Instruments, Inc., for the micro-gas-cell infrared spectra, to Professor R. M. Farquhar, Department of Physics, University of Toronto, for the conventional mass spectra, to Mr. R. Strom of this laboratory for the gas adsorption chromatographic analyses, to the Phillips Petroleum Company for the provision of the pure hydrocarbon samples used as standards, and to the Linde Air Products Company for providing samples of their molecular sieves.

REFERENCES

1. R. O. KING, S. SANDLER, and R. STROM. Can. J. Technol. **32**, 102 (1954).
2. R. O. KING, S. SANDLER, and R. STROM. Can. J. Chem. Eng. **35**, 33 (1957).
3. A. R. UBBELOHDE. Proc. Roy. Soc. (London), A, **152**, 378 (1935).
4. E. W. MALMBERG. J. Am. Chem. Soc. **76**, 980 (1954).
5. E. W. MALMBERG, E. L. FISHEL, M. L. SMITH, and W. C. DAVIS. Paper presented at Am. Chem. Soc. Meeting, Los Angeles, March, 1953.
6. C. R. YOKLEY and R. E. FERGUSON. Combustion and Flame, **2**, 117 (1958).
7. G. KYRYACOS, H. R. MENAPACE, and C. E. BOORD. Anal. Chem. **31**, 222 (1959).
8. K. J. HUGHES, R. W. HURN, and F. G. EDWARDS. Paper presented at the Second Intern. Symposium on Gas Chromatography, East Lansing, Michigan, June, 1959.
9. P. W. WEST and B. SEN. Z. anal. Chem. **153**, 177 (1956).
10. O. WIDMAIER and F. MAUSS. Rev. inst. franç. pétrole et Ann. combustibles liquides, **3**, 183 (1948).
11. R. S. GOHLKE. Anal. Chem. **31**, 535 (1959).
12. J. U. WHITE, N. L. ALPERT, W. M. WARD, and W. S. GALLOWAY. Anal. Chem. **31**, 1267 (1959).
13. C. E. BOORD. Advances in Chem. Ser. No. **20**, 5 (1958).

Can. J. Chem. Downloaded from www.nrcresearchpress.com by 210.87.254.42 on 09/05/12
For personal use only.

Can. J. Chem. Downloaded from www.nrcresearchpress.com by 210.87.254.40 on 09/05/12
For personal use only.

THE STRUCTURE OF MONOBROMINATED ETHYL INDOLE-3-CARBOXYLATE AND THE PREPARATION OF 7-BROMOINDOLE[1]

B. E. LEGGETTER AND R. K. BROWN

ABSTRACT

The compound reported by Majima and Kotake as ethyl 6-bromoindole-3-carboxylate, obtained from the monobromination of ethyl indole-3-carboxylate, when saponified, decarboxylated, and the product repeatedly crystallized from alcohol, actually gave a nearly equimolar mixture of 5- and 6-bromoindoles of constant melting point, 74–75°. 7-Bromoindole has been synthesized by two unambiguous routes.

INTRODUCTION

Majima and Kotake have reported the preparation of ethyl 6-bromoindole-3-carboxylate via bromination in acetic acid of ethyl indole-3-carboxylate (1). Their proof of structure rested upon the observation that dibromination, in acetic acid, of ethyl indole-3-carboxylate actually gave ethyl 5,6-dibromoindole-3-carboxylate, a fact established by the isolation of 5,6-dibromoisatin and 4,5-dibromo-2-amino-benzoic acid. Since the *mono*brominated compound gave a monobromoisatin quite different from the authentic 5-bromoisatin previously prepared by Borsche and Jacobs (2) and in view of the established structure of the dibrominated product, it was concluded that monobromination of ethyl indole-3-carboxylate had occurred at position 6. The discrepancy between the melting point of their "6-bromoisatin" (256–258°) and that of Ettinger and Friedlander's 6-bromoisatin (m.p. 263–264°) (3) was attributed to contamination of their monobromoisatin with some 5,6-dibromoisatin.

The monobrominated ethyl indole-3-carboxylate of Majima and Kotake, saponified and decarboxylated in this laboratory, gave a monobromoindole melting at 74–75° which, according to the assignment of the Japanese authors, should be 6-bromoindole. A recently reported unambiguous preparation of 6-bromoindole (4) melting at 94° casts doubt upon Majima and Kotake's structural assignment. This was further intensified by observation in this laboratory of a marked depression of the melting point of a mixture of these two bromoindoles. That the compound melting at 74–75° is neither 4- nor 5-bromoindoles is shown by comparison of their physical constants. Authentic 4-bromoindole (4) is a liquid which we found to boil at 89–92°/0.25 mm and which has a refractive index of 1.6566 at 21°, while 5-bromoindole melts at 88.5–89° (5). Furthermore, the infrared spectra of the 4-, 5-, and 6-bromoindoles failed to correspond with that obtained for the questionable bromoindole.

Since the possibility existed that the as yet unknown 7-bromoindole might actually be the compound synthesized by Majima and Kotake, its preparation was undertaken. The precursor, 7-bromoindole-2-carboxylic acid, was made by two unambiguous routes. The first method entailed the preparation of ethyl pyruvate 2-bromophenylhydrazone, which was then subjected to Fischer ring closure with polyphosphoric acid. The second method involved the conversion of 3-carboxy-2-nitrotoluene (6) to 3-bromo-2-nitrotoluene by the Hunsdiecker reaction (7). A Reissert condensation of 3-bromo-2-nitrotoluene with ethyl oxalate (5), affording optimum yields only after prolonged reaction between the ester and the nitrotoluene at room temperature, gave ethyl 3-bromo-2-nitrophenylpyruvate. This was converted to 7-bromoindole-2-carboxylic acid by the usual reductive ring closure.

[1]*Manuscript received May 6, 1960.*
Contribution from the Department of Chemistry, University of Alberta, Edmonton, Alberta.

The 7-bromoindole-2-carboxylic acid gave unsatisfactory decarboxylation by the usual procedures (4, 5, 8). However, a modified version of one method (8, 9), in which the acid was refluxed in synthetic quinoline for 48 hours while small amounts of copper chromite (10) were added at frequent intervals, gave a 48% yield of 7-bromoindole. This synthesis now makes available the last of the isomeric benzene ring-monobrominated indoles.

The infrared spectrum and melting point (42–43°) of 7-bromoindole showed conclusively that it was not the "6-bromoindole" derived from the "ethyl 6-bromoindole-3-carboxylate" of Majima and Kotake.

Comparison of the infrared spectra of 5- and 6-bromoindoles suggested that the unknown substance might be a mixture of the two. Accordingly, when samples containing various proportions of the two isomeric bromoindoles were prepared, it was found that a mixture of 45% of 5-bromoindole and 55% of 6-bromoindole gave a spectrum identical in every respect with that of the unknown. The bands at 1308 cm^{-1} for the 5-isomer and at 1329 cm^{-1} for the 6-isomer have nearly equal intensities and can be used as a reasonably good method for estimation of the relative amounts of these two isomers in a mixture. The two isomers can be clearly distinguished by the absorption bands shown in the following table.

Compound	Absorption bands at: (cm^{-1})						
6-Bromoindole	665 (w)	800 (s)	840 (m)	852 (w)	864 (w)	1305 (w)	1329 (s)
5-Bromoindole	664 (s)	788 (s)	Nil	Nil	864 (s)	1308 (s)	1329 (w)

NOTE: w, m, and s are respectively weak, medium, and strong.

Neither the melting point of this mixture (74–75°) nor its composition could be altered by repeated crystallization. Similar constant-melting mixtures of isomeric compounds have been recorded in the literature, a specific example being the isomeric 5- and 7-nitro-1,2,3,4-tetrahydrocarbazoles, a mixture of which crystallizes in equimolecular proportion from a variety of solvents to form a substance of constant composition and melting point (11). However, unlike the case of the tetrahydrocarbazoles, chromatography does not readily separate the 5-bromoindole from the 6-bromoindole. Since a single chromatographic operation using an alumina column did in fact achieve a partial separation, as shown by the change in the infrared spectra of the fractions, it is no doubt possible by repeated and careful chromatography to separate them completely.

We have repeated the bromination of ethyl indole-3-carboxylate as described in the literature and obtained the same results (1). Several crystallizations of the ethyl bromoindole-3-carboxylate from aqueous alcohol failed to alter the melting point of 134–137°. A sample of this substance, passed through a column of activated alumina, gave very little separation. Chromatography of the fractions obtained from this first attempt at separation also gave unsatisfactory results. However, since the melting points of the various fractions did in fact differ somewhat both in value and in range from each other it was assumed that, as for the case of the 5- and 6-bromoindoles, a separation could be achieved by painstaking care. It is to be noted that crystallization of each of these various fractions from diluted alcohol again gave the material of constant melting point of 134–137°.

Hydrolysis of the ester according to the literature (1) gave an acid which upon several crystallizations from 95% alcohol melted at 212°, a fact which had already been recorded (1). No attempt was made to separate this substance into its isomers. Our decarboxylation

Can. J. Chem. Downloaded from www.nrcresearchpress.com by 210.87.254.40 on 09/05/12
For personal use only.

of this compound in quinoline at 140° afforded a compound whose analysis, following several crystallizations from alcohol, agreed with that of a monobromoindole and is now known to be a nearly equimolar mixture of 5- and 6-bromoindoles (m.p. 74–75°).

This work indicates that not only do 5-bromoindole and 6-bromoindole form a constant-melting mixture, but that their precursors, 5- and 6-bromoindole-3-carboxylic acid and the ethyl ester, do likewise. Whether the precursors are nearly equimolar mixtures is uncertain. However, if that is so, then ease of bromination of ethyl indole-3-carboxylate is approximately equal for the 5 and the 6 positions.

EXPERIMENTAL

All melting points are uncorrected. The 4-bromoindole (4), 5-bromoindole (5), and 6-bromoindole (4) were prepared according to the published procedures.

3-Bromo-2-nitrotoluene

Bromine (24 g, 0.15 mole) was added slowly to a stirred suspension of 41.5 g (0.144 mole) of silver salt of 3-methyl-2-nitrobenzoic acid in anhydrous carbon tetrachloride (350 ml) at 25°. Following the addition, the mixture was heated to reflux for 3 hours, during which time carbon dioxide was evolved. The cooled solution was freed from silver salts and the filtrate washed first with aqueous sodium bisulphite, then with aqueous sodium bicarbonate, and finally with water, and then dried over anhydrous magnesium sulphate. Removal of the sulphate and ether afforded a brown oil which, when steam distilled, yielded 18.0 g of 3-bromo-2-nitrotoluene (58%) melting at 27°, lit. m.p. 27° (12).

Potassium Enolate of Ethyl 3-Bromo-2-nitrophenylpyruvate

Potassium (2.3 g, 0.059 mole) was dissolved in anhydrous ethanol (20 ml). To this solution, diluted with 100 ml of dry ether, was added 8.7 g (0.059 mole) of diethyloxalate and the mixture was then stirred gently for 15 minutes. The addition of an ether solution of 11.0 g (0.05 mole) of 3-bromo-2-nitrotoluene produced a deep orange solution which, left at 25° for 7 days, slowly deposited the potassium salt as an orange precipitate. The solid was collected, washed thoroughly with anhydrous ether, and air-dried, yielding 12.1 g (67%) of product.

Ethyl 3-Bromo-2-nitrophenylpyruvate

When a small portion of the above potassium salt was dissolved in water, cooled to 0°, and acidified carefully with 6 *N* hydrochloric acid, a bright yellow solid precipitated. Crystallization from ethanol gave a melting point of 114–115°, which further crystallization failed to alter. Calc. for $C_{11}H_{10}BrNO_5$: C, 41.84; H, 3.17; N, 4.43. Found: C, 41.83; H, 3.19; N, 4.24.

7-Bromoindole-2-carboxylic Acid

A solution of the potassium enolate of ethyl 3-bromo-2-nitrophenylpyruvate (3.0 g, 0.009 mole) in warm 4 *N* ammonium hydroxide (100 ml) was slowly added, with stirring, to a boiling suspension of ferrous hydroxide prepared by the addition of ammonium hydroxide (6 ml, $d = 0.880$) to a boiling solution of ferrous sulphate heptahydrate (14.0 g, 0.05 mole) in 100 ml of water. The resulting reduction mixture was maintained at 90° for 30 minutes and then filtered from the ferric oxide sludge. The sludge was extracted three times with boiling 2 *N* ammonium hydroxide and the combined filtrate and extracts cooled to 25° and acidified with 6 *N* hydrochloric acid. The solid, collected by suction filtration, when crystallized once from aqueous ethanol gave 1.2 g (60%) of 7-bromoindole-2-carboxylic acid melting at 236–239°. Repeated crystallization gave an

Can. J. Chem. Downloaded from www.nrcresearchpress.com by 210.87.254.40 on 09/05/12
For personal use only.

analytical sample of melting point 242–244°. Calc. for $C_9H_6BrNO_2$: C, 45.00; H, 2.50; N, 5.83. Found: C, 45.20; H, 2.58; N, 5.99.

7-Bromoindole

A solution of 7-bromoindole-2-carboxylic acid (2.9 g) in synthetic quinoline (20 ml) was refluxed for 48 hours, during which time small amounts of copper chromite (10) catalyst were added at frequent intervals. The cooled reaction mixture was poured into 350 ml of 1 *N* hydrochloric acid and the resulting solution extracted thrice with 150-ml portions of ether. The combined ether extracts, washed twice with 1 *N* hydrochloric acid, once with water, twice with 1 *N* ammonium hydroxide, and then with water, were dried over anhydrous magnesium sulphate. Removal of the ether yielded a yellow oil which was purified by chromatography on an alumina column, using *n*-pentane as eluant, giving 1.13 g (48%) of colorless crystals melting at 42–43°. Calc. for C_8H_6BrN: C, 48.98; H, 3.06; N, 7.14; Br, 40.81. Found: C, 49.08; H, 3.09; N, 7.13; Br, 40.42.

Ethyl Pyruvate 2-Bromophenylhydrazone

A solution containing ethyl pyruvate (15.3 g, 0.13 mole) (13), 2-bromophenylhydrazine (24.1 g, 0.13 mole) (14), and ethanol (50 ml) was refluxed for 1 hour, cooled, and poured into cold water. The precipitated yellow solid, when air-dried and crystallized for ethanol, gave 33.1 g (91%) of product melting at 44–46°. Calc. for $C_{11}H_{13}BrN_2O_2$: C, 46.32; H, 4.56; N, 9.86. Found: C, 46.36; H, 4.63; N, 9.78.

Ethyl 7-Bromoindole-2-carboxylate

A mixture of ethyl pyruvate 2-bromophenylhydrazone (33.1 g) and polyphosphoric acid* (40 g) was slowly heated. When the temperature of the mixture reached 70° a spontaneous exothermic reaction occurred raising the temperature to 150°. The reactants were kept at this temperature for 10 minutes, then cooled and poured into cold water. The ether extracts of this solution when dried with anhydrous magnesium sulphate gave a brown oil which solidified. Crystallization from ethanol yielded 14.3 g (46%) of product, m.p. 85–86°. Calc. for $C_{11}H_{10}BrNO_2$: C, 49.25; H, 3.73; N, 5.22. Found: C, 49.01; H, 3.74; N, 5.17.

When 14.3 g of ethyl 7-bromoindole-2-carboxylate was dissolved in a mixture of ethanol (200 ml) and 2.5 *N* aqueous sodium hydroxide solution (70 ml), refluxed for 2 hours, poured into cold water (1000 ml), and then acidified with 6 *N* hydrochloric acid, a solid deposited which after crystallization from ethanol afforded 7.1 g (55.5%) of product melting at 237–239°. This was found to be identical with the 7-bromoindole-2-carboxylic acid prepared above.

Decarboxylation of the Mixture of 5- and 6-Bromoindole-3-carboxylic Acids

Twelve grams of the monobromoindole-3-carboxylic acid mixture (m.p. 212°) (1) in 25 ml of quinoline was heated to 140° whereupon vigorous evolution of carbon dioxide ensued. The temperature was maintained at 140° for 2.5 hours, after which time no further evolution of carbon dioxide occurred. The reaction mixture was then poured into 300 ml of 1 *N* hydrochloric acid and a dark oil separated. The oil solidified and was collected, washed with 1 *N* hydrochloric acid, and then with water. Crystallization from aqueous alcohol yielded a product melting at 74–75°, which repeated crystallization from aqueous alcohol, skellysolve, or heptane failed to alter. Yield, 4.3 g (46%). Calc. for C_8H_6NBr: C, 49.0; H, 3.1. Found: C, 48.7; H, 2.9.

**Commercially available from Victor Chemical Works, Chicago, Illinois.*

Can. J. Chem. Downloaded from www.nrcresearchpress.com by 210.87.254.40 on 09/05/12
For personal use only.

ACKNOWLEDGMENTS

The authors wish to express their gratitude to the National Research Council of Canada and the National Cancer Institute of Canada for financial assistance throughout the course of this work.

REFERENCES

1. R. MAJIMA and M. KOTAKE. Ber. **63** B, 2237 (1930).
2. W. BORSCHE and W. JACOBS. Ber. **47**, 360 (1914).
3. L. ETTINGER and P. FRIEDLÄNDER. Ber. **45**, 2082 (1912).
4. H. PLIENINGER, F. SUEHIRO, K. SUHR, and M. DECKER. Ber. **88**, 370 (1955).
5. H. R. SNYDER, S. M. PARMERTER, and L. KATZ. J. Am. Chem. Soc. **70**, 222 (1948).
6. E. MULLER. Ber. **42**, 430 (1909).
7. C. V. WILSON. Organic reactions. Vol. 9. John Wiley & Sons, Inc., New York. 1957. p. 332.
8. H. N. RYDON and J. C. TWEDDLE. J. Chem. Soc. 3499 (1955).
9. D. G. HARVEY. J. Chem. Soc. 3760 (1958).
10. ORGANIC SYNTHESES. Coll. Vol. 2. John Wiley & Sons, Inc., New York. p. 142.
11. B. M. BARCLAY and N. CAMPBELL. J. Chem. Soc. 530 (1945).
12. L. A. ELSON, C. S. GIBSON, and J. D. A. JOHNSON. J. Chem. Soc. 2741 (1929).
13. ORGANIC SYNTHESES. Vol. 31. John Wiley & Sons, Inc., New York. p. 59.
14. M. BUSCH and E. MEUSSDÖRFER. J. prakt. Chem. **75**, 121 (1907).

Can. J. Chem. Downloaded from www.nrcresearchpress.com by 210.87.254.40 on 09/05/12
For personal use only.

Can. J. Chem. Downloaded from www.nrcresearchpress.com by 210.87.254.105 on 09/05/12
For personal use only.

SYNTHESES OF POLYURETHANES FROM HYDROXY-TERMINATED POLYESTERS[1]

PAUL E. GAGNON, JEAN-L. BOIVIN,[2] AND GEORGE W. HOUSE[3]

ABSTRACT

Hydroxy-terminated polyesters were synthesized by treating diols with the diethyl esters of dicarboxylic acids. Ethylene, diethylene, and triethylene glycols, four polyoxyethylene glycols ranging in molecular weight from 200 to 600, 1,2-propanediol, dipropylene glycol, five polyoxypropylene glycols ranging in molecular weight from 150 to 2025, 1,3-propanediol, 1,3-butanediol, 1,4-butanediol, 2,3-butanediol, 1,5-pentanediol, 2,2′-(methylimino)diethanol, 2,2′-(ethylimino)diethanol, 2,2′-(butylimino)diethanol, and 2,2′-thiodiethanol were condensed with diethyl succinate in the absence and presence of a catalyst, and with diethyl cyanomalonate, cyanosuccinate, and α-cyanoglutarate.

Polyurethanes were obtained from the various polyesters prepared by treatment with different quantities of 2,4-tolylene diiocyanate. In general, non-elastomeric products were obtained from polyesters of monomeric glycols, while elastomeric polyurethanes with the lowest brittle points were formed from polyoxyethylene glycol 400 and 600, and polyoxypropylene glycol 750, 1025, and 2025 polyesters. Also the succinate polyurethanes, which did not contain nitrile groups, had the greatest tendency to be elastomeric and had the lowest brittle points. For the nitrile containing polyurethanes, the cyanomalonates had the lowest tendency to be elastomeric and had the highest brittle points. The cyanosuccinate and α-cyanoglutarates had about the same properties.

INTRODUCTION

Polyesters constitute an important class of synthetic polymers employed as textiles, resins, and intermediates for the preparation of polyurethanes. They can be prepared by the reactions commonly used to obtain simple esters. Hydroxy-terminated polyesters are produced by heating diols in excess with dibasic acids or esters and by continuing the heating under vacuum to yield high molecular weight polymers (1).

Polyurethanes are made by reacting polyhydroxylated compounds or polyesters with diisocyanates. They have found extensive use as rubber substitutes (2, 3, 4, 5), foams (6), coatings (7), and adhesives (8).

In the present investigation, the main object was the synthesis of polyesters and polyurethanes, some containing nitrile groups, and the comparison of their properties.

RESULTS AND DISCUSSION

Polyesters

Polyesters were prepared by the transesterification of different diols with diethyl succinate, cyanomalonate, cyanosuccinate, and α-cyanoglutarate.

$$n\text{HOROH} + n\text{EtOOR'COOEt} \rightarrow \text{H(OROOCR'CO)}_n\text{OEt} + (2n-1)\text{EtOH}$$

It was observed that the general order of reactivity of diols was thus: (*a*) the basic and therefore self-catalyzed N-substituted iminodiethanols, (*b*) the other monomeric glycols bearing two primary hydroxyl groups, (*c*) monomeric glycols bearing one or two secondary hydroxyl groups, (*d*) polymeric glycols bearing solely primary hydroxyl groups, and (*e*)

[1]*Manuscript received April 22, 1960.*
Contribution from the Department of Chemistry, Laval University, Quebec, Que. This paper constitutes part of a thesis submitted to the Graduate School, Laval University, in partial fulfillment of the requirements for the degree of Doctor of Science.
[2]*Canadian Armament Research and Development Establishment, Valcartier, Que.*
[3]*Graduate student, holder of National Research Council of Canada Studentships in 1957–60.*

polymeric glycols bearing solely secondary hydroxyl groups. To terminate the chains by hydroxyl groups, an excess of glycol was added to the reaction mixture and heating continued.

$$H(OROOCR'CO)_nOEt + HOROH \rightarrow H(OROOCR'CO)_nOROH + EtOH$$

Then the reaction was driven towards completion and excess glycol was removed under vacuum.

Succinates

The reaction between diethyl succinate and the glycols in the absence of a catalyst proceeded only quite slowly and in most cases ethanol distilled at temperatures ranging from 155 to 215° C, and prolonged reaction times were necessary.

The molecular weights of the products, measured by hydroxyl end-group analysis, varied from 500 to 3540 but were for the most part between 800 and 2000. The values found for the polyesters of polyoxyethylene glycol 600 and polyoxypropylene glycols 425, 750, 1025, and 2025 were higher than the true molecular weight values because no excess glycol had been employed to assure the termination of polyester chains by hydroxyl groups. Furthermore, the values found for the polyesters of polyoxypropylene glycols 1025 and 2025 were certainly not high as compared to the molecular weights of the glycols themselves, indicating that very little reaction had taken place.

In order to investigate the effect of an ester interchange catalyst on the rate of the polyesterification reaction and on the molecular weight of the product, the syntheses of of the succinate polyesters were repeated in the presence of a sodium catalyst. It was observed that ethanol began to form at reaction temperatures well below those of the corresponding preparations carried out without catalyst, 70 to 90 degrees lower in most cases. Distillation was also much more rapid and complete with catalyst than without. In the case of 1,2-propanediol, for instance, without catalyst 25% of the theoretical amount of ethanol had collected after 114 hours of reaction time at 190° C, whereas with a catalyst 82% of the theoretical amount of ethanol had collected after 17 hours at the same temperature. The molecular weights of the products varied between 670 and 3620, although most lay in the region 1000 to 2000. In general, these molecular weights were higher than those of the corresponding products formed without catalyst. The viscosities of polyesters, which were of roughly the same molecular weight when prepared by either method, were higher for products prepared using catalyst than for those prepared without.

Cyanomalonates

Diethyl cyanomalonate was obtained from the reaction of the sodium derivative of ethyl cyanoacetate and ethyl chloroformate (9). The transesterification between diethyl cyanomalonate and the glycols proceeded quite rapidly, ethanol beginning to distill at reaction temperatures about the same as those in the syntheses of the corresponding succinate polyesters prepared with catalyst, and much lower than those in the syntheses of succinate polyesters prepared without catalyst. In addition, ethanol was collected more rapidly and more completely than in the syntheses of the corresponding succinate polyesters without catalyst. However, the molecular weights of the polyesters, based on hydroxyl end-group analysis and the assumption of two hydroxyl groups per molecule, were very low, below 500 in most cases. Thus it would appear that diethyl cyanomalonate, although much more reactive than diethyl succinate, gave polyesters of lower molecular weight.

Can. J. Chem. Downloaded from www.nrcresearchpress.com by 210.87.254.105 on 09/05/12
For personal use only.

The high reactivity of diethyl cyanomalonate ($pK_a = 4.76$ at 25° C) was explained by its acidity, which catalyzed the transesterification reaction with glycols. Furthermore, because of the acidity the central carbon atom of the ester was assumed to be alkylated by a glycol, with the formation of water.

$$\mathrm{HOROH + EtOOCCHCOOEt \rightarrow EtOOCC(ROH)COOEt + H_2O}$$

The resulting alkylated molecule, which possessed two ester groups and one hydroxyl group, would then undergo a series of transesterifications and alkylations. In the presence of excess glycol, polymeric cross-linked molecules containing many hydroxyl groups could build up.

The apparently low molecular weight of the cyanomalonate polyesters could thus be explained by the assumption that each molecule contained several rather than two hydroxyl groups. Because the average number of hydroxyl groups per molecule was not known, the cyanomalonate polyesters were reported as having a certain hydroxyl number rather than a certain molecular weight. The values found were above 200 for most polyesters prepared from monomeric glycols but lower for those derived from the higher molecular weight polymeric glycols and the N-substituted 2,2′-iminodiethanols. The lower hydroxyl number of polyesters of higher molecular weight polymeric glycols could be explained by the low proportion of trifunctional cyanomalonate in the polyester molecules. Also, polyesters of the N-substituted 2,2′-iminodiethanols could have low hydroxyl numbers because of salt formation between the ester and amine, which would prevent alkylations from taking place.

Cyanosuccinates

Diethyl cyanosuccinate, which was prepared by condensing the sodium derivative of ethyl cyanoacetate with ethyl chloroacetate (10), proved to be of the same order of reactivity as cyanomalonate, with respect to glycols.

α-Cyanoglutarates

Diethyl α-cyanoglutarate was synthesized by the Michael reaction between ethyl cyanoacetate and ethyl acrylate in the presence of a sodium ethoxide catalyst (11). The ester appeared to be slightly less reactive towards the glycols than was diethyl cyanosuccinate.

Polyurethanes

Polyurethanes were prepared by mixing the hydroxyl-terminated polyesters previously described with various quantities of 2,4-tolylene diisocyanate (TDI) and by allowing the mixture to cure at 100° C for 5 days in the presence of ferric acetylacetonate as a catalyst.

$$n\mathrm{HO{-}polyester{-}OH} + (n+1)\mathrm{OCNRNCO} \rightarrow \mathrm{OCNR(NHCOO{-}polyester{-}OOCNHR)_nNCO}$$

The varied consistencies of the products were classified into different categories, although completely distinct boundary lines did not exist between all of them.

It was found that, in general, more than the equivalent amount of TDI was required to cure a polyester to a solid polyurethane. It was also noted that the polyurethanes tended towards brittle solids as the amounts of TDI increased. The change from stringy to

Can. J. Chem. Downloaded from www.nrcresearchpress.com by 210.87.254.105 on 09/05/12
For personal use only.

leathery to resinous was often observed. Also for products which were elastomeric, the elongation at break normally decreased with increasing amount of TDI and in many cases the brittle point increased, although in some cases the reverse was true.

In general, non-elastomeric products were obtained from polyesters of monomeric glycols, while elastomeric polyurethanes with the lowest brittle points were formed from polyoxyethylene glycol 400 and 600 and polyoxypropylene glycol 750, 1025, and 2025 polyesters. Also, in general, the succinate polyurethanes, which did not contain nitrile groups, had the greatest tendency to be elastomeric and had the lowest brittle points (Tables VI and VII). For the nitrile containing polyurethanes, the cyanomalonates had the lowest tendency to be elastomeric and had the highest brittle points (Table VIII). The cyanosuccinates (Table IX) and α-cyanoglutarates (Table X) had about the same properties.

EXPERIMENTAL

Polyesters

Polyesters were prepared by condensing ethylene, diethylene, and triethylene glycols, four polyoxyethylene glycols ranging in molecular weight from 200 to 600, 1,2-propanediol, dipropylene glycol, five polyoxypropylene glycols ranging in molecular weight from 150 to 2025, 1,3-propanediol, 1,3-butanediol, 1,4-butanediol, 2,3-butanediol, 1,5-pentanediol, 2,2′-(methylimino)diethanol, 2,2′-(ethylimino)diethanol, 2,2′-(butylimino)diethanol, and 2,2′-thiodiethanol with diethyl succinate in the absence and presence of a sodium catalyst and with diethyl cyanomalonate (9), cyanosuccinate (10), and α-cyanoglutarate (11).

Equimolar quantities of a glycol and diethyl ester having a combined weight of about 150 grams were placed in a 300-ml three-necked round-bottomed flask. The flask was fitted with thermometer and gas delivery tube in the side necks and Claisen head in the center neck. A vertical condenser protected by a calcium chloride tube was fitted into the side neck of the Claisen head which had a distillate take-off tap mounted at the elbow. The contents of the flask were heated to a temperature in the region of 200° C under a steady stream of nitrogen, ethanol beginning to distill off at reaction temperatures ranging from 95 to 215° C. After a heating period of from 4 to 222 hours, by which time ethanol had ceased to distill, an excess of glycol was added to the reaction mixture in most cases and heating continued for another 4 to 70 hours, at which time ethanol no longer distilled. The contents of the flask, after being allowed to cool, were slowly heated to a temperature in the region of 200° C under a vacuum less than 1 millimeter of mercury for 4 to 12 hours, until no more distillate collected.

The kinematic viscosity of polyesters was measured at 20.0° C using Ostwald–Fenske viscometers. Several determinations were carried out on each sample and the average value computed. Viscosities above 30,000 centistokes were not measured but recorded only as being greater than this value.

The average molecular weight or, in the case of the cyanomalonates, the hydroxyl number of polyesters was determined by a hydroxyl end-group analysis based on acetylation with acetic anhydride in the presence of pyridine. Duplicate determinations were carried out on each polyester and an average taken of the two values obtained.

The individual syntheses of the various polyesters are given in detail as follows: succinates prepared without catalyst, Table I; succinates prepared using sodium catalyst, Table II; cyanomalonates, Table III; cyanosuccinates, Table IV; and α-cyanoglutarates, Table V.

Can. J. Chem. Downloaded from www.nrcresearchpress.com by 210.87.254.105 on 09/05/12
For personal use only.

Can. J. Chem. Downloaded from www.nrcresearchpress.com by 210.87.254.105 on 09/05/12
For personal use only.

TAB

Succinate polyesters

Starting material					Reaction temp., °C	Ethanol collected				Reaction time, hours
Glycol			Diethyl succinate			Initial temp., °C	Volume, ml	Yield		
Name	g	moles	g	moles				g	%	
Ethylene glycol	46.6	0.75	130.7	0.75	180	180	47	37	53	53
Diethylene glycol	63.7	0.60	104.5	0.60	210	180	54	42	77	16
Triethylene glycol	75.1	0.50	87.1	0.50	210	190	28	22	48	18
PEG* 200	100.0	0.50	87.1	0.50	215	195	13	10	22	90
300	100.0	0.33	58.1	0.33	215	200	17	13	43	40
400	100.0	0.25	43.6	0.25	215	210	10	8	34	40
600	120.0	0.20	34.8	0.20	215	215	5	4	21	127
1,2-Propanediol	49.5	0.65	113.2	0.65	190	190	17	13	22	84
Dipropylene glycol	67.1	0.50	87.1	0.50	210	195	15	12	26	128
PPG* 150	75.0	0.50	87.1	0.50	215	195	12	9	20	123
425	106.3	0.25	43.6	0.25	215	215	5	4	17	197
750	125.0	0.167	29.0	0.167	215	215	4	3	20	197
1,025	128.1	0.125	21.8	0.125	215	215	4	3	27	201
2,025	126.5	0.0625	10.9	0.0625	215	215	2	2	27	222
1,3-Propanediol	57.1	0.75	130.7	0.75	210	180	35	27	46	83
1,3-Butanediol	45.1	0.50	87.1	0.50	200	175	29	23	49	20
1,4-Butanediol	45.1	0.50	87.1	0.50	210	175	42	33	72	8
2,3-Butanediol	45.1	0.50	87.1	0.50	180	180	14	11	24	58
1,5-Pentanediol	52.1	0.50	87.1	0.50	210	190	27	21	46	54
2,2′-(Methylimino)-diethanol	59.6	0.50	87.1	0.50	180	155	36	28	61	21
2,2′-(Ethylimino)-diethanol	66.6	0.50	87.1	0.50	180	165	29	23	49	14
2,2′-(Butylimino)-diethanol	80.6	0.50	87.1	0.50	180	165	25	20	43	27
2,2′-Thiodiethanol	61.1	0.50	87.1	0.50	190	185	22	17	37	36

*Polyoxyethylene glycol (PEG), $HO(CH_2)_2[O(CH_2)_2]_nOH$, and polyoxypropylene glycol (PPG), $CH_3CHOHCH_2[OCH_2CH$ molecular weights were within a 5% tolerance of the values given.

TAB

Succinate polyesters prepare

Starting material					Sodium catalyst		Reaction temp., °C	Ethanol collected				Reaction time, hours
Glycol			Diethyl succinate					Initial temp., °C	Volume, ml	Yield		
Name	g	moles	g	moles	g	moles				g	%	
Ethylene glycol	46.6	0.75	130.7	0.75	0.50	0.022	180	105	71	56	81	4
Diethylene glycol	63.7	0.60	104.5	0.60	0.50	0.022	210	105	59	46	84	4
Triethylene glycol	75.1	0.50	87.1	0.50	0.50	0.022	210	105	47	37	80	4
PEG 200	100.0	0.50	87.1	0.50	0.50	0.022	210	105	50	39	85	4
300	100.0	0.33	58.1	0.33	0.50	0.022	210	115	32	25	82	5
400	100.0	0.25	43.6	0.25	0.50	0.022	210	120	25	20	85	7
600	100.0	0.167	29.0	0.167	0.50	0.022	210	125	14	11	72	6
1,2-Propanediol	57.1	0.75	130.7	0.75	0.50	0.022	190	110	60	47	68	10
Dipropylene glycol	67.1	0.50	87.1	0.50	0.50	0.022	210	110	43	34	73	4
PPG 150	75.0	0.50	87.1	0.50	0.50	0.022	210	110	44	35	75	4
425	106.3	0.25	43.6	0.25	0.50	0.022	210	130	21	16	72	5
750	125.0	0.167	29.0	0.167	0.30	0.013	210	145	8	6	41	5
1,025	128.1	0.125	21.8	0.125	0.20	0.009	210	155	7	5	48	7
2,025	126.5	0.0625	10.9	0.0625	0.10	0.004	210	145	2	2	27	8
1,3-Propanediol	57.1	0.75	130.7	0.75	0.50	0.022	210	100	73	57	83	4
1,3-Butanediol	45.1	0.50	87.1	0.50	0.50	0.022	200	105	48	38	82	4
1,4-Butanediol	45.1	0.50	87.1	0.50	0.50	0.022	210	100	49	38	83	3
2,3-Butanediol	45.1	0.50	87.1	0.50	0.50	0.022	180	110	32	25	54	10
1,5-Pentanediol	52.1	0.50	87.1	0.50	0.50	0.022	210	100	51	40	87	4
2,2′-(Methylimino)-diethanol	59.6	0.50	87.1	0.50	0.50	0.022	190	105	47	37	80	11
2,2′-(Ethylimino)-diethanol	66.6	0.50	87.1	0.50	0.50	0.022	200	105	40	31	68	11
2,2′-(Butylimino)-diethanol	80.6	0.50	87.1	0.50	0.50	0.022	210	110	42	33	72	4
2,2′-Thiodiethanol	61.1	0.50	87.1	0.50	0.50	0.022	210	105	42	33	72	4

*1,4-Butanediol. †The product was too dark for an accurate measurement.

Can. J. Chem. Downloaded from www.nrcresearchpress.com by 210.87.254.105 on 09/05/12
For personal use only.

LE I

prepared without catalyst

Excess glycol added			Further heating, hours	Total ethanol collected			Reaction mixture heated *in vacuo*			Weight distillate, g	Polyester		
				Volume,	Yield		Final	Pressure,	Time,		Yield,	Viscosity,	Molecular
g	moles	%		ml	g	%	temp., °C	mm	hours		g	cs 20° C	weight
46.6	0.75	100	30	55	43	62	190	0.1	7	54.0	97.4	Waxy	1,910
63.7	0.60	100	7	54	42	77	210	0.1	7	59.7	112.0	>30,000	2,730
75.1	0.50	100	37	34	27	58	210	0.1	7	67.2	120.5	13,100	1,670
10.0	0.050	10	10	15	12	26	210	0.2	6	15.1	142.9	630	1,120
10.0	0.033	10	10	18	14	46	210	0.5	6	3.0	127.1	990	1,560
10.0	0.025	10	10	11	9	37	210	0.5	6	1.6	130.0	900	1,580
Nil	Nil	Nil	Nil	5	4	21	215	0.2	6	0.1	134.5	Jelly	3,540
49.5	0.65	100	28	19	15	25	190	0.1	7	120.7	53.1	1,230	500
67.1	0.50	100	48	16	13	27	210	0.2	7	56.1	109.8	1,460	840
75.0	0.50	100	70	15	12	26	215	0.2	6	66.5	127.3	600	970
Nil	Nil	Nil	Nil	5	4	17	215	0.2	6	12.6	117.4	240	1,440
Nil	Nil	Nil	Nil	4	3	20	215	0.5	5	11.7	128.3	200	1,250
Nil	Nil	Nil	Nil	4	3	27	215	0.2	6	16.8	110.5	180	1,430
Nil	Nil	Nil	Nil	2	2	27	215	0.2	5	8.9	116.2	350	2,140
57.1	0.75	100	54	46	36	52	210	0.2	7	53.2	120.9	1,380	840
45.1	0.50	100	49	48	38	82	210	0.1	6	5.2	108.6	3,750	1,740
45.1	0.50	100	12	69	54	118	210	0.2	7	7.2	82.6	Waxy	1,900
45.1	0.50	100	46	20	16	34	180	0.5	6	81.6	51.8	560	890
52.1	0.50	100	48	36	28	61	210	0.2	6	21.5	114.8	1,010	840
59.6	0.50	100	7	48	38	82	180	0.1	6	28.6	110.4	>30,000	1,260
66.6	0.50	100	20	42	33	72	180	0.2	6	34.7	126.0	5,910	1,300
80.6	0.50	100	21	34	27	58	180	0.2	6	50.7	141.4	1,620	1,130
61.1	0.50	100	38	40	31	68	190	0.1	6	5.2	160.1	3,890	1,290

$(CH_3)]_nOCH_2CHOHCH_3$. These products were obtained from the Carbide Chemicals Company, Montreal, Que. Their average

LE II

using sodium catalyst

Excess glycol added			Further heating, hours	Total ethanol collected			Reaction mixture heated *in vacuo*			Weight distillate, g	Polyester		
				Volume,	Yield		Final	Pressure,	Time,		Yield,	Viscosity,	Molecular
g	moles	%		ml	g	%	temp., °C	mm	hours		g	cs 20° C	weight
46.6	0.75	100	6	83	65	94	190	0.1	4	41.3	107.1	Waxy	3,620
63.7	0.60	100	8	64	50	91	210	0.2	5	62.6	109.7	>30,000	2,380
75.1	0.50	100	5	54	42	92	210	0.5	4	77.7	107.6	>30,000	2,230
45.1*	0.50	100	5	55	43	94	210	0.6	6	49.0	127.5	~10,000†	1,770
30.0*	0.33	100	7	34	27	87	210	0.5	6	18.8	132.1	~3,000†	1,100
22.5*	0.25	100	4	26	20	89	210	0.5	4	13.7	123.9	~3,000†	1,160
15.0*	0.167	100	7	14	11	72	210	0.5	4	5.8	117.3	~3,000†	1,150
57.1	0.75	100	7	72	57	82	210	0.5	4	56.1	116.9	>30,000	1,630
67.1	0.50	100	12	49	38	83	210	0.5	5	65.4	106.7	>30,000	2,010
75.0	0.50	100	13	51	40	87	210	0.2	6	76.3	113.3	>30,000	2,730
22.5*	0.25	100	12	22	17	75	210	0.2	5	11.0	133.7	~600†	780
15.0*	0.167	100	15	9	7	46	210	0.2	5	9.9	145.1	390	1,120
11.3*	0.125	100	13	7	5	48	210	0.5	6	6.4	141.6	580	1,480
5.6*	0.0625	100	12	2	2	27	210	0.2	5	0.8	133.4	1,370	2,480
57.1	0.75	100	6	86	68	98	210	0.5	4	47.7	122.2	>30,000	1,700
45.1	0.50	100	8	54	42	92	210	0.2	4	40.6	86.4	>30,000	1,220
45.1	0.50	100	6	58	46	99	210	0.5	6	23.2	86.8	Waxy	1,520
45.1	0.50	100	7	37	29	63	180	0.5	6	75.7	64.0	>30,000	670
52.1	0.50	100	6	54	42	92	210	0.5	6	44.8	93.1	>30,000	1,240
59.6	0.50	100	7	60	47	102	180	0.5	5	22.3	108.5	>30,000	2,280
66.6	0.50	100	9	47	37	80	200	0.2	6	38.2	122.3	11,500	1,950
80.6	0.50	100	9	56	44	95	210	0.2	12	49.7	138.5	7,780	2,650
61.1	0.50	100	13	56	44	95	210	0.7	6	11.0	131.8	~10,000†	990

Can. J. Chem. Downloaded from www.nrcresearchpress.com by 210.87.254.105 on 09/05/12
For personal use only.

TAB

Cyanomalonat

Starting material					Reaction temp., °C	Ethanol collected				Reaction time, hours
Glycol			Diethyl cyanomalonate			Initial temp., °C	Volume, ml	Yield		
Name	g	moles	g	moles				g	%	
Ethylene glycol	37.2	0.60	111.1	0.60	180	100	45	35	64	8
Diethylene glycol	53.1	0.50	92.6	0.50	190	105	43	34	73	8
Triethylene glycol	67.6	0.45	83.3	0.45	200	105	44	35	83	8
PEG 200	80.0	0.40	74.1	0.40	200	105	36	28	77	8
300	90.0	0.30	55.6	0.30	190	105	25	20	71	8
400	80.0	0.20	37.0	0.20	190	105	18	14	77	8
600	90.0	0.15	27.8	0.15	190	105	11	9	62	8
1,2-Propanediol	45.7	0.60	111.1	0.60	180	110	55	43	78	13
Dipropylene glycol	64.4	0 48	88.9	0.48	190	115	42	33	74	8
PPG 150	67.5	0.45	83.3	0.45	190	115	30	24	57	13
425	85.0	0.20	37.0	0.20	190	110	11	9	47	13
750	90.0	0.12	22.2	0.12	190	140	7	5	50	14
1,025	102.5	0.10	18.5	0.10	190	145	6	5	51	14
2,025	101.3	0.050	9.3	0.050	190	145	1	1	17	14
1,3-Propanediol	45.7	0.60	111.1	0.60	190	105	42	33	60	7
1,3-Butanediol	49.6	0.55	101.8	0.55	190	105	46	36	71	7
1,4-Butanediol	49.6	0.55	101.8	0.55	190	95	65	51	101	6
2,3-Butanediol	49.6	0.55	101.8	0.55	180	110	47	37	73	15
1,5-Pentanediol	52.1	0.50	92.6	0.50	190	100	55	43	94	8
2,2′-(Methylimino)-diethanol	59.6	0.50	92.6	0.50	180	105	50	39	85	8
2,2′-(Ethylimino)-diethanol	63.9	0.48	88.9	0.48	180	100	46	36	82	7
2,2′-(Butylimino)-diethanol	64.5	0.40	74.1	0.40	180	110	40	31	85	8
2,2′-Thiodiethanol	61.1	0.50	92.6	0.50	180	95	43	34	73	8

*1,4-Butanediol.

TAB

Cyanosuccinat

Starting material					Reaction temp., °C	Ethanol collected				Reaction time, hours
Glycol			Diethyl cyanosuccinate			Initial temp., °C	Volume, ml	Yield		
Name	g	moles	g	moles				g	%	
Ethylene glycol	31.0	0.50	99.6	0.50	180	170	30	24	51	8
Diethylene glycol	53.1	0.50	99.6	0.50	210	170	36	28	61	13
Triethylene glycol	75.1	0.50	99.6	0.50	210	190	30	24	51	8
PEG 200	75.0	0.375	74.7	0.375	210	180	28	22	64	14
300	90.0	0.30	59.8	0.30	210	180	22	17	62	14
400	80.0	0.20	39.8	0.20	210	180	15	12	64	14
600	90.0	0.15	29.9	0.15	210	210	8	6	45	21
1,2-Propanediol	38.1	0.50	99.6	0.50	185	180	28	22	48	14
Dipropylene glycol	67.1	0.50	99.6	0.50	210	185	30	24	51	8
PPG 150	75.0	0.50	99.6	0.50	210	185	30	24	51	19
425 I	85.0	0.20	39.8	0.20	210	210	6	5	26	28
425 II	106.3	0.25	49.8	0.25	210	210	7	5	24	29
750 I	90.0	0.12	23.9	0.12	210	210	4	3	28	28
750 II	112.5	0.15	29.9	0.15	210	210	6	5	34	18
1,025 I	102.5	0.10	19.9	0.10	210	210	2	2	17	28
1,025 II	102.5	0.10	19.9	0.10	210	210	2	2	17	26
2,025 I	101.3	0.050	10.0	0.050	210	210	1	1	17	28
2,025 II	121.5	0.060	12.0	0.060	210	210	1	1	14	25
1,3-Propanediol	38.1	0.50	99.6	0.50	200	170	36	28	61	13
1,3-Butanediol	45.1	0.50	99.6	0.50	200	175	31	24	53	21
1,4-Butanediol	45.1	0.50	99.6	0.50	210	165	46	36	78	8
2,3-Butanediol	45.1	0.50	99.6	0.50	175	175	23	18	39	31
1,5-Pentanediol	52.1	0.50	99.6	0.50	210	180	33	26	56	8
2,2′-(Methylimino)-diethanol	59.6	0.50	99.6	0.50	180	110	50	39	85	8
2,2′-(Ethylimino)-diethanol	59.9	0.45	89.6	0.45	180	110	40	31	76	12
2,2′-(Butylimino)-diethanol	60.4	0.375	74.7	0.375	210	110	32	25	73	8
2,2′-Thiodiethanol	55.0	0.45	89.6	0.45	190	155	35	27	66	13

*1,4-Butanediol.

Can. J. Chem. Downloaded from www.nrcresearchpress.com by 210.87.254.105 on 09/05/12
For personal use only.

.E III

olyesters

Excess glycol added			Further heating, hours	Total ethanol collected			Reaction mixture heated *in vacuo*			Weight distillate, g	Polyester			
				Volume, ml	Yield		Final temp., °C	Pressure, mm	Time, hours		Yield, g	Viscosity, cs 20° C	Hydroxyl number	Acid number
g	moles	%			g	%								
37.2	0.60	100	6	57	45	81	180	0.1	5	35.3	43.9	>30,000	230	Nil
53.1	0.50	100	6	46	36	78	180	0.4	7	49.7	85.2	>30,000	470	39.6
67.6	0.45	100	7	47	37	89	180	0.4	7	58.1	105.9	>30,000	310	19.0
36.0*	0.40	100	7	63	49	134	180	0.4	7	22.3	79.7	890	240	3.7
27.0*	0.30	100	7	35	27	99	180	0.5	6	14.0	104.3	840	250	2.1
18.0*	0.20	100	7	21	16	89	180	0.4	6	7.8	90.1	830	200	3.1
13.5*	0.15	100	7	12	9	68	180	0.4	6	6.5	97.7	1,050	180	2.0
45.7	0.60	100	7	60	47	85	180	0.5	4	90.3	30.4	>30,000	240	6.6
64.4	0.48	100	7	46	36	82	180	0.3	6	70.2	81.2	>30,000	290	21.2
67.5	0.45	100	7	32	25	61	180	0.2	6	68.1	101.0	>30,000	240	23.3
18.0*	0.20	100	7	17	13	72	180	0.2	6	13.2	90.7	640	220	2.1
10.8*	0.12	100	7	8	6	57	180	0.2	6	4.5	96.7	430	210	25.8
9.0*	0.10	100	7	7	5	60	180	0.1	6	4.2	105.2	500	190	27.2
4.5*	0.05	100	7	1	1	17	180	0.2	6	3.3	102.4	720	91.1	5.5
45.7	0.60	100	7	60	37	67	180	0.5	7	55.6	77.5	>30,000	330	1.3
49.6	0.55	100	7	54	42	84	180	0.4	6	73.5	60.7	>30,000	250	2.0
49.6	0.55	100	6	99	78	153	180	0.5	4	11.7	34.3	>30,000	370	25.9
49.6	0.55	100	11	57	45	88	180	0.3	6	103.6	20.4	>30,000	330	8.3
52.1	0.50	100	8	74	58	126	180	0.4	6	35.8	69.2	5,200	290	9.6
59.6	0.50	100	6	51	40	87	180	0.5	6	65.3	39.0	>30,000	200	Nil
63.9	0.48	100	7	46	36	82	180	0.2	6	75.9	50.1	>30,000	84.2	Nil
64.5	0.40	100	7	41	32	87	180	0.2	5	71.8	57.2	4,650	110	Nil
61.1	0.50	100	7	47	37	80	180	0.4	6	40.9	83.1	2,130	230	Nil

.E IV

olyesters

Excess glycol added			Further heating, hours	Total ethanol collected			Reaction mixture heated *in vacuo*			Weight distillate, g	Polyester		
				Volume, ml	Yield		Final temp., °C	Pressure, mm	Time, hours		Yield, g	Viscosity, cs 20° C	Molecular weight
g	moles	%			g	%							
31.0	0.50	100	6	46	36	78	180	0.1	4	28.4	46.5	>30,000	850
53.1	0.50	100	8	45	35	77	210	0.3	6	59.9	92.6	>30,000	1,360
75.1	0.50	100	14	43	34	73	210	0.5	5	63.1	125.8	>30,000	1,220
33.8*	0.375	100	7	46	36	104	210	0.3	8	39.6	76.3	440	790
27.0*	0.30	100	7	33	26	94	210	0.2	6	15.5	106.1	300	740
18.0*	0.20	100	7	19	15	81	210	0.2	6	5.2	96.5	350	870
13.5*	0.15	100	14	10	8	57	210	0.1	6	9.4	98.3	290	920
38.1	0.50	100	6	35	27	60	185	0.1	4	71.6	35.2	>30,000	1,860
67.1	0.50	100	14	40	31	68	210	0.6	7	84.0	90.1	>30,000	1,140
75.0	0.50	100	14	40	31	68	210	0.5	7	88.2	106.0	>30,000	1,050
18.0*	0.20	100	14	12	9	51	210	0.1	6	35.5	75.1	140	620
Nil	Nil	Nil	Nil	7	5	24	210	0.1	5	8.6	129.7	440	1,340
10.8*	0.12	100	14	5	4	36	210	1.1	6	12.9	91.4	180	840
Nil	Nil	Nil	Nil	6	5	34	210	0.1	7	1.9	129.0	610	1,660
9.0*	0.10	100	14	4	3	34	210	0.1	6	13.0	104.5	230	1,100
Nil	Nil	Nil	Nil	2	2	17	210	0.1	5	1.8	113.4	380	1,770
4.5*	0.05	100	14	1	1	17	210	0.1	6	5.6	102.4	450	1,900
Nil	Nil	Nil	Nil	1	1	14	210	0.2	5	3.4	125.7	580	2,950
38.1	0.50	100	7	47	37	80	200	0.5	6	36.1	73.5	>30,000	1,870
45.1	0.50	100	7	39	31	66	200	0.5	6	64.2	61.7	>30,000	1,080
45.1	0.50	100	13	67	53	114	210	0.1	4	32.5	37.4	Waxy	2,290
45.1	0.50	100	9	24	19	41	175	0.1	5	74.5	57.8	>30,000	630
52.1	0.50	100	10	59	46	100	210	0.1	5	51.3	44.4	840	1,570
59.6	0.45	100	8	56	44	95	180	0.1	7	41.0	92.1	>30,000	1,090
59.9	0.45	100	7	43	34	81	180	0.1	7	42.9	97.0	>30,000	1,120
60.4	0.375	100	8	40	31	91	210	0.1	5	32.5	102.1	21,900	1,580
55.0	0.45	100	7	36	28	68	190	0.2	7	31.2	103.4	6,100	810

Can. J. Chem. Downloaded from www.nrcresearchpress.com by 210.87.254.105 on 09/05/12
For personal use only.

TA

α-Cyanoglutara

Starting material					Reaction temp., °C	Ethanol collected				Reactio time, hours
Glycol			Diethyl α-cyanoglutarate			Initial temp., °C	Volume, ml	Yield		
Name	g	moles	g	moles				g	%	
Ethylene glycol	31.0	0.50	106.6	0.50	180	175	30	24	51	21
Diethylene glycol	53.1	0.50	106.6	0.50	210	175	44	35	75	13
Triethylene glycol	60.7	0.40	85.3	0.40	210	190	36	28	77	12
PEG 200	80.0	0.40	85.3	0.40	210	190	18	14	38	30
300	100.0	0.33	71.1	0.33	210	190	23	18	59	32
400	100.0	0.25	53.3	0.25	210	190	18	14	61	33
600	100.0	0.167	35.5	0.167	210	210	9	7	46	36
1,2-Propanediol	38.1	0.50	106.6	0.50	190	185	30	24	51	32
Dipropylene glycol	67.1	0.50	106.6	0.50	210	190	27	21	46	35
PPG 150	60.0	0.40	85.3	0.40	210	190	23	18	49	35
425	106.3	0.25	53.3	0.25	215	215	9	7	31	35
750	125.0	0.167	35.5	0.167	215	215	5	4	26	35
1,025	123.0	0.12	25.6	0.12	215	215	4	3	28	35
2,025	141.8	0.070	14.9	0.07	215	215	2	2	24	35
1,3-Propanediol	38.1	0.50	106.6	0.50	200	170	29	23	49	35
1,3-Butanediol	45.1	0.50	106.6	0.50	200	175	44	35	75	32
1,4-Butanediol	45.1	0.50	106.6	0.50	210	170	52	41	89	17
2,3-Butanediol	45.1	0.50	106.6	0.50	180	180	14	11	24	35
1,5-Pentanediol	52.1	0.50	106.6	0.50	210	180	47	37	80	25
2,2′-(Methylimino)-diethanol	59.6	0.50	106.6	0.50	180	120	47	37	80	8
2,2′-(Ethylimino)-diethanol	66.6	0.50	106.6	0.50	180	120	47	37	80	14
2,2′-(Butylimino)-diethanol	64.5	0.40	85.3	0.40	210	120	35	27	75	23
2,2′-Thiodiethanol	55.0	0.45	96.0	0.45	190	155	28	22	53	21

*1,4-Butanediol.

Polyurethanes

A polyester sample (5 or 10 g) was thoroughly mixed in an aluminum foil moisture dish (60 mm diameter, 18 mm depth) with a quantity of 2,4-tolylene diisocyanate, TDI, which was roughly equivalent. The TDI employed contained 100 mg/kg of ferric acetylacetonate as a catalyst. In four other dishes the same amount of polyester was well mixed with quantities of TDI two, three, four, and five times that used for the first sample. Highly viscous polyesters were heated sufficiently that their viscosities were reduced to a few thousand centistokes and solid polyesters melted in order to permit mixing. The moisture dishes and their contents were placed in the oven and allowed to cure for 5 days at 100° C.

The varied consistencies of polyurethane products were classified into several categories, although completely distinct boundary lines did not exist between all of them. The distinguishing features of each category were (*a*) viscous, the sample was a viscous liquid; (*b*) stringy, the sample could be drawn out into threads; (*c*) cheesy, the sample broke cleanly with little or no resistance when a stretching force was applied; (*d*) gelatinous, the sample was a sticky jelly; (*e*) elastomeric, the sample recovered its shape on deformation; (*f*) leathery, the sample was both tough and flexible; on application of a stretching force, it offered resistance but broke without stretching; and (*g*) resinous, the sample was a brittle solid.

.E V

olyesters

Excess glycol added			Further heating, hours	Total ethanol collected			Reaction mixture heated *in vacuo*			Weight distillate, g	Polyester		
				Volume, ml	Yield		Final temp., °C	Pressure, mm	Time, hours		Yield, g	Viscosity, cs 20° C	Molecular weight
g	moles	%			g	%							
31.0	0.50	100	7	37	29	63	180	0.1	5	27.1	72.2	17,100	2,920
53.1	0.50	100	13	50	39	85	210	0.2	5	49.1	102.7	>30,000	1,310
50.7	0.40	100	21	39	31	83	210	0.2	7	52.2	109.4	~20,000	1,420
36.0*	0.40	100	34	29	23	62	210	0.5	5	62.4	69.1	160	540
30.0*	0.33	100	35	32	25	82	210	0.5	5	3.3	128.8	230	860
22.5*	0.25	100	32	22	17	75	210	0.5	5	2.8	122.1	300	950
15.0*	0.167	100	28	9	7	46	210	0.5	5	4.9	113.4	320	1,040
38.1	0.50	100	29	42	33	72	190	0.2	6	37.0	70.0	4,200	1,870
37.1	0.50	100	36	31	24	53	210	0.2	10	89.6	76.0	>30,000	530
60.0	0.40	100	28	25	20	53	210	0.2	10	60.8	108.6	8,780	460
22.5*	0.25	100	28	15	12	51	210	0.2	7	49.9	91.4	130	600
15.0*	0.167	100	28	8	6	41	210	0.2	6	19.8	127.1	170	890
10.8*	0.12	100	28	5	4	36	215	0.2	6	14.4	123.6	230	1,260
6.3*	0.070	100	28	2	2	24	210	0.2	6	6.7	140.6	450	2,070
38.1	0.50	100	14	40	31	68	200	0.5	7	36.2	79.7	26,100	1,960
45.1	0.50	100	29	44	35	75	200	0.1	6	50.7	73.5	~20,000	1,900
45.1	0.50	100	35	71	56	121	210	0.2	7	29.4	52.5	130	2,820
45.1	0.50	100	21	17	13	29	180	0.5	7	97.7	60.7	370	610
52.1	0.50	100	28	65	51	111	210	0.5	7	51.4	60.0	600	1,210
59.6	0.50	100	7	53	42	90	180	0.3	6	~70	88.0	14,900	2,120
36.6	0.50	100	14	48	38	82	180	0.2	8	63.3	99.9	3,800	2,130
34.5	0.40	100	28	37	29	79	210	0.5	8	28.2	116.7	3,360	2,450
55.0	0.45	100	13	28	22	53	190	0.1	8	44.2	98.7	1,460	1,480

The elongation at break of elastomeric polyurethanes was determined by measuring the increase in length which a uniform strip of sample (20 mm in length, 1–2 mm in breadth, and 2–4 mm in width) underwent before breaking when a stretching force was applied. Several determinations were made for each value calculated.

The brittle point of elastomeric polyurethanes was determined by measuring the maximum temperature at which a sample (4–5 mm in length, about 1 mm in breadth, and 1–3 mm in width), cooled in an acetone – dry ice bath, broke when a bending force was applied. Many determinations were made for each sample to establish the correct temperature. In some cases, when none of the samples formed from a particular polyester was elastomeric, the brittle point was measured on one of the samples which were either stringy, cheesy, or leathery.

The proportions of 2,4-tolylene diisocyanate and polyester employed to prepare the different polyurethanes are given together with their consistencies, elongations at break, and brittle points as follows: succinate polyurethanes from polyesters prepared without catalyst, Table VI; succinate polyurethanes from polyesters prepared using sodium catalyst, Table VII; cyanomalonate polyurethanes, Table VIII; cyanosuccinate polyurethanes, Table IX; and α-cyanoglutarate polyurethanes, Table X.

Can. J. Chem. Downloaded from www.nrcresearchpress.com by 210.87.254.105 on 09/05/12
For personal use only.

Can. J. Chem. Downloaded from www.nrcresearchpress.com by 210.87.254.105 on 09/05/12
For personal use only.

TABLE VI

Succinate polyurethanes from polyesters prepared without catalyst

Starting glycol for polyester	TDI per 10 g polyester, g	Consistency of polyurethane	Elongation at break, %					Brittle point, °C				
Ethylene glycol	1 2 3 4 5	r r r r r	—	—	—	—	—	—	—	—	—	—
Diethylene glycol	"	e e l l l	500	75	—	—	—	−23	−25	—	—	—
Triethylene glycol	"	s l l l r	—	—	—	—	—	—	—	—	—	—
PEG 200	"	v v e e l	—	—	175	75	—	—	—	−16	−14	—
300	"	v v e e l	—	—	100	50	—	—	—	−28	−26	—
400	"	v s e e e	—	—	125	25	25	—	—	−31	−35	−30
600	"	v s s e e	—	—	—	50	75	—	—	—	−42	−42
1,2-Propanediol	2 4 6 8 10	s r r r r	—	—	—	—	—	8	—	—	—	—
Dipropylene glycol	"	s l l l l	—	—	—	—	—	—	—	—	—	—
PPG 150	"	s s s s s	—	—	—	—	—	—	−2	—	—	—
425	1 2 3 4 5	v v c c e	—	—	—	—	75	—	—	—	—	−18
750	"	v s ec ec e	—	—	50	25	50	—	—	−34	−29	−24
1,025	"	v v ec ec ec	—	—	75	25	25	—	—	−37	−34	−30
2,025	"	v s s ec ec	—	—	—	25	25	—	—	—	−46	−45
1,3-Propanediol	2 4 6 8 10	s l l l r	—	—	—	—	—	—	—	—	—	—
1,3-Butanediol	1 2 3 4 5	v s e e l	—	—	200	100	—	—	—	−15	−18	—
1,4-Butanediol	"	r r r r r	—	—	—	—	—	—	—	—	—	—
2,3-Butanediol	2 4 6 8	s r r r	—	—	—	—		—	—	—	—	
1,5-Pentanediol	2 4 6 8 10	s e l l l	—	100	—	—	—	—	−29	—	—	—
2,2′-(Methylimino)-diethanol	1 2 3 4 5	s r r r r	—	—	—	—	—	—	—	—	—	—
2,2′-(Ethylimino)-diethanol	"	s s s l r	—	—	—	—	—	—	—	—	—	—
2,2′-(Butylimino)-diethanol	"	s s e l r	—	—	175	—	—	—	—	−20	—	—
2,2′-Thiodiethanol	"	s s e l l	—	—	75	—	—	—	—	−17	—	—

NOTE: v, s, c, e, l, and r signify viscous, stringy, cheesy, elastomeric, leathery, and resinous, respectively.

Can. J. Chem. Downloaded from www.nrcresearchpress.com by 210.87.254.105 on 09/05/12
For personal use only.

TABLE VII

Succinate polyurethanes from polyesters prepared using sodium catalyst

Starting glycol for polyester	TDI per 10 g polyester, g	Consistency of polyurethane	Elongation at break, %					Brittle point, °C			
Ethylene glycol	0.5 1 1.5 2 2.5	c l l l l	—	—	—	—	—	—	—	—	—
Diethylene glycol	1 2 3 4 5	s e l l r	—	50	—	—	—	—	−23	—	—	—
Triethylene glycol	"	v c c l l	—	—	—	—	—	—	—	—	—	—
PEG 200	"	s e l l l	—	150	—	—	—	—	−33	—	—	—
300	"	v s e l l	—	—	150	—	—	—	—	−33	—	—
400	"	v e e l l	—	250	50	—	—	—	−37	−43	—	—
600	"	v e l l l	—	800	—	—	—	—	−44	—	—	—
1,2-Propanediol	"	s e e l l	—	100	100	—	—	—	4	4	—	—
Dipropylene glycol	"	s e e l r	—	100	50	—	—	—	−14	−11	—	—
PPG 150	"	s e l l r	—	150	—	—	—	—	−19	—	—	—
425	2 4 6 8 10	s e l r r	—	100	—	—	—	—	−13	—	—	—
750	1 2 3 4 5	v s e e e	—	—	300	100	50	—	—	−34	−36	−35
1,025	"	v s e e l	—	—	200	75	—	—	—	−52	−51	—
2,025	"	s c e e l	—	—	50	50	—	—	—	−55	−58	—
1,3-Propanediol	"	s e e l r	—	400	50	—	—	—	−35	−27	—	—
1,3-Butanediol	"	s e e l r	—	300	50	—	—	—	−16	−13	—	—
1,4-Butanediol	"	r r l l r	—	—	—	—	—	—	—	—	—	—
2,3-Butanediol	2 4 6 8 10	s r r r r	—	—	—	—	—	—	—	—	—	—
1,5-Pentanediol	1 2 3 4 5	s e e l l	—	450	100	—	—	—	−59	−55	—	—
2,2′-(Methylimino)-diethanol	"	s c r r r	—	—	—	—	—	—	—	—	—	—
2,2′-(Ethylimino)-diethanol	"	s s l r r	—	—	—	—	—	—	—	—	—	—
2,2′-(Butylimino)-diethanol	"	v s l r r	—	—	—	—	—	—	—	—	—	—
2,2′-Thiodiethanol	2 4 6 8 10	s e l r r	—	150	—	—	—	—	−19	—	—	—

NOTE: v, s, c, e, l, and r signify viscous, stringy, cheesy, elastomeric, leathery, and resinous, respectively.

Can. J. Chem. Downloaded from www.nrcresearchpress.com by 210.87.254.105 on 09/05/12
For personal use only.

TABLE VIII

Cyanomalonate polyurethanes

Starting glycol for polyester	TDI per 10 g polyester, g	Consistency of polyurethane	Elongation at break, %					Brittle point, °C				
Ethylene glycol	3 6 9	r r r	—	—	—			—	—	—		
Diethylene glycol	4 8 12 16 20	r r r r r	—	—	—	—	—	—	—	—	—	—
Triethylene glycol	3 6 9 12 15	s r r r r	—	—	—	—	—	—	—	—	—	—
PEG 200	"	e r r r r	100	—	—	—	—	−11	—	—	—	—
300	"	v s l r r	—	—	—	—	—	—	7	—	—	—
400	2 4 6 8 10	v s s s e	—	—	—	—	100	—	—	—	—	4
600	"	v s s l l	—	—	—	—	—	—	—	—	−40	—
1,2-Propanediol	3 6	r r	—	—				—	—			
Dipropylene glycol	3 6 9 12 15	r r r r r	—	—	—	—	—	—	—	—	—	—
PPG 150	"	r r r r r	—	—	—	—	—	—	—	—	—	—
425	2 4 6 8 10	s e l r r	—	300	—	—	—	—	−7	—	—	—
750	"	s s e e e	—	—	200	200	150	—	—	−28	−26	−14
1,025	"	s c c ec ec	—	—	—	25	25	—	—	—	−25	−25
2,025	1 2 3 4 5	v e e e ec	—	800	200	150	100	—	−44	−41	−41	−43
1,3-Propanediol	3 6 9 12 15	s r r r r	—	—	—	—	—	5	—	—	—	—
1,3-Butanediol	"	c r r r r	—	—	—	—	—	13	—	—	—	—
1,4-Butanediol	4 8 20	s r r	—	—	—			10	—	—		
2,3-Butanediol	3 6	r r	—	—				—	—			
1,5-Pentanediol	3 6 9 12 15	s s r r r	—	—	—	—	—	—	8	—	—	—
2,2′-(Methylimino)-diethanol	2 4 6 8 10	r r r r r	—	—	—	—	—	—	—	—	—	—
2,2′-(Ethylimino)-diethanol	1 2 3 4 5	r r s r r	—	—	—	—	—	—	—	9	—	—
2,2′-(Butylimino)-diethanol	"	r r r r r	—	—	—	—	—	—	—	—	—	—
2,2′-Thiodiethanol	3 6 9 12 15	s r r r r	—	—	—	—	—	4	—	—	—	—

NOTE: v, s, c, e, l, and r signify viscous, stringy, cheesy, elastomeric, leathery, and resinous, respectively.

Can. J. Chem. Downloaded from www.nrcresearchpress.com by 210.87.254.105 on 09/05/12
For personal use only.

TABLE IX

Cyanosuccinate polyurethanes

Starting glycol for polyester	TDI per 10 g polyester, g	Consistency of polyurethane	Elongation at break, %					Brittle point, °C				
Ethylene glycol	2 3 4	r r r	—	—	—			—	—	—		
Diethylene glycol	1 2 3 4 5	s s s l l	—	—	—	—	—	—	—	8	—	—
Triethylene glycol	"	v e l l l	—	450	—	—	—	—	−3	—	—	—
PEG 200	2 4 6 8 10	v s s e l	—	—	—	100	—	—	—	—	5	—
300	"	v s s s e	—	—	—	—	100	—	—	—	—	−6
400	"	v s e e e	—	—	400	100	50	—	—	−14	−14	−16
600	"	v s e e l	—	—	200	100	—	—	—	−16	−19	—
1,2-Propanediol	1 3 5	s r r	—	—	—			—	—	—		
Dipropylene glycol	1 2 3 4 5	s s r r r	—	—	—	—	—	—	13	—	—	—
PPG 150	"	s s s r r	—	—	—	—	—	—	—	13	—	—
425 I	2 4 6 8 10	s e e l l	—	400	100	—	—	—	−8	−27	—	—
425 II	1 2 3 4 5	v v s e e	—	—	—	100	25	—	—	—	−2	3
750 I	2 4 6 8 10	s e e e e	—	200	100	100	25	—	−39	−22	−17	−16
750 II	1 2 3 4 5	v v s e e	—	—	—	100	25	—	—	—	−25	−17
1,025 I	"	v s e e e	—	—	200	100	100	—	—	−46	−46	−42
1,025 II	"	v s e e l	—	—	200	50	—	—	—	−29	−31	—
2,025 I	"	v e e e e	—	500	100	50	50	—	−63	−67	−69	−59
2,025 II	0.5 1 1.5 2 2.5	v g e e e	—	—	50	75	100	—	—	−56	−57	−57
1,3-Propanediol	1 2 3 4 5	s s r r r	—	—	—	—	—	—	11	—	—	—
1,3-Butanediol	"	s r r r r	—	—	—	—	—	7	—	—	—	—
1,4-Butanediol	1 2 3 5	s c c r	—	—	—	—		—	—	—	—	
2,3-Butanediol	1 2 3 4 5	r r r r r	—	—	—	—	—	—	—	—	—	—
1,5-Pentanediol	2 4	c c	—	—				—	—			
2,2′-(Methylimino)-diethanol	1 2 3 4 5	r r r r r	—	—	—	—	—	—	—	—	—	—
2,2′-(Ethylimino)-diethanol	"	s s s r r	—	—	—	—	—	—	—	14	—	—
2,2′-(Butylimino)-diethanol	"	s s r r r	—	—	—	—	—	—	—	—	—	—
2,2′-Thiodiethanol	2 4 6 8 10	s r r r r	—	—	—	—	—	—	—	—	—	—

NOTE: v, s, c, g, e, l, and r signify viscous, stringy, cheesy, gelatinous, elastomeric, leathery, and resinous, respectively.

Can. J. Chem. Downloaded from www.nrcresearchpress.com by 210.87.254.105 on 09/05/12
For personal use only.

TABLE X

α-Cyanoglutarate polyurethanes

Starting glycol for polyester	TDI per 10 g polyester, g	Consistency of polyurethane	Elongation at break, %					Brittle point, °C				
Ethylene glycol	1 2 3 4 5	v v s s c	—	—	—	—	—	—	—	—	—	4
Diethylene glycol	"	s e e l r	—	200	50	—	—	—	−14	−13	—	—
Triethylene glycol	"	s e e e e	—	800	400	200	100	—	−12	−15	−15	−15
PEG 200	3 6 9 12 15	v s r r r	—	—	—	—	—	—	8	—	—	—
300	2 4 6 8 10	v s s l r	—	—	—	—	—	—	−2	—	—	—
400	"	v s e l r	—	—	200	—	—	—	—	−9	—	—
600	1 2 3 4 5	s e e e e	—	500	100	50	50	—	−21	−24	−26	−20
1,2-Propanediol	"	v s l l r	—	—	—	—	—	—	—	—	—	—
Dipropylene glycol	3 6 9 12 15	s l r r r	—	—	—	—	—	0	—	—	—	—
PPG 150	"	e l l r r	125	—	—	—	—	−3	—	—	—	—
425	3 4.5 6 9 12	s e l l r	—	700	—	—	—	—	0	—	—	—
750	2 4 6 8 10	s e e l l	—	125	75	—	—	—	−58	−44	—	—
1,025	1 2 3 4 5	v s e e e	—	—	400	250	100	—	—	−25	−39	−34
2,025	"	v g c c ec	—	—	—	—	25	—	—	—	—	−43
1,3-Propanediol	"	s s r r r	—	—	—	—	—	—	0	—	—	—
1,3-Butanediol	"	s s l r r	—	—	—	—	—	—	—	—	—	—
1,4-Butanediol	1 1.5 2 2.5 3	v v v v e	—	—	—	—	50	—	—	—	—	−47
2,3-Butanediol	2 4 6 8 10	s s r r r	—	—	—	—	—	—	15	—	—	—
1,5-Pentanediol	2 3 4 5 6	v s s s c	—	—	—	—	—	—	—	—	—	−11
2,2′-(Methylimino)-diethanol	1 2 3 4 5	r r r r r	—	—	—	—	—	—	—	—	—	—
2,2′-(Ethylimino)-diethanol	"	v s s l r	—	—	—	—	—	—	—	−6	—	—
2,2′-(Butylimino)-diethanol	"	v s l r r	—	—	—	—	—	—	−17	—	—	—
2,2′-Thiodiethanol	"	v s s e l	—	—	—	75	—	—	—	—	−1	—

NOTE: v, s, c, g, e, l, and r signify viscous, stringy, cheesy, gelatinous, elastomeric, leathery, and resinous, respectively.

REFERENCES

1. W. H. CAROTHERS and G. A. ARVIN. J. Am. Chem. Soc. **51**, 2560 (1929).
2. B. A. DOMBROW. Polyurethanes. Reinhold Publishing Corp., New York. 1957.
3. O. BAYER, E. MÜLLER, S. PETERSEN, H. F. PIEPENBRINK, and E. WINDEMUTH. Angew. Chem. **62**, 57 (1950); Rubber Chem. and Technol. **23**, 812 (1950).
4. E. MÜLLER, O. BAYER, S. PETERSEN, H. F. PIEPENBRINK, F. SCHMIDT, and E. WEINBRENNER. Angew. Chem. **64**, 523 (1952); Rubber Chem. and Technol. **26**, 493 (1953).
5. N. V. SEEGER, T. G. MASTIN, E. E. FAUSER, F. S. FARSON, A. F. FINELLI, and E. A. SINCLAIR. Ind. Eng. Chem. **45**, 2538 (1953); Rubber Chem. and Technol. **27**, 430 (1954).
6. R. J. FERRARI, J. W. SINNER, J. C. BILL, and W. F. BRUCKSCH. Ind. Eng. Chem. **50**, 1041 (1958).
7. J. BJORKSTEN, H. TOVEY, and H. L. DOLLARD, JR. Modern Plastics, **31** (8), 143, 228 (1954).
8. A. C. STEVENSON. Rubber Age (N.Y.), **77**, No. 1, 63 (1955).
9. A. HALLER. Compt. rend. **105**, 169 (1887); Ann. chim. [6], **16**, 426 (1889).
10. A. HALLER and L. BARTHE. Compt. rend. **106**, 1413 (1888); Bull soc. chim. France, [3], **2**, 299 (1889); Ann. chim. [6], **18**, 281 (1889).
11. W. H. PERKIN, JR. and J. F. THORPE. J. Chem. Soc. **85**, 128 (1904).

Can. J. Chem. Downloaded from www.nrcresearchpress.com by 210.87.254.105 on 09/05/12
For personal use only.

Can. J. Chem. Downloaded from www.nrcresearchpress.com by 210.87.254.105 on 09/05/12
For personal use only.

DETERMINATION OF TRACE AMOUNTS OF SILVER IN GALENA ORES[1]

E. J. Bounsall and W. A. E. McBryde[2]

ABSTRACT

An analytical method is described for the determination of microgram amounts of silver in galena ores, based on the "reversion" of silver dithizonate. Silver is separated from relatively large amounts of lead by extraction as dithizonate into chloroform from an aqueous 1:99 nitric acid solution. Separation from mercury, which is also extracted under these conditions and would, if present, interfere in the analysis, is achieved by reverting the dithizonate solution with a 5% aqueous sodium chloride solution which is also 0.015 molar in hydrochloric acid. Following dilution of this aqueous solution and adjustment of pH, silver is again extracted into chloroform as the dithizonate, and determined absorptiometrically. Analyses of a number of galena ore samples showed a precision of within 3% for a silver content ranging from 0.03 to 0.4%.

Some other methods for isolating silver from these samples, which were tried but found unsatisfactory, are discussed.

INTRODUCTION

For an accurate and precise determination of trace amounts of silver in galena ores, a quantitative chemical method of analysis is necessary. Wasserstein (1), having completed a spectrographic analysis of galena (lead sulphide) ores, reported that the sensitivity of detection for the different elements was not the same, and that the role of silver could not be accurately assessed, as its sensitivity in the spectrographic examination did not allow the estimation of even very approximate amounts of this element. Several colorimetric procedures involving extraction and determination of microgram amounts of silver by a chloroform or carbon tetrachloride solution of dithizone have been outlined by Sandell (2). The technique of reversion introduced by Irving, Risdon, and Andrew (3), and later somewhat simplified by Maynes and McBryde (4), in our opinion is an improvement over other published procedures based on the use of dithizone. It eliminates the necessity of using dithizone solutions of exactly known or constant concentration, provides for maximum sensitivity, and is of real value when amounts of interfering metals are present and a reversion agent can be found which will revert the dithizonate of the metal being determined without affecting the other metallic dithizonates.

Since the extraction of lead by dithizone requires an alkaline medium, and since silver, copper, mercury, palladium, and gold are the only metals extracted by dithizone from mineral acid solution, extraction at low pH would be expected to separate silver from the relatively large amounts of lead present in galena, and from any other but the aforementioned elements. Of the latter, gold and palladium are extremely unlikely to be in galena ores, copper is sure to be present, and mercury may possibly be (5). A reversion agent was needed which would not revert copper and mercury, but which would quantitatively revert silver, subsequent to the separation of these metals from lead.

REAGENTS AND APPARATUS

Laboratory distilled water and nitric acid were distilled in borosilicate glass stills. C.P. sulphuric acid and perchloric acid were used without further purification. The 1:99 nitric acid was prepared by dilution of 1 volume of distilled nitric acid with 99 volumes of redistilled water. The 6 *N* hydrochloric acid was prepared from C.P. concentrated

[1]*Manuscript received April 21, 1960.*
Contribution from the Department of Chemistry, University of Toronto, Toronto 5, Ontario, Canada.
[2]*Present address of authors: Department of Chemistry, University of Waterloo, Waterloo, Ontario.*

acid, diluted 1:1 with doubly distilled water, and then twice distilled in a borosilicate glass still, with rejection of the first 20% and last 10% of the distillate.

Chloroform

Both U.S.P. and reclaimed chloroform were purified by the procedure outlined by Biddle (6), except that the calcium oxide was filtered out before distillation in a glass still.

Dithizone and Cotton

Purification of each was carried out by the procedure described by Maynes and McBryde (4). Dithizone solutions were prepared by dissolving approximately 10 mg of the purified reagent in 1 liter of chloroform. With experience, solutions of suitable concentration were prepared, by visually estimating the color of the solution, immediately before use.

Buffer and Reversion Agent Solutions

The analytical grade reagents were dissolved in redistilled water, and the solutions shaken with dithizone in chloroform to free them of heavy metals.

Potassium Chromate Solution

A 4% (w/v) solution was prepared from reagent grade potassium chromate and redistilled water.

Standard Solutions of Metals

The composition of these solutions was based on accurately known weights of (i) dried analytical reagent grade silver nitrate; (ii) Specpure lead; (iii) Specpure copper; (iv) doubly distilled mercury. The metals were dissolved in 1:1 nitric acid, and these solutions boiled to free them of oxides of nitrogen; the silver nitrate was dissolved in, and the solutions of all the nitrates made up to, known volumes with 1:99 nitric acid. From stock solutions so prepared, standard solutions of silver, mercury, and copper, containing about 10 μg of metal (accurately known) per ml, were prepared by dilution with 1:99 nitric acid. The standard lead solution contained about 100 mg of metal (accurately known) per ml.

From time to time, checks were made on the concentration of the standard silver solution by carrying out the reversion procedure described below on a measured volume of this solution. The reversion values for these samples were compared with the standard reversion working curve which had been determined when the solution was first prepared.

Spectrophotometer and Cells

All measurements of optical density were made with a Beckman Model DU spectrophotometer set at 610 mμ, the absorption maximum of dithizone. The optical cells were cylindrical, 1 cm in path length, with Corex glass windows, and ground-glass stoppers to minimize loss of chloroform by evaporation.

Glassware

Borosilicate glassware was used throughout. It was cleaned after each use in hot nitric and sulphuric acids, rinsed thoroughly with tap water, and then washed well with doubly distilled water. Extractions were carried out in Squibb-type separatory funnels. Aliquots of standard metal solutions were measured from 5-ml class A microburettes.

EXPERIMENTAL

Reversion Procedure

A cotton pledget was inserted in the stem of a clean, dry, 125-ml separatory funnel equipped with a 7-mm delivery tube. A measured volume of the standard silver solution

Can. J. Chem. Downloaded from www.nrcresearchpress.com by 210.87.254.105 on 09/05/12
For personal use only.

was transferred to the funnel, and the volume made up to 25 ml with 1:99 nitric acid. Sufficient dithizone solution was added to extract all of the silver present, and the funnel was shaken for 1 minute. When the phases separated, the dithizone–dithizonate extract was transferred to a 25-ml volumetric flask. The aqueous phase was washed twice with 8-ml portions of chloroform, and the washings were added to the volumetric flask to make the volume to 25 ml. A portion of this dithizone–dithizonate solution was added to one colorimeter cell. A second portion of approximately 5 to 7 ml was added to a 30-ml separatory funnel, and an equal volume of the reverting solution added. This funnel was shaken for 1 minute, the phases allowed to separate, and a few drops of the reverted dithizone solution allowed to flow through a fresh cotton pledget placed in the stem of the funnel. Sufficient of the reverted solution was then delivered to fill a second colorimeter cell. The spectrophotometer was set to read zero optical density for the first solution, and the apparent optical density of the reverted solution measured against this. This quantity is known as the *reversion value* of the silver solution.

Reversion Agent for Silver

The use of 6% (w/v) potassium iodide in 0.25 *N* sulphuric acid, first recommended as a reversion agent for silver (3), met with little success owing to decomposition of dithizone by free iodine. The addition of 0.1 *N* thiosulphate, suggested by Morrison and Paige (7), did not overcome this difficulty. A neutral 6% (w/v) potassium iodide solution yielded reversion values exhibiting quite poor precision, due perhaps to a solubility loss of dithizone to the neutral reverting medium. Reversions with a 6% (w/v) solution of potassium bromide in 0.1 *N* hydrochloric acid also yielded results with poor precision.

With 2.0 *N* hydrochloric acid as the reversion agent, a series of experiments on amounts of silver solution equivalent to from 5 to 50 μg of metal gave reversion values proportional to the quantity of silver taken. The average reversion value per microgram of silver was 0.0148 ± 0.0001 within a range of 0.0145 to 0.0150. Each reversion value was corrected for a blank amounting to 0.003 ± 0.001.

Test for Completeness of Extraction of Silver

Maynes and McBryde (4) suggested a convenient test for the completeness of extraction of a metal with dithizone. Applying their procedure, the molar extinction coefficient of dithizone in a chloroform solution was determined, from a solution whose composition was based on a direct weighing of dithizone, to be 3.77×10^4 liter/mole cm. The same quantity was then calculated from the reversion value obtained for a known amount of silver extracted by a known volume of dithizone solution, assuming the molar ratio of silver to dithizone in the dithizonate to be 1:1; this value was 3.94×10^4 liter/mole cm. The difference between the two values is 4%, and the sign of the difference indicates 104% recovery of silver. This difference is attributed to experimental error in the extinction coefficient obtained by direct measurement; the value obtained is somewhat lower than two other published values (4, 8), although the latter were each obtained with different instruments from that used here.

It was concluded that both the extraction of silver with dithizone and the reversion of silver using 2.0 *N* hydrochloric acid were complete; accordingly a standard reversion working curve of reversion plotted against micrograms of silver was prepared for this particular reversion agent and experimental conditions.

Extraction of Other Metals

Comparison with the standard reversion working curve showed that a slight reversion of mercury was also being obtained under the identical reversion conditions used for

Can. J. Chem. Downloaded from www.nrcresearchpress.com by 210.87.254.105 on 09/05/12
For personal use only.

silver. In the case of copper, it was found that not even microgram amounts were extracted by dithizone from 1:99 nitric acid, and that no extraction occurred until the pH of the solution was raised by ammonia to 4.2.

Complete extraction of microgram amounts of silver occurred, and no extraction of even microgram amounts from gram quantities of lead was detected at acid concentrations as low as 1:99 nitric acid and 0.1 *N* perchloric acid. Silver was not completely extracted from solutions of perchloric acid more concentrated than 2 normal.

Separation of Silver from Copper and Mercury

In the event that extraction of silver might be required from an acidic medium from which copper was also extracted, a reversion agent was sought which would completely revert silver but not copper or mercury. Friedeberg (9) found that silver could be separated from copper and mercury by selectively decomposing silver dithizonate with a 10% sodium chloride solution which was also 0.015 *N* in hydrochloric acid. The silver was subsequently extracted from this aqueous phase after it had been diluted 10-fold with water, or had its pH raised to between 3 and 3.5, into a solution of dithizone.

To obtain complete recovery of silver by this procedure we have been obliged to modify the directions slightly. The sodium chloride concentration of this reverting solution could be lowered to 5% while the hydrochloric acid concentration was kept unchanged. Copper and mercury dithizonates were completely unreverted by this solution. It was found that the subsequent re-extraction of silver with dithizone was incomplete unless the aqueous phase was both diluted 10-fold and treated to raise its pH to 4.6. The re-extraction of silver was incomplete when the pH was below 4.6 or when the aqueous solution was less dilute regardless of the pH.

Double Reversion Procedure

The recovery of silver and its separation from copper and mercury were tested by the following procedure.

A measured volume of the standard silver solution was transferred to a clean, dry, 125-ml separatory funnel, in the stem of which was a cotton pledget, and the volume made up to 50 ml with 1:99 nitric acid. Sufficient dithizone was added to extract all of the silver present, and the funnel was shaken for 1 minute. When the phases separated, the silver dithizonate–dithizone extract was transferred to another clean, dry, 125-ml separatory funnel, in which were 3 ml of the reversion agent (5% sodium chloride, 0.015 *N* hydrochloric acid). The aqueous phase in the first funnel was washed twice with 5-ml portions of chloroform, and the washings were combined in the second funnel, which was then shaken for 1 minute. When the phases separated, the chloroform phase containing the dithizone was discarded, and the pH of the aqueous phase (containing the silver) was adjusted with sodium acetate solution (1.6 g/liter) to 4.6, and the total volume was made up to 30 ml with redistilled water. Ten milliliters of the dithizone solution was added, and the funnel was shaken for 1 minute. The rest of the procedure was exactly as outlined in the original reversion procedure described above.

This procedure was carried out on amounts of standard silver solution containing the equivalent of from 5 to 45 μg of silver. The average recovery for nine determinations corresponding to 10 μg of silver was 9.97 μg with an average deviation of 0.29 μg. The range of these values was from 9.6 to 10.7 μg after correction for the blank, which was equivalent to 0.7 μg of silver.

Determination of Silver in the Presence of Mercury, Copper, and Lead

Results, corrected for the blank, for the determination of silver, according to the

Can. J. Chem. Downloaded from www.nrcresearchpress.com by 210.87.254.105 on 09/05/12
For personal use only.

double reversion procedure, from mixtures of standard solutions of silver, mercury, copper, and lead, in the proportion that these metals are likely to be present in galena ores, are given in Table I.

TABLE I

Results of analyses on make-up samples

	Grams of lead	Micrograms of mercury taken	Micrograms of copper taken	Micrograms of silver	
				Taken	Found
Sample 1	0.5	30	30	30	30.6
,, 2	0.5	30	100	30	29.1
,, 3	0.5	100	30	30	29.8
,, 4	0.5	30	100	15	15.6
,, 5	1.0	20	25	45	43.5
,, 6	0.5	30	50	20	20.0

Determination of Silver in Galena Ores

The usual method employed for the dissolving of galena ores is heating with hydrochloric acid. However, since even small amounts of chloride prevent the extraction of silver with dithizone, an acid other than hydrochloric must be used. When nitric acid was employed, it was found that, regardless of the temperature (from room temperature to 200° C) or the acid concentration (from concentrated to 1:9) used, a heavy, insoluble, white precipitate of lead sulphate formed during dissolving of the ore. Concentrated perchloric acid, however, at a temperature of 120° to 135° C, was found to be completely satisfactory, with a dissolving time of approximately two hours. When lower acid concentration or lower temperatures were used, a longer time was needed for dissolving. At temperatures above 135° C, regardless of the perchloric acid concentration, a fine white precipitate formed.

Procedure

A sample of ore weighing 0.02 to 0.06 g, after being crushed to a fine powder, was transferred to a 50-ml beaker and covered with a watch glass. Two milliliters of concentrated perchloric acid was added, and the sample heated at 120° to 135° C until dissolution was complete. After the solution was cooled, the watch glass and the sides of the beaker were washed with water, and the solution was evaporated almost to dryness. Sufficient 1:99 nitric acid was added, and the solution was heated just under boiling until all the salts had dissolved. After cooling, the solution was transferred to a 125-ml separatory funnel, and the volume made up to 50 ml with rinsings of 1:99 nitric acid. The double reversion procedure with dithizone was then carried out, and the amount of silver determined by comparison with the standard reversion working curve.

Since there were no standard galena samples available with which to check the accuracy of the new procedure, and since there was no trustworthy alternative procedure of analysis, known amounts ("spikes") of silver were added to various of the ore samples immediately after dissolving, as a means of checking the subsequent analysis. An amount of silver equal to the amount added as the "spike" was then subtracted from the value determined by the analysis.

As the percentage of lead sulphide actually in the ore samples differed widely among the samples, the concentration of silver was expressed as p.p.m. lead, rather than p.p.m. ore sample. A lead analysis for each silver determination was carried out, essentially

Can. J. Chem. Downloaded from www.nrcresearchpress.com by 210.87.254.105 on 09/05/12
For personal use only.

according to the chromate procedure outlined by Vogel (10), on the aqueous phase containing the lead from the double reversion procedure. The accuracy and precision of the chromate method for the determination of lead were established by analyzing three 3-ml samples of standard lead solution. The results obtained were 0.4% low, with no deviation.

Galena ore samples obtained from deposits at Broken Hill, N.S.W., Australia, were kindly made available for analysis by Professor R. M. Farquhar, Geophysics Laboratory, Department of Physics, University of Toronto. The results of the analyses, corrected for the blank and "spike", are shown in Table II. The samples marked with asterisks are

TABLE II

Results of galena ore analyses

Sample numbers	Silver in lead (p.p.m.)	Average
667	1211, 1241,* 1197, 1192	1200
668	427, 452, 422*	434
669	1197, 1246, 1247*	1230
670	572, 571, 578, 541*	566
671	699, 734, 711*	715
672	993,* 999, 971	988
723	728, 716, 698	714
725	437, 436, 443	439
726	852, 842, 858	851
912	1780, 1800, 1810	1800
913	3960, 3950	3960
917	307, 293	300

*A "spike" equivalent to 10 micrograms of silver was added.

those to which a "spike" equivalent to 10 micrograms of silver was added. The results of analyses are not listed for 12 samples on which only one determination was made.

The precision of the analyses is within 0.4 to 2.8% based on the average deviation. The determinations on samples to which "spikes" of silver were added do not differ appreciably within the above-stated limits of precision from those analyzed directly.

INVESTIGATION OF OTHER WAYS OF SEPARATING SILVER FROM COPPER AND MERCURY

Extraction of Silver with Diethylammonium Diethyldithiocarbamate

Maynes (11) found that mercury, copper, and only a slight trace of silver could be extracted by a chloroform solution of diethylammonium diethyldithiocarbamate (dithiocarbamate) from aqueous solutions 5.1 N in hydrochloric acid. Subsequent dilution of the aqueous phase to 1.5 N in hydrochloric acid permitted extraction of silver. A qualitative test for silver in the remaining aqueous phase by means of dithizone revealed no silver.

It was affirmed that no silver was extracted by dithiocarbamate from solutions 5.4 N in hydrochloric acid, but that the extraction was still incomplete (50%) when the hydrochloric acid was as dilute as 0.05 N. Thus a subsequent determination of silver, after separation of copper and mercury, could not conveniently be achieved if hydrochloric acid was present. Maynes' qualitative test for silver in 1.5 N hydrochloric acid employed dithizone, but, as previously described, even small amounts of hydrochloric acid prevent formation of silver dithizonate.

According to Luke (12) silver could be extracted by dithiocarbamate from 3.6 N

Can. J. Chem. Downloaded from www.nrcresearchpress.com by 210.87.254.105 on 09/05/12
For personal use only.

sulphuric acid. Wyatt (13) reported extraction of copper and mercury by the same reagent from 1 to 10 *N* sulphuric acid solutions. Our results for the extraction of silver by dithiocarbamate from sulphuric acid solutions of differing normality indicate that at low acid concentrations extraction is incomplete, and at high acid concentrations, at which copper and mercury are extracted, silver is as well. Thus a separation of silver from copper and mercury could not be effected.

Extraction with 1,10-Phenanthroline

This reagent forms intensely colored complex ions with iron (II) and copper (I), and the sterically hindered derivatives, 2,9-dimethylphenanthroline (neocuproine) and 2,9-dimethyl-4,7-diphenylphenanthroline (bathocuproine), in chloroform solution have been found specific for microgram amounts of copper (14, 15, 16). The greater selectivity is due presumably to steric hindrance to sixfold co-ordination. Thus, copper might possibly be separable from silver prior to the determination of the latter by the use of these reagents. However, it was found that varying amounts of silver were also extracted by a chloroform solution of 1,10-phenanthroline over the entire pH range below 7. One would expect the derivatives mentioned above to behave in a similar fashion since silver exhibits fourfold co-ordination as a maximum.

Anion Exchange Studies

Attempts with an anion exchange resin of the strongly basic type (Amberlite IRA-400) to remove chloride ion from a silver solution after its separation from mercury and copper (see page 1491) revealed that silver was also completely absorbed by the resin, indicating that silver was present in solution in some anionic form (probably $AgCl_2^-$).

ACKNOWLEDGMENTS

This investigation was made possible through generous support from the University of Toronto's Advisory Committee on Scientific Research. One author (E. J. B.) was assisted by an Eldorado Mining and Refining Geochemical Scholarship for which grateful thanks are tendered.

REFERENCES

1. B. WASSERSTEIN. Am. Mineralogist, **36**, 102 (1951).
2. E. B. SANDELL. Colorimetric determination of traces of metals. 3rd ed. Interscience Publishers Inc., New York. 1959. p. 812.
3. H. IRVING, E. J. RISDON, and G. ANDREW. J. Chem. Soc. 537 (1949).
4. A. D. MAYNES and W. A. E. MCBRYDE. Anal. Chem. **29**, 1259 (1957).
5. M. FLEISCHER. Econ. Geol., 50th Anniv. Vol. 975 (1955).
6. D. A. BIDDLE. Ind. Eng. Chem., Anal. Ed. **8**, 99 (1936).
7. S. L. MORRISON and H. L. PAIGE. Ind. Eng. Chem., Anal. Ed. **18**, 211 (1946).
8. S. S. COOPER and M. L. SULLIVAN. Anal. Chem. **23**, 613 (1951).
9. H. FRIEDEBERG. Anal. Chem. **27**, 305 (1955).
10. A. I. VOGEL. Quantitative inorganic analysis. 2nd ed. Longmans, Green & Co., London. 1951. p. 421.
11. A. D. MAYNES. Ph.D. Thesis, University of Toronto, Toronto, Ont. 1956.
12. C. L. LUKE. Anal. Chem. **28**, 1276 (1956).
13. P. F. WYATT. Analyst, **80**, 368 (1955).
14. G. F. SMITH and W. H. MCCURDY. Anal. Chem. **24**, 371 (1952).
15. G. F. SMITH and D. H. WILKINS. Anal. Chem. **25**, 510 (1953).
16. C. L. LUKE and M. E. CAMPBELL. Anal. Chem. **25**, 1588 (1953).

Can. J. Chem. Downloaded from www.nrcresearchpress.com by 210.87.254.105 on 09/05/12
For personal use only.

Can. J. Chem. Downloaded from www.nrcresearchpress.com by 210.87.254.105 on 09/05/12
For personal use only.

17α-HALOGENATED PROGESTERONES: ORALLY-ACTIVE PROGESTINS[1]

DAVID J. MARSHALL AND ROGER GAUDRY

ABSTRACT

17α-Chloroprogesterone, 6α-fluoro-17α-bromoprogesterone, 1-dehydro-6α-fluoro-17α-bromoprogesterone, and 6α-chloro-17α-bromoprogesterone have been synthesized. These compounds have been found to be orally-active progestins without androgenic properties.

In recent years, considerable effort has been devoted to the search for orally-active progestational agents to substitute for the natural hormone, progesterone. The newer synthetic progestogens which have acquired prominence because of their oral activity fall into two classes: 19-norsteroids such as 19-norprogesterone (1) and 17α-ethynyl-19-nortestosterone (2) and its $\Delta^{5(10)}$-isomer (3), and derivatives of progesterone containing a 17α-acetoxy substituent (4–7).

It has been shown recently that 17α-bromoprogesterone (8) is an orally-active progestogen (9), indicating that substituents other than acetoxyl at C-17 can enhance the very weak oral activity of progesterone. It was clearly of interest to prepare other 17α-halogenated progesterones, and to determine whether modifications in structure which enhance the activity of 17α-acetoxyprogesterone, such as the introduction of a 6α-halo substituent and a Δ^1-double bond (4, 5), would have a similar effect on the comparatively weak oral activity of 17α-bromoprogesterone.

In this paper, we record the synthesis and preliminary biological evaluation of 17α-chloroprogesterone and of the 6α-fluoro-, 1-dehydro-6α-fluoro-, and 6α-chloro-derivatives of 17α-bromoprogesterone.

17α-Chloroprogesterone

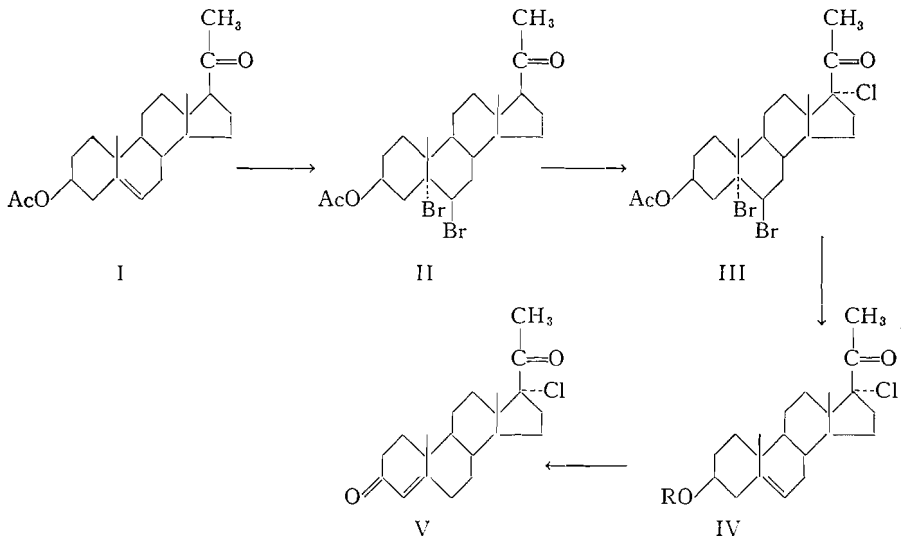
Pregnenolone acetate (I) was brominated at a low temperature, and the 5,6-dibromide II was allowed to react with chlorine in acetic acid. The resulting mixture of 17- and 21-chloro derivatives (III) was treated with sodium iodide in acetone which regenerated the 5,6-double bond and replaced chlorine at C-21 with iodine. Finally, the iodine at C-21 was removed by reduction with aqueous sodium bisulphite solution (10) and 17α-chloropregnenolone acetate (IV, R = Ac) was isolated after chromatographic purification. The α-configuration of the chlorine was inferred from the general preference for "back-side" attack and from the fact that bromination of 20-ketones has been clearly shown to result in the formation of 17α-bromo derivatives (11).

Acid-catalyzed hydrolysis of IV (R = Ac) yielded 17α-chloropregnenolone (IV, R = H), which, without purification, was oxidized with chromic acid in acetone (12). The shift of the double bond into conjugation with the carbonyl group to yield 17α-chloroprogesterone (V) was completed by treatment of the crude oxidation product with oxalic acid (13).

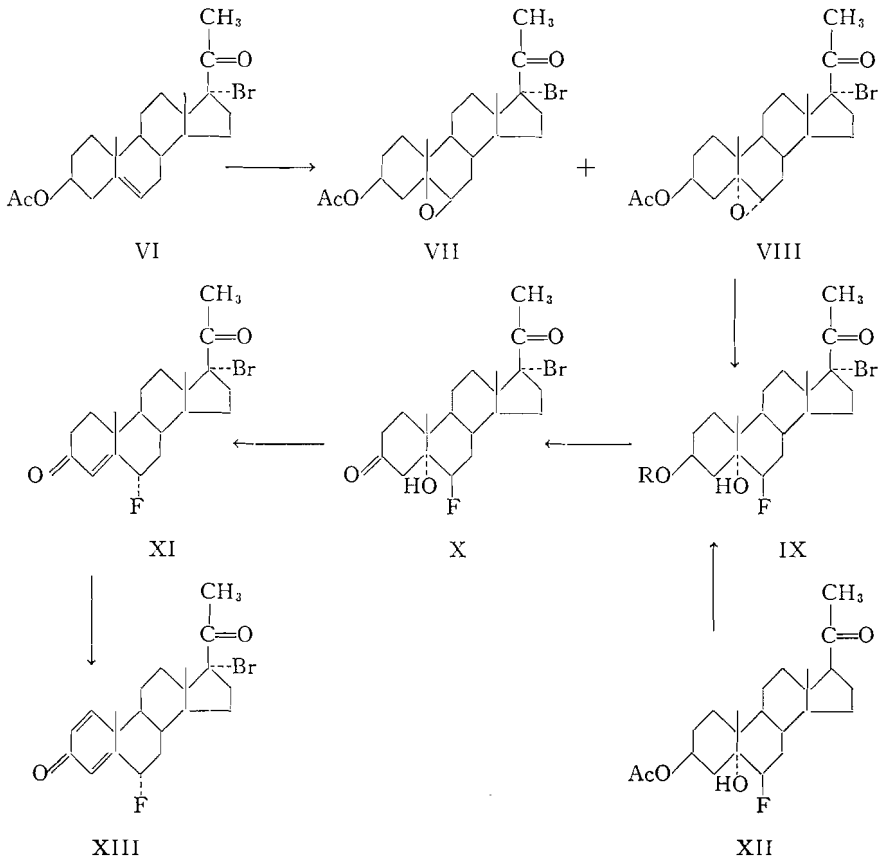
6α-Halo-17α-bromoprogesterones[2]

17α-Bromopregnenolone acetate (VI) (8, 10) was converted to a 6-fluoro derivative by conventional means (14). Epoxidation of VI with monoperphthalic acid gave a mixture of 5β,6β- and 5α,6α-epoxides, VII and VIII. The epoxides were separated by chromatog-

[1]*Manuscript received May 9, 1960.*
Contribution from the Ayerst Research Laboratories, P.O. Box 6115, Montreal, Que.
[2]*While this article was in manuscript, the synthesis of 6α-fluoro-17α-bromoprogesterone was reported by Ch. R. Engel and R. Deghenghi, Can. J. Chem.* **38**, *452 (1960).*

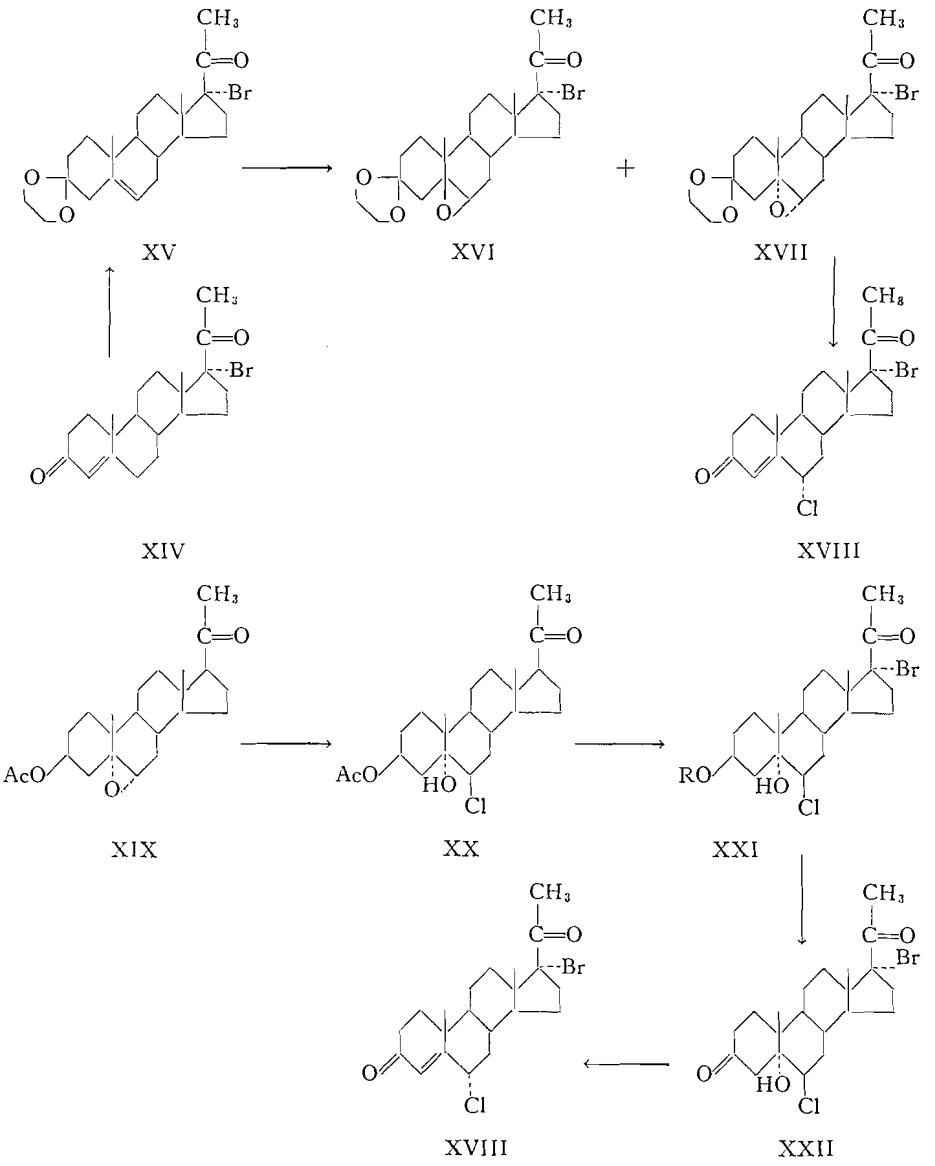


raphy on Florisil, and the more strongly adsorbed and more levorotatory isomer was assigned the α-structure by analogy with other pairs of epimeric 5,6-epoxides (15). Cleavage of the epoxide ring of VIII with anhydrous hydrogen fluoride (14, 16) gave the



Can. J. Chem. Downloaded from www.nrcresearchpress.com by 210.87.254.105 on 09/05/12
For personal use only.

5α-hydroxy-6β-fluoro derivative IX (R = Ac) in good yield. The alternative method of forming the fluorohydrin, reaction of the epoxide with boron trifluoride etherate (6, 15, 17–20), gave much less satisfactory results. The fluorohydrin acetate IX (R = Ac) was hydrolyzed with perchloric acid in methanol to the diol IX (R = H). Oxidation of the diol with sodium dichromate in acetic acid and dehydration of the resulting diketone X with anhydrous hydrogen chloride in chloroform gave 6α-fluoro-17α-bromoprogesterone (XI), λ_{max} 237 mμ, ε 17,800. The stability of XI to further treatment with acid and the value of the extinction coefficient (6β-fluoro-Δ^4-3-ketones have extinction coefficients of 10,000–13,000 (18)) served to establish that the expected inversion of C-6 had occurred, and that the fluorine was in the equatorial (6α) configuration.



Can. J. Chem. Downloaded from www.nrcresearchpress.com by 210.87.254.105 on 09/05/12
For personal use only.

Can. J. Chem. Downloaded from www.nrcresearchpress.com by 210.87.254.105 on 09/05/12
For personal use only.

The fluorohydrin IX (R = Ac) was also obtained, in good yield, by bromination of 3β-acetoxy-5α-hydroxy-6β-fluoropregnan-20-one (XII) (16, 17) with N-bromosuccinimide (21).

Dehydrogenation of XI with 2,3-dichloro-5,6-dicyanoquinone (22) yielded the 1-dehydro analogue XIII, which was also obtained, in lower yield, by reaction of XI with selenium dioxide.

For the synthesis of 6α-chloro-17α-bromoprogesterone, 17α-bromoprogesterone (XIV) was converted to the corresponding 3-monoethylene ketal XV by reaction with ethylene glycol and *p*-toluenesulphonic acid in refluxing toluene. Epoxidation of the ketal with monoperphthalic acid gave a mixture of 5β,6β- and 5α,6α-epoxides XVI and XVII, separated by chromatography on Florisil. The configurations of the epoxides were assigned on the basis of their relative behavior during chromatography and a comparison of optical rotations, since it is known (15) that in any pair of epimeric 3-ketal-5,6-epoxides, the α-epoxide is more polar toward adsorbents and is more levorotatory than the β-epimer.

Treatment of the α-epoxide XVII with anhydrous hydrogen chloride in chloroform resulted in cleavage of the epoxide linkage to form the 5α-hydroxy-6β-chloro derivative, hydrolysis of the ketal group, dehydration to the α,β-unsaturated ketone, and inversion of configuration at C-6, and 6α-chloro-17α-bromoprogesterone (XVIII) was isolated in 80% yield. The structure of XVIII was established by elemental analysis, by infrared and ultraviolet spectral data, and by the stability of the compound to acid.

In a second synthesis of XVIII, 3β-acetoxy-5α,6α-epoxypregnan-20-one (XIX) (16, 17) was allowed to react with hydrogen chloride in chloroform, and the resulting 5α-hydroxy-6β-chloro derivative XX was brominated at C-17 with N-bromosuccinimide to give XXI (R = Ac). Acid-catalyzed hydrolysis to the diol XXI (R = H), oxidation to the diketone XXII, and dehydration-inversion with hydrogen chloride then led to XVIII.

A crystalline product could not be obtained from attempted dehydrogenations of XVIII with selenium dioxide or 2,3-dichloro-5,6-dicyanoquinone.

Biological Activity

The progestational activity of the 17α-halogenated progesterones relative to progesterone (subcutaneous) and to 17α-ethynyl-19-nortestosterone (oral), as determined in the Clauberg assay, is summarized in Table I. It will be seen that chlorine has a smaller

TABLE I

Relative progestational activity (Clauberg assay)

	Subcutaneous	Oral
Progesterone	1.0	
17α-Ethynyl-19-nortestosterone		1.0
17α-Bromoprogesterone (XIV)	2.0	0.04
17α-Chloroprogesterone (V)	1.0	<0.04
6α-Fluoro-17α-bromoprogesterone (XI)	4.0	0.3
6α-Chloro-17α-bromoprogesterone (XVIII)	2.0	0.3

potentiating effect on the progestational activity than does bromine at C-17α of progesterone. But fluorine and chlorine at C-6α enhance the activity of 17α-bromoprogesterone to about the same extent as they enhance the activity of 17α-acetoxyprogesterone (6, 7). Preliminary assays indicated that the 1-dehydro derivative XIII was more active than XI.

There have been a number of reports recently that the administration of some synthetic progestins to rats (23) and to humans (24) during gestation can induce masculinization of female fetuses. For example, it has been found (23) that when pregnant rats are treated with relatively low doses of 17α-ethynyl-19-nortestosterone or 6α-methyl-17α-acetoxyprogesterone (5), serious masculinization occurs in the female offspring. It was therefore of interest to test some of the compounds made in this investigation for androgenic activity. The 17α-bromoprogesterones did not show androgenic properties in castrated male rats, nor was there any indication of masculinization in female offspring of pregnant rats which had been treated with high doses of XI or XIV.

The detailed results of the biological assays of these compounds will be published elsewhere (25).

EXPERIMENTAL

Melting points are uncorrected. Rotations were determined in chloroform solution at a concentration of about 1%, and ultraviolet spectra were taken in solution in 95% ethanol. The alumina used for chromatography was Merck chromatographic grade alumina which had been neutralized by being allowed to stand overnight in ethyl acetate and reactivated by heating *in vacuo* at 145° for 18 hours. Microanalyses were carried out in our analytical laboratory by Mr. W. J. Turnbull and associates.

17α-CHLOROPROGESTERONE

17α-Chloropregnenolone Acetate (IV, R = Ac*)*

To a stirred solution of 50.0 g of 3β-acetoxy-5-pregnen-20-one in 930 ml of chloroform cooled to −60° was added over a period of 2 hours 467 ml of a 0.3 *M* solution of bromine in carbon tetrachloride. After the solution was warmed to room temperature, the volume was reduced to about 100 ml *in vacuo* and the 5α,6β-dibromide II was precipitated by the addition of 350 ml of methanol. The yield was 60.4 g, m.p. 143–146° decomp.

To a solution of 14.0 g of II in 125 ml of acetic acid containing 0.1 ml of concentrated hydrochloric acid was added 78.4 g of a solution of chlorine in acetic acid (2.46 g chlorine per 100 g of solution) over a period of 1 hour. After 250 ml of water was added, the mixture was refrigerated overnight and the colorless solid was filtered and washed with water. Crystallization from methylene chloride – methanol yielded 10.3 g of a mixture of 17- and 21-chlorodibromides (III), m.p. 129–137° decomp. This product was dissolved in 100 ml of boiling acetone and a solution of 10 g of sodium iodide in 60 ml of acetone was added. After it was heated under reflux for 1 hour, under nitrogen, the mixture was cooled in ice and the iodine was reduced by the slow addition of 362 ml of 0.1 *N* sodium thiosulphate solution. The precipitated product was dissolved in 70 ml of ether, 10 ml of 10% sodium bisulphite solution was added, and the mixture was shaken intermittently for 30 minutes, after which no further iodine color developed on standing. The ether solution was washed with an additional portion of bisulphite solution and with water and was dried and concentrated to dryness. The resulting solid (6.8 g) could not be readily purified by crystallization.

A 1.87 g portion of this product was chromatographed on 65 g of alumina. Elution with 650 ml of benzene–petroleum ether 1:3 yielded 1.45 g of 3β-acetoxy-17α-chloro-5-pregnen-20-one (IV, R = Ac), m.p. 145–148°. Crystallization from methylene chloride – methanol gave an analytical sample, m.p. 147–149°, $[\alpha]_D$ −84.9°. Anal. Calc. for $C_{23}H_{33}ClO_3$: C, 70.30; H, 8.46; Cl, 9.02. Found: C, 70.41; H, 8.67; Cl, 9.18.

Can. J. Chem. Downloaded from www.nrcresearchpress.com by 210.87.254.105 on 09/05/12
For personal use only.

17α-Chloroprogesterone (V)

A mixture of 4.65 g of the acetate IV (R = Ac), 130 ml of methanol, and 4.65 ml of 70% perchloric acid was heated at the boiling point until the solid had dissolved and was then left at room temperature for 24 hours. Water (140 ml) precipitated 3.80 g of 17α-chloropregnenolone (IV, R = H), m.p. 120°, resolidifying and remelting at 156–161°, which was not further purified.

To a stirred solution of 3.48 g of 17α-chloropregnenolone in 140 ml of acetone cooled to 5° under nitrogen was added 2.78 ml of a chromic acid solution (26.72 g of chromium trioxide in 23 ml of sulphuric acid diluted to 100 ml with water). After the solution had been stirred for 5 minutes, 420 ml of water was added and the precipitated solid was filtered and dried (3.25 g). This product was dissolved in 43 ml of ethanol, 1.6 g of oxalic acid was added, and the solution was heated under reflux under nitrogen for 45 minutes. Water was added and the product was extracted with ether. The ether solution was washed with 5% sodium bicarbonate solution and with water, and the brown gum remaining after drying and evaporation of the solvent was adsorbed on 150 g of alumina in benzene – petroleum ether 1:1. Elution with 600 ml of benzene gave 1.14 g of colorless solid which was crystallized from aqueous methanol yielding 1.00 g of 17α-chloroprogesterone (V), m.p. 166–168°. Recrystallization from aqueous methanol gave an analytical sample, m.p. 168.5–170°, $[\alpha]_D$ +51.0°, λ_{max} 240 mμ (ε 17,900). Anal. Calc. for $C_{21}H_{29}ClO_2$: C, 72.31; H, 8.38; Cl, 10.12. Found: C, 72.63; H, 8.39; Cl, 10.31.

6α-FLUORO-17α-BROMOPROGESTERONE

Epoxidation of 17α-Bromopregnenolone Acetate

To a stirred, ice-cooled solution of 5.00 g of 3β-acetoxy-17α-bromo-5-pregnen-20-one in 75 ml of chloroform was added, over a period of 15 minutes, 102 ml of a 0.342 *M* solution of monoperphthalic acid in ether. After storage at 10° for 4 days, the mixture was filtered, and the filtrate was washed with 10% sodium bicarbonate solution and with water and dried over magnesium sulphate. The crude product obtained after evaporation of the solvent was dissolved in benzene and chromatographed on 150 g of Florisil. Two liters of benzene containing 1% ethyl acetate eluted 1.12 g of the *5β,6β-epoxide* VII, which was recrystallized from ethyl acetate, m.p. 158–160.5°, $[\alpha]_D$ −57.6°. Anal. Calc. for $C_{23}H_{33}BrO_4$: C, 60.92; H, 7.34; Br, 17.62. Found: C, 61.15; H, 7.22; Br, 17.57.

Elution of the column with 2 liters of benzene containing 5% ethyl acetate gave 2.82 g of the *5α,6α-epoxide* VIII, which, after recrystallization from ethyl acetate had a melting point of 192–193°, $[\alpha]_D$ −102.4°. Anal. Calc. for $C_{23}H_{33}BrO_4$: C, 60.92; H, 7.34; Br, 17.62. Found: C, 60.64; H, 7.12; Br, 17.31.

3β-Acetoxy-5α-hydroxy-6β-fluoro-17α-bromopregnan-20-one (IX)

A. From the Epoxide VIII

To 51.1 g of anhydrous hydrogen fluoride in a polyethylene bottle in a Dry Ice–acetone bath at −60° was added slowly, in turn, 102 g of dry tetrahydrofuran, 50 ml of chloroform, and a solution of 51.1 g of the epoxide VIII in 325 ml of chloroform. The solution was kept at −10° for 2 hours and was then poured, with stirring, into a mixture containing 200 g of potassium carbonate, 600 ml of water, ice, and 100 ml of chloroform. The chloroform solution was washed with sodium bicarbonate solution and with water, dried over magnesium sulphate, and evaporated to dryness *in vacuo*. Crystallization from methylene chloride – methanol yielded 34.7 g of the fluorohydrin IX, m.p. 170–171° decomp. The analytical sample, obtained by crystallization from the same solvent

Can. J. Chem. Downloaded from www.nrcresearchpress.com by 210.87.254.105 on 09/05/12
For personal use only.

mixture had a melting point of 173° decomp., $[\alpha]_D$ −78.3°. Anal. Calc. for $C_{23}H_{34}BrFO_4$: C, 58.34; H, 7.24; Br, 16.88; F, 4.01. Found: C, 58.32; H, 7.26; Br, 16.85; F, 3.89.

B. From 3β-Acetoxy-5α-hydroxy-6β-fluoropregnan-20-one (XII)

A mixture of 20.0 g of the fluorohydrin XII, 15.0 g of N-bromosuccinimide, and 500 ml of carbon tetrachloride was heated under reflux on the steam bath. When the solvent was boiling vigorously, the flask was irradiated with a 250-watt infrared lamp and refluxing was continued for 10 minutes. The flask was then cooled in an ice bath, the mixture was filtered, and the filtrate was washed with dilute sodium bisulphite solution and with water. The dried (Na_2SO_4) solution was evaporated to dryness *in vacuo* and 40 ml of methanol was added to the amorphous residue. The mixture was brought rapidly to the boiling point, cooled in ice, and the crystalline product was filtered and washed with methanol. The yield of 17α-bromo derivative IX was 15.1 g, m.p. 171.5° decomp., identical (mixed m.p. and infrared spectrum) with the product obtained in *A*.

In larger runs it was found desirable to have a small amount of pyridine present to inhibit the ionic bromination which sometimes occurred. Thus, a mixture of 100 g of IX, 75 g of N-bromosuccinimide, 2.5 liters of carbon tetrachloride, 24 g of pyridine, and 6 g of benzoyl peroxide heated under reflux for 15 minutes followed by working up as above, yielded 80 g of VI, m.p. 174° decomp.[3]

3β,5α-Dihydroxy-6β-fluoro-17α-bromopregnan-20-one (IX, R = H)

A mixture of 34.7 g of the acetate IX (R = Ac), 500 ml of methanol, and 12 ml of 70% perchloric acid was boiled until the steroid had dissolved (about 10 minutes) and was then left at room temperature for 17 hours. The solid obtained by the addition of 500 ml of water was crystallized from methanol, yielding 25.8 g of the diol IX (R = H), m.p. 174° decomp. Recrystallization from aqueous methanol gave the analytical sample, m.p. 176° decomp., $[\alpha]_D$ −65.2°. Anal. Calc. for $C_{21}H_{32}BrFO_3$: C, 58.46; H, 7.48; Br, 18.52; F, 4.40. Found: C, 58.22; H, 7.71; Br, 18.44; F, 4.56.

5α-Hydroxy-6β-fluoro-17α-bromopregnane-3,20-dione (X)

To a solution of 25.8 g of the diol IX (R = H) in 250 ml of acetic acid cooled to 15° was added with stirring a solution of 25.8 g of sodium dichromate dihydrate in 520 ml of acetic acid. After the mixture had been allowed to stand at room temperature for 16 hours, 50 ml of methanol was added, followed by 1300 ml of water. The finely divided solid was filtered and washed well with water. The wet product, which was difficult to dry, was dissolved in methylene chloride (in which it was only moderately soluble), and the solution was dried over sodium sulphate and concentrated. Crystallization from methylene chloride – methanol yielded 16.4 g of the diketone X, m.p. 174° decomp., and 2.8 g, m.p. 173° decomp. The analytical sample, m.p. 173.5–174.5° decomp., $[\alpha]_D$ −42.1°, was obtained by crystallization from *i*-propanol. Anal. Calc. for $C_{21}H_{30}BrFO_3$: C, 58.75; H, 7.04; Br, 18.61; F, 4.93. Found: C, 58.71; H, 6.91; Br, 18.90; F, 4.49.

6α-Fluoro-17α-bromoprogesterone (XI)

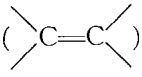
Anhydrous hydrogen chloride was passed for 1 hour through an ice-cooled suspension of 10.8 g of the diketone X in 200 ml of chloroform. The solid went rapidly into solution. After standing an additional hour in the ice bath, the orange solution was washed with water, 10% sodium bicarbonate solution, and again with water. Drying over sodium sulphate and evaporation of the solvent gave a solid which was crystallized from methylene chloride – methanol, yielding 6.5 g of 6α-fluoro-17α-bromo-4-pregnene-3,20-dione

[3]*We are indebted to Dr. Gordon Myers for carrying out this experiment.*

Can. J. Chem. Downloaded from www.nrcresearchpress.com by 210.87.254.105 on 09/05/12
For personal use only.

(XI) as colorless needles, m.p. 173–175.5° decomp. From the mother liquors, an additional 0.5 g of product was obtained, m.p. 171–173° decomp. Recrystallization from methylene chloride – methanol yielded an analytical sample, m.p. 176–177.5° decomp., $[\alpha]_D$ +17.0°, λ_{max} 236 mμ (ε 17,800). Anal. Calc. for $C_{21}H_{28}BrFO_2$: C, 61.34; H, 6.86; Br, 19.43; F, 4.62. Found: C, 61.51; H, 7.06; Br, 19.28; F, 4.42.

1-Dehydro-6α-fluoro-17α-bromoprogesterone (XIII)

A solution of 1.00 g of XI, 0.64 g of 2,3-dichloro-5,6-dicyanoquinone (22), and 26 mg of *p*-toluenesulphonic acid in 40 ml of benzene was heated under reflux for 18 hours. The cooled mixture was filtered, and the filtrate was diluted with 20 ml of ethyl acetate and washed (initially without shaking to avoid emulsions) with 10% sodium bicarbonate solution and with water. After drying over magnesium sulphate, the solvent was removed *in vacuo*, and the solid residue was chromatographed in benzene on 10 g of Florisil. Elution with 250 ml of benzene containing 5–10% ethyl acetate yielded 656 mg of pale yellow solid. Crystallization from methylene chloride – methanol (charcoal) gave 0.51 g of XIII as colorless plates, m.p. 181–182° decomp. The analytical sample was obtained by recrystallization from acetone–hexane and melted at 181–183° decomp., $[\alpha]_D$ −20.5°, λ_{max} 241 mμ (ε 18,200), $\nu_{max}^{CS_2}$ 1711 cm^{-1} (20-ketone), 1675 cm^{-1} (3-ketone), 1637 cm^{-1} (), 904 cm^{-1}. Anal. Calc. for $C_{21}H_{26}BrFO_2$: C, 61.63; H, 6.40; Br, 19.53; F, 4.64. Found: C, 61.52; H, 6.31; Br, 19.38; F, 4.78.

6α-CHLORO-17α-BROMOPROGESTERONE

3,3-Ethylenedioxy-17α-bromo-5-pregnen-20-one (XV)

A mixture of 10.0 g of 17α-bromoprogesterone, 310 ml of toluene, 80 ml of ethylene glycol, and 0.30 g of *p*-toluenesulphonic acid was heated under reflux under a water separator for 6 hours. After it was cooled in ice, the mixture was washed with 10% sodium bicarbonate solution and with water, and the solvent was removed *in vacuo*. Crystallization from methanol containing a few drops of pyridine yielded 5.0 g of the 3-ketal XV, m.p. 128–130°. The analytical sample was obtained by crystallization from methanol, m.p. 131–132°, $[\alpha]_D$ −84.0°. The infrared spectrum (CS_2) showed a single carbonyl band at 1705 cm^{-1}. Anal. Calc. for $C_{23}H_{33}BrO_3$: C, 63.16; H, 7.60; Br, 18.27. Found: C, 63.40; H, 7.60; Br, 18.56.

Epoxidation of XV

To a solution of 2.00 g of the bromoketal XV in 40 ml of chloroform cooled to −60° was added 47 ml of a 0.192 *M* solution of monoperphthalic acid in ether over a period of 20 minutes. After it had been stirred at −60° for 2 hours, the mixture was kept overnight at 0°, washed with 5% sodium carbonate solution and with water, dried over magnesium sulphate, and the solvent was removed. The crude product was chromatographed in benzene on 60 g of Florisil. Elution with benzene containing 2% ether gave the *5β,6β-epoxide* XVI, which was crystallized from methanol, yielding 0.70 g, m.p. 119–120°. Recrystallization from methanol gave an analytical sample, m.p. 120–121°, $[\alpha]_D$ −38.4°. Anal. Calc. for $C_{23}H_{33}BrO_4$: C, 60.92; H, 7.33; Br, 17.63. Found: C, 60.69; H, 7.23; Br, 17.74.

The *5α,6α-epoxide* XVII was obtained by elution of the column with benzene containing 10% ether. Crystallization from methanol gave 0.69 g of XVII, m.p. 180–182°. The analytical sample, obtained by recrystallization from methanol, had m.p. 182–183°,

Can. J. Chem. Downloaded from www.nrcresearchpress.com by 210.87.254.105 on 09/05/12
For personal use only.

$[\alpha]_D$ −88.4°. Anal. Calc. for $C_{23}H_{33}BrO_4$: C, 60.92; H, 7.33; Br, 17.63. Found: C, 60.72; H, 7.25; Br; 17.62.

3β-Acetoxy-5α-hydroxy-6β-chloropregnan-20-one (XX)

Hydrogen chloride was passed for 1 hour through a solution of 122 g of 3β-acetoxy-5α,6α-epoxypregnan-20-one (XIX) (18, 19) in 1 liter of chloroform. After an additional hour at room temperature, the solution was washed with water, 10% sodium bicarbonate solution, and water again, and dried over sodium sulphate. Removal of the solvent and crystallization from methylene chloride – methanol yielded two crops of XVI totalling 101 g, m.p. 230–233° decomp. Recrystallization from the same solvent combination raised the m.p. to 232–234° decomp., $[\alpha]_D$ +8.1°. Anal. Calc. for $C_{23}H_{35}ClO_4$: C, 67.22; H, 8.58; Cl, 8.63. Found: C, 67.41; H, 8.49; Cl, 8.67.

3β-Acetoxy-5α-hydroxy-6β-chloro-17α-bromopregnan-20-one (XXI, R = Ac)

A suspension of 101 g of the chlorohydrin XX and 101 g of N-bromosuccinimide in 2.6 liters of carbon tetrachloride was heated to the boiling point and irradiated with two 250-watt heat lamps for 15 minutes. The mixture was then cooled in ice and filtered, and the filtrate was washed with 5% sodium bisulphite solution, 10% sodium bicarbonate solution, and water. Drying over sodium sulphate and evaporation of the solvent *in vacuo* gave a crude product, which, on crystallization from aqueous methanol, yielded 80 g of XXI (R = Ac), m.p. 188–190° decomp. The analytical sample, m.p. 190–191° decomp., $[\alpha]_D$ −66.1, was obtained by recrystallization from aqueous methanol. Anal. Calc. for $C_{23}H_{34}BrClO_4$: C, 56.39; H, 7.00. Found: C, 56.10; H, 6.92.

3β,5α-Dihydroxy-6β-chloro-17α-bromopregnan-20-one (XXI, R = H)

Eighty grams of the acetate XXI (R = Ac) was dissolved in 2 l. of methanol by warming and 50 ml of 70% perchloric acid was added. The solution was left overnight at room temperature and the product was then precipitated by the addition of 1 liter of water. The yield of diol XXI (R = H) was 54 g, m.p. 175° decomp. After recrystallization from acetone–hexane, the diol melted at 175.5° decomp., $[\alpha]_D$ −70.7°, but it did not give a satisfactory analysis. Anal. Calc. for $C_{21}H_{32}BrClO_3$: C, 56.31; H, 7.20. Found: C, 56.94; H, 7.00.

5α-Hydroxy-6β-chloro-17α-bromopregnane-3,20-dione (XXII)

To a solution of 51.5 g of diol XXI (R = H) in 515 ml of acetic acid was added a solution of 25.75 g of sodium dichromate in 515 ml of acetic acid. The mixture was left for 4 hours at room temperature, 2 liters of water was added, and the precipitated solid was filtered and washed with water. The yield of diketone XXII was 42 g, m.p. 188–190° decomp. The analytical sample, m.p. 190° decomp., $[\alpha]_D$ −62.2°, was obtained by recrystallization from *i*-propanol. Anal. Calc. for $C_{21}H_{30}BrClO_3$: C, 56.57; H, 6.78. Found: C, 56.58; H, 6.75.

6α-Chloro-17α-bromoprogesterone (XVIII)

A. From the Epoxyketal XVII

Hydrogen chloride was passed for 1 hour through a solution of 1.3 g of XVII in 30 ml of chloroform. After it had been allowed to stand an additional hour, the solution was washed with water, with 5% sodium carbonate solution, and with water again and dried over magnesium sulphate. The product obtained on evaporation of the solvent was crystallized from acetone–hexane, yielding 0.98 g of 6α-chloro-17α-bromo-4-pregnene-3,20-dione (XVIII), m.p. 156–157°. Recrystallization from the same solvent mixture gave

Can. J. Chem. Downloaded from www.nrcresearchpress.com by 210.87.254.105 on 09/05/12
For personal use only.

an analytical sample, m.p. 157–158°, $[\alpha]_D$ +6.5°, λ_{max} 237 mμ (ε 16,200). Anal. Calc. for $C_{21}H_{28}BrClO_2$: C, 58.96; H, 6.60. Found: C, 59.02; H, 6.40.

B. From the Hydroxyketone XXII

An ice-cooled suspension of 3.0 g of XXII in 75 ml of chloroform was treated with hydrogen chloride for 1 hour, and, after an additional hour, the product was isolated as in *A*. Crystallization from acetone–hexane yielded 2.3 g of XVIII, m.p. 152–153°, identical by mixed m.p. and infrared spectrum with the product obtained in *A*.

ACKNOWLEDGMENTS

We wish to acknowledge the valuable technical assistance of T. F. Muther and J. Blackwell. We are indebted to Drs. C. Revesz and C. I. Chappel for the biological data, to Mr. M. Boulerice for the ultraviolet spectra, and to Dr. G. Papineau-Couture and Mrs. J. Jachner for numerous infrared spectra.

REFERENCES

1. C. Djerassi, L. Miramontes, and G. Rosencranz. J. Am. Chem. Soc. **75**, 4440 (1953). J. S. Mills, H. J. Ringold, and C. Djerassi. J. Am. Chem. Soc. **80**, 6118 (1958).
2. C. Djerassi, L. Miramontes, G. Rosencranz, and F. Sondheimer. J. Am. Chem. Soc. **76**, 4092 (1954). D. A. McGinty and C. Djerassi. Ann. N.Y. Acad. Sci. **71**, 500 (1958).
3. F. B. Colton. U.S. Patent No. 2,725,389 (1955). G. Pincus, M. Chang, M. X. Zarrow, E. S. E. Hafez, and A. Merrill. Science, **124**, 890 (1956); Endocrinology, **59**, 695 (1956).
4. R. B. Turner. J. Am. Chem. Soc. **75**, 3489 (1953). H. J. Ringold, B. Löken, G. Rosencranz, and F. Sondheimer. J. Am. Chem. Soc. **78**, 816 (1956). J. W. Goldzieher, W. F. Peterson, and R. A. Gilbert. Ann. N.Y. Acad. Sci. **71**, 722 (1958).
5. J. C. Babcock, E. S. Gutsell, M. E. Herr, J. A. Hogg, J. C. Stucki, L. E. Barnes, and W. E. Dulin. J. Am. Chem. Soc. **80**, 2904 (1958). S. P. Barton, B. Ellis, and V. Petrow. J. Chem. Soc. 478 (1959). H. J. Ringold, J. Perez Ruelas, E. Batres, and C. Djerassi. J. Am. Chem. Soc. **81**, 3712 (1959).
6. A. Bowers, L. C. Ibanez, and H. J. Ringold. J. Am. Chem. Soc. **81**, 5991 (1959).
7. H. J. Ringold, E. Batres, A. Bowers, J. A. Edwards, and J. A. Zderic. J. Am. Chem. Soc. **81**, 3485 (1959).
8. Ch. R. Engel and H. Jahnke. Can. J. Biochem. and Physiol. **35**, 1047 (1957).
9. C. Revesz, R. Herne, and C. I. Chappel. Proc. Can. Fed. Biol. Societies, First Annual Meeting, June 9–11, 1958. p. 41.
10. P. L. Julian and W. J. Karpel. J. Am. Chem. Soc. **72**, 362 (1950).
11. N. L. Wendler, R. P. Graber, and G. G. Hazen. Tetrahedron, **3**, 144 (1958).
12. C. Djerassi, R. R. Engle, and A. Bowers. J. Org. Chem. **21**, 1547 (1956).
13. L. F. Fieser. J. Am. Chem. Soc. **75**, 5421 (1953).
14. J. A. Hogg, G. B. Spero, J. L. Thompson, B. J. Magerlein, W. P. Schneider, D. H. Peterson, O. K. Sebek, H. C. Murray, J. C. Babcock, R. L. Pederson, and J. A. Campbell. Chem. & Ind. 1002 (1958).
15. A. Bowers, L. C. Ibanez, and H. J. Ringold. Tetrahedron, **7**, 138 (1959).
16. J. A. Campbell, J. C. Babcock, and J. A. Hogg. U.S. Patent No. 2,838,528 (1958).
17. A. Bowers and H. J. Ringold. Tetrahedron, **3**, 14 (1958).
18. J. S. Mills, A. Bowers, C. Casas Campillo, C. Djerassi, and H. J. Ringold. J. Am. Chem. Soc. **81**, 1264 (1959).
19. J. A. Edwards, A. Zaffaroni, H. J. Ringold, and C. Djerassi. Proc. Chem. Soc. 87 (1959).
20. H. B. Henbest and T. I. Wrigley. J. Chem. Soc. 4765 (1957).
21. R. U. Schock and W. J. Karpel. U.S. Patent No. 2,684,963 (1954).
22. D. Burn, D. N. Kirk, and V. Petrow. Proc. Chem. Soc. 14 (1960).
23. C. Revesz, C. I. Chappel, and R. Gaudry. Endocrinology, **66**, 140 (1960).
24. L. Wilkins, H. W. Jones, G. H. Holman, and R. S. Stempfel. J. Clin. Endocrinol. and Metabolism, **18**, 559 (1958). M. M. Grumbach, J. R. Ducharme, and R. E. Moloshok. J. Clin. Endocrinol. and Metabolism, **19**, 1369 (1959). L. Wilkins. J. Am. Med. Assoc. **172**, 1028 (1960).
25. C. Revesz, C. I. Chappel, and R. Gaudry. To be published.

Can. J. Chem. Downloaded from www.nrcresearchpress.com by 210.87.254.105 on 09/05/12
For personal use only.

Can. J. Chem. Downloaded from www.nrcresearchpress.com by 210.87.254.42 on 09/05/12
For personal use only.

SOME DEUTERIUM KINETIC ISOTOPE EFFECTS

II. α-DEUTERIUM EFFECTS IN THE WATER SOLVOLYSIS OF SOME ALKYL COMPOUNDS[1]

K. T. LEFFEK,[2] J. A. LLEWELLYN,[2] AND R. E. ROBERTSON

ABSTRACT

As an extension of previous work on methyl compounds, α-deuterium kinetic effects have been measured for ethyl, *n*-propyl, and isopropyl compounds. The effects can be accounted for in terms of current theory but a modification involving intramolecular van der Waals forces seems to provide a more satisfactory description of some of the processes involved in the production of the rate changes.

INTRODUCTION

When deuterium is substituted for a protium in compounds undergoing nucleophilic substitution reactions, the kinetic isotope effects (measured as the rate ratio k_H/k_D) may be greater or less than unity, i.e. deuteration may produce an increase or a decrease in rate of reaction (1). The reaction which we have studied is a simple hydrolysis in water symbolized by

$$RX + H_2O \rightarrow ROH + H^+ + X^-$$

where X, the leaving group, may be bromine, iodine, benzenesulphonate, substituted benzenesulphonate, or methanesulphonate. Earlier studies on a series of methyl compounds showed that increased reaction velocities were characteristic of the heavy analogues (2) but in this extension of that work we find effects in both directions when more complicated molecules are examined. The reaction rates were determined conductimetrically and the Guggenheim analysis (3) applied to the data to give pseudo-first order rate constants; the experimental techniques have been described in more detail elsewhere (4). Rate data are given in Table I. Several of the light analogues of the compounds examined in this investigation had already been studied and our current measurements are in excellent agreement with this data previously determined in this laboratory.

TABLE I

Deuterium isotope effect for more complicated compounds hydrolyzing in water

Compound	Solvolysis rates: Protium compound (k_1 sec^{-1})	Solvolysis rates: α-Deuterated compound (k_1 sec^{-1})	T (°C)	k_H/k_D
Ethyl *p*-toluenesulphonate	1.998×10^{-4}	1.925×10^{-4}	54.285	1.03_8
Ethyl methanesulphonate	1.957×10^{-4}	1.888×10^{-4}	60.003	1.03_7
Ethyl bromide	2.722×10^{-4}	2.769×10^{-4}	80.001	0.98_3
Ethyl iodide	1.554×10^{-4}	1.625×10^{-4}	80.000	0.96_6
Isopropyl *p*-toluenesulphonate	7.664×10^{-4}	6.757×10^{-4}	30.001	1.13_4
Isopropyl methanesulphonate	3.690×10^{-4}	3.229×10^{-4}	29.999	1.14_3
Isopropyl bromide	3.493×10^{-4}	3.269×10^{-4}	59.998	1.06_9
Isopropyl iodide	3.115×10^{-4}	2.967×10^{-4}	59.996	1.05_0
n-Propyl benzenesulphonate	2.042×10^{-4}	1.974×10^{-4}	54.192	1.03_4
n-Propyl methanesulphonate	1.370×10^{-4}	1.322×10^{-4}	60.004	1.03_6
n-Propyl bromide	1.629×10^{-4}	1.663×10^{-4}	80.009	0.98_0
n-Propyl iodide	2.230×10^{-4}	2.217×10^{-4}	90.003	1.00_6

[1]*Manuscript received May 27, 1960.*
Contribution from the Division of Pure Chemistry, National Research Council, Ottawa, Canada. Issued as N.R.C. No. 5774.
[2]*National Research Council Postdoctorate Fellow.*

Can. J. Chem. Downloaded from www.nrcresearchpress.com by 210.87.254.42 on 09/05/12
For personal use only.

DISCUSSION

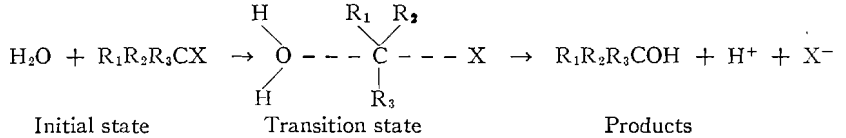
The general theory advanced for the α-deuterium effects observed with methyl compounds involved two opposing changes, both of which affected the frequencies of the fundamental modes of vibration and hence the activation energy via zero-point energy changes. It was postulated that:[3]

(A) The change in hybridization of the reacting carbon atom (sp^3 initially, sp^2 in the transition state) produced zero-point energy changes in a direction which tended to make the heavy compound react more slowly.

(B) The relative positions of entering and leaving groups will affect the ease with which the α-C—H bonds may be bent. Where crowding of the C—H bond is pronounced, fundamental modes involving C—H deformations in an important way will have higher characteristic frequencies, and the resulting zero-point changes might exceed those from factor A. In consequence the net effect would then be a more rapid reaction of the heavy compound.

If the transition state of reaction is more crowded than the initial state, then deuteration might be expected to produce an increased rate of reaction as a consequence of dominance by factor B. Such a situation would prevail where a high degree of nucleophilic assistance was required for reaction, as with the methyl halides, and the expected decrease in effect is observed as the interaction by the entering group is decreased by "better" leaving groups. As we alter the alkyl grouping by alpha methylation, nucleophilic assistance becomes less necessary and the crowding in the transition state (factor B) fades out. Eventually, factor A gives rise to an isotope effect (k_H/k_D) greater than unity. For a given alkyl group, similar changes with reversal of effect may be seen as the X group is varied.

Deutero-*n*-propyl bromide reacts more quickly than its light analogue ($k_H/k_D = 0.98_0$) whereas *n*-propyl methanesulphonate reacts more slowly when deuterated ($k_H/k_D = 1.03_6$). Again this change in the deuterium isotope effect is attributed to a more crowded transition state in the bromide reaction where nucleophilic interaction is greater than in the methanesulphonate reaction. For other alkyl groups the changes are parallel; the alpha-deuterium isotope effect increases as the transition state becomes less crowded, e.g. the rate ratios k_H/k_D for ethyl iodide, bromide, and methanesulphonate are 0.95_6, 0.98_3, and 1.03_7 respectively. In addition to these effects there is a third which is a simple consequence of the mass alteration produced by isotopic substitution. The thermodynamic properties of the molecules depend on the masses of the constituent atoms so that independently of zero-point effects there may be a "thermodynamic" isotope effect. It is difficult to state in a general way exactly what the consequences of isotope substitution will be on the contributions to the thermodynamic parameters from the various degrees of freedom. Some obvious expressions were given in an earlier paper on the methyl compounds (2), but calculations for more complicated molecules are frequently difficult and often impossible because of lack of information. Some general comments can be made, however. For reactions such as these where two molecules become partially bonded on passing to the



[3]*The suggestions concerning altered hybridization and modification of the effect by leaving group were first suggested by Streitwieser and co-workers (see ref. 8) and extended by us (ref. 2) to cover inverse isotope effects.*

Can. J. Chem. Downloaded from www.nrcresearchpress.com by 210.87.254.42 on 09/05/12
For personal use only.

transition state, then the effect of substitution with a heavier isotope on the translational contribution will always be in a direction such that k_H/k_D tends to exceed unity. For α-deuteration, a substitution close to reaction site, the center of gravity of the molecule will be brought closer to the point at which mass increase from reaction occurs, and the rotational entropy of activation will accordingly decrease, i.e. k_H/k_D tends to exceed unity. It seems reasonable to neglect changes in the vibrational contribution in this context, by comparison with the zero-point energy changes which will arise from the same source. Detailed calculations have been made in cases where it has been practical (2, 5) and the general conclusion is that the "thermodynamic" effect favors slower reaction for the heavy compound and is of a magnitude which is comparable with observed effects in some cases, but cannot account for inverse isotope effects.

Further Considerations

Interpretation in terms of factor A, the hybridization change, and B, crowding by the entering group, seemed reasonably satisfactory and led to a self-consistent scheme for the α-deuterium kinetic isotope effects. There are some aspects of factor A, however, which seem doubtful: the intermediate in an S_N1 reaction will be the carbonium ion so that the transition state will probably not have completely altered hybridization of the reacting carbon, and the more the molecule can accommodate the developing charge by internal stabilization the nearer will be the configuration to tetrahedral in the transition state (6). In an S_N2 reaction, however, the hybridization change will probably be complete in the transition state with the entering and leaving groups interacting with the p orbital and the C—H bonds sp^2 hybridized (7). Thus hybridization change will be most marked in S_N2 reactions although zero-point effects will be modified by the presence of the entering group. It seems that the hybridization change is a necessary part of the reaction but is not necessarily responsible for the decrease in zero-point sum which plays such an important part in our considerations of the α-isotope effect. The difficulty in connection with this latter point is well illustrated by Streitwieser's comment on the effect of assuming different models for the sp^2 C—H bond (8). Making the usual reservations concerning the comparison of force constants we can find (9) wide overlapping ranges of force constants for sp^2 and sp^3 bonds. Some of the confusion is undoubtedly the consequence of the application of varying force fields in the spectral analysis but some consistency does appear when similar treatments are applied; for example Table II shows an increase in stretching

TABLE II

Effect of bond type on C—H force constant (13)

System	Bond	Constant $\times 10^{-5}$ dyne/cm
CH	p	4.09
CH_4	sp^3	4.79
C_2H_4	sp^2	5.1
C_2H_2	sp	5.85

force constant with increased s character in the C—H bond, which contradicts the hypothesis A set up to explain the α-deuterium isotope effect.

The bending constants appear to change in the opposite direction. Using simple valence force fields, Linnett (10) quotes the bending constants given below. In contrast, using orbital valence force fields to analyze CH_4 spectra, C—H bond bending has a

TABLE III
S.V.F.F. bending constants

System	Bending constant (erg/radian^2×10^{11})
C—C$\diagup^{H}$	0.66
C=C$\diagup^{H}$	0.60
C≡C$\diagup^{H}$	0.24

constant 1.35×10^5 dyne/cm for doubly degenerate vibrations and 0.86×10^5 dyne/cm for triply degenerate vibrations whereas a comparable figure for ethylene is 0.95×10^5 and between 1.03 and 1.09×10^5 for formaldehyde, depending on the exact dimensions of the molecule which are taken in the analysis (10, 12). Thus the evidence that a hybridization change $sp^3 \rightarrow sp^2$ does produce the proposed zero-point change appears to be inconclusive. It is possible that the decrease in frequency springs from other sources, and one in particular seems worth considering.

Examination of vibrational spectra has shown that they may be satisfactorily accounted for by including potential energy terms for non-bonded atomic interactions comparable with those for intermolecular repulsions (10, 12–16). In molecules of the type XY_3, XY_4, XY_6, non-bonded interactions must be taken into account when considering molecular distortions. CH_4 could be treated neglecting H . . . H repulsion; it was assumed negligible in treatments of C_2H_4 and HCHO with some reservations, and it was found necessary to include H . . . O and H . . . C repulsion using a function $v = a/R^{12}$. Simanouti (17–19) has also successfully analyzed the vibrational spectra of numerous XABCD compounds using valence force field plus non-bonded interatomic repulsion terms of magnitude comparable to those used by Lennard-Jones to describe rare gas interatomic forces. Encouraging results have also attended correlations of molecular geometry with simple hard-sphere potential energy functions for non-bonded intramolecular interactions (20). In the reactions that we have studied, there is a movement of the X group away from the reaction center so that a reduction in intramolecular forces between this group and the α-hydrogen atoms might be expected. The magnitude of the change will depend on the increase in the H(α)—X distance and the degree of charge separation that has occurred, but will undoubtedly produce a significant decrease in the force field that governs vibrations involving the C—H bonds. It is postulated, therefore, that the increased H(α)—X distance in the transition state produces a decrease in the zero-point sum as a consequence of reduced intramolecular van der Waals forces. This postulate is really an extension of factor B in the earlier argument and the α-isotope effect now appears to be governed largely by steric effects. Obviously it is difficult to separate this possibility from that of altered hybridization but the proposed consequences of the $sp^3 \rightarrow sp^2$ hybridization change are not evident, whereas a zero-point decrease seems inevitable when non-bonded atomic interactions are reduced.

On this basis of varying intramolecular van der Waals forces it appears that the α-isotope effect can still be interpreted as a measure of the crowding about the carbon

Can. J. Chem. Downloaded from www.nrcresearchpress.com by 210.87.254.42 on 09/05/12
For personal use only.

atom which forms the reaction center. For entering and leaving groups of comparable sizes in different reactions k_H/k_D is interpreted as a measure of the extent to which bond-making and bond-breaking have occurred, with smaller ratios indicating predominance of bond-making processes and larger ratios indicating bond-breaking. Thus the alternative postulate does not materially alter the conclusions which were drawn from the observed effects but appears to offer a more satisfactory explanation of some of the changes involved in their production than does the original postulate concerning altered hybridization (8). This is not to say that the hybridization change does not occur; on the contrary it forms a very vital part of ideas on the nature of these reactions, but does say that the zero-point decrease is not an immediate and obvious consequence of the change.

EXPERIMENTAL

Ethyl-αd_2 alcohol (minimum 98% isotopic purity) supplied by Merck and Co. Ltd. was converted to ethyl-1d_2 *p*-toluenesulphonate by the method of Tipson (21). The crude product was distilled under vacuum; m.p. 30.0° C (uncorrected). A comparison of the nuclear magnetic resonance (N.M.R.) spectrum of this compound with that of an undeuterated sample indicated that the alpha carbon atom was fully deuterated.

Ethyl-αd_2 bromide and ethyl-αd_2 iodide were prepared by heating, to 50° C under a vacuum, ethyl-αd_2 *p*-toluenesulphonate with a 3-mole excess of the appropriate potassium halide in the presence of a small amount of triethylene glycol. The ethyl halide evolved was collected in a trap cooled with liquid N_2 and redistilled at reduced pressure.

Ethyl-αd_2 methanesulphonate was made by shaking, at room temperature for ca. 100 hours, an equimolar solution of ethyl-αd_2 bromide and silver methanesulphonate in acetonitrile. The precipitated silver bromide was removed by filtration and the remaining solution evaporated to dryness at reduced pressure. The residue was extracted with anhydrous ether and, after removal of the ether, the product was distilled under a vacuum. It is considered extremely unlikely that any deuterium exchange could take place during the conversion of the deuterated alkyl *p*-toluenesulphonates to the corresponding alkyl halides and methanesulphonates, for the alkyl groups which we have studied (24). The kinetic purity of the compound was verified by the straight-line kinetic plots which were obtained in all cases. With the techniques which have been developed in this laboratory this test has repeatedly proved to be more sensitive than the normal methods of analysis.

The reduction of acetone with lithium aluminum deuteride (minimum 97.4% isotopic purity) yielded isopropyl-αd alcohol. The reaction was carried out by the standard method, modified by the use of diethylene glycol diethyl ether as solvent and diethylene glycol monobutyl ether as the reagent to decompose the complex aluminum compounds (22, 23). The crude isopropyl-αd alcohol, recovered from the reaction mixture by a simple distillation, was redistilled; boiling range 83.5–85.0° C, $n_D^{22.5} = 1.3762$ (lit. $n_D^{20} = 1.3773$). The N.M.R. spectrum indicated that the alpha carbon atom was fully deuterated.

Isopropyl-αd *p*-toluenesulphonate, bromide, iodide, and methanesulphonate were prepared by a series of reactions analogous to that employed for the ethyl compounds.

n-Propyl-αd_2 bromide (minimum 98% isotopic purity) was purchased from Merck and Co. Ltd. The N.M.R. spectrum showed that the alpha carbon atom was ca. 90% deuterated. This bromide was converted into *n*-propyl-αd_2 benzenesulphonate and methanesulphonate by the silver sulphonate method as described for the ethyl compounds. The iodide was prepared from the benzenesulphonate and potassium iodide.

Can. J. Chem. Downloaded from www.nrcresearchpress.com by 210.87.254.42 on 09/05/12
For personal use only.

For each of the above preparations a parallel reaction was carried out with undeuterated compounds. The products were used to check the rate constants of the protium compounds which had been determined in the course of previous work under the same conditions. Good agreement was obtained in all cases.

ACKNOWLEDGMENTS

We are indebted to Mr. S. E. Sugamori for his skillful measurements of rate constants and would like to acknowledge discussion of synthetic methods with Dr. L. C. Leitch and the help of Dr. W. Raynes with the N.M.R. spectra.

REFERENCES

1. E. S. LEWIS and R. R. JOHNSON. Proc. Chem. Soc. 52 (1958).
2. J. A. LLEWELLYN, R. E. ROBERTSON, and J. M. W. SCOTT. Can. J. Chem. **38**, 222 (1960).
3. E. A. GUGGENHEIM. Phil. Mag. **2**, 538 (1926).
4. R. E. ROBERTSON. Can. J. Chem. **33**, 1536 (1955).
5. Unpublished work.
6. A. STREITWIESER. Chem. Revs. **56**, 639 (1956).
7. A. STREITWIESER. Chem. Revs. **56**, 576, 638 (1956).
8. A. STREITWIESER, R. H. JAGOW, R. C. FAHEY, and S. SUZUKI. J. Am. Chem. Soc. **80**, 2327 (1958).
9. T. Y. WU. Spectra of polyatomic molecules. J. W. Edwards, Ann Arbor, Michigan. 1946. Supplement pp. 362–363.
10. J. W. LINNETT, D. F. HEATH, and P. J. WHEATLEY. Trans. Faraday Soc. **45**, 832 (1949).
11. A. D. WALSH. Discussions Faraday Soc. **18**, 2 (1947).
12. J. W. LINNETT and P. J. WHEATLEY. Trans. Faraday Soc. **45**, 39 (1949).
13. D. F. HEATH and J. W. LINNETT. Trans. Faraday Soc. **44**, 878 (1948).
14. D. F. HEATH and J. W. LINNETT. Trans. Faraday Soc. **44**, 885 (1948).
15. D. F. HEATH and J. W. LINNETT. Trans. Faraday Soc. **44**, 561 (1948).
16. D. F. HEATH and J. W. LINNETT. Trans. Faraday Soc. **45**, 265 (1949).
17. T. SIMANOUTI. J. Chem. Phys. **17**, 245 (1949).
18. T. SIMANOUTI. J. Chem. Phys. **17**, 734 (1949).
19. T. SIMANOUTI. J. Chem. Phys. **17**, 848 (1949).
20. L. S. BARTELL. J. Chem. Phys. **32**, 827 (1960).
21. R. F. TIPSON. J. Org. Chem. **9**, 235 (1944).
22. R. F. NYSTROM, W. H. YANKO, and W. G. BROWN. J. Am. Chem. Soc. **70**, 441 (1948).
23. V. J. SHINER. J. Am. Chem. Soc. **74**, 5285 (1952).
24. L. C. LEITCH. Private communication.

Can. J. Chem. Downloaded from www.nrcresearchpress.com by 210.87.254.42 on 09/05/12
For personal use only.

Can. J. Chem. Downloaded from www.nrcresearchpress.com by 210.87.254.105 on 09/05/12
For personal use only.

ISOLATION AND PROPERTIES OF A GLUCOMANNAN FROM THE WOOD OF RED MAPLE (ACER RUBRUM L.)[1]

A. JABBAR MIAN AND T. E. TIMELL

ABSTRACT

A glucomannan has been isolated from the wood of red maple (*Acer rubrum* L.) in a yield corresponding to 92% of the mannose residues in this wood and with a ratio of mannose to glucose of 2:1. Partial hydrolysis of the polysaccharide yielded 4-*O*-β-D-mannopyranosyl-D-mannose, 4-*O*-β-D-mannopyranosyl-D-glucose, 4-*O*-β-D-glucopyranosyl-D-mannose, 4-*O*-β-D-glucopyranosyl-D-glucose, and *O*-β-D-mannopyranosyl-(1 → 4)-*O*-β-D-mannopyranosyl-(1 → 4)-D-mannose. The methylated glucomannan on hydrolysis gave a mixture of di-*O*-methylhexoses, 2,3,6-tri-*O*-methyl-D-mannose, 2,3,6-tri-*O*-methyl-D-glucose, and 2,3,4,6-tetra-*O*-methyl-D-glucose in a mole ratio of 7:29:13:1. The methylated polysaccharide contained 55 hexose residues per average molecule, while the corresponding value for the nitrate derivative was 67. It is concluded that the glucomannan is composed of a minimum of 70 glucose and mannose residues linked together by (1 → 4)-β-glycosidic bonds to linear molecules. The glucose residues are probably interposed between two or three contiguous mannose residues.

In the last few years, glucomannans have been isolated from the wood of many gymnosperms, where this polysaccharide constitutes the preponderant hemicellulose. Little attention has so far been directed towards the origin of the relatively few mannose residues present in the wood of the arborescent angiosperms. A glucomannan has been isolated from trembling aspen (1) and similar polysaccharides have been obtained also from red alder and from madrona (2). The isolation of a glucomannan from white birch was recently reported (3). This paper is concerned with the isolation of a glucomannan from red maple (*Acer rubrum* L.) and with the properties of this diheteroglycan.

RESULTS AND DISCUSSION

Red maple wood, containing 2.4% mannose residues, was delignified with acid chlorite (4) to give a holocellulose in a yield closely corresponding to the lignin content of the wood. The holocellulose was exhaustively extracted with 24% potassium hydroxide, which removed a pure methylglucuronoxylan. Subsequent extraction with sodium hydroxide – borate (5, 6) gave a mixture containing mannose and glucose residues in a ratio of 1.34:1 in addition to 14% of xylose. One treatment with barium hydroxide (7) removed the xylose containing polysaccharide and increased the above ratio to 1.94:1. The crude and purified products contained 95% and 92%, respectively, of the mannose residues originally present in the wood.

The pure glucomannan, $[\alpha]_D$ −31°, was a white powder, insoluble in water. When oxidized with periodate, it consumed 1.0 mole of oxidant per hexose residue. The number-average molecular weight of the nitrate derivative as determined by osmometry (8) was 18,200, corresponding to a degree of polymerization of 67. Boundary electrophoresis according to Tiselius (9) indicated that the polysaccharide was chemically homogeneous.

A portion of the glucomannan was partially hydrolyzed with aqueous formic acid to give a mixture of sugars which was resolved on a charcoal–Celite (10) column by gradient (11) elution with aqueous ethanol (12). The sugars obtained included D-mannose, 4-*O*-β-D-mannopyranosyl-D-mannose, 4-*O*-β-D-mannopyranosyl-D-glucose, 4-*O*-β-D-glucopyranosyl-D-mannose, 4-*O*-β-D-glucopyranosyl-D-glucose, and *O*-β-D-mannopyranosyl-(1 → 4)-*O*-β-D-mannopyranosyl-(1 → 4)-D-mannose. Mannobiose and glucosyl mannose

[1]*Manuscript received May 20, 1960.*
Contribution from the Pulp and Paper Research Institute of Canada and the Department of Chemistry, McGill University, Montreal, Que.

were isolated in the highest, cellobiose in the lowest, yield. Two tetraose compounds were also obtained crystalline, containing both glucose and mannose residues.

Another portion of the glucomannan was methylated to completion and subsequently hydrolyzed to a mixture of sugars which was resolved on a charcoal–Celite column. A mixture of di-*O*-methylhexoses, 2,3,6-tri-*O*-methyl-D-mannose, 2,3,6-tri-*O*-methyl-D-glucose, and 2,3,4,6-tetra-*O*-methyl-D-glucose was obtained in a mole ratio of 7:29:13:1. The tri-*O*-methylmannose was identified through its characteristic 1,4-di-*p*-nitrobenzoate derivative (13) and the tri- and tetra-*O*-methylglucoses crystallized. The methylated glucomannan contained 55 hexose residues per average molecule as estimated by osmometry.

From the above evidence a tentative structure can now be assigned to the glucomannan present in red maple wood. The large quantity of 2,3,6-tri-*O*-methylhexoses shows that the polysaccharide is composed of (1 → 4)-linked hexose residues and this conclusion is corroborated by the consumption of 1 mole of periodate per hexose residue. The negative rotation of the glucomannan suggests that the linkage is of the β-type. The isolation of 2,3,4,6-tetra-*O*-methyl-D-glucose indicates that most of the non-reducing end groups consist of glucose residues, one such end group being present per 50 anhydrohexose units. Since the average molecule contained 55 hexose residues, the glucomannan contained few, if any, branching points. The occurrence of the di-*O*-methylhexoses was probably due to demethylation during methanolysis and hydrolysis.

The above conclusions were corroborated by the nature of the oligosaccharides formed on partial hydrolysis of the glucomannan. The high yield of mannobiose and mannotriose as compared to the low yield of cellobiose suggests that few of the glucose residues were contiguous. Relatively more glucosyl mannose and more mannosyl glucose were isolated than have previously been obtained from softwood glucomannans (14–16). This is to be expected in view of the lower ratio of mannose to glucose in hardwood as compared with softwood glucomannans. Similarly, mannose has been found to form most of the non-reducing end groups in glucomannans from gymnosperms (16–21), while both the present glucomannan and a similar polysaccharide from white birch wood (22) seem to contain more glucose than mannose end groups.

The glucomannan contained approximately 70 hexose residues per average molecule. This value might not represent the molecular magnitude of the native polymer since acid chlorite was used to delignify the wood (23).

The present polysaccharide is the first representative hardwood glucomannan whose structure has been determined in detail, and direct comparison with other glucomannans of similar origin is therefore not possible. Methylation studies of the glucomannan previously isolated from aspen wood (1) indicated the presence of a (1 → 4)-linked polysaccharide with a ratio between glucose and mannose of 1:2. A glucomannan from western red alder (2) has been reported to contain glucose and mannose in a ratio of 1:1.5. For a birch glucomannan (3) this ratio was 1:1.1. Subsequent investigations of other hardwood glucomannans (24) have shown that while the ratio of mannose to glucose is close to 1.0 for birches, most other hardwoods exhibit a ratio of 1.5–2.

Glucomannans from gymnosperms usually contain approximately three times as many mannose as glucose residues. The glucomannans present in arborescent angiosperms appear to have a higher relative content of anhydroglucose units. Apart from this discrepancy, there seem to be few differences between hardwood and softwood glucomannans. Both types of polysaccharides consist of essentially linear macromolecules composed of 100–200 (1 → 4)-linked β-D-hexose residues, probably with many of the glucose residues interposed as single units between several contiguous mannose residues. Relative sugar

Can. J. Chem. Downloaded from www.nrcresearchpress.com by 210.87.254.105 on 09/05/12
For personal use only.

composition and relative abundance are therefore the only two respects in which softwood and hardwood glucomannans differ in any essential way.

EXPERIMENTAL

All specific rotations are equilibrium values unless otherwise stated and were determined at 20° C. Melting points are corrected. Evaporations were carried out *in vacuo* at 40–50° C.

Paper Chromatography

Solvent systems used for separating sugars were (v/v): (A) ethyl acetate – acetic acid – water (9:2:2), (B) butan-1-ol–pyridine–water (10:3:3), and (C) butanone–water (89:11). Whatman No. 1 filter paper and the descending technique were used. Paper electrophoresis was carried out with Whatman No. 3 MM filter paper in 0.05 *M* borate buffer at 750 volts. The spray reagent was *o*-aminodiphenyl (25).

Wood

Logs from a freshly cut red maple were barked, chipped, and converted to sawdust. The 20–80 mesh fractions were exhaustively extracted with ethanol–benzene (1:2 v/v), extracted with cold water, and dried in the air. The following data were obtained by standard analytical procedures: cellulose (44.1%), lignin (24.0%), ash (0.2%), acetyl (3.8%), uronic anhydride (3.5%), residues of galactose (0.6%), glucose (46.6%), mannose (2.4%), arabinose (0.5%), and xylose (14.8%).

Isolation of a Crude Glucomannan

Extractive-free wood meal (1080 g) was suspended with stirring in water (18 liters) at 70–80° C. Acetic acid (120 ml) and sodium chlorite (360 g) were added every hour for a total period of 7 hours (4). The reaction mixture was cooled, and the solids were washed by decantation with tap water. They were then transferred to a filter and washed with distilled water and ethanol. The white product was dried in the air to yield 840 g of holocellulose, 76% of the wood.

The holocellulose (840 g) was shaken in an atmosphere of nitrogen with 24% (w/w) aqueous potassium hydroxide (6 liters) at room temperature for 3 hours. The alkaline extract was removed by filtration through fritted glass and the residue was washed with water. The still wet residue was extracted in the same way with 17.5% sodium hydroxide to which 4% boric acid had been added (5, 6). The alkaline extracts and washings (8 liters) were poured into ethanol (30 liters) containing glacial acetic acid (3 liters). The precipitate formed was washed on the centrifuge with 80% aqueous ethanol, ethanol, and petroleum ether (b.p. 30–60° C), yielding a white powder (40.0 g). Sugar residues in the potassium hydroxide extract were xylose and uronic acids, in the alpha-cellulose (unextracted residue) glucose and traces of xylose. The alkaline borate extract (the crude glucomannan) contained mannose and glucose in a ratio of 1.31:1 and 14% xylose residues.

Purification of the Crude Glucomannan

Crude glucomannan (40 g) was dissolved in 10% sodium hydroxide (1 liter) and 5% aqueous barium hydroxide (2 liters) was added with constant stirring over a period of 2 hours. The precipitate formed was collected by centrifuging, washed twice with water, acidified with acetic acid, and poured into ethanol (5 liters). The precipitate was recovered in the usual way (35 g, 3.3% of the wood). Mannose/glucose: 1.94. Xylose: nil. $[\alpha]_D$ $-31°$ (*c*, 1.0 in 10% sodium hydroxide).

Can. J. Chem. Downloaded from www.nrcresearchpress.com by 210.87.254.105 on 09/05/12
For personal use only.

Partial Hydrolysis of the Glucomannan

Glucomannan (9.7 g) was dissolved in 90% formic acid (50 ml). Water (50 ml) was added and the solution was heated to 95–97° C for 3 hours (14). After cooling, the clear solution was removed by decantation and the solid residue was again hydrolyzed. This treatment was repeated twice. The solutions were combined and the formic acid was removed by evaporation with water. Formate esters were hydrolyzed with 0.5 *N* sulphuric acid at 100° for 10 minutes (100 ml). After neutralization with barium carbonate, filtration through Celite, and treatment with Amberlite IR-120 exchange resin, evaporation gave a clear sirup (7.5 g). Paper chromatography (solvents A and B) indicated the presence of hexoses and hexose oligosaccharides.

Resolution of the Hydrolyzate

The partial hydrolyzate (7.5 g) was dissolved in water (50 ml) and added to the top of a Darco G-60 – Celite column (10) (6×64 cm). Gradient elution (11) was carried out with 3 liters each of the following solvents: 2% aqueous ethanol → 10% ethanol, 10% ethanol → 20% ethanol, and 20% ethanol → 40% ethanol. Fractions, 25 ml each, were collected at an average rate of two per hour and the sugar content of every third fraction was estimated by paper chromatography (solvent B).

Identification of Sugars

All sugars moved on the paper chromatogram (solvents A and B) at the same rate as authentic specimens.

(1) Monosaccharides

Following a mixture of glucose and mannose with a trace of xylose (1.45 g), pure D-mannose (1.82 g) was eluted from the column, m.p. and mixed m.p. 132° C, $[\alpha]_D$ +12.8° (*c*, 2.3 in water). The mannose phenylhydrazone had a melting point and mixed melting point of 194° C.

(2) 4-O-β-D-Mannopyranosyl-D-mannose

Hydrolysis of this compound (790 mg) gave only mannose. The mannobiose, after recrystallization from methanol, had a melting point and mixed melting point of 200–201° C, $[\alpha]_D$ −8.5° (*c*, 1.0 in water).

(3) 4-O-β-D-Mannopyranosyl-D-glucose

Hydrolysis of this fraction (193 mg) gave equal amounts of mannose and glucose. After reduction with sodium borohydride, mannose only was obtained on hydrolysis. The compound, $[\alpha]_D$ +27° (*c*, 1.5 in water), could not be induced to crystallize, nor could the derived octaacetate derivative be obtained in crystalline form.

(4) O-β-D-Mannopyranosyl-(1 → 4)-O-β-D-mannopyranosyl-(1 → 4)-D-mannose

This fraction (171 mg) readily crystallized from methanol containing some water and butan-1-ol, m.p. and mixed m.p. 230–232° C, $[\alpha]_D$ −25° (*c*, 1.3 in water). Partial hydrolysis followed by examination by paper chromatography suggested the presence of unchanged mannotriose, mannobiose, and mannose. Complete hydrolysis gave mannose.

(5) 4-O-β-D-Glucopyranosyl-D-glucose

This disaccharide (30 mg) on recrystallization from aqueous methanol had melting point and mixed melting point 226–227° C, $[\alpha]_D$ +24° (*c*, 1.0 in water). Complete hydrolysis gave only glucose.

Can. J. Chem. Downloaded from www.nrcresearchpress.com by 210.87.254.105 on 09/05/12
For personal use only.

(6) 4-O-β-D-Glucopyranosyl-D-mannose

The disaccharide (663 mg) on hydrolysis gave equal amounts of glucose and mannose. The compound, when recrystallized from ethanol, had melting point and mixed melting point 137–138° C, $[\alpha]_D$ +11° → +6° (*c*, 1.0 in water).

(7) Hexotetraose Fraction

This fraction (23 mg) had a melting point of 237–238° C. Partial hydrolysis with formic acid gave glucosyl mannose, glucose, and mannose. The degree of polymerization was estimated as 4.1 (26).

(8) Hexotetraose Fraction

This compound had a melting point of 210–212° C (20 mg). Partial hydrolysis yielded a hexotriose, glucosyl mannose, glucose, and mannose. The degree of polymerization was 4.2 (26).

Methylation of the Glucomannan

Glucomannan (13 g) was dissolved in 40% (w/w) aqueous sodium hydroxide in an atmosphere of nitrogen and dimethyl sulphate (250 ml) was added dropwise over a period of 48 hours. This process was repeated three times. Solid sodium hydroxide (200 g) was added, followed by dimethyl sulphate (250 ml). This treatment was repeated six times, water being added whenever necessary for efficient stirring. The reaction mixture was neutralized with sulphuric acid to pH 4 and then heated to boiling. The precipitated polysaccharide was recovered by filtration and washed briefly with hot water. Yield, 7.5 g; OCH_3, 44.3%.

The material (7.0 g) was dissolved in dry dimethyl formamide (150 ml) (27) and treated with methyl iodide (50 ml) and silver oxide (50 g) for 48 hours at room temperature. The polysaccharide was recovered in the usual way (27) to yield 4.9 g of material. The infrared diagram indicated the absence of hydroxyl groups.

Hydrolysis of the Methylated Glucomannan and Resolution of the Hydrolyzate

Methylated glucomannan (3.5 g) was boiled under reflux with 0.7 *N* methanolic hydrogen chloride for 7 hours and subsequently with *N* hydrochloric acid for 7 hours. The solution was neutralized with silver carbonate, filtered through Celite, treated with hydrogen sulphide, again filtered through Celite, and finally evaporated to give a clear sirup (3.1 g). Paper chromatography (solvent C) indicated the presence of di-, tri-, and tetra-*O*-methylhexoses.

The hydrolyzate (3.0 g) was added to the top of a column (5×56 cm) containing a 1:1 mixture of Darco G-60 charcoal and Celite. Gradient elution was effected with 3 liters each of the following solvents: 5% aqueous ethanol → 10% ethanol, 10% ethanol → 30% ethanol, and 30% ethanol → 60% ethanol. The resolution was followed by paper chromatography (solvent C) and, for the tri-*O*-methylhexoses, by measuring the optical rotation of the fractions.

(1) Di-O-methylhexoses

This fraction (290 mg) on demethylation with hydrobromic acid (28) gave glucose and mannose on the paper chromatogram.

(2) 2,3,6-Tri-O-methyl-D-mannose

The sirup (1355 mg), $[\alpha]_D$ −12.5° (*c*, 1.2 in water), was converted to the characteristic di-*p*-nitrobenzoate derivative (13), m.p. and mixed m.p. 186–187° C after recrystallization from ethyl acetate, $[\alpha]_D$ +33° (*c*, 0.5 in chloroform).

Can. J. Chem. Downloaded from www.nrcresearchpress.com by 210.87.254.105 on 09/05/12
For personal use only.

(3) 2,3,6-Tri-O-methyl-D-glucose

This compound (640 mg), $[\alpha]_D$ +41° (*c*, 1.3 in water), could not be induced to crystallize. The 2,3,6-tri-*O*-methyl-D-glucose-1,4-di-*p*-nitrobenzoate (13) had melting point and mixed melting point 190° C, $[\alpha]_D$ −33° (*c*, 0.6 in chloroform).

2,3,4,6-Tetra-O-methyl-D-glucose

The last fraction (51 mg), on standing, crystallized. Recrystallization from hot petroleum ether gave melting point and mixed melting point 89–90° C. A portion of the original sirup on demethylation (28) yielded glucose and a trace of mannose. The fraction was thus mainly 2,3,4,6-tetra-*O*-methyl-D-glucose.

Periodate Oxidation of the Glucomannan

The glucomannan (150–200 mg) was oxidized in the dark for various lengths of time with 50.0 ml of 0.05 *M* sodium metaperiodate. Consumption of oxidant was measured by the excess arsenite method. Extrapolation to zero time indicated a consumption of periodate of 1.0 mole per hexose residue.

Determination of Number-Average Molecular Weights

The glucomannan was converted to its nitrate ester as described previously (30, 31). Osmotic pressure measurements were carried out as reported elsewhere (16, 29). The solvent for the methylated glucomannan was a 9:1 (v/v) mixture of chloroform and ethanol, and for the nitrate derivative *n*-butyl acetate. The experimental results are presented in Table I. Number-average molecular weights ($\bar{M}_n$) were calculated from the relationship $\bar{M}_n = 25{,}700/(h/w)_{w=0}$.

TABLE I

Osmometry data

Methylated glucomannan			Nitrated glucomannan		
w*	h†	h/w	w	h	h/w
2.464	5.791	2.350	3.368	5.077	1.508
1.896	4.375	2.307	3.356	4.900	1.460
1.662	4.030	2.425	2.262	3.206	1.417
1.020	2.385	2.338	1.124	1.625	1.445
0	—	2.32	0	—	1.41

*Concentration in grams/kilogram of solution.
†Osmotic height in centimeters of solution.

Boundary Electrophoresis

The glucomannan was dissolved to a concentration of 1–2% in a buffer solution containing 7.50 g of boric acid and 4.0 g of sodium hydroxide per liter (30). The instrument was a Spinco Model H apparatus. Only one maximum was observed at various intervals of time, in addition to a stationary salt boundary.

ACKNOWLEDGMENT

The authors wish to express their gratitude to the National Research Council of Canada for financial support.

REFERENCES

1. J. K. N. JONES, E. MERLER, and L. E. WISE. Can. J. Chem. **35**, 634 (1957).
2. J. K. HAMILTON and N. S. THOMPSON. Pulp Paper Mag. Can. **59** (10), 233 (1958); Tappi, **42**, 752 (1959).

Can. J. Chem. Downloaded from www.nrcresearchpress.com by 210.87.254.105 on 09/05/12
For personal use only.

3. T. E. TIMELL. Chem. & Ind. (London), 905 (1958).
4. L. E. WISE, M. MURPHY, and A. A. D'ADDIECO. Paper Trade J. **122** (2), 35 (1946).
5. J. K. N. JONES, L. E. WISE, and J. P. JAPPE. Tappi, **39**, 139 (1956).
6. J. K. HAMILTON and J. R. QUIMBY. Tappi, **40**, 781 (1957).
7. H. MEIER. Acta Chem. Scand. **12**, 144 (1958).
8. C. P. J. GLAUDEMANS and T. E. TIMELL. Svensk Papperstidn. **61**, 1 (1958).
9. A. TISELIUS and P. FLODIN. Advances in Protein Chem. **8**, 461 (1953).
10. R. L. WHISTLER and D. F. DURSO. J. Am. Chem. Soc. **72**, 677 (1950).
11. R. S. ALM. Acta Chem. Scand. **6**, 1186 (1952).
12. B. LINDBERG and B. WICKBERG. Acta Chem. Scand. **8**, 569 (1954).
13. P. A. REBERS and F. SMITH. J. Am. Chem. Soc. **76**, 6097 (1954).
14. J. K. N. JONES and T. J. PAINTER. J. Chem. Soc. 669 (1957); 573 (1959).
15. A. TYMINSKI and T. E. TIMELL. J. Am. Chem. Soc. In press.
16. M. O. GYAW and T. E. TIMELL. Can. J. Chem. In press. 1960.
17. I. CROON and B. LINDBERG. Acta Chem. Scand. **12**, 453 (1958).
18. J. K. HAMILTON, E. V. PARTLOW, and N. S. THOMPSON. J. Am. Chem. Soc. **82**, 451 (1960).
19. J. K. HAMILTON and H. W. KIRCHER. J. Am. Chem. Soc. **80**, 5703 (1958).
20. G. G. S. DUTTON and K. HUNT. J. Am. Chem. Soc. **80**, 5697 (1958).
21. I. CROON, B. LINDBERG, and H. MEIER. Acta Chem. Scand. **13**, 1299 (1959).
22. T. E. TIMELL. Unpublished results.
23. C. P. J. GLAUDEMANS and T. E. TIMELL. Svensk Papperstidn. **60**, 869 (1957).
24. T. E. TIMELL. Svensk Paperstidn. In press.
25. T. E. TIMELL, C. P. J. GLAUDEMANS, and A. L. CURRIE. Anal. Chem. **28**, 1916 (1956).
26. S. PEAT, W. J. WHELAN, and J. G. ROBERTS. J. Chem. Soc. 2258 (1956).
27. R. KUHN, H. TRISCHMANN, and I. LÖW. Angew. Chem. **67**, 32 (1955).
28. L. HOUGH, J. K. N. JONES, and W. H. WADMAN. J. Chem. Soc. 1702 (1950).
29. W. J. ALEXANDER and R. L. MITCHELL. Anal. Chem. **21**, 1497 (1949).
30. A. B. FOSTER. J. Chem. Soc. 982 (1953).

Can. J. Chem. Downloaded from www.nrcresearchpress.com by 210.87.254.105 on 09/05/12
For personal use only.

Can. J. Chem. Downloaded from www.nrcresearchpress.com by 210.87.254.6 on 09/05/12
For personal use only.

PROTONATION OF THE AMIDE GROUP

I. THE BASICITIES OF SUBSTITUTED BENZAMIDES[1]

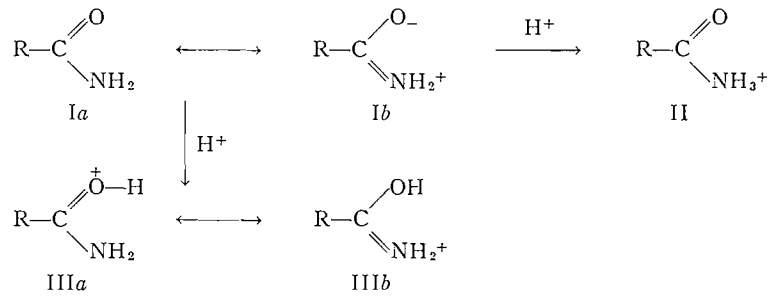
J. T. EDWARD,[2] H. S. CHANG,[2] K. YATES,[3] AND ROSS STEWART[3]

ABSTRACT

The basicities of benzamide and of 11 meta- and para-substituted benzamides in sulphuric acid media have been determined by a spectrophotometric method. The pK_{BH^+} values of the protonated benzamides were found to be proportional to the Hammett σ constants for the substituents, unlike the pK_{BH^+} values of the protonated benzaldehydes, acetophenones, and benzoic acids, which are approximately proportional to σ^+ constants. The lack of conjugation between the protonated amide group and the ring, which is indicated by these results, is most easily interpreted in terms of N-protonation although O-protonation cannot be completely excluded. Various other aspects of the problem of N- versus O-protonation are also discussed.

INTRODUCTION

While it has been known for a long time that amides behave as moderately strong Brønsted bases in mineral acids (1), taking up one proton (2, 3), the structure of the ion formed is still debated. Two alternative sites are available for attachment of the proton, the amino nitrogen or the carbonyl oxygen. In 1931 Hantzsch (4) presented evidence for the O-protonated form (III; R = Ph) for benzamide (I; R = Ph) in concentrated



sulphuric acid, by noting the similarity of the ultraviolet absorption spectrum of this solution with that of ethyl benzimidate in acid. The protonated form of the latter compound can only have the structure Ph—C(OEt)=NH_2^+. The later work of Mizushima *et al.*, who studied the ultraviolet absorption of N-methylacetamide in acid, appeared to indicate N-protonation (5), but has not been confirmed (6).

Huisgen and Brade (7) presented arguments in favor of O-protonation based on the orders of basicities of substituted amides. However, their arguments involve several questionable assumptions and cannot be considered conclusive. Further evidence for O-protonation has come from studies of amides in neutral and in acid solution by nuclear magnetic resonance (8, 9, 10, 11, 12). In neutral solution it can be shown that there is a barrier to rotation about the C–N linkage, presumably because of its partial double bond character due to the resonance (I*a* ↔ I*b*). A barrier to rotation is found also for

[1]*Manuscript received May 24, 1960.*
Contribution from the Departments of Chemistry, McGill University, Montreal, Que., and the University of British Columbia, Vancouver, B.C.
[2]*McGill University, Montreal, Que.*
[3]*University of British Columbia, Vancouver, B.C.*

amides in strong acid, as would be expected for the O-protonated form (III*a* ↔ III*b*), but not for the N-protonated form (II). However, in moderate concentrations of acid, nuclear magnetic resonance (n.m.r.) studies indicate that some N-protonation also occurs, although it has been considered that probably O-protonation predominates (11). This interpretation of the n.m.r. results has been criticized by Spinner (13), who has suggested that they are more in accord with N-protonation.

On theoretical grounds, it has been generally considered (14, 15) that the O-protonated form (III) should be preferred over the N-protonated form (II) because it preserves the resonance stabilization (III*a* ↔ III*b*) characteristic of the amide molecule itself (I*a* ↔ I*b*). Spinner, who has supported the concept of N-protonation (16), has taken the view that π electrons are not delocalized in conjugated systems (17). This idea, which will be unacceptable to many, should not be considered central to the problem. Undoubtedly, ion III possesses much more resonance energy than does ion II. The latter's total energy, however, may still be the lower of the two.

Evidence favoring N-protonation exists in the observed decreases in the N—H and increases in the C=O stretching frequencies in the infrared and Raman region (5, 16, 18, 19, 20). Particularly significant has been the evidence for an N-protonated structure for the urea cation (18), since it has been considered that for this ion the O-protonated structure is, even more than for amide conjugate acids, favored by the possibilities for resonance stabilization (15).*

It is apparent that further evidence on the structure of protonated amides is desirable. In the present paper we report the effect of meta- and para-substitution on the pK_{BH^+} of benzamide. If protonation takes place on the nitrogen, no direct resonance interaction between the charged center and the substituent is possible, and it should be expected that the pK_{BH^+} values should be proportional to σ, Hammett's constant for the substituent (22). On the other hand, if protonation takes place on the oxygen, then (as in the case of substituted acetophenones (23) and benzaldehydes (24)) direct resonance interaction is possible between the substituent and the charged carbonyl group, and one would expect pK_{BH^+} to be proportional to σ^+ (25, 26) or at least to deviate from a linear σ relation. This method has been used to show that carbonyl oxygen protonation occurs in the case of the carboxyl group since the pK_{BH^+} values are approximately proportional to σ^+ (27).

EXPERIMENTAL

Materials

N-Methyl- and N,N-dimethylbenzamide were prepared by the method of Galat and Elion (28) from benzamide and methylamine hydrochloride and from benzamide and dimethylamine hydrochloride respectively. The other amides were commercial products, or were prepared by standard methods from the acids or acid chlorides. N,N-Dimethylbenzamide was obtained as a liquid, b.p. 135°–137° C at 16 mm (lit. b.p. 132°–133° C at 15 mm (29)); its ultraviolet spectrum in water was identical with that found by Ley and Specker (30). The other amides were solids, and were recrystallized from alcohol to constant melting point, which in all cases was close to values reported in the literature. Sulphuric acid of various concentrations was prepared and standardized following methods already described (23, 24).

**The validity of the identification of the carbonyl stretching band in these salts is currently being tested with the use of oxygen-18 labelled compounds (21).*

Can. J. Chem. Downloaded from www.nrcresearchpress.com by 210.87.254.6 on 09/05/12
For personal use only.

Can. J. Chem. Downloaded from www.nrcresearchpress.com by 210.87.254.6 on 09/05/12
For personal use only.

Procedure

Absorption spectra of the benzamides in water and in various concentrations of sulphuric acid were measured at 25±0.1° according to published methods (23, 24). Solutions in water and in 59–69% acid (see Table I) were used to locate the wavelengths of

TABLE I

Absorption spectra of substituted benzamides and acetophenones

	Benzamides				Acetophenones†	
	In water		In 59.0% H_2SO_4*		in 44.0% H_2SO_4	
Substituent	λ_{max} (mμ)	ϵ_{max}	λ_{max} (mμ)	ϵ_{max}	λ_{max} (mμ)	ϵ_{max}
Hydrogen	225	9100	245 (*a*)	11950	250	11500
m-Methyl	231	9770	250	11500	252	7590
p-Methyl	238	11500	258 (*b*)	14400	260	
m-Methoxy	(231)‡	7240	251	8510	253	8910
p-Methoxy	253	14800	282	16900	282	13800
m-Chloro	(229)‡	7460	245 (*c*)	9530	248	8920
p-Chloro	237	12600	256	14800	258	15000
m-Bromo	(232)‡	8130	247	10000	248	8710
p-Bromo	242	13500	261	15500	270	
p-Fluoro	229	8860	248 (*c*)	11960	250	10980
m-Nitro	215	20600	229 (*d*)	21100	232	17000
p-Nitro	266	11200	264 (*e*)	14460	270	13500
N-Methyl	(226)‡	10000	242	12000		
N,N-Dimethyl	218	7250	236	8320		

*Except in the following instances: (*a*) 59.3% H_2SO_4, (*b*) 57.2% H_2SO_4, (*c*) 60.0% H_2SO_4, (*d*) 64.0% H_2SO_4, (*e*) 69.7% H_2SO_4.

†Ref. 23.

‡Shoulder.

maximal absorption of the unprotonated (λ_u) and protonated (λ_l) forms respectively. Distinct maxima were obtained in all cases except for the unionized forms of *m*-chloro- (Fig. 1), *m*-bromo-, *m*-methoxy-, and N-methyl-benzamide, which showed only shoulders on the sides of more intense peaks situated in the vacuum ultraviolet region. In these cases readings of the absorption of the unionized form were taken at several wavelengths in the vicinity of the shoulder, and those wavelengths chosen to represent λ_u which resulted in the smoothest plots of $\epsilon(\lambda_l) - \epsilon(\lambda_u)$ against H_0.

2-Furamide in water had λ_{max} 253 mμ, ϵ_{max} 12,400, and in 59.0% H_2SO_4 λ_{max} 275 mμ, ϵ_{max} 14,900, and was investigated in the same way as the benzamides.

Hydrolysis of the amides was shown to be negligible in the time required for measurements by periodic checks of the measurements of absorption in the acidity range known to give maximal rates of hydrolysis (31). After several hours standing these showed variations of less than 2%.

Calculation of pK_{BH^+} Values

The pK_{BH^+} values were determined by the graphical method of Davis and Geissman (32) as used previously by Stewart and Yates (23, 24), and are listed in Table II for the benzamides; 2-furamide had a pK_{BH^+} of −2.61. *m*-Nitrobenzamide in water showed two well-defined absorption peaks (Fig. 2), and two pK_{BH^+} values were obtained depending on the wavelength chosen for $\epsilon(\lambda_u)$. In the absence of medium effects these values should be identical; the difference between them is a measure of the precision of the

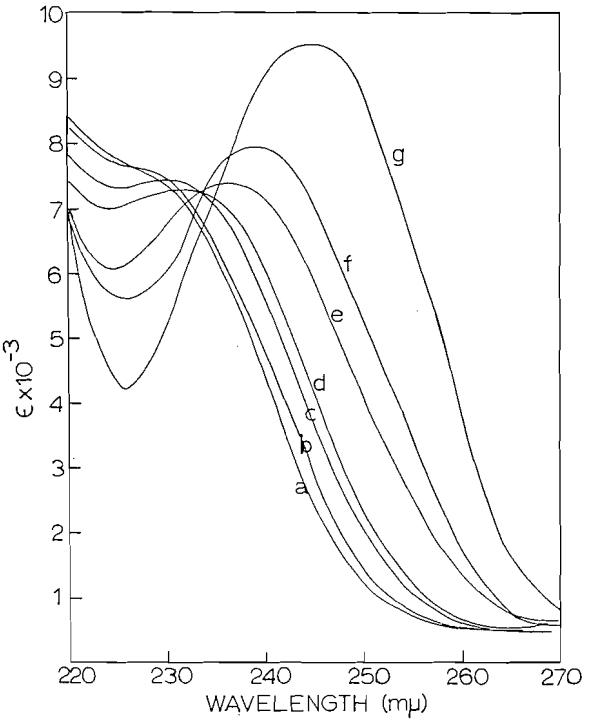


FIG. 1. Absorption spectra of *m*-chlorobenzamide in the following concentrations of aqueous sulphuric acid: *a*, 0%; *b*, 12.8%; *c*, 26.9%; *d*, 31.2%; *e*, 41.0%; *f*, 46.4%; *g*, 60.0%.

TABLE II

pK_{BH^+} values of substituted benzamides

Substituent		$-pK_{BH^+}$	Substituent constants*	
			σ	σ^+
Hydrogen		2.16	0	0
m-Methyl		2.15	−0.069	−0.066
p-Methyl		2.01	−0.170	−0.311
m-Methoxy		2.35	0.115	0.047
p-Methoxy		1.80	−0.268	−0.778
m-Chloro		2.59	0.373	0.399
p-Chloro		2.47	0.227	0.114
m-Bromo		2.75	0.391	0.405
p-Bromo		2.47	0.232	0.150
p-Fluoro		2.24	0.062	−0.073
m-Nitro	2.99 (*a*)† 3.14 (*b*)	3.07	0.710	0.674
p-Nitro		3.23	0.778	0.790
N-Methyl		2.13		
N,N-Dimethyl		1.62		

*Refs. 25, 26, and 33.

†(*a*) From plots of $\epsilon_{260} - \epsilon_{230}$ against H_0. (*b*) From plots of $\epsilon_{225} - \epsilon_{320}$ against H_0.

results. The basicities determined for benzamide and for *p*-methoxybenzamide differ slightly from values previously reported (31), probably in part because of the different graphical method used in analyzing the earlier results.

Can. J. Chem. Downloaded from www.nrcresearchpress.com by 210.87.254.6 on 09/05/12
For personal use only.

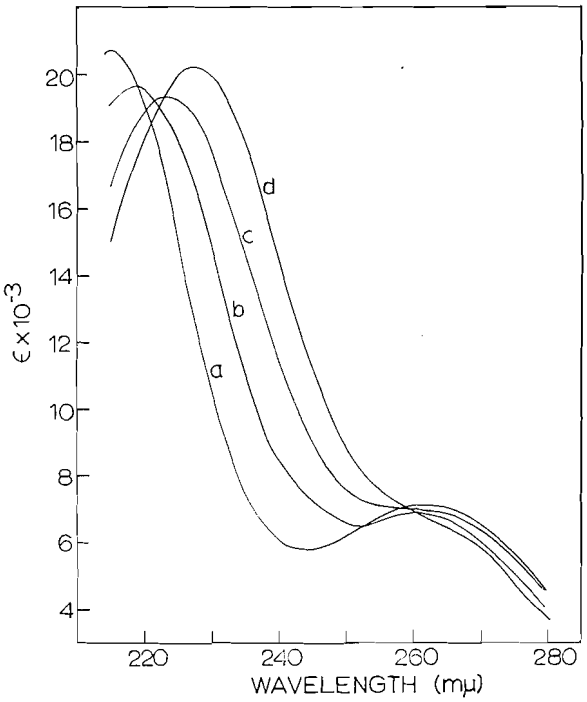


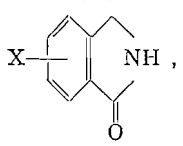
FIG. 2. Absorption spectra of *m*-nitrobenzamide in the following concentrations of aqueous sulphuric acid: *a*, 0%; *b*, 41.0%; *c*, 56.8%; *d*, 60.0%.

RESULTS AND DISCUSSION

The Basicities of Meta- and Para-Substituted Benzamides

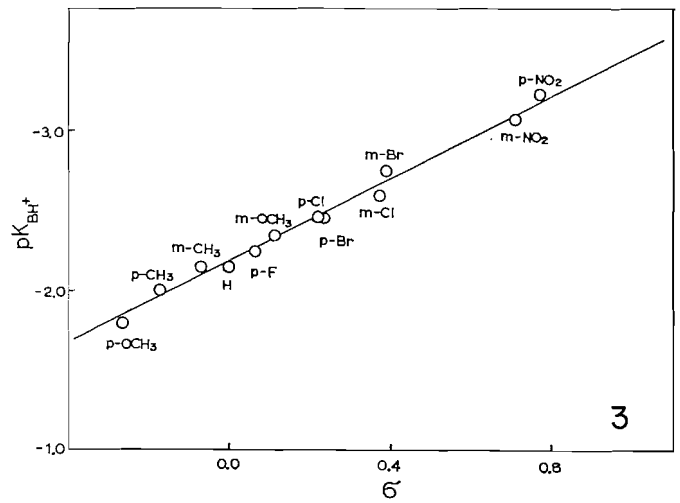
In Figs. 3 and 4 the pK_{BH^+} values of the substituted benzamides are plotted against σ and σ^+ respectively (33). It can be seen that in the first case a good linear relationship is obtained ($r = 0.988$) with the usual precision (34) found for this type of ionization. The value of ρ (by the method of least squares) is 1.30. The correlation of pK_{BH^+} with σ^+ (Fig. 4) is much poorer ($r = 0.958$). The straight line has been drawn with respect to the groups *m*-methyl, *m*-bromo, and hydrogen, since the σ and σ^+ values of these groups are very close. In this case a large deviation is observed for *p*-methoxy, which is able to supply electrons by resonance to the carbonyl group. A correlation with σ^+ can only be attributed to O-protonation. A correlation with σ tells us that para substituents are not in conjugation with the protonated amide group. The most attractive explanation for this is that N-protonation has occurred. It is conceivable, however, that O-protonation has taken place and the lack of conjugation is due to lack of planarity between the ring and the protonated amide group. In other words, the extra resonance stabilization provided by the ring and its substituents might not be sufficient to cause coplanarity.*

**An attempt has been made to eliminate this possibility by examining the phthalimidine series,*



in which coplanarity is enforced. However, the precision in measuring the basicities of phthalimidine ($pK_{BH^+} = -2.1$) and its 6-nitro derivating ($pK_{BH^+} \approx -3.1$) was found to be lower than for the benzamides and further work was not considered worth while (35).

Can. J. Chem. Downloaded from www.nrcresearchpress.com by 210.87.254.6 on 09/05/12
For personal use only.



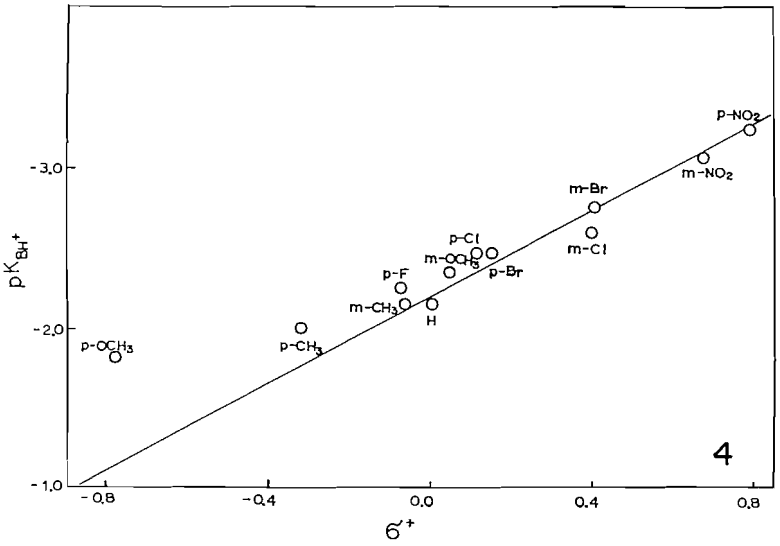
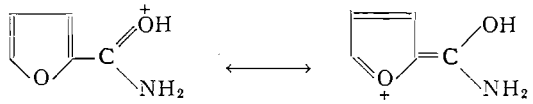


FIG. 3. pK_{BH^+} for substituted benzamides plotted against Hammett's σ constants.
FIG. 4. pK_{BH^+} for substituted benzamides plotted against Brown's σ^+ constants.

The Basicity of Furamide

Furoic acid is a stronger acid ($pK_{HA} = +3.18$) than benzoic acid ($pK_{HA} = +4.20$) (22), the net electron pull due to the inductive and resonance polar effects (36) of the furyl group evidently being greater than that of the phenyl group. This effect would be expected to make furamide a weaker base than benzamide, as is observed, if protonation takes place on the nitrogen and hence only inductive and resonance polar effects operate. In fact, we find that 2-furamide ($pK_{BH^+} = -2.61$) is a considerably weaker base than benzamide ($pK_{BH^+} = -2.15$). On the other hand, if protonation took place on the carbonyl oxygen the direct resonance interaction possible between the ring oxygen and the protonated carbonyl group (IV*a* ↔ IV*b*) would be expected to make furamide the stronger base.

Can. J. Chem. Downloaded from www.nrcresearchpress.com by 210.87.254.6 on 09/05/12
For personal use only.



IV*a* IV*b*

It turns out, in fact, that resonance of this type is not as important as we had expected it to be. This follows from the fact that 2-furoic acid and benzoic acid, both of which, one can assume, protonate at the carbonyl oxygen (27), actually have similar basicities, −7.3 for 2-furoic acid (35) and −7.2 for benzoic acid (27). It appears that the resonance effect is only large enough to cancel approximately the inductive and resonance polar effects. Thus the support for the N-protonated form provided by the furamide basicity cannot be considered unequivocal.

Ultraviolet Spectra of Protonated Benzamides

A comparison of the spectral characteristics of protonated benzamides with those of similarly substituted unprotonated acetophenones in 44.0% sulphuric acid (Table I) shows them to be closely similar, the positions of the absorption maxima in most cases being within 2–3 mμ of each other. The similarity extends to the general shape of the absorption curves, as shown for acetophenone and protonated benzamide in Fig. 5.

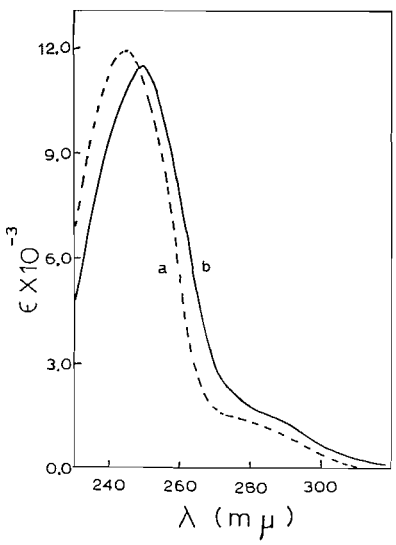


FIG. 5. Absorption spectra of benzamide in 59.3% sulphuric acid (*a*) and of acetophenone in 50% sulphuric acid (*b*). (Latter curve plotted from values from Flexser, Hammett, and Dingwall, J. Am. Chem. Soc. **57**, 2103 (1935).)

The same is true for protonated furamide (in 59.0% H_2SO_4: λ_{max} 275 mμ, ϵ_{max} 14,900), which closely resembles methyl 2-furyl ketone (in H_2O: λ_{max} 275 mμ, ϵ_{max} 13,900 (37)).

These results are to be expected for the N-protonated structures, since it has been observed that replacement of a methyl by an $-NH_3^+$ group has only a minor effect on the ultraviolet spectra of many aromatic compounds (38, 39, 40). It is evident that the absorption characteristics of protonated benzamide are equally compatible with an N- or an O-protonated structure, and are not exclusively in favor of the latter, as Hantzsch (4) assumed.

Can. J. Chem. Downloaded from www.nrcresearchpress.com by 210.87.254.6 on 09/05/12
For personal use only.

ACKNOWLEDGMENT

The financial aid of the National Research Council is gratefully acknowledged.

REFERENCES

1. N. F. HALL. J. Am. Chem. Soc. **52**, 5115 (1930) and references cited there to earlier literature.
2. G. ODDO and E. SCANDOLA. Z. physik. Chem. **66**, 138 (1909).
3. R. J. GILLESPIE and J. A. LEISTEN. Quart. Revs. **8**, 40 (1954).
4. A. HANTZSCH. Ber. **64**, 661 (1931).
5. S. MIZUSHIMA, T. SIMANOUTI, S. NAGAKURA, K. KURATANI, M. TSUBOI, H. BABA, and O. FUJIOKA. J. Am. Chem. Soc. **72**, 3490 (1950).
6. J. BELLO. J. Phys. Chem. **60**, 1341 (1956).
7. R. HUISGEN and H. BRADE. Chem. Ber. **90**, 1432 (1957).
8. J. D. ROBERTS. Nuclear magnetic resonance. McGraw-Hill Book Co., Inc., New York. 1959. p. 69.
9. H. S. GUTOWSKY and C. H. HOLM. J. Chem. Phys. **25**, 1228 (1956).
10. G. FRAENKEL and C. NIEMANN. Proc. Natl. Acad. Sci. U.S. **44**, 688 (1958).
11. A. BERGER, A. LOEWENSTEIN, and S. MEIBOON. J. Am. Chem. Soc. **81**, 62 (1959).
12. W. D. PHILLIPS. J. Chem. Phys. **23**, 1363 (1955).
13. E. SPINNER. J. Phys. Chem. **64**, 275 (1960).
14. L. PAULING. The nature of the chemical bond. Cornell University Press, Ithaca, New York. 1940. p. 208.
15. T. W. J. TAYLOR and W. BAKER. Sidgwick's organic chemistry of nitrogen. Oxford University Press. 1936. pp. 144, 284.
16. E. SPINNER. Spectrochim. Acta, **11**, 95 (1959).
17. E. SPINNER. J. Chem. Soc. 1226. 1960.
18. M. DAVIES and L. HOPKINS. Trans. Faraday Soc. **53**, 1563 (1957).
19. E. H. WHITE. J. Am. Chem. Soc. **77**, 6215 (1955).
20. M. DAVIES and H. E. HALLAN. Trans. Faraday Soc. **47**, 1170 (1951).
21. R. STEWART and L. J. MUENSTER. To be published.
22. L. P. HAMMETT. Physical organic chemistry. McGraw-Hill Book Co., Inc., New York. 1940. p. 184.
23. R. STEWART and K. YATES. J. Am. Chem. Soc. **80**, 6355 (1958).
24. R. STEWART and K. YATES. Can. J. Chem. **37**, 664 (1959).
25. N. C. DENO and W. L. EVANS. J. Am. Chem. Soc. **79**, 5804 (1957).
26. H. C. BROWN and Y. OKAMOTO. J. Am. Chem. Soc. **79**, 1913 (1957).
27. R. STEWART and K. YATES. J. Am. Chem. Soc. In press.
28. A. GALAT and G. ELION. J. Am. Chem. Soc. **65**, 1566 (1943).
29. H. L. WHEELER. Am. Chem. J. **23**, 139 (1900).
30. H. LEY and H. SPECKER. Ber. **72**, 192 (1939).
31. J. T. EDWARD and S. C. R. MEACOCK. J. Chem. Soc. 2000 (1957).
32. C. T. DAVIS and T. A. GEISSMAN. J. Am. Chem. Soc. **76**, 3507 (1954).
33. D. H. MCDANIEL and H. C. BROWN. J. Org. Chem. **23**, 420 (1958).
34. H. H. JAFFÉ. Chem. Revs. **53**, 191 (1953).
35. M. R. GRANGER and R. STEWART. Unpublished results.
36. R. W. TAFT. *In* Steric effects in organic chemistry. *Edited by* M. S. Newman. John Wiley and Sons, Inc., New York. 1956. p. 577 ff.
37. R. F. RAFFAUF. J. Am. Chem. Soc. **72**, 753 (1950).
38. R. N. JONES. Chem. Revs. **32**, 14 (1943).
39. L. DOUB and J. M. VANDENBELT. J. Am. Chem. Soc. **69**, 2714 (1947).
40. J. C. D. BRAND, W. C. HORNING, and M. B. THORNLEY. J. Chem. Soc. 1374 (1952).

Can. J. Chem. Downloaded from www.nrcresearchpress.com by 210.87.254.6 on 09/05/12
For personal use only.

Can. J. Chem. Downloaded from www.nrcresearchpress.com by 210.87.254.105 on 09/05/12
For personal use only.

A RADIOCHEMICAL TECHNIQUE FOR STUDYING RANGE–ENERGY RELATIONSHIPS FOR HEAVY IONS OF KEV ENERGIES IN ALUMINUM[1]

J. A. DAVIES, J. FRIESEN,[2] AND J. D. MCINTYRE[3]

ABSTRACT

A rapid technique has been developed for dissolving successive thin layers of metal from the surface of an aluminum foil: viz. electrochemical oxidation at constant voltage in aqueous ammonium citrate, followed by removal of the oxide film in a phosphoric acid – chromic oxide solution. Due to the highly protective nature of the aluminum oxide film, this two-step process enables very uniform surface layers of metal as thin as 1 $\mu g/cm^2$ to be removed. The total weight of aluminum dissolved increases with the applied anodic voltage at a rate of 0.30 $\mu g\ cm^{-2}\ volt^{-1}$ (approximately 11 Å per volt) over the range 0–150 volts. The technique should be sufficiently sensitive to study the depth of penetration in aluminum of radioactive ions with kinetic energies as low as a few kiloelectron volts.

An approximate value for the range of Na^{24} recoil atoms from the Al^{27} (n,α) reaction was obtained. A more extensive application to range studies is given in the next paper.

INTRODUCTION

A great deal of attention has been devoted in recent years to studying the interaction of charged particles with matter. However, in the energy region below 1 Mev very few experimental data have been obtained on the range of heavy ions. A knowledge of the depth of penetration of ions of kev energies injected into solid materials is of interest from several points of view. It is of value in interpreting radiation damage and sputtering phenomena, and in preparing targets for nuclear research. From a theoretical viewpoint, such an investigation is of primary interest in the determination of the screened-interaction potential and of the mechanism of energy transfer in the elastic nuclear scattering of charged particles.

The current lack of experimental data may be attributed largely to the difficulties encountered in trying to measure extremely small depths of penetration. The mean range of a 45-kev Cs^{137} ion in aluminum, according to the Bohr–Nielsen theory (1), is about 5 $\mu g/cm^2$, or 180 Å. Obviously, for ions of such short range, it would be difficult, if not impossible, to prepare sufficiently thin foils for studying the depth of penetration by conventional stacked-foil techniques.

The present work was undertaken in order to develop a sufficiently sensitive and reliable technique for carrying out range studies with heavy ions in the energy region 1–100 kev. The application of this technique in determining the range of alkali-metal ions as a function of energy will be presented in subsequent papers.

One approach to the problem has been reported recently by Baulch and Duncan (2). They used a gaseous absorber to study the range of radioactive recoil atoms from certain α-decay processes, and observed the effect of pressure on the number of recoil atoms reaching a collector plate. Unfortunately, the method is restricted to those few α-emitting nuclides that have a suitable radioactive daughter. Furthermore, since the energy of the recoil atom cannot be varied, the method is not capable of extensive application.

The approach in this laboratory has been to use a solid absorber, bombard it with a monoenergetic beam of radioactive ions, and then study the depth of penetration of

[1]*Manuscript received March 10, 1960.*
Contribution from the Research Chemistry Branch, Atomic Energy of Canada Limited, Chalk River, Ontario. Issued as A.E.C.L. No. 1059.
[2]*Present address: Department of Chemistry, University of Manitoba, Winnipeg, Manitoba.*
[3]*Present address: Department of Chemistry, Rensselaer Polytechnic Institute, Troy, N.Y., U.S.A.*

Can. J. Chem. Downloaded from www.nrcresearchpress.com by 210.87.254.105 on 09/05/12
For personal use only.

ions into the target by removing successive uniform layers of target material and determining the amount of radioactivity in each. It was evident that mechanical methods would be far too coarse to remove sufficiently thin layers. Direct chemical or electrochemical etching of the surface is sensitive enough, but would almost certainly be non-uniform; corrosion phenomena are known to occur at very different rates at grain boundaries and impurity centers. Bredov and Okuneva (3) used chemical etching in an attempt to study the range of 4-kev Cs^{134} ions in germanium. They found that approximately 25% of the ions were not dissolved even after prolonged etching, and concluded that some of the ions must have penetrated several thousand angstroms into the target. However, this abnormal result could equally well be attributed to non-uniform etching of the surface.

We therefore selected a two-stage process, electrochemical formation of a uniform protective film, followed by chemical removal of the film, as the most promising possibility for further study.

It is well known that certain metals such as aluminum produce a thin highly protective oxide film when subjected to anodic oxidation in a suitable buffered electrolyte. If the oxidation is carried out at constant voltage, then within a few minutes the film thickness approaches an almost constant value. This value increases almost linearly with the applied voltage up to several hundred volts. Furthermore, according to Charlesby (4) the anodic current forming the film depends so markedly on the voltage gradient that the resulting film should be extremely uniform in thickness. Finally, Lewis and Plumb (5) have shown that a hot aqueous solution of phosphoric acid and chromium trioxide will rapidly dissolve the aluminum oxide layer without appreciably attacking the underlying aluminum metal. By using P^{32} and Cr^{51}, they demonstrated that such a treatment replaced the anodic layer with a highly protective mixed oxide film approximately 10 Å thick.

Provided the mixed oxide does not interfere with subsequent anodic oxidation, it should be possible to remove successive uniform layers of aluminum by this two-step process. However, the relationship between film thickness and applied voltage had not been determined previously below 15 volts (approximately 200 Å). It was therefore necessary to investigate film thicknesses at lower voltages in order to obtain sufficient sensitivity for the proposed range studies.

EXPERIMENTAL

Materials

The aluminum targets used throughout this work were prepared from superpure aluminum foil, 0.020-in. thick, by careful manual polishing with successively finer grades of metallurgical paper and then electropolishing for 60 minutes in a perchloric acid – acetic anhydride bath, according to the method outlined by Tegart (6). The resulting surface had a mirror-like finish; and hence surface irregularities must be considerably less than the wavelength of visible light. Immediately before use, each foil was anodized at 100 volts and then dipped in hot phosphoric acid – chromium trioxide solution to remove the resulting thick layer of aluminum oxide. This preanodizing treatment reduced the effective surface area of the foil by approximately 30% (see Fig. 2), presumably by removing submicroscopic irregularities, and gave a reproducibly flat surface.

Anodizing Step

The anodizing bath consisted of an aqueous solution of C.P. ammonium citrate (30 g per liter), maintained at $25 \pm 0.5°$ C in a 200-ml aluminum beaker which served as cathode.

The aluminum sample to be anodized was suspended in the center of the beaker by an aluminum wire, and the desired voltage provided from a bank of storage batteries. In some of the early runs, a calomel reference electrode was occasionally inserted into the bath to measure the voltage across the anodic film. However, except at the start of a run, this voltage was very close to the total applied voltage across the cell; since chloride ion is small enough to penetrate the aluminum oxide film and thereby interfere with the electrolytic process, the use of a reference electrode was discontinued in subsequent runs, and the anodic voltage was assumed to be identical with the total applied voltage.

Film-Stripping Step

Rapid dissolution of these aluminum oxide layers was accomplished by immersing the anodized aluminum samples in a hot aqueous solution of orthophosphoric acid (50 g per liter) and chromium trioxide (30 g per liter). Provided the temperature of the solution was maintained above 90° C, a 2-minute treatment completely removed even a 100-volt film.

Aluminum Analysis

The thickness of the oxide layers was determined by neutron activation analysis. Three samples of known area were cut from each anodized foil, and inserted in a nylon capsule along with an aluminum standard (approximately 100 μg Al wire). The capsule was then irradiated for 30 seconds in the pneumatic carrier (7) of NRX at a flux of 6.8×10^{13} neutrons per square centimeter per second. After irradiation the anodized aluminum was placed in the stripping solution in order to dissolve the oxide layer, and the amount of Al^{28} activity in solution determined with a well-type NaI scintillation counter. By comparing this activity with that obtained from the aluminum standard, which had been dissolved in sodium hydroxide solution to provide comparable geometry and absorption, the amount of aluminum in the oxide layer can be readily calculated. Due to the high neutron flux and rapid delivery time available, the method was sufficiently sensitive to determine 0.1 μg of aluminum. In view of the short half-life of Al^{28} (2.3 minutes), this was considered quite satisfactory.

With the exception of the films formed at zero applied voltage, a standard deviation of less than 5% was obtained. At zero voltage, the deviation was much larger (approximately 20%). This is probably due to the presence of a thin highly protective film produced on the aluminum surface by CrO_3 (5) during the preanodizing treatment. In the absence of an applied potential, this film probably continues to exert sufficient protection, even after removal from the stripping solution, to inhibit partially the subsequent oxidation process.

RESULTS AND DISCUSSION

In order to determine how rapidly the phosphoric acid – chromic oxide stripping solution dissolved an aluminum oxide barrier layer, two pieces of aluminum were anodized at 25 volts, irradiated in NRX, and then immediately immersed in stripping solution, one at 50° C, and the other at 90° C. Aliquots were removed at various times, and counted to determine the amount of aluminum that had dissolved (Table I).

A standard 2-minute treatment is evidently sufficient to remove the oxide layer completely, provided the temperature is maintained at 90° C. At the lower temperature, however, stripping was far from complete, even after 10 minutes.

In order to investigate the relationship between oxide film thickness and anodic voltage, a series of foils were anodized at different voltages from 0 to 30 volts. In each case the electrolysis was carried out at constant voltage for approximately 10 minutes.

Can. J. Chem. Downloaded from www.nrcresearchpress.com by 210.87.254.105 on 09/05/12
For personal use only.

TABLE I

Efficiency of film stripping by H_3PO_4–CrO_3 solution

Time in H_3PO_4–CrO_3 solution (minutes)	c.p.m. of Al^{28} (normalized for decay)	
	At 50° C	At 90° C
0.5	—	42,300
1.0	3,140	42,000
2.0	5,600	43,200
5.0	18,100	44,000
10.0	35,500	43,300

A typical curve of current vs. time is shown in Fig. 1, with a change of abscissa after the first 60 seconds. It is evident that the rate of film formation, which is directly related to the anodic current, falls very rapidly in the first few seconds, but gradually approaches an almost constant value. Walkenhorst (8) showed that, after 1 hour, the rate of film

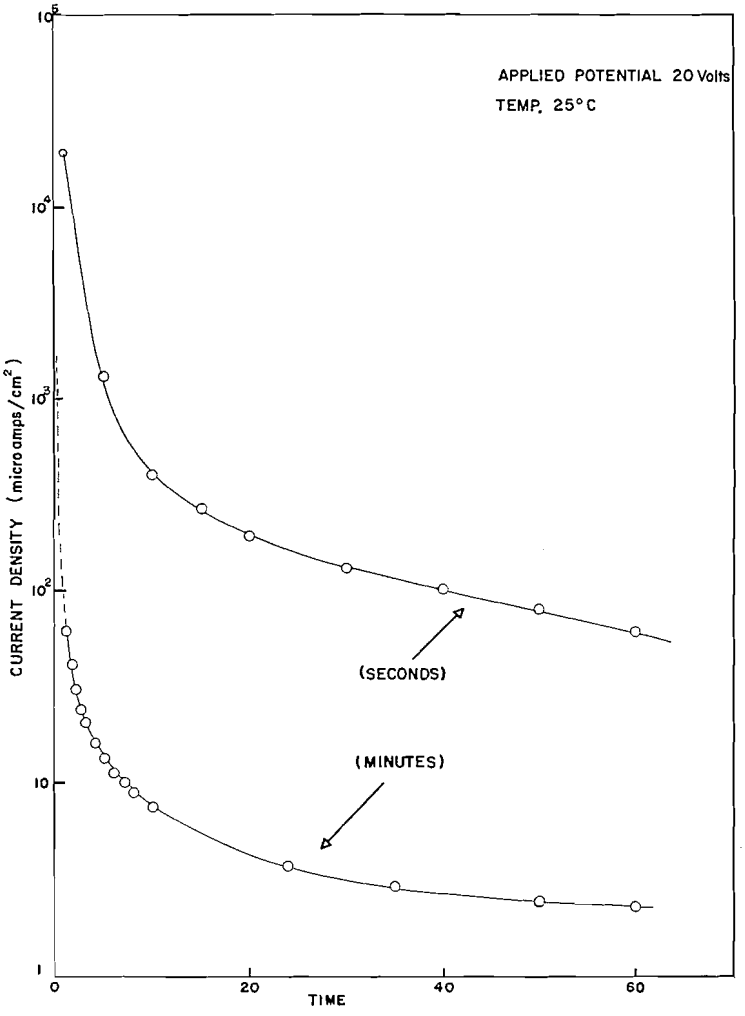


FIG. 1. Anodization of aluminum: current–time relationship.

Can. J. Chem. Downloaded from www.nrcresearchpress.com by 210.87.254.105 on 09/05/12
For personal use only.

growth had decreased to less than 1% per hour. A somewhat shorter time of 10 minutes was selected as the standard anodic treatment in the present investigation, so as to permit future range studies to be carried out with fairly short-lived isotopes. Even after 10 minutes, the film formation current had usually fallen below 7 microamperes/cm^2, which is equivalent to a rate of aluminum oxidation of less than 1 Å per minute.

The effect of voltage on film thickness is illustrated in Fig. 2. Some of the foils had not

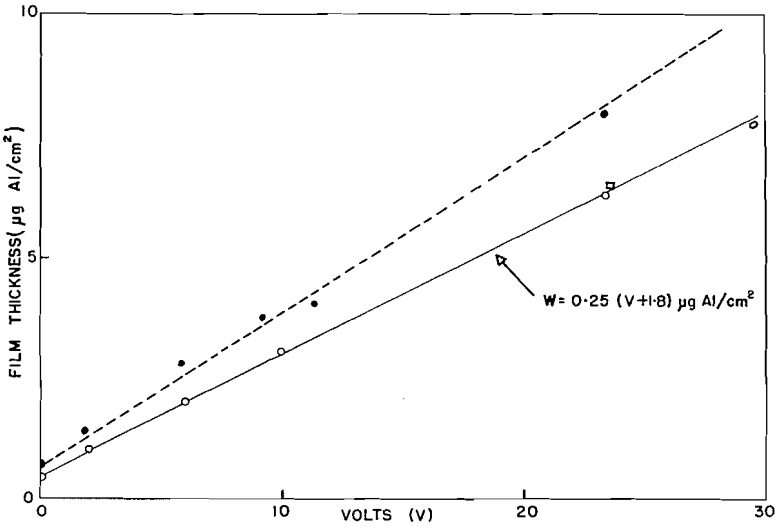


FIG. 2. Graph of film thickness (μg Al cm^{-2}) vs. the applied voltage (V). Number of preanodizing treatments: ● none, ○ one, □ four.

been subjected to any preanodizing treatment. In both cases, a linear relationship was observed. However, with preanodized foils, the slope was considerably less. This can probably be interpreted as a reduction in the true surface area caused by the removal of a thick uniform oxide layer in the preanodizing treatment. No further reduction in surface area occurred even after three additional preanodizing steps. It was concluded, therefore, that one such treatment was sufficient to produce a very reproducible surface. All further work was carried out only with preanodized foils.

The relationship between film thickness (W) in micrograms of aluminum per square centimeter and the applied voltage (V) may be expressed as follows:

$$W = 0.25\times(V+1.8). \qquad [1]$$

The "effective" voltage (1.8 volts) required to account for the observed thickness at zero applied voltage agreed quite closely with the standard electrochemical potential of aluminum of 1.66 volts.

If the oxide consists largely of unhydrated Al_2O_3, as X-ray studies on thicker films suggest (9), then the above value of 0.25 μg cm^{-2} volt^{-1} for the weight of aluminum in the oxide film is equivalent to a total oxide film thickness of 0.475 μg cm^{-2} volt^{-1}. This is in good agreement with previously published values of 0.47 to 0.50 μg cm^{-2} volt^{-1} (8, 10, 11) which were observed at much higher voltages (30–580 volts) by determining the decrease in weight on stripping off the oxide.

Can. J. Chem. Downloaded from www.nrcresearchpress.com by 210.87.254.105 on 09/05/12
For personal use only.

Can. J. Chem. Downloaded from www.nrcresearchpress.com by 210.87.254.105 on 09/05/12
For personal use only.

In order to study the depth of penetration of radioactive ions in aluminum, it is necessary to know the total amount of aluminum removed in the anodizing plus stripping operation. In the above experiments, we have investigated only the amount that is removed during the stripping process, i.e. the thickness of the protective oxide film produced during the anodic oxidation. However, it has been suggested (12, 13) that the efficiency of the anodic current in forming Al_2O_3 may be considerably less than 100%, and that a significant amount of aluminum ion may escape into solution during the anodic process. This would cause the total thickness of aluminum removed to be somewhat greater than that expressed by equation 1.

Several runs were therefore carried out to investigate the existence and importance of this effect. Pieces of aluminum foil were irradiated briefly in NRX, and were then subjected to anodic oxidation and film stripping as before. The amount of Al^{28} activity in both the anodizing and the stripping solutions was measured, and the results are tabulated in Table II. Over the range studied (18–100 volts), the ratio of Al^{28} activities in the

TABLE II

Loss of Al^{+++} during anodizing

Applied voltage, volts	Al^{28} activity (c.p.m.) in:		Ratio, A/B
	Anodizing solution	Stripping solution	
	A	B	
18	2010	9900	0.20
18	1080	5080	0.21
18	1260	7400	0.17
100	8730	41,000	0.21

two solutions remained constant; hence it is evident that a correction of 20% must be applied to equation 1 to account for the loss of aluminum during the anodizing step. The total weight (W) of aluminum removed by anodic oxidation plus film stripping may be expressed as

$$W = 0.30\ (V+1.8). \qquad [2]$$

Due to the short half-life of Al^{28}, the counting rates after 10-minute anodizing treatment had become very small and this investigation could not be extended to lower voltages. However, it would seem reasonable to assume that the fraction of aluminum ions lost in the anodizing step would remain almost constant over the total voltage range of interest to us.

It may be concluded, from the above studies, that layers of aluminum as thin as 1 μg cm^{-2} may be removed rapidly and reproducibly. This would permit range-distribution studies in aluminum to be carried out with radioactive ions having kinetic energies as low as a few kiloelectron volts (see following paper).

Na^{24} *Recoil Atoms*

An additional check on the reproducibility of the anodizing and film-stripping techniques for removing layers of aluminum of known thickness was obtained by studying the distribution of the Na^{24} atoms produced by the (n,α) nuclear reaction on aluminum. Samples of aluminum, wrapped in cadmium to prevent thermal neutron side-reactions, were irradiated for 15 hours in the NRX reactor, and allowed to decay for at least 12 hours to eliminate the short-lived Mg^{27} and Al^{28} activities. The Na^{24} distribution as a

function of depth was then determined by removing successive layers of aluminum of various thicknesses and counting the resulting solutions. A well-type NaI crystal was used as previously, but with a pulse-height selector set to record only those γ-pulses that exceeded 2.0 Mev. Under these conditions, the total contribution from the most significant impurities in superpure aluminum (14), viz. Cu, Ga, Sc, Mn, La, and Co, amounted to less than 0.05% of the Na^{24} activity. It should be noted that, due to the small cross section for the (n,α) reaction, low counting rates of Na^{24} were involved: for example, with a 20-volt film, the Na^{24} activity was approximately 100 c.p.m., which is only three times the background counting rate. Consequently, statistical counting errors were rather large, in some cases, as high as 15%. Thicker oxide films (up to 150 volts) were used in order to reduce this error.

The $Al^{27}(n,\alpha)Na^{24}$ reaction is endothermic by approximately 3.3 Mev, and can only occur with high-energy neutrons. Since fast neutrons are not significantly attenuated in passing through a thin foil of aluminum, it is evident that the rate of production of Na^{24} atoms will be uniform throughout the foil. However, those formed within their recoil range of the surface will have a finite probability of escaping. The Na^{24} distribution, therefore, should increase at first with increasing depth below the original surface, and gradually approach a constant value. A graph of the actual distribution observed in a typical run is shown in Fig. 3. The thickness of each layer was calculated from the anodic voltage by means of equation 2. After about 5000 Å of aluminum was removed, the Na^{24} content did approach a constant value. In Table III, this constant value is compared with the average Na^{24} content for the whole foil. The latter quantity was determined by

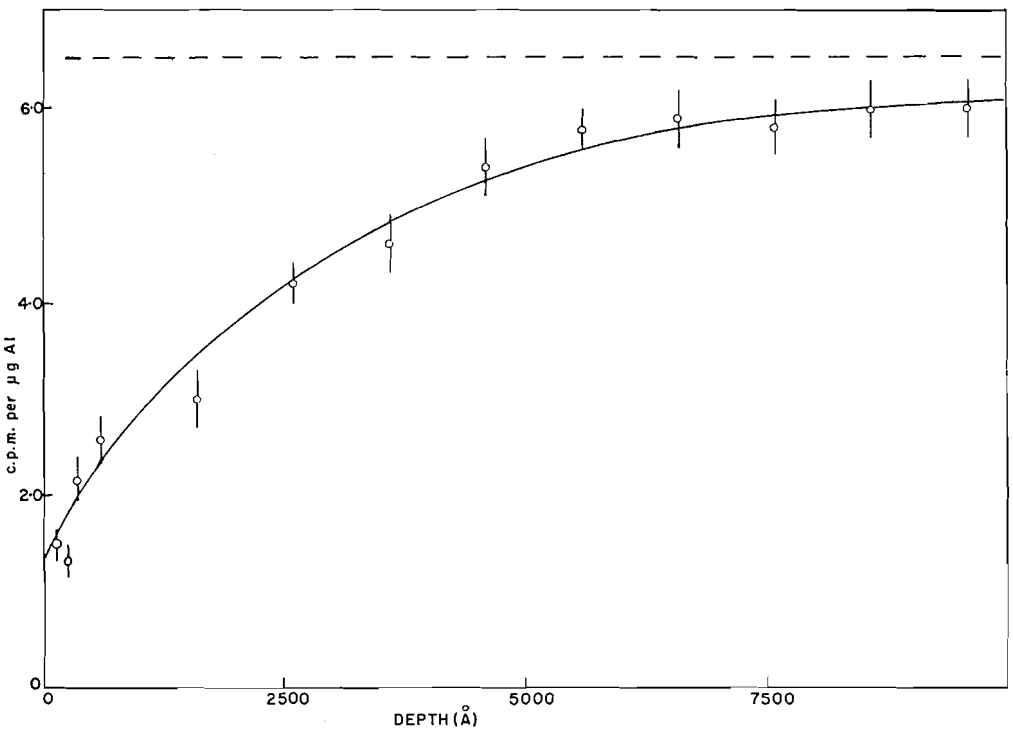


FIG. 3. Distribution of Na^{24} recoil atoms vs. depth below surface of foil. Dotted line represents average Na^{24} content of the whole foil.

Can. J. Chem. Downloaded from www.nrcresearchpress.com by 210.87.254.105 on 09/05/12
For personal use only.

TABLE III

Comparison of Na^{24} content in a thin layer with Na^{24} content for the whole foil

Run No.	Na^{24} content (c.p.m./μg Al) of:		Ratio, A/B
	Thin layer	Total foil	
	A	B	
2	5.49	5.78	0.95_0
3	4.34	4.62	0.94_0
4	4.55	4.89	0.93_0
5	5.50	5.40	1.0_2

completely dissolving a piece of the foil of known weight, and measuring the Na^{24} activity in a small aliquot. The agreement between the two confirms the validity of equation 2 up to at least 150 volts.

In one run, 25 successive layers were removed at an applied potential of 100 volts in order to test the reproducibility of the technique. In every fifth layer, the Na^{24} content was measured by counting both the anodizing and stripping solutions. Also, the foil was weighed in order to determine directly the average weight loss for the previous five layers. The results are summarized in Table IV. Both the weight loss and the Na^{24} content

TABLE IV

Reproducibility of anodizing process

Number of 100-v layers removed	Av. weight loss/100 v for previous five layers ($\mu g/cm^2$)	Na^{24} content in last layer (c.p.m./cm^2)
5	28.5	121
10	28.0	136
15	29.5	130
20	29.0	140
25	28.5	139
Calculated value per 100-v layer (from equation 2)	30.5	138

remained almost constant throughout, thereby indicating that the process may be repeated a large number of times without significantly affecting the voltage–thickness relationship. The somewhat lower value obtained in layer 5 for the Na^{24} content may be attributed to recoil loss which, according to Fig. 3, should be quite significant for the first six to eight layers. Good agreement was obtained between the observed values and those calculated from equation 2 both for the weight loss, and for the Na^{24} content per 100-volt layer. This provides an excellent cross-check on the validity of equation 2.

One might think that the variation of Na^{24} activity with depth, illustrated in Fig. 3, might be used to provide quantitative information about the range of the Na^{24} recoil atoms themselves; but, unfortunately, this was not possible. First of all, the recoil atoms were not collimated and therefore a geometric factor would have to be introduced to correlate the number of atoms escaping from a given depth below the surface with the range. This factor, in turn, would depend to some extent on the shape of the recoil track which, due to elastic scattering, would certainly not be linear.

Can. J. Chem. Downloaded from www.nrcresearchpress.com by 210.87.254.105 on 09/05/12
For personal use only.

Furthermore, the recoil atoms were not monoenergetic; their energy depended markedly on the energy of the incident neutron and on the angular correlation between it and the emitted α-particle. Using the most recent data for the (n,α) cross section (15) and for the neutron spectrum in NRX, it was estimated that 90% of the recoils would occur between 0.1 and 2.0 Mev, provided there is little or no correlation in the center of mass system between the direction of the incident neutron and the emitted α-particle. A strong angular correlation, although considered very unlikely in an (n,α) reaction, would shift the energy limits for the recoil atoms to much lower values (0.04 and 0.3 Mev, respectively).

It is evident from Fig. 3 that only a very small number of Na^{24} atoms, originating at a depth greater than 10,000 Å below the surface, manage to escape. This implies that the mean range of a 2-Mev Na^{24} atom in aluminum is somewhat less than 10,000 Å.

SUMMARY

Successive uniform layers of known thickness can be removed from an Al target by a two-stage process, consisting of anodic oxidation followed by chemical dissolving of the film. The thickness removed varies linearly with the applied voltage. Reproducible results were obtained with layers as thin as 1.0 μg per cm^2 (37 Å) of aluminum, which suggests that the method should be sufficiently sensitive for studying the range of radioactive ions with kinetic energies as low as a few kiloelectron volts.

ACKNOWLEDGMENTS

The authors would like to express their thanks to Dr. R. H. Betts for suggesting the problem, and for his interest and encouragement throughout the work.

REFERENCES

1. K. O. Nielsen. Electromagnetically enriched isotopes and mass spectrometry. Academic Press, Inc., New York; Butterworth and Co., London. 1956. pp. 68–81.
2. D. L. Baulch and J. F. Duncan. Australian J. Chem. **10**, 112 (1957).
3. M. M. Bredov and N. M. Okuneva. Doklady Akad. Nauk S.S.S.R. **113**, 795 (1957).
4. A. Charlesby. Atomic Energy Research Establ. (Gt. Brit.), Rept. M/R 714, 1951.
5. J. E. Lewis and R. C. Plumb. Intern. J. Appl. Radiation and Isotopes, **1**, 33 (1956).
6. W. J. McG. Tegart. Electrolytic and chemical polishing of metals. The Pergamon Press Ltd., London. 1956. p. 52.
7. E. C. Trapp. A pneumatic carrier for irradiation of materials in the NRX reactor. Atomic Energy Can. Ltd. Rept. CRL-53. 1958.
8. W. Walkenhorst. Naturwissenschaften, **34**, 373 (1947).
9. E. Brandenburger and R. J. Hafeli. Helv. Chim. Acta, **31**, 1168 (1948).
10. J. R. Young. Phys. Rev. **103**, 292 (1956).
11. L. Harris. J. Opt. Soc. Am. **45**, 27 (1955).
12. S. Anderson. J. Appl. Phys. **15**, 477 (1944).
13. G. Haas. J. Opt. Soc. Am. **39**, 532 (1948).
14. R. E. Jervis and W. D. Mackintosh. II Geneva Conference A/Conf.P-189, **28**, 470 (1958).
15. J. A. Grundl, R. L. Henkel, and B. L. Perkins. Phys. Rev. **109**, 428 (1958).

Can. J. Chem. Downloaded from www.nrcresearchpress.com by 210.87.254.105 on 09/05/12
For personal use only.

Can. J. Chem. Downloaded from www.nrcresearchpress.com by 186.148.149.217 on 09/04/12
For personal use only.

THE RANGE OF ALKALI METAL IONS OF KILOELECTRON VOLT ENERGIES IN ALUMINUM[1]

J. A. DAVIES, J. D. MCINTYRE,[2] R. L. CUSHING, AND M. LOUNSBURY

ABSTRACT

A simple electrostatic accelerator capable of producing a monoenergetic beam of alkali metal ions at energies up to 100 kev has been used to study the range of Cs^{137} ions in aluminum as a function of energy. The median range (R_M) increases linearly with energy as predicted from the Bohr–Nielsen equation, but has a value about twice that predicted by this equation. Furthermore, the observed straggling about the mean value is not Gaussian in shape, but consists of an asymmetric peak with a pronounced exponential "tail". The possible significance of these results is discussed. Preliminary results are given for the range of 30-kev Rb^{86} and Na^{24} ions in aluminum.

INTRODUCTION

The present study has been undertaken as part of a program to obtain precise experimental measurements on the penetration depth and distribution of heavy atomic particles in matter at bombardment energies up to 100 kev. As pointed out by Nielsen (1) this is a velocity region of very considerable importance, both from the theoretical and practical viewpoint. The ion is moving sufficiently slowly for elastic nuclear collision to predominate over ionization as the principal mode of energy loss; hence range studies are of considerable interest for comparison with theoretical predictions of the cross section and mechanics of energy transfer in the elastic scattering process. Furthermore, since nuclear collision is far more effective than ionization in producing atomic displacements, this is also the region in which maximum radiation damage and sputtering should occur.

However, because of the experimental difficulties associated with measuring small depths of penetration, there have been until now almost no reliable experimental results reported on the range of heavy particles below 100 kev.

Our experimental technique consists in bombarding an aluminum target with a monoenergetic beam of radioactive ions of desired energy, and then determining the distribution of radioactivity as a function of depth by dissolving successive very thin uniform layers of aluminum of known thickness—using the electrochemical method described in the previous paper (2).

EXPERIMENTAL

The accelerator used for producing the beam of radioactive ions was designed and constructed specially for these range studies. Considerable economy and flexibility in design were achieved by carrying out the acceleration in two separate stages (see Fig. 1). In the first or low-energy stage, a beam of positive ions is produced in a thermionic-emission ion source A of the single-filament type (3). It consists of a tantalum ribbon upon which is evaporated a solution containing approximately 10^{-7} g of $(Cs^{137})_2SO_4$, and produces a beam of Cs^{137} ions at currents up to 10^{-6} amp. The filament is maintained at a positive potential of up to 5 kv in order to provide the first stage of acceleration. In the second stage, the beam passes between a set of four monitoring plates F, each of which is connected to an electrometer, and is then accelerated towards the target G,

[1]*Manuscript received May 16, 1960.*
Contribution from Research Chemistry Branch, Atomic Energy of Canada Limited, Chalk River, Ontario. Issued as A.E.C.L. No. 1060.
[2]*Present address: Department of Chemistry, Rensselaer Polytechnic Institute, Troy, N.Y., U.S.A.*

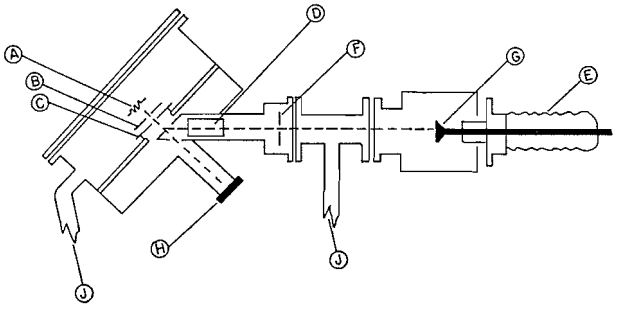


FIG. 1. Schematic diagram of ion accelerator: (A) ion filament, (B) grounded defining slit, (C), (D) beam-alignment plates, (E) high-voltage polystyrene insulator, (F) monitoring plates (4), (G) target, (H) Faraday cup, (J) to diffusion pumps.

which is maintained at any required negative potential up to 120 kv. In this way, the problem of maintaining an ion source at high voltage is eliminated. For energies up to 5 kev, the required voltage can be provided by the first stage alone, and in such cases the second stage is connected directly to ground.

Between the two stages, the beam passes between two pairs of plates C and D; an adjustable voltage is applied across each pair in order to align the beam on the target. One set of plates C deflects the beam through an angle of 30° in order to separate the ions completely from any neutral, and hence unaccelerated, atoms. The ion current is determined intermittently by reducing the deflecting voltage across C to zero, thereby permitting the ions to enter the Faraday cup H. The ion current is determined on a Keithley Electrometer Model 200 capable of measuring currents down to 10^{-13} amp with an accuracy of $\pm 2\%$.

In order to minimize radiation damage and contamination effects, it is desirable to bombard as large an area of the target as possible. Hence, there is no need to provide any focusing. Indeed, the cross-sectional area of the beam is considerably smaller than the normal target area (4 cm^2), and therefore, in most runs, the beam is traversed back and forth across the target to increase the bombarded area. This is accomplished by gradually varying the voltages on C and D during the bombardment until current begins to register on one or other of the monitoring plates at F. These four plates are positioned at 90° with respect to one another, and can be adjusted to define accurately the desired area of target to be bombarded. In Fig. 2, a curve of ion current falling on

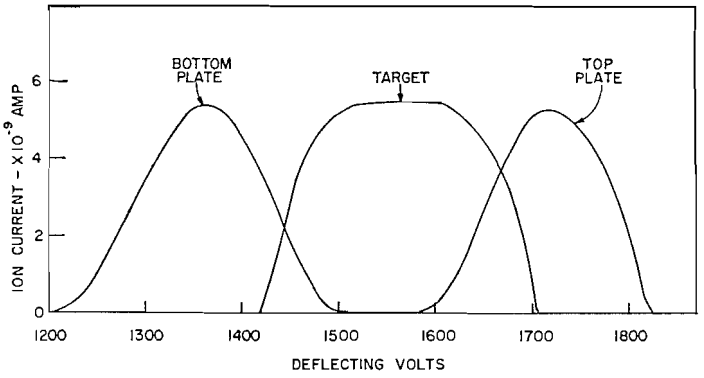


FIG. 2. Ion current on monitoring plates and target as a function of deflecting voltage. Accelerating voltage 3 kv.

Can. J. Chem. Downloaded from www.nrcresearchpress.com by 186.148.149.217 on 09/04/12
For personal use only.

two of these monitoring plates and on the target is shown as a function of the deflecting voltage across C.

A differential pumping system is used, consisting of two high-speed oil-diffusion pumps, one connected to the source chamber, and the other to the target chamber. The normal operating pressure along the path of the beam is about 2×10^{-6} mm. The total path length is 30 cm.

The adjustable accelerating voltage for the second stage is provided by a New Jersey Electronics 120-kv power supply Model HL-80 stabilized to $\pm2\%$.

PROCEDURE

Aluminum targets, approximately 2.5×2.5 cm, were cut from strips of 0.020-in. "super-pure" aluminum foil which had been carefully electropolished and preanodized to provide a reproducibly flat surface. The final stage of this treatment, removal of a thick anodic oxide film, was carried out immediately before the target was loaded into the accelerator in order to minimize the thickness of the surface oxide layer formed by action of air on the aluminum. After the bombardment was completed, the radioactivity of the target was measured to determine the number of Cs^{137} ions embedded in it, and then a series of uniform layers were removed by successive anodic oxidation and film stripping, as described in the preceding paper (2).

By varying the applied voltage in the oxidation step, layers of aluminum of any desired thickness from 37 Å to 1000 Å could be prepared for stripping. After one anodic oxide film had been stripped off, the target was rinsed with ethyl alcohol, allowed to dry, and counted. The process was then repeated until all the Cs^{137} ions had been removed from the target. The activity of the target was measured with an end-window flow-type proportional counter having a geometrical efficiency of approximately 30%.

The amount of Cs^{137} contained in each layer was determined from the decrease in the amount of residual radioactivity in the target. In some runs, to perform a mass balance, the Cs^{137} content in each layer was also determined directly by measuring the radioactivity in aliquots from the anodizing and film-stripping solutions. Good agreement was obtained between the two methods; however, in practice, the latter was much more tedious. Very small aliquots had to be used to avoid errors due to source thickness, and consequently the counting rates involved were very low. Therefore, in most of the runs, the Cs^{137} content per layer was determined solely from the decrease in target activity.

It should perhaps be noted that the depth of penetration of Cs^{137} ions into the target is sufficiently small to neglect any subsequent attenuation of the emitted β-particles. This was verified by placing a thin aluminum absorber (2 mg/cm^2) over the target. The counting rate decreased by 2.1%. Even at 50 kev, the average depth of penetration of Cs^{137} in aluminum was only 0.01 mg/cm^2, and hence the attenuation of β-particles was negligible.

RESULTS

A typical run illustrating the determination of the Cs^{137} distribution in a bombarded target is shown in Table I. The two different methods (columns 6 and 7) for obtaining the Cs^{137} activity in each layer are in satisfactory agreement. The thickness (W) per layer (column 3) has been calculated directly from the anodic voltage V by using the relationship from the preceding paper (2): viz. $W = 0.30\ (V+1.8)$. It will be noted that the first layer contains an extra 0.5 μg/cm^2. This represents a small correction term which is applied to all runs in order to take account of the oxygen that is present

Can. J. Chem. Downloaded from www.nrcresearchpress.com by 186.148.149.217 on 09/04/12
For personal use only.

TABLE I

Distribution of 50-kev Cs^{137} ions in aluminum target

(1)	(2)	(3)	(4)	(5)	(6)	(7)
					Cs^{137} activity (c.p.m.) per layer:	
Layer number	Anodic voltage	Amount of Al (W) in oxide layer ($\mu g/cm^2$)	Total amount removed ($\mu g/cm^2$)	Residual target activity (c.p.m.)	Calculated from col. 5	By direct measurement
0				59,920		
1	5.5	2.2+0.5	2.7	59,550	370	520
2	3.9	1.7	4.4	58,760	790	880
3	3.9	1.7	6.1	55,255	3505	3940
4	3.9	1.7	7.8	46,885	8370	8080
5	3.9	1.7	9.5	36,920	9965	9670
6	3.9	1.7	11.2	28,330	8590	8710
7	3.9	1.7	12.9	21,380	6950	6580
8	3.9	1.7	14.6	16,840	4540	4610
9	3.9	1.7	16.3	13,635	3205	3240
10	11.8	4.1	20.4	8,100	5535	5470
11	11.8	4.1	24.5	4,970	3130	3080
12	11.8	4.1	28.6	3,172	1798	1850
13	11.8	4.1	32.7	2,097	1075	1195
14	23.8	7.7	40.4	875	1222	1205
15	23.8	7.7	48.1	456	419	—
16	23.8	7.7	55.8	172	284	—
17	23.8	7.7	63.5	78	94	—
18	23.8	7.7	71.2	30	48	—

during the bombardment as an oxide layer on the target surface, and which contributes therefore to the slowing down of the ion beam. The aluminum content of this oxide layer is included in the above expression for W. It is assumed that the aluminum and oxygen atoms have comparable stopping power for heavy ions. This assumption should be valid provided the ion range is considerably greater than 0.5 $\mu g/cm^2$.

The actual distribution of Cs^{137} ions in the target was observed to be markedly asymmetric. This may be seen more clearly in Fig. 3, in which the Cs^{137} content in each successive layer is plotted against the depth beneath the original surface. The existence of an appreciable, highly penetrating "tail" in the distribution curve is a characteristic feature of these range studies; as a result, the median range R_M, i.e. the thickness required to stop 50% of the incident ions, is somewhat greater than the most probable value R_P. Both R_M and R_P increase linearly with energy (Table II).

Typical distribution curves for Cs^{137} ions of various energies are shown in Fig. 4, in

TABLE II

Range of Cs^{137} ions in aluminum

Energy (kev)	R_P/E ($\mu g\ cm^{-2}\ kev^{-1}$)	R_M/E ($\mu g\ cm^{-2}\ kev^{-1}$)	$X_{\frac{1}{2}}/E$ ($\mu g\ cm^{-2}\ kev^{-1}$)
2*	—	$0.3\pm.1_5$	$0.20\pm.05$
5*	—	$0.2\pm.06$	$0.12\pm.02$
20	$0.20\pm.03$	$0.24\pm.02$	$0.14_5\pm.01$
30	$0.19\pm.02$	$0.25\pm.01$	$0.13\pm.01$
50	$0.19\pm.01$	$0.23\pm.01$	$0.13\pm.01$

*Depth of penetration too small to observe R_P, as the first layer contained more than 50% of Cs^{137} ions. R_M was obtained from Fig. 4 by extrapolation.

Can. J. Chem. Downloaded from www.nrcresearchpress.com by 186.148.149.217 on 09/04/12
For personal use only.

Can. J. Chem. Downloaded from www.nrcresearchpress.com by 186.148.149.217 on 09/04/12
For personal use only.

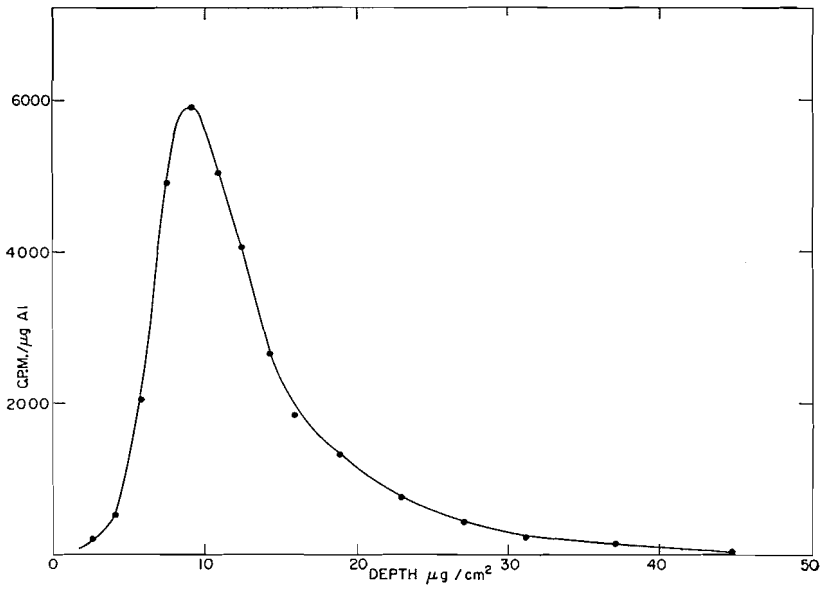


FIG. 3. Depth of penetration of 50-kev Cs^{137} ions in aluminum.

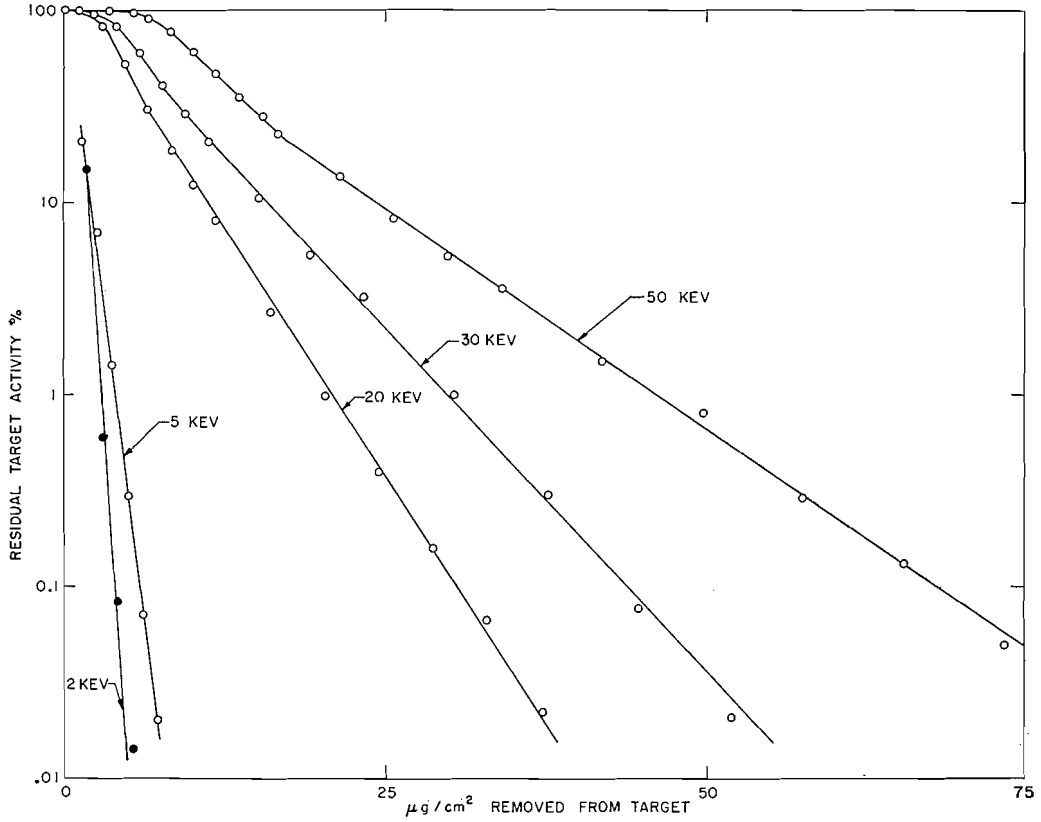


FIG. 4. Distribution curves for Cs^{137} ions of various energies in aluminum.

which the residual activity remaining in the target has been plotted against the total thickness of aluminum removed. In each case, apart from an initial region, the activity falls off exponentially with depth. The half-thickness, $X_{1/2}$, of this exponential region also was observed to increase linearly with the energy of the incident ion.

In order to test the reproducibility of the technique, several runs were carried out at 30 kev under various experimental conditions (see Table III).

TABLE III

Test of reproducibility: 30-kev Cs^{137} ions in aluminum

Run No.	Ion current (μamp)	Total number of Cs ions	R_P ($\mu g/cm^2$)
1	40	0.56×10^{13}	4.4
2	40	4.7	4.8
3	40	20*	4.8
4	600	3.8	4.5

*4.0×10^{13} Cs^{137} ions, plus 16.0×10^{13} Cs^{133} ions.

In the first three runs, the duration of the ion bombardment was varied by a factor of 30 to investigate whether sputtering or radiation damage could alter significantly the initial distribution of the incident ions. The results indicate that prolonged bombardment does not change appreciably the observed value for the most probable range. In run 3, a further check on the absence of significant sputtering was provided by carrying out the bombardment in two stages: 4×10^{13} ions of Cs^{137} in the first stage, followed by a much larger number of inactive Cs^{133} ions in the second one. The observed distribution of Cs^{137} as a function of depth was identical with that in run 2, which showed clearly that the subsequent bombardment by inactive cesium had not changed the distribution of Cs^{137}. Furthermore, the radioactivity of the target was measured immediately before and after the second bombardment to determine whether any Cs^{137} had been sputtered from the target by the Cs^{133} ions. The observed decrease in activity was extremely small (0.3%), and in fact was not significantly greater than the statistical counting errors involved.

The absence of detectable sputtering or other secondary radiation damage in these range–distribution studies is not unexpected; even in run 3, the total number of ions striking the target was only 2×10^{14} and those were distributed over an area of 4 cm^2. From the observed distribution curves for 30-kev ions in aluminum, it can readily be shown that the maximum ratio of cesium atoms to aluminum atoms in the target was less than 10^{-3}. Therefore, each cesium ion would have to eject an unreasonably large number of aluminum atoms from the target to reduce significantly the observed depth of penetration.

Run 4 was carried out at much higher ion current in order to investigate whether the observed distribution depended on the rate of energy deposition. It is true that in these experiments the rate of energy deposition was extremely small, usually less than 10 milliwatts; but, due to the short range of the incident ions, the kinetic energy is dissipated in an extremely small volume, equivalent to a power input of approximately one kilowatt per gram. It was thought that this high heat flux might give rise

Can. J. Chem. Downloaded from www.nrcresearchpress.com by 186.148.149.217 on 09/04/12
For personal use only.

to some secondary thermal effects. However, run 4 shows clearly that a 15-fold increase in the rate of energy deposition had no appreciable effect.

The distribution of Cs^{137} for each of the above runs is illustrated in Fig. 5. Within the statistical errors involved, the results for the four runs are indistinguishable.

Other Alkali Metal Ions

Some preliminary studies have also been carried out with 30-kev Na^{24} and Rb^{86} ions in aluminum. The results are illustrated in Fig. 6, and in Table IV. With both ions, a markedly asymmetric distribution curve is again observed. The energy dependence for these ions has not yet been investigated.

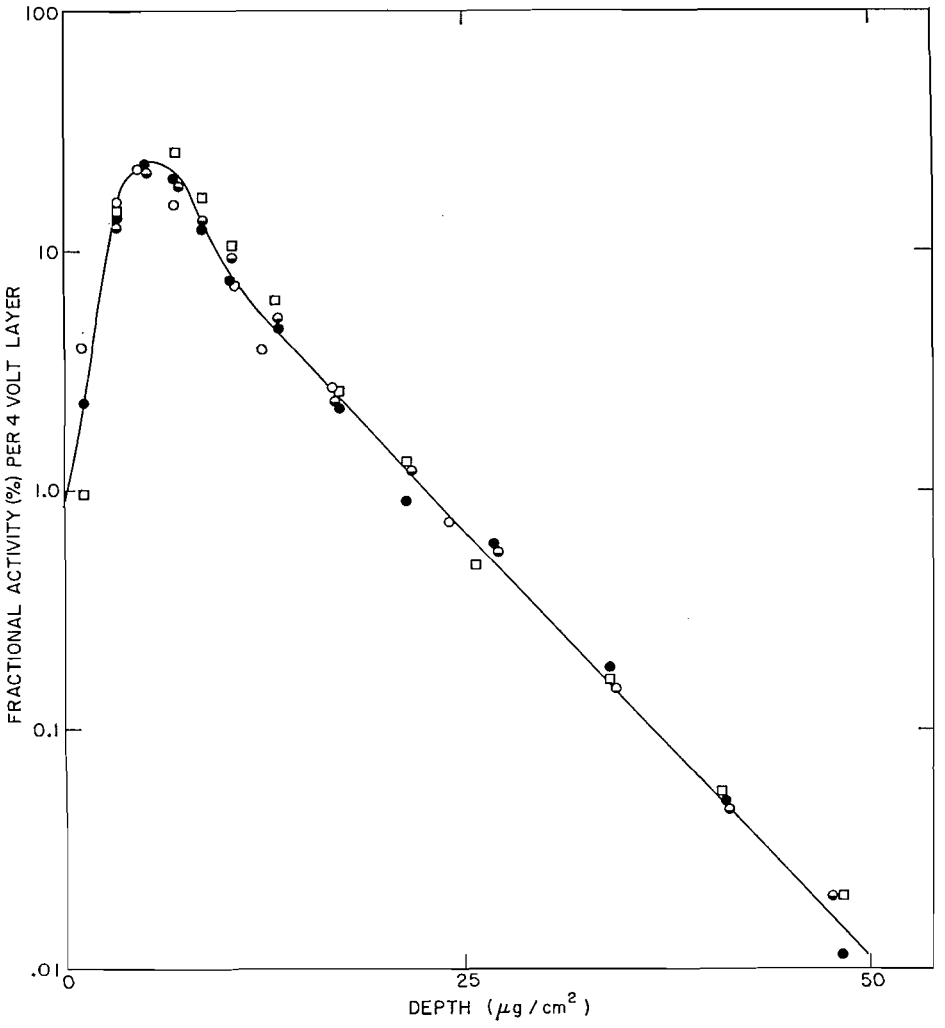


FIG. 5. Depth of penetration of 30-kev Cs^{137} ions in aluminum under different experimental conditions: ○ run 1, ◒ run 2, ● run 3, □ run 4.

Can. J. Chem. Downloaded from www.nrcresearchpress.com by 186.148.149.217 on 09/04/12
For personal use only.

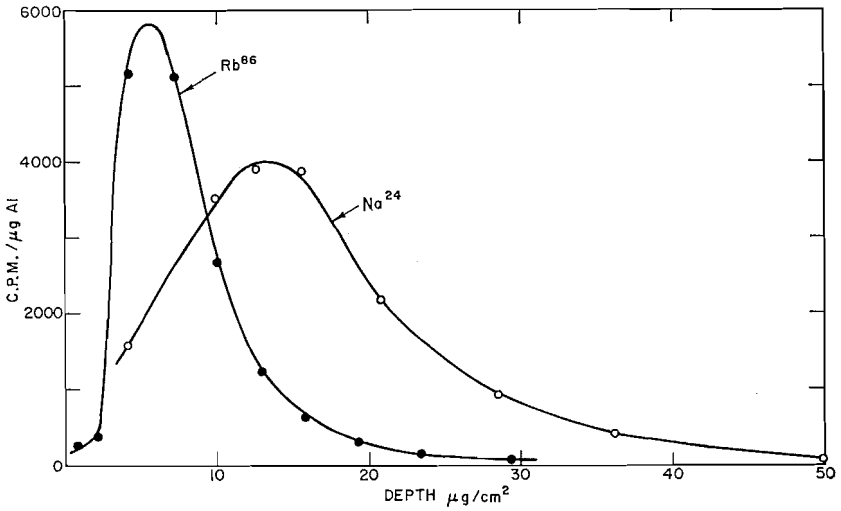


FIG. 6. Depth of penetration of 30-kev Rb^{86} and Na^{24} ions in aluminum.

TABLE IV

Range of 30-kev alkali-metal ions in aluminum

Ion	R_P (μg cm^{-2})	R_M (μg cm^{-2})	Range predicted by Bohr–Nielsen equation (μg cm^{-2})
Na^{24}	13.1	15.0	23.4
Rb^{86}	6.6	8.4	5.4
Cs^{137}	5.8	7.6	3.6
Na^{24}/Cs^{137}	2.2	2.0	6.5

DISCUSSION OF RESULTS

Bohr (4) has shown that the complicated many-body problem involved in slowing down an atomic particle can be simplified considerably by separating it into two distinct types of collision processes: electronic or inelastic collisions, in which energy is transferred to individual electrons, thereby causing ionization or atomic excitation; and nuclear or elastic collisions, in which momentum and kinetic energy are transferred to the stopping atom as a whole. The former process is the more important at high velocity such as in the initial portion of a fission-fragment or alpha-particle track; whereas, when the moving particle has a velocity less than that of the slowest orbital electrons in the stopping material (viz. $<2\times10^8$ cm/sec), nuclear collisions tend to predominate. The ion velocities used in the present work were considerably less than this critical velocity; hence, nuclear collisions should be the more significant process throughout the range.

Nuclear collisions may be subdivided further into various types depending on the relative magnitude of the collision diameter, the screening parameter, and the wavelength of the incident particle. A general treatment of the problem is therefore quite complicated. However, at the energies studied in the present work, it has been shown by Nielsen (1) that, over the entire range, the collision diameter, or minimum distance of approach in a head-on collision in an unscreened coulomb field, is considerably larger

Can. J. Chem. Downloaded from www.nrcresearchpress.com by 186.148.149.217 on 09/04/12
For personal use only.

Can. J. Chem. Downloaded from www.nrcresearchpress.com by 186.148.149.217 on 09/04/12
For personal use only.

than the screening parameter. Hence, the nuclear collisions occur in a screened coulomb field. Furthermore, over most of the range, the wavelength of the incident ion is much smaller than the screening parameter and classical orbital considerations may be applied. For such a system the following range–energy relationship has been developed (1, 5):

$$\frac{R}{E} = 0.60\,\frac{A_1+A_2}{A_1}\cdot\frac{A_2}{Z_2}\cdot\frac{(Z_1^{2/3}+Z_2^{2/3})^{\frac{1}{2}}}{Z_1}$$

where R is the range in $\mu g/cm^2$, E is the energy of the incident particles in kev, A_1, A_2 are the masses, and Z_1, Z_2 are the atomic numbers of the incident and target atoms respectively.

The predicted linear relationship between range and energy is observed for Cs^{137} ions in aluminum (Table II). A comparison of the absolute magnitude of the experimental and predicted values for the range of 30-kev alkali-metal ions is given in Table IV. Clearly, the theoretical values do have the correct order of magnitude, but the predicted variation from Na^{24} to Cs^{137} is several times larger than that observed. This discrepancy may be ascribed partly to the fact that the theory gives the total distance travelled by the particle in coming to rest, not merely the depth of penetration beneath the target surface. One important characteristic (1) of screened-field scattering is that the angular distribution is almost isotropic in the center-of-mass system, in contrast with coulomb scattering where small angular deflections predominate. As a result, the individual ion tracks will be far from linear; hence the predicted ranges must be reduced somewhat before comparing with the experimental values.

In the case of Cs^{137}, this correction term is quite small. The mass of the incident particle is more than five times that of the target atom; hence, to conserve momentum, it can be shown that the maximum deflection per collision is only 12°. On the other hand, with Na^{24}, where the mass ratio is close to unity, individual deflections as large as 90° are possible, and consequently the depth of penetration will be much less than the total path length.

Effect of Surface Area

One problem of some concern in the interpretation of these range studies is the possible effect of surface non-uniformity on the measured depth of penetration. Consider a small segment of surface (Fig. 7) inclined at an angle θ to the plane of the target. Let the area of the segment be ΔA. If the target is bombarded uniformly by a collimated beam of ions, then the number striking ΔA is given by $N(\Delta A \cos\theta/A')$ where N is the total number of ions striking the target and A' is the apparent or measured area. Each of these ions, in traversing a thin uniform layer of thickness δ, travels a distance $\delta/\cos\theta$. Hence, the sum of the distances travelled by all the ions striking the segment is given by $N(\Delta A/A').\delta$, which is independent of θ. Integrating over the whole target, and dividing by N, we find that the average distance travelled per ion is $\delta.(A/A')$, where A/A' is the ratio of the true to the apparent surface area of the target. It is obvious, therefore, that surface irregularities increase markedly the average path length travelled.

However, in calibrating the relationship between oxide film thickness and anodic voltage (2), it was not possible to measure the true film thickness δ, but only the apparent thickness δ'. It can readily be shown that $\delta' = \delta(A/A')$. Since the same type of surface was used in the preliminary calibration as in the subsequent depth of penetration studies, it can be seen that the average distance travelled per ion in traversing a uniform film is identical with the apparent film thickness. Consequently, the effects of non-uniformity cancel out in determining the average range.

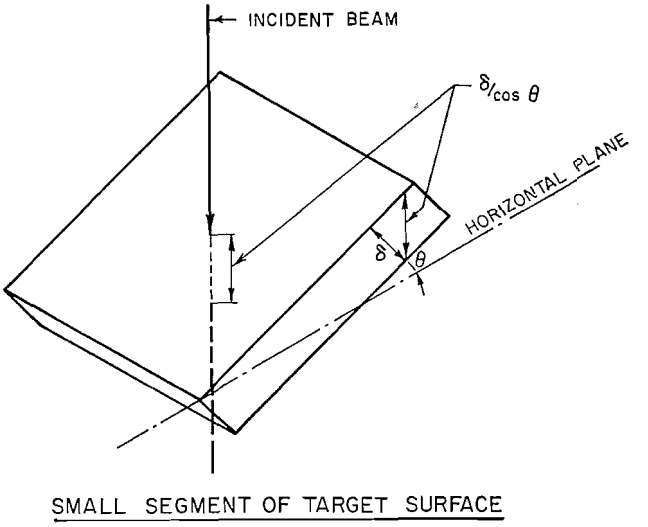


FIG. 7. Sketch to illustrate surface-area effect.

Of course, surface irregularities will introduce some straggling into the observed distribution, but this straggling should not be very marked: optically flat surfaces have been used throughout this work, and the preanodizing studies reported in the preceding paper (2) suggest that the ratio (A/A') is probably very close to unity.

A particularly interesting feature of our results is the observed asymmetric distribution. Some previous workers (6, 7) have assumed that the distribution of individual particle ranges about a mean value would be given approximately by an error curve:

$$W(R) = \frac{1}{\rho R_M \sqrt{2\pi}} \exp\left[-\frac{1}{2\rho^2}\cdot\left(\frac{R-R_M}{R_M}\right)^2\right]$$

with a straggling parameter

$$\rho^2 = \frac{4}{3}\frac{A_1A_2}{(A_1+A_2)^2}.$$

However, as noted by Bohr (4, p. 50), a Gaussian distribution occurs only when the maximum fractional energy transfer T_{max} per collision is very small: in other words, when $A_1 \gg A_2$. This assumption is certainly not valid when using an aluminum target. Even with Cs^{137}, where $A_1 = 5.1A_2$, T_{max} is almost 0.60; and, assuming isotropic scattering, T_{av} is approximately 0.30. Since the range varies linearly with the energy, this means that each ion, on the average, traverses one-third of its total range before the first collision. Furthermore, since the collision diameter increases with decreasing energy of the incident ion, the mean free path should decrease markedly with every collision. Obviously, the depth of penetration is determined primarily by the first few collisions. Under such conditions, it can be shown (see Fig. 8, and Appendix) that the distribution curve consists of an asymmetric peak with a highly penetrating exponential "tail"; the half-thickness of the exponential region is determined by the mean free path for the first collision.

With Cs^{137}, this exponential "tail" is in fact observed. Furthermore, the half-thickness varies linearly with the energy, as would be expected.

Can. J. Chem. Downloaded from www.nrcresearchpress.com by 186.148.149.217 on 09/04/12
For personal use only.

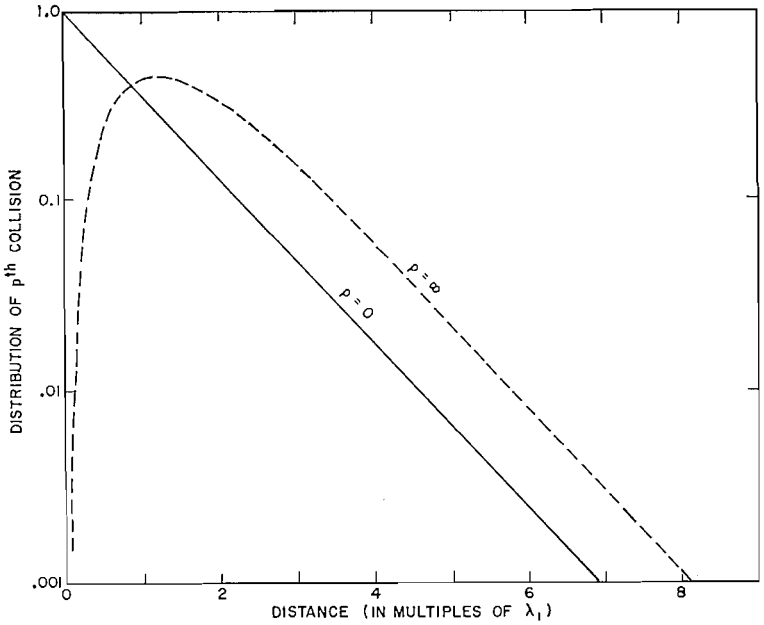


FIG. 8. Calculated distribution curves for large fractional energy loss per collision.

It is planned to extend these studies to somewhat higher energies, to other ions, and to other target materials in order to permit a more quantitative interpretation of the role of nuclear collisions in determining range–energy relations.

ACKNOWLEDGMENTS

The authors wish to acknowledge the invaluable assistance of Mr. G. Sims with the construction and operation of the ion accelerator, and with the subsequent radiochemical analyses. We are particularly indebted to Dr. R. H. Betts for his advice and encouragement throughout this work, and to Mr. G. C. Hanna for his help in developing the mathematical treatment in the Appendix.

REFERENCES

1. K. O. NIELSEN. *In* Electromagnetically enriched isotopes and mass spectrometry. *Edited by* M. L. Smith. Academic Press, New York. 1956. p. 68.
2. J. A. DAVIES, J. FRIESEN, and J. D. MCINTYRE. Can. J. Chem. **38**, 1526 (1960).
3. M. LOUNSBURY. Proc. Royal Soc. Can. **46**, 128 (1952).
4. N. BOHR. Kgl. Danske Videnskab. Selskab, Mat-fys. Medd. **18** (8) (1948).
5. J. LINDHARD and M. SCHARFF. Private communication (*quoted by* R. B. Leachman and H. Atterling. Arkiv. Fysik, **13**, 101 (1957)).
6. D. L. BAULCH and J. F. DUNCAN. Australian J. Chem. **10** (2), 112 (1957).
7. L. WINSBERG and J. M. ALEXANDER. UCRL-8618 (1958), p. 35.
8. H. BATEMAN. Proc. Cambridge Phil. Soc. **15**, 423 (1910).

APPENDIX

CALCULATED RANGE DISTRIBUTION FOR LARGE ENERGY TRANSFERS

Consider an experiment in which N particles have been shot into the absorbing material. Suppose $N_p(r)$ is the number of particles that made p collisions in penetrating a distance r. Then the number that reached $(r+dr)$ making p collisions is the sum of

Can. J. Chem. Downloaded from www.nrcresearchpress.com by 186.148.149.217 on 09/04/12
For personal use only.

those that reached r making p collisions without making a further collision in dr and those that reached r in $(p-1)$ collisions and did make a collision in dr. That is

$$[1] \qquad N_p(r+dr) = N_{p-1}(r)dr/\lambda_p + N_p(r)(1-dr/\lambda_{p+1})$$

where λ_p is the mean free path for the pth collision.

Writing $\mu = 1/\lambda$ gives

$$[2] \qquad (d/d_r)N_p(r) = \mu_p N_{p-1}(r) - \mu_{p+1}N_p(r).$$

This equation is the same, with r replacing time, as that governing a series of radioactive transformations, with the familiar solutions (8)

$$N_0(r) = Ne^{-\mu_1 r}$$

$$N_1(r) = N\mu_1\left(\frac{e^{-\mu_1 r}}{\mu_2-\mu_1}+\frac{e^{-\mu_2 r}}{\mu_1-\mu_2}\right)$$

etc.

and

$$[3] \qquad N_p(r) = N\mu_1\mu_2 \ldots \mu_p \sum_{n=1}^{p+1} \frac{e^{-\mu_n r}}{a_n}$$

where

$$a_n = \prod_{i=1}^{p+1} (\mu_i - \mu_n), \qquad i \neq n.$$

For the special case where the mean free path remains constant (i.e. where $\mu_1 = \mu_2 \ldots = \mu_p$), equation (3) becomes a Poisson distribution, which for large values of p is simply the familiar Gaussian curve. Such a condition would be approximately correct for a system in which the fractional energy loss per collision is small. However, where the energy transfer per collision is large, a very different type of distribution curve is obtained.

In order to illustrate this, let us take a somewhat idealized system in which the fractional energy transfer per collision is exactly 0.5. Clearly, in such a case, only the first few mean free paths contribute significantly to the total range. Since the mean free path is proportional to the energy, we may substitute in equation (3) the following relationship:

$$\mu_1 = \frac{1}{2}\mu_2 = \frac{1}{4}\mu_3 \ldots = \frac{1}{2^{n-1}}\cdot\mu_n.$$

The resulting series

$$\sum_{n=1}^{\infty} \frac{1}{a_n} [\exp -(2^{n-1})\mu_1 r]$$

is rapidly convergent and leads to the distribution shown in Fig. 8 by a dotted line: viz. an asymmetric peak, followed by an exponential region of half-thickness identical with that for the first collision.

The above treatment is greatly oversimplified and cannot be used for quantitative comparison with the observed distribution curves. No allowance has been made for variations in energy transfer from one collision to another, nor for the difference between the total path length and the depth of penetration.

Can. J. Chem. Downloaded from www.nrcresearchpress.com by 186.148.149.217 on 09/04/12
For personal use only.

Can. J. Chem. Downloaded from www.nrcresearchpress.com by 210.87.254.42 on 09/05/12
For personal use only.

ISOLATION AND STRUCTURE OF A NEW ALKALOID: ASPIDOCARPINE[1]

STEWART MCLEAN,[2] K. PALMER,[2] AND LÉO MARION

ABSTRACT

From the root bark of *Aspidosperma megalocarpon* Muell. Arg. a new alkaloid, aspidocarpine, has been isolated. It has the empirical formula $C_{22}H_{30}O_3N_2$ and contains an N-acetyl, one methoxyl group, and one active hydrogen. The alkaloid, a phenolic monoacidic tertiary base, has been shown by its properties, those of its derivatives, and the spectroscopic data, to contain an N-acetyl-6-methoxy-7-hydroxydihydroindole moiety. Oxidation of aspidocarpine with chromic acid gave rise to a product identical in all respects with apoaspidospermine obtained from the similar oxidation of aspidospermine. Since the structure of aspidospermine is known, the foregoing results establish the structure of the alkaloid aspidocarpine.

The root bark of *Aspidosperma megalocarpon* Muell. Arg., a tree that grows in British Guiana,[3] has been found to contain alkaloids. They mostly occur in the petroleum ether extract, and largely consist (0.06% of dry weight) of one base which it is proposed to designate aspidocarpine. Its empirical formula derived from the analytical figures of the base and its salts is $C_{22}H_{30}O_3N_2$. Aspidocarpine melts at 168.5–169.5°, and determination of functional groups revealed that it contains one acetyl group, one methoxyl, one additional C-methyl besides that arising from the acetyl, and one active hydrogen.

The ultraviolet spectrum of aspidocarpine contains maxima at λ_{max} 227 mμ, log ϵ 4.42, and λ_{max} 263.5 mμ, log ϵ 3.92. It resembles that of aspidospermine and suggests that the new alkaloid, like aspidospermine, contains the N-acetyl-indoline chromophore. The spectrum of aspidocarpine was not affected by the presence of mineral acid, but was profoundly changed by the addition of sodium hydroxide.

In the infrared the spectrum of aspidocarpine contains no apparent hydroxyl absorption, but shows a peak at 1632 cm^{-1} which, although weak and at a low wave-number, must be indicative of the carboxyl of an N-acetyl group. Since, however, the base does not contain a carboxylic group, but contains an active hydrogen and is soluble in sodium hydroxide, since, further, it produces a pale olive-green color with ferric chloride, it must be phenolic. If the phenolic hydroxyl and the N-acetyl group were located sufficiently close to one another to form a strong hydrogen bond the effect in the infrared would shift the hydroxyl and carbonyl absorption to lower wave-numbers. Hence any hydroxyl absorption would be shifted to and covered by the CH stretching absorption region. The situation would thus parallel that observed in demethylaspidospermine (1). Evidence that this assumption is indeed correct has been obtained by blocking the hydroxyl function and thus removing the possibility of hydrogen bonding. Acetylation of the hydroxyl group was carried out smoothly in acetic anhydride and pyridine. The product, O-acetylaspidocarpine ($C_{24}H_{32}O_4N_2$) shows bands in the infrared at 1768 cm^{-1} and 1204 cm^{-1} characteristic of a phenolic O-acetyl (2) and another band at 1666 cm^{-1} due to the carbonyl of the N-acetyl group.

The phenolic hydroxyl of aspidocarpine did not react with diazomethane under the usual conditions, a common occurrence with strongly hydrogen-bonded phenols, but methylation was readily effected by the use of alkaline dimethylsulphate at room tempera-

[1]*Manuscript received June 3, 1960.*
Contribution from the Division of Pure Chemistry, National Research Council, Ottawa, Canada.
Issued as N.R.C. No. 5775.
[2]*National Research Council Postdoctorate Fellow.*
[3]*The plant material was obtained through the courtesy of Mr. R. Smeathers, Conservator of Forests, Kingston, Georgetown, British Guiana.*

ture. The O-methylaspidocarpine ($C_{23}H_{32}O_3N_2$) thus produced showed a strong absorption band in the infrared at 1656 cm^{-1} due to the N-acetyl carbonyl. The ultraviolet spectra of both the O-acetyl and the O-methyl derivatives were not appreciably altered by sodium hydroxide. Thus when the phenolic hydroxyl is blocked and no hydrogen bonding is possible, the carbonyl absorption of the N-acetyl group in the infrared appears with its normal frequency and intensity.

The N-acetyl group was characterized by hydrolysis of the alkaloid with sulphuric acid, steam-distillation of the reaction mixture, and spot-testing of the ethylamine salt of the distilled acetic acid on a paper chromatogram.

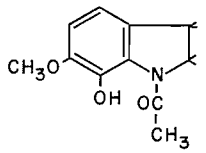
O-Methylaspidocarpine was hydrolyzed with 10% hydrochloric acid to O-methyl-deacetylaspidocarpine ($C_{21}H_{30}O_2N_2$). The infrared spectrum of this product no longer shows any carbonyl absorption, but contains a band at 3335 cm^{-1} attributable to an imino group. Treatment of the product with acetic anhydride and pyridine regenerates O-methylaspidocarpine, thus confirming the presence of an N-acetyl group in the alkaloid.

Treatment of aspidocarpine with hydrobromic acid produced an extremely unstable material which could not be crystallized. This material gives a blood red color with ferric chloride, which is consistent with an aminodihydric phenol. The material must be O-demethyl-N-deacetylaspidocarpine because on acetylation it is converted to O,O-diacetyl-O-demethylaspidocarpine ($C_{25}H_{32}O_5N_2$). The latter has an infrared absorption spectrum containing bands at 1777 and 1767 cm^{-1} (C=O) and 1204 cm^{-1} (C—O—) due to two phenolic O-acetyl groups, as well as a band at 1668 cm^{-1} attributable to the non-bonded carbonyl of the N-acetyl group. This observation places the original methoxyl group of aspidocarpine in the aromatic ring. In support of this conclusion it has proved possible to hydrolyze selectively the O-acetyl groups of O,O-diacetyl-O-demethylaspidocarpine and isolate pure O-demethylaspidocarpine, $C_{21}H_{28}O_3N_2$, which has the characteristics of a dihydric phenol. In the infrared spectrum of this compound, as expected, the carbonyl absorption shows the effect of hydrogen bonding, and the hydroxyl region contains an absorption band attributable to the non-hydrogen-bonded hydroxyl group. Treatment of O-demethylaspidocarpine with diazomethane did not affect the original hydroxyl, which had already been shown to resist methylation by this method, but methylated the second hydroxyl, thus regenerating aspidocarpine.

O-Demethylaspidocarpine behaves as an ortho-dihydric phenol as shown by the following observations. With ferric chloride it produces initially an intense blue-green color, which on addition of sodium carbonate, changes to a very deep red, a color sequence characteristic of catechols. In a series of tests on the compounds already described it was observed that coupling with diazotized sulphanilic acid occurred whenever either the hydroxyl or the indoline nitrogen was free, but did not occur when both were substituted. This indicates that the positions in the benzene ring para to these two functions are unsubstituted. Attempts to oxidize aspidocarpine or O-demethylaspidocarpine with periodate by the method of Adler and Magnusson (3) failed to give any crystallizable products, but produced color sequences indicative of the formation of an ortho-quinone. The condensation of either the presumed crude quinone with ortho-phenylenediamine, or of O-demethylaspidocarpine with phosgene led invariably to amorphous products of doubtful composition. The product of the reaction with phosgene, however, showed in the infrared a peak at 1835 cm^{-1}, a value indicative of the formation of a cyclic carbonate. It is of some interest that O-methylaspidocarpine gives no color in the brucine test with

Can. J. Chem. Downloaded from www.nrcresearchpress.com by 210.87.254.42 on 09/05/12
For personal use only.

nitric acid and acetic acid, an observation in accordance with the model experiments of Lyons, Perkin, and Robinson (4), whereas aspidocarpine and O-demethylaspidocarpine both give a deep red color different from the characteristic brucinequinone color. The best evidence in favor of the ortho arrangement of the hydroxyl groups in O-demethylaspidocarpine came from an application of Jurd's method (5), which is based on the effect of buffered boric acid on the ultraviolet spectrum of a compound. The ultraviolet spectrum of O-demethylaspidocarpine shows a dramatic change in the presence of buffered boric acid and parallel experiments show that catechol undergoes a similar change while the other dihydroxybenzenes are unaffected. The spectrum of aspidocarpine is unaffected by buffered boric acid. The sum of the evidence therefore strongly favors partial structure I as representing rings A and B of aspidocarpine. The nuclear magnetic resonance evidence, discussed later, also supports this conclusion.



I

The close similarity between the chemistry of aspidocarpine and that of aspidospermine, as well as in the spectral properties of both alkaloids, is quite striking. The relationship in rings A and B has already been demonstrated. In the study of the saturated moiety of the molecule it has been found that the reactions of aspidocarpine parallel exactly those of aspidospermine including the rather remarkable rearrangements known to take place in the latter (6).

In line with aspidospermine (6, 7) aspidocarpine showed a high analytical N-methyl value (76% of calculated figure for one N-methyl) which later proved spurious, and still in keeping with other *Aspidosperma* alkaloids, O-methylaspidocarpine gave an N-methyl value considerably lower than that obtained with the alkaloid (24% of calculated value for one such group).

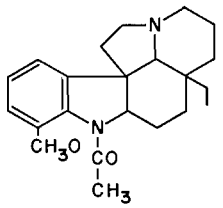
Aspidocarpine-N(*b*)-methiodide was readily prepared in dimethylformamide. It did not undergo the Hofmann degradation, however, but gave back aspidocarpine.

The von Braun degradation of aspidocarpine also produces a significant parallel with the behavior of aspidospermine in this reaction (6). Treatment of aspidocarpine with cyanogen bromide in chloroform (the reaction failed in benzene) gives rise to aspidocarpine bromocyanamide, $C_{23}H_{30}O_3N_3Br$, which exhibits the usual characteristics of this class of compounds, except that the normal solvolytic completion of the von Braun degradation fails since the bromocyanamide reverts to aspidocarpine even on reflux with ethanol.

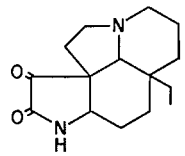
These similarities between aspidospermine and aspidocarpine, coupled with their botanical relationship, suggested the possibility that they might differ only insofar as ring A was concerned. Ewins (8) had oxidized aspidospermine with chromic acid and had obtained a product, m.p. 193°, to which he tentatively assigned the structure of a keto-lactam (apoaspidospermine) resulting from the oxidative degradation of the

Can. J. Chem. Downloaded from www.nrcresearchpress.com by 210.87.254.42 on 09/05/12
For personal use only.

aromatic ring. The structure of aspidospermine (II) recently determined by X-ray crystallography[4] (9) leads to structure III for apoaspidospermine,



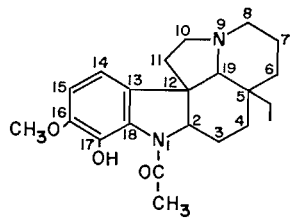
II



III

which should also be the product of the similar oxidation of aspidocarpine. Ewins' analytical figures were not in agreement with this structure but in our hands the oxidation of aspidospermine with chromic acid yielded a product, m.p. 224–225°, which gave analytical figures in excellent agreement with those required by III ($C_{15}H_{22}O_2N_2$). Both the infrared and ultraviolet spectra of the oxidation product were consonant with the presence of a five-membered keto-lactam in the molecule. This product was most probably identical with Ewins' apoaspidospermine, although it was purer as shown by the higher melting point. Aspidocarpine when oxidized with chromic acid yielded a product which had the same optical rotation and the same melting point as apoaspidospermine, alone or in admixture. The infrared spectra and the X-ray powder diagrams of both products were exactly superimposable.

The identity of the oxidation products of aspidocarpine and aspidospermine establishes the structure of the saturated moiety of the former, and this, together with the demonstration of the presence of a hydroxymethoxy-N-acetyl-indole in the molecule, affords conclusive proof that the structure of aspidocarpine is



IV

represented by formula IV. The assignment of the structure of the saturated part of the molecule depends on the X-ray crystallographic analysis of aspidospermine (9), and it follows from the identity of the oxidation products obtained from both alkaloids.

Aspidocarpine has proved very suitable for examination by nuclear magnetic resonance[5] especially since the spectrum can be compared with that of aspidospermine, the structure of which has been conclusively established (9, 10).

[4]*We acknowledge with thanks the courtesy of Professor N. S. Nyburg, who communicated to us the structure of aspidospermine in advance of his publication.*

[5]*Spectra were obtained with a Varian Associates high resolution nuclear magnetic resonance spectrometer operating at 60 Mc/s frequency. Chloroform was employed both as a solvent and as an internal reference; its proton resonance was assigned a value of zero c.p.s. and the scale was fixed from the position of the associated* C^{13} *(natural abundance) peaks which were shown to have a value of* ± 105 *c.p.s.*

Can. J. Chem. Downloaded from www.nrcresearchpress.com by 210.87.254.42 on 09/05/12
For personal use only.

Can. J. Chem. Downloaded from www.nrcresearchpress.com by 210.87.254.42 on 09/05/12
For personal use only.

The significant features of the spectrum of aspidocarpine are:

(1) A single sharp peak at −215 c.p.s. with area equivalent to one proton. This is attributed to the internally hydrogen-bonded phenolic OH group.

(2) A triplet with strong central peak at 44 c.p.s. This multiplet produced by the aromatic protons is of the AB type (11) with a very small chemical shift and $J = 9$ c.p.s. The total area is equivalent to two protons.

(3) A quartet at 193, 198, 202, and 208 c.p.s. with a total area equivalent to one proton. This is attributed to the proton at C2. The structure shows the effect of splitting by the adjacent methylene protons and demonstrates the rigidity of ring C.

(4) A single sharp peak at 211 c.p.s. of area equivalent to three protons. This is attributed to the protons of the methoxyl group.

(5) A multiplet at 247, 255, 258, and 263 c.p.s. of which the 258 c.p.s. peak is the strongest and sharpest. These signals are more difficult to assign to particular protons, but are probably to be associated with the protons on carbons adjacent to the nitrogen at position 9. From the area under the curve, two or at most three protons are involved with this resonance. Since ring size is known to affect the position of proton resonance in saturated heterocyclic systems (12) it would be expected that the signals of the protons at C8 would be separated from those at C10. The most likely situation is that the protons at C10 (in a five-membered ring) are involved with this multiplet while the C8 protons (in a six-membered ring) appear in the general absorption above 300 c.p.s. The sharp peak at 258 c.p.s. may be part of the C10 resonance or, if the total area does in fact represent three protons, it may be caused by the proton at C19, which is common to a five-membered and a six-membered ring and is isolated from protons which could cause splitting.

(6) A single sharp peak at 303 c.p.s. with an area equivalent to three protons. It is attributed to the protons of the N-acetyl group.

(7) A sharp peak at 400 c.p.s. with an area corresponding to about two protons, but the peak is probably associated with some of the adjacent structure and is attributed to the methyl protons of the ethyl group.

A comparison of the spectrum of aspidospermine with that of aspidocarpine shows almost all the expected relationships.

(1) The OH peak at −215 c.p.s. is absent.

(2) The aromatic protons (now three) show a multiplet of the ABC type centered on 32 c.p.s., but a complete analysis is not possible since only nine separate peaks are observed.

(3) The quartet associated with the proton at C-2 now appears at 165, 171, 175, and 182 c.p.s. The shift from the corresponding values in aspidocarpine is associated with the nature of the N-acetyl group. In aspidocarpine the carbonyl of this group is hydrogen-bonded with the C17 hydroxyl and this certainly pulls the oxygen away from the C2 proton. In aspidospermine, hydrogen bonding does not occur and it can readily be seen from models that the acetyl group will take up a less hindered conformation.[6] Since a shift occurs the important deduction that can be drawn is that the assignment of the quartet to the C2 proton resonance is confirmed.

The remainder of the spectrum of aspidospermine is essentially the same as that of aspidocarpine except that the N-acetyl protons appear at 8 c.p.s. lower in the latter, an

[6]*There are two less hindered conformations that can be taken up by the acetyl group. In one conformation the carbonyl and the* C2—H *bond have a cis relationship but are trans in the other. A cis relationship would cause a shift to higher frequency and since the observed shift is to lower frequency the trans relationship is more probable. Stereochemical predictions from scale models are in agreement with this.*

effect probably produced by the hydrogen bonding with the acetyl carbonyl in aspidocarpine.

The spectrum of O-methylaspidocarpine has also given interesting information. Since the phenolic hydroxyl is blocked, hydrogen bonding is excluded in this derivative and the spectrum is very similar to that of aspidospermine except that there are two methoxyl peaks (210 and 215 c.p.s.) and the aromatic proton region shows a complete AB type (11) quartet centered on 39 c.p.s. with an area equivalent to two protons (chemical shift = 11.5 c.p.s. and $J = 8$ c.p.s.). The quartet associated with the C2 proton (166, 172, 176, 182 c.p.s.) is essentially the same as in the spectrum of aspidospermine. The relationship between the spectra in the aromatic region of aspidocarpine and O-methylaspidocarpine affords supporting evidence for the assignment on chemical grounds of substituents to positions 16 and 17. Since the oxygen function at position 17 is considered to be conclusively established, the original methoxyl group must be located at one of the three positions (14, 15, or 16). Position 15 meta to position 17 is excluded because the spectrum requires two adjacent protons. If in O-methylaspidocarpine the original methoxyl were at position 14 the protons at 15 and 16 would have almost identical environment, and a very small chemical shift would be expected. In fact the chemical shift in the O-methylaspidocarpine spectrum is greater than in the spectrum of aspidocarpine and the methoxyl must therefore be placed at position 16. The small chemical shift for the aromatic protons in aspidocarpine is explainable by the fact that the effect of a hydroxyl group on a proton para to it (i.e., at position 14) is almost the same as the effect of a methoxyl group (position 16) on a proton at its ortho position (i.e. position 15).

Conroy and his co-workers (6) have made an analysis of the spectrum of aspidospermine using a 40 Mc/s instrument, and while the major features of their spectrum correspond to those of ours (after the appropriate conversions of scale, etc.) there are several important differences. The peaks that we have assigned to the C2 and C10 protons are not easily seen in their chloroform solution spectrum, but are more evident when they used carbon tetrachloride as solvent. The peaks close to the N-acetyl and methoxyl signals which they assign to the CH_2 groups and the CH adjacent to the nitrogen do not appear in our spectrum.

EXPERIMENTAL

Melting points were determined on a Kofler micro hot stage. The infrared spectra were obtained with a Perkin–Elmer model 21 spectrophotometer, and the absorption is reported in wave numbers followed by a bracketed (m) or (s) to indicate medium or strong absorption. The ultraviolet spectra unless otherwise stated were determined with a Beckman model DU spectrophotometer.

Isolation of Aspidocarpine

The root bark of *Aspidosperma megalocarpon* Muell. Arg. (83.2 kg) was ground to a powder and percolated with petroleum ether (b.p. 95°–110°). The petroleum ether extract was concentrated under reduced pressure and the concentrate deposited the crude alkaloid in crystalline form. Aspidocarpine was purified by recrystallization from heptane and from methanol from which it separated as colorless prisms (50 g), m.p. 168.5–169.5°, $[\alpha]_D^{25}$ +140° (*c*, 2.3 in chloroform), pK_a, 6.55 (by titration with *p*-toluenesulphonic acid). Found: C, 71.18, 71.13; H, 8.10, 8.11; N, 7.52; act. H, 0.26; CH_3CO, 10.06; C—CH_3, 6.34; OCH_3, 8.28, 8.29; N—CH_3, 3.09 (spurious result); mol. equiv. 371, 374 (acid titration). Calc. for $C_{22}H_{30}O_3N_2$; C, 71.32; H, 8.16; N, 7.56; 1 act. H, 0.27;

Can. J. Chem. Downloaded from www.nrcresearchpress.com by 210.87.254.42 on 09/05/12
For personal use only.

1 CH_3CO, 11.61; 2C.CH_3, 8.12; 1 OCH_3, 8.38; mol. wt. 370. Infrared in chloroform: 1632, 1603, 1582 cm^{-1}, in nujol: 1637, 1605, 1587 cm^{-1}. Ultraviolet spectrum in 95% ethanol: λ_{max}, 228 mμ, log ϵ 4.42, 263.5 mμ, log ϵ 3.92, λ_{min} 249 mμ, log ϵ 3.80; after addition of a drop of aqueous sodium hydroxide: λ_{max} 224 mμ, log ϵ 4.29, 238 mμ, log ϵ 4.29, 308 mμ, log ϵ 3.65.

Aspidocarpine perchlorate, prepared in the usual manner separated from methanol as colorless needles, m.p. 280–282° (decomp.). Found: C, 56.38; H, 6.29; N, 5.93. Calc. for $C_{22}H_{30}O_3N_2.HClO_4$: C, 56.11; H, 6.64; N, 5.95%. Ultraviolet spectrum in 95% ethanol: λ_{max} 227 mμ, log ϵ 4.28, 262 mμ, log ϵ 3.82; λ_{min} 250 mμ, log ϵ 3.68.

Aspidocarpine hydrochloride crystallized from ethyl acetate–ethanol as colorless prismatic needles, m.p. 224–230° (decomp.). Found: C, 64.47; H, 7.52. Calc. for $C_{22}H_{30}O_3N_2.HCl$: C, 64.93; H, 7.63%.

The hydrobromide separated from methanol as prismatic needles m.p. 288–290°. Found: C, 57.82; H, 6.68. Calc. for $C_{22}H_{30}O_3N_2.HBr.O.5H_2O$: C, 57.38; H, 7.00%.

Aspidocarpine hydriodide crystallized in rectangular plates from methanol, m.p. 272–274° (decomp.). Found: C, 52.17; H, 6.09. Calc. for $C_{22}H_{30}O_3N_2.HI.0.5H_2O$: C, 52.08; H, 6.35%.

O-Acetylaspidocarpine

Aspidocarpine (281 mg) was dissolved in acetic anhydride (3 ml) containing pyridine (0.8 ml) and allowed to stand at room temperature for 6 hours. The solution was evaporated to dryness under reduced pressure, the residue dissolved in benzene and chromatographed on neutral alumina. Careful elution with benzene and evaporation of the eluate gave a crystalline product which separated from hexane–ether as colorless prisms, m.p. 165–167°, $[\alpha]_D^{25}$ −8.4° (*c*, 0.81 in chloroform). Found: C, 69.90; H, 7.78; CH_3CO, 20.25. Calc. for $C_{24}H_{32}O_4N_2$: C, 69.88; H, 7.82; CH_3CO (one OAc+one NAc) 20.86%. Infrared in chloroform: 1768 (s), 1666 (s) cm^{-1}. Ultraviolet (95% ethanol; Cary model 11M): λ_{max} (log ϵ) 223 mμ (4.53), 253 mμ (3.98), 292 mμ (3.61); λ_{min} (log ϵ), 240 mμ (3.89), 272 mμ (3.28). The spectrum was not appreciably affected by the presence of base.

O-Methylaspidocarpine

Aspidocarpine (1.040 g) was dissolved in dilute hydrochloric acid (20 ml) and the solution made basic by the cautious addition with stirring of 20% aqueous sodium hydroxide. A precipitate was first formed which redissolved after the solution had become basic. Methylation was carried out with methyl sulphate (5 ml) in the usual manner. The product which separated as the reaction proceeded was filtered off and washed with water. After two crystallizations from aqueous methanol it consisted of prismatic needles (0.752 g) m.p. 152–154° $[\alpha]_D^{25}$ −94° (*c*, 1.15 in chloroform). Found: C, 71.44; H, 8.10; CH_3O, 16.58; CH_3N, 0.94 (spurious). Calc. for $C_{23}H_{32}O_3N_2$: C, 71.84; H, 8.39; $2CH_3O$, 16.14%. pK_a 6.9 (titration with *p*-toluenesulphonic acid in 50% ethanol).

Infrared (chloroform): 1660 (sh), 1645 (s) cm^{-1}; in carbon tetrachloride, 1663 (s) cm^{-1}; in nujol, 1656 (s) cm^{-1}. Ultraviolet in 95% ethanol: λ_{max} (log ϵ) 224 mμ (4.60), 252 mμ (4.07), 288 mμ (3.44), λ_{min} (log ϵ), 244 mμ (4.03), 279 mμ (3.41). The spectrum was not appreciably affected by base.

O-Methyldeacetylaspidocarpine

O-Methylaspidocarpine (107 mg) was dissolved in 10% hydrochloric acid (5 ml) and the solution refluxed in an atmosphere of nitrogen for 3 hours. The cooled solution was

Can. J. Chem. Downloaded from www.nrcresearchpress.com by 210.87.254.42 on 09/05/12
For personal use only.

made basic with solid sodium carbonate and immediately extracted with chloroform. After drying (sodium sulphate) the extract was evaporated to dryness and the residue dissolved in aqueous methanol from which it crystallized as white needles (50 mg), m.p. 151–152°. Recrystallization raised the melting point to 153–154°. $[\alpha]_D^{25}$ −4.9° (*c*, 1.03 in chloroform). pK_a 7.8 (titration with *p*-toluenesulphonic acid in 50% ethanol). Found: C, 73.95; H, 8.83; N, 8.65. Calc. for $C_{21}H_{30}O_2N_2$: C, 73.64; H, 8.83; N, 8.18%. Infrared in nujol 3335 cm^{-1}. Ultraviolet in 95% ethanol: strong end absorption, λ_{infl} 240 mμ, log ε 3.82, λ_{min} 268 mμ, log ε 2.97, λ_{max} 293 mμ, log ε 3.49. The spectrum was not appreciably affected by acid.

Treatment of a sample of O-methyldeacetylaspidocarpine with acetic anhydride and pyridine reconverted it to O-methylaspidocarpine in about 50% yield.

O,O-Diacetyl-O-demethylaspidocarpine

Aspidocarpine (731 mg) was refluxed with constant boiling hydrobromic acid (10 ml) in an atmosphere of nitrogen for 1 hour. The solution was evaporated to dryness under reduced pressure and the residue heated on the steam bath with acetic anhydride (15 ml) in an atmosphere of nitrogen for 3 hours. The solution was evaporated to dryness under reduced pressure and the residue dissolved in dilute aqueous sodium carbonate. This solution was extracted with ether and the extract washed with a little water and dried (sodium sulphate). Evaporation of the ether yielded a residue (757 mg) which crystallized from hexane–acetone as yellowish microcrystals (510 mg), m.p. 140–144°. After treatment with charcoal and recrystallization from the same solvent, the product consisted of colorless platelets, m.p. 144–145°, $[\alpha]_D^{25}$ +9.8° (*c*, 1.33 in chloroform). Found: C, 68.21; H, 7.19; CH_3CO, 30.36. Calc. for $C_{25}H_{32}O_5N_2$: C, 68.16; H, 7.32; $3CH_3CO$, 29.31%. Infrared in chloroform: 1777 (sh), 1767 (s), 1668 (s) cm^{-1} (in nujol, 1204 cm^{-1}).

O-Demethylaspidocarpine

The material was prepared first by controlled hydrolysis of O,O-diacetyl-O-demethylaspidocarpine but it was found more convenient to start with aspidocarpine and carry out the whole preparation in the same flask without isolating the intermediates in pure form.

Aspidocarpine (1.043 g) was treated successively with hydrobromic acid and acetic anhydride as described above for the preparation of the diacetyl derivative. After removal of the acetic anhydride, the crude residue was dissolved in methanol (25 ml) to which was added 20% aqueous sodium hydroxide (2.5 ml). The solution was refluxed in an atmosphere of nitrogen for 20 minutes and then evaporated under reduced pressure to a volume of about five milliliters. Crushed ice (ca. 5 g) was added, the solution made just acid with 5% sulphuric acid, then brought to pH 8 with aqueous sodium carbonate and finally thoroughly extracted with chloroform. The extract was dried (sodium sulphate) and the solvent removed by evaporation. The residue, a brown solid (0.845 g) was dissolved in a mixture of ether and benzene and passed through a short column of silica gel which was then eluted with a mixture of benzene (4 parts) and ether (1 part). Evaporation of the eluate yielded a colorless solid (0.676 g) which, on crystallization from aqueous methanol, formed needles, m.p. 130° with an apparent phase change and partial melting at 92–94°. Recrystallization from benzene produced colorless tablets, m.p. 130°, with softening above 125°. After drying *in vacuo*, found: C, 70.91; H, 8.17; N, 7.79. Calc. for $C_{21}H_{28}O_3N_2$: C, 70.76; H, 7.92; N, 7.86%. $[\alpha]_D^{25}$ +121° (*c*, 0.81 in chloroform). Infrared (nujol), 3330 (m), 1634 (s) cm^{-1}. Ultraviolet (pure ethanol): λ_{max} (log ε) 227 mμ (4.41),

Can. J. Chem. Downloaded from www.nrcresearchpress.com by 210.87.254.42 on 09/05/12
For personal use only.

262 mμ (4.01), λ_{min} (log ε) 248 mμ (3.86). In the presence of buffered boric acid: strong end absorption, λ_{infl} (log ε) 258 mμ (4.08), λ_{max} (log ε) 290 mμ (3.56).

For the determination of the ultraviolet spectra in the presence of buffered boric acid a stock solution of O-demethylaspidocarpine (2.0 mg) in pure ethanol (10 ml) was prepared. Simple dilution of the stock solution afforded the solution used in determining the spectrum of the untreated substance. For the spectrum in the presence of buffered boric acid, the stock solution (1 ml) was added to a saturated solution of boric acid in ethanol (2 ml) and diluted to 10 ml with ethanol. Excess anhydrous sodium acetate was added, and the mixture was thoroughly shaken and allowed to stand for 20 minutes before use.

Treatment of O-demethylaspidocarpine in methanol with an ethereal solution of diazomethane reconverted it to aspidocarpine in 60% yield.

Aspidocarpine-N(b)-methiodide

Aspidocarpine (258 mg) was dissolved in dimethylformamide (5 ml) containing methyl iodide (3 ml) and heated under reflux on a steam bath for 4 hours. The solution was evaporated to dryness on a rotary evaporator and the yellow residue crystallized from methanol from which it separated as yellowish crystals (170 mg), m.p. 280–284° (decomp.). Recrystallization from the same solvent gave colorless rectangular plates, m.p. 288–290° (decomp.). Found: C, 52.93; H, 6.26. Calc. for $C_{22}H_{30}O_3N_2.CH_3I.O.5H_2O$: C, 52.98; H, 6.57%.

Aspidocarpine-N(*b*)-methiodide (34 mg) was refluxed for 30 minutes with a solution of potassium hydroxide (70 mg) in 95% ethanol (5 ml) in an atmosphere of nitrogen. The solution was evaporated to dryness under reduced pressure and the yellowish residue dissolved in water (5 ml). The aqueous solution was thoroughly extracted with ether, the extract washed with a little water, dried (sodium sulphate), and evaporated to dryness. The residue was a slightly discolored crystalline solid (17 mg) which, on recrystallization, proved identical with an authentic sample of aspidocarpine.

von Braun Degradation: Aspidocarpine Bromocyanamide

Aspidocarpine (215 mg) was refluxed with cyanogen bromide (416 mg) in chloroform (10 ml) for 24 hours. Evaporation of the solution left a white residue which was triturated with ethyl acetate. The insoluble fraction (70 mg) proved to be aspidocarpine hydrobromide. The ethyl acetate solution when concentrated deposited a colorless crystalline solid (133 mg), m.p. 167–169°, which formed needles, m.p. 170–171° on recrystallization from methanol. Found: C, 58.45; H, 6.33; N, 8.93. Calc. for $C_{23}H_{30}O_3N_3Br$: C, 57.98; H, 6.35; N, 8.81%. Infrared (nujol): 2218(m), 1633(s) cm^{-1}.

In a subsequent preparation, the alkaloid hydrobromide was removed by dissolving the crude mixture in chloroform and chromatography on a short column of neutral alumina.

Aspidocarpine bromocyanamide (73 mg) was refluxed for 6 hours with 95% ethanol (9 ml) in an atmosphere of nitrogen. The solution was concentrated to a small volume under reduced pressure, diluted with a little water, made basic with solid sodium carbonate, and extracted with chloroform. The extract, after drying over sodium sulphate, was chromatographed on a short column of neutral alumina and eluted with chloroform. The eluate yielded a solid product (60 mg) which, on crystallization from methanol, formed colorless prisms identical in every respect with aspidocarpine.

Can. J. Chem. Downloaded from www.nrcresearchpress.com by 210.87.254.42 on 09/05/12
For personal use only.

Chromic Acid Oxidation

(a) Aspidocarpine

The alkaloid (1.131 g) was dissolved in water (17 ml) containing sulphuric acid (3 ml) and heated on a steam bath. Chromium trioxide (1.8 g) dissolved in a little water was cautiously added over a period of about one hour. Heating was continued for a further hour and the hot solution subsequently made basic with hot aqueous barium hydroxide and filtered. The yellow filtrate was exhaustively extracted with chloroform and the dried (sodium sulphate) extract evaporated. A semisolid residue was left (0.169 g) which was dissolved in benzene, chromatographed on neutral alumina, and crystallized in a mixture of hexane and acetone from which it separated as yellowish microcrystals (76 mg), m.p. 222–224°. Recrystallization from the same solvent gave pale yellowish rods, m.p. 224–225°, $[\alpha]_D^{25}$ −132° (*c*, 1.03 in chloroform). Found: C, 68.87; H, 8.52; N, 10.63. Calc. for $C_{15}H_{22}O_2N_2$: C, 68.67; H, 8.45; N, 10.68%. Infrared (chloroform): 3410 (w), 1762 (s), 1728 (vs) cm^{-1}. Ultraviolet (95% ethanol): λ_{min} 227 mμ log ϵ 3.31, λ_{max} 252 mμ log ϵ 3.55, 336 mμ, ϵ 59. In the presence of a drop of dilute aqueous potassium hydroxide: λ_{min} 234 mμ log ϵ 3.28, λ_{max} 268 mμ log ϵ 3.48 (longer wave-length absorption not measured).

(b) Aspidospermine

Aspidospermine obtained from Inland Alkaloid Co., and recrystallized (1.020 g) was treated with chromic acid as described above, except that heating was continued for 8 hours. The crude product (0.105 g) proved more difficult to purify than the oxidation product of aspidocarpine. The crystalline product, m.p. 223–225°, has $[\alpha]_D^{25}$ −128° (*c*, 0.47 in chloroform). Its infrared spectrum contained the same peaks as that of the oxidation product of aspidocarpine and the X-ray diffraction patterns of both compounds were identical.

ACKNOWLEDGMENTS

The authors acknowledge their indebtedness to Dr. Maria Przybylska for the X-ray powder patterns and Dr. R. Norman Jones and Mr. R. Lauzon for the infrared spectra.

REFERENCES

1. B. Witkop and J. B. Patrick. J. Am. Chem. Soc. **76**, 5603 (1954).
2. R. N. Jones and C. Sandorfy. *In* Chemical applications of spectroscopy. *Edited by* W. West. Interscience Publishers, Inc., New York. 1956. p. 483.
3. E. Adler and R. Magnusson. Acta Chim. Scand. **13**, 505 (1959).
4. F. Lyons, W. H. Perkin, and R. Robinson. J. Chem. Soc. **127**, 1158 (1925).
5. L. Jurd. Arch. Biochem. Biophys. **63**, 376 (1956).
6. H. Conroy, P. R. Brook, M. K. Rout, and N. Silverman. J. Am. Chem. Soc. **80**, 5178 (1958).
7. O. O. Orazi, R. A. Corral, J. S. E. Holker, and C. Djerassi. J. Org. Chem. **21**, 979 (1956).
8. A. J. Ewins. J. Chem. Soc. **105**, 2738 (1914).
9. J. F. D. Mills and S. C. Nyburg. Tetrahedron Letters, **11**, 1 (1959); J. Chem. Soc. 1458 (1960).
10. H. Conroy, P. R. Brook, and Y. Amiel. Tetrahedron Letters, **11**, 4 (1959).
11. J. A. Pople, W. G. Schneider, and H. J. Bernstein. High-resolution nuclear magnetic resonance. McGraw-Hill Book Co., Inc., New York. 1959. Chap. 6.
12. H. S. Gutowsky, R. L. Rutledge, M. Tamres, and S. Searles. J. Am. Chem. Soc. **76**, 4242 (1954)

Can. J. Chem. Downloaded from www.nrcresearchpress.com by 210.87.254.42 on 09/05/12
For personal use only.

Can. J. Chem. Downloaded from www.nrcresearchpress.com by 210.87.254.105 on 09/05/12
For personal use only.

THE ELECTROCHEMICAL BEHAVIOR OF THE NICKEL OXIDE ELECTRODE

PART II. QUASI-EQUILIBRIUM BEHAVIOR[1]

P. L. Bourgault and B. E. Conway

ABSTRACT

The electrode potential of the nickel oxide electrode has been determined as a function of water and solute activity in aqueous solutions of potassium hydroxide. The electrode, which was charged to a mean state of oxidation corresponding to 50% Ni II and 50% Ni III, was examined after long periods of time and by cathodic and anodic e.m.f. decay measurements after polarization in order to establish the quasi-reversible potentials by two methods. The results are discussed in terms of the stoichiometry of the potential-determining reaction, and distinction between mixed and true reversible potentials is made.

INTRODUCTION

We have previously examined in part I (1) the kinetic behavior of the "overcharged" nickel oxide electrode with regard to rates of self-discharge and oxygen evolution. In the present paper we present data on the quasi-equilibrium potentials of the nickel oxide electrode in aqueous potassium hydroxide solutions. The behavior of the electrodes is referred to as "quasi-equilibrium" since the electrodes are continuously losing charge on open-circuit by the corrosion type of process described previously (1).

This can affect the electrode in two ways: firstly to produce a continuous but slow decrease of the state of oxidation of the oxide and secondly to give rise to an electrode potential which is more cathodic than the true equilibrium potential corresponding to the formal state of oxidation of the oxide. In fact, the potentials measured on open-circuit are analogous to mixed potentials observed in corrosion, since there is a slow anodic evolution of oxygen and a corresponding cathodic self-reduction of the oxide. This factor does not seem to have been realized in previous work (2, 3, 4). However, by suitable choice of conditions and methods of study it is possible to determine the potential of the electrode under conditions very near to equilibrium. Thus, if the electrodes are left in dilute potassium hydroxide (0.001 M) for several days, the potential ceases to change by more than 0.1 mv per hour and the potential of the electrode may then be examined as a function of potassium hydroxide activity without further significant self-discharge during the measurements. Also in the solutions of higher alkali concentration the electrode is more stable* since the open-circuit potential becomes less anodic to the reversible oxygen potential and the rate of self-discharge (already allowed to become small in the 0.001 M solution) becomes negligible.

Electrode potentials and stoichiometric reactions for the potential-determining reaction at the nickel oxide electrode have been discussed in earlier work by Forster (2) and Zedner (3) and more recently by Kornfeil (4). A potential of 0.49 v has been attributed to the nickel oxide electrode by Latimer (5), but no evidence that the potential-determining species (e.g. NiO_2) are those written by Latimer (5) has been given; in fact there is no evidence that NiO_2 exists as such in the electrochemically active material in the nickel

[1]*Manuscript received April 22, 1960.*
Contribution from the Department of Chemistry, University of Ottawa, Ottawa, Ontario.

**This is not in contradiction to our previous findings (1); in the latter work we showed that the exchange currents for oxygen evolution became greater in the solutions of higher alkali concentration. In the present work the open-circuit potentials are lower in the stronger solutions so that the oxygen "overpotential" is relatively smaller and the self-discharge rate is hence less at the open-circuit potential.*

oxide electrode. The IV-valent state of nickel may exist in a non-stoichiometric oxide lattice in electrodes charged beyond the "$NiO_{1.5}$" composition but it is not possible at room temperature to achieve states of oxidation greater than about "$NiO_{1.7}$" (6), so that the oxide cannot be completely oxidized to the "NiO_2" state. In other work (2, 3) the stoichiometric reactions suggested are not in mutual agreement and the more recent work (4) contributes further serious discrepancies.

We have therefore examined the potential of partially charged nickel oxide electrodes at a controlled formal state of oxidation as a function of potassium hydroxide and water activity in aqueous alkali solutions by a polarization decay method in which the reversible potential is approached both from the anodic and cathodic directions. This method may be expected to give more reliable values of the electrode potential than those obtained by leaving the electrode on open-circuit for arbitrary periods of time. We have also compared data obtained by the decay method with the e.m.f. values from "stationary" potential measurements i.e. at very long times, and deduced the nature of the potentials which are measured by these procedures. From these determinations, the role of potassium hydroxide and water in the over-all potential-determining reaction can be evaluated.

EXPERIMENTAL

1. General

Nickel hydroxide electrodes were prepared in nickel sinters as described previously and charged anodically (7, 1) to the higher oxide for 30 hours at 25° C in aqueous potassium hydroxide (analytical grade) solutions of the concentrations indicated below, until an appreciable rate of oxygen evolution was maintained.

2. Reversible Potentials from Polarization Decay Measurements

Here the potentials of nickel oxide electrodes at a formal state of oxidation of $NiO_{1.25}$ were determined by extrapolating cathodic and anodic e.m.f. decay lines, plotted logarithmically in time, to the potential of their intersection. This procedure is analogous to the determination of reversible potentials by extrapolation of anodic and cathodic Tafel lines to zero overpotential (cf. 26).

The electrodes were prepared as described above and initially charged in solutions of KOH of various concentrations at 38.2 ma per gram of $Ni(OH)_2$ for 30 hours at 25° C. The electrodes were then left to stand on open-circuit to allow the surface pseudocapacity (8) to become discharged. The remaining bulk electrochemical capacity* was then determined by discharging the electrode at a constant rate such that the theoretical capacity (based on a state of oxidation "$NiO_{1.5}$") would be discharged in 5 hours. The observed charge held by the electrodes agreed with that expected theoretically to within 10% (this deviation simply means that a state of oxidation slightly different from $NiO_{1.5}$ is reached initially). On the basis of this determination, a charging rate i_c was then chosen such that the electrode would be oxidized to 50% Ni^{II}–Ni^{III} (i.e. $NiO_{1.25}$) in 1 hour. The charging was interrupted and the decay of potential was followed on open-circuit for 24 hours or more on a recording potentiometer. The charging was resumed at the rate i_c for 2 hours; after decay on open-circuit for several hours (to again discharge the surface capacity associated with oxygen evolution), discharging was commenced at the rate $-i_c$ for 1 hour so that the electrode regained a state of oxidation of "$NiO_{1.25}$". The discharging current was interrupted and the potential decay from this *cathodic*

**We use the term "capacity" here in the sense familiar in battery technology. We in fact determine the Faradaic charge, which can be withdrawn from the electrode by the current i_c passing for a measured period of time.*

Can. J. Chem. Downloaded from www.nrcresearchpress.com by 210.87.254.105 on 09/05/12
For personal use only.

polarization was followed for 24 hours, after which the remaining bulk electrochemical "capacity" was checked by complete discharge with the same current, $-i_c$.

This sequence of operations and the corresponding e.m.f.'s are shown schematically for a typical experiment (in 7.3 M KOH) in Fig. 1.

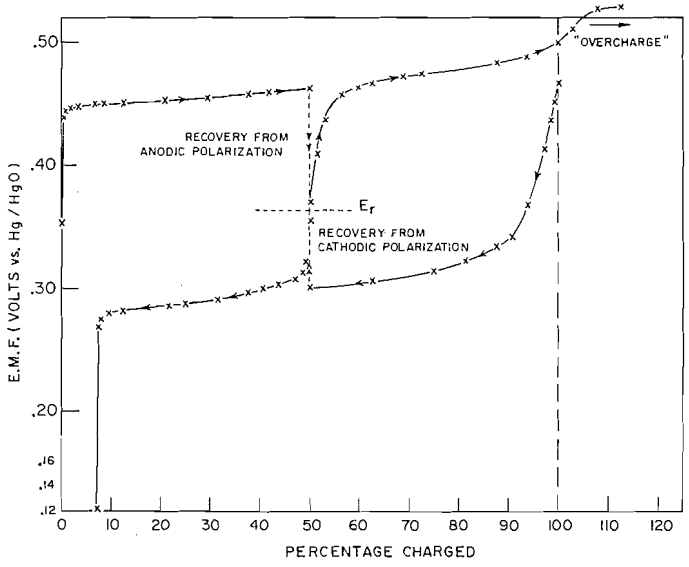


FIG. 1. Charging and discharging cycle for the nickel oxide electrode used in polarization decay studies.

3. Quasi-Equilibrium Potentials

In this series of measurements, electrodes were allowed to stand on open-circuit in 0.001 M aqueous KOH until the degree of charge corresponded to an approximate state of oxidation of "$NiO_{1.25}$". The electrodes were then transferred to other potassium hydroxide solutions by the following three alternative procedures:

(*a*) Six electrodes were transferred directly into solutions 14.6, 11.0, 7.3, 3.7, 1.46, and 0.146 M in KOH, respectively, which were stirred by bubbling purified oxygen. The e.m.f. of the electrodes was followed as a function of time (versus a Hg/HgO electrode) for 1 week.

(*b*) Six electrodes were transferred from the 0.001 M KOH to a solution of 14.6 M KOH where they were allowed to stand for about 24 hours; they were then transferred to solutions of 0.07, 0.146, 0.73, 1.46, 7.3, and 11 M KOH respectively and again the e.m.f. was recorded at regular intervals of time.

(*c*) (i) An electrode was taken from the 0.001 M KOH solution and then allowed successively to equilibrate in 0.07, 0.7, 3.65, 7.3, 11.0, and 14.6 M KOH solutions for periods of 2 hours during which the e.m.f. became constant to better than 0.5 mv per hour. A reverse series of measurements was then made by transferring the electrodes back from the concentrated to the more dilute solutions.

(ii) A similar series of e.m.f. values were obtained by transferring the electrode from the 0.001 M KOH directly to the strongest (14.6 M) solution and thence successively to the more dilute solutions and back again to the more concentrated ones.

From these measurements, the reversibility of the e.m.f. changes with changes of

Can. J. Chem. Downloaded from www.nrcresearchpress.com by 210.87.254.105 on 09/05/12
For personal use only.

concentration could be judged. The sequence of changes of conditions and corresponding e.m.f. values can be seen by reference to Fig. 2.

The degree of oxidation of the electrodes was measured after the e.m.f. runs by discharging the electrodes at a controlled current (30 ma per gram of $Ni(OH)_2$) and hence determining coulometrically their electrochemical "capacity".

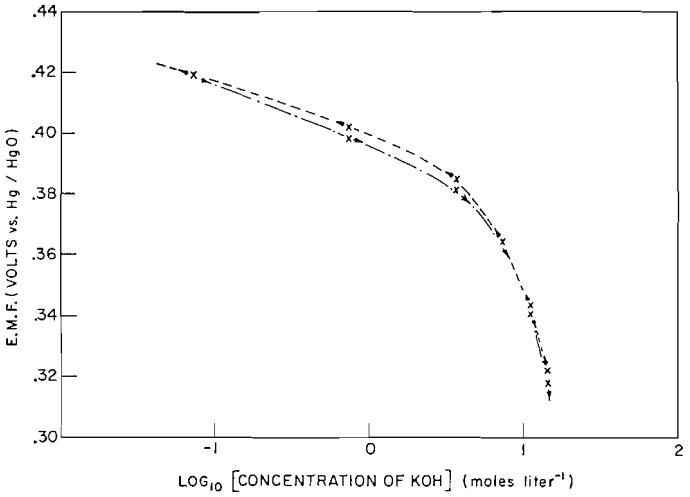


FIG. 2. Reversibility of e.m.f. of the nickel oxide electrode with successive changes of concentration. Arrows indicate sequence of changes for electrode initially put in strongest solution after being maintained in 0.001 *M* KOH.

4. Solutions

Aqueous solutions of analytical grade potassium hydroxide were made up by diluting a saturated (25° C) solution of potassium hydroxide kept in a "seasoned" closed "polythene" bottle. Concentrations were checked after runs by titration against standard acid. The water used had been prepared from distilled water by a further distillation from alkaline permanganate in a still provided with three glass spray traps. Use of potassium hydroxide recrystallized at −20° C gave results insignificantly different from those obtained with the analytical grade reagent.

Several experiments were also carried out in heavy water (99.76% D_2O) and in these cases, KOD solutions in D_2O were prepared by decomposing electrolytically prepared dry potassium amalgam with the heavy water. The nickel oxide electrodes for this part of the work were prepared by impregnating the sinters with a solution of nickel sulphate made up from the anhydrous substance by dissolution in deuterium oxide. The Ni_2SO_4 was obtained from the hexahydrate by heating it to constant weight (52 hours) at 600–700° C. Control runs were also carried out on electrodes prepared by the same method but using ordinary water as the solvent.

5. Measurement of e.m.f.

Potentials of the nickel oxide electrodes were measured against yellow mercuric oxide electrodes (9) in the same solutions by means of a Tinsley potentiometer and a Philips high input impedance recording potentiometer capable of measuring to 0.5 mv on a full scale of 100 mv on various voltage ranges.

Can. J. Chem. Downloaded from www.nrcresearchpress.com by 210.87.254.105 on 09/05/12
For personal use only.

Can. J. Chem. Downloaded from www.nrcresearchpress.com by 210.87.254.105 on 09/05/12
For personal use only.

RESULTS

1. Polarization Decay

The kinetic significance of measurements of decay of e.m.f. after cessation of a polarization has been treated previously (10, 11). Thus, the rate of decay of e.m.f. with (Naperian) logarithmic time gives the Tafel slope $-RT/\alpha F$ for the rate-determining mechanism involved in the discharge of the double-layer or surface capacity provided that this capacity is constant in the range of potentials over which the polarization decay occurs. At very long times of decay, the e.m.f. approaches the reversible potential asymptotically as discussed previously (11). Thus, plots of e.m.f. during decay from both anodic and cathodic polarization vs. the logarithm of the effective time of decay can be extrapolated to a potential where they intersect and this potential should approximate closely to the reversible potential E_r (unless other alternative processes can occur), which would theoretically be reached only after infinite time. Plots of decay of anodic and cathodic polarization as a function of time t plus θ, where θ is the semiempirical constant discussed previously (11, 1), are shown for the $NiO_{1.25}$ electrode in Figs. 3*a–d* and 4*a*, *b* for the indicated concentrations of potassium hydroxide. The quantity θ can be regarded as the time required for the potential of the electrode to fall from an infinite value to that at the commencement of decay of the polarization corresponding to passage of a current i_c. The constant θ is given by

$$\theta = Cb/2.3\ i_c \qquad [1]$$

where b is the Briggsian slope for the decay process and C is the capacity suffering discharge by the electrochemical process. The quantity θ is determined as described previously (1, 11) by an empirical procedure but is not involved in the kinetic equations determining the slope b and hence the extrapolated values of E_r.

In order to establish the effect of varying water activity at a constant KOH activity, one experiment was carried out in a saturated aqueous KF solution (25° C) 0.08 molar (i.e. approximately unit activity (see Discussion, Section 4)) in KOH. The anodic and cathodic decay lines are shown in Fig. 4*b*.

In the Figs. 3*a–d* and 4*a*, *b*, the extrapolated values of potential designated E_m or E_r (see below) are shown in the brackets on the ordinate axes and are indicated by dotted lines. Cases where inflections occur in the anodic lines are discussed in detail below.

Decay lines similar to those in Figs. 3*a–d* and 4*a*, *b* are also given in Fig. 5 for the nickel oxide electrodes in a 0.93 *M* KOD solution in deuterium oxide and the data shown are the means of two sets of values which agreed to ca. ±2 *mv*.

2. Quasi-Equilibrium Potentials

The potentials obtained by the procedure *c*(ii) described in Section 3 under Experimental are shown as a logarithmic function of molar concentration of KOH in Fig. 2. The results obtained from "backward" successive immersions agreed with those obtained by "forward" immersions as shown in this figure but some irreversibility occurs when the sequence of operations is carried out by immersing the electrode initially in dilute solutions (*c*(i)) followed successively by more concentrated solutions and then returned to the more dilute solutions. These values obtained in the "forward" direction by procedure *c*(i) are not therefore regarded as true equilibrium values.

In Fig. 6, comparison is made between the data obtained by procedure *b* (crosses)

Can. J. Chem. Downloaded from www.nrcresearchpress.com by 210.87.254.105 on 09/05/12
For personal use only.

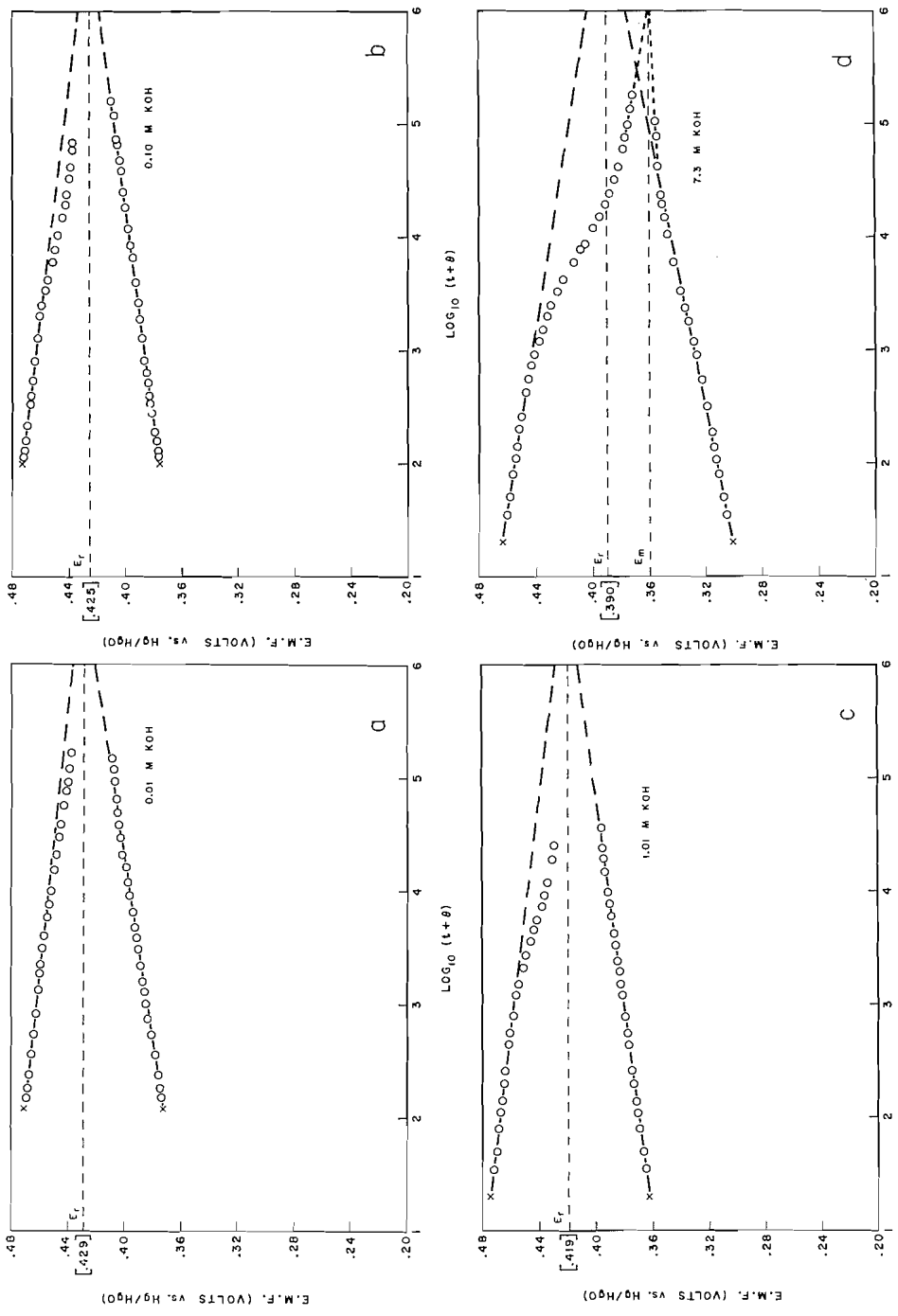


FIG. 3. Decay of e.m.f. from anodic and cathodic polarization as a logarithmic function of effective time of decay. (*a*) 0.01 *M* KOH; (*b*) 0.10 *M* KOH; (*c*) 1.01 *M* KOH; (*d*) 7.3 *M* KOH.

Can. J. Chem. Downloaded from www.nrcresearchpress.com by 210.87.254.105 on 09/05/12
For personal use only.

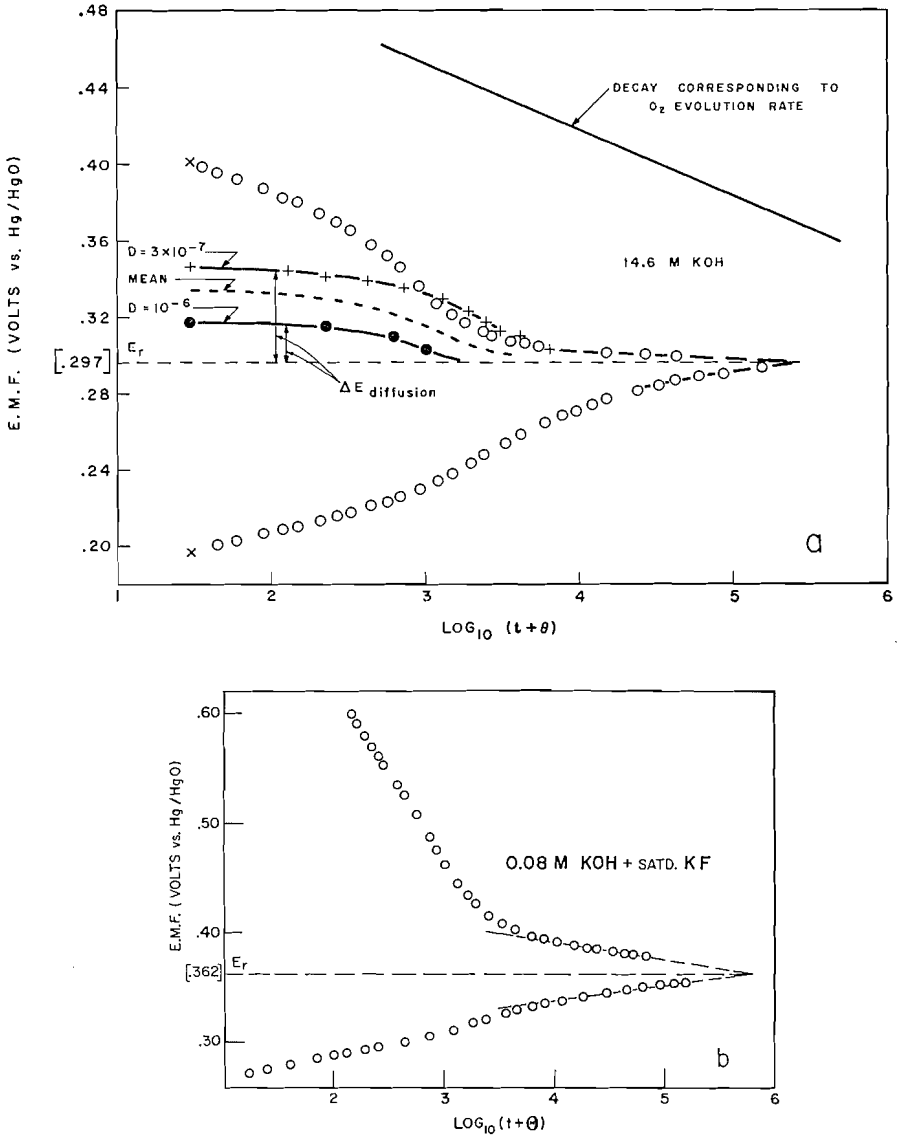


FIG. 4. Decay of e.m.f. from anodic and cathodic polarization as a logarithmic function of effective time of decay.

(*a*) 14.6 *M* KOH showing decay of concentration polarization, $\Delta E_{\text{diffusion}}$, and decay rate corresponding to rate of oxygen evolution.

(*b*) Saturated KF + 0.08 *M* KOH.

(taking the e.m.f. attained 24 hours* after transfer of an electrode from a strong solution to a more dilute one) and the polarization decay method (circles) and it is seen that the polarization decay values tend to be significantly more positive (ca. 15–30 mv) to the Hg/HgO electrode than those obtained by procedure *b*. This is in fact to be expected

**The e.m.f. values obtained by procedure c are not used for comparison with the decay values since the times of equilibration may have been too short for electrolyte diffusion effects to have become negligible in the strongest solutions (see Appendix).*

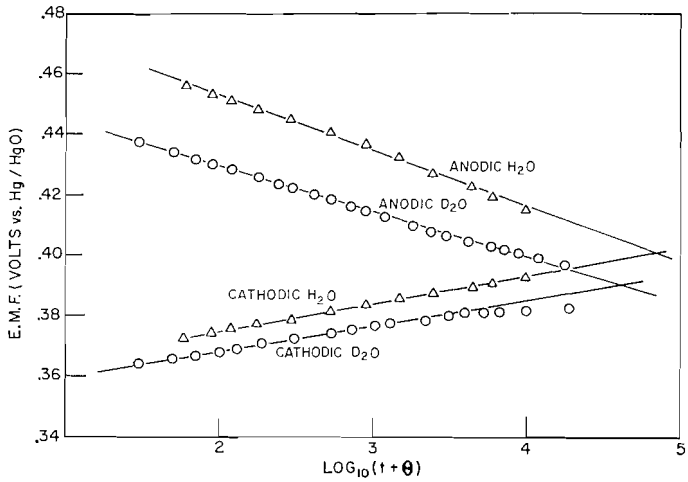


FIG. 5. Decay of e.m.f. from anodic and cathodic polarization in 0.93 *M* KOD/D_2O or KOH/H_2O.

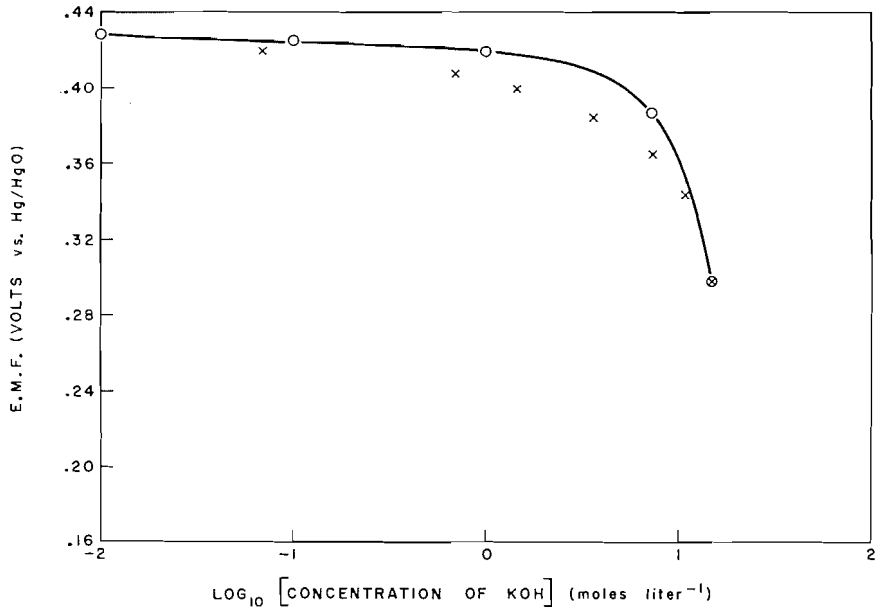


FIG. 6. Comparison of e.m.f. values obtained from "stationary" potential measurements (crosses) and from appropriate extrapolation of logarithmic decay lines (circles).

since the values obtained by the latter procedure are the mixed potentials and will be depressed from the true reversible potential by the small cathodic polarization impressed on the electrode by virtue of its finite rate of self-discharge by the corrosion-type of process discussed previously (1).

3. Accuracy and Reproducibility

Owing to kinetic self-discharge effects and to the relatively complex method (7, and above) of preparation of the electrodes at a controlled state of charge, reproducibility of

Can. J. Chem. Downloaded from www.nrcresearchpress.com by 210.87.254.105 on 09/05/12
For personal use only.

electrode potentials cannot be expected to be so good as that obtainable with primary standard half-cells, e.g. the Ag/AgCl electrode (12). However, replicate runs usually gave e.m.f. values (vs. the Hg/HgO electrode) reproducible to ±3 mv from either the polarization decay method or the procedure *b*.

The precision of the measurements was greater than this since potentials measured on the Tinsley and automatic recording potentiometers could be read to 0.2 mv and 0.5 mv, respectively, with a similar accuracy after standardization by means of a Weston cadmium cell. The temperature of the air thermostat used to house the cells during measurements was constant to ±0.1° C. The order of magnitude of the temperature coefficient of the e.m.f. of the nickel oxide – mercuric oxide electrode pair is 10^{-1} mv $°C^{-1}$ (13) so that the constancy of temperature provided was more than adequate to ensure insignificant errors of e.m.f. arising from temperature fluctuations.

DISCUSSION

1. *Nature of the Electrode Processes*

In the polarization decay studies, the aim was to disturb the equilibrium between reduced and oxidized forms of the nickel oxide in the semicharged electrode ("$NiO_{1.25}$") by passing an anodic or a cathodic current and then observing the decay towards the reversible potential of the oxide electrode. However, whilst passage of a current in either direction will cause a change in the formal degree of oxidation of the bulk material, for the reasons given below this process is found to be an *indirect* one.

The quantity θ, which can be determined empirically for the decay lines shown in Figs. 3 and 4, as described previously (11, 1), enables the surface capacity associated with the electrochemical processes involved in the decay of e.m.f. to be calculated (equation [1]) and the values found are between 500 (7 *M* KOH) and 3000 (0.01 *M* KOH) farads per gram of $Ni(OH)_2$. This capacity is very much larger by several orders of magnitude than any possible ionic double-layer capacity corresponding to the real area of the nickel in the sinter (5000 cm^2* in an electrode capable of supporting 1 g of $Ni(OH)_2$). On the other hand, the charge which can be withdrawn from this capacity over a given voltage range is very much smaller, by a factor of 50–100, than that which can be withdrawn as conventional electrochemical "capacity" from the bulk material over a comparable range of voltage.

The values of the capacity obtained from θ were checked by observations on the potential (E) – time (t) relations for build-up and forced decay of e.m.f. at constant current using the half-charged electrodes. Although there was some hysteresis between build-up and forced decay lines, the mean capacities obtained as $d(it)/dE$ from these measurements were comparable with the capacity values obtained from θ.

The above values of capacity must therefore be regarded as corresponding to a *surface* layer (14*a*) of intermediates (probably adsorbed radicals of OH or O) which participate in the process of oxidation of the bulk material. Conversely, the reduction of the bulk material proceeds by an opposite process, and the reactions observed in the cathodic and anodic polarization and their decay correspond, respectively, to removal and formation of this surface layer. The capacity associated with this layer may be referred to as a "surface capacity" in which the degree of charge must be changed before any chemical changes in the bulk oxide can be effected.

We may therefore qualitatively represent the behavior of the electrode upon charge or

**This value was kindly determined by Dr. C. Amberg of the National Research Council on an outgassed sample of sinter by the B.E.T. method.*

Can. J. Chem. Downloaded from www.nrcresearchpress.com by 210.87.254.105 on 09/05/12
For personal use only.

discharge by the electrical analogue shown in Fig. 7 where C_S is the surface capacity, C_B that corresponding to the electrochemically active bulk material, R_{O_2} the non-ohmic

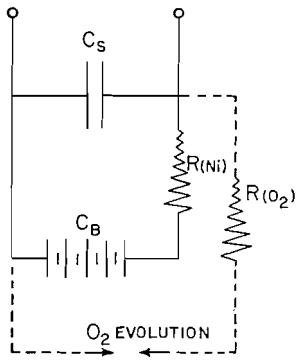


FIG. 7. Schematic equivalent circuit by which charging and discharging of electrode can be represented.

resistance corresponding to the reciprocal of the rate of electrochemical oxygen evolution, and R_{Ni} that corresponding to the reciprocal of the rate of oxidation or reduction of the bulk material by the chemisorbed species constituting the surface pseudocapacity.

When current is made to flow anodically into the system through the two schematic terminals at the top of the circuit (Fig. 7), C_S is first charged up and in the steady state, charge flows mainly through R_{Ni} with some "leakage" through R_{O_2}, giving, respectively, simultaneous oxidation of the bulk material (C_B) and some oxygen evolution. On open-circuit, following anodic polarization, oxygen evolution still occurs (but this can only be detected in the "over-charge" region (Fig. 1) as described previously (1)) and the remainder of the excess charge on C_S passes into C_B with resultant oxidation of the material. This indirect mechanism of charging is supported by the direction of the H/D isotope effect on the polarization on charging and discharging (Fig. 5), which is significantly *less* in D_2O than in H_2O. If H^+ or D^+ transfer steps (1, 6) were rate-determining in the oxidation or reduction of the bulk oxide the reverse isotope effect would be expected (20). The *faster* rate in D_2O is connected with the expected lower heat of solvation of OD^- than that of OH^- in the respective isotopic solvents (21).

Conversely, on cathodic polarization, C_S is discharged to potentials low enough for current to flow from C_B through R_{Ni} sufficient to maintain the current taken from the over-all system, the oxygen evolution rate then being negligible at these more cathodic potentials (it becomes significant in some cases only as the reversible or mixed potential is reached, e.g. in Fig. 3*d*). On open-circuit following cathodic polarization, C_S can be regarded as recharged by the current through R_{Ni} (less the small current corresponding to oxygen evolution) and this corresponds to the lower recovery lines shown in the Figs. 3*a–d* and 4*a*.

At long times after cessation of anodic or cathodic polarization, the potential across C_S would become equal to that set up across C_B if no leakage occurred through R_{O_2}, i.e. if no self-discharge were taking place, and the reversible potential of the electrochemically active material constituting C_B would then be measured by the potential at which the extrapolated logarithmic decay lines intersect. Inspection of the e.m.f. decay lines indicates, however, that in all but the most dilute solutions there are inflections in the anodic lines and at the highest concentrations (14.6 *M*) also in the cathodic line. This

Can. J. Chem. Downloaded from www.nrcresearchpress.com by 210.87.254.105 on 09/05/12
For personal use only.

raises the problem of how the extrapolations should be carried out, i.e. by extension of the upper lines in the region of low times (i.e. log $[t+\theta]$ in the range 1 to 3) or production of the lines after the longest periods of time (i.e. for log $[t+\theta] > 4$). We therefore now consider possible reasons for these inflections in the decay lines.

2. Form of the Decay Lines

(a) Oxygen Evolution Rates

The anodic decay lines for concentrations greater than 0.1 *M* KOH show an inflection from a low slope to a high slope with increasing time which is characteristic of *alternative* electrochemical reactions with different Tafel slopes as discussed by Parsons (14). From the foregoing, it is evident that the process alternative to the one with the lower slope could be oxygen evolution. At higher anodic potentials we have examined the kinetics of oxygen evolution (1, 15) and from these data it is possible to calculate what the rate of oxygen evolution will be in the range of potentials over which the polarization decay occurs at the semicharged electrodes. In Figs. 8*a* and 9*a* are shown the Tafel lines for the anodic oxidation (I) of the semicharged electrode and for oxygen evolution (II) in solutions of the same concentration. The solid lines show the polarization behavior based on i_0 and b values* for each of the alternative processes and the dotted line shows the calculated *total* rates† over the potential range where I and II have comparable rates. Figs. 8*b* and 9*b* show the same data plotted in terms of the e.m.f. decay lines, the dotted region corresponding to the total rate similarly drawn in Figs. 8*a* and 9*a* and the points the actual e.m.f.'s obtained during an experimental decay run. It is clear from these figures that between 0.1 *M* and 7.3 *M* the inflections in the anodic decay lines are adequately accounted for by the alternative oxygen evolution process which becomes (because of its higher b value) the predominant process at low potentials. We may note that the cathodic lines in Figs. 3*a–d* show no significant inflections; this would be expected since the alternative oxygen process is much slower at the more cathodic potentials. Calculations of the rates of the alternative oxygen evolution process indicate that the inflections in all the anodic decay plots up to 7.3 *M* KOH can be accounted for. However, in the 14.6 *M* KOH solution and in some experiments carried out at 0° C, the oxygen evolution rate is too slow by a factor of about 100 to influence the decay, yet an inflection is observed (Fig. 4*a*) and is also present now in the cathodic line. Furthermore, in the 14.6 *M* solution, the e.m.f. reached at long times is below the reversible oxygen potential so that the oxygen evolution process referred to above cannot be responsible for depressing the e.m.f. to this low value. The electrochemical charging or discharging reaction causes changes of the relative concentrations of water and KOH in the sinter (2, 3, 4) and we show in the Appendix that this effect brings about a concentration polarization in the porous electrode which falls off with time on open-circuit owing to diffusion and gives rise to the inflection in Fig. 4*a*.

(b) Mixed Potentials

From the above, it is seen that the potentials reached at the intersection of the decay lines for solutions up to 7.3 *M* in KOH (or at very long times) must be the mixed potentials corresponding to a finite rate of oxygen evolution and self-discharge on open-circuit. These potentials will be less anodic than the true reversible potentials. From the present data (Figs. 3*a–d*) and our other work (1, 15), we can obtain the polarization parameters

**The method of calculation of these parameters from the decay lines has been discussed previously (11, 1).*

†True surface areas of the oxide electrode being unknown, rates in these figures and in Fig. 10 are expressed in amp g^{-1} of $Ni(OH)_2$ *as discussed previously (1).*

Can. J. Chem. Downloaded from www.nrcresearchpress.com by 210.87.254.105 on 09/05/12
For personal use only.

Can. J. Chem. Downloaded from www.nrcresearchpress.com by 210.87.254.105 on 09/05/12
For personal use only.

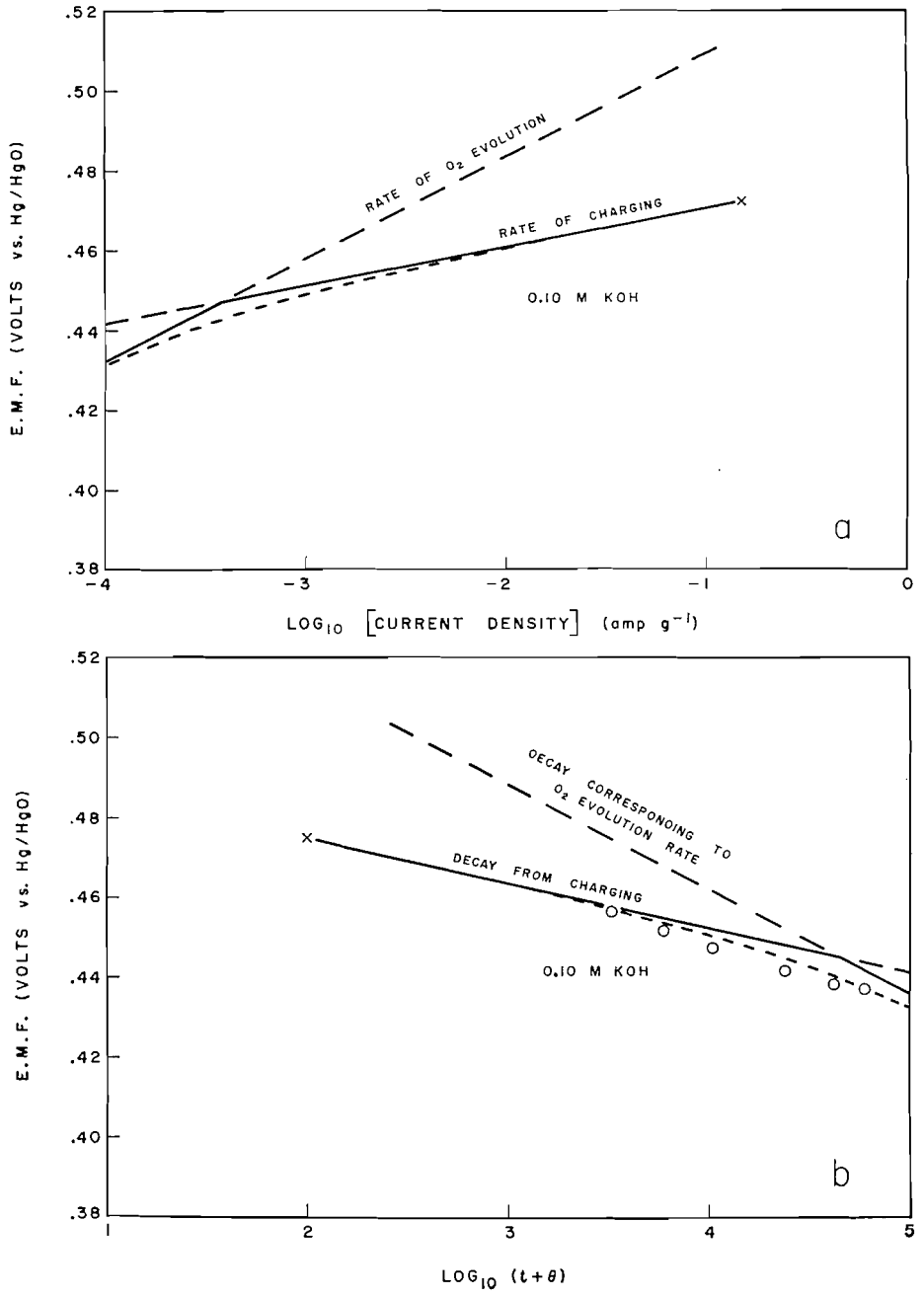


FIG. 8. (*a*) Tafel lines for anodic oxidation of the semicharged electrode and for O_2 evolution (0.1 *M* KOH). Line for *net* current density is broken.

(*b*) E.m.f. decay lines corresponding to rates of anodic charging and O_2 evolution: dotted line is resultant decay curve; circles, experimental points (0.1 *M* KOH).

Can. J. Chem. Downloaded from www.nrcresearchpress.com by 210.87.254.105 on 09/05/12
For personal use only.

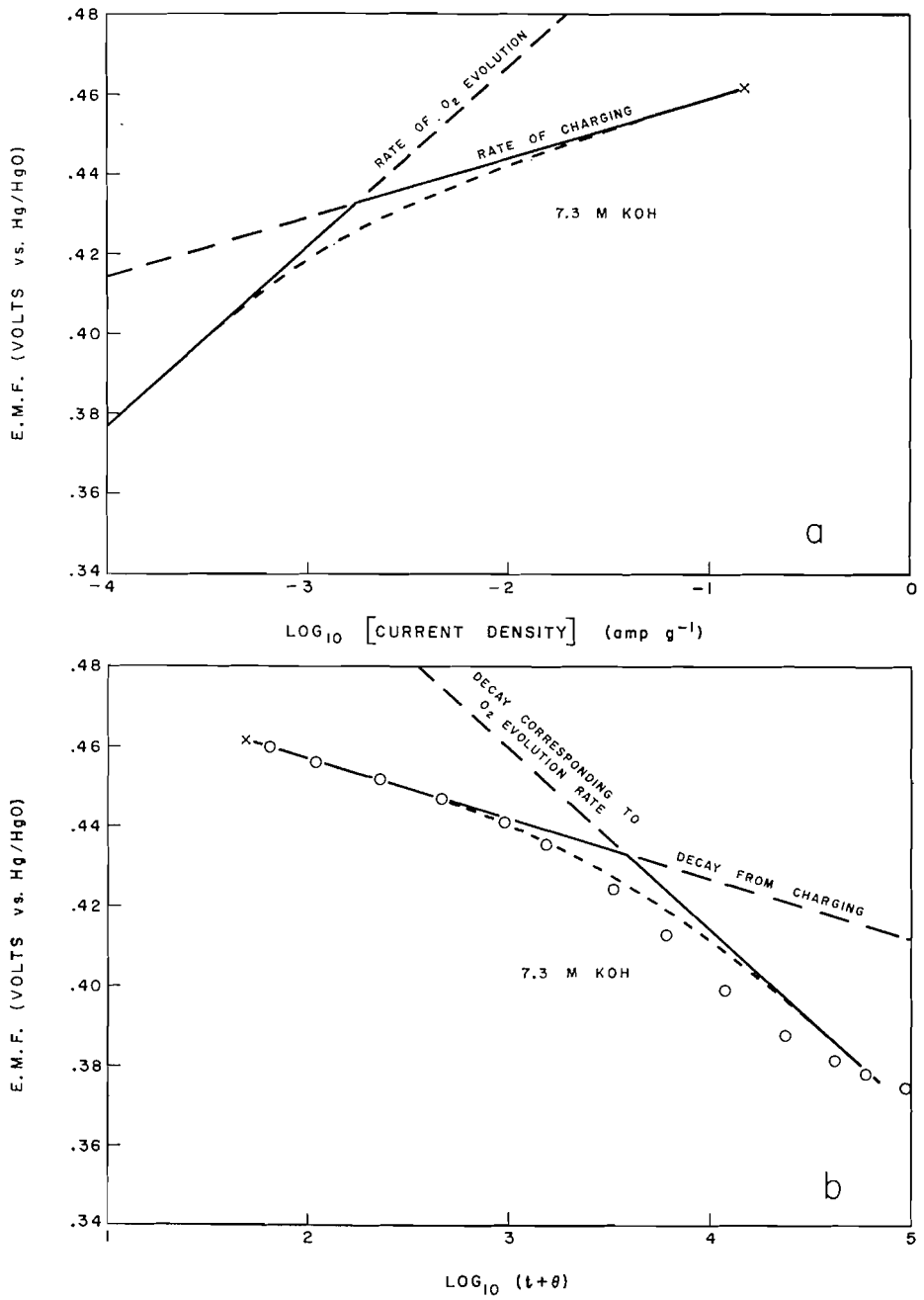


FIG. 9. (*a*) Tafel lines for anodic oxidation of the semicharged electrode and for O_2 evolution (7.3 *M* KOH). Line for *net* current density is broken.

(*b*) E.m.f. decay lines corresponding to rates of anodic charging and O_2 evolution: dotted line is resultant decay curve; circles, experimental points (7.3 *M* KOH).

i_0 and b for the cathodic and anodic partial "corrosion" reactions, respectively, in the self-discharge process; hence, the mixed potential and the net self-discharge rate at this potential may be calculated as shown in Fig. 10 for 7.3 M KOH solution. In this diagram,

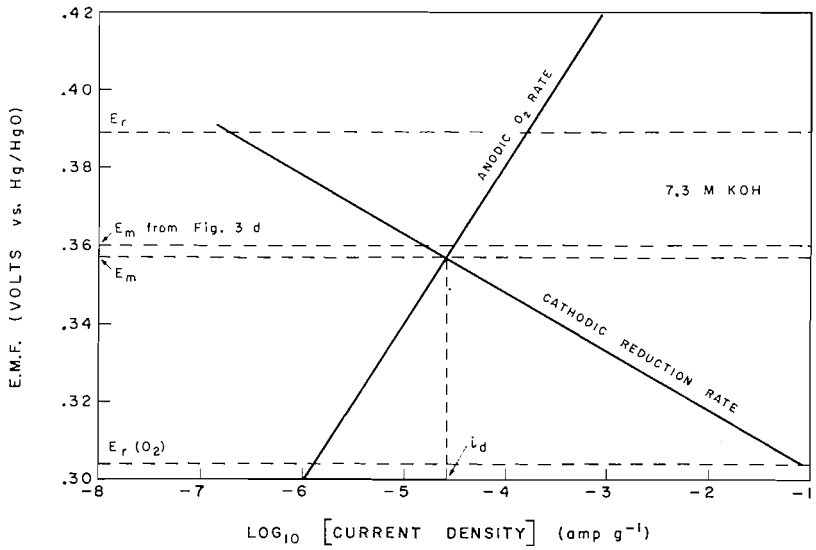


FIG. 10. Polarization lines for the partial reactions in the "corrosion" or self-discharge of the nickel oxide electrode in 7.3 M KOH (symbols are defined in text).

E_m is the steady-state mixed potential, E_r the ideal reversible potential, and i_d the net rate of "corrosion" or self-discharge. It is clear that any e.m.f. measurements (cf. 2, 3, 4) taken on open-circuit at long periods of time, except in the most concentrated solutions and at low temperatures, will not give the true reversible potential E_r but the steady-state *mixed* potential E_m, which will be lower than E_r by 5–30 mv. Similar figures to 10 may be drawn for the other concentrations of KOH and, except for the 14.6 M KOH solution, the extrapolated or long-time potentials will be E_m.

3. Assignment of Reversible Potentials

In solutions up to 7.3 M in KOH, the true reversible potentials E_r should be based on extrapolation of the whole region of the cathodic decay lines and that region of the anodic line before which oxygen evolution becomes a significant process, i.e. in the first 3.5 decades of $t+\theta$. The values of E_r thus obtained are shown as circles in Fig. 6 whilst the long-time values or those based on *all* the decay points (i.e. the E_m values) are indicated by crosses. They differ, as expected, by 5–30 mv. In the derivation of the Nernst equation for the electrode, it is clear that the E_r, and not the E_m values as usually used (2, 3, 4), must be considered.

In the 14.6 M KOH solution, the inflection in the decay line cannot be accounted for at all by the process of oxygen evolution, which is some 100 times too slow in the range of potentials concerned to affect the course of the decay curve. For this solution we can show (see Appendix) that the inflection arises from concentration changes in the electrode which fall off with increasing time after termination of the charging. In this solution and in the saturated KF, the values of potential corresponding to intersection of the cathodic

Can. J. Chem. Downloaded from www.nrcresearchpress.com by 210.87.254.105 on 09/05/12
For personal use only.

and anodic decay lines are therefore to be taken as the E_r values, there being no mixed potential in this case.

4. The Nernst Equation for the Electrode

From the above assignment of reversible potentials, we obtain a series of E_r values at various KOH concentrations. Using the data of Akerlöf and Bender (16), these E_r values can be expressed as logarithmic functions of activity of KOH and water. Three unknowns are then involved in the Nernst equation for the potential-determining electrode process viz., $E°$, and the two coefficients of the logarithmic activity terms. Using the data shown in Fig. 6 for E_r, we may obtain three (or more) simultaneous equations in E_r (experimentally determined), $E°$, ln a_{H_2O}, and ln a_{KOH}, which give, upon numerical solution, the following Nernst equation at 25° C for the cell

$$\text{Hg/HgO KOH } (a_{KOH}) \begin{cases} \text{NiO.OH*} \\ \text{Ni(OH)}_2\text{*} \end{cases}$$
$$\text{H}_2\text{O } (a_{H_2O})$$

where the * refers to unspecified and probably non-stoichiometric (22, 23, 24) quantities of associated water and adsorbed KOH:

[2] $$E_r = 0.420\ (\pm 0.002) - 0.004\ (\pm 0.001) \log_{10} [a_{KOH}] + 0.105\ (\pm 0.01) \log_{10} [a_{H_2O}],$$

which corresponds to the formal reaction

[3] $$[2\text{NiO.OH}]\ (0.14\text{KOH ads.}) + \text{Hg} + 3.56\text{H}_2\text{O} \rightleftarrows 2[\text{Ni(OH)}_2.1.28\text{H}_2\text{O}] + \text{HgO} + 0.14\text{KOH aq.}$$

It will be noted that in this equation terms both in KOH and water activity are required to represent the results, i.e. the dependence of E_r on KOH concentration cannot be quantitatively accounted for through the diminution of water activity with increasing KOH concentration. This residual dependence on KOH activity is consistent and in fair agreement with that deduced from previous work (4) and our own (see below) using a KOH/KF mixture. Chemically, adsorption of KOH at the higher oxide is not inconsistent with the general properties of higher oxides, which are usually more acidic than corresponding lower ones.

The dependence on water activity is, however, very much greater than that found in Kornfeil's work (4) and is moreover in the *opposite* direction to that found by him. Our results are in qualitative agreement with those of Zedner with regard to direction of the dependence of e.m.f. on water activity. It is unfortunate that Kornfeil's results are presented in an obscure fashion; thus, no *absolute* values of E_r as a function of concentration are stated and the dependence of e.m.f. upon concentration is expressed only as a fraction of the e.m.f. value for a 0.01 M KOH solution, i.e. $E°$ is not stated. Kornfeil's equation

[4] $$E = E° - 0.029\ (0.16 \log_{10} a_{H_2O} + 0.067 \log a_{KOH})$$

also predicts, using the data of Akerlöf and Bender (16), a minimum e.m.f. at 12 molal KOH, whereas in the present work and in that of Zedner (3) the e.m.f. continues to decrease rapidly with increasing concentration at high concentrations of KOH. Since we have no knowledge of the actual e.m.f. values in Kornfeil's work, it is difficult to seek an explanation of his anomalous results. It may be remarked, however, that the procedure used in his work was different to that used here and involved analytical determinations of the change of KOH and water concentrations relative to that of a KCl or KBr reference

Can. J. Chem. Downloaded from www.nrcresearchpress.com by 210.87.254.105 on 09/05/12
For personal use only.

electrolyte. The interpretation of results obtained by this method may be complicated by variation of adsorption of KCl on the electrode with changing KOH concentration and electrode potential. Thus it is well known that Cl^- ions are specifically adsorbed at electrodes particularly at potentials anodic to the potential of zero charge (25).

For the single electrode process at the nickel oxide electrode, equation [3] gives

[5] $[2NiO.OH]\ (0.14KOH\ ads.)+4.56H_2O+2e \rightleftarrows 2[Ni(OH)_2.1.28H_2O]+0.14KOH\ aq.+2OH^-.$

Equations derived by other workers expressed in corresponding form (cf. 4) to that of equation [5] are

$$2NiO.OH.H_2O+4H_2O+2e \rightleftarrows 2Ni(OH)_2.2H_2O+2OH^- \qquad \text{(Zedner)}$$

and

$$2NiO.OH.0.1H_2O+1.8H_2O+2e \rightleftarrows 2Ni(OH)_2+2OH^- \qquad \text{(Forster)}$$

from which it is seen that apart from the KOH adsorption not considered in the earlier work, our results with regard to dependence on water activity are in closest agreement with those of Zedner. Forster's results (2) differ from the above, possibly on account of the use of nickel oxide electrodes containing graphite. Kornfeil's equation

$$[2NiO.OH]\ (0.067KOH\ ads.)+0.84H_2O+2e \rightleftarrows 2Ni(OH)_2^*+2OH^-+0.067KOH$$

leads to an anomalously small role of water in the electrode process. Most of the above equations involve non-stoichiometric amounts of hydrate water and this is not inconsistent with available data (22, 23, 24) which indicate non-stoichiometric ranges of hydrate composition.

As an independent check on the validity of our equation [2], the measurements made (Fig. 4*b*) in saturated KF containing 0.08 *M* KOH enabled a value of E_r to be obtained at a low KOH activity (1.3*), and in which solution the water activity (determined directly by a differential vapor pressure measurement at 25° C) was also low at 0.30. The value of E_r observed experimentally in the KF/KOH mixture was 0.362 v whilst that calculated from equation [2] for the same conditions is 0.364 (6); the agreement is thus within the reproducibility claimed (see Results, Section 3)) in the present work.

Further work, in which the variation of e.m.f. has been studied with degree of oxidation, viz. at states of oxidation greater and less than "$NiO_{1.25}$" will be reported elsewhere.

APPENDIX

Diffusion Effects

We show here that the inflection in the anodic decay line for the 14.6 *M* KOH solution can be semiquantitatively accounted for by diffusion effects, which can arise in two ways: (i) from changes of e.m.f. of the electrode itself due to changes of KOH and water activity arising from Faradaic transport and the occurrence of the electrode reaction, and (ii) concentration polarization in the electrode arising secondarily from these concentration changes.

**The activity coefficient for* KOH *in the mixed electrolyte was taken as that for a solution of pure* KOH *having the same water activity as that (0.3) in the* KF *solution. This approximation is justified since at very high ionic strengths, the activity coefficient is determined to a large extent by ion–solvent interaction (19).*

Can. J. Chem. Downloaded from www.nrcresearchpress.com by 210.87.254.105 on 09/05/12
For personal use only.

During charging, the water and KOH activities near the interface of the electrode material will be higher and lower, respectively, than those in the bulk. After some time, a steady-state activity gradient of water and KOH will be set up in the electrode out towards the solution with a corresponding change in the electrode–solution potential difference. Upon termination of the charging, this activity gradient will fall to zero with attendant e.m.f. changes which will be superimposed on those arising from the "activation controlled" (17) electrode processes discussed above.

It is of interest to make a semiquantitative calculation to establish if these effects could account for the observed inflection in the decay lines in 14.6 *M* KOH.

(*a*) Model: a finite slab of thickness h is assumed (18) with homogeneous solutions at concentration C_b at the two slab–solution interfaces. (The porous electrode approximates to this since its dimensions were $2.5\times1.2\times0.1$ cm.) The integrated solution to the diffusion equation for this model is (18)

$$[6] \qquad \frac{\bar{C}-C_b}{C_1-C_b} = \frac{8}{\pi^2}\sum_{\nu=0}^{\infty}\frac{1}{(2\nu+1)^2}\exp\left[-\left(\frac{(2\nu+1)\pi}{h}\right)^2 Dt\right]$$

where $\bar{C}$ is the mean concentration of diffusing substance (diffusion constant D) at time t, C_1 the initial concentration (or in the present case, the mean steady state concentration of KOH during charging, prior to decay), and ν the order of the terms required in the Fourier solution of the diffusion equation.

(*b*) Calculation of concentration changes with time: we cannot make a rigorous calculation of concentration changes with time owing to the complexity of the diffusion problem in a real electrode. However, the following method involving two successive approximations will enable an estimate of the magnitude of the changes of concentration with time to be calculated. Diffusion will occur as soon as any changes of concentration are brought about by the electrolytic charging. At the end of this process, the average concentration in the sinter will hence be less than that which would have arisen had there been no diffusion *during* charging.

As a first approximation, we assume hypothetically that the latter condition obtains and that this results in a change of mean concentration $\Delta\bar{C}$. The fall of $\Delta\bar{C}$ (with no current passing) with time is then calculated from equation [6] and from this plot rates of change of mean concentration $d\bar{C}/dt$ can be calculated at various times. As a second approximation, we then obtain that value of $d\bar{C}/dt$ from the values discussed above, which corresponds to the rates of production of water and removal of KOH, respectively, during charging. This value of $d\bar{C}/dt$ will then be relevant to that time at which the current is interrupted for decay measurements. In the first approximation treatment, this rate of change of concentration would have been reached after a time t'. The subsequent decay of $\Delta\bar{C}$ with time t after the *actual* termination of charging is then calculated and plotted against t and this concentration change $\Delta\bar{C}$ after the times t would be equivalent to the same changes of concentration after times $t+t'$ in the first approximation calculation. This procedure will thereby allow approximately for the fact that during electrolysis some steady state change of concentration will tend to have been set up which will be less than that occurring if no diffusion took place. Two alternative values of D in equation [6] were taken as 10^{-6} and 3×10^{-7} cm^2 sec^{-1} in order to place limits on the resulting e.m.f. variation which could arise from uncertainties in the value of D. The above values were estimated from data at low concentration (19) by correction for the relative viscosity (η_r) of 14.6 *M* KOH ($\eta_r = 12$) and after empirical allowance

Can. J. Chem. Downloaded from www.nrcresearchpress.com by 210.87.254.105 on 09/05/12
For personal use only.

for the fact that, in the porous electrode, the diffusion path length will probably be somewhat longer than that corresponding to the free linear diffusion and the fact that the channel area available for diffusion out of the electrode will be less than the projected area of the electrode. The values of D taken are probably of the right order of magnitude but cannot be regarded as more precise than this.

From the changes of concentration calculated by the above procedure, the total change of e.m.f., ΔE_c, with time, due to diffusion effects, can be calculated using equations [2] and the data given by Akerlöf and Bender (16) for concentration cells in KOH and water.

The calculated values of ΔE_c are shown for 14.6 M KOH in Fig. 4*a* as a function of time during decay and is seen that ΔE_c is comparable with the total anodic polarization observed and can hence account fairly well for the form of the inflected decay line in 14.6 M KOH. Similar considerations apply to the cathodic line where effects in an opposite direction will occur. It may be noted that no value of θ exists which can lead to linearity of the decay curve in Figs. 4*a* or 4*b*.

We can therefore conclude that the potential to be taken as the reversible one in 14.6 M KOH (Fig. 4*a*) is that corresponding to the intersection of the anodic and cathodic decay lines after the longest times. The same conclusions will apply to the results in saturated KF solution (Fig. 4*b*).

Diffusion effects will be much less significant in the more dilute and less viscous solutions since it may readily be shown that ΔE_c values are much smaller and the times over which diffusion equilibration is occurring are much shorter (owing to the higher diffusion constants) than those for the 14.6 M solutions. For the more dilute solutions, the inflections arise, as discussed above, from the alternative oxygen evolution process.

It can be shown that these effects in dilute solution are operative over periods of time comparable to θ (the time correction applied to allow for a finite charging rate). Thus diffusion effects are absorbed in the empirical assignment of θ. This will introduce some uncertainty in its value but will have no significant effect on the slope of the anodic and cathodic decay lines since θ in these cases is not larger than about 100 seconds.

ACKNOWLEDGMENTS

We are indebted to the Defence Research Board, Department of National Defence, Canada, for financial assistance on Grant No. DRB 5480-12. One of us (P. L. B.) also wishes to acknowledge the award of a Cominco Scholarship held during part of the time during which this work was carried out.

REFERENCES

1. B. E. Conway and P. L. Bourgault. Can. J. Chem. **37**, 292 (1959).
2. F. Forster. Z. Elektrochem. **13**, 414 (1907); **14**, 285 (1908).
3. J. Zedner. Z. Elektrochem. **11**, 809 (1905); **12**, 463 (1906); **13**, 752 (1907).
4. F. Kornfeil. Proc. Ann. Battery Research Develop. Conf., 12th Conf. U.S. Army Signal Corps. 1958.
5. W. M. Latimer. Oxidation potentials. 2nd ed. Prentice-Hall. 1952.
6. G. W. D. Briggs and W. K. F. Wynne-Jones. Trans. Faraday Soc. **52**, 1272 (1956). E. Jones and W. K. F. Wynne-Jones. Trans. Faraday Soc. **52**, 1260 (1956).
7. E. J. Casey, P. L. Bourgault, and P. E. Lake. Can. J. Technol. **34**, 95 (1956).
8. K. Rozenthal, P. Dolin, and B. V. Erschler. Acta Physicochim. U.R.S.S. **21**, 213 (1946).
9. F. G. Donnan and A. Allmand. J. Chem. Soc. **99**, 845 (1911). F. Knobel. J. Am. Chem. Soc. **45**, 70 (1923).
10. G. Armstrong and J. A. V. Butler. Trans. Faraday Soc. **29**, 1261 (1933).
11. H. B. Morley and F. E. W. Wetmore. Can. J. Chem. **34**, 359 (1956).
12. H. Taniguchi and G. J. Janz. J. Electrochem. Soc. **104**, 123 (1957).
13. B. E. Conway and P. L. Bourgault. Unpublished: datum based on temperature coefficient of potential reached after long periods of standing in 1 M KOH.

Can. J. Chem. Downloaded from www.nrcresearchpress.com by 210.87.254.105 on 09/05/12
For personal use only.

14. R. PARSONS. J. chim. phys. C, **49**, 82 (1952).
14*a*. P. D. LUKOVTSEV and S. A. TEMERIN. Trudy Soveshchaniya Elektrokhim. Akad. Nauk S.S.R., Otdel. Khim. Nauk Moscow, 1950. 493 (1953).
15. B. E. CONWAY and P. L. BOURGAULT. Trans. Faraday Soc. In course of publication.
16. G. C. AKERLÖF and P. BENDER. J. Am. Chem. Soc. **70**, 2366 (1948).
17. J. O'M. BOCKRIS. Modern aspects of electrochemistry. Butterworths. 1954. Chap. 4.
18. W. JOST. Diffusion. Academic Press, New York. 1952.
19. R. A. ROBINSON and R. H. STOKES. Electrolyte solutions. Butterworths. 1955.
20. B. E. CONWAY. Proc. Roy. Soc. A, **247**, 400 (1959); A, **256**, 128 (1960).
21. O. REITZ and E. F. FORSTER. Z. Elektrochem. 44, 45 (1938).
22. N. V. SIDGWICK. Chemical elements and their compounds. Vol. II. Oxford. 1950.
23. J. W. MELLOR. A comprehensive treatise on inorganic and theoretical chemistry. Vol. XV. Longmans. 1936.
24. G. F. HÜTTIG and A. ZÖRNER. Z. anorg. Chem. **189**, 183 (1930).
25. D. C. GRAHAME. Chem. Revs. **41**, 441 (1947).
26. J. O'M. BOCKRIS and A. K. M. S. HUQ. Proc. Roy. Soc. A, **237**, 277 (1956).

Can. J. Chem. Downloaded from www.nrcresearchpress.com by 210.87.254.105 on 09/05/12
For personal use only.

Can. J. Chem. Downloaded from www.nrcresearchpress.com by 91.191.171.90 on 09/05/12
For personal use only.

HYDROGEN ATOM ABSTRACTION BY ETHYL-d_5 RADICALS. PART I[1]

P. J. Boddy[2] and E. W. R. Steacie

ABSTRACT

The photolysis of 3-pentanone-d_{10} has been used as a source of deuterated ethyl radicals and some of their hydrogen abstraction reactions studied over the temperature range 50–300° C.

The compounds neopentane, *n*-butane, and isobutane were chosen as representative of the basic structural features in the alkane series. The activation energies for abstraction ($E_8-\frac{1}{2}E_2$) are respectively 12.60±0.7, 10.4±0.75, and 8.9±0.6 kcal/mole and the pre-exponential factors ($\log_{10}(A_8/A_4)$) are 0.300±0.09, 0.082±0.09, and −0.334±0.066 where

$$2\ C_2D_5\cdot \rightarrow C_4D_{10}, \quad [2]$$

$$C_2D_5\cdot + \text{3-pentanone-}d_{10} \rightarrow C_2D_6, \quad [4]$$

$$C_2D_5\cdot + \text{hydrocarbon} \rightarrow C_2D_5H. \quad [8]$$

For abstraction of a deuterium atom from the ketone the values obtained are $E_4-\frac{1}{2}E_2 = 9.0\pm0.5$ kcal/mole and $(\log_{10}(A_4/A_2^{\frac{1}{2}})) = \bar{8}.36\pm0.20$ in agreement with previous investigations (1, 2).

The value of the disproportionation to combination ratio for C_2D_5 radicals is 0.0985±0.008 independent of temperature.

INTRODUCTION

Although a great deal of information has been obtained on the abstraction of hydrogen atoms from hydrocarbons by methyl radicals, there is little information on more complex alkyl radicals. The methyl radical work has led to the realization of a relationship between structural features of hydrocarbon molecule reactants and activation energy for abstraction of a hydrogen atom (3). This, however, has not in turn led to any good theoretical treatment of the problem probably, at least in part, because there is so little experimental data on the influence of the structure of the alkyl radical itself. There is published data on the abstraction by ethyl radicals from some unsaturated hydrocarbons in the C_6 and C_8 range (4) and this does throw light on the effect of bond multiplicity but not on the aspects of alkane structure.

The major difficulty with higher radicals is that of analysis of the reaction products. In the case of ethyl radicals, calculation of the rate constant for abstraction involves determination of small quantities of ethane, ethylene, and *n*-butane. This severely complicates investigation of some of the most interesting hydrocarbons.

The mechanism of 3-pentanone photolysis is known to be (5)

$$(C_2H_5)_2CO + h\nu \rightarrow 2C_2H_5\cdot + CO, \quad [1]$$

$$2C_2H_5\cdot \rightarrow C_4H_{10}, \quad [2]$$

$$2C_2H_5\cdot \rightarrow C_2H_6 + C_2H_4, \quad [3]$$

$$C_2H_5\cdot + (C_2H_5)_2CO \rightarrow C_2H_6 + \cdot C_2H_4COC_2H_5, \quad [4]$$

$$C_2H_5\cdot + \cdot C_2H_4COC_2H_5 \rightarrow C_4H_9COC_2H_5, \quad [5]$$

$$2\cdot C_2H_4COC_2H_5 \rightarrow (C_2H_4COC_2H_5)_2, \quad [6]$$

$$\cdot C_2H_4COC_2H_5 \rightarrow C_2H_4 + CO + C_2H_5\cdot, \quad [7]$$

$$C_2H_5\cdot + RH \rightarrow C_2H_6 + R\cdot. \quad [8]$$

[1]*Manuscript received April 27, 1960.*
Contribution from the Division of Pure Chemistry, National Research Council, Ottawa, Canada.
Issued as N.R.C. No. 5776.

[2]*N.R.C. Postdoctorate Fellow 1957–59. Present address: Bell Telephone Laboratories, Murray Hill, New Jersey, U.S.A.*

Under suitable conditions the ethane from [3], and [4] can be assessed and hence the rate of [8] determined.

The situation can be greatly simplified by the use of labelled species. The use of deuterated hydrocarbon molecules is possible but does not lead to results directly comparable with the large number of experiments carried out with methyl and perfluoralkyl radicals and hydrogenated molecules without making certain assumptions about the relative reactivities of C—H and C—D bonds. A study has been made of the reaction between ethyl radicals and deuterium molecules (6) and from this the activation energy for abstraction from a hydrogen molecule deduced. The value obtained agrees reasonably well with that determined experimentally for ethyl-d_5 radicals and hydrogen (7).

A preferable experiment involves the use of a deuterated radical source with hydrogenated molecules. Current evidence suggests that insofar as activation energy for hydrogen atom abstraction is concerned, deuterated radicals behave identically with their hydrogenated counterparts within the present limits of experimental error (4, 8, 9). Analysis of products is greatly simplified since only reactions [4] and [8] need to be considered and from the ratio of (in this case) C_2D_5H/C_2D_6 the activation energy difference between [4] and [8] may be determined. (C_2D_6 from [3] is easily estimated.)

The reasonable assumption is made here that the mechanism outlined above for 3-pentanone-d_0 is entirely applicable to the photolysis and subsequent reactions of 3-pentanone-d_{10}, although the rate constants for the individual steps will, of course, be different.

EXPERIMENTAL

A conventional high vacuum apparatus was used with sections for storage, purification, reaction, analysis, and sampling of gases as previously described in papers from this laboratory. Mercury cutoffs were used at all points where absorption of organic vapors could lead to error.

The reaction system was a 10-cm-long quartz cell with an all glass circulating pump in the connecting tubing, the total volume being 196 ml. Both the cell and the metal valves isolating it from the rest of apparatus were contained in an air thermostat. The cell itself was surrounded by a cylindrical electric furnace which was maintained to within 1° C of the required temperature. Pressures were measured on a quartz spiral gauge within the thermostat.

Radiation from a Hanovia S-500 lamp was collimated by an aluminum cylinder and then brought to a parallel beam, which just filled the cell, with a quartz lens. A 2-mm-thick "Pyrex" filter removed radiation below 2900 Å.

The reaction products were distilled several times at −80° C to remove most of the unphotolysed ketone and involatile products, and then passed through traps at −165° C, −125° C, and −215° C in that order. Carbon monoxide passed straight through. C_2 hydrocarbons were collected at −215° C. The fraction between −125° C and −165° C was n-butane-d_{10} (this was measured only in experiments where the ketone was photolysed alone).

MATERIALS

3-Pentanone-d_{10} was obtained from Merck of Canada. It was degassed and stored in a blackened bulb behind a mercury cutoff. Small samples were further degassed before each run. The purity of the ketone is discussed below.

Can. J. Chem. Downloaded from www.nrcresearchpress.com by 91.191.171.90 on 09/05/12
For personal use only.

Neopentane, *n*-butane, and isobutane were all Phillips Research Grade materials. They were degassed and stored in the same way as the ketone. Their purities exceeded 98%.

TREATMENT OF DATA

1. Ketone

The low energy (15 v) mass spectrum of the ketone, showing only parent peaks, gave the following analysis, assuming equal sensitivities:

(1) $C_4D_{10}CO$ 93.7%,
(2) C_4D_9HCO 5.95%,
(3) $C_4D_8H_2CO$ 0.34%.

The peaks were small due to the low sensitivities at 15 v and the smallest peak was difficult to measure.

The normal (70 v) spectrum gave information on the relative abundance of species 1 and 2.

Parent peaks	95 pk/96 pk = 5.25%.
Propionyl peaks	61 pk/62 pk = 2.8% (≡ 5.6% of species 2).
Ethyl peaks	33 pk/34 pk = 2.5% (≡ 5.0% of species 2).

The latter two ratios include the effect of species 3 but since the values lie on either side of the direct ratio of the parent peak the effect of this appears to be well within the experimental error. An average value of 5.3% of species 2 was adopted. In view of the relative abundances of species 2 and 3 it was assumed that 3 was largely $(C_2D_4H)_2CO$ (since 0.0595^2 is very close to 0.0034, the value obtained at low energy). In previous work with this ketone, prepared by the same method (heavy water exchange with $(CD_3CH_2)_2CO$), it was logically assumed that the H atoms were mainly in the primary position (1). A similar assumption is made here.

The composition of the ketone used in the following experiments was therefore taken to be:

(1) $(C_2D_5)_2CO$ 94.4%,
(2) $CD_2HCD_2COC_2D_5$ 5.3%,
(3) $(CD_2HCD_2)_2CO$ 0.28%.

The relative abundance of 3 has been adjusted to $.053^2$.

2. Butanes

The butane produced in reaction [2] should have an isotopic composition similar to that of the original ketone. Only the 70 v spectrum was taken so no butane with two H atoms could be detected with accuracy. The ratio C_4D_9H/C_4D_{10} was in good agreement with the expected value of 0.053 over the whole range of experimental conditions. C_4D_{10} was taken as 94.4% of total butane in most runs, but the ratio was checked at intervals and found to be constant. The uncertainty introduced by not analyzing the $C_4D_8H_2$ was negligible.

3. C_2 Hydrocarbons

(a) Ethanes

C_2D_6 can arise in three ways:

(i) $C_2D_5\cdot$ + ketone → C_2D_6, which we wish to determine.

Can. J. Chem. Downloaded from www.nrcresearchpress.com by 91.191.171.90 on 09/05/12
For personal use only.

(ii) $C_2D_5\cdot + C_2D_5\cdot \rightarrow C_2D_6 + C_2D_4$; this can be estimated from the C_2D_4 after correction has been made for other sources.

(iii) $C_2D_5\cdot + C_2D_4H\cdot \rightarrow C_2D_6 + C_2D_3H$; this can be estimated from the C_2D_3H yield.

C_2D_5H can arise from:

(iv) $C_2D_5\cdot$ + hydrocarbon $\rightarrow C_2D_5H$, which we wish to determine.

(v) $C_2D_5\cdot$ + ketone $\rightarrow C_2D_5H$; an empirical correction curve for this is described later.

(vi) $C_2D_4H\cdot$ + ketone $\rightarrow C_2D_5H$ assuming the ketone composition given above and assuming that there is no different rate of photolysis, or reaction of the two types of radical about 3.0% should be $C_2D_4H\cdot$. Hence C_2D_5H from (vi) should be 3.0% of C_2D_6 from (i).

Preliminary results showed that the ratio of disproportionation to combination for ethyl-d_5 was about 0.1 compared with 0.14 for ethyl-d_0 radicals (5). The activation energy for these reactions is very close to zero, and the collision numbers cancel from each ratio. Assuming that the steric factors for combination in the two cases are equal since the radicals are so similar, then on a collision-for-collision basis C—H bonds break 1.4 times more frequently than C—D bonds in the disproportionation reaction. If these relative rates hold good for abstraction from $CD_2HCD_2\cdot$ and bearing in mind the head-to-tail mechanism of disproportionation (2, 15), the relative rates of abstraction of D and H stand in the ratio 2:1.4. Since $C_2D_4H\cdot$ represents about 3.0% of the total radical concentration then reaction (iii) above should represent $((2/3.4)\times 3.0\% =)$ 1.75% of the total disproportionation reaction. Since C_2D_4 is produced in all disproportionation reactions except (iii) and in negligible amounts in other ways below 197° C, the C_2D_4 yield can be taken to represent the total disproportionation. Figure 1, in which C_2D_3H/C_2D_4 from a series of experiments with the ketone alone is plotted vs. temperature, shows that in the range 50–150° C the ratio comes close to that predicted. At 180° C and above

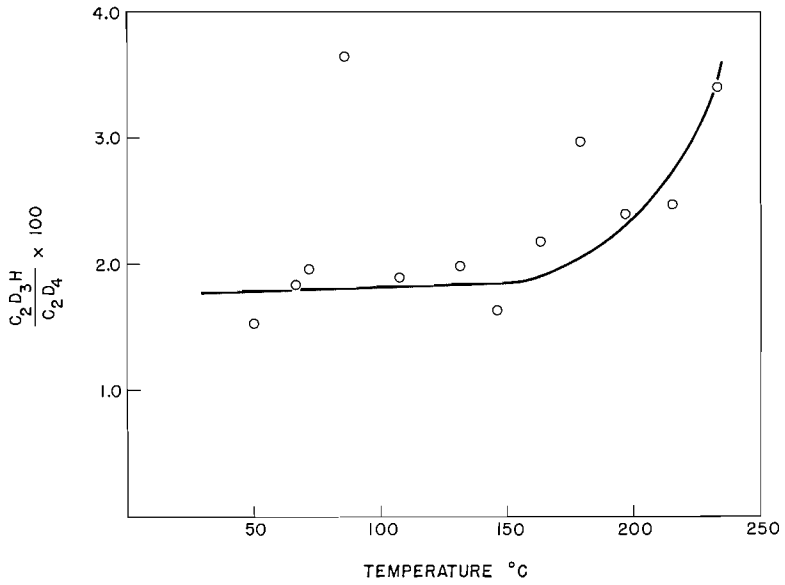


FIG. 1. Ratio of C_2D_3H to C_2D_4 in DEK-d_{10} photolysis.

Can. J. Chem. Downloaded from www.nrcresearchpress.com by 91.191.171.90 on 09/05/12
For personal use only.

the ratio increases, probably due to decomposition of pentanonyl radicals, which would be hydrogen enriched if the hydrogen is primary. If there is no isotope effect on the decomposition, about 3% of the ethylene from this source would be C_2D_3H.

(vii) $C_2D_5\cdot + CD_2HCD_2\cdot \rightarrow C_2D_5H + C_2D_4$; on the basis of the above discussion this should be $((1.4/3.4)\times 3.0\% =)$ 1.25% of the total disproportionation reaction.

(viii) $CD_2HCH_2\cdot + C_2D_5 \rightarrow C_2D_5H + C_2D_4$, 3.0% of the total disproportionation.

Since the $C_2D_4H\cdot$ concentration is relatively low, interactions between these radicals and with impure ketone are not considered.

(*b*) *Ethylenes*

C_2D_4 can arise in four ways:

(ii) $C_2D_5\cdot + C_2D_5\cdot \rightarrow C_2D_6 + C_2D_4$, the major source when (ix) is not significant.

(vii) $C_2D_5\cdot + C_2D_4H\cdot \rightarrow C_2D_5H + C_2D_4$, 1.25% of the total disproportionation.

(viii) $C_2D_4H\cdot + C_2D_5\cdot \rightarrow C_2D_5H + C_2D_4$, 3.00% of the total disproportionation.

(ix) $\cdot C_2D_4COC_2D_5 \rightarrow C_2D_4 + CO + C_2D_5\cdot$; this reaction is of little importance below 200° C. Under these circumstances 4.25% of the C_2D_4 arises from (vii) and (viii), the remainder from (ii).

C_2D_3H can arise only in (iii) and is discussed above.

On the basis of these corrections the data was treated in the following way. The measured $R_{C_2D_6}$ was converted to that produced in (i) by subtracting the $R_{C_2D_4}$ from (ii) (i.e. 95.75% of the total $R_{C_2D_4}$) and $R_{C_2D_3H}$. $R_{C_2D_5H}$ was corrected by subtracting 3.0% $R_{C_2D_6}$ (vi) and 4.25% of the total $R_{C_2D_6}$ (vii) and (viii).

When this procedure had been carried out for the experiments in which the ketone was photolysed alone there was a small residue of C_2D_5H. This could have been largely removed by adjustment of the correction factors but it was preferred to treat it as a separate temperature-dependent correction due to reaction (v). The function $(R_{C_2D_5H\ \text{residual}})/(R^{\frac{1}{2}}_{C_4D_{10}}[\text{ketone}])$ is plotted vs. $1/T$ in Fig. 2, which was used as a correction curve for subsequent experiments. The results are not sufficiently precise to ascribe an activation energy and hence check the position of the H atom in the ketone molecule.

While the corrections are complex, they are generally not large and the final results are not greatly affected by the approximate nature of some of the corrections.

RESULTS

Ketone Photolysis

The data obtained for photolysis of the ketone alone are presented in Table I. Columns 10, 11, and 12 have been corrected as described. In the region where reaction [7] is negligible column 12 represents k_3/k_2. Below 197° C the values are in good agreement (0.0985 ± 0.008) and independent of temperature. At higher temperatures this value of k_3/k_2 is used to calculate $R_{C_2D_6}$ from [2] by measurement of $R_{C_4D_{10}}$ from [3]. The corrections described in the previous section are valid only when $R_{C_2D_4}$ from [7] is negligible. Experiments were carried out up to a temperature where the activation energy plot showed a curvature (300° C) indicating the onset of a systematic error in the correction.

It can easily be shown that in the valid range $(k_4/k_2^{\frac{1}{2}}) = R_{C_2D_6\ \text{corrected}}/R^{\frac{1}{2}}_{C_4D_{10}}[\text{ketone}]$.

Can. J. Chem. Downloaded from www.nrcresearchpress.com by 91.191.171.90 on 09/05/12
For personal use only.

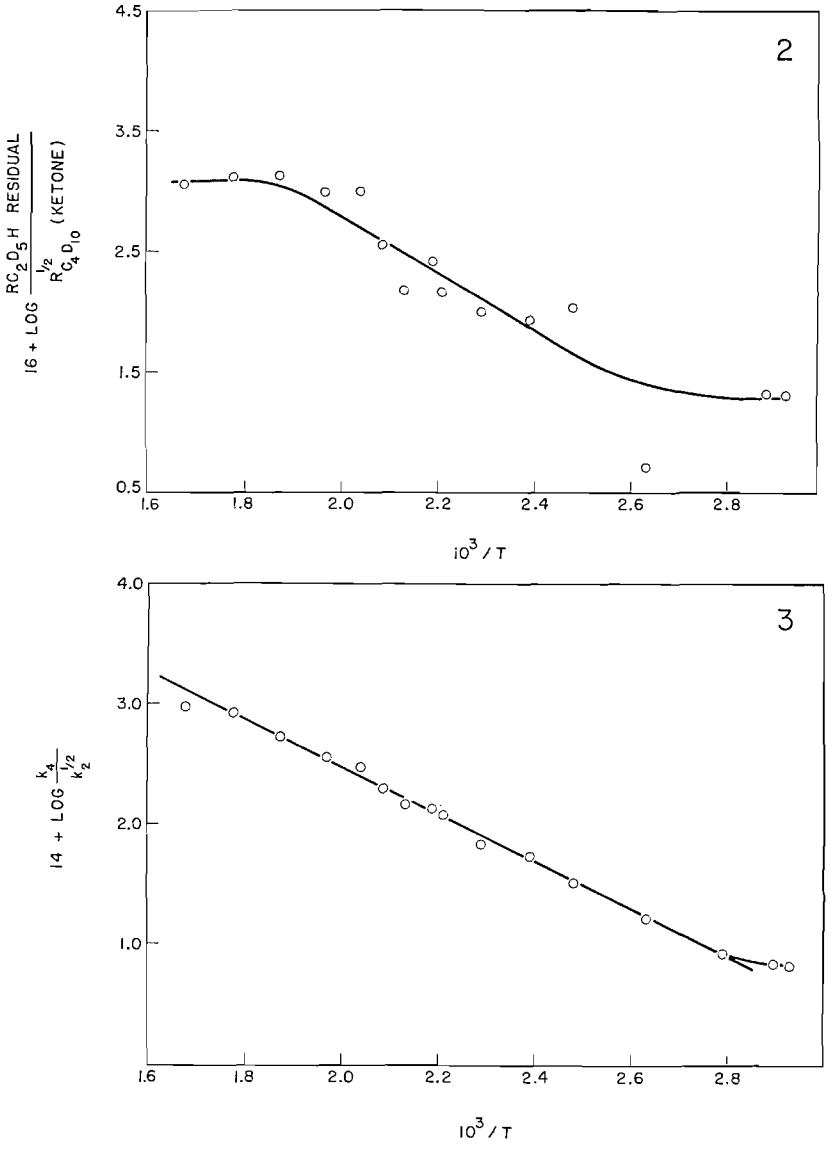


FIG. 2. Correction curve for residual C_2D_5H.
FIG. 3. Activation energy plot for C_2D_5+DEK-d_{10}.

The data are plotted vs. $1/T$ in Fig. 3. The results calculated by the least squares method are compared with previous values below:

		C	B	$13+\log_{10} A_4/A_2^{\frac{1}{2}}$	$E_4-\frac{1}{2}E_2$
(*a*)	Wijnen and Steacie	5.455	2.008	5.5±0.2	9.2±0.4
(*b*)	James and Steacie	5.750	2.113	5.7±0.2	9.6±0.4
(*c*)	Boddy and Steacie	5.360	1.948	5.4±0.2	9.0±0.5

In (*a*) 2,2′,4,4′-tetradeuterodiethyl ketone was used and the data refers to abstraction of α-D. In (*b*) and (*c*) the data refers to the over-all abstraction involving both α- and β-D.

Can. J. Chem. Downloaded from www.nrcresearchpress.com by 91.191.171.90 on 09/05/12
For personal use only.

Can. J. Chem. Downloaded from www.nrcresearchpress.com by 91.191.171.90 on 09/05/12
For personal use only.

TABLE I

Ketone, mol./ml $\times 10^{-17}$	Temp., °K	Time, sec	$R_{C_2D_6}$	$R_{C_2D_5H}$	$R_{C_2D_4}$	$R_{C_2D_3H}$	$R_{C_4D_{10}}$	R_{CO}	$R_{C_2D_6\ corr}$	$R_{C_2D_5H\ res}$	$\frac{R_{C_2D_4\ corr}}{R_{C_4D_{10}}}$	$16+\log\frac{R_{C_2D_5H\ res}}{R^{\frac{1}{2}}_{C_4D_{10}}[K]}$	$14+\log\frac{k_1}{k_2^{\frac{1}{2}}}$
			$\times 10^{-12}$ in mol./ml sec										
5.70	452	3600	1.28_2	0.0548	0.260	0.0077	2.32_6	—	1.026	0.0128	0.1067	2.1673	2.0712
7.34	437	3600	1.02	0.0456	0.272	0.0059	2.44_7	3.74_7	0.754	0.0113	0.1062	1.9924	1.8169
2.96	404	4410	0.295	0.0155	0.172	0.0034	1.77_3	3.04_5	0.127_3	0.0043	0.0926	2.0382	1.5091
6.00	380.5	3720	0.454	0.0182	0.296	0.0056	2.89_1	4.09_7	0.165_7	0.00053	0.0977	0.7153	1.2103
7.04	359	3960	0.474_6	0.0128	0.367	0.0134	3.45_4	4.93_5	0.110_7	—	0.1014	—	0.9273
17.26	470	3720	4.86_8	0.198_8	0.481	0.0115	3.11_8	7.98_8	4.397	0.0462	0.1473	2.1798	2.1741
7.38	419	3720	0.731	0.033	0.185	0.0030	1.82_1	2.70_1	0.551_3	0.0086	0.0964	1.9345	1.7423
12.60	339	3723	0.326_3	0.0166	0.210	0.0038	2.10_3	2.60	0.122	0.0039	0.0951	1.3308	0.8240
12.60	344.5	3600	0.338	0.0172	0.217	0.0040	2.10_5	2.55_2	0.126_8	0.0041	0.0984	1.3489	0.8414
8.59	489	3300	2.33_8	0.142_9	0.119_5	0.0029	0.729	—	2.22_1	0.074	0.1565	3.0000	2.4893
8.81	507.5	3600	2.51_8	0.143_1	0.0705	0.0024	0.575	2.55_2	2.44_9	0.067	0.1170	2.9560	2.5655
11.40	323	4780	0.231_6	0.013_5	0.177_7	0.0027	1.84_5	—	0.0592	0.0041	0.0919	1.4220	0.5834
8.68	534	2915	3.11	0.171	0.048_2	0.025	0.441	—	3.04_2	0.078	0.1045	3.1290	2.7218
8.23	563	4191	3.30_3	0.150	0.181	0.031	0.218	—	3.250	0.0515	0.795	3.1270	2.9273
10.17	456	3600	1.61_6	0.0775	0.109	0.0158	1.16	—	1.48_6	0.0278	0.0940	2.4090	2.1373
10.38	479	3600	1.93_6	0.0918	0.0905	0.0159	0.805	—	1.84_1	0.033	0.1075	2.5495	2.2961
10.68	597	3600	5.50	0.228	0.921	0.0917	0.262	—	5.38	0.0654	3.370	3.0630	2.9928

The constants are those in the expression $13+\log_{10}(k_4/k_2^{\frac{1}{2}}) = C-(B.10^3/T)$.

The present results confirm the conclusion that there is negligible effect of isotopic substitution on the reactivity of ethyl radicals. It was important to redetermine the ketone data here since subsequent activation energies were measured relative to this.

Ketone and Hydrocarbons

The data from the experiments with neopentane, *n*-butane, and isobutane appear in Tables II, III, and IV.

Activation energies may be obtained in two ways. The most precise way is to consider the reactions [4] and [8]. The activation energy difference E_8-E_4 may be obtained by plotting

$$\log_{10}\frac{R_{C_2D_5H\ \text{corrected}}}{R_{C_2D_6\ \text{corrected}}}\cdot\frac{[\text{ketone}]}{[\text{hydrocarbon}]}\ \text{vs.}\frac{1}{T} \qquad \text{(Fig. 4).}$$

The isobutane curve falls off below 110° C. This was due to the use of too low an isobutane to ketone ratio and hence to too low a $R_{C_2D_5H}$ to $R_{C_2D_6}$ ratio leading through small errors in the correction factors to a large systematic error in $R_{C_2D_5H\ \text{corrected}}$. Increase of the relative isobutane pressure gave the point close to the drawn line ($1/T = 2.64$).

Least squares calculation gives:

For neopentane

$E_{8a}-E_4 = 3.6\pm0.2$ kcal,
$\log_{10}(A_{8a}/A_4) = 0.30\pm0.09$;

hence $E_{8a}-\frac{1}{2}E_2 = 12.6\pm0.7$ kcal,
$(A_{8a}/A_4) = 2.00\pm0.5$.

For *n*-butane

$E_{8b}-E_4 = 1.38\pm0.25$ kcal,
$\log_{10}(A_{8b}/A_4) = 0.082\pm0.09$;

hence $E_{8b}-\frac{1}{2}E_2 = 10.4\pm0.75$ kcal,
$(A_{8b}/A_4) = 1.21\pm0.27$.

For isobutane

$E_{8c}-E_4 = 0.1\pm0.1$ kcal,
$\log_{10}(A_{8c}/A_4) = \bar{1}.666\pm0.066$;

hence $E_{8c}-\frac{1}{2}E_2 = 8.9\pm0.6$ kcal,
$(A_{8c}/A_4) = 0.464\pm0.07$.

Alternatively, $R_{C_2D_4}$ may be used to calculate $R_{C_4D_{10}}$ from k_3/k_2 and then by plotting $\log_{10}(R_{C_2D_5H\ \text{corrected}}/R_{C_4D_{10}}^{\frac{1}{2}}$ [hydrocarbon] vs. $1/T$, $E_8-\frac{1}{2}E_2$ may be obtained directly. This method suffers from the very unfavorable value of k_3/k_2 which multiplies errors in $R_{C_2D_4}$ in the final expression. This limits the range of validity of the experiments since it is so sensitive to $R_{C_2D_4}$ from [7] and also increases the scatter over the range where the analysis is valid. The results plotted in Fig. 5 are, however, compatible with those from the first method.

The data for abstraction from the ketone in the presence of hydrocarbons is plotted in Fig. 6. The line is drawn to correspond to that in Fig. 3. In view of the greater complexity of these systems the agreement is considered satisfactory.

Can. J. Chem. Downloaded from www.nrcresearchpress.com by 91.191.171.90 on 09/05/12
For personal use only.

Can. J. Chem. Downloaded from www.nrcresearchpress.com by 91.191.171.90 on 09/05/12
For personal use only.

TABLE II

Ketone, mol./ml $\times 10^{-17}$	Neopentane, mol./ml $\times 10^{-17}$	Temp., °K	Time, sec	$R_{C_2D_5H}$	$R_{C_2D_6}$	$R_{C_2D_4}$	$R_{C_2D_3H}$	$R_{C_2D_5H\ corr}$	$R_{C_2D_6\ corr}$	$2+\log\frac{k_{8a}}{k_4}$	$13+\log\frac{k_4}{k_2^{\frac{1}{2}}}$	$15+\log\frac{k_{8a}}{k_2^{\frac{1}{2}}}$
				$\times 10^{-12}$ in mol./ml sec								
5.26	11.9	556	4830	1.42_9	6.61	0.125	—	1.12_1	6.49	0.8837	—	—
5.79	13.0	525	4000	1.05_1	5.91_3	0.291	0.0313	0.756_5	5.60_1	0.7800	—	—
5.86_5	9.19	494	4565	0.481	4.06_2	0.342_6	0.007	0.283_5	3.72_8	0.6860	—	—
6.22	12.3_5	473	4250	0.379	3.22_3	0.508	0.0977	0.230	2.64	0.6425	—	—
5.61	18.8	452.5	4317	0.277	1.93_6	0.496_7	0.0182	0.187	1.44_1	0.5900	1.0590	1.6470
5.99	18.2	435	3935	0.173_6	1.51_3	0.497	0.0147	0.105_5	1.02_3	0.5300	0.8810	1.4116
8.35	66.7	358.5	3620	0.0295	0.258	0.107_2	0.00276	0.105_7	0.152	0.1106	0.1240	0.2330
9.09	51.5	377	3600	0.089	0.331_7	0.0880	0.0103	0.0236	0.237	0.2455	0.4400	0.6850
7.78	65.4_5	422	4440	0.144	0.544	0.0503	—	0.119_4	0.496	0.4580	0.9500	1.4065
5.24	32.5_5	575	3160	0.943	1.61_3	—	—	0.687	1.61_3	0.9731	—	—
6.07	37.1	597	3600	1.33_4	2.00_6	0.491	0.034	1.25	1.97_2	1.0157	—	—

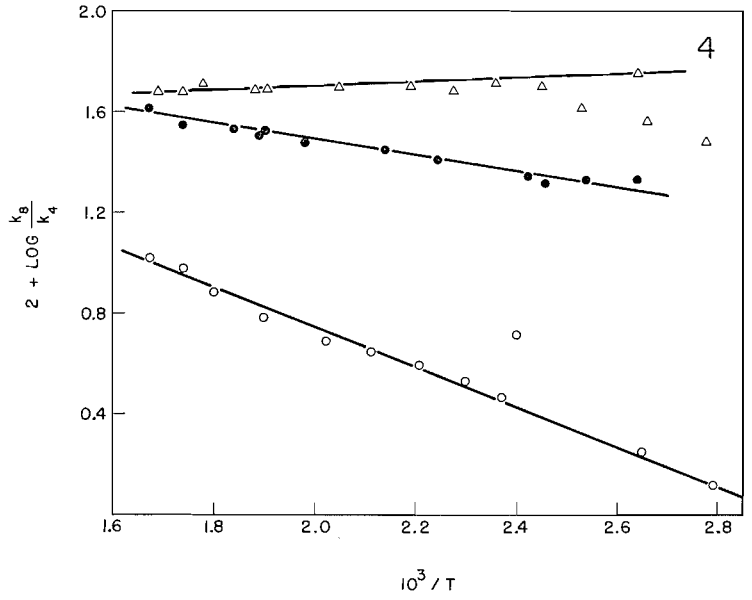
TABLE III

Ketone, mol./ml $\times 10^{-17}$	*n*-Butane, mol./ml $\times 10^{-17}$	Temp., °K	Time, sec	$R_{C_2D_5H}$	$R_{C_2D_6}$	$R_{C_2D_4}$	$R_{C_2D_3H}$	$R_{C_2D_5H\ corr}$	$R_{C_2D_6\ corr}$	$1+\log\frac{k_{8b}}{k_4}$	$13+\log\frac{k_4}{k_2^{\frac{1}{2}}}$	$13+\log\frac{k_{8b}}{k_2^{\frac{1}{2}}}$
				$\times 10^{-12}$ in mol./ml sec								
3.86	3.27	525.5	4000	1.30	4.01_8	0.0781	0.0239	1.11_3	3.91_9	0.5250	—	—
4.86	3.56	505	3700	1.07_5	3.99	0.195	0.0104	0.832_2	3.79_4	0.4757	—	—
4.73_5	2.85	467	3700	0.402_6	2.17	0.338	0.0152_4	0.307_8	1.83_2	0.4456	1.3198	1.7657
5.18	4.51	445.5	3600	0.414	1.87_8	0.441	0.0127	0.319_5	1.44_4	0.4074	1.0319	1.4370
5.68_5	4.46	406	7280	0.150	1.13_8	0.507_5	0.0195	0.102_3	0.633_8	0.3152	0.6912	1.0043
4.95	5.88	394	3600	0.125	0.898	0.566	0.0237	0.084	0.333_8	0.3243	0.2967	0.7747
2.60	60.5	379	3600	0.234_9	0.107_9	0.0643	—	0.230_1	0.0465	0.3269	0.3439	0.6721
9.13	43.5_5	412.5	3620	0.319_2	0.346_3	0.00561	—	0.303_6	0.292_7	0.3373	0.6286	0.9659
7.12	47.6	529	3600	2.04_7	0.950_4	—	—	2.00_3	0.950_4	0.4990	—	—
7.83	42.2	543	3600	2.55_2	1.37_2	—	—	2.49_4	1.37_2	0.5272	—	—
3.64	41.9	575	3600	3.670	0.898_7	—	—	3.63_4	0.898_7	0.5463	—	—
5.41	37.6	598	4310	4.86_4	1.71_8	0.887	0.597	4.86_4	1.71_8	0.6104	—	—

Can. J. Chem. Downloaded from www.nrcresearchpress.com by 91.191.171.90 on 09/05/12
For personal use only.

TABLE IV

Ketone, mol./ml $\times 10^{-17}$	Isobutane, mol./ml $\times 10^{-17}$	Temp., ° K	Time, sec	$R_{C_2D_5H}$	$R_{C_2D_6}$	$R_{C_2D_4}$	$R_{C_2D_3H}$	$R_{C_2D_5H\ corr}$	$R_{C_2D_6\ corr}$	$1+\log \frac{k_{8c}}{k_4}$	$13+\log \frac{k_4}{k_2^{\frac{1}{2}}}$	$13+\log \frac{k_{8c}}{k_2^{\frac{1}{2}}}$
				$\times 10^{-12}$ in mol./ml sec								
12.0_8	3.64_5	522	3610	2.54	12.8_9	0.0403	0.0326	12.8_2	1.90_5	0.6925	—	—
10.4_9	2.77	488	3725	0.974	5.72	0.598	0.0307_5	5.12	0.675_5	0.6989	—	—
15.7_7	2.58	456.5	3600	0.959	8.21	0.858	0.0575	7.23	0.601	0.7056	1.1900	1.8960
10.4_3	2.63	440	3600	0.565	4.01	0.781	0.032	3.23	0.392_5	0.6822	1.0422	1.7251
15.3_6	3.75	424.5	4630	0.587	4.15	0.973	0.0443	3.17_4	0.404	0.7165	0.8182	1.5349
11.1_6	2.96	408.5	3400	0.329_5	2.55_8	0.937_5	0.035	1.62_8	0.219_1	0.7065	0.6739	1.3791
6.01	10.7_7	562	3600	0.732	0.798	0.0435	—	0.757	0.707_8	0.7177	—	—
6.18	19.6_4	531	3640	1.41_8	0.896	—	—	0.896	1.39_1	0.6893	—	—
9.24	31.0_6	574	3000	2.45_4	1.48_6	—	—	1.48_6	2.41_1	0.6830	—	—
6.48	28.6_3	592	3600	2.08_2	0.957	—	—	0.957	2.05_3	0.6855	—	—
11.9_8	3.42	395	3600	0.261	2.37_7	1.05_6	0.0369	1.33	0.158	0.6191	0.5308	1.1501
11.8_3	3.78	375.5	3675	0.157	1.65_4	0.965	0.0365	0.697	0.082	0.5658	0.2747	0.8407
10.1_9	3.62	360	4400	0.092	1.21	0.861	0.0448	0.353	0.0385	0.4810	0.0682	0.5551
8.10	56.5_4	378	4370	1.07_4	0.445	0.192	—	0.261_6	1.05_5	0.7612	0.3636	1.1255



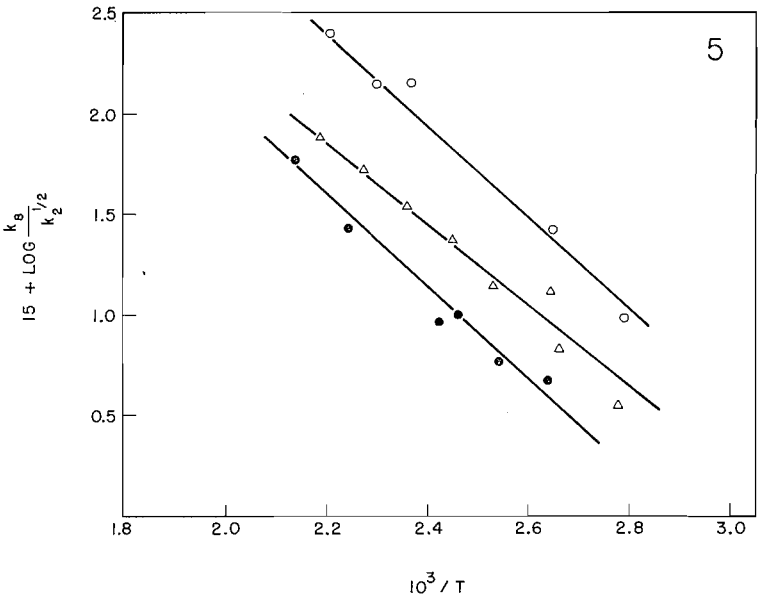


FIG. 4. Activation energy difference between C_2D_5+hydrocarbon → C_2D_5H and C_2D_5+DEK·d_{10} → C_2D_6.
FIG. 5. Activation energy plot for C_2D_5+hydrocarbons.

DISCUSSION

The results obtained for ethyl-d_5 radicals are compared below with those corresponding for methyl (9). In both cases the results are approximately corrected for the presence of primary hydrogen atoms in the two butanes by using the rate per primary hydrogen atom from the neopentane experiments. The behavior in the two cases is parallel in that there is a change in reactivity of about an order of magnitude as one goes from primary to secondary to tertiary hydrogen atoms.

Can. J. Chem. Downloaded from www.nrcresearchpress.com by 91.191.171.90 on 09/05/12
For personal use only.

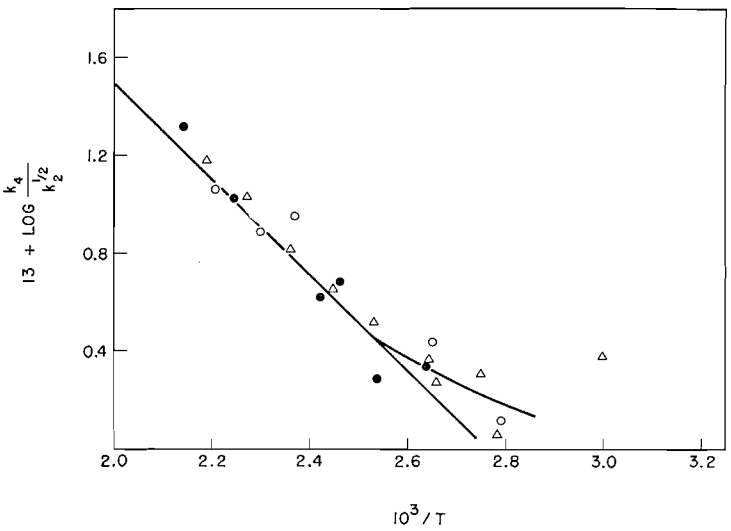


FIG. 6. Activation energy plot for C_2D_5+DEK·d_{10} in the presence of hydrocarbons.

TABLE V

	$C_2D_5\cdot$			$CH_3\cdot$		
	$E_8-\frac{1}{2}E_2$ in kcal	$k_8/k_2^{\frac{1}{2}}\times10^{13}$ at 182° C	$k_8/k_2^{\frac{1}{2}}\times10^{13}$ per "active" H atom	$E_1-\frac{1}{2}E_2$ in kcal	$k_1/k_2^{\frac{1}{2}}\times10^{13}$ at 182° C	$k_1/k_2^{\frac{1}{2}}\times10^{13}$ per "active" H atom
neo-C_5H_{12}	12.6	0.45	0.04	10.0	6.3	0.5
n-C_4H_{10}	10.4	3.15	0.70	8.3	21	4.5
iso-C_4H_{10}	8.9	6.1	5.7	7.6	42	37

NOTE: k_1 refers to $CH_3\cdot + RH \rightarrow CH_4 + R\cdot$.

The reduced activity of ethyl as compared with methyl is obvious but not surprising in view of the lower exothermicity of the ethyl abstractions. In fact, as can be seen from Fig. 7, the experimental values for both radicals lie on a good curve suggesting that at low values of ΔH both radicals have the same activation energy for the same value of ΔH based on some usually accepted figures for C—H bond energy (10). The uncertainty in the bond energies, however, introduces an uncertainty approaching 100% in the C—H bond energy difference for methane and ethane (ΔH). Electron impact methods although subject to criticism have been used to obtain more precise information on such differences (12). It can be seen from Table V that the activation energy difference (ΔE) for methyl and ethyl abstracting from neopentane is 2.6 kcal. It has been suggested that the constant α (in the expression $\Delta E = \alpha\Delta H$) should have a maximum value of 0.5 due to the symmetry of the reaction (11) and this leads to a minimum ΔH of 5.2 kcal. The same is true of the previously observed activation energies for abstraction by methyl from methane (16, 17) and ethane (18, 19), which also differ by about 2.6 kcal. The figure of 5.2 kcal is in excellent agreement with the electron impact value of 5.1±0.7 kcal. Hence the data suggests that α approaches a value of 0.5 at low negative values of ΔH and one assumes that this may be extended to endothermic reactions. The equation of the line is $E = 14.1+(\Delta H/2)$ (in kcal). The ΔE for methyl and ethyl abstractions from various hydrocarbons varies, but definitely seems to increase with the

Can. J. Chem. Downloaded from www.nrcresearchpress.com by 91.191.171.90 on 09/05/12
For personal use only.

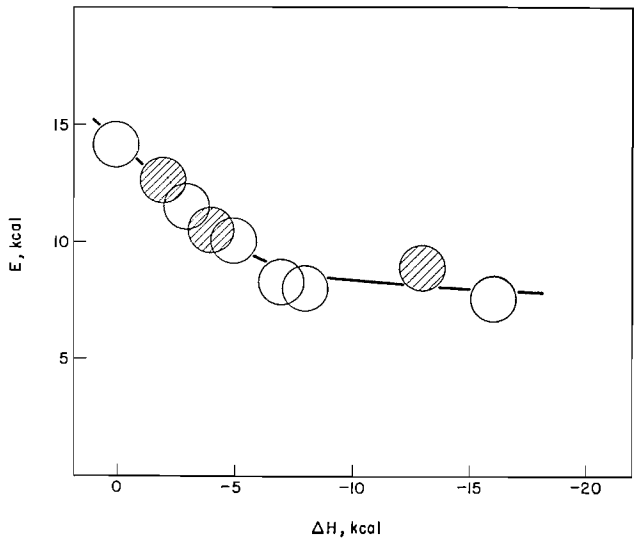


FIG. 7. Activation energy for H atom abstraction vs. ΔH, for CH_3 and C_2D_5 radicals.

strength of the bond broken. Since ΔE is 2.6 kcal for neopentane it should be at least this for ethane. Hence the activation energy for ethyl abstracting from ethane should be at least 14.1 kcal. (This is very close to the corresponding thermally neutral methyl abstraction from methane.) By assuming ΔH for ethane and neopentane to be 3.0 kcal (this is well within the accuracy of the photobromination experiments) and taking ΔH for methane and ethane as 5.2 kcal the following table may be constructed from the above equation.

TABLE VI

Radical abstracting from:	Activation energy in kcal		
	CH_4	C_2H_6	neo-C_5H_{12}
$CH_3\cdot$	14.1*	11.5*	10.0*
$C_2H_5\cdot$	16.7**	14.1	12.6*
neo-$C_5H_{11}\cdot$	18.2	15.6	14.1

Values marked * have been experimentally measured and agree closely with the equation. Value marked ** was estimated by the present authors to be greater than 16.0 kcal on the basis of an unsuccessful attempt to measure the activation energy of ethyl-d_5 abstracting from methane. The yield of C_2D_5H at the highest temperature was used with an assumed steric factor of 10^{-3} to calculate an approximate lower limit of the activation energy. Table VI is entirely consistent with the requirement that the activation energy difference between the forward and reverse reactions should equal ΔH.

An estimate is made of the activation energies for neopentyl radical abstractions. If these values are correct they may never be measured experimentally due to the radical decomposition and rearrangement occurring at the temperatures necessary to measure activation energies of this magnitude. There seems to be no reason not to include all alkyl radicals in this treatment since a ΔH of 5.0 kcal seems to make no difference in the methyl and ethyl case. Results with isopropyl and *tert*-butyl radicals are awaited

Can. J. Chem. Downloaded from www.nrcresearchpress.com by 91.191.171.90 on 09/05/12
For personal use only.

with interest. If the above argument is correct these radicals should have $\alpha = 0.5$ throughout almost the whole range of their abstraction from alkanes.

The result deduced in an earlier section that in the disproportionation of ethyl radicals C—H bonds break 1.4 times more frequently than C—D bonds is of particular interest. This figure is almost exactly equal to the ratio of C—H and C—D stretching frequencies in C_2H_6 and C_2D_6 (13). There is an empirical rule that in similar molecules corresponding vibrations stand in the same ratio (14). This is extended here to the assumption that the frequency ratio for a certain type of vibration in C_2H_6 and C_2D_6 is the same for a similar vibration in C_2H_5 and C_2D_5.

$$\frac{R_{\text{C—H break}}}{R_{\text{C—D break}}} = \frac{0.139}{0.0985} = 1.41.$$

	ν_1 (cm^{-1})	ν_5 (cm^{-1})
C—H stretch in C_2H_6	2899	2954
C—D stretch in C_2D_6	2083	2111
Ratio	1.39	1.40

It appears that there is good evidence here to definitely relate the steric factor of the reaction with the vibrational frequency of the reacting bond. There is probably at least one other term in the steric factor but here where the reactions are so similar it may be expected to be about equal in the two cases.

ACKNOWLEDGMENTS

The authors wish to express their thanks to Mrs. Berneice Riem, who carried out the mass-spectral analyses and to Mr. R. Renaud, who prepared samples of C_2D_5H and $C_2D_4H_2$.

REFERENCES

1. D. G. L. James and E. W. R. Steacie. Proc. Roy. Soc. (London), A, **245**, 470 (1958).
2. M. H. J. Wijnen and E. W. R. Steacie. Can. J. Chem. **29**, 1092 (1951).
3. A. F. Trotman-Dickenson and E. W. R. Steacie. J. Chem. Phys. **19**, 329 (1951).
4. D. G. L. James and E. W. R. Steacie. Proc. Roy. Soc. (London), A, **244**, 289 (1958).
5. K. O. Kutschke, M. H. J. Wijnen, and E. W. R. Steacie. J. Am. Chem. Soc. **74**, 714 (1952).
6. M. H. J. Wijnen and E. W. R. Steacie. J. Chem. Phys. **20**, 205 (1952).
7. P. J. Boddy and E. W. R. Steacie. To be published.
8. E. Whittle and E. W. R. Steacie. J. Chem. Phys. **21**, 993 (1953).
9. A. F. Trotman-Dickenson and E. W. R. Steacie. J. Chem. Phys. **19**, 163 (1951).
10. G. B. Kistiakowsky and E. R. Van Artsdalen. J. Chem. Phys. **12**, 469 (1944). Also see review in E. W. R. Steacie. Atomic and free radical reactions. Reinhold Pub. Co., New York. 1954. p. 80.
11. A. F. Trotman-Dickenson. Dicussions Faraday Soc. **10**, 111 (1951).
12. D. P. Stevenson. Discussions Faraday Soc. **10**, 113 (1951).
13. G. Herzberg. Infra-red and Raman spectra. Van Nostrand, New York. 1945. p. 345.
14. H. D. Noether. J. Chem. Phys. **10**, 693 (1942).
15. J. R. McNesby, C. M. Drew, and A. S. Gordon. J. Phys. Chem. **59**, 988 (1955).
16. F. S. Dainton, K. J. Ivin, and F. Wilkinson. Trans. Faraday Soc. **55**, 929 (1959).
17. J. R. McNesby and A. S. Gordon. J. Am. Chem. Soc. **76**, 4196 (1954).
18. J. R. McNesby and A. S. Gordon. J. Am. Chem. Soc. **77**, 4719 (1955).
19. M. H. J. Wijnen. J. Chem. Phys. **23**, 1357 (1955).

Can. J. Chem. Downloaded from www.nrcresearchpress.com by 91.191.171.90 on 09/05/12
For personal use only.

Can. J. Chem. Downloaded from www.nrcresearchpress.com by 210.87.254.105 on 09/05/12
For personal use only.

THE EFFECT OF SOLVENTS UPON EQUILIBRIA, SPECTRA, AND REACTION RATES[1]

S. BROWNSTEIN

ABSTRACT

It is shown that the effect of solvent upon a wide variety of equilibria, reaction rates, and spectral shifts may be described by the equation $\log (k_{solvent}/k_{ethanol}) = SR$. S is a constant related to the polarity of the solvent and R is a measure of the sensitivity of the system to change in solvent polarity. Tables of S and R are included.

INTRODUCTION

Many attempts have been made to correlate solvent effects with a physical property of the solvent (1–4). Most of these have involved a function of the dielectric constant of the solvent, but refractive index has also been used in an attempt to correlate spectral shifts (5). No satisfactory correlation with a physical property of the solvent could be obtained over an extended range of solvents, or solvent composition in a mixed solvent. This was attributed to specific solvent–solute interaction for some solvents and the ineffectiveness of dielectric constant as a measure of the hydrogen bonding ability of a solvent.

A linear relationship has been observed for the change in reaction rate of closely related reactions as the solvent is varied (6). However, by its nature it is limited to solvolysis reactions and hydroxylic solvents. A four-parameter equation has also been proposed for this group of reactions (7). A similar relationship has been observed in the solvent-dependent shift of certain infrared frequencies (8, 9). A correlation has also been found between solvent effects on solvolysis reactions, described by Y values (6), and ultraviolet spectral shifts, described by Z values (10). Again this cannot be readily extended, as it is formulated, to widely different situations. The success of Kosower's correlation of solvent effects upon solvolysis reactions and ultraviolet spectral shifts suggests the possibility of a semiquantitative correlation of solvent effect upon a wide variety of reactions, equilibria, and spectral shifts. Therefore, it should be possible to predict approximately the effect of changing solvent in a wide variety of cases.

It is the purpose of this paper to propose an equation for correlating solvent effects and to show how well this fits some of the results obtained by a variety of workers. Since the effect of solvent is to change the free energy of the product, activated complex, or excited state, relative to the initial state, a linear free-energy relationship similar to that proposed by Hammett for the reactions of substituted benzenes seems appropriate (11). Absolute ethanol will arbitrarily be chosen as the standard solvent. It appears suitable since much work has been done in this solvent and it is intermediate in dielectric constant and polarity.

Let us assume $\log(k_{solv}/k_{EtOH}) = SR$ where k is a reaction rate, equilibrium constant, or function of a spectral shift. S will be a constant characteristic of any given solvent or solvent mixture. For absolute ethanol it is defined as 0.000 by the above equation, since any other value would require all reactions to have $R = 0.000$. R is a constant characteristic of the sensitivity of a given reaction to solvent effects. The shift of the absorption maximum in 1-ethyl-4-carbomethoxypyridinium iodide (10) was arbitrarily chosen to have

[1]*Manuscript received April 29, 1960.*
Contribution from the Division of Applied Chemistry, National Research Council, Ottawa, Canada.
Issued as N.R.C. No. 5782.

$R = 1.000$. This reaction was chosen since data is available for a wider range of solvents than with most other reactions. With the choice of one standard solvent and one standard reaction, S and R values may be calculated for any reaction and any solvent. The present discussion is limited to a single temperature and 25° C, or room temperature, has been chosen. Although relative solvent polarities, and hence S values, will change with temperature the effect is probably small, since activation energies for a given reaction in various solvents are usually quite similar (6).

Reaction rates and equilibrium constants are exponentially proportional to the difference in free energy between initial and final states while shifts in frequency are directly proportional to energy differences. Therefore for shifts in spectral absorption

$$k = e^{\tilde{\nu}_{\text{max solv}}/\tilde{\nu}_{\text{max EtOH}}}.$$

Then

$$SR = \log \frac{e^{\tilde{\nu}_{\text{max solv}}/\tilde{\nu}_{\text{max EtOH}}}}{e^{\tilde{\nu}_{\text{max EtOH}}/\tilde{\nu}_{\text{max EtOH}}}}$$

$$= \frac{\tilde{\nu}_{\text{max solv}}}{\tilde{\nu}_{\text{max EtOH}}} - \frac{\tilde{\nu}_{\text{max EtOH}}}{\tilde{\nu}_{\text{max EtOH}}}$$

$$= \frac{\tilde{\nu}_{\text{max solv}} - \tilde{\nu}_{\text{max EtOH}}}{\tilde{\nu}_{\text{max EtOH}}}$$

In cases where the appropriate measurements have not been made in absolute ethanol as solvent, and it is not feasible to do them, the following procedure may be used.

$$S_1R = \log\left(\frac{k_{s1}}{k_{\text{EtOH}}}\right) = \log k_{s1} - \log k_{\text{EtOH}}$$

$$S_2R = \log\left(\frac{k_{s2}}{k_{\text{EtOH}}}\right) = \log k_{s2} - \log k_{\text{EtOH}}$$

Therefore

$$R(S_1 - S_2) = \log k_{s1} - \log k_{s2}$$

and

$$R = \frac{\log k_{s1} - \log k_{s2}}{S_1 - S_2}.$$

It is desirable to have results in several solvents grouped into two equal sets and use

$$R = \frac{\sum \log k_{s1} - \sum \log k_{s2}}{\sum S_1 - \sum S_2}.$$

In cases where k is a frequency this still does not remove the necessity of a measurement in absolute ethanol since

$$\log k_{s1} = \log e^{\tilde{\nu}_{\text{max } S_1}/\tilde{\nu}_{\text{max EtOH}}} = \frac{\tilde{\nu}_{\text{max } S_1}}{\tilde{\nu}_{\text{max EtOH}}}$$

and

$$R = \left\{\frac{\tilde{\nu}_{\text{max } S_1} - \tilde{\nu}_{\text{max } S_2}}{\tilde{\nu}_{\text{max EtOH}}}\right\}/(S_1 - S_2).$$

For these cases the data were plotted and the value found for the frequency at S equals zero was used for $\tilde{\nu}_{\text{max EtOH}}$.

EXPERIMENTAL

The data of Kosower (10) were used to determine 58 S values. In those cases where concentration of the pyridinium salt affected the spectral shift, the results were extrapolated to infinite dilution. Using these S values, R values were calculated for nine

Can. J. Chem. Downloaded from www.nrcresearchpress.com by 210.87.254.105 on 09/05/12
For personal use only.

Can. J. Chem. Downloaded from www.nrcresearchpress.com by 210.87.254.105 on 09/05/12
For personal use only.

TABLE I

S values

Aqueous solutions	
%[a]Ethanol	*S*
100	0
98	.00825
96	.0154
95	.0201
92	.0302
90	.0366
85	.0525
80	.0650
75	.0761
70	.0848
60	.0880
50	.1028
45	.1102
40	.1177
37.5	.1219
35	.1255
30	.1325
25	.1376
20	.1417
15	.1455
10	.1490
5	.1515

% Methanol	*S*
100	.0499
97.5	.0560
95	.0615
92.5	.0668
90	.0740
87.5	.0782
85	.0849
80	.0674
77	.0777
72	.0850
60	.0983
50	.1116
40	.1234
30	.1334
20	.1409
10	.1480

% Acetone	*S*
100	−.1748
99	−.1499
95	−.0848
93	−.0607
90	−.0388
85	−.0111
80	.0136
75	.0316
70	.0449
65	.0591
60	.0744
50	.0956
40	.1119
30	.1258
25	.1316
20	.1378
10	.1467
5	.1526

% Dioxane	*S*
100	−.179
90	−.0384
85	−.0056
80	.0071
75	.0268
70	.0413
60	.0766
50	.0947
40	.1108
30	.1250
20	.1369
10	.1464

% 2-Propanol	*S*
100	−.0413
95	−.0032
90	.0234
80	.0546

% Formic acid	*S*
100	.1139
95	.1170
90	.1185
80	.1212
66 2/3	.1250
50	.1303
33 1/3	.1390
25	.1430
14.3	.1470

% Pyridine	*S*
100	−.1970
95	−.1248
90	−.0830
80	−.0330

% Dimethyl formamide	*S*
100	−.1416
90	−.0762
80	−.0262

% *t*-Butanol	*S*
100	−.1047
95	−.0392
90	.0097
80	.0460

Acetic acid	*S*
100%	.0050
.50M H_2O	.0176
2.00M H_2O	.0326
4.00M H_2O	.0454
8.00M H_2O	.0621
16.00M H_2O	.0840
60%	.0990
50%	.1105
40%	.1210
25%	.1359

Other solutions	
Methanol–iso-octane	
%Methanol by volume	*S*
95	.0477
90	.0456
85	.0435
80	.0420

Pyridine–benzene	*S*
1:9	−.1913
1:99	−.1992

Chloroform–acetic acid	*S*
1:1	−.0420

Chloroform–iso-octane	*S*
1:1	−.1240

Propanol–toluene	*S*
1:9	−.1053

Acetic acid–formic acid	
% Acetic acid	*S*
75	.0518
50	.0778
25	.0875
10	.1085

Dioxane–formic acid	
% Dioxane	*S*
60	.0378
40	.0678
20	.0648

Pure solvents	*S*
1-Propanol	−.0158
1-Butanol	−.0240
Formamide	.0463
Acetonitrile	−.1039
Methyl cyclopropyl ketone	−.1788
Ethylene glycol	.0679
Water	.1540
Ethyl acetate	−.210
Isopropyl ether	−.229
Ether	−.277
n-Butyl ether	−.286
Triethylamine	−.285
Chloroform	−.2000
Methylene chloride	−.1890
Gas phase	−.556
Tetrachloroethylene	−.263
Carbon tetrachloride	−.245
Methyl iodide	−.170
Carbon disulphide	−.240
Nitromethane	−.134
Methylene bromide	−.095
Sym. tetrachloroethane	−.083
Bromoform	−.042
Ethylene dichloride	−.151
Methylene iodide	−.043
n-Heptane	−.337
n-Hexane	−.337
Cyclohexane	−.324
Nitrobenzene	−.218
Mesitylene	−.217
Anisole	−.214
Chlorobenzene	−.182
Bromobenzene	−.164
Toluene	−.237
Benzene	−.215
ψ Cumene	−.245
Aniline	.001
Pyrrole	.012

[a]Weight % is meant unless otherwise mentioned.

reactions and these in turn were used to calculate a total of 158 S values. These S values were then used to determine 78 R values. These figures are given in Tables I and II. This does not constitute an exhaustive survey of the literature but is sufficient to show the range of values which can be expected.

A minimum of nine points were used to determine R values of reactions which were subsequently utilized to determine further S values. If the average deviation for these reactions was large, results from two or three reactions were averaged to obtain the additional S values. For the carbonyl absorption of acetone, dimethyl formamide, and methyl acetate in the infrared, data were obtained for additional solvents in this laboratory using a Perkin–Elmer model 21 spectrophotometer with a rock salt prism. It was calibrated immediately before use.

TABLE II

R values

Reaction	R	Deviation	n	Reference
U.V. absorption of 1-methyl-4-carbomethoxypyridinium iodide	* .963	.088	19	(10)
U.V. absorption of 1-ethyl-4-cyanopyridinium iodide	1.076	.047	6	(10)
U.V. absorption of pyridine-1-oxide	.224	.092	12	(10)
Solvolysis of *t*-butyl chloride	*35.89	1.07	17	(3, 6)
Solvolysis of *t*-butyl bromide	29.9	4.1	20	(14)
Solvolysis of benzyhydryl chloride	22.8	6.3	19	(15)
Solvolysis of α-phenylethyl chloride	29.4	4.5	32	(14)
Solvolysis of α-phenylethyl bromide	26.6	3.7	20	(14)
Solvolysis of benzhydryl bromide	20.0	8.6	5	(15)
" of trityl fluoride	25.4	5.0	6	(7)
" of *p*-nitrobenzoyl chloride	8.3	2.3	5	(16)
" of *p*-nitrobenzoyl fluoride	20.2	5.6	7	(16)
" of benzoyl chloride	13.5	2.4	9	(16)
" of benzoyl fluoride	23.3	3.2	7	(16)
" of acetic anhydride	18.6	6.1	7	(17)
C=O absorption of acetone	*−.036	.021	10	(8)
C=O absorption of dimethyl formamide	−.045	.025	10	(8)
C=O absorption of methyl acetate	*−.057	.026	9	(8)
U.V. absorption of 2,6-dimethyl-4-seleno-γ-pyran	.822	.226	14	(18)
C=O absorption of cyclohexanone	−.021	.012	22	(8)
C=O " of benzophenone	−.045	.011	24	(8)
C=O " of acetophenone	−.020	.010	24	(8)
C=O " of acetyl chloride	−.017	.007	21	(8)
1867 cm^{-1} absorption of ethylene carbonate	−.054	.009	20	(8)
1758 cm^{-1} absorption of ethylene carbonate	.028	.014	20	(8)
N—H absorption of pyrrole	−3.19	0.81	17	(19)
Solvolysis of methane sulphonyl chloride	11.0	0.8	9	(20)
Solvolysis of ethyl chloroformate	9.9	0.5	12	(20)
Asymmetric N—H absorption of aniline	*−.079	.017	10	(19)
Symmetric N—H absorption of aniline	*−.194	.048	10	(19)
Asymmetric O—H stretch of water	−1.15	.25	11	(19)
Symmetric O—H stretch of water	−1.03	.22	11	(19)
B—H stretch of decaborane	−.059	.005	9	(19)
O—H stretch of phenol	−.484	.073	8	(19)
Racemization of 2-nitro-6-carboxy-2′-methoxybiphenyl	No correlation		6	(21)
Racemization of 2-nitro-6-carboxy-2′-ethoxybiphenyl	No correlation		6	(21)
Chemical shift difference of extra ring protons of benzyl alcohol	20.9	3.1	13	(22)
S=O frequency of dimethyl sulphoxide	−.140	.032	19	(23)
Phenyl frequency of diphenyl sulphoxide	−.026	.004	17	(23)
S=O frequency of diphenyl sulphoxide	−.063	.011	19	(23)
S=O frequency of thionyl chloride	−.037	.007	13	(23)
P=O frequency of phosphorous oxychloride	−.073	.015	10	(23)
Susceptibility corrected chemical shift of propargyl bromide CH_2	2.86	.27	8	(24)

Can. J. Chem. Downloaded from www.nrcresearchpress.com by 210.87.254.105 on 09/05/12
For personal use only.

TABLE II (*concluded*)

Reaction	R	Deviation	n	Reference
Susceptibility corrected chemical shift of propargyl bromide CH	3.32	.23	7	(24)
Chemical shift difference of CH_2 and CH protons of propargyl bromide	−.86	.07	7	(24)
C≡H stretch of propargyl bromide	−.044	.005	8	(24)
High frequency P=O stretch of dimethyl hydrogen phosphonate	−.099	.010	17	(23)
Low frequency P=O stretch of dimethyl hydrogen phosphonate	−.071	.007	17	(23)
Trans N=O stretch of methyl nitrite	−.051	.011	11	(23)
Third harmonic OH band of CH_3OH	−.048	.018	9	(25)
2nd OH overtone of phenol	−.203	.034	10	(26)
N—N band of dimethyl nitrosamine	.130	.028	14	(23)
Pseudo dimer N=O band of nitrosamine	No correlation		9	(23)
N=O band of dimethyl nitrosamine	−.071	.014	9	(23)
Trans N=O stretch of isopropyl nitrate	−.062	.017	11	(23)
Cis N=O stretch of isopropyl nitrate	−.016	.005	11	(23)
Rate of reaction of aniline with ω-bromoacetophenone	4.30	2.35	7	(27)
$\pi \rightarrow \pi^*$ transition of nitrobenzene	−.075	.035	5	(28)
$n \rightarrow \pi^*$ transition of nitromethane	.050	.022	7	(28)
$n \rightarrow \pi^*$ transition of crotonaldehyde	.26	.08	5	(28)
$n \rightarrow \pi^*$ transition of acetone	.097	.037	7	(28)
λ_{max} of phenol blue	*−.281	.081	15	(29)
5000 A° absorption of lycopene	.166	.088	11	(29)
4800 A° absorption of lycopene	.146	.060	9	(29)
4500 A° absorption of lycopene	.126	.050	9	(29)
Absorption of phenolphthalein	.192	.057	6	(29)
Absorption of *p*-rosaniline hydrochloride	.222	.240	9	(29)
Keto-enol equilibrium of ethyl acetoacetate	−3.48	3.48	14	(30)
Long wavelength absorption of mesityl oxide	.129	.045	9	(10)
Absorption of 2-methyl-4,6-diphenylpyridinium N^+N Betaine	.273	.108	10	(31)
Pyridine + ethyl iodide yields pyridinium iodide (rate)	3.01	1.87	7	(32)
Short wavelength absorption of mesityl oxide	No correlation		9	(10)
Proton resonance shift of water between vapor and solution	3.78	1.08	10	(33)
Fluorine resonance shift of benzotrifluoride	No correlation		8	(34)
Fluorine resonance shift of 1,2-di-fluorotetra-chloroethane	No correlation		8	(34)
Fluorine resonance shift of 1-fluoropentane	3.46	2.16	6	(34)
Reaction of trimethylamine and *o*-nitrobenzylchloride	No correlation		7	(35)
Reaction of trimethylamine and *m*-nitrobenzylchloride	No correlation		7	(35)
Reaction of trimethylamine and *p*-nitrobenzylchloride	No correlation		7	(35)
Decomposition of azodicarbonate ion	9.86	.06	7	(36)
Reaction of methyl iodide and silver nitrate	−2.82	1.72	6	(37)
1st dissociation constant of succinic acid	12.4	2.0	15	(38)
2nd dissociation constant of succinic acid	18.4	2.7	15	(38)
1st dissociation constant of azelaic acid	29.4	2.4	12	(38)
2nd dissociation constant of azelaic acid	33.8	2.6	12	(38)
Isomerization of *cis*-azobenzene	−1.6	0.8	9	(39, 40)
Racemization of *tris*-oxalato-chromium III	19.7	2.8	12	(41)

DISCUSSION

There is found to be a good fit of the proposed equation to the experimental data. Therefore, there is probably a characteristic of solvents, described here by S values, which is responsible for solvent effects in a wide variety of situations. However, this type of correlation necessarily averages out individual differences in solvents and reactions so it would be dangerous to attribute too much theoretical significance to the individual numbers. It obviously will not apply to measurements where there is a unique interaction between the solvent and the species which is being measured. Such a situation occurs with infrared spectral shifts when there is hydrogen bonding between the solvent

Can. J. Chem. Downloaded from www.nrcresearchpress.com by 210.87.254.105 on 09/05/12
For personal use only.

and some functional group of the substance whose spectrum is being determined. It also occurs when the solvent is able to complex with one of the species in a reaction whose rate is being determined. This type of correlation should nevertheless prove quite useful in transposing data, primarily spectroscopic, from one solvent system to another.

For the rates of 14 solvolysis reactions the average deviation from the individual R values was 19.4% for rates differing by up to 10,000 times. The R values for the individual reactions were all positive and varied between 9.9 and 35.9. For 32 infrared absorptions the average deviation from the individual R values was 27%. All R values were negative and ranged between -3.19 and $-.016$ except for two positive values and one case which did not fit the equation. These numbers correspond to a slight solvent shift and the experimental accuracy in determining the solvent shifts usually limited the accuracy with which the data fitted the equation.

For the spectral shifts of 15 ultraviolet absorptions the average deviation from the individual R values was 34%. There was no correlation in two instances. The R values were positive and ranged between .05 and 1.08 except for two negative values. It has been suggested that $\pi \rightarrow \pi^*$ transitions are affected differently by solvent change than $n \rightarrow \pi^*$ transitions (12). This can be stated more quantitatively by noting that $\pi \rightarrow \pi^*$ transitions are likely to have negative R values. The solvent corrections for Woodwards rules can also be stated in terms of R values (13). They correspond to saying the transitions usually have an R value of about 0.10, although chloroform does not seem to fit this scheme very well.

Magnetic-susceptibility-corrected solvent shifts of nuclear resonance spectra are also correlated by the same equation. The average deviation in individual R values for five proton resonance solvent shifts is only 13.6%. Little correlation is found with fluorine resonance shifts.

This type of correlation should be useful in correcting literature values of data in some solvent system to the system which an investigator finds convenient in his own work.

REFERENCES

1. (*a*) J. G. KIRKWOOD. J. Chem. Phys. **2**, 351 (1934).
   (*b*) S. GLASSTONE, K. J. LAIDLER, and H. EYRING. The theory of rate processes. McGraw-Hill Book Co., New York. 1941. p. 419.
2. K. J. LAIDLER. Chemical kinetics. McGraw-Hill Book Co., New York. 1950. p. 127.
3. A. H. FAINBERG and S. WINSTEIN. J. Am. Chem. Soc. **78**, 2770 (1956). (Good for earlier references.)
4. M. L. JOSIEN and N. FUSON. J. Chem. Phys. **22**, 1169 (1954).
5. N. S. BAYLISS, A. R. H. COLE, and L. H. LITTLE. Australian J. Chem. **8**, 26 (1955).
6. E. GRUNWALD and S. WINSTEIN. J. Am. Chem. Soc. **70**, 846 (1948).
7. C. G. SWAIN and R. B. MOSELY. J. Am. Chem. Soc. **77**, 3727 (1955).
8. L. J. BELLAMY and R. L. WILLIAMS. Trans. Faraday Soc. **55**, 14 (1959).
9. L. J. BELLAMY. Spectrochim. Acta, **14**, 216 (1959).
10. E. M. KOSOWER. J. Am. Chem. Soc. **80**, 3253 (1958).
11. L. P. HAMMETT. Physical organic chemistry. McGraw-Hill Book Co., New York. 1940. p. 184.
12. H. MCCONNELL. J. Chem. Phys. **20**, 700 (1952).
13. R. B. WOODWARD. J. Am. Chem. Soc. **63**, 1123 (1941).
14. A. H. FAINBERG and S. WINSTEIN. J. Am. Chem. Soc. **79**, 1597 (1957) et seq.
15. S. WINSTEIN, A. H. FAINBERG, and E. GRUNWALD. J. Am. Chem. Soc. **79**, 4146 (1957).
16. C. G. SWAIN, R. B. MOSELY, and D. E. BROWN. J. Am. Chem. Soc. **77**, 3731 (1955).
17. V. GOLD. Trans. Faraday Soc. **44**, 506 (1948).
18. M. ROLLA and P. FRANZOSINI. Gazz. chim. ital. **88**, 837 (1958).
19. L. J. BELLAMY, H. E. HALLAM, and R. L. WILLIAMS. Trans. Faraday Soc. **54**, 1120 (1958).
20. H. BOHME and W. SCHURHOFF. Ber. **84**, 28 (1951).
21. C. C. LI and R. ADAMS. J. Am. Chem. Soc. **57**, 1565 (1935).
22. P. L. CORIO, R. L. RUTLEDGE, and J. R. ZIMMERMAN. J. Mol. Spectroscopy, **3**, 592 (1959).
23. L. J. BELLAMY, C. P. CONDUIT, R. J. PACE, and R. L. WILLIAMS. Trans. Faraday Soc. **55**, 1677 (1959).
24. E. B. WHIPPLE, J. H. GOLDSTEIN, L. MANDELL, G. S. REDDY, and G. R. MCLURE. J. Am. Chem. Soc. **81**, 1321 (1959).

Can. J. Chem. Downloaded from www.nrcresearchpress.com by 210.87.254.105 on 09/05/12
For personal use only.

25. L. H. JONES and R. M. BADGER. J. Am. Chem. Soc. **73**, 3132 (1951).
26. R. MECKE. Discussions Faraday Soc. **9**, 161 (1950).
27. H. E. COX. J. Chem. Soc. **119**, 142 (1921).
28. N. S. BAYLISS and E. G. MCRAE. J. Phys. Chem. **58**, 1006 (1954).
29. A. L. LEROSEN and C. E. REID. J. Chem. Phys. **20**, 233 (1952).
30. K. H. MEYER. Ann. **380**, 212 (1911).
31. K. DIMROTH, G. ARNOLDY, S. v. EICKEN, and G. SCHIFFLER. Ann. **604**, 221 (1957).
32. J. F. NORRIS and S. W. PRENTISS. J. Am. Chem. Soc. **50**, 3042 (1928).
33. G. MAVEL. J. phys. radium, **20**, 834 (1959).
34. D. F. EVANS. J. Chem. Soc. 877 (1960).
35. H. MCCOMBIE, H. A. SCARBOROUGH, and F. F. P. SMITH. J. Chem. Soc. 802 (1927).
36. C. V. KING and J. J. JOSEPHS. J. Am. Chem. Soc. **66**, 767 (1944).
37. K. A. BURKE and F. G. DONNAN. J. Chem. Soc. 555 (1904).
38. M. YASUDA. Bull. Chem. Soc. Japan, **32**, 429 (1954).
39. G. S. HARTLEY. J. Chem. Soc. 633 (1938).
40. R. J. W. LEFEVRE and J. NORTHCOTT. J. Chem. Soc. 867 (1953).
41. G. K. SCHWEITZER and J. L. ROSE. J. Phys. Chem. **56**, 428 (1952).

Can. J. Chem. Downloaded from www.nrcresearchpress.com by 210.87.254.105 on 09/05/12
For personal use only.

Can. J. Chem. Downloaded from www.nrcresearchpress.com by 186.148.149.217 on 09/04/12
For personal use only.

THE FLUORINE RESONANCE SPECTRUM OF PERCHLORYL FLUORIDE[1]

S. BROWNSTEIN

ABSTRACT

The first instance of observable spin–spin coupling with a chlorine nucleus is found in the fluorine resonance of perchloryl fluoride. The explanations of this, and of the very large chemical shift, are given.

When a nucleus of non-zero spin is bonded directly, or with a few intervening atoms, to another nucleus of non-zero spin, coupling of the two nuclear spins occurs via the bonding electrons. If the spin-coupled nuclei are magnetically non-equivalent, the spin coupling manifests itself by a splitting of the observed nuclear resonance peaks (1, Chap. 8). When a nucleus of spin 1/2 is coupled to a nucleus with spin greater than 1/2, spin coupling is not always observed in the resonance spectrum of the nucleus with spin 1/2. This is attributed to a rapid relaxation of the nucleus with spin greater than 1/2 due to interaction of its quadrupole moment with an unsymmetric electric field gradient. One would expect to see spin coupling when there is spherical symmetry about the nucleus of spin greater than one half, and this is observed (2). If the symmetry is less, the individual lines broaden and eventually coalesce into a single sharp line when the relaxation is rapid.

No examples have been reported of observable spin coupling of nuclei with chlorine, but sharp single peaks are always observed. Both chlorine-35 and chlorine-37 have spin 3/2 and appreciable quadrupole moments. Since chlorine is quite electronegative, unsymmetric bonds are to be expected in most of its compounds and rapid relaxation of the chlorine nuclear spin occurs. Three oxygens and a fluorine are tetrahedrally arranged about a central chlorine in perchloryl fluoride and the compound has no observable dipole moment (3). Relaxation of the chlorine nuclear spin should not be too rapid in this compound.

The fluorine resonance spectrum of perchloryl fluoride is shown in Fig. 1. It has a

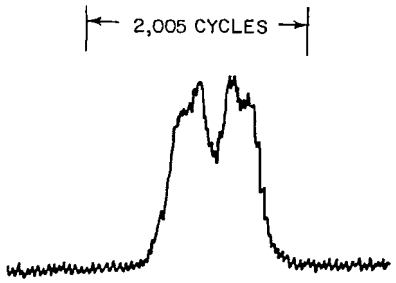


FIG. 1. Fluorine resonance of perchloryl fluoride.

chemical shift of 320 p.p.m. to low field from the fluorine resonance in trifluoracetic acid. The splitting between the two partially resolved lines is 310 cycles and the extrapolated line width, at half the height, for each line is 430 cycles. The signal is very weak requiring

[1]*Manuscript received June 6, 1960.*
Contribution from the Division of Applied Chemistry, National Research Council, Ottawa, Canada. Issued as N.R.C. No. 5778.

40 decibels more of radio-frequency power to obtain the same signal intensity as that of trifluoracetic acid.

A correlation of chemical shift with the electronegativity of the atom or group to which fluorine is bonded has been demonstrated (4). The shift to low field is greatest the lower the electron density about fluorine, with the spherically symmetric fluoride ion occurring at highest field. The fluorine resonance shift in perchloryl fluoride is to lower field than any compound of fluorine, except for molecular fluorine. The lack of dipole moment for perchloryl fluoride suggests that the electronegativity of the perchloryl group approaches that of fluorine. Therefore the chemical shift is in agreement with previous observations.

Four lines of equal intensity are to be expected in the spectrum of a nucleus spin coupled to one other of spin 3/2. Since both stable isotopes of chlorine have spin 3/2 two sets of four lines will be expected with $J_{Cl^{35}}/J_{Cl^{37}} = \mu_{Cl^{35}}/\mu_{Cl^{37}} = .821/.683$ (1, p. 188). The relative intensities will be three to one. Combining the individual spectra gives a composite spectrum in which the intensity between the outside peaks is greater than between the center ones. This is illustrated in Fig. 2 for triangular peaks. A Gaussian

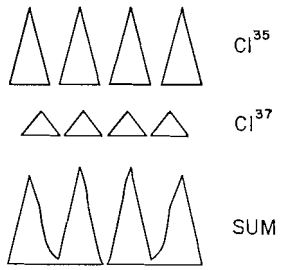


FIG. 2. Effect of isotopic composition upon the spectrum.

line shape would probably accentuate this. Possibly for this reason only two poorly resolved peaks are actually observed.

The lines of perchloryl fluoride have a width of 430 cycles whereas at the same sweep rate the resonance of trifluoracetic acid is immeasurably narrow. Therefore considerable broadening of the fluorine resonance is occurring due to rapid relaxation of the chlorine nuclear spin.

EXPERIMENTAL

Perchloryl fluoride was obtained from Pennsalt Chemicals Corporation, and used without further purification. The gas was condensed under vacuum into a 5-mm O.D. Pyrex tube which was then sealed. Upon warming to room temperature, a colorless mobile liquid remained in the sample tube.

The spectra were run on a Varian Associates high resolution nuclear magnetic resonance spectrometer Model V4300C operating at 56.4 Mc. The spectra were calibrated using audio side bands (5) counted with a Hewlett Packard Model 521C frequency counter. Since the observed chemical shift was beyond the normal sweep range of the instrument, the magnet current was varied after the instrument was calibrated. Because of hysteresis in the electromagnet, the chemical shift obtained in this manner will only be accurate within about 5 p.p.m. A radio-frequency power level of 50 db below 1/2 watt was required to produce an adequate signal. Variation of the power about this level gave no indication of saturation of the signal.

Can. J. Chem. Downloaded from www.nrcresearchpress.com by 186.148.149.217 on 09/04/12
For personal use only.

ACKNOWLEDGMENT

The author wishes to thank Dr. R. F. Grant for a wide line fluorine resonance spectrum.

REFERENCES

1. J. A. POPLE, W. G. SCHNEIDER, and H. J. BERNSTEIN. High resolution nuclear magnetic resonance. McGraw-Hill. 1959.
2. R. A. OGG and J. D. ROY. J. Chem. Phys. **26**, 1339 (1957).
3. BOOKLET DC-1819, Pennsalt Chemicals Corporation, Philadelphia, Pa.
4. H. S. GUTOWSKY and C. J. HOFFMAN. J. Chem. Phys. **19**, 1259 (1951).
5. J. T. ARNOLD and M. E. PACKARD. J. Chem. Phys. **19**, 1608 (1951).

Can. J. Chem. Downloaded from www.nrcresearchpress.com by 186.148.149.217 on 09/04/12
For personal use only.

Can. J. Chem. Downloaded from www.nrcresearchpress.com by 210.87.254.40 on 09/05/12
For personal use only.

THE PREPARATION OF CYCLIC PEROXIDES AND THEIR DECOMPOSITION IN SOLUTION[1]

K. E. Russell

ABSTRACT

The cyclic dimers of sebacyl, dodecanedioyl, and tetradecanedioyl peroxide have been prepared, together with high yields of the corresponding high molecular weight polymeric peroxides. The decomposition of these peroxides in styrene and benzene solution has been studied. The results show that if diradicals are formed in the breakdown of the cyclic peroxides, they undergo self-termination before reacting with a significant number of styrene molecules. In the presence of low concentrations of 1,1-diphenyl-2-picrylhydrazyl (DPPH) in benzene solution, self-termination of diradicals is preferred to reaction with the hydrazyl.

INTRODUCTION

The main objective of this investigation was to study the reactions of diradicals obtained by the thermal breakdown of cyclic peroxides. Previous work (1, 2) has shown that phthalyl peroxide may be readily prepared by the reaction of phthalyl chloride with sodium peroxide, but that its decomposition in solution may be complex (2, 3). It was thus not possible to reach firm conclusions concerning the reactions of diradicals from studies involving this aromatic peroxide. Some cyclic aliphatic peroxides have now been prepared using the same experimental method. Attempts were made to isolate succinyl, adipyl, suberyl, azelayl, sebacyl, dodecanedioyl, and tetradecanedioyl peroxides, but low molecular weight cyclic peroxides were only obtained in the last three cases. Polymeric peroxides of high molecular weight were always obtained as the major reaction products.

The decomposition of the cyclic and linear peroxides in benzene solution was studied by direct analysis in order to show that there is no fundamental difference in the primary step of the breakdown. Measurements were made of the rate of polymerization of styrene using the various peroxides as initiators to determine to what extent the radical intermediates grow to give high molecular weight polystyrene. The decomposition of the peroxides in benzene solutions of 1,1-diphenyl-2-picrylhydrazyl (DPPH) was studied to give information concerning the reactions of the radical intermediates with DPPH.

EXPERIMENTAL

Materials

Chloroform was treated with concentrated sulphuric acid to remove alcohol and was washed twice with distilled water. Reagent grade (Fisher) benzene was used for the kinetic studies. Styrene was distilled at 15 mm pressure and subjected to two bulb-to-bulb distillations on the high vacuum line. DPPH was prepared by the method of Goldschmidt and Renn (4); it was heated *in vacuo* to 90° for 1 hour to remove complexed solvent. Succinyl, adipyl, sebacyl, and hexanoyl chlorides were Eastman Kodak materials.

Suberic, azelaic, dodecanedioic, and tetradecanedioic acids were converted to the corresponding acid chlorides by reaction with thionyl chloride. Thionyl chloride (2.4 moles per mole of acid) was used and the reaction was allowed to proceed for 3 days at 40°; excess thionyl chloride was distilled off at reduced pressure. The light yellow product was treated with activated charcoal. (This modification of the usual method was suggested by R. F. Liming, Distillation Products Industries.) The purity of the acid chlorides was

[1]*Manuscript received May 13, 1960.*
Contribution from the Department of Chemistry, Queen's University, Kingston, Ontario.

shown to be greater than 98.5% by allowing them to react with 6 *N* sodium hydroxide, adding 6 *N* hydrochloric acid equivalent to the sodium hydroxide, and determining the hydrochloric and dibasic acids present.

Preparation of the Peroxides

The peroxides were prepared by stirring a dilute aqueous solution of sodium peroxide with a dilute chloroform solution of the acid chloride. In a typical preparation, 20 g of disodium hydrogen phosphate hexahydrate and 0.01 mole of sodium peroxide were added to 110 ml of water at 0° C. A solution of 0.015 mole of acid chloride in 250 ml of chloroform was added and the mixture stirred vigorously. Further quantities of sodium peroxide, up to a total of 0.025 mole, were added over a period of 20 minutes. Stirring was continued for a further 30 minutes.

The chloroform layer was separated and washed twice with water, and the chloroform was evaporated with a stream of dry air at room temperature. The white solid obtained was extracted twice with low-boiling petroleum ether.

Significant yields of low molecular weight peroxide soluble in petroleum ether were obtained only in the cases of sebacyl, dodecanedioyl, and tetradecanedioyl peroxides. These materials were purified by recrystallization from petroleum ether and dried *in vacuo* at room temperature. Molecular weights were determined by measurement of the depression of the freezing point of pure benzene, and peroxide contents were determined by the method of Wagner, Smith, and Peters (5). Sebacyl peroxide: yield 4–6%, m.p. 19–21°. Anal. Calc. for $C_{10}H_{16}O_4$: C, 60.0; H, 8.06; —O—O—, 16.0. Found: C, 60.16, 60.22; H, 8.07, 8.06; —O—O—, 15.8%. Mol. wt. 360, 370. Dodecanedioyl peroxide: yield 5–6%, m.p. 32–35°. Anal. Calc. for $C_{12}H_{20}O_4$: C, 63.15; H, 8.77; —O—O—, 14.0. Found: C, 63.17, 63.26; H, 8.78, 8.97; —O—O—, 13.8, 13.7%. Mol. wt. 429, 473. Tetradecanedioyl peroxide: yield 7–9%, m.p. 43–46°. Anal. Calc. for $C_{14}H_{24}O_4$: C, 65.56; H, 9.38; —O—O—, 12.5. Found: C, 65.54, 65.58; H, 9.65, 9.53; —O—O—, 12.1%. Mol. wt. 462.

In the attempted preparation of succinyl peroxide a low yield of chloroform-insoluble peroxide was obtained and very little peroxide remained in the chloroform layer even before evaporation. With other preparations the major product was a peroxide which was insoluble in petroleum ether. Molecular weight determination by depression of the freezing point of benzene indicated values greater than 3000; intrinsic viscosities of chloroform solutions of sebacyl, dodecanedioyl, and tetradecanedioyl peroxides varied between 0.3 and 0.5. These high molecular weight peroxides will be referred to as polymeric peroxides and individual peroxides as polysebacyl peroxide, etc. *When dry, polymeric peroxides explode on scratching or on heating. The sensitivity to percussion and the vigor of the explosion increase with the peroxide content of the polymeric peroxide.* Polyadipyl peroxide: yield 50%, m.p. 118–119° decomp. Polysuberyl peroxide: yield 75%, m.p. 116–118° decomp. Anal. Calc. for $C_8H_{12}O_4$: —O—O—, 18.6. Found: —O—O—, 18.3%. Polyazelayl peroxide: yield 70%, m.p. 104–105° decomp. Anal. Calc. for $C_9H_{14}O_4$: —O—O—, 17.2. Found: —O—O—, 17.0%. Polysebacyl peroxide: yield 85%, m.p. 112–113° decomp. Anal. Calc. for $C_{10}H_{16}O_4$: C, 60.0; H, 8.06; —O—O—, 16.0. Found: C, 60.12, 60.22; H, 8.07, 7.95; —O—O—, 15.9, 15.8%. Polydodecanedioyl peroxide: yield 80%, m.p. 108–109°. Anal. Calc. for $C_{12}H_{20}O_4$: —O—O—, 14.0. Found: —O—O—, 13.7%. Polytetradecanedioyl peroxide: yield 80%, m.p. 108–110°. Anal. Calc. for $C_{14}H_{24}O_4$: —O—O—, 12.5. Found: —O—O—, 11.9%.

Hexanoyl peroxide was prepared by the above method. Anal. Calc. for $C_{12}H_{22}O_4$: —O—O—, 13.9. Found: —O—O—, 13.4%. Mol. wt. 219.

Can. J. Chem. Downloaded from www.nrcresearchpress.com by 210.87.254.40 on 09/05/12
For personal use only.

Infrared spectra were taken of the low molecular weight and polymeric sebacyl, dodecanedioyl, and tetradecanedioyl peroxides in chloroform solution using a Perkin–Elmer Model 21 spectrometer.

Decomposition Studies

The rates of breakdown of the peroxides in benzene and styrene solutions were determined by peroxide analysis. For styrene as solvent, about 0.04 g of peroxide was weighed and introduced into a reaction tube. Approximately 4 g of styrene was distilled into the tube, and after it was sealed off, the tube was placed in a bath at 60° for 1 hour or 2 hours. The remaining peroxide was then estimated (5). For benzene as solvent, the solutions were degassed twice before being placed in the bath at 60°.

In the polymerization studies, solutions of peroxide in styrene were made up as described above, and the polymerization allowed to proceed at 60° for 2 hours. The high molecular weight polystyrene was precipitated in methanol, filtered, and dried *in vacuo* at 60°.

The rates of disappearance of DPPH were studied using benzene solutions which were approximately 0.0004 *M* in DPPH and 0.005 *M* in peroxide. The solutions were degassed and were heated to 60° for periods of 20 minutes. Readings of optical density were taken at a solution temperature of 20° using a Fisher electrophotometer with a 650 mμ filter. The optical densities of a series of DPPH solutions of known concentration were also determined.

RESULTS AND DISCUSSION

The Structures of the Peroxides

The major product of the reaction between a dibasic acid chloride and sodium peroxide under the experimental conditions used in this work is a polymeric peroxide. Good yields of polyadipyl, polysuberyl, polyazelayl, polysebacyl, polydodecanedioyl, and polytetradecanedioyl peroxides were obtained. The average molecular weights of the polymeric peroxides are probably between 5000 and 10,000. They are almost certainly linear polymers.

Small yields of low polymers of sebacyl, dodecanedioyl, and tetradecanedioyl peroxides were isolated. Analytical data and molecular weight determinations suggest that these low polymers are cyclic dimers. It is possible that the products are mixtures of low polymers, e.g., cyclic monomer, dimer, and trimer. However, fractional crystallization did not appreciably affect the melting points of the products and it is probable that the peroxides are largely, if not completely, cyclic dimers. Confirmatory evidence for the nature of the low molecular weight products is provided by their infrared spectra. The spectra of corresponding low and high molecular weight products are identical except for slight differences in the intensities of some bands. This indicates that similar structural units are present in the dimer and polymer. There is no absorption in the O—H stretching frequency region in any of the spectra; the cyclic dimer is therefore not seriously contaminated by low molecular weight linear peroxides.

The production of cyclic dimer instead of monomer in the case of sebacyl peroxide is not surprising in view of the strain normally involved in 12-membered rings. Overberger and Lapkin (6) obtained the cyclic dimer, 3,12,15,24-tetraphenyl-1,2,13,14-tetraaza-1,13-cyclotetracosatetradiene, when they attempted to prepare the monomeric 12-membered ring compound. A dimer was also formed when they attempted to prepare the corresponding 14-membered ring compound. In the present work it was hoped that the 16-membered

Can. J. Chem. Downloaded from www.nrcresearchpress.com by 210.87.254.40 on 09/05/12
For personal use only.

ring of monomeric tetradecanedioyl peroxide would be formed more readily, but the molecular weight evidence indicates that formation of dimer is preferred to that of monomer.

Decomposition of the Peroxides in Solution

The thermal decomposition of the peroxides in benzene and styrene solution was studied by peroxide analysis. The peroxides investigated were the cyclic dimers and the high molecular weight linear polymers of sebacyl, dodecanedioyl, and tetradecanedioyl peroxide. These six peroxides all decompose at rates within the range 5.5 to 8.5%/hour in the two solvents at 60°. Since the cyclic peroxides decompose at approximately the same rates as the linear peroxides, it is reasonable to assume that homolytic cleavage of the peroxide link occurs as the initial step in both cases. The radicals so formed may eliminate carbon dioxide. Thermal decomposition of the polymeric peroxides gives rise to monoradicals and decomposition of the cyclic peroxides leads to diradicals.

The Peroxides as Initiators for the Polymerization of Styrene

The three cyclic dimers and their long-chain linear analogues were used as initiators for the polymerization of styrene at 60°. The measured rates of polymerization were converted to rates of initiation R_i by means of the relationship (7)

$$[1] \qquad R_p^2 = 3\times10^{-2}R_i .$$

In this work concentrations are expressed in moles/liter and time in seconds; for the peroxides, concentrations are given in moles/liter of monomer units. Values of $R_i/(I)$, where (I) is the concentration of peroxide, are given in Table I.

TABLE I

Rates of initiation of polymerization of styrene and rates of disappearance of DPPH at 60°

	$10^6 R_i/(I)$ sec^{-1}	$10^6 R_{DPPH}/(I)$ sec^{-1}
Polysebacyl peroxide	8.0	12.1
Sebacyl peroxide (cyclic dimer)	0.22	0.5
Polydodecanedioyl peroxide	7.9	11.0
Dodecanedioyl peroxide (cyclic dimer)	0.21	0.35
Polytetradecanedioyl peroxide	8.2	11.4
Tetradecanedioyl peroxide (cyclic dimer)	0.37	0.6
Hexanoyl peroxide	13.8	18

The three polymeric peroxides have a value of $R_i/(I)$ of 8×10^{-6} sec^{-1} within experimental error. The polymeric peroxides differ only in the number of methylene groups joined together in their repeating units, and unless this number is very small, significant differences between the rates for the three peroxides would not be expected. The value of $R_i/(I)$ for hexanoyl peroxide, a simple linear peroxide, is 13.8×10^{-6} sec^{-1}.

The rates of initiation of polymerization of styrene are very much lower when the cyclic dimers are used as initiators. The maximum rate is observed with tetradecanedioyl peroxide and this is only 4.5% of the rate observed with the corresponding polymeric peroxide. If the cyclic dimers decompose to produce diradicals, these diradicals undergo self-termination before they add on a significant number of styrene units. Other workers have reached a similar conclusion on the basis of theoretical and experimental studies. Zimm and Bragg (8) predicted that even large polystyryl diradicals would undergo self-termination more rapidly than addition of a styrene monomer unit. Tobolsky and Russell

Can. J. Chem. Downloaded from www.nrcresearchpress.com by 210.87.254.40 on 09/05/12
For personal use only.

(9) showed that the photochemical breakdown of a cyclic disulphide in styrene gave very little high molecular weight polystyrene, in contrast with the result obtained using a linear disulphide. Overberger and Lapkin (6) observed that the thermal decomposition of a 24-membered ring azo compound in styrene gave a relatively low yield of high polymer, and Cohen *et al.* (10) observed that a 6-membered ring azo compound behaved in a similar manner.

In previous studies it was not clear whether the small amount of high polymer formed arose from the growth of diradicals or of monoradicals originating from an impurity. This point can be investigated by comparing the degree of polymerization of the polystyrene produced by a cyclic peroxide with that predicted by the equation (11)

$$[2] \qquad \frac{1}{P_n} = C_m + \frac{K_t}{K_p^2} \times \frac{R_p}{[M]^2}.$$

This relationship applies to initiators which produce monoradicals and which do not undergo chain transfer with polystyryl radicals. P_n is the number average degree of polymerization, C_m is the chain transfer constant for styrene, K_t is the termination rate constant, K_p is the propagation rate constant, and [M] is the concentration of styrene. For samples of polystyrene produced using the three cyclic peroxides as initiators, the experimental and calculated values of P_n are very close to one another (see Table II).

TABLE II

Experimental and calculated degrees of polymerization of polystyrene

	Experimental DP	Calculated DP
Sebacyl peroxide (cyclic dimer)	4460	4100
Dodecanedioyl peroxide (cyclic dimer)	3400	3370
Tetradecanedioyl peroxide (cyclic dimer)	3360	3310

Johnson and Tobolsky (12) have pointed out that polystyrene produced by diradicals which fail to undergo self-termination will have a much larger degree of polymerization than that predicted by the above relationship. The small amount of polystyrene produced when the cyclic peroxides are used as initiators therefore originates from a monoradical-producing compound, which is probably a linear peroxide present as impurity in the cyclic dimer. Diradicals formed in the breakdown of the cyclic dimers appear to have a negligible chance of growing to high polymer.

Decomposition of Peroxides in the Presence of DPPH

DPPH has been used to measure the rate of formation of free radicals in the thermal decomposition of benzoyl peroxide (13). The decomposition of the cyclic peroxides in the presence of DPPH was investigated to determine whether self-termination of diradicals occurred before they could react with DPPH. The linear polymeric peroxides and hexanoyl peroxide were used as standards of comparison. The results obtained for $R_{DPPH}/(I)$, where R_{DPPH} is the rate of disappearance of DPPH, are given in Table I. The reactions were zero order with respect to DPPH in the concentration range studied. The values of $R_{DPPH}/(I)$ for the polymeric peroxides are almost 50% greater than the values of $R_i/(I)$. This difference is not necessarily significant as there is some uncertainty in the choice of constant for equation (1) and the experimental error in the DPPH work may be as high as 10%.

Can. J. Chem. Downloaded from www.nrcresearchpress.com by 210.87.254.40 on 09/05/12
For personal use only.

The cyclic peroxides give very low values of $R_{DPPH}/(I)$. The observed rates may well be due to the reaction of DPPH with monoradicals from a small amount of linear peroxide present in the cyclic dimers. Diradicals from the cyclic peroxides thus undergo self-termination in preference to reaction with DPPH.

The high rate of self-termination of large diradicals is of importance in discussing the mechanism of the thermal polymerization of styrene. It appears likely that diradicals are formed in pure styrene (14), and that some of them have a sufficient lifetime to react with a further molecule of styrene (14) or with DPPH (15). This is only possible for small diradicals containing two styrene units where there are steric difficulties in self-termination. The probability of self-termination for larger diradicals is so great that the high polymer obtained in thermal polymerization must have been formed through an alternative monoradical process.

ACKNOWLEDGMENTS

The author is grateful to the National Research Council for financial assistance. The styrene used in this work was a gift of Dow Chemical of Canada Limited.

REFERENCES

1. H. KLEINFELLER and K. RADSTADTER. Angew. Chem. **65**, 543 (1953).
2. K. E. RUSSELL. J. Am. Chem. Soc. **77**, 4814 (1955).
3. F. D. GREENE. J. Am. Chem. Soc. **78**, 2246 (1956).
4. S. GOLDSCHMIDT and K. RENN. Ber. **55**, 628 (1922).
5. C. D. WAGNER, R. H. SMITH, and E. D. PETERS. Anal. Chem. **19**, 976 (1947).
6. C. G. OVERBERGER and M. LAPKIN. J. Am. Chem. Soc. **77**, 4651 (1955).
7. M. S. MATHESON, E. E. AUER, E. B. BEVILACQUA, and E. J. HART. J. Am. Chem. Soc. **73**, 1700 (1951).
8. B. H. ZIMM and J. K. BRAGG. J. Polymer Sci. **9**, 476 (1952).
9. K. E. RUSSELL and A. V. TOBOLSKY. J. Am. Chem. Soc. **76**, 395 (1954).
10. C. H. WANG, S. HSIAO, E. SKLAD, and S. G. COHEN. J. Am. Chem. Soc. **79**, 2661 (1957).
11. P. FLORY. Principles of polymer chemistry. Cornell Univ. Press, Ithaca, New York. 1953. p. 138.
12. D. H. JOHNSON and A. V. TOBOLSKY. J. Am. Chem. Soc. **74**, 938 (1952).
13. C. E. H. BAWN and S. F. MELLISH. Trans. Faraday Soc. **47**, 1216 (1951).
14. F. R. MAYO. J. Am. Chem. Soc. **75**, 6133 (1953).
15. K. E. RUSSELL and A. V. TOBOLSKY. J. Am. Chem. Soc. **75**, 5052 (1953).

Can. J. Chem. Downloaded from www.nrcresearchpress.com by 210.87.254.40 on 09/05/12
For personal use only.

Can. J. Chem. Downloaded from www.nrcresearchpress.com by 186.148.149.217 on 09/04/12
For personal use only.

DETERMINATION OF DIELECTRIC CONSTANT IN BINARY ORGANIC SYSTEMS[1]

C. G. MILLER[2] AND O. MAASS

ABSTRACT

Measurements of the dielectric constants of binary systems have been made; hexane, benzene, toluene, acetone, isopropyl alcohol, and nitrobenzene have been used two at a time. It was the purpose to obtain accurate data for the dielectric constants for the 15 systems over the whole range of concentrations from 0 to 100%, with the absolute accuracy of 0.1%. It is claimed that the relative accuracy is of this order. From the data obtained regularities have been found which are expressed in the form of empirical equations which summarize the data. Tentative suggestions regarding theoretical conclusions are made in a number of cases.

INTRODUCTION

There are already extensive data in the literature concerning the dielectric constants of binary organic mixtures (1). These data have been obtained over a period of years by a number of investigators and by a number of different techniques. While some of the systems investigated in the present work have been recorded elsewhere, in most cases these studies are isolated in the sense of dealing with a single system and in some cases only a relatively small concentration range has been considered within a given system. In addition the data are reported at various temperatures.

The initial objective of the authors was to build up a body of self-consistent dielectric constant data at a single temperature in those mixtures which would cover a wide range of dielectric constant, and over the complete range of concentration in a given system, with a view to investigating subsequently electrolytic conductivity in such mixtures.

In the furtherance of this objective, measurements were made of the dielectric constant in two-component systems which may be of interest per se. The 15 systems reported comprise a systematic study of mixtures of six compounds taken in pairs and cover a range of dielectric constant (ϵ) from 2 to 35. In this presentation it is considered an advantage for comparative purposes that all systems have been studied with the same apparatus and technique.

While the authors are interested in establishing the accuracy of the absolute values of their results, it may be pointed out that whatever error there may be in the measurements will be relative and will not affect the general nature of the conclusions drawn.

Those inferences drawn from the dielectric constant data in regard to certain regularities were so interesting that it was considered useful to record these regularities, although at this stage the authors do not contemplate making any theoretical deductions.

To assist in interpreting the results of the dielectric constant measurements, the densities of the various mixtures were required and were determined experimentally where adequate data were not readily available in the literature.

The technique of the measurement of dielectric constant follows fairly closely that of other investigators and whatever changes have been made are recorded in the experimental section.

[1]*Manuscript received May 19, 1960.*
Contribution from the Division of Pure Chemistry, National Research Council, Ottawa, Ontario.
Issued as N.R.C. No. 5922.
[2]*National Research Council Postdoctorate Fellow 1957–58.*

Can. J. Chem. Downloaded from www.nrcresearchpress.com by 186.148.149.217 on 09/04/12
For personal use only.

EXPERIMENTAL

A. Materials

Benzene and toluene (Mallinckrodt "Analytical Reagent"), normal hexane and cyclohexane (Phillips "Pure Grade") were all used without further purification. The dielectric constant was taken as the criterion of purity and its values for all the hydrocarbons agreed closely with the accepted values for the pure liquids.

Acetone (Mallinckrodt "Analytical Reagent") was dried by distillation from a large quantity of Drierite and allowed to stand over a small quantity of Drierite from which it was decanted for use.

Isopropanol (Eastman) was dried over freshly calcined lime and distilled from the lime immediately prior to each series of measurements.

Nitrobenzene (Eastman) was twice distilled in vacuum (less than 2 mm of mercury) and the distillate stored in a sealed container until used.

B. Apparatus and Procedure

The dielectric cell was of similar design and dimensions to that described by Gross and Taylor (2). The capacitor comprised two coaxial metallic cylinders, the medium under study filling the annular space between the cylinders. The outer cylinder was surrounded by a guard element which formed the body of the cell. These three elements were made from rhodium-plated brass. The assembly was held rigidly by teflon spacers and by a stainless steel lid which screwed down tightly and formed a part of the guard element. When assembled, the cell had an air capacitance of approximately 4.89 $\mu\mu$f and an internal volume of about 14 ml. The cell assembly was lowered into a grounded aluminum canister from which it was insulated electrically by a teflon ring, and the canister was immersed in a water thermostat maintained at 25°±0.01° C. The cell, once assembled and calibrated, was used for all measurements without disassembly.

Capacitance measurements were made by substitution on a capacitance bridge (General Radio type 716-C with guard circuit type 716-P4 and detector type 1231-BRF). Experiments on air and cyclohexane showed no variation in capacitance reading over the frequency range 1 kc/sec to 100 kc/sec. Accordingly the frequencies 1 kc/sec, 10 kc/sec, and 100 kc/sec were used indiscriminately throughout this work, the higher frequencies being preferred in the polar liquids where the dissipation factor was appreciable. All capacitance measurements were made by a reiterative method, sufficient readings being taken that the estimated probable error in the mean did not exceed 0.1% of the mean.

TABLE I

Cell capacitance using toluene

	C_i	B_0	Δ_{corr}	C_0	C_0-C_i
1	100.18	111.90	+0.02	111.92	11.74
2	199.96	211.70	−0.02	211.69	11.73
3	400.24	412.04	−0.01	412.03	11.79
4	599.58	611.34	+0.01	611.35	11.77
5	800.24	812.06	−0.02	812.04	11.80
6	1000.12	1011.90	+0.01	1011.91	11.79
	Mean				11.770±0.012

By way of illustration, in Table I is given the record of an actual experiment using toluene as the dielectric. In operation the variable capacitor of the capacitance bridge was set to an arbitrary value with the cell in parallel with it. The bridge was balanced, the

cell removed from the circuit, and the bridge rebalanced by means of increasing the capacitance of the variable capacitor. The difference in reading gives the capacitance of the cell. In Table I, C_1 is the reading of the variable capacitor with the cell in the circuit, B_0 the reading of the variable capacitor when the cell has been removed, Δ_{corr} the net correction as obtained from the bridge calibration and applied to B_0, C_0 the corrected value for B_0 (that is, $C_0 = B_0 + \Delta_{corr}$), and finally $C_0 - C_1$ represents the capacitance of the cell.

The probable error in the mean, ± 0.012, was estimated from the expression: $R = \pm 0.6745 \sqrt{\{\sum V^2/n(n-1)\}}$ where R is the probable error, V the individual deviations from the mean, and n the number of readings taken.

A correction for switch and lead capacitance was made by the same reiterative method and was applied to capacitance readings as follows:

Observed capacitance	$11.770 \pm 0.012\ \mu\mu f$
Switch correction	$-0.157_5 \pm 0.001_4\ \mu\mu f$
Net cell capacitance	$11.612 \pm 0.013\ \mu\mu f$
Cell constant (previously determined)	$4.887 \pm .005\ \mu\mu f$
Dielectric constant of toluene $\frac{11.612}{4.887}$	$= 2.376 \pm 0.005$

The dielectric cell was calibrated with air as the dielectric and cyclohexane was used as a secondary standard, as recommended by Hartshorn and his co-workers (3). Excellent agreement (0.1%) was obtained, and the true cell constant was taken as the mean, with the value obtained from cyclohexane given half-weight.

Density measurements were performed with a Westphal balance. The temperature of the liquid was measured to 0.2° C and the density corrected to 25.0° C, assuming the temperature coefficients of the pure liquids to persist in the mixtures.

All mixtures were prepared by volume, the temperature of the pure liquids being measured and the molar percentages calculated from the density data given by Timmermans (4).

RESULTS

A comparison between observed values of dielectric constant for the pure liquids (ϵ_{obs}) and the accepted values (ϵ_{ref}) as recorded by Maryott and Smith (5) is given in Table II. All the observed values are thought to be accurate to $\pm 0.2\%$ except that for

TABLE II

Dielectric constants of pure liquids at 25° C

Compound	ϵ_{obs}	ϵ_{ref}
n-Hexane	1.884 ± 0.004	1.882 ± 0.01
Benzene	2.281 ± 0.006	2.274 ± 0.002
Toluene	2.376 ± 0.005	2.379 ± 0.01
Isopropanol	19.13 ± 0.04	18.3 ± 0.4
Acetone	20.54 ± 0.04	$20.7_0 \pm 0.4$
Nitrobenzene	34.62 ± 0.07	34.82 ± 0.07

Can. J. Chem. Downloaded from www.nrcresearchpress.com by 186.148.149.217 on 09/04/12
For personal use only.

benzene, which is slightly high, due probably to a small amount of moisture in the sample. Hartshorn (3) has shown that traces of water in benzene cause a high dielectric constant and are extremely difficult to remove. No attempt was made to dry the benzene used in this work.

There is a notable discrepancy between the observed dielectric constant of isopropanol and that recorded by Maryott and Smith. However, these authors, when selecting the value 18.3 as the dielectric constant of isopropanol, neglected the value 20.1 recorded by Hennings (6) although they suggested that Hennings' value be considered in any future revision of the data. Since the interest in the present work lay largely in the relative variation of dielectric constant with composition, no attempt was made to resolve this discrepancy. All dielectric constant values, whether for mixtures or for pure liquids, are internally consistent to $\pm 0.1\%$.

In Table III (A, B, and C) are recorded the experimental determinations of the dielectric constants for the various mixtures. For each system the mole fraction refers to

TABLE IIIA

Dielectric constants of hydrocarbon systems
(experimental values)

Toluene in benzene		Benzene in hexane		Toluene in hexane	
Mol. Fr.	ϵ	Mol. Fr.	ϵ	Mol. Fr.	ϵ
0	2.281	0	1.884	0	1.884
0.173	2.290	0.269	1.945	0.235	1.967
0.358	2.312	0.495	2.024	0.451	2.063
0.556	2.329	0.688	2.102	0.648	2.161
0.770	2.350	0.855	2.186	0.831	2.266
1.00	2.376	1.00	2.281	1.00	2.376

TABLE IIIB

Dielectric constants of non-hydroxylic systems
(experimental values)

Acetone in hexane		Acetone in benzene		Acetone in toluene		Nitrobenzene in hexane	
Mol. Fr.	ϵ	Mol. Fr.	ϵ	Mol. Fr.	ϵ	Mol. Fr.	ϵ
0	1.88_4	0	2.28_1	0	2.37_6	0	1.88_4
0.308	4.40_0	0.232	4.99_7	0.265	4.98_5	0.242	6.17_1
0.542	7.69_6	0.446	8.12_2	0.490	8.19_7	0.460	11.92
0.727	11.68	0.644	11.85	0.742	13.24	0.657	19.04
0.876	16.01	0.828	15.97	0.852	16.07	0.836	26.65
1.00	20.54	1.00	20.54	1.00	20.54	1.00	34.62

Nitrobenzene in benzene		Nitrobenzene in toluene		Nitrobenzene in acetone	
Mol. Fr.	ϵ	Mol. Fr.	ϵ	Mol. Fr.	ϵ
0	2.28_1	0	2.37_6	0	20.54
0.178	6.58_3	0.206	6.72_0	0.152	23.36
0.367	11.90	0.409	11.99	0.324	26.00
0.566	18.26	0.609	18.45	0.519	28.75
0.776	25.65	0.806	25.81	0.742	31.46
1.00	34.62	1.00	34.62	1.00	34.62

Can. J. Chem. Downloaded from www.nrcresearchpress.com by 186.148.149.217 on 09/04/12
For personal use only.

TABLE IIIC

Dielectric constants of hydroxylic systems
(experimental values)

Isopropanol in hexane		Isopropanol in benzene		Isopropanol in toluene	
Mol. Fr.	ϵ	Mol. Fr.	ϵ	Mol. Fr.	ϵ
0	1.88_4	0	2.28_1	0	2.37_6
0.300	2.78_5	0.226	3.44_0	0.258	3.52_8
0.533	5.88_7	0.437	6.04_1	0.482	6.21_2
0.720	10.27	0.636	9.89_4	0.776	10.12
0.873	14.96	0.824	14.57	0.848	14.68
1.00	19.13	1.00	19.13	1.00	19.13

Nitrobenzene in isopropanol		Acetone in isopropanol	
Mol. Fr.	ϵ	Mol. Fr.	ϵ
0	19.13	0	19.13
0.158	20.08	0.207	17.62
0.333	21.98	0.410	17.34
0.529	24.91	0.610	17.95
0.749	28.93	0.806	19.26
1.00	34.62	1.00	20.54

the first named component and it is the more polar. Measured dielectric constants are plotted for selected systems in Fig. 1 (*a*, *b*, *c*). The curve for the nitrobenzene–acetone system is slightly convex upward; the system acetone–isopropanol exhibits a minimum in dielectric constant at about 0.35 mole fraction acetone; the system toluene–benzene shows a linear variation in dielectric constant with composition; all other systems studied show a downward convexity in the dielectric constant – composition curve. Typical examples of this latter behavior are shown in Fig. 1*a* for nitrobenzene–hexane and in Fig. 1*c* for the benzene–hexane and toluene–hexane systems.

Table IV (parts 1, 2, 3) contains the values of density (column 2) and dielectric constant (column 3) at the selected concentrations (column 1) of 0, 0.20, 0.40, 0.60, 0.80, and 1.00 mole fraction. As in Table III the mole fraction refers to the first-named component of each system. Experimental values of dielectric constant and density relative to molecular concentration were plotted on graphs from which the values at the selected concentrations were read. The error in the values thus derived can be expected to be at least as small as the error in any specific measurement.

Where density data for the mixtures were readily available no measurements were made. The density values taken from the literature were corrected by a constant amount over the whole concentration range in a given system in order to bring the densities of the pure liquids to the values given by Timmermans (4) and accepted in the remainder of this work. In only one system (acetone–benzene) was this correction of a significant magnitude, and amounted to about 0.2%. The systems so corrected were acetone–benzene (correction -0.0016) (7); nitrobenzene–benzene (correction 0.004) (7); and acetone–isopropanol (correction 0.0005) (8). Rakshit (9) has shown that density is a linear function of composition in the toluene–benzene system at 20° C. The densities for this system in Table IV have been calculated on the assumption of a similar linearity at 25° C.

For the remaining 11 systems the densities were determined experimentally as described

Can. J. Chem. Downloaded from www.nrcresearchpress.com by 186.148.149.217 on 09/04/12
For personal use only.

Can. J. Chem. Downloaded from www.nrcresearchpress.com by 186.148.149.217 on 09/04/12
For personal use only.

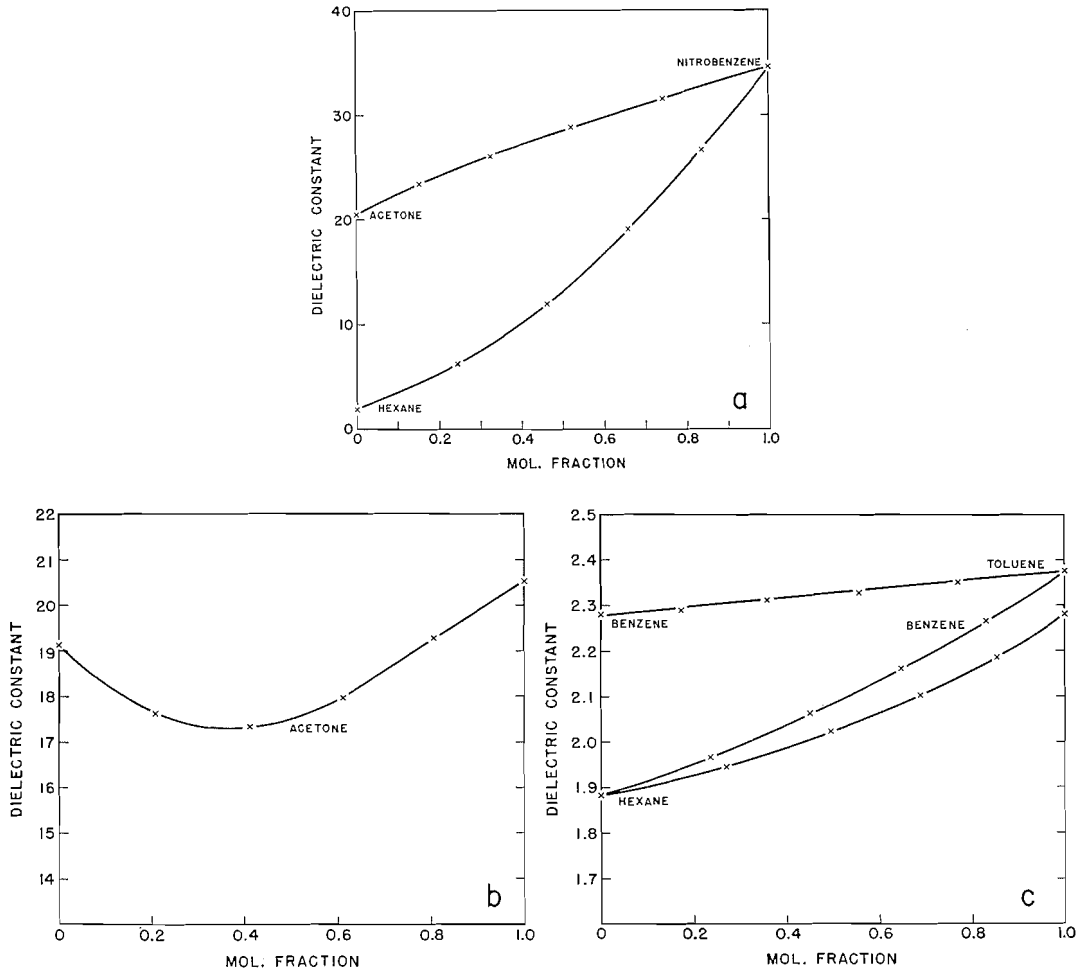
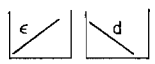
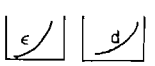
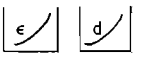
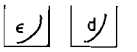
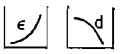
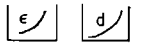
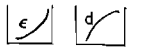
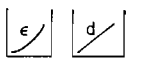
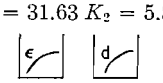


FIG. 1. (*a*) Measured dielectric constants in two nitrobenzene systems.
(*b*) Measured dielectric constants in acetone–isopropanol system.
(*c*) Measured dielectric constants in three hydrocarbon systems.

above. The temperature correction was small in all determinations and the accuracy of the density data is estimated at $\pm 0.1\%$ absolute.

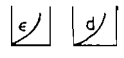
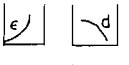
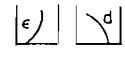
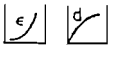
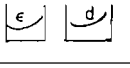
In addition to the columns relating to molecular concentration, density, and dielectric constant, Table IV contains several columns which will be described fully in the discussion but which may be mentioned briefly here. The fourth column shows calculated values of dielectric constant based on a relationship which will be dealt with later, and the difference between this value and the observed is given in the fifth column. The next two columns contain calculated values of the so-called molecular polarizations of the mixture and of the relatively more polar component respectively. Finally, the values of K_1 and K_2 from the empirical relationship to be discussed below, together with a qualitative indication of the relative variation of the dielectric constant and of the density over the whole range of concentration are shown in column eight.

TABLE IV

Mol. Fr.	Density	ϵ_{obs}	ϵ_{calc}	$\epsilon_{obs} - \epsilon_{calc}$	P_{12}	P_2	
				Part 1			
0.0	0.874	2.281			26.8		Toluene in benzene
0.2	0.871	2.298	2.298	0.0	28.0	33.2	$K_1 = 8.337$ $K_2 = 0$
0.4	0.869	2.319	2.319	0.0	29.4	33.4	
0.6	0.867	2.338	2.338	0.0	30.8	33.4	
0.8	0.864	2.357	2.357	0.0	32.1	33.5	
1.0	0.862	2.376			33.6	33.6	
0.0	0.655	1.884			29.9		Benzene in hexane
0.2	0.686	1.928	1.930	−.002	29.0	25.4	$K_1 = 1.451$ $K_2 = 1.665$
0.4	0.722	1.987	1.989	−.002	28.4	26.2	
0.6	0.763	2.060	2.060	±.000	27.8	26.4	
0.8	0.813	2.154	2.153	+.001	27.2	26.6	
1.0	0.874	2.281			26.8	26.8	
0.0	0.655	1.884			29.9		Toluene in hexane
2.0	0.691	1.955	1.956	−.001	30.6	33.0	$K_1 = 1.967$ $K_2 = 1.964$
4.0	0.728	2.034	2.034	±.000	31.2	33.0	
6.0	0.768	2.135	2.133	+.002	32.1	33.5	
8.0	0.813	2.247	2.244	+.003	32.8	33.6	
1.0	0.862	2.376			33.6	33.6	
				Part 2			
0.0	0.655	1.88			29.9		Acetone in hexane
0.2	0.667	3.39	3.33	+0.06	53.5	147.9	$K_1 = 115.3$ $K_2 = 214.8$
0.4	0.684	5.38	5.41	−0.03	65.0	107.6	
0.6	0.708	8.78	8.57	+0.21	70.7	97.8	
0.8	0.739	13.60	13.36	+0.24	69.6	79.5	
1.0	0.785	20.54			64.1	64.1	
0.0	0.874	2.28			26.8		Acetone in benzene
0.2	0.859	4.57	4.41	+0.16	46.9	127.4	$K_1 = 132.2$ $K_2 = 831.5$
0.4	0.842	7.35	7.34	+0.01	58.0	105.0	
0.6	0.824	10.87	10.90	−0.03	61.5	84.7	
0.8	0.805	15.31	15.17	+0.14	63.1	73.0	
1.0	0.785	20.54			64.1	64.1	
0.0	0.862	2.38			33.6		Acetone in toluene
0.2	0.852	4.26	4.23	+0.03	51.9	125.0	$K_1 = -171.4$ $K_2 = 829.0$
0.4	0.839	6.73	6.75	−0.02	61.4	108.1	
0.6	0.824	10.14	10.10	+0.04	64.5	86.8	
0.8	0.806	14.63	14.76	−0.13	66.0	74.1	
1.0	0.785	20.54			64.1	64.1	
0.0	0.655	1.88			29.9		Nitrobenzene in
0.2	0.747	5.30	5.27	+0.03	73.8	249.1	hexane
0.4	0.849	10.21	10.16	+0.05	89.7	179.3	$K_1 = 32.49$ $K_1 = 51.09$
0.6	0.961	16.74	16.55	+0.19	94.7	137.9	
0.8	1.076	24.96	24.55	+0.41	95.6	112.0	
1.0	1.148	34.62			94.3	94.3	
0.0	0.874	2.28			26.8		Nitrobenzene in
0.2	0.948	7.16	7.10	+0.06	61.8	202.6	benzene
0.4	1.016	12.80	12.97	−0.17	75.4	148.4	$K_1 = 54.33$ $K_2 = 165.3$
0.6	1.080	19.39	19.44	−0.05	83.7	121.6	
0.8	1.140	26.46	26.13	+0.33	89.6	105.2	
1.0	1.198	34.62			94.3	94.3	
0.0	0.862	2.38			33.69		Nitrobenzene in
0.2	0.929	6.44	6.53	−0.09	67.9	205.0	toluene
0.4	0.996	11.78	11.72	−0.04	82.1	154.8	$K_1 = 53.53$ $K_2 = 126.8$
0.6	1.064	18.19	18.26	−0.07	88.6	125.3	
0.8	1.130	25.60	25.82	−0.20	92.2	106.9	
1.0	1.198	34.62			94.3	94.3	
0.0	0.785	20.54			64.1		Nitrobenzene in
0.2	0.987	24.15	24.14	+0.01	70.1		acetone
0.4	0.992	27.18	27.20	−0.02	76.1		$K_1 = 31.63$ $K_2 = 5.829$
0.6	1.052	29.81	29.75	−0.06	83.6		
0.8	1.138	32.28	32.16	−0.12	88.3		
1.0	1.198	34.62			94.3		

Can. J. Chem. Downloaded from www.nrcresearchpress.com by 186.148.149.217 on 09/04/12
For personal use only.

TABLE IV (*concluded*)

Mol. Fr.	Density	ϵ_{obs}	ϵ_{calc}	$\epsilon_{obs}-\epsilon_{calc}$	P_{12}	P_2	
			Part 3				
0.0	0.655	1.88			29.9		Isopropyl alcohol in hexane $K_1 = 54.41$ $K_2 = 48.48$ 
0.2	0.668	2.28	2.67	−0.39	36.2	61.5	
0.4	0.686	3.83	4.16	−0.33	53.6	89.0	
0.6	0.711	7.37	7.32	+0.05	67.4	92.4	
0.8	0.742	12.68	11.45	+1.23	70.0	80.1	
1.0	0.781	19.13			66.0	66.0	
0.0	0.874	2.28			26.8		Isopropyl alcohol in benzene $K_1 = 38.3$ $K_2 = 1545.0$ 
0.2	0.856	3.27	3.49	−0.22	37.5	80.5	
0.4	0.837	5.40	5.61	−0.21	50.3	85.7	
0.6	0.819	9.17	9.03	+0.14	60.1	82.3	
0.8	0.801	14.96	14.00	+0.95	65.4	74.9	
1.0	0.781	19.13			66.0	66.0	
0.0	0.862	2.38			33.6		Isopropyl alcohol in toluene $K_1 = 48.48$ $K_2 = 1938.0$ 
0.2	0.848	3.11	3.46	−0.29	41.5	73.0	
0.4	0.834	4.98	5.24	−0.26	54.2	85.1	
0.6	0.820	8.46	8.09	+0.37	63.5	83.4	
0.8	0.802	13.33	12.31	+1.02	66.7	75.0	
1.0	0.781	19.13			66.0	66.0	
0.0	0.781	19.13			66.0		Nitrobenzene in isopropyl alcohol $K_1 = 0.24$ $K_2 = 21.76$ 
0.2	0.890	20.50	20.38	+0.12	70.8		
0.4	0.982	22.89	22.75	+0.14	76.4		
0.6	1.064	25.08	26.28	−0.20	81.8		
0.8	1.135	29.41	30.20	−0.75	88.1		
1.0	1.198	34.62			94.3		
0.0	0.781	19.13			66.0		Acetone in isopropyl alcohol $K_1 = 1345$ $K_2 = 2.444 \times 10^5$ 
0.2	0.780	17.65	17.56	+0.09	64.1		
0.4	0.780	17.28	17.17	+0.11	64.2		
0.6	0.780	17.98	18.40	−0.42	64.1		
0.8	0.782	19.28	20.29	−1.01	64.2		
1.0	0.785	20.54			64.1		

Also to be described in detail later is Fig. 2 in which are plotted the molecular polarization of the mixture and the molecular polarization of the more polar component as these are tabulated in columns 6 and 7, Table IV.

DISCUSSION

The application of the theory of dielectric constants of binary systems to the interpretation of experimental data has not been very fruitful. At best it can be said that theory has indicated certain trends which have been borne out. This is so, for instance, in regard to molecular polarization, which will be referred to later.

That density and dielectric constant of a medium are related has been indicated, at least in so far as pure compounds are concerned. In a two-component system certain relationships between dielectric constant and density have been suggested. Having this in mind, the relationship of dielectric constant with density which was observed was found to lend itself to algebraic expression within certain limits for a number of systems including those having a polar compound as one of the components.

In the following discussion ϵ_1 and ϵ_2 are the dielectric constants of the pure components of a binary mixture in which $\epsilon_2 > \epsilon_1$. The corresponding densities are d_1 and d_2; ϵ_{12} and d_{12} are dielectric constant and density respectively of the mixture. The first approach is that

$$\epsilon_{12} = \epsilon_1 + K(d_{12} - d_1). \qquad [1]$$

Can. J. Chem. Downloaded from www.nrcresearchpress.com by 186.148.149.217 on 09/04/12
For personal use only.

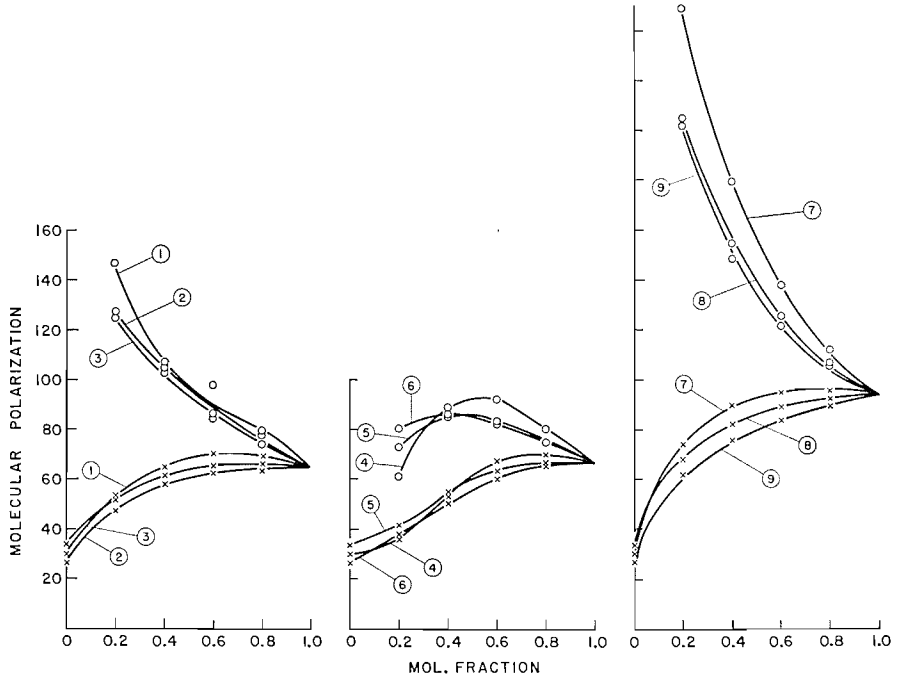


FIG. 2. Calculated values of molecular polarization.
$\times = P_{12}$, $\circ = P_2$. (1) Acetone–hexane. (2) Acetone–benzene. (3) Acetone–toluene. (4) Isopropanol–hexane. (5) Isopropanol–toluene. (6) Isopropanol–benzene. (7) Nitrobenzene–hexane. (8) Nitrobenzene–toluene. (9) Nitrobenzene–benzene.

This is in agreement within experimental error only in the system benzene–toluene. Even with the hexane–benzene and hexane–toluene systems this does not hold. However, if instead of the above simple relationship we use

$$[2] \qquad \epsilon_{12} = \epsilon_1 + K_1 (d_{12} - d_1) + K_2 (d_{12} - d_1)^2,$$

there is perfect agreement in the hydrocarbon systems betwen the calculated and observed results (Table IV, part 1).

Having found this perfect agreement between the empirical relationship (2) and the experimental results in a limited number of systems, an examination of the application of this to all the other systems examined was made.

From the qualitative graphical representation of the relation between dielectric constant and composition, and density and composition, respectively, made in the final column of Table IV it is obvious that the relative convex and concave curvature, as between dielectric constant and composition on the one hand and density and composition on the other, varies from system to system, and it might seem that no particular regularity could be expected. Nevertheless, when equation [2] is applied, this relationship is found to be in fairly good agreement with the experimental results as far as systems involving only one polar compound are concerned (Table IV, part 2) and even indicatively correct for systems involving two so-called polar compounds.

Calculations show that in the hydrocarbon systems (Table IV, part 1) equation [2] hold exactly. In Table IV (part 2) the average difference between observed and calculated values is 0.9% and in Table IV (part 3) 4.0%.

Can. J. Chem. Downloaded from www.nrcresearchpress.com by 186.148.149.217 on 09/04/12
For personal use only.

Reference to column 7, in Table IV, part 1, shows that the molecular polarization remains essentially constant with dilution for the hydrocarbons used in this work. This constancy can be made use of in the calculation of P_2, the molecular polarization of the more polar component.

Figure 2 contains three families of curves representing systems containing acetone, isopropanol, and nitrobenzene respectively. For each polar compound the three curves represent mixtures with the hydrocarbons taken in turn. These curves are plots of the calculated values of P_{12} and P_2 as given in Table IV (parts 2 and 3). There is an essential similarity for curves for all hydrocarbons. In benzene and toluene they are almost contiguous while an appreciable divergence is noted for hexane.

A difference in shape is noted in the P_2 curve for systems containing acetone and nitrobenzene as distinct from the systems containing isopropanol. The increase in molecular polarization of acetone and nitrobenzene with increasing dilution may be explained simply by postulating an association between the dipoles in concentrated solution, an association that results in a partial cancellation of the moments of the associated dipoles. As the dilution increases fewer of the molecules exist in the associated state and each exerts its own moment.

The behavior of isopropanol in giving maxima in the P_2 curves calculated for systems containing hydrocarbons is common to other alcohols as well (10). An explanation which has been advanced for this behavior in the past supposes that two different mechanisms of association exist in binary mixtures of alcohols and hydrocarbons. The first mechanism is similar to that advanced above and accounts for the portion of the P_2 curve to the right of the maximum. As the concentration of alcohol is still further reduced, however, the dominant form of association is one in which the alcohol molecules are lined up, perhaps in chains, in such a way that the moments reinforce each other. As this type of association is reduced with increasing dilution the effective moment of each molecule and hence the apparent molecular polarization is also reduced.

CONCLUSION

It has been shown that the dielectric constants of binary systems are dependent on their density and the polarity of each of the components. Certain regularities have been established by summarizing the results obtained in the form of empirical equations. Aberrations from these equations can in the main be attributed to so-called association of one of the components, an association that is affected by the concentration of the second component.

ACKNOWLEDGMENTS

The authors are indebted to Dr. D. W. Davidson, who suggested the design of the dielectric cell, and who provided much valuable discussion throughout the work, and to Mr. Gordon Graham for his technical assistance.

The rhodium-plating of the cell was very kindly undertaken by Avon Jewellery Limited, Belleville, Ontario.

REFERENCES

1. J. TIMMERMANS. Physico-chemical constants of binary systems in concentrated solutions. Interscience. 1959.
2. P. M. GROSS and R. C. TAYLOR. J. Am. Chem. Soc. **72**, 2675 (1950).
3. L. HARTSHORN, J. V. L. PARRY, and L. ESSEN. Proc. Phys. Soc. B, **68**, 436 (1955).

Can. J. Chem. Downloaded from www.nrcresearchpress.com by 186.148.149.217 on 09/04/12
For personal use only.

4. J. TIMMERMANS. Physico-chemical constants of pure organic compounds. Elsevier. 1950.
5. A. A. MARYOTT and E. R. SMITH. Table of dielectric constants of pure liquids. U.S. Natl. Bur. Standards Circ. 514. 1951.
6. C. HENNINGS. Z. physik. Chem. B, **28**, 267 (1935).
7. D. L. HAMMICK and L. W. ANDREW. J. Chem. Soc. 754 (1929).
8. G. S. PARKS and C. S. CHAFFEE. J. Phys. Chem. **31**, 439 (1927).
9. J. N. RAKSHIT. Z. Electrochem. **31**, 320 (1925).
10. C. P. SMYTH and W. N. STOOPS. J. Am. Chem. Soc. **51**, 3312 (1930).

Can. J. Chem. Downloaded from www.nrcresearchpress.com by 186.148.149.217 on 09/04/12
For personal use only.

Can. J. Chem. Downloaded from www.nrcresearchpress.com by 210.87.254.105 on 09/05/12
For personal use only.

THE POLYSACCHARIDES OF CRYPTOCOCCUS LAURENTII (NRRL Y-1401)

PART I[1]

M. J. Abercrombie, J. K. N. Jones, M. V. Lock,[2] M. B. Perry, and R. J. Stoodley

ABSTRACT

The extracellular polysaccharides produced by *Cryptococcus laurentii* have been isolated and shown to consist of (A) an acidic polysaccharide containing D-mannose, D-xylose, and D-glucuronic acid; (B) a neutral polysaccharide containing D-glucose only.

Preliminary structural studies on the acidic material suggest that it consists of a mannose-containing backbone with xylose and glucuronic acid as end groups, while the glucan contains $1 \rightarrow 3$, $1 \rightarrow 4$, $1 \rightarrow 2$, and (or) $1 \rightarrow 6$ linked residues.

INTRODUCTION

Much is known about the origin of sugars found in homopolysaccharides (1–11). On the other hand the origin of sugars in heteropolysaccharides has not been investigated to any great extent (12, 13).

As part of a program for investigating the biosynthesis of monosaccharides found in heteropolysaccharides, we have studied the extracellular polysaccharide produced by the yeast organism *Cryptococcus laurentii*.

This organism, kindly supplied by the United States Department of Agriculture, Peoria, Illinois, was chosen because it produced high yields of polysaccharides from a wide variety of sugar substances.

Cryptococcus laurentii was grown on an unbuffered casamino acids – salts medium with glucose as the main carbon source (14). An acidic and a neutral polysaccharide were isolated by the following procedure, which was considered unlikely to cause degradation of the polysaccharides. The cell-free solution was dialyzed and then passed through an ion exchange column to give a clear, light brown viscous solution. After the solution was concentrated, the polysaccharides were precipitated with ethanol and had $[\alpha]_D$ +27°. Chromatographic examination of the acid hydrolyzate showed sugars which moved at rates corresponding to mannose, xylose, glucuronic acid, and glucose. The sugars were obtained crystalline or as crystalline derivatives and were shown to be D-mannose, D-xylose, D-glucose, and D-glucuronic acid. The crude polysaccharide showed two peaks on electrophoresis in a veronal buffer. On addition of an aqueous solution of 'cetavlon' (cetyltrimethyl-ammonium bromide) to an aqueous solution of the polysaccharide an insoluble cetyltrimethyl-ammonium salt of an acidic polysaccharide was precipitated. This salt was dissolved in 10% aqueous sodium chloride solution and the sodium salt of the acidic polysaccharide was precipitated in ethanol. Chromatographic examination of the acid hydrolyzate of this material showed mannose, xylose, and glucuronic acid to be present. Electrophoresis in veronal and borate buffers showed a single peak: glass paper electrophoresis (17) showed a single spot. Further attempts at fractionation failed to give any separation. The supernatant from the cetyltrimethyl-ammonium precipitate was concentrated and added to ethanol. Mainly glucose and traces of mannose, xylose, and glucuronic acid were detected in the precipitated material (chromatography).

The acidic polysaccharide had $[\alpha]_D$ +21°; the molar ratio of mannose to xylose present

[1]*Manuscript received May 11, 1960.*
Contribution from the Department of Chemistry, Queen's University, Kingston, Ontario, Canada.
[2]*On leave of absence from British Rayon Research Association, Heald Green Laboratories, Wythenshawe, Manchester 22, England.*

in this material was found to be 5:2 (18); titration of the polysaccharide with standard sodium hydroxide gave a uronic acid content of 14.4%. Determination of uronic acid content by the carbazole method (19) gave 11.8%.

On oxidation with sodium metaperiodate the acid polysaccharide consumed 1.10 moles of sodium metaperiodate and liberated 0.58 mole of formic acid per sugar residue. These figures appear to indicate that end group or $1 \rightarrow 6$ linked hexose only is oxidized since a sugar which contains hydroxyl groups on each of three contiguous carbon atoms will reduce 2 moles of periodate and yield 1 mole of formic acid per mole. However, glucuronic acid is present as an end group which is known to overoxidize easily. Hence no exact interpretation can be placed on these results. The oxidized material was reduced with sodium borohydride and hydrolyzed: chromatographic examination of the hydrolyzate showed mannose to be the only sugar present.

Hydrolysis of the acidic polysaccharide in the presence of Amberlite 1R-120 (H) resin removed considerable quantities of xylose without liberating mannose or glucuronic acid. This treatment was repeated with fresh resin until no more xylose was liberated. Chromatographic examination of the hydrolyzate of the resin resistant polysaccharide showed mannose, glucuronic acid, and some xylose. The mannose to xylose molar ratio (18) was determined and found to be 25:3; thus about 66% of the xylose had been hydrolyzed.

The results obtained from sodium metaperiodate oxidation and resin hydrolysis suggest that the polysaccharide consists of a resistant mannose containing backbone with xylose and glucuronic acid as end groups.

The glucan had $[\alpha]_D$ $+180°$ but was contaminated with traces of the acidic polysaccharide. It did not give a blue color with iodine nor was it hydrolyzed by β-amylase.

On oxidation with sodium metaperiodate the polysaccharide consumed 0.83 ± 0.07 mole of metaperiodate and liberated 0.14 ± 0.04 mole of formic acid per anhydro hexose unit. These results indicate that about 1 glucose residue in 10 contains hydroxyl groups in each of three contiguous carbon atoms and that about 40% of the glucose residues do not contain adjacent hydroxyl groups. The oxidized material was reduced with sodium borohydride and hydrolyzed. Chromatographic examination of the hydrolyzate showed glucose, erythritol, and glycerol to be present, suggesting the presence of $1 \rightarrow 3$, $1 \rightarrow 4$, $1 \rightarrow 2$, and (or) $1 \rightarrow 6$ linked residues.

EXPERIMENTAL

The following solvent systems (v/v) were used to separate sugars on paper chromatograms: (A) butanol:pyridine:benzene:water, 5:3:3:1; (B) ethyl acetate:acetic acid:water, 9:2:2; (C) butanol:ethanol:water, 3:1:1. Sugars were detected on paper chromatograms by spraying the chromatograms with either *p*-anisidine hydrochloride (20) or alkaline silver nitrate (21). Solutions were evaporated under reduced pressure at ca. 40° C. All optical rotations were measured in aqueous solution at $23° \pm 3°$ C unless otherwise stated.

Growth of Cryptococcus laurentii and Isolation of the Polysaccharide

The following two media were prepared and each was electrometrically adjusted to pH 7.0 with dilute potassium hydroxide solution: (i) 'Difco' bactocasamino acids (15 g), potassium nitrate (5 g), potassium dihydrogen phosphate (20 g), dipotassium hydrogen phosphate (15 g), magnesium sulphate heptahydrate (2.5 g), thiamine hydrochloride (5 mg), trace element solution (25 ml) (15), water (4l); (ii) glucose (250 g), water (1 liter). The trace element solution contained zinc sulphate heptahydrate (2.0 g), copper

Can. J. Chem. Downloaded from www.nrcresearchpress.com by 210.87.254.105 on 09/05/12
For personal use only.

sulphate pentahydrate (0.1 g), manganese sulphate monohydrate (1.5 g), ferrous sulphate heptahydrate (2.0 g), and distilled water (1 liter).

Medium (i) was equally distributed between 10 conical flasks (1 liter), the necks of which were plugged with cotton wool. Both media were steam-sterilized for 15 minutes at a pressure of 15 p.s.i. Aliquots (ca. 100 ml) of the glucose solution were added to each flask under sterile conditions and the solutions were innoculated with an aqueous suspension of *Cryptococcus laurentii*. The flasks were swirled on a mechanical shaker at 20°±2° C for 14 days, after which the culture medium had become extremely viscous.

The combined solution was diluted with water (2 vol.) and centrifuged on a Sharples ultracentrifuge to remove suspended yeast cells. The supernatant was dialyzed against tap water (3 days) and distilled water (1 day). The clear, light brown solution was passed through an Amberlite IR-120 (H) resin column: since the solution was slightly cloudy it was again centrifuged on the Sharples ultracentrifuge. The solution was concentrated on a continuous evaporator at 35° C until a highly viscous solution was obtained. This solution was poured into ice-cold ethanol (6 vol. containing 1% hydrochloric acid) with vigorous stirring. The fibrous white product, suspended in ethanol, was broken up in a Waring Blender: the finely divided material was washed with ethanol until free of chloride ions. This material was collected by filtration, dried *in vacuo* over calcium chloride, and had $[\alpha]_D$ +27° (yield 19 g, 8% based on glucose).

Chromatographic examination of the polysaccharide hydrolyzate in solvents A and B indicated the presence of mannose, xylose, glucuronic acid, and glucose.

Neutral Component Sugars of the Polysaccharide

The polysaccharide (500 mg) was heated with *N* sulphuric acid (50 ml) for 24 hours on a boiling water bath. The solution was neutralized ($BaCO_3$), filtered, and deionized by passage through an Amberlite IR-120 (H) resin column. The solution was concentrated to a syrup and fractionated by paper chromatography using solvent A. Extraction of the appropriate sections of the paper afforded crystalline D-xylose, m.p. 142–143°, $[\alpha]_D$ +17.6°; D-glucose, m.p. 145°, $[\alpha]_D$ +50°, which gave a N-*p*-nitrophenyl-β-D-glucosylamine (22), m.p. 185°, $[\alpha]_D$ −200° (pyridine); D-mannose (crystallized after seeding and standing 4 weeks), m.p. 133° C, $[\alpha]_D$ +13°, which gave D-mannose phenylhydrazone, m.p. 188°–190° C (mixture melting points with authentic samples showed no depression). The glucuronolactone failed to crystallize. A spot of the D-glucose solution gave a positive test when sprayed with the glucose oxidase reagent (23).

Free Electrophoresis of the Polysaccharide

The polysaccharide in solution at a concentration of 1.0% in veronal buffer (0.1 *M* barbital/sodium hydroxide pH 9.5) was subjected to electrophoresis in a Perkin–Elmer Model 38-A moving boundary apparatus (1° C). The polysaccharide solution was dialyzed against the veronal buffer for 48 hours to gain full equilibration of the ionic concentrations prior to electrophoresis. Figure 1 is the diagram obtained in the descending arm after 5 and 60 minutes. Two peaks were observed, a fast-moving peak and a stationary small peak. Electrophoresis was continued until the fast-moving peak had moved off the screen. Chromatographic examination of the hydrolyzate of the solutions contained in the solution, buffer, and middle arms of the electrophoresis cell showed that the fast-moving peak was an acidic polysaccharide containing mannose, xylose, and glucuronic acid. The stationary peak was a polysaccharide containing mainly glucose.

Fractionation of the Polysaccharide

The polysaccharide mixture was dissolved in water (5 liters): to this solution was

Can. J. Chem. Downloaded from www.nrcresearchpress.com by 210.87.254.105 on 09/05/12
For personal use only.

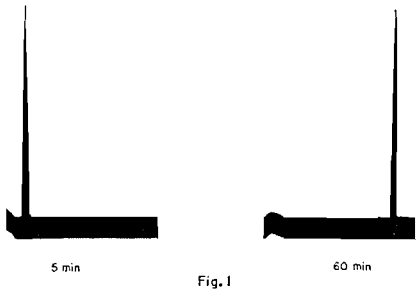


Fig. 1



Fig. 2

FIGS. 1 and 2. Free electrophoresis of polysaccharide.

added a 2.5% solution of 'cetavlon' with stirring until no further precipitate formed (15, 16). The white material was collected by centrifugation, washed well with water, and dissolved in 10% aqueous sodium chloride solution (500 ml). The solution was poured into ice-cold ethanol (6 vol.) and the precipitated polysaccharide was washed with 95% aqueous ethanol. The polysaccharide (sodium salt) was collected by filtration, dried *in vacuo* over calcium chloride, and had $[\alpha]_D$ +21°, ash 4.5%, and nitrogen content 0.1% (yield 17 g). Chromatographic examination of the hydrolyzate in solvents A and B indicated the presence of mannose, xylose, and glucuronic acid. The supernatant from the 'cetavlon' precipitate was dialyzed against tap water (4 days) and distilled water (1 day), concentrated, and poured into ice-cold ethanol. The small amount of white precipitate was collected by centrifugation, washed with ethanol, and dried (yield 1.0 g). Chromatographic examination of the hydrolyzate of this material indicated the presence of glucose and small quantities of mannose, xylose, and glucuronic acid.

Free Electrophoresis of the Acidic Polysaccharide

A 1% solution of the acidic polysaccharide in (i) borate buffer (0.05 *M* borate) and (ii) veronal buffer (as above) was subjected to electrophoresis. Figure 2 is the diagram obtained in the descending arm in each buffer: only a single peak was observed.

Glass Paper Electrophoresis

The glass paper electrophoresis was carried out as described by Smith and Lewis (17). A type 3371 B LKB power supply was used with 2 *N* sodium hydroxide as the electrolyte. The chromatogram was sprayed with sulphuric acid/*p*-anisidine. The electrophoresis was repeated (×4); in each case a single spot was observed.

Can. J. Chem. Downloaded from www.nrcresearchpress.com by 210.87.254.105 on 09/05/12
For personal use only.

Can. J. Chem. Downloaded from www.nrcresearchpress.com by 210.87.254.105 on 09/05/12
For personal use only.

Reduction of the Acidic Polysaccharide

The sodium salt of the acidic polysaccharide (100 mg, glucose-free) was dissolved in water (10 ml) and deionized by passing its solution through a small column of Amberlite IR-120 (H) resin. The solution was concentrated and lyophilized. The residual material was suspended in methanol and an ethereal solution of diazomethane was added with stirring until a permanent yellow color was obtained. The polysaccharide was collected by filtration, washed with methanol, and dissolved in water. An excess of sodium borohydride (50 mg) was added and the reaction was allowed to stand at room temperature for 5 hours. The excess sodium borohydride was destroyed by the addition of acetic acid: the solution was dialyzed against distilled water for 24 hours and then passed through an Amberlite IR-120 (H) resin column. The deionized solution was concentrated and the polysaccharide precipitated by pouring the solution into ice-cold ethanol. The polysaccharide was collected by centrifugation. A small portion of this (ca. 5 mg) was hydrolyzed with *N* sulphuric acid as previously described. Chromatographic examination of the hydrolyzate in solvent A indicated the presence of mannose, xylose, glucuronic acid, and glucose. When sprayed with the glucose oxidase spray (23), a spot of the hydrolyzate gave a positive reaction for glucose. The treatment with diazomethane and reduction with sodium borohydride was repeated twice until the chromatographic examination of the hydrolyzate showed that only a trace of glucuronic acid remained. The remainder of the polysaccharide (ca. 60 mg) was hydrolyzed with *N* sulphuric acid on a boiling water bath, neutralized ($BaCO_3$), filtered, and deionized by passage of the solution through an Amberlite IR-120 (H) resin column. The solution was concentrated to a syrup which was fractionated by chromatography on Whatman 3MM paper by the use of solvent A. The appropriate section of the paper containing glucose was eluted and the solution concentrated to a syrup. The syrup was dissolved in methanol (1 ml) containing a trace of hydrochloric acid and 10 mg of *p*-nitroaniline was added: the reaction mixture was heated on a boiling water bath for 10 minutes; on cooling yellow crystals appeared, m.p. 185° C (mixture melting point with authentic N-*p*-nitrophenyl-β-D-glucosylamine was not depressed).

Quantitative Estimation of the Component Sugars of the Acidic Polysaccharide

Samples of the polysaccharide (30–40 mg) were hydrolyzed in the usual way. The syrup obtained was fractionated by chromatography on Whatman 3MM paper by the use of solvent A. The appropriate sections of paper were eluted and the ratio of mannose to xylose was determined by the phenol – sulphuric acid method (18). The results indicated that mannose and xylose were present in the molar ratio 5:2.

The glucuronic anhydride content of the polysaccharide was determined by the carbazole method (19) and found to be 11.8%. The ash-free polysaccharide had an equivalent weight of 1215 (≡ 14.4% glucuronic anhydride), found by electrometric titration with standard alkali.

Sodium Metaperiodate Oxidation of the Acidic Polysaccharide

Accurately weighed samples of the polysaccharide (ca. 50 mg) were oxidized with aqueous sodium metaperiodate solution using standard procedures. The periodate uptake was estimated by the method of Neumuller and Vasseur (24) and the formic acid liberation by Andrews *et al.* (26). The results are collected in Table I.

When the oxidation with sodium metaperiodate was complete, ethylene glycol (3 ml) was added and the solution was dialyzed against distilled water for 24 hours. Sodium

TABLE I

Sodium metaperiodate oxidation of the acidic polysaccharide per anhydro residue

Time (hr)	HCOOH	IO_4
4.5	0.14	0.31
12.5	0.26	0.62
24.0	0.37	0.82
37.0	0.50	0.99
61.0	0.58	1.10
85.0	0.58	1.10
105.0	0.58	1.10

borohydride was added (50 mg) and the solution was left overnight and then dialyzed. The concentrated non-dialyzable material was hydrolyzed with *N* sulphuric acid in a sealed tube in a boiling water bath. Examination of the neutralized ($BaCO_3$) hydrolyzate on paper chromatograms showed mannose to be the only original sugar present.

Degradation of the Acidic Polysaccharide with Resin

The polysaccharide (500 mg) was dissolved in water (100 ml) and Amberlite IR-120 (H) resin (5 ml) was added. The reaction mixture was heated on a boiling water bath; at intervals, samples (ca. 1 ml) were withdrawn and examined chromatographically. Only xylose was detected; after 20 hours no apparent further release of xylose took place. The resin was removed by filtration and the solution concentrated and added to ice-cold ethanol, the precipitated polysaccharide (300 mg) was collected by centrifugation. The hydrolyzate of a small portion of this material (ca. 10 mg) was examined chromatographically; some xylose as well as mannose and glucuronic acid was present. The treatment with resin was repeated twice; only traces of xylose were removed by fresh resin: the weight of the polysaccharide remained constant during the two hydrolyses. The molar ratio of mannose to xylose was determined by the phenol – sulphuric acid method and found to be 25:3. Thus the hydrolysis of the polysaccharide with the resin had removed ca. 66% of the xylose without liberating mannose or glucuronic acid.

Examination of the Glucan

The glucan had $[\alpha]_D$ +180°: it did not give a blue color with iodine nor was it hydrolyzed with β-amylase.

Sodium Metaperiodate Oxidation of the Glucan

The oxidation of the glucan was carried out as described for the acidic polysaccharide. The results are collected in Table II. Extrapolation of the overoxidation part of the

TABLE II

The sodium metaperiodate oxidation of the glucan per anhydro hexose residue

Time (hr)	HCOOH	IO_4
2.75	—	0.65
5.75	—	0.78
10.50	0.14	0.84
25.00	0.20	0.98
54.50	0.24	1.06

Can. J. Chem. Downloaded from www.nrcresearchpress.com by 210.87.254.105 on 09/05/12
For personal use only.

curve to zero time gave a value corresponding to a metaperiodate uptake of 0.83±0.07 mole and a liberation of 0.14±0.04 mole of formic acid per anhydro hexose unit.

Hydrolysis of the Oxidized Glucan

The polysaccharide (50 mg) was oxidized with sodium metaperiodate as described. After 100 hours, ethylene glycol (5 ml) was added to destroy the excess periodate. The polyaldehyde was then reduced by the addition of a large excess of sodium borohydride and the solution stirred for 2 hours. The solution was acidified with dilute acetic acid and dialyzed against distilled water. The dialyzate, after concentration to dryness, was dissolved in *N* sulphuric acid and hydrolyzed for 10 hours. Chromatographic examination of the hydrolyzate in solvents A, B, and C, using *p*-anisidine hydrochloride and alkaline silver nitrate sprays, detected spots corresponding to glucose, glycerol, and erythritol.

Growth of Cryptococcus laurentii at pH 5, 7, and 9 and Isolation of the Polysaccharides

Culture media were prepared as before and each was adjusted to pH 5, pH 7, or pH 9. The media were treated in a similar manner to those described previously; after 12 days' shaking the solutions had become extremely viscous. The clear solutions were collected and the acidic polysaccharide and the glucan were isolated as previously described. The weights of the polysaccharides isolated from each growth media are shown in Table III.

TABLE III

Growth of *Cryptococcus laurentii* at various pH's

Initial pH of growth media	Yield of crude polysaccharide	Acidic polysaccharide	Glucan
5	12.0 g	6.5 g	4.0 g
7	10.0 g	9.0 g	0.2 g
9	7.0 g	6.5 g	—

ACKNOWLEDGMENTS

The authors are indebted to the National Research Council for grants and for the award of a scholarship (to M.J.A.): one of us (R.J.S.) thanks Queen's University for a R. S. McLaughlin Scholarship.

REFERENCES

1. G. A. GREATHOUSE *et al.* J. Am. Chem. Soc. **76**, 1658, 5052, 5157 (1954); **77**, 1244 (1955); **79**, 4505 (1957). Science, **117**, 553 (1953).
2. C. GILVARG. J. Biol. Chem. **199**, 57 (1952).
3. J. C. SOWDEN, S. FRANKEL, B. H. MOORE, and J. E. MCCLARY. J. Biol. Chem. **206**, 547 (1954).
4. V. GINSBURG and W. Z. HASSID. J. Biol. Chem. **223**, 277 (1956).
5. A. C. NEISH and S. A. BROWN. Can. J. Biochem. and Physiol. **32**, 170 (1954).
6. A. C. NEISH. Can. J. Biochem. and Physiol. **33**, 658 (1955).
7. H. A. ALTERMATT and A. C. NEISH. Can. J. Biochem. and Physiol. **34**, 405 (1956).
8. A. C. NEISH. Can. J. Biochem. and Physiol. **36**, 187 (1958).
9. J. ELDERMAN, V. GINSBURG, and W. Z. HASSID. J. Biol. Chem. **213**, 843 (1955).
10. C. G. SEEGMILLER, B. AXELROD, and R. M. MCCREADY. J. Biol. Chem. **217**, 765 (1955).
11. C. G. SEEGMILLER, R. JANG, and W. MANN. Arch. Biochem. Biophys. **61**, 422 (1956).
12. J. C. SOWDEN and S. FRANKEL. J. Biol. Chem. **221**, 587 (1956).
13. S. M. LESLEY and R. M. HOCHESTER. Can. J. Biochem. and Physiol. **31**, 513 (1959).
14. L. O. KRAMPITZ. Private communication.
15. B. C. BERA, A. B. FOSTER, and G. ZWEIFEL. Chem. & Ind. 330 (1957).
16. A. S. JONES. Biochim. et Biophys. Acta, **10**, 607 (1953).
17. F. SMITH and B. A. LEWIS. J. Am. Chem. Soc. **79**, 3929 (1957).

Can. J. Chem. Downloaded from www.nrcresearchpress.com by 210.87.254.105 on 09/05/12
For personal use only.

18. M. DUBOIS, K. A. GILLES, J. K. HAMILTON, P. A. REBERS, and F. SMITH. Anal. Chem. **26**, 350 (1956).
19. Z. DISCHE. J. Biol. Chem. **167**, 190 (1947); **183**, 489 (1950).
20. L. HOUGH, J. K. N. JONES, and W. H. WADMAN. J. Chem. Soc. 1702 (1950).
21. W. E. TREVELYAN, D. P. PROCTOR, and J. S. HARRISON. Nature, **166**, 444 (1950).
22. F. WEYGAND, W. PERKOW, and P. KUHNER. Ber. **84**, 594 (1951).
23. L. M. WHITE and G. E. SECOR. Science, **495**, 125 (1957).
24. G. NEUMULLER and E. VASSEUR. Arkiv Kemi, **2**, 235 (1953).
25. M. L. WOLFROM and K. ANNO. J. Am. Chem. Soc. **74**, 5583 (1952).
26. P. ANDREWS, L. HOUGH, and J. K. N. JONES. J. Chem. Soc. 806 (1954).

Can. J. Chem. Downloaded from www.nrcresearchpress.com by 210.87.254.105 on 09/05/12
For personal use only.

Can. J. Chem. Downloaded from www.nrcresearchpress.com by 210.87.254.105 on 09/05/12
For personal use only.

INDOLYL-3-PYRUVIC ACID OXIME AS THE PRECURSOR OF INDOLYL-3-ACETONITRILE[1]

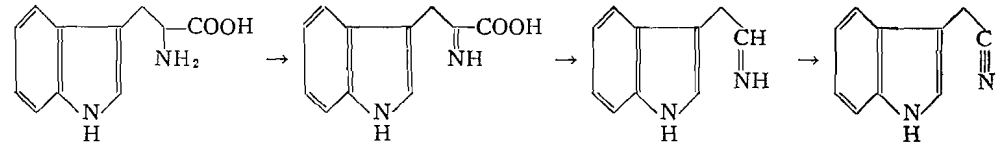
A. Ahmad and Ian D. Spenser

ABSTRACT

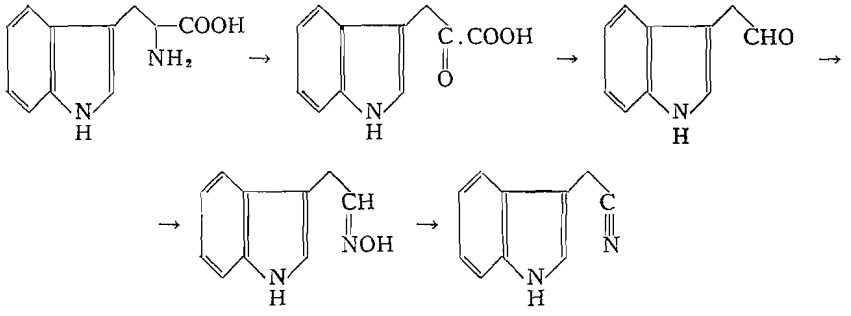
Chemical and chromatographic evidence is presented compatible with the hypothesis that the auxin indolyl-3-acetonitrile is derived in plants from indolyl-3-pyruvic acid oxime (anti HO– –COOH) by a concerted reaction.

Since the discovery that indolyl-3-acetonitrile (IAN) occurs naturally (1) and shows auxin activity in certain plant species, two hypotheses of its biosynthetic origin have been proposed. Both of these postulate tryptophan as the parent substance, but differ in the intermediate steps whereby the alanyl side chain of the amino acid is modified to $-CH_2-CN$ in the nitrile.

Sequence A was the first to be put forward (1).

(A) 

Experimental work (2) has established that IAN is indeed derived enzymatically from tryptophan in watermelon slices and in *Avena* coleoptiles. Incubation of the tissues with α-C^{14}-tryptophan, followed by paper chromatographic analysis of extracts, gave rise to a number of radioactive spots, one of which was assigned to IAN. Another highly active spot was tentatively ascribed to indolyl-3-pyruvic acid, whose occurrence in plant extracts (3) had been the subject of controversy (4, 5, 6). A modified sequence of steps (sequence B) for IAN biosynthesis was suggested as a result of this tracer work (2).

(B) 

Neither of the two hypotheses is entirely satisfactory. The first step of sequence A has many biochemical analogies, but amino acid oxidases, the type of enzyme required to catalyze such a reaction, are comparatively rare in plant tissues (7). The final step, dehydrogenation of an aldehyde imine to a nitrile, is without known chemical or biochemical precedent, and even the second step is unusual since in biochemical systems

[1]*Manuscript received May 20, 1960.*
Contribution from the Department of Chemistry, McMaster University, Hamilton, Ontario.

Can. J. Chem. Downloaded from www.nrcresearchpress.com by 210.87.254.105 on 09/05/12
For personal use only.

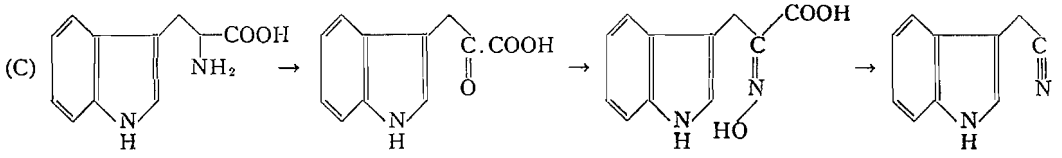
α-imino acids undergo rapid spontaneous hydrolysis to α-keto acids (8) rather than decarboxylation. The latter reaction is feasible, however, since in vitro primary amines catalyze α-keto acid decarboxylation (e.g. ref. 9) with the intermediate formation of N-substituted α-imino acids (Schiff's bases), which themselves readily decarboxylate (e.g. ref. 9). Such a mechanism, however, is no longer accepted for the enzymatic decarboxylation of α-keto acids (10).

Indirect evidence supporting the first step of sequence B, conversion of tryptophan to indolyl-3-pyruvic acid by transamination, has been accumulating (e.g. ref. 11). The only intermediate in sequence B which has not yet been found to occur is indolyl-3-acetaldoxime. Other oximes, and particularly α-keto acid oximes, have, however, been isolated from natural sources (e.g. ref. 12) and the formation of indolyl-3-acetaldoxime from indolyl-3-acetaldehyde and hydroxylamine is a tenable supposition, since indirect evidence for the occurrence of both these substances in plants is available (6 and 13 respectively). The fact that IAN biosynthesis from tryptophan is inhibited by dimedone, which is regarded as a specific aldehyde trapping agent, has been adduced as an important argument in favor of the implication of indolyl-3-acetaldehyde in the biogenetic sequence (14). The final step of sequence B, although easily accomplished chemically under vigorous, usually anhydrous, reaction conditions, is again without known biochemical analogy.

Neither sequence, however, accounts for the detection by Housley and Bentley (4, 15) of an acidic precursor of IAN in the water-soluble, ether-insoluble fraction of an extract of cabbage leaves. This precursor gave IAN when heated in aqueous solution pH 5.6 at 98–100° for 25 minutes. The same chemical reaction took place to some extent even at room temperature under basic, but particularly under acidic, conditions. Other data (16) also point to the occurrence of a water-soluble, ether-insoluble acidic precursor of IAN.

It should be noted that Housley and Bentley (15) do not present direct evidence bearing on the conversion of their precursor to the nitrile in vivo, but infer biological conversion on the basis of the precursor's growth-promoting properties and by analogy with its chemical behavior. Accepting this inference as a working hypothesis, it follows that any substance postulated as direct biological precursor of the nitrile should also be convertible to nitrile under mild chemical conditions. The identity of the precursor with either indolyl-3-acetaldehyde imine (sequence A) or indolyl-3-acetaldoxime (sequence B) must therefore be ruled out.

We have examined the chemical and chromatographic properties of synthetic indolyl-3-pyruvic acid oxime and have found them to be very similar to those of the IAN precursor described by Housley and Bentley. We wish to advance a new hypothesis for the biosynthesis of IAN (sequence C) with indolyl-3-pyruvic acid oxime as the key intermediate:



The first step in our sequence is identical with that of sequence B. The second step, in vivo conversion of α-keto acid to the corresponding oxime, is not a novel idea (13). Although indolyl-3-pyruvic acid oxime has not been isolated from natural sources, other

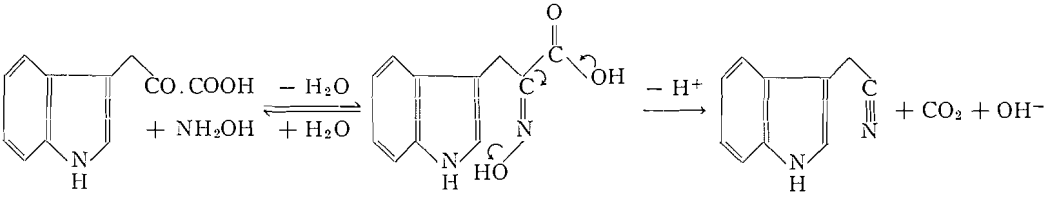
Can. J. Chem. Downloaded from www.nrcresearchpress.com by 210.87.254.105 on 09/05/12
For personal use only.

α-oximino acids have been obtained from plants (17) and from micro-organisms (e.g. ref. 12) and it has been shown that compounds of this type may be utilized biologically (18, 19), whereas oximes of carbonyl compounds other than α-keto acids are relatively inactive (18, 20). A transoximase system, catalyzing the transfer of =N–OH between α-keto acids, has been detected in a variety of tissues (21). α-Keto acid oximes are thus known as biochemical intermediates.

The novel feature of our sequence lies in the postulated concerted conversion of indolyl-3-pyruvic acid oxime to IAN. We have found that this reaction takes place readily in aqueous solutions pH 1 to 7 at moderate temperatures, as required for an IAN precursor by the results of Housley and Bentley.

Not only indolyl-3-pyruvic acid oxime, but all other α-keto acid oximes we have tested, yield the lower nitrile and CO_2 under these reaction conditions. The generality of this phenomenon was first recorded by Bouveault and Locquin (22) but has since been almost entirely overlooked, except in isolated instances (23). Considering the ease with which the conversion takes place it is not surprising that reaction of α-keto acids with hydroxylamine under the usual conditions gives oxime in poor yield only and that occasionally (e.g., indolyl-3-glyoxylic acid (24)) no oxime, but only nitrile is obtained. It is probable that Bauguess and Berg (25) obtained a very impure sample of indolyl-3-pyruvic acid oxime (m.p. indefinite, >175°) by this method. The compound (m.p. 154° (decomp.)) was obtained in 59% yield (26) by nitrosation of ethyl α-acetyl-β-(3-indolyl)-propionate.

When heated in 0.05 *M* H_2SO_4 for 3 hours, indolyl-3-pyruvic acid oxime is converted to IAN in 95% yield. The same product (60% yield) is obtained directly when equimolar amounts of indolyl-3-pyruvic acid and hydroxylamine hydrochloride are refluxed in aqueous solution, pH 1.



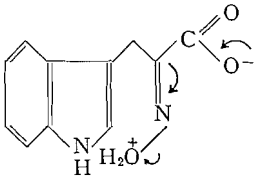
In further confirmation of the ease with which IAN formation takes place, decomposition of oxime to nitrile was found to occur readily even at low temperature. Table I

TABLE I

Yield of IAN on incubation at 41.5° for 24 hours of 20 mg indolyl-3-pyruvic acid oxime in buffer solutions, pH 1–7

Buffer	Initial pH	Final pH	IAN obtained	
			mg	% yield
HCl/KCl	1.0	1.0	6.44	45.0
HCl/KCl	1.6	1.6	7.36	51.4
HCl/KCl	2.0	2.0	7.51	52.5
Phthalic acid/hydrogen phthalate	3.1	3.0	6.73	47.0
Hydrogen phthalate/phthalate	4.0	3.6	5.41	37.8
Hydrogen phthalate/phthalate	5.0	4.5	1.85	12.9
$H_2PO_4^-/HPO_4^=$	7.0	6.3	0.78	5.5

shows the yields of nitrile at various pH values, when a dilute solution of oxime was incubated at 41.5° for 24 hours. The yield of product was optimal at pH 2, decreased at lower pH values, and dropped with rise in pH, but even at pH 7 nitrile was obtained. Although the decreased yields at pH <2 may be due entirely to side reactions leading to destruction of the indole nucleus, this is not likely in view of the good yield of IAN at pH 1 at 100° but may be a consequence of the existence at pH 2 of maximal amounts of the zwitterionic species, which would be the most favorable for a concerted elimination



of carbonic anhydride and water from the oxime. At pH <2 the carboxylate group (pK_a 3.4) would be more than 96% protonated, whereas at pH >2 the oxime OH is unlikely to bear a proton.

A concerted elimination of this type requires an anti (HO– –COOH) stereochemistry of the oxime. Only in very few instances (phenylglyoxylic acid (27), oxaloacetic acid (28), and possibly phenylpyruvic acid (29), glyoxylic acid (30), and α-ketoglutaric acid (19)) have syn- and anti-isomers of α-keto acid oximes been described. The stereochemistry of these oximes has not been reinvestigated by modern methods, and therefore remains uncertain, but on the basis of their classical investigations both Hantzsch (27, 28) and Meisenheimer (31) concur that, where only one isomer is known, the favored stereochemical arrangement of α-keto acid oximes is anti (HO– –COOH), as now required to account for the facility of their conversion to nitriles in aqueous solution by a concerted acid catalyzed mechanism.

Having established that indolyl-3-pyruvic acid oxime yields IAN under mild chemical conditions, as demanded for a precursor according to Housley and Bentley, it remained to compare the behavior on extraction and chromatography of Housley and Bentley's precursor with that of the oxime. In Table II the chromatographic behavior of indolyl-3-

TABLE II

	Precursor	Oxime	IAN
(1) R_f ranges			
2-PrOH/0.15 M NH_3 (4:1)	0.39–0.48	0.40–0.45	0.85–0.90
1-BuOH, saturated with 1.5 M NH_3	0.10–0.15	0.13–0.21	0.85–0.90
(2) Chromogenic sprays			
$FeCl_3/HClO_4$	Yellow	Mauve changing to greenish yellow	Violet blue changing to brown
HNO_2/HNO_3	Yellow	Yellow	Blue-purple changing to greenish yellow
p-Dimethylaminobenzaldehyde		Mauve changing to greenish yellow	Mauve changing to brown
(3) Fluorescence	Bluish-purple	Blue	Blue

pyruvic acid oxime is compared with that of Housley and Bentley's IAN precursor. The similarity of the R_f ranges of the two substances in the solvent systems used by Housley and Bentley is evident. Differences in color with Ehrlich's reagent and $FeCl_3$/perchlorate

Can. J. Chem. Downloaded from www.nrcresearchpress.com by 210.87.254.105 on 09/05/12
For personal use only.

Can. J. Chem. Downloaded from www.nrcresearchpress.com by 210.87.254.105 on 09/05/12
For personal use only.

may be accounted for by concentration effects. At low concentrations the mauve color given by indolyl-3-pyruvic acid oxime with these two reagents was exceedingly transient.

Complete analogy was found in the behavior of synthetic oxime and IAN precursor on partition between solvents: using a solution of indolyl-3-pyruvic acid oxime (20 mg in 15 ml 95% ethanol, adjusted to pH 3.2 with dilute sulphuric acid) we duplicated the operations performed by Housley and Bentley in their treatment of those fractions of cabbage extract which contained IAN precursor. The details of this comparison are set out in the experimental section. Housley and Bentley fractionated cabbage extract into ether-soluble neutral, ether-soluble acidic, and water-soluble fractions by extraction with ether after pH adjustment. Their IAN precursor was found, by chromatography and bio-assay, mainly in the water-soluble, but also in the acidic ether-soluble, fraction. Elution of the IAN precursor from chromatograms and rechromatography led to a decrease in IAN precursor and an appearance of indolyl-3-acetonitrile. When we applied Housley and Bentley's procedures to indolyl-3-pyruvic acid oxime, results analogous in all particulars were obtained. In a number of their chromatograms Housley and Bentley detected two other growth active substances (R_f 0.10–0.20 and R_f 0.55–0.65, respectively, in 2-PrOH/NH_3). Chromatography of the ether extract of an acidified 5% $NaHCO_3$ solution of indolyl-3-pyruvic acid oxime gave, in addition to the expected spots of starting material and IAN, two weakly Ehrlich-positive spots of unknown nature with R_f ranges, 0.11–0.18 and 0.60–0.70, similar to those of Housley and Bentley. These growth active zones may thus have been due to artifacts derived from their acidic IAN precursor during extraction and chromatography.

The inhibition of IAN formation by dimedone, which has already been referred to, requires explanation. Since under mild conditions dimedone reacts specifically with aldehydes (e.g. ref. 32) it would appear that an aldehyde is implicated in IAN formation. This consideration led Gordon (14) to reject indolyl-3-pyruvic acid oxime as a possible intermediate in IAN biosynthesis in favor of indolyl-3-acetaldehyde. Preliminary experiments have now shown that Gordon's inference was based on insufficient evidence: whereas incubation of indolyl-3-pyruvic acid oxime at pH 2.0 and at pH 5.0, yielded IAN in 52.5% and 12.9% yield respectively (Table I), incubation of the oxime under similar conditions in the presence of dimedone did not yield detectable amounts of nitrile. Instead, the neutral ether-soluble fraction contained an oily yellow material of unknown structure which had no trace of –CN absorption at 2250 cm^{-1}, and showed, in addition to the indole bands at 280–288 mμ, an absorption band at 410 mμ, which disappeared in alkaline solution. Incubation of indolyl-3-pyruvic acid with dimedone, either in the presence or absence of hydroxylamine, gave rise to a similar yellow substance. When indolyl-3-acetonitrile was incubated with dimedone, starting material was recovered in 95% yield. Although the nature of the yellow dimedone adducts of indolyl-3-pyruvic acid and its oxime is as yet undetermined, it is clear that dimedone inhibits their conversion to indolyl-3-acetonitrile. This is consistent with Gordon's experimental results (14) on the inhibition of IAN formation from tryptophan in the presence of dimedone in *Avena* coleoptiles.

The auxin activity of indolyl-3-pyruvic acid oxime was compared with that of IAN and of indolyl-3-acetic acid in the *Avena* section (straight growth) test.[2] The oxime was found to have from 25% to 20% of the auxin activity of indolyl-3-acetic acid (compared

[2]*We are greatly indebted to Drs. J. Shen and S. A. Gordon, Argonne National Laboratory, Lemont, Illinois, for this study.*

on a molar basis) over a concentration range of 10^{-4} to 10^{-2} gram moles per liter (Fig. 1).

The chemical reactivity of indolyl-3-pyruvic acid oxime, the behavior of this substance on chromatography and solvent partition, and its biological activity thus correspond to the properties of the IAN precursor described by Housley and Bentley.

The evidence is compatible with the hypothesis that indolyl-3-pyruvic acid oxime is the biochemical precursor of indolyl-3-acetonitrile.

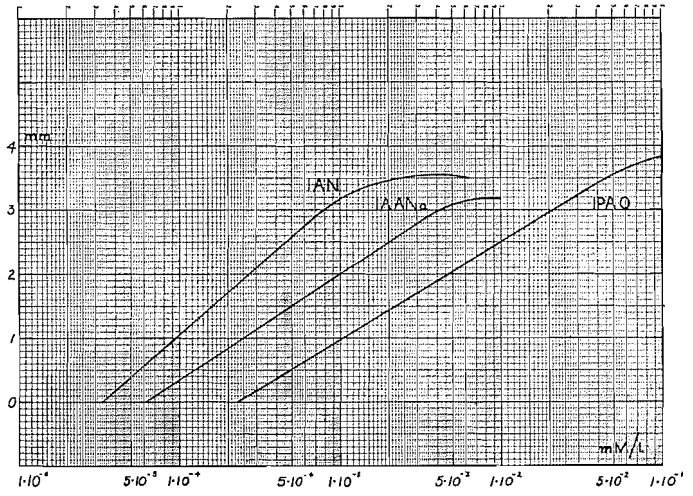


FIG. 1. Auxin activities of indolyl-3-acetonitrile (IAN), sodium indolyl-3-acetate (IAA.Na), and indolyl-3-pyruvic acid oxime (IPAO) in the *Avena* section (straight growth) test: 3-mm sections; medium: 0.01 *M* $NaHCO_3$, containing 2% w/v sucrose (2 ml); 20 hours.
Ordinate: mm increase over original length, corrected for control sections in medium alone (linear scale).
Abscissa: concentration of auxin in millimoles per liter (log scale).

EXPERIMENTAL

Indolyl-3-pyruvic acid was prepared according to Bentley *et al.* (5). Indolyl-3-pyruvic acid oxime was obtained from indolyl-3-pyruvic acid (25) and also by nitrosation of ethyl α-acetyl-β-(3-indolyl)-propionate (26), melting at 157°, pK' 3.4 (i.e., pH at half equivalence in saturated aqueous solution), infrared absorption (Nujol) (cm^{-1}): 3360(s), 1690(s), 1620(m); ultraviolet absorption (λ_{max}, mμ (log ϵ)): 225(4.13), 274(3.83), 282(3.84), 290(3.77).

Indolyl-3-acetonitrile

(1) *From Indolyl-3-pyruvic Acid*

Indolyl-3-pyruvic acid (0.400 g, 0.00197 mole) and hydroxylamine hydrochloride (0.136 g, 0.00197 mole) in 30 ml water were refluxed 2.5 hours. The solution, which contained a small amount of dark brown precipitate, was filtered, allowed to cool, and extracted with ether (5 times 10 ml). The ether extract was washed with 5% sodium bicarbonate solution and with water, dried over Na_2SO_4, and concentrated, yielding indolyl-3-acetonitrile as an oily residue. The product was distilled at 100° and 10^{-3} mm and was obtained as a yellow oil (0.184 g, 60%), whose infrared (in $CHCl_3$ (cm^{-1}): 3450(s), 2250(s), 1615(m), 1455(s), 1350(s), 1330(s)) and ultraviolet (λ_{max}, mμ (log ϵ) in MeOH: 220(4.50), 273(3.78), 279(3.80), 288(3.68)) absorption was identical with that of an authentic specimen melting at 35–36°, prepared from gramine methiodide (33). The oil crystallized on seeding with a few crystals of the authentic sample.

Can. J. Chem. Downloaded from www.nrcresearchpress.com by 210.87.254.105 on 09/05/12
For personal use only.

A small portion of the oily product was converted to the picrate, melting at 127–128° (33).

(2) *From Indolyl-3-pyruvic Acid Oxime*

(i) At 100°.—The oxime (0.100 g, 0.00046 mole) was dissolved in 20 ml 0.05 *M* H_2SO_4 (0.001 mole) and the solution refluxed 3 hours in an atmosphere of nitrogen. On cooling, a small amount of dark sediment was filtered off, the solution was extracted with ether, the ether extract washed with 5% bicarbonate solution and with water, dried over Na_2SO_4 and concentrated, and the oily residue distilled at 100° and 10^{-3} mm to yield 0.068 g (95%) indolyl-3-acetonitrile as a light yellow oil, crystallizing on seeding with an authentic specimen.

(ii) At 40°.—A solution of oxime (0.020 g, 0.000092 mole) in 20 ml buffer solution was allowed to stand 12 hours at room temperature and then 24 hours at 41.5°. Buffers used were those of Clark and Lubs, HCl/KCl (pH 1, 1.6, and 2), phthalate (pH 3, 4, and 5), and $H_2PO_4^-/HPO_4^=$ (pH 7). Some discoloration was observed at pH 1–4. The solution was extracted with ether; the extract washed with 5% bicarbonate and water, dried over Na_2SO_4, and concentrated; the residue was dissolved in $CHCl_3$ and identified as indolyl-3-acetonitrile by its infrared absorption. The yield was determined by measuring the intensity of the ultraviolet absorption at 288 mμ of the product in methanol at suitable dilution. Results are summarized in Table I. Incubation of the oxime in the presence of dimedone (0.200 g) was carried out similarly and the reaction mixture was worked up for neutral products in the same way, except that dilute NaOH, instead of $NaHCO_3$ solution, was used for washing, to remove unreacted dimedone.

Solvent Fractionation and Chromatography of Indolyl-3-pyruvic Acid Oxime

Chromatography.—Solvents used in ascending paper chromatography on Whatman No. 1 paper were (*a*) 2-propanol/0.15 *M* ammonia (1:4), and (*b*) 1-butanol, saturated with 1.5 *M* ammonia. Chromogenic reagents applied were (i) Salkowski reagent: ferric chloride/perchloric acid (100 ml 5% aqueous $HClO_4$ and 2 ml 0.05 *M* $FeCl_3$); (ii) nitrous acid/nitric acid (1 g KNO_2 in 200 ml HNO_3, sp. gr. 1.42, diluted 10 times); (iii) Ehrlich's reagent (2 g *p*-dimethylaminobenzaldehyde in a mixture of 80 ml absolute ethanol and 20 ml HCl, sp. gr. 1.18) (15).

Solvent fractionation of the oxime according to the procedure used by Housley and Bentley (15) for the investigation of cabbage extract.—For purposes of comparison Housley and Bentley's operations and results at each stage are quoted in square brackets.

Preliminary Fractionation

(A) Indolyl-3-pyruvic acid oxime (20 mg) in 15 ml 95% ethanol adjusted to pH 3.2 with 0.05 *M* H_2SO_4, was stirred at −10° for 40 hours (fraction 1). Chromatography in 2-PrOH/NH_3, R_f 0.42, i.e., unchanged oxime. [Frozen ground cabbage was extracted for 40 hours at −10° with 95% ethanol acidified to pH 3.2 with H_2SO_4. Not chromatographed.]

(B) The pH of the solution was adjusted to pH 5 by addition of saturated aqueous $Ba(OH)_2$, $BaSO_4$ was filtered off and ethanol removed from the filtrate *in vacuo* at 30° (fraction 2). Chromatography in 2-PrOH/NH_3 gave a spot at R_f 0.42, i.e., unchanged oxime. The residual solution was mixed with 3 ml phthalate buffer, pH 3, and allowed to stand at room temperature 24 hours. [$Ba(OH)_2$ solution was added adjusting the pH to pH 5, the extract was filtered, ethanol removed at 35° *in vacuo* and the pH of the residual solution adjusted to pH 3 with dilute H_2SO_4. Not chromatographed.]

(C) The solution was exhaustively extracted with ether, yielding ether extract (fraction 3) and aqueous layer (fraction 4). Chromatography of the ether layer in 2-PrOH/NH_3

Can. J. Chem. Downloaded from www.nrcresearchpress.com by 210.87.254.105 on 09/05/12
For personal use only.

gave spots R_f 0.42 (oxime) and R_f 0.90 (nitrile). The aqueous layer showed a spot at R_f 0.42 (oxime) only. [The solution was extracted with ether, yielding an ether-soluble fraction and a water-soluble fraction.]

The above experiments show that indolyl-3-pyruvic acid oxime is stable at pH 3.2–5 at $-10°$, but that it is partially converted to the nitrile at pH 3 and room temperature. They also show that the oxime is soluble both in ether and in water. Later steps were carried out with freshly prepared oxime in the requisite solvent.

Investigation of the "Ether-soluble" Fraction

(D) Indolyl-3-pyruvic acid oxime (10 mg) was dissolved in 5 ml ether giving a solution corresponding to fraction 3. This was extracted with 5% $NaHCO_3$ solution, yielding an ethereal and an aqueous layer. The ethereal layer was dried (fraction 6).

The aqueous bicarbonate layer was acidified to pH 3 with 0.05 *M* H_2SO_4. This solution was divided into two portions, one of which was extracted with ether immediately, and the ether layer washed and dried (fraction 5*a*), the other extracted with ether after 16 hours and the ether layer treated similarly (fraction 5*b*).

Chromatography of the "neutral" fraction 6 in 2-PrOH/NH_3 showed a single weak spot of R_f 0.90, i.e., indole-3-acetonitrile. The "acidic" fraction 5*b* showed an intense spot at R_f 0.90 (indole-3-acetonitrile), and a weak spot at R_f 0.41 (oxime). Fraction 5*a* showed a strong spot at R_f 0.90 (nitrile), a strong spot at R_f 0.42 (oxime), and in addition weakly Ehrlich-positive spots at R_f 0.60–0.70 (green, changing to yellow, changing to green), R_f 0.42–0.55 (purple, changing to green), and R_f 0.11–0.18 (blue green).

Evidently prolonged exposure to pH 3 had caused almost complete conversion of oxime to nitrile (fraction 5*b*), whereas during shorter contact with an acid medium (fraction 5*a*) conversion of oxime to nitrile was incomplete. The nature of the materials giving rise to the additional indolic spots in this fraction is obscure, but it is suggestive that Housley and Bentley report the occurrence, in a number of their chromatograms, of growth active materials of R_f 0.1–0.2 and 0.5–0.7 which could not be ascribed to recognized auxins. It is possible that these materials may have been breakdown products of their precursor, similar to the oxime breakdown products of fraction 5*a*. [The ether-soluble fraction from step C was washed, dried, concentrated, redissolved in ether, and extracted with bicarbonate solution. The ether layer gave a neutral fraction, containing growth active zones at R_f 0.46–0.90 (mainly IAN, but presumably some precursor, due to incomplete fractionation), whereas the bicarbonate layer, after acidification to pH 3, extraction into ether, and drying and evaporation of the ether layer, showed weak auxin activity at R_f 0.25–0.50 (precursor) and strong activity at R_f 0.54–0.89 (IAN).]

Investigation of the "Water-soluble" Fraction

(E) Indolyl-3-pyruvic acid oxime (10 mg) was dissolved in 5 ml water, giving a solution corresponding to fraction 4 (step C). Chromatography in 2-PrOH/NH_3 gave R_f 0.42 only. The area of the paper corresponding to the oxime was eluted with 4 ml water, and the eluate concentrated and rechromatographed with 2-PrOH/NH_3 and also with 1-BuOH/NH_3. The former chromatogram showed spots at R_f 0.42 (oxime) and R_f 0.90 (nitrile), the latter at R_f 0.16 (oxime) and R_f 0.90 (nitrile). During elution and rechromatography oxime had thus partially decomposed to nitrile. [The pH of the water-soluble fraction from step (C) was adjusted to pH 5.3 and the solution concentrated at 25°. Chromatography in 2-PrOH/NH_3 of the concentrate gave a precursor spot at R_f 0.4–0.5 and an IAN spot at R_f 0.8–0.9, the latter presumably due to previous acid treatment. The area on the chromatogram corresponding to precursor was eluted with 4 ml water at 5° and

Can. J. Chem. Downloaded from www.nrcresearchpress.com by 210.87.254.105 on 09/05/12
For personal use only.

the eluate rechromatographed with 2-PrOH/NH_3, where it showed R_f 0.4–0.5, and with *n*-BuOH/NH_3, where it gave R_f 0–0.15. In both the latter chromatograms an IAN spot at R_f 0.8–0.9 also appeared. Thus during elution and rechromatography precursor had partially decomposed to IAN.]

(F) Indolyl-3-pyruvic acid oxime (10 mg) was dissolved in 3 ml water and heated under reflux 25 minutes. On cooling, the solution was extracted with ether. Chromatography of the ether extract in 2-PrOH/NH_3 gave spots at R_f 0.42 (oxime) and R_f 0.90 (nitrile). Chromatography of the aqueous layer gave a weak spot, R_f 0.42 (oxime). [The pH of the water-soluble fraction from step C was adjusted to pH 5.3, the solution was concentrated at 25° and heated at 98–100° for 25 minutes, cooled, dissolved in 20 ml aqueous $NaHCO_3$, and the solution extracted with ether. Chromatography of the ethereal "neutral" fraction showed a weak auxin zone at R_f 0.29–0.44 (precursor which according to Housley and Bentley had entered this fraction due to incomplete separation) and a strong zone at R_f 0.7–0.95 (nitrile). Elution and rechromatography in 2-PrOH/NH_3 of the zone R_f 0.29–0.44 gave rise to more IAN. The aqueous phase was acidified to pH 3 and extracted with ether, yielding an "acidic" fraction, which on chromatography showed auxin activity at R_f 0.25–1.00 with activity peaks at R_f 0.85–0.92 (IAN, presumably derived from precursor due to acidification during fractionation) and at R_f 0.35–0.48 (presumably precursor, but ascribed by Housley and Bentley to indolyl-3-acetic acid, since this region gave a pink color with Salkowski's reagent).]

ACKNOWLEDGMENTS

We are greatly indebted to Dr. S. A. Gordon, Argonne National Laboratories, Lemont, Illinois, for placing at our disposal the manuscript, as yet unpublished, of a review on the biogenesis of auxin (14), and for testing the auxin activity of indolyl-3-pyruvic acid oxime.

Financial assistance by the National Research Council of Canada and by the Ontario Research Foundation is gratefully acknowledged. One of us (A. A.) wishes to thank the Colombo Plan authorities for financial support and the Pakistan Council of Scientific and Industrial Research for the award of a scholarship.

REFERENCES

1. E. R. H. Jones, H. B. Henbest, G. F. Smith, and J. A. Bentley. Nature, **169**, 485 (1952).
2. W. N. Dannenburg and J. L. Liverman. Plant Physiol. **32**, 263 (1957); J. L. Liverman and W. N. Dannenburg. Plant Physiol. **32**, xviii (1957).
3. B. B. Stowe and K. V. Thimann. Nature, **172**, 764 (1953); Arch. Biochem. Biophys. **51**, 499 (1954).
4. J. A. Bentley, S. Housley, and G. Britton. *In* The chemistry and mode of action of plant growth substances. *Editors* R. L. Wain and F. Wightman. Butterworth, London. 1956. p. 40.
5. J. A. Bentley, K. R. Farrar, S. Housley, G. F. Smith, and W. C. Taylor. Biochem. J. **64**, 44 (1956).
6. S. A. Gordon. *In* The chemistry and mode of action of plant growth substances. *Editors* R. L. Wain and F. Wightman. Butterworth, London. 1956. p. 65.
7. H. A. Krebs. *In* The enzymes. Vol. 2. *Editors* J. B. Sumner and K. Myrbäck. Academic Press, New York. 1951. p. 499.
8. B. M. Pitt. J. Am. Chem. Soc. **80**, 3799 (1958).
9. W. Langenbeck. Advances in Enzymol. **14**, 163 (1953).
10. R. Breslow. J. Am. Chem. Soc. **80**, 3719 (1958). R. Breslow and E. McNelis. J. Am. Chem. Soc. **81**, 3080 (1959).
11. B. B. Stowe. Biochem. J. **61**, ix (1955). D. G. Wilson, K. W. King, and R. H. Burris. J. Biol. Chem. **208**, 863 (1954).
12. A. I. Virtanen and N. E. Saris. Acta Chem. Scand. **9**, 337 (1955).
13. N. Rautanen. *In* Encyclopedia of plant physiology. *Editor* K. Mothes. Springer, Berlin. **8**, 212 (1958). P. W. Wilson. *In* Encyclopedia of plant physiology. *Editor* K. Mothes. Springer, Berlin. **8**, 9 (1958).

Can. J. Chem. Downloaded from www.nrcresearchpress.com by 210.87.254.105 on 09/05/12
For personal use only.

14. S. A. GORDON. Private communication; *In* Encyclopedia of plant physiology. *Editor* H. Burström. Springer, Berlin. **14** (in press).
15. S. HOUSLEY and J. A. BENTLEY. J. Exptl. Botany, **7**, 219 (1956).
16. E. K. BONDE. Botan. Gaz. **115**, 1 (1953). T. A. BENNET-CLERK and N. P. KEFFORD. Nature, **171**, 645 (1953).
17. A. I. VIRTANEN and T. LAINE. Biochem. J. **33**, 412 (1939). A. I. VIRTANEN, A. A. ARHIMO, J. SUNDMAN, and L. JANNES. J. prakt. Chem. **162**, 71 (1943).
18. J. G. WOOD and M. R. HONE. Australian J. Sci. Research, Ser. B, **1**, 163 (1948). J. H. QUASTEL, P. G. SCHOLEFIELD, and J. W. STEVENSON. Biochem. J. **51**, 278 (1952).
19. J. G. WOOD, M. R. HONE, M. E. MATTNER, and C. P. SYMONS. Australian J. Sci. Research, Ser. B, **1**, 38 (1948).
20. H. L. JENSEN. J. Gen. Microbiol. **5**, 360 (1951).
21. K. YAMAFUJI. Nature, **171**, 745 (1953). K. YAMAFUJI and M. ETO. Enzymologia, **16**, 247 (1953). K. YAMAFUJI, M. SHIMAMURA, and H. TAKAHASHI. Enzymologia, **17**, 110 (1954). K. YAMAFUJI, M. SHIMAMURA, and H. OMURA. Enzymologia, **17**, 359 (1956).
22. L. BOUVEAULT and R. LOCQUIN. Bull. soc. chim. France, [3], **31**, 1142 (1904).
23. E. E. BLAISE and H. GAULT. Bull. soc. chim. France, [4], **1**, 75 (1907); **9**, 451, 458 (1911). K. L. WATERS. Chem. Revs. **41**, 585 (1947).
24. R. MAJIMA, T. SHIGEMATSU, and T. ROKKAKU. Ber. **57**, 1453 (1924).
25. L. C. BAUGUESS and C. P. BERG. J. Biol. Chem. **104**, 675 (1934).
26. D. O. HOLLAND and J. H. C. NAYLER. J. Chem. Soc. 280 (1953).
27. A. HANTZSCH. Ber. **24**, 36 (1891).
28. A. HANTZSCH. Ber. **24**, 1192 (1891). C. CRAMER. Ber. **24**, 1198 (1891).
29. R. GAUDRY and R. A. MCIVOR. Can. J. Chem. **29**, 427 (1951).
30. C. CRAMER. Ber. **25**, 713 (1892). F. C. PALAZZO. Gazz. chim. ital. **43**, 51 (1913). F. C. PALAZZO and V. EGIDI. Gazz. chim. ital. **43**, 57 (1913).
31. J. MEISENHEIMER and W. THEILACKER. *In* Stereochemie. *Edited by* K. Freudenberg. F. Deuticke, Leipzig and Vienna, **3**, 1040 (1932).
32. E. HEUSER. *In* Houben-Weyl, Methoden der Organischen Chemie. *Edited by* E. Müller. G. Thieme, Stuttgart. **2**, 450 (1953).
33. H. B. HENBEST, E. R. H. JONES, and G. F. SMITH. J. Chem. Soc. 3796 (1953).

Can. J. Chem. Downloaded from www.nrcresearchpress.com by 210.87.254.105 on 09/05/12
For personal use only.

Can. J. Chem. Downloaded from www.nrcresearchpress.com by 91.191.171.90 on 09/05/12
For personal use only.

NOTES

A PROPOSED CRYOSCOPIC METHOD FOR DETERMINING THE HEAT OF COMPLEX FORMATION FOR A REACTION, $X + Y \rightleftharpoons Z$

P. A. D. DE MAINE*

Spectrophotometric methods (1, 2, 3) have been used frequently to determine equilibrium constant (K) and heat of formation (ΔH) values for complexes between dissimilar molecules in inert solvents. Scott (4) has reported that such values for K are not reliable; but he (4) and others (5, 6, 7) have noted that ΔH can be determined accurately with spectrophotometric data. Some workers (8, 9, 10) have suggested that the changes in absorption spectra used to determine ΔH (5, 6, 7, 4) arise from changes in the electrical properties of the solution and/or non-specific interactions between the unlike molecules. However, evidence that the changes in spectra are due to specific interactions between the molecules has been reported (11, 12, 13). Thus a non-spectrophotometric method for the determination of ΔH should prove helpful in elucidating the actual nature of the interactions.

If two unlike molecules, X and Y, interact thus,

$$X + Y \overset{K}{\rightleftharpoons} Z,$$

then

$$[1] \qquad K = N_Z/(N_X - N_Z)\,(N_Y - N_Z)$$

where N_Z, $(N_X - N_Z)$, and $(N_Y - N_Z)$ are the equilibrium concentrations in mole fraction units of Z, X, and Y respectively.

If K_f is the cryoscopic constant (degrees C/mole 100 grams of solvent) of the solvent, then for dilute solutions

$$[2] \qquad C_X + C_Y - C_Z = K_a(C_X + C_Y)/K_f,$$

where K_a is the apparent constant calculated for the mixed solute solution with the assumption that $C_Z = 0$.

$$[3] \qquad C_X = N_X\,100/M, \qquad C_Y = N_Y\,100/M, \qquad C_Z = N_Z\,100/M,$$

where M is the molecular weight of the pure solvent.

As N_X and N_Y are known, K and N_Z can be calculated for each mixed solute solution at its freezing point. With the van't Hoff equation (ΔH assumed to be independent of temperature) it can be shown that

$$[4] \qquad \Delta T_2 = \frac{\Delta H(\Delta T_1 - \Delta T_2)}{R(T_f - \Delta T_1)\ln\,(K_1/K_2)} + T_f.$$

K_1 and K_2 are values for the equilibrium constant, in mole fraction units, calculated for mixed solute solutions with freezing points of ΔT_1 and ΔT_2 °C, respectively, below the absolute freezing point (T_f °K) of the pure solvent.

*Present address: Chemistry Department, University of Mississippi, Oxford, Mississippi.

Plots of ΔT_2 versus $(\Delta T_1 - \Delta T_2)/\ln(K_1/K_2)$ for data with ΔT_1 constant should be linear with

$$\text{slope} = \Delta H/R\,(T_f - \Delta T_1), \quad [5]$$

$$T_f = \Delta T_2 \text{ intercept}. \quad [6]$$

Thus the absolute freezing point of the pure solvent (T_f °K) and ΔH can be determined with data obtained from measurements with a differential thermometer.

In deriving equations [4], [5], and [6] it has been assumed that (*a*) activities equal concentration; (*b*) ΔH is independent of temperature; and (*c*) both solutes have the same cryoscopic constant.

Thanks are due the Research Corporation for support of this work.

1. L. J. ANDREWS and R. M. KEEFER. J. Am. Chem. Soc. **73**, 4169 (1951).
2. H. A. BENESI and J. H. HILDEBRAND. J. Am. Chem. Soc. **71**, 2703 (1949).
3. J. A. A. KETELAAR, C. VAN DE STOLPE, A. GOUDSMIT, and W. DZCUBAS. Rec. trav. chim. **71**, 1104 (1952).
4. R. L. SCOTT. Rec. trav. chim. **75**, 787 (1956).
5. D. BOOTH, F. S. DAINTON, and K. J. IVIN. Trans. Faraday Soc. **55**, 1293 (1959).
6. P. A. D. DE MAINE and J. PEONE. J. Mol. Spectroscopy. **4**, 262 (1960).
7. R. M. KEEFER and L. J. ANDREWS. J. Am. Chem. Soc. **77**, 2164 (1955).
8. N. S. BAYLISS. J. Chem. Phys. **18**, 292 (1950).
9. L. E. ORGEL and R. S. MULLIKEN. J. Am. Chem. Soc. **79**, 4839 (1957).
10. K. SHINODA and J. H. HILDEBRAND. J. Phys. Chem. **62**, 295 (1958).
11. P. A. D. DE MAINE. J. Chem. Phys. **26**, 1199 (1957).
12. P. A. D. DE MAINE and P. J. SANTIAGO. Can. J. Chem. **38**, 157 (1960).
13. C. REID and R. S. MULLIKEN. J. Am. Chem. Soc. **76**, 3869 (1954).

RECEIVED FEBRUARY 25, 1960.
CHEMISTRY DEPARTMENT,
NEW YORK STATE UNIVERSITY COLLEGE OF EDUCATION,
135 WESTERN AVENUE, ALBANY 3, N.Y., U.S.A.

Can. J. Chem. Downloaded from www.nrcresearchpress.com by 91.191.171.90 on 09/05/12
For personal use only.

CRYSTALLINE *O*-METHYL ETHERS OF D-GALACTITOL*

C. T. BISHOP

During the course of some work on the separation of carbohydrate derivatives by gas–liquid partition chromatography it was found that anomeric methyl glycosides of methylated monosaccharides were separable (1). The ultimate objective of this work was application of gas–liquid partition chromatography to the structural investigation of polysaccharides; it appeared that the complex mixture of anomers that might be expected from methanolysis of a methylated polysaccharide could be avoided by reduction of the *O*-methyl monosaccharides to the sugar alcohols, which could then be separated as their acetates. It was later found that methanolysis of methylated polysaccharides did not yield as complex mixtures as had been anticipated so this approach was dropped. However, a number of partially methylated sugar alcohols were prepared for use as standard compounds; some of these are readily crystallized, sharp melting, and eminently suitable as characteristic derivatives of the parent monosaccharide. The opportunity is therefore taken to record the preparation and physical properties of 2,4-di-*O*-methyl-; 2,3,4-tri-*O*-methyl-; and 2,3,4,6-tetra-*O*-methyl-D-galactitol; these are derived from

*Issued as N.R.C. No. 5754.

Plots of ΔT_2 versus $(\Delta T_1 - \Delta T_2)/\ln(K_1/K_2)$ for data with ΔT_1 constant should be linear with

$$\text{slope} = \Delta H/R\,(T_f - \Delta T_1), \quad [5]$$

$$T_f = \Delta T_2 \text{ intercept}. \quad [6]$$

Thus the absolute freezing point of the pure solvent (T_f °K) and ΔH can be determined with data obtained from measurements with a differential thermometer.

In deriving equations [4], [5], and [6] it has been assumed that (*a*) activities equal concentration; (*b*) ΔH is independent of temperature; and (*c*) both solutes have the same cryoscopic constant.

Thanks are due the Research Corporation for support of this work.

1. L. J. ANDREWS and R. M. KEEFER. J. Am. Chem. Soc. **73**, 4169 (1951).
2. H. A. BENESI and J. H. HILDEBRAND. J. Am. Chem. Soc. **71**, 2703 (1949).
3. J. A. A. KETELAAR, C. VAN DE STOLPE, A. GOUDSMIT, and W. DZCUBAS. Rec. trav. chim. **71**, 1104 (1952).
4. R. L. SCOTT. Rec. trav. chim. **75**, 787 (1956).
5. D. BOOTH, F. S. DAINTON, and K. J. IVIN. Trans. Faraday Soc. **55**, 1293 (1959).
6. P. A. D. DE MAINE and J. PEONE. J. Mol. Spectroscopy. **4**, 262 (1960).
7. R. M. KEEFER and L. J. ANDREWS. J. Am. Chem. Soc. **77**, 2164 (1955).
8. N. S. BAYLISS. J. Chem. Phys. **18**, 292 (1950).
9. L. E. ORGEL and R. S. MULLIKEN. J. Am. Chem. Soc. **79**, 4839 (1957).
10. K. SHINODA and J. H. HILDEBRAND. J. Phys. Chem. **62**, 295 (1958).
11. P. A. D. DE MAINE. J. Chem. Phys. **26**, 1199 (1957).
12. P. A. D. DE MAINE and P. J. SANTIAGO. Can. J. Chem. **38**, 157 (1960).
13. C. REID and R. S. MULLIKEN. J. Am. Chem. Soc. **76**, 3869 (1954).

RECEIVED FEBRUARY 25, 1960.
CHEMISTRY DEPARTMENT,
NEW YORK STATE UNIVERSITY COLLEGE OF EDUCATION,
135 WESTERN AVENUE, ALBANY 3, N.Y., U.S.A.

Can. J. Chem. Downloaded from www.nrcresearchpress.com by 210.87.254.5 on 09/05/12
For personal use only.

CRYSTALLINE *O*-METHYL ETHERS OF D-GALACTITOL*

C. T. BISHOP

During the course of some work on the separation of carbohydrate derivatives by gas–liquid partition chromatography it was found that anomeric methyl glycosides of methylated monosaccharides were separable (1). The ultimate objective of this work was application of gas–liquid partition chromatography to the structural investigation of polysaccharides; it appeared that the complex mixture of anomers that might be expected from methanolysis of a methylated polysaccharide could be avoided by reduction of the *O*-methyl monosaccharides to the sugar alcohols, which could then be separated as their acetates. It was later found that methanolysis of methylated polysaccharides did not yield as complex mixtures as had been anticipated so this approach was dropped. However, a number of partially methylated sugar alcohols were prepared for use as standard compounds; some of these are readily crystallized, sharp melting, and eminently suitable as characteristic derivatives of the parent monosaccharide. The opportunity is therefore taken to record the preparation and physical properties of 2,4-di-*O*-methyl-; 2,3,4-tri-*O*-methyl-; and 2,3,4,6-tetra-*O*-methyl-D-galactitol; these are derived from

*Issued as N.R.C. No. 5754.

three *O*-methyl ethers of D-galactose which are found frequently as hydrolysis products of methylated polysaccharides (2).

EXPERIMENTAL

Reductions

The *O*-methyl-D-galactose (100 mg) was dissolved in methanol (3 ml) and potassium borohydride (15–16 mg) was added. The solution was kept at room temperature for 24 hours and then Amberlite IR-120 ion exchange resin was added with shaking until gas evolution ceased. The resin was filtered, washed with methanol, and filtrate plus washings were evaporated to dryness. Addition and evaporation of methanol were repeated six times to remove boric acid. The residues crystallized spontaneously when dried *in vacuo* over anhydrous calcium chloride. Yields were quantitative throughout.

2,4-Di-O-methyl-D-galactitol

This compound was prepared by reduction of 2,4-di-*O*-methyl-D-galactose, m.p. 103–104° C, $[\alpha]_D^{26} = +88° \pm 1°$ equilibrium value (*c*, 1.1% in water) (3). The crystalline reduction product was recrystallized from ethyl acetate to a constant melting point of 134–135° C (corr.), $[\alpha]_D^{28} = +23.5° \pm 0.5°$ (*c*, 2.04% in methanol). Anal. Calc. for $C_8H_{18}O_6$: C, 45.70%; H, 8.63%; OCH_3, 29.64%. Found: C, 45.59%; H, 8.31%; OCH_3, 29.80%.

2,3,4-Tri-O-methyl-D-galactitol

This compound was prepared by reduction of sirupy 2,3,4-tri-*O*-methyl-D-galactose, $[\alpha]_D^{25} = +110° \pm 2°$ (*c*, 1% in water), which had been characterized as its anilide (4, 5), m.p. 166–168° C, $[\alpha]_D^{26} = +42° \pm 3°$, equilibrium (*c*, 1% in methanol) and by conversion to 2,3,4-tri-*O*-methyl-D-galactonamide (5), m.p. 166–167° C, $[\alpha]_D^{26} = +35° \pm 3°$ (*c*, 0.8% in water). The crystalline reduction product was recrystallized from ethyl acetate to a constant melting point of 121–122° C, $[\alpha]_D^{26} = \pm 0°$ (*c*, 1.56% in methanol). Anal. Calc. for $C_9H_{20}O_6$: C, 48.20%; H, 8.93%; OCH_3, 41.50%. Found: C, 48.07%; H, 8.85%; OCH_3, 41.85%.

2,3,4,6-Tetra-O-methyl-D-galactitol

This compound was prepared by reduction of sirupy 2,3,4,6-tetra-*O*-methyl-D-galactose, $[\alpha]_D^{25} = +109° \pm 2°$ (*c*, 1% in water), which had been characterized as its anilide (6), m.p. 196.5–198° C, $[\alpha]_D^{25} = -137° \pm 1°$ (*c*, 2% in pyridine). The crystalline reduction product was recrystallized from cyclopentane to a constant melting point of 68–70° C, $[\alpha]_D^{27} = +12.5° \pm 0.5°$ (*c*, 2.25% in ethanol). Anal. Calc. for $C_{10}H_{22}O_6$: C, 50.40%; H, 9.31%; OCH_3, 52.32%. Found: C, 50.64%; H, 9.34%; OCH_3, 52.61%.

ACKNOWLEDGMENTS

The author is grateful to Mr. A. E. Castagne, Division of Applied Biology, National Research Council, for doing the microanalyses.

1. C. T. Bishop and F. P. Cooper. Can. J. Chem. **38**, 388 (1960).
2. F. Smith and R. Montgomery. Chemistry of plant gums and mucilages. Reinhold Publishing Corp., New York. 1959.
3. C. T. Bishop. Can. J. Chem. **35**, 1010 (1957).
4. D. McCreath and F. Smith. J. Chem. Soc. 387 (1939).
5. F. Smith. J. Chem. Soc. 1724 (1939).
6. J. C. Irvine and D. McNicoll. J. Chem. Soc. **97**, 1449 (1910).

Received April 11, 1960.
Division of Applied Biology,
National Research Council,
Ottawa, Ontario.

Can. J. Chem. Downloaded from www.nrcresearchpress.com by 210.87.254.5 on 09/05/12
For personal use only.

SPIROHEXANE

DONALD E. MCGREER

Can. J. Chem. Downloaded from www.nrcresearchpress.com by 91.191.171.90 on 09/05/12
For personal use only.

In 1953 Slobodin and Blinova (1) reported an attempt to synthesize spirohexane by the treatment with zinc dust of 1,1-bis-(bromomethyl)-cyclobutane prepared from the corresponding diol and phosphorus tribromide. The only product isolated in the dehalogenation reaction was methylenecyclopentane. Rearrangement may have occurred in the dehalogenation step since similar rearrangements have been observed to occur as in the preparation of spiropentane (2). It is also possible that treatment of the diol leads to a rearranged dibromide since rearrangement has been noted in the treatment of cyclobutyl carbinol with phosphorus tribromide (3).

Spirohexane has now been prepared in good yield from 1,1-bis-(iodomethyl)-cyclobutane (I) and zinc in the presence of tetrasodium ethylenediaminetetraacetate to remove the zinc ions as formed in the reaction. This method was recently developed by Applequist *et al.* for the synthesis of spiropentane from pentaerythrityl tetrabromide (2). The 1,1-bis-(iodomethyl)-cyclobutane was prepared by the method of Schubert and Leahy (4) and its structure was checked by N.M.R., which showed two unresolved peaks with an area ratio of 2:3 at 104 and 260 p.p.10^8 from water due to the $—CH_2I$ and cyclobutyl hydrogens, respectively. The spirohexane obtained by treatment of I with zinc dust showed no absorption in the infrared spectrum in the region for multiple bonds and had a N.M.R. spectrum which showed two peaks in an area ratio of 3:2 at 289 and 459 p.p.10^8 from water due to the cyclobutyl and cyclopropyl hydrogens, respectively (5).

Spirohexane has also recently been prepared by the reaction of methylenecyclobutane and methylene iodide in the presence of a zinc–copper couple (6).

EXPERIMENTAL

An "Aerograph" vapor chromatography unit fitted with a 10-ft Ucon Polar column was used with helium as the carrier gas. The N.M.R. spectra were determined on a 40-Mc/s Varian spectrophotometer with field stabilizer VK 3506, and methylene chloride was used as an external standard.

1,1-Bis-(iodomethyl)-cyclobutane (I)

1,1-Bis-(iodomethyl)-cyclobutane, b.p. 76–78° at 0.3 mm, was prepared in 50% yield by the method of Schubert and Leahy (4). A N.M.R. spectrum (0.5 ml/ml of carbon tetrachloride) showed two peaks at 104 and 260 p.p.10^8 from water with peak areas in the ratio of 2:3, respectively.

Spirohexane

In a 250-ml three-necked flask fitted with a reflux condenser, stirrer, and dropping funnel was placed 21 g of disodium dihydrogen ethylenediaminetetraacetate, a solution of 7.4 g of sodium hydroxide in 13 ml of water, 40 ml of 95% ethanol, and 0.6 g of sodium iodide. The mixture was heated to reflux and 5.5 g of zinc dust was added followed by 6.3 g of 1,1-bis-(iodomethyl)-cyclobutane which was added dropwise over a half-hour period. The mixture was refluxed an additional hour and distilled through a wire gauze column to give 2.8 g, b.p. 56–79°. Separation of the distillate by vapor chromatography gave 0.94 g (60%) of spirohexane, b.p. 70°, n_D^{22} 1.4245, D_4^{24} 0.855. Found: C, 87.65; H, 12.00%. Calc. for C_6H_{10}: C, 87.73, H, 12.27%.

The infrared spectrum (liquid film) showed no bands in the region from 1500 to 2800 cm^{-1}. The N.M.R. spectrum (neat) showed two peaks at 289 and 459 p.p.10^8 from water with peak areas in the ratio of 3:2 respectively.

In addition to spirohexane the chromatogram of the crude product showed ethanol and an unidentified component for which the peak area was less than 3% of that for spirohexane.

Support for this research was received from the National Research Council of Canada and is gratefully acknowledged.

1. Ya. M. Slobodin and M. V. Blinova. Zhur. Obshcheĭ Khim. **23**, 1994 (1953).
2. D. E. Applequist, G. F. Fanta, and B. W. Henrikson. J. Org. Chem. **23**, 1715 (1958).
3. H. G. Kuivila and W. L. Masterton. J. Am. Chem. Soc. **74**, 4953 (1952).
4. W. M. Schubert and S. M. Leahy, Jr. J. Am. Chem. Soc. **79**, 381 (1957).
5. D. E. Applequist and D. E. McGreer. J. Am. Chem. Soc. **82**, 1965 (1960).
6. D. E. Applequist and J. A. Landgrebe. Personal communication.

Received May 27, 1960.
Department of Chemistry,
University of British Columbia,
Vancouver 8, B.C.

Can. J. Chem. Downloaded from www.nrcresearchpress.com by 91.191.171.90 on 09/05/12
For personal use only.

AMINONITRILES. II. SOME DERIVATIVES OF 2-AMINO-3-CYANOINDENE*

D. L. Garmaise and S. Gelblum

As part of a study on the relation between chemical structure and bacteriostatic activity, a series of 2-arylamino- (and aralkylamino)-3-cyanoindenes was prepared from the readily accessible 2-amino-3-cyanoindene.

The replacement of the unsubstituted amino group in β-iminonitriles (α-amino-β-cyanoethylenes) by anilino groups is normally accomplished (1, 2) by reacting the iminonitrile with the substituted aniline in acetic acid solution. This procedure was found to give variable results when applied to 2-amino-3-cyanoindene, and, in the case of 3-nitroaniline, 3-nitroacetanilide was isolated as the major product. Better results were obtained by heating the iminonitrile and the amine without solvent in the presence of the amine hydrochloride. The superiority of strong acid catalysis is to be expected in this type of nucleophilic addition to α,β-unsaturated systems (3). 2-(3,4-Dichlorobenzylamino)-3-cyanoindene was obtained in 95% yield by heating the iminonitrile and 3,4-dichlorobenzylamine with 5 mole% 3,4-dichlorobenzylamine hydrochloride. The 3,4-dichloroanilino derivative was prepared by simply fusing the iminonitrile with 3,4-dichloroaniline hydrochloride.

Although the action of concentrated sulphuric acid on 2-amino-3-cyanoindene gives 2-amino-3-carboxyindene in good yield (4), similar treatment of 2-(3,4-dichlorobenzylamino)-3-cyanoindene yielded the corresponding amide, 2-(3,4-dichlorobenzylamino)-indene-3-carboxamide, as the only identifiable product. The same amide was unexpectedly obtained when 2-amino-3-carboxyindene was heated with a mixture of 3,4-dichlorobenzylamine and its hydrochloride.

**Report No. 26.*

The infrared spectrum (liquid film) showed no bands in the region from 1500 to 2800 cm^{-1}. The N.M.R. spectrum (neat) showed two peaks at 289 and 459 p.p.10^8 from water with peak areas in the ratio of 3:2 respectively.

In addition to spirohexane the chromatogram of the crude product showed ethanol and an unidentified component for which the peak area was less than 3% of that for spirohexane.

Support for this research was received from the National Research Council of Canada and is gratefully acknowledged.

1. Ya. M. Slobodin and M. V. Blinova. Zhur. Obshcheĭ Khim. **23**, 1994 (1953).
2. D. E. Applequist, G. F. Fanta, and B. W. Henrikson. J. Org. Chem. **23**, 1715 (1958).
3. H. G. Kuivila and W. L. Masterton. J. Am. Chem. Soc. **74**, 4953 (1952).
4. W. M. Schubert and S. M. Leahy, Jr. J. Am. Chem. Soc. **79**, 381 (1957).
5. D. E. Applequist and D. E. McGreer. J. Am. Chem. Soc. **82**, 1965 (1960).
6. D. E. Applequist and J. A. Landgrebe. Personal communication.

Received May 27, 1960.
Department of Chemistry,
University of British Columbia,
Vancouver 8, B.C.

AMINONITRILES. II. SOME DERIVATIVES OF 2-AMINO-3-CYANOINDENE*

D. L. Garmaise and S. Gelblum

As part of a study on the relation between chemical structure and bacteriostatic activity, a series of 2-arylamino- (and aralkylamino)-3-cyanoindenes was prepared from the readily accessible 2-amino-3-cyanoindene.

The replacement of the unsubstituted amino group in β-iminonitriles (α-amino-β-cyanoethylenes) by anilino groups is normally accomplished (1, 2) by reacting the iminonitrile with the substituted aniline in acetic acid solution. This procedure was found to give variable results when applied to 2-amino-3-cyanoindene, and, in the case of 3-nitroaniline, 3-nitroacetanilide was isolated as the major product. Better results were obtained by heating the iminonitrile and the amine without solvent in the presence of the amine hydrochloride. The superiority of strong acid catalysis is to be expected in this type of nucleophilic addition to α,β-unsaturated systems (3). 2-(3,4-Dichlorobenzylamino)-3-cyanoindene was obtained in 95% yield by heating the iminonitrile and 3,4-dichlorobenzylamine with 5 mole% 3,4-dichlorobenzylamine hydrochloride. The 3,4-dichloroanilino derivative was prepared by simply fusing the iminonitrile with 3,4-dichloroaniline hydrochloride.

Although the action of concentrated sulphuric acid on 2-amino-3-cyanoindene gives 2-amino-3-carboxyindene in good yield (4), similar treatment of 2-(3,4-dichlorobenzylamino)-3-cyanoindene yielded the corresponding amide, 2-(3,4-dichlorobenzylamino)-indene-3-carboxamide, as the only identifiable product. The same amide was unexpectedly obtained when 2-amino-3-carboxyindene was heated with a mixture of 3,4-dichlorobenzylamine and its hydrochloride.

**Report No. 26.*

Can. J. Chem. Downloaded from www.nrcresearchpress.com by 210.87.254.40 on 09/05/12
For personal use only.

Hydrogenation of 2-amino-3-carboxyindene with platinum oxide in ethanol at atmospheric pressure proceeded until 4 moles of hydrogen were absorbed. A single isomer of 1-carboxy-2-aminohydrindane, m.p. 171–172° C, was isolated.

2-(3,4-Dichlorobenzylamino)-3-cyanoindene was the only member of the series which showed appreciable bacteriostatic activity. It inhibited the growth of *M. pyogenes* var. *aureus*, *Sarcina lutea*, and *Streptococcus faecalis* at dilutions of 1:320,000, 1:160,000, and 1:40,000, respectively, as determined by the serial dilution tube technique. It was ineffective against Gram-negative organisms.

EXPERIMENTAL*

2-Amino-3-cyanoindene

o-Phenylenediacetonitrile (5) (31.1 g, 0.2 mole) was refluxed with sodium ethoxide (1.0 g, 0.015 mole) in ethanol (130 ml) for 1 hour. The product crystallized on cooling, yield 28.4 g (91%), m.p. 193–194° C (lit. reported m.p. 193° C (4)).

2-(3-Nitroanilino)-3-cyanoindene

A solution of 2-amino-3-cyanoindene (1.56 g, 0.01 mole) and 3-nitroaniline (1.38 g, 0.01 mole) in glacial acetic acid (30 ml) was refluxed for 2 hours. The solution was evaporated to dryness, and the residue was crystallized from dilute acetone to give 3-nitroacetanilide (1.32 g), m.p. 150–151° C, and the product (0.12 g, 4.4%), which melted at 225–226° C, after recrystallization from methanol. Anal. Calc. for $C_{16}H_{10}Cl_2N_2$: C, 63.80; H, 3.35; Cl, 23.54; N, 9.31. Found: C, 63.55; H, 3.35; Cl, 23.52; N, 9.54.

2-(3,4-Dichloroanilino)-3-cyanoindene

2-Amino-3-cyanoindene (1.56 g, 0.01 mole) and 3,4-dichloroaniline hydrochloride (1.98 g, 0.01 mole) were heated at 170–230° C for 25 minutes. Crystallization from ethanol gave the product melting at 200–203° C. Yield 2.27 g (75.5%). The analytical sample, m.p. 203–204° C, was prepared by recrystallization from methanol. Anal. Calc. for $C_{16}H_{10}Cl_2N_2$: C, 63.80; H, 3.35; Cl, 23.54; N, 9.31. Found: C, 63.55; H, 3.35; Cl, 23.52; N, 9.54.

2-(4-Chlorobenzylamino)-3-cyanoindene

A solution of 2-amino-3-cyanoindene (1.56 g, 0.01 mole) and 4-chlorobenzylamine (1.41 g, 0.01 mole) in glacial acetic acid (30 ml) was refluxed for 2 hours. The solution was evaporated to dryness and the residue was crystallized from dilute acetone to give the crude product, m.p. 164–167° C. Yield 1.51 g (54%). Crystallization from methanol raised the melting point to 173–174° C. Anal. Calc. for $C_{17}H_{13}ClN_2$: C, 72.73; H, 4.67; Cl, 12.63; N, 9.98. Found: C, 72.74; H, 5.02; Cl, 12.71; N, 10.15.

2-(3,4-Dichlorobenzylamino)-3-cyanoindene

A mixture of 2-amino-3-cyanoindene (15.6 g, 0.1 mole), 3,4-dichlorobenzylamine (17.4 g, 0.1 mole), and 3,4-dichlorobenzylamine hydrochloride (0.08 g, 0.005 mole) was stirred at 170–200° C for 1 hour. The mixture was cooled and triturated in ethanol (300 ml), giving the product melting at 178–179° C. Yield 30.0 g (95%). The analytical sample melted at 180–181° C after crystallization from dilute acetone. Anal. Calc. for $C_{17}H_{12}Cl_2N_2$: C, 64.77; H, 3.84; Cl, 22.50; N, 8.89. Found: C, 64.86; H, 4.08; Cl, 22.53; N, 8.92.

**All melting points are uncorrected. Microanalyses were performed by Micro-Tech Laboratories, Skokie, Illinois.*

Can. J. Chem. Downloaded from www.nrcresearchpress.com by 210.87.254.40 on 09/05/12
For personal use only.

2-Amino-3-carboxyindene

2-Amino-3-cyanoindene (2.0 g, 0.013 mole) was stirred in concentrated sulphuric acid (20 ml) for 1 hour, during which the temperature rose from 26° C to 35° C. The solution was poured onto crushed ice, and the resulting suspension was allowed to stand for 2 hours. The precipitate was filtered and extracted with 1 *N* sodium hydroxide solution (50 ml). Acidification of the alkaline extract gave the product melting at 186° C (decomp.). Moore and Thorpe (4) reported a melting point of 171° C. Anal. Calc. for $C_{10}H_9NO_2$: C, 68.55; H, 5.18; N, 8.00. Found: C, 68.38; H, 5.37; N, 8.17.

1-Carboxy-2-aminohydrindane

2-Amino-3-carboxyindene (0.485 g, 0.0028 mole) was hydrogenated at atmospheric pressure in ethanol (50 ml) in the presence of platinum oxide (5 mg). A total of 285 ml hydrogen (0.012 mole) was absorbed in 10 hours. The suspension was filtered and evaporated and the residue was crystallized from ethyl acetate (35 ml), giving the completely saturated product, m.p. 171–172° C. Yield 0.12 g (23.4%). Anal. Calc. for $C_{10}H_{17}NO_2$: C, 65.54; H, 9.35; N, 7.64. Found: C, 65.67; H, 9.51; N, 7.73.

A mixture of incompletely hydrogenated products, m.p. 121–123° C, was isolated from the mother liquors.

2-(3,4-Dichlorobenzylamino)-indene-3-carboxamide

I. 2-(3,4-Dichlorobenzylamino)-3-cyanoindene (4.0 g, 0.013 mole) was stirred in concentrated sulphuric acid (50 ml) for 2 hours. The solution was poured onto crushed ice, and the aqueous suspension was allowed to stand for 2 hours. The crude product was filtered and extracted with 1 *N* sodium hydroxide solution (50 ml). Crystallization of the insoluble fraction from methanol gave the pure amide, m.p. 164–165° C. Yield 0.84 g (20%). Anal. Calc. for $C_{17}H_{13}Cl_2NO_2$: C, 61.30; H, 4.24; Cl, 21.20; N, 8.41. Found: C, 61.20; H, 4.36; Cl, 21.04; N, 8.30.

Acidification of the alkaline extract did not yield any identifiable products.

II. 2-Amino-3-carboxyindene (1.0 g, 0.0057 mole), 3,4-dichlorobenzylamine (1.0 g, 0.0057 mole), and 3,4-dichlorobenzylamine hydrochloride (0.02 g, 0.0001 mole) were heated at 175° C for 20 minutes. The mixture was crystallized from ethanol (10 ml), giving the product melting at 164–165° C. Yield 0.90 g (47%). There was no depression on admixture with the product prepared as in I.

ACKNOWLEDGMENT

The authors wish to thank Dr. H. A. Baker, of Ayerst, McKenna and Harrison Limited, for determination of the bacteriostatic activities of these compounds.

1. E. von Meyer. J. prakt. Chem. (2) **78**, 497 (1908).
2. M. Lamant. Compt. rend. **238**, 1591 (1954).
3. C. K. Ingold. Structure and mechanism in organic chemistry. Cornell Univ. Press, Ithaca, New York. 1953. p. 695.
4. C. W. Moore and J. F. Thorpe. J. Chem. Soc. **93**, 165 (1908).
5. J. O. Halford and B. Weissman. J. Org. Chem. **17**, 1646 (1952).

Received May 26, 1960.
L. G. Ryan Research Laboratories,
Monsanto Canada Limited,
LaSalle, Que.

Can. J. Chem. Downloaded from www.nrcresearchpress.com by 210.87.254.40 on 09/05/12
For personal use only.

Can. J. Chem. Downloaded from www.nrcresearchpress.com by 210.87.254.6 on 09/05/12
For personal use only.

Canadian Journal of Chemistry

Issued by THE NATIONAL RESEARCH COUNCIL OF CANADA

VOLUME 38 OCTOBER 1960 NUMBER 10

Symposium on Some Fundamental Aspects of Atomic Reactions

The papers that follow were presented at a symposium held at McGill University, Montreal, on September 6 and 7, 1960, under the auspices of the Physical Chemistry Subject Division of the Chemical Institute of Canada and organized by the chairman of the symposium, Dr. J. C. Polanyi of the University of Toronto. A few of the papers presented are not published here because of prior commitments.

The executive committee of the subject division wishes to express its gratitude to the symposium chairman, to McGill University for its generous co-operation in the use of its facilities, and to the Editor-in-Chief and staff of the Canadian Journal of Chemistry for their valuable assistance.

THE TRANSFER REACTIONS OF HALOGEN ATOMS[1]

G. C. FETTIS, J. H. KNOX, AND A. F. TROTMAN-DICKENSON

ABSTRACT

Extensive results on the reactions of fluorine, chlorine, and bromine atoms with alkanes and with some other molecules have been obtained from the study of competitive halogenations. The comparison of the A factors of the reactions provides an excellent test of the transition state theory. The activation energies of the bromine atom reactions can be combined with measurements of the activation energies for the reactions of alkyl radicals with hydrogen bromide to yield unusually reliable values of bond strengths. Information on the influence of polar effects on the activation energies of atomic reactions can be obtained from results on the reactions of fluorine and chlorine atoms with methyl halides.

The reaction of a halogen with a pair of hydrocarbons can be represented by the following steps:

$$\begin{aligned} X + R^1H &= XH + R^1 \\ R^1 + X_2 &= R^1X + X \end{aligned} \qquad [1]$$

$$\begin{aligned} X + R^2H &= XH + R^2 \\ R^2 + X_2 &= R^2X + X \end{aligned} \qquad [2]$$

In this paper we shall be concerned with the rate constants and Arrhenius factors for reactions [1] and [2] and for those of the reverse processes [−1] and [−2]. The relative values of k_1 and k_2 can be found by competitive methods in two ways. The first is the consumption method in which the amounts of R^1H and R^2H removed from a mixture during reaction with a halogen are determined. Then

$$\frac{k_1}{k_2} = \frac{-d[R^1H]/dt.\ [R^2H]}{-d[R^2H]/dt.\ [R^1H]}.$$

In practice this relation is used in its integrated form and the conversions are kept below about 20–30%. This method was particularly attractive before the development of gas chromatography for it was much simpler to analyze for small quantities of R^1H and R^2H than of the corresponding halides. It was employed by Pritchard, Pyke, and Trotman-Dickenson (1) to study chlorine atom reactions and later by Mercer and Pritchard (2) to study fluorine atoms.

[1]*Contribution from the Chemistry Department, Edinburgh University, Edinburgh 9, Scotland; paper presented at the Symposium on the Fundamental Aspects of Atomic Reactions held at McGill University, Montreal, Que., September 1960.*

The second method depends upon the measurement of the rate of formation of the halides formed. The rate constants are then obtained from

$$\frac{k_1}{k_2} = \frac{d[R^1X]/dt.\ [R^2H]}{d[R^2X]/dt.\ [R^1H]}.$$

The integrated form of the equation need not be used as the percentage conversions should be kept very low to avoid secondary reactions of the halides. Fortunately halides are not more than 10 times as reactive as their parent alkanes. This approach was first used by Hass, McBee, and Weber (3) in their studies of chlorinations. Their work was done on a large scale in flow systems, so that sufficient chlorides were formed for analysis by distillation. They worked at high temperatures. Some isomerization of the chlorides probably occurred so that the results do not agree well with those of later workers. Knox (4) applied gas chromatography to the problem and was able to reduce the scale of reaction by about 10^4 and at the same time improve the accuracy. The method has the great advantage that isomeric products can be distinguished and reactivities directly assigned to specific types of hydrogen atom. The attack on hydrogen is not simply followed because hydrogen halides are not easily determined by gas chromatography and are produced in reactions of all hydrogen-containing compounds.

Relative rate constants obtained by competitive methods can be placed on an absolute scale if the constant for one member of the series can be absolutely determined. Fortunately the rate constant for the attack of a chlorine atom on molecular hydrogen has been determined by three groups of workers whose results are in good agreement. Kistiakowsky and Van Artsdalen have carefully measured the rate of reaction of bromine atoms with methyl bromide and methane (5). No rate constant for a fluorine atom reaction has been measured. In this work it has been assumed that the value of the A factor calculated for the reaction of fluorine atoms with ethane is correct and that the activation energies for attack on hydrocarbons heavier than ethane are zero. The justification for these assumptions will be apparent in what follows.

Table I summarizes the results that have been obtained at Edinburgh, together with

TABLE I

Rate constants, A factors, and activation energies for reactions of the type X + RH = HX + R

	Fluorine atoms (8)			Chlorine atoms (9)			Bromine atoms (10)		
RH	log k (25°)	log A	E	log k (25°)	log A	E	log k (100°)	log A	E
H_2	12.8	14.0	1.71[2]	9.8	13.9	5.50[7]	3.3[5]	13.7	17.5
CH_4	13.1	14.0	1.21	10.6	13.4	3.85[1]	3.3	14.0	18.3
Primary									
C_2H_6	13.5	13.7	0.28	13.2	14.0	1.04[1]	6.1	13.9	13.4
C_3H_8	13.4	13.4	0	13.3	14.0	1.00	—	—	—
n-C_4H_{10}	13.3	13.3	0	13.2	13.9	0.79	—	—	—
iso-C_4H_{10}	13.6	13.6	0	13.5	14.1	0.82	—	—	—
neo-C_5H_{12}	13.7	13.7	0	13.6	14.3	0.92	5.9	14.2	14.3
Secondary									
C_3H_8	13.0	13.0	0	13.3	13.9	0.68	7.7	13.7	10.1
n-C_4H_{10}	13.3	13.3	0	13.8	13.9	0.27	7.2	13.2	10.2
cyclo-C_3H_6	13.4	13.4	0	10.7	13.7	4.1	—	—	—
cyclo-C_4H_8	—	—	—	13.8	14.4	0.83	—	—	—
Tertiary									
iso-C_4H_{10}	12.8	12.8	0	13.2	13.2	0.02	8.9	13.3	7.5

NOTE: A and k are in $cm^3\ mole^{-1}\ sec^{-1}$; E is in kilocalories $mole^{-1}$.

Can. J. Chem. Downloaded from www.nrcresearchpress.com by 210.87.254.6 on 09/05/12
For personal use only.

a few other results of our own and of other workers. The experimental details and a full comparison of the results with the rather small number available from other sources are fully discussed in the original papers to which reference is made. With the notable exception of the bromination results of Van Artsdalen's group the present work is in excellent agreement with the small amount of recent work by other authors. Benson and Buss (6) have discussed at length the probable reasons for the unreliability of the results of Van Artsdalen's very careful work. These results were always suspect because they appeared to be out of line with those for all other atomic reactions.

The A Factors

According to transition state theory the A factor for a bimolecular reaction is given by

$$A = e^2.(kT/h) \exp [(\Delta S^{\ddagger}_{tr} + \Delta S^{\ddagger}_{rot} + \Delta S^{\ddagger}_{vib})/R].$$

The translational entropies of activation can be calculated exactly from the molecular weights of the reactants and complexes. The accuracy of the calculated value of the rotational entropy of activation is limited by the uncertainty of the exact configuration of the complex and, to a lesser degree, of the reactant. The C—H and C—C bond lengths have throughout been assumed to be 1.10 and 1.54 Å except that the half-order bonds $\diagdown$C—H—X$\diagup$ have been taken as 0.18 Å longer than the corresponding single bonds. The two extreme forms of the *n*-butane – halogen complexes in which the molecule is fully extended or completely curled up yield rotational entropies of activation that differ by less than 10%. Since intermediate configurations are much more profitable, it is unlikely that the error arising from assumptions about the configurations are as large as this.

The calculation of the vibrational entropies of activation is less certain and has a greater effect upon the result obtained. It has been assumed that many of the vibrations in RH will be little changed by the addition of the halogen atom and that their contributions to $\Delta S^{\ddagger}_{vib}$ will largely cancel. Only a few vibrations intimately connected with the part of the molecule to which the halogen atom is attached will give rise to important contributions. These vibrations are the C—H stretching and C—H wagging in the hydrocarbon which are replaced by five new vibrations in the activated complex. The C—H stretching becomes the reaction co-ordinate and the C—H wagging becomes the wagging of H—X against the rest of the hydrocarbon. The three additional vibrations are the symmetrical stretching of the C—H—X bonds and the doubly degenerate bending of the C—H—X bonds. Pitzer (11) deduced $\Delta S^{\ddagger}_{vib}$ for the reaction

$$Cl + H_2 = HCl + H$$

from the observed A factor and found that the bending and stretching frequencies were 560 cm^{-1} and 1460 cm^{-1} respectively. It has here been assumed that the force constants for these modes of vibration are the same for all the complexes and that the corresponding frequencies can therefore be calculated by classical mechanics for the different groups, R, and atoms, X.

The calculated and experimental A factors are compared for each type of halogen in Table II. In only one instance does A_{exp} differ from A_{calc} by more than a factor of 4. The transition state theory, therefore, accounts very well for the magnitude of the A factors. Even the deviations from the calculated values show a fairly regular pattern as can be seen by comparing the columns of ratios. This encourages us to think that the experimental results are adequate to sustain the test of a more precise theory if

Can. J. Chem. Downloaded from www.nrcresearchpress.com by 210.87.254.6 on 09/05/12
For personal use only.

TABLE II

A factors for halogen atom reactions

RH	log A_{exp}/A_{calc}		
	F	Cl	Br
H_2	+0.29	+0.01	+0.24
CH_4	+0.24	−0.68	−0.36
Primary C—H bonds			
C_2H_6	0.00*	−0.10	−0.41
C_3H_8	−0.05	+0.25	—
n-C_4H_{10}	−0.03	+0.20	—
iso-C_4H_{10}	+0.04	+0.24	—
neo-C_5H_{12}	+0.06	+0.31	+0.03
Secondary C—H bonds			
C_3H_8	−0.03	+0.52	+0.18
n-C_4H_{10}	+0.08	+0.50	+0.08
cyclo-C_3H_6	−0.17	−0.16	—
cyclo-C_4H_8	—	+0.56	—
Tertiary C—H bonds			
iso-C_4H_{10}	+0.15	+0.41	+0.12

*This value is assumed and the others for fluorine based on it.

one could be found. Since the deviations are more extreme for the heavier halogens, it is likely that the wagging of the H—X bond or the bending of the C—H—X bonds have not been correctly accounted for.

The Activation Energies

The activation energies of the reactions of the higher hydrocarbons with chlorine closely approach zero. It is not surprising that no differences between the activation energies for attack on the higher hydrocarbons by fluorine could be detected. There is probably no energy barrier to attack on these compounds.

The activation energies of the bromine atom reactions vary widely and are of greater interest because of the relation that they bear to the strengths of the bonds broken. The heat of reaction is related to the activation energies for the forward and reverse reactions by the equation

$$\Delta H_1 = E_1 - E_{-1}.$$

Since D(H—Br) is known, D(R^1—H) can be found if E_1 and E_{-1} are measured. At the moment, the values of E_{-1} are not accurately known and consequently the measurements do not yield the bond strengths directly. Until the E_{-1}'s have been determined it is convenient to use the Polanyi relation as a method of interpolation. This leads to the results shown below, which is based on the currently accepted values of D(Me—H) and D(Bu^t—H).

R	E_1	E_{-1}	D(R—H)
Me	18.3	1.8	102.5
Et	13.4	(2.5)	96.9
Pr^i	10.2	(3.1)	93.1
Bu^t	7.5	(3.6)	90.0

Information about E_{-1} can be obtained by photolysing a source of R^1 in a mixture of hydrogen bromide and iodine. The products are then analyzed for RH and RI. Hence

$$\frac{k_{-1}}{k_2} = \frac{R_{R^1H}}{R_{R^1I}} \frac{[I_2]}{[HBr]}$$

Can. J. Chem. Downloaded from www.nrcresearchpress.com by 210.87.254.6 on 09/05/12
For personal use only.

where k_3 refers to

$$R^1 + I_2 = R^1I + I. \quad [3]$$

So far preliminary experiments have been carried out with methyl ethyl ketone as the source of ethyl radicals. Hence we find that

$$E_{-1} - E_3 = 2.3 \text{ kcal mole}^{-1}.$$

It seems likely that the activation energies for the attack of radicals on iodine are very small and may well be zero. The value for ethyl agrees well with that listed above. Further investigations along these lines are clearly required.

Polar Effects

Although bond strengths largely determine the activation energies of the reactions of halogen atoms, polar effects are also important. This has been realized for some years. Recent experiments by Fredricks and Tedder (12) have extended our knowledge. We have attempted to study polar effects in the fluorination, chlorination, and less systematically, in the bromination of halogenated methanes. Fluorination is the most satisfactory because the reactions are so exothermic that the bond strengths are unlikely to be important, and all variations can be ascribed to the polar nature of the activated complexes. The available results are shown in Table III. The first conclusion to be drawn from the table is that more results are needed. The second is that there is little parallelism between the reactivities of the halogenated methanes and the α-hydrogen atoms in the halogenated *n*-butanes.

TABLE III

Relative rate constants for the reactions of halogen atoms with halogenated methanes

	F	Cl	Br
CH_4	1	1	1
CH_3Cl	0.33*	4.9, 0.7†	90, 34†
CH_2Cl_2	0.07*	7.5	—
$CHCl_3$	0.6*	3.9	—
CH_3Br	0.23*	0.3†	14
CH_3F	0.3†	0.9†	10†
Temp., °C	25	100, 146†	100, 146†

*Values obtained at Edinburgh by Dr. R. Foon.
†Reactivities of α-hydrogen atoms in halogenated butanes.

REFERENCES

1. H. O. PRITCHARD, J. B. PYKE, and A. F. TROTMAN-DICKENSON. J. Am. Chem. Soc. **77**, 2629 (1955).
2. P. D. MERCER and H. O. PRITCHARD. J. Phys. Chem. **63**, 1468 (1959).
3. H. B. HASS, E. T. MCBEE, and P. WEBER. Ind. Eng. Chem. **27**, 1190 (1935); **28**, 333 (1936).
4. J. H. KNOX. Chem. & Ind. 1631 (1955).
5. G. B. KISTIAKOWSKY and E. R. VAN ARTSDALEN. J. Chem. Phys. **12**, 479 (1944).
6. S. W. BENSON and J. H. BUSS. J. Chem. Phys. **28**, 301 (1958).
7. P. G. ASHMORE and J. CHANMUGAM. Trans. Faraday Soc. **49**, 254 (1953).
8. G. C. FETTIS, J. H. KNOX, and A. F. TROTMAN-DICKENSON. J. Chem. Soc. 1064 (1960).
9. J. H. KNOX and R. L. NELSON. Trans. Faraday Soc. **55**, 937 (1959).
10. G. C. FETTIS, J. H. KNOX, and A. F. TROTMAN-DICKENSON. Submitted for publication.
11. K. S. PITZER. J. Am. Chem. Soc. **79**, 1804 (1957).
12. P. S. FREDRICKS and J. M. TEDDER. J. Chem. Soc. 144 (1960).

Can. J. Chem. Downloaded from www.nrcresearchpress.com by 210.87.254.6 on 09/05/12
For personal use only.

Can. J. Chem. Downloaded from www.nrcresearchpress.com by 210.87.254.5 on 09/05/12
For personal use only.

SURFACE-CATALYZED ATOM RECOMBINATIONS THAT PRODUCE EXCITED MOLECULES[1]

PAUL HARTECK, ROBERT R. REEVES, AND GENE MANNELLA

ABSTRACT

Various metal surfaces such as nickel, cobalt, copper, and silver give rise to a reddish uminosity in a stream of N- and O-atoms. Spectroscopic and photographic analysis of these glows indicate the formation of electronically excited molecules on the metal surface which diffuse into the gas phase and radiate. Two parallel processes are involved: the formation of an NO($B\,^2\Pi$), which results in NO β radiation, and the formation of an $N_2(A\,^3\Sigma_u^+)$, which, in collision, crosses into the $N_2(B\,^3\Pi_g)$ state and then radiates back to the $A\,^3\Sigma_u^+$, giving the N_2 first positive system. The N_2 first positive system observed here shows the strongest bands from $v' = 8$ and 6; these vibrational levels straddle the $A\,^3\Sigma_u^+$–$B\,^3\Pi_g$ potential energy curve crossing point. This crossing-over of N_2 molecules into the $(B\,^3\Pi_g)$ at this point may explain the observed strong $v' = 6$ transition in normal N-atom recombination if it is assumed that some of the N-atoms recombine into the $A\,^3\Sigma_u^+$ in addition to the $^5\Sigma_g^+$ state.

The N_2 second positive system ($C\,^3\Pi_u \rightarrow B\,^3\Pi_g$) has also been observed over copper in an N- and O-atom stream. This is most surprising since the $N_2(C\,^3\Pi_u)$ has about 1.4 ev more than D_{N_2}.

INTRODUCTION

A program of research in upper atmosphere chemistry has been underway in this laboratory for the past several years. This investigation has centered about the reactions of N-atoms and O-atoms. The results of this study to date have included determinations of the rate coefficients of the following reactions (1, 2, 3).

$$NO + O + M \rightarrow NO_2 + M \quad [1]$$

$$N + N + M \rightarrow N_2 + M \quad [2]$$

$$O + O + M \rightarrow O_2 + M \quad [3]$$

In order to determine the absolute atom concentrations necessary to obtain the rate constant in the second-order reactions [2] and [3], gas-phase titration procedures were developed for each of the atom species. A modified procedure was then developed which permitted the titration of mixed N- and O-atom streams in a single step. During some of the work with mixed N- and O-atom streams, silver foil was used to catalytically recombine the O-atoms, leaving the N-atoms unchanged. It was noticed in this work that a reddish glow appeared adjacent to the silver surface, particularly if the silver had contacted the orthophosphoric acid used to condition the walls of the decay tube. Further investigation showed that the glow was definitely in the gas phase and was not a corona, since it slowly faded out with the afterglows if the discharges were turned off. Further study of this glow showed it to be due to the surface-catalyzed recombination of N- and O-atoms to form electronically excited molecules.

DISCUSSION

It was subsequently discovered that cobalt and nickel also produced the luminosity, but much brighter than over the silver. The glow grew in size with decreasing pressure

[1]*Contribution from the Rensselaer Polytechnic Institute, Troy, New York; paper presented at the Symposium on the Fundamental Aspects of Atomic Reactions held at McGill University, Montreal, Que., September 1960. The research reported in this document has been sponsored by the Geophysics Research Directorate of the Air Force Cambridge Research Center, Air Research and Development Command, under Contract No. AF19(604)-6128.*

and was unaffected by magnetic fields. Spectroscopic analysis showed the first positive system of N_2 and the NO β bands. The mixing of N- and O-atom streams had been observed to produce the same band systems by the gas-phase reactions

$$N(^4S) + N(^4S) + M \rightarrow N_2(^5\Sigma_g^+) + M \quad [2a]$$

$$N_2(^5\Sigma_g^+) \rightarrow N_2(B\ ^3\Pi_g)_{v=12} \quad [2b]$$

$$N_2(B\ ^3\Pi_g) \rightarrow N_2(A\ ^3\Sigma_u^+) + h\nu \text{ (1st positive)} \quad [2c]$$

and

$$N(^4S) + O(^3P) + M \rightarrow NO(B\ ^2\Pi) + M \quad [4]$$

$$NO(B\ ^2\Pi) \rightarrow NO(X\ ^2\Pi) + h\nu\ (\beta \text{ bands}) \quad [4a]$$

However, several important differences were apparent in the spectral analysis of the glows produced over the metals. The radiation from [2*c*] showed the strongest transitions to be from $v' = 12, 11, 10 \ldots$ The spectrum of the glow showed the most intense bands to be from $v' = 8$ and 6. Also, the mixing of N- and O-atom streams is observed to produce NO γ bands in addition to the β bands. No γ bands were observable on our plates.

Thus, it was apparent that the metal surface was catalytically recombining atoms into an electronically excited state. This molecule, instead of giving its energy of excitation and coming off the surface in the ground state, was actually diffusing into the gas phase and radiating. Since both N- and O-atoms appeared necessary to produce the glow, it was postulated that the primary molecule being formed was the $NO(B\ ^2\Pi)$. This species could be formed on the metal surface, diffuse into the gas phase, and then radiate or react with an N-atom to form $N_2(B\ ^3\Pi_g)$, which then radiated. The early work done on nickel produced glows which were several millimeters thick and the lifetime estimated from the diffusion distance was not inconsistent with the available estimates of the lifetime of the $NO(B\ ^2\Pi)$. However, cobalt produced a very enhanced glow at 1 mm pressure, which was 10–15 mm thick and which required only a very small amount of O-atoms. Photographic analysis of this glow using red and blue filters showed two parallel radiations: an intense blue extending only a few millimeters into the gas phase, and a red which extended very far out into the gas phase and which showed an unsymmetry due to the flowing stream which was not visible to the unaided eye. When nickel was used, a strong blue was evident and only a medium red; when cobalt was used, practically no blue appeared but the red was very large.

From these results it was concluded that two parallel processes were occurring on the surface. One involved the formation of $NO(B\ ^2\Pi)$ via [4]. This molecule leaves the surface and goes into the gas phase where it radiates. The thickness of the blue radiation is in excellent agreement with the diffusion distance calculated using the lifetime of 10^{-6} sec recently reported in the literature (4).

The second process occurring must involve the formation of an excited N_2 as the primary product. It is possible to explain the strong radiation from $v' = 8$ and 6 and the long lifetime of the species responsible for the glow by assuming that an $N_2(A\ ^3\Sigma_u^+)$ is formed on the surface. (In the case of cobalt, the small amount of O-atoms necessary to enhance the glow are probably required to condition the metal surface and permit the absorbed N-atoms which eventually form the excited molecule to be attached with an electron volt or less.) The $N_2(A\ ^3\Sigma_u^+)$ and $(B\ ^3\Pi_g)$ potential energy curves cross at

Can. J. Chem. Downloaded from www.nrcresearchpress.com by 210.87.254.5 on 09/05/12
For personal use only.

about 8.5–9.0 ev or $v' = 8$–6. The metastable $N_2(A\ ^3\Sigma_u^+)$, which is the upper level of the well-known Vegard–Kaplan system, forms on the metal surface, diffuses into the gas phase and, by collision, crosses into the $(B\ ^3\Pi_g)$ state. This crossing-over would be at $v' = 8$–6 and the $N_2(B\ ^3\Pi_g)$ would immediately radiate back to the $(A\ ^3\Sigma_u^+)$. The lifetime of the species responsible for the red glow as calculated both from the diffusion distances and the linear velocity of the gas stream and the unsymmetry of the glow is about 10^{-3} sec. This would represent the time required by the $N_2(A\ ^3\Sigma_u^+)$ to relax vibrationally to the crossing point and by collision cross into the $(B\ ^3\Pi_g)$ state. Since the radiative lifetime of the $(A\ ^3\Sigma_u^+)$ is reported to be at least 10^{-2} sec (5), the time interval of 10^{-3} sec is sufficient for any necessary relaxation and the crossing-over to occur.

The $N_2(A\ ^3\Sigma_u^+)$–$(B\ ^3\Pi_g)$ crossing may have another interesting ramification in the presently accepted theory on N-atom recombination as outlined in [2*a*], [2*b*], and [2*c*] (6, 7). This theory postulates the $N_2(^5\Sigma_g^+)$–$(B\ ^3\Pi_g)$ crossing to be at $v' = 12$ and is supported by observations that bands from $v' = 12$, 11, and 10 are the most intense and the transition from $v' = 13$ is never observed in the nitrogen afterglow. However, an unusually intense band from $v' = 6$ has been discussed by several authors (8, 9). No really conclusive explanation has ever been offered for this observation. It is suggested that the lower levels of the $(B\ ^3\Pi_g)$ are populated by an analogous mechanism via the formation of a certain percentage of $(A\ ^3\Sigma_u^+)$ molecules in normal N-atom recombination.

From the observations and comparison of glows over cobalt and nickel, it appears that cobalt favors the formation of $N_2(A\ ^3\Sigma_u^+)$, while nickel favors the $NO(B\ ^2\Pi)$. The glows over nickel always appear a little bluish to the eye. In the case of $N_2(A\ ^3\Sigma_u^+)$ formation on the surface of cobalt, the reaction

$$N_2(A\ ^3\Sigma_u^+) + O\ ^3P \rightarrow NO(B\ ^2\Pi) + N(^4S) \qquad [5]$$

could account for some of the small amount of blue observed over cobalt. The $NO(B\ ^2\Pi)$ over nickel could similarly react,

$$NO(B\ ^2\Pi) + N(^4S) \rightarrow N_2(B\ ^3\Pi_g) + O(^3P), \qquad [6]$$

accounting for some of the first positive bands there. To what extent these exchange reactions occur is not known at the present.

A red glow with N- and O-atoms similar to those produced over silver, nickel, and cobalt has also been produced over copper, although it has been reported in the literature that electrolytically deposited copper can be used to extinguish the nitrogen afterglow (10, 11). The copper surface is slightly attacked. However, if the copper is maintained at approximately 15–20° C in a stream of N-atoms alone, the blue glow of the second positive system of nitrogen appears $(C\ ^3\Pi_u \rightarrow B\ ^3\Pi_g)$. This blue glow is less intense than the red glows observed earlier and extends about 2 mm into the gas phase. Transitions from the $(C\ ^3\Pi_u)$ state are indeed very striking, since the excitation of this level is about 11.2 ev, compared with D_{N_2}, which is only 9.76 ev. The mechanism for such a reaction must then necessarily involve three atoms or two excited species.

CONCLUSIONS

Surface-catalyzed excitation of N- and O-atoms can give rise to a number of excited species. What we originally believed to be a rather singular effect must now include the formation of $NO(B\ ^2\Pi)$, $N_2(A\ ^3\Sigma_u^+)$, and even $N_2(C\ ^3\Pi_u)$. We believe that this is the first recognition of this effect.

Can. J. Chem. Downloaded from www.nrcresearchpress.com by 210.87.254.5 on 09/05/12
For personal use only.

REFERENCES

1. P. HARTECK, R. R. REEVES, and G. MANNELLA. J. Chem. Phys. **29**, 1333 (1958).
2. P. HARTECK, R. R. REEVES, and G. MANNELLA. J. Chem. Phys. **29**, 608 (1958).
3. R. R. REEVES, G. MANNELLA, and P. HARTECK. J. Chem. Phys. **32**, 946 (1960).
4. J. C. KECK *et al.* Ann. Phys. (N.Y.), **7**, 1 (1959).
5. W. LICHTEN. J. Chem. Phys. **26**, 306 (1957).
6. J. BERKOWITZ, W. A. CHUPKA, and G. B. KISTIAKOWSKY. J. Chem. Phys. **25**, 457 (1956).
7. A. G. GAYDON. Dissociation energies. Dover, New York. 1950.
8. O. OLDENBERG. Phys. Rev. **90**, 727 (1953).
9. G. CARIO and J. KAPLAN. Z. Physik, **58**, 769 (1920).
10. RAYLEIGH. Proc. Roy. Soc. A, **85**, 219 (1911).
11. E. J. B. WILLEY. J. Chem. Soc. 2188 (1927).

Can. J. Chem. Downloaded from www.nrcresearchpress.com by 210.87.254.5 on 09/05/12
For personal use only.

Can. J. Chem. Downloaded from www.nrcresearchpress.com by 210.87.254.5 on 09/05/12
For personal use only.

ON THE EXCITATION OF THE EMISSION SPECTRUM OF NCO IN SOLID MATRICES CONDENSED AT 4° K[1]

R. W. NICHOLLS[2] AND S. L. N. G. KRISHNAMACHARI[3]

ABSTRACT

Seventeen broad (~50 Å wide) spectral features have been excited in emission between 3000 Å and 4600 Å in the products of a microwave discharge through N_2 deposited on a cold (4° K) surface on which the discharge products of CO + N_2 had been previously condensed. The features which lie between 3650 Å and 4470 Å show close agreement with those observed in absorption by Dixon during the flash photolysis of NCO and assigned to the $A\ ^2\Sigma$–$X\ ^2\Pi_i$ transition. It therefore seems likely that the emission features arise from NCO also as a result of the reaction

$$N(^2P) + CO(X\ ^1\Sigma^+) \rightarrow NCO \begin{cases} A\ ^2\Sigma^+ \\ B\ ^2\Pi_i \end{cases}$$

at the solid surface.

1. INTRODUCTION

During the past few years, extensive spectroscopic studies have been made upon the luminosities arising from solids condensed between 1° K and 80° K from the products of microwave discharges maintained in a variety of gases, but mostly in N_2, A, O_2, and mixtures of them (1, 2, 3, 4, 5). Much of the work has been carried out with N_2–A mixtures (sometimes including a small oxygen impurity) (3, 5) and the spectra in these cases consisted almost entirely of atomic features of NI and OI and specific band systems of N_2, O_2, NO, and NO_2. Nearly all of the spectral features so far identified arise from transitions which, in the gas phase at least, are relatively forbidden (e.g. the "α" (^2D–^4S), and "μ" (^2P–^4S) features of NI; the "β" (^1S–^1D) feature of OI; the Vegard–Kaplan ($A\ ^3\Sigma_u^+$–$X\ ^1\Sigma_g^+$) system of N_2; the Herzberg ($A\ ^3\Sigma^+$–$X\ ^3\Sigma_g^-$) system of O_2; and the "M" ($^4\Pi$–$^2\Pi$) system of NO). Some allowed transitions (e.g. NO β ($B\ ^2\Pi$–$X\ ^2\Pi$); NO γ ($A\ ^2E$–$X\ ^2\Pi$) systems) have been reported (3). In general, however, the forbidden transitions predominate in the spectra of the solids because short-lived excited species decay radiatively during transit between the discharge and the cooled surface, while the longer lived metastable excited species are deposited and isolated from radiationless de-excitation influences before they can loose their energy.

It has therefore been thought worth while to attempt to excite forbidden transitions of other molecules, particularly those containing carbon, and also to attempt to excite in emission the spectra of polyatomic species. Most of the work on polyatomic spectra of low temperature solid matrices has so far been in absorption (6) although the "B" bands of NO_2 have been recognized in emission for some time.

This paper therefore describes some experiments with discharged N_2 + CO and the conditions under which NCO may be excited in the condensed solid. A subsequent paper (7) will discuss conditions under which CO_2^+ spectra can be excited.

The electronic spectrum of NCO was first observed in emission at low dispersion both in fluorescence from, and in discharges through, C_2H_5NCO, and later in absorption at much higher dispersion by flash photolysis of the same compound (8). Subsequent high dispersion studies by Dixon (9), of the absorption spectrum arising from flash photolysis of HNCO, lead to definitive identifications and rotational analysis of bands of the

[1]*Contribution from the National Bureau of Standards, Washington, D.C.; paper presented at the Symposium on the Fundamental Aspects of Atomic Reactions held at McGill University, Montreal, Que., September 1960.*
[2]*Temporarily on leave of absence from The University of Western Ontario, London, Ontario.*
[3]*Temporarily on leave of absence from the Indian Atomic Energy Laboratories, Bombay.*

$A\ ^2\Sigma^+$–$X\ ^2\Pi_i$ transition between 3603 Å and 4484 Å. Dixon (10) has recently analyzed bands of the $B\ ^2\Pi_i$–$X\ ^2\Pi_i$ transition between 2650 Å and 3200 Å using the same technique. Robinson and McCarty (11) have also reported identification of one strong absorption feature (at 4400 Å) of NCO in a low temperature solid condensed at 4.2° K from a discharge through N_2, O_2, and CH_4.

2. EXPERIMENTAL PROCEDURE AND RESULTS

Our experiments were carried out in a pyrex dewar flask, which has been described by Schoen *et al.* (12), in which the bottom of the central liquid helium container was a wedge-shaped "finger" on which the deposits were formed. All of the helium container except the terminal finger was protected against thermal radiation by a concentric cylindrical pyrex shield which contained liquid nitrogen. N_2 and CO gas flows were individually controlled by needle valves and were measured by floating ball flowmeters. The gas mixture was passed through a 2450 Mc/sec microwave discharge maintained at a few millimeters of pressure, and the discharge products flowed upwards through a "Wood" type light trap onto the liquid helium cooled finger. Prior to starting the discharge, the space around the finger was maintained at a vacuum of better than 10^{-6} mm Hg. During deposition it is believed that the pressure does not rise above 1 micron Hg.

The solid deposit formed on the pyrex finger exhibited a feeble blue luminescence over a wide range of N_2:CO mixtures. Its spectrum appears to be CO_2^+ and will be described elsewhere (7). After the solid condensed from the mixed gas stream had been built up for a few minutes, the CO flow was stopped and the deposition of discharged N_2 was continued. A marked surface color change from blue to bright yellow occurred in the luminescence from the deposit and the spectrum was easily recorded in a few minutes exposure of Kodak 103-F emulsion in a Hilger F/4 quartz spectrograph.

A typical spectrum is shown in Fig. 1 together with a mercury arc calibration. The spectrum consists of the atomic features "μ" (^2P–^4S) of NI at 3478 Å, "α" (^2D–^4S) of NI at 5228 Å, "β" (^1S–^1D) of OI at 5549 Å together with 18 broad (50 Å) features between 3000 Å and 4600 Å. Fifteen of these features (3206 Å–4600 Å) are relatively strong and three (3000 Å–3206 Å) are extremely weak. The wavelengths of the bands including their widths and estimates of intensity on a scale of 0 to 5 are given in Table I, and,

TABLE I

Wavelengths and identification

Wavelength range (Å) and eye estimate intensities on a scale of 0–5	NCO band-head wavelengths (Å) and eye estimate intensities on a scale of 0–100 (9, 10)	Transition (9, 10)	Comments
3000–3015 (0)			CO_2^+
3075–3090 (0)			
3140–3165 (0)	3150 (strong) 3148	$B\ ^2\Pi_i$–$X\ ^2\Pi_i$ (0,0,0–0,0,0)	See (10)
3206–3230 (1)			
3240–3250 (2)			CO_2^+
3270–3305 (2)		All following transitions	
3335–3380 (3)		are $A\ ^2\Sigma$–$X\ ^2\Pi_i$	
3410–3460 (3)			
3480–3500 (4)			CO_2^+; NI (μ)
3500–3545 (4)			
3570–3630 (5)			Weak (<5) $A\ ^2\Sigma$–$X\ ^2\Pi_i$ feature 3603–3630 Å

Can. J. Chem. Downloaded from www.nrcresearchpress.com by 210.87.254.5 on 09/05/12
For personal use only.

TABLE I (*concluded*)

Wavelength range (Å) and eye estimate intensities on a scale of 0–5	NCO band-head wavelengths (Å) and eye estimate intensities on a scale of 0–100 (9, 10)	Transition (9, 10)	Comments
3650–3710 (5)	3642 (20)	$0,0^0,2\ ^2\Sigma^+–0,0^1,0\ ^2\Pi_i$	
	3655 (10)	$0,0^0,2\ ^2\Sigma^+–0,0^1,0\ ^2\Pi_i$	
3750–3800 (4)	3733 (15)	$0,2^0,1\ ^2\Sigma^+–0,0^1,0\ ^2\Pi_i$	
	3786 (15)	$1,0^0,1\ ^2\Sigma^+–0,0^1,0\ ^2\Pi_i$	
	3787 (10)	$0,2^0,1\ ^2\Sigma^+–0,0^1,0\ ^2\Pi_i$	
	3800 (10)	$1,0^0,1\ ^2\Sigma^+–0,0^1,0\ ^2\Pi_i$	
3800–3830 (5)			CO^+_2
3860–3920 (5)	3927 (5)	$1,2^0,0\ ^2\Sigma^+–0,0^1,0\ ^2\Pi_i$	Weak (<5) $A\ ^2\Sigma–X\ ^2\Pi_i$ bands 3874–3907 Å
3940–4025 (4)	3949 (5)	$0,1^1,1\ ^2\Pi–0,1^0,0\ ^2\Sigma^+$	
	3956 (20)	$0,1^1,1\ ^2\Pi–0,1^2,0\ ^2\Delta_i$	
	3971 (15)		
	3977 (40)	$0,1^1,1\ ^2\Pi–0,1^2,0\ ^2\Delta_i$	
	3981 (10)	$0,0^0,1\ ^2\Sigma–0,0^1,0\ ^2\Pi_i$	
	3993 (40)	$0,0^0,1\ ^2\Sigma–0,0^1,0\ ^2\Pi_i$	
4080–4120 (3)	4099 (5)	$0,3^1,0\ ^2\Pi–0,1^0,0\ ^2\Sigma^+$	
	4106 (10)	$0,3^1,0\ ^2\Pi–0,1^2,0\ ^2\Delta_i$	
	4122.6 (10)	$1,1^1,0\ ^2\Pi–0,1^0,0\ ^2\Sigma^+$	
	4122.7 (10)	$0,3^1,0\ ^2\Pi–0,1^2,0\ ^2\Delta_i$	
	4128 (5)	$1,1^1,0\ ^2\Pi–0,1^2,0\ ^2\Delta_i$	No comparable features observed in solid spectrum
	4134.6 (30)	$0,2^0,0\ ^2\Sigma^+–0,0^1,0\ ^2\Pi_i$	
	4137 (10)	$0,2^0,0\ ^2\Sigma^+–0,0^1,0\ ^2\Pi_i$	
4145–4180 (1)	4144 (5)	$1,1^1,0\ ^2\Pi–0,1^2,0\ ^2\Delta_i$	
	4150.1 (30)	$1,0^0,0\ ^2\Sigma^+–0,0^1,0\ ^2\Pi_i$	
	4150.25 (30)	$0,2^0,0\ ^2\Sigma^+–0,0^1,0\ ^2\Pi_i$	
	4154 (10)	$1,0^0,0\ ^2\Sigma^+–0,0^1,0\ ^2\Pi_i$	
	4167 (30)	$1,0^0,0\ ^2\Sigma^+–0,0^1,0\ ^2\Pi_i$	
4180–4220 (1)			CO^+_2
4275–4370 (2)	4257 (10)	$0,1^1,0\ ^2\Pi–0,0^1,0\ ^2\Pi_i$	
	4275 (10)	$0,1^1,0\ ^2\Pi–0,0^1,0\ ^2\Pi_i$	
	4328 (5)	$0,2^2,0\ ^2\Delta–0,2^3,0\ ^2\phi_i$	
	4348 (30)	$0,1^1,0\ ^2\Pi–0,1^0,0\ ^2\Sigma^+$	
	4350 (20)	$0,1^1,0\ ^2\Pi–0,1^0,0\ ^2\Sigma^+$	
	4351 (10)	$0,1^1,0\ ^2\Pi–0,1^0,0\ ^2\Sigma^+$	
	4357 (30)	$0,1^1,0\ ^2\Pi–0,1^2,0\ ^2\Delta_i$	
	4361 (5)	$0,1^1,0\ ^2\Pi–0,1^2,0\ ^2\Delta_i$	
	4375 (30)	$0,1^1,0\ ^2\Pi–0,1^2,0\ ^2\Delta_i$	
	4385 (100)	$0,0^0,0\ ^2\Sigma^+–0,0^1,0\ ^2\Pi_i$	
4400–4470 (1)	4389 (30)	$0,0^0,0\ ^2\Sigma^+–0,0^1,0\ ^2\Pi_i$	
	4404 (100)	$0,0^0,0\ ^2\Sigma^+–0,0^1,0\ ^2\Pi_i$	
	4409 (10)	$0,0^0,0\ ^2\Sigma^+–0,0^1,0\ ^2\Pi_i$	
4560–4600 (1)			

as is discussed below, there are good reasons for thinking that 17 of the bands are due to NCO. Owing to the diffuseness of the features there is perhaps a 10 Å uncertainty in the wavelengths.

DISCUSSION

Dixon's band-head wavelengths, transition assignments, and rough intensity estimates for the NCO $A\ ^2\Sigma^+–X\ ^2\Pi_i$ system are also given in Table I grouped for ease of comparison with our features. He used an intensity scale of 0 to 100 and we have only included bands with intensities greater than 5. Not only is a very strong correlation seen

Can. J. Chem. Downloaded from www.nrcresearchpress.com by 210.87.254.5 on 09/05/12
For personal use only.

Can. J. Chem. Downloaded from www.nrcresearchpress.com by 210.87.254.5 on 09/05/12
For personal use only.

PLATE I

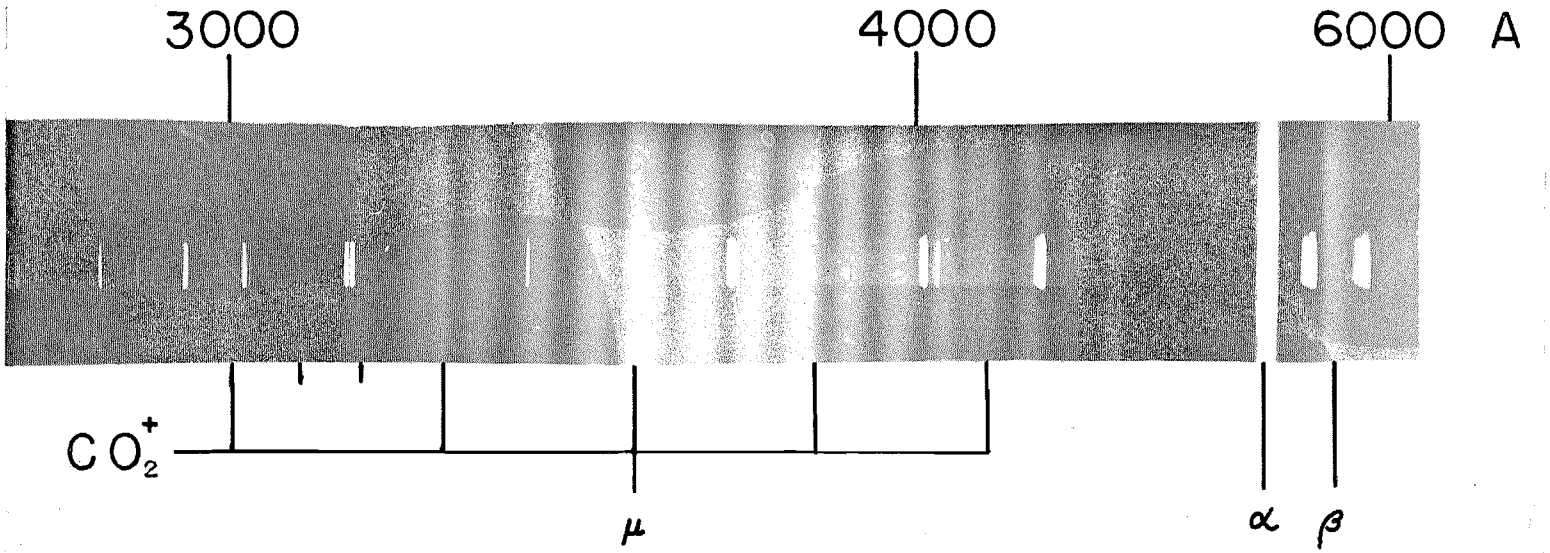


FIG. 1. Spectrum of luminosity arising from the action of discharged nitrogen on CO at 4° K.

in Table I between groups of Dixon's band heads and each of our features between 3650 Å and 4470 Å, but there is also good correlation between the spaces between our features and the regions where Dixon records absence of bands or very weak bands.

On this basis it seems very plausible to assign not only those of our features with which there is a strong correlation with those of Dixon to overlaps of strong NCO bands but also to assign those which lie between 3000 Å and 3630 Å and between 4560 Å and 4600 Å (which lie outside the range reported in absorption) to the same emitter.

Each of our features undoubtedly arises from the overlap of a number of adjacent bands whose rotational structure is not very extensive at the low temperature of the source. It will be observed in Fig. 1 that all or part of each of five features has been assigned to bands of CO_2^+. These assignments derive from experiments referred to above (7) on the spectra of condensed discharged CO + N_2. One CO_2^+ feature in Fig. 1 is also assigned in part to "μ" of NI. The three features between 3000 Å and 3165 Å are extremely weak and there is a possibility that there is a contribution to them from bands of the $B\,^2\Pi_i$–$X\,^2\Pi_i$ system of NCO reported by Dixon (10) to lie between 2677 Å and 3167 Å. In particular the 3140–3165 feature may be the strong 000–000 transition of this system. Alternatively these bands may be a continuation of the $A\,^2\Sigma$–$X\,^2\Pi_i$ system.

While the flash photolysis experiments involve the decomposition of HNCO into fragments, the mechanism operative in our experiments is almost certainly one of synthesis of NCO [either in the gas phase near the cold finger (no NCO spectrum is seen from the discharge itself), or as is more likely, on the surface of the cold finger itself]. This surface was prepared by deposition of discharged CO + N_2 and will therefore have a high concentration of ground state ($X\,^1\Sigma^+$) CO molecules on it. The surface was then treated with the discharge products of N_2, a significant number of which are N atoms in ^2P, ^2D, and ^4S (ground) states as is shown by the presence of "α" and "μ" in the spectra. Thus N + CO collisions occur at the surface. Dixon has pointed out (9) that

$$N(^2D) + CO(X\,^1\Sigma^+) \rightarrow NCO(X\,^2\Pi) \qquad [1]$$

and

$$N(^2P) + CO(X\,^1\Sigma^+) \rightarrow NCO\begin{cases} A\,^2\Sigma^+ \\ B\,^2\Pi_i \end{cases} \qquad [2]$$

are energetically possible and plausible processes. Before collision, the CO molecules were most probably in the $v = 0$ level, but the N atoms will collide with the kinetic energy of the discharge ($T \sim 300$–$400°$ K). NCO can therefore be formed in excited vibrational levels such as is required by the identifications of Table I. It may be remarked in passing that the possibility of forming NCO ($B\,^2\Pi_i$) by equation [2] makes reasonably plausible the possible assignment of our 3140–3165 feature to the strong (000–000) transition of the $B\,^2\Pi$–$X\,^2\Sigma$ transition.

It should not be overlooked that it may also be possible to form CON and CNO in the collision mechanism (equation [2]) and with our experimental arrangement. Further work on these possibilities is in progress.

ACKNOWLEDGMENTS

We should like to acknowledge the valuable technical assistance of Mr. G. E. Beale, Jr. One of us (S. L. N. G. K.) acknowledges the award of an I. C. A. fellowship during the tenure of which this work was performed.

Can. J. Chem. Downloaded from www.nrcresearchpress.com by 210.87.254.5 on 09/05/12
For personal use only.

REFERENCES

1. A. Bass and H. P. Broida. The trapping of free radicals at low temperatures. Academic Press, Inc., New York. 1960.
2. A. Bass and H. P. Broida. Phys. Rev. **101**, 1740 (1956).
3. M. Peyron and H. P. Broida. J. Chem. Phys. **30**, 139 (1959).
4. M. Peyron, I. Hörl, H. Brown, and H. P. Broida. J. Chem. Phys. **30**, 1304 (1959).
5. H. P. Broida and M. Peyron. J. Chem. Phys. **32**, 1068 (1960).
6. D. A. Ramsay. Optical spectroscopy of free radicals. 1960. p. 169. Ref. 1.
7. S. L. N. G. Krisnamachari and R. W. Nicholls. To be published. 1960.
8. R. Holland, D. W. G. Style, R. N. Dixon, and D. A. Ramsay. Nature, **182**, 336 (1958).
9. R. N. Dixon. Phil. Trans. Roy. Soc. A, **252**, 165 (1960).
10. R. N. Dixon. Can. J. Phys. **38**, 10 (1960).
11. M. McCarty, Jr. and G. W. Robinson. J. chim. phys. **56**, 721 (1959).
12. L. J. Schoen, L. E. Kuentzel, and H. P. Broida. Rev. Sci. Instr. **29**, 633 (1958).

Can. J. Chem. Downloaded from www.nrcresearchpress.com by 210.87.254.5 on 09/05/12
For personal use only.

Can. J. Chem. Downloaded from www.nrcresearchpress.com by 210.87.254.42 on 09/05/12
For personal use only.

ABSOLUTE RATE MEASUREMENTS OF O-ATOM REACTIONS WITH ETHYLENE AND WITH BUTANE[1]

L. Elias and H. I. Schiff

ABSTRACT

The absolute rate constants for the primary reactions of O-atoms with ethylene and with butane have been determined in a fast-flow system. The O-atoms were produced by electrodeless discharge of O_2 and allowed to react with the hydrocarbon introduced downstream. Addition of a small amount of NO to the gas stream enabled a photometric monitoring of the O-atoms in the reaction zone. The initial atom concentration was determined by NO_2 titration. The reaction could be stopped at any point in the reaction zone by means of a movable surface of cobalt oxide. The hydrocarbon concentration at any point could then be determined by condensation downstream and analysis of the products.

Rate measurements were carried out over the temperature range $-50°$ to $200°$ C. The rates were found to be consistent with a two-body mechanism. For O-atoms with ethylene,

$$k = 1.8(\pm 0.6)\times 10^{-11}\, e^{-1600/RT}\ \text{cm}^3\ \text{molecule}^{-1}\ \text{sec}^{-1}$$

and for O-atoms with butane,

$$k = 5.0(\pm 1.6)\times 10^{-11}\, e^{-4200/RT}\ \text{cm}^3\ \text{molecule}^{-1}\ \text{sec}^{-1}.$$

INTRODUCTION

Cvetanović has recently measured relative rate constants for the reactions of oxygen atoms with a series of olefins (1). This study enabled him to make interesting deductions about the effect of structure on the rates and mechanisms of these reactions. Absolute rate constants were estimated by comparison with the value for the reaction $O + NO_2$ reported by Ford and Endow (2), which was, in turn, based on the rate constant for the reaction $O + O_2 + M$, obtained by Benson and Axworthy (3) from their mechanism for the thermal decomposition of ozone.

Notwithstanding the high caliber of the work of these authors, it seemed desirable to measure the absolute value of the rate constant directly for one of these olefin reactions. It also seemed important to determine its activation energy and steric factor, since such data are virtually non-existent.

The present paper reports the measurement of the absolute rate constant and its temperature dependence for the reaction of O-atoms with ethylene. For comparison purposes, similar measurements were also obtained for the reaction of O-atoms with *n*-butane.

Principle of the Method

The rate constant of interest is that of the initial attack of an O-atom on an olefin molecule. The subsequent reactions are complicated and lead to a variety of products which depend on the ratio of atomic to molecular oxygen. Cvetanović has found, however, that the presence of molecular oxygen does not affect the rate of consumption of the olefin (4), which indicates that the initial O-atom attack is rate-determining. Consequently, no attempt was made in this work at a detailed product analysis.

[1]*Contribution from the Upper Atmosphere Chemistry Group, Physical Chemistry Laboratory, McGill University, Montreal, Que.; paper presented at the Symposium on the Fundamental Aspects of Atomic Reactions, held at McGill University, Montreal, Que., September 1960. This work has been supported in part by the Air Force Cambridge Research Center under Contract No. AF19(604)-4104, and in part by the Defence Research Board of Canada.*

The rate of disappearance of hydrocarbon can then be represented by a simple bimolecular equation,

$$[1] \qquad -\frac{d[\mathrm{RH}]}{dt} = k[\mathrm{O}][\mathrm{RH}].$$

Integration of this equation between reaction time limits t_1 and t_2 gives

$$[2] \qquad \ln\frac{[\mathrm{RH}]_1}{[\mathrm{RH}]_2} = k\int_{t_1}^{t_2}[\mathrm{O}]dt.$$

As a result of secondary reactions, [O] will be a complex function of time. However, in a well-defined flow system, time can be related to distance. [O] can then be measured along the length of the reaction vessel and the integral evaluated graphically. The rate constant is then obtained from the measurement of [RH] at times t_1 and t_2 and the value of the integral in that time interval.

The only assumptions involved in this method for determining k are that RH is neither reformed nor consumed in the secondary reactions. It is extremely unlikely that RH will be the product of any reaction of radicals resulting from the attack of O-atoms on the hydrocarbon. The radicals are also much more likely to react with O_2, which is present in large excess, than with the parent hydrocarbon. The validity of these assumptions, as well as the independence of the rates on $[O_2]$, is attested to by the good agreement of the relative rate constants for butane and ethylene obtained in this work with that obtained by Cvetanović (4) using a completely different technique, and in the absence of O_2.

EXPERIMENTAL

Apparatus

A conventional fast-flow system was used which incorporated the usual arrangement of fine-control needle valves and calibrated flowmeters. Molecular oxygen was dissociated to the extent of a few per cent by a microwave discharge in the manner described previously (5). Precautions were taken to exclude mercury vapor from the apparatus. The discharge tube was connected to the reaction vessel represented in Fig. 1. The latter consisted of a pyrex tube 16 mm i.d. and 30 cm long, surrounded by an outer jacket through which tap water could be flowed. The reaction vessel was thermostatted at higher temperatures by the vapors of appropriate liquids boiling in a flask attached to the apparatus at F and refluxing in a condenser attached at C. To achieve temperatures below 20° C, the outer jacket was replaced by a double-walled vacuum jacket, open at the top, into which could be placed suitable mixtures of ethanol and powdered dry ice.

A movable coil of platinum wire D_1, coated with cobalt oxide, served to remove all the atoms from the gas stream (5). It was mounted on a glass rod which could be moved axially along the reaction tube by rotation of the tygon-covered rod T, which pressed against it. This device was used to stop the reaction at selected positions, and thereby permitted an accurate control of the reaction time.

D_2 was a similar movable coil of copper wire (a less efficient catalyst for O-atom recombination) which was used to decrease the oxygen atom concentration by lowering it into the gas stream.

The hydrocarbon was introduced through the multiple jet J_1, which consisted of a small bulb in which five equally spaced small holes were blown in a plane transverse to the direction of the oxygen stream.

Can. J. Chem. Downloaded from www.nrcresearchpress.com by 210.87.254.42 on 09/05/12
For personal use only.

Can. J. Chem. Downloaded from www.nrcresearchpress.com by 210.87.254.42 on 09/05/12
For personal use only.

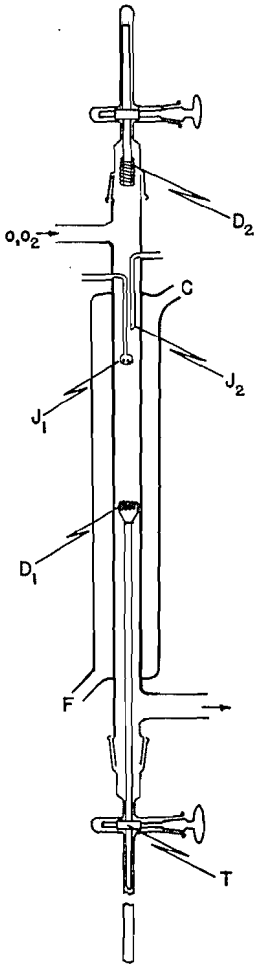


FIG. 1. Reaction vessel.

Materials

Linde tank oxygen rated to contain less than 0.1% N_2 was used without further purification. Matheson reagent grade ethylene and butane were 'trap-to-trap' distilled before use. Nitric oxide, also a Matheson product, was freed of NO_2 by passage through Caroxite, a commercial CO_2 absorbent. NO_2 was prepared by addition of O_2 to NO and stored with a small excess of O_2.

O-*Atom Measurement*

In previous studies in this laboratory (5, 6), O-atom concentrations were measured with an isothermal calorimeter. This technique could not be used in the present study, since preliminary experiments indicated that species produced in the secondary reactions liberated heat to the calorimeter. Consequently, a small amount of NO was added to the gas stream through J_2, and the resulting light emission used to monitor the O-atom concentration along the reaction tube. The change in [O] with time was measured photometrically in the manner suggested by Kaufman (7). The feasibility of this method depends on the following facts:

(1) The consumption of O-atoms by NO is relatively slow at these pressures, since it can be represented as occurring by the three-body process

$$O + NO + M \rightarrow NO_2 + M.$$

(2) The subsequent reaction

$$O + NO_2 \rightarrow NO + O_2$$

is fast and regenerates the NO so that the NO concentration remains essentially constant.

(3) The light emission is independent of the amount and nature of any third body and can be represented by

$$O + NO \rightarrow NO_2 + h\nu.$$

Thus for a given amount of NO the intensity depends only on the partial pressure of O-atoms.

The relative light intensity was measured by means of a IP21 photomultiplier tube. The phototube housing was mounted on rails and could be moved parallel to the reaction vessel. Collimating slits were used to limit detection of light from a 2-mm section of the reaction tube.

To convert the photometer readings to atom concentrations, it was only necessary to know the absolute value of [O] at one point in the reaction vessel. The value of $[O]_0$, the atom concentration at the inlet J_1, was determined by NO_2 titration. The NO flow was stopped, and an excess amount of NO_2 was added through J_1. The NO produced, which equals $[O]_0$, was trapped downstream with the excess NO_2. The trapped NO was determined by the amount of oxygen consumed in converting the mixture of the oxides to NO_2. It was found that NO could be trapped quantitatively at liquid nitrogen temperature only if the ratio of NO_2 to NO in the oxygen stream was greater than 2. Use of lower ratios resulted in some loss of NO by pumping and by oxidation in the trap. Blank experiments, in which synthetic mixtures of NO_2 and NO were introduced through J_1 with a molecular oxygen stream, showed that the uncertainty in the analysis was less than 2%.

The use of a Wratten 23A filter in front of the collimating slits of the phototube ensured that signal from the weak 'blue' flame resulting from the O-hydrocarbon reaction was negligible relative to that from the O–NO emission.

The presence of the small amount of NO did not affect the rate of the reaction under study, as evidenced from the constancy of the rate constant and the [O] decay curves when the NO flow was changed by a factor of 10 or more. In some experiments with butane the reaction flame was so feeble that the trace of NO formed in the discharge from the N_2 impurity in the oxygen was sufficient for accurate phototube readings. Rate constants determined using this 'afterglow' to monitor [O] were identical with those obtained when the glow was greatly enhanced by addition of NO.

This technique also provided a very sensitive visual test for the efficiency of coil D_1 in removing the atoms and stopping the reaction. A sharp discontinuity of the glow at the top of the coil indicated complete atom consumption. This discontinuity became more diffuse and extended further down the coil at higher atom flows.

Experimental Procedure

In a typical experiment the oxygen was passed through the discharge and the reaction tube for at least an hour to ensure that steady conditions had been achieved; $[O]_0$ was then determined by NO_2 titration. NO was then added through J_2, hydrocarbon

Can. J. Chem. Downloaded from www.nrcresearchpress.com by 210.87.254.42 on 09/05/12
For personal use only.

Can. J. Chem. Downloaded from www.nrcresearchpress.com by 210.87.254.42 on 09/05/12
For personal use only.

through J_1, and the O-atom profile determined photometrically. The NO flow was stopped, and the coil D_1 was introduced to stop the reaction at some position in the reaction tube. The products were then trapped downstream at liquid nitrogen temperature and removed for analysis when a sufficiently large sample had been collected. During this removal the gas leaving the reaction vessel was made to bypass the trap in order to leave the gas flow undisturbed.

The products were then distilled at $-90°$ C through a column of Caroxite. Mass spectrometric and gas chromatographic analyses showed that the effluent gas consisted only of unreacted hydrocarbon. This indicated that the Caroxite absorbed the oxygen-containing products which were volatile at $-90°$ C. The measurement of unconsumed hydrocarbon could thus be effected in a matter of minutes.

The procedure was then repeated with the coil D_1 at some new position. The determination of [RH] at several positions down the reaction tube permitted the evaluation of k by equation [2] for a variety of time intervals.

The presence of the coil D_1 in the reaction zone should not affect the rate measurements if it recombines atoms much faster than it catalyzes the reaction of O-atoms with the hydrocarbon on its surface. That this condition was fulfilled was shown by the following experiment. A reactant flow could be chosen which resulted in the complete consumption of O-atoms within the length of the reaction tube. For such experiments the coil D_1 was not needed to define the reaction zone. Since [O] decays to zero, no explicit knowledge of t_2 is required to evaluate the integral in equation [2]. The values of $[RH]_1$ and $[RH]_2$ are the concentrations at the inlet and that remaining after all the atoms are consumed. The rate constants obtained in these experiments were indistinguishable from those obtained when the coil was present. Although the presence of the coil evidently does not affect the initial reaction, it might well influence the course of the secondary reactions.

Since the reactions under study were quite exothermic, it was necessary to limit the reactant flow rates to prevent temperature rises which would increase the measured rate constant. Temperature measurements were effected by replacing the D_1 coil asesmbly by a thermocouple well. For the butane reaction, the flow rates used were such that the temperature increase in the reaction zone did not exceed 3 C°. Due to the lower activation energy of the ethylene reaction, a temperature rise of 10 C° could be tolerated without noticing an increase in the measured rate.

RESULTS AND DISCUSSION

Table I shows the results of an experiment in which the ethylene flow rate was sufficiently large to consume all the atoms within the reaction vessel. Columns 2 and 3 show the decrease in [O] and $[C_2H_4]$ with time. The coil D_1 was used to stop the reaction at positions 1, 2, and 5 cm from the jet J_1. The last number in column 3 is the value of $[C_2H_4]$ recovered in the absence of the coil. The rate constants shown in column 6 were calculated from equation [2] for the distance intervals shown in column 5. These results show that the presence of the coil does not affect the rate measurement and that there is no trend in the value of k with a 13-fold change in reaction time. These results also afford a very stringent test on the method, since the ratio of reactant concentrations differ by several orders of magnitude over the time intervals used. It will be noted that the ratio of O-atoms consumed to ethylene consumed (column 4) is never less than one. This is consistent with the basic assumption of the method, viz., that the ethylene is attacked only in the initial reaction. The fact that this ratio decreases and approaches unity at

TABLE I

Rate constant k as a function of reaction time for the reaction $O + C_2H_4$

Distance from J_1 (cm)	10^{-14} [O] (molecule cm^{-3})	10^{-14} [C_2H_4] (molecule cm^{-3})	$\frac{\Delta[O]}{\Delta[C_2H_4]}$	Distance interval used to calculate k (cm)	10^{12} k (cm^3 molecule^{-1} sec^{-1})
0	4.5_6	4.62			
			2.3	0–1	0.9
1	0.8_9	3.05			
			1.2	1–2	1.2
2	0.4_2	2.65			
3	0.2_1		1.0	2–5	1.2
5	0.0_7	2.30			
7	0.0_4				
9	0.0_2		1	5–13	1.1
11	0.00				
13	0.00	2.19		0–13	1.0

NOTE: Temperature, 20° C; pressure, 1.0 mm Hg; linear flow, 515 cm/sec.

TABLE II

Effect of pressure on $k(O + C_2H_4)$

Pressure (mm)	0.25	0.49	1.0	2.0	3.4	4.9	7.5
10^{12} k (cm^3 molecule^{-1} sec^{-1}	1.2	1.0	1.0	1.2	1.1	1.4	1.3

NOTE: Temperature, 20° C.

TABLE III

Effect of pressure on $k(O + C_4H_{10})$

Pressure (mm)	0.22	0.45	1.0	2.0	3.5	4.2
10^{14} k (cm^3 molecule^{-1} sec^{-1})	2.4	2.4	2.4	2.3	2.2	2.4

NOTE: Temperature, 7° C.

TABLE IV

Effect of variation of initial reactant concentrations on $k(O + C_2H_4)$

Expt. No.	10^{-14} $[O]_0$ (molecule cm^{-3})	10^{-14} $[C_2H_4]_0$ (molecule cm^{-3})	10^{12} k (cm^3 molecule^{-1} sec^{-1})
A_1	6.1	1.8	1.0
A_2	3.0	1.8	1.0
A_3	2.0	1.8	1.2
A_4	1.0	1.8	1.1
B_1	3.0	1.7	1.1
B_2	1.5	1.7	1.2
C_1	1.6	3.6	1.1
C_2	1.6	1.8	1.0
C_3	1.6	.9	1.1
D_1	3.2	3.9	$.9_3$
D_2	3.2	1.6	1.1

NOTE: A and C series: temperature, 20° C; pressure, 3.4 mm.
B and D series: temperature, 20° C; pressure, 1.0 mm.

the end of the reaction suggests (*a*) that O-atom consumption by free radicals becomes less efficient at low values of [O] and (*b*) that free radicals react with O_2 in preference to ethylene.

The independence of the rate constant on total pressure is shown in Table II for the C_2H_4 reaction, and in Table III for the C_4H_{10} reaction. The pressure was mainly due to

Can. J. Chem. Downloaded from www.nrcresearchpress.com by 210.87.254.42 on 09/05/12
For personal use only.

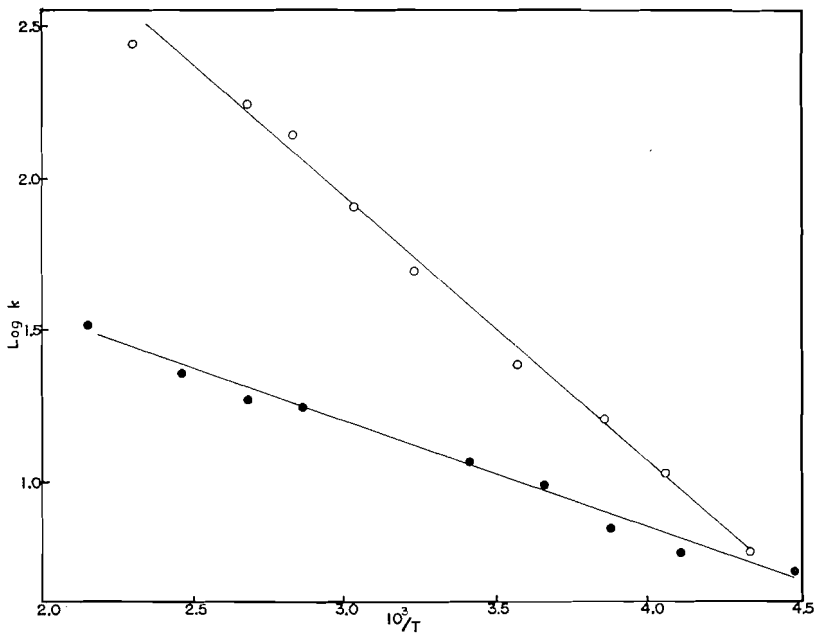


FIG. 2. Arrhenius plots. ○ 10^{14} k for O + C_4H_{10}; ● 10^{13} k for O + C_2H_4.

TABLE V

Effect of variation of initial reactant concentrations on k(O + C_4H_{10})

Expt. No.	10^{-14} $[O]_0$ (molecule cm^{-3})	10^{-14} $[C_4H_{10}]_0$ (molecule cm^{-3})	10^{14} k (cm^3 $molecule^{-1}$ sec^{-1})
E_1	4.0	1.6	8.0
E_2	2.0	1.6	8.0
E_3	1.0	1.6	7.7
E_4	.7	1.6	8.0
F_1	1.5	10.0	2.5
F_2	1.5	4.2	2.5
F_3	1.5	1.8	2.1

NOTE: E series: temperature, 57° C; pressure, 0.47 mm.
F series: temperature, 7° C; pressure, 0.22 mm.

O_2. Similar constancy for the value of k was obtained when the pressure was increased by addition of large amounts of inert gas to the oxygen. This result is significant since it has been shown that discharged oxygen contains a proportion of excited oxygen O_2*, which decreases with addition of helium (8). If ethylene were attacked by O_2* differences in k might be expected when helium is added. Constant values of k were, however, obtained with O_2–He mixtures from 3.5 to 100 mole% O_2.

Tables IV and V show the independence of k on the reactant concentrations for the C_2H_4 and C_4H_{10} reactions respectively.

These results clearly indicate that the rate-controlling steps in these reactions are second order, first order in each of the reactants.

Rate constants were determined for the C_2H_4 reaction over the temperature range −50° C to 192° C and for the n-C_4H_{10} reaction from −42° C to 160° C. Account was taken in the calculations of the effect of temperature on the concentrations and linear velocities of the reactants. The results are shown in Tables VI and VII and the Arrhenius plots in Fig. 2. These curves yield activation energies of 1.6±0.2 and 4.2±0.2 kcal/mole

Can. J. Chem. Downloaded from www.nrcresearchpress.com by 210.87.254.42 on 09/05/12
For personal use only.

Can. J. Chem. Downloaded from www.nrcresearchpress.com by 210.87.254.42 on 09/05/12
For personal use only.

TABLE VI

Variation of k with temperature ($O + C_2H_4$)

Temp. (°C)	Pressure (mm)	Total flow (μmolecules sec^{-1})	10^{-14} [O]$_0$ (molecule cm^{-3})	$10^{-12}\int O dt$ (molecule cm^{-3} sec^{-1})	10^{-14} [C_2H_4]$_0$ (molecule cm^{-3})	$\frac{[C_2H_4]_1}{[C_2H_4]_2}$	10^{12} k (cm^3 molecule^{-1} sec^{-1})
−50	0.97	53	3.32	1.91	2.76	2.85	0.55
−50	0.97	53	4.15	1.88	4.03	2.52	0.50
−30	0.97	53	4.12	1.24	5.50	2.05	0.58
−15	0.97	51	5.25	2.12	3.77	4.16	0.67
−15	0.93	48	2.38	0.95_0	3.42	1.93	0.69
0	1.00	52	2.20	0.80_5	2.75	2.15	0.95
20			(cf. Tables I, II, and IV)				1.1_5
77	1.02	51	1.80	0.49_2	2.64	2.37	1.7_5
100	1.03	51	2.39	0.69_6	2.56	3.33	1.7_2
100	1.03	51	2.64	0.53_2	3.53	2.61	1.8_0
134	1.04	51	1.61	0.37_5	2.32	2.32	2.2_4
192	1.05	51	1.87	0.32_2	2.80	2.58	2.9_4
192	1.05	51	1.87	0.36_7	2.22	3.44	3.3_6

TABLE VII

Variation of k with temperature ($O + C_4H_{10}$)

Temp. (°C)	Pressure (mm)	Total flow (μmolecules sec^{-1})	10^{-14} [O]$_0$ (molecule cm^{-3})	$10^{-12}\int O dt$ (molecule cm^{-3} sec^{-1})	10^{-14} [C_4H_{10}]$_0$ (molecule cm^{-3})	$\frac{[C_4H_{10}]_1}{[C_4H_{10}]_2}$	10^{14} k (cm^3 molecule^{-1} sec^{-1})
−42	0.43	18.5	4.2	13.9	1.86	1.08_5	0.58
−27	0.45	18.5	4.4	12.0	1.95	1.13_5	1.0_5
−14	0.43	18.5	3.8	9.7_0	1.69	1.16_7	1.5_8
7			(cf. Tables III and V)				2.4
36	0.45	17.0	4.3	4.07	1.80	1.22_0	4.9
57			(cf. Table V)				8.0
80	0.47_5	18.0	2.9	1.71	1.63	1.26_5	$13._7$
100	0.47_5	18.0	2.8	1.32	1.60	1.26_2	$17._5$
100	0.48	18.5	2.3	1.02	1.90	1.20_6	$17._8$
160	0.49	17.0	3.0	1.21	1.34	1.46_0	$27._7$

for the C_2H_4 and n-C_4H_{10} reactions respectively, with corresponding pre-exponential factors of $1.8(\pm 0.6)\times 10^{-11}$ and $5.0(\pm 1.6)\times 10^{-11}$ cm^3 molecule^{-1} sec^{-1}.

The rate constant of 1.2×10^{-12} cm^3 molecule^{-1} sec^{-1} obtained for the C_2H_4 reaction at 25° C can be compared with Cvetanović's figure of 0.29×10^{-12} (1) and that of Ford and Endow of 0.76×10^{-12} (9). Since the last two values are derived indirectly from relative measurements using quite different experimental techniques, the agreement can be considered to be satisfactory.

The ratio of the rate constants for the ethylene and butane reactions was found to be 28 ± 3 at 25° C. Cvetanović (4) found this ratio to be 22 ± 5 from relative rate measurements. Again, the agreement is quite satisfactory.

Cvetanović (1) has suggested that the trend in rate constants for O-atom reactions with olefins is due to a trend in activation energy alone. On this basis his data would imply that the ethylene reaction has an activation energy 2.8 kcal greater than that of the 2,3-dimethylbutene-2 reaction. This is clearly inconsistent with the absolute value of 1.6 ± 0.2 kcal/mole for the value of E for the ethylene reaction found in the present work. It would therefore appear that the trend in k's for the olefin series must also involve a trend in steric factors.

REFERENCES

1. R. J. Cvetanović. J. Chem. Phys. **30**, 19 (1959).
2. H. W. Ford and N. Endow. J. Chem. Phys. **27**, 1156 (1957).
3. S. W. Benson and A. E. Axworthy, Jr. J. Chem. Phys. **26**, 1718 (1957).
4. R. J. Cvetanović. J. Chem. Phys. **23**, 1375 (1955).
5. L. Elias, E. A. Ogryzlo, and H. I. Schiff. Can. J. Chem. **37**, 1680 (1959).
6. E. A. Ogryzlo and H. I. Schiff. Can. J. Chem. **37**, 1690 (1959).
7. F. Kaufman. Proc. Roy. Soc. (London), A, **247**, 123 (1958).
8. E. A. Ogryzlo. Ph.D. Thesis, McGill University, Montreal, Que. 1958.
9. H. W. Ford and N. Endow. J. Chem. Phys. **27**, 1277 (1957).

Can. J. Chem. Downloaded from www.nrcresearchpress.com by 210.87.254.42 on 09/05/12
For personal use only.

Can. J. Chem. Downloaded from www.nrcresearchpress.com by 210.87.254.5 on 09/05/12
For personal use only.

PRESSURE DEPENDENCE OF ROTATIONALLY PERTURBED LINES IN THE ULTRAVIOLET BAND SPECTRUM OF CN[1]

H. P. Broida and Sidney Golden[2]

ABSTRACT

Intensity measurements of the components of rotationally perturbed lines ($K' = 4$, 7, 11, and 15) in the 0,0 transition of the violet system ($B\ ^2\Sigma^+$–$X\ ^2\Sigma^+$) of the CN formed in an "active" nitrogen flame have been made at pressures from 0.1 to 100 mm Hg. A simple kinetic model considering competition between formation, radiation, and collisional interchange of states gives a reasonable fit to the data over the entire range of measured pressures. At high pressures the intensity ratios of the components of rotationally perturbed lines depend only upon the radiative transition probabilities and at low pressures, only upon the relative rates at which they are populated. At intermediate pressures, the intensity ratios depend upon the collision frequency for the interchange of the rotationally perturbed states. The collision frequency determined in this manner is of the same order of magnitude as the gas kinetic collision frequency.

INTRODUCTION

The violet bands of CN ($B\ ^2\Sigma^+$–$X\ ^2\Sigma^+$) show intensity anomalies originating in the $v' = 0$ level of the $B\ ^2\Sigma^+$ state caused by perturbations of rotational levels with the $v' = 10$ level of the $A\ ^2\Pi_i$ state. Herzberg (1) first noticed that lines $K' = 4$, 7, and 15 of the 0,0 band of the violet system were greatly enhanced at low pressures in discharges and in "active" nitrogen flames. Beutler and Fred (2) found that the enhanced lines consisted of doublets and suggested that the anomalously high intensities of these lines are caused by interaction of these rotational levels with corresponding rotational levels of the $v' = 10$ (3)* level of the $A\ ^2\Pi_i$ state. This suggestion was confirmed by Wager's measurements (4, 5) of the perturbations in both the 10,4 band of the red system and the 0,0 band of the violet system. In addition he found another rotationally perturbed level, $K' = 11$, also consisting of a doublet. Recently, Kiess and Broida (6, 7) found that the enhancement of the perturbed lines was increased greatly at pressures below 1 mm Hg and that under conditions in which transitions from the $K' = 4$, 7, and 15 levels are enhanced in the violet system, lines from corresponding rotational levels in the $v' = 10$ state of the red system ($A\ ^2\Pi_i$–$X\ ^2\Sigma^+$) are weakened.

This paper reports the intensity measurements of the so-called *main* and *extra* lines of the rotationally perturbed pairs in the 0,0 transition of the violet system over a pressure range from 0.1 to 100 mm Hg. The *main* lines correspond to normally allowed transitions; the *extra* lines correspond to normally forbidden transitions. A mathematical model developed on the basis of kinetic considerations has been devised to fit the data. The ratio of the intensity of the extra line to that of the main line is expressed as a function of three parameters and the pressure. One parameter, $2k_M/k_E$, is the ratio of the radiative transition probability of the main line to that of the extra line. The factor of two appears as a result of the fact that the main line itself is an unresolved doublet. The k_M/k_E ratios found from measurements of the pressure variation of the intensity ratios for the lines $K' = 7$, 11, and 15 are in good agreement with the determinations of Wager (5) found from measure-

[1]*Contribution from the National Bureau of Standards, Washington D.C.; presented at the Symposium on the Fundamental Aspects of Atomic Reactions held at McGill University, Montreal, Que., September 1960.*

[2]*Brandeis University, Waltham, Massachusetts.*

**The vibrational numbering of bands from the red system in earlier work must be increased by one unit (see, for example, Herzberg et al. (3)).*

ments of perturbed line displacements. Another parameter, α, is interpreted to mean that CN is formed in the upper state of the extra line at approximately three times the rate that CN is formed in the upper state of the main line. The third parameter, k_c/k_M, gives a rate of collisional depopulation compared with the rate of radiative transition.

EXPERIMENTAL PROCEDURE

CN emission was obtained by mixing "active" nitrogen with gases of compounds containing carbon in a simple reaction chamber similar to that of Wager (5) and of Kiess and Broida (6). Bright flames were observed at the point of mixing, and at lower pressures the flame filled the entire reaction tube (300 mm long and 45 mm diameter). Prepurified nitrogen (stated by the manufacturer to be of 99.997% purity) was taken from cylinders through float-ball flowmeters by means of Tygon tubing and was admitted by a stopcock into the discharge region. Pyrex glass (washed with soap, rinsed with a 12% solution of HF, and then rinsed with distilled water) was used in the remainder of the apparatus. Because CH_2Cl_2 gave the brightest flames in this burner (particularly at pressures below 1 mm Hg), it was used for most experiments. CH_2Cl_2 vapor was admitted to the reaction chamber through a stopcock from a graduated tube containing liquid CH_2Cl_2 (C.P.).

In most experiments, a 2450-megacycle electrodeless discharge (125 watts) was used to dissociate the nitrogen. A small percentage of nitrogen atoms (8) found in such discharges at pressures near 1 mm Hg. For pressures above 20 to 30 mm Hg, it was necessary to use a 800-watt generator.* In addition for some work below 0.2 mm, a spark discharge using 7μf and 3000 volts at 1 kilowatt with aluminum electrodes about 1 meter apart was found to give brighter reactions.

Pressure was measured with a Bourdon gauge which could be read to 0.05 mm Hg. A McLeod gauge was used for calibration and for measuring nitrogen pressures below 1 mm.

Spectra were recorded with a high resolution grating monochromator with photomultiplier detection.† This instrument, used with 7 micron slits, is able to resolve lines of 0.03 Å separation. Since peak heights were used for intensity measurements, relative intensities of lines closer than about 0.1 Å were not reliable.

Under the best conditions, for pressures between 0.2 and 20 mm Hg and for values greater than 0.1, intensity ratios were reproducible to about $\pm 2\%$. However, for weak flames at very low and very high pressures the reliability was not as good. For pressures lower than 0.1 mm Hg, errors of 50% in the intensity ratio were possible. These errors are associated with the very weak signals obtained.

EXPERIMENTAL DATA

Figures 1 and 2 illustrate the effect of pressure on the perturbed lines. With decreasing pressure the main lines, M, become increasingly enhanced so that at very low pressures they are more than 10 times the intensity of their neighbors. The extra lines, E, increase relative to the main lines. The extra lines occur on the short wavelength side of the main lines for $K' = 7$, 11, and 15 and on the long wavelength side of $K' = 4$. At the very lowest pressures, below 0.1 mm Hg, the extra lines at $K' = 7$, 11, and 15 were more than twice the intensity of the main lines.

Wager (5) has measured the separations of the extra lines from the perturbed main

*We wish to thank the Raytheon Manufacturing Company for the loan of a 800-watt microwave power generator.

†This monochromator was constructed by Leeds and Northrup Company and loaned to the National Bureau of Standards on a field trial basis.

Can. J. Chem. Downloaded from www.nrcresearchpress.com by 210.87.254.5 on 09/05/12
For personal use only.

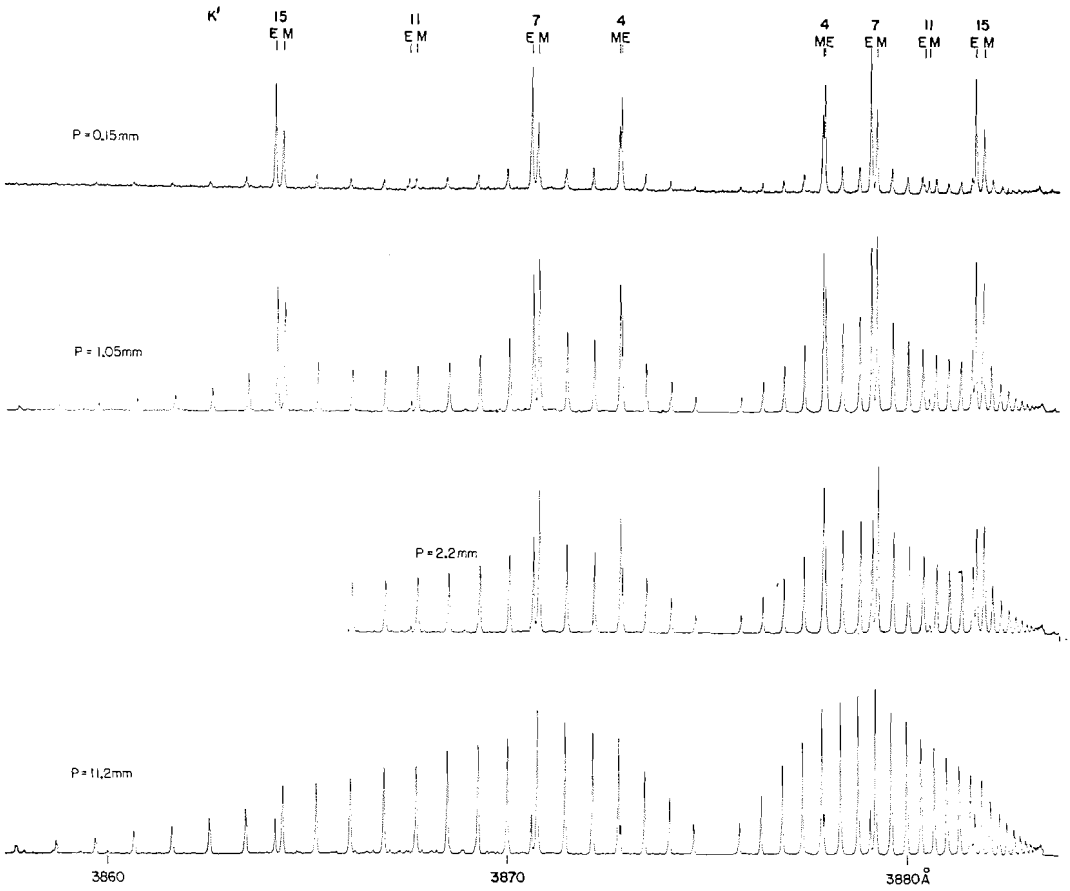


FIG. 1. Spectra of the violet CN emission from "active" nitrogen flames at several pressures.

lines to be -0.352, $+0.938$, $+1.177$, and $+1.212$ cm^{-1} respectively for $K' = 4, 7, 11$, and 15. Since the separation of lines from $K' = 4$ levels were not sufficiently resolved for reliable intensity measurements, intensity measurements on these lines have been excluded from detailed analysis.

Measured ratios of the intensity of the extra line, I_E, to the intensity of the main line, I_M, as obtained from peak height measurements at pressure from 0.08 to 100 mm Hg are shown in Figs. 3, 4, and 5. Pressure is the variable having the largest influence on I_E/I_M. The data have been obtained over a period of 18 months. Small effects on I_E/I_M caused by different relative amounts of CH_2Cl_2 and N_2 were noticeable but were too small for systematic measurement. No effects on the ratio were found to be caused by the type of discharge, the power in the discharge, the size or type of reaction chamber, flow rate, or the reactant.

The addition of appreciable amounts of argon or helium had a small but measureable effect on the ratio between 2 and 20 mm Hg. This is illustrated in Table I where I_E/I_M is given for various proportions of added helium. The effect of rare gas is the same whether it is added before or after the discharge. Other gases—N_2, O_2, CO, or CO_2—had little effect (much less than the rare gases) on I_E/I_M.

Can. J. Chem. Downloaded from www.nrcresearchpress.com by 210.87.254.5 on 09/05/12
For personal use only.

Can. J. Chem. Downloaded from www.nrcresearchpress.com by 210.87.254.5 on 09/05/12
For personal use only.

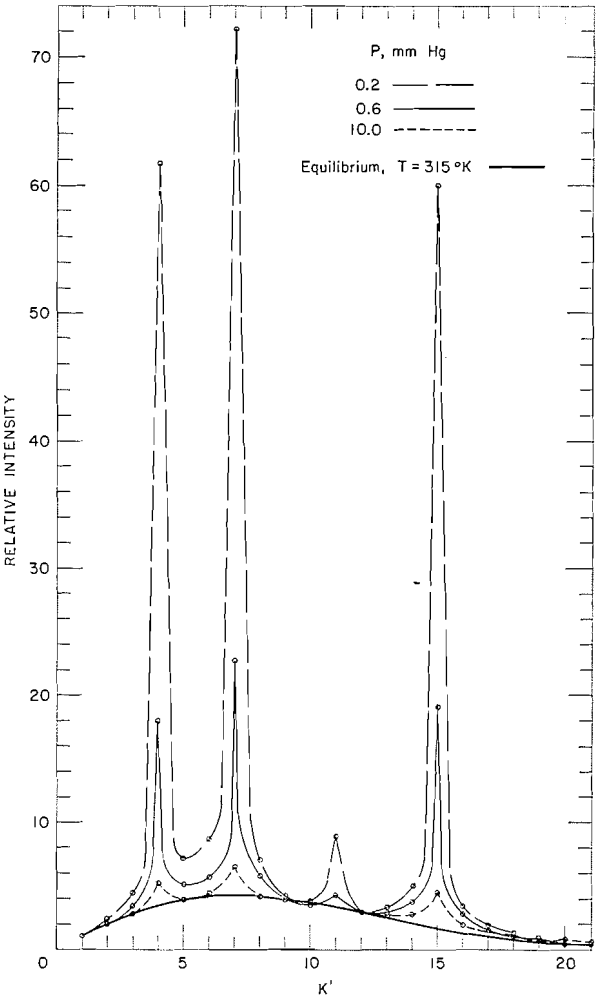


FIG. 2. Effect of pressure on the enhancement of the perturbed lines; the sum of the extra and the main lines is used. For comparison with the measured intensities, there also is shown a Boltzmann distribution calculated for the measured (6) gas temperature of 300° K.

TABLE I

Measured values of I_E/I_M for $K' = 15$ as affected by added helium

Total pressure, mm Hg	Ratio of helium to nitrogen			
	0	1	10	100
0.8	1.39		1.35	
1.4	1.14	1.16	1.13	
2.2	.93	.93	.97	
3.4	.76	.82	.84	
5.0	.62	.71	.72	.75
7.5	.51	.61	.61	.63
10	.45	.52	.57	.57
15	.38	.44	.47	.47
20	.34	.39	.42	.40
25	.32	.33	.39	.38
30	.29	.29		.33
40	.285			.31
45	.28			.30

Can. J. Chem. Downloaded from www.nrcresearchpress.com by 210.87.254.5 on 09/05/12
For personal use only.

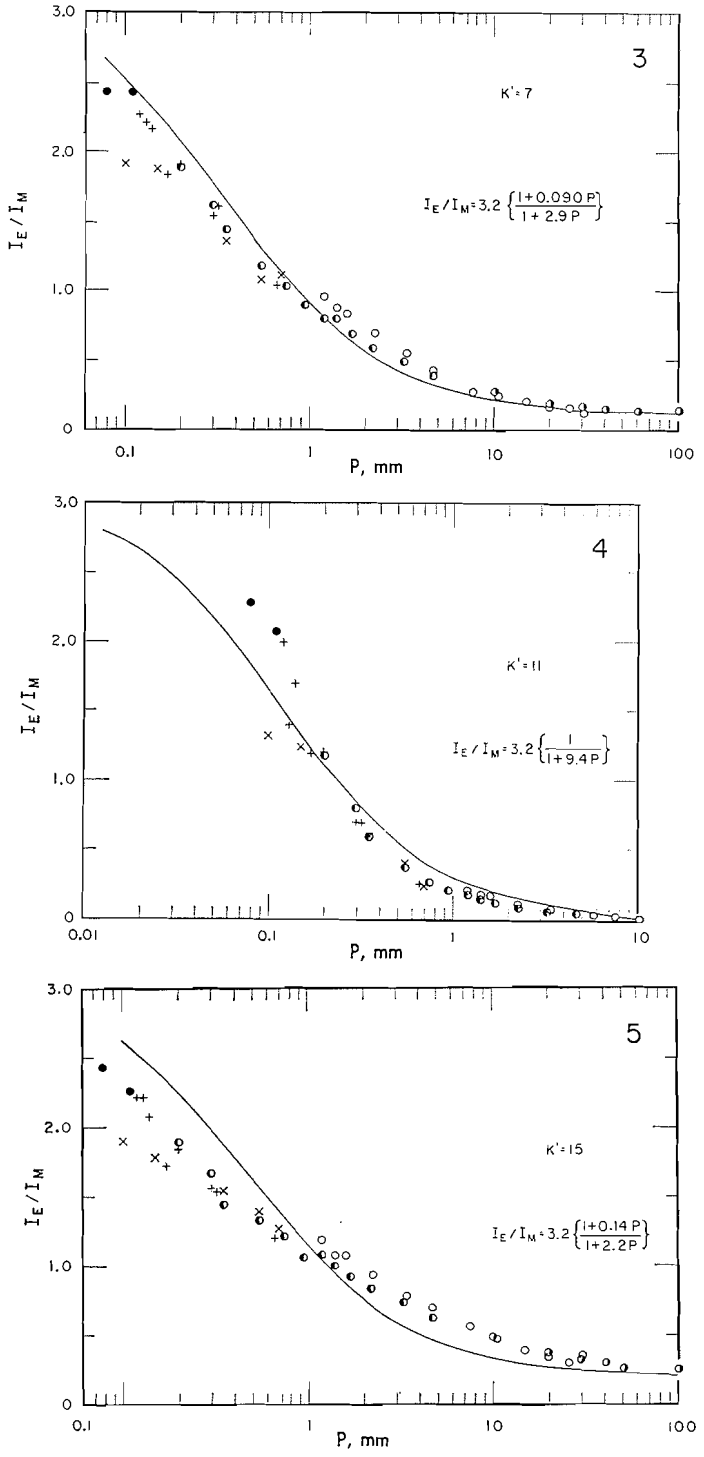


FIG. 3. Measured intensity ratios, I_E/I_M, for $K' = 7$ at various pressures and the curve calculated from equation [13] and the parameters listed in Table II.

FIG. 4. Measured intensity ratios, I_E/I_M, for $K' = 11$ at various pressures and the curve calculated from equation [13] and the parameters listed in Table II.

FIG. 5. Measured intensity ratios, I_E/I_M, for $K' = 15$ at various pressures and the curve calculated from equation [13] and the parameters listed in Table II.

Can. J. Chem. Downloaded from www.nrcresearchpress.com by 210.87.254.5 on 09/05/12
For personal use only.

THEORETICAL MODEL

The model to be elaborated here is concerned mainly with the formation of CN molecules in those states which are affected by rotational perturbations. The energy relations of those states has been discussed in some detail by Wager (5). The upper states involved are degenerate doublets (or nearly so). However, only one of the spin components in the $B\ ^2\Sigma$ state and only one of the Λ components in the $A\ ^2\Pi$ state interact via a rotational perturbation (9). Thereby, the component derived from the $A\ ^2\Pi$ state acquires an enormously increased probability of transition to the ground state: this transition corresponds to the extra line. The other component of the $A\ ^2\Pi$ state is unaffected and has negligible intensity. By contrast, both components of the $B\ ^2\Sigma$ state have large transition probabilities, so that the main line that they produce is an unresolved doublet. However, the relative intensity of these doublets depends upon the relative rates at which they are being populated.

Figure 6 is a simplified energy level diagram indicating that the transitions associated with the doublets observed in the violet CN bands may be presumed to involve not only the radiative transitions, M and E, but also those ascribable to the formation of the CN molecule in the various states and those ascribable to non-radiative transitions. For simplicity, only non-radiative transitions between the members of each group of upper states are taken into account explicitly. The remaining possible non-radiative transitions are considered collectively in terms of the otherwise net rate of production into each of the pair of rotationally perturbed excited states. A diagram like Fig. 6 is applicable to each rotationally perturbed pair of states and the associated unperturbed state.

It is assumed that the various processes indicated schematically by the diagram occur with rates which are simply proportional to the appropriate concentration of relevant species. Thus, for example, the emission from the normally allowed member of the perturbed pair ($V' \rightarrow V$) would have an intensity equal to $k'_M[V']$, where $[V']$ is the concentration of CN molecules occupying the indicated state. Similarly, the rate at which CN molecules experience collisions which take them from one of the pair of perturbed states to the other, say ($V' \rightarrow R'$), is given by $k_{-c}\,[V']\,[N_T]$, where $[N_T]$ is the total concentration of species which are effective in inducing these non-radiative transitions.*

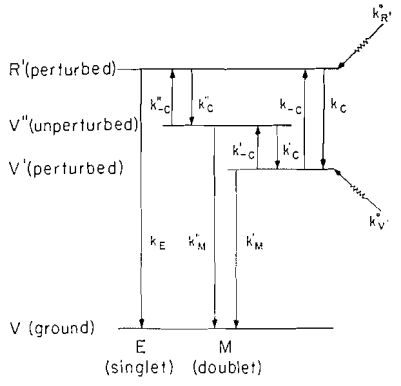


FIG. 6. Simplified energy level diagram, illustrating the transitions explicitly considered in the theoretical model involving the rotationally perturbed states of CN. The various k's refer to rate constants employed in the text.

**It may be noted that a more satisfactory expression which would take into account the different effectiveness of the individual species comprising the system would be exhibited in the form of a linear combination of their respective concentrations. Alternatively, the present simple form ascribes a composition dependence to the collisional rate constants.*

Because of the complexity of the production processes, the rates associated with them will not be given explicitly. Instead, $k^0_{R'}$ and $k^0_{V'}$ will be taken as the net rate of production into states R' and V' (apart from processes of collisional exchange) and will be assumed to depend upon the concentration and composition of the system. All rates are to be understood in terms of changes in concentration per unit time.

The intensity of radiation (neglecting self-absorption) emitted from the perturbed component of the main line ($V' \rightarrow V$) is given by

$$I'_{\mathrm{M}} = k'_{\mathrm{M}}[V'], \tag{1}$$

while for the unperturbed component ($V'' \rightarrow V$)

$$I''_{\mathrm{M}} = k''_{\mathrm{M}}[V'']. \tag{2}$$

Clearly, the intensity of the observed unresolved main line corresponds to

$$I_{\mathrm{M}} = I'_{\mathrm{M}} + I''_{\mathrm{M}}. \tag{3}$$

The intensity of the extra line ($R' \rightarrow V$) is given by

$$I_{\mathrm{E}} = k_{\mathrm{E}}[R']. \tag{4}$$

At any instant, the rates of change of molecules in the excited states are

$$\frac{d[V']}{dt} = k^0_{V'} + k_{\mathrm{c}}[R'][N_{\mathrm{T}}] + k'_{\mathrm{c}}[V''][N_{\mathrm{T}}] - k_{-\mathrm{c}}[V'][N_{\mathrm{T}}] - k'_{-\mathrm{c}}[V'][N_{\mathrm{T}}] - k'_{\mathrm{M}}[V'], \tag{5}$$

$$\frac{d[V'']}{dt} = k''_{\mathrm{c}}[R'][N_{\mathrm{T}}] + k'_{-\mathrm{c}}[V'][N_{\mathrm{T}}] - k'_{\mathrm{c}}[V''][N_{\mathrm{T}}] - k''_{-\mathrm{c}}[V''][N_{\mathrm{T}}] - k''_{\mathrm{M}}[V''], \tag{6}$$

$$\frac{d[R']}{dt} = k^0_{R'} + k_{-\mathrm{c}}[V'][N_{\mathrm{T}}] + k''_{-\mathrm{c}}[V''][N_{\mathrm{T}}] - k_{\mathrm{c}}[R'][N_{\mathrm{T}}] - k''_{\mathrm{c}}[R''][N_{\mathrm{T}}] - k_{\mathrm{E}}[R']. \tag{7}$$

The solution of these equations will give the dependence of the line intensities upon the total concentration and, hence, the pressure of the system.

However, it is not possible to solve the preceding equations without some explicit statement regarding the rates of production. In addition the complete solution of the equations is of interest only for transient circumstances, whereas the experimental conditions dealt with here are practically stationary. As a consequence, attention will be devoted only to the stationary solutions of the equations. To solve the equations, several assumptions will be introduced:

stationary hypothesis:

$$\frac{d[V']}{dt} = \frac{d[V'']}{dt} = \frac{d[R']}{dt} = 0; \tag{8}$$

collision hypothesis:

$$\begin{cases} k_{\mathrm{c}} = k_{-\mathrm{c}} \\ k'_{\mathrm{c}} = k'_{-\mathrm{c}} \\ k''_{\mathrm{c}} = k''_{-\mathrm{c}} \end{cases} \tag{9}$$

and

$$k_{\mathrm{c}} = k'_{\mathrm{c}} = k''_{\mathrm{c}}; \tag{10}$$

production hypothesis:

$$k^0_{R'} = \alpha k^0_{V'}, \qquad \alpha \text{ constant.} \tag{11}$$

Can. J. Chem. Downloaded from www.nrcresearchpress.com by 210.87.254.5 on 09/05/12
For personal use only.

The first assumption is justified on the basis of the experimental conditions. The second assumption partly conforms to microscopic reversibility which, however, is strictly applicable for conditions close to equilibrium. Equation [10] is introduced for simplicity. The third assumption also is introduced for simplicity. However, it is to be expected that the relative rates of production of CN molecules into the pair of perturbed states will vary with the mode of their production, especially when the latter is altered markedly (i.e., discharge vs. flame production). Since the radiative transition probabilities of the two components of the main line are the same,

$$k'_{M} = k''_{M} = k_{M}. \qquad [12]$$

Equations [5]–[7] are greatly simplified by substituting equations [8]–[12] and can be solved for the measured intensity ratio,

$$I_{E}/I_{M} = \frac{\alpha+(1+\alpha)(k_{c}/k_{M})[N_{T}]}{1+2(1+\alpha)(k_{c}/k_{E})[N_{T}]}. \qquad [13]$$

For indefinitely great pressures

$$(I_{E}/I_{M}) \rightarrow 1/2(k_{E}/k_{M}), \qquad [N_{T}] \rightarrow \infty, \qquad [14]$$

a result that is in accord with the notion that an equilibrium distribution among the various states should be achieved by the CN molecules at sufficiently high pressures. For extremely low pressures, on the other hand,

$$I_{E}/I_{M} \rightarrow \alpha, \qquad [N_{T}] \rightarrow 0, \qquad [15]$$

which is consistent with the hypothesis of production expressed in equation [11]. For sufficiently low pressures, one may expect that the rate of collisions in altering the populations in the various states becomes negligibly small, in which case the steady production must be equated to the rate of radiative transitions.

Equation [13] can be rearranged in a variety of ways and one form which is convenient for the subsequent analysis is the following:

$$\frac{\alpha-(I_{E}/I_{M})}{(I_{E}/I_{M})-1/2(k_{E}/k_{M})} = 2(1+\alpha)(k_{c}/k_{E})[N_{T}]. \qquad [16]$$

ANALYSIS OF EXPERIMENTAL DATA

The measured values of the intensity ratios have been subjected to an analysis in the light of the foregoing section and a reasonable fit is found. However, any fit of the data involving the empirical evaluation of three parameters cannot be weighted too heavily in judging the soundness of the theory. To achieve more confidence in the model described previously, the parameters must be compared with estimates of their values obtained from entirely different considerations of the phenomena. Such comparisons will be made in the course of the present section and give increased confidence in the general model.

Preliminary efforts at a least-squares analysis for the parameters were made but this approach was discarded because erratic values for the parameters resulted, one group of experimental data giving values of parameters seemingly unrelated to another group of data. Such discrepancies were caused by small effects due to changes in mixtures and flow rates of the reactants and to an inability to make sufficiently precise pressure measurements at low pressures.

The procedure employed to evaluate the parameters was an iterative one. It is evident

Can. J. Chem. Downloaded from www.nrcresearchpress.com by 210.87.254.5 on 09/05/12
For personal use only.

that the asymptotic behavior at high and low pressures of the ratio of intensity I_E/I_M will give two parameters in equation [13]. Thus a preliminary value of α could be estimated from an extrapolated value of I_E/I_M at low pressures. The resulting value was employed in equation [16] to yield an expression which gave a linear extrapolation to high pressures, permitting an estimate to be made of k_E/k_M. The value resulting was then employed to obtain an expression which gave a linear extrapolation to low pressures, permitting a redetermination of the value of α. The iteration needed repetition only once to yield parameters which remained unchanged (to within 10%). With the final values of α and k_E/k_M obtained, the remaining parameter could be determined as an average value for all of the data. This procedure was carried through for the lines with $K' = 7$ and 15. The final plots for $K' = 7$ are given in Figs. 7 and 8 to illustrate the procedure for obtaining the asymptotic limits.

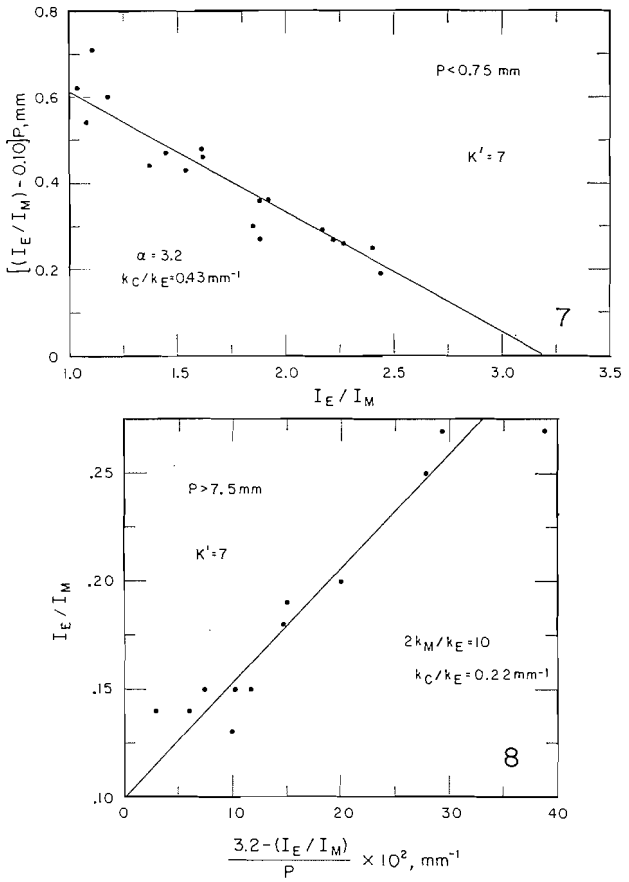


FIG. 7. The use of equation [13] to determine α.
FIG. 8. The use of equation [13] to determine $2k_M/k_E$.

The values of α which were obtained, as already indicated by the original data, suggested that the various lines exhibited a more-or-less uniform value of this parameter. To establish this, and eliminate the experimental uncertainties in the values of the pressure (at low pressures), the data were treated as in Fig. 9. The ratios of intensities of the lines

Can. J. Chem. Downloaded from www.nrcresearchpress.com by 210.87.254.5 on 09/05/12
For personal use only.

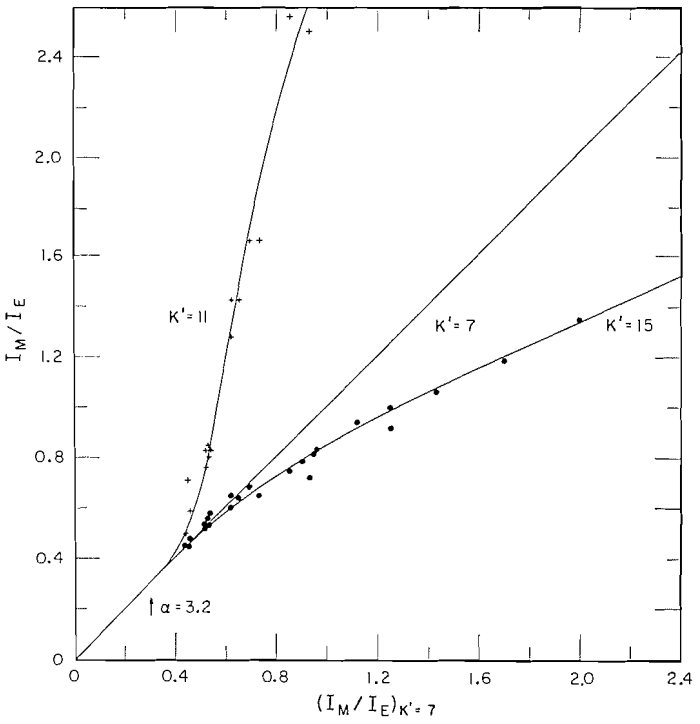


FIG. 9. Relations between intensity ratios at the same pressure for $K' = 7$, 11, and 15.

corresponding to $K' = 11$ and 15 have been plotted against the value for $K' = 7$, each point corresponding to the *same* value of the pressure, but differing, for any pair of lines, from point to point. It seems reasonable to suppose that for $K' = 7$, 11, and 15, α is approximately 3.2 since the curves for $K' = 11$ and 15 extrapolate smoothly to the value found for $K' = 7$.

With a more-or-less uniform value of α taken as 3.2 the analysis can be carried out to estimate k_E/k_M for the lines $K' = 7$, 11, 15 by extrapolation to high pressures. However, it is immediately apparent that the data for $K' = 11$ have a very small value of k_E/k_M from the low values of I_E/I_M at high pressures. The accuracy of the data do not permit a reliable estimate of k_E/k_M to be made for this line. As can be seen from equation [16], small values of k_E/k_M yield a pressure dependence (i.e. $[N_T]$) which is more reliably given by

$$\alpha-(I_E/I_M) \sim 2(1+\alpha)\,(k_c/k_E)[N_T](I_E/I_M), \qquad [17]$$

providing $k_E/k_M \ll 1$, which is apparently valid in the range of data where reliable estimates of I_E/I_M can be made. As a result k_c/k_E can be estimated from the data, but not k_c/k_M. The results obtained are summarized in Table II where $[N_T]$ has been measured in millimeters of mercury, for the lines with $K' = 7$, 11, 15.

The values of k_M/k_E obtained here from intensity measurements are uniformly one-half the values previously obtained by Wager (5) from wavelength measurements. However, Wager failed to consider that the main lines actually consist of doublets, only one component of which is affected by the rotational perturbation. It is evident that the frequency

Can. J. Chem. Downloaded from www.nrcresearchpress.com by 210.87.254.5 on 09/05/12
For personal use only.

TABLE II

Summary of the parameters

K'	α	$2k_M/k_E$	k_M/k_E (Wager)	k_c/k_M, mm^{-1}	k_c/k_E, mm^{-1}
7	3.2	10	10.6	0.068	0.34
11	3.2	>100 (est.)	130	—	1.13
15	3.2	5	5.6	0.104	0.26

displacements will be greater than those observed for the unresolved main line. Consequently the mixing of the two perturbed states will be greater than the values obtained by Wager, resulting in a smaller value of k_M/k_E. Better measurements of the perturbed line displacements should be possible from spectra obtained from flames at pressures near 0.1 mm Hg, so that the displacement of the main line will be less influenced by the unperturbed component.

The parameters have been incorporated into equation [13] for the ratio of intensities and the calculated curves are compared with the data in Figs. 3, 4, and 5 for pressures less than 100 mm, beyond which value the change in intensity ratio with pressure is very small. The fit to the data is relatively good.

One additional piece of information may be obtained from the data. The quantity k_c can be determined if the value of k_M is known (or that of k_E) or estimated. Since the ratio gives, when multiplied by the pressure, a measure of the ratio of collision frequency to the reciprocal of the radiative lifetime, these quantities may be evaluated independently. It is estimated from kinetic theory that a molecule of CN has approximately 10^6 collisions per second at 1 mm pressure and 300° K. Thus, for a radiative lifetime of 10^{-7} to 10^{-8} sec, it is estimated that $(k_c/k_M) \sim 0.1-0.01$ substantially in agreement with the observed values. Therefore, k_c is in fact a collision frequency corresponding essentially to the kinetic theory value. It seems unlikely that any more precise comparison can be made with the values obtained from our present analysis and those obtained otherwise. Rare gases (Table I) decrease k_c as compared with nitrogen.

DISCUSSION

The analysis of the experimental data provides support for the simple model which has been assumed; a competition between formation rates, radiative transitions, and collisional interchanges between the components of rotationally perturbed states seems adequate to account in a general way for the effect of pressure upon the relative intensities of the perturbed and extra lines in the emission spectrum of CN ($B\,^2\Sigma^+$–$X\,^2\Sigma^+$).

Nevertheless, the mathematical model, which has been presented, represents a great simplification of the actual state of affairs. This can be seen in part from the trends in the disparity between the data and the fitted curves. A more detailed examination would reveal that the parameters which have been used are better to be regarded as depending somewhat upon other parameters such as pressure. For example, k_c/k_E for the low-pressure extrapolation (Fig. 7) differs by about a factor of two from that for the high-pressure extrapolation (Fig. 8); fitting the whole range of pressures (Fig. 3 and Table II) gives intermediate values. Thus the results reported here represent some sort of average value. However, we should emphasize that the parameter α has been weighted in terms of low-pressure behavior. There seems to be no simple way of determining this quantity reliably under the opposite extreme of pressure.

Can. J. Chem. Downloaded from www.nrcresearchpress.com by 210.87.254.5 on 09/05/12
For personal use only.

Because the model, which has been considered, has not dealt with the relative intensities of lines of different K's, the analysis is far from complete. In fact, since the anomalous intensities of the rotationally perturbed lines would seem to depend upon the actual rates of forming the CN in the several excited states, the present analysis, dealing with the *relative* rates of formation of specific pairs of these states, can only have a minor influence on that problem. Indeed the tacit use of a more-or-less constant value of α itself raises questions to which we have no ready answer.

REFERENCES

1. G. HERZBERG. Z. Physik, **52**, 815 (1928).
2. H. BEUTLER and M. FRED. Phys. Rev. **61**, 107 (1942).
3. G. HERZBERG and J. G. PHILLIPS. Astrophys. J. **108**, 163 (1948).
4. A. T. WAGER. Phys. Rev. **61**, 107 (1942).
5. A. T. WAGER. Phys. Rev. **64**, 18 (1943).
6. N. H. KIESS and H. P. BROIDA. Seventh Symposium on Combustion. Butterworth Scientific Publications, London. 1959. p. 207.
7. N. H. KIESS and H. P. BROIDA. To be published.
8. J. T. HERRON, J. L. FRANKLIN, P. BRADT, and V. H. DIBELER. J. Chem. Phys. **30**, 879 (1959).
9. G. HERZBERG. Molecular spectra and molecular structure. I. Spectra of diatomic molecules. D. Van Nostrand Co., Inc., New York. 1950. p. 286.

Can. J. Chem. Downloaded from www.nrcresearchpress.com by 210.87.254.5 on 09/05/12
For personal use only.

Can. J. Chem. Downloaded from www.nrcresearchpress.com by 210.87.254.105 on 09/05/12
For personal use only.

ELECTROPHILIC CHARACTER OF OXYGEN ATOMS[1]

R. J. CVETANOVIĆ

ABSTRACT

The relative rates of reactions of oxygen atoms with a number of olefins in the vapor phase determined in previous work are summarized and supplemented by some additional results. The uncertainty in the values of the relative rate constants is now believed to be reduced to only a few per cent. A number of simple correlations observed previously have been re-examined on the basis of the more complete and more accurate list of values available at present. These correlations show a distinct electrophilic character of oxygen atoms in their reactions with olefins and their potential significance for the understanding of the finer details of these addition processes is discussed.

INTRODUCTION

Possibilities of finding simple correlations between reaction rates and physical properties of the reactants have been extensively explored at various times in the past with the object of establishing the factors which contribute to chemical reactivity. Thus, for example, considerations of the likely potential energy changes when two molecules interact have suggested linear dependence of activation energies on such quantities as heats of reaction or singlet–triplet excitation energies (1–6). In the case of metathetical reactions such views have found little experimental support. Some addition reactions, on the other hand, at least those involving a number of aromatic hydrocarbons (5, 6) and a somewhat restricted group of olefins (7), appear to show simple relations of this kind.

Reactions of atoms with series of structurally related compounds are particularly attractive for this type of investigation, especially if they can be studied under conditions where complications from solvent effects of variable magnitude can be eliminated. Solvent effects are of course absent in vapor phase reactions, but until very recently there were essentially no rate data for series of addition reactions in the vapor phase. An exception to this represented the reactions of H-atom additions to olefins, investigated by Robb and Melville (8). However, the work now in progress in this laboratory on these reactions at higher pressures and with the use of a different technique (9) reveals some differences in the values of the rate constants from those obtained by these authors. A discussion of the trends in reactivity in this reaction series has, therefore, to be delayed until the current work is completed.

Although free atoms as a rule possess unpaired electrons and thus have free radical character, they may be expected to react in particular reactions as either electrophilic, nucleophilic, or radical reagents. The type of the reactant character exhibited will be largely determined by the relative values of the electron affinities and ionization potentials of the atoms and their reaction partners.

In the past several years extensive information on the vapor phase reactions of oxygen atoms with olefins has been accumulated in this laboratory. Both the mechanism (10, 11) and the relative rates (12) have been investigated in considerable detail. The results of these studies show that ground-state oxygen atoms, which are diradicals, behave as distinctly electrophilic reagents in their reactions with olefins. The relative rates were found to exhibit approximate simple correlations with some physical properties of olefins

[1]*Contribution from the Division of Applied Chemistry, National Research Council, Ottawa, Canada; presented at the Symposium on the Fundamental Aspects of Atomic Reactions held at McGill University, Montreal, Que., September 1960.*
Issued as N.R.C. No. 5770.

and also to give linear "free energy" plots with the corresponding rates of some other electrophilic reagents studied in solutions. All such correlations show as a rule smaller or greater individual deviations from the basic trends. These deviations are only partly ascribable to experimental errors. In the present paper the earlier findings are summarized and supplemented by some additional experimental results with the particular object of obtaining further information on the extent and the nature of deviations from some of the observed correlations.

EXPERIMENTAL

Oxygen atoms were generated by mercury-photosensitized decomposition of nitrous oxide and the nitrogen produced served as an internal actinometer. A detailed study of this reaction (13) had shown that in this decomposition only nitrogen and oxygen atoms were initially formed. The oxygen atoms are in all probability in their ground, triplet $O(^3P)$ state. This is required by the spin conservation rule and is confirmed by comparisons with the analogous reactions with oxygen atoms generated by photolysis of nitrogen dioxide (14).

A circulating reaction system of total volume of 415 ml was used. The gases were circulated by means of an all-glass vertical plunger pump. The reaction cell was cylindrical, 5 cm in diameter and 10 cm long, and was illuminated by two low-pressure mercury lamps, one at each end of the cell. The reactant olefins were measured manometrically on a constant volume burette. By using mercury cutoffs instead of stopcocks the reactant olefins were kept from coming in contact with stopcock grease during the transfer into the reaction system and the run. Nitrous oxide was measured manometrically on a volume of 1000 ml before its introduction into the reaction vessel.

The rate constants of oxygen atom additions to olefins were measured relative to that of cyclopentene. In the cyclopentene reaction, ethylene is an important product while with the other olefins studied it is not formed or is produced at best only in very small amounts. At various olefin-to-cyclopentene ratios various amounts of ethylene are produced and the ratio of the rate constants can be calculated from the expression*

$$[1] \qquad k_1/k_2 = \log\{1-[\Delta N_2/(a_1)_1]+[\Delta C_2H_4/\alpha_2(a_1)_1]\}/\log\{1-[\Delta C_2H_4/\alpha_2(a_2)_1]\},$$

where subscript 2 refers to cyclopentene; $(a_1)_1$ and $(a_2)_1$ are the initial amounts of the competing olefin and cyclopentene, respectively; ΔN_2 and ΔC_2H_4 are the respective amounts of N_2 and C_2H_4 produced; and α_2 is C_2H_4/N_2 in the reaction of oxygen atoms with cyclopentene alone. In separate experiments α_2 has been found to be 0.270 at 26° C. The values of ΔC_2H_4 used in equation [1] have to be corrected for any ethylene produced from the competing olefin in the absence of cyclopentene. This is done by using the expression†

$$[2] \qquad (\Delta C_2H_4)_{\text{corrected}} = [(\Delta C_2H_4)_{\text{total}} - \beta\Delta N_2]/(1-\beta/\alpha_2),$$

where β is C_2H_4/N_2 in the absence of cyclopentene. In view of the relative magnitudes of α_2 and β these corrections are very small.

Of the reaction products only N_2 and C_2H_4 were of interest in the present work. Analyses were made therefore only for the non-condensible gases and the C_2 fraction. Both fractions were measured manometrically on a constant volume burette. The former was further analyzed by the use of a Cu–CuO furnace at about 250° (to remove CO and any H_2)

*Equation (5) of reference 12.
†Rearranged equation (2) of reference 12.

Can. J. Chem. Downloaded from www.nrcresearchpress.com by 210.87.254.105 on 09/05/12
For personal use only.

followed by mass spectrometric analysis to determine the small amount of CH_4 in the recovered N_2. The C_2 fraction was analyzed by mass spectrometer. A Le Roy still (15) followed by a "pump-out" trap was used to separate the two fractions from the rest of the products and the excess reactants present.

The reactants were of the best available grade and were degassed and bulb-to-bulb distilled *in vacuo* before use. Peroxides were removed from cyclopentene by filtering through an activated alumina column and rapid introduction into the vacuum apparatus. Large excess of nitrous oxide and high total pressures ensured no interference from chemical quenching reactions by the olefins.

RESULTS AND DISCUSSION

In the earlier work (12) it was found that *trans*-2-butene reacted somewhat more rapidly with oxygen atoms than *cis*-2-butene. However, the difference was almost comparable to the cumulative uncertainty in these determinations at that time and the reality of this observation was therefore in doubt. For this reason the relative rates of these two olefins have been redetermined with the use of the cyclopentene technique. This technique and the additional improvements in the handling of the reactants and the products have permitted appreciably more accurate determination of the relative rates than was originally possible. The results are given in Table I, in which the rate constants are determined relative to that of cyclopentene. It is seen that the rate of

TABLE I

Determination of relative rate constants for *cis*-2-butene, *trans*-2-butene, and *n*-1-hexene
(The amounts of the reactants and of the nitrogen produced are given in millimeters in 415 ml at 25° C; the amounts of the other products are given relative to the nitrogen produced; a_2 = cyclopentene)

Run	Temp., °C	$\frac{(a_1)_i}{(a_2)_i}$	$(a_1)_i$ (mm)	$(a_2)_i$ (mm)	N_2O (mm)	Irradiation (minutes)	ΔN_2 (mm)	$\frac{CO}{N_2}$	$\frac{CH_4}{N_2}$	$\frac{C_2H_6}{N_2}$	$\frac{C_2H_4}{N_2}$	$\frac{k_1}{k_2}$
						(I) a_1 = *cis*-2-Butene						
169	(27.4)		4.17	—	495.2	60	1.529	.017	.007	.094	.012	—
170	27.3	3.09	21.06	6.81	497.9	60	1.463	.019	.008	.060	.085	.801
171	26.0	1.69	12.44	7.38	496.9	90	2.251	.019	.010	.047	.122	.774
172	25.9	.97	8.26	8.50	495.0	90	2.297	.019	.006	.032	.154	.808
173	26.7	.74	8.08	10.89	490.8	90	2.281	.021	.007	.027	.170	.822
Mean	26.5											0.801±.014
						(II) a_1 = *trans*-2-Butene						
177	(24.5)		8.20	—	496.2	90	2.388	.020	.006	.069	.016	—
180	(26.8)		8.58	—	499.1	90	2.314	.021	.004	.070	.016	—
176	26.8	2.01	16.87	8.38	489.1	90	2.232	.019	.005	.039	.101	.954
175	25.5	1.19	9.68	8.14	495.2	90	2.309	.019	.005	.031	.130	1.010
174	26.4	1.18	9.26	7.82	493.7	90	2.298	.018	.005	.032	.131	.995
178	26.0	1.02	8.23	8.08	508.0	90	2.322	.018	.005	.025	.148	.878
179	26.8	.61	7.85	12.80	493.7	90	2.262	.020	.005	.016	.176	.919
Mean	26.3											0.951±.042
						(III) a_1 = *n*-1-Hexene						
182	(27.5)		9.12	—	497.7	90	2.272	.022	—	—	—	—
185	25.6	4.82	22.63	4.69	496.9	90	2.092	.017	—	—	.130	.215
183	26.8	4.52	20.27	4.48	494.5	90	2.086	.018	—	—	.128	.222
186	24.1	3.90	20.27	5.19	494.5	90	2.075	.019	—	—	.139	.222
184	25.2	2.73	20.65	7.55	504.3	90	2.060	.017	—	—	.165	.215
181	26.6	.69	9.00	13.07	494.5	90	2.168	.021	—	—	.234	.214
Mean	25.7											0.218±.004

Can. J. Chem. Downloaded from www.nrcresearchpress.com by 210.87.254.105 on 09/05/12
For personal use only.

addition of oxygen atoms to *trans*-2-butene is about 15% greater than it is for *cis*-2-butene. This is in approximate agreement with the previous finding although the difference between the two olefins is now found to be slightly smaller than in the earlier work.

Table I also includes the results of the determinations of the relative rate of reaction of oxygen atoms with *n*-hexene-1, which was not measured before. The particular interest in this compound in connection with the present work will be evident from the discussion which follows.

The temperature dependence of the relative rates of addition of oxygen atoms to several representative olefins has been recently determined. A full report on this work is being published elsewhere (16) and only a summary of the Arrhenius parameters obtained is given in Table II. In all cases the ratio of the pre-exponential factors (relative

TABLE II

Ratios of the Arrhenius pre-exponential factors and the differences in activation energies

(The subscript CP refers to cyclopentene, and TME to tetramethyl ethylene)

Olefin	A/A_{CP}	$E-E_{CP}$ (cal/mole)	$E-E_{TME}$ (kcal/mole)
Ethylene	1.01	2008	2.60
1-Butene	.74	803	1.40
1,3-Butadiene	1.14	205	.80
Cyclopentene	1	0	.60
Cyclohexene	.89	−13	.58
Isobutene	.67	−130	.47
Trimethyl ethylene	1.18	−485	.11
Tetramethyl ethylene	1.25	−596	0

to cyclopentene) is very close to unity. Within the experimental error the differences in reactivities in this reaction series appear then to be essentially entirely due to differences in the activation energies. In view of this any correlation of the logarithms of the rate constants for these reactions is to a good approximation equivalent to a correlation of the activation energies.

A list of the values available at present of the relative rate constants of the reactions of oxygen atoms with olefins at 25° C is given in Table III. As indicated in the table, besides several new determinations, most of these values are recent redeterminations and they agree very well with the previous values (12) which were in most cases obtained by

TABLE III

Relative rates of addition of oxygen atoms to olefins at 25° C

(The value for isobutene is taken as unity)

Olefin	Relative rate constant	Olefin	Relative rate constant
Ethylene	0.040[a]	*cis*-2-Pentene	0.90[b]
Propylene	0.23[b]	Cyclopentene	1.19[a]
1-Butene	0.23[a]	Cyclohexene	1.08[a]
1-Hexene	0.26[c]	Trimethyl ethylene	3.17[a]
Isobutene	1.00	Tetramethyl ethylene	4.07[a]
cis-2-Butene	0.95[c]	1,3-Butadiene	0.97[a]
trans-2-Butene	1.13[c]		

[a]Reference 16. [b]Reference 12. [c]Present work.

Can. J. Chem. Downloaded from www.nrcresearchpress.com by 210.87.254.105 on 09/05/12
For personal use only.

quite different techniques. The only exception to this is provided by *cis*-2-butene for which the rate constant determined in the present work is about 12% greater than previously found (12). It is believed that the present figures are accurate to within a few per cent in contrast to the previously estimated uncertainty of 10 to 15%.

The electrophilic character of oxygen atoms in their reactions with olefins is evident from the continuous increase in reactivity with increasing number of alkyl substituents on the doubly bonded carbon atoms, which primarily determine the electron-donating power, i.e. the basicity of olefins. Furthermore, in agreement with the electrophilic character of oxygen atoms their rate of addition to butadiene is comparable to that of two-substituted ethylenes while for radical reagents it would be expected to be much larger.

The logarithms of the relative rate constants of the reactions of oxygen atoms with olefins were previously found to be approximately linearly correlated with the following physical properties of the olefins (12): ionization potentials, heats of hydrogenation, and spectroscopic excitation energies. Also approximate linear free energy plots were obtained with some other series of electrophilic reactions (12), as well as approximate linear correlations with the theoretically derived excitation energies and bond orders (17). In view of the more complete and more accurate list of the relative rate constants for this reaction series now available (Table III), and additional literature information for some of the other reaction series considered, it is necessary to examine these correlations in somewhat greater detail.

In Fig. 1 are plotted logarithms of the relative rate constants for several series of electrophilic reactions against the ionization potentials of olefins. Of these series the oxygen atom additions to olefins are the only series of vapor phase reactions. The CCl_2 and CBr_2 series will be disregarded for the moment. It is seen that the bromination reactions give a good linear correlation. However, information is lacking for a greater variety of compounds that would permit finding out whether deviations shown by the oxygen atom and the peracetic acid series would appear in this case as well. In the latter two series it is found that the values of the rate constants for all the singly substituted ethylenes remain essentially constant and thus do not follow the trend in the ionization potentials. The same holds also for the two-substituted ethylenes.

In Fig. 2 relative rate constants are plotted against the excitation energies obtained by molecular orbital calculations (17). Excellent linear correlation is shown by the peracetic acid series. The same is also largely true for the oxygen atom and the bromination series, although in the former the value for tetramethyl ethylene is somewhat low and in the latter there is perhaps suggestion of a slight curvature. The value for the reaction of oxygen atoms with butadiene does not fit into this plot, although it does fit quite well into the ionization potential plot in Fig. 1 and the plot of the log k values against the bond orders in Fig. 3 (in these plots butadiene is indicated by squares instead of circles). The bond orders have been obtained by molecular orbital calculations (17) and they correlate well with the logarithms of the rate constants for the peracetic acid, oxygen atom, and bromination series, although the plots are slightly curved.

The deviations from the straight line plots in Fig. 1 for the oxygen atom and the peracetic acid series are as a rule larger for bigger substituents. Thus, for example, in the oxygen atom series the deviations for the monosubstituted ethylenes are in the order propylene < 1-butene < *n*-1-hexene, and similarly for the peracetic acid series the order is propylene < *n*-1-pentene < *n*-1-hexene < *n*-1-octene < *n*-1-decene. In view of this, the deviations could perhaps be ascribed to steric hindrance. However, it is significant that these deviations disappear in the plots against the theoretically derived excitation

Can. J. Chem. Downloaded from www.nrcresearchpress.com by 210.87.254.105 on 09/05/12
For personal use only.

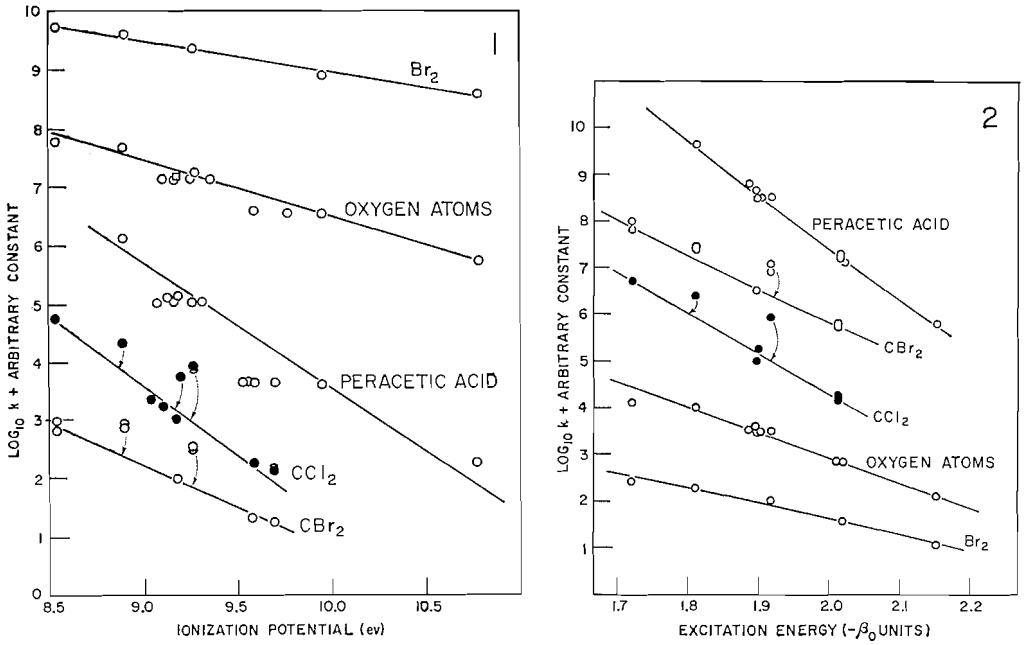


FIG. 1. Plot of log k values against the ionization potentials. (Source of data: Ionization potentials—J. Collin and F. P. Lossing. J. Am. Chem. Soc. **81**, 2064 (1959); R. E. Honig. J. Chem. Phys. **16**, 105 (1948). *Bromination reactions*—S. V. Anantakrishnan and C. K. Ingold. J. Chem. Soc. 984, 1396 (1935). *Peracetic acid reactions*—J. Boeseken and J. Stuurman. Rec. trav. chim. **56**, 1034 (1937); J. Boeseken and C. J. A. Hanegraaff. Rec. trav. chim. **61**, 69 (1942); D. Swern. J. Am. Chem. Soc. **69**, 1692 (1947). CBr_2 *and* CCl_2 *reactions*—W. von E. Doering and Wm. A. Henderson, Jr. J. Am. Chem. Soc. **80**, 5274 (1958) with some results for CBr_2 reactions from P. S. Skell and A. Y. Garner. J. Am. Chem. Soc. **78**, 5430 (1956). *Oxygen atom reactions*—taken from Table III of the present work.)

FIG. 2. Plot of log k values against the excitation energies. (Source of data: excitation energies, reference 17; rate constants, as given in caption of Fig. 1.)

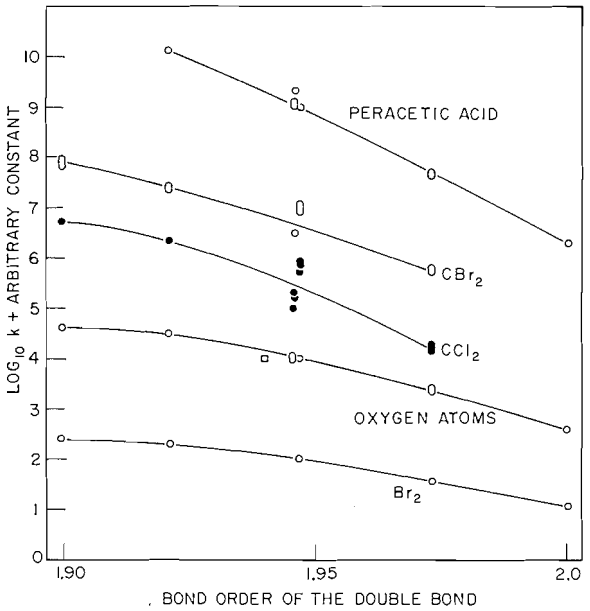


FIG. 3. Plot of log k values against the bond orders of the olefinic double bonds. (Source of data: bond orders, reference 17; rate constants, as given in caption of Fig. 1.)

Can. J. Chem. Downloaded from www.nrcresearchpress.com by 210.87.254.105 on 09/05/12
For personal use only.

energies and bond orders. The same is true for the "free energy" plots shown in Fig. 4. The plot of log k values for the peracetic acid reactions vs. log k_O (the values for the oxygen atom reactions) shows no deviations of this kind. It appears, therefore, that the trend in the ionization potentials is only an approximate measure of the basicity of olefins as determined, for example, by the trends in the oxygen atom reactions.

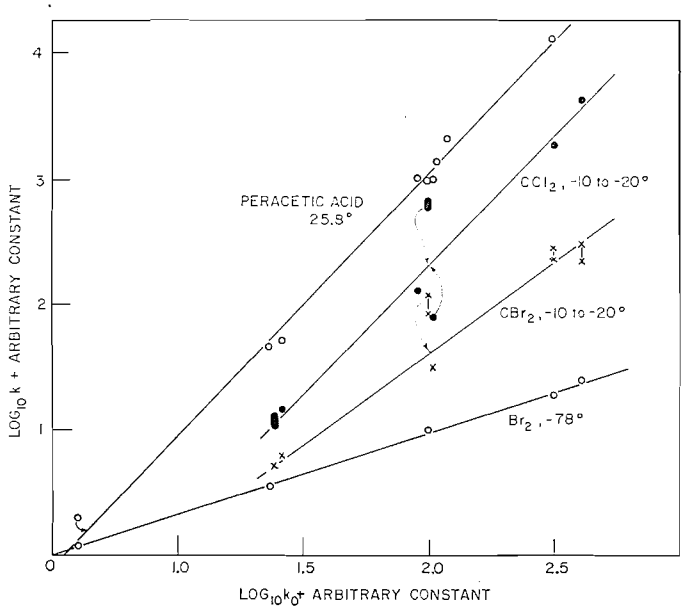


FIG. 4. Free energy plots for bromination, peracetic acid, CBr_2, CCl_2, and oxygen atom reactions with olefins. (Source of data: as given in caption of Fig. 1.)

There is little quantitative information on the basicity of olefins. The basicity towards silver ion was found by Winstein and Lucas (18) to decrease rather than increase with increasing alkyl substitution, presumably because of steric hindrance to the approach of the large ion to the π-electrons of the olefin. Brown and Brady (19) have measured Henry's law constants for olefin–HCl mixtures at −78° and the order of basicity found by these authors is qualitatively the same as the order of reactivity for the considered electrophilic reactions. Unfortunately the data cannot be used for a quantitative correlation. West (20) has recently obtained some quantitative information for the basicity of a number of olefins towards phenols from the shifts in the frequency of the O—H infrared band due to hydrogen bond formation. Plots of log k values against the frequency shifts due to hydrogen bonding of olefins with p-fluorophenol are given in Fig. 5. For the bromination series the available information is very incomplete. For the oxygen atom and the peracetic acid series there is a good correlation except that the shifts are exceptionally large for the α,α-disubstituted olefins* and therefore these compounds show large deviations. In addition to this irregularity, the experimental uncertainty in these values of about ± 6 cm^{-1} is relatively large for the purpose of quantitative correlations of this kind.

The mechanisms of reactions of electrophils with aromatic compounds have been extensively investigated. The mechanism of electrophilic aromatic substitution has been

**Possible reasons for this are discussed in reference 20. In Fig. 5 the frequency shift for 2-methyl-1-butene has been used for isobutene, for which the frequency shift was not determined.*

Can. J. Chem. Downloaded from www.nrcresearchpress.com by 210.87.254.105 on 09/05/12
For personal use only.

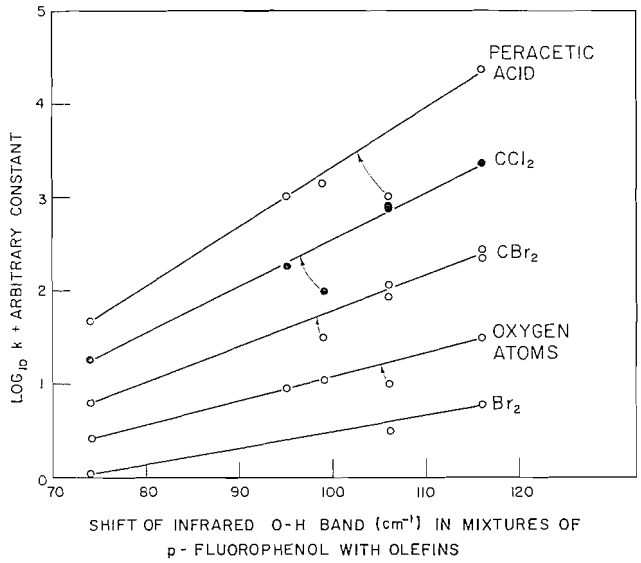


FIG. 5. Plot of log k values against the frequency shift of infrared O—H band in mixtures of p-fluorophenol with olefins. (Source of data: frequency shifts, reference 20; rate constants, as given in caption of Fig. 1.)

recently discussed by Brown (21) with the conclusion that it involves unsymmetrical inner charge-transfer complexes (or σ complexes) as stable intermediates, rather than outer complexes (or π complexes), in which only slight charge transfer to the electrophil occurs. He derived certain theoretical quantities (Z values) as indices of chemical reactivities of positions in aromatic compounds for a given electrophil. These are largely determined by the difference of the electron affinity of the electrophil and the ionization potentials of the aromatic compounds. An extension of this treatment to some electrophilic addition reactions appears to be contemplated.

In the case of oxygen atom addition to olefins there is indication that the rate of addition and the orientation are not governed by the same factors. This conclusion is based on the observation (11, 12) that in 2-pentene the addition takes place exclusively at the doubly bonded C-atom to which methyl group is attached (and not to the one to which ethyl group is attached) although the rates of addition to propylene and to 1-butene are the same and in both cases terminal addition occurs. Similarly the rates of addition to 2-butene and 2-pentene are again about the same. If the same factors governed the over-all reactivity and the orientation, about equal addition to the two doubly bonded C-atoms in 2-pentene would be expected. For these reasons it appears that the transition state responsible for the observed activation energies must occur quite early in the reaction process, perhaps as shown qualitatively in Fig. 6.

In their approach to an olefinic double bond, oxygen atoms experience at first a repulsion, but already at relatively large distances the electrostatic interaction leads to a lowering of the potential energy of the system. It seems necessary to assume that at this stage the atoms are not localized on one of the two doubly bonded C-atoms and the minimum at A in Fig. 6 is visualized as perhaps corresponding to a charge-transfer complex (using this term somewhat loosely). In this particular process the very exothermic transformation to the intermediate B is believed to occur rapidly and does not influence

Can. J. Chem. Downloaded from www.nrcresearchpress.com by 210.87.254.105 on 09/05/12
For personal use only.

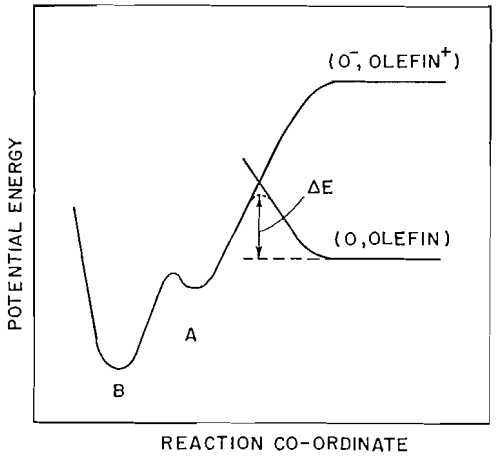


FIG. 6. Potential energy – reaction co-ordinate schematic diagram for the reaction of oxygen atoms with olefins.

the over-all rate of addition. In B the oxygen atom is localized on one of the two double-bond C-atoms and this intermediate is believed to be a triplet biradical (probably with some Zwitterion character) when the oxygen atoms reacting with the olefin are in their ground state (^3P). In agreement with this, both *cis*- and *trans*-epoxides are formed from internal olefins, and also intramolecular rearrangements to carbonyl compounds take place (11).

It is also possible that in some cases the transformation from A to B in Fig. 6 may be rather slow, in which case the observed rate is a composite quantity, as discussed in connection with a study of the rates of ozone addition to olefins in the vapor phase (22).

The diagram in Fig. 6 is of the type discussed in the Introduction and one could, therefore, adopt the usual assumptions (1–6) and from simple geometrical considerations arrive at the prediction of approximate linear dependence of the activation energies on such a property of the olefins as, for example, the ionization potentials. At the same time, some of these assumptions are very arbitrary and can only be justified by extensive agreement of experimental observations with the predictions. Moreover, the exact significance of the experimentally observed approximate linear correlations is uncertain since several physical properties of the olefins show approximately parallel trends.

The significance of the free energy plots in Fig. 4 has been discussed in some detail previously (12). In as much as in a plot of log k_1 vs. log k_2 the linear correlation persists over a temperature range, then in each one of the two reaction series either (*a*) the entropies of activation are to a good approximation equal for all the members of the series (isoentropic series), (*b*) the enthalpies of activation are equal (isoenthalpic series), or (*c*) there is linear correlation between the enthalpies and entropies of activation (compensating or additive enthalpy–entropy effect). In view of this, the slope of the free energy plot for peracetic acid and oxygen atoms represents the constant ratio of the activation energy differences for equal structural changes in the olefins multiplied by the inverse ratio of the absolute temperatures at which rate determinations have been made in the two series (cf. equation (14*a*) of reference 12) since both these series of reactions are approximately isoentropic. Any contributions of the solvent effects to the activation energies of the peracetic acid reactions must be small or to a good approximation constant

Can. J. Chem. Downloaded from www.nrcresearchpress.com by 210.87.254.105 on 09/05/12
For personal use only.

for the considered cases. These conclusions perhaps also approximately apply to the other series of reactions considered here, although their temperature coefficients at sufficiently large temperature intervals are not known.

The good correlations in the free energy plots in Fig. 4 for the peracetic acid and bromination reactions, when plotted against the logarithms of the rate constants of the oxygen atom reactions, show that these values can serve as an empirical measure of the basicity of olefins as it manifests itself in such addition reactions. This is equivalent to defining Hammett σ and ρ functions for these processes (12).

The series of CBr_2 and CCl_2 reactions with olefins have been considered here for the sake of completeness. They show general electrophilic trends but at the same time there are some large systematic deviations in the plots in Figs. 1–5. Thus, for example, in Fig. 4 the rate constants for cyclohexene are too low and for isobutene they are too high. In the plot in Fig. 5, the discrepancy for cyclohexene remains while it disappears for the α,α-disubstituted olefins. This is due to the exceptionally high values obtained for infrared O—H band frequency shifts in mixtures of phenols with these latter compounds and it may perhaps be fortuitous. There is need for more extensive experimental information on these reaction series in order to ascertain in greater detail the extent and the nature of the deviations.

ACKNOWLEDGMENTS

The author is indebted to Mr. L. C. Doyle for assistance with the experimental work and to Dr. A. W. Tickner for mass spectrometer analyses.

REFERENCES

1. R. A. Ogg, Jr. and M. Polanyi. Trans. Faraday Soc. **31**, 604 (1935).
2. M. G. Evans and M. Polanyi. Trans. Faraday Soc. **34**, 11 (1938).
3. M. G. Evans. Discussions Faraday Soc. **2**, 271 (1947).
4. M. G. Evans, J. Gergely, and E. C. Seaman. J. Polymer Sci. **3**, 866 (1948).
5. M. Levy and M. Szwarc. J. Am. Chem. Soc. **77**, 1949 (1955).
6. M. Szwarc. J. Phys. Chem. **61**, 40 (1957); J. H. Binks and M. Szwarc. J. Chem. Phys. **30**, 1494 (1959).
7. C. Walling. J. Phys. Chem. **64**, 166 (1960).
8. H. W. Melville and J. C. Robb. Proc. Roy. Soc. (London), A, **196**, 445, 466, 479, 494 (1949).
9. K. R. Jennings and R. J. Cvetanović. To be published.
10. R. J. Cvetanović. J. Chem. Phys. **25**, 376 (1956).
11. R. J. Cvetanović. Can. J. Chem. **36**, 623 (1958).
12. R. J. Cvetanović. J. Chem. Phys. **30**, 19 (1959).
13. R. J. Cvetanović. J. Chem. Phys. **23**, 1203 (1955).
14. S. Sato and R. J. Cvetanović. Can. J. Chem. **36**, 279, 970, 1668 (1958); **37**, 953 (1959).
15. D. J. Le Roy. Can. J. Research, B, **28**, 492 (1950).
16. R. J. Cvetanović. J. Chem. Phys. In press.
17. S. Sato and R. J. Cvetanović. J. Am. Chem. Soc. **81**, 3223 (1959).
18. S. Winstein and H. J. Lucas. J. Am. Chem. Soc. **60**, 836 (1938).
19. H. C. Brown and J. D. Brady. J. Am. Chem. Soc. **74**, 3570 (1952).
20. R. West. J. Am. Chem. Soc. **81**, 1614 (1959).
21. R. D. Brown. J. Chem. Soc. 2224 (1959).
22. T. Vrbaski and R. J. Cvetanović. Can. J. Chem. **38**, 1053 (1960).

Can. J. Chem. Downloaded from www.nrcresearchpress.com by 210.87.254.105 on 09/05/12
For personal use only.

Can. J. Chem. Downloaded from www.nrcresearchpress.com by 210.87.254.40 on 09/05/12
For personal use only.

ATOMIC REACTIONS IN THE UPPER ATMOSPHERE[1]

JOSEPH KAPLAN, WILLIAM J. SCHADE, CHARLES A. BARTH, AND ALVIN F. HILDEBRANDT

ABSTRACT

The reaction rates of nine upper atmosphere chemical reactions have been analyzed with a digital computer. The dependence of the loss rates of atomic nitrogen and atomic oxygen as well as the relative concentrations of nitric oxide and nitrogen dioxide in the upper atmosphere are given. Using a flow system, nitrogen atoms were produced and then titrated by the addition of NO. The resulting nitrogen and oxygen atom densities were measured with an e.p.r. spectrometer. The dependence of the intensities of the nitrogen afterglow and the NO afterglow were related to the atom densities. An excitation mechanism for OI 5577 has been determined from the relation of the intensity of λ 5577 to the atom densities.

ATOMIC REACTIONS IN THE CHEMOSPHERE

In the upper half of the earth's chemosphere between 65 and 120 km, reactions involving atomic species constitute the predominant chemical activity. The atoms involved are those produced by the solar photodissociation of the molecular atmospheric gases, nitrogen, oxygen, and hydrogen. The atoms react with one another and with the remaining molecules that are present. The dominant upper atmosphere reactions between atomic nitrogen and atomic oxygen and their various molecular forms are described by the following nine equations:

$$N + N + M \rightarrow N_2 + M \quad [1]$$

$$N + O + M \rightarrow NO + M \quad [2]$$

$$O + O + M \rightarrow O_2 + M \quad [3]$$

$$N + NO \rightarrow N_2 + O \quad [4]$$

$$N + O_2 \rightarrow NO + O \quad [5]$$

$$O + O_2 + M \rightarrow O_3 + M \quad [6]$$

$$O + O_3 \rightarrow O_2 + O_2 \quad [7]$$

$$NO + O + M \rightarrow NO_2 + M \quad [8]$$

$$NO_2 + O \rightarrow NO + O_2 \quad [9]$$

In the first three reactions, atomic nitrogen and atomic oxygen recombine in three-body reactions. Atomic nitrogen also reacts rapidly with nitric oxide and more slowly with molecular oxygen in reactions 4 and 5. The formation and destruction of ozone are governed by reactions 6 and 7 and the formation and destruction of nitrogen dioxide, by reactions 8 and 9. The rate coefficients for reaction 1 and reactions 4 through 9 are available in the recent literature (1, 2). Recently, in an experiment at the Jet Propulsion Laboratory, the rate coefficients of reactions 2 and 3 have been measured (3).

The differential equations describing the rates of change of density of the various species are the following:

$$-[\dot{N}] = 2k_1[N]^2[M] + k_2[N][O][M] + k_4[N][NO] + k_5[N][O_2] \quad [10]$$

$$-[\dot{O}] = k_2[N][O][M] + 2k_3[O]^2[M] - k_4[N][NO] - k_5[N][O_2] + k_6[O][O_2][M] + k_7[O][O_3] + k_8[NO][O][M] + k_9[NO_2][O] \quad [11]$$

[1]*Contribution from the Institute of Geophysics, University of California, Los Angeles, California, and the Jet Propulsion Laboratory, California Institute of Technology, Pasadena, California; paper presented at the Symposium on the Fundamental Aspects of Atomic Reactions held at McGill University, Montreal, Que., September 1960. The research reported in this paper was sponsored in part by the Geophysics Research Directorate, Air Force Cambridge Research Center, Air Research and Development Command, under Contract No. AF 19(604)-2143, and in part by the National Aeronautics and Space Administration at the Jet Propulsion Laboratory.*

$$-[\dot{N}O] = -k_2[N][O][M] + k_4[N][NO] - k_5[N][O_2] + k_8[NO][O][M] - k_9[NO_2][O] \quad [12]$$

$$-[\dot{O}_2] = -k_3[O]^2[M] + k_5[N][O_2] + k_6[O][O_2][M] - 2k_7[O][O_3] - k_9[NO_2][O] \quad [13]$$

$$-[\dot{O}_3] = -k_6[O][O_2][M] + k_7[O][O_3] \quad [14]$$

$$-[N\dot{O}_2] = -k_8[NO][O][M] + k_9[NO_2][O] \quad [15]$$

This set of simultaneous, non-linear differential equations has been numerically integrated for several different initial conditions on the Jet Propulsion Laboratory's IBM 704 digital computer (3). The results of one of these numerical calculations may be seen in Fig. 1. Although the atom densities used in this calculation pertain to a laboratory

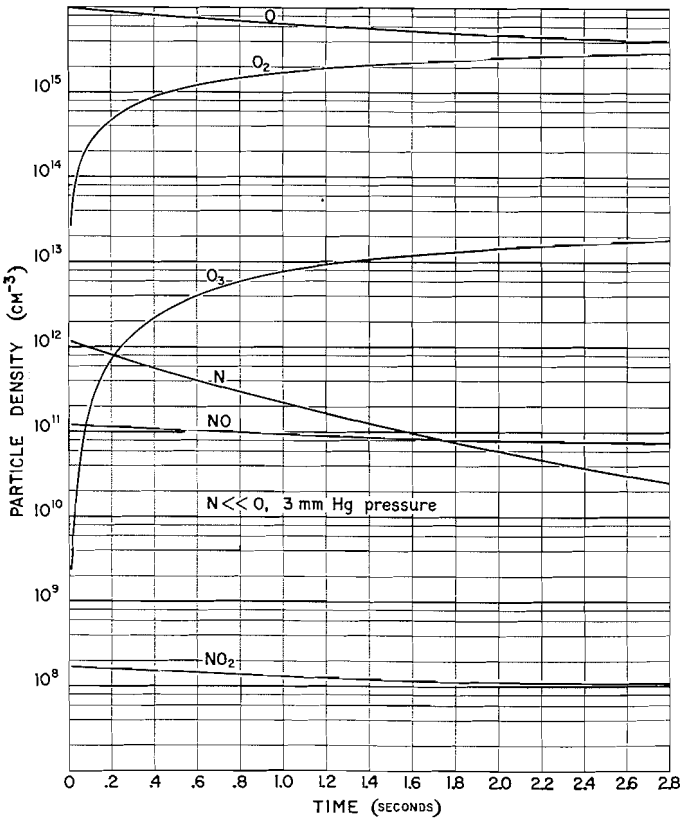


FIG. 1. Change of particle densities with time.

experiment, the conditions are analogous to those of the upper atmosphere in that the density of oxygen atoms is much greater than the density of nitrogen atoms. An analysis of the results of this numerical integration when applied to the chemosphere between 80 and 120 km gives the following results:

1. The rate of loss of atomic nitrogen is governed by its reaction with molecular oxygen, reaction 5.

2. The concentration of nitric oxide is determined by reaction 5 and the reaction of atomic nitrogen with nitric oxide, reaction 4. The density of nitric oxide is much less than, and proportional to, the density of the molecular oxygen present.

$$[NO] = k_5/k_4[O_2] \quad [16]$$

Can. J. Chem. Downloaded from www.nrcresearchpress.com by 210.87.254.40 on 09/05/12
For personal use only.

3. The concentration of nitrogen dioxide in the upper atmosphere is governed by the reactions of atomic oxygen with nitric oxide and nitrogen dioxide, reactions 8 and 9. The density of nitrogen dioxide is less than, and proportional to, the density of nitric oxide.

$$[NO_2] = (k_8/k_9)[M][NO] \qquad [17]$$

4. The rate of loss of atomic oxygen is determined by its three-body recombination, reaction 3.

ATOM DENSITY MEASUREMENTS

In some recent work at the Jet Propulsion Laboratory, atom densities of mixtures of nitrogen atoms and oxygen atoms have been measured with an electron paramagnetic resonance spectrometer (4). With this technique, atom densities as low as 5×10^{12} atoms/cm^3 have been determined. The nitrogen atoms are produced in a flow system by a 2450-mc microwave discharge operating at a total pressure of 3 mm Hg. The oxygen atoms were produced by titrating the atomic nitrogen with nitric oxide. The resulting mixture of atoms was pumped through the e.p.r. resonant cavity, which is located between the pole faces of an electromagnet. It is in this cavity that the atom densities are measured. The ground state of atomic nitrogen is ^4S with $J = 3/2$ and a Lande g factor of 2. Atomic oxygen has a ^3P ground state with a Lande g factor of 3/2. Both the $J = 2$ and $J = 1$ states of oxygen are measured.

The results of this study are shown in Fig. 2. The atom densities are plotted along the

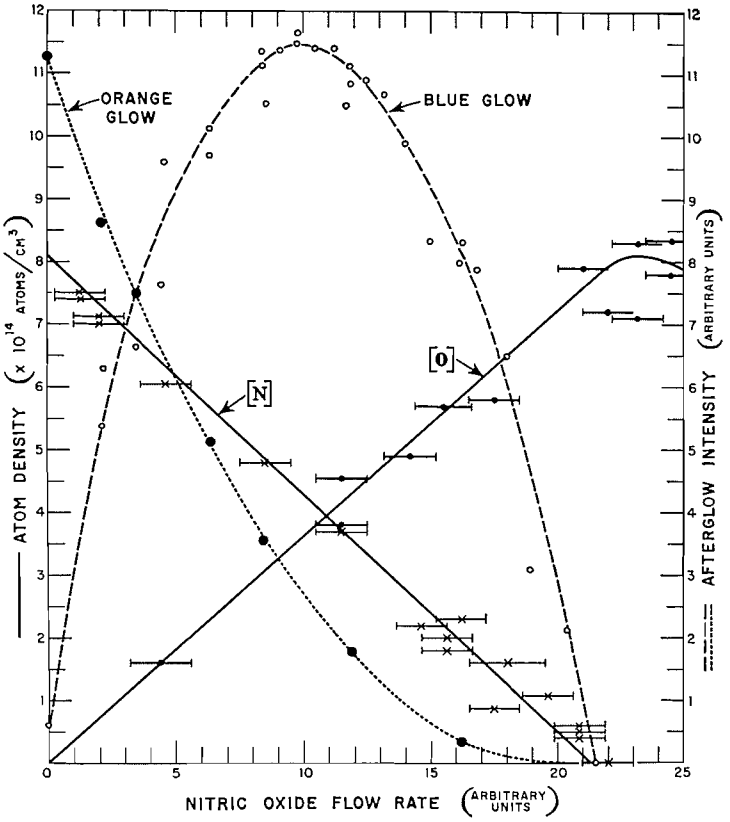


FIG. 2. Dependence of afterglow intensities on atom densities.

Can. J. Chem. Downloaded from www.nrcresearchpress.com by 210.87.254.40 on 09/05/12
For personal use only.

ordinate and the amount of NO added is plotted along the abscissa. Since the atomic nitrogen – nitric oxide reaction is very fast (1), for every nitric oxide molecule added, a nitrogen atom is converted into an oxygen atom before the gas enters the resonant cavity. Hence, the straight lines with slopes of 45° and −45° for the oxygen and nitrogen atom densities, respectively. Nitric oxide was continued to be added after all the nitrogen atoms were consumed. The loss of oxygen atoms on the right-hand side of the figure is governed by the nitric oxide – atomic oxygen reaction which is still taking place as the gas is pumped through the resonant cavity. Figure 1 is a decay study of the experimental conditions occurring near the minimum of nitrogen atom density and the maximum of oxygen atom density.

AFTERGLOW INTENSITY MEASUREMENTS

The intensity of the molecular nitrogen first positive bands that are emitted by the nitrogen afterglow is proportional to the square of the nitrogen atom density (5). In some work at the University of California, Los Angeles, it has been shown that the intensity of the nitric oxide beta bands is proportional to the product of the nitrogen atom density and the oxygen atom density (6). Using the preceding technique of addition of NO to atomic nitrogen, the atomic nitrogen density was decreased and the atomic oxygen density was increased. A simultaneous photometric recording of the intensities of the N_2 first positive bands and the NO beta bands provides data for interpreting the dependence of the intensity of the NO beta bands on the relative atomic densities of oxygen and nitrogen. A plot of I_b (intensity of NO beta bands) against the square root of the intensity of the N_2 first positive bands then yields a parabolic curve. This curve is consistent with the interpretation that the fast reaction 4 produces an increase in the atomic oxygen density which is equal in magnitude to the decrease in atomic nitrogen density, i.e.,

$$d[O] = -d[N]. \qquad [18]$$

Integration of 18 gives

$$[O] = [N_0] - [N], \qquad [19]$$

in which $[N_0]$ is the initial atomic nitrogen density before addition of NO and the initial atomic oxygen density is zero. Assuming that the emission of the beta bands follows a recombination of type 2, the intensity of the beta bands can be written

$$I_b = k_b[N][O][M]. \qquad [20]$$

Substitution of [19] into [20] gives

$$I_b = k_b[M][N]([N_0] - [N]) \qquad [21]$$

so that a plot of [21] against [N] produces the same parabolic curve obtained experimentally. The afterglow recombination mechanism 2 was also concluded in previous work (7). The dependence of the intensity of the N_2 first positive bands and the nitric oxide beta bands is plotted in Fig. 2 against flow rate of added nitric oxide. The parabolic shape of these curves illustrates their relationship to the nitrogen and oxygen atom densities.

Excitation of the atomic oxygen green line, OI 5577, which is a prominent spectral feature emanating from the upper atmosphere, has been studied recently by the addition of NO to active nitrogen (6). When atomic oxygen is added to atomic nitrogen by reaction 4, OI 5577 is found to be excited. As more NO is added to the system, the intensity of λ 5577 goes through a maximum value and decreases rapidly as the atomic nitrogen

Can. J. Chem. Downloaded from www.nrcresearchpress.com by 210.87.254.40 on 09/05/12
For personal use only.

density approaches zero. An excitation mechanism which is consistent with the relation between the intensity of λ 5577 and the variation of the atomic species is found to be

$$N + N + O \rightarrow N_2 + O(^1S) \quad [22]$$

$$O(^1S) \rightarrow O(^1D) + \lambda\ 5577 \quad [23]$$

in which ^1S is the upper state and ^1D the lower state of atomic oxygen for the emission of λ 5577. When sufficient NO is added to the system so that all atomic nitrogen has been removed, a condition is obtained in which the only remaining atomic species is that of oxygen so that $[O] = [N_0]$ (see Fig. 2). Under this condition the excitation of OI 5577 should take place by the reaction

$$O + O + O \rightarrow O_2 + O(^1S) \quad [24]$$

$$O(^1S) \rightarrow O(^1D) + \lambda\ 5577 \quad [25]$$

which was proposed for the excitation occurring in the upper atmosphere (8). It has been found in the laboratory that reaction 22 is much more efficient than reaction 24 in the excitation of the ^1S state of atomic oxygen.

REFERENCES

1. G. B. KISTIAKOWSKY and G. G. VOLPI. J. Chem. Phys. **27**, 1141 (1957); **28**, 665 (1958).
2. F. KAUFMAN. J. Chem. Phys. **28**, 352 (1958).
P. HARTECK, R. R. REEVES, and G. MANELLA. J. Chem. Phys. **29**, 608 (1958).
J. F. HERRON, J. L. FRANKLIN, P. BRADT, and V. H. DIBELER. J. Chem. Phys. **30**, 879 (1959).
R. R. REEVES, G. MANELLA, and P. HARTECK. J. Chem. Phys. **32**, 632 (1960).
S. KRONGELB and M. W. P. STRANDBERG. J. Chem. Phys. **31**, 1196 (1959).
S. W. BENSON and A. E. AXWORTHY. J. Chem. Phys. **26**, 1718 (1957).
H. W. FORD and N. ENDOW. J. Chem. Phys. **27**, 1156 (1957).
3. C. A. BARTH. J. Chem. Phys. Submitted for publication.
4. A. F. HILDEBRANDT and C. A. BARTH. J. Chem. Phys. Submitted for publication.
5. J. BERKOWITZ, W. A. CHUPKA, and G. B. KISTIAKOWSKY. J. Chem. Phys. **25**, 457 (1956).
6. W. J. SCHADE and J. KAPLAN. To be published.
7. F. KAUFMAN and J. R. KELSO. J. Chem. Phys. **27**, 1209 (1957).
F. KAUFMAN. J. Chem. Phys. **28**, 992 (1958).
C. A. BARTH, W. J. SCHADE, and J. KAPLAN. J. Chem. Phys. **30**, 347 (1959).
8. S. CHAPMAN. Phil. Mag. **23**, 657 (1937).

Can. J. Chem. Downloaded from www.nrcresearchpress.com by 210.87.254.40 on 09/05/12
For personal use only.

Can. J. Chem. Downloaded from www.nrcresearchpress.com by 210.87.254.6 on 09/05/12
For personal use only.

THREE-BODY RECOMBINATION OF GASEOUS IONS[1]

TAKAYUKI FUENO, HENRY EYRING, AND TAIKYUE REE

ABSTRACT

The recombination of gaseous ions in the presence of third bodies is assumed to follow a sequence of two bimolecular steps: $M + X^+ \rightleftharpoons MX^+$ and $MX^+ + Y^- \rightarrow XY + M$. The termolecular rate constants of the over-all processes are calculated for several ionized gases at various temperatures. For the calculation, the equilibrium internuclear separation and the corresponding binding energy of a complex ion, MX^+, are obtained by minimizing the interaction energy between M and X^+, which is approximated to the sum of the Lennard-Jones potential for the M–X interaction and the polarization energy between M and X^+. The recombination coefficients of some ionized gases at 288° K and various pressures are calculated and compared with the observed data. The agreement is found to be satisfactory. The limitations of this theoretical approach are discussed.

INTRODUCTION

The surplus energy evolved by the neutralization (or recombination) between positive and negative ions in a gaseous phase can be removed as radiation or taken up as the energy of excitation or homolytic dissociation of the recombination product (1, 2). Thomson (3) developed a gas-kinetic theory of the ion recombination occurring by the three-body process. The theory was based on the concept that two ions of opposite signs are only capable of recombination if either of the two ions collides with an uncharged molecule within a certain maximum distance from the other. The theory has proved very successful in the pressure range from 100 to 1000 mm Hg.

Recently, Bunker and Davidson (4) have proposed a kinetic theory to account for the rates of halogen atom recombinations in the presence of various third bodies. The theory assumes that an equilibrium concentration of intermediate complex is formed between halogen atoms and third bodies and that the collisions of the complexes with halogen atoms result in the halogen atom recombinations, releasing the third-body molecules. The dependence of the termolecular reaction rate constants upon temperature and third body has thus been interpreted quantitatively.

The present paper outlines a theoretical method of predicting the rates of the three-body recombinations of gaseous ions. The treatment pursues essentially the Bunker–Davidson theory for atom recombinations (4), except that, in our approach, the electrostatic nature of the recombining species is also taken into account. The theory is successfully applied to the calculation of the recombination coefficients for some ionized gases.

CALCULATION METHOD

An over-all three-body process of ion recombination, $X^+ + Y^- + M \rightarrow XY + M$, is assumed to be divided into a sequence of two bimolecular steps:

$$M + X^+ \underset{k_{-1}}{\overset{k_1}{\rightleftharpoons}} MX^+ \qquad [i]$$

$$MX^+ + Y^- \xrightarrow{k_2} XY + M \qquad [ii]$$

where M denotes a third body. If MX^+ is a loose complex and M is in a large excess

[1]*Contribution from the Department of Chemistry, University of Utah, Salt Lake City, Utah; paper presented at the Symposium on the Fundamental Aspects of Atomic Reactions held at McGill University, Montreal, Que., September 1960.*

compared with X^+ and Y^-, then MX^+ will be in equilibrium with X^+ and M, undisturbed by step [ii]. Then the rate constant, k_t, for the over-all termolecular process can be approximated as (4, 5)

$$[1] \qquad k_t = K_1 k_2,$$

K_1 being the equilibrium constant for step [i].

Assuming that the complex MX^+ is an ion cluster, we now calculate the equilibrium constant, K_1. The complex may be loose enough so that M and X^+ are free to rotate and vibrate within the complex (6). Then, all the internal parts of the partition functions of the separated reactants will also appear in the partition function of the complex and will cancel out in the expression of the equilibrium constant, K_1, in terms of partition functions. Thus,

$$[2] \qquad K_1 = \frac{F_{t,MX^+} F_{v,MX^+} F_{r,MX^+}}{F_{t,M} F_{t,X^+}} e^{\epsilon_m/kT}$$

where ϵ_m is the binding energy of MX^+, and the subscripts t, v, and r indicate that the F's are respectively the translational, vibrational, and rotational partition functions of the substances indicated.

If we assume that the complex is a rigid rotor as well as a harmonic oscillator and that neither of the rotational and vibrational energies of the complex can exceed the binding energy ϵ_m, then (7)

$$[3] \qquad F_{r,MX^+} = \frac{8\pi^2 \mu_+ r_m^2 kT}{h^2} (1 - e^{-\epsilon_m/kT})$$

and

$$[4] \qquad F_{v,MX^+} = \frac{1 - e^{-\epsilon_m/kT}}{1 - e^{-\epsilon_v/kT}}$$

where μ_+ is the reduced mass of the complex, r_m the equilibrium internuclear distance between M and X^+ in the complex, and ϵ_v the vibrational quantum of the $M—X^+$ bond. Substituting all the partition functions into eq. 2, we obtain

$$[5] \qquad K_1 = \frac{h^3}{(2\pi\mu_+ kT)^{3/2}} \cdot \frac{8\pi^2 \mu_+ r_m^2 kT}{h^2} \cdot \frac{(1 - e^{-\epsilon_m/kT})^2 e^{\epsilon_m/kT}}{1 - e^{-\epsilon_v/kT}}.$$

For step [ii] of the recombination we assume that every collision between MX^+ and Y^- leads to the neutralization with the liberated energy which is carried away by the third body, M. Then, assuming that the steric factor for the collision is unity, we can write

$$[6] \qquad k_2 = Q \left\{ \frac{8kT(m + m_+ + m_-)}{\pi(m + m_+) m_-} \right\}^{\frac{1}{2}},$$

where Q is the effective collision cross section, and m, m_+, and m_- are the masses of M, X^+, and Y^-, respectively.

The feature of the collision cross section for ion recombinations is largely different from that of the usual gas-kinetic collisions, because of a considerable extent of coulombic attraction between the two recombining ionic partners. One charged particle can be captured by the other when the attraction exceeds the relative kinetic energy of the ion pair. If the gaseous ions are in thermal agitation, the largest permissible distance of approach, δ, for ions to recombine is (3)

$$[7] \qquad \delta = \frac{2e^2}{3kT},$$

Can. J. Chem. Downloaded from www.nrcresearchpress.com by 210.87.254.6 on 09/05/12
For personal use only.

where e is the electronic charge and δ is of the order of 10^{-6} cm at ordinary temperatures. The effective cross section, Q, for the ion recombination is given by

$$[8] \qquad Q = \pi\delta^2 = \frac{4\pi e^4}{9k^2T^2}.$$

From eqs. 1, 5, 6, and 8 we finally obtain the termolecular rate constant, after the proper cancellation,

$$[9] \qquad k_t = \frac{32\pi h e^4 r_m^{\,2}(m+m_+ +m_-)^{\frac{1}{2}}}{9\mu_+^{\frac{1}{2}} m_-^{\frac{1}{2}}(m+m_+)^{\frac{1}{2}}k^2T^2} \cdot \frac{(1-e^{-\epsilon_m/kT})^2 e^{\epsilon_m/kT}}{1-e^{-\epsilon_v/kT}}.$$

In order to obtain the values of k_t for recombining systems from eq. 9 it is necessary to evaluate the three parameters, r_m, ϵ_m, and ϵ_v. For evaluating the r_m and ϵ_m, both the X^+ and M are idealized as rigid spheres. If X and M are molecules with little or no permanent dipole, then the potential of interaction between X^+ and M will be reasonably approximated to the sum of the Lennard-Jones potential of interaction between the two neutral molecules and the polarization energy, i.e., the attraction between the static charge on X^+ and the dipole moment induced on M

$$[10] \qquad \epsilon_L(r) = 4\epsilon_0\left\{\left(\frac{\sigma}{r}\right)^{12} - \left(\frac{\sigma}{r}\right)^{6}\right\} - \frac{\alpha e^2}{2r^4}.$$

Here ϵ_0 and σ respectively denote the maximum depth of the potential well and the closest approach for the interaction between X and M, r is the internuclear separation of the MX^+ complex, and α is the angle-average polarizability of M. The equilibrium distance, r_m, and the corresponding binding energy, ϵ_m, of the complex can be obtained by minimizing the $\epsilon_L(r)$ with respect to r, provided that the values of ϵ_0, σ, and α are known.

The vibrational quantum, ϵ_v, can be calculated from [8]

$$[11] \qquad \epsilon_v = 2a\,(\epsilon_r\epsilon_m)^{\frac{1}{2}}$$

where $\epsilon_r = h^2/8\pi^2\mu_+ r_m^2$ and a is a parameter appearing in the Morse potential function for the complex in the form

$$[12] \qquad \epsilon_M(r) = \epsilon_m[\{1-e^{-a[(r/r_m)-1]}\}^2 - 1].$$

The value of a is obtainable, in principle, by making the Morse potential curve (eq. 12) fit the Lennard-Jones-type potential curve (eq.10). A practical method employed here for this purpose is setting the bond-stretching force constant, f_M, derived from the Morse function

$$[13] \qquad f_M = \left[\frac{d^2\epsilon_M(r)}{dr^2}\right]_{r=r_m} = \frac{2a^2\epsilon_m}{r_m^{\,2}}$$

equal to the force constant, f_L, from the Lennard-Jones-type function

$$[14] \qquad f_L = \left[\frac{d^2\epsilon_L(r)}{dr^2}\right]_{r=r_m} = \frac{24\epsilon_0}{r_m^{\,2}}\left\{26\left(\frac{\sigma}{r_m}\right)^{12} - 7\left(\frac{\sigma}{r_m}\right)^{6}\right\} - \frac{10\alpha e^2}{r_m^{\,6}}.$$

Thus, the three parameters, r_m, ϵ_m, and ϵ_v, involved in eq. 9 can straightforwardly be evaluated for the interacting systems for which the data of the relevant parameters, ϵ_0, σ, and α are available.

Can. J. Chem. Downloaded from www.nrcresearchpress.com by 210.87.254.6 on 09/05/12
For personal use only.

COMPARISON WITH EXPERIMENTS

It is experimentally established that the rates of recombination of gaseous ions are of a first order with respect to each concentration of positive and negative ions. The bimolecular rate constants, ρ, defined as

$$[15] \qquad \frac{d(X^+)}{dt} = \frac{d(Y^-)}{dt} = -\rho(X^+)(Y^-),$$

are usually called the recombination coefficients (1, 2). If the recombination takes place by the two-step mechanism assumed in this paper, the recombination coefficient should be equal to the product of the termolecular rate constant and the third-body concentration, i.e.

$$[16] \qquad \rho = k_t(M).$$

Over the pressure range from 100 to 760 mm Hg, the values of ρ for the recombinations in familiar gases such as CO, CO_2, SO_2, N_2O, and air have been observed to be proportional to the gas pressure (9). This observation indicates that over this pressure range the three-body process is the most important for the recombinations of ions at least in the cases of the above-mentioned molecular gases.

In order to obtain the value of ρ for recombining ions in a given gas, molecular configurations of X^+ and Y^- need to be specified. According to the mass spectroscopic experiments, most of the positive ions formed by electron impact with molecules are, in general, of the simple molecular type, i.e., the lowest appearance potential of a positive ion from a molecule corresponds to the simple removal of an electron without dissociation (10). Probably, a similar generalization applies to the ionizations of molecular gases resulting from the action of X-rays, a method which was often employed in earlier years (9, 11). Thus, it is assumed throughout the present paper that X^+ is the molecular ion formed by the removal of an electron from M.

Negative ions can be formed by the collisions of electrons with neutral molecules. However, it is not, as a rule, obvious what products result from the collisions. The best information has been given by mass spectroscopic studies. For instance, the most prominent negative ion observed in air and oxygen under pressures of 0.1 to 10 mm Hg has been identified to be O^-, instead of O_2^- (12). The atomic ion O^- is found to be the most abundant (or the only) negative ion also in the cases of CO (13), CO_2 (14), N_2O (15), NO (13, 15), NO_2 (16), and SO_2 (17). Thus, it appears very likely that the gaseous oxide molecules as well as oxygen molecules produce negative ions most effectively by the "resonance electron-capture dissociation (18)." In our calculation, therefore, Y^- is assumed to be the atomic ion O^- for all of the oxygen-containing molecules investigated.

According to the procedure described in the preceding section, all the potential parameters associated with the M—X^+ interactions were calculated for various gases. The data of the Lennard-Jones potential parameters, σ and ϵ_0, and the polarizability, α, for these gases were taken from the literature (19). All of the parametric values obtained are summarized in Table I.

Figure 1 shows the potential curves of interaction between CO_2^+ and CO_2 as a typical example of the M—X^+ interaction curves. The potential parameters used for drawing these curves are those listed in Table I. It is seen in Fig. 1 that the Morse curve somewhat deviates from the Lennard-Jones-type curve when the internuclear separation is fairly large compared with the equilibrium separation. However, any further modification of

Can. J. Chem. Downloaded from www.nrcresearchpress.com by 210.87.254.6 on 09/05/12
For personal use only.

TABLE I

Potential parameters for the ion–molecule interaction

Gas	σ^* (Å)	ϵ_0/k^* (°K)	$\alpha\times10^{24}$† (cm^3)	r_m (Å)	$\epsilon_m\times10^{13}$ (erg)	$f_L\times10^3$ (dyne cm^{-1})	a	$\epsilon_v\times10^{14}$ (erg)
H_2	2.928	37.0	0.79	2.591	1.561	11.90	5.058	8.894
O_2	3.433	113	1.60	3.342	1.350	6.627	5.236	1.659
N_2	3.681	91.5	1.76	3.576	1.146	4.801	5.176	1.509
Air	3.617	97.0	1.73‡	3.516	1.189	5.216	5.207	1.551
CO	3.706	88.0	1.95	3.567	1.231	5.230	5.198	1.665
CO_2	3.897	213	2.65	3.972	1.341	4.899	5.369	1.217
SO_2	4.290	252	3.72	4.431	1.312	3.919	5.415	0.9016
N_2O	3.879	220	3.00	3.827	1.502	8.976	6.788	1.690

*Reference 19, p. 1111.
†Reference 19, p. 950.
‡Obtained by taking the weighted average of the data for O_2 and N_2.

the a-value in this respect will not be made here because it does not yield any serious change in the results obtained from the present approximation.

Using the parametric values given in Table I, the values of the equilibrium constant, K_1, and the reaction rate constants, k_2 and k_t, were calculated for several gases at 288, 600, and 1000° K. The results are given in Table II.

TABLE II

Calculated values of K_1, k_2, and k_t

Gas	Temp. (°K)	$K_1\times10^{21}$ (cm^3 $molecule^{-1}$)	$k_2\times10^6$ (cm^3 ion^{-1} sec^{-1})	$k_t\times10^{26}$ (cm^3 ion^{-1} $molecule^{-1}$ sec^{-1})
H_2	288	4.697	9.970	4.683
	600	0.4291	3.315	0.1422
	1000	0.1382	1.541	0.02130
O_2	288	4.152	3.231	1.342
	600	0.6404	1.074	0.06878
	1000	0.2493	0.4993	0.01245
Air	288	3.296	3.266	1.076
	600	0.5868	1.086	0.06373
	1000	0.2361	0.5048	0.01192
CO	288	2.578	3.277	0.8448
	600	0.4409	1.090	0.04806
	1000	0.1756	0.5064	0.008892
CO_2	288	5.850	3.142	1.838
	600	0.9339	1.045	0.09759
	1000	0.3681	0.4855	0.01787
SO_2	288	5.536	3.064	1.696
	600	0.9241	1.019	0.09417
	1000	0.3693	0.4735	0.01749
N_2O	288	4.845	3.142	1.522
	600	0.6479	1.045	0.06771
	1000	0.2444	0.4855	0.01187

Inspection of the data in Table II indicates that the negative temperature-dependence of k_t is not only a consequence of the decreasing nature of K_1 with increasing temperature but it is also due to the same tendency of k_2. In fact, at relatively high temperatures, the latter constant appears to depend upon the temperature to the same extent as the former does.

Can. J. Chem. Downloaded from www.nrcresearchpress.com by 210.87.254.6 on 09/05/12
For personal use only.

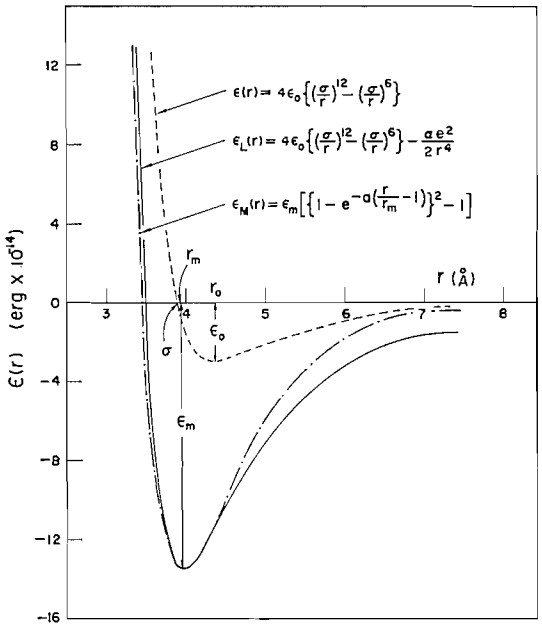


FIG. 1. The potential curves of interaction between CO_2 and CO_2^+.

TABLE III

Calculated and observed ion-recombination coefficients at 288° K

Gas	Pressure (mm Hg)	$\rho_{calc} \times 10^6$ ($cm^3\ ion^{-1}\ sec^{-1}$)	$\rho_{obs} \times 10^{6*}$ ($cm^3\ ion^{-1}\ sec^{-1}$)	$\frac{\rho_{obs}}{\rho_{calc}}$
H_2	760	1.19	1.44†	1.2
O_2	760	0.342	1.61†	4.7
Air	743	0.268	1.68	6.3
	662	0.239	1.48	6.2
	462	0.167	1.03	6.2
	363	0.131	0.83	6.3
	307	0.111	0.73	6.6
	197	0.0711	0.44	6.2
CO	757	0.215	0.87	4.1
	690	0.196	0.77	3.9
	556	0.158	0.63	4.0
	409	0.116	0.45	3.9
	247	0.0700	0.22	3.1
CO_2	729	0.449	1.65	3.7
	614	0.379	1.45	3.8
	498	0.307	1.20	3.9
	373	0.230	0.93	4.0
	265	0.163	0.67	4.1
	175	0.108	0.49	4.5
SO_2	680	0.387	1.32	3.4
	504	0.287	1.08	3.8
	444	0.253	0.91	3.6
	338	0.192	0.73	3.8
	200	0.114	0.42	3.7
	83.5	0.0475	0.26	5.5
N_2O	749	0.382	1.36	3.6
	596	0.304	1.15	3.8
	430	0.220	0.81	3.7
	294	0.150	0.53	3.5
	200	0.102	0.33	3.2

*Reference 9, unless otherwise noted.
†Reference 20.

Can. J. Chem. Downloaded from www.nrcresearchpress.com by 210.87.254.6 on 09/05/12
For personal use only.

For the gases listed in Table II, the values of ion-recombination coefficients, ρ, were calculated under varying pressures at 288° K. In Table III, the calculated values are compared with the observed data (9). Except for H_2 and air, the calculated values of ρ are too small by a roughly constant factor of 4. In the case of air the factor is about 6. Yet, the disagreement is not as bad as it sounds, in view of the crudeness of the approximations involved in the present theory. Generally the calculated values agree with experiment at least in order of magnitude. In this sense, therefore, the coincidence found for H_2 is considered as accidental.

DISCUSSION

(A) Termolecular Reaction and the Steady-State Treatment

Under the assumption of the stationary concentration of MX^+, the over-all rate of ion recombinations is expressed by

$$v = \frac{k_1 k_2 (M)(X^+)(Y^-)}{k_{-1} + k_2 (Y^-)}, \qquad [17]$$

which can be kinetically third order if $k_{-1} \gg k_2\,(Y^-)$. The last condition is fulfilled in the recombining systems investigated, in the following way:

Since k_{-1} is the rate constant for the unimolecular decomposition of MX^+, one may expect that $k_{-1} \simeq 10^{13} e^{-\epsilon_m/kT}\,\mathrm{sec}^{-1}$. If we choose $\epsilon_m = 1.4\times10^{-13}$ erg for a complex ion, then k_{-1} comes out to be ca. 3×10^{11} sec^{-1} at ordinary temperatures. On the other hand, the bimolecular rate constant, k_2, at 288° K is approximately 3×10^{-6} cm^3 ion^{-1} sec^{-1} for most gases investigated, as seen in Table II. Therefore, k_{-1} will be larger than $k_2\,(Y^-)$ until (Y^-) exceeds 10^{17} ions cm^{-3} (or 3.7×10^{-3} in mole fraction in a gas at the normal temperature and pressure). In many ionization phenomena the ion concentrations are much smaller than this limiting concentration, and so it is very probable that $k_2\,(Y^-)$ is sufficiently small compared with k_{-1}. In addition, the condition $k_{-1} \gg k_2\,(Y^-)$ is favored by high temperatures and low pressures, because k_2 has a negative temperature coefficient and (Y^-) will become smaller with decreasing pressure.

Obviously the theory is subjected to a serious restriction concerned with the steady-state hypothesis. In order that the time lag between the formation and destruction of MX^+ is negligible, the concentration of MX^+ as an intermediate should be at all times much less than that of X^+ as a reactant. To check this point, the concentration ratios, $(MX^+)/(X^+)$, were calculated from

$$\frac{(MX^+)}{(X^+)} = K_1(M) \qquad [18]$$

for the gases in question, using the values of K_1 given in Table II. The calculated ratios at 288° K and 1 atmosphere pressure are: H_2, 0.119; O_2, 0.106; air, 0.084; CO, 0.066; CO_2, 0.149; SO_2, 0.141; N_2O, 0.124. Although these ratios are not actually small compared with unity, they do appear to be small enough to neglect for the present purpose. This situation becomes more serious under higher pressures, because the concentration ratio increases proportionally with the increasing pressure. Therefore, under pressures much higher than 1 atmosphere, the over-all recombination cannot be approximated by $K_1 k_2 (M)(X^+)(Y^-)$ even if the condition $k_1 \gg k_2(Y^-)$ is satisfied.

Moreover, it has been shown experimentally that, although the recombination coefficients increase linearly with the increasing pressure up to approximately 1000 mm Hg, they attain the maximum values around this limiting pressure and then decrease

Can. J. Chem. Downloaded from www.nrcresearchpress.com by 210.87.254.6 on 09/05/12
For personal use only.

gradually as the pressure increases further (1, 2). Apparently, the latter phenomenon is not attributable to the three-body process. It is thus concluded that the present theory does not apply to the ion recombinations occurring under gas pressures higher than 1000 mm Hg.

(B) The Potential Parameters

As has already been described, all the potential parameters necessary for the calculation of K_1 are obtainable from the interrelations among these parameters provided that the values for ϵ_0, σ, and α are known. Thus the calculated data for the ion-recombination coefficients are essentially dependent upon these three parameters. Of the three, ϵ_0 is the least important, because the equilibrium separation, r_m, of an M—X^+ binding is usually close to σ where the Lennard-Jones potential is zero as seen in Table I. In other words, the maximum binding energy of the complex is mainly due to the polarization force at the separation, r_m, and it can even be approximated with a reasonable accuracy to the polarization force at the internuclear separation of σ (see Fig. 1 as an example). Thus, it should be noticed that the calculated values of the recombination coefficients are particularly sensitive to the empirical values of σ chosen.

The close agreement between theory and experiment found for the ρ's for hydrogen will break down with a more reasonable choice of the σ-value. In the calculation, σ (= 2.928 Å) was the closest approach for elastic collisions between hydrogen molecules, and the ion cluster H_2—H_2^+ was assumed to be stable at an internuclear separation, 2.591 Å, which was obtained by using the above value of σ. According to Eyring, Hirschfelder, and Taylor (6), however, an irreversible process

$$H_2 + H_2^+ \rightarrow H_3^+ + H \qquad [iii]$$

can take place very rapidly. Actually, it has been deduced from experiments that reaction [iii] occurs in nearly every collision between H_2 and H_2^+ (21). If we consider that the pre-neutralization equilibrium in the case of hydrogen is

$$H_2 + H_3^+ \rightleftharpoons H_2—H_3^+ \qquad [iv]$$

rather than

$$H_2 + H_2^+ \rightleftharpoons H_2—H_2^+, \qquad [v]$$

then the equilibrium internuclear separation in the intermediate complex will be larger on account of more bulkiness of H_3^+ than that of H_2^+. As a result, the binding energy of the complex and consequently the calculated values of K_1 and ρ will become correspondingly smaller.

(C) An Alternative Mechanism

So far the discussion has been confined to the recombination mechanism in which positive ions, X^+, are assumed to be equilibrated with their ion clusters prior to the neutralization with negative ions, Y^-. However, there is no definite reason why an alternative mechanism

$$M + Y^- \rightleftharpoons MY^- \qquad [vi]$$

$$MY^- + X^+ \rightarrow XY + M \qquad [vii]$$

can be eliminated from the consideration. Nevertheless, the mechanism does not seem very likely, because there would be a large possibility that the detachment of electrons (or ionization of MY^-) occurs on the collisions of MY^- with M. The possibility of this ionizaton is much larger than that of the second step [vii], because of the presence of a

Can. J. Chem. Downloaded from www.nrcresearchpress.com by 210.87.254.6 on 09/05/12
For personal use only.

large excess of M and the small electron affinities of the negative ions in general. The electrons thus liberated could collide with M to reproduce the negative ions Y^-, the concentration of which would therefore be maintained until they are neutralized with the partners, MX^+. There is then no participation of step [vii] in the ion recombinations. This point is, of course, still open to question and needs further consideration in the future.

ACKNOWLEDGMENTS

The authors wish to express their appreciation to the Office of Ordnance Research, United States Army, for partial support of the present work under Contract No. DA-04-495-ORD-959. The work was also supported in part by the United States Air Force under Contract No. AF 04(647)-177, to whom the authors are gratefully indebted.

REFERENCES

1. H. S. W. Massey and E. H. S. Burhop. Electronic and ionic impact phenomena. Oxford at the Clarendon Press. 1952. Chap. 10.
2. A. von Engel. Ionized gases. Oxford at the Clarendon Press. 1955. Chap. 6.
3. J. J. Thomson. Phil. Mag. **47**, 337 (1924).
4. D. L. Bunker and N. Davidson. J. Am. Chem. Soc. **80**, 5090 (1958).
5. S. W. Benson. The foundations of chemical kinetics. McGraw-Hill Book Co., Inc., New York. 1960. p. 306.
6. H. Eyring, J. O. Hirschfelder, and H. S. Taylor. J. Chem. Phys. **4**, 479 (1936).
7. D. Britton. J. Phys. Chem. **63**, 1464 (1959).
8. A. G. Gaydon. Dissociation energies. Dover Publishers, Inc., New York. 1950. p. 29.
9. H. Thirkill. Proc. Roy. Soc. A, **88**, 477 (1913).
10. J. J. Thomson and G. P. Thomson. Conduction of electricity through gases. Vol. 1. 3rd ed. Cambridge. 1933. Chap. 3.
11. J. J. Thomson and G. P. Thomson. Conduction of electricity through gases. Vol. 2. 3rd ed. Cambridge. 1928. Chap. 2.
12. H. S. W. Massey. Negative ions. 2nd ed. Cambridge. 1950. p. 2.
13. H. S. W. Massey. Negative ions. 2nd ed. Cambridge. 1950. p. 58.
14. J. D. Craggs and B. A. Tozer. Proc. Roy. Soc. A, **254**, 229 (1960).
15. B. E. Knox and B. P. Burtt. J. Chem. Phys. **28**, 1256 (1958).
16. R. E. Fox. J. Chem. Phys. **32**, 285 (1960).
17. H. Neuert and O. Rosenbaum. Naturwissenschaften, **41**, 85 (1954).
18. F. H. Field and J. L. Franklin. Electron impact phenomena. Academic Press, Inc., New York. 1957. p. 25.
19. J. O. Hirschfelder, C. F. Curtiss, and R. B. Bird. Molecular theory of gases and liquids. John Wiley & Sons, Inc., New York. 1954.
20. K. T. Compton and I. Langmuir. Revs. Mod. Phys. **2**, 123 (1930).
21. J. O. Hirschfelder, C. F. Curtiss, and R. B. Bird. Molecular theory of gases and liquids. John Wiley & Sons, Inc., New York. 1954. p. 1095.

Can. J. Chem. Downloaded from www.nrcresearchpress.com by 210.87.254.6 on 09/05/12
For personal use only.

Can. J. Chem. Downloaded from www.nrcresearchpress.com by 210.87.254.6 on 09/05/12
For personal use only.

A COMBINED FLASH PHOTOLYSIS AND SHOCK WAVE METHOD FOR THE STUDY OF BROMINE ATOM RECOMBINATION OVER A WIDE TEMPERATURE RANGE[1]

GEORGE BURNS AND D. F. HORNIG

ABSTRACT

A combined flash photolysis shock wave experiment is described in which bromine is first flash photolyzed, then compressed and heated by a shock wave, and finally allowed to recombine at the high temperature. Some of the problems connected with working in a shock tube used as a photolysis vessel are analyzed. The apparatus was used to measure recombination rates with argon as a third body at room temperature, to estimate the efficiency of bromine as a third body at room temperature, and to obtain a preliminary measurement of the recombination rate of bromine in the presence of argon at 950° K.

INTRODUCTION

The rate of the three-body recombination of both iodine and bromine atoms has been measured as a function of temperature between 300° K to 550° K by the flash photolysis method (1–4). Recombination rates have also been calculated from rates of dissociation and equilibrium constants in iodine, bromine, and oxygen (5–12). In every case the rate of recombination decreases with increasing temperature.

The source of this temperature effect has been the subject of considerable theoretical discussion and it may arise from several sources.

(*a*) An approximately $1/T$ temperature dependence appears in the statistical theories of Wigner (13) and of Keck (14).

(*b*) The fact that for attracting molecules the collision cross section decreases with increasing molecular velocity will produce a decrease in the rate as the mean velocity increases, similar to the effect on gaseous viscosities (15).

(*c*) If the reaction proceeds through the sequence

$$A + M \rightleftarrows AM$$

$$AM + A \rightarrow A_2 + M,$$

the fall-off may be attributed to the decreasing equilibrium concentration of the complex AM. This latter suggestion has been particularly in vogue recently (16–19). However, the existing experimental data do not cover a wide enough temperature range to make any unambiguous choices so it seemed important to extend the temperature range of direct recombination rate measurements.

It seemed possible to do this by using flash photolysis to dissociate the halogen molecule and a shock wave to heat the gas. Several variations of such an experiment might be considered.

1. If the gas is initially photolyzed and then heated, the photolysis is carried out at the initial gas density and the recombination is carried out at a gas density two to four times higher. This results in faster recombination, an important feature since it is only possible to maintain the high temperature for a limited time in the shock tube. An intrinsic limitation of this approach is that in order to observe recombination, the photolytic dissociation must exceed the equilibrium thermal dissociation behind the shock wave. In

[1]*Contribution from the Frick Chemical Laboratory, Princeton University, Princeton, N.J.; paper presented at the Symposium on Fundamental Aspects of Atomic Reactions held at McGill University, Montreal, Que., September 1960.*

most experimental arrangements this would make it possible to reach temperatures in the vicinity of 2000° C.

2. If the gas is initially heated and then photolyzed the upper temperature limitation of the first approach is removed since the photolytic dissociation is added to the thermal dissociation. However, in this case the rates are from 2^3 to 4^3 lower for comparable initial conditions because of the density effect.

3. Either of the first two methods can be applied to a reflected shock wave. Reflected shocks have the advantage that higher temperatures and gas densities may be reached while at the same time the gas behind the reflected wave is not in motion. However, a variety of problems involving shock wave dynamics have complicated previous experiments with reflected waves (20, 21).

In designing an experiment, then, one must arrive at a suitable compromise among a variety of factors.

APPARATUS

A diagram of the apparatus utilized is shown schematically in Fig. 1. The low-pressure section, a 3-in. diameter pyrex glass shock tube, was filled with the bromine–argon mixture to be studied. When a cellulose acetate diaphragm (X), separating the low-pressure section from the helium-filled high-pressure section was punctured, a shock wave was sent through the low-pressure gas, compressing it and heating it to the desired temperature.

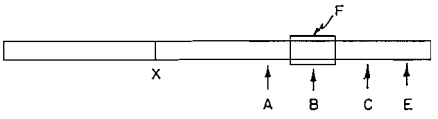


FIG. 1. Diagram of the apparatus.

By the time the disturbance reached station A a shock wave had been formed. Station A activated the time delay circuits which triggered the flash lamps (F), started the oscilloscope sweeps, etc. When the shock was about to enter the illuminated region the high-voltage condensers were discharged through the flash lamp, dissociating about 20% of the Br_2. The partially dissociated gas was subsequently compressed and heated by the shock wave. Since the gas behind the shock front was in motion the dissociated gas was carried down the tube and the optical absorption, from which the concentration of Br_2 could be measured, was studied at successive times by stations C and E.

The distance between the electrodes of the flash lamps was 25 cm; they were made of 1.9-cm diameter quartz tubes filled with xenon at a pressure of 100 mm Hg. The electrodes were made of 1/4-in. tungsten rods. In order to minimize the inductance the return lead from each lamp was made of copper foil covering the outer half of each tube. These lamps had an inductance of 1.8 microhenries and a resistive impedance of 1 ohm. The light pulse had a width at half peak intensity of 7 microseconds when a 3.75-μf condenser was discharged through a single lamp. The resistance and inductance of the rest of the circuit was negligible compared with those of the lamp.

Up to eight of these lamps were arranged in a ring, each parallel to the shock tube and separated from it by 1/8 inch, inside a reflecting box. They were operated in parallel and were capable of dissipating up to 4000 joules/flash in less than 10 microseconds. In order to make absorption measurements the eight lamps were separated into two groups of

Can. J. Chem. Downloaded from www.nrcresearchpress.com by 210.87.254.6 on 09/05/12
For personal use only.

four and the measuring beam (B) was directed through the gap, at right angles to lamps and shock tube.

The flash lamps were each connected to separate capacitors. They were fired simultaneously by triggered spark gaps connected in series with the lamps. The spark gap electrodes consisted of a 1/4-in. diameter nickel hemisphere and a plane nickel electrode. The 2-mm diameter trigger electrode was inserted in a 4-mm diameter hole in the plane electrode. The trigger electrodes were pulsed by transformers which delivered approximately 6 kv with a rise time of 10 ± 1 microseconds. Using separate thyratrons to pulse the primaries it was possible to fire the eight flash lamps with a simultaneity of less than one microsecond.

Each measuring station (A, B, C, and E) consisted of a photomultiplier, an optical system, and an incandescent lamp source. Stations C and E were used to follow the changes in bromine concentration and to measure the shock velocity; A was used to trigger the flash lamps and to measure shock velocity. B was used only to study flash photolysis at room temperature. The rise time of the photomultiplier circuits was less than one microsecond and a square wave decayed 0.5% in 1 millisecond. Over the range of light intensities used the intensity measurements were accurate to within 1%.

At station B the intensity of the flash was roughly 10^5 times that of the incandescent source in the measuring circuit. Therefore care had to be taken to minimize the effect of scattered light which could damage the photomultiplier tube or at least affect its sensitivity. Aside from the strong peak there was a "tail" continuing for another 150 microseconds or so, which interfered with subsequent measurements. It was not established whether this was caused by continuing light output from the gas or by luminescence of the quartz walls of the flash lamps.

The main source of scattering was the glass wall of the shock tube. The effect of scattering was minimized by using a well-collimated optical system, relatively low photomultiplier voltage (190 v), and a relatively intense light source for the measuring circuit (8 v, 18-amp tungsten ribbon lamp). Measurements were all made at 4420 Å through an interference filter. The signal-to-noise ratio at station B was over 1000. Stations C and E were well removed from the flash lamps so that the problem of scattered light was less severe. The signal-to-noise ratio at these stations was about 300.

The low-pressure section of the shock tube was an 11-ft section of 3-in. I.D. pyrex pipe. The high-pressure section was a 6-ft section of 3-in. I.D. brass fitted with a knife-type plunger used to break the diaphragm, made of 10 or 15 mil cellulose acetate. The density in the flows in the shock wave was constant to within $\pm3\%$. This was probably the largest single experimental uncertainty leading to scatter in the experimental results.

The pressure of inert gas in the low-pressure section was measured with a mercury manometer and that of bromine, by a butyl phthalate manometer buffered with argon. The gases were thoroughly mixed in a 3-liter flask.

Although the system was originally vacuum tight, the strong shocks used caused leaks between sections of the shock tube which were very hard to eliminate. It is not believed that the air which was admixed with the argon could have produced an error over 1%.

STATIC EXPERIMENTS

In order to test the apparatus, measurements were first carried out at room temperature in a closed cell 3 inches in diameter and 27 cm long. Recombination constants in the rate equation $d[Br_2]/dt = k_{app}[Ar][Br]^2$ were measured over a 15-fold range in the [Br]/[Ar] ratio. All of the measurements were made at station B (Fig. 1). At each concentration

Can. J. Chem. Downloaded from www.nrcresearchpress.com by 210.87.254.6 on 09/05/12
For personal use only.

ratio at least five traces of the scattered light and of scattered light plus deflection due to the changing Br_2 concentration were taken.

Further room temperature experiments were carried out using the shock tube itself as a reaction vessel (but with no shock wave). The results obtained in all of the static experiments are given in Table I. Both the absolute value of the experimental rate constant and the scatter in our data compare well with previously published work.

TABLE I

Rate of recombination of bromine atoms at room temperature

	$[Br_2]\times10^4$ moles/liter	Diluent gas $\times10^2$ moles/liter	Diluent	No. of runs	$k_{app}(\times10^{-9}$ l^2 $mole^{-2}$ $sec^{-1})$
This work[a]	0.96	0.66	Ar	11	3.47±0.2
"	"	1.50	"	6	3.24±0.3
"	"	2.50	"	8	2.9±0.3
"	"	3.67	"	5	2.9±0.3
"	1.92	0.639	"	5	2.9±0.3
"	"	1.48	"	9	3.5±0.3
"	"	2.57	"	7	3.0±0.2
"	"	3.68	"	5	3.5±0.1
"	1.55	0.639	"	6	3.4±0.4
"	"	1.51	"	5	2.95±0.2
"	"	2.50	"	5	3.04±0.2
"	"	3.68	"	11	3.2±0.2
This work[b]	2.05	3.76	"	10	$(3.1^d-3.7^e)\pm0.3$
"	0.78	3.88	"	6	$(3.4^d-3.6^e)\pm0.3$
Givens and	1.57	3.72	"		2.9
Willard (4)	2.4	2.08	"		4.6
"	2.2	1.05	"		5.6
"	2.7	0.675	"		12.7[c]
"	3.36	0.55	"		19
Rabinowich and Wood (mean value)(22)			"		2.4±0.5
This work[b]	1.10	3.92	He	5	$1.3^e\pm0.1$
Rabinowich and Wood (mean value) (22)			"		1.35±0.15

[a]Closed vessel.
[b]Open cell (shock tube).
[c]At 37° C.
[d]Assuming no expansion.
[e]Assuming equilibrium expansion.

On the other hand, our data are in rather serious disagreement with those of Givens and Willard (4) as regards the dependence of the experimental rate constant on the $[Br_2]/[Ar]$ ratio. When this ratio was high our records showed a definite effect of heating by the flash and wave systems were set up in the closed reaction vessel (Fig. 2). We have

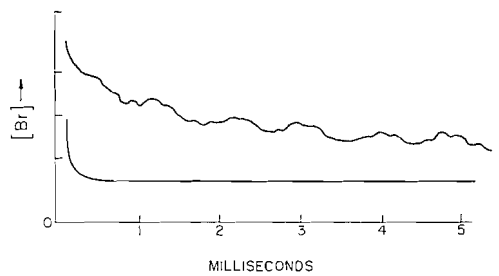


FIG. 2. Oscilloscope traces showing scattered light and recombination of bromine atoms in a closed vessel containing 1.92×10^{-4} moles/liter of Br_2 and 6.39×10^{-3} moles/liter of Ar. Vertical scale 4.5×10^{-6} moles/liter Br per small division.

Can. J. Chem. Downloaded from www.nrcresearchpress.com by 210.87.254.6 on 09/05/12
For personal use only.

used the midpoint of the waves for measurement and it is hard to see how this can account for the disagreement. On the other hand, as regards this dependence, our results agree reasonably well with those of Strong and Basila (23) and Christie, Roy, and Thrush (24).

If both Br_2 and Ar act as third bodies for the recombination, the apparent rate constant is given by

$$[1] \qquad k_{app} = k_{Ar} + \frac{[Br_2]}{[Ar]} k_{Br_2}$$

so that the rate constant for Br_2 acting as a third body is obtained from the slope of Fig. 3. We have not taken enough data at high $[Br_2]/[Ar]$ ratios to obtain a reliable value of k_{Br_2}. It is plain, though, that the ratio of k_{Br_2}/k_{Ar} from our results (ca. 20) is much smaller than that of Givens and Willard (4). The values of k_{Br_2} reported recently are summarized in Table II.

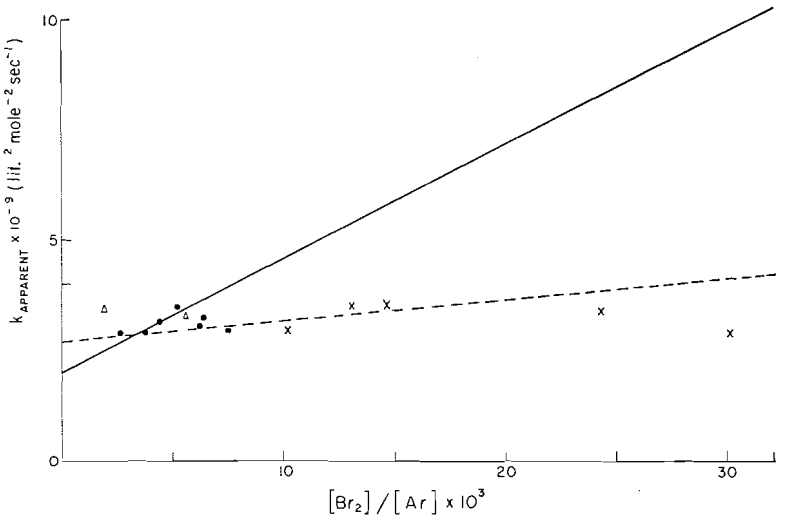


FIG. 3. Dependence of the recombination rate constant upon $[Br_2]/[Ar]$. Closed circles, oscilloscope trace shows no detectable waves; crosses, waves can be observed; triangles, experiments in shock tube used as a reaction vessel; solid line, dependence predicted from reference 4; dashed line, dependence predicted from reference 23 and reference 24.

TABLE II

Rate constant for bromine atom recombination with Br_2 as third body

Investigators	k_{Br_2}, l^2 mole^{-2} sec^{-1}
Strong and Basila (1958) (23)	49×10^9
Givens and Willard (1959) (4)	260×10^9
Christie, Roy, and Thrush (1959) (24)	48×10^9
This work	$<50 \times 10^9$

In order to determine this rate constant accurately more data must be taken at higher values of the $[Br_2]/[Ar]$ ratio. It would be particularly advantageous to use He instead of Ar as the diluent in such studies since He is about three times less efficient than Ar as a third body. In this case the slope of a plot similar to Fig. 3 could be determined with about three times more precision.

Can. J. Chem. Downloaded from www.nrcresearchpress.com by 210.87.254.6 on 09/05/12
For personal use only.

Can. J. Chem. Downloaded from www.nrcresearchpress.com by 210.87.254.6 on 09/05/12
For personal use only.

THERMAL EFFECTS

Heating by the Flash

When the flash dissociates the Br_2 the bromine atoms are released with a kinetic energy equal to the difference between the photon energy and the energy necessary to produce two $^2P_{3/2}$ atoms (45.6 kcal) or most often a $^2P_{1/2}$ and a $^2P_{3/2}$ atom (56.05 kcal). This excess kinetic energy is degraded to heat in a very few collisions. As a consequence the gas is heated from a few degrees to as much as 100° C, depending on the dilution and flash intensity, within the duration of the flash.

In a closed cell experiment in which the illumination is absolutely uniform, the only result is that the recombination is measured at a higher temperature. If the illumination is non-uniform there are further effects. The temperature, and hence the pressure, are increased more in the region of most intense illumination so that compression waves are propagated into the regions of less intense illumination, giving rise to oscillations in the record as sound waves are reflected back and forth through the cell. This phenomenon is illustrated in Fig. 2. Even if the wave motion is averaged there is an effect since the more intensely illuminated regions gradually expand while the less intensely illuminated regions are compressed, giving rise to a local gas density different from that to which the cell was filled. In particular, if the illumination is symmetrical about the midpoint of a cylindrical cell, the density, ρ_f, is given by the expression

$$\frac{\rho_f}{\rho_0} = \left(\frac{\bar{P}_f}{P_i}\right)^{1/\gamma} \qquad [2]$$

where $\bar{P}_f$ is the average final pressure in the tube, P_i is that immediately after the flash, and ρ_0 the gas density before the flash.

$$P_i = \rho_0 R T_i \quad \text{and} \quad \bar{P}_f = \rho_f R \bar{T}_f. \qquad [3]$$

Finally,

$$\begin{aligned} T_i - T_0 &= Q/C_v \\ \bar{T}_f - T_0 &= \bar{Q}/C_v \end{aligned} \qquad [4]$$

where Q is the excess kinetic energy produced in the Br atoms and C_v is the heat capacity. In a typical case in the experiments described in the last section, the illumination at the ends of the closed 27-cm cell was about 75% of that in the center. At the highest Br_2/Ar ratio $T_i - T_0$ was about 10° C while the corresponding $\bar{T}_f - T_0$ was about 9.1° C. In that case $\bar{P}_f/P_i = 0.993$ and $\rho_f/\rho_0 = (0.993)^{0.6} = 0.996$. The resultant errors are therefore not serious. We have not pursued this matter in the present experiments.

When the cell is open ended, as in a shock tube, the effects are much larger. In that case the initially heated gas expands until its pressure is back to the initial pressure so that equation [2] becomes

$$\rho_f = \rho_0 (P_i/P_0)^{1/\gamma} \qquad [5]$$

and for 10° C heating, $\rho_f = 0.98\rho_0$. Since a 2% density change by expansion would produce a change in the bromine absorption comparable to that produced by dissociation, it was considered necessary to study this initial heating experimentally in the shock tube.

The initial heating was studied under conditions where it would be maximized and the rate of recombination would be made negligible during the experiment, namely in pure bromine at low concentration ($0.44\text{–}0.77 \times 10^{-5}$ moles/liter). When pure Br_2 was photolyzed in the shock tube, a bromine absorption record similar to that in Fig. 4 was obtained

at station B. There was an abrupt decrease in the Br_2 concentration immediately following the flash because of the photolytic dissociation. This was followed by a slow further decrease which became much more rapid during the first millisecond. After about two milliseconds the gas was completely expanded and a new, relatively constant, value of $[Br_2]$ was reached.

It was clear that the second process was the anticipated expansion since the time at which it occurred was almost exactly equal to the expected time of arrival (1.3 milliseconds) of a sound wave from the edge of the illuminated region (where the expansion would be initiated). This conclusion was checked further by adding helium to the bromine to increase the velocity of sound and in that case the final plateau of Fig. 4 was reached in less than one millisecond.

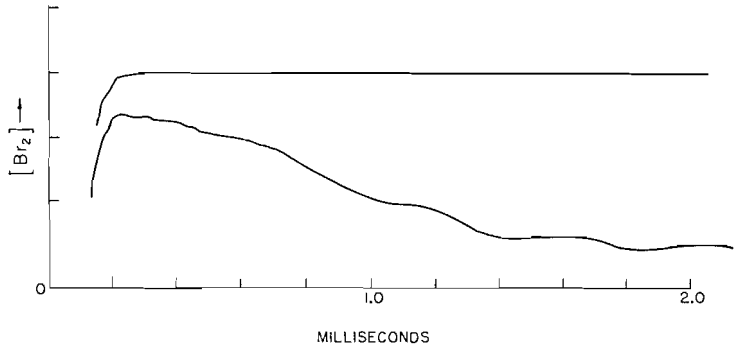


FIG. 4. Oscilloscope trace showing scattered light and expansion of bromine due to initial heating. Shock tube filled with 0.7×10^{-4} moles/liter Br_2. Vertical scale: 7.7×10^{-6} moles/liter Br_2 per division.

A final check that the phenomenon observed was indeed the expansion was obtained by observing the compression wave which the expanding gas in the illuminated region sent through the unilluminated part of the tube. The disturbance was observed at stations C and E; it was found that it propagated at a velocity almost exactly equal to that of sound in bromine and had its origin in the illuminated region at the time of the flash.

It was possible, therefore, to estimate the initial heating quantitatively from these experiments. The initial concentration, $[Br_2]_0$, was known from the initial pressure as well as from the optical absorption. The concentration, $[Br_2]_1$, immediately after the flash could be determined by extrapolating the record back to $t = 0$. Consequently

$$[Br]_1 = 2([Br_2]_0 - [Br_2]_1) \qquad [6]$$

and the degree of dissociation was

$$\alpha = ([Br_2]_0 - [Br_2]_1)/[Br_2]_0 \qquad [7]$$

If Q calories were released for each molecule dissociated, the temperature after the flash was

$$T_1 = T_0 + \frac{Q\alpha[Br_2]_0}{(1-\alpha)[Br_2]_0 C_{Br_2} + 2\alpha C_{Br}} . \qquad [8]$$

Can. J. Chem. Downloaded from www.nrcresearchpress.com by 210.87.254.6 on 09/05/12
For personal use only.

Hence Q could be determined if T_1 was known. T_1 could be determined from the temperature after the adiabatic expansion since

$$\frac{T_1}{T_t} = \left(\frac{[Br_2]_1}{[Br_2]_t}\right)^{\gamma-1}, \tag{9}$$

and T_t was known from the equation of state (if the final pressure equals the initial pressure),

$$\frac{T_t}{T_0} = \frac{[Br_2]_0}{[1+2\alpha][Br_2]_t}. \tag{10}$$

Hence Q could be determined from a single record similar to Fig. 4 since $[Br_2]_t$ could be measured from the final plateau.

Five experiments in pure Br_2 at a concentration of 0.75×10^{-4} moles/liter with four lamps firing yielded $Q = 9.6$ kcal/mole. Another set of four experiments at a concentration 0.48×10^{-4} moles/liter gave $Q = 5.7$ kcal/mole although the scatter among the determinations, using from one to four lamps, was only about 10%. The reason for the discrepancy is not known. However, the presence of as much as 1 mm Hg of air in the tube would account for it.

Because of the uncertainty in α caused by the difficulty in extrapolating to $t = 0$, another set of experiments was carried out in which argon was added to almost atmospheric pressure (3.88×10^{-2} moles/liter). The rate constant was determined in the usual way by plotting 1/Br vs. time. Extrapolating this straight line to $t = 0$ gave the initial concentration of Br atoms (8.6×10^{-7} moles/liter per flash lamp). Using the value of α determined in this way to fix the $t = 0$ point on another set of 35 runs in pure Br_2 at a concentration of 0.7×10^{-4} moles/liter gave $Q = 8.5$ kcal/mole.

These experiments were not carried further because our main interest was in high-dilution experiments where the heating and expansion effects were very small. Their importance lies in the fact that they show that the expansion is a smooth process and that it is possible to work quantitatively under conditions where the heating and expansion are large.

Recombination Heating

When recombination takes place the heat evolved warms the gas and in an open tube the consequent expansion may produce large effects. If the expansion is rapid enough so that inertial forces are significant the hydrodynamic conservation equations must be applied (8). When that is not the case there will be a free expansion of the heated gas at a constant pressure. We then have

$$\dot{[Br_2]} = \left(\frac{\partial Br_2}{\partial \alpha}\right)_{T,P}\dot{\alpha} + \left(\frac{\partial Br_2}{\partial T}\right)_{P,\alpha}\dot{T}. \tag{11}$$

For a three-body recombination

$$\left(\frac{\partial Br_2}{\partial \alpha}\right)_{T,P}\dot{\alpha} = k[Br]^2[M]. \tag{12}$$

From the equation of state

$$\left(\frac{\partial Br_2}{\partial T}\right)_{P,\alpha} = -\frac{[Br_2]}{T}. \tag{13}$$

Can. J. Chem. Downloaded from www.nrcresearchpress.com by 210.87.254.6 on 09/05/12
For personal use only.

For a constant pressure process

$$\dot{H} = \dot{q},$$

so that

$$[15] \qquad ([Br_2]C_{pBr_2}+[Br]C_{pBr}+[M]C_{pM})\,\dot{T} = Dk[Br]^2[M].$$

Therefore equation [11] becomes simply

$$[16] \qquad [\dot{Br_2}] = k[Br]^2[M]\left(1-\frac{D[Br_2]}{([Br_2]C_{pBr_2}+[Br]C_{pBr}+[M]C_{pM})T}\right).$$

Under conditions of high dilution this simplifies to

$$[17] \qquad [Br_2] = k[Br]^2[M]\left(1-\frac{D[Br_2]}{[M]C_{pM}T}\right).$$

It should be noted, therefore, that as recombination proceeds the Br_2 concentration may either decrease or increase. A similar situation exists for dissociation reactions and there both cases have been observed experimentally (8). In general, though, the bromine molecule concentration will increase during recombination when the gas is sufficiently dilute and decrease for pure Br_2 at any practicable temperature.

Cooling by the Walls

Norrish *et al.* (16) have called attention to the problem created by cooling at the walls. In a conventional photolysis cell the observations are made longitudinally. Cooling at the walls results in increased gas density near the walls and decreased density in the center of the tube where observations are made. In our apparatus observations were made transversely so that in first approximation the effect of cooling at the walls is averaged out, providing the cell is long enough so that the end walls are far removed. Consequently, we have for the present neglected this effect.

HIGH-TEMPERATURE MEASUREMENTS

Recombination measurements were made at 950° K in mixtures of 0.6% Br_2 in Ar. The low-pressure section of the shock tube was filled with bromine at a concentration of $(3.7\pm.05)\times10^{-5}$ moles/liter and argon at a concentration of $(6.05\pm.05)\times10^{-3}$ moles/liter. The total pressure was 11.4 cm Hg. The high-pressure section was filled with He at a pressure of three atmospheres. The strength of the shock wave produced when the diaphragm was ruptured was determined by measuring the time of passage between stations A, B, C, and E. All three shocks had an average velocity of 0.90 mm/microsecond over the 964-mm path from A to C. The third shock showed an average velocity of 0.92 mm/microsecond over the total path of 1297 mm so that its apparent velocity over the last 333 millimeters was 0.98 mm/microsecond. It is not yet known whether this represents experimental error or whether there was a genuine acceleration of the shock. Using the velocity 0.90 mm/microsecond (Mach number = 2.80), the compression ratio across the shock was 2.89 and the temperature behind the shock was 950° K. If the velocity was as high as 0.97 mm/microsecond (Mach number = 3.00) the corresponding numbers would be 2.99 and 1060° K.

The photolysis was carried out with eight lamps discharging a total of 32.25 mf at 10.4 kv. Since station B was not used, the initial Br atom concentration was determined in a separate photolysis on pure bromine at room temperature (no shock). Bromine

Can. J. Chem. Downloaded from www.nrcresearchpress.com by 210.87.254.6 on 09/05/12
For personal use only.

molecules (22%) were dissociated in the photolysis. The initial heating amounted to 5.3° C. The subsequent expansion would amount to 1% at 300° K and 0.34% at 950° K. Since the expansion should have been complete after about 750 microseconds it took place partially before and partially after the arrival of the shock wave at about 200 microseconds. Because of the high degree of dissociation the expansion had only a very minor effect on these measurements.

The rate constants were obtained from the initial bromine concentration, determined separately, and corrected for the expansion and the recombination which occurred before arrival of the shock (6%), plus the bromine atom concentration at the center of the pulse when it arrived at stations C (0.76 millisecond later) and E (1.30 milliseconds). The rate constants were corrected for the recombination heating, a correction of 7.7%.

The rate constants obtained on three high-temperature experiments were:

Expt.	Time range, milliseconds	k, l² mole⁻² sec⁻¹
I	0–0.76	6.4×10^8
	0.76–1.3	7.9×10^8
II	0–0.76	9.0×10^8
III	0.76–1.3	9.7×10^8
		Average $8.2\pm1.1\times10^8$

DISCUSSION

The most striking feature of previous work on bromine and iodine is that it was difficult to fit the low-temperature flash photolysis data and the high-temperature shock wave data to a single k vs. T curve. It was hoped that an intermediate temperature point might indicate where the difficulty lay. Furthermore, the various theoretical approaches suggest different forms of the k vs. T curve. The complex mechanism yields a function $k = Ae^{E/RT}$ whereas most other considerations yield functions of the form $k = B/T^n$.

The various measurements are therefore plotted as a function of temperature in Fig. 5; a straight line on the three representations shown would correspond to the functions: (A) $k = B/T^n$, (B) $k = Ae^{E/RT}$, and (C) $k = Ae^{-BT}$. The present work agrees reasonably well with the results of Willard and co-workers at room temperature but the rate constant at 950° K is substantially higher than would be predicted by extrapolation of their data.

A point of some interest is the fate of the $^2P_{1/2}$ atoms, which comprise roughly 50% of those produced in the initial photolysis, since they cannot lead directly to the formation of ground state molecules. If they were collisionally degraded to the $^2P_{3/2}$ state the 10.4 kcal released ought to appear in our experiments as heat and this does not seem to have been the case. They might, however, undergo a radiative transition and lose the energy as a photon. If their lifetime exceeds the recombination time (ca. 1 millisecond), though, all flash photolysis results would be in error unless the lifetime of the excited molecules produced from these atoms is short compared with the recombination time. This problem has been considered previously (16) but the evidence for neglecting this possibility does not seem conclusive to us.

If the $^2P_{1/2}$ atoms do not enter the observed recombination, the rate constants would be about four times greater and it should be noted that since the corresponding problem does not arise in thermal dissociation (e.g. in shock waves) this would help bring the flash photolysis and shock wave results into better agreement.

Can. J. Chem. Downloaded from www.nrcresearchpress.com by 210.87.254.6 on 09/05/12
For personal use only.

Can. J. Chem. Downloaded from www.nrcresearchpress.com by 210.87.254.6 on 09/05/12
For personal use only.

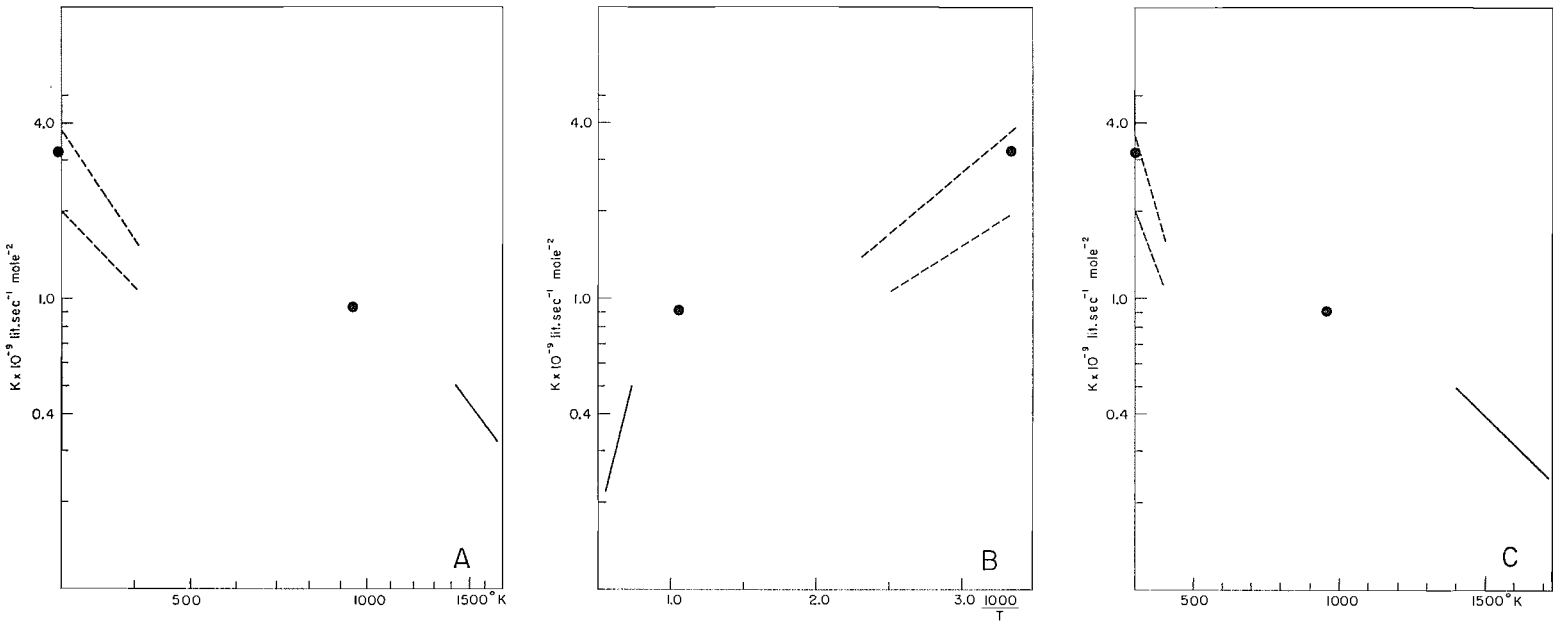


FIG. 5. Temperature dependence of recombination rate constant. (A) Log–log representation; (B) Arrhenius representation; (C) log k vs. T representation. Closed circles, present experiment; solid line, estimated from reference 12; upper dashed line, estimated from reference 2; lower dashed line, estimated from reference 4.

CONCLUSIONS

The combination of flash photolyses with the shock tube to obtain recombination rates at high temperatures appears quite feasible. All of the major problems, such as the various thermal effects, appear soluble and it has been possible to obtain preliminary results of reasonable accuracy for bromine recombination at 950° K. It now seems possible to reach higher temperatures, to improve the accuracy, and to work at lower dilutions.

ACKNOWLEDGMENTS

One of us (G. Burns) is indebted to the General Electric Company and to the Gulf Research and Development Company for fellowships. The work was supported in part by the Office of Naval Research and the California Research Corporation.

REFERENCES

1. K. E. Russel and J. Simons. Proc. Roy. Soc. A, **217**, 271 (1953).
2. R. L. Strong, J. C. W. Chien, P. E. Graf, and J. E. Willard. J. Chem. Phys. **26**, 1287 (1957).
3. D. L. Bunker and N. Davidson. J. Am. Chem. Soc. **68**, 5085 (1958).
4. W. G. Givens, Jr. and J. E. Willard. J. Am. Chem. Soc. **81**, 4773 (1959).
5. D. Britton, N. Davidson, W. Gehman, and G. Schott. J. Chem. Phys. **25**, 804 (1956).
6. D. Britton and N. Davidson. J. Chem. Phys. **25**, 810 (1956).
7. D. F. Hornig. Ann. N. Y. Acad. Sci. **67**, 463 (1957).
8. H. B. Palmer and D. F. Hornig. J. Chem. Phys. **26**, 98 (1957).
9. D. L. Matthews. Phys. Fluids, **2**, 170 (1959).
10. S. R. Byron. J. Chem. Phys. **30**, 1380 (1959).
11. R. Engleman and N. Davidson. J. Am. Chem. Soc. In press. (1960).
12. D. Britton. J. Phys. Chem. In press. (1960).
13. E. P. Wigner. J. Chem. Phys. **5**, 720 (1937).
14. J. C. Keck. J. Chem. Phys. **32**, 1035 (1960).
15. J. O. Hirshfelder. Molecular theory of gases and liquids. Wiley, New York. 1954. pp. 552–559.
16. M. T. Christie, A. J. Harrison, R. G. W. Norrish, and G. Porter. Proc. Roy. Soc. A, **231**, 446 (1955).
17. D. L. Bunker and N. Davidson. J. Am. Chem. Soc. **80**, 5090 (1958).
18. O. K. Rice. Monatsh. Chem. **90**, 330 (1959).
19. D. L. Bunker. J. Chem. Phys. **32**, 1001 (1960).
20. J. P. Toennies and P. F. Greene. J. Chem. Phys. **26**, 665 (1957).
21. R. A. Strehlow and A. Cohen. J. Chem. Phys. **28**, 983 (1958).
22. E. Rabinowitch and W. C. Wood. Trans. Faraday Soc. **32**, 907 (1936).
23. M. R. Basila. The flash photolysis and recombination of bromine. Ph.D. Thesis, Rensselaer Polytechnic Institute. August 1958.
24. M. T. Christie, R. S. Roy, and B. A. Thrush. Trans. Faraday Soc. **55**, 1139 (1959).

Can. J. Chem. Downloaded from www.nrcresearchpress.com by 210.87.254.6 on 09/05/12
For personal use only.

Can. J. Chem. Downloaded from www.nrcresearchpress.com by 210.87.254.5 on 09/05/12
For personal use only.

THE ROLE OF Hg 6^3P_0 ATOMS IN MERCURY PHOTOSENSITIZATION

I. REACTIONS IN THE PRESENCE OF NITROGEN[1]

G. H. KIMBELL AND D. J. LE ROY

ABSTRACT

A quantitative investigation has been made of the factors affecting the concentration of mercury 6^3P_0 atoms formed by collisions of the second kind between mercury 6^3P_1 atoms and nitrogen. The absorption of 4047 Å (6^3P_0–7^3S_1) and the emission of 2656 Å (6^3P_0–6^1S_0) were studied in the pressure range 0.06 mm to 140 mm. Both types of measurement indicate that the forbidden line arises from spontaneous as well as collision-induced emission. The lifetime for spontaneous emission is estimated to be 4.2×10^{-4} sec.

The production of mercury 6^3P_0 atoms by collisions of the second kind between 6^3P_1 atoms and nitrogen is well known. The methods used to study their relative concentration and reactivity are of five main types.

The absorption of the line 4047 Å, corresponding to the transition 6^3P_0–7^3S_1, was first observed by Wood and Gaviola (1), and has been applied quantitatively by a number of others (2, 3, 4, 5). Correlation of the apparent concentration of 6^3P_0 atoms with cell geometry suggested that these atoms have a relatively long lifetime and are deactivated on the wall (2). With increasing nitrogen pressure the concentration reaches a maximum (3) and shows some indication of a fall-off at pressures above 20 mm (4).

As a result of the absorption of 4047 Å there is an increase in the population of the 7^3S_1 level. The intensity of the resulting emission of 4358 Å (7^3S_1–6^3P_1) and 5461 Å (7^3S_1–6^3P_2) has been used as a measure of the 6^3P_0 concentration (6).

Elevation of 6^3P_0 atoms to the 6^3P_1 level requires only 5 kcal per mole and can be brought about by collisions with nitrogen molecules. Because of the long lifetime of the former compared with that of the latter (1.1×10^{-7} sec), the emission of 2537 Å will continue for some time after the exciting radiation of that wavelength is cut off; its intensity can then be correlated with the concentration of 6^3P_0 atoms (5, 7, 8).

The liberation of electrons when 6^3P_0 atoms collide with metal plates has been used as a quantitative measure of their concentration (9, 10, 11), but the method may be complicated by the fact that Hg_2^+ ions appear to be produced homogeneously (4).

Although the transition 6^3P_0–6^1S_0 is forbidden by the usual selection rules, it has been observed by Wood (12) and others. Its wavelength *in vacuo* (2656.39 Å) lies close to the pseudotriplet, 2655.92, 2654.47, 2652.83, arising from transitions between the levels 7^1D_2, 7^3D_1, 7^3D_2, and the 6^3P_1 level, and can be separated from these only with a spectrograph of high dispersion. Laroze and Cojan (13) have tried to get around this difficulty by passing the light from the primary lamp through a filter designed to reduce the intensity of the pseudotriplet, relative to that of 2537 Å, by a large factor. Unfortunately, while this would reduce the rate of formation of $7D$ atoms from 6^3P_1 atoms, it would not affect their rate of formation by such processes as the absorption of 2535.5 Å by 6^3P_0 atoms to give 7^3D_1 atoms. Indeed, it was found in the present work that the intensity of the line 2654.47 Å increased very markedly in the presence of small amounts

[1]*Contribution from the Department of Chemistry, University of Toronto, Toronto, Ontario; presented at the Symposium on the Fundamental Aspects of Atomic Reactions held at McGill University, Montreal, Que., September 1960.*

of nitrogen and was reduced below that of the forbidden line only at relatively high pressures.

EXPERIMENTAL

The apparatus in its present form was designed to permit measurements of the absorption of 4047 Å as well as of the emission of the forbidden line; its main features may be seen in Fig. 1. Two primary lamps of the low-pressure mercury-rare gas type were used.

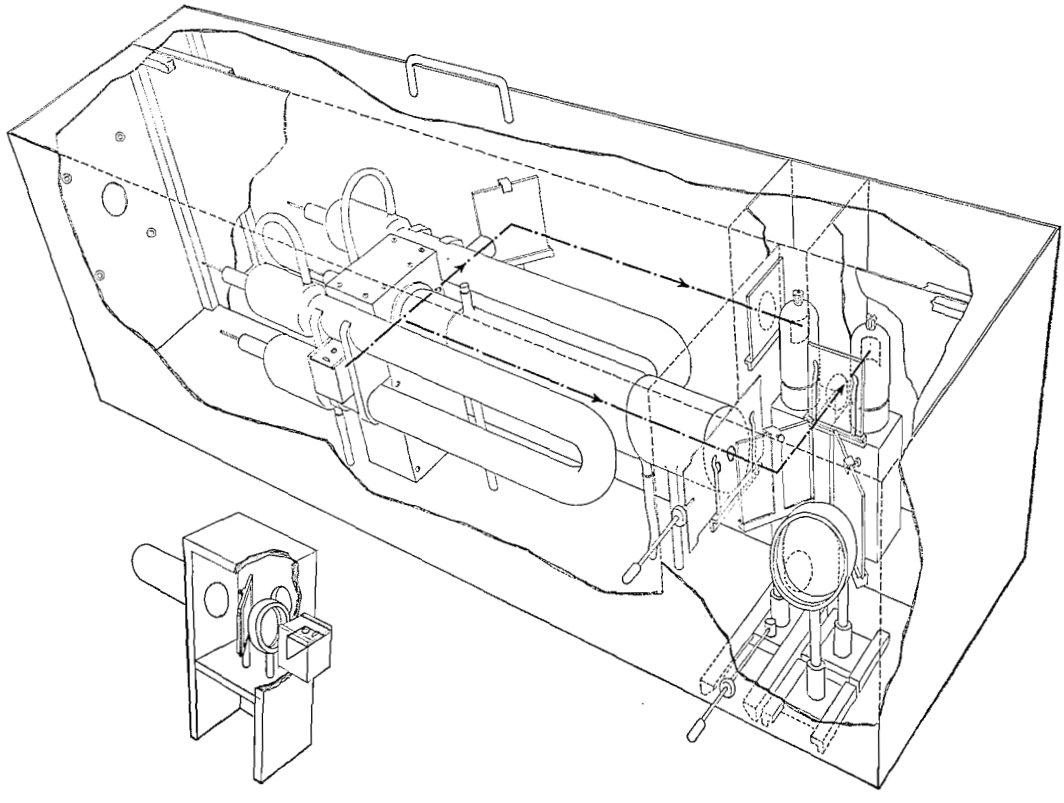


FIG. 1. Apparatus for studying absorption of 4047 Å and emission of 2656 Å by mercury 6^3P_0 atoms.

These were made entirely of fused quartz, including the jacketed electrode chambers, which were maintained at 29° C. The lamps were U-shaped and were mounted with their long axes parallel to that of the cell. The latter was also of fused quartz, and consisted of an outer tube 28 cm long and 5.5 cm O.D. and an inner tube 20 cm long and 3.1 cm I.D. The annular space between the tubes was filled with a filter solution of aqueous nickel sulphate, which removed essentially all of the 4047 Å radiation coming from the primary lamps (14). Close-fitting metal cylinders covered each end of the cell, leaving a central portion 18 cm long exposed to the light from the two lamps. Nitrogen and mercury vapor entered and left the cell through blackened side arms at each end of the cell, adjacent to the plane quartz windows.

Can. J. Chem. Downloaded from www.nrcresearchpress.com by 210.87.254.5 on 09/05/12
For personal use only.

To study the absorption of 4047 Å a beam of light from the end of one of the lamps was rendered parallel and then split into two roughly equal beams by a partially transmitting first surface mirror. One served as a reference beam, the other was passed longitudinally through the cell. The analysis beam was circular in cross section and 0.6 cm in diameter. By means of Corning filters each beam was made monochromatic before falling on separate GL-935 photocells. The photocell circuit used to measure the absorption of 4047 Å was similar to that described previously (15) except that the electrometer was a General Radio Type 1230-A.

The cell, lamps, photocells, etc. were mounted inside a metal box which was separated into lighttight shielded compartments by metal partitions. The cell compartment was flushed continuously with nitrogen to eliminate ozone formation.

Our procedure differed from that of previous workers in that we allowed the nitrogen and mercury vapor to flow through the cell continuously in order to avoid the build-up of impurities which might come off the walls of the cell. Nitrogen of the highest purity obtainable was passed over copper oxide at 250° C, over copper filings at 900° C, and then through a trap cooled with liquid air. After the gas had passed through a capillary flowmeter incorporating a mercury U-tube manometer, its pressure was lowered to the desired value by passing it through an Edwards LB-1 needle valve. An excess of mercury vapor was then added to the gas by passing it through a trap maintained at 40° C and containing a pool of mercury in the bottom and adherent drops of mercury on the sides. The mercury concentration in the gas was then adjusted to a value corresponding to saturation at 15.0° C by passing it through two long narrow traps kept at this temperature. After the gas had passed through the cell its pressure was lowered to the operating value for the diffusion pump by means of a second valve. The pressure in the cell was measured by a variable range mercury manometer connected to the cell through a stopcock connected to the exit tube.

Apparent concentrations of 6^3P_0 atoms (hereafter referred to as Hg^0 for simplicity) were obtained in terms of the optical density, $K^0L(Hg^0) = \log_{10}(I_0/I_t)$, in which K^0 is the extinction coefficient for the absorption of 4047 Å by Hg^0 atoms and L is the length of that part of the cell illuminated by the lamps. The measurements corresponding to I_0 (100%) were made by closing the needle valve on the upstream side of the cell and pumping continuously. Tests showed that no correction needed to be made for scattered light.

In making measurements on the emission of the forbidden line the diameter of the exit diaphragm of the cell was increased from 0.6 to 1.0 cm, the mirror which reflected the analysis beam of 4047 Å onto its photocell was slid out of place and the emitted light was allowed to fall on a quartz lens mounted over a hole in the side of the metal box. The conjugate foci of this lens were at the center of the cell and the slit of the spectrograph.

The spectrograph was of the Littrow type and had one 60° and one 30° prism. In the wavelength region of the forbidden line the dispersion was approximately two angstroms per millimeter. Plates were monitored by a recording microphotometer. Individual values of γ were obtained for each plate, using as standards the intensity of the forbidden line at a fixed pressure of nitrogen and various exposure times. Correction for the failure of the reciprocity law was made by using calibrated screens placed at the exit diaphragm of the cell. The screens were calibrated *in situ* using the optical arrangement for 4047 Å transmission measurements. The intensities of the forbidden line at various pressures of nitrogen were computed relative to the intensity for the standard pressure.

Can. J. Chem. Downloaded from www.nrcresearchpress.com by 210.87.254.5 on 09/05/12
For personal use only.

RESULTS AND DISCUSSION

The results on the absorption of 4047 Å for a wide range of nitrogen pressures are shown in Fig. 2. Assuming that K^0 is independent of nitrogen pressure, a dangerous

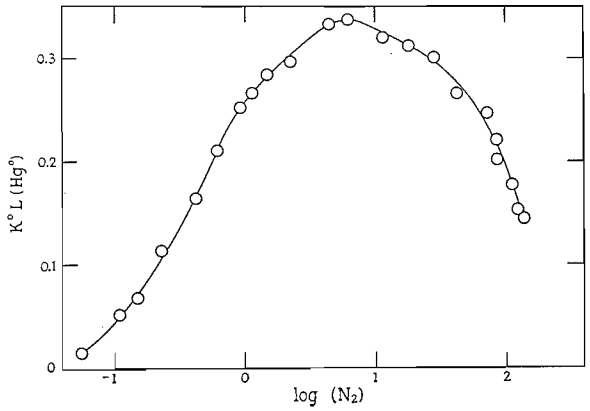


FIG. 2. Optical density, $K^0L(Hg^0)$, for the absorption of 4047 Å by mercury 6^3P_0 atoms as a function of nitrogen pressure.

assumption, it would appear that (Hg^0) reaches a maximum at about 5–10 mm and then falls off. On the other hand, the intensity of the forbidden line, shown in Fig. 5, is constant in the region 10–150 mm.

In order to make a kinetic analysis of the steady-state processes occurring in the cell under constant illumination the following reactions are considered; for simplicity 6^3P_1 atoms are referred to as Hg*, 6^1S_0 atoms as Hg.

$$Hg + h\nu^* = Hg^* \quad [1]$$

$$Hg^* = Hg + h\nu^* \quad [2]$$

$$Hg^* + N_2 = Hg + N_2 \quad [3]$$

$$Hg^* + N_2 = Hg^0 + N_2 \quad [4]$$

$$Hg^0 = Hg \text{ (on wall)} \quad [5]$$

$$Hg^0 = Hg + h\nu^0 \quad [6]$$

$$Hg^0 + N_2 = Hg + N_2 \quad [7]$$

$$Hg^0 + N_2 = Hg^* + N_2 \quad [8]$$

$$Hg^0 + N_2 = Hg + h\nu^0 + N_2 \quad [9]$$

Since the rate of [5] will be inversely proportional to the pressure of nitrogen it will be written as $k_5(Hg^0)/(N_2)$. The reactivation of Hg^0 atoms to the Hg* level by collisions with nitrogen has been observed by Samson (8) and others. The energy requirement would be 5.0 kcal per mole, close to the excess energy of the N_2 molecule formed in reaction [4]. However, the probability of such a molecule being deactivated by collisions with normal nitrogen molecules is far greater than its probability of undergoing reaction [8], except at very low pressures. Similar considerations apply to the excited nitrogen molecules formed in reactions [3] and [7]. It will therefore be assumed that the energy distribution in the nitrogen is essentially Boltzmann, and that the rate of reaction [8]

Can. J. Chem. Downloaded from www.nrcresearchpress.com by 210.87.254.5 on 09/05/12
For personal use only.

will be given by $k_8(Hg^0)(N_2)$, with an activation energy of at least 5.0 kcal per mole.

For the steady state the above mechanism yields the following relation between (Hg^0) and (N_2):

$$\text{(i)} \qquad 1/K^0L(Hg^0) = A/(N_2)^2+B/(N_2)+C+D(N_2),$$

in which

$$A = k_2k_5/k_4I_a{}^*K^0L,$$

$$B = [(k_3+k_4)k_5+k_2k_6]/k_4I_a{}^*K^0L,$$

$$C = [(k_3+k_4)k_6+k_2(k_7+k_8+k_9)]/k_4I_a{}^*K^0L,$$

$$D = [(k_3+k_4)(k_7+k_8+k_9)-k_4k_8]/k_4I_a{}^*K^0L,$$

and $I_a{}^*$ is the rate of formation of Hg* atoms by reaction [1]. It is convenient to use an expression for $1/K^0L(Hg^0)$ rather than for $1/(Hg^0)$ since the former is obtained directly from the transmission measurements; consideration will be given later to the possible variation of K^0 with pressure.

(a) Absorption Measurements

While the general shape of the curve in Fig. 2 is in agreement with a function of the form given in (i), more detailed information can be obtained by examining the low-, medium-, and high-pressure regions. In Fig. 3 the quantity $(N_2)^2/K^0L(Hg^0)$ is plotted

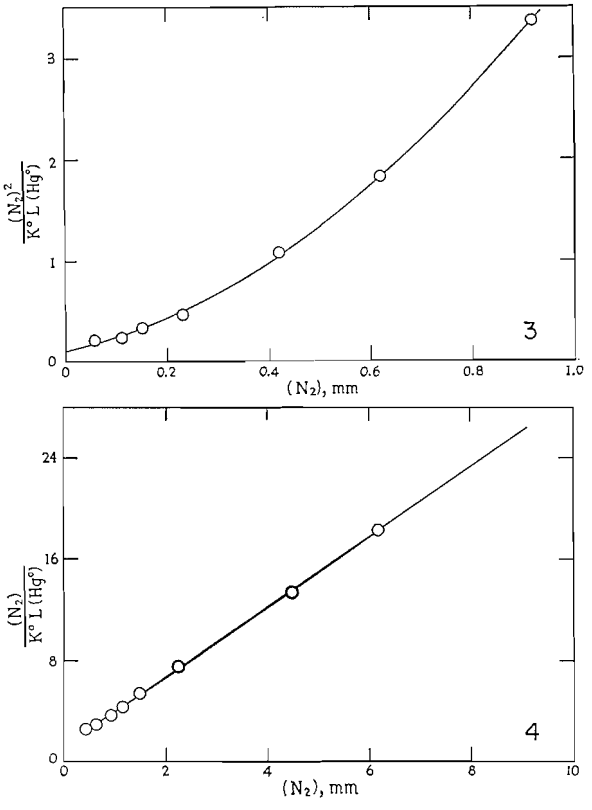


FIG. 3. $(N_2)^2/K^0L(Hg^0)$ as a function of nitrogen pressure in the low-pressure range.
FIG. 4. $(N_2)/K^0L(Hg^0)$ as a function of nitrogen pressure in the medium-pressure range.

Can. J. Chem. Downloaded from www.nrcresearchpress.com by 210.87.254.5 on 09/05/12
For personal use only.

against (N_2) for pressures below 1 mm. The smooth curve is plotted from the function $A+B(N_2)+C(N_2)^2$ in which the constants $A = 0.0974$ mm², $B = 1.171$ mm, $C = 2.597$ were obtained by the method of least squares.

In Fig. 4 the function $(N_2)/K^0L(Hg^0)$ is plotted against (N_2) for the pressure region 0.62 to 6.17 mm. The smooth curve is a plot of $A/(N_2)+B+C(N_2)$, in which $A = 0.0974$ as derived previously, $B = 1.116$, and $C = 2.780$. In this case the values of B and C were obtained by applying the method of least squares to the function $(N_2)/K^0L(Hg^0) - 0.0974/(N_2)$. To avoid crowding together of experimental points the lower part of the curve of Fig. 4, including the turnup is not shown. Although there is relatively little difference between the two sets of values of B and C, we prefer to use those corresponding to Fig. 4, since it is in this region that they play their most important role.

The value of D was obtained by taking the simple average of the quantity $[1/K^0L(Hg^0) - 0.094/(N_2)^2 - 1.116/(N_2) - 2.780]/(N_2)$ in the pressure region 9.26 to 137.0 mm; this was equal to 0.023 mm^{-1} with a mean deviation of 0.004.

Matland (16) obtained a value of approximately 0.4×10^{-16} cm² for σ^2 for the quenching of 2537 Å by nitrogen, corresponding to a value of 2.1×10^5 mm^{-1} sec^{-1} for (k_3+k_4). From the work of Alpert, McCoubrey, and Holstein (17) it would appear that with the mercury concentration and cell dimensions used in the present work there should be a negligible amount of imprisonment, and hence k_2 will be approximately 10^7 sec^{-1}. The quantity $(k_3+k_4)/k_2$ will then be 2.1×10^{-2} mm^{-1}. Since $B/A = (k_3+k_4)/k_2+k_6/k_5 = 11.4$, it follows that the first term can be neglected and that k_6/k_5 is equal to 11.4 mm^{-1}.

In order to evaluate k_6 it is necessary to obtain a relation between k_5 and the diffusion coefficient of Hg^0 atoms in nitrogen. Under steady illumination the relation between (Hg^0) and r, the radial distance from the axis of the cylindrical reaction cell is given by

$$\partial^2(Hg^0)/\partial r^2+(1/r)\partial(Hg^0)/\partial r-a(Hg^0)+b = 0, \tag{ii}$$

in which $a = [k_6+(k_7+k_8+k_9)(N_2)]/D^0$; $b = k_4(Hg^*)(N_2)/D^0$; and D^0 is the diffusion coefficient of Hg^0 atoms in nitrogen.

Since the cell is more or less uniformly irradiated by the four arms of the two U-shaped lamps, the radius of the cell is only 1.55 cm, and the partial pressure of mercury corresponded to saturation at 15° C, we feel justified in assuming that I_a^*, and hence (Hg^*), is uniform throughout the cell. This is supported by the work of Pinder and Le Roy (18) on the extinction coefficient for the absorption of 2537 Å by mercury, in which they used a lamp similar to those used in the present work. Actually, any decrease in (Hg^*) as r approaches zero will be partially compensated by an increase in the rate of reaction [8], since (Hg^0) will increase as r approaches zero.

The solution of (ii) is

$$(Hg^0) = \frac{b}{a}\left[1-\frac{\Sigma(\alpha\rho^2/4)^n/(n!)^2}{\Sigma(\alpha/4)^n/(n!)^2}\right], \tag{iii}$$

in which $\alpha = aR^2$, $\rho = r/R$, R is the radius of the cell, and the summations are for all integral values of n from zero to infinity. Since D^0 is inversely proportional to (N_2) it follows that a and α will approach zero as (N_2) approaches zero. Hence, at low pressures,

$$(Hg^0) \rightarrow bR^2(1-\rho^2)/4 \rightarrow \frac{k_4I_a^*(N_2)}{4k_2D^0}(1-\rho^2) \tag{iv}$$

or, at the axis of the cell,

$$(Hg^0) \rightarrow \frac{k_4I_a^*(N_2)}{4k_2D^0}. \tag{v}$$

Can. J. Chem. Downloaded from www.nrcresearchpress.com by 210.87.254.5 on 09/05/12
For personal use only.

Since the radius of the analysis beam is approximately one-fifth that of the cell, the average value of (Hg^0) in the beam will differ from that at the axis by a negligible amount. Comparison of (v) with the limiting low-pressure value of (Hg^0) given by (i) shows that

$$k_5 = 4D^0(N_2)/R^2. \qquad \text{(vi)}$$

Since there are no certain values of D^0 in the literature, we have used the data of Spier (19) on the diffusion coefficient of Hg in nitrogen. These were obtained under conditions similar to those of the present experiments: 1.12 to 1.75 mm pressure and 292.2° to 298.7° K. Assuming a square law dependence of D^0 on the temperature, and an inverse first-power dependence on the pressure, the average value of D^0 at 1 mm pressure and 25° C is 124 $cm^2\ sec^{-1}$, from which k_5 is calculated to be 206 $mm\ sec^{-1}$.

From this value of k_5 and the empirical values of A, B, and C, the following kinetic parameters were obtained: $k_6 = 2.35\times10^3\ sec^{-1}$ (i.e. natural lifetime is 4.25×10^{-4} sec); $(k_7+k_8+k_9) = 5.84\times10^3\ mm^{-1}\ sec^{-1} = 1.09\times10^{11}\ cm^3\ mole^{-1}\ sec^{-1}$. Assuming that $k_4 \gg k_3$ and that the coefficient D is not invalidated by pressure broadening, values of (k_7+k_9) and k_8 are found to be $2.32\times10^3\ mm^{-1}\ sec^{-1}$ and $3.52\times10^3\ mm^{-1}\ sec^{-1}$, respectively. Assuming that reactions [7] and [9] have no activation energy, their mean value of σ^2 is $4.5\times10^{-19}\ cm^2$. The value of σ^2 for reaction [8] is $31.5\times10^{-16}\ cm^2$, assuming an activation energy of 5.0 kcal per mole in the expression, $k_8 = \sigma^2(8\pi RT/\mu)^{1/2}e^{-E/RT}$; this appears to be high; whether or not this is the result of incomplete deactivation of excited N_2 molecules formed in reactions such as [3], [4], or [7] cannot be established until the possible influence of pressure broadening is ascertained.

The absorption measurements clearly indicate the occurrence of [6]; the lifetime of the 6^3P_0 state, with respect to emission was found to be 4.25×10^{-4} sec. This value was derived from experiments at pressures less than 1 mm, where errors from pressure broadening should be negligible, but involved the assumption that Hg^0 and Hg have the same diffusion coefficient. Whether or not we can conclude that there is also a collision-induced emission by reaction [9] is open to some question. Even if we neglect pressure-broadening effects in the high-pressure region it is possible to evaluate (k_7+k_9), but not k_9 alone. The constant intensity of the forbidden line in the high-pressure region, as shown in Fig. 5, would obtain if both k_7 and k_9 were equal to zero, but this would imply a very strong dependence of K^0 on nitrogen pressure in the region 10 to 137 mm.

(b) Emission Measurements

The effect of nitrogen pressure on the intensity of the forbidden line is shown in Fig. 5. According to the present mechanism the intensity should be proportional to $[k_6+k_9(N_2)](Hg^0)$. Qualitatively the results are in agreement with a relation of this form in which (Hg^0) is related to the nitrogen pressure by equation (i). However, it was necessary to assume a much larger value of D than that derived from the absorption measurements. The best agreement was obtained by using $A = 0.0974$, $B = 1.116$, $C = 2.78$, and $D = 2.0$, together with a value of 0.4 for k_6/k_9. The value of the latter is not in serious disagreement with that derived from the absorption measurements, which gave a value of 1.0 for $k_6/(k_7+k_9)$.

In comparing the results of the two series of experiments it must be borne in mind that although there is unequivocal evidence for pressure-dependent emission of the forbidden line, any conclusions about the particular form of the emission process will be influenced by the interpretation of the data given in Figs. 2 and 5. If the fall-off in

Can. J. Chem. Downloaded from www.nrcresearchpress.com by 210.87.254.5 on 09/05/12
For personal use only.

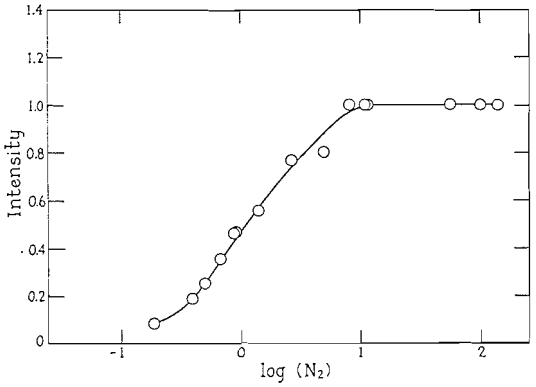


FIG. 5. Intensity of the forbidden line, 2656 Å, in arbitrary units as a function of nitrogen pressure.

$K^0L(Hg^0)$ at high pressures is due only to pressure broadening effects, then the coefficient D in equation (i) is actually zero; in which case all of the emission would have to be by reaction [6]. However, this would predict a considerably higher emission intensity below 10 mm than was actually found. On the other hand, if all emission is assumed to occur by reaction [9] it would not be possible to interpret the results of the absorption measurements in the low-pressure regions where pressure broadening effects are not likely to be serious. One factor that has not been taken into consideration is that the lamps were operated on 60-cycle alternating current, which might invalidate the use of the steady-state assumption.

Although it is evident that further work will have to be done in order to resolve the quantitative discrepancies between the two sets of measurements, the present work has shown that in any future attempt to interpret the behavior of mercury 6^3P_0 atoms cognizance must be taken of the spontaneous and collision-induced emission of the forbidden line.

The authors are grateful to the National Research Council of Canada for a Studentship (held by G. H. K.) and for a grant-in-aid of the research.

REFERENCES

1. R. W. WOOD and E. GAVIOLA. Phil. Mag. **6**, 271 (1928).
2. E. GAVIOLA. Phil. Mag. **6**, 1154, 1167 (1928).
3. H. KLUMB and P. PRINGSHEIM. Z. Physik, **52**, 610 (1928).
4. J. A. BERBERET and K. C. CLARK. Phys. Rev. **100**, 506 (1955).
5. M. L. POOL. Phys. Rev. **33**, 22 (1929); **38**, 955 (1931).
6. T. ASADA, R. LADENBURG, and W. TIETZE. Z. Physik, **29**, 549 (1928).
7. H. W. WEBB and H. A. MESSENGER. Phys. Rev. **40**, 466 (1932).
8. E. W. SAMSON. Phys. Rev. **40**, 940 (1932).
9. S. SONKIN. Phys. Rev. **43**, 788 (1933).
10. J. H. COULLIETTE. Phys. Rev. **32**, 636 (1928).
11. B. DE B. DARWENT and F. G. HURTUBISE. J. Chem. Phys. **20**, 1684 (1952).
12. R. W. WOOD. Proc. Roy. Soc. **106**, 679 (1924).
13. G. LAROZE and J. L. COJAN. Compt. rend. 995 (1958).
14. M. KASHA. J. Opt. Soc. Am. **38**, 929 (1948).
15. M. J. DIGNAM, W. G. FORBES, and D. J. LE ROY. Can. J. Chem. **35**, 1341 (1957).
16. C. G. MATLAND. Phys. Rev. **92**, 637 (1953).
17. D. ALPERT, A. O. MCCOUBREY, and T. HOLSTEIN. Phys. Rev. **76**, 1257 (1949).
18. J. A. PINDER and D. J. LE ROY. Can. J. Chem. **35**, 588 (1957).
19. J. L. SPIER. Physica, **7**, 381 (1940).

Can. J. Chem. Downloaded from www.nrcresearchpress.com by 210.87.254.5 on 09/05/12
For personal use only.

Can. J. Chem. Downloaded from www.nrcresearchpress.com by 210.87.254.40 on 09/05/12
For personal use only.

HIGH ENERGY REACTIONS OF ATOMIC HYDROGEN[1]

MICHAEL HENCHMAN,[2] DAVID URCH,[3] AND RICHARD WOLFGANG

ABSTRACT

The chemistry of hot hydrogen atoms has been studied using tritium of high kinetic energy as produced by nuclear recoil. The possibilities and limitations of this technique are discussed using a collision theory for reactions of atoms having a very high initial energy. Using this theory and certain experimental data, it is concluded that hot hydrogen atoms react to combine with organic molecules at very high collision efficiency (of the order of approximately 0.2 to 0.4) in the energy range 3–10 ev. There is no indication that collisions at much higher energies lead to combination. With most systems, e.g. alkanes, a wide variety of reactions is observed. The systematics of these hot reactions is discussed and evidence on their detailed mechanism is presented. It appears that most products are formed by a fast displacement of an atom or group by the hot hydrogen. There is no evidence for the formation of a common, internally equilibrated, collision complex which decays on a statistically determined basis to the various products. Instead, the course of the reactions seems largely governed by the direction and point of impact of the hot atom. Thus, stereochemical evidence indicates that axial approach of the hot hydrogen atom along the C—H bond axis leads to abstraction while approach at large angles to this axis results in displacement without Walden inversion. In some cases sufficient excitation energy is introduced in the hot displacement process to cause further decomposition of the primary product. This model of high-energy reactions is compared with that of thermal reactions and its general implications are briefly discussed.

Perhaps the severest limitation on the study of chemical kinetics has been the scarcity of data on high-energy interactions. Little information on such interactions is obtainable from results on thermally excited species. Thermal reactions generally have very low collision efficiencies which are sensitively dependent on the activation energy. As a consequence only those reaction modes with minimum activation energies are observed. In a sense these modes are only limiting cases of the high-energy situation. Here activation energies are no longer large compared with the energies available; consequently collision efficiencies should be higher and a much wider variety of reactions may be expected.

Thus up to a few years ago, the only known reaction between atomic hydrogen and methane was simple abstraction, as it proceeds with thermal hydrogen (1, 2)

$$D + CH_4 \rightarrow HD + CH_3\cdot$$

But other reactions of hydrogen atoms are quite conceivable; for instance, exchange

$$D + CH_4 \rightarrow CH_3D + H$$

or perhaps

$$D + CH_4 \rightarrow H_2 + CH_2D\cdot$$

and so on. These reactions are interesting and a priori one might expect them to occur at higher energies, where the system may follow paths on the reaction surface other than those going through the lowest saddle point.

There has been no shortage of interest in possible high-energy reactions. Rather, what has been lacking is the means of producing high energy or "hot" species under controlled conditions, where their elementary reactions might be studied. Some work has been done, generating hot atoms and radicals by photochemical dissociation; but, in general, these have still not been of sufficient energy to react in a qualitatively different manner from their low-temperature thermal counterparts (3). In principle, the ideal system for the

[1]*Contribution No. 1625 from the Sterling Chemistry Laboratory, Yale University, New Haven, Connecticut; paper presented at the Symposium on the Fundamental Aspects of Atomic Reactions held at McGill University, Montreal, Que., September 1960.*

[2]*Studies carried out in partial fulfillment of the requirements for the Ph.D. degree.*

[3]*Present address: Department of Chemistry, Queen Mary College, Mile End Road, London E1, U.K.*

study of high kinetic energy atoms and other species would be monoenergetic molecular beams of controllable energy. However, for work in what is chemically perhaps the most interesting energy range—of the order of 1 to 20 ev—it does not appear that present beam techniques are likely to give useful results for some time.

In the meantime it appears that high-energy recoils from certain nuclear reactions may provide systems in which high-energy atomic reactions may be studied under controlled conditions. In our laboratory we have used recoil tritium from the nuclear reaction $He^3(n,p)T$ as a source of hot atoms. This paper briefly surveys our recent and largely unpublished results and uses them as a basis for discussion of a model of hot atom reactions.

METHOD

The principle of the recoil method as used for hot hydrogen atoms is very simple (4). He^3 is mixed in a quartz ampoule with the gas whose reactions with hot hydrogen are to be studied. (A lithium salt may be substituted for He^3 in condensed systems.) Hot hydrogen in the form of recoil tritium is generated by exposure to neutrons. This will react to form trace quantities of various products which are labeled due to the radioactivity of the contained tritium. These products are then separated, generally by gas chromatography, and assayed using an internal flow proportional counter attached to the chromatography unit (5, 6). Any of the products may then be degraded to determine the intramolecular position of the tritium.

While this method is basically simple there are a number of pitfalls to be avoided. In the first place unless the nuclear reaction gives rise to a well-defined species, it becomes a difficult problem in itself simply to determine the nature of the reactant. Thus radiative neutron capture (n,γ reaction) usually yields a recoil species with an energy between 1 and 1000 ev, which may or may not be charged, and which may or may not be neutralized before undergoing "chemical" reaction. Fortunately the $He^3(n,p)T$ reaction yields ions of very high energy, 2×10^5 ev; neutralization of these ions occurs at 10^4 ev in non-ionic media; in an energy range well above that in which they may react to become chemically bound (4). This nuclear reaction is thus a well-defined source of atoms of essentially infinite energy, which lose energy by collision until they react or are reduced to thermal energies.

Secondly, the high-energy release associated with the nuclear reactions will cause gross radiation damage to the system and may build up a significant level of reactive impurities. This effect is controlled by using only a trace amount of recoil tritium—of the order of 10^{14} atoms—a device made possible, of course, by its radioactivity. The tracer level experiment has the further advantage of eliminating the confusing type of secondary process where more than one hydrogen atom is involved.

A final important point of technique is being able to distinguish between hot reactions and the thermal reactions of those atoms which have been collisionally deactivated (7). These thermal reactions are effectively eliminated by the addition of a small concentration of a scavenger, such as I_2, with which the thermalized species will react preferentially. On the other hand the hot reactions are unaffected since hot atoms have an effective lifetime of only a few collisions and are therefore unlikely to encounter the scavenger.

COLLISION KINETICS AND ENERGY DEPENDENCE

The main disadvantage of using nuclear recoil as a source of hot atoms is that the reactions occur over a range of energies, from the highest possible energy where combination may take place down to (but not including) the thermal region. It is for this reason that molecular beams are, in principle, preferable; they would make possible a direct and

Can. J. Chem. Downloaded from www.nrcresearchpress.com by 210.87.254.40 on 09/05/12
For personal use only.

Can. J. Chem. Downloaded from www.nrcresearchpress.com by 210.87.254.40 on 09/05/12
For personal use only.

explicit measurement of reaction probability as a function of energy. However, even if recoil atoms cannot be used to study reactions at a single energy, their distribution of energies is well defined and their collision kinetics can thus be treated analytically (7). In a sense the collision theory of hot atoms, briefly outlined below, is quite analogous to collision theories of thermal species whose Boltzmann energy distribution yields expressions such as the Arrhenius equation.

Kinetic Theory

Consider a system (7) of hot atoms which lose energy in successive collisions but may react to combine between energies E_2 and E_1. Above E_2 the collisions are too energetic to result in stable combination and E_1 is the minimum energy required for reaction. Let $n(E)dE$ be the differential probability of collision at energy E, f the probability that a collision will be with a reactive species, and $p(E)$ the probability that such a collision at energy E will result in combination. Then the total probability P that the hot atom will react during its lifetime is given by

$$P = \int_{E_2}^{E_1} fp(E)n(E)dE. \qquad [1]$$

$n(E)$ is evaluated assuming that the initial energy is much greater than E_2, that the reaction threshold E_1 is above thermal energies, and that the energy loss is as by elastic collisions. P can then be evaluated (7)

$$P = 1-\exp\left[-\frac{f}{\alpha} I\right] \qquad [2]$$

$$I = \int_{E_1}^{E_2} \frac{p(E)}{E} dE \qquad [3]$$

where α is the average logarithmic energy loss per collision. P, the total probability of hot reaction, is experimentally measurable and f and α may be calculated from the composition of the system. Similar considerations (7) lead to expressions for the total probability of hot reaction P_i to give a specific product i.

This detailed theory has been tested (7) using the reactions

$$CH_4 + T \rightarrow CH_3T + H, \qquad [4]$$

$$CH_4 + T \rightarrow CH_2T\cdot + H_2. \qquad [5]$$

f and α were varied by adding rare gas moderators. The effect of these is to reduce the total probability of hot reactions by reducing the number of collisions of the hot atom with methane. Figure 1 shows the probability of formation of CH_3T in the presence of

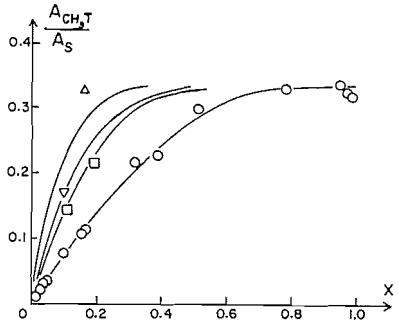


FIG. 1. Plot of the relative yield of labeled methane as function of the mole fraction of methane. Moderators: helium ○, neon □, argon ▽, xenon △.

Can. J. Chem. Downloaded from www.nrcresearchpress.com by 210.87.254.40 on 09/05/12
For personal use only.

various amounts of He, Ne, A, and Xe. The points are experimental and the lines through them calculated from the kinetic theory. The fit is good within experimental error and the treatment is evidently a valid representation of the system.[4]

Energy Dependence

This model of hot reactions makes it clear that high-energy recoil atoms cannot supply explicit and absolute information on the energy dependence of the collision efficiency $p(E)$. As obtained from this treatment $p(E)$ is wrapped up in the definite integral I. The only energy information that can be directly obtained from the detailed theory is on the relative average energies at which various products are formed in a given system (7). Thus it appears that the two hot atom reactions of methane ([4] and [5]) proceed at about the same average energy.

Information on the energy range in which hot reactions can occur must come from calculations on the dynamics of the collision (which are quite difficult) and from the character of the reactions which are observed. Data on the lower energy limit (E_1) comes from experiments in which Hamill *et al.* (3) have observed that the hydrogen displacement reaction does not occur with photochemically generated hydrogen atoms of 1 to 2 ev. At the other limit, the only conceivable way in which a very high-energy hydrogen atom (>10–20 ev) can undergo displacement reaction [4] is by transferring most of its kinetic energy to the ejected hydrogen in a quasi-elastic or billiard-ball (8) collision. This would leave the incoming atom with sufficiently little energy so that it could be captured by the methyl group. (Such a process can be considered as essentially an atom–atom collision, where one of the atoms is held in a relatively shallow potential well to the rest of the molecule, with which it is then only weakly coupled.)

It has been calculated by Cross (9) that if displacement reaction [4] with CH_4 and CD_4 occurs by such a pure billiard-ball mechanism, there should be an isotope effect of about 3. No such large effect is experimentally observed, indicating that this type of mechanism is not important (9). Apparently reaction occurs in an energy range where valence bond coupling is strong, i.e. as far as transfer of momentum is concerned the incoming atom collides with the molecule, or a large part of it, instead of a single atom within it. This finding was not unexpected in view of the earlier observation that alkyl groups and halogen atoms as well as hydrogen atoms could be displaced. The tritium must therefore have a kinetic energy of the order of magnitude of valence bond energies. This conclusion is consistent with the products observed from other systems, for the energy deposited in a hot displacement reaction appears to be insufficient to cause extensive decomposition or rearrangement. This topic will be discussed later in this paper.

Collision Efficiencies

If, therefore, the conclusion is that the hot hydrogen reacts to combine while between 2 and 20 ev or, more likely still, while between 3 and 10 ev, the kinetic theory can be used to calculate collision efficiencies. From equation [3] the collision efficiency $p(E)$ averaged over the entire energy interval E_2 to E_1 is

$$\overline{p(E)} = \frac{I}{\ln(E_2/E_1)} \qquad [6]$$

For the methane system I has been measured to be 0.4 (7). Fortunately $\overline{p(E)}$ is quite insensitive to the energy range E_2/E_1. Using the values just quoted we find that for hot

[4]*Conversely, these considerations provide a further proof that the reactions studied are indeed hot. A fit cannot be obtained even if there is only a small contribution by thermal processes (7).*

atom reactions collision efficiencies are of the order of 0.2 to 0.4. These values are several orders of magnitudes higher than those for thermal reactions of a similar nature and are one of the distinguishing characteristics of hot atom reactions.

SYSTEMATICS OF HOT HYDROGEN ATOM REACTIONS

The reaction of hot tritium with hydrocarbons (4, 10, 11, 12, 13), alcohol (14), acetone (14), carboxylic acids (15), and various solid compounds (16) has been investigated. The types of reactions found are quite similar in all those systems. We can therefore use the results of a recent study (13) we have made of the alkane system as a representative example of the systematics of hot hydrogen displacement reactions. (Hot hydrogen addition reaction, as studied in alkenes (10), is a separate class of mechanism and will not be discussed here.)

As in most systems about two-thirds to three-quarters of hot hydrogen atoms in pure alkanes will undergo reaction before reaching thermal energies. The types of reactions found are as follows, in decreasing order of relative importance (butane is used as example):

(I) Hydrogen atom abstraction. This reaction, the only one observed at thermal energies, also occurs with hot hydrogen (although with a much higher collision yield).

$$T^* + CH_3CH_2CH_2CH_3 \rightarrow \begin{matrix} CH_3CH_2\dot{C}HCH_3 \\ CH_3CH_2CH_2CH_2\cdot \end{matrix} + HT.$$

(II) Hydrogen atom displacement:

$$T^* + CH_3CH_2CH_2CH_3 \rightarrow \begin{matrix} CH_3CH_2CH_2CH_2T \\ CH_3CH_2CHTCH_3 \end{matrix} + H.$$

(III) Replacement of alkyl group to form a degraded alkane:

$$T^* + CH_3CH_2CH_2CH_3 \rightarrow \begin{matrix} CH_3T \\ CH_3CH_2T \\ CH_3CH_2CH_2T \end{matrix}$$

(IV) Replacement of two groups to form a radical. Either two hydrogen atoms or a hydrogen atom and an alkyl group may be displaced by the hot tritium atom, e.g.,

$$T^* + CH_3CH_2CH_2CH_3 \rightarrow CH_3CH_2CH_2CHT\cdot.$$

The resulting radical may combine with iodine scavenger to form alkyl iodide. Alternatively it may decompose into a smaller radical and an alkene by breaking a C—C bond without rearrangement, e.g.,

$$CH_3CH_2CH_2CHT\cdot \rightarrow CH_3CH_2\cdot + CH_2CHT.$$

(This type of decomposition has also been observed with similar radicals made by hot atom addition to alkenes (10).)

These reactions account for essentially the entire yield. No built-up or rearranged products are formed. The relative importance of these various types of reactions with the alkanes are given in Table I. However, their relative probabilities vary sharply and in a specific manner from system to system. It is in this variation that we must look for clues to the mechanism.

MECHANISM

We have mentioned earlier that in high-energy processes the activation energies should become less important in determining the path of a reaction. This is reflected in the

Can. J. Chem. Downloaded from www.nrcresearchpress.com by 210.87.254.40 on 09/05/12
For personal use only.

result that 90±2% of the hot reactions are hydrogen abstraction or displacement and less than 10% involve displacement of an alkyl group. In other words the probability of C—H bond rupture is about four times greater than with the weaker C—C bond. This finding also implies that hot displacement reactions do not pass through a common intermediate or collision complex of sufficient lifetime to permit internal equilibration of energy, as has been suggested (17, 18). Such an intermediate would certainly be expected to decompose at least as often by breaking a weaker rather than a stronger bond. There appears to be no data supporting the supposition that hot displacement reactions do go through such quasi-equilibrated intermediates. For instance, if HT and $CH_2T\cdot$ were produced from methane by decomposition of a common activated complex, in which the incident and the CH_4 hydrogen atoms have become indistinguishable

$$T + CH_4 \rightarrow (CH_4T) \rightarrow \begin{matrix} CH_2T\cdot + H_2 \text{ or } CH_3\cdot + HT \\ CH_3T + H \quad \text{or } CH_4 + T \end{matrix}$$

their ratio $HT/CH_2T\cdot$ would be expected, on a purely statistical basis, to be 2:3. Even allowing for possible isotope effects the observed ratio of 9:1 hardly supports such a mechanism (4). Instead, all results are consistent with the hypothesis that the displacement reaction is a fast, direct, localized event occurring on a time scale comparable to a bond vibration ($\sim 10^{-14}$ sec).[5]

Stereochemistry of Hot Atom Displacement

If hot reactions are thus not controlled by energetics, or the statistically determined decay of a common collision complex, we must turn to stereochemical factors affecting displacement and abstraction processes, as the major determinant of hot atom reactions. For example, it appears to be a reasonable hypothesis that the C—H bond is attacked more readily than the C—C bond because of its greater exposure. Two related questions then arise: (*a*) Does hydrogen displacement proceed by a Walden inversion mechanism? and (*b*) What determines whether the hydrogen atom is displaced or abstracted? The answers to these questions have been sought in experiments on the retention of spatial configuration during hydrogen displacement.

The first experiment performed using hot tritium indicated that configuration was retained during hydrogen displacement. The system was glucose (19, 20) and it yielded a substantial amount of glucose labeled at hydrogen atoms attached to asymmetric carbon atoms. Had inversion occurred, other labeled hexoses would have been obtained instead. Retention of configuration has also been demonstrated in displacement at the hydrogen attached to the asymmetric center in alanine (21). However, since these experiments were carried out in the solid phase, they left open the possibility that the molecule was constrained to keep its configuration only by the crystal structure.

Experiments were therefore carried out on the retention of configuration in the vapor phase. The displacement reaction for gaseous optically active *sec*-butyl alcohol was studied. There is no change in configuration about the asymmetric carbon atom during the displacement of both the hydrogen bonded directly to it and those in the methyl and ethyl groups. These results actually show 90±10% retention of configuration.

With this information we can now discuss a more detailed model for the hydrogen abstraction and displacement, which together account for 90% of the hot reactions in

[5]*It is interesting to compare the fast displacement reactions with the addition reactions of hot hydrogen to double bonds in alkenes. In the latter case it can be clearly shown that a long-lived radical intermediate is formed (10). These well-defined intermediates may each decompose into two or three sets of alternative products.*

Can. J. Chem. Downloaded from www.nrcresearchpress.com by 210.87.254.40 on 09/05/12
For personal use only.

alkanes. If Walden inversion is unimportant, it can be postulated that to react with a bound hydrogen, the incoming hot hydrogen must approach within a wide cone about the C—H bond axis (see Fig. 2). However, if the approach is directly along the C—H bond

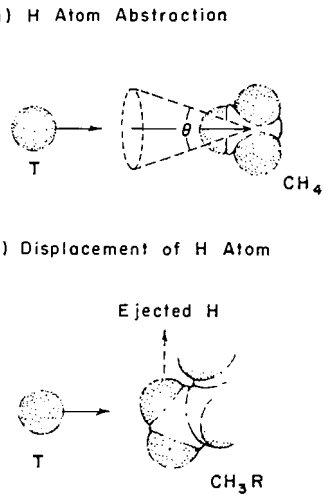


FIG. 2. Stereochemistry of the abstraction and displacement of hydrogen from an alkane.

axis, displacement could not occur as it would be difficult to juxtapose the positions of the H and T atoms. But abstraction of the H atom should be entirely possible for this approach. This is in accord with calculations of Gorin *et al.* (22), showing that axial attack along the C—H bond is the most favorable route for hydrogen abstraction. This mechanism is also consistent with the finding that abstraction from CH_2D_2 yields equal amounts of HT and DT (23). Thus we arrive at the tentative conclusion that hot hydrogen attack at small angles to the C—H bond, within a small inner cone about the bond axis, normally leads to abstraction, whereas approach at large angles, within a larger co-axial cone, usually results in displacement (see Fig. 2).

This model is crude and obviously oversimplified. But it can be tested. Consider a particular C—H in an alkane. Methyl or methylene groups attached to the carbon will obstruct those approaches of the hot atom at large angles to the C—H bond axis and will reduce the amount of displacement. Approaches at small angles will not be affected and hence there will be no steric obstruction of the abstraction reaction. We consider that the displacement reaction in methane is unobstructed and that replacement of one of these hydrogens by a methyl or methylene group reduces the amount of displacement at one of the remaining hydrogens, relative to that of abstraction, by a factor $(1-\Omega)$. Experimentally the ratio abstraction/displacement is found to be unity for methane. On this simple picture, for an alkane containing n hydrogens, of which n_1 are primary, n_2 secondary, and n_3 tertiary,

$$\frac{\text{abstraction}}{\text{displacement}} = \frac{n}{n_1(1-\Omega)+n_2(1-\Omega)^2+n_3(1-\Omega)^3}.$$

The experimental and calculated values of this ratio are plotted in Fig. 3 for all the alkanes listed in Table I and for cyclopentane. The value $\Omega = 0.45$ for the obstruction

Can. J. Chem. Downloaded from www.nrcresearchpress.com by 210.87.254.40 on 09/05/12
For personal use only.

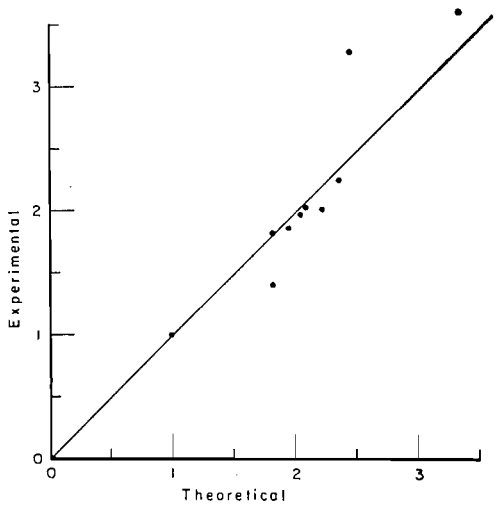


FIG. 3. Comparison of the theoretical and experimental values of the ratio of hydrogen abstraction to hydrogen displacement for cyclopentane and the alkanes listed in Table I. The obstruction parameter $\Omega = 0.45$.

TABLE I

Summary of product distribution from non-cyclic alkanes (relative to yield of labeled parent molecule)

	T-Labeled product	Corresponding replacement	Molecule reacting with hot hydrogen								
			CH_4	C_2H_6	∧	∧∨	⟩—	∧∧	⟩—\	+	∧∧∨
I	HT	Abstraction	1.0	1.82	1.97	1.99	1.92	2.37	2.03	1.40	3.28
II	Parent molecule	H atom	1.0	1.0	1.0	1.0	1.0	1.0	1.0	1.0	1.0
III	Degraded alkane	Alkyl group	—	0.12	0.15	0.15	0.17	0.19	0.21	0.23	0.31
IV	Methyl iodide[a] (initially $CH_2T\cdot$)	Alkyl group[b] + H atom or two H atoms	0.12[b]	0.14	0.06	0.09	0.05	0.08	0.09	0.09	0.07
IV	Alkene (initially radical)	Alkyl group + H atom	—	0.11	0.08	0.08	0.09	0.10	0.09	~0.05	0.12
	Rearranged and built-up products	Unaccounted for[c]	—	~0.03	0.00	0.01	0.01	0.00	0.00	0.01	0.02

[a]In presence of I_2 scavenger only.
[b]2H displacement in case of CH_4.
[c]Not compatible with formation as direct consequence of a hot displacement reaction.

parameter gives the best fit. This is a simple-minded calculation with obvious shortcomings. The principal one is that it attributes the same amount of obstruction to any attached group, regardless of whether it is, say, methyl or isopropyl. Nevertheless, we suggest that the excellent correlation between calculation and experiment provides evidence for the detailed model used for hydrogen abstraction and displacement as well as the more general postulate that the course of the reaction depends primarily on the angle of approach and the point of impact of the hot atom.

Alkyl Group Displacement

It is tempting to try and generalize the hydrogen displacement mechanism for the displacement of larger atoms and groups. Such replacement has been shown to occur. Odum (24) finds that fluorine, chlorine, bromine, and iodine in alkyl halides have a high probability of being displaced by a hot hydrogen atom.

$$T^* + CH_3X \rightarrow CH_3T + X$$

Can. J. Chem. Downloaded from www.nrcresearchpress.com by 210.87.254.40 on 09/05/12
For personal use only.

Rowland and co-workers have demonstrated the occurrence of hot hydrogen displacements of halogens and also of nitro groups in aromatic systems (25).

This would seem to indicate that degraded alkanes are formed by direct alkyl group displacement (reaction type III), e.g.,

$$CH_3CH_2CH_2CH_3 \rightarrow CH_3T \text{ or } CH_3CH_2T \text{ or } CH_3CH_2CH_2T.$$

In this single-step mechanism it is postulated that the hot hydrogen attacks the C—C bond in a direction nearly perpendicular to the bond axis. It would displace one group and combine with the other. This mechanism is consistent with the following results for the alkane system (13).

1. Displacement of an alkyl group is less probable than that of an H atom. This may be correlated with the greater steric obstruction of the C—C bond.

2. The amount of an alkane RT formed depends on the number of R groups in the reacting molecule. Thus the amount of methane formed from the pentanes increases in the order cyclopentane $<$ *n*-pentane $<$ isopentane $<$ neopentane.

3. In attacking a C—C bond the tritium preferentially combines with the smaller of the groups joined by the bond. This bias is more pronounced if the two groups are very dissimilar in size. Thus neopentane yields eight times as much methane-T as isobutane-T.

Although direct alkyl group displacement is not the only possible mechanism for the formation of the degraded alkanes (see footnote 6) it appears to be the most likely. Its validity would be established by showing that configuration is retained in the formation of the degraded alkanes.

The direct displacement mechanism can also account for the production of radicals (reaction type IV). Two atoms or groups would have to be displaced, e.g.,

$$T^* + CH_3CH_2CH_2CH_3 \rightarrow H_2 + CH_3CH_2CH_2CHT.$$

This mechanism is plausible but there is as yet insufficient evidence to regard it as more than a tentative hypothesis.

EXCITATION ENERGY IN PRIMARY PRODUCT OF HYDROGEN DISPLACEMENT

It is likely that some of the energy of the incident hot atom will remain as excitation in the product of the displacement process. Although we have presented evidence that the point and direction of impact is the primary determinant of the reaction path, this excitation energy may also be a factor in determining the final product. That this energy is very unlikely to be large (of the order of 10 ev) is indicated by the very small yields of products requiring multiple bond rupture for their formation. Thus only traces of acetylene are formed by hot hydrogen reaction with alkanes; similarly, the yield of methylacetylene and allene by reaction with alkenes is less than 1% (10, 11, 13).

The excitation energy is sufficient to cause some decomposition of the product of the primary displacement especially in sensitive systems. Thus carboxylic acids tend to decarboxylate following hot hydrogen displacement (15), e.g.,

$$CH_3COOH + T^* \rightarrow CH_2TCOOH^* \rightarrow CH_3T.$$

The resulting decarboxylated hydrocarbon can presumably also be produced by direct displacement of —COOH. But the yield of this product decreases very rapidly with increasing chain length. This indicates that most of it must have been formed by decomposition of excited acid molecules. As the size of such molecules increases so does their lifetime (26) and it becomes more likely that they lose their energy by collision rather than decomposition.

Other systems also provide evidence for deposition of moderate amounts of excitation

Can. J. Chem. Downloaded from www.nrcresearchpress.com by 210.87.254.40 on 09/05/12
For personal use only.

energy on displacement. When a hydrogen atom bound to the sp^2 carbon atom in cis and trans dichloroethylenes is replaced, configuration is lost in 30% of the events (13). This loss is probably due to rotation about the double bond requiring an activation energy of about 2 ev.

Reaction of hot hydrogen with cyclopropane yields at least 15% as much propylene as substituted cyclopropane (13, 17). The isomerization of cyclopropane to propylene has an activation energy of 3 ev. At the pressures at which the experiment was carried out, this would mean that about 4 ev of excitation had been introduced during hydrogen atom displacement.

The examples quoted are particularly sensitive systems, and even in them the fraction of the total products formed by rearrangement or decomposition of a species excited in the initial displacement is not large. In the more stable alkane systems, the only significant products, which could plausibly be formed by such decomposition, are the alkyl radicals (Systematics, reaction type IV), e.g.,

$$T^* + CH_3CH_2CH_3 \rightarrow CH_2TCH_2CH_3^* \rightarrow CH_2TCH_2\cdot + CH_3\cdot.$$

Radicals account for only about 5% of the total yield from alkanes and they could also have been produced by the two group displacement mechanism mentioned earlier.[6]

CONCLUSION

While the studies briefly outlined here represent only a small start towards understanding the chemical properties of hot hydrogen atoms, it does appear that the broad outlines of a mechanism are emerging. The significance of our findings may be summarized by comparing the model for hot reactions with that for thermal processes.

In thermal reactions only a small fraction $e^{-\Delta E/kT}$ (where ΔE is the activation energy) of species have sufficient energy for reaction. Even these species have barely sufficient energy and their only possible path over the energy surface must pass through a saddle point. This is evidenced by the fact that only a small fraction of collisions between species of sufficient energy result in reaction. This fraction p is, of course, the so-called steric factor and $pe^{-\Delta E/kT}$, the collision efficiency, is thus usually a very small number. By contrast we have shown that when a hydrogen atom with a kinetic energy of the order of 3 to 10 ev strikes a molecule, there is a high probability, approaching one-half, that it will react. This must in part simply result from the fact that all systems have energy in excess of the minimum activation energy, so that the factor $e^{-\Delta E/kT}$ approaches unity. What is more significant, however, is that many of the hot atoms have considerably more than the minimum energy for reaction. As a result, their possible paths over the reaction energy surface are not restricted to passage through the lowest saddle point, and a much wider

[6]*It may be proposed that degraded alkanes (Systematics, reaction type III) can be produced as a result of excitation energy left in hydrogen displacement and not by direct alkyl displacement. If decomposition of the primary product could yield hot radicals, these could form degraded alkane molecules by hydrogen abstraction (even in the presence of scavenger), e.g.,*

$$T^* + CH_3CH_2CH_2CH_3 \rightarrow CH_3CHTCH_2CH_3^* \rightarrow CH_3CHT\cdot^* \xrightarrow{\text{H abstraction}} CH_3CH_2T$$

This mechanism has difficulties however. An excited radical normally decomposes to a smaller radical and an alkene (10). To abstract hydrogen, the radical would therefore have to have kenetic rather than internal energy. The production of such species is rather improbable. Furthermore, to account for the distribution of products, e.g. the 8:1 ratio of methane-T: isobutane-T from neopentane, it would have to be postulated that the C—C bond broken was nearly always that closest to the site of the original displacement; in other words that there was little intramolecular energy transfer. Even so it is very difficult to account for the relative constancy, or even increase, in the ratio of total degraded alkanes to hydrogen substitution, that is observed with increasing chain length of the reacting alkane (Table I). However, a final decision on this mechanism must await data on the retention of configuration of the degraded alkanes. This and other alternative mechanisms can be finally excluded if it is shown that configuration is retained in alkyl displacement.

Can. J. Chem. Downloaded from www.nrcresearchpress.com by 210.87.254.40 on 09/05/12
For personal use only.

range of impact parameters can lead to reaction. Many different kinds of reactive collisions become possible. A variety of products may result, as illustrated by the alkane data, and their relative yields are not primarily governed by energy considerations. As a consequence, differences in chemical reactivity as conventionally understood become unimportant: for example, hydrogen atoms are about equally well displaced whether they are aromatic or aliphatic (23). Furthermore, the availability of excess energy may result in the products of the initial displacement being left with a range of excitation energies. There is, however, considerable evidence to suggest that these excitation energies are quite moderate. This is not unexpected for, in collisions, where the hot hydrogen has too much energy, it cannot lose enough momentum to combine.

This model is not consistent with the view that the course of hot reactions is governed by the statistically determined decay of a common intermediate or collision complex. Such a mechanism is essentially an extension of transition state theory of unimolecular decompositions. It has recently been proposed by Magee and Hamill (18) as possibly accounting for the reactions of low-energy hot atoms of photochemical origin. It seems unlikely that such a theory could be a valid representation of the reactions of atoms having more than about 2 ev of energy. Because of this excess kinetic energy, passage along the reaction co-ordinate is so rapid that there is insufficient time for internal equilibration of energy in the collision complex. The fate of this complex thus cannot be predicted by calculating the relative probabilities of decomposition, through various channels, of an equivalent internally equilibrated complex. Instead, the manner in which the collision complex disintegrates is determined by the particular manner in which it was put together.[7]

We thus postulate that the initial hot displacement reaction occurs by a fast ($\sim 10^{-14}$ sec) localized "direct" displacement. The course of this process is governed primarily by the direction and point of impact. These stereochemical considerations are of a different nature than that encountered in the "steric factor" of thermal reactions. In the thermal case it was simply a matter that with the minimal energy available only a certain approach could lead to reaction. With hot hydrogen, reaction appears likely for many types of approaches. What is governed by the stereochemistry is not so much whether reaction will take place but what kind of reaction will take place. An example is provided by the situation with alkanes, where approach co-axial to a C—H bond leads to abstraction, whereas approach at a larger angle results in displacement.

ACKNOWLEDGMENTS

The authors wish to thank Dr. John Chesick for many stimulating discussions. This work was supported by the U.S. Atomic Energy Commission under Contract No. AT(30-1)-1957.

REFERENCES

1. M. R. Berlie and D. J. Le Roy. Can. J. Chem. **32**, 650 (1954).
2. R. Klein, J. R. McNesby, M. D. Scheer, and L. J. Schoen. J. Chem. Phys. **30**, 58 (1959).
3. R. J. Carter, W. H. Hamill, and R. R. Williams. J. Am. Chem. Soc. **77**, 6457 (1955).
4. M. Amr El-Sayed, P. J. Estrup, and R. Wolfgang. J. Phys. Chem. **62**, 1356 (1958).
5. R. Wolfgang and F. S. Rowland. Anal. Chem. **30**, 903 (1958).
6. R. Wolfgang and C. F. MacKay. Nucleonics, **16**, 69 (1958).
7. P. J. Estrup and R. Wolfgang. J. Am. Chem. Soc. **82**, 2661, 2665 (1960).
8. W. F. Libby. J. Am. Chem. Soc. **69**, 2523 (1947).

[7]*However, hot* addition *reactions of hydrogen to double bonds yield excited radicals of relatively long life. The subsequent decomposition of these radicals can presumably be treated by absolute rate theory of unimolecular reactions.*

Can. J. Chem. Downloaded from www.nrcresearchpress.com by 210.87.254.40 on 09/05/12
For personal use only.

9. J. CROSS and R. WOLFGANG. Unpublished work.
10. D. URCH and R. WOLFGANG. J. Am. Chem. Soc. **81**, 2025 (1959).
11. J. K. LEE, B. MUSGRAVE, and F. S. ROWLAND. *From* preprint of article submitted to J. Am. Chem. Soc.
12. M. C. SAUER, JR. and J. E. WILLARD. J. Phys. Chem. **64**, 359 (1960).
13. D. URCH and R. WOLFGANG. Unpublished work.
14. W. F. HOFF, JR. and F. S. ROWLAND. J. Am. Chem. Soc. **79**, 4867 (1957).
15. A. M. ELATRASH, R. H. JOHNSEN, and R. WOLFGANG. J. Phys. Chem. **64**, 785 (1960).
16. F. S. ROWLAND and R. WOLFGANG. Nucleonics, **14**, 58 (1956).
17. J. K. LEE, B. MUSGRAVE, and F. S. ROWLAND. J. Am. Chem. Soc. **81**, 3803 (1959).
18. J. L. MAGEE and W. H. HAMILL. J. Chem. Phys. **31**, 1380 (1959).
19. F. S. ROWLAND, C. N. TURTON, and R. WOLFGANG. J. Am. Chem. Soc. **78**, 2354 (1956).
20. H. KELLER and F. S. ROWLAND. J. Phys. Chem. **62**, 1373 (1958).
21. J. G. KAY, R. P. MALSAN, and F. S. ROWLAND. J. Am. Chem. Soc. **81**, 5050 (1959).
22. E. GORIN, W. KAUZMANN, J. WALTER, and H. EYRING. J. Chem. Phys. **7**, 633 (1939).
23. W. G. BROWN and J. L. GARNETT. Int. J. Appl. Rad. and Isotopes, **5**, 114 (1959).
24. R. ODUM and R. WOLFGANG. Unpublished results.
25. R. M. WHITE and F. S. ROWLAND. Unpublished results.
26. L. S. KASSEL. J. Phys. Chem. **32**, 225 (1928).

Can. J. Chem. Downloaded from www.nrcresearchpress.com by 210.87.254.40 on 09/05/12
For personal use only.

Can. J. Chem. Downloaded from www.nrcresearchpress.com by 210.87.254.42 on 09/05/12
For personal use only.

THE REACTIONS OF HYDROGEN ATOMS WITH SOME ORGANIC LIQUIDS[1]

R. B. INGALLS AND J. R. HARDY

ABSTRACT

Measurements have been made of isotopic exchange and deuterium pressure change during deuterium atom bombardment of *o*-terphenyl, toluene, and eicosane just above their melting points. The number of molecules of HD formed was larger than the number of molecules lost or gained by the gas phase. A mechanism of reaction of deuterium atoms with aromatic liquids is proposed.

INTRODUCTION

During studies of the radiation chemistry of some aromatic liquids (1), a need for a better understanding of the reactions of hydrogen atoms with aromatic molecules became apparent. There have been a number of studies of the action of hydrogen or deuterium atoms with aromatic or double-bond systems in the gas and solid phases reported (2), but reactions of hydrogen atoms in organic liquids have been largely neglected. Experimental difficulties encountered in such studies may be in part responsible for this state of affairs.

Hydrogen atoms are important intermediates in the radiation-induced formation of both high molecular weight products and hydrogen gas in aromatic and vinyl hydrocarbon systems (3). Therefore, a knowledge of their reactions is necessary for an understanding of the radiation chemistry of these materials. A knowledge of hydrogen atom reactions would also contribute indirectly to our knowledge of energy transfer and other important processes in radiation chemistry by allowing the separation of these reactions from other effects (4).

The work reported here is part of an effort to gain better understanding of the reactions of hydrogen atoms with aromatic materials by direct experimentation. Purified deuterium gas was dissociated into atoms on a hot tungsten filament. The gas, containing a small fraction of atoms, was cooled by indirect momentum transfer with thermostatted walls of the reaction vessel before impinging on the surface of the liquid under investigation. The gas consumed or formed during the reaction was measured, and the formation of HD was determined by mass spectroscopy.

EXPERIMENTAL

Deuterium gas, obtained from Stuart Oxygen Company, was further purified by storage as uranium deuteride. Its isotopic purity was determined by mass spectroscopy to be 99.5%.

Reagent grade toluene, obtained from Mallinckrodt, was distilled through a $2\frac{1}{4}$-ft glass-helix packed column and dried over calcium hydride. No impurities were detectable by gas–liquid partition chromatography.

Eastman Kodak white label eicosane and *o*-terphenyl were used without further purification. High-temperature gas–liquid partition chromatography indicated no impurities in the *o*-terphenyl and 2.4% of lower boiling impurities in the eicosane.

[1]*Contribution from the Research Department of Atomics International, A Division of North American Aviation, Inc., Canoga Park, California; paper presented at the Symposium on the Fundamental Aspects of Atomic Reactions held at McGill University, Montreal, Que., September 1960. Work performed under A.E.C. Contract AT(11-1)-GEN-8.*

An appropriate quantity of deuterium gas was measured into the system and pumped into a 2-liter measuring volume and micromanometer head. The 2-liter volume and the micromanometer head were maintained constant within 0.2° C at about 36° C. After a period of about 15 minutes was allowed for temperature equilibration, the micromanometer head was isolated and the main portion of the gas was pumped into a 5-liter storage bulb. During the run, the deuterium gas was circulated from this bulb through the reaction cell (see drawing of reaction cell, Fig. 1). The storage bulb was designed so that mixing of the gas occurred during circulation.

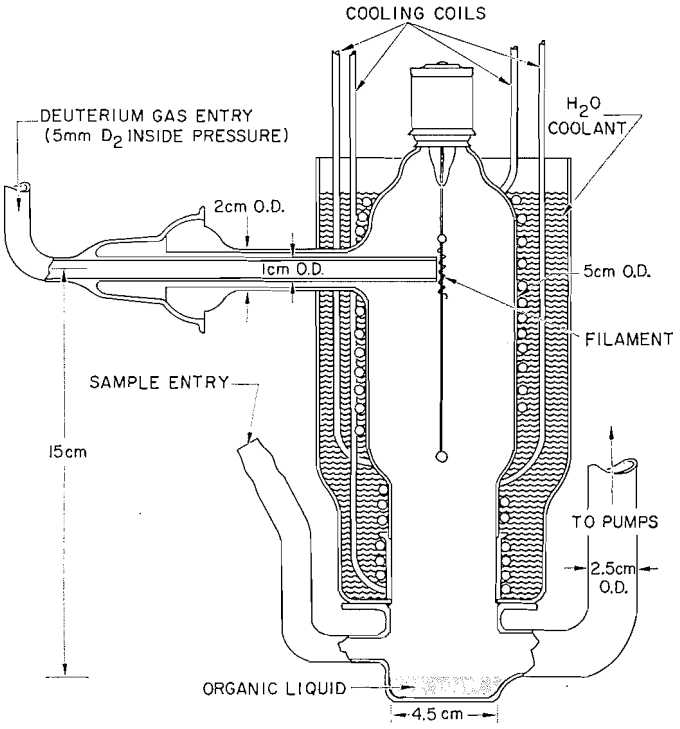


FIG. 1. Reaction cell.

It is important to understand that the pressure in the reaction cell during the run was about 5 mm of Hg* and that at this pressure, the mean free path of deuterium is nearly three orders of magnitude smaller than the dimensions of the reaction cell. Therefore, many of the deuterium atoms are prevented from getting to the wall to recombine while traveling the 15 centimeters from the filament to the surface of the liquid reactant. Indirect thermal contact with the thermostatted walls of the reaction cell does cool the gas, however, to within a degree or so of the temperature of the wall.

In order to prevent back diffusion of the organic vapors to the filament, a degassed sample was introduced into the reaction cell while the deuterium gas was being circulated. The reaction cell was brought to a constant temperature somewhat above the melting

**In order to pump deuterium rapidly at 5 mm, two mercury diffusion pumps were used in series. One was an 80-liter per second, three-stage pump and the other was a single-stage pump designed to pump into pressures up to 20 mm of Hg. The gas was pumped through the reaction cell at about 2 liters per minute when the inlet pressure to the big pump was maintained at about 0.2 mm of Hg by a controlled leak. Three traps were maintained at liquid nitrogen temperatures throughout the experiments.*

Can. J. Chem. Downloaded from www.nrcresearchpress.com by 210.87.254.42 on 09/05/12
For personal use only.

point of the sample which was stirred magnetically to increase the heat transfer with the bath. The filament was then brought up to temperature for an appropriate length of time. The gas was then pumped into the 2-liter bulb, permitted to come to temperature, and allowed to equilibrate with only one side of the micromanometer head. In this way, the pressure change which occurred during the reaction could be measured directly with the micromanometer to a precision greater than one part in a thousand. A sample of the gas was analyzed by mass spectroscopy for isotopic composition.

RESULTS

The experimental results are given in Table I. The values reported in the column headed % pressure per minute are equal to $(\Delta P \times 100)/(P \times T)$, where ΔP is the observed pressure change during the run, P is the pressure in the 2-liter measuring volume, and T is the length of the run in minutes. The corrected* increase in percentage of HD in the D_2 during the run divided by the time of the run in minutes is reported in the column headed % HD per minute.

A change in the geometry of the apparatus occurred between *o*-terphenyl runs 5 and 6. This did not significantly affect the ratio of HD formation to pressure change, although the rates of conversion dropped by approximately a factor of 4. Total conversion of the deuterium gas was about 10% in the runs with *o*-terphenyl and toluene, but was considerably less in the runs with eicosane. Blank runs with helium and *o*-terphenyl prove that cracking of the organic on the filament does not contribute to the results. This is not surprising in view of the low vapor pressure (less than 10 microns) of the materials at their melting point.† For the same reason, a gas phase reaction of organic vapors and deuterium atoms does not contribute significantly to the results.

The organic materials were examined by gas chromatography after reaction. A comparison of the sensitivity of the starting *o*-terphenyl and a 4.8-g sample from which 2.2×10^{-4} moles of HD had been produced indicated that exchange of deuterium for hydrogen had occurred in the *o*-terphenyl during the reaction. Using internal standards for comparison (5), the area under the curve for the starting material was $0.5\% \pm .05\%$ less than the area under the curve of the reacted material. This can be explained in terms of an increase in heat capacity and resulting increase in thermal conductivity of the *o*-terphenyl upon substitution of deuterium for some of the hydrogen (6).

No internal standard was used in the examination of the eicosane since impurities of the order of 2.4% were found in the unreacted material. The area under the curve for the impurity peaks was significantly reduced relative to the eicosane peaks in the reacted material. This effect may be due in part to substitution of deuterium and in part due to the selective reaction of the impurities.

Gas chromatographic examination of the reacted toluene revealed low yields of higher-boiling products. Bibenzyl was the major product, but its yield corresponded to only 1 mole per 10^4 moles HD formed. This indicates that abstraction of hydrogen from toluene is not important at these low temperatures (−80° C).

The values reported for the runs made with eicosane and toluene are preliminary and are intended only to support in a general way the results obtained with *o*-terphenyl. The eicosane results are open to question on two counts:

1. The conversions were low, decreasing our accuracy.

**A small correction for exchange on the walls was made based on results from blank runs.*

†This type of experiment is limited in applicability to materials of extremely low vapor pressures at the temperature of the reaction.

Can. J. Chem. Downloaded from www.nrcresearchpress.com by 210.87.254.42 on 09/05/12
For personal use only.

2. The 2.4% impurities in the eicosane may have been consumed disproportionately during the reaction.

The toluene runs were made at an earlier date and are more difficult experimentally so that the accuracy is probably not as high as in the runs with *o*-terphenyl.

A more detailed study of these materials as well as several other classes of organic compounds is being planned.

DISCUSSION

The reaction of thermal deuterium atoms with liquid *o*-terphenyl at 60° to 75° C produces more molecules of HD than there are molecules lost from the gas phase. Similar results were obtained with toluene at −88° to −79° C (see Table I). We propose the following mechanism for these systems:

$$\dot{D} + \phi = \dot{\phi}D \qquad k_1 = 10^9 \exp -[(3\times10^3)/RT] \qquad [1a]$$

$$\dot{\phi}D + (n-1)\phi = \dot{\phi}_nD \quad n = 1, 2, 3, \ldots \qquad [1b]$$

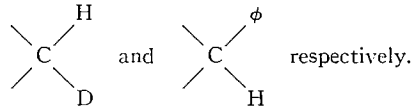
$$\dot{D} + \dot{\phi}_nD = HD + \phi_n \qquad k_2 = 4\times10^{10} \qquad [2]$$

$$\dot{D} + \dot{\phi}_nD = \phi_nD_2 \qquad k_3 = 10^7 \qquad [3]$$

$$\dot{\phi}_nD + \dot{\phi}_nD = \text{high molecular weight products} \qquad k_4 = 10^6 \qquad [4]$$

$$\dot{D} + \dot{D} = D_2 \qquad k_5 = 10^{11} \qquad [5]$$

In this set of equations, ϕ represents a molecule of the substrate, $\dot{\phi}D$ and $\dot{\phi}_nD$ represent free radicals containing the structure



respectively.

The formation of D_2 by a reaction analogous to reaction [2] does occur, but it is slower than the production of HD for two reasons:

1. an isotope effect is expected for the reaction with $\dot{\phi}D$, which will favor the formation of HD (7); and
2. in reactions with $\dot{\phi}_nD$, $n = 2, 3, \ldots$, the deuterium is not likely to be in an activated position.

The production of D_2 by a reaction analogous to reaction [2] is not equivalent to reaction [5] since its rate depends on $(\dot{D})$ $(\dot{\phi}_nD)$ instead of $(\dot{D})^2$. However, we chose to neglect it in this treatment since its effects are small.

The values of the specific reaction rate constants chosen for reactions [4] and [5] are in agreement with the theory of bimolecular combination of two radicals (8). However, the rate constants for reactions [1*a*], [1*b*], [2], and [3] require some comment. Reaction [1*b*] is not specified since its value is not needed for the calculations we have made. It has been assumed that the rate constants for the reactions of $\dot{\phi}_nD$ are independent of n in order to simplify the treatment. The activation energy for reaction [1*a*] was chosen to be consistent with the values observed for the addition of hydrogen to double bonds (2), assuming reaction [3], which is a radical combination reaction, to have zero activation

Can. J. Chem. Downloaded from www.nrcresearchpress.com by 210.87.254.42 on 09/05/12
For personal use only.

energy. k_3 and the pre-exponential term in k_1 were chosen slightly lower than would be predicted theoretically in order to keep the value of k_2 (which as calculated depends on k_3 and k_1) well below the rate of collision between two particles.

TABLE I

Filament temperature, °K	Temperature of liquid reactant, °C	% Pressure per minute	% HD per minute	% HD / % Pressure
(A) Terphenyl				
1705	59.5	−0.27	0.38	−1.78
*1744	62.0	−0.22	0.66	−3.00
1800	75.0	−0.23	0.78	−3.36
*1755	75.0	−0.25	0.74	−2.56
1805	75.0	−0.29	0.63	−2.24
1855	59.0	−0.07	0.35	−4.32
1890	60.0	−0.04	0.29	−7.15
*1895	60.0	−0.04	0.15	−3.45
				Average 3.48±1.12
(B) Eicosane				
1733	37.5	+0.03	0.05	+1.67
*1827	37.0	+0.03	0.10	+3.33
*1816	37.0	+0.04	0.09	+2.25
				Average 2.42±0.61
(C) Toluene				
2095	−79	−.04	.45	−11.8
*2137	−79	−.086	.14	− 1.57
2060	−79	−.05	.18	− 3.21
*2067	−79	−.02	.07	− 3.61
2070	−88	−.03	.32	−11.4
*2087	−88	−.07	.15	− 2.09
				Average 5.61±3.99

*These rows refer to runs made using the same sample of organic liquid as used in the preceding run without purification.

The value of k_2 can be calculated from the experimental data in the following manner: HD is produced about three times as fast as molecules are lost from the gas phase in the experiments with *o*-terphenyl (see Table I). Therefore one can write the following relationship:

$$[6] \qquad k_2(\dot{\mathrm{D}})\,(\dot{\phi}_n\mathrm{D}) = 2\times 3\,[(k_1(\dot{\mathrm{D}})\,(\phi)+k_3\,(\dot{\mathrm{D}})\,(\dot{\phi}_n\mathrm{D})-k_2\,(\dot{\mathrm{D}})\,(\dot{\phi}_n\mathrm{D})].$$

Solving for k_2, we obtain

$$[7] \qquad k_2 = \frac{k_1(\phi)+k_3(\dot{\phi}_n\mathrm{D})}{7/6(\dot{\phi}_n\mathrm{D})}.$$

This expression for k_2 may then be substituted in the following steady-state equations:

$$[8] \qquad \frac{d(\dot{\mathrm{D}})}{dt} = I-k_1(\dot{\mathrm{D}})(\phi)-(k_2+k_3)(\dot{\mathrm{D}})(\dot{\phi}_n\mathrm{D})-k_5(\dot{\mathrm{D}})^2 = 0$$

and

$$[9] \qquad \frac{d(\dot{\phi}_n\mathrm{D})}{dt} = k_1(\dot{\mathrm{D}})(\phi)-(k_2+k_3)(\dot{\mathrm{D}})(\dot{\phi}_n\mathrm{D})-k_4(\dot{\phi}_n\mathrm{D})^2 = 0,$$

Can. J. Chem. Downloaded from www.nrcresearchpress.com by 210.87.254.42 on 09/05/12
For personal use only.

where I = rate of initiation of deuterium atoms in the liquid, to obtain the following set of equations:

$$I = (\dot{D})\,[(13/7k_1\,(\phi)+13/7k_3\,(\dot{\phi}_n D)+k_5\,(\dot{D})], \tag{10}$$

$$k_4\,(\dot{\phi}_n D)^2+13/7k_3\,(\dot{D})\,(\dot{\phi}_n D)-1/7k_1\,(\phi)\,(\dot{D}) = 0. \tag{11}$$

A numerical value of I which is necessary for the solution of equations [10] and [11] may be obtained by the following series of approximations.

The half life of the deuterium atoms is less than 10^{-7} seconds* in the reaction with *o*-terphenyl. Therefore the steady-state concentration of deuterium atoms is a strong function of the distance from the surface where the atoms are introduced into the liquid. An exact mathematical description of this reaction including the spatial distribution of radical concentrations is not available at this writing. We will therefore assume the reaction to be homogeneous in a small volume near the surface of the liquid.

The reaction volume, V, has been estimated to be about 10^{-4} cc.† The rate of initiation of deuterium atoms, I, is taken to be the number of moles of deuterium atoms that react per second divided by the reaction volume V. Therefore,

$$I = (10^{-7}\text{ mole sec}^{-1})/10^{-4}\text{ cc} = 10^{-3}\text{ mole sec}^{-1}\text{ cc}^{-1} = 1\text{ mole sec}^{-1}\text{ liter}^{-1}.$$

Using this value of I, equations [10] and [11] can be solved simultaneously by numerical methods yielding the values of 1.4×10^{-7} moles liter^{-1} and 8.8×10^{-4} moles liter^{-1} for the steady-state concentrations of deuterium atoms and $(\dot{\phi}_n D)$ radicals. $k_2 = 3.9\times10^{10}$ mole liter^{-1} sec^{-1} can now be obtained from equation [7]. This value of k_2 corresponds to a steric factor of about 0.1 if the reaction is considered to have a zero activation energy. There is some question as to whether this value is reasonable since there have been no values reported in the literature for analogous reactions. Even the steric factors for abstraction reactions from saturated hydrocarbons are not known unequivocally since various results have been reported (10).

Using this mechanism, results, qualitatively similar to those observed with *o*-terphenyl, are expected for toluene, if it is assumed that abstraction from the methyl group is not important at −80°C. This assumption can be justified as follows: It has been shown by several workers that, in a series of related elementary reactions, the energy of activation,

**Most of the deuterium atoms that enter the liquid react by reaction [1a] at the initiation rates used in the experiment. (This can easily be ascertained, assuming the proposed mechanism to be correct, by multiplying together the rate constants and appropriate steady-state concentrations to obtain actual reaction rates.) Therefore, the half life of the deuterium atoms in o-terphenyl is determined mainly by reaction [1a]. $k_1(\phi)$ is a pseudo first-order rate constant with a value of 4×10^7. Thus, the half life of a deuterium atom in o-terphenyl is approximately $\ln 2/k_1(\phi) \sim 10^{-7}$ sec.*

†A value for the volume V in which the reaction is considered to proceed is equal to the product of the surface area of the liquid (5 cm²) and the distance, Δx, the atoms diffuse in a time equal to their half life in the substrate (about 10^{-7} sec). To find Δx, we substitute approximate values for each of the terms in Ficks first law of diffusion

$$D\frac{d(\dot{D})}{dx} = F.$$

The numerical value of D, the Ficks law diffusion coefficient for the diffusion of deuterium atoms in liquid o-terphenyl, was found to have the approximate value of $D = 2\times10^{-3}$ by the absolute reaction rate theory (9). An approximation for the gradient of the deuterium atom concentration $d(\dot{D})/dx$ is the steady-state concentration of deuterium atoms in the reaction volume divided by Δx. An approximation of the steady-state concentration is the flux of deuterium atoms into the reaction volume (10^{-7} moles/sec) times the half life of the deuterium atoms (10^{-7} sec) divided by the reaction volume (5 cm² Δx). The flux F diffusing into the reaction volume from the surface is 10^{-7} moles/5 cm² sec.

Substituting these values into the diffusion equation, we obtain

$$2\times10^{-3}\frac{(10^{-7}\times10^{-7}-0)/5\Delta x}{\Delta x} = 10^{-7}/5.$$

Thus $\Delta x = 1.4\times10^{-5}$ and the reaction volume $V = 7\times10^{-5}$ cc $\sim 10^{-4}$ cc.

Can. J. Chem. Downloaded from www.nrcresearchpress.com by 210.87.254.42 on 09/05/12
For personal use only.

E, of the reaction can be related empirically to the heat of reaction in a simple manner (11). For abstraction reactions, there is some evidence (12) for the relationship

$$E = 11.5 - 0.25Q$$

where Q is the exothermic heat of reaction in kilocalories per mole.

Taking the value 77.5 kcal for the heat of dissociation of the C—H bonds of the methyl group of toluene, the heat of reaction Q for

$$C_6H_5CH_3 + H = C_6H_5CH_2 + H_2 \quad + Q_1 \qquad [12]$$

is $Q_1 = 24.9$ kcal.* Thus, the activation energy for the abstraction of hydrogen from the methyl group of toluene is about 5.3 kcal, which is about 2.3 kcal higher than the activation energy required for reaction [1a] (see pp. 7 and 8). Therefore at −80° C reaction [1a] should be almost 400 times as fast as abstraction from the methyl group if the pre-exponential terms are equal. Low yields of bibenzyl (see p. 6) also indicate that abstraction from the methyl group is unimportant. The assumption that abstraction from the methyl group of toluene does not compete effectively with reaction [1a] therefore seems reasonable.

In calculating the products to be expected from the reaction with toluene, the only parameter which is not already specified is the initiation rate. The value of I for the work with toluene is probably quite similar to that for the experiments with *o*-terphenyl since $\ln 2/k_1$ (ϕ) and the net rate of deuterium conversion is similar. Thus, the initiation rate is probably similar and the ratio of the products is expected to be only slightly different due to the difference in k_1 at the lower temperature. Experimental results for toluene reported in Table I are similar to those of *o*-terphenyl within experimental error.

In the reaction with eicosane the ratio of the percentage of HD produced to the percentage of pressure increase is not very different from 2, the value to be expected if abstraction of hydrogen from the substrate were the only reaction involving deuterium atoms. This is not surprising since the abstraction of hydrogen by a deuterium atom from a saturated hydrocarbon proceeds with an activation energy of about 9 kcal (13), so that the lifetime of a deuterium atom in eicosane at 37° C should be about 10^{-4} seconds. Thus the reaction volume is some three orders of magnitude larger than in the case of *o*-terphenyl, and the initiation rate is therefore correspondingly lower. It can be shown that smaller amounts of products formed by the reaction of deuterium atoms with other radicals are to be expected at these lower initiation rates (14). Thus, the results obtained with eicosane are consistent with the concepts upon which the proposed mechanism is based.

The proposed mechanism has the additional advantage that it is in general accord with a number of seemingly unrelated results reported in the literature.

1. Very low values of the pre-exponential terms in the rate constants for addition reactions of atoms (and radicals) to double bonds have often been reported (12). These values correspond to steric factors of 10^{-3} to 10^{-5}.
This addition reaction

$$2\dot{D} + \phi = \phi D_2$$

is probably a two-step process composed of reactions [1a] and [3]. Since the second step is in strong competition with equations [2] and [4], the steric factor for the over-all hydrogenation reaction would be expected to be low. Thus, the low steric factors previously reported can be accounted for.

**If 89.9 kcal/mole is taken to be the value for the heat of dissociation of the methyl* C—H *bonds,* Q_1 *is 13.5 kcal.*

Can. J. Chem. Downloaded from www.nrcresearchpress.com by 210.87.254.42 on 09/05/12
For personal use only.

2. Deuterium-hydrogen exchange during the hydrogenation of olefins by atomic hydrogen at −195° C has been recently reported (15), indicating that HD can be formed by a low activation energy process. Since reaction [2] is strongly exothermic, it is likely to have a low activation energy.

3. In the radiation chemistry of benzene, it has been found that the formation of hydrogen gas increases more rapidly than does polymer formation with increasing L.E.T. (16). This increased hydrogen formation relative to polymer formation with increasing L.E.T. corresponds to an increase of products formed by reaction [2] relative to products formed by reactions [1*b*] and [4] as the initiation rate is increased. Thus, these results may be accounted for by the mechanism proposed in this paper.

4. During radiolysis experiments at low hydrogen atom initiation rates, exchange with perdeutero aromatic additives occurs to a very limited extent (17).

This mechanism predicts a value of the steady-state concentration of $\dot{\phi}_n$D which is subject to experimental verification. An attempt to test the mechanism by studying the steady-state concentration of the $\dot{\phi}_n$D radicals in this system by electron spin resonance spectroscopy will be made.

ACKNOWLEDGMENTS

We are grateful to R. A. Meyer for the mass spectrometric analyses, to R. H. Shudde for programming the numerical solutions of the steady-state equations for an IBM 709, and to R. C. Shepard for the gas chromatographic analyses.

REFERENCES

1. R. B. Ingalls. Hydrogen formation in the radiolysis of liquid toluene. To be published.
J. G. Burr and J. M. Scarborough. J. Phys. Chem. In press.
2. B. de B. Darwent and R. Roberts. Discussions Faraday Soc. **14**, 55 (1953).
H. W. Melville and J. C. Robb. Proc. Roy. Soc. A, **202**, 181 (1950).
P. E. Allen, H. W. Melville, and J. C. Robb. Proc. Roy. Soc. A, **218**, 311 (1953).
R. Klein and M. D. Scheer. J. Phys. Chem. **62**, 1011 (1958).
3. E. Collinson and A. J. Swallow. Chem. Revs. **56**, 471 (1956).
4. M. Burton and W. N. Patrick. J. Phys. Chem. **58**, 421 (1954).
W. N. Patrick and M. Burton. J. Phys. Chem. **58**, 424 (1954).
5. R. A. Baxter and R. T. Keen. Anal. Chem. **31** (1959).
R. T. Keen, R. A. Baxter, M. A. Rotheram, J. L. Miller, and R. C. Shepard. Naa-SR-4356. Methods of analysis of polyphenyl reactor coolants.
6. R. B. Ingalls, R. H. Shudde, and R. Shepard. Analysis of isotopic composition of organic materials by thermal conductivity using gas chromatography. To be published.
7. K. B. Wiburg. Chem. Revs. **55**, 713 (1955).
8. A. F. Trotman-Dickenson. Free radicals: an introduction. Methuen & Co., Ltd., London. 1959. p. 35.
9. A. Glasstone, K. J. Laidler, and H. Eyring. The theory of rate processes. McGraw-Hill Book Co., Inc., New York. 1941.
10. M. R. Berlie and D. J. Le Roy. J. Chem. Phys. **20**, 200 (1952).
D. J. Le Roy. Discussions Faraday Soc. **14**, 120 (1953).
B. de B. Darwent and R. Roberts. Discussions Faraday Soc. **14**, 55 (1953).
11. M. G. Evans and M. Polanyi. Trans. Faraday Soc. **32**, 1933 (1936); **34**, 11 (1938).
E. T. Butler and M. Polanyi. Trans. Faraday Soc. **39**, 19 (1943).
H. Steiner and A. R. Watson. Discussions Faraday Soc. **2**, 88 (1947).
N. N. Tikhomirova and V. V. Voevodskii. Doklady Akad. Nauk S.S.S.R. **79**, 993 (1951). English translation, Natl. Research Council Can. TT-260 (1951).
12. A. N. N. Seminov. Some problems of chemical kinetics and reactivity. Pergamon Press, London. 1958.
13. B. de B. Darwent and R. Roberts. Discussions Faraday Soc. **14**, 55 (1953).
14. R. B. Ingalls and R. H. Shudde. Hydrogen atom reactions in organic radiation chemistry. To be published.
15. F. G. Ponomarev and V. L. Talrose. Doklady Akad. Nauk S.S.S.R. **130**, 1 (120–121) (1960).
16. W. G. Burns. The irradiation of polyphenyls with different types of radiation. Presented at Congress Scientifico, Seziane Nucleare, Rome (1959).
17. P. V. Phung and M. Burton. Radiation Research, **7**, 199 (1957).
M. Burton and W. N. Patrick. J. Phys. Chem. **58**, 421 (1954).
W. N. Patrick and M. Burton. J. Phys. Chem. **58**, 424 (1954).

Can. J. Chem. Downloaded from www.nrcresearchpress.com by 210.87.254.42 on 09/05/12
For personal use only.

Can. J. Chem. Downloaded from www.nrcresearchpress.com by 210.87.254.5 on 09/05/12
For personal use only.

AN IMPROVED TECHNIQUE FOR THE OBSERVATION OF INFRARED CHEMILUMINESCENCE: RESOLVED INFRARED EMISSION OF OH ARISING FROM THE SYSTEM H + O_2[1]

P. E. Charters and J. C. Polanyi

ABSTRACT

A multiple reflection apparatus for the observation of infrared chemiluminescence is described. By means of this apparatus infrared emission from the system H + O_2 has been identified as being due to vibrationally excited OH radicals in levels $v = 1$, 2, and 3 of the ground electronic state. The resolved infrared spectrum of the OH fundamental has been observed for the first time without interference from other emission. The most likely source of excited OH is the reaction H + $HO_2 \rightarrow OH\dagger + OH$. The vibrational 'temperature' of OH† (vibrationally excited OH in its ground electronic state) in our system is in the region of $T_V = 2240°$ K. These findings are discussed in relation to Krassovsky's suggestion that reaction between H and O_2 could account for the Meinel hydroxyl bands in the night sky.

INTRODUCTION

Infrared emission arising from the gaseous system H + O_2, at room temperature, has been reported by Cashion and Polanyi (1). The emission consisted principally of three broad unresolved bands extending from 3400 to 4000 cm^{-1}, with maxima at 3600, 3730, and 3830 cm^{-1} (2.78, 2.68, and 2.61 μ). The intensity of the first peak could be varied, by varying reagent flows, independently of the other two, indicating that it was due to a separate emitting species. It was thought that this might be the hydroxyl radical, OH, with ν_0 for $v = 1 \rightarrow v = 0$ at 3570 cm^{-1} (2). The other two maxima were of constant relative intensity and it was suggested that these might be either the Q and R branches of the ν_3 O—H stretching fundamental of water (ν_0 at 3755.8 (3)) or alternatively the O—H stretching fundamental of the HO_2 radical. In either case the P branch would presumably be masked by the other emission, attributed to the hydroxyl radical.

Prior to the work described above, McKinley, Garvin, and Boudart (4) had observed visible and photographic-infrared regions of the spectrum from OH formed in the reaction H + O_3. They failed, however, to observe any emission whatever from the system H + O_2. They concluded, in agreement with suggestions made by Bates and Nicolet (5), and by Herzberg (6), that the reaction H + O_3 was responsible for the Meinel hydroxyl bands in the airglow (7). This result later received further support from a careful re-examination of the visible and photographic-infrared emission (8) and recently an examination of the infrared emission (9).

Krassovsky (10), however, has put forward the view (criticized by Bates and Moiseiwitsch (11)) that the evidence concerning the Meinel hydroxyl bands is more consistent with the formation of excited OH in a reaction H + O_2. He considered that this reaction, to be sufficiently exothermic, would have to involve vibrationally excited O_2. At first sight the results of Cashion and Polanyi (1) might appear to lend support to Krassovsky's view. The present investigation was undertaken in the hope of clarifying this point. In order to do this it was necessary in the first place to establish that the system H + O_2 does in fact give rise to vibrationally excited hydroxyl, and that the excited hydroxyl is present as a result of chemical reaction, not as a result of diffusion of reagents or products into the discharge or spreading of the discharge into the reaction zone. Once this has been

[1]*Contribution from the Department of Chemistry, University of Toronto, Toronto, Ontario; presented at the Symposium on the Fundamental Aspects of Atomic Reactions held at McGill University, Montreal, Que., September 1960.*

done a comparison of the distribution of excited OH among vibrational levels with that observed in the upper atmosphere might help to decide whether the reaction could account for the Meinel hydroxyl bands.

At the same time it was hoped that the identity of the 3730 and 3830 cm^{-1} emission, due it was thought to H_2O or HO_2, could be established.

The apparatus used in this investigation represents a major departure from that used by Cashion and Polanyi; it will therefore be described in some detail. The system $H + O_2$ was used for the first trial of this apparatus since the reagents are relatively non-corrosive. In work presently being undertaken in this laboratory the same apparatus is being used for a re-investigation of the infrared emission from $H + Cl_2$ at pressures several orders of magnitude less than those at which detectable emission was obtained in the experiments of Cashion and Polanyi (12).

EXPERIMENTAL

Reaction Cell

A diagram of the reaction cell is given in Fig. 1. Partially dissociated hydrogen entered the cell from four Wood discharge tubes through 6 mm I.D. nozzles that protruded into

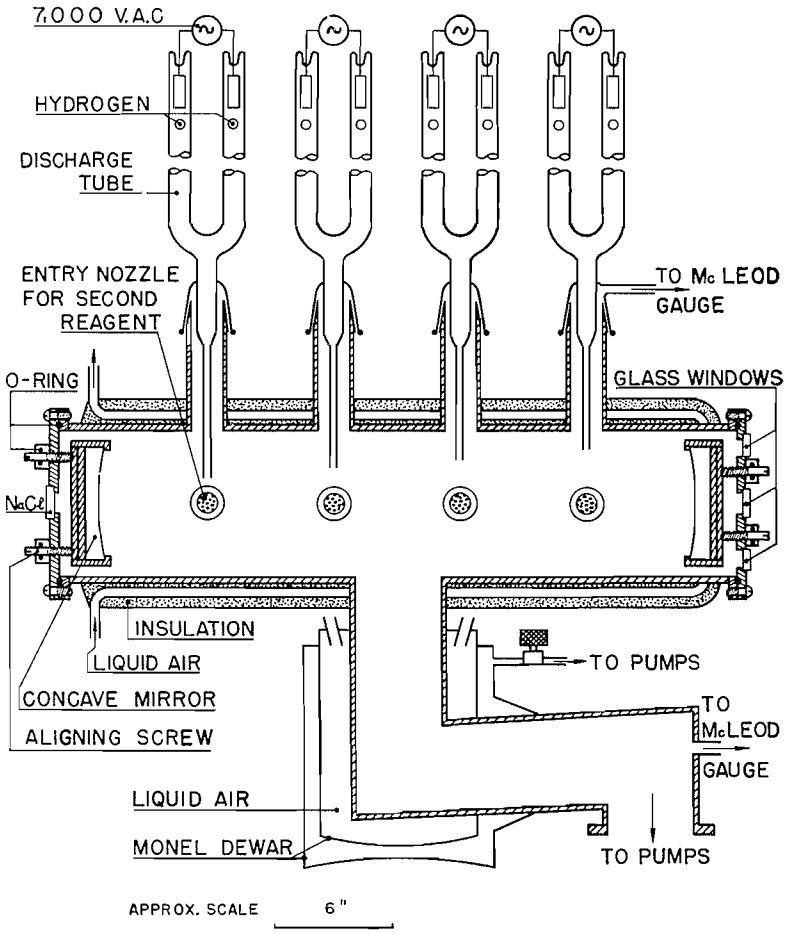


FIG. 1. Cross section of the reaction cell.

Can. J. Chem. Downloaded from www.nrcresearchpress.com by 210.87.254.5 on 09/05/12
For personal use only.

the cell to a point just above the cone of radiation visible to the spectrometer. Before use the discharge tubes (made from pyrex) were washed with dilute hydrofluoric acid and coated with an approximately 60% solution of phosphoric acid. The other reactant (in this case oxygen) diffused into the cell through sintered glass plugs placed in four side arms. These side arms ended flush with the walls of the reaction cell, since the cone of light with multiple reflection extended laterally across the entire diameter of the mirrors (see below). In each of the eight side arms linking the glass part of the apparatus to the reaction vessel, the connection was made through a 40/50 standard-taper metal cone and glass socket.

The cell itself consisted of a monel tube $6\frac{1}{4}$ in. I.D. $\times$ $23\frac{1}{2}$ in. long. The ends were sealed by $8\frac{1}{2}$ in. diameter monel plates held against "O" rings. The emission was viewed by the spectrometer through a sodium chloride window in the center of the front plate, the plate nearest the spectrometer. A vertical row of three glass windows in the back plate facilitated the alignment of the mirrors, mounted internally at either end of the reaction cell.

The reaction products passed out of the cell through a centrally located 4 in. I.D. monel pipe welded to the cell. A fixed metal dewar surrounded this pipe almost to the point where it entered an N.R.C. O.B.-4 booster pump (4 in. I.D.; 240 l./sec at 10^{-2} mm, falling to 50 l./sec at 10^{-1} mm). An Edwards "Speedivac" ISC450B pump (450 l./min) provided the backing pressure, and was connected to the diffusion pump through a Veeco valve ($1\frac{1}{2}$ in. port opening) and a length of $1\frac{1}{2}$ in. I.D. flexible steel tubing.

Monel was used throughout the cell and exit pipe to reduce corrosion when studying reactions involving halogens, and also to permit coating with phosphoric acid without deterioration of the metal surface. In practice it was found that phosphoric acid slowly reacted with the surface, and in the experiments described in this paper the cell was coated first with a thin layer of polystyrene and then with phosphoric acid over this base layer.

By switching leads on the four high-voltage transformers the reaction cell could be made earth for the high-voltage alternating current. The discharge then struck directly down into the reaction cell, filling the cell with the pink atomic hydrogen glow that was normally restricted to the U of the discharge tube.

Provision was made for cooling the entire cell by blowing liquid air through copper coils which followed a path back and forth along the length of the cell. The coils were clamped against the cell and were insulated by $1\frac{1}{2}$ inches of glass wool.

The mirror system consisted of four concave mirrors, all four having very closely matched radii of curvature; the system was identical with that suggested by Welsh and co-workers (13, 14) for use in high-resolution Raman spectroscopy. The radius of curvature of the mirrors in our system was 50.094 cm, diameter 14 cm, and average thickness 1.5 cm. The mirrors were made for us by the Perkin–Elmer Company of Norwalk, Conn., U.S.A. The dimensions were chosen so that the 15° cone of radiation accepted by the $f/4$ optical system of our spectrometer very nearly filled the back mirrors (furthest from the spectrometer). Each "pair" of mirrors (one pair at either end of the cell) was made from a single mirror which had been cut along a vertical axis so that the two halves could be adjusted separately and light could pass through a 0.5–2.0 mm (adjustable) slit-like gap between them. Under operating conditions the source optics of the spectrometer had its focal plane at a point centrally placed in the gap between the front pair of mirrors, on a level with the silvered surface of these mirrors. If the mirrors had not been present, only emitters within the 15° cone of light centered on the focal plane, emitting in the direction defined by the cone, would have contributed to the observed emission. With the

Can. J. Chem. Downloaded from www.nrcresearchpress.com by 210.87.254.5 on 09/05/12
For personal use only.

mirrors present, a succession of such cones displaced laterally from one another fell within the line-of-sight of the spectrometer. This was the origin of the gain in intensity.

The mirror mounts, made entirely from monel, were based on a design due to Welsh and Shepherd (15). Each of the four mirrors, backed by springs, was held by clips to a plate. This plate was held by screws to a backing plate, the two plates being free to slide over each other for coarse horizontal and vertical alignment of the mirrors. The backing plate in turn was held down by springs on to three metal columns, two of adjustable height and a fixed one surmounted by a ball bearing. The adjustable columns extended into rods which passed through "O" rings and fine threads in the external end plates. By adjusting the two rods appropriate to any one of the four mirrors, that mirror could be aligned while the apparatus was under vacuum, and while chemiluminescent emission was being observed.

We wish to acknowledge here the skilled machining of Mr. Hans Hellenkamp, who constructed the reaction cell.

The efficiency of the multiple reflection system is markedly dependent on the reflectivity of the mirrors, approaching $1/1-r$ (r is the reflectivity) when the number of reflections is large. The mirrors in this apparatus were in contact with the reacting gases. To minimize deterioration they were first front-surface coated with silver (reflectivity 98.8% at 3 μ (16)) and then coated with ca. 1700 Å layer of cryolite or magnesium chloride. Coating was either carried out on an apparatus kindly made available by Professor H. L. Welsh and Professor J. C. Stryland of the Department of Physics, or was carried out professionally by Canadian Arsenals Ltd., Toronto.

Spectrometer

The spectrometer was a model 112G Perkin–Elmer double-pass grating instrument employing a Bausch and Lomb 300 groove/mm plane grating blazed at 3 μ in the first order. Several modifications were made in the instrument. A liquid-air-cooled lead sulphide detector was installed in the position provided by the makers for "external detectors". The housing for the cooled lead sulphide cell was identical with that described in a recent communication (17) .The detector itself has a sensitive surface 2.5 mm × 0.25 mm, sandwiched between two layers of sapphire. It was mounted *in vacuo* behind a sapphire window. The detector, made by Infrared Industries Inc., Waltham, Mass., U.S.A., had one half of peak sensitivity at 3.3 μ (ref. 17).

The source optics supplied by the makers was replaced by optics of slightly different design; the sequence of mirrors was reversed so that incoming radiation encountered first a spherical concave mirror (80 mm diameter, 294 mm radius) and then a plane mirror (55 mm square) placed close to the concave mirror. The source optics housing could then be reduced in size to 22 cm × 17 cm, eliminating the space between source optics and foreprism monochromater, normally occupied by an absorption cell. The source optics focus remote from the foreprism monochromater slit then fell at a point 14 cm from the front of the source optics housing, instead of being 2–3 cm from the housing as in the normal instrument. This alteration was necessary since the focal plane of the source optics must be brought to a point on a level with the front surface of the mirrors inside the reaction cell, 5.6 cm from the front (sodium chloride) window of the cell.

The gap between the front window of the cell and the front window of the source optics housing was bridged by a tube which was continuously flushed with dry air, as was the whole of the remainder of the path traversed by the radiation from the reaction cell through the spectrometer to the lead sulphide cell. This was of importance since

Can. J. Chem. Downloaded from www.nrcresearchpress.com by 210.87.254.5 on 09/05/12
For personal use only.

emission was to be observed in regions of the spectrum where water vapor absorbs strongly.

To permit calibration without interference with the closed optical path linking the spectrometer to the reaction cell, the source optics was provided with a sodium chloride window at one side. A diagonal mirror within the source optics housing, mounted on an externally actuated swivel, could be swung into the optical path so that either a mercury lamp (for wavelength calibration) or a globar (for sensitivity calibration) could be viewed by the spectrometer.

The spectrometer was mounted on a table with provision for hydraulic lifting, and also for lateral and to-and-fro movement of the table top by means of adjusting screws. This degree of adjustment was required since the reaction vessel was rigidly attached to a separate rack carrying the reagent flow system and pumps. To facilitate the alignment of the spectrometer to the reaction cell, and the alignment of the multiple reflection system within the reaction cell, a light bulb was mounted permanently inside the spectrometer on a solenoid arm so that it could be moved into a position behind the foreprism monochrometer slit by closing a switch. This made possible rapid checks of alignment during the course of an experiment; at the same time a check could be made for deterioration of the mirrors, by counting the number of images formed at the front mirrors by the multiple cones of light within the cell (13, 14).

In the 112G spectrometer the grating table can swing through an angle of no more than 12°; to cover one order of the grating it is therefore necessary to insert "pins" into the grating table and thus obtain a coarse change in the range of angles being scanned. Changing pins necessitates removal of the entire grating monochromater housing, exposing the optics to the atmosphere. To avoid this we duplicated the pin mechanism at the lower end of the grating table shaft, beneath the instrument. Pins could then be rapidly inserted and removed without interfering with the flow of dry air through the apparatus.

Reagents

The hydrogen and oxygen flows were metered by measuring the pressure drops across two calibrated capillaries. Absolute pressure could be measured on a McLeod gauge just ahead of the cell and on one just beyond it (see Fig. 1); both of these pressure points were linked by wide tubing to the cell. The two pressures differed only slightly, but the former was taken as the true value since this measuring point was linked directly to the reaction cell through tubing in which no flow took place.

In most experiments the hydrogen was Dominion Oxygen Co. Electrolytic grade, 99.8% minimum purity. This was passed through a Deoxo unit guaranteed to reduce oxygen concentration to less than one part per million. In some experiments water was frozen out in a liquid air trap. The oxygen in most experiments was Linde Air Products Co., U.S.P. grade. However, to check for possible effects of slight impurities a portion of spectrum was retraced replacing both reagents simultaneously with Matheson research grade reagents. This grade of hydrogen contains less than the following mol.% impurities; oxygen 0.001%, nitrogen 0.03%, carbon dioxide 0.005%, water 0.001%. The oxygen contains less than the following percentage impurities; carbon dioxide 0.1%, carbon monoxide 0.01%, argon 0.01%, nitrogen 0.05%, hydrogen 0.01%, water 0.0002%.

RESULTS AND DISCUSSION

Figures 2 and 3 are reproductions of actual traces of the emission obtained in the 2950–3800 cm^{-1} (3.39–2.63 μ) and the 6600–7150 cm^{-1} (1.52–1.40 μ) regions of the spectrum. Four different grating slit widths were used in making these traces, varying from 0.400 mm for the strongest emission (section A of the trace) to 2.000 mm for the

Can. J. Chem. Downloaded from www.nrcresearchpress.com by 210.87.254.5 on 09/05/12
For personal use only.

Can. J. Chem. Downloaded from www.nrcresearchpress.com by 210.87.254.5 on 09/05/12
For personal use only.

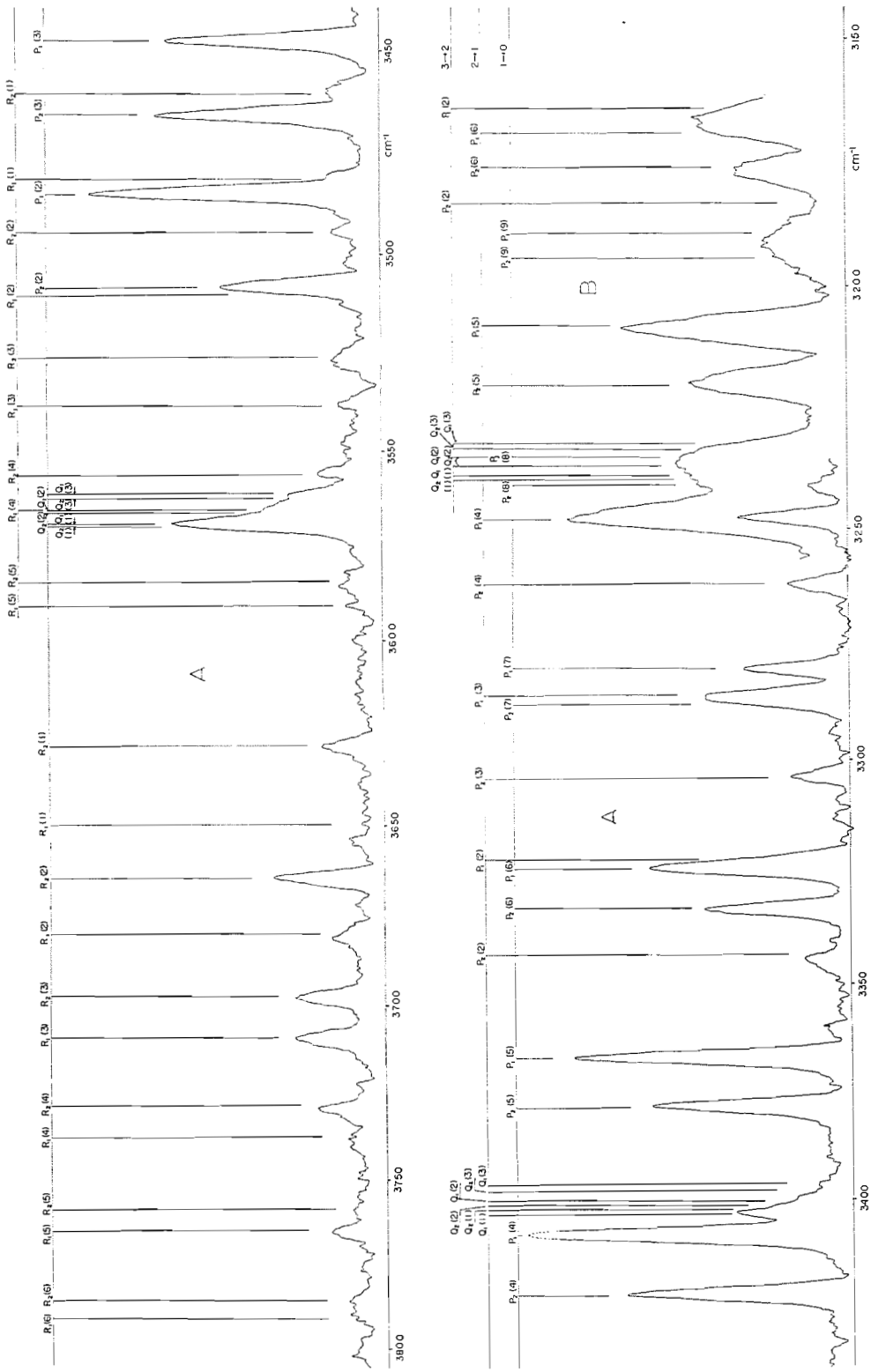


FIG. 2. The fundamental ($\Delta v = 1$) OH emission spectrum from the system $H + O_2$. A, slit width 0.400 mm. B, slit width 1.000 mm.

Can. J. Chem. Downloaded from www.nrcresearchpress.com by 210.87.254.5 on 09/05/12
For personal use only.

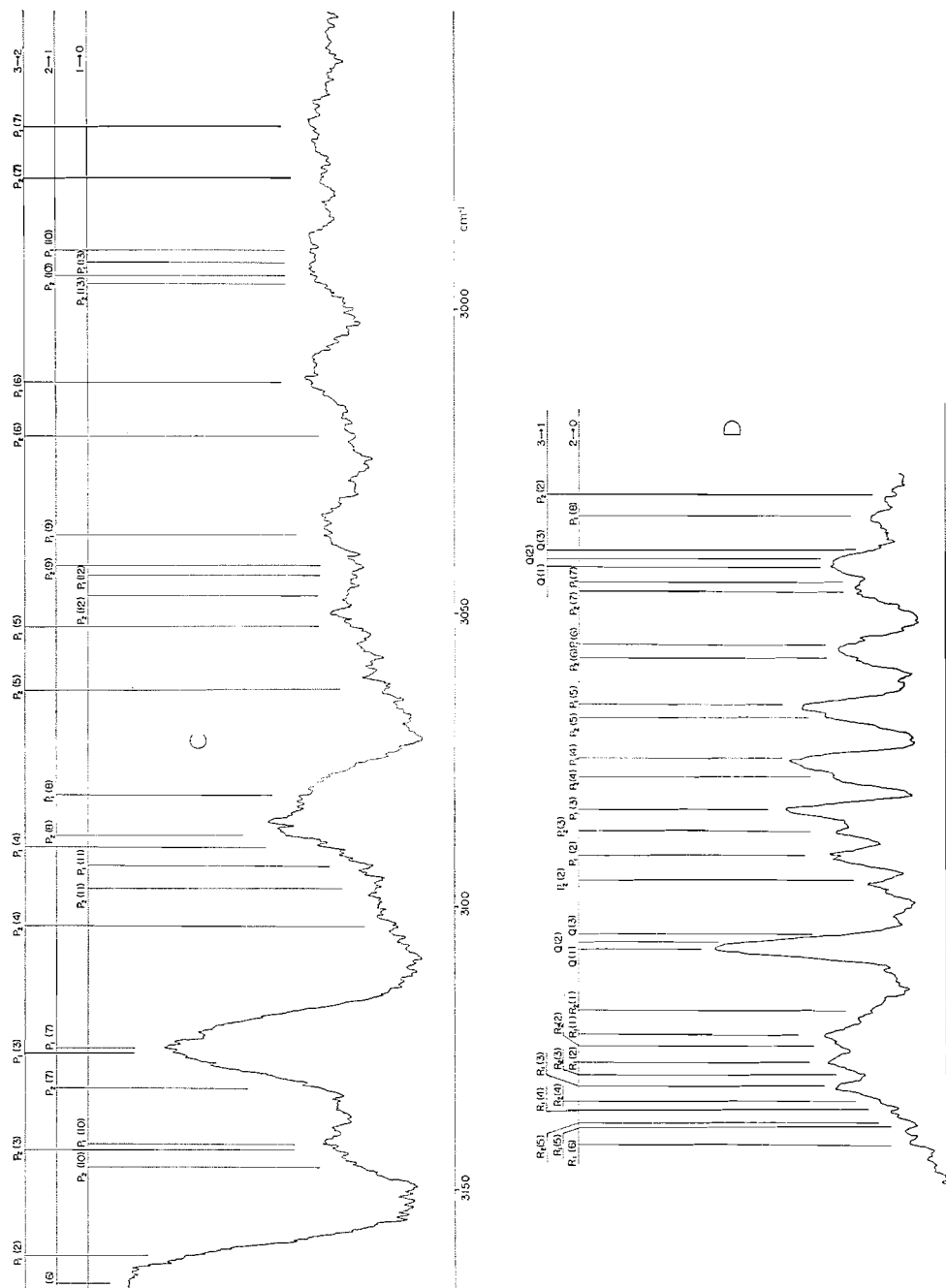


FIG. 3. The fundamental ($\Delta v = 1$) and first overtone ($\Delta v = 2$) OH emission spectrum from the system $H + O_2$. C, slit width 2.000 mm D (overtone), slit width 1.100 mm.

weakest (section C of the trace). These data are recorded beneath the figures. No other emission was observed, though attempts were made to detect emission in the 3700–4000 cm^{-1} region, where Cashion and Polanyi observed emission (due to water vapor or HO_2) and at 5333 cm^{-1} where these workers observed emission due to atomic hydrogen. The experimental conditions applicable to these traces were hydrogen flow 2500 μmoles/sec, oxygen flow 1200 μmoles/sec, pressure in the reaction vessel 4.0 mm Hg, pumping by mechanical pump only, transit time through cone-of-sight 0.15 second. Reagents were standard grade hydrogen and oxygen used without drying of either reagent. The reaction cell was at room temperature and the mirrors were freshly coated.

Standard grade reagents were used since in a separate experiment it was shown that use of Matheson research grade reagents made no difference to the emission. Passing both reagents through liquid air traps also had no effect on the emission. Deliberately saturating both hydrogen and oxygen streams with water vapor, so that the partial pressure of water vapor in the discharge tube and reaction vessel became ca. 0.13 mm Hg, caused a 30% drop in emission intensity (in the region from 3400–3500 cm^{-1} that was scanned) but otherwise had no effect.

The region of spectrum from 3400–3500 cm^{-1} was traced at five total pressures ranging from 4.0 mm to 0.51 mm, while the molar inflow ratio of reagents was kept constant. The intensity of the emission was found to vary approximately linearly with total pressure.

An attempt was made to estimate the H atom concentration by measuring the heat liberated by atoms recombining at a hot tungsten filament placed in the reaction cell. The method used (Tollefson and Le Roy (18)) was first to clean the wire by prolonged heating in a stream of hydrogen passing through the cell, and then, by means of an a-c. bridge, to measure the rise in temperature of the wire as atoms recombined on it. Next, in the absence of H atoms, an external current was passed through the wire, and the current required to heat the wire to the same temperature as before was accurately measured. Knowing the resistance of the wire, the power liberated by the passage of the current could be calculated; this was identical with the power liberated by the recombining atoms. Knowing the surface area of the wire and assuming recombination at every collision the pressure of H in the gas could be calculated. The pressure measured was only ca. 5.10^{-3} mm of H at 4.0 mm total H_2 pressure with two discharge tubes running. We would expect 1.10^{-2} mm with all four tubes running. This constitutes a lower limit, but if correct it would mean that our H atom pressure may be only in the region of one third to one tenth of that obtained by Cashion and Polanyi (12, 17).

The spectrometer was calibrated using the lines of a low-pressure mercury lamp. The calibration was made under different conditions of slit width and chart speed to the actual trace. As a result the observed spectrum was found to be shifted bodily by 3 cm^{-1} to higher frequencies than the published values for OH. Accepting the published value (see below) for one line in the fundamental region ($P_1(2)$ of $1 \rightarrow 0$) and one in the overtone region (P_1 (3) of $2 \rightarrow 0$) and applying a correction for this apparent small shift, the remaining ca. 35 sharpest peaks fell within ± 0.5 cm^{-1} of the published values. The OH line frequencies were taken from an extensive compilation of OH frequencies made by Dr. H. P. Gush and Dr. E. H. Richardson on the University of Toronto digital computer. The calculation was based on spectroscopic constants obtained by Dieke and Crosswhite (19) and by Herman and Hornbeck (20). We are most grateful to Dr. Gush and Dr. Richardson for providing us with a copy of these tables.

The correspondence of the calculated frequencies with our observed lines leaves no doubt that we are observing emission due to three bands within the fundamental of OH

Can. J. Chem. Downloaded from www.nrcresearchpress.com by 210.87.254.5 on 09/05/12
For personal use only.

in its ground electronic state ($^2\Pi$, $v(1 \rightarrow 0)$, $v(2 \rightarrow 1)$, $v(3 \rightarrow 2)$) and two bands in the first overtone region ($^2\Pi$, $v(2 \rightarrow 0)$, $v(3 \rightarrow 1)$). At the narrower slit widths used in this work the lines of each band are well resolved into spin (but not lambda) doublets. All the lines in the spectrum can be accounted for as OH lines.

A striking feature of the spectrum is the complete absence of emission due to water vapor. The only previous observation of the fundamental infrared spectrum of OH has been in emission from flames, particularly in the work of Plyler and co-workers (21, 22, 23). The hydroxyl emission is accompanied by a strong water emission that tends to overlap many OH lines, and makes observation of the R branch of $1 \rightarrow 0$ impossible. Since water will be present in most systems in which OH is being formed, including the reaction system H + O_2 which we have studied, any non-specific method of excitation (thermal excitation, or excitation by electrical discharge) will give rise at the same time to H_2O and OH emission. In our system we are bound to postulate a highly specific method of excitation; this, of course, is most likely to be a chemical reaction. The specific nature of chemical reaction may well make infrared emission from chemical systems a valuable spectroscopic source of "clean" infrared spectra (cf. 24).

In some experiments the discharge was made to strike down into the reaction cell. Emission due to vibrationally excited water vapor was then observed. The appearance of water vapor emission could be due to physical excitation of the water molecules in the discharge.

We are able positively to identify this discharged-induced emission as being due to excited water molecules. If the unidentified emission observed by Cashion and Polanyi was also due to water, the question arises as to why water emission was not observed in the present investigation, under normal operating conditions. The answer may possibly lie in the fact that our reaction cell and discharge in normal operation are separated by 15–20 cm of narrow (6 mm I.D.) tubing and 15 cm of 28 mm I.D. tubing, whereas in Cashion and Polanyi's apparatus the discharge was separated by only 0.5 cm of 28 mm I.D. tubing from the cell. Back diffusion of water vapor into the discharge could perhaps have given rise to the emission observed by the earlier workers. However, this is far from certain. Our system also differs from theirs in other notable respects; the pressure in the present work was 10 times as high (but attempts to observe H_2O emission at lower pressure failed), the transit time was 0.25–0.10 times as great in our experiments, and the H atom pressure may have been as little as 0.1 times Cashion and Polanyi's.

The proximity of the discharge to the reaction cell in the work of Cashion and Polanyi probably accounts for the fact that they observed emission due to atomic hydrogen. They believed that this emission arose from electronically excited atomic hydrogen in their reaction cell, and not to reflected light from the discharge. This is in accord with the finding that in our system, where the discharge is removed to a distance from the reaction cell, emission from atomic hydrogen is absent. Moreover in our system the atomic hydrogen emission can be made to appear if the discharge is struck down into the reaction cell.

In our experiments we found no trace of any emission, either under normal operating conditions or with the discharge striking into the reaction cell, that could have been ascribed to the hydroperoxy radical, HO_2.

For reasons outlined above we consider that the vibrationally excited OH in our system is present as a result of some chemical reaction. The reaction between atomic hydrogen and ozone is a well-established source of vibrationally excited hydroxyl. However, it can be excluded in our system on several counts. The reagents entering the reaction cell

Can. J. Chem. Downloaded from www.nrcresearchpress.com by 210.87.254.5 on 09/05/12
For personal use only.

certainly contained no ozone. It might be argued that after entering the reaction cell a very small amount of oxygen might have diffused up into the discharge and been converted to ozone. The argument would rest upon the fact that in a system such as ours traces of ozone might produce enough OH† (vibrationally excited hydroxyl in its ground electronic state) to account for the observed emission. But Herron and Schiff (25) have shown that the passage of pure oxygen at 2 mm pressure through a Wood discharge tube produces an amount of ozone which is below the limit of detection of a mass spectrometer. Furthermore, back diffusion into the discharge must be slight, and a very large gain in intensity would be expected if the discharge were brought down into the reaction cell. However, if there was an increase in the intensity of the OH† emission on striking the discharge down into the cell, it was a small increase (2 times or less, masked by water emission). Finally it should be noted that the vibrational "temperature" of OH† in our system (see below) is one-quarter that observed by Garvin, Broida, and Kostkowski in a recent examination of the H + O_3 emission in the infrared (their analysis was based on overtone transitions since they did not observe the OH fundamental bands) (9). Since their experiments were made in the same region of total pressures as ours, with considerable amounts of H_2, H_2O, and O_2 present in the system (ozone amounted to a few per cent), it seems most probable that the difference in vibrational temperature of the OH† in the two systems is due to a difference in the chemical processes by which it is produced.

The possibility exists that traces of NO_2 in the system might give rise to the observed weak emission since Cashion and Polanyi (26) found that this is a rapid reaction producing strong OH and H_2O emission. NO_2 would have to be formed in the discharge from air leaking into the apparatus. (An upper limit for the pressure of NO_2 that could conceivably be formed in this way is $\sim 10^{-5}$ mm.) However, in this case the emission should persist even if the O_2 flow is cut off, whereas the emission disappeared when this was done.

It would appear that the emission arises in some way from reaction between atomic hydrogen and molecular oxygen.

Reference has already been made to Krassovsky's (10) suggestion that reaction between atomic hydrogen and vibrationally excited oxygen might lead to the formation of vibrationally excited hydroxyl,

$$H + O_2\dagger \rightarrow OH\dagger + O \qquad Q = -16.7 \text{ kcal/mole.} \qquad [1]$$

Q is the heat of reaction assuming reagent and product molecules to be in their ground vibrational levels (D(O—O) = 118.0 (27), D(O—H) = 101.3 kcal/mole (28)). To account for the formation of OH† in $v = 3$ ($E(v = 3)$ = 29.2 kcal/mole) the oxygen molecule would have to have 45.9 kcal of vibrational energy. Recombination of atomic oxygen could lead to the formation of such highly vibrating molecules. (Fairly direct evidence for the formation of highly vibrating molecules as product of atomic association is to be found in reference 17.) Formation and recombination of O atoms should become far more important if the discharge strikes down into the reaction cell where O_2 is in plentiful supply. However, as already observed, no more than a small increase in intensity was obtained when this was tried.

It appears more probable that the primary reaction is

$$H + O_2 + M \rightarrow HO_2 + M \qquad Q = 47 \text{ kcal/mole,} \qquad [2]$$

for which strong evidence has been found by a number of authors. The work of Foner and Hudson (29) comes closest to our experimental conditions. They brought together

Can. J. Chem. Downloaded from www.nrcresearchpress.com by 210.87.254.5 on 09/05/12
For personal use only.

atomic H from a Wood discharge tube and oxygen at room temperature and examined the reaction mixture mass spectrometrically. At 30–40 mm pressure they obtained HO_2, OH, and H_2O as products, in the ratio 1.4:30:92. At 1 mm pressure (30) they detected no HO_2 but substantial amounts of OH and H_2O. It seems likely that HO_2 was also being formed in their low-pressure experiments, but was rapidly consumed. Foner and Hudson (30) have in fact suggested that at low pressure ($\sim$1 mm) HO_2 is formed, not, however, in the gas phase but at the wall. The HO_2, they believe, will then react with H at the wall, forming OH if the wall is at room temperature, or H_2O_2 if the wall is at liquid air temperature. We have tried cooling our reaction cell to liquid air temperature but have failed to obtain reproducible results, perhaps due to changes in mirror alignment or reflectivity. Nonetheless on three occasions out of four we have observed stronger OH emission from the cold cell (temperature $-185°$ C, measured on a thermocouple attached to the cell wall—the mirrors were probably only at $-10°$ to $-20°$ C). This increase in intensity is surprising in view of the fact that Foner and Hudson found that no OH is formed in a cold cell.

The volume-to-surface ratio in our cell is much greater than that in Foner and Hudson's small reaction tube. Taking our value for H (which is a minimum) we calculate that each HO_2 suffers at least 23 collisions with H for each wall collision. Burgess and Robb (31) have found the collision efficiency of this reaction at room temperature to be unity. If this is correct to within an order of magnitude, most HO_2 radicals in the room temperature system will react in the gas phase before reaching the wall. Foner and Hudson's suggestion that in the room temperature system OH is formed at the wall would require in the present case either that OH emits while adsorbed on the mirror surface (the only part of the "wall" in the line-of-sight) or that hydroxyl is desorbed at high vibrational temperature, i.e. as OH†. Neither of these processes seems likely, but neither can definitely be excluded.

Subsequent gas phase reactions, following the formation of HO_2, which could result in the production of vibrationally excited hydroxyl are

$$H + HO_2 \rightarrow OH\dagger + OH \qquad Q = 38 \text{ kcal/mole} \qquad [3]$$

$$H_2 + HO_2 \rightarrow OH\dagger + H_2O \qquad Q = 53 \text{ kcal/mole} \qquad [4]$$

with a very minor contribution from

$$2H + OH \rightarrow H_2 + OH\dagger \qquad Q = 103 \text{ kcal/mole.} \qquad [5]$$

($D(H—O_2) = 47 \pm 2$ kcal/mole is from Foner and Hudson (32), $D(HO—O) = 63$ kcal/mole from thermodynamic data (33).) Reaction [5] must be of relatively little importance in view of the fact that it involves a ternary reaction between three species present only in low concentration. The relative importance of [3] and [4] cannot easily be assessed. Using the data of Burgess and Robb (31), [3] is favored by having a collision efficiency 60 times that of [4]; however, this advantage may be offset in our system by a concentration ratio (upper limit) of H_2:H = 400:1. Leaving aside the uncertain question of the relative over-all rates of [3] and [4], reaction [3] seems a much more likely source of vibrationally excited hydroxyl since it conforms to the pattern followed by all known exothermic exchange reactions which produce vibrationally excited products: vibrational excitation appears in the new bond being formed and little if any appears in the residue of the molecule under attack.

Reaction [3] is of special interest since it is one in which an activated complex splits into two fragments of identical composition. It would be interesting to know whether

Can. J. Chem. Downloaded from www.nrcresearchpress.com by 210.87.254.5 on 09/05/12
For personal use only.

these fragments are identical also in internal energy. If [3] is the origin of the OH† that we observe in $v = 3$ (and $v = 2$) we can confidently say that the internal energy is unequally distributed since even distribution would necessitate an endothermic reaction which would be slow at room temperature. This is shown in Table I. In the table Q_{TRV}

TABLE I

Heats of reactions forming OH† ($v = 2$, $v = 3$) from H + HO_2

Products of the reaction	Q_{TR} (= $Q_{TRV} - E(v)$) kcal/mole
Even distribution of vibration	
[3] *a* 2OH† ($v = 3$)	−20
[3] *b* 2OH† ($v = 2$)	−2
Uneven distribution of vibration	
[3] *c* OH† ($v = 3$) + OH† ($v = 2$)	−11
[3] *d* OH† ($v = 3$) + OH† ($v = 1$)	−1
[3] *e* OH† ($v = 3$) + OH	9
[3] *f* OH† ($v = 2$) + OH† ($v = 1$)	8
[3] *g* OH† ($v = 2$) + OH	18

is the total heat of reaction (called Q above). Q_{TR} is the heat of reaction available for translation and rotation after the stated amount of energy has gone into vibration. It is clear from the table that the fastest reactions producing OH† in $v = 2$ and $v = 3$ involve uneven distribution of energy among the otherwise identical products. If then H + HO_2 is the principal source of OH† in $v = 2$ and $v = 3$ it would follow that the activated complex HOOH dissociates preferentially to OH† + OH. This would be in accord with the suggestion (Polanyi (34)) that in the activated complex of the exothermic exchange reaction the new bond being formed is extended relative to normal internuclear separation for the isolated product molecule, and that this extension persists in a large measure as the complex disintegrates forming highly vibrating product. For reaction [3] this might be written as, H + O—OH → H- - -O—OH → H—O† + OH.

Evidence has been adduced above which contradicts Krassovsky's suggestion that the reaction between atomic hydrogen and vibrationally excited oxygen could constitute an important source of vibrationally excited hydroxyl. In our view the most likely source of OH† is the reaction between atomic hydrogen and HO_2. This would rule out the possibility that reactions involving H and O_2 could account for the Meinel hydroxyl bands, since these bands involve OH† in vibrational levels $v \leqslant 9$, whereas the room-temperature reaction H + HO_2 could only produce OH† in levels $v \leqslant 4$.

There remains the possibility that the Meinel hydroxyl bands originating in vibrational levels $v \leqslant 4$ may arise, to a greater or lesser extent, from reaction between H and O_2. To investigate this possibility we have calculated the approximate relative population distribution among vibrational levels of OH in our system. The calculation has been made by comparing the intensities of corresponding rotational lines within different bands of the $\Delta v = 1$ sequence. The lines in question, their measured areas, their areas corrected to a common scale (corrected for change in slit width, transmissivity of the instrument, and sensitivity of the detector), the ratios of intensities (taken from these corrected areas), the ratios of transition probabilities, the ratios of populations, and the derived vibrational 'temperatures', T_V, are shown in Table II. The areas were corrected for change in transmissivity of the instrument and changing sensitivity of the detector, from one wavelength to another, by comparing an experimental trace of the globar taken with

Can. J. Chem. Downloaded from www.nrcresearchpress.com by 210.87.254.5 on 09/05/12
For personal use only.

TABLE II

Relative populations in levels $v = 1$, $v = 2$, and $v = 3$ of OH†

Line	Area (arbitrary units)	Corrected area	Intensity ratio	Transition probability ratio	Population ratio	T_V (°K)
				$A_{2,1}/A_{1,0}$	N_2/N_1	
P_1 (5) [2 → 1]	38.7	134	5.02	1.83	9.19	2215
P_1 (5) [1 → 0]	32.1	673				
P_2 (5) [2 → 1]	23.9	82.9	5.25	1.83	9.61	2170
P_2 (5) [1 → 0]	21.4	435				
P_2 (4) [2 → 1]	28.8	99.8	4.69	1.83	8.58	2288
P_2 (4) [1 → 0]	24.1	468				
				$A_{3,1}/A_{1,0}$	N_3/N_1	
P (6)*[3 → 2]	19.5	46.8	20.3	2.75	55.8	2379
P (6)*[1 → 0]	45.7	948				
						Mean T_V = 2240

*$P_1(6) + P_2(6)$.

the lead sulphide detector (at the same slit width as the chart being calibrated), with the theoretical trace to be expected from a detector of uniform sensitivity and a spectrometer of uniform transmissivity. The theoretical trace was calculated from the black-body formula using the temperature of the globar as measured on a calibrated optical pyrometer, and taking the emissivity of the globar at various wavelengths from the data of Silverman (35). Relative populations ($N_{v'}$) were then obtained from the relative intensities ($I^K_{v',v''}$) by means of the relation

$$\frac{(N_{v'})_2}{(N_{v'})_1} = \frac{(I^K_{v',v''})_2 \cdot (\nu^K_{v',v''} \cdot A_{v',v''})_1}{(I^K_{v',v''})_1 \cdot (\nu^K_{v',v''} \cdot A_{v',v''})_2}$$

where $(\nu^K_{v',v''})_1$ and $(\nu^K_{v',v''})_2$ are the frequencies of the lines being compared, and $(A_{v',v''})_1$ and $(A_{v',v''})_2$ are the Einstein transition probabilities appropriate to the bands. Ratios of Einstein transition probabilities were calculated from data given by Garvin and coworkers (8, 9). Our calculation involves the assumption that the rotational temperature is the same in all three bands, $v(1 \rightarrow 0)$, $v(2 \rightarrow 1)$, $v(3 \rightarrow 2)$. We neglect the effect of vibration–rotation interaction on the rotational line strength.

The distribution of vibrators among vibrational levels clearly corresponds to a lower temperature, $T_V \approx 2240 \pm 60°$ K at 4 mm pressure, than that derived by Chamberlain and Smith (36) for $v = 1$, 2, 3 of OH in the night sky, $T_V \approx 8000°$ K at a pressure of about 10^{-2} mm, or that obtained from the reaction H + O_3 in the laboratory, $T_V \approx 9250°$ K at pressures in the range 2–5 mm (9). Of the two laboratory systems, H + O_3 corresponds much more closely in vibrational temperature of the OH† product to the Meinel bands. However, the significance of this correspondence will remain uncertain until the H + O_3 system has been examined at a pressure in the region of 10^{-2} mm. We plan an investigation on these lines, making use of the apparatus described here.

ACKNOWLEDGMENTS

The authors wish to thank Professor H. L. Welsh and Professor H. P. Gush of the Physics Department, University of Toronto, and Dr. D. J. Le Roy of the Chemistry Department, for advice and assistance which has contributed very greatly to this work.

Can. J. Chem. Downloaded from www.nrcresearchpress.com by 210.87.254.5 on 09/05/12
For personal use only.

They are also indebted to Professor P. A. Giguère of Laval University and Dr. E. K. Plyler of the National Bureau of Standards for helpful discussions. They thank the Alfred P. Sloan Foundation for the award of a Fellowship to one of them (J. C. P.) and the National Research Council of Canada and Defence Research Board for grants-in-aid of this research.

REFERENCES

1. J. K. Cashion and J. C. Polanyi. J. Chem. Phys. **30**, 316 (1959).
2. G. Herzberg. Spectra of diatomic molecules. D. Van Nostrand Co., Inc., New York. 1950.
3. G. Herzberg. Infrared and Raman spectra. D. Van Nostrand Co., Inc., New York. 1945.
4. J. D. McKinley, D. Garvin, and M. J. Boudart. J. Chem. Phys. **23**, 784 (1955).
5. D. R. Bates and M. Nicolet. J. Geophys. Research, **55**, 301 (1950).
6. G. Herzberg. J. Roy. Astron. Soc. Can. **45**, 100 (1951).
7. A. B. Meinel. Astrophys. J. **111**, 555 (1950); **112**, 120 (1950).
8. D. Garvin. J. Am. Chem. Soc. **81**, 3173 (1959).
9. D. Garvin, H. P. Broida, and H. J. Kostkowski. J. Chem. Phys. **32**, 880 (1960).
10. V. I. Krassovsky. The airglow and aurora. Pergamon Press, London. 1956. p. 197.
11. D. R. Bates and B. L. Moiseiwitsch. J. Atmospheric and Terrest. Phys. **8**, 305 (1956).
12. J. K. Cashion and J. C. Polanyi. J. Chem. Phys. **29**, 455 (1958); **30**, 1097 (1959).
13. H. L. Welsh, C. Cumming, and E. J. Stansbury. J. Opt. Soc. Am. **41**, 712 (1951).
14. H. L. Welsh, E. J. Stansbury, J. Romanko, and T. Feldman. J. Opt. Soc. Am. **45**, 338 (1955).
15. G. G. Shepherd. Ph.D. Thesis, Department of Physics, University of Toronto, Toronto, Ont. 1956.
16. D. M. Gates, C. C. Shaw, and D. Beaumont. J. Opt. Soc. Am **48**, 88 (1958).
17. J. K. Cashion and J. C. Polanyi. Proc. Roy. Soc. (London). In press.
18. E. L. Tollefson and D. J. Le Roy. J. Chem. Phys. **16**, 1057 (1948).
19. G. H. Dieke and H. M. Crosswhite. Bumble bee report No. 87. Johns Hopkins University. 1948.
20. R. C. Herman and G. A. Hornbeck. Astrophys. J. **118**, 214 (1953).
21. E. K. Plyler and J. J. Ball. J. Chem. Phys. **20**, 1178 (1952).
22. H. C. Allen, Jr., L. R. Blaine, and E. K. Plyler. Spectrochim. Acta, **9**, 126 (1957).
23. E. K. Plyler and E. D. Tidwell. J. Research Natl. Bur. Standards, **61**, 263 (1958).
24. J. K. Cashion and J. C. Polanyi. J. Chem. Phys. **30**, 317 (1959).
25. J. T. Herron and H. I. Schiff. Can. J. Chem. **36**, 1159 (1958).
26. J. K. Cashion and J. C. Polanyi. Unpublished work.
27. T. L. Cottrell. The strengths of chemical bonds. Butterworth Scientific Publications, London. 1958.
28. R. F. Barrow and A. R. Downie. Proc. Phys. Soc. (London), A, **69**, 178 (1956).
29. S. N. Foner and R. L. Hudson. J. Chem. Phys. **21**, 1374, 1608 (1953).
30. S. N. Foner and R. L. Hudson. J. Chem. Phys. **23**, 1974 (1955).
31. R. H. Burgess and J. C. Robb. Chem. Soc. (London), Spec. Publ. No. 9, 167 (1958).
32. S. N. Foner and R. L. Hudson. J. Chem. Phys. **23**, 1364 (1955).
33. Natl. Bur. Standards (U.S.), Circ. 500, February (1952).
34. J. C. Polanyi. J. Chem. Phys. **31**, 1338 (1959).
35. S. Silverman. J. Opt. Soc. Am. **38**, 989 (1948).
36. J. W. Chamberlain and C. A. Smith. J. Geophys. Research, **64**, 611 (1959).

Can. J. Chem. Downloaded from www.nrcresearchpress.com by 210.87.254.5 on 09/05/12
For personal use only.

Can. J. Chem. Downloaded from www.nrcresearchpress.com by 210.87.254.40 on 09/05/12
For personal use only.

HOT ATOM REACTIONS AND RADIATION-INDUCED EFFECTS IN THE REACTIONS OF RECOIL TRITIUM WITH CYCLOPROPANE[1]

J. K. Lee, Burdon Musgrave, and F. S. Rowland

ABSTRACT

Recoil He^3 (n, p) tritium atoms have been reacted with cyclopropane in the gas phase under a variety of experimental conditions. The labeled hydrocarbon and molecular hydrogen products have been separated by gas chromatography and assayed by gas proportional counting.

The observed products show a strong dependence upon irradiation dose—cyclopropane is very inert toward reactions with hydrogen atoms and organic radicals, and the labeled olefinic products react preferentially, in effect as scavengers, with the reactive species from radiolysis of the parent molecule.

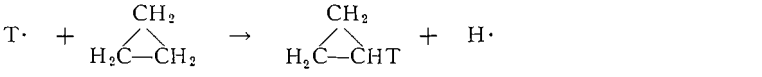
Energetic tritium atoms are able to react with cyclopropane to give labeled cyclopropane as a product without causing isomerization or decomposition of the molecule. The relative yields of cyclopropane and propylene are dependent upon the average collisional de-excitation times, indicating that a fraction of the labeled cyclopropane molecules are decomposing in times of approximately 10^{-9} seconds. Cyclopropane, propylene, ethylene, hydrogen, and small amounts of allene and methylacetylene are observed as "hot" products in the presence of gaseous free radical scavengers. Many additional compounds are found as the result of free radical and/or radiolysis reactions in the absence of scavengers.

The "hot" reactions are explained in terms of the single-step interactions of high kinetic energy tritium atoms with the cyclopropane molecules—the energy for endothermic and high activation energy processes is obtained from the recoil energy. The kinetic energy of the recoil atom at reaction is estimated to be of the order of 130 kcal/mole for some of the observed labeled compounds.

INTRODUCTION

The reactions of recoil tritium atoms from the nuclear reaction $He^3(n,p)T$ with saturated and unsaturated aliphatic hydrocarbons have been studied in detail in several laboratories, and the general outline of behavior is now well known (1–9). It will be assumed from these experiments, and from similar experiments with recoil tritium atoms from the $Li^6(n,\alpha)T$ reaction in condensed phases (10), that the recoiling atoms react predominantly while still "hot" in the sense of possessing excess kinetic energy from the nuclear recoil. As a result of this excess kinetic energy, the tritium atom is able to react at many positions in the molecule which are inaccessible to thermal hydrogen atoms (25° C) because of the high activation energies involved.

The cyclopropane molecule offers an interesting opportunity for further elucidation of the nature of these "hot" reactions because of its relatively high activation energy for substitution reaction—no deuterated cyclopropane was observed in mixtures of thermal deuterium atoms and cyclopropane (11)—and its ready thermal isomerization to propylene at temperatures in the range of 400–500° C (12). Preliminary experiments have already been reported which demonstrated that tritium-labeled cyclopropane can readily be obtained in good yield from the reactions of recoil tritium atoms with cyclopropane, as in reaction [1] (13).



[1]

More detailed experiments have now been carried out on the mechanism of reaction of energetic tritium atoms with cyclopropane. The most pertinent variables in these

[1]*Contribution from the Department of Chemistry, University of Kansas, Lawrence, Kansas; paper presented at the Symposium on Fundamental Aspects of Atomic Reactions held at McGill University, Montreal, Que., September 1960. Research supported by A.E.C. Contract No. AT-(11-1)-407.*

experiments have been the length of the irradiation, the pressure of cyclopropane, and the absence or presence of other gases, especially nitric oxide and/or helium, during the irradiation.

EXPERIMENTAL

The experimental conditions of these experiments are quite similar to those established previously in our studies of olefinic hydrocarbons (9). Mixtures of He^3, cyclopropane, and any other gases to be added were prepared in a vacuum system, and sealed into irradiation tubes made of 20-mm I.D. Pyrex 1720 glass, in lengths of about 5–8 cm. He^3 was obtained from Oak Ridge and freed from tritium-labeled impurities by combustion over CuO at 600° C, and passage through a liquid nitrogen trap (14). The level of radioactive impurity gases in the He^3 after this purification was less than 50 d.p.m./cc S.T.P. of (T_2 + HT), and less than 50 d.p.m./cc S.T.P. of CH_3T or other aliphatic hydrocarbons. These activity levels are negligible in comparison to the neutron-induced radioactivity in each of the irradiated samples. The other gases were all obtained from the Matheson Company and have quoted purities of >99% for He and NO, and >99.5% for cyclopropane. Our measurements on the cyclopropane showed no detectable hydrocarbon impurities as large as 0.01%.

The irradiation tubes were exposed to neutrons in the instrument tunnel facility of the Brookhaven National Laboratory, which has a nominal flux of 2.8×10^9 n/cm² sec and an ambient temperature of about 30° C. Irradiations were carried out for periods of time varying from 2 hours to 6 days in this facility. The actual neutron flux during irradiation was somewhat reduced by neutron absorption in the Pyrex 1720 glass, and by self-shielding during simultaneous irradiation of many samples. Neutron flux calculations based on the observed tritium radioactivity fall in the range $0.5–1.0\times10^9$ n/cm² sec, as shown in Table I.

The distribution of radioactivity among molecular hydrogen and the various hydrocarbon molecules was obtained for each irradiated sample by gas chromatographic separation and flow proportional counting of the chromatographic effluent gas. Two or more aliquots were run on each sample, usually a large aliquot on a 50-ft dimethylsulpholane (DMS) column at 25° C, and a smaller aliquot on 10 ft silica gel at 85° C. The counting gas consisted of the helium carrier gas and methane in about a 50–50 mixture, the methane being added after the carrier gas had passed through a thermal conductivity detector for determination of macroscopic radiation damage. Further details have been given previously (15, 16).

Aliquots of some samples were run through a 50-ft safrole column in order to determine the relative contributions of *n*-butane – neopentane and cyclopropane–acetylene. In the usual dimethylsulpholane runs, the former pair are unseparated and acetylene is obscured by the large cyclopropane peak immediately preceding it. Acetylene contributions are also measured on the silica gel column, although they are partially obscured when propane is present in large amounts. The parent peaks usually overload the DMS column and emerge somewhat early; other components are practically unaffected by the overload of the parent compound.

RESULTS

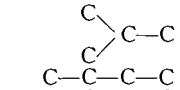
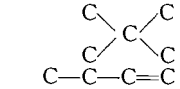
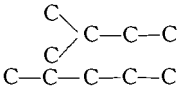
Variation in Length of Irradiation

The yields of tritium radioactivity found in various molecules, measured relative to cyclopropane as 100, are shown in Table I for a series of irradiations carried out under

Can. J. Chem. Downloaded from www.nrcresearchpress.com by 210.87.254.40 on 09/05/12
For personal use only.

TABLE I

Distribution of tritium radioactivity from $He^3(n,p)T$ in cyclopropane: effect of length of irradiation
(Yields relative to cyclopropane = 100)

Gas, Δ	70.4	72.4	72.1	78.1	76.7	80.4	74.5	73.2
Pressure He^3	2.0	2.0	2.0	1.3	2.0	1.3	2.0	1.3
Irradiation time, hours	138	48	48	48	24	8	4	2
Neutron flux (from T product on) counts observed			8×10^8	7×10^8	6×10^8	9×10^8	7×10^8	7×10^8
In Δ peak	29,000	6,000	25,500	16,800	8,650	2,530	1,900	660
Product, Δ	100	100	100	100	100	100	100	100
HT	141	138	138	159	147±2	140±5	153±6	150±10
CH_3T	11	11	9					
C—C	28	26	22	25	22±1	16±1	11±2	33±5
C=C	7	9	10	11	10±1	10±1	12±2	
C≡C	2	2	2	2	2	—	—	—
C—C—C	54	52	48	51	44±2	37±2	20±2	23±5
C—C=C	9	15	15	19	22±1	31±2	49±3	54±5
C=C=C	1	1	1	1	2±1	2±2	2±2	—
	13	15	14	13	16±1	21±2	7±2	29±5
C—C—C—C	39	35	30	29	25±1	15±1	7±2	9±3
	1	2	2	2	3±0.5	3±1	5±1	—
	24	28	23	21	22±1	17±2	7±1	—
C—C—C—C—C	6	9	5	5	4±0.5	5±2		—
Δ—C	3	3	4	5	4±0.5	3±1	2±1	—
"170"*	—	12	10	10	10±1	12±2	9±2	

*C_6 peak at 170 minutes or DMS; not conclusively identified.

nearly constant conditions except for the length of the irradiation. As can readily be seen, the relative yields of several labeled unsaturated molecules fall, and the yields of the corresponding saturated aliphatic products increase, with increasing radiation time. The total number of counts actually measured in the cyclopropane peak and the flux estimate from the total observed tritium activity are also given in Table I for the irradiations. The shortest irradiations did not create much tritium radioactivity, and the quoted errors are calculated from the statistical uncertainty of the observed counts. For runs of 48 hours or longer, the statistical uncertainty is probably less than other possible errors. The irradiation times were varied from 2 to 138 hours; duplicate samples at 48 hours were separately irradiated several months apart and analyzed on both the dimethylsulpholane and safrole columns.

Nitric Oxide Experiments

The observed tritium distributions are given in Table II for a series of experiments carried out in the presence of nitric oxide. The usual role of nitric oxide in these experiments is to react with free radicals and thermal hydrogen atoms, and to remove them from the reacting system, thus protecting other recoil reaction products, e.g. propylene and ethylene, from secondary reactions with radiation-induced species. At the same time, all labeled compounds are eliminated which involve thermal atoms or radicals in

Can. J. Chem. Downloaded from www.nrcresearchpress.com by 210.87.254.40 on 09/05/12
For personal use only.

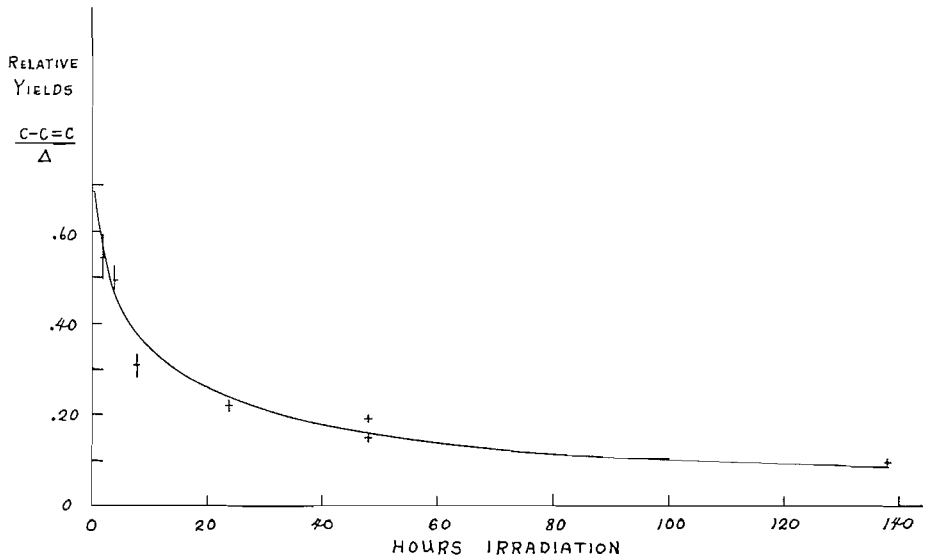


FIG. 1. Propylene yield vs. irradiation time. $G(H) = 5$, $G(olefin) = 4$. $k_4/k_7 = 8\times10^{-5}$.

TABLE II

Distribution of tritium radioactivity from $He^3(n,p)T$ in cyclopropane – nitric oxide mixtures

Gas, Δ	72.7	66.4	40.6	33.2	19.9	21.4
Pressures He^3	1.9	1.9	1.8	1.8	1.6	1.6
NO	5.0	7.7	4.3	5.0	2.1	1.8
	Neutron flux $\sim 10^9$ n/cm² sec					
Counts observed in Δ peak*	19,000	66,000	56,000	12,000	22,000	17,000
Irradiation time, hours	48	138	138	48	48	138
HT	131	131	131	133	133	131
CH_3T	2	2	2			2
C=C	6	6	7	6	7	7
C—C=C	7	16	35	7	30	38
Δ	100	99	97	92	93	90
C≡C	1	1	1	1	1	1
C=C=C	1	1	2	1	1	—
Δ—C	1	1	1	1	0	—
"125"†	2	5	6	7	2	—
"140"†	1	1	1	1	1	—

NOTE: C–C–C=C ~ 0.3, "168" ~ 0.3, others <0.1.

*Since the sample aliquots were not all of the same size, the listed observed counts show only the statistical counting accuracy of the analysis, and not the total or relative specific activities.

†Peaks at 125 minutes and 140 minutes on DMS not yet conclusively identified. C=C–C=C and C–C≡C or C–C–C=C–C have the correct retention times.

their production. Those labeled compounds which are unaffected by the presence of a radical scavenger are then assumed to be obtained from direct recoil reaction. A possible exception could occur if the direct reaction created a "hot" radical (e.g. ·CHT·), which was able to react very efficiently with the hydrocarbon molecule.

The nitric oxide experiments confirm hydrogen, ethylene, propylene, and cyclopropane

Can. J. Chem. Downloaded from www.nrcresearchpress.com by 210.87.254.40 on 09/05/12
For personal use only.

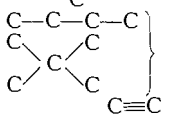
as products of recoil reaction, although the amounts observed are not always found in consistent ratios.

Pressure Effects

The tritium distributions have also been measured with a series of samples irradiated at various cyclopropane pressures from 7.9 to 80 cm Hg (plus 1–2 cm Hg of He^3) and are recorded in Table III. The practice of expressing all products in terms of the parent

TABLE III

Distribution of tritium radioactivity from $He^3(n, p)T$ in cyclopropane: pressure effects
(Neutron flux $\sim 10^9$ n/cm^2 sec)

Gas, Δ	72.4	70.4	50.9	48.7	17.3	18.1	7.9	9.2
He^3, cm	2.0	2.0	1.7	1.7	1.7	1.7	2.1	2.1
Counts in Δ peak	6,000	28,000	27,000	80,000	28,000	27,000	14,000	11,000
Irradiation time, hours	48	138	48	138	48	138	48	138
Product, Δ	100	100	100	100	100	100	100	100
C—C—C	52	54	54	58	71	72	77	88
C—C=C	15	9	16	7	13	9	14	7
HT	138	141	142	(143)	156	154	159	180
CH_3T	11	11	11		12	13	14	12
C—C	26	28	27	28	33	32	34	39
C=C	9	7	8	6	10	10	13	10
	15	13	16	16	22	22	25	21
	35	39	36	46	50	52	53	70 —
C≡C	2	2	—	—	2	—	—	2
Δ—C	3	3	4	3	3	3	2	—
	28	24	27	30	37	38	41	44
C—C—C—C—C	9	6	7	9	9	9	15	11
Estimated relative parent activity	100	100	98	98	92	91	87	80

yield is not very satisfactory for Tables II and III, for a comparison of the actual amounts of radioactivity observed in various compounds indicates that the percentage of labeled parent compound falls off with decreasing pressure. This parent fall-off is accompanied by an increase in the percentage of radioactivity observed as propane. There is no compound whose activity is necessarily constant through the pressure changes, although hydrogen is experimentally observed to be nearly so. We have chosen to hold the cyclopropane activity as 100 for comparison purposes. The column labeled estimated relative parent activity represents an estimate of the absolute change in the activity as cyclopropane.

Helium Moderator

The results of a series of runs carried out in the presence of moderator He^4, with and without nitric oxide as a scavenger, are shown in Table IV. The actual yield of labeled hydrogen is not very much affected by changes in He^4/cyclopropane ratio, but the yield of labeled cyclopropane falls markedly. Both propane and *n*-butane increase as the He^4/parent ratio is increased.

Can. J. Chem. Downloaded from www.nrcresearchpress.com by 210.87.254.40 on 09/05/12
For personal use only.

TABLE IV

Distribution of tritium radioactivity from $He^3(n,p)T$ in cyclopropane–He^4 mixtures
(Neutron flux $\sim 10^9$ n/cm^2 sec)

Gas, Δ	52.5	23.8	22.6	7.8	10.1
He^3, cm	2.0	1.6	1.6	1.5	1.5
He^4	20.0	45.0	44.5	66.0	66.7
Counts in Δ peak	51,000	11,000	27,000	11,000	14,000
Irradiation time, hours	138	48	138	48	138
Product, Δ	100	100	100	100	100
HT	141	182	186	275	270
CH_3T	11	16	13	15	17
C—C	27	35	42	70	70
C=C	8	14	9	29	20
C≡C	9	6	8	14	13
C—C—C	49	74	81	110	115
C—C=C	15	19	10	26	16
	12	23	21	32	27
	43	60	92	115	124 —
Δ—C	5	5	3	4	—
	30	46	49	76	73
C—C—C—C—C	7	10	13	17	20

DISCUSSION

The distribution of tritium activity among the various possible molecular forms in a given system depends upon three separate steps:

(*a*) The primary reaction of the recoil tritium with a molecule of the medium. If, as is frequently true, this reaction occurs while the tritium atom possesses excess kinetic energy, this attack can be expected to be rather indiscriminate upon all species in the system. In lightly irradiated systems such as these, the "hot" reaction would then be with cyclopropane almost exclusively, for the total concentration of degradation products, free radicals, ions, etc. is always very small in comparison to the cyclopropane concentration. These "hot" reactions produce the initial recoil tritium yields.

(*b*) The "hot" product may itself be quite reactive, and be able to participate in further reactions in the system. This can happen if the "hot" product is either a labeled free radical, such as the $CH_2T\cdot$ or *sec*-$C_4H_8T\cdot$ suggested for other hydrocarbons (1, 3, 9), or if it is a molecule sufficiently vibrationally excited to undergo decomposition or isomerization. The identified stable labeled molecule will depend in each case on the further reactions of the radical or excited molecule involved. These reactions, unlike the "hot" reactions, can be strongly influenced by the presence or absence of reactive ions, atoms, and molecules from radiation degradation.

It is also possible to form a stable molecule in temperature equilibrium with the system which is able to undergo thermal chemical reactions with other molecules present. There have been no experimental indications of any such molecules in any of the hydrocarbon systems investigated in our laboratory. Furthermore, the known hydrocarbons do not react or undergo isotopic exchange over a period of several months at room

Can. J. Chem. Downloaded from www.nrcresearchpress.com by 210.87.254.40 on 09/05/12
For personal use only.

temperature, as confirmed by samples irradiated in duplicate and analyzed several months apart.

(*c*) The final distribution that is observed may also reflect subsequent alteration of the products of (*a*) and (*b*) by continued exposure to a radiation field. The perturbing effect of such radiation-induced reactions can readily be minimized, if the parent molecule is reasonably reactive toward radiation-produced species. If the parent molecule is rather inert, however, the brunt of the radiation damage may be borne by reactive product molecules present in low concentration, e.g. olefins, and will result in appreciable alteration in the observed amounts of these products.

The nitric oxide – scavenger experiments of Table II demonstrate that labeled hydrogen, cyclopropane, propylene, ethylene, and other molecules are all formed in the initial reaction of the "hot" tritium atom with cyclopropane. The experiments in the absence of nitric oxide show an appreciably different spectrum of labeled hydrocarbons, including substantial yields of a number of saturated aliphatic molecules that arise from the reactions of excited species, as in (*b*), or radiation alteration, as in (*c*).

Since reactions in both categories (*b*) and (*c*) are quite sensitive to the presence of radiation-produced reactive species in the rather unreactive cyclopropane, we must consider the radiation chemistry of the recoil system as well as the initial "hot" reactions with cyclopropane itself.

Radiation Effects

I. Ionization Processes

The recoil triton and proton from the $He^3(n,p)T$ reaction dissipate a total of 0.78 Mev for each tritium atom produced, and almost all of this energy is released as ionization and excitation in the gas phase. The identity of the ions, radicals, and atoms created by radiation effects can be estimated from the 70-volt mass spectra, as in the calculations of Futrell on *n*-hexane (17). Such a calculation, with the additional assumption that the ion–molecule reactions of $C_3H_5^+$ and $C_3H_6^+$ with cyclopropane go approximately as well as the corresponding reactions with propylene (18–20), clearly indicates the formation of substantial quantities of radiation produced ethylene and hydrogen atoms, as well as smaller yields of methyl and other radicals. Additional hydrogen atoms and or radicals will arise from the ion–electron or ion–ion recombination reactions.

II. Reactions of Hydrogen Atoms and Radicals

In pure cyclopropane, abstraction reactions such as [4] and [5] are the only important reactions that can occur for H atoms or radicals, except recombination as in [6].

$$H\cdot + \underset{H_2C-CH_2}{\overset{CH_2}{\diagup\diagdown}} \xrightarrow{k_4} H_2 + C_3H_5\cdot \qquad [4]$$

$$R\cdot + \underset{H_2C-CH_2}{\overset{CH_2}{\diagup\diagdown}} \xrightarrow{k_5} RH + C_3H_5\cdot \qquad [5]$$

$$R\cdot + R'\cdot \xrightarrow{k_6} R{-}R' \text{ (R can be H)} \qquad [6]$$

As irradiation proceeds and olefinic products begin to accumulate, the atoms and radicals may react with them, too, as in [7] and [8], and the actual course of reaction will depend upon the relative rates of the individual reactions [4] to [9] for the various radicals involved.

Can. J. Chem. Downloaded from www.nrcresearchpress.com by 210.87.254.40 on 09/05/12
For personal use only.

$$H\cdot + C_nH_{2n} \xrightarrow{k_7} C_nH_{2n+1}\cdot \quad [7]$$

$$R\cdot + C_nH_{2n} \xrightarrow{k_8} R{-}C_nH_{2n}\cdot \quad [8]$$

Experimentally, it is observed that the sum of the relative yields of propylene and propane in Table I is reasonably constant over a factor of 70 in irradiation times, although the individual yields are changing. This observation strongly suggests that the most probable reaction for the removal of propylene from the system, and its lowered relative yield, is reaction [7] followed by the further addition of another hydrogen atom, probably by reaction [5] for the C_nH_{2n+1} radical. The sum of the yields for ethane plus ethylene is also nearly constant for different irradiation times—the ethylene concentration does not fall as smoothly as the propylene yield, but there are difficulties in separating the ethane and ethylene radioactivity at these low count rates.

A crude calculation of the kinetic behavior of atoms and radicals in the cyclopropane system can be made by assuming that

(*a*) H atoms and olefin are produced continuously by radiation effects on cyclopropane;

(*b*) olefin is removed only by reaction with H atoms, as in reaction [7], followed by reaction [5];

(*c*) H atoms are removed only by reactions [4] and [7], and rapidly reach a steady-state equilibrium.

Such assumptions lead to a predicted curve of olefin concentration versus time of irradiation which depends on the parameters: (1) radiation G values of hydrogen and olefin, and (2) the ratio k_4/k_7. The olefin reaches a steady-state concentration eventually, and since the total radioactivity produced rises linearly with time, the fraction of radioactivity found as olefin falls steadily (21).* The propylene yields of Table I agree quite well with the crude estimate obtained using the parameters: $k_4/k_7 = 8\times10^{-5}$, $G(H) = 5$, and $G(\text{olefin}) = 4$. These G values are reasonable ones, and the value of k_4/k_7 used is in good agreement with measured values for this ratio (11, 22, 23). The intercept for the propylene yield at zero irradiation time corresponds to zero initial production of labeled propane, and allows the additional conclusion that the sum of propylene plus propane yields is a satisfactorily accurate measure of the *total* production of propylene in the system by "hot" reactions. In the subsequent discussion of the "hot" reactions themselves, we shall use this sum of yields as a measure of the labeled propylene production in comparison to the labeled cyclopropane yield.

Tritium Reactions at High Kinetic Energy

Previous gas-phase experiments have led to a hypothesis for the reactions of high-energy recoil atoms with hydrocarbons that is able to explain the observed effects quite satisfactorily (1–9). The most important characteristics of this hypothesis are that the tritium atoms react

(*a*) as neutral atoms—the predominant charge state for a moving hydrogen nucleus at energies from 10^4 ev down;

(*b*) while possessing kinetic energy greatly in excess of average thermal energies, and hence are able to both react in a very few collisions and to undergo reactions that are highly endothermic and/or have high activation energies. Essentially, all positions in

**K. Yang and P. Gant (J. Chem. Phys. (in press)) have reported steady-state concentrations of ethylene in cyclopropane of about $10^{-3}\,x(\text{cyclo-}C_3H_6)$ for cyclopropane irradiated with beta particles from tritium decay.*

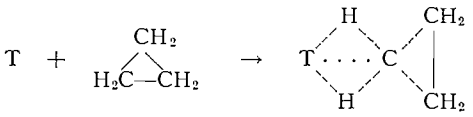
Can. J. Chem. Downloaded from www.nrcresearchpress.com by 210.87.254.40 on 09/05/12
For personal use only.

a molecule are approximately equally subject to attack by, and reaction with, the recoil tritium atom.

(*c*) the reaction usually takes place so rapidly that only one parent molecule is involved—the reaction is completed before energy can be removed from the system by collisions.

(*d*) the reaction takes place through a transition complex and does not require "cages" or combination with other radicals in order to produce most of the observed radioactive molecules.

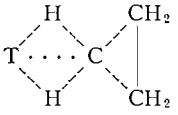
The recoil tritium reactions with both saturated and unsaturated positions of aliphatic molecules have been interpreted as involving momentarily a transition complex including the tritium recoil atom and all of the previously bonded substituents. This complex then decomposes by breaking one (or more) of these bonds, often leading to a stable molecule as a result. With cyclopropane, such a complex might be pictorially written as in [9] (without intending to indicate any specific details about the geometry and bonding involved).

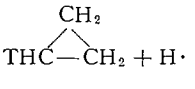


[9]

The lifetime of this complex is very short—it may only exist for one vibration or so, and equilibration of energy among the vibrated co-ordinates of the complex does not occur. The C_3H_6T complex above can break one of the bonds to the attacked carbon atom, with four possible reactions.

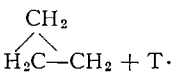
$$\rightarrow \quad HT + C_3H_5\cdot \qquad [10]$$





[11]

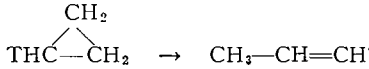
$$\rightarrow \quad CH_2T—CH_2—CH_2\cdot \qquad [12]$$



[13]

The tritium atom emerging from reaction [13] will usually be degraded in energy and will react again as a "hot" atom or a thermal atom depending upon the energy remaining. Undoubtedly a relatively high activation energy is required for the tritium atom to penetrate into the molecule far enough to bond even briefly to one of the carbon atoms. The relative yields of equations [10]-[13] may very well be strongly energy dependent.

The tritium-labeled cyclopropane from reaction [11] will usually be produced in an excited vibrational state, and, if this energy is sufficient, can undergo the isomerization reaction [14] for which the activation energy is 65 kcal/mole (24). Some tritium would be



[14]

expected in all hydrogen positions of the propylene. The labeled *n*-propyl radical from reaction [12] must be excited since the reaction is highly exothermic as shown in Table V.

Can. J. Chem. Downloaded from www.nrcresearchpress.com by 210.87.254.40 on 09/05/12
For personal use only.

TABLE V

Energetics of formation of "hot" products in recoil tritium reactions with cyclopropane

Reaction	ΔH (kcal/mole)
$T + \underset{H_2C-CH_2}{\overset{CH_2}{\diagup\diagdown}} \rightarrow$	
$\underset{H_2C-CHT}{\overset{CH_2}{\diagup\diagdown}} + H$	~0
$CH_3-CH=CHT + H$	−8
$CH_2=CHT + CH_3\cdot$	−20
$CH_2=CHT + \cdot CH_2 + H\cdot$	+83
$CH_2T-C\equiv CH + H_2 + H\cdot$	+31
$CH_2T-C\equiv CH + 3H\cdot$	+135
$CH_2=C=CHT + H_2 + H\cdot$	+32
$CH_2=C=CHT + 3H\cdot$	+136
ΔHf° used (isotopic differences ignored) (25–27)	
$\underset{H_2C-CH_2}{\overset{CH_2}{\diagup\diagdown}}$	+12.7
$CH_3-CH=CH_2$	+4.9
$CH_2=CH_2$	+12.5
$CH_3-C\equiv CH$	+44.3
$CH_2=C=CH_2$	+45.3
H	+52.1
$CH_3\cdot$	32.0
$\cdot CH_2$	83

This energy is sufficient to permit decomposition to labeled methyl and ethylene to occur readily,

$$CH_2T-CH_2-CH_2\cdot \rightarrow CH_2T\cdot + C_2H_4; \quad [15]$$

to hydrogen and propylene to occur less readily,

$$CH_2T-CH_2-CH_2\cdot \rightarrow CH_2T-CH=CH_2 + H\cdot, \quad [16]$$

and perhaps to decompose as in reaction [17] to a hydrogen atom and the trimethylene radical,

$$CH_2T-CH_2-CH_2\cdot \rightarrow \cdot CHT-CH_2-CH_2\cdot + H\cdot. \quad [17]$$

"Hot" Products

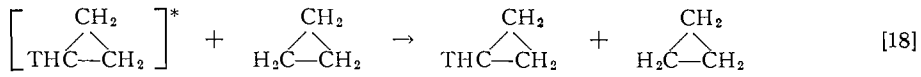
Cyclopropane

The identification of labeled cyclopropane among the radioactive products immediately indicates that reaction [1]—presumably by steps [9] plus [11]—is able to take place without further isomerization as in [14]. This failure to isomerize can be expected if the tritiated molecule is left with less vibrational energy than the 65 kcal/mole activation energy, or if the excess energy is not too great and can be removed by collision before isomerization.

The data of Table III show that the fraction of tritium activity found as labeled cyclopropane is greater at high pressures. (The results of Table IV show that the changes in He/Δ ratio of Table III are insufficient to explain the observed decreases in cyclopropane yield with decreased pressure during irradiation.) The increased cyclopropane

Can. J. Chem. Downloaded from www.nrcresearchpress.com by 210.87.254.40 on 09/05/12
For personal use only.

yield at higher pressures is readily explained as a competition between the isomerization reaction [14] and the removal of excitation by collision:



[18]

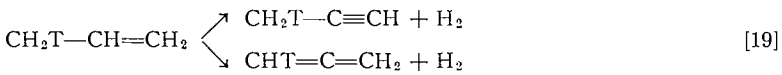
De-excitation of the excited *n*-propyl radical is not a satisfactory mechanism, for this de-excitation will not lead to labeled cyclopropane, but rather to an aliphatic hydrocarbon.

An estimate of the excitation energy required for reactions [14] and [15] to be competitive depends on the efficiency of collisions in removing excess vibrational energy. Since the excess energy is quite large, the collision efficiency is probably very high, approaching unity. The rate of isomerization must then be of the order of 10^9 sec^{-1} in order to be competitive with gas collisions at 0.1 to 1.0 atmosphere pressure. Such a rate requires an excitation energy roughly double the activation energy for a molecule with 13 active degrees of freedom, and hence approximately 130 kilocalories/mole of internal energy. Almost all of this energy must be supplied from the original kinetic energy of the tritium, which must then have been at least 6–7 ev at the time of reaction. The possible alternate path to propylene by reactions [9] and [16] prevents additional conclusions about higher vibrational energies from being drawn from the experimental observation that substantial yields of propylene (plus propane) are found at the highest pressures used. Some information on the relative importance of the two paths to propylene formation could be obtained in principle by degradation of the propylene molecules in order to determine the intramolecular tritium distribution.

Ethylene, Allene, Methylacetylene, and Hydrogen

The unsaturated molecules ethylene, allene, and methylacetylene are all obtained in low yield from the recoil reactions in the presence of nitric oxide, as well as in its absence. Each of these molecules could arise from the decomposition of the excited intermediate by reactions other than [9] to [13], or by further decomposition of the propylene of [14] or [16], of the trimethylene radical from [17], or of the *n*-propyl radical from reaction [12].

Both allene and methylacetylene must be formed by a highly endothermic reaction, as shown in Table V. If the three hydrogen atoms that must be lost from the transition complex are all lost as separate atoms, a kinetic energy of more than 135 kcal/mole must be supplied by the recoiling tritium atom. The second possibility exists that two of these hydrogens are given off as H_2, as in reactions [19], from the unimolecular elimination of molecular hydrogen from an excited propylene molecule.



[19]

The over-all path by this sequence of reactions is only 31 and 32 kcal/mole endothermic, respectively. However, reactions such as [19] can be expected to have activation energies of the order of 40–60 kcal/mole, and again roughly double this energy would be required for decomposition before collisional deactivation. Hence, for either possible path to labeled methylacetylene or allene, an energy of about 120+ kcal/mole must be supplied from the kinetic energy of the recoil tritium. The unscavenged HT found in the nitric oxide systems may arise from an energetic hydrogen abstraction reaction. An alternate path that may be very important would be the intramolecular elimination of HT instead of H_2 from the excited propylene molecule, as in [19].

Can. J. Chem. Downloaded from www.nrcresearchpress.com by 210.87.254.40 on 09/05/12
For personal use only.

The excited *n*-propyl radical decomposition is exothermic over all in going to methyl plus ethylene, but the sequence of reaction [9] followed by [15] leads only to labeled methyl radical in the absence of some hydrogen transfer reactions in the excited radical. The decomposition of trimethylene diradical as in [20] is quite endothermic, but the energy requirements are no more severe than those for the formation of the other

$$\cdot CH_2—CH_2—CHT\cdot \rightarrow \cdot CH_2 + CH_2{=}CHT \qquad [20]$$

"hot" products. Since this reaction does not involve hydrogen transfer, it may be able to compete successfully. Furthermore, in the presence of so much excess vibrational energy, an excited trimethylene diradical for reaction [20] can probably be obtained readily by direct opening of the cyclopropane ring, as in [21]:

$$\begin{array}{l} CH_2 \\ /\ \backslash \\ H_2C—CHT \end{array} \rightarrow \cdot CH_2—CH_2—CHT\cdot \qquad [21]$$

Methylcyclopropane and Butene-1

Methylcyclopropane could presumably arise in this system by any of these three reactions:

$$\cdot CHT + \begin{array}{l} CH_2 \\ /\ \backslash \\ H_2C—CH_2 \end{array} \rightarrow \begin{array}{l} CH_2 \\ /\ \backslash \\ CH_2T—HC—CH_2 \end{array} \qquad [22]$$

$$CH_2T\cdot + \begin{array}{l} CH_2 \\ /\ \backslash \\ H_2C—CH_2 \end{array} \rightarrow \begin{array}{l} CH_2 \\ /\ \backslash \\ CH_2T—HC—CH_2 \end{array} + H\cdot \qquad [23]$$

$$CH_2T\cdot + \begin{array}{l} \cdot CH \\ /\ \backslash \\ H_2C—CH_2 \end{array} \rightarrow \begin{array}{l} CH_2 \\ /\ \backslash \\ CH_2T—HC—CH_2 \end{array} \qquad [24]$$

The recent experiments of Butler and Kistiakowsky demonstrate that a mixture of butenes would also be expected from reaction [22] under these experimental conditions (28). Since the yields of isobutylene and *cis*- and *trans*-butene-2 are negligible, the methylene insertion reaction is probably negligible, too. Reaction [23] is endothermic and would require a "hot" $CH_2T\cdot$ group. The observation of some labeled butene-1 in the presence of radical scavenger (Table II) is consistent with this reaction.

The radical recombination reaction seems quite likely since $C_3H_5\cdot$ radicals (of unspecified structure) will be expected in good yield from the abstraction reactions [4] and [5] by hydrogen atoms and radicals, respectively. Similarly, the recombination of methyl with allyl radical [26] is probably the source of the labeled butene-1 found in this system.

$$CH_2T\cdot + CH_2{=}CH—CH_2\cdot \rightarrow CH_2T—CH_2—CH{=}CH_2 \qquad [26]$$

Moderator Effect

Qualitatively, the changes in yields of cyclopropane and other molecules in the presence of He^4 (Table IV) are consistent with the removal of the excess kinetic energy of the recoil tritium in elastic collisions with the helium moderator. The energy loss reduces the probability of a large excess of vibrational energy, and hence of isomerization; it also reduces the probability of a successful reaction while still possessing the necessary activation energy for reaction with the cyclopropane molecule to form HT or labeled parent molecule. The more rapid decrease in the yield of labeled cyclopropane than of HT implies that the activation energy for the former is larger, as is also indicated by the thermal deuterium experiments of Schiff and Steacie.

Can. J. Chem. Downloaded from www.nrcresearchpress.com by 210.87.254.40 on 09/05/12
For personal use only.

Wolfgang and Estrup have presented a theory of high-energy kinetics and have applied it quite successfully to the recoil reactions of tritium with methane (4). The reactions in the cyclopropane system are sufficiently complicated, however, that additional experiments are required on radiation effects and on collisional de-excitation in He^4–Δ mixtures before a suitable test of the applicability of the theory to this system can be made.

REFERENCES

1. M. El-Sayed and R. Wolfgang. J. Am. Chem. Soc. **79**, 3286 (1957).
2. M. El-Sayed, P. J. Estrup, and R. Wolfgang. J. Phys. Chem. **11**, 1356 (1958).
3. D. Urch and R. Wolfgang. J. Am. Chem. Soc. **81**, 2025 (1959).
4. P. Estrup and R. Wolfgang. J. Am. Chem. Soc. In press.
5. D. Urch and R. Wolfgang. Am. Chem. Soc. 136th Meeting, Atlantic City, 1959.
6. A. A. Gordus, M. C. Sauer, Jr., and J. Willard. J. Am. Chem. Soc. **79**, 3284 (1957).
7. J. B. Evans, J. Quinlan, M. C. Sauer, Jr., and J. Willard. J. Phys. Chem. **11**, 1351 (1958).
8. M. C. Sauer, Jr. and J. Willard. J. Phys. Chem. **64**, 359 (1960).
9. J. K. Lee, B. Musgrave, and F. S. Rowland. Am. Chem. Soc., 134th Meeting, Chicago, 1958; J. Am. Chem. Soc. In press.
10. W. J. Hoff, Jr. and F. S. Rowland. J. Am. Chem. Soc. **79**, 4867 (1957).
11. H. I. Schiff and E. W. R. Steacie. Can. J. Chem. **29**, 1 (1951).
12. H. O. Pritchard, R. G. Sowden, and A. F. Trotman-Dickenson. Proc. Roy. Soc. (London), A, **217**, 563 (1953).
13. J. K. Lee, B. Musgrave, and F. S. Rowland. J. Am. Chem. Soc. **81**, 3803 (1959).
14. J. K. Lee and F. S. Rowland. J. Inorg. & Nuclear Chem. **10**, 336 (1959).
15. R. Wolfgang and F. S. Rowland. Anal. Chem. **30**, 903 (1958).
16. J. K. Lee, B. Musgrave, and F. S. Rowland. Am. Chem. Soc. 137th Meeting, Cleveland, 1960.
17. J. H. Futrell. J. Am. Chem. Soc. **81**, 5921 (1959).
18. D. P. Stevenson. J. Phys. Chem. **61**, 1453 (1957).
19. D. O. Schissler and D. P. Stevenson. J. Chem. Phys. **24**, 926 (1956).
20. F. W. Lampe and F. H. Field. Tetrahedron, **7**, 189 (1959).
21. K. Yang and P. Gant. J. Chem. Phys. In press.
22. P. E. Allen, H. Melville, and J. C. Robb. Proc. Roy. Soc. A, **218**, 311 (1953).
23. B. Darwent and R. Roberts. Discussions Faraday Soc. **14**, 55 (1953).
24. H. O. Pritchard, R. G. Sowden, and A. F. Trotman-Dickenson. Proc. Roy. Soc. A, **217**, 563 (1953).
25. A. F. Trotman-Dickenson. Free radicals: an introduction. Methuen. 1959.
26. S. W. Benson. The foundations of chemical kinetics. McGraw-Hill. 1960.
27. A. F. Trotman-Dickenson. Gas kinetics. Butterworth. 1955.
28. J. Butler and G. Kistiakowsky. J. Am. Chem. Soc. **82**, 759 (1960).

Can. J. Chem. Downloaded from www.nrcresearchpress.com by 210.87.254.40 on 09/05/12
For personal use only.

Can. J. Chem. Downloaded from www.nrcresearchpress.com by 210.87.254.42 on 09/05/12
For personal use only.

VIBRATIONAL DISEQUILIBRIUM IN REACTIONS BETWEEN ATOMS AND MOLECULES[1]

N. Basco and R. G. W. Norrish

ABSTRACT

Observations on the production of vibrationally excited oxygen molecules in the flash photolysis of nitrogen peroxide and of ozone have extended previous work on these systems. In the case of nitrogen peroxide it has been shown that oxygen molecules possessing the entire exothermicity of the reaction in the form of vibrational energy are produced. A new class of reactions is reported in which vibrationally excited hydroxyl radicals are produced under isothermal conditions by the reaction $O(^1D) + RH \rightarrow OH^* + R$, in which the energy for excitation is contributed by the electronic energy of the oxygen atom.

These and other cases of non-equilibrated energy distributions in reaction products and theories accounting for this phenomenon are reviewed.

The first clear indication that the energy distribution in a chemical reaction between an atom and a polyatomic molecule can differ appreciably both from equipartition and from the Maxwell–Boltzmann law was obtained by McKinley, Garvin, and Boudart (8), who showed that in the reaction

$$H + O_3 \rightarrow OH + O_2 \qquad + 80 \text{ kcal}$$

the hydroxyl radical was produced with up to nine quanta of vibrational energy (75 kcal). Soon after, Lipscomb, Norrish, and Thrush (4) detected oxygen molecules with up to eight quanta of vibrational energy (34 kcal) in the isothermal flash photolysis of nitrogen dioxide and chlorine dioxide and showed that these were produced in the reactions

$$O + NO_2 \rightarrow O_2 + NO \qquad + 46 \text{ kcal},$$

and

$$O + ClO_2 \rightarrow O_2 + ClO_2 \qquad + 61 \text{ kcal}.$$

Other examples of this process viz.

$$O + O_3 \rightarrow O_2^* + O_2$$
$$Cl + O_3 \rightarrow ClO^* + O_2$$
$$Br + O_3 \rightarrow BrO^* + O_2$$

were found by McGrath and Norrish (1, 6, 7) in the flash photolysis of ozone and of chlorine and bromine in the presence of ozone. From these results they arrived at the general conclusion (1) that the exothermic reaction between an atom and a triatomic molecule

$$A + BCD = AB + CD \qquad + Q \text{ kcal}$$

could lead to the accumulation of most of the energy Q in the newly formed bond AB.

More recently, several other examples have been reported by Cashion and Polanyi (2, 13, 14, 15), by Kaufman and Kelso (16), by Dressler (17), and by Thrush (18). These and other examples of this type of reaction are listed in Table I, which shows the exothermicity of the reactions (Q kcal/mole) together with the highest vibrational level observed.

The subject has been reviewed by McGrath and Norrish (1) and discussed from theoretical points of view by Polanyi (2) and by Smith (3). It is the purpose of this paper

[1]*Contribution from the Department of Physical Chemistry, University of Cambridge, Lensfield, Cambridge, England; paper presented at the Symposium on the Fundamental Aspects of Atomic Reactions held at McGill University, Montreal, Que., September 1960.*

TABLE I

Reaction	Q (kcal)	Highest level observed and energy in kcal/mole	Reference
$O + ClO_2 \rightarrow O_2^* + ClO$	61	8 = 34	4
$O + NO_2 \rightarrow O_2^* + NO$	46 (48)?	8 = 34	4
		11 = 45½ (12 = 49)?	5
$O + O_3 \rightarrow O_2^* + O_2$	138 $O(^1D)$	17 = 66½	6,7
	93 $O(^3P)$	19(?20) = 73	5
$Br + O_3 \rightarrow BrO^* + O_2$	19 $Br(P^{3/2})$	4 = 8	1, 6
	29½ $Br(P^{1/2})$		
$Cl + O_3 \rightarrow ClO^* + O_2$	40 $Cl(P^{3/2})$	5? = 11	1, 6
	42½ $Cl(P^{1/2})$		
$O + H_2 \rightarrow OH^* + H$	43		
$O + HCl \rightarrow OH^* + Cl$	44		
$O + H_2O \rightarrow OH^* + OH$	29 $O(^1D)$	2 = 19.8	5
$O + NH_3 \rightarrow OH^* + NH_2$	45		
$O + CH_4 \rightarrow OH^* + CH_3$	45		
$H + O_3 \rightarrow OH^* + O_2$	80	9 = 75	8–12
$H + Cl_2 \rightarrow HCl^* + Cl$	45	6 = 45	13, 14
$H + Br_2 \rightarrow HBr^* + Br$	41	5 = 34	2
$H + HO_2 \rightarrow OH^* + OH$	38	1 = 9.9	15
$N + NO \rightarrow N_2^* + O$	70	1 = 6.6	16, 17
$H + F_2 \rightarrow HF^* + F$	98	9 = 86	18
$X + Na_2 \rightarrow NaX^* + Na$	81 (X = Cl)		
	71 (X = Br)		
	54 (X = I)		
$Na + ClX \rightarrow NaX^* + Cl$	52? (X = Cl)	At least 48½	20
	39? (X = Br)		
	53? (X = I)		
$Na + HgX \rightarrow NaX^* + Hg$	75 (X = Cl)		
	71? (X = Br)		

to discuss various aspects of the production of vibrationally excited molecules in the reaction between an atom and a molecule in the light of our more recent results, which will now be briefly reported.

In the flash photolysis of ozone in the presence of ammonia, hydrogen, hydrogen chloride, methane, and water under isothermal conditions, we have observed in each case vibrationally excited hydroxyl radicals. So far, only the first and second excited levels have been detected, but further work is in progress. We suggest that the reaction in which they are produced is of the type

$$O(^1D) + RH \rightarrow OH^* + R.$$

These reactions are of particular interest for two reasons. Firstly, methane and ammonia provide the first examples of this type of reaction involving molecules more complex than triatomic and, secondly, because it is the first time that the electronic energy of the approaching atom has been shown to appear as vibrational energy of the product in otherwise thermoneutral or endothermic reactions. It should be noted that, though in the photolysis of ozone the reaction

$$O(^1D) + O_3 \rightarrow O_2^* + O_2$$

has been shown to be responsible for the production of O_2^*, the degree of vibrational excitation so far observed can be accounted for without involving the electronic energy. The observation of OH* in the systems described confirms the place ascribed to the $O(^1D)$ atom in the photolysis of ozone by McGrath and Norrish (7).

Can. J. Chem. Downloaded from www.nrcresearchpress.com by 210.87.254.42 on 09/05/12
For personal use only.

Can. J. Chem. Downloaded from www.nrcresearchpress.com by 210.87.254.42 on 09/05/12
For personal use only.

The question of the extent to which the heat of reaction in the general case

$$A + BCD \rightarrow AB + CD$$

can appear as vibrational energy in the products has interested us for some time. We considered it likely that the species AB could be formed with any allowed vibrational energy up to the maximum. Where the highest permitted vibrational level has not so far been observed, we suspected that this might be a consequence of experimental difficulties. Accordingly, we have started reinvestigating some of the systems previously studied by flash photolysis. In the photolysis of NO_2 and ClO_2 (4) it seemed rather a coincidence that the highest vibrational level of O_2* observed was 8 in each case though the exothermicities for the reactions

$$O + NO_2 \rightarrow O_2^* + NO$$

and

$$O + ClO_2 \rightarrow O_2^* + ClO$$

differed by 15 kcal.

In preliminary experiments with NO_2, we have now observed the 9th, 10th, and 11th (and 12th?) vibrational levels, the energy of the 11th level being equal to the exothermicity of the reaction. We have also observed very faintly the first and possibly the second vibrationally excited levels of NO, though this has yet to be confirmed.

In further studies on the flash photolysis of ozone, we have been able to observe the 18th and, very faintly, the 19th (and 20th?) vibrational level of O_2*. Further work on this system is expected to provide evidence in connection with the reaction,

$$O_2^{*}{}_{(v=7)} + O_3 \rightarrow O(^1D) + 2O_2,$$

which McGrath and Norrish (7) have proposed, to explain the high quantum yield in the photolysis of ozone with ultraviolet radiation. We have also extended observation to shorter wavelengths and have observed the 11th and 10th (9th?) vibrationally excited levels of O_2.

In reactions of the type

$$A + BCD \rightarrow AB + CD \quad + Q \qquad [1]$$

the evidence for the accumulation of most of the energy Q in the bond is thus quite convincing. We believe that the evidence now permits the generalization that, in all exothermic abstraction reactions, the heat of reaction will appear largely as vibrational energy of the products. However, the need for more experimental evidence is apparent and perhaps best illustrated by the fact that no reaction conforming strictly to equation [1] is yet known, B and D being either both hydrogen or oxygen atoms.

There is equally a need for theoretical treatments of the problem and here Polanyi (2) and Smith (3) have made significant contributions. Polanyi's valence bond resonance description of the activated complex ABC in the reaction

$$A + BC \rightarrow AB + C$$

leads to the prediction that almost the entire heat of reaction will appear as vibrational energy of the bond AB. The transition complex is presumed to be most stable when the two resonance forms

$$AB—C$$

and

$$A—BC$$

have equal energy. Since in an exothermic reaction the bond AB is stronger than BC, the internuclear separation AB in the complex will be larger than in the isolated molecule, while the internuclear distance in B—C will be that of the isolated molecule. Since the energy of the complex is generally accepted to be only 5 ± 5kcal greater than of the two resonance forms and assuming that the probability of the transfer of an appreciable amount of energy to C is very small, even when there is a chemical affinity between them, the molecule AB will be formed with very nearly the entire heat of reaction in vibration.

As well as the detection of molecules AB possessing nearly all the heat of reaction as vibrational energy, the most important experimental test of this model is to demonstrate that initially all the molecules are formed in the highest observed vibrational state. So far, in all cases, a distribution of energies has been observed and though, in the case of the reaction studied by Polanyi (14),

$$H + Cl_2 \rightarrow HCl^* + Cl$$

the energy distribution is reported (2) as corresponding qualitatively with a system relaxing from a high vibrational level, there is no certainty that all the HCl is initially formed with $v = 6$. Further, evidence has been furnished by Garvin, Broida, and Kostkowski (12) that in the reaction

$$H + O_3 \rightarrow OH^* + O_2$$

there is an appreciable production in all levels $v \leqslant 9$.

Restricted to the case A+BC, this model is a very plausible one and the experimental evidence strongly supports the idea that it is possible for at least some molecules to possess the entire heat of reaction.

It is not immediately apparent to what extent the model applies to the more general case

$$A + BCD \rightarrow AB + CD.$$

The probability of energy transfer between AB and CD in the transition complex may well be higher in this case, and this could result in the production of some molecules AB with appreciably less than the maximum possible vibrational excitation.

In a molecule of type BCB, the strength of the CB bond is not necessarily the same as in the isolated molecule CB. Where they differ appreciably, as, for example, in ozone and nitrogen peroxide, a considerable reorganization of the CB bonds must take place when an atom is abstracted. We consider it reasonable to suppose that the ease with which this reorganization takes place could depend on the nature of the molecule BCB and of the atom A and, perhaps more important, on the relative spacial configuration of the atoms at the moment of impact. The effect of this reorganization would be to reduce on the average the amount of energy available for vibrational excitation of the AB molecule, though, in any particular collision, there would always be a definite probability of producing the molecule AB vibrationally excited to the fullest extent. Thus, on this model the observed population of all possible vibrational levels is a consequence of the nature of the reaction itself rather than of deactivation of molecules initially produced entirely in the highest vibrational level. A quantitative estimate of the relative initial population of the various vibrational levels will have to take into account the variation in reaction probability with the direction of approach of the atom relative to the configuration of the molecule BCD and it seems likely that the reaction is most probable when there is the most favorable configuration for maximum vibrational excitation of AB.

Can. J. Chem. Downloaded from www.nrcresearchpress.com by 210.87.254.42 on 09/05/12
For personal use only.

Can. J. Chem. Downloaded from www.nrcresearchpress.com by 210.87.254.42 on 09/05/12
For personal use only.

For a non-linear molecule BCD, it is reasonable to expect a fraction (not necessarily constant) of the heat of reaction to appear as rotational energy as well as translational energy of AB and CD and this should also be true for an oblique collision of an atom with a linear triatomic molecule. It also seems possible on this model for the molecule CD to be vibrationally excited to some extent.

Smith (3) postulates a definite maximum value for the fraction of the heat of reaction which can appear as vibration. This is limited by a kinematic factor $\sin^2\beta$, where β is the angle of rotation required to take a co-ordinate system describing the reactants into one suitable for describing the products. The kinematic factor depends only on the masses M_A, M_B, M_C, and M_D of the atoms involved and can be calculated for the reaction

$$A + BC \rightarrow AB + C \left[\tan^2\beta = \frac{M_B}{M_A} + \frac{M_B}{M_C} + \frac{M_B^2}{M_A M_C} \right]$$

and

$$A + BCD \rightarrow AB + CD \left[\tan^2\beta' = \frac{M_B}{M_A} + \frac{M_B}{M_C + M_D} + \frac{M_B^2}{M_A(M_A + M_C)} \right].$$

The theoretical maximum value of the fraction of energy appearing as vibration in the second case then lies in the range $\sin^2\beta' - \sin^2\beta$, the latter value applying if the influence of D is neglected.

The model is a remarkably simple one and predicts accurately in several cases where good experimental data is available, e.g., 0.96–0.97 for

$$H + O_3 \rightarrow OH^* + O_2$$

and 0.986 for

$$H + Cl_2 \rightarrow HCl^* + Cl$$

compared with experimental values of 0.94 and 1.0.

He points out that it fails in the case of

$$I + Na_2 \rightarrow NaI^* + Na$$

where the predicted value of 0.576 gives the NaI* molecule insufficient energy for the reactions

$$NaI^* + Na \rightarrow NaI + Na^*$$
$$Na^* \rightarrow Na + h\nu$$

and suggests that there is either some peculiarity in the potential energy surface or the mechanism is in fact

$$Na + I_2 \rightarrow NaI^* + I$$

where $\sin^2\beta = 0.9$, but this is in disaccord with Evans' and Polanyi's original conclusion (20).

We consider that it again appears inadequate in the reaction

$$O + NO_2 \rightarrow O_2^* + NO$$

where it predicts a maximum value of the vibrational energy of 31–35.2 kcal, agreeing very well with the value of 34 kcal ($v = 8$) previously reported (4). Now that we have observed the 9th, 10th, and 11th vibrational levels, it seems that the agreement was fortuitous in this case. The agreement of theory with experiment in the case of ozone

is again not conclusive, since the evidence is strong in favor of the O atom being in the (^1D) state (7), whereas the exothermicity was calculated for the reaction of the O(^3P) atom. Further, since molecules with more than 17 quanta may react rapidly with O_3 (7) in the reaction

$$O_2^* + O_3 \rightarrow O(^1D) + 2O_2$$

the failure in previous work to detect them spectroscopically was evidence for their taking part in this reaction rather than for their not being produced. As we have shown, the threshold is not sharp and molecules with 18 and more quanta have now been observed.

Finally, the values of $\sin^2 \beta$ for the reactions of the type

$$O(^1D) + RH \rightarrow OH^* + R$$

described earlier are insufficient, except in the case of H_2, for the observed production of the vibrationally excited hydroxyl radical.

A third model accounting for the production of vibrationally excited molecules in the reaction

$$A + BCD \rightarrow AB^* + CD$$

has recently been proposed by Simons (21). He visualizes the atom A approaching B with such a velocity that, when A is finally brought to rest relative to B, the internuclear distance of A—B is very short compared with the equilibrium distance, so that on separation the molecule AB is vibrationally hot. The conditions necessary to achieve this are that the B—C bond is weak relative to AB so that dissociation of the complex (ABCD) occurs easily and little of the impact of A on B is transmitted to the C—D bond. There must be also an attractive force between A and B to overcome the normal repulsion of non-interacting particles. This model accounts for the ready production of O_2^* in the reactions

$$O(^3P) + NO_2 \rightarrow O_2^* + NO$$
$$O(^3P) + ClO_2 \rightarrow O_2^* + ClO$$

on the basis of electrons pin coupling between the paramagnetic species O(^3P) and NO_2 or ClO_2 resulting in attraction. In the case of ozone, the diamagnetic ozone molecule is considered as a weakly bound complex of $O_2(^3\Sigma)$ and O(^3P). Since the O_2—O bond is weak, the large internuclear distance favors the electron spin coupling. On this model the reaction

$$I + Na_2 \rightarrow NaI^* + Na$$

is particularly favored both on account of the low bond energy of the Na_2 molecule and the strong coulombic attraction between Na and I. Only qualitative tests of this model are possible and the author cites the reactions

$$O + SO_2 \rightarrow SO + O_2$$

and

$$O + Cl_2O \rightarrow O_2 + Cl_2$$

as being cases where the necessary conditions do not obtain, and therefore where vibrationally excited molecules should not be produced. He considers the failure of Oldershaw and Norrish (22) and of Edgecombe, Norrish, and Thrush (23) to observe O_2^* in these systems as evidence for the model. In our opinion, a more detailed consideration of the

Can. J. Chem. Downloaded from www.nrcresearchpress.com by 210.87.254.42 on 09/05/12
For personal use only.

Can. J. Chem. Downloaded from www.nrcresearchpress.com by 210.87.254.42 on 09/05/12
For personal use only.

experimental conditions under which both these reactions could have occurred shows that in neither case could an appreciable concentration of O_2^* have been produced for reasons quite unconnected with the proposed model. Firstly, in the photolysis of SO_2 itself, the oxygen atom produced is necessarily $O(^3P)$ and O_2^* could obviously not be produced in the reaction

$$O(^3P) + SO_2 \rightarrow SO + O_2 \qquad -12 \text{ kcal.}$$

In the photolysis of SO_3, the sequence

$$SO_3 \rightarrow SO_2 + O(^1D)$$
$$O(^1D) + SO_2 \rightarrow O_2 + SO \qquad +33 \text{ kcal}$$

would, we believe, result in the production of O_2^* ($v \ll 7$) if it occurred. Considering the low absorption coefficient of SO_3 and the possible alternative primary photolysis step

$$SO_3 + h\nu \rightarrow SO + O_2$$

only low concentrations of SO_2 and $O(^1D)$ would be present. It is therefore unlikely that a detectable concentration of O_2^* would be produced in this system even if the reaction itself were efficient. In any case, the oxygen atoms would probably react preferentially with the much larger amount of SO_3 present than with SO_2. One should also take into account that observation below about 2270 Å was particularly difficult in view of the continuous absorption and, at longer wavelengths, transitions from $v'' < 4$ are weak. It would therefore have been difficult to detect a low concentration of O_2^*.

A somewhat stronger case might have been made for failure of the reaction

$$O + SO_3 \rightarrow O_2^* + SO_2$$

to produce a detectable concentration of O_2^*, but even here some of the above arguments still apply and provide a satisfactory explanation which does not involve the inherent unlikelihood of the reaction itself.

In the other example quoted by Simons, the photolysis of Cl_2O, it should be noted that the reaction

$$O + Cl{-}O{-}Cl \rightarrow O_2 + Cl_2 \qquad +76 \text{ kcal}$$

is not of the type A + BCD. Requiring the breaking of two bonds, it is easy to visualize that the entire exothermicity of the reaction is not, in any case, available for vibrational excitation of the oxygen molecule.

There are other good reasons accounting for the failure to observe excited species in this system. The primary reaction might well be

$$Cl_2O \xrightarrow{h\nu} Cl + ClO$$

as well as

$$Cl_2O \rightarrow 2Cl + O$$

and the oxygen atom concentration may be low and would be further reduced by the reaction

$$O + Cl_2O \rightarrow 2ClO,$$

the concentration of ClO* being below detectable limits.

In our opinion, therefore, the negative evidence from the two systems considered does not test the model proposed by Simons. Objections to it are firstly that the argument he applies to the reaction

$$O + O_3 \rightarrow O_2^* + O_2$$

does not seem plausible when the atom involved is the $O(^1D)$ and, secondly, that it appears impossible to reconcile it with the occurrence of the reactions

$$O(^1D) + RH \rightarrow OH^* + R$$

It is profitable to consider further to what extent the available experimental evidence provides tests for theoretical models. The information required is:

1. Conclusive evidence of the reaction in which the vibrationally excited species is produced.
2. Certainty that all the vibrational levels produced have been observed or, failing that, a convincing explanation of the absence of certain levels.
3. The relative populations of the various vibrational levels and this as a function of experimental conditions; in particular, the distribution of vibrational energies in the molecules at the instant of formation and the subsequent variation with time.
4. The presence or absence of vibrational energy in the other species produced in the case of an atom and a polyatomic molecule.
5. Whether the electronic and kinetic energy of the abstracting atom can contribute to the vibrational energy of the bond formed.

The evidence for the proposed mechanism of formation of the excited species in the reactions considered is on the whole quite strong but, in some cases, far from conclusive. Even where the mechanism is well established, it is worth while to re-examine the arguments in favor of the proposed mechanism and to consider alternatives.

The production of O_2^* in the flash photolysis of NO_2 and of ClO_2 provides particularly well-established examples of the reaction

$$O + OXO \rightarrow O_2^* + XO.$$

An alternative mechanism, considered at the time, was that the O_2 molecule was initially formed in the $^1\Delta_g$ or $^1\Sigma_g^+$ electronic states and that the higher vibrational levels of the $^3\Sigma_g^-$ ground state were populated by collision-induced radiationless transitions, or by magnetic dipole radiation. This was rejected on the ground that such transitions, involving the breaking of two selection rules, would be unlikely to occur sufficiently rapidly to account for the results. Whether these rules are relaxed sufficiently in the presence of low pressures of ClO_2 and ClO or of NO_2 and NO is again doubtful, except, possibly, while the configuration approximates closely to the transition complex (O—O—X—O). In the extreme this reduces to the accepted mechanism and could only be distinguished from it if the calculated distribution of vibrational energies differed in the two cases.

In the case of ozone, the evidence (7) strongly supports the proposed mechanism

$$O(^1D) + O_3 \rightarrow O_2^* + O_2 \qquad +138 \text{ kcal.}$$

The possibility of the reaction,

$$O(^1D) + O_3 \rightarrow O_2(^3\Sigma_g^-) + O_2(^3\Sigma_u^-) \qquad -3 \text{ kcal,}$$

postulated by Benson (24) in connection with a photon-propagated chain decomposition of ozone, is, however, worth considering.

Population of high values of v'' by the process

$$O_2(^3\Sigma_u^-)(v' = 0) \rightarrow O_2(^3\Sigma_g^-)$$

is expected on the Franck–Condon principle and the observed apparent maximum in the

Can. J. Chem. Downloaded from www.nrcresearchpress.com by 210.87.254.42 on 09/05/12
For personal use only.

vibrational energy distribution at $v'' = 13$ or 14 may be consistent with this mechanism. The endothermicity of the reaction is not a strong contrary argument in view of a probable low or zero value for the activation energy.

In most cases, vibrational levels corresponding in energy to the full exothermicity of the reaction have not been observed. It seems that the reason for this is more likely to be found in the limitations of present experimental techniques rather than in any fundamental restriction on the proportion of energy which can appear as vibration.

We hope to test this both by further work on systems previously studied by flash photolysis and by investigating new systems. As we have seen, preliminary results in the NO_2 system show that all energetically possible vibrational levels are produced and that the ClO_2 system should be capable of providing a definite test. The ozone system is much more difficult and the evidence available strongly suggests that direct observation of vibrational levels appreciably higher than those already reported is unlikely. On account of the diffuseness of the threshold, it should be possible to follow the decay of molecules with vibrational energy $\geqslant 70$ kcal which seem to participate in the reaction,

$$O_2^*(v'' > 17) + O_3 \rightarrow 2O_2 + O(^1D),$$

and so provide a direct test of this reaction. So far, only the 18th level has been observed with sufficient intensity for quantitative measurements; but it may be possible to achieve this with the 19th and 20th levels. It is again doubtful whether possible failure to observe vibrational levels higher than the second in the reaction

$$O(^1D) + RH \rightarrow OH^* + R$$

will be theoretically significant because of rapid physical deactivation and chemical reaction. The concentration of molecules in these levels is likely to be small and the low transition probabilities for absorption from those levels makes the systems experimentally difficult.

There is little definite information on the initial distribution of vibrational energy and on its variation with time. In spite of the theoretical advantage of better time resolution in flash photolysis, the only indication that the distribution changes with time is to be found in the observation of Lipscomb, Norrish, and Thrush (4) that the half-lives for the levels with $v'' > 6$, which are slightly shorter than those with $v'' = 6$, which are likewise shorter than those with $v'' < 6$. The same authors concluded from the slow rate of vibrational energy transfer that the energy distribution observed at the shortest time was that actually produced in the reaction. The closely similar distribution for the ClO_2 and the NO_2 systems at the shortest times is equally significant. No marked changes of intensity distribution with time in the case of O_2^* formed from ozone have been reported, though it is evident that in all cases much more detailed information is needed. The experimental difficulties are, however, considerable. It may well be possible to extrapolate the results obtained in flow systems to infinite flow rate and zero pressures and an attempt to do this had been planned (14). Provided that this can be unambiguously correlated with zero time, important information may be expected.

In flash photolysis, completely reliable information could only be expected when the half-life of the excited species is very long compared with the flash times and, except in the case of O_2^* produced in the ClO_2 system, it is not clear that this condition has not so far been met. As well as the errors involved in long extrapolations and the averaging effect if the flashes are comparatively long, the possibility that the initial distribution may be changed by absorption of radiation may have to be considered. The present evidence,

Can. J. Chem. Downloaded from www.nrcresearchpress.com by 210.87.254.42 on 09/05/12
For personal use only.

from flash photolysis, incomplete as it is, supports the hypothesis of an initial distribution rather than population of all levels from the highest observed level.

On any model which predicts that, in some collisions, only part of the energy can appear as vibration in AB, the question of whether any part of the excess can appear as vibration in the bond C—D can be considered. The suggestion cannot be directly tested in the case of ozone itself and the presence of ClO* and NO* has not been reported in the ClO_2 and NO_2 systems, nor of O_2*, in the reactions of chlorine and bromine atoms with ozone. In the last-mentioned case, this could be a consequence of the experimental conditions and might also be explained in the case of ClO_2 by the approximate equality of the ClO bond strengths in ClO and ClO_2. In the case of NO_2, the probable rapid deactivation of NO* by NO_2 and the experimental difficulty of observing a weak NO* spectrum in the presence of a strong O_2* spectrum makes the negative evidence of its not having been reported previously inconclusive on this point. The observation of the first and possibly also the second excited vibrational levels of NO in our reinvestigation of this system is also inconclusive, as it has not been possible yet to show definitely how they are produced. The other case where there is evidence of vibrational energy in the bond CD is equally uncertain. Oldershaw and Norrish (22) in the flash photolysis of SO_3 observed bands arising from the levels $v'' = 0$, 1, 2, and 3 of SO, though the system was at near room temperature, and they suggested that this might arise from the reaction

$$O(^1D) + SO_2 \rightarrow SO^* + O_2 \qquad +33 \text{ kcal}$$

As we have pointed out, this reaction is an unlikely source of a detectable concentration of O_2*, but it is conceivable that, under their experimental conditions, a probably smaller concentration of SO* could be observed. It is also possible that SO* may be produced in the initial photochemical split

$$SO_3 \xrightarrow{h\nu} SO + O_2.$$

The participation of the electronic energy of the approaching atom in the vibrational energy of the bond formed is an interesting possibility. It can easily be imagined in the case of ozone if the oxygen molecule formed in the excited $^3\Sigma_u^-$ electronic state, but, unfortunately, it cannot be directly proved in this case unless the vibrational energy of the oxygen can be shown to exceed 93 kcal. In the absence of a convenient electronic state, the evidence is limited to the reactions

$$O(^1D) + RH \rightarrow OH^* + R$$

where the energy of vibration must come from the $O(^1D)$ atom if this mechanism is accepted. There seems to be, at present, no evidence for the participation of the kinetic energy of the approaching atom in vibrational excitation, except possibly the observation of the 12th vibrational level of oxygen in the flash photolysis of nitrogen peroxide (5). Recent work (19) has established the first N—O bond strength in NO_2 to be not greater than 71.2 kcal/mole and this makes the exothermicity of the reaction

$$O + NO_2 \rightarrow NO + O_2$$

a maximum of 48 kcal, which is insufficient in itself to excite the 12th vibrational level in oxygen (49 kcal/mole).

The production of vibrationally excited species under isothermal conditions both by flash photolysis and the atomic flame technique provides a potentially powerful method for studying vibrational energy transfer and the chemical reactions of these species.

Can. J. Chem. Downloaded from www.nrcresearchpress.com by 210.87.254.42 on 09/05/12
For personal use only.

There is reason to believe that endothermic reaction is facilitated if one of the molecules possesses vibrational energy, e.g., in the reactions

$$H + O_2 \rightarrow OH + O \qquad [25]$$

$$O_2 + O_2 \rightarrow O + O_3 \qquad [26]$$

$$O_2 + O_3 \rightarrow 2O_2 + O(^1D) \qquad -69 \text{ kcal} \qquad [27]$$

though there is no evidence from the flash photolysis of ozone for the reaction

$$O_2 + O_3 \rightarrow 2O_2 + O(^3P) \qquad -24 \text{ kcal}$$

and the effect of this reaction, if it occurs, on the observed population of the various vibrational levels of O_2* has not been considered in the preceding discussion.

The reaction

$$OH(v'' \geqslant 2) + H_2 \rightarrow H_2O + H \qquad +16 \text{ kcal}$$

has been proposed by Garvin, Broida, and Kostowsky (12) in the H atom / ozone flame to account for the large increase in line intensities of the upper levels as the mole fraction of hydrogen increases. According to their views, the lower levels, being present in higher concentrations, are preferentially removed, and the upper levels are repopulated by further reaction of the hydrogen atoms with ozone. However, it is not clear if this explanation is satisfactory if, as was reported, the hydrogen atoms were initially present in excess. It is hoped that more evidence will be obtained from a further study of the O_3/RH systems by flash photolysis.

Finally, the field covered by this review is an exciting one and much remains to be done. We are confident that the work now being planned in various laboratories will lead in the near future to a greatly increased understanding of the important fundamental principles involved.

ACKNOWLEDGMENT

One of us (N. B.) wishes to thank Imperial Chemical Industries for the award of a Fellowship.

REFERENCES

1. W. D. McGrath and R. G. W. Norrish. Z. physik. Chem. **15**, 245 (1958).
2. J. C. Polanyi. J. Chem. Phys. **31**, 1338 (1959).
3. F. T. Smith. J. Chem. Phys. **31**, 1352 (1959).
4. F. J. Lipscomb, R. G. W. Norrish, and B. A. Thrush. Proc. Roy. Soc. A, **233**, 455 (1956).
5. N. Basco and R. G. W. Norrish. To be published.
6. W. C. McGrath and R. G. W. Norrish. Proc. Roy. Soc. A, **242**, 265 (1957).
7. W. D. McGrath and R. G. W. Norrish. Proc. Roy. Soc. A, **254**, 317 (1960).
8. J. D. McKinley, D. Garvin, and M. J. Boudart. J. Chem. Phys. **23**, 784 (1955).
9. T. M. Cawthorn and J. D. McKinley. J. Chem. Phys. **25**, 583 (1956).
10. F. Kraus. Z. Naturforsch. **12***a*, 479 (1957).
11. D. Garvin. J. Am. Chem. Soc. **81**, 3173 (1959).
12. D. Garvin, H. P. Broida, and H. J. Kostkowski. J. Chem. Phys. **32**, 880 (1960).
13. J. K. Cashion and J. C. Polanyi. J. Chem. Phys. **29**, 455 (1958).
14. J. K. Cashion and J. C. Polanyi. J. Chem. Phys. **30**, 1097 (1959).
15. J. K. Cashion and J. C. Polanyi. J. Chem. Phys. **30**, 316 (1959).
16. F. Kaufman and J. R. Kelso. J. Chem. Phys. **28**, 510 (1958).
17. K. Dressler. J. Chem. Phys. **30**, 1621 (1959).
18. B. A. Thrush. 7th International Symposium on Combustion. 1959. p. 243.
19. H. P. Broida, H. I. Schiff, and T. M. Sugden. To be published.
20. M. G. Evans and M. Polanyi. Trans. Faraday Soc. **35**, 178 (1939).
21. J. P. Simons. Nature, **186**, 551 (1960).
22. G. A. Oldershaw and R. G. W. Norrish. Proc. Roy. Soc. A, **249**, 498 (1958).
23. F. H. C. Edgecombe, R. G. W. Norrish, and B. A. Thrush. Proc. Roy. Soc. A, **243**, 24 (1957).
24. S. W. Benson. J. Chem. Phys. **26**, 1351 (1957).
25. F. L. Schott and J. L. Kinsey. J. Chem. Phys. **29**, 1177 (1958).
26. W. Jost. 7th International Symposium on Combustion. 1959. p. 190.

Can. J. Chem. Downloaded from www.nrcresearchpress.com by 210.87.254.42 on 09/05/12
For personal use only.

Can. J. Chem. Downloaded from www.nrcresearchpress.com by 210.87.254.105 on 09/05/12
For personal use only.

SEVEN MECHANISMS IN THE PHOTOLYSIS OF NO_2 BETWEEN 3100 AND 3700 Å[1]

HADLEY FORD

ABSTRACT

Nitrogen dioxide has been photolyzed by various investigators under seven different limiting conditions, all at wavelengths between 3100 and 3700 Å. The results are reviewed and discussed in terms of two general mechanisms, both of which quantitatively relate the experimental data. The mechanisms differ in that one postulates that atomic oxygen attacks NO_2 in two ways, yielding NO and O_2 in one case and excited NO_3 in the other. The excited NO_3 can decompose to form atomic oxygen and NO_2; it can be deactivated, or it can react with NO_2. The second mechanism postulates a single mode of attack on NO_2 by atomic oxygen, again yielding excited NO_3. The NO_3 can decompose to form NO and O_2; it can be deactivated, or it can react with NO_2. Of the two mechanisms the first seems more consistent with the thermal reactions of NO_2 and NO_3. It is believed that both the linear and the triangular NO_3 play important roles in the photolysis.

INTRODUCTION

The photolysis of nitrogen dioxide has been investigated (1–7) at various wavelengths of light and with varying pressures of NO_2 and inert gases. Quantum yield measurements are reasonably complete and consistent. It now appears that below 3700 Å atomic oxygen is an important product of the primary photochemical process. This report discusses the photolysis in terms of the following reactions:[2,3]

$$h\nu + NO_2 \rightarrow NO + O \quad [1]$$

$$O + O_2 + M \rightarrow O_3 + M \quad [2]$$

$$O + NO_2 + M \rightarrow NO_3 + M \quad [3]$$

$$O + NO_2 \rightarrow NO_3^* \quad [3a]$$

$$NO_3^* + M \rightarrow NO_3 + M \quad [3b]$$

$$O + NO_2 \rightarrow O_2 + NO \quad [4]$$

$$NO_3^* \rightarrow O_2 + NO \quad [4a]$$

$$NO_3^* \rightarrow NO_2 + O \quad [4b]$$

$$O + NO + M \rightarrow NO_2 + M \quad [5]$$

$$NO_3 + NO \rightarrow 2NO_2 \quad [6]$$

$$O_3 + NO \rightarrow NO_2 + O_2 \quad [7]$$

$$NO_3 + NO_2 \rightarrow N_2O_5 \quad [8]$$

$$N_2O_5 \rightarrow NO_3 + NO_2 \quad [9]$$

$$O + NO_2 + NO_2 \rightarrow O_2 + NO + NO_2 \quad [11]$$

$$NO_3^* + NO_2 \rightarrow O_2 + NO + NO_2 \quad [11a]$$

$$O_3 + NO_2 \rightarrow NO_3 + O_2 \quad [12]$$

Some of these reactions have been studied by Ford and Endow (6), who obtained the relative rates of reactions [2], [3], [4], and [5]. Using Benson and Axworthy's (9) rate

[1]*Contribution from the Jet Propulsion Laboratory, California Institute of Technology. This paper presents the results of one phase of research carried out at the Jet Propulsion Laboratory, California Institute of Technology, under joint sponsorship of the Department of the Army, Ordnance Corps (under Contract No. DA-04-495-Ord 18), and the Department of the Air Force; presented at the Symposium on Fundamental Aspects of Atomic Reactions held at McGill University, Montreal, Que., September 1960.*

[2]*The numbering of reactions is consistent with ref. 6.*

[3]*It is entirely possible that some of the reactions can be replaced by alternatives which will also explain the results.*

constant for reaction [2], a quantitative mechanism was proposed. Since then, the rate constants have been measured and reported by others (9–12), and agreement is quantitative within the limits of precision for each rate constant.

Later (7), it was shown that the relative concentration of atomic oxygen calculated from k_1, k_2, k_3, k_4, and k_5 was actually observed over a wide range of concentrations of NO_2, NO, and O_2. This meant that k_3+k_4 was correct, relative to k_2 and k_5. Other work has isolated k_4 from k_3, and the value of k_4 has been independently determined and found to agree with the value previously reported.

As has been emphasized by Leighton and Perkins (13), however, it is possible that none of the assumed reaction mechanisms is precisely correct. It is the purpose of this report to discuss the interrelationships of the various reactions and to show how they relate experimental results in the photolysis of NO_2 below 3700 Å.

Seven mechanisms are discussed which have many steps in common; and, in general, as experimental variables are gradually changed, the shift from one mechanism to another is also gradual. Each mechanism is a special case of a generally satisfactory mechanism. It is assumed in the discussion that in the wavelength region of from 3100 to 3700 Å the mechanisms are not wavelength dependent. Even so, small changes in the primary quantum yield with wavelength would produce small changes in the rate constants.

Because of the great complexity of the many interrelated mechanisms and reactions, the mechanisms are discussed in the order of increasing complexity, rather than decreasing generality. It is believed that this should make for easier reading.

THE PRIMARY PROCESS

The appearance of fluorescence at wavelengths above 3700 Å, but not at shorter wavelengths, led Norrish (14) to the hypothesis that dissociation occurred only on the short-wavelength side of 3700 Å.

$$h\nu + NO_2 \rightarrow NO + O \qquad [1]$$

To test this hypothesis Norrish photolyzed NO_2 in the presence of hydrogen, and since water was not produced, he concluded that reaction [1*a*] was the primary process at all wavelengths.

$$h\nu + NO_2 \rightarrow NO_2^* \qquad [1a]$$

Norrish then assumed oxygen was produced by

$$NO^* + NO_2 \rightarrow NO + NO + O_2. \qquad [14]$$

This is analogous to a similar reaction in the thermal decomposition of NO_2:

$$NO_2 + NO_2 \rightarrow NO + O_2 + NO. \qquad [14a]$$

Light in reactions [1*a*] and [14] provides the energy for activation which is provided by thermal collisions in reaction [14*a*]. A rate constant for reaction [14] can be estimated by assuming it is the same as, or greater than, the pre-exponential factor of reaction [14*a*]. Thus from the data of Rosser and Wise (15)

$$k_{14} \geqslant 3 \times 10^9 \text{ liter mole}^{-1} \text{ sec}^{-1}.$$

The absence of water as noted by Norrish is explained by the extremely small collision yield for the reaction of atomic oxygen with hydrogen when compared with the collision

Can. J. Chem. Downloaded from www.nrcresearchpress.com by 210.87.254.105 on 09/05/12
For personal use only.

yield with NO_2. No water would be expected even if reaction [1] proceeded with a quantum yield of unity.

Hall (4), on the other hand, found that when mixtures of isotopically enriched oxygen and normal NO_2 were irradiated at 3130 Å, isotopic scrambling occurred to about the extent expected from the data of Ogg (16). Essentially no scrambling was present at 4047 Å. Hall concluded that reaction [1] was the primary process at 3130 Å and that reaction [1*a*] was the process at 4047 Å.

Later, Ford and Endow photolyzed NO_2 at 3660 Å, using trace amounts of NO_2 in nitrogen at 1 atm pressure, and found a quantum yield of 0.69 for NO_2 disappearance. Under these conditions

$$NO_2^* + M \rightarrow NO_2 + M \qquad [15]$$

should remove reaction [14] as a possibility. The authors assumed that reaction [1] had a quantum yield of one, and that reaction [3] followed by reaction [6] led to a decreased efficiency, which, by reaction [4], would otherwise have led to $\Phi = 2$ for nitrogen dioxide disappearance.[4] The agreement between the rate constant the authors reported for reaction [3] and that reported by Kaufman (10) for

$$O + SO_2 + M \rightarrow SO_3 + M \qquad [16]$$

$$k_3 = 1.0\times10^{11} \text{ liter}^2 \text{ mole}^{-2} \text{ sec}^{-1}$$

$$k_{16} = 3.0\times10^{10} \text{ liter}^2 \text{ mole}^{-2} \text{ sec}^{-1}$$

gives credence to the belief that the inefficiency is caused by reaction [3] and not by a decrease in the rate of reaction [1] with increasing pressure.

DISCUSSION OF MECHANISMS

Mechanism I

This is the limiting mechanism for the condition $(NO)/(NO_2) \rightarrow \infty$ in the presence of a third body. The mechanism is given by reactions [1] and [5],[5] which predict a quantum yield of zero. Experimentally, the conditions of mechanism I have been approached by Ford and Endow (6), who found the following relationship when trace amounts of NO_2 were photolyzed in nitrogen at 1 atm pressure:

$$\text{(A)} \qquad \frac{1}{\Phi_{NO_2}} = 1.45+0.178\frac{NO}{NO_2}.$$

Thus for high values of $(NO)/(NO_2)$, $\Phi_{NO_2} \rightarrow 0$. Since the rate of reaction [5] is now well known (7–12), mechanism I becomes an important source of atomic oxygen at known, low concentrations.

In the limiting case of $(NO)/(NO_2) \rightarrow \infty$ the concentration of atomic oxygen is given by

$$\text{(B)} \qquad (O) = \frac{KI\Phi(NO_2)}{k_5(NO)(M)}.$$

The absorption coefficient has been measured by Hall and Blacet (17); the light intensity can be measured by any one of several methods, and k_5 has been reported by several investigators.

[4]Φ *is the over-all quantum yield of* NO_2 *disappearance;* Φ_{O_2} *is the over-all quantum yield of oxygen production.*
[5]*Although this is the simplest mechanism discussed, at least one alternative is possible. A discussion of the alternative mechanism is given in ref. 11.*

Can. J. Chem. Downloaded from www.nrcresearchpress.com by 210.87.254.105 on 09/05/12
For personal use only.

Author	Reference	k_5
Kaufman	10	2.0×10^{10}
Ford and Endow[6]	7	1.8×10^{10}
Ogryzlo and Schiff	11	1.8×10^{10}
Harteck, Reeves, and Manella	12	2.7×10^{10}

A value of k_5 of 6×10^9 was measured at 900 to 1000° K by Kaufman, Gerri, and Bowman (8), indicating a small, negative temperature coefficient. A value of 4.6×10^{13} calculated from the results of Kistiakowski and Volpi (18) is apparently in error, probably because the equations of a stirred flow reactor were not applicable as had been assumed. Since the values of k_5 of ref. 7, 9, and 10 cover a pressure interval of a few millimeters to 1 atm, the third-body dependence of reaction [5] is well established. Since the rate of reaction [17] is also known (7), reactions [1], [5], and [17] can be used to measure third-body efficiencies in reaction [5].

$$O + \textit{cis}\text{-2-pentene} \rightarrow \text{products} \qquad [17]$$

Mechanism II

This mechanism represents the low-pressure limit in the photolysis of NO_2. Following photolysis, NO and NO_2 would compete for atomic oxygen in bimolecular reactions. If Kaufman (19) is correct and reaction [5*a*] occurs only once in 10^7 collisions, restrictions on (NO/NO_2) should not be severe.

$$O + NO \rightarrow NO_2 + h\nu \qquad [5a]$$

The mechanism is given by reaction [1] followed by reaction [4], or alternatively, reaction [1] followed by reactions [3*a*] and [4*a*]. Kistiakowski and Volpi (18) reported a lower limit for the rate of reaction [4], which can be compared with that from ref. 7:

$$\text{Kistiakowski and Volpi: } k_4 > 9.5\times10^8 \text{ liter mole}^{-1} \text{ sec}^{-1},$$

$$\text{Ford and Endow: } \qquad k_4 = 2.1\times10^9 \text{ liter mole}^{-1} \text{ sec}^{-1}.$$

Because of the obviously large error in the value of reaction [5] calculated from the work of Kistiakowski and Volpi, the agreement may well be fortuitous. In the absence of presently unknown radiative processes, the conditions of mechanism II should lead to a quantum yield of two.

Mechanism III

Experimental conditions: trace concentrations of nitrogen dioxide, swamping concentrations of oxygen

$$[(NO_2)/(O_2) < 2\times10^{-6}]$$

at high third-body pressures (e.g., 1 atm). This condition is frequently found in the lower atmosphere and can be described by reactions [1], [2], and [7]. Since the rates of reactions [2] and [7] are both known (5, 9, 11, and 20) and the rate of reaction [1] can presumably be determined from the light intensity, the concentrations of atomic oxygen, ozone, nitric oxide, and nitrogen dioxide can be calculated for steady state and for approach to steady state. Since the rate of reaction [2] is known with much more accuracy than that

[6]*The value of k_2 reported in ref. 7 depends on the method of extrapolation of k_2 from the temperatures used by Benson and Axworthy to room temperature. From Benson and Axworthy $k_2 = 6.00\pm0.33\times10^7$ exp (600/RT) liter^2 mole^{-2} sec^{-1}; k_2 was obtained by direct substitution of the temperature (300° K) and with no assumption of a temperature dependence in the pre-exponential portion of k_2.*

Can. J. Chem. Downloaded from www.nrcresearchpress.com by 210.87.254.105 on 09/05/12
For personal use only.

of reaction [7], calculated values of the steady-state concentrations of atomic oxygen should be considerably more accurate than those for ozone. Using Johnston and Crosby's (20) value for k_7 and assuming a primary quantum yield of unity, the ozone concentrations calculated were equal to those observed within a rather large combined experimental error (5).

Mechanism IV

Experimental conditions are the same as for mechanism III except that $(NO_2)/(O_2) > 10^{-6}$. Under these conditions when nitrogen dioxide is photolyzed below 3700 Å, the ozone concentration does not reach a constant steady-state value, but rather rapidly approaches a maximum concentration, and then this quasi-steady-state level gradually decreases. This decay is caused by atomic oxygen attacking nitrogen dioxide and converting the latter into nitric oxide. This, in turn, increases the rate of disappearance of ozone, by reaction [7], and causes the ozone level to decrease gradually. The mechanism, given in the terms of Ford and Endow, is [1], [2], [4], and [7]. In the same terms, reaction [3] followed by reaction [6] can be neglected. The reason for neglecting reactions [3] and [6] is that they have the effect of slightly decreasing the light intensity and not otherwise appreciably affecting the kinetics. Reactions [4] and [7], on the other hand, while proceeding even more slowly than reactions [3] and [6], have a profound effect on the steady-state ozone concentrations. The conditions of mechanism IV are the only known high-pressure conditions under which reaction [4] can be studied independently of reaction [3].

The observed rate of decay of the ozone concentration (17) and mechanism IV confirm that the rate of reaction [4] in nitrogen at 1 atm pressure was that reported by Ford and Endow (6). However, the relative concentrations of atomic oxygen observed in ref. 7 cannot be accounted for by reaction [4] alone. This is confirming evidence for the existence of reaction [3]. In polluted urban atmospheres generally $(NO_2)/(O_2) < 10^{-6}$, so that the conditions of mechanism IV are not met under average conditions.

Since steady-state conditions are not rapidly attained, (O) and (O_3) are functions of time over long time intervals. Atomic oxygen concentrations are given by

$$(O) = \frac{KI(NO_2)}{k_2(O_2)(M)} \qquad (C)$$

provided reaction [2] is fast compared with reactions [3] and [4]. Thus the concentration of atomic oxygen can be calculated if I, (NO_2), and (O_2) are known. The ozone concentration is approximated at any time by

$$(O_3)_t \cong \frac{KI(NO_2)_t}{k_7(NO)_t} \qquad (D)$$

and the rate of change of the steady-state ozone concentration by

$$\frac{d(O_3)_{ss}}{dt} \cong \frac{KIk_4(O)(NO_2)(NO_2)_1}{k_7(NO)^2}. \qquad (E)$$

The decay is slow because reaction [2] leads to a very low concentration of atomic oxygen. Reference 21, which will be published, discloses a more elegant approximation to the rate of ozone decay by this mechanism.

Mechanism V

Experimental conditions are the same as for mechanism III but with ozone added in trace amounts. The effect of added ozone on ozone formed during photolysis can be

Can. J. Chem. Downloaded from www.nrcresearchpress.com by 210.87.254.105 on 09/05/12
For personal use only.

explained only if reactions [1], [6], [7], [8], [9], and [12] are considered. Reaction [2] can be assumed to be fast (22). In this case the rate at which ozone is formed is given by reaction [1], which is known, and its rate of disappearance by reactions [7] and [12]. The over-all effect of photolysis is to suppress the ozone – nitrogen dioxide reaction. This is shown by the cancellation of all species in the following reactions:

$$h\nu + O_2 + NO_2 \rightarrow O_3 + NO \qquad [1a]$$

$$O_3 + NO_2 \rightarrow O_2 + NO_3 \qquad [12]$$

$$NO_3 + NO \rightarrow 2NO_2 \qquad [6]$$

The extent of this suppression was used to measure k_6k_8/k_9. Since k_8/k_9 is the equilibrium constant for the dissociation of nitrogen pentoxide, k_6 can be calculated using the value of K_{eq} reported by Schott and Davidson (25). Thus $k_6K_{eq} = 0.44\ sec^{-1}$ is in reasonable agreement with the value of $1.0\ sec^{-1}$ reported by Hisatsune, Ogg, and Crawford (23). This agreement gives quantitative confirmation of the validity of mechanism V. The resulting derived value of k_6 is 3.4×10^9 liter $mole^{-1}$ sec^{-1}.

Mechanism VI

This is the mechanism for the photolysis of nitrogen dioxide for conditions most frequently used and not involving trace reactant concentrations (1–4). The mechanism covers the millimeter pressure range for nitrogen dioxide with and without added inert gases. The following experimental facts must be explained:

1. In the millimeter pressure range the quantum yield of nitrogen dioxide disappearance[7] is constant and nearly equal to 2 (1–4).

2. In the photolysis of NO_2 in the millimeter pressure range the reciprocal of the quantum yields (either oxygen formation or nitrogen dioxide disappearance) is proportional to the pressure of added inert gas. Hall (4) has shown that

$$1/\Phi_{O_2} = 1+k(M).$$

3. At atmospheric pressure of inert gas, the quantum yield decreases with decreasing concentrations of NO_2, extrapolating to a finite value as $(NO_2) \rightarrow 0$, as shown by the data of refs. 4 and 6.

4. In the photolysis of NO_2 in the millimeter pressure range, the concentration of atomic oxygen is independent of the pressure of added inert gas. Proof of this seems definite if indirect. This conclusion is drawn from the data of Cvetanović (24), who photolyzed mixtures of *cis*-2-pentene, nitrogen dioxide, and nitrogen. Such directly found products as *cis*- and *trans*-β-pentene oxide formed at a rate which was independent of the pressure of added nitrogen over the internal of 0–400 mm. It is probable that the *cis*-2-pentene formed the oxides as a result of attack by atomic oxygen.

The facts can be explained by a variety of mechanisms, some of which can be ruled out on other grounds. The mechanism proposed by Ford and Endow for their conditions should be considered since their mechanism, consisting of [1], [3], [4], and [6], appears to yield quantitatively valid results.

Thus,

$$(F) \qquad 1/\Phi_{O_2} = 1+k_3(M)/k_4.$$

This is in the form reported by Hall. If it is assumed that NO_2, CO_2, and N_2 all have about the same efficiency as a third body, then from ref. 6,

$$(G) \qquad 1/\Phi_{O_2} = 1+2.6\times10^{-3}P_{NO_2,CO_2,N_2}$$

[7]*This assumes the previously mentioned stoichiometry:* $2NO_2 \rightarrow 2NO + O_2$.

Can. J. Chem. Downloaded from www.nrcresearchpress.com by 210.87.254.105 on 09/05/12
For personal use only.

where the pressure is given in millimeters of mercury. Assuming quantum yield measurements are precise to within 10%, the effect of NO_2 pressure on the quantum yield would not be noticeable below 20 mm of NO_2. For CO_2 and propane being used as inert gases, the data from the work of Hall is shown in Fig. 1. The line calculated, using Ford and

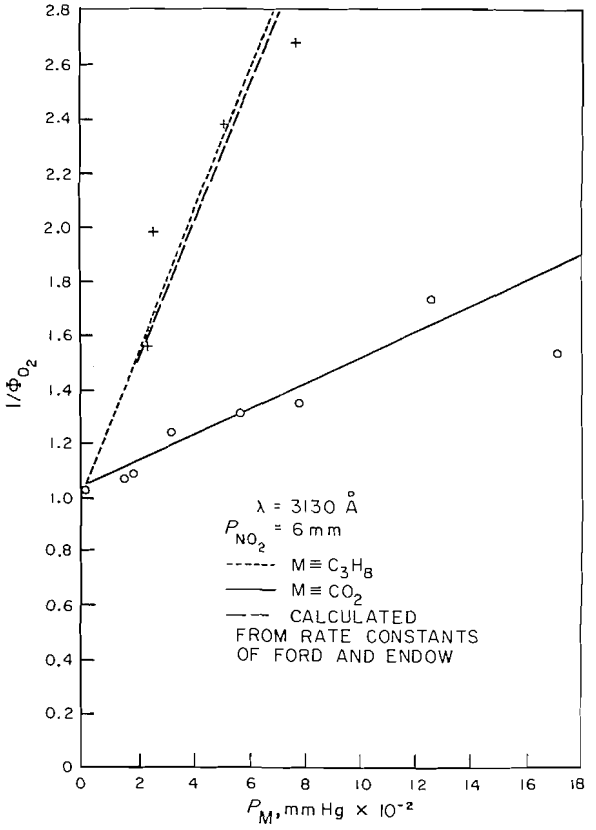


FIG. 1. Recpirocal quantum yield of oxygen appearance as a function of the pressure of added CO_2 and C_3H_8 from the data of hall.

Endow's values for k_3 and k_4 where nitrogen was used as a third body, is shown for comparison. It is obvious that CO_2 is not as efficient a third body as might reasonably have been expected from the rate constants of Ford and Endow and the mechanism given above. The mechanism predicts that the dependence of the quantum yield on added inert gas would be independent of the NO_2 concentration. This prediction is contrary to experimental results. Furthermore, according to this mechanism, the concentration of atomic oxygen is pressure dependent,

$$(H) \qquad (O) = \frac{KI}{k_3(M)+k_4},$$

neglecting the case where large amounts of NO are present and reaction [5] is important. With the values of k_3 and k_4 reported by Ford and Endow, the concentration of atomic oxygen would decrease by a factor of two in going from 0 mm to 400 mm of N_2. This is contrary to the observations of Cvetanović (24).

Can. J. Chem. Downloaded from www.nrcresearchpress.com by 210.87.254.105 on 09/05/12
For personal use only.

The facts can be explained by at least two mechanisms which have several steps in common. The two mechanisms are given below for direct comparison:

Mechanism VIA	Mechanism VIB
$h\nu + NO_2 \rightarrow NO + O$	$h\nu + NO_2 \rightarrow NO + O$
$O + NO_2 \rightarrow NO_3^*$	$O + NO_2 \rightarrow NO_3^*$
$NO_3^* + NO_2 \rightarrow NO + O_2 + NO_2$	$NO_3^* + NO_2 \rightarrow NO + O_2 + NO_2$
$NO_3^* + M \rightarrow NO_3 + M$	$NO_3^* + M \rightarrow NO_3 + M$
$NO_3^* \rightarrow NO + O_2$	$NO_3^* \rightarrow NO_2 + O$
	$O + NO_2 \rightarrow O_2 + NO$

The remaining steps, consisting of reactions [2], [5], [6], [7], [8], [9], and [12], would be common to both mechanisms. If the usual steady state can be assumed for NO_3, mechanism VIA gives

$$(I) \qquad 1/\Phi_{NO_2} = 1/2 + \frac{\frac{1}{2}k_{3b}(M)}{k_{4a} + k_{11a}(NO_2)}$$

or

$$(J) \qquad 1/\Phi_{O_2} = 1 + \frac{k_{3b}(M)}{k_{4a} + k_{11a}(NO_2)}.$$

So far as is known, the quantum yields at high pressures (e.g., 1 atm) decrease with decreasing NO_2 concentration and approach a finite value as $(NO_2) \rightarrow 0$. Equations (I) and (J) give the correct pressure dependence and the correct quantum yield at low third-body pressure.

Quantatively the significance of mechanism VIA can be seen from the work of Hall (4). Besides obtaining the data represented in Fig. 1, Hall measured the quantum yields of O_2 appearance at 1 atm total pressure of propane and at various partial pressures of NO_2. A summary of his data is given below:

Condition	$2\Phi_{O_2} = \Phi_{NO_2}$
1 atm CO_2, 6 mm NO_2	1.4
1 atm propane, 6 mm NO_2	0.7
1 atm propane, $P_{NO_2} \rightarrow 0$	0.2

The value of 0.2 was extrapolated from Hall's data by the author. From this data and equation (J)

$$k_{3b}(C_3H_8)_{1\text{ atm}} = 9.0k_{4a},$$

$$k_{11a}(NO_2)_{6\text{ mm}} = 3.8k_{4a},$$

$$k_{3b}(CO_2)_{1\text{ atm}} = 1.9k_{4a},$$

$$k_{3b}(N_2)_{1\text{ atm}} = 1.9k_{4a} \text{ (see ref. 7).}$$

If the mechanism is correct, CO_2 and N_2 are equally effective in deactivating excited NO_3. The pressure dependence of the quantum yield at constant NO_2 concentration and the dependence of the quantum yield on the concentration of NO_2 at 1 atm total pressure of propane give the same ratio for k_{11a} to k_{4a} within experimental error. At least formally,

Can. J. Chem. Downloaded from www.nrcresearchpress.com by 210.87.254.105 on 09/05/12
For personal use only.

the assumed mechanism and measured rate constants determine the quantum yield for all pressures of CO_2, N_2, and propane and for all concentrations of NO_2, provided the system is at room temperature and the concentrations are in the regions that have been most frequently studied. The dependence of the quantum yields on third-body pressure and on NO_2 concentration at 1 atm pressure of added gas are given in Figs. 2 and 3.

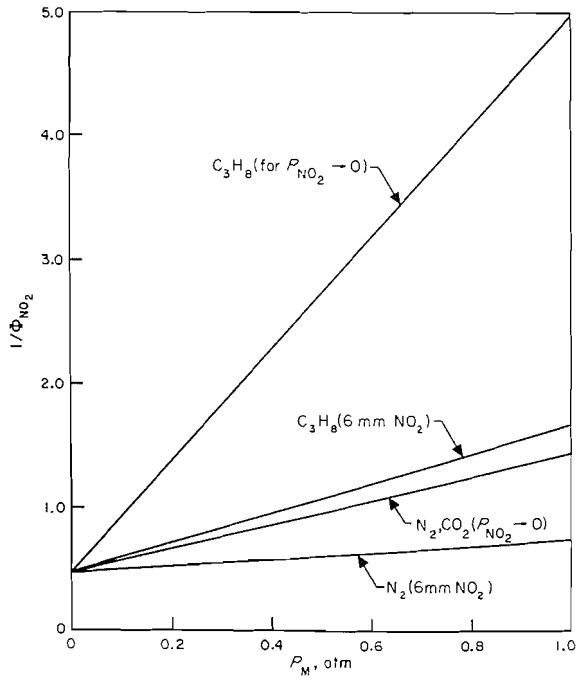


FIG. 2. Reciprocal quantum yields of NO_2 disappearance as a function of pressure of added gas.

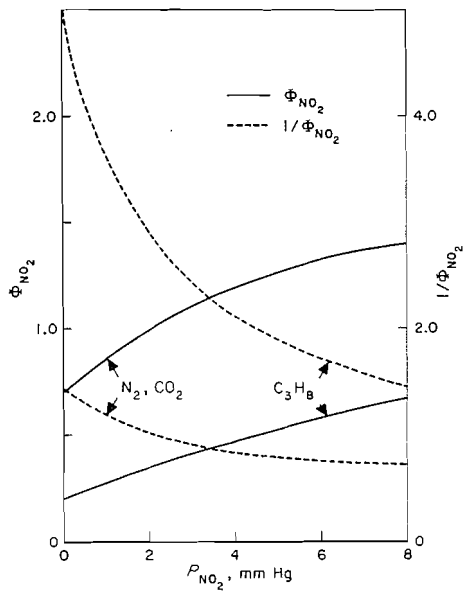


FIG. 3. Quantum yields of NO_2 disappearance as a function of NO_2 partial pressure.

Can. J. Chem. Downloaded from www.nrcresearchpress.com by 210.87.254.105 on 09/05/12
For personal use only.

In the absence of appreciable amounts of NO or O_2 the concentration of atomic oxygen is simply KI/k_{3a}, and therefore independent of pressure, as required.

Mechanism VIB requires one more reaction than VIA, gives less clear-cut results, and requires more assumptions but nevertheless seems to be the more convincing of the two mechanisms. In the absence of appreciable NO and O_2, and making the reasonable assumption that $k_{3c} \gg k_{3b}(M)$

$$\text{(K)} \qquad \frac{1}{\Phi_{NO_2}} = 1/2+\frac{\frac{1}{2}k_3(M)}{k_4+[k_4+k_{3a}][k_{11a}/k_{3c}](NO_2)}.$$

To fit the data of Hall to that of Ford and Endow

$$\text{(L)} \qquad [k_4+k_{3a}]k_{11a}/k_{3c} = 2.6\times10^{13} \text{ liter}^2 \text{ mole}^{-2} \text{ sec}^{-1}.$$

At trace concentrations equation (K) reduces to the form given by the mechanism of Ford and Endow,

$$\text{(M)} \qquad \frac{1}{\Phi_{NO_2}} = 1/2+\frac{k_3(M)}{2k_4}.$$

Thus, in fitting the two sets of data no changes are required in the values of k_3 and k_4 reported by the latter authors. This means that k_4 in equation (K) is known, leaving three unknowns in the one equation. The quantity, k_{3a}, is probably of the order of 5×10^{11} liter mole^{-1} sec^{-1} so that $k_4 \ll k_{3a}$. Or $k_{11a}/k_{3c} \cong 50$. A unimolecular decomposition of a diatomic molecule that might be of the order of 10^{13} sec^{-1}, whereas k_{3c} might be estimated at 10^9.

In this case $k_{11a} = 5\times10^{10}$ compared with a pre-exponential factor of 4×10^9 for the equivalent thermal reaction. It is, of course, easy to speculate about the relative values of the rate constants in equation (L), but the important point is that neither rate constants nor simple rate constant ratios can be calculated from available experimental data without additional assumptions. Quantum yields can be calculated and give the same dependence on pressure as shown by mechanism VIA (Fig. 2). Both mechanisms (VIA and VIB) can be used to calculate the dependence of the quantum yields on NO_2 concentration at 1 atm pressure of inert gas (Fig. 3).

For low concentrations of O_2 and NO, and for $k_{3b}(M) \ll k_{3c}$ the atomic oxygen concentration has the following dependence based on mechanism VIB:

$$\text{(N)} \qquad \text{(O)} = \frac{KI[k_{3c}+k_{11a}(NO_2)]}{k_4k_{3c}+k_{11a}[k_{3a}+k_4]}.$$

Thus, the concentration of atomic oxygen is not pressure dependent. The two mechanisms will be considered in more detail following a discussion of mechanism VII.

Mechanism VII

This mechanism is based on a study of the photolysis of nitrogen dioxide at trace concentrations in nitrogen at atmospheric pressure and with varying amounts of added oxygen, nitric oxide, and *cis*-2-pentene. The latter was used as a tracer for atomic oxygen (6, 7). The mechanism incorporates reaction [5] into the general scheme and permits quantitative evaluation of the rate of reactions [3], [4], and [5], or, alternatively, [3*a*]

Can. J. Chem. Downloaded from www.nrcresearchpress.com by 210.87.254.105 on 09/05/12
For personal use only.

and [5] from Benson and Axworthy's rate constant for reaction [2]. Under the experimental conditions, all reactions except perhaps [11*a*] were playing a significant role. Quantum yield measurements were delayed so that reactions [6], [7], [8], [9], and [12] would have gone to completion. Therefore the significant steps in interpreting the experimental results are either reactions [1], [2], [3*a*], [3*b*], [4*a*], and [5], or [1], [2], [3], [4], and [5]. The latter mechanism was proposed by Ford and Endow and is consistent with mechanism VIA.

Experimentally, Ford and Endow found that $1/\Phi_{NO_2}$ was proportional to $(NO)/(NO_2)$ and to $(O_2)/(NO_2)$, and they measured the proportionality constants. Extrapolating $(NO)/(NO_2)$ and $(O_2)/(NO_2)$ to zero separately, they obtained a limiting quantum yield of 0.69 for NO_2 disappearance. The following relation was derived:

$$(O) \qquad 1/\Phi_{NO_2} = 1/2+\frac{k_3(M)}{2k_4}+\frac{k_5(M)(NO)}{2k_4(NO_2)}+\frac{k_2(M)(O_2)}{2k_4(NO_2)},$$

based on reactions [1], [2], [3], [4], and [5]. An analogous expression, based on reactions [1], [2], [3*a*], [3*b*], [4*a*], and [5] is given by

$$(P) \qquad 1/\Phi_{NO_2} = 1/2+\frac{k_{3b}(M)}{2k_{4a}}+\frac{(k_{4a}+k_{3b})k_5(NO)(M)}{2k_{4a}k_{3a}(NO_2)}+\frac{(k_{4a}+k_{3b})k_2(O_2)(M)}{2k_{4a}k_{3a}(NO_2)}.$$

At low values of $(NO)/(NO_2)$ and $(O_2)/(NO_2)$

$$(Q) \qquad 1/\Phi_{NO_2} = 1.45 = \frac{k_{4a}}{k_{3b}(M)}.$$

Also

$$(R) \qquad \frac{k_5(M)[k_{4a}+k_{3b}(M)]}{k_{4a}k_{3b}} = 1.33\times10^{-3}$$

and

$$(S) \qquad \frac{k_2(M)[k_{4a}+k_{3b}(M)]}{k_{4a}k_{3b}} = 0.36.$$

From these ratios and Benson and Axworthy's rate constant k_2, the value of k_{3a} can be calculated:

$$k_{3a} = 6.0\times10^9 \text{ liter mole}^{-1} \text{ sec}^{-1}.$$

Beyond that, the data only give the ratio of k_{4a} to k_{3b}.

From the mechanism (reactions [1], [2], [3*a*], [3*b*], [4*a*], and [5]):

$$(T) \qquad k_4 = \frac{k_{4a}k_{3a}}{k_{4a}+k_{3b}(M)},$$

$$(W) \qquad k_3 = \frac{k_{3a}k_{3b}}{k_{4a}+k_{3b}(M)},$$

$$(X) \qquad k_{11} = \frac{k_{3a}k_{11a}}{k_{4a}+k_{3b}(M)}.$$

Can. J. Chem. Downloaded from www.nrcresearchpress.com by 210.87.254.105 on 09/05/12
For personal use only.

Thus k_{3a} is the low-pressure limit of k_4. The variations of k_4, k_3, and k_{11} as functions of the third-body pressure and of the pressure of NO_2 are given in Figs. 4 through 7.

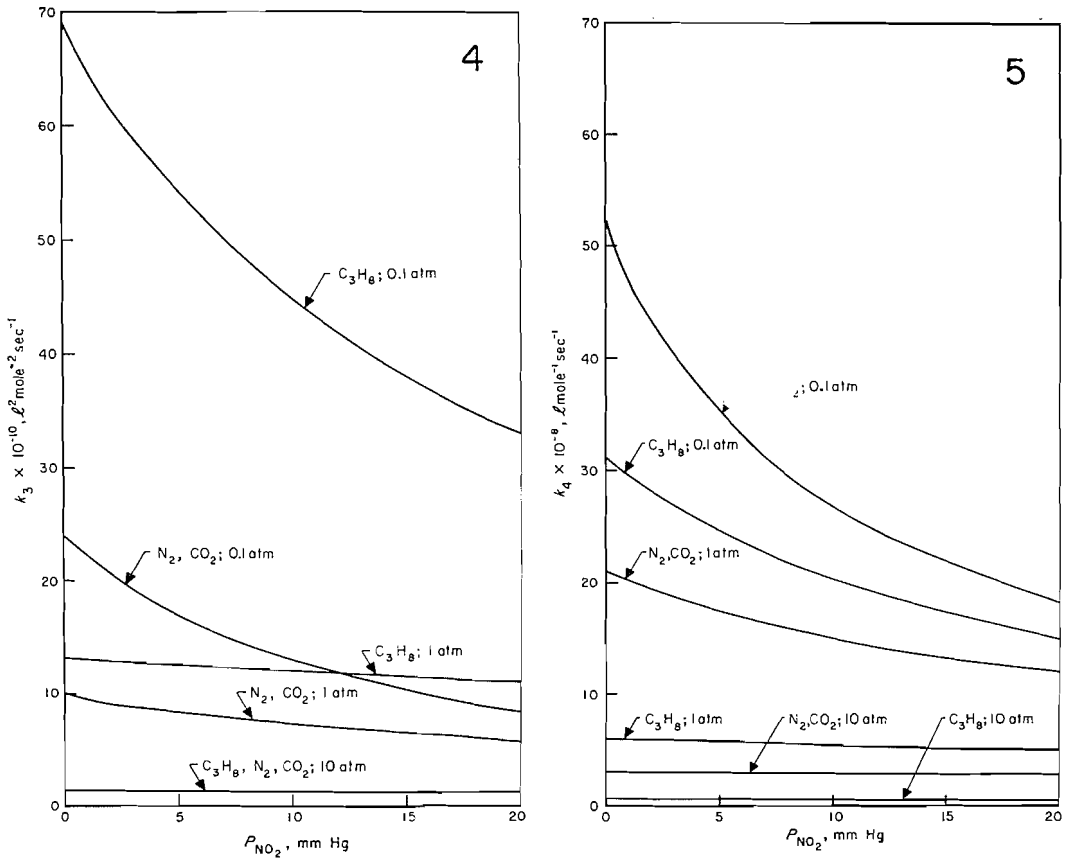


FIG. 4. Dependence of k_3 on NO_2 partial pressure at various partial pressures of matrix gas.
FIG. 5. Dependence of k_4 on NO_2 partial pressure at various partial pressures of matrix gas.

As it turns out, k_3, as given is constant with mechanism VIA. However, k_3 has a different definition consistent with VIB.

$$k_3 = \frac{k_{3a}k_{3b}}{k_{4b}+k_{3b}(\mathrm{M})}. \qquad \text{(Y)}$$

For the usual case $k_{4b} \gg k_{3b}(\mathrm{M})$ the three-body recombination reaction would have the usual form, and k_3 would be independent of pressure in the region of interest.

In both equations (W) and (Y) the steady-state concentration of NO_3^* was calculated neglecting reaction [11*a*], and consequently k_2 is a limiting value as $(NO_2) \rightarrow 0$.

Can. J. Chem. Downloaded from www.nrcresearchpress.com by 210.87.254.105 on 09/05/12
For personal use only.

Can. J. Chem. Downloaded from www.nrcresearchpress.com by 210.87.254.105 on 09/05/12
For personal use only.

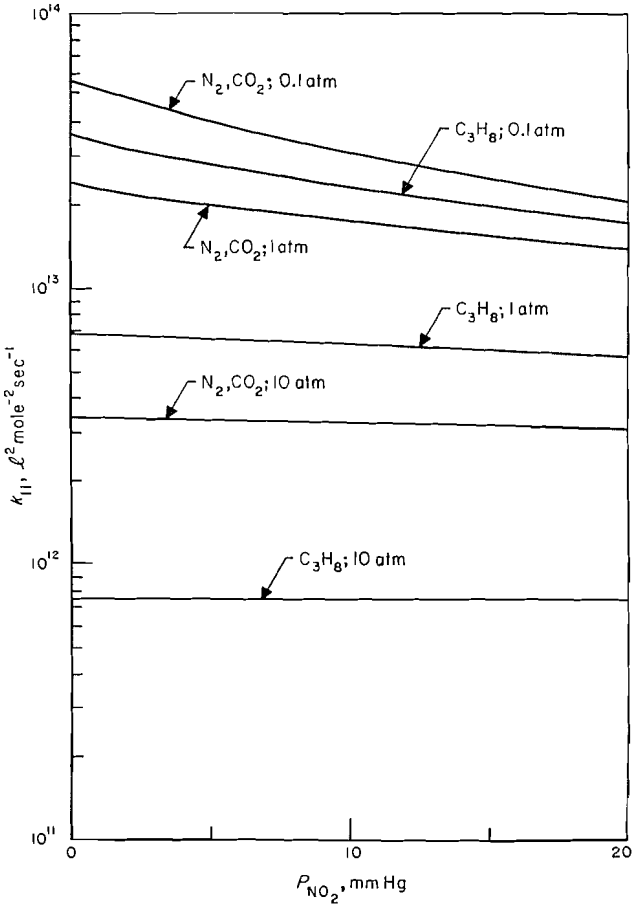


FIG. 6. Dependence of k_{11} on NO_2 partial pressure at various partial pressures of added gas.

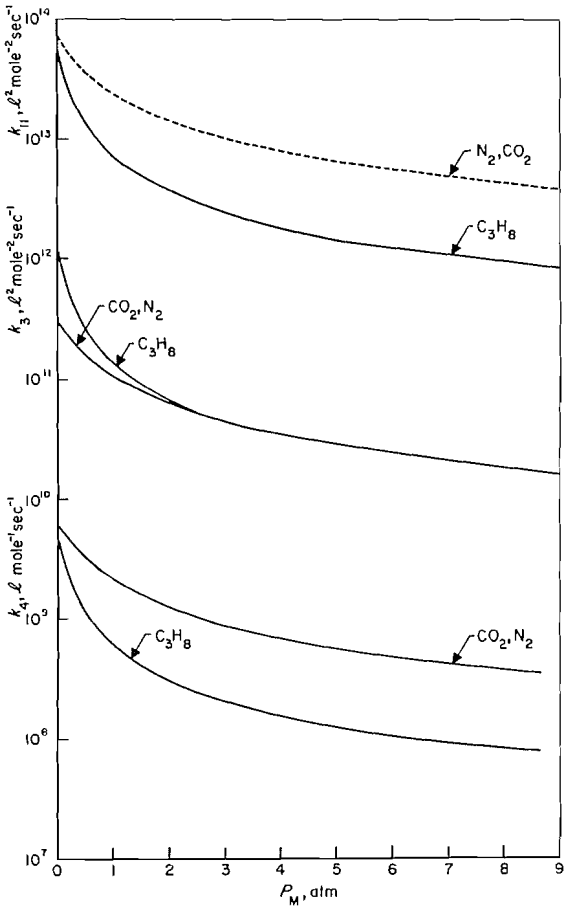


FIG. 7. Effective values of k_3, k_4, and k_{11}, based on the assumption that the excited-molecule mechanism is correct, for the case of $NO_2 \rightarrow 0$.

DISCUSSION

The difficulties and ambiguities in the mechanism can be summarized with the question: What happens when atomic oxygen attacks NO_2? The photolysis of NO_2 provides no definite answer. The situation can be somewhat clarified by considering other reactions of NO_2. Thus Schott and Davidson (25) agree with Ashmore and Levitt (26) that both of the following reactions occur in the thermal decomposition of NO_2:

$$NO_2 + NO_2 \rightarrow 2NO + O_2 \quad [10]$$

$$NO_2 + NO_2 \rightarrow NO_3 + NO \quad [13]$$

Similarly Huffman and Davidson (27) agree with Johnston (28) that the following reactions are important in the thermal decomposition of N_2O_5:

$$NO_3 + NO_2 \rightarrow NO + O_2 + NO_2 \quad [14]$$

$$NO_3 + NO_2 \rightarrow N_2O_5 \quad [8]$$

It is therefore of interest that Ford and Endow also postulated two reactions of atomic oxygen with NO_2:

$$O + NO_2 \rightarrow O_2 + NO \quad [4]$$

$$O + NO_2 + M \rightarrow NO_3 + M \quad [3]$$

The following appears to be a reasonable explanation of these reactions. When O, NO_2, or NO_3 attack NO_2, the approach to the NO_2 can follow either of two paths. The activated complex for each of the above cases would then be of the forms given below:

Reaction No.	Activated complex	Subsequent intermediate
[10]	ONOONO	OONO
[13]	$ONON\begin{matrix}O\\O\end{matrix}$	
[14]	$\begin{matrix}O\\O\end{matrix}NOONO$	OONO
[8]	$\begin{matrix}O\\O\end{matrix}NON\begin{matrix}O\\O\end{matrix}$	
[4]	OONO	OONO
[3]	$ON\begin{matrix}O\\O\end{matrix}$	

When the activated complex is of the peroxy form, decomposition either occurs to give OONO or O_2 and NO. Evidence for the peroxy form of NO_3 has been found by Benson (29), who has shown that the activation energy of [14] is less than the endothermicity by about 2 kilocalories. Benson explains this by a two-step process:

$$\begin{matrix}O\\O\end{matrix}NO + ONO \rightarrow ONO + OONO \quad [15]$$

$$OONO + M \rightarrow O_2 + NO + M. \quad [16]$$

Reaction [14] would be unusual as an elementary reaction because NO_2 is both a reactant and a product. According to this explanation, reaction [14] is composite, the first step consisting of an abstraction reaction which results in the peroxy form of NO_3. A similar explanation applies to the attack of atomic oxygen and NO_2 on NO_2.

Can. J. Chem. Downloaded from www.nrcresearchpress.com by 210.87.254.105 on 09/05/12
For personal use only.

In distinguishing between mechanisms, it would seem that [4*b*] is much more probable than [4*a*]. An attack on NO_2 by atomic oxygen by two paths rather than one has a geometrical and structural basis, and is analogous to the other reactions mentioned above. In the opinion of the author mechanism VII and the equivalent mechanism VIB best conform to our present understanding of the chemistry of NO_2.

REFERENCES

1. H. H. Holmes and F. Daniels. J. Am. Chem. Soc. **56**, 630 (1934).
2. R. G. Dickinson and W. P. Baxter. J. Am. Chem. Soc. **50**, 774 (1928).
3. R. G. W. Norrish. J. Chem. Soc. **51**, 1158 (1929).
4. T. C. Hall, Jr. Ozone catalysis of isotope exchange between molecular oxygen species. Ph.D. dissertation, University of California, Los Angeles. October, 1953.
5. H. W. Ford, G. J. Doyle, and N. Endow. J. Chem. Phys. **26**, 1337 (1957).
6. H. W. Ford and N. Endow. J. Chem. Phys. **27**, 1156 (1957).
7. H. W. Ford and N. Endow. J. Chem. Phys. **27**, 1277 (1957).
8. F. Kaufman, N. J. Gerri, and R. F. Bowman. J. Chem. Phys. **25**, 106 (1956).
9. S. W. Benson and A. E. Axworthy. J. Chem. Phys. **26**, 1718 (1957).
10. F. Kaufman. J. Chem. Phys. **28**, 352 (1958).
11. E. A. Ogryzlo and H. I. Schiff. Can. J. Chem. **37**, 1690 (1959).
12. P. Harteck, R. R. Reeves, and G. Mannela. J. Chem. Phys. **26**, 1333 (1957).
13. P. A. Leighton and W. A. Perkins. Photochemical secondary reactions in urban air. Rept. No. 24. Air Pollution Foundation, San Marino, California. August, 1958.
14. R. G. W. Norrish. J. Chem. Soc. **51**, 1604 (1929).
15. W. A. Rosser, Jr. and H. Wise. J. Chem. Phys. **24**, 493 (1956).
16. R A. Ogg and W. T. Sutphen. J. Chem. Phys. **21**, 2078 (1953).
17. T. C. Hall and F. E. Blacet. J. Chem. Phys. **21**, 1745 (1952).
18. G. B. Kistiakowsky and G. G. Volpi. J. Chem. Phys. **27**, 1141 (1957).
19. P. Kaufman. Proc. Roy. Soc. A, **247**, 123 (1958).
20. H. S. Johnston and H. J. Crosby. J. Chem. Phys. **22**, 689 (1954).
21. H. W. Ford, G. J. Doyle, and N. Endow. The reaction of atomic oxygen with nitrogen dioxide. To be published.
22. H. W. Ford, G. J. Doyle, and N. Endow. J. Chem. Phys. **32**, 1256 (1960).
23. I. C. Hisatsune, R. A. Ogg, Jr., and B. Crawford, Jr. J. Am. Chem. Soc. **79**, 4648 (1957).
24. S. Sato and R. J. Cvetanović. Can. J. Chem. **37**, 953 (1959).
25. G. Schott and N. Davidson. J. Am. Chem. Soc. **80**, 1841 (1958).
26. P. G. Ashmore and B. P. Levitt. Research (London), **9**, S25 (1956).
27. R. E. Huffman and N. Davidson. J. Am. Chem. Soc. **81**, 2311 (1959).
28. H. S. Johnston. J. Am. Chem. Soc. **73**, 4542 (1951).
29. S. W. Benson. The foundations of chemical kinetics. McGraw-Hill, New York. 1960; and private communication.

Can. J. Chem. Downloaded from www.nrcresearchpress.com by 210.87.254.105 on 09/05/12
For personal use only.

Can. J. Chem. Downloaded from www.nrcresearchpress.com by 210.87.254.105 on 09/05/12
For personal use only.

THE PRODUCT EMITTER DIFFUSION FLAME: THE REACTION OF NITRIC OXIDE WITH OXYGEN ATOMS[1]

DAVID GARVIN, PAUL P. GWYN, and JULES W. MOSKOWITZ

ABSTRACT

The use of the Polanyi diffusion flame technique as a diagnostic test for the identification of reactions that lead to light emission is presented. There is developed the mathematical model needed for the interpretation of such flames in which a product is responsible for the emission that is studied. The method is applied to the systems in which oxygen atoms and nitrogen atoms react with nitric oxide. The rate constant of the reaction $O + NO + M \rightarrow NO_2 + M$ at 293° K was determined as $k = 1.4 \times 10^{17}$ (cc/mole)^2 sec^{-1}.

INTRODUCTION

The Polanyi diffusion flame technique has been used numerous times for the measurement of rates of very fast reactions (1–5). It is applied here to a system in which several reactions of nitric oxide occur, both to determine rates and as a diagnostic tool to determine the probable reaction, which is studied directly. In part, this paper presents an experimental confirmation for the mechanism of the 'airglow' or 'oxygen afterglow' that has been identified and studied intensively in the past few years (6–10), and, in addition, there is presented the model needed for the interpretation of diffusion flames in which a product is the emitting species. This model is applied to a determination of the rate of the O+NO reaction as it may be studied in two systems. Finally, there are reported several qualitative observations on related reactions.

DIAGNOSTIC STUDIES

It is usually essential that the elementary reactions that are studied by the diffusion flame technique be established by some independent means. In some cases an a priori knowledge of the possible reactions is sufficient, and in others product analysis is helpful. In any case, such information is needed for the interpretation of the experiments because the lifetime or spatial distribution of a very reactive species is used as the basis for the quantitative measurements.

The special geometry of the diffusion flame system imposes severe conditions on the reactions that can be studied: they must be very fast, i.e., occur at least once in 10^5 collisions, and must be homogeneous. In this method one reagent (y) is fed in small amounts through an orifice into a low pressure atmosphere containing its reaction partner (z) in considerable excess. At the low pressures employed y penetrates the atmosphere principally by diffusion and reacts with z before reaching any wall surface.

If, in a given system, one reaction leads to immediate emission of light, and the spatial distribution of this emission is to be studied, the particular reaction that is responsible for it can be identified by employing as y and z the possible reactant pairs in the system. The light-emitting reaction will give a small, well-defined zone of emission near the orifice while the other reactions will give, at best, a diffuse emission throughout the reactor. Where several sets of reagent pairs lead to emission, other criteria (such as rate and spectral studies) must also be used.

[1]*Contribution from the Frick Chemical Laboratory, Princeton University, Princeton, N.J. Based in part on theses submitted in partial fulfillment of the requirements for the degree of Bachelor of Arts at Princeton University by Jules W. Moskowitz, May 1956, and by Paul P. Gwyn, May 1957; presented at the Symposium on the Fundamental Aspects of Atomic Reactions held at McGill University, Montreal, Que., September 1960.*

A favorable case for the application of this type of test is the system in which nitric oxide may react either with oxygen or nitrogen atoms. The following reactions have been shown to be important.

$$O + NO \rightarrow NO_2^* \quad [1]$$

$$NO_2^* \rightarrow NO_2 + h\nu \quad [2]$$

$$O + NO_2 \rightarrow O_2 + NO \quad [3]$$

$$N + NO \rightarrow N_2 + O \quad [4]$$

$$N + NO_2 \rightarrow NO + NO \quad [5]$$

$$\rightarrow N_2 + O_2 \quad [6]$$

The rate of [1] has been determined independently by Kaufman (8) and by Harteck, Reeves, and Mannella (10). NO_2 is the probable emitter, but has not been positively identified. Reaction [3] has been studied by the flash photolysis technique and an excited oxygen molecule shown to be a primary product (11). Dressler (12) found evidence for [4] in the nitrogen 'afterglow', the nitrogen molecule being in an excited state. Also, limited emission of the oxygen 'afterglow' (1) in systems containing nitrogen atoms and nitrogen dioxide require consideration of reactions [5] and [6]. The sequence [1], [2], [3] is generally considered to explain the long-lived 'afterglow' in impure oxygen in which traces of NO are produced along with much larger quantities of oxygen atoms by an electric discharge.

TABLE I

Observations of reaction zones in systems related to the NO–O reaction

Nozzle reagent	Atmosphere	Appearance of reaction zone
(*a*) $O + O_2$	Air	Diffuse glow throughout reactor
(*b*) NO	$O + O_2$	Diffuse glow throughout reactor
(*c*) $O + O_2$	NO (excess)	Stable flame, small zone near nozzle
	$NO + N_2$	
(*d*) $O + O_2$	NO_2 (excess)	No glow
(*e*) $O + O_2$	NO_2 (limited)	Glowing zone with dark center
(*f*) $N + N_2$ (active nitrogen)	N_2	Active nitrogen color, difficult to restrict
(*g*) $N + N_2$	NO (excess)	Stable flame, spectrum same as that of (*c*)
(*h*) $N + N_2$	NO_2	No zone, active nitrogen color diminished

Table I summarizes a number of observations made on these reactions using the usual diffusion flame arrangement. The behavior of (*c*) and (*b*) are consistent with the oxygen 'afterglow' mechanism. Reactions (*d*) and (*e*) agree with results found in oxygen atom titration experiments (8,10,13), and the behavior of (*e*) is to be interpreted as a sequence of [3] and [1]–[2]. Reaction (*g*) could be interpreted in terms of emission in [4], but the fact that the spectrum of (*g*) in the visible region is the same continuum as that produced by (*c*) is an argument in favor of the sequence [4]–[3]–[1]–[2]. This is in agreement with the other studies mentioned above.

These observations offer direct evidence that the reaction leading to emission in systems containing O and N atoms and an excess of NO is [1]–[2]. (When the supply of NO is limited and there is an abundant supply of N atoms the bands of NO are produced by atom recombination (14). These were not observed here.)

Can. J. Chem. Downloaded from www.nrcresearchpress.com by 210.87.254.105 on 09/05/12
For personal use only.

Can. J. Chem. Downloaded from www.nrcresearchpress.com by 210.87.254.105 on 09/05/12
For personal use only.

SPECTRA

Since our conclusions depend upon observation of the spectrum of the radiation produced in (*c*) and (*g*), the results of such studies are summarized here. Comparative spectra of the reaction zones in (*c*) and (*g*) were taken with a medium quartz Hilger Cornu type spectograph using Eastman Kodak type F plates to emphasize the red end of the spectrum. A continuum with faint banded structure extended from about 4400 Å to the plate limit (about 6600 Å). The intensity was not uniform, but the variations with wavelength were characteristic of the sensitivity of the emulsion, not of the flame. Similar spectra have been reported many times (7,8). A more extensive study of the airglow spectrum was made using a large aperture spectograph designed at the National Bureau of Standards (15).* With this instrument and films sensitive to the visible and the near infrared region the airglow spectrum was surveyed to beyond 11,000 Å. The continuum is strong out to the limit of the I-N emulsion (about 8900 Å) and continues to about 10,900 Å. No intensity measurements were made, but it was apparent that the continuum intensity was decreasing more rapidly than was the emulsion sensitivity as the long wavelength limit was approached. This spectrum should be studied in detail in any reinvestigation of the nitrogen dioxide spectrum.

System (*h*) was studied because reaction (5) is sufficiently exothermic to permit the production of NO in excited vibrational states that could lead to emission in the 1–2 micron region. An exposure of 144 minutes on I-Z film did not reveal any bands attributable to NO.

REACTION RATES: THE PRODUCT EMITTER DIFFUSION FLAME MODEL

There is presented in this section the mathematical model needed for the interpretation of diffusion flames in which a product molecule emits the radiation that is monitored. It has been used previously for the analysis of the $H+O_3$ system (16), and a similar treatment has been used recently by Rapp and Johnston (17) in connection with the nitric oxide – fluorine flame. The equations for the spatial distribution of reagents and intermediates are developed for the cases that may be applied to O+NO and N+NO. The modifications that must be introduced when the flame is photometered or photographed are then presented. In a following section the application to these systems is discussed.

The reaction scheme that is applicable to the O+NO system is

$$y+z \rightarrow w^* \qquad \text{rate} = k_1\,[z][y]$$

$$w^* \rightarrow w+h \qquad = k_2\,[w^*]$$

$$w^*+M \rightarrow w+M \qquad = k_3[M][w^*]$$

in which y is the nozzle reagent, z the atmosphere reagent (present at constant concentration), and M is any 'third body'. Following the development used for the temperature pattern method (3), treating the nozzle as a point source, the steady-state diffusion equations are

$$[7] \qquad -D_y\Delta^2[y] = -k_1[z][y]$$

$$[8] \qquad -D_w\Delta^2[w^*] = -(k_2+k_3[M])[w^*]+k_1[z][y]$$

We are indebted to the National Bureau of Standards for the opportunity to use this instrument, and to Dr. A. M. Bass for conducting these experiments.

with the boundary conditions

$$y \rightarrow 0 \quad \text{as} \quad r \rightarrow \infty, \qquad b = \int_0^\infty k_1[\mathrm{z}][\mathrm{y}]\, dV$$

$$w^* \rightarrow 0 \quad \text{as} \quad r \rightarrow \infty, \qquad b = \int_0^\infty (k_2 + k_3[M])[\mathrm{w}^*]\, dV$$

where D is a diffusion coefficient, b is the molar flow rate of the nozzle reagent, V is the volume, and r the radial distance from the nozzle. Spherical symmetry is assumed and equations [7] and [8] are solved in sequence by standard techniques. The solutions that satisfy the boundary conditions are

[9] $$[\mathrm{y}] = be^{-cr}/4\pi D_y r, \text{ where } c^2 = k_1[\mathrm{z}]/D_y$$

[10] $$[\mathrm{w}^*] = \frac{b}{4\pi D_w} \cdot \frac{c^2}{(a^2 - c^2)} \cdot \frac{e^{-cr} - e^{-ar}}{r}$$

where $$a^2 = (k_2 + k_3[\mathrm{M}])/D_w.$$

If w^* were stable and the nozzle reagent concentration were studied, as in the sodium diffusion flames, equation [9] would be used for the analysis. Where w^* is the emitter and the emission pattern is studied, two simple cases can be distinguished. If $a \gg c$, that is instantaneous emission or destruction,

[11] $$[\mathrm{w}^*] = \frac{b}{4\pi D_w} \cdot \frac{c^2 e^{-cr}}{a^2 r}$$

and then if $k_3[\mathrm{M}] \ll k_2$

[12] $$k_2[\mathrm{w}^*] = \frac{bc^2 e^{-cr}}{4\pi r}.$$

If $a = c$, i.e., the rates of formation and destruction of w^* are equivalent, the general expression for w^* goes to a limit of

[13] $$[\mathrm{w}^*] = \frac{bce^{-cr}}{8\pi D_w}$$

and then, if $k_3[\mathrm{M}] \ll k_2$

[14] $$k_2[\mathrm{w}^*] = \frac{bc^3 e^{-cr}}{8\pi}.$$

A scheme that is applicable to the case of N + NO is

$$y + z \rightarrow p + I$$

$$p + z \rightarrow w^* \qquad \text{rate} = k_4[\mathrm{z}][\mathrm{p}]$$

$$w^* \rightarrow w + h$$

$$w^* + M \rightarrow w + M$$

where I is an inert product, the other symbols have the meanings previously assigned,

Can. J. Chem. Downloaded from www.nrcresearchpress.com by 210.87.254.105 on 09/05/12
For personal use only.

and the same rate notation is associated with the same reagents. The diffusion equations for this case are [7] and

$$[15] \qquad -D_p\Delta^2[\mathrm{p}] = -k_4[\mathrm{z}][\mathrm{p}]+k_1[\mathrm{z}][\mathrm{y}]$$

$$[16] \qquad -D_w\Delta^2[\mathrm{w}^*] = -(k_2+k_3[\mathrm{M}])+k_4[\mathrm{z}][\mathrm{p}]$$

with the additional boundary condition

$$p \to 0 \quad \text{as} \quad r \to \infty, \qquad b = \int_0^\infty k_4[\mathrm{z}][\mathrm{p}]\, dV.$$

The solution of [7] remains the same, the solution of [15] is of the same form as [8], except that p replaces w^* and a new parameter $f^2 = k_4[\mathrm{z}]/D_p$ replaces a. (The last retains its same significance here, see eq. [10].) The solution for w^* is

$$[17] \qquad [\mathrm{w}^*] = \frac{bc^2f^2[(f^2-c^2)e^{-ar}+(a^2-f^2)e^{-cr}-(a^2-c^2)e^{-fr}]}{4\pi D_w r(f^2-c^2)(a^2-c^2)(a^2-f^2)}.$$

We record here both the simplification that corresponds to rapid formation of p, $c \gg f$, and a

$$[18] \qquad [\mathrm{w}^*] = \frac{bf^2[e^{-fr}-e^{-ar}]}{4\pi D_w(a^2-f^2)r},$$

which is of the same form as the general solution in the first case considered [10], and the simplification that specifies rapid destruction of w^* under the conditions leading to [18] $a \gg f$

$$[19] \qquad [\mathrm{w}^*] = bf^2e^{-fr}/4\pi D_w a^2 r$$

and if, as before $k_3[\mathrm{M}] \ll k_2$

$$[20] \qquad k_2[\mathrm{w}^*] = bf^2e^{-fr}/4\pi r,$$

which is identical in form with [12].

This completes the development of the concentration and emission density expressions needed here. Other less limited cases differ only in the terms preceding the exponentials.

We now turn to the question of the form of the pattern recorded on a photograph of such an emission zone, or, indeed, of the resonance zone produced in sodium diffusion flames. Ideally, such a photograph is a plane representation of the three dimensional zone, at each point of which there is an emission density $k_2[\mathrm{w}^*]$. Each point on the film represents a summation of the emission from a sequence of points in the flame. We shall assume that these points lie on a chord of the sphere that runs perpendicular to the plane of the film, and that all such points contribute radiation in proportion to their values of $k_2[\mathrm{w}^*]$. Since the flame is 'focused' onto the film, these assumptions should be moderately good. If v represents a distance from the center of the reaction zone in the plane parallel to the film, and u a distance perpendicular to this plane, the integration of the emitter density along u yields the emission recorded by the film (or a number proportional to it).

$$F(cv, av) = 2\int_0^\infty k_2[\mathrm{w}^*]\, du = \frac{bk_2c^2}{2\pi D_w(a^2-c^2)}\int_0^\infty \frac{e^{-cr}-e^{-ar}}{r}\, du$$

Can. J. Chem. Downloaded from www.nrcresearchpress.com by 210.87.254.105 on 09/05/12
For personal use only.

which becomes upon substitution of $u = v \sinh$ and integration (for w^* given by [10] or [18] with f replacing c)

$$[21] \qquad F(cv,av) = \frac{bk_2c^2}{2\pi D_w(a^2-c^2)} [K_0(cv)-K_0(av)]$$

where $K_0(x)$ is a modified Bessel function of the second kind, for which tabulated values are available (18). For the case of instantaneous emission, equations [11] and [19], a particularly simple result is obtained

$$[22] \qquad F(cv) = bc^2K_0(cv)/2\pi.$$

When $a = c$ and equation [14] is employed

$$[23] \qquad F(cv) = bc^3vK_1(cv)/4\pi.$$

The general equation [21] can be simplified when emitter densities at large values of cv are considered. Then, the function $K_0(cv)$ is closely approximated by c^2e^{-cv}/v.

While the treatment given above completes the presentation needed here, its relationship to the classical sodium diffusion flame deserves mention (2). In such studies the 'edge' of the flame, that point at which the sodium resonance emission is just visible, is determined. This is compared to that concentration of sodium that is just visible in static experiments under similar conditions. Thus, instead of using the integral criterion

$$\int_0^\infty [y]\, du = A \int_0^\infty (e^{-cr}/r)\, du$$

the expression

$$[y]_R = A' e^{-cR}$$

is used. Since the factor c^2 present in [22] does not enter here (it must be considered in any analysis based on an absolute value of [y] or [w*]), the approximation is probably no worse than the neglect of spherical symmetry.

The important difference between the sodium flame and the product emitter flame is that in the latter a decrease in c or a reduces the apparent size of the reaction zone, while in the former a reduction in c may produce an apparent enlargement. In this respect, the product emitter flame behaves in a manner opposite to that of the sodium flame.

REACTION RATES: APPLICATION TO NITRIC OXIDE SYSTEMS

Studies of the O+NO and the N+NO systems were made in a conventional low-pressure flow system. In both cases the atom-bearing stream was the nozzle reagent and either pure NO or NO diluted with nitrogen formed the atmosphere. The NO (Matheson) was fractionally distilled before use. Tank oxygen was dried but not purified further. Nitrogen was passed over heated copper and dried before use. All gases were fed through critical orificii into the low pressure system from reservoirs, the pressures of which were adjusted to provide the desired flow rates. The reactor was a 4-in. diameter cylinder with plate glass ends through which the flame was photographed. The nozzles through which reagent y was introduced were pyrex tubes drawn down to an i.d. of 1 to 2.2 mm. The reactor pressure could be controlled by a valve near the mechanical oil pump that maintained the flow. Pressures within the reactor ranged from 0.5 to 2 mm Hg and were adjusted to provide flames 2 to 5 cm in diameter. In all cases higher pressures were needed to restrict the flames in the NO–N_2 mixtures than in pure NO.

Can. J. Chem. Downloaded from www.nrcresearchpress.com by 210.87.254.105 on 09/05/12
For personal use only.

The O+NO flames were photographed with a Leica IIe 35 mm camera, and the N+NO flames were recorded with a Zeiss $2\frac{1}{4}\times3\frac{1}{4}$ film pack camera. In both cases the ranges were adjusted so that the flame filled most of the film. In both cases Eastman Kodak XXX panchromatic film was used. For each set of flame pictures there was prepared a film calibration made by exposing a strip of film through a calibrated step wedge. The calibrations were processed at the same time as the corresponding flame pictures.

The flame negatives were densitometered using a Leeds and Northrup microdensitometer, traverses being taken across several regions of each flame so density maps could be prepared. These maps showed a slight elongation of the flame along the nozzle axis, this being noticeable only at small distances from the nozzle tip. After the plate densities were converted to exposures, plots of exposure versus distance from the center of the flame pattern were prepared. For this purpose only exposure values were used that were taken from points near a line perpendicular to the nozzle axis and passing through the center of the pattern.

These exposure–distance plots were analyzed in terms of the models presented in the last section. Examination of either equation [21] or [22] reveals that the *shape* of the function is determined by the behavior of the modified Bessel function. Thus, if a parameter c or two parameters, c and a, can be chosen so that the shape of the experimental curve can be reproduced, the rate constants may be obtained without knowledge of the molar flow rate of atoms through the nozzle. In this case, and in others involving unstable species, this is advantageous.

In all the cases studied here it was feasible to reproduce the experimental exposure–distance curves by means of a formula such as [22] containing only one rate parameter. For this reason, the general relation [21] has not been applied. The results of the experiments are given in Table II. The 'shape parameter' column may be interpreted as

TABLE II

Product emitter flame measurements of rates of the reaction of nitric oxide with oxygen atoms

Mole fractions		Nozzle flow / Total flow	Pressure (mm Hg)	Shape parameter (cm^{-1})	$k/D'\times10^{-7}$ (cm/mole at 1 mm Hg)
NO	N_2				
(*a*) With oxygen atoms and molecules as nozzle reagent					
0.882	0	0.135	0.65	0.7	2.4
0.886	0	0.129	0.64	1.1	6.0
0.518	0.349	0.15	1.57	1.35	2.6
0.565	0.286	0.176	1.34	1.23	2.7
0.557	0.281	0.192	1.43	2.02	6.6
(*b*) With active nitrogen (N and N_2) as nozzle reagent					
0.414	0.568	0.262	1.95	2.86	8.7
0.427	0.573	0.359	1.50	1.84	6.4
0.220	0.780	0.225	1.40	0.81	2.8
0.220	0.780	0.225	1.40	0.75	2.4
0.762	0.238	0.238	1.25	1.66	4.1
0.762	0.238	0.238	1.25	1.54	3.7

NOTE: Mole fractions based on the sum of atmosphere flow and nozzle flow. All experiments at room temperature, 293° K.

c, a, or f. The final column represents $k/D = c^2/[z]$, see equation [9] where z is the NO concentration and the diffusion coefficient would have its value for a pressure of 1 mm Hg (that is, the reciprocal pressure dependence of the diffusion coefficient has been factored out). The average of k/D' for set a is $(4.1\pm2.4)\times10^7$, and for set b is $(4.7\pm2.0)\times10^7$ (arithmetic errors).

Can. J. Chem. Downloaded from www.nrcresearchpress.com by 210.87.254.105 on 09/05/12
For personal use only.

Can. J. Chem. Downloaded from www.nrcresearchpress.com by 210.87.254.105 on 09/05/12
For personal use only.

DISCUSSION OF RATE MEASUREMENTS

The equality of the average values of k/D' for the experiments using O and N atoms indicate that the same process is controlling in both systems. The spread of values in set *a*, Table II, must be attributed to experimental error. The spatial resolution on the 35-mm films used here was considerably less than for set *b*, where the larger films were used. In the latter the reproducibility in equivalent is much better. Here there is a slight suggestion that k/D' varies with the NO pressure, but this is far from certain.

For set *a*, the shape parameter may be identified as *c* as defined by equation [9] and for set *b* as *f* defined immediately before [17]. These then apply to equation [1], or its equivalent

$$O + NO + M \rightarrow NO_2 + M. \qquad [24]$$

In either case a value for the diffusion coefficient, D', must be supplied if the rate constant is to be extracted. This number is uncertain, due to our poor knowledge of the diameter of the oxygen atom. Here we assume a value of $250 = D'$. Then for equation [1], $k_1 = 1\times10^{10}$ cc/mole-sec. This value is tenable for the type of reaction considered but is 1000 times larger than other estimates (8,10). If [24] is assumed to dominate, $k_{24} = 1.4\times10^{17}$ $(cc/mole)^2$ sec^{-1} based on set *b*. This value is fivefold greater than that reported by Kaufman (8) and by Harteck, Reeves, and Mannella (10).

(An alternative interpretation of the shape parameter may be made because of the symmetry of the equations. If it is considered to be *a*, equation [10], either a value of $k_2 = 4\times10^2$ sec^{-1} or $k_3 = 7\times10^9$ $(cc/mole)^2$ sec^{-1}. The former is improbable for the decay of an excited NO_2, the latter is very low for a three-body recombination coefficient. Neither is tenable here.)

The interpretation of these flames in terms of [24] and the comparison with previous work provides an adequate justification for the model developed here for the product emitter flame. It is apparent that, as presently used as a photographic method, the precision is not high. A photometric application should markedly improve the technique. The fact that the rate, k_{24}, reported here is larger than has been determined earlier deserves some comment. The product emitter flame is a limiting case of a few oxygen atoms reacting with a large excess of NO. The more accurate work on this system has employed the reverse condition, a small amount of NO for many oxygen atoms. If there should be systematic errors in that work (and we have not found them), particularly reactions in the cycle that destroys and regenerates NO whose rates have not been considered but are only moderately fast, they would tend to reduce the apparent value of the rate. Some of the discrepancy may lie here, but most or all of it should be attributed to as yet unevaluated factors in this diffusion flame method.

REFERENCES

1. H. VON HARTEL and M. POLANYI. Z. physik. Chem. B, **11**, 97 (1931).
2. J. F. REED and B. S. RABINOVITCH. J. Phys. Chem. **61**, 598 (1957).
3. D. GARVIN and G. B. KISTIAKOWSKY. J. Chem. Phys. **20**, 105 (1952).
4. F. T. SMITH and G. B. KISTIAKOWSKY. J. Chem. Phys. **31**, 621 (1959).
5. F. T. SMITH. J. Chem. Phys. **22**, 1605 (1954). R. J. CVETANOVIĆ and D. J. LE ROY. Can. J. Chem. **29**, 597 (1951).
6. M. L. SPEALMAN and W. H. RODEBUSH. J. Am. Chem. Soc. **57**, 1475 (1935).
7. A. G. GAYDON. Proc. Roy. Soc. (London), A, **183**, 111 (1944).
8. F. KAUFMAN. J. Chem. Phys. **28**, 352, 992 (1958).
9. H. W. FORD and N. ENDOW. J. Chem. Phys. **27**, 1156 (1957).
10. P. HARTECK, R. R. REEVES, and G. MANNELLA. J. Chem. Phys. **29**, 1333 (1958).

11. F. J. LIPSCOMB, R. G. W. NORRISH, and B. A. THRUSH. Proc. Roy. Soc. (London), A, **223**, 455 (1956).
12. K. DRESSLER. J. Chem. Phys. **30**, 1621 (1959).
13. G. B. KISTIAKOWSKY and G. G. VOLPI. J. Chem. Phys. **27**, 1141 (1957); **28**, 665 (1958).
14. F. KAUFMAN and J. R. KELSO. J. Chem. Phys. **27**, 1209 (1957).
15. A. M. BASS and K. G. KESSLER. J. Opt. Soc. Am. **49**, 1223 (1959).
16. D. GARVIN and J. D. MCKINLEY, JR. J. Chem. Phys. **24**, 1256 (1956).
17. D. RAPP and H. S. JOHNSTON. Final Report on Contract Nonr 222(56), Project NR 051-246, Department of Chemistry, University of California, Berkeley, California. March 10, 1960.
18. BRITISH ASSOCIATION for the Advancement of Science. Mathematical Tables. Vol. VI. Bessel Functions, Part I. Cambridge Univ. Press. 1937. pp. 266–268.

Can. J. Chem. Downloaded from www.nrcresearchpress.com by 210.87.254.105 on 09/05/12
For personal use only.

Can. J. Chem. Downloaded from www.nrcresearchpress.com by 210.87.254.6 on 09/05/12
For personal use only.

SOME OBSERVATIONS ON THE RADIATIVE COMBINATION OF ATOMIC HYDROGEN WITH ATOMIC HALOGENS IN BURNER FLAMES[1]

L. F. PHILLIPS AND T. M. SUGDEN

ABSTRACT

When small quantities of gaseous molecular halogens chlorine, bromine, and iodine are introduced into the supply to premixed hydrogen–oxygen–nitrogen flames one of the most important spectroscopic features appearing is an apparently continuous emission in the visible, sometimes extending into the near ultraviolet. The intensity of this continuous emission has been studied as a function of amount of halogen, and of temperature, composition, and position with respect to the reaction zone in a wide variety of flames. In oxygen-rich flames it has been attributed to an over-all process,

$$X + X \rightarrow X_2 + h\nu,$$

where X denotes an atom of halogen; one of the atoms may be in an excited state. Most of the work concerns hydrogen-rich flames, where a very strong correlation between the intensity and the product [H][X] is obtained. The over-all process may be written as

$$H + X \rightarrow HX + h\nu.$$

The efficiency of this over-all process is measured as 1 quantum emitted for about 10^{10} ordinary kinetic collisions of the atoms. The mechanism is discussed from the aspects of direct radiative recombination and of stabilization by collision of an intermediate excited HX* before radiation.

INTRODUCTION

A rather convenient method for studying some gaseous reactions at high temperatures has been shown to be the addition of the reactant or reactants in small amount to premixed flames of hydrogen, oxygen, and nitrogen at atmospheric pressure (1, 2). Variation of the amounts of hydrogen and nitrogen relative to oxygen enables a range of burnt gas temperatures from 1500° to 2500° K to be covered. The composition of the flame gas may also be varied isothermally. Little or no disturbance is produced in such gases by small amounts of additives, and the main flame gases can be regarded as a medium or 'solvent' in which the reactions of the additive take place.

Hydrogen–oxygen–nitrogen flames have two advantages over most other flames for this kind of work. Firstly, a great deal is known about the burnt gases and the reactions proceeding in them in the absence of additives, and secondly, the radiation from such flames is either very weak or confined to rather narrow regions of the spectrum in the visible and contiguous near ultraviolet and infrared.

The premixed flame has a narrow reaction zone close to the burner, followed by a zone of hot burnt gas extending several centimeters downstream. The use of sintered metal or Mèker-type burners allows this reaction zone to be made almost flat, and parallel with the burner surface, and it is then possible to use the downstream direction as a variable for following reactions with time. The scale is such that 1 cm corresponds with times of about 1 millisecond. The effects of entrained air from the surroundings can be reduced by shielding the flame containing the trace additive with a second flame of similar composition but without additive. In this way the inner flame is protected over a distance of several centimeters.

The major part of the burning takes place in the reaction zone in a distance of a fraction of a millimeter. The relevant properties of the burnt gases are as follows. In general, the

[1]*Contribution from the Department of Physical Chemistry, University of Cambridge, Lensfield, Cambridge; paper presented at the Symposium on the Fundamental Aspects of Atomic Reactions held at McGill University, Montreal, Que., September 1960.*

amounts of the free radicals H and OH emerging from the reaction zone are very much in excess (up to 1000 times for cooler flames) of the equilibrium ones for the measured temperatures (3, 4). This occurs because of the branched chain nature of the main process of combustion. These radicals recombine relatively slowly, as they proceed downstream, by reactions

$$H + H + M \rightarrow H_2 + M$$
$$H + OH + M \rightarrow H_2O + M$$

where M is a third body. This third body is usually a molecule of a major constituent of the burnt gases and, in the case of fuel-rich flames, as normally used in this work, will be H_2O, N_2, or H_2. Certain rapid, reversible, bimolecular reactions can occur, however, at such speeds that definite relations hold between the concentrations of the burnt gas molecules. The most important of these is (1, 5)

$$H + H_2O \rightleftharpoons OH + H_2; \qquad K_0 = ([OH][H_2])/([H][H_2O]).$$

This reaction proceeds so rapidly that the concentrations of H and OH are related to each other at all points in the burnt gases by the equilibrium law for K_0, in terms of $[H_2]$ and $[H_2O]$, both of which are large, and known with reasonable accuracy for fuel-rich flames.

Flame photometric methods for measuring [H] and [OH], based on the addition of very small amounts (1 part in 10^6 or less) of various metallic compounds to the flame gases, have been devised, and shown to be consistent and reliable (3, 6, 7, 8). The temperature of the flame gases (about 2000° K) can be measured to within 10° C. It can thus be seen that the flame gases can be used as a fairly controlled source of atomic hydrogen and hydroxyl radicals.

The other great advantage of these flames is that their normal radiation is limited to strong emission from OH in the near ultraviolet, H_2O vibration–rotation bands in the far red and near infrared, and a very weak, apparently continuous, spectrum extending across most of the visible region (9). This last has been shown by Padley to arise from (10)

$$H + OH \rightarrow H_2O + h\nu$$

although whether this is a true radiative combination, or whether an excited H_2O^* is formed and stabilized by collision, is not fully established. Spectra arising from additives often stand out strongly and allow of photometric investigations.

The emission resulting from addition of amounts up to 2% of the halogens chlorine, bromine, and iodine to hydrogen–nitrogen–oxygen flames, mainly fuel-rich, is discussed in this paper. Figure 1 shows typical exposures for the reaction zone of a flame of this kind with small additions of these halogens. The addition of iodine produces the well-known IO band system (11) in the visible quite strongly, and the addition of bromine produces the BrO bands (12), weakly. No ClO bands were detected in this work, although such a system has been found in other circumstances (13, 14). These halogen oxide bands became much weaker downstream from the reaction zone, presumably because of the decrease of atomic oxygen with distance.

The most important feature from the present aspect is, however, an apparently continuous spectrum extending from the red into the ultraviolet. In the case of chlorine it is clearly visible at shorter wavelengths than the (0,0) bandhead of OH at 3064 Å, but no very sharp short wavelength cutoff can be ascribed to it. These continua persist, with some reduction in intensity, into the burnt gas. This general type of continuous spectrum appears to be quite a common feature of flames. In particular, they occur when

Can. J. Chem. Downloaded from www.nrcresearchpress.com by 210.87.254.6 on 09/05/12
For personal use only.

nitric oxide (15, 16), carbon monoxide (17, 18, 19), and alkali metals (8) are added in small quantities, and in these cases have been ascribed to

$$NO + O \rightarrow NO_2 + h\nu$$
$$CO + O \rightarrow CO_2 + h\nu$$
$$Na + OH \rightarrow NaOH + h\nu$$

respectively. The atomic hydrogen–hydroxyl continuum has been mentioned above (10). It is not known in most cases whether an excited intermediate molecule is stabilized. Better resolution of the spectra might show discrete structure, which would be evidence in favor of this stabilization.

These apparently continuous spectra given by the halogens have been studied in a wide variety of flames, their intensities being measured as functions of wavelength, flame gas composition, temperature, and position in the flame gases.

EXPERIMENTAL

The burner consisted of a bundle of fine silica tubes, each of about 0.5 mm internal and 1.0 mm external diameter. The whole bundle was 1.2 cm in diameter. It was supplied with premixed hydrogen, nitrogen, and air, which were individually metered by calibrated capillary-type flowmeters. The gases were mixed before passing to the burner. A diagram of the burner and its supply lines is shown in Fig. 2. Silica tubes were used in preference to metal ones on account of possible corrosion by the halogens, which were also supplied to the gas mixture before it entered the burner. The bundle of tubes was held together by Araldite cement. This 'experimental' flame was surrounded by a shield flame supplied by a similar gas mixture, except for the halogen, to reduce the effects of entrained air on the inner flame. The tubing for the shield flame was stainless steel hypodermic tube, again cemented with Araldite. The arrangement gave a stable, laminar flame with primary reaction cones about 0.5 mm high, i.e. the reaction zone was almost flat. The burner was water-cooled. The total flow to the burner was of the order of 1 cubic foot/minute and was adjusted to give a stable flame for each composition.

The temperature of the burnt gas was measured by the sodium D-line reversal method (20), which has been established to be reliable for these flames provided the measurements are made more than 1 cm downstream from the reaction zone, so as to avoid effects due to chemiluminescent excitation of the sodium (2). Sodium was added as a fine spray of concentrated aqueous sodium chloride solution from an atomizer operated by part of the air supply. Measurements of the reversal were made visually, using a tungsten strip filament lamp which was calibrated with a Cambridge optical pyrometer. A Hilger, glass prism, constant deviation spectroscope was used. The temperatures ranged from 1500° K to 2300° K, depending on the composition of the mixture; most of the flames were fuel-rich. Reproducibility was to within 10° C. The potassium resonance doublet at 7665 and 7699 Å is considerably less liable to chemiluminescence, as compared with thermal excitation (5), and was used photometrically to extend temperature measurements closer to the reaction zone than 1 cm.

Measurements of the concentration of atomic hydrogen in the burnt gas were made by the Na–Li method of James and Sugden (3, 21). This involves flame photometry of

FIG. 1. Emission spectra for addition of halogen to an H_2–O_2–N_2 flame. Hilger Medium Quartz Spectrometer with Ilford H.P.3 Plates. Exposures 1 hour. Observations made on the reaction zone. Flame $H_2/O_2/N_2 = 3/1/4$, $T \sim 2300°$ K. The extension of continua into the ultraviolet below 3064 Å is only visible on the original plate. The minimum in the green corresponds with a region of low plate sensitivity.

Can. J. Chem. Downloaded from www.nrcresearchpress.com by 210.87.254.6 on 09/05/12
For personal use only.

Can. J. Chem. Downloaded from www.nrcresearchpress.com by 210.87.254.6 on 09/05/12
For personal use only.

PLATE I

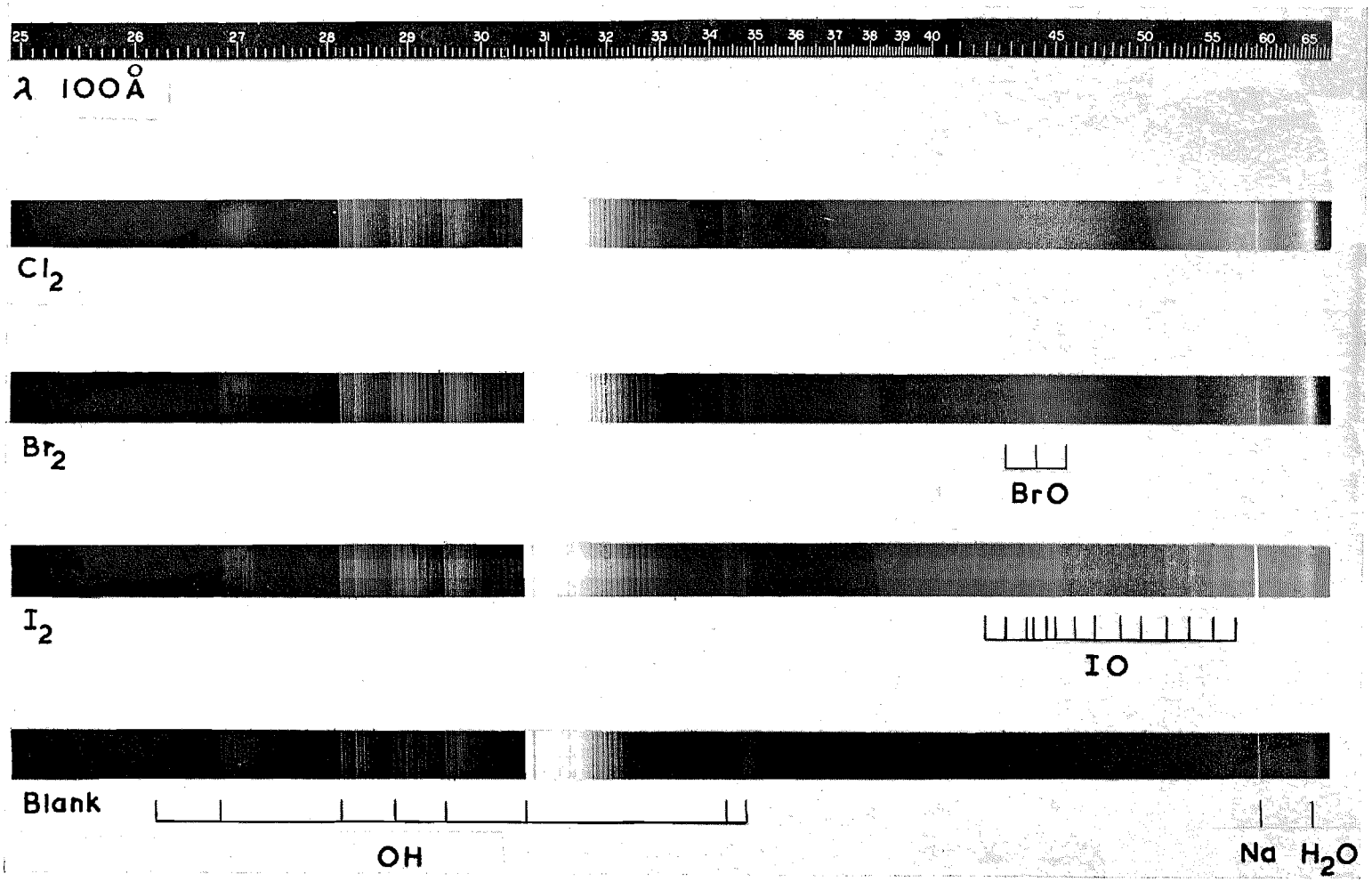


FIG. 1.

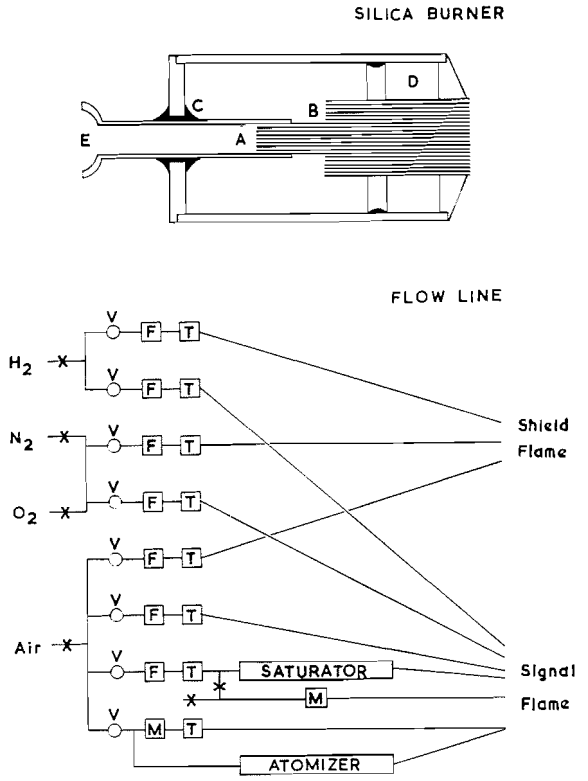


FIG. 2. Burner and supply lines. A is the 'experimental' flame with silica tubes, supplied from E. B indicates the stainless steel tubes for the shield flame (supply tubes not shown). C is a wax seal to eliminate strain. D is the water-cooling jacket, X tap, V needle valve, F flowmeter, M mercury manometer, T trap.

the emission from the resonance lines when equal amounts of sodium and lithium are introduced as salt sprays into the flame supply, the concentrations being sufficiently low to make self-reversal negligible. A significant amount of the lithium is removed as the very stable gaseous compound LiOH by the balanced reversible reaction

$$Li + H_2O \rightleftharpoons LiOH + H.$$

The NaOH molecule is much less stable, and the amounts of it formed can be neglected. The method leads to absolute values of [H] correct to within $\pm 20\%$, and to relative values for a series of flames to within $\pm 5\%$. The equilibrium constant of the reaction was calculated from a formula given by Smith and Sugden (22), with thermochemical data from Gaydon and Wolfhard (20), modified to correspond with a heat of dissociation of OH of 102.5 kcal/mole, as recommended by Gray (23). The method yields values of [H] in accordance with equilibrium ones in circumstances where equilibrium is known to obtain, i.e. at temperatures above 2400° K and at 3 cm from the reaction zone. It is valid provided that the emission of the resonance lines is thermal, a condition which holds reasonably well 1 cm or more downstream from the reaction zone.

To obtain [H] nearer to the reaction zone, the CuH photometric method of Bulewicz and Sugden (6) was adopted, as recommended by Padley and Sugden (2). This method is not absolute, but can be calibrated against the Li–Na method. It is apparently not subject to difficulties arising from chemiluminescence.

Can. J. Chem. Downloaded from www.nrcresearchpress.com by 210.87.254.6 on 09/05/12
For personal use only.

All photometric measurements were made by chopping the light from the flame with a sector disk at a frequency of 600 cycles/second before it fell on the entrance slit of the Hilger constant deviation glass spectrometer fitted with an IP 21 photomultiplier as detector. The output from this was amplified by a homodyne system, a reference signal being taken from the same chopping disk, and was finally presented as a meter reading. The wavelength sensitivity was obtained by calibration with a tungsten strip filament lamp running at known temperatures. The spatial resolution of the optical system allowed a section of the 'experimental' flame about 0.5 mm in height to be studied. The burner was mounted horizontally so that the image of a cross section of the flame filled the vertical entrance slit of the spectrometer.

Elementary halogens were added by the following means. For chlorine, cylinder supplies were transferred to a gas aspirator, where they were stored over brine. The gas was passed into the main flame gas supply by displacing the brine with a metered stream of air. Liquid bromine was contained over a sintered glass disk in a thermostatted saturator. A very small, measured proportion of the air supply was diverted through the sintered disk, and became saturated with Br_2 vapor. Independent tests showed saturation to be efficient. Iodine was contained in a similar saturator immersed in glycerol at 130° C, whereby it could be kept in liquid form. It was necessary to heat the connecting tubes to within a short distance of the burner to reduce condensation on the walls. Even so, some difficulty was experienced from this source. Vapor pressure data were taken from the International Critical Tables.

RESULTS AND CONCLUSIONS

1. *The Effect of Halogens on Temperature and Flame Composition*

The first point to be established is whether the addition of the halogen has any marked effect on the parameters of the main flame gases. Two of these have been examined, as being the most important—the temperature and the concentration of atomic hydrogen. Addition of 2% of chlorine causes an increase of temperature of 20–30° C. Since most of the measurements were made with amounts below 1%, the effects of change of temperature can be neglected, in first approximation. The addition of bromine and iodine had much smaller effects on the temperature than did that of chlorine. The effect of the addition of halogen on the concentration of atomic hydrogen has been estimated indirectly, since it is not possible to use the Li–Na method or the CuH method in the presence of halogen, on account of the formation of alkali halides in the one case, and of emission from gaseous cuprous halides in the other.

Addition of chlorine in amounts of the order of 0.1–1% of the gases causes a reduction of the intensity of the sodium D-line provided by adding a very small (1 part in 10^8) portion of sodium salt because of the formation of gaseous sodium chloride. By far the most stable compound of chlorine in hydrogen-rich flame gases is hydrogen chloride, and the added chlorine will be expected (see below) to be almost entirely in this form. The reaction by which sodium chloride is made will be the rapid reversible one of Na with HCl

$$Na + HCl \rightleftharpoons NaCl + H; \qquad \text{eq. const. } K_1.$$

This balance will be set up in the flame gases within a few microseconds. If [H] remains unchanged on addition of chlorine, then a plot of (I_0/I) against $[Cl]_0$ should be a straight line, where I_0 and I are the intensities of the sodium D-lines in emission without and with total added chlorine $[Cl]_0$ respectively, since $[Cl]_0 \sim [HCl]$, and thus

Can. J. Chem. Downloaded from www.nrcresearchpress.com by 210.87.254.6 on 09/05/12
For personal use only.

$$[Na]_0/[Na] = 1+(K_1[Cl]_0)/[H].$$

I is proportional to [Na] for sufficiently low concentrations of sodium to make self-reversal negligible. If [H] is dependent on $[Cl]_0$, curved plots should be obtained.

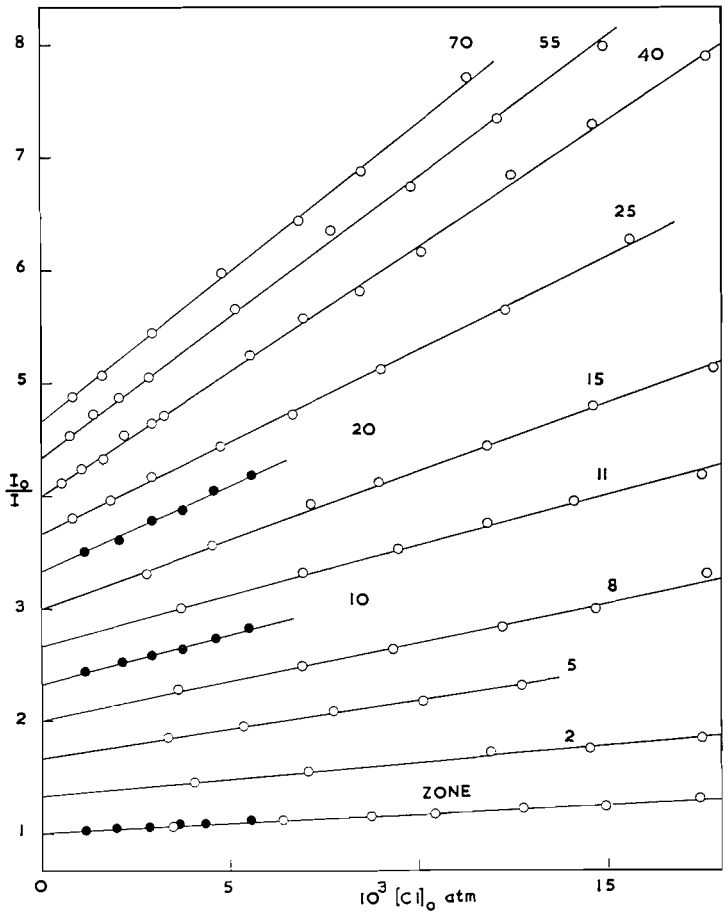


FIG. 3. (I_0/I) sodium D-lines against total added chlorine $[Cl]_0$ for a flame with $H_2/O_2/N_2 = 3/1/4$. The open circles are for addition of chlorine gas, and the full circles for addition of chlorine as chloroform. The numbers on the plots give distance in millimeters from the reaction zone. The lines (apart from that for the reaction zone) have been displaced vertically for clarity: without such displacement they have a common intercept. $M/1000$ NaCl solution sprayed from the atomizer.

Figure 3 shows typical plots of (I_0/I) against $[Cl]_0$. They are good straight lines. In the case illustrated they give evidence of decrease of [H] with increasing distance from the burner. There is thus good evidence that [H] is not significantly altered by the amounts of chlorine used. Earlier work (3) showed a slight initial curvature of plots of this kind, but this has been shown to arise from faults in the method of adding the halogens. Results with the same implication, that [H] is unaffected, hold for addition of bromine and iodine up to 0.5%. This greatly simplifies the analysis of the results to be described, insofar as they are connected with the concentration of atomic hydrogen. Some observations have also been made on the effect of chlorine on the intensity in emission of the (0,0) band of OH at 3064 Å. Two per cent of chlorine produced no significant effect. This is in agree-

Can. J. Chem. Downloaded from www.nrcresearchpress.com by 210.87.254.6 on 09/05/12
For personal use only.

ment with the absence of change in [H], since the two radicals are related to each other and the major constituents by

$$H_2O + H \rightleftharpoons H_2 + OH,$$

which is balanced.

2. The Halogen 'Continua'

Figure 4 shows some results on the emission from various hydrogen–oxygen–nitrogen flames to which amounts of less than 1% of chlorine, bromine, or iodine were added. They were taken at wavelengths, and in positions in the flame gases, where interference

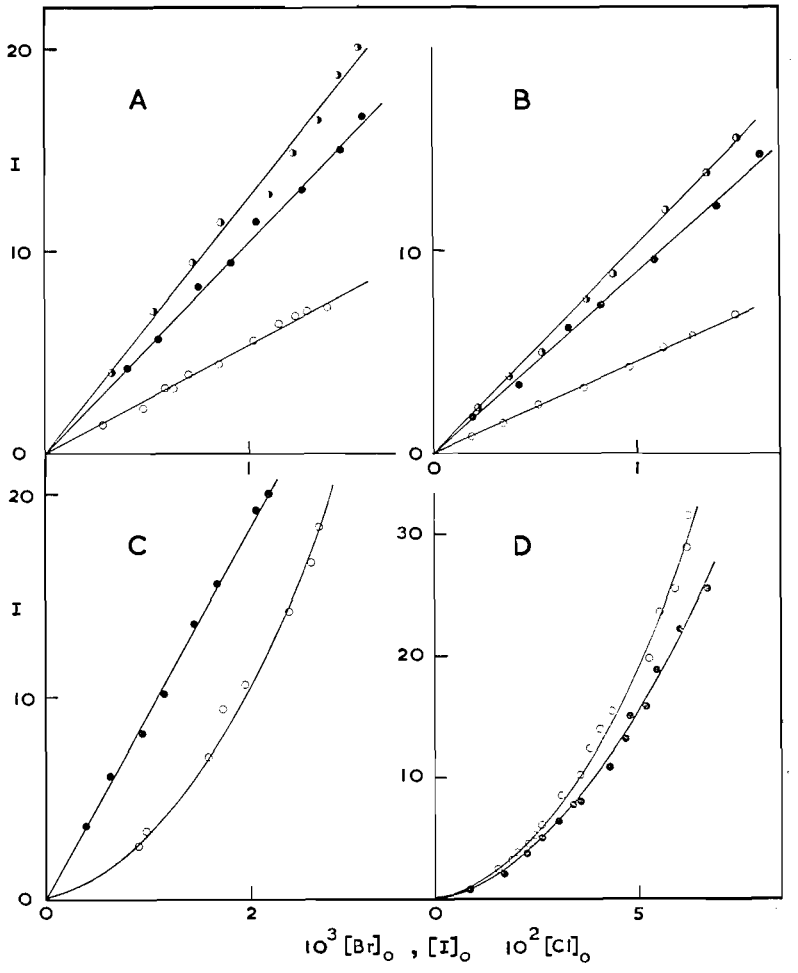


FIG. 4. Plots of intensity of halogen continua in H_2–O_2–N_2 flames as functions of total added halogen $[X]_0$. Waveband observed about 50 Å wide.

(A) Addition of chlorine. ○, flame $H_2/O_2/N_2 = 3/1/4$ at 10 mm from the reaction zone; ●, flame $H_2/O_2/N_2 = 3.5/1/5$ at 4 mm; ◑, flame $H_2/O_2/N_2 = 4.5/1/6$ at 2 mm. All at 4900 Å.

(B) Addition of bromine, all at 2 mm from reaction zone. Flame $H_2/O_2/N_2 = 3.5/1/5$: ○, for 6400 Å; ●, for 5500 Å; ◑, for 4900 Å.

(C) Addition of iodine. ○, flame $H_2/O_2/N_2 = 1/1/4$ at 8 mm; ●, flame $H_2/O_2/N_2 = 3/1/4$ at 2 mm. Both plots for 6400 Å.

(D) Flame $H_2/O_2/N_2 = 1/1/4$ at 8 mm and 4900 Å. ○, for addition of chlorine; ●, for addition of bromine.

Can. J. Chem. Downloaded from www.nrcresearchpress.com by 210.87.254.6 on 09/05/12
For personal use only.

from known discrete spectra (such as that of IO) was negligible. The intensity of emission without added halogen was subtracted directly from the total reading. Wide slits were used, so that a section of about 50 Å was observed.

An important relation to the general flame composition is at once apparent. When a fuel-rich flame is used there is a direct proportionality between the observed intensity I and the total halogen $[X]_0$, whereas for a very oxygen-rich flame, I is proportional to $[X]_0^2$.

The heats of dissociation of X_2 halogen molecules are such that at flame gas temperatures, and with the amounts of halogen used, the proportion which would be expected, on thermodynamic grounds, to be present as X_2 are negligible. Molecules of this type entering the reaction zone would immediately be decomposed by reaction with atomic hydrogen, of which a great deal is present,

$$X_2 + H \rightarrow HX + X.$$

A subsequent very rapid, reversible, reaction

$$HX + H \rightleftharpoons H_2 + X; \qquad \text{eq. const. } K_2$$

then sets up a balance between atomic X and the hydride HX

$$[HX]/[X] = [H_2]/K_2[H]$$

and

$$[X]_0 = [HX] + [X].$$

The ratio $[HX]/[X]$ may thus be obtained from the known values of the equilibrium constant K_2, and the concentrations $[H_2]$ and $[H]$. The former of these concentrations is readily calculable for a fuel-rich flame with sufficient accuracy, and the latter has been measured. The result is that $[HX]/[X] \gg 1$ for chlorine in fuel-rich flames, $\ll 1$ for iodine, and is not far from unity for bromine. In oxygen-rich flames the value of this ratio will be very severely reduced since molecular hydrogen now becomes a very minor constituent and in this case hardly any hydride HX is expected, and for all the halogens $[X] \sim [X]_0$. Consideration of the dissociation energies of the XO molecules (24) shows that they will not take up an appreciable part of the total halogen in any of the present flames.

It is therefore suggested that the observed dependence of I on $[X]_0^2$ in a very oxygen-rich flame arises from the radiation being associated with an over-all process

$$X + X \rightarrow X_2 + h\nu.$$

Whether X_2^* is stabilized by collision with other molecules before emission ensues (i.e. whether X_2^* is associated with a potential curve with a minimum) cannot be decided from the observations, since at the flame temperatures the discrete structure expected in this event would be so rich as not to be resolvable by the spectrometer. It is interesting to note that Kondratiev and Leipunski (25) observed an apparently continuous spectrum from heated halogens in this region (blue-green). This they attributed to recombination of excited and normal halogen atoms. Similar continua were observed by Ludlam, Reid, and Soutar (26) in H_2–Cl_2 diffusion flames, and by Urey and Bates (27) in H_2–Cl_2 and H_2–O_2–X_2 flames, and were associated with the same origin.

The main interest of this paper, however, centers on the emission from hydrogen-rich

Can. J. Chem. Downloaded from www.nrcresearchpress.com by 210.87.254.6 on 09/05/12
For personal use only.

flames, where the results of Fig. 4 exclude the possibility of radiative recombination of two halogen atoms. The direct dependence of I on $[X]_0$ implies that the radiation emerges from a molecule or process in which only one atom of halogen is concerned. On an a priori basis the over-all effect

$$H + X \rightarrow HX + h\nu$$

deserves consideration, since Padley (10) has shown that in these flames a very similar spectrum arises from

$$H + OH \rightarrow H_2O + h\nu.$$

Neither the results of Ludlam *et al.* nor those of Urey and Bates exclude the possibility that such an effect gave rise to some of the emission which they observed.

3. Dependence of Intensities on [H]

The total halogen is effectively distributed between [X] and [HX] in fuel-rich flames,

$$[X]_0 = [X] + [HX] = [X]\{1+([H_2]/K_2[H])\}.$$

Then, if the intensity $I = k[H][X]$

$$I = (k[H][X_0])/\{1+([H_2]/K_2[H])\}.$$

In the case of chlorine $[HX]/[X] = [H_2]/K_2[H] \gg 1$, so that

$$I = (kK_2[H]^2[Cl]_0)/[H_2]$$

whereas for iodine $[H_2]/K_2[H] \gg 1$, and

$$I = k[H][I]_0.$$

One way of testing these expressions is to observe I as a function of distance downstream from the reaction zone. The decrease in [H] as this distance increases, due to recombination of the excess radicals, may be followed by flame photometric methods. The most convenient one is the CuH method of Bulewicz and Sugden (6), referred to in the experimental section. The intensity of the CuH band at 4280 Å when a very small amount of copper salt is added to the flame is directly proportional to [H]. Thus, the lowest plot of Fig. 5 is effectively one of $1/[H]$ against distance from the reaction zone for a particular flame. It is a straight line with slope characteristic of the velocity constants of the ternary recombination processes such as

$$H + H + M \rightarrow H_2 + M$$

The first plot of Fig. 5 is of $(1/I)^{\frac{1}{2}}$ for the chlorine continuum: it is linear, and has the same (slope/intercept) as the $1/[H]$ plot at the bottom. The third plot is of $(1/I)$ for the iodine continuum, and is again of the same form as the $1/[H]$ plot. Thus the predictions based on the law $I = k[H][X]$ are borne out. Both $(1/I)$ and $(1/I)^{\frac{1}{2}}$ are plotted for bromine. The former is a little too steep, and the latter not nearly steep enough. This is in good agreement with the calculated values of $[HX]/[X]$ in this flame at 6 mm of 22.5, 0.55, and 2×10^{-4} for X = Cl, Br, and I respectively.

Can. J. Chem. Downloaded from www.nrcresearchpress.com by 210.87.254.6 on 09/05/12
For personal use only.

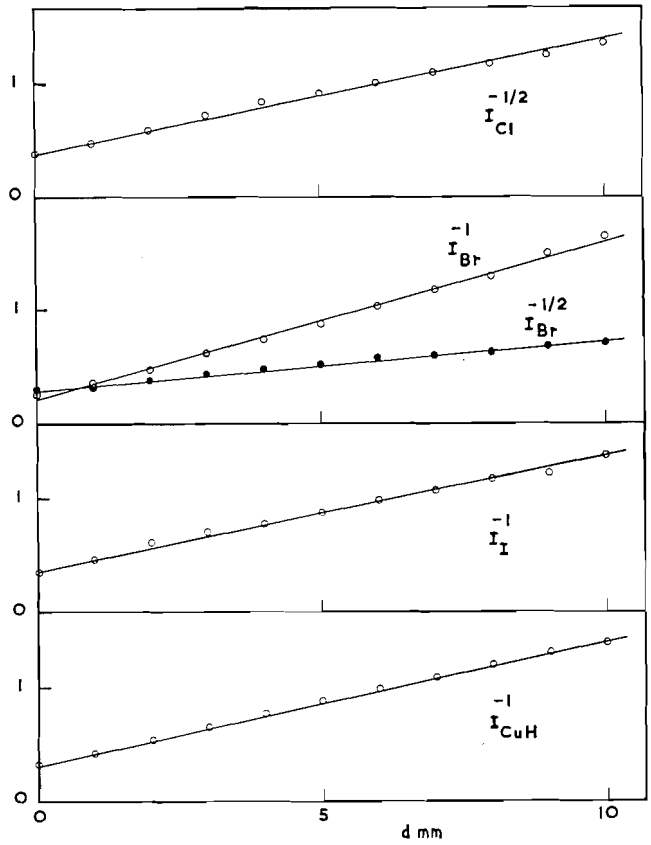


FIG. 5. Decay of intensity of I halogen continua with distance from the reaction zone for flame $H_2/O_2/N_2$ = 3.5/1/5, $T \sim 2000°$ K. Observed at 4900 Å for Cl_2 and Br_2 addition and at 6400 Å for iodine. $[Cl]_0 = 2 \times 10^{-2}$ atm, $[Br]_0 = [I]_0 = 2 \times 10^{-3}$ atm. Compared with decay of [H] as given by the intensity of the CuH band at 4280 Å.

A more complete test of the correlation of I with [H] (for iodine) or with $[H]^2$ (for chlorine) is obtained by plotting the values of all these quantities for the reaction zone (defined here as the point of maximum [H]) for a wide series of flames. One of the most convincing ways of doing this is to use the method of 'families', first introduced by James and Sugden (8). A 'family' is a set of flames for which $[N_2]/[O_2]$ in the unburnt gas is constant, usually integral: the flames within it have various $[H_2]/[O_2]$ values, ranging in this work from 2.5 (hot end of family) to 4.5 (cold end). Their properties are plotted conveniently against $1/T$, a line connecting members of a particular family. Thus figure 6 shows such plots for the functions $[H]_0$ and $[H]_0^2/[H_2]$, $[H]_0$ denoting the value of [H] in the reaction zone. It will be seen that one function gives clearly separated families, while the other produces characteristic overlapping. Figure 7 shows the intensity of the continua for chlorine, bromine, and iodine at constant total halogen concentration, plotted in the same way. The correlation of the iodine pattern with $[H]_0$, and that of the chlorine pattern with $[H]_0^2/[H_2]$ is very striking. Bromine is again intermediate in behavior. The case that the observed emission is given by $k[H][X]$ is thus a very strong one.

Can. J. Chem. Downloaded from www.nrcresearchpress.com by 210.87.254.6 on 09/05/12
For personal use only.

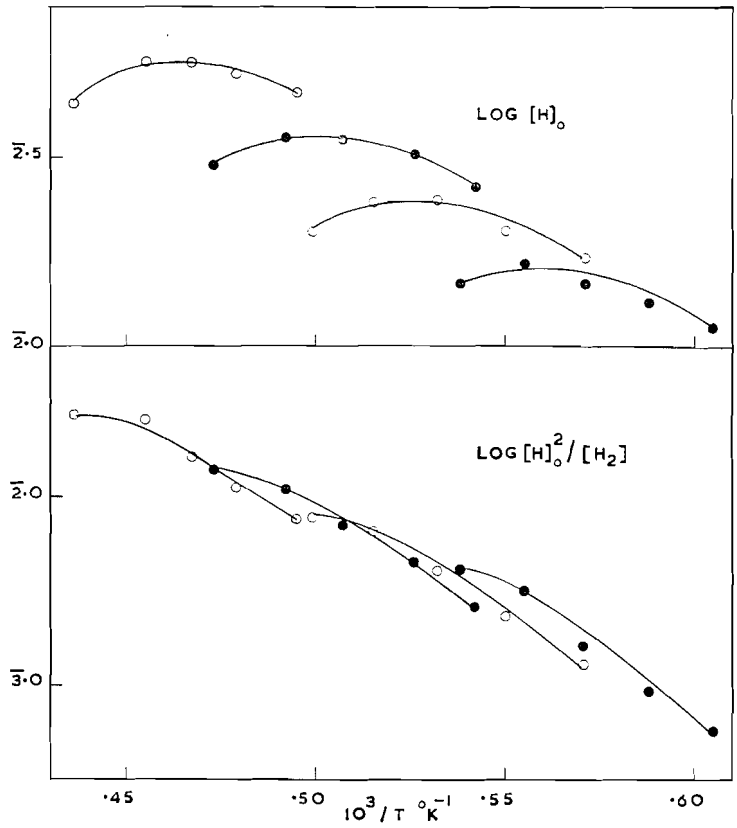


FIG. 6. Variation of $[H]_0$ and $[H]_0^2/[H_2]$ with flame composition. $[H]_0$ is the partial pressure (in atmospheres) of hydrogen atoms in the reaction zone. Flame families (N_2/O_2 in unburnt gas) 4, 5, 6, and 7. Points in each family are for unburnt H_2/O_2 ratios 2.5, 3, 3.5, 4, and 4.5. The temperature indicated is the steady value reached in the burnt gases after a time of ~1 millisecond.

4. The Efficiency of Emission in the Continuum

A figure for the number of quanta emitted per cubic centimeter/second, can be obtained by suitable integration over the whole of the continuum, and comparing the result with the known thermal emission from the sodium D-lines under conditions of known sodium concentration and no self-reversal. The result of this measurement is to establish that 1 quantum in the continuum for HCl is emitted for every 4×10^{10} normal kinetic collisions of H and Cl atoms in a flame at ca. 2300° K. This figure is subject to a number of limitations. Firstly, the intensity was only observed from about 3000 Å, where it becomes very weak, to 6500 Å, where it is still quite strong; any infrared contribution is ignored. Secondly, a mean collision diameter of 3 Å for H and Cl has been assumed in calculating the frequency of 'normal' collisions. Nevertheless, the above result for the "efficiency" of emission should be correct to an order of magnitude.

Figure 8 shows plots of relative k (where $I = k[H][X]$) obtained by computing $(I/[H][X])$, and indicates the way in which k varies with temperature. The plots show that it decreases markedly with increasing temperature for chlorine, at a rate corresponding to an exponential term with an energy of about 15 kcal/mole. The corresponding

Can. J. Chem. Downloaded from www.nrcresearchpress.com by 210.87.254.6 on 09/05/12
For personal use only.

Can. J. Chem. Downloaded from www.nrcresearchpress.com by 210.87.254.6 on 09/05/12
For personal use only.

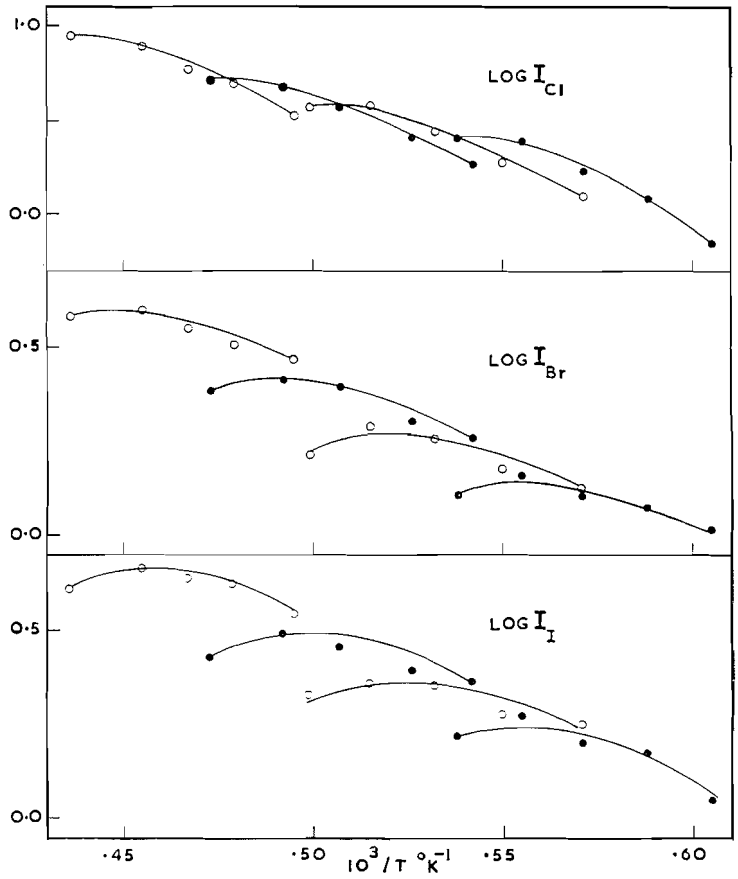


FIG. 7. Variation of intensities of halogen continua in reaction zone with flame composition. Families as in Fig. 6. $[Cl]_0 = 2\times10^{-2}$ atm, $[Br]_0 = [I]_0 = 2\times10^{-3}$ atm.

decrease for bromine is much smaller, and no decrease is observed for iodine, although in this case there is quite a high scatter on the points. These results do not refer to complete wavelength scans, but only to the emission at 4900 Å for chlorine and bromine, and 6400 Å for iodine. They must be interpreted with caution since the dependence of intensity distribution on temperature has not yet been fully explored.

DISCUSSION

Given that the intensity of the emission is proportional to [H][X], two types of mechanism appear possible.

(i) Direct radiative recombination from an upper electronic state which is arrived at by collision of atoms (ground state H and $^2P_{3/2}$ or $^2P_{1/2}$ atoms of halogen), without the intervention of any third body.

(ii) Stabilization of an intermediate HX* formed by collision of the atoms in the presence of a third body M. A typical scheme may be written

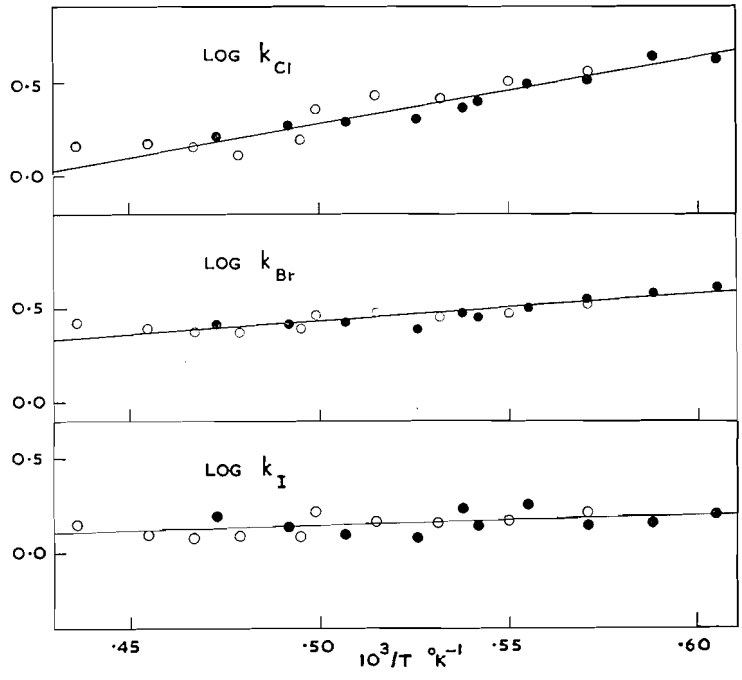


FIG. 8. Dependence of relative k, defined by I (continuum) = k[H][X] on temperature for the halogen continua in hydrogen-rich flames.

$$H + X + M \xrightarrow{k_1} HX^* + M,$$

$$HX^* + M \xrightarrow{k_{-1}} H + X + M,$$

$$HX^* + M \xrightarrow{k_2} HX + M,$$

$$HX^* \xrightarrow{k_3} HX + h\nu.$$

If the mean kinetic energy of approach of H and X, given by kT, is small compared with the vibrational spacing in the ground electronic state, then some fluctuations in intensity of emission corresponding with this spacing might be expected in case (i). It is interesting that Weizel, Wolff, and Binkele (28) observed multiple maxima in apparently continuous emission between the green and 2500 Å with hydrogen bromide in a weak uncondensed discharge. At flame temperatures kT is about one half of the vibrational spacing and such maxima might be obscured, giving an apparently smooth continuum. Case (ii) might be expected to give a somewhat more discrete spectrum, but if HX* has only a shallow minimum a large number of its vibrational states would be occupied, which, together with the number of rotational levels involved at flame temperatures could well make the result indistinguishable, with our resolution, from case (i).

The previously observed absorption spectra are of little use here, since only continua have been observed. Goodeve and Taylor (29, 30) obtain absorption continua for HBr and HI, which they consider are connected with dissociation to H($^2S_{1/2}$), Br($^2P_{3/2}$), and I($^2P_{3/2}$). Unfortunately the long wavelength limits lie above the dissociation energy, and

Can. J. Chem. Downloaded from www.nrcresearchpress.com by 210.87.254.6 on 09/05/12
For personal use only.

it is then impossible to say whether the HX* is in a completely repulsive state or not. These observations, as well as others by Trivedi (31), are discussed by Finkelnburg (32).

From the general kinetic point of view, case (i) leads to

$$I = k[H][X]$$

where k is the velocity constant of a single process, whereas case (ii) leads to

$$I = (k_3k_1[H][X][M])/(k_{-1}[M] + k_2[M])$$

provided that radiation is only a minor source of removal of HX* molecules. M may be different for the reactions leading to dissociation and deactivation of HX*, and so does not cancel directly. If dissociation predominates, $k_{-1}[M] \gg k_2[M]$ and [M] then cancels. Writing K_1, the equilibrium constant of $H + X \rightleftharpoons HX^*$, for k_1/k_{-1}, we have

$$I = k_3K_1[H][X] \quad \text{and} \quad k = k_3K_1.$$

If the heat of dissociation of HX* into $H(^2S_{1/2}) + X(^2P_{3/2})$ is ΔE^*, a positive quantity, then K_1 may be written

$$K_1 = Q_1 \exp(\Delta E^*/RT)$$

and a rough calculation, with reasonable rotational and vibrational parameters, leads to

$$K_1 = 10^{-23} \exp(\Delta E^*/RT) \text{ cm}^{-3}.$$

The experimental values of k are of the order of 10^{-21} cm^3 sec^{-1}, so that if $\Delta E^* =$ 10 kcal/mole, at 2000° the value of k_3 will be of order 10 sec^{-1}. This implies a highly forbidden transition; reference to the states indicating that $^3\Pi \rightarrow {}^1\Sigma$ would be the only one to fulfil such a requirement. Increments of ΔE^* by units of 10 kcal/mole have the effect of decreasing k_3 approximately by orders of magnitude, but the absence of discrete spectra implies that HX* cannot be very stable.

If deactivation predominates over dissociation, i.e. $k_2[M] \gg k_{-1}[M]$, k_3 is correspondingly increased, and the radiative lifetime shortened. It is improbable that this inequality would amount to a sufficient factor to make the radiative lifetime short enough for a fully allowed transition (order of 10^{-8} sec).

A very crude analysis of case (i) can be made as follows. The period of a molecular vibration is of the order of 10^{-13} sec, and this can be taken as the duration of a collision for a repulsive state. A normal radiative lifetime for electronic transition (10^{-8} sec) would then give an efficiency of order 10^{-5}, corresponding with k of order 10^{-15} cm^3 sec^{-1}. Again, therefore, the transition must be a highly forbidden one.

It is considered that the different variations with temperature found for the various halogens probably favor case (ii) insofar as ΔE^* could readily show a range of 15 kcal/mole among the halogens. No great temperature dependence of k_3 would be expected, nor of k for case (i), but the evidence presented here is not sufficient to allow of a final decision. It is of interest that the NO–O 'continuum' in flames has recently been shown (33) to derive, at least to some extent, from a mechanism of the general type (ii).

One of us (L. F. P.) is grateful for the award of a Shell Commonwealth Scholarship (New Zealand). We also wish to express our thanks to our colleagues in the Department of Physical Chemistry for useful discussions.

Can. J. Chem. Downloaded from www.nrcresearchpress.com by 210.87.254.6 on 09/05/12
For personal use only.

REFERENCES

1. T. M. SUGDEN. Trans. Faraday Soc. **52**, 1465 (1956).
2. P. J. PADLEY and T. M. SUGDEN. Proc. Roy. Soc. A, **248**, 248 (1958).
3. E. M. BULEWICZ, C. G. JAMES, and T. M. SUGDEN. Proc. Roy. Soc. A, **235**, 89 (1956).
4. E. M. BULEWICZ and T. M. SUGDEN. Trans. Faraday Soc. **54**, 1855 (1958).
5. P. J. PADLEY and T. M. SUGDEN. Symposium on Combustion. 7th Symposium. Butterworth Scientific Publications, London. 1959. p. 235.
6. E. M. BULEWICZ and T. M. SUGDEN. Trans. Faraday Soc. **52**, 1475 (1956).
7. E. M. BULEWICZ and T. M. SUGDEN. Trans. Faraday Soc. **52**, 1481 (1956).
8. C. G. JAMES and T. M. SUGDEN. Proc. Roy. Soc. A, **248**, 238 (1958).
9. A. G. GAYDON. The spectroscopy of flames. Chapman & Hall, London. 1957.
10. P. J. PADLEY. Trans. Faraday Soc. **56**, 449 (1960).
11. E. H. COLEMAN, A. G. GAYDON, and W. M. VAIDYA. Nature (London), **162**, 108 (1948).
12. E. H. COLEMAN and A. G. GAYDON. Discussions Faraday Soc. **2**, 166, 176 (1947).
13. G. PANNETIER and A. G. GAYDON. Nature (London), **161**, 242 (1948).
14. G. PORTER. Discussions Faraday Soc. **9**, 60 (1950).
15. A. G. GAYDON. Proc. Roy. Soc. A, **183**, 111 (1944).
16. A. G. GAYDON. Trans. Faraday Soc. **42**, 292 (1946).
17. H. P. BROIDA and A. G. GAYDON. Trans. Faraday Soc. **49**, 1190 (1953).
18. H. P. BROIDA and A. G. GAYDON. Proc. Roy. Soc. A, **222**, 181 (1954).
19. W. E. KASKAN. Combustion and Flame, **3**, 39 (1959).
20. A. G. GAYDON and H. G. WOLFHARD. Flames. Chapman & Hall, London. 1960.
21. C. G. JAMES and T. M. SUGDEN. Proc. Roy. Soc. A, **227**, 312 (1955).
22. H. SMITH and T. M. SUGDEN. Proc. Roy. Soc. A, **219**, 204 (1953).
23. P. GRAY. Trans. Faraday Soc. **55**, 408 (1959).
24. A. G. GAYDON. Dissociation energies. 2nd ed. Chapman & Hall, London. 1953.
25. V. KONDRATIEV and A. LEIPUNSKI. Z. Physik, **50**, 366 (1928).
26. E. B. LUDLAM, H. G. REID, and G. S. SOUTAR. Proc. Roy. Soc. Edinburgh, **49**, 156 (1929).
27. H. C. UREY and J. R. BATES. Phys. Rev. **34**, 1541 (1929).
28. W. WEIZEL, H. W. WOLFF, and H. E. BINKELE. Z. physik. Chem. B, **10**, 459 (1930).
29. C. F. GOODEVE and A. W. C. TAYLOR. Proc. Roy. Soc. A, **152**, 221 (1935).
30. C. F. GOODEVE and A. W. C. TAYLOR. Proc. Roy. Soc. A, **154**, 181 (1936).
31. H. TRIVEDI. Proc. Natl. Acad. Sci. India, **6**, 18 (1936).
32. W. FINKELNBURG. Kontinuierliche Spektren. Julius Springer, Berlin. 1938. p. 155.
33. H. P. BROIDA, H. I. SCHIFF, and T. M. SUGDEN. To be published.

Can. J. Chem. Downloaded from www.nrcresearchpress.com by 210.87.254.6 on 09/05/12
For personal use only.

Can. J. Chem. Downloaded from www.nrcresearchpress.com by 210.87.254.5 on 09/05/12
For personal use only.

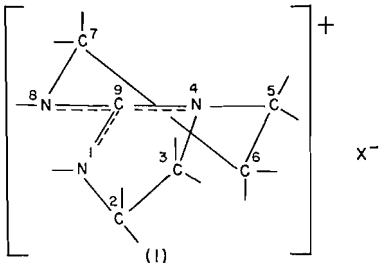
NITRATION OF BICYCLIC GUANIDINES[1]

A. F. McKay and M.-E. Kreling

ABSTRACT

The course of the nitration of a bicyclic guanidine system has been shown to depend on substitution at an adjacent carbon atom. The pyrimidine ring in 5-keto-2,3,6,7-tetrahydro-5(H)-thiazolo(3,2-*a*)pyrimidine is opened more rapidly by benzylamine and ethanolic hydrogen chloride than the pyrimidine ring in 5-keto-2,3,6,7-tetrahydro-1(H),5(H)-imidazo(1,2-*a*)pyrimidine. These effects are interpreted in terms of the resonance ion structure at the ring junctions.

The bicyclic guanidine, 2,3,6,7-tetrahydro-1(H),5(H)-imidazo(1,2-*a*)pyrimidine,[2] has been converted into 1-nitro-2,3,6,7-tetrahydro-1(H),5(H)-imidazo(1,2-*a*)pyrimidinium nitrate by nitration in absolute nitric acid – acetic anhydride medium (1). Nitration of the 2,3,6,7-tetrahydro-1(H),5(H)-imidazo(1,2-*a*)pyrimidinium ion is consistent with the presence of the guanidinium ion in its structure. The model of this bicyclic guanidinium ion may be represented diagrammatically by structure I. Atoms 1, 2, 3, 4, 5, 8, and 9 are



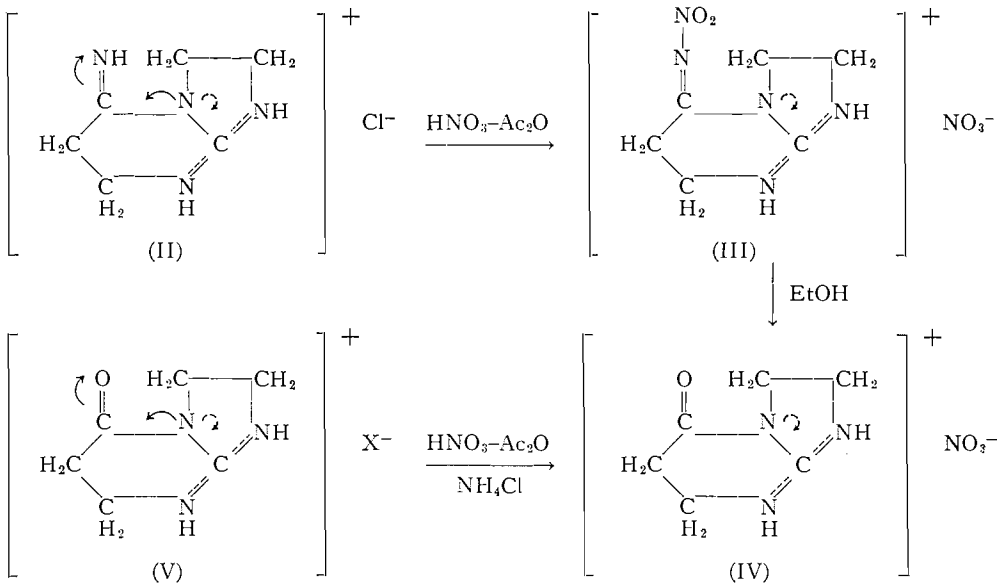
(I)

in the same plane, since the five-membered ring can be considered to be planar. A slight deviation of C atoms 2 or 3 from the plane of the ring would not contribute much to a relief of strain within this structure. A continuation of nitration studies on the 2,3,6,7-tetrahydro-1(H),5(H)-imidazo(1,2-*a*)pyrimidine system has shown that an electronegative substituent such as oxygen or nitrogen on C_5 affects the nitration of the guanidine structure.

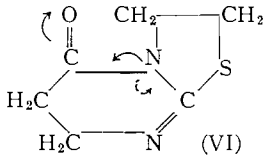
Nitration of 5-imino-2,3,6,7-tetrahydro-1(H),5(H)-imidazo(1,2-*a*)pyrimidinium chloride (II) in absolute nitric acid – acetic anhydride medium gave 5-nitrimino-2,3,6,7-tetrahydro-1(H),5(H)-imidazo(1,2-*a*)pyrimidinium nitrate (III). The failure of the guanidine structure to nitrate is explained by the electron displacements within structure II. There are two opposing electron attractive forces working on N_4; one involves its participation in the guanidinium ion and the other in the electron displacement indicated by the curved unbroken arrows in structure II. These opposing forces give the resonance ion structure more of an amidinium ion character than a guanidinium ion character and the amidinium ion does not nitrate. Thus nitration occurs only on the 5-imino nitrogen. The same explanation is given for the failure of 5-keto-2,3,6,7-tetrahydro-1(H),5(H)-imidazo(1,2-*a*)pyrimidine to nitrate.

5-Nitrimino-2,3,6,7-tetrahydro-1(H),5(H)-imidazo(1,2-*a*)pyrimidinium nitrate (III) is converted into 5-keto-2,3,6,7-tetrahydro-1(H),5(H)-imidazo(1,2-*a*)pyrimidinium nitrate (IV) on crystallization from ethanol. Because of this easy replacement of the nitrimino group, extreme care was required in the preparation of a pure sample of compound III.

[1]*Manuscript received June 8, 1960.*
Contribution No. 27 from the L. G. Ryan Research Laboratories of Monsanto Canada Limited, LaSalle, Que.
[2]*Named in accordance with the rules on nomenclature of fused ring systems given in The ring index, Am. Chem. Soc. 2nd ed., 1960. This compound was referred to as* Δ^8*-hexahydro-1,4,8-pyrimidazole in ref. 1.*



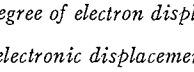
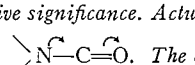
When 5-keto-2,3,6,7-tetrahydro-5(H)-thiazolo(3,2-*a*)pyrimidine (VI) was treated with an ethanolic solution of hydrogen chloride, a quantitative yield of 2-(β-carbethoxyethylamino)-2-thiazoline was obtained. Similarly benzylamine opened the pyrimidine ring of VI to give 2-(β-(N-benzylcarbamyl)-ethylamino)-2-thiazoline (2). Both ethanolic hydrogen chloride and benzylamine failed to open the pyrimidine ring of 5-keto-2,3,6,7-tetrahydro-1(H),5(H)-imidazo(1,2-*a*)pyrimidine (V) under similar conditions. The greater resistance of the pyrimidine ring to opening in V than in VI is due to the relative ease of electron displacements towards the carbonyl oxygen atom in these two systems. In V the opposing electron attractive force to the electron displacement indicated by the solid arrows[3] is greater than the opposing electron attractive force in VI. This is probably the main factor contributing to relative ease of opening the pyrimidine ring in these compounds although the slight difference in the conformations of the two ring systems also may make some contribution.



EXPERIMENTAL[4]

5-Keto-2,3,6,7-tetrahydro-1(H),5(H)-imidazo(1,2-a)pyrimidine

2-(β-Carboxyethylamino)-Δ²-1,3-diazacyclopentene (m.p. 209–211° C with decomp.) was prepared in 73.2% yield and the acid was esterified with ethanolic hydrogen chloride as previously described (3). On evaporation of the ethanolic solution 2-(β-carbethoxyethylamino)-Δ²-1,3-diazacyclopentene hydrochloride was obtained as a viscous oil.

[3]*The solid and broken arrows in the graphic formulas are used only for differentiation in discussion and they have no quantitative significance. Actually the degree of electron displacement in the*  *system is greater than in*  . *The effects of electronic displacements and resonance on the chemical reactivity of the bicyclic guanidines are under investigation.*

[4]*All melting points are uncorrected. Analyses were performed by Micro-Tech Laboratories, Skokie, Illinois.*

Can. J. Chem. Downloaded from www.nrcresearchpress.com by 210.87.254.5 on 09/05/12
For personal use only.

The above ester hydrochloride (10.3 g, 0.0465 mole) in absolute methanol (200 ml) was passed through a column of IRA-400 resin in the hydroxyl form. The resin column had been previously washed with absolute methanol. After the resin had been washed with absolute methanol (150 ml), the eluate and washings were evaporated to dryness *in vacuo*. The white crystalline residue weighed 6 g (92.8% yield). It melted at 141° C, resolidified, and melted at 148–149° C. This melting point was not changed by crystallization from absolute ethanol – ether (1:2) solution. Anal. Calc. for $C_6H_9N_3O$: C, 51.78; H, 6.52; N, 30.20%. Found: C, 51.53; H, 6.31; N, 30.34%.

The picrate (m.p. 248–249° C) of 5-keto-2,3,6,7-tetrahydro-1(H),5(H)-imidazo(1,2-*a*) pyrimidine was prepared in 95% yield from ethanol solution. Anal. Calc. for $C_{12}H_{12}N_6O_8$: C, 39.14; H, 3.29; N, 22.82%. Found: C, 38.93; H, 3.41; N, 22.75%.

5-Keto-2,3,6,7-tetrahydro-1(H),5(H)-imidazo(1,2-a)pyrimidinium Nitrate

5-Keto-2,3,6,7-tetrahydro-1(H),5(H)-imidazo(1,2-*a*)pyrimidine (0.695 g, 0.005 mole) was added to a nitration medium consisting of 98% nitric acid (2.33 ml, 0.05 mole), acetic anhydride (4.72 ml, 0.05 mole) and ammonium chloride (0.6 g, 0.011 mole). After the reaction mixture was stirred at 32° C for 2 hours, it was poured into cold absolute ether (75 ml). The ether was decanted from the oil, which was washed twice with fresh portions of absolute ether. After the oil was triturated with absolute ethanol, crystals (m.p. 129.5–131° C) separated from the oil, yield 0.57 g (56.4%). One crystallization from absolute ethanol raised the melting point to 132–133° C. Anal. Calc. for $C_6H_{10}N_4O_4$: C, 35.65; H, 4.99; N, 27.71%. Found: C, 35.56; H, 4.88; N, 27.38%.

The picrate (m.p. 247–249° C), which was prepared from absolute ethanol solution in 91.8% yield, did not depress the melting point of a known sample of 5-keto-2,3,6,7-tetrahydro-1(H),5(H)-imidazo(1,2-*a*)pyrimidine picrate (m.p. 248–249° C).

5-Imino-2,3,6,7-tetrahydro-1(H),5(H)-imidazo(1,2-a)pyrimidine

2-Methylmercapto-2-imidazolinium iodide (14.64 g, 0.06 mole) and β-aminopropionitrile (4.2 g, 0.06 mole) in absolute ethanol (15 ml) were refluxed for 7 hours. Crystals (m.p. 192–198° C) separated from the solution on cooling, yield 7.43 g (46.5%). Several crystallizations from absolute ethanol raised the melting point to 201–203° C. Anal. Calc. for $C_6H_{11}IN_4$: C, 27.08; H, 4.17; N, 21.06; I, 47.69%. Found: C, 27.26; H, 4.08; N, 20.86; I, 47.43%.

Decreasing the reflux period in the above reaction in individual runs to 2 and 5.5 hours lowered the yields of 5-imino-2,3,6,7-tetrahydro-1(H),5(H)-imidazo(1,2-*a*)pyrimidinium iodide to 37.6 and 41% respectively.

The picrate (m.p. 228–231° C) was formed from aqueous solution. Recrystallization from water–ethanol (1:1) solution raised the melting point to 248–249° C. This picrate was shown by analysis and a mixed melting point determination to be identical with the picrate (m.p. 248–249° C) from 5-keto-2,3,6,7-tetrahydro-1(H),5(H)-imidazo(1,2-*a*) pyrimidine. Thus the imino group of the original compound was hydrolyzed to a keto group during the formation of the picrate in aqueous solution.

A sample of 5-imino-2,3,6,7-tetrahydro-1(H),5(H)-imidazo-(1,2-*a*)pyrimidinium iodide (9.1 g, 0.034 mole) in absolute methanol (180 ml) was passed through a column of IRA-400 resin (Cl^- form) which had been washed thoroughly with absolute methanol. The column was washed with absolute methanol (150 ml) and the eluate was taken to dryness *in vacuo* under nitrogen. The hydrochloride salt was obtained in 98.9% (5.90 g) yield. One crystallization from absolute methanol – ether (1:1) gave crystals melting at 193–194° C. Anal. Calc. for $C_6H_{11}ClN_4$: C, 41.27; H, 6.35; Cl, 20.30; N, 32.09%. Found: C, 41.42; H, 6.36; Cl, 20.44; N, 31.89%.

Can. J. Chem. Downloaded from www.nrcresearchpress.com by 210.87.254.5 on 09/05/12
For personal use only.

An ethanolic solution of a sample of 5-imino-2,3,6,7-tetrahydro-1(H),5(H)-imidazo (1,2-*a*)pyrimidinium chloride on treatment with ethanolic picric acid gave a dipicrate (m.p. 218–220° C) in 77% yield. Anal. Calc. for $C_{18}H_{16}N_{10}O_{14}$: C, 36.25; H, 2.74; N, 23.49%. Found: C, 36.50; H, 2.96; N, 23.38%.

5-Nitrimino-2,3,6,7-tetrahydro-1(H),5(H)-imidazo(1,2-a)pyrimidinium Nitrate

5-Imino-2,3,6,7-tetrahydro-1(H),5(H)-imidazo(1,2-*a*)pyrimidinium chloride (0.75 g, 0.0043 mole) was added to a nitration medium of 98% nitric acid (2.0 ml, 0.043 mole), acetic anhydride (4.06 ml, 0.043 mole), and ammonium chloride (0.3 g, 0.0056 mole) at 0° C. The temperature was raised to 32° C and the stirred solution was maintained at this temperature for 2.5 hours. When the solution was poured into cold absolute ether (75 ml) a sticky crystalline mass separated. The ether solution was decanted from the solid, which was washed with absolute ether (3×50 cc) by decantation. The solid was triturated with absolute ethanol (50 cc) and the crystals were recovered by filtration. After this process was repeated, the crystals were dried *in vacuo* at room temperature. The crystals melted at 152.5–153° C with decomposition, yield 0.45 g (42.6%). Anal. Calc. for $C_6H_{10}N_6O_5$: C, 29.27; H, 4.10; N, 34.13%. Found: C, 29.27; H, 4.32; N, 34.47%.

After a sample of the 5-nitrimino-2,3,6,7-tetrahydro-1(H),5(H)-imidazo(1,2-*a*)pyrimidinium nitrate was refluxed in ethanol for 1.5 hours, the crystals obtained on cooling the solution melted at 131–133° C. These crystals did not depress the melting point of a known sample of 5-keto-2,3,6,7-tetrahydro-1(H),5(H)-imidazo(1,2-*a*)pyrimidine nitrate (m.p. 132–133° C). The infrared spectra of these two samples were also identical.

Attempts to Open the Pyrimidine Ring of 5-Keto-2,3,6,7-tetrahydro-1(H),5(H)-imidazo-(1,2-a)pyrimidine

(*A*) *With Benzylamine*

5-Keto-2,3,6,7-tetrahydro-1(H),5(H)-imidazo(1,2-*a*)pyrimidine (0.556 g, 0.004 mole) and benzylamine (0.43 g, 0.004 mole) in absolute ethanol (7 ml) were allowed to stand at room temperature for 17 hours. The solution was concentrated to 3 ml *in vacuo* and ether was added. The crystals (m.p. 141° C and 148–149° C) on admixture with the starting material gave no depression in melting point, yield 0.506 g (91%).

A similar experiment in which the reactants in ethanolic solution were refluxed for 3.5 hours gave an 81% recovery of starting material.

(*B*) *With Ethanolic Hydrogen Chloride*

A solution of 5-keto-2,3,6,7-tetrahydro-1(H),5(H)-imidazo(1,2-*a*)pyrimidine (0.278 g, 0.002 mole) in ethanolic hydrogen chloride (10 ml of absolute ethanol containing 79 mg, 0.0022 mole of hydrogen chloride) was refluxed for 2.5 hours. The cooled solution was divided into two equal parts. One part on treatment with ethanolic picric acid solution gave 5-keto-2,3,6,7-tetrahydro-1(H),5(H)-imidazo(1,2-*a*)pyrimidine picrate (m.p. 248–249° C) in 98% (0.36 g) yield. This picrate did not depress the melting point of a known sample of 5-keto-2,3,6,7-tetrahydro-1(H),5(H)-imidazo(1,2-*a*)pyrimidine picrate (m.p. 248–249° C).

The second portion on standing in the cold gave crystals melting at 251.5–252.5° C, yield 120 mg (68.4%). The melting point of this sample of 5-keto-2,3,6,7-tetrahydro-1(H), 5(H)-imidazo(1,2-*a*)pyrimidinium chloride was not changed by crystallization from ethanol–ether solution. Anal. Calc. for $C_6H_{10}ClN_3O$: C, 41.04; H, 5.74; Cl, 20.19; N, 23.93%. Found: C, 41.18; H, 5.91; Cl, 20.00; N, 23.34%.

REFERENCES

1. A. F. McKay and M.-E. Kreling. Can. J. Chem. **35**, 1438 (1957).
2. A. F. McKay, D. J. Whittingham, and M.-E. Kreling. J. Am. Chem. Soc. **80**, 3339 (1958).
3. A. F. McKay and W. G. Hatton. J. Am. Chem. Soc. **78**, 1618 (1956).

Can. J. Chem. Downloaded from www.nrcresearchpress.com by 210.87.254.5 on 09/05/12
For personal use only.

Can. J. Chem. Downloaded from www.nrcresearchpress.com by 210.87.254.5 on 09/05/12
For personal use only.

THE STRUCTURE OF LYCODINE[1]

W. A. Ayer and G. G. Iverach

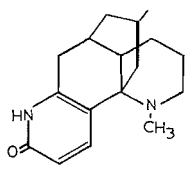
ABSTRACT

The molecular formula of the *Lycopodium* alkaloid lycodine has been revised to $C_{16}H_{22}N_2$. Transformation of β-obscurine (I) into N-methyl lycodine has shown that lycodine is the pyridine analogue of des-N-methyl-β-obscurine and is represented by structure II (R = H). The transformation of β-obscurine into α-obscurine is also described.

The alkaloid lycodine was first isolated from *Lycopodium annotinum* L. in 1958 by Anet and Eves (1), who assigned to it a molecular formula $C_{17}H_{24}N_2$. Lycodine was shown to be a tetracyclic diacidic base containing a secondary nitrogen atom, a 5,6,7,8-tetrahydroquinoline system unsubstituted in the heterocyclic ring, and a C-methyl group.

When structure I was advanced for β-obscurine (2) it was suggested that lycodine is formed by a similar biogenetic path,[2] with the exception that N-methylation has not occurred, and is represented by structure II (R = H). The correctness of this structure has now been confirmed by a series of experiments which are described in this communication.

The isolation of lycodine from *L. annotinum* L. involves a rather extended separation procedure (1). We have found that lycodine also occurs in *L. obscurum* L. and is readily separable by chromatography of the crude bases over alumina. Some lycodine was obtained directly by crystallization of the eluates. The remainder was separated from contaminating bases (mainly lycopodine and annotinine) by lithium aluminum hydride reduction, which transformed the contaminants into hydroxylic materials but did not affect the lycodine, followed by chromatography. The total yield of lycodine from dried plant material was approximately 0.003%.



I



II

Structure II (R = H) requires that the formula of lycodine be revised to $C_{16}H_{22}N_2$. The analytical results quoted by Anet and Eves (1), especially those for the dipicrate of lycodine and the picrate of N-acetyl lycodine, do not clearly differentiate between the two possibilities. Our analytical results with lycodine and N-methyl lycodine, together with the preparation of N-methyl lycodine from β-obscurine ($C_{17}H_{24}ON_2$) described below, confirm the 16 carbon formulation. The proposed structure differs in two other respects from the partial structure advanced by Anet and Eves (1). Firstly, the more strongly basic nitrogen is attached to a carbon α to the pyridine ring. This attachment

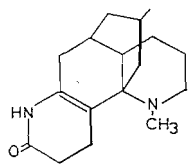
[1]*Manuscript received June 13, 1960.*
Contribution from the Department of Chemistry, University of Alberta, Edmonton, Alberta. This work forms a portion of a thesis to be submitted by G. G. Iverach in partial fulfillment of the requirements for the degree of Master of Science.

[2]*Recently, Professor H. Conroy (3) has outlined a biogenetic scheme which accounts for the formation, from acetate units and ammonia, of all the Lycopodium alkaloids of known structure.*

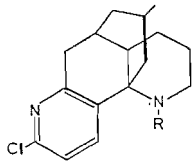
Can. J. Chem. Downloaded from www.nrcresearchpress.com by 210.87.254.5 on 09/05/12
For personal use only.

was regarded as improbable by the previous workers on the basis of a comparison of the pK_a's of the pyridine nitrogen atoms in lycodine and nicotine. We believe that the greater basicity (pK_a 3.97) of the pyridine nitrogen in lycodine as compared with that in nicotine (pK_a 3.35) is explained by the presence in lycodine of an electropositive substituent in the 2-position of the pyridine ring (4). Secondly, the C-methyl group of lycodine is not attached to a quaternary carbon atom. The assignment of the C-methyl group to such a grouping was made on the basis of the fact that the C-methyl peak in the nuclear magnetic resonance spectrum of lycodine is unsplit (1). The failure of the $\rangle CHCH_3$ peak to split is possibly attributable to the proximity of the aromatic ring, since in β-obscurine (I) the C-methyl peak is also unsplit, whereas in α-obscurine (III) the usual splitting occurs (2). In this connection, it is interesting to note that reduction of β-obscurine (I) with lithium and ammonia, a reagent which has been shown (5) to selectively reduce α-pyridones to the corresponding 3,4-dihydro-α-pyridones, yields α-obscurine (III).

It seemed at this point that structure II could be confirmed by direct transformation of β-obscurine (I) into lycodine (II, R = H) or, since some difficulty was anticipated in the removal of the N-methyl group of β-obscurine, into N-methyl lycodine (II, R = CH_3).



III



IV

Treatment of lycodine with formaldehyde and formic acid gave, in good yield, N-methyl lycodine (II, R = CH_3). The new base had no NH stretching band in the infrared and the ultraviolet spectrum was almost identical with that of lycodine. The nuclear magnetic resonance spectrum was similar to that of lycodine (1), with the addition of a strong (3-proton) signal at τ = 7.38 due to the N-methyl group (6). The C-methyl peak (at τ = 9.21) was again unsplit.

The transformation of an α-pyridone into the corresponding 2-chloropyridine is usually accomplished by the treatment with phosphorus oxychloride, phosphorus pentachloride, or a mixture of these two reagents (7). β-Obscurine was recovered unchanged after prolonged refluxing with phosphorus oxychloride and phosphorus oxychloride – phosphorus pentachloride. However, treatment with phosphorus pentachloride at 200° or, preferably, with phenylphosphonic dichloride (8) yielded an oily product whose spectral properties (ultraviolet maximum at 275 mμ, peak in the infrared at 1565 cm^{-1}) were consistent with those expected for the desired chloropyridine IV. The crude chloro compound was hydrogenated over platinum in acetic acid. Chromatography of the products gave N-methyl lycodine (41% yield from β-obscurine) and, unexpectedly, lycodine (23% yield). Presumably, loss of the N-methyl group occurred during the treatment with phenylphosphonic dichloride and the oily product was a mixture of the chloropyridines IV (R = CH_3) and IV (R = H). The appearance of a weak NH band at 3330 cm^{-1} in the infrared spectrum of the crude product is consistent with this view.

This transformation establishes that lycodine is the pyridine analogue of des-N-methyl-β-obscurine and, on the basis of the proposed (2) structure for β-obscurine, is represented by structure II (R = H).

Can. J. Chem. Downloaded from www.nrcresearchpress.com by 210.87.254.5 on 09/05/12
For personal use only.

EXPERIMENTAL

Ultraviolet spectra were measured in ethanol and, unless otherwise stated, infrared spectra in chloroform. Microanalyses are by Pascher Mikroanalytisches Laboratorium, Bonn, West Germany, and Micro-Tech Laboratory, Skokie, Illinois.

Isolation of Lycodine

Finely ground *L. obscurum* L. (10 kg) was extracted by the procedure of Manske and Marion (9). The crude alkaloids (9.3 g) yielded some lycopodine (2.0 g) on crystallization from ether. The mother liquors were dissolved in chloroform and placed on a column of basic alumina (150 g). Thorough elution with chloroform gave 3.75 g of basic material which was rechromatographed over alumina (100 g). Fraction A (2.1 g), eluted with benzene (900 ml), was mainly lycopodine. Fraction B (0.63 g), eluted with ether (850 ml), was a mixture of lycopodine and lycodine (as shown by infrared and ultraviolet measurements). Fraction C (0.17 g), eluted with 1:1 ether – methylene chloride (500 ml), contained annotinine, lycodine, and unidentified carbonyl-containing compounds. Crystallization of fraction B from pentane gave lycodine (172 mg). The residues from the crystallization were combined with fraction C, dissolved in ether, and reduced with lithium aluminum hydride in the usual manner. The product was chromatographed over alumina. Elution with benzene–ether gave crystalline lycodine (130 mg). The combined lycodine was recrystallized several times from pentane to give colorless blocks, m.p. 118–119°. Calc. for $C_{16}H_{22}N_2$: C, 79.29; H, 9.15; N, 11.56%. Found: C, 79.49, 79.33; H, 9.13, 9.09; N, 11.61, 11.47%; no N-methyl.

N-*Methyl Lycodine*

Lycodine (52 mg) was dissolved in 98% formic acid (0.25 ml) and formalin (0.25 ml) added. The solution was refluxed for 2 hours, then maintained at 50° for 12 hours. The reaction mixture was diluted with water (50 ml), basified with concentrated ammonium hydroxide, and extracted several times with chloroform. Evaporation of the dried chloroform extracts gave a pale yellow oil (0.05 g) which solidified on standing. Three recrystallizations from acetone gave N-methyl lycodine as colorless blocks (23 mg), m.p. 91–92°. Calc. for $C_{17}H_{24}N_2$: C, 79.63; H, 9.44; N, 10.93; one N—CH_3, 5.86%. Found: C, 79.61, 79.59; H, 9.36, 9.27; N, 11.25, 10.75; N—CH_3, 5.19%. Ultraviolet spectrum: λ_{max} 268 mμ (log ϵ = 3.61), shoulder at 275 mμ (log ϵ = 3.49). Infrared spectrum (Nujol): γ_{max} 3040, 1574, 1472, 812, 737 cm^{-1} (pyridine ring).

N-*Methyl Lycodine and Lycodine from β-Obscurine*

A solution of β-obscurine (168 mg, isolated from *L. annotinum* L. by established procedures (10, 11)) in phenylphosphonic dichloride (50 ml) was maintained at 200–210° for 45 minutes. The reaction solution was decomposed with ice and water and made basic by the addition of concentrated ammonium hydroxide. Chloroform extraction yielded the crude chloro compounds IV (R = CH_3) and IV (R = H) as a pale yellow oil (0.16 g), ultraviolet maximum 275 mμ, infrared peaks at 3330 cm^{-1} (NH) and 1565 cm^{-1} (pyridine ring). The oil was dissolved in glacial acetic acid and shaken with hydrogen (50 p.s.i.) in the presence of Adam's catalyst (100 mg) for 3 hours. The catalyst was filtered off and the filtrate concentrated, diluted with water, made basic with ammonium hydroxide, and extracted thoroughly with chloroform. Removal of the chloroform left a viscous yellow oil (0.12 g) which was chromatographed over basic alumina (3 g). Elution with benzene and crystallization from acetone gave N-methyl lycodine (65 mg), m.p. 91–92°. This did not depress the melting point of the N-methyl compound prepared from lycodine and their infrared spectra were identical.

Elution of the column with ether yielded a fraction (35 mg) which crystallized from acetone as colorless blocks, m.p. 115–116°. The infrared spectrum was identical with that of lycodine and a mixture melting point was undepressed.

α-Obscurine from β-Obscurine

A solution of β-obscurine (31 mg) in dry tetrahydrofuran (100 ml) was added during 1/2 hour to a vigorously stirred solution of lithium (0.1 g) in ammonia (40 ml). The solution was stirred for a further $2\frac{1}{2}$ hours, then the reaction mixture was evaporated to dryness. The residue was dissolved in aqueous HCl, washed with chloroform, basified, and extracted with chloroform. Evaporation of the chloroform left a solid residue which was chromatographed over alumina (1 g). Elution with chloroform and crystallization from methanol gave α-obscurine (20 mg), m.p. 285–287° (uncorrected). The mixture melting point with authentic α-obscurine was undepressed, and the infrared spectra of the two were identical.

Further elution of the column with chloroform–methanol (4:1) gave a fraction (7 mg) whose spectral properties were identical with those of β-obscurine.

ACKNOWLEDGMENTS

We wish to thank the National Research Council for financial support, Professor Z. Valenta for the nuclear magnetic resonance spectrum, and Mr. R. N. Swindlehurst for many of the ultraviolet and infrared spectra.

REFERENCES

1. F. A. L. Anet and C. R. Eves. Can. J. Chem. **36**, 902 (1958).
2. W. A. Ayer and G. G. Iverach. Tetrahedron Letters. In press.
3. H. Conroy. Tetrahedron Letters. In press.
4. E. A. Braude and F. C. Nachod. Determination of organic structures by physical methods. Academic Press, New York. 1955. p. 597.
5. J. A. Berson and J. S. Walia. J. Org. Chem. **24**, 756 (1959).
6. L. M. Jackman. Applications of nuclear magnetic resonance spectroscopy in organic chemistry. Pergamon Press, New York. 1959. p. 56.
7. R. C. Elderfield. Heterocyclic compounds. Vol. 1. John Wiley and Sons, New York. 1950. p. 513.
8. Z. Valenta, H. Yoshimura, E. F. Rogers, M. Ternbah, and K. Wiesner. Tetrahedron Letters. In press.
9. R. H. F. Manske and L. Marion. Can. J. Research, B, **20**, 87 (1942).
10. R. H. F. Manske and L. Marion. Can. J. Research, B, **21**, 92 (1943).
11. B. P. Moore and L. Marion. Can. J. Chem. **31**, 952 (1953).

Can. J. Chem. Downloaded from www.nrcresearchpress.com by 210.87.254.5 on 09/05/12
For personal use only.

Can. J. Chem. Downloaded from www.nrcresearchpress.com by 210.87.254.105 on 09/05/12
For personal use only.

SOME EQUILIBRIUM CONSTANTS OF TRANSITION METAL HALIDES[1]

M. W. Lister and P. Rosenblum

ABSTRACT

Measurements are reported on the formation of complex ions in solutions containing cupric and chloride or bromide ions, and solutions of nickel or cobalt with chloride. In each case the halide was present in very low amount. With copper a spectrophotometric method was used, and a cell voltage method with nickel and cobalt. The ionic strength was kept constant, but the temperature was varied. The data show difficulties of interpretation if it is assumed that only MX^+ ions (M is the metal, X is the halogen) are formed, the difficulties arising from the anomalous variation of the equilibrium constant with temperature, and from the general drift of the calculated constants from the e.m.f. measurements. Various explanations are considered and it is shown that postulation of M_2X^{+3} ions is at least a possible explanation.

A considerable number of measurements have been made on the dissociation constants of complex ions in aqueous solution, particularly those containing transition metals. In many cases, however, no very precise values have been obtained, or the effect of varying conditions, and especially the effect of temperature, has not been examined. The object of the present paper is to report results on the ions $CoCl^+$, $NiCl^+$, $CuCl^+$, and $CuBr^+$. The previous work on these ions will be briefly reviewed as each one is considered. The present work shows that the apparent equilibrium constants for $CuBr^+$, and to a lesser extent for $CuCl^+$, change with temperature in an anomalous manner. The possible cause of this is considered in some detail, since it is relevant to the use of spectrophotometric measurements generally for determining equilibrium constants.

The copper chloride and bromide systems were examined by means of a spectrophotometer, and the cobalt chloride and nickel chloride by means of cell voltages. The results on copper chloride and bromide will be given first, and then their explanation will be considered.

COPPER CHLORIDE MEASUREMENTS

This system has been the subject of many investigations of which the earlier ones are largely qualitative. Of recent investigations the most notable are those of Näsänen (1), who found a value of $K_1 = [CuCl^+]/[Cu^{++}].[Cl^-] = 0.90$ at 25° C; and of McConnell and Davidson (2), who found K_1 to be 1.30 at 25.2° C and 1.39 at 46.9° C, both at an ionic strength of 1.0. The discrepancy between these determinations was attributed by Kruh (3) to neglect of molecules of $CuCl_2$ (or other higher complexes) in Näsänen's calculations.

The present work largely confirms McConnell and Davidson's values. The experimental details are as follows. The optical densities of the solutions were measured by means of a Beckmann DU spectrophotometer, modified to allow water at constant temperature to circulate round the absorption cells. The temperature of the solutions being measured was thereby controlled to ±0.05° C or better.

The materials used were copper perchlorate and sodium perchlorate, supplied by the G. Frederick Smith Co.; sodium chloride (British Drug House's "analar" grade), twice recrystallized; and perchloric acid (Baker "analyzed" reagent). A stock solution of copper perchlorate (about 0.4 *M*), containing 0.1 *M* perchloric acid, was prepared, and analyzed iodometrically; other solutions were prepared by diluting the stock solution.

[1]*Manuscript received March 31, 1960.*
Contribution from the Department of Chemistry, University of Toronto, Toronto, Ontario.

The results are given below in the form of tables of optical density at various copper concentrations. These original data are included because, as will be seen later, there are some difficulties in their interpretation, and their explanation is not entirely certain. Hence the original data are given so that any other possible explanations can be checked against them. All results were at an ionic strength of 2.00 (adjusted by sodium perchlorate), with a perchloric acid concentration of 0.300 M, and a sodium chloride concentration of 0.00748 M. The light path was 1.000 cm. Table I gives the optical densities. The comparison cell contained the same solution without the sodium chloride. Each measurement was repeated, and the setting at zero optical density for the comparison cell was checked after each measurement.

TABLE I

Optical densities of copper chloride at various wave lengths

Temp., °C	Total Cu, M	300 mμ	295	290	285	280	275	270	265	260	255
12.0	.07877	.025	.035	.048	.068	.099	.145	.215	.310	.413	.498
	.09452	.031	.042	.057	.081	.117	.172	.255	.366	.488	.588
	.1103	.035	.048	.065	.093	.135	.199	.294	.422	.561	.675
	.1260	.039	.055	.074	.104	.152	.225	.332	.424	.631	.754
	.1339	.041	.057	.077	.109	.159	.235	.349	.498	.662	.791
	.1417	.045	.061	.083	.116	.168	.248	.367	.522	.698	.826
	.1575	.050	.066	.090	.126	.184	.272	.402	.576	.759	.899
	.1732	.054	.072	.098	.138	.201	.298	.437	.625	.825	.976
	.1891	.057	.178	.105	.148	.216	.319	.469	.670	.876	1.044
25.0	.07877	.038	.054	.072	.102	.148	.216	.315	.439	.570	.670
	.09452	.045	.062	.085	.119	.172	.251	.363	.510	.660	.777
	.1103	.052	.070	.098	.136	.198	.290	.420	.588	.760	.889
	.1260	.059	.081	.111	.154	.225	.329	.477	.662	.860	1.000
	.1339	.061	.084	.115	.162	.236	.344	.499	.697	.900	1.044
	.1417	.066	.090	.122	.171	.249	.363	.526	.732	.946	1.092
	.1575	.073	.099	.133	.187	.271	.396	.571	.797	1.033	1.180
	.1732	.078	.107	.144	.204	.296	.432	.623	.869	1.121	1.274
	.1891	.085	.114	.154	.217	.316	.460	.663	.923	1.188	1.334
40.0	.07877	.059	.081	.111	.156	.226	.325	.462	.629	.795	.911
	.09452	.071	.097	.131	.185	.267	.384	.545	.741	.934	1.064
	.1103	.081	.110	.150	.211	.304	.438	.625	.849	1.072	1.207
	.1260	.092	.123	.168	.238	.342	.492	.698	.952	1.191	1.318
	.1339	.098	.130	.177	.251	.360	.519	.737	1.002	1.261	1.402
	.1417	.103	.137	.187	.263	.376	.542	.769	1.049	1.305	1.424
	.1575	.111	.150	.204	.288	.415	.598	.843	1.147	1.417	1.492
	.1732	.121	.162	.220	.311	.444	.645	.907	1.237	1.518	1.556
	.1891	.129	.174	.237	.333	.479	.689	.981	1.321	1.599	—

COPPER BROMIDE MEASUREMENTS

As with copper chloride, earlier measurements were largely qualitative. Riley and Smith (4) used a cell, $Cu/CuSO_4/KNO_3/CuSO_4 + NaBr/Cu$, to obtain successive equilibrium constants; their value for K_1 was 2.1×10^6. Job (5) used spectrophotometric measurements to get 0.063 for K_1 (the first equilibrium constant). Näsänen (6), using a spectrophotometer, found K_1 to be 0.94 at 25° C. Farrington (7), in 1952, obtained 2.1 ± 0.25 for K_1, at $22\pm2°$ C and at unit ionic strength.

In the present work the reagents and method were the same as for copper chloride, except that recrystallized sodium bromide was used in place of sodium chloride. The results in Table II are for an ionic strength of 2.00, with perchloric acid at 0.300 M, and sodium bromide at 0.00839 M. As before, the light path was 1.000 cm, and the comparison cell contained the same solution without the sodium bromide.

Can. J. Chem. Downloaded from www.nrcresearchpress.com by 210.87.254.105 on 09/05/12
For personal use only.

TABLE II

Optical densities of copper bromide at various wave lengths

Temp., °C	Total Cu, M	305 mμ	300	295	290	285	280	275	270	265
12.0	.1260	.154	.191	.230	.263	.287	.291	.273	.237	.191
	.1496	.182	.224	.270	.308	.336	.340	.319	.278	.224
	.1732	.208	.256	.309	.353	.383	.389	.364	.317	.257
	.1969	.253	.287	.344	.395	.429	.435	.405	.351	.285
	.2205	.257	.317	.382	.437	.475	.481	.450	.390	.316
	.2441	.280	.343	.415	.475	.518	.525	.491	.427	.345
	.2677	.303	.373	.450	.515	.562	.570	.532	.462	.373
	.2914	.324	.399	.479	.550	.597	.605	.566	.492	.401
	.3149	.346	.427	.512	.590	.639	.648	.604	.523	.422
25.0	.1260	.213	.261	.311	.350	.376	.376	.348	.300	.239
	.1496	.249	.304	.361	.408	.436	.437	.404	.350	.280
	.1732	.287	.349	.414	.469	.500	.501	.463	.398	.320
	.1969	.317	.386	.460	.519	.556	.556	.512	.440	.350
	.2205	.348	.426	.505	.572	.610	.610	.565	.486	.388
	.2441	.379	.464	.552	.623	.668	.668	.618	.530	.426
	.2677	.408	.498	.590	.667	.714	.714	.659	.567	.456
	.2914	.435	.530	.627	.712	.763	.764	.705	.607	.488
	.3149	.462	.564	.668	.757	.810	.811	.751	.642	.515
40.0	.1260	.308	.370	.435	.483	.509	.501	.458	.386	.306
	.1496	.358	.429	.505	.562	.593	.583	.534	.452	.358
	.1732	.409	.490	.573	.639	.674	.662	.604	.511	.406
	.1969	.455	.545	.637	.710	.748	.735	.670	.469	.455
	.2205	.498	.602	.702	.784	.827	.815	.744	.630	.502
	.2441	.545	.656	.768	.858	.903	.890	.807	.685	.544
	.2677	.587	.710	.827	.925	.981	.965	.877	.742	.593
	.2914	.629	.756	.888	.998	1.050	1.033	.939	.795	.637
	.3149	.665	.801	.940	1.055	1.112	1.093	.997	.841	.674
12.0	.1255	.155	.191	.231	.263	.286	.291	.272	.237	.191
20.0		.194	.237	.285	.321	.346	.347	.321	.276	.219
25.0		.214	.262	.311	.351	.376	.376	.349	.300	.240
30.0		.242	.296	.348	.392	.419	.416	.381	.325	.256
35.0		.270	.328	.385	.432	.457	.451	.415	.352	.279
40.0		.307	.469	.433	.481	.505	.500	.454	.385	.304
12.0	.1961	.232	.286	.344	.394	.428	.434	.405	.353	.285
20.0		.288	.351	.423	.475	.513	.514	.476	.409	.325
25.0		.316	.385	.459	.518	.554	.554	.514	.440	.352
30.0		.355	.436	.513	.578	.616	.612	.562	.480	.379
35.0		.400	.485	.570	.640	.677	.668	.612	.519	.413
40.0		.455	.548	.642	.715	.751	.740	.673	.570	.452

DISCUSSION OF RESULTS

If we assume that, because of the high copper and low halide concentration, the only complex ion present is CuX^+ (X = Cl or Br), then the law of mass action gives

$$\frac{D/\epsilon_1}{(a-D/\epsilon_1)(b-D/\epsilon_1)} = K_1$$

where a is the total copper concentration,
b is the total halide concentration,
D is the optical density,
ϵ_1 is the extinction coefficient,
K_1 is the equilibrium constant for $Cu^{++} + X^- \rightleftharpoons CuX^+$.

Can. J. Chem. Downloaded from www.nrcresearchpress.com by 210.87.254.105 on 09/05/12
For personal use only.

If $a \gg b$, this can be rearranged (as was first done by Rabinowitch and Stockmayer for an analogous system (8)) to give

$$\frac{a}{D} = \frac{1}{K_1 b \epsilon_1} + \frac{a}{b\epsilon_1}.$$

Hence a plot of a/D for any wave length against a should give a straight line, from the slope and intercept of which K_1 and ϵ_1 can be found. The present data give at least nearly straight lines for this plot. If the best straight lines are drawn through the data by the method of least squares the calculated values of K_1 and ϵ_1 are as given in Table III.

TABLE III
Values of K_1

Compound	Temp., °C	295	290	285	280	275	270	265	260	Mean	
Copper chloride	12	—	—	1.01	0.98	0.88	0.99	1.07	1.28	1.03	
	25	—	1.29	1.13	1.11	1.14	1.24	1.30	1.32	1.22	
	40	1.28	1.25	1.24	1.36	1.29	1.38	1.35	—	1.31	
		305	300	295	290	285	280	275	270	265	Mean
Copper bromide	12	.689	.708	.732	.682	.709	.709	.740	.764	.743	0.72
	25	.923	.939	.984	.921	.943	.943	.946	.997	.952	0.95
	40	.913	.870	.884	.807	.804	.805	.844	.846	—	0.85

Two comments can be made on these results. At any one temperature, the K_1 values usually drift in a characteristic way with wave length, being higher at the high and low wave lengths and lower in the middle. This drift is not large, but it seems to be definite. Secondly, the average K_1 values give a rather unexpected change with temperature, in that the usual log K against $1/T$ plot is not linear. This is particularly marked with copper bromide, where K_1 at first rises with temperature and then falls. This is confirmed from the results in Table II, where the optical densities were followed in a more detailed way over a range of temperature. The mean values of K_1 calculated from Table II are

temp.:	12.0	20.0	25.0	30.0	35.0	40.0,
K_1:	0.72	0.85	0.98	0.96	0.89	0.83.

The corresponding values of the extinction coefficient for CuX^+ ions are given in Table IV.

TABLE IV
Extinction coefficients of CuX^+ ions

Ion	Temp., ° C	305 mμ	300	295	290	285	280	275	270	265	260	255
$CuCl^+$	12.0	—	—	—	—	121	176	256	383	555	753	923
	25.0	—	—	—	111	153	222	326	477	669	866	1055
	40.0	—	—	116	158	223	324	464	664	902	1161	—
$CuBr^+$	12.0	222	274	332	376	411	417	392	342	276	—	—
	20.0	240	292	353	396	428	429	397	341	271	—	—
	25.0	238	292	349	390	419	420	388	337	268	—	—
	30.0	267	328	326	435	463	460	423	361	285	—	—
	35.0	321	389	457	513	543	536	491	416	331	—	—
	40.0	388	467	547	609	640	630	573	486	385	—	—

Can. J. Chem. Downloaded from www.nrcresearchpress.com by 210.87.254.105 on 09/05/12
For personal use only.

With $CuCl^+$ the absorption band advances steadily towards the red as the temperature is raised; this is what is to be expected if the band is widened at higher temperatures. However, with $CuBr^+$ the absorption maximum rises slowly at first and then rapidly at higher temperatures.

These results, particularly the effect of temperature on K_1, need further explanation. Various possibilities will now be considered.

1. Rapidly Changing Heat of Reaction

The equation $d \ln K/dt = \Delta H/RT^2$ will, of course, only give a linear relation between $\ln K$ and $1/T$, if it is assumed that ΔH is independent of temperature. If C is the specific heats of the products minus those of the reagents, ΔH will be of the form $\Delta H = B+CT$, where B is a constant. If C is assumed to be independent of temperature, then integration gives $\ln K = A - B/RT + (C/R) \ln T$, where A is an integration constant. Hence measurements of K at three (or more) temperatures will allow A, B, and C to be evaluated. If this is done for the K_1 values quoted above, for temperatures 12.0, 25.0, and 40.0° C, the results are

$$\Delta H = 30040 - 95.5T \qquad \text{for } Cu^{++}+Cl^- \rightleftharpoons CuCl^+$$
$$\Delta H = 134200 - 446.5T \qquad \text{for } Cu^{++}+Br^- \rightleftharpoons CuBr^+$$

or if T is in °C: $CuCl^+$: $\Delta H = 3960 - 95.5T$ (°C); $CuBr^+$: $\Delta H = 12260 - 446.5T$ (°C).

These values of C seem impossibly high, since C is the difference in specific heats of relatively simple ions in solution. It is true that the sign of C makes the specific heat of the two simple ions larger than that of the complex ion, as might be expected, but the difference seems impossibly large. If these effects are genuine, it might be expected that they would also show up in the specific heats of copper chloride solutions, on which some data are available. Marignag (9) gives the specific heat of copper chloride solutions as

molar ratio, water/copper chloride:	25	50	100,
specific heat/g solution:	.779	.864	.920 cal/°C.

It is very uncertain how these figures should be interpreted, but if the concentrations of Cu^{++}, $CuCl^+$, and Cl^- ions are calculated in each solution, and if it is assumed that each ion has a certain specific heat/gram molecule, and that these are strictly additive (the specific heat of the water present being taken as that in pure water), then the above results require the specific heats/gram molecule of each ion to be $Cu^{++}-171$, $CuCl^+-21$, Cl^-+49 cal/°C. Hence the difference in specific heats between $CuCl^+$ and $Cu^{++} + Cl^-$ is +101 cal/°C. Although this is large, it is of the wrong sign to explain the equilibrium constant results. Thus quite apart from the question of the justification of treating specific heat results in this simplified way, the specific heats do not support the view that the heat of reaction changes rapidly with temperature.

2. Deviations from the Beer–Lambert Law

It is necessary to assume the accuracy of the Beer–Lambert law in colorimetric investigations of complex ions, since otherwise no evaluation of equilibrium constants would be possible. Evidence for the Beer–Lambert law is obtained from the internal consistency of results, but it is usual to avoid having any very high concentration of the colored species present, since deviations are generally small at low concentrations. In the present work, the $CuCl^+$ concentration varied from about 7 to 15×10^{-4} M, and the $CuBr^+$ concentration

Can. J. Chem. Downloaded from www.nrcresearchpress.com by 210.87.254.105 on 09/05/12
For personal use only.

from 8 to 18×10^{-4} M. It can be calculated that if the equilibrium constant for $CuBr^+$ was really unchanged with temperature, and its apparent rise and fall were entirely due to variations in the extinction coefficient, then the extinction coefficient of $CuBr^+$ would have to change by about 10% over the range of concentration given above (at any one temperature). This seems to be too rapid a change for such small concentrations.

3. Occurrence of Other Complex Ions

Another, and perhaps more plausible, possibility is that some other complex ion occurs in those solutions. Since the copper concentration is high and halide low, the only reasonable suggestion is that the ion Cu_2X^{+3} (where X is a halogen) is present. Ions of this type have not been often postulated, but they are not really inherently improbable, since halogen atoms are known to hold two metal atoms together in various compounds, for instance Al_2Cl_6. One other consideration shows that this is a possible ionic type: suppose that CuX^+ is purely an ion pair association, with r the distance between ionic centers, then the electrostatic energy of formation of CuX^+ is $2e^2/r$, where e is the electron charge. Similarly for Cu_2X^{+3} the energy is $2e^2/r$, but for Cu_3X^{+5}, assumed to be flat, it would be $-0.93e^2/r$. Hence CuX^+ and Cu_2X^{+3} might be stable, but probably not Cu_3X^{+5}. This, of course, is an oversimplified picture, since covalent binding is ignored, but it gives a qualitative indication of what to expect.

If we postulate the existence of Cu_2X^{+3}, then this introduces a new equilibrium constant $K_2 = [Cu_2X^{+3}]/[Cu^{++}]^2[X^-]$ and the extinction coefficient for Cu_2X^{+3}. Using the same nomenclature as earlier, this modifies the equation for a/D to

$$\frac{a}{D} = \frac{1+K_1a+K_2a^2}{b(K_1\epsilon_1+K_2\epsilon_2a)}$$

and if K_2 and a are not too large this gives approximately

$$\frac{a}{D} = \frac{1}{bK_1\epsilon_1}\left\{1+\left(K_1-\frac{K_2\epsilon_2}{K_1\epsilon_1}\right)a+\left[K_2-\frac{K_2\epsilon_2}{\epsilon_1}+\left(\frac{K_2\epsilon_2}{K_1\epsilon_1}\right)^2\right]a^2\right\}.$$

In theory any four measurements should suffice to evaluate K_1, K_2, ϵ_1, and ϵ_2, but it is better to combine all the data at one wave length to get the best values of these quantities. The plots of a/D against a are nearly straight lines, but many of them show a slight curvature. Accordingly the best equation of the type $a/D = A+Ba+Ca^2$ was fitted by the method of least squares to the experimental data, thus giving numerical values of A, B, and C. A comparison of the two expressions for a/D shows that

$$K_2-K_1\left(\frac{B}{A}\right) = \frac{C}{A}-\left(\frac{B}{A}\right)^2.$$

A, B, and C, of course, vary with wave length. Hence a graph of B/A against $C/A-(B/A)^2$ should give a straight line, using data at one temperature but various wave lengths, since K_1 and K_2 are constants. As will be seen, these graphs were in fact moderately good straight lines, although the points were somewhat scattered. The small curvature of the original a/D graph makes the accuracy rather low. The best straight line was drawn through the values of B/A plotted against $C/A-(B/A)^2$; this gives K_1 and K_2, and the extinction coefficients can be found as $\epsilon_1 = 1/K_1Ab$, and $\epsilon_2 = (K_1-B/A)/K_2Ab$.

Can. J. Chem. Downloaded from www.nrcresearchpress.com by 210.87.254.105 on 09/05/12
For personal use only.

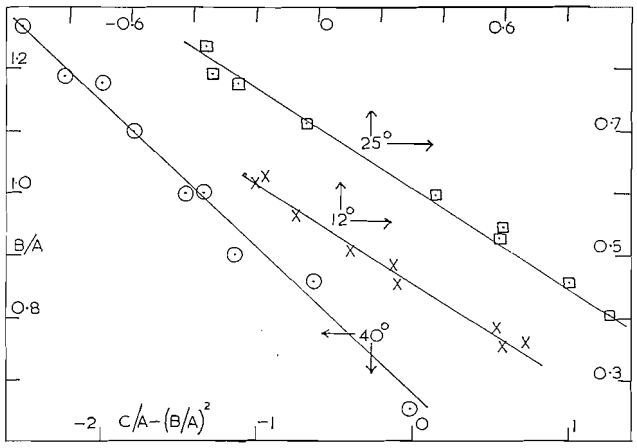


FIG. 1. Copper bromide.

The results of this treatment were as follows. Figure 1 gives the graph of B/A plotted against $C/A-(B/A)^2$ for copper bromide at various temperatures. The points are at least approximately linear. The constants calculated from these lines are as follows:

Copper bromide			Copper chloride		
Temp.	K_1	K_2	Temp.	K_1	K_2
12° C	3.08	1.73	12° C	3.92	3.40
25° C	3.56	2.31	25° C	5.47	5.21
40° C	4.15	2.77	40° C	7.35	7.79

For copper bromide, log K_1 plotted against $1/T$ gives a reasonably good straight line corresponding to $\Delta H = 1.9$ kcal; log K_2 gives only a moderately straight line corresponding to ΔH of about 3.0 kcal. For copper chloride, these give reasonably linear log K against $1/T$ plots: ΔH from K_1 is 4.0 kcal, and 5.2 kcal from K_2.

The calculated extinction coefficients are as follows:

Copper bromide		305 mμ	300	295	290	285	280	275	270	265
ϵ_1	12° C	50	68	75	86	94	95	91	78	62
	25° C	66	82	98	109	118	120	110	97	77
	40° C	78	91	113	125	131	127	120	99	77
ϵ_2	12° C	244	278	359	396	438	440	395	349	301
	25° C	267	315	374	431	444	431	384	330	268
	40° C	384	479	502	555	600	601	517	467	377

Copper chloride		295 mμ	290	285	280	275	270	265	260
ϵ_1	12° C	16	22	31	46	66	98	144	187
	25° C	17	23	35	50	71	106	152	192
	40° C	—	28	39	57	82	116	158	194
ϵ_2	12° C	68	87	113	158	259	375	496	758
	25° C	93	123	142	196	342	494	620	887
	40° C	—	163	239	328	477	682	948	1293

Can. J. Chem. Downloaded from www.nrcresearchpress.com by 210.87.254.105 on 09/05/12
For personal use only.

Although the behavior of the equilibrium constants is as might be expected, the extinction coefficients are sufficiently surprising to cast doubt on the interpretation of the experimental results through the postulation of Cu_2X^{+3} ions. In particular the absorption maxima for $CuBr^+$ and Cu_2Br^{+3} increase with temperature, and for Cu_2Br^{+3} the increase is disproportionately large at 40° C. The copper chloride results are less unusual, since the absorption only shifts to longer wave lengths at higher temperatures. However, in both cases ϵ_2/ϵ_1 seems unduly large, particularly at the absorption maximum for copper bromide.

To sum up, the linearity of the plots of B/A against $C/A-(B/A)^2$, and the more regular behavior of K_1 and K_2 with temperature favor an explanation in terms of Cu_2X^{+3}; against it is the anomalous behavior of the extinction coefficients. Thus, although there is some support for a suggestion of Cu_2X^{+3} ions, the matter cannot be definitely decided.

Cobalt and Nickel Chloride

Because of the striking color change when cobaltous ions form complexes with chloride, this system has been the subject of considerable investigation, starting with the early work on ion migration by Donnan and Bassett (10). Job (11), using a spectrophotometer, obtained evidence for $CoCl^+$ and $CoCl_3^-$, with K_1 for $CoCl^+$ equal to 4.5×10^{-3}. In 1949, Bobtelsky and Spiegler (12) investigated cobalt chloride in ethanol water mixtures, and similar measurements were made by Katzin and Gebert (13), and by Barvinok (14): these workers all found evidence of $CoCl_2$ and $CoCl_4^{--}$. Moore and Kraus (15) used anion exchange resins to investigate cobalt (II) in hydrochloric acid solutions, and obtained evidence for $CoCl_3^-$ and $CoCl_4^{--}$. However, Moore, Gootman, and Yates found evidence only for $CoCl_2$ from vapor pressure measurements (16).

The situation with respect to nickel chloride is similar, though there is less early work. Kiss and Csokan in 1941 (17) investigated nickel chloride in hydrochloric acid, obtaining evidence for $NiCl_4^{--}$ in concentrated solution. Moore and Kraus (15) examined its ion exchange behavior, obtaining evidence that anionic species were formed only to a very small extent. Beaver, Trevorrow, Estill, Yates, and Moore (18) examined nickel chloride in 2-octanol obtaining evidence for $NiCl_2$ and $(NiCl_2)_n$, and for complex ions. Herber and Irvine in 1956 (19) found evidence for $NiCl_3^-$ and $NiCl_4^{--}$ by ion exchange, but optical measurements indicated only $NiCl^+$ up to high hydrochloric acid concentrations.

The present work was undertaken initially to investigate the extent of formation of the first complex, $CoCl^+$ or $NiCl^+$, and the variation of this with temperature. However, as will be seen below, the results also provide evidence of the existence of ions of the type M_2Cl^{+3}, where M is the metal.

In the first instance, spectrophotometric measurements were made. However, even up to 0.12 M chloride, the effect of chloride was so slight over the range 240–900 mμ, that this method seemed to offer no prospects of success. In fact, one must conclude either that $NiCl^+$ is not formed, or that its absorption spectrum is very like that of Ni^{++}. The situation with cobalt was found to be very similar. Accordingly measurements were made by another method, by the use of the e.m.f. of cells, to decide between these two alternatives. Here evidence for MCl^+ was obtained, and it seems to be necessary to conclude that for both nickel and cobalt the spectrum of MCl^+ is very like that of M^{++}.

Apparatus and Method

The measurements made were on the e.m.f. of the cell: Ag, AgCl/NaCl+$M(ClO_4)_2$+$NaClO_4$/NaCl+$NaClO_4$/AgCl, Ag, where M is cobalt or nickel. The two electrolytes

Can. J. Chem. Downloaded from www.nrcresearchpress.com by 210.87.254.105 on 09/05/12
For personal use only.

were adjusted to the same ionic strength and acidity by means of sodium perchlorate and perchloric acid. The sodium chloride concentrations in the two solutions were the same; so the only difference was the presence in one side of cobalt or nickel perchlorate, with an adjustment of the sodium perchlorate concentration to keep the ionic strengths equal. The sodium perchlorate was much more concentrated than the chloride (0.008 *M*).

The silver/silver chloride electrodes were prepared as recommended by Janz and Taniguchi (20). The electrodes so prepared gave voltages of 0.02 mv or less when placed in the same solution, this difference being found and allowed for in the subsequent calculations. The two sodium chloride solutions were separated by a salt bridge, sodium perchlorate being used for this. The voltage was measured on a Leeds and Northrup K-2 potentiometer. The cell, of course, was at constant temperature during use. Nickel and cobalt perchlorate from the G. Frederick Smith Co. were used in making up the solutions: the concentrations of the solutions were determined by E.D.T.A. titration for cobalt with murexide indicator (21), and by dimethylglyoxime for nickel.

RESULTS

The observed e.m.f. are given in Table V. In interpreting these results it has to be assumed that the liquid junction potentials cancel as a result of the similar concentrations and ionic strengths of the solutions on each side of the salt bridge. This assumption is

TABLE V

Cell voltages in millivolts

Compound	*T*, ° C	0.0999 *M*	0.1497	0.1748	0.1997	0.2247	0.2496	0.2746	0.2995	0.3245
Cobalt chloride	12	1.53	2.28	2.69	3.04	3.46	3.86	4.24	4.62	5.02
	25	1.72	2.58	3.06	3.44	3.90	4.35	4.78	5.21	5.61
	40	1.91	2.94	3.44	3.90	4.39	4.85	5.35	5.82	6.34
		0.1208 *M*	0.1451	0.1932	0.2175	0.2416	0.2659	0.2900	0.3139	
Nickel chloride	12	1.56	1.97	2.63	3.01	3.41	3.78	4.09	4.51	
	25	1.83	2.25	3.05	3.44	3.84	4.29	4.61	5.05	
	40	2.10	2.55	3.43	3.87	4.31	4.77	5.22	5.73	

NOTE: Ionic strength = 2.0; $[HClO_4] = 0.300$ *M*.

supported by the consistency of the equilibrium constants calculated from the results. The voltages were very steady with time, which supports this assumption. In the calculations below it was assumed that the great excess of sodium perchlorate made it the effective conductor of the current. Since all runs were made with very low chloride concentration and relatively high metal, it is reasonable to assume (as for copper) that the complex ions are MCl^+ (formation constant K_1) and M_2Cl^{+3} (formation constant K_2). If, as before, a is the total metal concentration, and b the total chloride, and if $a \gg b$, and if u is the concentration of free chloride in the solution containing cobalt or nickel, then it is easily shown that $b/u = 1+K_1a+K_2a^2$. But b/u is the ratio of the chloride in the two solutions, and, assuming that the activity coefficients are equal at the same ionic strengths, then

$$E = \frac{RT}{nF} \ln(b/u)$$

where E is the cell voltage. Hence b/u can be found. The first equation can be rewritten: $(b/u-1)/a = K_1+K_2a$. If only MCl^+ is formed $(b/u-1)/a$ will be constant; otherwise

Can. J. Chem. Downloaded from www.nrcresearchpress.com by 210.87.254.105 on 09/05/12
For personal use only.

it should increase linearly with a. Table VI gives the calculated values of $(b/u-1)/a$.

These values of $(b/u-1)/a$ are approximately linear when plotted against a, although there is evidently some random error. If the best straight line is drawn through them by the method of least squares, the following constants are obtained.

Compound	Temp.	K_1	K_2
$CoCl_2$	12° C	.611	.263
	25° C	.666	.274
	40° C	.711	.327
$NiCl_2$	12° C	.508	.426
	25° C	.569	.407
	40° C	.620	.409

The K_1 values give ΔH as 1.0 kcal for $Co^{++} + Cl^- \rightarrow CoCl^+$, and 1.25 kcal for $Ni^{++} + Cl^- \rightarrow NiCl^+$. It is impossible to calculate heats of reaction for the formation of M_2Cl^{+3}, except to say that here ΔH must be very small. Thus, if this interpretation of the results is correct, the complexes M_2Cl^{+3} are formed nearly as easily as MCl^+. While this interpretation is certainly possible, it cannot be considered as proved.

TABLE VI

Values of $(b/u-1)/a$

Compound	T, °C		.0999 M	.1497	.1748	.1997	.2247	.2496	.2746	.2995	.3245
Cobalt chloride	12	$(b/u-1)/a$	.643	.645	.661	.659	.672	.681	.685	.690	.698
	25		.693	.705	.723	.717	.729	.739	.744	.750	.751
	40		.734	.768	.777	.778	.785	.788	.798	.803	.815
	T, °C		.1208 M	.1451	.1932	.2175	.2416	.2659	.2900	.3139	
Nickel chloride	12		.542	.575	.584	.599	.616	.625	.624	.641	
	25		.611	.631	.652	.658	.667	.683	.677	.691	
	40		.669	.682	.701	.708	.716	.726	.734	.753	

REFERENCES

1. R. NÄSÄNEN. Acta Chem. Scand. 4, 140 (1950).
2. H. MCCONNELL and N. DAVIDSON. J. Am. Chem. Soc. **72**, 3164, 3168 (1950).
3. R. KRUH. J. Am. Chem. Soc. **76**, 4865 (1954).
4. H. L. RILEY and H. C. SMITH. J. Chem. Soc. 1448 (1934).
5. P. JOB. Compt. rend. **198**, 827 (1934).
6. R. NÄSÄNEN. Acta Chem. Scand. 4, 816 (1950).
7. P. S. FARRINGTON. J. Am. Chem. Soc. **74**, 966 (1952).
8. E. RABINOWITCH and W. H. STOCKMAYER. J. Am. Chem. Soc. **64**, 335 (1942).
9. C. MARIGNAG. Ann. chim. et phys. Ser. 5, **8**, 410 (1876).
10. F. G. DONNAN and H. BASSETT. J. Chem. Soc. **81**, 939 (1902).
11. P. JOB. Compt. rend. **196**, 181 (1933).
12. M. BOBTELSKY and R. S. SPIEGLER. J. Chem. Soc. 143 (1949).
13. L. I. KATZIN and E. GEBERT. J. Am. Chem. Soc. **72**, 5464 (1950).
14. M. S. BARVINOK. Zhur Obshchei Khim. **20**, 1947 (1950).
15. G. E. MOORE and K. A. KRAUS. J. Am. Chem. Soc. **74**, 843 (1952).
16. T. E. MOORE, E. A. GOOTMAN, and P. C. YATES. J. Am. Chem. Soc. **77**, 298 (1955).
17. A. V. KISS and P. CSOKAN. Z. anorg. u. allgem. Chem. **245**, 355 (1941).
18. W. D. BEAVER, L. E. TREVORROW, W. E. ESTILL, P. C. YATES, and T. E. MOORE. J. Am. Chem. Soc. **75**, 4556 (1953).
19. R. H. HERBER and J. W. IRVINE. J. Am. Chem. Soc. **78**, 905 (1956).
20. G. J. JANZ and H. TANIGUCHI. Chem. Revs. **53**, 397 (1953).
21. G. SCHWARZENBACH. Complexometric titrations. Methuen and Co. Ltd., London. 1957. p. 78.

Can. J. Chem. Downloaded from www.nrcresearchpress.com by 210.87.254.105 on 09/05/12
For personal use only.

Can. J. Chem. Downloaded from www.nrcresearchpress.com by 210.87.254.105 on 09/05/12
For personal use only.

THE STUDY OF HYDROGEN BONDING AND RELATED PHENOMENA BY ULTRAVIOLET LIGHT ABSORPTION

PART V. INTRAMOLECULAR HYDROGEN BONDING IN ANILINES AND PHENOLS[1]

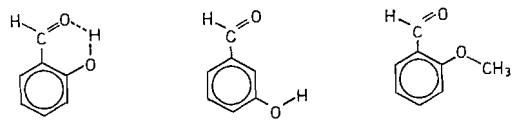
J. C. Dearden[2] and W. F. Forbes[3]

ABSTRACT

Information concerning intramolecular hydrogen bonding in phenols and anilines can be obtained from ultraviolet spectra by a variety of methods. One method is to note the spectral changes observed between the corresponding *o*-substituted phenols and anisoles. A second method is to compare the spectral changes between *o*-substituted phenols or anilines and the corresponding meta isomers. A third method is to note the absence of an appreciable spectral change, on altering the solvent conditions, which may also indicate the formation of an intramolecular hydrogen bond. The conclusions deduced from the three methods confirm previously stated generalizations concerning the nature of the hydrogen bond. One notable exception is that the spectral changes ascribed to the intramolecular hydrogen bond in *o*-nitrophenol can be explained in terms of an electrostatic model of the hydrogen bond.

INTRODUCTION

Intramolecular hydrogen bonds are known to cause bathochromic wavelength displacements in some of the absorption bands of the ultraviolet spectra. In order to obtain a quantitative measure of this effect for intramolecularly bonded phenols or anilines such as salicylaldehyde (IA), a reference compound must be available against which the wavelength displacement can be measured. This reference compound may be provided either by the corresponding *m*-isomer, for example *m*-hydroxybenzaldehyde (IB), or by the otherwise similar O-methyl- or N-methyl-substituted compound, for example *o*-methoxybenzaldehyde (IC). In the absence of interfering interactions both methods

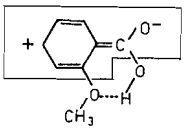


IA IB IC

should afford similar results. Moreover, some of the absorption bands of systems containing an intramolecular hydrogen bond should be less affected by competitive intermolecular hydrogen bonding between solute and solvent molecules than otherwise similar, but non-intramolecularly bonded, molecules.

However, the following considerations may affect the reliability of the observed spectral changes: (i) The absorption band under consideration may be determined by that part of the chromophoric system which does not contain the intramolecular hydrogen bond and consequently this absorption band will not be appreciably affected by intramolecular hydrogen bonding. For example, the similarity of the benzoic acid *B*-bands for *o*-methoxybenzoic acid and benzoic acid is explained by assuming that the intramolecular hydrogen bond in *o*-methoxybenzoic acid does not appreciably affect the

[1]*Manuscript received March 8, 1960.*
Contribution from the Memorial University of Newfoundland, St. John's, Newfoundland, and from the Division of Protein Chemistry, C.S.I.R.O., Melbourne, Australia.
[2]*Present address: "Shell" Research Limited, P.O. Box 1, Chester, England.*
[3]*Present address: Division of Protein Chemistry, C.S.I.R.O., 343 Royal Parade, Parkville, N.2. (Melbourne), Victoria, Australia. All correspondence should be addressed to this author.*



II

resonance form of type II, which can be assumed to determine predominantly the observed absorption band (see ref. 1). (ii) Steric interactions and other proximity effects, which almost always operate in *o*-disubstituted benzene derivatives, may be appreciably different in the intramolecularly hydrogen-bonded compound and in the reference compound. For example, in cyclohexane solution the nitrobenzene *B*-band of *o*-nitroanisole shows a hypsochromic wavelength displacement of ca. 11.5 mμ from this same band in *m*-nitroanisole (2*a*). This hypsochromic displacement is associated with steric and other short-range interactions between the methoxy and the nitro groups. It follows that *o*-nitroanisole cannot be assumed to provide a satisfactory reference compound for estimating intramolecular hydrogen bonding in *o*-nitrophenol. (iii) The absence of spectral changes with change of solvent may be caused by a strong intermolecular hydrogen bond, but it may *also* be caused by steric hindrance preventing solvent–solute interaction. For example, *o*-substituted phenols such as 2,6-di-*tert*.butyl phenol in which the ortho substituents are large, do not show the usual wavelength displacements if the spectra are determined in cyclohexane and ethanol solution, presumably because the large *o*-substituents prevent solvent–solute interactions (cf. ref. 2*b* and references cited there).

The purpose of the present paper is to summarize the spectral changes which can be ascribed with some degree of confidence to intramolecular hydrogen bonding, and to deduce from the data certain generalizations concerning the intramolecular hydrogen bond in phenols and anilines.

THE INTRAMOLECULAR HYDROGEN BOND IN SOME ORTHOSUBSTITUTED PHENOLS AND ANILINES

Salicylaldehyde

The relevant ultraviolet and infrared spectra of salicylaldehyde (IA) and *m*-hydroxybenzaldehyde (IB) are listed in Table I. The intense infrared carbonyl band at 1666 cm^{-1} for salicylaldehyde occurs at lower frequency than for *m*-hydroxybenzaldehyde (1700 cm^{-1}) or for benzaldehyde (1709 cm^{-1}) (see Table I) and this then indicates an intramolecular hydrogen bond in salicylaldehyde (cf. also refs. 3, 4, 5, 6).* It may also be noted that the O—H stretching frequencies of phenol and salicylaldehyde occur near 3600 and 3200 cm^{-1} respectively (7). Salicylaldehyde may therefore be taken as an example of an intramolecularly hydrogen-bonded compound where, moreover, steric interactions are likely to be small. In *n*-hexane solution, the benzaldehyde ultraviolet *B*-band of salicylaldehyde shows a slight bathochromic wavelength displacement compared with the same *B*-band in *m*-hydroxybenzaldehyde and this displacement is accompanied by an increase in the maximal extinction coefficient (ϵ_{max}) from 9500 to 11,700 (see Table I). In the corresponding methoxybenzaldehydes no significant wavelength displacement is

**The other infrared bands listed in Table I are presumably to be associated with aromatic* C—H *vibrations which usually occur in this region; it is worth noting that for benzaldehyde and salicylaldehyde at least three fairly intense bands occur in this region. It is therefore possible, though considered unlikely, that the band at 1644 cm^{-1} in salicylaldehyde also represents a carbonyl band.*

Can. J. Chem. Downloaded from www.nrcresearchpress.com by 210.87.254.105 on 09/05/12
For personal use only.

TABLE I

Main ultraviolet maxima and infrared bands in the 1700–1560 cm^{-1} region for salicylaldehyde and reference compounds*†

		Ultraviolet maxima‡						Infrared bands in carbon tetrachloride	
		Phenol or anisole *B*-band		Benzaldehyde *B*-band		*C*-band		Carbonyl band	Other bands in the 1700–1560 cm^{-1} region
Compound	Solvent	$\lambda_{max}(m\mu)$	ϵ_{max}	$\lambda_{max}(m\mu)$	ϵ_{max}	$\lambda_{max}(m\mu)$	ϵ_{max}	$\nu_{max}(cm^{-1})$	$\nu_{max}(cm^{-1})$
Salicylaldehyde	Hexane	215§	17,000	251 258	11,000 11,700	327	3,600	1,666(s)	1,644(s) 1,618(m) 1,576(m)
m-Hydroxybenzaldehyde	Hexane	213	19,000	245 251	9,500 9,500	305 ca. *311*	2,900 *2,850*	1,700(m)	1,683(m)
Benzaldehyde	Hexane	—	—	242 *248*	14,000 *12,000*	279–280 289	1,200 1,000	1,709(s)	1,649(m) 1,581(m) 1,569(m)
o-Methoxybenzaldehyde	Hexane (2*a*)	211	20,000	247 ca. *254*	10,500 *8,500*	309 ca. *317*	4,600 4,200	—	—
Salicylaldehyde	Ether	218	15,000	ca. *251* 255–256	*10,500* 10,700	325	3,500	—	—
m-Hydroxybenzaldehyde	Ether			249 *253–254*	9,700 *9,200*	308 *311* *316*	3,250 *3,200* *3,050*	—	—

*See also ref. 2*b*. †Band nomenclature in this and subsequent tables is as generally used in ref. 2. ‡Values in italics represent inflections in this and subsequent tables. §In 0.1 *N* ethanolic NaOH this band occurs at ca. 232 mμ. It is therefore believed to be a phenolic *B*-band (see ref. 2*b*).

observed between the *o*- and *m*-isomers and the increase in ϵ_{max} on passing from the *m*- to the *o*-isomer is from 9200 to 10,500, that is, somewhat less than for the hydroxybenzaldehydes (see ref. 2*a*). Since, therefore, steric interactions in *o*-methoxybenzaldehyde do not give rise to appreciable wavelength displacements, the small wavelength displacement in the *B*-bands between salicylaldehyde and *m*-hydroxybenzaldehyde may be taken as an indication of intramolecular hydrogen bonding in salicylaldehyde as shown in IA.

The phenolic *B*-band also shows a slight bathochromic displacement (2 mμ) relative to the same band in *m*-hydroxybenzaldehyde and this displacement may also be related to hydrogen-bond formation. Three possible factors may account for this latter spectral change: (i) the displacement may occur because the hydrogen atom tends to become detached from the phenolic hydroxy group in the course of hydrogen-bond formation and hence the absorption maximum may tend towards that of the phenolate ion, (ii) the displacement may occur because of steric or other reasons since the hydrogen bond may cause the hydroxy group to rotate from its normal position in phenol (cf. ref. 2*b*), and (iii) the hydrogen bond may affect the vibrational levels of the hydroxy group in such a way as to cause the observed spectral change. *C*-Band data of salicylaldehyde and the other compounds studied are listed in Table I and subsequent tables. Their significance will be discussed in the Concluding Remarks.

The spectrum of salicylaldehyde compared with that of *o*-methoxybenzaldehyde is altered in a similar way. That is, compared with *o*-methoxybenzaldehyde both *B*-bands are again shifted to longer wavelength and these wavelength displacements are of the same order as between salicylaldehyde and *m*-hydroxybenzaldehyde (see Table I).

Next, it may be noted that the ultraviolet spectra of salicylaldehyde in cyclohexane and ether solution are more similar than, for example, the spectra of *m*-hydroxybenzalde-

Can. J. Chem. Downloaded from www.nrcresearchpress.com by 210.87.254.105 on 09/05/12
For personal use only.

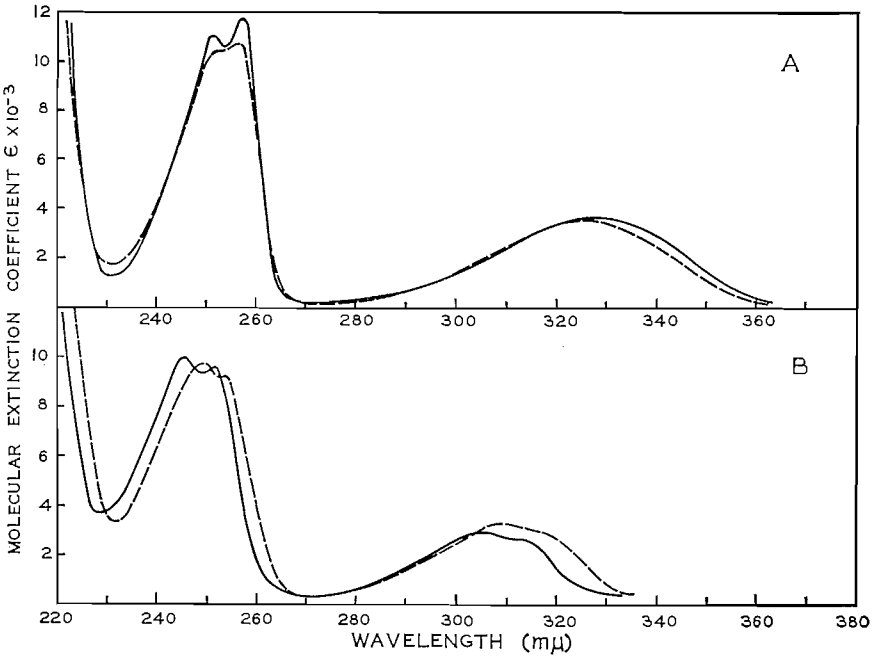


FIG. 1. The spectra of (A) salicylaldehyde and (B) *m*-hydroxybenzaldehyde in *n*-hexane (———) and ether (– – –) solutions.

hyde in these two solvents (see Fig. 1). The lack of any appreciable spectral change, particularly in the *C*-band, accompanying the solvent change for the spectrum of salicylaldehyde may again be ascribed to the presence of a strong intramolecular hydrogen bond.

All the above-mentioned spectral changes for salicylaldehyde can therefore be rationalized in terms of an intramolecular hydrogen bond, which can be schematically represented as shown in structure III.



III IV

TABLE II

Main ultraviolet maxima for *o*-hydroxyacetophenone and reference compounds

		Phenol or anisole *B*-band		Acetophenone *B*-band		*C*-band	
Compound	Solvent	λ_{max}(mμ)	ϵ_{max}	λ_{max}(mμ)	ϵ_{max}	λ_{max}(mμ)	ϵ_{max}
o-Hydroxyacetophenone	Cyclohexane	213	22,200	249.5 256	9,000 8,700	324 331	3,750 3,550
m-Hydroxyacetophenone	Cyclohexane	211	20,500	243 249	8,650 7,150	300.5 ca. *309*	2,550 *2,100*
Acetophenone	Cyclohexane	—	—	238	12,500	279	900
o-Methoxyacetophenone	Cyclohexane	211	20,300	ca. *238* 242.5	*8,100* 8,350	298 ca. *308*	3,550 *2,500*
o-Hydroxyacetophenone	Ether	214	16,000	250 ca. *254*	9,000 *8,550*	324 ca. *330*	3,700 *3,500*
m-Hydroxyacetophenone	Ether			246 ca. *252*	8,900 7,000	304 ca. *310*	2,900 *2,600*

Can. J. Chem. Downloaded from www.nrcresearchpress.com by 210.87.254.105 on 09/05/12
For personal use only.

o-Hydroxyacetophenone

The relevant ultraviolet spectral data are listed in Table II. The infrared spectrum of *o*-hydroxyacetophenone again shows the presence of an intramolecular hydrogen bond (cf. refs. 8, 9, and references cited there). It may also be noted that whereas the carbonyl band of *o*-hydroxyacetophenone does not show a doublet, the infrared carbonyl bands of compounds like *m*-hydroxyacetophenone (ν_{max} 1688 and 1678 cm^{-1}), *o*-chloro- and *o*-bromo-acetophenone (10) do show doublets in carbon tetrachloride solution. If structure IV indeed represents the predominant form of *o*-hydroxyacetophenone one would anticipate a number of similarities between the ultraviolet spectra of salicylaldehyde and *o*-hydroxyacetophenone and these are in fact observed (see Table II and cf. Table I).*

o-Nitrophenol

The infrared hydroxyl band of *o*-nitrophenol shows one intense band at 3209 cm^{-1} with only low-intensity absorption at higher frequency (see Fig. 2). The position of this band (see ref. 9, p. 84, Table VI and refs. 11 and 12) as also the absence of any observed concentration dependence of the band (see Experimental) indicates that the band corresponds to an intramolecularly hydrogen-bonded form. The NO_2-valence

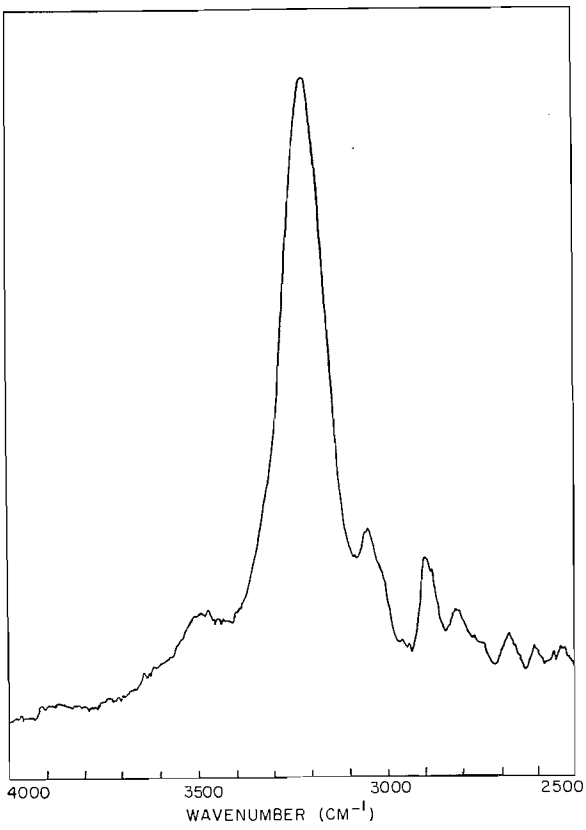


FIG. 2. The —OH stretching absorption band (3209 cm^{-1}) of *o*-nitrophenol, due to intramolecular hydrogen bonding (0.20 molar solution in carbon tetrachloride).

**The slightly greater displacement in o-hydroxyacetophenone compared with the o-methoxy compound is probably caused by steric interactions in the latter compound. This suggestion also receives support since for o- and m-methoxyacetophenones the acetophenone B-bands are no longer similar as they are for the corresponding benzaldehydes, but the o-isomer now absorbs at shorter wavelength indicative of steric interactions (see ref. 2a).*

Can. J. Chem. Downloaded from www.nrcresearchpress.com by 210.87.254.105 on 09/05/12
For personal use only.

vibration, for reasons which will be discussed later, is not particularly influenced by intramolecular hydrogen bonding (cf. ref. 12).

TABLE III

Main ultraviolet maxima for *o*-nitrophenol and reference compounds

Compound	Solvent	Phenol or anisole *B*-band		Nitrobenzene *B*-band		*C*-band	
		$\lambda_{max}(m\mu)$	ϵ_{max}	$\lambda_{max}(m\mu)$	ϵ_{max}	$\lambda_{max}(m\mu)$	ϵ_{max}
o-Nitrophenol	Cyclohexane	ca. *231*	*4,000*	271	7,350	346	3,700
m-Nitrophenol	Cyclohexane	222	10,200	258.5	6,100	312	2,170
Nitrobenzene (2*c*)	Cyclohexane	—	—	252	9,000	ca. *285*	*1,500*
o-Nitroanisole	Cyclohexane			250	3,400	307	2,500
m-Nitroanisole	Cyclohexane	223	13,000	261.5	6,100	316	2,400
o-Nitrophenol	Ether	ca. *234*	*3,000*	271	6,900	346	3,550
o-Nitrophenol	Ethanol	ca. *231*	*3,550*	272.5	6,050	347	3,250
o-Nitroanisole	Ether	ca. *229*	*5,500*	252–253	3,050	312	2,300
o-Nitroanisole	Ethanol	ca. *231*	*5,000*	257	3,200	319	2,350

The relevant ultraviolet data are listed in Table III and again confirm the presence of an intramolecular hydrogen bond in *o*-nitrophenol. The nitrobenzene *B*-band of *o*-nitrophenol compared with that of *m*-nitrophenol is more appreciably displaced (by 12.5 mμ) and intensified (see Table III). Compared with *o*-nitroanisole even larger wavelength displacements are observed but steric interactions preclude the use of *o*-nitroanisole as a suitable reference compound (see Introduction). The phenolic *B*-band data (see Table III) also show the anticipated wavelength displacements (see previous sections) but show a surprisingly large decrease in the ϵ_{max} value for the *o*-isomer. Next, the absence of appreciable wavelength changes for *o*-nitrophenol on changing the solvent from cyclohexane to ether and ethanol may also again be taken as evidence for a strong intramolecular hydrogen bond (see Table III and Fig. 3).

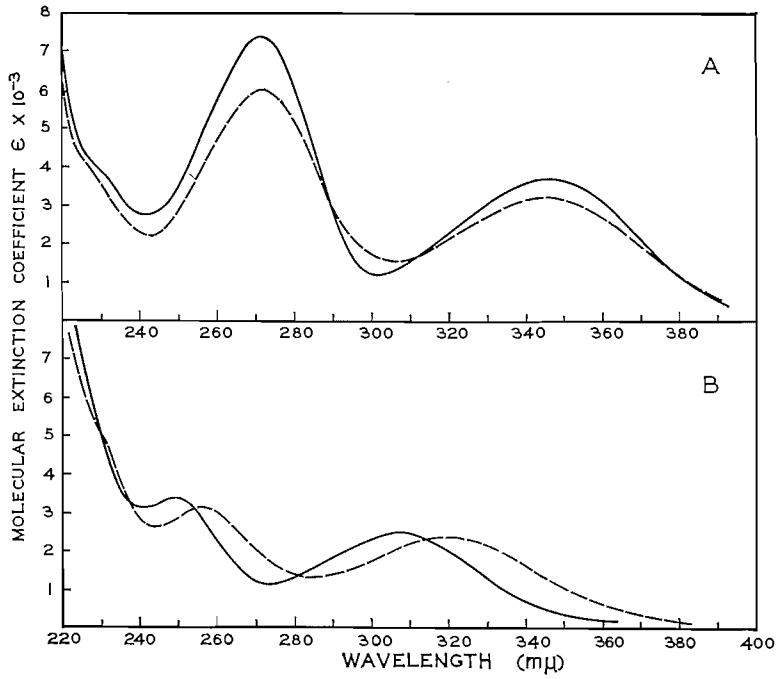


FIG. 3. The spectra of (A) *o*-nitrophenol and (B) *o*-nitroanisole in cyclohexane (———) and ethanol (– – –) solutions.

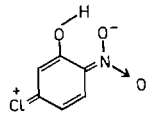
Can. J. Chem. Downloaded from www.nrcresearchpress.com by 210.87.254.105 on 09/05/12
For personal use only.

Can. J. Chem. Downloaded from www.nrcresearchpress.com by 210.87.254.105 on 09/05/12
For personal use only.

As previously shown, the wavelength displacement between *o*-nitrophenol and *o*-nitroanisole cannot be used directly as a measure of the intramolecular hydrogen bonding because of steric interactions in *o*-nitroanisole. However, additional substituents in the benzene ring, not vicinal to the nitro or methoxy substituents, are unlikely to affect these steric interactions; hence the above-mentioned wavelength displacements may be used as a measure of the strength of the intramolecular hydrogen bond in compounds of the type as listed in Table IV, where comparison with a *m*-isomer is not possible. The spectra of the compounds listed in Table IV were collected in order to investigate whether a substituent in the absence of additional steric interactions affects the strength of an intramolecular hydrogen bond.

The infrared frequency displacements listed in Table IV indicate that the intramolecular hydrogen bond is progressively strengthened by a chloro and a methoxy substituent, if these substituents are *para* with respect to the nitro group (cf. ref. 9, p. 84, Table VI). This strengthening of the intramolecular hydrogen bond, for a *p*-methoxy substituent, would also have been anticipated from benzoic acid data since a *p*-methoxy substituent apparently strengthens the dimeric hydrogen bond in benzoic acid (1). Moreover, using resonance symbols, both *p*-chloro- and *p*-methoxy substituents would be anticipated to give rise to increased contributions of resonance forms of type V which might be expected to favor the formation of an intramolecular hydrogen bond.

The ultraviolet spectral changes (if expressed in wave numbers) show approximately parallel effects. That is, 5-chloro or 5-methoxy substituents give rise to slightly larger



V

frequency displacements between the nitrobenzene *B*-bands of the phenol and the anisole (indicative of a stronger intramolecular hydrogen bond) whereas the opposite effect is observed for 4-methyl, 4-methoxy, or 4-chloro substituents (see Table IV). The data in Table IV also show that the spectra of intramolecularly hydrogen-bonded compounds are again generally only slightly affected on being determined in ethanol solution.

A simple explanation to rationalize the spectral changes is as follows: The negative charge on the NO_2 oxygen atom is increased by a *p*-methoxy or a *p*-chloro substituent and this enhanced charge formation occurs for *both* nitrophenol and nitroanisole; it accounts for the bathochromic displacement in the ultraviolet nitrobenzene *B*-band for 5-methoxy- and 5-chloro-nitrophenol and for the corresponding anisoles relative to these bands in nitrophenol or nitroanisole. This increased negative charge on the NO_2 oxygen atom, only for the *o*-nitrophenol, now also attracts the hydrogen atom of the hydroxyl group and this accounts for the lower frequency of the O—H vibration in both 5-methoxy- and 5-chloro-2-nitrophenol relative to *o*-nitrophenol. The closer proximity of the hydrogen atom, however, does not apparently affect appreciably the negative charge on the NO_2 group in the ground state (see below), and this phenomenon can be explained by assuming an electrostatic model for *this* hydrogen bond.* This model for *o*-nitrophenol also accounts for the infrared NO_2 vibrational frequencies which are remarkably constant (1530 ± 2 cm^{-1}) for the following compounds: *o*-nitrophenol, *o*-nitroanisole (cf. also ref. 12 for the

*Since a "covalent" contribution would be anticipated to affect the negative charge on the nitro group it should be noted that this model does of course not necessarily hold for other intramolecularly bonded systems (cf., for example, the carbonyl bands described in the previous section which are appreciably affected by a vicinal hydroxy group).

Can. J. Chem. Downloaded from www.nrcresearchpress.com by 210.87.254.105 on 09/05/12
For personal use only.

TABLE IV

Wavelength displacements between *o*-nitrophenols and *o*-nitroanisoles and infrared hydroxyl frequencies of *o*-nitrophenols

Compound	Solvent	Phenol or anisole *B*-band		Nitrobenzene *B*-band			*C*-band			Infrared hydroxyl band (in carbon tetrachloride)	
		λ_{max}(mμ)	ϵ_{max}	λ_{max}(mμ)	ϵ_{max}	Wavelength displacement relative to anisole	λ_{max}(mμ)	ϵ_{max}	Wavelength displacement relative to anisole	ν_{max}(cm^{-1})	Frequency displacement relative to *o*-nitrophenol (cm^{-1})
o-Nitrophenol	Cyclohexane	ca. *231*	*4,000*	271	7,350	21 mμ (3100 cm^{-1})	346	3,700	39 mμ (3670 cm^{-1})	3,209	—
o-Nitroanisole	Cyclohexane			250	3,400	—	307	2,500	—	—	—
4-Methyl-2-nitrophenol	Cyclohexane	ca. *234*	*3,650*	274–275	7,250	21 mμ (3020 cm^{-1})	359–360	3,600	41 mμ (3580 cm^{-1})	3,218	+9
4-Methyl-2-nitrophenol	Ethanol	ca. *234*	*4,000*	276	6,200	—	359–360	3,150	—	—	—
4-Methyl-2-nitroanisole	Cyclohexane			253.5	3,000	—	318–319	2,450	—	—	—
4-Methoxy-2-nitrophenol	Cyclohexane	244	5,900	277	6,500	21 mμ (2960 cm^{-1})	388–389	4,000	50 mμ (3810 cm^{-1})	3,216	+7
4-Methoxy-2-nitrophenol	Ethanol	244	5,850	278–279	5,600	—	388	3,400	—	—	—
4-Methoxy-2-nitroanisole	Cyclohexane	ca. *237*	*6,300*	*256*	*2,100*	—	338.5	2,650	—	—	—
4-Methoxy-2-nitroanisole	Ethanol	ca. *238*	*6,000*	ca. *264*	*2,300*	—	353	2,550	—	—	—
4-Chloro-2-nitrophenol	Cyclohexane			267	6,700	19 mμ (2870 cm^{-1})	359	3,500	39 mμ (3390 cm^{-1})	3,216	+7
4-Chloro-2-nitrophenol	Ethanol			265	5,100	—	353	3,000	—	—	—
4-Chloro-2-nitroanisole	Cyclohexane			ca. *248*	*3,100*	—	320	2,350	—	—	—
4-Chloro-2-nitroanisole	Ethanol			ca. *256*	*2,750*	—	342	2,350	—	—	—
5-Methoxy-2-nitrophenol	Cyclohexane	233 237	5,300 5,100	307 339–340	8,500 9,050	34.5 mμ (4120 cm^{-1})	—	—	—	3,144	−65
5-Methoxy-2-nitrophenol	Ethanol	232 ca. *237*	4,750 *4,650*	ca. *314* 341	*8,150* 9,350	—	—	—	—	—	—
5-Methoxy-2-nitroanisole	Cyclohexane	231	8,700	272.5 308	6,000 5,450	—	—	—	—	—	—
5-Chloro-2-nitrophenol	Cyclohexane			281	9,700	23.5 mμ (3240 cm^{-1})	340	5,200	33 mμ (3160 cm^{-1})	3,182	−27
5-Chloro-2-nitroanisole	Cyclohexane			257.5	5,400	—	307	3,500	—	—	—

reported, but unexplained similarity of the NO_2 vibrational frequency for these two compounds), 5-methoxy-2-nitrophenol, 4-methoxy-2-nitrophenol, 4-methyl- and 5-methyl-2-nitrophenol, and 4-chloro-2-nitrophenol* (see also Concluding Remarks) and ref. 13 for a discussion of the infrared N—O stretching frequencies).

Salicylic Acid

The relevant ultraviolet and infrared spectra are listed in Table V. The monomeric infrared carbonyl band for salicylic acid occurs at lower frequency than for benzoic acid or for *o*-methoxybenzoic acid (see Table V) and this then again indicates an intramolecular hydrogen bond involving the carbonyl oxygen atom (see also refs. 6, 14).

TABLE V

Ultraviolet *B*-bands and infrared carbonyl bands of salicylic acid and reference compounds

Compound	Solvent	Ultraviolet maximum*		Infrared carbonyl band† (in carbon tetrachloride), ν_{max} (cm^{-1})
		λ_{max}(mμ)	ϵ_{max}	
Salicylic acid	Cyclohexane	239	8,000	1,691
m-Hydroxybenzoic acid	Cyclohexane containing ca. 1% ether	233–234	6,800	Insufficiently soluble
Benzoic acid	Cyclohexane	230	12,500	1,744
o-Methoxybenzoic acid	Cyclohexane	230	8,300	1,749

*Spectra are determined at concentrations at which the monomeric species are believed to predominate (see ref. 1).
†Monomeric bands from ref. 1.

Supporting evidence for this hydrogen bonding is also obtained from the ultraviolet data listed in Table V, which show that the benzoic acid *B*-band in salicylic acid is bathochromically displaced compared with the same band in *m*-hydroxybenzoic acid; for the *o*- and *m*-isomers of methoxybenzoic acid on the other hand, the *m*-isomer absorbs at slightly longer wavelength (2*a*). Moreover, salicylic acid in ether is reported to absorb maximally at 237 mμ, ϵ = 7800 (15) which is close to the absorption of the monomeric species in cyclohexane solution (see Table V).†

TABLE VI

Main ultraviolet maxima for *o*-aminobenzaldehyde and reference compounds

Compound	Solvent	Aniline *B*-band		Benzaldehyde *B*-band		*C*-band	
		λ_{max}(mμ)	ϵ_{max}	λ_{max}(mμ)	ϵ_{max}	λ_{max}(mμ)	ϵ_{max}
o-Aminobenzaldehyde	Cyclohexane			256 ca. *263*	5,600 *3,400*	356	4,700
m-Aminobenzaldehyde*	Cyclohexane containing ca. 0.2% ether	228	17,500	ca. *244* ca. *257*	*9,000* *7,500*	331.5	2,000
Benzaldehyde	Hexane	—	—	242 *248*	14,000 *12,000*	279–280 289	1,200 1,000
Aniline*	Cyclohexane	234	9,000	—	—	289	1,900

*Data from ref. 2*e*.

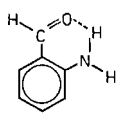
**The same band in 5-chloro-2-nitrophenol occurs only at slightly lower frequency (ν_{max} 1521 cm^{-1}). It might also be noted that the infrared* O—H *vibrational frequencies listed in Table IV for various substituted nitrophenols are not proportional to the relevant* σ *values.*

†*Dannenberg (15) assumes that the intramolecular hydrogen bond causes a wavelength displacement of 16* mμ *but this value is probably too large since it is obtained by comparing the maximal absorptions of salicylic and o-methoxybenzoic acids; that is steric interactions, as mentioned in the Introduction may operate in the latter compound and these will tend to increase the apparent wavelength displacement ascribed to the intramolecular hydrogen bond.*

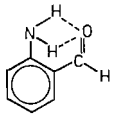
Can. J. Chem. Downloaded from www.nrcresearchpress.com by 210.87.254.105 on 09/05/12
For personal use only.

o-Aminobenzaldehyde

The relevant ultraviolet data are listed in Table VI, and these data show that the wavelength displacements between the *o*- and *m*-isomers may again be taken as evidence of intramolecular hydrogen bonding. An interesting difference between the spectra of amino and hydroxy compounds is that only for the amino compounds are the ϵ_{max} values of the benzaldehyde *B*-band substantially decreased in the *o*-isomer compared with the ϵ_{max} values of the *m*-isomer (see Table VI, and compare also later tables). A possible explanation is that the intramolecular hydrogen bond prevents the alignment of the carbonyl group in the same plane as the benzene ring since steric interactions are well known to give rise to intensity decreases. A coplanar alignment would be expected to lead to a large ϵ_{max} value, and hydrogen bonding of type VI would have been expected to facilitate this same alignment. However, if the above explanation (i.e. the hydrogen bond preventing coplanar alignment) concerning the ϵ decrease is correct, it is necessary to postulate that the six-membered ring system, involving the intramolecular hydrogen bond as shown in structure VI, is not entirely coplanar. Another more general interpretation is that the coplanar hydrogen-bonded confirmation causes some of the "normal" transitions to be "forbidden." A third explanation may be provided by supposing that



VI



VII

there is a tendency for *both* N-hydrogen atoms to form intramolecular hydrogen bonds as shown in structure VII, and that in this process both the NH_2 and CHO groups are twisted out of the plane of the benzene ring. A similar explanation—that is, *two* hydrogen bonds being formed at the expense of coplanarity—may also hold for the intensity decrease observed for the *B*-band of *o*-aminobenzoic acid (see Table IX) and for the ϵ decrease as observed for the phenolic *B*-band in *o*-nitrophenol (see Table III and also Concluding Remarks).

o-Aminoacetophenone

Infrared data have previously indicated (10, 16) the presence of an intramolecular hydrogen bond for this compound and the present ultraviolet spectra support this hypothesis (see Table VII); that is, the acetophenone *B*-band relative to the same band

TABLE VII

Main ultraviolet *B*-bands and infrared carbonyl bands of *o*-aminoacetophenone and reference compounds

		Ultraviolet maxima						Infrared carbonyl bands* (in carbon tetrachloride)	
		Aniline *B*-band		Acetophenone *B*-band		*C*-band			
Compound	Solvent	$\lambda_{max}(m\mu)$	ϵ_{max}	$\lambda_{max}(m\mu)$	ϵ_{max}	$\lambda_{max}(m\mu)$	ϵ_{max}	$\nu_{max}(cm^{-1})$	$\epsilon_{max}^{(a)}$ (mean)
o-Aminoacetophenone	Cyclohexane	224	23,500	253	5,500	351	4,350	1,653	549
m-Aminoacetophenone	Cyclohexane	226	26,500	*247*	*9,000*	323	2,500	1,689	540
Acetophenone	Cyclohexane	—	—	238	12,500	279	900	1,691	650
o-Aminoacetophenone	Ethanol	226	21,000	255	5,600	363	4,350	—	—
m-Aminoacetophenone	Ethanol	231	23,000	ca. *256*	*7,000*	341	1,900	—	—

*Data from ref. 10.

Can. J. Chem. Downloaded from www.nrcresearchpress.com by 210.87.254.105 on 09/05/12
For personal use only.

in the *m*-isomer is bathochromically displaced. The intensity of the *B*-band in *o*-aminoacetophenone is again decreased (cf. Table VI). Although the ultraviolet spectrum of *o*-aminoacetophenone is not completely unaffected on altering the solvent from cyclohexane to ethanol, the observed spectral changes are less than for the corresponding *m*-isomer and particularly the ϵ values remain strikingly similar.

The ultraviolet data for this compound have also been determined by Lutskii and Dorofeev (17), who obtain spectral data similar to those obtained by us for *o*- and *m*-aminoacetophenone. Lutskii and Dorofeev also show that for the corresponding N,N-dimethyl derivatives a *hypsochromic* wavelength displacement is obtained in the acetophenone *B*-band if the spectrum of the *o*-isomer is compared with that of the *m*-isomer. This is not unexpected and suggests the presence of steric interactions in the *o*-isomer of N,N-dimethylaminoacetophenone. It follows that the latter compound is unsuitable as a reference compound for measuring the strength of the intramolecular hydrogen bond in *o*-aminoacetophenone.

o-Nitroaniline

Infrared data for *o*-nitroaniline, as judged primarily from the N—H stretching frequencies, have been assumed to show the *absence* of an intramolecular hydrogen bond in this compound (18, 19). The NO_2 vibrational frequencies are again only slightly, or not at all, lowered in the *o*-isomer compared with these same frequencies in the *m*-isomer of nitroaniline (12, 18, 19). However, this evidence cannot perhaps be regarded as entirely conclusive since some interaction would be expected to occur between the two *o*-substituents in *o*-nitroaniline, and since also there is some evidence for this interaction from other infrared data (see refs. 20, 21). The question whether a hydrogen bond exists in the ground state of *o*-nitroaniline must therefore remain undecided although, as pointed out by Dyall and Hambly (18), there is at present no unambiguous evidence of such a hydrogen bond in *o*-nitroaniline.

TABLE VIII

Main ultraviolet maxima for *o*-nitroaniline and reference compounds

Compound	Solvent	Aniline *B*-band		Nitrobenzene *B*-band		*C*-band	
		$\lambda_{max}(m\mu)$	ϵ_{max}	$\lambda_{max}(m\mu)$	ϵ_{max}	$\lambda_{max}(m\mu)$	ϵ_{max}
o-Nitroaniline	Cyclohexane	228	18,000	271	5,000	375	5,000
m-Nitroaniline	Cyclohexane	234	15,300	ca. *266*	*4,000*	345	1,950
Nitrobenzene	Cyclohexane	—	—	252	9,000	ca. *280*	*1,500*
o-Nitroaniline	Ethanol	232	17,000	279	5,000	408	5,500
m-Nitroaniline	Ethanol	234	18,000			380	1,600
m-Nitroaniline	Ether	235	19,000	ca. *277*	*4,600*	373	1,800

This uncertainty is also reflected in the ultraviolet spectra (see Table VIII). On the one hand, a bathochromic wavelength displacement (of ca. 5 mμ) between the *o*- and *m*-isomers is observed in the nitrobenzene *B*-band; on the other hand, this *B*-band spectral change is less for *o*-nitroaniline than for *o*-aminoacetophenone, and on changing the solvent from cyclohexane to ethanol both *B*- and *C*-bands are appreciably more displaced for *o*-nitroaniline than for *o*-nitrophenol or *o*-aminoacetophenone.

A possible explanation is that the electronic perturbations, loosely ascribed to intramolecular hydrogen bonding, are of only minor importance *in the ground state* (cf. ref. 18 and also the dipole moment data for 2,4-dinitroaniline of Smith and Walshaw (22)), but

Can. J. Chem. Downloaded from www.nrcresearchpress.com by 210.87.254.105 on 09/05/12
For personal use only.

that these perturbations become more important in the electronic excited state and in this way give rise to the observed ultraviolet spectral changes. Even on this interpretation, however, it seems probable that intramolecular "hydrogen bonding" in *o*-nitroaniline is weaker than in most of the other *o*-amino or *o*-hydroxy compounds discussed in this paper.

o-Aminobenzoic Acid

The wavelength displacements between *o*- and *m*-isomers of aminobenzoic acid in ether and ethanol solution are ca. 8 and 6.5 mμ, respectively, for the ultraviolet benzoic acid *B*-band. The *C*-band ϵ_{max} values are appreciably larger in the *o*-isomer (see Table IX). These observations can in a general way be related to the existence of intramolecular hydrogen bonding or related interactions in *o*-aminobenzoic acid.

TABLE IX

Main ultraviolet maxima for *o*-aminobenzoic acid and reference compounds*

		Benzoic acid *B*-band		*C*-band	
Compound	Solvent	λ_{max}(mμ)	ϵ_{max}	λ_{max}(mμ)	ϵ_{max}
o-Aminobenzoic acid	Ether	252	7,400	333	5,200
m-Aminobenzoic acid	Ether	244	7,800	320	2,800
o-Aminobenzoic acid	Ethanol	248.5	6,700	336	4,500
m-Aminobenzoic acid	Ethanol	ca. *242*	*7,000*	323	2,100

*Data from ref. 2*e*.

CONCLUDING REMARKS

In all the above *o*-substituted anilines or phenols, which may contain an intramolecular hydrogen bond, a bathochromic wavelength displacement of between 5 and 12.5 mμ (690 and 1780 cm^{-1}) is observed in the *B*-band compared with the *B*-band absorption in the corresponding *m*-isomer. (See Tables I–IX; the *B*-band referred to is the *B*-band associated with transitions involving predominantly that mono-substituted benzene derivative in which the substituent is electron-withdrawing.) Since for most of these compounds an intramolecular hydrogen bond is generally believed to be present, this suggests that intramolecular hydrogen bonding or related interactions contribute to this wavelength displacement. If this interpretation is correct this also indicates that intramolecular hydrogen bonding or related interaction give rise to approximately the *same* amount of electronic perturbation for most of the compounds discussed ($\Delta\nu$ = 1175 ±215 cm^{-1}), except that for *o*-nitroaniline the observed wavelength displacement is smaller (690 cm^{-1}) and larger for *o*-nitrophenol (1780 cm^{-1}).

Evidence which can be interpreted in terms of an intramolecular hydrogen bond affecting *all* the above-mentioned compounds in a similar manner can also be deduced from the corresponding *C*-band spectral changes (see Tables I to IX). Apart from bathochromic wavelength displacements, the intensity of the *C*-band is also consistently increased in the *o*-isomer but this increase is not exclusively caused by intramolecular hydrogen bonding since it is very pronounced for *o*-nitroaniline compared with *m*-nitroaniline, although *o*-nitroaniline is not believed to contain a strong intramolecular hydrogen bond. Moreover, this intensity increase in the *C*-band is also observed for compounds like *o*-methoxyacetophenone compared with *m*-methoxyacetophenone (2*a*) although *no* intramolecular hydrogen bond is possible in the former compound. This suggests that *C*-band spectral changes are less reliable than *B*-band spectral changes in estimating the strength of an intramolecular hydrogen bond (cf. also ref. 2*d*).

Can. J. Chem. Downloaded from www.nrcresearchpress.com by 210.87.254.105 on 09/05/12
For personal use only.

Can. J. Chem. Downloaded from www.nrcresearchpress.com by 210.87.254.105 on 09/05/12
For personal use only.

The absence of an appreciable spectral change on determining the ultraviolet spectrum of a molecule in cyclohexane and ether or ethanol solution also provides support for the supposed presence of a strong intramolecular hydrogen bond. This argument is particularly convincing if the *m*-isomer or other reference compound shows an appreciable spectral change on altering the solvent in an identical manner (see Figs. 1 and 3 and Tables I, II, III, IV, and VII); only for *o*-nitroaniline the observed wavelength displacements point *against* the presence of an intramolecular hydrogen bond (the intensity values, however, again remain similar for the spectrum of *o*-nitroaniline in cyclohexane and ethanol). As anticipated, the concept of competitive hydrogen bonding is also indicated by some of the infrared data. For example, on determining the O—H vibrational band for a number of phenols under various solvent conditions, phenol affords frequency displacements of up to 300 cm^{-1}, *p*-nitrophenol affords frequency displacements of over 400 cm^{-1}, whereas the frequency displacements in *o*-nitrophenol for the same solvent range are never greater than 66 cm^{-1} (11). For salicylaldehyde both carbonyl band frequencies as also band intensities remain similar in carbon tetrachloride, chloroform, *n*-butanol, and even in acetonitrile (23).

There is also other evidence that the above eight compounds do not contain a similar intramolecular hydrogen bond. For example for phenols the ϵ_{max} value of the *B*-band not associated with the phenol or aniline system is usually increased substantially in the *o*-isomer compared with the same band in the *m*-isomer (see Tables I to V), but this same ϵ_{max} value is generally *reduced* for *o*-substituted anilines. Next, the other *B*-band, associated with the phenol or aniline chromophore, is only slightly affected if the spectrum of the *o*-isomer is compared with that of the *m*-isomer; however, a small *bathochromic* wavelength displacement is usually observed for the *o*-substituted phenol (see Tables I–III), whereas a small *hypsochromic* displacement is observed for *o*-aminoacetophenone (see Table VII). *o*-Nitroaniline may be exceptional since a slight bathochromic displacement is observed relative to the *m*-isomer and also since for *o*-nitroaniline the ϵ_{max} value of this band is increased (cf. Table VIII and other tables). Moreover, infrared spectral changes are also dissimilar. For example, the data in reference 6 show that the estimated frequency displacements of the O—H stretching bands are different for *o*-nitrophenol, salicylaldehyde, and salicylic acid. The reason for these differences remains obscure. A possible partial explanation is that the formation of N—H- - -O bonds tends to twist the carbonyl group out of the plane of the benzene ring, possibly to form hydrogen bonds or related interactions with *both* of the hydrogen atoms of the NH_2 group as shown in structure VII. This could account for some of the spectral differences observed between *o*-substituted anilines and phenols, but does not account for the anomalous spectral changes in *o*-nitroaniline. There is incidentally no evidence that an intramolecular O—H- - -O bond is stronger than an intramolecular N—H- - -O bond although precisely this relationship is indicated for the corresponding *inter*molecular hydrogen bonds (24).

Perhaps the most important deduction is that the data provide no evidence for other than an electrostatic linkage in the compounds discussed in this paper. That is, covalent-type hydrogen-bonded structures tend to be excluded for *o*-nitrophenols because the N—O stretching vibrations remain practically unaffected by the intramolecular hydrogen bond or related interactions for a number of substituted *o*-nitrophenols and for *m*-nitrophenol. (A covalent-type linkage would be expected to affect the N—O bond order and consequently the infrared stretching bands.) For some of the other compounds studied in this paper, for example *o*-hydroxy- and *o*-amino-acetophenone, the carbonyl

stretching vibration *is* altered, presumably by the formation of the intramolecular hydrogen bond or related interaction, but this does not necessarily provide evidence for a covalent linkage since an electrostatic linkage might also affect the negative charge on the carbonyl oxygen atom and hence the bond order of the carbonyl group.* In fact it must be supposed that the N—O bond order remaining unaffected in *o*-nitrophenol represents a somewhat exceptional behavior which *cannot* be explained readily in terms of a covalent linkage; it *can*, however, be explained in terms of an electrostatic linkage if it is assumed that the relatively large negative charge on the NO_2 oxygen atom is only slightly affected by the comparatively smaller positive charge on the neighboring hydrogen atom of the OH or NH_2 groups. For other compounds a variety of evidence has been obtained; some indicates a covalent type of linkage or at least that covalent forces play a considerable part (cf. for example, refs. 1, 6, 26), while other evidence, like the present data, may be assumed to indicate a predominantly electrostatic type of linkage (25).

Assuming that the change in the O—H stretching vibration provides the most sensitive method of determining the strength of an intramolecular "hydrogen bond" we may now attempt to summarize our observations. We can thus suppose that the interactions loosely referred to as intramolecular hydrogen bonding tend to attract the hydrogen atom(s) of the OH or NH_2 groups towards the adjoining negative center; this gives rise to the changes in bond order of the O—H or N—H bonds and consequently to the changes in the corresponding infrared vibrational bands. The bond order of the group containing the negative charge is not necessarily affected in the ground state but appears to be affected in the electronic excited state. Such a mechanism accounts for the ultraviolet spectral changes and also seems reasonable since the presence of a vicinal positive charge on the hydrogen atom might be expected to affect the bond order of the N—O bond to a greater extent in the electronic excited state than in the ground state.

EXPERIMENTAL

The ultraviolet absorption spectra were determined as described in previous parts of this series of papers (1, 24).

The infrared spectra were determined on a Unicam SP100 double-beam spectrophotometer using a NaCl prism and diffraction grating at the following solute concentrations: The spectrum of *o*-nitrophenol was determined at solute concentrations of 0.2 *M* and 1.0 *M*, and the spectra of the other *o*-nitrophenols were determined at concentrations of 0.2 *M*. The spectrum of salicylaldehyde was determined at solute concentrations of 0.05 and 0.25 *M*, the spectrum of benzaldehyde at 0.05 *M* and the spectra of *m*-hydroxybenzaldehyde and *m*-hydroxyacetophenone were determined in saturated solutions.

The phenols and anilines were either commercially available materials or prepared by standard methods as described in the literature. The compounds were purified by distillation or recrystallization until their melting points or boiling points and refractive indices showed them to be sufficiently pure. The solvents used were spectroanalyzed cyclohexane (Fisher), spectroanalyzed carbon tetrachloride, or commercially available absolute ethanol suitable for spectroscopy.

**However, intramolecularly hydrogen-bonded systems containing a carbonyl group have been reported in which no effect of the hydrogen bonding on the carbonyl stretching frequency was observed (25).*

Can. J. Chem. Downloaded from www.nrcresearchpress.com by 210.87.254.105 on 09/05/12
For personal use only.

ACKNOWLEDGMENTS

The authors are greatly indebted to Mr. D. L. Coffen for very competent technical assistance in the preparation of some of the compounds and in the determination of the infrared spectra. Thanks are also due to Miss N. Joan Smith for determining some of the ultraviolet absorption spectra.

The authors also wish to thank the Fisheries Research Board of Canada for financial support, since part of this work was carried out under a contract between the Fisheries Research Board of Canada and the Memorial University of Newfoundland. Finally, the assistance of the National Research Council in support of these studies is again gratefully acknowledged.

REFERENCES

1. W. F. Forbes, A. R. Knight, and D. L. Coffen. Can. J. Chem. **38**, 728 (1960).
2. (*a*) J. C. Dearden and W. F. Forbes. Can. J. Chem. **37**, 1305 (1959).
   (*b*) J. C. Dearden and W. F. Forbes. Can. J. Chem. **37**, 1294 (1959).
   (*c*) W. F. Forbes. Can. J. Chem. **36**, 1350 (1958).
   (*d*) W. F. Forbes, W. A. Mueller, A. S. Ralph, and J. F. Templeton. Can. J. Chem. **35**, 1049 (1957).
   (*e*) W. F. Forbes and I. R. Leckie. Can. J. Chem. **36**, 1371 (1958).
3. P. M. G. Bavin and W. J. Canady. Can. J. Chem. **35**, 1555 (1957).
4. H. Tsubomura. J. Chem. Phys. **24**, 927 (1956).
5. S. Pinchas. Anal. Chem. **29**, 334 (1957).
6. K. Nakamoto, M. Margoshes, and R. E. Rundle. J. Am. Chem. Soc. **77**, 6480 (1955).
7. P. J. Krueger and H. W. Thompson. Proc. Roy. Soc. A, **250**, 22 (1959).
8. M. St. C. Flett. Spectrochim. Acta, **10**, 21 (1957).
9. L. J. Bellamy. The infrared spectra of complex molecules. Methuen & Co. Ltd., London. 1954.
10. R. N. Jones, W. F. Forbes, and W. A. Mueller. Can. J. Chem. **35**, 504 (1957).
11. L. J. Bellamy and H. E. Hallam. Trans. Faraday Soc. **55**, 220 (1959).
12. B. Franck, H. Hörmann, and S. Scheibe. Ber. **90**, 330 (1957).
13. T. Urbanski. Roczniki Chem. **31**, 37 (1957); **32**, 241 (1958).
14. M. Neuilly. Compt. rend. **238**, 781 (1954).
15. H. Dannenberg. Z. Naturforsch. **4b**, 327 (1949).
16. A. N. Hambly and J. Bonnyman. Australian J. Chem. **11**, 529 (1958).
17. A. E. Lutskii and V. V. Dorofeev. Zhur. Obshchei Khim. **27**, 1059 (1957); Cf. Chem. Abstr. **52**, 881 (1958).
18. L. K. Dyall and A. N. Hambly. Australian J. Chem. **11**, 513 (1958).
19. T. Urbanski and U. Dabrowska. Chem. & Ind. (London), 1206 (1958).
20. R. D. Kross, V. A. Fassel, and M. Margoshes. J. Am. Chem. Soc. **78**, 1332 (1956).
21. R. J. Francel. J. Am. Chem. Soc. **74**, 1265 (1952).
22. J. W. Smith and S. M. Walshaw. J. Chem. Soc. 4527 (1957).
23. H. Yamada. Bull. Chem. Soc. Japan, **32**, 1051 (1959).
24. J. C. Dearden and W. F. Forbes. Can. J. Chem. **38**, 896 (1960).
25. N. Mori, Y. Tsuzuki, and H. Tsubomura. Nippon Kagaku Zasshi, **77**, 459 (1956); Cf. Chem. Abstr. **52**, 7858 (1958).
26. E. W. Gill and E. D. Morgan. Nature, **183**, 248 (1959).

Can. J. Chem. Downloaded from www.nrcresearchpress.com by 210.87.254.105 on 09/05/12
For personal use only.

Can. J. Chem. Downloaded from www.nrcresearchpress.com by 210.87.254.5 on 09/05/12
For personal use only.

THE STUDY OF HYDROGEN BONDING AND RELATED PHENOMENA BY ULTRAVIOLET LIGHT ABSORPTION

PART VI. THE EFFECT OF STERIC INTERACTIONS ON THE INTRAMOLECULAR HYDROGEN BOND IN *o*-NITROPHENOL[1]

J. C. DEARDEN[2] AND W. F. FORBES[3]

ABSTRACT

Intramolecular hydrogen bonding occurring in *o*-nitrophenol is discussed with special reference to the effects of the steric interactions on the absorption bands and on the bonding. An alkyl substituent vicinal to the OH group, or a methyl group vicinal to the NO_2 group appears to strengthen the intramolecular hydrogen bond in *o*-nitrophenol. The O—H vibrational stretching frequency in *o*-nitrophenol appears to be more susceptible to steric than to mesomeric interactions, and a methyl substituent vicinal to the nitro group in *o*-nitrophenols is found to give rise to a characteristic O—H stretching vibration band. For 6-*t*-butyl-2-nitrophenol, a special, "protected" hydrogen bond is postulated. In some of the *o*-nitrophenols, intermolecular hydrogen bonding gives rise to appreciable ultraviolet intensity decreases presumably because of increased steric interactions.

INTRODUCTION

In the previous paper (1), it was shown that spectral data confirm the generally held opinion that *o*-nitrophenol possesses an intramolecular hydrogen bond; it was also shown that the spectral effects ascribed to this hydrogen bonding could be adequately explained in terms of an electrostatic model. That is, it may be assumed that the NO_2-group because of its negative charge merely attracts the hydrogen atom of the OH-group and that there is no need to postulate the presence of a covalent contribution since the infrared NO_2 stretching bands remain practically unaffected for a number of substituted *o*-nitrophenols, for *o*-nitroanisole, and for *m*-nitrophenol.

The purpose of the present paper is to investigate how steric interactions affect the spectral changes ascribed to intramolecular hydrogen bonding in various sterically hindered nitrophenols.

THE SPECTRA OF *o*-NITROPHENOL AND *o*-NITROANISOLE

The greatly reduced maximal extinction coefficient in the nitrobenzene *B*-band (for band nomenclature used, see ref. 2 and other papers in that series of papers, and ref. 3) of *o*-nitroanisole (λ_{max} 250 mμ, $\epsilon = 3400$) compared with that of *o*-nitrophenol (λ_{max} 271 mμ, $\epsilon = 7350$), *m*-nitrophenol (λ_{max} 258.5 mμ, $\epsilon = 6100$), and *m*-nitroanisole (λ_{max} 262 mμ, $\epsilon = 6100$) (all in cyclohexane solution) suggests the operation of steric interactions in *o*-nitroanisole. If intramolecular hydrogen bonding were wholly responsible for the relative intensity increase in *o*-nitrophenol compared with the intensity in *o*-nitroanisole, a similar intensity increase should be observed for *o*-nitrophenol compared with *m*-nitrophenol but this is not found to be so. Since, further, a hypsochromic wavelength displacement of 21 mμ occurs for this same band in *o*-nitroanisole compared with *o*-nitrophenol (12 mμ compared with *m*-nitroanisole), whereas the infrared NO_2 stretching vibrations remain approximately constant (1530 ± 2 cm^{-1}) this suggests that the energy levels of the nitrobenzene groups in the two compounds are as shown in Fig. 1.

[1]*Manuscript received May 2, 1960.*
Contribution from the Memorial University of Newfoundland, St. John's, Newfoundland, and from the Division of Protein Chemistry, C.S.I.R.O., Melbourne, Australia.
[2]*Present address: "Shell" Research Limited, P.O. Box 1, Chester, England.*
[3]*Present address: Division of Protein Chemistry, C.S.I.R.O., 343 Royal Parade, Parkville, N.2 (Melbourne), Victoria, Australia. All correspondence should be addressed to this author.*

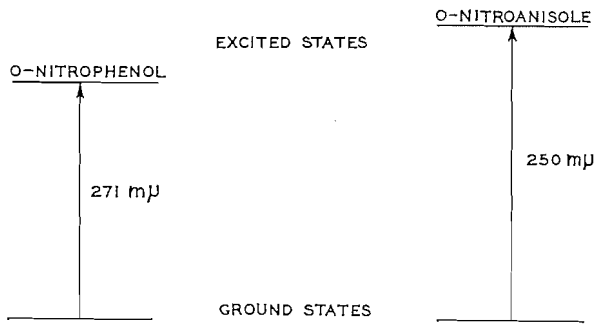


FIG. 1. Schematic representation of ground and excited states for nitrophenol and nitroanisole.

Figure 1 illustrates that the ultraviolet hypsochromic wavelength displacement is to be ascribed to the potential energy being raised predominantly in the electronic excited state of *o*-nitroanisole, and a contributing factor to this may be a slight twist in the interplanar angle between the NO_2-group and the benzene ring. Moreover, this slight change in interplanar angle may cause some of the transitions in *o*-nitroanisole to become "forbidden" and this may contribute to the observed loss of absorption intensity in this compound (4, 5, 6). It remains to explain the well-known appreciable frequency displacement in carbon tetrachloride solution for the infrared O—H band in *o*-nitrophenol (ν_{max} 3209 cm^{-1}) compared with that of *m*-nitrophenol (ν_{max} ca. 3500 cm^{-1}) on the basis of this model, but this has previously been done (1) by assuming that the negative charge on the NO_2-group attracts the hydrogen atom and thus weakens the O—H bond and consequently causes absorption at lower frequency.

THE SPECTRA OF *o*-NITROPHENOL, 6-METHYL-2-NITROPHENOL, AND 6-*t*-BUTYL-2-NITROPHENOL

The spectra of *o*-nitrophenol, 6-methyl-2-nitrophenol, and 6-*t*-butyl-2-nitrophenol are listed in Table I.

Table I shows that, as judged by the infrared O—H stretching bands, an alkyl substituent ortho to the OH group in *o*-nitrophenol apparently strengthens the intramolecular hydrogen bond. Moreover, this effect, associated with strengthening of the intramolecular hydrogen bond, is more pronounced for a *t*-butyl than for a methyl substituent. The effect of the alkyl substituents on the infrared O—H band is also paralleled by the effect on the ultraviolet maximal wavelengths, which are progressively displaced to longer wavelength (i.e. to lower frequency) with increased size of the alkyl substituent (see Table I). The above spectral changes therefore suggest that the introduction of alkyl substituents vicinal to the OH group in *o*-nitrophenol may be assumed to provide an example of steric facilitation of hydrogen bonding (for other examples of steric facilitation of hydrogen bonding see ref. 7 and cf. also refs. 8, 9, and footnote 14 of ref. 10).

However, there are some significant differences between the spectra of 6-methyl-2-nitrophenol and 6-*t*-butyl-2-nitrophenol (see Table I). First, doublet formation occurs in both infrared stretching bands for the 6-methyl compound but not for 6-*t*-butyl-2-nitrophenol or *o*-nitrophenol. The most obvious cause of this observed band splitting is conformational heterogeneity, but it is difficult to conceive of two different conformational isomers in 6-methyl-2-nitrophenol. Next, the ultraviolet data show that for *o*-nitrophenol and 6-*t*-butyl-2-nitrophenol the maximal wavelengths are altered only

Can. J. Chem. Downloaded from www.nrcresearchpress.com by 210.87.254.5 on 09/05/12
For personal use only.

Can. J. Chem. Downloaded from www.nrcresearchpress.com by 210.87.254.5 on 09/05/12
For personal use only.

TABLE I

Absorption spectra of *o*-nitrophenol, 6-methyl-2-nitrophenol, and 6-*t*-butyl-2-nitrophenol

	Infrared spectra				Ultraviolet spectra					
					o-Nitrophenol		6-Methyl-2-nitrophenol		6-*t*-Butyl-2-nitrophenol	
Bands	*o*-Nitrophenol, ν_{max}	6-Methyl-2-nitrophenol, ν_{max}	6-*t*-Butyl-2-nitrophenol, ν_{max}	Bands	λ_{max} (mμ)	ϵ_{max}	λ_{max} (mμ)	ϵ_{max}	λ_{max} (mμ)	ϵ_{max}
Spectrum in carbon tetrachloride				Spectrum in cyclohexane						
				Nitrobenzene *B*-band	271	7,350	281	7,850	283	6,900
				C-band	346	3,700	354	3,400	357	3,550
O—H bands (in cm^{-1})	3,209(s)	3,078(w)* 3,154(m)	3,067(m)							
				Spectrum in ethanol						
NO_2 bands (in cm^{-1})	1,532(s) 1,316(s)	1,534(m) 1,552(m) 1,309(m) 1,327(m)	1,536(s) 1,333(m)	Nitrobenzene *B*-band	272.5	6,050	274	6,850	285	6,500
				C-band	347	3,250	341	2,750	358	3,350

*Band assignment doubtful; this band may be a —C—H stretching band, or may correspond to associated molecules.

slightly on changing the solvent from cyclohexane to ethanol. However, for 6-methyl-2-nitrophenol an appreciable wavelength change is observed with change of solvent (see Table I), and incidentally the ϵ_{max} values are greatest for the *B*-band and smallest for the *C*-band of 6-methyl-2-nitrophenol. These changes can partly be explained by assuming that competitive intermolecular hydrogen bonding occurs for 6-methyl-2-nitrophenol (which gives rise to the observed wavelength displacement on determining the spectrum in cyclohexane and ethanol), but that such competitive intermolecular hydrogen bonding does not occur for 6-*t*-butyl-2-nitrophenol presumably because of the bulk effect of the *t*-butyl group. If this interpretation is correct it must also be assumed that for *o*-nitrophenol competitive intermolecular hydrogen bonding is of less importance. The reason for this may be that only for 6-methyl-2-nitrophenol (in which steric facilitation of hydrogen bonding occurs), but not for *o*-nitrophenol, steric interactions are increased by this competitive intermolecular hydrogen bonding. It may be noted that 6-*t*-butyl-2-nitrophenol therefore occupies a somewhat unique position among *o*-nitrophenols possessing adjacent alkyl groups (see also following sections), since only for this compound is there observed no wavelength displacement on determining the ultraviolet spectrum in cyclohexane and ethanol. This, in turn, suggests a stronger, "protected" hydrogen bond and this hypothesis also receives support from the greater frequency displacement (142 cm^{-1}) observed for the O—H stretching band and from examination of scale models of 6-*t*-butyl-2-nitrophenol.

THE SPECTRA OF *o*-NITROPHENOL, 3-METHYL-2-NITROPHENOL, AND 3,4-DIMETHYL-2-NITROPHENOL

The relevant spectral data are listed in Table II.

It may first be noted that the infrared O—H stretching vibration bands of all *o*-nitrophenols containing a methyl group vicinal to the nitro-group are different from these bands in other *o*-nitrophenols. This is illustrated in Fig. 2.

Figure 2 shows that 3-methyl-substituted 2-nitrophenols afford a broad O—H absorption band in the 3350–2900 cm^{-1} region as opposed to the more intense, sharp bands observed for the other *o*-nitrophenols. This broadness of the bands suggests that 3-methyl-substituted *o*-nitrophenols give rise to strong intramolecular bonds (cf. ref. 11), presumably again because of steric facilitation of the hydrogen bond. Apart from these diffuse O—H stretching bands, 3-methyl-substituted 2-nitrophenols also afford a sharp band which occurs at lower frequency, and which is ascribed to —C—H stretching bands. The displacement of the infrared O—H stretching band for 3-methyl-2-nitrophenol ($\Delta\nu = +41$ cm^{-1}) again indicates steric facilitation of hydrogen bonding but the displacement for the O—H band of 3,4-dimethyl-2-nitrophenol ($\Delta\nu = -136$ cm^{-1}) is in the opposite direction. This suggests that buttressing interactions also affect the intramolecular hydrogen bond in some way (see below). The infrared NO_2 symmetrical stretching band of 3-methyl- and 3,4-dimethyl-2-nitrophenol again shows some signs of band splitting. Moreover, there is some indication that in sterically hindered *o*-nitrophenols the intensity of the symmetrical NO_2 stretching band decreases slightly relative to the same band in *o*-nitrophenol, presumably because of steric interactions (cf. ref. 13).

The ultraviolet spectra in cyclohexane solution first indicate that a 3-methyl group causes a slight twist of the nitro-group away from the plane of the benzene ring as judged by the reduced ϵ_{max} value of the nitrobenzene *B*-band (see Table II). The ϵ_{max} value of 3-methyl-2-nitrophenol is slightly *greater* than that of *o*-methylnitrobenzene in isooctane

Can. J. Chem. Downloaded from www.nrcresearchpress.com by 210.87.254.5 on 09/05/12
For personal use only.

Can. J. Chem. Downloaded from www.nrcresearchpress.com by 210.87.254.5 on 09/05/12
For personal use only.

TABLE II

Absorption spectra of *o*-nitrophenol, 3-methyl-2-nitrophenol, and 3,4-dimethyl-2-nitrophenol

Bands	Infrared spectra: *o*-Nitrophenol, ν_{max}	Infrared spectra: 3-Methyl-2-nitrophenol, ν_{max}	Infrared spectra: 3,4-Dimethyl-2-nitrophenol, ν_{max}
Spectrum in carbon tetrachloride			
O—H bands (in cm^{-1})	3,209(s)	ca. 3,168 (m; diffuse) 3,042(sh)*	ca. 3,345 (m; diffuse) ca. 3,150(sh)*
NO_2 bands (in cm^{-1})	1,532(s) 1,316(s)	1,534(m) 1,325(m) 1,335(w; sh)	1,524(s) 1,325(m) 1,310(vw)

Bands	Ultraviolet spectra: *o*-Nitrophenol λ_{max} (mμ)	*o*-Nitrophenol ϵ_{max}	3-Methyl-2-nitrophenol λ_{max} (mμ)	3-Methyl-2-nitrophenol ϵ_{max}	3,4-Dimethyl-2-nitrophenol λ_{max} (mμ)	3,4-Dimethyl-2-nitrophenol ϵ_{max}
Spectrum in cyclohexane						
Nitrobenzene *B*-band	271	7,350	278	6,500	280	5,000
Second *B*-band	ca. *231*	*4,000*†	ca. *234*	*3,400*†	243	3,200
C-band	346	3,700	351	2,900	361	2,600
Spectrum in ethanol						
Nitrobenzene *B*-band	272.5	6,050	270	1,750	275	1,650
Second *B*-band	ca. *231*	*3,550*†	ca. *241*	*1,750*†	251	1,425
C-band	347	3,250	ca. *340*	*725*†	ca. *345* ca. *359*	*550*† *500*
Spectrum in ether						
Nitrobenzene *B*-band	271	6,900	278.5	3,300		
Second *B*-band	ca. *234*	*3,000*†	ca. *236*	*2,600*†		
C-band	*346*	*3,550*	348	1,400		

*Band assignment doubtful; this band may be a —C—H stretching band, or may correspond to associated molecules.
†Values in italics represent inflections in this and subsequent tables.

Can. J. Chem. Downloaded from www.nrcresearchpress.com by 210.87.254.5 on 09/05/12
For personal use only.

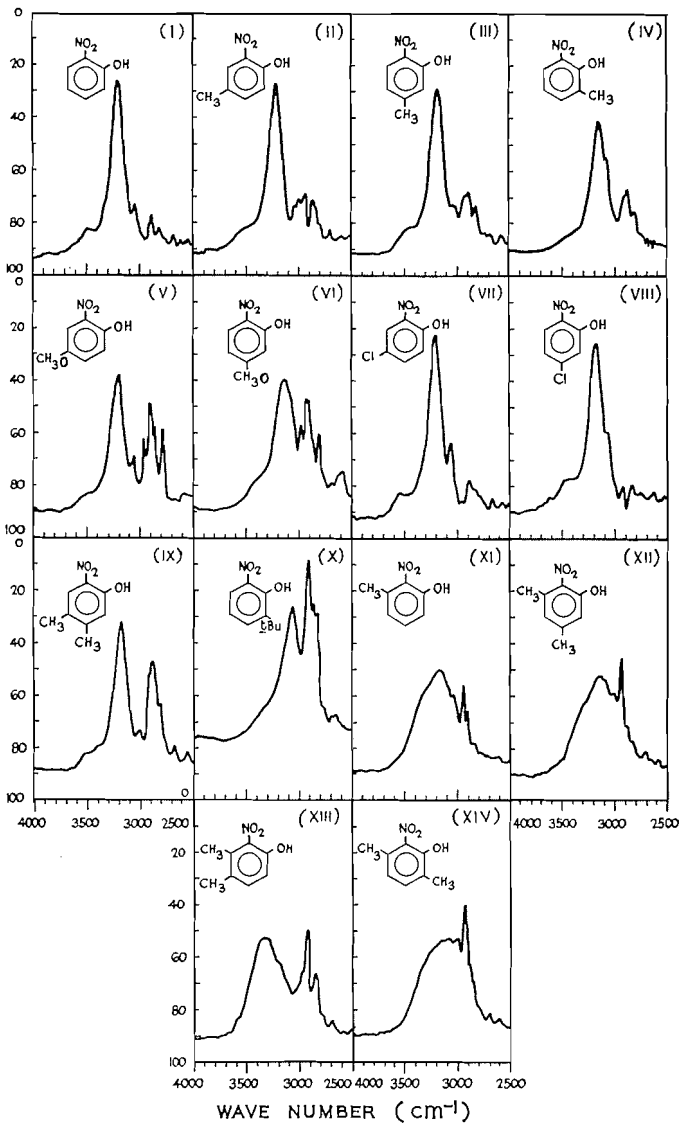


FIG. 2. The infrared O—H stretching vibration bands at concentrations of 0.2 molar in carbon tetrachloride solution of (i) *o*-nitrophenol, (ii) 4-methyl-2-nitrophenol, (iii) 5-methyl-2-nitrophenol, (iv) 6-methyl-2-nitrophenol, (v) 4-methoxy-2-nitrophenol, (vi) 5-methoxy-2-nitrophenol, (vii) 4-chloro-2-nitrophenol, (viii) 5-chloro-2-nitrophenol, (ix) 4,5-dimethyl-2-nitrophenol, (x) 6-*t*-butyl-2-nitrophenol, and (xi) 3-methyl-2-nitrophenol, (xii) 3,5-dimethyl-2-nitrophenol, (xiii) 3,4-dimethyl-2-nitrophenol, (xiv) 3,6-dimethyl-2-nitrophenol. (Fine structure observed in these O—H bands may be caused by intermolecular hydrogen bonding.)

solution whereas in cyclohexane solution the ϵ_{max} value of *o*-nitrophenol is less than that of nitrobenzene (cf. Table II and ref. 2), and this may imply that the intramolecular hydrogen bonding tends to keep the NO_2-group in a position coplanar with that of the benzene ring. In 3,4-dimethyl-2-nitrophenol the ϵ_{max} value of the nitrobenzene *B*-band is yet further decreased, indicative of a buttressing effect of the 4-methyl on the 3-methyl

group (see Table II and cf. ref. 12). In ethanol solution, the ϵ_{max} values of all three bands in both 3-methyl- and 3,4-dimethyl-2-nitrophenol are drastically reduced, and a similar but less pronounced effect is observed for 3-methyl-2-nitrophenol in ether solution (see Table II and Fig. 3). Both 3-methyl- and 3,4-dimethyl-2-nitrophenol again give rise to

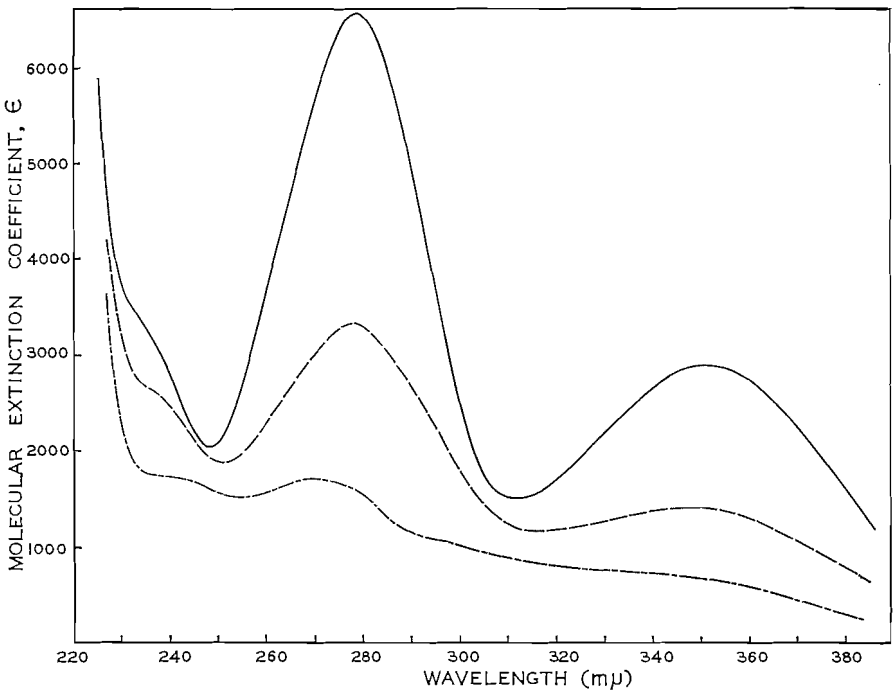
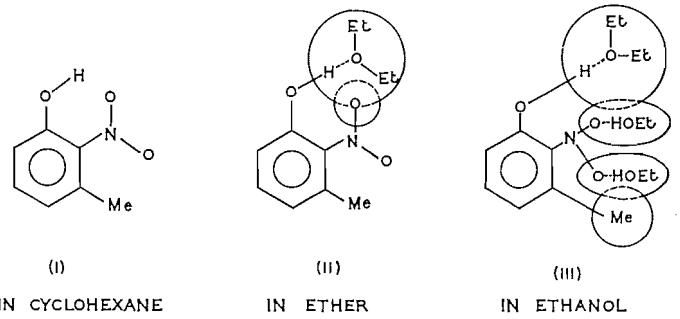


FIG. 3. The spectrum of 3-methyl-2-nitrophenol in cyclohexane (———), ether (– – –), and ethanol (– · – · –).

appreciable wavelength displacements when the solvent is altered, which indicates competing solvent–solute interactions.

The hypothesis of a coplanar conformation facilitating hydrogen bonding also receives support since this coplanarity is disturbed in ethanol *or* ether solution, as judged by the greatly reduced ϵ_{max} values of the 3-methyl-substituted compounds (see Table II), although ether presumably interacts predominantly with the OH-group only. It may thus be assumed that ether interacts competitively with the OH-group and in this way weakens the intramolecular hydrogen bonding, and that as a result of this weakening, there occurs the above-mentioned non-planarity between the nitro-group and the benzene ring. This is further illustrated by structures I, II, and III, which schematically indicate the effect of competing intermolecular hydrogen bonding on the intramolecular hydrogen bond and on the steric interactions present in 3-methyl-2-nitrophenol (cf. also the *B*-band intensities of *o*-nitrophenol in different solvents and later discussion). The steric facilitation of hydrogen bonding relative to *o*-nitrophenol, which is again observed for 3-methyl-2-nitrophenol as judged from the infrared O—H bands, may be ascribed to the NO_2-group – OH-group distance being decreased probably through the NO_2-group being *bent* towards the OH-group.

Can. J. Chem. Downloaded from www.nrcresearchpress.com by 210.87.254.5 on 09/05/12
For personal use only.



THE SPECTRA OF 3-METHYL-2-NITROPHENOL, 3,5-DIMETHYL-2-NITROPHENOL, 4,5-DIMETHYL-2-NITROPHENOL, AND 3,6-DIMETHYL-2-NITROPHENOL

The relevant spectral data are listed in Table III.

The infrared O—H vibrational stretching frequencies of the compounds listed in Table III again afford the expected changes in as much as only 4,5-dimethyl-2-nitrophenol, which does not possess a 3-methyl substituent, shows a sharp absorption band (see Fig. 2). It may be noted that the effect of steric interactions on this O—H band is larger than the effect of mesomeric interactions on the same band. Thus, the data in Tables II and III show that only in 4,5-dimethyl-2-nitrophenol is the O—H stretching band (ν_{max} 3191 cm^{-1}) reasonably close to that in *o*-nitrophenol (ν_{max} 3209 cm^{-1}) and in the previous paper of this series it was shown that the O—H bands in 4-chloro-2-nitrophenol (ν_{max} 3216 cm^{-1}), 4-methoxy-2-nitrophenol (ν_{max} 3216 cm^{-1}), 4-methyl-2-nitrophenol (ν_{max} 3218 cm^{-1}), and 5-chloro-2-nitrophenol (ν_{max} 3182 cm^{-1}), 5-methoxy-2-nitrophenol (ν_{max} 3144 cm^{-1}), 5-methyl-2-nitrophenol (ν_{max} 3185 cm^{-1}) all occur fairly close to the O—H band in *o*-nitrophenol (see ref. 1), whereas steric interactions give rise to larger frequency displacements (cf. Tables I, II, and III). It is also worth noting that in dimethyl-substituted *o*-nitrophenols frequency displacements in the infrared O—H stretching band are approximately additive, except as for the previously mentioned 3,4-dimethyl compound. Thus, relative to the O—H band in *o*-nitrophenol, the O—H band in 3-methyl-2-nitrophenol is displaced by 41 cm^{-1} and the relevant band in 5-methyl-2-nitrophenol by 24 cm^{-1}. Adding these displacements affords a calculated value of 65 cm^{-1} for the frequency displacement in 3,5-dimethyl-2-nitrophenol, which is identical with the observed frequency displacement of the infrared O—H band in 3,5-dimethyl-2-nitrophenol relative to the same band in *o*-nitrophenol. Similarly, for 3,6-dimethyl-2-nitrophenol the "calculated" frequency displacement is 96 cm^{-1} while the observed frequency displacement is 109 cm^{-1}, and the "calculated" frequency displacement for 4,5-dimethyl-2-nitrophenol is 15 cm^{-1} while the observed displacement is 18 cm^{-1}. These displacements incidentally are not quantitatively related to the wavelength displacements observed in the ultraviolet *B*-bands; at best, a rough semiquantitative relation holds for compounds where there is no steric effect, that is, for *o*-nitrophenols which have substituents only in the 4- or 5-positions.

Next, a substituent in the 4-position causes absorption at slightly higher frequency, whereas a substituent in the 5-position causes absorption at slightly lower frequency than for 2-nitrophenol (cf. ref. 1). This latter observation may in general terms be related to the ability of an electron-donating substituent in the 5-position to enhance the negative

Can. J. Chem. Downloaded from www.nrcresearchpress.com by 210.87.254.5 on 09/05/12
For personal use only.

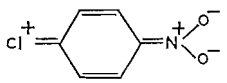
Can. J. Chem. Downloaded from www.nrcresearchpress.com by 210.87.254.5 on 09/05/12
For personal use only.

TABLE III

Absorption spectra of 3-methyl-2-nitrophenol, 3,5-dimethyl-2-nitrophenol, 3,6-dimethyl-2-nitrophenol, and 4,5-dimethyl-2-nitrophenol

	Infrared spectra					Ultraviolet spectra							
						3-Methyl-2-nitrophenol		3,5-Dimethyl-2-nitrophenol		4,5-Dimethyl-2-nitrophenol		3,6-Dimethyl-2-nitrophenol	
Bands	3-Methyl-2-nitrophenol, ν_{max}	3,5-Dimethyl-2 nitrophenol, ν_{max}	4,5-Dimethyl-2-nitrophenol, ν_{max}	3,6-Dimethyl-2-nitrophenol, ν_{max}	Bands	λ_{max}(mμ)	ϵ_{max}	λ_{max}(mμ)	ϵ_{max}	λ_{max}(mμ)	ϵ_{max}	λ_{max}(mμ)	ϵ_{max}
Spectrum in carbon tetrachloride					Spectrum in cyclohexane								
					Nitrobenzene *B*-band	278	6,500	289	8,250	284	8,700	286	6,700
					Second *B*-band	ca. *234*	*3,400*	ca. *258*	*3,000*	ca. *255*	*3,600*	ca. *241*	*2,300*
O—H bands (in cm^{-1})	ca. 3,168(m; diffuse) 3,042(sh)*	ca. 3,144(m; diffuse) 3,006(w)*	3,191(s)	ca. 3,100(m; diffuse) 3,007(w)*	*C*-band	351	2,900	351	3,500	357	4,250	358	2,650
					Spectrum in ethanol								
					Nitrobenzene *B*-band	270	1,750	279	2,350‡			280	2,750‡
NO_2 bands (in cm^{-1})	1,534(m) 1,325(m) 1,335(w;sh)	1,533(m) 1,331(m) 1,315(w;sh)	1,525(s) 1,300(s)	1,539(s) 1,327(m)†	Second *B*-band	ca. *241*	*1,750*	245	2,100			ca. *245*	*1,550*
					C-band	ca. *340*	*725*	341	1,200			347	1,200

*Band assignment doubtful; this band may be a C—H stretching band or may correspond to associated molecules.
†Band is slightly unsymmetrical.
‡Some fine structure occurs on the longer wavelength side.



(IV)

charge on the NO_2-group by means of mesomeric interaction as shown in structure IV, which, as discussed in ref. 1, tends to facilitate the intramolecular hydrogen bond.

Related, though less pronounced effects are observed for the NO_2 stretching vibrations as follows. The asymmetrical NO_2 stretching vibrational frequency remains approximately constant, although it may be noted that for 4,5-dimethyl-2-nitrophenol the band occurs at slightly lower frequency (1525 cm^{-1}; see Table III) than for *o*-nitrophenol (ν_{max} 1532 cm^{-1}). This may be a general effect for *o*-nitrophenols possessing a substituent in the 4- or 5- positions since 3,4-dimethyl-2-nitrophenol (ν_{max} 1524 cm^{-1}), 4-methoxy-2-nitrophenol (ν_{max} 1528 cm^{-1}), and 4-chloro-2-nitrophenol (ν_{max} 1530 cm^{-1}) also absorb at slightly lower frequency than *o*-nitrophenol. 4-Methyl-2-nitrophenol absorbs at ν_{max} 1532 cm^{-1} like *o*-nitrophenol, and *o*-nitrophenols possessing *only* a substituent in the 5-position also tend to absorb at lower frequency than *o*-nitrophenol, for example 5-chloro-2-nitrophenol (ν_{max} 1521 cm^{-1}), 5-methyl-2-nitrophenol (ν_{max} 1529 cm^{-1}), and 5-methoxy-2-nitrophenol (ν_{max} 1529 cm^{-1}), but all other *o*-nitrophenols discussed show the asymmetric NO_2 stretching band at higher frequency.

Similar effects are observed for the symmetrical NO_2 stretching vibration near 1315 cm^{-1} except that comparisons are sometimes more difficult because of band splitting and also because 5-methoxy-2-nitrophenol absorbs at slightly higher frequency (1317 cm^{-1}) than *o*-nitrophenol, although it might have been expected to absorb at lower frequency. Thus it seems that the effect of both electronic and steric interactions on the NO_2 vibrational stretching bands are small but that there is a tendency for electron-donating substituents in the 4- or 5-positions to cause absorption at lower frequency and for steric interactions, brought about by substituents in the 3- or 6-positions, to cause absorption at higher frequency.

The ultraviolet spectra listed in Table III give rise to the expected wavelength displacements when it is remembered that the ultraviolet *B*-bands are particularly susceptible to mesomeric interactions. This presumably accounts for the nitrobenzene *B*-band absorption at longer wavelength for 3,5-dimethyl-2-nitrophenol in cyclohexane solution. In ethanol solution the previously discussed decrease in the ϵ values of the 3-methyl-substituted 2-nitrophenols is again observed (see Table III). The spectral changes with change of solvent for a number of *o*-nitrophenols and *o*-nitroanisoles are also listed in Table IV.

Table IV shows that changing the solvent from cyclohexane to ethanol causes a bathochromic wavelength displacement of ca. 6 mμ (ca. 900 cm^{-1}) in nitrobenzene accompanied by a slight intensity decrease (2). In sterically hindered nitrobenzenes, such as 2,4- or 2,5-dimethoxynitrobenzene, this bathochromic wavelength displacement of the nitrobenzene *B*-band appears to be increased to ca. 8–10 mμ (ca. 1200–1300 cm^{-1}). In cyclohexane solution, an intensity decrease occurs for this band in 2,4-dimethoxynitrobenzene relative to the same band in nitrobenzene and this decrease is considerably more pronounced in the 2,6-dimethoxynitrobenzene. An intermediate intensity value is observed in the 2,5-isomer, probably because of a buttressing effect (cf. ref. 12) and because in 2,4-dimethoxy-, but not in 2,5-dimethoxy-benzene, can the mesomeric effect of the

Can. J. Chem. Downloaded from www.nrcresearchpress.com by 210.87.254.5 on 09/05/12
For personal use only.

TABLE IV

Ultraviolet absorption maxima of nitrobenzenes in cyclohexane and ethanol

Compound	Absorption band	Cyclohexane		Ethanol	
		λ_{max} (mμ)	ϵ_{max}	λ_{max} (mμ)	ϵ_{max}
Nitrobenzene	*B*-band	252	9,000	258	8,000
2,4-Dimethoxy-nitrobenzene	*B*-band	272	6,000	282	5,200
	2nd *B*-band	308	5,500	321	6,100
2,5-Dimethoxy-nitrobenzene	*B*-band	ca. *256*	*2,100*	ca. *264*	*2,200*
	C-band	339	2,650	353	2,550
2,6-Dimethoxy-nitrobenzene	*B*-band	279	1,650		
	C-band	ca. *343*	*200*		
o-Nitrophenol	*B*-band	271	7,350	272.5	6,050
	C-band	346	3,700	347	3,250
5-Methyl-2-nitrophenol	*B*-band	281	9,000	284	7,600
	C-band	ca. *336*	*4,200*	345	4,200
		347	4,500		
6-Methyl-2-nitrophenol	*B*-band	281	7,850	274	6,850
	C-band	354	3,400	341	2,750
3-Methyl-2-nitrophenol	*B*-band	278	6,500	270	1,750
	C-band	351	2,900	ca. *340*	*725*
2-Nitroresorcinol	*B*-band	314.5	10,800	308	4,000
	C-band	406	1,600		

p-methoxy substituent be expected to cause increased double-bond character in the C—N bond, which in turn may lead to increased coplanarity and increased absorption intensity. The low intensity value of the 2,6-isomer shows that two substituents, one on either side of the nitro-group, produce a much larger steric effect than one such substituent, which in turn implies that the interactions on the nitro-group do not only involve a twisting effect on a symmetrical nitro-group. (If these interactions merely caused a symmetrical nitro-group to twist out of the plane of the benzene ring, two like substituents would be expected to cause changes in the conformation of the nitro-group similar to those caused by a single substituent.) Changing the solvent incidentally does not appreciably affect the absorption intensity for 2,4-dimethoxy- or 2,5-dimethoxynitrobenzene. Next, for intramolecularly hydrogen-bonded molecules, such as *o*-nitrophenol and 5-methyl-2-nitrophenol, only small wavelength changes and small intensity decreases are observed on changing the solvent from cyclohexane to ethanol. For 6-methyl-2-nitrophenol a hypsochromic wavelength displacement is observed on changing the solvent from cyclohexane to ethanol and this suggests, as previously noted, that the intramolecular hydrogen bond has been affected by the 6-methyl substituent. It may be noted that the wavelength displacements are in a different direction from those observed for ordinary nitrobenzenes, and this could be because the intramolecular hydrogen bond in 6-methyl-2-nitrophenol is partially inhibited by changing the solvent. Direct steric interactions, it may be noted, are unlikely to be entirely responsible for this hypsochromic wavelength displacement since changing the solvent affects the absorption intensity only slightly.

In 3-methyl-2-nitrophenol, however, changing the solvent from cyclohexane to ethanol produces a very large intensity decrease comparable to the intensity decrease observed for 2,6-dimethoxynitrobenzene in cyclohexane solution, and this may be related to the observation that in both compounds the nitro-group has two large neighboring groups.

Can. J. Chem. Downloaded from www.nrcresearchpress.com by 210.87.254.5 on 09/05/12
For personal use only.

In this case, however, it must further be assumed that the ethanol molecule attaches itself to the OH-group, and in this way increases the effective size of the OH-group. These general hypotheses are supported by the *B*-bands of 2-nitroresorcinol in cyclohexane and ethanol solution since in the latter there occurs a hypsochromic wavelength displacement accompanied by a considerable intensity decrease; steric interactions and the inhibition of part of the intramolecular hydrogen bonding would be expected to give rise to precisely these spectral changes.

Summarizing, the above-mentioned and previous data all suggest that in most 3-methyl-substituted 2-nitrophenols the NO_2-group is partly twisted out of the plane of the benzene ring, and also that solvent–solute interactions become important for 3-methyl- or 6-methyl-substituted 2-nitrophenols. These latter interactions tend to weaken the intramolecular hydrogen bond and may also increase the effective size of the NO_2- and OH-groups.

EXPERIMENTAL

The ultraviolet absorption spectra were determined by standard methods using a Unicam SP500 spectrophotometer as described in previous parts of this series of papers (1, and references cited there). For each compound at least two independent sets of observations were made. The accuracy of λ_{max} values is estimated to be ± 1 mμ, and the precision of ϵ_{max} values $\pm 5\%$ or better. Values were reproducible in most cases to $\pm 2\%$.

The infrared spectra were determined on a Unicam SP100 double beam spectrophotometer using a NaCl prism and diffraction grating. The day-to-day reproducibility was better than ± 2 cm^{-1} for sharp bands. The spectra were determined in carbon tetrachloride at solute concentrations of about 0.2 *M* in cells of path lengths of 0.1 and 0.5 cm.

Most of the compounds were synthesized according to directions obtained from the literature. All the compounds, except 6-*t*-butyl-2-nitrophenol, have previously been described in the literature. 6-*t*-Butyl-2-nitrophenol, prepared by a modification of the method of Gibson (14) distilled under vacuum as a bright golden oil, b.p. 122° at 7 mm, $n_D^{22.5}$ 1.5562. Found: C, 61.7; H, 6.9; N, 7.5%. $C_{10}H_{13}O_3N$ requires C, 61.5; H, 6.7; N, 7.2%.

The solvents used were spectroanalyzed cyclohexane (Fisher), spectroanalyzed carbon tetrachloride, and commercially available absolute ethanol suitable for spectroscopy.

ACKNOWLEDGMENTS

The authors are greatly indebted to Mr. D. L. Coffen for very competent technical assistance in the preparation of some of the compounds and in the determination of the infrared spectra, and to Miss N. Joan Smith for determining some of the ultraviolet absorption spectra. Thanks are also due to Dr. A. W. Baker, Dow Chemical Company, Pittsburgh, California, U.S.A., for a generous sample of 3,5-dimethyl-2-nitrophenol.

The authors also wish to thank the Fisheries Research Board of Canada for financial support, since part of this work was carried out under a contract between the Fisheries Research Board of Canada and the Memorial University of Newfoundland. Finally the assistance of the National Research Council in support of these studies is again gratefully acknowledged.

Can. J. Chem. Downloaded from www.nrcresearchpress.com by 210.87.254.5 on 09/05/12
For personal use only.

REFERENCES

1. J. C. DEARDEN and W. F. FORBES. Can. J. Chem. **38**, 1837 (1960).
2. W. F. FORBES. Can. J. Chem. **36**, 1350 (1958).
3. W. F. FORBES and R. SHILTON. ASTM Bull. (1960).
4. E. A. BRAUDE, F. SONDHEIMER, and W. F. FORBES. Nature, **173**, 117 (1954).
5. E. A. BRAUDE and F. SONDHEIMER. J. Chem. Soc. 3754 (1955).
6. W. F. FORBES and R. SHILTON. J. Am. Chem. Soc. **81**, 786 (1959).
7. I. M. HUNSBERGER, H. S. GUTOWSKY, W. POWELL, L. MORIN, and V. BANDURCO. J. Am. Chem. Soc. **80**, 3294 (1958).
8. L. P. KUHN. J. Am. Chem. Soc. **80**, 5950 (1958).
9. S. MARCINKIEWICZ and J. GREEN. J. Chem. Soc. 849 (1959).
10. A. W. BAKER and A. T. SHULGIN. J. Am. Chem. Soc. **80**, 5358 (1958).
11. L. J. BELLAMY. The infra-red spectra of complex molecules. Methuen & Co. Ltd., London 1954. p. 84.
12. W. F. FORBES and W. A. MUELLER. J. Am. Chem. Soc. **79**, 6495 (1957).
13. R. N. JONES and C. SANDORFY. *In* Chemical applications of spectroscopy. *Edited by* W. West. Interscience Publishers, Inc., New York. 1956. pp. 540–541.
14. G. P. GIBSON. J. Chem. Soc. **127**, 42 (1925).

Can. J. Chem. Downloaded from www.nrcresearchpress.com by 210.87.254.5 on 09/05/12
For personal use only.

Can. J. Chem. Downloaded from www.nrcresearchpress.com by 210.87.254.5 on 09/05/12
For personal use only.

RADICAL TERMINATION MECHANISMS IN BULK POLYMERIZATION[1]

B. L. Funt and W. Pasika[2]

ABSTRACT

The termination mechanism in the bulk polymerization of styrene and vinyl acetate initiated by α,α'-azobisisobutyronitrile has been investigated. C^{14}-Labelled initiators were employed and activities of samples were determined by internal liquid scintillation counting. Measurements of fractionated and unfractionated polystyrene showed an average of 1.94 and 2.04 tagged fragments per molecule, respectively, and indicated termination by combination at 60° C. For polyvinyl acetate 1.06 fragments were found per molecule, indicating termination by disproportionation at 60° C.

One of the features of vinyl addition reactions, which is still subject to considerable uncertainty, is the mode of termination of growing chains. It is universally accepted that termination reactions must occur as the result of the interaction of two radicals, but the mechanism of this termination, whether by direct combination or by disproportionation, has only been investigated for a few systems, and has not been proved unequivocally even for these.

Nevertheless the mode of termination is of primary importance in kinetic analysis of data, in the assignment of termination constants and the prediction of molecular weights. Unless the mode of termination is understood, these quantities are subject to an uncertainty of a factor of two.

Two sensitive methods exist for the solution of this problem. Bamford and Jenkins (1) have described a technique of coupling preformed polymer possessing suitably reactive end groups. Alternatively with the use of radioactive initiators, it is possible to determine the number of initiator fragments present per polymer molecule (2, 3, 4). Since each initiator fragment found generated a chain, then in the final polymer the presence of two initiator fragments per polymer molecule would indicate the exclusive occurrence of combination, and of one initiator fragment of disproportionation.

Previous studies have not yielded completely conclusive results. For methyl methacrylate, the monomer subjected to the most intensive study, early work by Arnett and Peterson (5) using tagged initiators, indicated combination, whereas Bevington *et al.* (3) found a predominance of disproportionation. Ayrey and Moore (6) also found disproportionation and combination, but their results were not in exact agreement with those of Bevington.

It is reasonable to assume that for most monomers, termination reactions by combination and disproportionation can be considered as competitive reactions, each with a definite rate constant and activation energy. It is our intention to investigate this problem in detail, and the present report represents our first work in this direction.

The systems styrene and vinyl acetate, initiated with α,α'-azobisisobutyronitrile (AIBN), were chosen for this preliminary study.

EXPERIMENTAL

Materials

α,α'-Azobisisobutyronitrile (AIBN) dicyano C^{14} was obtained from the Commissariat à L'Énergie Atomique, Saclay, France, and possessed a specific activity of 200 μc/g. It

[1]*Manuscript received June 3, 1960.*
Contribution from the Department of Chemistry, University of Manitoba, Winnipeg, Manitoba.
[2]*Present address: Department of Chemistry, University of Alberta, Edmonton, Alberta.*

was suitably diluted with inactive AIBN, dissolved in benzene to an activity of 1 μc/ml, and the mixture purified by the method of Ikamura and Motoyama (7).

Styrene, obtained through the courtesy of the Dow Chemical Company, was washed three times with 5% NaOH solution, three times with distilled water, dried over $CaSO_4$, slightly prepolymerized, and then distilled under reduced pressure (8).

Vinyl acetate, obtained from Carbide and Carbon Chemicals, was twice distilled at atmospheric pressure under an argon atmosphere. Prior to the second distillation it was refluxed for 1 hour under argon to destroy peroxides.

Scintillation grade *p*-terphenyl and 1,4-di-2-(5 phenyl oxazolyl)benzene (POPOP) were obtained from Nuclear Enterprises Ltd., Winnipeg, and were employed without further purification.

Methods

Polymerization

The monomers, with appropriate amounts of initiator added, were placed in Pyrex tubes and degassed by a series of freezing–thawing cycles under vacuum. The tubes were evacuated and sealed, and the 20-ml charges placed into a thermostatted water bath at 60.0° C. Samples were polymerized to approximately 10% conversion and blank experiments (without initiator) were performed for all samples to determine whether thermal uninitiated polymerization was also occurring.

In order to determine that the polymerizations were following established mechanisms, samples were isolated and weighed at different degrees of conversion, and it was found that the kinetics accurately obeyed the expected linear dependence of rate of polymerization on the square root of the AIBN concentration.

Isolation and Purification of Polymers

After polymerization the polystyrene was dissolved in methyl ethyl ketone and precipitated in methanol. Polyvinyl acetate was precipitated in a 25/75 methanol–water mixture (5), redissolved in acetone, and precipitated in *n*-hexane. The polymer was finally isolated by the freeze-drying method (9).

Molecular Weights

Molecular weights were primarily determined by viscometry, employing an Ubbelohde viscometer, with benzene and acetone as solvents for polystyrene and polyvinyl acetate respectively.

Values of K and α employed in the Staudinger equation were 1.03×10^{-4} and 0.74, respectively, for fractionated polystyrene (10), 2.62×10^{-4} and .68 for unfractionated polystyrene (11), and 1.76×10^{-4} and .68 for fractionated polyvinyl acetate (12). At a later stage a bank of five Stabin–Immergut osmometers was in operation in our laboratory (13), and where the amount of sample available was sufficient, number average molecular weights were also obtained by osmometry.

Radioassay Technique

One of the objectives of this work was to test the suitability of internal liquid scintillation counting techniques for tracer studies of this type. The scintillation counting method provides a greater inherent sensitivity, will accommodate larger samples and hence of lower specific activity, and allows energy discrimination and the concomitant reduction in background counting rate. A further important advantage in the present work is that it eliminates the necessity of sample combustion, and purification of CO_2 gas required for Geiger techniques.

Can. J. Chem. Downloaded from www.nrcresearchpress.com by 210.87.254.5 on 09/05/12
For personal use only.

The active samples of polymer were dissolved directly in 20 ml of a liquid scintillator containing 2.0% *p*-terphenyl and 0.04% POPOP in xylene and counted.

The counting assembly consisted of a DuMont 6292 photomultiplier, a cathode follower, linear non-overloading amplifier, a pulse height analyzer, a scaler, and a stabilized high-voltage supply, and was similar to units employed in previous work (14). The liquid scintillator cell was $1\frac{1}{2}$ inches in diameter and 2 inches high. It was surrounded by a magnesium oxide powder reflector and was fitted with a bubbling device for the removal of dissolved oxygen (15, 16) to improve its luminescent output.

RESULTS

It was first necessary to determine whether the quenching effects of added polymer would seriously affect the counting rates and thus lead to spurious results. Figure 1 shows

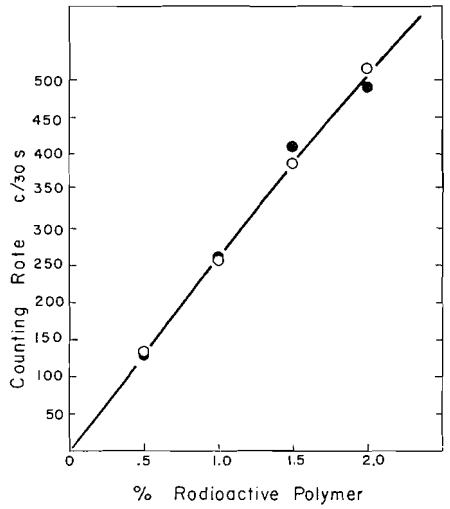


FIG. 1. Proportionality between counting rate and concentration of radioactive polymer. Solid and open circles denote duplicate experiments.

the data obtained for a tagged polystyrene sample and it can be seen that the counting rate is proportional to the amount of active polymer up to 2% concentration. It was therefore considered convenient and satisfactory to work with solutions of 1% polymer in the liquid scintillator.

The efficiency of separation of polymer from occluded initiator was tested by adding 0.2 μc of active AIBN to 0.5 g of inactive polystyrene and repeatedly precipitating the polymer from methyl ethyl ketone with methanol. For no separation one would expect 13,200 c.p.m. per 0.1500 g polymer. The counts obtained were 76 c.p.m. after one precipitation and 20 c.p.m. after two precipitations. This indicated that a double precipitation was adequate.

For the polymer samples a pulse height analyzer lower gate of 15 kev was employed and checks were made with an internal standard of C^{14} (17, 18) to detect any possible variations in counting efficiencies due to electronic drift or quenching action.

The results for unfractionated polystyrene are presented in Table I.

In order to determine whether the number of AIBN fragments incorporated in the final polymer was influenced by molecular weight, a sample of polystyrene prepared with

Can. J. Chem. Downloaded from www.nrcresearchpress.com by 210.87.254.5 on 09/05/12
For personal use only.

TABLE I

Determination of number of initiator fragments per polymer molecule in unfractionated polystyrene at 60° C

Sample No.	AIBN concentration (g/l.)	Intrinsic viscosity	Molecular weight	Weight of sample counted (g)	Counts/g min	No. of initiator fragments per polymer molecule
16	6.30	0.446	56,200	0.1718	3,749	2.02
18	4.50	0.480	64,500	0.1718	3,166	1.95
19	3.40	0.536	74,100	0.1718	2,771	1.96
20	2.70	0.585	85,100	0.1718	2,514	2.04
21	1.80	0.677	104,700	0.1718	2,165	2.14
22	0.90	0.835	141,000	0.1718	1,582	2.13
Initiator	—	—	—	—	1,274,000	—
					Average	2.04

TABLE II

Determination of number of initiator fragments per polymer molecule in fractionated polystyrene at 60° C

Sample No.	Intrinsic viscosity	Molecular weight	Weight of sample counted (g)	Counts/g min	No. of initiator fragments per polymer molecule
0	0.485	64,000	0.1720	4,884	1.97
1	0.550	109,500	0.1719	3,133	2.16
2	0.253	38,800	0.1719	7,199	1.76
1A	0.780	174,000	0.1290	2,052	2.24
1B	0.684	144,000	0.1719	2,240	2.04
1C	0.591	100,000	0.1718	2,789	1.76
1D	0.405	70,800	0.1719	3,754	1.64
Initiator	—	—	0.00045	1,953,000	—
				Average	1.94

TABLE III

Determination of number of initiator fragments per polymer molecule in fractionated vinyl acetate at 60° C

Sample No.	Intrinsic viscosity	Molecular weight	Weight of sample counted (g)	Counts/g min	No. of initiator fragments per polymer molecule
9-1	1.235	456,000	0.1639	425	1.26
10-1	1.510	602,000	0.1627	286	1.14
11-1	1.290	490,000	0.1683	350	1.14
12-1	1.370	525,000	0.1648	275	0.96
9-1-2	0.867	263,000	0.1648	575	1.00
10-1-2	1.177	426,000	0.1682	401	1.12
11-1-2	1.050	354,000	0.1645	463	1.08
12-1-2	1.046	355,000	0.0930	410	0.96
Initiator	—	—	0.00045	2,050,000	—
9-1-2-3	0.570	145,000	0.1189	1,113	0.96
10-1-2-3	0.750	214,000	0.1095	891	—
11-1-2-3	0.690	195,000	0.1241	790	1.14
Initiator	—	—	0.00045	1,850,000	0.94
				Average	1.06

active AIBN was separated into four fractions, by incremental precipitation from methyl ethyl ketone. The results are summarized in Table II, and it is evident that the results are essentially unchanged from those obtained with unfractionated material. The original sample, designated as 0, was separated into two fractions labelled 1 and 2 representing the

Can. J. Chem. Downloaded from www.nrcresearchpress.com by 210.87.254.5 on 09/05/12
For personal use only.

high and low molecular weight material, respectively, and sample 1 was fractionated into four parts labelled 1A to 1D.

The data for polyvinyl acetate polymerized at 60.0° C are presented in Table III.

DISCUSSION

The data in Tables I and II indicate that in the thermal reactions polystyrene radicals terminate by mutual combination and that the method of termination is independent of molecular weight over the range investigated. These findings are in agreement with Bevington's studies of the photopolymerized system (3), and with Bamford and Jenkins conclusions based on coupling of preformed polymer (1). Although early work (19, 20, 21) had assumed termination by combination, this cannot be construed to be the current picture, and the present results are therefore considered to extend and confirm the current views of the mechanism of termination in styrene.

In many respects the data presented here for styrene appear to be in surprisingly close agreement with the simple picture presented. It is recognized that the presence of thermal reaction, or of chain transfer to polymer or initiator, could tend to vitiate the results. After this investigation had been essentially completed it was possible to check the molecular weights of a few samples by osmometry, although the amounts of samples available were not sufficiently large for optimum conditions of osmotic measurement. Sample 16, for example, yielded a molecular weight of 61,700 by osmometry vs. 56,200 from viscosity data. The agreement is within 10% and is well within the limits necessary to discard a disproportionation mechanism in favor of one by combinaion.

The results for vinyl acetate, in Table III, indicate one initiator fragment per polymer molecule and hence the occurrence of disproportionation. Previous investigation of this system by Burnett, George, and Melville (22) indicated an unusual variation in the number of fragments from 1.6 to 6.0 per molecule at temperatures from +27 to −38° C.

Chain transfer to polyvinyl acetate is known to occur and might be expected to affect the results. However, it should be noted that if a growing radical $IR\cdot$ were to abstract an H atom from a dead polymer molecule then $IR\cdot_m + IR_n \rightarrow IR_{(n+r)} + IR_m$ one initiator fragment per molecule would still remain and the results would be indistinguishable from those in the absence of branching if disproportionation is predominant.

A few preliminary experiments with vinyl acetate performed at 30° C showed spurious results and indicated an increase in the number of tagged fragments above a value of 3. Time did not permit an investigation of this effect in further detail as part of this work, and the few results obtained were considered tentative and were not included in the tabular presentation. A more detailed study of the variation of termination mechanism with temperature and of the determination of competitive rate constants for termination by combination and disproportionation for some systems has now begun in our laboratories.

ACKNOWLEDGMENTS

We gratefully acknowledge the financial assistance of Imperial Oil Ltd. in the support of this work, and of the National Research Council of Canada in providing summer stipends and grants-in-aid.

REFERENCES

1. C. H. BAMFORD and A. D. JENKINS. Nature, **176**, 78 (1955).
2. I. M. KOLTHOFF, P. R. O'CONNOR, and J. L. HANSEN. J. Polymer Sci. **15**, 459 (1955).
3. J. C. BEVINGTON, H. W. MELVILLE, and R. P. TAYLOR. J. Polymer Sci. **12**, 449 (1954).
4. J. C. BEVINGTON, H. W. MELVILLE, and R. P. TAYLOR. J. Polymer Sci. **14**, 463 (1954).

Can. J. Chem. Downloaded from www.nrcresearchpress.com by 210.87.254.5 on 09/05/12
For personal use only.

5. L. M. ARNETT and J. H. PETERSON. J. Am. Chem. Soc. **74**, 2031 (1952).
6. G. AYREY and G. G. MOORE. J. Polymer Sci. **36**, 41 (1959).
7. S. IKAMURA and T. MOTOYAMA. J. Polymer Sci. **17**, 428 (1955).
8. B. L. FUNT and E. COLLINS. J. Polymer Sci. **28**, 97 (1958).
9. F. R. MAYO and F. M. LEWIS. Ind. Eng. Chem. Anal. Ed. **17**, 134 (1945).
10. C. E. H. BAWN, R. F. J. FREEMAN, and A. R. KAMALIDDIN. Trans. Faraday Soc. **46**, 1107 (1950).
11. J. C. BEVINGTON, G. M. GUZMAN, and H. W. MELVILLE. Proc. Roy. Soc. A, **221**, 453 (1954).
12. R. N. WAGNER. J. Polymer Sci. **2**, 21 (1947).
13. B. L. FUNT and F. D. WILLIAMS. J. Polymer Sci. In press.
14. B. L. FUNT and A. HETHERINGTON. Internat. J. Appl. Radiation and Isotopes, **4**, 189 (1959).
15. R. W. PRINGLE, D. BLACK, B. L. FUNT, and S. SOBERING. Phys. Rev. **92**, 1582 (1953).
16. B. L. FUNT and E. NEPARKO. J. Phys. Chem. **60**, 267 (1956).
17. F. N. HAYES. Internat. J. Appl. Radiation and Isotopes, **1**, 46 (1956).
18. J. D. DAVIDSON and P. FEIGELSON. Internat. J. Appl. Radiation and Isotopes, **2**, 1 (1957).
19. C. H. BAMFORD and M. J. S. DEWAR. Proc. Roy. Soc. A, **192**, 308 (1948).
20. H. W. MELVILLE and L. VALENTINE. Trans. Faraday Soc. **46**, 210 (1950).
21. G. M. BURNETT. Trans. Faraday Soc. **46**, 772 (1950).
22. G. M. BURNETT, M. M. GEORGE, and H. W. MELVILLE. J. Polymer Sci. **16**, 31 (1955).

Can. J. Chem. Downloaded from www.nrcresearchpress.com by 210.87.254.5 on 09/05/12
For personal use only.

THE SEPARATION OF SOME INORGANIC IONS BY HIGH-VOLTAGE ELECTROMIGRATION IN PAPER[1]

R. A. BAILEY[2,3] AND L. YAFFE

ABSTRACT

A number of inorganic ions have been separated by high-voltage electromigration in paper. The systems considered include some of particular radiochemical interest, such as Sr–Y, Ba–La, Mo–Tc, Pb–Bi–Po, as well as the alkali metals, some elements of the first long period, and other metals. Background electrolytes were usually solutions of complex-forming organic acids.

INTRODUCTION

Numerous references to the separation of inorganic ions by electromigration in paper (paper electrophoresis) have appeared over the last 10 years. The present work deals with a number of separations which were performed while making a general study of the method with a view to applying it to routine radiochemical separations. As such, it deals with a fairly large number of systems, and is a preliminary survey. It does not consider in detail the effects of varying such factors as the concentration and pH of the background electrolyte solution, which would be necessary if the optimum conditions for any separation were to be determined. Nevertheless, some striking results were obtained even with this rather arbitrary choice of conditions, illustrating the power of the method. The technique of electromigration has some specialized advantages. However, as a general method of separating small amounts of inorganic material, it can compete with other means, such as ion exchange, only on the basis of speed. Therefore a very high voltage technique was adopted, and solutions of low conductivity were used. This has permitted a number of separations to be made in 10 minutes or less.

Many of the ions studied are of adjacent atomic number, since these are often of chief interest radiochemically.

EXPERIMENTAL

The technique used was basically the same as that employed for quantitative measurements of zone mobility (1). An apparatus capable of withstanding much higher voltages was used, however, and for these qualitative results much less attention was paid to details which are important for zone mobility determinations.

A closed strip technique was used wherein the paper was placed between two cooling plates. These were of aluminum, $40\times10\times1/4$ in. in size. Copper tubing was bolted to the backs of both plates to allow the circulation of cooling water. Electrical insulation was provided by a strip of mica 4 in. wide running the length of each plate. This was extended to the edges of the plates at the high-voltage end to prevent arcing from the paper. Mica combines a higher electrical breakdown potential with a greater heat conductivity than most other practical materials. The strip was built up as a lamination of thin sheets 4×4 in. in size glued together; the thickness was 0.016 in. at the high-voltage end but somewhat less over most of its length. This insulation proved to be quite suitable. It could withstand a potential of 10,000 volts, and it had the additional advantage that, if the paper did char, the mica was not damaged. The mica was protected by a thin sheet of polyethylene or polyvinylchloride which could be replaced readily.

[1]*Manuscript received May 26, 1960.*
Contribution from the Radiochemistry Laboratory, Department of Chemistry, McGill University, Montreal, Que., with financial assistance from the National Research Council of Canada.
[2]*Holder of a National Research Council Studentship.*
[3]*Present address: Department of Chemistry, University College, University of London, London, England.*

Can. J. Chem. Downloaded from www.nrcresearchpress.com by 210.87.254.5 on 09/05/12
For personal use only.

In order to obtain the good contact between the paper and the cooling surface, which is necessary at high voltages, about 140 lb of lead weights was placed on the upper plate.

No electrolyte reservoirs were employed. The electrodes were of platinum foil and were in direct contact with the ends of the paper strip. They could be placed at any distance from the ends of the plates to give any desired migration distance up to the full length of the plates. Electrical connections were made to them by means of aluminum or copper ribbons. Products of electrolysis were trapped by means of suitable buffer solutions.

A d-c. power supply giving a continuously variable, well-filtered output of up to 10 kv was used as a source of voltage.

A number of the ions studied were radioactive; such substances are easily detected and identified. They were located after separation by means of a Geiger counter for β-radiation, or a scintillation counter for γ-rays. The strip was either cut into sections, 1 cm broad, or measured intact with a scanning device. The latter is much less tedious, but it is not as sensitive toward very low levels of radioactivity such as may be found if a zone 'trails'. Alpha particles were detected by a 2π-proportional counter operated at its α-plateau voltage. In all cases the identity of the various zones was confirmed by means of the γ-ray spectra of the migrants, or by their relative rates of decay.

Many experiments were carried out with inactive migrants when radioactive nuclides were not available and when simple chemical tests could be used. Such tests may fail to show low-concentration regions, but they are satisfactory in most cases, and are fast and simple. The reagents used were rubeanic acid – NH_3 for Co(II) and Ni(II); NH_4SCN for Fe(III); alizarin–NH_3 for Al(III), Ga(III), and In(III); and dithizone for the remainder of the inactive ions.

The concentration of the inactive solutions was 0.01 M or less, while the radioactive solutions were much more dilute. Most ions were in solution as the nitrate, sometimes with a slight excess of nitric acid, but with other substances capable of forming stable complexes absent. Ten microliters of each migrant solution was normally used.

A number of temperatures were employed in this work. The comparatively low temperatures, which many workers have used to achieve adequate cooling, were found to be unnecessary with our apparatus; the best operation was obtained at 35–40° C. Since higher temperatures lead to higher zone mobilities, they may result in more rapid separations.

RESULTS AND DISCUSSIONS

The separations made with inactive materials are shown as reproductions of a tracing of the strip; those with radioactive substances are shown as histograms. The heavy vertical line in the former indicates the starting position. The relative heights of the peaks on the histograms are not significant since the detection efficiency varies for the different nuclides. The conditions of each separation are indicated in the figure captions. Except where indicated otherwise, Whatman No. 3MM chromatography paper was used, and the absorbance used was about 1.1 ml/g.

The first series of separations are of the following groups of cations in several organic acid background electrolytes:

(*a*) Fe(III), Co(II), Ni(II), Cu(II), Zn(II), Ga(III);
(*b*) Ag(I), Cd(II), In(III);
(*c*) Hg(II), Tl(I), Pb(II), Bi(III);
(*d*) Zn(II), Cd(II), Hg(II);
(*e*) Al(III), Ga(III), In(III).

Can. J. Chem. Downloaded from www.nrcresearchpress.com by 210.87.254.5 on 09/05/12
For personal use only.

Oxalic acid gave the best results in most cases, but citric, tartaric, and lactic acids were investigated as well. The latter two gave superior separations of aluminum, gallium, and indium. Complex formation occurs in most of these systems, although often it is not strong enough to cause the migrant to behave as an anion. Table I gives the migration sequences in the systems used. Figures 1 to 3 illustrate some of the separations achieved.

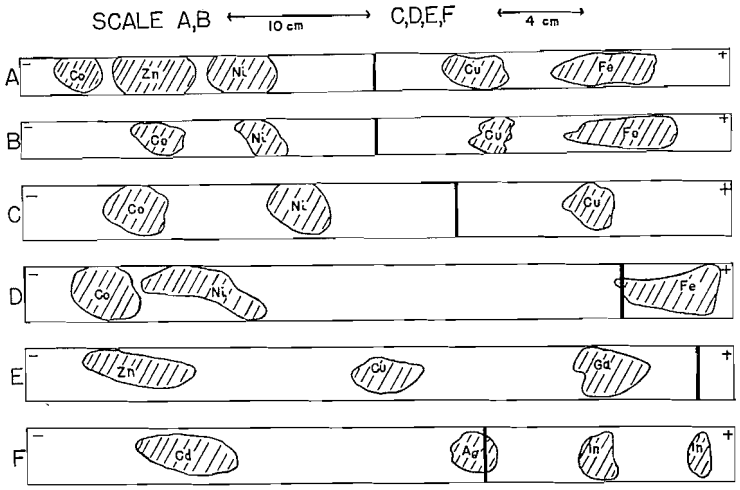


FIG. 1. (A) Separation of Fe(III), Co(II), Ni(II), Cu(II), and Zn(II) in 0.01 *M* oxalic acid; 60 v/cm, 55 minutes, 39° C.

(B) Separation of Fe(III), Co(II), Ni(II), and Cu(II) in 0.01 *M* oxalic acid; 150 v/cm, 15 minutes, 35° C.

(C) Separation of Co(II), Ni(II), and Cu(II) in 0.01 *M* oxalic acid; 160 v/cm, 10 minutes, 35° C.

(D) Separation of Co(II), Ni(II), and Fe(III) in 0.015 *M* citric acid; 160 v/cm, 10 minutes, 39° C.

(E) Separation of Zn(II), Cu(II), and Ga(III) in 0.1 *M* tartaric acid; 80 v/cm, 28 minutes, 25° C.

(F) Separation of Ag(I), Cd(II), and In(III) in 0.01 *M* oxalic acid; 120 v/cm, 9 minutes, 39° C.

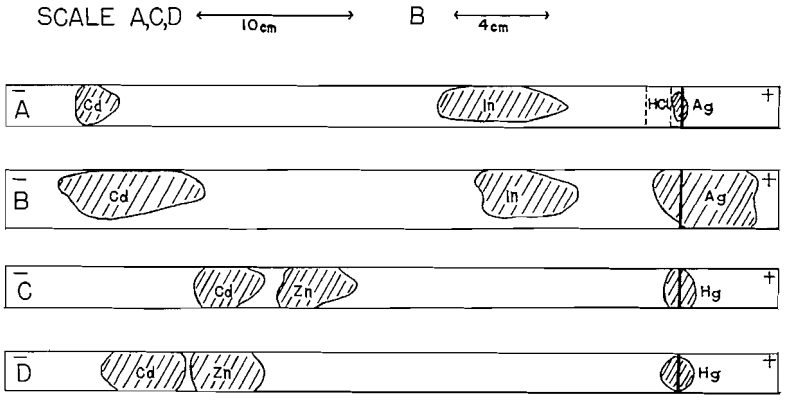


FIG. 2. (A) Separation of Ag(I), Cd(II), and In(III), utilizing a zone of HCl to prevent streaking of silver; 0.1 *M* lactic acid, 80 v/cm, 31 minutes, 35° C.

(B) Separation of Ag(I), Cd(II), and In(III) with KCN added to the migrant solution before application; 0.1 *M* tartaric acid, 80 v/cm, 24 minutes, 35° C.

(C) Separation of Zn(II), Cd(II), and Hg(II) in 0.1 *M* tartaric acid; 80 v/cm, 29 minutes, 25° C.

(D) Separation of Zn(II), Cd(II), and Hg(II) in 0.1 *M* lactic acid; 80 v/cm, 29 minutes, 25° C.

Can. J. Chem. Downloaded from www.nrcresearchpress.com by 210.87.254.5 on 09/05/12
For personal use only.

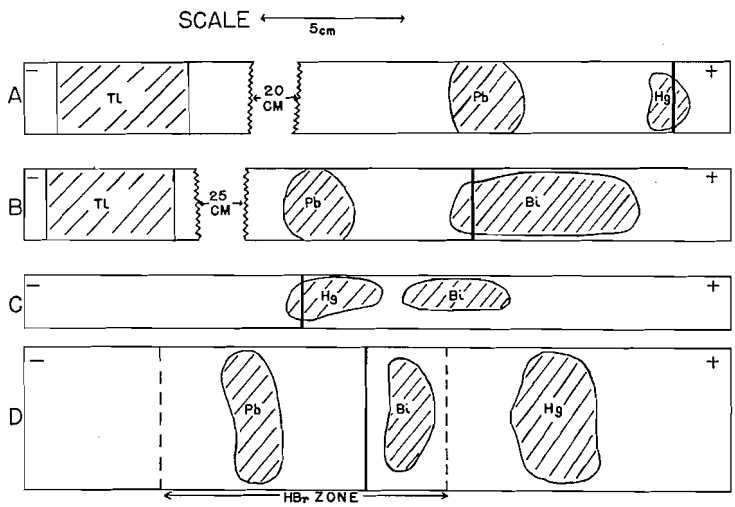


FIG. 3. (A) Separation of Hg(II), Tl(I), and Pb(II) in 0.01 *M* oxalic acid; 200 v/cm, 7 minutes, 41° C.
(B) Separation of Tl(I), Pb(II), and Bi(III) in 0.01 *M* oxalic acid; 200 v/cm, 6 minutes, 41° C.
(C) Separation of Hg(II) and Bi(III) in Reeve Angel 934 AH glass fiber paper with 0.1 *M* tartaric acid; 24 v/cm, 43 minutes, 25° C.
(D) Separation of Hg(II), Pb(II), and Bi(III) using a zone of 0.1 *M* HBr in a strip moistened with 0.01 *M* oxalic acid; nominal voltage gradient 80 v/cm, 30 minutes, 39° C. Tl(I) was separated in the same experiment, but is not shown; it has moved far toward the negative electrode.

TABLE I

Migration sequences of a number of ions in several electrolyte solutions

Acetic acid of concentration 1–2 *M* Tl(I), Co(II), Ni(II), Zn(II), Ga(III), Cd(II), Pb(II), Cu(II), In(III), Fe(III):
0.01 *M* oxalic acid Tl(I), Cd(II), Co(II), Zn(II), Ni(II), Pb(II): In(III), Cu(II), Al(III), [Ga(III)+Fe(III)], In(III)
0.015 *M* citric acid Tl(I), Cd(II), Co(II), [Ni(II)+Zn(II)] [Pb(II)+Cu(II)]: Fe(III), [Al(III)+In(III)], Ga(III)
0.1 *M* tartaric acid Tl(I), Cd(II), [Co(II)+Zn(II)], Ni(II), Pb(II), Cu(II), Al(III), In(III), Ga(III): Fe(III)
0.1 *M* lactic acid Tl(I), Cd(II), [Co(II)+Zn(II)], Ni(II), Pb(II), Cu(II), Al(III), [Fe(III)+Ga(III)]:
In addition, Ag(I), Hg(II), and Bi(III) are adsorbed by the paper and are found near the starting position in these electrolytes.

NOTE: Ions in parentheses have similar mobilities; the relative rates were not determined.
The starting point is indicated by the symbol :. Ions to the left of this move as cations, those to the right as anions.

No difficulty was encountered in separating most of these ions in at least one of the electrolytes used. Ternary mixtures could be resolved very rapidly. Only systems involving silver, or mercury and bismuth, gave difficulty. These ions are strongly adsorbed by the paper and either will not move from the starting position, or trail back to it. In the case of silver, this may be the result of a reduction of small amounts of the silver by certain groups in the paper. In 0.01 *M* oxalic acid, indium formed two anionic zones, indicating that two complex species are formed which are not in rapid exchange with one another. This does not interfere with separations. The results can also indicate the relative tendency

Can. J. Chem. Downloaded from www.nrcresearchpress.com by 210.87.254.5 on 09/05/12
For personal use only.

of complex formation of some of the ions. Thus, zinc seems to form stronger complexes than cadmium, and gallium stronger complexes than aluminum or indium, in the solutions used here.

Silver, when present in small enough amounts, remains at the starting position except when complexed strongly, as with ammonia. As the amount of silver present is increased, it tends to move toward the cathode, but leaves a low-concentration trail back to the starting point. The latter was detectable when radioactive Ag^{110} was used. Although in the separation of silver, cadmium, and indium no difficulty is encountered if a very small amount of silver is present (Fig. 1F), the extended zone formed with a larger quantity may overlap the zones of the other ions, since the mobility of the moving silver is high. In order to achieve a satisfactory separation in the latter case, some means of retaining all of the silver near the starting position is required.

By adding hydrochloric acid to a narrow zone on the cathode side of the starting position, all of the silver is precipitated or adsorbed between this zone and the initial position. If the hydrochloric acid is sufficiently dilute that complex formation with the other ions is slight, these ions pass through this zone with little interference (although the indium zone does tend to become elongated). A second procedure consists of adding a little potassium cyanide to the migrant solution before application to the paper. The $Ag(CN)^-$ ion is sufficiently stable to prevent any cationic motion of the silver. Separations utilizing these techniques are illustrated in Figs. 2A and 2B respectively.

Since both Hg(II) and Bi(III) remain near the starting position, they cannot be separated from one another in the electrolytes used here with ordinary filter paper. That the failure to move is due to interaction with the cellulose is shown by the results in 0.1 *M* tartaric acid in glass fiber filter paper (Fig. 3C). Both ions are anionic here, and they are separated. In the same electrolyte with cellulose paper, bismuth forms a streak toward the anode but does not leave the starting point entirely, while the mercuric ion moves scarcely at all. Glass paper may also yield a separation of lead from mercury and bismuth, but the fourth member of this group, thallium, is adsorbed and trails, hence overlapping the lead zone. Separation of all four ions in cellulose paper can be brought about by utilizing the bromide complexes, which were studied for mercury, lead, and bismuth by Pucar (2). A small zone of 0.1 *M* hydrogen bromide serves to separate these ions (Fig. 3D). The part of the strip moistened with another electrolyte (oxalic acid in this case) serves for the migration of any ion which leaves the hydrogen bromide zone without involving the high conductance of a strip completely moistened with hydrogen bromide. Tl(I) is a much faster cation than the rest and is readily separated from them.

A number of ions considered above were also studied in lactic acid by Sato *et al.* (3).

The behavior of Cr(III), Mn(II), Fe(III), and Co(II) in the strong chelating agents ethylenediaminetetraacetic acid (EDTA), nitrilotriacetic acid (NTA), hydroxyethylethylenediaminetriacetic acid (HEDTA), and 1,2-diaminocyclohexanetetraacetic acid (DCTA) was investigated and a number of separations accomplished. Examples are shown in Fig. 4. Further data on the electromigration in these systems are given in Table II. The anionic complexes formed are slow and hence do not lend themselves to rapid separations. Diffuse and multiple zones were also encountered.

Separation of the alkali metals was also attempted. Potassium, rubidium, and cesium have very similar mobilities, and could not be completely separated under the conditions employed. Sodium was readily separated from the rest. Other workers have obtained similar results (4, 5, 6). Only Gross (7) has reported a separation of potassium, rubidium,

Can. J. Chem. Downloaded from www.nrcresearchpress.com by 210.87.254.5 on 09/05/12
For personal use only.

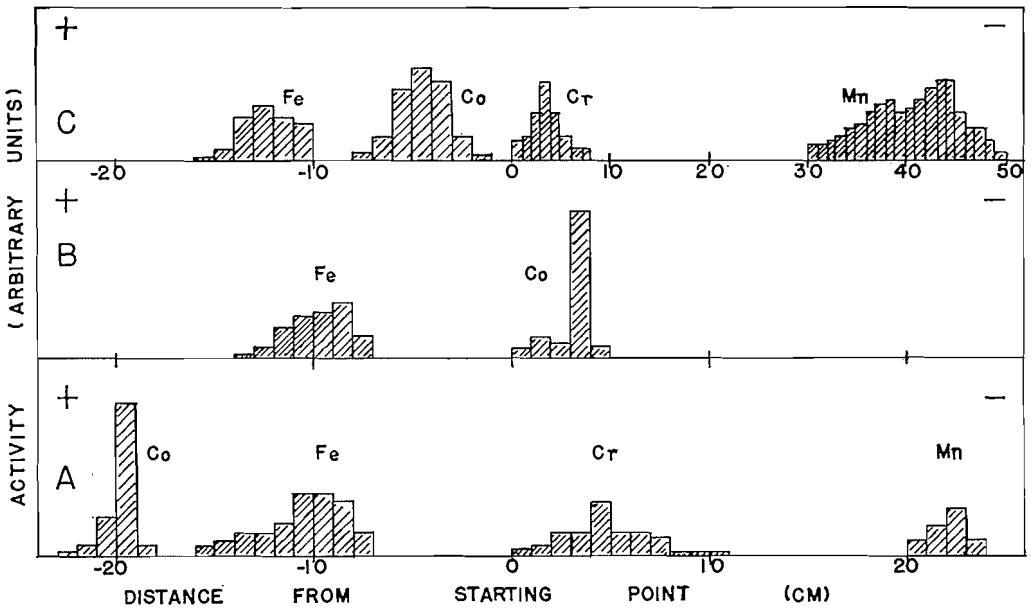


FIG. 4. (A) Separation of Cr(III), Mn(II), Fe(III), and Co(II) in 0.01 *M* HEDTA – 0.06 *M* NH_4OH; 80 v/cm, 114 minutes, 25° C.

(B) Separation of Fe(III) and Co(II) in a saturated solution of NTA in water; 70 v/cm, 140 minutes, 25° C.

(C) Separation of Cr(III), Mn(II), Fe(III), and Co(II) in 0.01 *M* NTA – 0.06 *M* NH_4OH; 75 v/cm, 116 minutes, 25° C.

TABLE II

Migration sequences of Cr(III), Mn(II), Fe(III), and Co(II) in some complexone electrolyte solutions

Complexone solution	Migration sequence	Remarks
Saturated EDTA in H_2O	Mn : (Cr+Co), Fe	Co, Cr have same mobility
Saturated NTA in H_2O	Mn, Cr, Co : Fe	Mn, Cr not complexed; Co near start
0.01 *M* HEDTA in H_2O	Mn, Cr : Fe, Co	Mn, Cr not complexed; Fe zone diffuse about start
0.01 *M* EDTA in 0.06 *M* NH_4OH	Cr : Mn, (Fe+Co)	
0.01 *M* NTA in 0.06 *M* NH_4OH	Mn, Cr : Co, Fe	
0.01 *M* HEDTA in 0.06 *M* NH_4OH	Mn, Cr : Fe, Co	Cr zone diffuse
0.01 *M* DCTA in 0.06 *M* NH_4OH	: Mn, (Cr+Fe+Co)	Cr zone diffuse; Fe, Co of same mobility
0.01 *M* EDTA in 1.2 *M* NH_4OH	: Cr, (Mn+Fe), Co	
0.01 *M* NTA in 1.2 *M* NH_4OH	: Cr, (Co+Mn+Fe)	
0.01 *M* HEDTA in 1.2 *M* NH_4OH	Cr : Co, Cr, (Mn+Fe)	Cr forms two zones; Mn zone diffuse
0.01 *M* DCTA in 1.2 *M* NH_4OH	: (Cr+Fe), Co, Cr, Mn	Cr forms two zones; one remains at start and overlaps Fe
0.03 *M* EDTA in 0.1 *M* NH_4OH	: Mn, Cr, Fe, Co	Cr zone diffuse, tends to overlap Mn
0.03 *M* NTA in 0.1 *M* NH_4OH	Mn : (Cr+Co), Fe	Cr, Co zones diffuse; Cr tends to spread on both sides of start
0.04 *M* EDTA in 0.1 *M* NH_4OH	: Mn, (Cr+Fe), Co	Cr tends to be diffuse

NOTE: Parentheses indicate the enclosed ions have very similar mobilities.
The starting point is represented by the symbol : . Ions to the left of this move as cations, those to the right as anions.

and cesium. Figure 5 shows typical results obtained. Alkali metal ions are readily separated from others in strong complexing agents. Figure 6 shows some separations of alkali metals and other univalent cations in NH_4OH–EDTA solutions. Silver forms multiple zones in this electrolyte, probably because of competition between the EDTA and the ammonia in forming complexes.

Can. J. Chem. Downloaded from www.nrcresearchpress.com by 210.87.254.5 on 09/05/12
For personal use only.

Can. J. Chem. Downloaded from www.nrcresearchpress.com by 210.87.254.5 on 09/05/12
For personal use only.

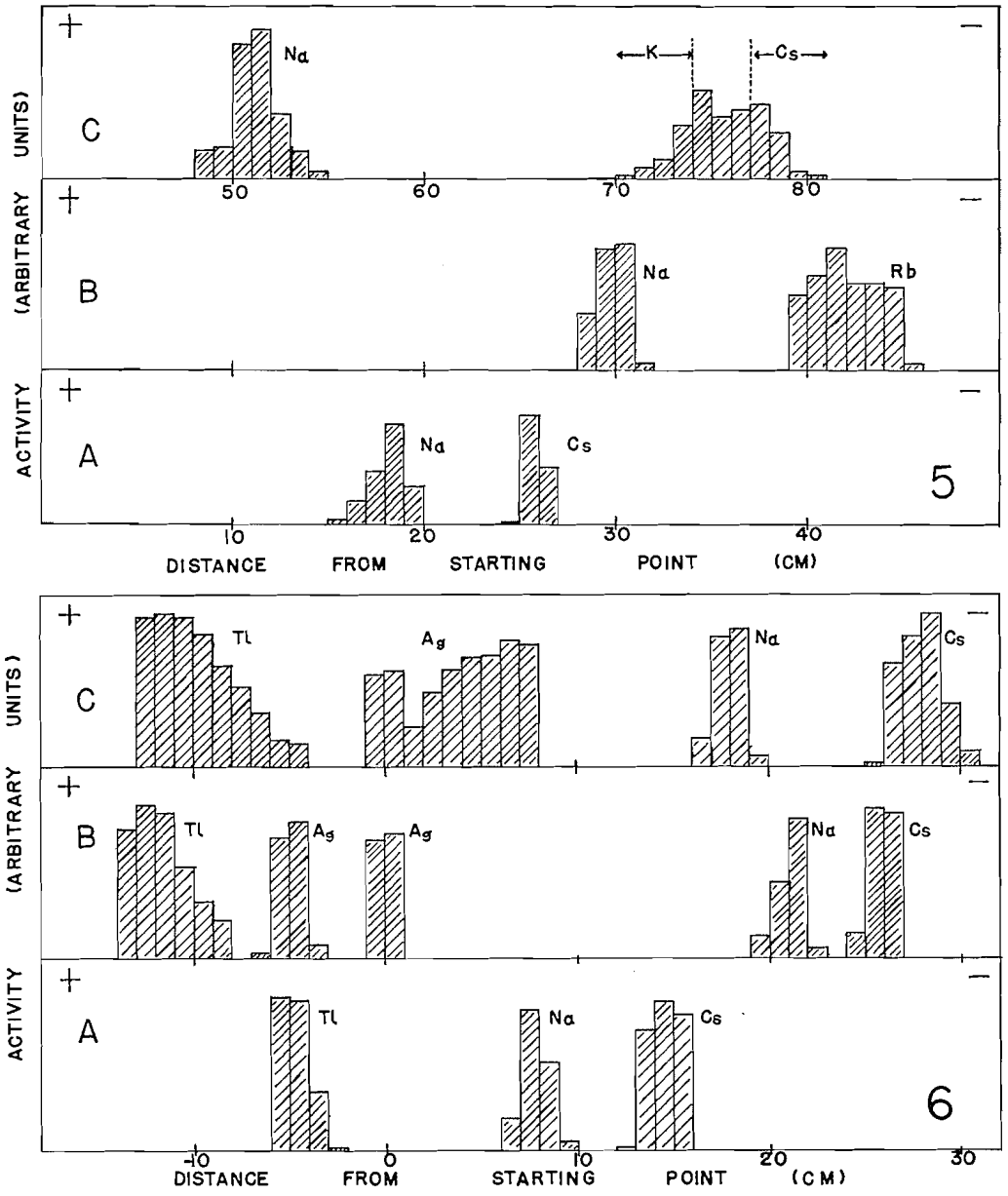


FIG. 5. (A) Separation of Na^+ and Cs^+ in 2.36 *M* acetic acid; 35 v/cm, 50 minutes, 25° C.
(B) Separation of Na^+ and Rb^+ in 1.18 *M* acetic acid; 80 v/cm, 28 minutes, 25° C.
(C) Separation of Na^+, K^+, and Cs^+ in 0.15% ammonium acetate solution; 60 v/cm, 63 minutes, 25° C.

FIG. 6. Separation of some univalent cations.
(A) Na^+, Cs^+, and Tl^+ in 0.01 *M* EDTA – 6.1 *M* NH_4OH; 20 v/cm, 27 minutes, 25° C. Whatman No. 52 paper.
(B) Na^+, Cs^+, Tl^+, and Ag^+ in 0.1 *M* EDTA – 1.2 *M* NH_4OH; 50 v/cm, 24 minutes, 25° C. Whatman No. 52 paper.
(C) Na^+, Cs^+, Tl^+, and Ag^+ in 0.01 *M* EDTA – 6.1 *M* NH_4OH; 50 v/cm, 38 minutes, 25° C. Whatman No. 52 paper.

Can. J. Chem. Downloaded from www.nrcresearchpress.com by 210.87.254.5 on 09/05/12
For personal use only.

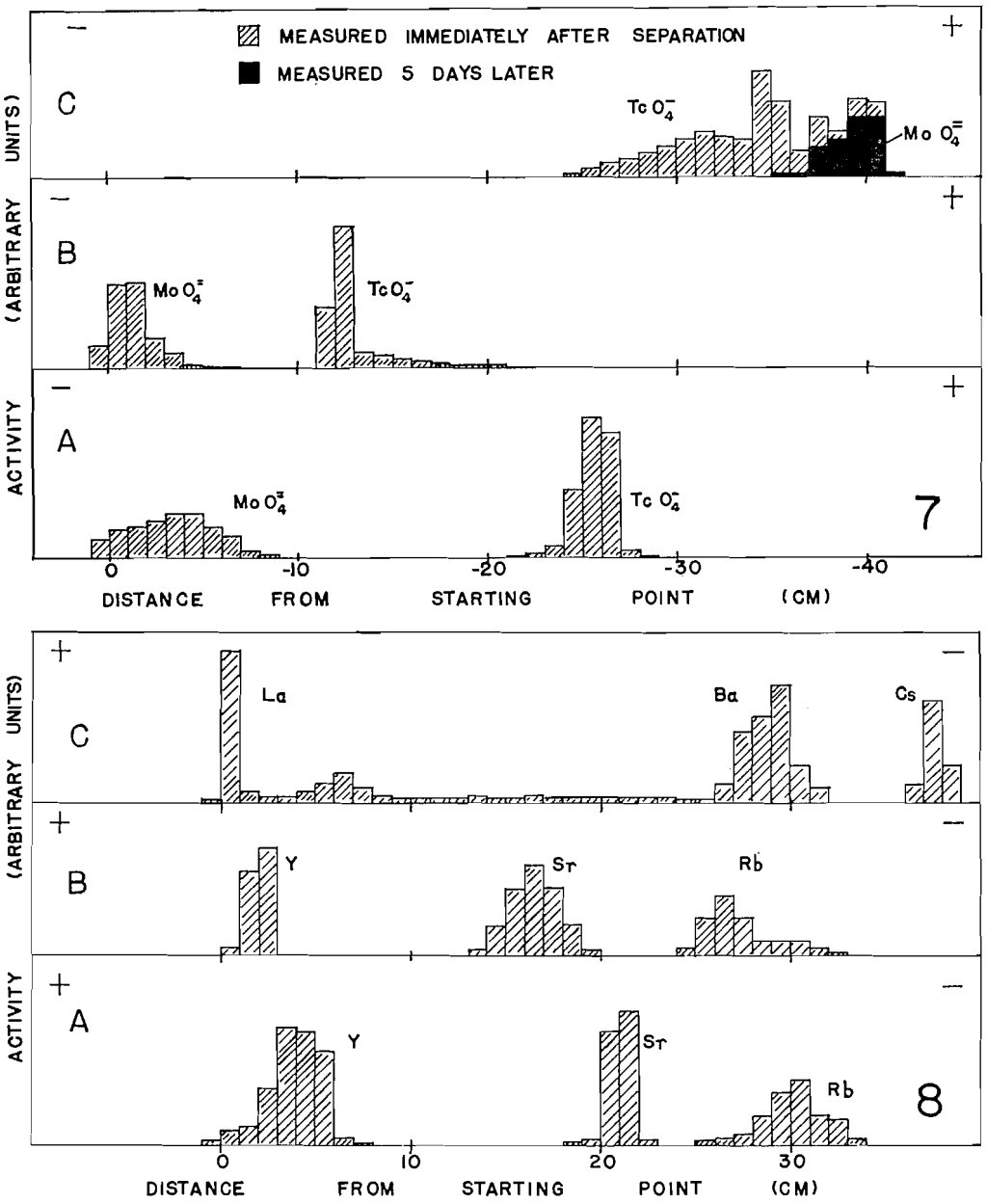


FIG. 7. Separation of molybdenum and technetium as the molybdate and pertechnate ions.
(A) In 0.15% ammonium acetate solution; 60 v/cm, 55 minutes, 30° C.
(B) In 1.18 *M* acetic acid; 100 v/cm, 25 minutes, 30° C.
(C) In 1.2 *M* NH_4OH; 80 v/cm, 45 minutes, 30° C.

FIG. 8. (A) Separation of Rb, Sr, and Y in 1.18 *M* acetic acid; 120 v/cm, 8 minutes, 35° C.
(B) Separation of Rb, Sr, and Y in 0.015 *M* citric acid; 180 v/cm, 5 minutes, 35° C.
(C) Separation of Cs, Ba, and La in 1% citric acid; 160 v/cm, 8 minutes, 33° C.

Separation of the molybdate and pertechnate ions are shown in Fig. 7. The former, as Mo^{99}, was obtained as a product of nuclear fission, while Tc^{99m} is its radioactive daughter, and is present in 'carrier-free' form. In non-basic solution, the $MoO_4^=$ ion may be precipitated as molybdic acid, which probably accounts for its occurrence near the starting position in ammonium acetate and acetic acid solutions. Figure 7C shows its migration in NH_4OH, where no precipitation takes place. $MoO_4^=$ is slightly faster than TcO_4^- but, even after a movement of 40 cm, they are not completely separated. The cross-hatched region, measured immediately after separation, includes both molybdenum and technetium

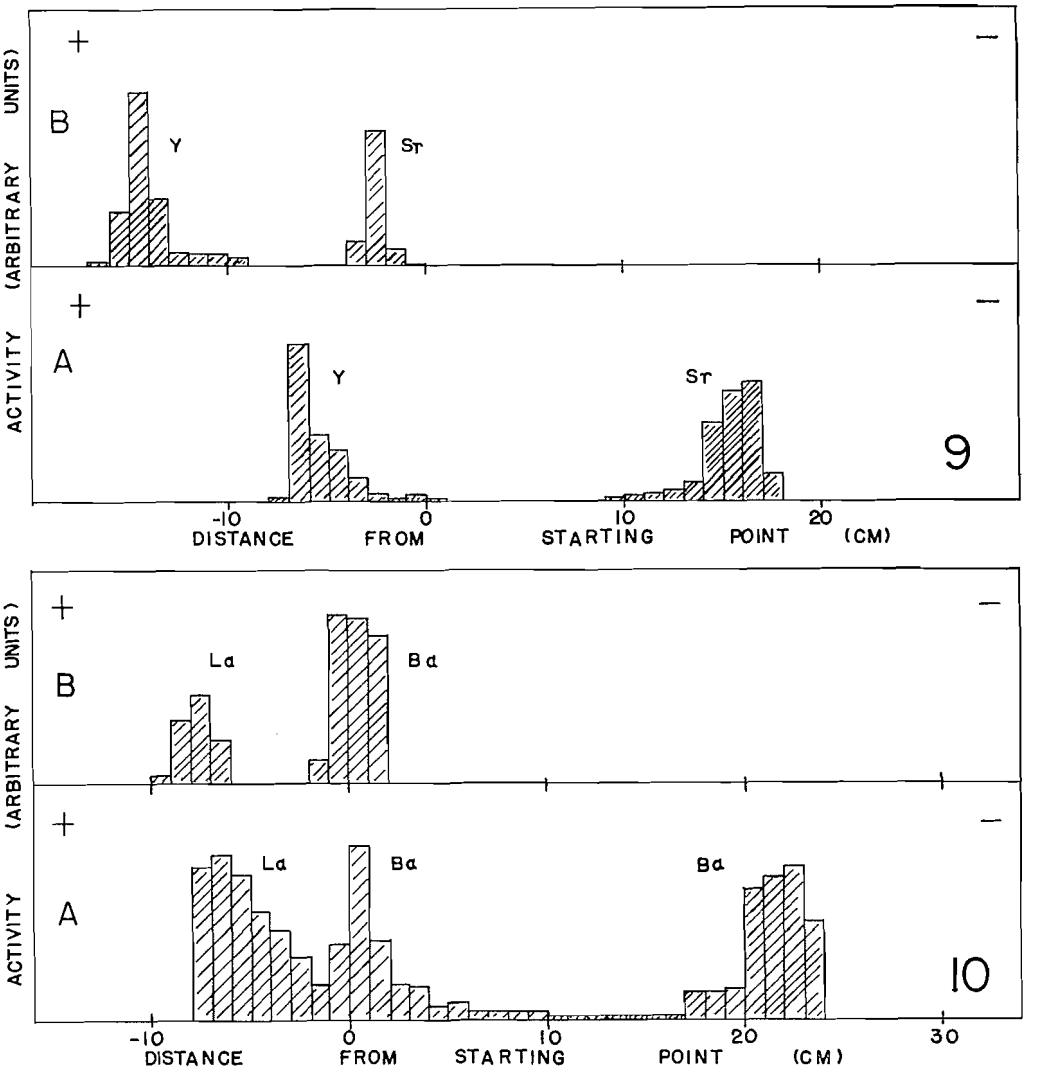


FIG. 9. Separation of Sr and Y in EDTA background electrolytes.
(A) A saturated solution of EDTA in water; 120 v/cm, 8.5 minutes, 30° C.
(B) 0.01 EDTA – 1.2 *M* NH_4OH; 75 v/cm, 35 minutes, 30° C.

FIG. 10. Separation of Ba and La in EDTA background electrolytes.
(A) A saturated solution of EDTA in water; 180 v/cm, 9 minutes, 33° C.
(B) 0.01 *M* EDTA – 1.2 *M* NH_4OH; 80 v/cm, 37 minutes, 33° C.

Can. J. Chem. Downloaded from www.nrcresearchpress.com by 210.87.254.5 on 09/05/12
For personal use only.

activities, while the blackened region, measured 5 days later, includes none of the technetium present initially, since the half-life of Tc^{99m} is only 6 hours. Tc^{99} was not detected.

Separations of rubidium, strontium, and yttrium in acetic and citric acids are shown in Figs. 8A and 8B. Similar separations of cesium, barium, lanthanum were attempted, but barium invariably exhibited a trail back to the starting point when it moved as a cation (Fig. 8C). The cause of this is not known, but it may be due to precipitation of small amounts of barium by traces of sulphate in the paper. Further separations of strontium and yttrium, and of barium and lanthanum, in EDTA solutions, are shown in Figs. 9 and 10 respectively. In all of these experiments, the yttrium and the lanthanum were 'carrier-free'.

The separation of RaD, RaE, and RaF (Pb^{210}, Bi^{210}, and Po^{210}) was also investigated. Both bismuth and polonium tend to be adsorbed by the paper and trail. RaD can be separated from the other two in oxalic, citric, tartaric, lactic, or acetic acids, and separation of RaF from the rest may be accomplished in EDTA solution. In this, and in the other chelating agents used, RaD and RaE move with similar mobilities, so that it was not found possible to separate all three ions in one run under these conditions.

Sato *et al.* (3, 8) have reported the separation of lead, bismuth, and polonium in lactic acid, but the bismuth and polonium zones seem to overlap here also.

ACKNOWLEDGMENT

One of us (R.A.B.) wishes to thank the National Research Council of Canada for Studentships held during the years 1957–58, 1958–59, and 1959–60.

REFERENCES

1. R. A. Bailey and L. Yaffe. Can. J. Chem. **37**, 1527 (1959).
2. Z. Pucar. Anal. Chim. Acta, **18**, 290 (1958).
3. T. R. Sato, W. P. Norris, and H. H. Strain. Anal. Chem. **26**, 267 (1954).
4. S. Harasawa and T. Sakamoto. J. Chem. Soc. Japan, Pure Chem. Sect. **74**, 862 (1953).
5. G. H. Evans and H. H. Strain. Anal. Chem. **28**, 1560 (1956).
6. O. Schier. Angew. Chem. **68**, 63 (1956).
7. D. Gross. Nature, **180**, 596 (1957).
8. T. R. Sato, W. P. Norris, and H. H. Strain. Anal. Chem. **27**, 521 (1955).

Can. J. Chem. Downloaded from www.nrcresearchpress.com by 210.87.254.5 on 09/05/12
For personal use only.

Can. J. Chem. Downloaded from www.nrcresearchpress.com by 210.87.254.105 on 09/05/12
For personal use only.

RELAXATION OF SURFACE PRESSURE AND COLLAPSE OF UNIMOLECULAR FILMS OF STEARIC ACID[1]

W. Rabinovitch, R. F. Robertson, and S. G. Mason

ABSTRACT

A study has been made of the time variations of π–A isotherms of stearic acid films at air/water interfaces using an automatic recording surface balance of the vertical pull type. The existence of coherent films below molecular areas of 22 sq. Å/molecule has been found to be dependent on the temperature, rate of compression, and the history of compression of a given film. The behavior at or near collapse, the decrease in π with time after sudden compression (relaxation), and the increase in π with time after sudden expansion (recovery) have been studied.

The results have been interpreted on the basis of structural changes in the monolayer.

INTRODUCTION

Although extensive studies have been made on the pressure–area (π–A) isotherms of simple long-chain fatty acids spread as unimolecular films at the air/water interface, little attention has been given to the possible time-dependency of these mechanical properties. By analogy with three-dimensional viscoelastic systems, it is not surprising that the π–A isotherms of two-dimensional systems should be time-dependent. This dependency has been observed experimentally under conditions of slow manual compression for stearic and other fatty acid films (1, 2, 3) and with automatic compression and surface pressure recording techniques for films of palmitic (4) and stearic (5, 6) acids.

The collapse of stearic acid films may occur with compression to 19 sq. Å/molecule surface area (5, 6, 7) or before this area is attained (1). In more definitive studies of collapse Muller (8) has suggested that a stearic acid film collapses by a stepwise wrinkling leading to the formation of numerous strata. Kimball and Ries (9) have reported the appearance of long wrinkles two molecules deep (100 Å) in electron micrographs of collapsed hexatricontanoic acid monolayers.

In the present study the π–A – time relations of stearic acid films have been investigated up to and beyond the collapse region in an attempt to elucidate the molecular processes associated with the formation and collapse of unimolecular films. Studies have been made of: (*a*) the effect of compression rate on the π–A isotherm, (*b*) the variation of π with time after repeated compressions and expansions of the film at molecular areas between 19 and 24 sq. Å, and (*c*) the effect of repeated compressions on the π–A isotherm of the same film.

EXPERIMENTAL PART

The Film Balance

Description

The surface pressure measurements were made with an automatically recording film balance of the Wilhelmy type. The balance incorporated a null-balance feature activated by the electronic servo-mechanism of Mauer (10) applied to a chainomatic balance. This surface balance was found to be capable of rapid and precise response to increasing or decreasing surface pressure.

[1]*Manuscript received June 10, 1960.*

Contribution from the Department of Chemistry, McGill University, and the Pulp and Paper Research Institute of Canada, Montreal, Que. Based on work conducted under Extramural Grant No. 2031-08 of the Defence Research Board of Canada. Presented at 43rd Annual Conference, Chemical Institute of Canada, Ottawa, Ontario, June 1960.

A Wilhelmy dipping plate is suspended by a nichrome wire from the bottom of the left-hand pan of a chainomatic balance. A galvanometer mirror attached at the fulcrum of the balance beam reflects a light beam from a source onto the separate twin cathodes of a phototube in a bridge circuit. The phototube senses the magnitude and direction of minute displacements of the balance arm from a given equilibrium position and translates the displacements into a proportional electrical voltage of corresponding polarity. By applying this voltage to the input of a direct-coupled amplifier an output current of corresponding magnitude and phase is obtained. This current is led through a solenoid whose field exerts a force on a magnet concentric with the solenoid and suspended from the right-hand pan connection of the chainomatic balance. The magnet is so oriented in the solenoid that the polarity opposes the displacement of the balance beam from equilibrium. When a vertical force is applied to the balance pan the system can be maintained continuously in equilibrium by this instantaneous self-balancing action. The balancing current was passed through a decade resistance and the resulting voltage was recorded by a multiple-span strip chart recorder (Minneapolis-Honeywell-Brown, Extended Range, Type 153).

Calibration

A clean dipping plate suspended from the nichrome wire was allowed to dip into a clean substrate surface and the initial zero reading of the balance was obtained after taring. A calibrating weight was placed on the balance pan and the positive deflection of the recorder was adjusted to full scale by the decade resistance. Normally the calibrating weight was chosen to give $\pi = 25$ or 50 dynes/cm for the full 10 in. chart width; however, the multiple-span feature of the recorder made it possible to extend the range to 50 inches when desired.

Characteristics of the Surface Balance

The surface balance response was highly stable over long periods of time (10 hours) and was linear within 0.1% for loads from 0 to 300 mg. Beyond 300 mg the instrument was not self-balancing with the size of magnet (1/4×3 in.) employed. The response time of the balance to rapidly changing surface pressure was limited by the response time (4.5 seconds) of the recorder pen for full-scale deflection.

With the conventional Wilhelmy surface balance in which the depth of immersion is changed by manipulation, measurement of decreasing values of π becomes uncertain since the downward movement of the dipping plate into the substrate may cause the contact angle to deviate from zero (11, 12). Since, however, vertical movement is negligible ($<10^{-2}$ cm) in this balance it was possible to measure both increasing and decreasing π to within ± 0.1 dynes/cm.

The Trough Assembly

A description of the air thermostat and barriers employed can be found in earlier publications (13, 14). The film area could be varied by stepwise manual compression or by a motor-driven barrier-moving device which provided either a fixed trough traverse time of 10 seconds or a variable traverse time of from 10 minutes to several hours.

Materials

The stearic acid (m.p. 69° C) used in these experiments was obtained from the Defence Research Chemical Laboratories, Ottawa, Canada. A stock solution of 0.00418 M stearic acid was prepared in benzene and used in all experiments. At the standard initial area of 880.9 sq. cm, 0.1 ml of this solution formed a film at 35 sq. Å/molecule initial area. All substrates were 0.01 N HCl aqueous solution.

Can. J. Chem. Downloaded from www.nrcresearchpress.com by 210.87.254.105 on 09/05/12
For personal use only.

Experimental Techniques

The dipping plate and teflon-coated trough and barriers were cleaned with chromic acid and rinsed with copious quantities of distilled water. After the trough and barriers were placed in the thermostat, the substrate solution was added, the dipping plate installed, and the balance brought to its equilibrium zero position. The surface was then checked for contamination by advancing the barrier from its initial position to one corresponding to an area 1/4 to 1/8th of the initial area. An increase in pressure of less than 0.25 dyne/cm during this compression was taken as the criterion of a clean surface. The system was left for several hours for temperature equilibration with the barrier at its initial position and then checked for surface contamination again before a film was spread.

RESULTS

Effect of Compression Rate on the π–A Isotherms

The pressure–area (π–A) isotherms were obtained on 0.01 N HCl substrates at 25° C over a range of compression rates from 0.04 to 2.43 sq. Å/molecule per minute. The results for three freshly spread monolayers are given in Fig. 1. Curve 1 of this figure is the

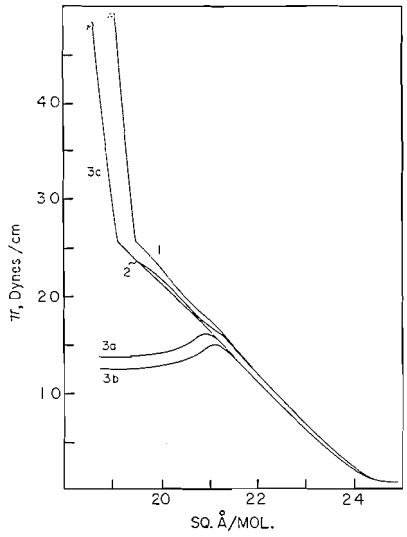


FIG. 1. Isotherms (25° C) of stearic acid monolayers determined at the following continuous compression rates in sq. Å per molecule/minute: 2.43 (curve 1), 0.213 (curve 2), 2.43 after a 7-hour rest period (curve 3). Curves 3*a* and 3*b* were obtained by slow manual stepwise compression as explained in the text, and 3*c* by recompression at 2.43 sq. Å/molecule per minute after expansion and resting for 7 hours at 35 sq. Å/molecule.

isotherm obtained from a film initially at a molecular area of 35 sq. Å under continuous compression at a rate of 2.43 sq. Å/molecule per minute and curve 2 is the isotherm of a similar film compressed at the rate of 0.213 sq. Å/molecule per minute. The isotherms represented by curves 3*a* and 3*b* were obtained by 30 stepwise compressions, each of 0.2 sq. Å/molecule, in the range 25 to 19 sq. Å/molecule of the surface area. The film initially at 35 sq. Å/molecule was compressed rapidly to 25 sq. Å/molecule and then by steps with 5 minutes between each compression. The surface pressure was noted immediately after each compression and immediately before the next. Curves 3*a* and 3*b* are the isotherms obtained on plotting these two values of the surface pressure. After the slow stepwise

Can. J. Chem. Downloaded from www.nrcresearchpress.com by 210.87.254.105 on 09/05/12
For personal use only.

compression the film was rapidly expanded to 35 sq. Å/molecule, left for 7 hours, and then recompressed continuously at a rate of 2.43 sq. Å/molecule per minute to obtain curve 3*c*. The significance of these observations is discussed later.

Surface Pressure Relaxation and Recovery

A study was made of the variation with time of the surface pressure at constant area after sudden compression and expansion. Adopting the customary nomenclature, the decrease in π with time after rapid compression is called pressure relaxation, and the increase in π with time after rapid expansion is called recovery.

All experiments were made at 25° C with the film at an initial area of 35 sq. Å/molecule. This monolayer was rapidly compressed or expanded between molecular areas of 24 and 21 sq. Å, and the pressure recorded as a function of time t at each intermediate area. The details of the experimental operations for one typical film are given in Table I and the results are given as plots of π vs. t in Figs. 2 (A, B, C, D), 3, and 4.

TABLE I

Stepwise compression and expansion of stearic acid film

Step	Sq. Å/molecule Initial	Final	Operation	Process studied	Duration of observation (minutes)	Figure	Curve
1	35	24	Compression	Relaxation	15	2A	1
2	24	23	"	"	12	2B	2
3	23	22	"	"	11	2C	3
4	22	23	Expansion	Recovery	11	2B	4
5	23	24	"	"	10	2A	5
6	24	23	Compression	Relaxation	10	2B	6
7	23	22	"	"	10	2C	7
8	22	23	Expansion	Recovery	11	2B	8
9	23	24	"	"	10	2A	9
10	24	23	Compression	Relaxation	10	2B	10
11	23	22	"	"	10	2C	11
12	22	21	"	"	13	2D	12(*a*)
13	21	21	None	Relaxation	120	3	12(*b*)
14	21	22	Expansion	Recovery	53	4	13
15	22	23	"	"	19	4	14
16	23	24	"	"	10	2A	15
				Total time = 335			

NOTE: Initial area = 35 sq. Å/molecule. Initial π = 0.17 dynes/cm. Temperature = 25° C.

At areas of 24, 23, and 22 sq. Å/molecule the pressure relaxation is shown in Figs. 2 and 3 to be 0.13 dyne/cm in 10 minutes. At 21 sq. Å/molecule, however, the relaxation is 1.7 dynes/cm in 10 minutes (a 10-fold increase) and after 2 hours the pressure has decayed by about 5 dynes/cm. On subsequent expansion the pressure recovery is of the same order as the relaxation (Fig. 4). The curves obtained for both the relaxation and recovery seem to indicate that these two phenomena reflect properties of the monolayer and are not the result of slow solution and diffusion of film molecules into the substrate.

Surface Pressure Relaxation at 19 sq. Å/molecule

At a compression rate of 2.43 sq. Å/molecule per minute the monolayer attained a surface pressure before collapse in excess of 45 dynes/cm at a molecular area of about 19.5 sq. Å (Fig. 1, curve 1). Other workers (5–7) have reported maximum surface pressures from 55 to 62 dynes/cm at molecular areas near 18.5 sq. Å for stearic acid films compressed

Can. J. Chem. Downloaded from www.nrcresearchpress.com by 210.87.254.105 on 09/05/12
For personal use only.

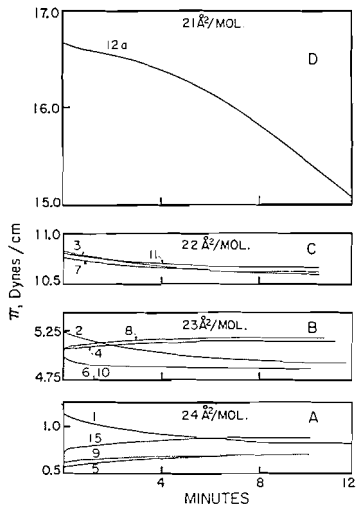


FIG. 2. Relaxation and recovery curve over 10 to 12 minutes. See Table I for details of curves.

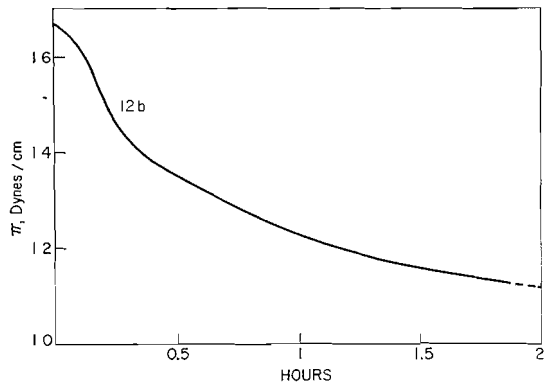


FIG. 3. Relaxation curve over a 2-hour period at 21 sq. Å/molecule (see Table I).

at rates in excess of 3 sq. Å/molecule per minute. To examine pressure relaxation at the pressure maximum obtained on rapid compression, a film initially at an area of 35 sq. Å/molecule was compressed at a rate of 2.43 sq. Å/molecule per minute until the pressure maximum was attained and the surface pressure recorded with time at constant area. Figure 5 shows the π–A isotherm (part A) and the relaxation plot (part B), respectively, for a film at an initial pressure maximum of 45 dynes/cm and a molecular area of 19.2 sq. Å.

It is apparent from Fig. 5 that on decreasing the molecular area from 19.5 to 19.2 sq. Å during compression, 7.5 seconds were required for the film pressure to increase from 25 to 45 dynes/cm, but on stopping the barrier 12 seconds were required for the pressure to decay from 45 to 25 dynes/cm at 19 sq. Å/molecule. The rate of pressure decay changed markedly (20-fold) at 25 dynes/cm reflecting the similar discontinuity in the isotherm at 25 dynes/cm pressure. This behavior was demonstrated a number of times with different films.

Can. J. Chem. Downloaded from www.nrcresearchpress.com by 210.87.254.105 on 09/05/12
For personal use only.

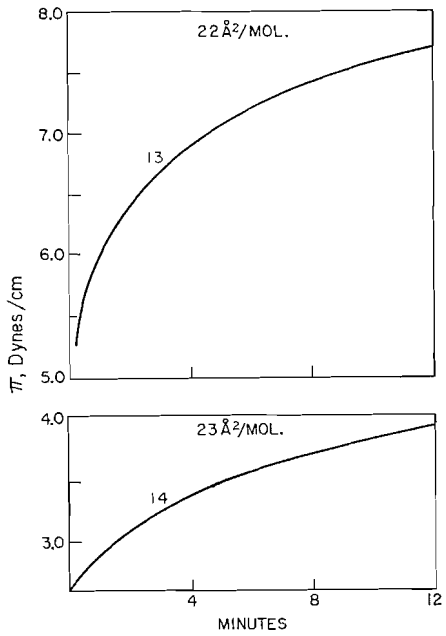


FIG. 4. Surface pressure recovery curves. See Table I for details of curves.

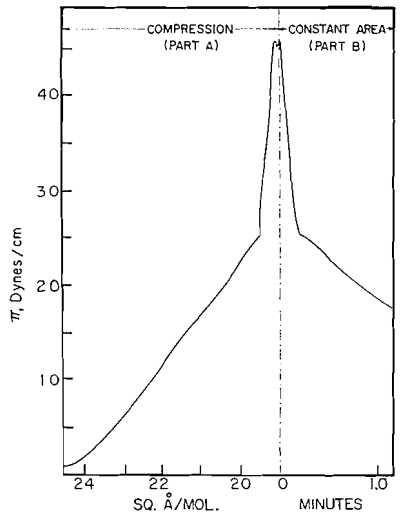


FIG. 5. Part A: π–A isotherm at a compression rate of 2.43 sq. Å per molecule/minute until an area of 19.2 sq. Å/molecule was reached.
Part B: Relaxation of π at constant area of 19.2 sq. Å/molecule.

Isotherms on Repeated Compressions and Expansions

The π–A isotherms were obtained for films subjected to repeated compressions and expansions. After spreading a film to an initial area of 35 sq. Å/molecule the monolayer was compressed at a rate of 2.43 sq. Å/molecule per minute to the maximum pressure and immediately re-expanded to 35 sq. Å/molecule and left at this molecular area for

Can. J. Chem. Downloaded from www.nrcresearchpress.com by 210.87.254.105 on 09/05/12
For personal use only.

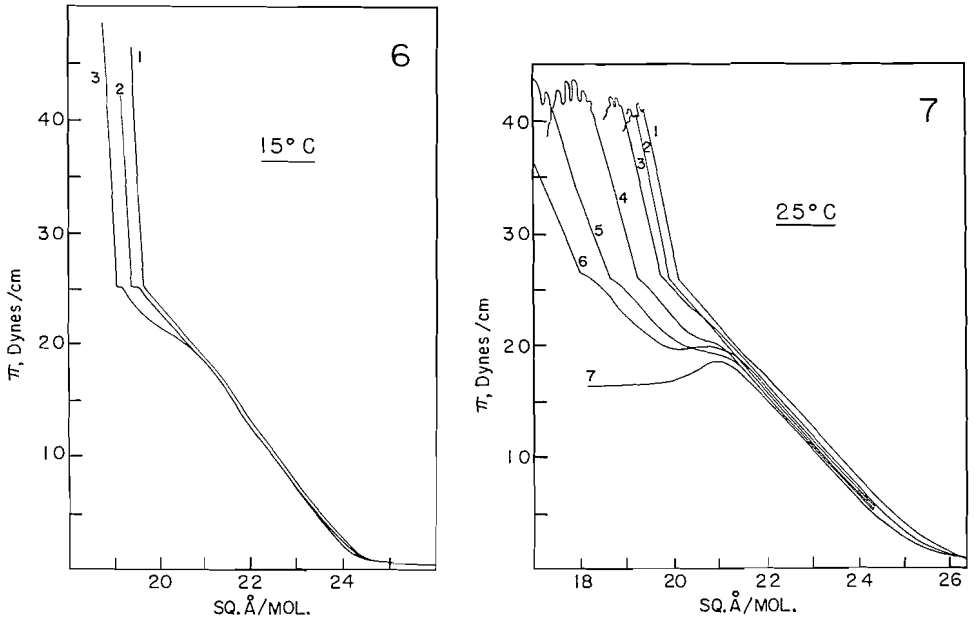


FIG. 6. Isotherms of a repeatedly compressed and expanded film at 15° C. Curve numbers represent the sequence of compressions.

FIG. 7. Isotherms of repeatedly compressed and expanded film at 25° C. Curve numbers represent the sequence of compressions.

1 hour to permit respreading. After this time interval the film was recompressed as before. Figures 6 and 7 are the isotherms obtained from such a series of compressions and subsequent expansions at 15° C and 25° C respectively. The curves are numbered according to the sequence of compressions.

The isotherms obtained with successive compressions are very similar to those obtained by varying the rate of compression (Fig. 1). The highly incompressible solid phase persists on the 15° C isotherm after three compressions but is shifted to smaller molecular areas with each compression (Fig. 6). The shift in area results from a change in the slope of the isotherm just before the appearance of the solid phase of constant compressibility similar to that apparent in Fig. 1. At 25° C the shift of the solid phase to progressively smaller areas with succeeding compressions becomes strikingly evident (Fig. 7). Not only does a marked change occur in the shape of the isotherm before the appearance of the solid phase, as found in varying the compression rate (Fig. 1), but the slope of the isotherm and hence the compressibility of the solid phase change with each compression and finally the phase disappears (Fig. 7, curve 7). There is some indication of a change in slope in the solid phase isotherm itself (Fig. 7, curve 5).

DISCUSSION

Heller (4) has reported that the shape of the π–A isotherm of palmitic acid monolayers depends on the rate of compression of the film. A similar dependence with stearic acid monolayers is indicated in Fig. 1, in which substantially the same film compressibility from molecular areas of 24.5 to 21 sq. Å is shown; below 21 sq. Å/molecule, however, a

Can. J. Chem. Downloaded from www.nrcresearchpress.com by 210.87.254.105 on 09/05/12
For personal use only.

marked divergence is apparent in the shape and slope of the curves. At the highest compression rate (2.43 sq. Å/molecule per minute) the highly incompressible solid phase of stearic acid monolayer is evident (Fig. 1, curve 1). When the compression rate was reduced to 0.213 sq. Å/molecule per minute (Fig. 1, curve 2) the isotherm was identical with curve 1 until a 21 sq. Å/molecule area was reached and a more compressible intermediate film appeared. With slow manual compression (Fig. 1, curves 3*a*, 3*b*) the slope of the isotherm was again identical with the others until reaching 21 sq. Å/molecule, but on further reduction of the molecular area neither the solid film nor the intermediate film appeared. Further, pressure relaxation, essentially absent at molecular areas greater than 21 sq. Å/molecule, became measurable at smaller molecular areas when slow compression was used (Fig. 1, curves 3*a*, 3*b*).

The absence of the solid phase in curves 2, 3*a*, 3*b* of Fig. 1 seems to be associated with the compression rate, since 7 hours after slow compression the film readily exhibited the highly incompressible solid phase (Fig. 1, curve 3*c*). The maximum pressure attained before collapse seems similarly dependent on the rate of compression (Fig. 1); collapse occurred at surface pressures varying from 15 to 49 dynes/cm and from 21 to 19.4 sq. Å/molecule as the rate of compression was increased. The work of Dervichian (6) on stearic acid films, which reports a pressure maximum of 61 dynes/cm at 18.6 sq. Å/molecule under an estimated compression rate of 18 sq. Å/molecule/min, corroborates these findings.

The point of collapse near 21 sq. Å/molecule for slowly compressed monolayers appeared as an inflection on the isotherm obtained under rapid compression (Fig. 1). Inflections of this type have been reported for stearic acid (15) and behenic acid (16) and have been related to the appearance of a second-order phase transition in the film. The nature of this transition point is obscure, Adam (17) suggesting that the head group packing beneath the film is responsible for the effect.

According to Vold (18) a molecular cross-sectional area of 25.2 sq. Å can be calculated from the volume swept out during the rotation of vertically oriented fatty acid molecules of the stearic type with the head groups close-packed and planar in the water surface (Fig. 8(*a*)). The discontinuity found at 25 sq. Å/molecule in the π–A isotherms of stearic acid monolayers is assumed to reflect the appearance of such a surface configuration with free rotation permitted. When the film molecules are identically oriented on the surface but no longer free to rotate, the molecular cross-sectional area, now ovoid, is calculated to be 20.5 sq. Å for the most efficient packing (Fig. 8(*b*)). The π–A isotherm of stearic acid on compression from 25 to 21 sq. Å/molecule can be assumed to reflect the progressive inhibition of free rotation until at the lower area rotation is completely restricted. At this point the compressibility of the film would depend on the compressibility of the head groups only and should decrease markedly. The discontinuity in the π–A isotherm at 21 sq. Å/molecule does in fact reflect this change to a lower compressibility. As the lateral compression continues and the film approaches collapse, the planar configuration of the head groups (Fig. 8(*c*)) should give way to a multiplanar one as head groups are forced to a position either above or below the original plane (Fig. 8(*d*)). Finally some of the stearic acid molecules may invert under lateral compression to form a second molecular layer (Fig. 8(*e*, *f*)) with ensuing collapse.

If the inversion process requires time, the appearance of the solid film on rapid compression may be the consequence of insufficient time for inversion between the moment at which 21 sq. Å/molecule area was reached and the moment of general collapse of the film.

Can. J. Chem. Downloaded from www.nrcresearchpress.com by 210.87.254.105 on 09/05/12
For personal use only.

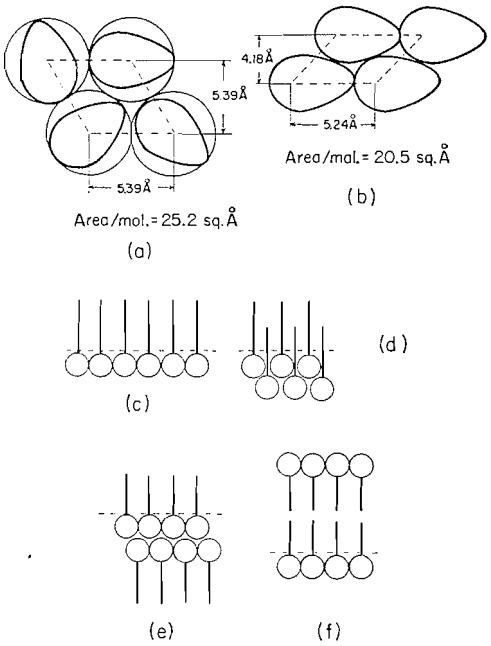


FIG. 8. Possible configuration of stearic acid monolayers.
(*a*) At 25 sq. Å/molecule, free rotation (18). (*b*) At 21 sq. Å/molecule, no rotation (18).
(*c*) Planar configuration at 21 sq. Å/molecule. (*d*) Below 21 sq. Å before inversion.
(*e*, *f*) Possible modes of inversion below 21 sq. Å/molecule.

As the compression rate is decreased the time per unit change in area after attaining 21 sq. Å/molecule increases and the time available for inversion increases. Consequently the inversion process can occur to an extent dependent on the particular compression rate employed. With intermediate compression rates a competition can occur between the processes of solid film formation and inversion resulting in the π–A isotherm of variable compressibility found by experiment. At very low rates of compression the time available for inversion is so great that the film molecules can invert at a rate at least equal to the compression rate and no solid or intermediate film is formed.

The variation in slope and hence compressibility illustrated in Figs. 6 and 7, obtained by successive compressions and expansions, can also be explained by a process of inversion. With rapid compression to areas below 21 sq. Å/molecule a small fraction of the molecules may invert but not in sufficient numbers to alter the apparent compressibility of the solid phase. With subsequent expansion the inversion process may be reversed but the molecules involved retain a configuration on the surface favorable to rapid inversion on subsequent compression. On immediate recompression these molecules rapidly invert and others follow, thus increasing the fraction of film molecules conditioned for rapid inversion in the next expansion–compression cycle. The over-all effect of this mechanism would be an apparent increase in the inversion rate with each successive compression until the rate of the inversion process approaches the rate of compression and no solid film appears (Fig. 7).

Can. J. Chem. Downloaded from www.nrcresearchpress.com by 210.87.254.105 on 09/05/12
For personal use only.

REFERENCES

1. W. D. HARKINS and G. C. NUTTING. J. Am. Chem. Soc. **61**, 1180 (1939).
2. W. D. HARKINS and R. J. MYERS. J. Chem. Phys. **4**, 716 (1936).
3. N. K. ADAM. Proc. Roy. Soc. A, **101**, 452 (1922).
4. S. HELLER. Kolloid-Z. **136**, 120 (1954).
5. E. STENHAGEN. The Svedberg. (Almquist & Wiksells Boktryckeri Ab) Uppsala, Sweden. 1944. p. 31.
6. D. G. DERVICHIAN. J. phys. Radium, Ser. 7, Vol. 6. 221 (1935).
7. D. G. DERVICHIAN. Ann. phys. **8**, 361 (1937).
8. F. H. MULLER. Z. Elektrochem. **59**, 316 (1955).
9. W. A. KIMBALL and H. E. RIES, Jr. Intern. Congr. Surface Activity. 2nd Congr. Vol. 1. Butterworth Scientific Publications, London. 1957. p. 75.
10. F. A. MAUER. Rev. Sci. Instr. **25**, 598 (1954).
11. W. D. HARKINS and T. F. ANDERSON. J. Am. Chem. Soc. **59**, 2189 (1937).
12. E. STENHAGEN. The Svedberg. (Almquist & Wiksells Boktryckeri Ab) Uppsala, Sweden. 1944. p. 29.
13. R. F. ROBERTSON, C. A. WINKLER, and S. G. MASON. Can. J. Chem. **34**, 718 (1956).
14. W. RABINOVITCH, R. F. ROBERTSON, and S. G. MASON. J. Colloid Sci. **13**, 600 (1958).
15. D. G. DERVICHIAN. J. Chem. Phys. **7**, 931 (1939).
16. E. STENHAGEN and S. STALLBERG-STENHAGEN. Nature, **159**, 814 (1947).
17. N. K. ADAM. The physics and chemistry of surfaces, 3rd ed. Oxford Univ. Press. 1941.
18. M. J. VOLD. J. Colloid Sci. **7**, 196 (1952).

Can. J. Chem. Downloaded from www.nrcresearchpress.com by 210.87.254.105 on 09/05/12
For personal use only.

Can. J. Chem. Downloaded from www.nrcresearchpress.com by 210.87.254.42 on 09/05/12
For personal use only.

ANIONIC POLYMERIZATION OF STYRENE[1]

D. J. Worsfold and S. Bywater

ABSTRACT

A study of the kinetics of the initiation and propagation reactions in the polymerization of styrene by butyllithium in benzene solution has been made. The initiation has been shown to be first order in styrene and 0.155 order in butyllithium, the propagation to be first order in styrene and half order with respect to active chain ends. The apparent activation energies of the two reactions have been shown to be 18,000 calories and 14,300 calories respectively. The ultraviolet absorption spectra of colored species produced has been measured and compared with others found in similar systems.

The polymerization of styrene by butyllithium in benzene solution is an anionic chain reaction comprising initiation and propagation steps. Chain termination is negligible if the starting materials are rigorously purified and the reaction is carried out in a high vacuum system. Previous kinetic studies on this system have followed only the rate of monomer consumption (1, 2). Since, however, the reaction is complicated by the fact that initiation and propagation rates are of comparable magnitude under many experimental conditions, it seemed desirable to study the initiation and propagation steps separately. The method employed to follow the reaction was photometric using the known absorption bands of styrene and the absorption band of the polystyryl anion measured as described later. Because of the high extinction coefficient of both compounds, the concentration ranges studied were lower than previously used or overlapped their lower concentration range.

EXPERIMENTAL

The butyllithium was supplied by Foote Mineral Company as a 16% solution in a heptane/pentane solvent mixture.

The purification of the styrene has been described before (3).

Reagent grade benzene was stirred for a week with concentrated sulphuric acid, washed with water, with dilute sodium hydroxide solution, and again with water. It was distilled from phosphorus pentoxide onto calcium hydride, degassed, and stored under vacuum. The benzene was distilled in the vacuum system as needed to a smaller reservoir containing butyllithium from which the solvent had been removed by pumping. From here it was transferred to the reaction vessel by distillation.

The techniques used in the handling of the reactants under high vacuum have been described before (3) and entailed using small fragile glass bulbs of the reactants, and glass-covered magnetic bars for breaking them. All reaction vessels were washed with a solution of butyllithium in benzene and rinsed by refluxing as before, after all the reactant bulbs had been sealed inside and the vessels evacuated.

It was necessary to dilute the stock butyllithium solution by a factor of 50 or more before it could be used. A milliliter of the stock solution was transferred by hypodermic syringe in a dry nitrogen box to a fragile glass bulb, connected to a stopcock, that previously had been evacuated and reopened in the dry box. The bulb was then pumped and sealed off. This butyllithium was diluted 50 times and sealed into a large number of similar bulbs in a vacuum apparatus by the methods referred to above. It had been

[1]*Manuscript received June 3, 1960.*
Contribution from the Division of Applied Chemistry, National Research Council, Ottawa, Canada.
Issued as N.R.C. No. 5921.

determined previously that handling 1 milliliter of the stock solution by syringe in this manner destroyed less than 2% of the butyllithium.

Lithium analyses were performed spectrophotometrically using a solution of "Thorin" on aliquots of the lithium polystyryl solution after the benzene had been evaporated on a hot plate, and the polymer burned off at a temperature of less than 500°. Higher temperatures seemed to cause loss of lithium. The analysis is reputed to have an accuracy of 3%.

The optical cells used were made of 1-cm sq. clear quartz tubing, and could be converted to 1-mm cells with appropriate square quartz blocks. The cells were calibrated with potassium chromate solution. The spectra were measured on a Beckman DU spectrophotometer.

To show that the absorption band of the polystyryl salt obeyed Beer's law, the optical cell was connected to a graduated tube, with benzene in a reservoir joined to the cell and tube. The optical density of a solution of the polystyryl lithium salt at 335 mμ was measured over a 10-fold range of dilution, and the dependence was shown to be linear. Styrene was estimated at 291 mμ after a correction for the tail of the polystyryl ion band was applied.

The vessels used for the kinetic experiments, and for the determination of the spectra of the lithium polystyryl salt, are shown in Fig. 1, which is thought to be self-explanatory. The volume of reaction mixture was about 50 milliliters. Only one bulb of catalyst was used, but successive additions of styrene were achieved by breaking in turn up to three bulbs of styrene. This enabled the propagation step to be followed separately after

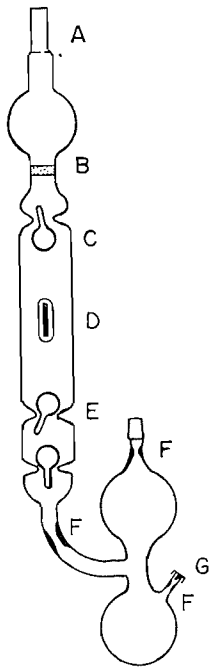


FIG. 1. Reaction vessel.

A. Optical cell.
B. Filter
C. Diluted catalyst solution.
D. Breaker.
E. Styrene.
F. Constrictions for sealing off.
G. Serum cap to introduce butyllithium solution to wash apparatus.

Can. J. Chem. Downloaded from www.nrcresearchpress.com by 210.87.254.42 on 09/05/12
For personal use only.

measurements of the optical density at 335 mμ had indicated that chain initiation was complete. The breaking of successive bulbs of styrene after this point could sometimes decrease the optical density by 1 to 2% due to the presence of residual impurities. Otherwise once it had attained a steady value, it remained constant during the course of a kinetic run (about 4 hours) and only decreased slowly over a period of weeks. This indicates that chain termination is negligible in this system under the experimental conditions used.

The reactions were carried out at 30.3°, except those for the temperature dependence, which were carried out over the range 10.0°–30.3°.

RESULTS

The spectrum of the colored species produced by the action of butyllithium on styrene in benzene solution was found to consist of a single absorption band centered at 334 mμ, with a long wavelength wing extending into the visible region which gives the solution its yellow color. The short wavelength wing was lost in the accompanying polystyrene bands below 280 mμ. Assuming that the structure of this species is $[\text{———}CH_2CHPhCH_2\overset{-}{C}HPh.\overset{+}{L}i]$, the extinction coefficient of the polystyryl ion was determined by analysis of the solution for lithium. The results are shown in Table I.

TABLE I

Extinction coefficient of lithium polystyryl salt

[Li], moles/liter $\times 10^4$	ϵ, $\times 10^{-4}$
2.61	1.32
6.07	1.28
7.14	1.33
8.53	1.27

To confirm that each butyllithium molecule initiated one polymer molecule, the molecular weights of three of the polymers from the kinetic experiments were determined viscometrically using a viscosity – molecular weight relationship determined using monodisperse polystyrenes (4). The conditions of preparation were such that the initiation reaction was completed rapidly compared with the propagation reaction, and the three polymers could be expected to have a low $\bar{M}_w/\bar{M}_n$ ratio. The molecular weights calculated from the butyllithium and total styrene concentrations, assuming no chain transfer, are compared with the experimental values in Table II. The first two polymers were terminated by methanol, the third by exposure to air. The last entailed two separate additions of styrene.

TABLE II

Molecular weights of polystyrenes

[Lithium butyl], moles/liter $\times 10^4$	[Styrene], moles/liter $\times 10^2$	Molecular weight	
		Calculated	Experimental
3.11	13.9	46,700	48,000
1.07	3.48	33,900	35,000
0.45	3.57	82,700	84,000

Can. J. Chem. Downloaded from www.nrcresearchpress.com by 210.87.254.42 on 09/05/12
For personal use only.

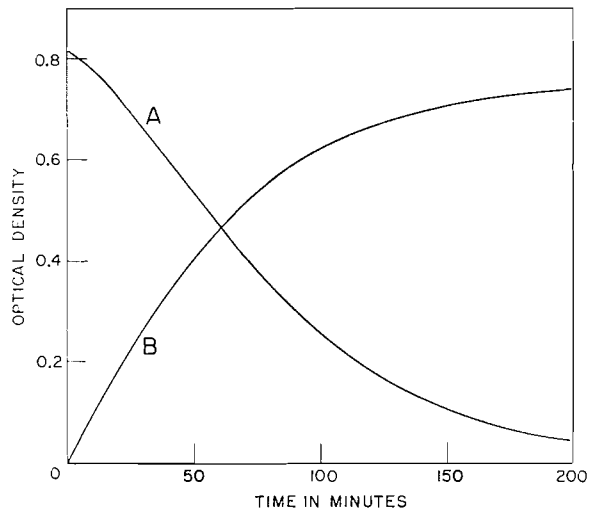


FIG. 2. Typical reaction curves of initiation reaction.
A. Disappearance of styrene measured at 291 mμ.
B. Appearance of polystyryl ion at 335 mμ.
Initially, [styrene] = 1.39×10^{-2} moles/liter; [butyllithium] = 1.10×10^{-3} moles/liter.

The reagent consumption curves of a typical initiation reaction are shown in Fig. 2.

The initial rates of formation of the colored species were determined from the plots of optical density versus time. The plots are usually not strongly curved and the initial tangent could probably be drawn with an accuracy of 5% or better. The results are shown in Table III.

Consideration of the first section suggests that the rate of formation of polystyryl

TABLE III
Initiation of styrene by butyllithium

[BuLi], moles/liter $\times10^4$	[Styrene], moles/liter $\times10^3$	Initial rate, moles/liter min^{-1} $\times10^6$	Initial rate / [Styrene] $\times10^4$	k_1, $liters^{1/6}$ $mole^{-1/6}$ min^{-1} $\times10^3$
6.07	27.6	11.4	4.14	1.42
6.65	7.67	3.14	4.09	1.38
7.14	6.73	2.86	4.25	1.42
8.09	3.50	1.57	4.50	1.47
6.68	2.83	1.23	4.35	1.46
6.65	7.67	3.14	4.09	1.38
60.0	9.23	5.30	5.74	1.35
388.	8.75	6.76	7.73	1.32
22.2	4.96	2.41	4.87	1.35
11.8	27.4	12.6	4.60	1.42
11.0	13.9	6.63	4.78	1.49
2.61	19.4	6.93	4.60	1.42
0.93	1.85	.581	3.14	1.48
0.675	2.73	.725	2.66	1.32
0.166	1.88	.324	1.73	1.08
0.155	2.28	.292	1.28	0.81

Can. J. Chem. Downloaded from www.nrcresearchpress.com by 210.87.254.42 on 09/05/12
For personal use only.

anions is first order in styrene, the second section shows the rate to increase very slowly with butyllithium concentration. A plot of $\log_{10}$ (initial rate/[styrene]) against $\log_{10}$ [butyllithium] is relatively insensitive at such low orders, but appears to give $0.155 \pm 10\%$ for the order with respect to the butyllithium for concentrations between 5×10^{-5} M and 4×10^{-2} M (Fig. 3). This is close to an order of 1/7 or 1/6, and for convenience, and with

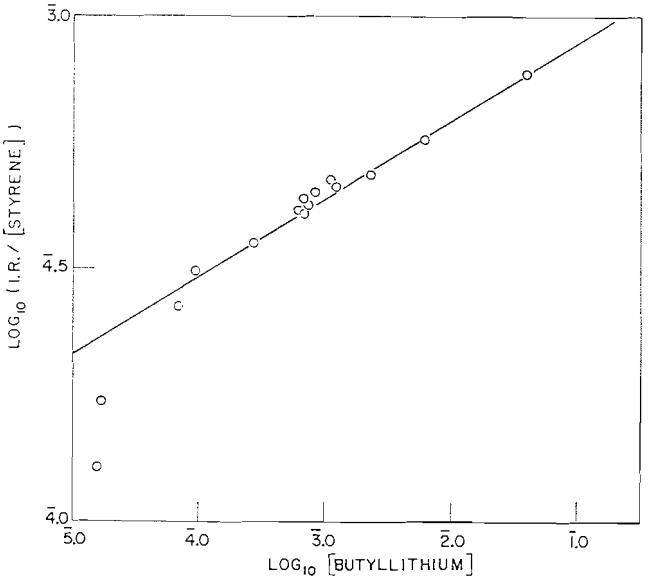


FIG. 3. Dependence of initiation rate on butyllithium concentration.

some theoretical justification the latter figure has been used subsequently. The two runs at concentration below 2×10^{-5} M showed deviation from this behavior, their rates being too low.

Plotting initial rate/[lithium butyl]$^{1/6}$ against [styrene] for the seven runs with butyllithium concentration between 6×10^{-4} M and 1.2×10^{-3} M gives a good straight line over the range of styrene concentration 3×10^{-3} M to 3×10^{-2} M (Fig. 4). Thus the over-all expression for the initial rate of formation of polymer chains, or consumption of butyllithium is given by

$$d\,[\text{butyllithium}]/dt = -k_1\,[\text{butyllithium}]^{1/6}\,[\text{styrene}]$$

and the values of k_1 calculated for individual kinetic experiments are given in Table III.

If sufficient monomer were present, the optical density at 335 mμ would increase to a maximum and then remain constant, at which point it was assumed that all the butyllithium had reacted to form active chains. The propagation reaction, once all the chains had been initiated, was followed by the consumption of the residual monomer, or by the consumption of further bulbs of styrene broken into the reaction mixture. Here, of course, the method of initial rates could not be used. The rate of consumption of monomer, however, followed a first-order course over a matter of at least four half-life times, at which point the precision of the analysis was the limiting factor. A logarithmic plot of this first-order rate against the initial butyllithium concentration (equal to the number

Can. J. Chem. Downloaded from www.nrcresearchpress.com by 210.87.254.42 on 09/05/12
For personal use only.

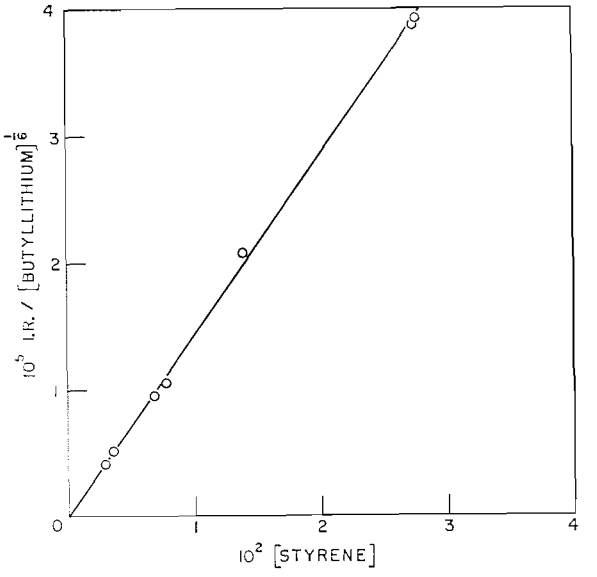


FIG. 4. Dependence of intiation rate on styrene concentration.

of polystyryl ions present) showed a good half-order dependence of the rate on the butyllithium concentration (Fig. 5). The kinetic equation for the propagation reaction is then

$$d\,[\text{styrene}]/dt = -k_2\,[\text{styrene}]\,[\text{butyllithium}]^{1/2}.$$

The temperature dependence of the initiation reaction was found to correspond to an apparent activation energy of 18,000 calories, that of the propagation reaction to 14,300

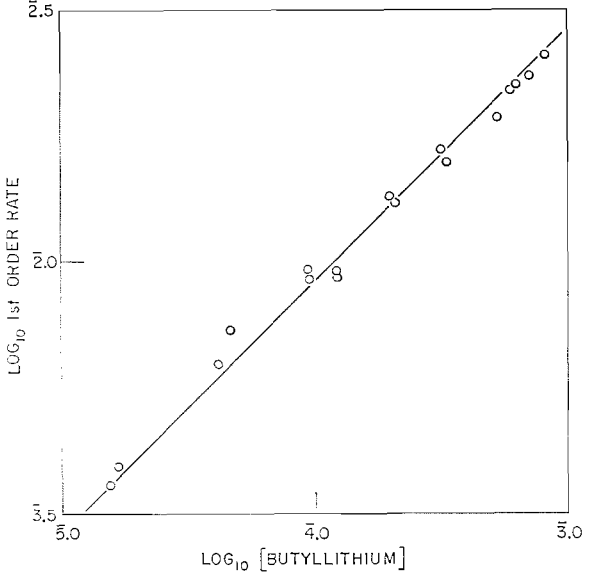


FIG. 5. Dependence of propagation rate on butyllithium concentration.

Can. J. Chem. Downloaded from www.nrcresearchpress.com by 210.87.254.42 on 09/05/12
For personal use only.

calories, for the temperature range 10.0°–30.3°. The appropriate mean rate constants calculated assuming the same kinetics apply at the lower temperatures are shown in Table IV. The half-order dependence on the butyllithium concentration of the first-order disappearance of monomer in the pure propagation reaction was confirmed at all four lower temperatures, but not the orders of the initiation step.

DISCUSSION

The absorption band of the lithium polystyryl compound in benzene with a maximum at 334 mμ is very similar to the absorption band of the similarly prepared compound in tetrahydrofuran, which has a maximum at 340 mμ and extends rather more into the visible region. The absorption bands of the lithium compounds cut off much more sharply than do the absorption bands of the sodium and potassium polystyryl salts in tetrahydrofuran which have a maximum at 343 mμ and extend so far into the visible region to give their solution a red color, whereas the lithium salts are yellow. All the bands are sufficiently similar to suppose that they are due to the same species, the polystyryl anion, somewhat modified by the environment composed of the solvent and gegenion. The integrated area under the band of the lithium polystyrene salt in benzene, extrapolated where it is lost in the bands of polystyrene, has about 85% of the corresponding area of the sodium compound in tetrahydrofuran. If the arguments of Evans *et al.* (5) concerning similar bands of carbonium ions are valid, this would suggest that the ionic nature of the C—metal bond is very little reduced in changing to the less favorable conditions of dielectric constant and alkali metal ion. There was no change in the optical density of solutions at 335 mμ in the temperature range 10° to 30°, suggesting that there is no temperature-dependent equilibrium between ionic and nonionic forms in this range.

The most straightforward schemes that can be suggested to explain the kinetics found for the reaction of butyllithium with styrene are as follows:

$$\text{Initiation}\begin{cases}(\text{Li Bu})_6 \rightleftharpoons 6\ \text{Li Bu} & [1]\\ \text{Li Bu} + \text{styrene} \rightarrow \text{Bu(M)}_1^-\ \text{Li}^+ & [2]\end{cases}$$

$$\text{Propagation}^*\begin{cases}(a)\begin{cases}[\text{Bu (M)}_n^-\ \text{Li}^+]_2 \rightleftharpoons 2\text{Bu(M)}_n^-\ \text{Li}^+ & [3]\\ \text{Bu (M)}_n^-\ \text{Li}^+ + \text{styrene} \rightarrow \text{Bu(M)}_{n+1}^-\ \text{Li}^+ & [4]\end{cases}\\ (b)\begin{cases}\text{Bu (M)}_n^-\ \text{Li}^+ \rightleftharpoons \text{Bu(M)}_n^- + \text{Li}^+ & [5]\\ \text{Bu (M)}_n^- + \text{styrene} \rightarrow \text{Bu(M)}_{n+1}^- & [6]\end{cases}\end{cases}$$

The subscript 6 applied to the butyllithium aggregate is probably an average.

A strong argument in favor of the first propagation scheme can be made on the basis of the behavior in the sodium naphthenide catalyzed polymerization of α-methylstyrene in tetrahydrofuran. Here the propagation step is close to first order in initiator (6). Conductivity measurements on the sodium polystyryl salt (3) indicate that it exists largely in the form of ion pairs in this solvent. Both facts suggest that the ion pair is the reactive species in this solvent. Molecular weight determinations in boiling ether (7) suggest that lithium benzyl and lithium phenyl exist in the form of dimers so presumably lithium polystyryl would be expected also to be dimerized in solvents of low dielectric constant. The heat of dissociation of the dimer $(\text{Bu(M)}_n^-\text{Li}^+)_2$ would have to be in this

**In the first scheme (a) it is assumed that the reaction is due solely to ion pairs in equilibrium with ion pair dimers, and in the second scheme (b) it is due solely to the extremely low concentration of free ions which are in equilibrium with the ion pairs. The equilibria 1, 3, and 5 are normally predominantly on the left-hand side of the equations.*

Can. J. Chem. Downloaded from www.nrcresearchpress.com by 210.87.254.42 on 09/05/12
For personal use only.

case somewhat over 10 kilocalories as the apparent activation energy of the propagation step (14,300 calories) would be composed of its heat of dissociation and the actual activation energy of the propagation step. The latter is presumably low as was the case in tetrahydrofuran solution. A heat of dissociation of this magnitude is not incompatible with the apparent high stability of alkyl and aryl lithium complexes in solutions of low dielectric constant. On the other hand, similar arguments applied to the second propagation step infer a similar heat of dissociation of the ion pair into kinetically free ions. This appears to be much too low for this process in benzene solution.

The activation energy of the initiation step of 18,000 calories would consist of an activation energy and a dissociation energy of the same type. The activation energy of attack of the comparatively covalent butyllithium on styrene would be expected to be higher than that of the propagation step, thus allowing a similar heat of dissociation of butyllithium. One difficulty which applies to the initiation scheme is the great dilutions at which the butyllithium aggregates must remain in the form of hexamers. The experimental results suggest no significant breakdown above a concentration of 5×10^{-5} M. Several studies of the degree of association of ethyllithium and butyllithium in ether and benzene by measurement of freezing point depression or boiling point elevation (8, 9, 7) have indicated a value of about six in the concentration range down to 1/10th molar. One other study under identical conditions (10) indicated a degree of association of two. A study of the infrared spectra of ethyllithium and butyllithium (11) was interpreted to show that in benzene or hexane on dilution, the hexamer fairly rapidly dissociated to dimer and monomer in the same concentration range. Further work on this topic is obviously desirable before adequate comment can be made on the low order of the initiation step with respect to butyllithium.

An attempt can be made at analysis of the system for the over-all disappearance of monomer during the period which both consecutive reactions are occurring. Whatever the detailed mechanism, the kinetic scheme may be written

$$C+M \rightarrow M_1^- \quad \frac{d[\mathrm{M}^-]}{dt} = k_1[\mathrm{C}]^{1/6}[\mathrm{M}]$$

$$M_n^- + M \rightarrow M_{n+1}^- \quad \frac{d[\mathrm{M}]}{dt} = -k_2[\mathrm{M}^-]^{1/2}[\mathrm{M}]$$

where $[\mathrm{M}^-] = \Sigma[\mathrm{M}_n^-]$, using the rate constants shown in Table IV.

TABLE IV

Summary of rate constants

Temp., °C	$k_1\times10^4$, liters$^{1/6}$ mole$^{-1/6}$ min^{-1}	k_2, liters$^{1/2}$ mole$^{-1/2}$ min^{-1}
30.3	14.0	0.929
25.0		0.563
20.0	4.68	0.387
15.0		0.265
10.0	1.45	0.155

The complete solution of the differential equations of consecutive, competing reactions is only available for the simplest of cases, and not for this particular case. It is possible to obtain a partial solution by eliminating the variable time, leaving C and M as the variables, and also with the simplification of ignoring monomer consumption in the

Can. J. Chem. Downloaded from www.nrcresearchpress.com by 210.87.254.42 on 09/05/12
For personal use only.

initiation stage. Then by treating the resultant equation as two separate binomial series it is possible to obtain

$$[M_0-M] = \frac{k_2}{k_1} C_0^{4/3}\left(\frac{2}{3}\left[\frac{M^-}{C_0}\right]^{3/2}+\frac{1}{15}\left[\frac{M^-}{C_0}\right]^{5/2}+\frac{1}{36}\left[\frac{M^-}{C_0}\right]^{7/2}+\frac{91}{5832}\left[\frac{M^-}{C_0}\right]^{9/2}\cdots\right)$$

for $0 \leqslant M^- < C_0$

and

$$[M_0-M] = \frac{k_2}{k_1}C_0^{4/3}\left(\frac{6}{5}\left[\frac{C_0-M^-}{C_0}\right]^{5/6}-\frac{6}{22}\left[\frac{C_0-M^-}{C_0}\right]^{11/6}-\frac{6}{136}\left[\frac{C_0-M^-}{C_0}\right]^{17/6}-\frac{6}{368}\left[\frac{C_0-M^-}{C_0}\right]^{23/6}\cdots\right)$$

for $0 < M^- \leqslant C_0$.

The latter expression converges more rapidly than the first, but taking the first part for $0 \leqslant M^- \leqslant C_0/2$ and the second for $C_0 \geqslant M^- \geqslant C_0/2$, only four terms or less are necessary to evaluate either.

From these equations it should be possible to plot $[M_0-M]$ against the computed values of the right-hand side for values $[M^-/C_0]$ in the initiation reaction, and thus evaluate k_2/k_1 from the resultant straight lines. This was done whenever possible and the value of k_2/k_1 at 30.3° for eight of the runs was 522, compared with 665 obtained from the k_1 of the initial rates, and the k_2 of the pure propagation reaction. Again at the lowest butyllithium concentration the ratio was abnormal being twice the mean, and not included in the the mean.

The discrepancy between the two values of k_2/k_1 is probably no more than the experimental error, but it could be due to the excess butyllithium complexing with the propagating species and depressing the rate, as was suggested by Tobolsky (1). This would lower the k_2/k_1 ratio obtained under conditions where both reactions were occurring simultaneously. But for the reaction with the highest concentration of lithium butyl (3.88×10^{-2} moles/liter), where it is in large excess (only 2% reacted whilst most of the monomer was consumed), the value of k_2/k_1 is only 30% lower than the mean, although it had the largest deviation by a factor of two. This is taken to indicate that the propagation reaction is very largely independent of the excess butyllithium, because if the kinetics were changed appreciably the equations above would not hold as well as they do.

From the form of these equations it is seen that, as is expected of a reaction with an order of less than one, the initiation reaction goes to completion at a finite monomer consumption. For any given starting butyllithium concentration, it is possible to calculate the required initial monomer concentration to ensure all the butyllithium has reacted, with the qualification that when the unreacted butyllithium concentration approaches 10^{-5} M, the kinetic scheme is no longer valid. For an initial catalyst concentration C_0 to react completely, the monomer concentration must equal $0.84\ C_0^{4/3}\ k_2/k_1$. Taking a mean value at 30° of 600 for k_2/k_1 and a value of $C_0 = 0.01$ M, the initial monomer concentration must be 1.08 M for complete reaction; for 50% of the butyllithium to react the monomer concentration must be 0.326 M. At points before all the butyllithium has reacted, it is possible to compute that the ratio $\bar{M}_w/\bar{M}_n \sim 1.28$; further consumption of monomer will decrease this ratio.

This implies that at initiator concentrations greater than 0.01 molar and using a molar solution of monomer the reaction will exhibit the combined characteristics of the initiation

Can. J. Chem. Downloaded from www.nrcresearchpress.com by 210.87.254.42 on 09/05/12
For personal use only.

and propagation reaction. It will not be possible to study the propagation reaction separately even at later stages in the reaction. Due to the low order in butyllithium the rate of styrene consumption will appear to be largely independent of initiator concentration. A semiquantitative study of the complex kinetic equations shows that the percentage conversion will be a linear function of time over a fairly wide conversion range and that the apparent order with respect to initial monomer concentration will be between one and two. Generally speaking therefore our kinetic scheme is compatible with the results of O'Driscoll and Tobolsky (1) even though we have postulated a different propagation step and the absence of chain termination.

A comparison with the paper of Welch (2) is somewhat more difficult. Although he claims to have followed the propagation reaction only, it seems from the analysis given above that his highest concentration reactions were performed under such conditions that he could not free the propagation reaction from the initiation reaction by his experimental procedure. This is supported by the appearance of his typical first-order polymerization plot at the highest concentration, which curves in a way that would be predicted. The apparent change to zero order in butyllithium at concentrations above 0.02 M could well be due to the reasons outlined above. It should be noted, however, that our experiments do not show that a decrease in order of the propagation reaction at these concentrations does not occur, as all the kinetic runs on this reaction were conducted well below them. In fact such a decrease in order is quite possible as higher aggregates are likely to form in more concentrated solutions, although the measurements of Wittig *et al.* (7) did not show this.

The first-order dependence found by Welch for the propagation step on lower concentrations of butyllithium is at variance with the half order found in this work. The reason for this probably lies in the different methods of analysis for active chain ends. The optical method used here is simpler and more direct than that used by Welch since he calculated the butyllithium concentration from the viscosity of the polymer produced. Although the method of Welch is basically sound, it would require a far more rigorous technique to be truly effective. This Welch demonstrated when, using as he described extreme precautions in his procedure, he found agreement with the molecular weight–viscosity relationship of Szwarc *et al.* (12), who noted a discrepancy of a factor of about two between it and the true relationship. By picking individual points from the graph in the paper of Welch, it is possible to calculate the rate constants to fit the kinetic equation in this paper, and it is found that they are generally about 25% lower than the constant found at 20° here. Although his results for the lower half of his concentration range show considerable scatter, they are a reasonable extension of the half-order dependence on butyllithium.

REFERENCES

1. K. F. O'Driscoll and A. V. Tobolsky. J. Polymer Sci. **35**, 259 (1959).
2. F. J. Welch. J. Am. Chem. Soc. **81**, 1345 (1959).
3. D. J. Worsfold and S. Bywater. J. Chem. Soc. In press.
4. J. M. Cowie, D. J. Worsfold, and S. Bywater. Trans. Faraday Soc. In press.
5. A. Bentley, A. G. Evans, and J. Halpern. Trans. Faraday Soc. **47**, 711 (1951).
6. D. J. Worsfold and S. Bywater. Can. J. Chem. **36**, 1141 (1958).
7. G. Von Wittig, F. J. Meyer, and G. Lange. Ann. **571**, 167 (1951).
8. F. Hein and H. Schramm. Z. physik. Chem. **151**, 234 (1930).
9. T. L. Brown and M. T. Rogers. J. Am. Chem. Soc. **79**, 1859 (1957).
10. K. B. Piotrovsky and M. P. Ronina. Doklady Akad. Nauk S.S.S.R. **115**, 737 (1957).
11. A. N. Rodionov, D. N. Shigorin, T. V. Talalaeva, and K. A. Kocheshkov. Izvest. Akad. Nauk S.S.S.R. **22**, 1110 (1958).
12. R. Waak, A. Rembaum, J. D. Coombes, and M. Szwarc. J. Am. Chem. Soc. **79**, 2026 (1957).

Can. J. Chem. Downloaded from www.nrcresearchpress.com by 210.87.254.42 on 09/05/12
For personal use only.

HYDROGEN BONDING IN THE AMINE HYDROHALIDES

III. NEAR-INFRARED SPECTRA OF ALIPHATIC AMINE HYDROHALIDES[1]

P. SAUVAGEAU AND C. SANDORFY

ABSTRACT

The first overtones of the $\overset{+}{N}H_n$ (n = 3, 2, or 1) stretching fundamentals are very weak and difficult to locate. Binary combinations between $\overset{+}{N}H_n$ stretching and $\overset{+}{N}H_n$ bending vibrations and also $\overset{+}{N}H_n+CH_n$ stretching–bending combinations fall into the 4600–4400 cm^{-1} area for primary and secondary amine hydrohalides and are much stronger. The intensity of these combination bands is not due to the anharmonicity of the potential surface but to the electrical anharmonicity of bending vibrations.

INTRODUCTION

There is a fargoing analogy between the vibrations of $\overset{+}{N}H_3$ and $\overset{+}{N}H_2$ groups on the one hand and CH_3 and CH_2 vibrations on the other and the most characteristic bands of the near-infrared spectra of both aliphatic hydrocarbons and alkylammonium ions are combinations between CH_n and $\overset{+}{N}H_n$ stretching and CH_n and $\overset{+}{N}H_n$ bending vibrations (n = 3, 2, or 1).

Let us suppose first that these vibrations are completely localized in the respective functional groups. Then, as a CH_3 group has C_{3v} symmetry, the asymmetric stretching vibrations (near 2967 cm^{-1}) will be doubly degenerate and the symmetric one (near 2872 cm^{-1}) non-degenerate. The first overtone of the former may split into two levels, belonging to irreducible representations A_1 and E because of anharmonicity. The latter will give one overtone of symmetry A_1. Transitions from the ground state to all these levels are allowed. The combination of the two stretching vibrations (E) is also allowed. Thus we expect to find four bands in the 5800 cm^{-1} area. This argument holds for the $\overset{+}{N}H_3$ group as well. For the hydrogen bonded species the asymmetric and symmetric stretching vibrations appear to be close to each other. They are also close to the stretching vibrations of the CH_3 group (1, 2, 3).

For the CH_3 bending vibrations again the asymmetrical one (near 1460 cm^{-1}) is degenerate (E) and the symmetrical one (near 1375 cm^{-1}) is non-degenerate (A_1). Thus again there are four binary combinations. The same applies to the $\overset{+}{N}H_3$ group with its bending bands lying close to 1600 and 1500 cm^{-1}.

Combinations between one stretching and one bending vibration yield certain new features. If the two asymmetrical vibrations are combined, A_1, A_2, and E states result. Transition from the ground state to A_2 is forbidden, so two bands remain. The two symmetrical vibrations would give one allowed totally symmetrical combination. The sum of the asymmetrical stretching vibration and the symmetrical bending vibration would give one level (E); the sum of the symmetrical stretching vibration and the asymmetrical bending vibration would also give one level. Together, five bands would result.

[1]*Manuscript received June 6, 1960.*
Contribution from Département de Chimie, Université de Montréal, Montréal, Qué.

Can. J. Chem. Vol. 38 (1960)

The situation is simpler for localized CH_2 or $\overset{+}{N}H_2$ vibrations. Under C_{2v} symmetry all vibrations are non-degenerate and all binary combinations between stretching and bending bands are allowed. This would yield three bands due to combinations of the stretching vibrations, one overtone for the bending vibration and two stretching–bending combinations. (As a general reference see (4).)

Analogous combinations between one $\overset{+}{N}H_n$ and one CH_n vibration are also expected to occur and could fall into the same part of the spectrum.

Interactions between individual groups in the molecule and between molecules in the crystal may split the bands and further complicate the spectrum. All intermolecular effects are much more likely to influence $\overset{+}{N}H_n$ vibrations than CH_n vibrations, as the former are affected by hydrogen bonding.

Under the resolution of our instrument, separation of all the expected bands would be impossible and we have to restrict ourselves to interpret the most conspicuous features of the spectra.

EXPERIMENTAL

The near-infrared spectra were measured by a Beckman DK-1 spectrometer, mounted with a fused-silica prism. The hydrohalides were taken in the form of hexachlorobutadiene mulls. With some of these compounds it is quite difficult to obtain spectra which are free of scattered light. For this reason no complete series of hydrochloride, hydrobromide, and hydriodide spectra could be obtained in every case.

The fundamentals were measured previously in this laboratory, using a Perkin–Elmer model 112 instrument with LiF and CaF_2 prisms.

RESULTS

Cyclohexylamine, piperidine, and triethylamine hydrohalides were chosen as representatives of aliphatic primary, secondary, and tertiary amine hydrohalides. Figures 1, 2, and 3 give the near-infrared spectra of one of the hydrohalides measured as a hexachlorobutadiene mull together with the spectrum of the related amine in liquid phase. The spectra of some other hydrohalides and of some related hydrocarbons were measured as well and will be referred to incidentally in the text. No detailed discussion of these seems to be warranted, however.

No originality is claimed for the spectra of the amines and the hydrocarbons. As to previous literature concerning them, we deem it sufficient to refer to review papers by Kaye (5) and Wheeler (6).

Tables I, II, and III summarize the fundamentals and binary combinations relevant to the discussion. Care should be exercised in considering the exact values of the frequencies of the fundamentals. There is a considerable amount of band overlapping in these spectra, especially in the 3000–2800 cm^{-1} region. Bands due to hydrogen bonded $\overset{+}{N}H_n$ groups are usually quite broad and carry several other bands atop themselves, making assignments difficult. Furthermore, it may be said because of reasons given in the introduction that the hydrohalide spectra offer many opportunities for Fermi resonance and the apparent peaks might be modified by it. Fermi resonance is very likely to occur frequently in the near-infrared spectra too, where binary combinations often coincide with ternary and

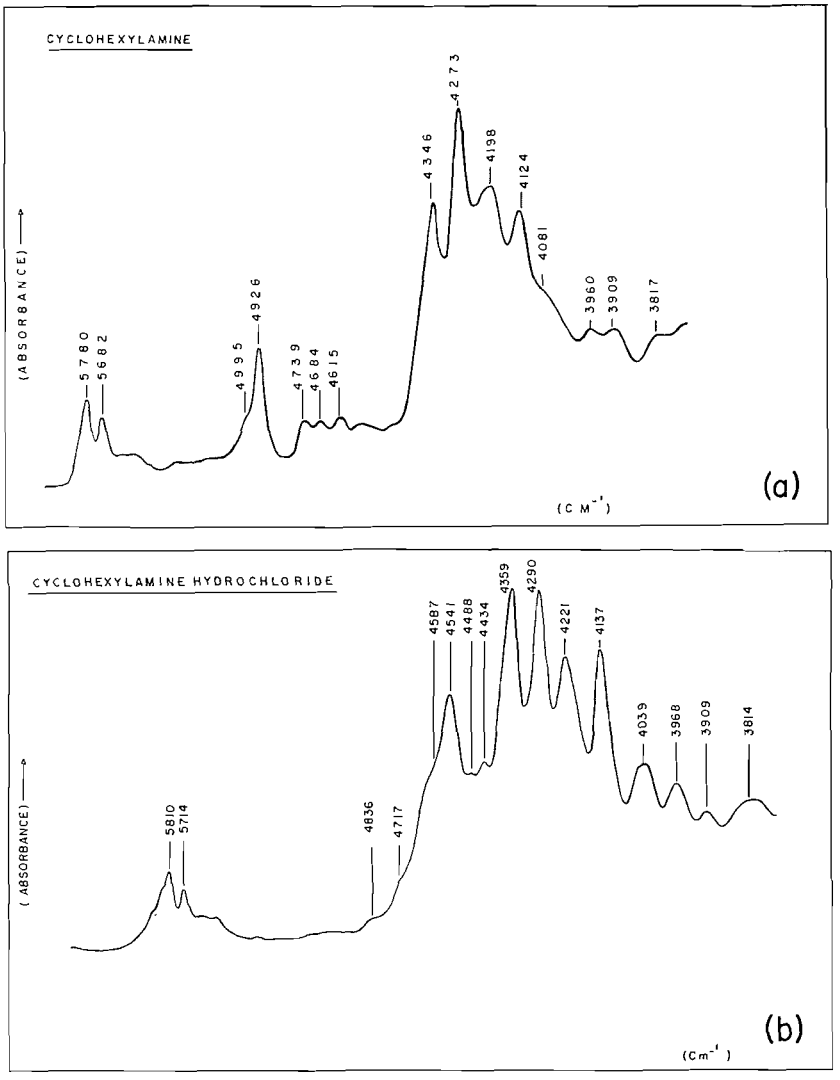


FIG. 1. Near-infrared spectra of cyclohexylamine (above) and cyclohexylamine hydrochloride (below).

other higher combinations. The tables do not contain all the observed bands, only those necessary to discuss our specific problem, the assignment of the first $\overset{+}{N}H_n$ overtones, the $\overset{+}{N}H_n$ stretching plus $\overset{+}{N}H_n$ bending combinations, and the analogous $CH_n+\overset{+}{N}H_n$ combinations. They should be regarded together with the respective figures. Intensities are given by usual symbols. Capital letters are used for the fundamental region, lower case letters for the overtone region. There is a factor of about 100 between the two scales. A "very strong" overtone would be considered as "weak" (at most) on the scale applied to the fundamentals. Indexes *a* and *s* stand for asymmetrical and symmetrical respectively.

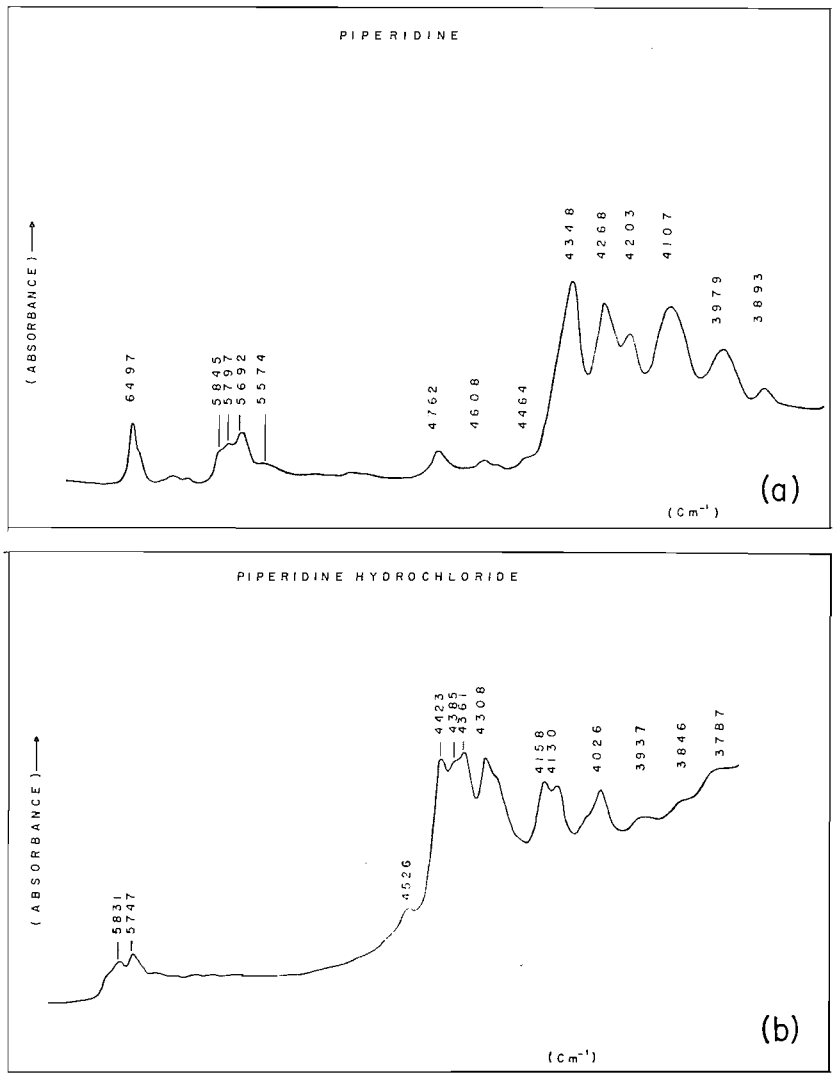


FIG. 2. Near-infrared spectra of piperidine (above) and piperidine hydrochloride (below).

DISCUSSION

G. and L. Herzberg examined the near-infrared spectrum of methyl iodide in the vapor state and established the main features pertaining to the methyl group (7). (For other methyl halides see ref. 4, p. 312.) The near-infrared spectra of liquid paraffins exhibit similar characteristics. There is a series of strong bands between 4400 and 4000 cm^{-1} due to combinations between a CH_n stretching vibration from the 2900 cm^{-1} area and a CH_n deformation vibration. These bands are much stronger than the first overtones of the stretching vibrations which are near 5800 cm^{-1}. In methyl iodide (7) the shift of the latter bands from the sum of the observed fundamentals is of the order of 40 to 50

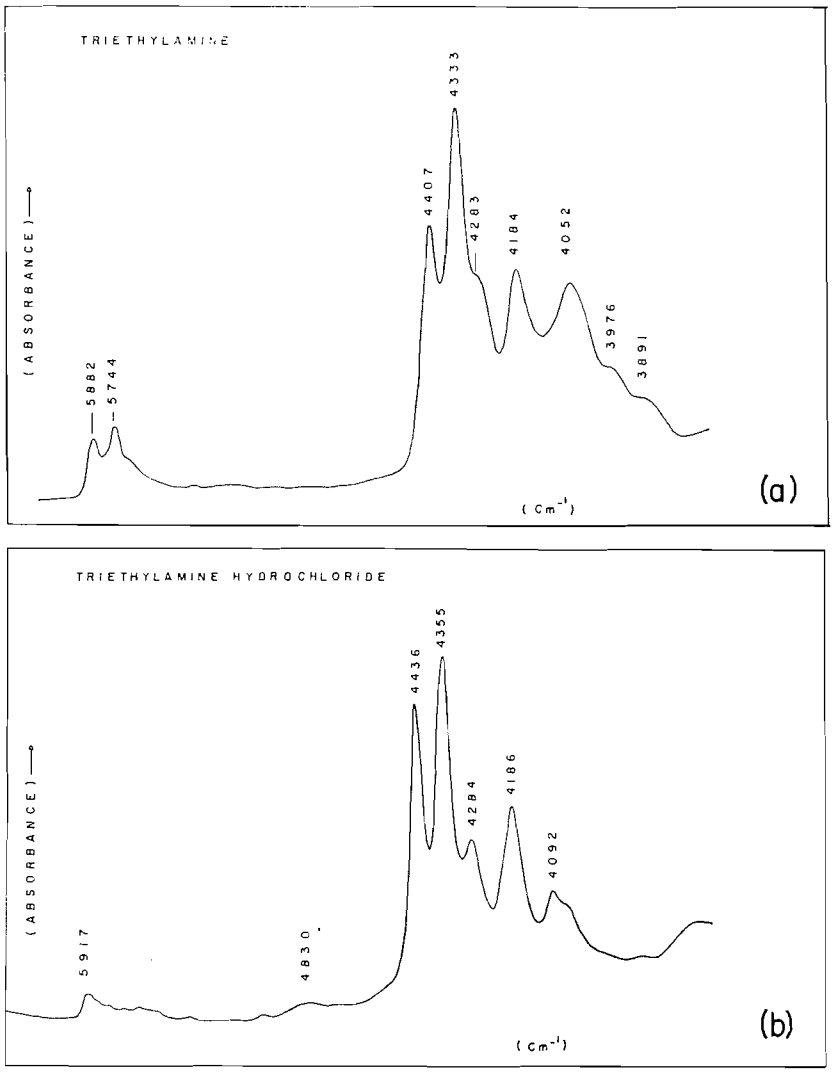


FIG. 3. Near-infrared spectra of triethylamine (above) and triethylamine hydrochloride (below).

cm^{-1}, while for the former it is only of the order of 10 to 30 cm^{-1}. This is related to the expected higher mechanical anharmonicity of the stretching vibrations but it also shows that the relatively high intensity of the combination tones in the 4400–4000 cm^{-1} area is not due to mechanical anharmonicity or, in particular, to high anharmonicity constants between stretching and bending vibrations. Therefore, electrical anharmonicity of the bending vibrations involved should explain the higher intensity of these bands.

It is important that no strong band appears above about 4400 cm^{-1} in saturated hydrocarbons. In the hydrohalides these CH_n stretching+CH_n bending summation bands

TABLE I

	Cyclohexane		Cyclohexylamine		Hydrochloride		Hydrobromide		Hydriodide	
	cm^{-1}	I	cm^{-1}	I	cm^{-1}	I	cm^{-1}	I	cm^{-1}	I
$\nu_a(\overset{+}{N}H_3)$					2980	VS	2996	VS	3011	VS
$\nu_s(\overset{+}{N}H_3)$										
$\nu_a(CH_2)$	2923	VS	2915	VS	2934	VS	2932	VS	2935	S
$\nu_s(CH_2)$	2951	S	2846	S	2859	S	2857	S	2855	M
$\delta_a(\overset{+}{N}H_3)$					1620, 1618		1609, 1601		1594, 1588	
					1615, 1610	W	1591	W		M
$\delta_s(\overset{+}{N}H_3)$					1505, 1498	M	1497, 1490	M	1487, 1483	M
$\delta(CH_2)$	1453	M	1451	S	1458	M	1457	M	1457	Several weak bands
$2\nu(\overset{+}{N}H_3)$					Probably 6000 to 5800			w	broad	
$2\nu_a(CH_2)$	5780	w	5780	w	5810	w	5817	w	5848	w
$\nu_a(CH_2)+\nu_s(CH_2)$	5692	w	5682	w	5714	w	5717	w	5747	w
$\nu_a(\overset{+}{N}H_3)+\delta_a(\overset{+}{N}H_3)$					4587	sh	4593	s	4591	s
					4541	s	4541	s	4525	s
$\nu_a(CH_2)+\delta_a(\overset{+}{N}H_3)$					4488	w	4476	w	4484	sh
$\nu_a(\overset{+}{N}H_3)+\delta_s(\overset{+}{N}H_3)$					4434	w	4424	sh	4464	sh
$\nu_a(CH_2)+\delta(CH_2)$	4344	s	4346	s	4359	s	4363	s	4357	s
$\nu_s(CH_2)+\delta(CH_2)$	4277	s	4273	s	4290	s	4288	s	4288	s
$2\delta_a(\overset{+}{N}H_3)$					3223	s	3203	s	3181	s
$\delta_a(\overset{+}{N}H_3)+\delta_s(\overset{+}{N}H_3)$					3112	s	3096	s	3078	s

TABLE II

	Piperidine		Hydrochloride		Hydrobromide	
	cm^{-1}	I	cm^{-1}	I	cm^{-1}	I
$\nu_a(\overset{+}{N}H_2)$			2944	VS	2944	VS
$\nu_s(\overset{+}{N}H_2)$						
$\nu_a(CH_2)$	2928	VS	2925	VS	2926	S
$\nu_s(CH_2)$	2851	S	2843	S	2837	S
$\delta(\overset{+}{N}H_2)$			1593	M	1590	M
$\delta(CH_2)$	1468, 1454		1464, 1461		1463, 1457	
	1444, 1437	M	1455	M	1449, 1437	M
$2\nu(\overset{+}{N}H_2)$			Probably 6000 to 5800			w, broad
$2\nu_a(CH_2)$	5797	w	5831	w	5845	w
$\nu_a(CH_2)+\nu_s(CH_2)$	5692	w	5747	w	5747	w
$\nu_a(\overset{+}{N}H_2)+\delta_a(\overset{+}{N}H_2)$			4526	w	4519	w
$\nu_a(\overset{+}{N}H_2)+\delta(CH_2)$			4423	s	4419	s
$\nu_s(CH_2)+\delta(\overset{+}{N}H_2)$			4385	sh	4382	sh
$\nu_a(CH_2)+\delta(CH_2)$	4348	s	4361	s	4357	s
$\nu_s(CH_2)+\delta(CH_2)$	4268	s	4308	s	4305	s

TABLE III

	Triethylamine		Hydrochloride		Hydrobromide		Hydriodide	
	cm^{-1}	I	cm^{-1}	I	cm^{-1}	I	cm^{-1}	I
$\nu(\overset{+}{N}H)$			2600	VS	2668	VS	2760	VS
$\nu_a(CH_3)$	2967	S	2972	S	2962	M	2964	S
$\nu_s(CH_3)$	2874	M	2878	M	2877	M	2873	M
$\nu_a(CH_2)$	2930	S	2935	VS	2929	S	2932	VS
$\nu_s(CH_2)$	2798	S						
$\delta(\overset{+}{N}H)$			1446	M	1435	M	1424	M
$\delta_a(CH_3)$	1464	M	1476	M	1474	M	1464	M
$\delta_s(CH_3)$	1380	S	1399	M	1398	M	1399	M
$\delta(CH_2)$	1453, 1443	M	1480	M	1476	M	1468	M
$2\nu_a(CH_3)$	5882	w	5917	w	5917	w	5920	w
$\nu_a(CH_3)+\nu_s(CH_3)$	5744	w	sh		sh		sh	
$2\nu(\overset{+}{N}H)$			4830?	w, broad				
$\nu_a(CH_3)+\delta_a(CH_3)$	4407	s	4436	s	4425	s	4425	s
$\nu_a(CH_3)+\delta(CH_2)$	4333	vs	4355	s	4348	vs	4348	s
$\nu_a(CH_3)+\delta_s(CH_3)$	4283	sh	4284	m	4264	m	4274	m

are sometimes found as high as 4430 cm^{-1}. We shall not discuss here ternary and higher combinations.

Cyclohexylamine Hydrohalides

In liquid cyclohexylamine (Fig. 1) the 4400–4000 cm^{-1} and the 5800 cm^{-1} areas are very similar to what they are in the spectra of the hydrocarbons and must be due mainly to binary combinations of CH_n vibrations. A medium strong band at 4926 cm^{-1} (with a shoulder at about 4995 cm^{-1}) represents the expected NH_2 stretching+NH_2 bending combinations. Combinations between NH_2 stretching and CH_2 bending vibrations can explain the weaker bands at 4739, 4684, 4615 cm^{-1}. The first NH_2 overtone is at 6502 cm^{-1} (not shown in the figure).

A conspicuous new feature in the spectrum of cyclohexylamine hydrochloride is a strong band at 4541 cm^{-1} with several shoulders and weaker bands at 4488 and 4434 cm^{-1} (Fig. 1).

The asymmetrical $\overset{+}{N}H_3$ stretching band near 2980 cm^{-1} and the asymmetrical $\overset{+}{N}H_3$ bending band near 1615 cm^{-1} are very probably split by removal of their degeneracy, and their frequencies are modified by Fermi resonance with other close-lying bands. Instead of the bending band we actually find a group of four bands at 1620, 1618, 1615, and 1610 cm^{-1}.

Table I contains the fundamentals and the main binary combinations down to about 4300 cm^{-1} with the proposed assignments. The main contributor to the 4600–4500 cm^{-1} absorption is very likely the asymmetrical $\overset{+}{N}H_3$ stretching+asymmetrical $\overset{+}{N}H_3$ bending combination (or combinations). The second largest contribution appears to come from the CH_2 stretching+$\overset{+}{N}H_3$ asymmetrical bending combinations. Minor contributions may come from many other combinations.

In other instances there are two well-defined peaks in this area:

Cyclohexylamine	hydrochloride	4587 sh	4541
	hydrobromide	4593	4541
	hydriodide	4630 sh	4525
		4591	
Tertiary butylamine	hydrochloride	4625 sh	4505
		4575	
	hydrobromide	4625	4484
		4566	
	hydriodide	4612	4468
		4570	
		4535	
Ethylamine	hydrochloride	4598	4525
	hydrobromide	4619	4525
	hydriodide	4617	4521

No one is a single band. This is clearly seen in the case of tertiary butylamine hydriodide where the higher frequency band is split into three well-distinguishable bands.

The value of the 4600–4500 cm^{-1} area for the identification of *primary* amine hydrohalides should be emphasized.

We have to look now for the first overtones of (and combination between) the $\overset{+}{N}H_3$ stretching vibrations. No significant band appears, however. One explanation may be that they coincide with the CH_3 and CH_2 overtones. This is how Waldron (1) interpreted the near-infrared spectrum of methylamine hydrochloride.

Assigning the 4600–4500 cm^{-1} bands to the stretching overtones (and not to the stretching–bending combinations as we did) does not seem to be reasonable. We measured the spectrum of 1.28 *M* ethanol in carbon tetrachloride. The associated OH stretching fundamental is at 3360 cm^{-1}, its first overtone at 6329 cm^{-1}. This amounts to a shift of about 400 cm^{-1} from the sum of the fundamentals. If the overtones for $\overset{+}{N}H_3$ are at 4600 cm^{-1}, this would correspond to a shift of almost 1400 cm^{-1}.

Thus we are led to think that the $\overset{+}{N}H_3$ stretching overtones are covered by the CH_2 overtones being broad an even weaker than the latter. The weakness of the overtones and their slight anharmonic shift shows that in this case hydrogen-bonding causes only a slight increase in mechanical anharmonicity. In complete analogy with the hydrocarbons the electrical anharmonicity of the bending vibrations appears again as mainly responsible for the relatively high intensity of the combination tones. This is in line with our previous conclusions relative to the infrared spectra of amine hydrohalides (3).

Reference should be made here to papers by Russell and Thompson (8) and Moccia and Thompson (9), who stressed the importance of electrical anharmonicity for the intensity of the overtones in the case of the NH and OH groups respectively.

Piperidine Hydrohalides

In the near-infrared spectrum of piperidine (Fig. 2, Table II), the first overtone of the NH stretching vibration is at 6497 cm^{-1}, the CH_2 stretching overtones are at their usual

places, the band at 4762 cm^{-1} may be assigned to the NH stretching + NH bending summation tone (this frequency seems to be somewhat low). The weaker bands at 4608 and 4464 cm^{-1} represent probably $NH+CH_2$ combinations. The strong CH_2 combination tones do not go higher than 4348 cm^{-1}.

In the spectrum of the hydrochloride a strong new band appears at 4423 cm^{-1} (with a shoulder at 4385 cm^{-1}) which must be due to the $\overset{+}{N}H_2$ stretching + CH_2 bending combinations. There is a weak band at 4526 cm^{-1} to which the $\overset{+}{N}H_2$ stretching + $\overset{+}{N}H_2$ bending and the CH_2 stretching + $\overset{+}{N}H_2$ bending combinations must contribute.

In diethyl amine hydrohalides the band between 4600 and 4500 cm^{-1} is stronger but still much weaker than in the primary amine hydrohalides. This must be linked to the lack of degenerate asymmetrical $\overset{+}{N}H_n$ stretching and bending vibrations.

The first overtones of the $\overset{+}{N}H_2$ stretching vibrations are again apparently too weak and are hidden by the CH_2 stretching overtones.

Triethylamine Hydrohalides

In the amine itself the strong CH_n combination tone of highest frequency is at 4407 cm^{-1} and shifts to 4436 cm^{-1} in the hydrochloride. In the hydrochloride the $\overset{+}{N}H$ stretching fundamental is near 2600 cm^{-1} and the $\overset{+}{N}H$ deformation band of highest frequency is at 1446 cm^{-1}. Therefore, we would expect an $\overset{+}{N}H$ stretching + $\overset{+}{N}H$ bending summation band near 4000 cm^{-1} and the overtone of the $\overset{+}{N}H$ stretching band well below 5200 cm^{-1}. No one of them can be clearly distinguished, however (Fig. 3, Table III). There are several broad but weak bands between 5600 and 4600 cm^{-1} and the one at 4830 might well be the $\overset{+}{N}H$ stretching overtone. A look at the spectrum shows, however, that this cannot be asserted with any degree of certainty. Nor can we say whether there is a splitting due to a double well potential surface, which is a possibility here as the tertiary amine hydrohalides form significantly stronger hydrogen bonds than the primary and secondary ones (2, 3). The $\overset{+}{N}H$ stretching + bending combination should coincide with a CH_n combination band between 4100 and 4000 cm^{-1}. Actually, the shape of the latter undergoes changes due to hydrohalide formation. CH_n stretching + $\overset{+}{N}H$ bending combinations could explain a shoulder near 4370 cm^{-1} in the hydrobromide and hydriodide.

The weakness of the first overtones of the $\overset{+}{N}H_n$ fundamentals appears to be a common phenomenon for all aliphatic amine hydrohalides.

ACKNOWLEDGMENTS

We acknowledge financial help from the National Research Council of Canada and we express our thanks to Mrs. I.-R. Jegyud for assistance in the preparation of our manuscript.

REFERENCES

1. R. D. WALDRON. J. Chem. Phys. **21**, 734 (1953).
2. B. CHENON and C. SANDORFY. Can. J. Chem. **36**, 1181 (1958).
3. C. BRISSETTE and C. SANDORFY. Can. J. Chem. **38**, 34 (1960).

4. G. HERZBERG. Molecular spectra and molecular structure. Vol. II. Infrared and raman spectra of polyatomic molecules. D. Van Nostrand Co., New York. 1945. pp. 101, 126, 129, 252.
5. W. KAYE. Spectrochim. Acta, **6**, 257 (1954).
6. O. H. WHEELER. Chem. Revs. **59**, 629 (1959).
7. G. HERZBERG and L. HERZBERG. Can. J. Research, B, **27**, 332 (1949).
8. R. A. RUSSELL and H. W. THOMPSON. Proc. Roy. Soc. A, **234**, 318 (1956).
9. R. MOCCIA and H. W. THOMPSON. Proc. Roy. Soc. A, **243**, 154 (1958).

Can. J. Chem. Downloaded from www.nrcresearchpress.com by 210.87.254.105 on 09/05/12
For personal use only.

SPHERICAL AGGLOMERATION OF BARIUM SULPHATE[1]

H. M. SMITH[2] AND I. E. PUDDINGTON

ABSTRACT

The mechanical agglomeration of barium sulphate suspended in organic media into essentially spherical masses has been studied. The presence of a small quantity of water is necessary for the phenomenon to occur. This is regarded as a bridging agent that forms liquid lenses between the particles and binds them together. An equilibrium is set up for this water between the surface of the solid and the bulk suspending medium. The methods of formation of the spherical agglomerates are discussed and their properties examined.

INTRODUCTION

Flocculation of the solid constituents, which is frequently desirable to promote more rapid settling in suspension, almost invariably results in a large increase in the final volume of the sediment obtained. An exception to this general behavior was reported by Stock (1), who observed that when dried, finely divided barium sulphate suspended in dry benzene in cylindrical containers was shaken with a reciprocating motion, discrete spheres of 0.5 to 1.0 mm in diameter were formed. These settled rapidly to a volume considerably less than that obtained from an equal amount of the suspension that had not been shaken. It was tentatively suggested that the phenomenon was owing to the tendency of the hydrophilic barium sulphate to aggregate in such a way that a minimum surface was exposed to the hydrophobic benzene. Thus the phenomenon was considered to be somewhat analogous to the formation of droplets when two immiscible liquids are shaken together.

The pronounced flocculating influence of small quantities of water on suspensions of solids having hydrophilic surfaces in organic media has been frequently reported (2, 3, 4, 5). A few preliminary experiments demonstrated that the phenomenon observed by Stock (1) did not occur if the system were thoroughly dry and the present work was undertaken to ascertain the conditions necessary for the formation of spherical agglomerates with barium sulphate suspended in benzene and, if possible, to give an indication of how the technique might be applied to other systems.

EXPERIMENTAL

Procedure

Suspensions were prepared by weighing 4-g portions of pure barium sulphate directly into sample holders which were subsequently sealed to a vacuum system equipped with facilities for B.E.T. surface area measurements. The barium sulphate was freed from water by heating the samples to 200° C and reducing the pressure to about 10^{-5} mm Hg. B.E.T. surface areas (6) were determined in the usual way. The nitrogen adsorption isotherms were all of the reversible S-type, characteristic of adsorption on a non-porous solid. A known volume of benzene, usually about 20 ml, was then condensed from a doser into the sample holder and, similarly, water was added if desired in quantities from 2 mg upwards. After being sealed off, the vessel was shaken for a period of 12 hours or more. For most of the work a mechanical horizontal shaker that had a frequency of

[1]*Manuscript received May 13, 1960.*
Contribution from the Division of Applied Chemistry, National Research Council, Ottawa, Canada.
Issued as N.R.C. No. 5909.
[2]*N.R.C. Postdoctorate Fellow, 1957–59, National Research Council, Ottawa, Canada.*

4 cycles per second with a displacement of 6 cm was used. Visual observation of the specimens usually showed no further change after about half an hour but the longer shaking period was convenient and it ensured that equilibrium was reached. The sedimentation volume of the barium sulphate was determined from calibrations on the sample container. Readings were taken after the suspension had been allowed to settle under gravity for a week although little change was observed after 48 hours.

A number of qualitative experiments were also carried out using flat-bottomed, stoppered cylindrical containers in which 4 g of the barium sulphate had been dried in an oven at 200° C overnight and cooled in a vacuum desiccator. The liquids were added rapidly and the tubes quickly stoppered before they were placed in the shaker. This method enabled a wider range of systems and conditions to be studied without the tedious experimentation with the vacuum system. Blank runs were always performed in order to check against accidental contamination from the atmosphere. Twenty milliliters of the suspending liquid was normally used with 0.1 ml of bridging agent.

Water in the supernatant benzene was determined by the Karl Fischer method (7). The saturation value of water in benzene at 25° C determined in the work was 0.046% w/v. This value is the same as that calculated from the nomogram given by Davis (8) based on data determined by Jones and Taylor (9) using a tritium oxide analysis method.

Preparation of Materials

Reagent grade, thiophene-free benzene was shaken and left in contact with calcium hydride for 2 weeks. After the benzene was passed through a column containing dried silica gel, alumina, and calcium hydride into a distillation flask containing more calcium hydride, it was finally distilled into a storage vessel which had been previously dried by heating under reduced pressure. Benzene was distilled from the storage vessel into the prepared system when required.

Other organic liquids were reagent grade and dried for several weeks over anhydrous calcium sulphate before use.

Deionized water was obtained from an Amberlite MB1, mixed bed ion exchange column and placed in a small water storage flask. Dissolved gases were substantially removed from the water by evacuation of the system for 1/2 hour.

Barium sulphate was prepared from reagent grade barium chloride. The chloride was first dried at 140° C and then washed with absolute ethyl alcohol to remove traces of strontium and calcium, followed by drying again at 140° C. It was dissolved in warm water and reagent grade concentrated sulphuric acid was added with stirring. After settling, the barium sulphate was washed many times with distilled water and finally with equilibrium water. Spectrographic analysis revealed fewer impurities in the specimen than the reference material (Johnson, Matthey & Co. Ltd. spectroscopically pure barium carbonate). The purified barium sulphate was crushed in an agate mortar and passed through a 200-mesh sieve before being sealed onto the vacuum system in its container. Electron micrographs showed that the particle size was mostly in the range 0.2 to 1 micron diameter. The particles were approximately spherical but had some flat faces on them extending up to 0.5 micron in length.

RESULTS

Preliminary runs showed that no agglomeration took place when the system contained no water. With small additions of water voluminous flocs were formed after agitation but it was only with further additions of water that spherical agglomerates were apparent.

Can. J. Chem. Downloaded from www.nrcresearchpress.com by 210.87.254.105 on 09/05/12
For personal use only.

Experiments were conducted with identical 4-g portions of barium sulphate using different amounts of benzene and water to determine the distribution of water between the barium sulphate and benzene. The results are given in Table I. From the analyses of the supernatant liquid, the water associated with the barium sulphate was calculated.

TABLE I

Distribution of water between barium sulphate and benzene

Benzene used, ml	Total water added, g	Water in benzene, % w/v	Water with $BaSO_4$, g/100 g	Water in benzene / Total water
18.35	0.0049	0.013	0.0633	0.026
18.10	0.0069	0.017	0.0953	0.025
35.25	0.0110	0.016	0.1333	0.015
16.52	0.0097	0.019	0.1633	0.020
36.91	0.0219	0.041	0.1695	0.019
34.27	0.0288	0.046	0.3258	0.016
17.61	0.0231	0.046	0.3743	0.020
17.53	0.0235	0.041	0.4083	0.017

The ratio water in benzene (g/ml)/total water added (g) was found to be approximately constant below the saturation point of the benzene, the average value being 0.020.

Further experiments established the amount of water associated with the barium sulphate over the complete range of water content where flocculation and spherical agglomeration occur. Figure 1 shows the sedimentation volume of the settled barium sulphate

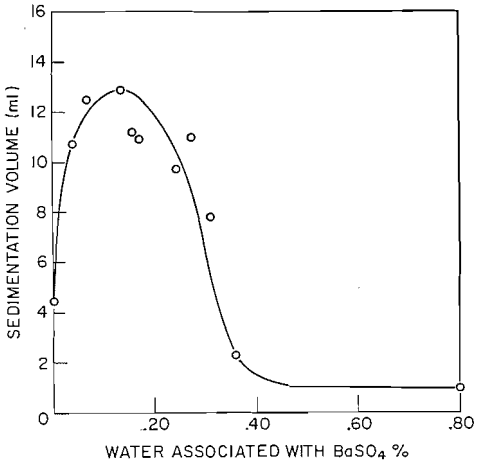


FIG. 1. The effect of water on the sedimentation volume of barium sulphate.

as a function of its water content. It is seen that, with the first additions of water, flocculation causes the settled volume to increase. On further additions the volume decreases with some of the particles forming spherical-shaped clusters. Finally, when enough water has been added, good spherical agglomerates are formed. For the area of barium sulphate considered here, 18 sq. meter/g, the necessary amount of water to form completely spherical agglomerates is 0.3125 g/100 g. If the water is less than this amount, only partial spherical agglomeration occurs. Taking the area of the water

Can. J. Chem. Downloaded from www.nrcresearchpress.com by 210.87.254.105 on 09/05/12
For personal use only.

molecule as 10.5 sq. Å, the above water is only sufficient to give an average monolayer coverage of about 60% with the specimen considered here.

Qualitative experiments were carried out using benzene to which small amounts of nitromethane, nitrobenzene, or acetonitrile were added. These three substances would not promote the spherical agglomeration without a small quantity of added water. However, since much less water was necessary under these conditions to give agglomeration, these three substances enhanced considerably the effect of the water.

Good spheres of barium sulphate were formed on agitation when the following liquids containing the appropriate amount of water were substituted for benzene: toluene, nitrobenzene, diethyl ether, chloroform, carbon tetrachloride, *n*-hexane, cyclohexane. If systems were rigorously dried, however, no agglomerates were apparent.

The effect of shaking at reduced temperatures was studied using the technique of the qualitative experiments with toluene as the suspending medium. The tubes were cooled by placing them in a copper jacket which had circulating ethylene glycol in a surrounding cooling coil. A run at $-2°$ C gave the same result as the blank shaken at room temperature with good agglomerates being formed. A run held over the range $-17°$ to $-20°$ C gave no spheres and the barium sulphate remained virtually unchanged. It is to be noted that collision of the particles probably causes the temperature at the point of impact to rise and, although the outside of the tube was kept below $-17°$ C, higher temperatures may have existed at the interfaces of colliding particles. The conclusion may be drawn from the above experiments, however, that for spherical agglomeration to occur the water must be in a liquid form and free to form the linkages between the particles.

Knacke and Pohl (10) report that in the formation of granules by standard pelletization processes, added salts in the binding liquid result in stronger granules. The increased strength was attributed to salt bridges being formed. Experiments using normal and saturated (25° C) reagent grade sodium chloride solutions in place of water gave agglomerates which appeared not to differ from the blank run where only water was used.

The effect of different modes of shaking for the production of the spheres was reviewed. Although a detailed study involving different rates of motion was not made, each method was tested under conditions which appeared most favorable for the formation of agglomerates. Reciprocating horizontal shaking as described gave the best results. Rolling end-over-end gave good agglomerates but rather smaller in size. With horizontal rolling, dense agglomerates formed which were less spherical and uniform in size than those given by the other methods of agitation. Longitudinal rocking through a circular path gave few agglomerates and these were neither spherical nor uniform in size. Vibration applied to the tube gave negative results. Apparently motion that allows the initial flocs to roll with not too much impact or shear is desirable for the densification to occur. No difference in behavior was noted when the diameter of the cylindrical glass containers was varied from 15 to 45 mm, each being filled to the same height. Rendering the surfaces of the tubes lyophobic with "dri-film" eliminated the very fine coating of barium sulphate that normally occurs. It is probable that in all the experiments with untreated tubes, the glass surface adsorbs water which binds a small amount of the barium sulphate. The amounts of water and barium sulphate involved with this effect were not important in the over-all quantitative runs, however.

When the spherical agglomerates were drained of their supernatant liquid and left to dry in the air, good free-flowing particles were obtained. They could be transferred without dusting and withstood a force of the order of 10^5 dynes before being crushed. No difference was observed when the particles were maintained for 24 hours at a pressure

Can. J. Chem. Downloaded from www.nrcresearchpress.com by 210.87.254.105 on 09/05/12
For personal use only.

of 10^{-5} mm Hg, and heating at 200° C for 24 hours at this pressure produced no visible effect.

When immersed in water, some of the dried spheres rapidly shattered but most remained unaltered. There was no change after 24 hours. This shattering was probably due to a large hydrostatic pressure being set up in any small pores present. Similar results were obtained when benzene was added to the dried spheres. It is apparent that, once formed, the spherical aggregates retain their shape when allowed to air-dry, the ultimate particles being held together by fairly strong forces.

If the barium sulphate spheres were drained of their supernatant liquid and, before they had dried, a large volume of water was added, the particles lost their spherical shape leaving a creamy suspension of barium sulphate. The bridging liquid appears to bind the particles into agglomerates by virtue of surface tension forces which disappear when the interface is removed through the addition of excess bridging liquid.

X-Ray analysis showed no detectable change in crystal structure or cell size with the formation of the spheres. It appeared, however, that the spheres were of somewhat greater crystalline perfection than the original material and thus the treatment appears to have stimulated a recrystallization or its equivalent.

Increasing amounts of water beyond the minimum necessary for spherical aggregation increases the diameter of the agglomerates. The results were somewhat erratic, however, due to differences with the initial formation. If particles group in different ways initially, a direct relationship between added water and diameter of formed spheres would not be expected. With a run in which 0.50 g of water was added, the barium sulphate formed into one sphere of approximately 1.2 cm in diameter. Further additions of water resulted in the solid adhering to the walls of the tube in a sticky mass, the spherical form of the agglomerate being lost. A continued increase of water resulted in a separate aqueous phase in which the barium sulphate remains.

Apparent density measurements on two groups of six particles, having mean diameters of 0.3 and 0.8 mm, respectively, gave values of 2.7 and 2.9 g per cc. The void volume of the spheres is therefore about 30 to 35%. The two samples, examined microscopically, were remarkably good spheres and quite uniform in diameter. A possible mechanism by which the spheres grow was suggested by the examination of a third sample, where, apparently, slightly more water was present in the system than the amount required for the compact spheres that were initially formed and sufficient excess was available to flocculate a number of these spheres into groups of two, three, or four by the Kruyt and van Selms mechanism. Further agitation had compressed these into dumbells, disks, tetrahedra, etc. in which the outlines of the original spheres were clearly visible. Obviously further mechanical action could form these into new spheres with volumes approximately simple multiples of the spheres originally formed. Were the process to be carried out on a lyophilic suspension in which the particles become partially desolvated by the bridging liquid, considerable increase in the size of the spheres might be expected with continued shaking owing to the excess of bridging liquid made available by the shrinkage of the solid.

DISCUSSION

Apparently the added small quantity of water displaces organic solvent from part of the barium sulphate surface. An equilibrium is set up between the water molecules on the barium sulphate surface and in the organic solvent. When the solid particles are brought in sufficiently close proximity by the agitation, the adsorbed water links the

Can. J. Chem. Downloaded from www.nrcresearchpress.com by 210.87.254.105 on 09/05/12
For personal use only.

particles by forming a water lens or bridge between them. With the first additions of water, the particles are held together in loose clusters, voluminous flocs being formed. However, with further additions of water more linkages are possible and with the aid of mechanical agitation the particles are able to assume a more closely packed pattern and ultimately an over-all compact, spherical shape. The flat faces of the ultimate particles may have some significance in the amount of bridging liquid necessary. As still more water is added larger spheres which require more junctions per unit volume are formed with the extra bridging liquid. Where organic liquids, along with water, act as a bridging agent, it is probable that the water promotes the adsorption of both species on the solid surface. There is, as before, an equilibrium set up with the organic suspending medium.

The barium sulphate/benzene/water system is well suited for the observation of the phenomenon. The barium sulphate has a very low solubility in both benzene and water as well as being chemically inert to both liquids. The water acting as the bridging agent has a low solubility in the benzene and in this system the benzene is saturated with water before spherical agglomerates are formed. This is not regarded as being essential to the phenomenon but depends on the relative affinities of the solid and organic medium for the bridging liquid.

Other systems meeting these requirements should show the phenomenon and the success of obtaining the spherical agglomerates will depend on how readily these factors are met.

ACKNOWLEDGMENT

Grateful acknowledgment is made to J. R. Farnand for continued help and many useful suggestions in this work.

REFERENCES

1. D. I. Stock. Nature, **170**, 423 (1952).
2. W. D. Harkins and D. M. Gans. J. Phys. Chem. **36**, 86 (1932).
3. H. R. Kruyt and F. G. van Selms. Rec. trav. chim. **62**, 415 (1943).
4. A. E. J. Eggleton and I. E. Puddington. Can. J. Chem. **32**, 86 (1954).
5. M. J. Vold. J. Colloid Sci. **14**, 168 (1959).
6. S. Brunauer, P. H. Emmett, and E. Teller. J. Am. Chem. Soc. **60**, 309 (1938).
7. K. Fischer. Angew. Chem. **48**, 394 (1935).
8. D. S. Davis. Chem. Process Eng. **38**, 341 (1957).
9. G. G. Joris and H. S. Taylor. J. Chem. Phys. **16**, 45 (1948).
10. O. Knacke and H. Pohl. Chem. Ing. Tech. **31**, 50 (1959).

Can. J. Chem. Downloaded from www.nrcresearchpress.com by 210.87.254.105 on 09/05/12
For personal use only.

Can. J. Chem. Downloaded from www.nrcresearchpress.com by 210.87.254.105 on 09/05/12
For personal use only.

A NEW SYNTHESIS OF METHYL β-D-GULOPYRANOSIDE[1]

N. J. Antia and M. B. Perry

ABSTRACT

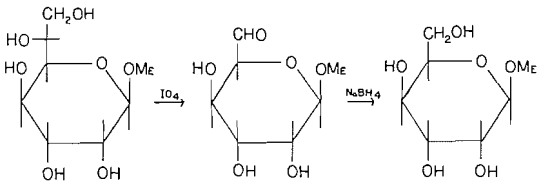
The oxidation of 1 mole of β-D-glycero-D-gulo-heptopyranoside with 1 mole of sodium metaperiodate, followed by reduction with sodium borohydride, gave rise to crystalline methyl β-D-gulopyranoside. The method provides a new synthetic route to the D-guloside and, thence, to D-gulose. The possibility of utilizing this reaction scheme as a general convenient method for preparing the relatively rare aldohexoses as well as for "labelling" carbon atom 1 of these compounds is discussed.

It was shown recently by Perry and Pietak (1) that the periodate oxidation of aldoheptoses proceeds in nearly discrete stages, with the sugars being oxidized in their cyclic forms. Consumption of the first mole of oxidant per mole was correlated with the almost exclusive scission of the C_6–C_7 (exocyclic) bond of the heptose. This observation appeared to be of great potential value for the facile synthesis of hexoses not readily available. The controlled oxidation of 1 mole of the heptose with 1 mole of periodate would be expected to yield the corresponding hexodialdose, which would require a selective reduction of the —CHO group at C_6 to give the corresponding hexose. The reduction step was considered to present insuperable difficulties and, accordingly, we turned our attention to the application of the reaction sequence to the heptosides, where such selective reduction would not be required. An analogous series of reactions was used by Foster, Davies, and Crumpton (2) in their conversion of heptose units in polysaccharides to hexose units.

Methyl β-D-glycero-D-gulo-heptopyranoside had been prepared by Fisher (3) and a proof of its pyranoside structure had been offered by Haworth, Hirst, and Stacey (4). We have prepared the heptoside by the method of the latter authors, but have found difficulty in separating it from contaminating heptose. One mole of the methyl β-D-glycero-D-gulo-heptopyranoside (I) was oxidized with 1 mole of sodium metaperiodate in unbuffered medium, and the product (II) was directly reduced with an excess of sodium borohydride. After deionization with ion-exchange resins, crystalline methyl β-D-gulopyranoside (III) was isolated in 30% yield. Attempts to isolate the guloside from the borohydride reduction reaction without recourse to resin deionization, by acetylation with acetic anhydride/pyridine or by *p*-nitrobenzoylation, failed to yield crystalline material. The D-guloside was shown (*a*) to be homogeneous, by paper chromatography in three solvent systems, and (*b*) to be identical with a sample obtained from Dr. Isbell (5, 6). The identity was established by comparison of infrared spectra and by mixed melting point determination. The pyranoside structure of the D-guloside was confirmed by periodate oxidation studies (2 moles of periodate consumed, 1 mole of formic acid liberated). Mineral acid hydrolysis of the D-guloside gave predominantly a reducing sugar identified as gulose from paper chromatographic evidence.

The synthesis reported above suggests that other heptosides may similarly be converted to the corresponding hexosides, and the method appears to offer a convenient, general, synthetic route for the conversion of heptoses to hexoses. The particular value of this synthetic method lies in (*a*) the simplicity and ease of preparation, in quantity, of the relatively rare hexoses, and (*b*) the possibility of selectively "labelling" a hexose

[1]*Manuscript received May 16, 1960.*
Contribution from the Chemistry Department, Queen's University, Kingston, Ontario.



I II III

at carbon atom 1 by starting with a *1*-C^{14}-heptose. Obviously the preparative value of the method will be governed by the ease of availability of aldoheptoses. Both classical Kiliani/Fischer cyanohydrin synthetic method (7) and the more recent nitromethane/Nef reaction scheme of synthesis (8) provide convenient preparative routes to aldoheptoses from aldohexoses. Both of these methods effect the addition of a one-carbon fragment to the carbon atom 1 of the hexose. The incoming carbon atom may be "labelled" by the use of $HC^{14}N$ or $C^{14}H_3NO_2$. In this way, a readily available hexose (e.g., D-glucose) may be converted to a *1*-C^{14}-aldoheptose (e.g., D-glycero-D-gulo-heptose) which, by the application of the synthetic scheme described above, may be further converted to the desired *1*-C^{14}-hexose (e.g., D-gulose).

EXPERIMENTAL

All melting points reported are uncorrected.

Paper chromatography was performed by the descending method on Whatman No. 1 paper, using the following solvent systems:

solvent I: 1-butanol/ethanol/water (3:1:1 v/v);
solvent II: 1-butanol/pyridine/water (10:3:3 v/v);
solvent III: ethyl acetate/acetic acid/water (9:2:2 v/v).

The following sprays were used to detect the sugars on the chromatograms: (A) 2% solution of *p*-anisidine hydrochloride in 1-butanol, (B) 1% solution of silver nitrate in acetone, followed by 2% ethanolic sodium hydroxide, and (C) saturated aqueous solution of potassium periodate followed, 6 minutes later, by benzidine reagent (9). The rate of movement of the sugars on the chromatograms is given relative to that of 2,3,4,6-tetra-*O*-methyl-D-glucose (R_{TMG}) or of rhamnose (R_{Rha}).

Methyl β-D-Glycero-D-gulo-heptopyranoside

The glycoside was prepared by refluxing D-glycero-D-gulo-heptose (m.p. 190–192°) with 3–5% methanolic hydrogen chloride for 24–48 hours. Yields of the crude crystalline product were of the order obtained by Haworth, Hirst, and Stacey (4). After two recrystallizations from alcohol, the glycoside had a melting point of 166–168°, $[\alpha]_D^{20}$ −72°±2° (*c*, 1.1 in water). Paper chromatography in solvents I and II showed the presence of a heptose. Treatment of the glycoside in aqueous solution with Dowex 1-X2(OH) (by agitation with the resin at room temperature for 20 hours, followed by passage of the solution down a column of the resin) effected removal of most of the contaminating heptose, but traces were still detectable. The treated glycoside crystallized from alcohol as colorless prisms with the same melting point and optical rotation as given above. The following R_{TMG} values were observed for the heptoside: solvent I, 0.33; solvent II, 0.35; solvent III, 0.41.

Can. J. Chem. Downloaded from www.nrcresearchpress.com by 210.87.254.105 on 09/05/12
For personal use only.

Can. J. Chem. Downloaded from www.nrcresearchpress.com by 210.87.254.105 on 09/05/12
For personal use only.

Methyl β-D-Gulopyranoside

The calculated quantity of an aqueous solution of sodium metaperiodate (49.18 ml, 0.045 *M* $NaIO_4$) was added slowly to a stirred solution of methyl β-D-glycero-D-gulo-heptopyranoside (0.4935 g) in water (25 ml) cooled to 0°. After addition was complete, the solution was agitated for 2 hours at room temperature and allowed to stand overnight. The solution was next cooled to 0°, and a solution of sodium borohydride (0.8 g) in water (25 ml) was added slowly, with mechanical agitation. The solution was agitated for 2 hours at room temperature and allowed to stand overnight. The pH of the solution was adjusted to 5 by the addition of 50% aqueous acetic acid with mechanical agitation and cooling. After 1 hour at room temperature, a test sample showed no reduction of Fehling's solution (absence of reducing sugar as well as of borohydride). The solution (160 ml) was divided into halves at this stage. One half was used for the attempted isolation of the D-guloside by (*a*) acetylation and (*b*) *p*-nitrobenzoylation. The other half was passed successively through columns of Amberlite IR-120(H) and Duolite A-4(OH) ion-exchange resins. The pH of the eluent from the latter column was ca. 3–4 and it was found necessary to deionize the solution further by passing it through Dowex 1-X2(OH) resin. This solution (pH7) was evaporated to dryness *in vacuo* and the residual boric acid was removed as methyl borate by repeated evaporation *in vacuo* with methanol. The residue was next extracted with ethanol, the ethanol-insoluble material being rejected (negative reaction to Molisch reagent). The ethanol extract (0.22 g) was taken up in boiling ethanol, allowed to cool, and ethyl acetate was added to incipient turbidity. The solution was allowed to crystallize at 0–5° for 4 days. Methyl β-D-gulopyranoside crystallized as prisms (0.065 g), m.p. 178–180°, $[\alpha]_D^{20}$ −87.9° (*c*, 1.03 in water). The mother liquors failed to yield any further crystalline product. The over-all yield of the D-guloside was ca. 30% of the theoretical. Isbell (6) has given the following constants for the D-guloside, m.p. 176°, $[\alpha]_D^{20}$ −83°. A mixed melting point determination of the D-guloside with Isbell's sample showed no depression. The infrared spectra (KBr disk) of the D-guloside samples were identical.

The attempted acetylation of the D-guloside with acetic anhydride and pyridine failed to give a crystalline product, although Isbell (5) has described a crystalline tetraacetate.

Paper chromatography of the D-guloside showed (*a*) complete absence of reducing sugars, and (*b*) a homogeneous product having the following R_{TMG} values: solvent I, 0.44; solvent II, 0.51; solvent III, 0.51.

Periodate oxidation studies: The D-guloside (19.4 mg) was oxidized at 0–4° with an aqueous solution of sodium metaperiodate (5 ml, 0.1 *M* $NaIO_4$), the total volume of the reaction mixture being adjusted to 100 ml with distilled water. Aliquots (5 ml) of the reaction mixture were taken at the time intervals stated in Table I, in order to determine the periodate consumed and the formic acid liberated. These determinations were carried out by standard methods.

TABLE I

Periodate oxidation of methyl β-D-gulopyranoside

Oxidation period, hours	Periodate uptake, moles per mole	Formic acid release, moles per mole
1	1.92	0.94
2	2.02	0.94
4	2.02	0.96
21	1.98	0.96

D-Gulose

The D-guloside (10 mg) was hydrolyzed with *N* HCl (10 ml) (refluxed for 2 hours), the mineral acid was neutralized with silver carbonate, and the product was worked up in the usual manner. No attempt was made to crystallize the D-gulose or to prepare a derivative.

Paper chromatography of the product showed the presence of a reducing sugar as the major component, along with traces of what may be 1,6-anhydro-D-gulose, oligosaccharides, and polymeric material formed by the acid treatment. The reducing sugar was identified as D-gulose by comparison of R_{Rha} values with those of D-mannose (see Table II). Thomas (10) has shown that these two sugars are virtually inseparable on paper chromatograms in the solvent systems used.

TABLE II

R_{Rha} values of some reducing sugars

Sugar	Solvent system		
	I	II	III
D-Gulose	0.54	0.52	0.74
D-Mannose	0.62	0.55	0.80
D-Glycero-D-gulo-heptose	0.41	0.31	0.69

ACKNOWLEDGMENTS

The authors wish to express their thanks to the National Research Council for financial assistance (Grant No. 706); to Dr. H. S. Isbell, National Bureau of Standards, Washington, D.C., for kindly supplying an authentic specimen of methyl β-D-gulopyranoside; and to Professor J. K. N. Jones, for his interest and advice.

REFERENCES

1. M. B. Perry and T. Pietak. The periodate oxidation of aldoheptoses. Paper presented to the Royal Society of Canada, June Meeting, Kingston, Ontario. 1960.
2. A. B. Foster, D. A. L. Davies, and M. J. Crumpton. Nature, **181**, 412 (1958).
3. E. Fischer. Ber. **28**, 1156 (1895).
4. W. N. Haworth, E. L. Hirst, and M. Stacey. J. Chem. Soc. 2864 (1931).
5. H. S. Isbell. J. Research Natl. Bur. Standards, **8**, 1 (1932).
6. H. S. Isbell. Proc. Natl. Acad. Sci. U.S. **16**, 699 (1930).
7. C. S. Hudson. Advances in Carbohydrate Chem. **1**, 1 (1945).
8. J. C. Sowden. Advances in Carbohydrate Chem. **6**, 291 (1951).
9. J. A. Cifonelli and F. Smith. Anal. Chem. **26**, 1132 (1954).
10. G. H. S. Thomas. Studies on Polyuronides. M.A. Thesis, Queen's University, Kingston, Ontario. 1956.

Can. J. Chem. Downloaded from www.nrcresearchpress.com by 210.87.254.105 on 09/05/12
For personal use only.

Can. J. Chem. Downloaded from www.nrcresearchpress.com by 210.87.254.105 on 09/05/12
For personal use only.

EXPERIMENTAL STUDIES OF SOLUTION PROCESSES

VI. EFFECT OF SOLVENT ON INFRARED ABSORPTION SPECTRA[1]

P. A. D. DE MAINE,[2] L. H. DALY, AND M. M. DE MAINE[2]

ABSTRACT

Here are reported infrared absorption data between 4000 cm^{-1} and 700 cm^{-1} near 19° C for methanol, *n*-propanol, isopropanol, cyclohexanol, benzyl alcohol, diethyl ether, anisole, 1,4-dioxane, diisopropyl ether, nitromethane, acetone, *p*-xylene, benzene, and hexane as pure substances and in carbon tetrachloride solution. Band frequencies accurate to within 1 cm^{-1} are reported. Except for the 3340 cm^{-1} band in dilute MeOH solutions no frequency shifts were observed even with gross changes of the electrical properties of the solutions. Molar extinction coefficients at absorption maxima are discussed briefly.

INTRODUCTION

During the last 5 years several workers have reported results of experimental and theoretical investigations of solvent effects on infrared absorption spectra. Excellent summaries of these data are found in Spectrochimica Acta (1, 2, 3, 4, 5) and in Annual Reports of the Chemical Society (6). Thompson (5), la Lau (4), and Bellamy (1) have shown that the Kirkwood–Bauer–Magat equation (7, 8) cannot be used to explain many frequency shifts observed for different solvents. Bellamy *et al.* (9, 10) have demonstrated that the frequency shifts observed for X—H and carbonyl stretching vibrations result from specific interactions between solute and solvent molecules.

De Maine (11) has reported that all the band frequencies for nitromethane dissolved in carbon tetrachloride do not shift even for gross changes in solution composition. However, Brown (2) has quoted the work of Bayliss *et al.* (12) as evidence that for non-polar solvents the frequency shifts appear to depend only on the dielectric constant of the solvent, as predicted by the Kirkwood–Bauer–Magat equation (7, 8).

La Lau (4) has shown that the Debye (13) or Onsager (14) equations for the integrated band intensities must be replaced by a more complicated expression which cannot be handled easily. Coulson (3) has attributed changes of the integrated band intensities with solvent to small changes in the term $\partial\mu/\partial Q$ (μ, dipole moment; Q, normal co-ordinate) which does not necessarily cause a frequency shift. Thompson (5) has quoted numerous workers to support his assertion that neither the Debye equation (13) nor the Onsager equation (14) gives a satisfactory explanation for changes in band intensities with solvent.

In this work we report band frequencies for five alcohols, four ethers, acetone, benzene, nitromethane, *p*-xylene, and hexane as pure substances and in carbon tetrachloride solution. No frequency shifts are observed even with gross changes in the composition of the solutions.

EXPERIMENTAL

Solutions were made by diluting the pure substance with carbon tetrachloride to the required volumes. Actual concentrations were calculated with density data for the pure solvents (15) as described elsewhere (16). The concentration ranges and number of samples studied are given in Table I.

[1]*Manuscript received April 11, 1960.*
Contribution from the Chemistry Department, New York State College for Teachers, State University of New York, Albany, New York.
[2]*New address: Chemistry Department, University of Mississippi, Oxford, Mississippi.*

TABLE I

Data of experiments with the solvents indicated

Compound	Source	Grade	Concentration range (moles/l.)	Cell length	No. of samples
Carbon tetrachloride	Fisher	Spectrograde	—	.028	—
Methanol	Fisher	Spectrograde	.019–24.75	.028, 5.00	36
n-Propanol	Fisher	Cert. reagent	.107–13.39	.028	13
Isopropanol	Fisher	Cert. reagent	.105–13.08	.028	13
Cyclohexanol	Fisher	Reagent	.095–12.10	.028	12
Benzyl alcohol	Fisher	Cert. reagent	.078–9.70	.028	12
Diethyl ether	Mallinckrodt	Anal. reagent	.077–9.63	.028	12
Diisopropyl ether	Eastman Kodak	Red Label	.057–7.10	.028	12
1,4-Dioxane	Fisher	Spectrograde	.094–11.70	.028	12
Anisole	Fisher	Reagent	.074–9.21	.028	12
Nitromethane	Eastman Kodak	Spectrograde	.278–18.51	.028	20
Actone	Fisher	Cert. reagent	.109–13.64	.028	11
p-Xylene	Eastman Kodak	White Label	.065–8.11	.028	11
Benzene	Mallinckrodt	Reagent	.090–11.25	.028	11
Hexane	Fisher	Spectrograde	.061–7.65	.028	11

All measurements were made with a Perkin–Elmer Model 21 double-beam infrared spectrophotometer with sodium chloride optics. Absorption by carbon tetrachloride was cancelled by use of a variable path-length cell filled with pure carbon tetrachloride in the reference beam. Base lines were obtained with both cells filled with carbon tetrachloride before each set of measurements. Samples were run starting with the most dilute and increasing the concentration of solute. The decreasing concentration of solvent was compensated for by a decrease in the path length of the cell in the reference beam.

Each sample was scanned from 4000 cm^{-1} to 700 cm^{-1}. The temperature was $19\pm2°$ C. Repeated measurements showed that band frequencies between 2000 cm^{-1} and 700 cm^{-1} could be reproduced to within 1 cm^{-1}. At higher frequencies (4000 to 2000 cm^{-1}) reproducibility was within 4 cm^{-1}. No changes in the spectra of samples were observed even after 8 hours.

RESULTS

Dielectric constants, refractive indices, and observed band frequencies for the 15 pure solvents studied are given in Table II. Except for the center of the hydrogen bond band (near 3340 cm^{-1} in pure alcohols), no measurable frequency shifts were observed for any band of any solute – carbon tetrachloride pair studied, even for large changes in the electrical properties of the solutions.

In agreement with other workers, we observed that the broad band with center near 3340 cm^{-1}, which is common to all alcohols (Table II), does not shift measurably in passing from the pure alcohol to carbon tetrachloride solutions with near 0.200 mole per liter of methanol, *n*-propanol, isopropanol, cyclohexanol, or benzyl alcohol. Figure 1 provides data for the methanol – carbon tetrachloride system. In carbon tetrachloride solutions with alcohol concentration less than about 0.200 M, the hydrogen bond band first changes shape and on further dilution, it disappears. Figure 2 illustrates these changes for methanol – carbon tetrachloride, together with the isolation of a weak band near 3640 cm^{-1} which is observed first in a 1.485 M methanol solution and which shows no measurable frequency shift on further dilution of the methanol solution with carbon tetrachloride.

Extinction coefficients at all absorption maxima were calculated for all solutions studied.

Can. J. Chem. Downloaded from www.nrcresearchpress.com by 210.87.254.105 on 09/05/12
For personal use only.

TABLE II

Dielectric constants (ϵ), refractive indices (η), and observed band frequencies for the pure liquids indicated near 20° C

CCl_4	MeOH	*n*-Propyl alcohol	Isopropyl alcohol	Cyclo-hexanol	Benzyl alcohol	Ethyl ether	Isopropyl ether	Dioxane	Anisole	Nitro-methane	Acetone	*p*-Xylene	Benzene	Hexane
975	1030	855	812	842	695	842	845	874	880	850	895	955	845	880
1002	1110	885	950	860	729	914	903	885	994	875	1085	1020	1034	900
1215	1450	901	1102	886	812	930	1010	1047	1020	917	1215	1039	1174	949
1250	2058	965	1126	924	840	1021	1106	1083	1041	1099	1359	1100	1390	980
1555	2228	1013	1158	969	906	1040	1123	1121	1075	1378	1415	1116	1480	1035
	2520	1051	1300	1025	1013	1075	1166	1254	1105	1400	1430	1180	1525	1062
	2838	1095	1340	1065	1031	1116	1186	1289	1150	1425	1710	1219	1616	1131
	2955	1232	1378	1135	1055	1150	1301	1322	1170	1565	2004	1240	1669	1170
	3340	1344	1405	1171	1076	1278	1368	1365	1180	1830	2140	1378	1746	1291
		1381	1465	1235	1205	1295	1379	1454	1245	2040	2260	1450	1810	1340
		1455	1758	1255	1300	1350	1466	1720	1286	2300	2438	1516	1967	1376
		1940	1900	1294	1330	1381	1804	1900	1301	2470	2578	1630	2210	1460
		2874	2080	1346	1380	1414	1910	1965	1335	2800	2928	1786	3040	2720
		2960	2190	1365	1455	1444	2630	2130	1390	2942	2970	1830	3080	2844
		3340	2400	1451	1495	1487	2880	2222	1440	3050	3002	1890		2960
			2657	1696	1586	1970	2936	2280	1453		3400	2100		
			2875	2660	1606	2280	2978	2572	1466		3520	2310		
			2920	2860	1704	2600	3160	2685	1496		3610	2404		
			2970	2940	1804	2858		2850	1588			2580		
			3340	3340	1874	2930		2910	1600			2724		
					1956	2970		2962	1690			2862		
					2400	3482			1765			2922		
					2865				1832			3000		
					2920				1930					
					3024				2040					
					3040				2082					
					3340				2288					
									2480					
									2540					
									2838					
									2944					
									3020					
ϵ 2.219[a]	31.20[a]	22.20[a]	17.95[a]	14.96[c]	13.10[c]	4.376[a]	—	2.235[a]	—	34.093[a]	21.45[a]	2.270[c]	2.2925[a]	1.904[a]
η 1.4104[a]	1.331[a]	1.385[a]	1.394[a]	1.466[b]	1.5396[b]	1.350[a]	—	1.420[a]	1.518[c]	1.5526[a]	1.3616[a]	1.4958[c]	1.5011[a]	1.3749[a]

[a]B. E. Conway. Electrochemical data. Elsevier Publ. Co., London. 1952.
[b]Handbook of chemistry and physics. 35th ed. Chemical Rubber Pub. Co., Cleveland. 1954.
[c]Langes Handbook of chemistry. 9th ed. Handb. Publ. Inc., Sandusky, Ohio. 1956.

Can. J. Chem. Downloaded from www.nrcresearchpress.com by 210.87.254.105 on 09/05/12
For personal use only.

Can. J. Chem. Downloaded from www.nrcresearchpress.com by 210.87.254.105 on 09/05/12
For personal use only.

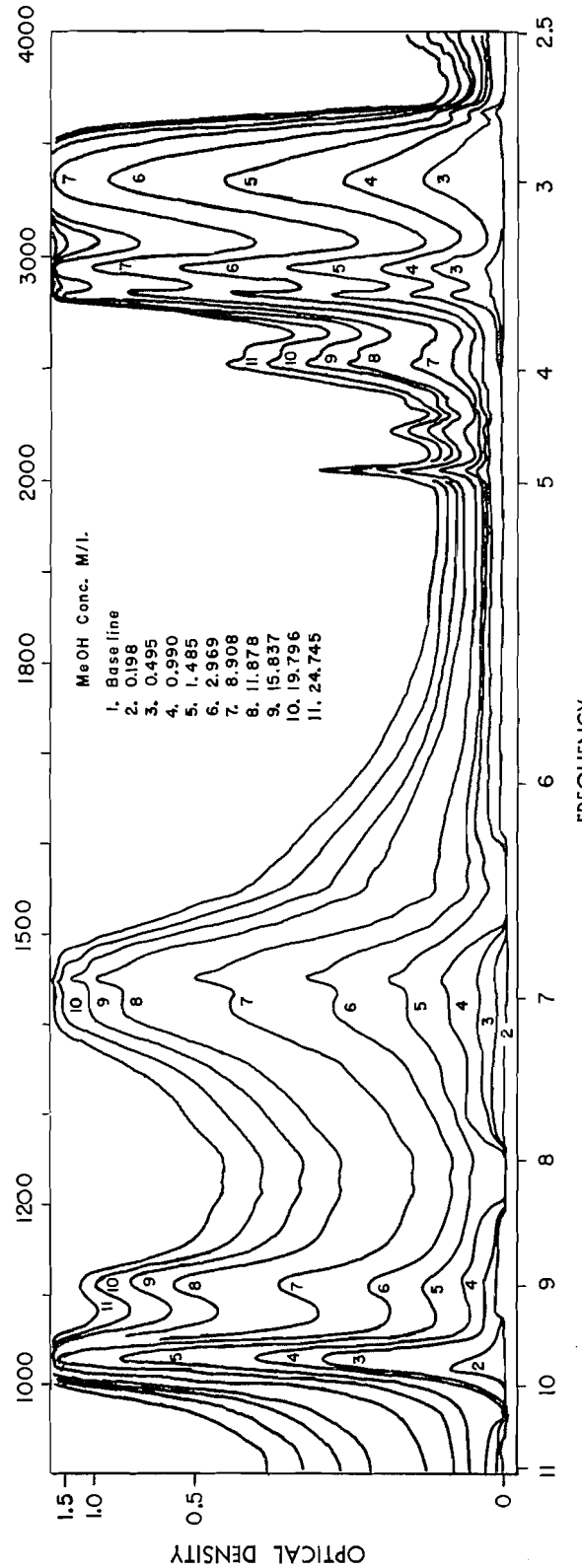


FIG. 1. Infrared absorption spectra between 800 cm^{-1} and 4000 cm^{-1} for pure methanol and for methanol dissolved in carbon tetrachloride near 19° C. Absorption by carbon tetrachloride has been subtracted. The methanol concentrations (in moles/liter) are indicated. Cell length is 0.028 mm.

Can. J. Chem. Downloaded from www.nrcresearchpress.com by 210.87.254.105 on 09/05/12
For personal use only.

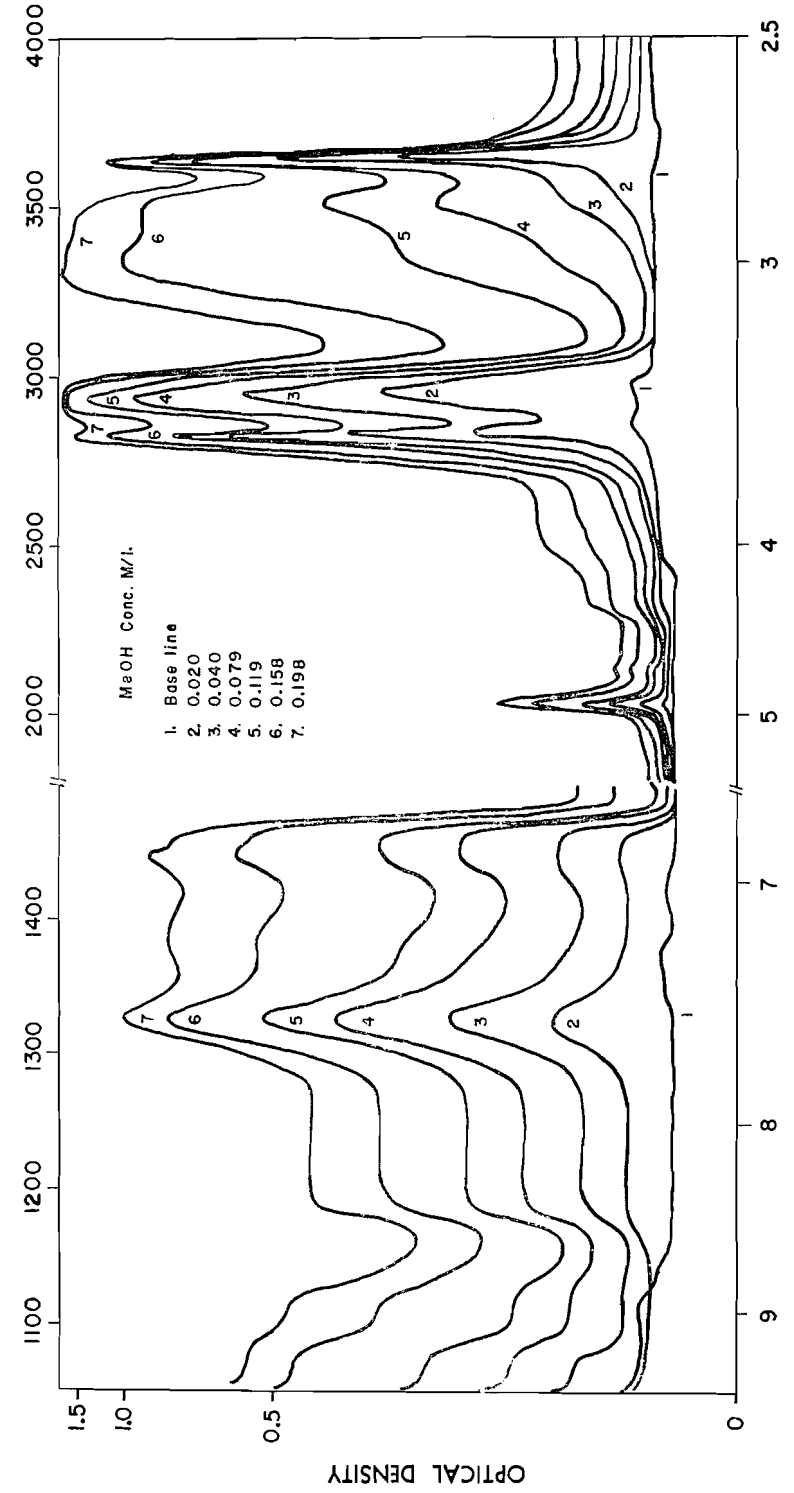


FIG. 2. Infrared absorption spectra between 1275 cm^{-1} and 4000 cm^{-1} for dilute solutions of methanol in carbon tetrachloride near 19° C. Absorption by carbon tetrachloride has been subtracted. Cell length is 5.000 mm. Methanol concentrations are indicated.

Within a 10% limit of reliability all bands between 3100 and 800 cm^{-1} for methanol, *n*-propanol, isopropanol, cyclohexanol, benzyl alcohol, nitromethane, acetone, hexane, and *p*-xylene obey Beer's law. In agreement with other workers we observed that the broad band with center near 3340 cm^{-1} (hydrogen bond band) increases with increasing alcohol concentration. This increase together with the changes in band shape reported for the dilute methanol solutions can be explained in terms of partial and reversible polymerization of alcohol molecules. The weak band with center near 3640 cm^{-1}, reported for the dilute methanol solutions, appears to obey Beer's law.

At increased concentrations of the ethers and of benzene, the extinction coefficients measured at the band centers decrease uniformly. For diethyl ether, anisole, benzene, 1,4-dioxane, and diisopropyl ether, average decreases of 50, 25, 24, 21, and 20%, respectively, were observed in the concentration range of 0.1 *M* to pure substance.

DISCUSSION

These data cannot be explained with the Kirkwood–Bauer–Magat equation (7, 8) or with any modification of this equation (17) since the band frequencies are independent of the electrical properties of the solutions. As a variety of alcohols have been examined, and as the 3340 cm^{-1} band common to all is not perturbed at alcohol concentrations greater than near 0.20 *M*, it seems that frequency shifts previously reported may arise from specific interactions between solute and solvent molecules rather than from the average electrical properties of the solution.

Inherent difficulties already described by la Lau and Thompson have prevented a thorough examination of theories which predict intensity variations with solution changes. That all the bands for alcohols (except 3340 cm^{-1}) apparently obey Beer's law, while those of the ethers and benzene do not, may be of special interest.

ACKNOWLEDGMENT

Special thanks are due to Dr. F. C. Nachod of Sterling-Winthrop Research Institute, Rensselaer, N.Y., for the loan of a variable path-length cell.

REFERENCES

1. L. J. Bellamy. Spectrochim. Acta, **14**, 192 (1959).
2. T. L. Brown. Spectrochim. Acta, **10**, 149 (1957).
3. C. A. Coulson. Spectrochim. Acta, **14**, 161 (1959).
4. C. la Lau. Spectrochim. Acta, **14**, 181 (1959).
5. H. W. Thompson. Spectrochim. Acta, **14**, 145 (1959).
6. I. M. Mills. Ann. Repts. on Progr. Chem. (Chem. Soc. London), **55**, 55 (1958).
7. E. Bauer and M. Magat. J. Phys. radium, **9**, 319 (1938).
8. J. G. Kirkwood. J. Chem. Phys. **5**, 14 (1937).
9. L. J. Bellamy, H. E. Hallam, and R. L. Williams. Trans. Faraday. Soc. **54**, 1120 (1958).
10. L. J. Bellamy and R. L. Williams. Trans. Faraday Soc. **55**, 14 (1959).
11. P. A. D. de Maine. J. Mol. Spectroscopy, **4**, 407 (1960).
12. N. S. Bayliss, A. R. H. Cole, and L. H. Little. Australian J. Chem. **8**, 26 (1955).
13. P. Debye. Handb. Radiol. **6**, 69 (1933).
14. L. Onsager. J. Am. Chem. Soc. **58**, 1496 (1936).
15. International Critical Tables. McGraw-Hill Book Co., Inc., New York. 1926.
16. P. A. D. de Maine. J. Chem. Phys. **26**, 1192 (1957).
17. D. H. Wiffen. Quart. Revs. (London), **4**, 131 (1950).

Can. J. Chem. Downloaded from www.nrcresearchpress.com by 210.87.254.105 on 09/05/12
For personal use only.

ALKALOIDS OF LYCOPODIUM FAWCETTII. PART II[1, 2]

R. H. BURNELL, B. S. MOOTOO, AND D. R. TAYLOR

β-Lofoline and fawcettiine are shown to be identical. Hydrolysis of bases from *Lycopodium fawcettii* gave rise to lycofoline and a smaller amount of an α-obscurine like base. Milder extraction procedures afford four new bases, base M, $C_{17}H_{27}NO_2$; base O, $C_{20}H_{31}NO_5$; base K, which is acetylfawcettiine, $C_{20}H_{31}NO_4$; and base N, which is diacetyllycofoline, $C_{20}H_{29}NO_4$. The isolation of fawcettiine from *Lycopodium clavatum Linn.* gathered in Jamaica is also reported.

Can. J. Chem. Downloaded from www.nrcresearchpress.com by 210.87.254.42 on 09/05/12
For personal use only.

After the initial extraction of this species (1) it was decided that a detailed study of deacetylfawcettiine was necessary and a slightly modified procedure was used to isolate this base. The stronger bases from the plant were hydrolyzed before being separated and the deacetylfawcettiine was then obtained by chromatography over alumina. These operations afforded another crystalline base, $C_{16}H_{25}NO_2$ (m.p. 140–141°), which we had not previously isolated. From the infrared spectrum and analyses it was learned that base H is an unsaturated tertiary base containing two hydroxyl groups. In a recent paper on the alkaloids of *Lycopodium annotinum* (2), Anet and Khan described an unsaturated base, lycofoline, which is identical with that described above.

Small quantities of another base which shows a great similarity to α-obscurine (3) were also obtained but insufficient material prevents a positive identification at this stage.

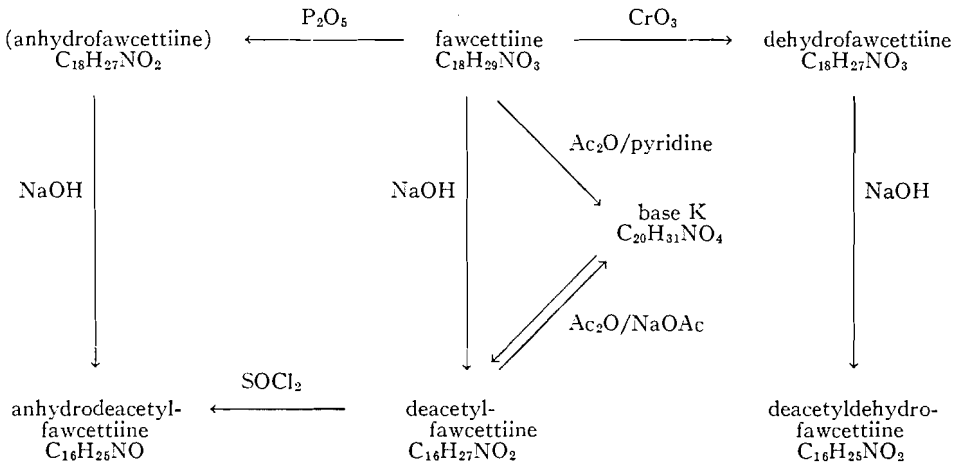
Using the procedures of Manske and Marion (4) for the extraction of lycopodiums affords an extremely dark crude product, a large portion of which proves to be intractable. We have found that cold percolation with dilute tartaric acid gives not only a cleaner, more readily purified extract but also affords a higher yield of tractable base. The new procedure gives rise to different proportions of the previously recorded bases (1) but base B (Marion's L.30 (5)) has not been found. Base E, $C_{17}H_{25}NO_2$, was not found in any quantity but a very similar substance base M, $C_{17}H_{27}NO_2$, was obtained. This base gives by far the least soluble perchlorate and can only be satisfactorily recrystallized from water. Like base E, base M shows a distinguishing ammonium band at 2000 cm^{-1} in the infrared (as does lycopodine).

The crude base from the tartaric acid extraction was distributed between chloroform and buffer in nine funnels and from this operation a significant quantity of a crystalline base (base J) was obtained. Analyses show a molecular formula $C_{18}H_{29}NO_3$ and melting point, mixed melting point, and infrared comparison have shown the substance to be β-lofoline, also reported by Anet and Khan (2). β-Lofoline perchlorate is indistinguishable from fawcettiine perchlorate in the infrared and shows the same melting point but fawcettiine had never been obtained crystalline and its perchlorate consistently analyzed for the monohydrate, $C_{18}H_{29}NO_3 . HClO_4 . H_2O$, whereas using the same conditions for drying prior to analysis, β-lofoline perchlorate analyses for $C_{18}H_{29}NO_3 . HClO_4$. However, a mixed melting point determination on the two perchlorates gave no depression, showing the two to be identical. We would like to retain the name fawcettiine for this base since it represents the major alkaloid of the species. Hydrolysis of crystalline β-lofoline gives deacetylfawcettiine (1).

Oxidation of fawcettiine with chromium trioxide gave a six-membered ring ketone,

[1]*Manuscript received June 1, 1960.*
Contribution from Chemistry Department, University College of West Indies, Jamaica, B.W.I.
[2]*Part I: Burnell, reference 1.*

dehydrofawcettiine ($C_{18}H_{27}NO_3$) which could be readily hydrolyzed to deacetyldehydrofawcettiine, $C_{16}H_{25}NO_2$, m.p. 145–147°. The more readily eliminated hydroxyl group in deacetylfawcettiine has been shown to be that present as the free hydroxyl in fawcettiine since the dehydration product from fawcettiine can be hydrolyzed to the previously obtained anhydrodeacetylfawcettiine, $C_{16}H_{25}NO$. These, and other transformations mentioned later, may be summarized:



The most highly oxygenated base isolated from *L. fawcettii*, base O (m.p. 181–182°), has the molecular formula $C_{20}H_{31}NO_5$ and from spectral and analytical results contains two O-acetyl residues and a hydroxyl group.

The greatest difference between the methanol and tartaric acid extractions was found in the weaker bases. Base F was obtained only in small amounts while two diacetate bases not previously described represented the bulk of the weak base fraction. Countercurrent distribution over 120 tubes did not completely separate these two bases and since neither crystallizes nor forms the usual crystalline salts, characterization was extremely difficult. Neither compound shows hydroxyl absorption in the infrared but both show bands corresponding to O-acetyl frequencies. Hydrolysis of one, base K ($C_{20}H_{31}NO_4$), affords deacetylfawcettiine and O-acetyl determinations show two such residues to be present in the base. Acetylation of fawcettiine with acetic anhydride and pyridine gave rise to base K, which can also be prepared from deacetylfawcettiine by refluxing in acetic anhydride containing sodium acetate.

The other diacetate weak base, present in much smaller quantity, gives rise to lycofoline on hydrolysis and the absence of hydroxyl absorption in the infrared, supported by the analogy of the other acetylated bases shown to be present in the plant, suggests that this unstable compound is represented by the formula $C_{20}H_{29}NO_4$, i.e. diacetyllycofoline.

Tartaric acid extraction of locally collected *L. clavatum* Linn. led to the isolation of fawcettiine and smaller quantities of lycopodine. Several other bases which have been obtained from this plant will be described in a future publication.

EXPERIMENTAL

All melting points are uncorrected and the infrared spectral figures are for Nujol mulls unless otherwise stated. Paper chromatography means in all cases No. 4 Whatman

Can. J. Chem. Downloaded from www.nrcresearchpress.com by 210.87.254.42 on 09/05/12
For personal use only.

paper employing pyridine, ethyl acetate, water (2.3:7.5:1.65), the bases being spotted as the hydrochlorides.

Base H *(Lycofoline)*

The stronger bases from a methanolic extraction (see ref. 1) were hydrolyzed with 5% methanolic sodium hydroxide. The base was extracted (3.9 g) and then run over a column of ethyl acetate washed alumina in benzene. Elution with 20% chloroform in benzene gave white crystals (1.0 g), m.p. 140°, a sample of which was sublimed for analysis, m.p. 141°. Calc. for $C_{16}H_{25}NO_2$: C, 73.0; H, 9.6; N, 5.3; O, 12.2. Found: C, 73.0; H, 9.4; N, 5.2; O, 12.3.

The infrared showed both absorption in the OH stretching region (3350 cm^{-1}) and a weak band due to unsaturation (1675 cm^{-1}). The trace was identical with that published for lycofoline (2) and a mixed melting point (140–141°), kindly performed by Dr. Anet, with lycofoline (m.p. 142°) showed no depression.

Base I

Elution of the column (above) with 50% chloroform in benzene afforded another crystalline base (100 mg), m.p. 300° (decomp.). The ultraviolet spectrum showed λ_{max} 252 mμ, log ϵ (based on the molecular weight of α-obscurine) 3.77. The infrared spectrum, which was not identical with that of α-obscurine, had peaks at 3480 (OH), 3200 (NH), and 1662 (lactam C:O) cm^{-1}.

Further elution of the column with chloroform gave deacetylfawcettiine (1.1 g).

Extraction of L. fawcettii with Tartaric acid

The dried, ground plant (18 kg) was percolated with 3% tartaric acid solution and the aqueous percolate then evaporated at 40° to a manageable volume. Neutral impurities were removed by ether extraction and after basification with ammonia, the crude base (28.0 g) was obtained by ether extraction. The base was shaken between chloroform and phosphate buffer, pH 5.3, in nine 1-liter separatory funnels, and the stronger bases in funnels 1–7 (12.4 g) was distributed again between chloroform and acetate buffer, pH 5.6, in a 120-tube multiple extractor. The weight curve (Fig. 1) showed three peaks but paper chromatography showed a larger number of bases to be present.

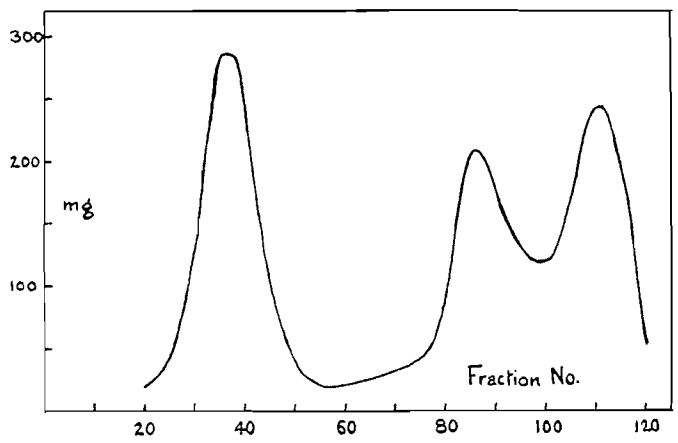


FIG. 1. Countercurrent distribution of strong bases with the system chloroform–buffer of pH 5.6.

Can. J. Chem. Downloaded from www.nrcresearchpress.com by 210.87.254.42 on 09/05/12
For personal use only.

Can. J. Chem. Downloaded from www.nrcresearchpress.com by 210.87.254.42 on 09/05/12
For personal use only.

Base A

Tubes 25-50 contained only base A (1).

The material from tubes 77–97 (3.18 g) was a mixture of three bases as shown by paper chromatography, so it was shaken between chloroform and phosphate buffer, pH 5.9, for 60 transfers. Complete separation was not obtained but from the central part of the distribution a crystalline base appeared.

Base O

The base was sublimed for analysis, m.p. 181–182°. Found: C, 65.7; H, 8.7; N, 3.9; O, 22.1; O—Ac, 23.9. $C_{20}H_{31}NO_5$ requires: C, 65.7; H, 8.6; N, 3.8; O, 21.9; $(O—Ac)_2$, 23.6. Infrared peaks at 3180 (bonded OH) and 1725 and 1235 (O—Ac) cm^{-1}.

Base M

The acetone mother liquors from base O were made slightly acidic with perchloric acid affording a sparingly soluble perchlorate, m.p. 280–282° (from water). Found: C, 54.1; H, 7.2; N, 3.8; O, 25.3; Cl, 9.3. $C_{17}H_{27}NO_2.HClO_4$ requires: C, 54.0; H, 7.4; N, 3.7; O, 25.4; Cl, 9.4. Infrared peaks at 3420 (OH), 2010 (NH), and 1692 (C:O) cm^{-1}.

The third base in this fraction is as yet uncharacterized.

The material (4.18 g) from the third peak of the first distribution (tubes 99-120, Fig. 1) was shown to contain one major and one minor component by paper chromatography, other than smaller amounts of the bases found in the second peak. Distribution between chloroform and phosphate buffer, pH 7.4, gave a central peak fraction containing the major base (2.33 g), which crystallized from an acetone solution.

β-Lofoline (*Fawcettiine*)

The base was sublimed for analysis, m.p. 172–173°. Calc. for $C_{18}H_{29}NO_3$: C, 70.3; H, 9.5; N, 4.6; O, 15.6; active H, 0.33. Found: C, 70.4; H, 9.6; N, 4.5; O, 15.8; active H, 0.34. Infrared peaks at 3470 and 3100 (OH) and at 1730 and 1710 (C:O) cm^{-1}. In carbon tetrachloride solution the infrared spectrum showed only weak hydroxyl absorption and only one carbonyl band at 1733 cm^{-1}.

The methiodide was prepared in methanol, m.p. 293–296°. Calc. for $C_{19}H_{32}NO_3I$: C, 50.8; H, 7.2; N, 3.1; I, 28.2; N—Me, 3.2. Found: C, 51.1; H, 7.2; N, 3.2; I, 28.4; N—Me, 3.0.

The perchlorate was recrystallized from acetone, m.p. 272–275°. Calc. for $C_{18}H_{29}NO_3.HClO_4$: C, 53.0; H, 7.8; N, 3.4; Cl, 8.7. Found: C, 53.2; H, 7.5; N, 3.4; Cl, 8.5. Mixed melting point with fawcettiine perchlorate (m.p. 272-275°) gave no depression.

Hydrolysis of β-Lofoline

β-Lofoline (175 mg) was hydrolyzed in methanolic sodium hydroxide giving white solids (160 mg), m.p. 207–208°. A sublimed sample gave an infrared spectrum identical with that of deacetylfawcettiine, and admixture with an authentic sample caused no lowering of the melting point.

Anhydrodeacetylfawcettiine from Fawcettiine

Excess phosphorus pentoxide was added to fawcettiine (100 mg) in dry benzene and the mixture gently refluxed for 6 hours and then allowed to stand at room temperature overnight. The mixture was poured into cold water, and the solution was then made basic with solid sodium carbonate and the organic base removed by extraction with carbon tetrachloride. The pale oil obtained could not be made to crystallize nor could the perchlorate be obtained crystalline so the product was sublimed and then hydrolyzed

Can. J. Chem. Downloaded from www.nrcresearchpress.com by 210.87.254.42 on 09/05/12
For personal use only.

in ethanolic sodium hydroxide. The base, extracted with chloroform after dilution of the reaction mixture with water, gave a crystalline hydrochloride showing an infrared spectrum superimposable on that of anhydrodeacetylfawcettiine hydrochloride (1).

Dehydrofawcettiine

Fawcettiine (530 mg) in pyridine (8 ml) was added to excess chromium trioxide / pyridine complex prepared in the usual manner. After 1 hour at room temperature, the reaction mixture was poured into water, made strongly basic with ammonia, and extracted with chloroform. The chloroform solution was extracted with 10% hydrochloric acid, which was then basified with ammonia and re-extracted with chloroform giving a dark brown oil (300 mg) which showed, in addition to unchanged fawcettiine, another spot of greater R_f on paper. The crude product was chromatographed on ethyl acetate washed alumina and afforded, in the benzene eluate, a colorless oil (220 mg) which solidified on standing. The solid was sublimed, m.p. 134–137°. Found: C, 71.0; H, 9.4; N, 4.5; O, 15.5; C—Me, 9.4. $C_{18}H_{27}NO_3$ requires: C, 70.8; H, 8.9; N, 4.6; O, 15.7; $(C—Me)_2$, 9.8. Infrared peaks at 1700 (six-membered ring ketone) and 1725, 1240, and 1220 (O—Ac) cm^{-1}. No absorption in the hydroxyl region.

The methiodide was recrystallized from methanol/acetone, m.p. 267–268° (inserted at 240°).

Deacetyldehydrofawcettiine

Dehydrofawcettiine (120 mg) was dissolved in methanol (5 ml) and a solution of sodium hydroxide (1 g) in methanol (3 ml) and water (5 ml) was added. After 6 hours at room temperature, the solution was diluted with water and extracted with chloroform, yielding a white solid which after sublimation, melted over the range 145–147°. The acetate peaks were absent in the infrared spectrum but both hydroxyl (3080 cm^{-1}) and carbonyl bands (1708 cm^{-1}) were present. The substance was characterized as the methiodide prepared from the base (20 mg) in methanol (10 ml) and recrystallized from methanol/acetone, m.p. 308–309° (inserted at 240°). Found: C, 50.0; H, 7.0; N, 3.6; I, 31.8. $C_{16}H_{25}NO_2.CH_3I$ requires: C, 50.4; H, 7.0; N, 3.5; I, 31.3.

Acetylfawcettiine

Fawcettiine (100 mg) was acetylated in acetic anhydride/pyridine at room temperature for 12 hours. The product was sublimed to remove traces of pyridine and a white semisolid (m.p. ca. 110°) was obtained. In the infrared the substance showed no hydroxyl absorption but could not be crystallized from any solvent. A portion was sublimed for analysis, m.p. 116–117°. Found: O—Ac, 25.4. $C_{20}H_{31}NO_4$ requires: $(O—Ac)_2$, 24.6. Mixed melting point, paper chromatography and identical infrared spectra show acetylfawcettiine to be base K (see below).

Weak Bases

The weak base from the nine-funnel distribution (11 g) was distributed between chloroform and acetate buffer, pH 3.2, for 120 transfers. The first 27 tubes contained neutral material (1.96 g) and no significant quantities of base were encountered until tubes 52–78 (0.75 g) containing base N and 84–102 (1.91 g) mostly base K.

Base N

This substance failed to crystallize or form crystalline salts. It was not completely stable to sublimation but showed only one relatively slow-moving spot on paper. Hydrolysis (of tube 52) in methanolic sodium hydroxide for 24 hours at room temperature gave

a solid base which sublimed readily, m.p. 140°. Comparison of the infrared spectrum of the hydrolysis product with that of lycofoline showed them to be identical and a mixed melting point confirmed this. The infrared spectrum of base N shows no hydroxyl peak but a broad carbonyl band 1725–1740 cm^{-1} with complementary absorption at 1235 cm^{-1}. A shoulder at 1660 cm^{-1} is due to the carbon–carbon double bond.

Base K

The material (1.91 g) was run over alumina in benzene giving a white solid which solidified after sublimation, showed homogeneity on paper, but did not crystallize from solvents. The base was resublimed for analysis, m.p. 117°. Found: O—Ac, 24.7; N, 3.8. $C_{20}H_{31}NO_4$ requires: $(O—Ac)_2$, 24.6; N, 4.0. Infrared absorption at 1725 (C:O) and a broad peak at 1240 cm^{-1}.

Hydrolysis of base K gave an almost quantitative yield of deacetylfawcettiine as shown by the infrared spectrum, m.p. 207° and mixed melting point 207°. Base K was the major product when deacetylfawcettiine was acetylated in refluxing acetic anhydride containing sodium acetate.

Extraction of L. clavatum Linn.

Through the dried, ground plant material (4.5 kg) was percolated aqueous 3% tartaric acid solution until no alkaloid could be detected using a potassium iodide/platinic chloride spray. The crude base (7.5 g) was obtained as described earlier and then distributed between chloroform and phosphate buffer, pH 5.3 (25 transfers). Three distinct fractions were obtained, tubes 20–25 (fraction A, 2.89 g) containing one main strongly basic component. Tubes 5–19 were combined (fraction B, 1.71 g) as were tubes 1–4, but this last fraction has not been investigated further.

Fawcettiine

Fraction A (2.18 g) was distributed between chloroform and phosphate buffer, pH 7.17 (20 transfers), and from the weight curve and paper chromatography it appeared that tubes 9–15 contained a single component. The perchlorates obtained from these tubes were combined and recrystallized from acetone/ether, m.p. 271–275° (500 mg). Mixed melting point and infrared comparison showed this derivative to be fawcettiine perchlorate.

Lycopodine

Fraction B (1.71 g) after countercurrent extraction afforded a perchlorate, m.p. 281–282° (550 mg). The infrared spectrum and no depression in the melting point on admixture with an authentic sample showed this to be lycopodine perchlorate.

ACKNOWLEDGMENTS

The authors express their thanks to Dr. F. A. L. Anet, Ottawa, for performing the mixed melting points and one of the authors (D. R. T.) wishes to acknowledge financial support in the form of a Postgraduate Scholarship from T. Geddes Grant Ltd., Kingston, Jamaica.

REFERENCES

1. R. H. Burnell. J. Chem. Soc. 3091 (1959).
2. F. A. L. Anet and N. H. Khan. Can. J. Chem. **37**, 1587 (1959).
3. B. Moore and L. Marion. Can. J. Chem. **31**, 952 (1953).
4. R. H. F. Manske and L. Marion. Can. J. Research, B, **24**, 57 (1946).
5. G. S. Perry and D. B. MacLean. Can. J. Chem. **34**, 1189 (1956).

Can. J. Chem. Downloaded from www.nrcresearchpress.com by 210.87.254.42 on 09/05/12
For personal use only.

Can. J. Chem. Downloaded from www.nrcresearchpress.com by 210.87.254.5 on 09/05/12
For personal use only.

SYNTHÈSES D'ACIDES AMINOBUTYRIQUES

1. ACIDES ALKYLAMINO-2 AMINO-4 BUTYRIQUES[1]

RÉAL LALIBERTÉ ET LOUIS BERLINGUET

ABSTRACT

The syntheses of eight 2-alkylamino-4-aminobutyric acids are described. The starting material is 4-butyrolactone, which is opened with potassium phthalimide to give 4-phthalimidobutyric acid. After bromination the 2-bromo-4-phthalimidobutyric acid, obtained in excellent yield, is treated with aliphatic amines in alcoholic medium to give the desired substituted 2,4-diaminobutyric acids, which were characterized as the monohydrochlorides and the di(phenylcarbamates). Three of them cyclized easily to give the corresponding hydantoins. In the course of the reaction, substituted diamides of phthalic acid were isolated and characterized.

INTRODUCTION

Les dérivés aminés de l'acide *n*-butyrique retiennent l'attention depuis quelques années. En particulier, on connaît maintenant le rôle très important de l'acide amino-4 butyrique (GABA) (1, 2) dans le système nerveux central des mammifères et sa distribution généralisée chez tous les êtres vivants: levures (3), plantes et protéines animales (4). Des études ont aussi été faites sur les propriétés physiques et le rôle biologique de l'acide amino-2 butyrique ainsi que des acides amino-2 hydroxy-4 butyrique (5) et diamino-2,4 butyrique (6). Ces substances sont des intermédiaires normaux dans le métabolisme de quelques acides aminés. L'acide diamino-2,4 butyrique est absorbé très rapidement par la cellule intacte (7).

Vu l'importance biologique de ces composés, nous avons voulu préparer une série de dérivés N-alkylés de l'acide diamino-2,4 butyrique pour les soumettre à des essais biologiques.

La synthèse de ces dérivés présente des difficultés. Si l'on désire obtenir l'acide diamino-2,4 butyrique symétriquement substitué, on peut, en théorie, utiliser un acide butyrique dihalogéné. Mais des essais récents (8, 9, 10) montrent qu'une amination directe en position 4 est difficile à cause de réactions secondaires.

Si l'on veut obtenir l'acide diamino-2,4 butyrique substitué sur l'un des azotes, il faut, lors de la synthèse, bloquer l'atome d'azote qui doit rester exempt de substituants. Ainsi Christensen (7), en partant de dérivés *p*-toluène-sulfonyles de l'acide diamino-2,4 butyrique, a préparé quelques dérivés méthylés, soit en position 2, soit en position 4.

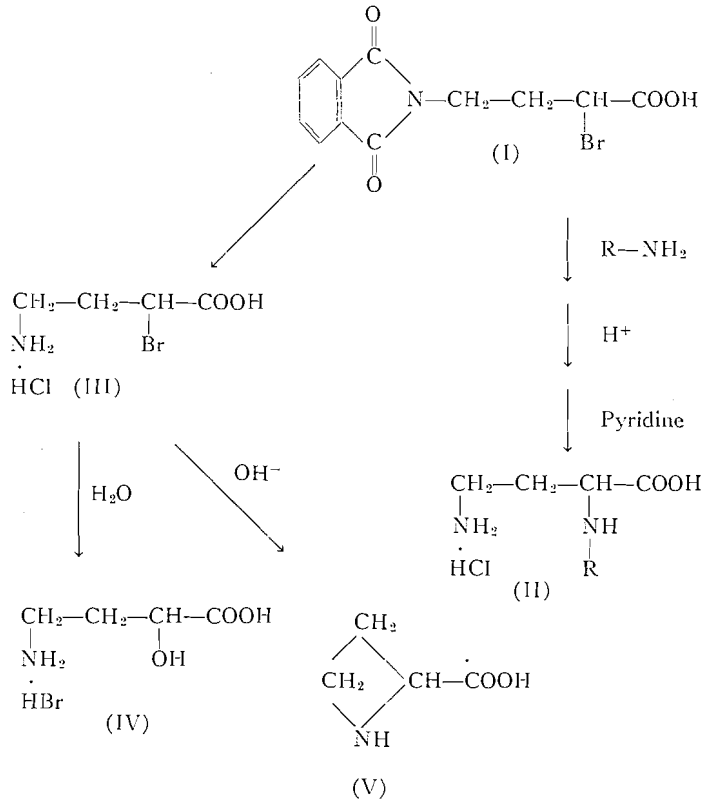
Nous avons voulu utiliser comme produit de départ une substance facilement accessible: la butyrolactone-4. Talbot, Gaudry et Berlinguet (11), Frankel (6) ainsi que Zaoral (12) ont préparé avec de bons rendements l'acide phtalimido-4 butyrique. Nous avons bromé cet acide (Zaoral) (12) en position 2, puis nous avons remplacé l'halogène par réaction avec les amines aliphatiques voulues.

La fonction amine primaire en position 4 se trouve protégée par le radical phtalimidé, lequel peut être hydrolysé une fois la réaction terminée ou peut être scindé par aminolyse lors de la réaction pour donner le diamide de l'acide phtalique.

Théoriquement, dans cette synthèse à partir de l'acide bromo-2 phtalimido-4 butyrique (I), plusieurs réactions sont possibles. Il peut y avoir amination, hydroxylation si la réaction se fait en milieu aqueux ou encore cyclisation si le groupe phtalimide est scindé.

[1]*Manuscrit reçu le 26 mai 1960.*
Contribution du Département de Biochimie, Faculté de Médecine, Université Laval, Québec, Qué.

En plus de l'acide diamino-2,4 butyrique substitué désiré (II) on peut donc avoir, comme produit de la réaction, l'acide hydroxy-2 amino-4 butyrique (IV), l'acide bromo-2 amino-4 butyrique inchangé (III) et l'acide azétidine-carboxylique-2 (V) (9).



Dans les synthèses rapportées ici, la chromatographie et l'électrophorèse sur papier nous ont permis de constater la présence, après hydrolyse des produits d'amination, d'une faible quantité d'acide hydroxy-2 amino-4 butyrique en plus de l'acide diamino-2,4 butyrique voulu. La purification de ce dernier produit se fait facilement par cristallisation dans l'éthanol.

Zaoral (12) n'a pas réussi à substituer l'atome de brome de l'acide bromo-2 phtalimido-4 butyrique par de l'ammoniaque. Nous avons repris cette réaction et, à l'aide de la chromatographie sur papier, nous avons pu mettre en évidence la présence dans ces conditions d'une grande quantité d'acide hydroxy-2 amino-4 butyrique ainsi qu'un peu des acides bromo-2 amino-4 butyrique et diamino-2,4 butyrique. Il semble qu'avec l'ammoniaque il y ait hydrolyse du groupe phtalimidé et hydroxylation en position 2 plutôt que substitution comme dans le cas des amines.

Pour favoriser l'amination nous avons condensé les amines en milieu alcoolique. Sauf dans le cas de la méthylamine et de l'éthylamine, les rendements sont meilleurs en solution alcoolique qu'en solution aqueuse.

Certaines amines sont des bases assez fortes pour couper le radical phtalimidé en milieu alcoolique. Dans ces cas on recueille, après la réaction, les diamides correspondants de l'acide phtalique. Nous avons caractérisé les diamides suivants: N,N′-dibutyl phtalamide, N,N′-dicyclohexyl phtalamide et N,N′-diisopropyl phtalamide.

Can. J. Chem. Downloaded from www.nrcresearchpress.com by 210.87.254.5 on 09/05/12
For personal use only.

La température optimum pour les substitutions semble être 20° C. Les rendements sont sensiblement les mêmes, que l'on utilise l'acide halogéné ou son ester méthylique.

Nous avons caractérisé huit nouveaux acides amino-4 butyriques portant en position 2 une fonction amine secondaire ou tertiaire. Nous en avons fait les di(phénylcarbamates) et nous avons noté que trois d'entre eux se cyclisent très facilement pour donner les hydantoïnes correspondantes.

PARTIE EXPÉRIMENTALE

Acide phtalimido-4 butyrique

On peut faire la réaction dans la diméthylformamide (Talbot, Gaudry et Berlinguet) (11) ou sans solvant (Zaoral) (12). Dans ce cas, on ajoute lentement (30 minutes) à de la butyrolactone-4 (70.0 g, 0.81 mole) maintenue entre 180° et 200° de la phtalimide de potassium (150.0 g, 0.81 mole). On chauffe le mélange pendant 30 minutes, puis on dissout la masse dans 1 litre d'eau. On ajoute alors 200 ml d'éthanol et on refroidit. L'addition lente d'acide chlorhydrique concentré accompagnée d'une forte agitation précipite l'acide phtalimido-4 butyrique. Rendement brût: 160 g (85%). Il n'est pas nécessaire de recristalliser le produit pour les manipulations suivantes, p.f. 112°–115°* (lit. p.f. 117°–118°) (13). Anal. Calc. pour $C_{12}H_{11}O_4N$: N, 6.00%. Trouvé: N, 6.31%.

Acide bromo-2 phtalimido-4 butyrique

Dans un ballon muni d'un réfrigérant, on place 62 g (0.27 mole) d'acide phtalimido-4 butyrique, 1 g de tribromure de phosphore, 1 g de phosphore rouge amorphe et 250 g (1.55 moles) de brome dissous dans 200 ml de CCl_4. On chauffe à reflux pendant 18 heures. Après avoir évaporé le solvant et l'excès de brome, on lave le solide avec du benzène. Le résidu est dissous à chaud dans l'éthanol. L'addition d'eau permet la cristallisation de l'acide bromo-2 phtalimido-4 butyrique. Rendement: 80 g (96%), p.f. 150–152°. Une seconde cristallisation dans l'acétate d'éthyle donne un point de fusion de 157° (lit. 157–158°) (12). Anal. Calc. pour $C_{12}H_{10}BrO_4N$: N, 4.5; Br, 25.6%. Trouvé: N, 4.5; Br, 25.7%.

Acides alkylamino-2 amino-4 butyriques

On place dans une fiole conique 40 g (0.125 mole) d'acide bromo-2 phtalimido-4 butyrique et 200 ml d'éthanol. À la suspension refroidie, on ajoute en agitant un excès d'amine (environ 1.0 mole). La méthylamine, l'éthylamine et la diméthylamine sont en solution aqueuse de sorte que le mélange réactionnel est un mélange eau–alcool. Les autres amines réagissent en milieu alcoolique. On laisse en contact en agitant de temps à autre. Après 5 jours, les solutions sont évaporées à sec sous vide. On hydrolyse à reflux le résidu avec 500 ml d'acide chlorhydrique concentré pendant 12 heures. En refroidissant, l'acide phtalique cristallise. Après l'avoir filtré (21 g) on évapore à sec sous vide. On dissout le dichlorhydrate de l'acide diaminé dans l'éthanol chaud. On précipite le monochlorhydrate par addition de 9 ml de pyridine. Le monochlorhydrate obtenu est recristallisé deux fois par dissolution dans 75 ml d'eau chaude et addition de 400 ml d'éthanol. Le Tableau I contient la liste des acides alkylamino-2 amino-4 butyriques préparés. Dans le cas de la diméthylamine, il faut substituer la triéthylamine à la pyridine pour isoler l'acide diméthylamino-2 amino-4 butyrique libre.

Di(phénylcarbamates) des acides alkylamino-2 amino-4 butyriques

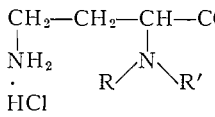
On peut caractériser les acides diaminés en les transformant en di(phénylcarbamates). Dans 5 ml de NaOH 4 *N* (0.02 mole), on dissout 1.68 g (0.01 mole) du monochlorhydrate

**Les points de fusion ne sont pas corrigés.*

Can. J. Chem. Downloaded from www.nrcresearchpress.com by 210.87.254.5 on 09/05/12
For personal use only.

TABLEAU I

Acides alkylamino-2 amino-4 butyriques



R	R′	Rendement, %	R_f‡	P.f., °C	N % Trouvé	N % Théorie	Cl % Trouvé	Cl % Théorie
—CH_3	—H	60	0.11	262–263	16.3	(16.6)	20.8	(21.0)
—C_2H_5	—H	55	0.20	277	15.2	(15.3)	19.6	(19.4)
n—C_3H_7	—H	55	0.27	280–282	14.1	(14.2)	17.9	(18.0)
iso—C_3H_7	—H	25	0.28	246–248	14.1	(14.2)	18.1	(18.0)
n—C_4H_9	—H	55	0.35	286	13.1	(13.2)	17.1	(16.8)
—C_6H_{11}	—H	80	0.36	259	11.7	(11.8)	15.0	(14.9)
—CH_3	—CH_3*	70	0.16	231–233	19.1	(19.1)	Base libre	
—C_2H_5	—C_2H_5†	30	0.28	205–206	11.3	(11.5)	28.6	(28.6)

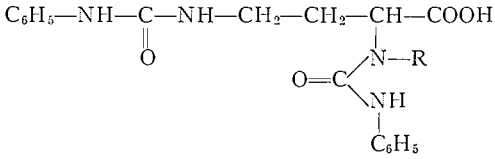
*Le monochlorhydrate a été préparé par Christensen (6), p.f. 213–215° C.
†Le dichlorhydrate cristallise lentement dans l'alcool anhydre.
‡Dans la pyridine à 80%.

de l'acide méthylamino-2 amino-4 butyrique puis on ajoute en agitant à froid 2.39 g (0.02 mole) d'isocyanate de phényle. Après avoir agité et filtré, on précipite le di(phénylcarbamate) par un excès d'acide chlorhydrique. On recristallise le produit dans un mélange d'acétone et d'éther de pétrole. Rendement: 70%.

En procédant de façon identique, on obtient les di(phénylcarbamates) des autres acides diamino-2,4 butyriques dont les constantes sont données au Tableau II. Dans

TABLEAU II

Di(phénylcarbamates) des acides alkylamino-2 amino-4 butyriques



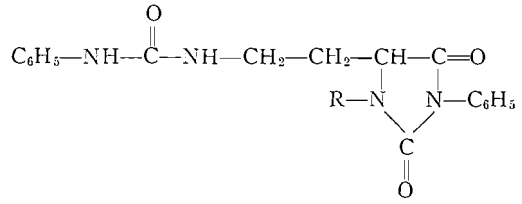
R	P.f., °C	N % Trouvé	N % Théorie
—CH_3	56–57	14.8	15.0
—C_2H_5	103	14.1	14.5
n-C_3H_7	149–150	14.0	14.0
iso-C_3H_7	102–103	13.9	14.0
n-C_4H_9	118–119	13.5	13.5
—C_6H_{11}	115	12.5	12.7

le cas des acides diamino-2,4 butyriques portant en position 2 un groupe méthyle, éthyle ou cyclohexyle, le chauffage du di(phénylcarbamate) dans l'acétone lors de la recristallisation provoque une cyclisation. On obtient alors les alkyl-1 phényl-3 hydantoïnes-5 correspondantes. Les constantes physiques de ces hydantoïnes sont données dans le Tableau III.

Can. J. Chem. Downloaded from www.nrcresearchpress.com by 210.87.254.5 on 09/05/12
For personal use only.

TABLEAU III

Alkyl-1 phényl-3 (phénylcarbamate amino-2 éthyl)-5 hydantoïnes



R	P. f., °C	N % Trouvé	N % Théorie
—CH_3	173–174	15.8	15.8
—C_2H_5	153–154	14.9	15.2
—C_6H_{11}	172	13.3	13.3

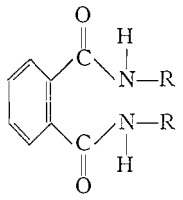
Le groupe phénylcarbamate en position 2 de la chaîne éthyle placée en position 5 du noyau de l'hydantoïne peut être hydrolysé par ébullition avec l'acide chlorhydrique concentré. On obtient ainsi le chlorhydrate de la méthyl-1 phényl-3 (amino-2 éthyl)-5 hydantoïne. On peut le cristalliser de l'alcool par addition d'éther, p.f. 227–228°. Anal. Calc. pour $C_{12}H_{16}N_3O_2Cl$: N, 15.6; Cl, 13.2%. Trouvé: N, 15.4; Cl, 13.3%.

Diamides de l'acide phtalique

Lors de la condensation de l'acide bromo-2 phtalimido-4 butyrique avec les amines primaires en solution alcoolique, il y a aminolyse du groupe phtalimidé et formation des diamides correspondants. On les isole en ajoutant à la solution 300 ml d'eau. On peut obtenir ainsi les N,N′-dibutyl phtalamide, N,N′-dicyclohexyl phtalamide et N,N′-diisopropyl phtalamide. Ces composés peuvent être recristallisés dans l'isopropanol. Leurs constantes physiques sont données dans le Tableau IV.

TABLEAU IV

Diamides de l'acide phtalique



R	P. f., °C	N % Trouvé	N % Théorie	Rendement, %
iso-C_3H_7	218	11.5	11.3	45
n-C_4H_9	103–104	10.0	10.1	90
—C_6H_{11}	253	8.6	8.5	95

Chromatographie et électrophorèse

Les acides alkylamino-2 amino-4 butyriques migrent vers la cathode à l'électrophorèse

Can. J. Chem. Downloaded from www.nrcresearchpress.com by 210.87.254.5 on 09/05/12
For personal use only.

sur papier à pH 8.6. Ils donnent une coloration pourpre à la ninhydrine. Les distances de migration (R_f) pour un mélange pyridine et eau (80:20) sont données au Tableau I.

REMERCIEMENTS

Les auteurs remercient le Conseil National de Recherches pour une bourse accordée à l'un d'eux (R. L.) ainsi que l'Institut National du Cancer pour aide financière.

BIBLIOGRAPHIE

1. F. BRÜCKE (*Editeur*). Comptes rendus des travaux du Quatrième Congrès International de Biochimie. Symposium III. Biochimie du système nerveux central. Pergamon Press, London. 1958. pp. 213–278.
2. R. A. SALVADOR et W. R. ALBERS. J. Biol. Chem. **234**, 923 (1959).
3. L. J. REED. J. Biol. Chem. **183**, 451 (1950).
4. A. I. VIRTANEN et J. K. MIETTINEN. Biochim. et Biophys. Acta, **12**, 181 (1953).
5. H. S. MUDD. J. Biol. Chem. **234**, 1784 (1959).
6. D. H. PETERSON et L. M. REINEKE. J. Biol. Chem. **181**, 95 (1949).
7. H. N. CHRISTENSEN et R. RIGGS. J. Biol. Chem. **220**, 265 (1956).
8. M. FRANKEL, Y. KNOBLER et T. SHERADSKY. Bull. Research Council Israel, A, **7**, 173 (1958).
9. L. FOWDEN. Biochem. J. **64**, 323 (1956).
10. L. BERLINGUET et R. LALIBERTÉ. Ann. Acfas, **25**, 84 (1959).
11. G. TALBOT, R. GAUDRY et L. BERLINGUET. Can. J. Chem. **36**, 593 (1958).
12. M. ZAORAL. Chem. listy, **52**, 2338 (1958).
13. S. GABRIEL et J. COLMAN. Ber. **41**, 513 (1908).

Can. J. Chem. Downloaded from www.nrcresearchpress.com by 210.87.254.5 on 09/05/12
For personal use only.

Can. J. Chem. Downloaded from www.nrcresearchpress.com by 210.87.254.105 on 09/05/12
For personal use only.

CONDUCTANCES OF AQUEOUS SOLUTIONS OF SODIUM HEXANOATE (SODIUM CAPROATE) AND THE LIMITING CONDUCTANCES OF THE HEXANOATE ION, AT 25° C AND 35° C[1]

A. N. Campbell and J. I. Friesen[2]

ABSTRACT

The equivalent conductances, densities, and viscosities of aqueous solutions of sodium hexanoate have been determined at 25° C and 35° C at concentrations ranging from 0.0003 *M* to saturation.

The limiting equivalent conductances of the hexanoate ion have been determined as 27.37±0.04 mhos at 25° C and 34.69±0.05 mhos at 35° C.

The Robinson–Stokes and the Falkenhagen–Leist equations have been applied to the data. The Robinson–Stokes equation reproduces the data within 0.7 mho up to 0.5 *M* at 25° C when $\mathring{a}$ = 13 Å. At 35° C the data are reproduced within 0.5 mho up to 0.05 *M* with $\mathring{a}$ = 10 Å. The Falkenhagen–Leist equation reproduces the data at 25° C within 0.4 mho up to 0.1 *M* with $\mathring{a}$ = 5.5 Å. An $\mathring{a}$ = 4.0 Å reproduces the 35° C data within 0.5 mho up to 0.05 *M*.

From the form of the conductance curves and from an estimation of the apparent molecular weight it was concluded that the hexanoate ion does not form ionic micelles.

This research, in which the conductances of sodium hexanoate solutions have been determined, was part of a program in which it was intended to measure the conductances of the sodium salts of the fatty acids. It was thought that, proceeding up the homologous series, the increasing size of the anions might eventually lead to a situation where the anion was essentially motionless and non-conducting. On the other hand, it was known that, after a certain number of carbon atoms in the chain is reached, micelle formation occurs and that therefore the increasing size of the anion might be to some extent counterbalanced by the increased electrical charge; hence, even the largest ions would exhibit appreciable conductance. The limiting conductances of the hexanoate ion at two temperatures were determined, from the results in very dilute solution, and the results from concentrated solutions were compared with results calculated by means of the Wishaw–Stokes (1) and the Falkenhagen–Leist (2) equations. These equations have been quoted so frequently by us that they need not be stated again here.

EXPERIMENTAL

n-Hexanoic acid was obtained from the Eastman Kodak Company and purified by redistillation. The refractive index agreed very closely with the figure given in the literature. To prepare the sodium salt the acid was neutralized with an alcoholic solution of sodium hydroxide and the solution was evaporated until the salt crystallized out. The salt was then recrystallized twice from alcohol, dried at 110° C, ground in an agate mortar, and stored in an oven at 110° C.

Attempts to determine the purity of the salt by titration with hydrochloric acid, using a Fisher titrimeter, failed. Finally, the salt was analyzed by conversion to sulphate. The method, which is crude, gave a result corresponding to 99.5% sodium hexanoate. Had the salt contained either sodium carbonate or sodium hydroxide, the result would have been high rather than low.

Solutions were prepared in two ways. For concentrations ranging from 0.02 *N* to saturation, at least 2.3 g was weighed to 0.2 mg and the resulting solution weighed to

[1]*Manuscript received May 16, 1960.*
Contribution from the Chemistry Department, University of Manitoba, Winnipeg, Manitoba.
[2]*Holder of N.R.C. Bursary, 1959–60.*

0.2 mg, if it weighed less than 120 g, or to 10 mg, if it weighed more than 120 g; all weighings were reduced to vacuum. The weight concentration was therefore known to 0.01%. Dilute solutions were prepared by successive additions of salt to a known amount of water. At least 0.02 g of salt was weighed on a microbalance to 2μg. A maximum of six additions was made so that the weight concentrations were known to 0.01%.

For the more concentrated solutions, distilled water, having a specific conductance less than 5×10^{-6} mhos/cm, at 25° C, was used as solvent. For the medium concentration range, water from a Barnstead still was first passed through an Amberlite N-3 mixed bed ion exchange resin and then "equilibrated" with the carbon dioxide of the atmosphere by shaking for at least half an hour. The specific conductance was then about $2\text{–}3\times10^{-6}$ mhos/cm, at 25° C. For the very dilute region, water from the still was purified by bubbling purified nitrogen through it for several hours. The specific conductance was then 2 to 3×10^{-7} mhos/cm.

The electrical measurements were made on a Jones bridge and all the refinements of good work were applied. The technique has been described frequently. Four conductance cells, all of the type described by Jones and Bollinger (3), were used, and they had cell constants varying from 1.4409 to 443.76.

The conductances of very dilute solutions were determined in a cell of the Shedlovsky type (4). The constant of this cell was determined with potassium chloride, using the equation of Fuoss (5)

$$\Lambda = 149.93 - 94.65\sqrt{C} + 58.74C \log C + 198.4C.$$

From this equation, Λ for KCl at 25° C can be calculated for any given low concentration. But

$$\Lambda = 1000\, A/CR$$

where R is the measured resistance of the cell and A the cell constant. In this way the cell constant for the Shedlovsky cell was found to be 0.43246. We have pointed out, in previous papers, that it is easy to show, by means of the Washburn equation (6) that the effect of temperature on cell constant is, for cells of conventional geometry, exceedingly slight. In the present case, the constant of the Shedlovsky cell changes by 0.004%, for a 10-degree rise in temperature. It is therefore quite permissible to use, at 35° C, cell constants determined at 25° C.

For the more concentrated solutions, thermostats of conventional type were used. All thermometers were calibrated against a platinum-resistance thermometer. For the very dilute solutions, where the Shedlovsky cell was used, a more complicated thermostat, containing about six gallons of bleached petroleum oil and housed in a double-walled insulated box, was used. Stirring was by means of a circulating pump. Temperature was controlled by a mercury–toluene regulator and thyratron relay as described by Swinehart (7) and it was read directly on a platinum-resistance thermometer. In all cases, the temperature was known to about 0.005° C and it was constant within 0.002° C. When this thermostat was operated at 35° C, the air above the bath was maintained just above 35° C to prevent distillation of solvent into the exposed section of the cell.

Viscosity measurements were made with two viscometers of the Cannon and Fenske type (8), in which drainage and kinetic energy corrections are negligible. They were calibrated with water at the two temperatures. The reproducibility of run times was not better than 0.05%. Density and viscosity measurements were not made on the six most dilute solutions, since these were made up by successive additions of salt to the Shedlovsky-type cell.

Can. J. Chem. Downloaded from www.nrcresearchpress.com by 210.87.254.105 on 09/05/12
For personal use only.

Can. J. Chem. Downloaded from www.nrcresearchpress.com by 210.87.254.105 on 09/05/12
For personal use only.

EXPERIMENTAL RESULTS

TABLE I

Densities, viscosities, and conductances of sodium hexanoate at 25° C

Concentration (moles/liter)	Density (g/ml)	Relative viscosity	Specific conductance (mhos/cm×10^4)	Equivalent conductance (mhos)
0.000250	—	—	0.19197	76.56
0.000632	—	—	0.48207	76.04
0.000968	—	—	0.73337	75.65
0.001579	—	—	1.1889	75.16
0.002320	—	—	1.7350	74.69
0.003249	—	—	2.4128	74.18
0.019937	0.99788	1.014	13.876	69.57
0.049792	0.99896	1.035	32.648	65.55
0.099588	1.00075	1.067	61.299	61.54
0.50023	1.01527	1.374	231.01	46.18
0.98536	1.03233	1.875	350.52	35.57
2.0019	1.05917	4.606	498.53	24.89
2.6215	1.07242	11.654	531.99	20.29
2.9987	1.08127	21.64	521.35	17.38
3.4487	1.09058	39.27	477.78	13.85

TABLE II

Data for sodium hexanoate at 35° C

Concentration (moles/liter)	Density (g/ml)	Relative viscosity	Specific conductance (mhos/cm×10^4)	Equivalent conductance (mhos)
0.000611	—	—	0.5782	94.31
0.001164	—	—	1.0925	93.64
0.001604	—	—	1.4973	93.16
0.002241	—	—	2.0783	92.60
0.002926	—	—	2.6983	92.08
0.003014	—	—	3.5845	91.45
0.019875	0.99480	1.015	17.087	85.91
0.049637	0.99585	1.033	40.204	80.96
0.092732	0.99759	1.064	—	—
0.49838	1.01152	1.341	288.06	57.79
0.98092	1.02768	1.778	455.42	45.40
1.9909	1.05335	4.202	643.49	32.31
2.6061	1.06612	10.14	688.89	26.43
2.9803	1.07473	17.46	682.15	22.88
3.4238	1.08270	30.26	635.93	18.57

DISCUSSION

After a careful consideration of all possible errors, we conclude that our equivalent conductances have a maximum possible error of $\pm 0.1\%$.

Limiting equivalent conductances are usually obtained either by the classical Kohlrausch method, in which equivalent conductance is plotted against the square root of the concentration, or by the Shedlovsky (4) or some other, method of extrapolation. Both the Kohlrausch and the Shedlovsky methods were used by us. In very dilute solutions hydrolysis is appreciable and correction was made for this by the method of Campbell and Bock (9). This method calculates x, the degree of hydrolysis, from the expression

$$x = -\frac{K_h}{2C} + \sqrt{\frac{K_h^2}{4C^2} + \frac{K_h}{C}},$$

where K_h is the hydrolysis constant and C is the stoichiometric concentration, and assumes that the equivalent conductance of free acid or base, as the case may be, is the limiting equivalent conductance of acid or base. It then follows that

$$\Lambda_{exp} = (1-x)\Lambda_{corr}+x\Lambda_{base}.$$

Thus Λ_{corr}, the equivalent conductance of the unhydrolyzed salt, can be calculated. The hydrolysis constants were obtained from the data of Everett, Landsman, and Pinsent (10). At 25° C, $K_h = 7.25\times10^{-10}$ and at 35° C, $K_h = 1.57\times10^{-9}$.

The Kohlrausch method gave for the limiting equivalent conductance of sodium hexanoate at 25° C a value of 77.47±0.04 mhos, and at 35° C a value of 96.23±0.05 mhos. The Shedlovsky extrapolation method gave the values 77.84 and 96.71 mhos, respectively. The Shedlovsky values are distinctly higher. Similar behavior was observed by Bock (9) for ammonium salts. Since the Shedlovsky method is empirical and the deviations from a straight line in the Kohlrausch plot are small (maximum deviation 0.05%, by the method of least squares), we think the Kohlrausch values are the ones that should be accepted.

The limiting conductances of the sodium ion, according to Benson and Gordon (11), are 50.10 mhos at 25° C and 61.54 mhos at 35° C. Subtracting these values from the values obtained for sodium hexanoate, the limiting conductance of the hexanoate ion results as 27.37±0.04 mhos at 25° C and 34.69±0.05 mhos at 35° C.

It now appears that there is little theoretical justification for the application of Wishaw–Stokes and the Falkenhagen–Leist equations to the region of concentrated solution. Nevertheless, the manner in which these equations predict the experimental results is surprising. We note in particular the results of Campbell and Paterson on lithium chlorate (12) where the observations were pushed right up to the molten salt, without serious discrepancy. We therefore find it of interest to apply these equations to our results and we have done so in the present instance. In this case, however, both equations appear to be useless. Both conductance equations were programmed on a Bendix G-15 D computer, in such a way that the best $\mathring{a}$ was found for each concentration. An $\mathring{a}$ value was then chosen in the dilute region (usually about 0.1 N), and this $\mathring{a}$ value was then used to calculate a conductance value for each concentration.

TABLE III

Calculated equivalent conductances at 25° C

Concentration (moles/liter)	Equivalent conductance (mhos)	Calculated equivalent conductance			
		Robinson–Stokes (mhos)		Falkenhagen–Leist (mhos)	
		$\mathring{a}$ = 13.0 Å	$\mathring{a}$ = 20.0 Å	$\mathring{a}$ = 5.5 Å	$\mathring{a}$ = 7.0 Å
0.000250	76.56	76.31	76.34	76.52	76.52
0.000632	76.04	75.67	75.75	75.96	75.98
0.000968	75.65	75.28	75.40	75.62	75.64
0.001579	75.16	74.73	74.91	75.11	75.15
0.002301	74.69	74.23	74.48	74.63	74.69
0.003249	74.18	73.72	74.04	74.13	74.20
0.019937	69.57	69.56	70.63	69.59	69.95
0.049792	65.55	66.17	67.81	65.50	66.19
0.099588	61.54	62.58	64.65	61.14	62.18
0.50023	46.18	45.52	47.78	42.65	44.49
0.98536	35.57	32.19	33.69	29.81	31.53
2.0019	24.89	12.39	12.55	11.58	12.45
2.6215	20.29	4.739	4.622	4.503	4.867
2.9987	17.38	2.500	2.362	2.406	2.608
3.4487	13.85	1.342	1.208	1.315	1.430

Can. J. Chem. Downloaded from www.nrcresearchpress.com by 210.87.254.105 on 09/05/12
For personal use only.

TABLE IV

Calculated equivalent conductances at 35° C

Concentration (moles/liter)	Equivalent conductance (mhos)	Calculated equivalent conductances			
		Robinson–Stokes (mhos)		Falkenhagen–Leist (mhos)	
		$\mathring{a}$ = 10 Å	$\mathring{a}$ = 17 Å	$\mathring{a}$ = 4.0 Å	$\mathring{a}$ = 6.0 Å
0.000611	94.31	93.97	94.07	94.37	94.40
0.001164	93.64	93.17	93.37	93.69	93.74
0.001604	93.16	92.67	92.93	93.24	93.31
0.002241	92.60	92.14	92.45	92.71	92.81
0.002926	92.08	91.58	91.99	92.21	92.34
0.003914	91.45	90.94	91.46	91.60	91.77
0.019875	85.91	85.58	87.21	85.98	86.64
0.049637	80.96	81.04	83.54	80.48	81.78
0.49838	57.79	55.65	59.82	51.18	55.21
0.98092	45.40	40.31	43.52	35.90	39.94
1.9909	32.31	16.16	17.14	14.06	16.24
2.6061	26.43	6.514	6.755	5.661	6.638
2.9803	22.88	3.721	3.786	3.240	3.827
3.4238	18.57	2.106	1.620	1.842	2.194

The 25° C data, based on the Wishaw–Stokes equation, are given in columns 3 and 4 of Table III. Two values of $\mathring{a}$, viz. 13 Å and 20 Å, were used in these calculations. Even in the very dilute region, the calculated and observed conductances differ by as much as 0.3 mho. When $\mathring{a}$ = 13 Å is used, the calculated and observed conductances agree within 0.7 mho up to a concentration of 0.5 M but for higher concentrations the calculated values differ markedly from the experimental results. For $\mathring{a}$ = 20 Å, the deviation becomes large for a concentration of 0.02 M. Below this concentration, the agreement is similar to that observed for $\mathring{a}$ = 13 Å. The reason for the similarity in the dilute region, despite the large difference in $\mathring{a}$ values, is that the equation becomes very insensitive to a change in $\mathring{a}$ value at lower concentrations.

The results with the Wishaw–Stokes equation at 35° C are given in columns 3 and 4 of Table IV, using $\mathring{a}$ values of 10 and 17 Å. Again, the agreement between observed and calculated values in the dilute region is only within 0.5 mho. For $\mathring{a}$ = 10 Å, the conductance values are reproduced within 0.5 mho up to a concentration of 0.05 M. For $\mathring{a}$ = 17 Å, the agreement is somewhat better in the dilute region but the region now extends only to 0.004 M. The calculated values for the higher concentrations again deviate very markedly from the experimental values.

The results of the calculations at 25° C based on the Falkenhagen–Leist equation are given in columns 5 and 6 of Table III. In the dilute region this equation reproduces the data rather well, the deviations being less than 0.1 mho up to 0.05 M and 0.4 mho at 0.1 M, when $\mathring{a}$ = 5.5 Å. For the larger value, $\mathring{a}$ = 7.0 Å, the deviation becomes appreciable at 0.02 M. Above 0.1 M, the equation fails rather badly.

Columns 5 and 6 of Table IV give the 35° C data obtained with the Falkenhagen–Leist equation. Behavior similar to that observed at 25° C is also observed here. The data are reproduced within 0.5 mho up to 0.05 M, with $\mathring{a}$ = 4.0 Å, and within 0.8 mho, for $\mathring{a}$ = 6.0 Å.

Compared with their behavior in regard to lithium chlorate, both equations perform very poorly. Moreover, the $\mathring{a}$ values are so large as scarcely to have any physical significance, at least with the Wishaw–Stokes equation, where the best value of $\mathring{a}$ is 10 Å, or greater. All conductance equations for the region of higher concentration must contain some function of the viscosity since undoubtedly a moving ion encounters a greater

Can. J. Chem. Downloaded from www.nrcresearchpress.com by 210.87.254.105 on 09/05/12
For personal use only.

resistance than it would in pure water or a very dilute solution. In the absence of a precise knowledge of the form of the viscosity function, theoretical investigators have been reduced to the necessity of dividing their calculated result by the relative viscosity of the solution and this has of course been done in all the calculations given here. If this were not done, a ludicrous result would be obtained for the very concentrated and very viscous solutions. In this connection it is perhaps significant that while the viscosity of sodium hexanoate solutions does not rise as high, at saturation, as that of lithium chlorate at saturation (an ideal salt for this kind of treatment), at comparable concentrations the viscosity of sodium hexanoate is much higher than that of lithium chlorate. This is exemplified in Fig. 1, where the viscosities of the aqueous solutions of the salts, at 25° C,

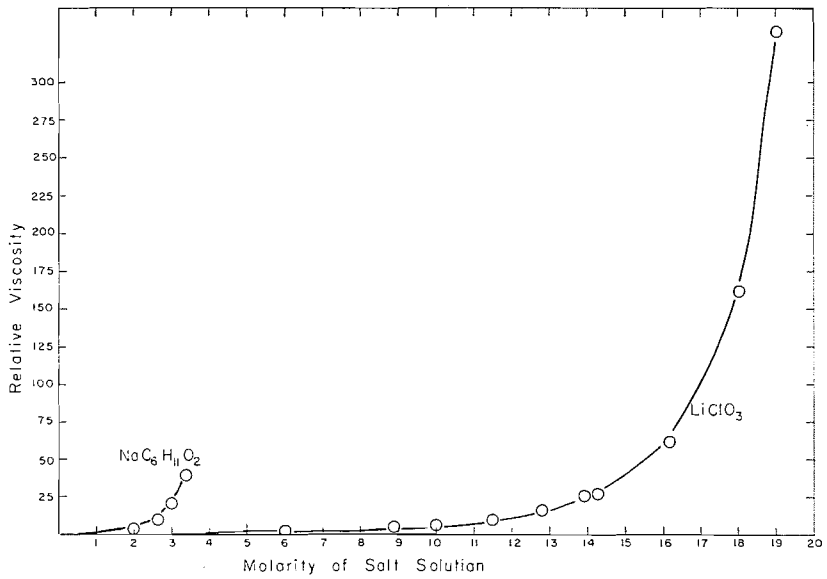


FIG. 1. Viscosity of sodium hexanoate and of lithium chlorate solution at 25° C.

are plotted against molar concentration. The graph shows that a saturated, or almost saturated, aqueous solution of sodium hexanoate, has a molarity of 3.45 but its viscosity equals that of a 15 *M* solution of lithium chlorate. If some power of the viscosity other than unity were used, the results might be brought into harmony, not only with one another, but with smaller $\mathring{a}$ values. In the absence, however, of any theoretical indication as to what form the viscosity correction should take, there seems no point in further speculation.

An obvious explanation of the large $\mathring{a}$ values would appear to exist in the assumption of micelle formation. According to McBain (13), solutions of colloidal electrolytes exhibit approximately ideal behavior until a certain concentration, characteristic of the substance, is reached. Marked deviation from ideal behavior then sets in rather suddenly. The sodium salts of the fatty acids belong to the class of compounds which exhibit this behavior. Smith and Robinson (14), employing the isopiestic vapor pressure method, conclude that the butyrate ion is the first of the fatty acid series to exhibit tendency toward micelle formation: micelle formation was observed for the hexanoate ion. On the other hand, McBain and co-workers (15) measured the conductance of the potassium

Can. J. Chem. Downloaded from www.nrcresearchpress.com by 210.87.254.105 on 09/05/12
For personal use only.

salts of the fatty acids and observed that anomalous curves were first obtained with potassium laurate (C_{12}). When our own figures for the equivalent conductance of sodium hexanoate are plotted against concentration, the curves do not show the minima characteristic of salts which form micelles. Again, if the specific conductance is plotted against concentration, there should be a "break" or sharp change of direction, at the critical micelle concentration, but no such "breaks" occur.

To clinch the question of whether or not micelle formation occurs in solutions of sodium hexanoate, we determined the apparent molecular weight of sodium hexanoate in solutions of different concentration, by the method of freezing point lowering. The liquid in equilibrium with ice at various temperatures was analyzed by evaporation to dryness. The results are given in Table V. The apparent molecular weights correspond to

TABLE V

Concentration, g salt/100 g H_2O	Apparent molecular weight
1.0517	69.2
5.1895	67.0
10.287	63.0
17.298	59.5

complete dissociation of the salt and give no evidence of micelle formation. It is strange that the apparent molecular weights decrease with increasing concentration but colligative behavior cannot be expected at these high concentrations and the activity coefficients are not known. Hence, in our opinion, micelle formation cannot be considered an explanation of the very large values of $\mathring{a}$.

REFERENCES

1. B. F. Wishaw and R. H. Stokes. J. Am. Chem. Soc. **76**, 2065 (1954).
2. H. Falkenhagen, M. Leist, and G. Kelbg. Ann. Physik, **11** (6), 51 (1952); H. Falkenhagen and M. Leist. Naturwiss. **24**, 570 (1954); Z. physik. Chem. **205**, 16 (1955).
3. G. Jones and G. M. Bollinger. J. Am. Chem. Soc. **53**, 411 (1931).
4. T. Shedlovsky. J. Am. Chem. Soc. **54**, 1411 (1932).
5. J. E. Lind, Jr., J. J. Zwolenik, and R. M. Fuoss. J. Am. Chem. Soc. **81**, 1557 (1959).
6. E. W. Washburn. J. Am. Chem. Soc. **38**, 2431 (1916).
7. D. F. Swinehart. Anal. Chem. **21**, 1577 (1949).
8. M. J. Cannon and M. R. Fenske. Ind. Eng. Chem., Anal. Ed. **10**, 299 (1938).
9. A. N. Campbell and E. Bock. Can. J. Chem. **36**, 330 (1958).
10. D. H. Everett, D. A. Landsman, and B. R. W. Pinsent. Proc. Roy. Soc. A, **215**, 403 (1952).
11. G. C. Benson and A. R. Gordon. J. Chem. Phys. **13**, 473 (1945).
12. A. N. Campbell and W. G. Paterson. Can. J. Chem. **36**, 1004 (1958).
13. M. E. L. McBain and E. Hutchinson. Solubilisation and related phenomena. Academic Press Inc., New York. 1955.
14. E. R. B. Smith and R. A. Robinson. Trans. Faraday Soc. **38**, 70 (1942).
15. J. W. McBain, M. E. Laing, and A. F. Titley. J. Chem. Soc. **115**, 1279 (1919).

Can. J. Chem. Downloaded from www.nrcresearchpress.com by 210.87.254.105 on 09/05/12
For personal use only.

Can. J. Chem. Downloaded from www.nrcresearchpress.com by 210.87.254.42 on 09/05/12
For personal use only.

THE PREPARATION OF L-ARGINYL DIPEPTIDES OF ASPARAGINE, GLUTAMINE, AND SOME BASIC AMINO ACIDS[1]

CASIMIR BERSE, LUCIEN PICHÉ, AND AKIRA UCHIYAMA

ABSTRACT

The synthesis of the following dipeptides is described: L-arginyl-L-asparagine acetate, L-arginyl-L-glutamine acetate, L-arginyl-L-lysine diacetate, and L-arginyl-L-ornithine diacetate. The two former were prepared by coupling a mixed anhydride of α-carbobenzoxy-ω-nitro-L-arginine directly with L-asparagine or with L-glutamine; catalytic hydrogenolysis of the resulting intermediates gave the dipeptides. The two others were obtained by combining α-carbobenzoxy-L-arginine with ω-carbobenzoxy-L-lysine methyl ester hydrochloride or with ω-carbobenzoxy-L-ornithine methyl ester hydrochloride in the presence of N,N′-dicyclohexylcarbodiimide; saponification and hydrogenation was necessary to uncover the resulting dipeptides.

Arginine is a universal constituent of proteins and is found in most of the physiologically active polypeptides. Its introduction in synthetic peptides has presented unusual difficulties caused by the strongly basic character of the guanidino group (1). The arginyl peptides, in which the carboxyl group of arginine is involved, were not prepared until three groups of workers reported initial success almost at the same time in 1953 (2, 3, 4). Although a variety of these compounds have now been synthetized by appropriate methods (5–8), the arginyl dipeptides containing basic amino acids have not hitherto been described; L-arginyl-L-arginine is the only exception (9).

Two methods were adapted to the combination of arginine with L-asparagine and L-glutamine or with L-lysine and L-ornithine respectively. In the first of these, α-carbobenzoxy-ω-nitro-L-arginine (6, 10) was converted to a mixed anhydride (11) by the action of ethyl chloroformate in the presence of an equimolar amount of tri-*n*-butylamine; it was then condensed directly with L-asparagine or with L-glutamine in alkaline solution. Catalytic hydrogenolysis of the resulting intermediates removed the carbobenzoxyl and nitro groups and resulted in the respective dipeptides; these were crystallized as the acetates.

The synthesis of L-arginyl-L-lysine and of L-arginyl-L-ornithine was attempted by the same procedure: the mixed anhydride of ethyl carbonate and α-carbobenzoxy-ω-nitro-L-arginine was condensed with ω-carbobenzoxy-L-lysine methyl ester hydrochloride and with ω-carbobenzoxy-L-ornithine methyl ester hydrochloride. Saponification of the resulting covered dipeptide esters was successful but the carboxylic compounds resisted hydrogenolysis in acidic, neutral, or basic media.

An alternate procedure based on the previous experience of Boissonnas *et al.* (15) was adopted. In this procedure the guanido group of α-carbobenzoxy-L-arginine is protected by a proton (2, 3) while condensation is carried out with N,N′-dicyclohexylcarbodiimide (12). Use of the proton to cover the guanido group avoided the necessity for hydrogenolysis of the nitro group and in contrast to previous experience of the authors (7) gave satisfactory yields of the protected dipeptides. The esters obtained by condensation of α-carbobenzoxy-L-arginine with ω-carbobenzoxy-L-lysine methyl ester or with ω-carbobenzoxy-L-ornithine methyl ester were saponified in the usual manner. Hydrogenation in 10% acetic acid over palladium catalyst converted the carboxylic intermediates into arginyl dipeptides; these were isolated as the diacetates.

[1]*Manuscript received in original form February 1, 1960, and, as revised, July 11, 1960.*
Contribution from the Department of Chemistry, Université de Montréal, Montreal, Que.

Can. J. Chem. Downloaded from www.nrcresearchpress.com by 210.87.254.42 on 09/05/12
For personal use only.

EXPERIMENTAL

*α-Carbobenzoxy-ω-nitro-*L*-arginyl-*L*-asparagine*

Ethyl chloroformate (2.44 ml, 20 mmoles) was added to a solution of α-carbobenzoxy-ω-nitro-L-arginine (7.06 g, 20 mmoles) (5, 6, 10) and tri-*n*-butylamine (2.8 ml, 20 mmoles) in dry dioxane (50 ml). After 10 minutes, L-asparagine (2.64 g, 20 mmoles) in 0.4 *N* sodium hydroxide (50 ml) was added to the mixture at 10°. Carbon dioxide gas was given off vigorously. The mixture was shaken for 15 minutes at 10°, and then it was acidified to Congo red with *N* hydrochloric acid. Dioxane was evaporated *in vacuo* in the water bath, water was decanted, and the resulting oily product was triturated with cold acetonitrile until crystallization occurred. The compound was recrystallized from a mixture of N,N-dimethylformamide and acetonitrile. Yield 4.6 g (48%), m.p. 201°, $[\alpha]_D^{25}$ +6.2 (*c*, 4.17 in N,N-dimethylformamide). Anal. Calc. for $C_{18}H_{25}O_8N_7$: C, 46.25; H, 5.39; N, 20.98. Found: C, 46.27; H, 5.46; N, 20.88.

L-*Arginyl-*L*-asparagine Acetate*

α-Carbobenzoxy-ω-nitro-L-arginyl-L-asparagine (2.12 g, 4.53 mmoles) was dissolved in 0.1 *N* sodium hydroxide (4.65 ml). Palladium catalyst was added and the mixture was shaken with hydrogen for 5 hours. The catalyst was filtered off; pH of the solution was 8.6; it was brought to 5–6 with glacial acetic acid, then the solvent was evaporated until dryness *in vacuo* at 30–40°. The resulting product was washed with absolute ethanol and treated with N,N-dimethylformamide. On standing, the residue crystallized. The compound was recrystallized from aqueous methanol. Yield 1.2 g (75%), m.p. 260° (decomp.), $[\alpha]_D^{25}$ +11.1° (*c*, 0.83 in water). Anal. Calc. for $C_{12}H_{24}O_6N_6$: C, 41.34; H, 6.95; N, 24.13. Found: C, 41.32; H, 7.07; N, 24.16.

*α-Carbobenzoxy-ω-nitro-*L*-arginyl-*L*-glutamine*

This compound was prepared from α-carbobenzoxy-ω-nitro-L-arginine (3.53 g, 10 mmoles) and L-glutamine (1.46 g, 10 mmoles) in the manner described for α-carbobenzoxy-ω-nitro-L-arginyl-L-asparagine; the product was crystallized several times from a mixture of a small amount of absolute ethanol and methylene chloride. Yield 2.8 g (45%), m.p. 168°, $[\alpha]_D^{25}$ −0.5° (*c*, 3.8 in N,N-dimethylformamide). Anal. Calc. for $C_{19}H_{27}O_8N_7$ (1/2 H_2O): C, 46.65; H, 5.72; N, 19.99. Found: C, 46.72; H, 5.91; N, 19.97.

L-*Arginyl-*L*-glutamine Acetate*

α-Carbobenzoxy-ω-nitro-L-arginyl-L-glutamine (2 g, 4.16 mmoles) was dissolved in a mixture of water (2 ml), methanol (2 ml), and glacial acetic acid (20 ml). The compound was hydrogenated for 12 hours at room temperature and at atmospheric pressure over 1 g of 10% palladium on carbon. The catalyst was filtered off and the solvent was evaporated *in vacuo* at 40–50°. The residue was crystallized from methanol–acetone. Yield 1.0 g (66%), m.p. 160°, $[\alpha]_D^{25}$ +19.2° (*c*, 3.87 in water). Anal. Calc. for $C_{13}H_{26}O_6N_6$ (1/2 H_2O): C, 42.16; H, 7.35; N, 22.65. Found: C, 42.34; H, 7.11; N, 22.67.

*α-Carbobenzoxy-ω-nitro-*L*-arginyl-ω-carbobenzoxy-*L*-lysine Methyl Ester*

α-Carbobenzoxy-ω-nitro-L-arginine (3.53 g, 10 mmoles) was dissolved in dry dioxane (100 ml) and tri-*n*-butylamine (2.4 ml, 10 mmoles) was added. The solution was cooled to 10° C; ethyl chloroformate (0.96 ml, 7.8 mmoles) was added with stirring and the solution was kept at 11–12° for 15 minutes. The product was then added to 150 ml of N,N-dimethylformamide containing 3.31 g (10 mmoles) of ω-carbobenzoxy-L-lysine methyl ester hydrochloride (13, 14). The mixture was shaken for 2 hours at room temperature and the solvent was evaporated at 40–50°. The residue was dissolved in ethyl acetate,

and the solution was washed successively with *N* hydrochloric acid, water, *N* sodium bicarbonate and water, dried over sodium sulphate, and evaporated to dryness *in vacuo*; it was then treated with isoamyl alcohol – methylene chloride (1:50). The resulting crystals were washed with ether and recrystallized from N,N-dimethylformamide–water. Yield 3.9 g (62%), m.p. 104°, $[\alpha]_D^{25}$ −2.5° (*c*, 4.64 in N,N-dimethylformamide). Anal. Calc. for $C_{29}H_{39}O_9N_7$: C, 55.35; H, 6.25; N, 15.58. Found: C, 55.28; H, 6.32; N, 15.39.

*α-Carbobenzoxy-ω-nitro-*L*-arginyl-ω-carbobenzoxy-*L*-lysine*

α-Carbobenzoxy-ω-nitro-L-arginyl-ω-carbobenzoxy-L-lysine methyl ester (6.35 g, 10.01 mmoles) was dissolved in methanol (20 ml) and *N* sodium hydroxide (20 ml, 20 mmoles) was added. The mixture was shaken for 3 hours; the alkaline solution was washed with ethyl acetate, then acidified to Congo red with *N* hydrochloric acid; the oily residue crystallized on standing. It was recrystallized from hot water or aqueous methanol. Yield 4.7 g (77%), m.p. 159°, $[\alpha]_D^{25}$ +3.8° (*c*, 1.44 in N,N-dimethylformamide). Anal. Calc. for $C_{28}H_{37}O_9N_7$: C, 54.80; H, 6.07; N, 15.93. Found: C, 54.55; H, 6.19; N, 15.74.

*α-Carbobenzoxy-*L*-arginyl-ω-carbobenzoxy-*L*-lysine Methyl Ester Hydrochloride*

α-Carbobenzoxy-L-arginine (3.08 g, 10 mmoles) (15, 17) and ω-carbobenzoxy-L-lysine methyl ester hydrochloride (3.65 g, 11 mmoles) were suspended in N,N-dimethylformamide (10 ml) containing diethyl phosphite (2 ml) and the mixture was stirred for 2 hours (15). To this solution was added N,N-dicyclohexylcarbodiimide (3.10 g, 15 mmoles). The mixture was stirred for 2 days at room temperature, then it was cooled to −10°; N,N-dicyclohexylurea precipitated and was filtered off. The urea was washed with a small amount of N,N-dimethylformamide which was combined with the filtrate. The solvent was removed *in vacuo*. The residue was triturated several times with anhydrous ether; it was then dissolved in methylene chloride (200 ml). The solution was washed with *N* ammonium hydroxide, water, *N* hydrochloric acid and water, and it was dried over sodium sulphate; the solvent was removed *in vacuo*. The crude product thus obtained was crystallized from methylene chloride – ether. It was recrystallized from the same solvent and again recrystallized from ethanol–ether. Yield 4.05 g (65%), m.p. 131°, $[\alpha]_D^{25}$ +9.9° (*c*, 5.69 in N,N-dimethylformamide). Anal. Calc. for $C_{29}H_{41}O_7N_6Cl$: C, 56.00; H, 6.66; N, 13.62. Found: C, 57.40; H, 7.01; N, 13.88.*

*α-Carbobenzoxy-*L*-arginyl-ω-carbobenzoxy-*L*-lysine Hydrochloride*

Sodium hydroxide (4 *N*, 2 ml, 8 mmoles) was added to α-carbobenzoxy-L-arginyl-ω-carbobenzoxy-L-lysine methyl ester hydrochloride (2.6 g, 4.2 mmoles) dissolved in methanol. The mixture was shaken at room temperature for 2 hours. The solution was diluted with water (2 ml), acidified with concentrated hydrochloric acid under cooling. Methanol was evaporated *in vacuo*. The product precipitated as an oil and crystallized on standing. It was recrystallized from hot water. Yield 1.53 g (60%), m.p. 205° $[\alpha]_D^{25}$ +27.8° (*c*, 1.82 in N,N-dimethylformamide). Anal. Calc. for $C_{28}H_{39}O_7N_6Cl$: C, 55.50; H, 6.50; N, 13.83. Found: C, 56.19; H, 7.12; N, 13.83.*

L-*Arginyl-*L*-lysine Diacetate*

(*a*) A number of attempts towards the hydrogenation of α-carbobenzoxy-ω-nitro-L-arginyl-ω-carbobenzoxy-L-lysine in methanol containing acetic acid or ammonium hydroxide or in neutral methanol, over palladium catalyst in the usual manner, were unsuccessful.

**In view of the poor agreement of the analytical data the other properties of the compound are subject to question. However, the intermediate at this stage of purity was suitable for the synthesis of* L*-arginyl-*L*-lysine diacetate.*

Can. J. Chem. Downloaded from www.nrcresearchpress.com by 210.87.254.42 on 09/05/12
For personal use only.

(*b*) α-Carbobenzoxy-L-arginyl-ω-carbobenzoxy-L-lysine hydrochloride (1 g, 1.64 mmoles) was dissolved in methanol (20 ml) containing 10% by volume of glacial acetic acid. The compound was hydrogenated for 3 hours at room temperature and atmospheric pressure over palladium catalyst. The catalyst was removed by filtration and the filtrate was evaporated to dryness *in vacuo*. The residue was crystallized from methanol–acetone. Yield 0.41 g (58%), m.p. 167°, $[\alpha]_D^{25}$ +5.1 (*c*, 3.41 in water). Anal. Calc. for $C_{16}H_{33}O_7N_6$: C, 45.48; H, 8.11; N, 19.99. Found: C, 45.59; H, 8.24; N, 20.61.

α-Carbobenzoxy-ω-nitro-L-arginyl-ω-carbobenzoxy-L-ornithine Methyl Ester

This compound was prepared from α-carbobenzoxy-ω-nitro-L-arginine (3.53 g, 10 mmoles) and ω-carbobenzoxy-L-ornithine methyl ester hydrochloride (3.46 g, 10 mmoles) (16) in the manner described for α-carbobenzoxy-nitro-L-arginyl-ω-carbobenzoxy-L-lysine methyl ester hydrochloride. The product was recrystallized from methanol – methylene chloride (1:100 by volume). Yield 3.53 g (58%), m.p. 88°, $[\alpha]_D^{25}$ −16.2° (*c*, 1.0 in N,N-dimethylformamide). Anal. Calc. for $C_{28}H_{37}O_9N_7$: C, 54.70; H, 6.06; N, 15.91. Found: C, 54.35; H, 6.20; N, 15.85.

α-Carbobenzoxy-ω-nitro-L-arginyl-ω-carbobenzoxy-L-ornithine

α-Carbobenzoxy-ω-nitro-L-arginyl-ω-carbobenzoxy-L-ornithine methyl ester (7.00 g, 14 mmoles) was dissolved in methanol (20 ml) and *N* sodium hydroxide (20 ml, 20 mmoles) was added. The mixture was shaken for 3 hours. The product was isolated in the usual manner and recrystallized from hot water. Yield 4.9 g (72%), m.p. 185°, $[\alpha]_D^{25}$ −12.7° (*c*, 0.77 in N,N-dimethylformamide). Anal. Calc. for $C_{27}H_{35}O_9N_7$: C, 54.00; H, 5.86; N, 16.31. Found: C, 53.81; H, 5.84; N, 16.25.

α-Carbobenzoxy-L-arginyl-ω-carbobenzoxy-L-ornithine Methyl Ester Hydrochloride

This compound was prepared from α-carbobenzoxy-L-arginine (3.08 g, 10 mmoles) and ω-carbobenzoxy-L-ornithine methyl ester hydrochloride (3.80 g, 11 mmoles) in the manner described for α-carbobenzoxy-L-arginyl-ω-carbobenzoxy-L-lysine methyl ester hydrochloride. The crude product was precipitated from ethanol–ether and was recrystallized from methylene chloride – ether. Yield 3.73 g (62%), m.p. 122°, $[\alpha]_D^{25}$ +4.6 (*c*, 4.78 in N,N-dimethylformamide). Anal. Calc. for $C_{28}H_{39}O_7N_6Cl$: C, 55.30; H, 6.48; N, 13.85. Found: C, 55.51; H, 6.60; N, 13.88.

α-Carbobenzoxy-L-arginyl-ω-carbobenzoxy-L-ornithine Hydrochloride

α-Carbobenzoxy-L-arginyl-ω-carbobenzoxy-L-ornithine methyl ester hydrochloride (1.00 g, 1.75 mmoles) was saponified in the manner described for α-carbobenzoxy-L-arginyl-ω-carbobenzoxy-L-lysine hydrochloride. The product was recrystallized from hot water. Yield 0.61 g (58%), m.p. 103–106°, $[\alpha]_D^{25}$ +3.5° (*c*, 1.72 in N,N-dimethylformamide). Anal. Calc. for $C_{27}H_{37}O_7N_6Cl$: C, 54.70; H, 6.29; N, 14.17. Found: C, 54.48; H, 7.03; N, 13.80.

L-Arginyl-L-ornithine Diacetate

α-Carbobenzoxy-L-arginyl-ω-carbobenzoxy-L-ornithine hydrochloride (1.00 g, 1.68 mmoles) was dissolved in methanol (10 ml) containing 10% by volume of glacial acetic acid. The compound was hydrogenated for 3 hours at room temperature and atmospheric pressure over the palladium catalyst. The final product was obtained in the manner described for L-arginyl-L-lysine diacetate. Yield 0.53 g (77%), hygroscopic. The crude product (0.52) in 5% acetic acid (50 ml) was applied to the top of the curtain of the continuous flow paper electrophoresis cell (Spinco Model CP) and was carried downward by acetic acid solution (5%, 16 liters). Sample feed rate was 0.8 ml/hour. The acetic

Can. J. Chem. Downloaded from www.nrcresearchpress.com by 210.87.254.42 on 09/05/12
For personal use only.

acid solution was maintained at 1° C and the curtain temperature was 10° C. Power supply was 30 milliamperes and 500 volts. The curtain came to equilibrium after 2 hours. Collection of the sample solution was started 1/2 hour after the first fraction reached the drip point. Thirty-two (32) test tubes were used to collect the solution. Duration of a typical run was 65 hours. The curtain was then dried and developed with ninhydrin.

The sample solution in test tubes No. 27 to 32 was combined and the solvent was evaporated *in vacuo* at 40–50° C. The residue was precipitated from methanol–ether. Yield 0.36 g (53.9%), $[\alpha]_D^{25}$ +9.6 (*c*, 2.9 in water). Anal. Calc. for $C_{15}H_{22}O_7N_6$: C, 44.11; H, 7.90; N, 20.60. Found: C, 44.14; H, 8.05; N, 20.49.

ACKNOWLEDGMENTS

This research was supported by a grant of the National Research Council of Canada. One of us (A. U.) held a Canadian Industries Limited Fellowship during part of the period of work. The authors wish to express their appreciation of this support.

REFERENCES

1. J. S. FRUTON. Advances in Protein Chem. **51** (1949).
2. G. W. ANDERSON. J. Am. Chem. Soc. **75**, 6081 (1953).
3. D. T. GISH and F. H. CARPENTER. J. Am. Chem. Soc. **75**, 5872 (1953).
4. K. HOFMANN, W. D. PECKHAM, and A. RHEINER. J. Am. Chem. Soc. **75**, 6083 (1953).
5. H. O. VAN ORDEN and E. L. SMITH. J. Biol. Chem. **208**, 751 (1954).
6. K. HOFMANN, W. D. PECKHAM, and A. RHEINER. J. Am. Chem. Soc. **78**, 238 (1956).
7. C. BERSE and L. PICHÉ. J. Org. Chem. **21**, 808 (1956).
8. N. IZUMIYA and S. MAKISUMI. J. Chem. Soc. Japan, **78**, 1768 (1957).
9. L. ZERVAS, T. OTANI, M. WINITZ, and J. P. GREENSTEIN. Arch. Biochem. Biophys. **75**, 290 (1958).
10. M. BERGMANN, L. ZERVAS, and H. RINKE. Z. physiol. Chem. **224**, 40 (1934).
11. R. A. BOISSONNAS. Helv. Chim. Acta, **34**, 874 (1951).
12. J. C. SHEENAN and G. P. HESS. J. Am. Chem. Soc. **77**, 1067 (1955).
J. C. SHEENAN, M. GOODMAN, and G. P. HESS. **78**, 1367 (1956).
13. A. NEUBERG and F. SANGER. Biochem. J. **37**, 515 (1943).
14. M. BERGMANN, L. ZERVAS, and F. WILLIAM. J. Biol. Chem. **111**, 249 (1935).
15. R. A. BOISSONNAS, ST. GUTTMANN, R. L. HUGUENIN, P. A. JAQUENOUD, and ED. SANDRIN. Helv. Chim. Acta, **41**, 1867 (1958).
16. R. L. M. SYNGE. Biochem. J. **42**, 100 (1948).
17. M. BERGMANN and L. ZERVAS. Ber. **65**, 1199 (1932).

Can. J. Chem. Downloaded from www.nrcresearchpress.com by 210.87.254.42 on 09/05/12
For personal use only.

Can. J. Chem. Downloaded from www.nrcresearchpress.com by 210.87.254.105 on 09/05/12
For personal use only.

PROTON MAGNETIC RESONANCE ABSORPTION IN ANHYDROUS POTASSIUM STEARATE[1]

R. F. GRANT[2] AND B. A. DUNELL

ABSTRACT

The proton magnetic resonance absorption in anhydrous potassium stearate has been measured over the temperature range −190° C to 182° C. Abrupt changes in line width have been found between 55° C and 62° C, and between 170° C and 171° C; these changes correspond approximately to known phase transitions. The reduction in line width and second moment with rising temperature is discussed.

INTRODUCTION

Like other alkali metal salts of long-chain fatty acids, potassium stearate passes through several transitions between solid state phases that exist in successive temperature ranges below the melting point. These transitions have been observed by various experimental methods, dilatometry (1, 2), differential calorimetry (3), and light transmission studies (4). They are, however, not so well understood in potassium stearate as in the sodium salts, for which it has been shown that the lowest temperature transitions (from a crystalline or curd phase to a waxy phase) correspond to the appearance of considerable structural disorder in the paraffin chain portion of the molecules (5, 6, 7). One infers from this appearance of disorder that the low-temperature transition may represent the onset of considerable motion in the paraffin chains. Since proton magnetic resonance has been useful in determining the nature of molecular motion in solid long-chain paraffin compounds (8, 9, 10), a magnetic resonance investigation of the lower-temperature transitions in anhydrous potassium stearate was made.

EXPERIMENTAL METHOD AND RESULTS

The potassium stearate used in this investigation was prepared from Eastman Kodak White Label grade stearic acid. This acid, which had a freezing point of 68.1° C, was purified by repeated crystallization at −20° C from freshly distilled acetone (11) until the freezing point was raised to 69.1° C. The purified acid was dissolved in hot ethanol and titrated with an ethanolic solution of potassium hydroxide, using phenolphthalein as the indicator. The potassium stearate precipitate was dried at 105° C and then fused under vacuum to remove traces of water and alcohol. When cool, the fused soap was crushed and fused again under vacuum in 10-mm o.d. Pyrex sample tubes; dry nitrogen was admitted to the vacuum system and the sample tubes were sealed off.

The nuclear magnetic resonance spectrometer and sample thermostat have been described previously (12). The temperature of the sample was measured with a thermocouple inserted in a well in the side of the sample tube.

Figure 1 shows the variations of the proton magnetic resonance line width of potassium stearate as a function of temperature. Following the common usage, we have taken the line width as the separation, in gauss, of the points of maximum and minimum slope

[1]*Manuscript received June 24, 1960.*
Contribution from the Department of Chemistry, University of British Columbia, Vancouver 8, British Columbia.
[2]*Holder of National Research Council Studentships. Present address: Division of Applied Chemistry, National Research Council, Ottawa, Canada.*

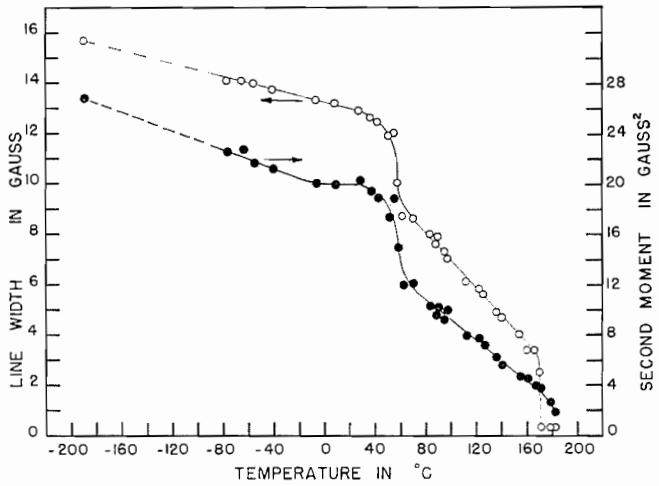


FIG. 1. Line width and second moment of potassium stearate as functions of temperature. Open circles, line width; filled circles, second moment.

on the resonance absorption line. Figure 1 also shows the corresponding variations of the second moment values with temperature. The second moments were obtained from the experimental derivative curves by the convenient method described by Powles (13) and were corrected for the effects of modulation (14).

It can be seen from Fig. 1 that there is an abrupt change in both line width and second moment between about 55° and 62° C and that there is a second discontinuity in line width between 170° and 171° C. At 171° C the line width is determined by depth of modulation and field inhomogeneity. The second moment shows no abrupt change at this temperature since the wings of the resonance line are only slightly narrowed, or decreased in intensity, as Fig. 2 shows.

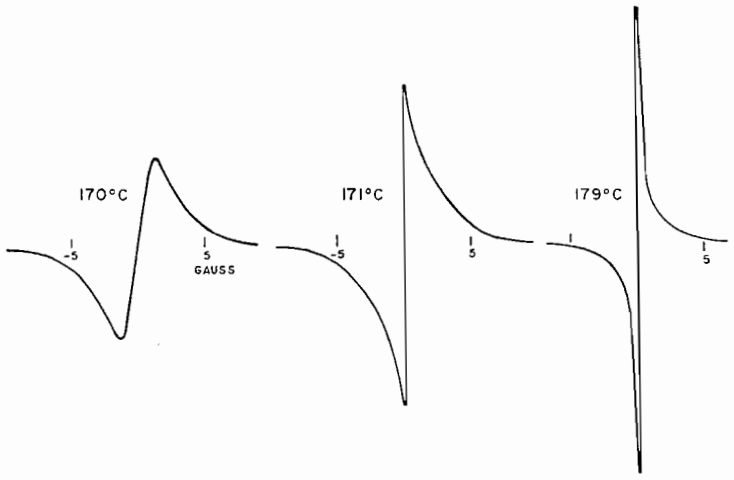


FIG. 2. Line shapes for potassium stearate near the phase transition at 170° C.

Can. J. Chem. Downloaded from www.nrcresearchpress.com by 210.87.254.105 on 09/05/12
For personal use only.

Can. J. Chem. Downloaded from www.nrcresearchpress.com by 210.87.254.105 on 09/05/12
For personal use only.

DISCUSSION

It is generally agreed that anhydrous potassium stearate passes through at least three phase transitions before melting (1–4). The lowest-temperature transition is variously located between 50° and 80° C; dilatometrically at 51° C by Vold (1) and with two changes in density at 65° and 80° C by Puddington and his co-workers (2), calorimetrically at 57° C by Ravich and Nechitaylo (3), and with X-ray studies at 78° C by Lomer (15), who has also measured the lattice parameters of the crystalline lower temperature B phase and crystalline higher temperature C phase. At least two other transitions occur before the substance melts to an isotropic liquid at 353° C (4), one in the range 160° to 170° C, and the other in the range 265° to 270° C (1–4). The positions at 160° and 170° C of the discontinuities observed in the n.m.r. line width agree with the transition temperatures observed by other techniques. Some indication of the nature of the low-temperature transition and of the solid phases may be obtained from a study of the second moment of the n.m.r. signal.

It can be shown that the rigid lattice second moment of the proton magnetic resonance for a polycrystalline sample (16, 17) is given by

$$S = \frac{716}{N} \sum_{j>k} r_{jk}^{-6}$$

where N is the number of protons whose interactions are considered and r_{jk} is the distance in angstrom units between any two protons j and k (9). In using this particular formula, it is assumed that the interactions of magnetic nuclei other than the protons in potassium stearate, such as the potassium nuclei and the nuclei of C^{13} and O^{17} in natural abundance, make a negligible contribution to the second moment.

An X-ray diffraction investigation of the A form of potassium caprate has indicated that the alternate carbon atoms in the zigzag paraffin chain are 2.60 Å apart (18), which would suggest that the bond angles differ slightly from the tetrahedral angle usually considered for long-chain paraffins. Moreover, electron diffraction studies on solid paraffin compounds have shown that the H—C—H bond angle may be about 107° and that the C—H bond length is about 1.12 Å (19, 20). A model of the paraffin chain part of potassium stearate, constructed using these bond parameters, and assuming that the C—C bond length is 1.54 Å (20), yields an intramolecular second moment of 18.0 gauss^2. The model in which tetrahedral bond angles and a C—H bond length of 1.094 Å are used gives an intramolecular second moment of 18.9 gauss^2. The intermolecular contribution will differ even less from the contribution for the non-tetrahedral model, and the total difference in second moments between the two is approximately within the error of experimental determination of second moment. If the experimental second moment of 26.8 gauss^2 at −190° C represents rigid lattice conditions, then the intermolecular second moment should be about 8.8 gauss^2.

Only the unit cell dimensions and the angle of tilt of the paraffin chains have been reported for potassium stearate (15). However, in the solid, the soap molecules are usually arranged such that the carboxylate ends form an electrically balanced ionic double layer, with the paraffin chains sticking out parallel to each other from both sides of this layer. If the paraffin chains were arranged parallel to one another with their long axes parallel to the *ac* planes and tilted at the angle $\tau = 53°$ (15) to the plane *ab* containing

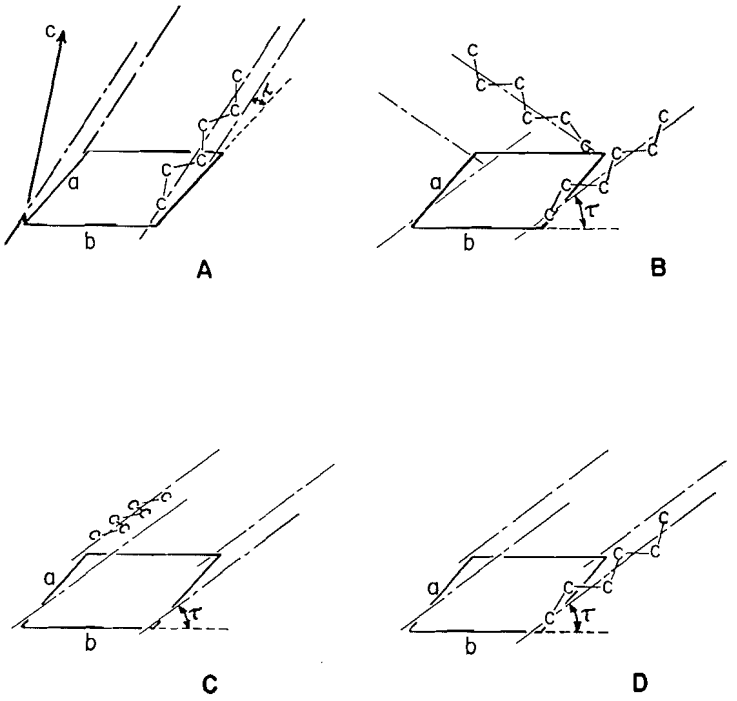


FIG. 3. Possible orientations of the hydrocarbon chains in the potassium stearate unit cell. The dot-and-dash lines — - — - represent the long axes of the hydrocarbon chains, and τ is the angle of tilt of 53° with respect to the plane *ab*.

the polar ends, as shown in Fig. 3A, some of the interhydrogen distances between chains would be reduced to values much less than the van der Waals diameter for a hydrogen atom, 2.4 Å (21). This arrangement has been dismissed as highly improbable. If the paraffin chains are inclined at 53° to the *ab* plane and arranged with their long axes parallel to *bc* planes, at least three reasonable values of the intermolecular second moment at 25° C may be obtained: 5.9 gauss^2 if the chains are not parallel to one another but are arranged in a crisscross fashion (Fig. 3B) as in the A phase of potassium caprate (18), 6.6 gauss^2 if the chains are parallel to one another and the plane of the C—C—C bonds is parallel to the *a*-axis (Fig. 3C), and 8.1 gauss^2 if the chains are parallel to one another and the plane of the C—C—C bonds is parallel to the *b*-axis (Fig. 3D). At −190° C the values are 6.2, 8.7, and 8.9 gauss^2 if one corrects the unit cell dimensions for thermal contraction using the coefficient of expansion given by Lomer (15). The first of these possibilities is considered less probable than either of the other two because of the poorer agreement between its calculated second moment of either 24.2 gauss^2 or 25.1 gauss^2 (non-tetrahedral or tetrahedral bond angles, respectively) at −190° C and the observed value of 26.8 gauss^2. The difference between the two remaining arrangements decreases with decreasing temperature because dimensional change in the *a* direction is much greater than in the *b* direction (15). The calculated value of the rigid lattice second moment may, then, be given as 27.2±0.5 gauss^2 depending mainly on whether or not tetrahedral bond angles are assumed in the hydrocarbon chain, and based on the arrangement of chains in the unit cell which gives best agreement with the experimental second moment of 26.8 gauss^2.

Can. J. Chem. Downloaded from www.nrcresearchpress.com by 210.87.254.105 on 09/05/12
For personal use only.

Can. J. Chem. Downloaded from www.nrcresearchpress.com by 210.87.254.105 on 09/05/12
For personal use only.

In considering the decrease of the line width and of the experimental second moment with increasing temperature, one must take note of recent modifications of the theory of Gutowsky and Pake (22), according to which theory both of these phenomena are to be expected as molecular reorientation becomes sufficiently rapid. Andrew and Newing (23) have discussed in detail the argument that the second moment must theoretically remain constant independent of the extent of molecular motion, pointing out that although the main central portion of the spectrum narrows, there is increased intensity in the wings of the spectral line because of production of side bands by modulation of the Larmor frequency by the molecular reorientation. Under some experimental conditions, however, the intensity of the side bands or the wings of the spectral line is comparable to or less than the noise level in the spectrometer. Thus the wings, which keep the second moment at its rigid lattice value, are not observable experimentally and the experimental second moment falls according to the earlier theory of Gutowsky and Pake. In the spectra of potassium stearate there were no indications of extended wings from the spectrometer with signal-to-noise ratio of 30. Further, the change of second moment with temperature effectively parallels the change in line width. Correlation frequencies can be calculated from the change of line width, which is not affected by the side bands, with temperature following the theory of Gutowsky and Pake (22). These agree substantially with correlation frequencies calculated from change of the observed second moment with temperature. One concludes, then, that the sensitivity and noise level of the spectrometer used in this work were such that side bands were not observed under any conditions, and our interpretation follows that of the original theory.

The experimental second moment at 25° C is 20 gauss^2, whereas the predicted rigid lattice value at this temperature is between 24.6 and 27 gauss^2 depending on the structure assumed. If the end methyl groups in potassium stearate reorient about their C_3 axes, a form of motion which is probably the first to take place with rising temperature in paraffins (9), the intramolecular second moment is reduced to 16.3 gauss^2 (17.1 gauss^2 for tetrahedral bond angles) (24). If the intermolecular contribution is reduced by a corresponding proportion, the total second moment should be between 22.2 and 24.4 gauss^2. Although zero-point vibrational motions may decrease the calculated second moment a little more (25), it will probably not be sufficient to give agreement with the experimental value of 20.0 gauss^2 at 25° C (12). It is suggested that the paraffin chains twist about their longitudinal axes in a torsional oscillation with amplitude somewhat in excess of the zero-point rocking vibration of the CH_2 groups. The relationship of the reduction of second moment to the amplitude of such oscillation has been calculated (8). Since each paraffin chain is clamped at one end in a strongly bonded salt layer, the amplitude of oscillation should increase along the chain with distance from this layer.

The line width and second moment change between 55° C and 62° C probably corresponds to the transition between the B and C crystalline phases (1, 2, 4). The known unit cell dimensions at 75° C (15) give an intermolecular second moment of about 6 gauss^2 if the paraffin chains are tilted at 53° C to *ab* and lie parallel to the *bc* plane. Thus the predicted rigid lattice second moment changes by about 2 gauss^2 between 25° C and 75° C, whereas the experimentally observed change is about 10 gauss^2. On going from the B to the C phase between 55° C and 62° C the experimental second moment is reduced by about 7 gauss^2, and hence greatly increased molecular motion, corresponding to more than 5 gauss^2 decrease in second moment, must accompany this change in structure. The complete reorientation of the potassium stearate molecules about the longitudinal axes of the paraffin chain portions would reduce the intramolecular second moment to 5.0

gauss^2 if reorientation of the end methyl groups about their C_3 axes also occurred (22, 24). The total second moment would then be 6.7 gauss^2 (8), which is the value at 130° C. There would be a further reduction of the second moment if there were reorientation about other axes in the molecule (24), which might be brought about by a bending motion of the twisting or rotating chain.

The sudden narrowing of the line width between 170° C and 171° C is probably associated with the phase transition reported to occur between 160° C and 170° C. This narrow line width must indicate comparatively great freedom of molecular motion in all directions, for most of the interaction between the proton pairs has been averaged out. However, the small change in the second moment at 171° C suggests that the molecules maintain their mean positions in the lattice (26) and that molecular motion is not yet isotropic. Infrared (6) and X-ray studies (7) on some sodium soaps suggest that a similar change in structure occurs when the temperature is raised above the "supercurd sub-waxy" transition at about 117° C. The transition between 160° C and 170° C reported in potassium stearate may therefore represent the beginning of a waxy-type phase.

ACKNOWLEDGMENTS

We thank the National Research Council for a Studentship awarded to one of us (R. F. G.) and for a grant-in-aid of the research. We are also indebted to Professor C. A. McDowell for his interest in this work.

REFERENCES

1. R. D. Vold, M. Macomber, and M. J. Vold. J. Am. Chem. Soc. **63**, 168 (1941); R. D. Vold and M. J. Vold. J. Phys. Chem. **49**, 42 (1945).
2. D. P. Benton, P. G. Howe, R. Farnand, and I. E. Puddington. Can. J. Chem. **33**, 1798 (1955).
3. G. B. Ravich and N. A. Nechitaylo. Doklady Akad. Nauk S.S.S.R. **83**, 117 (1952).
4. D. P. Benton, P. G. Howe, and I. E. Puddington. Can. J. Chem. **33**, 1384 (1955).
5. H. Nordsieck, F. B. Rosevear, and R. H. Ferguson. J. Chem. Phys. **16**, 175 (1948).
6. D. Chapman. J. Chem. Soc. 784 (1958).
7. A. Skoulios and V. Luzzati. Nature (London), **183**, 1310 (1959).
8. E. R. Andrew. J. Chem. Phys. **18**, 607 (1950).
9. F. A. Rushworth. Proc. Roy. Soc. (London), A, **222**, 526 (1954).
10. S. Kojima and S. Ogawa. J. Phys. Soc. Japan, **8**, 283 (1953).
11. J. B. Brown and D. K. Kolb. Progress in the chemistry of fats and other lipids. Vol. 3. Pergamon, London. 1955. p. 58.
12. R. F. Grant and B. A. Dunell. Can. J. Chem. **38**, 359 (1960).
13. J. G. Powles. Brit. J. Appl. Phys. **9**, 299 (1958).
14. E. R. Andrew. Phys. Rev. **91**, 425 (1953).
15. T. R. Lomer. Acta Cryst. **5**, 11 (1952).
16. J. H. Van Vleck. Phys. Rev. **74**, 1168 (1948).
17. H. S. Gutowsky, G. B. Kistiakowsky, G. E. Pake, and E. M. Purcell. J. Chem. Phys. **17**, 972 (1949).
18. V. Vand, T. R. Lomer, and A. Lang. Acta Cryst. **2**, 214 (1949).
19. B. K. Vainshtein and A. N. Lobachev. Doklady Akad. Nauk S.S.S.R. **120**, 3 (1958).
20. B. K. Vainshtein, A. N. Lobachev, and M. M. Stasova. Kristallographia, **3**, 452 (1958).
21. L. Pauling. The nature of the chemical bond. Cornell University Press. 1948. p. 189.
22. H. S. Gutowsky and G. E. Pake. J. Chem. Phys. **18**, 162 (1950).
23. E. R. Andrew and R. A. Newing. Proc. Phys. Soc. B, **72**, 959 (1958).
24. J. G. Powles and H. S. Gutowsky. J. Chem. Phys. **21**, 1704 (1953).
25. J. A. Ibers and D. P. Stevenson. J. Chem. Phys. **28**, 929 (1958).
26. E. R. Andrew. Bristol Conference on Defects in Crystalline Solids, July 1954. The Physical Society, London. p. 60.

Can. J. Chem. Downloaded from www.nrcresearchpress.com by 210.87.254.105 on 09/05/12
For personal use only.

Can. J. Chem. Downloaded from www.nrcresearchpress.com by 210.87.254.40 on 09/05/12
For personal use only.

CONSTITUTION OF A GLUCOMANNAN FROM THE WOOD OF EASTERN WHITE PINE (PINUS STROBUS L.)[1]

M. O. Gyaw and T. E. Timell

ABSTRACT

Glucomannans have been isolated from the wood of eastern white pine (*Pinus strobus* L.) by two different methods, the ratios of mannose to glucose being 3.8:1 and 2.7:1, respectively. The yields, based on the mannose content of the wood, were 70 and 50%. Partial acid hydrolysis gave 4-*O*-β-D-mannopyranosyl-D-mannose, 4-*O*-β-D-mannopyranosyl-D-glucose, 4-*O*-β-D-glucopyranosyl-D-mannose, 4-*O*-β-D-glucopyranosyl-D-glucose, *O*-β-D-mannopyranosyl-(1 → 4)-*O*-β-D-mannopyranosyl-(1 → 4)-D-mannose, and *O*-β-D-mannopyranosyl-(1 → 4)-*O*-β-D-mannopyranosyl-(1 → 4)-*O*-β-D-mannopyranosyl-(1 → 4)-D-mannose. The fully methylated polysaccharide on hydrolysis gave a mixture of di-*O*-methylhexoses, 2,3,6-tri-*O*-methyl-D-mannose, 2,3,6-tri-*O*-methyl-D-glucose, and 2,3,4,6-tetra-*O*-methylhexose (mostly mannose) in a mole ratio of 4:61:21:1. The number-average degrees of polymerization of the methylated and the nitrated glucomannans were 96 and 93. On the basis of this and other evidence it is concluded that the glucomannan contains at least 90 mannose and glucose residues linked together by (1 → 4)-β-glycosidic bonds to linear macromolecules. The nature and relative composition of the oligosaccharides obtained on partial hydrolysis indicate that very few of the glucose residues are contiguous. The glucomannan is compared with similar polysaccharides from the wood of other gymnosperms.

In recent years it has become evident that the mannose residues in the wood of gymnosperms largely originate from glucomannan (1) or galactoglucomannan (2) heteropolymers. Glucomannans are the main hemicelluloses of softwoods and have lately been isolated from several species. A previous investigation (3) dealt with an arabino-4-*O*-methylglucuronoxylan from the wood of white pine (*Pinus strobus* L.). The present paper is concerned with the isolation and properties of a glucomannan from the same species.

RESULTS AND DISCUSSION

White pine wood (11.7% mannose residues) was delignified with acid chlorite (4) to give a holocellulose which still contained at least 5% lignin. Extraction with aqueous sodium hydroxide containing borate (5) gave a mixture of hemicelluloses which was not amenable to resolution by complexing with copper (6). Better results were obtained by the barium hydroxide method (7), but the precipitated glucomannan still contained 6.4% galactose residues which could not be removed by further treatments.

A glucomannan from Scots pine (*Pinus sylvestris* L.) was recently also found to retain galactose residues which could be removed only after complete elimination of residual lignin (8). The present crude glucomannan had an ultraviolet spectrum indicative of the occurrence of lignin, and the latter was accordingly eliminated by treatment with chlorine and ethanolamine (9). The hemicellulose obtained on copper complexing of the delignified material contained less than 2% galactose residues. Evidently, the lignin left in the crude hemicellulose acted as a binding agent between the main glucomannan component and other polysaccharides containing galactose residues. Whether the association was of a chemical or physical nature could not be decided on the basis of the present evidence.

The purified glucomannan, $[\alpha]_D$ −32°, contained glucose and mannose residues in a ratio of 1:3.8 and amounted to 10.6% by weight of the wood. Osmotic pressure measure-

[1]*Manuscript received May 20, 1960.*
Contribution from the Pulp and Paper Research Institute of Canada and the Department of Chemistry, McGill University, Montreal, Que.

Can. J. Chem. Downloaded from www.nrcresearchpress.com by 210.87.254.40 on 09/05/12
For personal use only.

ments on the nitrate derivative (10) gave a number-average degree of polymerization of 82. The polysaccharide consumed 1.0 mole of periodate per hexose residue, thus suggesting the presence of (1 → 4)-glycosidic bonds.

In an alternative method of isolation of the glucomannan, wood meal was delignified with acid chlorite until the Klason lignin content was less than 1%. A hemicellulose mixture containing 5 parts of pentosan and 3 parts of hexosan was removed by extraction with aqueous potassium hydroxide. The residue, when extracted with sodium hydroxide containing borate, gave a hexosan containing only 3% xylose residues in a yield of 7% of the original wood. One precipitation with barium hydroxide lowered this yield to 6%. The glucomannan thus obtained contained 3% galactose residues and had a ratio of mannose to glucose of 2.7. Its number-average degree of polymerization was 93.

It is evident from this and other investigations (1, 11, 12) that the relative proportions of mannose and glucose residues in glucomannans are apt to vary considerably with the mode of isolation of these hemicelluloses. Of the two methods used here, the second was by far the least time-consuming and is preferable in spite of the somewhat lower yield. It is well known that prolonged treatment of wood with acid chlorite entails loss of carbohydrates (13, 14). In isolation of softwood hemicelluloses, this factor has to be weighed against the desirability of eliminating the lignin as completely as possible.

A portion of the glucomannan isolated by the first method was partially hydrolyzed with aqueous formic acid (15). The sugar mixture obtained was resolved on a column of charcoal–Celite (16) by gradient elution (17) with aqueous ethanol (18). Twelve oligosaccharides were collected, some of which were further purified by paper chromatography. Five of the oligosaccharides were crystallized and were fully identified, namely 4-*O*-β-D-mannopyranosyl-D-mannose (mannobiose), 4-*O*-β-D-glucopyranosyl-D-mannose, 4-*O*-β-D-glucopyranosyl-D-glucose (cellobiose), *O*-β-D-mannopyranosyl-(1 → 4)-*O*-β-D-mannopyranosyl-(1 → 4)-D-mannose, and *O*-β-D-mannopyranosyl-(1 → 4)-*O*-β-D-mannopyranosyl-(1 → 4)-*O*-β-D-mannopyranosyl-(1 → 4)-D-mannose. Two sugars could not be crystallized but were tentatively characterized as a (1 → 4)-β-linked *O*-mannosyl glucose and an *O*-glucosyl-*O*-mannosyl mannose. The paucity of material available prevented a characterization of the other oligosaccharides, all of which were evidently tri- or tetrasaccharides.

The mannobiose, mannosyl glucose, and glucosyl mannose have previously been isolated from many coniferous woods (12, 15, 19–24). The mannotriose has been obtained crystalline from loblolly pine (15) and white spruce wood (24) and was probably also present in glucomannan hydrolyzates from western hemlock (21), red cedar (22), and spruce sulphite pulp (23). The mannotetraose has been isolated previously only from vegetable ivory (25) and from white spruce wood (24). A mixed trisaccharide, apparently very similar to the compound obtained here, has been obtained from a spruce pulp (23).

The mannobiose was obtained in the highest yield (14.7%), followed by glucosyl mannose (5.4%), mannotriose (3.8%), mannotetraose (2.3%), mannosyl glucose (1.0%), and cellobiose (0.3%). Some of these results can undoubtedly be explained by the different stability towards acids of the glycosidic bonds, for example the five times higher yield of glucosyl mannose as compared with mannosyl glucose. This explanation cannot account, however, for the low yield of cellobiose which probably is more stable towards acids than any other of the oligosaccharides isolated. Low yields of cellobiose have been noticed on several occasions when softwood glucomannans were partially hydrolyzed (15, 23, 24, 26).

Can. J. Chem. Downloaded from www.nrcresearchpress.com by 210.87.254.40 on 09/05/12
For personal use only.

The glucomannan was methylated to completion and subsequently hydrolyzed to a mixture of sugars which was resolved on a charcoal–Celite column by gradient elution with aqueous ethanol. A mixture of di-*O*-methylhexoses, a tri-*O*-methylmannose, a tri-*O*-methylglucose, and a mixture of tetra-*O*-methylhexoses were obtained in a molar ratio of 4:61:21:1. The first fraction probably contained 2,6-di-*O*-methyl-D-glucose as its main component (8, 27). The following, and main, fraction was identified as 2,3,6-tri-*O*-methyl-D-mannose through its crystalline aniline and di-*p*-nitrobenzoate derivatives (28, 29). The tri-*O*-methylglucose crystallized and was also identified through its di-*p*-nitrobenzoate ester as 2,3,6-tri-*O*-methyl-D-glucose (29). The last fraction on demethylation gave mannose and a small quantity of glucose. Treatment with aniline, followed by repeated recrystallization, gave pure 2,3,4,6-tetra-*O*-methyl-*N*-phenyl-D-mannosylamine (30). This fraction consisted therefore predominantly of 2,3,4,6-tetra-*O*-methyl-D-mannose. The molar amount of this compound corresponded to one non-reducing end group per 87 hexose residues.

From the evidence adduced a simplified structure can now be assigned to the glucomannan present in the wood of white pine. The isolation of the two 2,3,6-tri-*O*-methyl-D-hexoses shows that the polysaccharide is composed of $(1 \rightarrow 4)$-linked D-mannopyranose and D-glucopyranose residues. The negative rotation of the original and the methylated hemicelluloses indicates that the hexose residues are present in the β-modification. The average number of hexose residues present in the methylated macromolecule was 96 while 87 such residues occurred for each non-reducing end group. An average number of 0.10 branch points per molecule was thus indicated. This number is so low, however, that the glucomannan might be regarded as essentially linear. Mannose residues apparently constituted the preponderant portion of the non-reducing end groups.

The nature of the hexose oligosaccharides isolated corroborate these conclusions. The low yield of cellobiose, in conjunction with the absence of any higher glucose oligosaccharides, show that very few of the glucose residues in the glucomannan were contiguous. The relatively high yields of mannobiose, mannotriose, and mannotetraose indicate that the glucose residues were probably interposed between blocks of contiguous mannose residues.

The mannose-to-glucose ratios of 2.7 and 3.8 found here are similar to those reported for other softwood glucomannans, such as (2.5) red cedar (22), (3) western hemlock (1, 21), (2.7) loblolly pine (15), (3.1–3.7) Scots pine (8, 31), (3.5–4) Norway spruce (27, 32), (2.5) Sitka spruce (12), and (3) white spruce (24, 33).

The evidence presently available concerning the linear or branched nature of softwood glucomannans is not conclusive. Glucomannans from red cedar (22), western hemlock (21), and Sitka spruce (12) are stated to be essentially linear, whereas similar glucomannans from Scots pine (8) and Norway spruce (27) are reported to be branched. The number-average degree of polymerization found here (93) is within the same range as the values observed for glucomannans from (130) western hemlock (21), (70–115) Scots pine (32), (68–100) Norway spruce (27), and (107) white spruce (24). All these polysaccharides were obtained after delignification of the wood with acid chlorite. In view of the now well-established depolymerizing action of this reagent on polysaccharides (9, 34), it seems almost certain that none of the above values represented the molecular magnitude of the native glucomannans. On the basis of previous results (34), an original number-average degree of polymerization of 200 for the present glucomannan does not appear unlikely.

Can. J. Chem. Downloaded from www.nrcresearchpress.com by 210.87.254.40 on 09/05/12
For personal use only.

CONCLUSIONS

The main structural features of the two preponderant hemicelluloses in the wood of white pine have now been established. One of these polysaccharides, which amounts to approximately 7% of the wood, is a (1 → 4)-β-linked xylan containing numerous single side chains of either (1 → 2)-α-linked 4-*O*-methyl-D-glucuronic acid or (1 → 3)-linked L-arabinofuranose residues. The other hemicellulose, which accounts for 10–14% of the wood, is a neutral (1 → 4)-linked hexosan containing about three times as many β-D-mannose as β-D-glucose residues. Both polysaccharides are linear or only slightly branched and both contain at least 100 but probably closer to 200 sugar residues in their native state.

The occurrence in the wood of gymnosperms of a predominant, neutral glucomannan together with an arabino-4-*O*-methylglucuronoxylan is apparently of early botanical origin. The same arrangement is found also for the wood of the now monotypical *Ginkgo biloba* (35), a phylogenetically far older gymnosperm (upper Carboniferous) than the present-day conifers. In contrast, the hemicelluloses of the botanically much younger arborescent angiosperms are characterized by the presence of a predominating 4-*O*-methylglucuronoxylan while the neutral glucomannan here has been relegated to a much more inconspicuous role.

EXPERIMENTAL

All specific rotations are equilibrium values and were determined at 20° C. Melting points are corrected. Evaporations were carried out *in vacuo* at 40–50° C.

Paper Chromatography

The following solvent systems (v/v) were used for separating the sugars: (A) ethyl acetate – acetic acid – water (9:2:2), (B) butan-1-ol – pyridine – water (10:3:3), (C) butan-1-ol – pyridine – water (6:4:4), and (D) butanone–water (89:11). Whatman No. 1 or, for preparative purposes, No. 3MM filter papers were used. Paper electrophoresis was carried out with Whatman No. 3MM filter paper in 0.05 *M* borate buffer at 750 or 2000 volts. *o*-Aminodiphenyl was used as a spray reagent and also for quantitative sugar analysis (36).

Isolation of a Mixture of Hemicelluloses

The preparation and properties of the wood sawdust used have been described previously (3). Extractive-free wood meal (40–60 mesh, 200 g) was suspended with stirring in water at 75–80° C. Acetic acid (20 ml) and sodium chlorite (60 g) were added and the reaction was allowed to proceed for 1 hour, when the same amounts of reagents were added. After a total time of 4 hours, the holocellulose was recovered by filtration, washed with water and then with ethanol, and dried in the air. Yield: 151 g, 75.5% of the wood. This process was repeated several times with new wood.

Chlorite holocellulose (300 g) was shaken with 17.5% (w/w) aqueous sodium hydroxide, to which 4% of boric acid had been added, in an atmosphere of nitrogen at room temperature for 3 hours. The alkaline solution was removed by filtration through fritted glass and the solid residue was washed with 17.5% sodium hydroxide (3 liters). Washing with aqueous acetic acid, water, and ethanol gave an alpha-cellulose (109 g). The alkaline solutions were poured into ice-cold ethanol (15 liters) containing glacial acetic acid (3 liters). The precipitate formed was recovered by filtration, washed in succession with

80% aqueous ethanol, ethanol, and petroleum ether (b.p. 30–60° C), and finally dried *in vacuo* to give a crude hemicellulose (118 g, 29.7% of the wood). Constituent sugars were galactose (3%), glucose (13%), mannose (41%), arabinose (8%), and xylose (35%).

Isolation of a Crude Glucomannan

The mixture of hemicelluloses (100 g) was dissolved in 5% sodium hydroxide (4 liters). The solution was centrifuged and a minor amount of insoluble material was removed. Saturated aqueous barium hydroxide (4 liters) was added dropwise with constant stirring (7). The precipitate formed was recovered on the centrifuge, washed twice with 5% sodium hydroxide, suspended in ice water, and acidified with acetic acid. The solution was poured into four times its volume of ethanol and the precipitate was recovered in the usual way. Yield: 68 g, 20.2% of the wood. Constituent sugars were galactose (6.4%), glucose (17.5%), mannose (70.3%), and xylose (5.8%). Further treatments with barium hydroxide or Fehling's solution (6) failed to alter the galactose content. The ultraviolet spectrum of the product exhibited a band at 280 mμ.

Purification of the Glucomannan

Glucomannan (35 g) was dissolved in water (3 liters). Gaseous chlorine was introduced into the solution at +6° C for 5 minutes (9). The solution was poured into ethanol (12 liters) and the recovered hemicellulose was suspended in ethanol (3 liters) containing 3% monoethanolamine for 5 minutes at 70° C. The polysaccharide was recovered by centrifuging and washed three times with ethanol after which it was added to water (3 liters). This delignification process was repeated three times. The polysaccharide was finally treated twice with Fehling's solution to yield a purified product (18 g, 10.4%). Analysis indicated the presence of galactose (2%), glucose (20%), and mannose (78%).

Isolation of a Glucomannan by an Alternative Method

Extractive-free wood meal (1385 g) was delignified with acid chlorite in the usual way (4) for 4 hours. The holocellulose (962 g, 69.6%) was extracted with 24% potassium hydroxide as described previously (3) to yield a mixture of hemicelluloses (155 g, 15.0%), containing 37% of hexosans. The solid residue (780 g) was shaken with 17.5% aqueous sodium hydroxide, to which 4% boric acid had been added, at room temperature for 5 hours. The alkaline solution was recovered by filtration and the residue was washed thoroughly with water. The filtrate and washings were poured into four times their volume of a 4:1 mixture of ethanol and acetic acid. The precipitate was recovered in the usual way to give a glucomannan (96 g, 7.0% of the wood), containing glucose and galactose (23%), mannose (68%), and xylose (3%). One precipitation with barium hydroxide (7) gave a product (83 g, 6.0%) which contained galactose (3%), glucose (26%), and mannose (71%). Specific rotation, $[\alpha]_D$ −32° (*c*, 1.0 in 10% sodium hydroxide).

Partial Hydrolysis of the Glucomannan and Resolution of the Hydrolyzate

A portion of the glucomannan obtained by the first method (10 g) was dissolved in 90% formic acid and diluted with water to 45% (100 ml). The solution, $[\alpha]_D$ −27°, was heated at 97° C for 3 hours when the specific rotation was +15° (after heating for 7 hours, $[\alpha]_D$ was +39°, equilibrium). Formic acid was removed by repeated evaporation from water after which the residue was boiled under reflux with 0.5 *N* sulphuric acid (320 ml) for 10 minutes for elimination of formate esters. The acid was neutralized with barium

Can. J. Chem. Downloaded from www.nrcresearchpress.com by 210.87.254.40 on 09/05/12
For personal use only.

carbonate and the solution obtained after filtration through Celite was deionized with Amberlite IR-120 (H^+) and Dowex 1-X4 (acetate) exchange resins.

A portion of the hydrolyzate (7.5 g) was added to the top of a Darco G-60 charcoal – Celite column (9) (1:1, w/w, 6×64 cm) and the sugars were removed by gradient elution (17) with aqueous ethanol (18) in the following order: water → 2% aqueous ethanol (3 liters each), 2% ethanol → 10% ethanol (4 liters), 10% ethanol → 20% ethanol (4 liters), and 20% ethanol → 40% ethanol (2 liters). The eluate was collected in 20-ml fractions at intervals of 30 minutes.

Identification of Sugars

All sugars were chromatographically identical with authentic specimens (solvents A, B, and C).

(1) Monosaccharides

A mixture of glucose and mannose in addition to minor amounts of xylose (2890 mg) was first obtained. The sugars were characterized only by paper chromatography (solvents A and B).

(2) 4-O-β-D-Mannopyranosyl-D-mannose

Hydrolysis of this fraction (1015 mg), the first oligosaccharide to be removed from the charcoal column, indicated the presence of mannose only. The mannobiose, after recrystallization from methanol, had a melting point and a mixed melting point of 209–210° C, $[\alpha]_D$ −8° (*c*, 3.5 in water) (37). The X-ray diffraction pattern and infrared diagram were identical with those from an authentic specimen.

(3) 4-O-β-D-Mannopyranosyl-D-glucose

This sirupy disaccharide (73 mg) had $[\alpha]_D$ +29° (*c*, 2.4 in water) (38) and on hydrolysis yielded equal amounts of glucose and mannose. After reduction with sodium borohydride only mannose was obtained on hydrolysis. The mannosyl glucose could not be induced to crystallize.

(4) 4-O-β-D-Glucopyranosyl-D-glucose

This fraction (107 mg) was a mixture of a disaccharide and a tetraose. Resolution by paper chromatography (solvent C) gave pure cellobiose (23 mg), $[\alpha]_D$ +35° (*c*, 1.0 in water). Recrystallization from methanol gave a melting point and a mixed melting point of 234–235° C (39).

(5) O-β-D-Mannopyranosyl-(1 → 4)-O-β-D-mannopyranosyl-(1 → 4)-D-mannose

This trisaccharide (262 mg) on hydrolysis gave mannose and on partial hydrolysis mannobiose and mannose. Analysis by the method of Peat, Whelan, and Roberts (40) suggested a degree of polymerization of 2.8. The product crystallized from ethanol, m.p. and mixed m.p. 165–168° C, $[\alpha]_D$ −25° (*c*, 2.4 in water) (41).

(6) 4-O-β-D-Glucopyranosyl-D-mannose

Hydrolysis of this disaccharide (373 mg) gave equal amounts of glucose and mannose. The compound crystallized from ethanol, m.p. and mixed m.p. 134–137° C, $[\alpha]_D$ +10° (*c*, 4.0 in water) (42). The octaacetate derivative had a melting point and a mixed melting point of 201° C, $[\alpha]_D$ +34° (*c*, 1.0 in chloroform).

(7) O-Glucosyl-O-mannosyl Mannose

This fraction (285 mg), $[\alpha]_D$ −8° (*c*, 6.6 in water), on hydrolysis yielded glucose and mannose in a ratio of 1:2. Reduction with sodium borohydride followed by hydrolysis

Can. J. Chem. Downloaded from www.nrcresearchpress.com by 210.87.254.40 on 09/05/12
For personal use only.

gave equal amounts of glucose and mannose. The degree of polymerization of the compound was 2.9 (40). Partial hydrolysis with formic acid gave mannobiose, glucosyl mannose, glucose, and mannose.

*(8) O-β-*D*-Mannopyranosyl-(1 → 4)-O-β-*D*-mannopyranosyl-(1 → 4)-O-β-*D*-mannopyranosyl-(1 → 4)-*D*-mannose*

At this stage, elution of the column gave a mixture of trisaccharides which was not further examined (941 mg). Subsequent elution gave a mixture of higher oligosaccharides (1034 mg) which, on resolution by paper chromatography (solvent C), yielded a pure mannotetraose (114 mg). The compound on recrystallization from aqueous ethanol had a melting point and a mixed melting point of 232–234° C, $[\alpha]_D$ −31° (*c*, 1.0 in water) (25). Partial hydrolysis gave mannotriose, mannobiose, and mannose.

Methylation of the Glucomannan

Glucomannan (19 g) was dissolved in 30% (w/w) aqueous sodium hydroxide (400 ml) in an atmosphere of nitrogen, and dimethyl sulphate (200 ml) was added dropwise at 0° C over a period of 8 hours (43). This treatment was repeated twice. The reaction mixture was neutralized with sulphuric acid, concentrated to 1 liter, and dialyzed against running water for 1 week. The polysaccharide solution was concentrated to 200 ml and freeze-dried for 2 days, yielding a powder of partially methylated glucomannan (18 g, OCH_3, 26.8%). The product was dissolved in dry dimethyl formamide (44). Silver oxide (50 g) and methyl iodide (50 ml) were added and the mixture was shaken at 30° C for 20 hours. The same amounts of reagents were added and the reaction mixture was again shaken for 20 hours. The insoluble, grayish mass was washed on the centrifuge with chloroform. The solution obtained was washed with 5% aqueous potassium cyanide (3×300 ml) and then with water (3×500 ml). After drying over anhydrous sodium sulphate, the chloroform solution was concentrated to 200 ml and poured slowly with stirring into petroleum ether (2 liters) to yield a white powder (14 g).

After one more methylation as above, the product was methylated according to Purdie (45) with methyl iodide (200 ml) and silver oxide (80 g). The final product had $[\alpha]_D$ −21° (*c*, 1.0 in chloroform). Anal. Calc. for a fully methylated glucomannan: OCH_3, 45.3%. Found: OCH_3, 45.0%. The infrared spectrum of the polysaccharide indicated the absence of hydroxyl groups.

Hydrolysis of the Methylated Glucomannan and Resolution of the Hydrolyzate

The fully methylated polysaccharide (4.0 g) was boiled under reflux with 0.7 *N* methanolic hydrogen chloride for 12 hours. Most of the methanol was removed and *N* hydrochloric acid (120 ml) was added. The solution was refluxed for 7 hours, neutralized with silver carbonate, filtered through Celite, treated with hydrogen sulphide, and again filtered. Chromatographic examination (solvent D) of the sirupy hydrolyzate (3.6 g) revealed the presence of di-, tri-, and tetra-*O*-methylhexoses.

A portion of the sirup (3.4 g) was added to the top of a Darco G-60 charcoal – Celite column (5×56 cm) and subjected to gradient elution with 4 liters each of 5% aqueous ethanol → 20% ethanol and 20% ethanol → 40% ethanol.

Preliminary Characterization of Di-O-methylhexoses

Paper electrophoresis indicated the presence of three components in the fraction first eluted from the charcoal column (156 mg). The principal component gave only glucose

Can. J. Chem. Downloaded from www.nrcresearchpress.com by 210.87.254.40 on 09/05/12
For personal use only.

on demethylation with hydrobromic acid (46). It was chromatographically and electrophoretically indistinguishable from 2,6-di-*O*-methyl-D-glucose. The other two components were electrophoretically similar to 2,4- and 3,6-di-*O*-methylglucose.

Identification of 2,3,6-Tri-O-methyl-D-mannose

The second fraction (2400 mg) was further purified by paper chromatography (solvent D). The sirup had $[\alpha]_D$ −12.6° (*c*, 2.6 in water) (47). A portion of the compound (100 mg) was converted to the 1,4-di-*p*-nitrobenzoate derivative (80 mg), m.p. and mixed m.p. 187–188° C, $[\alpha]_D$ +33° (*c*, 1.0 in chloroform), after recrystallization from ethanol (29). Recrystallization from ethyl acetate gave needles, m.p. 187–188° C. The 2,3,6-tri-*O*-methyl-*N*-phenyl-D-mannopyranosylamine had a melting point of 125° C, $[\alpha]_D$ −152° (*c*, 0.6 in methanol) (28).

Identification of 2,3,6-Tri-O-methyl-D-glucose

The third fraction (814 mg) on recrystallization from ethyl ether had a melting point and a mixed melting point of 120–121° C, $[\alpha]_D$ +70° C (*c*, 1.0 in water) (47). The 1,4-di-*p*-nitrobenzoate derivative (29), on recrystallization from methanol, had a melting point and a mixed melting point of 189–190° C, $[\alpha]_D$ −34° (*c*, 0.7 in chloroform).

Identification of 2,3,4,6-Tetra-O-methyl-D-mannose

The fourth fraction (43.7 mg) on demethylation yielded glucose and mannose and was a mixture of the 2,3,4,6-tetra-*O*-methyl derivative of glucose and mannose, $[\alpha]_D$ +4.8° (*c*, 4.4 in water). The infrared spectrum of the sirup agreed closely with that of 2,3,4,6-tetra-*O*-methyl-D-mannose. Treatment with aniline gave 2,3,4,6-tetra-*O*-methyl-*N*-phenyl-D-mannosylamine, m.p. and mixed m.p. 145–146° C (30), after three recrystallizations from ethyl ether.

Periodate Oxidation of the Glucomannan

Glucomannan (150–200 mg) was oxidized for various lengths of time in the dark at 30° C with 0.05 *M* sodium metaperiodate (50 ml). The consumption of periodate was measured by the excess arsenite method. The molar consumption of periodate per hexose residue was 1.0.

Preparation of the Nitrate Derivative of the Glucomannan

Glucomannan (1 g) was treated with a mixture of nitric acid, phosphoric acid, and phosphorus pentoxide (64:26:10, w/w) at +17° C for 1 hour (48). The reaction mixture was poured into aqueous acetic acid (1:1) cooled to −16° C. The nitrate was recovered by filtration and washed with water until the washings were neutral. Yield, 90%; nitrogen content (49), 13.56%. A duplicate experiment gave a product with the same nitrogen content and in the same yield.

Determination of the Number-Average Molecular Weight of the Methylated and the Nitrated Glucomannans

The osmometers were of the modified (49) Zimm–Myerson (50) type. The membranes were of gel cellophane and the solvent was a mixture of chloroform and ethanol (9:1, v/v) for the methylated and *n*-butyl acetate for the nitrated glucomannan. The temperature was 30±0.01° C and the static method of measuring the osmotic height was used. The results obtained are summarized in Table I.

Can. J. Chem. Downloaded from www.nrcresearchpress.com by 210.87.254.40 on 09/05/12
For personal use only.

TABLE I

Osmometry data

Nitrate ester				Methyl ether	
Preparation I*		Preparation II†			
w‡	h/w§	w	h/w	w	h/w
4.429	1.176	5.004	1.026	2.511	1.444
2.218	1.163	3.151	1.018	1.952	1.363
2.198	1.139	2.225	0.991	1.399	1.343
1.121	1.108	1.330	1.006	0.823	1.334
0	1.11	0	0.98	0	1.31

*Glucomannan isolated by first method.
†Glucomannan isolated by second method.
‡Concentration in grams/kilogram of solution.
§Osmotic height in centimeters of solution/concentration.

ACKNOWLEDGMENT

M. O. Gyaw wishes to express his gratitude to the Technical Co-operation Service of the Department of Trade and Commerce for financial assistance through the Colombo plan.

REFERENCES

1. J. K. HAMILTON, H. W. KIRCHER, and N. S. THOMPSON. J. Am. Chem. Soc. **78**, 2508 (1956).
2. J. K. HAMILTON, E. V. PARTLOW, and N. S. THOMPSON. J. Am. Chem. Soc. **82**, 451 (1960).
3. S. K. BANERJEE and T. E. TIMELL. Tappi. In press.
4. L. E. WISE, M. MURPHY, and A. A. D'ADDIECO. Paper Trade J. **122**, No. 2, 35 (1946).
5. J. K. N. JONES, L. E. WISE, and J. P. JAPPE. Tappi, **39**, 139 (1956).
6. E. SALKOWSKI. Ber. **27**, 497 (1894).
7. H. MEIER. Acta Chem. Scand. **12**, 144 (1958).
8. H. MEIER. Acta Chem. Scand. **12**, 1911 (1958).
9. T. E. TIMELL and E. C. JAHN. Svensk Papperstidn. **54**, 831 (1951).
10. C. P. J. GLAUDEMANS and T. E. TIMELL. Svensk Papperstidn. **61**, 1 (1958).
11. G. G. S. DUTTON and K. HUNT. J. Am. Chem. Soc. **80**, 5697 (1958).
12. G. O. ASPINALL, R. A. LAIDLAW, and R. B. RASHBROOK. J. Chem. Soc. 4444 (1957).
13. B. L. BROWNING and L. O. BUBLITZ. Tappi, **36**, 452 (1953).
14. H. O. BOUVENG and H. MEIER. Acta Chem. Scand. **13**, 1884 (1959).
15. J. K. N. JONES and T. J. PAINTER. J. Chem. Soc. 669 (1957); 573 (1959).
16. R. L. WHISTLER and D. F. DURSO. J. Am. Chem. Soc. **72**, 677 (1950).
17. R. S. ALM. Acta Chem. Scand. **6**, 1186 (1952).
18. B. LINDBERG and B. WICKBERG. Acta Chem. Scand. **8**, 569 (1954).
19. J. G. LEECH. Tappi, **35**, 249 (1952).
20. A. ANTHIS. Tappi, **39**, 401 (1956).
21. J. K. HAMILTON and H. W. KIRCHER. J. Am. Chem. Soc. **80**, 5703 (1958).
22. J. K. HAMILTON and E. V. PARTLOW. J. Am. Chem. Soc. **80**, 4880 (1958).
23. E. MERLER and L. E. WISE. Tappi, **41**, 80 (1958).
24. A. TYMINSKI and T. E. TIMELL. J. Am. Chem. Soc. 82 (1960).
25. G. O. ASPINALL, R. B. RASHBROOK, and G. KESSLER. J. Chem. Soc. 215 (1958).
26. J. K. HAMILTON, E. V. PARTLOW, and N. S. THOMPSON. Tappi, **41**, 803 (1958).
27. I. CROON and B. LINDBERG. Acta Chem. Scand. **12**, 453 (1958).
28. W. N. HAWORTH, E. L. HIRST, and H. R. L. STREIGHT. J. Chem. Soc. 1349 (1931).
29. P. A. REBERS and F. SMITH. J. Am. Chem. Soc. **76**, 6097 (1954).
30. W. N. HAWORTH, R. L. HEATH, and S. PEAT. J. Chem. Soc. 833 (1941).
31. I. CROON, B. LINDBERG, and H. MEIER. Acta Chem. Scand. **13**, 1299 (1959).
32. B. LINDBERG and H. MEIER. Svensk Papperstidn. **60**, 785 (1957).
33. T. E. TIMELL and A. TYMINSKI. Tappi, **40**, 519 (1957).
34. C. P. J. GLAUDEMANS and T. E. TIMELL. Svensk Papperstidn. **60**, 869 (1957).
35. A. JABBAR MIAN and T. E. TIMELL. Unpublished results.
36. T. E. TIMELL, C. P. J. GLAUDEMANS, and A. L. CURRIE. Anal. Chem. **28**, 1916 (1956).
37. R. L. WHISTLER and J. Z. STEIN. J. Am. Chem. Soc. **73**, 4169 (1951).
38. F. SMITH and H. C. SRIVASTAVA. J. Am. Chem. Soc. **78**, 1404 (1956).
39. Z. H. SKRAUP and J. KÖNIG. Monatsh. **22**, 1011 (1901).

Can. J. Chem. Downloaded from www.nrcresearchpress.com by 210.87.254.40 on 09/05/12
For personal use only.

40. S. PEAT, W. J. WHELAN, and J. G. ROBERTS. J. Chem. Soc. 2258 (1956).
41. R. L. WHISTLER and C. G. SMITH. J. Am. Chem. Soc. **74**, 3795 (1952).
42. M. BERGMAN and H. SCHOTTE. Ber. **54**, 1564 (1921).
43. W. N. HAWORTH. J. Chem. Soc. **107**, 8 (1915).
44. R. KUHN, H. TRISCHMANN, and I. LÖW. Angew. Chem. **67**, 32 (1955).
45. T. PURDIE and J. C. IRVINE. J. Chem. Soc. **83**, 1021 (1903); **85**, 1049 (1904).
46. L. HOUGH, J. K. N. JONES, and W. H. WADMAN. J. Chem. Soc. 1702 (1950).
47. J. C. IRVINE and E. L. HIRST. J. Chem. Soc. **121**, 1213 (1922).
48. W. J. ALEXANDER and R. L. MITCHELL. Anal. Chem. **21**, 1497 (1949).
49. J. V. STABIN and E. H. IMMERGUT. J. Polymer Sci. **14**, 209 (1954).
50. B. H. ZIMM and I. MYERSON. J. Am. Chem. Soc. **68**, 911 (1946).

Can. J. Chem. Downloaded from www.nrcresearchpress.com by 210.87.254.40 on 09/05/12
For personal use only.

CATIONIC POLYMERIZATION OF ETHYLENE OXIDE

IV. THE PROPAGATION REACTIONS[1]

G. T. MERRALL, G. A. LATRÉMOUILLE, AND A. M. EASTHAM

ABSTRACT

Studies of the boron-fluoride-catalyzed reaction of ethylene oxide with simple alcohols and low molecular weight polyglycols indicate three ways in which chain growth could occur, but only one of these is considered to be important after the initial stages of polymerization. The rate of disappearance of monomer reaches a maximum at a molecular weight of about 400. A mechanism is proposed to account for both polymerization and depolymerization and it is shown how equilibrium between these two reactions could result.

Can. J. Chem. Downloaded from www.nrcresearchpress.com by 210.87.254.6 on 09/05/12
For personal use only.

The polymerization of ethylene oxide by boron fluoride is a complex process in which the propagation reaction must compete with an apparently independent depolymerization reaction. The depolymerization process, as discussed in the previous paper (1), breaks down the polyglycol to dioxane seemingly through a chain reaction propagated by oxonium ions acting upon the ether linkages in the polymer molecule. The polymerization on the other hand appears to occur through a stepwise addition of monomer to the terminal hydroxyls of the polymer chain. A study was therefore undertaken of the reaction of ethylene oxide with alcohols in the presence of boron fluoride in an effort to obtain a mechanism for the propagation and to observe the transition from propagation to depolymerization. This paper presents the results of these studies.

EXPERIMENTAL

Ethylene chloride, ethylene oxide, and boron fluoride were prepared for use as previously described (2). Volatile alcohols were dried by distillation from their magnesium alcoholates in the usual way and ethers were dried over sodium metal or calcium hydride. Wherever the reactants were sufficiently volatile they were stored on the vacuum system and transferred by distillation. The polyglycols were either stirred under high vacuum for several hours or dissolved in dry ethylene chloride and pumped free from solvent before use.

Molecular weights were determined by viscosity measurements as before, but in a few cases were confirmed by freezing point depressions in benzene. Where hydroxyl content of the polymer was important, end group analysis by acetylation with acetyl chloride in pyridine, according to the method of Smith and Bryant (3), was used. All three methods gave satisfactory agreement.

Reactions were carried out in ethylene chloride solution at 20° C. Rates were followed either by the decrease in vapor pressure of ethylene oxide as described in the earlier work, or by a dilatometric method. The dilatometers were so constructed that they could be dried and filled under vacuum and then transferred to a constant temperature bath while exposing only the capillary tip to the atmosphere. Absolute contractions were not determined but the contraction per unit of oxide appeared to be constant over the range of the experiments. The two methods gave good agreement wherever they could be compared.

[1]*Manuscript received May 13, 1960.*
Contribution from the Division of Applied Chemistry, National Research Council, Ottawa, Canada.
Issued as N.R.C. No. 5932.

RESULTS AND DISCUSSION

Before discussing the reaction of ethylene oxide with alcohols, it is necessary to draw some conclusions as to the probable distribution of boron fluoride in a system containing both hydroxyl and ether groups. We know (4) that boron fluoride with water forms both monohydrates and dihydrates and that the second molecule of water is held, at least in the crystal, as the hydronium ion,

$$BF_3 \overset{H_2O}{\rightleftharpoons} BF_3{:}H_2O \overset{H_2O}{\rightleftharpoons} H_3\overset{+}{O} \ldots \overset{-}{B}F_3OH.$$

The dihydrate is much the more stable of the two complexes but in the corresponding alcoholates this difference in stability appears to be much smaller. Ethers yield 1:1 compounds with boron fluoride but in the presence of alcohols they yield ternary complexes, analogous to the dihydrates, in which the ether is held by hydrogen bonding,

$$ROH{:}BF_3 + R'_2O \rightleftharpoons RO{:}BF_3 \ldots HOR'_2 \rightleftharpoons ROH + R'_2O{:}BF_3.$$

Obviously then, in a solution of hydroxyl and ether groups such as one has with the polyglycols, the boron fluoride will be present as an equilibrium mixture of several complexes and, since the reaction rates will depend on the concentrations and reactivities of the various species present, a rigorous interpretation of the kinetics will require an accurate knowledge of all the equilibrium constants. Information of this kind is not available nor is it likely to be for some time to come so a few simple experiments were conducted in an effort to obtain some idea of the relative importance of the various complexes.

The relative basicities of a few ethers towards boron fluoride were examined by equilibrating the ethers in ethylene dichloride solution against dimethyl ether and boron fluoride. The concentration of free dimethyl ether in solution was obtained from its vapor pressure and the position of the equilibrium was then calculated from the known initial concentrations of all reactants. Constants obtained in this way held very well over about a fivefold range of concentrations and, where comparison could be made, were in good agreement with values calculated from the data of Brown and Adams (5) for the thermal dissociation of boron fluoride etherates. A few values of the relative basicities are listed in Table I.

TABLE I

Dimethyl ether	1
Di-*n*-butyl ether	0.16
Dioxane (molar basis)	0.115
Tetrahydrofurane	25.

Ethylene oxide unfortunately could not be examined because of its high reactivity, but the dimethyl ether of diethylene glycol, $CH_3OCH_2CH_2OCH_2CH_2OCH_3$, is of some interest because of its similarity to the polyglycols. In our experiments this molecule was found to add only two molecules of boron fluoride and of these one seemed to be held quite loosely. At low boron fluoride concentrations, however, the triether was quite basic with a relative basicity, on a molar basis, of about 0.4. In a similar manner a little information was obtained about the ternary complexes. If one adds dimethyl ether to a solution of equimolar amounts of boron fluoride and *n*-butanol, then an amount of ether equal to

Can. J. Chem. Downloaded from www.nrcresearchpress.com by 210.87.254.6 on 09/05/12
For personal use only.

the boron fluoride is removed from the solution. Since addition of further alcohol regenerates some ether, an equilibrium of the type

$$ROBF_3 \ldots H \ldots OR'_2 + ROH \rightleftharpoons ROBF_3 \ldots H \ldots HOR + R'_2O$$

seems indicated so, on the assumption that any binary complexes present are in low concentration compared with the ternaries, an equilibrium constant can be obtained. This constant was found to hold surprisingly well over the short range of concentrations which could be examined and indicated that the dimethyl ether was about 1.5 times as basic as *n*-butanol towards the acid ROH:BF_3. From subsequent experiments it seems likely that at high ratios of ether to alcohol serious interference from the binary ether – boron fluoride complex may occur, but as much of our work has been carried out at low values of this ratio, we feel justified in assuming that the catalyst will be present largely as the ternary complex in most of our reaction mixtures. Furthermore, as alcohols and ethers seem to have rather similar basicities, we must expect that a mixture of ternary complexes will be present.

Ethylene oxide reacts with simple alcohols to give the β-alkoxyethanols which can in turn react with further monomer. Since the latter reaction is several times more rapid than the initial one, rates must be obtained either from initial slopes or from experiments at high alcohol/oxide ratios. The results obtained with *n*-butanol are shown in Table II

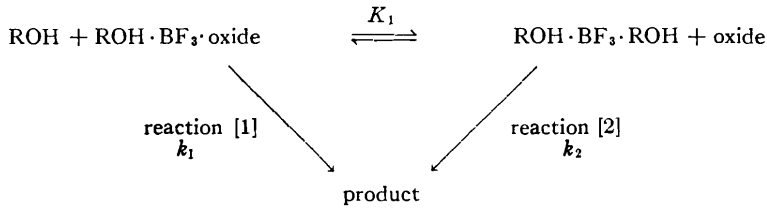
TABLE II

Reaction of *n*-butanol with ethylene oxide

Butanol	Oxide	BF_3	Initial rate, moles liter^{-1} min^{-1} Observed	Calculated
		Vapor pressure method		
0.26	1.10	.0093	.025	.0285
0.26	1.10	.0150	.040	.046
0.52	0.50	.0121	.0095	.0107
0.52	0.55	.0191	.017	.0202
0.52	0.52	.0191	.0175	.0192
0.52	1.10	.0066	.013	.0128
0.52	1.10	.0099	.019	.0192
0.52	1.10	.0166	.0335	.0322
0.52	1.10	.0188	.040	.0365
0.52	1.64	.0190	.062	.0502
1.0	0.52	.0220	.014	.0142
1.0	0.535	.0218	.015	.0145
1.0	1.10	.0117	.0155	.0152
1.0	1.10	.0160	.020	.0208
1.0	1.10	.0208	.030	.0270
1.0	1.56	.0069	.0115	.0123
1.0	1.56	.0118	.021	.0210
1.0	1.56	.0118	.0205	.0210
1.0	1.56	.0127	.022	.0226
1.0	1.56	.0203	.0435	.036
1.4	1.52	.0121	.018	.0172
		Dilatometric method		
0.52	1.110	.0095	.00184	.00218
0.62	0.233	.0104	.0041	.00435
1.0	0.083	.0181	.00202	.00195
1.0	0.115	.0109	.00125	.00161
1.43	0.102	.0153	.00156	.00160
1.43	0.116	.0146	.00162	.00173

Can. J. Chem. Downloaded from www.nrcresearchpress.com by 210.87.254.6 on 09/05/12
For personal use only.

but essentially similar results were obtained with ethanol. The rate of the reaction decreases with increasing alcohol concentration. From our previous discussion it seems most probable that this decrease is due to an increase in the concentration of boron fluoride dialcoholate, so we may suppose that the rate is governed by the following reactions,



where reaction [1] is the unimolecular rearrangement of a ternary complex of all three reactants while reaction [2] is a bimolecular reaction between ethylene oxide and the boron fluoride dialcoholate. The rate expression for this system, assuming only ternary complexes, is found to be

$$-\frac{d(\text{oxide})}{dt} = (BF_3)(\text{oxide})\,\frac{k_1K_1+k_2(\text{ROH})}{K_1(\text{oxide})+(\text{ROH})}$$

which, when assigned the following values for the constants, $K_1 = 0.1$, $k_1 = 9$ min^{-1}, and $k_2 = 0.4$ liter mole^{-1} min^{-1}, gives the calculated rates shown in Table II. The agreement with the experimental values is good but since there are three constants to adjust such agreement does not mean a great deal. The real test of the mechanism would perhaps be an independent measurement of the equilibrium constant K_1, i.e. of the basicity of ethylene oxide and this, as noted above, we were unable to obtain. The above kinetic value of K_1 suggests that the oxide is about 1/10th as basic as *n*-butanol and hence about 15 times less basic than dimethyl ether, so is in agreement with qualitative experiments (6) which indicate that epoxides are among the least basic of the simple ethers.

The reaction of ethylene oxide with a simple alcohol is the first step in an addition polymerization in which the second and third steps can be represented by the reactions of the monoethyl ethers of glycol (Cellosolve) and diethylene glycol (Carbitol), respectively. The results of some dilatometric experiments with these alcohols are shown in Fig. 1; vapor pressure measurements were in reasonable agreement with the dilatometric measurements at the higher alcohol concentrations but diverged at the lower ones. The rate measurements show a minimum with both Cellosolve and Carbitol at low alcohol concentration. We have examined this region carefully and feel that the minimum is probably real but admittedly it could be due to a breakdown of the dilatometric method in this region or to experimental errors which tend to accumulate at low alcohol concentrations. If it is real, it would appear that the increasing rate at very low hydroxyl concentrations corresponds to an extension of the curve for *n*-butanol to low alcohol concentrations, i.e. to a region where reaction [1] is dominant. This view receives some support from the fact that no minimum is evident in runs with a polyglycol of molecular weight 600 (Fig. 1) where the contribution from reaction [1] would be reduced markedly by the competition of the polymer ether groups for the boron fluoride. While the presence of the minimum is disturbing, its presence should not be allowed to obscure the most important conclusion from these results, namely, that a clear change in mechanism, not

Can. J. Chem. Downloaded from www.nrcresearchpress.com by 210.87.254.6 on 09/05/12
For personal use only.

Can. J. Chem. Downloaded from www.nrcresearchpress.com by 210.87.254.6 on 09/05/12
For personal use only.

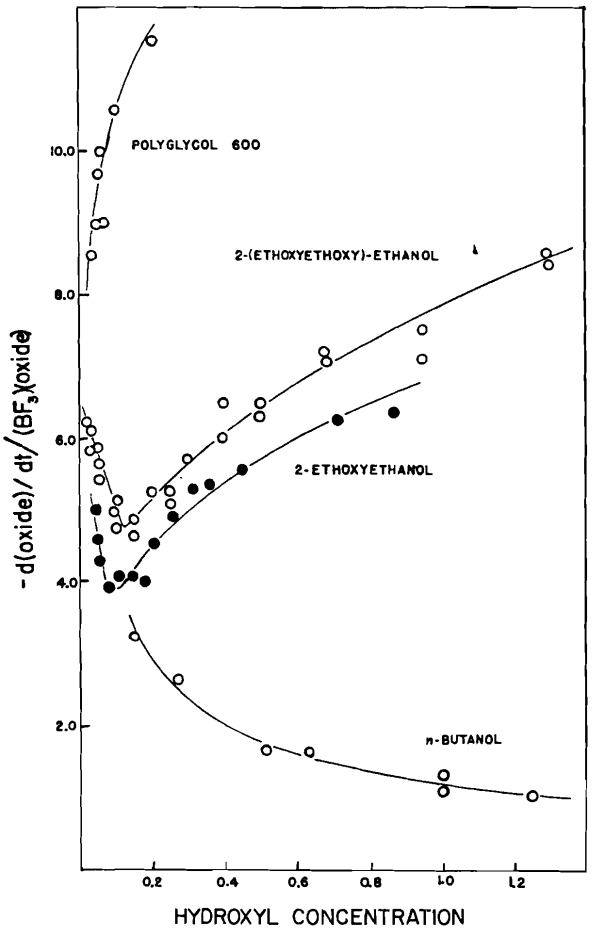
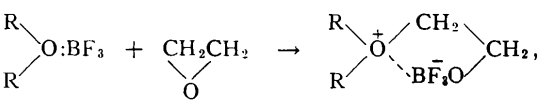


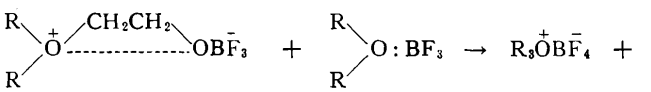
FIG. 1.

merely a change in rate, has occurred in passing from the simple alcohols to the β-ether alcohols. This change must be due to the presence of the ether groups and suggests that an oxonium ion type of reaction is important even at this early stage of the polymerization.

Meerwein and his co-workers have shown (7) that epoxides react, both rapidly and quantitatively, with anhydrous ethers and boron fluoride to form the inner oxonium salts,



which can then react with further etherate to form the tertiary salts,



The inner salts differ from the tertiaries in being very unstable and insoluble so most probably account for the precipitation and discoloration we observe in the absence of

hydroxyl groups. It may be that the hydroxyl groups decompose the inner salts as formed, but an alternative explanation is possible and would account for other aspects of the polymerization process. Klages and Meuresch (8) showed that ether complexes of very strong acids will react with diazomethanes to form tertiary oxonium salts, both rapidly and quantitatively,

$$R_2O\text{-------}HBF_4 \quad + \quad R'CHN_2 \quad \rightarrow \quad R_2\overset{+}{O}CH_2R'\text{-------}\overline{BF_4} \quad + \quad N_2.$$

The acid–ether complexes here are closely similar to the alcohol–ether – boron fluoride complexes encountered in the present work so if ethylene oxide could replace the diazomethane, tertiary oxonium ions would be formed directly according to the reaction

$$RO{:}BF_3\text{--------}H\text{-------}OR'_2 \quad + \quad \underset{\diagdown O \diagup}{CH_2-CH_2} \quad \xrightarrow{k_4} \quad R'_2\overset{+}{O}CH_2CH_2OH\text{--------}\overline{BF_3}OR. \qquad [4]$$

A reaction of this form seems best able to account for the rapid reaction of ethylene oxide with the lower ether alcohols and may be considered as an exact analogue of reaction [2], differing from it only in the stability of the product; in reaction [2] the catalyst is regenerated immediately

$$RO{:}\overline{BF_3}\text{-------}H\text{—}\overset{H^+}{\underset{|}{O}}R \quad + \quad \underset{\diagdown O \diagup}{CH_2CH_2} \quad \xrightarrow{k'_2} \quad RO\overset{H^+}{\underset{|}{C}}H_2CH_2OH\text{--------}\overline{BF_3}OR \qquad [2]$$

whereas in reaction [4] the oxonium ion is sufficiently stable that it must be decomposed by reaction with a hydroxyl group, i.e.

$$R'_2\overset{+}{O}CH_2CH_2OH \quad + \quad ROH \quad \xrightarrow{k_5} \quad R'_2O \quad + \quad RO\overset{H^+}{\underset{|}{C}}H_2CH_2OH. \qquad [5]$$

The net effect of this formation and destruction of the oxonium ion is to lengthen a chain by one oxide unit so we now have three processes which can lead to chain growth, reactions [1], [2], and [4, 5], all of which must be considered as important in the reaction of Cellosolve and Carbitol. The system is obviously too complex for complete kinetic analysis but under conditions of high alcohol/oxide ratios, as in some of the dilatometric experiments, reaction [1] should not be important and the boron fluoride will be distributed between two ternary complexes,

$$ROH\cdot BF_3\cdot\text{alcohol}/ROH\cdot BF_3\cdot\text{ether} = K_2,$$

according to whether hydrogen bonding takes place at an alcohol or ether group. The value of K_2 will be governed by the ratio of ether to alcohol groups in the molecule and not by the concentration of the ether–alcohol; it will decrease as the chain grows longer. If steady-state conditions were to apply to the oxonium ion, the rate expression for the system would be

$$-\frac{d(\text{oxide})}{dt} = \frac{k'_2K_2+k_4k_5}{K_2+1+\dfrac{k_4(\text{oxide})}{k_5(ROH)}}(BF_3)(\text{oxide}),$$

or if reaction [5] were very rapid compared with [4]

$$-\frac{d(\text{oxide})}{dt} = \frac{k'_2K_2+k_4}{K_2+1}(BF_3)(\text{oxide}).$$

Can. J. Chem. Downloaded from www.nrcresearchpress.com by 210.87.254.6 on 09/05/12
For personal use only.

These very similar expressions are in agreement with the observed first-order dependence on boron fluoride and ethylene oxide but require that the rate be independent of hydroxyl concentration. It is evident in Fig. 1 that at the higher alcohol concentrations where reaction [1] can be disregarded, the rates do in fact tend towards such independence without actually achieving it. This failure of the rate expressions is probably due to the high rate of reaction [4], which invalidates the assumptions used in deriving them.

Extension of these results to low molecular weight polymers is not simple. Rate expressions of the type just considered suggest that as the molecular weight increases and K_2 becomes very small, the reaction should reduce to a simple second-order process. In fact, however, at high molecular weights (3000–4000) the rate of oxide disappearance becomes very slow and independent of monomer concentration. For reasons detailed in the previous paper (1), we believe that this slow zero-order rate is due to the formation of stable oxonium ions which do not react directly with ethylene oxide with the result that reaction [5] becomes rate controlling. (In solutions of high molecular weight polymer the hydroxyl concentration is, of necessity, low.) Between the two extremes of the very low and the high molecular weight polyglycols the rate of reaction of oxide with the glycols, at constant hydroxyl concentration, passes through a maximum at a molecular weight of about 400. The order in oxide at moleculer weights below the maximum is always one or nearly so, but at higher molecular weights it drops off steadily. If, as we believe, the order is determined by the relative rates of reactions [4] and [5], then it is legitimate to compare initial rates of oxide disappearance and this is done in Fig. 2 for initial concentrations of boron fluoride and ethylene oxide of 0.012 M and 0.55 M, respectively.

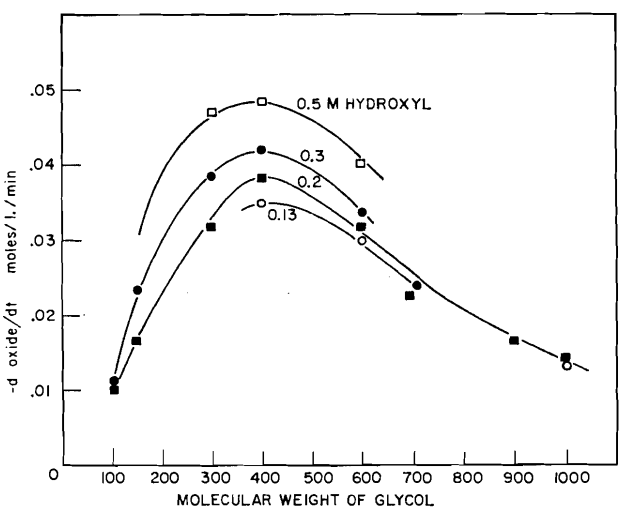
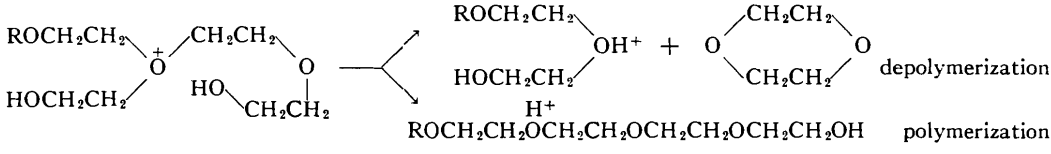


FIG. 2.

It was stated earlier that the increase in rate in passing from the simple alcohols to the ether alcohols is most probably due to a contribution from a reaction proceeding via oxonium ions. On the other hand, the decrease in both rate and order at higher molecular weights is almost certainly due to the presence of stable oxonium ions, so the problem is to resolve this apparent conflict in a way which will account for the rate maximum at molecular weight 400. Dilatometric experiments with low molecular weight polymer and very small amounts of monomer suggest strongly that reaction [4], oxonium ion formation,

Can. J. Chem. Downloaded from www.nrcresearchpress.com by 210.87.254.6 on 09/05/12
For personal use only.

is very fast even at molecular weights well above 400 (Fig. 1), so the over-all rate must be governed largely by reaction [5]. It follows that reaction [5] must be especially rapid in the molecular weight range 200–400 and since there seems no reason why reaction between an oxonium ion and *any* terminal hydroxyl group should be molecular weight dependent, this conclusion suggests that internal reaction, i.e. reaction of the oxonium ion with the hydroxyls of its own chain, is important at low molecular weights. Once reached, this conclusion seems quite reasonable for we know that an oxonium ion readily attacks the oxygen atoms of its own chain (dioxane formation), so with low molecular weight polymer there is a high probability that the oxygen attacked will be that of a hydroxyl group. With triethylene glycol, for example ($HOCH_2CH_2OCH_2CH_2OCH_2CH_2OH$, mol. wt. 150), no other reaction is possible, but with higher polymers one or more dioxane units may have to be eliminated before the attack at hydroxyl is possible. The reaction could take place in two ways, one leading to polymerization and the other to depolymerization,



$ROCH_2CH_2OCH_2CH_2OCH_2CH_2OCH_2CH_2OH$

but from the point of view of rate it does not matter which occurs since both lead to destruction of the oxonium ion. Our evidence suggests, however, that polymerization is favored for we could detect no dioxane in the product of the reaction between the monoethylether of triethylene glycol and an equimolar amount of triethyloxonium fluoroborate.

According to the reaction scheme here proposed, the increasing rate at low molecular weights is due primarily to a transition from reaction [2] to reaction [4]. With continued chain growth, however, reaction [5], which is composed of two parts corresponding to internal and external termination, becomes steadily slower as internal termination becomes less and less probable. Since the probability of internal termination should be inversely related to the molecular weight, it is not surprising that the maximum rate occurs at a definite molecular weight at all hydroxyl concentrations. More surprising perhaps is the relatively small contribution of the external to the total termination.

With a reaction mechanism for guidance, the conditions governing molecular weight equilibrium can be considered. If equilibrium were to occur at molecular weights above about 1500, the situation would be relatively simple because it could be assumed that all termination occurred by the external route and the order in oxide could be taken as zero, with all the catalyst in the form of oxonium ion. The rates of dioxane formation and monomer disappearance would be given approximately by

$$d(\text{dioxane})/dt = k_6(\text{oxonium ion}),$$

$$-d(\text{oxide})/dt = k_7(\text{oxonium ion})(\text{ROH}),$$

and would be related at equilibrium as

$$2d(\text{dioxane})/dt = -d(\text{oxide})dt.$$

It follows that equilibrium would occur at a hydroxyl concentration equal to $2k_6/k_7$ but it would be an equilibrium in the sense that if a polymer were added to the reaction so as to give a hydroxyl concentration of $2k_6/k_7$, then that polymer would neither grow nor depolymerize. At higher hydroxyl concentrations growth would occur and at lower concentrations the polymer would disappear.

Can. J. Chem. Downloaded from www.nrcresearchpress.com by 210.87.254.6 on 09/05/12
For personal use only.

Can. J. Chem. Downloaded from www.nrcresearchpress.com by 210.87.254.6 on 09/05/12
For personal use only.

In practice equilibrium occurs at molecular weights where the order in oxide is less than about 0.5 but certainly not zero, and where internal termination is still a major part of the total termination. If the oxide concentration were important in determining the equilibrium, then the molecular weight should rise to a maximum in the course of a polymerization and fall off again as the monomer concentration declines. We have found some evidence for a maximum of this kind but it is scarcely greater than the error in the weight measurements, so the concentration of oxide will be ignored in the present discussion. The contribution of internal termination to the equilibrium, on the other hand, cannot be ignored and unfortunately cannot be expressed with our present information. It obviously will become smaller as the molecular weight increases and may perhaps be roughly inversely proportional to the molecular weight, in which case the total termination rate would be given by

$$-d(\text{oxonium ion})/dt = [k_7(\text{ROH}) + k_8/(\text{mol. wt.})](\text{oxonium ion})$$

which in turn, assuming that reaction [5] is rate controlling, would be the rate of oxide disappearance. Accordingly at equilibrium

$$2k_6(\text{oxonium ion}) = [k_7(\text{ROH}) + k_8/(\text{mol. wt.})](\text{oxonium ion})$$

giving

$$(\text{mol. wt.})_{\text{equilib}} = k_8/[2k_6 - k_7(\text{ROH})].$$

This treatment is obviously exceedingly crude but is interesting in that it suggests that the equilibrium molecular weight should be somewhat dependent on the hydroxyl concentration for this in fact seems to be the case (Table III).

TABLE III

Hydroxyl concentration	Approx. final molecular wt.
0.03	525
0.06	600
0.12	750
0.20	800
0.61	1000

A reaction as complex as this one will require a great deal of work before it yields any exact solutions and we do not pretend that the reaction schemes presented in this and the preceding paper are any more than preliminary ones. They do, however, seem to account in a qualitative and fairly logical way for almost all of our observations on the boron fluoride catalyzed polymerization of ethylene oxide. Perhaps the most interesting problem which remains unexplained is the difference in behavior of the various Friedel–Crafts catalysts in this polymerization, for the reaction schemes proposed do not seem to account satisfactorily for the fact that stannic chloride, and perhaps antimony pentachloride, can produce much higher molecular weight polymer than boron fluoride.

REFERENCES

1. G. A. LATRÉMOUILLE, G. T. MERRALL, and A. M. EASTHAM. J. Am. Chem. Soc. **82**, 120 (1960).
2. D. J. WORSFOLD and A. M. EASTHAM. J. Am. Chem. Soc. **79**, 900 (1957).
3. D. M. SMITH and W. M. D. BRYANT. J. Am. Chem. Soc. **57**, 61 (1935).
4. N. N. GREENWOOD and R. L. MARTIN. Quart. Rev. **8**, 1 (1954).
5. H. C. BROWN and R. M. ADAMS. J. Am. Chem. Soc. **64**, 2557 (1942).
6. S. SEARLES and M. TAMRES. J. Am. Chem. Soc. **73**, 3704 (1951).
7. H. MEERWEIN, E. BATTENBURG, H. GOLD, E. PFEIL, and G. WILLFANG. J. prakt. Chem. **154**, 83 (1939).
8. F. KLAGES and H. MEURESCH. Ber. **85**, 863 (1952); **86**, 1322 (1953).

Can. J. Chem. Downloaded from www.nrcresearchpress.com by 210.87.254.6 on 09/05/12
For personal use only.

AN IMPROVED PREPARATION OF ω-HYDROXY ALIPHATIC ACIDS AND THEIR ESTERS[1]

D. G. M. Diaper and D. L. Mitchell[2]

ABSTRACT

Reductive cleavage of the ozonides of aliphatic acids and their esters by sodium borohydride or by hydrogenation produces ω-hydroxy aliphatic acids and ω-hydroxy aliphatic esters, respectively, in high yields.

INTRODUCTION

ω-Difunctional aliphatic compounds have found much employment in the synthesis of higher aliphatic compounds. Among these, substances having two different terminal functions are the most favored, and probably the most important reagents for chain extension are the esters of the ω-halogeno acids. These compounds, in various chain-lengths, were required for condensation with malonic ester derivatives in the preparation of branched alkanedioic acids (1, 2, 3, 4) in this laboratory. With the exception of those members of the series of very short chain-length, only one ω-bromo acid, 11-bromo-undecanoic, is easily available and this substance is best prepared by the peroxide-catalyzed addition of hydrogen bromide to 10-undecenoic acid (5). The latter compound is unique among the terminal unsaturated acids in that it is available in quantity and this method of preparation cannot be regarded as a method of general applicability. Use of the more common unsaturated acids with non-terminal olefinic linkages as starting materials for the preparation of ω-hydroxy acids and ω-bromo acids was first explored by Adams (6, 7), who ozonized the esters and isolated ω-aldehydo esters. These compounds were then reduced to give the esters of the ω-hydroxy acids. A practical difficulty in preparations of this type is the inevitable oxidation of a portion of the aldehydo ester to the half ester of the corresponding dicarboxylic acid. Contamination of intermediates with substances in the dicarboxylic acid series is undesirable as such compounds are usually high melting and insoluble and therefore difficult to remove. It is desirable, therefore, to obviate the sensitive aldehyde intermediate by exploitation of the new metal hydride reagents (8) and by selective reductive cleavage of the ozonide-ester prepare the hydroxy ester without isolation of the aldehyde. A similar observation on the preparation of primary alcohols by the borohydride cleavage of ozonides appeared while this work was in progress (9).

We have compared the high-pressure hydrogenolysis of certain ozonides with their reductive cleavage by sodium borohydride and the results are summarized in Table I. Yields of hydroxy ester were found to be superior when the borohydride was used and the products were also of higher purity as indicated by a narrow boiling range and ease of crystallization of the phenylurethane. When the scale of the preparation was increased, the yield by borohydride cleavage remained the same but the yield by high-pressure hydrogenation diminished. Sodium borohydride is still an expensive reagent and it may therefore be more economical to use the hydrogenation method on a large scale.

[1]*Manuscript received June 20, 1960.*
Contribution from the Department of Chemistry, Royal Military College of Canada, Kingston, Ontario. The financial support for this work was supplied by the Defence Research Board under D.R.B. Grant No. 9530-17.
[2]*Defence Research Board of Canada Postdoctorate Fellow, 1959–60.*

TABLE I

Olefinic substrate	Product isolated	Yield	
		Method (*a*)*	Method (*b*)
10-Undecenoic acid (undecylenic acid)	10-Hydroxydecanoic acid	91	56
Ethyl 10-undecenoate	Ethyl 10-hydroxydecanoate	94	71
9,12-Octadecadienoic acid (linoleic acid)	9-Hydroxynonanoic acid	42	—
cis-9-Octadecenoic acid (oleic acid)	9-Hydroxynonanoic acid	50	—
trans-9-Octadecenoic acid (elaidic acid)	9-Hydroxynonanoic acid	74	—
Methyl 9,12-octadecadienoate	Methyl 9-hydroxynonanoate	78	78
Ethyl 9,12-octadecadienoate	Ethyl 9-hydroxynonanoate	74	66
Methyl 9-octadecenoate (methyl oleate)	Methyl 9-hydroxynonanoate	88	66
Isopropyl 9-octadecenoate	Isopropyl 9-hydroxynonanoate	70.5	—
(+)-12-Hydroxy-9-octadecenoic acid (ricinoleic acid)	(−)-Nonane-1,3-diol	72	—

*Method (*a*) by sodium borohydride reduction, method (*b*) by Raney nickel catalyzed hydrogenation.

The working solvent employed for ozonizations has customarily been chloroform, carbon tetrachloride, acetic acid, ethyl acetate, or light petroleum. We have found absolute methanol, ethanol, and isopropanol to be convenient solvents and have used sodium borohydride in the same solvent, thus performing the ozonization and reductive cleavage in one sequence. The alcohol chosen as a solvent for the ozonolysis of an ester was that corresponding to its alkyl radical for it was found that transesterification took place if a different alcohol was employed. Presumably the basic environment of the borohydride reduction step made this transesterification possible.

A limitation on the use of methanol as a solvent is the rapid decomposition of sodium borohydride in this solvent. This can be obviated by reversing the usual order of addition and employing solid borohydride in place of an alcoholic solution.

It may be seen that 9-hydroxynonanoic acid may be obtained either from oleic acid or from linoleic acid. Using the former starting material, difficulties were encountered in freeing the hydroxy acid from the concomitant nonan-1-ol either by the method of Sousa and Bluhm (8) or by the steam-distillation method here described. When linoleic acid is the starting material, the other cleavage products are of lower molecular weight and therefore more easily removed.

10-Hydroxydecanoic acid was obtained in two ways from 10-undecenoic acid. The direct ozonization–borohydride method gives good yields and a high degree of purity. In the second method, undecenoic acid was esterified and reduced by the Bouveault–Blanc process, giving 10-undecen-1-ol without saturation or migration of the olefinic linkage. The acetate of the latter was then ozonized and the aldehyde thus obtained was oxidized to the corresponding acid, 10-acetoxydecanoic acid. This was then saponified. In the first method the carboxylic acid function of the starting material is retained and in the second it becomes the primary alcohol function of the end product.

The structure of (+)-ricinoleic acid as 12-hydroxy-9-octadecenoic acid (10) and most likely possessing the D-configuration (11) has been established by degradation studies (12, 13) and by synthesis (14, 15, 16). Early ozonolysis experiments performed on ricinoleic acid produced 3-hydroxy-nonanoic and nonanedioic acids and the corresponding aldehydes, which were characterized by the formation of crystalline derivatives (17, 18). These experiments supported the Goldsobel formula. We have found that sodium borohydride reduction of the ozonide of (+)-ricinoleic acid formed a hitherto unknown laevorotatory diol with boiling point, refractive index, and infrared spectrum very similar to those of racemic (±)-nonane-1,3-diol. The latter compound was synthesized by a

Can. J. Chem. Downloaded from www.nrcresearchpress.com by 210.87.254.6 on 09/05/12
For personal use only.

Reformatsky condensation of *n*-heptanal and ethyl bromoacetate followed by lithium aluminum hydride reduction of the intermediate ethyl 3-hydroxynonanoate which was not isolated. Although racemic (±)-nonane-1,3-diol formed a crystalline mono-*N*-phenylcarbamate and bis-*N*-phenylcarbamate, attempts to form these crystalline derivatives from the optically active isomer were unsuccessful.

EXPERIMENTAL

Melting points were uncorrected. Infrared spectra were determined on 5% solutions in chloroform. Hydrogenations were carried out in a high-pressure autoclave equipped with a stirrer.*

10-Hydroxydecanoic Acid by the Sodium Borohydride Reduction Method

A stream of ozonized oxygen was bubbled through a solution of 10-undecenoic acid (undecylenic acid, b.p. 176–178° C/23 mm, 39.7 g) in absolute methanol (40 ml) at 0° C until an aliquot test portion no longer decolorized a dilute solution of bromine in a glacial acetic acid. The ozonide solution was then added dropwise to an ice-cold solution of sodium hydroxide (12.5 g) and sodium borohydride (17 g) in 50% aqueous ethanol (300 ml). A gentle evolution of hydrogen resulted and stirring was continued at room temperature for at least 10 hours. The methanol and ethanol were removed by distillation under reduced pressure and at a bath temperature of 40° C or less, and the alkaline aqueous solution was then added dropwise with stirring to an excess of ice-cold dilute hydrochloric acid (1.5 liters). The precipitated 10-hydroxydecanoic acid was collected by suction filtration, washed thoroughly with portions of ice-cold water, and dried under reduced pressure to constant weight (37.0 g, 91%). The yield was not reduced when the scale of the experiment was doubled. Recrystallization twice from benzene gave a product of constant melting point, 77° C, and mixed melting point 75.5–77° C (lit. 75.5–76.5° C (19)).

10-Hydroxydecanoic Acid by the Pressure Hydrogenolysis Method

A solution of the ozonide from 10-undecenoic acid (37.4 g) in ethanol was hydrogenated at room temperature and 2000 p.s.i. for 3 hours using Raney nickel W-2 catalyst (20). The temperature was increased to 130–150° C and the hydrogenation was continued a further 5 hours. The product was isolated by solvent removal, conversion to the sodium salt, and precipitation by pouring the alkaline solution into ice-cold dilute hydrochloric acid. The slightly syrupy crude product (33.6 g) was recrystallized from benzene – light petroleum to give a product (21.4 g, 56%) with a melting point of 75° C.

Ethyl 10-Hydroxydecanoate

The ozonide from ethyl 10-undecenoate (ethyl undecylenate) (20.4 g) in absolute ethanol (200 ml) was prepared according to the above method. The solution was added to sodium borohydride (6.0 g) in absolute ethanol (300 ml) as before and allowed to stand for 24 hours in a loosely stoppered flask at 5° C. After removal of most of the ethanol under reduced pressure, the product was taken up in ether (1500 ml), washed with acid and alkali in the usual manner, and dried. The product (19.7 g, 94%) distilled† at 114–115° C/0.07 mm and crystallized in the refrigerator (m.p. 15° C, thermometer immersed), n_D^{24} 1.4460.

Reduction of the ozonide from methyl 10-undecenoate (24.9 g) with a cold (3%)

*Superpressure Division of American Instrument Company, Inc., Silver Springs, Maryland, U.S.A.

†*A test for ozonide (i.e. starch iodide paper) and a safety shield are recommended for this distillation. In a preliminary experiment, when the borohydride reduction step was acidified after 5 minutes of reduction, the isolated crude product decomposed explosively during distillation presumably due to unreduced ozonide present.*

Can. J. Chem. Downloaded from www.nrcresearchpress.com by 210.87.254.6 on 09/05/12
For personal use only.

ethanolic solution of sodium borohydride (9 g) for 30 hours produced ethyl 10-hydroxydecanoate (22.2 g, 82%). The derived *N*-phenylcarbamate had a melting point and a mixed melting point of 52–54° C.

The derived *N*-phenylcarbamate of ethyl 10-hydroxydecanoate melted at 52–54° C after two recrystallizations from heptane. The ethyl ester of 10-hydroxydecanoic acid was prepared; it formed a *N*-phenylcarbamate of melting point 52–54° C and mixed melting point 52–54° C. Both specimens gave an identical infrared absorption spectrum. Anal. Calc. for $C_{19}H_{29}O_4N$: C, 68.1; H, 8.7; N, 4.2. Found: C, 67.4; H, 8.8; N, 4.3.

Ethyl 10-hydroxydecanoate was also prepared from ethyl 10-undecenoate (25.2 g) by the ozonolysis–hydrogenation method described above. The product (18.4 g, 71%) was purified by two distillations and had a boiling point of 106–108° C/0.04 mm and n_D^{22} 1.4410.

Large-scale experiments (ca. 100 g of ozonide) produced a less pure product boiling over a 10° C range in yields of 40 to 66%.

The derived *N*-phenylcarbamate (m.p. 52–54° C) was prepared but did not crystallize readily.

9-Hydroxynonanoic Acid

The ozonide from linoleic acid* (50 g) in absolute ethanol (100 ml) was added dropwise to an aqueous alcoholic solution (1:1, 100 ml) of sodium hydroxide (20 g) and sodium borohydride (15 g). The solution was stirred for 48 hours, and it was acidified and extracted with ether (3×200 ml). The ethereal extracts were steam distilled until most of the alcohols had been removed. The product was recovered by ether extraction, was crystallized from benzene – light petroleum (13 g, 42%) and had a melting point of 43–45° C. Recrystallization from ethyl acetate raised the melting point to 50–51° C [lit. m.p. 53–54° C (corr.) (6), and m.p. 51–51.5° C (21)].

When the above procedure was carried out with oleic and elaidic acids, crude 9-hydroxynonanoic acid was obtained in 50% and 74% yields, respectively. The product obtained from oleic acid was difficult to purify by crystallization. Poor yields and resinous products in the ozonization of oleic acid and its esters have been attributed to excessive temperatures of ozonization (22).

Methyl 9-Hydroxynonanoate

Methyl oleate (20.6 g) in methanol (200 ml) was ozonized as described above. To minimize the borohydride–methanol reaction, however, the order of addition was reversed, the borohydride (9 g) being added in 0.5-g portions during 5 hours. Distillation at 0.1 mm produced two fractions: (*a*) b.p. 80–100° C (7.2 g) (72%), n_D^{22} 1.4340 (lit. for nonan-1-ol, n_D^{20} 1.4338 (23)); (*b*) b.p. 103–109° C/0.1 mm, 11.75 g (88%), n_D^{21} 1.4433. The derived *N*-phenylcarbamate melted at 53–54° C and had a mixed melting point of 53.5–55.5° C [lit. methyl 9-hydroxynonanoate *N*-phenylcarbamate 53–54° C (6)].

Methyl 9-hydroxynonanoate was also prepared from methyl oleate by the ozonization–hydrogenation technique and from methyl linoleate by the borohydride and catalytic hydrogenation methods. The yields are listed in Table I. Examination of the forerun (b.p. 80–105° C/0.2 mm) from the latter preparation by gas-liquid chromatography indicated the presence of at least two components.

Ethyl 9-Hydroxynonanoate

The ozonide from ethyl linoleate (b.p. 148–153° C/0.4 mm, n_D^{20} 1.4573) (50.15 g) in absolute ethanol was divided equally into two parts. One part was reduced by the dropwise

**Nutritional Biochemicals Corporation, Cleveland 28, Ohio (linoleic acid, 75%).*

Can. J. Chem. Downloaded from www.nrcresearchpress.com by 210.87.254.6 on 09/05/12
For personal use only.

addition to sodium borohydride in absolute ethanol and gave a product (12.1 g, 73%) with a boiling point of 110–118° C/0.2 mm and n_D^{21} 1.4441. Anal. Calc. for $C_{11}H_{22}O_3$: C, 65.3; H, 11.0. Found: C, 65.6; H, 11.0. The second portion was reduced by the two-stage hydrogenation described above and gave a product (10.8 g, 65%) with a boiling point of 110–120° C/0.1 mm and n_D^{18} 1.4415.

When both specimens were warmed with one-half by weight of phenyl isocyanate, the derived *N*-phenylcarbamate was obtained (m.p. 59–60° C). Recrystallization from 2,2,4-trimethylpentane – benzene raised the melting point to 60–61.5° C. Anal. Calc. for $C_{18}H_{27}O_4N$: C, 67.3; H, 8.5; N, 4.5. Found: C, 67.5; H, 8.6; N, 4.7.

Isopropyl 9-Hydroxynonanoate

The ozonide from isopropyl oleate (b.p. 225–227° C/22 mm, n_D^{22} 1.4491) (32 g) was reduced with sodium borohydride in isopropanol according to the above method. The product (15 g, 70.5%) had a boiling point of 116–120° C/0.4 mm and $n_D^{25.5}$ 1.4399. Anal. Calc. for $C_{12}H_{24}O_3$: C, 66.6; H, 11.2. Found: C, 66.8; H, 11.3.

The derived *N*-phenylcarbamate was recrystallized from 2,2,4-trimethylpentane and had a melting point of 66.5–68° C. Anal. Calc. for $C_{19}H_{29}O_4N$: C, 68.1; H, 8.7; N, 4.2. Found: C, 68.3; H, 8.8; N, 4.1.

10-Hydroxydecanoic Acid by the Ozonization of the Acetate of 10-Undecen-1-ol

10-Undecen-1-ol (from ethyl undecylenate by Bouveault–Blanc reduction (24)) was acetylated by the acetic anhydride method of Chuit (25) in 83–86% yield. The acetate was ozonized in 20-g portions in acetic acid (40 cc) and the ozonide was reduced by the zinc dust – ether – water method of Adams (7). 10-Acetoxydecanal was obtained as a pungent oil, b.p. 113–118° C/0.3 mm, and was not purified before oxidation. Its oxime was obtained from ethanol as colorless prisms, m.p. 67.5–68° C. Anal. Calc. for $C_{12}H_{23}O_3N$: C, 63.0; H, 10.0; N, 6.1. Found: C, 63.0; H, 9.85; N, 5.7. Its *p*-nitrophenylhydrazone was obtained as yellow needles from aqueous acetic acid, m.p. 118° C. Anal. Calc. for $C_{18}H_{27}O_4N_3$: C, 61.9; H, 7.75; N, 12.0. Found: C, 61.8; H, 7.65; N, 11.5.

Oxidation of 10-acetoxydecanal (15 g) to the corresponding acid was performed in 65–68% yield by passing air through a rapidly stirred mixture of the aldehyde with 200 cc of 20% aqueous manganous chloride solution. The product, 10-acetoxydecanoic acid, isolated with the aid of ether and potassium carbonate, melted at 34.5–36° C and a 15–30% recovery of unchanged aldehyde was effected. By saponification of 10-acetoxydecanoic acid in aqueous–ethanolic potassium hydroxide, 10-hydroxydecanoic acid, m.p. 74–74.5°, was obtained and found to be identical with the product described above.

(−)-Nonane-1,3-diol

After ozonolysis of ricinoleic acid (26 g, $[\alpha]_D^{22}$ 16.3°, *c*, 14.1, ethanol) and sodium borohydride reduction in aqueous alkaline methanol as described above, there was obtained an aqueous solution which was extracted with ether. From the extract of non-acidic products was obtained (−)-nonane-1,3-diol (10.0 g, 72%, b.p. 98–105°/0.1 mm). Two further distillations produced a colorless liquid with a boiling point of 97–99° C/0.1 mm, $n_D^{23.5}$ 1.4506, $[\alpha]_D^{22}$ −6.0° (neat liquid), and $[\alpha]_D^{22}$ −6.3° (*c*, 10, ethanol).

The product had an infrared absorption spectrum identical with that of (±)-nonane-1,3-diol prepared by the method described below. The infrared spectrum was also very similar to those of octan-1-ol and octan-2-ol with the major difference being a stronger absorption at the stretching frequency due to hydroxyl (3420 cm^{-1}).

Can. J. Chem. Downloaded from www.nrcresearchpress.com by 210.87.254.6 on 09/05/12
For personal use only.

Examination of the product by gas–liquid chromatography indicated the presence of at least three impurities which constituted approximately 6% of the product. This material was fractionally distilled in a Piros–Glover microdistillation still* with seven fractions being collected with n_D^{25} 1.4483, 1.4490, 1.4495, 1.4500, 1.4500, 1.4500, 1.4500, respectively. Anal. Calc. for $C_9H_{20}O_2$: C, 67.45; H, 12.6. Found: C, 67.3; H, 12.6.

Attempts to prepare the *N*-phenylcarbamate from fractions 4, 5, 6, or 7 resulted in the formation of a gel. This phenomenon of gel formation was also observed on the slightly impure product.

(±)-Nonane-1,3-diol

n-Heptanal (57 g) and ethyl 1-bromoacetate (83.5 g) were condensed by a standard Reformatsky procedure. After the reaction was complete, the solution was filtered from the unreacted zinc granules and the volume of the filtrate was adjusted to 300 ml with dry ether. The ethereal solution was added dropwise to an ethereal suspension of excess lithium aluminum hydride at such a rate that a gentle reflux was maintained. After the solution had been heated under reflux for an additional 2 hours, the residual lithium aluminum hydride was decomposed by the addition of excess ethyl acetate (100 ml). After 0.5 hour, water was added and a voluminous froth developed. The froth was suspended in ether and cold dilute hydrochloric acid was added until the solution was strongly acidic. The ethereal layer was separated and washed successively with water, sodium hydrogen carbonate solution, and water. Evaporation of the ether left an oil which distilled at 97–99° C/0.04 mm (42 g, 52.5%). A second distillation gave a main fraction with a boiling point of 97–99° C/0.1 mm and n_D^{23} 1.4512. Anal. Calc. for $C_9H_{20}O_2$: C, 67.45; H, 12.6. Found: C, 67.4; H, 12.6.

Bis-N-phenylcarbamate of (±)-Nonane-1,3-diol

Equal weights of phenyl isocyanate and (±)-nonane-1,3-diol were warmed to 60° C for 8 hours. Upon cooling, the product crystallized and was recrystallized from 2,2,4-trimethylpentane, m.p. 85–85.5° C. Examination of the infrared spectrum indicated the absence of the hydroxyl band. Anal. Calc. for $C_{23}H_{30}O_4N_2$: C, 69.3; H, 7.6; N, 7.0. Found: C, 69.3; H, 7.7; N, 7.2.

N-Phenylcarbamate of (±)-Nonane-1,3-diol

(±)-Nonane-1,3-diol was mixed with one-half by weight of phenyl isocyanate and the solution was stored at room temperature for 6 hours, then gently warmed to 60° C for 0.5 hour. The crystalline product was recrystallized from 2,2,4-trimethylpentane and melted at 83–84.5° C. The melting point was depressed upon admixture with the above bis-*N*-phenylcarbamate. Examination of the infrared spectrum indicated the presence of bands due to OH and NH stretching frequencies in approximately equal intensity. Anal. Calc. for $C_{16}H_{25}O_3N$: C, 68.8; H, 9.0; N, 5.0. Found: C, 69.0; H, 9.1; N, 5.0.

ACKNOWLEDGMENTS

The authors wish to thank Dr. C. T. Bishop, National Research Council, Ottawa, and Mr. S. Gunner, Queen's University, Kingston, for gas chromatographic data and Mr. M. V. Schwemin for technical assistance.

H. S. Martin and Co., Evanston, Illinois, U.S.A.

Can. J. Chem. Downloaded from www.nrcresearchpress.com by 210.87.254.6 on 09/05/12
For personal use only.

REFERENCES

1. A. C. Cope, H. L. Holmes, and H. O. House. Org. Reactions, IX, 107 (1957).
2. D. G. M. Diaper and A. Kuksis. Chem. Revs. **59**, 89 (1959).
3. R. Adams and R. M. Kamm. Organic syntheses. Coll. Vol. I. John Wiley and Sons, Inc., New York. 1941. p. 250.
4. W. J. Gensler. Chem. Revs. **57**, 191 (1957).
5. R. Ashton and J. C. Smith. J. Chem. Soc. 435 (1934).
6. W. H. Lycan and R. Adams. J. Am. Chem. Soc. **51**, 625 (1929).
7. C. R. Noller and R. Adams. J. Am. Chem. Soc. **48**, 1074 (1926).
8. N. G. Gaylord. Reduction with complex metal hydrides. Interscience Publishers, New York. 1956. p. 708.
9. J. A. Sousa and A. L. Bluhm. J. Org. Chem. **25**, 108 (1960).
10. A. G. Goldsobel. Ber. **27**, 3121 (1894).
11. K. Serck-Hanssen and E. Stenhagen. Acta Chem. Scand. **9**, 866 (1955).
12. J. T. Scanlan and D. Swern. J. Am. Chem. Soc. **62**, 2309 (1940).
13. St. E. Brady. J. Am. Chem. Soc. **61**, 3464 (1939).
14. L. Crombie and A. G. Jacklin. J. Chem. Soc. 1740 (1955).
15. A. S. Bailey, V. G. Kendall, P. B. Lumb, J. C. Smith, and C. H. Walker. J. Chem. Soc. 3027 (1957).
16. W. J. Gensler and C. B. Abrahams. Chem. & Ind. (London), 47 (1957).
17. A. Haller and A. Brochet. Compt. rend. **150**, 496 (1910).
18. A. C. Noorduyn. Rec. trav. chim. **38**, 327 (1919).
19. A. Grün and T. Wirth. Ber. **55**, 2211 (1922).
20. R. Mozingo. Organic syntheses. Vol. 21. John Wiley and Sons, Inc., New York. 1941. p. 15.
21. P. Chuit and J. Hausser. Helv. Chim. Acta, **12**, 463 (1929).
22. E. H. Pryde, D. E. Anders, H. M. Teeter, and J. C. Cowan. J. Org. Chem. **25**, 618 (1960).
23. V. J. Harding and C. Weizmann. J. Chem. Soc. 304 (1910).
24. L. Bouveault and G. Blanc. Bull. soc. chim. France, **31**, 1210 (1904).
25. P. Chuit. Helv. chim. Acta, **9**, 1074 (1926).

Can. J. Chem. Downloaded from www.nrcresearchpress.com by 210.87.254.6 on 09/05/12
For personal use only.

STEROIDS

PART IV. CONDENSATION OF CHOLESTAN-3-ONE AND CHOLESTANE-3,6-DIONE WITH FORMALDEHYDE[1,2]

TED H. WAID AND ALFRED TAURINS

ABSTRACT

Cholestan-3-one and cholestane-3,6-dione were allowed to react under the conditions of the Mannich reaction with paraformaldehyde and amine hydrochlorides. The products obtained proved to be methylene-bis-ketones, and were formulated as di(2,2′-3-oxocholestanyl)methane and di(4,4′-3,6-dioxocholestanyl)methane respectively.

Can. J. Chem. Downloaded from www.nrcresearchpress.com by 210.87.254.6 on 09/05/12
For personal use only.

DISCUSSION

In the steroid series, the Mannich reaction has been applied to compounds containing an activated methylene group in ring D, or in the aliphatic side chain attached to C_{17} (1, 2) and also to certain estrogens (3). A 21-aminomethyl, and several 16-aminomethyl and 2-dialkylaminomethyl steroid derivatives, have been prepared in this way.

The present investigation was undertaken in order to study, by means of the Mannich reaction, the reactivity of hydrogen atoms in rings A and B of certain steroidal ketones. The steroidal materials selected for study were 5-cholesten-3-one (I) (4), 4,4-dimethyl-5-cholesten-3-one (II) (5), 4-cholesten-3-one (III) (4, 6), cholestan-3-one (IV) (7, 8), and cholestane-3,6-dione (V) (9).

The procedure used for the Mannich condensations that were attempted consisted in allowing the amine and paraformaldehyde to react, then adding the keto compound gradually. Paraformaldehyde was used instead of a 40% aqueous solution of formaldehyde because of the very low solubility of oxosteroids in water. The amines and hydrochlorides used in the reactions were morpholine, piperidine, and dimethylamine.

It was thought that if the isomerization of the double bond in 5-cholesten-3-one (I) from C_5 to C_4 could be avoided, then the hydrogen at C_4 should be particularly active due to the activation by the adjacent double bond and the keto group. In all the attempts to react morpholine with the Δ^5-3-one (I) and paraformaldehyde, brown, viscous oils, which could not be crystallized, and did not contain nitrogen, were obtained. Efforts to condense piperidine under similar conditions, using absolute ethanol, *n*-butyl alcohol, and isoamyl alcohol as solvents, also resulted in the formation of oils. When morpholine, piperidine, or dimethylamine hydrochloride was used in place of the free amine in the foregoing reaction, a viscous oil was obtained, and the unreacted amine hydrochloride was recovered in high yield.

In view of these results, it was felt that the high degree of reactivity of the methylene group in position 4 of 5-cholesten-3-one (I) might be responsible for the rapid formation of oily substances under various conditions. It was decided, therefore, to examine the reactivity of the methylene group in 2-position in a compound in which position 4 would be rendered inactive. Under conditions similar to those employed previously, 4,4-dimethyl-5-cholesten-3-one (II) failed to react with morpholine, piperidine, their hydrochlorides, or

[1]*Manuscript received May 2, 1960.*
Contribution from the Department of Chemistry, McGill University, Montreal, Que., with financial assistance from the National Research Council of Canada, Ottawa.
[2]*Steroids. Part III. T. H. Waid and A Taurins, Can. J. Chem.* **38**, *987 (1960).*

dimethylamine hydrochloride, and was recovered unchanged after 4 hours refluxing in isoamyl alcohol.

Unreacted starting material also was recovered in high yield from the reactions of 4-cholesten-3-one (III) with paraformaldehyde and morpholine or piperidine. Since bromination of III occurs under enolizing conditions (10), it was concluded that the ketone was not sufficiently enolized by the secondary amines to participate in the reaction. In the reactions of III with morpholine, piperidine, and dimethylamine hydrochlorides, after refluxing for 1/2 hour in isoamyl alcohol, *n*-butyl alcohol, or absolute ethanol, non-crystalline oils were isolated. The absence of the characteristic odor of formaldehyde in the reaction mixtures indicated that the oils were a condensation product of III with formaldehyde.

By analogy with the acid-catalyzed halogenation of ketones (11, 12), an electrophilic substitution, it was presumed that the Mannich condensation in the cases of cholestan-3-one (IV) and cholestane 3,6-dione (V) would proceed via enolization of the ketones. Since the enol forms of IV and V were not stabilized by conjugation, as was the case in the unsaturated ketones, it was expected that the acidic hydrogen atoms of the saturated ketones would exhibit less reactivity.

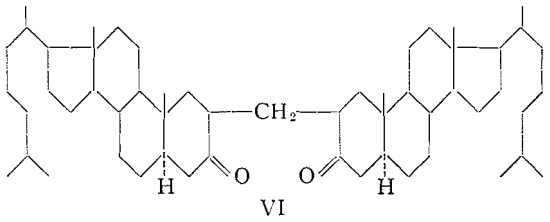
When cholestan-3-one (IV) was refluxed in isoamyl alcohol for 20–30 minutes with paraformaldehyde and morpholine hydrochloride, a product melting at 208–210° and containing no nitrogen was obtained in a 35% yield. An identical material was produced when piperidine hydrochloride was substituted for the morpholine hydrochloride. The product appeared to be a condensation product of IV with formaldehyde and, on the basis of the analytical results and a comparative study of infrared spectra, was formulated as a methylene-bis-ketone. In the infrared spectrum of cholestan-3-one (IV), the carbonyl band appeared at 1710 cm^{-1}. The band of medium intensity present at 1425 cm^{-1} was considered to be due to the C–H scissoring vibrations in an unsubstituted methylene group at C_2 or C_4 in a 3-oxosteroid (13, 14). In the spectrum of the reaction product, two carbonyl bands occurred at 1735 cm^{-1} and 1700 cm^{-1}. The absorption due to methylene groups adjacent to the ketone appeared at 1413 cm^{-1}, and was of weak intensity. This spectroscopic evidence was interpreted as indicating that the new compound contained two residues of cholestan-3-one joined by a methylene bridge in either 2 or 4 position. It was noted that bromination of cholestan-3-one with bromine in acidic medium takes place in 2-position (15). Since an aldol condensation in basic or acidic medium proceeds through enolization, it is reasonable to postulate that the linkage in the methylene-bis-ketone is between the carbon atoms in 2-position. Consequently the compound was designated as di(2,2′-3-oxocholestanyl)methane (VI).

When morpholine and piperidine were used in place of their hydrochlorides in the foregoing reaction, the starting material IV was recovered unchanged. Both the ketone (IV) and the amine could be considered as competing nucleophilic reactants with regard to the electrophilic reagent formaldehyde. When the amine hydrochloride was used in the reaction, the ketone was the only nucleophilic species present, and condensation with the formaldehyde occurred.

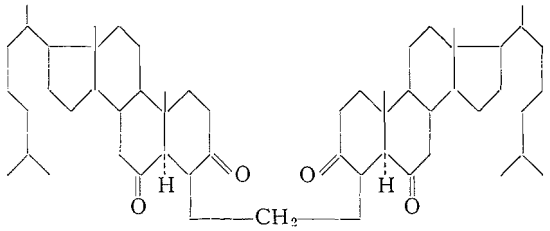
A non-nitrogenous product melting at 242–242.5° was obtained in a 21% yield (based on V) when cholestane-3,6-dione (V) was refluxed with paraformaldehyde and morpholine or piperidine hydrochloride for 45 minutes in isoamyl alcohol. The analytical results and the infrared absorption spectrum inferred a methylene-bis-ketone structure. In the infrared, the dione (V) absorbed at 1710 cm^{-1} and with low intensity at 1420 cm^{-1}. The

Can. J. Chem. Downloaded from www.nrcresearchpress.com by 210.87.254.6 on 09/05/12
For personal use only.

spectrum of the condensation product exhibited two bands in the carbonyl region at 1727 cm^{-1} and 1710 cm^{-1}. The band due to methylene groups was shifted to 1425 cm^{-1} and existed as a shoulder on the more intense band at 1465 cm^{-1}. In V, there are methylene groups at positions 2, 4, and 7 adjacent to keto functions. The reactivity of the hydrogen atoms belonging to these methylene groups was evaluated by a consideration of other substitution reactions. Bromination of the dione (V) with 3 moles of bromine in acidic medium leads to the formation of 4,7-dibromo-4-cholestene-3,6-dione (VII) (16). Apparently an initial electrophilic attack occurs at position 4 in this reaction. Therefore it was considered that the linkage in the methylene-bis-ketone was between the carbon atoms in 4-position, and the compound was formulated as di(4,4′-3,6-dioxocholestanyl) methane (VIII).



VI



VIII

When the free amines were used in place of their hydrochloride salts, the unreacted dione (V) was recovered. The ketones IV and V also were recovered unchanged when they were allowed to react with paraformaldehyde in neutral or acidic media.

Two alternative mechanisms are offered to explain the condensation of cholestan-3-one (IV) and cholestane-3,6-dione (V) with formaldehyde. Scheme A (Fig. 1) represents an abnormal Mannich condensation in an acid–base catalyzed system. Although there is no proof of an intermediate Mannich base, several similar reactions leading to methylene-bis-molecular compounds are known to respond to alkaline and acidic catalysis in much the same manner as the Mannich reaction (17–20). According to the mechanism (Fig. 1), a carbonium ion (ix) is formed from formaldehyde and the secondary amine through the intermediate methylene-bis-amine (v) or methylolamine (vi). This cation combines then with the anion (iv) derived from the ketone as in a normal Mannich reaction. Formation of the cation (ix) is promoted by hydrochloric acid, and that of the anion (iv) by the amine present in the system. Then cleavage of the C—N bond occurs with the loss of amine and formation of the carbonium ion (xii). Such a possibility has been clearly demonstrated by Hellman (21), who reviewed and studied extensively the use of Mannich bases for alkylations. In the final step, the cation (xii) condenses with the anion (iv) to give the methylene-bis-ketone (xiii).

Can. J. Chem. Downloaded from www.nrcresearchpress.com by 210.87.254.6 on 09/05/12
For personal use only.

Can. J. Chem. Downloaded from www.nrcresearchpress.com by 210.87.254.6 on 09/05/12
For personal use only.

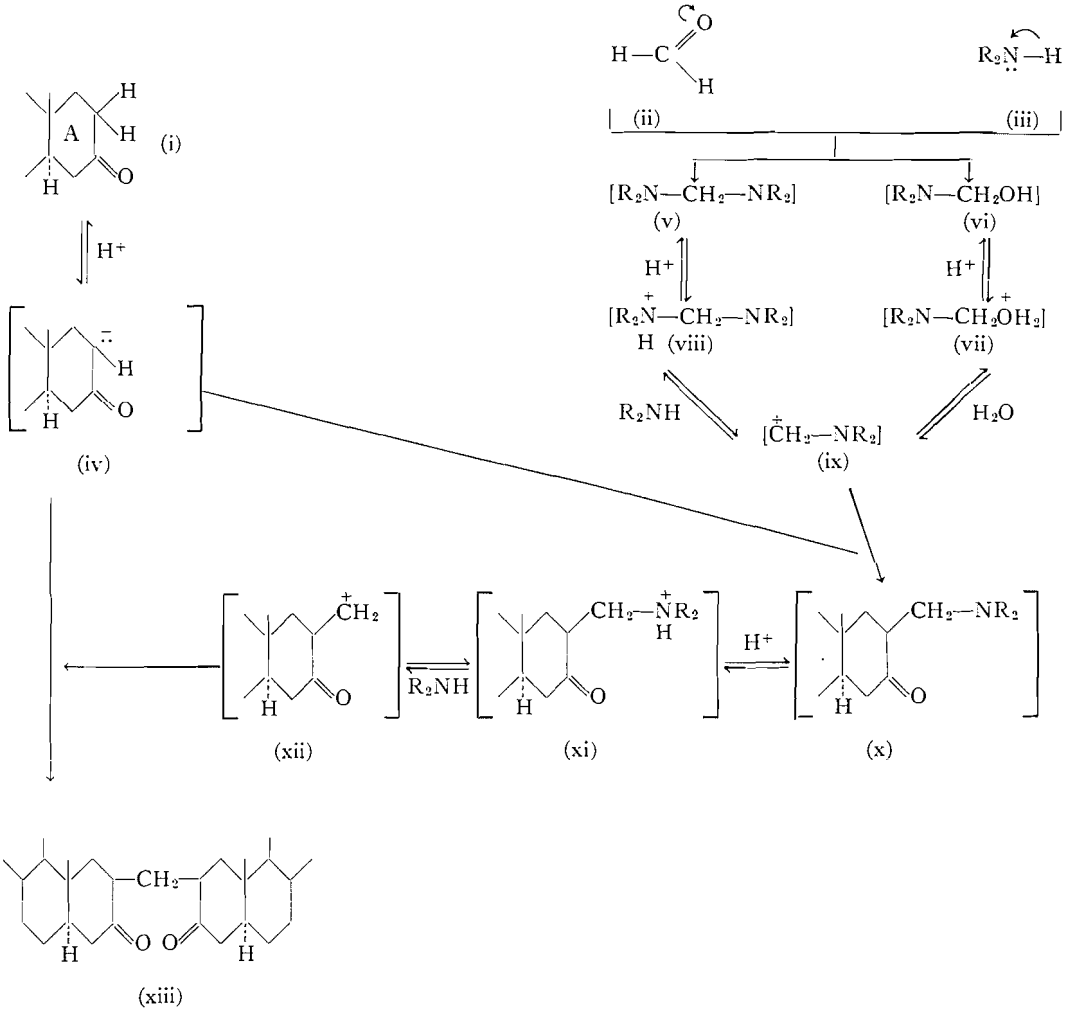


FIG. 1. Scheme A: mechanism proposed for an abnormal Mannich reaction.

The alternative mechanism is presented (Fig. 2) in view of the uncertainty about whether a secondary amine derived from its hydrochloride participates actively in the reaction or acts only as a buffer toward the hydrochloric acid. This mechanism accounts for an acid-induced aldol condensation of formaldehyde with the oxosteroid. In the first step, a transition state complex (ii) is formed which rearranges to a β-ketomethylol (iii). The latter is unstable in acidic medium, and gives, upon protonation, an oxonium ion (iv) which by loss of a molecule of water affords a carbonium ion (v). Finally the carbonium ion combines with the carbanion (vi) derived from the ketone (i) to give the methylene-bis-ketone (vii).

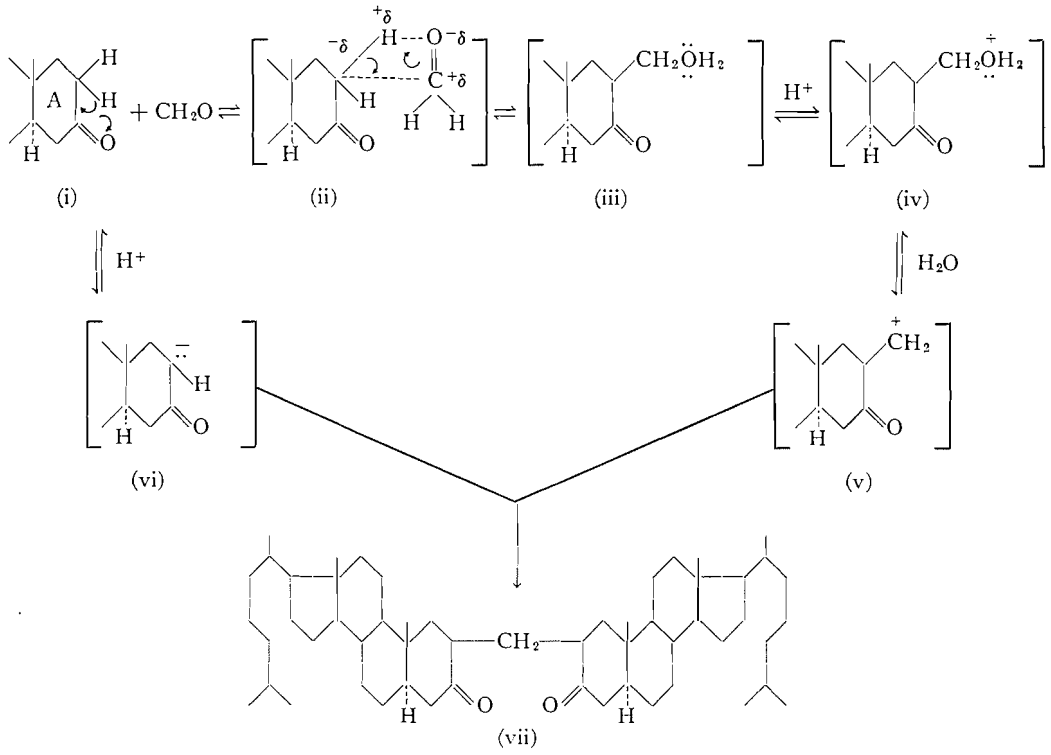


FIG. 2. Scheme B: mechanism proposed for an abnormal Mannich reaction.

EXPERIMENTAL

The melting points were determined in a Thiele-Dennis melting-point tube containing Dow Corning silicone fluid No. D.C. 550 and are uncorrected. The analyses were performed by the Schwarzkopf microanalytical laboratory, Woodside, N.Y., U.S.A. All infrared spectra were determined on a Perkin–Elmer Model 21 double-beam spectrometer equipped with a sodium chloride prism.

The secondary amines were dried by refluxing over sodium hydroxide pellets for 6 hours, distilling, and storing over solid sodium hydroxide. The hydrochloride salts of the amines were prepared by addition of a calculated amount of dilute hydrochloric acid to the amine with cooling, evaporation to dryness, and recrystallization from absolute ethanol.

Attempted Condensation of 5-Cholesten-3-one (I) with Paraformaldehyde and Secondary Amine Hydrochlorides

In a nitrogen atmosphere, morpholine hydrochloride (0.185 g), paraformaldehyde (0.04 g), and isoamyl alcohol (6 ml) were stirred for 20 minutes at room temperature. The mixture was heated to reflux, and all solids dissolved. During the next hour, 5-cholesten-3-one (I) (0.58 g) was added in portions, and refluxing was continued for an additional hour. The brown solution was allowed to cool to room temperature, and the long needles which separated were filtered off and dried. The material (0.15 g) melted at 171–172°, and the mixed melting point with an authentic sample of morpholine hydrochloride was

Can. J. Chem. Downloaded from www.nrcresearchpress.com by 210.87.254.6 on 09/05/12
For personal use only.

undepressed. The filtrate was shaken with 4% hydrochloric acid (10 ml), diluted with water, and extracted with ether. The brown ethereal extract was dried, and then allowed to stand with decolorizing carbon Nuchar-C190-N for a few hours at room temperature with occasional shaking. After filtration, the solvent was evaporated *in vacuo*, and the tarry brown residue was dried over phosphorus pentoxide. The oil contained no nitrogen, possessed a tendency to form films, and resisted all attempts of crystallization.

The aqueous layer was made alkaline with saturated sodium carbonate solution, and extracted again with ether. The ethereal extract was washed with water, dried, and evaporated to dryness. No residue remained.

Similar results were obtained when the molar ratios of the ketone, paraformaldehyde, and morpholine hydrochloride were varied from 1:1:1 to 1:2:3 and 1:5:7.5. The refluxing time was varied from 15 minutes to 2 hours in each case. The results were not affected when absolute ethanol or *n*-butanol was substituted for isoamyl alcohol under the previously described conditions. When dimethylamine and piperidine hydrochlorides were used in place of morpholine hydrochloride in the foregoing experiments, film-forming oils which could not be crystallized resulted in all cases. These oils contained no nitrogen. In each experiment, the major part of the amine salt was recovered.

Attempted Condensation of 4,4-Dimethyl-5-cholesten-3-one (II) with Paraformaldehyde and Morpholine Hydrochloride

When II, morpholine hydrochloride, and paraformaldehyde were heated in isoamyl alcohol for 4 hours under the conditions described in the previous procedure, morpholine hydrochloride was recovered in a 75% yield.

Similar results were obtained when piperidine and dimethylamine hydrochlorides were used in place of morpholine hydrochloride, and also when morpholine itself was used.

Attempted Condensation of 4-Cholesten-3-one (III) with Paraformaldehyde and Secondary Amine Hydrochlorides

The procedure outlined for the attempted condensations of 5-cholesten-3-one (I) was followed, and morpholine, piperidine, and dimethylamine hydrochlorides were used. The molar ratios of the ketone, paraformaldehyde, and amine salts were varied from 1:1:1 to 1:2:3 and 1:5:7.5. Absolute ethanol, *n*-butanol, and isoamyl alcohol were employed as solvents, and the refluxing time was varied from 1/2 hour to 2 hours in each case. Brown viscous oils, possessing film-forming tendencies were the only isolable products in all instances. The oils contained no nitrogen, and could not be crystallized.

Attempted Condensation of 4-Cholesten-3-one (III) with Paraformaldehyde and Secondary Amines

When the conditions outlined for the condensation reaction of 5-cholesten-3-one (I) were employed, using either piperidine or morpholine, an 80% recovery of the starting material III was achieved. When the refluxing time was extended to 2 hours or longer, a brown amorphous material which could not be crystallized resulted in each case. Varying the molar ratios of the reactants did not affect the course of the reaction.

Di(2,2'-3-oxocholestanyl)methane (VI)

A mixture of cholestan-3-one (IV) (0.58 g), paraformaldehyde (0.05 g), morpholine hydrochloride (0.2 g), and isoamyl alcohol (2.5 ml) was heated to reflux, with stirring, in a nitrogen atmosphere. All solids dissolved when the temperature reached 115°, after 5 minutes heating. When the solution had been refluxed for 20–30 minutes, solid material precipitated. The mixture was allowed to cool to room temperature, and was refrigerated

Can. J. Chem. Downloaded from www.nrcresearchpress.com by 210.87.254.6 on 09/05/12
For personal use only.

overnight. The product (0.33 g) was isolated. It was a white crystalline solid, melting at 205–207° to a deep brown liquid. Recrystallization from benzene provided di(2,2′-3-oxocholestanyl)methane (VI), m.p. 208–210°, ν_{max} 1725, 1700 cm^{-1} (C=O). Anal. Calc. for $C_{55}H_{92}O_2$: C, 84.18; H, 11.73. Found: C, 83.86; H, 11.64%.

A similar yield of VI was obtained in an analogous reaction in which piperidine hydrochloride was substituted for morpholine hydrochloride.

When the reaction was carried out in absolute ethanol, and refluxing was maintained for 2 hours, unreacted cholestan-3-one (IV) was recovered in 95% yield. The yield of product was unaffected by a change in the molar ratio of ketone (IV) to paraformaldehyde from 1:1 to 2:1.

Di(4,4′-3,6-dioxocholestanyl)methane (VII)

In a nitrogen atmosphere, a mixture of cholestane-3,6-dione (VI) (0.60 g), paraformaldehyde (0.05 g), morpholine hydrochloride (0.2 g), and isoamyl alcohol (3 ml) was stirred, and heated to reflux. All solids dissolved when the temperature reached 105°. After 45 minutes refluxing, the solution was dark yellow. Crystalline material separated on cooling of the solution to room temperature. The mixture was treated with water (0.5 ml), and the organic layer was separated, dried over anhydrous magnesium sulphate, and evaporated to dryness *in vacuo*. The solid residue was crystallized from acetone (250 ml) yielding soft needles (0.254 g) melting at 214–217°. Recrystallization from acetone provided di(4,4′-3,6-dioxocholestanyl)methane (VII), m.p. 242–242.5°, ν_{max}^{nujol} 1727, 1710 cm^{-1} (C=O). Anal. Calc. for $C_{55}H_{88}O_4$: C, 82.51; H, 11.83. Found: C, 82.09; H, 11.82%.

The yield of product was not affected by varying the molar ratio of ketone and paraformaldehyde from 1:1 to 2:1. In dioxane the reaction was complete after 60–70 minutes' refluxing. The yield of product was considerably lower than when isoamyl alcohol was the solvent.

ACKNOWLEDGMENT

The authors wish to acknowledge the assistance of Dr. B. G. Ketcheson in the preparation of this manuscript.

REFERENCES

1. P. L. Julian, E. W. Meyer, and H. C. Printy. J. Am. Chem. Soc. **70**, 3872 (1948).
2. P. L. Julian, E. W. Meyer, and H. C. Printy. U.S. Patent No. 2,562,194 (1951): Chem. Abstr. **46**, P. 1598 (1952).
3. T. L. Patton. Chem. & Ind. 923 (1959).
4. L. F. Fieser. J. Am. Chem. Soc. **75**, 5421 (1953).
5. R. V. Oppenauer. Rec. trav. chim. **56**, 137 (1937).
6. H. H. Inhoffen, W. Logemann, W. Hohlweg, and A. Serini. Ber. **71**, 1032 (1938).
7. E. B. Hershberg, E. Oliveto, M. Rubin, H. Staendle, and L. Kuhlen. J. Am. Chem. Soc. **73**, 1144 (1951).
8. Organic Syntheses, **17**, 43 (1937).
9. L. F. Fieser. J. Am. Chem. Soc. **75**, 4381 (1953).
10. I. Heilbron, E. R. H. Jones, and G. F. Woods. J. Chem. Soc. 461 (1953).
11. A. J. Lapworth. J. Chem. Soc. **85**, 30 (1904).
12. P. D. Bartlett and R. H. Rosenwald. J. Am. Chem. Soc. **56**, 1990 (1934).
13. R. N. Jones and A. R. H. Cole. J. Am. Chem. Soc. **74**, 5648 (1952).
14. R. N. Jones, A. R. H. Cole, and B. Nolin. J. Am. Chem. Soc. **74**, 6321 (1942).
15. A. Butenandt and A. Wolff. Ber. **68**, 2091 (1935).
16. A. Butenandt, G. Schramm, and H. Kudssus. Ann. **531**, 176 (1937).
17. J. R. Feldman and E. C. Wagner. J. Org. Chem. **7**, 31 (1942).
18. G. B. Backmann and M. T. Atwood. J. Am. Chem. Soc. **78**, 484 (1956).
19. R. D. Desai. J. Indian Chem. Soc. **10**, 663 (1933).
20. E. C. Horning and M. G. Horning. J. Org. Chem. **11**, 95 (1946).
21. H. Hellmann. Angew. Chem. **65**, 473 (1953).

Can. J. Chem. Downloaded from www.nrcresearchpress.com by 210.87.254.6 on 09/05/12
For personal use only.

Can. J. Chem. Downloaded from www.nrcresearchpress.com by 210.87.254.42 on 09/05/12
For personal use only.

CATALYTIC OXIDATION OF CARBON MONOXIDE PRESENT IN LOW CONCENTRATIONS[1]

S. Sourirajan[2] and Mauro A. Accomazzo

ABSTRACT

The oxidation of carbon monoxide present in low concentrations has been studied in the presence of the CuO–Al_2O_3 (1:1) catalyst using 1,000–10,000 p.p.m. of CO in air in the temperature range 120°–322° C, and gas space velocities ranging from 8,000–16,000 hr^{-1}. It was found that for the entire concentration range studied, the percentage of oxidation of CO at a given temperature was independent of its initial concentration and at temperatures above 200° C, more than 95% of CO was removed by oxidation at all gas space velocities up to 16,000 hr^{-1}. A simple first-order rate equation was found to fit the experimental data well. The presence of water vapor in the reactant gas was found to have no effect on the efficiency of the catalyst at temperatures above 225° C. The possible practical utility of the above catalyst for the removal of carbon monoxide present in auto exhaust gases was tested using a six-cylinder Chevrolet engine run on leaded gasoline fuel. It was found that under all conditions of engine operation, more than 99% of carbon monoxide present in the exhaust gases was removed by catalytic oxidation when the initial temperature of the catalyst bed was kept at or above 220° C.

INTRODUCTION

The development of suitable catalysts for the efficient oxidation of carbon monoxide present in low concentrations in the exhaust gases emanating from various combustion sources is of particular importance as a possible method of air pollution control. An extensive literature is available on the heterogeneous oxidation of carbon monoxide (1, 2). The object of this investigation is to study the efficiency and the practical utility of the copper oxide – alumina (1:1) catalyst for the oxidation of low concentrations of carbon monoxide, in view of the proved effectiveness of the above catalyst for the total oxidation of hydrocarbons (3).

EXPERIMENTAL DETAILS

The apparatus used was similar to the one described earlier (3). The carbon monoxide gas was mixed with air before entering the catalyst bed, which was placed in a vycor glass reactor tube enclosed in a furnace. The gas flow rates were measured by appropriate flowmeters which were initially calibrated. The lower section of the vycor tube, filled with porcelain beads, served as a preheater for the reactant gases. The temperature of the catalyst bed was measured by means of a thermocouple. The gases flowing through the preheater and reactor tube could be sampled both immediately before and after passing through the catalyst bed. The carbon monoxide content of the samples was analyzed by a combustible analyzer developed by Miller (4). It consisted essentially of two cells constituting the two arms of a Wheatstone bridge arrangement; the combustion of the gas sample material took place on the surface of a hot platinum wire in one of the cells, and the resistance change resulting from the increase in temperature due to combustion measured the concentration of the combustibles in the gas mixture entering or leaving the catalyst bed. The instrument, coupled to an automatic recorder, was initially calibrated for different concentrations of carbon monoxide. The analyzer gave results reproducible within 1%.

The concentration of carbon monoxide in the reactant gas ranged from 1,000–10,000 p.p.m. in diluent air. The temperature of the catalyst bed was varied from 120°–322° C

[1]*Manuscript received June 24, 1960.*
Contribution from the Department of Engineering, University of California, Los Angeles 24, California.
[2]*Present address: Institute of Geophysics, University of California, Los Angeles 24, California.*

and the gas space velocities (volume of gas per hour per volume of catalyst) ranged from 8,000 to 16,000 hr^{-1}. During the reaction, the furnace controls were set so that the temperature gradient across the different parts of the catalyst bed was less than 10° C. Under steady-state conditions, the highest temperature of the catalyst bed (taken as the reaction temperature), the gas flow rate, and the carbon monoxide concentrations in the gases entering and leaving the catalyst bed were recorded and the efficiency of the catalyst for the oxidation of carbon monoxide was evaluated.

The catalyst was prepared as follows. Copper hydroxide was precipitated on the alumina carrier from a hot dilute aqueous solution of copper nitrate by the addition of an excess of sodium hydroxide. The precipitate was then filtered and washed free of alkali. The wet solid mass was then extruded, dried, and pelleted. The composition of the catalyst was $CuO:Al_2O_3 = 1:1$. The catalyst material was heated in the reactor at 450° C for a period of 12 hours in a current of air before use in the experiments. The surface area of the catalyst, as determined by the B.E.T. method, was 128 square meters/g, and its pore volume, as determined by the helium–mercury method, was 0.56 cc/g. The mean radius of the pores in the catalyst, as calculated from its known surface area and pore volume measurements assuming cylindrical pores, was 87 Å. Twenty-five cubic centimeters of catalyst material was used in all these experiments.

EXPERIMENTAL RESULTS AND DISCUSSION

Efficiency of the Catalyst

Tables I and II give the experimental results obtained on the oxidation of carbon monoxide present in the concentration range of 1,000 to 10,000 p.p.m. in diluent air in the presence of the copper oxide – alumina catalyst described above. Figures 1 and 2 show the effect of temperature and gas space velocity, respectively, on the extent of oxidation. Most of the experiments were carried out at a gas space velocity of 10,000 hr^{-1} or more in order to simulate comparable conditions for practical utilization of the catalyst in air pollution control devices. The results showed that (i) for the entire concentration range studied, the percentage of oxidation of CO at a given temperature was independent of its initial concentration and (ii) at temperatures above 200° C, more than 95% of CO was removed by oxidation at all gas space velocities up to 16,000 hr^{-1}. Thus, the above copper oxide – alumina catalyst was found to be a very efficient one for the oxidation of CO present in low concentrations.

Rate Equation for Reactor Design

Garner, Gray, and Stone (5) investigated the nature of the interaction of carbon monoxide and oxygen on the surface of the copper oxide catalyst through surface conductivity and heat of adsorption measurements. They found that in the temperature range 100°–270° C, the rate-controlling step in the adsorption of oxygen on plane surfaces was first order. When a mixture of carbon monoxide and oxygen was admitted to the catalyst surface, the first process was always the saturation of the surface with carbon monoxide. They also observed that the rate of oxidation of carbon monoxide in the presence of the copper oxide catalyst was independent of carbon monoxide pressure and proportional to the oxygen pressure. They hence concluded that the $CO–O_2$ reaction occurred on the catalyst surface saturated with carbon monoxide.

The experimental data obtained in this work, however, show that the rate of catalytic oxidation of CO present in low concentrations by excess oxygen, is more nearly first order

Can. J. Chem. Downloaded from www.nrcresearchpress.com by 210.87.254.42 on 09/05/12
For personal use only.

Can. J. Chem. Downloaded from www.nrcresearchpress.com by 210.87.254.42 on 09/05/12
For personal use only.

TABLE I

Data on the oxidation of carbon monoxide present in low concentrations in the presence of the CuO–Al_2O_3 (1:1) catalyst

t, °C	X_0, p.p.m.	X_1, p.p.m.	% oxidation	Q, liters/hour	SV, hr^{-1}
120	1,000	728	27	250	10,000
140	1,000	447	55	250	10,000
160	1,000	346	66	250	10,000
180	1,000	148	85	250	10,000
200	1,000	25	98	250	10,000
268	1,000	21	98	250	10,000
120	2,000	1,760	12	250	10,000
146	2,000	1,200	38	250	10,000
160	2,000	873	57	250	10,000
170	2,000	700	65	250	10,000
186	2,000	196	90	250	10,000
200	2,000	41	98	250	10,000
304	2,000	25	99	250	10,000
124	5,000	4,420	11	250	10,000
140	5,000	3,230	35	250	10,000
168	5,000	2,060	59	250	10,000
190	5,000	780	84	250	10,000
210	5,000	154	97	250	10,000
322	5,000	72	99	250	10,000
120	10,000	8,900	11	250	10,000
140	10,000	7,500	25	250	10,000
160	10,000	3,390	65	250	10,000
190	10,000	542	94	250	10,000
242	10,000	268	97	250	10,000
200	2,000	60	97	200	8,000
200	2,000	24	99	300	12,000
200	2,000	35	98	400	16,000

TABLE II

Data on the oxidation of carbon monoxide present in low concentrations in the presence of the CuO–Al_2O_3 (1:1) catalyst

X_0, p.p.m.	t, °C	Q, liters/hour	Z	$(T/T_1)\ln[1/(1-Z)]$	$(V_R/Q)\times10^4$	$k'\times10^{-3}$
2,000	128	200	0.258	0.403	1.250	
2,000	128	250	0.230	0.350	1.000	3.33
2,000	128	300	0.210	0.318	0.833	
2,000	128	400	0.133	0.188	0.625	
2,000	146	200	0.440	0.812	1.250	
2,000	146	250	0.384	0.674	1.000	6.67
2,000	146	300	0.355	0.613	0.833	
2,000	146	400	0.256	0.412	0.625	
2,000	160	200	0.626	1.420	1.250	
2,000	160	250	0.565	1.208	1.000	
2,000	160	300	0.485	0.957	0.833	11.50
2,000	160	350	0.430	0.815	0.714	
2,000	160	400	0.385	0.706	0.625	
2,000	170	200	0.722	1.890	1.250	
2,000	170	250	0.650	1.551	1.000	14.70
2,000	170	350	0.500	1.022	0.714	
2,000	170	450	0.417	0.785	0.556	

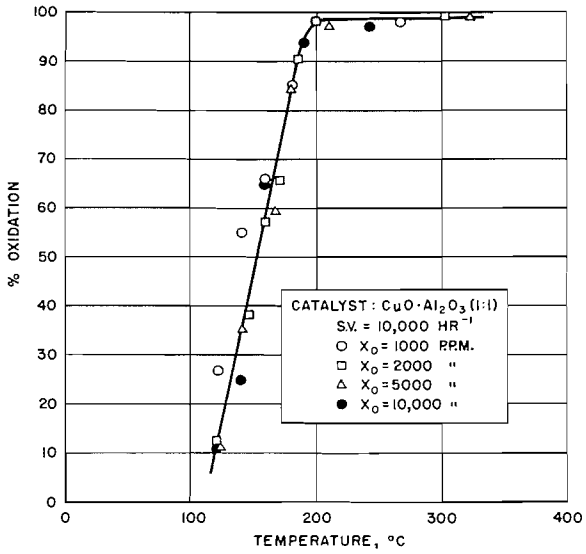


FIG. 1. Effect of CO concentration and temperature on the catalytic oxidation of carbon monoxide.

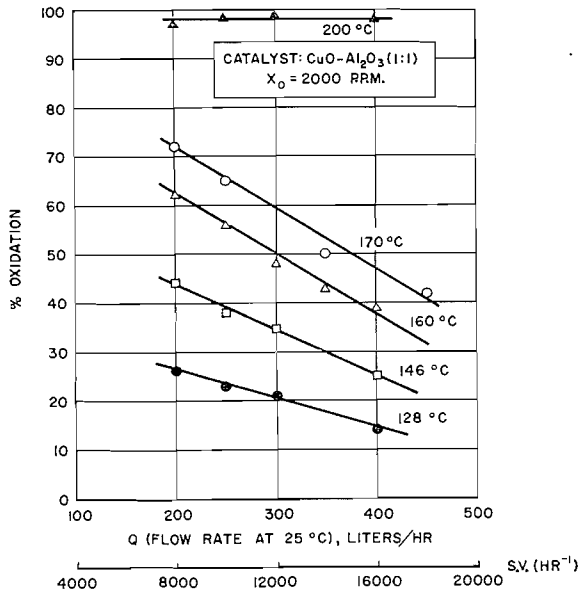


FIG. 2. Effect of gas flow rate and temperature on the catalytic oxidation of carbon monoxide.

with respect to CO concentration. For the purpose of reactor design, an empirical rate equation for the catalytic oxidation of CO by excess air can be derived as follows to fit the experimental data reported above.

Can. J. Chem. Downloaded from www.nrcresearchpress.com by 210.87.254.42 on 09/05/12
For personal use only.

Can. J. Chem. Downloaded from www.nrcresearchpress.com by 210.87.254.42 on 09/05/12
For personal use only.

For flow reactors,

$$[1] \qquad \frac{V_R}{F} = \int_0^Z \frac{dZ}{r},$$

$$[2] \qquad r = -\frac{dC}{d\theta} = kC^nC_{O_2}^m.$$

When the oxygen concentration is much in excess,

$$[3] \qquad kC_{O_2}^m \approx k' = f(T)$$

therefore

$$[4] \qquad \frac{V_R}{F} = \int_0^Z \frac{dZ}{k'C^n}.$$

At any point in the reactor where a conversion of fraction Z has taken place, the concentration of carbon monoxide can be written as

$$[5] \qquad C = C_0(1-Z).$$

Hence at constant temperature,

$$[6] \qquad \frac{V_R}{F} = \frac{1}{k'C_0^n}\int_0^Z \frac{dZ}{(1-Z)^n}$$

$$[7] \qquad = \frac{1}{k'C_0}\ln\frac{1}{1-Z} \qquad \text{for } n = 1.$$

Since

$$[8] \qquad F = QC_0\frac{T}{T_1}$$

equation [7] becomes

$$[9] \qquad k'\frac{V_R}{Q} = \frac{T}{T_1}\ln\frac{1}{(1-Z)}.$$

Hence a plot of V_R/Q vs. $(T/T_1)\ln[1/(1-Z)]$ should be a straight line (with slope = k') passing through the origin. Such plots are shown in Fig. 3, and the graphs obtained are seen to be nearly straight lines justifying the essential validity of equation [9].

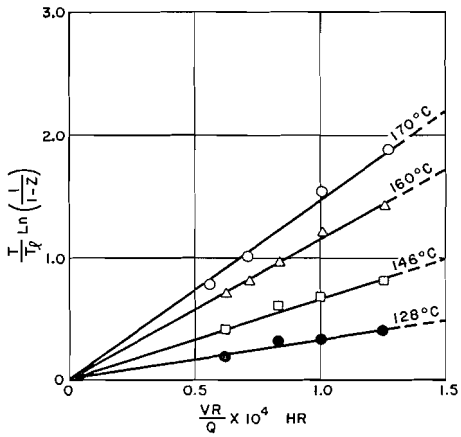


FIG. 3. Apparent first-order plot for the catalytic oxidation of carbon monoxide present in low concentrations.

Assuming

$$k' = f(T) = Ae^{-E/RT} \quad [10]$$

the plot of ln k' vs. $1/T$ should be a straight line with slope $= -E/R$. Such a plot is shown in Fig. 4 which is also seen to be nearly a straight line giving an apparent activation

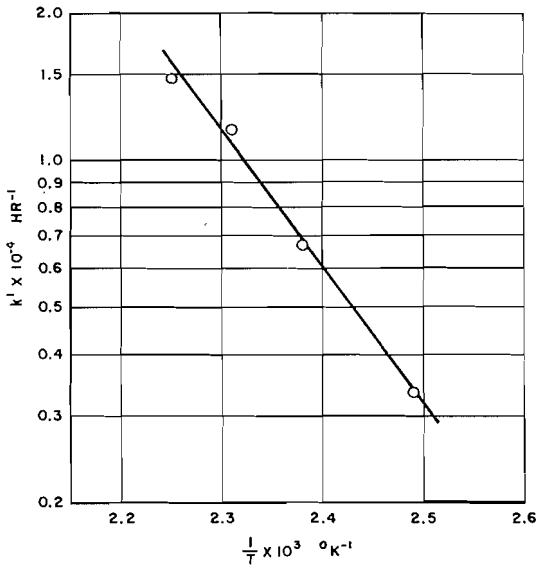


FIG. 4. Variation of reaction rate constant with temperature.

energy of 12.8 kcal/g.mole with $A = 3.1\times10^{10}$ hr^{-1}. Thus

$$r = Ae^{-E/RT}C \quad [11]$$

is found to be a simple rate equation useful for reactor design applicable to the experimental data reported previously for the catalytic oxidation of carbon monoxide present in low concentrations.

Experiments with Water Vapor in Reactants

It is known that water vapor retards the catalytic oxidation of carbon monoxide (6). Since considerable amounts of water vapor may be present in gases issuing from various air-polluting sources, it is important to consider the efficiency of the above CuO–Al_2O_3 catalyst for the oxidation of CO in presence of water vapor. With 2000 p.p.m. of CO in air saturated with water vapor at the laboratory temperature (i.e., with water vapor in the feed = 3.0%) experiments were carried out on the effect of temperature on the extent of oxidation at a gas space velocity of 10,000 hr^{-1}. The results obtained are given in Fig. 5.

It was found that the presence of water vapor did retard the rate of reaction at lower temperatures, but it had no effect at temperatures higher than 225° C. Thus, at temperatures higher than 225° C, CO present in air in low concentrations, even with a large relative proportion of water vapor, was almost completely removed by oxidation in presence of the above CuO–Al_2O_3 catalyst.

Can. J. Chem. Downloaded from www.nrcresearchpress.com by 210.87.254.42 on 09/05/12
For personal use only.

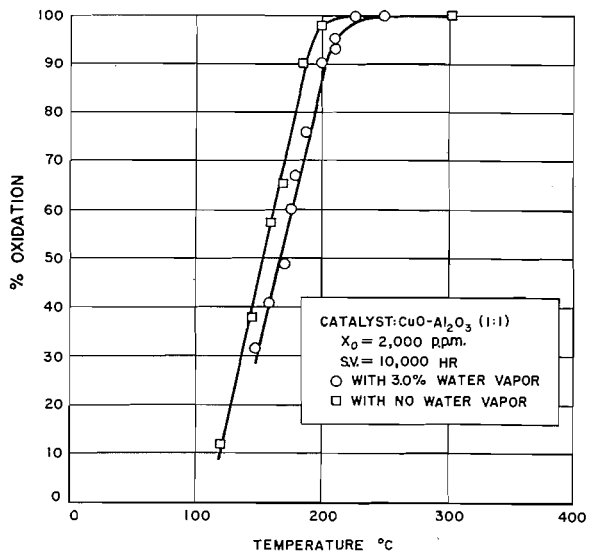


FIG. 5. Effect of water vapor and temperature on the catalytic oxidation of carbon monoxide.

Experiments with Auto Exhaust Gases

The possible practical utility of the above catalyst for the removal of carbon monoxide present in auto exhaust gases was then tested. For this purpose, a 1955 six-cylinder Chevrolet engine coupled to an eddy current dynamometer was used. The engine was run on leaded gasoline fuel. The air/fuel ratio in the engine was determined by a DuMont type 932 exhaust gas analyzer. Part of the exhaust gases from the engine was cooled to room temperature, mixed with excess air (2 to 4 times that needed for complete combustion), and then passed through the catalyst bed initially kept at 200°–220° C, at a gas space velocity of 10,000 hr^{-1} at 25° C. The amount of carbon monoxide present in the engine exhaust gases was determined by orsat analysis, and that present in the gases leaving the catalyst bed was determined by means of a Mines Safety Appliance carbon monoxide indicator (using hopcalite catalyst) capable of analyzing CO within 50 p.p.m. Under the different engine conditions tested, the concentration of CO in the exhaust gases ranged from 1.5–7%; as soon as the air-mixed exhaust gases from the engine entered the reactor, the temperature of the catalyst bed increased rapidly due to reaction and attained steady-state conditions within 10 minutes. The experimental results obtained under the varying conditions of engine operation are recorded in Table III. It was found

TABLE III

Data on the use of the CuO–Al_2O_3 (1:1) catalyst for the removal of carbon monoxide present in auto engine exhaust gases

Engine conditions					Catalyst performance					
r.p.m.	Air/fuel ratio	Cylinder vacuum, in. of Hg	hp	% CO in exhaust	t_0, °C	t, °C	X_0, p.p.m.	X_1, p.p.m.	% oxidation	SV, hr^{-1}
580	12.0	19.8	0.00	7.0	200	600	49000	<50	>99	10000
1050	12.2	19.2	1.17	5.5	220	579	38000	<50	>99	10000
1000	12.5	19.2	2.50	4.5	210	448	31000	<50	>99	10000
1300	13.5	19.5	2.93	3.0	220	400	24000	<50	>99	10000
1600	14.0	19.2	6.00	1.5	210	400	12600	<50	>99	10000

Can. J. Chem. Downloaded from www.nrcresearchpress.com by 210.87.254.42 on 09/05/12
For personal use only.

that under all conditions of engine operation, more than 99% of carbon monoxide present in the exhaust gases was removed by catalytic oxidation. Thus, the above CuO–Al_2O_3 (1:1) catalyst was found to be practically useful for the almost complete removal of CO present in the auto exhaust gases. Coupled with the fact that the above catalyst was already shown to be effective for the removal of hydrocarbons present in low concentrations (3), the experimental results reported in this paper indicate the possibility of developing a practical antismog catalyst containing copper oxide for the simultaneous oxidation of both hydrocarbons and carbon monoxide present in low concentrations in gases issuing from various air-polluting sources.

SYMBOLS

A	constant;
C	concentration of carbon monoxide at any time θ, in moles/cc;
C_0	concentration of carbon monoxide in the gas entering the catalyst bed, in moles/cc;
C_1	concentration of carbon monoxide in the gas leaving the catalyst bed, in moles/cc;
C_{O_2}	concentration of oxygen at anytime θ, in moles/cc;
E	apparent activation energy in cal/g.mole;
F	carbon monoxide feed rate, in moles/hour;
hp	engine load in horse power;
k	constant;
k'	constant;
m	order of reaction with respect to oxygen;
n	order of reaction with respect to carbon monoxide;
p.p.m.	parts per million by volume;
Q	gas flow rate at laboratory temperature;
r	reaction rate in moles/hour cc;
R	universal gas constant in cal/g.mole °K;
r.p.m.	engine revolutions per minute;
SV	space velocity, in hr^{-1};
t	maximum temperature of catalyst bed under steady-state reaction conditions, in °C;
t_0	initial temperature of the catalyst bed under no reaction conditions, in °C;
T	t in °K;
T_1	laboratory temperature in °K;
V_R	volume of catalyst bed;
X_0	concentration of carbon monoxide in the gas entering the catalyst bed, in p.p.m.;
X_1	concentration of carbon monoxide in the gas leaving the catalyst bed, in p.p.m.;
Z	fraction oxidation of carbon monoxide.

ACKNOWLEDGMENTS

This investigation forms part of the catalysis studies in the Air Pollution Research program being supported by the State of California. The authors are grateful to Professor L. M. K. Boelter and Professor W. C. Hurty for their continued support and encouragement to this work. Our thanks are due to Mr. David Cahn for his valuable assistance in this project and to Mr. Delmar J. Albright, who fabricated the glass apparatus.

Can. J. Chem. Downloaded from www.nrcresearchpress.com by 210.87.254.42 on 09/05/12
For personal use only.

REFERENCES

1. S. BERKMAN, J. C. MORELL, and G. EGLOFF. Catalysis. Reinhold Publ. Corp., New York. 1940. pp. 775–780.
2. M. KATZ. Advances in catalysis. Vol. V. Academic Press Inc., New York. 1953. pp. 177–216.
3. S. SOURIRAJAN, M. A. ACCOMAZZO, and K. NOBE. Proc. Intern. Congr. on Catalysis. 2nd. Paris, paper 130, 1960.
4. J. MILLER. The measurement of combustibles by a hot wire method. M. S. Thesis, Department of Engineering, University of California, Los Angeles, Calif. 1958.
5. W. E. GARNER, T. J. GRAY, and F. S. STONE. Disc. Faraday Soc. **8**, 246 (1950); Proc. Roy. Soc. A, **197**, 294 (1949).
6. C. J. ENGELDER and L. E. MILLER. J. Phys. Chem. **36**, 1345 (1932).

Can. J. Chem. Downloaded from www.nrcresearchpress.com by 210.87.254.42 on 09/05/12
For personal use only.

Can. J. Chem. Downloaded from www.nrcresearchpress.com by 210.87.254.6 on 09/05/12
For personal use only.

A CHEMICAL PROCEDURE FOR DETERMINATION OF THE C^{14} DISTRIBUTION IN SOME LABELLED CARBOHYDRATES[1]

M. J. Abercrombie and J. K. N. Jones

ABSTRACT

A chemical procedure for the determination of the labelling in the terminal carbon atoms of some unsubstituted carbohydrates using 20 mg of material is described. The procedure has been tested on D-glucose-1-C^{14}, D-glucose-6-C^{14}, D-glucose-2-C^{14}, and D-glucuronolactone-6-C^{14} with satisfactory results.

A procedure based on the work of Smith *et al.* for the degradation of hexoses via the methyl glucopyranosides is described and has been applied to D-glucose-1-C^{14} and D-glucose-6-C^{14} with satisfactory results. These procedures have been designed to give barium carbonate as the final product in each determination.

INTRODUCTION

There are many procedures for determining C^{14} distribution in carbohydrates described in the literature (1–14), but of these only two afford a complete determination of the labelling on a millimole scale (11, 13). The remainder either require large amounts of material or do not give the labelling in all of the carbon atoms. Gunsalus and Gibbs have described a fermentation procedure with *Leuconostoc mesenteroides* (11) for the degradation of glucose and Altermatt, Blackwood, and Neish (12) have extended the method to the degradation of xylose. Although this procedure yields satisfactory results it is limited to those sugars which the organism will ferment. Boothroyd, Brown, Thorn, and Neish have described chemical procedures for the determination of the C^{14} labelling in glucose (13) and xylose (14) (see also 10). This method is applicable to many sugars.

A limitation to the methods available for radioactive degradation procedures is the type of counting apparatus available. If counting of barium carbonate plates is the only method available then the combustion of large molecules, such as dimedone and phenylhydrazone derivatives, is not always suitable, since the labelled moiety becomes diluted with large quantities of unlabelled carbon material.

The first part of this paper describes a method by which the C^{14} labelling in the terminal position of any unsubstituted carbohydrate may be determined on a minimum of material (20 mg). This quantity is the amount required to give 30 mg of barium carbonate for each of the three determinations involved.

The sodium metaperiodate oxidation of sugars has (16, 17) been extensively studied in this (15) and other laboratories. It has been shown that complete oxidation of an aldohexose to 5 moles of formic acid (C 1–5) and 1 mole of formaldehyde (C-6) takes place rapidly at pH 8.0 (15) (phosphate buffer). Hough *et al.* (17) have shown that the oxidation of glucuronic acid proceeds smoothly to give 1 mole of carbon dioxide (C-6) and 5 moles of formic (C 1–5) at pH 3.6 (acetate buffer). The borohydride reduction of oligosaccharides and subsequent metaperiodate oxidation carried out *in situ* without isolation of the intermediatory glycitol derivative has been studied (18). These methods when applied to monosaccharides gave a method for determining the labelling in the terminal carbon atoms.

The specific activity of the sugar can be determined by the complete combustion of the material to carbon dioxide (C 1–6). Metaperiodate oxidation and oxidation of the formic acid liberated to carbon dioxide with mercuric acetate (7) gives the specific activity of carbon atoms 1–5. Similarly reduction with borohydride and metaperiodate oxidation

[1]*Manuscript received May 11, 1960.*
Contribution from the Department of Chemistry, Queen's University, Kingston, Ontario, Canada

of the glycitol *in situ* gives the specific activity of carbon atoms 2–5. Thus by difference the labelling in C-1 and C-6 can be determined. Although the determination of activities by difference has been criticized by many workers it can be seen from Table II that the results obtained from the above procedure are within ±2% of those expected. The figures in Table I show that the results are reproducible within ±2% except in the determinations where the activity is very small.

TABLE I

Determination of C^{14} in terminal carbon atoms of glucose and glucuronolactone

		D-Glucose-1-C^{14},* counts/min mg $BaCO_3$	D-Glucose-1-C^{14},† counts/min mg $BaCO_3$	D-Glucose-6-C^{14},† counts/min mg $BaCO_3$	D-Glucose-2-C^{14},† counts/min mg $BaCO_3$	D-Glucurono-lactone-6-C^{14},† counts/min mg $BaCO_3$
Van Slyke (C 1–6)	(i)	425	137.0	174.7	23.0	754.0
	(ii)	413	136.6	176.8	22.7	760.0
	(iii)	420	—	—	23.3	—
Mean		419±1.5%	136.8±1%	175.7±0.6%	23.0±1.5%	757.0±0.5%
$NaIO_4$ (C 1–5)	(i)	515	159.0	2.6	28.4	4.0
	(ii)	506	161.4	1.9	—	2.5
	(iii)	512	162.3	—	—	
Mean		511±1.0%	160.9±1%	2.3±15%	28.4	3.25±25%
$NaBH_4$ $NaIO_4$ (C 2–5)	(i)	5	1.3	1.10	33.9	—
	(ii)	4	—	—	—	—
Mean		4.5±9%	1.3	1.10	33.9	—

*Degradation by method A. †Degradation by method B.

The above method requires a minimum of material since the activity of the formic acid and not the formaldehyde is determined. The quantity of formic acid liberated is fivefold that of the formaldehyde in the metaperiodate oxidation and twice that of the formaldehyde in the borohydride/metaperiodate oxidation. Thus the same quantity of barium carbonate is obtained from a fifth and a half as much sugar respectively.

The second part of this paper describes a chemical method for the degradation of any aldohexose, using a single sample of material, for determination of the activity in each of the six positions.

The method is outlined in Fig. 1. Smith *et al.* have studied the metaperiodate oxidation of methyl glycosides (19) and have isolated the dialdehyde (II), characterized the triol (III), and isolated derivatives of glycerol and glycolic aldehyde (IV). Neish *et al.* (13) attempted to make use of these products for a degradation procedure, but found that C-2 was contaminated by C-1 due to enolization of the glycolic aldehyde.

In the present work the procedure was carried a stage further to give glycerol and ethylene glycol (V). These compounds have been characterized as glycerol tris-*p*-nitrobenzoate and ethylene glycol-bis-*p*-nitrobenzoate. The glycerol / ethylene glycol mixture is obtained in high yield (95% based on the methyl glycoside).

A considerable amount of time was spent devising methods for the separation of glycerol and ethylene glycol. The best method of separation would be to use gas-phase chromatography with a column that could separate milligram quantities. Separation on resin columns (20) has been attempted but only a partial separation has been obtained to date. The components can be separated satisfactorily on a cellulose column using butanol/ethanol/water, 6:2:1. Excellent separation is achieved by paper chromatography when the same solvent mixture was used but in the ratio 3:1:1. In the latter two

Can. J. Chem. Downloaded from www.nrcresearchpress.com by 210.87.254.6 on 09/05/12
For personal use only.

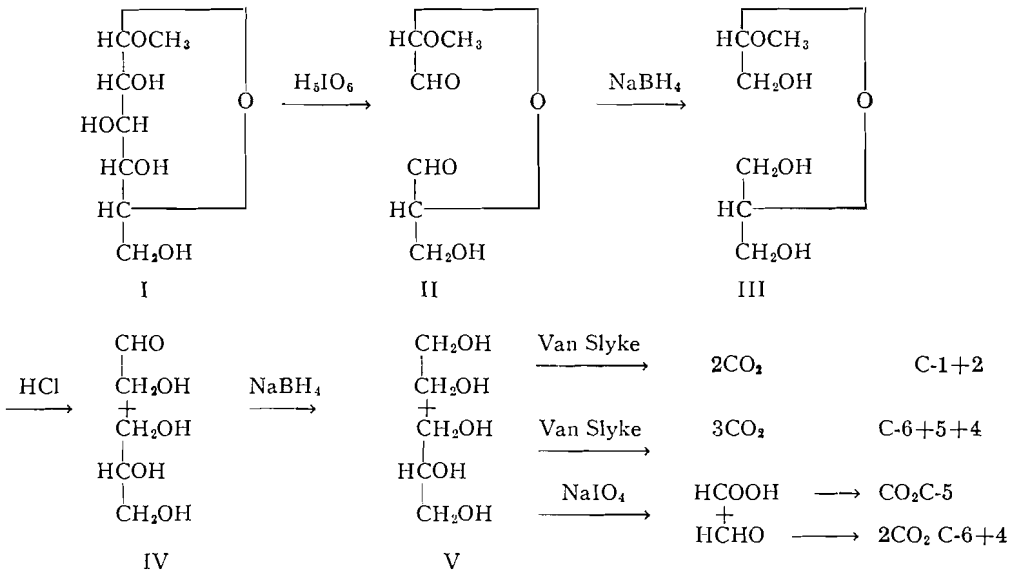


FIG. 1.

techniques 95% or better recovery of glycerol was obtained but the recovery of ethylene glycol was considerably less (50–65%).

The activity of the ethylene glycol was determined by combustion (C 1+2). The glycerol was oxidized with aqueous sodium metaperiodate to give 2 moles of formaldehyde (C 6+4) and 1 mole of formic acid (C-5). This degradation procedure gives us the labelling in C (1+2), C-3, C-5, and C (4+6). Since the labelling in C-1 and C-6 can be obtained from a small quantity of material as described at the beginning of this paper the C^{14} labelling in all six carbon atoms of the aldohexose can be determiued. The results are collected in Table II.

TABLE II

Determination of C^{14} distribution in D-glucose and D-glucuronolactone

		D-Glucose-1-C^{14}*		D-Glucose-1-C^{14}†		D-Glucose-6-C^{14}		D-Glucose-2-C^{14}†		D-Glucurono-lactone-6-C^{14}†	
		Counts/ min mg glucose	% Total	Counts/ min mg glucose	% Total	Counts/ min mg glucose	% Total	Counts/ min mg glucose	% Total	Counts/ min mg glucurono-lactone	% Total
Van Slyke	C 1–6	2750	100.0	881	100.0	1152	100.0	151	100.0	768	100.0
$NaIO_4$	C 1–5	2780	101.0	881	100.0	12	1.1	155	102.0	3	0.4
BH_4*/IO_4*	C 2–5	21	0.7	6	0.7	5	0.4	149	98.5	—	—
Methyl-α-D-glucoside	C-3			4	0.4	5	0.4				
Glycerol											
Van Slyke	C 4–6			2	0.2	1140	99.0				
IO_4*	C-5			—	—	5	0.4				
Ethylene glycol											
Van Slyke	C 1–2			872	98.5	11	1.0				
	C-1		100.3		99.3		0.7		1.5		↑
	C-2		↑		(−0.8)		0.3		↑		↑
	C-3		0.7		0.4		Nil		98.5		0.4
	C-4		↓		>0.2		(−0.3)		↓		↓
	C-5				>0.2		0.4				
	C-6		(−1.0)		Nil		98.9		(−2)		99.6

*See Table I. †See Table I.

Can. J. Chem. Downloaded from www.nrcresearchpress.com by 210.87.254.6 on 09/05/12
For personal use only.

The above methods have been used in studying the biosynthesis of the sugars found in the polysaccharides produced by *Cryptococcus laurentii*. Details of this work will be published shortly.

METHODS

The chromic acid reagent used for the complete combustion of organic samples was prepared according to the directions given by Van Slyke (21).

The mercuric acetate/acetic acid reagent used for the oxidation of formic acid to carbon dioxide was prepared by the method of Bernstein (7). These oxidations were carried out in an apparatus which is a slightly modified form of that described by Johansson *et al.* (22) for the determination of uronic acid.

The radioactive sugars used in the experiments described in this paper were purchased from Isbell (National Bureau of Standards, Washington).

The separation of glycerol and ethylene glycol was carried out on Whatman 3MM paper which had been washed with acid, water, and solvent. The following solvent system was used for the chromatographic separation: butanol–ethanol–water, 3:1:1. The glycols were detected on the chromatograms by spraying them with the metaperiodate / *p*-anisidine hydrochloride reagent described by Bragg *et al.* (23).

Measurement of C^{14} *in Barium Carbonate Samples*

The barium carbonate plates were prepared by the method of Calvin *et al.* (24) and each sample was plated in triplicate (ca. 10 mg barium carbonate on each plate).

The activity of the barium carbonate plates was measured in a proportional methane gas flow counter comprised of the following: the detector, model CFIS2, purchased from the Atomic Energy of Canada Limited and a preamplifier, scaler, and high-voltage assembly manufactured by the Atomic Instrument Co.

The background count was determined and a standard C^{14} plate was counted before and after each counting period. The barium carbonate plates were counted until 1000–1200 counts had accumulated; each plate was counted in triplicate. A correction factor for self-absorption of the barium carbonate was applied.

EXPERIMENTAL

Degradation of Glucose-1-C^{14} *(method A)*

The total activity (C 1–6) of the glucose sample was determined in the usual way by use of the Van Slyke reagent.

Metaperiodate Oxidation (C 1–5)

The glucose (6–7 mg) was dissolved in phosphate buffer solution pH 8.0 (*M*/20) and 2 ml of 0.3 *M* aqueous sodium metaperiodate was added. The oxidation was allowed to proceed in the dark for 2 hours. An excess (×10) of sodium borohydride was added to destroy the remaining metaperiodate; after 15 minutes 2 *N* sulphuric acid was added until the solution was acidic (pH 2.0). The formic acid was separated from the inorganic material by steam distillation (7), the mercuric acetate/acetic acid reagent (9 ml) was added to the distillate, and after the apparatus was flushed with nitrogen for 10 minutes the reaction mixture was boiled for 20 minutes with constant stirring. The barium carbonate was collected and prepared for counting as described above.

Reduction with Sodium Borohydride and Oxidation with Sodium Metaperiodate (C 2–5)

Glucose (7–8 mg) was dissolved in water (2 ml) and sodium borohydride (9 mg) was

Can. J. Chem. Downloaded from www.nrcresearchpress.com by 210.87.254.6 on 09/05/12
For personal use only.

added; the solution was allowed to stand for 12 hours. The excess sodium borohydride was destroyed by making the solution acidic (pH 2.0) with 2 *N* sulphuric acid. Sodium hydroxide (2 *N*) solution was added until the pH of the solution was ca. 7.0, 10 ml of phosphate buffer solution and 2 ml of 0.3 *M* aqueous sodium metaperiodate were added, and the solution was left in the dark for 2 hours. The metaperiodate was destroyed with excess sodium borohydride and the oxidation was continued as before.

Degradation of Glucose-1-C^{14}, -6-C^{14}, *and* -2-C^{14} *(method B)*

The total activity (C 1–6) of the glucose samples was determined as above.

Metaperiodate Oxidation (C 1–5)

The metaperiodate oxidation and addition of sodium borohydride was carried out as described in method A. The excess sodium borohydride was destroyed by the addition of 2 *N* sulphuric acid and the mercuric acetate/acetic reagent (10 ml) was added. A bright red precipitate of mercuric salts was formed, the apparatus was flushed out with nitrogen, and the oxidation continued as described above.

Reduction with Sodium Borohydride and Oxidation with Sodium Metaperiodate (C 2–5)

The reaction was carried out in a similar manner to that described above, i.e. without distillation of the formic acid.

Degradation of Glucuronolactone-6-C^{14}

The total activity (C 1–6) was determined as usual.

Metaperiodate Oxidation (C 1–5)

The glucuronolactone solution (7 mg in 3 ml of water) was titrated to neutrality with 0.01 *N* sodium hydroxide solution. The acetate buffer, pH 3.65 (10 ml), and 2 ml of 0.3 *M* aqueous sodium metaperiodate were added. The reaction mixture was kept in the dark for 6.5 hours, after which ethylene glycol was added to destroy the excess metaperiodate. After 10 minutes the acidic solution was gently boiled to drive off carbon dioxide (C-6) the solution was cooled and the mercuric acetate/acetic acid reagent (9 ml) was added. The oxidation was continued in the usual manner.

*Preparation of Methyl-α-*D*-glucopyranoside*

The methyl-α-D-glucopyranoside was prepared by the standard method (25). The product was recrystallized from a mixture of equal parts of ethanol and methanol until a constant melting point of 164–165° C was obtained.

*Periodic Acid Oxidation of Methyl-α-*D*-glucopyranosides*

A solution of methyl-α-D-glucopyranoside (194 mg) in water (3 ml) was treated with 0.4 *M* periodic acid (5.5 ml) at room temperature for 3 hours. The solution was then passed through a column of Duolite A-4 (OH) resin (1.9×6 cm). The column was washed with distilled water until the total volume of the eluate reached 110 ml. This eluate, which contained the dialdehyde (II) (Fig. 1), was concentrated to ca. 25 ml, sodium borohydride (60 mg) was added, and the reduction to the triol (III) (Fig. 1) was allowed to proceed overnight. The excess sodium borohydride was destroyed by making the solution acidic with 2 *N* hydrochloric acid. The triol was hydrolyzed to glycerol and glycolic aldehyde (IV) (Fig. 1) by adding 2 *N* hydrochloric acid (4 ml) and warming at 60° C for 20 minutes. After the solution was cooled 2 *N* sodium hydroxide solution was added until the pH of the solution was 6.0–6.5. Sodium borohydride (40 mg) was added to reduce the glycolic aldehyde to ethylene glycol (V) (Fig. 1); the reaction mixture

Can. J. Chem. Downloaded from www.nrcresearchpress.com by 210.87.254.6 on 09/05/12
For personal use only.

was allowed to stand for 2 hours. The excess sodium borohydride was destroyed by making the solution acid with 2 *N* hydrochloric acid. The solution was brought to neutrality by the addition of 2 *N* sodium hydroxide solution and concentrated *in vacuo* to 15 ml.

Separation of Glycerol and Ethylene Glycol from the Inorganic Material

The glycerol and ethylene glycol were separated from the inorganic material by passing the solution through a Dowex 50W (8% D.V.B.) resin column (Ba^{++}) (20×115 cm) (20). The eluate was collected in the tubes of a fraction collector. The tubes containing the glycerol and ethylene glycol were combined and evaporated to dryness. Boric acid was still present in the fractions and was removed by codistillation with methanol (×2). A pale yellow syrup was obtained (146 mg). This syrup was passed through a short mixed resin column (Amberlite IR-120 (H) and Duolite-A-4 (OH)) and again evaporated to dryness. The colorless mobile syrup was taken up in methanol, filtered through a celite/charcoal pad, and again evaporated to dryness. A colorless, clear mobile syrup was obtained (134 mg, 100%). Chromatographic examination of an aliquot of this syrup showed spots which moved at rates corresponding to those of ethylene glycol and glycerol. A small quantity of a third material, which moved at a slower rate than glycerol, was detected. This material is probably a tetritol derived from the dimerization of glycolic aldehyde.

*Separation of Glycerol (*C-6, C-5, *and* C-4*) and Ethylene Glycol (*C-1 *and* C-2*)*

The syrup (134 mg) was fractionated by placing it on Whatman 3MM paper and by chromatography of the mixture with the neutral solvent. The appropriate portions of the paper containing the glycerol and ethylene glycol were eluted with water and evaporated to dryness. The syrups obtained were dissolved in water, deionized on mixed ion-exchange resin columns, and evaporated to dryness. These syrups were taken up in methanol (3 ml) filtered through small celite/charcoal pads, and evaporated to dryness. The fraction corresponding to glycerol weighed 92 mg (100%) and that corresponding to ethylene glycol 27 mg (65%). Both fractions were clear, colorless, mobile syrups. On chromatographic examination each showed a single spot which moved at a rate corresponding to either glycerol or ethylene glycol.

Identification of Glycerol and Ethylene Glycol

Each fraction was treated with a 50% molar excess of *p*-nitrobenzoylchloride (recrystallized) in pyridine (freshly dried and distilled) according to the method of Smith *et al.* (26). The glycerol fraction gave crystalline glycerol-tris-*p*-nitrobenzoate, m.p. 198–199° C; the ethylene glycol fraction gave crystalline ethylene glycol-bis-*p*-nitrobenzoate, m.p. 143–144° C. (Mixture melting points with authentic samples were not depressed.)

*Degradation of Methyl-α-*D*-glycopyranoside-*1-C^{14} *and* -6-C^{14}

Each sample (100 mg and 57 mg) was subjected to the degradation procedure described above and afforded 65 mg (95%) and 36 mg (100%) of the glycerol/ethylene glycol mixtures.

Determination of C^{14} *in* C-3 *(13)*

After removal of the dialdehyde, the resin column was washed with a further 50 ml of water and the washings were discarded. The formic acid was eluted from the column with 0.25 *N* barium hydroxide (20 ml) solution followed by water (30 ml). The alkaline

Can. J. Chem. Downloaded from www.nrcresearchpress.com by 210.87.254.6 on 09/05/12
For personal use only.

barium formate solution was acidified with 2 *N* sulphuric acid. The formic acid in the solution was then oxidized to carbon dioxide by refluxing it for 20 minutes with mercuric acetate. The barium carbonate was collected and assayed for C^{14} as described above.

Radiographic Examination of the Glycerol/Ethylene Glycol Mixtures

Each of the two samples was chromatographed on Whatman 3MM paper in the neutral solvent. An X-ray film was left in contact with the chromatogram for 4 weeks. On development the radiogram showed one band corresponding to the position of glycerol from the methyl-α-D-glycopyranoside-6-C^{14} and one band corresponding to the position of ethylene glycol from methyl-α-D-glucopyranoside-1-C^{14}, the latter also showed a weak band corresponding to the position of the tetritol discussed earlier. The positions of the non-radioactive samples of glycerol and ethylene glycol were determined in the usual manner. The appropriate sections of the paper were eluted and purified as described above.

The methyl-α-D-glucopyranoside-1-C^{14} yielded glycerol, 40 mg (84%), and the ethylene glycol, 10 mg (46%). The methyl-α-D-glucopyranoside-6-C^{14} yielded glycerol, 25 mg (92%), and ethylene glycol, 5 mg (40%).

Degradation of Glycerol and Ethylene Glycol

The samples of ethylene glycol (5 mg) were totally combusted in the normal manner. The total activities of the glycerol samples were determined in a similar fashion. The glycerol derived from the methyl-α-D-glucopyranoside-6-C^{14} was further degraded to determine the radioactivity in C-5. Glycerol (15 mg) was oxidized with aqueous 0.3 *M* metaperiodate in a similar manner to that described for the metaperiodate oxidation of glucose-1-C^{14} (method B).

ACKNOWLEDGMENTS

The authors are grateful to Dr. G. Krotkov of the Biology Department of Queen's University for making available the counting apparatus. We thank the National Research Council of Canada for financial assistance and (M. J. A.) thanks them for the award of a scholarship.

REFERENCES

1. H. N. Barnet and A. N. Wick. J. Biol. Chem. **185**, 657 (1950).
2. D. A. Rappopart, H. A. Barker, and W. Z. Hassid. Arch. Biochem. Biophys. **31**, 326 (1951).
3. Y. J. Topper and A. B. Hastings. J. Biol. Chem. **179**, 1255 (1949).
4. S. Abraham, I. L. Chaikoff, and W. Z. Hassid. J. Biol. Chem. **195**, 567 (1952).
5. S. Aronoff, H. A. Barker, and M. Calvin. J. Biol. Chem. **169**, 459 (1947).
6. H. G. Wood, N. Lifson, and V. Larber. J. Biol. Chem. **159**, 475 (1945).
7. I. A. Bernstein. J. Biol. Chem. **205**, 309 (1953).
8. H. L. Frush and H. S. Isbell. J. Research Natl. Bur. Standards, **51**, 167 (1953).
9. C. T. Bishop. Science, **117**, 715 (1953).
10. J. C. Bevington, E. J. Bourne, and C. N. Turton. Chem. & Ind. 1390 (1953).
11. I. C. Gunsalus and M. Gibbs. J. Biol. Chem. **194**, 871 (1952).
12. H. A. Altermatt, A. C. Blackwood, and A. C. Neish. Can. J. Biochem. and Physiol. **33**, 622 (1955).
13. B. Boothroyd, S. A. Brown, J. A. Thorn, and A. C. Neish. Can. J. Biochem. and Physiol. **33**, 62 (1955).
14. S. A. Brown. Can. J. Biochem. and Physiol. **33**, 368 (1955).
15. M. B. Perry. Personal communication.
16. G. Neumüller and E. Vasseur. Arkiv Kemi, **5**, 235 (1953).
17. L. Hough, J. Taylor, G. H. S. Thomas, and B. M. Woods. J. Chem. Soc. **239**, 1212 (1958).
18. L. Hough, B. M. Woods, and M. B. Perry. Chem. & Ind. 1100 (1957).
19. M. Abdel-Akher, J. E. Cadotte, R. Montgomery, F. Smith, J. W. Van Cleve, and B. A. Lewis. Nature, **171**, 474 (1953).
20. J. K. N. Jones, R. A. Wall, and (*in part*) A. O. Pittet. Chem. & Ind, 1196 (1959).

Can. J. Chem. Downloaded from www.nrcresearchpress.com by 210.87.254.6 on 09/05/12
For personal use only.

21. D. D. VAN SLYKE, J. PLAZIN, and J. R. WEISIGER. J. Biol. Chem. **192**, 299 (1951).
22. A. JOHANSSON, B. LINDBERG, and O. THEANDER. Svensk Papperstidn. **57**, 41 (1954).
23. P. D. BRAGG and L. HOUGH. J. Chem. Soc. 4050 (1958).
24. M. CALVIN, C. HEIDELBERGER, J. C. REID, B. TOLBERT, and P. F. YANKERVICH. Isotopic carbon. John Wiley & Sons, Inc., New York. 1949. p. 116.
25. E. FISCHER. Ber. **28**, 1145 (1895).
26. F. SMITH and J. W. VAN CLEVE. J. Am. Chem. Soc. **77**, 3091 (1955).

Can. J. Chem. Downloaded from www.nrcresearchpress.com by 210.87.254.6 on 09/05/12
For personal use only.

Can. J. Chem. Downloaded from www.nrcresearchpress.com by 210.87.254.105 on 09/05/12
For personal use only.

THE POLYSACCHARIDES OF CRYPTOCOCCUS LAURENTII (Y1401)

PART II. BIOSYNTHESIS OF THE CARBOHYDRATES FOUND IN THE ACIDIC POLYSACCHARIDE[1]

M. J. Abercrombie, J. K. N. Jones, and M. B. Perry

ABSTRACT

Cryptococcus laurentii was grown on media which contained D-glucose-1-C^{14}, D-glucose-6-C^{14}, D-mannose-1-C^{14}, D-galactose-1-C^{14}, D-xylose-1-C^{14}, and L-arabinose-1-C^{14}. The radioactive polysaccharides were isolated and hydrolyzed. The distribution of the radioactivity in D-mannose, D-xylose, and D-glucuronic acid isolated from the polysaccharides was determined.

The results show that (A) D-mannose and D-glucuronic acids are formed from the hexoses without any appreciable breakdown of the hexose skeleton; (B) D-xylose is formed from the hexoses mainly by a process involving loss of carbon-6; (C) D-xylose and L-arabinose are both converted to D-mannose, D-xylose, and D-glucuronic acid with rearrangement of the pentose skeleton that may involve the action of transaldolase and transketolase.

INTRODUCTION

In Part I of this series of papers (1) the growth, isolation, and preliminary structural investigation of the polysaccharides produced by *Cryptococcus laurentii* were reported. It was shown that two polysaccharides were present: an acidic polysaccharide containing D-mannose, D-xylose, and D-glucuronic acid and a neutral polysaccharide which consisted of D-glucose only.

In this paper the biosynthesis of the monosaccharides found in the acidic polysaccharide is discussed.

EXPERIMENTAL

Materials

D-Glucose-1-C^{14}, D-glucose-6-C^{14}, D-xylose-1-C^{14}, and L-arabinose-1-C^{14} were purchased from the National Bureau of Standards, Washington. D-Mannose-1-C^{14} and D-galactose-1-C^{14} were purchased from Merck & Co., Montreal. The uniformly labelled D-glucose-C^{14} was provided by Dr. G. Krotkov, Department of Biology, Queen's University, Kingston.

The purity of these compounds was checked by chromatographic and radioautographic examination.

Growth of Cryptococcus laurentii and Isolation of the Polysaccharide

The organism was grown on the media described in Part I (1). The aqueous solution containing the carbon-14 labelled sugar and the growth solution were steam sterilized in separate vessels. These solutions were combined in a sterile 250-ml, two-necked round-bottom flask. The final strength of the solution was $2\frac{1}{2}\%$ with respect to the sugar. A slow stream of sterilized, carbon dioxide free air was drawn through the solution; the carbon dioxide evolved was collected in a trap which contained 200 ml of 2 *N* sodium hydroxide solution. The media were inoculated from a freshly prepared slope on which the yeast organism was growing. The slope contained the same sugar as the growth media which were to be inoculated.

The growth of the organism was followed by sampling the carbon dioxide evolved. When the sodium carbonate content of the aqueous sodium hydroxide trap reached a constant value the growth was stopped. The conversion of carbohydrate to carbon dioxide

[1]*Manuscript received May 11, 1960.*
Contribution from the Department of Chemistry, Queen's University, Kingston, Ontario, Canada.

reached a constant value at about 55% of the theoretical assuming complete oxidation of carbohydrate to carbon dioxide (see Table I). The average growth time was 7 days.

The growth solution was diluted to 50 ml with water and the solution was shaken to wash the viscous material from the wall of the reaction vessel. The yeast cells were removed by centrifugation and the cells were washed with water (2×20 ml). The supernatant and the washings were combined and diluted to 100 ml.

A 5-ml sample of this solution was deionized by passing the solution through a small mixed bed ion-exchange resin column (Amberlite IR-120 (H)/Duolite-A-4 (OH)). The eluate was concentrated *in vacuo* to a small volume and was examined by chromatography and radioautography. In most experiments a spot moving at the same speed as the free sugar which formed part of the original substrate was the only compound detected by either method. In the other experiments no spots were observed (see Table I).

The remainder of the supernatant (95 ml) was dialyzed against distilled water (2 liters) in which was suspended mixed ion-exchange resins (as above) for 2 days. The dialyzed solution, which had become cloudy, was filtered through a small pad of "Celite" to give a clear filtrate. The pad of "Celite" was washed with a further 50 ml of water and the washings were combined with the filtrate. The solution was concentrated to about 10 ml; the polysaccharide was precipitated by addition of 75 ml of ice-cold ethanol which contained 1% of hydrochloric acid. The polysaccharide was collected by centrifugation, washed with ethanol, and dried *in vacuo*. The yields are recorded in Table I.

TABLE I

Incorporation of C^{14} into the polysaccharides produced by *Cryptococcus laurentii*

Compound fed	mg of compound	μc* of C^{14}	Time of growth (days)	Yield				% CO_2 evolved	Radioactive yield ×100/ dry weight yield	Sugar remaining in substrate
				mg	%	μc*	%			
D-Glucose-E-C^{14}										
I	200	67.6	10½	9.0	4.5	2.22	3.3	—	80.0	Glucose
II	200	33.8	10½	5.5	2.8	0.71	2.1	—	83.5	Glucose
III	400	106.0	7	31.5	7.8	6.2	5.9	—	83.0	Glucose
D-Glucose-1-C^{14}	400	150.0	7	57.7	14.0	11.3	7.6	53.0	45.5	Nil
D-Glucose-6-C^{14}	400	147.0	7	48.2	12.0	7.3	5.0	52.6	41.5	Nil
D-Mannose-1-C^{14}	408	150.0	7	27.8	7.0	6.2	4.1	51.5	59.0	Mannose
D-Galactose-1-C^{14}	400	103.0	7	33.5	8.5	5.3	5.2	55.0	60.0	Galactose†
D-Xylose-1-C^{14}	400	104.0	7	42.0	10.5	6.9	6.7	59.0	64.0	Xylose†
L-Arabinose-1-C^{14}	400	50.0	7	34.0	8.5	2.3	4.5	58.0	53.0	Nil

* μc=microcuries of activity.
† Showed substances other than galactose or xylose which were not identified.

Hydrolysis of the Polysaccharides

The polysaccharides isolated from media which had contained D-xylose-1-C^{14} or L-arabinose-1-C^{14} were hydrolyzed for 24 hours with ca. 7 ml of *N* sulphuric acid in sealed glass tubes which were suspended in a boiling-water bath. The hydrolyzates were diluted to 50 ml with water, neutralized with barium carbonate, filtered through beds of "Celite", and deionized by passage through small columns of Amberlite IR-120 (H) ion-exchange resin. These solutions were made up to a known volume (100 ml). Aliquots of each solution were then dried on aluminum disks and counted. The total activity of the hydrolyzates and the radioactive yields are recorded in Table I. Since there appeared

Can. J. Chem. Downloaded from www.nrcresearchpress.com by 210.87.254.105 on 09/05/12
For personal use only.

Can. J. Chem. Downloaded from www.nrcresearchpress.com by 210.87.254.105 on 09/05/12
For personal use only.

to be a considerable loss of material due to degradation during hydrolysis the remaining samples of polysaccharides were hydrolyzed by the following procedure.

The polysaccharides were hydrolyzed with ca. 5 ml of 2% methanolic hydrogen chloride in sealed glass tubes in a boiling-water bath for 15 hours. After the tubes had cooled they were opened and the solutions were evaporated to dryness under a stream of air. To the residues 5 ml of *N* hydrochloric acid was added, the tubes were sealed, and the methyl glycosides were hydrolyzed in a boiling-water bath for 5 hours. After cooling, the hydrolyzates were diluted to 50 ml with water and silver carbonate was added to neutralize the hydrochloric acid. The insoluble salts were removed by filtration and the filtrates were deionized by passage through small Amberlite IR-120 (H) ion-exchange resin columns. The solutions were diluted to known volumes and counted as before. The results are collected in Table I.

The hydrolyzates of the polysaccharides produced from the media containing uniformly labelled glucose-1-C^{14} had recoveries of ca. 80% based on the dry weight of the polysaccharides. The recoveries from the polysaccharides derived from D-glucose-1-C^{14}, D-glucose-6-C^{14}, D-mannose-1-C^{14}, and D-galactose-1-C^{14} were rather less. This is attributed to the fact that when the hydrolyzates were fractionated by chromatography considerable quantities of methyl glycosides were detected and the fractions had to be eluted from the paper and rehydrolyzed with *N* hydrochloric acid.

Isolation of the Radioactive Carbohydrates

The 3MM Whatman paper on which the hydrolyzate mixtures were fractionated was washed with acid, water, and solvent before use. Chromatographic fractionations were carried out using the following solvent system (v/v) *n*-butanol:pyridine:benzene:water, 5:3:3:1. After the chromatograms had been developed for ca. 30 hours they were dried and placed in contact with X-ray films for 9 days. The bands corresponding to the portions of mannose, xylose, glucose, and uronic acids (present on the base line) were eluted and the eluates were diluted to known volumes. Aliquots of each solution were then dried on aluminum disks and counted. The solutions were concentrated *in vacuo* at 35° C to a small volume and applied to the base line on sheets of Whatman 3MM paper (treated as above). The chromatograms were developed in ethyl acetate : acetic acid : water, 9:2:2 (v/v). The chromatograms were radioautographed and the sugars eluted and counted as before. The results are collected in Table II. The solutions of the neutral radioactive carbohydrates were passed through small columns of mixed ion-exchange resins (as

TABLE II

Total activities (μc) found in isolated monosaccharides

Compound fed	D-Mannose	D-Xylose	D-Glucose	D-Glucuronic acid A	D-Glucuronic acid B	Total	D-Mannose / D-Xylose
D-Glucose-E-C^{14}							
I	1.03	0.34	0.05	0.38	—	1.75	3.02/1.0
II	0.35	0.11	0.02	0.11	—	0.55	3.10/1.0
III	2.54	0.75	0.16	0.91	—	4.36	3.40/1.0*
D-Glucose-1-C^{14}	3.00	1.18	0.32	1.22	0.40	5.72	2.56/1.0
D-Glucose-6-C^{14}	4.10	0.09	0.25	1.01	0.29	5.45	45.0/1.0
D-Mannose-1-C^{14}	2.10	0.58	0.24	0.84	0.13	3.76	3.6/1.0
D-Galactose-1-C^{14}	1.70	0.40	0.17	0.43	0.29	2.70	4.25/1.0
D-Xylose-1-C^{14}	3.70	1.23	0.19	1.10	0.44	6.20	3.00/1.00
L-Arabinose-1-C^{14}	1.25	0.43	0.03	0.35	0.15	1.81	2.85/1.00

*Analysis of mannose/xylose ratio by colorimetric method of Smith (5) gave 3.10/1.00.

above) to remove traces of ash which were present. The radioactive monosaccharides were diluted with the quantity of cold material required for the degradation procedures.

Degradation of the Sugars

The radioactive content of the carbon atoms of D-mannose and D-glucuronic acid and of the terminal carbon atoms of D-xylose were determined by methods described previously by the authors (2). The radioactive content of the carbon atoms 3 and 4 of D-xylose were determined by methods described in the literature (3, 4). The results are collected in Table III.

TABLE III

Distribution of C^{14} in D-mannose, D-xylose, and D-glucuronic acid isolated from the polysaccharide produced by *Cryptococcus laurentii*

		C^{14} as % total in monosaccharide					
Compound fed	Sugar isolated	Carbon-1	Carbon-2	Carbon-3	Carbon-4	Carbon-5	Carbon-6
D-Glucose-1-C^{14}	D-Mannose	83.8	←	5.8		→	10.4
	D-Xylose	93.6	←	4.7	→	1.7	—
	D-Glucuronic acid	86.6	←	7.4		→	7.0
D-Glucose-6-C^{14}	D-Mannose	6.3	←	2.5		→	91.2
	D-Xylose	37.0	←	21.0	→	42.0	—
	D-Glucuronic acid	2.6	←	2.0		→	95.6
D-Mannose-1-C^{14}	D-Mannose	81.7	←	3.3		→	15.0
	D-Xylose	85.6	←	5.4	→	9.0	—
	D-Glucuronic acid	26.3	←	26.3		→	47.2
D-Galactose-1-C^{14}	D-Mannose	76.8	←	7.2		→	16.0
	D-Xylose	93.7	←	4.1	→	2.8	—
	D-Glucuronic acid	55.0	←	24.0		→	21.0
D-Xylose-1-C^{14}	D-Mannose	48.1	1.1	24.5	13.0	3.5	13.5
	D-Xylose	56.9	2.6	30.0	9.0	1.5	—
	D-Glucuronic acid	53.0	←	38.5		→	8.5
L-Arabinose-1-C^{14}	D-Mannose	50.9	0.2	27.7	9.8	2.8	7.1
	D-Xylose	56.0	0.5	32.5	7.5	4.5	—
	D-Glucuronic acid	48.5	←	45.0		→	6.5

RESULTS

The percentage yields of polysaccharides shown in the fifth column of Table I indicate that D-glucose may be a more efficient precursor for polysaccharide formation than the other sugars; however, there is little to choose between them.

In the last column of Table II the ratio of D-mannose to D-xylose in the polysaccharides from the growths on uniformly labelled D-glucose is shown to be approximately 3:1 (w/w). This is in agreement with the value obtained from the colorimetric procedure (5) which was determined on the same sample of polysaccharide. Allowing for the difficulties encountered during the hydrolysis of the radioactive polysaccharides the ratios of D-mannose to D-xylose in the other experiments are in the region of 3:1 except for the polysaccharide grown from substrate containing D-glucose-6-C^{14} where the apparent ratio is 45:1. This result shows that the main pathway for the conversion of D-glucose (or hexose) to D-xylose is via a pathway which involves the loss of carbon-6. This is in agreement with the results of previous workers (9, 14).

Columns A and B (Table II) show the total activities of the uronic acid fraction from the hydrolyzate of the polysaccharides after the first and second fractionation by paper chromatography. Column A shows the total uronic acid residue content (mono-, di-, and tri-uronic acid residues) and column B shows the amount of D-glucuronic acid obtained

Can. J. Chem. Downloaded from www.nrcresearchpress.com by 210.87.254.105 on 09/05/12
For personal use only.

from these fractions. The radioautograms showed that there was at least one aldobiouronic acid and one aldotriuronic acid plus other minor components. These figures show that in all cases the D-glucuronic acid content was 50% or less of the uronic acid containing fraction first isolated from the hydrolyzate.

Table III shows the distribution of C^{14} in D-mannose, D-xylose, and D-glucuronic acid.

The conversion of the hexoses to D-mannose is primarily a direct conversion with at least 76% retention of labelling in the original position. The bulk of the remainder of the labelling is in the other terminal carbon. This supports the conclusion of other workers (6–15, 26) that the Embden–Meyerhof glycolytic pathway is also utilized. It is interesting to note that the carbon-1 to carbon-6 rearrangement of the hexoses is greater for D-galactose and for D-mannose than for D-glucose. This is of special interest since it indicates that some of the D-mannose is not incorporated directly into the mannose-containing backbone of the polysaccharide via the mannosyl phosphate or guanosine diphosphate – mannose (16, 17) but that it is probably in equilibrium with D-fructose 1,6-diphosphate.

The distribution of C^{14} in the samples of D-xylose further supports the theory that D-xylose may arise from the hexoses via loss of carbon-6.

It has been postulated (18, 19) that uronic acids in pectin are derived from hexoses by direct oxidation of carbon-6 without significant breakdown of the carbon skeleton. The C^{14} labelling in D-glucuronic acid derived from D-glucose-1-C^{14} and D-glucose-6-C^{14} supports this theory. The D-glucuronic acid derived from D-mannose-1-C^{14} and D-galactose-1-C^{14} while retaining approximately 50% of the activity in carbon-1 also has a considerable distribution of activities in the other carbons. Thus in these cases there must be a significant amount of breakdown of the carbon skeleton to fragments followed by resynthesis.

L-Arabinose was not converted directly to D-xylose as was found by Neish (14). From the results it seems probable that L-arabinose is converted into a hexose which is the common precursor for the formation of D-mannose, D-glucuronic acid (via oxidation of carbon-6), and D-xylose via oxidation and decarboxylation of carbon-6. D-xylose follows a similar pathway to that of L-arabinose.

DISCUSSION

The topic *Biosynthesis of Monosaccharides* has been recently reviewed (20, 21, 22).

The results presented in this paper support the theory that hexoses are readily interconvertible with only a small amount of cleavage of the carbon skeleton occurring (6–15, 27). The probable intermediates for such conversions are shown in Fig. 1 (20).

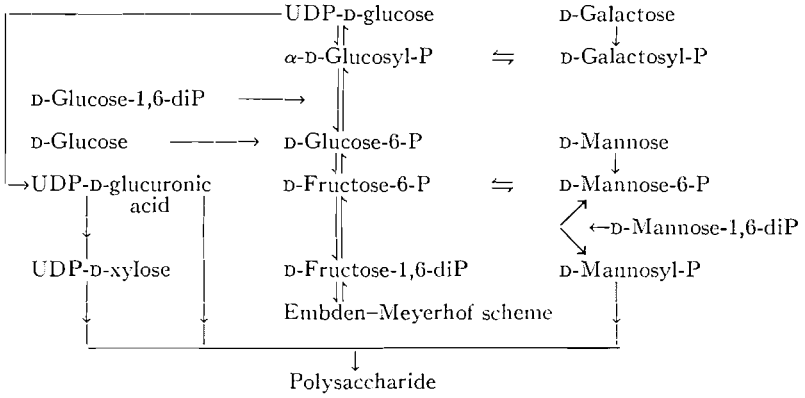


FIG. 1. The interconversion of hexoses. P = phosphate; UDP = uridine diphosphate.

Can. J. Chem. Downloaded from www.nrcresearchpress.com by 210.87.254.105 on 09/05/12
For personal use only.

Can. J. Chem. Downloaded from www.nrcresearchpress.com by 210.87.254.105 on 09/05/12
For personal use only.

The results show that the conversion of D-galactose to the D-glucose intermediate takes place without appreciable breakdown of the carbon skeleton, probably via a "galactowaldenase" enzyme system (23). The D-glucose intermediate is epimerized to D-mannose; the over-all retention of activity in carbon-1 for the conversion of D-galactose to D-mannose is 77%. The bulk of the remainder of the activity (16%) is present in carbon-6 as would be expected if the Embden–Meyerhof pathway was operative.

The formation of D-xylose from hexoses by loss of carbon-6 is apparent, since the D-xylose derived from D-glucose-6-C^{14} contains only 6.5% of the activity that it would have contained had it been derived from D-glucose-1-C^{14}. The D-xylose derived from D-glucose-1-C^{14}, D-mannose-1-C^{14}, and D-galactose-1-C^{14} retains 85–94% of its activity in carbon-1. Similar results were obtained by other workers (12, 14, 9).

It is possible that D-xylose and D-glucuronic acid derived from D-glucose-1-C^{14} and D-glucose-6-C^{14} had the same UDP-hexuronic acid precursor since the retention of activity in carbon-1 in the former is very high. In the latter the D-glucuronic acid had 4.4% of its activity in carbons 1–5 and the D-xylose contained 6.5% of activity in carbons 1–5 as mentioned above.

The D-xylose and D-glucuronic acid derived from D-mannose-1-C^{14} and D-galactose-1-C^{14} do not come from the same UDP-hexuronic acid precursor since the retention of activity in carbon-1 of the D-xylose is high (85–93%), but the activity in the D-glucuronic acid is much more widely distributed through the molecule.

The conversion of D-xylose-1-C^{14} and L-arabinose-1-C^{14} into the polysaccharide constituents takes place with much breakdown of the pentose carbon skeleton and resynthesis to pentose, hexose, and hexuronic acid. Gibbs and Horecker (24) showed that D-ribose-5-phosphate was converted to hexose monophosphate via a pathway involving transketolase and transaldolase (Fig. 2). The results collected in Table III show that the distribution of the activity in D-mannose, D-xylose, and probably D-glucuronic acid agree with the results expected from this pathway if it is assumed that D-xylose is derived from a hexose precursor by loss of carbon-6. Neish (12, 13) and Hassid *et al.* (9) found with wheat seedlings that D-xylose was metabolized by such a pathway but L-arabinose was not (14). It was proposed that UDP-L-arabinose was formed as an intermediate which could be converted to UDP-D-xylose which was incorporated directly into the xylan. Neish suggested that the enzyme systems for converting free D-xylose into UDP-D-xylose were not present in wheat seedlings and that it was metabolized by the following scheme:

$$\text{D-xylose} \xrightarrow[\text{transaldolase}]{\text{transketolase}} \text{hexose} \rightarrow \text{UDP-hexuronic acid} \rightarrow \text{UDP-D-xylose} \rightarrow \text{xylan.}$$

It is apparent that in the growth media of *Cryptococcus laurentii* although there is an enzyme system for converting D-galactose → D-glucose → D-mannose there is no such system for the similar L-arabinose → D-xylose conversion. The results in Table III indicate that L-arabinose and D-xylose are metabolized through the same intermediates. Recently Horecker *et al.* (25) have shown that D-ribose, D-xylose, and L-arabinose are interconvertible through the scheme showed in Fig. 3.

It is now recognized that D-threopentulose-5-phosphate, not D-erythropentulose-5-phosphate, is the substrate of transketolase in animals and microorganisms (22).

Since D-xylose and L-arabinose are metabolized by *Cryptococcus laurentii* via the same intermediates then it would be reasonable to propose that the enzyme systems responsible for the intermediates involved in Fig. 3 and Fig. 2 must be present.

Can. J. Chem. Downloaded from www.nrcresearchpress.com by 210.87.254.105 on 09/05/12
For personal use only.

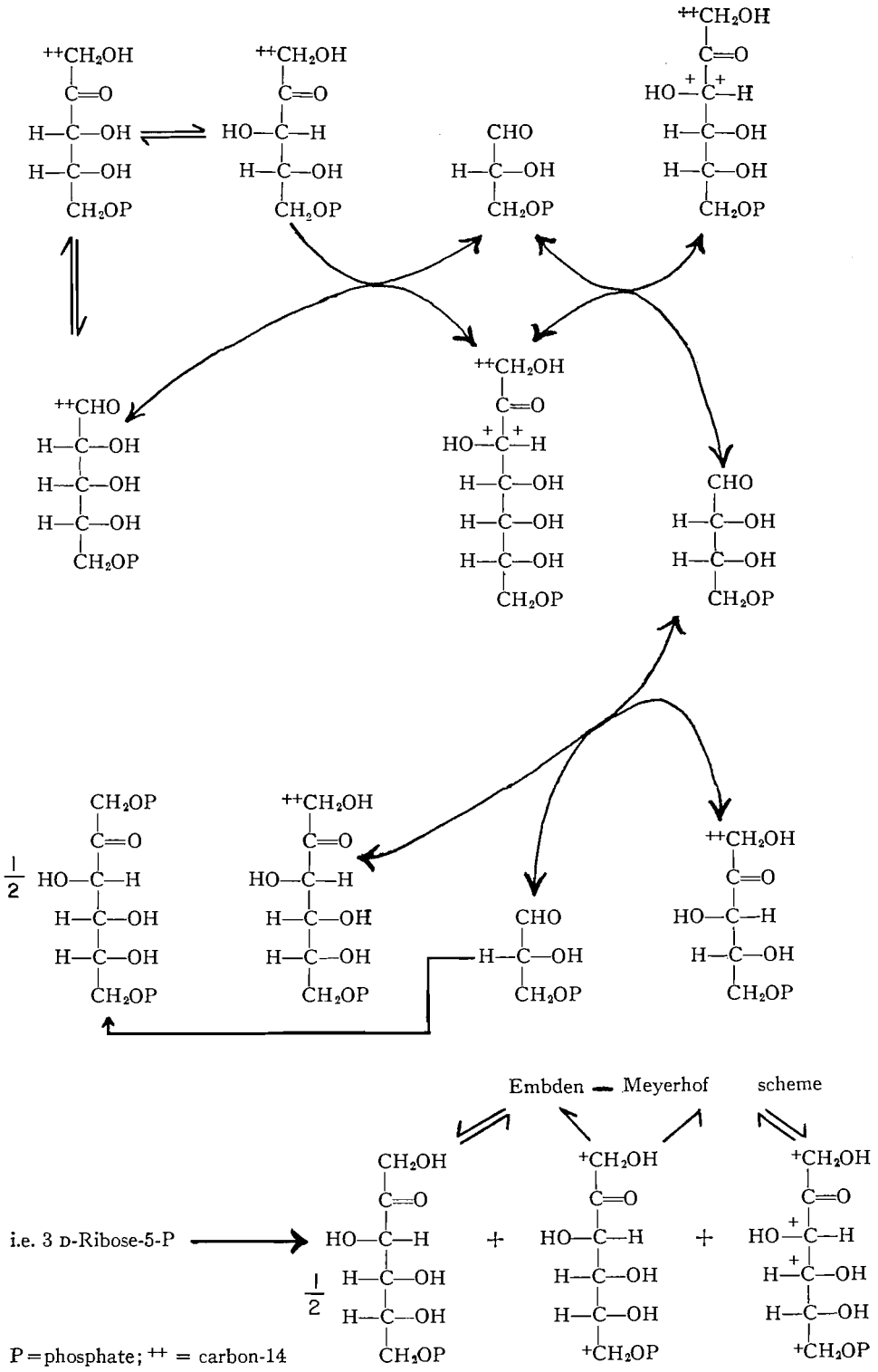


FIG. 2

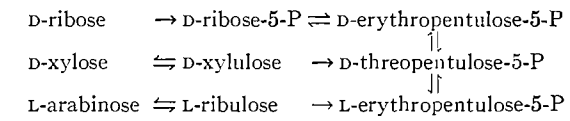


FIG. 3.

ACKNOWLEDGMENTS

The authors are indebted to the National Research Council for grants and for the award of a scholarship (to M.J.A.).

REFERENCES

1. M. J. ABERCROMBIE, J. K. N. JONES, M. V. LOCK, M. B. PERRY, and R. J. STOODLEY. Can. J. Chem. **38**, 1617 (1960).
2. M. J. ABERCROMBIE and J. K. N. JONES. This issue.
3. S. A. BROWN. Can. J. Biochem. and Physiol. **33**, 368 (1955).
4. Y. J. TOPPER and A. B. HASTINGS. J. Biol. Chem. **179**, 1255 (1949).
5. M. DUBOIS, K. A. GILLES, J. K. HAMILTON, P. A. REBERS, and F. SMITH. Anal. Chem. **26**, 350 (1956).
6. G. A. GREATHOUSE *et al.* J. Am. Chem. Soc. **76**, 1658, 5052, 5157 (1954); **77**, 1244 (1955); **79**, 4505 (1957); Science, **117**, 553 (1953).
7. C. GILVARG. J. Biol. Chem. **199**, 57 (1952).
8. J. C. SOWDEN and S. FRANKEL. J. Biol. Chem. **221**, 587 (1956).
9. V. GINSBURG and W. Z. HASSID. J. Biol. Chem. **223**, 277 (1956).
10. J. ELDERMAN, V. GINSBURG, and W. Z. HASSID. J. Biol. Chem. **213**, 843 (1955).
11. S. A. BROWN and A. C. NEISH. Can. J. Biochem. and Physiol. **32**, 170 (1954).
12. A. C. NEISH. Can. J. Biochem. and Physiol. **33**, 658 (1955).
13. H. A. ALTERMATT and A. C. NEISH. Can. J. Biochem. and Physiol. **34**, 405 (1956).
14. A. C. NEISH. Can. J. Biochem. and Physiol. **36**, 187 (1958).
15. J. C. SOWDEN and S. FRANKEL. J. Biol. Chem. **221**, 587 (1956).
16. E. CABIB and L. F. LELOIR. J. Biol. Chem. **206**, 779 (1954).
17. C. W. CHUNG and W. J. NICKERSON. J. Biol. Chem. **208**, 395 (1954).
18. C. G. SEEGMILLER, B. AXELROD, and R. M. MCCREADY. J. Biol. Chem. **217**, 765 (1955).
19. C. G. SEEGMILLER, R. JANG, and W. MANN. Arch. Biochem. Biophys. **61**, 422 (1956).
20. L. HOUGH and J. K. N. JONES. Advances in Carbohydrate Chem. **11**, 185 (1956).
21. S. BAYNE. Rare sugars. Ann. Rept. Chem. Soc. 1958.
22. B. L. HORECKER and A. H. MEHLER. Ann. Rev. Biochem. **24**, 207 (1955).
23. L. F. LELOIR *et al.* J. Biol.Chem. **179**, 497 (1949); **184**, 333 (1950); Biochem. J. (London), **51**, 426 (1952); Nature, **165**, 191 (1950).
24. M. GIBBS and B. L. HORECKER. J. Biol. Chem. **208**, 813 (1954).
25. E. C. HEATH, J. HURWITZ, B. L. HORECKER, and A. GINSBURG. J. Biol. Chem. **231**, 1009 (1958).
26. S. L. CHEN. Biochim. et Biophys. Acta, **32**, 486 (1959).

Can. J. Chem. Downloaded from www.nrcresearchpress.com by 210.87.254.105 on 09/05/12
For personal use only.

Can. J. Chem. Downloaded from www.nrcresearchpress.com by 210.87.254.5 on 09/05/12
For personal use only.

PHASE EQUILIBRIUM RELATIONSHIPS IN THE BINARY SYSTEM METHYL ETHYL KETONE – WATER[1]

IRWIN SIEGELMAN[2] AND C. H. SORUM[3]

ABSTRACT

A complete investigation of the phase equilibrium relationships in the binary system of the partially miscible liquid pair methyl ethyl ketone – water is presented. The system shows a minimum azeotrope at 73.35±0.05° C with a composition of 88.45±0.15 wt.% ketone. The azeotrope falls outside of the miscibility gap for this system. The liquid–vapor curves intersect the miscibility gap at the temperature of 73.60±0.05° C at which two conjugate solutions of compositions 18.10±0.10 and 87.78±0.15 wt.% ketone, respectively, are in equilibrium with a vapor phase of composition 88.00±0.15 wt.% ketone. The partially miscible liquid pair shows an upper consolute temperature of 139±0.5° C at a composition of 44.9±0.2 wt.% ketone. The liquid–liquid curves intersect the solid–liquid curves at a temperature of −6.0±0.5° C at which two conjugate solutions of composition 40.0±0.2 and 78.0±0.2 wt.% ketone, respectively, are in equilibrium with ice. A binary eutectic exists at a temperature of −89.0±0.5° C with composition of the eutectic solid equal to 99.4±0.4 wt.% ketone. The freezing point of pure, dry methyl ethyl ketone is determined to be −83.5±0.5° C.

INTRODUCTION

Discrepancies in the literature data (1–8) on mutual solubility studies for the system methyl ethyl ketone – water, as shown in Fig. 1, and similar discrepancies in the literature

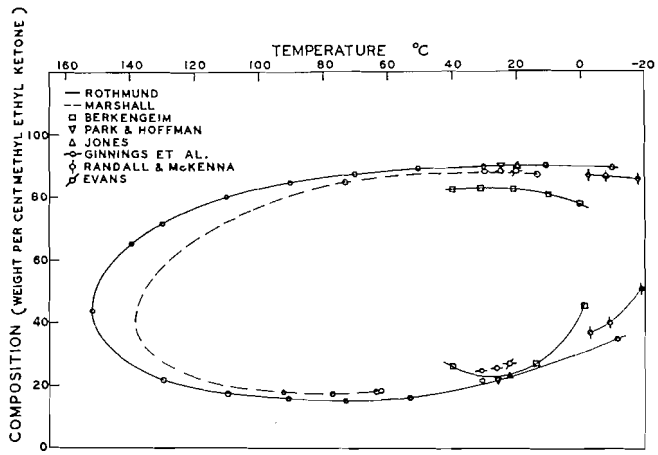


FIG. 1. Mutual solubility data as reported in the literature.

(9, 10, 11) on liquid–vapor studies of this system, as shown in Fig. 2, prompted this present work. This paper presents, then, the results of a reinvestigation of the mutual solubility and liquid–vapor relationships found in the system methyl ethyl ketone – water plus a study of the solid–liquid equilibria for a complete picture of the phase equilibrium relationships in this system.

[1]*Manuscript received April 7, 1960.*
Contribution from the Department of Chemistry, University of Wisconsin, Madison, Wisconsin. The work described herein was included in a thesis submitted by Siegelman to the University of Wisconsin in partial fulfillment of the requirements for the degree of Doctor of Philosophy.
[2]*Present address: John Harrison Laboratory of Chemistry, University of Pennsylvania, Philadelphia, Pennsylvania.*
[3]*Department of Chemistry, University of Wisconsin, Madison, Wisconsin.*

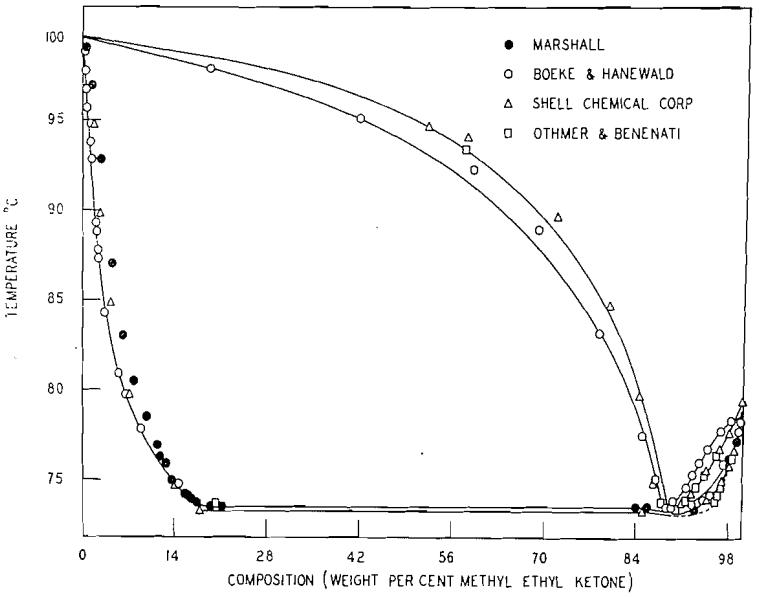


FIG. 2. Liquid–vapor data as reported in the literature.

EXPERIMENTAL

A. Materials

The water used in these studies was distilled water from the laboratory tap which was redistilled from alkaline permanganate solution. Constancy of freezing point was used as a criterion of purity.

Commercial methyl ethyl ketone (minimum purity 99.0% by weight, b.p. 79.0–81.0° C), a straw yellow in color, was dried following the technique found in Weissberger's standard work (12). Middle fractions of doubly distilled water-clear ketone (b.p. 79.60± 0.05° C) were collected and stored over anhydrous potassium carbonate in the dark. (Methyl ethyl ketone is subject to slow photolysis.) A combination of physical techniques and visual observation used indicated a ketone purity of not less than 99.6% and probably of the order of 99.9%. As will be noted below, in the section pertaining to solid–liquid studies, the freezing point of methyl ethyl ketone as prepared for this work is further evidence of its high purity and dryness.

B. Thermometers

Throughout these studies temperatures were measured by use of conventional liquid-in-glass thermometers. The mercury-in-glass instruments (Brooklyn Thermometer Company precision grade) used between 0° C and 140° C were calibrated against a National Bureau of Standards' certified platinum resistance thermometer. The petrolate-in-glass instruments (Brooklyn Thermometer Company) used between 0° C and −90° C were calibrated and certified by the National Bureau of Standards.

C. Determination of the Liquid–Vapor Curves

The Othmer equilibrium still (13) was used to determine the liquid–vapor curves for this system. In order to present data at 1 atmosphere it was necessary to use the still in conjunction with a simple pressure line capable of maintaining the pressure in the still at 760±1 mm. Compositional analyses of boiling liquids and their condensed vapors were made by measurement of their relative refractive indices which were then compared

Can. J. Chem. Downloaded from www.nrcresearchpress.com by 210.87.254.5 on 09/05/12
For personal use only.

to working curves of relative readings of refractive index versus percentage composition of known solutions. An interesting result obtained for refractive index of ketone-rich solutions at 25° C is that a maximum occurs in the curve in the vicinity of 90% ketone (Fig. 3). Data obtained by the Shell Chemical Company (14) do not show such a maximum.

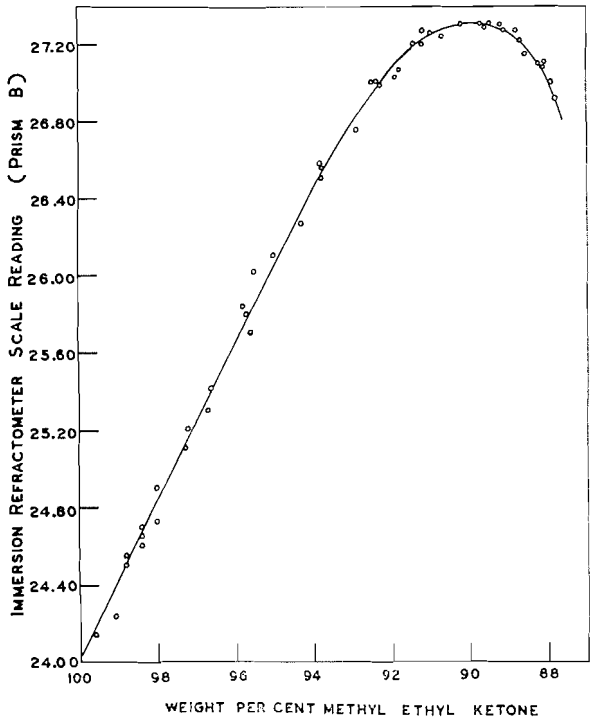


FIG. 3. Working curve of refractive index for ketone-rich solutions.

For most solutions tapped from the Othmer still no further treatment beyond cooling them to 25° C was necessary prior to relative refractive index measurement. In some cases, however, the condensed vapors were heterogeneous and had to be mechanically agitated until equilibrium was attained. In those cases also, known weights of water were added until a homogeneous solution prevailed and then relative refractive indices were taken. A simple back calculation gave the compositional analyses for the original heterogeneous samples.

The data found for the liquid–vapor curves in the system are presented in Table I and Fig. 4. The most interesting point on this aspect of the system is that the minimum azeotrope, which occurs at 73.35±0.05° C at a composition of 88.45±0.15 wt.% methyl ethyl ketone, falls just outside of the intersection of the miscibility gap and the boiling point curve. This intersection, an invariant point of the system, occurs at 73.60±0.05° C where conjugate solutions of compositions 18.10±0.10 and 87.78±0.15 wt.% ketone, respectively, are in equilibrium with a vapor of composition 88.00±0.15 wt.% ketone.

D. Determination of the Solid–Liquid Curves

The method of thermal analysis was used throughout the study of the solid–liquid equilibria. The freezing point cell was capped with a teflon stopper through which the low-temperature thermometer and all glass stirring rod were fitted. The latter was, in

Can. J. Chem. Downloaded from www.nrcresearchpress.com by 210.87.254.5 on 09/05/12
For personal use only.

TABLE I

Vapor and liquid compositions of mixtures of methyl ethyl ketone and water

B.p.[a] (°C, 1 atm)	Wt.% methyl ethyl ketone		B.p. (°C, 1 atm)	Wt.% methyl ethyl ketone	
	Liquid	Vapor		Liquid	Vapor
100.00	0.00	0.00	73.35[d]	88.45	88.40
98.50	0.26	21.00	73.35[d]	88.45	88.65
97.30	0.54		73.60	81.10[b]	88.02
92.10	1.42			87.80[b]	
90.30	1.70	67.74[c]	73.80	93.55	91.90
85.00	2.89	78.42[c]	73.90	94.55	91.40
84.20	4.23		74.00	95.10	92.55
82.35	4.88		74.60	96.80	92.93
80.10	6.38	84.32[c]	74.80	96.55	93.25
78.20	8.58		75.30	97.10	94.20
77.00	10.34	86.24[c]	75.45	97.27	94.13
75.90	12.36	86.83[c]	77.05	98.80	96.50
73.55	18.06[b]	87.90	77.20	98.80	96.95
	87.76[b]		79.35	99.95	100.00
			79.35	99.85	100.00
			79.60	100.00	100.00

[a]To ±0.05° C.
[b]Two liquid layers and homogeneous condensed vapor.
[c]Dilution with water required to obtain homogeneity; calculated values.
[d]Minimum azeotrope.

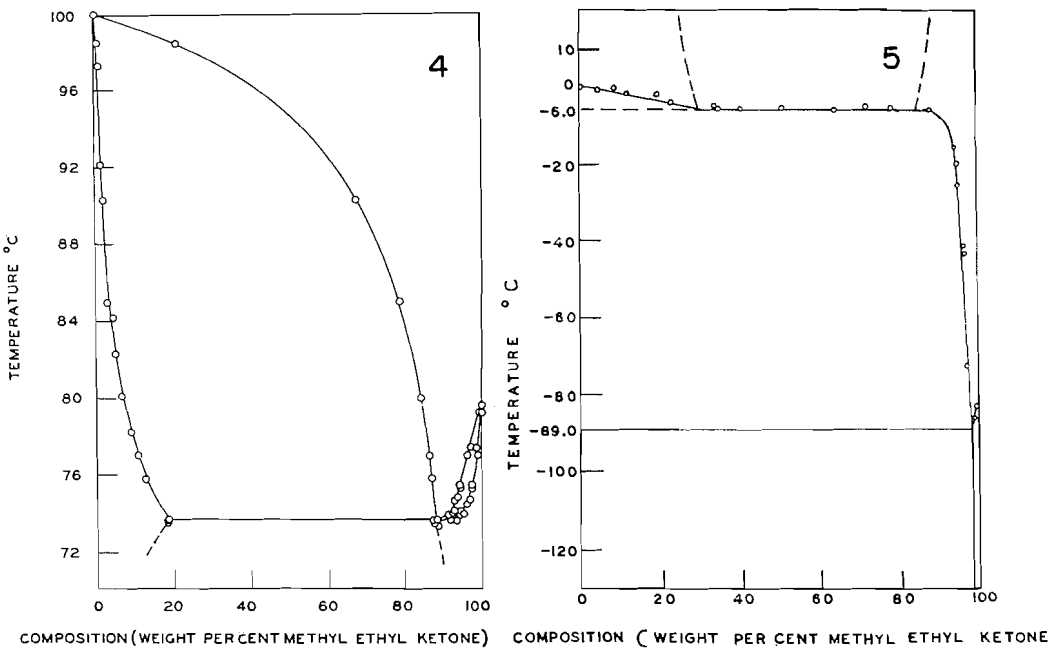


FIG. 4. Liquid–vapor phase equilibria.
FIG. 5. Solid–liquid phase equilibria.

turn, fitted with a semiball joint and spun in contact with the self-lubricating teflon stopper. This allowed for efficient mechanical agitation of the synthetic mixtures in the cell, particularly if they were heterogeneous, and at the same time provided a confined system, thereby preventing any loss of material through vaporization.

The temperature-controlling system employed was relatively crude. The cooling mixes

Can. J. Chem. Downloaded from www.nrcresearchpress.com by 210.87.254.5 on 09/05/12
For personal use only.

chosen were an ice slurry (for cooling to 0° C), a trichloroethylene – dry ice mix (for cooling in the range of 0° to −35° C), and liquid air (for cooling to very low temperatures). Manual raising and lowering of the cooling mix was chosen to establish a fairly well-regulated rate of cooling. Each synthetic mixture was thermally analyzed at least twice.

The data found for the solid–liquid curves in the system are presented in Table II

TABLE II

Freezing points of mixtures of methyl ethyl ketone and water

F.p.[a] (°C)	Wt.% ketone	F.p. (°C)	Wt.% ketone
0.00	0.00	−9.0	92.14
−0.05	8.63	−9.0	92.87
−2.0	11.45	−9.5	92.88
−2.5	19.19	−16.0	94.36
−4.5	22.95	−20.5	94.95
−6.0	33.72	−26.0	95.35
−5.5	34.71	−42.0	96.46
−6.0	40.34	−44.0	97.08
−6.0	51.10	−72.5	97.48
−7.0	64.20	−73.0	97.56
−6.0	71.98	−73.0	97.58
−6.0	78.30	−86.5	99.34
−6.5	87.15	−89.0[b]	99.4[b]
−8.5	91.96	−83.5	100.00

[a]All but first two to ±0.5° C.
[b]Eutectic point by extrapolation.

and Fig. 5. The first invariant point for the solid–liquid curves occurs at −6.0±0.5° C, at which a pair of conjugate solutions are in equilibrium with ice. The approximate compositions of the conjugate solutions were determined by extrapolation to be 36% and 80% by weight of methyl ethyl ketone, respectively. As a result of the liquid–liquid studies reported below, these compositions were determined with greater accuracy. The second invariant point for the solid–liquid curves occurs at −89.0±0.5° C, the eutectic point. It was impossible to determine the eutectic composition by any means other than extrapolation since this composition lies so close to that of pure ketone. Such extrapolation would indicate the eutectic composition to be 99.4±0.4% by weight methyl ethyl ketone. This piece of data would seem to account for the low freezing points of methyl ethyl ketone (−86° C to −86.9° C) as reported in standard reference tabulations (15, 16, 17). This work reports a freezing point for pure, *dry* methyl ethyl ketone of −83.5 ± 0.5° C.

E. Determination of the Liquid–Liquid Curves

The "thermostatic method" of Hill (18) was used primarily to determine the liquid–liquid curves. Two separate Hill method analyses were run. The results of those analyses are reported in Table III and Fig. 6. The Hill method allows for the calculation of the mean compositions of the conjugate liquid pair. Such calculations were made and plotted as a function of temperature. This was done in order to ascertain the general vicinity of the upper consolute temperature for the system. According to a variation of the law of Cailletet and Mathias (19) such calculations should lead to a straight line passing through the consolute point. The results of these calculations are also given in Table III and Fig. 6. From them the upper consolute temperature for this system appeared to be near 140° C at a composition of 40–45% by weight methyl ethyl ketone. In order to determine the upper consolute point more closely, several more points on the liquid–liquid curve

Can. J. Chem. Downloaded from www.nrcresearchpress.com by 210.87.254.5 on 09/05/12
For personal use only.

TABLE III

Mutual solubility of methyl ethyl ketone and water: Hill method

Temperature (°C)[a]	Calculated wt.% ketone[b,c]		Mean composition (wt.%)
	Lower layer	Upper layer	
7.50	32.9	85.4	59.7
9.50	32.3	85.1	58.7
11.00	31.1	87.1	59.1
11.00	28.7	89.0	58.8
18.00	28.6	90.1	59.4
18.50	28.3	87.6	57.9
30.50	24.0	91.4	57.7
35.00	22.4	91.2	56.8
40.00	21.1	91.0	56.0
45.00	21.0	89.6	55.3
56.00	18.8	89.3	54.0
62.00	18.6	88.7	53.7
71.00	17.6	88.4	53.0
83.00	17.5	84.0	52.8

[a] ±0.05° C.

[b] ±0.2%.

[c] First four figures are for experiment in which the two synthetic mixtures were composed of 7.1266 g ketone/8.2682 g water, and 6.9349 g ketone/9.3329 g water. All other figures are for sealed experiments in which the two synthetic mixtures were composed of 7.0760 g ketone/12.6050 g water, and 9.8135 g ketone/9.6782 g water.

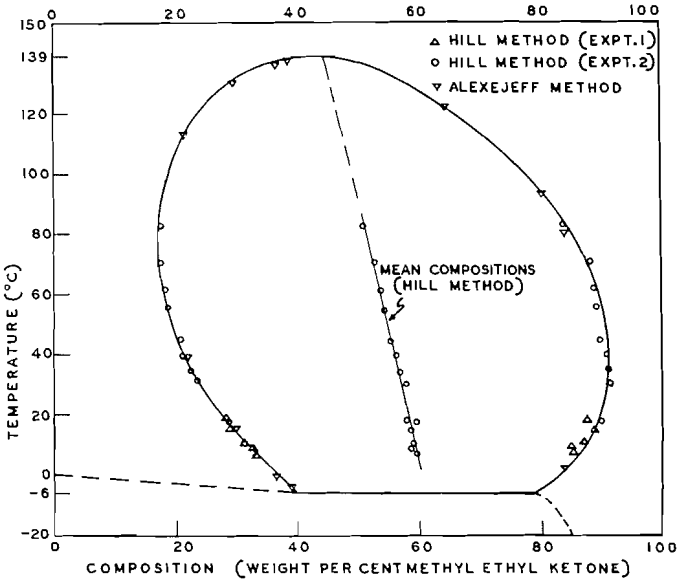


FIG. 6. Liquid–liquid phase equilibria.

were determined using the familiar "synthetic method" (cloud-clear points) of Alexejew (20). These results are given in Table IV and also shown on Fig. 6.

With the additional points obtained from the cloud-clear point analyses, the extrapolated Cailletet–Mathias plot indicates that the upper consolute temperature for this system occurs at 139.0±0.5° C at a composition of 44.9±0.2% by weight of methyl ethyl ketone.

Can. J. Chem. Downloaded from www.nrcresearchpress.com by 210.87.254.5 on 09/05/12
For personal use only.

TABLE IV

Mutual solubility of methyl ethyl ketone and water: Alexejew method

Wt.% ketone	Cloud points[a] (°C)[b]		Clear points[a] (°C)[b]	
	Upper	Lower	Upper	Lower
21.72	113.0	39.5	115.0	39.0
29.83	132.0	15.5	131.0	16.0
36.82	137.0	−0.5	135.5	0.0
38.96	138.0	−4.0	136.5	−4.5
65.43	122.0	[c]	120.0	[c]
80.98	93.0	−2.5	91.0	−2.0
83.88	81.0	3.0	80.0	2.5

[a]Average of two experiments.
[b]±0.5° C.
[c]Ice formed at −6.0±0.5° C.

It was indicated in the solid–liquid section of this paper (Section D) that the miscibility gap intersects the freezing point curves in the vicinity of 36% and 80% by weight methyl ethyl ketone, respectively. From the liquid–liquid work a very short extrapolation to the freezing point curves indicates that these invariant points have the more accurately determined values of 40.0±0.2% and 78.0±0.2% by weight methyl ethyl ketone, respectively, at the temperature of −6.0±0.5° C.

DISCUSSION

A summary of all the equilibrium phase relationships for the binary system, methyl ethyl ketone – water, as found in this study is given by a total phase diagram shown in Fig. 7.

From the liquid–vapor studies, the results of this work (Table I and Fig. 4) compare quite well with the data reported by the Shell Chemical Corporation (10) and, earlier, by Marshall (2). The minimum azeotrope found in this study, at a temperature of 73.35±0.05° C and a composition of 88.45±0.15% by weight methyl ethyl ketone, is consistent with their reported figures of 73.4° C and 73.6° C, and 88.7% and 88.62% by weight, respectively. Othmer and Benenati (11) report a higher composition, 89.1%, while Boeke and Hanewald (9) report a lower figure, 87.8%.

From the liquid–liquid studies given here (Tables III and IV and Fig. 4) agreement with Marshall's studies (2) from 20° C to approximately 100° C is found. However, the enhanced solubility of methyl ethyl ketone in water and vice versa at temperatures below 20° C found in this work are at variance with Marshall's data for the same temperature region, but are in close agreement with the solubilities found by Ginnings *et al.* (6). It appears probable that the results reported in other previous investigations (1, 3, 4, 5, 7, 8) are in error. The most recent investigation on this aspect of the system is that of Campbell *et al.* (21), which is less extensive than the present work. Their work agrees closely with the combined data of Marshall and Shell Chemical Corporation investigators (22) with which this work is in some slight disagreement at temperatures near the upper consolute point. In particular, the initial study on the mutual solubilities to be reported for this system by Rothmund (1) is further shown to be incorrect by consideration of the upper consolute point. The data of this study, 139.0±0.5° C and 44.9±0.2% by weight methyl ethyl ketone, and that of Campbell *et al.* (21) and the Shell Chemical Corporation (22), 143° C and 45% by weight ketone, would indicate that Rothmund's data of 151.8° C and 44.2% by weight ketone is probably in error.

Can. J. Chem. Downloaded from www.nrcresearchpress.com by 210.87.254.5 on 09/05/12
For personal use only.

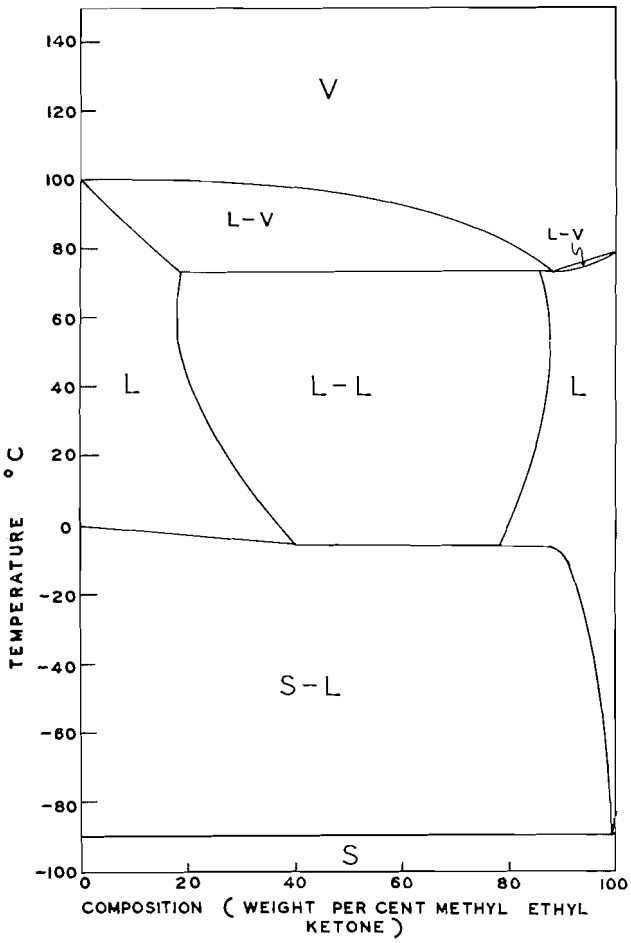


FIG. 7. Summary phase equilibria diagram.

The solid–liquid studies reported here (Table II and Fig. 5) are in good agreement with those of Randall and McKenna (7), who report the eutectic temperature to be $-88.88\pm0.01°$ C at a composition of 99.91% by weight methyl ethyl ketone, while this work reports values of $-89.0\pm0.5°$ C and $99.4\pm0.4\%$ by weight ketone.

ACKNOWLEDGMENTS

We wish to thank Dr. Charles C. Price, Chairman, and members of the Staff of the Department of Chemistry at the University of Pennsylvania for their encouragement and material aid which allowed this work to be completed.

REFERENCES

1. V. ROTHMUND. Z. physik. Chem. 26 (1898).
2. A. MARSHALL. J. Chem. Soc. **89**, 1350 (1906).
3. T. I. BERKENGEIM. Chem. Abstr. **40**, 6961 (1946).
4. J. G. PARK and H. E. HOFFMAN. Ind. Eng. Chem. **24**, 132 (1932).
5. D. C. JONES. J. Chem. Soc. 799 (1929).
6. P. M. GINNINGS, D. PLONK, and E. CARTER. J. Am. Chem. Soc. **62**, 1923 (1940).
7. M. RANDALL and F. E. MCKENNA. J. Am. Chem. Soc. **73**, 4859 (1951).

Can. J. Chem. Downloaded from www.nrcresearchpress.com by 210.87.254.5 on 09/05/12
For personal use only.

8. T. W. EVANS. Ind. Eng. Chem. Anal. Ed. **8**, 206 (1936).
9. J. BOEKE and K. H. HANEWALD. Rec. trav. chim. **61**, 881 (1942).
10. SHELL CHEMICAL CORPORATION. Methyl ethyl ketone. 2nd ed. New York. 1950. p. 68.
11. D. OTHMER and R. BENENATI. Ind. Eng. Chem. **37**, 299 (1945).
12. A. WEISSBERGER (*Editor*). Techniques of organic chemistry. Vol. VII. Organic solvents. 2nd ed. Interscience Publishers, Inc., New York. 1955. p. 382.
13. D. F. OTHMER, *et al.* Ind. Eng. Chem. **20**, 743 (1928); **37**, 299, 895 (1945); **40**, 168 (1948); Ind. Eng. Chem. Anal. Ed. **4**, 232 (1932).
14. Shell Chemical Corporation. Methyl ethyl ketone. 2nd ed. New York. 1950. p. 66.
15. N. LANGE (*Editor*). Handbook of chemistry. 9th ed. Handbook Publishers, Inc., Sandusky, Ohio. 1956. p. 604.
16. THE HANDBOOK OF CHEMISTRY AND PHYSICS. 35th ed. Chemical Rubber Publishing Co., Cleveland, Ohio. 1953. p. 808.
17. THE MERCK INDEX OF CHEMICALS AND DRUGS. 6th ed. Merck and Co., Inc., Rahway, N.J. 1955. p. 382.
18. A. E. HILL. J. Am. Chem. Soc. **45**, 1143 (1923).
19. S. GLASSTONE. Textbook of physical chemistry. 2nd ed. D. Van Nostrand Co., Inc., New York. 1946. p. 431.
20. W. ALEXEJEW. Bull. soc. chim. France, **38**, 145 (1882); Ann. phys. chim. **28**, 305 (1886).
21. A. N. CAMPBELL, E. M. KARTZMARK, and W. E. FALCONER. Can. J. Chem. **36**, 1475 (1958).
22. Shell Chemical Corporation. Methyl ethyl ketone. 2nd ed. New York. 1950. p. 67.

Can. J. Chem. Downloaded from www.nrcresearchpress.com by 210.87.254.5 on 09/05/12
For personal use only.

Can. J. Chem. Downloaded from www.nrcresearchpress.com by 210.87.254.42 on 09/05/12
For personal use only.

NOTES

VAPOR/LIQUID PARTITION OF TRITIUM IN TRITIATED WATER

O. Sepall and S. G. Mason

INTRODUCTION

In a study of the exchange of tritium between cellulose and tritiated water, it was necessary to extend the published data on the ratio of isotopic concentrations $[H^3]/[H^1]$ in the saturated vapor and liquid phases of tritiated water so as to cover the temperature range 0° to 90° C.

METHOD

Isotopic concentrations in tritiated water were determined by the gas counting method of Robinson (3) in which the hydrogen in the water is converted to methane by reaction with methyl grignard. Vapor samples were obtained by an equilibrium distillation technique.

The distillations were carried out in the arrangement shown in Fig. 1. The tritiated

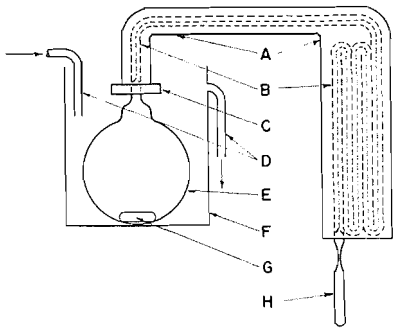


Fig. 1. Equilibrium distillation apparatus.
A. Asbestos covering with heater wire.
B. Capillary tube.
C. Rubber isolating disk between water and heater.
D. Recirculation lines for temperature regulated water.
E. 100-ml flask.
F. Copper vessel.
G. Magnetic stirrer.
H. Sample collecting tube.

water was contained in the flask E, immersed in a constant temperature bath. The vapor was distilled through the capillary tube B into a collecting tube H. The capillary served to restrict the distillation rate and to prevent diffusion back from the collecting tube to the flask. As the temperature was raised, the length of capillary was increased so as to ensure equilibrium distillation. The complete length of tubing was heated electrically by a resistance wire embedded in the asbestos covering to avoid condensation.

For a distillation, 50 ml of tritiated water (0.8 μcurie/g, $[H^3]/[H^1] = 10^{-10}$) were introduced into the flask. This quantity was large enough that concentration changes during distillation were negligible. The system was evacuated through the sampling tube until all air had been removed, and the sample tube was sealed off. The capillary heater was adjusted to give a temperature about 30° C higher than the saturation temperature for the experiment. A sample of 0.3 ml was then distilled over by immersing the collecting tube in liquid air. The length and size of the capillary had been selected so that

distillation time was at least 30 minutes. Longer times gave the same result. The sample was then isolated by sealing off the constriction in the tube.

RESULTS AND DISCUSSION

The measured ratios of isotopic concentrations in vapor and liquid are listed in Table I, and are seen to agree with the values of Brown (2). They are much higher than those of Price (1), which are concluded to be in error.

TABLE I

Isotopic ratios in tritiated water vapor and liquid

Temperature, °C	$\frac{[H^3]/[H^1]_{vapor}}{[H^3]/[H^1]_{liquid}}$	
	Present data	Brown (2)
0 ±0.5	0.86±0.005	
0.5		.88
14	0.90	
19.5		.91
20	0.91	
30	0.92	
50	0.94	
56.5		.945*
70	0.96	
90	0.97	

*From reference 4.

The accuracy of the data is limited by the gas-counting assay for tritium. The results of this analysis show a scatter with a standard deviation of 0.6%. The data reported here are averages of duplicate determinations and have been rounded off to the nearest 0.5%.

The procedure used in this work was found to be quite satisfactory. The results were reproducible for distillation times of 30 minutes or longer. For times as short as 5 minutes, the ratios tended to rise, indicating a non-equilibrium distillation.

This technique could readily be adapted for measurements above 100° C by making provision for the pressure developed.

1. A. H. Price. Nature, **181**, 262 (1958).
2. R. M. Brown. Atomic Energy of Canada, Ltd. Private communication. 1960.
3. C. V. Robinson. Nucleonics, **13** (11), 90 (1955).
4. E. C. Bertsche. U.S. Atomic Energy Commission Rept. DP325. 1958.

Received June 3, 1960.
Physical Chemistry Division,
Pulp and Paper Research Institute of Canada,
and
Department of Chemistry,
McGill University,
Montreal, Que.

THE REACTION OF THE *O*- AND *N*-METHYL DERIVATIVES OF AROMATIC KETOXIMES WITH CARBON MONOXIDE AND HYDROGEN

Alex Rosenthal

It has been previously shown that benzophenone oxime cyclizes with carbon monoxide containing about 1% hydrogen to yield 3-phenylphthalimidine in high yield (1). The

Can. J. Chem. Downloaded from www.nrcresearchpress.com by 210.87.254.42 on 09/05/12
For personal use only.

distillation time was at least 30 minutes. Longer times gave the same result. The sample was then isolated by sealing off the constriction in the tube.

RESULTS AND DISCUSSION

The measured ratios of isotopic concentrations in vapor and liquid are listed in Table I, and are seen to agree with the values of Brown (2). They are much higher than those of Price (1), which are concluded to be in error.

TABLE I

Isotopic ratios in tritiated water vapor and liquid

Temperature, °C	$\frac{[H^3]/[H^1]_{vapor}}{[H^3]/[H^1]_{liquid}}$	
	Present data	Brown (2)
0	±0.5	0.86±0.005	
0.5			.88
14		0.90	
19.5			.91
20		0.91	
30		0.92	
50		0.94	
56.5			.945*
70		0.96	
90		0.97	

*From reference 4.

The accuracy of the data is limited by the gas-counting assay for tritium. The results of this analysis show a scatter with a standard deviation of 0.6%. The data reported here are averages of duplicate determinations and have been rounded off to the nearest 0.5%.

The procedure used in this work was found to be quite satisfactory. The results were reproducible for distillation times of 30 minutes or longer. For times as short as 5 minutes, the ratios tended to rise, indicating a non-equilibrium distillation.

This technique could readily be adapted for measurements above 100° C by making provision for the pressure developed.

1. A. H. Price. Nature, **181**, 262 (1958).
2. R. M. Brown. Atomic Energy of Canada, Ltd. Private communication. 1960.
3. C. V. Robinson. Nucleonics, **13** (11), 90 (1955).
4. E. C. Bertsche. U.S. Atomic Energy Commission Rept. DP325. 1958.

Received June 3, 1960.
Physical Chemistry Division,
Pulp and Paper Research Institute of Canada,
and
Department of Chemistry,
McGill University,
Montreal, Que.

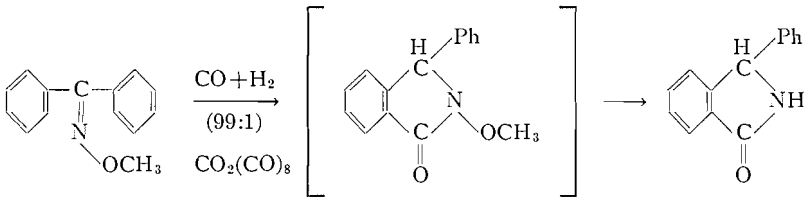
THE REACTION OF THE *O*- AND *N*-METHYL DERIVATIVES OF AROMATIC KETOXIMES WITH CARBON MONOXIDE AND HYDROGEN

Alex Rosenthal

It has been previously shown that benzophenone oxime cyclizes with carbon monoxide containing about 1% hydrogen to yield 3-phenylphthalimidine in high yield (1). The

Can. J. Chem. Downloaded from www.nrcresearchpress.com by 210.87.254.5 on 09/05/12
For personal use only.

present work was initiated in an attempt to devise a method for obtaining *N*-hydroxyphthalimidines using similar high-pressure reactions described before (1). It was hoped that by blocking the labile hydroxyl group on the oxime with an *O*-methyl ether group concurrent or subsequent elimination of the former group would be prevented, without obstruction of the cyclization with carbon monoxide. Thus, reaction of *O*-methylbenzophenone oxime with carbon monoxide might be expected to yield *N*-methoxy-3-phenylphthalimidine (I) as shown below:

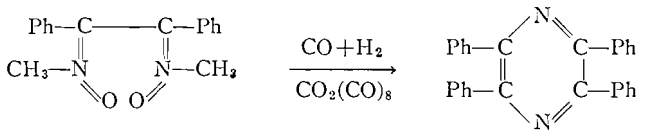


I II

Subsequent demethylation of the latter might produce *N*-hydroxy-3-phenylphthalimidine since the lactam ring is stable to acid hydrolysis.

When a benzene solution of *O*-methylbenzophenone oxime was reacted with a mixture of carbon monoxide and hydrogen (99:1) at about 300 atmospheres and at about 220° for 70 minutes in the presence of preformed dicobalt octacarbonyl the main product was 3-phenylphthalimidine (II). Compound II was characterized by direct comparison (mixed melting point and infrared) with an authentic sample (2). No attempt was made to determine whether the cleavage of the ether took place prior or subsequent to the cyclization with carbon monoxide.

As carbon monoxide cyclized readily with nitrogen (in the trivalent state) to the aromatic ring (1), it seemed of interest to determine if the nitrogen in the *N*-methyl ether might undergo a similar attachment to the aromatic ring. When α-benzildioxime *N*,*N*′-dimethyl ether was reacted with carbon monoxide and hydrogen at about 225° for 2 hours the main product was tetraphenylpyrazine (III) as shown below:



III

The structure of compound III was unequivocally established by direct comparison (mixed melting point and infrared) with an authentic sample (3).

Various analyses were carried out in an attempt to ascertain the mechanism of formation of the unexpected tetraphenylpyrazine. Three moles of gases per mole of substrate was consumed in the reaction. Reaction of the gases with dilute hydrochloric acid gave a trace amount of a crystalline salt melting at approximately the correct temperature for ammonium chloride. Treatment of the salt with sodium hydroxide produced a gas which turned red litmus blue. Gas chromatographic analyses of the liquid component of the reaction mixture showed only benzene to be present. The residual organic material remaining after extraction of tetraphenylpyrazine appeared to be polymeric in nature as evidenced by the fact that the residue was insoluble in organic solvents. Since none of these experiments shed any light on the mechanism, further work was abandoned.

Can. J. Chem. Downloaded from www.nrcresearchpress.com by 210.87.254.5 on 09/05/12
For personal use only.

EXPERIMENTAL

General Considerations

The equipment was described previously (1).

Reaction of O-Methylbenzophenone Oxime with Carbon Monoxide and Hydrogen

1. Preparation of O-Methylbenzophenone Oxime

Benzophenone (20 g) and *O*-methylhydroxylamine hydrochloride (14 g) were refluxed for 4 hours with 20 ml of pyridine and 200 ml of ethanol. The ethanol was then removed under reduced pressure. Slow addition of water with stirring caused the product to crystallize (87% yield). *O*-Methylbenzophenone oxime was twice recrystallized from acetone–methanol–water according to the method described by Hauser and Hoffenberg (4), m.p. 60–61°; reported m.p. 60–61° (4).

2. Carbonylation of O-Methylbenzophenone Oxime

To a solution of *O*-methylbenzophenone oxime (10.5 g, 0.05 mole) and dicobalt octacarbonyl (0.026 mole) in 50 ml of purified thiophene-free benzene contained in a glass liner in the bomb was added a mixture of carbon monoxide and hydrogen (99:1) at 2300 p.s.i. The bomb was rocked and heated at 220° for 70 minutes. The over-all pressure drop was 125 p.s.i. measured at 0° C (1.3 moles of gas per mole of substrate). After the dicobalt octacarbonyl was decomposed at 70–80°, the benzene was removed under reduced pressure. The solid residue was extracted with two 100-ml portions of ether. The remaining residue was extracted with hot chloroform. After the chloroform was evaporated the residue was recrystallized from ethanol to yield 3-phenylphthalimidine, m.p. 218–220°, mixed melting point with an authentic sample of 3-phenylphthalimidine (2), 218–220°.

After removal of the catalyst and solvent, a portion of the crude product (0.55 g) in 10 ml of benzene was added to the top of a glass column containing a 80×38 mm (diameter) adsorbent column of alumina. Elution of the column with 200 ml of benzene gave a trace of brown oil. An amount of 0.40 g (about 75%) of 3-phenylphthalimidine was eluted using benzene–ethanol (9:1) as developer.

When the reaction product (after removal from the bomb) was fractionated on alumina using benzene as developer, an unstable brown organo–cobalt complex was eluted which on being warmed in petroleum ether became insoluble. Attempts to characterize this material were unsuccessful.

Reaction of α-Benzildioxime N,N′-Dimethyl Ether with Carbon Monoxide and Hydrogen

In a similar way a mixture of 5.9 g of α-benzildioxime *N,N′*-dimethyl ether (5) in 60 ml benzene containing 2 g of dicobalt octacarbonyl as catalyst was reacted with 3800 p.s.i. of carbon monoxide and hydrogen (99:1), at 225–230° for about 2 hours. The over-all pressure drop was 130 p.s.i. measured at room temperature. The gaseous product was bubbled through dilute hydrochloric acid. Evaporation of the solvent left a few milligrams of a crystalline product which melted at 300–340°. Treatment of the salt with dilute sodium hydroxide evolved a gas which was basic to litmus paper.

An aliquot of the reaction mixture was allowed to stand at room temperature until the catalyst was decomposed. Vapor phase chromatography of the distillate showed benzene only to be present.

After the catalyst was decomposed, the crude product (0.75 g) was fractionated by chromatography on alumina (85×38 mm diameter) using benzene ethanol (99.5:0.5) as developer. Evaporation of the eluate from the main zone gave a faint yellow residue (0.28 g, about 55% yield) which after several recrystallizations from acetone yielded pure

Can. J. Chem. Downloaded from www.nrcresearchpress.com by 210.87.254.5 on 09/05/12
For personal use only.

tetraphenylpyrazine (III), m.p. 252–253°. The mixed melting point of the main fraction and an authentic sample of tetraphenylpyrazine (3) was 252–253°. The infrared spectra of both compounds were identical. Anal. Found: C, 87.86; H, 5.29; N, 7.26. Calc. for $C_{28}H_{20}N_2$: C, 87.48; H, 5.24; N, 7.29. Infrared of II (KBr): 3040(m), 1625(w), 1580(w), 1448(s), 1393(s), 1215(m), 1160(m), 1107(s).

A second minor component could not be purified.

ACKNOWLEDGMENTS

The preliminary experimental work on *O*-methylbenzophenone oxime was done by Mr. J. P. O'Donnell.

Grateful acknowledgment is made to the National Research Council for financial support of part of this work. This research was also supported in part by a grant from the Petroleum Research Fund administered by the American Chemical Society. Grateful acknowledgment is hereby made to the donors of the fund.

1. A. ROSENTHAL, R. F. ASTBURY, and A. HUBSCHER. J. Org. Chem. **23**, 1037 (1958); A. ROSENTHAL and J. P. O'DONNELL. Can. J. Chem. **38**, 457 (1960).
2. R. E. ROSE. J. Am. Chem. Soc. **33**, 388 (1911).
3. D. DAVIDSON, M. WEISS, and M. JELLING. J. Org. Chem. **2**, 328 (1937).
4. C. R. HAUSER and D. S. HOFFENBERG. J. Org. Chem. **20**, 1482 (1955).
5. O. L. BRADY and H. M. PERRY. J. Chem. Soc. **127**, 2874 (1925).

RECEIVED JUNE 23, 1960.
DEPARTMENT OF CHEMISTRY,
UNIVERSITY OF BRITISH COLUMBIA,
VANCOUVER 8, BRITISH COLUMBIA.

STOICHIOMETRY OF THE REACTION OF CHROMYL CHLORIDE WITH CYCLOHEXENE

R. A. STAIRS

In the reactions of chromyl chloride with hydrocarbons, brown precipitates of unknown structure, that have been formulated in most cases as $(HC).2CrO_2Cl_2$, are obtained (1). However, where the hydrocarbon is an olefin, analysis of the precipitate has led to very uncertain results. Cristol and Eilar have suggested (2) that only one molecule of chromyl chloride is essential. A simple experiment has been performed that strongly supports this suggestion, consisting of a calorimetric "titration" of cylohexene with chromyl chloride in carbon tetrachloride solution. The two solutions were mixed in various proportions in a crude calorimeter, the temperature rise was measured, and the quantity of heat liberated in the reaction was calculated and plotted against the logarithm of the molar ratio in each mixture. The result, shown in the figure, indicates a pronounced maximum. This was located at $\log_{10} R = 0 \pm .02$ by linear extrapolation of the two branches, corresponding to $R = 1.00 \pm 0.05$. This may be compared with results from analysis of precipitates, which yield values of r from 1.2 to 2.3 depending on the conditions, and on whether chlorine or chromium content is the basis of calculation (2).

In the figure the solid curves represent the theoretical effect of a heat of reaction of 50 kcal/mole. (The asymmetry arises from the inequality of the concentrations of the two reagent solutions.)

It is apparent that an additional heat effect is present when chromyl chloride is in excess. Comparison with the analyses suggests that further attack by chromyl chloride on the main product occurs, leading to chlorination, as all the results reported (2) are high in chlorine. To avoid this in preparative use of this reaction, it should be carried out at as low a temperature as possible and with the olefin always in excess.

Can. J. Chem. Downloaded from www.nrcresearchpress.com by 210.87.254.5 on 09/05/12
For personal use only.

tetraphenylpyrazine (III), m.p. 252–253°. The mixed melting point of the main fraction and an authentic sample of tetraphenylpyrazine (3) was 252–253°. The infrared spectra of both compounds were identical. Anal. Found: C, 87.86; H, 5.29; N, 7.26. Calc. for $C_{28}H_{20}N_2$: C, 87.48; H, 5.24; N, 7.29. Infrared of II (KBr): 3040(m), 1625(w), 1580(w), 1448(s), 1393(s), 1215(m), 1160(m), 1107(s).

A second minor component could not be purified.

ACKNOWLEDGMENTS

The preliminary experimental work on *O*-methylbenzophenone oxime was done by Mr. J. P. O'Donnell.

Grateful acknowledgment is made to the National Research Council for financial support of part of this work. This research was also supported in part by a grant from the Petroleum Research Fund administered by the American Chemical Society. Grateful acknowledgment is hereby made to the donors of the fund.

1. A. ROSENTHAL, R. F. ASTBURY, and A. HUBSCHER. J. Org. Chem. **23**, 1037 (1958); A. ROSENTHAL and J. P. O'DONNELL. Can. J. Chem. **38**, 457 (1960).
2. R. E. ROSE. J. Am. Chem. Soc. **33**, 388 (1911).
3. D. DAVIDSON, M. WEISS, and M. JELLING. J. Org. Chem. **2**, 328 (1937).
4. C. R. HAUSER and D. S. HOFFENBERG. J. Org. Chem. **20**, 1482 (1955).
5. O. L. BRADY and H. M. PERRY. J. Chem. Soc. **127**, 2874 (1925).

RECEIVED JUNE 23, 1960.
DEPARTMENT OF CHEMISTRY,
UNIVERSITY OF BRITISH COLUMBIA,
VANCOUVER 8, BRITISH COLUMBIA.

STOICHIOMETRY OF THE REACTION OF CHROMYL CHLORIDE WITH CYCLOHEXENE

R. A. STAIRS

In the reactions of chromyl chloride with hydrocarbons, brown precipitates of unknown structure, that have been formulated in most cases as $(HC).2CrO_2Cl_2$, are obtained (1). However, where the hydrocarbon is an olefin, analysis of the precipitate has led to very uncertain results. Cristol and Eilar have suggested (2) that only one molecule of chromyl chloride is essential. A simple experiment has been performed that strongly supports this suggestion, consisting of a calorimetric "titration" of cylohexene with chromyl chloride in carbon tetrachloride solution. The two solutions were mixed in various proportions in a crude calorimeter, the temperature rise was measured, and the quantity of heat liberated in the reaction was calculated and plotted against the logarithm of the molar ratio in each mixture. The result, shown in the figure, indicates a pronounced maximum. This was located at $\log_{10} R = 0 \pm .02$ by linear extrapolation of the two branches, corresponding to $R = 1.00 \pm 0.05$. This may be compared with results from analysis of precipitates, which yield values of r from 1.2 to 2.3 depending on the conditions, and on whether chlorine or chromium content is the basis of calculation (2).

In the figure the solid curves represent the theoretical effect of a heat of reaction of 50 kcal/mole. (The asymmetry arises from the inequality of the concentrations of the two reagent solutions.)

It is apparent that an additional heat effect is present when chromyl chloride is in excess. Comparison with the analyses suggests that further attack by chromyl chloride on the main product occurs, leading to chlorination, as all the results reported (2) are high in chlorine. To avoid this in preparative use of this reaction, it should be carried out at as low a temperature as possible and with the olefin always in excess.

Can. J. Chem. Downloaded from www.nrcresearchpress.com by 210.87.254.42 on 09/05/12
For personal use only.

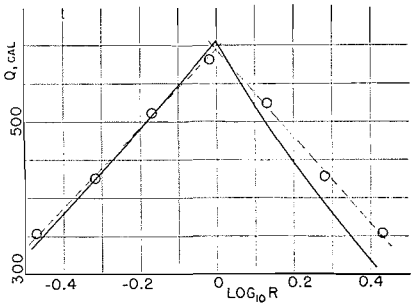


FIG. 1. Heat evolved on mixing vs. the logarithm of the molar ratio $R = (CrO_2Cl_2)/(C_6H_{10})$.

EXPERIMENTAL

Solutions were prepared as follows:

(A) Cyclohexene (Matheson, once distilled, b.p. 82.0–82.8° C, 755 mm) made up by direct weighing, 0.197±0.002 mole/l., and (B) chromyl chloride (prepared from CrO_3 and dry HCl, b.p. 115.5–117° C, 755 mm) standardized iodometrically, 0.134±0.001 mole/l., both in reagent CCl_4 dried over calcium sulphate.

A certain volume of solution B was measured into a Dewar flask (the calorimeter), and a volume of solution A to make the total 150 ml was measured into another Dewar vessel. In view of other inaccuracies in the method, and to avoid stopcock troubles and lessen troubles from evaporation these volumes were measured with graduated cylinders.

The temperature of each was read, A was poured into B, and the mixture was stirred. Temperature readings were taken about every half minute until successive readings agreed to 0.2° C (about 5 minutes). Temperature rises of 5 to 10 degrees were observed. No attempt was made to correct for the effects of stirring or of heat exchange with the room, since these systematic errors would not affect the conclusions respecting stoichiometry.

The approximate heat evolved, Q, was calculated by the formula

$$Q = K[t(V_A+V_B+C)-t_AV_A-t_B(V_B+C)],$$

where t_A and t_B, V_A and V_B are the initial temperatures and volumes of the solutions, C is the CCl_4 equivalent of the calorimeter (estimated to be 30±15 ml, from the water equivalent found by students in teaching laboratory), and K is the volume specific heat of carbon tetrachloride, about 0.32 cal ml^{-1} deg^{-1}.

1. W. H. HARTFORD and M. DARRIN. Chem. Revs. **58**, 1 (1958).
2. S. J. CRISTOL and L. D. EILAR. J. Am. Chem. Soc. **72**, 4353 (1950).

RECEIVED MAY 20, 1960.
DEPARTMENT OF CHEMISTRY,
QUEEN'S UNIVERSITY,
KINGSTON, ONTARIO.

3,5-DI-*O*-METHYL-D-GALACTOSE, A NEW METHYLATED SUGAR FROM A FULLY METHYLATED POLYSACCHARIDE OF GIBBERELLA FUJIKUROI (FUSARIUM MONILIFORME)*

I. R. SIDDIQUI AND G. A. ADAMS

During methylation studies of the extracellular acidic polysaccharide of *Gibberella fujikuroi* A.T.T.C. 10052 (*Fusarium moniliforme*), a di-*O*-methyl fraction was obtained

**Issued as N.R.C. No. 5911.*

Can. J. Chem. Downloaded from www.nrcresearchpress.com by 210.87.254.42 on 09/05/12
For personal use only.

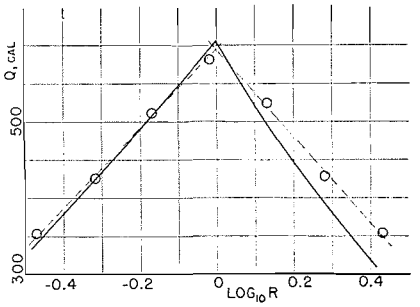


FIG. 1. Heat evolved on mixing vs. the logarithm of the molar ratio $R = (CrO_2Cl_2)/(C_6H_{10})$.

EXPERIMENTAL

Solutions were prepared as follows:

(A) Cyclohexene (Matheson, once distilled, b.p. 82.0–82.8° C, 755 mm) made up by direct weighing, 0.197±0.002 mole/l., and (B) chromyl chloride (prepared from CrO_3 and dry HCl, b.p. 115.5–117° C, 755 mm) standardized iodometrically, 0.134±0.001 mole/l., both in reagent CCl_4 dried over calcium sulphate.

A certain volume of solution B was measured into a Dewar flask (the calorimeter), and a volume of solution A to make the total 150 ml was measured into another Dewar vessel. In view of other inaccuracies in the method, and to avoid stopcock troubles and lessen troubles from evaporation these volumes were measured with graduated cylinders.

The temperature of each was read, A was poured into B, and the mixture was stirred. Temperature readings were taken about every half minute until successive readings agreed to 0.2° C (about 5 minutes). Temperature rises of 5 to 10 degrees were observed. No attempt was made to correct for the effects of stirring or of heat exchange with the room, since these systematic errors would not affect the conclusions respecting stoichiometry.

The approximate heat evolved, Q, was calculated by the formula

$$Q = K[t(V_A+V_B+C)-t_AV_A-t_B(V_B+C)],$$

where t_A and t_B, V_A and V_B are the initial temperatures and volumes of the solutions, C is the CCl_4 equivalent of the calorimeter (estimated to be 30±15 ml, from the water equivalent found by students in teaching laboratory), and K is the volume specific heat of carbon tetrachloride, about 0.32 cal ml^{-1} deg^{-1}.

1. W. H. HARTFORD and M. DARRIN. Chem. Revs. **58**, 1 (1958).
2. S. J. CRISTOL and L. D. EILAR. J. Am. Chem. Soc. **72**, 4353 (1950).

RECEIVED MAY 20, 1960.
DEPARTMENT OF CHEMISTRY,
QUEEN'S UNIVERSITY,
KINGSTON, ONTARIO.

3,5-DI-*O*-METHYL-D-GALACTOSE, A NEW METHYLATED SUGAR FROM A FULLY METHYLATED POLYSACCHARIDE OF GIBBERELLA FUJIKUROI (FUSARIUM MONILIFORME)*

I. R. SIDDIQUI AND G. A. ADAMS

During methylation studies of the extracellular acidic polysaccharide of *Gibberella fujikuroi* A.T.T.C. 10052 (*Fusarium moniliforme*), a di-*O*-methyl fraction was obtained

**Issued as N.R.C. No. 5911.*

Can. J. Chem. Downloaded from www.nrcresearchpress.com by 210.87.254.105 on 09/05/12
For personal use only.

which gave, *inter alia*, a di-*O*-methyl sugar which has been identified as 3,5-di-*O*-methyl-D-galactose. This is a new sugar derivative and proof of its identification is provided by the following evidence.

The aforementioned di-*O*-methyl sugar showed $[\alpha]_D^{26}$ $-24.8°\pm0.5°$ in water and a methoxyl content of 28.7%; a di-*O*-methyl hexose requires OMe, 29.8%. On demethylation (1) it gave only galactose as the parent sugar. The di-*O*-methyl galactose moved as a single spot on paper electrophoresis (2) in borate buffer and on paper chromatograms in three different solvent systems.

In addition to indicating homogeneity the results of these experiments also suggested that the di-*O*-methyl galactose was in the furanose rather than in the pyranose ring form. None of the reported di-*O*-methyl-D-galactopyranoses show negative rotation (3). The di-*O*-methyl galactose gave a higher M_g value (0.66) on paper electrophoresis in borate (2) than is to be expected for a di-*O*-methyl hexopyranose (4). The R_g value (0.65) on paper chromatography in *n*-butanol:ether:water (5:1:4) was much higher than reported for the known di-*O*-methyl galactopyranoses (5).

Confirmation of the furanose structure was obtained by methylation and oxidation studies. Complete methylation by Purdie's method of the glycoside of the di-*O*-methyl galactose yielded the glycoside of 2,3,5,6-tetra-*O*-methyl-D-galactose as shown by gas–liquid partition chromatography (6, 7). Oxidation of the di-*O*-methyl galactose with bromine water afforded a crystalline lactone which showed the slow hydrolysis in water typical of γ-lactones (8). An additional piece of evidence in support of the γ-lactone structure was provided by the infrared spectrum of the compound. It showed a strong C=O stretching peak at 1786 cm^{-1}. For comparison the infrared spectra of 2,5-di-*O*-methyl-L-arabonolactone and gluconic acid δ-lactone were also examined. The former compound showed the C=O stretching peak at 1772 cm^{-1} while in the latter it occurred at 1720 cm^{-1}. These values are in agreement with those given by Bellamy (9) for γ- and δ-lactones respectively. Barker *et al.* have also pointed out that in the five-membered lactone rings the increase of strain results in an increase of the C=O stretching frequency from 1733 cm^{-1} in δ-hexanolactone to 1770 cm^{-1} in γ-butyrolactone (10). The γ-lactone was converted by methanolic ammonia into a crystalline amide which gave a positive Weerman test (11), thereby proving the presence of a free hydroxyl group at position 2.

Finally, reduction of the di-*O*-methyl-D-galactose by potassium borohydride (12) yielded a crystalline di-*O*-methyl hexitol having the same melting point and equal but opposite specific rotation as 2,4-di-*O*-methyl-D-galactitol (13). The infrared spectrum of this hexitol and authentic 2,4-di-*O*-methyl-D-galactitol were superimposable. These findings proved that the derived galactitol was 2,4-di-*O*-methyl-L-galactitol, which is the same as 3,5-di-*O*-methyl-D-galactitol. Hence the parent sugar was 3,5-di-*O*-methyl-D-galactose.

EXPERIMENTAL

The organic phases of the following solvents (v/v) were used for paper chromatographic separations: (A) *n*-butanol:ethanol:water (5:1:4); (B) benzene:ethanol:water:ammonia (200:47:14:1); (C) 2-butanone saturated with water containing 2% ammonia; (D) pyridine : ethyl acetate : water (1:2.5:2.5). Sugars were detected on chromatograms by spraying with *p*-anisidine hydrochloride spray reagent. Infrared spectra were measured using the Nujol mull technique and a microcell. Measurements were made in the frequency range 3800–600 cm^{-1}.

The di-*O*-methyl sugar under consideration was found as a product of hydrolysis of

Can. J. Chem. Downloaded from www.nrcresearchpress.com by 210.87.254.105 on 09/05/12
For personal use only.

the methylated polysaccharide from *Gibberella fujikuroi*. It was separated from other di-*O*-methyl hexoses by preparative paper chromatography using solvent C.

*3,5-Di-O-methyl-*D*-galactose*

The syrupy di-*O*-methyl sugar showed $[\alpha]_D^{26}$ $-24.8°\pm0.5°$ (*c*, 1.935 in water) and a methoxyl content of 28.7%; a di-*O*-methyl hexose requires OMe, 29.8%. Paper chromatographic analysis of this sugar in solvents A, B, and C gave R_g values of 0.64, 0.23, and 0.41 respectively. Paper electrophoretic (2) examination of this sugar in borate buffer, pH 10, showed a single component (M_g, 0.66). A small quantity of the syrup (1–2 mg) was dissolved in dichloromethane (0.2 ml) and was demethylated (1) with boron trichloride (0.5 ml) at −70° C. Paper chromatographic analysis of the demethylated sugar in solvent D showed that only galactose was the parent sugar. The di-*O*-methyl sugar (ca. 1 mg) was heated in a sealed tube with 4% methanolic hydrogen chloride for 24 hours, neutralized with silver carbonate, filtered, evaporated, and methylated by Purdie's reagents (silver oxide ca. 20 mg + methyl iodide 2 ml). Examination of the fully methylated sugar by gas–liquid partition chromatography, using a 4-ft column of 20% Apiezon M on Celite 545 at 150° C and an argon flow rate of 150 ml/minute, showed that the relative retention time of the sample with respect to quinoline was 1.54. The authentic methyl glycoside of 2,3,5,6-tetra-*O*-methyl-D-galactose gave a retention time of 1.52 under the same conditions.

*3,5-Di-O-methyl-*D*-galactitol*

Di-*O*-methyl-D-galactose (35 mg) in water (2 ml) was mixed with a solution of potassium borohydride (12) (75 mg in 1 ml) and the solution was left overnight. Excess borohydride was destroyed with glacial acetic acid (few drops) and the solution was deionized with Amberlite resins IR-120 and IR-4B. The resulting hexitol crystallized when kept as a syrup overnight. It was recrystallized from ethyl acetate containing a little methanol. The crystals showed a melting point of 134–135° C, $[\alpha]_D^{26}$ $-23.7°\pm1°$ (*c*, 1.01 in methanol). Anal. Calc. for $C_8H_{18}O_6$: C, 45.71%; H, 8.63%. Found: C, 45.92%; H, 8.32%. Reported values for 2,4-di-*O*-methyl-D-galactitol are m.p. 134–135° C, $[\alpha]_D^{28}$ $+23.5°\pm0.5°$ (*c*, 2.04 in methanol) (13). The unknown hexitol and 2,4-di-*O*-methyl-D-galactitol showed superimposable infrared spectra.

*3,5-Di-O-methyl-*D*-galactonic Acid Lactone*

3,5-Di-*O*-methyl-D-galactose (180 mg) in water (4 ml) was oxidized with bromine (15 drops), in the presence of barium carbonate (100 mg), for 60 hours. Bromine was removed by aeration and the solution was extracted with chloroform for 3 days. The chloroform extract was dried with anhydrous sodium sulphate and concentrated to a syrup which was lactonized by distillation (bath temperature 130–160° C/0.02 mm). Crystallization of the syrup from ether : petroleum ether containing a few drops of methanol gave 3,5-di-*O*-methyl-D-galactonic acid-γ-lactone; m.p. 89.5–91° C; $[\alpha]_D^{26}$ $-72.9°\pm2° \rightarrow -49.2°\pm2°$, 18 days (incomplete) (*c*, 1.015 in water); ν_{max} 1786 cm^{-1}. Anal. Calc. for $C_8H_{14}O_6$: C, 46.60%; H, 6.84%. Found: C, 46.84%; H, 6.93%.

*3,5-Di-O-methyl-*D*-galactonamide*

3,5-Di-*O*-methyl-D-galactonic acid lactone (15 mg) was kept in methanol saturated with ammonia at 5° C for 24 hours. Removal of the solvent gave a syrup which crystallized when scratched. Recrystallization from ethanol:ether gave the amide, m.p. 131–133° C; $[\alpha]_D^{27}$ $+9.2°\pm2°$ (c, 0.87 in methanol). Anal. Calc. for $C_8H_{17}O_6N$: N, 6.27%. Found: N, 6.26%.

Can. J. Chem. Downloaded from www.nrcresearchpress.com by 210.87.254.105 on 09/05/12
For personal use only.

A portion of the amide (ca. 4 mg) was oxidized with sodium hypochlorite and on addition of semicarbazide hydrochloride (14) gave a white precipitate of hydrazodicarbonamide.

ACKNOWLEDGMENTS

The authors wish to thank A. E. Castagne for the microanalytical determinations.

1. S. Allen, T. G. Bonner, E. J. Bourne, and N. M. Saville. Chem. & Ind. (London), 630 (1958).
2. A. B. Foster. J. Chem. Soc. 982 (1953).
3. D. J. Bell. Advances in Carbohydrate Chem. **6**, 1 (1951).
4. S. A. Barker, A. B. Foster, I. R. Siddiqui, and M. Stacey. J. Chem. Soc. 2358 (1958).
5. E. L. Hirst and J. K. N. Jones. Discussions Faraday Soc. **7**, 268 (1949).
6. A. G. McInnes, D. H. Ball, F. P. Cooper, and C. T. Bishop. J. Chromatog. **1**, 556 (1958).
7. C. T. Bishop and F. P. Cooper. Can. J. Chem. **38**, 388 (1960).
8. H. D. K. Drew, E. H. Goodyear, and W. N. Haworth. J. Chem. Soc. 1237 (1927).
9. L. J. Bellamy. The infrared spectra of complex molecules. Methuen & Co. Ltd., London. 1954. p. 153.
10. S. A. Barker, E. J. Bourne, and D. H. Whiffen. Methods of Biochem. Anal. **3**, 213 (1956).
11. M. R. A. Weerman. Rec. trav. chim. **37**, 16 (1918).
12. M. Abdel-Akher, J. K. Hamilton, and F. Smith. J. Am. Chem. Soc. **73**, 4691 (1951).
13. C. T. Bishop. Can. J. Chem. **38**, 1636 (1960).
14. J. I. Cunneen and F. Smith. J. Chem. Soc. 1146 (1948).

Received July 5, 1960.
Division of Applied Biology,
National Research Council,
Ottawa, Canada.

Can. J. Chem. Downloaded from www.nrcresearchpress.com by 210.87.254.105 on 09/05/12
For personal use only.

Can. J. Chem. Downloaded from www.nrcresearchpress.com by 210.87.254.105 on 09/05/12
For personal use only.

Canadian Journal of Chemistry

Issued by THE NATIONAL RESEARCH COUNCIL OF CANADA

VOLUME 38 NOVEMBER 1960 NUMBER 11

NUCLEOPHILIC DISPLACEMENT OF METHYL SULPHONIC ESTERS BY HYDROXIDE ION IN WATER[1]

S. HARTMAN[2] AND R. E. ROBERTSON

ABSTRACT

Rate data for the reaction between OH^- and methyl benzenesulphonate, methyl methanesulphonate, and dimethyl sulphate in water are determined for a series of temperatures. The corresponding k_{OH^-}/k_{H_2O} ratio are found to be 3 to 6 times smaller than those values characterizing the reaction for the methyl halides, and the ratios in all cases are temperature dependent. While the stability of the initial state solvation shell undoubtedly contributes to the difference between the halides and sulphonates in these reactions, it is probable that differences in nucleophilic interaction between the oxygen of the water molecule and the partially empty p orbital of the methyl carbon is a more important factor in determining the characteristic difference.

In a recent paper (1) Fells and Moelwyn-Hughes suggested that the rough constancy of the k_{OH^-}/k_{H_2O} ratio of ~216 for the three methyl halides be taken as evidence for the similarity of the two reactions

$$R{-}X + H_2O = ROH + H^+ + X^-, \quad [1]$$

$$R{-}X + OH^- = ROH + X^-. \quad [2]$$

Extending this argument, the fact that the corresponding value for the above ratio for methyl benzenesulphonate was calculated to be 75 (2) would suggest some marked difference in mechanism between the methyl benzenesulphonate and the methyl halides in one or both of the above reactions. The aim of this work was to determine the rate of base-catalyzed hydrolysis for the methyl benzenesulphonate, methyl methanesulphonate, and dimethyl sulphate and to examine any differences in the k_{OH^-}/k_{H_2O} ratio between these values and the corresponding values reported by Moelwyn-Hughes for the methyl halides in terms of current mechanistic ideas.

EXPERIMENTAL METHOD

The experimental method adopted for the determination of the rate of bimolecular displacement of sulphonate ions from methyl esters by hydroxide was the classical one involving the use of ampoules containing a measured aliquot of the reaction mixture. Since the methyl sulphonic esters are relatively involatile at the temperatures studied, the presence of a small vapor space above the solution would not introduce the errors noted by Moelwyn-Hughes (3). There can be no doubt that there is a great need for the development of a method for obtaining bimolecular rate data such as sought here by some means which does not involve a sampling technique. However, the tube method

[1]*Manuscript received May 27, 1960.*
Contribution from the Division of Pure Chemistry, National Research Council, Ottawa, Canada.
Issued as N.R.C. No. 5954.
[2]*Summer student, 1959. Present address: Queen's University, Kingston, Ontario.*

was used in this instance in spite of its shortcomings because the rate data so obtained would be accurate enough as a basis for our conclusions. The methyl benzenesulphonate, methyl methanesulphonate, and dimethyl sulphate were from the same samples as had been purified for detailed study of the temperature dependence of the rate of hydrolysis of these compounds (4, 5, 6) and were used without further purification. The reaction mixture was made up to 0.02 N in NaOH and 0.01 M with respect to ester. Aliquots of 5 cc$\pm$0.007 were added to ampoules with a semiautomatic tube filler, the filling temperature being held at approximately 0° C in the case of the dimethyl sulphate. Rates were determined by immersing the required number of tubes simultaneously in the bath, with shaking, and, after allowing sufficient time for temperature equilibrium, initial tubes were chilled and analyzed for residual base. A series of such analysis over a suitable range of time, combined with corresponding solvolytic rates, provided the necessary data for calculation of the bimolecular rate of reaction, according to the following equation (7):

$$k_2 = \frac{1}{(a-b)t} \ln \frac{b(a-x)}{a(b-x)} - \frac{k_1}{a-x}.$$

Typical data for the hydrolysis of methyl benzenesulphonate at 30.0° C are given in Table I.

TABLE I

Typical kinetic data for the reaction of methyl benzenesulphonate and OH^- in water at 30.00° C

Time, seconds	Concentration of: Base a, moles/liter	Ester b, moles/liter	$k_2 \times 10^3$, liters/mole sec
0	0.01671	0.00646	
7200	0.01490	0.00465	1.46
9000	0.01451	0.00426	1.51
14400	0.01368	0.00343	1.37
16200	0.01339	0.00314	1.42
18000	0.01312	0.00287	1.46
19800	0.01289	0.00264	1.47
21610	0.01272	0.00247	1.42
23400	0.01254	0.00229	1.43
25200	0.01241	0.00216	1.37
27000	0.01218	0.00193	1.46
∞	0.01025	0	
	$k_1 = 2.146 \times 10^{-5}$*		
	k_2(av.) $= 1.44 \times 10^{-3}$ liters/mole sec		

*Reference 4.

RESULTS AND DISCUSSION

A summary of the rate data for the three compounds methyl methanesulphonate, methyl benzenesulphonate, and dimethyl sulphate is given in Table II for several temperatures. By combining these values with those for the hydrolytic process in the absence of base the corresponding k_{OH^-}/k_{H_2O} ratios may be calculated. In Table III these are compared with the corresponding values for the methyl halides from the work of Moelwyn-Hughes (7). The difference in the value of this ratio between the methyl halides and that for methyl benzenesulphonate from the early work of Praetorius (8) is seen to be confirmed and, if we may generalize from three examples, represents a general difference between the relative reactivity of the halides and sulphonates in respect to one or both reactions [1] and [2].

Can. J. Chem. Downloaded from www.nrcresearchpress.com by 210.87.254.105 on 09/05/12
For personal use only.

TABLE II

Summary of rate data for hydrolysis of methyl esters

Ester	Temp., °C	k_1, mole/liter sec	k_2, sec^{-1}	k_2 (average)	k_2/k_1
Me methanesulphonate	30.00	$9.32_5\times10^{-6}$	6.95×10^{-4} 7.13×10^{-4}	7.04×10^{-4}	76
	40.00	$2.93_5\times10^{-5}$	1.96×10^{-3} 1.96×10^{-3} 1.97×10^{-3}	1.96×10^{-3}	67
	50.00	$8.43_8\times10^{-5}$	5.44×10^{-3} 5.42×10^{-3}	5.43×10^{-3}	64
Me benzenesulphonate	30.00	$2.14_6\times10^{-5}$	1.437×10^{-3} 1.441×10^{-3}	1.44×10^{-3}	67
	40.00	$6.78_0\times10^{-5}$	4.27×10^{-3} 4.16×10^{-3}	4.22×10^{-3}	62
	50.00	$1.96_4\times10^{-4}$	1.09×10^{-2} 1.09×10^{-2} 1.07×10^{-2}	1.09×10^{-2}	55
Dimethyl sulphate	5.00	$1.12_3\times10^{-5}$	9.222×10^{-4} 8.94×10^{-4}	9.08×10^{-4}	81
	10.00	$2.30_5\times10^{-5}$	1.73×10^{-3} 1.62×10^{-3}	1.67×10^{-3}	73

TABLE III

A comparison of reactivity relative to methyl chloride for reactions [1] and [2]

RX	$k_X/k_{Cl}(OH^-)$	$k_X/k_{Cl}(H_2O)$
MeCl	1	1
MeBr	6.0	14.6
MeI	6.6	3.5
Me methanesulphonate	11.1	111.4
Me benzenesulphonate	22	260
Me methoxysulphonate	(363)	(3552)
Me phosphate	(13.5)	(0.36)

Normal experience would suggest that individual differences would be more apparent for reaction with the weaker nucleophile (water), and support for this conclusion may be found in Table IV where the relative reactivity of the methyl esters is compared with

TABLE IV

Dependence of relative reactivity on displaced anion for methyl compounds in hydrolysis

Anion	k_{OH^-}/k_{H_2O}*	k_H/k_D‡
Methoxysulphonate	47†	0.97
Benzenesulphonate	50	0.96
Methanesulphonate	56	0.96
Chloride	180	0.92
Bromide	226	0.90
Iodide	300	0.87

*Approximate values for 60° C.
†Estimated from data at lower temperature.
‡Secondary deuterium isotope effect from fully deuterated methyl esters (6).

Can. J. Chem. Downloaded from www.nrcresearchpress.com by 210.87.254.105 on 09/05/12
For personal use only.

Can. J. Chem. Downloaded from www.nrcresearchpress.com by 210.87.254.105 on 09/05/12
For personal use only.

that of methyl chloride for the two types of reaction. For nucleophilic displacement by OH^-, individual differences as a consequence of differences in the C—X bond being broken are surprisingly small (column 1, Table III). The differences in relative reactivity for hydrolysis show a slightly greater range of values for hydrolysis through the three halides (column 2, Table III) but a 10-fold increase in reactivity between the halides and the sulphonates. Hence, assuming that the difference is quantitative rather than qualitative, the reduced value of the k_{OH^-}/k_{H_2O} ratio noted in Table IV is the consequence of the relatively greater increase in the reactivity of the sulphonic esters for hydrolysis, in the absence of strong base.

Since a value of the k_{OH^-}/k_{H_2O} ratio > 1 indicates (9) some degree of nucleophilic interaction in the activation process for hydrolysis, the reduced values of this term for the sulphonates (Table IV) would suggest that bond making is less advanced in the transition state for these compounds than for the halides. The inverse secondary deuterium isotope effect ($k_H/k_D < 1$) recently reported by Llewellyn, Robertson, and Scott (6) for the hydrolysis of the above compounds leads to the same conclusion. Thus, the sharing of the p orbital between the entering and leaving groups leads to crowding of the transition state which will vary with the degree of overlap required of the former in the transition state and so leads to a proportional increase in the C—H bending frequencies and corresponding changes in the zero-point energy terms. Gratifying confirmation of this interpretation is seen in the linear correlation between the k_H/k_D and k_{OH^-}/k_{H_2O} ratios for a series of methyl esters (Fig. 1).

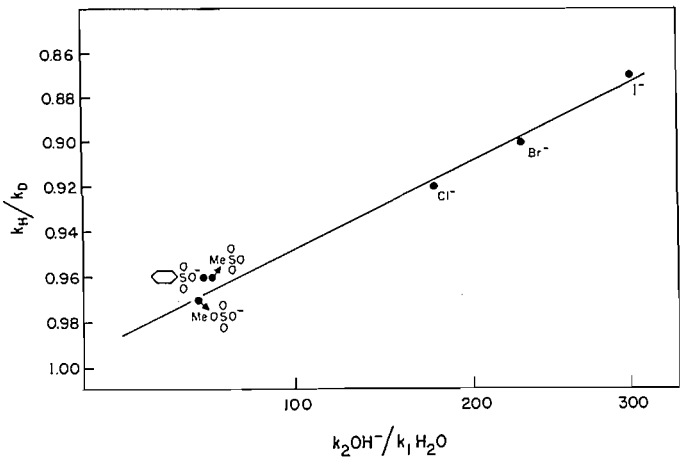


FIG. 1. A correlation of α-deuterium isotope effect with the k_{OH^-}/k_{H_2O} ratio.

The temperature dependence of the k_{OH^-}/k_{H_2O} ratio follows directly from the fact that reaction [1] is characterized by a large negative heat capacity of activation (6) while it would appear that this factor is small for reaction [2] (13).

Differences in the stability of the initial state solvation shell about the two types of esters will also contribute to the difference in reactivity but it is difficult to evaluate the relative importance of this factor. Thus the medium isotope effect which appears to depend on the relative stability of the initial state solvation shell in light and heavy water is, for the sulphonates, but one-half the average value for the halides (10, 11) and shows a much lower temperature dependence as would be expected (12). Evidence for

modification of the initial state solvation shell by the nature of the sulphonate grouping may be also obtained by considering the relative heat capacity changes ($\Delta C_p^{\ddagger}$) which characterize the hydrolysis of corresponding sulphonic and halide esters (4). The latter terms, which appear to be determined to an important degree by the temperature dependence of the stability of the initial state solvation shell, have less negative values for the sulphonic esters than for the halides, a result quite consistent with the indications of the medium isotope effect and supported by the value of $\delta_X \Delta H^{\ddagger}$ (below). Against such arguments favoring the importance of initial state solvation differences in determining differences in reactivity must be considered the position of methyl phosphate in such reactions. Thus judging from the medium isotope effect (k_{D_2O}/k_{H_2O}) the methyl phosphate would appear to have reduced the stability of the initial state solvation shell in a manner analogous to the sulphonates (11) (k_{D_2O}/k_{H_2O} for methyl methanesulphonate and methyl phosphate being identical, 0.94). The relative reactivity of the methyl phosphate, however, is but one-third that of methyl chloride in hydrolysis, while methyl methanesulphonate reacts 100 times faster (Table III).

While no particular significance can be attached to small differences in the values of the enthalpy and entropy corresponding to the reaction of the sulphonates and the halides with hydroxide (Table V), there is, approximately, a regular decrease in enthalpy

TABLE V

Thermodynamic parameters for the reaction of a series of methyl esters with OH^- and H_2O in water

	Base attack			Hydrolysis		
MeX	$\Delta H^{\ddagger}$, kcal/mole	$\Delta S^{\ddagger}$, cal/deg mole	Ref.	$\Delta H^{\ddagger}$, cal/mole	$\Delta S^{\ddagger}$, cal/deg mole	Ref.
Chloride	22,855	−5.5	(7)	25.263	−8.89	(14)
Bromide	21,575	−3.5	(7)	24.142	−6.65	(14)
Iodide	20,795	−8.0	(7)	25.950	−3.94	(14)
Methanesulphonate	19,500	−8.72	(*)	20.441	−14.08	(15)
Benzenesulphonate	19,180	−8.30	(*)	20.597	−11.58	(4)
Methoxysulphonate	(18,500)	(−5.81)	(*)	(19.918)	(−8.87)	(5)

*This paper.

with increasing reactivity in contrast to the 4–5 kcal difference ($\delta_X \Delta H^{\ddagger}$) between the values for the halides and the sulphonates in the hydrolysis reactions. With the exception of the iodide, the entropy change associated with the displacement by OH^- is 3–5 e.u. more positive than for the corresponding hydrolysis, as is required by the difference in the charge distribution in the initial and transition states.

ACKNOWLEDGMENT

The authors wish to acknowledge the technical assistance received from Mr. S. Sugamori during the initial stages of this investigation.

REFERENCES

1. I. Fells and E. A. Moelwyn-Hughes. J. Chem. Soc. 398 (1959).
2. A. J. Streitwieser. J. Chem. Revs. **56**, 571 (1956).
3. E. A. Moelwyn-Hughes. Trans. Faraday Soc. **37**, 279 (1941).
4. R. E. Robertson. Can. J. Chem. **35**, 613 (1957).
5. R. E. Robertson. Unpublished work.
6. J. A. Llewellyn, R. E. Robertson, and J. M. Scott. Can. J. Chem. **38**, 222 (1960).
7. E. A. Moelwyn-Hughes. Proc. Roy. Soc. A, **196**, 540 (1949).
8. A. Praetorius. Monatsh. **26**, 1 (1905).

Can. J. Chem. Downloaded from www.nrcresearchpress.com by 210.87.254.105 on 09/05/12
For personal use only.

9. C. K. INGOLD. Structure and mechanism in organic chemistry. Cornell Univ. Press, Ithaca, N.Y. 1953. Chap. 7.
10. P. M. LAUGHTON and R. E. ROBERTSON. Can. J. Chem. **34**, 1714 (1956).
11. R. E. ROBERTSON and P. M. LAUGHTON. Can. J. Chem. **35**, 1319 (1957).
12. P. M. LAUGHTON and R. E. ROBERTSON. Can. J. Chem. **37**, 1491 (1959).
13. D. N. GLEW and E. A. MOELWYN-HUGHES. Proc. Roy. Soc. A, **211**, 254 (1952).
14. R. L. HEPPOLETTE and R. E. ROBERTSON. Proc. Roy. Soc. A, **252**, 273 (1959).
15. P. W. C. BARNARD and R. E. ROBERTSON. Unpublished work.

Can. J. Chem. Downloaded from www.nrcresearchpress.com by 210.87.254.105 on 09/05/12
For personal use only.

Can. J. Chem. Downloaded from www.nrcresearchpress.com by 210.87.254.42 on 09/05/12
For personal use only.

THE CHEMISTRY OF ETHYLENE OXIDE

VI. THE ACID-CATALYZED REACTION OF ETHYLENE OXIDE WITH ETHANOL–WATER MIXTURES[1]

R. K. Brown and A. M. Eastham

ABSTRACT

The rate of reaction of ethylene oxide with alcohol–water mixtures at 25° C has been determined. The ratio of glycol to ethoxyethanol in the product was determined for each mixture and found to be approximately equal to the molecular ratio of water to ethanol in the solvent.

Ethylene oxide reacts with water to form ethylene glycol and with ethanol to form 2-ethoxyethanol. The uncatalyzed and alkali-catalyzed reactions are very slow at ordinary temperatures but the acid-catalyzed reactions are rapid and suitable for kinetic measurements because they can be followed easily by the dilatometric method. Rate data are well established for the water reaction (1, 2, 3) but not for ethanol so this paper records the results of some measurements in ethanol and ethanol–water mixtures.

EXPERIMENTAL

Anhydrous ethanol was prepared from the commercial anhydrous material by distillation from sodium and ethyl phthalate (4). No aldehydes could be detected with Tollen's reagent.

Commercial ethylene oxide having a purity of over 99% was used as received.

Stock solutions of perchloric acid in alcohol were prepared from the 70% acid (perchloric acid dihydrate) and anhydrous ethanol and were found to be stable for several weeks. All titrations were made with a pH meter as most acid–base indicators give unsatisfactory end points.

Sodium perchlorate was dried by heating at 110° C for 24 hours, then over phosphorus pentoxide. It is sparingly soluble in dry ethanol so was used only with solutions containing at least 1% water.

Lithium perchlorate was dried under vacuum for 8 hours at 100° C, then was held for 10 hours at 160° C in a stream of thoroughly dry air. The product was immediately dissolved in dry ethanol and used as a solution.

For all reactions in aqueous ethanol the amount of glycol in the product was determined by the periodic acid – arsenite method (5). The remainder of the ethylene oxide was assumed to form ethoxyethanol.

For the rate measurements, acid and salt were dissolved in the appropriate alcohol–water mixture in a dry container attached to the dilatometer. A small glass vial containing a weighed quantity of ethylene oxide was introduced and the solution was then degassed by slight suction. The solution was brought to constant temperature (25.0° C) in a water bath, the vial of oxide was broken by means of a plunger, and the solution was then forced into the dilatometer by air pressure. The concentration of oxide in all experiments was between 0.01 and 0.06 M and its rate of disappearance showed excellent first-order dependence under all conditions. Rates were evaluated by the Guggenheim method (6).

[1]*Manuscript received July 7, 1960.*
Contribution from the Division of Applied Chemistry, National Research Council, Ottawa, Canada. Issued as N.R.C. No. 5944.

Can. J. Chem. Downloaded from www.nrcresearchpress.com by 210.87.254.42 on 09/05/12
For personal use only.

RESULTS

As the acid-catalyzed hydration of ethylene oxide shows a marked salt effect, it was desirable to evaluate this effect in ethanol so a series of runs were made with varying concentrations of lithium perchlorate and a constant acid concentration of 0.0034 *M*. The results were quite erratic possibly due to traces of water (see below), but indicated a strong positive salt effect. All points within the concentration range 0.005 *M* to 0.12 *M* of perchlorate ion were accounted for within ±3% by a rate constant having the value

$$k_{H^+} = 5.9+16.\,c \text{ liter mole}^{-1} \text{ min}^{-1},$$

where c is the total concentration of perchlorate ion. However, the data suggest that the salt effect may be even greater at lower salt concentration (compare the results for reaction of acetaldehyde in ethanol – hydrogen chloride solutions (7)).

The corresponding expression for the salt effect upon the hydration of ethylene oxide at 25° C was found to be (2)

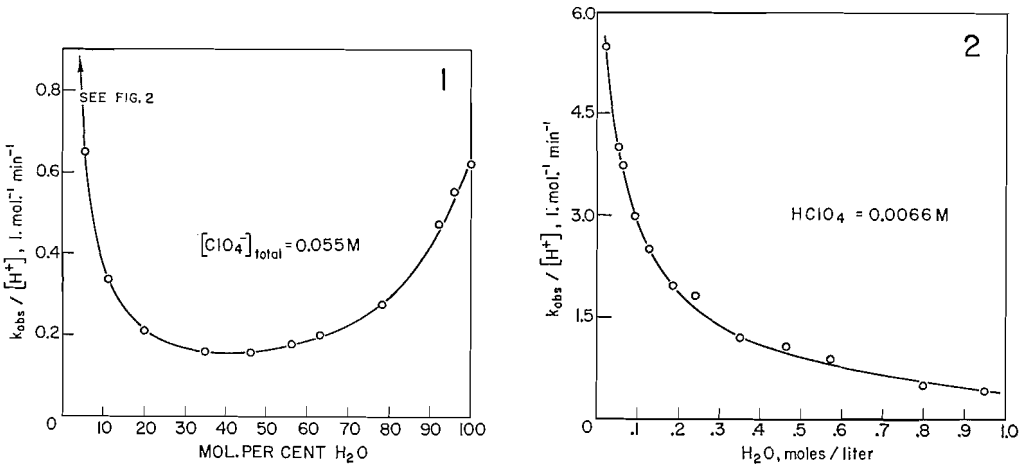
$$k_{H^+} = 0.55+0.48\,c,$$

so the rate of reaction with ethanol is much faster than with water and shows a salt effect which is in the same direction but proportionately about three times as large as that in water. The subsequent runs in water–ethanol mixtures were conducted at a constant concentration of perchlorate ion (0.055 *M*) but the magnitude of the salt effect was not determined for each composition. It cannot be assumed that salt effects do not make at least a minor contribution to the shape of the curve in Fig. 1; presumably they make a larger contribution to the rate at the higher alcohol concentrations.

TABLE I
Composition of the product in alcohol–water mixtures

Molarity H_2O	Mole% H_2O	Mole% glycol in product
1	5.7	~8
2	11	13
4	20	26
8	35	37
12	46	47
16	56	51
20	63	60.5
30	78	70
43	92	86
49	96	92
52	98	95
—	100	101

The rates of reaction of ethylene oxide with water–ethanol mixtures containing up to 95 mole % of ethanol are shown in Fig. 1. Each point represents the average of several runs at acid concentrations varying from about 0.01 to 0.06 *M*. The rates decrease to a minimum at about 40 mole % (ca. 15 wt.%) of water from either pure water or pure ethanol. Throughout this range the ratio of glycol to ethoxyethanol is approximately equal to the molecular ratio of water to alcohol in the solvent (Table I), which might indicate a reaction independent of the concentration of nucleophilic reagent. In other studies of competition between reactants for ethylene oxide in acid solution, however, it was found that the rate was markedly dependent upon nucleophilicity (2), so one must conclude that water and ethanol are about equally reactive under the present conditions.



FIGS. 1 AND 2.

It follows that the shape of the curve in Fig. 1 must be determined primarily by medium effects and by variations in the acid–base equilibria due to changes in the ratio of the ions H_3O^+ and $C_2H_5OH_2^+$.

At water concentrations below about one molar, the rate increases very sharply with further reduction in the water concentration (Fig. 2). The extent of the increase cannot be estimated from the present data because solutions made up from 70% perchloric acid always contain small amounts of water, but it is at least 10-fold on reducing the water concentration from 1 *M* to about 0.015 *M*. Similar observations have been made by Deyrup (7) in studies of the acid-catalyzed reaction of acetaldehyde in ethanol solution and by Goldschmidt and his co-workers (8) in studies of acid-catalyzed esterifications in ethanol. The usual explanation is due to Goldschmidt and accounts for the decreasing rate with increasing water as due to the replacement of the ion $C_2H_5OH_2^+$ by the less acidic and therefore less catalytic ion, H_3O^+. So far as we are aware, however, this phenomenon has been observed only in ethanol; in the reaction of acetaldehyde with methanol the effect of small amounts of water ought to be very large if the above explanation is correct, because the rate in pure methanol is greater than that in water by a factor of 10^3 (9).

REFERENCES

1. J. N. BRONSTED, M. KILPATRICK, and M. KILPATRICK. J. Am. Chem. Soc. **51**, 428 (1929).
2. A. M. EASTHAM and G. A. LATRÉMOUILLE. Can. J. Chem. **30**, 169 (1952).
3. H. J. LICHTENSTEIN and G. H. TWIGG. Trans. Faraday Soc. **44**, 905 (1948).
4. H. MANSKE. J. Am. Chem. Soc. **53**, 1106 (1931).
5. ORGANIC REACTIONS. Vol. II. John Wiley & Sons, Inc., New York. 1947.
6. E. A. GUGGENHEIM. Phil. Mag. **2**, 538 (1926).
7. A. J. DEYRUP. J. Am. Chem. Soc. **56**, 60 (1934).
8. H. GOLDSCHMIDT and E. SUNDE. Ber. **39**, 711 (1906); H. GOLDSCHMIDT and O. UDBY. Z. physik. Chem. **60**, 728 (1907).
9. G. W. MEADOWS and B. DE B. DARWENT. Trans. Faraday Soc. **48**, 1015 (1952).

Can. J. Chem. Downloaded from www.nrcresearchpress.com by 210.87.254.42 on 09/05/12
For personal use only.

Can. J. Chem. Downloaded from www.nrcresearchpress.com by 210.87.254.5 on 09/05/12
For personal use only.

THE PREPARATION OF SUBSTITUTED THIONOCARBAMATES[1]

A. F. McKay, D. L. Garmaise, G. Y. Paris, S. Gelblum, and R. J. Ranz

ABSTRACT

The preparations and properties of a number of substituted thionocarbamates are described.

The thionocarbamate derivatives in Tables I–IV were prepared by one of the following three methods:

$$ROH + CSCl_2 \xrightarrow{-HCl} ROC(S)Cl + R'NH_2 \xrightarrow{-HCl} R'NHC(S)OR, \quad [1]$$

$$ROH + R'NCS \xrightarrow{(C_2H_5)_3N} R'NHC(S)OR, \quad [2]$$

$$ROH + R'NCS \xrightarrow{NaH} R'NHC(S)OR. \quad [3]$$

Route 1 was used to prepare both the aryl arylthionocarbamates and the aryl aralkylthionocarbamates. Procedure 2 gave good results with aralkyl isothiocyanates but triethylamine did not catalyze the addition of aryl isothiocyanates to phenols under the conditions employed in this study. All of the benzyl N-substituted thionocarbamates were prepared by procedure 3.

Harris and Fischback (1) reported the preparation of thionocarbamates by the reaction of amines with methyl xanthates. An attempt to prepare phenyl 3,4-dichlorobenzylthionocarbamate from S-methyl phenylxanthate by this procedure gave methyl 3,4-dichlorobenzyldithiocarbamate. Thus the phenoxy group was replaced more readily by 3,4-dichlorobenzylamine than the methylmercapto group. However, if 3,4-dichlorobenzylamine is added to S-methyl ethylxanthate the methylmercapto group is replaced and ethyl 3,4-dichlorobenzylthionocarbamate is formed. These reactions are represented by equations 4 and 5.

$$RNH_2 + \langle\bigcirc\rangle\!-\!OC(S)SCH_3 \longrightarrow RNHC(S)SCH_3 + \langle\bigcirc\rangle\!-\!OH \quad [4]$$

$$RNH_2 + C_2H_5OC(S)SCH_3 \longrightarrow RNHC(S)OC_2H_5 + CH_3SH \quad [5]$$

$R = 3,4\text{-}Cl_2C_6H_3CH_2-$

The thiolcarbamates in Table V were prepared by treating the corresponding phenyl chlorothiolformates with the appropriate amines. The phenyl chlorothiolformates were obtained by treating the lead salts of the thiophenols with phosgene by the method of Rivier (2).

An attempt to prepare phenyl 3,4-dichlorobenzylthionocarbamate by heating a methanolic solution of methyl 3,4-dichlorobenzyldithiocarbamate in the presence of Amberlite IRA-400 resin saturated with phenol gave methyl 3,4-dichlorobenzylthionocarbamate in 48% yield.

The aryl chlorothionoformates, which were isolated during these studies, are described in Table VI.

[1]*Manucript received July 8, 1960.*
Contribution No. 28 from the L. G. Ryan Research Laboratories of Monsanto Canada Limited, LaSalle, Que.

Can. J. Chem. Downloaded from www.nrcresearchpress.com by 210.87.254.5 on 09/05/12
For personal use only.

EXPERIMENTAL[2]

Di-3,4-dichlorobenzylamine

A mixture of 3,4-dichlorobenzyl chloride (9.75 g, 0.05 mole) and 3,4-dichlorobenzylamine (35.2 g, 0.20 mole) was heated on the steam bath for 2 hours. Ether (200 ml) and 10% sodium hydroxide solution (50 ml) were added, and the ether layer was washed with water and dried over anhydrous sodium sulphate. Fractionation of the ether extract yielded 15 g (85.2%) of unchanged 3,4-dichlorobenzylamine (b.p. 93–100°/1 mm) and di-3,4-dichlorobenzylamine (b.p. 175–180°/1 mm, n_D^{25} 1.60665, D_4^{27} 1.3690), yield 10 g (59.7%). Anal. Calc. for $C_{14}H_{11}Cl_4N$: C, 50.20; H, 3.31; Cl, 42.34; N, 4.18. Found: C, 50.68; H, 3.44; Cl, 42.00; N, 4.13.

A solution of the amine (0.61 g, 0.0018 mole) in absolute ethanol (30 ml) was acidified with hydrogen chloride. Di-3,4-dichlorobenzylamine hydrochloride (m.p. 228–229°) was recovered by filtration, yield 0.21 g (33%). Anal. Calc. for $C_{14}H_{12}Cl_5N$: C, 45.26; H, 3.26; Cl, 47.72; N, 3.77. Found: C, 45.17; H, 3.09; Cl, 47.80; N, 3.98. N-4-Chlorobenzylaniline (3) (b.p. 155°/0.5 mm) and di-4-chlorobenzylamine (m.p. 30–32°) were prepared in the same way in 62.8% and 60% yield respectively. A melting point of 31° has been reported (4) for di-4-chlorobenzylamine.

2-(3,4-Dichlorophenyl)-acetonitrile

A solution of 3,4-dichlorobenzyl chloride (48.87 g, 0.25 mole) in ethanol (50 ml) was added during 30 minutes to a stirred solution of potassium cyanide (19.50 g, 0.30 mole) in water (15 ml) at 60°. The mixture was refluxed for 4 hours, and then cooled and filtered. The filtrate was concentrated *in vacuo* and the residue was extracted with ether (100 ml). The ether solution was dried and evaporated, and the residue was distilled to give the product (b.p. 106–108°/0.1 mm; m.p. 35.5–38.5°), yield 37.6 g (81%). Recrystallization from ether – petroleum ether raised the melting point to 39.5–40.5°. Anal. Calc. for $C_8H_5Cl_2N$: C, 51.65; H, 2.71; Cl, 38.12; N, 7.53. Found: C, 51.81; H, 2.92; Cl, 38.14; N, 7.56.

2-(3,4-Dichlorophenyl)-ethylamine

Aluminum chloride (6.66 g, 0.05 mole) in ether (150 ml) was added to a suspension of lithium aluminum hydride (1.99 g, 0.05 mole) in ether (100 ml) maintained in a nitrogen atmosphere. A solution of 2-(3,4-dichlorophenyl)-acetonitrile (9.3 g, 0.05 mole) in ether (200 ml) was added dropwise to the stirred mixture, and the stirring was continued for 30 minutes. Water was added cautiously to destroy the excess lithium aluminum hydride and after further addition of water (total 140 ml) and 6 *N* sulphuric acid (140 ml), the aqueous layer was separated and washed with ether (100 ml). The aqueous layer was basified with 40% sodium hydroxide solution at 0°, and the free base was extracted with ether (3×150 ml). Fractionation of the dried ether extract yielded the product (b.p. 100–102°/0.12 mm), yield 6.75 g (71%). Anal. Calc. for $C_8H_9Cl_2N$: C, 50.56; H, 4.78; Cl, 37.32; N, 7.37. Found: C, 50.25; H, 4.92; Cl, 37.16; N, 7.22.

The amine in aqueous ethanol was converted into its picrate (m.p. 199–200°, decomp.) in the usual manner, yield 67.5%. Anal. Calc. for $C_{14}H_{12}Cl_2N_4O_7$: C, 40.12; H, 2.89; Cl, 16.92; N, 13.37. Found: C, 40.15; H, 3.14; Cl, 17.06; N, 13.50.

3-(3,4-Dichlorophenyl)-propionic Acid

3,4-Dichlorobenzaldehyde was converted to 3,4-dichlorocinnamic acid (m.p. 214–217° C) in 69.2% yield by the method of Walling and Wolfstirn (5).

[2]*All melting points are uncorrected. Microanalyses were performed by Micro-Tech Laboratories, Skokie, Illinois.*

3,4-Dichlorocinnamic acid (58.5 g, 0.27 mole) in glacial acetic acid (1500 ml) was hydrogenated at atmospheric pressure in the presence of 5% palladium on charcoal (5.8 g). The absorption of hydrogen ceased after 10.5 hours (6 liters). The solution was filtered and evaporated, and the residue was crystallized from water to give the product (m.p. 90–93°), yield 53.0 g (90%). Recrystallization from ethanol raised the melting point to 96–97°. Anal. Calc. for $C_9H_8Cl_2O_2$: C, 49.34; H, 3.68; Cl, 32.37. Found: C, 49.07; H, 3.68; Cl, 32.41.

3-(3,4-Dichlorophenyl)-propionamide

A solution of 3-(3,4-dichlorophenyl)-propionic acid (53.0 g, 0.24 mole) and thionyl chloride (119 g, 1.0 mole) in benzene (100 ml) was allowed to stand overnight, and was then evaporated to dryness. The oily residue was added in portions to 28% aqueous ammonia (270 ml) with stirring at 20–25° and the mixture was stirred for 4 hours. The product (m.p. 76–80°) was recovered by filtration, yield 45.5 g (86.3%). Recrystallization from benzene – petroleum ether raised the melting point to 80–81°. Anal. Calc. for $C_9H_9Cl_2NO$: C, 49.56; H, 4.16; Cl, 32.51; N, 6.42. Found: C, 49.78; H, 4.22; Cl, 32.67; N, 6.42.

3-(3,4-Dichlorophenyl)-propionitrile

A solution of the amide (37.9 g, 0.174 mole) and thionyl chloride (119 g, 1.0 mole) in benzene (200 ml) was refluxed for 5 hours, and the solution was then evaporated. Distillation of the residue yielded crude 3-(3,4-dichlorophenyl)-propionitrile (b.p. 140–158°/1 mm), yield 30.8 g (88%). Redistillation gave the pure product (b.p. 121°/0.4 mm, n_D^{25} 1.55403; d_{20} 1.2742). Anal. Calc. for $C_9H_7Cl_2N$: C, 54.02; H, 3.53; Cl, 35.44; N, 7.01. Found: C, 54.24; H, 3.66; Cl, 35.38; N, 7.03.

3-(3,4-Dichlorophenyl)-propylamine

3-(3,4-Dichlorophenyl)-propionitrile (18.0 g, 0.09 mole) was reduced by lithium aluminum hydride – aluminum chloride in ether exactly as described above for 2-(3,4-dichlorophenyl)-acetonitrile. The product (b.p. 120–125°/1 mm) was obtained in 17.3 g (95%) yield. A redistilled sample (b.p. 104°/0.4 mm, n_D^{27} 1.55487, d_{20} 1.2082) was submitted for analysis. Anal. Calc. for $C_9H_{11}Cl_2N$: C, 52.96; H, 5.43; Cl, 34.75; N, 6.87. Found: C, 53.08; H, 5.45; Cl, 34.73; N, 7.09.

The picrate of the amine, which was prepared in quantitative yield from water, melted at 150–151° after recrystallization from hot water. Anal. Calc. for $C_{15}H_{14}Cl_2N_2O_7$: C, 41.59; H, 3.26; Cl, 16.37; N, 12.93. Found: C, 41.69; H, 3.21; Cl, 16.53; N, 12.84.

Preparation of 4-n-Alkylphenols

A series of 4-*n*-alkylphenols, three of which are new, was prepared by the general method of Sandulesco and Girard (6).

4-n-Hexylphenol

4-*n*-Hexylphenol (b.p. 135–136°/0.4 mm) was prepared in 72.6% yield from *p*-caproylphenol. The reported (6) boiling point at 10 mm is 146–147°.

4-n-Decylphenol

Decanoyl chloride (69 g, 0.35 mole) was heated with phenol (32.9 g, 0.35 mole) at 120° for 1 hour. The crude phenyl decanoate was added during a 30-minute period to a suspension of anhydrous aluminum chloride (56 g, 0.42 mole) in carbon disulphide (100 ml). The reaction was exothermic and the solvent began to reflux during the addition. Refluxing was continued for 2 hours. The solution was then evaporated to dryness, and the residue was heated at 150° for 2 hours. Hydrochloric acid (200 ml of 18% HCl) was added cautiously

Can. J. Chem. Downloaded from www.nrcresearchpress.com by 210.87.254.5 on 09/05/12
For personal use only.

and the mixture was diluted with water (150 ml). The oily product was extracted with chloroform (200 ml) and the chloroform solution was dried and evaporated. Fractionation of the residue yielded 2-decanoylphenol (b.p. 130–133°/0.25 mm), yield 42.8 g (49.4%), and 4-decanoylphenol (b.p. 194–195°/0.4 mm), yield 15 g (17.3%). The *p*-isomer (m.p. 59–60°) crystallized in the receiver. Anal. Calc. for $C_{16}H_{24}O_2$: C, 77.38; H, 9.74. Found: C, 77.26; H, 9.79.

4-Decanoylphenol (10 g, 0.04 mole) in ethanol (50 ml) was added to a vigorously stirred suspension of amalgamated zinc (70 g) in 18% hydrochloric acid (140 ml) and the reaction mixture was refluxed for 2 hours. The mixture was extracted with toluene (100 ml) and the toluene solution was dried and evaporated. Fractionation of the residue gave 7.8 g (83%) of 4-*n*-decylphenol (b.p. 146–148°/0.75 mm). The product crystallized (m.p. 54–56°) on standing. Anal. Calc. for $C_{16}H_{26}O$: C, 82.00; H, 11.19. Found: C, 81.83; H, 11.01.

4-n-Dodecylphenol

Phenol was heated with dodecanoyl chloride under similar conditions to form phenyl dodecanoate, which was rearranged to yield 51% of 2-dodecanoylphenol (b.p. 140–165°/0.75 mm), and 29.5% of 4-dodecanoylphenol (b.p. 198°/0.25 mm). Reduction of 4-dodecanoylphenol with amalgamated zinc and hydrochloric acid gave 4-*n*-dodecylphenol (b.p. 154°/3 mm, m.p. 65–67°), yield 81%. Anal. Calc. for $C_{18}H_{30}O$: C, 82.38; H, 11.53. Found: C, 82.48; H, 11.58.

4-n-Octadecylphenol

A mixture of stearic acid (113 g, 0.4 mole) and thionyl chloride (143 g, 1.2 mole) was refluxed for 1 hour. The mixture was distilled to give octadecanoyl chloride (b.p. 159–162°/0.1 mm), yield 87.9 g (72.5%). The acid chloride was converted to phenyl *n*-octadecanoate, which was rearranged to 31.6% of 2-*n*-octadecanoylphenol (b.p. 164–182°/0.15 mm) and 28% of 4-*n*-octadecanoylphenol (b.p. 209–212°/0.15 mm). Reduction of the para-isomer gave 4-*n*-octadecylphenol (b.p. 182–187°/0.15 mm, m.p. 65–67°) in 83% yield. Anal. Calc. for $C_{24}H_{42}O$: C, 83.18; H, 12.22. Found: C, 83.10; H, 12.00.

Aryl Thionocarbamates

Method A: 4-n-Propylphenyl 3,4-Dichlorophenylthionocarbamate

4-*n*-Propylphenol (20.43 g, 0.15 mole) in 3% sodium hydroxide solution (200 ml) was added to a stirred solution of thiophosgene (17.25 g, 0.15 mole) in chloroform (200 ml) at 0–10° during a period of 30 minutes. The stirring was continued for 30 minutes and the chloroform layer was separated, dried, and evaporated. Distillation of the residue gave 4-*n*-propylphenyl chlorothionoformate (b.p. 101–102°/0.8 mm), yield 24 g (74.7%).

3,4-Dichloroaniline (16.2 g, 0.1 mole) in chloroform (150 ml) was added to a stirred solution of 4-*n*-propylphenyl chlorothionoformate (10.73 g, 0.05 mole) in chloroform (200 ml) at 25° during a period of 30 minutes. The stirring was continued for 1 hour, and the precipitated 3,4-dichloroaniline hydrochloride (9.6 g, 97%) was removed by filtration. The filtrate was concentrated to a volume of 200 ml and petroleum ether (300 ml) was added to give the product (m.p. 150–151°), yield 12.6 g (74%). Recrystallization from the same solvents did not raise the melting point. When the phenol was insoluble in dilute sodium hydroxide, the dried sodium phenoxide was reacted with thiophosgene in chloroform suspension.

The compounds listed in Tables I and III, and those compounds in Table II for which no other method is noted, were prepared by this general procedure.

Can. J. Chem. Downloaded from www.nrcresearchpress.com by 210.87.254.5 on 09/05/12
For personal use only.

Can. J. Chem. Downloaded from www.nrcresearchpress.com by 210.87.254.5 on 09/05/12
For personal use only.

TABLE I

Aryl arylthionocarbamates, RNHC(S)OR′

R	R′	Yield, %	M.p., °C	Formula	C		H		Cl		N		S	
					Calc.	Found	Calc.	Found	Calc.	Found	Calc.	Found	Calc.	Found
3,4-Dichlorophenyl	Phenyl	44	156–157[a]	$C_{13}H_9Cl_2NOS$	52.36	52.37	3.04	3.12	23.78	24.19	4.70	4.73	10.75	10.82
3,4-Dichlorophenyl	4-Methylphenyl	53	173–174[b]	$C_{14}H_{11}Cl_2NOS$	53.86	53.63	3.55	3.84	22.71	22.83	4.49	4.62	10.27	10.18
3,4-Dichlorophenyl	4-Ethylphenyl	52	158–159[b]	$C_{15}H_{13}Cl_2NOS$	55.22	55.37	4.02	4.13	21.74	21.76	4.29	4.34	9.83	10.02
3,4-Dichlorophenyl	4-*n*-Propylphenyl	74	159–161[b]	$C_{16}H_{15}Cl_2NOS$	56.48	56.73	4.44	4.50	20.84	21.07	4.12	4.24	9.42	9.61
3,4-Dichlorophenyl	4-*n*-Butylphenyl	48	125–126[c]	$C_{17}H_{17}Cl_2NOS$	57.63	57.39	4.84	4.84	20.01	20.13	3.95	4.17	9.05	9.18
3,4-Dichlorophenyl	2,6-di-*t*-Butyl-4-methylphenyl	24	139–140[c]	$C_{22}H_{27}Cl_2NOS$	62.26	62.67	6.41	6.40	16.71	16.00	3.30	3.29	7.55	7.22
3,4-Dichlorophenyl	4-Methoxyphenyl	57	167–168[d]	$C_{14}H_{11}Cl_2NO_2S$	51.24	50.97	3.38	3.43	21.61	21.61	4.27	4.42	9.76	9.62
3,4-Dichlorophenyl	4-Ethoxyphenyl	64	173–175[a]	$C_{15}H_{13}Cl_2NO_2S$	52.64	52.46	3.84	3.92	20.72	20.73	4.09	4.45	9.37	9.48
3,4-Dichlorophenyl	3,4-Dichlorophenyl	91	142–143[a]	$C_{13}H_7Cl_4NOS$	42.54	42.16	1.92	2.02	38.65	37.68	3.82	4.23	8.74	8.38
3,4-Dichlorophenyl	3-Nitrophenyl	85	135–136[b]	$C_{13}H_8Cl_2N_2O_3S$	45.50	45.70	2.35	2.64	20.66	20.74	8.17	8.24	9.34	9.38
2,4-Dichlorophenyl	2,4-Dichlorophenyl	68	142–143[e]	$C_{13}H_7Cl_4NOS$	42.54	42.77	1.92	2.10	38.65	38.85	3.82	4.23	8.74	8.38
4-Methoxyphenyl	4-Methoxyphenyl	87	175–176[b]	$C_{15}H_{15}N_2O_3S$	62.26	62.44	5.23	5.34	—	—	4.84	4.85	11.08	11.05
4-Ethoxyphenyl	4-Ethylphenyl	61	118–119[b]	$C_{17}H_{19}NO_2S$	67.75	67.43	6.35	6.41	—	—	4.65	4.64	10.63	10.56
3-Nitrophenyl	4-Ethylphenyl	58	104–105[b]	$C_{15}H_{14}N_2O_3S$	59.58	59.66	4.67	4.62	—	—	9.27	9.13	10.60	10.49
3-Nitrophenyl	3-Nitrophenyl	67	157–158[f]	$C_{13}H_9N_3O_5S$	48.90	49.24	2.84	3.09	—	—	13.16	13.06	10.04	10.13
3-Phenyl-6-hydroxyphenyl	4-Methoxyphenyl	57	139–140[a]	$C_{20}H_{17}NO_3S$	68.36	68.28	4.88	5.12	—	—	3.99	4.18	9.12	9.41

[a]Crystallized from chloroform. [b]Chloroform – petroleum ether. [c]Petroleum ether. [d]Benzene – petroleum ether. [e]Ether – petroleum ether. [f]Benzene.

Can. J. Chem. Downloaded from www.nrcresearchpress.com by 210.87.254.5 on 09/05/12
For personal use only.

TABLE II

Aryl aralkylthionocarbamates, RNHC(S)OR′

R	R′	Yield, %	M.p., °C	Formula	C		H		Cl		N		S	
					Calc.	Found	Calc.	Found	Calc.	Found	Calc.	Found	Calc.	Found
Benzyl	Phenyl	46	82–83[b]	$C_{14}H_{13}NOS$	69.11	69.32	5.38	5.69	—	—	5.76	5.63	13.18	13.17
4-Nitrobenzyl	Phenyl	81	110–111[c]	$C_{14}H_{12}N_2O_3S$	58.32	58.36	4.20	4.32	—	—	9.72	9.65	11.12	11.15
4-Chlorobenzyl	Phenyl	82	119–120[d]	$C_{14}H_{12}ClNOS$	60.56	60.69	4.36	4.28	12.77	12.72	5.04	5.05	11.54	11.40
4-Chlorobenzyl	3,4-Dichlorophenyl	80	90–91[e]	$C_{14}H_{10}Cl_3NOS$	48.51	48.84	2.91	2.81	30.68	30.75	4.04	4.25	9.25	9.13
3,4-Dichlorobenzyl	Phenyl	89	104–105[c]	$C_{14}H_{11}Cl_2NOS$	53.85	53.98	3.55	3.70	22.71	22.48	4.49	4.31	10.27	10.06
3,4-Dichlorobenzyl	2-Methylphenyl	34[a]	89–90[b]	$C_{15}H_{13}Cl_2NOS$	55.25	55.14	4.02	4.41	21.75	21.94	4.29	4.32	9.83	9.90
3,4-Dichlorobenzyl	4-Methylphenyl	68[a]	118–119[b]	$C_{15}H_{13}Cl_2NOS$	55.25	55.08	4.02	4.10	21.75	21.60	4.29	4.17	9.83	9.75
3,4-Dichlorobenzyl	4-Ethylphenyl	59[a]	97–98[e]	$C_{16}H_{15}Cl_2NOS$	56.48	56.54	4.44	4.45	20.84	20.84	4.12	4.32	9.42	9.41
3,4-Dichlorobenzyl	4-*n*-Propylphenyl	14[a]	81[c]	$C_{17}H_{17}Cl_2NOS$	57.64	57.88	4.84	4.86	20.02	20.01	3.95	4.13	9.05	8.86
3,4-Dichlorobenzyl	4-*n*-Butylphenyl	42	90–91[b]	$C_{18}H_{19}Cl_2NOS$	58.70	58.53	5.20	5.36	19.25	19.35	3.80	3.91	8.71	8.69
3,4-Dichlorobenzyl	4-*n*-Hexylphenyl	49	87–88[e]	$C_{20}H_{23}Cl_2NOS$	60.61	60.81	5.85	6.24	17.89	17.81	3.53	3.63	8.09	8.38
3,4-Dichlorobenzyl	4-*n*-Decylphenyl	81	85–86[e]	$C_{24}H_{31}Cl_2NOS$	63.71	63.74	6.91	6.78	15.67	15.74	3.09	3.32	7.09	7.08
3,4-Dichlorobenzyl	4-*n*-Dodecylphenyl	70	87.5–88.5[c]	$C_{26}H_{35}Cl_2NOS$	64.48	64.81	7.34	7.33	14.76	14.96	2.91	3.10	6.67	6.67
3,4-Dichlorobenzyl	4-*n*-Octadecylphenyl	60	86–87[e]	$C_{32}H_{47}Cl_2NOS$	68.06	67.29	8.39	8.08	12.56	13.21	2.48	2.61	5.68	6.01
3,4-Dichlorobenzyl	2,6-di-*t*-Butyl-4-methylphenyl	65	113–114[b]	$C_{23}H_{29}Cl_2NOS$	63.01	62.92	6.67	6.67	16.17	16.22	3.19	3.03	7.31	7.26
3,4-Dichlorobenzyl	4-Methoxyphenyl	75	107–108[c]	$C_{15}H_{13}Cl_2NO_2S$	52.64	52.93	3.83	4.07	20.72	21.07	4.09	4.09	9.37	9.58
3,4-Dichlorobenzyl	4-Ethoxyphenyl	80	88–89[c]	$C_{16}H_{15}Cl_2NO_2S$	53.95	53.92	4.25	4.41	19.91	20.08	3.93	4.06	9.00	9.03
3,4-Dichlorobenzyl	3-Nitrophenyl	89	123–124[f]	$C_{14}H_{10}Cl_2N_2O_3S$	47.07	47.04	2.82	2.97	19.85	20.31	7.84	7.65	8.98	9.07
3,4-Dichlorobenzyl	β-Naphthyl	78	124–125[e]	$C_{18}H_{13}Cl_2NOS$	59.61	59.74	3.61	3.73	19.58	19.60	3.87	3.98	8.85	8.86
3,4-Dichlorobenzyl	4-Fluorophenyl	63	123–124[c,g]	$C_{14}H_{10}Cl_2FNOS$[h]	50.94	50.95	3.05	3.12	21.48	21.26	4.26	4.34	9.71	9.78
3,4-Dichlorobenzyl	4-Chlorophenyl	72	135–136[c]	$C_{14}H_{10}Cl_3NOS$	48.51	48.49	2.91	3.04	30.68	30.53	4.04	3.97	9.25	9.17
3,4-Dichlorobenzyl	2,4-Dichlorophenyl	85	154–155[c]	$C_{14}H_9Cl_4NOS$	44.13	44.13	2.38	2.55	37.23	37.46	3.68	3.70	8.41	8.26
3,4-Dichlorobenzyl	3,4-Dichlorophenyl	20	95–96[c]	$C_{14}H_9Cl_4NOS$	44.13	44.07	2.38	2.56	37.23	37.10	3.68	3.70	8.41	8.38
3,4-Dichlorobenzyloxy	Phenyl	50	67–68[b]	$C_{14}H_{11}Cl_2NO_2S$	51.22	51.39	3.38	3.13	21.60	21.78	4.27	4.29	9.77	9.87
2-(3,4-Dichlorophenyl)-ethyl	Phenyl	81	84–85[b]	$C_{15}H_{13}Cl_2NOS$	55.23	55.13	4.02	4.04	21.74	21.71	4.29	4.25	9.83	9.78
3-(3,4-Dichlorophenyl)-propyl	Phenyl	35	64–65[c]	$C_{16}H_{15}Cl_2NOS$	56.46	56.79	4.44	4.66	20.84	20.62	4.12	4.20	9.42	9.15

[a]Prepared by adding 3,4-dichlorobenzyl isothiocyanate to the appropriate phenol. [b]Crystallized from ether – petroleum ether. [c]Petroleum ether – chloroform. [d]Chloroform. [e]Petroleum ether. [f]Benzene. [g]Polymorphic modification, m.p. 108–109°. [h]Calc.: F, 5.76. Found: F, 5.73.

Can. J. Chem. Downloaded from www.nrcresearchpress.com by 210.87.254.5 on 09/05/12
For personal use only.

TABLE III

Aryl disubstituted thionocarbamates, RR'NC(S)OR''

R	R'	R''	Yield, %	M.p., °C	Formula	C		H		Cl		N		S	
						Calc.	Found	Calc.	Found	Calc.	Found	Calc.	Found	Calc.	Found
Phenyl	4-Chlorobenzyl	Phenyl	41	138–139[a]	$C_{20}H_{16}ClNOS$	67.87	67.99	4.56	4.59	10.02	10.00	3.96	4.08	9.06	8.92
4-Chlorobenzyl	4-Chlorobenzyl	Phenyl	34	114–115[b]	$C_{21}H_{17}Cl_2NOS$	62.70	62.82	4.26	4.34	17.63	17.67	3.48	3.46	7.97	7.90
4-Chlorobenzyl	4-Chlorobenzyl	β-Naphthyl	46	117–118[b]	$C_{25}H_{19}Cl_2NOS$	66.36	66.56	4.23	4.53	15.68	15.38	3.10	3.15	7.09	6.92
3,4-Dichloro-benzyl	3,4-Dichlorobenzyl	Phenyl	26	120–121[b]	$C_{21}H_{15}Cl_4NOS$	53.51	53.74	3.21	3.15	30.10	30.61	2.97	3.33	6.80	6.93

[a]Crystallized from acetone. [b]Acetone–water.

TABLE IV

Aralkyl aralkylthionocarbamates, RNHC(S)OR'

R	R'	Yield, %	M.p., °C	Formula	C		H		Cl		N		S	
					Calc.	Found	Calc.	Found	Calc.	Found	Calc.	Found	Calc.	Found
Benzyl	2,4-Dichlorobenzyl	84	107–108[a]	$C_{15}H_{13}Cl_2NOS$	55.22	55.16	4.02	4.08	21.74	22.22	4.29	4.14	9.83	9.51
3,4-Dichlorobenzyl	4-Chlorobenzyl	77	73–74[b]	$C_{15}H_{12}Cl_3NOS$	49.93	50.29	3.36	3.24	29.49	29.39	3.88	3.64	8.89	8.77
3,4-Dichlorobenzyl	2,4-Dichlorobenzyl	72	104–105[a]	$C_{15}H_{11}Cl_4NOS$	45.59	45.76	2.81	2.95	35.90	36.17	3.55	3.38	8.11	8.11
3,4-Dichlorobenzyl	3,4-Dichlorobenzyl	80	79–80[b]	$C_{15}H_{11}Cl_4NOS$	45.59	45.49	2.81	2.76	35.90	35.20	3.55	3.45	8.11	7.92

[a]Crystallized from acetone–water. [b]Ethanol–water.

Method B: 4-Methylphenyl 3,4-Dichlorobenzylthionocarbamate

A mixture of 3,4-dichlorobenzyl isothiocyanate (4.36 g, 0.02 mole), *p*-cresol (2.16 g, 0.02 mole), and triethylamine (0.04 g, 0.0004 mole) was heated in a sealed tube at 80° for 4 hours. The reaction mixture was dissolved in ether (100 ml) and the ether solution was washed with 2% sodium hydroxide solution and with water. The residue obtained on evaporation of the ether solution (5.8 g, m.p. 92–96°) was recrystallized from petroleum ether (40 ml) to give the product melting at 115–117°, yield 4.4 g (67.5%). One crystallization from ether – petroleum ether solvent raised the melting point to 118–119°. This reaction was found to be generally applicable to the addition of phenols to aralkyl isothiocyanates. Compounds prepared by this method are included in Table II.

Aralkyl Thionocarbamates

3,4-Dichlorobenzyl 3,4-Dichlorobenzylthionocarbamate

Sodium hydride (0.48 g of a 50% dispersion, 0.01 mole) was added to 3,4-dichlorobenzyl alcohol (1.77 g, 0.01 mole) in benzene (30 ml). The mixture was stirred at room temperature until the evolution of hydrogen ceased, after which it was briefly heated to boiling. The cooled suspension of sodium 3,4-dichlorobenzyloxide was treated with 3,4-dichlorobenzyl isothiocyanate (2.18 g, 0.01 mole) in benzene (10 ml) and the mixture was stirred overnight. The precipitated sodio derivative (4.18 g) was dissolved in acetone and the solution was filtered clear of insoluble impurities (0.34 g). Acidification of the filtrate with aqueous acetic acid precipitated the product (m.p. 103–104°), yield 2.86 g (72.1%). Recrystallization from aqueous acetone raised the melting point to 104–105°.

All of the compounds listed in Table IV were prepared by this procedure.

1,4-Phenylene Di-(3,4-dichlorobenzylthionocarbamate)

A mixture of 3,4-dichlorobenzyl isothiocyanate (2.18 g, 0.01 mole), hydroquinone (1.10 g, 0.01 mole), and triethylamine (0.01 g, 0.0001 mole) was heated in a sealed tube at 144° for 3 hours. The crude product was triturated in ether (100 ml) to give 1.79 g (65.6%) of product (m.p. 165–170°). Recrystallization from aqueous acetone raised the melting point to 170–171°, yield 1.25 g (45.8%). Anal. Calc. for $C_{22}H_{16}Cl_4N_2O_2S_2$: C, 48.38; H, 2.95; Cl, 25.96; N, 5.13; S, 11.74. Found: C, 48.49; H, 3.13; Cl, 25.98; N, 5.27; S, 11.73.

1,4-Phenylene Di-(benzylthionocarbamate)

A mixture of benzyl isothiocyanate (3.83 g, 0.026 mole), hydroquinone (1.41 g, 0.013 mole), and triethylamine (0.023 g, 0.0023 mole) was heated in a sealed tube at 144° for 3 hours. The crude product was extracted with ether, and the residue was recrystallized from aqueous acetone to give crystals melting at 171–172°, yield 0.24 g (4.6%). Recrystallization from acetone raised the melting point to 178–179°. Anal. Calc. for $C_{22}H_{20}N_2O_2S_2$: C, 64.67; H, 4.94; N, 6.86; S, 15.70. Found: C, 64.93; H, 5.07; N, 6.67; S, 15.79.

Aryl Thiolcarbamates

Phenyl chlorothiolformate (b.p. 90–95°/13 mm) was prepared in 18% yield by the method of Rivier (2).

The chlorothiolformate (3.40 g, 0.02 mole) in chloroform (30 ml) was added dropwise to a stirred solution of 3,4-dichlorobenzylamine (4.30 g, 0.04 mole) in chloroform (10 ml) at 25°. The reaction mixture was allowed to stand overnight, and the precipitated 3,4-dichlorobenzylamine hydrochloride (2.87 g, 100%) was recovered by filtration. The residue obtained on evaporation of the filtrate was crystallized from benzene – petroleum ether to give crystals melting at 101–102°, yield 2.65 g (55%).

Can. J. Chem. Downloaded from www.nrcresearchpress.com by 210.87.254.5 on 09/05/12
For personal use only.

Can. J. Chem. Downloaded from www.nrcresearchpress.com by 210.87.254.5 on 09/05/12
For personal use only.

TABLE V

Aryl N-substituted thiolcarbamates, RNHC(O)SR′

R	R′	Yield, %	M.p., °C	Formula	C		H		Cl		N		S	
					Calc.	Found	Calc.	Found	Calc.	Found	Calc.	Found	Calc.	Found
4-Chlorobenzyl	4-Chlorophenyl	82	192–193[a]	$C_{14}H_{11}Cl_2NOS$	53.85	53.98	3.55	3.68	22.71	22.73	4.49	4.54	10.27	10.02
3,4-Dichlorobenzyl	Phenyl	55	101–102[b]	$C_{14}H_{11}Cl_2NOS$	53.85	53.68	3.55	3.60	22.71	23.07	4.49	4.70	10.27	10.01
3,4-Dichlorobenzyl	4-Chlorophenyl	57	149–150[c]	$C_{14}H_{10}Cl_3NOS$	48.59	48.49	2.91	2.88	30.68	30.92	4.04	4.13	9.25	9.06
3,4-Dichlorophenyl	4-Chlorophenyl	70	209–210[d]	$C_{13}H_8Cl_3NOS$	46.94	47.20	2.42	2.45	31.98	32.23	4.21	4.43	9.64	9.58

[a]Crystallized from ethanol–water. [b]Benzene – petroleum ether. [c]Dioxane – petroleum ether. [d]Dioxane–water.

TABLE VI

Aryl chlorothionoformates, ROC(S)Cl

R	Yield, %	B.p., °C/mm Hg	Formula	C		H		Cl		S	
				Calc.	Found	Calc.	Found	Calc.	Found	Calc.	Found
4-Ethoxyphenyl	90.5	100–104/0.2	$C_9H_9ClO_2S$	49.89	49.67	4.19	4.01	16.36	16.27	14.80	14.48
4-Methylphenyl	92.0	62–65/0.25	C_8H_7ClOS	51.93	51.93	3.78	4.03	19.00	18.45	17.18	16.39
4-*n*-Propylphenyl	74.7	101–102/0.1	$C_{10}H_{11}ClOS$	55.94	56.07	5.16	5.00	16.52	16.62	14.93	14.70
4-Methoxyphenyl	84.8	96/0.4	$C_8H_7ClO_2S$	47.40	47.46	3.48	3.56	17.50	17.40	15.82	15.67
3-Nitrophenyl	54.0	128/0.1[a]	$C_7H_4ClNO_3S$[c]	38.63	39.36	1.85	2.16	16.29	15.90	14.73	14.18
4-Nitrophenyl	44.6	—[b]	$C_7H_4ClNO_3S$[d]	38.63	38.83	1.85	1.91	16.29	16.22	14.71	14.60

[a]M.p. 64–65°. [b]M.p. 59–60°. [c]Calc.: N, 6.44. Found: N, 6.39. [d]Calc.: N, 6.44. Found: N, 6.62.

4-Chlorophenyl chlorothiolformate (b.p. 145–155°/30 mm) was prepared in 67.5% yield from lead 4-chlorophenylmercaptide and phosgene, according to Rivier's method (2). Condensation with the appropriate amine as described above yielded the other thiolcarbamates listed in Table V.

S-*Methyl Phenylxanthate*

The reaction between carbon disulphide and potassium phenolate in ethanol (7) was found to yield only potassium ethylxanthate. Replacement of the ethanol by dimethylformamide yielded the desired potassium phenylxanthate.

Carbon disulphide (6.09 g, 0.08 mole) was added during a 30-minute period to potassium phenolate (10.58 g, 0.08 mole) in dimethylformamide (80 ml) at 20°. Methyl chloride was bubbled through the reaction mixture for 30 minutes at 30°. Water (1500 ml) was added, and the mixture was extracted with ether (5×100 ml). The ether extracts were combined and washed with 5% sodium hydroxide solution, 5% hydrochloric acid, and water. Fractionation of the dried ether solution yielded S-methyl phenylxanthate (b.p. 82–84°/0.11 mm, n_D^{25} 1.62189), yield 6.0 g (41.8%). Anal. Calc. for $C_8H_8OS_2$: C, 52.15; H, 4.38; S, 34.80. Found: C, 52.15; H, 4.45; S, 34.19.

Methyl 3,4-Dichlorobenzyldithiocarbamate

Method A.—3,4-Dichlorobenzylamine (2.58 g, 0.146 mole) was added to S-methyl phenylxanthate (2.7 g, 0.0146 mole) at room temperature. The temperature rose to 42°, and the mixture gradually solidified. Crystallization from chloroform – petroleum ether yielded methyl 3,4-dichlorobenzyldithiocarbamate (m.p. 98–100°), yield 3.37 g (74.1%). Recrystallization from chloroform – petroleum ether gave the analytical sample melting at 100–101°. Anal. Calc. for $C_9H_9Cl_2NS_2$: C, 40.61; H, 3.41; Cl, 26.64; N, 5.26; S, 24.08. Found: C, 41.11; H, 3.44; Cl, 26.07; N, 5.42; S, 24.14.

Method B.—Carbon disulphide (16.75 g, 0.22 mole) was added to a stirred mixture of sodium hydroxide (8.8 g, 0.22 mole) in water (14 ml) and 3,4-dichlorobenzylamine (35.21 g, 0.20 mole) in ether (100 ml) at 0–5°. The mixture was stirred for 1 hour at room temperature, and the sodium 3,4-dichlorobenzyldithiocarbamate (40.7 g, 75%) was recovered by filtration. The sodium salt (13.71 g, 0.05 mole) was added to a solution of methyl iodide (7.10 g, 0.05 mole) in methanol (150 ml) and the mixture was allowed to stand for 1 hour. The solution was concentrated and diluted with water, giving methyl 3,4-dichlorobenzyldithiocarbamate (m.p. 95–100°). Recrystallization from benzene yielded the pure product (9.0 g, 71%), melting point and mixed melting point with the product described above in A was 100–101°.

Methyl 3,4-Dichlorobenzylthionocarbamate

A solution of methyl 3,4-dichlorobenzyldithiocarbamate (1.33 g, 0.005 mole) in methanol (50 ml) was refluxed for 1 hour in the presence of Amberlite IRA-400 resin (25 ml) which had been saturated with phenol. The solution was filtered and evaporated. Crystallization of the residue from chloroform – petroleum ether yielded methyl 3,4-dichlorobenzylthionocarbamate (m.p. 75–76°), yield 0.60 g (48%). Anal. Calc. for $C_9H_9Cl_2NOS$: C, 42.23; H, 3.63; Cl, 28.35; N, 5.60; S, 12.82. Found: C, 42.23; H, 3.90; Cl, 28.60; N, 5.39; S, 12.59.

Ethyl 3,4-Dichlorobenzylthionocarbamate

The procedure is essentially that of Harris and Fischback (1). Methyl chloride was passed through a solution of potassium ethylxanthate (0.20 mole) in ethanol (200 ml) for 1 hour at 25–30°. 3,4-Dichlorobenzylamine (35.2 g, 0.20 mole) was added and the

Can. J. Chem. Downloaded from www.nrcresearchpress.com by 210.87.254.5 on 09/05/12
For personal use only.

solution was maintained at 40° for 30 minutes. The solution was evaporated, and the residue was dissolved in chloroform (200 ml). The chloroform solution was extracted with 5% sodium hydroxide solution, 5% hydrochloric acid, and water. The chloroform solution was dried and evaporated to give ethyl 3,4-dichlorobenzylthionocarbamate (m.p. 55–58°), yield 16 g (30.3%). Anal. Calc. for $C_{10}H_{11}Cl_2NOS$: C, 45.46; H, 4.19; Cl, 26.84; N, 5.30; S, 12.14. Found: C, 45.39; H, 4.30; Cl, 27.00; N, 5.70; S, 12.10.

REFERENCES

1. G. H. HARRIS and B. C. FISCHBACK. U.S. Patent No. 2,691,635; Chem. Abstr. **49**, 11696 (1955).
2. H. RIVIER. Bull. soc. chim. France, **1** (4), 733 (1907).
3. H. D. LAW. J. Chem. Soc. **101**, 154 (1912).
4. J. VON BRAUN, M. KUHN, and J. WEISMANTEL. Ann. **449**, 249 (1926).
5. C. WALLING and K. B. WOLFSTIRN. J. Am. Chem. Soc. **69**, 852 (1947).
6. G. SANDULESCO and A. GIRARD. Bull. soc. chim. France, **47** (4), 1300 (1930).
7. P. SACCARDI. Ital. Patent No. 432,082; Chem. Abstr. **43**, 8604 (1949).

Can. J. Chem. Downloaded from www.nrcresearchpress.com by 210.87.254.5 on 09/05/12
For personal use only.

Can. J. Chem. Downloaded from www.nrcresearchpress.com by 210.87.254.5 on 09/05/12
For personal use only.

ORGANOPHOSPHORUS COMPOUNDS

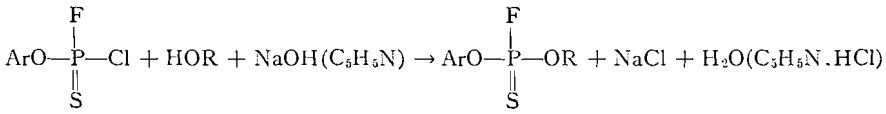
VIII. O-ALKYL, O′-ARYL PHOSPHOROFLUORIDOTHIOATES AND O-ARYL N-ALKYL PHOSPHORAMIDOFLUORIDOTHIOATES[1, 2]

G. A. Olah and A. A. Oswald[3]

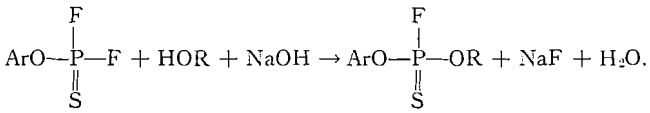
O-Alkyl, O′-aryl phosphorofluoridothioates and O-aryl N-alkyl phosphoramidofluoridothioates were prepared from the corresponding aryl phosphorochlorofluoridothioates and aryl phosphorodifluoridothioates.

In a previous paper (1) the preparation of aryl phosphorochlorofluoridothioates and aryl phosphorodifluoridothioates was described. Using these compounds as starting materials, it was now possible to prepare the previously unknown O-alkyl, O′-aryl phosphorofluoridothioates and O-aryl N-alkyl phosphoramidofluoridothioates.

O-Alkyl, O′-aryl phosphorofluoridothioates have been obtained in good yields by reacting aryl phosphorochlorofluoridothioates with sodium alcoholates, or with alcohols in the presence of NaOH or pyridine.



Aryl phosphorodifluoridothioates react in a similar manner:

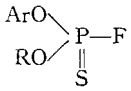


The yields with this method, however, are in general slightly smaller than with aryl phosphorochlorofluoridothioates.

The following O-alkyl, O′-aryl phosphorofluoridothioates were prepared: O-ethyl, O′-phenyl-; O-methyl, O′-*p*-tolyl-; O-ethyl, O′-α-naphthyl-; and O-methyl, O′-*p*-chlorophenyl-phosphorofluoridothioates. Some physical properties and analytical data are shown in Table I.

TABLE I

O-Alkyl, O′-aryl phosphorofluoridothioates



Ar	R	Yield,* %	B.p., °C/mm	n_D^{20}	Fluorine	
					Calculated	Found
Phenyl	Ethyl	77	75–76/3	1.5019	8.62	8.74
p-Tolyl	Methyl	91	79–80/3	1.5069	7.62	7.83
α-Naphthyl	Ethyl	73	124–125/2	1.5730	7.03	7.16
p-Chlorophenyl	Methyl	85	81–82/3	1.5241	7.89	7.89

*Obtained by the reaction of aryl phosphorochlorofluoridothioates with sodium alcoholates.

[1]*Manuscript received May 31, 1960.*
Contribution No. 13 from the Exploratory Research Laboratory, Dow Chemical of Canada, Limited, Sarnia, Ontario, Canada.
[2]*Part VII: J. Org. Chem.* **25**, *603 (1960).*
[3]*Present address: Research Department, Imperial Oil Limited, Sarnia, Ontario, Canada.*

Can. J. Chem. Downloaded from www.nrcresearchpress.com by 210.87.254.5 on 09/05/12
For personal use only.

Alkyl esters of phosphoramidofluoridic acid were prepared by Saunders (2), Schrader (3), and Sartori (4) to combine the rapid toxic action and miotic effect of the dialkyl phosphorofluoridates and of the high toxicity of some of the phosphorodiamidofluoridates. The synthesis started from phosphorus oxydichlorofluoride and was carried out without the isolation of the ethyl phosphorofluoridochloridate intermediate according to the following sequence of reactions (5):

$$POCl_2F + C_2H_5OH \rightarrow C_2H_5OPOClF + HCl \xrightarrow{3C_6H_5NH_2} \begin{matrix} C_2H_5O \\ C_6H_5NH \end{matrix}\!\!>\!POF + 2C_6H_5NH_2.HCl.$$

Similar reactions starting from phosphorus thiodichlorofluoride were used for the preparation of the alkyl esters of phosphoramidofluoridothioic acids as described in a previous paper of this series (6). No aryl esters of either phosphoramidofluoridic or phosphoramidofluoridothioic acid were reported.

In this work aryl esters of N-alkyl phosphoramidofluoridothioic acid were prepared by reacting aryl phosphorochlorofluoridothioates with a primary or secondary amine according to the following equation:

$$ArO{-}\overset{\overset{F}{|}}{\underset{\underset{S}{\|}}{P}}{-}Cl + 2HNR_2 \rightarrow ArO{-}\overset{\overset{F}{|}}{\underset{\underset{S}{\|}}{P}}{-}NR_2 + R_2NH.HCl.$$

Aryl phosphorodifluoridothioates react with amines in a similar manner to yield O-aryl N-alkyl phosphoroamidofluoridothioates and amine hydrofluorides:

$$ArO{-}\overset{\overset{F}{|}}{\underset{\underset{S}{\|}}{P}}{-}F + 2HNR_2 \rightarrow ArO{-}\overset{\overset{F}{|}}{\underset{\underset{S}{\|}}{P}}{-}NR_2 + R_2NH.HF.$$

Syntheses starting from aryl phosphorodifluoridothioates required somewhat higher reaction temperatures and gave slightly lower yields.

In the place of the second mole of amine, pyridine (or another organic base) can be used to bind the halogen hydrogen formed in the reaction

$$ArO{-}\overset{\overset{F}{|}}{\underset{\underset{S}{\|}}{P}}{-}Cl + H_2NR + C_5H_5N \rightarrow ArO{-}\overset{\overset{F}{|}}{\underset{\underset{S}{\|}}{P}}{-}NHR + C_5H_5N.HCl.$$

Yields and purity of compounds were equivalent to previous methods.

TABLE II

O-Aryl N-alkyl phosphoramidofluoridothioates

$$ArO{-}\overset{\overset{F}{|}}{\underset{\underset{S}{\|}}{P}}{-}N\begin{matrix}R_1\\R_2\end{matrix}$$

Ar	R_1	R_2	B.p., °C/mm	n_D^{20}	Yield,* %	Fluorine	
						Calculated	Found
Phenyl	Metyhl	Methyl	93–93.5/3	1.5268	92	8.66	8.76
o-Tolyl	Methyl	Methyl	91.5–92/3	1.5251	90	8.14	8.10
o-Tolyl	Methyl	Hydrogen	110–110.5/3	1.5299	92	8.19	8.35
Phenyl	*t*-Butyl	Hydrogen	123–124/2.5	1.5338	75	7.68	7.84

*Obtained by the reaction of aryl phosphorochlorofluoridothioates with amines.

The following O-aryl N-alkyl phosphoramidofluoridothioates were prepared: O-phenyl N,N-dimethyl-; O-*o*-tolyl N,N-dimethyl-; amido-, O-*o*-tolyl N-ethyl-; and O-phenyl N-*t*-butyl-phosphoramidofluoridothioates. The yields and some of the properties of the compounds prepared are shown in Table II.

All derivatives are colorless liquids. They are fairly resistant to hydrolysis. Therefore, they can be prepared also in water media in satisfactory yields.

EXPERIMENTAL

O-Alkyl, O'-Aryl Phosphorofluoridothioates

(A) From Aryl Phosphorochlorofluoridothioates with Alcoholates

Aryl- (phenyl-, *p*-tolyl-, α-naphthyl-, and *p*-chlorophenyl-) phosphorochlorofluoridothioate (0.1 mole) was dissolved in 100 ml of benzene (ether could be also used as an alternate solvent) and placed in a 500-ml three-necked flask equipped with a stirrer, dropping funnel, and thermometer. The other reagent, 0.1 mole of sodium alcoholate (methylate and ethylate), was dissolved in the corresponding alcohol. The sodium alcoholate solution was then added in small portions to the aryl phosphorochlorofluoridate while the reaction mixture was stirred and cooled in an ice bath. Sodium chloride precipitated instantly. After the reaction mixture was allowed to stand for 2 hours, it was washed with three volumes of water, then with 2.5% sodium carbonate solution, and then again with water. The mixture was dried over anhydrous sodium sulphate, and the solvent was removed by distillation at atmospheric pressure and then the remaining product was fractionated *in vacuo*. For yields, physical and analytical data see Table I.

(B) From Aryl Phosphorochlorofluoridothioates with Alcohols

A solution of 0.1 mole of aryl phosphorochlorofluoridothioate in 50 ml of the corresponding alcohol (methanol or ethanol in our experiments) was placed into a 200-ml flask equipped with a mechanical stirrer, dropping funnel, and thermometer. To the alcoholic solution, an aqueous solution of 4.0 g (0.1 mole) of sodium hydroxide (in 15 ml of water) was added dropwise, with effective stirring and ice-water cooling. After the addition, the reaction mixture was allowed to stand overnight at room temperature and then extracted with 150 ml of ether. The ether solution was washed with water, 1% aqueous sodium hydroxide solution, and then again with water. The ether solution was then dried over anhydrous sodium sulphate, the solvent was removed by distillation at atmospheric pressure, and the remaining raw O-alkyl, O'-aryl phosphorofluoridothioate was purified by fractionation *in vacuo*.

In the presence of pyridine.—To a solution of 0.1 mole of aryl phosphorochlorofluoridothioate in 50 ml of the corresponding alcohol, a solution of 0.1 mole of pyridine in 100 ml of ether was added slowly with shaking. After the addition, the reaction mixture was allowed to stand overnight, diluted with 200 ml of water and 100 ml of ether. The ether phase was washed successively with water, 5% aqueous sodium carbonate, and water and then dried over sodium sulphate. The solvent was removed by distillation, and the O-alkyl, O'-aryl phosphorofluoridothioate was obtained by fractionation *in vacuo*.

(C) From Aryl Phosphorodifluoridothioates

Aryl (α-naphthyl-, and *p*-chlorophenyl-) phosphorodifluoridothioate (0.1 mole) was dissolved in 100 ml of benzene and reacted with an alcoholic solution of 0.1 mole of sodium alcoholate (methylate and ethylate) as described under method (*A*).

Can. J. Chem. Downloaded from www.nrcresearchpress.com by 210.87.254.5 on 09/05/12
For personal use only.

O-Aryl N-Alkyl Phosphoramidofluoridothioates

(A) From Aryl Phosphorochlorofluoridothioates with Amines

To a solution of 0.1 mole of aryl- (phenyl-, *o*-tolyl-) phosphorochlorofluoridothioate in 100 ml of benzene (or toluene), 0.2 mole of the corresponding alkylamine (methyl, dimethyl, *t*-butyl) in 100 ml of benzene was added with cold water cooling and stirring. The amine hydrochloride precipitated instantly. The reaction mixture was allowed to reach room temperature and to stand overnight. The amine hydrochloride was then removed by filtration and washed with benzene. The combined filtrate was distilled; at first the benzene solvent was removed at atmospheric pressure and then the raw O-aryl N-alkyl phosphoramidofluoridothioate was fractionated *in vacuo*. Yields and physical and analytical data are shown in Table II.

(B) From Aryl Phosphorochlorofluoridothioates with Amines and Pyridine

To a solution of 0.1 mole of aryl phosphorochlorofluoridothioate in 150 ml of benzene, a mixture of 0.1 mole of alkylamine and 0.1 mole of pyridine was added dropwise with stirring. The reaction mixture was warmed to 50° C and kept at that temperature for an hour. Then the pyridine hydrochloride precipitate was removed by filtration and washed with benzene. The combined benzene filtrates were washed with water, dried over anhydrous sodium sulphate and distilled.

(C) From Aryl Phosphorodifluoridothioate

To a benzene solution of 0.1 mole of phenyl phosphorodifluoridothioate, 0.2 mole of alkylamine (dimethyl and *t*-butyl) in 100 ml of benzene was added with stirring. The reaction mixture was heated to 50° C and kept at that temperature for an hour. Then it was worked up as described under method (*A*).

REFERENCES

1. G. A. Olah and A. A. Oswald. J. Org. Chem. **25**, 603 (1960).
2. B. C. Saunders. Some aspects of the chemistry and toxic action of organic compounds containing phosphorus and fluorine. Cambridge at the University Press. 1957. p. 90.
3. G. Schrader. Die Entwicklung neuer Insektizide auf Grundlage organischer Fluor- und Phosphoverbindungen, 2. Aufl., Verlag Chemie GmbH., Weinheim. 1952.
4. M. F. Sartori. Chem. Revs. **48**, 225 (1951).
5. H. G. Cook, J. D. Flett, B. C. Saunders, G. J. Stacey, H. G. Watson, I. G. E. Wilding, and S. J. Woodcock. J. Chem. Soc. 2921 (1949).
6. G. Olah, A. Oswald, and A. Mlinko. Ann. **602**, 123 (1957).

Can. J. Chem. Downloaded from www.nrcresearchpress.com by 210.87.254.5 on 09/05/12
For personal use only.

Can. J. Chem. Downloaded from www.nrcresearchpress.com by 210.87.254.42 on 09/05/12
For personal use only.

THE DETERMINATION OF THE AREAS OF RESOLVED AND PARTIALLY RESOLVED CHROMATOGRAPHY PEAKS[1]

JOHN C. BARTLET AND D. MORISON SMITH

ABSTRACT

Gas chromatographic peaks were demonstrated to have the form of normal distribution curves. A mathematical treatment has been developed which permits the calculation of the areas of these curves from the statistical parameters, height of the mode (peak height), and standard deviation σ. The standard deviation equals the width of the peak at 0.882 of peak height. Methods given for the evaluation of the mutual effects of overlapping peaks have made it possible to obtain corrected peak heights. The standard deviation of the gas chromatography peak has been found to vary linearly with the retention time, thus permitting the graphical estimation of σ for use with corrected peak heights in the calculation of true areas for overlapping peaks. The method has also been extended to the treatment of skewed, overlapping peaks. The variation of σ with retention time, its constancy, and its relationship to the number of theoretical plates are discussed.

INTRODUCTION

In quantitative gas chromatography using a differential detector, the area under the peak corresponding to a compound is proportional to the amount of that compound present in the gas stream. Area measurements are therefore fundamental.

Various procedures have been proposed for the measurement of peak areas. The integrator built into the recorder is the least laborious, but suffers from obvious disadvantages if there is a base-line drift or if there are overlapping peaks. The triangulation procedure (1) gives a good first approximation. Another procedure which has been widely used is to cut out the peaks or a tracing of the peaks, and to weigh the cut paper. Planimeter tracing has also been used. With all these procedures, precision and accuracy suffer when the peaks are very narrow or if two or more peaks have a moderate overlap.

AREA OF SYMMETRICAL PEAKS

(a) Isolated Peaks

It has been pointed out and developed theoretically (2, 3, 4) that the peaks obtained with a well-designed chromatograph closely approximate a normal or Gaussian distribution curve as shown in Fig. 1. The equation for this type of curve is given by Goulden (5) as

$$Y = \frac{N}{\sigma\sqrt{2\pi}} \cdot e^{-\frac{1}{2}(x/\sigma)^2} \qquad [1]$$

where Y is the height of the curve measured at a distance x from the mean, N is the number of variates, which, for our purposes may be taken as the area, A, and σ is the standard deviation. At the mean or central peak of the curve, $x = 0$, $Y = h$ or peak height, and equation [1] becomes

$$h = \frac{A}{\sigma\sqrt{2\pi}} \qquad [2]$$

or

$$A = h\sigma\sqrt{2\pi} = 2.507h\sigma. \qquad [3]$$

[1]*Manuscript received June 30, 1960.*
Contribution from Food and Drug Directorate, Department of National Health and Welfare, Ottawa, Canada. Presented in part at the Ottawa Meeting of the Chemical Institute of Canada, June 14, 1960.

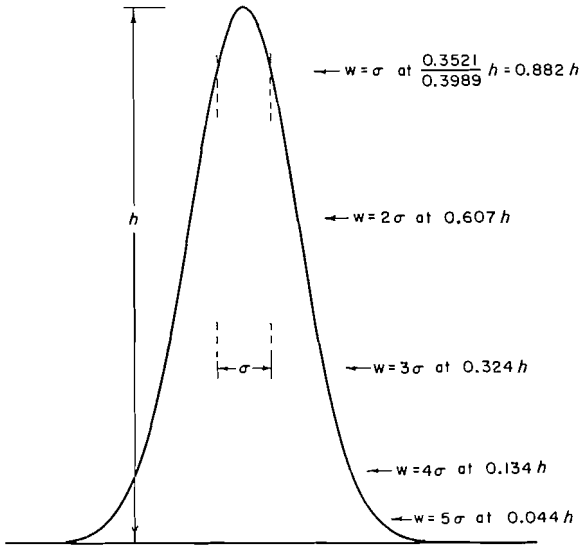


FIG. 1. The normal distribution curve.

For a normal distribution curve, σ may easily be determined, as shown in Fig. 1, by any one of the formulae which have been derived from Sheppard's tables of the Probability Integral (Biometrika Tables) (6). Thus, for an isolated peak, the area may be calculated, without construction, by simply measuring the peak height and the σ derived from the peak width at $0.607h$ or $0.324h$ and substituting in equation [3]. For accuracy, the peak width measurements for σ should be made using a magnifying viewer with reticle such as the Bausch and Lomb spectrum measuring magnifier No. 81-34-97-20.

The conformity of the peaks to the normal distribution curve can be tested by measuring the peak width of an isolated peak at the various heights listed in Fig. 1. The σ obtained should be constant or nearly constant to a peak width of 4σ.

Figure 2 gives a typical chromatogram for which the σ of the various peaks are indicated. Some of these values and others taken from other chromatograms using pure standard substances on the same column have been plotted against retention time in Fig. 3. As may be seen from the figure, the function is linear. In this way, the value for σ may be obtained from the graph for peaks which are insufficiently resolved for accurate measurement. These values of σ can be used directly in equation [3] for resolved peaks.

(b) Unresolved Peaks

If distances along the x axis are measured in terms of σ and the area is taken as 1 (i.e., a standardized normal distribution) then equation [2] becomes

$$h = \frac{1}{\sqrt{2\pi}} \qquad [4]$$

and the ordinate Y becomes Z (5). Then

$$Z = \frac{e^{-\frac{1}{2}(x/\sigma)^2}}{\sqrt{2\pi}}. \qquad [5]$$

Note that $Z = h = 1/\sqrt{2\pi}$ when $x = 0$.

Can. J. Chem. Downloaded from www.nrcresearchpress.com by 210.87.254.42 on 09/05/12
For personal use only.

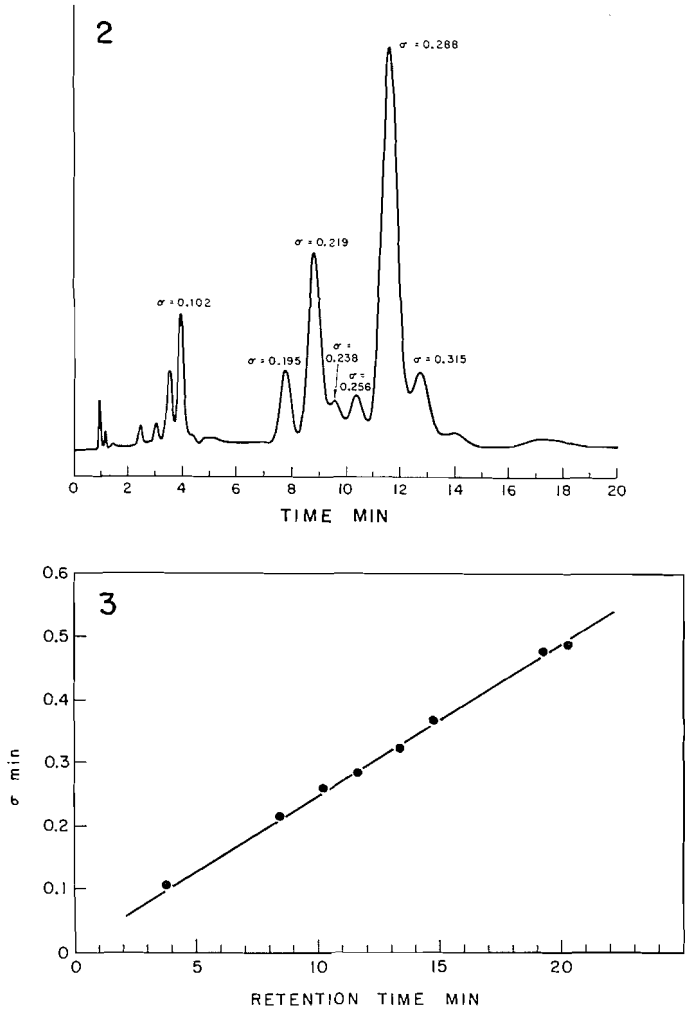


FIG. 2. Gas chromatogram of peppermint oil. Temperature of column, 170°; flow rate, 80 ml/minute of helium; packing, 20% SAIB on Chromosorb W, 2½ meters long.
FIG. 3. Relationship of σ, standard deviation, to retention time, t_r.

The values for Z may be found in Sheppard's table (5) for a standardized normal distribution curve. These values have been converted to percentage of peak height h at a distance x from the mean. Figure 4 gives these percentage corrections at separations, x, measured in units of the σ of the interfering peak.

When there are two incompletely resolved peaks as in Figs. 5 and 6, it is possible to calculate the height of the curve due to one component at the position of the other peak, and thus the contribution of one component to the observed peak height of the other.

For example, let us consider two peaks, a and b, of peak heights h_a and h_b separated by x (measured in units of σ_a and hence called x_a) as shown in Fig. 5. The ordinate Y of the curve of peak a at a distance x_a from the mean is given by substituting h_a for $N/\sigma\sqrt{2\pi}$ in equation [1].

Can. J. Chem. Downloaded from www.nrcresearchpress.com by 210.87.254.42 on 09/05/12
For personal use only.

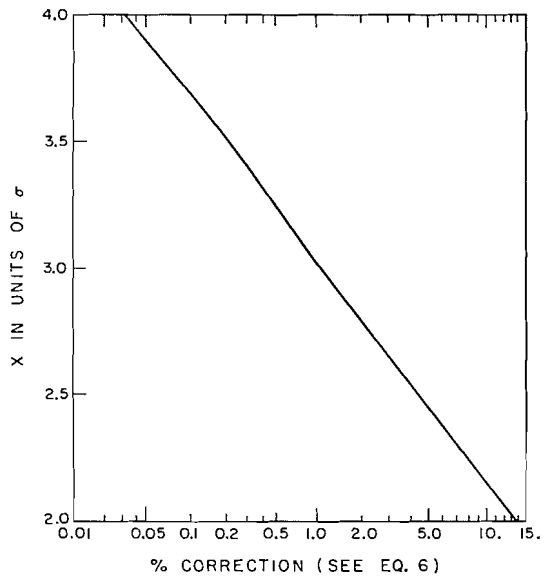


FIG. 4. Peak height corrections for given separations measured in units of the σ of the interfering peak.

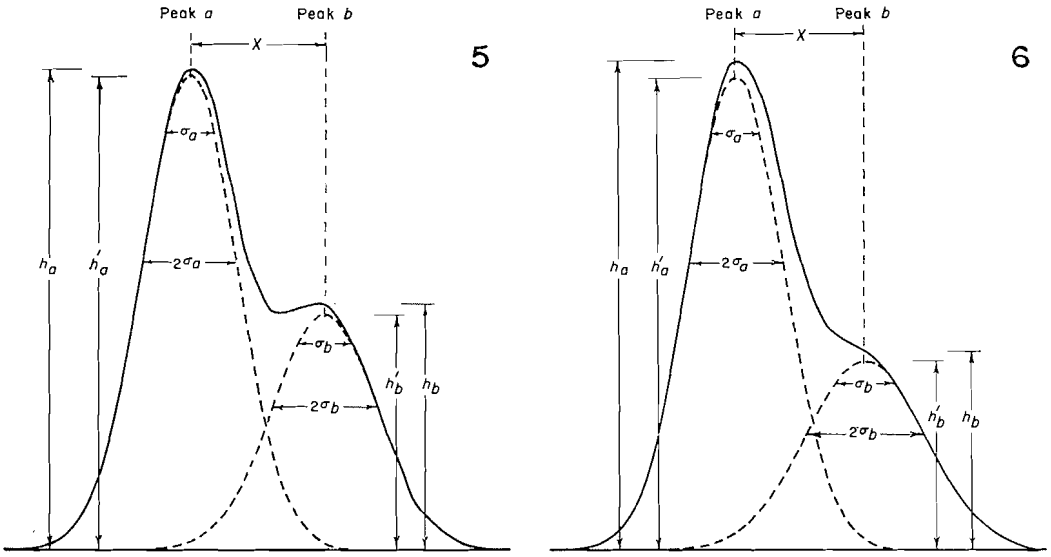


FIG. 5. Symmetrical peak with partially resolved side peak.
FIG. 6. Symmetrical peak with unresolved shoulder.

[6] $$Y = h_a e^{-\frac{1}{2}(x_a/\sigma_a)^2}$$

and the corrected height of peak b, h_b', becomes

[7] $$h_b' = h_b - h_a e^{-\frac{1}{2}(x_a/\sigma_a)^2}$$

and the area, A_b, becomes

[8] $$A_b = h_b' \sigma_b \sqrt{2\pi} = 2.507\, h_b' \sigma_b.$$

Can. J. Chem. Downloaded from www.nrcresearchpress.com by 210.87.254.42 on 09/05/12
For personal use only.

This is obviously the first member of a series of iterative approximations, whose later members are usually too small to be considered. However, if both h_a and h_b are large and x is small, it may be necessary to carry through the corrections a second time using h_a' in place of h_a in equation [7] and h_b' in the corresponding correction for h_b.

To simplify the correction for peak height, Fig. 4 or Sheppard's table (6) may be used to obtain the percentage of the height of the interfering peak to be subtracted from the peak under consideration. If the separation is greater than 4σ, the correction is usually negligible even though the valley between the peaks does not return to the base line. In the above example h_a can similarly be corrected for the effect of peak b, using x measured in units of σ_b. Note that if peak b comes after peak a, σ_b will be greater than σ_a as shown in Figs. 5 and 6, x_b will be less than x_a, and the percentage of h_b to be subtracted from h_a will be greater than the percentage correction of h_a on h_b. In Fig. 6 the correction for h_b on h_a is actually larger even though the peak b is smaller.

Figure 5 shows two symmetrical peaks, which, although overlapping, are still well enough separated so that the peak positions can be determined.

Figure 6 shows an extreme case where peak b appears only as a shoulder. The corrections can still be applied provided the retention time of the second compound relative to the first is known from other data. This is necessary so that the distance x can be measured accurately.

Note that although in both Figs. 5 and 6 there is serious overlap, there is still only a relatively small correction on peak height. However, as may be seen from these figures a serious error would be introduced if the σ used in the calculations were taken from the curve. In the case of overlapping peaks the σ to be used must be derived from a graph of the type of Fig. 3 for accurate results.

ASYMMETRICAL PEAKS

A peak may be skewed and still have some of the properties of a normal distribution curve. Skewed peaks which will be considered in detail are of the type shown in Fig. 7

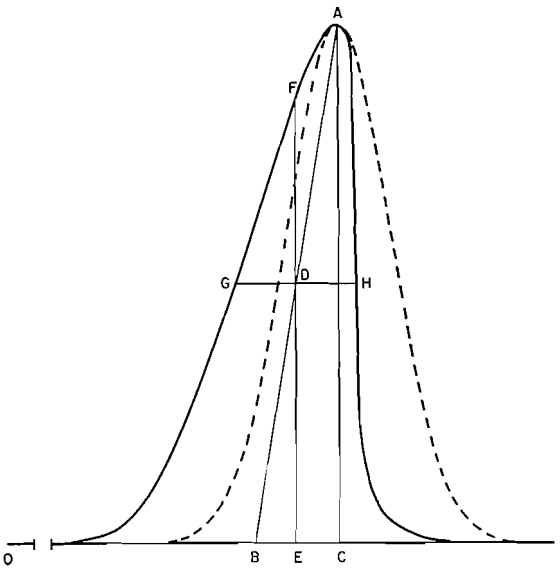


FIG. 7. Comparison of skewed and symmetrical distribution curves.

Can. J. Chem. Downloaded from www.nrcresearchpress.com by 210.87.254.42 on 09/05/12
For personal use only.

and have the following properties:

1. The asymmetry is such that the locus of the midpoint of the peak width at all heights is a straight line (AB in Fig. 7).
2. The peak width measured at the various heights listed on Fig. 1 shall yield a constant value for σ.

Skewness has been defined by Pearson (7) as (mean$-$mode)/σ where the mean is the value which vertically bisects the area and the mode is the position of peak height. Figure 7 shows a skewed curve of the type described, along with a symmetrical normal distribution curve with arbitrary origin at 0. Line AC gives peak height h and line AB is the locus of the midpoint between the ascending and descending portions of the curve. The mode is given by point C. To a first approximation the mean or vertical bisector EDF of the area can be obtained from the half height, GDH, at its intersection, D, of line AB, thus, an approximate skewness, Sk, is given by

$$[9] \qquad Sk = \frac{OE-OC}{\sigma} = \frac{EC}{\sigma} \quad \text{or} \quad \frac{\frac{1}{2}BC}{\sigma}.$$

If the distance BC is less than σ the error of this estimate of the mean is negligible.

The distance BC cannot exceed 1.66σ for any curve which satisfies the conditions of a straight line for the midpoint locus, AB, or a constant value for σ at various points on the curve. Thus, the skewness, Sk, which can be treated, will be -0.83 to $+0.83$ (using the approximate mean derived from the above construction).

(*a*) *Area of isolated asymmetrical peaks.*—As may be seen from Fig. 7, the areas of the symmetrical and the asymmetrical peaks are virtually identical. The area may therefore be calculated from equation [3] where $h = AC$ (Fig. 7).

(*b*) *Area of overlapping asymmetrical peaks.*—If two peaks, only one of which is skewed, overlap, the area of the asymmetrical peak can be calculated using the corrections for the contribution of the symmetrical peak to the peak height of the other as described in the previous section.

The correction for the contribution of an asymmetrical peak to the height of either a symmetrical or skewed peak is more complicated and requires a series of successive approximations. In the remainder of this section, points and lines referred to are taken from Fig. 7. The distance between the peaks is measured in terms of the σ of the asymmetrical peak from the midpoint of the base line (point B) rather than from the mode (point C) to the mode of the second peak. The ordinate, Y, of the curve at the distance x can be calculated in the same way as for a symmetrical peak. The intersection of this height Y with the midpoint locus (line AB) is determined, and a new value for the distance x is measured from this point to the mode of the second peak. The height, Y, is recalculated using the corrected distance, and the entire operation is repeated if necessary.

These corrections, after the successive approximations, are given in terms of percentage of the interfering peak for various values of skewness, Sk, in Table I. The distance x between peaks is given in terms of σ of the interfering peak measured from the midpoint locus intersection with the base line (point B) to the mode of the peak under consideration. The corrections to be applied for symmetrical peaks ($Sk = 0$) have also been plotted on probability paper in Fig. 4.

DISCUSSION

The calculation for area using this method eliminates the subjective errors of construction in the triangulation method or of cutting in the paper weighing method. It is a

Can. J. Chem. Downloaded from www.nrcresearchpress.com by 210.87.254.42 on 09/05/12
For personal use only.

Can. J. Chem. Downloaded from www.nrcresearchpress.com by 210.87.254.42 on 09/05/12
For personal use only.

TABLE I

Peak height corrections[a] in percentage of peak height of interfering peak

Distance[c] between peaks	Skewness[b]																
	0.83	0.70	0.60	0.50	0.40	0.30	0.20	0.10	0.0	0.10	0.20	0.30	0.40	0.50	0.60	0.70	0.83
	Gently sloping side of curve									Steeply sloping side of curve							
2.0	9.7	10.2	10.4	10.8	11.2	11.7	12.3	12.8	13.5	14.4	15.2	16.3	17.5	19.4	22.2	26.0	Very large
2.1	8.2	8.5	8.8	9.1	9.4	9.7	10.1	10.5	11.0	11.6	12.2	12.9	13.6	14.7	16.2	18.6	21.0
2.2	6.8	7.1	7.3	7.5	7.8	8.0	8.3	8.6	8.9	9.3	9.7	10.1	10.6	11.2	12.0	12.9	14.8
2.3	5.7	5.8	6.0	6.1	6.3	6.5	6.7	6.9	7.1	7.4	7.6	7.9	8.2	8.5	8.9	9.4	10.5
2.4	4.6	4.7	4.9	5.0	5.1	5.2	5.4	5.5	5.6	5.8	5.9	6.1	6.2	6.5	6.7	7.0	7.5
2.5	3.8	3.8	3.9	4.0	4.1	4.2	4.3	4.3	4.4	4.5	4.6	4.7	4.8	4.9	5.0	5.2	5.5
2.6	2.9	3.0	3.1	3.1	3.2	3.2	3.3	3.3	3.4	3.4	3.5	3.6	3.7	3.7	3.8	3.9	4.0
2.7	2.3	2.3	2.4	2.4	2.5	2.5	2.5	2.6	2.6		2.6	2.7	2.8	2.8	2.8	2.9	3.0
2.8	1.8	1.8	1.9	1.9	1.9	1.9	2.0		2.0		2.0	2.1	2.1	2.1	2.2	2.2	2.2
2.9	1.4	1.4	1.4	1.4	1.5				1.5			1.5	1.6	1.6	1.6	1.6	1.6
3.0	1.0	1.0	1.1						1.1						1.1	1.2	1.2
3.1	0.8								0.8								0.8
3.2									0.6								
3.3									0.4								
3.4									0.3								
3.5									0.2								
3.6									0.2								
3.7									0.1								
3.8									0.1								
3.9									0.05								
4.0									0.03								

[a]Unfilled spaces, corrections same as center column.

[b]Skewness, $Sk = \frac{1}{2} BC/\sigma$ (see Fig. 7).

[c]Distance measured in terms of σ from midpoint locus intercept with base line of interfering peak to mode of peak being measured.

reasonably rapid procedure for isolated peaks requiring only the measurement of peak height and the determination of σ, either from the chromatogram itself by direct measurement or from a graph similar to Fig. 3 constructed from such measurements. For overlapping peaks the area determination is much less subjective than by any other method, and can be done quickly after practice.

A probability treatment for gas chromatography has been worked out by Sen (8). The values of the position of the peak (here called t_r) and of σ, the standard deviation, are stated to "completely define the distribution curve or the macroscopic behaviour of the column". Difficulty is frequently encountered in repeating work on two different columns which apparently have been made up identically. The same conditions of flow rate and temperature do not produce the same results due to microscopic differences in packing, etc. With proper manipulation of the adjustable variables, it is possible to reproduce the probability and distribution of successes, that is, curves with the same t_r and σ. This should be aimed at, rather than duplication of flow rate, temperature, etc., since this also corresponds to duplication of the number of theoretical plates, r, for, as pointed out by Schmauch (9),

$$r = \left(\frac{t_r}{\sigma}\right)^2. \qquad [10]$$

Another way of presenting this data is in a plot of σ versus t_r (both in minutes) as given in Fig. 3. By reversing the criteria in the above paragraph, deterioration of the column packing can be detected. Thus, the constancy of the σ versus t_r plot obtained under fixed conditions will indicate that the column is still in its original state.

If a measured value of σ for a given peak falls off the plot of σ versus retention time, two or more compounds have emerged together. Figure 2 gives the plot for a single SAIB column (10) obtained from a large number of chromatograms of peppermint oil. The σ obtained for one peak was invariably well off the curve even though the peak was often reasonably symmetrical. Further investigation showed that two compounds with nearly identical retention volumes were responsible for the wider peak. By a series of successive approximations using equation [3], it was possible to make an estimate of the two areas.

For all calculations in this paper, it has been assumed that the normal distribution curve holds true. Factors affecting the peak shape such as detector volume and sample size have been discussed by Johnson and Stross (11) and others. If both are kept small the curves obtained are sufficiently close to the normal curve for the use of these calculations. The peaks often obtained from highly polar compounds such as water, ammonia, amines, alcohols, etc. are too badly skewed to treat by calculations in this paper.

Using these calculations it is possible to obtain a great deal of information from chromatograms with incompletely resolved peaks. Thus it may be unnecessary to use long columns, a variety of packings, or long elution times to complete a difficult analysis.

SYMBOLS USED

A = area.
h = peak height.
r = number of theoretical plates.
t_r = time between introduction of the sample and the peak emergence.
w = peak width at any specified height.
x = distance from a peak center measured in units of its σ.
Y = the ordinate of the curve at a distance x from peak center.
Z = the special case of Y when $A = 1$.
σ = standard deviation.

Can. J. Chem. Downloaded from www.nrcresearchpress.com by 210.87.254.42 on 09/05/12
For personal use only.

ACKNOWLEDGMENTS

The authors wish to thank Mr. J. M. Airth and Dr. Leo Levi, of this Directorate, for valuable discussion and criticism during the development of the method.

REFERENCES

1. A. I. M. KEULEMANS. Gas chromatography. Reinhold Publishing Corp., New York. 1957. p. 32.
2. A. I. M. KEULEMANS. Gas chromatography. Reinhold Publishing Corp., New York. 1957. p. 111.
3. A. KLINKENBERG and F. SJENITZER. Chem. Eng. Sci. **5**, 258 (1956).
4. D. W. GRANT and G. A. VAUGHAN. J. Appl. Chem. **10**, 181 (1960).
5. C. H. GOULDEN. Methods of statistical analysis. 2nd ed. John Wiley and Sons Inc., New York. 1952. p. 30.
6. BIOMETRIKA TABLES FOR STATISTICIANS. Vol. 1. Cambridge University Press, London. 1954. p. 104.
7. K. PEARSON. *In* Methods of statistical analysis. 2nd ed. C. H. Goulden. John Wiley and Sons Inc., New York. 1952. p. 33.
8. B. SEN. Anal. Chim. Acta **22**, 130 (1960).
9. L. J. SCHMAUCH. Anal. Chem. **31**, 225 (1959).
10. D. M. SMITH, J. C. BARTLET, and L. LEVI. Anal. Chem. **32**, 568 (1960).
11. H. W. JOHNSON and F. H. STROSS. Anal. Chem. **31**, 1206 (1959).

Can. J. Chem. Downloaded from www.nrcresearchpress.com by 210.87.254.42 on 09/05/12
For personal use only.

Can. J. Chem. Downloaded from www.nrcresearchpress.com by 210.87.254.6 on 09/05/12
For personal use only.

SOLVENT EFFECTS AS AN AID IN THE ANALYSIS OF THE PROTON MAGNETIC RESONANCE SPECTRUM OF VINYL BROMIDE[1]

T. SCHAEFER[2] AND W. G. SCHNEIDER

ABSTRACT

By making use of specific solvent effects it has been possible to vary the relative chemical shift between the *geminal* protons of vinyl bromide from about +10 cycles/sec to −4 cycles/sec (at 60 Mc/sec) and to study the resultant changes in the proton resonance spectrum in the limiting region of zero chemical shift. Of particular interest is the growth and displacement of the combination lines, which appear in the resonance signals of the proton bonded to the same carbon atom as the bromine. From the variation of the six possible lines in this region it was confirmed that the *cis* and *trans* proton coupling constants must have the same sign. The intensity distribution of the lines in the *geminal* proton region require the *geminal* coupling constant to be of opposite sign to the other two.

INTRODUCTION

Recent studies of specific solvent interactions (1) have shown that, within limits, it is possible to vary the relative chemical shifts of protons in certain molecules in a continuous and controlled manner by altering the solvent conditions. This provides a very useful aid in arriving at an assignment and analysis of the proton spectrum, as well as a convenient method of studying the pronounced changes of the spectrum in the limit as the relative chemical shift is progressively reduced to zero. Solvent-induced shifts of this kind are generally observed for unsaturated molecules containing a strongly electronegative or electropositive substituent (1). Vinyl bromide, CH_2:CHBr, chosen for the present work, fulfills these conditions. Its proton spectrum is typical of a three-spin system and has been discussed by several authors (2, 3, 4, 5). Depending on the relative proton chemical shifts such spectra may be classed as ABX, ABC, or AB_2 types and are observed in the resonance spectra of many common molecules (2, 4, 5, 6, 7). In general vinyl compounds belong to the type ABC when observed at a measuring frequency of 40 Mc/sec, and usually also at 60 Mc/sec, although a rough analysis is often possible on the basis of an ABX type (8).

Lately it has become a matter of theoretical interest to determine, if not the absolute sign, at least the relative signs of the three coupling constants involved (9, 10, 12). Theory indicates that if the coupling constant is small between protons it may be negative, whereas if it is large it is probably positive (12). The coupling constant between the *geminal* protons in vinyl compounds is small, about 0 to 2 cycles/sec. The *trans* coupling constant is over 10 cycles/sec and often over 15 cycles/sec as compared with about 5 to 10 cycles/sec for the *cis* coupling constant (8). An exact analysis of the proton spectrum involves a numerical solution of the case ABC. This has been done for a number of vinyl compounds by means of a computer (11, 12). In particular, the proton spectrum of vinyl bromide requires the *cis* and *trans* coupling constants to be of the same sign but of opposite sign to the *geminal* coupling constant, the latter being small and presumably negative.

It is the purpose of the present work to present an experimental method for the determination of the relative signs of the *cis* and *trans* coupling constants in vinyl

[1]*Manuscript received June 21, 1960.*
Contribution from the Division of Pure Chemistry, National Research Council, Ottawa, Canada.
Issued as N.R.C. No. 5953.
[2]*Research Associate, summer 1959. Permanent address: Department of Chemistry, University of Manitoba, Winnipeg, Manitoba.*

bromide and to illustrate the appearance and growth of the combination lines as the relative electronic screening of the protons is changed.

EXPERIMENTAL

Measurements of the proton resonance spectra of vinyl bromide in the pure state and at various concentrations in solvents were made at 60 Mc/sec on a Varian n.m.r. spectrometer. The vinyl bromide was distilled before use and the solvents used were acetone, hexane, and benzene. The concentrations in acetone and hexane were 5 mole% but the solutions in benzene were made up approximately by volume. Since vinyl bromide boils below room temperature the pure substance was contained in a sealed tube. The solutions could be measured in an open tube.

RESULTS AND DISCUSSION

(a) Pure Vinyl Bromide

The observed spectrum of pure vinyl bromide is shown in Fig. 1 together with the proton assignment and the spectrum calculated as an ABC case. The resultant chemical shifts and spin-coupling constants are compared with those derived by Sheppard (11) and by Karplus, Grant, and Gutowsky (12) in Table I. Chemical shifts have been converted to 60 Mc/sec. It should be noted that Sheppard's parameters apply to a 10% solution in carbon tetrachloride.

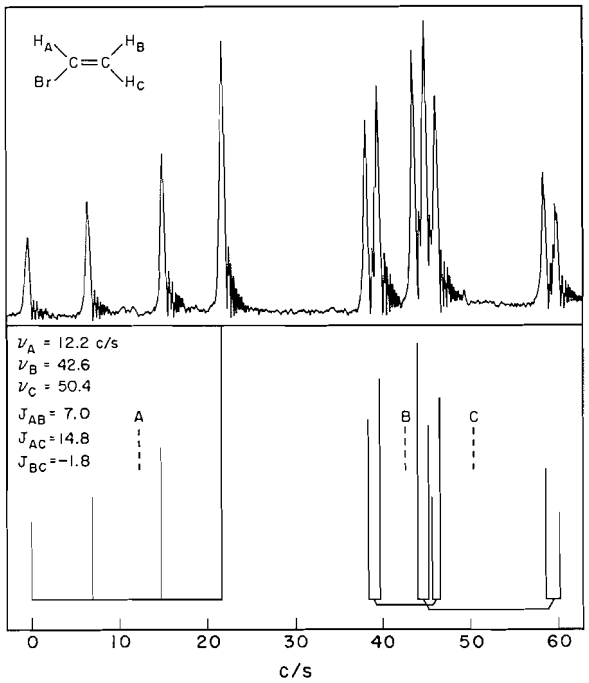


FIG. 1. Observed and calculated proton spectra of vinyl bromide at 60 Mc/sec. Increasing applied field is from left to right.

The opposite signs between J_{BC} and J_{AC} is not obvious from the spectrum at 60 Mc/sec because of the overlap of the two lines at about 45 cycles/sec in the observed spectrum. The relative positions of the lines can be fitted with all coupling constants of the same

Can. J. Chem. Downloaded from www.nrcresearchpress.com by 210.87.254.6 on 09/05/12
For personal use only.

TABLE I

Chemical shifts and spin-coupling constants (in cycles/sec) of pure vinyl bromide

	Sheppard,* cycles/sec	Karplus *et al.*, cycles/sec	This paper, cycles/sec
$\nu_C-\nu_B$†	7.3	8.1	8.1
$\nu_C-\nu_A$†	36.2	36.2	38.0
J_{AB}	7.1	6.9	7.0
J_{AC}	15.0	14.3	14.8
J_{BC}	−1.7	−1.8	−1.8

*10% in CCl_4.
†At 60 Mc/sec; notation of Fig. 1.

sign and with slight changes in the values of the parameters. However, at 40 Mc/sec there is no overlap and from the intensity distribution of the lines the other workers deduced the correct sign relationship. It is actually the pair of B lines at high field which decides the matter. In many of the spectra in Fig. 3 it is clear that in this pair the line at low field is much weaker than its neighbor. J_{BC} must be of opposite sign to J_{AC} and J_{AB} if this situation is to be met, together with the right intensities for the other lines arising from transitions of protons B and C.

(b) Relative Signs of J_{AB} and J_{AC}

Considerable labor is involved in the determination of the relative signs of the coupling constants even if a computer is available. It would be of value if there were a way of deciding, before the numerical work is begun, which of the coupling constants have the same sign. An examination of the spectra in Fig. 3 below suggests such a possibility. Note, first, that the most widely separated lines in the A region maintain a constant separation even though $\nu_C-\nu_B$ changes from positive to negative values. Then consider the line separations for the corresponding region for the case XBC given below in Part (*c*) (see also p. 134 of reference 7). One pair of lines (1 and 4 below) is separated by $|J_{AB}+J_{AC}|$ and since coupling constants are independent of chemical shift* this pair of lines should maintain a constant separation as $\nu_C-\nu_B$ is varied. If the line positions (as compared with the line intensities) of the vinyl bromide spectrum approximate sufficiently closely to an XBC spectrum, it follows that the pair of lines maintaining a constant separation in the A region of the observed spectra (X region in the case XBC) must be spaced by $|J_{AB}+J_{AC}|$. Evidently this is the case. In the seven spectra in Figs. 2 and 3 the two outside lines in the A region have a separation of between 21.7 and 22.2 cycles/sec (the variation can be attributed to experimental error and to the fact that we are really dealing with the case ABC). The other lines in the A region vary greatly in position as $\nu_C-\nu_B$ changes.

Hence $|J_{AB}+J_{AC}| \approx 22$ cycles/sec and if J_{AB} and J_{AC} are both less than 22 cycles/sec in magnitude, as seems clear, they must have the same sign. This fact reduces the four possible sign permutations in the three-spin system to two. If, in addition, the change in intensity distribution of the lines in the 40 cycles/sec region with change in $\nu_C-\nu_B$

It is, of course, well known that the chemical shift is directly proportional to the applied magnetic field while the coupling constants are independent of the latter. However, when the relative *electronic shielding of protons in a solute molecule is changed rather drastically by perturbations from solvent molecules, it is not inconceivable that the coupling constants will change somewhat because of a "selective perturbation" of the various bonds in the solute molecule. Experiments along these lines are being made.*

Can. J. Chem. Downloaded from www.nrcresearchpress.com by 210.87.254.6 on 09/05/12
For personal use only.

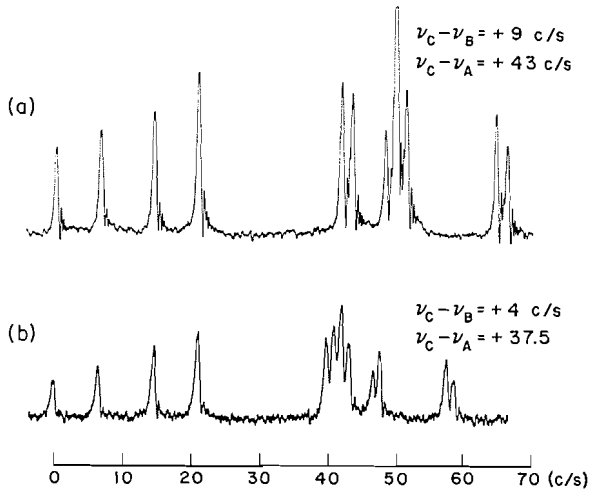


FIG. 2. Proton resonance spectrum of 5 mole% solution of vinyl bromide in (*a*) acetone and (*b*) *n*-hexane.

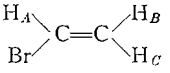
is taken into account, an a priori sign permutation can be arrived at by inspection of solvent effects on the spectrum.

(c) Combination Lines

The manner in which the relative chemical shifts of the protons in vinyl bromide are altered in different solvents is illustrated by the results shown in Table II. The

TABLE II

Proton chemical shifts of vinyl bromide in various solvents: concentration, 5 mole% (in cycles/sec at 60 Mc/sec, relative to external $CHCl_3$, and corrected for differences in bulk susceptibility)



Solvent	Chemical shift (cycles/sec)			
	Proton *A*	Proton *B*	Proton *C*	$\nu_C-\nu_B$
Benzene	114	149	145	−4
n-Hexane	62.5	96	100	+4
Acetone	48	82	91	+9

nature of these solvent effects has been discussed elsewhere (1, 14, 15). Figure 2 shows the proton resonance spectra of vinyl bromide in acetone and hexane solutions and Fig. 3 shows the corresponding spectra for different concentrations of vinyl bromide in benzene. The relative chemical shifts of protons H_B and H_C are roughly indicated. As $\nu_C-\nu_B$ becomes small enough, two extra lines appear in the A region (Fig. 3(*a*)). As $\nu_C-\nu_B$ is further decreased and made negative they approach one another in position, coalesce, and then separate again (Figs. 3(*b*)–3(*e*)). For purposes of discussion it is appropriate to consider this region of the spectrum as the X region of an XBC spectrum. The exact (ABC) calculation in Fig. 1 agrees well with the approximate XBC calculation

Can. J. Chem. Downloaded from www.nrcresearchpress.com by 210.87.254.6 on 09/05/12
For personal use only.

Can. J. Chem. Downloaded from www.nrcresearchpress.com by 210.87.254.6 on 09/05/12
For personal use only.

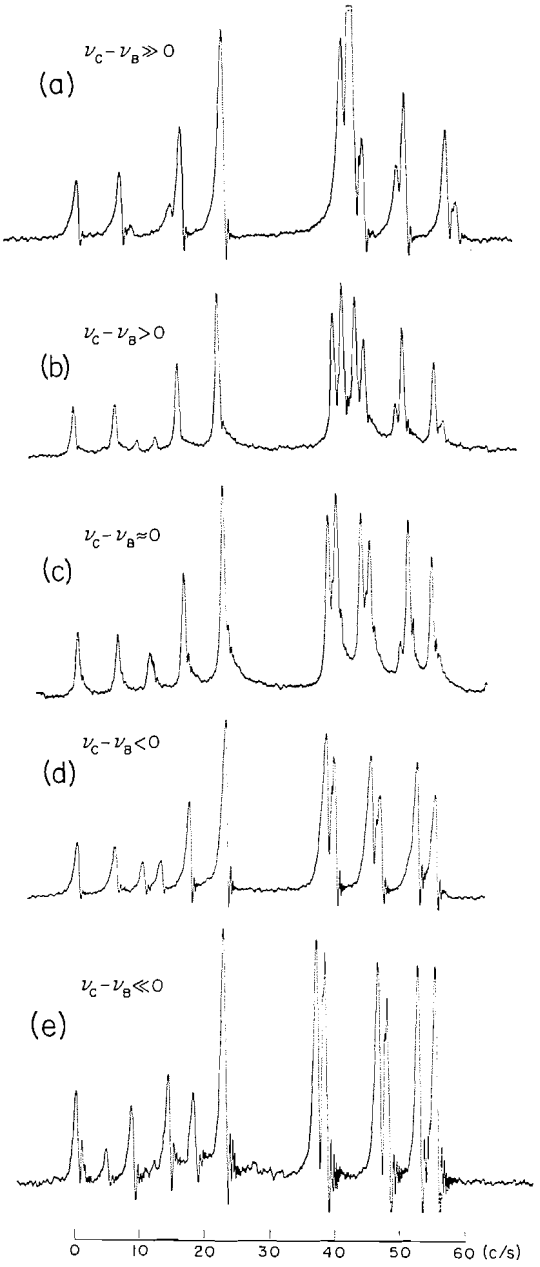


FIG. 3. Proton resonance spectrum of vinyl bromide at various concentrations in benzene. Approximate ratios (by volume) of vinyl bromide to benzene in the solutions are as follows: (*a*) 1:1, (*b*) ~2:3, (*c*) ~1:2, (*d*) ~1:3, (*e*) ~1:20.

in the prediction of the line *positions* in this region of the spectrum. The comparison in Fig. 5 between one of the observed spectra and the spectrum calculated using the parameters indicated is intended to show that the position of the predicted combination lines again agrees well with the *XBC* prediction. There is some disagreement in other

line positions but this only means that the chemical shifts employed in the calculated spectrum are not quite correct: the shift between protons B and C is no doubt not quite zero.

In the present notation the six transitions in the X (or A) region are then written relative to the origin of the lines as:

	Energy	Relative intensity
1.	$-\frac{1}{2}(J_{AB}+J_{AC})$	1
2.	D_+-D_-	$\cos^2(\phi_+-\phi_-)$
3.	$-D_++D_-$	$\cos^2(\phi_+-\phi_-)$
4.	$\frac{1}{2}(J_{AB}+J_{AC})$	1
5.	$-D_+-D_-$	$\sin^2(\phi_+-\phi_-)$
6.	D_++D_-	$\sin^2(\phi_+-\phi_-)$

The positive quantities D_+, D_- and angles ϕ_+, ϕ_- are defined by

$$D_+ \cos 2\phi_+ = \tfrac{1}{2}(\nu_C-\nu_B)+\tfrac{1}{4}(J_{AB}-J_{AC}),$$
$$D_+ \sin 2\phi_+ = \tfrac{1}{2}J_{BC},$$
$$D_- \cos 2\phi_- = \tfrac{1}{2}(\nu_C-\nu_B)-\tfrac{1}{4}(J_{AB}-J_{AC}),$$
$$D_- \sin 2\phi_- = \tfrac{1}{2}J_{BC}.$$

In these expressions $\nu_C-\nu_B$ has the same meaning as in the discussion above, namely, the relative chemical shift between protons C and B in cycles per second.

On this energy level scheme lines 1 and 4 are independent of $\nu_C-\nu_B$ and they are the lines at 0 and about 22 cycles/sec in the observed spectra. The predicted intensities are clearly wrong but they are much more sensitive to the correct wave functions than are the line positions and the main points of the discussion will still be valid.

Figure 4 gives a plot of the energy levels when $\nu_C-\nu_B$ is varied from 10 to 0 cycles/sec with J_{AB} = 7.0, J_{AC} = 14.8, J_{BC} = −1.8 cycles/sec. The plot as $\nu_C-\nu_B$ varies from 0 to −10 cycles/sec is the mirror image of Fig. 4. The combination lines 5 and 6 reach

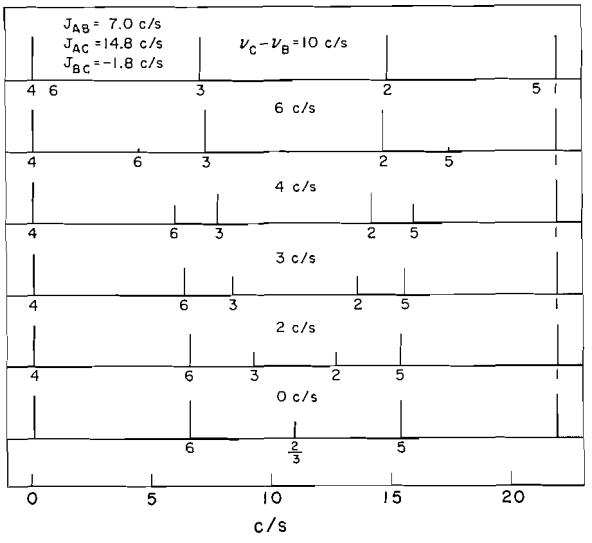


FIG. 4. The X part of an XBC spectrum calculated with the spin-coupling constants given and various values of the relative chemical shift $\nu_C-\nu_B$.

Can. J. Chem. Downloaded from www.nrcresearchpress.com by 210.87.254.6 on 09/05/12
For personal use only.

a measurable intensity for the given values of the coupling constants when $\nu_C - \nu_B$ is in the region of 5 cycles/sec. They derive this intensity at the expense of lines 2 and 3 (at about 7 and 15 cycles/sec in Fig. 1). When $\nu_C - \nu_B$ becomes less than 5 cycles/sec, lines 5 and 6 become effectively A lines. When $\nu_C - \nu_B = 0$, lines 2 and 3 coalesce, as is clear from the definitions of D_+ and D_-, and are in effect combination lines. When $\nu_C - \nu_B$ becomes less than zero, lines 2 and 3 separate and recede and eventually become A lines again, while 5 and 6 once more take on the role of combination lines. The sign of J_{BC} does not affect the predicted intensities.*

In the observed spectra this course of events is not followed exactly but is clearly similar. The combination lines arise at about the same value of $\nu_C - \nu_B$ (Fig. 3(a)) and coalesce when $\nu_C - \nu_B \approx 0$ (Fig. 3(c) and Fig. 5). The intensity distribution is, however,

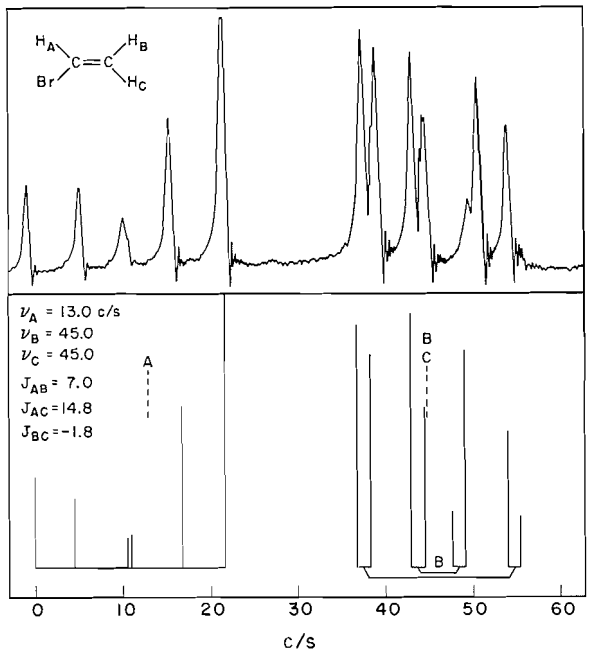


FIG. 5. The observed and calculated spectrum of vinyl bromide diluted in benzene. The spectrum was calculated as an XBC type with $\nu_C - \nu_B = 0$.

not in agreement with the XBC calculation. When $\nu_C - \nu_B$ becomes less than zero the effective combination lines are receding in the direction from which they appeared and have decreased in intensity.† The solvent effects are not large enough to eliminate them entirely.

**It should perhaps be noted that it is only when $\frac{1}{2}|J_{BC}| \approx \frac{1}{4}|J_{AB} - J_{AC}|$ that the combination lines have a large predicted intensity. This is immediately clear from the definitions and expressions for the intensities above. If, on the other hand, $|J_{BC}| \gg |J_{AB} - J_{AC}|$ the predicted spectrum would in effect be one of three equally spaced lines when $\nu_C - \nu_B = 0$. These lines would have the intensity ratio 1:2:1 and this could lead to a wrong determination of coupling constants. Such an effect has been discussed and illustrated with actual spectra for p-fluorotoluene (13).*

†In Fig. 3(e) the couplings between C^{13} and H^1 nuclei in the benzene solvent produce a "hump" in the 15–20 cycles/sec region of the spectrum and obscure the true intensity relations of the lines. This effect could be eliminated by using the expensive C_6D_6 as a solvent.

Can. J. Chem. Downloaded from www.nrcresearchpress.com by 210.87.254.6 on 09/05/12
For personal use only.

REFERENCES

1. T. SCHAEFER and W. G. SCHNEIDER. J. Chem. Phys. **32**, 1218, 1224 (1960).
2. W. A. ANDERSON. Phys. Rev. **102**, 151 (1956).
3. M. K. BANERJEE, T. P. DAS, and A. K. SAHA. Proc. Roy. Soc. A, **226**, 490 (1954).
4. H. S. GUTOWSKY, C. H. HOLM, A. SAIKA, and G. A. WILLIAMS. J. Am. Chem. Soc. **79**, 4596 (1957).
5. H. J. BERNSTEIN, J. A. POPLE, and W. G. SCHNEIDER. Can. J. Chem. **35**, 65 (1957).
6. R. E. RICHARDS and T. SCHAEFER. Mol. Phys. **1**, 331 (1958).
7. J. B. LEANE and R. E. RICHARDS. Trans. Faraday Soc. **55**, 707 (1959).
8. J. A. POPLE, W. G. SCHNEIDER, and H. J. BERNSTEIN. High resolution nuclear magnetic resonance. McGraw-Hill Book Co., Inc., New York. 1959. Chap. 2.
9. M. KARPLUS. J. Chem. Phys. **30**, 11 (1959).
10. H. M. MCCONNELL. J. Chem. Phys. **30**, 126 (1959).
11. N. SHEPPARD. Private communication.
12. M. KARPLUS, D. GRANT, and H. S. GUTOWSKY. ONR Report No. 17, University of Illinois. 1959.
13. T. SCHAEFER and W. G. SCHNEIDER. Can. J. Chem. **37**, 2078 (1959).
14. A. D. BUCKINGHAM. Can. J. Chem. **38**, 300 (1960).
15. A. D. BUCKINGHAM, T. SCHAEFER, and W. G. SCHNEIDER. J. Chem. Phys. **32**, 1227 (1960).

Can. J. Chem. Downloaded from www.nrcresearchpress.com by 210.87.254.6 on 09/05/12
For personal use only.

Can. J. Chem. Downloaded from www.nrcresearchpress.com by 210.87.254.6 on 09/05/12
For personal use only.

SOME FACTORS AFFECTING THE ZONE MOBILITY OF INORGANIC IONS DURING ELECTROMIGRATION IN PAPER[1]

R. A. BAILEY[2,3] AND L. YAFFE

ABSTRACT

A number of factors which affect the zone mobilities of inorganic ions were investigated. The influence of temperature was that expected from its effect on the conductance in free solution. The zone mobility tends to decrease, and the zone size to increase, with increasing migrant concentration. Excess foreign ions in the initial migrant zone can have a similar result. Experiments in the presence of the swelling agent thiourea indicate that swelling has at least a constant and perhaps a negligible influence on the obstructive factor. Finally, variation of the zone mobility with paper type was considered in relation to the ion-exchange capacity. Of the ions studied, only copper showed any correlation. Some observations were made using ion-exchange papers.

INTRODUCTION

The study of the electromigration of ions in moist paper has received considerable attention from the point of view of a separatory technique, but comparatively little has been done to try to understand the interactions between the ions and the porous supporting medium in this process. It is well known that many physical variables affect the zone mobility. However, very little work, aimed at investigating these variables thoroughly, has appeared. This paper will attempt to show quantitatively the effects of some of these variables with regard to inorganic ions.

The following are the factors which can have a direct influence on the zone mobility of an ion in paper.

1. Temperature

Since the conductance in free solution (and hence the mobility) of an ion increases with increasing temperature, a similar effect should be expected for the mobility in paper. This has been found by a few workers (1, 2, 3). Although the mobility values actually obtained may be questionable, the temperature coefficient seems to be similar in free solution and in paper, or about 2% per degree centigrade.

2. Absorbance

As the absorbance (the volume of liquid present per gram of paper) increases, so does the zone mobility. This factor was considered in a previous paper (4).

3. The Nature of the Supporting Medium

The zone mobility varies with the supporting medium, even when two papers are compared at corresponding values of absorbance. Although some effects might result from different fiber structure, this should be small, at least as long as only cellulose papers are considered. Most of the influence is more probably due to specific interactions of the ions with paper itself. This in turn could be different for various papers because of differences in the manufacturing process. In particular, the number of carboxyl groups which are present, and which can take part in ion-exchange reactions with the migrant ions, may differ from paper to paper. The fact that acid-washed paper yields larger

[1]*Manuscript received June 3, 1960.*
Contribution from the Radiochemistry Laboratory, Department of Chemistry, McGill University, Montreal, Que., with financial assistance from the National Research Council of Canada.
[2]*Holder of National Research Council Studentships, 1957–58, 1958–59, and 1959–60.*
[3]*Present address: Department of Chemistry, University College, University of London, London, England.*

values of zone mobility than the same paper without acid washing (3, 5) has been interpreted as implying that exchange processes are important. Exchange presumably takes place more readily between the migrant cation and the metal cation impurity than between the migrant ion and the hydrogen ion which would be on the carboxyl group in the absence of impurities. Examples of the effect of ion-exchange capacity will be shown later.

4. The Concentration and Composition of the Migrant Solution

The concentration of the migrant solution itself can have an effect on the resulting migration, but most studies on this have taken place in complex-forming media. Miller (6), Sato (7), and Strain (8) claimed that if the migrant ion is not adsorbed, the zone mobility is independent of the concentration unless this is greater than that of the background electrolyte solution. When it is greater, the size of the spot increases markedly, and the zone mobility decreases. In cases where small amounts of the migrant are strongly adsorbed by the paper, an increase in migrant concentration may result in an increased over-all mobility because of the more rapid motion of the non-adsorbed part. Such cases usually exhibit trailing. The increase in size of the zone when the migrant concentration exceeds that of the background electrolyte has been noted many times, and has been predicted theoretically by Edward (9).

The actual composition of the migrant solution apart from its concentration may be important also, since interactions between the components may give rise to their anomalous behavior. This may be an effect of ionic strength, or a specific chemical interaction, but the latter need not concern us here.

5. The Background Electrolyte Solution

The ionic strength and viscosity of the background electrolyte solution can affect the mobility of an ion moving in it. This will occur in free solution as well as in paper, as was brought out in a previous communication (4) where the calculation of zone mobilities was discussed. A more important effect of the background solution lies in its ability to form complexes with the migrant ions. If complexing occurs, the mobility observed will depend on the stability of the complex formed, as well as on the mobility of the complexed and non-complexed species present. It can be calculated in principle.

Berbalk and Schier (10) showed that the zone mobility of a weakly dissociated substance such as a weak acid depends on its degree of dissociation b. The zone mobility is given by

$$U_z = b\rho U_F \qquad [1]$$

where ρ is a factor for the slowing of the ions by the paper, and U_F is the actual speed of the ion formed by dissociation. For a weak acid, for example, this could be determined from the limiting conductance of the anion. Equation [1] is equivalent to the statement that the zone mobility is given by the speed of the mobile form and the fraction of time which the migrant spends in that form.

We can extend this to complex-forming systems where a number of mobile species are present in a rapid dynamic equilibrium. In the simplest case, suppose the forms present are M_1 and M_2, and the fraction of the migrant present as M_1 is b_1, and as M_2 is $b_2 = 1-b_1$. If the mobilities in free solution are U_{F_1} and U_{F_2}, respectively, then

$$\begin{aligned} U_z &= \rho[b_1U_{F_1}+b_2U_{F_2}] \\ &= \rho[b_1(U_{F_1}-U_{F_2})+U_{F_2}] \end{aligned} \qquad [2]$$

Can. J. Chem. Downloaded from www.nrcresearchpress.com by 210.87.254.6 on 09/05/12
For personal use only.

if we neglect specific adsorption effects. If n species are present,

$$[3] \qquad U_z = \rho\left[\sum_{i=1}^{n} b_i U_{F_1}\right].$$

This takes into account adsorbed and non-ionized forms, since for these $U_F = 0$.

In practice, values of b and the free solution mobility of complex species usually are not known, so that this equation cannot be used to estimate the zone mobility. However, if more were known about ρ, this treatment might provide a means of obtaining information about the stabilities of complexes.

Extraneous factors such as evaporation and flow of background electrolyte solution in the strip can affect the zone mobility very much. Unless such factors are eliminated or corrected for, the zone mobilities obtained have no meaning. The chief factors of this sort which may be encountered are electroosmotic flow of electrolyte solution, flow of electrolyte from the ends toward the center of the strip (due to either evaporation from the strip or initial unsaturation of it), changes in concentration of electrolyte in the strip due to evaporation and non-uniform absorbance. These are problems of experimental technique.

From a very simple model (11) it can be shown that the zone mobility U_z may be given by the expression

$$[4] \qquad U_z = \rho U_F$$

where U_F is the mobility in free solution, and ρ is the obstructive factor which accounts for the tortuous path followed by a particle migrating through a medium such as wet paper. If adsorption effects are neglected, a semiempirical expression can be deduced for the obstructive factor (4, 12). For fibers which do not swell in the presence of the solution, this is

$$[5] \qquad \rho = \alpha\left(\frac{a}{a+v_s}\right) = \alpha\epsilon$$

where a is the absorbance, v_s is the specific volume of the fibers, and ϵ is the void fraction or porosity. Here, α is a constant equal to 0.96. For fibers which do swell,

$$[6] \qquad \rho = \alpha\left(\frac{a-2v_sX}{a+v_s}\right)$$

where X is the fractional increase in volume on swelling. The latter expression would be expected to apply to cellulose papers in aqueous solution, but X is not known.

We may define an apparent obstructive factor

$$[7] \qquad \rho_{app} = \frac{U_z}{U_F}.$$

The term ρ_{app} includes all factors which tend to slow an ion moving through a porous medium—adsorption as well as mechanical obstruction. This gives a means of comparing the hindrance encountered by different ions moving under various conditions.

If r represents an adsorption or hindrance factor,

$$[8] \qquad \rho_{app} = r\rho$$

where ρ is the mechanical obstructive factor calculated from equation [5] or [6]. For a given paper, r may vary with the migrant and the background electrolyte. In effect, r represents the fraction of time during which the ion is free to move.

Can. J. Chem. Downloaded from www.nrcresearchpress.com by 210.87.254.6 on 09/05/12
For personal use only.

Attempts have been made to account for adsorption effects by means of the chromatographic R_f factor, which is defined as

$$R_f = \frac{\text{distance moved by zone of substance}}{\text{distance moved by advancing solvent front}}.$$

This was used by Yasunaga and Shimomura (13) and Pucar and Jakovac (14). Since the conditions in paper chromatography and electromigration are not the same, and since the R_f factor is notoriously variable with minor changes in experimental technique, this is not satisfactory. An approach by Maki (15) based on partition chromatography is of interest, but it has not been sufficiently tested. Thus, although there are available a few values of ρ_{app} obtained under conditions such that all of the variables concerned were fixed (4), there is as yet no independent means of obtaining a value for r even if ρ can be calculated.

EXPERIMENTAL

A closed strip technique was used in which the paper was placed between metal plates and kept at a constant temperature. The paper was moistened to the desired absorbance by means of a pipette. Electrodes were placed in direct contact with the paper, and the electrolytic products were prevented from entering the central part of the strip by having suitable buffer solutions at the ends. Normally, no motion of background electrolyte could be detected.

Radioactive migrants were detected by measuring 1-cm broad segments of the strip with a Geiger counter, while inactive migrants were located by suitable chemical means. The migrant concentrations were very low, and small volumes were used. With inactive materials, 10 microliters of 0.001 M solution were used. The concentrations of the radioactive solutions were much lower.

Complete details of the technique and apparatus are given in a previous publication (4).

RESULTS AND DISCUSSION

The variation of zone mobility with temperature in several systems is illustrated in Fig. 1. The effect is that expected from the variation of the conductance. The temperature coefficient over the range 25° C to 39° C is about 2% per degree centigrade in all cases except that of Cu(II) moving in an oxalic acid background electrolyte solution. Here, the copper is present as a negatively charged complex. The increase in zone mobility (expressed as a negative number since the motion is anionic) is only 1.6% per degree centigrade, appreciably less than in the other examples. This would be the expected behavior if the complex were less stable at higher temperatures. There seems to be no change in the interaction of the ions with the paper over this temperature range. In those cases for which U_F could be found, the value of ρ_{app} did not change with temperature. This is shown in Table I.

The effect of migrant concentration was studied for Na^+ in 2.36 M acetic acid. The results are shown in Figs. 2 and 3. The first of these shows that the zone mobility decreases with increasing migrant concentration. This decrease is linear with the square root of the concentration, at least as long as this is greater than the ionic strength of the background electrolyte. In Fig. 3, the size of the zone relative to that given by 'carrier-free' Na^+ also yields a plot which is linear with the square root of the Na^+ concentration in this region.

Can. J. Chem. Downloaded from www.nrcresearchpress.com by 210.87.254.6 on 09/05/12
For personal use only.

Can. J. Chem. Downloaded from www.nrcresearchpress.com by 210.87.254.6 on 09/05/12
For personal use only.

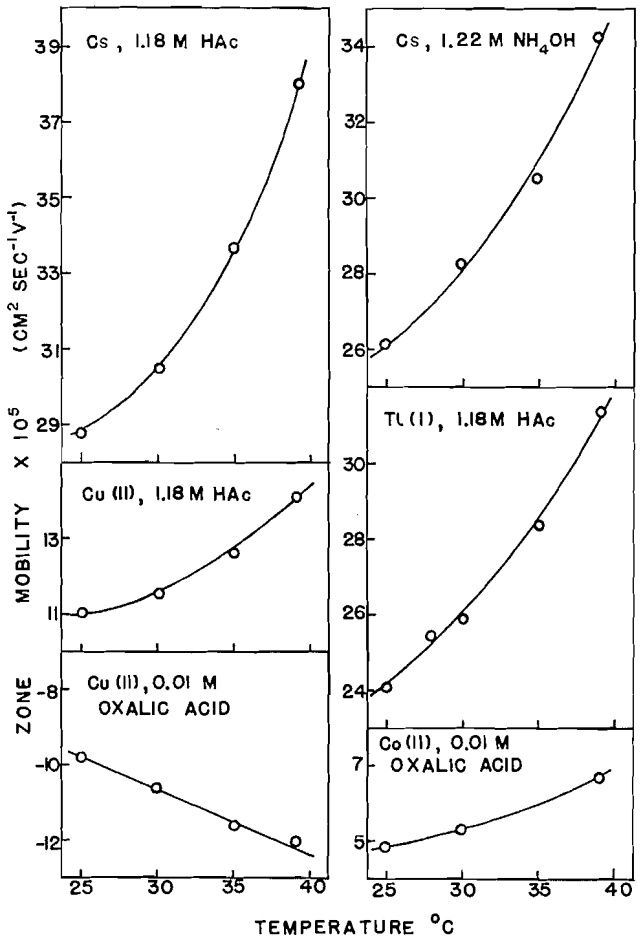


FIG. 1. Zone mobility vs. temperature for several ions in various background electrolytes; absorbance 0.96 ml/g, Whatman No. 52 paper.

TABLE I

Effect of temperature on zone mobility and apparent obstructive factor for Cs^+

Background electrolyte	Temperature, °C	U_z, $cm^2\ v^{-1}\ sec^{-1} \times 10^5$	ρ_{app}
1.18 *M* acetic acid	25	28.8	0.43
	30	30.5	0.42
	35	33.7	0.42
	39	38.0	0.42
1.22 *M* NH_4OH	25	26.1	0.35
	30	28.2	0.35
	35	30.5	0.35
	39	34.3	0.36

Further results on the variation of zone size with migrant concentration are shown in Table II. In both sodium and potassium acetate background solutions, the zone size

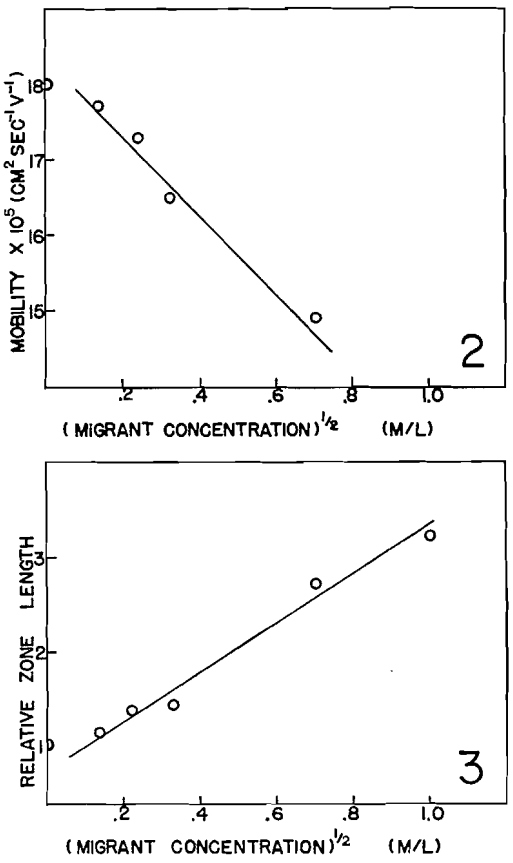


FIG. 2. Zone mobility vs. the square root of the migrant concentration for Na^+ in 2.36 *M* acetic acid; absorbance 0.96 ml/g, Whatman No. 52 paper, 25.0±0.5° C.

FIG. 3. Relative zone length vs. the square root of the migrant concentration for Na^+ in 2.36 *M* acetic acid; absorbance 0.96 ml/g, Whatman No. 52 paper, 25.0±0.5° C.

TABLE II

Variation of size of zone with initial concentration of migrant solution

Background electrolyte solution	Zone length (cm) with initial Na^+ concentration of:		
	0 *M**	0.005 *M*	0.025 *M*
0.005 *M* sodium acetate	4.0	4.0	5.8
0.01 *M* sodium acetate	2.5	2.5	4.5
0.005 *M* potassium acetate	3.5	4.5	8.5
0.01 *M* potassium acetate	2.5	4.0	7.0

NOTE: Migrant is Na^+ in solution as sodium acetate. Absorbance 0.96 ml/g, Whatman No. 52 paper, 25.0±0.5° C.
*'Carrier-free' solution.

becomes quite large when the concentration of the migrant Na^+ is greater than that of the background.

In Table III, the variation of zone mobility and size when the migration of 'carrier-free' Na^+ was carried out in the presence of increasing amounts of HCl in the initial

Can. J. Chem. Downloaded from www.nrcresearchpress.com by 210.87.254.6 on 09/05/12
For personal use only.

TABLE III

Effect of excess foreign ions present in the initial migrant solution on the zone mobility and zone size of Na^+

Initial concentration of HCl in migrant solution, moles/liter	U_z of Na^+, $cm^2\ v^{-1}\ sec^{-1} \times 10^5$	Relative zone length*
0	20.7	1
0.001	20.7	1.1
0.012	19.9	1.3
0.12	16.7†	2.0

NOTE: Background electrolyte 1.18 *M* acetic acid, absorbance 0.96 ml/g, Whatman No. 52 paper, 25.0±0.5° C.
*Relative to zone length given by 'carrier-free' Na^+ with no HCl present.
†Zone elongated with trailing.

zone is shown. The behavior can be due only to ionic strength effects here, since the moving zone of sodium is freed rapidly from excess H^+ and Cl^- ions. When the HCl concentration is increased to 0.12 *M*, the zone mobility decreases appreciably, while the zone itself becomes longer. Most of this effect is due to a low concentration tail from the main peak, which does not seem to be influenced very much.

Thiourea is a substance which, in aqueous solution, enhances the swelling of cellulose fibers. Determination of values of ρ_{app} in the presence of thiourea accordingly might give some information about the effect of swelling on a migrating ion. Values of ρ_{app} for Cs^+ and Na^+ in 1.18 *M* acetic acid are compared with those in 1.18 *M* acetic acid in 1 *M* thiourea in Table IV. As is evident, there is no increase in hindrance when

TABLE IV

Variation of the apparent obstructive factor in the presence of the swelling agent thiourea

		1.18 *M* acetic acid		1.18 *M* acetic acid in 1 *M* thiourea	
Ion	Paper (Whatman)	U_z, $cm^2\ v^{-1}\ sec^{-1} \times 10^5$	ρ_{app}	U_z, $cm^2\ v^{-1}\ sec^{-1} \times 10^5$	ρ_{app}
Na^+	52	20.7	0.48	21.4	0.51
	31 double thickness	17.3	0.40	18.8	0.45
	3 MM	19.8	0.46	21.4	0.51
Cs^+	52	28.8	0.43	29.1	0.45
	31 double thickness	24.6	0.35	27.2	0.42
	3 MM	27.5	0.41	30.7	0.47

NOTE: Absorbance 0.96 ml/g, 25.0±0.5° C.

thiourea is present for any of the three papers used. There may even be a slight decrease in those which are not hardened. This may be interpreted as indicating that the swelling is accompanied by an increase in the fractional volume of the fibers now permeable to the ions (16, 17), or to reduced adsorption which counteracts the effects of swelling. However, these results are in agreement with those of Vacik *et al.* (18, 19) which indicate that there is no decrease in void fraction, and hence in ρ, with wet (swollen) paper.

The above authors have studied a number of chromatography papers, and for Whatman No. 52, that used for most of our experiments, they found that ϵ, the porosity or void fraction, of the wet paper was 0.74. The value of ϵ calculated from equation [5] is 0.77

Can. J. Chem. Downloaded from www.nrcresearchpress.com by 210.87.254.6 on 09/05/12
For personal use only.

at the appropriate absorbance (2.05 ml/g). Although no value of X is known, any calculation using equation [6] would give a lower value for ρ. A value of X of 0.2, for instance, a reasonable estimate from previous work, would yield a result of 0.68. Values of X determined empirically (4) include adsorption effects as well as swelling. Moreover, the results of these workers indicate that the void fraction of wet paper is greater than that of dry paper, implying that, whatever swelling may occur, it does not decrease the void fraction on a molecular scale, and hence does not contribute to enhanced mechanical hindrance. This is in agreement with the values obtained for ρ_{app} in the presence of thiourea. These data indicate that the mechanical obstructive factor may be calculated reasonably well from equation [5], even for cellulose papers, and the specific effects of adsorption may be taken care of in the hindrance factor r. It remains possible that the fraction of the fibers, permeable to the migrant ions (16, 17), may show some specific nature.

For a given ion and background electrolyte, the zone mobility, and hence also ρ_{app}, may vary with the type of paper used, even if measurements are carried out at the same value of absorbance. Data on this are given in Table V. Of the properties of the

TABLE V

Variation of zone mobility with paper type for several ions

Whatman chromatography paper No.	Exchange capacity, meq/g	U_z, $cm^2\ v^{-1}\ sec^{-1} \times 10^5$				ρ_{app}			
		Cu^{++}	Zn^{++}	Cd^{++}	Na^+	Cu^{++}	Zn^{++}	Cd^{++}	Na^+
7	0.0027	8.4	12.2	11.1	16.5	0.20	0.31	0.30	0.43
52	0.0028	9.0	12.6	11.6	18.1	0.21	0.32	0.32	0.48
42	0.0029	8.2	13.5	11.8	—	0.19	0.34	0.32	—
4	0.0049	9.2	13.5	12.0	—	0.22	0.34	0.33	—
1	0.0056	7.5	10.1	8.5	—	0.18	0.26	0.23	—
20	0.0089	4.9	12.5	11.1	16.9	0.12	0.32	0.30	0.44

NOTE: Background electrolyte 2.36 M acetic acid, absorbance 0.96 ml/g, 25.0±0.5° C.

paper which may influence the mobility of an ion, adsorption by ion-exchange processes seems to be one of the most probable (15, 20). The values of the exchange capacity included in the table were determined by the method of Ultee (21); this is claimed to give a measure of the carboxyl content, and hence the ion-exchange capacity, of the paper. As is evident, the effects on ρ_{app} are very specific. There is no correlation between ρ_{app} and the exchange capacity except in the case of Cu(II). With this ion, ρ_{app} decreases roughly linearly as the exchange capacity increases (Fig. 4). Copper is more hindered than the other ions considered (ρ_{app} is smaller), indicating that more interaction is taking place. It appears that copper undergoes a different type of reaction with the paper and, although this seems to take place with the ion exchange sites, it may not be an ion-exchange process.

Jakovac and Lederer (22) have proposed from electromigration studies that copper, like a few other ions, forms complexes with cellulose. However, evidence indicates that these form with the hydroxyl groups on adjacent carbon atoms, rather than with carboxyl groups which are the chief ion-exchange sites.

Copper is also more hindered than zinc in Reeve Angel 934AH glass fiber filter paper. The zone mobilities and apparent obstructive factors of these ions in acetic acid are given in Table VI; the calculated obstructive factor is 0.86. This is considerably larger

Can. J. Chem. Downloaded from www.nrcresearchpress.com by 210.87.254.6 on 09/05/12
For personal use only.

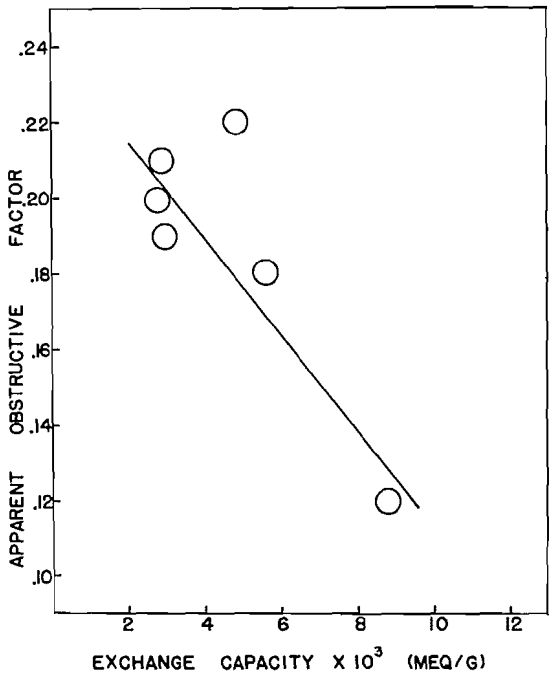


FIG. 4. Apparent obstructive factor vs. exchange capacity of the paper for Cu^{++}; background electrolyte 2.36 *M* acetic acid, absorbance 0.96 ml/g, 25.0±0.5° C.

TABLE VI

Zone mobilities of Cu^{++} and Zn^{++} in Reeve Angel 934AH glass fiber paper in acetic acid background electrolyte

Ion	Concentration of acetic acid, moles/liter	U_z, $cm^2\ v^{-1}\ sec^{-1} \times 10^5$	ρ_{app}
Zn^{++}	0.01	ca. 34	ca. 0.6
	0.12	34.0	0.66
	0.59	31.2	0.64
	2.36	25.9	0.66
	5.89	19.0	0.66
Cu^{++}	0.01	ca. 22	ca. 0.4
	0.12	23.0	0.42
	0.59	21.4	0.40
	2.36	17.1	0.43
	5.89	11.8	0.38

NOTE: Absorbance 3.96 ml/g, 25±0.5° C.

than any value of ρ_{app} for these ions, and indicates a good deal of adsorption. However, in cellulose acetate paper,* zinc and copper have similar mobilities. Although accurate measurements could not be made because of electroosmosis and difficulties in establishing a known, uniform absorbance, ρ_{app} was fairly close to the calculated value of ρ for copper, zinc, and sodium in acetic acid background electrolyte.

**'Oxoid electrophoresis strips' manufactured by Courtaulds Limited for Oxo Limited.*

Can. J. Chem. Downloaded from www.nrcresearchpress.com by 210.87.254.6 on 09/05/12
For personal use only.

Can. J. Chem. Downloaded from www.nrcresearchpress.com by 210.87.254.6 on 09/05/12
For personal use only.

Further experiments were carried out in paper loaded with Amberlite ion-exchange resins, and with cellulose ion-exchange papers. In Reeve Angel SA-2 papers which have strong cation exchange properties, cobalt, zinc, copper, and cesium all had very low mobilities in acetic acid. The mobilities in Reeve Angel WA-2 paper, a weakly acid exchanger, were higher under similar conditions, implying weaker adsorption. This is reasonable, since the carboxyl groups of this material are not strongly ionized in an acid solution. The bivalent ions showed similar behavior in Whatman P20 cellulose phosphate paper, and in Whatman CM50 carboxymethyl cellulose paper (strong and weak cation exchangers, respectively), but the univalent ions were comparatively faster. In the former, the zone mobility of Na^+ was about 10×10^{-5} cm^2 v^{-1} sec^{-1} in 2.36 M acetic acid at an absorbance of 0.98 ml/g. All mobilities in these materials were much lower than in ordinary papers, but this cannot be attributed completely to ion-exchange adsorption. In Whatman DE 20 diethylaminoethyl cellulose paper, an anion exchanger, the zone mobility of Na^+ was only 8.3×10^{-5}, and that of Zn^{++} and Cu^{++} about 3.7×10^{-5} and 1×10^{-5} cm^2 v^{-1} sec^{-1}, respectively, under similar conditions. These figures are not too significant because of factors such as electroosmosis, but they do show that even in this material copper is more hindered than zinc.

In anion-exchange resin loaded paper (Reeve Angel SB-2) the zone mobilities of cations are still much lower than in ordinary paper, although they are larger than in the cation-exchange papers. Jakubovic *et al.* (23) have reported some ionic mobilities in ion-exchange resins which indicate that bivalent ions in particular are hindered a great deal.

Most of the above work in ion-exchange papers, and in cellulose acetate, is only qualitative. Flow of background electrolyte is often different in these materials from that in ordinary paper; in some cases this was clearly evident from the visible distribution of liquid in the strip after electromigration. This was especially marked with cellulose acetate. Although in this instance the flow was measured with H_2O_2, uncertainties in corrections obtained from such measurements, and the non-uniform absorbance which was set up, make the figures obtained for U_z have little quantitative value. They do indicate, however, that this material offers less hindrance by non-mechanical effects (adsorption) than do the other materials studied. The zones, especially of sodium, were very sharp.

Ion-exchange papers may prove useful for separations, although the higher obstruction which they in general seem to possess is a disadvantage. A few preliminary experiments with cobalt and zinc in Reeve Angel SA-2, WA-2, and SB-2 papers showed that separations were possible in suitable complexing agents, but ordinary papers gave as good or better results.

REFERENCES

1. M. Maki. Japan Analyst, **3**, 311 (1954).
2. S. Yasunaga and O. Shimomura. J. Pharm. Soc. Japan, **74**, 62 (1954).
3. S. Achiwa. J. Electrochem. Soc. Japan, **25**, 266 (1957).
4. R. A. Bailey and L. Yaffe. Can. J. Chem. **37**, 1527 (1959).
5. S. Achiwa. J. Electrochem. Soc. Japan, **25**, 131 (1957).
6. J. Miller, W. F. Pickering, and F. L. Ward. Anal. Chim. Acta, **14**, 538 (1956).
7. T. R. Sato, W. P. Norris, and H. H. Strain. Anal. Chem. **27**, 521 (1955).
8. H. H. Strain. Anal. Chem. **24**, 356 (1952).
9. J. T. Edward. Chem. & Ind. (London), 276 (1958).
10. H. Berbalk and O. Schier. Monatsh. Chem. **88**, 1095 (1957).
11. H. G. Kunkel and A. Tiselius. J. Gen. Physiol. **35**, 89 (1951).
12. R. Crawford and J. T. Edward. Anal. Chem. **29**, 1543 (1957).

13. S. YASUNAGA and O. SHIMOMURA. J. Pharm. Soc. Japan, **74**, 321 (1954).
14. Z. PUCAR and Z. JAKOVAC. J. Chromatog. **2**, 320 (1959).
15. M. MAKI. Japan Analyst, **5**, 26 (1956).
16. J. J. BIKERMAN. J. Phys. Chem. **46**, 724 (1942).
17. D. A. I. GORING and S. G. MASON. Can. J. Research, B, **28**, 307 (1950).
18. J. VACIK and J. CABICAR. Collection Czechoslov. Chem. Communs. **25**, 404 (1960).
19. J. VACIK, O. GRUBNER, and J. DVORAK. Collection Czechoslov. Chem. Communs. **25**, 625 (1960).
20. M. MAKI. Japan Analyst, **5**, 23 (1956).
21. A. J. ULTEE and J. HARTEL. Anal. Chem. **27**, 557 (1955).
22. Z. JAKOVAC and M. LEDERER. J. Chromatog. **2**, 658 (1959).
23. A. O. JAKUBOVIC, G. J. HILLS, and J. A. KITCHENER. Trans. Faraday Soc. **55**, 1570 (1959).

Can. J. Chem. Downloaded from www.nrcresearchpress.com by 210.87.254.6 on 09/05/12
For personal use only.

Can. J. Chem. Downloaded from www.nrcresearchpress.com by 210.87.254.40 on 09/05/12
For personal use only.

LA RÉACTION DE REFORMATSKY APPLIQUÉE À L'OXO-2 CYCLOHEXANE-PROPIONITRILE ET À DES CÉTO-NITRILES ANALOGUES[1]

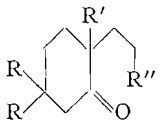
F. BRUDERLEIN,[2] HÉLÈNE BRUDERLEIN,[3] H. FAVRE, R. LAPIERRE[3] ET Y. LEFEBVRE[4]

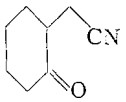
RÉSUMÉ

L'action du bromo-acétate d'éthyle et du zinc sur l'oxo-2 cyclohexane-propionitrile, le diméthyl-4,4 oxo-2 cyclohexane-propionitrile et l'oxo-2 cyclohexane-acétonitrile est discutée; en plus de l'hydroxy-ester-nitrile attendu, on obtient divers composés: lactones-esters et acides carboxyliques. Les acides méthylène-2 cyclohexane-propionique, diméthyl-4,4 méthylène-2 cyclohexane-propionique et méthylène-2 cyclohexane-acétique sont décrits.

Pour des fins de synthèse dans le domaine des terpènes nous avons examiné les produits résultant de l'action du bromo-acétate d'éthyle et du zinc sur quelques céto-nitriles: oxo-2 cyclohexane-propionitrile (I) (1), diméthyl-4,4 oxo-2 cyclohexane-propionitrile (II) et oxo-2 cyclohexane-acétonitrile (III) (2). Baumgarten et Eifert (3) ont rapporté que la réaction de Reformatsky appliquée à l'acétyl-4 valéronitrile conduisait au composé normalement attendu, l'ester éthylique de l'acide cyano-6 hydroxy-3 diméthyl-3,4 hexanoïque, avec un rendement de 35%.

Nous attribuons la constitution II au produit de monocyanoéthylation de la diméthyl-3,3 cyclohexanone selon la méthode de Stork (1), parce que l'hydrolyse de ce céto-nitrile conduit à l'acide cétonique IV, p.f. 61–62°, que l'on obtient également par hydrolyse du composé V, issu de la cyanoéthylation de l'ester éthylique de l'acide diméthyl-4,4 oxo-2 cyclohexane-carboxylique.[5] La constitution du composé V est établie par le fait que ce céto-ester ne donne plus de réaction colorée avec le chlorure ferrique alcoolique: il n'est donc plus énolisable (voir (6)).





III

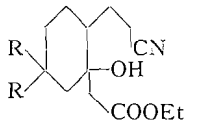
I	R = R' = H	R'' = CN	
II	R = CH_3	R' = H	R'' = CN
IV	R = CH_3	R' = H	R'' = COOH
V	R = CH_3	R' = COOEt	R'' = CN

La réaction de Reformatsky, à partir des cétones cyanoéthylées I et II, conduit à trois types de composés facilement séparables les uns des autres: 1) les hydroxy-ester-nitriles VI et VII; malgré plusieurs tours de distillation ils n'ont pu être obtenus tout à fait purs, mais leurs spectres infrarouges montrent bien leurs bandes nitrile, hydroxyle et ester; 2) les lactone-esters IX et X, caractérisées par une bande unique dans la région carbonyle du spectre infrarouge (1730 cm^{-1}, ester et δ-lactone); 3) des acides carboxyliques:

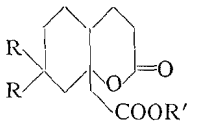
[1]*Manuscrit reçu le 6 juillet 1960.*
Contribution du Département de Chimie de l'Université de Montréal, Montréal, Qué. Ce mémoire a été présenté en partie au Congrès de l'Institut de Chimie du Canada, Vancouver, 3–5 juin 1957; il est tiré en partie de la thèse de doctorat de Y.L. et du mémoire de maîtrise de F.B.
[2]*Boursier du Conseil National de Recherches du Canada, 1957–1960.*
[3]*Madame Bruderlein et R. Lapierre ont reçu une bourse de l'Office de la Recherche Scientifique de la Province de Québec, 1956–1959.*
[4]*Boursier du Conseil National de Recherches du Canada 1953–1957. Adresse actuelle: Ayerst, McKenna & Harrison Ltd., Montréal, Qué.*
[5]*Pour la synthèse de ce céto-ester, voir (4, 5).*

(*a*) dans la série diméthylée l'acide est solide, de formule $C_{13}H_{22}O_5$, p.f. 144.5–145.5°; nous lui attribuons la constitution XIII bien supportée par un spectre infrarouge; il se décompose par chauffage en acide diméthyl-4,4 méthylène-2 cyclohexane-propionique (XV), dont la constitution est discutée plus loin.

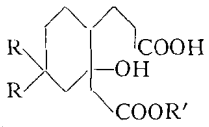
(*b*) dans la série non méthylée les acides par chauffage se décomposent soit en acide méthylène-2 cyclohexane-propionique (XIV) dont la constitution est prouvée plus loin, soit en (éthoxycarbonyl-méthyl)-8*a* oxo-2 perhydro-chromanne (IX), identique à celui obtenu plus haut en 2); comme ces acides sont des huiles qui résistent à toute tentative de cristallisation leur nature exacte n'a pu être déterminée. La fraction acide qui se décarboxyle en acide à double liaison semicyclique pourrait renfermer soit le diacide hydroxylé XI par analogie avec la série diméthylée, soit un diacide déshydraté (du type XVII avec double liaison sur le cycle), soit encore l'acide VIII; tous ces composés sont susceptibles d'engendrer par chauffage une double liaison semicyclique (7, 8, 9, 10, 11). L'acide qui engendre la lactone IX serait l'ester XII. Ces fractions acides sont certainement des mélanges des isomères cis et trans.



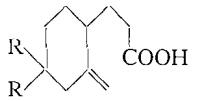
VI R = H
VII R = CH_3



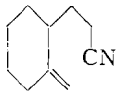
VIII R = H R′ = H
IX R = H R′ = C_2H_5
X R = CH_3 R′ = C_2H_5



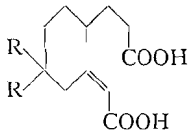
XI R = R′ = H
XII R = H R′ = C_2H_5
XIII R = CH_3 R′ = H



XIV R = H
XV R = CH_3



XVI



XVII R = H
XVIII R = CH_3

Les deux acides à insaturation semicyclique XIV et XV ont dans leurs spectres infrarouges les bandes caractéristiques, 1645 et 890 cm^{-1}, de la double liaison méthylénique, comme Stauffacher et Schinz (11) l'ont mentionné pour l'acide diméthyl-6,6 méthylène-2 cyclohexane-propionique. La formaldéhyde formée, selon le mode opératoire de Seidel, Schinz et Ruzicka (12), indique une teneur de 87% en liaison méthylénique chez l'acide XIV; cet acide fut obtenu également, avec un rendement global de 7–10%, en faisant réagir le méthylène-triphényl-phosphorane (13)[6] sur l'oxo-2 cyclohexane-propionitrile (I) et en saponifiant le nitrile méthylénique XVI brut.

L'hydrolyse (hydroxyde de potassium–méthanol) des lactone-esters IX et X conduit à des diacides que nous formulons comme XVII et XVIII rsepectivement, après examen de leurs spectres ultraviolets caractéristiques d'acides cyclohexylidène-acétiques (15) (XVII: λ_{max} 220.5 mμ, log ϵ = 4.11; XVIII: λ_{max} 221.5 mμ, log ϵ = 4.10) et de leurs spectres infrarouges montrant deux sortes de groupes carbonyles.

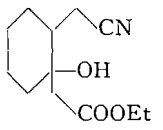
La saponification de l'hydroxy-ester-nitrile XI conduit à un acide brut, p.f. 124–137°, qui, traité par de l'acide chlorhydrique conduit à un carboxyméthyl-8*a* oxo-2 perhydro-chromanne (VIII), p.f. 150°; cette constitution est établie par spectroscopie infrarouge et par titrage alcalimétrique. Cet acide se décarboxyle difficilement par

[6]*Pour cette nomenclature, voir (14).*

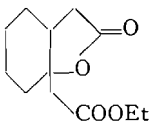
Can. J. Chem. Downloaded from www.nrcresearchpress.com by 210.87.254.40 on 09/05/12
For personal use only.

chauffage en acide méthylène-2 cyclohexane-propionique (XIV) (rendement de 20%) et en divers autres composés que nous n'avons pas étudiés plus à fond. La pyrolyse de l'acide brut, p.f. 124–127°, mène à l'acide XIV avec un rendement voisin de 60%; il se forme également dans cette réaction des traces de γ-lactones et de δ-lactones, décelées par spectroscopie infrarouge.

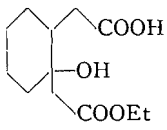
À partir de l'oxo-2 cyclohexane-acétonitrile (III) la réaction de Reformatsky donne trois composés également: l'hydroxy-ester-nitrile XIX, dont le spectre infrarouge est typique pour ces groupes fonctionnels; l'ester lactonique XX, dont le spectre infrarouge présente les deux bandes caractéristiques de la γ-lactone et de l'ester; et une fraction acide, probablement XXI, qui donne XX par chauffage. L'hydrolyse de l'hydroxy-ester-nitrile XIX donne un mélange d'acides (diacide hydroxylé correspondant à XXI et acides non saturés XXII, selon le spectre infrarouge et le titrage alcalimétrique) qui se décarboxylent pour donner l'acide méthylène-2 cyclohexane-acétique (XXIII); cet acide a été caractérisé par son sel de benzyl-iso-thio-uronium; il est identique à celui que l'on obtient à partir du nitrile XXIV (préparé par la réaction de Wittig (13) au départ du céto-nitrile III). L'ozonolyse de cet acide XXIII confirme sa structure; le spectre infrarouge présente les bandes (1645 et 892 cm^{-1}) caractéristiques de la double liaison semi-cyclique.



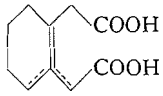
XIX



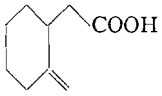
XX



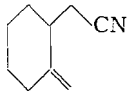
XXI



XXII

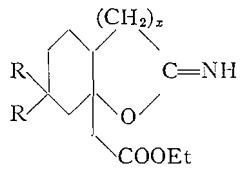


XXIII



XXIV

La façon dont les divers produits de réaction se forment doit être soulignée. Une fois la condensation terminée et le composé zincique décomposé par de l'acide sulfurique on ne retrouve dans la phase organique, lors des extractions usuelles, que l'hydroxy-ester-nitrile. L'ester-lactone et la fraction acide se séparent peu à peu de la phase aqueuse acide sous forme d'une huile rouge; il faut donc admettre que ces derniers composés, solubles dans les solvants organiques, n'existent pas comme tels au moment de la décomposition du composé zincique, sans quoi on les retrouverait dans la phase organique à côté de l'hydroxy-ester-nitrile; nous formulons un composé intermédiaire basique formé dans le milieu anhydre requis par la condensation, puis retenu dans les eaux acides sous forme de sel, s'hydrolysant enfin petit à petit en lactone-ester et en acides carboxyliques; ce composé basique est une imino-O-lactone du type:[7]



R = H ou CH_3

x = 1 ou 2

[7]*Les sels des imino-éthers s'hydrolysent en esters en milieu aqueux lorsque le catalyseur est un acide minéral fort (16, 17, 18, 19).*

Can. J. Chem. Downloaded from www.nrcresearchpress.com by 210.87.254.40 on 09/05/12
For personal use only.

Can. J. Chem. Downloaded from www.nrcresearchpress.com by 210.87.254.40 on 09/05/12
For personal use only.

PARTIE EXPÉRIMENTALE[8]

1. Diméthyl-4,4 oxo-2 cyclohexane-propionitrile (II)

1.1. La diméthyl-3,3 cyclohexanone est préparée d'après la méthode de Frank et Hall (20), selon le mode opératoire décrit en (21) pour la préparation de l'homocamphre.

1.2. Selon la technique de Cohen et Witkop (22) on prépare avec un rendement de 93.5% la N-(diméthyl-5,5 cyclohexényl-1) pyrrolidine, à partir de diméthyl-3,3 cyclohexanone et de pyrrolidine. C'est un liquide incolore, p. é. 125° sous 18 mm, brunissant très rapidement. Calculé pour $C_{12}H_{21}N$: C, 80.38; H, 11.81; N, 7.81%. Trouvé: C, 80.47; H, 11.55; N, 7.97%. Cette ène–amine est cyanoéthylée selon la technique décrite en (22). On obtient avec un rendement de 73% le *diméthyl-4,4 oxo-2 cyclohexane-propionitrile* qui, purifié par distillation, présente les constantes: p. é. 97–98° sous 0.55 mm, $n_D^{29} = 1.4640$. Calculé pour $C_{11}H_{17}NO$: C, 73.70; H, 9.56; N, 7.81%. Trouvé: C, 73.94; H, 9.47; N, 7.92%. Spectre infrarouge: —CN, 2250 cm^{-1}; =C=O, 1700 cm^{-1}. Dinitro-2,4 phénylhydrazone: aiguilles orangé, p.f. 148.5–149.5° (CH_3OH–$CHCl_3$). Calculé pour $C_{17}H_{21}N_5O_4$: C, 56.81; H, 5.89; N, 19.49%. Trouvé: C, 56.90; H, 5.93; N, 19.46%.

1.3. Le céto-nitrile précédent (1 g) est chauffé à reflux avec 625 mg d'hydroxyde de potassium dans 6.25 ml d'eau pendant 20 heures. Après refroidissement, on extrait par de l'éther pour éliminer les composés neutres, refroidit la solution aqueuse alcaline à 5°, ajoute lentement de l'acide chlorhydrique concentré refroidi à 5° jusqu'au virage bleu du rouge congo. On extrait l'acide libéré par de l'éther; on lave deux fois la solution éthérée avec de l'eau, sèche sur sulfate de sodium et distille l'éther; le résidu est recristallisé dans un mélange d'éther et d'éther de pétrole (p. é. 40–60°): on obtient 1 g d'acide diméthyl-4,4 oxo-2 cyclohexane propionique (IV), p.f. 61–62°, ne donnant pas de dépression avec l'acide préparé en 2.

2. Acide diméthyl-4,4 oxo-2 cyclohexane-propionique (IV)

On ajoute à 58 g de diméthyl-4,4 oxo-2 cyclohexane-carboxylate d'éthyle, dans 77 g de *tert*-butanol, 2 ml de Triton B (solution aqueuse d'hydroxyde de benzyl-triméthyl-ammonium à 40%), puis, goutte à goutte, en maintenant la température à 25°, 20 g d'acrylo-nitrile. Il y a précipitation abondante; on fait passer le précipité en solution par adjonction de 40 ml de benzène anhydre. Après 4 heures d'agitation le catalyseur est neutralisé par de l'acide chlorhydrique; la solution benzénique est lavée à neutralité. On distille le solvant et recristallise le résidu dans un mélange d'éther et d'éther de pétrole: 73 g (98% de rendement) d'éthoxycarbonyl-7 diméthyl-4,4 oxo-2 cyclohexane-propionitrile, p.f. 63°. Calculé pour $C_{14}H_{21}NO$: N, 5.57%. Trouvé: N, 5.62%. On hydrolyse le tout en chauffant à reflux avec 82.5 g d'hydroxyde de potassium dans 825 ml d'eau. Après 24 heures de chauffage on isole comme plus haut en 1.3, 55 g d'acide diméthyl-4,4 oxo-2 cyclohexane-propionique brut, p.f. 59°. On en prépare l'ester éthylique (méthode ordinaire à l'alcool éthylique et l'acide sulfurique) que l'on saponifie (méthode habituelle par KOH) et obtient ainsi l'acide plus pur, p.f. 62°; P.M. calculé 198.27; trouvé 197.3. Calculé pour $C_{11}H_{18}O_3$: C, 66.64; H, 9.15%. Trouvé: C, 66.43%; H, 9.05%.

[8]*Les points de fusion (p.f.) ont été déterminés en tubes capillaires, le thermomètre étant étalonné avec des substances de point de fusion connu (Bureau des Standards de Washington). Les spectres infrarouges ont été déterminés à l'aide d'un spectromètre Perkin–Elmer, modèle 21, optique* NaCl*; les liquides étaient sous forme de film, les solides en suspension dans le nujol; seules les bandes servant à l'identification des composés sont indiquées: les valeurs en cm^{-1} correspondent aux maxima d'absorption, sauf celles qui correspondent aux groupes* —OH *des acides carboxyliques et qui montrent la région entière de l'absorption. Les spectres ultraviolets ont été déterminés au moyen d'un spectromètre Beckman DK1, dans l'éthanol 95%. Les poids moléculaires (P.M.) des acides ont été déterminés par titrages alcalimétriques. Les analyses sont de Geller Laboratoires, Hackensack, N.J., et de W. Manser, Herrliberg, Suisse.*

Dinitro-2,4 phénylhydrazone de l'ester méthylique.—En traitant l'acide oxo-2 cyclohexane-propionique par une quantité équimoléculaire de dinitro-2,4 phénylhydrazine dans 20 fois son poids de méthanol contenant 4% d'acide chlorhydrique concentré on obtient la dinitro-2,4 phénylhydrazone de l'ester méthylique correspondant, aiguilles jaunes (MeOH), p.f. 110–111°. Calculé pour $C_{18}H_{24}N_4O_6$: C, 55.09; H, 6.16%. Trouvé: C, 55.15; H, 6.07%.

3. Action du bromo-acétate d'éthyle sur l'oxo-2 cyclohexane-propionitrile en présence de zinc

3.1. Dans un ballon rond à deux tubulures, surmonté d'un refrigérant et d'une ampoule à robinet, on introduit 33.3 g (0.510 mole) de zinc en fine grenaille, préalablement lavé avec de l'acide chlorhydrique à 5% et à l'eau et séché sous 12 mm à 100° en présence d'un petit cristal d'iode. On fait couler dans le ballon 40 ml du mélange: 70 g (0.463 mole) d'oxo-2 cyclohexane-propionitrile, 92.7 g (0.555 mole) de bromo-acétate d'éthyle, 140 ml de benzène et 93 ml de toluène anhydres. On amorce la réaction en chauffant légèrement et on fait couler, goutte à goutte, le reste du mélange, de façon à maintenir une douce ébullition. À la fin de l'addition on reprend le chauffage et maintient l'ébullition à reflux durant 2 heures 30 minutes. On abandonne ensuite la solution à 25° pendant 12 heures. On projette alors le tout sur 800 g de glace concassée et on ajoute 750 ml d'acide sulfurique 2 *N*. On obtient deux phases limpides que l'on agite vivement, sépare par décantation et examine séparément.

3.2. Examen de la phase organique.—Elle est lavée successivement par des solutions d'acide sulfurique à 5%, de carbonate de sodium à 10% et par de l'eau jusqu'à neutralité. Après séchage sur sulfate de sodium, on élimine les solvants par distillation et rectifie le résidu sous vide; fraction I: p. é. 96–149° sous 0.6 mm, 7 g, formée principalement par le céto-nitrile non entré en réaction; fraction II: p. é. 149–152° sous 0.6 mm, 21.9 g, constituée essentiellement de l'*ester éthylique de l'acide (cyano-2 éthyl)-2 hydroxy-1 cyclohexane-acétique* (VI), p. é. 128–130° sous 0.15 mm, n_D^{23} = 1.4782, après redistillation. Calculé pour $C_{13}H_{21}NO_3$: C, 65.24; H, 8.85; N, 5.85%. Trouvé: C, 65.92; H, 8.96; N, 5.04%. Spectre infrarouge: —OH (—COOH), 3400–2400 cm^{-1}; —OH (alcool), 3500 cm^{-1}; —CN, 2552 cm^{-1}; =CO ester, 1730 cm^{-1}.

3.3. Examen de la phase aqueuse.—Elle laisse déposer peu à peu une huile rouge, qui, après 8 heures, est extraite par de l'éther. La solution éthérée est lavée avec une solution d'hydroxyde de sodium à 10%, ce qui permet d'en extraire une fraction acide. Ce qui reste dans l'éther est isolé, après séchage de la solution et évaporation du solvant, et rectifié par distillation: l'*(éthoxycarbonyl-méthyl)-8a oxo-2 perhydro-chromanne* (IX) est un liquide incolore, p. é. 138° sous 0.4 mm, n_D^{27} = 1.4842. Calculé pour $C_{13}H_{20}O_4$: C, 64.97; H, 8.39. Trouvé: C, 64.82; H, 8.26%. Spectre infrarouge: =CO ester et δ-lactone, 1730 cm^{-1}.

La fraction acide est isolée en acidifiant les eaux alcalines et en extrayant l'huile formée par de l'éther. L'huile obtenue après distillation de l'éther ne cristallise pas. Par chauffage à 165°, sous vide de 0.1 mm, cette fraction acide se décompose en acide *méthylène-2 cyclohexane-propionique* (XIV) (voir plus loin en 5.2).

3.4. Au cours de certaines réactions de Reformatsky la fraction acide ne se décarboxyle pas en acide méthylène-2 cyclohexane-propionique, mais conduit à la lactone ester IX mentionnée en 3.3, p. é. 135° sous 0.3 mm, n_D^{26} = 1.4842 (identité prouvée par spectres infrarouges). Le spectre infrarouge de cette fraction acide montre une bande à 3520 cm^{-1} (—OH, alcool), une région d'absorption prononcée de 3400 à 2500 cm^{-1} (—OH, acide carboxylique), une bande large dans la région du groupe carbonyle, maximum à 1730 cm^{-1}, provenant des groupes —COOH et COOEt.

Can. J. Chem. Downloaded from www.nrcresearchpress.com by 210.87.254.40 on 09/05/12
For personal use only.

4. Carboxyméthyl-8a oxo-2 perhydro-chromanne (VIII)

On chauffe à l'ébullition à reflux durant 24 heures 5 g d'ester éthylique de l'acide (cyano-2 éthyl)-2 hydroxy-1 cyclohexane-acétique avec 5 g d'hydroxyde de potassium dans 50 ml d'eau. Après refroidissement on extrait par de l'éther pour éliminer les parties neutres; on acidifie par de l'acide chlorhydrique concentré la solution alcaline et on extrait les acides précipités par de l'éther; la solution éthérée est lavée à l'eau, séchée sur du sulfate de sodium et évaporée. Le résidu (4.18 g, 90%) se solidifie lentement. Après quatre cristallisations dans le mélange acétone – éther de pétrole le point de fusion s'étend de 124° à 137°. Le composé ainsi obtenu (14.2 g) est chauffé, 2 heures durant, sous un séparateur d'eau, dans 350 ml de benzène contenant 2 ml d'acide chlorhydrique concentré. Après distillation du benzène on recueille 14.0 g d'acide, p.f. brut 144–146°, montant à 150° après cristallisation dans le mélange acétone – éther de pétrole. P.M. trouvé 210.7; calculé 212.25. Calculé pour $C_{11}H_{16}O_4$: C, 62.25; H, 7.60%. Trouvé: C, 62.16; H, 7.68%. Spectre infrarouge: —OH (COOH), 3400–2400 cm^{-1}; bande forte à 1700 cm^{-1} (=C=O, acide) avec fort épaulement à 1730 cm^{-1} (δ-lactone).

5. Acide méthylène-2 cyclohexane-propionique (XIV)

5.1. Première méthode.—À une solution 14.3 g (0.170 mole) de phényl-lithium dans 150 ml d'éther on ajoute 61 g (0.170 mole) de bromure de méthyl-triphényl-phosphonium) puis on agite 1 heure à reflux sous atmosphère d'azote; à la solution rouge-brique refroidie à 0°, on ajoute goutte à goutte 25.7 g (0.170 mole) d'oxo-2 cyclohexane-acétonitrile; on chauffe à reflux pendant 3 heures, puis centrifuge et lave le précipité à l'éther. Les solutions éthérées réunies sont lavées à l'eau, séchées sur sulfate de sodium. Le résidu de la distillation de l'éther est distillé plusieurs fois pour fournir une fraction, p. é. 110–112° sous 0.5 mm, présentant des bandes à 2250 cm^{-1} (—CN) et 890 cm^{-1} (double liaison semicyclique), donc riche en méthylène-2 cyclohexane-propionitrile. Ce nitrile (3 g) est hydrolysé par chauffage avec 3 g d'hydroxyde de sodium dans 50 ml d'eau, pendant 24 heures. On isole à la manière habituelle 2.1 g d'acide; l'acide méthylène-2 cyclohexane-propionique pur présente les constantes suivantes: p. é. 108° sous 0.7 mm, $n_D^{25} = 1.4810$. Calculé pour $C_{10}H_{16}O_2$: C, 71.39; H, 9.59%. Trouvé: C, 71.29; H, 9.59%. Spectre infrarouge: OH (—COOH), 3400–2400 cm^{-1}; =CO acide, 1715 cm^{-1}; insaturation semi-cyclique, 1650 et 890 cm^{-1}.

5.2. Deuxième méthode.—En la chauffant à 165° sous vide de 0.1 mm, dans un ballon de Claisen, la fraction acide décrite plus haut en 3.3 se décarboxyle pour donner l'acide méthylène-2 cyclohexane-propionique, p. é. 107–109° sous 0.7 mm, $n_D^{21} = 1.4838$.

5.3. Troisième méthode.—En le chauffant à 165° sous 0.1 mm dans un ballon de Claisen le carboxyméthyl-8*a* oxo-2 perhydro-chromanne brut décrit en 4, p.f. 124–137°, se décarboxyle pour donner l'acide méthylène-2 cyclohexane-propionique qui distille; acide purifié par distillation, p. é. 104–114° sous 1.0 mm, $n_D^{23.5} = 1.4840$. Rendement de l'opération: 61%. Le spectre infrarouge montre des épaulements, sur la bande à 1715 cm^{-1} vers 1735 (δ-lactone) et 1770 (γ-lactone). En pyrolysant le carboxyméthyl-8*a* oxo-2 perhydro-chromanne, p.f. 150° (décrit en 4), on obtient à côté de l'acide méthylène-2 cyclohexane-propionique, p. é. 102° sous 0.4 mm, $n_D^{25} = 1.4842$ (25%), une fraction huileuse importante, p. é. 185°, dont le spectre infrarouge montre des bandes à 1740 et 1770 cm^{-1} indiquant une forte teneur en δ- et γ-lactones.

5.4. Sel de benzyl-iso-thio-uronium.—Aiguilles (MeOH), p.f. 145–145.5°. Calculé pour $C_{18}H_{26}N_2O_3S$: C, 64.64; H, 7.84%. Trouvé: C, 64.73; H, 7.90%.

5.5. Ozonolyse.—En suivant fidèlement la technique et les proportions indiquées par

Can. J. Chem. Downloaded from www.nrcresearchpress.com by 210.87.254.40 on 09/05/12
For personal use only.

Can. J. Chem. Downloaded from www.nrcresearchpress.com by 210.87.254.40 on 09/05/12
For personal use only.

Stauffacher et Schinz (11) 250 mg d'acide méthylène-2 cyclohexane-propionique ont donné 130 mg du dérivé formaldéhyde-dimédon (soit une teneur de 87% en liaison méthylénique) et 40 mg d'acide oxo-2 cyclohexane-propionique, p.f. 62.5°, ne donnant pas de dépression de point fusion en mélange avec l'acide authentique, p.f. 64° (23).

6. Acide carboxyméthylène-2 cyclohexane-propionique (XVII)

On chauffe sur un bain-marie, durant 2 heures 1 g d'(éthoxycarbonyl-méthyl)-8*a* oxo-2 perhydro-chromanne (IX), 1 g d'hydroxyde de potassium dans 20 ml de méthanol. On distille le méthanol et projette le résidu sur 50 g de glace. On acidifie la solution par de l'acide chlorhydrique concentré, jusqu'au virage bleu du rouge congo. L'acide carboxyméthylène-2 cyclohexane-propionique qui précipite (918 mg) est cristallisé dans l'eau, p.f. 161–162°. P.M. trouvé 211.8; calculé 212.24. Spectre ultraviolet: λ_{max} 220.5 mμ, log ϵ = 4.11. Spectre infrarouge: —OH (—COOH) 3400–2400 cm^{-1}; 1714 cm^{-1}, =CO acide non conjugué; 1690 cm^{-1}, =CO acide conjugué; 1623 cm^{-1}, double liaison conjuguée. Calculé pour $C_{11}H_{16}O_4$: C, 62.25; H, 7.60%. Trouvé: C, 62.11; H, 7.59%.

7. Action du bromo-acétate d'éthyle sur le diméthyl-4,4 oxo-2 cyclohexane-propionitrile en présence de zinc

En procédant comme plus haut en 3, on ajoute à 18.3 g de zinc un mélange de 44.4 g de diméthyl-4,4 oxo-2 cyclohexane-propionitrile, 51.8 g de bromo-acétate d'éthyle, 100 ml de benzène et 66 ml de toluène anhydres. On recueille (*a*) dans la phase organique 17 g de céto-nitrile de départ, p. é. 104–118°, et 4.8 g d'un mélange riche en ester éthylique de l'*acide (cyano-2 éthyl)-2 hydroxy-1 diméthyl-5,5 cyclohexane-acétique* (VII), p. é. 140–150° sous 0.45 mm. Calculé pour $C_{15}H_{25}NO_3$: C, 67.38; H, 9.43; N, 5.24%. Trouvé: C, 68.70; H, 9.16; N, 4.05%. Spectre infrarouge: —OH, 3505 cm^{-1}; —CN, 2268 cm^{-1}; =CO ester non conjugué, 1729 cm^{-1}; on décèle également une bande faible à 1717 cm^{-1}. (*b*) Dans la phase aqueuse acide (séparation en composés acide et neutre comme en 3.3) on recueille: l'*acide carboxyméthyl-2 hydroxy-2 diméthyl-4,4 cyclohexane-propionique* (XIII), 8.5 g, p.f. 144.5–145.5°. Anal. Calculé pour $C_{13}H_{22}O_5$: C, 60.45; H, 8.58%. Trouvé: C, 60.55; H, 8.58%. Spectre infrarouge: —OH (—COOH), 3400–2400 cm^{-1}; —OH (hydroxyle), 3505 cm^{-1}; =CO acide, 1700 cm^{-1} et l'*(éthoxycarbonyl-méthyl)-8a diméthyl-7,7 oxo-2 perhydro-chromanne* (X), qui après redistillation présente les constantes suivantes: p. é. 137° sous 0.3 mm; n_D^{22} = 1.4847. Calculé pour $C_{15}H_{24}O_4$: C, 67.14; H, 9.01%. Trouvé: C, 66.91; H, 8.90%. Spectre infrarouge: =CO ester et δ-lactone, 1731 cm^{-1}.

8. Acide diméthyl-4,4 méthylène-2 cyclohexane-propionique (XV)

L'acide carboxyméthyl-2 hydroxy-2 diméthyl-4,4 cyclohexane-propionique (XIII) (8.5 g) est chauffé dans un ballon de Claisen jusqu'à 165° à pression atmosphérique, puis à 0.6 mm jusqu'à 220°. Le vide varie de 0.6 à 2.7 mm, puis revient à 2 mm. En même temps un liquide incolore distille, p. é. 117–124° (3 g ou 48% de rendement); l'acide diméthyl-4,4 méthylène-2 cyclohexane-propionique redistillé présente les constantes: p. é. 102–103° sous 0.2 mm, n_D^{25} = 1.4755. Calculé pour $C_{12}H_{20}O_2$: C, 73.43; H, 10.27%. Trouvé: C, 73.35; H, 10.23%. Spectre infrarouge OH (acide) 3400–2400 cm^{-1}; =CO acide, 1706 cm^{-1}; double liaison semicyclique, 1647 et 894 cm^{-1}.

9. Acide carboxyméthylène-2 diméthyl-4,4 cyclohexane-propionique (XVIII)

Comme décrit en 6, la saponification de 11 g d'(éthoxycarbonyl-méthyl)-8*a* diméthyl-7,7 oxo-2 perhydro-chromanne (X) conduit à 9.2 g d'acide carboxyméthylène-2 diméthyl-4,4 cyclohexane-propionique. Le point de fusion brut 136–138° passe à 135–140° par

cristallisation dans un mélange d'acétone et d'éther de pétrole et à 137–140° par cristallisation dans l'eau. P.M. trouvé 246.2; calculé 240.30. Spectre ultraviolet: λ_{max} 221.5 mμ, log ϵ = 4.10. Spectre infrarouge: —OH (—COOH) 3400–2400 cm^{-1}; =CO acide conjugué, 1678 cm^{-1}; =CO acide non conjugué, 1707 cm^{-1}; double liaison conjuguée, 1629 cm^{-1}. Calculé pour $C_{13}H_{20}O_4$: C, 64.98; H, 8.39%. Trouvé: C, 64.91; H, 8.42%.

10. Action du bromo-acétate d'éthyle sur l'oxo-2 cyclohexane-acétonitrile en présence de zinc

Selon la technique décrite en 3, on ajoute à 37.3 g de zinc un mélange de 71 g d'oxo-2 cyclohexane-acétonitrile, 104 g de bromo-acétate d'éthyle, 150 ml de benzène et 100 ml de toluène anhydres. On examine immédiatement la phase organique et au bout de 24 heures la phase aqueuse.

(*A*) La phase organique contient 23 g d'*ester éthylique de l'acide cyanométhyl-2 hydroxy-1 cyclohexane-acétique* (XIX) qui après distillation présente les constantes: p. é. 128° sous 0.3 mm, n_D^{24} = 1.4788. Calculé pour $C_{12}H_{19}NO_3$: C, 63.97; H, 8.50; N, 6.22%. Trouvé: C, 63.98; H, 8.47; N, 6.06%. Spectre infrarouge: —OH, 3500 cm^{-1}; —CN, 2260 cm^{-1}; =CO 1720 cm^{-1}.

(*B*) La phase aqueuse abandonne: (*a*) 54.5 g d'*(éthoxy-carbonyl-méthyl)-7a oxo-2 oxa-1 perhydro-indène* (XX), p. é. 132° sous 0.5 mm, n_D^{22} = 1.4788. Calculé pour $C_{12}H_{18}O_4$: C, 63.70; H, 8.02%. Trouvé: C, 63.65; H, 7.94%. Spectre infrarouge: =CO (γ-lactone) 1780 cm^{-1}; =CO (ester) 1735 cm^{-1}. (*b*) 2.2 g d'acide qui par distillation donne 1.2 g d'un composé dont le spectre infrarouge est superposable à celui de l'(éthoxycarbonyl-méthyl)-7*a* oxo-2 oxa-1 perhydro-indène (XX).

11. Acide mthyélène-2 cyclohexane-acétique (XXIII)

11.1. Première méthode.—Selon le mode opératoire décrit en 5.1, on ajoute 15.4 g d'oxo-2 cyclohexane-acétonitrile dans 120 ml d'éther anhydre à une solution éthérée préparée à partir de 40.0 g de bromure de méthyl-triphényl-phosphonium, 2.4 g de lithium et 27 g de bromobenzène dans 106 ml d'éther. On chauffe à reflux, en atmosphère d'azote, pendant 3 heures. On obtient après extraction et distillation 2.2 g (15) d'un liquide incolore, jaunissant très rapidement, p. é. 95–105° sous 25 mm. Bande —CN à 2254 cm^{-1} et bandes à 1645 et 892 cm^{-1} (double liaison semicyclique) dans le spectre infrarouge. On hydrolyse immédiatement ce nitrile: 3 g sont chauffés à reflux durant 24 heures avec 3.8 g d'hydroxyde de potassium dans 10 ml d'eau. L'acide méthylène-2 cyclohexane-acétique, extrait à la manière habituelle, est un liquide, p. é. 139° sous 11 mm, n_D^{25} = 1.4814. P.M. trouvé 156.9; calculé 154.21. Calculé pour $C_9H_{14}O_2$: C, 70.10; H, 9.15%. Trouvé: C, 70.13; H, 9.16%. Spectre infrarouge: —OH (—COOH) 3400–2400 cm^{-1}; =CO acide, 1700 cm^{-1}; double liaison semicyclique, 1646 et 892 cm^{-1}.

11.2. Deuxième méthode.—Selon le mode opératoire décrit plus haut en 4, 20.8 g d'ester éthylique de l'acide cyanométhyl-2 hydroxy-1 cyclohexane-acétique (XIX) sont saponifiées par 20.8 g d'hydroxyde de potassium dans 200 ml d'eau. On obtient 17 g d'acides, cristallisant en partie dans le nitrométhane, p.f. 153.5–154.5°. P.M. trouvé: 208.8. Calculé pour l'acide hydroxy-1 cyclohexane diacétique-1,2, 216.24, et pour l'acide déshydraté correspondant XXII, 198.22. La littérature (24) donne pour un mélange des acides XXII isomères un point de fusion de 164–166°. En chauffant 125 g de l'acide, p.f. 153.5–154.5°, à 250° sous pression atmosphérique, puis sous 11 mm dans un ballon de Claisen, on recueille un distillat de 204 mg, p. é. 125–139°, n_D^{24} = 1.4795. On reprend cet acide par de l'éther; on lave la solution avec une solution aqueuse $NaHCO_3$ 10% refroidie à 5°; on libère l'acide méthylène-2 cyclohexane-acétique par HCl 10% (température 5°) que l'on isole à la manière habituelle par de l'éther. Le spectre infrarouge de cet acide est superposable à celui obtenu par la première méthode.

Can. J. Chem. Downloaded from www.nrcresearchpress.com by 210.87.254.40 on 09/05/12
For personal use only.

11.3. Sel de benzyl-iso-thio-uronium.—Après trois cristallisations dans l'acétone, aiguilles p.f. 159–160° (première méthode), 158–158.5° (deuxième méthode); pas de dépression en mélange. Calculé pour $C_{17}H_{24}N_2O_2S$: C, 63.72; H, 7.55; N, 8.74%. Trouvé: C, 63.71; H, 7.54; N, 8.69%.

11.4. Ozonolyse.—Selon le mode opératoire mis en œuvre en 5.5, 254 mg d'acide méthylène-2 cyclohexane-acétique donnent 150 mg de dérivé formaldéhyde-dimédon, p.f. 189–190°, soit un rendement de 34.2% correspondant à une teneur de 102.6% en insaturation semicyclique.

REMERCIEMENTS

Nous remercions le Conseil National de Recherches du Canada de son aide financière (subvention de recherches (H.F.) et bourses d'études (F.B. et Y.L.)), ainsi que l'Office de Recherches Scientifiques de la Province de Québec pour des bourses d'études à H.B. et R.L. Nous remercions aussi M. le Professeur C. Sandorfy de son aide dans l'étude des spectres infrarouges.

BIBLIOGRAPHIE

1. G. Stork, R. Terrell et J. Szmuszkovicz. J. Am. Chem. Soc. **76**, 2029 (1954).
2. B. Belleau. Can. J. Chem. **35**, 651 (1957).
3. H. E. Baumgarten et R. L. Eifert. J. Org. Chem. **18**, 1177 (1935).
4. R. Adams, S. Loewe, C. W. Theobald et C. M. Smith. J. Am. Chem. Soc. **64**, 2653 (1942).
5. A. Brenner et H. Schinz. Helv. Chim. Acta, **35**, 1333 (1952).
6. D. Stauffacher et H. Schinz. Helv. Chim. Acta, **37**, 1223 (1954).
7. N. A. Abraham et M. Vilkas. Compt. rend. **248**, 2880 (1959).
8. O. Wallach. Ann. **360**, 26 (1908).
9. B. Willhalm, U. Steiner et H. Schinz. Helv. Chim. Acta, **41**, 1359 (1958).
10. H. Favre et H. Schinz. Helv. Chim. Acta, **41**, 1368 (1958).
11. D. Stauffacher et H. Schinz. Helv. Chim. Acta, **37**, 1227 (1954).
12. C. F. Seidel, H. Schinz et L. Ruzicka. Helv. Chim. Acta, **32**, 1739 (1949).
13. G. Wittig et U. Schollkopf. Chem. Ber. **87**, 1318 (1954).
14. J. Levisalles. Bull. soc. chim. France, [5], 1021 (1958).
15. A. T. Nielsen. J. Org. Chem. **22**, 1539 (1957).
16. J. Stieglitz. Am. Chem. J. **39**, 29, 166, 402 (1908).
17. I. H. Derby. Am. Chem. J. **39**, 437 (1908).
18. W. McCracken. Am. Chem. J. **39**, 586 (1908).
19. H. I. Schlesinger. Am. Chem. J. **39**, 719 (1908).
20. R. L. Frank et H. K. Hall. J. Am. Chem. Soc. **72**, 1645 (1950).
21. H. Favre, B. Marinier et J. C. Richer. Can. J. Chem. **34**, 1329 (1956).
22. L. A. Cohen et B. Witkop. J. Am. Chem. Soc. **77**, 6595 (1955).
23. R. D. Haworth et C. R. Mavin. J. Chem. Soc. 1012 (1933).
24. C.-K. Chuang et C.-M. Ma. Ber. B, **68**, 871 (1935).

Can. J. Chem. Downloaded from www.nrcresearchpress.com by 210.87.254.40 on 09/05/12
For personal use only.

Can. J. Chem. Downloaded from www.nrcresearchpress.com by 210.87.254.105 on 09/05/12
For personal use only.

SELECTIVE ENZYMOLYSIS OF POLY-β-D-GLUCANS, AND THE STRUCTURE OF THE POLYMERS[1]

F. W. PARRISH,[2] A. S. PERLIN, AND E. T. REESE[3]

ABSTRACT

The soluble poly-β-D-glucan from oats has been subjected to degradation by two different types of enzymes. "Cellulase" converts the polysaccharide to a trisaccharide, 4-*O*-β-D-laminaribiosyl-D-glucose, and two tetrasaccharides, 3′-*O*-β-D-cellobiosyl-D-cellobiose and 4′-*O*-β-D-laminaribiosyl-D-cellobiose.* Degradation by the second enzyme, "laminarinase", produces a trisaccharide, 3-*O*-β-D-cellobiosyl-D-glucose, and a tetrasaccharide, 3-*O*-β-D-cellotriosyl-D-glucose.† These products, which account for 75–85% of the polymer in each experiment, have been characterized by chemical methods. The data show that the glucan is composed almost entirely of two types of structural sequences: one is a tetrameric unit in which a single β-(1 → 3) linkage alternates with two β-(1 → 4) linkages, and the other, a pentameric unit in which a single β-(1 → 3) linkage alternates with three consecutive β-(1 → 4) linkages.

The soluble poly-β-D-glucan from barley has been shown by enzymolysis with the "cellulase" to be closely related in detailed structure to the oat polymer.

Steric aspects of the enzymic degradations are discussed.

The grains of oats and barley contain water-soluble polysaccharides which are composed of β-D-glucopyranosyl units (1, 2, 3, 4, 5). In barley, the polyglucan appears to be closely associated with the malting process, during which there occurs a large increase in the proportion of the water-soluble polymer. Results from several investigations (6, 7, 8, 9) have shown that these polysaccharides are linear and that the monomeric units are joined by either (1 → 3) or (1 → 4) β-D-glycosidic linkages. An examination by Peat, Whelan, and Roberts (9) of the products formed by partial acid hydrolysis of oat glucan, has demonstrated clearly that both types of linkage occur together in the same chain, and that a major proportion of the polymer may be represented by a tetrameric repeating unit (I) in which two (1 → 4) linkages and a (1 → 3) linkage alternate. Lichenin, a poly-β-D-glucan from Iceland moss, was found also by this approach to be constituted in a closely similar fashion (9).

In the current study, the β-D-glucans from oats and barley have been degraded selectively with two different enzymic preparations, a "cellulase" and a "laminarinase". From the identity of the products formed detailed information about the structure of the polysaccharides has been obtained. The basic type of formula (I) advanced by Peat, Whelan, and Roberts has been confirmed for the oat glucan, and shown to apply also for barley glucan, and additional data about the constitution of these polymers provided.

$$G_p1 \rightarrow 3\ G_p1 \rightarrow 4\ G_p1 \rightarrow 4\ G_p$$

I

[1]*Manuscript received June 27, 1960.*

Contribution from the National Research Council of Canada, Prairie Regional Laboratory, Saskatoon, Saskatchewan, and the Microbiology Laboratory, Quartermaster Research and Engineering Center, Natick, Massachusetts.

Issued as N.R.C. No. 5975.

[2]*National Research Council of Canada Postdoctorate Fellow, 1959–1960.*

[3]*Microbiology Laboratory, Quartermaster Research and Engineering Center, Natick, Massachusetts.*

**For the sake of brevity, trivial names are used where possible in describing the oligosaccharides reported in this paper. More formal descriptions of the trisaccharide and two tetrasaccharides, respectively, are: O-β-D-glucopyranosyl-(1 → 3)-O-β-D-glucopyranosyl-(1 → 4)-D-glucose; O-β-D-glucopyranosyl-(1 → 4)-O-β-D-glucopyranosyl-(1 → 3)-O-β-D-glucopyranosyl-(1 → 4)-D-glucose; and O-β-D-glucopyranosyl-(1 → 3)-O-β-D-glucopyranosyl-(1 → 4)-O-β-D-glucopyranosyl-(1 → 4)-D-glucose.*

†*O-β-D-Glucopyranosyl-(1 → 4)-O-β-D-glucopyranosyl-(1 → 3)-D-glucose and O-β-D-glucopyranosyl-(1 → 4)-O-β-D-glucopyranosyl-(1 → 4)-O-β-D-glucopyranosyl-(1 → 3)-D-glucose, respectively.*

Can. J. Chem. Downloaded from www.nrcresearchpress.com by 210.87.254.105 on 09/05/12
For personal use only.

Enzymic Degradation by Cellulase

The glucans were found to be hydrolyzed rapidly and extensively by a cellulase isolated from *Streptomyces* sp. QM B814. This enzyme preparation hydrolyzes cellulose in high yield to cellobiose and cellotriose (10). Under conditions expected to minimize transglycosylation side-reactions, the products formed from both glucans were mainly one tri- and two tetra-saccharides, and only minor or trace proportions of higher oligosaccharides, disaccharides, and glucose were detected. The products (Table I) were isolated by preparative paper chromatography.

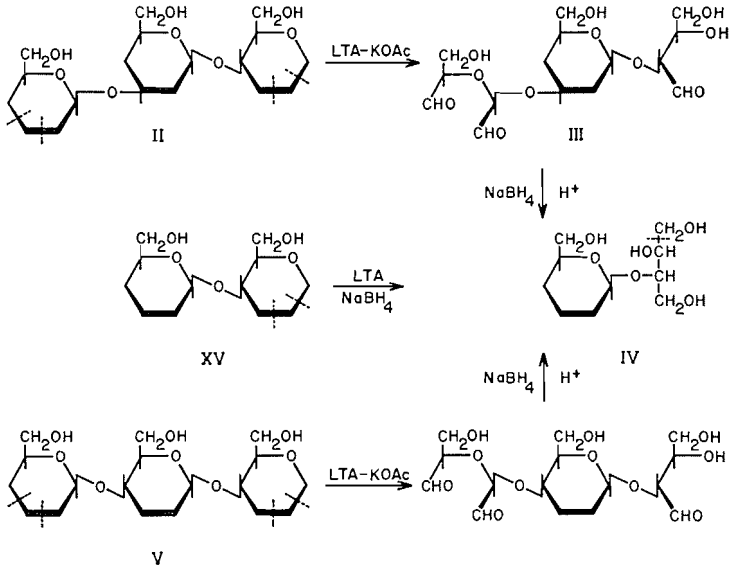
TABLE I

Yields of products from enzymolysis of poly-β-D-glucans*

	Cellulase		Laminarinase
Fraction	Barley glucan	Oat glucan	Oat glucan
Trisaccharide	628 } (2.7)	638 } (2.5)	520 } (2.3)
Tetrasaccharides	303 }	337 }	302 }
Disaccharide	68	75	61
Glucose	9	8	81
Unidentified†	93	67	—

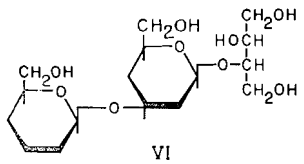
*Milligrams of crude product/1.0 g polyanhydroglucose. Figures in parentheses are moles trisaccharide : moles tetrasaccharide.
†Components remaining close to the origin on paper chromatograms.

The major product obtained from each glucan (yield, about 60%) was an amorphous trisaccharide, which was purified by conversion to a crystalline acetate. The physical constants of the derived acetate corresponded to those reported for 4-*O*-β-D-laminaribiosyl-D-glucose undecaacetate (9), and the free trisaccharide was found to possess this structure (II)* in the following way. On treatment with lead tetraacetate in the presence of potassium acetate the compound produced formic acid at the same rate as cellotriose (11), and consumed 4 moles of oxidant, consistent with the formulation of a

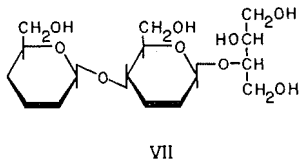


**All hexopyranosyl units represented by these formulae possess the* D-*gluco-configuration.*

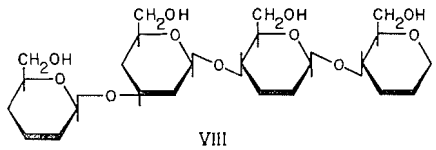
4-substituted reducing end-unit, and the production of III. The oxidation product was reduced with sodium borohydride (12), and selectively hydrolyzed with acid under the conditions recommended by Smith and co-workers (13), yielding 2-*O*-β-D-glucopyranosyl-D-erythritol (IV) (14). Hence the central unit of the original trisaccharide was attached to the reducing end-unit by a β-(1 → 4) linkage. The validity of this degradation procedure was checked with cellotriose (V), which also yielded IV since the central unit in this trisaccharide is resistant to lead tetraacetate oxidation under the conditions used (11). In the absence of potassium acetate, a relatively slow uptake of about 1.7 moles of lead tetraacetate was observed with II, characteristic of a 4-substituted D-glucose (14), and reduction of the product afforded 2-*O*-β-D-laminaribiosyl-D-erythritol (VI). Presence of the β-(1 → 3) linkage in II was confirmed by partial hydrolysis, which afforded laminaribiose, characterized as the octaacetate.



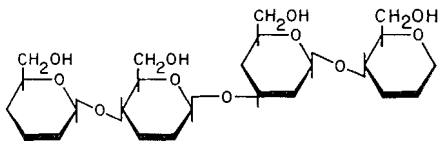
VI



VII



VIII



IX

The amorphous tetrasaccharide fraction obtained from the oat and barley glucans accounted for about 30% of the original polysaccharides. Oxidation of each fraction with lead tetraacetate – potassium acetate, followed by reduction of the oxidized tetramer with sodium borohydride and selective acid hydrolysis (13), yielded two products in a ratio of approximately 3 to 2. The major product was 2-*O*-β-D-cellobiosyl-D-erythritol (VII) and the other, 2-*O*-β-D-laminaribiosyl-D-erythritol (VI). Isolation of these two triitols showed that the tetrasaccharide fractions contained two components (not separable by paper chromatography), one containing a central β-(1 → 4) linkage and the other a central β-(1 → 3) linkage, and both having a β-(1 → 4) linkage adjacent to the reducing end-unit. One of these components was isolated by fractional crystallization,* and when degraded according to the reaction sequence described above afforded VII. Also, on reduction followed by partial acid hydrolysis, the crystalline tetrasaccharide gave laminaribiose, cellobiose, and trisaccharide (II). These properties therefore characterized the compound as 4′-*O*-β-D-laminaribiosyl-D-cellobiose (VIII). The second tetrasaccharide component was amorphous. However, it was shown to be 3′-*O*-β-D-cellobiosyl-D-cellobiose (IX), since it yielded VI on selective degradation (as above), and after reduction followed by partial hydrolysis it afforded cellobiose, laminaribiose, and trisaccharide (X).

A detailed structure for the major proportion (about 85%) of the oat and barley β-D-glucans may clearly be formulated from the identity of the three oligosaccharides obtained by enzymolysis. Since the molar ratio of trisaccharide to tetrasaccharide formed

**Two modifications of this tetrasaccharide were obtained, the α-anomer and a dihydrate of the β-anomer.*

Can. J. Chem. Downloaded from www.nrcresearchpress.com by 210.87.254.105 on 09/05/12
For personal use only.

is about 2.5 to 1, and since (on the average) about seven glucose units are linked by (1 → 4) bonds and three by (1 → 3) bonds, a structural relationship between polymer and products may be depicted as in Fig. 1.* According to this scheme, the polymers

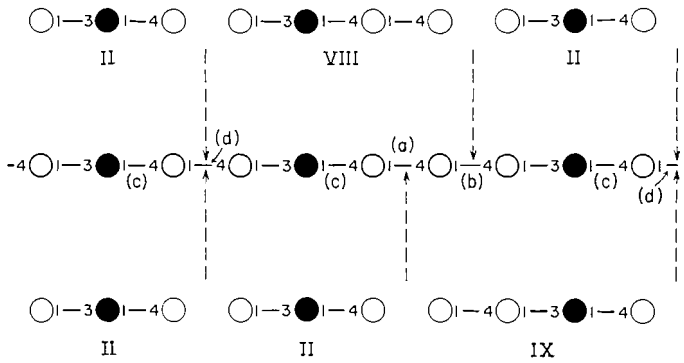


FIG. 1. Structural relationship between oat and barley poly-β-D-glucan (central row of circles) and oligosaccharides produced by the action of "cellulase". All circles represent β-D-glucopyranosyl units; those units which are bonded glycosidically through positions-1 and -3 are in black, for contrast.

contain two types of repeating units represented by (*a*) a tetrameric unit (I, page 2094) in which a single β-(1 → 3) linkage alternates with two consecutive β-(1 → 4) linkages (9), and (*b*) a pentameric unit in which a single β-(1 → 3) linkage alternates with three consecutive β-(1 → 4) linkages. The (1 → 3) bonds occur solely in isolated positions, but there can be few, if any, isolated (1 → 4) bonds in the molecule.† Rather, the (1 → 4) linkages are found most frequently in pairs and less often as a sequence of three, but the available evidence suggests that there are never more than three (1 → 4) linkages in consecutive order along the polymer chain.

Formation by the cellulase of the two tetrasaccharides VIII and IX appears to involve cleavage of bond (*b*) or (*a*), respectively (Fig. 1), 2 moles of trisaccharide II being formed in either instance. Since more of VIII than IX is produced, bond (*a*) is the more easily cleaved although the difference is rather small (ratio of 3.5 to 2). However, it may be noted that bond (*c*) is *not* cleaved by the enzyme, although it is also of the β-(1 → 4) type usually associated with cellulase action. As noted elsewhere (15), the D-glucosyl unit to the left of bond (*c*) is substituted at position-3, rather than at position-4, making for a "(→ 3)-β-(1 → 4)" relationship. By contrast, linkages (*a*), (*b*), and (*d*), which possess a "(→ 4)-β-(1 → 4)" arrangement, all are cleaved by the cellulase.

Enzymic Degradation by Laminarinase

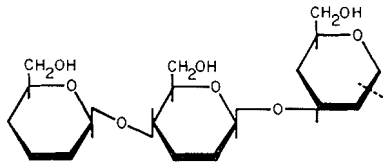
A second type of enzyme, classified as a "laminarinase" by Reese and Mandels (16) since it shows high specificity for laminarin, was also found capable of rapidly degrading the β-D-glucans. This glycosidase is an endo-enzyme produced by *Rhizopus arrhizus* QM 1032. Acting on laminarin, it yields laminaribiose and laminaritriose as the dominant products (16). With the oat polymer, a tri- and tetra-saccharide were detected in the hydrolyzate together with a small proportion of laminaribiose. The major product, which

**For simplicity, the ratio of tri- to tetra-saccharide in Fig. 1 is 2 to 1. However, closer agreement is obtained with the ratio found experimentally by considering a larger repeating structure (e.g., one containing 20–25 units). The molecular weight of the polysaccharides was not estimated, but the low yield of formic acid produced during periodate oxidation of the materials (experimental section) indicated a D.P. value of not less than 50–100 units.*

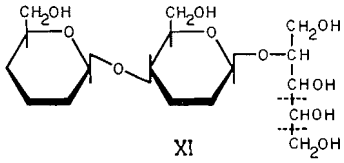
†Oligosaccharides having D.P. greater than 4, which were formed in low yield (Table I), were not examined and may represent minor structural sequences not accommodated by Fig. 1.

Can. J. Chem. Downloaded from www.nrcresearchpress.com by 210.87.254.105 on 09/05/12
For personal use only.

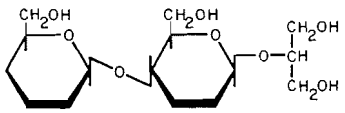
accounted for about 50% of the glucan, was an amorphous trisaccharide, characterized as the derived acetate. This trisaccharide was shown to be 3-*O*-β-D-cellobiosyl-D-glucose (X)* by the following reactions. It rapidly consumed 1 mole of lead tetraacetate per mole and yielded an equivalent of pentose showing that the reducing end-unit was substituted at position-3 (14). In agreement with this assignment the compound migrated on an electrophoretogram (18) at a rate close to that of laminaribiose. The oxidized trisaccharide was reduced to the corresponding glycitol (XI, not isolated) which was treated in turn with 2 moles of lead tetraacetate, followed by a second reduction. This degradation procedure had been used earlier to convert a 3-linked hexose disaccharide to a 2-*O*-glycosyl-glyceritol (19). Accordingly, the final product obtained was 2-*O*-β-D-cellobiosyl-glyceritol (XII).



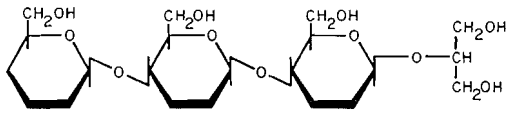
X



XI



XII



XIII

The tetrasaccharide, which accounted for 30% of the polymer, was crystalline. Its behavior on oxidation with lead tetraacetate and ionophoresis paralleled that of the trisaccharide (X) (above), showing that this compound also possesses a 3-substituted reducing end-unit. By selectively degrading the reducing end-unit to a 2-substituted glyceritol unit (as for X to XI), 2-*O*-β-D-cellotriosyl-glyceritol (XIII) was obtained. Accordingly, the tetrasaccharide produced by laminarinase action is 3-*O*-β-D-cellotriosyl-D-glucose (XIV, Fig. 2).

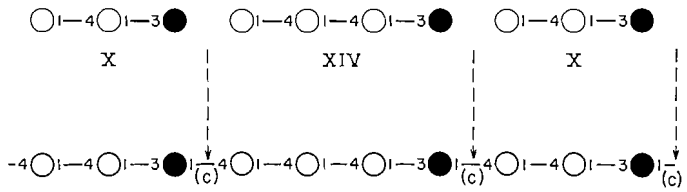


FIG. 2. Structural relationship between oat poly-β-D-glucan (lower row of circles) and oligosaccharides produced by the action of "laminarinase". All circles represent β-D-glucopyranosyl units; those units which are bonded glycosidically through positions-1 and -3 are in black, for contrast.

Together, the tri- and tetra-saccharide account for about 80% of the original oat β-D-glucan and are produced in a molar ratio of about 2.3 to 1. As shown in Fig. 2, formation of these products can readily be accommodated by the polymeric structure

Two sets of physical constants have been reported for the undecaacetate of this compound: m.p. 110° C, $[\alpha]_D$ −8° (9) and m.p. 183° C, $[\alpha]_D$ −22° (17). (The acetate obtained in the current study has the same properties as recorded in reference 9.) Consequently, a confirmation of the structure of X appeared necessary, and is reported herein.

Can. J. Chem. Downloaded from www.nrcresearchpress.com by 210.87.254.105 on 09/05/12
For personal use only.

already depicted in Fig. 1.* With laminarinase, cleavage was specific for linkage (*c*), i.e., one adjacent to a β-D-glucosyl unit *substituted at position-3*, rather than the β-(1 → 3) bond itself (15). Hence, in contrast to the action of cellulase, only one tetrasaccharide was obtained. These results, therefore, fully complement those obtained by enzymolysis of the β-D-glucans with cellulase, and show clearly that the major proportion of the polysaccharides is constituted as depicted in Figs. 1 and 2. It is possible that the glucans comprise a mixture of molecules, some of which contain only the tetrameric repeating unit and others only the pentameric unit. However, formation of the two tetrasaccharides by the "cellulase" is accommodated most readily by assuming that both types of repeating units occur interspersed within the same molecule. Of possible significance in this connection is the fact that fractional precipitation of barley glucan yielded several fractions, each of which was hydrolyzed to the same degree by cellulase and gave the same mixture of products.

EXPERIMENTAL

Paper chromatography was carried out with ethyl acetate:pyridine:water (10:4:3) as solvent (20); for preparative chromatography Whatman 3MM paper was used. Spray reagents used were aniline oxalate (21) and ammoniacal silver nitrate (22). R_G represents the rate of travel of a compound on a chromatogram relative to the rate for glucose.

Paper electrophoresis (18) was carried out using borate buffer (pH 9.2 (23)) at 10 volts per centimeter.

Copper-reducing power was measured by the method of Nelson (24).

Solutions were evaporated at 40–50° C, and optical rotations were measured at approximately 25° C. Melting points are corrected.

Oat flour was milled from Fortune oats grown at the University of Saskatchewan, and barley flour from husky six-rowed barley grown in the Saskatoon area.

Isolation of Polyglucans

A combination of the procedures described by Morris (2) and by Meredith, Watts, and Anderson (5) was used. Oat or barley flour (3 kg), previously heat-inactivated with boiling 80% ethanol, was extracted with water (24 liters) for 3 hours in the presence of papain (6 g). The digest was centrifuged and ammonium sulphate (2200 g) was added to the supernatant solution causing flocculation of the polyglucan. The latter was collected, washed with 50% ethanol until sulphate-free, then with acetone, and air-dried. The barley glucan (19.0 g) was a white powder, $[\alpha]_D^{22}$ −13.1° (*c*, 0.9, H_2O). Found: anhydroglucose (copper-reducing power after hydrolysis), 89.0%; N, 0.37%; ash, 0.81%; moisture, 12.4%. The oat glucan (26.0 g) was a white fibrous material, $[\alpha]_D^{27}$ −8.3° (*c*, 0.9, H_2O). Found: anhydroglucose, 86.9%; N, 0.36%; ash, 0.17%; moisture, 10.2%.

Periodate Oxidation of Polyglucans

By oxidation of the polyglucans with 2 molar equivalents of sodium metaperiodate at 20° C in the dark, the following results were obtained:

Periodate consumed by barley glucan (moles/mole (hours)): 0.72 (20), 0.73 (45), 0.79 (95), 0.81 (141). Formic acid production (moles/mole) at 20 and 141 hours was 0.005 and 0.055, respectively, giving a corrected value of about 0.75 mole periodate consumed per anhydroglucose unit at 141 hours.

Closely similar data were obtained with the oat glucan. Periodate consumption (moles/

*See footnote, p. 2097.

Can. J. Chem. Downloaded from www.nrcresearchpress.com by 210.87.254.105 on 09/05/12
For personal use only.

mole (hours)): 0.65 (23), 0.76 (47), 0.77 (102), 0.80 (143). At 47 hours the yield of formic acid was 0.016 mole/mole.

Degradation of Barley Glucan Fractions with Cellulase

Ethanol was added dropwise to a vigorously stirred barley glucan solution (500 mg, 22.5 ml). Precipitates obtained (weights in parentheses) between zero and 17% ethanol (115 mg), 17–23% (276 mg), 23–31% (57 mg), 31–47% (21 mg), and 47–64% (5 mg) were collected and dried. The first four fractions (18 mg) were incubated in water (1.7 ml) at 48° C and pH 6 with cellulase (6 mg). No difference was observed between fractions in rate of hydrolysis (copper-reducing power). In addition, when the reducing power became constant (at glucose equivalent of 25%, 2 hours), paper chromatographic examination of the digests showed the presence in each of two main products, corresponding to a tri- and tetra-saccharide, respectively (R_G 0.45 and 0.22). Of the three minor products detected, two were indistinguishable from glucose and cellobiose, and the third had R_G 0.10.

Further experiments with the unfractionated glucan showed that the glucan:cellulase ratio could be increased to 8:1 with little effect on the degree of hydrolysis attained and the type of products formed.

Degradation of Oat and Barley Glucans with Cellulase

Oat or barley glucan (1.0 g) in water (100 ml) was incubated at 48° C with cellulase (0.12 g) for 5 hours. The enzyme was then inactivated by heating the digest for 10 minutes on the boiling-water bath, the digest was filtered, concentrated, and the syrup obtained was chromatographed on Whatman 3 MM paper sheets. After elution from the papers with water, the sugars were purified by use of mixed-bed ion-exchange resins. Yields of individual sugars are given in Table I.

Products from the Cellulase Degradation of Barley Glucan

4-O-β-D-Laminaribiosyl-D-glucose (II)

The trisaccharide fraction was chromatographically homogeneous containing neither laminaritriose nor cellotriose, $[\alpha]_D$ +11.6° (*c*, 1.3, H_2O). Partial hydrolysis of the material yielded cellobiose, laminaribiose, and glucose (paper chromatogram). On treatment with lead tetraacetate the rate of uptake of oxidant was closely similar to that of cellotriose and cellobiose (11, 14), and in the presence of potassium acetate the lead tetraacetate oxidation characteristics were those of a hexopyranosyl trisaccharide possessing a 4-linked reducing end-unit (11).

4-O-β-D-Laminaribiosyl-β-D-glucose Undecaacetate

A portion (53 mg) of II was heated at 100° C for 2 hours with acetic anhydride containing anhydrous sodium acetate. After evaporation of the acetic anhydride the product was isolated by extraction into chloroform and crystallized from ethanol (weight, 75 mg), m.p. 120–122° C and $[\alpha]_D$ −20.0° (*c*, 1.5, $CHCl_3$) (lit. (9) m.p. 121–123° C and $[\alpha]_D$ −22.2°). Calculated for $C_{40}H_{54}O_{27}$: C, 49.69%; H, 5.63%; acetyl, 48.98%. Found: C, 49.55%; H, 5.70%; acetyl, 49.10%.

Deacetylation of the material in the mother liquors, followed by paper chromatography, indicated the presence of II only.

Degradation of II *to 2-O-β-D-Glucopyranosyl-D-erythritol*

The amorphous material (149 mg) in water (1 ml) was taken up in acetic acid (9 ml) and treated with a solution of lead tetraacetate (660 mg, 5 molar proportions) and potassium acetate (400 mg) in acetic acid (27 ml). After 11 hours the excess tetravalent

Can. J. Chem. Downloaded from www.nrcresearchpress.com by 210.87.254.105 on 09/05/12
For personal use only.

Can. J. Chem. Downloaded from www.nrcresearchpress.com by 210.87.254.105 on 09/05/12
For personal use only.

lead was reduced with a 10% solution of oxalic acid in acetic acid (0.2 ml), and the solution was treated with excess Amberlite IR-120 and concentrated. By repeated addition of ethanol and toluene to the residue, and evaporation, the last traces of acetic acid were removed. The final residue was dissolved in water (5 ml) and added slowly to a solution of sodium borohydride (150 mg) in ice water (5 ml). After 16 hours, sodium ions were removed with Amberlite IR-120 and borate as the volatile methyl ester, and the reduced product was treated with 0.1 *N* sulphuric acid at room temperature for 16 hours (13). The hydrolyzate was neutralized with Dowex-1 resin and concentrated, and was found by paper chromatographic examination to contain two main components indistinguishable from 2-*O*-β-D-glucosyl-D-erythritol and glycerol. This mixture (105 mg) was fractionated on a column of coconut charcoal (25) (5 g) by gradient elution with aqueous ethanol up to a concentration of 20% ethanol, affording 2-*O*-β-D-glucopyranosyl-D-erythritol (40 mg), m.p. 191–194° C and $[\alpha]_D$ −15.2° (*c*, 1.3, H_2O). The X-ray diffraction pattern of the compound was indistinguishable from that of an authentic sample (14). Calculated for $C_{10}H_{20}O_9$: C, 42.25%; H, 7.09%. Found: C, 42.42%; H, 7.39%.

Degradation of II *to Laminaribiose*

A portion (800 mg) of II was hydrolyzed with 0.33 *N* sulphuric acid (30 ml) for 1 hour at 100° C, the hydrolyzate was neutralized, concentrated, and fractionated on a cellulose column using butanol saturated with water as solvent. Laminaribiose (117 mg) was isolated and characterized by conversion to the β-octaacetate, m.p. 163–165° C and $[\alpha]_D$ −26.2° (*c*, 2, $CHCl_3$), which gave an X-ray powder diagram indistinguishable from that of an authentic specimen. Calculated for $C_{28}H_{38}O_{19}$: C, 49.56%; H, 5.65%. Found: C, 49.38%; H, 5.78%.

2-O-β-D-Laminaribiosyl-D-erythritol (VI)

4-*O*-β-D-Laminaribiosyl-D-glucose (II) (200 mg) in water (0.5 ml) was taken up in acetic acid (30 ml) and oxidized with lead tetraacetate (320 mg). After 5 hours excess tetravalent lead was reduced and divalent lead precipitated by addition of excess 10% oxalic acid in acetic acid. The product was reduced with sodium borohydride and crystallized from methanol–ethanol, m.p. 164–166° C and $[\alpha]_D$ −23.8° (*c*, 1.5, H_2O). Calculated for $C_{16}H_{30}O_{14}$: C, 43.05%; H, 6.77%. Found: C, 42.84%; H, 7.08%.

2-O-β-D-Cellobiosyl-D-erythritol (VII) *and 2-O-β-D-Laminaribiosyl-D-erythritol* (VI) *from the Tetrasaccharide Fraction*

The tetrasaccharide fraction appeared to be chromatographically homgeneous, $[\alpha]_D$ +9° (*c*, 3.1, H_2O). The copper-reducing power ratio before and after acid hydrolysis was 1:3.9 (requires 4.0).

A portion (229 mg) of the material was oxidized in 90% acetic acid with lead tetraacetate (916 mg, 6 molar proportions) in the presence of potassium acetate (440 mg) for 11.5 hours. By the procedure described above, the oxidation product was recovered, reduced with sodium borohydride, and partially hydrolyzed. Paper chromatographic examination of the hydrolyzate showed the presence of two triitol components which, after separation by preparative paper chromatography, were found to be:

(*a*) *2-O-β-D-Laminaribiosyl-D-erythritol* (VI) (29 mg).—Crystallized from methanol–ethanol, it had a melting point of 171–173° C and gave an X-ray powder diagram indistinguishable from that of the authentic material.

(*b*) *2-O-β-D-Cellobiosyl-D-erythritol* (VII) (65 mg)—which, after crystallization from aqueous methanol, had a melting point of 209–211° C, $[\alpha]_D$ −8.3° (*c*, 1.2, H_2O), and gave an X-ray powder diagram indistinguishable from that of a specimen prepared from

cellotriose* (27). Calculated for $C_{16}H_{30}O_{14}$: C, 43.05%; H, 6.77%. Found: C, 42.86%; H, 6.84%.

Isolation of these two products showed that the original fraction contained two tetrasaccharide components. The ratio of the triitols, estimated by the anthrone method (26) after elution of the products from paper chromatograms, was 1.8 to 1.

*4'-O-β-*D*-Laminaribiosyl-α-*D*-cellobiose* (VIII)

The tetrasaccharide fraction (243 mg) afforded crystalline material (120 mg) from solution in aqueous methanol, m.p. 221–224° C (decomp.), $[\alpha]_D$ +12.9° (2 minutes) → +10.6 (45 minutes, constant) (*c*, 3.6, H_2O). Calculated for $C_{24}H_{42}O_{21}$: C, 43.24%; H, 6.35%. Found: C, 43.16%; H, 6.67%.

Degraded by the procedure described in the previous section, the crystalline tetrasaccharide afforded 2-*O*-β-D-cellobiosyl-D-erythritol (VII), but no laminaribiosyl-erythritol. Reduction of the tetrasaccharide with sodium borohydride, followed by partial acid hydrolysis with 0.33 *N* sulphuric acid at 100° C for 1 hour, yielded glucose, laminaribiose, cellobiose, and 4-*O*-β-D-laminaribiosyl-D-glucose (II) (paper chromatographic and electrophoretic evidence).

*3'-O-β-*D*-Cellobiosyl-*D*-cellobiose* (IX)

After separation of the crystalline tetrasaccharide (VIII) a second crop of impure VIII was precipitated by addition of ethanol to the mother liquor. Concentration of the supernatant solution afforded an amorphous product (80 mg), $[\alpha]_D$ +19.8° (*c*, 1.6, 90% CH_3COOH). On oxidation with lead tetraacetate – potassium acetate followed by reduction and partial hydrolysis, this material was found chromatographically to account for the production of 2-*O*-β-D-laminaribiosyl-D-erythritol (VI) from the tetrasaccharide fraction; a minor proportion of the cellobiosyl-erythritol (VII) was also detected. The material was reduced with sodium borohydride, then hydrolyzed with hot 0.33 *N* sulphuric acid for 1 hour, yielding glucose, laminaribiose, cellobiose, and 3-*O*-β-D-cellobiosyl-D-glucose (X) (paper chromatographic and electrophoretic evidence).

Products from the Cellulase Degradation of Oat Glucan

*4-O-β-*D*-Laminaribiosyl-D-glucose* (II)

This product, which was chromatographically homogeneous, was characterized by conversion to the β-undecaacetate (540 mg from 310 mg of free sugar), m.p. 120–122° C and $[\alpha]_D$ −22.7° (*c*, 1.5, $CHCl_3$). Calculated for $C_{40}H_{54}O_{27}$: C, 49.69%; H, 5.63%; acetyl, 48.98%. Found: C, 49.77%; H, 5.55%; acetyl, 48.73%.

Tetrasaccharide Fraction

The amorphous product afforded crystalline material from aqueous methanol, m.p. 223–227° C (decomp.), indistinguishable from VIII by comparison of X-ray diffraction powder diagrams. Calculated for $C_{24}H_{42}O_{21}$: C, 43.24%; H, 6.35%. Found: C, 43.04%; H, 6.38%.

In one experiment, a second crystalline modification of this tetrasaccharide was obtained and found to be a dihydrate of the β-anomer, m.p. 180–181° C and $[\alpha]_D$ +7° (2 minutes) → +10° (constant) (*c*, 2, H_2O). Calculated for $C_{24}H_{42}O_{21}.2H_2O$: C, 41.02%; H, 6.60%. Found: C, 41.05%; H, 6.76%. By seeding, the higher-melting α-form (m.p. 221–223° C) of the tetrasaccharide obtained from barley glucan (above) was converted to this lower-melting modification.

By the degradative procedure described above the original, amorphous, tetrasaccharide

**2-O-β-D-Cellobiosyl-D-erythritol was prepared from cellotriose by oxidation with 1.8 molar proportions of lead tetraacetate followed by reduction with sodium borohydride, as in the conversion of cellobiose to 2-O-β-D-glucopyranosyl-D-erythritol (14).*

Can. J. Chem. Downloaded from www.nrcresearchpress.com by 210.87.254.105 on 09/05/12
For personal use only.

fraction was shown (chromatographically) to yield both cellobiosyl-erythritol and laminaribiosyl-erythritol in a ratio of 1.7 to 1 (anthrone method (26)).

Enzymic Degradation of Oat Glucan with Laminarinase

Oat glucan (9.3 mg) in water (1.5 ml) was incubated at 40° C with laminarinase (1, 2 or 3 mg). At the two highest levels of enzyme concentration the copper-reducing power was virtually constant in 2 to 3 hours, when the apparent conversion to glucose was about 25%. A substantially slower reaction was observed at the substrate:enzyme ratio of 9:1. Examined by paper chromatography, all three digests were found to contain two major components which corresponded to a tri- and tetra-saccharide, respectively (R_G 0.47 and 0.22). Minor components detected were glucose, laminaribiose, and material having R_G 0.04.

Oat glucan (1.5 g) in water (100 ml) was incubated with laminarinase (0.25 g) for 2.5 hours. The digest was heated on the boiling-water bath for 7 minutes, filtered, and concentrated. The sugar mixture was fractionated by preparative paper chromatography; individual components were eluted and purified with mixed ion-exchange resins. Yields of the products are given in Table I.

3-O-β-D-Cellobiosyl-D-glucose (X)

The amorphous trisaccharide fraction was chromatographically and electrophoretically homogeneous, $[\alpha]_D$ +12.1° (*c*, 1.7, H_2O). On oxidation with lead tetraacetate in 97% acetic acid an uptake of 0.8 mole of oxidant per mole was found in 15–30 minutes and, in 90% acetic acid and in the presence of potassium acetate, the consumption of lead tetraacetate was 2.9 moles per mole. In both oxidations, approximately 1 mole of pentose (estimated colorimetrically (28)) was produced per mole of trisaccharide, the over-all data being consistent with presence of a 3-linked reducing end D-glucose unit.

Acetylation of the material (225 mg) with hot acetic anhydride – sodium acetate yielded a β-undecaacetate (340 mg), m.p. 104–105° C and $[\alpha]_D$ −9.7° (*c*, 1.6, $CHCl_3$). Calculated for $C_{40}H_{54}O_{27}$: C, 49.69%; H, 5.63%; acetyl, 48.98%. Found: C, 49.42%; H, 5.69%; acetyl, 49.37%.

2-O-β-D-Cellobiosyl-glyceritol (XII)

Trisaccharide X (264 mg) in water (1.5 ml) was taken up in acetic acid (50 ml) and treated with lead tetraacetate (232 mg, 1 molecular proportion) for 2 hours. Excess oxalic acid was added to precipitate the divalent lead, and the filtrate was concentrated. The residue in water (2 ml) was neutralized with sodium bicarbonate and the solution added dropwise to ice-cold sodium borohydride solution (264 mg, 12 ml). After 16 hours the reaction mixture was worked up, affording a solid product (227 mg), which was treated in 97% acetic acid (24 ml) with lead tetraacetate (424 mg, 2 molar proportions) for 16 hours. A second reduction with sodium borohydride followed, and the final product was crystallized from aqueous ethanol, m.p. 138–141° C and $[\alpha]_D$ −15.6° (*c*, 2.5, H_2O). The compound gave an X-ray diffraction pattern indistinguishable from that of an authentic sample* (27). Calculated for $C_{15}H_{28}O_{13}$: C, 43.27%; H, 6.78%. Found: C, 43.00%; H, 6.83%.

3-O-β-D-Cellotriosyl-α-D-glucose (XIV)

The tetrasaccharide fraction readily crystallized from solution in hot aqueous ethanol, m.p. 241–245° C (decomp.) and $[\alpha]_D$ +11.4° (5 minutes) → +8.4° (3 hours, constant)

**Prepared from 2-O-β-D-cellobiosyl-D-erythritol* (VII) *by oxidation with 1 molar proportion of lead tetraacetate followed by reduction with sodium borohydride, as in the degradation of 2-O-β-D-glucopyranosyl-D-erythritol to 2-O-β-D-glucopyranosyl-glyceritol (14).*

Can. J. Chem. Downloaded from www.nrcresearchpress.com by 210.87.254.105 on 09/05/12
For personal use only.

(*c*, 2.7, H_2O). Calculated for $C_{24}H_{42}O_{21}$: C, 43.24%; H, 6.35%. Found: C, 43.19%; H, 6.37%.

Treated in 97% acetic acid with 3 molar proportions of lead tetraacetate, the tetrasaccharide (20 mg) consumed 0.91, 0.96, and 0.99 mole of oxidant/mole at 5, 15, and 30 minutes, respectively, and yielded 1.0 mole of pentose/mole. Hydrolysis of the oxidation product with 0.33 *N* sulphuric acid at 100° C for 1 hour yielded arabinose, glucose, cellobiose, and cellotriose as well as two pentose-containing oligosaccharides (detected chromatographically).

*2-O-β-*D*-Cellotriosyl-glyceritol* (XIII)

Tetrasaccharide XIV (157 mg) was degraded as described above for the conversion of X to XI. The procedure involved, successively, oxidation with 1 molar proportion of lead tetraacetate, reduction with sodium borohydride, oxidation with 2 molar proportions of lead tetraacetate, and reduction with sodium borohydride. The final product was crystallized from aqueous ethanol (weight, 122 mg), m.p. 234–237° C; the X-ray powder diagram was indistinguishable from that of 2-*O*-β-D-cellotriosyl-glyceritol* (27), $[\alpha]_D$ −12.4° (*c*, 1.4, H_2O). Calculated for $C_{21}H_{38}O_{18}$: C, 43.60%; H, 6.62%. Found: C, 43.16%; H, 6.87% (hygroscopic material).

ACKNOWLEDGMENTS

The authors gratefully acknowledge the technical assistance of Mr. J. W. L. C. Christ. Barley flour was kindly provided by Mr. R. Teed, University of Saskatchewan, and a sample of Fortune oats by Dr. D. Knott, University of Saskatchewan. Microanalyses were performed by M. Mazurek, and X-ray diffraction patterns prepared by Miss Inez Gaffney.

REFERENCES

1. C. O'Sullivan. J. Chem. Soc. 41, 24 (1882).
2. D. L. Morris. J. Biol. Chem. **142**, 881 (1942).
3. I. A. Preece and K. G. Mackenzie. J. Inst. Brewing, **58**, 353 (1952).
4. I. A. Preece and R. Hobkirk. J. Inst. Brewing, **59**, 385 (1953).
5. W. O. S. Meredith, T. A. Watts, and J. A. Anderson. Can. J. Chem. **31**, 653 (1953).
6. K. Gilles, W. O. S. Meredith, and F. Smith. Cereal Chem. **29**, 314 (1952).
7. G. O. Aspinall and R. G. J. Telfer. J. Chem. Soc. 3519 (1954).
8. R. A. Aitken, B. P. Eddy, M. Ingram, and C. Weurman. Biochem. J. **64**, 63 (1956).
9. S. Peat, W. J. Whelan, and J. G. Roberts. J. Chem. Soc. 3916 (1957).
10. E. T. Reese, E. Smakula, and A. S. Perlin. Arch. Biochem. Biophys. **85**, 171 (1959).
11. A. S. Perlin and A. R. Lansdown. Can. J. Chem. **34**, 451 (1956).
12. M. L. Wolfrom and H. B. Wood. J. Am. Chem. Soc. **73**, 2933 (1951).
13. I. J. Goldstein, G. W. Hay, B. A. Lewis, and F. Smith. American Chemical Society, 135th Meeting, Abstracts, 3D (1959).
14. A. J. Charlson and A. S. Perlin. Can. J. Chem. **34**, 1200 (1956).
15. F. W. Parrish and A. S. Perlin. Nature. In press.
16. E. T. Reese and M. Mandels. Can. J. Microbiol. **5**, 173 (1959).
17. H. Ono and M. Dazai. Nature, **183**, 1055 (1959).
18. A. B. Foster. J. Chem. Soc. 982 (1953).
19. A. J. Charlson, P. A. J. Gorin, and A. S. Perlin. Can. J. Chem. **35**, 365 (1957).
20. M. A. Jermyn and F. A. Isherwood. Biochem. J. **44**, 402 (1949).
21. R. H. Horrocks. Nature, **164**, 444 (1949).
22. S. M. Partridge. Nature, **158**, 270 (1946).
23. J. L. Frahn and J. A. Mills. Australian J. Chem. **12**, 65 (1959).
24. N. Nelson. J. Biol. Chem. **158**, 375 (1944).
25. F. W. Barth and T. E. Timell. Can. J. Chem. **36**, 1321 (1958).
26. D. L. Morris. Science, **107**, 254 (1948).
27. P. A. J. Gorin and A. S. Perlin. Unpublished results.
28. W. R. Fernell and H. K. King. Analyst, **78**, 80 (1953).

**Prepared from cellotetraose by a sequence of reactions involving two oxidations with lead tetraacetate and two reductions with sodium borohydride, the procedure being the same as used in degrading cellobiose* (XV) *to 2-O-β-*D*-glucopyranosyl-glyceritol (14), and cellotriose to 2-O-β-*D*-cellobiosyl-glyceritol (see above).*

Can. J. Chem. Downloaded from www.nrcresearchpress.com by 210.87.254.105 on 09/05/12
For personal use only.

Can. J. Chem. Downloaded from www.nrcresearchpress.com by 210.87.254.5 on 09/05/12
For personal use only.

STRUCTURE OF BRIDGMAN'S BLACK CARBON DISULPHIDE[1]

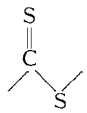
E. WHALLEY

ABSTRACT

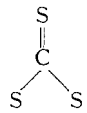
The infrared spectrum of black carbon disulphide dispersed in a potassium bromide disk has been examined. The blackness and the infrared spectrum are consistent with its being a linear polymer, $-(C{=}S.S)_n-$.

1. INTRODUCTION

Bridgman (1) found that carbon disulphide transformed slowly to a black solid at pressures of about 45 kilobars and temperatures over 175° C. When heated to about 200° C at normal pressure it decomposed to carbon and sulphur. It was denser than either graphite or sulphur, and it gave a broad, diffuse X-ray diffraction pattern. He suggested that the structure might be similar to that of silicon dioxide, i.e. a three-dimensional network of carbon and sulphur atoms linked by single bonds. It is difficult to see how a substance with this structure would be black. The blackness of black carbon disulphide demands a highly polarizable system, probably a conjugated one. The simplest that can be envisaged is a linear structure with the unit



repeated indefinitely. The group



is a strong chromophore (2, 3) and thiophene is an aromatic compound, so it seems very likely that the C—S—C group can conjugate with the C=S group. It is difficult to imagine any other structure which is conjugated and in which the atoms are not formally charged.

In order to test this structure, we have investigated the infrared spectrum of black carbon disulphide.

2. EXPERIMENTS AND RESULTS

A small amount of black carbon disulphide was made by subjecting carbon disulphide to a pressure of about 55 kilobars at 185° C in a simple squeezer (4). About 0.1 to 0.2 mg were incorporated into a disk with 400 mg of potassium bromide; more than this amount in the disk caused too much scattering. The spectra were recorded with a Perkin–Elmer Model 21 double-beam infrared spectrophotometer with a sodium chloride prism and with a Beckman IR-4 double-beam spectrophotometer with a cesium bromide prism. Many of the absorption bands observed were very weak and so a 10-times scale expansion was used, and the transmission of a disk containing the sample was divided

[1]*Manuscript received July 8, 1960.*
Contribution from the Division of Applied Chemistry, National Research Council, Ottawa, Canada.
Issued as N.R.C. No. 5946.

point by point by the transmission of a disk containing only potassium bromide. Calibration was conveniently done on the 10-times scale by using incompletely compensated atmosphere bands. The spectrum is shown in Fig. 1. A strong band of variable relative

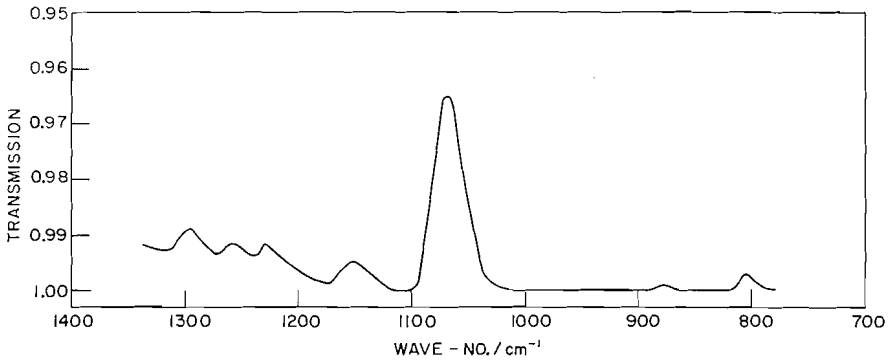


FIG. 1. Infrared spectrum of black carbon disulphide dispersed in a potassium bromide disk.

intensity was always present at $1502\pm\sim5\ cm^{-1}$. It could be removed by prolonged evacuation and gentle warming either before or after making the potassium bromide pellet, and it is attributed to unchanged carbon disulphide. The small shift from the vapor frequency, which is $1522\ cm^{-1}$, indicates that the carbon disulphide is not very strongly attached to the black carbon disulphide. The difficulty of removing it is therefore probably due to slow diffusion through the black carbon disulphide. The other bands were of constant relative intensity, and are listed in Table I.

TABLE I

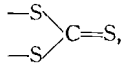
Infrared bands of black carbon disulphide

Frequency cm^{-1}	Rough relative intensity	Assignment
$1286\pm\sim5$	w	O—H bending, end group?
$1250\pm\sim5$	w	C—O stretching, end group, and bands due to imperfections in the chain?
$1220\pm\sim5$	w	
$1144\pm\sim5$	w	
$1063\pm\sim5$	vs	C═S stretching
$870\pm\sim10$	vw	C—S stretching
$806\pm\sim5$	m	

In order to avoid confusion with graphite, the spectrum of graphite was recorded in a similar manner; no bands were observed. The spectrum is discussed in another publication.

3. DISCUSSION

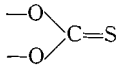
If black carbon disulphide has the structure suggested here then it should show a C═S stretching band. It is well established that compounds that contain the group



such as the trithiocarbonates (5, 6, 7), have a strong infrared band near $1060\ cm^{-1}$

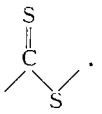
Can. J. Chem. Downloaded from www.nrcresearchpress.com by 210.87.254.5 on 09/05/12
For personal use only.

which is due to the C═S stretching vibration. The strong band in the spectrum of black carbon disulphide at 1063 cm^{-1} is very strong evidence for the presence of this group, in agreement with our expectation. The decrease of frequency of the C═S stretching vibration from its value of about 1220 cm^{-1} in compounds (7) with the group



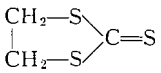
is consistent with a decrease of force constant due to conjugation with the singly bonded sulphur atoms.

If the chain of black carbon disulphide is mainly planar, as it probably is in order to facilitate conjugation, the repeating unit is



In an isolated chain, the only infrared-active vibrations are those that are in phase in each repeating unit, and so the factor group of the line group that describes the symmetry of the chain is appropriate for analyzing the spectrum. There are two parallel reflection planes, one through the S═C group and one through the singly bonded S atom, both perpendicular to the plane of the chain, and a reflection plane in the plane of the chain. There are, of course, twofold axes at the junctions of the planes. The corresponding point group is therefore C_{2v}. There are three atoms in the repeating unit and so there are $(3\times3-4) = 5$ fundamental vibrations that are potentially active. These can be described approximately as a C═S stretching vibration of species a_1, two C—S stretching vibrations of species a_1 and b_1, an S—C═S in-plane bending vibration of species b_1, and an S—C═S out-of-plane bending vibration of species b_2. All are active in infrared absorption.

It is likely that the medium band at 806 cm^{-1} is due to one of the C—S stretching vibrations, and perhaps the very weak band at 870 cm^{-1} is due to the other. There is almost no published information about similar vibrations in simple molecules. The only relevant spectra the author knows of is that of ethylene trithiocarbonate



which was deposited with the Chemical Society by Haszeldine and Kidd (5). There is a moderate band at about 870 cm^{-1} which may correspond to the C—S stretching vibration. The stretching frequency of an unconjugated C—S bond is usually between 700 and 600 cm^{-1} according to Bellamy (8), but conjugation with C═S will probably increase the force constant and so increase the frequency. Our assignment of the 806-cm^{-1} and perhaps the 870-cm^{-1} band to the C—S vibrations seems therefore to be reasonable. The bending vibrations are probably of lower frequency, and are probably weak. They are not observed.

The remaining bands, which are all very weak, cannot be certainly assigned, but plausible guesses can be made. Although it is possible that the chains end in free radicals, as presumably sometimes occurs with the sheets of graphite, it is also possible that

Can. J. Chem. Downloaded from www.nrcresearchpress.com by 210.87.254.5 on 09/05/12
For personal use only.

chemically saturated end groups are present. A possible complete structure is

$$HO\left(\begin{matrix}S\\ \|\\ C-S\end{matrix}\right)_nH,$$

the end groups being derived from a molecule of water, in a similar manner to the polyaldehydes (9). The 1286-cm^{-1} band is perhaps an OH deformation and one of the bands at somewhat lower frequency (1144 cm^{-1}?) is perhaps a C—O stretching vibration. No OH stretching band was observed, though this is not surprising in view of the greater scattering in this region and the presence of adsorbed water. Some of the other bands could be due to imperfections in the chain such as a —C—S— group the wrong way round, but because there are few published spectra of model simple compounds detailed speculation is fruitless.

The author is indebted to Mr. A. Lavergne for help with the high-pressure experiments and to Mr. R. Ironside for taking the infrared spectra.

REFERENCES

1. P. W. Bridgman. Proc. Am. Acad. Arts Sci. **74**, 399 (1941).
2. J. E. Purvis, H. O. Jones, and H. S. Tasker. J. Chem. Soc. **97**, 2287 (1910).
3. E. A. Challenger, E. A. Mason, E. C. Holdsworth, and R. Emmett. J. Chem. Soc. 292 (1953).
4. D. T. Griggs and G. C. Kennedy. Am. J. Sci. **254**, 722 (1956).
5. R. N. Haszeldine and J. M. Kidd. J. Chem. Soc. 3871 (1955).
6. W. I. Jones, W. Kynaston, and J. L. Hales. J. Chem. Soc. 614 (1957).
7. R. Mecke, R. Mecke, and A. Lüttringhaus. Z. Naturforsch. B, **10**, 367 (1955).
8. L. J. Bellamy. The infra-red spectra of complex molecules. 2nd ed. Methuen & Co., Ltd., London. 1958. p. 353.
9. A. Novak and E. Whalley. Trans. Faraday Soc. **55**, 1490 (1959); Can. J. Chem. **37**, 1710, 1718, 1722 (1959).

Can. J. Chem. Downloaded from www.nrcresearchpress.com by 210.87.254.5 on 09/05/12
For personal use only.

Can. J. Chem. Downloaded from www.nrcresearchpress.com by 210.87.254.105 on 09/05/12
For personal use only.

IONIZATION OF ORGANIC COMPOUNDS IN ACID

I. ALIPHATIC KETONES[1]

H. J. CAMPBELL[2] AND J. T. EDWARD

ABSTRACT

The changes in the ultraviolet absorption spectra of aliphatic ketones in aqueous sulphuric acid have been followed as the acid strength is increased from 0 to 98%. With increase in strength up to 65% the weak peak at about 270 mμ is shifted to shorter wavelengths by a medium effect. However, with further increase in acid strength the peak disappears altogether because of protonation of the carbonyl group. The pK_{BH^+} values of several ketones have been calculated from the spectrophotometric results to be about −7. The pK_{BH^+} values of cyclic ketones vary systematically with ring size. The significance of the present work to recent studies on the rate of enolization of acetone is discussed.

INTRODUCTION

In absolute sulphuric acid, aliphatic and aromatic ketones (B) are essentially completely protonated to form the conjugate acid (BH^+) (1). The extent of protonation of the ketone in a less concentrated acid solution may be determined by the ultraviolet absorption at a given wavelength, according to the equation

$$[1] \qquad [B]/[BH^+] = (\epsilon_{BH^+}-\epsilon)/(\epsilon-\epsilon_B)$$

where ϵ_B, ϵ_{BH^+}, and ϵ are the molecular extinction coefficients of the unprotonated ketone, the protonated ketone, and the ketone in the test solution, and the quantities in brackets represent concentrations (2, 3). From the variation of $[B]/[BH^+]$ with the acidity function H_0 (4, 5) of the acid solvent, the protonation constant (pK_{BH^+}) of BH^+, defined by

$$[2] \qquad pK_{BH^+} = H_0 - \log [B]/[BH^+],$$

may be determined. For acetophenone Hammett (2) found a pK_{BH^+} of −6.03, recalculated as −6.15 by use of a corrected acidity function scale (5). This value was confirmed recently by Stewart and Yates (6).

By analogy with the behavior of other aliphatic and aromatic oxygen bases, e.g. benzoic acid ($pK_{BH^+} = -7.38$) and acetic acid ($pK_{BH^+} = -6.2$ (5)), the pK_{BH^+} values of aliphatic ketones would also be expected to be about −6. This view finds support in measurements of the relative basicities of various ketones from their effect on the rate of the acid-catalyzed etherification of benzhydrol in refluxing benzene (7), which indicated cyclopentanone, cyclohexanone, and diethyl ketone to have about the same basicity as *p*-methylacetophenone ($pK_{BH^+} = -5.47$ (6)). Furthermore, Lemaire and Lucas (8) observed no measurable protonation of acetone, acetophenone, and benzophenone by small concentrations of perchloric acid in acetic acid, and concluded that these compounds must have pK_{BH^+} values below −4.5. On the other hand, Nagakura, Minegishi, and Stanfield (9) recently reported a spectrophotometric determination of a pK_{BH^+} of −1.58 for acetone. This unexpectedly high basicity has prompted our reinvestigation by spectrophotometry of the ionization of acetone and other aliphatic ketones. We have found that protonation of the ketones occurs only in much more concentrated acids than those investigated by Nagakura *et al.*, and that in fact most aliphatic ketones have pK_{BH^+} values of about −7.

[1]*Manuscript received in original form March 28, 1960, and, as revised, August 2, 1960. Contribution from the Department of Chemistry, McGill University, Montreal 2, Que.*
[2]*Holder of C.I.L. Scholarship, 1959–60.*

Can. J. Chem. Downloaded from www.nrcresearchpress.com by 210.87.254.105 on 09/05/12
For personal use only.

EXPERIMENTAL

Materials

Chemically pure acetone and methyl ethyl ketone were purified by treatment with potassium permanganate according to Vogel (10), followed by fractionation through a 25×1 cm vacuum-jacketed column packed with glass helices, the middle fraction being taken. Cyclobutanone (Aldrich Chemical Co.) was distilled, and the middle fraction, b.p. 98–99° C at 759 mm, was used. Methyl isopropyl ketone, methyl *t*-butyl ketone, cyclopentanone, cyclohexanone, cycloheptanone (Aldrich), and cyclooctanone (Aldrich) were purified via their semicarbazones (11), which were recrystallized to constant melting point and then decomposed with 10% sulphuric acid. The ketones were removed by steam distillation, dried over magnesium sulphate, and then distilled as above.

The acid solutions were obtained by dilution of Nichols C.P. Reagent sulphuric acid (95.5–96.5%) and Baker and Adamson Reagent perchloric acid (70–72%), and the concentrations determined by titration with standard alkali. Sulphuric acid (98%) was prepared by adding 30% fuming sulphuric acid (Baker and Adamson Reagent) to 96% sulphuric acid. The corresponding H_0 values were read from large scale plots of H_0 against acid concentration, constructed from the data of Paul and Long (5).

Apparatus

Most measurements were made with a Beckmann Model DU spectrophotometer using quartz cells of 1 cm light path. The cell compartment was maintained at 25±0.1° C by thermospacers. With this instrument measurements could be taken down to a wavelength of about 220 mμ. For a few measurements down to wavelengths of about 185 mμ, a Unicam SP 500 spectrophotometer was used. There was no temperature control in the cell compartment of this instrument; the temperatures of the solutions in these cases were about 22±3° C.

Procedure

Solutions were made up by weighing the ketone (10–20 mg) directly into a 10-ml volumetric flask containing about 2 ml of the acid solution to be used as solvent, and swirling to mix the solution. In this manner weighing errors due to evaporation of the ketone were reduced. The solutions were made up to volume, mixed, and their extinction coefficients at various wavelengths measured. A solvent blank of acid of the same concentration as that containing the ketone was used.

RESULTS AND DISCUSSION

A selection of curves for the absorption above 220 mμ of acetone (Figs. 1A and 1B) and of cyclohexanone (Figs. 1C and 1D) in various strengths of sulphuric acid is shown. The family of curves over this range of wavelengths for methyl ethyl ketone in 0 to 65.3% acid resembled that of acetone; those for the other ketones resembled more that of cyclohexanone. The positions of the long wavelength peaks in water and in 65.3% sulphuric acid are given in Table I. The spectra of solutions of acetone in 0–66.6% perchloric acid varied with acid concentration in a fashion similar to that shown in Fig. 1A for solutions in sulphuric acid.

Extent of Condensation Reactions in Strong Acid Solution

Acetone in 96% sulphuric acid, when in fairly high concentration, is converted to mesityl oxide, phorone, and other compounds having strong ultraviolet absorption (9). However, it is believed that following the experimental procedure given above such condensation reactions are almost negligible, because of the great dilution almost

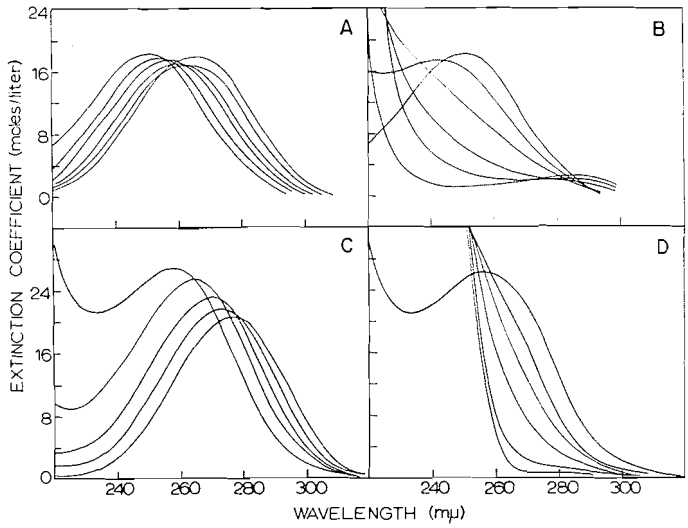


FIG. 1. Ultraviolet absorption curves of ketones in sulphuric acid solutions.
(A) Acetone in dilute acid: 0, 24.0, 41.7, 50.7, 58.8, and 65.3% H_2SO_4 reading from right to left, respectively.
(B) Acetone in concentrated acid: 65.3, 74.1, 80.0, 84.7, 89.2, and 98.2% H_2SO_4 respectively.
(C) Cyclohexanone in dilute acid: 0, 32.2, 44.9, 57.2, and 65.3% H_2SO_4 respectively.
(D) Cyclohexanone in concentrated acid: 65.3, 72.2, 76.3, 81.3, 87.0, and 98.6% H_2SO_4 respectively.

TABLE I

Wavelengths (in mμ) of peaks for $n \rightarrow \pi^*$ transitions of ketones in different media

Ketone	In inert solvent	In water	In 65.3% H_2SO_4
Acetone	277[a]	266	250
Methyl ethyl ketone	278[b]	268	254
Methyl isopropyl ketone	285[b]	275	259
Methyl *t*-butyl ketone	288[c]	278	262
Cyclobutanone	280[d]	274	255
Cyclopentanone	300,[c] 299,[d] 295[b]	281	261
Cyclohexanone	285,[d] 288[b]	277	262
Cycloheptanone	281[e]	278	259
Cyclooctanone	290[c]	277	(<260)[f]

[a]In cyclohexane, ref. 21. [b]In ethylene dichloride, ref. 22. [c]In cyclohexane. [d]In hexane, ref. 11. [e]In hexane, ref. 23. [f]Submerged by edge of much more intense peak at ca. 185 mμ due to $\pi \rightarrow \pi^*$ transition.

instantaneously achieved by the ketone in the acid solutions. (The importance of the dilution effect has been emphasized by Grace and Symons (12).) Thus, when a solution of acetone in 98% sulphuric acid was diluted to give an acid concentration of 50%, the spectrum was practically identical with that of a solution prepared directly from 50% acid; the latter preparation would almost certainly be free from condensation products. However, it seems likely that the small peak found at about 280 mμ for solutions of acetone, methyl ethyl ketone, and cyclooctanone in the stronger acid solutions (see Fig. 1B for acetone) comes from condensation products. Mesityl oxide in concentrated sulphuric acid has λ_{max} at 284 mμ (9); the condensation to mesityl oxide of 0.03% of the acetone dissolved in 98.2% sulphuric acid would suffice to give the molecular extinction coefficient observed by us (Fig. 1B) at 284 mμ. This portion of the spectrum, further-

Can. J. Chem. Downloaded from www.nrcresearchpress.com by 210.87.254.105 on 09/05/12
For personal use only.

more, was found to have an optical density which increased very slowly with time; however, the portion from 220–260 mμ, which furnished the values of the extinction coefficient for the calculations mentioned below, did not change with time.

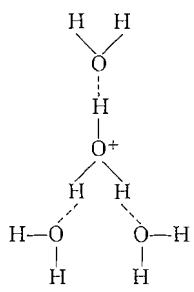
While we may conclude that the spectra obtained in the present instance are substantially those of the ketones themselves and not of condensation products, the reverse has been true for the spectra previously reported for aliphatic ketones in concentrated acid solution (13).

Gillespie, Hughes, and Ingold (14), in cryoscopic studies of very dilute solutions of acetone in absolute sulphuric acid, assumed that no destruction of the ketone was taking place, although the condensation of two molecules of acetone to form one molecule of mesityl oxide and one molecule of water would have led to no change in the cryoscopic behavior of the solution. However, the present work shows their assumption to have been justified.

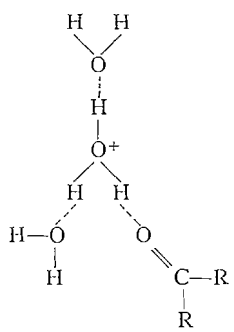
Effect of Acid Strength on the $n \rightarrow \pi^*$ Transition of Ketones

The weak, long wavelength absorption of aliphatic ketones is ascribed to the excitation of an electron from a non-bonding (n) orbital of the oxygen to an antibonding (π^*) orbital of the carbonyl group (15). The absorption peak is shifted to shorter wavelengths (a "blue shift") with increasing polarity of the solvent, because of the preferential stabilization of the ground state of the carbonyl group by dipole–dipole interactions or by hydrogen-bonding with a solvent molecule (16, 17, 18, 19, 20). This effect accounts for the different wavelengths of the absorption peaks of the ketones in hydrocarbon or other inert solvents and in water (Table I).

It has long been known that the 265 mμ peak of acetone in water undergoes a further blue shift to 261 mμ in 5 *M* aqueous calcium chloride (24); we have found the peak also at 261 mμ in 15 *M* lithium bromide. In these concentrations of electrolyte a fair proportion of the water is bound in the primary or secondary hydration shells of the cations (25). The polarization of these water molecules, induced by the charge of the cation, should increase the strengths of the hydrogen bonds to the carbonyl oxygen (26). The progressive blue shifts produced by increasing hydronium ion concentration in going from 0 to 65.3% sulphuric acid (Table I and Figs. 1A and 1C) and from 0 to 66.6% perchloric acid are also best explained by a progressive increase in the strength of the hydrogen-bonding of solvent molecules to ketone. In dilute aqueous solution the hydronium ion exists as the relatively stable ion $H^+.4H_2O$ (I) (27, 28). However, in 65.3% sulphuric acid only 3 moles of water are present for each mole of acid, so that it is possible that in this strength of acid the ketone molecules are for the most part associated directly with hydronium ions as pictured in (II).



I



II

Can. J. Chem. Downloaded from www.nrcresearchpress.com by 210.87.254.105 on 09/05/12
For personal use only.

Can. J. Chem. Downloaded from www.nrcresearchpress.com by 210.87.254.105 on 09/05/12
For personal use only.

Nagakura, Minegishi, and Stanfield (9) have interpreted the blue shifts of acetone with increasing acid concentration as due to protonation of the ketone. However, their arguments for this interpretation are unsound for the following reasons:

1. They claim that a simple equilibrium between two species of molecules is shown by the presence of an isobestic point in the family of absorption curves. However, only the curves for acetone (Fig. 1A) and methyl ethyl ketone show an approximation to an isobestic point (cf. Fig. 1C).

2. They point out that the pK_B ($= -pK_{BH^+}$) values for acetone calculated from extinction coefficients at various wavelengths, and on both sides of the isobestic point, are approximately constant, varying from 1.39 to 1.72. However, they restricted their attention to solutions having $H_0 = -2.32$ or more. Over this limited range of acidities the absorption of acetone and methyl ethyl ketone (but *not* of the other ketones) does indeed change with H_0 according to equations 1 and 2. However, this correspondence of experimental results with those expected for a $pK_{BH^+} = -1.58$ for acetone is limited to the region above $H_0 = -2.3$, and is not found if one takes account of the absorption in more acidic solutions of $H_0 = -3$ to -5.

It seems more reasonable to associate protonation of the ketone with the disappearance of the long wavelength peak (16) as the sulphuric acid concentration is increased from 65% to 98% (Figs. 1B and 1D), a region of acid concentrations not investigated by Nagakura *et al.* This explanation is confirmed by the fact that in this region of acid concentrations the changes in absorption *for all ketones* follow approximately the changes in acidity function according to equations 1 and 2. This is shown in Figs. 2A and 2B

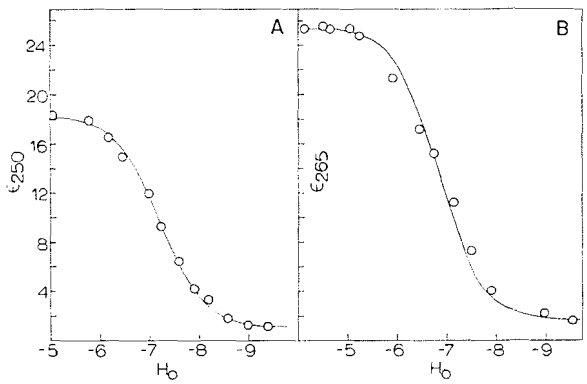


FIG. 2. (A) Ionization of acetone in H_2SO_4. Theoretical curve for equations 1 and 2, with $pK_{BH^+} = -7.2$.
(B) Ionization of cyclohexanone in H_2SO_4. Theoretical curve for $pK_{BH^+} = -6.8$.

for acetone and cyclohexanone, in which the molecular absorption coefficients at 250 mμ and 265 mμ, respectively, have been plotted against the values of the acidity function of the solutions. The experimental values fit reasonably well with the theoretical curve calculated from equations 1 and 2, using the values of ϵ_B and ϵ_{BH^+} recorded in Table II. Plots of ϵ at other wavelengths against H_0 indicated slightly different pK_{BH^+} values. Those for acetone (wavelengths given) were: -7.4 (245 mμ), -7.3 (248 mμ), -7.1 (252 mμ), -7.0 (255 mμ). However, the fit of the experimental points to the theoretical curve was less satisfactory than that found taking ϵ at 250 mμ. It was assumed that these deviations were caused by the medium effect (2), and the wavelength chosen (λ, Table II) was that which afforded the best fit of experimental points to the theoretical curve. However

TABLE II

Basicities of ketones

Ketone	λ (mμ)	ϵ_B	ϵ_{BH^+}	$-pK_{BH^+}$
Acetone	250	18.2	1.2	7.2
Methyl ethyl ketone	250	21.8	0.9	7.2
Methyl isopropyl ketone	260	34.0	3.2	7.1
Methyl *t*-butyl ketone	265	36.5	1.8	7.1
Cyclobutanone	260	33.0	3.0	9.5
Cyclopentanone	260	24.8	1.8	7.5
Cyclohexanone	265	25.4	1.8	6.8
Cycloheptanone	265	32.3	3.8	6.6
Cyclooctanone	270	24.5	6.4	6.2

it seems likely that because of the uncertainty in allowing for the medium effect the precision of the pK_{BH^+} values cannot be better than about ±0.2 unit. These values, listed in Table II, were all obtained by this graphical method. Graphical analysis of the absorption results by the slightly different method of Davis and Geissman (29) gave substantially the same pK_{BH^+} values.

It is apparent that unstrained cyclic and acyclic ketones all have pK_{BH^+} values of about −7. Contrary to the evidence of Pratt and Matsuda (7), the basicities of cyclopentanone and cyclohexanone differ considerably from that of *p*-methylacetophenone; however, it is not to be expected that exactly the same order of basicities will be shown in aqueous acids and in benzene.

In the series acetone, methyl ethyl ketone, methyl isopropyl ketone, and methyl *t*-butyl ketone, it is probable that the tendency for basicity to be increased by the inductive effect of an increasing number of alkyl groups on the α-carbon atom is offset by the effect of these groups in restricting the stabilization of the protonated ketone by solvation (30). The increase in basicity with ring size on going from cyclobutanone to cyclooctanone agrees with recent findings that the strengths of hydrogen bonds between these ketones and methanol or chloroform increase in the same order (31). These changes in basicity parallel changes in the infrared stretching frequency of the carbonyl group, as shown in Fig. 3. A similar change has been noted in both basicity and infrared frequency

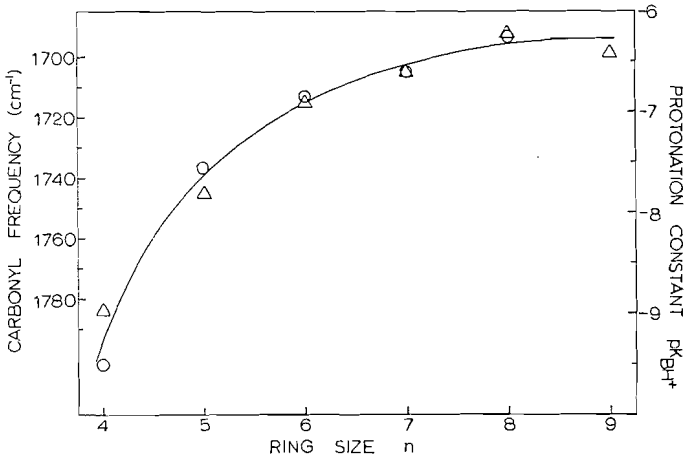


FIG. 3. Change of infrared stretching frequency (△) and pK_{BH^+} (○) with number of carbon atoms (*n*) in cyclic ketones.

Can. J. Chem. Downloaded from www.nrcresearchpress.com by 210.87.254.105 on 09/05/12
For personal use only.

of the carbonyl group of benzlactams with increasing ring size (32), while Stewart and Yates (6) have shown a linear relationship between the basicity and carbonyl frequency of *meta*- and *para*-substituted acetophenones.

The simple aliphatic ketones of Table II are much weaker bases than enolized β-diketones such as 5,5-dimethylcyclohexane-1,3-dione (pK_{BH^+} −0.8) and acetylacetone (pK_{BH^+} −3.7) (33); this is to be expected because of the resonance stabilization of the protonated forms of the latter compounds (e.g., V).



Va Vb

Effect of Acid on the $\pi \rightarrow \pi^*$ Transition of Aliphatic Ketones

Besides the $n \rightarrow \pi^*$ transition, ketones show a more intense absorption at shorter wavelengths due to a $\pi \rightarrow \pi^*$ transition. In the case of α,β-unsaturated ketones the change from an inert solvent to a hydrogen-bonding (17, 24, 34) or protonating solvent (9) causes a red shift in this peak, but acetone shows a blue shift on changing the solvent from isooctane (λ_{max} 187.6 mμ (34)) to water (34, 35). It has been claimed that this differing behavior is to be expected for two-center (36) and four-center (9) $\pi \rightarrow \pi^*$ transitions. However, the $\pi \rightarrow \pi^*$ peak for cyclohexanone showed a red shift on protonation (Table III). Unfortunately, with the spectrophotometers available it was not

TABLE III

Molecular extinction coefficients at 190 mμ of ketones in various solvents

Ketone	Solvent			
	Cyclohexane	Water	65% H_2SO_4	96% H_2SO_4
Acetone	1060[a]	148	34	340
Cyclohexanone	440	800	1540	2520[b]
Cyclooctanone	2900	1360	2400	3610

[a]At 194 mμ. [b]$\lambda_{max} \simeq 192$ mμ (flat peak); $\epsilon_{max} = 2520$.

possible to measure the absorption at low enough wavelengths to define this peak for the protonated forms of acetone and cyclooctanone. However, it seems likely, from the change in extinction coefficient at 190 mμ (Table III) that it undergoes a red shift on protonation in these cases also. The results in Table III indicate that the spectra of the non-protonated ketones vary with the solvent in an irregular fashion.

The Basicity and Rate of Enolization of Acetone

The enolization of ketones is known to involve the participation of one or more water molecules in addition to the protonated ketone molecule in the rate-determining step (37). However, Archer and Bell (38) recently showed that if a pK_{BH^+} of −1.58 were accepted for acetone, then its rate of enolization in 1–8 *M* hydrochloric acid is approximately proportional to the fraction of the compound protonated. According to the Hammett–Zucker hypothesis (39, 40), this would indicate that the reaction does *not*

Can. J. Chem. Downloaded from www.nrcresearchpress.com by 210.87.254.105 on 09/05/12
For personal use only.

involve a water molecule in rate-determining step, and hence the results were interpreted as a disproof of the hypothesis. However, it seems likely that Archer and Bell's correlation is fortuitous because of the limited range of acid concentrations investigated by them. In fact, accepting a pK_{BH^+} of -7.2, a better correlation of their enolization rates with changing acidity is obtained by plotting $\log k_\psi + H_0$, where k_ψ is the experimental first-order rate constant based on the concentration of acetone, against $\log a_{H_2O}$, where a_{H_2O} is the activity of the water in the various concentrations of hydrochloric acid. The points fit closely to a straight line of slope 3.7. Bunnett (41) has recently shown that such a relation is more general than the Hammett–Zucker relations, and that the slope of the curve defines a hydration parameter w for the reaction, which is related to the number of water molecules in the transition state of the rate-determining step.

ACKNOWLEDGMENTS

We are grateful to the National Research Council for generous financial help.

REFERENCES

1. R. J. Gillespie and J. A. Leisten. Quart. Revs. (London), **8**, 40 (1954).
2. L. A. Flexser, L. P. Hammett, and A. Dingwall. J. Am. Chem. Soc. **57**, 2103 (1935).
3. L. A. Flexser and L. P. Hammett. J. Am. Chem. Soc. **60**, 885 (1938).
4. L. P. Hammett. Physical organic chemistry. McGraw-Hill, New York. 1940. p. 262.
5. M. A. Paul and F. A. Long. Chem. Revs. **57**, 1 (1957).
6. R. Stewart and K. Yates. J. Am. Chem. Soc. **80**, 6355 (1958).
7. E. F. Pratt and K. Matsuda. J. Am. Chem. Soc. **75**, 3739 (1953).
8. H. Lemaire and H. J. Lucas. J. Am. Chem. Soc. **73**, 5198 (1951).
9. S. Nagakura, A. Minegishi, and K. Stanfield. J. Am. Chem. Soc. **79**, 1033 (1957).
10. A. I. Vogel. Practical organic chemistry. Longmans, Green & Co., London. 1956. p. 171.
11. S. W. Benson and G. B. Kistiakowsky. J. Am. Chem. Soc. **64**, 80 (1942).
12. J. A. Grace and M. C. R. Symons. J. Chem. Soc. 958 (1959).
13. L. C. Anderson and C. M. Gooding. J. Am. Chem. Soc. **57**, 999 (1935).
14. R. J. Gillespie, E. D. Hughes, and C. K. Ingold. J. Chem. Soc. 2473 (1950).
15. H. L. McMurry and R. S. Mulliken. Proc. Natl. Acad. Sci. **26**, 312 (1940). H. L. McMurry. J. Chem. Phys. **9**, 231, 241 (1941).
16. M. Kasha. Discussions Faraday Soc. **9**, 14 (1950).
17. H. McConnell. J. Chem. Phys. **20**, 700 (1952).
18. N. S. Bayliss and E. G. McRae. J. Phys. Chem. **58**, 1002 (1954).
19. G. J. Brealey and M. Kasha. J. Am. Chem. Soc. **77**, 4462 (1955).
20. G. C. Pimentel. J. Am. Chem. Soc. **79**, 3323 (1957).
21. T. M. Lowry and R. E. Lishmund. J. Chem. Soc. 1313 (1935).
22. M. F. Hawthorne and W. D. Emmons. J. Am. Chem. Soc. **80**, 6399 (1958).
23. A. Castille and E. Ruppol. Bull. soc. chim. biol. **10**, 623 (1928).
24. G. Scheibe. Ber. **58**, 588 (1925).
25. J. O'M. Bockris. Quart. Revs. (London), **3**, 173 (1949).
26. C. A. Coulson. Research (London), **10**, 149 (1957).
27. E. Wicke, M. Eigen, and T. Ackermann. Z. physik. Chem. **1**, 340 (1954).
28. K. N. Bascombe and R. P. Bell. Discussions Faraday Soc. **24**, 158 (1957).
29. C. T. Davis and T. A. Geissman. J. Am. Chem. Soc. **76**, 3507 (1954).
30. H. C. Brown, D. H. McDaniel, and O. Häfliger. *In* Determination of organic structures by physical methods. *Edited by* E. A. Braude and F. C. Nachod. Academic Press, New York. 1955. p. 567.
31. M. Tamres and S. Searles. J. Am. Chem. Soc. **81**, 2100 (1959).
32. R. Huisgen, I. Ugi, H. Brade, and E. Rauenbusch. Ann. **586**, 30 (1954).
33. B. Eistert, E. Merkel, and W. Reiss. Chem. Ber. **87**, 1513 (1954).
34. E. M. Kosower. J. Am. Chem. Soc. **80**, 3261 (1958).
35. H. Ley and B. Arends. Z. physik. Chem. B, **12**, 132 (1931).
36. L. Goodman. Footnote (44) in ref. 34.
37. C. G. Swain, A. J. DiMilo, and J. P. Cordner. J. Am. Chem. Soc. **80**, 5983 (1958).
38. G. Archer and R. P. Bell. J. Chem. Soc. 3228 (1959).
39. L. Zucker and L. P. Hammett. J. Am. Chem. Soc. **61**, 2791 (1939).
40. F. A. Long and M. A. Paul. Chem. Revs. **57**, 935 (1947).
41. J. F. Bunnett. J. Am. Chem. Soc. **82**, 500 (1960).

Can. J. Chem. Downloaded from www.nrcresearchpress.com by 210.87.254.105 on 09/05/12
For personal use only.

Can. J. Chem. Downloaded from www.nrcresearchpress.com by 210.87.254.105 on 09/05/12
For personal use only.

THE USE OF THE HELLMANN–FEYNMAN THEOREM TO CALCULATE MOLECULAR ENERGIES[1]

RICHARD F. W. BADER

ABSTRACT

The Hellmann–Feynman theorem has been employed to calculate the repulsion between two helium atoms and the molecular energies of H_2 and H_3. The method of molecular orbitals was used to determine the necessary expressions for the electron densities. The screening constants of the atomic orbitals comprising the molecular orbitals were treated as functions of the internuclear separation according to an empirical expression which duplicates very closely the "best" values for these parameters as determined by the variational method. The results of the calculations indicate that the present method is capable of yielding estimates of molecular energies which are comparable to those obtained by the more elaborate and time-consuming variational methods.

I. THE ELECTROSTATIC METHOD OF CALCULATING MOLECULAR ENERGIES

The Hellmann–Feynman theorem states that the x-component of the force acting on the αth nucleus, considered as occupying some fixed position in a molecule, is

$$[1] \qquad F_{\alpha x} = \frac{\partial}{\partial x_\alpha}\left(\sum_{\beta(\neq\alpha)} \frac{Z_\alpha Z_\beta e^2}{r_{\alpha\beta}}\right) - \int \rho \mathfrak{E}_{\alpha x}\, d\mathbf{r}$$

where Z_α is the nuclear charge of nucleus α, $r_{\alpha\beta}$ an internuclear separation, ρ is the electron density at the point (x, y, z), and $\mathfrak{E}_{\alpha x}$ is the electric field produced by the αth nucleus in the x-direction at the position of the ith electron (1). Equation [1] states that the force $F_{\alpha x}$ acting on a nucleus in any system of nuclei and electrons is simply the sum of the classical electrostatic forces due to the other nuclei and to the electron charge distribution. Thus, once the electronic charge density $\rho(x, y, z)$ has been determined by the methods of quantum mechanics, the forces acting on the nuclei are interpretable entirely in terms of classical electrostatics. The wave function for a molecule containing n electrons is a function of $3n$ space co-ordinates. However, due to the equivalence of all the electrons in a molecule, the electron density at any point is a three-dimensional quantity of physical significance. Because of this the formulation given by equation [1] of the forces which bind a molecule together is conceptually simpler than the more usual discussion in terms of the energies involved.

Hurley, in a series of papers (2, 3, 4, 5), has given a reformulation of the Hellmann–Feynman theorem together with a very thorough comparison of the electrostatic method of calculating molecular energies with the more usual method employing the Ritz variational procedure. Hurley has shown that if the exact wave function is used in equation [1] then the forces acting on the nucleus as calculated by the electrostatic method will agree precisely with those calculated from the results obtained by the variational procedure. However, when an approximation is made to the wave function, either in terms of molecular orbitals or Heitler–London functions, the two methods will not necessarily agree. Hurley has examined this question and has shown that when all of the variable parameters in the wave function, excluding the scale factor (the orbital exponent in hydrogen-like atomic orbitals), are determined by the variational procedure, the electrostatic and the conventional methods will lead to identical results. Variation of the scale factor as well insures that the results will be consistent with the virial theorem.

[1]*Manuscript received July 5, 1960.*
Contribution from the Department of Chemistry, University of Ottawa, Ottawa, Ontario.

Although not always thought of as such, the internuclear distance is a variable parameter in a valence bond or molecular orbital wave function. Thus to insure agreement between the electrostatic and the variational methods it is necessary to employ so-called floating wave functions. These are wave functions which allow for the possibility of the electron charge detaching itself from the nucleus and taking up an optimum position along the internuclear axis, thus in effect making the internuclear separation a parameter to be varied in terms of the *electronic* co-ordinates.

There is no reason a priori to prefer the variational method to the electrostatic method in the calculation of molecular energies. One is forced to employ approximate wave functions in both methods and the ultimate test is the agreement with experiment. Thus there is no need to employ floating wave functions in electrostatic calculations in order to insure that the results of such a calculation will agree with those obtained from the conventional method.* In fact it is well known that a wave function based on the molecular orbital approximation leads to incorrect results at large internuclear distances when this wave function is employed in a variational type of calculation. If this same simple molecular orbital formulation is used to approximate the electron density for use in equation [1] this difficulty does not arise as the function leads to the correct expression for the electron density at infinite internuclear separation. Thus to employ a floating wave function in an electrostatic calculation would but reintroduce the errors of the conventional method when molecular orbitals were employed.

Hurley (2) has employed the simple molecular orbital approximation in the electrostatic calculations for the hydrogen molecule and for the repulsion between two helium atoms. The agreement of these calculations with the experimental results was fair. The great merit of the electrostatic calculations lies in their great simplicity and the case with which they may be carried out. It would be of great value, therefore, if they could be improved to the point where the accuracy of their results would justify their application to systems which at present are too complicated by the conventional methods. Such calculations would also be very useful for rapid estimates of the properties of transition-state molecules with reference to absolute rate theory and isotope effects.

It is the purpose of the present investigation to show that an improvement may be obtained in the calculation of molecular energies by the electrostatic method by employing molecular orbitals in which certain of the parameters are adjusted empirically so as to give a wave function which approximates very closely the one obtained by a variational calculation. The great beauty of the variational method whereby parameters may be varied to minimize the energy is of course not found in the electrostatic method. Instead some means must be devised to adjust the parameters in the wave function empirically. The most suitable parameters to vary in a simple molecular orbital function are the orbital exponents or screening constants. This is the procedure that has been adopted in the present calculations.

The expression for the electron density to be substituted into equation [1] was determined by the methods of molecular orbitals. The molecular orbitals were taken as linear combinations of Slater atomic orbitals. The screening constant $Z(R)$ in the atomic orbitals is treated as a parameter, a function of the internuclear separation, R. The empirical rule used to govern the variation of $Z(R)$ with R is

$$[2] \qquad Z(R) = Z_s - \Delta Z e^{-R}$$

**Shull and Ebbing (19) have in fact shown that much of the previously published numerical work involving floating wave functions is in error, and that very little improvement in energy results from allowing the orbitals to float.*

Can. J. Chem. Downloaded from www.nrcresearchpress.com by 210.87.254.105 on 09/05/12
For personal use only.

where R is expressed in atomic units (a.u.). Z_s is the value of the screening constant for the separated atoms (when R equals infinity) and $\Delta Z = Z_s - Z_u$, Z_u being the screening constant for the united atom (when R equals zero). It is well known from variational calculations that the value of $Z(R)$ varies in a smooth fashion from the value for the separated atoms to that for the united atom. Equation [2] reproduces the values obtained for $Z(R)$ by the variational method in a very striking fashion. The merits of this function have been previously discussed by Musulin (6).

II. AN ELECTROSTATIC CALCULATION OF THE ENERGY OF THE HYDROGEN MOLECULE

The hydrogen molecule correlates with the ^1S state of the helium atom. Thus for this calculation $Z_s = 1$, $Z_u = 2$, and the expression for $Z(R)$ becomes

$$Z(R) = 1+e^{-R}.$$

If we let the atomic orbital centered on nucleus α be represented by ϕ_α and that on nucleus β by ϕ_β then the electron density for the hydrogen molecule, as given by the molecular orbital theory, is

[3] $$\rho = (1+s)^{-1}(\phi_\alpha^2+\phi_\beta^2+2\phi_\alpha\phi_\beta)$$

where s is the overlap integral between ϕ_α and ϕ_β. When this expression for the electron density is substituted into equation [1] the following expression is obtained for the force in atomic units acting on nucleus α in the line of the nuclei which is taken as the x-axis,

[4] $$F_{\alpha x} = \frac{1}{R^2} - (1-s)^{-1}[\langle\phi_\beta\phi_\beta|\cos\theta_{\alpha i}/r_{\alpha i}^2\rangle+2\langle\phi_\alpha\phi_\beta|\cos\theta_{\alpha i}/r_{\alpha i}^2\rangle],$$

where $\theta_{\alpha i}$ and $r_{\alpha i}$ are the polar co-ordinates of the ith electron with origin at nucleus α. All of the integrals occurring in equation [4] have been evaluated analytically by Coulson (7). Equation [4] together with equation [3] allows one to calculate the force acting on nucleus α for any value of R. The results of the calculation are shown in Fig. 1

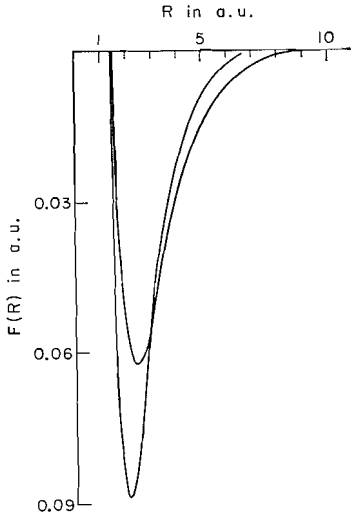


FIG. 1. Experimental (lowest curve at 2 a.u.) and calculated force curves for H_2.

Can. J. Chem. Downloaded from www.nrcresearchpress.com by 210.87.254.105 on 09/05/12
For personal use only.

Can. J. Chem. Downloaded from www.nrcresearchpress.com by 210.87.254.105 on 09/05/12
For personal use only.

together with the experimental curve obtained from the derivative of the Morse potential for the hydrogen molecule. It is seen that the force predicted by equation [4] is too large at large distances and not quite large enough at shorter distances. The agreement, however, is very good and represents a substantial improvement over the earlier electrostatic calculations and over the variational method. The energy of the hydrogen molecule as obtained from an integration of the calculated curve together with the equilibrium internuclear distance is compared in Table I with the experimental values and with those obtained by other methods as indicated.

TABLE I

	Present calc.	Hurley (2)	Simple M.O. (8)	Expt. (9)
Binding energy (in a.u.)	0.158	0.136	0.098	0.174
R_e (in a.u.)	1.56	1.8	1.6	1.4

III. AN ELECTROSTATIC CALCULATION OF THE REPULSION BETWEEN TWO HELIUM ATOMS

The approach of two normal helium atoms results in the molecular state $(\sigma_g 1s)^2\ (\sigma_u 1s)^2\ {}^1\Sigma_g^+$. For very small internuclear separations this state will correlate with the $1s\sigma^2 2p\sigma^2\ {}^1\Sigma_g^+$ state, which in the limit of the united atom reverts to the $1s^2 2p^2$ electronic configuration of the beryllium atom. However, the splitting of a beryllium atom with a $1s^2 2s^2$ electronic configuration will also give rise to a ${}^1\Sigma_g^+$ molecular state, which for small internuclear separations must lie lower than the state resulting from the $1s^2 2p^2$ configuration (9). This second ${}^1\Sigma_g^+$ state correlates with two separated helium atoms in ${}^3S$ states and thus for large internuclear separations it must possess a higher energy than the state resulting from the configuration $(\sigma_g 1s)^2\ (\sigma_u 1s)^2$. It is evident from these considerations that for large separations the molecular orbitals of the He_2 system are best considered as $\sigma_g 1s$ and $\sigma_u 1s$ while for very close approach of the two nuclei the system is more faithfully represented by an electronic configuration of the form $(\sigma_g 1s)^2\ (\sigma_g 2s)^2$.

Buckingham (20) and Wu (10) have pointed out that all of the quantum mechanical calculations performed so far for the He_2 system have used an upper molecular orbital of σ_u character. This, they feel, explains why all such calculations have been in serious error for small values of R. Much better results should be obtained if instead one employed an orbital with more $\sigma_g 2s$ character for small internuclear separations.

We have employed two wave functions in the electrostatic calculations for the He_2 system. The first is similar to that employed by Huzinaga (11) in the best variational treatment so far performed for He_2. It is derived from the electronic configuration $(\sigma_g 1s)^2\ (\sigma_u 1s)^2$. The second was used in calculations for very small values of R and thus employed the $\sigma_g 2s$ orbital in place of the $\sigma_u 1s$ orbital.

In this case it is necessary to employ two screening constants, one for the σ_g orbital and one for the σ_u orbital. The value of Z_s for the σ_g orbital is 1.70, the value of the screening constant for the helium atom. The screening constant for the united atom is taken equal to 4.00, the nuclear charge for the beryllium atom.* The expression for the screening constant for the σ_g orbital, $Z(R)_g$ is

$$Z(R)_g = 1.70 + 2.30e^{-R}.$$

The presence of the second electron in the orbital is not taken into account in determining the screening constant for the united atom. Thus Z_u in the case of H_2 was taken as 2.00, not as 1.70, and for the helium atoms, Z_u is given a value of 4.00, not 3.70. This procedure is followed simply because the values so obtained for the energies are in better agreement with the experimental ones and Z(R) is in any event an empirical parameter.

The screening constant for the σ_u orbital goes to the same limit for infinite internuclear separation as it does for the σ_g orbital, i.e., 1.70. However, the united atom limit for the σ_u orbital is a $2p$ atomic orbital of a beryllium atom, screened by two $1s$ electrons. Thus $Z_u = 2.30/2$. (The result is divided by 2, the principal quantum number, as required by the Slater recipe.) The screening constant for the σ_u orbital, $Z(R)_u$, is

$$Z(R)_u = 1.70 - 0.55e^{-R}.$$

There are thus two atomic orbital functions necessary for each helium atom. They are of the form

$$\phi_{\alpha g} = (Z(R)_g^3/\pi)^{1/2} \exp(-Z(R)_g r_\alpha),$$
$$\phi_{\alpha u} = (Z(R)_u^3/\pi)^{1/2} \exp(-Z(R)_u r_\alpha).$$

The wave function for a system of two helium atoms is

$$\Psi = (4!)^{-1/2} \sum (-1)^p P \sigma_g(1)\sigma_g(2)\sigma_u(3)\sigma_u(4)\alpha(1)\beta(2)\alpha(3)\beta(4)$$

where σ_g and σ_u are the orthonormal molecular orbitals

$$\sigma_g = (2+2s_g)^{-1/2}(\phi_{\alpha g} + \phi_{\beta g}); \qquad \sigma_u = (2-2s_u)^{-1/2}(\phi_{\alpha u} - \phi_{\beta u})$$

and s_g and s_u are the appropriate overlap integrals. The electron density resulting from this wave function is

$$\rho = (1+s_g)^{-1}(\phi_{\alpha g}^2 + \phi_{\beta g}^2 + 2\phi_{\alpha g}\phi_{\beta g}) + (1-s_u)^{-1}(\phi_{\alpha u}^2 + \phi_{\beta u}^2 - 2\phi_{\alpha u}\phi_{\beta u})$$

and thus the force exerted on nucleus α along the line of approach of the two atoms is

$$[5] \qquad F_{\alpha x}(R) = \frac{1}{R^2} - 2(1+s_g)^{-1}[\langle \phi_{\beta g}\phi_{\beta g} | \cos\theta_{\alpha i}/r_{\alpha i}^2\rangle + 2\langle \phi_{\alpha g}\phi_{\beta g} | \cos\theta_{\alpha i}/r_{\alpha i}^2\rangle]$$
$$- 2(1-s_u)^{-1}[\langle \phi_{\beta u}\phi_{\beta u} | \cos\theta_{\alpha i}/r_{\alpha i}^2\rangle - 2\langle \phi_{\alpha u}\phi_{\beta u} | \cos\theta_{\alpha i}/r_{\alpha i}^2\rangle]$$

where the symbols have the same significance as previously. Again, as in the case of the hydrogen molecule, only one- and two-center one-electron integrals arise which are easily evaluated. The results of the calculation are shown in Fig. 2 together with the best variational calculation that has so far been performed (11) and the experimental results of Amdur and Harkness (12). The electrostatic calculations in this case almost duplicate the variational treatment. It is evident that the repulsion predicted by the electrostatic and the variational calculations at small values of R is far too extreme. This is to be expected of a wave function with σ_u character in the light of the opening discussion on the He_2 system. If we assume that for small values of R we are justified in excluding all σ_u character and instead employ a wave function resulting from the electronic configuration $(\sigma_g 1s)^2 (\sigma_g 2s)^2$, then a separate electrostatic calculation may be performed. From this we may hope to determine whether or not the contribution from the $\sigma_g 2s$ orbital does improve the calculation to a point where it gives results of the right order of magnitude and at the same time gain some idea of where the transition from $\sigma_u 1s$ to $\sigma_g 2s$ character occurs. Both of these features would be of value in a more refined variational treatment which took account of the $\sigma_g 2s$ contribution.

We begin by assigning the four electrons to two orthogonal molecular orbitals

$$\Psi = (4!)^{-1/2} \sum (-1)^p P \sigma_g(1)\sigma_g(2)\sigma_{g0}(3)\sigma_{g0}(4)\alpha(1)\beta(2)\alpha(3)\beta(4)$$

Can. J. Chem. Downloaded from www.nrcresearchpress.com by 210.87.254.105 on 09/05/12
For personal use only.

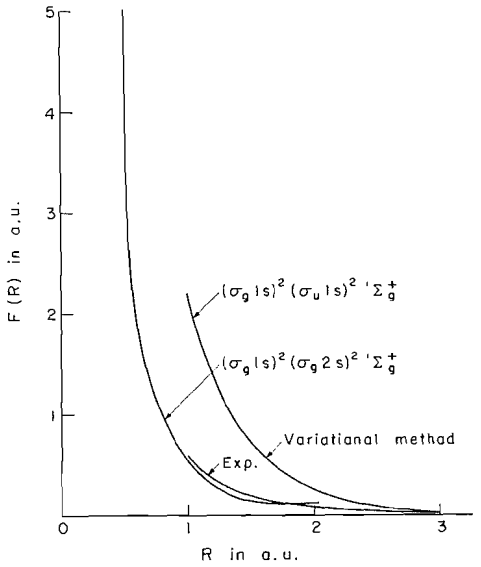


FIG. 2. Force curves for He_2. The curve of the results obtained by the variational method (3 a.u.→1 a.u.) is identical with that obtained by the indicated electrostatic method to the accuracy of this plot.

where σ_g is identical with the corresponding orbital employed above and σ_{g0} is given by

$$\sigma_{g0} = (\sigma_{g'} - s_{gg'}\sigma_g)(1-s_{gg'}^2)^{-1/2}.$$

The $\sigma_{g'}$ molecular orbital is composed of atomic $2s$ orbitals and is of the form

$$\sigma_{g'} = (2+2s_{g'})^{-1/2}(X_\alpha + X_\beta)$$

where

$$X_\alpha = (Z_{g'}^5/3\pi)r_\alpha \exp(-Z_{g'}r_\alpha).$$

The electron density for the system is then found to be

$$\rho = (\sigma_g^2 + \sigma_{g'}^2 - 2s_{gg'}\sigma_{g'}\sigma_g)(1-s_{gg'}^2)^{-1}.$$

The expression for the force on nucleus α is obtained in the same manner as previously, but due to the lack of orthogonality between the σ_g and $\sigma_{g'}$ orbitals is too cumbersome to be set down here. Since the Slater method of assigning screening constants does not differentiate between orbitals of the same principal quantum number, i.e., the $2s$ and $2p$ of the united atom beryllium, we have employed the same value for $Z_{g'}$ as was employed for Z_u.

The results of the calculations are given in Fig. 2. Obviously the answer to improving the calculations for He_2 does depend upon the inclusion of the $\sigma_g 2s$ orbital. The electrostatic calculations now predict a repulsion which is actually slightly less than that obtained experimentally for small values of R. It is only for values of R less than 3 a.u. that the function with σ_u character diverges seriously. Any contribution from this function must be small in the region of 1 a.u. A calculated point has been included for 0.5 a.u., a region which is not covered by experiment. The force of repulsion is seen to rise very steeply in this region to a value of 5.02 a.u.

Can. J. Chem. Downloaded from www.nrcresearchpress.com by 210.87.254.105 on 09/05/12
For personal use only.

Can. J. Chem. Downloaded from www.nrcresearchpress.com by 210.87.254.105 on 09/05/12
For personal use only.

IV. AN ELECTROSTATIC CALCULATION OF THE ENERGY OF THE H_3 MOLECULE

The electronic energy of a system of three hydrogen atoms has been the subject of many theoretical investigations. The most recent of these calculations was carried out by Boys and Shavitt (13), who employed the method of molecular orbitals with the superposition of configurations. This very extensive variational calculation demanded the use of an electronic computer. It is of interest to compare with their results those which can be obtained by an electrostatic calculation, a calculation which is easily carried out using a desk computer.

The three hydrogen atoms are arranged in a linear symmetric fashion as shown:

$$\underset{\alpha}{\cdot}\overset{\leftarrow R \rightarrow}{\text{———}}\underset{\beta}{\cdot}\text{———}\underset{\gamma}{\cdot}$$

The two internuclear distances $R_{\alpha\beta}$ and $R_{\beta\gamma}$ are maintained equal to each other ($= R$) and varied from infinity to the equilibrium value R_e. For any value of R the force exerted on nucleus α is equal and opposite to the force exerted on nucleus γ. There is no net force acting on nucleus β in the linear symmetrical configuration. The energy of H_3 in this configuration can thus be obtained by the integration of the force acting on nucleus α as the three atoms are brought together in the symmetric fashion from infinity to the equilibrium separation R_e.

The correlation diagram for the approach of three hydrogen atoms (the system at all times possessing $D_{\infty h}$ symmetry) is shown in Fig. 3. Two molecular orbitals will be

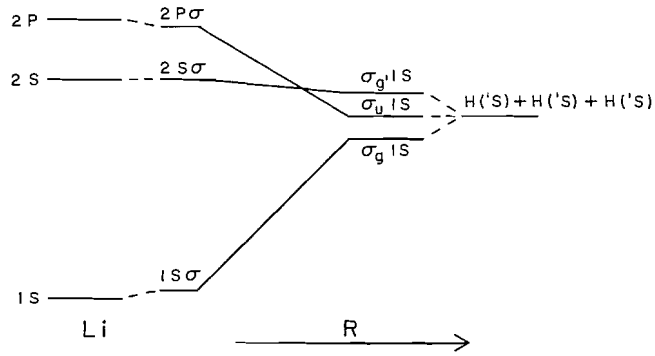


FIG. 3. Correlation diagram for H_3 in the $D_{\infty h}$ nuclear configuration.

occupied in the ground electronic configuration, a σ_g and a σ_u orbital. The value of Z_s for all three of the molecular orbitals will be unity and Z_u will equal 3.00 and 0.65 for the σ_g and σ_u orbitals, respectively. The screening constants for the two occupied orbitals are therefore,

$$Z(R)_g = 1+2e^{-R} \qquad \text{and} \qquad Z(R)_u + 1 - 0.35e^{-R}.$$

The forms of the three molecular orbitals which result from the linear combinations of the hydrogen 1s atomic orbitals are

$$\sigma_g = N_g(\phi_{\alpha g}+\lambda\phi_{\beta g}+\phi_{\gamma g})$$

$$\sigma_u = N_u(\phi_{\alpha u}-\phi_{\gamma u})$$

$$\sigma_{g'} = N_g'(\phi_{\alpha g}'-\lambda'\phi_{\beta g}'+\phi_{\gamma g}')$$

where the N_i are normalizing factors and the ϕ's are again normalized atomic orbitals of the Slater type. The ground state wave function for linear symmetric H_3 is

$$\Psi = (3!)^{-1/2}\sum (-1)^p P\sigma_g(1)\sigma_g(2)\sigma_u(3)\alpha(1)\beta(2)\alpha(3)$$

and this results in an electron density

$$\rho = 2[2+2S^g_{\alpha\gamma}+2\lambda(S^g_{\alpha\beta}+S^g_{\beta\gamma})]^{-1}[\phi_{\alpha g}{}^2+\lambda^2\phi_{\beta g}{}^2+\phi_{\gamma g}{}^2+2\lambda\phi_{\alpha g}\phi_{\beta g} + 2\lambda\phi_{\beta g}\phi_{\gamma g}+2\phi_{\alpha g}\phi_{\gamma g}]+[2-2S^u_{\alpha\gamma}]^{-1}[\phi_{\alpha u}{}^2+\phi_{\gamma u}{}^2-2\phi_{\alpha u}\phi_{\gamma u}].$$

The five necessary atomic orbitals will be of the forms

$$\phi_{\alpha g} = (Z(R)_g{}^3/\pi)^{1/2}\exp(-Z(R)_g r_\alpha) \qquad \text{for the } \sigma_g \text{ orbital,}$$

$$\phi_{\alpha u} = (Z(R)_u{}^3/\pi)^{1/2}\exp(-Z(\mathrm{R})_u r_\alpha) \qquad \text{for the } \sigma_u \text{ orbital.}$$

The application of the Hellmann–Feynman theorem gives the following expression for the force acting on nucleus α along the line of centers

$$F_{\alpha z}(R) = \frac{1.25}{R^2} - 2N_g^2\{\langle\phi_{\beta g}\phi_{\beta g}|\cos\theta_{\alpha i}/r^2_{\alpha i}\rangle+\langle\phi_{\gamma g}\phi_{\gamma g}|\cos\theta_{\alpha i}/r^2_{\alpha i}\rangle + 2\lambda\langle\phi_{\alpha g}\phi_{\beta g}|\cos\theta_{\alpha i}/r^2_{\alpha i}\rangle+2\lambda\langle\phi_{\beta g}\phi_{\gamma g}|\cos\theta_{\alpha i}/r^2_{\alpha i}\rangle + 2\langle\phi_{\alpha g}\phi_{\gamma g}|\cos\theta_{\alpha i}/r^2_{\alpha i}\rangle\} - N_u^2\{\langle\phi_{\gamma u}\phi_{\gamma u}|\cos\theta_{\alpha i}/r^2_{\alpha i}\rangle - 2\langle\phi_{\alpha u}\phi_{\gamma u}|\cos\theta_{\alpha i}/r^2_{\alpha i}\rangle\}.$$

All but one of the integrals occurring in equation [6] are similar to the ones previously encountered. The one new integral is

$$\langle\phi_\beta\phi_\gamma|\cos\theta_{\alpha i}/r^2_{\alpha i}\rangle.$$

This is a three-center one-electron integral and it possesses no analytical solution. The integral represents the interaction of an ideal dipole centered on nucleus α with the charge distribution arising from the overlap of the atomic orbitals on nuclei β and γ. The value of this integral can be approximated by a transformation to known integrals of the type $\langle\phi_\beta\phi_\beta|\cos\theta_{\alpha i}/r^2_{\alpha i}\rangle$ using an expansion first suggested by Mulliken (14) and later commented on and discussed by Rüdenberg (15) and Csavinszky (16). Both ϕ_β and ϕ_γ are expanded in terms of an orthonormal set of hydrogenic wave functions centered on the opposite atom, i.e.,

$$\phi_\beta = \sum_j S_{\beta\gamma(j)}\phi_{\gamma(j)} \qquad \text{and} \qquad \phi_\gamma = \sum_i S_{\gamma\beta(i)}\phi_{\beta(i)}$$

where the coefficients of the expansion, $S_{\beta\gamma(j)}$, are the corresponding overlap integrals

$$\langle\phi_\beta|\phi_{\gamma(j)}\rangle.$$

With this expansion $\phi_\beta\phi_\gamma$ becomes

$$\phi_\beta\phi_\gamma = 1/2S_{\beta\gamma(1)}(\phi_\beta\phi_{\beta(1)}+\phi_\gamma\phi_{\gamma(1)})+1/2S_{\beta\gamma(2)}(\phi_\beta\phi_{\beta(2)}+\phi_\gamma\phi_{\gamma(2)})+\ldots\ .$$

Rüdenberg has pointed out that this expansion is best for small values of R. Under these conditions the coefficients $S_{\beta\gamma(j)}$, $j \neq 1$ become vanishingly small because of their near orthogonality. As a guide to the approximation we have employed the same

Can. J. Chem. Downloaded from www.nrcresearchpress.com by 210.87.254.105 on 09/05/12
For personal use only.

expansion to approximate the known integral $\langle\phi_\alpha\phi_\beta|\cos\theta_\alpha/r_{\alpha i}^2\rangle$. Out to 4 a.u. the major portion is contributed by the leading term as is to be expected. Beyond 4 a.u. the contributions from terms of larger j values became increasingly important and made the approximation prohibitive. Instead, it was found that the known integral was very well approximated by the values of

$$R^{-1/2}S_{\alpha\beta}\langle\phi_\beta\phi_\beta|\cos\theta_{\alpha i}/r_{\alpha i}^2\rangle.$$

For values of $R > 4$ a.u. this same form was used to approximate the three-center integral as well.

The value which is to be given to the parameter λ, which occurs in the expression for the σ_g orbital, is yet to be determined. In variational calculations the energy is minimized with respect to λ and its optimum value is thus determined. The parameter λ possesses no optimum value in an electrostatic calculation, the force exerted on nucleus α by the electrons in the σ_g orbital increasing to a limiting value of $2\langle\phi_\beta\phi_\beta|\cos\theta_\alpha/r_\alpha^2\rangle$ as the value of λ is increased. However, a lower limit can be given to λ even in the electrostatic calculations. For large values of R, λ must approach the value $\sqrt{2}$ if the wave function is to give the correct electron density for large separations. Walsh and Matsen (17) have carried out a variational calculation for H_3 using the wave function employed in this investigation and have found the optimum value for λ to be 1.5 when the effective nuclear charges were simultaneously varied. It is to be expected that λ will have a value greater than $\sqrt{2}$ as charge is forced onto the central atom from the two neighboring atoms as the internuclear separation is decreased.*

TABLE II

	Present calc.		Simple M.O. (17)	M.O. with C.I. (13)	Expt. (13)
	$\lambda = \sqrt{2}$	$\lambda = 1.5$			
Binding energy (in a.u.)	0.1307	0.1482	0.0733	0.1278	0.1625
R_e (in a.u.)	1.66	1.61	1.82	1.779	—

The energy of H_3 has been determined for λ equal to $\sqrt{2}$ and to 1.5, that is, the lower limiting value and a higher one, consistent with that found from a variational calculation. The results of the calculations are given in Table II. The electrostatic calculation with $\lambda = \sqrt{2}$ (equivalent to treating λ as a constant in a variational calculation) is seen to far surpass the simple molecular orbital approach and to match the more elegant calculation of Boys and Shavitt which included the contributions from configurational interaction. When the value of λ is increased to 1.5, only a 9% error remains in the calculated energy, and of course this is a more realistic value of λ than is $\sqrt{2}$. The values of the frequencies for the symmetrical stretch ω_1 and the bending vibration ω_2 of the H_3 molecule are easily determined from the results of the electrostatic calculation. The value of the frequency for the antisymmetric stretching vibration cannot, unfortunately, be determined in these calculations unless some additional assumptions are made. The frequencies obtained, together with those determined by Boys and Shavitt (13) and by Weston (18) are given in Table III. The values reported by Weston were obtained by an application of Sato's method for determining potential energy surfaces, in this

*The parameter λ was not treated as a function of R in the electrostatic calculations. A variation of λ from 1.5 at $R = 2$ to $\lambda = \sqrt{2}$ at $R = \infty$ would not significantly change the result since the variation is slight and since the major change brought about by a change in λ is in the region of $R = 2$.

Can. J. Chem. Downloaded from www.nrcresearchpress.com by 210.87.254.105 on 09/05/12
For personal use only.

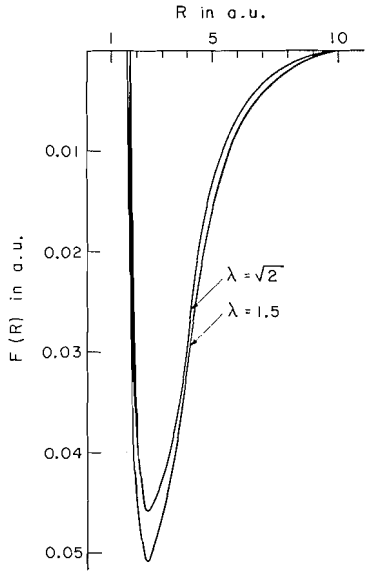


FIG. 4. Force curves for H_3 for two values of the parameter λ.

TABLE III

	Present calc.		Boys and Shavitt (13)	Weston (18)
	λ = √2	λ = 1.5		
ω_1 (cm^{-1})	2066	2093	1945	2108
ω_2 (cm^{-1})	1292	1307	952	877

case applied to the H + H_2 reaction. The values for ω_1 are seen to be in fair agreement with the other calculations, while a higher value is predicted for the bending vibration.

V. DISCUSSION

The results of the present calculations indicate that the electrostatic method, when complemented with the empirical expression [2] for determining the screening constant, is capable of giving very reliable estimates of binding energies and force constants. Furthermore, these results may be obtained with relative ease and in a short period of time. This method should be of value in the calculation of the properties of transition states where calculations capable of giving reliable results would be of great help.

It should be pointed out that the use of equation [2] need not necessarily be considered an empirical correction. Since it reproduces the "best" wave functions as determined by the variational procedure to such a remarkable degree, it can be argued that its use is simply to provide the electrostatic method with the best possible wave function obtainable from the variational method.

REFERENCES

1. J. O. HIRSCHFELDER, C. F. CURTISS, and R. B. BIRD. Molecular theory of gases and liquids. John Wiley & Sons, Inc., New York. 1954. p. 934.
2. A. C. HURLEY. Proc. Roy. Soc. A, **226**, 170 (1954).
3. A. C. HURLEY. Proc. Roy. Soc. A, **226**, 179 (1954).
4. A. C. HURLEY. Proc. Roy. Soc. A, **226**, 193 (1954).

Can. J. Chem. Downloaded from www.nrcresearchpress.com by 210.87.254.105 on 09/05/12
For personal use only.

5. A. C. HURLEY. Proc. Roy. Soc. A, **235**, 224 (1956).
6. B. MUSULIN. J. Chem. Phys. **25**, 801 (1956).
7. C. A. COULSON. Proc. Cambridge Phil. Soc. **38**, 210 (1942).
8. H. HELLMANN. Einführung in die Quantum-chemie. Leipzig. 1937.
9. G. HERZBERG. Molecular spectra and molecular structure I. Spectra of diatomic molecules. Van Nostrand, New York. 1950.
10. TA-YOU WU. J. Chem. Phys. **28**, 986 (1958).
11. S. HUZINAGA. Progr. Theoret. Phys. (Kyoto), **18**, 139 (1957).
12. I. AMDUR and A. L. HARKNESS. J. Chem. Phys. **22**, 664 (1954).
13. S. F. BOYS and I. SHAVITT. Tech. Rept. WIS-AF-13, Ser. 3, AF 33 (616)-3414, March, 1959.
14. R. S. MULLIKEN. J. chim. phys. **46**, 500 (1949).
15. K. RÜDENBERG. J. Chem. Phys. **19**, 1433 (1951).
16. P. CSAVINSKY. J. Chem. Phys. **28**, 996 (1958).
17. J. M. WALSH and F. A. MATSEN. J. Chem. Phys. **19**, 526 (1951).
18. R. E. WESTON. J. Chem. Phys. **31**, 892 (1959).
19. H. SHULL and D. D. EBBING. J. Chem. Phys. **28**, 866 (1958).
20. R. A. BUCKINGHAM. Trans. Faraday Soc. **54**, 453 (1958).

Can. J. Chem. Downloaded from www.nrcresearchpress.com by 210.87.254.105 on 09/05/12
For personal use only.

Can. J. Chem. Downloaded from www.nrcresearchpress.com by 210.87.254.40 on 09/05/12
For personal use only.

THE REACTIONS OF PERFLUOROETHYL RADICALS WITH HYDROGEN AND METHANE[1]

S. J. W. PRICE[2] AND K. O. KUTSCHKE

ABSTRACT

The reactions of C_2F_5 radicals, produced by the photolysis of $(C_2F_5)_2CO$, with methane and hydrogen have been studied. Assuming zero activation energy for $2C_2F_5 \rightarrow C_4F_{10}$ the activation energies for $C_2F_5 + CH_4 \rightarrow C_2F_5H + CH_3$ and $C_2F_5 + H_2 \rightarrow C_2F_5H + H$ are 10.6 kcal/mole and 11.9 kcal/mole respectively. The present results have been correlated with data on the reactions of CF_3, C_3F_7, and CH_3 radicals with H_2, D_2, CH_4, and C_2H_6. Taking $E_{recombination} \approx 0$ in all cases and assuming the frequency factor for the recombination reaction varies little from radical to radical, the order of ease of hydrogen abstraction from a given substrate is $CF_3 > C_2F_5 > C_3F_7 > CH_3$. Similarly the ease of hydrogen abstraction from a substrate by a given fluorinated radical is $C_2H_6 > H_2 > CH_4 > D_2$. A calculation based on very limited data indicates the reaction $CH_3 + C_2F_5COC_2F_5 \rightarrow CH_3COC_2F_5 + C_2F_5$ may occur with an activation energy of approximately 7 kcal/mole.

INTRODUCTION

The availability of CF_3 and n-C_3F_7 radicals from the photolysis of the appropriate ketone (1, 2) has led to the study of the reactions of these radicals with simple hydrocarbons, hydrogen, and deuterium (3, 4, 5, 6). Recently C_2F_5 radicals have been obtained by the photolysis of $(C_2F_5)_2CO$ (7). In the present work the reactions of this radical with hydrogen and with methane have been studied.

As was the case in the study of n-C_3F_7 radical reactions the condensable product could not be separated quantitatively from the ketone by low-temperature distillation. A combination of gas phase adsorption chromatography and mass spectrometry has been used in an attempt to obtain complete analysis of the reaction products.

EXPERIMENTAL

Apparatus

The photolysis apparatus was similar to that employed in similar investigations in this laboratory (2, 5). The quartz reaction cell (optical path 10 cm, 190 cc) was mounted inside a hot box which could be controlled to $\pm 0.1°$ C. It was fully illuminated by a parallel beam of light in the 3130 Å region obtained via a standard set of filters (8) from a Hanovia S500 lamp operated on a regulated supply. The cell was connected to the vacuum system through a mercury cutoff mounted immediately below the hot box. The volume of the connecting tubing and a small Dewar sealed to the top of the reaction cell, both of which were outside the irradiated region, was approximately 20 cc thus giving a total volume of 210 cc for the reaction system.

Materials

The perfluorodiethyl ketone used in this work was supplied by Merck and Company of Canada. The ketone contained significant quantities of benzene and some unidentified bromine compound. These impurities were removed in the later stages of the work by a method described previously (7). Phillips Research Grade methane was used without further purification. Hydrogen was purified by passage through a palladium thimble.

[1]*Manuscript received July 20, 1960.*
Contribution from the Division of Pure Chemistry, National Research Council, Ottawa, Canada.
Issued as N.R.C. No. 5965.
[2]*National Research Council Postdoctorate Fellow 1958–59. Present address: Chemistry Department, Essex College, Assumption University, Windsor, Ontario.*

C_2F_5H for calibration of the mass spectrometer and the chromatographic columns was prepared by photolysis of $(C_2F_5)_2CO$ (80 mm) with hydrogen (160 mm) at 250° C and low light intensity (approximately 0.8×10^{12} quanta/cc sec). The mass spectrum of C_2F_5H is given in Table I.

TABLE I

Mass spectrum of C_2F_5H*

Mass No.	Relative height	Probable positive ion
31	8.33	CF
32	2.68	CFH
44	3.80	C_2FH
50	2.88	CF_2
51	100.00	CF_2H
69	27.60	CF_3
100	2.16	C_2F_4
101	47.0	C_2F_4H
119	1.53	C_2F_5

*The isotope peaks are not recorded.

Procedure

Perfluorodiethyl ketone was admitted to the reaction zone and to connecting tubing of the mixing volume, and its pressure read on a mercury manometer. The ketone was condensed in a side arm of the mixing chamber which then was isolated from the measuring volume. Hydrogen or methane was admitted and measured in a similar manner. The ketone was warmed and transferred back to the measuring volume by means of a Toepler pump. After they were mixed 10 times by expansion into the Toepler pump the mixed gases were compressed to their original volume. The reaction zone was isolated by raising the mercury in the cutoff below the hot box and the experiment was started by removing a stop from the light beam. The experiments were allowed to proceed to 2.5% to 10% decomposition of the ketone, most experiments being in the region of 5% decomposition.

Analysis

(*i*) $(C_2F_5)_2CO + CH_4$

The products of the photolysis were passed through two traps at −120° C to remove the bulk of the ketone and then through a trap at −210° C to remove the remaining condensable materials. Carbon monoxide and methane were transferred to a copper oxide furnace at 300° C. After 2 hours, during which time the gases in the copper oxide furnace were mixed several times, the mixture in the furnace was condensed at −196° C and the methane pumped off. The CO_2 was measured in a gas burette.

Since C_4F_{10} and the ketone cannot be separated readily by low-temperature distillation, the entire mixture of condensable products was transferred to a gas chromatographic apparatus where it was analyzed using a 3-ft alumina column (4 mm I.D.) maintained at 25° C. Hydrogen was used as a carrier gas at a flow rate of approximately 60 cc per minute. Exact retention volumes or appearance times cannot be given as these varied considerably with the moisture content of the alumina and the age of the column. As far as could be ascertained the ketone is completely absorbed on the column. Because of this the columns have a useful life of approximately 15 analyses. During this time the sensitivity based on peak height increases by as much as a factor of two.

Can. J. Chem. Downloaded from www.nrcresearchpress.com by 210.87.254.40 on 09/05/12
For personal use only.

The elution times similarly decrease. However, for a given column at a fixed temperature and flow rate, the relative elution times remain constant as does the sensitivity based on peak area (this latter point was checked by running a standard C_4F_{10} sample immediately after each analysis). In all cases the products appeared in the order C_2H_6, C_4F_{10}, a peak initially unidentified which was later shown to be C_2F_5Br, and a peak consisting of a mixture of C_2F_5H and $C_2F_5CH_3$. Under the stated conditions the appearance time of C_4F_{10} varied from column to column and with column age over the approximate range 10 minutes to 30 minutes. When the appearance time for C_4F_{10} was about 10 minutes the following approximate appearance times were observed: C_2H_6, 1 minute; C_2F_5Br, 17 minutes; $C_2F_5H + C_2F_5CH_3$, 35 minutes.

The mass spectrum of accumulated C_2F_5Br peaks is shown in Table II.

TABLE II

Mass spectrum of C_2F_5Br

Mass No.	Relative peak height	Probable positive ion
31	20.0	CF
50	10.7	CF_2
69	44.9	CF_3
79	5.9	Br
81	6.1	Br
91	1.1	CBr
93	1.1	CBr
100	4.9	C_2F_4
110	2.0	CFBr
112	2.0	CFBr
119	100	C_2F_5
129	30.6	CF_2Br
131	30.0	CF_2Br
141	.05	C_2F_2Br
143	.05	C_2F_2Br
160	.17	C_2F_3Br
162	.17	C_2F_3Br
179	13.9	C_2F_4Br
181	13.5	C_2F_4Br
198	17.7	C_2F_5Br
200	19.0	C_2F_5Br

The mixture of C_2F_5H and $C_2F_5CH_3$ was collected as it was eluted from the column, its volume measured in a gas burette, and the mixture analyzed on a mass spectrometer using the mass 51 (CF_2H) and mass 101 (C_2F_4H) peaks for C_2F_5H and the mass 65 (CF_2CH_3) peak for $C_2F_5CH_3$. The mass spectrometer was calibrated using C_2F_5H. Hence C_2F_5H was determined directly and the $C_2F_5CH_3$ calculated by difference. In each case the relative sensitivity to C_2F_5H (based on mass 51) and $C_2F_5CH_3$ (based on mass 65) was 0.63:1.00. During the course of the work a new element was installed in the mass spectrometer. This changed the sensitivity to CH_4 (using mass 15) from approximately 7 cm peak height per micron to 24 cm peak height per micron but had no apparent effect on the relative sensitivity of C_2F_5H to $C_2F_5CH_3$ (as based on masses 51 and 65). The mass spectrum of $C_2F_5CH_3$ obtained by subtracting the C_2F_5H spectrum from that of a mixture of the compounds is given in Table III. Virtually the same $C_2F_5CH_3$ spectrum is obtained using any of the analyses carried out in the course of the work.

(*ii*) $(C_2F_5)_2CO + H_2$

The condensable products were trapped out as described in Section (*i*). Carbon monoxide and hydrogen were oxidized to carbon dioxide and water in a copper oxide furnace

Can. J. Chem. Downloaded from www.nrcresearchpress.com by 210.87.254.40 on 09/05/12
For personal use only.

TABLE III

Mass spectrum of $C_2F_5CH_3$ obtained by subtracting the C_2F_5H spectrum from the spectrum of a mixture of these compounds

Mass No.	Relative height	Probable positive ion
15	1.7	CH_3
31	1.9	CF
44	12.0	CFCH
45	15.5	$CFCH_2$
50	0.2	CF_2
64	5.6	CF_2CH_2
65	100.0	CF_2CH_3
69	13.0	CF_3
115	5.2	$C_2F_4CH_3$
119	10.0	C_2F_5
134	3.2	$C_2F_5CH_3$

and the CO_2 was estimated by transferring it to a gas burette. Several degassings of the water–CO_2 mixture were carried out to obtain as complete a separation as possible. During removal of CO_2 the CO_2–water mixture was kept at $-90°$ C. Since $C_2F_5CH_3$ is not formed in this photolysis complete analysis of the condensable products was carried out using the gas chromatographic system described in Section (*i*).

RESULTS

The observed products of the photolyses may be accounted for qualitatively by the following mechanisms:

(*a*) *Photolysis in the presence of methane.*—

$$C_2F_5COC_2F_5 + h\nu \rightarrow 2C_2F_5 + CO,$$

$$C_2F_5 + CH_4 \rightarrow C_2F_5H + CH_3, \quad [1]$$

$$2C_2F_5 \rightarrow C_4F_{10}, \quad [2]$$

$$C_2F_5 + CH_3 \rightarrow C_2F_5CH_3, \quad [4]$$

$$2CH_3 \rightarrow C_2H_6. \quad [5]$$

For the unpurified ketone two additional reactions are required:

$$C_2F_5 + \text{impurity} \rightarrow C_2F_5H + \text{radical}, \quad [6]$$

$$C_2F_5 + \text{impurity} \rightarrow C_2F_5Br + \text{radical}. \quad [7]$$

The impurities shown in equations [6] and [7] are not necessarily the same. The exact nature of the contaminants was not established; however, mass spectrometric analyses and infrared experiments suggest benzene as one possible impurity in which case the "radical" in equation [6] would be the phenyl radical, which would presumably either dimerize or abstract from methane regenerating benzene. The impurity containing bromine may possibly be present as bromobenzene in which case the radical in equation [7] would also be the phenyl radical. When impure ketone was used, the material balance was always low, i.e., less product was found than is compatible with the production of $2C_2F_5$ per CO. This fact also suggests an unsaturated impurity.

(*b*) *Photolysis in the presence of hydrogen.*—

$$C_2F_5COC_2F_5 + h\nu \rightarrow 2C_2F_5 + CO,$$

$$C_2F_5 + H_2 \rightarrow C_2F_5H + H, \quad [3]$$

$$H + C_2F_5 \rightarrow C_2F_5H, \quad [4]$$

Can. J. Chem. Downloaded from www.nrcresearchpress.com by 210.87.254.40 on 09/05/12
For personal use only.

plus reactions [2], [6], and [7]. It has been assumed that [10] is of negligible importance under the experimental conditions used (5).

$$H + H + M \rightarrow H_2 + M. \qquad [10]$$

If this reaction did contribute appreciably then all values reported for $k_3/k_2^{\frac{1}{2}}$ should be increased by a factor lying between one and two.

The results of the photolyses in the presence of methane are given in Table IV and those for the photolyses in the presence of hydrogen in Table V. Except as noted the

TABLE IV

The reaction of C_2F_5 radicals with methane

Temp., °C	Length of run, 10^3 sec	Ketone	CH_4	CO	C_2F_5H	C_4F_{10}	C_2H_6	$C_2F_5CH_3$	C_2F_5Br
		10^{-6} mole/cc†		10^{-6} mole					
272	59.16	1.50	1.37	10.8	23.8	4.62	0.10	4.60	0.70
255	18.60	1.30	1.18	18.6	15.4	13.5	—	3.40	0.83
255	16.74	1.24	1.18	15.2	11.9	9.98	0.23	3.16	1.50
240*	11.46	1.36	1.73	8.20	8.05	6.40	0.047	1.78	0.00
235	14.70	1.21	1.74	13.0	10.0	8.50	0.28	2.80	0.86
229	18.96	1.34	1.28	20.8	10.0	15.8	0.17	3.70	1.45
211	19.44	1.45	1.76	18.8	9.35	14.5	0.16	2.95	0.89
212	22.38	1.37	3.24	20.0	18.44	12.9	0.38	5.76	0.83
212	18.00	1.49	0.795	—	4.45	15.0	0.05	1.25	1.37
212	71.64	1.45	1.29	13.8	12.2	10.4	0.25	2.20	0.80
212	40.08	1.45	1.32	21.7	11.5	17.5	0.10	3.00	1.13
210	16.50	1.30	2.15	14.8	8.42	10.7	0.32	2.80	0.76
191	18.54	1.23	2.02	16.9	6.00	13.1	0.29	2.10	1.67
184*	14.22	1.46	2.16	11.1	3.86	9.65	0.065	1.40	0.00
184*	68.52	1.46	1.35	11.9	5.68	10.33	0.055	1.53	0.00
160	18.00	1.49	2.32	18.0	3.85	12.40	0.31	1.17	1.24
159	17.64	1.88	1.82	18.7	3.60	14.3	0.11	1.30	0.94
150	22.02	1.33	2.90	24.0	4.95	17.0	0.33	1.55	—

*Runs with pure $C_2F_5COC_2F_5$. †Volume of reaction zone 190 cc.

TABLE V

The reaction of C_2F_5 radicals with hydrogen

Temp., °C	Length of run, 10^3 sec	Ketone	H_2	C_2F_5H	C_2F_5Br	C_4F_{10}	CO
		10^{-6} mole/cc†		10^{-6} mole			
237	12.60	1.20	1.22	20.8	1.12	1.57	13.6
212	12.60	1.30	1.39	16.5	1.36	2.62	13.2
193*	12.12	1.48	1.08	10.3	0.00	4.89	10.2
193	12.72	1.35	1.38	13.2	1.73	4.38	13.8
174*	12.18	1.32	0.40	3.00	0.00	8.37	9.80
174	13.20	1.30	0.49	4.54	1.74	8.93	13.1
174	13.26	1.35	1.35	9.70	1.46	6.35	13.4
174*	11.94	1.38	1.45	10.3	0.00	6.45	10.9
174	13.20	1.25	4.28	18.8	1.35	2.83	13.9
154	13.50	1.49	1.44	6.70	1.63	9.73	14.5
138*	9.42	1.58	2.25	3.58	0.00	5.82	7.57
137	13.02	1.15	1.70	4.11	0.92	7.00	11.50

*Runs with pure ketone. †Volume of reaction zone 190 cc.

experiments were done using the slightly impure ketone. Since it had been found previously that the photolysis of the impure ketone gave C_2F_5H as a product (unpublished results of work carried out in connection with reference 7), a correction for this was made as follows.

Can. J. Chem. Downloaded from www.nrcresearchpress.com by 210.87.254.40 on 09/05/12
For personal use only.

$$R_{C_2F_5H} = k_6[C_2F_5][\text{impurity}]+k_1[C_2F_5][CH_4]$$

$$R_{C_2F_5H}/R_{C_4F_{10}}^{\frac{1}{2}} = (k_6/k_2^{\frac{1}{2}})([\text{impurity}]/[\text{ketone}])[\text{ketone}]+(k_1/k_2^{\frac{1}{2}})[CH_4].$$

From experiments in the absence of CH_4

$$(k_6/k_2^{\frac{1}{2}})([\text{impurity}]/[\text{ketone}]) = \text{antilog}\ (\bar{3}.987+461/T)$$

(second-order rate constants are expressed in $(\text{mole/cm}^3)^{-1}\ \text{sec}^{-1}$). Hence values of $k_1/k_2^{\frac{1}{2}}$ could be calculated. As may be seen from Fig. 1, the ratios $k_1/k_2^{\frac{1}{2}}$ obtained in this manner are in excellent agreement with those calculated from data taken with the purified ketone. A similar correction was applied to the data from the hydrogen – impure ketone system; good agreement was also achieved with data obtained when purified ketone was used. In the hydrogen system

$$\tfrac{1}{2}R_{C_2F_5H}/R_{C_4F_{10}}^{\frac{1}{2}} = \tfrac{1}{2}(k_6/k_2^{\frac{1}{2}})([\text{impurity}]/[\text{ketone}])[\text{ketone}]+(k_3/k_2^{\frac{1}{2}})[H_2].$$

With a ketone concentration of approximately 1.45×10^{-6} mole/cc, varying the methane concentration from 0.80×10^{-6} to 3.24×10^{-6} mole/cc had no apparent effect on $k_1/k_2^{\frac{1}{2}}$ ($t = 212°$ C). Similarly with a ketone concentration of approximately 1.3×10^{-6} mole/cc, a variation in the hydrogen concentration from 0.40×10^{-6} to 4.28×10^{-6} mole/cc did not alter the value of $k_1/k_3^{\frac{1}{2}}$ ($t = 174°$ C).

DISCUSSION

The following values have been obtained from Fig. 1:

$$E_1-\tfrac{1}{2}E_2 = 10.62\ \text{kcal/mole};\qquad A_1/A_2^{\frac{1}{2}} = 4.17\times10^4\ (\text{mole/cm}^3)^{-\frac{1}{2}}\ \text{sec}^{-\frac{1}{2}};$$

$$E_3-\tfrac{1}{2}E_2 = 11.90\ \text{kcal/mole};\qquad A_3/A_2^{\frac{1}{2}} = 5.25\times10^5\ (\text{mole/cm}^3)^{-\frac{1}{2}}\ \text{sec}^{-\frac{1}{2}}.$$

By analogy with other simple radicals the activation energy for the recombination of two C_2F_5 radicals may be expected to be very small (9, 10, 11, 12, 13). Therefore the observed activation energies should be approximately those for the hydrogen abstraction reactions.

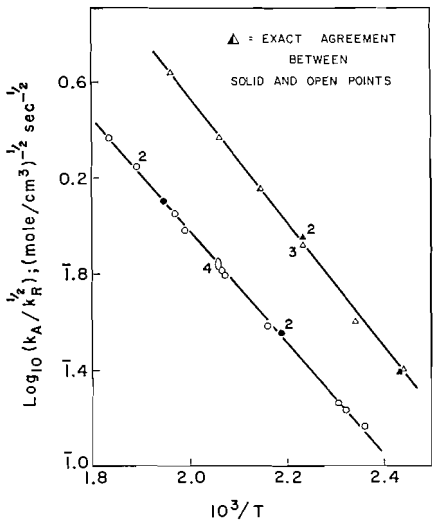


FIG. 1. Arrhenius plots for the reactions of C_2F_5 radicals with methane (○) and with hydrogen (△). Solid points refer to runs using the purified ketone. Subscripts refer to number of experiments averaged to obtain a point; the maximum and minimum values of each set lie within the point.

Can. J. Chem. Downloaded from www.nrcresearchpress.com by 210.87.254.40 on 09/05/12
For personal use only.

TABLE VI

Summary of data on reactions $R + R^1H \rightarrow RH + R^1$

R =	CH_3			C_3F_7			C_2F_5			CF_3		
R^1H	E	log A	k	E	log A	k	E	log A	k	E	log A	k
C_2H_6	10.4	4.45*	.276	9.20	5.24‖	6.41	—	—	—	7.50	4.97‡	22.8
H_2	10.0	4.65†	.675	12.3	5.64**	0.96	11.9	5.74‡‡	1.82	8.80	4.92††	7.94
CH_4	13.0	4.41‡	.014	9.5	3.99††	0.41	10.6	4.62‡‡	0.55	10.3	4.99‡	1.74
D_2	12.2	4.71§	.068	13.8	5.78**	.107	—	—	—	9.70	4.77††	1.25

NOTE: In each case $E = E_1 - \frac{1}{2}E_2$, $\log A = A_1/(A_2)^{\frac{1}{2}}$, and $k = k_1/k_2^{\frac{1}{2}}$ where the subscript 1 refers to the abstraction reaction and the subscript 2 to the reaction $R + R \rightarrow R_2$. Units: E kcal/mole; A_1, A_2, k_1, and k_2 (moles $cm^{-3})^{-1}$ sec^{-1}; all k's refer to 200° C.

*Reference 14. These values actually refer to $CD_3 + C_2H_6$; however, the limited data available indicates that rates of abstraction by CH_3 and CD_3 do not differ greatly. †Reference 15. ‡Reference 3. §Reference 16. ‖Reference 4. **Reference 5. ††Reference 6. ‡‡Present work.

In Table VI the present results are compared with those obtained with similar radicals and substrates. As indicated in the footnotes of Table VI, the tabulated E values are $E_{\text{abstraction}} - \frac{1}{2}E_{\text{recombination}}$; however, in the ensuing discussion it will be assumed that $E_{\text{recombination}}$ is effectively zero in each case. The further assumption will be made that $A_{\text{recombination}}$ is approximately the same for the four radicals considered. This has been borne out by experiment for CH_3 and CF_3 (9, 10, 11); it might not be true for C_2F_5 and C_3F_7 recombinations but will serve as a basis for discussion, any errors thus introduced being remedied easily when experimental values become available. As may be seen from Table VI there is no consistent trend in either activation energies or frequency factors. However, there is a marked and in fact almost unique pattern in the values of k calculated at 200° C. In many of these investigations the exact slope of the Arrhenius curve is somewhat doubtful. Since the A factors are calculated using the experimental E, compensation between A and E must occur if E is incorrectly calculated. However, provided k values are calculated from these A and E values within or close to the experimental temperature range, much less relative error is to be expected in these than in A or E separately. Using k as a measure of the relative radical reactivity with respect to hydrogen abstraction, the following sequence is observed for all four substrates: $CF_3 > C_2F_5 > C_3F_7 > CH_3$. Although this order is obtained from k's at 200° C the convergence of values with temperature is so small that it apparently should hold over all readily accessible temperatures, except in the case of C_3F_7 and C_2F_5, which would apparently replace each other in the reactivity series below approximately 70° C. Similarly, for all three fluorinated radicals the ease of hydrogen abstraction from a given substrate is observed to be $C_2H_6 > H_2 > CH_4 > D_2$. It is assumed that the abstraction by C_2F_5 from C_2H_6 and from D_2 would follow this pattern although at present this is not known.

Although the data are extremely limited another point may be considered. In the photolysis of azomethane in the presence of hexafluoro-acetone, Pritchard and Steacie (17) found that the over-all reaction $CH_3 + CF_3COCF_3 \rightarrow CH_3COCF_3 + CF_3$ had an activation energy of approximately 6 kcal/mole. In the three runs with pure $C_2F_5COC_2F_5$ in the presence of methane the following material balance was expected:

$$(C_4F_{10} + \tfrac{1}{2}C_2F_5H + \tfrac{1}{2}C_2F_5CH_3)/CO = 1, \quad \text{(i)}$$

$$(2C_2H_6 + C_2F_5CH_3)/C_2F_5H = 1. \quad \text{(ii)}$$

Can. J. Chem. Downloaded from www.nrcresearchpress.com by 210.87.254.40 on 09/05/12
For personal use only.

However, it was observed that (i) exceeded unity and (ii) was much less than unity. The total radical balance

$$(C_4F_{10} + C_2F_5CH_3 + C_2H_6)/CO = 1 \qquad \text{(iii)}$$

was obeyed experimentally (1.002 ± 0.001). This suggests that [9] occurs. The reaction merely exchanges free radicals so that (iii) should be obeyed whereas (i) and (ii) should not.

$$CH_3 + C_2F_5COC_2F_5 \rightarrow C_2F_5 + CH_3COC_2F_5 \qquad [9]$$

The reaction might proceed via an addition complex but the lifetime of the complex must be sufficiently small that it will not scavenge free radicals to form an ether.

Considering reactions [9], [2], and [4]

$$(R_{C_4F_{10}} \cdot R_{exchange})/R_{C_2F_5CH_3} = \{(k_2^{\frac{1}{2}}k_9)/k_4\}[C_2F_5COC_2F_5]$$

and assuming k_2 and k_4 to be temperature independent, the value of E_9 is found to be 7 ± 1 kcal/mole where, noting that the result is based on only three experiments, the limits of error are rather arbitrary. In principle it would also be possible to use reactions [9] and [5] to calculate this quantity. However, the quantities of C_2H_6 are very small and the accuracy of their analysis is questionable. Therefore any calculations employing ethane yields would be of very doubtful value.

In the photolyses with H_2 it was expected that $(\frac{1}{2}C_2F_5H + C_4F_{10})/CO = 1$. This was indeed the case when purified ketone was used. Thus the analogue with H of reaction [9],

$$H + C_2F_5COC_2F_5 \rightarrow C_2F_5CHO + C_2F_5,$$

does not occur.

Consideration of reactions [2], [4], and [5] indicates that

$$R_{C_2F_5CH_3}/(R_{C_4F_{10}}R_{C_2H_6})^{\frac{1}{2}} = k_4/(k_2k_5)^{\frac{1}{2}},$$

which should be a constant equal to about 2.5 if $E_2 = E_4 = E_5 = 0$ and if the collision theory cross-sections are related by $\sigma_4 = (\sigma_2\sigma_5)^{\frac{1}{2}}$. The data for all the experiments, except that at the highest temperature, give values of the left side of this expression in the range 2 ± 1. A slight trend toward larger values at the higher temperatures was noted, but the lack of good precision in the ethane analysis, leading to considerable scatter, prevents the drawing of a definite conclusion in this regard.

ACKNOWLEDGMENTS

The authors wish to express their thanks to Mrs. R. H. Riem for the mass spectrometric analyses and to Dr. R. N. Jones for infrared experiments on the impure ketone. We also wish to thank Dr. E. W. R. Steacie for many stimulating discussions during the course of this work.

REFERENCES

1. P. B. Ayscough and E. W. R. Steacie. Proc. Roy. Soc. A, **234**, 476 (1956).
2. G. H. Miller, G. O. Pritchard, and E. W. R. Steacie. Z. physik. Chem. **15**, 262 (1958).
3. E. W. R. Steacie. J. Chem. Soc. 3991 (1956).
4. G. Giacometti and E. W. R. Steacie. Can. J. Chem. **36**, 1493 (1958).
5. G. H. Miller and E. W. R. Steacie. J. Am. Chem. Soc. **80**, 6486 (1958).
6. G. O. Pritchard, H. O. Pritchard, and A. F. Trotman-Dickenson. Trans. Faraday Soc. **52**, 849 (1956).

Can. J. Chem. Downloaded from www.nrcresearchpress.com by 210.87.254.40 on 09/05/12
For personal use only.

7. G. GIACOMETTI, H. OKABE, S. J. W. PRICE, and E. W. R. STEACIE. Can. J. Chem. **38**, 104 (1960).
8. P. B. AYSCOUGH, J. C. POLANYI, and E. W. R. STEACIE. Can. J. Chem. **33**, 743 (1955).
9. G. B. KISTIAKOWSKY and E. K. ROBERTS. J. Chem. Phys. **21**, 1637 (1953).
10. A. SHEPP. J. Chem. Phys. **24**, 939 (1956).
11. P. B. AYSCOUGH. J. Chem. Phys. **24**, 944 (1956).
12. A. SHEPP and K. O. KUTSCHKE. J. Chem. Phys. **26**, 1020 (1957).
13. S. G. WHITEWAY and C. R. MASSON. J. Chem. Phys. **25**, 233 (1956).
14. A. F. TROTMAN-DICKENSON, J. R. BIRCHARD, and E. W. R. STEACIE. J. Chem. Phys. **19**, 163 (1951).
15. E. WHITTLE and E. W. R. STEACIE. J. Chem. Phys. **21**, 993 (1953).
16. S. DAVIDSON and M. BURTON. J. Am. Chem. Soc. **74**, 498 (1952). *See also* M. H. J. WIJNEN and E. W. R. STEACIE. Discussions Faraday Soc. **14**, 118 (1953).
17. G. O. PRITCHARD and E. W. R. STEACIE. Can. J. Chem. **35**, 1216 (1957).

Can. J. Chem. Downloaded from www.nrcresearchpress.com by 210.87.254.42 on 09/05/12
For personal use only.

Can. J. Chem. Downloaded from www.nrcresearchpress.com by 210.87.254.42 on 09/05/12
For personal use only.

ÉTARD REACTION

III. NATURE OF THE COMPLEX[1]

OWEN H. WHEELER

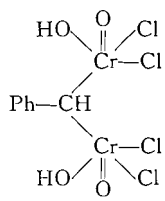
ABSTRACT

Magnetic susceptibility measurements have shown that the chromium atoms in the toluene – chromyl chloride complex are tetravalent. The structure of the complex and the reaction mechanism are discussed. Spectroscopic evidence has been found of the initial formation of a π-complex. The products of reaction of chromyl chloride and ethylbenzene, isopropylbenzene, tetralin, and indane have been determined.

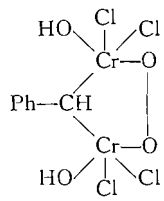
An insoluble dark-brown complex is formed as an intermediate in the Étard oxidation of toluenes with chromyl chloride (1, 2, 3), and although a number of structures have been suggested for the complex (3) no positive evidence has been published concerning its structure.

The analysis of the complex formed with toluene agrees with the empirical formula $C_7H_8.2CrO_2Cl_2$. The complexes are generally sparingly soluble in organic solvents and are decomposed by water to give benzaldehydes and to liberate chromium in a valence state of +4 or +5 (1). The chromium atoms in the complex must thus have some valency from four to the six of the original chromyl chloride.

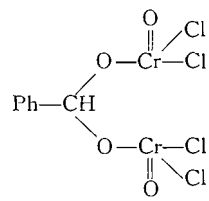
Hartford and Darrin (3) have suggested structures involving hydrogen bonding between two hydrogen atoms of the methyl group of toluene and two chlorine or oxygen atoms of two molecules of chromyl chloride. Structure I, proposed by Rhode (4), also involves Cr^{VI} but with the rather improbable co-ordination number of 5.



I

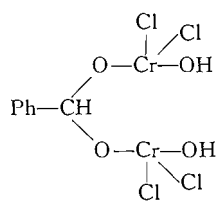


II



III

Two structures (II and III) can be envisaged for pentavalent chromium. However, the former (II) again has a co-ordination number of 5. In structure III the Cr^{V} has a co-ordination number of 4, and, although the molecule lacks two hydrogen atoms, the formula could be accommodated by the analysis. Étard (5) and later Westheimer (6) proposed structure IV involving tetravalent and tetraco-ordinate chromium.



IV

[1]*Manuscript received in original form October 13, 1959, and, as revised, May 30, 1960.*
Contribution from the Departments of Chemistry of Dalhousie University, Halifax, N.S., and the College of Agriculture and Mechanic Arts, University of Puerto Rico, Mayaguez, Puerto Rico. Presented in part at the VII Congreso Latinoamericano de Química, in Mexico City, March 1959. Part II: Can. J. Chem. **36**, *667 (1958).*

In order to determine the valency state of the chromium atoms the magnetic susceptibility (7) of the toluene complex was measured and it gave a value of 3.16 Bohr magnetons per chromium atom. This value (Table I) can only correspond to two unshared electrons

TABLE I

Magnetic susceptibilities of chromium*

	n†	μ_{calc}‡	μ_{obs}§
Cr^{VI}	0	0	0
Cr^{V}	1	1.73	1.7–1.8
Cr^{IV}	2	2.83	2.8–3.1
Cr^{III}	3	3.87	3.85–3.9

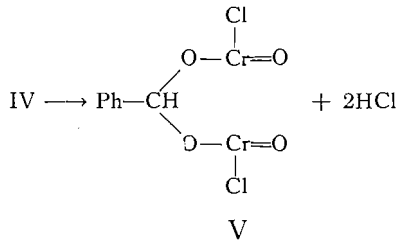
*Values for covalent atoms, from ref. 8. †Number of unshared electrons. ‡Magnetic moment calculated from $\mu = \sqrt{\{n(n+2)\}}$. §Magnetic moments observed in covalent bond complexes of Cr and other atoms with the same number of unshared electrons.

per atom. The fact that the value is a little higher than that usually found is probably due to the approximations involved in determining the susceptibility of a solid, or to interaction between the two chromium atoms in the same molecule. The chromium atoms must thus be tetravalent and the complex must have structure IV.

The infrared spectrum of the complex, either as a Nujol mull or as a potassium bromide disk, was rather ill-defined but showed evidence of the presence of a hydroxyl group (maxima at 2.35, 9.3, and 9.7 μ, which may be due to OH stretching and deformation vibrations).

It might be expected that the third hydrogen atom of toluene would be displaced, but the product of the Étard reaction is always a benzaldehyde and not a benzoic acid. The fact that the reaction terminates after displacing two hydrogen atoms probably has its origin in the low solubility of the complex formed with two molecules of chromyl chloride, although a more important factor is probably a steric one. The commonest stereochemical configuration of co-ordination number four is the square planar (dsp^2) form (8), and with two such planes joined to a carbon atom, together with the benzene ring in IV, the third hydrogen atom will be completely hindered to displacement by the bulky chromyl chloride molecule. In the alternative tetrahedral (d^3s) form of the complex the molecule would be even more crowded. It may be noted that ortho-substituted toluenes with large substituents, such as an iodo-atom or nitro-group, give much lower yields of benzaldehydes than their para isomers (1) and this is no doubt largely due to steric hindrance.

The structure IV is in accord with the reactions of the complex, since hydrolysis of the chromium–oxygen bonds will give benzaldehyde (initially as its hydrate). The loss of half the chlorine as hydrogen chloride on heating the complex (3) is also easily explained since a structure with tetravalent chromium atoms such as V could be readily formed.



V

Can. J. Chem. Downloaded from www.nrcresearchpress.com by 210.87.254.42 on 09/05/12
For personal use only.

As has been already suggested (1) the first stage in the reaction of chromyl chloride and a toluene will be the formation of a π-complex, the chromyl chloride acting as a Lewis acid and the aromatic ring as the corresponding base. The formation of such a π-complex accounts for the initial exothermic reaction observed (1, 3) and spectroscopic evidence for this complex has now been obtained (Fig. 1). A solution of chromyl chloride in carbon tetrachloride has maxima at 290 and 415 mμ (curve II), while a solution of toluene has no significant absorption above 270 mμ (curve I). On mixture of the two solutions, the intensity near 290 mμ increases while the intensity at 415 mμ decreases (curve III). This is consistent with the reaction of the chromyl chloride (decrease in intensity of visible band) with the toluene to form a π-complex with a maximum near 300 mμ. When the mixture is allowed to stand, a precipitate forms and the intensity of both bands decreases, although the greatest decrease is observed at 300 mμ (curve IV) since the π-complex is transformed into the insoluble reaction complex.

The oxidation of a methyl group to an aldehyde is not the only reaction which can take place between an aromatic compound and chromyl chloride. In a previous publication (2) it was shown that the methylene groups in 9,10-dihydroanthracene, phenanthrene, and fluorenene could be oxidized to quinones and that 9-methylanthracene was oxidized to anthraquinone. The products of the oxidation of ethylbenzene have been found to be acetophenone (oxidation of methylene group) and phenylacetaldehyde (oxidation of terminal methyl group) in about equal quantities. It has been reported (12) that benzaldehyde is also formed but this could not be detected in the infrared spectrum of the products. Isopropylbenzene similarly afforded acetophenone (displacement of a methyl group, cf. 9-methylanthracene) and α-phenyl propionaldehyde (oxidation of terminal methyl group) again in about equal amounts (cf. 13). Under the same conditions tert-butylbenzene was unaffected. It has also been found that the oxidation of tetralin gave about equal amounts of α- and β-tetralone. The formation of two products again illustrates the high reactivity of chromyl chloride since the chromic oxide oxidation of tetralin gives only α-tetralone (14). Indane similarly gave apparently a mixture of α- and β-indanone, although the yield was very low and a large amount of polymer was formed.

EXPERIMENTAL

Toluene Complex

Toluene (2.5 g, 0.027 mole) in carbon tetrachloride (20 ml) was treated dropwise with stirring with chromyl chloride (9) (7.75 g, 0.05 mole) in carbon tetrachloride (30 ml) during 1/2 hour, stirred for a further 2 hours, and allowed to stand at room temperature overnight. The suspension was filtered and the precipitate washed with carbon tetrachloride until the washings were colorless, and then dried in a vacuum (9.3 g). Analysis: found, Cl = 34.5, 34.8%; calc. for C_7H_8 $(Cr\ O_2Cl_2)_2$, Cl = 35.16%.

Reaction of benzene (3.9 g) in a like manner gave an oily precipitate (0.20 g) which fumed in air.

Similarly reaction of *tert*-butylbenzene (5.0 g) gave a dark-black precipitate (0.8 g) which decomposed on standing.

Magnetic Measurements

The magnetic susceptibility (χ) was determined by the method of Gouy (7). $X = (a+b\ \delta w)/W$ (10), where $a = k.v$ (k = volume susceptibility of air, v = volume of specimen) and $b = 2\ gv/AH^2$ (A = cross-sectional area and H = field strength). The

Can. J. Chem. Downloaded from www.nrcresearchpress.com by 210.87.254.42 on 09/05/12
For personal use only.

susceptibility (diamagnetic) of air is very small and the formula can be reduced to $X = b\ \delta w/W$. For two specimens occupying the same volume, this becomes

$$\chi_1/\chi_2 = \delta w_1 . W_2/\delta w_2 . W_1.$$

Ferrous ammonium sulphate ($\chi = 9500\times10^{-6}/(T+1)$ (11)) was used to calibrate the apparatus. The molecular susceptibility ($\chi_M = \chi \times$ mol. wt.) was corrected for the diamagnetic susceptibility of the other atoms using the values of Pascal (7) and the corrected value was halved to obtain the atomic susceptibility (χ_A) of each chromium atom. The atomic magnetic moment (μ_A) was then calculated using the Langevin formula,

$$\mu_A = \sqrt{(3\,RT\,\chi_A/N)}.$$

Spectroscopic Measurements

The ultraviolet and visible spectra (Fig. 1) were determined in stoppered Corex cells using carbon tetrachloride as solvent. Chromyl chloride had two maxima, at 290 mμ (ϵ = 3600) and 415 mμ (ϵ = 2900).

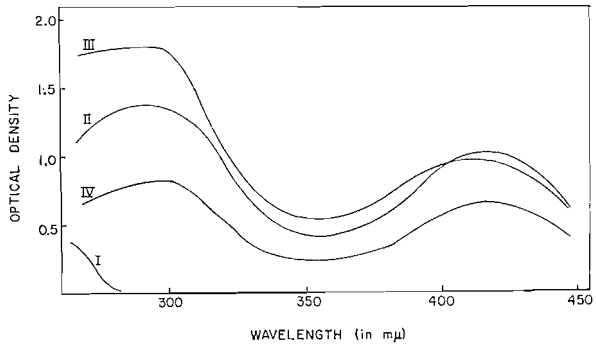


FIG. 1. Spectra of complex. (I) Toluene (1.3×10^{-3} M) in CCl_4. (II) CrO_2Cl_2 (4×10^{-4} M) in CCl_4. (III) Toluene (1.3×10^{-3} M) + CrO_2Cl_2 (4×10^{-4} M). (IV) Same after 24 hours.

The infrared spectrum of the toluene complex was determined in a Nujol mull and as a potassium bromide disk.

The principal maxima and their most probable assignments (values in microns and relative intensities in parenthesis) are:

Nujol mull	2.35 (m)	6.26 (m)	6.58 (m)	—	6.85 (s)
KBr disk	—	6.25 (s)	6.54 (s)	6.68 (m)	—
Assignment	OH?	Benzene	Benzene	Benzene	Nujol
Nujol mull	7.26 (s)	8.49 (w)	9.33 (w)	9.74 (w)	
KBr disk	—	8.47 (m)	9.29 (m)	9.74 (m)	
Assignment	Nujol	Mono-sub. benzene	OH?	OH?	

Reactions with Aromatic Hydrocarbons

(Ultraviolet spectra determined in ethanol solution and infrared spectra in carbon tetrachloride.)

Ethylbenzene

Ethylbenzene (21 g) in carbon tetrachloride (100 ml) was treated dropwise with stirring and cooling to 20–25° with chromyl chloride (60 g) in carbon tetrachloride (100 ml) during 1 hour, stirred for 2 hours more, and allowed to stand at room temperature overnight. The reaction mixture was decomposed by being poured into excess aqueous sodium

Can. J. Chem. Downloaded from www.nrcresearchpress.com by 210.87.254.42 on 09/05/12
For personal use only.

bisulphite solution and the organic phase separated and dried. After removal of the solvent, the residue was distilled to give a product (10.5 g), b.p. 76–80° at 100 mm, with infrared maxima at 5.85 and 5.97 μ (acetophenone and benzaldehyde have bands at 5.97 and 5.75 μ, respectively). Ultraviolet absorption λ_{max} 242 mμ, ϵ = 7500 corresponding to 59% acetophenone (242 mμ, ϵ = 12,700). A small sample gave a precipitate with 2,4-dinitrophenylhydrazone sulphate solution, which was separated by chromatography on a long column of alumina and elution with benzene, into two fractions; one melting point 247° (from ethyl acetate) (mixed melting point with acetophenone derivative 246–247°) and a second melting point 108–110° (mixed melting point with phenyl acetaldehyde derivative 110–111°).

Isopropylbenzene

Isopropylbenzene (16 g) in carbon tetrachloride (40 ml) was treated dropwise with chromyl chloride (43 g) in carbon tetrachloride (50 ml) over 1 hour at 20–25°. The mixture was stirred for 2 hours, allowed to stand overnight, and worked up as usual, giving a fraction (5.5 g), b.p. 80–85° at 100 mm, having infrared bands at 5.85 and 5.98 μ. Ultraviolet absorption λ_{max} 242 mμ, ϵ = 5850 corresponding to 46% acetophenone. A small sample gave a mixture of 2,4-dinitrophenylhydrazones, separated by chromatography on alumina and elution with benzene into a fraction, m.p. 246° (from ethyl acetate) (no depression on admixture with authentic derivative of acetophenone), and another, m.p. 227–233° (mixed melting point with derivative of α-phenylpropionaldehyde (m.p. 238°) 235–237°).

tert-Butylbenzene

Reaction of *tert*-butylbenzene (20 g) in the same manner gave recovered material (18.5 g), b.p. 168–170°, which showed a very weak carbonyl infrared band, but gave no precipitate with 2,4-dinitrophenylhydrazine reagent.

Tetralin

Freshly distilled tetralin (10 g) in carbon tetrachloride (50 ml) was treated with chromyl chloride (25 g) in carbon tetrachloride (50 ml) at 0° during 2 hours and stirred at 0° for a further 5 hours. Decomposition of the complex in the usual manner gave unchanged tetralin (2 g) and a mixture of α- and β-tetralones (5.6 g), b.p. 112–124° at 10 mm, which had infrared bands at 5.85 and 5.97 μ (authentic α-tetralone had a band at 5.98 μ), and ultraviolet absorption of λ_{max} 242 mμ, ϵ = 5300 (α-tetralone showed λ_{max} 248 mμ, ϵ = 11,400). A small sample gave a 2,4-dinitrophenylhydrazone, m.p. 200–215°, separated as above, into a fraction, m.p. 272° (from ethyl acetate) (mixed melting point with the derivative of α-tetralone 270–271°) and another melting point, 250° (mixed melting point with the derivative of β-tetralone 251–252°).

The main portion (5.2 g) was shaken with an excess of 10% aqueous sodium bisulphite and allowed to stand overnight. The precipitate was filtered, washed with ether, and decomposed with acid, giving β-tetralone (2.5 g), b.p. 123° at 10 mm, 2,4-dinitrophenylhydrazone, melting point and mixed melting point 251°. The ether washings yielded α-tetralone (2.3 g), b.p. 120° at 10 mm, 2,4-dinitrophenylhydrazone melting point and mixed melting point 271°.

Indane

Indane (5.5 g) (prepared by Clemmensen reduction of α-indanone) in carbon tetrachloride (50 ml) was reacted, as above with chromyl chloride (17.0 g) in carbon tetrachloride (50 ml) giving a mixture of α- and β-indanones (0.8 g), b.p. 130–132° at 25 mm,

Can. J. Chem. Downloaded from www.nrcresearchpress.com by 210.87.254.42 on 09/05/12
For personal use only.

having infrared maxima at 5.73 and 5.86 μ (α-indanone showed a band at 5.86 μ) and ultraviolet absorption λ_{max} 245 mμ, ϵ = 4100. The amount of product was insufficient to identify it completely. (α-Indanone showed λ_{max} 250 mμ, ϵ = 10,800.)

ACKNOWLEDGMENTS

The author is grateful to Dr. D. A. Ryan, Dalhousie University, for the loan of the Gouy balance and Dr. J. L. Mateos, University of Mexico, for determining the infrared spectra of the toluene complex.

REFERENCES

1. O. H. WHEELER. Can. J. Chem. **36**, 667 (1958).
2. O. H. WHEELER. Can. J. Chem. **36**, 949 (1958).
3. W. H. HARTFORD and M. DARRIN. Chem. Revs. **58**, 1 (1958).
4. G. ROHDE. Sammlung chemische und chemisch-technischer Vortrage. Vol. VI. F. Enke, Stuttgart. 1901. p. 241–302.
5. A. ÉTARD. Ann. chim. et phys. [5] **22**, 218 (1881).
6. F. H. WESTHEIMER. Chem. Revs. **45**, 419 (1949).
7. P. W. SELWOOD. Magnetochemistry. Interscience Publishers, Inc., New York. 1956.
8. R. S. NYHOLM. Quart. Revs. (London), **7**, 377 (1953).
9. H. H. SISLER. Inorganic syntheses. Vol. 2. McGraw-Hill Book Company, New York. 1946. p. 205.
10. F. G. BADDAR, O. M. M. HITAL, and S. SUDGEN. J. Chem. Soc. 132 (1949).
11. L. C. JACKSON. Phil. Trans. Roy. Soc. London, A, **224**, 1 (1923).
12. W. VON MILLER and G. ROHDE. Ber. **23**, 1070 (1890).
13. W. VON MILLER and G. ROHDE. Ber. **23**, 1356 (1890).
14. I. N. NAZAROV and M. S. BURMISTROVA. Zhur. Obshcheĭ Khim. **20**, 1304 (1950).

Can. J. Chem. Downloaded from www.nrcresearchpress.com by 210.87.254.42 on 09/05/12
For personal use only.

Can. J. Chem. Downloaded from www.nrcresearchpress.com by 210.87.254.105 on 09/05/12
For personal use only.

THE SOLID–LIQUID EQUILIBRIUM BETWEEN ANHYDROUS MAGNESIUM CHLORIDE AND N,N-DIMETHYLFORMAMIDE[1]

DENYS COOK

ABSTRACT

The solid–liquid equilibrium between anhydrous magnesium chloride and N,N-dimethylformamide has been investigated between −58° and +97° C, and up to 25 mole% in magnesium chloride by the techniques of thermal analysis. The following compounds and their melting points have been noted: $MgCl_2.12DMF$, 8.7°; $MgCl_2.6DMF$, 35.0° (incongruent); $MgCl_2.5DMF$, 51.0°; $MgCl_2.4DMF$, 69.0° C. Infrared examination of some of the compounds suggests that co-ordination is through the carbonyl group.

INTRODUCTION

Anhydrous magnesium chloride is known to form complexes with a variety of molecules such as H_2O (1), NH_3 (2), etc. These are usually of the form $Mg6X.Cl_2$ where the cation is octahedrally surrounded by six equivalent donor molecules. These can be thermally degraded and lose some or all of the donor molecules. The thermodynamic properties of this process for the hexahydrate (1) and diammonate (2) have been known for some time.

Because of an interest in the remarkable solvent properties of N,N-dimethylformamide (DMF) it was decided to investigate the solid–liquid equilibrium of the $MgCl_2$–DMF system. It was hoped that specific information concerning the possible formation of an octahedral complex of DMF around Mg^{++} would result. This was of interest since the DMF molecule is a good deal larger than either H_2O or NH_3 mentioned previously, and steric factors could easily play a part in the equilibrium. It was also hoped to ascertain the site of the donor center in DMF.

EXPERIMENTAL

To establish the phase boundaries, the method of thermal analysis of cooling curves of mixtures of $MgCl_2$ and DMF was employed (3). A pyrex cooling cell was constructed, provided with an efficient, magnetically operated stirring system, and a thin-walled tube to accommodate a copper–constantan thermocouple. A Brown strip-chart recorder traced the temperature–time cooling curves.

A weighed amount of $MgCl_2$ was placed in the cell and the proper amount of DMF was added. These operations were performed in a dry box. This mixture was outgassed and then heated to dissolve the $MgCl_2$. A cooling curve was started when all the $MgCl_2$ was in solution. A jacket, which could be evacuated, was placed round the cell, and the appropriate refrigerant surrounded this. The melting point was always easily discernible, particularly as with many mixtures supercooling, occasionally up to 10° C, was observed. The eutectic points, however, were much more elusive and few were recorded with any confidence.

Originally, mixtures were made up by adding further DMF to a known mixture, but some irreproducibility seemed to be introduced by this technique, so subsequently mixtures were freshly and individually prepared.

Between three and five cooling curves were recorded for each mixture and the average

[1]*Manuscript received July 27, 1960.*
Contribution No. 33 from the Exploratory Research Laboratory, Dow Chemical of Canada, Limited, Sarnia, Ontario.

melting point taken. Temperatures could be read to about 0.5° C but points were reproducible to probably 1–2° C.

RESULTS

The results obtained are shown in Table I and are plotted in Fig. 1. Table II shows the melting points of compounds as determined by the dystectic points of the curves.

TABLE I
Melting points of mixtures

Mole% $MgCl_2$	M.p., °C	Mole% $MgCl_2$	M.p., °C
0.0	−58.0	14.65	40.0
4.2	−21.5	15.95	50.0
5.93	+ 2.3	16.79	50.5
7.70	8.7	17.37	56.0
9.15	5.2	18.50	66.0
10.08	4.7	20.68	67.5
11.12	17.0	21.22	78.0
12.02	29.5	22.52	79.5
13.54	33.0	23.85	96.5
14.07	35.0	24.47	89.7

TABLE II
Melting points of compounds

Compound	Mole% $MgCl_2$	M.p., °C	Remarks
$MgCl_2$.12DMF	7.70	8.7	
$MgCl_2$.6DMF	14.28	35.0	Incongruent
$MgCl_2$.5DMF	16.33	51.0	
$MgCl_2$.4DMF	20.00	69.0	

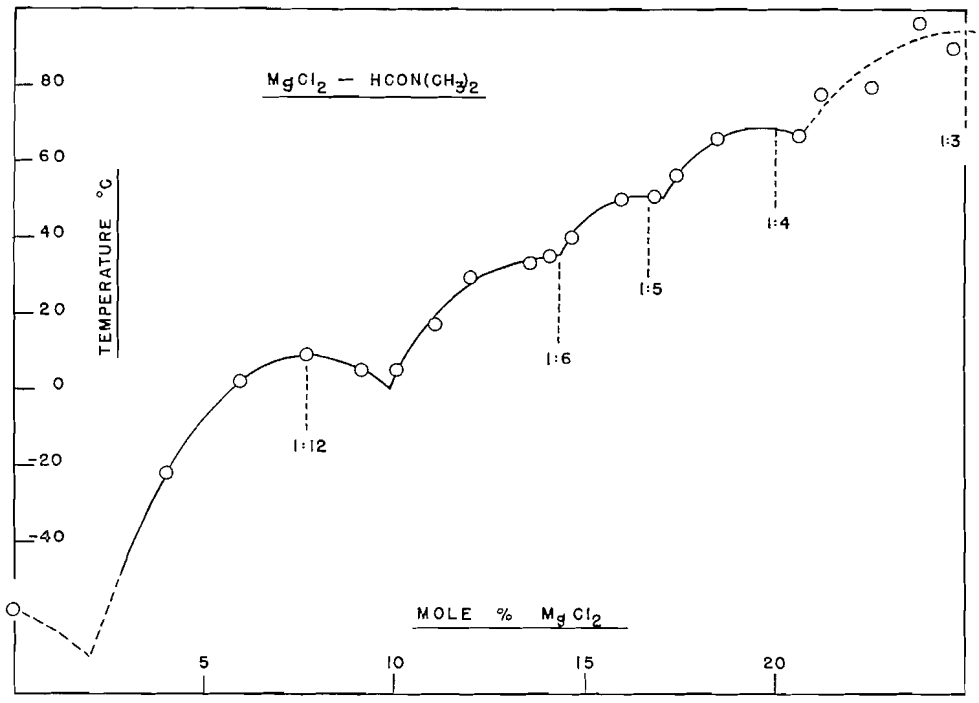


FIG. 1.

Can. J. Chem. Downloaded from www.nrcresearchpress.com by 210.87.254.105 on 09/05/12
For personal use only.

Can. J. Chem. Downloaded from www.nrcresearchpress.com by 210.87.254.105 on 09/05/12
For personal use only.

DISCUSSION

The appearance of a compound albeit of incongruent melting point at a molecular ratio of 1:6, i.e. $MgCl_2.6DMF$, indicates that even a relatively large molecule like DMF can co-ordinate, probably octahedrally, round the Mg^{++}. (A powder X-ray diffraction pattern of the 1:6 compound showed marked differences from those of anhydrous $MgCl_2$ or the hexahydrate.) The compounds with fewer DMF molecules are probably derived from this compound by successive loss of a DMF molecule from the co-ordination shell at higher temperatures. A 1:3 compound has been tentatively shown in Fig. 1. It probably exists but, in this temperature region, the reproducibility of the melting points was growing worse. There is a strong possibility that thermal decomposition may be a factor at these elevated temperatures.

For all these mixtures, in the crystallization period, especially if supercooling occurred, the first crystals observed were nearly transparent and had a cubic structure. Furthermore, when a mixture of approximately 14.28 mole% $MgCl_2$ was made up, heated to dissolve all the $MgCl_2$, and then cooled slowly, a mass of poorly shaped crystals grew. But by leaving them in a place exposed to weak sunlight, after a few days, a portion of a beautiful cubic crystal grew on top of the other crystals, with an edge of about 6 mm. This cubic structure could be consistent with octahedral co-ordination around the Mg^{++} ion.

Infrared examination of the 4:1 and 3:1 complexes showed a spectrum very similar to that of DMF except that its carbonyl frequency was displaced to lower frequencies by about 46 cm^{-1}. This phenomenon is well known to occur when there is an interaction with the carbonyl oxygen, as in hydrogen bond formation, or Lewis acid–base interaction (4). It is concluded, therefore, that the carbonyl group is the donor group in DMF in this case. Very similar results have been obtained recently for the DMF_2:$TiCl_4$ complex, in which the carbonyl frequency was some 30 cm^{-1} lower than in DMF (5).

The 1:12 compound was rather unexpected, although a compound of the same constitution is observed in the $MgCl_2$–H_2O system. On freezing the $MgCl_2.12DMF$ compound, a mass of small white crystals appeared with no supercooling so observation of their shape was difficult. Their appearance was different enough from the $MgCl_2.6DMF$, or lower compounds, to infer a difference in lattice type. While conjecture on the structure is quite speculative, it seems most unlikely that this could be a Mg^{++} with 12 DMF molecules co-ordinated around it. What is more likely is a six co-ordinated Mg^{++} with six further DMF molecules not interacting with the cation but incorporated in the lattice. Since this compound melted at 9° C it was not possible to take the infrared spectrum to see if two carbonyl bands were present due to two environmentally different DMF molecules.

Finally, a rough estimate of the stability of the 1:6 compound can be deduced from the following evidence. Treatment of a solution of $MgCl_2$ in DMF with NH_3 gave a slow-forming white precipitate, which settled very slowly. By contrast, a solution of $MgCl_2$ in water which is, in effect, $Mg(6H_2O)^{++}$, $2Cl^-$, when treated with NH_3 gave an immediate, copious white precipitate of $MgCl_2.6NH_3$, identified by its infrared spectrum. This is a rough indication that the stability of the $MgCl_2.6DMF$ is intermediate between $MgCl_2.6NH_3$ and $MgCl_2.6H_2O$.

ACKNOWLEDGMENT

The author is indebted to Miss C. D. Anderson for preparing the infrared spectra.

REFERENCES

1. C. H. SHOMATE and E. H. HUFFMAN. J. Am. Chem. Soc. **65**, 1625 (1943).
2. W. BILTZ and G. F. HÜTTIG. Z. anorg. u. allgem. Chem. **119**, 115 (1921).
3. D. COOK, Y. LUPIEN, and W. G. SCHNEIDER. Can. J. Chem. **34**, 957 (1956).
4. D. COOK. Can. J. Chem. **37**, 48 (1959).
5. J. ARCHAMBAULT and R. RIVEST. Can. J. Chem. **36**, 1461 (1958).

Can. J. Chem. Downloaded from www.nrcresearchpress.com by 210.87.254.105 on 09/05/12
For personal use only.

Can. J. Chem. Downloaded from www.nrcresearchpress.com by 210.87.254.6 on 09/05/12
For personal use only.

SEARCH FOR INDEPENDENT FORMATION OF Cs^{134m} IN FISSION[1]

A. P. Baerg,[2] R. M. Bartholomew, and R. H. Betts

ABSTRACT

The independent yield of Cs^{134m} in thermal neutron fission of U^{235} is less than 1.7×10^{-6} of the mass 134 chain yield and that of Cs^{136} was found to be $(0.94\pm0.04)\times10^{-3}$ of the mass 136 chain yield. The half-life for Cs^{134m} was measured as 2.91 ± 0.01 hours.

INTRODUCTION

The principal mode of formation of the shielded nuclide Cs^{134} in neutron-irradiated uranium is generally thought to be by neutron capture in Cs^{133}. This latter nuclide is a fission product of high yield which builds up in the uranium during a long irradiation. However, recent unpublished work (1) involving highly irradiated uranium dioxide has shown that, in some cases at least, the amount of Cs^{134} is apparently considerably larger than that expected from the 30-barn (2) neutron capture cross section of Cs^{133}. One explanation suggested to account for this anomaly was that the independent fission yield of Cs^{134} may be unexpectedly large; a value of about $7\times10^{-3}\%$ would account for the "excess" Cs^{134} found.

Although it would be very difficult in a short irradiation to detect independent formation of the order of $7\times10^{-3}\%$ yield for 2.2-year Cs^{134} in the presence of other fission product cesium isotopes, it would be readily observable as the high-spin Cs^{134m} isomer (3 hours half-life), if this were formed in amounts comparable with that of the 2.2-year ground state. Judging from the limited information available on isomer ratios of independently formed fission products (3, 4) this is not an unlikely situation. This paper reports on the results of a search which was made for Cs^{134m} formed directly in thermal neutron fission of U^{235}.

EXPERIMENTAL

The method consisted of extracting carrier-free fission product cesium from a sample of uranium which had been irradiated for a short time only to avoid production of Cs^{134m} through neutron capture in fission-produced Cs^{133}. Samples of the carrier-free material were counted in a 4π beta proportional counter to determine the Cs^{134m} relative to Cs^{136} and Cs^{137}. The counting efficiency for the low-energy electrons from the isomeric transition in Cs^{134m} was determined in separate experiments by a coincidence counting method, using Cs^{134m} produced by neutron capture in Cs^{133}.

Irradiation and Purification

Approximately 1 g samples of natural uranium, as UO_2, were sealed in quartz capsules and irradiated in a self-serve position of the Chalk River, NRX reactor. The neutron flux was about $10^{13}/cm^2$ sec and the irradiations were limited to 3 hours. The purification of the cesium, requiring about 3 hours, was delayed 12 hours to permit 32-minute Cs^{138} and 9-minute Cs^{139} to decay to negligible levels.

The irradiated UO_2 was dissolved in a solution 9 *N* in hydrochloric and 3 *N* in nitric

[1]*Manuscript received July 13, 1960.*
Contribution from the Chemistry and Metallurgy Division, Research Chemistry Branch, Atomic Energy of Canada Limited, Chalk River, Ontario.
Issued as A.E.C.L. No. 1099.
[2]*Present address: National Research Council, Ottawa, Ontario.*

acid. This solution was evaporated and the residue taken up in 10 ml of 1 *M* sodium citrate buffer solution adjusted to pH 6 with nitric acid. The cesium was extracted, carrier-free, from this solution with an amyl acetate solution 0.05 *M* in sodium tetraphenyl boron (5). After scrubbing with water the cesium was backwashed with 3 *N* hydrochloric acid and the latter scrubbed with pure amyl acetate. This acid solution was again evaporated and the extraction procedure repeated three times.

It was found that carrier-free silver is also extracted very efficiently in this procedure and so an ion-exchange purification step was introduced. The cesium, in 0.1 *N* hydrochloric acid, was adsorbed on a 200–400 mesh Dowex-50 (8% cross-linked) cation resin column, 10 cm long and 3 mm in diameter. The column was washed, first with 3 ml of 0.1 *N* hydrochloric acid which removed all the silver.* This was followed by about 24 ml of 0.5 *N* hydrochloric acid and finally the cesium was collected in about 2 ml of this eluant. This cesium fraction was further purified by two more extractions with sodium tetraphenyl boron and another cation resin column elution. An additional check on the purity was made in each experiment by adding cesium carrier to a portion of the sample and precipitating cesium silicotungstate (6). These several samples always showed identical decay characteristics and gamma-ray spectra.

Samples of Cs^{134m} for determination of counting efficiency were prepared by irradiation of approximately 1 mg of "spec-pure" CsCl, sealed in a quartz ampoule. The irradiated cesium was purified by several elutions from a cation resin column (see above). Purity checks were made by precipitation of a portion of the cesium with silicotungstic acid and comparison of the decay characteristics.

Counting

Samples of the fission product cesium were prepared for 4π beta counting by evaporating aliquots onto VYNS films. These films were rendered conducting by evaporated gold (10 $\mu g/cm^2$) (7). The dried sources were covered with a similar film. Frequent counts were taken during the first day after the purification, accumulating a minimum of 10^6 counts in each measurement. Subsequently the decay was followed over a period of about 2 months to determine the relative amounts of Cs^{136} and Cs^{137}.

The 4π beta proportional counter-efficiency for the detection of Cs^{134m} was determined by a coincidence technique, using about 1 μg samples of irradiated Cs^{133} mounted in the same way as the fission product samples. Coincidence counting equipment similar to that described by Campion (8) was used. In Fig. 1 is given the decay scheme for Cs^{134m}

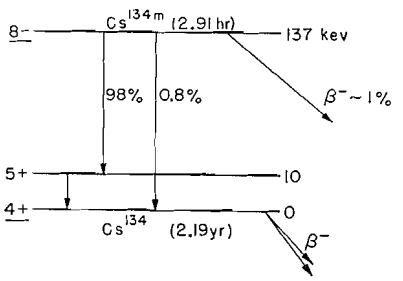


FIG. 1. Disintegration scheme of Cs^{134m}.

**The silver was found by gamma-energy analysis and half-life measurements to be of very high purity. Decay of the Ag^{111}, observed over a period of 60 days, yielded a half-life of 7.45±0.01 days. The purification described appears to be an excellent one for both carrier-free silver as well as for cesium.*

Can. J. Chem. Downloaded from www.nrcresearchpress.com by 210.87.254.6 on 09/05/12
For personal use only.

(9) showing 98% of the transitions going to the 10.5-kev level. The transitions from this level are essentially 100% converted in the L shell (10) giving rise to 4.5- to 6.2-kev electrons. The detection efficiency for these electrons was determined by counting in coincidence with the 127-kev gamma rays from those transitions to the 10.5-kev level which are not themselves converted. Provided these low-energy electrons are detected with good efficiency, it is reasonable to assume nearly 100% efficiency for the other conversion electrons which are of much higher energy.

Treatment of Data

The total disintegration rate of the fission product cesium samples at any time, t, following the irradiation is given by

$$[1] \qquad Cs_{total} = Cs_0^{137}e^{-\lambda_7 t} + Cs_0^{136}e^{-\lambda_6 t} + Cs_0^{134m}e^{-\lambda_4 t}$$

where the subscripts 0 denote initial disintegration rates and λ_7, λ_6, and λ_4 are the respective disintegration constants. No contribution from Cs^{138} and Cs^{139} is indicated in the equation because the purification was delayed long enough to allow these to decay. Since the irradiations were of short duration no significant amount of Cs^{134} would have been formed by neutron capture in fission-produced Cs^{133}. The contribution to the observed counting rate is also negligible from Cs^{135}, due to its long half-life (2×10^6 years).

In the long-term counting data there is no contribution from Cs^{134m} and equation [1] may be rearranged to

$$[2] \qquad Cs_{total}e^{\lambda_7 t} = Cs_0^{136}e^{(\lambda_7-\lambda_6)t} + Cs_0^{137}$$

so that if the total observed count, multiplied by $e^{\lambda_7 t}$, is plotted versus $e^{(\lambda_7-\lambda_6)t}$, a straight line should result having a slope equal to Cs_0^{136} and a zero intercept equal to Cs_0^{137}.

Having determined Cs_0^{136} and Cs_0^{137}, the initial counting rate of Cs^{134m} may be determined by rearrangement of equation [1] as follows,

$$[3] \qquad (Cs_{total} - Cs_0^{137}e^{-\lambda_7 t})e^{\lambda_6 t} = Cs_0^{136} + Cs_0^{134m}e^{(\lambda_6-\lambda_4)t},$$

and plotting the term on the left versus $e^{(\lambda_6-\lambda_4)t}$. The slope of the straight line then represents Cs_0^{134m} and the zero intercept represents Cs_0^{136}.

RESULTS AND DISCUSSION

Two measurements on the Cs^{134m} yield were made, treating in each case first the long-term counting data according to equation [2] to determine the Cs^{136} and Cs^{137} content of the samples. This treatment of the data is illustrated in Fig. 2. The values of Cs_0^{136} and Cs_0^{137} thus obtained were then used in equation [3] and the short-term counting data plotted as shown in Fig. 3. The errors indicate the standard deviation of the observed count. It is evident from this figure that the contribution of Cs^{134m} to the observed counting rate is very small indeed and that at best an upper limit may be set for the yield of this isomer. This limit is estimated to be $<1.3\times10^{-5}\%$. The parameters used in arriving at this value are given in Table I. The results of the counting data are summarized in Table II, together with the estimated limits. These limits will, however, depend on various factors including the Cs^{134m} counting efficiency, the accuracy of the Cs^{136} and Cs^{137} determinations, and the half-life values used in the calculations.

The detection efficiency of the 4π beta counter for the conversion electrons from the 10.5-kev transition in Cs^{134m} was found, in three separate experiments, to be $(86\pm2)\%$. In view of this fairly high efficiency the conversion electrons from the 127-kev transition

Can. J. Chem. Downloaded from www.nrcresearchpress.com by 210.87.254.6 on 09/05/12
For personal use only.

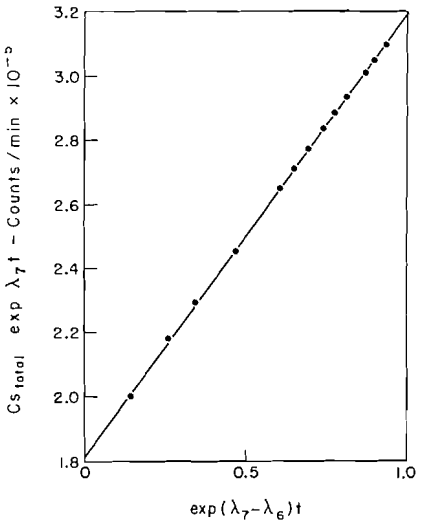


FIG. 2. Long-term decay of fission product cesium.

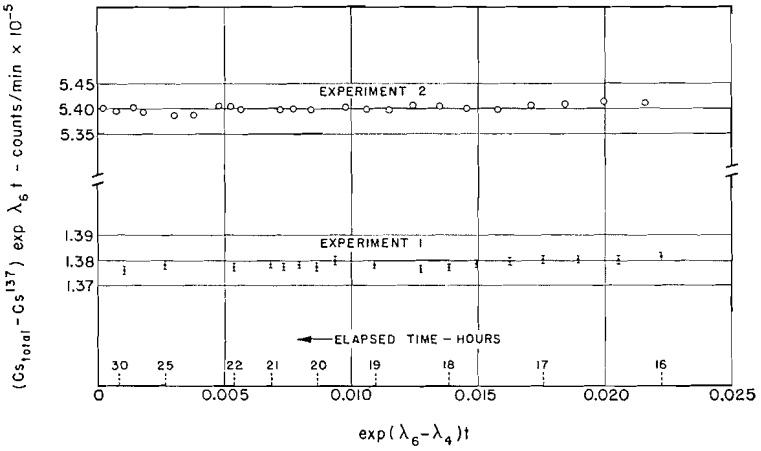


FIG. 3. Short-term decay of fission product cesium.

TABLE I

Values of parameters used to estimate the yield of Cs^{134m}

Irradiation time	3 hours
Half-life of Cs^{136}	12.9 days (11)
Half-life of Cs^{137}	30.0 years (12)
Correction to Cs^{137} activity	0.909 (12)
Half-life of Cs^{134m}	2.91 hours
Counting efficiency of Cs^{134m}	0.974

were assumed to be detected with 100% efficiency. These transitions are 86.9% converted in the K and L shells. The conversion coefficient for the 137-kev transition is not known. It constitutes only 0.8% of all transitions and was assumed not detected. The 1% abundant beta transition was taken to be detected with 100% efficiency. These considerations then lead to an over-all counting efficiency of 97.4% for the Cs^{134m}.

Can. J. Chem. Downloaded from www.nrcresearchpress.com by 210.87.254.6 on 09/05/12
For personal use only.

TABLE II

Experimental data and results

Experiment	Cs_0^{137}, counts/min	Cs_0^{136}, counts/min	Cs_0^{134m}, counts/min	Fission yield ratios	
				Cs^{136}/Cs^{137}	Cs^{134m}/Cs^{136}
1	1.81×10^5	1.38×10^5	$<0.2\times10^5$	0.99×10^{-3}	$<2\times10^{-3}$
2	7.12×10^5	5.40×10^5	$<0.9\times10^5$	0.98×10^{-3}	$<2.2\times10^{-3}$

	Fission yields*	
	% Yield	Fraction of mass chain
Cs^{136}	$(6.1\pm0.24)\times10^{-3}$	$(0.94\pm0.04)\times10^{-3}$
Cs^{134m}	$<1.3\times10^{-5}$	$<1.7\times10^{-6}$

*Taking the cumulative yields of Cs^{137}, mass 136, and mass 134 to be 6.15%, 6.44%, and 8.03% respectively (13).

The counting efficiency for Cs^{136} and Cs^{137} was taken to be 100%. This is believed not to be in error by more than 4% and it is expected that these nuclides were counted with equal efficiency within 1%. In the two measurements a value of 0.76 was obtained for the counting ratio Cs_0^{136}/Cs_0^{137}, with an estimated error of 4%. After a correction factor of 0.909 is applied to the counting rate of Cs^{137} for Ba^{137m} (12), the yield of Cs^{136} becomes $(0.94\pm.04)\times10^{-3}$ as the fraction of the mass 136 chain yield. This value agrees favorably with that of 1×10^{-3} given by Grummitt and Milton (14).

The decay of Cs^{134m}, obtained from the irradiated and purified Cs^{133}, was followed over at least eight half-lives in each of the three counting efficiency measurements. These data yielded a half-life of 2.91 ± 0.01 hours, the value that was used in the calculation. It is somewhat lower than the accepted one of 3.2 hours (9).

The largest error in estimating the Cs^{134m} arises from errors in the value of the term Cs_0^{136} and in the half-life of Cs^{136}. Neither of these is believed to be greater than 5%. It is estimated that even a 10% error in either Cs_0^{136} or its half-life would not change the present results for the Cs^{134m}/Cs^{136} yield ratio by more than a factor of two.

The upper limit for the yield of Cs^{134m} relative to the mass 134 cumulative yield becomes $<1.7\times10^{-6}$ taking the yields of masses 134, 136, and 137 as given in Table II. Extrapolation of existing correlations (14) for independent fission yields suggests a value for Cs^{134} of the order of 5×10^{-6}. The present results then do not indicate any unusual behavior in the independent formation of Cs^{134m} in fission.

REFERENCES

1. R. C. Hawkings. A.E.C.L. Rept. PR-CM-17. March, 1959.
2. D. J. Hughes and R. B. Schwartz. U.S. Atomic Energy Rept. BNL 325.
3. Sylvia Mae Bailey. U.S. Atomic Energy Rept. UCRL-8710. Unpublished.
4. R. A. Sharp and A. C. Pappas. J. Inorg. & Nuclear Chem. **10**, 173 (1959).
5. T. Prach, C. Auerbach, and H. L. Finston. Brookhaven Natl. Lab. Unpublished.
6. Rosalie M. Bartholomew and A. P. Baerg. Can. J. Chem. **34**, 201 (1956).
7. B. D. Pate and L. Yaffe. Can. J. Chem. **33**, 15 (1955).
8. P. J. Campion. Intern. J. Appl. Radiation and Isotopes, **4**, 232 (1959).
9. D. Strominger, J. M. Hollander, and G. T. Seaborg. Revs. Modern Phys. **30**, No. 2, Part 2 (1958).
10. A. N. Sunyar, J. W. Mihelich, and M. Goldhaber. Phys. Rev. **95**, 570 (1954).
11. J. L. Olsen and G. D. O'Kelley. Phys. Rev. **95**, 1539 (1954).
12. F. Brown, G. R. Hall, and A. J. Walter. J. Inorg. & Nuclear Chem. **1**, 241 (1955).
13. J. A. Petruska, H. G. Thode, and R. H. Tomlinson. Can. J. Phys. **33**, 693 (1955).
14. W. E. Grummitt and Gwen M. Milton. J. Inorg. & Nuclear Chem. **5**, 93 (1957).

Can. J. Chem. Downloaded from www.nrcresearchpress.com by 210.87.254.6 on 09/05/12
For personal use only.

Can. J. Chem. Downloaded from www.nrcresearchpress.com by 210.87.254.42 on 09/05/12
For personal use only.

TRYPTAMINES, CARBOLINES, AND RELATED COMPOUNDS

PART VIII. δ-CARBOLINE[1, 2]

R. A. Abramovitch, K. A. H. Adams, and A. D. Notation

ABSTRACT

The first unambiguous synthesis of δ-carboline has been achieved starting with 3-amino-2-phenylpyridine. This was converted to the azide which was thermally cyclized to δ-carboline. The carboline gave a *py*-*N*-methiodide which was converted to the anhydronium base. The pK_a of the anhydronium base was determined and its significance is discussed. The anhydronium base formed a methiodide which, on dry distillation, gave *ind*-*N*-methyl-δ-carboline. The spectral properties of the various derivatives of δ-carboline were examined and the bond structures of the anhydronium base and the methiodides are discussed.

Whereas the chemistry of α-, β-, and γ-carboline has been well studied and a number of unambiguous methods are available for the synthesis of these ring systems practically nothing is known concerning δ-carboline (I). There has appeared only one reference to the synthesis of the parent compound and that to the Graebe–Ullmann cyclization of 1-β-pyridylbenztriazole by Späth and Eiter (1), who obtained a mixture of β-carboline and what was tentatively identified as δ-carboline (since it was not identical with either α-, β-, or γ-carboline) in unspecified low yield. *N*-3-Pyridylaniline was also obtained in this reaction. Subsequently, Eiter (2) was unable to obtain any of the supposed δ-carboline by carrying out this reaction on a larger scale. A similar cyclization of 4-methyl-1-β-pyridylbenztriazole gave 5-methyl-β-carboline as the main product together with a small amount of a compound for which the structure 5-methyl-δ-carboline was suggested (3). Gulland, Robinson, Scott, and Thornley (4) were unable to degrade 3,4-methylenedioxyquindoline to δ-carboline. However, oxidation of this compound with nitric acid gave 7-nitro-δ-carboline-2-carboxylic acid in low yield.

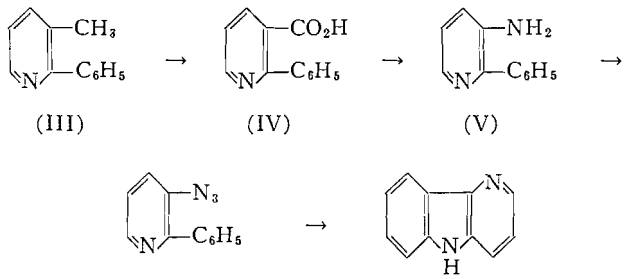
Apart from the fact that it is the only member of the carboline family whose chemistry has not been studied to any degree δ-carboline is interesting from a number of other points of view. It is present in the ring system of the alkaloid cryptolepine (5), which is noteworthy from a biogenetic point of view (6). Also, the relative basicities of α-, β-, and γ-carboline anhydronium bases have been measured by Gray (7), who proposed an explanation for the observed order of base strengths (β- > γ- > α-) and suggested, on the basis of considerations outlined below, that the δ-carboline anhydronium base should have a dissociation constant almost as high as that of the β-isomer. It was of interest to try and test this prediction experimentally.

Smith and Boyer (8) attempted to cyclize 2-*o*-azidophenylpyridine to δ-carboline but obtained instead 2-*o*-aminophenylpyridine.* When 2-*o*-nitrophenylpyridine was heated with ferrous oxalate, cyclization took place preferentially at the pyridine nitrogen atom to give pyrid[1,2-*b*]indazole (9). The Pschorr-type cyclization of 2-amino-*N*-methyl-*N*-3′-pyridylaniline gave a relatively good yield of *ind*-*N*-methyl-δ-carboline (II) (together with some *ind*-*N*-methyl-β-carboline) (10*a*) but attempted *N*-demethylation using a variety of procedures failed (10*b*).

δ-Carboline has now been synthesized unambiguously from 3-amino-2-phenylpyridine

[1]*Manuscript received June 6, 1960.*
Contribution from the Department of Chemistry, University of Saskatchewan, Saskatoon, Saskatchewan. Presented at the 43rd Annual Meeting of the Chemical Institute of Canada in Ottawa, June 1960.
[2]*Part VII: Can. J. Chem.* **38**, *2273 (1960).*
**Our results in this reaction differ from those of Smith and Boyer and will be reported in a subsequent paper.*

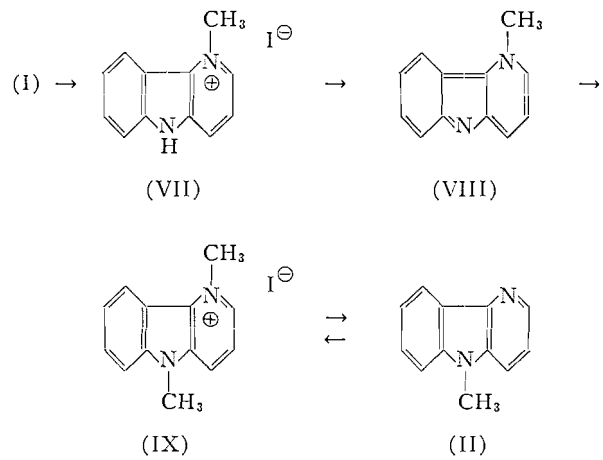
(V). The amine was obtained from 2-phenyl-3-picoline (III), which was oxidized to the carboxylic acid (IV) (11); this was transformed into the amine (V) via the acid chloride and the Curtius reaction. It could also be obtained directly by the action of phenyllithium on 3-aminopyridine (12). It was diazotized and converted to 3-azido-2-phenylpyridine (VI), which on being heated in decalin, gave variable yields of δ-carboline (I).



(III) (IV) (V)

(VI) (I)

The base formed a yellow methiodide (VII) readily but resisted all attempts at *ind-N*-methylation. Treatment of the methiodide with alkali gave the orange anhydronium base (VIII); this gave a yellow methiodide (IX) identical with that obtained from *ind-N*-methyl-δ-carboline (II), thus establishing conclusively the structure which had been assigned (10*a*) to (II), as well as the fact that methylation of the anhydronium base occurs at the *ind-N*-atom. Finally, dry distillation of the methiodide (IX) gave *ind-N*-methyl-δ-carboline (II) identical with the sample obtained from the Pschorr reaction (10*a*).



(VII) (VIII)

(IX) (II)

Ultraviolet Absorption Spectra and pK_a

Gray (7) obtained the following values for the pK_a's of the carboline anhydronium bases: α-, 7.75; β-, 11.11; and γ-, 10.54. The greater basicity of the β-derivative was ascribed to a lower stabilization energy of the β-carboline anhydronium base indicated from a consideration of the relative contributions made by quinonoid canonical forms. The low basic strength of the α- as compared with the γ-derivative was interpreted on

Can. J. Chem. Downloaded from www.nrcresearchpress.com by 210.87.254.42 on 09/05/12
For personal use only.

the basis of two complementary factors: (*a*) a much increased stability of the α-anhydronium base as a result of the juxtaposition of the oppositely charged centers; and (*b*) a reduced stability of the α-carboline salt owing to the inductive effect of the indole nitrogen attached to the same carbon as the positively charged pyridine nitrogen. Support for point (*a*) comes from the fact that pyrid[1,2-*b*]indazole, in which the charged centers are even closer together, is very reluctant to form a methiodide at all (9). A consideration of the basicities of the pyridonimines led Gray to suggest that there is some slight evidence that the aromatic charge-separated forms more nearly represent the properties of all three anhydronium bases. Additional support for this suggestion comes from the high dipole moment of sempervirine (13). Paoloni and Marini-Bettòlo (14) have argued that it is unnecessary to write a formula bearing separated charges for the β-carboline anhydronium base as suggested by Schwarz (15), and have carried out calculations using the LCAO method on 1-methyl-7-azaindole and on 7-methyl-7H-pyrrolo[2,3-*b*]pyridine, the results of which they say support their contention. It was hoped that the determination of the pK_a and spectral properties of the δ-carboline anhydronium base would shed some light on this problem and also verify or disprove Gray's suggestion concerning its base strength.

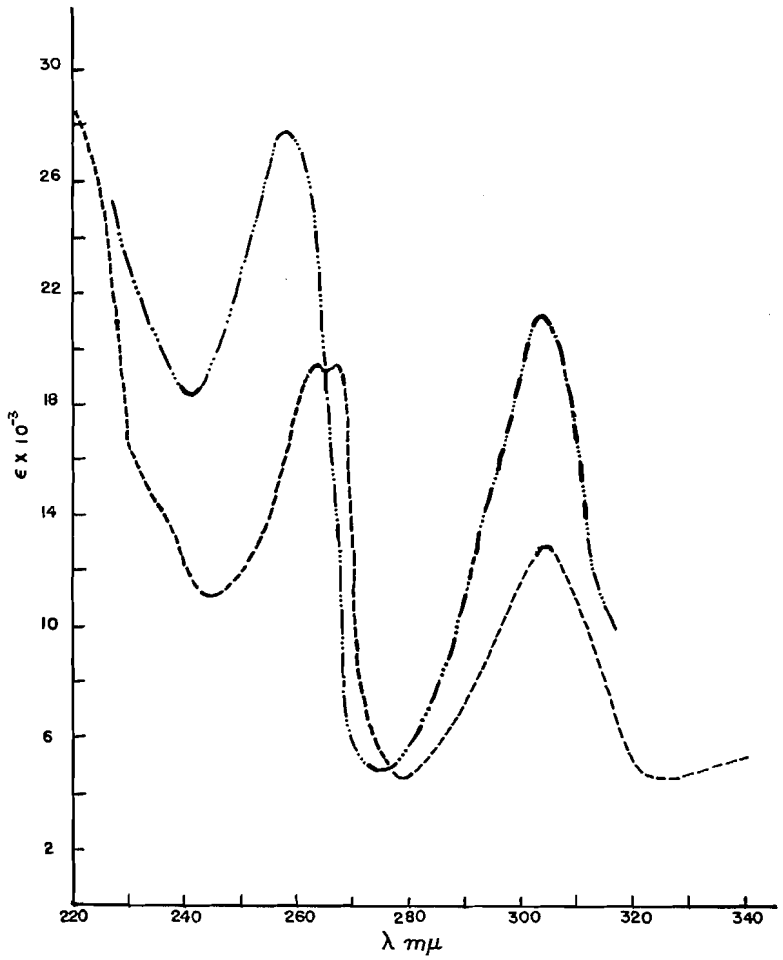
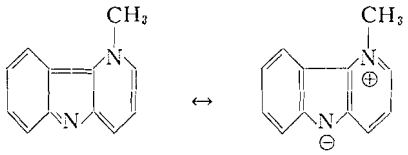


FIG. 1. —·—·— δ-Carboline in 95% ethanol. – – – *ind*-*N*-Methyl-δ-carboline in 95% ethanol.

Can. J. Chem. Downloaded from www.nrcresearchpress.com by 210.87.254.42 on 09/05/12
For personal use only.



A A′

The pK_a's of the anhydronium bases prepared from the methosalts of α-, β-, and δ-carboline were determined both spectroscopically and by potentiometric titration of the methiodides in 60% ethanol with 0.1 *N* sodium hydroxide, the pH at half neutralization being taken as the pK_a value, no correction for the ionic strength being applied. The average values of several determinations are given in Table I.

TABLE I

Anhydronium base	*py*-*N*-Methyl-α-carboline	*py*-*N*-Methyl-β-carboline*	*py*-*N*-Methyl-δ-carboline
pK_a	7.55	10.88	10.77

*Methiodide kindly supplied by Dr. I. D. Spenser, McMaster University, Hamilton, Ontario.

The values for the α- and β-bases are somewhat lower than those reported by Gray (7) but, as suggested by him, *py*-*N*-methyl-δ-carboline anhydro-base is almost as strong a base as its β-isomer. This result would seem to favor the quinonoid structure A as being an important contributor to the structure of the base, resulting in its having a lower stabilization energy as compared with its salt in which the benzenoid structure is preserved.* The infrared spectrum of *py*-*N*-methyl-δ-carboline anhydronium base afforded some slight tentative *negative* evidence in support of this suggestion. In the infrared spectra of two compounds, pyrid[1,2-*b*]indazole (9) and anthranil (16) in which the grouping $C_6H_4N^{\ominus}$ is known to make a strong, if not predominant contribution, bands have been observed at 1650 and 1642 cm^{-1}, respectively, which have been tentatively assumed to be characteristic of such a grouping. No such band was observed for the δ-carboline anhydronium base. A medium band at 1619 cm^{-1} might be ascribed to a highly conjugated C=N as would be present in A, or alternatively to an aromatic ring vibration as is present in A′. *py*-*N*-Methyl-α-carboline anhydronium base exhibits a band at 1630 cm^{-1} which is intermediate between the above values as might be expected from the suggested structure for this compound in which the benzenoid structure remains unchanged and in which the dipolar structure makes an important contribution. The evidence seems to indicate a mesomeric structure A ↔ A′ for the δ-anhydronium base with the quinonoid structure A making perhaps the weightier contribution to the ground state.

The analysis values of *py*-*N*-methyl-δ-carboline anhydronium base were unsatisfactory, but this seems to be characteristic of this type of compound (17). Its anhydro-base character was confirmed by its ultraviolet absorption spectrum (Fig. 2) compared with that of *py*-*N*-methyl-δ-carbolinium iodide; the bands for the anhydro-base exhibited the usual bathochromic shifts. The colors of the methiodides and anhydronium bases and of their solutions are of interest. Thus, both *py*-*N*-methyl-β- and -δ-carbolinium iodide are yellow in the solid state whereas the unmethylated bases are colorless and

**That disruption of the benzenoid structure is an important factor in the destabilization of the bases is shown by the recent work of Adler and Albert on the ionization constants of the diazaindenes (21) where this factor is not present and the order of base strengths is 1,5 > 1,6 > 1,4 > 1,7.*

Can. J. Chem. Downloaded from www.nrcresearchpress.com by 210.87.254.42 on 09/05/12
For personal use only.

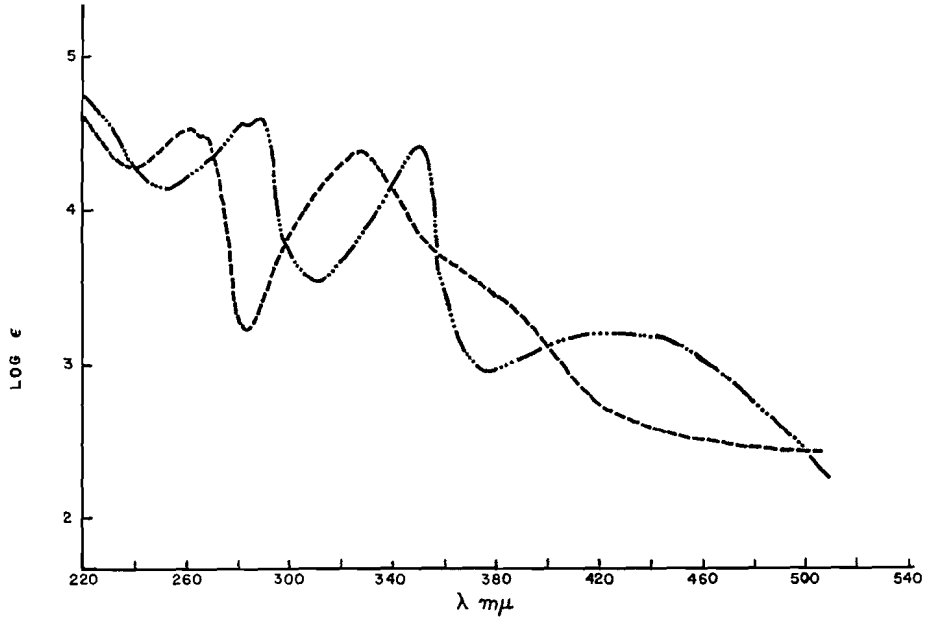


FIG. 2. *py-N*-Methyl-δ-carbolinium iodide. - - - In acidified 95% ethanol. —·· — In alkaline 95% ethanol.

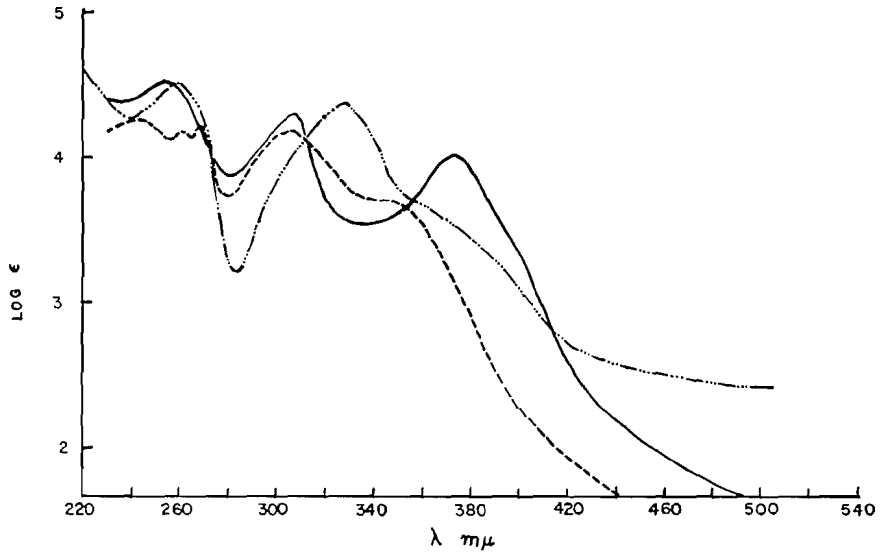


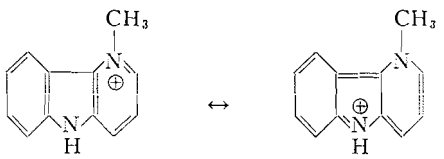
FIG. 3. - - - *py-N*-Methyl-α-carbolinium iodide (in 95% ethanol). ——— *py-N*-Methyl-β-carbolinium iodide (in 95% ethanol). —·· — *py-N*-Methyl-δ-carbolinium iodide (in 95% ethanol).

the α-methiodide is cream-colored (see Fig. 3). The anhydronium bases are all orange-colored and give yellow solutions in hydroxylic solvents. The ultraviolet spectra of *py-N*-methyl-δ-carbolinium iodide and of its anhydronium base in 95% ethanol are identical, indicating the ease with which the anhydronium base reverts to the more stable salt structure (compare the case of the β-carboline anhydro-base (18, and references

Can. J. Chem. Downloaded from www.nrcresearchpress.com by 210.87.254.42 on 09/05/12
For personal use only.

Can. J. Chem. Downloaded from www.nrcresearchpress.com by 210.87.254.42 on 09/05/12
For personal use only.

cited therein)). On the other hand, solutions of *py-N*-methyl-δ-carboline anhydronium base in non-polar solvents such as ether are darker in color than those in hydroxylic solvents and this is reflected in the ultraviolet absorption spectrum of an ethereal solution of this compound when the bands at 282, 289, 350, and 422 mμ (in alkaline 95% ethanol) are shifted to 289, doublet at 295 and 300, 362 and 464 mμ (in ether) respectively. This contrasts with the behavior of the β-carboline anhydro-base whose spectrum in alkaline ethanol is reported to be the same as that in ether solution despite the fact that the latter solution is darker than the former (18). For the δ-carboline anhydro-base the deepening of the yellow color on passing from aqueous ethanolic alkali to ether solution is undoubtedly due to the fact that the color is due to an $n \rightarrow \pi$ transition and that in aqueous ethanolic alkali the unshared electrons of the nitrogen atoms are stabilized in the ground state by hydrogen bonding. As regards the bands in the 282–350 mμ region the bathochromic shift is in the *opposite* direction to that expected for *K*-bands (19) which arise from $\pi \rightarrow \pi$ transitions. Such a blue shift on passing from a non-polar to a polar solvent might indicate an appreciable instantaneous change in polarity from the ground state to the excited state causing the solvating molecules of a polar solvent to be more disoriented than those of a non-polar one during such a transition. If this conclusion is valid it could be taken as providing some tenuous support for the suggestion that structure A is the more important of the two structures contributing to the resonance hybrid. Some comment may also be made concerning the yellow color of the δ-carboline methiodide as compared with the unmethylated base and the α-carboline methiodide. It seems likely that a structure such as (VII′) is contributing to the structure of the ground



VII ↔ VII′

state of the δ-carboline methiodide, the introduction of a positive charge on the *py-N*-atom producing a strong perturbation of the π-electron cloud. Similar comments will apply to the β-carboline methiodide. Due to the closeness of the two nitrogen atoms the perturbation in the α-carboline methiodide case is not as great (this is reflected in the lower pK_a of this compound).

In connection with the ultraviolet absorption spectra of the δ-carbolines it is of interest to note that Eiter and Nezval (3) claimed to have prepared 5-methyl-δ-carboline (no analysis given) and reported that this compound had two bands at 351 and 288 mμ in the ultraviolet. δ-Carboline itself has two bands at 303 and 258 mμ (Fig. 1); furthermore, the shape of the absorption curve given by Eiter and Nezval is quite different from that of δ-carboline reported here, but resembles that of 5-methyl-β-carboline (3). Horner compared the ultraviolet spectra of α- and β-carboline and found them to be similar (20). Both, however, are substantially different from the spectrum of δ-carboline. It seems unlikely therefore, that the compound isolated in very low yield by Eiter and Nezval was really 5-methyl-δ-carboline.

EXPERIMENTAL

Melting points are uncorrected. Infrared spectra were measured with a Perkin–Elmer

Model 21 spectrometer using sodium chloride optics. Ultraviolet absorption spectra were recorded on a Beckman DK2 spectrophotometer.

3-Amino-2-phenylpyridine

2-Phenylpyridine-3-carboxylic acid (11) (0.5 g) was kept at room temperature with thionyl chloride (3.5 ml) for ½ hour. The excess thionyl chloride was removed under vacuum, the residue dissolved in dry acetone, and the solvent evaporated leaving the acid chloride behind as a powder. This was dissolved in dry acetone (9 ml) and sodium azide (0.5 g) in water (1 ml) was stirred into the solution, the temperature being maintained below 20°. After 15 minutes, water (14 ml) was added and the mixture basified with 2 *N* sodium hydroxide. The mixture was heated on a steam bath for 3 hours, cooled, and extracted with ether. The combined extracts were dried (Na_2SO_4) and evaporated to give crude 3-amino-2-phenylpyridine (0.4 g; 92% yield) which was distilled under vacuum and had a boiling point of 119–121°/0.35 mm. The distillate solidified on cooling, and was recrystallized from benzene – light petroleum (b.p. 40–60°) to give colorless crystals, m.p. 62–64°, whose infrared spectrum was identical with that of a sample prepared from 3-aminopyridine and phenyllithium (12). The picrate, m.p. 204–206° (from ethanol), was identical (mixed melting point) with that of the specimen prepared by the 3-aminopyridine method (12).

δ-Carboline

3-Amino-2-phenylpyridine (1.0 g) was dissolved in concentrated hydrochloric acid (2.6 ml) and water (1 ml). A solution of sodium nitrite (0.41 g) in water (1 ml) was added with stirring and cooling on ice to the above solution at such a rate that the temperature remained below 3°. The excess nitrous acid was destroyed by the addition of urea and then a solution of sodium azide (0.45 g) in water (1.5 ml) was added below 3°. At the completion of this addition the solution gave a negative alkaline β-naphthol coupling test. The reaction mixture was allowed to stand at 0° for 1 hour, the solution was then made alkaline with cold sodium hydroxide solution (temperature kept below 5° at all times) and the aqueous solution was then extracted with ether repeatedly. Acidification of the aqueous layer caused the precipitation of 3-hydroxy-2-phenylpyridine (0.3 g; 33% yield), m.p. 206–207°, undepressed on admixture with an authentic specimen (12). The dried (Na_2SO_4) ether extract was evaporated to give the crude azide (0.67 g) as a reddish oil which could not be purified but was used as such in the next stage. Infrared spectrum (liquid film): 2120 (s) (azide), 1580 (m), 1285 (s) (broad), 1185 (m), 802 (m), 735 (s), 695 cm^{-1} (s).

The crude 3-azido-2-phenylpyridine (0.67 g) was dissolved in redistilled decalin (70 ml) and heated at 155–170° for 3 hours. Nitrogen was evolved smoothly at this temperature. On cooling of the reaction mixture, some crystals of δ-carboline separated. The whole mixture was extracted with dilute hydrochloric acid, the acid extracts made alkaline, and the solution extracted with ether. The dried (Na_2SO_4) ether extract was evaporated to give *δ-carboline* (0.44 g), which was recrystallized from benzene to give colorless needles, m.p. 216°. Calc. for $C_{11}H_8N_2$: C, 78.55; H, 4.79. Found: C, 78.15; H, 4.72. The *monopicrate* was recrystallized from ethanol and had a melting point of 277–279°. Calc. for $C_{11}H_8N_2$, $C_6H_3O_7N_3$: C, 51.39; H, 2.79. Found: C, 51.69; H, 2.78. The yields of δ-carboline obtained in several runs varied appreciably, the one reported above being the highest obtained. In some runs, some 3-amino-2-phenylpyridine, formed undoubtedly by hydrogen abstractions from the solvent, was isolated.

Can. J. Chem. Downloaded from www.nrcresearchpress.com by 210.87.254.42 on 09/05/12
For personal use only.

py-N-Methyl-δ-carbolinium Iodide (VII)

δ-Carboline (110 mg) in 95% ethanol (1 ml) was treated with an excess of methyl iodide (2 ml) and the solution kept overnight at room temperature. The precipitate (200 mg) was filtrated and recrystallized from methanol to give the *methiodide* as light yellow needles, m.p. 250–252°. Calc. for $C_{12}H_{11}N_2I$: C, 46.47; H, 3.57. Found: C, 46.27; H, 3.70. λ_{max} 262, 328 mμ; λ_{infl} 266, 348 mμ; log ε 4.53, 4.50, 4.35, 3.70 (in 95% ethanol).

py-N-Methyl-δ-carboline Anhydronium Base (VIII)

The above methiodide (50 mg) was dissolved in hot water (2 ml) and the solution treated with a warm 20% aqueous solution of sodium hydroxide (4 ml). The yellow precipitate (22.6 mg) which separated from the cooled suspension was filtered off and washed with a little cold water. The combined filtrates were extracted repeatedly with ether, the extracts dried (Na_2SO_4), and the ether evaporated to yield a further small quantity of base. The combined solids were recrystallized from anhydrous benzene to give the *anhydronium base* as orange-yellow plates which became almost black at ca. 200° and melted at 204–205°. The microanalytical values were unsatisfactory as is common for such substances (17). Calc. for $C_{12}H_{10}N_2$: C, 79.09; H, 5.53. Found (average of two determinations): C, 71.33; H, 6.00. Infrared spectrum (KBr disk) (main peaks only): 1619 (m), 1588 (m), 1335 (s), 797 (m), and 718 cm^{-1} (ms). λ_{max} 282, 290, 350, 422 mμ; log ε 4.56, 4.60, 4.38, 3.20 (in alkaline 95% ethanol).

ind-N-Methyl-δ-carboline py-N-Methiodide (IX)

A benzene solution of *py-N*-methyl-δ-carboline anhydronium base was treated with an excess of methyl iodide to give an immediate precipitate of the *methiodide* which was recrystallized from 95% ethanol and formed light yellow needles, m.p. 270.5–271.5°, identical with the authentic specimen obtained by treating *ind-N*-methyl-δ-carboline (10*a*) in 95% ethanol with methyl iodide and allowing the solution to stand at room temperature overnight. The melting points of the two specimens were undepressed on admixture and their infrared spectra were identical. Calc. for $C_{13}H_{13}N_2I$: C, 48.14; H, 4.01. Found: C, 48.08; H, 4.12.

ind-N-Methyl-δ-carboline (II)

The anhydro-base methiodide (IX) (13.7 mg) was heated at 300–310°/0.15 mm in a microsublimation apparatus. The methiodide decomposed smoothly and practically no residue was left. The condensate was washed off with ether and the ether evaporated to give the demethylated product (6.3 mg; 82% yield) as a colorless oil which crystallized on standing to a colorless solid, m.p. 77.5–78.5°, undepressed on admixture with an authentic specimen (10*a*). The two samples had identical infrared spectra.

pK_a *Determinations*

The titrimetric determinations were carried out by dissolving the methiodides (ca. 26 mg) in carbon-dioxide-free 60% aqueous ethanol (6 ml) and titrating with 0.998 *N* sodium hydroxide. The pH measurements were carried out with a Leeds–Northrup pH meter equipped with micro pH electrodes; the solution being titrated was stirred by means of a magnetic stirrer. The *py-N*-methyl-δ-carboline anhydronium base was similarly titrated with 0.989 *N* sulphuric acid.

The spectrophotometric determinations were carried out by measuring the extinction coefficients of acid, alkaline, and buffered (pH 10.61) solutions of the methiodides at two or more wavelengths.

Can. J. Chem. Downloaded from www.nrcresearchpress.com by 210.87.254.42 on 09/05/12
For personal use only.

ACKNOWLEDGMENTS

The authors are indebted to Drs. L. Vining and J. E. Newell for the use of recording ultraviolet spectrophotometers. This work was carried out during the tenure (by (K. A. H. A.) of a Canadian Kodak Fellowship and (by A. D. N.) of the Thorvaldson Scholarship. Financial support from the National Research Council is gratefully acknowledged.

REFERENCES

1. E. Späth and K. Eiter. Ber. **73**, 719 (1940).
2. K. Eiter. Monatsh. **79**, 17 (1948).
3. K. Eiter and A. Nezval. Monatsh. **81**, 404 (1950).
4. J. M. Gulland, R. Robinson, J. Scott, and S. Thornley. J. Chem. Soc. 2924 (1929).
5. E. Gellért, Raymond-Hamet, and E. Schlittler. Helv. Chim. Acta, **34**, 642 (1951).
6. R. Robinson. Structural relations of natural products. Oxford University Press. 1955. p. 105.
7. A. P. Gray. J. Am. Chem. Soc. **77**, 5930 (1955).
8. P. A. S. Smith and J. H. Boyer. J. Am. Chem. Soc. **73**, 2626 (1951).
9. R. A. Abramovitch. Chem. & Ind. 422 (1957).
10. R. A. Abramovitch. (*a*) Can. J. Chem. Submitted. (*b*) Unpublished observations.
11. R. A. Abramovitch, A. D. Notation, and Giam Choo Seng. Tetrahedron Letters, **8**, 1 (1959).
12. R. A. Abramovitch and A. D. Notation. Can. J. Chem. **38**, 1445 (1960).
13. B. Witkop. J. Am. Chem. Soc. **75**, 3361 (1953).
14. L. Paoloni and G. B. Marini-Bettòlo. Nature, **179**, 41 (1957).
15. H. Schwarz. Experientia, **6**, 330 (1950).
16. R. A. Abramovitch. Proc. Chem. Soc. 8 (1957).
17. H. Schwarz and E. Schlittler. Helv. Chim. Acta, **34**, 629 (1951).
18. I. D. Spenser. J. Chem. Soc. 3659 (1956).
19. A. E. Gillam and E. S. Stern. An introduction to electronic absorption spectroscopy in organic chemistry. Edward Arnold & Co., London. 1957. p. 303.
20. L. Horner. Ann. **540**, 73 (1939).
21. T. K. Adler and A. Albert. J. Chem. Soc. 1794 (1960).

Can. J. Chem. Downloaded from www.nrcresearchpress.com by 210.87.254.42 on 09/05/12
For personal use only.

Can. J. Chem. Downloaded from www.nrcresearchpress.com by 210.87.254.6 on 09/05/12
For personal use only.

THE PHOTOLYSIS OF DEUTERATED ACETONE AND OF DEUTERATED ACETONE–HYDROGEN MIXTURES[1]

J. F. HENDERSON[2] AND E. W. R. STEACIE

ABSTRACT

The photolyses of acetone, acetone-d_6, and acetone-d_6 – hydrogen mixtures were investigated at 471° K. The rates of formation of methane, ethane, and carbon monoxide and the ratio $R_{\text{methane}}/R_{\text{ethane}}^{\frac{1}{2}}$ were independent of the fractional amount of acetone which photolyzed, as measured by $100[CO]/[A]_0$, which was varied from <1% to 18%. When the acetone-d_6 – hydrogen mixtures were photolyzed, $R_{CD_4}/R_{C_2D_6}^{\frac{1}{2}}[A]_0$, $R_{CD_3H}/R_{C_2D_6}^{\frac{1}{2}}[H_2]_0$, and R_{CD_3H}/R_{CD_4} $[A]_0/[H_2]_0$ were observed to be functions of $[A]_0$ and $[H_2]_0$. It is postulated that some of the CD_4 and CD_3H was formed by a reaction between methyl radicals and an excited molecule which contained both C—D and C—H bonds.

INTRODUCTION

The results of many investigations indicate that, during the photolysis of acetone and acetone–hydrogen mixtures, methane and ethane are formed by the following reactions (1, 2, 3, 4, 5):

$$CD_3 + CD_3 \rightarrow C_2D_6, \qquad (a)$$

$$CD_3 + CD_3COCD_3 \rightarrow CD_4 + CD_2COCD_3, \qquad (b)$$

$$CD_3 + H_2 \rightarrow CD_3H + H. \qquad (c)$$

Hence

(i) $$R_{CD_4}/R_{C_2D_6}^{\frac{1}{2}}[A] = k_b/k_a^{\frac{1}{2}},$$

(ii) $$R_{CD_3H}/R_{C_2D_6}^{\frac{1}{2}}[H_2] = k_c/k_a^{\frac{1}{2}},$$

(iii) $$R_{CD_3H}/R_{CD_4}[A]/[H_2] = k_c/k_b.$$

It has been suggested by Long that, in addition to these reactions, methane is formed by reaction between methyl radicals and the ethane formed by step (*a*), and that this reaction is important even when the amount of acetone decomposed is small, e.g. <5% (6). Kutschke and Steacie have summarized evidence which indicates that reaction between methyl radicals and the product ethane is negligible under these conditions (7).

If Long's suggestion were correct, the rate constants calculated by equations (i), (ii), and (iii) would be functions of the length of photolysis. However, in none of the many investigations which have been made has this question been subjected to a detailed experimental test. Consequently, experiments have been carried out here to determine whether these rate constants vary with the extent of decomposition of the acetone.

[1]*Manuscript received July 20, 1960.*
Contribution from the Division of Pure Chemistry, National Research Council, Ottawa, Canada.
Issued as N.R.C. No. 5976.
[2]*National Research Council Postdoctorate Fellow 1957–59. Present address: Polymer Corporation Limited, Sarnia, Ontario.*

Can. J. Chem. Downloaded from www.nrcresearchpress.com by 210.87.254.6 on 09/05/12
For personal use only.

EXPERIMENTAL

The apparatus and methods of analysis were similar to those described elsewhere (2). The cracking pattern for CD_3H suggested by McNesby and Gordon was used when determining the isotopic composition of the methane fractions mass spectrometrically (4).

The reaction cell, which was 10 cm in length and 5 cm in diameter (195 cc volume), was filled with a nearly parallel beam of light from B.T.H. ME/D 250-w mercury lamp. The light was filtered either by a Corning filter 9863 in combination with a solution of potassium chromate (filter A) or a Corning filter 7910 (filter B) (8). The light intensity was varied either by neutral density filters or wire gauzes and both gave similar results. In some experiments the light absorption was measured by a photocell placed at the rear of the cell.

Reagent grade acetone (Merck), deuterated acetone (Merck of Canada; 98.2% acetone-d_6 and 1.8% acetone-d_5), and the hydrogen were purified by methods described earlier (2). Perfluoro-*n*-butane (Minnesota Mining and Manufacturing Co.) was outgassed at $-160°$ C.

In a few experiments, the methyl ethyl ketone produced during the photolysis of acetone was analyzed by gas chromatography on a 30-ft column consisting of 30% dinonyl phthalate on firebrick held at 94° C.

The temperature of the reaction cell was controlled by a Fenwal 560 temperature regulator, and the experiments were done at $471 \pm 0.5°$ K.

RESULTS

Deuterated acetone was photolyzed at pressures of 50 mm and 100 mm Hg, and the results are shown in Table I. The extent of the decomposition of the acetone, measured by 100 $[CO]/[A]_0$, was varied over a considerable range, and $R_{CD_4}/R^{\frac{1}{2}}_{C_2D_6}[A]_0$, R_M/R_E, and $(R_M+2R_E)/R_{CO}$ were independent of the conversion except at the very low conversions. It is interesting to note that at a given light intensity the rates of formation of methane, ethane, and carbon monoxide were independent of the length of photolysis. The light absorption, measured in a few experiments, was also independent of time for conversions up to 18%.

To determine more about the decrease in $R_{CD_4}/R^{\frac{1}{2}}_{C_2D_6}[A]_0$ at very low conversions, light acetone at 100 mm Hg was photolyzed, and the results are shown in Fig. 1. When

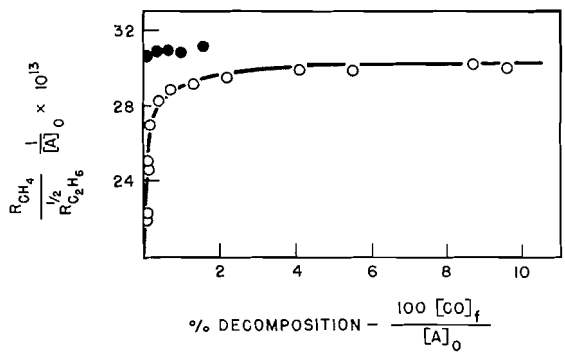


FIG. 1. Variation of $R_{CH_4}/R^{\frac{1}{2}}_{C_2H_6}[A]_0$ with percentage of decomposition of acetone.
○ Analysis by distillation. ● Mass spectrometric analysis.

TABLE I

The photolysis of deuterated acetone

Run	Time, seconds	Molecules/cc sec $\times 10^{-12}$ CO	Methane	Ethane	$\frac{R_{CD_3H}}{R_{CD_4}}$	$\frac{R_{C_2D_5H}}{R_{C_2D_6}}$	$\frac{(R_M/R_E^{\frac{1}{2}})}{(1/[A]_0)\times 10^{13}}$	$\frac{(R_{CD_4}/R_{C_2D_6}^{\frac{1}{2}})}{(1/[A]_0)\times 10^{13}}$	$\frac{R_M}{R_E}$	$\frac{100[CO]}{[A]_0}$
					Filter A					
					(Mean conc. *d*-acetone 1.07×10^{18} molecules/cc)					
32	3600	3.13	1.08	2.17	.0198	.0157	6.87	6.77	.498	1.05
33	5400	2.89	1.02	1.95	.0189	.0163	6.89	6.81	.523	1.47
27	7200	3.31	1.14	2.27	.0203	.0156	7.05	6.99	.502	2.23
31	9000	3.55	1.17	2.46	.0196	.0159	6.96	6.91	.476	2.99
26	10800	3.80	1.22	2.66	.0200	.0158	7.06	6.99	.459	3.87
30	12600	3.21	1.09	2.17	.0195	.0157	6.93	6.85	.502	3.77
25	14400	3.81	1.27	2.68	.0202	.0160	7.23	7.13	.474	5.13
29	16200	3.67	1.20	2.54	.0203		7.06		.472	5.56
28	19800	3.16	1.11	2.15	.0205	.0155	7.07	7.00	.516	5.84
24	21600	3.66	1.20	2.54	.0198	.0140	6.97	6.92	.472	7.31
					(Mean conc. *d*-acetone 2.16×10^{18} molecules/cc)					
3	1800	7.69	3.21	4.76			6.81		.674	.641
5	1800	6.76	2.95	4.12			6.82		.716	.572
6	1800	7.03	3.04	4.17			6.80		.729	.578
21	3600	6.18	2.79	3.68	.0206		6.74		.758	1.04
22	7200	6.10	2.82	3.60	.0201	.0169	6.79	6.73	.783	2.02
24	9000	6.41	2.99	3.74	.0310	.0163	6.95	6.87	.799	2.62
20	10800	5.97	2.78	3.57		.0172	6.90		.779	3.03
					(Mean conc. *d*-acetone 2.16×10^{18} molecules/cc)					
12	12600	7.07	3.20	4.28		.0166	6.97		.748	4.01
19	14400	6.05	2.85	3.60	.0196	.0169	6.99	6.90	.792	4.05
18	18000	6.66	2.97	3.97	.0198	.0153	6.97	6.89	.748	5.61
17	21600	5.84	2.68	3.40	.0206	.0150	6.87	6.78	.788	5.95
					Filter B					
					(Mean conc. *d*-acetone 1.48×10^{18} molecules/cc)					
63	1920	10.6	2.84	8.07	.0216	.0141	6.75	6.66	.460	2.84
					(Mean conc. *d*-acetone 2.13×10^{18} molecules/cc)					
85	300	9.53	3.28	6.74			5.93		.487	.134
82	300	9.43	3.15	6.77			5.98		.465	.139
83	450	9.92	3.62	6.74			6.54		.537	.210
81	600	10.5	3.73	7.21			6.51		.517	.295
75	600	13.4	4.19	9.77	.0237	.0157	6.23	6.14	.429	.375
65	1320	14.6	4.68	10.3	.0212	.0154	6.84	6.73	.454	.898
78	1800	10.9	4.06	7.31	.0241		6.98		.555	.916
76	3600	8.60	3.47	5.46	.0216	.0148	6.97	6.90	.636	1.45
51	3600	16.2	4.94	11.7	.0247	.0174	6.83	6.77	.422	2.74
53	7200	15.9	4.93	11.7	.0213	.0174	6.76	6.79	.421	5.37
					(Mean conc. *d*-acetone 2.13×10^{18} molecules/cc)					
69	9000	13.9	4.53	9.67	.0209	.0170	6.84	6.76	.468	5.86
52	10800	18.2	5.31	13.4	.0213	.0152	6.81	6.72	.396	9.21
68	19800	13.3	4.42	9.09	.0208	.0155	6.87	6.81	.486	12.3
56	18000	15.3	4.79	10.9	.0205	.0151	6.81	6.77	.439	13.0
55	21600	17.7	5.21	12.7	.0209	.0149	6.83	6.73	.410	17.8

the mixtures of methane, ethane, and carbon monoxide were analyzed by distillation, $R_{CH_4}/R_{C_2H_6}^{\frac{1}{2}}[A]_0$ decreased rapidly at low conversions, but this was not observed when these mixtures were analyzed by mass spectrometric analyses. It is concluded that a small but constant amount of methane was being occluded in the solid nitrogen trap

Can. J. Chem. Downloaded from www.nrcresearchpress.com by 210.87.254.6 on 09/05/12
For personal use only.

used to separate methane and carbon monoxide from ethane by distillation, and at low conversions this was appreciable relative to the total yields of methane and ethane. The amount of methane occluded varied with the temperature of the solid nitrogen. Recently similar observations were made elsewhere (9).

A few experiments were done in which the methyl ethyl ketone produced during the photolysis of acetone was determined, and the results (Table II) agree with those of Mandelcorn and Steacie (10).

TABLE II

The formation of methyl ethyl ketone during the photolysis of acetone

Run	Time, seconds	Molecules/cc sec $\times 10^{-12}$ CO	Methane	Ethane	MEK	$\frac{R_M+R_{MEK}+2R_E}{2R_{CO}}$	$\frac{R_{CH_4}}{R_{C_2H_6}^{\frac{1}{2}}}$	$\frac{1}{[A]_0}$	$\frac{100[CO]}{[A]_0}$
				(Conc. acetone 2.13×10^{18} molecules/cc)					
108	1320	14.3	12.4	4.03	7.17	0.93	29.0		.886
106	4500	11.3	10.8	2.95	6.14	0.98	29.5		2.38
105	10800	10.8	10.6	2.79	5.33	0.96	29.8		5.48
103	14400	12.9	12.1	3.54	5.83	0.94	30.2		8.70

Mixtures of deuterated acetone and hydrogen at pressures of 100 mm Hg and 50 mm Hg, respectively, were photolyzed, and the results are shown in Table III. The two

TABLE III

The photolysis of deuterated acetone in the presence of hydrogen

Run	Time, seconds	Molecules/cc sec $\times 10^{-12}$ CO	Methane	Ethane	$\frac{R_{CD_3H}}{R_{CD_4}}$	$\frac{R_{C_2D_5H}}{R_{C_2D_6}}$	$\frac{(R_{CD_4}/R_{C_2D_6}^{\frac{1}{2}})}{(1/[A]_0)\times10^{13}}$	$\frac{(R_{CD_3H}/R_{C_2D_6}^{\frac{1}{2}})(1/[H_2]_0)\times10^{13}}{\text{Method I}}$	Method II	$\frac{R_M}{R_E}$	$\frac{100[CO]}{[A]_0}$
						Filter A					
		(Mean conc. *d*-acetone 2.15×10^{18} molecules/cc; mean conc. hydrogen 1.02×10^{18} molecules/cc)									
40	1800	4.54	4.88	1.64	1.63	.0186	6.78	23.3	23.4	2.98	.390
39	3600	4.62	5.12	1.54	1.66	.0132	7.28	26.3	25.3	3.32	.770
38	5400	4.69	5.23	1.43	1.72	.0214	7.55	27.8	26.4	3.66	1.18
35	7200	4.89	5.28	1.65	1.82	.0192	7.15	26.4	25.8	3.20	1.76
45	9000	5.45	5.85	1.82	1.68	.0223	7.60	28.2	26.7	3.21	2.27
42	10800	4.99	5.50	1.73	1.72	.0237	7.23	26.3	25.5	3.18	2.51
43	14400	4.31	4.79	1.36	1.68	.0226	7.22	26.3	25.4	3.52	2.89
46	16200	4.66	5.03	1.56	1.73	.0263	6.97	25.7	25.1	3.22	3.52
44	18000	4.62	5.10	1.48	1.72	.0278	7.29	26.5	25.5	3.45	3.87
41	19800	4.64	5.06	1.50	1.70	.0274	7.23	26.1	25.2	3.37	4.27
37	21600	4.85	5.02	1.54	1.71	.0267	7.06	25.0	24.7	3.26	4.87
						Filter B					
61	3600	17.2	12.7	8.81	1.66	.0195	7.56	27.7	26.1	1.44	2.87
49	7200	17.3	12.8	8.73	1.68	.0222	7.57	28.1	26.6	1.47	5.76
60	11040	15.8	11.9	7.91	1.69	.0235	6.75	27.3	27.5	1.50	8.09
57	14460	14.7	11.7	7.12		.0247		28.8		1.64	9.86
50	14400	18.8	13.9	10.0	1.71	.0267	7.66	28.9	27.3	1.39	12.6
59	21660	16.5	12.7	8.57	1.66	.0300	7.70	28.4	26.6	1.48	16.6

Can. J. Chem. Downloaded from www.nrcresearchpress.com by 210.87.254.6 on 09/05/12
For personal use only.

procedures called methods I and II for calculating $R_{CD_3H}/R^{\frac{1}{2}}_{C_2D_6}[H_2]_0$ are the same as those used by Whittle and Steacie (2). The formation of CD_3H was determined either by using results obtained when deuterated acetone was photolyzed alone (method I) or by mass spectrometric analyses of the methane fractions (method II). The CD_3H arising from the small amount of acetone-d_5 present in the deuterated acetone was evaluated by equation (iv) and subtracted from the total CD_3H formed

$$\text{(iv)} \qquad R_{CD_3H}/R^{\frac{1}{2}}_{C_2D_6} = 0.014[A]_0 \times 10^{-12}(\text{molecules/cc})^{\frac{1}{2}}\ \text{sec}^{-\frac{1}{2}}.$$

No CD_2H_2 could be detected.

The values of $R_{CD_4}/R^{\frac{1}{2}}_{C_2D_6}[A]_0$, $R_{CD_3H}/R^{\frac{1}{2}}_{C_2D_6}[H_2]_0$, R_{CD_3H}/R_{CD_4}, R_M/R_E, and $(2R_E+R_M)/R_{CO}$ were independent of the fraction of the acetone that was photolyzed, and again the rates of formation of methane, ethane, and carbon monoxide were independent of conversion. The addition of hydrogen to deuterated acetone caused the ratio $R_{C_2D_5H}/R_{C_2D_6}$ to increase very slightly.

In both the presence and absence of hydrogen the formation of methane and ethane during the photolysis of deuterated acetone was linear in the carbon monoxide produced (Fig. 2).

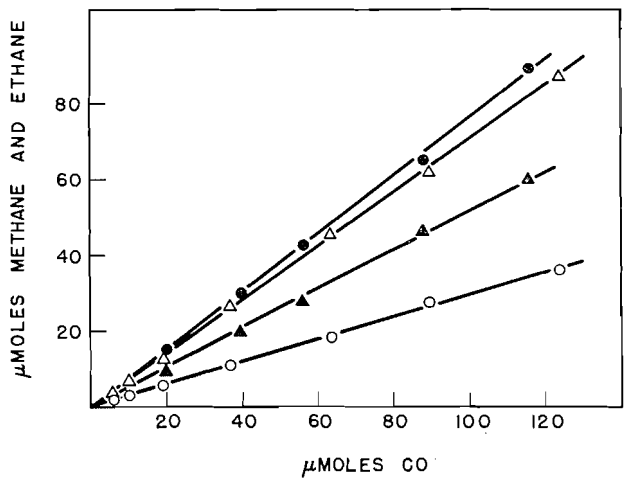
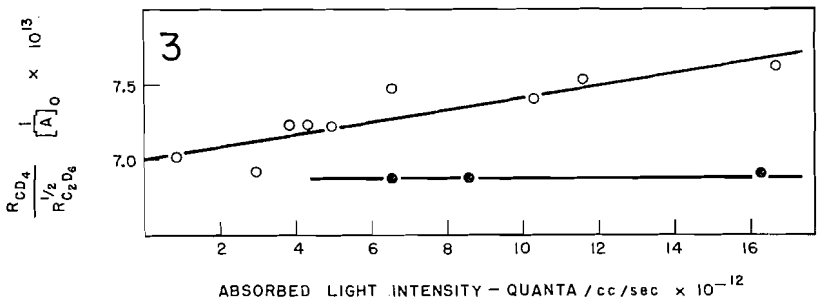


FIG. 2. Variation of the yields of methane and ethane with carbon monoxide.
○ CD_4 from 100 mm Hg *d*-acetone. △ C_2D_6 from 100 mm Hg *d*-acetone.
● Methane from 100 mm Hg *d*-acetone and 50 mm Hg hydrogen.
▲ Ethane from 100 mm Hg *d*-acetone and 50 mm Hg hydrogen.

It is interesting to note that in the presence of hydrogen $R_{CD_4}/R^{\frac{1}{2}}_{C_2D_6}[A]_0$ and $R_{CD_3H}/R^{\frac{1}{2}}_{C_2D_6}[H_2]_0$ but not R_{CD_3H}/R_{CD_4} depended on the light intensity. Experiments were made to investigate this effect in more detail, and the results are shown in Figs. 3 and 4. At zero light intensity, differences between the results calculated by methods I and II became very small.

Can. J. Chem. Downloaded from www.nrcresearchpress.com by 210.87.254.6 on 09/05/12
For personal use only.



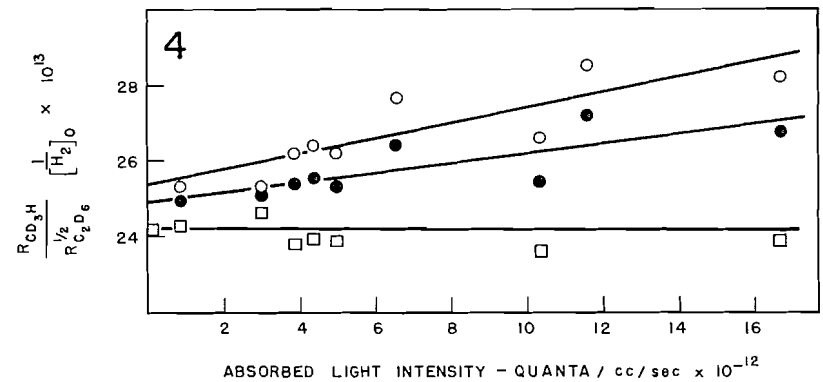


FIG. 3. Variation of $R_{CD_4}/R^{\frac{1}{2}}_{C_2D_6}[A]_0$ with light intensity.
● 100 mm Hg *d*-acetone.
○ 100 mm Hg *d*-acetone and 50 mm Hg hydrogen.

FIG. 4. Variation of $R_{CD_3H}/R^{\frac{1}{2}}_{C_2D_6}[H_2]_0$ with light intensity.
○ Method I. ● Method II.
□ $(R_{CD_3H}/R_{CD_4})\,([A]_0/[H_2]_0)\times 6.83\times 10^{-13}$.

Some experiments were carried out to determine the variations, if any, of $(R_{CD_4}/R^{\frac{1}{2}}_{C_2D_6})(1/[A]_0)$, $R_{CD_3H}/R^{\frac{1}{2}}_{C_2D_6}[H_2]_0$, and $(R_{CD_3H}/R_{CD_4})\,([A]_0/[H_2]_0)$ with the pressures of deuterated acetone and hydrogen. The results, shown in Figs. 5, 6, and 7, are rather surprising. Although the photolysis of deuterated acetone alone was not affected by the addition of perfluoro-*n*-butane, both $R_{CD_4}/R^{\frac{1}{2}}_{C_2D_6}[A]_0$ and $R_{CD_3H}/R^{\frac{1}{2}}_{C_2D_6}[H_2]_0$ were decreased when this substance was added to the deuterated acetone–hydrogen mixtures.

In one experiment, following the photolysis of deuterated acetone alone, about 50 mm Hg of hydrogen was added to the system, and it was shown that this had no effect on the analyses of the methane and ethane.

DISCUSSION

The object of this investigation, as mentioned earlier, was to determine the importance of the reaction between methyl radicals and the ethane produced during the photolysis of acetone or acetone–hydrogen mixtures.

If this reaction were important, then, $R_{CD_4}/R^{\frac{1}{2}}_{C_2D_6}[A]_0$, $R_{CD_3H}/R^{\frac{1}{2}}_{C_2D_6}[H_2]_0$, R_M/R_E, and

Can. J. Chem. Downloaded from www.nrcresearchpress.com by 210.87.254.6 on 09/05/12
For personal use only.

Can. J. Chem. Downloaded from www.nrcresearchpress.com by 210.87.254.6 on 09/05/12
For personal use only.

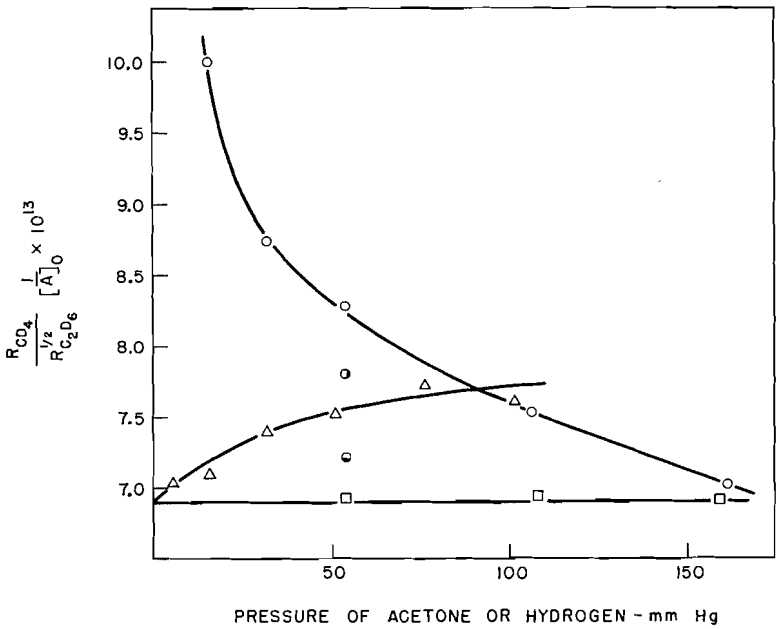


FIG. 5. Variation of $R_{CD_4}/R^{\frac{1}{2}}_{C_2D_6}[A]_0$ with *d*-acetone, hydrogen, and perfluoro-*n*-butane pressure.
○ 50 mm Hg hydrogen, *d*-acetone pressure varied.
△ 100 mm Hg *d*-acetone, hydrogen pressure varied.
□ 100 mm Hg *d*-acetone, perfluoro-*n*-butane pressure varied.
◑ 50 mm Hg *d*-acetone, 50 mm Hg hydrogen, and 50 mm Hg perfluoro-*n*-butane.
◒ 50 mm Hg *d*-acetone, 50 mm Hg hydrogen, and 150 mm Hg perfluoro-*n*-butane.

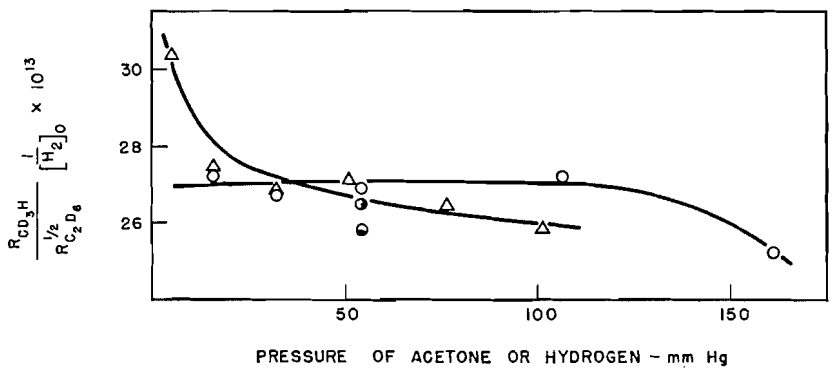


FIG. 6. Variation of $R_{CD_3H}/R^{\frac{1}{2}}_{C_2D_6}[H_2]_0$ with *d*-acetone, hydrogen, and perfluoro-*n*-butane pressure.
○ 50 mm Hg hydrogen, *d*-acetone pressure varied.
△ 100 mm Hg *d*-acetone, hydrogen pressure varied.
◑ 50 mm Hg *d*-acetone, 50 mm Hg hydrogen, and 50 mm Hg perfluoro-*n*-butane.
◒ 50 mm Hg *d*-acetone, 50 mm Hg hydrogen, and 150 mm Hg perfluoro-*n*-butane.

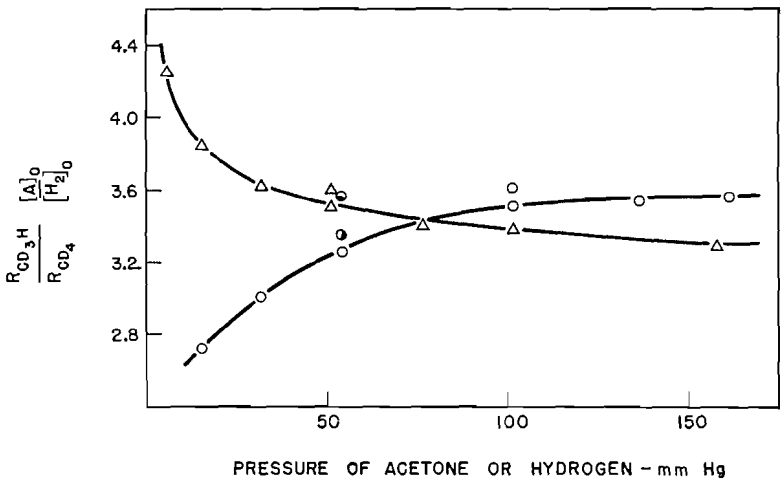


FIG. 7. Variation of R_{CD_3H}/R_{CD_4} $[A]_0/[H_2]_0$ with *d*-acetone, hydrogen, and perfluoro-*n*-butane pressure.
○ 50 mm Hg hydrogen, *d*-acetone pressure varied.
△ 100 mm Hg *d*-acetone, hydrogen pressure varied.
◑ 50 mm Hg *d*-acetone, 50 mm Hg hydrogen and 50 mm Hg perfluoro-*n*-butane.
◒ 50 mm Hg *d*-acetone, 50 mm Hg hydrogen, and 150 mm Hg perfluoro-*n*-butane.

R_{CD_3H}/R_{CD_4} in all probability would have been functions of the length of photolysis, but this was not observed. Furthermore, in the presence of hydrogen, a larger yield of C_2D_5H than was found would be expected due to the reaction of C_2D_5 radicals with hydrogen. Finally, the linear relations between both the methane and ethane and the carbon monoxide produced (Fig. 2) would not have been observed.

Both these observations and the evidence already summarized (7) make it apparent that this reaction of methyl radicals with the ethane, though possible under certain conditions, is negligible when the decomposition of the acetone is small.

It is difficult to discuss the observed independence of the absorbed light intensity and of the rates of formation of methane, ethane, and carbon monoxide with time as the length of photolysis was increased. Very many reactions become possible at the larger conversions due to the accumulation of products.

It is apparent that the results observed during the photolysis of the deuterated acetone–hydrogen mixtures are not predicted by reactions (*a*), (*b*), and (*c*) alone. The fact that the ratio (R_{CD_3H}/R_{CD_4}) $([A]_0/[H_2]_0)$ varies with $[H_2]_0$ and $[A]_0$ but is independent of conversion suggests that the anomalous behavior cannot be ascribed entirely to the production of ethane by a reaction other than (*a*) or by the consumption of ethane by radical attack. Consequently, it is postulated that appreciable amounts of methane were formed by reactions in addition to (*b*) and (*c*), and equations (i) and (ii) should be rewritten as follows:

$$(v) \qquad (R_{CD_4}/R^{\frac{1}{2}}_{C_2D_6})_{meas} = (k_b/k_a^{\frac{1}{2}})[A]_0 + (R_{CD_4}/R^{\frac{1}{2}}_{C_2D_6})_{excess},$$

$$(vi) \qquad (R_{CD_3H}/R^{\frac{1}{2}}_{C_2D_6})_{meas} = (k_c/k_a^{\frac{1}{2}})[H_2]_0 + (R_{CD_3H}/R^{\frac{1}{2}}_{C_2D_6})_{excess}.$$

Although neither $(R_{CD_4}/R^{\frac{1}{2}}_{C_2D_6})_{excess}$ nor $(R_{CD_3H}/R^{\frac{1}{2}}_{C_2D_6})_{excess}$ could be estimated with high

Can. J. Chem. Downloaded from www.nrcresearchpress.com by 210.87.254.6 on 09/05/12
For personal use only.

precision, they were found to be approximately equal in all the experiments and tended to zero at zero light intensity, zero hydrogen pressure, and infinite acetone pressure.

To account for these observations it is proposed that the excess methane was produced by reaction of methyl radicals with an activated molecule X* which was formed by a reaction involving hydrogen atoms, and this contained both C—H and C—D bonds.

$$CD_3 + X^* \rightarrow CD_4 + R \qquad (d)$$

$$\rightarrow CD_3H + R' \qquad (e)$$

$$X^* + M \rightarrow X + M \qquad (f)$$

If the reactivities of both hydrogen atoms and methyl radicals toward acetone are similar, some hydrogen atoms would be available for combination with methyl and acetonyl radicals to form CD_3H^* and $CD_3COCD_2H^*$. Very little quantitative information is available for the reaction between hydrogen atoms and acetone, but it can be shown that hydrogen atoms are about 10 times more reactive toward ethane at 471° K than are methyl radicals (11, 12). If CD_3H^* is unlikely because of the rapidity of

$$H + CD_3COCD_3 \rightarrow HD + CD_2COCD_3$$

then the formation of $CD_3COCD_2H^*$ must be rejected for a similar reason. On the other hand, if CD_3H^* and $CD_3COCD_2H^*$ are formed, it is likely that they would be partially stabilized very rapidly though it is possible that many collisions (10^6) may be required before they are deactivated to their ground vibrational states (13).

If X* represents an excited molecule of CD_3H, reaction (*d*) would give rise to CD_2H radicals, and some would undoubtedly combine with CD_3 radicals to form C_2D_5H. It was observed, however, that although $(R_{CD_4}/R^{\frac{1}{2}}_{C_2D_6})_{excess}$ was independent of the conversion and increased with increasing light intensity, the small yield of C_2D_5H increased with increasing conversion and decreased with increasing light intensity. Furthermore, due to reaction (*f*) the addition of a third body to the reaction mixture would cause the ratio $(R_{CD_3H}/R^{\frac{1}{2}}_{C_2D_6})_{excess}/(R_{CD_4}/R^{\frac{1}{2}}_{C_2D_6})_{excess}$ to increase and this was not observed.

On the other hand, if X* represents an excited molecule of $CD_3COCD_2H^*$ the observed kinetics are predicted. However, more direct evidence is required before it will be possible to identify the excited molecule X* with any degree of certainty.

The formation of some such excited molecule during the photolysis of acetone–hydrogen mixtures will account for the observations made here. It also suggests an explanation for the differing values obtained here, and earlier (1, 2), by methods I and II for the rate constant for the reaction of methyl radicals with hydrogen. Such an explanation could also account for the lowering of the apparent value of the activation energy of the reaction of methyl radicals with acetone as observed by Whittle and Steacie (2) for the two systems, acetone-d_6 – hydrogen and acetone–deuterium. It is possible that for the same reason the activation energies reported for the reaction of methyl radicals with hydrogen are slightly low, for example, by about 1 kcal/mole.

ACKNOWLEDGMENTS

We wish to thank Drs. K. O. Kutschke and K. J. Laidler for their interest in this work, Mrs. R. H. Riem for the mass spectrometric analyses, and Mr. R. Pilon for the gas chromatographic analyses.

Can. J. Chem. Downloaded from www.nrcresearchpress.com by 210.87.254.6 on 09/05/12
For personal use only.

REFERENCES

1. T. G. MAJURY and E. W. R. STEACIE. Can. J. Chem. **30**, 800 (1952).
2. E. WHITTLE and E. W. R. STEACIE. J. Chem. Phys. **21**, 993 (1953).
3. J. R. MCNESBY, A. S. GORDON, and S. R. SMITH. J. Am. Chem. Soc. **78**, 1287 (1956).
4. J. R. MCNESBY and A. S. GORDON. J. Am. Chem. Soc. **76**, 1416 (1954).
5. E. W. R. STEACIE. Atomic and free radical reactions. Reinhold Publishing Corp., New York. 1954.
6. L. H. LONG. J. Phys. Chem. **61**, 821 (1957).
7. K. O. KUTSCHKE and E. W. R. STEACIE. J. Phys. Chem. **62**, 866 (1958).
8. M. KASHA. J. Opt. Soc. Am. **38**, 929 (1948).
9. J. HEICKLEN and W. A. NOYES, JR. J. Am. Chem. Soc. **81**, 3858 (1959).
10. L. MANDELCORN and E. W. R. STEACIE. Can. J. Chem. **32**, 79 (1954).
11. M. R. BERLIE and D. J. LE ROY. Discussions Faraday Soc. No. 14, **50** (1953).
12. J. R. MCNESBY and A. S. GORDON. J. Am. Chem. Soc. **77**, 4719 (1955).
13. B. H. MAHON. J. Phys. Chem. **62**, 100 (1958).

Can. J. Chem. Downloaded from www.nrcresearchpress.com by 210.87.254.6 on 09/05/12
For personal use only.

Can. J. Chem. Downloaded from www.nrcresearchpress.com by 210.87.254.5 on 09/05/12
For personal use only.

SOME DEUTERIUM KINETIC ISOTOPE EFFECTS

IV. β-DEUTERIUM EFFECTS IN WATER SOLVOLYSIS OF ETHYL, ISOPROPYL, AND *tert*-BUTYL COMPOUNDS[1]

K. T. LEFFEK,[2] J. A. LLEWELLYN,[2] AND R. E. ROBERTSON

ABSTRACT

The secondary β-deuterium isotope effects have been measured in the water solvolytic reaction of alkyl halides and sulphonates for primary, secondary, and tertiary species. In every case the kinetic isotope effect was greater than unity ($k_H/k_D > 1$). This isotope effect may be associated with varying degrees of hyperconjugation or altered non-bonding intramolecular forces. The experiments make it difficult to decide which effect is most important.

As an extension of our work (1, 2, 3) on deuterium kinetic isotope effects we have measured the kinetic consequences of β-deuteration for a series of compounds solvolyzing in water,

$$RX + H_2O \rightarrow ROH + H^+ + X^- \qquad [1]$$

The kinetic effect produced by substituting deuterium for β-hydrogen in molecules undergoing solvolytic substitution has been studied by Shiner (4, 5, 6), Lewis *et al.* (7, 8, 9), Streitwieser *et al.* (10), and others (11, 12, 13). This paper presents a survey for a series of alkyl halides and sulphonates and the results of these measurements have been collected in Table I.

DISCUSSION

It will be noted that in all cases the deuterated compounds react more slowly than their protium analogues, the magnitude of the total isotope effect increasing both absolutely and relatively as the transition state becomes more ionic. Thus the effect of deuteration for a given alkyl group is greater in the sulphonates than for the halides and increases with increasing α-methylation. Since some of the compounds have been extensively deuterated, it will be necessary to consider as sources of the observed isotope effect not only those factors involved in the activation process contributing to changes in the zero-point energy such as changes in hyperconjugation and non-bonded interaction but also the consequence of mass increase. This factor has been discussed by us in an earlier paper as a "thermodynamic" effect involving changes in translational and rotational properties which affect the thermodynamic properties of the molecule independently of the zero-point energy shifts.

"Thermodynamic" Factors

Although a detailed evaluation of these elements is not yet possible, the relative values of k_H/k_D evident in Table I provide a basis for a semiquantitative discussion of the importance of possible contributors to the deuterium isotope effect.

[1]*Manuscript received August 4, 1960.*
Contribution from the Division of Pure Chemistry, National Research Council, Ottawa, Canada. Presented in part at the Chemical Institute of Canada Meeting in Ottawa, June 1960.
Issued as N.R.C. No. 5969.
[2]*National Research Council Postdoctorate Fellow.*

TABLE I

Secondary β-deuterium isotope effects in the water solvolysis of some alkyl compounds

Compound	$10^4 k_H$ (sec^{-1})	$10^4 k_D$ (sec^{-1})	Temp., ° C	k_H/k_D
Ethyl *p*-toluenesulphonate	3.480	3.420	59.93_5	1.01_8
Ethyl methanesulphonate	1.958	1.907	60.00_0	1.02_7
Ethyl bromide	2.722	2.636	80.00_1	1.03_3
Ethyl iodide	1.554	1.499	80.00_0	1.03_7
Isopropyl *p*-toluenesulphonate	7.664	4.942	30.00_1	1.55_1
Isopropyl methanesulphonate	3.686	2.386	30.00_1	1.54_5
Isopropyl bromide	3.448	2.580	59.93_2	1.33_6
Isopropyl iodide	3.125	2.380	60.00_3	1.31_3
t-Butyl chloride	9.860	3.840	2.07_0	2.56_8

In order to consider these effects, it is necessary to postulate models for initial and transition states of reaction. Obviously there is scope for considerable conjecture here, and it appears advisable to set limits where possible by oversimplification, and thereby obtain maximum values. For these reactions, the C—X bond (X represents the leaving group) is undoubtedly stretched almost to breaking; the number and role of the water molecules in the transition state form a field for speculation. Consider first translational changes: a simple ionization with no water involved and bond stretching in the transition state would have zero translational contribution to the isotope effect. For an extensively solvated transition state and an unsolvated initial state (almost as unrealistic a model as the first (14)), the translational differences will approximate to those in the initial state. This contribution will tend to slow the reaction for the heavy compound and a maximum value of about 86 cal/mole ($\Delta F_H^{\ddagger} - \Delta F_D^{\ddagger}$) can be calculated for *tert*-butyl chloride at 273° K. Initial-state solvation, which is undoubtedly important in these reactions, will serve to reduce this effect considerably. Rotational changes may be considered for similar models. Simple C—X extension if carried sufficiently far might produce an inverse effect ($k_H/k_D < 1$) by displacing the center of gravity in a direction away from the site of isotopic substitution. For more complicated models the expression for the rotational contribution (eq. 2) may be examined as follows in order to assess its maximum contribution

$$[2] \qquad k_H/k_D(\text{rotation}) = \left[\frac{\Pi I_D}{\Pi I_H}\frac{\Pi I_H^{\ddagger}}{\Pi I_D^{\ddagger}}\right]^{\frac{1}{2}}.$$

The maximum value for the second factor in the square bracket (referring to the transition state) is unity. Such a condition would exist for a massive, highly solvated transition state when deuteration made a negligible contribution to the mass. Thus the maximum value of the rotational contribution is now dependent on the ratio of the initial-state terms to the one-half power so that in case of a doubling of this inertial product by deuteration the maximum rotational isotope effect would be $k_H/k_D = \sqrt{2}$. Rough estimates for *t*-butyl and isopropyl halides indicate smaller effects which would again be further reduced by initial-state solvation. If rotational contributions were important, a decrease in isotope effect would be expected to follow substitution of toluenesulphonate for a halide as leaving group. Such changes do occur for the ethyl compounds, suggesting that inertial changes cannot be neglected. For the *n*-propyl series (3), and more particularly for higher members of the α-methylated series, such a change in the leaving group produces an increase in k_H/k_D, which becomes more marked as the transition state becomes more ionic indicating that other more powerful factors are determining the larger isotope effects.

Can. J. Chem. Downloaded from www.nrcresearchpress.com by 210.87.254.5 on 09/05/12
For personal use only.

As usual we neglect the thermodynamic contribution from vibrations in comparison with the zero-point energy change coming from the same source.

Zero-Point Effects

The factors involved here may be conveniently considered in three groups.

Protium–Deuterium

(a) Inductive and Hyperconjugative Differences

Halevi and co-workers have focussed attention on the fact that the mean lengths of bonds to hydrogen and deuterium are different (15). This arises as a consequence of effect of a lower ground-state potential energy for the deuterium-containing molecule, allied with the asymmetry of the potential surface describing the energy of the molecule with respect to displacements of the atoms in bond-stretching and bond-shortening directions. Since the potential surface rises more steeply for bond shortening, the mean positions of atoms for a molecule in a given vibrational state will correspond to increasing bond distances as the energy of the state increases, so that the lower potential energy deuterium compound will have effectively shorter bonds than the protium compound. As a consequence of this altered bond length, dipolar and other interactions will be altered and the behavior of C—H bonds and C—D bonds with respect to inductive and hyperconjugative effects will be different, quite apart from the consequences of altered vibrations produced by the activation process.* From experiment (16, 17, 18, 19) Halevi deduces that hyperconjugative electron release is reduced in the CD_3 group, whereas inductive release is increased in the CD_3 group, compared with the CH_3 group. It might therefore be expected that these differences would be most marked where charge separations are greatest, and vice versa. Our experiments show that the magnitude of the isotope effect k_H/k_D increases in cases where the electron deficiency is expected to be greater and hyperconjugation more powerful.

(b) Non-bonding Interactions

As a consequence of the isotopic alteration in bond length there will be differences in non-bonding forces in the two species (20) but there are other larger changes which might produce zero-point variations (3). Almost all activation processes produce alterations in the molecular geometry and the hydrolyses which have been examined involve changes in the position of the leaving group, the possible insertion of the nucleophile, and the movement of three of the groups attached to the reaction-center carbon atom from tetrahedral positions to something approaching coplanarity. This latter movement will affect intramolecular non-bonded forces between β-hydrogen atoms. If we compare the geometry about the tertiary carbon atom in *tert*-butyl chloride (21, 22, 23) with that about the central carbon in a coplanar carbonium ion we find the methyl groups are about 12% farther apart (as measured by the separation of their respective carbon atoms) even when 0.05 Å is allowed for the bond contraction for C—C sp^3–sp^2 bonding (24) in the transition state. When the high inverse power expressions for non-bonding repulsions are applied to this change in separation, it is obvious that forces affecting vibrations may be considerably reduced. The magnitude of this reduction will depend on other modifying factors such as the proximity of the nucleophile and the leaving group and it is interesting to note the qualitative inverse relationship between the

This aspect of the secondary deuterium isotope effect has been criticized by Weston (Tetrahedron, **6, 31 (1959)), who showed that isotopic perturbation of the potential energy hypersurface is negligible. Since Halevi considers that these effects (difference in bond lengths) arise in the lowest vibrational state as a result of anharmonicity, the isotopic invariance of the potential energy hypersurface will still be consistent with his hypothesis.*

Can. J. Chem. Downloaded from www.nrcresearchpress.com by 210.87.254.5 on 09/05/12
For personal use only.

magnitude of k_H/k_D and the expected proximity of these groups, with k_H/k_D per D greatest for that system which of those examined best fits the S_NI case with decreasing values as this description becomes increasingly less apt and the transition state becomes more crowded.

(c) Hyperconjugative Effects

The work of Lewis and Shiner and their respective groups has established that substitution of D for H in hyperconjugative positions usually produces kinetic isotope effects. The weakening of the C—H link, which is represented in valence bond theory by the contribution of non-bonded structures to the hybrid, is thought to decrease zero-point energy by facilitating the vibrations which involve relative extensive movement of β-hydrogens. The isotope effects which we have observed are consistent with such a hypothesis. The direction of the effect and its order of magnitude are in agreement with previous work in other solvents, e.g. 2-pentyl-βd_5 bromide and *p*-toluenesulphonate solvolyzing in formic acid have isotope rate ratios k_H/k_D 1.39 and 1.69, respectively (7), which can be composed with our values for isopropyl-βd_6 bromide (k_H/k_D = 1.34) and *p*-toluenesulphonate (k_H/k_D = 1.54) solvolyzing in water. For tertiary compounds a comparison may be made between *t*-amyl-βd_8 chloride solvolyzing in 80% aqueous alcohol with a rate ratio k_H/k_D = 2.35 (4) and *t*-butyl-βd_9 chloride solvolyzing in water (k_H/k_D = 2.57). The larger β-deuterium isotope effects in formic acid are consistent with the expectation that ionization was more advanced at the transition state in formic acid than in H_2O where some degree of nucleophilic interaction between oxygen and the reactive carbon will be expected, even for the isopropyl compounds. Although water is a better ionizing medium than 80% ethanol it is not possible to decide whether the small increase in k_H/k_D observed by us is to be attributed to increased charge development in the transition state or some other solvation effect. Experimental temperature differences will also make a minor contribution.

The increase in the stability of carbonium ions along the series ethyl, isopropyl, *tert*-butyl is usually associated with an increase in both the inductive and hyperconjugative effects. The expected increase in the β-deuterium isotope effect from ethyl to *tert*-butyl as a consequence of the increase in hyperconjugation is exemplified by the k_H/k_D rate ratios for ethyl and isopropyl bromide and *tert*-butyl chloride, which are 1.03_3, 1.33_6, and 2.56_8 respectively. Differences in the rate ratios are also found when the ease of formation of the carbonium ion is altered by changing the anionic group. Thus, isopropyl methanesulphonate, which is considered to be more easily ionized than the bromide, has a rate ratio $k_H/k_D = 1.54_5$ compared with 1.33_6 for the bromide.

In a discussion of the β-deuterium isotope effect in solvolysis the possible occurrence of an olefin-forming elimination reaction accompanying substitution must be examined. Where the mechanism of the reaction is such that the formation of the olefin takes place after the transition state (e.g. *tert*-butyl chloride) olefin production will not affect the k_H/k_D ratio. However, for reactions where this is not so (E_2) the elimination reaction would exhibit a primary deuterium isotope effect with a rate ratio k_H/k_D of the order of 4 to 6, since an isotopically substituted β-C—H bond is breaking. This would affect the measured k_H/k_D ratio to an extent depending on what fraction of the total reaction was elimination. We have measured the percentage of elimination occurring in the solvolysis of the compounds studied. These results are shown in Table II.

Even in the case of the ethyl compounds where the β-deuterium isotope effects are small, the amount of elimination which takes place concurrently with substitution is insufficient to account for the observed k_H/k_D values.

Can. J. Chem. Downloaded from www.nrcresearchpress.com by 210.87.254.5 on 09/05/12
For personal use only.

TABLE II

Olefin formation in the solvolysis in water of some alkyl compounds

Compound	Reaction time, hours	Temp., °C	% Olefin formed
Ethyl *p*-toluenesulphonate	1	100	<0.2
Ethyl methanesulphonate	1	100	~0.0
Ethyl bromide	1	100	~0.0
Ethyl iodide	1	100	<0.3
Isopropyl *p*-toluenesulphonate	16	60	2.5±0.2
Isopropyl methanesulphonate	16	60	0.7±0.2
Isopropyl bromide	16	60	0.7±0.1
Isopropyl iodide	16	60	1.5±0.2
t-Butyl chloride	<1	25	2.9±0.2

The most commonly accepted theoretical mechanism for hyperconjugation is the treatment due to Mulliken *et al.* (25), although an alternative model has been set up by Kreevoy and Eyring (26) which these authors call α-hydrogen bonding. Application of this latter model to β-deuterium isotope effects would require an interaction between the β-hydrogen orbital and the developing p orbital on the electron deficient α-carbon atom. One advantage of this treatment is its ability to explain the greater effectiveness of hydrogen in hyperconjugation as compared with carbon–carbon hyperconjugation. With this model the reduction in β-hydrogen vibration frequencies on activation can occur for bending modes and is therefore in harmony with Streitwieser's treatment of β-deuterium isotope effects (10). Kreevoy and Eyring have pointed out (26) that their model for hyperconjugation is closely related to neighboring group participation as described by Winstein and co-workers (27). Neighboring hydrogen participation, however, only occurs in situations favoring skeletal rearrangement of the reacting molecule whereas α-hydrogen bonding is much more widespread, does not involve rearrangement, and gives smaller effects.

Thus, although it is not possible to choose between Mulliken's model for hyperconjugation and that of Kreevoy and Eyring from the measurement of β-deuterium isotope effects, the latter is attractive in that it is able to link qualitatively the two fields of hyperconjugative effects and neighboring group participations.

CONCLUSION

It appears that hyperconjugative and non-bonding interactions are the principal sources of these isotope effects, with small modifications arising from rotational–translational inertia changes. The role of non-bonding interactions ("intramolecular van der Waals forces" (2, 3)) has been discussed by Bartell (20) and he has shown that they can be sufficiently large to account for a major portion of the observed effects. As far as hyperconjugation is concerned the relationships are largely qualitative since no calculations appear to have been made which would even establish the order of magnitude of the consequences of hyperconjugation on isotope effects. Despite this the evidence is moderately convincing (29), isotope rate effects usually being observed for hyperconjugative sites of substitution with magnitudes varying in the way which would be expected from considerations of hyperconjugative change. The jump in isotope effect observed on passing from an isotopically substituted group on the para position of an aromatic ring to a site adjacent to the reaction center (5, 28) seems large even allowing for the damping action of the ring. This may represent the effect of changing non-bonded forces arising

Can. J. Chem. Downloaded from www.nrcresearchpress.com by 210.87.254.5 on 09/05/12
For personal use only.

from the change from tetrahedral to trigonal configuration, which will be insignificant for the para position compared with that for the site adjacent to the reaction center. For the particular effects described in this paper it is difficult to decide which contribution is greater, hyperconjugation or intramolecular van der Waals forces, but undoubtedly both are present and make the major contribution to the isotopic rate change.

EXPERIMENTAL

Ethyl-βd_3 alcohol was prepared by a lithium aluminum hydride reduction of acetic-βd_3 acid (30). The redistilled product, boiling range 79.5–81.5° C, was converted to ethyl-βd_3 *p*-toluenesulphonate by reaction with *p*-toluenesulphonyl chloride in dry pyridine (31). The crude ester (m.p. 30.6° C) was purified by distillation under a vacuum. A comparison of the N.M.R. spectrum of this compound with that of an undeuterated sample indicated that the β-carbon atom was fully deuterated.

Ethyl-βd_2 iodide, bromide, and methanesulphonate were made from the *p*-toluenesulphonate by the methods previously described for the corresponding ethyl-αd_2 compounds (2).

Isopropyl-βd_6 alcohol was obtained by the reduction of acetone-βd_6 with lithium aluminum hydride (32). The crude product was redistilled, boiling range 83.5–84.5° C, and converted to the bromide by the phosphorus tribromide method. The N.M.R. spectrum of this compound showed that the β-carbon atom was fully deuterated.

Isopropyl-βd_6 methanesulphonate, *p*-toluenesulphonate, and iodide were prepared from the bromide by the methods used in the preparation of the deuterated ethyl compounds.

Tertiary butyl-βd_9 chloride (minimum isotopic purity 99%) was purchased from Merck and Co.

For all of the above deuterated compounds the protium analogues were prepared by parallel reactions and were used to check the rate constants which had been determined in the course of previous work under the same conditions (14). Excellent agreement was obtained in all cases.

The rate measurements were made conductometrically as described previously (3).

The following procedure was used for the olefin determinations. Water (75 ml) was placed in a 100-ml bulb fitted with a break-seal. Samples of 0.05 to 0.1 g of the sulphonate or halide were weighed in a weight pipette and introduced into the bulb. The system was then sealed and allowed to react. After reaction the break-seal side arm was fused to a distillation system consisting of a short column and condenser with an outlet passing under the absorbing solution of Byrne and Johnson (33). A slow stream of dry nitrogen was introduced through a mercury trap above the bulb. After opening the bulb, the reacted solution was boiled for 15 minutes. The amount of olefin was determined by back-titration with thiosulphate, suitable corrections being made for a blank in the presence of the alcohol produced and the original unreacted ester.

ACKNOWLEDGMENTS

Thanks are due to Dr. W. Raynes for the N.M.R. measurements, to Mr. S. Sugamori for the careful kinetic measurements, and to Mr. R. Maillet for the olefin determinations.

REFERENCES

1. J. A. Llewellyn, R. E. Robertson, and J. M. W. Scott. Can. J. Chem. **38**, 222 (1960).
2. K. T. Leffek, J. A. Llewellyn, and R. E. Robertson. Can. J. Chem. **38**, 1505 (1960).
3. K. T. Leffek, J. A. Llewellyn, and R. E. Robertson. J. Am. Chem. Soc. In press.

Can. J. Chem. Downloaded from www.nrcresearchpress.com by 210.87.254.5 on 09/05/12
For personal use only.

4. V. J. SHINER. J. Am. Chem. Soc. **75**, 2925 (1953).
5. V. J. SHINER. J. Am. Chem. Soc. **76**, 1603 (1954).
6. V. J. SHINER. J. Am. Chem. Soc. **78**, 2653 (1956).
7. E. S. LEWIS and C. E. BOOZER. J. Am. Chem. Soc. **76**, 791 (1954).
8. E. S. LEWIS and G. M. COPPINGER. J. Am. Chem. Soc. **76**, 4495 (1954).
9. E. S. LEWIS, R. R. JOHNSON, and G. M. COPPINGER. J. Am. Chem. Soc. **81**, 3140 (1959).
10. A. STREITWIESER, R. H. JAGOW, R. C. FAHEY, and S. SUZUKI. J. Am. Chem. Soc. **80**, 2326 (1958).
11. S. WINSTEIN and J. TAKAHASHI. Tetrahedron, **2**, 316 (1958).
12. M. L. BENDER, M. S. FENG, and J. M. JONES. Chem. & Ind. 1350 (1959).
13. W. H. SAUNDERS, S. ASPERGER, and D. H. EDISON. Chem. & Ind. 1417 (1957).
14. R. E. ROBERTSON. Suomen Kemistilehti, A, **33**, 63 (1960).
15. E. A. HALEVI. Intern. J. Appl. Radiation and Isotopes, **7**, 192 (1960).
16. E. A. HALEVI. Tetrahedron, **1**, 174 (1957).
17. E. A. HALEVI. Tetrahedron, **5**, 352 (1959).
18. E. A. HALEVI and N. NUSSIM. Bull. Research Council Israel, Sect. A, **5**, 263 (1956).
19. E. A. HALEVI and N. NUSSIM. Bull. Research Council Israel, Sect. A, **6**, 167 (1957).
20. L. S. BARTELL. Tetrahedron Letters, No. 6, 13 (1960).
21. J. W. COUTTS and R. L. LIVINGSTON. J. Am. Chem. Soc. **75**, 1542 (1953).
22. J. Y. BEACH and D. P. STEVENSON. J. Am. Chem. Soc. **60**, 475 (1938).
23. O. BASTIANSEN and L. SMEDVIK. Acta Chem. Scand. **7**, 652 (1953).
24. L. E. SUTTON. Tetrahedron, **5**, 118 (1959).
25. R. S. MULLIKEN, C. A. RIEKE, and W. G. BROWN. J. Am. Chem. Soc. **63**, 41 (1941).
26. M. M. KREEVOY and H. EYRING. J. Am. Chem. Soc. **79**, 5121 (1957).
27. M. SIMONETTA and S. WINSTEIN. J. Am. Chem. Soc. **76**, 18 (1954).
28. V. J. SHINER and C. J. VERBANIC. J. Am. Chem. Soc. **79**, 373 (1957).
29. E. S. LEWIS. Tetrahedron, **5**, 143 (1959).
30. R. OSTWALD, P. T. ADAMS, and B. M. TOLBERT. J. Am. Chem. Soc. **74**, 2425 (1952).
31. R. S. TIPSON. J. Org. Chem. **9**, 235 (1944).
32. V. J. SHINER. J. Am. Chem. Soc. **74**, 5285 (1952).
33. R. E. BYRNE, JR. and J. B. JOHNSON. Anal. Chem. **28**, 126 (1956).

Can. J. Chem. Downloaded from www.nrcresearchpress.com by 210.87.254.5 on 09/05/12
For personal use only.

Can. J. Chem. Downloaded from www.nrcresearchpress.com by 210.87.254.5 on 09/05/12
For personal use only.

HYDROGENOLYSIS OF CARBOHYDRATES

IX. FORMATION OF 2,6-ANHYDRO-β-D-FRUCTOFURANOSE AND ETHYL α- AND β-D-FRUCTOFURANOSIDE FROM SUCROSE[1]

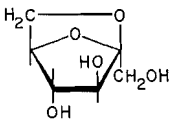
H. R. GOLDSCHMID[2] AND A. S. PERLIN

ABSTRACT

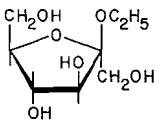
A compound formed during the hydrogenolysis of sucrose in ethanol or dioxane at 180° C, in the presence of copper chromium oxide catalyst, has been characterized as 2,6-anhydro-β-D-fructofuranose (2,5-anhydro-α-D-fructopyranose), a new type of anhydro-ketose. Ethyl α- and β-D-fructofuranosides are also produced when the hydrogenolysis reaction is carried out in ethanol, and various derivatives of these anomeric ketosides have been prepared.

Earlier papers of this series have described the hydrogenolysis of alkyl glycopyranosides in the presence of copper chromium oxide catalyst (1) at moderate temperature and pressure (2, 3, 4, 5, 6). A major effect observed in these reactions is the isomerization of carbinol groups but, particularly at temperatures above 180–200° C, glycosidic linkages also become unstable and extensive hydrogenolysis of hydroxyl groups occurs. Methyl β-L-arabopyranoside, for example, is isomerized to a mixture of methyl pentopyranosides at 180° C (4), whereas at 240° C it is converted in high yield to a mixture of 1,5-anhydro-2-deoxy-DL-pentitols (2, 5). In current studies the behavior of furanose glycosides towards these conditions of hydrogenolysis is being examined, and sucrose has been selected as a readily available substrate containing a furanosyl moiety.

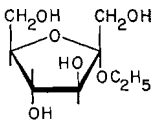
In ethanol at 180° C,* sucrose readily afforded three derivatives of D-fructose, each in about 10% yield (based on the fructose unit of sucrose). Detected initially on paper chromatograms as compounds having high R_F values (relative to that of sucrose) and giving a typical ketohexose test with urea oxalate (7), these products have been isolated by column chromatography on charcoal (8) and cellulose (9) and characterized as 2,6-anhydro-β-D-fructofuranose (I) (2,5-anhydro-α-D-fructopyranose), and ethyl α- and β-D-fructofuranoside (III and II).



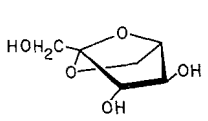
I



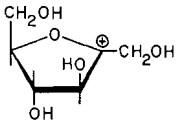
II



III



IV



V

[1]*Manuscript received July 4, 1960.*
Contribution from the National Research Council of Canada, Prairie Regional Laboratory, Saskatoon, Saskatchewan. Presented in part to the Organic Chemistry Division, Chemical Institute of Canada, 43rd Annual Conference, Ottawa, June 13–15, 1960.
Issued as N.R.C. No. 5974.
[2]*National Research Council of Canada Postdoctorate Fellow, 1958–1960.*
**By analogy with the behavior of methyl α-D-glucopyranoside (3), the α-D-glucopyranosyl unit of sucrose was expected to be stable at 180° C.*

Can. J. Chem. Downloaded from www.nrcresearchpress.com by 210.87.254.5 on 09/05/12
For personal use only.

The anhydride, m.p. 118–119° C, was found by the isothermal distillation method (10) to be monomeric. It did not reduce hot Fehling's solution nor react with sodium borohydride and, since it was recovered unchanged after prolonged treatment with methanolic ammonia, did not appear to contain an epoxy group. At room temperature, it was easily hydrolyzed by 0.1 *N* sulphuric acid affording D-fructose as the sole product. Tritylation of the anhydride in pyridine proceeded very slowly at room temperature, and two crystalline derivatives were isolated in low yield, one being a monotrityl and the other a ditrityl ether. The compound was resistant also to tosylation but, on prolonged treatment with tosyl chloride in pyridine, yielded a syrupy diester which, however, did not react with sodium iodide. These properties suggested that only the relatively unreactive C-1-carbinol group and/or secondary hydroxyl groups of the anhydride were being substituted, and hence that the normally reactive 6-position was involved in ring formation.

Attempts to methylate the anhydride fully with dimethyl sulphate – sodium hydroxide or with methyl iodide – silver oxide were unsuccessful, but several treatments with potassium in liquid ammonia (11) followed with methyl iodide under reflux, yielded a syrupy trimethyl derivative. On acid hydrolysis this ether afforded crystalline 1,3,4-tri-*O*-methyl-D-fructose (12), showing that both the 5- and 6-hydroxyl groups of the anhydride are involved in ring formation, and hence that the anhydride is 2,6-anhydro-D-fructofuranose (2,5-anhydro-D-fructopyranose).

Since the specific rotation of the anhydride, $[\alpha]_D$ −107°, is more strongly levorotatory than D-fructose itself, the 2,6-oxygen bridge of the compound appears to possess the β-configuration. The β-assignment is strongly supported by an examination of molecular models, which shows also that the 2,6-anhydro ring assumes a boat conformation (as in IV). The eclipsing of bonds and distortion of bond angles in such a molecule could account for the observed ease of acid hydrolysis of the anhydride, as had been anticipated by Mills (13), which contrasts with the relatively high acid stability of other anhydro sugars (epoxides excepted). That the 2,6-pyranoid ring of the compound is much less stable than the five-membered 2,5-ring (see 14, 15) was indicated by the rapid formation of ethyl α- and β-D-fructofuranoside when the anhydride was treated with ethanolic hydrogen chloride at room temperature. Moreover, the α-D-anomer predominated initially, which was to be expected from scission of a β-D-anhydro ring (16), and the observed rate of formation of the mixture of furanosides (rate of rotational change) closely paralleled that found with ethyl β-D-fructofuranoside.

The anhydride consumed no periodate, although it possesses a free glycol group (the *trans*-3,4-diol group), and with lead tetraacetate in acetic acid only a slow uptake of oxidant was found, caused most probably by gradual opening of the anhydro ring. This behavior is in accord with the recent report by Angyal and Young (17) that the camphane-2,3-*trans*-diols are virtually unoxidized by glycol-cleaving agents since the structure of the anhydride is closely analogous to that of the camphane diols. Dimler (18) has suggested that the 2,3-*trans*-diol group of 1,6-anhydro β-D-gluco- and α-galactofuranose, situated on a fused bicyclic system, resists glycol scission most probably because it is fixed rigidly in an arrangement highly unfavorable for complexing by the oxidants. The *trans*-glycol groups of the camphane-*trans*-diols and the anhydrofructose appear to possess a similar spatial arrangement, and their unreactivity can therefore be interpreted in the same way.*

Recently it has been found (H. R. Goldschmid and A. S. Perlin. Can. J. Chem. **38, 2178 (1960)) that these compounds are cleaved oxidatively by lead tetraacetate using pyridine as solvent (27).*

It may be noted, however, that some *vic–trans*-diols which are not located on bicyclic ring compounds, i.e., the 2,3-*trans*-glycol groups on internal (1 → 4)-linked units of oligosaccharides, are also resistant to attack by lead tetraacetate (19).

Several dimeric anhydrides of D-fructose are known to be formed by acid hydrolysis of D-fructans (20) and a 2,3-anhydro monomeric derivative of D-fructofuranose, as well as dimeric anhydrides, has been found recently among the products of direct nitration of D-fructose (21). The compound described here is yet another type of D-fructose anhydride. Also, it represents a class of rare anhydro-sugars, namely, that having the 1,4(2,5)-1,5(2,6)-bridged system. One other member of this class, 1,5-anhydro-β-D-ribofuranose, has been synthesized recently by Vis and Fletcher (22), and also has been converted to the 2,3-*O*-isopropylidene derivative, which proved to be indistinguishable from a compound described several years earlier but only tentatively identified (23). Derivatives of three related glycosans have been reported but incompletely characterized (see 14); these are 1,5-anhydro-2,3,6-tri-*O*-methyl-β-D-glucofuranose (24) and -α-L-idofuranose (25), and 2,3-di-*O*-acetyl-1,5-anhydro-β-L-rhamnofuranose (26).

Although 2,6-anhydro-β-D-fructofuranose cannot be regarded as a *hydrogenolysis* product derived from sucrose, it was not obtained when the reaction was carried out in the presence of argon rather than hydrogen. Considerable charring occurred under these latter conditions, however, and ethyl β-D-fructopyranoside was isolated from the reaction mixture, the furanosides being relatively minor products. Hence the hydrogenolysis conditions used may prevent decomposition of labile compounds, rather than serve directly in promoting formation of the furanose products. The occurrence together of the anhydride and of the anomeric furanosides suggests the possibility that all three products are formed from a carbonium-ion intermediate of the type encountered in the acid-catalyzed solvolysis of glycosides (see 15). A protonated form such as V, by reaction with the solvent, could yield the anomeric furanosides (II and III), and through intramolecular attack by the C-6-carbinol group give the 2,6-anhydride. Formation of an acyclic carbonium-ion intermediate (15) appears less likely in these reactions, since ethyl pyranosides would then be expected to predominate among the products at the high temperatures used. That the anhydride may be derived directly from sucrose rather than from the glycosides was shown by its formation also when the hydrogenolysis reaction was carried out in dioxane as solvent in place of ethanol. The anhydride itself undergoes ethanolysis readily by heat in the absence of added acid catalyst to yield the anomeric furanosides. Hence, the glycosides isolated from the hydrogenolysis mixture may be produced by solvolysis of the anhydride, as well as via a carbonium-ion intermediate such as V.

The α- and β-anomers of ethyl D-fructofuranoside were isolated as analytically pure syrups,* the β-anomer being readily cleaved by invertase. On tosylation, the β-glycoside furnished a crystalline diester which was converted by treatment with sodium iodide in acetone to a syrupy, monoiodo monotosyl derivative. In pyridine solution (27) the ditosylate consumed 1 mole of lead tetraacetate, in agreement with the expectation that the ester groups were located at positions-1 and -6; presumably, that at position-1 is not readily replaceable by iodide ion (28, 29). The β-anomer also furnished a crystalline 1,6-di-*O*-trityl derivative, the terminal location of the ether groups being shown by the fact that the compound, in pyridine, consumed a mole of lead tetraacetate; the ditrityl ether was characterized further as a crystalline diacetate. Tritylation of the α-glycoside

**The α-anomer of methyl D-fructofuranoside has been obtained in crystalline form (30).*

Can. J. Chem. Downloaded from www.nrcresearchpress.com by 210.87.254.5 on 09/05/12
For personal use only.

followed by acetylation afforded a crystalline di-*O*-acetyl dityrityl ether. After deacetylation the dityrityl ether was shown, also by oxidation with lead tetraacetate in pyridine, to be the 1,6-derivative.

No ethyl D-glucosides were detected among the reaction products, in accord with the expectation that the D-fructofuranosyl linkage should be cleaved preferentially. Further, as shown by the formation of D-sorbitol, the D-glucosyl unit appeared to be converted mainly to the free sugar and then reduced. The presence of D-mannitol in the mixture suggested that some D-fructose also was formed during the reaction. In addition to these products, glycerol and a small proportion of erythritol were isolated, but the origin of these fragments was not determined.

In contrast to the behavior of sucrose, the derived octaacetate was completely stable to the hydrogenolysis conditions, even at 240° C. The (2 → 6)-linked poly-D-fructan, inulin, although converted in small proportion in ethanol to the furanosides, appeared to yield none of the anhydride.

EXPERIMENTAL

Paper chromatography was carried out with butan-1-ol:ethanol:water (40:11:19) as solvent, and with urea oxalate (7) and ammoniacal silver nitrate (31) as spray reagents.

Column chromatography on cellulose was carried out using benzene:ethanol:water (500:50:1), (500:100:1) and ethanol.

Evaporations were carried out at 40–50° C, and optical rotations were measured at approximately 25° C. Melting points are corrected, and boiling points recorded are air-bath temperatures.

Hydrogenolysis of Sucrose in Ethanol and Separation of the Products

Sucrose (20 g) in absolute ethanol (75 ml) was heated at 180° C and a pressure of 1100 p.s.i. of hydrogen in the presence of copper chromium oxide catalyst (2 g) for 6 hours. The catalyst was filtered off and the filtrate concentrated, yielding a colorless syrup. Paper chromatographic examination of the syrup indicated the presence of the following components: hydroxymethylfurfural; glycerol; erythritol; ketohexose derivatives at R_F 0.60, 0.48, and 0.35; fructose; mannitol; sorbitol; sucrose; and slower-moving materials streaking to the origin.

The syrupy reaction product was chromatographed on a column of coconut charcoal (32). The glycerol (0.35 g) and erythritol (0.25 g) (m.p. 120° C, undepressed) were eluted with water.

By adding 5% ethanol to the column and then fractionating the mixture of eluted products on a cellulose column, the following were obtained: component R_F 0.60 (0.85 g), fructose (0.5 g), glucose (2.0 g), and admixed D-mannitol and D-sorbitol (1.5 g). D-Mannitol (m.p. 166° C, undepressed) was isolated by fractional crystallization, and D-sorbitol was characterized as the hexaacetate (m.p. 99° C, undepressed).

The charcoal column was washed finally with 10% ethanol yielding a mixture of products. This mixture was resolved on a cellulose column, giving component R_F 0.48 (0.9 g), component R_F 0.35 (0.85 g), and unchanged sucrose (9.5 g).

*2,6-Anhydro-β-*D*-fructofuranose* (I)

The chromatographically pure syrup (component R_F 0.35) solidified on prolonged storage, and was recrystallized from acetone, m.p. 118–119° C and $[\alpha]_D$ −107° (*c*, 1, H_2O) (no mutarotation). Calculated for $C_6H_{10}O_5$: C, 44.44%; H, 6.22%; mol. wt., 162. Found:

Can. J. Chem. Downloaded from www.nrcresearchpress.com by 210.87.254.5 on 09/05/12
For personal use only.

C, 44.49%; H, 6.37%; mol. wt., 157 (by isothermal distillation (10) in methanol at 50° C).

The compound did not reduce Fehling's solution, was unaffected by treatment under reflux for 6 hours with 1% methanolic ammonia, and also by treatment for 3 days at room temperature with aqueous sodium borohydride. With sodium metaperiodate no uptake of oxidant was found in 24 hours reaction time, and with lead tetraacetate in acetic acid the consumption of oxidant was 0.1 mole in 8 hours reaction time.

In 0.05 *N* sulphuric acid at 25° C the observed rotation of the anhydride solution (1.0%) decreased slightly from α_D −1.00° (3 minutes) → α_D −0.97° (5 hours, constant, 1 dcm tube). Paper chromatographic examination showed that most of the anhydride was hydrolyzed in 2 hours, and that conversion to fructose was complete within 5 hours; accordingly, the calculated $[\alpha]_D$ of the hydrolyzate was −89° (D-fructose shows $[\alpha]_D$ −92°). The product was characterized further by conversion to D-glucose phenylosazone, m.p. 209° C (decomp.), and indistinguishable from an authentic sample by X-ray diffraction.

The observed rotation of the anhydride in ethanolic hydrogen chloride (0.5%) at room temperature rose rapidly to $[\alpha]_D$ +0.44° (7 minutes), then decreased slowly to −0.09° (18 hours) (*c*, 1.2, 1 dcm tube). Paper chromatographic examination of the reaction mixture indicated that ethyl α-D-fructofuranoside was formed as the major product during the first 10 minutes reaction time. Under similar conditions, rotational changes shown by ethyl β-D-fructofuranoside were a rapid rise to $[\alpha]_D$ +0.32° (9 minutes), then dropping slowly to 0.03° (19 hours); ethyl α-D-fructofuranoside showed $[\alpha]_D$ +0.22° (2 minutes)→ −0.07° (20 hours), D-fructose, $[\alpha]_D$ +0.18° (14 minutes)→ −0.24° (18 hours). These values are similar to the data reported by Purves and Hudson (30, 33) for the methyl D-fructofuranosides and D-fructose.

Acetylation of the anhydride with acetic anhydride – pyridine at room temperature afforded a triacetate, b.p. 110–120° C at 0.05 mm, $[\alpha]_D$ −108° (*c*, 1.3, $CHCl_3$). Calculated for $C_{12}H_{16}O_8$: C, 50.00%; H, 5.60%; acetyl, 44.8%. Found: C, 50.17%; H, 5.79%; acetyl (sapon.), 44.4%.

Treated with benzoyl chloride and pyridine in cold chloroform, the anhydride yielded an amorphous tribenzoate, $[\alpha]_D$ −163° (*c*, 1.1, $CHCl_3$). Calculated for $C_{27}H_{22}O_8$: C, 68.35%; H, 4.67%. Found: C, 67.90%; H, 4.73%.

*1,3,4-Tri-O-methyl-*D*-fructose*

The anhydride (0.20 g) was dissolved in liquid ammonia (20 ml) and potassium was added portionwise until a stable blue color developed in the solution. After evaporation of the ammonia, methyl iodide (3 ml) was added and the solution heated under reflux for 3 hours and then stored at room temperature for 18 hours. The methyl iodide was evaporated off, the methylation procedure repeated twice, and the final reaction mixture was extracted with chloroform. The chloroform extract afforded a syrup which was distilled, b.p. 60–70° C at 0.05 mm. Paper chromatographic examination of the distillate showed the presence of a major component and a minor, slower-moving component which corresponded to 1,3,4-tri-*O*-methyl-D-fructose (below), indicative of partial hydrolysis. Calculated for $C_9H_{16}O_5$: methoxyl, 45.6%. Found: (two preparations) methoxyl, 42.9%, 41.7%.

The distillate (105 mg) was hydrolyzed with *N* sulphuric acid, the solution was neutralized with barium carbonate and extracted with chloroform. On evaporation, the aqueous layer yielded a syrup (99 mg) which consisted of a single component (paper chromatogram). Purified by distillation (b.p. 115–120° C at 0.05 mm) the product solidi-

Can. J. Chem. Downloaded from www.nrcresearchpress.com by 210.87.254.5 on 09/05/12
For personal use only.

fied, and was recrystallized from carbon tetrachloride, m.p. 72–73° C and $[\alpha]_D$ −49.6° (*c*, 1.3, H_2O) (lit. (12), m.p. 73° C and $[\alpha]_D$ −51.8° (H_2O)). Calculated for $C_9H_{18}O_6$: C, 48.36%; H, 8.3%; methoxyl, 41.89%. Found: C, 48.34%; H, 8.17%; methoxyl, 41.79%.

In acetic acid, the trimethyl D-fructose consumed no lead tetracetate in 4 hours reaction time, showing the absence of a free *vic*-diol at the 2,3-position (34) and also at the 1,2-position (35). After reduction with sodium borohydride, 1 mole of formaldehyde was produced (chromotropic acid method (36)) in 1 hour reaction time. This behavior showed the absence of methoxyl groups at positions-2, -5, and -6, and hence confirmed that the product was the 1,3,4-tri-*O*-methyl derivative.

Tritylation of 2,6-Anhydro-β-D-fructofuranose

In a preliminary experiment, using 2.2 moles of trityl chloride per mole of anhydride in pyridine at room temperature, some unchanged anhydride was present in the reaction mixture after 1 week (paper chromatogram). The anhydride (162 mg) in pyridine (4 ml) was treated at room temperature for 10 days with triphenylchloromethane (615 mg). Ice water was added, the reaction mixture was extracted with benzene, and the extract washed successively with water, sodium bicarbonate solution, and water, then dried over sodium sulphate, and the benzene was evaporated off. The oily product (720 mg) was fractionated on a column of reagent silicic acid using chloroform as the solvent. After elution of triphenylcarbinol, a ditrityl derivative (85 mg) was isolated and recrystallized from ethanol, m.p. 224–226° C and $[\alpha]_D$ −38.5° (*c*, 0.8, $CHCl_3$). Calculated for $C_{44}H_{38}O_5$: C, 81.75%; H, 5.92%; mol. wt., 643. Found: C, 81.88%; H, 6.00%; mol. wt., 621 (melting point depression in camphor).

Continued washing of the column with chloroform eluted a monotrityl derivative (145 mg) which, after recrystallization from dichloromethane – *n*-hexane, had a melting point of 150–153° C, $[\alpha]_D$ −43.7° (*c*, 1.0, $CHCl_3$). Calculated for $C_{25}H_{24}O_5$: C, 74.24%; H, 5.98%. Found: C, 74.24%; H, 5.98%.

Di-O-tosyl-2,6-anhydro-β-D-fructofuranose

The anhydride (200 mg) in pyridine (5 ml) was treated with *p*-toluenesulphonyl chloride (500 mg) at room temperature for 18 hours. A few drops of water were added, and after 30 minutes the reaction mixture was poured into ice water and extracted with benzene. After successive washings with water, sodium bicarbonate solution, and water, the benzene extract was dried and concentrated affording a glass (139 mg). The product, treated in acetone with sodium iodide in a sealed tube at 100° C, yielded only a trace of sodium *p*-toluenesulphonate in 24 hours reaction time, $[\alpha]_D$ −29.1° (*c*, 1.4, $CHCl_3$). Calculated for $C_{20}H_{22}O_9S_2$: C, 51.04%; H, 4.71%; S, 13.62%. Found: C, 51.60%; H, 4.91%; S, 14.17%.

Ethyl β-D-Fructofuranoside (II)

The syrupy, chromatographically pure glycoside had $[\alpha]_D$ −36° (*c*, 1, H_2O), was readily degraded to fructose by treatment with invertase, and was hydrolyzed to fructose at room temperature within 2 days by 0.1 *N* sulphuric acid. It consumed 1.0 mole of sodium periodate per mole.

On acetylation with acetic anhydride in pyridine at room temperature, the glycoside (200 mg) afforded a tetraacetate (310 mg), b.p. about 150° C at 0.06 mm, $[\alpha]_D$ −25° (*c*, 1.1, $CHCl_3$). Calculated for $C_{16}H_{24}O_{10}$: C, 51.06%; H, 6.43%; acetyl, 45.8%. Found: C, 51.07%; H, 6.52%; acetyl (sapon.), 46.1%.

Can. J. Chem. Downloaded from www.nrcresearchpress.com by 210.87.254.5 on 09/05/12
For personal use only.

Can. J. Chem. Downloaded from www.nrcresearchpress.com by 210.87.254.5 on 09/05/12
For personal use only.

1,6-Di-O-trityl Ethyl β-D-Fructofuranoside

The glycoside II (200 mg) in pyridine (4 ml) was treated at room temperature with trityl chloride (600 mg) for 48 hours. Isolated after treatment with ice water and extraction into benzene, the product (490 mg) was crystallized from ethanol, m.p. 180–183° C and $[\alpha]_D$ −2.3° (*c*, 1.0, $CHCl_3$). Calculated for $C_{46}H_{44}O_6$: C, 79.74%; H, 6.40%. Found: C, 79.91%; H, 6.60%.

Treated with lead tetraacetate in pyridine (27) at 0° C the ditrityl derivative consumed 1 mole of oxidant per mole in 0.5 hour.

The ditrityl glycoside (100 mg) treated with acetic anhydride – pyridine afforded a diacetate (95 mg) which, after recrystallization from ethanol, had a melting point of 207–208° C, $[\alpha]_D$ +35.8° (*c*, 1.3, $CHCl_3$). Calculated for $C_{50}H_{48}O_8$: C, 77.30%; H, 6.23%. Found: C, 77.07%; H, 6.29%.

1,6-Di-O-tosyl Ethyl β-D-Fructofuranoside

To the glycoside II (400 mg) in pyridine (5 ml) at 0° C was added a solution of *p*-toluenesulphonyl chloride (750 mg) in chloroform (10 ml). After 2 hours at 0° C and 18 hours at 25° C the reaction mixture was diluted with chloroform (30 ml), treated with a few drops of water, and 30 minutes later was washed successively with ice water, copper sulphate, sodium bicarbonate, and water. The solution was dried over sodium sulphate and concentrated, yielding a crystalline product (230 mg) which was recrystallized from ethanol – *n*-hexane, m.p. 125–127° C (decomp.), $[\alpha]_D$ −12.8° (*c*, 1.0, $CHCl_3$). Calculated for $C_{22}H_{28}O_{10}S_2$: C, 51.15%; H, 5.46%; S, 12.41%. Found: C, 51.02%; H, 5.46%; S, 12.13%.

In pyridine, the ditosyl derivative consumed 1.0 mole of lead tetraacetate per mole in 1 hour reaction time.

The ditosylate (100 mg) was heated at 100° C with sodium iodide (75 mg) in acetone (6 ml) for 24 hours. Sodium *p*-toluenesulphonate (35 mg), which crystallized out on cooling, was filtered off. After evaporation of the acetone, the residue was taken up in chloroform, washed with water, and recovered as an oil (72 mg), $[\alpha]_D$ −22.5° (*c*, 1.0, $CHCl_3$). Calculated for $C_{15}H_{21}O_7SI$: S, 6.79%; I, 26.87%. Found: S, 6.68%; I, 25.94%.

Ethyl α-D-Fructofuranoside (III)

The syrupy, chromatographically pure material showed $[\alpha]_D$ +65° (*c*, 1, H_2O), was not attacked by invertase, and was hydrolyzed to D-fructose within 15 hours at room temperature by 0.1 *N* sulphuric acid. It consumed 1 mole of sodium periodate per mole. Calculated for $C_8H_{16}O_6$: C, 46.15%; H, 7.75%; ethoxyl, 21.6%. Found: C, 45.98%; H, 8.13%; ethoxyl, 21.1%.

Acetylated at 25° C with acetic anhydride – pyridine, the glycoside yielded a tetraacetate, b.p. about 135° C at 0.01 mm, $[\alpha]_D$ +76° (*c*, 1.4, $CHCl_3$). Calculated for $C_{16}H_{24}O_{10}$: C, 51.06%; H, 6.43%; acetyl, 45.8%. Found: C, 51.22%; H, 6.65%; acetyl (sapon.), 45.8%.

3,4-Di-O-acetyl-1,6-di-O-trityl Ethyl α-D-Fructofuranoside

The glycoside III (205 mg) was treated with trityl chloride (615 mg) in pyridine (4 ml) at room temperature for 7 days, and the reaction mixture was worked up as described previously. The syrupy product (722 mg) was fractionated on a silicic acid column using chloroform as solvent, affording a crystalline ditrityl ether (260 mg) and, by continued elution, an oily product which probably was a monotrityl derivative. Despite repeated recrystallization from ethanol the ditrityl ether had a broad melting point (about

140–150° C). On acetylation at 100° C with acetic anhydride – sodium acetate, a di-*O*-acetyl di-*O*-trityl derivative was obtained, m.p. 142–144° C and $[\alpha]_D$ +44.7° (*c*, 1.4, $CHCl_3$). Calculated for $C_{50}H_{48}O_8$: C, 77.30%; H, 6.23%. Found: C, 77.32%; H, 6.32%.

The product was deacetylated with sodium methoxide in chloroform–methanol, the solvent was evaporated, and the residue treated at 0° C with lead tetraacetate in pyridine. Found: 1.0 mole of oxidant consumed per mole in 0.5 hour.

Hydrogenolysis of Sucrose in Dioxane

Sucrose (5 g) and copper chromium oxide catalyst (0.5 g) in dioxane (75 ml) were heated for 6 hours at 180° C under hydrogen at 1100 p.s.i. An oil consisting mainly of unchanged sucrose separated out on cooling, and the dioxane solution was evaporated. The residue (2.9 g) showed heavy streaking on a paper chromatogram. By chromatography on a cellulose column, a fraction corresponding (paper chromatogram) to the anhydride (I) was isolated (167 mg). After recrystallization from acetone, the product had a melting point of 118–119° C, undepressed. The X-ray diffraction powder diagram of the product was indistinguishable from that of the anhydride (I).

Ethanolysis of Sucrose

Sucrose (10 g) in dry ethanol (75 ml) was heated for 6 hours at 180° C in an atmosphere of argon (10 p.s.i.). The resulting dark-brown solution was concentrated to a syrup which, from paper chromatographic examination, appeared to contain hydroxymethylfurfural, ethyl D-fructofuranosides (II and III), a trace of anhydride (I), fructose, and sucrose. By column chromatography on cellulose the glycoside mixture was found to contain ethyl β-D-fructopyranoside (105 mg), m.p. 150–151° C and $[\alpha]_D$ −160° (*c*, 1.0, H_2O). Calculated for $C_8H_{16}O_6$: C, 46.15%; H, 7.75%. Found: C, 46.21%; H, 7.86%. The derived tetraacetate had a melting point of 83–84° C and $[\alpha]_D$ −127° (*c*, 1.2 $CHCl_3$). Calculated for $C_{16}H_{24}O_{10}$: C, 51.06%; H, 6.43%. Found: C, 51.33%; H, 6.57%.

ACKNOWLEDGMENTS

The authors gratefully acknowledge the technical assistance given by Mr. J. W. L. C. Christ, and helpful suggestions made by Dr. P. A. J. Gorin. Microanalyses were performed by Mr. M. Mazurek, and X-ray powder diagrams and infrared absorption spectra were prepared by Miss Inez Gaffney.

REFERENCES

1. W. H. ZARTMAN and H. ADKINS. J. Am. Chem. Soc. **55**, 4559 (1933).
2. H. F. BAUER and D. E. STUETZ. J. Am. Chem. Soc. **78**, 4097 (1956).
3. E. VON RUDLOFF, H. F. BAUER, and D. E. STUETZ. Can. J. Chem. **35**, 315 (1957).
4. A. S. PERLIN, E. VON RUDLOFF, and A. P. TULLOCH. Can. J. Chem. **36**, 921 (1958).
5. T. FRANCIS and A. S. PERLIN. Can. J. Chem. **37**, 1229 (1959).
6. P. A. J. GORIN. Can. J. Chem. **38**, 641 (1960).
7. E. L. HIRST, D. I. MCGILVRAY, and E. G. V. PERCIVAL. J. Chem. Soc. 1297 (1950).
8. R. L. WHISTLER and D. F. DURSO. J. Am. Chem. Soc. **72**, 677 (1950).
9. L. HOUGH, J. K. N. JONES, and W. H. WADMAN. J. Chem. Soc. 2511 (1949).
10. C. E. CHILDS. Anal. Chem. **26**, 1963 (1954).
11. I. E. MUSKAT. J. Am. Chem. Soc. **56**, 693 (1934).
12. H. HIBBERT, R. S. TIPSON, and F. BRAUNS. Can. J. Research **4**, 221 (1931).
13. J. A. MILLS. *In* Advances in carbohydrate chemistry. Vol. 10. Academic Press, Inc., New York. 1955. p. 1.
14. S. PEAT. *In* Advances in carbohydrate chemistry. Vol. 2. Academic Press, Inc., New York. 1947. p. 37.
15. F. SHAFIZADEH. *In* Advances in carbohydrate chemistry. Vol. 13. Academic Press, Inc., New York. 1958. p. 9.
16. R. U. LEMIEUX. *In* Advances in carbohydrate chemistry. Vol. 9. Academic Press, Inc., New York. 1954. p. 1.

Can. J. Chem. Downloaded from www.nrcresearchpress.com by 210.87.254.5 on 09/05/12
For personal use only.

17. S. J. ANGYAL and R. J. YOUNG. J. Am. Chem. Soc. **81**, 5467 (1959).
18. R. J. DIMLER. *In* Advances in carbohydrate chemistry. Vol. 7. Academic Press, Inc., New York. 1952. p. 37.
19. A. S. PERLIN and A. R. LANSDOWN. Can. J. Chem. **34**, 451 (1956).
20. E. J. MCDONALD. *In* Advances in carbohydrate chemistry. Vol. **2**. Academic Press, Inc., New York. 1947. p. 253.
21. M. SAREL-IMBER and J. LEIBOWITZ. J. Org. Chem. **24**, 1897 (1959).
22. E. VIS and H. G. FLETCHER, JR. J. Am. Chem. Soc. **79**, 1182 (1957).
23. P. A. LEVENE and E. T. STILLER. J. Biol. Chem. **102**, 187 (1933).
24. K. FREUDENBERG and E. BRAUN. Ber. **66**, B, 780 (1933).
25. K. HESS and F. NEUMANN. Ber. **68**, B, 1360 (1935).
26. F. MICHEEL and H. MICHEEL. Ber. **63**, 2862 (1930).
27. R. C. HOCKETT and D. F. MOWERY, JR. J. Am. Chem. Soc. **65**, 403 (1943).
28. R. S. TIPSON. *In* Advances in carbohydrate chemistry. Vol. 8. Academic Press, Inc., New York. 1953. p. 107.
29. R. U. LEMIEUX and J. P. BARRETTE. J. Am. Chem. Soc. **80**, 2243 (1958).
30. C. B. PURVES. J. Am. Chem. Soc. **56**, 1969 (1934).
31. S. M. PARTRIDGE. Nature, **158**, 270 (1946).
32. F. W. BARTH and T. E. TIMELL. Can. J. Chem. **36**, 1321 (1958).
33. C. B. PURVES and C. S. HUDSON. J. Am. Chem. Soc. **56**, 1973 (1934).
34. A. S. PERLIN and C. BRICE. Can. J. Chem. **34**, 541 (1956).
35. B. LINDBERG and B. WICKBERG. Acta Chem. Scand. **7**, 969 (1953).
36. M. LAMBERT and A. C. NEISH. Can. J. Research, B, **28**, 83 (1950).

Can. J. Chem. Downloaded from www.nrcresearchpress.com by 210.87.254.5 on 09/05/12
For personal use only.

Can. J. Chem. Downloaded from www.nrcresearchpress.com by 210.87.254.42 on 09/05/12
For personal use only.

REACTION OF OXYGEN ATOMS WITH BUTADIENE[1]

R. J. Cvetanović and L. C. Doyle

ABSTRACT

Reaction of oxygen atoms with 1,3-butadiene has been investigated at room temperature. It is found that it conforms to the general mechanism established previously for the analogous reactions of monoolefins. Only 1,2-addition occurs, and the addition products, butadiene monoxide and 3-butenal, possess excess energy when formed as a result of high heats of reaction. The pressure dependence of the formation of the addition products yields the values of the "lifetimes" of the initially produced "hot" molecules. The relative rate constants have been determined at 25 and 127° C and from these the relative values of the Arrhenius parameters have been calculated.

INTRODUCTION

The general mechanism of reaction of oxygen atoms with alkenes has recently been established in this laboratory (1) and the trends in the relative rate constants (2) demonstrated the electrophilic character of the ground-state oxygen atoms in these reactions. As an extension of this work the present study of the analogous reaction with 1,3-butadiene, as the simplest representative of conjugated diolefins was carried out.

The particular questions which the present investigation was hoped to answer are: first, whether conjugated diolefins in their reactions with oxygen atoms follow the general mechanism established for monoolefins; secondly, whether only 1,2- or also 1,4-addition products are formed; and lastly, whether the value of the rate constant of the reaction of oxygen atoms with 1,3-butadiene is such as might be expected in view of the trends and relations established in the case of monoolefins (2). Affirmative answers to these questions have been obtained and only the two 1, 2-addition products predicted on the basis of the rules formulated for the monolefins (1), butadiene monoxide and 3-butenal, the latter readily isomerizing to the more stable crotonaldehyde, have been observed. The 1,4-addition product, 2,5-dihydrofuran, is not formed.

The pronounced pressure effect observed in the present work illustrates particularly well initial formation of "hot" addition products and the consequent "pressure-dependent fragmentation" (1) in the reactions of oxygen atoms with olefins. As a result, in some of these reactions, including 1,3-butadiene itself, the addition products are essentially completely decomposed at pressures of a few millimeters and are then not observable experimentally. This feature and some other difficulties inherent in the electrical discharge method for production of oxygen atoms, as discussed recently elsewhere (3), are believed to be responsible for the entirely different conclusions from the present ones arrived at by Avramenko and Kolesnikova (4) in what seems to be the only other attempt reported in the literature to study the reaction of oxygen atoms with butadiene. These differences are of a general character and are not limited to the case of butadiene.

Oxygen atoms were generated by mercury-photosensitized decomposition of nitrous oxide, as described in the previous work (1, 2), and nitrogen liberated provided a quantitative measure of the oxygen atoms consumed in the reaction.

EXPERIMENTAL

The apparatus used in this work consisted of a cylindrical quartz reaction cell 5 cm in diameter and 10 cm long, connected in series with an all-glass vertical plunger-type

[1]*Manuscript received August 8, 1960.*
Contribution from the Division of Applied Chemistry, National Research Council, Ottawa, Canada.
Issued as N.R.C. No. 5978.

Can. J. Chem. Downloaded from www.nrcresearchpress.com by 210.87.254.42 on 09/05/12
For personal use only.

circulating pump. The circulating reaction system had a total volume of 415 ml. It was connected by means of mercury cutoffs to a constant volume burette for measuring the amounts of reactant hydrocarbons (butadiene, cyclopentene) to the analysis system and to the vacuum manifold. Nitrous oxide was measured manometrically on a volume of 1000 ml and then was frozen over into the reaction vessel.

The analysis system consisted of a Le Roy still (5), followed by a "pump-out" trap and then by a constant volume burette and outlets for transfer of samples to the gas–liquid chromatographic apparatus (GLC), mass spectrometer, and infrared spectrometer. The Le Roy still was used in particular for the separation of the more volatile fractions. The noncondensable gases, N_2, CO, CH_4, and H_2, were analyzed by the use of a copper oxide tube to oxidize CO and H_2. The CO_2 formed was measured manometrically and mass spectra were taken of the residual N_2 and CH_4. Hydrogen, the amount of which was determined by difference, was at best formed only in trace amounts in the present work. The "pump-out" trap ensured quantitative retention of C_2H_4 which, together with C_2H_6 and traces of CH_4 and N_2O, was eluted from the Le Roy still at $-180°$. This fraction was further analyzed mass spectrometrically. No appreciable amounts of methane, ethylene, or ethane were formed in the reaction of oxygen atoms with butadiene. Ethylene formed from cyclopentene served for the determination of the relative rate constants, as described before (2).

After removal of excess N_2O and a part of the butadiene, the remainder was run on a 4-ft GLC column consisting of about 4 weight per cent dimethyl sulpholane on glass beads (passing 270 mesh). Infrared and mass spectra of the major reaction products were taken after their elution from the GLC column.

An air-cooled low-pressure mercury lamp was used as source of the mercury resonance radiation. In most experiments the large excess of N_2O employed ensured only negligible quenching by butadiene and separate experiments showed that mercury-photosensitized decomposition of butadiene itself was not important under conditions of the present experiments. The reactants were of the best available grade and were degassed and bulb-to-bulb distilled *in vacuo* in the usual manner before use.

In the reaction of oxygen atoms with butadiene only two addition products were detected by GLC analysis (using dimethyl sulpholane column): butadiene monoxide and crotonaldehyde. They had GLC elution times, infrared spectra, and mass spectra identical with those of the respective commercial samples (a sample of butadiene monoxide was kindly supplied by Columbia-Southern Chemical Corp.). The GLC analysis of the condensable products showed also small amounts of what appeared to be three compounds eluting much faster than the two addition products. These were formed in too small amounts to be identified by the analytical techniques used but are believed to be the products of fragmentation of the "hot" addition products, as will be discussed in the following section. No 2,5-dihydrofuran, a potential 1,4-addition product, was detected.* The quantitative data on the products observed by GLC are based on calibrations made with butadiene monoxide and crotonaldehyde and with the assumption that the fragmentation products had equal response per unit area of the peaks to that of butadiene monoxide. Only the total sum of the fragmentation products observed by GLC is reported here since individually they were present in most cases in little more than trace amounts.

In the reaction of oxygen atoms with butadiene there was evidence for the formation

**The authors are very grateful to Dr. E. C. Horswill of these laboratories for synthesizing a sample of 2,5-dihydrofuran in order that its absence in the reaction products could be verified directly.*

of a deposit (referred to in the following as the "polymer") which was not removed, or was removed only extremely slowly, from the reaction vessel by evacuation or freezing out. No attempt was made to obtain qualitative and quantatitive information on this material.

RESULTS

The results of several experiments carried out at 25±2° at constant pressures of nitrous oxide and butadiene, 300 and 30 mm, respectively, but at varying exposure times are presented in Fig. 1. They show that within the investigated range the rates of formation of the products are independent of the reaction time.

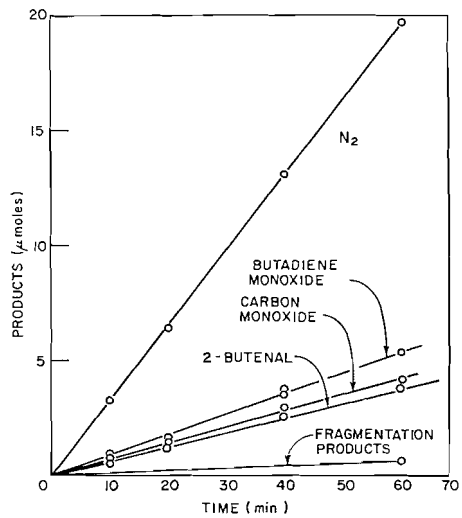


FIG. 1. Variation of the amounts of products formed with irradiation time. (Pressure of N_2O 299±2 mm, pressure of butadiene 31±2 mm, temperature 25±2° C. "Fragmentation products" refer to the unidentified condensable products of pressure-dependent fragmentation as observed by GLC.)

In the experiments shown in Fig. 1 exceptionally large amounts of butadiene were employed, about 10 times as large as in most of the other experiments. Even then no products other than those usually observed were detected. The only effect of variation in butadiene concentration reflected itself in a slight variation in the number of oxygen atoms generated (as measured by nitrogen formation) because of some competitive quenching by the diolefin. This is shown in Table I where more than fourfold increase

TABLE I

Dependence of the amounts of products formed on the initial concentration of butadiene

			Products				
Run	Butadiene, mm	Butadiene / N_2O	N_2, μmoles	CO / N_2	Epoxide / N_2	2-Butenal / N_2	Frag. products* / N_2
86	2.49	0.0073	12.8	0.22	0.27	0.19	0.04
88	5.48	0.0173	12.7	0.22	0.29	0.20	0.04
87	8.21	0.0265	12.5	0.22	0.27	0.19	0.04
85	11.10	0.0355	12.3	0.21	n.d.	0.20	0.05

NOTE: Temperature 25±1° C; irradiation time 40 minutes; N_2O pressure 303±1.5 mm.
*Condensable fragmentation products observed by GLC.
n.d. = not determined.

Can. J. Chem. Downloaded from www.nrcresearchpress.com by 210.87.254.42 on 09/05/12
For personal use only.

in butadiene concentration did not affect the rates of formation of the products per oxygen atom consumed (R/R_{N_2}) and only slightly decreased nitrogen production. This decrease is of correct magnitude to be entirely explainable as due to competitive quenching by butadiene. At the relatively high total pressures employed in the present work the energy transferred by quenching to butadiene is likely to be rapidly dissipated through collisional deactivation, as is usually the case with olefins, without causing any substantial decomposition of butadiene. Small amounts of a butadiene dimer, identified as such mass spectrometrically, were occasionally observed by GLC analysis of the products. This compound was found, however, to be present as a minor impurity in the butadiene used and was initially introduced together with the butadiene into the reaction system.

The effect of pressure on the products formed is very pronounced, as is shown in Fig. 2. In these experiments the pressure of butadiene was kept approximately constant

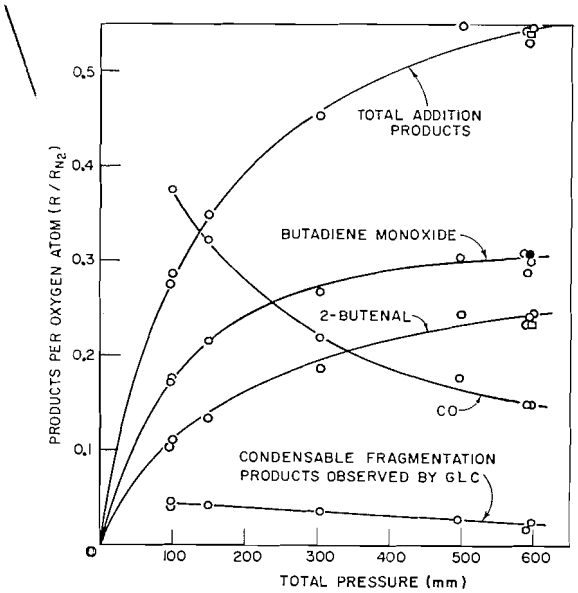


FIG. 2. Rates of product formation per oxygen atom consumed (R/R_{N_2}) at various total pressures. (Pressure of butadiene 3.0±0.5 mm, exposure 40 minutes, temperature 26±1° C. Filled circle and squares indicate initially added 3 mm of O_2.)

at about 3 mm, the exposure was 40 minutes so that between 11 and 13 μmoles of nitrogen were produced, and the temperature was 26±1°. The total pressure was varied by varying the partial pressure of nitrous oxide.

The general behavior in the case of butadiene is quite similar to that observed previously with propylene (1): with increasing pressure the amounts of the addition products, butadiene monoxide and crotonaldehyde, increase while at the same time those of the fragmentation products decrease. The reaction of oxygen atoms with butadiene provides therefore another good illustration of the pressure-dependent fragmentation in the reactions of oxygen atoms with olefins: at higher pressures greater number of the initially produced "hot" addition products is deactivated and less fragmentation of these products occurs.

An initial addition of 3 mm of molecular oxygen to 3 mm of butadiene and 587 mm

Can. J. Chem. Downloaded from www.nrcresearchpress.com by 210.87.254.42 on 09/05/12
For personal use only.

of nitrous oxide did not affect the formation of butadiene monoxide and crotonaldehyde, as shown by filled circle and squares in Fig. 2, and eliminated the condensable fragmentation products. No attempt was made to measure directly N_2 and CO in this case because of large excess of O_2 present. Nitrogen was estimated from comparable runs done in the absence of molecular oxygen.

The rate constants of the reaction of oxygen atoms with butadiene (k_B) were determined relative to those of cyclopentene (k_C) at 25.4±1° and 126.8±2° C. The experimental details and the results are given in Table II. The rate constants have been

TABLE II

Determination of the relative rate constant for butadiene and cyclopentene

Run	Butadiene / Cyclopentene	Butadiene, mm	Cyclopentene, mm	N_2O, mm	Gaseous products: N_2, mm	C_2H_4/N_2	CO/N_2	k_B/k_C
				(I) 25.4±1° C				
60	0.84	6.88	8.17	507.2	2.12	0.160	0.075	0.810
62	1.74	18.57	10.66	499.1	1.94	0.113	0.094	0.808
65	1.79	13.15	7.35	502.8	1.81	0.112	0.092	0.776
64	3.75	30.99	8.26	465.3	1.68	0.0685	0.117	0.845
61		29.73	—	503.3	1.94	—	0.143	
							Mean	0.810±.018
				(II) 126.8±2° C				
66	1.17	10.84	9.28	504.5	1.69	0.133	0.112	0.905
69	1.72	13.91	8.11	501.4	1.64	0.109	0.128	0.876
67	2.13	19.36	9.11	501.6	1.64	0.0962	0.136	0.869
71	2.63	21.64	8.23	505.5	1.62	0.0822	n.d.	0.879
68	3.07	28.64	9.34	507.5	1.54	0.0734	0.145	0.892
70		27.88	—	506.3	1.58	—	0.181	
							Mean	0.884±.011

NOTE: Exposure 60 minutes; quantities are given in millimeters in 415.1 ml at 25° C.

calculated from the rates of ethylene production in the manner described previously (2). From the mean values of the relative rate constants at the two temperatures the relative values of the Arrhenius parameters are found to be $E_B - E_C = 0.20$ kcal/mole and $A_B/A_C = 1.14$.

DISCUSSION

The products formed in the reaction of oxygen atoms with butadiene indicate that this diolefin conforms to the general mechanism established before (1) for the reaction of oxygen atoms with monoolefins. In the case of butadiene this mechanism requires the formation of butadiene monoxide and 3-butenal as the initial addition products. Actually crotonaldehyde (2-butenal) was observed after elution from the dimethyl sulpholane GLC column instead of 3-butenal. However, infrared absorption spectra of the condensable products taken *before* passage through GLC show that crotonaldehyde is not the primary product of the reaction but is formed during passage through GLC by isomerization of an aldehyde which has the carbonyl stretching absorption band at about 1745 cm^{-1} instead of a doublet at about 1720 cm^{-1} present in crotonaldehyde. Both aldehydes have the C=C stretching absorption band at about 1650 cm^{-1}. *After* GLC the infrared spectra of the products show only the presence of butadiene monoxide and crotonaldehyde, the latter at the expense of the aldehyde initially present, from which it is apparently formed by isomerization. We believe that the initially formed aldehyde

Can. J. Chem. Downloaded from www.nrcresearchpress.com by 210.87.254.42 on 09/05/12
For personal use only.

is 3-butenal. Some additional evidence for this was obtained by separating from a polypropylene glycol column a compound with an infrared spectrum similar to that of the initially formed aldehyde. This compound elutes much faster than crotonaldehyde but has a mass spectrum essentially the same as crotonaldehyde.

The isomerization of the initially produced aldehyde to crotonaldehyde apparently takes place quite readily on passage through GLC. Also there appeared to be as a rule slight and sometimes quite appreciable isomerization even in the course of the regular handling of the products in the vacuum apparatus before passage through GLC. While the information on 3-butenal available in the literature is somewhat limited, it would seem that an isomerization to the more stable 2-butenal under present conditions could readily take place.

A 1,4-addition of oxygen atoms to butadiene would produce 2,5-dihydrofuran. However, this compound is not observed so that 1,4-addition does not occur. The assumed primary intermediate in these reactions is a triplet biradical (1). There is evidence that this is extremely short-lived, since the distribution of the products differs somewhat between the two 2-butene isomers (1). Also, in view of the pronounced electronegativity of oxygen, the initial "biradical" is likely to have some zwitterion character. The formation of the 1,2- rather than 1,4-adduct with oxygen atoms in the case of 1,3-butadiene may then be understandable both on kinetic and energetic grounds.

The observed pressure effect in the reaction of oxygen atoms with 1,3-butadiene is very interesting and, together with the corresponding reaction of propylene (1), it illustrates well one of the fundamental features of these addition processes. As a result of high heats of reaction the products formed are "hot" to the extent of about 115 kcal/mole in the case of carbonyl compounds and probably about 80 to 90 kcal/mole in the case of the epoxides. Depending largely on the number of degrees of freedom available, various average time intervals will be required before sufficient excess energy is concentrated in a critical bond to break it. In the meantime the molecule will tend to become stabilized through collisional deactivation. In the case of ethylene, decomposition largely predominates at the usual pressures (6), while the products from the butenes are stabilized already at about 10 to 30 mm (7). Propylene exhibits an intermediate behavior and the same is now found to be true for 1,3-butadiene as well.

For a kinetic treatment of the observed pressure effect the following reaction scheme, based on the general mechanism of reaction of oxygen atoms with olefins, is considered.

$$N_2O + Hg(^3P_1) \rightarrow N_2 + O + Hg(^1S_0) \qquad (i)$$

$$CH_2{=}CH{-}CH{=}CH_2 + O \rightarrow (CH_2{=}CH{-}\dot{C}H{-}CH_2O\cdot) \rightarrow \alpha BO^* + \beta BA^* + X \qquad [1]$$

$$BO^* \rightarrow \gamma CO + \text{other decomposition products} \qquad [2]$$

$$BO^* + M \rightarrow BO + M \qquad [2a]$$

$$BA^* \rightarrow \delta CO + \text{other decomposition products} \qquad [3]$$

$$BA^* + M \rightarrow BA + M \qquad [3a]$$

where BO stands for butadiene monoxide, BA for butenal, X for any unknown products of reaction [1], and the asterisk indicates "hot" molecules. Steady-state treatment leads to the following expressions:

[1] $$\frac{R_{N_2}}{R_{BO}} = \frac{1}{\alpha}\left(1 + \frac{k_2}{k_{2a}(M)}\right),$$

[2] $$\frac{R_{N_2}}{R_{BA}} = \frac{1}{\beta}\left(1 + \frac{k_3}{k_{3a}(M)}\right)$$

Can. J. Chem. Downloaded from www.nrcresearchpress.com by 210.87.254.42 on 09/05/12
For personal use only.

and

$$[3] \qquad \frac{R_{CO}}{R_{N_2}} = \frac{\gamma\alpha}{1+k_{2a}(M)/k_2} + \frac{\delta\beta}{1+k_{3a}(M)/k_3}.$$

Plots of R_{N_2}/R_{BO} and R_{N_2}/R_{BA} against 1/(M) are given in Fig. 3. From these the

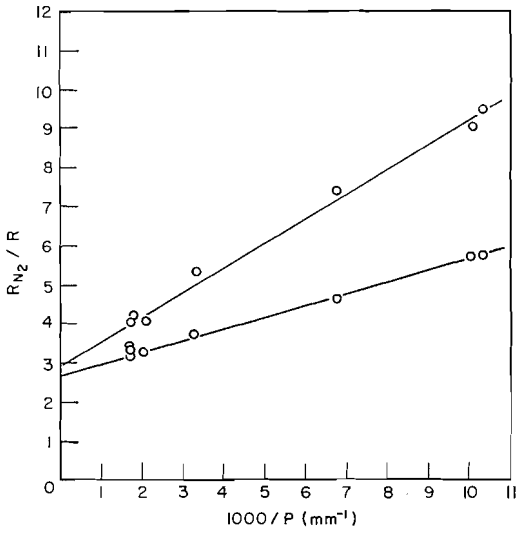


FIG. 3. Plots of R_{N_2}/R_{BO} and R_{N_2}/R_{BA} against reciprocal total pressure (equations [1] and [2]).

following values are obtained: $k_2/k_{2a} = 3.7\times10^{18}$ cc/molecule, $k_3/k_{3a} = 7.2\times10^{18}$ cc/molecule, $\alpha = 0.38$, $\beta = 0.34$.

In Fig. 4 R_{N_2}/R_{CO} is seen to be a linear function of (M) and this simple relation requires

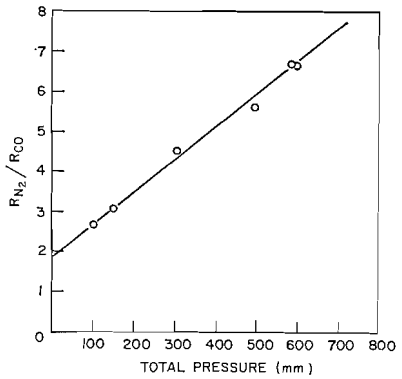


FIG. 4. Plot of R_{N_2}/R_{CO} against total pressure (equation [3a]).

simplification of equation [3]. The slope-to-intercept ratio of the plot in Fig. 4 indicates a k/k_a value of 7.3×10^{18} cc/molecule which is essentially the same as that obtained for k_3/k_{3a} from the plot in Fig. 3. In view of this it would appear that CO is produced by decomposition of "hot" butenal and not to any important extent from decomposition of "hot" butadiene monoxide, i.e., that in equation [3] $\gamma = 0$ and therefore

$$[3a] \qquad R_{CO}/R_{N_2} = \delta\beta/(1+k_{3a}(M)/k_3).$$

Can. J. Chem. Downloaded from www.nrcresearchpress.com by 210.87.254.42 on 09/05/12
For personal use only.

The plot in Fig. 4 is in agreement with equation [3*a*]. The intercept gives 0.54 for the value of $\delta\beta$, i.e. the value of R_{CO}/R_{N_2} as $P \rightarrow 0$. If CO is formed only from "hot" butenal such a high value of $\delta\beta$ is inconsistent with the value $\beta = 0.34$ from the plot in Fig. 3 since δ cannot be larger than unity. Additional CO is not produced in a pressure-independent fragmentation, as is evident from the alternative plot of equation [3*a*] in Fig. 5. The

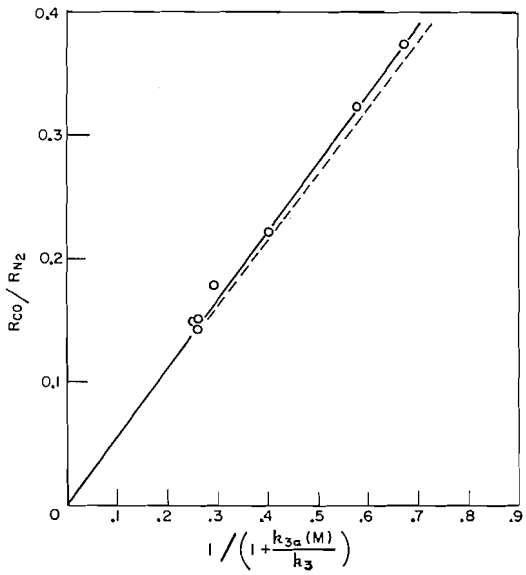


FIG. 5. Plot of R_{CO}/R_{N_2} against $1/(1+k_{3a}(M)/k_3)$ (rearranged equation [3*a*]).

values for k_3/k_{3a} have been taken as 7.2×10^{18} (broken line) as found above and 6.6×10^{18} cc/molecule (full line), the latter to show the relatively small effect of an appreciable variation in the value selected for k_3/k_{3a}. As $P \rightarrow \infty$ R_{CO}/R_{N_2} approaches zero or a value very close to it. The difficulty could be formally resolved by assuming that a constant fraction (37%) of the collisionally deactivated BA* molecules are not recovered as butenal but polymerize instead, either during the reaction or in subsequent handling of the products. This would also bring up the material balance of the oxygen atoms used in the reaction as $P \rightarrow \infty$ from about 70 to 75% to about 90 to 95%, which is satisfactory in view of the long extrapolations made to obtain the intercepts. In this connection it is of interest that Farberov and Ustavshchikov (8) have recently observed that 3-butenal resinifies rapidly on standing. However, it was not feasible in the present work to obtain quantitative estimates of the polymer formed and the suggested explanation must be regarded as only speculative.

Besides carbon monoxide only small amounts of other fragmentation products are observed. This is probably due to the scavenging action of butadiene for H atoms and free radicals with eventual formation of higher molecular weight compounds not directly observable by the analytical techniques used.

If it is assumed approximately that $k_{2a} = k_{3a} = 10^{-10}$ cc molecule^{-1} sec^{-1}, i.e. that deactivation occurs at approximately every collision, then the lifetimes of the "hot" butadiene monoxide and 3-butenal are calculated to be, respectively, $1/k_2 = 2.7\times10^{-9}$ and $1/k_3 = 1.4\times10^{-9}$ sec. From the plots in earlier work (1) the lifetime for the "hot" propanal is similarly found to be 8.0×10^{-9} and that of the "hot" propylene oxide

Can. J. Chem. Downloaded from www.nrcresearchpress.com by 210.87.254.42 on 09/05/12
For personal use only.

5.8×10^{-9} sec, although in this latter case on the basis of a very limited number of experiments the pressure dependence appeared to be more complex. For the hot addition products of the reaction of oxygen atoms with butene-1 and isobutene lifetimes an order of magnitude greater were indicated by the complete suppression of pressure-dependent fragmentation at pressures as low as 10 to 30 mm (7). The exceptionally short lifetimes of butadiene monoxide and in particular of 3-butenal considering the number of degrees of freedom available in these compounds are understandable since breakage of bonds may lead to the resonance stabilized allylic and substituted allylic radicals.

The rate constant of the reaction of oxygen atoms with butadiene is very close to that of isobutene and other two-substituted ethylene derivatives as may be expected in view of the electrophilic character of oxygen atoms in their reactions with olefins (2, 9). The temperature coefficient of the rate constant will be discussed elsewhere together with the data obtained for a number of monoolefins (10).

It is evident from the present work that at pressures as low as a fraction of a millimeter to several millimeters essentially complete decomposition of the "hot" addition products should occur and the primary step of the process, addition of oxygen atoms to the double bond, would no longer be directly observable. Under such conditions only fragmentation products would be produced and in particular their derivatives from secondary reactions with molecular oxygen, even when the latter is present only in small amounts, or with other active species which may be present. On this basis the entirely different results from the present ones obtained by Avramenko and Kolesnikova (4) are understandable, as well as the conclusions of these authors that oxygen atoms exhibit a versatility of behavior in their reactions with some organic compounds, and with olefins as well. These conclusions have not been born out by investigations in this laboratory, which show instead an electrophilic addition of the ground-state oxygen atoms to the double bond as the only primary reaction with olefins at room temperature.

ACKNOWLEDGMENTS

The authors are grateful to Dr. A. W. Tickner for mass spectrometric analyses and to the Analytical Section of this Division for the infrared analyses.

REFERENCES

1. R. J. CVETANOVIĆ. Can. J. Chem. **36**, 623 (1958).
2. R. J. CVETANOVIĆ. J. Chem. Phys. **30**, 19 (1959).
3. J. M. S. JARVIE and R. J. CVETANOVIĆ. Can. J. Chem. **37**, 529 (1959).
4. L. I. AVRAMENKO and R. V. KOLESNIKOVA. Voprosy Khimicheskoi Kinetiki Kataliza i Reaktsionnoi Sposobnosti. Akad. Nauk S.S.S.R., Moscow. 1955. p. 7; N.R.C. of Canada Technical Translation 789, Ottawa. 1959.
5. D. J. LE ROY. Can. J. Research, B, **28**, 492 (1950).
6. R. J. CVETANOVIĆ. J. Chem. Phys. **23**, 1375 (1955).
7. S. SATO and R. J. CVETANOVIĆ. Can. J. Chem. **36**, 970 (1958).
8. M. I. FARBEROV and B. F. USTAVSHCHIKOV. J. Gen. Chem. U.S.S.R. **25**, 2025 (1955). (English translation, Consultants Bureau, New York, N.Y. 1956.)
9. S. SATO and R. J. CVETANOVIĆ. J. Am. Chem. Soc. **81**, 3223 (1959).
10. R. J. CVETANOVIĆ. J. Chem. Phys. In press.

Can. J. Chem. Downloaded from www.nrcresearchpress.com by 210.87.254.42 on 09/05/12
For personal use only.

Can. J. Chem. Downloaded from www.nrcresearchpress.com by 210.87.254.105 on 09/05/12
For personal use only.

DECOMPOSITION PRESSURES OF FERRIC SULPHATE AND ALUMINUM SULPHATE[1]

N. A. WARNER[2] AND T. R. INGRAHAM[3]

ABSTRACT

The gas pressures over samples of anhydrous ferric sulphate and anhydrous aluminum sulphate have been measured in a static system, using a mercury manometer in which the exposed surface was covered with a flexible Pyrex bellows. The calculated ΔH for the decomposition of $Fe_2(SO_4)_3$ was +135.4 kcal/mole. It was not possible to calculate the ΔH for the $Al_2(SO_4)_3$ decomposition, because a discrete aluminum oxide with singular thermodynamic properties was not obtained.

In the $Fe_2(SO_4)_3$ system, the fraction of SO_3 in the gas phase was found to be almost constant over the range of temperature and pressure changes used in the study.

At any given temperature, the decomposition pressure over a ferric sulphate sample is greater than that over an aluminum sulphate sample, thus indicating that preferential decomposition of ferric sulphate should be thermodynamically feasible in mixtures of ferric sulphate and aluminum sulphate.

INTRODUCTION

When metallic sulphates are heated *in vacuo* or in a neutral atmosphere, they can be decomposed to oxides, e.g.,

$$MSO_4 \rightleftharpoons MO + SO_3,$$

$$M_2(SO_4)_3 \rightleftharpoons M_2O_3 + 3SO_3.$$

The ease with which this decomposition can be brought about varies widely with the different metallic sulphates. This variation has been utilized commercially in the separation of some sulphates. For example, copper sulphate is more stable than ferric sulphate. Hence, when some ores which contain copper and iron compounds are roasted in controlled sulphating atmospheres, it is possible to prepare copper sulphate almost selectively, while the iron is retained as oxide. Simple leaching techniques effectively separate the soluble copper sulphate from the insoluble iron oxide. The same basic principle of selective sulphate formation or decomposition has been applied industrially for the separation of cadmium and zinc compounds when they occur together in smelting dusts (1).

One of the recently patented methods for separating the constituents of clays and shales (2) would seem to depend on the fact that aluminum sulphate is more stable than ferric sulphate. Since the problem of utilizing the constituents of shale is an important one, the literature was searched to determine whether this assumption were true. Very little information is available on the stability of either compound, and the published data (3) fail to satisfy the critical tests of Kelley (4). Hence, it seemed worth while to measure the decomposition pressures of both of these compounds to determine whether the separation would be thermodynamically possible.

APPARATUS AND PROCEDURE

Because of its simplicity, a static method was chosen for measuring the equilibrium dissociation pressures of the sulphates. The apparatus assembled for the measurements

[1]*Manuscript received July 13, 1960.*
Contribution from the Extraction Metallurgy Division, Mines Branch, Department of Mines and Technical Surveys, Ottawa, Canada.
[2]*Postdoctorate Research Fellow of the National Research Council of Canada, assigned to the Mines Branch. Present address: School of Metallurgy, University of New South Wales, Australia.*
[3]*Head, Research Subdivision.*

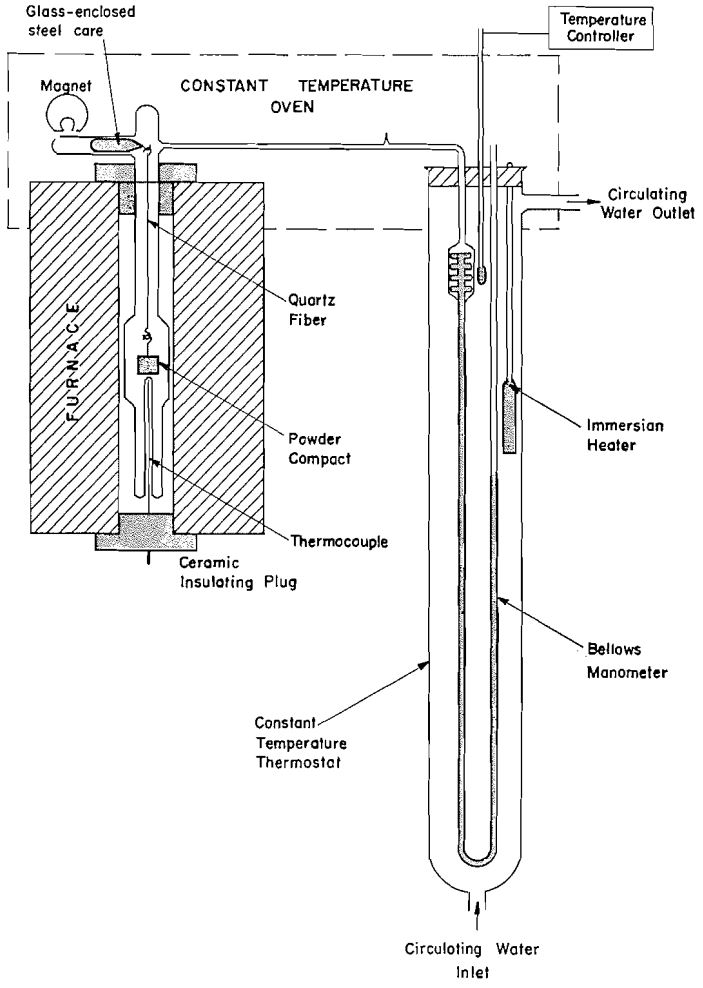


FIG. 1. Apparatus for measuring decomposition pressures of anhydrous sulphates.

is shown diagrammatically in Fig. 1. The most important feature of the apparatus is the glass-bellows mercury manometer. The design of the manometer is based on one originated by Spence (5). However, in the present version the mercury displacement has been modified from horizontal to vertical, and an appreciable increase in sensitivity has resulted (6).

The apparatus was constructed entirely from Pyrex and Vycor glass. The Vycor section extended out to the cool zone of the furnace, where it was joined through graded seals to the Pyrex part of the apparatus.

To avoid complications that might be introduced by the condensation of sulphur trioxide, the bellows manometer and the connecting tubing were thermostatically controlled at a temperature of 60° C.

For convenience in handling, powder compacts of anhydrous ferric sulphate and aluminum sulphate were pressed with a small platinum wire anchored in the pellet. The pellets were suspended by this platinum wire and a small quartz fiber which was attached

Can. J. Chem. Downloaded from www.nrcresearchpress.com by 210.87.254.105 on 09/05/12
For personal use only.

to a magnetically moveable hook. The hook was made moveable to permit free access for installing and removing the pellet through the top of the furnace tube.

After installation of each pellet, the reaction tube was sealed and the apparatus was evacuated. During the period of evacuation the pellet was heated to a temperature of about 650° C to remove the last traces of moisture. After several hours at this temperature, the vacuum line was sealed and the temperature raised to the point at which displacement of the mercury column indicated that decomposition of the sulphate had begun. Readings of the pressure were made at 24-hour intervals in the study of the ferric sulphate system, and at 48-hour intervals in the study of the aluminum sulphate system. The experiment was continued until a steady state had been reached.

Displacement of the mercury column in the manometer was observed with a cathetometer, and was corrected for changes in barometric pressure. With small changes in pressure, some sticking of the mercury in the column was noted. Sticking was relieved by rapping the manometer sharply just before readings were made.

RESULTS AND DISCUSSION

The results obtained in experiments with ferric sulphate, with aluminum sulphate, and with 1:1 mole mixtures of aluminum sulphate with iron oxide are shown in Table I.

TABLE I

Decomposition pressures over ferric sulphate, aluminum sulphate, and an aluminum sulphate – iron oxide mixture

Ferric sulphate		Aluminum sulphate		Aluminum sulphate – ferric oxide (mole ratio 1:1)	
Temp. (°C)	Pressure (cm of Hg)	Temp. (°C)	Pressure (cm of Hg)	Temp. (°C)	Pressure (cm of Hg)
				627	1.0
630*	7.3				
638	8.4				
		652*	1.4		
658	14.7				
660*	16.8				
		673*	2.4		
				679	3.2
680*	27.1	680	2.4		
685	28.6				
		694	3.6		
700	41.9				
705*	48.1				
		708	4.5		
715	61.1				
724	72.0			724	14.1
		730	7.8		
				736	49.6
				742	54.3
		743	13.5		
				752	71.7
		753	19.4		
		762	28.2		
		769	40.0		
		777	72.0		

*Measurements made with temperature decreasing. All other measurements made with temperature increasing.

Can. J. Chem. Downloaded from www.nrcresearchpress.com by 210.87.254.105 on 09/05/12
For personal use only.

Ferric Sulphate

When the results shown in Table I were plotted on a log p versus reciprocal of absolute temperature graph, Fig. 2 was obtained. It will be noted from Fig. 2 that the linearity

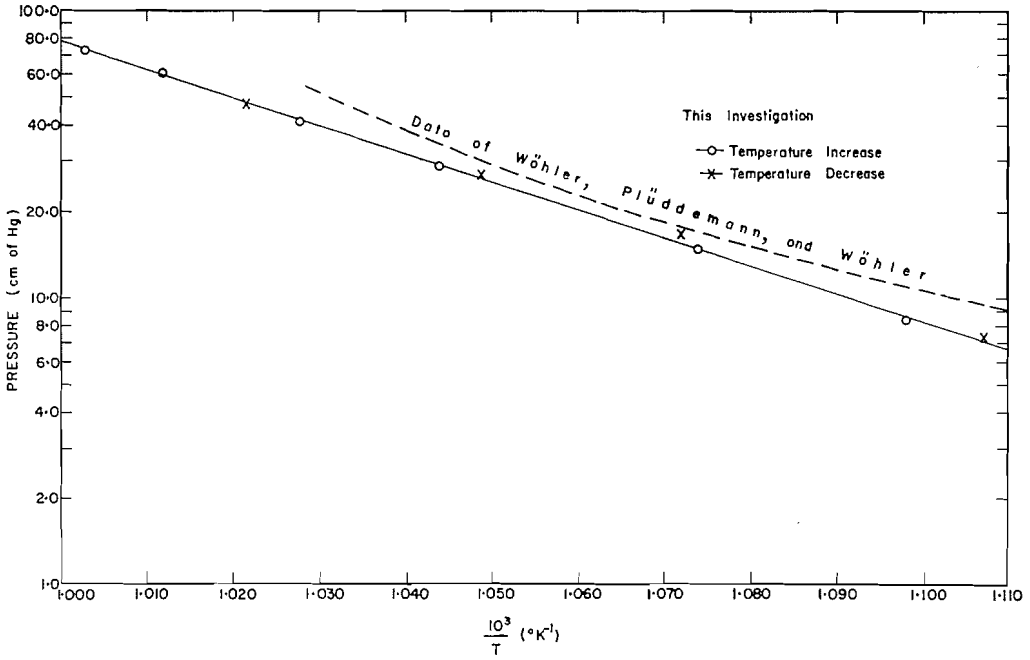


FIG. 2. Pressure vs. reciprocal temperature relationship for anhydrous ferric sulphate.

of the results is good, thus indicating that over the temperature range of the experiments there is not an appreciable change in the heat of the decomposition reaction. The linearity of the results and the demonstrated reversibility of the system indicate that true equilibrium had been reached in the experiments and that the gas phase probably contained only SO_2, SO_3, and O_2. It seems unlikely that polymers of SO_3 were present. The iron oxide product was identified as hematite.

When the static method of measuring the decomposition pressures was selected, the selection was made with some misgiving. From preliminary experiments it had been established that the dynamic method might be subject to substantial errors, because the rate of attainment of equilibrium decreases as equilibrium is approached, and it would be easy to assume that equilibrium had been reached, when in fact the reaction was still proceeding slowly.

Alternatively, the measurement of pressures in a static system containing a substantial temperature gradient and gases of different molecular weights is also subject to error. In this instance, due to thermal diffusion, the lighter molecules tend to congregate in the hotter zone. This means that the 2:1 molar ratio of SO_2:O_2, produced by the decomposition of SO_3, is reduced to somewhat less than 2:1 in the hot zone, and increased to somewhat more than 2:1 in the cold zone. This departure from exact stoichiometry can lead to errors in any quantities, e.g. degree of dissociation, etc., calculated on the basis of the 2:1 stoichiometry.

Can. J. Chem. Downloaded from www.nrcresearchpress.com by 210.87.254.105 on 09/05/12
For personal use only.

Can. J. Chem. Downloaded from www.nrcresearchpress.com by 210.87.254.105 on 09/05/12
For personal use only.

The magnitude of the error caused by thermal diffusion is difficult to assess on a purely theoretical basis (7), but the linearity of the results shown in Fig. 2 would favor the conclusion that the error is small or at least comparable with the other errors of measurement. Recently a novel method of studying sulphate equilibria, through the measurement of only one gas pressure, was developed by Kellogg (8). It is expected that when similar systems have been examined by both methods, it may be possible to assess the magnitude of the thermal diffusion error.

Having measured the decomposition pressure exerted by the mixed gases SO_3, SO_2, and O_2, over a ferric sulphate sample, it was of interest to calculate the heat of the decomposition reaction

$$Fe_2(SO_4)_3 \rightleftharpoons Fe_2O_3 + 3SO_3 \qquad [1]$$

from the variation of the equilibrium constant of the reaction with temperature. For this calculation it was necessary to know p_{SO_3}, since $K'_p = p^3_{SO_3}$ for reaction 1. The magnitude of p_{SO_3} was calculated on the assumption that p_{SO_3} satisfied both equation 1 and the equation for the decomposition of SO_3,

$$2SO_3 \rightleftharpoons 2SO_2 + O_2. \qquad [2]$$

The calculation was made by obtaining the equilibrium constant K_p, for reaction 2, from the data of Evans and Wagman (9) and converting this K_p to K_x (the equilibrium constant in terms of mole fractions) by dividing by the total pressure at each of a series of temperatures. For convenience and to minimize errors, interpolated temperatures from Fig. 2 were used.

When K_x had been calculated, it was equated to the equilibrium constant which was set up in mole fraction form on the basis that α is the fraction of 1 mole of SO_3 dissociated at a given temperature. Thus, $\{2(1-\alpha)\}/\{(2+\alpha)\}$ represents the mole fractions of SO_3, and $K_x = 4\alpha^3/(4\alpha^3-12\alpha+8)$. It should be noted that in this calculation an exact SO_2:O_2 ratio of 2:1 is implicitly assumed.

When K_x was calculated, it was found to be almost constant, with an average deviation of 1% over the temperature range 920 to 1000° K. The average K_x was used in calculations, and $\alpha = 0.538$ and a mole fraction of $SO_3 = 0.364$ were obtained.

The implications of the constancy of the mole fraction of SO_3 are of interest. Once the value 0.364 is known, the pressure of SO_3 in a system can be set very conveniently by including an excess of ferric sulphate in the system and then heating the system until the total pressure, reduced by the factor 0.364, produces the required partial pressure of SO_3.

When $\log K'_p = p^3_{SO_3}$ was plotted against reciprocal absolute temperature, a linear relationship was obtained. The relationship can be described by the equation:

$$\log K'_p = 28.34-(29{,}600/T).$$

When this equation was used to calculate the heat of reaction for the dissociation of ferric sulphate, a ΔH of +135.4 kcal was obtained.

Aluminum Sulphate

The results obtained from a study of the decomposition of aluminum sulphate and 1:1 mole mixtures of aluminum sulphate with ferric oxide are shown in Table I and as a log P versus reciprocal temperature relationship in Fig. 3. The curvature of the relationship indicates that the type of treatment accorded the ferric sulphate results to obtain a heat of decomposition would not be valid for the aluminum sulphate systems. It would

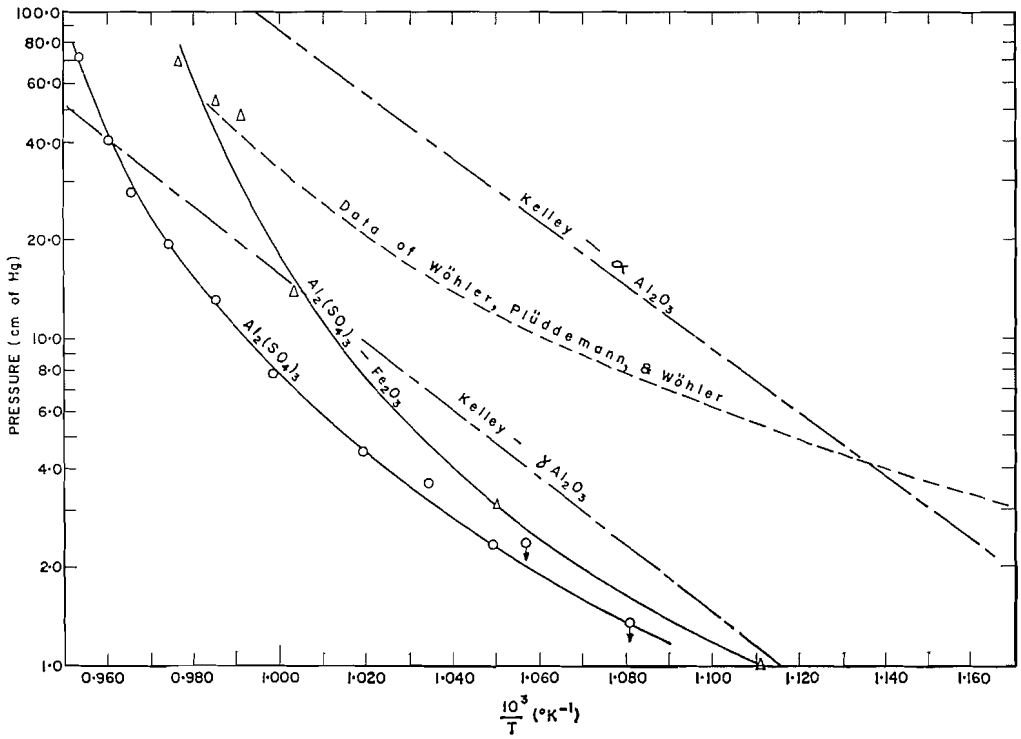


FIG. 3. Pressure vs. reciprocal temperature relationship for anhydrous aluminum sulphate and aluminum sulphate – iron oxide mixtures.

therefore seem sufficient to seek an explanation for the lack of linearity of the results, and to compare the pressures with the corresponding pressures for ferric sulphate, under similar conditions of temperature.

When the partly decomposed and completely decomposed pellets of aluminum sulphate were examined by X-ray diffraction, it was observed that gamma alumina was present. In one pellet which had been heated for a long time at a high temperature, alpha alumina was found. This is in general agreement with the observations of Kelley (10): "In actual decomposition of $Al_2(SO_4)_3$, there is not obtained Al_2O_3 (alpha) but a less stable variety usually designated Al_2O_3 (gamma). Unfortunately the latter appears not to have unique thermodynamic properties; available information indicates that there may be two varieties of Al_2O_3 (gamma) or at any rate that its properties depend upon the temperature to which it is heated and the time of heating." From the foregoing, it would seem possible that the results shown in Fig. 3 represent steady-state pressures over a metastable system of aluminum sulphate and some modification of gamma alumina. The curvature of the line in Fig. 3 could be interpreted as representing the presence of an increasingly stable modification of alumina, as the temperature of the experiments was increased. From a few experiments, there was an indication that the pressure measurements, although steady, were not readily reversible if the temperature of the specimen had previously been raised to appreciably above the temperature of the measurement. This would tend to confirm the presence of the more stable form of alumina at higher temperatures. Time did not permit a more extensive investigation of this point.

It is of interest to note, in Fig. 3, that the stable pressures over the aluminum sulphate –

Can. J. Chem. Downloaded from www.nrcresearchpress.com by 210.87.254.105 on 09/05/12
For personal use only.

ferric oxide system are, at all temperatures, greater than those over pure aluminum sulphate. This has been resolved by considering that ferric oxide acts as a catalyst in promoting the formation of the more stable forms of alumina. Higher equilibrium pressures are to be expected over the more stable forms of alumina.

Finally, it is of interest to compare, in Table I, the steady-state pressures over the ferric sulphate and aluminum sulphate systems at various temperatures. The comparison shows clearly that at all temperatures the pressure at any given temperature is always greater over the ferric sulphate system than over an aluminum sulphate system.

TABLE II

Calculations made to determine ΔH for the reaction $Fe_2(SO_4)_3 \rightleftharpoons Fe_2O_3 + 3SO_3$

T (°K)	K_p	P (atm)	K_x	α	N_{SO_3}	K'_p
920	0.0415	0.1466	0.283			1.519×10^{-4}
940	0.0706	0.2480	0.284			7.356×10^{-4}
960	0.1172	0.4046	0.290	0.538	0.364	3.194×10^{-3}
980	0.1914	0.6650	0.288			1.418×10^{-2}
1000	0.3050	1.047	0.291			5.535×10^{-2}
			Average 0.287 ± 0.003			

CONCLUSIONS

From an examination of the steady-state gas pressures over ferric sulphate and aluminum sulphate samples heated in a closed system, it has been concluded that the pressure at any given temperature is always substantially greater over a ferric sulphate sample. Hence, it would seem thermodynamically feasible to separate aluminum sulphate from ferric sulphate by roasting the compounds under conditions selected to decompose the ferric sulphate only, and then leaching the water-soluble aluminum sulphate from the roasted mixture. The practical limitations affecting the application of this approach will be discussed in a later communication.

ACKNOWLEDGMENT

The authors wish to express their thanks to Mr. George Ensell, glassblower at the National Research Council of Canada, for the construction of the bellows manometer used in this project.

REFERENCES

1. R. E. Lund and D. E. Warnes. Trans. AIME, **209**, 608 (1957).
2. R. C. Haff. U.S. Patent No. 2,551,944 (April, 1947).
3. L. Wöhler, W. Plüddemann, and P. Wöhler. Ber. deut. chem. Ges. **41**, 703 (1908).
4. K. K. Kelley. U.S. Bur. Mines, Bull. No. 406, 66, 89 (1937).
5. R. Spence. Trans. Faraday Soc. **36**, 417 (1940).
6. S. N. Flengas and T. R. Ingraham. Can. J. Chem. **38**, 813 (1960).
7. Sir James Jeans. An introduction to the kinetic theory of gases. Cambridge Univ. Press, London. 1959. p. 251.
8. H. H. Kellogg. Private communication.
9. W. E. Evans and D. D. Wagman. J. Research Natl. Bur. Standards, **49**, 141 (1952).
10. K. K. Kelley. U.S. Bur. Mines, Tech. Papers, No. 688, 58 (1946).

Can. J. Chem. Downloaded from www.nrcresearchpress.com by 210.87.254.105 on 09/05/12
For personal use only.

Can. J. Chem. Downloaded from www.nrcresearchpress.com by 210.87.254.42 on 09/05/12
For personal use only.

STUDIES ON IONIC SOLVATION

PART III. NEW THEORY FOR CALCULATING HEATS OF HYDRATION OF MONOVALENT IONS AT 25° C[1]

A. M. AZZAM

ABSTRACT

From Part I of this series, the structure of solution around a completely hydrated monovalent ion could be visualized. On the basis of this picture, the ionic heats of hydration is to be due to three terms. These three terms are critically discussed and evaluated for the case of alkali metals and halide ions.

The present theory shows that the Born–Bjerrum term contributes a significant part to the heat and that the ionic radius value included in this term must be dependent only on the charge and not on the ionic size. The most probable value is 2.4 Å for the positive ions and 2.9 Å for the negative ions.

The calculated ionic heats of hydration, which are in good agreement with the experimental values, are compared with those of previous theories.

1. INTRODUCTION

The heat of solvation of an ion, which does not combine chemically with the solvent, depends upon the difference in its potential energy in vacuum and in solution. Knowledge of values of ionic heats of solvation is of great importance in the calculation of several physical properties of ionic solutions (9, 12, 15, 37, 41, 42, 44).

Using experimental data on the heats of solution (13, 14, 31), together with the crystal lattice energy values (8, 9, 10, 11, 16), and following Born–Haber cycle, the heats of hydration of alkali halides (see Table I) had been calculated (5, 12). There is no simple

TABLE I

Heats of hydration calculated from the different experimental values of the lattice energy and the heat of solution

Salt \ Reference	(12, 19, 31)	(5)	(37)	(40)
LiF	245.9	246	241.8	
LiCl	211.3	208.8	208.6	213
LiBr	202.5	199.9	197.6	202
LiI	192.4	189.1		191
NaF	217.6	213.9	214.7	
NaCl	184.2	182.4	181.5	183
NaBr	177.6	174.9	175.3	
NaI	167.0	165.5		
KF	198.8	194.6	193.1	206
KCl	165.2	161.5	159.9	159
KBr	157.7	154.5	148	153
KI	147	145.9		
RbF	190.7	187.9		
RbCl	158.9	156.4		
RbBr	151	147.2		
RbI	142.7	138.8		137
CsF		182.4		
CsCl		147.4		
CsBr		139.7		
CsI		131.1		133

[1]*Manuscript received April 14, 1960.*
Contribution from the Chemistry Department, Faculty of Science, A'in Shams University, Cairo, Egypt.

way of dividing these sums into the hydration energies of the separate ions. However, several attempts (3, 5, 6) have been made to deduce from these experimental values the corresponding ionic heats of solvation. None of these methods is completely satisfactory (12, 19, 20, 21).

Moreover, several workers (1, 2, 3, 4, 5, 6, 29, 33) have theoretically calculated the ionic heats of solvation with widely divergent results (see Table II). However, certain features of this work are not entirely satisfactory (7, 18, 19, 24, 46).

TABLE II

Theoretical values of ionic heats of solvation as calculated by different authors

Author / Ion	Group I		Group II				
	Bernal and Fowler (4)	Eley and Evans (3)	Latimer, Pitzer, and Slansky (5)	Verwey (6)	Miscenko (29)	Average of all methods	Azzam
Li^+	136	133	121.2		125	128.8	139.0
Na^+	114	115	94.6		98	105.4	107.9
K^+	94	90	75.8	75	78	83.3	84.6
Rb^+	87	81	69.2			79.4	79.5
Cs^+	80	73	62	53		67	75.1
F^-	97	91	122.6	122		108.2	106.7
Cl^-	65	59	88.7		88	75.2	71.7
Br^-	57	52	81.4		77	66.8	68.0
I^-	47	45	72.1	72	66	60.4	63.7

Recently, the present author (7, 36) suggested a new method for the calculation of ionic solvation number by applying statistical-mechanical analysis to a postulated structure of the solution around an ion. The good agreement between the calculated values and those obtained by several experimental methods is a strong evidence for the validity of the suggested physical approach of the molecular structure of the solvent (7, 36).

The present theory is an attempt to calculate the heats of hydration of alkali metals and halide ions at 25° C.

2. ORIENTATION OF A SOLVENT MOLECULE NEXT TO AN ION

It seems to be generally agreed (3, 4, 7, 46, 47, 49) that the orientation for a water molecule next to a positive ion is as shown in case I, Fig. 1. On the other hand, it has been assumed by previous theories (3, 4, 6, 47, 49) that the orientation for a water molecule next to a negative ion is as shown in case IV, Fig. 1. This configuration was criticized and critically discussed by the present author (7, 18). Accordingly, it was suggested that the most probable structure of the solvated negative ion is as shown in case III, Fig. 1.

A similar conclusion was reached recently by Buckingham (46). In conclusion, cases I and III are energetically more favorable. Less familiar orientations (6, 26, 34) have been already criticized (19, 24).

3. STRUCTURE OF SOLUTION AROUND AN ION

The most outstanding problem, which is connected with the calculation of ionic heats of hydration, lies in the need of definite quantitative knowledge of the structure of solution around an ion. A simple model for the structure of solution around an ion could

Can. J. Chem. Downloaded from www.nrcresearchpress.com by 210.87.254.42 on 09/05/12
For personal use only.

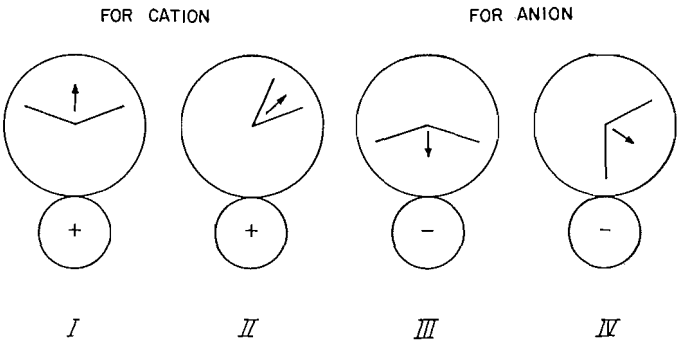


FIG. 1. Orientation of a water molecule next to an ion.

I	II	III	IV
Bernal and Fowler (4), 1933 Eley and Evans (3), 1938 Haggis *et al.* (49), 1952 Azzam (7), 1954 Buckingham (46), 1957	Verwey (6), 1941	Azzam (7), 1954 Buckingham (46), 1957	Bernal and Fowler (4),1933 Eley and Evans (3), 1938 Verwey (6), 1941 Haggis *et al.* (49), 1952

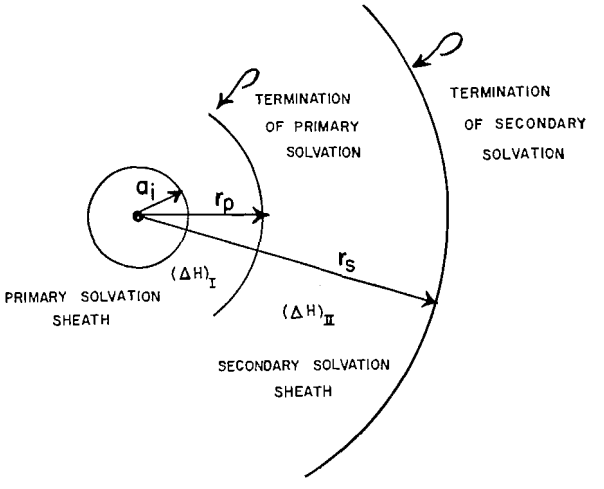


FIG. 2. The proposed structure of solution around a monovalent ion.
a_i = crystallographic radius of the ion,
r_p = radius of the primary solvated ion,
r_s = radius of the completely solvated ion.

be visualized from the present author's statistical–mechanical analysis (7) for the distribution of solvent dipoles around an ion.

The model suggested by these results is shown diagrammatically in Fig. 2. The firmly bound water molecules will be those constituting the primary solvation sheath (the innermost region). Beyond this sheath, there is the secondary solvation sheath with less firmly bound water molecules and finally there is the main bulk of the solvent (for definition see 7, 36).

Frank and Evans, from a re-analysis of the entropy of hydration (43), have developed a fundamentally similar picture. These authors claim that the ion is surrounded by three

Can. J. Chem. Downloaded from www.nrcresearchpress.com by 210.87.254.42 on 09/05/12
For personal use only.

concentric regions which are: the immobilization of water molecules, the structure-breaking and the structurally "normal" water regions. These three zones seem very probable to correspond with the three layers of the preceding model (see Fig. 2).

4. NEW THEORY FOR CALCULATING HEATS OF HYDRATION

From the proposed structure of ionic solution, the ionic heat of hydration is represented essentially by the sum of three terms corresponding to the three zones around an ion (see Fig. 2). It follows that

$$[1] \qquad \Delta H = (\Delta H)_{I} + (\Delta H)_{II} + (\Delta H)_{III}$$

where $(\Delta H)_{I}$ represents the contribution of water dipoles in the primary solvation sheath to (ΔH),

$(\Delta H)_{II}$ represents the contribution of water dipoles in the secondary solvation sheath to (ΔH),

$(\Delta H)_{III}$ represents the contribution of water dipoles beyond the solvation sheaths to (ΔH). In other words, it is the contribution of transferring an ion from the gas phase into solution.

The magnitudes of various contributions to ΔH for alkali metals and halide ions are discussed in Section 5 of this paper.

Concerning the structure of the primary solvation shell, a very clear physical picture, which is suitable for our purpose, is known from the present author's previous results (7). This is discussed in Section 3 of this paper. Accordingly the most probable value of $(\Delta H)_{I}$ could be evaluated.

The secondary solvation layer (see Fig. 2) is the intermediate zone between the frozen water (7, 18, 19, 41, 43) region and the normal structure region. Calculation of the term $(\Delta H)_{II}$ requires definite and quantitative knowledge of the structure-breaking effect (43, 48). Such a knowledge is not available. Any attempt to estimate the numerical magnitude of this structure-breaking effect must be based on rather arbitrary assumptions for which in the first instance no strict justification can be given.

As long as we consider the alkali metals and halide ions, it is not known whether or not, and to what extent, this structure-breaking effect is important in the calculation of heats of hydration. It seems very probable that such an order–disorder phenomenon is of significant importance for the calculations of entropies but not for the calculation of heats (49).

In the present theory, we will follow the most physical approach which was adopted by Buckingham (46) and treat the solvent beyond the primary solvation shell as a continuous dielectric, that is, a dielectric constant which can vary with the electric field strength.

We do not know how much error is involved in this approximation, but the effect is in any case of insignificant magnitude and could be checked in the following way.

CsI is usually regarded as having the relatively most marked structure-breaking effect (43, 45). In this case, $(\Delta H)_{II}$ contributes 8.7% to the total (ΔH). Assuming, as the result of neglecting the structure-breaking effect, a maximum of 25% error in the value of $(\Delta H)_{II}$, this will give rise to a maximum error of about 2.2% in the value of $(\Delta H)_{total}$.

A serious difficulty in the previous theories (3, 4, 5, 6, 8) is the choice of dielectric model. This problem was treated to a first approximation on the basis that very near to the ion the dielectric constant is taken as 1 and for layers of water molecules outside the first

Can. J. Chem. Downloaded from www.nrcresearchpress.com by 210.87.254.42 on 09/05/12
For personal use only.

layer it is taken as 80. In the present theory a less approximate treatment of the dielectric constant difficulty has been attempted by the application of Webb's analysis (2). It must be pointed out here that the structure-breaking effect, which is neglected in the present theory, is either partially or completely covered on using Webb's values for the dielectric constant as a function of distance.

5. VARIOUS CONTRIBUTIONS TO (ΔH)

(a) Evaluation of the Term $(\Delta H)_{\mathrm{I}}$

Consider an element volume (dv) at a distance (r) from an ion in the primary solvation sheath. If $(ds)_r$ is the number of dipoles associated with the ion in this element volume and $(u)_r$ is the ion–dipole interaction, it follows that

$$d(\Delta H) = (ds)_r\, u_r. \qquad [2]$$

The present author's statistical–mechanical analysis (7) showed that the number of dipoles associated with the ion in a concentric shell at a uniform distance (r) from the ion and of thickness (dr) is given by

$$(ds)_r = 4\pi n_0\, e^{-\{(w_r - w_0)/kT\}} r^2\, dr \qquad [3]$$

where

n_0 is the number of water molecules per cubic centimeter in the bulk of solution,
w_0 is the potential of a water molecule in the bulk of solution,
w_r is the net potential energy of a solvent dipole at a distance (r) from the ion.

Taking into account the specific factors on which the solvation number depends (7, 18), together with the suggested structure of a solvated ion, the net interaction energy term (w_r) could be evaluated from the following equation.

$$w_r = (u_1 - u_2 - u_3)_r \qquad [4]$$

where

u_1 is the ion–dipole interaction energy,
u_2 is the electrostatic potential due to the presence of the two water molecules attached to the dipole which is associated with the ion (3, 4, 7, 36), and
u_3 is to allow for the mutual effect of the co-ordinated water molecules.

Substituting from [3] into [2]

$$d(\Delta H_{\mathrm{I}})_r = 4\pi n_0\, u_r\, e^{-\{(w_r - w_0)/kT\}} r^2\, dr. \qquad [5]$$

The contribution of water molecules in the primary solvation sheath could be evaluated by integrating equation [5] over the volume of the solvent that surrounds the ion from a_1 to r_{p} (limits of primary solvation (see Fig. 1)).

$$(\Delta H)_{\mathrm{I}} = 4\pi n_0 \int_{a_1}^{r_{\mathrm{p}}} u_r\, e^{-\{(w_r - w_0)/kT\}} r^2\, dr. \qquad [6]$$

(b) Evaluation of the Term $(\Delta H)_{\mathrm{II}}$

This term could be evaluated in a similar manner as in the case of $(\Delta H)_{\mathrm{I}}$. The main differences between the two cases lie in the values of the limits of integration and also in the expression of the term (w_r). A solvent molecule in the secondary solvation sheath is no longer associated with the ion (4, 7, 12, 19) but it is only under the influence of its field.

Can. J. Chem. Downloaded from www.nrcresearchpress.com by 210.87.254.42 on 09/05/12
For personal use only.

[7] $$d(\Delta H)_{II} = 4\pi n_0 u_r e^{-\{(u_r - w_0)/kT\}} r^2 dr.$$

The integration will be carried out over the volume of the solvent that surrounds the ion from the distance at which the primary solvation ceases (r_p) to the distance at which secondary solvation terminates (r_s).

From the above discussion, it follows that

[8] $$(\Delta H)_{II} = 4\pi n_0 \int_{r_p}^{r_s} u_r e^{-\{(u_r - w_0)/kT\}} r^2 dr.$$

(c) Evaluation of the Term $(\Delta H)_{III}$

Whenever an ion passes from the gas phase into solution, the free energy of this process is best given by Born expression (1),

[9] $$\Delta G = -\frac{N(Ze)^2}{2x}\left(1-\frac{1}{D}\right),$$

where N is the Avogadro's number,
Ze is the charge of the ion,
x is the radius of the ion,
D is the dielectric constant of the medium.

The corresponding heat of hydration (Q) is obtained from the Gibbs–Helmholtz equation as

[10] $$Q = -\frac{N(Ze)^2}{2x}\left\{1-\frac{1}{D}-\frac{T}{D^2}\left(\frac{\partial D}{\partial T}\right)_p\right\}$$

(Born–Bjerrum equation) (32).

The term $(\Delta H)_{III}$ of the present theory (see equation [1]) can be evaluated from equation [10] provided that the selected value of "x" will be taken as r_s (the termination of solvation). It follows that

[11] $$(\Delta H)_{III} = -\frac{N(Ze)^2}{2r_s}\left\{1-\frac{1}{D}-\frac{T}{D^2}\left(\frac{\partial D}{\partial T}\right)_p\right\}.$$

(d) Evaluation of the Ionic Heats of Hydration

On substituting from equations [6], [8], and [11] into (1), the total ionic heat of hydration is given by

[12] $$(\Delta H)_{total} = 4\pi n_0 \int_{a_1}^{r_p} u_r e^{-\{(w_r - w_0)kT\}} r^2 dr + 4n_0 \int_{r_p}^{r_s} u_r e^{-\{(u_r - w_0)kT\}} r^2 dr + \frac{N(Ze)^2}{2r_s}\left\{1-\frac{1}{D}-\frac{T}{D^2}\left(\frac{\partial D}{\partial T}\right)_p\right\}.$$

6. METHOD OF CALCULATION

Methods of evaluations of u_1, u_2, u_3, r_p, r_s, n_0, w_0, and w_r have already been critically discussed in a previous paper (7) by the present author. It must be pointed out that in these calculations, microscopic values of the dielectric constant (2, 7) of water at different distances from the ion are used.

The integration terms of equation [12] cannot be evaluated directly. However, these integrations were solved graphically.

Can. J. Chem. Downloaded from www.nrcresearchpress.com by 210.87.254.42 on 09/05/12
For personal use only.

All data which are needed for the calculation of the term $(\Delta H)_{\mathrm{I}}$ are recorded in Table III. The corresponding relation

$$u_r e^{-\{(w_r-w_0)/kT\}r^2} - r,$$

which is required for the graphical evaluation of $(\Delta H)_{\mathrm{I}}$ (see equation [6]), is plotted in Fig. 3.

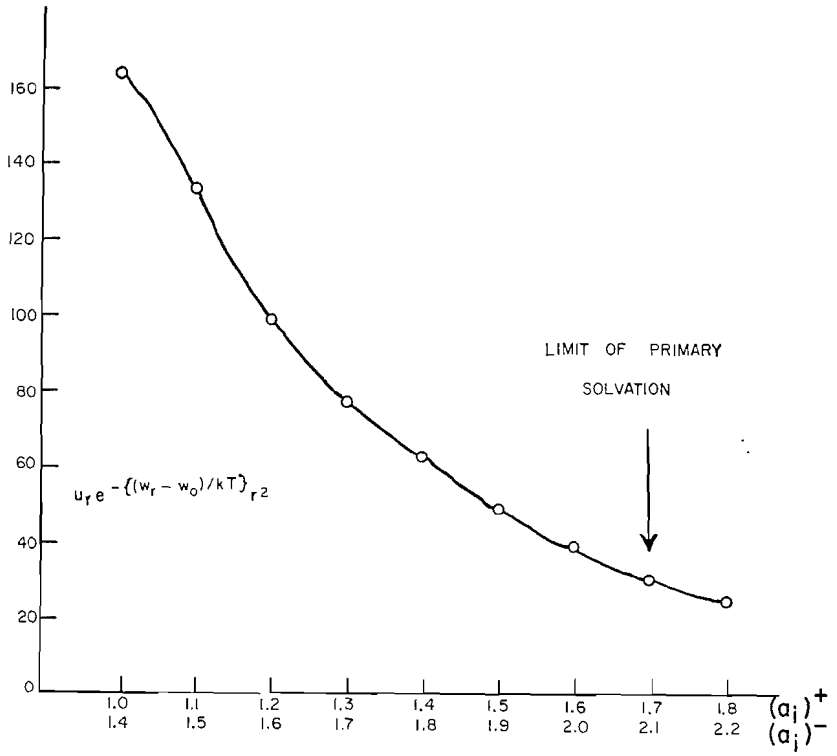


FIG. 3. The relation between $u_r e^{-\{(w_r-w_0)/kT\}r^2}$ and ionic radii.

TABLE III

Data needed for the calculation of $(\Delta H)_{\mathrm{I}}$

a_i	u_1	u_2	u_3	$e^{-\{(w_r-w_0)/kT\}r^2}$	$u_r e^{-\{(w_r-w_0)/kT\}r^2}$, kg cal/g ion	$(\Delta H)_{\mathrm{I}}$
1.0	0.1490	0.012	0.0291	76.5	164.14	6.93
1.1	0.1323	0.0116	0.0194	70.1	133.36	5.63
1.2	0.1168	0.0113	0.0138	59.5	99.74	4.22
1.3	0.1047	0.011	0.0094	51.6	77.8	3.28
1.4	0.0937	0.0107	0.0061	47.1	63.55	2.68
1.5	0.0836	0.0105	0.0044	41.2	49.6	2.09
1.6	0.0751	0.0104	0.0032	36.7	39.69	1.68
1.7	0.0667	0.0102	0.0025	32.3	31.02	1.31
1.8	0.06	0.0101	0.0019	29.6	25.58	1.08

The area underneath this curve between the specific limits is equal to $(\Delta H)_{\mathrm{I}}/4\pi n_0$. Similarly, all data which are required for the evaluation of the term $(\Delta H)_{\mathrm{II}}$ are given in Table IV and the required graphical relation is plotted in Fig. 4. The area underneath

Can. J. Chem. Downloaded from www.nrcresearchpress.com by 210.87.254.42 on 09/05/12
For personal use only.

Can. J. Chem. Downloaded from www.nrcresearchpress.com by 210.87.254.42 on 09/05/12
For personal use only.

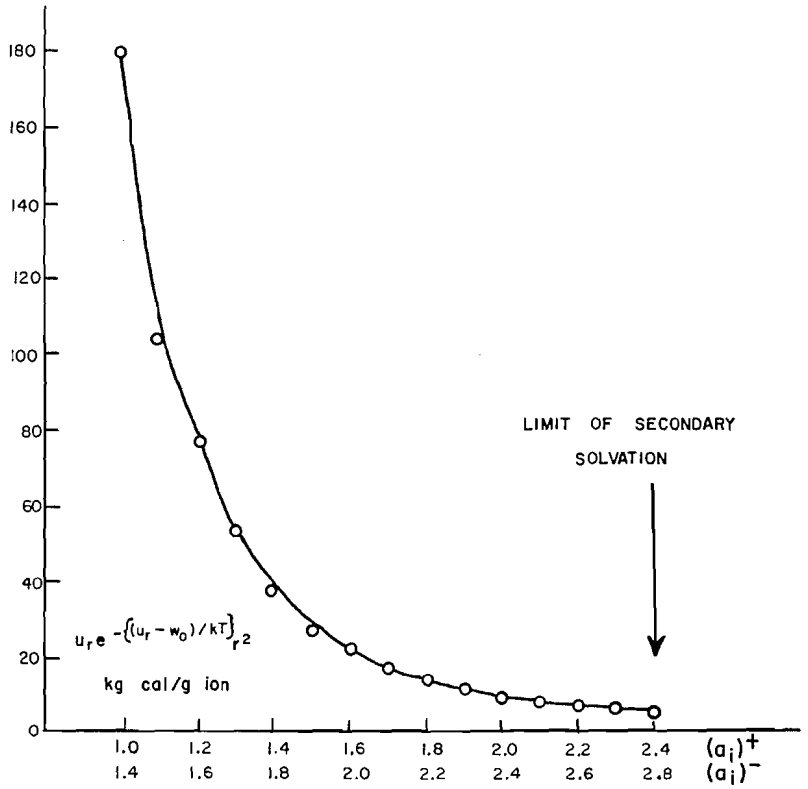


FIG. 4. The relation between $u_r e^{-\{(u_r - w_0)/kT\}} r^2$ and ionic radii.

TABLE IV

Data needed for the calculation of $(\Delta H)_{II}$

a_i	u_1	$e^{-\{(u_r - w_0)/kT\}} r^2$	$u_r e^{-\{(u_r - w_0)/kT\}} r^2$ kg cal/g ion	$(\Delta H)_{II}$
1.0	0.1490	198.0	179.3	48.6
1.1	0.1323	141.6	113.9	35.4
1.2	0.1168	109.4	77.6	25.8
1.3	0.1047	83.5	53.3	19.9
1.4	0.0937	67.0	38.1	15.2
1.5	0.0836	54.3	27.6	12.9
1.6	0.0751	49.5	22.6	9.1
1.7	0.0667	42.8	17.5	6.9
1.8	0.0600	38.7	14.1	5.2
1.9	0.0539	35.3	11.6	3.9
2.0	0.0482	32.5	9.5	2.9
2.1	0.0437	30.7	8.2	2.0
2.2	0.0399	29.7	7.2	1.2
2.3	0.0369	28.5	6.3	0.6
2.4	0.0322	27.2	5.2	0.0

this curve between the specific limits is equal to $(\Delta H)_{II}/4\pi n_0$. The theoretically calculated values of $(\Delta H)_I$, $(\Delta H)_{II}$, $(\Delta H)_{III}$, and $(\Delta H)_{total}$ for all the alkali metals and the halide ions are shown in Table V and the corresponding relationships to ionic radius are represented graphically in Fig. 5.

Can. J. Chem. Downloaded from www.nrcresearchpress.com by 210.87.254.42 on 09/05/12
For personal use only.

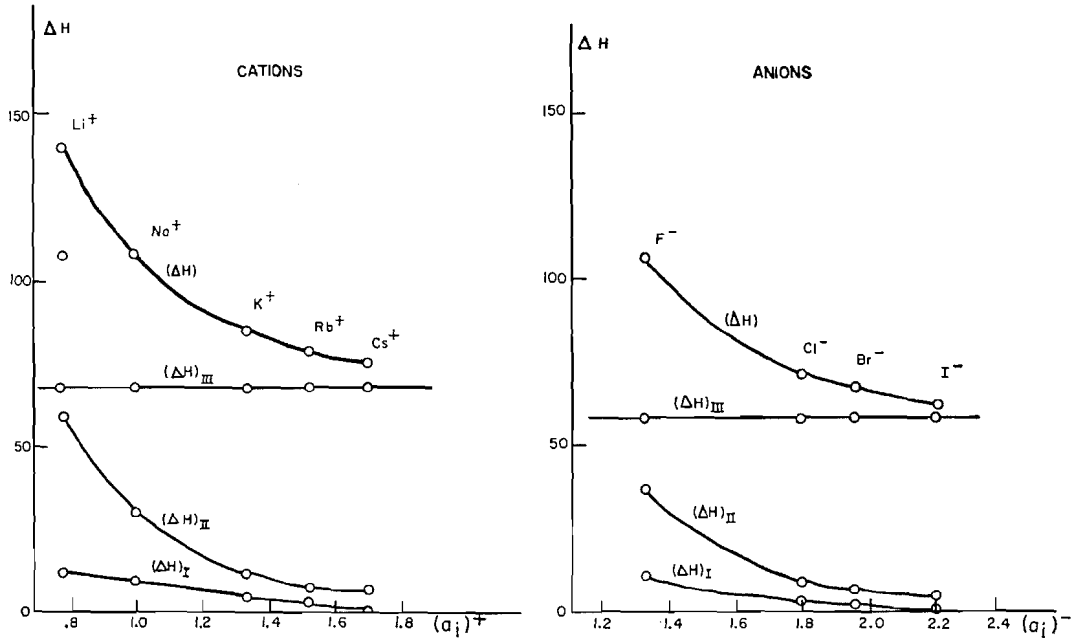


FIG. 5. Theoretically calculated values of $(\Delta H)_{I}$, $(\Delta H)_{II}$, $(\Delta H)_{III}$, and $(\Delta H)_{total}$ for the alkali metals and halide ions.

TABLE V

Theoretically calculated ionic heats of solvation using equation [12] (in kg cal/g ion at 25° C)

	Cations					Anions			
	Li^+	Na^+	K^+	Rb^+	Cs^+	F^-	Cl^-	Br^-	I^-
a_i	0.78	1.00	1.33	1.52	1.7	1.33	1.8	1.96	2.2
$(\Delta H)_{I}$	12.6	9.7	4.5	2.8		11.2	3.7	2.5	
$(\Delta H)_{II}$	59.0	30.0	12	7.5	6.9	37	9.5	7.0	5.2
$(\Delta H)_{III}$	68.2	68.2	68.2	68.2	68.2	58.5	58.5	58.5	58.5
$(\Delta H)_{total}$	139.8	107.9	84.7	78.5	75.1	106.7	71.7	68.0	63.7

7. DISCUSSION

The various theoretical calculations of ionic heats of solvation (3, 4, 5, 6, 29) do not give values which are in good agreement (see Table IV). However, some measure of agreement is obtained among the results if they are classified in such a way as to compare theories which are self-consistent. Accordingly, previous theories could be divided into two main groups:

group I: (1) Bernal and Fowler theory, (2) Eley and Evan theory;
group II: (1) Latimer *et al.* theory, (2) Verwey theory, (3) Miscenko theory.

A comparison between the results of the present theory and those of previous theories is of interest. The most important fact which arises from this analysis is that theories of group I give higher values for the positive ions, lower values for the negative ion while theories of group II show the reverse. It follows that the agreement of the present calculation with the average values of all previous theories is good (see Table II).

Can. J. Chem. Downloaded from www.nrcresearchpress.com by 210.87.254.42 on 09/05/12
For personal use only.

The numerically calculated values of ionic heats of hydration from the theories of group II (mainly that of Latimer *et al.*) disagree with those of the present theory. Their values for the positive ions are smaller by about 10–18 kg cal/g ion. On the other hand, their values for the negative ions are higher by about 10–18 kg cal/g ion. This is mainly due to an incorrect assumption in the method of calculation (19, 21). However, these authors claim that the validity of their theories rest upon the comparison of their values with experimental values which have been obtained by a procedure in which the validity of the theory under test is assumed (12, 18, 19, 20, 21, 23, 24). Moreover, their results disagree markedly with those of theories of group I which are apparently theoretically valid.

It is of interest to compare values obtained from the present theory with those from theories of group I. Table IV shows that all the group I values of the negative ions are lower by about 10–18 kg cal/g ion^{-1}. The fundamental reason for this difference is that the orientation of a water molecule near an anion, which is postulated in the present work, differs from that of authors of theories of group I (see Fig. 1) (7, 46). However, if the present author's model, which was successfully used in the calculation of ionic solvation number (7), is used in these authors procedures, values of the correct order could be obtained.

On the other hand, numerical values of Bernal and Fowler for the case of cations are in agreement with those of the present theory. The model of orientation of a water molecule near a cation is the same in both theories of Bernal and Fowler, and theories of the present author. This fact is a further supporting evidence for the explanation of the discrepancy found in the case of anions.

Using the same model as that of Bernal and Fowler, but subjecting the theory to a more vigorous treatment, Eley and Evans' calculated values show a better agreement with those of the present theory (see Table IV).

The small difference in the case of cations between the present theory and those of the theories of group I may be the consequence of the very approximate treatment given by these authors to the variation of dielectric constant with distance in which two zones were considered. The first layer near an ion is assumed to have $D = 1$ whereas the value $D = 80$ is used elsewhere. This picture is oversimplified (2, 7, 12, 18, 19, 27, 28, 35).

In conclusion, there is an essential agreement between the results of the present theory and those of the more reliable theories of group I.

It is to be stressed that some of the previous theories suffer from mixing of heat and free energy terms which may introduce an ambiguity of 3 to 30 kcal (19). However, this was avoided in the present theory (38).

The real test is to compare theoretically calculated and experimental values, but experimental values of ionic heats of hydration cannot be directly measured. The problem of evaluating individual heats of solvation depends on the assumption used in dividing up the experimental values. None of these methods can be considered as completely satisfactory (12, 19, 20, 21, 46). This difficulty hinders the checking of the theoretical values. However, the present theory can be verified by adding up the calculated ionic values to give values for the corresponding salts which can be then compared with the most reliable experimental results. This method of checking can only be applied to the present theory and to Eley and Evans' theory since all the other theories are semi-empirical ones (they depend on experimental values).

The good agreement which is shown in Table VI is a further indication of the validity of the present theory.

TABLE VI

Comparison between the theoretically calculated and experimentally determined values of heats of hydration of alkali halides

Salt	Results of experimental methods (mean of four sets (see Table I))	Theoretically calculated values	
		Azzam	Eley and Evans' theory (3)
LiF	244.4	245.7	224
LiCl	210.4	210.7	192
LiBr	200.5	207	185
LiI	190.8	202.7	178
NaF	215.4	214.6	206
NaCl	182.8	179.6	174
NaBr	175.9	175.9	167
NaI	166.3	171.6	160
KF	198.1	191.3	185
KCl	161.4	156.3	153
KBr	153.5	152.6	146
KI	146.5	148.3	139
RbF	189.3	186.2	172
RbCl	157.6	151.2	140
RbBr	149.1	147.5	133
RbI	139.1	143.2	126
CsF	182.4	181.8	164
CsCl	147.4	146.8	132
CsBr	139.7	143.1	125
CsI	132.0	138.8	118

8. "THE THIRD TERM OF EQUATION 12" BORN'S HEAT TERM

One of the most important conclusions arising from the present work is that the third term of equation [12] makes a significant contribution to the ionic heats of solvation (see Table V). Accordingly, a discussion of this term which has been used in all previous theories (1, 2, 3, 4, 5, 6) is of interest.

The main difficulty, which arises in the application of equations [9] and [10] in the calculation of ionic solvation energies, is the choice of the ionic radius (term x).

A list of the selected values of "x" in the different theories, which calculated the ionic solvation energies of alkali metal and halide ions, is as follows:

Theory	Selected value of x in Å	Remarks
Born (1)	a_i	Crystallographic radius
Latimer *et al.* (5)	$a_i+0.1$ (for anions) $a_i+0.85$ (for cations)	Assuming that $[\Delta G\ \alpha(1/r)]$
Eley and Evans (3)	$a_i+2r_{H_2O}$ ($2r_{H_2O} = 2.76$)	Arbitrary
Verwey (6)	$a_i+2r_{H_2O}$	Arbitrary
Bernal and Fowler (4)	2.9	Empirically
Azzam	2.4 (for cations) 2.8 (for anions)	Statistical–mechanical limit of solvation

With the exception of Bernal and Fowler and the present author's theories, the selected value of (x) is a function of the crystallographic ionic radii. Evidence given by these

Can. J. Chem. Downloaded from www.nrcresearchpress.com by 210.87.254.42 on 09/05/12
For personal use only.

authors in support of their selections are not completely satisfactory and have been criticized (4, 12, 19, 21, 22).

Bernal and Fowler suggested that "x" should represent the radius of the saturation sphere around the ion and pointed out that it must be dependent only on the charge and not on the ionic size. A similar picture has been given by Passynaski (39).

Bernal and Fowler suggested the value of 2.9 Å as the radius of the saturation sphere. There is an essential agreement between Bernal and Fowler's value and those of the present theory. The small differences in these values may arise from the very approximate treatment given by Bernal and Fowler (7, 19). Furthermore, Bernal and Fowler have derived their value 2.9 Å empirically while the values given in the present theory (2.4 and 2.8 Å) were calculated statistically–mechanically. Moreover, Bernal and Fowler did not differentiate between the case of cations and anions as in the present theory. However, due to the difference in the mode of orientation of water dipoles in the case of cations and the case of anions we should expect different values of the radius of the saturation sphere.

9. GENERAL REMARKS

It must be pointed out that all calculations of this kind by the author and by previous workers are beset with inherent difficulties (46, 47). The most important ones are probably the ordered structure of water, the effect of ions on it, and the time factors involved in the movement of water molecules near an ion.

This is mainly due to our incomplete state of knowledge of polar dielectrics. However, with the aid of some reasonable assumptions, it has been found possible to make successful attempts. These limitations must be borne in mind in judging the quantitative conclusions for such calculations.

10. CONCLUSIONS

1. Three layers around an ion contribute to ionic heats of solvation. These layers are:
   - (*a*) primary solvation sheath with contribution = $(\Delta H)_{\mathrm{I}}$,
   - (*b*) secondary solvation sheath with contribution = $(\Delta H)_{\mathrm{II}}$,
   - (*c*) main body of water with contribution = $(\Delta H)_{\mathrm{III}}$.
2. The following critical conditions have been derived:

Conditions	Remarks	$(\Delta H)_{\text{total}}$
Monovalent cations with radius less than 1.7 Å Monovalent anions with radius less than 2.1 Å	Primary and secondary hydrated	$(\Delta H)_{\mathrm{I}}+(\Delta H)_{\mathrm{II}}+(\Delta H)_{\mathrm{III}}$
Monovalent cations with radius less than 2.4 and greater than 1.7 Å Monovalent anions with radius less than 2.8 and greater than 2.1 Å	Secondary hydrated	$(\Delta H)_{\mathrm{II}}+(\Delta H)_{\mathrm{III}}$
Monovalent ions with radius beyond the above-mentioned limits	Unhydrated	$(\Delta H)_{\mathrm{III}}$

Can. J. Chem. Downloaded from www.nrcresearchpress.com by 210.87.254.42 on 09/05/12
For personal use only.

3. Both $(\Delta H)_{I}$ and $(\Delta H)_{II}$ can be calculated by statistical-mechanical analysis, while $(\Delta H)_{III}$ is best obtained from the Born-Bjerrum equation.

4. The effective radius term of Born-Bjerrum term is theoretically found to be 2.4 Å for cations and 2.8 Å for anions.

5. Theoretically calculated ionic heats of solvation are in good agreement with experimental values.

6. This theory supports the suggested physical approach concerning the orientation of a water molecule next to an ion and the structure of ionic solutions.

REFERENCES

1. M. Born. Verhandl. deut. physik. Ges. **21**, 13, 679 (1919).
   F. Haber. Verhandl. deut. physik. Ges. **21**, 750 (1919).
   K. Fajans. Verhandl. deut. physik. Ges. **21**, 549, 709 (1919).
   M. Born. Z. physik, **1**, 45 (1920).
2. T. J. Webb. J. Am. Chem. Soc. **48**, 2589 (1926).
3. D. D. Eley and M. G. Evans. Trans. Faraday Soc. **34**, 1093 (1938).
4. J. D. Bernal and R. H. Fowler. J. Chem. Phys. **1**, 515 (1933).
5. W. M. Latimer, K. S. Pitzer, and C. M. Slansky. J. Chem. Phys. **7**, 108 (1939).
   W. M. Latimer, K. S. Pitzer, and W. V. Smith. J. Am. Chem. Soc. **60**, 1829 (1938); J. Chem. Phys. **23**, 90 (1955).
   R. E. Powell and W. Latimer. J. Chem. Phys. **9**, 1139 (1951).
6. E. J. W. Verwey. Rec. trav. chim. **61**, 127 (1942).
   E. J. W. Verwey. Rec. trav. chim. **60**, 887 (1941).
7. A. M. Azzam. Z. Elektrochem. **58**, 889 (1954).
8. M. L. Huggins. J. Chem. Phys. **5**, 143 (1937).
9. H. Falkenhagen. Electrolyte, Leipzig. 1953.
10. E. Lange. Z. physik. Chem. **116**, 337 (1925).
11. J. Slater. Phys. Rev. **23**, 488 (1924).
12. G. Kortüm and J. Bockris. Textbook of electrochemistry. Elsevier. 1951.
13. F. Bichowski and F. D. Rossini. Thermochemistry of chemical substances. New York. 1936.
14. Landolt-Börnstein. Physikalisch-Chemische Tabellen. Springer, Berlin. p. 1505.
15. E. A. Moelwyn-Hughes. Physical chemistry. Cambridge University Press. 1947.
16. A. E. Van Arkel and J. H. de Boer. Chemical binding. Leipzig. 1931.
17. E. A. Moelwyn-Hughes. Proc. Cambridge Phil. Soc. **45**, 477 (1949).
18. A. M. Azzam. Thesis, London. 1949.
19. J. Bockris. Modern aspects of chemistry. London. 1954.
20. K. Fajans. Z. Elecktrochem. **34**, 502 (1928).
21. A. N. Frumkin. J. Chem. Phys. **7**, 552 (1939).
22. Strehlow. Z. Elecktrochem. **56**, 119 (1952).
23. D. Eley. Trans. Faraday Soc. **35**, 1281 (1939).
24. E. S. Compell. J. Chem. Phys. **20**, 1411 (1952).
25. Symposium on Hydrophobic Colloids, Utrecht. 53 (1937).
26. E. J. W. Verwey. Chem. Weekblad, **37**, 530 (1940).
27. H. Franck. J. Am. Chem. Soc. **63**, 1789 (1941).
28. J. Malsch. Z. Physik, **30**, 837 (1929).
29. K. P. Miscenko. Acta Physicochim. U.R.S.S. **3**, 693 (1935).
30. O. Klein and E. Lange. Z. Elecktrochem. **43**, 570 (1937).
31. G. Scatchord. J. Chem. Phys. **9**, 34 (1941).
    A. Eucken. Test book of chemical physics II, 2, 992. Leipzig. 1944.
    G. Scatchord. J. Am. Chem. Soc. **53**, 2037 (1931).
32. N. Bjerrum and Larsson. Z. physik. Chem. **127**, 358 (1927).
33. E. A. Moelwyn-Hughes. Proc. Cambridge Phil. Soc. **45**, 477 (1949).
34. J. Lennard-Jones and J. A. Pople. Proc. Roy. Soc. (London), A, **205**, 155, 161 (1951).
35. Debye. Marx Handbuch der Radiologie. Leipzig. 6, 618, 680. 1925.
    C. H. Collie, J. B. Hasted, and D. M. Ritson. J. Chem. Phys. **16**, 1 (1948).
    G. Schwartzenbach. Z. phys. Chem. A, **176**, 133 (1936).
36. A. M. Azzam. Can. J. Chem. **38**, 993 (1960).
37. J. A. V. Butler. Chemical thermodynamics. Macmillan, London. 1946.
38. H. Remy. Inorganic chemistry, Elsevier. 1956.
39. A. Passynsky. Acta Physicochim. U.R.S.S. **8**, 385 (1938).
40. P. Darmois. J. phys. radium, **2**, 2 (1941).
41. Interaction in Ionic Solutions. Discussions Faraday Soc. No. 24 (1957).
42. G. Milazzo. Elecktrochemie, Theoretische Grundlagen und Anwendunigen. Vienna. 1952.
    H. Harned and B. Owen. The physical chemistry of electrolytic solutions. Reinhold, New York. 1950.
43. H. S. Frank and M. G. Evans. J. Chem. Phys. **13**, 507 (1945).
    H. S. Robinson and A. L. Robinson. J. Chem. Phys. **8**, 933 (1940).
    H. S. Frank and Wen-Yang Wen. Discussions Faraday Soc. No. 24, 133 (1957).

Can. J. Chem. Downloaded from www.nrcresearchpress.com by 210.87.254.42 on 09/05/12
For personal use only.

44. R. GURNEY. Ionic processes in solution. McGraw-Hill, New York. 1953.
45. D. D. ELEY. Discussions Faraday Soc. No. 24, 219 (1957).
46. A. D. BUCKINGHAM. Discussions Faraday Soc. No. 24, 151 (1957).
47. C. A. COULSON and D. H. EVERETT. Trans. Faraday Soc. **36**, 633 (1940).
48. A. EUCKEN. Z. Elektrochem. **51**, 6 (1948).
49. G. H. HAGGIS, J. B. HASTED, and T. J. BUCHANAN. J. Chem. Phys. **20**, 1452 (1952).

Can. J. Chem. Downloaded from www.nrcresearchpress.com by 210.87.254.42 on 09/05/12
For personal use only.

Can. J. Chem. Downloaded from www.nrcresearchpress.com by 210.87.254.6 on 09/05/12
For personal use only.

2,3-*O*-ISOPROPYLIDENE-L-ERYTHROTETRURONIC ACID AND -L-ERYTHROSE, AND THE METHYL D-ERYTHRO- AND D-THREO-TETROFURANOSIDES[1]

J. N. BAXTER[2] AND A. S. PERLIN

ABSTRACT

Oxidation of 2,3-*O*-isopropylidene-β-L-rhamnose (I) with hypoiodite, followed by periodate cleavage of the derived aldonic acid, affords 2,3-*O*-isopropylidene-L-*erythro*tetruronic acid. Reduction of I with sodium borohydride and periodate oxidation of the resulting glycitol gives 2,3-*O*-isopropylidene-L-erythrose. Both products have been obtained in high yield, and are readily hydrolyzed to L-*erythro*tetruronic acid and L-erythrose, respectively.

Methyl α- and β-D-*erythro*- and D-*threo*-tetrofuranosides have been prepared by the Fischer glycoside synthesis from D-erythrose- and D-threose-formates, respectively. A notable anomeric difference in the lead tetraacetate oxidation behavior of the methyl D-threosides has been observed, the β-anomer being more reactive than the α-anomer.

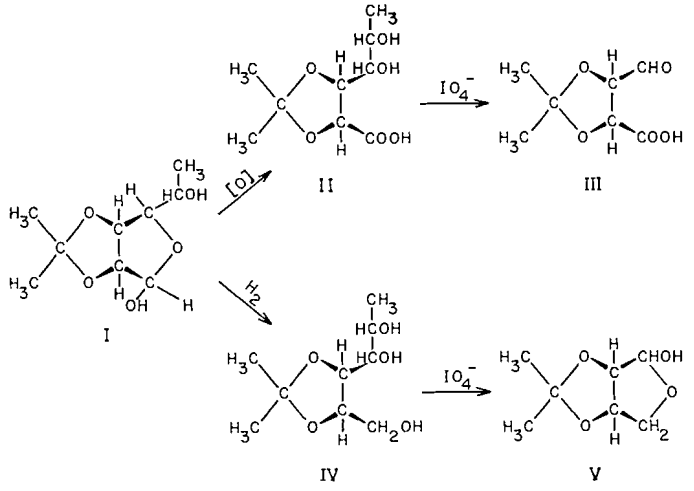
In continuing earlier studies in this laboratory on the chemistry of the tetrose sugars (1, 2, 3, 4) several new tetrose derivatives have been prepared and are described in the current paper.

Stepwise degradation of D-glucuronic and D-galacturonic acids to D-*erythro*- and D-*threo*-tetruronic acids, respectively, by lead tetraacetate oxidation has been described previously (3). Since the L-isomers of these hexuronic acids are rare compounds, they do not provide practical sources of the L-tetruronic acids. The L-*threo*-isomer has been prepared by selective reduction of 2,3-di-*O*-acetyl-L-tartaric anhydride (5) and by oxidative degradation of D-glucosaccharo-γ-lactone (6), but the L-*erythro*-acid does not appear to have been reported. In the current paper a method is described for preparing L-*erythro*tetruronic acid from readily available 2,3-*O*-isopropylidene-L-rhamnose (7) (I). The latter derivative also has been utilized to prepare L-erythrose in high yield.

Acetonation of L-rhamnose in the presence of hydrogen chloride (7) appears to yield the 2,3-*O*-isopropylidene derivative almost exclusively. Two crystalline forms of monoacetone L-rhamnose have been described (8, 9) but only the β-anomer (9) has been isolated in the present study. The isopropylidene derivative (I) was oxidized with hypoiodite (10) to the L-rhamnonate (II) and the latter, which was not isolated, was degraded by periodate cleavage. From the reaction mixture crystalline 2,3-*O*-isopropylidene-L-*erythro*tetruronic acid (III) was isolated in about 75% yield. Chromatographically pure L-*erythro*tetruronic acid was readily obtained by autohydrolysis of III in aqueous solution.

Reduction of isopropylidene-β-L-rhamnose (I) to the rhamnitol derivative (IV), followed by periodate oxidation, afforded crystalline 2,3-*O*-isopropylidene-L-erythrose (V) in about 80% yield. The L-glycitol derivative (IV) was obtained as a syrup by catalytic hydrogenation but, with sodium borohydride reduction, attempts to isolate it resulted in partial hydrolysis of the isopropylidene group. For preparation of V, however, it was most convenient to carry out the reduction with borohydride and, after neutralizing the reaction mixture, to continue directly with the periodate cleavage step. Such a procedure was used by Ballou (11) in converting 3,4-*O*-isopropylidene-D-arabinose to the D-isomer

[1]*Manuscript received June 23, 1960.*
Contribution from the National Research Council of Canada, Prairie Regional Laboratory, Saskatoon, Saskatchewan. Presented in part at the 4th Western Regional Conference, Chemical Institute of Canada, Winnipeg, September 4, 1958.
Issued as N.R.C. No. 5988.
[2]*National Research Council of Canada Postdoctorate Fellow, 1956–1958.*

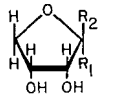


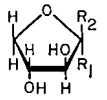
of V. Ballou's method, it will be noted, can also readily furnish V itself by starting with L-arabinose, but the required isopropylidene-pentose derivative is less readily prepared than is the monoacetone-L-rhamnose used in the current study.

Hydrolysis of 2,3-*O*-isopropylidene-L-erythrose with dilute acid afforded chromatographically pure L-erythrose. The calculated $[\alpha]_D$ of the latter sugar was +39°, somewhat higher numerically than most values reported earlier for the D- or L-isomer (see ref. 1 and references cited therein), but close to the value of $[\alpha]_D$ −41° found by Schaffer for D-erythrose derived from crystalline 2,4-*O*-ethylidene-D-erythrose dimer (12). These higher values, together with rotational data obtained by hydrolysis of the methyl D-erythrosides (see below), indicate that the specific rotation of D- or L-erythrose is −38° or +38° (±3°).

The current procedure for preparing L-erythrose may be found more satisfactory than previous means for obtaining this tetrose. Of other methods available the sulphone degradation (13) of diethyl dithio-L-arabinose affords the highest over-all yield of chromatographically pure L-erythrose (13), although the low specific rotation ($[\alpha]_D$ +23°) recorded for the syrupy product (13) suggests the presence of an undetected impurity.

Hockett and Maynard (15) found that D-erythrose reacts with methanolic hydrogen chloride (16) to form a mixture of the α- and β-furanosides (VII and VIII) rather than the dimethyl acetal or dimeric products, in this respect resembling more closely the higher-order sugars rather than DL-glycerose (17). In the current study it was of interest to isolate the isomeric tetrosides, which represent the simplest of the true glycosides. Di-*O*-formyl-D-erythrose (1), in 1% methanolic hydrogen chloride at room temperature, was rapidly deacylated and converted to a mixture of the glycosides. The anomeric compounds were readily distinguished on paper chromatograms (which showed also that





VI $R_1 = OCH_3$, $R_2 = H$

VII $R_1 = H$, $R_2 = OCH_3$

VIII $R_1 = OCH_3$, $R_2 = H$

IX $R_1 = H$, $R_2 = OCH_3$

Can. J. Chem. Downloaded from www.nrcresearchpress.com by 210.87.254.6 on 09/05/12
For personal use only.

Can. J. Chem. Downloaded from www.nrcresearchpress.com by 210.87.254.6 on 09/05/12
For personal use only.

other products were produced in only minor proportions), and were separated by chromatography on a cellulose column. The ratio of α- to β-anomer formed was about 1 to 3, whereas Hockett and Maynard found the ratio to be about 4 to 5 (15) and, recently, Ballou (18) has reported that the β-anomer is produced almost exclusively. In all three instances the reaction conditions used appear to have been similar and no explanation is offered to account for these wide variations. It may be noted, however, that the *trans*-β-glycoside always predominates in the mixtures.

Both glycosides were isolated as analytically pure syrups and characterized by optical properties and glycol-cleavage oxidation. Methyl β-D-erythroside was smoothly converted to a 2,3-cyclic carbonate, and a di-*p*-nitrobenzoate of the α-anomer was prepared. On hydrolysis with dilute aqueous acid each glycoside afforded chromatographically pure D-erythrose, the calculated specific rotation of the latter being $[\alpha]_D$ $-36°$ to $-39°$.

For the preparation of methyl α- and β-D-*threo*-tetrofuranosides (IX and X), di-*O*-formyl-D-threose (2) was treated with methanolic hydrogen chloride as for the corresponding D-erythrose derivative. The specific rotation of the syrupy product and of the dialdehydes derived by periodate oxidation indicated that the α- and β-glycosides were formed in a ratio of about 3 to 2. The mixture was not well resolved on paper chromatograms and only a partial separation was effected on a cellulose column. Presence of two major components in the reaction mixture in the ratio given above was demonstrated more satisfactorily by gas–liquid chromatography* and small analytically pure samples of the α- and β-threosides were obtained by this chromatographic method. Methyl α-D-threoside was isolated also via the mixture of derived di-*p*-nitrobenzoates by fractional crystallization and deacylation.

The possibility of preparing methyl α-D-threoside by means of the Koenigs–Knorr reaction (20) was examined briefly. Extensive studies on the halides of *O*-acyl-pentofuranoses (21) have shown that the 1,2-*trans*-glycoside is generally formed starting with either the α- or β-halide. Applied to the D-*threo*furanose series, formation of the α-glycoside was to be expected. Tri-*O*-acetyl-D-threofuranose (22) was accordingly treated with hydrogen bromide in acetic acid, yielding an unstable syrupy product which appeared to contain both anomeric bromides. Reaction of this material with methanol, either in the presence or absence of silver oxide, led to formation of the mixed α- and β-glycosides, with the former predominating. Under the conditions used, therefore, the reaction was less stereospecific than usually encountered with the higher sugars and did not constitute a satisfactory preparative procedure.

The behavior of the various glycosides towards glycol scission by lead tetraacetate in acetic acid (23) was in general accord with the oxidation characteristics of related five-membered ring compounds. The steric arrangement of the *vic*-diol group of the D-erythrosides should correspond closely to that found in cyclopentane-*cis*-1,2-diol (24) and 1,4-anhydro erythritol (25) and, accordingly, these glycosides consumed oxidant extremely rapidly (Table I), as already shown for the mixed anomers (15). Similarly, as with cyclopentane-*trans*-1,2-diol (23) and 1,4-anhydro-L-threitol (26, 27), the D-threosides were attacked relatively slowly (Table I). The oxidation rates for the anomeric forms differed substantially, however, in contrast to the more uniform behavior of anomeric pyranose glycosides towards lead tetraacetate.†

**This technique has been shown to be highly effective for separating the anomeric forms of some methyl hexoside methyl ethers (19).*

†*A notable exception is the observation that the α-anomer of methyl 2-deoxy-D-erythropentopyranoside consumes lead tetraacetate almost twice as rapidly as does the β-anomer (28). In the periodate oxidation of* sterically rigid *bicyclic methyl glycosides, substantial anomeric differences have been observed (29).*

TABLE I

Properties of the methyl D-tetrofuranosides

Isomer	$[\alpha]_D^{25}$	$[\alpha]_D^{25}$ dialdehyde*	Oxidation rate (k)†
α-D-*Erythro*-(VII)	+133°	+121°	Fast (0°)‡
β-D-*Erythro*-(VIII)	−148°	−119°	Fast (0°)‡
α-D-*Threo*-(IX)	+97°	+113°	0.084 (25°)§
β-D-*Threo*-(X)	−193°	−116°	0.49 (25°)§

*D'- of L'-Methoxy-diglycolic aldehyde formed by periodate oxidation. Derived from crystalline methyl pentosides, these dialdehydes show $[\alpha]_D^{20}$ ±122–124° (37, 38).

†Rate of lead tetraacetate oxidation in mole^{-1} liter minute^{-1}. Cyclopentane-*trans*-1,2-diol gives $k_{20°}$ 12.8 (24).

‡One mole of oxidant per mole was consumed within 45 seconds.

§The compound was not hydrolyzed when kept in acetic acid at 25° C for 6 hours.

EXPERIMENTAL

Paper chromatography was carried out using as solvents (A) ethyl acetate – acetic acid – formic acid – water (18:3:1:4), (B) butan-1-ol – ethanol – water (40:11:19), and (C) ethyl acetate – pyridine – water (100:40:30).

Gas–liquid chromatography was carried out as described by Craig and Murty (30), using a succinate – ethylene glycol polyester on Chromosorb W at a column temperature of 205° and a helium flow of 60 ml/minute.

Solutions were concentrated *in vacuo* at 40° C. Melting points are corrected. Boiling points cited are air-bath temperatures. Optical rotations were measured at approximately 25°.

2,3-O-Isopropylidene-L-*rhamnose* (I)

A slight modification of the procedure of Fischer (16) was used. L-Rhamnose hydrate (30 g) was dehydrated by heating *in vacuo* at 100° C for 3 hours. Dry acetone (300 ml) was added, followed by a solution of acetone (20 ml) containing hydrogen chloride (1.5 g), and the mixture was shaken at room temperature until the solid dissolved (1–2 hours). Excess ammonia was bubbled into the solution, the ammonium chloride filtered off, and the filtrate concentrated. The syrupy residue was dissolved in water (50 ml), extracted twice with ethyl acetate (100 ml), and the extract was washed twice with water (25 ml), dried over sodium sulphate, and concentrated. Weight, 19.0 g, $[\alpha]_D$ +6° (c, 4.3, H_2O). Paper chromatographic examination of the syrupy product and of the aqueous fractions indicated that the former consisted almost exclusively of monoacetone L-rhamnose (R_F 0.9, solvent B) and the latter mainly of L-rhamnose. Five grams of 2,3-*O*-isopropylidene-β-L-rhamnose, m.p. 88–90° C, $[\alpha]_D$ +17° (equilibrium value) (c, 2, H_2O), was obtained from a solution of the syrup in ether–hexane, but prolonged storage of the mother liquor in the cold failed to yield additional crystalline material. (For further examination of the syrupy residue, see below.)

2,3-O-Isopropylidene-L-*erythruronic Acid* (III)

2,3-*O*-Isopropylidene-β-L-rhamnose (1.0 g) was dissolved in water (50 ml), 0.1 N iodine (110 ml containing 2.4 g of potassium iodide) was added, and the solution cooled in an ice bath. Sodium hydroxide (N, 17.0 ml) was added dropwise with good stirring during a period of 15 minutes. At 45 minutes, titration of a portion of the reaction mixture showed that the consumption of hypoiodite was 1.0 mole/mole. A few drops of 0.1 N thiosulphate was added to decolorize the solution, silver acetate (7.0 g) was added and the suspension stirred at room temperature for 15 minutes, and sodium chloride solution

Can. J. Chem. Downloaded from www.nrcresearchpress.com by 210.87.254.6 on 09/05/12
For personal use only.

Can. J. Chem. Downloaded from www.nrcresearchpress.com by 210.87.254.6 on 09/05/12
For personal use only.

then added to remove excess silver ion. The suspension was filtered, the filtrate cooled to 5° C, and powdered sodium periodate (1.0 g) added. After 30 minutes, the oxidation mixture (which gave a faint test for excess periodate) was concentrated to a volume of 200 ml, acidified with Amberlite IR-120, and the solution and resin were extracted 5 times with ethyl acetate (50 ml). The combined extract was washed twice with water (25 ml) and dried over sodium sulphate. Evaporation of the solvent afforded a syrup which rapidly solidified (weight, 0.65 g), m.p. 92–98° C. (R_F 0.85, solvent A, yellow color with *p*-anisidine hydrochloride spray (31).) Recrystallized from ethyl acetate – hexane, the product had a melting point of 103–104° C, $[\alpha]_D$ +1.4° (*c*, 1.4, H_2O). Calculated for $C_7H_{10}O_5$: C, 48.27%; H, 5.79%. Found: C, 48.05%; H, 5.76%.

L-*Erythrotetruronic Acid*

Monoacetone L-erythruronic acid (28 mg) in water (2.0 ml) was heated on the steam bath: α_D +0.02° (1 dm, initial) → α_D −0.20° (60 minutes, constant); $[\alpha]_D$ −18° (calc.). (D-Erythruronic acid has $[\alpha]_D$ +18° (3).) Chromatographic examination of the hydrolyzate indicated the presence of one component travelling at the rate of D-*erythro*tetruronic acid (R_{gal} 1.4, solvent A) and giving an intense yellow color (which appears in the cold and intensifies on heating) with *p*-anisidine hydrochloride spray.

D-*Erythrono-γ-lactone*

Monoacetone L-erythruronic acid (0.3 g) was reduced with sodium borohydride (0.3 g) in water–methanol (2:1). The isopropylidene group of the syrupy product was hydrolyzed at 100° C in 80% acetic acid for 1.5 hours, affording D-erythrono-γ-lactone (0.1 g), which, recrystallized from ethanol, had a melting point of 100–102° C, undepressed, $[\alpha]_D$ −73° (*c*, 2.4, H_2O). (Lit. (1): m.p. 103–104° C; $[\alpha]_D$ −72°.) Calculated for $C_4H_6O_4$: C, 40.68%; H, 5.12%. Found: C, 40.69%; H, 5.16%.

2,3-O-Isopropylidene-L-*erythrose* (V)

2,3-*O*-Isopropylidene-L-rhamnose (2.0 g) in water (80 ml) was added dropwise to a well-stirred solution of sodium borohydride (0.8 g) in ice water (40 ml). After 4 hours at room temperature, acetic acid was added slowly to destroy excess borohydride and to adjust the pH to 6. The solution was cooled externally to 10° C, and powdered sodium periodate (2.2 g) was added portionwise over a period of 15 minutes. The reaction mixture was kept at 25° C for 3 hours (it then gave a faintly positive test for periodate), then concentrated to a volume of about 25 ml, and the slurry extracted 4 times with ethyl acetate (50 ml). After the extract was washed twice with water (15 ml) and dried over sodium sulphate, the solvent was evaporated off affording a clear, colorless syrup* (1.3 g) (R_F 0.8, solvent B) which solidified almost completely when stored overnight at 3° C. The crystalline material melted at 27–30° C. After distillation (60–70° C (bath) at 10 mm) the product still contained a small proportion of liquid, and the crystalline material melted at 29–31° C, $[\alpha]_D$ +72° (*c*, 2.4, CH_3OH) (no mutarotation observed). Calculated for $C_7H_{12}O_4$: C, 52.49%; H, 7.55%. Found: C, 52.53%; H, 7.56%.

2,3-O-Isopropylidene-L-*erythrose from Syrupy Monoacetone* L-*Rhamnose*

A sample (1.0 g) of the material remaining after crystallization of I (above) was treated with sodium borohydride followed by periodate oxidation, as in the preparation of V. The syrupy product (0.8 g) was distilled (50–70° C (bath) at 2 mm) affording a colorless syrup which solidified almost completely at 3° C. The melting point of the crystalline

**This product is moderately volatile, and hence should not be dried for a prolonged period in vacuo.*

material was 27–31° C. In addition to V, the product was found chromatographically to contain a minor component (R_F 0.9, solvent B) that was detected with aniline oxalate but did not give the tetrose color. Attempts to purify the monoacetone-L-erythrose by recrystallization from various solvent systems were unsuccessful.

L-Erythrose

2,3-*O*-Isopropylidene-L-erythrose (19.3 mg) in 0.1 *N* sulphuric acid (1 ml) was heated on the steam bath: α_D +1.22° (1 dm, initial) → +0.97° (30 minutes, constant); $[\alpha]_D$ +39° (calc.). After neutralization with Dowex-1 resin (bicarbonate form) the hydrolyzate was found chromatographically (solvent C) to contain a single component travelling at the rate of D-erythrose and giving the typical tetrose fluorescence under ultraviolet with aniline oxalate spray (32). The infrared absorption spectrum (potassium bromide disk) of the product was indistinguishable from that of D-erythrose. Reduction of the product with aqueous sodium borohydride yielded chromatographically pure erythritol, m.p. 118–120° C, undepressed. Calculated for $C_4H_{10}O_4$: C, 39.34%; H, 8.25%. Found: C, 39.43%; H, 8.30%.

2,3-O-Isopropylidene-L-rhamnitol

2,3-*O*-Isopropylidene-L-rhamnose (0.5 g) in absolute ethanol (10 ml) was heated at 100° C for 8 hours at a pressure of 1400 p.s.i. of hydrogen in the presence of Raney nickel catalyst (0.3 g). The catalyst was filtered off and the filtrate evaporated, affording a colorless syrup (0.5 g) which gave a single spot on a paper chromatogram (R_F 0.7, solvent B, ammoniacal silver nitrate spray (33)), $[\alpha]_D$ +5.5° (*c*, 4.1, CH_3OH). Presence of an isopropylidene group was indicated by the infrared absorption spectrum. The product consumed 1.0 mole of periodate per mole, affording 2,3-*O*-isopropylidene-L-erythrose. Acetylation and benzoylation gave amorphous products.

Reaction of Di-O-formyl-D-erythrose with Methanolic Hydrogen Chloride

Di-*O*-formyl-D-erythrose syrup (1) (3.2 g) in methanol (50 ml) (α_D +0.14°) was treated with 2.5% methanolic hydrogen chloride (35 ml) at 25° C, the observed rotation changing to α_D −1.65° (5 minutes, constant). Excess silver carbonate was added, the neutral filtrate was treated with hydrogen sulphide and again filtered, and the solution was concentrated to yield a colorless syrup (2.2 g), $[\alpha]_D$ −49° (*c*, 4.4, CH_3OH). Examined by paper chromatography (solvent B), the syrup was found to contain two main components (R_F 0.59 (major) and R_F 0.66), a small proportion of free erythrose, and two trace components (R_F 0.74 and R_F 0.79).

Methyl β-D-Erythrotetrofuranoside (II)

Methyl D-erythroside syrup (5.5 g) was chromatographed on a cellulose column using benzene–ethanol–water (500:50:1) as solvent. The component (R_F 0.59) was eluted from the column first and isolated as a colorless syrup (3.5 g), b.p. 80–90° C at 0.5 mm; n_D 1.4630, $[\alpha]_D$ −148° (*c*, 1.5, H_2O). (Ballou reports $[\alpha]_D$ −149° (*c*, 1, $CHCl_3$) (18).) Calculated for $C_5H_{10}O_4$: C, 44.77%; H, 7.52%. Found: C, 44.30%; H, 7.62%.

The glycoside was hydrolyzed with 0.1 *N* sulphuric acid at 100° C to constant rotation in 30 minutes. Calculated for chromatographically pure D-erythrose formed $[\alpha]_D$ −36° (in the acid solution, and after treatment with Dowex-1 resin (bicarbonate form)).

Oxidized with sodium periodate, the uptake by the glycoside was 1.0 mole/mole, and the observed rotation changed from α_D −2.55° (*c*, 1.75) to −2.06° (20 minutes, constant). Calculated for dialdehyde formed $[\alpha]_D$ −119°.

Can. J. Chem. Downloaded from www.nrcresearchpress.com by 210.87.254.6 on 09/05/12
For personal use only.

Can. J. Chem. Downloaded from www.nrcresearchpress.com by 210.87.254.6 on 09/05/12
For personal use only.

Methyl β-D-Erythrofuranoside-2,3-carbonate

Methyl β-D-erythroside (0.9 g) was dissolved in pyridine (30 ml) and to the stirred solution was added dropwise a solution of phosgene (0.75 g) in toluene (35 ml) (34). After 18 hours the solid pyridine hydrochloride was filtered off, the filtrate concentrated, and the residue taken up in chloroform. The chloroform solution was washed twice with copper sulphate solution, then with bicarbonate solution, twice with water, dried over sodium sulphate, and concentrated. The syrupy product (1.0 g) solidified, and recrystallization was effected from ethyl acetate – hexane, m.p. 73° and $[\alpha]_D$ −152° (*c*, 2.4, $CHCl_3$). Calculated for $C_6H_8O_5$: C, 45.00%; H, 5.01%. Found: C, 44.81%; H, 5.01%. The infrared absorption spectrum showed a major broad peak at 1790–1795 cm^{-1}, characteristic of a cyclic, rather than acyclic, carbonate group (35).

Methyl α-D-Erythrotetrofuranoside (I)

Following elution of the β-glycoside from the cellulose column, a fraction consisting mainly of the α-anomer was obtained (0.6 g), rechromatographed on the cellulose column, and distilled (b.p. 65–85° C at 0.2 mm); n_D 1.4665, $[\alpha]_D$ +133° (*c*, 1.2, H_2O). Calculated for $C_5H_{10}O_4$: methoxyl, 23.1%. Found: methoxyl, 22.8%.

On hydrolysis with 0.1 *N* sulphuric acid at 100° C to constant rotation, the observed value corresponded to $[\alpha]_D$ −37° for chromatographically pure D-erythrose formed; after neutralization with Dowex-1 (bicarbonate form), $[\alpha]_D$ −39°.

Treated with sodium periodate, the glycoside consumed 1.0 mole/mole, the observed rotation changing from α_D +1.71° → +1.48° (10 minutes, constant). Calculated for the dialdehyde formed, $[\alpha]_D$ +121°.

Methyl α-D-Erythrofuranoside Di-p-nitrobenzoate

Methyl α-D-erythroside (0.10 g) in pyridine (5 ml) was treated with *p*-nitrobenzoyl chloride (0.65 g) at 55° C for 4 hours. On addition of aqueous sodium bicarbonate, a solid product was obtained (0.30 g) and was recrystallized from ethyl acetate – hexane, m.p. 109–110° C and $[\alpha]_D$ −17.3° (*c*, 1.7, $CHCl_3$). Calculated for $C_{19}H_{16}O_{10}N_2$: C, 52.78%; H, 3.73%. Found: C, 52.84%; H, 3.60%.

Reaction of D-Threose Formate with Methanolic Hydrogen Chloride

D-Threose formate syrup (2) (4.5 g), treated with methanolic hydrogen chloride as described above, afforded a colorless syrup (2.6 g). Purified by distillation (b.p. 75–90° C at 0.2 mm) the product had $[\alpha]_D$ +7.9° (*c*, 2.4, H_2O) and, examined by paper chromatography (solvent B), was found to contain two major tetrose components (R_F 0.65 and 0.62; overlapping, with the former predominant) and a minor tetrose component (R_F 0.75). On treatment with periodate the mixture consumed 0.9 mole of oxidant per mole, the calculated value of $[\alpha]_D$ +33° for the dialdehydes formed corresponding to an α,β-mixture of about 3 to 2. Calculated for $C_5H_{10}O_4$: methoxyl, 23.1%. Found: methoxyl, 24.6%.

Methyl α- and β-D-Threotetrofuranosides

Vapor phase chromatography of the syrupy mixture of D-threosides readily separated the two major components from each other, and showed them to be present in a ratio of about 3 to 2 (α- to β-). On a preparative scale, 50–100 mg of each component was isolated by repeated chromatographic runs, and purified by distillation.

The first of the two components to emerge from the column was the *β-anomer* (R_F 0.62, b.p. 80–90°/0.2 mm), $[\alpha]_D$ −193° (*c*, 1.1, H_2O). The glycoside consumed 1.0 mole of

periodate per mole, affording a dialdehyde having $[\alpha]_D$ −116° (calculated). Calculated for $C_5H_{10}O_4$: C, 44.77%; H, 7.52%. Found: C, 44.60%; H, 7.48%.

The *α-anomer* (R_F 0.65, b.p. 85–100°/0.2 mm) had $[\alpha]_D$ +97° (*c*, 1.6, H_2O). It consumed 1.0 mole of periodate per mole, yielding a dialdehyde having $[\alpha]_D$ +113° (calculated). Calculated for $C_5H_{10}O_4$: C, 44.77%: H, 7.52%. Found: C, 44.73%; H, 7.31%.

Methyl α-D-Threofuranoside Di-p-nitrobenzoate and Methyl α-D-Threofuranoside

The mixture of α- and β-D-threosides (0.5 g) was treated with *p*-nitrobenzoyl chloride as described above, and the amorphous product (1.2 g) was taken up in ethyl acetate – hexane. Crystalline material (0.6 g) was deposited and recrystallized twice from the same solvent, m.p. 131–133° C and $[\alpha]_D$ −115° (*c*, 2.0, $CHCl_3$). Calculated for $C_{19}H_{16}O_{10}N_2$: C, 52.78%; H, 3.78%. Found: C, 52.80%; H, 3.65%.

The di-*p*-nitrobenzoate (0.3 g) suspended in methanol (20 ml) was treated under reflux with sodium methoxide (0.1 *N*, 2 ml). Acetic acid was added to neutrality, the methanol evaporated off, and the residue taken up in water and extracted three times with benzene. The aqueous layer was concentrated, and the product distilled, $[\alpha]_D$ +96° (*c*, 2.2, H_2O). The infrared absorption spectrum of the syrup was indistinguishable from that of methyl α-D-threoside and different from that of the β-glycoside.

Methyl β-D-Threofuranoside Di-p-nitrobenzoate

A syrup consisting mainly of methyl β-D-threofuranoside ($[\alpha]_D$ −165°) was obtained by partial separation of the mixed threosides on a cellulose column using benzene–ethanol–water (1000:15:0.5). Treatment with *p*-nitrobenzoyl chloride afforded a di-*p*-nitrobenzoate which, when crystallized from ethyl acetate – pentane, had a melting point of 55–57° C, $[\alpha]_D$ −213° (*c*, 1.6, $CHCl_3$). Calculated for $C_{19}H_{16}O_{10}N_2$ (containing a mole of ethyl acetate): C, 53.05%; H, 4.62%; N, 5.38%; acetyl, 8.27%. Found: C, 53.03%; H, 4.63%; N, 5.21%; acetyl, 7.81%.

Preparation of the Methyl D-Threosides via Acetobromo-D-threose

Tri-*O*-acetyl D-threose (22) (0.50 g) in chloroform (4 ml) ($[\alpha]_D$ +35°) was treated with hydrogen bromide (2 ml, 40% in acetic acid). Within 5 minutes the observed rotation was constant, giving a calculated value of $[\alpha]_D$ −10°. The solution was quickly concentrated, toluene being added 4 times in completing the evaporation of solvent, affording a pale yellow syrup (0.54 g). (Attempts to dry a portion thoroughly for analysis resulted in rapid darkening, and no crystalline product could be isolated from cold ether–hexane.)

The syrup (0.1 g) in methanol (5 ml) was shaken for 18 hours with silver oxide (0.3 g) and Drierite (0.7 g). Found: $[\alpha]_D$ −5° (calculated for methyl tetroside). In the absence of silver oxide and Drierite the observed rotation of the solution was constant in 10 minutes, $[\alpha]_D$ −6° (calculated for methyl tetroside). Both products were deacylated with sodium methoxide, and found by paper chromatography to contain mainly methyl threoside, $[\alpha]_D$ +25° (*c*, 1, H_2O). The infrared absorption spectra of the deacetylated products were closely similar to that of methyl α-D-threoside. Examined by vapor phase chromatography the α- and β-anomers were detected in the products in a ratio of about 3 to 1.

Lead Tetraacetate Oxidations

The methyl D-erythrosides (40 mg) in 5 ml of acetic–propionic acid mixture (75:25) (2) were each treated at 0° C with lead tetraacetate solution (50 mg in 4 ml of the same solvent). Oxidation of the methyl D-threosides was carried out in acetic acid at 25° C,

Can. J. Chem. Downloaded from www.nrcresearchpress.com by 210.87.254.6 on 09/05/12
For personal use only.

using the same concentration of reactants. Reaction rates were measured as described by Criegee (36).

ACKNOWLEDGMENTS

The authors are grateful to Dr. B. M. Craig for carrying out the vapor phase chromatographic separations reported, and to Mr. J. W. L. C. Christ for technical assistance. Microanalyses were carried out by Mr. M. Mazurek, and infrared absorption spectra were prepared by Miss Inez Gaffney.

REFERENCES

1. A. S. PERLIN and C. BRICE. Can. J. Chem. **33**, 1216 (1955).
2. A. S. PERLIN and C. BRICE. Can. J. Chem. **34**, 85 (1956).
3. P. A. J. GORIN and A. S. PERLIN. Can. J. Chem. **34**, 693 (1956).
4. J. N. BAXTER, A. S. PERLIN, and F. J. SIMPSON. Can. J. Biochem. and Physiol. **37**, 199 (1959).
5. H. J. LUCAS and W. BAUMGARTEN. J. Am. Chem. Soc. **63**, 1653 (1941).
6. O. T. SCHMIDT and P. GÜNTHERT. Ber. **71**, 493 (1938).
7. E. FISCHER. Ber. **28**, 1145 (1895).
8. K. FREUDENBERG and A. WOLF. Ber. **59**, 836 (1926).
9. P. A. LEVENE and J. COMPTON. J. Biol. Chem. **114**, 9 (1936).
10. R. WILLSTÄTER and G. SCHUDEL. Ber. **51**, 780 (1918).
11. C. E. BALLOU. J. Am. Chem. Soc. **79**, 165 (1957).
12. R. SCHAFFER. J. Am. Chem. Soc. **81**, 2838 (1959).
13. D. L. MACDONALD and H. O. L. FISCHER. J. Am. Chem. Soc. **74**, 2087 (1952).
14. L. HOUGH and T. J. TAYLOR. J. Chem. Soc. 1212 (1955).
15. R. C. HOCKETT and C. W. MAYNARD, JR. J. Am. Chem. Soc. **61**, 2111 (1939).
16. E. FISCHER. Ber. **26**, 2400 (1893).
17. H. O. L. FISCHER and C. TAUBE. Ber. **60**, 1706 (1927).
18. C. E. BALLOU. J. Am. Chem. Soc. **82**, 2585 (1960).
19. A. G. MCINNES, D. H. BALL, F. P. COOPER, and C. T. BISHOP. J. Chromatog. **1**, 556 (1958).
20. W. KOENIGS and E. KNORR. Ber. **34**, 957 (1901).
21. R. K. NESS and H. G. FLETCHER, JR. J. Am. Chem. Soc. **80**, 2007 (1958); and references cited therein.
22. R. C. HOCKETT. J. Am. Chem. Soc. **57**, 2260 (1935).
23. R. CRIEGEE. Ber. **64**, 260 (1931).
24. R. CRIEGEE, E. BÜCHNER, and W. WALTHER. Ber. **73**, 571 (1940).
25. R. E. REEVES. J. Am. Chem. Soc. **72**, 1499 (1950).
26. H. KLOSTERMAN and F. SMITH. J. Am. Chem. Soc. **74**, 5336 (1952).
27. J. S. BRIMACOMBE, A. B. FOSTER, M. STACEY, and D. H. WHIFFEN. Tetrahedron, **4**, 351 (1958).
28. R. E. DERIAZ, W. G. OVEREND, M. STACEY, and L. F. WIGGINS. J. Chem. Soc. 2836 (1949).
29. J. HONEYMAN and C. J. G. SHAW. J. Chem. Soc. 2454 (1959).
30. B. M. CRAIG and N. L. MURTY. Am. Oil Chemists' Soc. **36**, 549 (1959).
31. L. HOUGH, J. K. N. JONES, and W. H. WADMAN. J. Chem. Soc. 1702 (1950).
32. R. H. HORROCKS. Nature, **164**, 444 (1949).
33. S. M. PARTRIDGE. Nature, **158**, 270 (1946).
34. B. J. LUDWIG and E. C. PIECH. J. Am. Chem. Soc. **73**, 5779 (1951).
35. L. HOUGH, J. E. PRIDDLE, R. S. THEOBALD, G. R. BARKER, T. DOUGLAS, and J. W. SPOORS. Chem. & Ind. London, 148 (1960).
36. R. CRIEGEE. Ann. **495**, 211 (1932).
37. E. L. JACKSON and C. S. HUDSON. J. Am. Chem. Soc. **59**, 994 (1937).
38. F. SMITH and J. W. VAN CLEVE. J. Am. Chem. Soc. **77**, 3901 (1955).

Can. J. Chem. Downloaded from www.nrcresearchpress.com by 210.87.254.6 on 09/05/12
For personal use only.

CHEMICAL SHIFTS IN THE N.M.R. SPECTRA OF SUBSTITUTED XYLENES[1]

ROBERT R. FRASER

ABSTRACT

The complete results of analysis of the N.M.R. spectra of twelve 2,6-dimethyl-1-substituted benzenes are reported. The results are interpreted as evidence that the ability of the substituent to donate or withdraw electrons by resonance interaction with the benzene ring is a major factor in determining the position of absorption of the protons attached to the ring. The chemical shifts and coupling constants for nitroethylene are also reported.

The study of the effect of a substituent on the position of absorption in the N.M.R. spectra of protons attached to a benzene ring has been greatly hindered by the complexity of the spectra of monosubstituted benzenes. These spectra generally fall in the classification AB_2C_2 following the nomenclature of Bernstein, Pople, and Schneider (1). Analysis of such a five-spin system is extremely tedious even in the case of pyridine, which belongs to the slightly simpler AB_2X_2 system (2). For this reason little work has appeared in the literature on the correlation of chemical shifts of protons on a benzene ring with substituents since the first report by Corio and Dailey (3). These authors reported the values δ_o, δ_m, δ_p for the chemical shifts of the ortho, meta, and para protons in the N.M.R. spectra of 22 monosubstituted benzenes. Their analysis was of a qualitative nature on spectra whose resolution was limited by the use of a transmission frequency of 30.00 Mc/sec. Furthermore Bothner-By and Glick subsequently showed that solvent effects were responsible for inaccuracies of as much as 0.07 p.p.m. in the values for δ_p (4). Correlation of their δ values with Hammett's σ constants gave only rough agreement although Taft later showed that agreement to within 0.07 p.p.m. could be obtained employing the equation* $\delta_p = +0.40\sigma_I + 1.04\sigma_R^0 + 0.02$ (5). In this equation σ_I is the inductive substituent constant of Taft (6) and σ_R^0 is the resonance substituent constant corrected for isovalent conjugation (5). Taft has interpreted this agreement to be an indication that polarization effects in the transition state are sufficiently similar to those in the ground state to give the correlation between σ and δ_p (7).

An alternative theory of the origin of chemical shift differences in the ring protons of monosubstituted benzenes has been suggested in a recent article by Buckingham (8). He proposes that the screening constant for each proton is determined by the "internal electric field" of the molecule. In addition polarization of the surrounding solvent by the solute produces a "reaction field" whose effect combines with that of the electric field to give the total effect on the screening constants. He has derived expressions for these two fields in terms of the dipole moment of the solute, its refractive index, and the dielectric of the solution from which screening constants can be directly calculated. Calculations for nitrobenzene gave values of -0.69, -0.40, and -0.51 p.p.m. relative to benzene for the ortho, meta, and para protons in fair agreement with the values -0.97, -0.30, and -0.42 observed by Corio and Dailey. In order to provide data which might aid in the elucidation of the cause of chemical shift differences with different substituents, a series

[1]*Manuscript received June 29, 1960.*
Contribution from the Department of Chemistry, University of Ottawa, Ottawa, Ontario. This paper was presented at the 43rd Annual Conference of the Chemical Institute of Canada, Ottawa, June 13–15, 1960.

**It should be noted that Corio and Dailey employ $\delta_p = 10^6\{(H_{ref}-H)/H_{ref}\}$, which causes negative signs to represent shifts to higher field.*

of 2,6-dimethyl-1-substituted-benzenes were synthesized and their spectra obtained with a Varian V-4302 spectrometer using a 60 Mc/sec r.f. unit. These xylene derivatives were selected for study since they provide spectra which can be accurately analyzed.

RESULTS AND DISCUSSION

The results of analysis of the spectra of 12 substituted xylenes are given in Table I.

TABLE I

Results of analysis of twelve 2,6-dimethyl-1-substituted benzenes (substituent σ values are also given)

Substituent	$\Delta\nu_m$*	$\Delta\nu_p$*	$\Delta\nu_m'$	σ_m	σ_p	σ_R	τ_{CH_3}†
CN	12.9	0.3	2.6	0.62	0.68	0.10	7.52
Br	16.8	16.8	6.5	0.39	0.23	−0.22	7.61
I	18.4	14.4	8.1	0.35	0.28	−0.11	7.54
F	22.5	26.5	12.2	0.35	0.08	−0.44	7.76
D	24.8	14.5	14.5	0.00	0.00	0.00	7.73
OH	25.8	39.0	15.5	0.08	−0.35	−0.60	7.88
NH_2	29.0	47.2	18.7	−0.15	−0.66	−0.76	7.89
NO_2	12.5	5.2	2.2			+0.05	7.68
COOH	16.0	7.0	5.7			+0.06	7.55
OCH_3	23.5	29.0	13.2			−0.20	7.75
$NHCH_3$	25.5	35.8	15.2			−0.39	7.76
$N(CH_3)_2$	26	26	15.7			−0.21	7.76

NOTE: All the σ values for the first seven substituents are taken from R. W. Taft, Jr., N. C. Deno, and A. S. Skell. Ann. Rev. of Phys. Chem. **9**, 292 (1958). The σ_R values for the last five substituents are calculated from normal σ_R values by correcting for the percentage of steric inhibition of resonance. The percentage inhibition was taken from the following sources: R. W. Taft, Jr. and H. D. Evans. J. Chem. Phys. **27**, 1427 (1957), who reported NO_2 (67%), OCH_3 (59%), and $N(CH_3)_2$ (75%); B. M. Wepster. Rev. trav. chim. **76**, 335, 357 (1957), who found NO_2 (69%), $N(CH_3)_2$ (80%), and $NHCH_3$ (60%); A. Burawoy and J. T. Chamberlain. J. Chem. Soc. 2310 (1952), from whose results the value 62% is calculated for OCH_3; and G. M. Moser and A. I. Kohlenburg. J. Chem. Soc. 805 (1957), from whose data the value 50% is estimated for COOH. For a discussion of steric inhibition of resonance in these compounds see B. M. Wepster. Progress in stereochemistry. Vol. 2. *Edited by* W. Klyne and P. B. D. de la Mare. Butterworths Scientific Publications, London. 1958.

*$\Delta\nu_m$ and $\Delta\nu_p$ are the chemical shifts in cycles/sec at 60 Mc/sec relative to the internal reference benzene for the meta and para protons.

†τ_{CH_3} gives the chemical shift of the ortho methyls expressed as parts per million with tetramethylsilane assigned a value 10.00.

The protons attached to the aromatic ring appeared in all but three cases as an AB_2 pattern whose general solution has been reported in reference 1. The spectrum consists of eight transitions whose energies and intensities are dependent only on the ratio $J_{AB}/\Delta\nu_{AB}$.* In Fig. 1 the spectra of 2,6-dimethylphenol, 2,6-dimethylanisole, and N,N-dimethyl-2,6-dimethylaniline are shown. They illustrate cases where the ratio is less than one, about one, and much greater than one, respectively. In 2,6-dimethylphenol, as in all AB_2 systems, line 3 gives the position of chemical shift for the A nucleus, unmodified by spin coupling. The corresponding position for the B nuclei is the mean of transitions 5 and 7. Thus $\Delta\nu_{AB} = \Delta\nu_p - \Delta\nu_m$ can be obtained directly from the spectrum. In the spectrum of this compound transitions 5 and 6 could not be resolved. To insure accurate results, theoretical spectra were calculated for various ratios of $J/\Delta\nu_{AB}$ until agreement with the observed spectra to within 0.4 cycle/sec for each transition was obtained. In most spectra the agreement was within 0.2 cycle/sec for each transition. In all spectra J_{AB} was found to be 7.7 cycles/sec. The spectra of N,N-dimethyl-2,6-dimethylaniline and 2,6-dimethylbromobenzene showed only a single observable peak under high gain and it is estimated that the chemical shift of the meta and para protons in these two compounds is the same to within 3.0 cycles/sec.

**J_{AB} is the coupling constant between the para (A) and meta (B) protons. $\Delta\nu_{AB} = \nu_A - \nu_B$ represents the chemical shift between the meta and para protons. The symbol $\Delta\nu$ is used to denote chemical shifts in units of cycles per second as recommended by Pople, Schneider, and Bernstein (11).*

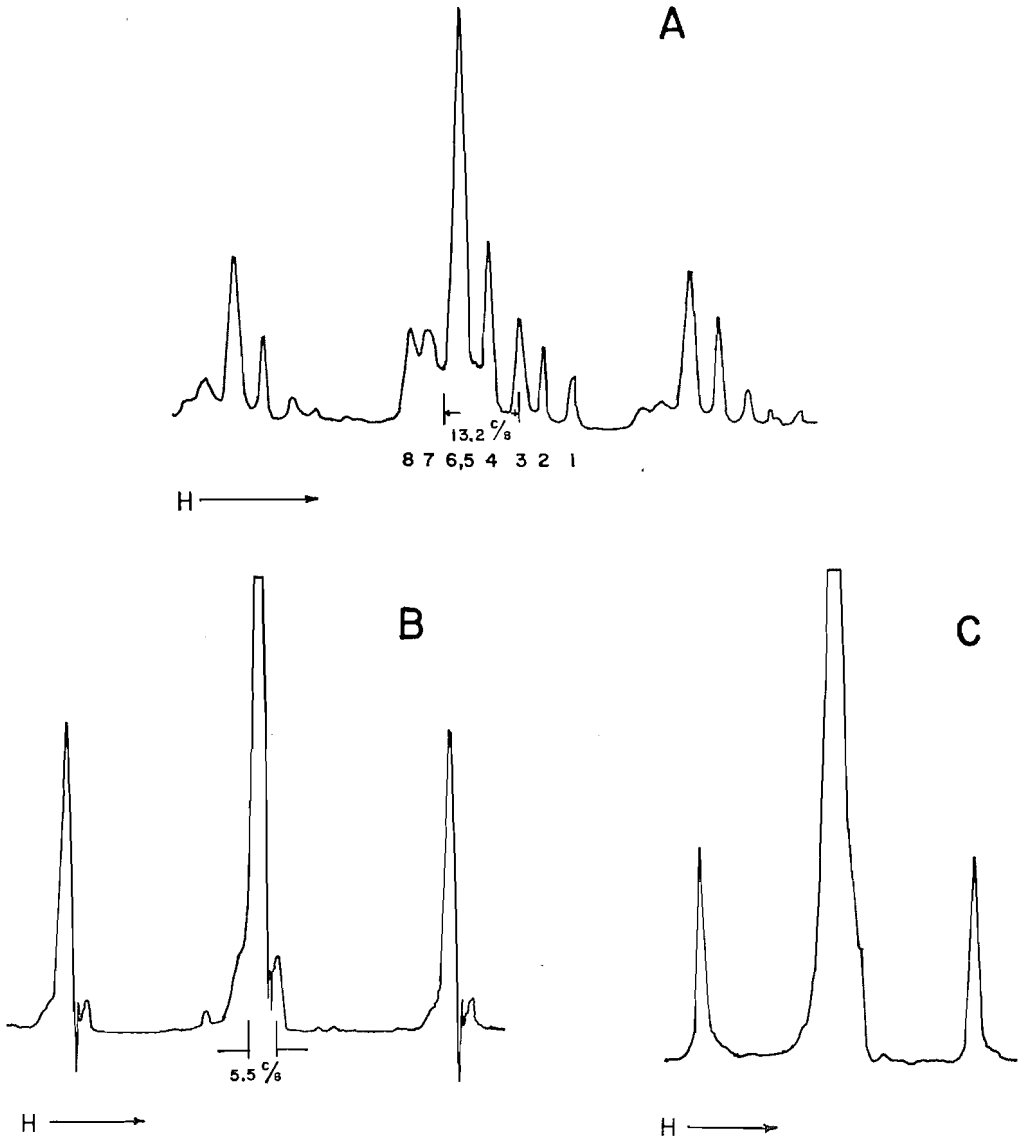


FIG. 1. (A) Aromatic proton absorption of 2,6-dimethylphenol (side bands at 40.0 cycles/sec) as a 10% solution in carbon tetrachloride. (B) Aromatic protons of 2,6-dimethylanisole (side bands at 35.1 cycles/sec) and (C) N,N-dimethyl-2,6-dimethylaniline (side bands at 25.0 cycles/sec) as 10% solutions in carbon tetrachloride.

In 2,6-dimethylfluorobenzene coupling of the fluorine atom with the meta and para protons resulted in the more complex spectrum shown in Fig. 2. By neglecting coupling of the methyl groups with the ring protons we can classify the aromatic protons and the fluorine nucleus as an AB_2X system. In order to simplify the calculations we have considered the aromatic proton spectrum as the sum of two AB_2 systems. This type of simplification has been employed previously by Anet in the analysis of the 2,3-dibromobutanes (9). When the X nucleus, fluorine, has a spin of $+1/2$ the aromatic protons will form one AB_2 system. When fluorine has a spin of $-1/2$ the aromatic protons comprise

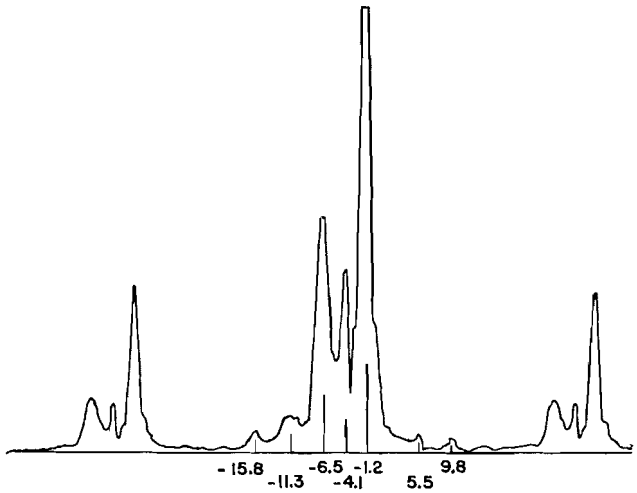


FIG. 2. Aromatic absorption of 2,6-dimethylfluorobenzene (side bands at 30.0 cycles/sec) as a 10% solution in carbon tetrachloride.

a second AB_2 system of equal total intensity. From the experimentally determined spectrum we found the chemical shift for the widely separated AB_2 system to be 8.6 cycles/sec. Using the values $J_{FH_B} = 7.0$ cycles/sec, $J_{FH_A} = \pm 2.2$ cycles/sec, and $J_{AB} = 7.7$ cycles/sec, it was then possible to calculate the complete spectrum for the aromatic protons. Two solutions were obtained, one for the case where the coupling constants between fluorine and the meta and para protons are of opposite sign (Fig. 3A) and one where the coupling constants are of the same sign (Fig. 3B). The numerical values for the fluorine–hydrogen coupling constants were chosen from the results of Gutowsky, Holm, Saika, and Williams, who observed the coupling between the ring protons and fluorine in fluoromesitylene to be 7.0 cycles/sec and the coupling between fluorine and a para proton to be 2.2 cycles/sec in several fluorinated benzenes (10). The line width of the strongest peak in the observed spectrum suggests that it is due to an AB_2 system having a very large ratio of $J/\Delta\nu_{AB}$ as depicted in Fig. 3A. In addition failure to observe the transition at $+2.2$ cycles/sec shown in Fig. 3B further indicates that the observed spectrum is due to a system in which the two fluorine–proton coupling constants are of opposite sign. Unfortunately an element of doubt remains as the differences between the two theoretical spectra are not large. The spectrum of 2,6-dimethylfluorobenzene was also measured in acetone, methylene iodide, dimethylsulphoxide, and aqueous methanol. Only in acetone was the spectrum altered significantly, $\Delta\nu_{AB}$ for the well-resolved AB_2 system being increased to 10.1 cycles/sec. Again better agreement between observed and calculated spectra was obtained assuming the fluorine–hydrogen coupling constants to be of opposite sign. With the values chosen in Fig. 3A, the chemical shift difference between the meta and para protons is found to be 4.0 cycles/sec with the para proton at higher field. The alternative assumption increases the difference to 6.2 cycles/sec. The methyl groups in 2,6-dimethylfluorobenzene appeared as a doublet of spacing 2.05 cycles/sec due to coupling with the fluorine nucleus.

Before the results are examined it is necessary to make a correction in the $\Delta\nu_m$ values. The spectrum of 2,6-dimethyldeuterobenzene shows that the meta protons are shifted 10.3 cycles/sec more to high field than the para ones by the methyl groups. Whatever

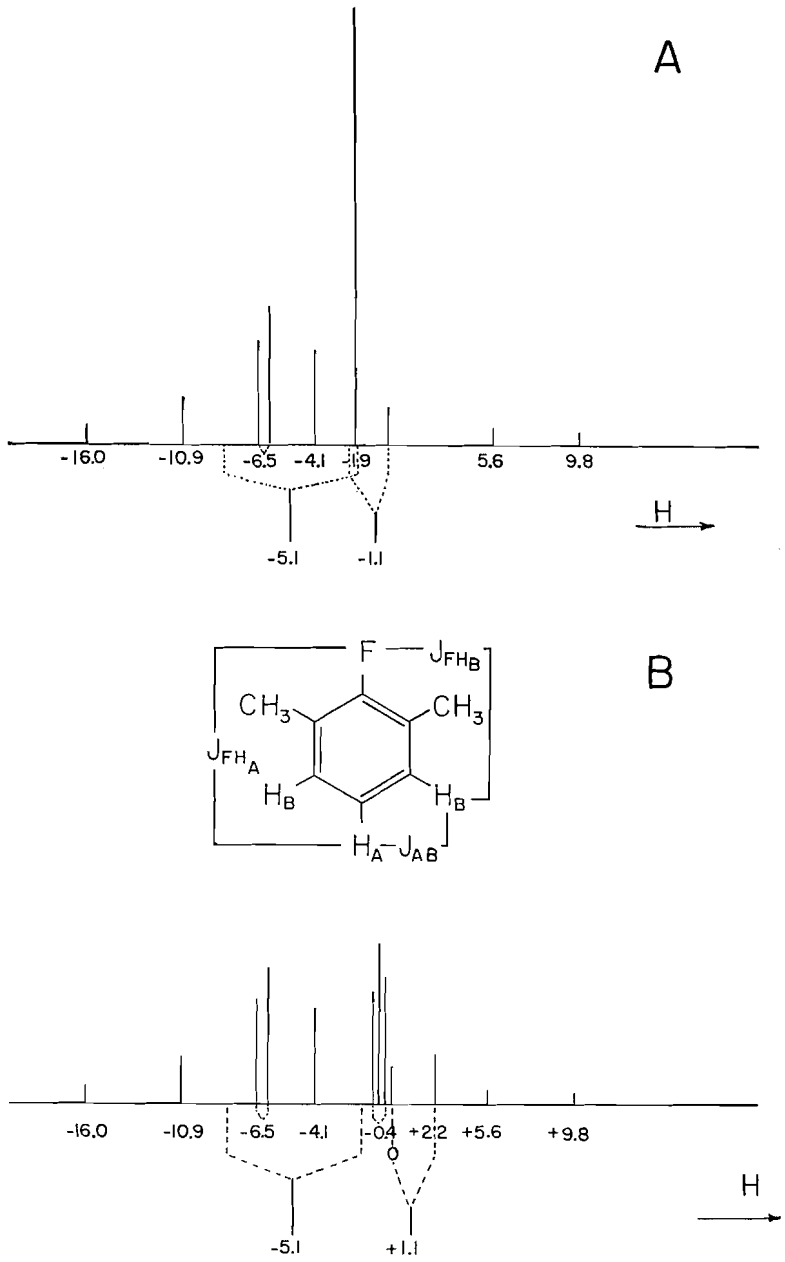


FIG. 3. Theoretical spectra of aromatic protons in 2,6-dimethylfluorobenzene.
(A) For $J_{AB} = 7.7$ cycles/sec, $J_{F-H_B} = 7.0$ cycles/sec, $J_{F-H_A} = -2.2$ cycles/sec, $\Delta\nu_{obs} = 8.6$ cycles/sec.
(B) For $J_{AB} = 7.7$ cycles/sec, $J_{F-H_B} = 7.0$ cycles/sec, $J_{F-H_A} = 2.2$ cycles/sec, $\Delta\nu_{obs} = 8.6$ cycles/sec.
In this diagram transitions of intensity less than 40% of band at +5.6 are not included. The positions of the A and B nuclei in the absence of coupling are shown below the abscissa.

the origin of this preferential shift, it is necessary to assume that it remains constant throughout the series of compounds measured. If this is true we can assign $\Delta\nu_m'$ values = $\Delta\nu - 10.3$ to the meta protons. Now the effect of the methyls is removed and the substituent

effect of a deuterium atom appears the same at the meta and para positions. The $\Delta\nu_m'$ values are also given in Table I. Let us now consider the chemical shifts observed in 2,6-dimethylaniline and its N,N-dimethyl derivative. The para proton in 2,6-dimethylaniline occurs at 47.2 cycles/sec relative to benzene, the meta proton at 29.0 cycles/sec relative to benzene. The value $\Delta\nu_p - \Delta\nu_m'$ shows that the amino substituent causes the para proton to be shifted 28.5 cycles/sec to higher field relative to the meta, which is corrected for the effect of the methyl group. On the other hand the dimethylamino substituent can be seen to cause only a 10.3 cycles/sec preferential shift of the para proton to higher field. It has been established by ultraviolet spectroscopy and by chemical reactivity (see references 1 and 2 in Table I) that two methyl groups ortho to a dimethylamino group greatly inhibit its resonance interaction with the benzene ring by preventing it from attaining coplanarity with the ring. The large difference in chemical shifts in 2,6-dimethylaniline can be explained by a resonance effect. That is to say the nitrogen atom donates its electrons to the para position more than to the meta position in the ground state and the increase in electron density results in a shift to higher field. The resonance interaction of the dimethylamino group with the ring is greatly decreased and so the effect on the shielding of the para and meta protons is also greatly diminished. The screening at the meta and para positions in the two compounds was calculated from the equations derived by Buckingham. The values 1.62 and 0.94, which Fischer found (12) for the dipole moments of 2,6-dimethylaniline and N,N-dimethyl-2,6-dimethylaniline, were used in the calculation. The dielectric constants for 5% solutions in carbon tetrachloride were estimated to be 2.5 and 2.4 respectively.

For 2,6-dimethylaniline the equations of Buckingham give values for $\Delta\nu_m'$ and $\Delta\nu_p$ of 6.4 cycles/sec and 7.2 cycles/sec. For the N,N-dimethyl derivative values of 3.7 and 4.1 cycles/sec were obtained. When these are compared with our experimental results it can be seen that the agreement is very poor.

A more obvious contradiction of the electric field effect is seen in the data for 2,6-dimethylfluorobenzene. Its dipole moment will most certainly be greater than zero with the negative end directed away from the ring.* Electric field theory then predicts that the para protons will be less screened than the meta when, in fact, the opposite situation has been found.

A plot of $\Delta\nu_m'$ and $\Delta\nu_p$ against the Hammett sigma constants for each substituent is shown in Fig. 4. No linear relationship is seen as the strongly electron-donating substituents appear at too high field. The same type of behavior was found for the F^{19} chemical shifts determined by Gutowsky (14). However, Taft later showed that the observed chemical shifts could be correlated with the inductive and resonance substituent constants σ_I and σ_R (7). The measured chemical shifts for the seven compounds whose substituents are free of steric inhibition of resonance were tested for correlation by the equation $\Delta\nu = \alpha\sigma_I + \beta\sigma_R + \gamma$ where α and β represent the susceptibility of the chemical shift to inductive and resonance effects of the substituent, respectively, and γ represents the constant methyl group effect. The chemical shifts for the meta protons are correlated by the equation $\Delta\nu_m' = 14.5 - 17\sigma_I - 10\sigma_R$, with the maximum error being 2.4 cycles/sec in the case of the bromo compound. The equation $\Delta\nu_p = 14.5 - 17\sigma_I - 46\sigma_R$ gives a better correlation, the maximum error being 1.7 cycles/sec in the iodo compound. As an illustration of the greater susceptibility of the para protons to σ_R, the value $\Delta\nu_p - \Delta\nu_m'$ for each

*The only available dipole moment data on fluorobenzenes is that of Everard, Kumar, and Sutton (13), who found the dipole moment of fluorobenzene to be 1.48 Debye units. The introduction of two methyl groups could lower the dipole moment by no more than 0.6 Debye unit which would lead to a minimum estimate of 0.88 Debye unit for 2,6-dimethylfluorobenzene.

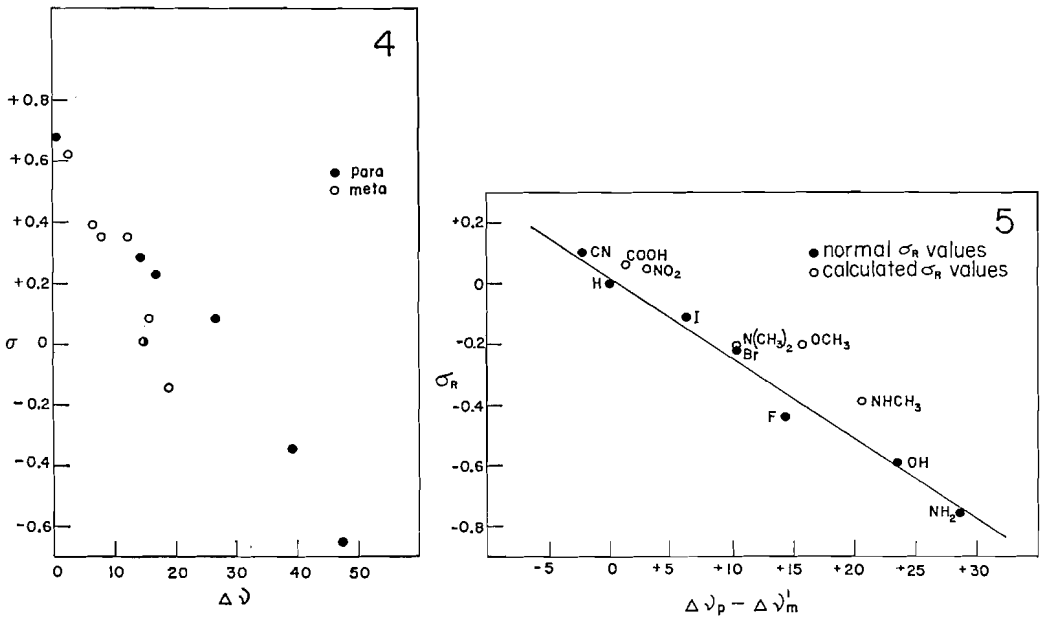


FIG. 4. Correlation of the shielding of the meta and para protons expressed in cycles per second at 60 Mc/sec from benzene by Hammett's σ's.
FIG. 5. Correlation of the separation in cycles per second at 60 Mc of the meta and para protons by Taft's σ_R.

compound is plotted against the σ_R value of the substituent in Fig. 5.* The linear relationship is obeyed to within 2.5 cycles/sec for those substituents free from resonance inhibition by the adjacent methyl groups. The substituents for which there is experimental evidence of steric inhibition of resonance are also plotted on the graph using σ_R values corrected for the percentage of inhibition as listed in Table I. The points for these substituents do not give a good linear plot, which might be interpreted as failure of the spectral and chemical methods to give a quantitative measure of the steric inhibition of resonance. Indeed the theoretical interpretation of the observed decrease in intensity of the ultraviolet absorption spectrum with increasing resonance inhibition, which was proposed by Braude, Sondheimer, and Forbes (15), has been invalidated by the recent work of Waight and Erskine (16). They observed no change in intensity of the ultraviolet spectra of a series of ortho-methylacetophenones with a 216° temperature change, a finding which contradicts Braude and co-worker's theory. It would be too presumptuous on the basis of our limited findings to propose corrected values for resonance inhibition by assuming the linear relationship to be valid for our compounds. It is sufficient to say that the deviation of these compounds from linearity does not refute the proposal that chemical shifts are determined by the inductive and resonance effects of the substituents.

Our findings can be compared with those of Corio and Dailey for the meta and para protons. The absence of ortho protons in our spectra is unimportant as Jackman has pointed out that the ortho shieldings are in many instances misleading (17). Jackman has found that each of the groups CN, Br, COOH, COCl, $COCH_3$, CHO in 2-substituted-1-propenes causes a shift of the proton cis to it to lower field relative to the trans proton.

*$If\ \Delta\nu_m' = \alpha\sigma_I+\beta\sigma_R+\gamma\ and\ \Delta\nu_p = \alpha\sigma_I+\beta'\sigma_R+\gamma\ then\ \Delta\nu_p-\Delta\nu_m' = (\beta'-\beta)\sigma_R\ and\ so\ a\ linear\ relationship\ between\ \Delta\nu_p-\Delta\nu_m'\ and\ \sigma_R\ should\ be\ found.$

The magnitude of the effect varies from 0.05 to 0.5 p.p.m. We have found that the nitro group has an even greater effect. Nitroethylene as a 10% solution in carbon tetrachloride gave a spectrum with well-separated absorption peaks. Assignments were made by assuming the coupling to be greater between protons trans to one another than cis and the results of analysis by first-order perturbation theory are given in Fig. 6. The

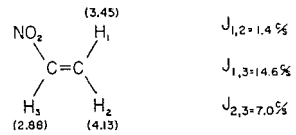


FIG. 6. Chemical shifts (τ values) and coupling constants for nitroethylene.

proton cis to the nitro group appears 0.68 p.p.m. to lower field than the proton trans to the nitro group. This effect of substituents will undoubtedly also be present in monosubstituted benzenes and will result in ortho protons appearing to lower field than in the absence of the effect. In instances where the effect is large, e.g. nitro, it could also be significant in the meta position even though it should fall off with the cube of the distance (11, p. 176). Our results are generally in agreement with those of Corio and Dailey although they show much greater sensitivity. For example, phenol showed no resolvable fine structure at 30 Mc/sec whereas 2,6-dimethylphenol showed signals for the meta and para protons separated by 13.2 cycles/sec. There is a discrepancy in the case of the iodo substituent. The values assigned to the para and meta protons in iodobenzene were +.10 and +.17 p.p.m. or 6.0 and 10.2 cycles/sec at 60 Mc/sec respectively. By subtracting the effect of the methyl groups our results for iodobenzene would be −0.1 and −6.4 cycles/sec respectively. Presumably, the discrepancy is due to those factors mentioned earlier, solvent effects and approximate analysis.

In conclusion it can be stated that our findings are not explainable by the Buckingham electric field theory. They are in agreement with the proposal of Taft that the observed shifts at the meta and para positions are determined by both the inductive and resonance effects of the substituent. The theoretical basis for such a relationship has been clearly discussed by Taft (7). In spite of our findings it should be emphasized that the quantitative value of the correlations is questionable. The meta protons are subject to only small shifts which could easily be overwhelmed by solvent or anisotropy effects. Indeed the recent work of Schneider (18) points out the need for caution. He found that the chemical shifts of the C^{13} nuclei in monosubstituted benzenes show appreciable variation due to resonance at the para position and even larger variation due to resonance and anisotropy effects at the ortho positions. At the meta position the variation in chemical shift was extremely small and not interpretable by resonance effects.

EXPERIMENTAL

The spectra were measured with a Varian V-4302 high-resolution N.M.R. spectrometer. Every result reported is the average of at least three determinations. Peak separations were determined by the side-band technique (11, p. 74) employing a Hewlett–Packard wide-range oscillator. The frequency of the side band was counted after each determination with a Hewlett–Packard 521C frequency counter with an accuracy of ±0.1 cycle/sec. If a broad peak was being measured the calibration was carried out by superposition of the reference signal on the desired peak. Alternatively, several of the spectra were calibrated by recording the spectrum of the reference and aromatic compound and their

side bands, then measuring the separation by interpolation. Both methods were used on 2,6-dimethylphenol and were found to agree to within 0.2 cycle/sec. All calibrations with respect to the internal reference were made employing 5% solutions of the aromatic compound in carbon tetrachloride containing 1% of benzene as internal reference. Measurements of the aromatic proton absorption of 2,6-dimethylanisole were made on 20%, 10%, and 5% solutions in carbon tetrachloride. From complete analysis of the multiplet system it was found that the chemical shift between the meta and para protons changed only 0.4 cycle/sec over the range studied. The check on effect of dilution was made since it was necessary to employ a concentration of 10% of some compounds in order to get reproducible measurements of the AB_2 system. For analysis of the deutero, dimethylamino, carboxyl, bromo, and methoxy compounds 5% solutions were employed. It is estimated from the average standard deviation for all compounds that the measured chemical shift between meta and para protons is accurate to within 0.4 cycle/sec and that the same accuracy was obtained for reference measurements. This would lead to a maximum possible error of ± 0.8 cycle/sec for the chemical shifts in Table I. The τ values for the methyl groups as listed in the table were obtained from measurements on 5% solutions in carbon tetrachloride containing 1% of tetramethylsilane. The nitroethylene spectrum was obtained from a 10% solution in carbon tetrachloride containing 1% of tetramethylsilane.

2,6-Dimethylaniline

Reagent grade 2,6-dimethylaniline (Eastman Kodak Co.) was freshly distilled from zinc dust to give a liquid, b.p. 79–80°, 6 mm, n_D^{25} 1.5588 (literature b.p. 216°, 747 mm, n_D^{20} 1.5602 (19)).

2,6-Dimethylnitrobenzene

Practical grade 2,6-dimethyl-1-nitrobenzene (Eastman Kodak Co.) was distilled before use to give a light yellow liquid, b.p. 81°, 7 mm, n_D^{25} 1.5203 (literature b.p. 225°, 744 mm (20, Vol. 3, p. 815)).

2,6-Dimethylphenol

Reagent grade 2,6-dimethylphenol (Eastman Kodak Co.) was twice sublimed before use to give white crystals, m.p. 43–44.5° (literature m.p. 49° (20, Vol. 4, p. 680)).

2,6-Dimethylanisole

Methylation of 2,6-dimethylphenol with dimethyl sulphate in alkali (21, p. 58) gave 69% of product from which a portion was redistilled to give a colorless liquid, b.p. 54°, 6 mm, n_D^{23} 1.5024 (literature b.p. 66–67°, 11 mm, n_D^{25} 1.5003 (22)).

N-*Methyl-2,6-dimethylaniline*

A mixture of 2.55 g (0.021 mole) of 2,6-dimethylaniline and 3.2 g (0.023 mole) of methyl iodide was heated under reflux for 30 minutes. The solid which formed was recrystallized from chloroform and acetone. The purified solid, 2.7 g, was then dissolved in 10% sodium bicarbonate and the solution extracted twice with ether. The ether extracts were dried over magnesium sulphate, then filtered, and the filtrate was distilled to remove the ether. The residue, 1.1 g (37%), was distilled through a Holtzmann column to give N-methyl-2,6-dimethylaniline, b.p. 73.5–74°, 6 mm, n_D^{25} 1.5347 (literature b.p. 87°, 13 mm (12)).

N,N-*Dimethyl-2,6-dimethylaniline*

Following the procedure of Brown and Grayson (19), N,N-dimethyl-2,6-dimethylaniline was prepared in 41% yield. The product distilled at 64–64.5°, 5 mm, n_D^{24} 1.5136 (literature b.p. 195°, 740 mm, n_D^{25} 1.5133 (19)).

2,6-Dimethylbenzonitrile

The nitrile was obtained in 37% yield from 2,6-dimethylaniline by diazotization and treatment with cuprous cyanide (21, p. 514). The product melted from 88–89.3° (literature m.p. 90–91° (23)).

2,6-Dimethylbenzoic Acid

The nitrile was converted to the amide by treatment with concentrated sulphuric acid and thence to the acid by heating with 100% phosphoric acid as described by Berger and Olivier (24). The acid after recrystallization from benzene melted from 115.5–116.5° (literature m.p. 115–116° (24)).

2,6-Dimethyliodobenzene

Following the procedure used for the preparation of iodobenzene (25, p. 351), 2,6-dimethylaniline was converted to the iodo compound in 14% yield. The product was a liquid, b.p. 98–99°, 9 mm (literature b.p. 228–230° (20, Vol. 3, p. 49)). Calc. for C_8H_9I: C, 41.4; H, 3.9. Found: C, 41.6; H, 3.7.

2,6-Dimethylbromobenzene

The procedure used for the conversion of *o*-toluene to *o*-bromotoluene (21, p. 135) was employed to convert 2,6-dimethylaniline into 2,6-dimethylbromobenzene in 15% yield. The product was a liquid, b.p. 74.5–75°, 7 mm, n_D^{25} 1.5532 (literature b.p. 206° (20, p. 379)). Calc. for C_8H_9Br: C, 51.8; H, 4.9. Found: C, 52.4, 51.9; H, 5.0, 5.0.

2,6-Dimethylfluorobenzene

This compound, although not previously prepared, was readily obtained from 2,6-dimethylaniline following exactly the procedure for the conversion of aniline to fluorobenzene (25, p. 295). The product was obtained in 40% yield as a liquid, b.p. 85°, 115 mm, n_D^{28} 1.4762. Calc. for C_8H_9F: C, 77.4; H, 7.3. Found: C, 77.6; H, 7.4.

2,6-Dimethylbenzene-1-d

The procedure for the preparation of this compound was kindly provided by Dr. L. C. Leitch (26). A mixture of 5 g of 2,6-dimethylaniline and 8 ml of heavy water (99.9%) containing a pellet of sodium hydroxide was stirred for 8 hours at 80°. The heavy water was separated in a separatory funnel and the exchange procedure was repeated twice more with fresh heavy water. The amine, 4.18 g (0.035 mole), was added to 12.1 ml of completely deuterated 50% hypophosphorous acid and 6.2 ml of heavy water and the mixture was cooled to −5° in an ice–salt bath. To this was added dropwise a solution of 2.38 g (0.035 mole) of sodium nitrite in 4.2 ml of heavy water keeping the temperature below 0°. The resultant solution was kept at 0° for 20 hours then extracted with ether. The extracts were dried over magnesium sulphate, filtered, and after removal of the ether under reduced pressure, distillation of the residue gave 0.7 g of colorless liquid, b.p. 65° (80 mm), whose N.M.R. spectrum gave no indication of contamination by other products.

Nitroethylene

This compound was prepared by the sequence recommended by Noland (27). The product was a lachrymatory yellow liquid, b.p. 43°, 90 mm, (literature b.p. 38–39°, 80 mm (28)).

ACKNOWLEDGMENTS

The author is grateful to Dr. W. G. Schneider for his helpful discussions. The author wishes to thank Dr. L. C. Leitch for providing the method of preparation of 2,6-dimethylbenzene-1-*d* and for a gift of deuterated hypophosphorous acid. The financial assistance

of the National Research Council of Canada is gratefully acknowledged. The author is also indebted to Mrs. V. Nicolson for technical assistance and to Miss E. Busk for the microanalyses.

REFERENCES

1. H. J. BERNSTEIN, J. A. POPLE, and W. G. SCHNEIDER. Can. J. Chem. **35**, 65 (1957).
2. W. G. SCHNEIDER, H. J. BERNSTEIN, and J. A. POPLE. Ann. N.Y. Acad. Sci. **70**, 806 (1958).
3. P. L. CORIO and B. P. DAILEY. J. Am. Chem. Soc. **78**, 3043 (1956).
4. A. A. BOTHNER-BY and R. E. GLICK. J. Chem. Phys. **26**, 1651 (1957).
5. R. W. TAFT, JR., S. EHRENSON, J. C. LEWIS, and R. E. GLICK. J. Am. Chem. Soc. **81**, 5352 (1959).
6. R. W. TAFT, JR. *In* Steric effects in organic chemistry. *Edited by* M. S. Newman. John Wiley and Sons, Inc., New York. 1956. p. 594.
7. R. W. TAFT, JR. J. Am. Chem. Soc. **79**, 1045 (1957).
8. A. D. BUCKINGHAM. Can. J. Chem. **38**, 300 (1960).
9. F. A. L. ANET. Proc. Chem. Soc. 327 (1959).
10. H. S. GUTOWSKY, C. H. HOLM, A. SAIKA, and G. A. WILLIAMS. J. Am. Chem. Soc. **79**, 4596 (1957).
11. J. A. POPLE, W. G. SCHNEIDER, and H. J. BERNSTEIN. High-resolution nuclear magnetic resonance. McGraw-Hill Book Co., Inc., New York. 1959. p. 88.
12. I. FISCHER. Acta Chem. Scand. **4**, 1197 (1950).
13. K. B. EVERARD, L. KUMAR, and L. E. SUTTON. J. Chem. Soc. 2807 (1951).
14. H. S. GUTOWSKY, D. W. MCCALL, B. R. MCGARVEY, and L. H. MEYER. J. Am. Chem. Soc. **74**, 4809 (1952).
15. E. A. BRAUDE, F. SONDHEIMER, and W. F. FORBES. Nature, **173**, 117 (1954).
16. E. S. WAIGHT and R. L. ERSKINE. Absorption spectra of conjugated carbonyl compounds. *In* Steric effects in conjugated systems. Butterworths Scientific Publications, London. 1958. p. 75.
17. L. M. JACKMAN. Applications of nuclear magnetic resonance spectroscopy in organic chemistry. Pergamon Press, New York. 1959. p. 123.
18. W. G. SCHNEIDER. To be published.
19. H. C. BROWN and M. GRAYSON. J. Am. Chem. Soc. **75**, 20 (1953).
20. I. HEILBRON and H. M. BUNBURY. Dictionary of organic compounds. Eyre and Spottiswoode Ltd., London. 1953.
21. ORGANIC SYNTHESES. Coll. Vol. I, p. 58.
22. D. Y. CURTIN and R. R. FRASER. J. Am. Chem. Soc. **80**, 6016 (1958).
23. R. SCHOLL and F. KACER. Ber. **36**, 327 (1903).
24. G. BERGER and S. C. J. OLIVIER. Rec. trav. Chim. **46**, 600 (1927).
25. ORGANIC SYNTHESES. Coll. Vol. II. p. 351.
26. L. C. LEITCH. Private communication.
27. W. E. NOLAND, H. I. FREEMAN, and M. S. BAKER. J. Am. Chem. Soc. **78**, 188 (1956).
28. N. LEVY and C. W. SCAIFE. J. Chem. Soc. 1471 (1947).

Can. J. Chem. Downloaded from www.nrcresearchpress.com by 210.87.254.40 on 09/05/12
For personal use only.

THE MECHANISMS OF PERMANGANATE OXIDATION

VI. THE OXIDATION OF CYANIDE ION[1, 2]

ROSS STEWART AND R. VAN DER LINDEN[3]

ABSTRACT

Kinetic and oxygen-18 tracer experiments have been used in an attempt to elucidate the mechanism(s) of permanganate oxidation of cyanide. From pH 12 to 14.6 the oxidation is represented by the equation,

$$2MnO_4^- + CN^- + 2OH^- \rightarrow 2MnO_4^{=} + NCO^- + H_2O.$$

From pH 12 to 6 the reaction was found to be complex and unstoichiometric yielding cyanate, carbon dioxide, cyanide ion, and finally cyanogen at pH 9 to 6.

The rate of reduction of permanganate, as followed iodometrically and spectrophotometrically, is found to be markedly dependent on the pH of the medium and reactant concentration. The rate is negligible in acid solution but rapid in basic media.

At pH greater than 12 two parallel processes are indicated which have been designated as reaction A and reaction B. Reaction A appears at low reactant concentrations $<0.0004\ M$ cyanide and higher hydroxyl ion concentrations >pH 13 and is represented by the kinetic expression

$$\left(-\frac{d[MnO_4^-]}{dt}\right)_A = k_2[MnO_4^-][CN^-]$$

where k_2 is independent of hydroxyl ion concentration and is insensitive to the presence of manganate and barium ions. A positive salt effect is observed and labeling experiments using permanganate enriched in oxygen[18] showed that the oxygen introduced into the product cyanate comes mainly from the oxidant (70%–80% oxygen-18 transferred).

The existence of a second process reaction B was indicated by the changing kinetics at higher reactant concentrations and lower basicities, by the non-linear Arrhenius plots, and by the observation that only 15–25% oxygen-18 transfer from permanganate to substrate had occurred at pH 13. The rate of this latter process is approximately represented by the kinetic expression

$$\left(-\frac{d[MnO_4^-]}{dt}\right)_B = \frac{k_3[MnO_4^-][CN^-]^2}{[OH^-]}.$$

These reactions are discussed in terms of mechanism.

INTRODUCTION

The permanganate oxidation of cyanide ion in basic solution is known to be a quantitative reaction and has been used by Drummond and Waters (5) in their studies of the oxidation of organic compounds by various compounds of manganese. Little is known about the mechanism of this reaction, however. Preliminary work in these laboratories (6) indicated that a transfer of oxygen occurs since oxidation with permanganate enriched in oxygen-18 produced cyanate containing an excess of oxygen-18. The present work was undertaken to elucidate the mechanism of this reaction.

After this work was completed a report of a kinetic study of the permanganate–cyanide reaction by Freund appeared (7). He studied the reaction in the 0.035–0.18 M hydroxyl ion region and obtained the rate law

$$-d[MnO_4^-]/dt = k_2[MnO_4^-][CN^-]$$

with an energy of activation of 9.0 kcal/mole^{-1}.

[1]*Manuscript received June 27, 1960.*

Contribution from the Department of Chemistry, University of British Columbia, Vancouver, B.C. From part of the thesis presented by R. V. der L. in partial fulfillment of the requirements for the Ph.D. degree, 1960.

[2]*The paper "The mechanism of the permanganate oxidation of fluoro alcohols in aqueous solution" by Ross Stewart and R. Van der Linden, Discussions Faraday Soc.* **29** *(1960), should be considered as Part V of this series. For earlier papers see references 1 to 4.*

[3]*Present address: Imperial Oil Co., Sarnia, Ontario.*

Can. J. Chem. Downloaded from www.nrcresearchpress.com by 210.87.254.40 on 09/05/12
For personal use only.

EXPERIMENTAL

Product Analysis

1. Cyanogen

A method developed by Rhodes (8) for detecting cyanogen was used. Nitrogen gas was bubbled through the cooled, acidified reaction mixture after the oxidation displacing the gaseous cyanogen. This was washed free of hydrocyanic acid by passing the gas flow through two tubes containing acidified 10% silver nitrate solution, and then was passed into two tubes containing 0.5 *M* sodium hydroxide which can hydrolyze cyanogen quantitatively to cyanide and cyanate (9). Cyanide was then determined by a Liebig titration (10). Yields of cyanogen were much lower if the permanganate oxidation was carried out at room temperature or if the reaction mixture was allowed to stand for any length of time before acidification, owing mainly to extensive hydrolysis under these conditions. If the oxidation was carried out at pH 9 at room temperature no cyanogen was found nor was cyanogen found when freshly precipitated manganese dioxide was used as the oxidizing agent. Paracyanogen or cyanogen polymer could not be observed when the reaction mixture after oxidation was slightly acidified and the manganese dioxide reduced with sodium bisulphite to obtain a clear solution.

2. Cyanate

(*a*) Cyanic acid was converted quantitatively (11) to carbon dioxide and ammonia by acid hydrolysis and the latter was determined by the usual Kjeldahl method. Cyanogen was removed from the reaction solutions before carrying out the Kjeldahl analysis.

(*b*) A gravimetric method, found to be reliable, involved the precipitation of cyanate as the silver salt after neutralization of the alkaline reaction mixtures to pH 5. This method cannot be used when the oxidation is carried out below pH 11, since cyanide, recovered in the reaction mixture, is precipitated as silver cyanide.

3. Carbon Dioxide

The total CO_2 content of the reaction mixtures was determined by using the same technique as for the analysis of cyanogen. Nitrogen was bubbled through the acidified oxidation mixture in which the cyanate has been hydrolyzed to CO_2, then through an acidified 10% silver nitrate solution into two tubes containing standard barium hydroxide solution. The unneutralized barium hydroxide was then titrated with standard acid. The amount of carbon dioxide which is produced in the oxidation at a given pH is the total amount minus the amount produced by cyanate hydrolysis.

4. Cyanide

Cyanide was analyzed by the usual Liebig titration. Below pH 12, where a 2:3 molar ratio of permanganate–cyanide is used, the precipitated MnO_2 was first removed by filtration. Above pH 12, where a 2:1 molar ratio is used, barium nitrate was added initially to the reaction mixture to precipitate insoluble barium manganate, which was then removed by filtration.

Reagents

Reagent grade chemicals were used. Potassium permanganate–O^{18} was prepared as previously described (1).

Alkaline manganate solutions were prepared by the method of Pode and Waters (12). The oxidizing power and alkalinity of the solutions were determined by an iodometric and hydrochloric acid titration methods respectively. A small correction to the alkalinity is required due to disproportionation of manganate. When manganate solutions were diluted, the solution was not allowed to become less basic than 0.01 *M* sodium hydroxide.

Can. J. Chem. Downloaded from www.nrcresearchpress.com by 210.87.254.40 on 09/05/12
For personal use only.

Kinetic Methods

Iodometric and spectrophotometric methods were used to follow the rate of reduction of permanganate and an argentimetric method was used to follow the rate of oxidation of cyanide.

1. Iodometric Method

In a typical kinetic run 50-ml samples were pipetted into 125-ml glass-stoppered Erlenmeyers and the Erlenmeyers brought to a temperature of 25±0.05° in a constant temperature bath. After addition of the permanganate these aqueous solutions became 0.1 *M* in KOH, 0.00024 *M* in KCN, 0.0005 *M* in $KMnO_4$, and 0.0363 *M* in K_2SO_4 ($\mu = 0.2$).

The reaction was initiated by introducing 4.73 ml of 0.00574 *M* permanganate solution with manual stirring from a rapid delivery pipette. The reaction was quenched at a given time interval with an acidified potassium iodide solution and the liberated iodine was titrated immediately with thiosulphate solution. In most cases at least eight points were obtained for the kinetic plots. The procedure for following the rate of manganate oxidation of cyanide was similar except that equimolar concentrations of reactants were used.

2. Spectrophotometric Method

This was essentially the same as that previously described with light absorption measurements being made at 522 and 426 mμ (3).

3. Argentimetric Method

In a typical kinetic method for following the rate of oxidation of cyanide the solutions were made up as for the iodometric method. Then 4.92 ml of 0.0116 *M* permanganate solution was added to each solution to start the reaction. The reaction was timed and then quenched with 1 drop of 30% hydrogen peroxide and the manganese dioxide filtered off. The clear solution was then titrated for cyanide by the Liebig method using 0.05 *M* silver nitrate solution.

4. Fast Reaction Kinetics

For very fast reactions the disappearance of permanganate was followed with the aid of an automatic quenching and timing device like that described by Sheppard and Wahl (13).

Oxygen-18 Tracer Techniques

1. Oxidation of Cyanide with Permanganate–O^{18}

Procedure (a): Silver cyanate obtained under stoichiometric reaction conditions.—A typical experiment was performed as follows. Over-all conditions: volume of solution 55 ml; approximate alkalinity 4 *M*; $[CN^-]_0 = 0.0195$ *M*. To a 125-ml glass-stoppered Erlenmeyer was added 0.304 gram of potassium permanganate (0.00192 mole; 1.114% enriched in O^{18}) dissolved in 25 ml boiled distilled water, 10 ml of 0.2 *M* barium nitrate solution, and 14 ml of 15.8 *M* sodium hydroxide carbonate free solution. The solution was cooled and immediately 5.5 ml of 0.195 *M* (0.00107 mole) potassium cyanide solution was pipetted into the stirred alkaline permanganate solution. The reaction mixture was allowed to stand for approximately 5 minutes at room temperature. The solution was centrifuged and the supernatant liquid filtered through a sintered glass funnel to remove the remaining insoluble barium manganate. The clear alkaline solution was then neutralized to pH 5 with dropwise addition of 4 *M* nitric acid. The neutralizing mixture was cooled in an ice bath while the solution was vigorously stirred with a magnetic stirring arrangement. Four milliliters of 0.5 *M* silver nitrate solution was added, silver cyanate was allowed to

settle and filtered on a sintered glass funnel, washed, and then dried over P_2O_5 under vacuum.

Procedure (b): Silver cyanate obtained using a twofold excess permanganate-O^{18}.—When a twofold excess of labeled permanganate was used, the excess permanganate was reduced with a few drops of 30% hydrogen peroxide after the reaction mixture was allowed to stand for 2 minutes. After filtration and centrifugation of the managanese dioxide – barium manganate precipitate, the solution was neutralized and the silver cyanate precipitated as in the previous procedure.

Procedure (c): Silver cyanate obtained under dilute reaction conditions.—Over-all conditions: volume of solution 500 ml of water; alkalinity 0.2 M; $[CN^-]_0 = 2.2\times10^{-3}$ M; $[MnO_4^-]_0 = 2.27\times10^{-3}$ M. To a 1000-ml stoppered Erlenmeyer was added 0.172 (0.00109 mole) of labeled permanganate dissolved in 300 ml of water, 5.6 grams of barium nitrate dissolved in 150 ml of water, than 49 ml of 2.04 M sodium hydroxide solution. To the vigorously stirred mixture was added 10 ml of 0.1088 M (0.00109 mole) potassium cyanide solution. The reaction mixture was allowed to stand until the permanganate color had disappeared (approximately 15 minutes) and then the combined silver cyanide – silver cyanate precipitate was obtained as before.

2. Determination of Oxygen Exchange Between Cyanate and H_2O^{18}

A typical experiment was performed as follows: A sample of recrystallized potassium cyanate (0.092 gram, 0.00113 mole) was weighed into a 4-ml stoppered flask and dissolved with 2 ml of water (>1.4% enriched in O^{18}). The pH of the solution, as measured on a Beckman Model G pH meter, was varied by addition of concentrated sodium hydroxide or dilute nitric acid. The solution was allowed to stand in a constant temperature bath at 25° for 30 minutes. The acidified solution was transferred to a 5-ml centrifuge tube and the cyanate precipitated with silver nitrate solution. The precipitate was centrifuged, the liquid decanted, and the solid washed with water. The wet precipitate was transferred to a 5-ml beaker, dried over calcium chloride and then over P_2O_5 under vacuum.

3. O^{18} *Analysis of Silver Cyanate*

Two methods, sulphuric acid decomposition and pyrolysis, were found suitable for converting silver cyanate to carbon dioxide which could be conveniently analyzed for O^{18} content by mass spectrometric analysis.

Method (a).—The silver cyanate was dropped on to concentrated sulphuric acid and the evolved carbon dioxide was collected. This method is similar to that previously used (12) except that break seals were used to transfer the gas to the mass spectrometer. The amount of excess O^{18} found in the silver cyanate can be calculated using the following equation (1); natural abundance of O^{18} = 0.204%.

$$\%\ \text{O from permanganate} = \frac{2y-0.408}{x-0.204}\times 100,$$

where

$$2y = \frac{I_{\text{mass}}46}{I_{\text{mass}}44 + I_{\text{mass}}46},$$

$$x = \%\ O^{18}\ \text{in}\ KMnO_4 = 1.114.$$

Method (b).—The silver cyanate samples were decomposed under a low flame using the same apparatus as for the previous method. The carbon dioxide produced was collected and analyzed in a mass spectrometer. Other gases were produced in the decomposition as

Can. J. Chem. Downloaded from www.nrcresearchpress.com by 210.87.254.40 on 09/05/12
For personal use only.

observed by scanning the mass spectrum of the gaseous material but unlabeled silver cyanate on decomposition gave the expected normal isotopic abundance for O^{18}. The amount of O^{18} found in the silver cyanate can be calculated using a similar equation except that now all the oxygen in the carbon dioxide comes from the silver cyanate.

$$\% \ O^{18} \text{ from permanganate} = \frac{y-0.204}{x-0.204} \times 100,$$

where

$$2y = \frac{I_{mass}46}{I_{mass}46 + I_{mass}44},$$

$$x = \% \ O^{18} \text{ in } KMnO_4 = 1.114.$$

Similar results were obtained when samples of silver cyanate were subjected to analysis by both methods.

RESULTS

Kinetic Results

The rate constants were calculated using the following equations (1). For the iodometric method

$$k_2 = \frac{1}{[CN^-]_0 \times t} \times \frac{V_0 - V_t}{V_t - 4/5 V_0}$$

where V is the volume of thiosulphate solution required in the titration. When $(V_0 - V_t)/(V_t - 4/5 V_0)$ was plotted against time, linear plots were obtained over a limited reactant and hydroxyl ion concentration range. Linear second-order rate plots were obtained in some cases to 70% completion of the reaction although most plots were taken to 50% completion. Second-order rate constants (k_2, liter mole^{-1} sec^{-1}) were calculated from the slopes.

For the spectrophotometric method the following equation was used, where D is optical density at the indicated wavelength (3):

$$[MnO_4^-] = \frac{D_{522} - 0.282 D_{426}}{2248}.$$

The usual integrated second-order rate expression was applied to the rate data.

Plots of reciprocal of the permanganate concentration versus time were found to be linear up to approximately 50% reaction (Fig. 1) and second-order rate constants were calculated. The plots become non-linear and variable if the reaction was taken beyond 50% completion of the reaction possibly from light scattering due to precipitation of manganese dioxide caused by disproportionation of manganate.

The rate expression

$$-\frac{d[MnO_4^-]}{dt} = k_2[CN^-]\,[MnO_4^-]$$

is in agreement with the observed kinetics over a limited reactant and hydroxyl ion concentration range. The second-order rate constants k_2, liter mole^{-1} sec^{-1}, obtained by both spectrophotometric and iodometric kinetic methods are in good agreement and indicate that the rate constants, calculated from the rate plots, are reliable (Table I).

Can. J. Chem. Downloaded from www.nrcresearchpress.com by 210.87.254.40 on 09/05/12
For personal use only.

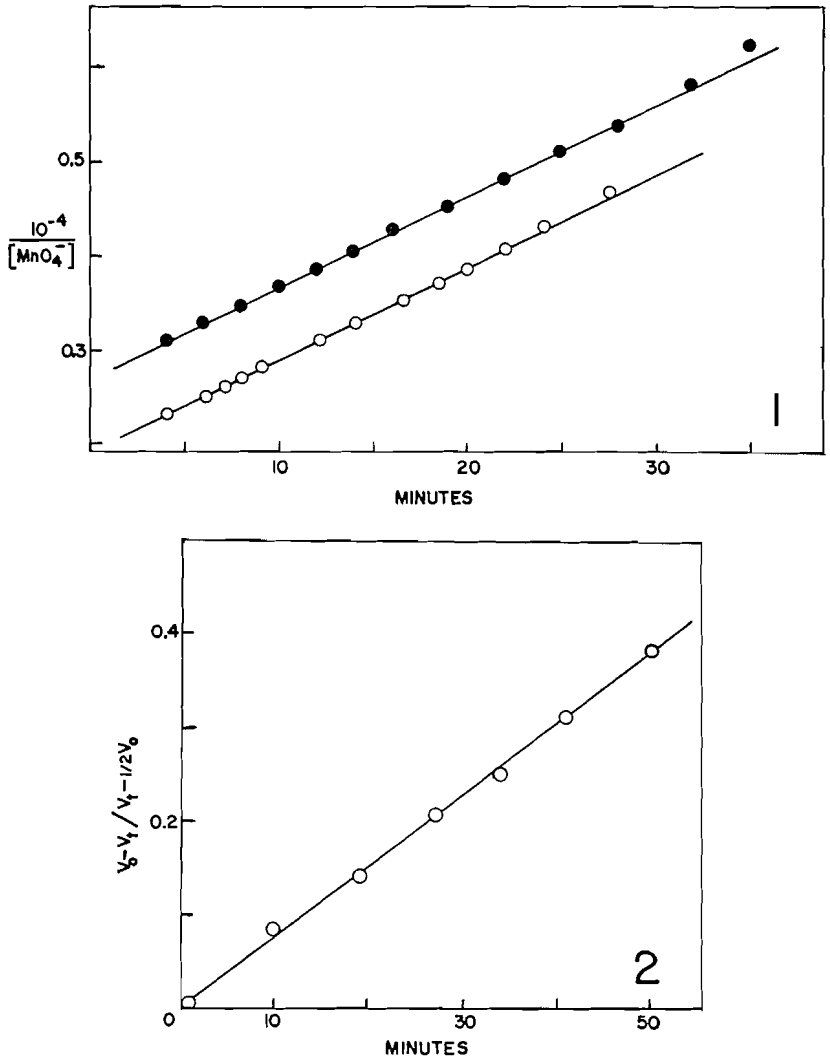


FIG. 1. Second-order rate plots for the permanganate–cyanide reaction by the spectrophotometric method.
$[OH^-] = 0.1\ M$, $T = 25°$, $k_2 = 3.20$ l. mole^{-1} sec^{-1}. ● $[MnO_4^-]_0 = 2[CN^-]_0 = 3.67\times10^{-4}$ mole/l.; ○ $[MnO_4^-]_0 = 2[CN^-]_0 = 5.13\times10^{-4}$ mole/l.

FIG. 2. Second-order rate plot for the manganate–cyanide reaction.
$[MnO_4^-]_0 = [CN^-]_0 = 3.27\times10^{-3}$ mole/l., $[OH^-] = 0.125\ M$, $T = 25°$, $k_2 = 0.039$ l. mole^{-1} sec^{-1}.

Observation of Table II with reference to Table I indicates that the second-order rate constants are relatively insensitive to additions of initial amounts of manganate ions and barium ions. Strontium nitrate was used to replace barium nitrate in one experiment in order to keep the ionic strength constant. Addition of initial amounts of manganate to the reaction mixture was possible since this species oxidizes cyanide 80 times slower than permanganate (Fig. 2).

Can. J. Chem. Downloaded from www.nrcresearchpress.com by 210.87.254.40 on 09/05/12
For personal use only.

TABLE I

Table of second-order rate constants for the permanganate–cyanide reaction under various conditions

Method	$[CN^-]_0$, M	$[OH^-]$, M	μ	k_2, l. mole^{-1} sec^{-1}
S	1.84×10^{-4}	0.1	0.1	3.2
S	2.57×10^{-4}	0.1	0.1	3.2
I	2.44×10^{-4}	0.1	0.1	2.9*
I	4.50×10^{-4}	0.1	0.2	4.0†
I	2.44×10^{-4}	0.1	0.2	3.9*
S	1.74×10^{-4}	0.2	0.2	3.7
I	2.44×10^{-4}	0.2	0.2	3.7‡
I	2.53×10^{-4}	0.06	0.1	3.0†
S	1.84×10^{-4}	0.06	0.1	3.4

NOTE: I = iodometric method, S = spectroscopic method, $[MnO_4^-]_0 = 2[CN^-]_0$; temperature = 25±0.05°.

*Average of two determinations.

†Rate constant obtained from the linear portion of the plot.

‡Average of three determinations.

TABLE II

Effect of initial amounts of manganate and barium nitrate on the second-order rate constants

$[CN^-]_0$, M	$[MnO_4^=]_0$, M	$[OH^-]$, M	μ	k_2,* l. mole^{-1} sec^{-1}
1.84×10^{-4}	1.78×10^{-4}	0.1	0.1	2.60
1.84×10^{-4}	3.55×10^{-4}	0.1	0.1	2.60
2.20×10^{-4}	2.13×10^{-4}	0.1	0.1	2.90

$[CN^-]_0$, M	$[Ba(NO_3)_2]$, M	$[OH^-]$, M	μ	k_2,† l. mole^{-1} sec^{-1}
2.53×10^{-4}	0.005	0.2	0.215	4.10
2.53×10^{-4}	—	0.2	0.215	3.50‡
2.53×10^{-4}	0.005	0.2	0.215	3.70

*Spectrophotometric kinetic method.

†Iodometric kinetic method; $[MnO_4^-]_0 = 2[CN^-]_0$; temperature = 25±0.05°.

‡0.005 M $Sr(NO_3)_2$ used in this experiment.

Data from Table I and Table III indicate that the second-order reaction is independent of the hydroxyl ion concentration under constant ionic strength conditions. For example, a 25-fold change in hydroxyl ion concentration does not change k_2 appreciably.

If increasing amounts of an inert electrolyte (potassium sulphate or potassium nitrate) are added to the reaction mixtures an increase in rate is observed at 0.1 M potassium hydroxide (Table IV and Table III). A primary positive salt effect is observed when log k_2 is plotted against $\sqrt{\mu}$ giving a straight line of slope +1 (Fig. 3). This agreement with the value expected from the Brönsted–Debye–Hückel relationship is rather surprising since this is a region of high ionic strength.

In order to determine the activation parameters a temperature study was done at 0.1 M and 0.2 M potassium hydroxide (Fig. 4 and Table V). When Arrhenius-type plots were made, linear plots were not obtained indicating that a more complex process was taking place than was implied by the simple rate expression given previously.

Since the kinetics indicate the presence of more than one mode of oxidation of cyanide by permanganate, the reaction conditions under which the second-order process (referred

Can. J. Chem. Downloaded from www.nrcresearchpress.com by 210.87.254.40 on 09/05/12
For personal use only.

TABLE III

Table of second-order rate constants for the permanganate–cyanide reaction under saturated salt* conditions

$[CN^-]_0$, M	$[OH^-]$, M	k_2, l. mole^{-1} sec^{-1}
4.04×10^{-4}	0.1†	8.2
2.02×10^{-4}	0.1*†	6.4
4.04×10^{-4}	0.2†	8.3
2.02×10^{-4}	0.2†	6.4
4.04×10^{-4}	0.53†	6.0
4.04×10^{-4}	1.55†	6.6
4.04×10^{-4}	2.41	7.8
4.04×10^{-4}	3.36	13.7±10%
4.04×10^{-4}	3.65	20.0±20%
4.04×10^{-4}	0.03†	16.5 } Initial rates taken from the
4.04×10^{-4}	0.03	16.5 } non-linear plots

*Use of 2 M KNO_3 gave a limiting reaction rate, i.e. further increases in salt concentration did not increase rate of reaction. Iodometric method, procedure 4; temperature = 25±0.05°.

†Ionic strength = 2.0; $[MnO_4^-]_0 = 2[CN^-]_0$.

TABLE IV

Rate constant as a function of ionic strength

Ionic strength	k_2, l. mole^{-1} sec^{-1}
0.1	2.90
0.1	2.80
0.133	3.20
0.166	3.40
0.166	3.67
0.200	3.90
0.200	3.90

NOTE: $[OH^-] = 0.1$ M; $[CN^-]_0 = 2.44\times10^{-4}$ M; $[MnO_4^-]_0 = 2[CN^-]$; potassium sulphate used to vary μ; temperature = 25±0.05; iodometric method.

TABLE V

Table of second-order rate constants at various temperatures

Temperature	0.1 M KOH k_2, l. mole^{-1} sec^{-1}	0.2 M KOH k_2, l. mole^{-1} sec^{-1}
10°±0.05	—	1.84
10°±0.05	—	1.88
15°±0.05	2.30	2.20
15°±0.05	2.20	2.16
20°±0.05	2.60	2.62
20°±0.05	—	2.64
30°±0.05	3.50	4.40
35°±0.05	4.3	5.80
35°±0.05	5.0	5.76

NOTE: $[MnO_4^-]_0 = 2[CN^-]_0 = 2.44\times10^{-4}$ M. Refer to Table I for 25° temperature points.

to herein as reaction A) is observed are summarized as follows:

when (*a*) $[MnO_4^-] = 2[CN^-]$ is less than 8×10^{-4} M;

(*b*) $[OH^-]$ is greater than or equal to 0.1 M;

(*c*) temperature is 25°.

Can. J. Chem. Downloaded from www.nrcresearchpress.com by 210.87.254.40 on 09/05/12
For personal use only.

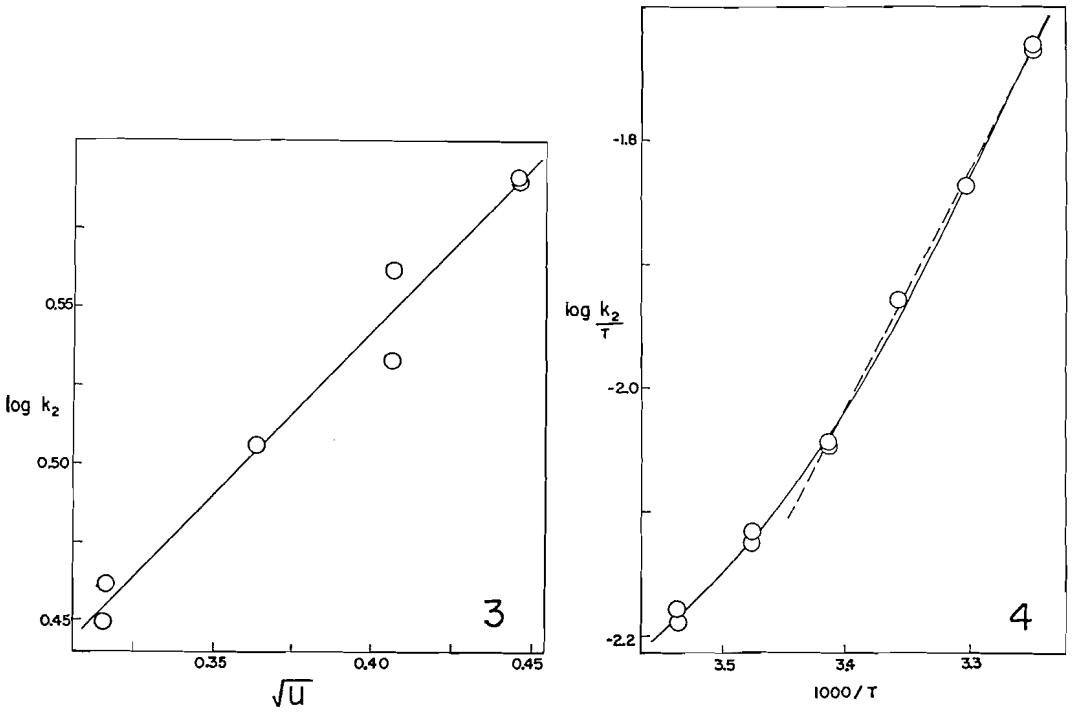


FIG. 3. Log k_2 vs. the square root of the ionic strength for the alkaline permanganate oxidation of cyanide. Slope = 1.0.

FIG. 4. Effect of temperature change on the rate of the permanganate–cyanide reaction in 0.2 *M* KOH. The straight line gives $\Delta H^{\ddagger} = 8.7$ kcal mole^{-1} and $\Delta S^{\ddagger} = -27$ e.u.

If second-order rate plots are attempted at higher concentration of reactants at the *same alkalinity* (Fig. 5) or lower alkalinities at the *same concentration of reactants* (Fig. 6), non-linear second-order rate plots are obtained and the rate was found to decrease with time. Under intermediate conditions (Fig. 6) the initial second-order rate plots are non-linear, becoming linear when the concentration of the reactants has been reduced.

The presence of a second mode of oxidation of cyanide is indicated (reaction B). Its rate appears to be a different function of concentration than the second-order process observed at lower concentrations and its rate is inhibited by high hydroxyl ion concentration. In an attempt to separate the two suspected reactions, concentration versus time plots were made for the rate data (Fig. 7) which gave non-linear second-order kinetics. These curves were smoothed and the slopes $(-d[MnO_4^-]/dt)_{A+B}$ obtained at various times.

Consider two parallel reactions contributing to the over-all rate,

$$\left(-\frac{dMnO_4^-}{dt}\right)_{A+B} = \left(-\frac{dMnO_4^-}{dt}\right)_A + \left(-\frac{dMnO_4^-}{dt}\right)_B,$$

where

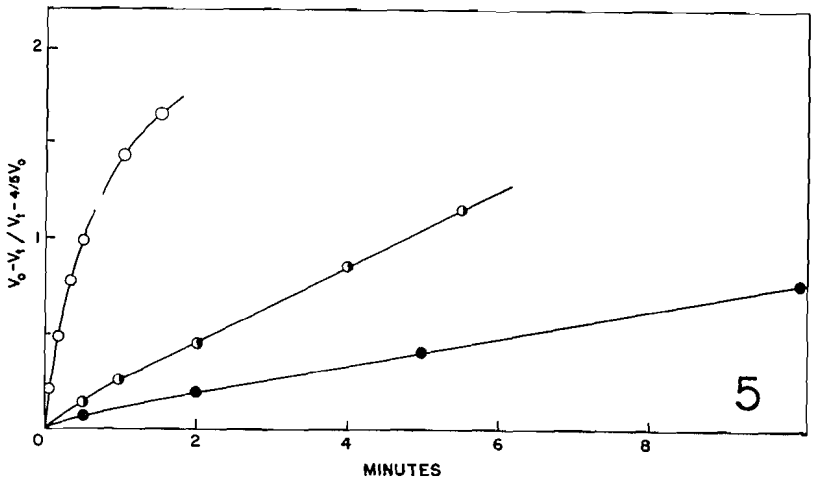
$$\left(-\frac{dMnO_4^-}{dt}\right)_A = \tfrac{1}{2}k_2[MnO_4^-]^2,$$

and

$$\left(-\frac{d[MnO_4^-]}{dt}\right)_B \propto [MnO_4^-]^n.$$

Can. J. Chem. Downloaded from www.nrcresearchpress.com by 210.87.254.40 on 09/05/12
For personal use only.

Can. J. Chem. Downloaded from www.nrcresearchpress.com by 210.87.254.40 on 09/05/12
For personal use only.



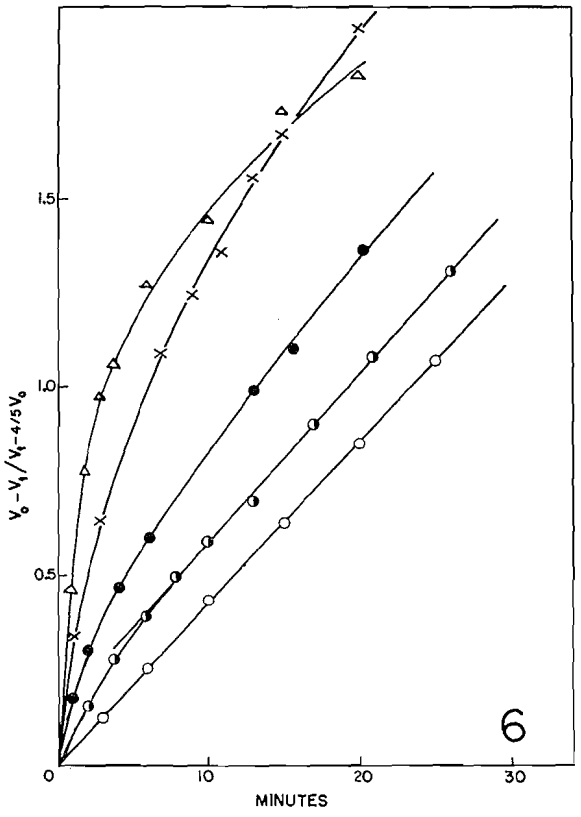


FIG. 5. Variation of the second-order rate function with reactant concentration in 0.1 M NaOH. $T = 25°$, $\mu = 2(KNO_3)$, $[MnO_4^-]_0 = 2[CN^-]_0$. ○ $[CN^-]_0 = 7.49\times10^{-4}$; ◑ $[CN^-]_0 = 4.04\times10^{-4}$; ● $[CN^-]_0 = 2.02\times10^{-4}$ mole/l.

FIG. 6. Variation of the second-order rate function with hydroxyl ion concentration. $[MnO_4^-] = 2[CN^-]_0 = 5.06\times10^{-4}$ mole/l., $\mu = 0.1$ (K_2SO_4), $T = 25°$. Δ = 0.01 M KOH; × = 0.02; ● = 0.04; ◑ = 0.06; ○ = 0.10.

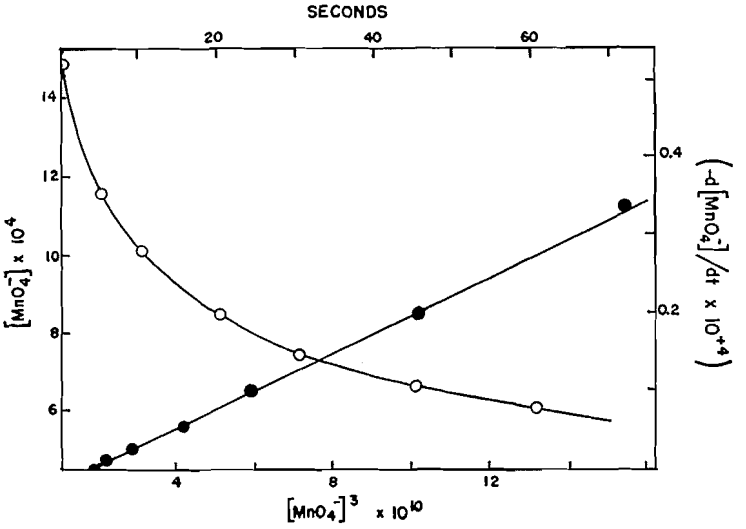


FIG. 7. Concentration vs. time (○) and the third-order rate plot (●) for the permanganate–cyanide reaction.
$[CN^-]_0 = 7.49\times10^{-4}$ mole/l., $[OH^-] = 0.1\ M$, $\mu = 2.0$.

Substituting for reaction A in the above equation and rearranging

$$\left(-\frac{d[MnO_4^-]}{dt}\right)_B = \left(-\frac{d[MnO_4^-]}{dt}\right)_{A+B} - \tfrac{1}{2}k_2[MnO_4^-]^2.$$

Therefore if k_2 is known at the same ionic strength and temperature and since reaction A is found to be independent of hydroxyl ion concentration, the rate of reaction A can be subtracted from the over-all rate.

A plot of $(-d[MnO_4^-]/dt)_B$ versus $[MnO_4^-]^3$ gives a straight line (Fig. 7). This technique was applied to a number of rate plots which gave non-linear second-order kinetics. The results although qualitative indicated that the reaction is third order and that the reaction is inhibited by hydroxyl ions.

Thus
$$\left(-\frac{d[MnO_4^-]}{dt}\right)_B = k_3[MnO_4^-]^3.$$

In order to determine the dependence of rate of reaction B on hydroxyl ion concentration more accurately, another plot using initial rates as obtained from the rate data from pH 12 to 13 was made. The initial point of the concentration–time plot was used to obtain $(-d[MnO_4^-]/dt)_{A+B}$ (Table VI).

TABLE VI
Initial rate as a function of hydroxyl ion concentration*

$[OH^-]$, M	$(-d[MnO_4^-]/dt)_{A+B\ (initial\ rate)}$	$[OH^-]\times$initial rate
0.01	0.034×10^{-4}	3.4×10^{-8}
0.02	0.021×10^{-4}	4.2
0.04	0.012×10^{-4}	4.8
0.05	0.0082×10^{-4}	4.1
0.06	0.0053×10^{-4}	3.2
0.10	0.0033×10^{-4}	3.3

*$[CN^-]_0 = 2.53\times10^{-4}$ mole/l.; $\mu = 0.1$; temperature = 25°.

Can. J. Chem. Downloaded from www.nrcresearchpress.com by 210.87.254.40 on 09/05/12
For personal use only.

The data in Table VI show that the initial rate multiplied by the hydroxyl ion concentration is very roughly a constant indicating that

$$k_3 \approx \frac{k_3'}{[OH^-]}.$$

The next stage in the investigation of this third-order process (reaction B) was to examine the kinetics of the very fast reaction when a 10-fold excess cyanide was used. Though the results are only qualitative a plot of log $[MnO_4^-]$ versus time (Fig. 8) at 0.03 *M* NaOH was approximately first order in permanganate after the first 5 seconds.

In an attempt to determine whether manganate was involved in a prior equilibrium step barium ions were added initially to the kinetic mixture. No marked change in rate was observed at 0.01 *M* and 0.04 *M* sodium hydroxide when insoluble barium manganate was precipitated. Also checks were made under various conditions using strontium nitrate to keep the ionic strength constant with no variation in rate being observed.

The spectrophotometric kinetic method led to marked non-linear second-order rate plots only at lower hydroxyl ion concentration, e.g. (0.02 *M* sodium hydroxide, μ = 0.1), since the permanganate and cyanide concentration used in this method were necessarily lower than those concentrations used in the iodometric method. It was observed that reaction B was greatly accelerated by increases in ionic strength.

Reduction of manganese to a lower valence state was considered as a possible cause for the observed faster reactions at lower alkalinities and higher reactant concentrations. If a deep-seated oxidation was taking place reducing permanganate or manganate to

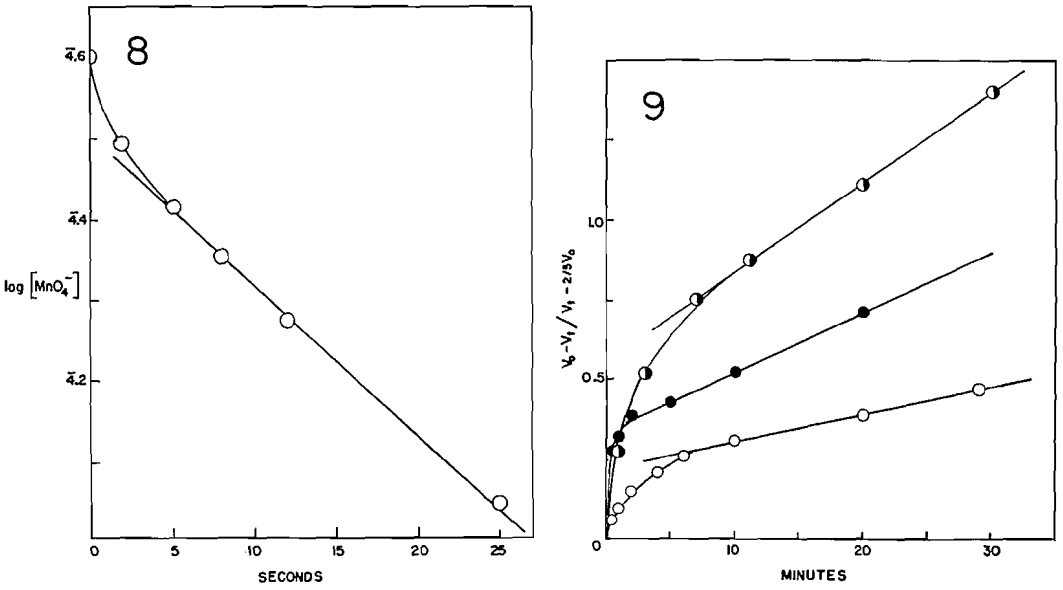


FIG. 8. Rate of disappearance of permanganate in presence of excess cyanide.
$[CN^-]_0 = 20.3 \times 10^{-4}$ mole/l., $[MnO_4^-]_0 = 4.03 \times 10^{-4}$ mole/l., $[OH^-] = 0.03$ mole/l., $T = 25°$, $k_1 = 0.0336$ sec^{-1}.

FIG. 9. Second-order rate function vs. time for the permanganate–cyanide reaction in weakly basic solution.
$[MnO_4^-]_0 = 2/3[CN^-]_0$, $\mu = 0.1$ (K_2SO_4), $T = 25°$, ○ pH = 10.4, $[CN^-]_0 = 2.67 \times 10^{-4}$ mole/l., $k_2 = 0.54$ l. mole^{-1} sec^{-1}; ● pH = 10.4, $[CN^-]_0 = 5.43 \times 10^{-4}$ mole/l., $k_2 = 0.59$ l. mole^{-1} sec^{-1}; ◑ pH = 9.8, $[CN^-]_0 = 2.52 \times 10^{-4}$ mole/l., $k_2 = 1.92$ l. mole^{-1} sec^{-1}.

Can. J. Chem. Downloaded from www.nrcresearchpress.com by 210.87.254.40 on 09/05/12
For personal use only.

lower oxidation states, an excess of cyanide over permanganate should be observed as reaction proceeds. Therefore, the argentimetric method for following the rate of oxidation of cyanide was developed. Observation of the concentration–time plots, obtained by both argentimetric and iodometric methods for the faster process at 0.1 *M* and 0.01 *M* sodium hydroxide, indicate that the stoichiometric concentrations (in this case $[MnO_4^-]$:$[CN^-]$ 2:1 molar ratio) holds throughout a major portion of the plot.

Early in the kinetic study a number of rate plots were obtained for the reaction at low pH's, and a few of these plots are presented (Fig. 9). Since the kinetics were more complex than those studied in more basic solution, a relative rate study was undertaken. This was accomplished by measuring the rate of the permanganate–cyanide reaction over a wide pH range, stopping the reactions at a given time interval. The extent of the reduction of permanganate was determined in an iodometric titration and $V_0 - V_t$ plotted against pH for a number of reaction conditions (Fig. 10).

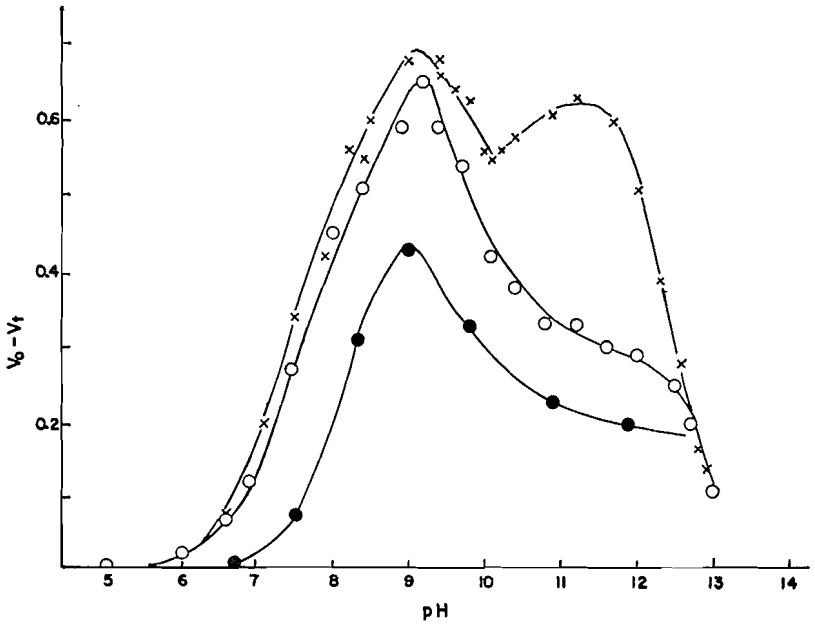


FIG. 10. Volume of thiosulphate consumed in a fixed time interval for the permanganate–cyanide reaction.

$T = 25°$, $\mu = 0.1$. ● $[CN^-]_0 = 3/2[MnO_4^-]_0 = 2.53\times10^{-4}$ mole/l., time interval = 2 minutes; ○ $[CN^-]_0 = 3/2[MnO_4^-]_0 = 2.09\times10^{-4}$ mole/l., time interval = 5 minutes; × $[CN^-]_0 = \frac{1}{2}[MnO_4^-]_0 = 2.09\times10^{-4}$ mole/l., time interval = 2 minutes.

Two important results might be noted:

(*a*) The rate of the permanganate-cyanide reaction is negligible in acid solution and increases markedly with increasing basicity.

(*b*) The maximum rate of the relative rate plots appears at the pK_a of HCN (pH = 9).

Oxygen-18 Tracer Results

Observation of Table VII shows that a transfer of oxygen has occurred from the oxidizing agent permanganate to the substrate cyanide. The percentage of O^{18} transferred appears to depend on the molar ratio and concentration of reactants as well as the alkalinity used in the experiments.

Can. J. Chem. Downloaded from www.nrcresearchpress.com by 210.87.254.40 on 09/05/12
For personal use only.

TABLE VII

Percentage O^{18} transferred from permanganate to cyanide under various reaction conditions

Alkalinity, M	$[MnO_4^-]_0/[CN^-]_0$	% O^{18} transferred (mean)	% O^{18} transferred (maximum)*
6	2/1†	—	80
4	2/1	70‡	78§, ‖
3	2/1	60¶	70
1.5	2/1	—	55
1	2/1	—	31
0.4	2/1	22**	25
0.1	2/1	20¶	23††
0.4	2/1	—	20
4	4/1	—	71‡‡
0.1	4/1	—	49‡‡
0.5	1/1	—	47§§
0.02	1/1	—	16§§
pH = 11.2	2/3	—	14
= 10	2/3	—	19
= 8	2/3	—	10

*$[CN^-]_0$ = 0.019 M; CO_2 obtained by pyrolysis of AgOCN. †Approximately 5% excess cyanide used in these experiments. ‡Average of five determinations. §76% obtained by the sulphuric acid method with the same sample. ‖82% transferred when the reaction was carried out at 50°. ¶Average of two determinations. **Average of three determinations. †† 26% transferred under saturated salt conditions, i.e., ionic strength 4, KNO_3. ‡‡$[CN^-]_0$ = 0.013 M. §§$[CN^-]_0$ = 0.0023 M.

In order to determine whether the product cyanate exchanges its oxygen with the solvent, cyanate was equilibrated with H_2O^{18} (<1.4% enriched) for 30 minutes at 25° at various acidities (six experiments were performed over a pH range from 5 to 14.6). In all experiments a negligible amount of O^{18} (0 to 2%) was found in the cyanate recovered as the silver salt, indicating that cyanate does not exchange its oxygen with the solvent in the time required to perform the oxidation.

The variation in the amount of O^{18} transferred under apparently similar conditions (e.g., 4 M sodium hydroxide) is difficult to explain but it should be pointed out that exchange reactions (14) can serve only to decrease the apparent transfer of O^{18} and, therefore, the maximum percentage transfer at any given pH can be used as a criterion of mechanism.

The O^{18} tracer and kinetic data will be discussed in terms of mechanism further in the paper, but the important features of the tracer data might be itemized as follows:

(*a*) The maximum percentage of O^{18} transferred in any experiment was 82% in 4 M sodium hydroxide at 50°.

(*b*) A general increase in percentage of O^{18} transferred is observed as the alkalinity is increased from 0.04 M to 6 M sodium hydroxide, i.e., fourfold increase (Fig. 11).

(*c*) The low percentage of O^{18} transferred at 0.1 M sodium hydroxide is not affected when the reaction is carried out at high ionic strength, i.e., $\mu = 4$.

(*d*) Almost a twofold increase in O^{18} transfer occurred on diluting the reaction mixture by eightfold at 0.4–0.5 M sodium hydroxide whereas at 0.02–0.04 M sodium hydroxide no change in percentage transfer took place.

(*e*) No further increase in O^{18} transfer is observed when the reaction is carried out with excess permanganate–O^{18} at 4 M base whereas an approximate twofold increase is observed at 0.1 M sodium hydroxide.

(*f*) In weakly basic solution, pH <12, only a small percentage of the oxygen introduced into cyanate originates from the oxidant.

Can. J. Chem. Downloaded from www.nrcresearchpress.com by 210.87.254.40 on 09/05/12
For personal use only.

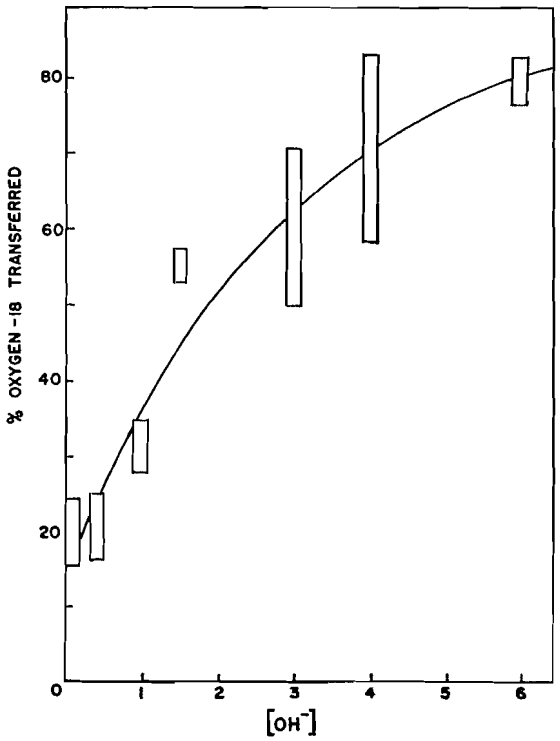


FIG. 11. Percentage of oxygen-18 transferred from permanganate to cyanide as a function of the molarity of hydroxyl ion.
$[MnO_4^-]_0 = 2[CN^-]_0$. The bar heights represent the variations found in different experiments.

DISCUSSION

The correlation of kinetic, oxygen-18 tracer, and analytical data which were of necessity obtained under different reaction conditions presents considerable difficulty. The kinetic data could only be conveniently obtained under low reactant concentration conditions where the rate was relatively small, whereas oxygen[18] tracer and analytical experiments necessitated in most cases considerably higher reactant concentrations.

The main features of the analytical data obtained for the permanganate–cyanide reaction over the pH range 6 to 14.6 are the following: Above pH 12 the sole product of the reaction is cyanate in almost quantitative yield; below pH 12 the reaction becomes increasingly unstoichiometric, yielding cyanate, carbon dioxide, cyanide, and finally cyanogen, which is isolated at pH 9 to 6. Cyanogen is presumably formed at higher basicities in these reaction mixtures but hydrolysis is very rapid at any pH greater than 9.

A fair material balance was obtained for the reaction over most of the pH range studied except for nitrogen (Table VIII). The presence of cyanogen in the reaction mixture (15) gives a ready explanation for the production of carbon dioxide through a deep-seated oxidation with permanganate and consequent recovery of cyanide, since cyanogen is known to hydrolyze readily in aqueous solutions to a number of easily oxidizable compounds (16, 17). As a consequence most of the kinetic and oxygen-18 tracer experiments were performed in alkaline solution above pH 12.

The rate of permanganate oxidation of cyanide is found to be markedly dependent on

Can. J. Chem. Downloaded from www.nrcresearchpress.com by 210.87.254.40 on 09/05/12
For personal use only.

TABLE VIII

Product yields for the permanganate–cyanide reaction

pH	13	12	11	10	9	8	7
% OCN^- Kjeldahl method	94		84	40	35	30	12
% OCN^- as AgOCN	98	96					
% Total CO_2*		99	96	71	50		46
% CO_2 produced in the reaction*		—	12	31	15†		24
% CN^- recovered			—	27	41		46
%$(CN)_2$	—	—	—	—	Trace	11	28

NOTE: Cyanide concentration approximately 0.02 *M* in the analytical experiments; 3:2 molar ratio of cyanide to permanganate used below pH 12; 1:2 molar ratio used at pH 12 and above.

*Total CO_2 includes that formed by complete hydrolysis of cyanate during the analysis plus that formed by the oxidation reaction. (See experimental section.)

†Weighed as barium carbonate.

the pH of the medium and on the reactant concentrations. Thus the rate of reaction is negligible in acid solution at pH 6 or less, and above pH 7 the rate increases rapidly as the solution becomes more alkaline, reaching a maximum rate at pH 9.1. At this point the rate decreases again as the alkalinity is increased and at pH 13 (depending on reactant concentration) the rate levels off and becomes independent of pH except for an ionic strength effect (Fig. 29).

Two reaction paths, A and B, are indicated. Since the experimental evidence for reaction A is more clear-cut, this process will be discussed first.

Route A

(1) Second-order kinetics are observed over a limited reactant and hydroxyl ion concentration range indicating that the rate expression

$$\left(-\frac{d[MnO_4^-]}{dt}\right)_A = k_2[MnO_4^-]\,[CN^-]$$

holds for reaction A.

(2) A primary positive salt effect was observed indicating that the slow step was between two like singly charged ions, presumably permanganate and cyanide ions. This result is surprising in this case in view of the fact that the Brönsted–Debye–Hückel relationship normally holds for reactions carried out under more dilute aqueous conditions. Though the result is qualitatively correct, the close correlation to theory may be the result of an increased contribution from reaction B which is strongly ionic strength dependent.

(3) At constant ionic strength or under saturated salt conditions k_2 is found to be independent of the hydroxyl ion concentration, i.e., from 0.1 *M* to 2.4 *M* sodium hydroxide at low reactant concentrations. An increase in rate is observed at high alkalinities but in this region the effect of various electrolytes on the activity coefficients of the reacting molecules is difficult to predict and this effect will not be considered further here.

(4) The rate is not affected by the presence of initial quantities of manganate or barium ions. If an equilibrium was present such as

$$MnO_4^- + CN^- \rightleftharpoons MnO_4^{=} + CN\cdot,$$

an initial concentration of manganate should retard the reaction whereas the presence of barium ions would precipitate barium manganate and thereby increase the rate of reaction.

(5) The oxygen introduced into the product cyanate comes predominantly *from* the oxidizing agent rather than from the solvent. The maximum percentage of O^{18} transferred,

Can. J. Chem. Downloaded from www.nrcresearchpress.com by 210.87.254.40 on 09/05/12
For personal use only.

Can. J. Chem. Downloaded from www.nrcresearchpress.com by 210.87.254.40 on 09/05/12
For personal use only.

80%, occurred when the tracer experiments were carried out at high alkalinities, e.g., 4 *M* sodium hydroxide. An explanation is necessary at this point. Most of the kinetic data was obtained in the low hydroxyl ion concentration region, 0.1 to 0.2 *M* potassium hydroxide, where only 15 to 25% O^{18} transfer was observed. The discrepancy between the kinetic and O^{18} results at low base concentrations is probably due to the large reactant concentration difference which exists between the two series of experiments, e.g., 0.02 *M* cyanide for the tracer experiments and 0.0004 *M* cyanide for the kinetic experiments. When the alkalinity is increased in the O^{18} tracer experiments, a gradual increase in percentage of O^{18} transfer is observed (Fig. 11) whereas k_2 remains essentially constant (Table III) for the same increase in base concentration, thus indicating that reaction A (the second-order process) involves the oxygen transfer mechanism. The changing kinetics at higher reactant concentrations at 0.1 to 0.2 *M* potassium hydroxide tends to confirm these ideas. In this connection a twofold increase in percentage of O^{18} transferred was observed at 0.5 *M* sodium hydroxide when the reactants were diluted eightfold as would be expected if reaction A was favored at the lower reactant concentrations.

(6) Though Arrhenius-type plots were made using the rate constants obtained under conditions where apparently only one reaction process was present, non-linear plots were observed. Approximate values of $\Delta H^{\ddagger} = 8.7$ kcal/mole and $\Delta S^{\ddagger} = -27$ e.u. were obtained for the study at 0.2 *M* potassium hydroxide. This enthalpy of activation corresponds very closely to that calculated from Freund's results (7), and the entropy of activation is reasonable for a reaction between two anions. The significant curvature observed in the plots further indicates the possibility that two processes are present each with a different activation energy.

A mechanism which fits most of the data for reaction A is the following:

$$MnO_4^- + CN^- \xrightarrow{k_2} (NC - - - O - - - MnO_3)^= \rightarrow MnO_3^- + {}^-OCN,$$

$$MnO_3^- + MnO_4^- + 2OH^- \xrightarrow{\text{fast}} 2MnO_4^= + H_2O.$$

The existence of a Mn(V) species as a reaction intermediate in permanganate oxidations has been well established (18).

Route B

Although the kinetic data for reaction B is of a qualitative nature certain aspects of this study, in particular, the O^{18} tracer experiments and the observation that cyanogen was produced in the reaction at lower pH, suggest a reasonable reaction path.

Linear third-order kinetic plots were obtained for some of the rate data. In some instances a much faster decrease in rate with time was observed for the initial portions of the rate plots than would be predicted for a third-order process, thus indicating that still more complex processes were occurring.

If the third-order kinetic relation is assumed to be due to a first-order dependence on permanganate ion and a second-order dependence on cyanide ion and if the approximately inverse dependence on hydroxyl ion is indeed correct the following relations hold for route B:

$$(-d[MnO_4^-]/dt)_B = k_3[MnO_4^-][CN^-]^2$$

$$= k_3' \frac{[MnO_4^-][CN^-]^2}{[OH^-]} \qquad \text{since } k_3 = k_3'/[OH^-]$$

$$= \frac{k_3' K_a}{K_w} [MnO_4^-][HCN][CN^-],$$

where K_a and K_w are the ionization constant and ion product of hydrocyanic acid and water, respectively.

A possible mechanism for route B is the following:

$$MnO_4^- + HCN + CN^- \xrightarrow{\text{slow}} MnO_4^{=} + (CN)_2^- + H^+$$

$$(CN)_2^- + MnO_4^- \xrightarrow{\text{fast}} (CN)_2 + MnO_4^{=}$$

$$(CN)_2 + 2OH^- \xrightarrow{\text{fast}} CN^- + NCO^- + H_2O$$

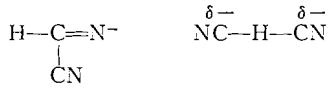
In this connection Adamson (19) has suggested that $(CN)_2^-$ is present as an intermediate in the ferricyanide oxidation of cyanide.

It is worth comparing the behavior of permanganate towards cyanide ion and towards formate ion. The latter has been shown by Taylor and Halpern to be oxidized by permanganate about 2000 times faster at room temperature than the neutral formic acid molecule (20). This is a rather similar situation to the cyanide reaction, the difference being that for the latter a path involving both a HCN molecule and a cyanide ion appears to exist (route B). If a species $H(CN)_2^-$ is in equilibrium with HCN and CN^- it could be oxidized by permanganate by a hydride transfer mechanism which would produce Mn (V) and cyanogen, which would then yield the observed reaction products.

$$HCN + CN^- \rightleftharpoons H(CN)_2^-$$

$$MnO_4^- \overset{\curvearrowleft}{H}\text{—}(CN)_2^- \rightarrow HMnO_4^{=} + (CN)_2 \rightarrow \text{products}$$

The hypothetical species $H(CN)_2^-$ might have either of the following structures,* the second being merely a hydrogen-bonded form.



An electron transfer from cyanide ion to permanganate ion is probably not an energetically reasonable step although electron transfer from hydroxyl ion to permanganate ion appears to take place in strongly basic solution (21, 22).

Finally it should be mentioned that hydrogen cyanide can be added to the list of compounds for which the anion reacts very much faster with permanganate ion than does the neutral molecule (23). These include alcohols (3, 24), formic acid (2, 20), and water (21, 22).

ACKNOWLEDGMENT

The financial assistance of the National Research Council is gratefully acknowledged. One of us (R. V. der L.) is grateful for the award of the Cominco Fellowship and the Shell Oil Fellowship.

REFERENCES

1. K. B. WIBERG and R. STEWART. J. Am. Chem. Soc. **77**, 1786 (1955).
2. K. B. WIBERG and R. STEWART. J. Am. Chem. Soc. **78**, 1214 (1956).
3. R. STEWART. J. Am. Chem. Soc. **79**, 3057 (1957).

A dimer of HCN *exists. It hydrolyzes in water and is believed to be iminoformyl isocyanide with structure* H—C(NC)=NH (25).

Can. J. Chem. Downloaded from www.nrcresearchpress.com by 210.87.254.40 on 09/05/12
For personal use only.

4. K. B. WIBERG and K. A. SAEGEBARTH. J. Am. Chem. Soc. **79**, 2822 (1957).
5. A. Y. DRUMMOND and W. A. WATERS. J. Chem. Soc. 435 (1953).
6. R. I. CARLSON, W. A. BRYCE, and R. STEWART. Unpublished results.
7. T. FREUND. J. Inorg. & Nuclear Chem. **13** (1960).
8. F. H. RHODES. Ind. Eng. Chem. **4**, 652 (1912).
9. B. RICCA. Ann. chim. appl. **16**, 83 (1926).
10. A. I. VOGEL. Quantitative inorganic analysis. Longmans, Green & Co., Inc., Toronto. 1951. p. 263, 275.
11. A. R. AMELL. J. Am. Chem. Soc. **78**, 6234 (1956).
12. J. S. F. PODE and W. A. WATERS. J. Chem. Soc. 717 (1956).
13. J. C. SHEPPARD and A. C. WAHL. J. Am. Chem. Soc. **79**, 1021 (1957).
14. M. C. R. SYMONS. J. Chem. Soc. 3676 (1954).
15. B. RICCA and F. PIRRONE. Ann. chim. appl. **18**, 550 (1928).
16. V. MIGRDICHIAN. The chemistry of organic cyanogen compounds. Reinhold Publishing Corp., New York. 1947. p. 10.
17. H. E. WILLIAMS. Cyanogen compounds. Edward Arnold and Co., London. 1948. p. 3.
18. J. S. F. PODE and W. A. WATERS. J. Chem. Soc. 3373 (1956).
19. A. W. ADAMSON. J. Phys. Chem. **56**, 858 (1952).
20. S. M. TAYLOR and J. HALPERN. J. Am. Chem. Soc. **81**, 2933 (1959).
21. M. C. R. SYMONS. J. Chem. Soc. 3956 (1956).
22. K. A. K. LOTT and M. C. R. SYMONS. Discussions Faraday Soc.
23. J. W. LADBURY and C. F. CULLIS. Chem. Revs. **58**, 403 (1958).
24. R. STEWART and R. VAN DER LINDEN. Discussions Faraday Soc. **29** (1960).
25. L. E. HINKEL and R. J. DUNN. J. Chem. Soc. 1834 (1930).

Can. J. Chem. Downloaded from www.nrcresearchpress.com by 210.87.254.40 on 09/05/12
For personal use only.

Can. J. Chem. Downloaded from www.nrcresearchpress.com by 210.87.254.40 on 09/05/12
For personal use only.

THE ROLE OF REACTION PRODUCTS IN THE SILVER-CATALYZED OXIDATION OF ETHYLENE[1]

KENNETH E. HAYES[2]

ABSTRACT

Initial-rate studies of the kinetics of the silver-catalyzed oxidation of ethylene oxide and carbon dioxide in a flow system have been made. It was found that, using carefully purified reactants, the effect of added carbon dioxide was to suppress the formation of ethylene oxide only. The initial rate of the formation of ethylene oxide is given by the equation

$$r = r^0\left(m + \frac{n}{1+kP_{CO_2}}\right) = r^0\left(\frac{1+mkP_{CO_2}}{1+kP_{CO_2}}\right)$$

where r^0 is the initial rate in the absence of CO_2; m, n, and k are constants with $m+n = 1$.

These results together with the results of oxygen exchange reactions between O^{18} and $C_2H_4O^{16}$, CO_2^{16} and H_2O^{16} are interpreted mechanistically.

INTRODUCTION

The silver-catalyzed oxidation of ethylene has been investigated by a large number of workers in the last 10 years: the researches of Twigg (1), Murray (2), and Orzechowski and MacCormack (3) should particularly be mentioned. At the time that this investigation was started there was no quantitative information regarding the influence of the reaction products on the reaction. This investigation was undertaken with a view to rectifying this omission, and also with the hope of obtaining a more detailed knowledge of the mechanism of the reaction.

EXPERIMENTAL

The apparatus used to investigate the role of carbon dioxide and water vapor on the rates of formation of ethylene oxide and carbon dioxide was essentially a conventional flow system as shown schematically in Fig. 1.

The nitrogen, oxygen, and ethylene, all of a nominal purity of 99.5% or better, were passed from their respective cylinders through purification trains consisting of (A) anhydrous magnesium perchlorate (anhydrone), (B) activated charcoal, (C) KOH pellets, (D) silver turnings, and then through U-tubes immersed in solid carbon dioxide/isopropyl alcohol at −80° C. From the purification trains the gases passed through their respective capillary flowmeters, the flow being controlled by "Edward's LB2" fine control needle valves; through more silver turnings; and then through a further set of U-tubes at −80° C. The oxygen and nitrogen were mixed and passed through a preheater filled with silver turnings before entering the reactor. The ethylene was admitted to the reactor at the same gas inlet.

The carbon dioxide was passed through a similar purification train except for the omission of the KOH and the first cold trap. After the carbon dioxide was passed through a flowmeter, it was admitted to the nitrogen stream at a point prior to the second cold trap in the nitrogen line.

Water vapor was admitted to the system by passing the purified ethylene through a

[1]*Manuscript received in original form June 29, 1959, and, as revised, June 1, 1960.*
Contribution from the Division of Applied Chemistry, National Research Council, Ottawa, Canada. Presented at the annual meeting of the Chemical Institute of Canada, Halifax, May 1959.
Issued as N.R.C. No. 6010.
[2]*National Research Council Postdoctorate Fellow 1954–1956. Assistant Research Officer 1956–1958. Present address: Chemistry Department, Dalhousie University, Halifax, N.S.*

series of large bubblers containing triple-distilled water. These bubblers were immersed in two thermostats, the first held approximately 1° C above the temperature of the second which was maintained within ±0.01° C of the temperature required to give the desired partial pressure of water vapor.

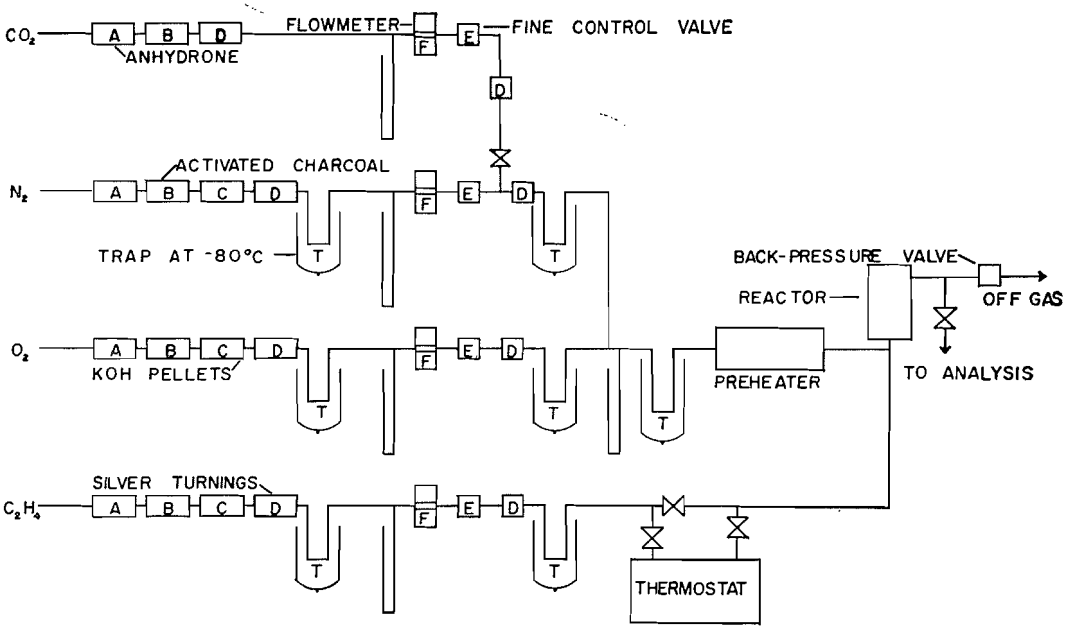


FIG. 1. Schematic diagram of apparatus.

The reactor is shown in detail in Fig. 2. For the preliminary experiments and for the comparison of various alloy catalysts, Part 2 was fabricated entirely from No. 304

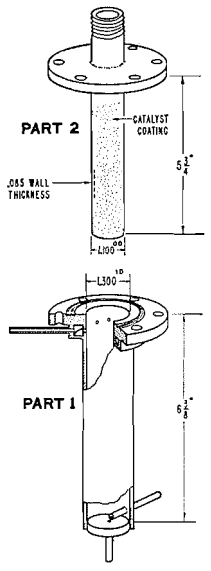


FIG. 2. Reactor in detail.

Can. J. Chem. Downloaded from www.nrcresearchpress.com by 210.87.254.40 on 09/05/12
For personal use only.

Can. J. Chem. Downloaded from www.nrcresearchpress.com by 210.87.254.40 on 09/05/12
For personal use only.

stainless steel, as was Part 1. For the detailed examination of the effect of CO_2 and H_2O on the reaction, the steel barrel of Part 2 was replaced by a sealed tube of "Mint Grade" silver. A 0.030-in. ring of annealed silver was used as a gasket between the two portions of the reactor. Temperature control was maintained by a mixture of Dowtherm A and E boiling under a pressure of nitrogen inside Part 2, heat being supplied by a sealed cartridge heater immersed in the Dowtherm. A copper condenser was attached to the reactor by means of the threads on Part 2. The temperatures reported in this work are the temperatures of the heat exchange medium measured by a chromel alumel thermocouple inserted into the boiling liquid. The temperature of the Dowtherm could be maintained within $\pm 1°$ C of a desired value. The temperature of the gas entering the reactor could also be measured by inserting a thermocouple into the thermocouple well situated right over the gas inlet of Part 1.

Samples of the gases issuing from the reactor were withdrawn by a similar technique to that described by Orzechowski and MacCormack (3) and the ethylene oxide and carbon dioxide were estimated in the customary manner by absorption in Lubatti reagent (4) and sodium hydroxide solution respectively. The absorbing solutions were added to the absorption bubblers by weight pipettes and the subsequent back titrations performed using weight burettes.

The catalysts used in this investigation were based on the "Cambron" (5) silver–calcium catalyst; 40- to 200-mesh 8.5% calcium in silver alloy was sprayed, under an atmosphere of nitrogen, onto the external surface of Part 2 of the reactor, this part being turned in a lathe during the spraying. The catalyst was cooled and then it was activated by the steam and acetic acid treatment already described (6). The reactor was then assembled and sealed into the system in the shortest possible time to avoid air-borne contamination.

Two other catalysts were examined in this investigation: a 1 wt.% gold in silver–8.5% calcium and a 1 wt.% antimony in silver – 8.5% calcium alloy. In each case the percentage of either gold or antimony was based on the amount of silver present and not on the combined silver–calcium weight. Both of these catalysts were sprayed and activated in the same manner as normal calcium–silver alloys.

The flow rates used in the investigation were multiples of 2/10/20 and 2/10/25 liters at S.T.P./hour for ethylene/oxygen/nitrogen. The maximum flow rates that could be conveniently handled were 7/35/70 and 6/30/75 liters at S.T.P./hour. Hence, for those experiments involving the catalyst deposited on the silver tube, the degree of reaction could be measured for values of M/F (where M is catalyst mass and F the total flow rate), varying between 0.191 and 0.669 and 0.193 and 0.578 g hour per liter for the two feeds, since the catalyst mass was 21.4 g and contained 0.083% calcium. When CO_2 was added to the feed it was added at the expense of the nitrogen thus maintaining the total flow rates at standard levels. The amount of CO_2 added to the feed was based on the ethylene in the feed. It then follows that when we speak of those experiments involving 10% CO_2 for example, the gas flow rates will be multiples of 2/10/19.8/0.2 and 2/10/24.8/0.2 liters at S.T.P./hour for $C_2H_4/O_2/N_2/CO_2$.

As has been shown by previous authors (3) the silver–calcium catalysts require approximately 75–100 hours operation under standard conditions before settling down to steady values of ethylene oxide and carbon dioxide produced. All of the results reported in this communication are for catalysts conditioned at standard flow rates of 2/10/20 liters at S.T.P./hour for at least 100 hours. It required a minimum of 3 hours for a

Can. J. Chem. Downloaded from www.nrcresearchpress.com by 210.87.254.40 on 09/05/12
For personal use only.

catalyst to settle down to a steady state after the flow conditions had been altered.

The preliminary experiments were performed at a total pressure of 1200 mm Hg; the experiments involving CO_2 and H_2O additions to the feed were made at both 1200 mm Hg and 850 mm Hg. The series of experiments involving CO_2 additions were made in one continuous operation—the reactor was not shut down for any purpose until the conclusion of the series; the same tank of ethylene was used throughout this series and necessary replacement of oxygen or nitrogen tanks was made at such times as coincided with the necessary changes in flow conditions. All of these experiments were made using the bracketing technique. At the end of the CO_2 series the reactor was shut down under a gas stream of 2/10/20 and then stored under nitrogen for a few days. The experiments on the addition of water vapor were then started and carried out in one continuous operation.

The exchange reactions between ^{18}O and C_2H_4O, CO_2, and H_2O were carried out in the same conventional high-vacuum apparatus that was used in the study of the decomposition of nitrous oxide on these silver–calcium catalysts (6). Ten millimeters of $^{18}O_2$-enriched oxygen, prepared by the electrolysis of H_2O^{18} (10%), was admitted to 10 g of an activated silver–calcium powder containing 0.43% calcium, and, after sufficient time had elapsed for adsorption equilibrium to be attained, 10 mm of either C_2H_4O, CO_2, or H_2O vapor (all purified by repeated distillation) was added, small gas samples being removed periodically for mass spectrographic analysis.

RESULTS

The preliminary experiments indicated that the results obtained for the percentage ethylene converted to ethylene oxide and carbon dioxide were reproducible to better than 3%, both for repeated experiments at a constant flow rate and for experiments at this flow after operations at different flows. This is shown for a typical catalyst in Table I.

In addition to illustrating the reproducibility obtainable in this system, Table I

TABLE I

$C_2H_4/O_2/N_2$ flow rates in liters at S.T.P./hour	Run No.	% C_2H_4 converted to:	
		C_2H_4O	CO_2
2/10/20	1	47.4	21.8
2/10/20	2	47.7	21.3
4/10/40	3	28.4	12.5
4/10/40	4	28.2	12.3
3/15/30	5	33.6	15.4
3/15/30	6	34.1	15.9
2.5/12.5/25	7	40.6	—
2.5/12.5/25	8	41.0	17.0
2.5/12.5/25	9	40.4	17.4
5/25/50	10	24.7	10.4
5/25/50	11	24.4	9.7
2/10/20	12	45.4	23.0
2/10/20	13	45.1	22.7
4/20/30	14	26.4	12.8
4/20/30	15	26.4	12.9
3/15/30	16	33.0	15.9
5/25/50	17	22.2	11.6
2/10/20	23	45.7	22.7

NOTE: Preliminary runs with 20 g of silver catalyst, % calcium, 0.1. Total pressure = 1200 mm Hg. Temperature, 250° for runs 1–11. Temperature, 245° for runs 12–23 after shutdown for major repairs. All analyses performed at 24-hour intervals.

also shows how easily the reaction level may be altered by uncontrolled changes in operating conditions. After run No. 11, a broken N_2 line resulted in a high concentration of ethylene and oxygen in the reactor leading to a runaway temperature and presumably causing sintering of the catalyst surface.

Table II compares the results obtained with normal calcium–silver catalysts and the special 1% gold–silver–calcium and 1% antimony–silver–calcium alloys. All of the results are for fully conditioned catalysts operating at 1200 mm Hg pressure, under standard conditions of 2/10/20 liters at S.T.P./hour.

TABLE II

The effect of alloying constituents on selectivity

Catalyst	% Calcium	Temp., °C	Cat. wt., g	% C_2H_4 converted to:		% Selectivity
				C_2H_4O	CO_2	
1% Sb–Ag	<0.01	243	20.0	15.4	35.5	30
1% Au–Ag	<0.01	225	17.0	19.8	57.7	25
Ag (1)	Appr. 0.1	250	20.0	47.4	21.3	69
Ag (2)	Appr. 0.1	250	20.0	40.4	14.9	72

It is seen from Table II that the presence of small quantities of gold or antimony in the silver alloy causes a marked decrease in the selectivity, although a high total activity is maintained. It is to be noted that the calcium content of these two catalysts is very low; as will be shown later, we would expect that the selectivity for these two "binary" catalysts containing calcium as the "impurity" should be low. However, if the calcium content is increased, the effect of the gold or antimony will be masked. Unpublished data of the author have shown that gold- and antimony-containing silver catalysts, containing also appreciable quantities of calcium, act as catalysts in the N_2O decomposition as though they were binary calcium–silver alloys containing less calcium, e.g. a 1% gold – 0.43% calcium in silver alloy acts as a calcium–silver alloy containing approximately 0.3% calcium.

Preliminary studies of the effect of CO_2 on the reaction showed that, within the limits of experimental error, added CO_2 had only a limited effect on the production of ethylene oxide, and no effect at all on the production of carbon dioxide. The quantitative results for the effect of CO_2 on ethylene oxide production are given in Table III and are illustrated in Fig. 3. The data of Table III are for four separate series of experiments, with flows which were multiples of 2/10/20, and 2/10/25 liters at S.T.P./hour for $C_2H_4/O_2/N_2$ and total pressures of 1200 and 850 mm Hg.

In Table IV the results of the effect of water vapor on the reaction are given. The temperatures refer to the temperature of the water in the saturators. Room temperature was between 25 and 27° during these runs; consequently, 22° C was the highest practical saturation temperature that could be used without heating the gas lines. It is apparent that, within the limits of experimental error, the addition of water vapor to the feed gas has no effect on the production of either ethylene oxide or carbon dioxide.

In Fig. 4, the results of the exchange between $^{18}O_2$-enriched oxygen chemisorbed in a silver catalyst and ethylene oxide, carbon dioxide, and water vapor are illustrated. It will be observed that the exchange involving ethylene oxide is much more rapid than that involving either of the other two gases. Of far greater importance is the fact that,

Can. J. Chem. Downloaded from www.nrcresearchpress.com by 210.87.254.40 on 09/05/12
For personal use only.

under similar experimental conditions, no oxidation of the ethylene oxide was observed until a temperature of 220° C had been reached, some 150° C above the temperature at which exchange takes place readily.

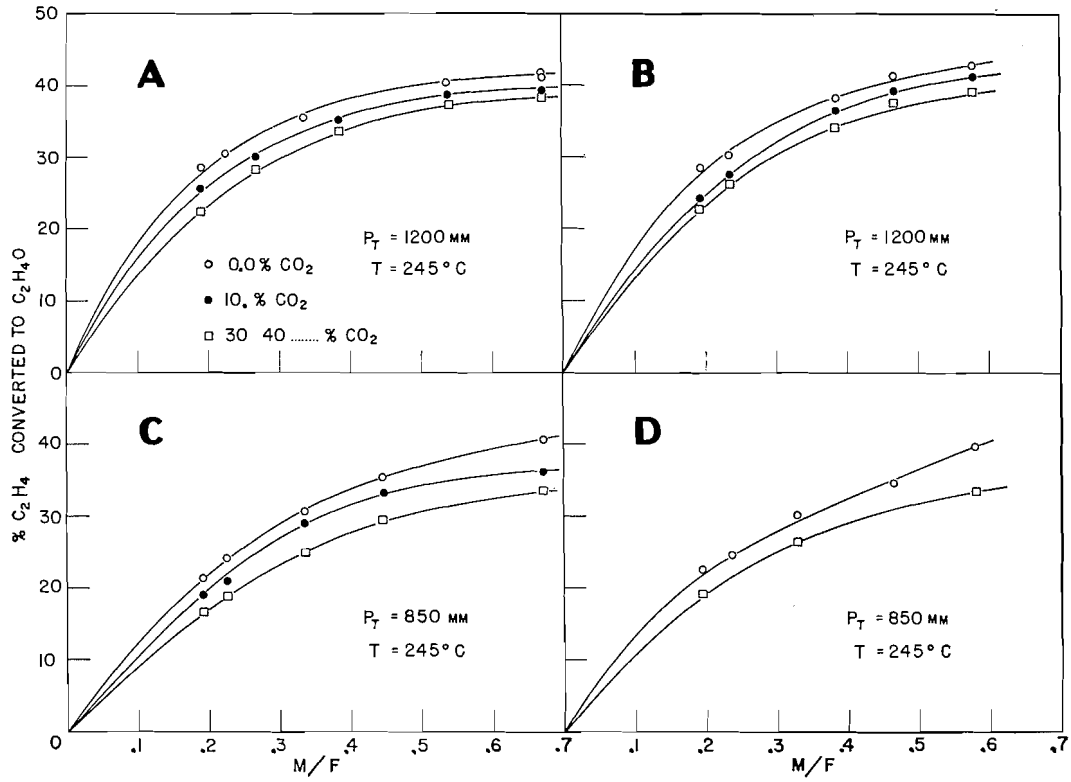


FIG. 3. Percentage conversion of C_2H_4 to C_2H_4O in the presence of CO_2.

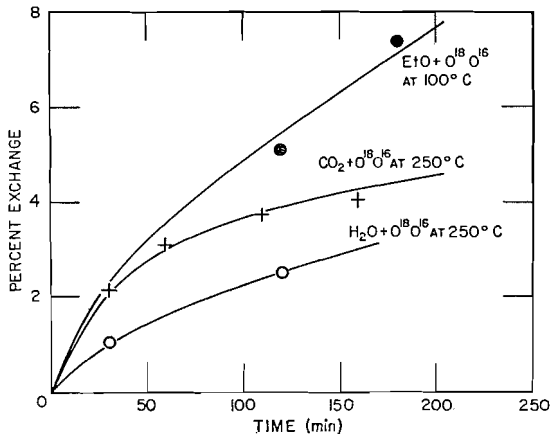


FIG. 4. Exchange between C_2H_4O, CO_2 and H_2O and O^{18} on silver–calcium alloy.

Can. J. Chem. Downloaded from www.nrcresearchpress.com by 210.87.254.40 on 09/05/12
For personal use only.

TABLE III

The effect of CO_2 on ethylene oxide production
(% conversion of ethylene to ethylene oxide)

$\frac{M}{F}$ \ $\frac{100\ CO_2}{C_2H_4}$ in feed	0	10	30	40
(A) Total pressure 1200 mm Hg				
M/F obtained from flow rates of X (2/10/20) liters at S.T.P./hour				
0.669	41.6	39.4	38.6	
0.535	40.3	38.9	37.4	37.9
0.446	38.4			
0.382		35.2	33.6	
0.334	35.3			
0.268		30.0	28.2	
0.223	30.0			
0.191	28.4	25.8	22.2	22.0
(B) Total pressure 1200 mm Hg				
M/F obtained from flow rates of X (2/10/25) liters at S.T.P./hour				
0.578	42.5	41.5	39.0	
0.463	41.2	39.3	37.5	
0.386	38.2	36.6	34.0	
0.231	31.9	27.6	26.3	
0.193	27.8	24.1	22.8	
(C) Total pressure 850 mm Hg				
M/F obtained from flow rates of X (2/10/20) liters at S.T.P./hour				
0.669	40.6	36.0	33.6	
0.446	35.3	33.2	29.4	
0.334	30.5	28.9	24.9	
0.223	23.9	21.0	18.9	
0.191	21.4	19.2	16.6	
(D) Total pressure 850 mm Hg				
M/F obtained from flow rates of X (2/10/25) liters at S.T.P./hour				
0.578	39.6		33.2	
0.463	34.4		—	
0.331	31.1		26.1	
0.231	24.6		—	
0.193	22.5		19.1	

NOTE: Catalyst, 21.4 g of 0.083% calcium in silver. Temperature, 245° C.

TABLE IV

The effect of water vapor on ethylene oxide production

$C_2H_4/O_2/N_2$ flow rates in liters at S.T.P./hour	No H_2O added	10° C	22° C
(A) % Ethylene converted to ethylene oxide			
2/10/20	38.5	38.5	38.7
7/35/70	23.6	24.4	24.0
(B) % Ethylene converted to CO_2			
2/10/20	35.8	—	35.3 (after 80 hours)

DISCUSSION

The experimental results of the silver-catalyzed oxidation of ethylene have been interpreted by two postulated mechanisms. The first, due to Twigg (1), assumed that ethylene oxide was formed by the interaction of ethylene with a single oxygen adatom;

Can. J. Chem. Downloaded from www.nrcresearchpress.com by 210.87.254.40 on 09/05/12
For personal use only.

Can. J. Chem. Downloaded from www.nrcresearchpress.com by 210.87.254.40 on 09/05/12
For personal use only.

and that deep oxidation was caused by the interaction of ethylene with a pair of suitably disposed oxygen adatoms. Orzechowski and MacCormack (3), on the other hand, interpreted their results on the basis of interaction between ethylene and chemisorbed oxygen atoms alone.

In 1952, DeBoer and Fortiun postulated (7) the existence of oxygen molecule ions O_2^- chemisorbed on silver, to account for the silver-catalyzed oxidation of cumene to cumene hydroperoxide. It was later postulated in this laboratory that chemisorbed O_2^- ions might be responsible for the deep oxidation of ethylene, with chemisorbed O^- ions being responsible for the formation of ethylene oxide. This viewpoint has subsequently been put forward by workers in this field. The conductivity measurements of Ljuburskij (8) have shown that oxygen abstracts electrons from a silver surface and this has been confirmed by the surface potential measurements of Kummer (9). In this latter paper, Kummer has also presented direct evidence for the existence of chemisorbed O_2^- ions on silver.

If oxygen is chemisorbed on silver, initially in the form of O_2^- ions, and subsequently as two O^- ions, we would expect that the addition of other components to the silver to decrease the work function would result in an increase in selectivity for the ethylene oxidation. A lowering of the work function would enhance the dissociation of O_2^- ions into O^- ions. Increasing the work function, on the other hand, would be expected to give the opposite effect, resulting in a lowering of the selectivity. The author has already shown (6), as a part of this investigation, that the addition of gold to silver increases the activation energy of the silver-catalyzed decomposition of N_2O. Since the rate-determining step in this decomposition involves the donation of an electron from the catalyst to the N_2O, an increase in activation energy is equivalent to an increase in work function. This same investigation also showed that by increasing the residual calcium in the catalyst (the silver–calcium alloys) the work function could be lowered.

The results in Table II show how the selectivities of the 1% gold in silver and 1% antimony in silver catalysts are markedly lower than the selectivities obtained from normal calcium–silver alloys. It is to be regretted that lowering the work function will not bring about as great an increase in selectivity under normal flow conditions, as we postulate that O^- ions are also responsible for the further oxidation of ethylene oxide to CO_2 and H_2O. A forthcoming publication (10) dealing with *initial-rate studies* on the silver-catalyzed oxidation of ethylene in a circulating system, in which the products are removed from the gas phase as they are formed, will show how the selectivity may be increased from 45% for pure silver to 65% for a 0.1% calcium in silver alloy.

If we now consider the poisoning of the reaction by added CO_2, we see from Fig. 4 that increasing the CO_2/C_2H_4 ratio in the feed gas over 0.30 has no further effect on the production of ethylene oxide. This means in effect that the initial rate of C_2H_4O formation in the presence of CO_2 falls to a steady value, greater than zero, as the partial pressure of CO_2 is increased. The data were analyzed in a manner similar to that used by Orzechowski and MacCormack, i.e., by considering the steady-state concentrations of the various adsorbed species (3). The two simplest assumptions regarding the adsorption of CO_2 are that CO_2 is either adsorbed on the free surface, at the expense of oxygen, or that it is adsorbed on top of the chemisorbed oxygen film at the expense of ethylene. Neither of these assumptions leads to a rate equation which fits our experimental data, since both derived rate equations require that the rate of production of C_2H_4O shall fall to zero if the CO_2 pressure is sufficiently high. If, on the other hand, it is assumed that the adsorption of CO_2 requires both a free surface site and an adsorbed O^- ion, leading

to a CO_3^- ion as the adsorption complex, then the initial-rate equation may be shown to be of the form

$$r_{EtO} = r^0_{EtO}\left(m+\frac{n}{1+kP_{CO_2}}\right) = r^0_{EtO}\left(\frac{1+k'P_{CO_2}}{1+kP_{CO_2}}\right)$$

where m, n, and k are constants, with $m+n = 1$ and $k' = mk$.

r_{EtO} = initial rate of C_2H_4O production in the presence of CO_2,

r^0_{EtO} = initial rate of C_2H_4O production in the absence of CO_2.

The rates, r, are given by the relation

$$r = \left(\frac{dx}{d(M/F)}\right)V_E$$

where x = fraction of ethylene converted to C_2H_4O,

M = catalyst weight in grams,

F = total flow rate in liters at S.T.P./hour,

and V_E = volume fraction of ethylene in the feed.

The constants m, n, and k were obtained from the data given in Table III(A). Values of $[dx/d(M/F)]V_E$ were then computed for the experimental conditions of Table III, (B), (C), and (D). The results are shown in Fig. 5, where the solid lines were calculated from the fitted points of A, the circles represent the experimentally determined points. The agreement is satisfactory.

Although the effect of added ethylene oxide on the production of ethylene oxide was not determined in this investigation, it has been shown by Roginskii and Margulis (11) that added C_2H_4O decreases the rate of production of C_2H_4O. This result could have been inferred from the exchange behavior of ethylene oxide with chemisorbed ^{18}O. We may visualize the exchange taking place as follows:

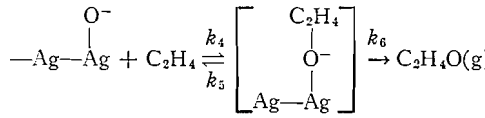
$$\begin{array}{l} {}^{18}O^- \\ |\\ -Ag-Ag- \end{array} + C_2H_4{}^{16}O \rightleftharpoons \begin{array}{c} CH_2-CH_2 \\ | \quad\times\quad | \\ {}^{18}O \qquad {}^{16}O \\ | \qquad\quad | \\ -Ag- \quad -Ag- \end{array} \rightleftharpoons \begin{array}{l} {}^{16}O^- \\ | \\ Ag-Ag \end{array} + C_2H_4{}^{18}O.$$

In view of the exchange behavior of water vapor, in which exchange possibly takes place via the formation of two OH^- ions in the surface, it is perhaps surprising that added water vapor has no apparent effect on either C_2H_4O and CO_2 production. It is possible, however, that water does inhibit the formation of ethylene oxide, in a manner analogous to that shown by CO_2, but the effect of water is so small that the water formed in the normal course of the reaction is sufficient to saturate the surface with respect to water vapor. We can summarize the basic postulates of this paper in the following reaction schemes:

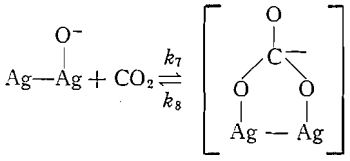
$$-Ag-Ag- + O_2 \rightleftharpoons \left[\begin{array}{c} O_2^- \\ -Ag-Ag- \end{array}\right] \rightleftharpoons \begin{array}{l} O^- \quad O^- \\ | \quad\quad | \\ Ag-Ag-Ag \end{array} \qquad [1]$$

$$\left[\begin{array}{c} O_2^- \\ Ag-Ag \end{array}\right] + C_2H_4 \underset{k_2}{\overset{k_1}{\rightleftharpoons}} \left[\begin{array}{c} C_2H_4 \\ O_2^- \\ Ag-Ag \end{array}\right] \overset{k_3}{\rightarrow} CO_2 + H_2O \qquad [2]$$

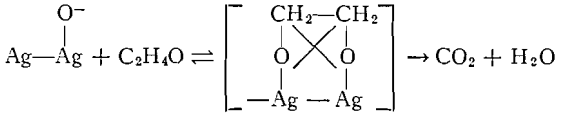
Can. J. Chem. Downloaded from www.nrcresearchpress.com by 210.87.254.40 on 09/05/12
For personal use only.



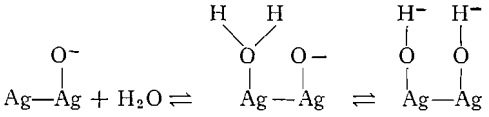
[3]



[4]



[5]



[6]

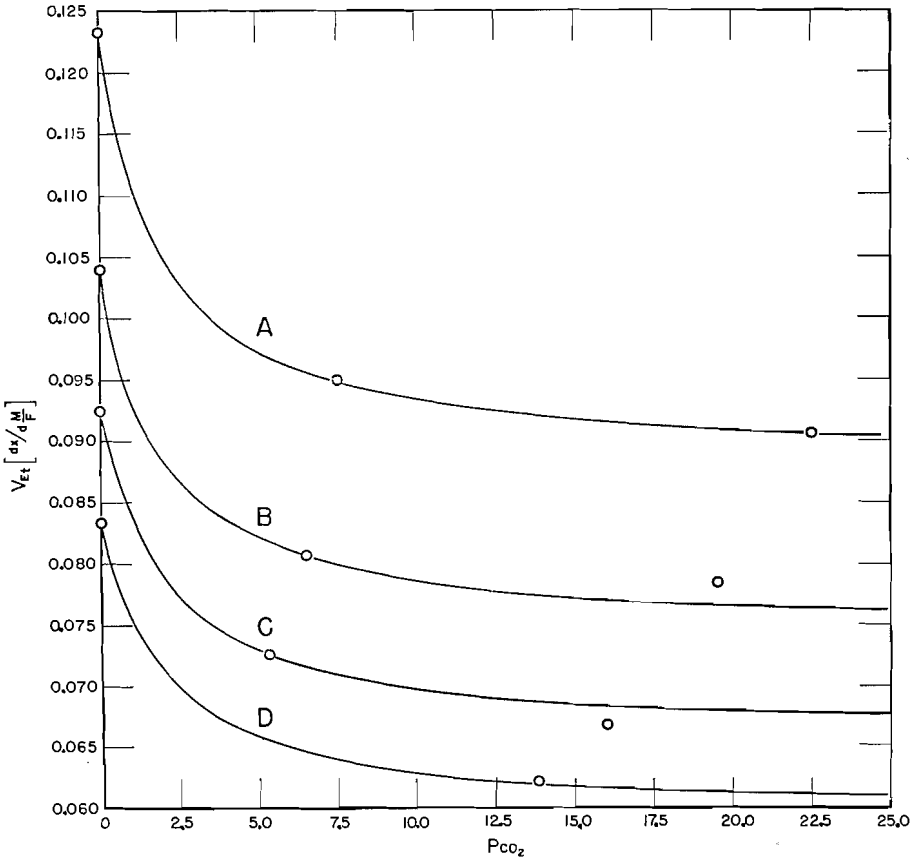


FIG. 5. Initial rates for the conversion of C_2H_4 to C_2H_4O as a function of the partial pressure of CO_2.

Can. J. Chem. Downloaded from www.nrcresearchpress.com by 210.87.254.40 on 09/05/12
For personal use only.

Can. J. Chem. Downloaded from www.nrcresearchpress.com by 210.87.254.40 on 09/05/12
For personal use only.

In applying the steady-state treatment to this postulated mechanism it is possible to treat the surface in two ways; this in effect means that we can treat the adsorption of oxygen in two ways. The first is to assume that any part of the surface is capable of holding the adsorbed oxygen as either O_2^- or O^-, and the second is to assume that, because of marked a priori heterogeneity, only certain portions of the surface can hold adsorbed oxygen as O_2^- and that other portions can hold adsorbed oxygen as O^-. The first treatment is far more complicated than the second, and while it shows that the selectivity of the reaction is a function of oxygen pressure (10), it also shows that the effect of added CO_2 under *all possible* circumstances is to reduce the rate of production of both CO_2 and EtO to zero if the pressure of CO_2 is sufficiently high.

The second treatment, while being perhaps more naive, satisfactorily accounts for most of the data published to date. We assume that the rates of formation of both adsorbed O_2^- and O^- may be considered as independent of each other and that the two species are found on different portions of the surface. We further assume that *all* of the CO_2 produced in the *early stages of the reaction* comes from interaction between ethylene and adsorbed O_2^-, i.e., there is no formation of CO_2 by a secondary oxidation of EtO.

Let θ be fraction of surface covered by O_2^- and θ' be fraction of surface covered by O^- under steady-state conditions. Further, let α be the fraction of the O_2^--covered surface covered by adsorbed ethylene, and β be the fraction of the O^--covered surface covered by adsorbed ethylene under steady-state conditions.

Following Orzechowski and MacCormack (3), we shall assume further that the rates of formation of the adsorbed oxygen species are given by the simple form of the Elovic equation.

Then the steady-state concentration of adsorbed O_2^- is given, ignoring desorption of oxygen, by

$$jP_O(1 - m\theta) + k_2\alpha\theta = k_1P_{Et}(1 - \alpha)\theta, \qquad [1]$$

where P_O and P_{Et} are the pressures of oxygen and ethylene respectively. Similarly the steady-state concentration of adsorbed O^- is given by

$$j'P_O(1 - m'\theta') + k_5\beta\theta' = k_4P_{Et}(1 - \beta)\theta'. \qquad [2]$$

The steady-state concentration of ethylene adsorbed on the O_2^- is given by

$$k_1P_{Et}(1 - \alpha)\theta = (k_2 + k_3)\alpha\theta. \qquad [3]$$

and steady-state concentration of ethylene adsorbed on the O^- by

$$k_4P_{Et}(1 - \beta)\theta' = (k_5 + k_6)\beta\theta'. \qquad [4]$$

Hence the rate of formation of CO_2 is given by

$$r^0_{CO_2} = k_3\alpha\theta = \frac{k_3\alpha jP_O}{(k_3\alpha + jmP_O)}. \qquad [5]$$

and the rate of formation of ethylene oxide by

$$r^0_{EtO} = k_6\beta\theta' = \frac{k_6\beta j'P_O}{(k_6\beta + j'm'P_O)}. \qquad [6]$$

We see immediately that the selectivity S, equal to $r^0_{EtO}/(r^0_{EtO} + r^0_{CO_2})$ is given by

$$S = \frac{j'\left(1 + \frac{jmP_O}{k_3\alpha}\right)}{\left[j\left(1 + \frac{jmP_O}{k_3\alpha}\right) + j'\left(1 + \frac{j'm'P_O}{k_6\beta}\right)\right]} \qquad [7]$$

or at constant ethylene pressure, as α and β are constants, the selectivity is a function of the oxygen pressure. From equations 5 and 6 we see that

[8] $$r^0_{EtO} = \frac{k_6 j' B P_O P_{Et}}{k_6 B P_{Et} + j' m' P_O + j' m' B P_O P_{Et}}$$

and

[9] $$r^0_{CO_2} = \frac{k_3 j A P_O P_{Et}}{k_3 A P_{Et} + j m P_O + j m A P_O P_{Et}}$$

where

$$A = \frac{k_1}{k_2 + k_3}$$

and

$$B = \frac{k_4}{k_5 + k_6}.$$

Equations 8 and 9 will then apply to those situations where the rate of oxygen adsorption is of the same order of magnitude as the rate of production of CO_2 and EtO. If now the rate of adsorption of oxygen becomes the limiting rate of the reaction it is permissible to suppose that in this case θ and θ' will be very small and that α and β both approach unity so that the rate of production of EtO will be independent of P_{Et} and,

[10] $$r^0_{EtO} = \frac{k_6 j P_O}{k_6 + j' m' P_O} \sim K P_O^{1/n}$$

[11] $$r^0_{CO_2} = \frac{k_3 j P_O}{k_3 + j P_O m} \sim K' P_O^{1/m}$$

Similarly, if the rate of adsorption of oxygen is faster than r^0_{EtO} or $r^0_{CO_2}$, then we can expect that the over-all rate, r^0_{EtO} or $r^0_{CO_2}$, to be functions only of the ethylene pressure; this has been found by Kurilenko (12).

If we now consider the effect of CO_2 on r^0_{EtO} and $r^0_{CO_2}$, we find that the postulate of adsorption of CO_2 on either O^-(ads.) or on the free surface will lower the activity to zero at sufficiently high CO_2 pressures. Similarly, in general, two point attachment of CO_2 involving both O^- adsorption and a free site will lower the activity to zero. However, for a special case, two point attachment will lower r_{EtO} only, and that to a limiting value greater than zero.

Let us suppose that a fraction γ of the O^--covered surface is covered with CO_2 under steady-state conditions, then a fraction $\gamma\theta'$ of the free surface will be used to obtain two point attachment.

The general equations 1, 2, 3, and 4 now become

[12] $$jP_O(1 - m\theta - \gamma\theta') + k_2\alpha\theta = k_1 P_{Et}(1 - \alpha)\theta$$

[13] $$j'P_O(1 - m'\theta' - \gamma\theta') + k_5\beta\theta' = k_4 P_{Et}(1 - \beta)\theta'$$

[14] $$k_1 P_{Et}(1 - \alpha)\theta = (k_2 + k_3)\alpha\theta$$

[15] $$k_4 P_{Et}(1 - \beta - \gamma)\theta' = (k_5 + k_6)\beta\theta'$$

and for the adsorption of CO_2

[16] $$k_7 P_{CO_2}(1 - \beta - \gamma)\theta'(1 - (\theta' + \theta) - \gamma\theta') = k_8\gamma\theta'.$$

The equations are difficult to solve (without making assumptions as to the relative value of second and third degree terms), but predict that the effect of CO_2 in general

Can. J. Chem. Downloaded from www.nrcresearchpress.com by 210.87.254.40 on 09/05/12
For personal use only.

will be to inhibit both CO_2 and EtO production. A similar series of equations predict the same behavior for both added EtO and H_2O. This type of behavior, namely complete inhibition by reaction products, in the order $EtO > CO_2 > H_2O$, would have been predicted on the basis of the isotope-exchange studies and has been found by Kurilenko (12) and more recently by Gorokhovatskii (13).

The results of this paper may be rationalized by assuming, (*a*) two-site adsorption of CO_2; (*b*) that the amount of adsorbed CO_2 is sufficiently small that no sites on which O_2^- (ads.) may be formed are destroyed, and (*c*) that the adsorption of CO_2 on the O^- (ads.) layer does not effect the adsorption of ethylene on this layer. The steady-state equations comparable to 13, 15, and 16 then become

$$j'P_O(1 - m'\theta' - \gamma\theta') + k_5\beta\theta' = k_4P_{Et}(1 - \beta)\theta', \quad [17]$$

$$k_4P_{Et}(1 - \beta)\theta' = (k_5 + k_6)\beta\theta', \quad [18]$$

$$k_7P_{CO_2}(1 - \gamma)\theta'(1 - \theta' - \gamma\theta') = k_8\gamma\theta'. \quad [19]$$

On solving these equations, with the further assumption that $(\theta')^2$ and $\gamma^2(\theta')$ may be neglected, we find that r_{EtO} is given by

$$r_{EtO} = \frac{k_6\beta j'P_O\left[1+\frac{k_7}{k_8}P_{CO_2}\right]}{k_6\beta\left(1+\frac{k_7}{k_8}P_{CO_2}\right)+j'm'P_O\left[1+\frac{k_7}{k_8}\left(\frac{m'+1}{m'}\right)P_{CO_2}\right]}. \quad [20]$$

For given values of P_O and P_{Et} equation 6 may be transformed to

$$\frac{1}{r^0_{EtO}} = \frac{k_6\beta+j'm'P_O}{k_6\beta j'P_O} = \frac{a}{r^0_{EtO}}+\frac{b}{r^0_{EtO}} \quad [21]$$

where a and b are fractions and $a+b = 1$. Comparison of 20 and 21 then gives, after some rearranging,

$$r_{EtO} = r^0_{EtO}\left[\frac{\left(1+\frac{k_7}{k_8}P_{CO_2}\right)}{\left\{1+\frac{k_7}{k_8}\left(\frac{m'+b}{m'}\right)P_{CO_2}\right\}}\right]. \quad [22]$$

Equation 22 then satisfactorily accounts for the data of this paper.

REFERENCES

1. G. H. Twigg. Proc. Roy. Soc. A, **188**, 92, 105, 123 (1946).
2. K. E. Murray. Australian J. Sci. Research, A, **3**, 433 (1950).
3. A. Orzechowski and K. E. MacCormack. Can. J. Chem. **32**, 388, 415, 432, 443 (1954).
4. O. F. Lubatti. J. Soc. Chem. Ind. (London), **51**, 361 (1933).
5. A. Cambron and F. L. W. McKim. U.S. Patent No. 2, 563,857 (1951); Can. Patent No. 475, 366 (1951).
6. K. E. Hayes. Can. J. Chem. **37**, 583 (1959).
7. J. H. DeBoer. Advances in catalysis. Vol. 8. Academic Press, Inc., New York, p. 79.
8. G. D. Ljuburskij. Doklady Akad. Nauk S.S.S.R. **110**, 112 (1956).
9. J. T. Kummer. J. Phys. Chem. **63**, 460 (1959).
10. J. B. Chenier, R. J. Cvetanović, and K. E. Hayes. To be published.
11. S. Z. Roginskii and L. Y. Margulis. Doklady Akad. Nauk S.S.S.R. **89**, 515 (1953).
12. A. I. Kurilenko *et al.* Zhur. Fiz. Khim. **32**, 797 (1958).
13. Ya. B. Gorokhovatskii *et al.* Doklady Akad. Nauk S.S.S.R. **125**, 171 (1959).

Can. J. Chem. Downloaded from www.nrcresearchpress.com by 210.87.254.40 on 09/05/12
For personal use only.

Can. J. Chem. Downloaded from www.nrcresearchpress.com by 210.87.254.6 on 09/05/12
For personal use only.

NOTES

ON THE EXISTENCE OF TERNARY COMPOUNDS IN THE SYSTEM NH_3–H_2O_2–H_2O

K. E. MIRONOV

Recently a note was published in this Journal (1) on the existence of ternary compounds in the system NH_3–H_2O_2–H_2O. On the basis of appearance of maxima in the melting-point curve along the plane $H_2O_2 \cdot 2H_2O$–NH_3 it was concluded that two compounds are formed, namely $NH_3 \cdot 3H_2O_2 \cdot 6H_2O$, m.p. −28.9° C, and $(NH_4)_2O_2 \cdot 2H_2O$, m.p. around 15° C. That this conclusion is erroneous may be gathered from an investigation of the whole liquidus surface of that system (2).

Indeed, there are two maxima in the above-mentioned plane (Fig. 1, p. 2270), but these maxima provide no evidence for ternary compounds since the said plane is not a singular or stable one (3). The first maximum at −29° C comes from intersection of the ridge in crystallization field of ice, while the second maximum comes from crystallization of the the compound $NH_3 \cdot H_2O_2$.

There were indications (1) from the infrared spectrum of the presumed compound at 32% NH_3 that it contained the NH_4^+ ion as well as water of crystallization. As may be judged from Fig. 1, the infrared investigation is consistent with the presence in that solid of the compound $NH_3 \cdot H_2O_2$ (4, 5) together with ice. On the other hand, the conclusion (1) regarding the non-ionic nature of the compound $2NH_3 \cdot H_2O_2$ seems correct in view of its limited range of existence, from −93.5° to −107° C (6). There are no ternary compounds in the system NH_3–H_2O_2–H_2O.

The author is grateful to I. I. Vol'nov for drawing his attention to paper (1).

1. P. A. GIGUÈRE and D. CHIN. Can. J. Chem. **37**, 2064 (1959).
2. K. E. MIRONOV. Dissertation. The diagram of phase conversions in the system NH_3–H_2O_2–H_2O and characteristics of compound $NH_3 \cdot H_2O_2$. (In Russian.) Referat. Zhur. Khim. No. 3 (1953). Ref. 2835D.
3. V. YA. ANOSOV and S. A. POGODIN. Fundamental principles of physico-chemical analysis. (In Russian.) Moscow, Leningrad. 1947. p. 576.
4. A. SIMON and A. KRIEGSMANN. Naturwiss. **42**, 14 (1955).
5. O. KNOP and P. A. GIGUÈRE. Can. J. Chem. **37**, 1794 (1959).
6. K. E. MIRONOV. Zhur. Neorg. Khim. **4**, 153 (1959).
7. A. G. ROLLET and G. VUILLARD. Compt. rend. **243**, 383 (1956).

RECEIVED MAY 30, 1960.
CANDIDAT OF CHEMICAL SCIENCES,
SIBERIAN DIVISION OF THE ACADEMY OF SCIENCES OF U.S.S.R.,
NOVOSIBIRSK, 49, KRASNY PROSPEKT,
U.S.S.R. DOM 163, KW. 114.

Can. J. Chem. Downloaded from www.nrcresearchpress.com by 210.87.254.6 on 09/05/12
For personal use only.

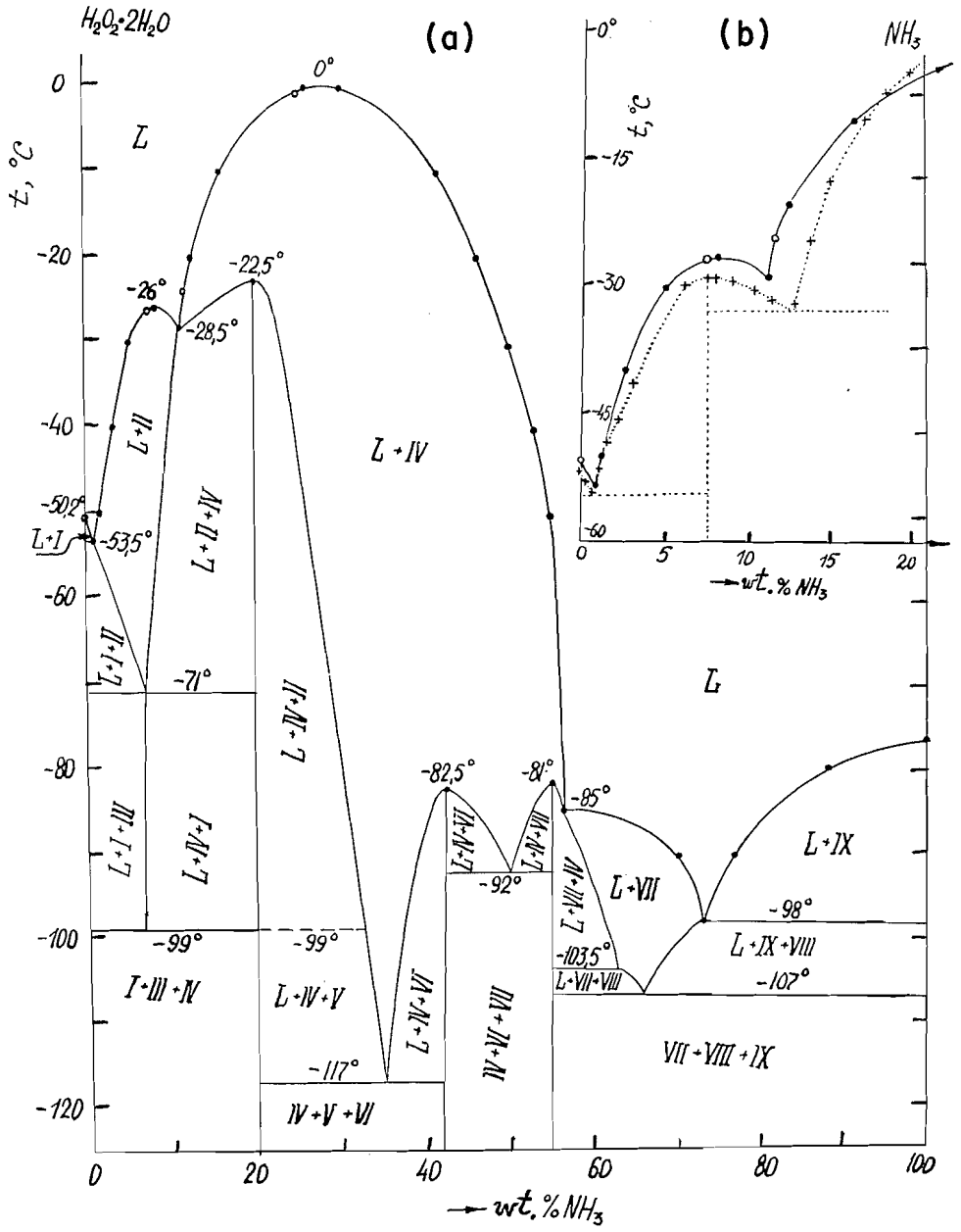


FIG. 1. (*a*) Melting-point diagram in the plane $H_2O_2 \cdot 2H_2O$–NH_3. (*b*) Comparison of liquidus diagrams in that plane.

Symbols: ○ liquidus from experimental data, ● liquidus from isotherms in the ternary system (2), + liquidus from the data of reference 1, ··· liquidus and solidus from reference 1, – – – more precise liquidus data from reference 7. L, liquid; I, $H_2O_2.2H_2O$; II, ice; III, H_2O_2; IV, $NH_3.H_2O_2$; V, $NH_3.2H_2O$; VI, $NH_3.H_2O$; VII, $2NH_3.H_2O$; VIII, $2NH_3.H_2O_2$; IX, NH_3.

APPLICATION OF THE HAMMETT EQUATION TO THE HYDROLYSIS OF SUBSTITUTED BENZAMIDES

J. T. EDWARD,* H. S. CHANG,* K. YATES,† AND ROSS STEWART†

The hydrolysis of amides is believed to take place by the two-stage mechanism (1, 2, 3):

$$RCONH_2 + H^+ \underset{\text{fast}}{\rightleftharpoons} RCONH_3^+ \qquad [1]$$

$$RCONH_3^+ + H_2O \xrightarrow[\text{slow}]{k_2} RCO_2H_2^+ + NH_3 \qquad [2]$$

Recently Leisten (4), by working with acid solutions which he considered concentrated enough to have all the amide present as $RCONH_3^+$, has attempted to obtain the rate constants k_2 for various substituted benzamides in the second rate-determining step:

$$\text{rate of reaction } v = k_2[RCONH_3^+].$$

(The concentration of water was not included in the kinetic equation since it was effectively constant in the experiments carried out in any one acid concentration.)

Leisten used 5.86 *M*, 7.19 *M*, and 8.54 *M* perchloric acid at 95° C. He gives reasons for believing that the pK_{BH^+} values of amides at this temperature will be about the same as at room temperature. On the basis of early estimates (3) of the basicities of benzamides, these concentrations of acid were assumed to be sufficient for essentially complete protonation of the compounds listed in Table I. However, the pK_{BH^+} values

TABLE I

Corrected rate constants k_2 (in hr^{-1}) for the hydrolysis of substituted benzamides in perchloric acid

	Acid concentration		
Substituent	5.86 *M*	7.19 *M*	8.54 *M*
p-Methoxy	0.238	0.073	0.026
p-Methyl	0.437	0.131	
m-Methyl		0.192	0.057
Hydrogen	0.805	0.234	0.073
p-Bromo		0.410	
m-Bromo		0.627	0.174
p-Nitro		1.77	0.545
m-Nitro	6.33	1.34	0.455

now reported for these compounds (5) show this assumption to be incorrect. Consequently, the experimental rate constants k_e (3), based on the stoichiometric concentration of amide and defined by

$$v = k_e([RCONH_2]+[RCONH_3^+]),$$

are not equal to k_2, which in fact is given by

$$[3] \qquad k_2 = k_e([RCONH_2]+[RCONH_3^+])/[RCONH_3^+] = k_e(K_{BH^+}+h_0)/h_0$$

*McGill University, Montreal, Que.
†University of British Columbia, Vancouver, B.C.

Can. J. Chem. Downloaded from www.nrcresearchpress.com by 210.87.254.42 on 09/05/12
For personal use only.

where $K_{BH^+} = -$antilog pK_{BH^+} and h_0 is Hammett's acidity function in its non-logarithmic form. The values of k_2 obtained from Leisten's results using eq. 3 are given in Table I.

The slopes of the least-squares plots of log k_2 against the σ values of the substituents (Fig. 1) give the values of the reaction constant ρ_2 for eq. 2 (6). These are listed below,

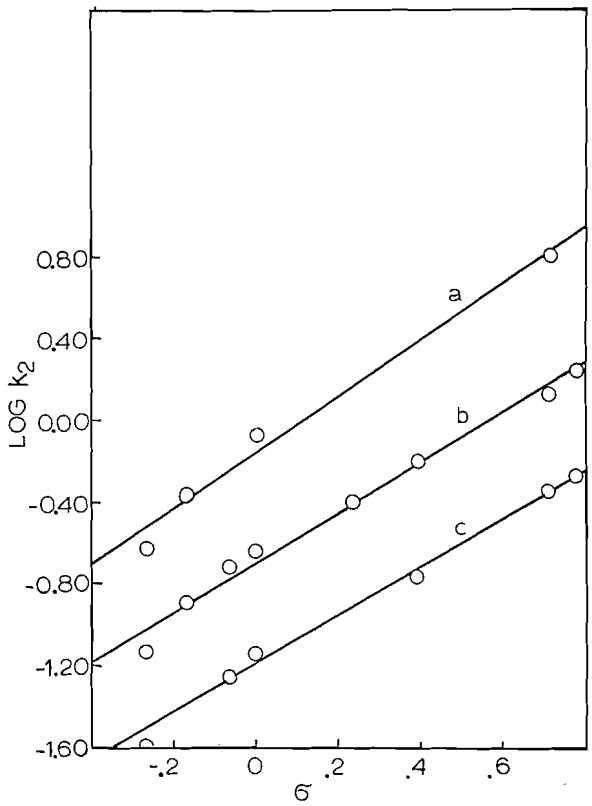


FIG. 1. Plots against Hammett's σ constants of log k_2 for substituted benzamides in the following concentrations of perchloric acid: *a*, 5.86 *M*; *b*, 7.19 *M*; *c*, 8.54 *M*.

with the number of results from which ρ_2 was determined (n), the standard deviation (s), and the correlation coefficient (r).

$HClO_4$ (M)	ρ_2	n	s	r
5.86	1.39	4	0.162	0.916
7.18	1.23	8	0.057	0.992
8.54	1.19	6	0.070	0.989

These values, slightly different from those of Leisten, are in better agreement with the value (1.42) calculated from the equation

[4] $$\rho_{0v} = \rho_1 + \rho_2$$

where ρ_{0v} is the reaction constant for the rates of hydrolysis of substituted benzamides in dilute acid (0.118, ref. 6), and ρ_1 ($= -1.30$) is the reaction constant recently determined (5) for eq. 1 in the direction shown.

Can. J. Chem. Downloaded from www.nrcresearchpress.com by 210.87.254.42 on 09/05/12
For personal use only.

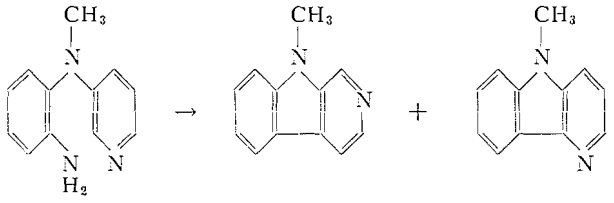
1. C. K. INGOLD. Structure and mechanism in organic chemistry. Bell & Sons, Ltd., London. 1953. p. 785.
2. M. L. BENDER and R. D. GINGER. J. Am. Chem. Soc. 77, 348 (1955).
3. J. T. EDWARD and S. C. R. MEACOCK. J. Chem. Soc. 2000 (1957).
4. J. A. LEISTEN. J. Chem. Soc. 765 (1959).
5. J. T. EDWARD, H. S. CHANG, K. YATES, and R. STEWART. Can. J. Chem. **38**, 1518 (1960).
6. L. P. HAMMETT. Physical organic chemistry. McGraw-Hill Book Co., Inc., New York. 1940. p. 184.

RECEIVED JULY 26, 1960.
DEPARTMENT OF CHEMISTRY,
MCGILL UNIVERSITY,
MONTREAL, QUE.,
AND
UNIVERSITY OF BRITISH COLUMBIA,
VANCOUVER, BRITISH COLUMBIA.

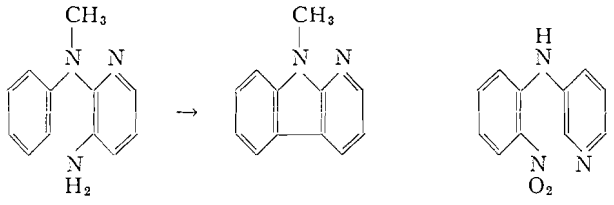
TRYPTAMINES, CARBOLINES, AND RELATED COMPOUNDS
PART VII. INTERNUCLEAR CYCLIZATION ONTO A PYRIDINE RING*†

R. A. ABRAMOVITCH

On the basis of two examples of internuclear cyclization of the Pschorr type onto a pyridine ring (1, 2) (one involving predominant electrophilic attack at the ring nitrogen) it was suggested (3) that the pyridine ring is more difficult to attack than a benzene ring in such reactions. The cyclization of 2-amino-*N*-methyl-*N*-3′-pyridylaniline (I) was studied to examine whether this was indeed so, as well as to provide a route to the δ-carboline ring system. Also, some evidence might thus be obtained to suggest a mechanism for the Pschorr reaction when carried out under such conditions, for the pyridine ring is known to be deactivated towards electrophilic substitution under mild conditions, but not towards homolytic attack. Should cyclization occur readily it was of interest to determine the orientation of the products since the isomer ratios for free radical phenylation of pyridine are in the order $\alpha > \beta > \gamma$ (4).



(I) (II) (III)



(IV) (V) (VI)

*Presented at the Atlantic City Meeting of the American Chemical Society on September 14, 1959.
†Part VI: Can. J. Chem. **38**, 557 (1960).

Can. J. Chem. Downloaded from www.nrcresearchpress.com by 210.87.254.42 on 09/05/12
For personal use only.

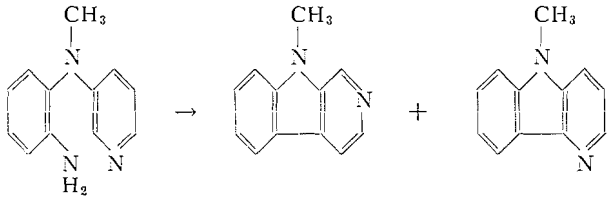
1. C. K. INGOLD. Structure and mechanism in organic chemistry. Bell & Sons, Ltd., London. 1953. p. 785.
2. M. L. BENDER and R. D. GINGER. J. Am. Chem. Soc. 77, 348 (1955).
3. J. T. EDWARD and S. C. R. MEACOCK. J. Chem. Soc. 2000 (1957).
4. J. A. LEISTEN. J. Chem. Soc. 765 (1959).
5. J. T. EDWARD, H. S. CHANG, K. YATES, and R. STEWART. Can. J. Chem. **38**, 1518 (1960).
6. L. P. HAMMETT. Physical organic chemistry. McGraw-Hill Book Co., Inc., New York. 1940. p. 184.

RECEIVED JULY 26, 1960.
DEPARTMENT OF CHEMISTRY,
MCGILL UNIVERSITY,
MONTREAL, QUE.,
AND
UNIVERSITY OF BRITISH COLUMBIA,
VANCOUVER, BRITISH COLUMBIA.

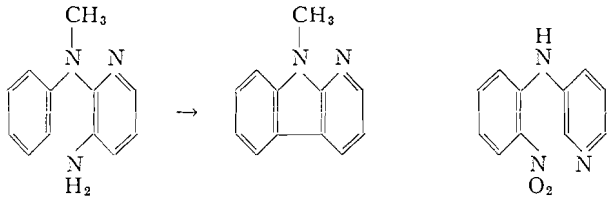
TRYPTAMINES, CARBOLINES, AND RELATED COMPOUNDS
PART VII. INTERNUCLEAR CYCLIZATION ONTO A PYRIDINE RING*†

R. A. ABRAMOVITCH

On the basis of two examples of internuclear cyclization of the Pschorr type onto a pyridine ring (1, 2) (one involving predominant electrophilic attack at the ring nitrogen) it was suggested (3) that the pyridine ring is more difficult to attack than a benzene ring in such reactions. The cyclization of 2-amino-*N*-methyl-*N*-3′-pyridylaniline (I) was studied to examine whether this was indeed so, as well as to provide a route to the δ-carboline ring system. Also, some evidence might thus be obtained to suggest a mechanism for the Pschorr reaction when carried out under such conditions, for the pyridine ring is known to be deactivated towards electrophilic substitution under mild conditions, but not towards homolytic attack. Should cyclization occur readily it was of interest to determine the orientation of the products since the isomer ratios for free radical phenylation of pyridine are in the order $\alpha > \beta > \gamma$ (4).



(I) (II) (III)



(IV) (V) (VI)

*Presented at the Atlantic City Meeting of the American Chemical Society on September 14, 1959.
†Part VI: Can. J. Chem. **38**, 557 (1960).

Can. J. Chem. Downloaded from www.nrcresearchpress.com by 210.87.254.5 on 09/05/12
For personal use only.

Decomposition of the aqueous diazonium sulphate of 2-amino-*N*-methyl-*N*-3′-pyridylaniline (I) with copper powder at room temperature resulted in a good yield of a mixture of cyclized products which was separated into *ind*-*N*-methyl-δ-carboline (III) (47.5% yield) and *ind*-*N*-methyl-β-carboline (II) (25.5% yield) by chromatography on a column of alumina. The structure of (III) was confirmed by the analytical results and by its infrared spectrum, which showed no monosubstituted phenyl bands, thus eliminating the possibility that the substance isolated was the deaminated product. Its ultraviolet absorption spectrum was very similar to that of an authentic specimen of δ-carboline obtained by an unambiguous synthesis (5). The structure was finally proved by comparison with an authentic specimen whose preparation from δ-carboline is described in the next part of this series (5). The total yield of cyclized product (73%) is comparable with that obtained (78%) when *N*-(3-amino-2-pyridyl)-*N*-methylaniline (IV) is ring-closed to *ind*-*N*-methyl-α-carboline (V) (2), i.e. a similar cyclization, with similar internuclear separation (6), onto a benzene ring. This clearly indicates that in the present case the pyridine ring is not deactivated towards nuclear attack and that under these very mild reaction conditions free radical intermediates (perhaps bound in some way with the copper catalyst) may be involved. An amino substituent in the pyridine is known to facilitate electrophilic attack of the ring due to the mesomeric effect of the electron pair of the amino nitrogen atom. Phenyl substitution at the 3-amino group is expected, however, to decrease the activating effect of this group and *o*-diazotization to decrease it still further. An attempt to eliminate this possible source of ambiguity by replacing the *N*-methyl group in (I) by an acyl grouping was made. 2-Nitro-*N*-3′-pyridylaniline (VI), however, resisted all attempts at acetylation, tosylation, or mesylation, so that the required starting material could not be obtained.

It is very likely (7) that in the absence of copper powder and at the boiling point of the aqueous acid the cyclization involves cationic intermediates so that in such a case, though the reaction conditions are more severe than in the one where copper powder is used, the yield of cyclized product would be expected to fall due to the resistance of the pyridine ring to electrophilic substitution. This was indeed found to be the case, the over-all yield of carbolines being 47.2%: *ind*-*N*-methyl-δ-carboline (33%), *ind*-*N*-methyl-β-carboline (14.2%). A product, whose picrate analyzed for that of the deaminated product, was also obtained under these conditions. It is to be noted, however, that in contrast to the above results ring closure of 2-amino-*N*-methyldiphenylamine under both sets of conditions gave comparable yields of *N*-methylcarbazole (6). Thus, by the action of copper powder on the cold solution of the diazonium sulphate a 66% yield of cyclized product was obtained; the action of heat upon the aqueous diazonium sulphate solution in the absence of copper resulted in a 60% yield of *N*-methylcarbazole. Here there is no decrease in yield on passing from a heterolytic to a presumably homolytic process since the benzene, unlike the pyridine ring, is not deactivated towards electrophilic attack. These observations also support the suggestion that the side-chain tertiary amino group is probably not activating the ring towards electrophilic attack in such aqueous acid solutions.

EXPERIMENTAL

Melting points and boiling points are uncorrected. Ultraviolet absorption spectra were measured on a Beckman DK 2 recording spectrophotometer. For the chromatographic separations alumina supplied by Peter Spence and Sons, Ltd., as activated alumina type H, 100/200 mesh, was used.

Can. J. Chem. Downloaded from www.nrcresearchpress.com by 210.87.254.5 on 09/05/12
For personal use only.

N-Methyl-2-nitro-N-3′-pyridylaniline

A mixture of 3-bromopyridine (3.2 g), *N*-methyl-*o*-nitraniline (2.3 g), anhydrous potassium carbonate (2 g), and copper bronze (100 mg) in nitrobenzene (12 ml) was boiled under reflux for 24 hours. The suspension was steam-distilled and the residue extracted with chloroform, the extract dried ($MgSO_4$) and evaporated. The residue was distilled *in vacuo* giving a red viscous oil (1.4 g), b.p. 140–150°/2×10^{-2} mm, which formed a glass on cooling. The product was analyzed as *the picrate* which crystallized from ethanol as yellow needles, m.p. 168°. Found: C, 46.90; H, 2.99. Calc. for $C_{12}H_{11}O_2N_3$, $C_6H_3O_7N_3$: C, 47.17; H, 3.06.

2-Amino-N-methyl-N-3′-pyridylaniline

The above nitro compound (2.7 g), Raney nickel (1 g), and 100% hydrazine hydrate (10 ml) in alcohol (50 ml) were boiled under reflux for 15 minutes, the suspension filtered, and the filtrate evaporated to dryness leaving an oil (1.77 g) which slowly solidified. Vacuum distillation gave the *amine* as a colorless oil, b.p. 140–143°/0.4 mm, which solidified to a colorless solid. This was recrystallized from benzene – light petroleum (b.p. 60–80°) giving colorless needles, m.p. 93–94°. Found: C, 71.98; H, 6.24; N, 20.60. Calc. for $C_{12}H_{13}N_3$: C, 72.33; H, 6.57; N, 21.10.

Decomposition of the Aqueous Diazonium Sulphate of 2-Amino-N-methyl-N-3′-pyridylaniline

(i) With Copper Powder at Room Temperature

The amine (1.9 g) in concentrated sulphuric acid (4 ml) and water (50 ml) was diazotized at 0–5° with sodium nitrite (2 g) in water (20 ml), stirring at 0–5° being continued for ½ hour. Urea (1.5 g) was added to the clear solution to decompose the excess nitrous acid, and then copper powder (2 g) was gradually stirred in. The decomposition was complete in ½ hour as indicated by the cessation of effervescence and a negative alkaline β-naphthol test. The suspension was stirred at room temperature for a further ½ hour and then it was filtered from the copper, made alkaline with an excess of concentrated ammonia, and extracted with chloroform (2×200 ml). The dried ($MgSO_4$) extract was evaporated and the tarry black residue was taken up in benzene and chromatographed on a column of alumina (70 g). Elution with benzene first gave a colorless oil (0.82 g, 47%) which soon solidified, and had a melting point of 73–74°. Recrystallization from light petroleum (b.p. 60–80°) gave *ind-N-methyl-δ-carboline* as colorless plates, m.p. 74°. Found: C, 78.75; H, 5.72. Calc. for $C_{12}H_{10}N_2$: C, 79.09; H, 5.53. λ_{max} 263, 267, 306 mμ; λ_{infl} 235, 249 mμ; $\epsilon\times10^{-3}$ 18.92, 18.80, 11.83, 13.35, 10.62 (in ethanol). Infrared spectrum (Nujol mull) (main peaks only): 1628 (m), 1595 (m), 774 (m), 750 (m), 727 (s). The *picrate* separated from alcohol and was recrystallized from dioxane giving fine yellow needles, m.p. 229–230°. Found: C, 52.60; H, 3.0. Calc. for $C_{12}H_{10}N_2$, $C_6H_3O_7N_3$: C, 52.56; H, 3.19.

Further elution with benzene gave a brown oil which solidified very slowly. The solid was recrystallized from light petroleum (b.p. 60–80°) giving *ind-N*-methyl-β-carboline as colorless plates, m.p. 97° (0.45 g, 25%), undepressed on admixture with an authentic sample (8). Further recrystallization from light petroleum raised the melting point to 106–107°. Found: C, 79.03; H, 5.4. Calc. for $C_{12}H_{10}N_2$: C, 79.09; H, 5.53. The picrate separated from alcohol and was recrystallized from acetone giving fluffy yellow needles, m.p. 258°. Found: C, 52.31; H, 3.20. Calc. for $C_{12}H_{10}N_2$, $C_6H_3O_7N_3$: C, 52.56; H, 3.19. (Lit. (8) gives a melting point of 258°.)

Can. J. Chem. Downloaded from www.nrcresearchpress.com by 210.87.254.5 on 09/05/12
For personal use only.

(ii) By Boiling Without Copper Powder

The amine (2.0 g) was diazotized as before and the filtered diazonium solution was boiled under reflux for 10 hours. The cold solution was made just alkaline with aqueous sodium hydroxide and extracted with chloroform. The dried ($MgSO_4$) chloroform extract was evaporated, the residue taken up in benzene, and chromatographed on alumina as before. Elution with benzene gave first *ind-N*-methyl-δ-carboline (0.60 g, 33%), m.p. 73°, and then *ind-N*-methyl-β-carboline (0.26 g, 14.2%) as a very crude oil characterized as the picrate, m.p. and mixed m.p. 258°. Elution with ether gave a brown oil (0.10 g) which formed a picrate from alcohol. This picrate was recrystallized from acetone giving small yellow needles, m.p. 202–203° (decomp.), which analyzed for the *picrate* of *N*-methyl-*N*-3′-pyridylaniline. Found: C, 52.09; H, 3.14; N, 17.30. Calc. for $C_{12}H_{12}N_2$, $C_6H_3O_7N_3$: C, 52.21; H, 3.32; N, 16.94.

2-Nitro-N-3′-pyridylaniline

3-Aminopyridine (0.94 g), *o*-bromonitrobenzene (2.02 g), anhydrous potassium carbonate (2 g), and copper bronze (0.05 g) in xylene (20 ml) were boiled under reflux for 6 hours. The solvent was decanted off and the residue extracted repeatedly with boiling benzene, the combined extracts were treated with dilute hydrochloric acid, the acid solution made alkaline, saturated with sodium chloride, and extracted with benzene. The benzene solution was chromatographed on a short column of alumina. Elution with ether gave *2-nitro-N-3′-pyridylaniline* (0.62 g) as a dark red solid, m.p. 90°, which crystallized from water containing a little ethanol in slender orange-red needles, m.p. 95–96°. Found: C, 61.50; H, 4.51. Calc. for $C_{11}H_9O_2N_3$: C, 61.39; H, 4.42.

Attempted Tosylation of 2-Nitro-N-3′-pyridylaniline

The nitro compound (60 mg) and tosyl chloride (60 mg) in 2 ml of redistilled pyridine were boiled under reflux for 24 hours. Addition of water and recovery of the solid which precipitated gave unchanged starting material, m.p. 95–96°.

Similar results were obtained on attempted mesylation and acetylation (even in the presence of perchloric acid).

ACKNOWLEDGMENTS

Part of this work was carried out during the tenure of an I.C.I. Research Fellowship at King's College, London, England. The author is grateful to Dr. I. D. Spenser for an authentic specimen of *ind-N*-methyl-β-carboline and to Dr. L. Vining for the use of a recording Beckman DK 2 spectrophotometer.

1. D. H. Hey and J. M. Osbond. J. Chem. Soc. 3164 (1949).
2. R. A. Abramovitch, D. H. Hey, and R. D. Mulley. J. Chem. Soc. 4263 (1954).
3. H. Plieninger and M. Schach von Wittenau. Ber. **91**, 1903 (1958).
4. D. H. Hey, C. J. M. Stirling, and G. H. Williams. J. Chem. Soc. 3936 (1955).
5. R. A. Abramovitch, K. A. H. Adams, and A. D. Notation. Can. J. Chem. **38**, 2152 (1960).
6. D. H. Hey and R. D. Mulley. J. Chem. Soc. 2276 (1952).
7. D. F. Detar. Organic reactions. Vol. IX. John Wiley & Sons, Inc., New York. 1957. p. 409.
8. E. Späth and E. Lederer. Ber. **63**, 2102 (1930).

Received April 20, 1960.
Chemistry Department,
University of Saskatchewan,
Saskatoon, Saskatchewan,
and
King's College,
London, W.C.2, England.

Can. J. Chem. Downloaded from www.nrcresearchpress.com by 210.87.254.5 on 09/05/12
For personal use only.

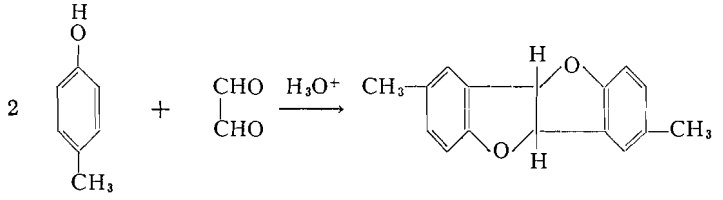
THE CONDENSATION OF GLYOXAL WITH *p*-CRESOL

ALEX ROSENTHAL AND ALEC ZAIONCHKOVSKY

The preparation of condensation products from glyoxal and phenolic substances has been of considerable interest in the past decade. Chwala and Bartek (1) reported the condensation of glyoxal sulphate with phenol in the presence of mineral acids to yield a resin. At about the same time, Stevens and Dubbs (2) found that the reaction of 2-*tert*-butyl-4-methylphenol with glyoxal in the presence of acetic acid, hydrochloric acid, and zinc chloride afforded water-insoluble compounds. They also isolated, in unspecified yield, a substituted benzofuro[2,3-*b*]benzofuran. Groote and Keiser (3) have reported that the condensation of glyoxal with a phenol yielded low-stage resins.

In our investigation on the condensation of glyoxal with *p*-cresol, we employed two different reaction media. In the first runs, the reactants were condensed in an aqueous system using acetic acid and sulphuric acid as catalyst, whereas in later experiments the condensations were carried out in bis-(2-ethoxyethyl) ether using *p*-toluenesulphonic acid as catalyst.

When equimolar ratios of glyoxalmonohydrate and *p*-cresol were heated in aqueous acetic acid containing sulphuric acid as catalyst, a 70% yield of a crystalline material was obtained. Recrystallization of this substance from ethanol afforded 5,5¹-dimethyl-coumarano-3¹,2¹,2,3-coumaran (I). The structure of compound I was confirmed by direct comparison with an authentic sample (4).



(I)

It is interesting to compare the prominent infrared spectral bands of 5,5¹-dimethyl-coumarano-3¹,2¹,2,3-coumaran (listed in the experimental) with those of other cyclic as well as straight-chain ethers. The fact that the coumarano-coumaran exhibited pronounced absorption at 1250 cm^{-1} provides additional confirmation for the generalization that the C—O—C of ring compounds probably absorbs at something like the same frequency as it does in open-chain products (5, 6). The band at 1095 cm^{-1} is ascribed to the asymmetrical ring stretching vibration (7).

Repeated attempts to condense anhydrous glyoxal with *p*-cresol in bis-(2-ethoxyethyl) ether using *p*-toluenesulphonic acid as catalyst, under various temperatures and in closed and open systems, were unsuccessful. Almost quantitative conversion of glyoxal into polymeric form occurred.

EXPERIMENTAL

Anhydrous glyoxal was prepared by heating glyoxalmonohydrate with phosphorus pentoxide in a dry all-glass apparatus fitted with a condensing trap cooled in dry ice.

Condensation of Glyoxal with p-Cresol

Procedure A.—Glyoxal monohydrate (2.6 g) dissolved in 15 ml water, and *p*-cresol

Can. J. Chem. Downloaded from www.nrcresearchpress.com by 210.87.254.40 on 09/05/12
For personal use only.

(3.6 g) dissolved in 10 ml glacial acetic acid, were mixed and placed in an apparatus fitted with a condenser. To the stirred preheated mixture, 5 ml of concentrated sulphuric acid was added dropwise. The voluminous precipitate was removed by filtration, washed with hot water, and dried: yield, 3.5 g. The material was recrystallized several times from ethanol, m.p. 192–194° C; mixed m.p. with an authentic sample of 5,5¹-dimethylcoumarano-3¹,2¹,2,3-coumaran (4), 191–194° C; infrared data in Nujol: 1600 (w), 1495 (s), 1330 (w), 1250 (m), 1195 (w), 1130 (w), 1095 (w), 990 (s). Anal. Calc. for $C_{16}H_{14}O_2$: C, 80.65; H, 5.88. Found: C, 80.66; H, 6.26.

Procedure B.—Glyoxal monohydrate (5.3 g), *p*-cresol (7.1 g), and *p*-toluenesulphonic (0.25 g) were heated in a sealed Carius tube at 102° C for 14 hours. The product was extracted with acetone and precipitated by addition of water. Recrystallization of the product from ethyl alcohol gave 0.85 g of 5,5¹-dimethylcoumarano-3¹,2¹,2,3-coumaran.

Procedure C.—Fusion of the same reactants as described in procedure B at 130–140° C for 10 minutes gave 0.2 g of the coumaran.

Procedure D.—A solution of anhydrous glyoxal (0.72 g), *p*-cresol (1.30 g), and *p*-toluenesulphonic acid (0.050 g) dissolved in 15 ml of anhydrous bis-(2-ethoxyethyl) ether was allowed to react at 0° C in a sealed Carius tube for 24 hours. Addition of petroleum ether (200 ml) to the reaction mixture caused a precipitate (0.72 g) to form, m.p. 140–150° C (decomp.). This material showed strong absorption in the infrared at about 3400 cm^{-1}. The product, when heated to a temperature above 170° C, gave off yellowish fumes of glyoxal. When anhydrous gloxal was reacted with *p*-cresol in bis-(2-ethoxyethyl) ether at elevated temperatures only polymerized glyoxal was obtained.

ACKNOWLEDGMENT

The authors are indebted to the National Research Council of Canada for support of this research.

1. A. Chwala and W. Bartek. Monatsh. **82**, 652 (1951); Chem. Abstr. **47**, 7443 (1953).
2. D. R. Stevens and A. C. Dubbs. U.S. Patent No. 2,515,909 (July 1950); Chem. Abstr. **44**, 94, 83 (1950).
3. M. De Groote and B. Keiser. U.S. Patent No. 2,564,192 (August 1951); Chem. Abstr. **45**, 9254 (1951).
4. O. Anselmino. Ber. **41**, 621 (1908).
5. L. J. Bellamy. Infrared spectra of complex molecules. Methuen & Co. Ltd., London. 1958. p. 119.
6. R. Norman Jones and Camille Sandorfy. Chemical applications of spectroscopy. Interscience Publishers, New York. 1956. p. 438.
7. G. M. Barrow and S. Searles. J. Am. Chem. Soc. **75**, 1175 (1953).

Received July 18, 1960.
Department of Chemistry,
The University of British Columbia,
Vancouver, British Columbia.

NUCLEAR MAGNETIC RESONANCE SPECTRA OF SOME MODEL INDOLINE DERIVATIVES*

Stewart McLean†

The nuclear magnetic resonance spectra of three model indoline derivatives have been analyzed in order to obtain support for the assignment of certain N.M.R. peaks to particular structural features in dihydroindole alkaloids under investigation.

*Issued as N.R.C. No. 6012.
†National Research Council Postdoctorate Fellow. Present address: Department of Chemistry, University of Toronto, Toronto, Ontario.

Can. J. Chem. Downloaded from www.nrcresearchpress.com by 210.87.254.40 on 09/05/12
For personal use only.

(3.6 g) dissolved in 10 ml glacial acetic acid, were mixed and placed in an apparatus fitted with a condenser. To the stirred preheated mixture, 5 ml of concentrated sulphuric acid was added dropwise. The voluminous precipitate was removed by filtration, washed with hot water, and dried: yield, 3.5 g. The material was recrystallized several times from ethanol, m.p. 192–194° C; mixed m.p. with an authentic sample of 5,5¹-dimethylcoumarano-3¹,2¹,2,3-coumaran (4), 191–194° C; infrared data in Nujol: 1600 (w), 1495 (s), 1330 (w), 1250 (m), 1195 (w), 1130 (w), 1095 (w), 990 (s). Anal. Calc. for $C_{16}H_{14}O_2$: C, 80.65; H, 5.88. Found: C, 80.66; H, 6.26.

Procedure B.—Glyoxal monohydrate (5.3 g), *p*-cresol (7.1 g), and *p*-toluenesulphonic (0.25 g) were heated in a sealed Carius tube at 102° C for 14 hours. The product was extracted with acetone and precipitated by addition of water. Recrystallization of the product from ethyl alcohol gave 0.85 g of 5,5¹-dimethylcoumarano-3¹,2¹,2,3-coumaran.

Procedure C.—Fusion of the same reactants as described in procedure B at 130–140° C for 10 minutes gave 0.2 g of the coumaran.

Procedure D.—A solution of anhydrous glyoxal (0.72 g), *p*-cresol (1.30 g), and *p*-toluenesulphonic acid (0.050 g) dissolved in 15 ml of anhydrous bis-(2-ethoxyethyl) ether was allowed to react at 0° C in a sealed Carius tube for 24 hours. Addition of petroleum ether (200 ml) to the reaction mixture caused a precipitate (0.72 g) to form, m.p. 140–150° C (decomp.). This material showed strong absorption in the infrared at about 3400 cm^{-1}. The product, when heated to a temperature above 170° C, gave off yellowish fumes of glyoxal. When anhydrous gloxal was reacted with *p*-cresol in bis-(2-ethoxyethyl) ether at elevated temperatures only polymerized glyoxal was obtained.

ACKNOWLEDGMENT

The authors are indebted to the National Research Council of Canada for support of this research.

1. A. Chwala and W. Bartek. Monatsh. **82**, 652 (1951); Chem. Abstr. **47**, 7443 (1953).
2. D. R. Stevens and A. C. Dubbs. U.S. Patent No. 2,515,909 (July 1950); Chem. Abstr. **44**, 94, 83 (1950).
3. M. De Groote and B. Keiser. U.S. Patent No. 2,564,192 (August 1951); Chem. Abstr. **45**, 9254 (1951).
4. O. Anselmino. Ber. **41**, 621 (1908).
5. L. J. Bellamy. Infrared spectra of complex molecules. Methuen & Co. Ltd., London. 1958. p. 119.
6. R. Norman Jones and Camille Sandorfy. Chemical applications of spectroscopy. Interscience Publishers, New York. 1956. p. 438.
7. G. M. Barrow and S. Searles. J. Am. Chem. Soc. **75**, 1175 (1953).

Received July 18, 1960.
Department of Chemistry,
The University of British Columbia,
Vancouver, British Columbia.

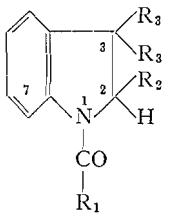
NUCLEAR MAGNETIC RESONANCE SPECTRA OF SOME MODEL INDOLINE DERIVATIVES*

Stewart McLean†

The nuclear magnetic resonance spectra of three model indoline derivatives have been analyzed in order to obtain support for the assignment of certain N.M.R. peaks to particular structural features in dihydroindole alkaloids under investigation.

*Issued as N.R.C. No. 6012.
†National Research Council Postdoctorate Fellow. Present address: Department of Chemistry, University of Toronto, Toronto, Ontario.

Can. J. Chem. Downloaded from www.nrcresearchpress.com by 210.87.254.5 on 09/05/12
For personal use only.



I (*a*) $R_1 = CH_3$; $R_2 = R_3 = H$
(*b*) $R_1 = CH_3CH_2$; $R_2 = R_3 = H$
(*c*) $R_1 = R_2 = R_3 = CH_3$

The aromatic protons of N-acetylindoline (I*a*) appeared in two parts of the spectrum, the C_7 proton (split by the other protons in the ring) as a doublet centered at −0.93 p.p.m. (spacing of 8.5 c.p.s.) and the remaining ring protons as a complex multiplet centered at about 0.22 p.p.m.* The corresponding peaks in N-propionylindoline (I*b*) were at −0.94 p.p.m. (spacing of 8.5 c.p.s.) and at about 0.27 p.p.m., and in N-acetyl-2,3,3-trimethylindoline (I*c*) at −0.52 p.p.m. (unresolved) and at about 0.35 p.p.m. The appearance of the C_7 proton signal at low field is potentially diagnostic for the absence of other substitution at the equivalent position in alkaloids of this partial structure. The protons at positions 2 and 3 in both I*a* and I*b* gave rise to the pair of triplets predicted for an A_2B_2 system approaching the A_2X_2 limit (2). The low-field signal was centered at 3.27 p.p.m. in the former and at 3.43 p.p.m. in the latter, and the high-field signals were centered at 4.15 p.p.m. and 4.28 p.p.m., respectively (the spacing was 8.5 c.p.s. for both). The proton at position 2 in I*c* gave rise to the A part of an AX_3 system (the C_2—CH_3 is the X part) and appeared as a quartet centered at 3.28 p.p.m. (J = 6.5 c.p.s.), supporting the assignment made to the corresponding proton in aspidocarpine (3).

The acetyl protons of I*a* and I*c* gave rise to single sharp peaks at 5.10 and 5.08 p.p.m., respectively. The propionyl protons of I*b* produced the expected quartet (two protons of CH_2) centered at 5.00 p.p.m. and triplet (three protons of CH_3) centered at 6.13 p.p.m. (J = 8 c.p.s.).

The methyl groups at positions 2 and 3 of I*c* produced three sharp peaks (total area equivalent to nine protons) at 6.05, 6.18, and 6.30 p.p.m. with relative intensities 2:3:1, which could be accounted for in the following way. The C_2 methyl group split by the C_2 proton formed a doublet at 6.18 and 6.30 p.p.m., one peak of which accidentally overlapped the peak at 6.18 p.p.m. produced by one of the C_3 methyl groups. The second C_3 methyl group produced the peak at 6.05 p.p.m.

EXPERIMENTAL

N-*Acetylindoline*— m.p. 106–106.5°, was prepared from indoline and acetic anhydride (4).

N-*Propionylindoline*— white needles, m.p. 104.5–105° from 95% ethanol, was prepared from indoline and propionic anhydride. Anal. Calc. for $C_{11}H_{13}ON$: C, 75.40; H, 7.48; N, 7.99. Found: C, 75.68; H, 7.49; N, 8.26.

N-*Acetyl-2,3,3-trimethylindoline*.—2,3,3-Trimethylindolenine (Aldrich Chemical Co.) (232 mg) was hydrogenated with pre-reduced platinum oxide catalyst in acetic anhydride. One mole of hydrogen was taken up rapidly. The catalyst was removed by filtration and

**Spectra were obtained with a Varian Associates high-resolution nuclear magnetic resonance spectrometer operating at 60 Mc/sec frequency. Chloroform was employed both as a solvent and as an internal reference; its proton resonance was assigned a value of zero part per million and the scale was fixed from the position of the associated C^{13} (natural abundance) peaks which were shown to have a value of ±1.75 p.p.m. Solutions were approximately 0.5 M and solvent effects were neglected. Accuracy to ±0.04 p.p.m. was anticipated on this scale. Chloroform has the value 2.75 p.p.m. on the Tiers scale (1).*

Can. J. Chem. Downloaded from www.nrcresearchpress.com by 210.87.254.5 on 09/05/12
For personal use only.

the filtrate was warmed and evaporated under reduced pressure. A chloroform solution of the residue was washed with dilute sulphuric acid and then with dilute sodium carbonate solution. The solution was dried (sodium sulphate) and evaporated. The residue, a yellow oil, distilled under reduced pressure, yielded an almost colorless oil (230 mg), b.p. 70–72°/10^{-1} mm, showing strong absorption at 1644 cm^{-1} in the infrared. Anal. Calc. for $C_{13}H_{17}ON$: C, 76.81; H, 8.43; N, 6.89. Found: C, 76.98; H, 8.43; N, 6.84.

ACKNOWLEDGMENT

Helpful discussion with Dr. H. J. Bernstein is acknowledged.

1. G. V. D. TIERS. J. Phys. Chem. **62**, 1151 (1958).
2. J. A. POPLE, W. G. SCHNEIDER, and H. J. BERNSTEIN. Can. J. Chem. **35**, 1060 (1957).
3. S. MCLEAN, K. PALMER, and L. MARION. Can. J. Chem. **38**, 1547 (1960).
4. G. M. BENNET and M. M. HAFEZ. J. Chem. Soc. 287 (1941).

RECEIVED AUGUST 15, 1960.
DIVISION OF PURE CHEMISTRY,
NATIONAL RESEARCH COUNCIL,
OTTAWA, CANADA.

Can. J. Chem. Downloaded from www.nrcresearchpress.com by 210.87.254.5 on 09/05/12
For personal use only.

SCISSION OF STERICALLY HINDERED *vic*-DIOLS*

H. R. GOLDSCHMID† AND A. S. PERLIN

The scission of *vic*-diols by lead tetraacetate (1) and periodic acid (2, 3) is strongly rate dependent on the stereochemistry of the glycol group attacked. This property has led to the view (4), now generally accepted, that the reaction usually involves formation of a coplanar cyclic intermediate complex between the glycol and oxidant. Complexing of this type is unlikely to occur if the projected valency angle of the glycol group is held rigidly in the region of 120–180° (5, 6, 7). Such a steric arrangement is found in several compounds that contain a *trans*-glycol group situated in a fused or bridged ring system, and the fact that these compounds fail to react with lead tetraacetate or periodate is in excellent agreement with the concept of the cyclic intermediate.‡ In this group of sterically hindered glycols are 1,6-anhydro-β-D-glucofuranose and -α-D-galactofuranose (8), the two *trans*-2,3-camphanediols (9), cholestane-3β,6β,7α-triol (10), 4,6-*O*-benzylidene methyl α-D-altropyranoside (11), and 2,6-anhydro-β-D-fructofuranose (12).

Steric effects that are strongly evident for oxidations with lead tetraacetate in acetic acid were noted by Hockett and Mowery (13) to be much less marked when pyridine was used as solvent. This observation suggested that the steric requirements for lead tetraacetate oxidation are less critical in pyridine than under the more usual reaction conditions, and prompted us to test the stability of the sterically hindered glycols towards lead tetraacetate in pyridine. Several of these compounds have now been examined and found, in fact, to be oxidized readily (Table I). That the reactions constitute true glycol cleavage is indicated by the degradation of 4,6-*O*-benzylidene methyl α-D-altropyranoside (I) (as well as the corresponding D-glucoside) to the dialdehyde isolated, as the hemialdal hydrate

**Issued as N.R.C. No. 5973.*
†*National Research Council of Canada Postdoctorate Fellow, 1958–1960.*
‡*Trans-9,10-Decalindiol also appears unable to attain such a transition state but is nevertheless oxidized by lead tetraacetate, possible via an acyclic pathway (7). However, this compound resists attack by periodate (10).*

the filtrate was warmed and evaporated under reduced pressure. A chloroform solution of the residue was washed with dilute sulphuric acid and then with dilute sodium carbonate solution. The solution was dried (sodium sulphate) and evaporated. The residue, a yellow oil, distilled under reduced pressure, yielded an almost colorless oil (230 mg), b.p. 70–72°/10^{-1} mm, showing strong absorption at 1644 cm^{-1} in the infrared. Anal. Calc. for $C_{13}H_{17}ON$: C, 76.81; H, 8.43; N, 6.89. Found: C, 76.98; H, 8.43; N, 6.84.

ACKNOWLEDGMENT

Helpful discussion with Dr. H. J. Bernstein is acknowledged.

1. G. V. D. Tiers. J. Phys. Chem. **62**, 1151 (1958).
2. J. A. Pople, W. G. Schneider, and H. J. Bernstein. Can. J. Chem. **35**, 1060 (1957).
3. S. McLean, K. Palmer, and L. Marion. Can. J. Chem. **38**, 1547 (1960).
4. G. M. Bennet and M. M. Hafez. J. Chem. Soc. 287 (1941).

Received August 15, 1960.
Division of Pure Chemistry,
National Research Council,
Ottawa, Canada.

Can. J. Chem. Downloaded from www.nrcresearchpress.com by 210.87.254.6 on 09/05/12
For personal use only.

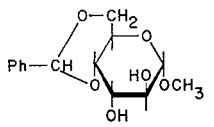
SCISSION OF STERICALLY HINDERED *vic*-DIOLS*

H. R. Goldschmid† and A. S. Perlin

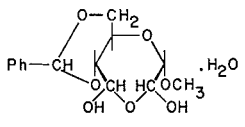
The scission of *vic*-diols by lead tetraacetate (1) and periodic acid (2, 3) is strongly rate dependent on the stereochemistry of the glycol group attacked. This property has led to the view (4), now generally accepted, that the reaction usually involves formation of a coplanar cyclic intermediate complex between the glycol and oxidant. Complexing of this type is unlikely to occur if the projected valency angle of the glycol group is held rigidly in the region of 120–180° (5, 6, 7). Such a steric arrangement is found in several compounds that contain a *trans*-glycol group situated in a fused or bridged ring system, and the fact that these compounds fail to react with lead tetraacetate or periodate is in excellent agreement with the concept of the cyclic intermediate.‡ In this group of sterically hindered glycols are 1,6-anhydro-β-D-glucofuranose and -α-D-galactofuranose (8), the two *trans*-2,3-camphanediols (9), cholestane-3β,6β,7α-triol (10), 4,6-*O*-benzylidene methyl α-D-altropyranoside (11), and 2,6-anhydro-β-D-fructofuranose (12).

Steric effects that are strongly evident for oxidations with lead tetraacetate in acetic acid were noted by Hockett and Mowery (13) to be much less marked when pyridine was used as solvent. This observation suggested that the steric requirements for lead tetraacetate oxidation are less critical in pyridine than under the more usual reaction conditions, and prompted us to test the stability of the sterically hindered glycols towards lead tetraacetate in pyridine. Several of these compounds have now been examined and found, in fact, to be oxidized readily (Table I). That the reactions constitute true glycol cleavage is indicated by the degradation of 4,6-*O*-benzylidene methyl α-D-altropyranoside (I) (as well as the corresponding D-glucoside) to the dialdehyde isolated, as the hemialdal hydrate

*Issued as N.R.C. No. 5973.
†*National Research Council of Canada Postdoctorate Fellow, 1958–1960.*
‡*Trans-9,10-Decalindiol also appears unable to attain such a transition state but is nevertheless oxidized by lead tetraacetate, possible via an acyclic pathway (7). However, this compound resists attack by periodate (10).*



I



II

TABLE I

Scission of *vic*-diols by lead tetraacetate in pyridine (moles of oxidant consumed/mole at 0° C)

Time (minutes)	2,6-Anhydro-β-D-fructofuranose		*trans*-2-Exo-3-endo-camphanediol*	
	(2 moles)†	(4.5 moles)	(3 moles)	(4.5 moles)
15	0.11	0.60	0.35	0.83
30	0.19	0.69	0.42	0.93
60	0.29	0.81	0.50	1.00
180	0.44	1.02	—	1.06
480	0.57	1.30	—	1.08

	4,6-*O*-Benzylidene methyl α-D-glycopyranoside	
	D-Altro-	D-Gluco-
	(5 moles)	
5	0.51	1.01
15	0.71	1.02
30	0.82	1.07
60	1.03	—
180	1.04	1.16

	Ethyl β-D-fructofuranoside and derivatives			
	1,6-Di-*O*-trityl-‡		1,6-Di-*O*-tosyl-	Glycoside‡
	(1.6 moles)§	(5 moles)	(1.7 moles)§	(2.0 moles)
15	0.54	1.02	—	0.88
30	0.63	0.98	0.95	1.03
60	0.72	1.00	0.96	1.18
90	0.74	—	1.04	1.21

*Closely similar data were obtained for the 2-endo-3-exo-isomer.
†Figures in parentheses give the number of moles of lead tetraacetate used per mole of substrate.
‡Closely similar data were obtained for the α-anomer.
§Temperature, 25° C.

(II) (14), formed by periodate oxidation of 4,6-*O*-benzylidene methyl α-D-glucopyranoside* (14, 15, 16).†

A normally "slow" diol (17), *trans*-1,2-cyclopentanediol, was very rapidly oxidized, the observed uptake being 0.9 to 1.0 mole of lead tetraacetate per mole in 5 minutes reaction time, irrespective of whether the excess of oxidant used was 0.25, 1.0, or 3.0 moles per mole. By contrast, the rate of oxidation of the hindered diols fell off sharply at well below

4,6-O-Benzylidene methyl α-D-glucopyranoside is oxidized at an unusually slow rate by periodate (11, 16). It also is extremely resistant to attack by lead tetraacetate in acetic acid, a property that is exhibited also by e,e trans-diols situated on 1,4-bonded central units of oligosaccarides (18). In pyridine, however, the benzylidene derivative is rapidly oxidized by lead tetraacetate (Table I and Experimental section).

†*Cholestane-3β,6β,7α-triol (10) (a sample of which was kindly provided by Prof. S. J. Angyal) is more resistant to oxidation than the other compounds examined: the observed rate of lead tetraacetate uptake (mole/mole(min)) was 0.34 (15), 0.55 (90), and 0.80 (360). This result contrasts strongly with the behavior of I (Table I), which also contains a diaxal glycol group, and may be related to the greater rigidity of ring B in the cholestane derivative than of the pyranoside ring in I.*

Can. J. Chem. Downloaded from www.nrcresearchpress.com by 210.87.254.6 on 09/05/12
For personal use only.

the theoretical level if an excess of only 1 to 2 moles of lead tetraacetate was used (Table I). With an excess of 3 to 4 moles the data were much more satisfactory (Table I). The marked drop in reaction rate at the lower level of concentration may possibly be related to Criegee's suggestion (4) that acetic acid, formed in the reduction of lead tetraacetate to the diacetate, can depress the rate of oxidation in a solvent other than acetic acid by a mass-action effect. Such an effect would be most readily apparent with the most highly hindered glycols.

Although the stoichiometry of the various reactions examined is close to the theoretical value under suitable conditions, slow overoxidation is always evident (Table I). Because of this non-specific overoxidation several hydroxylated compounds, other than 1,2-glycols, were examined. In this group were 1,2,3,4- and 2,3,4,6-tetra-*O*-acetyl-D-glucopyranose; 1,3-dihydroxypropane; 1,3-dihydroxy-2,2-dimethylpropane; pentaerythritol; 1,6-dihydroxyhexane; 2,5-dihydroxyhexane; and 1,3,6-trihydroxyhexane. Of these compounds, only 1,3-dihydroxypropane was attacked to a significant degree during the period of 1 to 2 hours (Table I) required for complete oxidation of the hindered glycols, the consumption in 2 hours reaction time being 0.12 mole of lead tetraacetate per mole. With a more prolonged oxidation period (8 to 24 hours), several of the compounds reduced a small proportion of oxidant (0.1 to 0.2 mole/mole), and with pentaerythritol the consumption reached a value of 0.6 mole/mole in 24 hours. It is clear, therefore, that in testing for the presence of a 1,2-diol group in an unknown compound with lead tetraacetate in pyridine, prolonged reaction periods should be avoided.

Pyridine is particularly suitable for the glycol-cleavage oxidation of certain classes of compounds which might be unstable or poorly soluble in media used more commonly. Hockett and co-workers (13, 19) first employed this solvent for lead tetraacetate oxidation of sucrose and trityl ethers of methyl D-arabopyranoside, compounds unstable in acetic acid. Similarly, we have found these conditions of oxidation useful for determining the structure of trityl- and tosyl-derivatives of ethyl α- and β-D-fructofuranoside (12). The 1,6-ditrityl ether of these glycosides exhibited behavior that is characteristic of the highly hindered diols described above, in that their oxidation rates dropped sharply when a small excess of lead tetraacetate was used (Table I). As shown by Smith and co-workers (20), periodate oxidation may be inhibited when a trityl or phenyl group is in close proximity to the *vic*-diol, the effect being attributed to steric interference. However, interference by bulky substituents does not appear to account fully for the retarded oxidation rate of the ditrityl-D-fructofuranosides, because the corresponding 1,6-ditosyl derivative reacts readily and quantitatively (Table I).

EXPERIMENTAL

Lead tetraacetate was dried *in vacuo* over solid potassium hydroxide, and pyridine was freshly distilled over solid potassium hydroxide.

Measurement of Lead Tetraacetate Uptake

The stopping solution (1) used (per milliliter of reaction mixture) contained potassium iodide (1.0 g), sodium acetate (2.7 g, anhydrous) in water (10 ml). Acetic acid (3 ml) was added to the stopping solution immediately before an aliquot of the oxidation mixture in order to complete the liberation of iodine. A bulky yellow precipitate is formed when lead tetraacetate in pyridine is mixed with the stopping solution; determination of the iodine with thiosulphate was facilitated by adding starch indicator at the outset, the suspension being titrated until the pea-green color was discharged.

Can. J. Chem. Downloaded from www.nrcresearchpress.com by 210.87.254.6 on 09/05/12
For personal use only.

In a typical experiment, 2,6-anhydro-β-D-fructofuranose (13.0 mg) in pyridine (4 ml) was treated at 0° C with a solution of lead tetraacetate (160 mg) in pyridine (6 ml). (The solution of lead tetraacetate in pyridine is deep brown in color, and the intensity of the color diminishes as oxidant is used up.) At chosen intervals, 1-ml portions of the reaction mixture were transferred to the stopping solution, and the liberated iodine was titrated immediately with thiosulphate.

Oxidation of 4,6-O-Benzylidene Methyl α-D-Altropyranoside (I)

To a solution of the benzylidene glycoside (282 mg) in pyridine (15 ml), lead tetraacetate (1.32 g) was added. After 25 minutes at room temperature the reaction mixture was treated with oxalic acid dihydrate (4.0 g) and a few drops of water. The precipitate was filtered off, the filtrate concentrated *in vacuo* at 45° C, and the residue obtained was taken up in hot aqueous acetone. A crystalline product (201 mg) was deposited from the cooled solution, and after recrystallization from aqueous acetone the product II (14) had a melting point of 130–133° C and $[\alpha]_D^{27}$ +62.8° (*c*, 1.9, pyridine). Calculated for $C_{14}H_{18}O_7 \cdot H_2O$: C, 53.16%; H, 6.37%. Found: C, 53.25%; H, 6.44%.

On treatment with hot phenylhydrazine acetate the product yielded glyoxal bis-phenylhydrazone, m.p. 164–166° C, undepressed.

The above hemialdal hydrate furnished a bis-cyclohexylamine derivative (14) with a melting point of 115–117° C and $[\alpha]_D^{27}$ −32.6° (*c*, 1.2, pyridine). Calculated for $C_{26}H_{38}O_4N_2$: C, 70.55%; H, 8.65%. Found: C, 70.48%; H, 8.86%.

Oxidation of 4,6-O-Benzylidene Methyl α-D-Glucopyranoside

The benzylidene glycoside (282 mg) was treated in pyridine (10 ml) with lead tetraacetate (618 mg) for 15 minutes at room temperature. Excess oxidant was reduced with oxalic acid, and the reaction mixture was worked up, affording compound II (14), m.p. 130–133° C, undepressed, and $[\alpha]_D^{27}$ +63.0° (*c*, 1.8, pyridine). Calculated for $C_{14}H_{18}O_7 \cdot H_2O$: C, 53.16%; H, 6.37%. Found: C, 53.54%; H, 6.16%.

On treatment with hot phenylhydrazine acetate the product yielded glyoxal bis-phenylhydrazone, m.p. 164–166° C, undepressed.

The derived bis-cyclohexylamine derivative (14) had a melting point of 115–117° C, undepressed and $[\alpha]_D^{27}$ −31.9° (*c*, 1.2, pyridine). Calculated for $C_{26}H_{38}O_4N_2$: C, 70.55%; H, 8.65%. Found: C, 70.56%; H, 8.59%.

The X-ray powder diagrams obtained from the above hemialdal hydrate and its bis-cyclohexylamine derivative were indistinguishable from the corresponding materials obtained from 4,6-*O*-benzylidene methyl α-D-altropyranoside.

The authors gratefully acknowledge a gift of *trans*-2-exo-3-endo- and -2-endo-3-exo-camphanediol from Prof. S. J. Angyal, and of 4,6-*O*-benzylidene methyl α-D-altropyranoside from Dr. A. C. Neish. They also thank Mr. J. W. L. C. Christ for technical assistance. Microanalyses were performed by Mr. M. Mazurek and X-ray powder diagrams were prepared by Miss Inez Gaffney.

1. R. CRIEGEE. Ber. **64**, 260 (1931).
2. L. MALAPRADE. Bull. soc. chim. France, **39**, 325 (1926).
3. P. F. FLEURY and J. LANGE. Compt. rend. **195**, 1395 (1932).
4. R. CRIEGEE, L. KRAFT, and B. RANK. Ann. **507**, 159 (1933).
5. R. E. REEVES. *In* Advances in carbohydrate chemistry. Vol. 6. Academic Press, Inc., New York. 1951. p. 107.
6. R. J. DIMLER. *In* Advances in carbohydrate chemistry. Vol. 7. Academic Press, Inc., New York. 1952. p. 37.

Can. J. Chem. Downloaded from www.nrcresearchpress.com by 210.87.254.6 on 09/05/12
For personal use only.

7. R. CRIEGEE, E. HÖGER, G. HUBER, P. KRUCK, F. MARKTSCHEFFEL, and H. SCHELLENBERGER. Ann. **599**, 81 (1956).
8. R. J. DIMLER, H. A. DAVIS, and G. E. HILBERT. J. Am. Chem. Soc. **68**, 1377 (1946).
9. S. J. ANGYAL and R. J. YOUNG. J. Am. Chem. Soc. **81**, 5467 (1959).
10. S. J. ANGYAL and R. J. YOUNG. J. Am. Chem. Soc. **81**, 5251 (1959).
11. J. HONEYMAN and C. J. G. SHAW. J. Chem. Soc. 2454 (1959).
12. H. R. GOLDSCHMID and A. S. PERLIN. Can. J. Chem. This issue.
13. R. C. HOCKETT and D. F. MOWERY, JR. J. Am. Chem. Soc. **65**, 403 (1943).
14. R. D. GUTHRIE and J. HONEYMAN. J. Chem. Soc. 2441 (1959).
15. J. W. ROWEN, R. E. REEVES, and F. H. FORZIATI. J. Am. Chem. Soc. **73**, 4484 (1951).
16. J. BADDILEY, J. G. BUCHANAN, and L. SZABO. J. Chem. Soc. 3826 (1954).
17. R. CRIEGEE, E. BÜCHNER, and W. WALTHER. Ber. **73**, 571 (1940).
18. A. S. PERLIN and A. R. LANSDOWN. Can. J. Chem. **34**, 451 (1956).
19. R. C. HOCKETT and M. ZIEF. J. Am. Chem. Soc. **72**, 2130 (1950).
20. E. F. GARNER, I. J. GOLDSTEIN, R. MONTGOMERY, and F. SMITH. J. Am. Chem. Soc. **80**, 1206 (1958).

RECEIVED JULY 25, 1960.
NATIONAL RESEARCH COUNCIL OF CANADA,
PRAIRIE REGIONAL LABORATORY,
SASKATOON, SASKATCHEWAN.

Can. J. Chem. Downloaded from www.nrcresearchpress.com by 210.87.254.6 on 09/05/12
For personal use only.

Can. J. Chem. Downloaded from www.nrcresearchpress.com by 210.87.254.5 on 09/05/12
For personal use only.

Canadian Journal of Chemistry

Issued by THE NATIONAL RESEARCH COUNCIL OF CANADA

VOLUME 38 DECEMBER 1960 NUMBER 12

THE SEPARATION OF SUGARS ON ION-EXCHANGE RESINS

PART I. SEPARATION OF OLIGOSACCHARIDES[1]

J. K. N. JONES, R. A. WALL, AND (*in part*) A. O. PITTET[2]

ABSTRACT

Fractionation according to molecular size has been achieved by development of oligosaccharide mixtures with water on columns of neutral salt forms of sulphonic acid type ion-exchange resins. The method was used to separate a synthetic mixture of raffinose, sucrose, and glucose and a number of hydrolyzates of polysaccharides to give clean, salt-free fractions of high purity. The procedure is rapid and economical and provides a useful extension of older methods of separating such mixtures.

INTRODUCTION

One of the major problems of carbohydrate chemistry is the separation of mixtures of sugars from hydrolyzates and synthetic reactions. Resolution is commonly achieved by using variations of the charcoal–celite columns of Whistler and Durso (1) or partition chromatography on cellulose columns (2). These procedures are usually very efficient and several grams of material can be separated per run, but the time required for fractionation may be of the order of weeks or even months. Moreover, the larger fragments are usually eluted at the end of the process, a reversal of the most desirable order.

The work of Wheaton and Bauman (3) and Samuelson *et al.* (4, 5, 6) on equilibria between aqueous solutions of polyhydroxy organic compounds and ion-exchange resins pointed the way to a new method of fractionation according to molecular bonding or size. It could be inferred from these data that small molecules are much more strongly attracted to the resin than are large molecules, and that column development of a mixture should result in the largest molecules appearing first in the eluate. Any further speculations had to be based on extrapolation, as no data were available for compounds of more than six carbon atoms (although Moore and Stein (7) were able to separate peptides by a similar process), but it seemed clear that bonding could vary greatly with the cross-linkage and salt form of the resin.

This extension of the data of Samuelson and Wheaton and Bauman was shown to be correct and separation of oligosaccharides and monosaccharides according to molecular size has been achieved on Dowex 50W (2% DVB, 200–400 mesh, Li^+ form). Many other types of ion exchangers with different degrees of cross-linking and in different salt forms were tried but were less satisfactory.

Synthetic mixtures of mono-, di-, and tri-saccharides and various polysaccharide hydrolyzates have been separated on the resin columns. Surprisingly, the same 2% DVB resin columns also gave some resolution of mixtures of *O*-alkylated monosaccharides,

[1]*Manuscript received December 28, 1959.*
Contribution from the Department of Chemistry, Gordon Hall, Queen's University, Kingston, Ontario. A summary of this work was given at the Atlantic City meeting of the American Chemical Society, September 1959.
[2]*Present address: Chemistry Department, Ohio State University, Columbus, Ohio.*

an interesting point being that the size order was reversed with these derivatives so that the most highly substituted molecules were eluted last.

The developing solvent was distilled water for most of the separations on the 2% DVB Dowex 50W columns, although 50% aqueous ethanol was used for some preliminary experiments. As predicted by theory the material of highest molecular weight was eluted first followed by lower oligosaccharides and continuing the order down to glycerol and ethylene glycol, which were partially separable. Fractionations were rapid (24–48 hours for complete elution) and the method is economical since the columns could be used many times and water was the only solvent used. The sugars were eluted in relatively concentrated aqueous solution such that direct spotting for paper chromatography was possible without evaporation of the eluate fractions.

EXPERIMENTAL

General Methods

Aqueous solutions were evaporated under reduced pressure at ca. 40° C. All melting points are uncorrected and were measured on a Kofler hot stage.

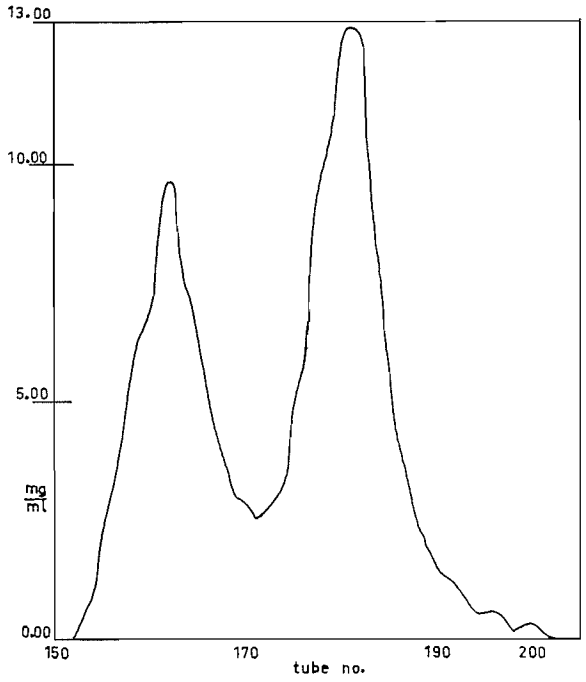


FIG. 1. Separation of raffinose (91 mg) and melibiose (130 mg); flow rate was 1.0 ml per 15-minute fraction. Recoveries calculated from the colorimetric analysis (9) were: raffinose 102% and melibiose 99%. Tubes 154–167 were concentrated to a syrup, and trituration with alcohol–acetone induced crystallization of prisms, m.p. 127–130° and mixed m.p. 131–135°, with authentic recrystallized raffinose of melting point 132–135° (seeded with the 127–130° material). The recovered compound had $[\alpha]_D^{23°}$ +115° (*c*, 1.2 in water) and an infrared spectrum (potassium bromide pellet) identical with that of authentic raffinose pentahydrate in the 700–1500 cm^{-1} region. Trituration with alcohol of the syrup from the contents of tubes 176–189 gave prisms which had a melting point of 181–184°, which was not depressed on admixture with authentic anhydrous melibiose.

Can. J. Chem. Downloaded from www.nrcresearchpress.com by 210.87.254.5 on 09/05/12
For personal use only.

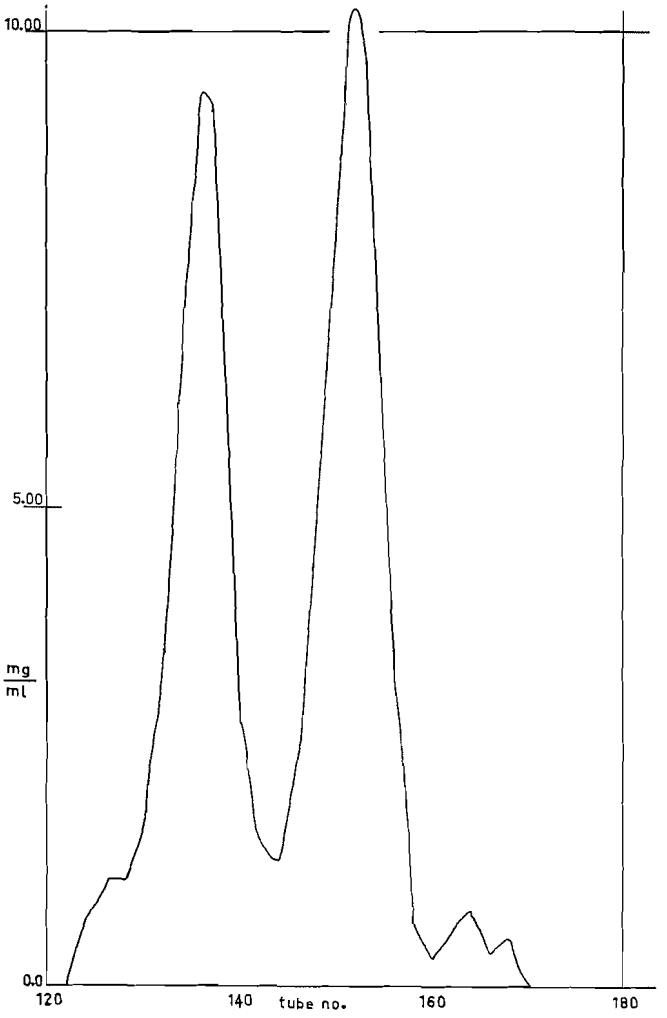


FIG. 2. Separation of D-glucose (115 mg) and maltose (115 mg) at a flow rate of 1.45 ml per 15-minute fraction. Calculated recoveries were: glucose 99% and maltose 97%. Treatment of the contents of tubes 131–140 as before gave prisms which had a melting point of 125–129° and an infrared spectrum (potassium bromide pellet) identical with that of authentic β-maltose hydrate. These crystals had $[\alpha]_D^{22°}$ +118° (10 minutes) → +131° (24 hours) (*c*, 1.1 in water) and gave on acetylation a crystalline acetate of melting point 161–163°, which did not depress the melting point of authentic α-maltose octaacetate. Crystalline D-glucose was obtained in a similar manner from the contents of tubes 148–160 and had a melting point and mixed melting point of 142–145°.

Preparation of Columns

Columns were sealed at the bottom with plugs of ½-in. thick polyurethane foam held in place with a tightly fitting rubber stopper with a short piece of glass capillary tubing through it. The capillary outlet was attached to a 4-ft length of 0.022 by 0.042 in. teflon tubing with a No. 24 syringe needle. This procedure allowed regulation of the rate of flow by changing the hydraulic head and gave very even flow.

A slurry of the resin (Dowex 50W X2, 200–400 mesh, Li^+ for oligosaccharides and *O*-alkylated monosaccharides) in water was poured into a glass tube of the desired size

Can. J. Chem. Downloaded from www.nrcresearchpress.com by 210.87.254.5 on 09/05/12
For personal use only.

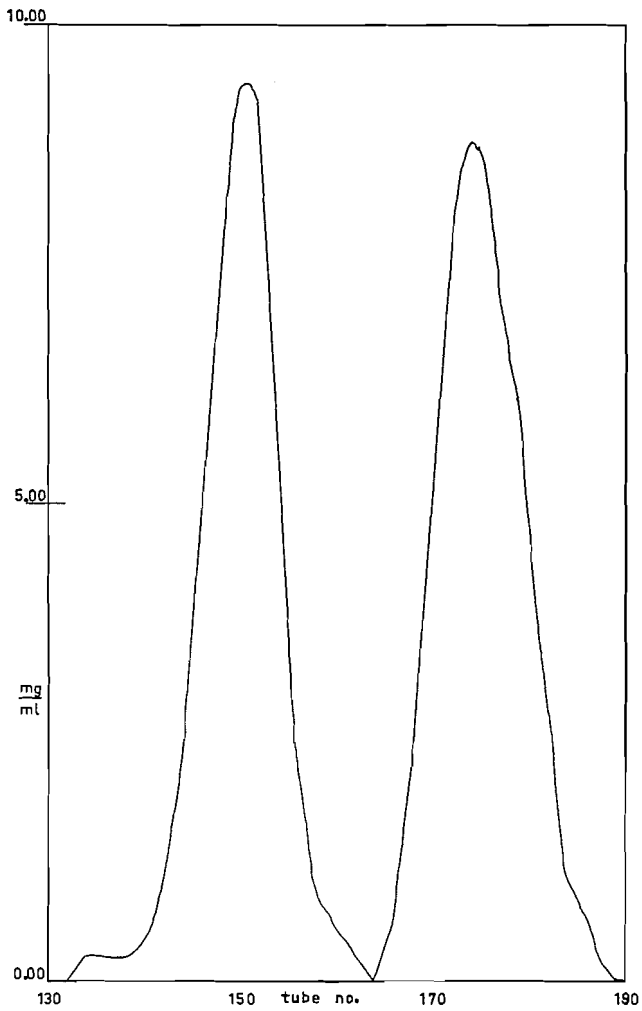


FIG. 3. Separation of lactose (94 mg) and D-galactose (108 mg) at a flow rate of 1.10 ml per 15-minute fraction. Calculated recoveries were: galactose 100% and lactose 105%. Treatment as before of the contents of tubes 141–160 gave crystalline α-lactose, m.p. and mixed m.p. 210–214° and $[\alpha]_D^{21°}$ +81.9° (9 minutes) → +60.6° (2 hours) → +56° (45 hours) (*c*, 2.4 in water). Crystalline α-D-galactose, m.p. and mixed m.p. 164–168°, was similarly obtained from the contents of tubes 165–180.

and backwashed for several hours at a rate sufficient to expand the bed to twice its final dimensions. After the fines, air bubbles, etc. had been removed, the backwashing was stopped and the resin was allowed to settle overnight by gravity. This slow settling is essential and should not be hastened by packing under pressure.

Different batches of both the Dowex 50W X2 used in the experiments detailed in this paper and the Dowex 50W X8 used in Part II were utilized at various times. No variation in separating power was ever found.

Oligosaccharide Separations

The first successful experiments with the new method were done by Dr. Pittet, who used Amberlite CG-120 (type 1, H^+) with 50% aqueous ethanol as the developing

Can. J. Chem. Downloaded from www.nrcresearchpress.com by 210.87.254.5 on 09/05/12
For personal use only.

solvent. Using this procedure he was able to separate completely glucose and maltose and to resolve partially the higher oligosaccharides from an enzymatic starch digest (335 mg on a 90×1 cm column). A larger column was used to fractionate a mixture (750 mg) of L-arabinose and an arabinosyl-arabinose obtained from partial hydrolysis of cherry gum. Crystalline L-arabinose (187 mg), m.p. 156° and mixed m.p. 159°, and a syrup (225 mg) having $[\alpha]_D^{21°}$ +165° (water) were isolated in this manner. The syrup gave a crystalline osazone, m.p. 238–241° (decomp.), which had an infrared spectrum identical with that of authentic 3-*O*-β-L-arabopyranosyl-L-arabinose phenylosazone. Unfortunately, use of the resin in the acid form gave rise to partial hydrolysis of labile oligosaccharides such as sucrose and raffinose, and modifications to reduce this difficulty were sought.

The most satisfactory resin was found to be Dowex 50W X2 (200–400 mesh, Li^+), and it was possible to separate in 48 hours raffinose, sucrose, and glucose (200 mg each) on a column (95×1.8 cm) with water as the sole developing solvent.

Elution diagrams of separations achieved in this manner are given in Figs. 1–3; the fractionations were followed with a modification of the orcinol reaction (9) and were all done on a column (112×1.8 cm) with flow rates of 1 to 2 ml per 15-minute fraction.

Separation of O-Alkylated Sugars

A hydrolyzate of fully methylated starch (1.0 g) was separated on a column (100 ×2.2 cm) of Dowex 50W X2 (200–400 mesh, Li^+) with water as sole developing solvent. The first run gave two fractions: the first contained mono-, di-, and tri-*O*-methyl-glucoses and the second apparently equal quantities of tri- and tetra-*O*-methyl-glucoses. This second fraction was refractionated on the same column and in this manner a syrup was obtained from which crystalline 2,3,4,6-tetra-*O*-methyl-D-glucose (60 mg) was isolated. Sublimation at room temperature and pressure of this material gave colorless needles of 2,3,4,6-tetra-*O*-methyl-α-D-glucose, m.p. and mixed m.p. 89–91°. The main fraction was stored as a viscous syrup and over a period of some months a tri-*O*-methyl-glucose of melting point 108–110° was obtained; presumably this was the expected 2,3,6-tri-*O*-methyl-D-glucose, but the melting point could not be raised to the literature (10) value of 121 to 123° by recrystallization.

ACKNOWLEDGMENTS

The authors thank Queen's University and the National Research Council for financial assistance (N.R.C. T-39 and N.R.C. M-749).

REFERENCES

1. R. F. WHISTLER and D. F. DURSO. J. Am. Chem. Soc. **72**, 677 (1950).
2. L. HOUGH, J. K. N. JONES, and W. H. WADMAN. J. Chem. Soc. 2511 (1949).
3. R. M. WHEATON and W. C. BAUMAN. Ann. N.Y. Acad. Sci. **57**, 159 (1953).
4. H. RÜCKERT and O. SAMUELSON. Svensk Kem. Tidskr. **66**, 12 (1954).
5. M. MATISSON and O. SAMUELSON. Acta. Chem. Scand. **12**, 1386 (1958).
6. M. MATISSON and O. SAMUELSON. Acta. Chem. Scand. **12**, 1404 (1958).
7. C. H. W. HIRS, W. H. STEIN, and S. MOORE. J. Biol. Chem. **219**, 623 (1956).
8. F. SMITH and A. M. UNRAU. Chem. & Ind. (London), 881 (1959).
9. R. J. WINZLER. *In* Methods of biochemical analysis. Vol. 2. Interscience, New York. 1955. p. 290.
10. W. N. HAWORTH, E. L. HIRST, and J. I. WEBB. J. Chem. Soc. 2681 (1928).

Can. J. Chem. Downloaded from www.nrcresearchpress.com by 210.87.254.5 on 09/05/12
For personal use only.

Can. J. Chem. Downloaded from www.nrcresearchpress.com by 210.87.254.42 on 09/05/12
For personal use only.

THE SEPARATION OF SUGARS ON ION-EXCHANGE RESINS

PART II. SEPARATION OF MONOSACCHARIDES[1]

J. K. N. JONES AND R. A. WALL

ABSTRACT

Columns of neutral salt forms of sulphonic acid type ion-exchange resins have been shown to be useful in separations of monosaccharide mixtures with water as the developing solvent. A number of synthetic mixtures and a series of plant extracts have been resolved into clean, salt-free fractions by use of the new technique. The procedure is analogous to column partition chromatography, but in many cases it is more rapid and gives a useful extension of separability.

INTRODUCTION

During the initial investigations of the separation of oligosaccharides on acidic ion-exchange resin columns (1*a*, 1*b*) it was observed that the fructose produced by partial hydrolysis of the sucrose and raffinose standards was always partially separated from the glucose also present in the standard mixture. This observation was confirmed by examination of the behavior of a series of monosaccharides and by the publication of Felicetta and co-workers (2) of a successful separation of D-xylose and L-arabinose on columns of Dowex 50W X8 (50–100 mesh, Ca^{++}) with water as the development solvent. This article prompted study of the separation of a series of monosaccharides using columns of a slightly more efficient resin, Dowex 50W X8 (200–400 mesh, Ba^{++}).

Table I gives the effluent volume at which maximum concentration of the given sugar is reached on a column (70×2.2 cm) of the above resin with water as the sole developing solvent. Experience has shown that if the difference between two effluent volumes is more than 25 ml, it can be predicted that the corresponding sugars are readily separable, e.g. D-ribose and D-xylose are completely separable, but L-arabinose and D-xylose are not.

TABLE I

Sugar	Volume (ml)	Sugar	Volume (ml)
D-Glucose	157	D-Lyxose	188
N-Acetyl-D-glucosamine	160	D-Mannitol	198
D-Sorbose	164	D-Fructose	200
D-Galactose	170	D-Glycero-D-galacto-heptitol (perseitol)	238
D-Xylose	171	Dulcitol	241
D-Manno-heptulose	176	D-Sorbitol	252
D-Mannose	181	D-Xylitol	257
D-Altro-heptulose (sedoheptulose)	183	D-Ribose	342
L-Arabinose	188	D-Galacturonic acid	350

A series of determinations of percentage recoveries of amounts ranging from 50 mg to 1 g per component gave better than 85% recovery and 90–95% was usual. Separation of a mixture of D-sorbitol and *N*-acetyl-D-glucosamine (1 g each) on the above column gave ca. 90% recovery of each component in a crystalline, chromatographically pure state.

Methods were worked out for the concentration of sedoheptulose from sedum extracts; D-manno-heptulose and perseitol from the avocado pear; and the main products, D-talose and D-tagatose, from the epimerization of D-galactose.

[1]*Manuscript received December 28, 1959.*
Contribution from the Department of Chemistry, Gordon Hall, Queen's University, Kingston, Ontario. A summary of this work was given at the Atlantic City meeting of the American Chemical Society, September 1959.

Can. J. Chem. Downloaded from www.nrcresearchpress.com by 210.87.254.42 on 09/05/12
For personal use only.

EXPERIMENTAL

General Methods

All columns were made and used as previously described (1) but using the 8% DVB, Ba^{++} resin mentioned before. The values quoted in Table I were obtained by analysis of mixtures of two known components by paper electrophoresis with borate buffers (3) or by use of paper chromatography on Whatman No. 1 paper using the following solvent systems (v/v ratio):

(A) *n*-butanol:ethanol:water, 3:1:1;
(B) *n*-butanol:pyridine:water, 5:3:2;
(C) *t*-butanol:acetic acid:water, 4:1:1;
(D) ethyl acetate:acetic acid:formic acid:water, 18:3:1:4.

Reducing sugars were detected on chromatograms by the *p*-anisidine hydrochloride spray reagent (4). Non-reducing compounds were detected on chromatograms and electrophorograms by silver nitrate:sodium hydroxide (5) and potassium permanganate:sodium metaperiodate (6) sprays. The orcinol:trichloroacetic acid (7) spray was used to detect ketoses on chromatograms. Aqueous solutions were concentrated under reduced pressure at ca. 40° C on a rotary film evaporator. All melting points are uncorrected and were measured on a Kofler hot stage.

Separation of Standard Mixtures

Figure 1 illustrates the complete separation of D-xylose (179 mg) and D-ribose (178 mg) on the resin column (112×1.8 cm) at a flow rate of 4.0 ml per 15-minute fraction. The colorimetric analysis (benzidine – acetic acid reagent (8)) gave calculated recoveries: D-xylose 99% and D-ribose 99%. Trituration of the syrup obtained on evaporation of the tubes corresponding to the first peak with alcohol–acetone gave crystalline D-xylose, m.p. and mixed m.p. 142–145°. The syrup obtained similarly from the tubes corresponding to the second peak crystallized slowly on trituration with *n*-propanol and seeding with authentic D-ribose to give rosettes of needles which had a melting point and mixed melting point of 84–86°.

Figures 2A and 2B demonstrate the partial separation of a mixture of D-glucose (58 mg) and D-galactose (67 mg) on a column (112×1.8 cm) at an elution rate of 1.5 ml per 15-minute fraction. The sugars were determined colorimetrically using the orcinol reagent (9); the chromatogram shows that even with this poor separation ca. 25% of the individual components could be recovered chromatographically pure.

Experiments on the separation of natural and synthetic mixtures were also carried out, using a three-step column (29.5×2.2 cm, 27.5×1.65 cm, and 21.0×1.2 cm) to sharpen the fractionation (cf. Hagdahl (10)).

Fractionation of Sedum Extract

An extract (700 mg) of *Sedum* sp. prepared by the method of Benson (11) was separated on the three-step column to give three main fractions which contained: (A) aldohexose and aldopentose, (B) heptulose, and (C) ketohexose. There was considerable overlap of the components, but a refractionation of the main fraction (B) gave a syrup (400 mg) which contained traces of hexose and pentose; paper chromatography showed it to be ca. 90% heptulose. Treatment of an aliquot of the syrup with acid according to Hudson (12) gave sedoheptulosan, m.p. and mixed m.p. 154–156°, $[\alpha]_D^{25°}$ −138° (*c*, 1.2 in water) after two recrystallizations from *n*-propanol.

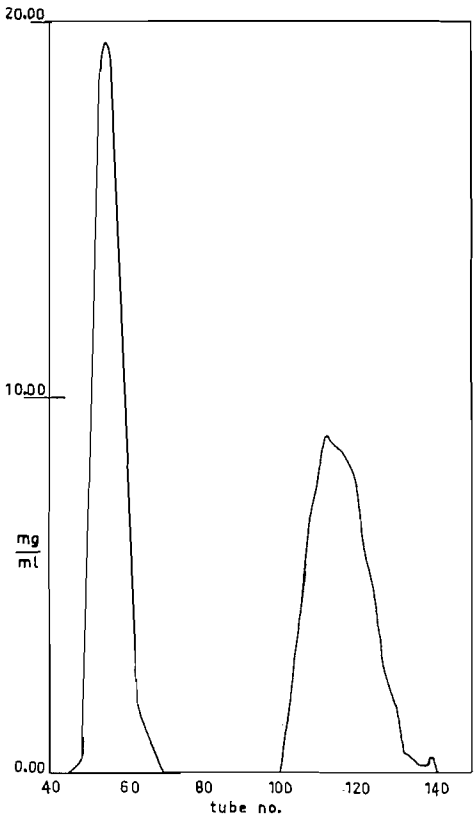


FIG. 1.

Fractionation of Avocado Extract

The acidic components of an alcoholic extract of the flesh of two ripe avocado pears were removed on a column (50×1.4 cm) of Amberlite CG-400 (type I, acetate) and the concentrated neutral effluent was passed down the three-step column to give four main fractions. These had as chief constituents: (A) disaccharide, (B) heptulose and aldohexose, (C) heptitol and ketohexose, and (D) ketohexose and unidentified reducing materials. The syrups obtained after several refractionations of mixtures (B) and (C) crystallized on standing overnight. In this manner D-manno-heptulose (2.2 g) was isolated from (B); it had a melting point and mixed melting point of 152–154.5° and $[\alpha]_D^{25°}$ +30° (10 minutes) (*c*, 2.4 in water) after two recrystallizations from ethanol. Mixture (C) gave rise to D-glycero-D-galacto-heptitol (0.5 g) of melting point 184–185° after two recrystallizations from aqueous methanol. The perseitol isolated in this experiment gave a heptaacetate of melting point 115.5–118.5° and $[\alpha]_D^{22°}$ −13.8° (*c*, 2.02 in chloroform) on treatment with acetic anhydride and pyridine.

Separation of the Epimerization Products of D-*Galactose*

D-Galactose (10 g) was epimerized by heating its solution in pyridine (100 ml) according to Karabinos (13). The published method was followed to the stage of removal of D-galactose by dilution with hot ethanol, and the resultant filtrate was evaporated under

Can. J. Chem. Downloaded from www.nrcresearchpress.com by 210.87.254.42 on 09/05/12
For personal use only.

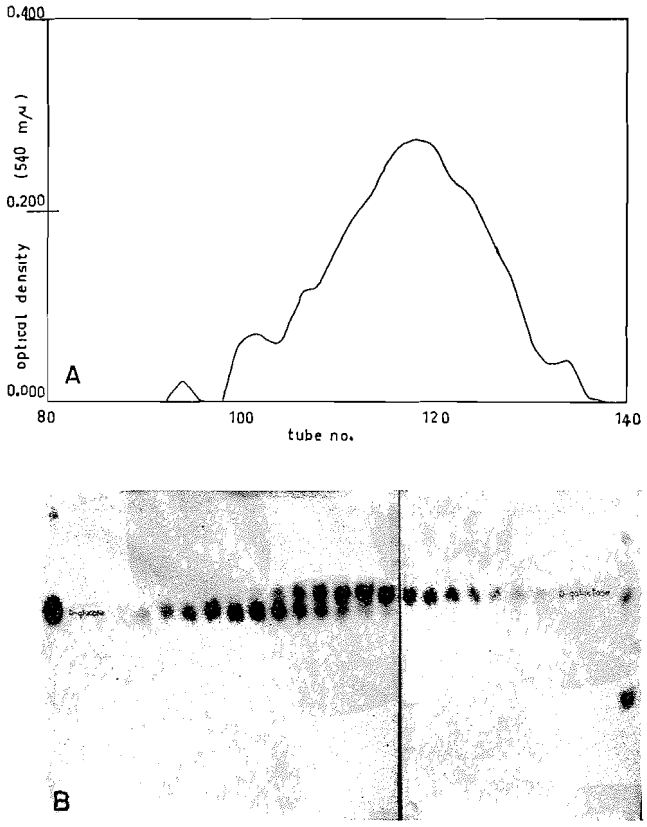


FIG. 2.

reduced pressure to a syrup which was dissolved in water (4 ml) and this solution was fractionated on the three-step column. The first separation gave three main fractions: (A) aldohexose and ketohexose, (B) ketohexose, and (C) aldohexose, of which only (C) was pure enough to crystallize directly from the syrup. Dissolution of (C) in hot ethanol left a small amorphous residue, which was removed by filtration. Colorless prisms (32 mg), which had a melting point and mixed melting point with authentic D-talose of 125.5 to 127.5° and $[\alpha]_D^{20°}$ +25° (10 minutes) (*c*, 1.0 in water), slowly crystallized from the clear filtrate. Refractionation of (A) and (B) gave syrups which crystallized on standing overnight. The solid from (A) was shown to be D-galactose, m.p. and mixed m.p. 162–166°, and $[\alpha]_D^{24°}$ +81° (10 minutes) (*c*, 1.2 in water). After two recrystallizations from ethanol the chief component of (B) was found to be D-tagatose (0.68 g), m.p. and mixed m.p. 130–132°, and its infrared spectrum (potassium bromide pellet) was identical with that of authentic D-tagatose; 85% of the initial D-galactose was recovered in a crystalline form.

ACKNOWLEDGMENTS

The authors thank Queen's University and the National Research Council for financial assistance (grant N.R.C. M-749).

Can. J. Chem. Downloaded from www.nrcresearchpress.com by 210.87.254.42 on 09/05/12
For personal use only.

REFERENCES

1*a*. J. K. N. JONES, R.A. WALL, and (in part) A. O. PITTET. This issue.
1*b*. J. K. N. JONES, R. A. WALL, and (in part) A. O. PITTET. Chem. & Ind. (London), 1196 (1959).
2. V. F. FELICETTA, M. LUNG, and J. L. MCCARTHY. Tappi, **42**, 496 (1959).
3. A. B. FOSTER. Chem. & Ind. (London), 828 (1952).
4. L. HOUGH, J. K. N. JONES, and W. H. WADMAN. J. Chem. Soc. 1702 (1950).
5. W. E. TREVELYAN, D. P. PROCTOR, and J. S. HARRISON. Nature, **166**, 444 (1950).
6. R. U. LEMIEUX and H. F. BAUER. Anal. Chem. **26**, 920 (1954).
7. A. BEVENUE and K. T. WILLIAMS. Arch. Biochem. Biophys. **34**, 225 (1951).
8. J. K. N. JONES and J. B. PRIDHAM. Biochem. J. **58**, 288 (1954).
9. R. J. WINZLER. *In* Methods of biochemical analysis. Vol. 2. Interscience, New York. 1955. p. 290.
10. L. HAGDAHL. Acta. Chem. Scand. **2**, 574 (1948).
11. A. NORDAL and A. A. BENSON. J. Am. Chem. Soc. **76**, 5054 (1954).
12. J. W. PRATT, N. K. RICHTMYER, and C. S. HUDSON. J. Am. Chem. Soc. **74**, 2200 (1952).
13. J. V. KARABINOS. *In* Advances in carbohydrate chemistry. Vol. 7. Academic Press, New York. 1952. p. 113.

Can. J. Chem. Downloaded from www.nrcresearchpress.com by 210.87.254.42 on 09/05/12
For personal use only.

Can. J. Chem. Downloaded from www.nrcresearchpress.com by 210.87.254.40 on 09/05/12
For personal use only.

PRIMARY QUANTUM EFFICIENCIES IN THE REACTION OF CYCLOPENTANE WITH MERCURY 6($^3P_1$) ATOMS[1]

RICHARD L. STOCK AND HARRY E. GUNNING

ABSTRACT

An investigation has been made of the reaction of cyclopentane with Hg 6($^3P_1$) atoms at a substrate pressure of 107 mm, under static conditions at 24° C. Low light intensities were used in order to minimize secondary reactions.

The products of the reaction, for small extents of decomposition, have been shown to be exclusively hydrogen, bicyclopentyl, and cyclopentene. With increasing duration of exposure, the cyclopentene-to-cyclopentane ratio achieves a steady-state value of 5.7×10^{-3}. Furthermore, it has been found that the same ratio is ultimately reached, upon prolonged exposure of a substrate initially containing cyclopentene at a concentration higher than the steady-state value. In the runs with added cyclopentene, a fourth product appeared in measurable quantities. Its molecular weight corresponded to the formula, $C_{10}H_{16}$, and it was assumed to be a cyclopentyl cyclopentene. The same compound appears in extensive decomposition of the pure substrate.

The addition of small amounts of nitric oxide was found to have a marked inhibiting effect on the reaction. Bicyclopentyl formation was completely suppressed when 0.7 mole% of nitric oxide was present; and the cyclopentene yield was reduced to one-fifth of its value for the pure substrate, by adding 0.98 mole% of nitric oxide.

In order to obtain primary quantum yields for the reaction, a series of runs were performed of 1 to 33 minutes in duration, with a cyclopentane which had been purified by gas–liquid chromatography. By a short extrapolation of the mean quantum yields of product formation to zero extent of reaction, it was found that the primary quantum yields for hydrogen, bicyclopentyl, and cyclopentene were respectively 0.8, 0.4, and 0.4.

On the basis of a simple four-step paraffinic mechanism, taken in conjunction with the primary quantum yield data, it is concluded that the reaction has a primary quantum yield of substrate decomposition of 0.8, and that cyclopentyl radicals have the same rates for disproportionation and recombination at 24° C.

INTRODUCTION

In two previous investigations (1, 2) of the reaction of cyclopentane vapor with Hg 6($^3P_1$) atoms, under static conditions, at 30° C, it was shown that the primary process involves scission of the C—H bond with formation of cyclopentyl radicals and H atoms. The products of the reaction were found to be hydrogen, bicyclopentyl, and cyclopentene. In the more recent of the two studies (2), limiting quantum yield values, at high substrate pressures, were used, in conjunction with a simple paraffinic free radical mechanism, to obtain values of 0.49 for the primary quantum yield, and 5.3 for the ratio of the rates of recombination to disproportionation for cyclopentyl radicals. The results reported in this paper represent the first phase in a study of the reaction as a function of temperature. In order to obtain more direct values for the primary quantum yields, the reaction has been studied at small extents of decomposition and low light intensities. The details of the investigation follow.

EXPERIMENTAL

The experiments were performed in cylindrical, fused, quartz reaction cells, 10 cm in length and 5 cm in diameter. For each run a breakseal, product trap, and filling tube were connected to the stem of the reaction cell. The product trap consisted of a short length of 7 mm O.D. tubing, with a constriction to facilitate removal by flame-cutting. In order to introduce the cyclopentane vapor, the cell was connected via the filling tube,

[1]*Manuscript received June 27, 1960.*
Contribution from the Department of Chemistry, University of Alberta, Edmonton, Alberta. This work was supported in part by the National Research Council, under Block Term Grant No. B.T.-74. This support is gratefully acknowledged.

of 3 mm I.D. capillary, to the vacuum manifold, and pumped down to at least 10^{-3} μ. Mercury vapor for the reaction was supplied by placing several drops of mercury in a small depression in the connecting tube of the product trap. In all runs the cell was filled with cyclopentane vapor at a pressure of 107 mm, by placing an ice bath around the reservoir of liquid cyclopentane. After being filled, the cell was flame-cut from the manifold and placed in an oven which was maintained at 24±0.5° C, for the present series of runs.

The 2537-Å resonance radiation was supplied by a Hanovia, Sc-2537 source, which was wound in the form of a five-turn helix. The lamp was rigidly positioned with respect to the cell, in order to assure constant light input. The oven was provided with a filter of Vycor, 7910 glass, to prevent 1849-Å radiation from entering the cell.

At the end of each run, products condensable in liquid nitrogen were frozen into the product trap. In order to assure that high-boiling products were quantitatively transferred to the trap, the remainder of the cell was heated to 250° C during the transfer process. By connecting the cell, via its breakseal, to an analytical system, the non-condensable gases could be transferred, by means of a Toepler pump, to a gas burette. The hydrogen was determined by standard procedures involving combustion over heated copper oxide at 250° C.

The product trap, containing the condensable products, was flame-cut from the cell, and placed in a 4-in. length of 3/8-in. copper tubing, which, in turn fitted into a special sample-insertion device. This device was provided with double-compression fittings, a thumbscrew for shattering the product trap, and a preheater.

The sample-insertion device was placed in series with the hydrogen gas stream to a special gas–liquid chromatographic (G.L.C.) unit. The katharometer was of the Gow-Mac, T/C type, with temperature regulation. Ten-foot chromatographic columns were used, containing 30–60 mesh, silica gel. The analyses were made with the katharometer at 106° C.

The cyclopentane and cyclopentene used were Phillips, Research Grade (P.R.G.). G.L.C. analysis of the cyclopentane showed that the only impurity was 0.051 mole% of cyclopentene. For one series of runs at low conversion, the cyclopentane was further purified by isolating the G.L.C. fraction. This sample showed no detectable impurities. It is estimated that the purity was at least 99.999 mole%. The nitric oxide used was Matheson, C.P. grade, of 99 mole% purity. The gas was further purified by trap-to-trap distillation.

RESULTS

In order to minimize complexities associated with the localized build-up of products in the reaction zone, the runs were carried out at a low absorbed light intensity. By using propane as an actinometer (3), the absorbed light intensity was found to be $3.75\pm0.05\times10^{-7}$ einstein/minute. All quantum yields reported here are based on this light intensity.

In Fig. 1, the relations are shown between product yield and duration of exposure, for a series of runs with P.R.G. cyclopentane. The cyclopentene yields were corrected for the small amount of cyclopentene present initially in the substrate. From the graph, it is apparent that the rate of bicyclopentyl production is constant throughout the range of duration of exposure studied. For hydrogen production, there is a slight indication of a decreased rate in the runs of long duration. The fact that cyclopentene achieves a steady-state concentration after approximately 120 minutes of exposure is shown clearly in

Can. J. Chem. Downloaded from www.nrcresearchpress.com by 210.87.254.40 on 09/05/12
For personal use only.

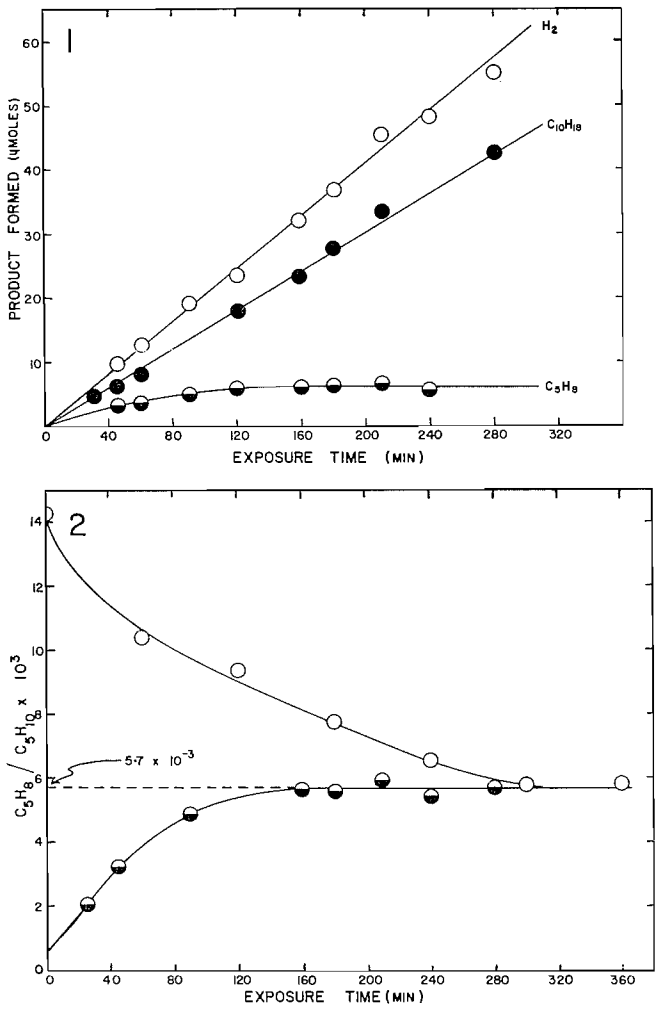


FIG. 1. Yields, in micromoles, for hydrogen, bicyclopentyl, and cyclopentene vs. exposure time in the mercury-photosensitized decomposition of Phillips, Research Grade (P.R.G.) cyclopentane.

FIG. 2. The change in the cyclopentene-to-cyclopentane ratio with increasing exposure time in the mercury-photosensitized decomposition of cyclopentane: ◒ P.R.G. cyclopentane, ○ cyclopentane containing 1.43 mole% of cyclopentene.

Fig. 1. In the runs exceeding about 200 minutes in duration, small amounts of a fourth product were detected in the G.L.C. analyses. This product is discussed in more detail below.

The lower curve in Fig. 2 shows the behavior of the cyclopentene-to-cyclopentane ratio, as a function of exposure time, for P.R.G. cyclopentane. The steady-state value for the $(C_5H_8)/(C_5H_{10})$ ratio was found to be $5.7\pm0.1\times10^{-3}$. In order to determine whether the same steady-state would be achieved with added cyclopentene, a series of runs were done with a sample of cyclopentane for which the $(C_5H_8)/(C_5H_{10})$ ratio was initially 14.3×10^{-3}. It can be seen from the upper curve in Fig. 2 that the same steady-state value is ultimately reached, as with the P.R.G. cyclopentane.

In the runs with added cyclopentene, it was noted that a fourth product appeared in

Can. J. Chem. Downloaded from www.nrcresearchpress.com by 210.87.254.40 on 09/05/12
For personal use only.

measurable quantities. In the G.L.C. analysis, the retention time for this product was identical with that of the minor peak obtained in runs of long duration with the P.R.G. substrate. The product was isolated, and a parent-peak determination was made on a mass spectrometer. The molecular weight corresponded to the formula $C_{10}H_{16}$. It was concluded that the product was likely a cyclopentyl cyclopentene. On the assumption that the $C_{10}H_{16}$ product had the same sensitivity as bicyclopentyl (4), the $(C_{10}H_{16})/(C_5H_{10})$ ratio could be estimated. These values, together with the $(C_5H_8)/(C_5H_{10})$ ratios, are given in Table I, for the runs with added cyclopentene. It can be seen from the table that the $(C_{10}H_{16})/(C_5H_{10})$ ratio reaches a steady-state value of $1.6\pm0.1\times10^{-3}$. It should further be noted that the $C_{10}H_{16}$ product and cyclopentene reach their respective steady-state concentrations in essentially the same period of time.

TABLE I

Quantum yields and steady-state concentrations for runs with added cyclopentene*

Exp. time, minutes	Quantum yields			$(C_5H_8)/(C_5H_{10})$ $\times10^3$	$(C_{10}H_{16})/(C_5H_{10})$ $\times10^3$
	C_5H_8	$C_{10}H_{18}$	$C_{10}H_{16}$		
0				14.3	
60	−0.173	0.37	0.016	10.4	0.28
120	−0.116	0.40	—	9.4	—
180	−0.124	0.46	—	7.7	—
240	−0.114	0.35	—	6.5	—
300	−0.090	0.43	0.015	5.8	1.3
360	−0.076	0.40	0.014	5.8	1.6
420	−0.065	0.36	0.013	5.8	1.6
420	—	0.38	0.011	—	1.6

*Initial cyclopentane pressure = 107 mm. Absorbed light intensity = 3.75×10^{-7} einstein/minute.

The data in Table I also show clearly that the quantum yield of bicyclopentyl formation is invariant in exposure time at 0.39 ± 0.03.

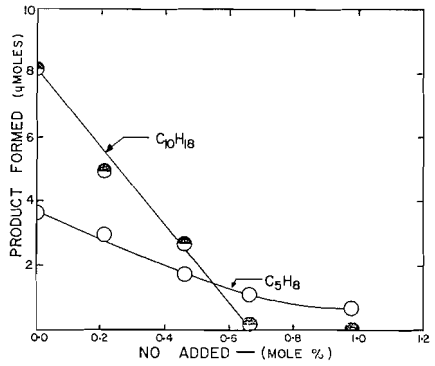


FIG. 3. The effect of added nitric oxide on the yields, in micromoles, of bicyclopentyl, and cyclopentene for 1-hour runs in the mercury-photosensitized decomposition of P.R.G. cyclopentane.

In Fig. 3 the effect is shown of the addition of small amounts of nitric oxide on the yields of cyclopentene and bicyclopentyl. The data are for 1-hour runs. The results demonstrate rather strikingly the free radical nature of the reaction. With 0.7% nitric oxide present, no bicyclopentyl is formed. With 0.98% added nitric oxide, the cyclopentene yield is reduced to 18% of its value for the pure substrate. In the 1-hour run,

Can. J. Chem. Downloaded from www.nrcresearchpress.com by 210.87.254.40 on 09/05/12
For personal use only.

with 0.98% nitric oxide, the total yield of cyclopentene was only 0.66 μmole. This small value is liable to considerable error, since correction must be made for the cyclopentene present in the P.R.G. substrate, apart from the inherent error in the determination. It can be concluded that the presence of approximately 1% nitric oxide completely inhibits bicyclopentyl formation, and reduces the cyclopentene yield to a very low value.

In Fig. 4, the mean quantum yields for the formation of hydrogen, bicyclopentyl, and cyclopentene are shown as a function of the exposure time, for P.R.G. cyclopentane. It should first be noted that the quantum yield of bicyclopentyl formation does not change with duration of exposure, maintaining throughout a constant value of 0.40±0.01. Reference to Table I shows that the value is the same as that obtained in the runs with added cyclopentene, within the experimental error. Extrapolation of the mean quantum yields of cyclopentene formation to $t = 0$ suggests a value of 0.4 for $\phi_{C_5H_8}$. From the stoichiometry $\phi^0_{H_2}$ must be 0.8.

In order to obtain more accurate data on the primary quantum yields of the reaction, a special batch of P.R.G. cyclopentane was purified by G.L.C. This ultrapure material showed no detectable impurities, and it was estimated that total impurities could not exceed 0.001 mole%. Runs were made with exposure times from 1.4 to 33 minutes. The

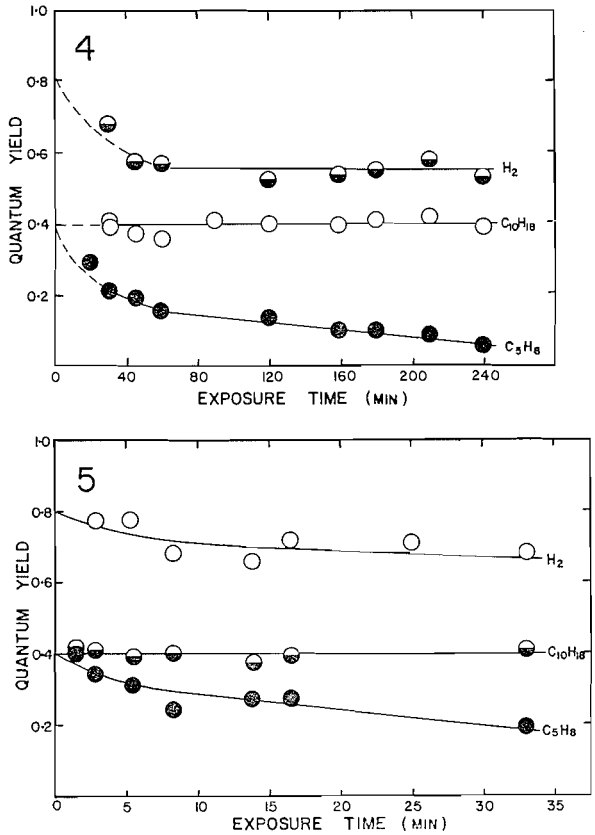


FIG. 4. The mean quantum yields of formation for hydrogen, bicyclopentyl, and cyclopentene vs. exposure time in the mercury-photosensitized decomposition of P.R.G. cyclopentane.

FIG. 5. The mean quantum yields of formation of hydrogen, bicyclopentyl, and cyclopentene vs. exposure time in the mercury-photosensitized decomposition of cyclopentane containing less than 0.001 mole% of impurities.

Can. J. Chem. Downloaded from www.nrcresearchpress.com by 210.87.254.40 on 09/05/12
For personal use only.

mean quantum yields vs. exposure time are shown in Fig. 5. Again the invariance of the quantum yield of bicyclopentyl formation at 0.40 is to be noted. The extrapolation of $\phi_{C_5H_8}$ to $t = 0$ can now fairly confidently be said to lead to a value of 0.4 for $\phi^0_{C_5H_8}$. Under such conditions, $\phi^0_{H_2}$ must be 0.8, and an inspection of Fig. 5 shows that 0.8 is a reasonable extrapolation of the actual data on the mean quantum yield of hydrogen formation to $t = 0$.

DISCUSSION

As in the previous two studies (1, 2) on the cyclopentane reaction, the mechanism under initial conditions will be represented by the following paraffinic sequence:

$$C_5H_{10} + Hg\ 6(^3P_1) \rightarrow C_5H_9 + H + Hg\ 6(^1S_0) \quad [1]$$

$$H + C_5H_{10} \rightarrow C_5H_9 + H_2 \quad [2]$$

$$2(C_5H_9) \rightarrow C_5H_8 + C_5H_{10} \quad [3]$$

$$2(C_5H_9) \rightarrow C_{10}H_{18} \quad [4]$$

The above four-step sequence should apply only in the limiting case of zero extent of reaction. A steady-state treatment leads to the following expressions for the primary quantum yields: $\phi^0_{H_2} = K$, $\phi^0_{C_5H_8} = K[1/(1+r)]$, $\phi^0_{C_{10}H_{18}} = K[r/(1+r)]$, and $\phi^0_{C_5H_{10}} = K[(1+2r)/(1+r)]$. The constant K represents the fraction of the primary quenching collisions which lead to reaction, and r is the ratio k_4/k_3, or the relative rate of recombination to disproportionation for cyclopentyl radicals. Both K and r can now be obtained from the primary quantum yields of formation of hydrogen, cyclopentene, and bicyclopentyl, which, in turn, were derived by short extrapolations of the mean quantum yields of product formation for ultrapure cyclopentane, as shown in Fig. 5. Thus taking $\phi^0_{H_2} = 0.8$, and $\phi^0_{C_{10}H_{18}} = \phi^0_{C_5H_8} = 0.4$, we find that $K = 0.8$ and $r = k_4/k_3 = 1.0$. The data would therefore indicate that the primary chemical efficiency of the reaction is 80%, and that cyclopentyl radicals have the same rates for disproportionation and recombination.

In the earlier study of the cyclopentane reaction at 30° C by Beck, Kniebes, and Gunning (2), the primary quantum yields, and the efficiency constant, K, were calculated from the limiting high-pressure values for the mean quantum yields. Their data were obtained for runs of 60-minute duration, at an absorbed light intensity of 2.5×10^{-6} einstein/minute. It was further assumed that the cyclopentene achieved a steady-state concentration by the reaction

$$C_5H_8 + H \rightarrow C_5H_9. \quad [5]$$

In this study we have measured directly the change in cyclopentene concentration with increasing duration of exposure, at an absorbed light intensity of 3.75×10^{-7} einstein/minute. The data, represented in Fig. 2, as a plot of the ratio $(C_5H_8)/(C_5H_{10})$ vs. the duration of exposure, show unequivocally that a steady-state concentration is indeed achieved, after approximately 160 minutes of irradiation. The steady-state value of $(C_5H_8)/(C_5H_{10})$ was found to be 5.7×10^{-3}. At an absorbed light intensity of 2.5×10^{-6} einstein/minute, with all other reaction parameters remaining constant, we would expect the steady-state to be reached in ca. $160(3.75\times10^{-7})/(2.5\times10^{-6}) = 24$ minutes. If reaction [5] is assumed to be the only method whereby cyclopentene is consumed, then the conditions in the previous study (2) should indeed represent a steady-state situation for cyclopentene. However, in the present investigation, we have found that

Can. J. Chem. Downloaded from www.nrcresearchpress.com by 210.87.254.40 on 09/05/12
For personal use only.

prolonged irradiation leads to the formation of an additional product, $C_{10}H_{16}$, which is assumed to be a cyclopentyl cyclopentene.

This product can be accounted for by the reactions

$$H + C_5H_8 \rightarrow C_5H_7 + H_2, \quad [6]$$

$$C_5H_7 + C_5H_9 \rightarrow C_{10}H_{16}, \quad [7]$$

where C_5H_7 represents a cyclopentenyl radical. Now, if hydrogen, cyclopentene, and bicyclopentyl are the only products of the reaction, the stoichiometry would demand that the mean quantum yields for hydrogen and bicyclopentyl formation approach each other with increasing exposure. From Fig. 4, it can be seen that the mean quantum yield of hydrogen formation is slightly larger than that calculated from the quantum yields of cyclopentene and bicyclopentyl. The discrepancy, furthermore, becomes greater with increasing duration of exposure. It should also be emphasized that the invariance of the quantum yield of bicyclopentyl formation strongly suggests that the secondary product, $C_{10}H_{16}$, arises by the decomposition of cyclopentene, rather than from bicyclopentyl. The most compelling evidence, however, for ascribing $C_{10}H_{16}$ formation to the secondary decomposition of cyclopentene is presented in Table I, and also in the upper curve of Fig. 2. For the series of runs in which cyclopentene was initially added, the $C_{10}H_{16}$ product becomes considerably more important than in the runs with the P.R.G. cyclopentane.

In comparing the results obtained in the previous investigation (2) with those in the present study, there is another factor which should be considered. In mercury photosensitization, the zone of reaction is concentrated near the window through which the radiation enters the cell. With increasing light intensity, there will be a localized build-up of reaction products near this incident window. Secondary reactions should therefore assume greater importance at higher light intensities. In the previous study (2), the light intensity was 6.7 times higher than in the present work.

Probably the most interesting result of this study is the fact that cyclopentyl radicals, at 24° C, have equal rate constants for recombination and disproportionation. There seems little doubt that the ratio k_3/k_4 is at least 1.0, and by inspection of Fig. 5, it can be seen that the initial rate of cyclopentene formation could conceivably be slightly greater than that for bicyclopentyl. That these rates are essentially identical might suggest that both recombination and disproportionation proceed through the same reaction intermediate.

The results of the runs with added nitric oxide demonstrate rather strikingly the free radical nature of the reaction. From Fig. 3, it can be seen that bicyclopentyl formation is completely suppressed by the addition of 0.7% of nitric oxide. With 1% nitric oxide present in the cyclopentane, there is no bicyclopentyl present after a 1-hour run, and the cyclopentene yield is reduced to about 18% of its value for the pure substrate. Such behavior would indicate that there is a fairly stable compound formed when cyclopentyl radicals interact with nitric oxide. A possible explanation would be that the $C_5H_9.NO$ intermediate rearranges to the stable cyclopentanone oxime,

$$C_5H_9.NO \rightarrow C_5H_8{:}NOH. \quad [8]$$

The fact that cyclopentene formation is not completely suppressed would suggest that the intermediate has an alternate mode of decomposition,

$$C_5H_9.NO \rightarrow C_5H_8 + NOH. \quad [9]$$

Can. J. Chem. Downloaded from www.nrcresearchpress.com by 210.87.254.40 on 09/05/12
For personal use only.

From the data represented in Fig. 2, for the change in the $(C_5H_8)/(C_5H_{10})$ ratio with duration of exposure, it is apparent that the same steady-state concentration of cyclopentene is ultimately achieved, regardless of the initial cyclopentene concentration. If we assume that the over-all reaction in the steady-state region can be described by steps [1] through [7], we find that the steady-state value, $(C_5H_8)/(C_5H_{10})_{SS}$, is related to the rate constants by the equation

$$(C_5H_8)/(C_5H_{10})_{SS} = k_2/(2k_6+k_5).$$

Now k_6, the rate constant for the abstraction reaction, should be considerably smaller than that for the addition reaction, k_5. To a first approximation, therefore,

$$(C_5H_8)/(C_5H_{10})_{SS} = k_2/k_5 = 5.7\times10^{-3}.$$

In other words, our results would indicate that reaction [5] is about 175 times faster than reaction [2].

CONCLUSIONS

As a result of this study, it has been shown that the reaction of cyclopentane vapor with Hg $6(^3P_1)$ atoms leads to the formation of cyclopentyl radicals and H atoms with a primary quantum efficiency of at least 80%. The complete free radical nature of the reaction has been demonstrated by showing that as little as 0.7 mole% of added nitric oxide leads to a complete inhibition of bicyclopentyl formation. From the fact that cyclopentene and bicyclopentyl have the same primary quantum yields, it is concluded that cyclopentyl radicals have identical rates for disproportionation and recombination at 24° C. The results of the investigation would further suggest that meaningful values for the ratio of the rates of disproportionation to recombination for free radicals can only be obtained when the reaction in question is studied at low light intensities and at very short durations of exposure.

REFERENCES

1. G. A. Allen, D. L. Kantro, and H. E. Gunning. J. Am. Chem. Soc. **72**, 3588 (1950).
2. P. W. Beck, D. V. Kniebes, and H. E. Gunning. J. Chem. Phys. **22**, 678 (1954).
3. S. Bywater and E. W. R. Steacie. J. Chem. Phys. **19**, 319 (1951).
4. A. E. Messner, D. M. Rosie, and P. A. Argabright. Anal. Chem. **31**, 230 (1959).

Can. J. Chem. Downloaded from www.nrcresearchpress.com by 210.87.254.40 on 09/05/12
For personal use only.

Can. J. Chem. Downloaded from www.nrcresearchpress.com by 210.87.254.42 on 09/05/12
For personal use only.

THE NATURE OF POLYMERIZATION CATALYSTS PREPARED FROM METAL ALKYLS AND TITANIUM HALIDES[1]

M. H. JONES, U. MARTIUS, AND M. P. THORNE

ABSTRACT

A study has been made of the composition and structure of the insoluble complexes formed in the reaction of aluminum triisobutyl or lithium *n*-butyl with titanium tetrachloride or trichloride in heptane at room temperature by chemical and X-ray diffraction analyses. For the tetrachloride systems it has been shown that, with metal alkyl:titanium tetrachloride ratios of 0.5 to 4, at least 50% of the titanium is present in the tetravalent state and that there is considerable loss of chlorine and alkyl groups. The aluminum complexes are amorphous except at component ratios of 0.5 to 1, where the X-ray pattern indicated traces of titanium trichloride.

With the aluminum triisobutyl – titanium trichloride system, X-ray evidence has shown that the titanium trichloride remains essentially unchanged. This result, together with the low aluminum content (less than 0.5%), is consistent with Natta's suggestion that this catalyst for olefine polymerization consists of a trichloride surface on which small quantities of aluminum alkyl are chemisorbed.

The reaction between lithium butyl and titanium trichloride at ratios above unity results in the formation of a new crystalline compound having a sodium chloride type lattice with a lattice spacing of 5.20 Å. The compound is thought to be a double salt of the type $(LiCl)_n$. $TiCl_2$ or $(LiCl)_n$.TiCl. Evidence of a second crystalline component was also noted but it could not be identified.

Tentative reaction schemes are proposed for the formation of the various complexes and their structures are considered in relation to their ability to polymerize 1-butene.

INTRODUCTION

During the past five years widespread interest has been shown in new catalysts available for the polymerization of α-olefines and dienes which are also capable of controlling the orientation of the monomer units entering the polymer chain, so that long sequences of units in a head-to-tail arrangement have the same configuration. One type of such catalysts, first reported by Ziegler (1), is obtained by the interaction in a hydrocarbon solvent of an alkyl of a metal from groups one to three of the periodic table with a halide, or other derivative, of a transition metal from groups four to eight. Although considerable information is available in the literature on the use of different catalyst combinations of this kind for polymerization, and on the nature of the polymers, less attention has been directed towards their composition and structure.

The catalyst system AlR_3–$TiCl_4$ has been studied in most detail and it is considered that complex formation occurs by reduction of the transition metal to a lower valency state by the metal alkyl (2, 3). Chemical analyses of the insoluble complexes (3, 4, 5) have shown that they contain aluminum, titanium, chlorine, and alkyl groups, the composition depending on the starting ratio of aluminum alkyl to titanium tetrachloride and the temperature of preparation. Some doubt exists as to the valency state of the titanium in the complexes and its relationship to catalytic activity both for this system and that in which lithium alkyls are used (2, 6). However, it has been established that catalysts which show the greatest stereospecificity in the polymerization of α-olefines are those derived from lower titanium halides (3).

From these and other considerations several suggestions (3, 7, 8, 9) have been made concerning the nature of the active species and the mechanism by which stereoregular

[1]*Manuscript received July 11, 1960.*
Contribution from the Departments of Chemistry and Metallurgy, Ontario Research Foundation, Toronto 5, Ontario. Presented at the Ninth Canadian High Polymer Forum held at The Guild Inn, Scarborough, Ontario, October 26–28, 1959.

polymers are formed. In general, for heterogeneous catalysts, the active sites for stereospecific polymerization are believed to be locations on a reduced titanium halide surface where the metal alkyl is chemisorbed, the resultant complex and the electron characteristics of the adjacent surface providing control of the monomer orientation during the propagation step.

In the present work additional information concerning the nature of complexes prepared from aluminum triisobutyl or lithium butyl with titanium tetrachloride or trichloride has been obtained from chemical analyses and X-ray diffraction studies, and is considered in relation to their activity as catalysts for the polymerization of 1-butene.

EXPERIMENTAL

Preparation of Reagents

(1) Solvent.—High-purity heptane (Distillation Products Inc.), b.p. 96–97° C, was purified by shaking with concentrated sulphuric acid, washing with 2% sodium hydroxide solution and water, and drying over calcium chloride and metallic sodium. After distillation from a piece of sodium in a nitrogen-flushed apparatus, the heptane was stored over sodium wire.

(2) Nitrogen.—Before use, Linde nitrogen (99.99%) containing a maximum of 15 grains water per 1000 cu. ft, was passed over heated copper and magnesium perchlorate to remove traces of oxygen and moisture.

(3) Aluminum triisobutyl.—A 25% solution in heptane of a mixture of approximately 60% triisobutyl aluminum and 40% diisobutyl aluminum hydride (Hercules Powder Company) was distilled under reduced pressure in a nitrogen atmosphere. The solvent was removed at low temperature and the aluminum triisobutyl distilled as a colorless liquid, b.p. 55° C, at 1.5 mm. The diisobutyl aluminum hydride, having an appreciably lower vapor pressure, remained in the high-boiling residue. The aluminum content of the trialkyl, which was stored as an approximately 45% (w/w) solution, was determined gravimetrically with 8-hydroxyquinoline after hydrolysis in aqueous sulphuric acid (found: Al, 13.4%; calc.: Al, 13.8%).

(4) Lithium butyl.—Lithium butyl was prepared by treating a 20% solution of *n*-butyl chloride in heptane with lithium wire (15% excess over the theoretical quantity) in an argon atmosphere. Close to 100% yields were obtained if the reaction mixture was cooled to −20° C during the addition of the lithium and allowed to heat up to room temperature slowly. After the solution of lithium alkyl was shaken for 24 hours it was filtered under nitrogen and analyzed by titration of the lithium hydroxide produced on hydrolysis.

(5) Titanium halides.—Fisher C.P. grade titanium tetrachloride was distilled in an inert atmosphere before use. Solutions in heptane were water-white. The violet titanium trichloride obtained from the Stauffer Chemical Company was pumped under vacuum to remove traces of the tetrachloride. Analysis gave a composition of $TiCl_{2.72}$.

Preparation of the Catalysts

Boston round bottles fitted with self-sealing butyl rubber gaskets protected by neoprene were used for preparation of solutions and catalyst suspensions. Particular care was taken to ensure that all the apparatus and solvent was thoroughly flushed with nitrogen before use.

For the titanium tetrachloride catalysts a concentrated solution containing about $1.5.10^{-3}$ moles ml^{-1} was prepared by addition of the pure titanium tetrachloride to a weighed quantity of solvent. The bottle was then flushed with nitrogen, capped, reweighed,

Can. J. Chem. Downloaded from www.nrcresearchpress.com by 210.87.254.42 on 09/05/12
For personal use only.

and pressurized with nitrogen. Samples were withdrawn with a hypodermic syringe for use in individual catalyst preparations. These titanium tetrachloride solutions could be used over a period of about 4 days, provided the cap was renewed each time a sample was removed.

For the titanium trichloride catalysts a separate suspension of the solid in heptane was prepared for each catalyst sample. The trichloride (1–2 g) was transferred to weighed bottles in a dry box, which was continuously flushed with nitrogen and gave a maximum dew point of −40° C. After reweighing the bottles, the heptane was added by means of a syringe.

All catalysts were prepared by injection of the metal alkyl solution into the solution or suspension of the halide in heptane. The bottles were shaken by hand during the addition of the alkyl. Concentrations of the catalysts, based on the amount of halide in the solvent, were of the order of 0.2 to 0.3 molar. The catalysts were aged for at least 1 hour before use.

Analysis of the Catalysts

X-Ray diffraction analyses were carried out on suspensions of the complexes in heptane using filtered copper radiation and a powder camera of 114.6 mm diameter. The diffraction patterns were measured and evaluated according to A.S.T.M. procedures. A nitrogen-flushed 0.5 mm bore Lindemann glass capillary tube was filled by lowering it into a sample of the suspension contained in a small tube blanketed by nitrogen. The capillary was sealed in a luminous flame. With careful manipulation no change in the appearance of a catalyst suspension could be detected. Also, once sealed, the complexes were stable over a period of at least several days as indicated by the reproducibility of the diffraction patterns.

For chemical analysis the complexes were isolated by filtration under nitrogen, washed with heptane, and dried under vacuum. About 1 g of dried solid was then hydrolyzed in 50 ml of 2 *N* sulphuric acid, also in a nitrogen atmosphere, and aliquot samples analyzed for titanium, chlorine, and aluminum or lithium.

Reduced titanium in the trivalent state was determined by running aliquot samples into an excess of ferric ammonium sulphate and estimating the ferrous iron thus produced by titration with 0.3 *N* potassium permanganate. Oxidation of the chloride ion in the solution was prevented by addition of an excess of a Zimmermann-Reinhardt solution (containing 50 g $MnSO_4.4H_2O$, 100 ml 98% H_2SO_4, and 100 ml 85% H_3PO_4 in 500 ml water). The total titanium was determined by a similar method after passing aliquot samples through a Jones' reductor.

Chlorine was determined by Volhard's method.

The aluminum analyses were carried out spectrographically* on a mixture of titanium and aluminum oxides obtained by precipitation with ammonium hydroxide and subsequent ignition.

Lithium was determined by flame photometry at a wavelength of 671 mμ.

Polymerizations

Butene polymerizations were carried out in a nitrogen atmosphere at 40° C in bottles with self-sealing gaskets. Matheson C.P. grade 1-butene, dried by passage through anhydrous calcium sulphate and phosphorus pentoxide, was condensed in the solvent at −30° C, the excess being allowed to boil off before capping the bottles. The catalyst

*Analyses made by Laboratories Branch, Department of Mines, Province of Ontario.

Can. J. Chem. Downloaded from www.nrcresearchpress.com by 210.87.254.42 on 09/05/12
For personal use only.

suspensions were added with a syringe at room temperature. In cases where no polymerization occurred at 40° C the temperature was raised to 80° C.

Ethylene polymerizations were carried out at room temperature in a three-necked flask fitted with neoprene rubber stoppers containing inlet tubes for nitrogen and ethylene. The solvent and catalyst components were introduced and the ethylene bubbled in at approximately 50 ml min^{-1}.

At the end of a polymerization reaction the catalyst was killed by the addition of ethanol to the reaction mixture. Decomposition of the catalyst and removal of the solvent were effected by stirring the jelly-like mass in a 10- to 20-fold excess of ethanol in a Waring Blendor. The polymer was filtered and dried under vacuum.

RESULTS

Catalytic Activity of the Complexes

Table I shows the results of a comparative study of the activity of the four catalyst systems towards the polymerization of 1-butene. The aluminum triisobutyl – titanium trichloride complexes are active over the widest range of initial alkyl:halide ratios,

TABLE I

Activity of Ziegler–Natta type complexes towards polymerization of 1-butene, at 40° C

	Alkyl:halide ratio			
	Below 0.5:1	0.5:1	1:1	Above 1:1
$Al(iBu)_3$–$TiCl_3$		+	+	+
$Al(iBu)_3$–$TiCl_4$	–	–	+	+
LiBu–$TiCl_3$	–	–	–	–
LiBu–$TiCl_4$	–	–	–	+ (if prepared in presence of monomer)

NOTE: Catalyst concentration: 2.10^{-2}–$3.5.10^{-2}$ moles (Ti halide)l^{-1}.

while the lithium systems only give polybutene under special conditions, i.e. with titanium tetrachloride at ratios above 1 provided the complex is prepared in the presence of the monomer. However, under these conditions, polymerization is rapid and almost complete for molar ratios of monomer to titanium up to at least 100. Polyethylene was obtained at ratios of unity and above from LiBu–$TiCl_4$ complexes prepared in the presence or absence of the monomer, but the LiBu–$TiCl_3$ complexes were completely inactive towards both ethylene and 1-butene.

Valency State of Titanium in Complexes

The method employed for the determination of reduced titanium cannot be used to establish the valency state of the metal since, on acid hydrolysis, divalent titanium is rapidly oxidized to the trivalent form (10), viz.

$$2Ti^{2+} + 2H_2O \rightarrow 2Ti^{3+} + 2OH^- + H_2.$$

However, from the two titanium analyses, an estimate of the residual tetravalent titanium can be made. These values for the insoluble products obtained from the reaction of lithium butyl or aluminum triisobutyl with titanium tetrachloride are plotted in Fig. 1 as a function of the initial component ratio. It is apparent that for both systems the titanium is present largely in the tetravalent state. With the LiBu–$TiCl_4$ complexes there is a trend to higher percentages of Ti^{4+} as the component ratio increases, while for the $Al(iBu)_3$–$TiCl_4$ complexes the percentage of Ti^{4+} remains essentially constant.

Can. J. Chem. Downloaded from www.nrcresearchpress.com by 210.87.254.42 on 09/05/12
For personal use only.

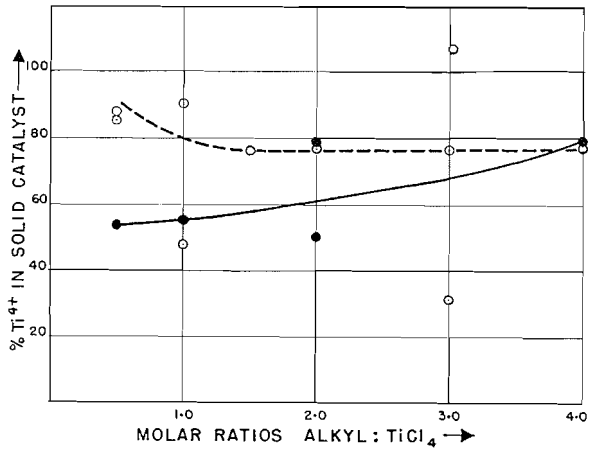


FIG. 1. Percentage of titanium in tetravalent state as function of component ratio. ○ $Al(iBu)_3$–$TiCl_4$, ● LiBu–$TiCl_4$.

Similar results for the lithium system have been reported by Friedlander and Oita (2) but with aluminum triisobutyl they found almost complete reduction of the titanium at component ratios above unity. In early experiments, where no special precautions were taken to ensure rapid dispersion of the metal alkyl during addition to the titanium tetrachloride solution, considerable reduction of titanium was noted (low values of Ti^{4+} at $Al(iBu)_3$:$TiCl_4$ ratios of 1 and 3). This may be one of the factors accounting for the discrepancy between the two results. Recently, it has been found that 90% of the titanium in the soluble complexes formed from these components at −78° C is in the tetravalent state (11).

Titanium, chlorine, and aluminum or lithium were found in all the solids analyzed. In calculating the elemental ratios in the insoluble reaction products, the alkyl content was taken as the difference between the weight of complex hydrolyzed and the total analysis of the other elements.

The Aluminum Triisobutyl – Titanium Trichloride System

Addition of the aluminum triisobutyl solution to a suspension of titanium trichloride in heptane resulted in the formation of a brown mixture which, on standing, settled into two layers consisting of a violet precipitate and a dark brown supernatant liquid. No marked difference in appearance was observed at $Al(iBu)_3$:$TiCl_3$ ratios in the range of 1 to 5. The dried solids were violet color and gave violet solutions on hydrolysis.

The chemical analyses for a series of the reaction products are recorded in Table II.

TABLE II

Analysis of aluminum triisobutyl – titanium trichloride complexes

$Al(iBu)_3$:$TiCl_3$	% Ti total	% Cl	% Al	% R	Atomic ratios Al:Ti	Cl:Ti	R:Ti	R:Al
0.5	33.7	65.3	0.24	0.8	0.012	2.62	0.02	1.5
1.0	31.7	64.6	0.26	3.4	0.014	2.75	0.09	6.3
2.0	31.8	65.9	0.42	1.9	0.023	2.80	0.05	2.1
5.7	31.5	65.5	0.51	2.5	0.029	2.81	0.07	2.3

Can. J. Chem. Downloaded from www.nrcresearchpress.com by 210.87.254.42 on 09/05/12
For personal use only.

The results show that the products consist principally of $TiCl_3$, independent of the initial $Al(iBu)_3$:$TiCl_3$ ratio, the aluminum content always being less than 0.5%. Similarly, the X-ray diffraction patterns of the various samples gave only lines of the violet form of titanium trichloride.

The Aluminum Triisobutyl – Titanium Tetrachloride System

The reaction of aluminum triisobutyl with titanium tetrachloride in heptane yields a precipitate whose color changes from a light reddish-brown to dark brown as the $Al(iBu)_3$:$TiCl_4$ ratio is increased. After filtration and vacuum drying, the color of the solid varies from light brown to purplish-black.

X-Ray analysis of suspensions of the complexes showed traces of titanium trichloride at initial component ratios of 0.5 and 1, but there was no indication of crystallinity at ratios below 0.5. Above the equimolar ratio the complexes were entirely amorphous. Natta *et al.* (12) have also reported that the complexes from the $Al(Et)_3$–$TiCl_4$ system are amorphous at component ratios above 0.7.

The results of the chemical analyses of a number of solids prepared at $Al(iBu)_3$:$TiCl_4$ ratios of 0.5 to 4 are given in Table III. The values for the atomic ratios are based on the

TABLE III

Analysis of aluminum triisobutyl – titanium tetrachloride complexes

	% Ti					Atomic ratios			
$Al(iBu)_3$:$TiCl_4$	Red.	Total	% Cl	% Al	% R	Al:Ti	Cl:Ti	R:Ti	R:Al
0.5	5.4	30.6	49.0	7.86	12.4	0.46	2.16	0.34	0.75
0.5	3.2	23.0	39.1	—	—	—	2.30	—	—
1.0	—	26.5	46.4	6.10	21.0	0.41	2.37	0.67	1.63
1.0	14.5	27.9	42.8	—	—	—	2.07	—	—
1.5	6.4	27.6	48.2	7.14	17.1	0.46	2.36	0.52	1.13
2.0	6.5	28.0	31.9	7.94	32.1	0.50	1.54	0.96	1.91
3.0	19.6	28.7	34.8	8.00	28.5	0.49	1.64	0.83	1.69
3.0	6.2	26.3	39.9	—	—	—	2.05	—	—
4.0	6.6	28.0	35.2	11.02	25.7	0.70	1.70	0.77	1.10

analyses for "total" titanium. It is apparent that there is an initial decrease in the Cl:Ti ratio and that the values lie between 2.5 and 1.5 over the whole range of compositions studied. These figures are considerably lower than those reported by Cooper and Rose (5) for similar catalyst systems. The low values for the Al:Ti and R:Ti ratios suggest that only a small proportion of the aluminum triisobutyl or its reaction products takes part in the formation of the precipitate, while the R:Al ratios, lying between 1.2 and 2.0, indicate loss of alkyl groups during the reaction. At least part of this loss is accounted for by the formation of C_4 hydrocarbons which were detected in gas chromatographic analysis of a sample of the vapor phase above a reaction mixture. Isobutane and isobutylene or 1-butene were the major constituents. A positive identification of the olefine could not be made, but it is probably isobutylene. Trace amounts of C_3 hydrocarbons were also detected.

Analyses of some of the filtrates from the complexes gave Cl:Ti ratios which steadily increased with increasing initial component ratio, having a value of 69 for an $Al(iBu)_3$:$TiCl_4$ ratio of 4. This implies that chlorine compounds soluble in heptane are formed during

Can. J. Chem. Downloaded from www.nrcresearchpress.com by 210.87.254.42 on 09/05/12
For personal use only.

the reaction. In addition, the valency state of titanium found in the filtrate was observed to change with component ratio. For an $Al(iBu)_3$:$TiCl_4$ ratio of 0.5, 98% of the titanium in the filtrate was present as Ti^{4+}, but at a ratio of 3 all the titanium was in the reduced state. At the higher component ratio, the titanium in the filtrate presumably represents soluble titanium compounds or finely divided titanium trichloride which passed through the filter.

The Lithium Butyl – Titanium Trichloride System

The reaction between lithium butyl and titanium trichloride in heptane is highly exothermic and the violet form of the trichloride is converted to an insoluble green complex.

The X-ray diffraction patterns of the complexes were obtained under identical experimental conditions over the whole range of LiBu:$TiCl_3$ ratios from 0.5 to 4. At a ratio of 4 the diffraction pattern could not be identified by comparison with the reference data of the A.S.T.M. index and, consequently, an attempt was made to index the pattern from basic principles. Using the graphic method it was found to consist of two separate compounds, one of them being cubic and having a sodium chloride type lattice with a lattice constant of 5.20 Å. This is appreciably larger than the lattice constant of lithium chloride (5.14 Å), and the compound is considered to be a mixed crystal of lithium and titanium chlorides, probably of composition $(LiCl)_n.TiCl_2$ or $(LiCl)_n.TiCl$. Although alkali metal complexes of both tetravalent and trivalent titanium halides are known, none have been reported in which titanium is in a lower valent state. The pattern of the second component could not be identified, but its higher symmetry suggests that it may be an alkylated compound. Both compounds were also found at component ratios of 2 and 1. At the equimolar ratio the two strongest lines of titanium trichloride were also evident and at ratios of less than one the X-ray diffraction patterns consisted of the trichloride lines only. The *d* values and approximate line intensities of the patterns obtained at ratios of 2 and 4 are given in Table IV and those for lithium chloride are included for comparison. From the table it is apparent that the relative line intensities of the cubic

TABLE IV

X-Ray diffraction patterns of complexes from LiBu–$TiCl_3$ system

Relative intensity of component ratio				LiCl*		
"*d*"	2:1	4:1	*hkl*	"*d*"	Rel. int.	*hkl*
6.00	80	40				
3.15	40	20				
3.01	60	60	111	2.967	100	111
2.61	100	100	200	2.570	86	200
2.00	10	—				
1.84	90	80	220	1.817	58	220
1.76	10	—				
1.57	10	10	311	1.550	29	311
1.50	30	20	222	1.484	16	222
1.30	10	10	400	1.285	4	400
				1.1791	10	331
1.16	20	10	420	1.1493	12	420
1.06	20	10	422	1.0491	8	422

*A.S.T.M. index (4-0664).

Can. J. Chem. Downloaded from www.nrcresearchpress.com by 210.87.254.42 on 09/05/12
For personal use only.

component and lithium chloride differ appreciably. This can be due to the different scattering power of the mixed crystal or to preferred orientation. Comparison of the patterns for the 2:1 and 4:1 complexes indicate that superposition of diffraction lines of the cubic component and the unknown constituent is not an important factor.

Hydrolysis of the dried solids in 2 *N* sulphuric acid was accompanied by considerable gas evolution, producing violet-colored solutions. In addition, at ratios of unity and above, increasing amounts of an insoluble blue solid were obtained, constituting, at the highest ratio, about 20% of the original weight of the complex. The compound was stable in air and different samples contained 55–61% titanium. Spectrographic analysis showed only traces of lithium. The X-ray diffraction pattern had considerable background scattering and was different from that of the complex before hydrolysis. This hydrolysis product is probably a hydrated form of one of the lower titanium oxides, i.e. of composition between Ti_2O_3 and TiO_2. Stable oxides of a similar color, corresponding to the nominal formulae Ti_3O_5 and Ti_7O_{12}, have been prepared (13) and are also resistant to strong acids except concentrated sulphuric acid.

The results of the chemical analysis of the reaction products for this system are given in Table V. The values for the 2.46 and 4.0 ratios are those for the solution with a correc-

TABLE V

Analysis of lithium butyl – titanium trichloride complexes

					Atomic ratios			
$LiBu:TiCl_3$	% Ti total	% Cl	% Li	% R	Li:Ti	Cl:Ti	R:Ti	R:Li
0.5	30.9	63.8	3.42	1.9	0.76	2.78	0.05	0.07
0.5	31.5	63.7	2.37	2.4	0.52	2.72	0.06	0.12
1.0	29.5	57.0	5.77	8.7	1.35	2.61	0.25	0.18
1.0	29.5	63.6	4.51	2.4	1.06	2.91	0.07	0.07
2.0	23.6	50.5	—	—	—	2.89	—	—
2.46	23.9	52.5	7.30	16.3	2.11	2.97	0.57	0.25
4.0	23.8	52.4	10.34	12.5	2.99	2.97	0.44	0.15

tion for the titanium present in the insoluble material formed during hydrolysis. It can be seen that the Cl:Ti ratio remains essentially constant while there is a progressive increase in the Li:Ti and R:Ti ratios. It is apparent, also, that there is a considerable loss of alkyl on formation of the complexes. Again, gas chromatographic analysis has shown that, at least in part, this appears as *n*-butane and 1-butene or isobutylene, probably the former.

The Lithium Butyl – Titanium Tetrachloride System

The reaction between lithium butyl and titanium tetrachloride is exothermic, and brown, jelly-like precipitates are formed, the color darkening as the proportion of lithium butyl is increased.

X-Ray examination did not show the presence of any crystalline component at $LiBu:TiCl_4$ ratios of less than 1. However, at ratios of 1 and above, a faint diffraction pattern was observed, showing two broad lines in the position of the two main lines of the cubic compound found in the trichloride system.

There appears to be a small decrease in the Cl:Ti ratio with increasing proportion of lithium butyl, but within the range studied it remains above 3. The Li:Ti ratio increases

Can. J. Chem. Downloaded from www.nrcresearchpress.com by 210.87.254.42 on 09/05/12
For personal use only.

TABLE VI
Analysis of lithium butyl – titanium tetrachloride complexes

	% Ti					Atomic ratios			
$LiBu:TiCl_4$	Red.	Total	% Cl	% Li	% R	Li:Ti	Cl:Ti	R:Ti	R:Li
0.5	9.82	21.0	53.3	4.07	21.6	1.34	3.43	0.86	0.65
1.0	10.6	23.5	58.5	4.61	13.4	1.35	3.36	0.48	0.35
2.0	10.5	21.1	56.2	6.31	16.4	2.06	3.60	0.65	0.32
2.0	4.57	23.2	48.1	6.41	22.3	1.91	2.80	0.81	0.42
4.0	4.97	23.0	50.6	9.91	14.5	2.97	3.09	0.53	0.18

progressively with the initial component ratio and is at a much higher level than the corresponding relationship for the $Al(iBu)_3$–$TiCl_4$ complexes. It is very similar to that for the $LiBu$–$TiCl_3$ system. The low R:Li ratios indicate that considerable alkyl is lost in the formation of the complexes. The principal hydrocarbons found in the vapor phase above the reaction mixtures were *n*-butane and 2-butene (cis and trans). In addition, small amounts of 1-butene or isobutylene, C_3, and C_2 hydrocarbons were detected.

It was noted that, on hydrolysis of the insoluble complexes in sulphuric acid solution, a greasy deposit formed on the side of the flask. A few milligrams of a white insoluble material recovered from the flask was shown to be a hydrocarbon product, indicating the formation of a small amount of polymer.

DISCUSSION

The chemical and X-ray diffraction analyses of the $Al(iBu)_3$–$TiCl_3$ catalysts are in agreement with Natta's observations (3, 14) for a similar system in that they consist essentially of unchanged titanium trichloride on which a residual amount of the metal alkyl is chemisorbed. The precision of the aluminum and alkyl contents of the catalysts given in Table II is low because of the small amounts present, but the values are similar to those reported where C^{14}-labelled aluminum triethyl was used (14). This system is one of the simplest in providing a guide to the requirements for catalytic activity and the mechanism by which control of the steric configuration of the monomer units in the polymer chain is achieved. Titanium trichloride has a layered lattice structure and it has been postulated (3) that the active sites are defect locations, or the boundaries of crystal faces, where the metal alkyl can enter into a co-ordination complex with the transition metal atom, the two dissimilar metal atoms being bridged through chlorine or alkyl groups. Polymer growth probably occurs at the aluminum atom although evidence from other catalyst systems (15, 16) suggests that a Ti—C bond may be involved. Steric control during the propagation step is visualized as resulting from the localization of the monomer units in a particular configuration as they enter the complex.

The $Al(iBu)_3$–$TiCl_4$ system is more complex and any mechanism proposed to account for the formation of the complexes must take into consideration the following factors:

(i) the high percentage of Ti^{4+} in the solids,

(ii) the loss of chlorine from the solids,

(iii) the loss of alkyl from the solids.

Can. J. Chem. Downloaded from www.nrcresearchpress.com by 210.87.254.42 on 09/05/12
For personal use only.

These factors can be accounted for, in a very general way, by the reaction scheme given below, which is based on suggestions by Natta (3) and Uelzmann (8).

$$TiCl_4 + AlR_3 \longrightarrow (TiCl_3)^+(AlR_3Cl)^- \quad [1]$$

$$(TiCl_3)^+(AlR_3Cl)^- \text{ decomp.} \begin{cases} \nearrow TiCl_3 + AlR_2Cl + R\cdot \\ \searrow TiCl_2 + AlR_2Cl + RCl \end{cases} \quad [2]$$

$$TiCl_4 + 2AlR_3 \begin{cases} \nearrow (TiCl_2R)^+(AlR_3Cl)^- + AlR_2Cl \\ \searrow (TiCl_2)^{2+}(AlR_3Cl)^-_2 \end{cases} \quad [3]$$

$$(TiCl_2R)^+(AlR_3Cl)^- \text{ decomp.} \begin{cases} \nearrow TiCl_2 + AlR_2Cl + 2R\cdot \\ \searrow TiCl + AlR_2Cl + RCl + R\cdot \end{cases} \quad [4]$$

Equations [1] and [3] represent the initial complex-forming reaction with increasing concentration of aluminum alkyl in which the titanium is stabilized in the tetravalent state. Decomposition of the first complex according to reaction [2] would account for the presence of crystalline titanium trichloride at low initial ratios of aluminum alkyl to titanium tetrachloride. Both the decomposition steps [2] and [4] can account for the loss of chlorine and alkyl through the formation of hydrocarbons and soluble halides. The detection in the reaction products of isobutane and a C_4 unsaturate which is probably isobutylene indicates that the isobutyl radicals undergo a disproportionation reaction. Part of the isobutane could also result from a hydrogen abstraction reaction with the solvent or metal alkyl. Also, the presence of alkyl chloride has been reported (17) in the reaction product from the $Al(Et)_3$–$TiCl_4$ system at low component ratios. However, it is obviously difficult to equate the analyses shown in Table III with the above scheme if the high Ti^{4+} content is related solely to this type of complex.

Uelzmann (8, 11) has proposed that the ionic complexes furnish the active polymerization sites but an alternative explanation is that they are formed by adsorption of alkyl upon the lower valent titanium halides formed in the decomposition steps, in analogy with the $Al(i\text{Bu})_3$–$TiCl_3$ system.

The catalysts from titanium tetrachloride give faster rates for the polymerization of 1-butene than the trichloride catalysts and yield polymers that are less crystalline. They are highly complex mixtures which presumably contain active sites of different configuration. Evidence for this suggestion (18) has come from an extensive study of the molecular weight distribution of polyethylene prepared from similar catalysts. The high degree of polydispersity observed is not compatible with a polymerization mechanism involving a single, well-defined catalyst site.

Since lithium is considerably more electropositive than titanium it is probable that the titanium is bound in complex anions and an acceptable mechanism to account for the

Can. J. Chem. Downloaded from www.nrcresearchpress.com by 210.87.254.42 on 09/05/12
For personal use only.

experimental observations on the two lithium systems, which is based on suggestions by Uelzmann, would be as follows:

$$LiR + TiCl_4 \longrightarrow Li^+(TiCl_4R)^- \quad [5]$$

$$Li^+(TiCl_4R)^- \xrightarrow{\text{decomp.}} \begin{matrix} LiCl.TiCl_3 + R\cdot \\ LiCl.TiCl_2 + RCl \end{matrix} \quad [6]$$

$$2LiR + TiCl_4 \longrightarrow (Li^+)_2(TiCl_4R_2)^= \quad [7]$$

$$(Li^+)_2(TiCl_4R_2)^= \xrightarrow{\text{decomp.}} \begin{matrix} 2LiCl.TiCl_2 + 2R\cdot \\ 2LiCl.TiCl + 2RCl \end{matrix} \quad [8]$$

or, considering the trichloride complexes:

$$LiR + TiCl_3 \longrightarrow Li^+(TiCl_3R)^- \quad [9]$$

$$Li^+(TiCl_3R)^- \xrightarrow{\text{decomp.}} LiCl.TiCl_2 + R\cdot \quad [10]$$

$$2LiR + TiCl_3 \longrightarrow (Li^+)_2(TiCl_3R_2)^= \quad [11]$$

$$(Li^+)_2(TiCl_3R_2)^= \xrightarrow{\text{decomp.}} 2LiCl.TiCl + 2R\cdot \quad [12]$$

The complex-forming reactions represented by the steps [5] and [7] would account for the preservation of titanium in the tetravalent state in the LiBu–$TiCl_4$ system, while the decomposition reactions [6], [8], [10], and [12] provide an explanation for the loss of alkyl either through the formation of hydrocarbon products or an alkyl chloride. The formation of an alkyl chloride may also account for the loss of chlorine in the tetrachloride complexes. The identification of the C_4 olefine in the tetrachloride catalyst as 2-butene is surprising since in a disproportionation reaction between *n*-butyl radicals this would involve a hydrogen atom rearrangement. The fact that only traces of 1-butene were detected in this case is consistent with its removal by polymerization.

Again, it is difficult to reconcile the low R:Ti ratio with the high percentage of tetravalent titanium, particularly for complexes with higher initial component ratios. A possible explanation for this inconsistency, which also appears in the Al(*i*Bu)$_3$–$TiCl_4$ system, is that certain complex anions or cations of titanium in a valency state of less than three may give tetravalent titanium on hydrolysis in acid media, the normal step preceding analysis. The formation of an oxide of probable composition between Ti_2O_3 and TiO_2 on hydrolysis of the LiBu–$TiCl_3$ complexes provides evidence for this suggestion since it indicates that oxidation can proceed beyond the trivalent stage. Also, similar behavior has been reported for halides of divalent zirconium and hafnium which are the next elements to titanium in group IVA of the periodic table. The lower valency states of titanium are progressively less stable and the simple monovalent titanium halides have

Can. J. Chem. Downloaded from www.nrcresearchpress.com by 210.87.254.42 on 09/05/12
For personal use only.

not been isolated. As these will be odd electron compounds they are likely to exist only in dimeric form and will be extremely reactive.

The inability of the LiBu–$TiCl_3$ system to initiate polymerization may be attributable to the fact that the well-ordered crystalline compound formed does not provide the type of support on which a catalyst site of suitable configuration can form. It will be noted that this complex has the symmetrical sodium chloride type lattice as opposed to the layered lattice structure of titanium trichloride. Evidence for the formation of the same compound in the LiBu–$TiCl_4$ system, although to a lesser degree, may also be the explanation of the inactivity of these catalysts for the polymerization of 1-butene if prepared prior to the addition of the monomer. However, they will polymerize ethylene but at a much slower rate than when prepared in its presence. These differences in activity imply that the olefine can take part in complex formation, presumably leading to catalysts of somewhat different structure.

ACKNOWLEDGMENTS

This work was made possible by a research grant to the Ontario Research Foundation by the Province of Ontario.

NOTE ADDED

Since this paper was submitted for publication Dr. N. F. H. Bright* and Mr. R. C. Garvie* have completed an examination of one of our X-ray diffraction patterns of the blue solid obtained on hydrolysis in aqueous sulphuric acid of a complex prepared in the reaction of lithium butyl with titanium trichloride. They find that, although the pattern is ill-defined, it indicates that the crystalline constituents of the solid are titanium sesquioxide (Ti_2O_3) and rutile (TiO_2). As the titanium content (55%) of this particular sample is less than that of the higher oxide (TiO_2) they suggest that some amorphous hydrated TiO_2 is probably present. Evidence of an amorphous material was noted in the X-ray pattern.

Dr. Bright and Mr. Garvie also comment on the unusual fact that the TiO_2 content is in the rutile form. Normally, anatase is the crystal form in which TiO_2 is obtained when precipitated chemically.

REFERENCES

1. K. Ziegler. Belgium Patent No. 533,362 (Nov. 16, 1954). K. Zeigler, E. Holzcamp, and H. Martin. Angew. Chem. **67**, 541 (1955).
2. H. N. Friedlander and K. Oita. Ind. Eng. Chem. **49**, 1885 (1957).
3. G. Natta. J. Inorg. & Nuclear Chem. **8**, 589 (1958).
4. W. M. Saltman, W. E. Gibbs, and J. Lal. J. Am. Chem. Soc. **80**, 5616 (1958).
5. M. L. Cooper and J. B. Rose. J. Chem. Soc. 795 (1959).
6. D. B. Ludlum, A. W. Anderson, and C. E. Ashby. J. Am. Chem. Soc. **80**, 1380 (1958).
7. F. Eirich and H. Mark. J. Colloid Sci. **11**, 748 (1956).
8. H. Uelzmann. J. Polymer Sci. **32**, 457 (1958).
9. A. Gilchrist. J. Polymer Sci. **34**, 49 (1959).
10. G. Patscheke and W. Schaller. Z. anorg. Chem. **235**, 257 (1938).
11. H. Uelzmann. J. Polymer Sci. **37**, 561 (1959).
12. G. Natta, L. Porri, A. Mazzei, and D. Morero. Chim. e. ind. **41**, 398 (1959).
13. Gmelins Handbuch. Vol. 8. System No. 41 (Titan). 1951. p. 212.
14. G. Natta. J. Polymer Sci. **34**, 21 (1959).
15. C. van Heerden. J. Polymer Sci. **34**, 46 (1959).
16. W. L. Carrick, F. J. Karol, G. L. Karapinka, and J. J. Smith. J. Am. Chem. Soc. **82**, 1503 (1960).
17. A. Malatesta. Can. J. Chem. **37**, 1176 (1959).
18. H. Wesslau. Makromol. Chem. **26**, 102 (1958).

**Mineral Sciences Division, Mines Branch, Department of Mines and Technical Surveys, Ottawa, Ontario.*

Can. J. Chem. Downloaded from www.nrcresearchpress.com by 210.87.254.42 on 09/05/12
For personal use only.

Can. J. Chem. Downloaded from www.nrcresearchpress.com by 210.87.254.5 on 09/05/12
For personal use only.

REARRANGEMENT STUDIES WITH C^{14}

X. ETHANOL-2-C^{14} FROM THE IRRADIATION OF ETHANOL-1-C^{14} WITH Co^{60} GAMMA RAYS[1]

C. C. Lee and D. G. Lee[2]

ABSTRACT

The irradiation of aqueous solutions of ethanol-1-C^{14}, containing about 2% ethanol by weight, with up to 58.0 million rads of Co^{60} γ-rays led to the formation of up to 0.49% ethanol-2-C^{14} in the alcohol recovered after irradiation. The G value of this isotope position rearrangement was about 0.04 and amounted to approximately 2% of the G value for the total amount of ethanol decomposed. Possible mechanisms for the rearrangement are discussed.

In a review in 1956, Collinson and Swallow (1) pointed out that radiolysis of alcohols follows the general pattern of a fission of an α-carbon – hydrogen bond to give an α-hydroxyalkyl radical which can either dimerize to a glycol or be further oxidized to a carbonyl compound. In the case of ethanol, this generalization can be applied to account satisfactorily for the formation of the chief products derived from the ethanol, namely, acetaldehyde and 2,3-butanediol (2–6).

While a number of minor products have been quantitatively estimated for the radiolysis of pure ethanol with α-particles (3), the irradiation of dilute aqueous solutions of ethanol with X or Co^{60} γ-rays was reported to give, besides hydrogen and hydrogen peroxide, only acetaldehyde in the presence of oxygen and acetaldehyde and 2,3-butanediol in deaerated solutions (2, 5, 6). The organic products can, therefore, be regarded as being formed from the α-hydroxyethyl radical. The most recently suggested mechanism for the radiolysis of aqueous solutions of ethanol postulated reactions of H or OH radicals with the solute to give α-hydroxyethyl from the breaking of an α-carbon – hydrogen bond (6). No rupture of the carbon–oxygen bond was envisaged. In the present study, dilute aqueous solutions of ethanol-1-C^{14} was irradiated with Co^{60} γ-rays to ascertain whether any isotope position rearrangement to ethanol-2-C^{14} would result. Detection of such a rearrangement could possibly be regarded as indicating some rupture of the carbon–oxygen bond to give an ethyl radical followed by a 1,2-hydrogen shift in the radical analogous to 1,2-hydride shifts observed in certain reactions involving the ethyl cation (7, 8, 9).

A stock solution containing 2.02% ethanol by weight was made up with distilled water and ethanol-1-C^{14}.* Its C^{14} content was about 10 μc/ml. Three-milliliter aliquots were placed in 4-ml glass vials, stoppered and sealed with wax, and then irradiated at room temperature in fixed positions near a 90-curie Co^{60} source. The dose rates were measured by determining the ferric ions formed upon irradiating solutions of ferrous ammonium sulphate (10). Under the conditions of the present experiments, the dose rates were of the order of 1200 rads/minute.

After irradiation, the samples were analyzed for total decomposition of ethanol and for the presence of isotopically rearranged ethanol-2-C^{14} in the recovered alcohol. Before and after irradiation, equal aliquots of the solution were diluted with exactly the same amounts of absolute ethanol as a carrier. The diluted solutions were converted to ethyl

[1]*Manuscript received June 6, 1960.*
Contribution from the Department of Chemistry, University of Saskatchewan, Saskatoon, Saskatchewan.
[2]*Holder of the Thorvaldson Scholarship, 1959–60.*
**Obtained from Atomic Energy of Canada Limited, Chalk River, Ontario. To minimize any radiolytic effects of its own radiation, the stock solution was prepared within a few days after receipt of the ethanol-1-C^{14}.*

3,5-dinitrobenzoate and to iodoform. The decrease in activity in the ethyl 3,5-dinitrobenzoate after irradiation represented the ethanol decomposed during the irradiation. The ethanol so decomposed most likely was chiefly converted to the known products, acetaldehyde and 2,3-butanediol. The activity in the iodoform corresponded to the C^{14} in the C-2 position of ethanol and thus would be a measure of the rearrangement to ethanol-2-C^{14}. The results are summarized in Table I.

TABLE I

Decomposition and rearrangement in the irradiation of ethanol-1-C^{14}

Dose (10^6 rads)	Derivative counted[a]	Activity[b] (mμc/mmole)	Decomposition of EtOH		Rearrangement to EtOH-2-C^{14}[c]	
			%	G_d	%	G_r
0	Benzoate	690				
	CHI_3	0.15				
41.8	Benzoate	572	17.1	1.7		
	CHI_3	2.98			0.41	0.04
44.1	Benzoate	562	18.5	1.8		
	CHI_3	2.60			0.39	0.04
52.0	Benzoate	516	25.2	2.0		
	CHI_3	3.56			0.49	0.04
58.0	Benzoate	517	25.1	1.8		
	CHI_3	3.18			0.44	0.03

[a]Benzoate designates ethyl 3,5-dinitrobenzoate.
[b]C^{14} activity in millimicrocuries per millimole of sample was assayed as CO_2 gas with a vibrating reed electrometer.
[c]Corrected for the activity of iodoform from the ethanol before irradiation.

It may be noted that the iodoform obtained from degradation of the commercial ethanol-1-C^{14} before irradiation showed a small amount of radioactivity (Table I). This was subtracted from the activity of iodoform derived from the irradiated ethanol before rearrangement to ethanol-2-C^{14} was calculated.

In some preliminary experiments with radiation dosages of up to 7 million rads, only about 0.1% rearrangement to ethanol-2-C^{14} was indicated. With higher radiation doses as tabulated in Table I, more significant amounts of rearrangement were observed. The activities of iodoform from these experiments were quite large, being some 20 to 30 times that of background depending on the size of sample counted. Moreover, all iodoform samples were shown to have practically constant specific activity on repeated recrystallization, indicating that the iodoform activity was not due to contamination. It is, therefore, reasonable to conclude that rearrangement of ethanol-1-C^{14} to ethanol-2-C^{14} actually occurred during the irradiation. The G_r value, designating the number of molecules of ethanol-1-C^{14} rearranged to ethanol-2-C^{14} per 100 electron volts of energy absorbed, was calculated to be about 0.04. The ratio of G_r to G_d was of the order of 0.02, indicating that rearrangement to ethanol-2-C^{14} occurred only to about 2% of the extent of total decomposition.

Two possible explanations for the observed formation of ethanol-2-C^{14} from ethanol-1-C^{14} may be suggested. Firstly, minute amounts of ethylene could be produced during irradiation which remained in solution and subsequently reacted with water to give ethanol-1-C^{14} and ethanol-2-C^{14}.

$$CH_3C^*H_2OH \longrightarrow\!\!\!\!\sim\!\!\!\!\sim\!\!\!\!\sim

though no attempts have been made to detect or estimate ethylene in studies with aqueous ethanol (5, 6). The formation of some alcohol, assumed to be ethanol, upon gamma irradiation of mixtures of ethylene and oxygen in water under pressure has been reported by Henley and co-workers (11, 12). However, similar studies by Clay, Johnson, and Weiss (13) on the action of Co^{60} γ-radiation on aqueous solution of ethylene at different pressures did not report ethanol as a product. Considering this somewhat conflicting evidence from the literature, it is reasonable to conclude that upon irradiation of a dilute aqueous solution of ethanol, formation of ethylene followed by rehydration back to ethanol does not occur extensively. Neverthless, it is possible that such a process may take place to a minor extent during irradiation. Reaction sequence [1] given above is, therefore, a plausible explanation for the formation of the small amount of ethanol-2-C^{14} from the irradiation of ethanol-1-C^{14}.

A second explanation for the observed isotope position rearrangement involves the postulation of a 1,2-hydrogen shift in an ethyl radical. The chemical effects of ionizing radiation in dilute aqueous solutions are generally considered to be due primarily to the action of H and OH radicals from the net process

$$H_2O \longrightarrow H\cdot + OH\cdot . \qquad [2]$$

A mechanism for the rearrangement of ethanol-1-C^{14} to ethanol-2-C^{14} may then be postulated as follows:

$$CH_3C^*H_2OH + H\cdot \rightarrow CH_3C^*H_2\cdot + H_2O \qquad [3]$$

$$CH_3C^*H_2OH + OH\cdot \rightarrow CH_3C^*H_2\cdot + H_2O_2 \qquad [4]$$

$$CH_3C^*H_2\cdot \xrightarrow[\text{shift}]{\text{1,2-H}} \cdot CH_2C^*H_3 \qquad [5]$$

$$C^*H_3CH_2\cdot + H_2O \longrightarrow C^*H_3CH_2OH + H\cdot \qquad [6]$$

The G_r value for the rearrangement is low because the chief effects in the radiolysis of dilute aqueous ethanol result from the breaking of the α-carbon – hydrogen bond rather than the carbon–oxygen bond. Moreover, the H produced in reaction [6] does not necessarily have to propagate a chain leading to a high yield of ethanol-2-C^{14} because the H atoms can enter into other processes such as its reaction with ethanol to give the α-hydroxyethyl radical (6).

The 1,2-shift depicted in reaction [5] is not unreasonable as a number of reported isomerizations induced by irradiation have been explained in a similar way. The formation of isopropyl chloride from irradiation of *n*-propyl chloride (14) and of *t*-butyl chloride and bromide from isobutyl chloride and bromide, respectively (15, 16), were postulated to take place through rearrangement of the *n*-propyl to isopropyl and isobutyl to *t*-butyl radicals, processes which involve 1,2-hydrogen shifts.

In conclusion, the present work has shown that Co^{60} γ-irradiation of a 2.02% aqueous solution of ethanol-1-C^{14} led to the formation of some ethanol-2-C^{14}, the G value for this isotope position rearrangement being about 0.04. Two plausible explanations for the rearrangement have been suggested. From the present data, however, it is not possible to decide whether only one or both of the suggested mechanisms actually accounted for the observed formation of ethanol-2-C^{14} from ethanol-1-C^{14}.

ACKNOWLEDGMENT

The financial support given by the National Research Council of Canada is gratefully acknowledged.

Can. J. Chem. Downloaded from www.nrcresearchpress.com by 210.87.254.5 on 09/05/12
For personal use only.

REFERENCES

1. E. COLLINSON and A. J. SWALLOW. Chem. Revs. **56**, 471 (1956).
2. A. J. SWALLOW. Biochem. J. **54**, 253 (1953).
3. W. R. MCDONELL and A. S. NEWTON. J. Am. Chem. Soc. **76**, 4651 (1954).
4. J. G. BURR. J. Phys. Chem. **61**, 1477 (1957).
5. G. G. JAYSON, G. SCHOLES, and J. WEISS. J. Chem. Soc. 1358 (1957).
6. J. T. ALLAN, E. M. HAYON, and J. WEISS. J. Chem. Soc. 3913 (1959).
7. J. D. ROBERTS and J. A. YANCEY. J. Am. Chem. Soc. **74**, 5943 (1952).
8. R. M. ROBERTS, G. A. ROPP, and O. K. NEVILLE. J. Am. Chem. Soc. **77**, 1764 (1955).
9. C. C. LEE, M. C. HAMBLIN, and N. JAMES. Can. J. Chem. **36**, 1597 (1958).
10. J. WEISS, A. O. ALLEN, and H. A. SCHWARZ. Proc. Intern. Congr. Peaceful Uses Atomic Energy, **14**, 179 (1956).
11. E. J. HENLEY and J. P. SCHWARTZ. J. Am. Chem. Soc. **77**, 3167 (1955).
12. E. J. HENLEY, W. P. SCHIFFRIES, and N. F. BARR. A.I.Ch.E. Journal, **2**, 211 (1956).
13. P. G. CLAY, G. R. A. JOHNSON, and J. WEISS. J. Chem. Soc. 2175 (1958).
14. R. H. WILEY, C. H. JARBOE, J. R. HARRELL, and D. J. PARISH. Proc. Chem. Soc. 347 (1957).
15. W. S. WILCOX. Radiation Research, **10**, 112 (1959).
16. E. B. DISMUKES and W. S. WILCOX. Radiation Research, **11**, 754 (1959).

Can. J. Chem. Downloaded from www.nrcresearchpress.com by 210.87.254.5 on 09/05/12
For personal use only.

ELECTRONIC STATES OF HYDRATED VANADIUM (II) ION[1]

RUTH M. BENNETT AND O. G. HOLMES

ABSTRACT

The optical absorption of a single crystal of $VSO_4.7H_2O$ was measured in the range 9000–35,000 cm^{-1}. The three observed bands were assigned to transitions between the four orbital levels resulting from cubic electrostatic perturbation of the spherical terms of configuration $3d^3$. Values of $Dq = 1200$ cm^{-1} and $E = 10{,}000$ cm^{-1} were derived from the spectral analysis.

INTRODUCTION

Ligand field theory has been applied with success to the hydrates and other complexes of ions of the first transition group metals. Several reviews of this work are available (1, 2, 3). The usual procedure is to consider the effect of the electrostatic potential generated by the ligands upon the electronic states of the central ion. Energy levels, magnetic and optical properties, etc. can then be evaluated for the perturbed ion. Some authors (4, 5, 6) have allowed for the possibility of covalent bonding by constructing appropriate molecular orbitals.

Inadequate optical data for hydrated V^{++} ion has led to some confusion about its electronic levels. We have therefore prepared $VSO_4.7H_2O$ crystals of sufficient size and purity for the accurate measurement of its optical absorption spectrum in the region 9000–35000 cm^{-1}. The observed bands have been assigned to transitions between levels derived from configuration $3d^3$ by a perturbing electrostatic field of cubic symmetry. Since both the "weak field" and "strong field" formalisms have become popular, we shall present both, even though they lead to identical results.

EXPERIMENTAL WORK

(a) Preparation of Hydrated Vanadium (II) Ion

The method of Jones and Colvin (7) was used for the preparation of $VSO_4.7H_2O$. Fisher reagent vanadium pentoxide was suspended in a sulphuric acid solution. Sulphur dioxide was bubbled through to reduce the vanadium to the plus four state (vanadyl). The filtered vanadium (IV) solution was reduced electrolytically at a mercury cathode to V^{++}. This solution was transferred to a flask under an atmosphere of nitrogen and ethyl alcohol poured over the surface. Over a period of several hours large well-formed violet crystals of $VSO_4.7H_2O$ deposited.

The total reducing power of the vanadium in the crystal was determined by titration to the plus five state with standard $KMnO_4$ (titer A). The vanadium concentration was found by reducing back to vanadium (IV) with sulphur dioxide and reoxidizing with $KMnO_4$ (titer B). The concentrations of V^{++} and V^{+++} were then calculated from titers A and B. The titration procedure was that suggested by Treadwell (8).

(b) Absorption Spectrum of Hydrated Vanadium (II) Ion

Figure 1 shows the optical absorption spectrum of a single crystal of $VSO_4.7H_2O$. These data were obtained with a Beckman DU spectrophotometer. Salient features of the spectrum are summarized in Table I.

[1]*Manuscript received June 27, 1960.*
Contribution from the Department of Chemistry, Regina College, University of Saskatchewan, Regina, Sask.

Can. J. Chem. Vol. 38 (1960)

Can. J. Chem. Downloaded from www.nrcresearchpress.com by 210.87.254.105 on 09/05/12
For personal use only.

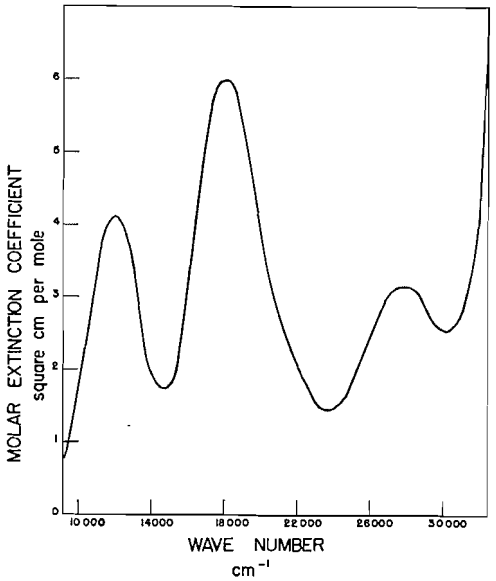


FIG. 1. Absorption spectrum of $VSO_4.7H_2O$.

TABLE I

Electronic transitions of hydrated V^{++}

Band peak, cm^{-1}	Peak extinction coefficient	f-Number	Transition	Calculated energy levels	
				E = 11,320 cm^{-1}	E = 10,000 cm^{-1}
12000	4.1	0.5×10^{-4}	$^4A_2$–$^4T_2$	(12000)	(12000)
18200	6.0	0.9×10^{-4}	$^4A_2$–$^4T_1$	18400	18000
27800	3.1	0.3×10^{-4}	$^4A_2$–$^4T_1$	28900	28000

The principal difficulty in measuring this absorption spectrum lies in the inevitable presence of V^{+++} generated by the very powerful reducing agent V^{++}. Since hydrated V^{+++} exhibits absorption bands at 17,800 and 25,700 cm^{-1}, respectively, with maximum extinction coefficients of 3.5 and 6.6 cm^2 per mole, as reported by Hartman and Schlafer (9), it interferes seriously with the spectral measurements.

For the spectrum in Fig. 1, a crystal of $VSO_4.7H_2O$ was chosen in which 97±1% of the vanadium was present as V^{++} with the V^{+++} concentration then being spectroscopically negligible.

ASSIGNMENT OF ABSORPTION BANDS

(a) Weak Field Treatment

Configuration $3d^3$ of V^{++} yields several terms which are separated by Coulombic electron interactions. However, only the ground state term ^4F and an upper ^4P term have the maximum spin multiplicity of four. If intercombination transitions are unimportant, all the other terms from $3d^3$ can be ignored.

In the heptahydrates of the transition ions for which the crystal structures are known, the central ion is surrounded by six water molecules at the corners of a regular octahedron,

Can. J. Chem. Downloaded from www.nrcresearchpress.com by 210.87.254.105 on 09/05/12
For personal use only.

with the seventh water molecule occupying a distant interstitial site. The electrostatic potential which perturbs the central ion has cubic symmetry and is of the form

$$V = D(x^4+y^4+z^4-\tfrac{3}{5}\bar{r}^4). \quad [1]$$

Such a field splits the ground term ^4F of V^{++} into three terms belonging to the cubic representations $^4A_2$, $^4T_2$, and $^4T_1$. The $^4A_2$ term is orbitally non-degenerate, the $^4T_2$ and $^4T_1$ terms threefold degenerate. The higher ^4P term is not split by V, but follows the representation $^4T_1$.

Thus a field with cubic symmetry produces four energy levels from the spin quartet terms. The three observed bands are then due to transitions between the $^4A_2$ ground level and the other three levels.

The matrix elements of V for the cubic orbitals are given in Table II, where D is the

TABLE II
Energy matrices for $3d^3$ in cubic field

	Weak field			
	$^4A_2$	$^4T_2$	$^4T_1(^4F)$	$^4T_1(^4P)$
$^4A_2$	$-12\,Dq$			
$^4T_2$		$-2\,Dq$		
$^4T_1(^4F)$			$6\,Dq$	$4\,Dq$
$^4T_1(^4P)$			$4\,Dq$	E
	Strong field			
	$^4A_2(t_2^3)$	$^4T_2(t_2^2e)$	$^4T_1(t_2^2e)$	$^4T_1(t_2e^2)$
$^4A_2(t_2^3)$	$-12\,Dq$			
$^4T_2(t_2^2e)$		$-2\,Dq$		
$^4T_1(t_2^2e)$			$-2\,Dq+12\,B$	$6\,B$
$^4T_1(t_2e^2)$			$6\,B$	$-8\,Dq+3\,B$

field parameter and $q = (2/105)\bar{r}^4$. Details of this treatment are given by Finkelstein and Van Vleck (10). The term separation matrix has been added to that for V, and appears as E, which is the $^4F-^4P$ energy in the absence of the cubic field.

Table III shows the cubic energy level diagram which results from the solution of the

TABLE III
Energy levels of hydrated V^{++}

Weak field origin	Cubic field	Strong field origin
^4P and ^4F	$^4T_1$	$3dt_2\ 3de^2$
^4F	$^4T_1$	$3dt_2^2\ 3de$
	$^4T_2$	
	$^4A_2$	$3dt_2^3$

secular determinant. The $^4A_2$ level is located at $-12\,Dq$, with respect to the free ion ^4F energy, and the $^4T_2$ level at $-2\,Dq$. The first observed transition energy 12,000 cm^{-1} is then $10\,Dq$, fixing Dq at 1200 cm^{-1}. The two $^4T_1$ levels depend upon the value of E. Table I shows the calculated positions of these levels with E = 11,320 cm^{-1}, which is the free ion value, and with E = 10,000 cm^{-1}, which gives the least difference between calculated and observed $^4T_1$ levels.

Can. J. Chem. Downloaded from www.nrcresearchpress.com by 210.87.254.105 on 09/05/12
For personal use only.

(b) Strong Field Treatment

In a cubic field the five $3d$ orbitals convert into an orbital triplet t_2 and an orbital doublet e at energy higher by 10 Dq. The ground state of V^{++} then is the term of highest multiplicity from $3dt_2^3$, which is $^4A_2$. Configuration $3dt_2^2 3de$ gives rise to $^4T_2$ and $^4T_1$ cubic terms, while $3dt_2 3de^2$ yields a $^4T_1$ term. No other spin quartet terms are possible.

The observed absorption bands are then allotted to transitions between the ground state $^4A_2$ and the three higher levels, these transitions involving the promotion of one or two t_2 electrons to e orbitals.

Tanabe and Sugano (11) have given the matrix elements for V between the strong field states. These elements have been added to the Coulombic repulsion elements in Table II, where $B = F_2 - 5F_4$, the F_n being Slater–Condon integrals. The identity of the roots of the strong field and weak field secular equations is apparent since $^4F - {}^4P = E = 15B$.

DISCUSSION

The dearth of optical data on the complexes of V^{++} has resulted in differing interpretations of their electronic states. Owen (4) assumed that the absorption bands of aqueous V^{++} reported by Dreisch and Kallscheuer (12) at 12,200 and 18,200 cm^{-1} corresponded to the two $^4A_2$–$^4T_1$ transitions and that another band should lie in the infrared region. This led to values for the parameters $Dq = 760\ cm^{-1}$ and $E = 9000\ cm^{-1}$.

On the other hand Jörgenson (2) used the band energies of 12,600, 18,200, and 26,500 cm^{-1} with the same assignment as presented here to calculate $Dq = 1260\ cm^{-1}$ (13).

On the basis of the spectrum of spectroscopically pure $VSO_4.7H_2O$, the "best values" we propose are $Dq = 1200\ cm^{-1}$ and $E = 10{,}000\ cm^{-1}$, which gives Racah's parameter $B = 670\ cm^{-1}$.

The decrease in E upon hydrating an ion such as V^{++} has been attributed by Owen (4) to covalent bonding between the central ion and the ligands. This would require that a small contribution from ligand orbitals be added to the $3d$ orbitals of the central ion to give the appropriate molecular orbitals. Then the distance between electrons would be increased and Coulombic interaction decreased, thus reducing term separations. Our results indicate that this effect is not so great for V^{++} as estimated by Owen.

The f-numbers for the three bands are listed in Table I. The value for the transition at 27,800 is not very reliable because the band is a shoulder on the strong charge transfer absorption and its area must be estimated. The relative intensities of the transitions are roughly 0.5:0.9:0.3. The higher T_1 band would be expected to have the lowest intensity since it requires that two $3dt_2$ electrons be promoted while the other transitions require only one promotion.

Nickel (II) with configuration $3d^8$ in $NiSO_4.7H_2O$ has the same energy level pattern as V^{++} and its three observed bands have f-numbers in order of increasing energy, 0.45×10^{-4}, 0.35×10^{-4}, and 0.6×10^{-4} (14). In this case contrary to expectations the higher transition $^3A_2$–$^3T_1$ has the greatest intensity. Several authors (see, for example, McClure (15)) have shown that this band includes transitions from the $^3A_2$ to $^1A_1$, $^1T_1$, and $^1T_2$ as well as $^3T_1$. However, Ballhausen and Liehr (16) have calculated recently that the intercombination transitions have negligible intensity for Ni^{++}, and that the intensity ratios can be explained with fair agreement by d–p mixing introduced through vibrational-electronic interaction. Calculations are under way to see if a similar mechanism applies to V^{++}.

Can. J. Chem. Downloaded from www.nrcresearchpress.com by 210.87.254.105 on 09/05/12
For personal use only.

ACKNOWLEDGMENT

One of us (O. G. H.) wishes to thank the National Research Council of Canada for financial assistance in the form of a Research Grant.

REFERENCES

1. W. Low. Ann. N. Y. Acad. Sci. **72**, 69 (1958).
2. C. K. Jörgenson. Report to the Tenth Solvay Council, Brussels. 1956.
3. P. George and D. S. McClure. Progress in inorganic chemistry. Vol. 1. Interscience Publishers, Inc., New York. 1959.
4. J. Owen. Proc. Roy. Soc. (London), A, **227**, 183 (1955).
5. J. S. Griffiths. J. Inorg. & Nuclear Chem. **2**, 1 (1956).
6. T. M. Dunn. J. Chem. Soc. 623 (1959).
7. G. Jones and J. H. Colvin. J. Am. Chem. Soc. **66**, 1563 (1944).
8. F. P. Treadwell. Analytical chemistry. Vol. 2. John Wiley & Sons, Inc., New York. 1935. p. 575.
9. H. Hartman and H. L. Schlafer. Z. Naturforsch. Pt. a, **6**, 760 (1951).
10. R. Finkelstein and J. H. Van Vleck. J. Chem. Phys. **8**, 790 (1940).
11. Y. Tanabe and S. Sugano. J. Phys. Soc. Japan, **9**, 753 (1954).
12. T. Dreisch and O. Kallscheuer. Z. physik. Chem. (Leipzig), B, **45**, 19 (1939).
13. L. E. Orgel. J. Chem. Phys. **23**, 1004 (1955).
14. O. G. Holmes and D. S. McClure. J. Chem. Phys. **26**, 1686 (1957).
15. D. S. McClure. J. Phys. and Chem. Solids, **3**, 311 (1957).
16. C. J. Ballhausen and A. D. Liehr. Mol. Phys. **2**, 123 (1959).

Can. J. Chem. Downloaded from www.nrcresearchpress.com by 210.87.254.105 on 09/05/12
For personal use only.

Can. J. Chem. Downloaded from www.nrcresearchpress.com by 210.87.254.42 on 09/05/12
For personal use only.

CELLULOSE COLUMN CHROMATOGRAPHIC SEPARATION OF LIGNIN OXIDATION PRODUCTS[1]

J. M. Pepper and M. Siddiqueullah[2]

ABSTRACT

A brief review is presented of the chemical nature and the methods of separation of those lignin derivatives obtained by the oxidation and/or alkaline hydrolysis of woody plants and isolated lignin or lignosulphonates. Nine such closely related derivatives, vanillin, syringaldehyde, *p*-hydroxybenzaldehyde, acetovanillone, acetosyringone, *p*-hydroxyacetophenone, vanillic acid, syringic acid, and *p*-hydroxybenzoic acid, were selected for a detailed study of their separation by cellulose column chromatography. Methods are presented whereby, by either a one- or two-stage process, a mixture of from any two to all nine of these compounds may be separated and the components recovered, using solvent systems which are suitable for subsequent quantitative spectrophotometric analysis. The application to a study of lignin chemistry is discussed.

INTRODUCTION

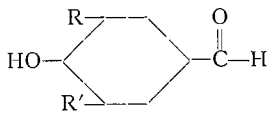
In recent years considerable attention has been given to the chromatographic separation of the products of oxidation and/or alkaline hydrolysis of the lignin component of woody plants and cereal straws. From the earlier work the characterization of these various lignin derivatives has contributed substantially to the present knowledge regarding the aromatic nature of lignin. More recently this phase of lignin research has been stimulated by an increased study of the fate of various C^{14}-labelled compounds which have been introduced into growing plants in a study of the biosynthetic pathway leading to lignin. The only reliable method whereby proof is obtained that the C^{14} has been incorporated into the lignin has been to obtain, from this fraction, purified degradation products whose specific activity may be measured. The larger the isolated lignin fragment the greater the structural significance that may be given to it and the more valuable the information that may be obtained from the position of the C^{14}-labelling. To date one of the more fruitful of such degradation studies has been the oxidation of lignin and, in particular, that using alkaline nitrobenzene as the oxidant system (1). By such means substantial yields of vanillin and a mixture of vanillin and syringaldehyde have been obtained from gymnosperms and angiosperms respectively. Along with both these compounds much smaller yields of *p*-hydroxybenzaldehyde have been found in the oxidation products of monocotyledons. This technique has been used by several workers interested in lignin chemistry and from various lignified materials the following other derivatives have been isolated and characterized (2, 3, 4): vanillic acid, syringic acid, *p*-hydroxybenzoic acid, acetovanillone, acetosyringone, 5-carboxyvanillin, 5-carboxyvanillic acid, 5-formylvanillin, 5-formylvanillic acid, dehydrodivanillin, and dehydrodivanillic acid.

In a series of investigations by both Pearl and McCarthy and their co-workers (5, 6, 7, 8, 9) using the alkaline cupric oxide, silver oxide, and mercuric oxide oxidations of lignosulphonates, many lignin degradation products have been obtained. These include

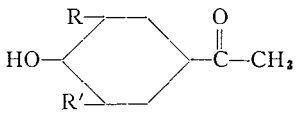
[1]*Manuscript received July 4, 1960.*
Contribution from the Department of Chemistry, University of Saskatchewan, Saskatoon, Saskatchewan. This paper constitutes part of the thesis submitted by M. Siddiqueullah in partial fulfillment of the requirements for the Ph.D. degree (1960). Presented, in part, at the 43rd Annual Conference, Chemical Institute of Canada, at Ottawa, June 13–15, 1960.
[2]*Colombo Plan Student in Canada at the University of Saskatchewan, 1957–1960.*

vanillin, syringaldehyde, vanillic acid, syringic acid, *p*-hydroxybenzoic acid, acetovanillone, acetosyringone, ferulic acid, *p*-coumaric acid, 5-carboxyvanillin, 5-carboxyvanillic acid, dehydrodivanillin, dehydrodivanillic acid, vanillil, 5-formylvanillin, 4,4′-dihydroxy-3,3′-dimethoxychalcone, vanillovanillone, and vanilloyl formic acid.

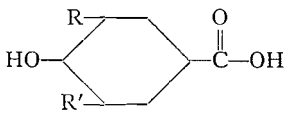
Apart from these lignin fragments that have been obtained from lignin under oxidizing conditions, many of the same compounds have been obtained by alkaline hydrolysis of the whole wood or of an isolated lignin. Hibbert (10, 11) early isolated vanillin and syringaldehyde by the alkaline hydrolysis of the lignin sulphonates from a deciduous wood. Smith (12) has reported the isolation of *p*-hydroxybenzoic acid from the products of a similar hydrolysis of the "native" lignin of *Populus tremula*. In another extensive investigation of the alkaline hydrolysis of various hardwoods and palms, Pearl and coworkers (13, 14, 15, 16, 17) isolated several phenolic compounds which may have arisen from the lignin fraction. The following such substances were identified: vanillin, syringaldehyde, *p*-hydroxybenzaldehyde, vanillic acid, syringic acid, *p*-hydroxybenzoic acid, ferulic acid, *p*-coumaric acid, acetovanillone, and acetosyringone. Stanek (18) using only an aqueous extraction, at 170°, of pre-extracted aspen wood obtained vanillin, syringaldehyde, coniferyl aldehyde, sinapaldehyde, vanillic acid, syringic acid, and *p*-hydroxybenzoic acid. Tanaka and Kondo (2) have reported the isolation also of both pyrogallol-1,3-dimethyl ether and 3,3′-dimethoxy-4,4′-dihydroxystilbene from the alkaline hydrolysis products of *Fagus cremata* and of the latter compound from red pine sawdust.



(I) R = H, R′ = OCH_3
(II) R = R′ = OCH_3
(III) R = R′ = H



(IV) R = H, R′ = OCH_3
(V) R = R′ = OCH_3
(VI) R = R′ = H



(VII) R = H, R′ = OCH_3
(VIII) R = R′ = OCH_3
(IX) R = R′ = H

Several methods have been devised for the separation of these compounds. Hibbert (19, 20, 21) reported separations of guaiacyl and syringyl compounds based upon the differential solubilities of their potassium and ammonium salts, upon fractional sublimation in high vacuum, and upon their conversion to the *p*-nitrobenzoate derivatives. The *m*-nitrophenylhydrazones of the phenolic aldehydes have been used also to assist in their separation (22). A qualitative paper chromatographic separation of vanillin and syringaldehyde was effected in 1949 by Bland (23). Later in 1951, a similar separation was reported by Pearl and Dickey (24) using a column of acid-washed Magnesol and Celite. Using benzene–ethanol (20:1) as the developer, Pearl and Beyer (25) were able to separate vanillic acid and protocatechuic acid on a similar type column. Stone and Blundell (26) further developed the paper chromatographic separation of the phenolic aldehydes into a quantitative analytical procedure. *n*-Butyl ether saturated with water separated vanillin and syringaldehyde but if *p*-hydroxybenzaldehyde were also present a suitable solvent system was petroleum ether (100–120°):*n*-butyl ether (6:1) saturated with water. These authors were the first to apply this method to the quantitative analyses of the products of the alkaline nitrobenzene oxidation of protolignin. In 1955, Brown and Neish (27) reported a partition chromatographic separation of these three aldehydes on a column of acid-washed Celite 535 using a two-step elution technique, i.e. isooctane

Can. J. Chem. Downloaded from www.nrcresearchpress.com by 210.87.254.42 on 09/05/12
For personal use only.

containing 10% benzene and saturated with water to elute vanillin and syringaldehyde, followed by benzene saturated with water for elution of the *p*-hydroxybenzaldehyde. To separate the various combinations of the alkaline hydrolyses products referred to earlier, the principal method has been paper chromatography with a variety of developers. The following solvent systems have been used: butanol saturated with 2% ammonia (13, 16, 17, 18), butanol:pyridine:water (10:3:3) (13, 16, 17), *n*-heptane:*n*-butyl ether:water (6:1:1) (15, 17), benzene saturated with formic acid (11), *n*-butyl ether saturated with water (18). Stanek (18) also used petroleum ether (65–110°):ethanol (50:1) as the developer for an acid-washed Magnesol column.

In 1953, Newcombe and Reid (28) reported the complete separation of vanillin, acetovanillone, verataldehyde, and acetoveratrone using chromatographic paper that had been sprayed with dilute sodium bisulphite and a solvent system consisting of hexane:chloroform:water (9:1:10). Later Pearl (7) employing a paper that had been sprayed only partially with sodium bisulphite, and developing with *n*-heptane:*n*-butyl ether:water (6:1:1) successfully separated vanillin, syringaldehyde, acetovanillone, and acetosyringone. Leopold (3) found that a phosphate-buffered paper (pH 7.5) was advantageous for the separation of acids.

Three other analytical procedures have been applied to the separation of lignin oxidation products. Cellulose column chromatography using butanol – 2% aqueous ammonia as the developer has been used by Pearl and Beyer (5, 29). McCarthy *et al.* effected a separation using anion exchange resins and also electrophoresis. Recently Kratzl and Puschmann (30) have applied the semimicro thin-layer chromatographic technique, developed by Stahl, to the separation of C^{14}-labelled oxidation products.

It was therefore clear that in an extensive study of the products of lignin oxidation, the large variety of such possible derivatives had to be considered and any quantitative procedure for their estimation must ensure no interference of one with another. Starting with the established method of Stone and Blundell (26) using the solvent system of petroleum ether (100–120°):*n*-butyl ether:water (6:1:1) (15 hours), the possible interference of vanillic, syringic, *p*-hydroxybenzoic acids on the separation of vanillin and syringaldehyde was investigated. The vanillin and *p*-hydroxybenzaldehyde, which moved the farthest, were well resolved but the syringaldehyde, which moved only slightly, was not separated distinctly from the acids which tended to tail from the base line. This may account, in part, for the usually poorer reproducibility of the syringaldehyde analysis by this method if applied to the oxidation of lignin materials. Subsequently, a study of the separation of the three aldehydes (I, II, III) and the three ketones (IV, V, VI) showed that using the same solvent system (16 hours) the aldehyde and its corresponding ketone had similar R_f values. It became clear that the quantitative analysis for vanillin, syringaldehyde, and *p*-hydroxybenzaldehyde by the Stone and Blundell method would be inaccurate should the conditions of oxidation be such that some of these other substances were also produced.

In an attempt to solve these interference problems and at the same time to devise a system whereby the products of large-scale oxidation may be separated, attention was directed to the use of cellulose column chromatography. Since usually not more than half of the original lignin can be accounted for in the form of the lower molecular weight oxidation products of the types outlined, it was hoped that this method would permit of the removal and separation of these units so that attention could then be directed to the purified lignin residues left on the column. The research reported here was limited to the study of the cellulose column chromatographic separation of the nine related possible

Can. J. Chem. Downloaded from www.nrcresearchpress.com by 210.87.254.42 on 09/05/12
For personal use only.

products of lignin oxidation: vanillin (I), syringaldehyde (II), *p*-hydroxybenzaldehyde (III), acetophenone (IV), acetosyringone (V), *p*-hydroxyacetophenone (VI), vanillic acid (VII), syringic acid (VIII), and *p*-hydroxybenzoic acid (IX). The study was conducted in three parts: (*a*) the resolution of a mixture of aldehydes alone, ketones alone, or acids alone; (*b*) the resolution of a mixture of any six components comprising the aldehydes and ketones, aldehydes and acids, or ketones and acids; and (*c*) the resolution of a mixture of all nine compounds. The synthetic mixtures were prepared from highly purified compounds using amounts ranging from 2 to 5 mg. The mixture of pure compounds was charged at the top of columns prepared from partially hydrated cellulose powder and the eluting solvents collected in 5-ml fractions. The presence of the phenolic substances was detected using the method of Barton *et al.* (31). In each case blanks using the individual pure compound were run to determine the order of elution.

Separation of Three-component Mixtures

Using the recommended (26) solvent system for the separation of aldehydes by paper chromatography (petroleum ether (100–120°):*n*-butyl ether:water (6:1:1) (organic phase)) good resolution was achieved on the cellulose column. A second developing system was found which resulted in an even more efficient separation using a shorter column. By this procedure the column was first eluted with cyclohexane saturated with water to remove and separate the vanillin (I) and syringaldehyde (II), and then with cylohexane: diethyl ether:water (6:1:1) (organic phase) (or an 8:1:1 mixture) to remove the *p*-hydroxybenzaldehyde (III). It is of interest to note the inversion in the order of elution of II and III using the two different solvents. The three ketones were separated in a similar manner. The elution and separation of the three acids was found to be best accomplished using a cyclohexane:diethyl ether:water (8:1:1) system to remove first the vanillic acid (VII) and then the *p*-hydroxybenzoic acid (IX). By increasing the solvent power using a similar system but in a 4:1:1 ratio, the syringic acid (VIII) was readily removed.

Separation of Six-component Mixtures

Since it was not possible to separate the aldehydes from the ketones by any of the solvent systems studied, recourse was made to the principle outlined by Newcombe and Reid (28) whereby the movement of aldehydes may be preferentially retarded using a sodium-bisulphite-sprayed paper. It was found that an effective separation may be obtained by using the technique whereby the six components were added to a cellulose column at the top of which was a small section containing cellulose saturated with sodium bisulphite. By first developing with the cyclohexane:water system the acetovanillone (IV) and the acetosyringone (V) were eluted and resolved in that order. The *p*-hydroxyacetophenone (VI) was then removed by changing to a cyclohexane:diethyl ether:water (8:1:1) system. Under these conditions it was proved, by a series of separate experiments, that no aldehydes were removed from the column nor were any ketones left on the column. To release, recover, and resolve the aldehydes, hydrochloric acid was added, the aldehydes washed through the column using diethyl ether, and then subsequently separated on a second column as described above.

In the case of the mixture of aldehydes and acids or ketones and acids the two-column technique was not necessary. Using the one cellulose column, and the following series of solvent changes, a complete separation and recovery of each compound of either six-component mixture was achieved. This was accomplished by using first the cyclohexane: water system to elute vanillin (I) (or acetovanillone IV), followed by syringaldehyde (II)

Can. J. Chem. Downloaded from www.nrcresearchpress.com by 210.87.254.42 on 09/05/12
For personal use only.

(or acetosyringone V), then the cyclohexane:diethyl ether:water (8:1:1) mixture to remove the *p*-hydroxybenzaldehyde (III) (or *p*-hydroxyacetophenone (VI)), the vanillic acid (VII), and the *p*-hydroxybenzoic acid (IX) in that order, and finally using cyclohexane:diethyl ether:water (4:1:1) to elute the syringic acid (VIII).

Separation of the Nine-component Mixture

To separate the components of a mixture of all nine components (I through IX), a two-stage procedure was required. A column of cellulose was used on the top of which was a smaller layer of cellulose saturated with sodium bisulphite. Elution of the ketones was done using cyclohexane–water to resolve the acetovanillone (IV) and acetosyringone (V) followed by cyclohexane:diethyl ether:water (8:1:1) to remove the *p*-hydroxyacetovanillone (VI). The three acids were then washed through the column with diethyl ether and the aldehydes first released by the addition of hydrochloric acid and then also washed through using ether. The recombined acids and aldehydes were charged to a second column and eluted and separated as described earlier.

This technique has been applied to the analysis of the products of the alkaline nitrobenzene oxidation, at 180°, of aspen wood lignin. Under these conditions no ketones were detected and hence this aspect of the interference objections raised earlier to Stone and Blundell's method is not valid. However, this does not mean that under either milder or stronger conditions of oxidation, the proportions of aldehydes, ketones, and acids may not vary and then this technique for their separation would become of value. This may be important for those studies requiring the isolation of purified C^{14}-labelled compounds especially of the C_6–C–C type. It is becoming evident that the other products of lignin oxidation, formed concurrently with the simple units discussed here, must be studied. It should be possible using this general technique to remove all the smaller molecular weight products from a cellulose column and thus leave behind the larger units which may subsequently be washed through and their structure investigated.

EXPERIMENTAL

Reagents

Genuine Whatman cellulose powder, standard grade, was obtained from W. and R. Balston, Ltd., England.

The syringaldehyde and acetosyringone were synthesized by previously reported methods (32, 33). All other chemicals were obtained from commercial sources and highly purified before use.

General Chromatographic Procedure

Preparation of Columns

The chromatographic columns were made of tubing 18 mm I.D. and 55 cm long, fitted at the lower end with a perforated disk immediately above a stopcock. The preferred method of packing the column was as follows. To each 10 g of cellulose powder was added 2.5 ml water and this mixture was intimately mixed until wetting was uniform and complete. This hydrated cellulose powder was then mulled using cyclohexane saturated with water (10 ml) and any lumps well broken before it was charged into the column using the wet method. Occasional pressing down of the cellulose during addition was beneficial. Each 10 g of cellulose packing was equivalent to about 3 inches in length.

The sodium bisulphite "traps" were prepared as follows. Each 2 g of cellulose powder was thoroughly mixed with a slurry of 1 g of sodium bisulphite in 1 ml of water. This mixture was then added onto the top of a cellulose column as described above for those

Can. J. Chem. Downloaded from www.nrcresearchpress.com by 210.87.254.42 on 09/05/12
For personal use only.

separations involving aldehydes and ketones. Such a "trap" was approximately 0.5 inch in length.

Charging of Synthetic Mixtures

The samples were added in concentrated ether solution to 1 g of cellulose powder which had been thoroughly mixed with 0.5 ml water. After the ether had evaporated, the powder was moistened with a few drops of cyclohexane saturated with water before packing onto the top of the column as described above.

Nature of Eluting Solvents

Solvent A = petroleum ether (100–120°):*n*-butyl ether:water (6:1:1) (organic phase).
Solvent B = cyclohexane saturated with water.
Solvent C = cyclohexane:diethyl ether:water (6:1:1) (organic phase).
Solvent D = solvent C (8:1:1).
Solvent E = solvent C (4:1:1).

Elution Technique

The eluting solvent was allowed to pass through the column while under a slight positive pressure of nitrogen so that the rate of elution varied from approximately 0.5 drop/second for the short columns to 1 drop/second for the longer columns. For those experiments which required changing of the solvent, the first solvent was allowed to flow until its upper level coincided with the top of the packing, before addition of the second solvent system. All eluates were collected in 5-ml fractions and the presence of each phenolic substance was determined using the ferric chloride – potassium ferricyanide spray reagent described by Barton *et al.* (31).

Chromatographic Separation of Three-component Mixtures

Aldehydes

To a 50-g column a mixture of vanillin (I) (4.48 mg), syringaldehyde (II) (5.48 mg), and *p*-hydroxybenzaldehyde (III) (4.65 mg) was added. Upon development using solvent A, I appeared in fractions 25–36, III in 45–67, and II in 75–107.

A second resolution of these aldehydes was made using a 20-g column and a mixture of I (4.5 mg), II (4.1 mg), and III (3.8 mg). By eluting first with solvent B, I appeared in fractions 13–23, II in 44–75, but even after a further 150 fractions III did not appear. After changing to solvent C, III was found in fractions 7–12.

Ketones

To a 10-g column a mixture of acetovanillone (IV) (5.6 mg), acetosyringone (V) (5.4 mg), and *p*-hydroxyacetophenone (VI) (5.0 mg) was added. Using solvent B, IV appeared in fractions 4–12 and V in fractions 21–39. Then solvent C was used whereupon VI appeared in fractions 2–5.

Acids

To a 25-g column a mixture of vanillic acid (VII) (1.1 mg), syringic acid (VIII) (5.1 mg), and *p*-hydroxybenzoic acid (IX) (2.9 mg) was added. Using solvent D, VII appeared in fractions 58–85 and IX in 90–130. After changing to solvent E, VIII appeared in fractions 21–76.

Chromatographic Separation of Six-component Mixtures

Aldehydes and Ketones

To a 10-g cellulose column on top of which was a 2-g cellulose – sodium bisulphite column, a mixture of vanillin (I) (4.65 mg), syringaldehyde (II) (4.10 mg), *p*-hydroxybenzaldehyde (III) (4.18 mg), acetovanillone (IV) (4.34 mg), acetosyringone (V) (4.23

Can. J. Chem. Downloaded from www.nrcresearchpress.com by 210.87.254.42 on 09/05/12
For personal use only.

mg), and *p*-hydroxyacetophenone (VI) (4.48 mg) was added. Using solvent B, IV appeared in fractions 5–18 and V in 28–55. After changing to solvent D, VI appeared in fractions 5–11. Excess hydrochloric acid (2 ml conc. in 6 ml water) was then added to the top of the column and forced through by means of nitrogen pressure. The released aldehydes were washed through the column using diethyl ether, the ether solution dried over anhydrous $MgSO_4$ and then concentrated to 1 ml. This sample was then charged to a 10-g column. Using solvent B, I appeared in fractions 3–19, and II in 25–48. After changing to solvent D, III appeared in fractions 4–13.

Aldehydes and Acids

(See procedure below.)

Ketones and Acids

To a 25-g column a mixture of acetovanillone (IV) (4.97 mg), acetosyringone (V) (4.68 mg), *p*-hydroxyacetophenone (VI) (5.06 mg), vanillic acid (VII) (0.9 mg), syringic acid (VIII) (3.29 mg), and *p*-hydroxybenzoic acid (IX) (3.64 mg) was added. Using solvent B, IV appeared in fractions 22–35 and V in 68–110. By changing then to solvent D, VI appeared in fractions 15–23, VII in 70–102, and IX in 115–175. After changing again to solvent E, VIII appeared in fractions 18–76.

Chromatographic Separation of Aldehydes, Ketones, and Acids

To a 10-g column, on top of which was a 2-g cellulose – sodium bisulphite column, a mixture of vanillin (I) (5.00 mg), syringaldehyde (II) (4.89 mg), *p*-hydroxybenzaldehyde (III) (5.62 mg), acetovanillone (IV) (5.42 mg), acetosyringone (V) (5.55 mg), *p*-hydroxyacetophenone (VI) (5.05 mg), vanillic acid (VII) (1.08 mg), syringic acid (VIII) (3.08 mg), and *p*-hydroxybenzoic acid (IX) (3.32 mg) was added. Using solvent B, IV appeared in fractions 6–20 and V in fractions 26–64. After changing to solvent D, VI appeared in fractions 6–12.

Diethyl ether (200 ml) was passed through the column to wash out the free acids. Excess hydrochloric acid (2 ml conc. HCl in 6 ml water) was added to the top of the column and passed through using slight nitrogen pressure. The released aldehydes were washed from the column using ether. The combined ether extracts were dried over anhydrous magnesium sulphate and concentrated to 1 ml. This sample was charged to a 25-g cellulose column. Using solvent B, I appeared in fractions 18–32 and II in fractions 58–90. After changing to solvent D, III appeared in fractions 14–22, VII in 73–112, and IX in 124–181. After changing again to solvent E, VIII appeared in fractions 23–73.

ACKNOWLEDGMENTS

We wish to express our thanks for the assistance given to one of us (M. S.) by the Pakistan Council of Scientific and Industrial Research during the tenure of a Colombo Plan Scholarship. We also gratefully acknowledge the support of the National Research Council, and the donation of vanillin from Howard Smith Chemicals Limited and of acetovanillone from the Ontario Paper Company, Limited.

REFERENCES

1. F. E. BRAUNS. The chemistry of lignin. Academic Press Inc., New York. 1952. Chap. XIX.
2. J. TANAKA and T. KONDO. Mokuzai Gakkaishi, **3**, 28 (1957) (Chem. Abstr. **51**, 11711 (1957)); Mokuzai Gakkaishi, **4**, 34 (1958) (Chem. Abstr. **52**, 11410 (1958)); Mokuzai Gakkaishi, **5**, 105 (1959) (Chem. Abstr. **53**, 22919 (1959)); Parupukami Kogyo Zasshi, **11**, 29 (1957) (Chem. Abstr. **52**, 6784 (1958)).
3. B. LEOPOLD. Acta Chem. Scand. **6**, 38 (1952).
4. J. C. PEW. J. Am. Chem. Soc. **77**, 2831 (1955).

Can. J. Chem. Downloaded from www.nrcresearchpress.com by 210.87.254.42 on 09/05/12
For personal use only.

5. I. A. PEARL and D. L. BEYER. J. Am. Chem. Soc. **76**, 6106 (1954).
6. I. A. PEARL and D. L. BEYER. Tappi, **39**, 171 (1956).
7. I. A. PEARL and D. L. BEYER. Tappi, **42**, 800 (1959).
8. D. W. GLENNIE, H. TECHLENBERG, E. T. REAVILLE, and J. L. MCCARTHY. J. Am. Chem. Soc. **77**, 2409 (1955).
9. R. E. DAVIS, E. T. REAVILLE, O. P. PENISTON, and J. L. MCCARTHY. J. Am. Chem. Soc. **77**, 2405 (1955).
10. F. LEGER and H. HIBBERT. Can. J. Research, B, **16**, 151 (1938).
11. W. L. HASKINS, G. F WRIGHT, and H. HIBBERT. J. Am. Chem. Soc. **59**, 2447 (1937).
12. D. C. C. SMITH. J. Chem. Soc. 2347 (1955).
13. I. A. PEARL, D. L. BEYER, B. JOHNSON, and S. WILKINSON. Tappi, **40**, 374 (1957).
14. I. A. PEARL. Tappi, **41**, 621 (1958).
15. I. A. PEARL, D. L. BEYER, and B. JOHNSON. Tappi, **41**, 255 (1958).
16. I. A. PEARL, D. L. BEYER, S. S. LEE, and D. LASKOWSKI. Tappi, **42**, 61 (1959).
17. I. A. PEARL, D. L. BEYER, and D. LASKOWSKI. Tappi, **42**, 779 (1959).
18. D. A. STANEK. Tappi, **41**, 601 (1958).
19. M. J. HUNTER and H. HIBBERT. J. Am. Chem. Soc. **61**, 2190 (1939).
20. J. J. PYLE, L. BRICKMAN, and H. HIBBERT. J. Am. Chem. Soc. **61**, 2198 (1939).
21. R. H. J. CREIGHTON, J. L. MCCARTHY, and H. HIBBERT. J. Am. Chem. Soc. **63**, 3049 (1941).
22. K. KRATZL. Mikrochim. Acta, 159 (1956).
23. D. E. BLAND. Nature, **164**, 1093 (1949).
24. I. A. PEARL and E. E. DICKEY. J. Am. Chem. Soc. **73**, 863 (1951).
25. I. A. PEARL and D. L. BEYER. Anal. Chem. **24**, 1366 (1952).
26. J. E. STONE and M. J. BLUNDELL. Anal. Chem. **23**, 771 (1951).
27. S. A. BROWN and A. C. NEISH. Can. J. Biochem. and Physiol. **33**, 948 (1955).
28. A. G. NEWCOMBE and S. G. REID. Nature, **172**, 455 (1953).
29. I. A. PEARL and D. L. BEYER. J. Am. Chem. Soc. **76**, 2224 (1954).
30. VON K. KRATZL and G. PUSCHMANN. Holzforschung, **14**, 1 (1960).
31. G. BARTON, R. S. EVANS, and J. A. F. GARDNER. Nature, **170**, 249 (1952).
32. J. M. PEPPER and J. A. MACDONALD. Can. J. Chem. **31**, 476 (1953).
33. L. W. CRAWFORD, E. O. EATON, and J. M. PEPPER. Can. J. Chem. **34**, 1562 (1956).

Can. J. Chem. Downloaded from www.nrcresearchpress.com by 210.87.254.42 on 09/05/12
For personal use only.

Can. J. Chem. Downloaded from www.nrcresearchpress.com by 210.87.254.6 on 09/05/12
For personal use only.

PHOTOLYSIS OF AZOISOPROPANE[1]

R. H. RIEM[2] AND K. O. KUTSCHKE

ABSTRACT

The photolysis of azoisopropane has been reinvestigated in an attempt to obtain a better understanding of the discrepancies found between the behavior of *sec*-propyl radicals produced from this source (1) and other sources under similar experimental conditions.

Analytical difficulties encountered in an earlier investigation (1) were avoided through the extensive use of gas chromatography.

It was found necessary to include an internal conversion reaction among the primary processes to explain the observed phenomena. A rough estimate of $E_{\text{internal conversion}} - E_{\text{dissociation}} = (1.99 \pm 0.72)$ kcal/mole has been deduced. This is believed to be the first observation of $E_{\text{internal conversion}} > E_{\text{dissociation}}$. An explanation of this observation remains a matter of conjecture though a tentative suggestion is offered.

The data also leads to results in agreement with those found for other azo compounds and in agreement with the rates of reactions of *sec*-propyl radicals obtained from other sources under similar conditions.

INTRODUCTION

Recent studies of the rates of reactions of *sec*-propyl radicals (2, 3, 4) present a slightly different picture to that obtained by Durham and Steacie (1) in the photolysis of azoisopropane. To some extent these differences can be traced back to the analytical difficulties encountered by Durham and Steacie. Since many of these difficulties can now be avoided, a reinvestigation of the photolysis of azoisopropane, making extensive use of gas chromatography, was undertaken. A further reason for the reinvestigation was the rather poor agreement at lower temperatures between the mechanism proposed and the experimental data obtained by Durham and Steacie (1).

EXPERIMENTAL

The high-vacuum apparatus was in general of the design usually employed in these laboratories; however, stopcocks and oil diffusion pumps were used in order to obtain a mercury-free system. Part of the analytical line, consisting of a simple mercury-containing system used to handle noncondensable reaction products, was connected to the mercury-free system in the manner described by McElcheren, Wijnen, and Steacie (5).

The quartz reaction cell, 10 cm in length with a volume of 180 cc, was enclosed in a thermostatted hot box in which the temperature could be controlled to within 1/2° C. A medium pressure Hanovia S500 mercury arc was employed as the light source. This, in conjunction with the filter A described by Kasha (6), supplied incident radiation consisting of the 3662.9 Å and 3663.3 Å lines. The ultraviolet absorption spectrum of azoisopropane shows one large band extending from 2900 Å to 3900 Å with a flat maximum at 3540 Å. A 935 phototube positioned behind the reaction cell and outside the hot box was coupled to a sensitive galvanometer to measure the transmitted intensity. By using azomethane in the reaction cell as an actinometer and making the assumption that, with this compound, $\Phi_{N_2} = 1$ (7), it was possible to correlate directly the difference in galvanometer readings obtained with the empty cell and the filled cell with the number of quanta absorbed per cubic centimeter per second. The error introduced into the actinometer

[1]*Manuscript received August 5, 1960.*
Contribution from the Division of Pure Chemistry, National Research Council, Ottawa, Canada.
Issued as N.R.C. No. 6006.
[2]*National Research Council of Canada Postdoctorate Fellow, 1958–60.*

measurements by any slight deviation from unity in the quantum yield of nitrogen for azomethane is felt to be no larger than the errors involved in the use of an external actinometer. Reproducibility in these measurements was found to be 3%.

A small cold finger attached to the reaction cell protruded slightly beyond the hot box; as this construction entailed a considerable amount of tubing outside the illuminated volume, the reactant was continuously circulated during a run by means of a small impeller. In an actual run the contents of the cell were condensed into the finger prior to opening the cell to the analytical line. By allowing the finger subsequently to warm very slowly, an effective separation of the noncondensables from the rest of the material, which shows a very strong tendency to occlusion, was obtained. In this manner it was found possible to obtain a quantitative separation in a reasonable time (1 hour). The analytical line consisted of two traps and a Ward–Le Roy still after which a two-way stopcock was placed to enable the products to be diverted either into the continuation of the mercury-free system to the introduction trap of a gas chromatography column, or into the small oil diffusion pump forming the first part of the bridge section (5) leading to the mercury system. The mercury system also consisted of a toepler pump, gas burette, and a mass spectrometer take-off.

The following fractions were removed and analyzed:

Noncondensables.—This contained only nitrogen, which was removed at −198° C and measured in the gas burette.

Second fraction −135° C.—This fraction consisted of C_3H_6 and C_3H_8. Analysis was done by mass spectrometry after the total pressure had been measured in the gas burette.

Liquid products.—All further material was introduced onto a 15-ft column (8) of 1/4-in. O.D. copper tubing packed with 30% bis-2,2-methoxyethoxyethylether (Eastman Kodak) on 30–60 mesh (Johns-Manville) Chromosorb (temperature, 40° C; flow, 64 ml H_2/minute). The reaction product 2,3-dimethylbutane emerged after 1/2 hour while the excess unreacted azoisopropane was retained for 2 hours. Though it was clearly not necessary to use such a long column for this separation, this length was necessary to obtain a separation between acetone and azoisopropane. This situation arose when purifying the starting material. The azoisopropane employed in this work was shown by gas chromatography to contain trace quantities of amines or hydrazines (mass spectrometric identification), 2,3-dimethylbutane, and approximately 5% acetone. As the separation of acetone from azoisopropane proved impossible by means of a Ward still distillation at −85° C (1) all material used in these experiments was purified by gas chromatography on the column described previously. Azoisopropane purified in this manner showed only a single peak when passed through a 10-ft column, 5 mm internal diameter, containing 25% dinonylphthalate + 5% glycerol on fire brick (temperature, 29° C; flow, 45 ml H_2/minute).

Azoisopropane has been subjected to thermal decomposition at different pressures at 127° C. Within the range of time employed in the photolytic experiments there was no evidence of thermal decomposition of azoisopropane.

RESULTS AND DISCUSSION

The following mechanism is proposed to explain the results obtained in the photolysis of azoisopropane between 34.7° C and 127° C. In the mechanism AIP refers to the normal ground-state molecule of azoisopropane while AIP* refers to an electronically excited state.

Can. J. Chem. Downloaded from www.nrcresearchpress.com by 210.87.254.6 on 09/05/12
For personal use only.

Can. J. Chem. Downloaded from www.nrcresearchpress.com by 210.87.254.6 on 09/05/12
For personal use only.

$AIP \xrightarrow{h\nu} AIP^*$	I_a		
$AIP^* \rightarrow N_2 + 2sec\text{-}C_3H_7$	k_1	[1]	Primary processes
$AIP^* + AIP \rightarrow 2AIP$	k_2	[2]	Primary processes
$AIP^* \rightarrow AIP$	k_t	[6]	Primary processes
$2sec\text{-}C_3H_7 \rightarrow C_3H_6 + C_3H_8$	k_3	[3]	Secondary processes
$2sec\text{-}C_3H_7 \rightarrow C_6H_{14}$	k_4	[4]	Secondary processes
$sec\text{-}C_3H_7 + C_3H_7NNC_3H_7 \rightarrow C_3H_8 + C_3H_6NNC_3H_7$	k_5	[5]	Secondary processes

Primary Processes

Assuming a steady-state concentration of AIP* (10) one arrives at the following expression for the reciprocal quantum yield of nitrogen:

$$[I] \qquad 1/\Phi_{N_2} = 1+(k_2/k_1)[AIP]+k_t/k_1.$$

A plot of the reciprocal quantum yield of nitrogen against [AIP], at each temperature measured, should be linear with intercepts of $1+(k_t/k_1)$. The experimental data from Table I (units employed are quanta, cubic centimeters, seconds, and molecules) plotted in this manner in Fig. 1 do in fact give five lines with intercepts significantly larger than unity. Moreover, the values of these intercepts increase in a continuous manner with increasing temperature, this in contrast to the decreasing intercepts found with azoethane

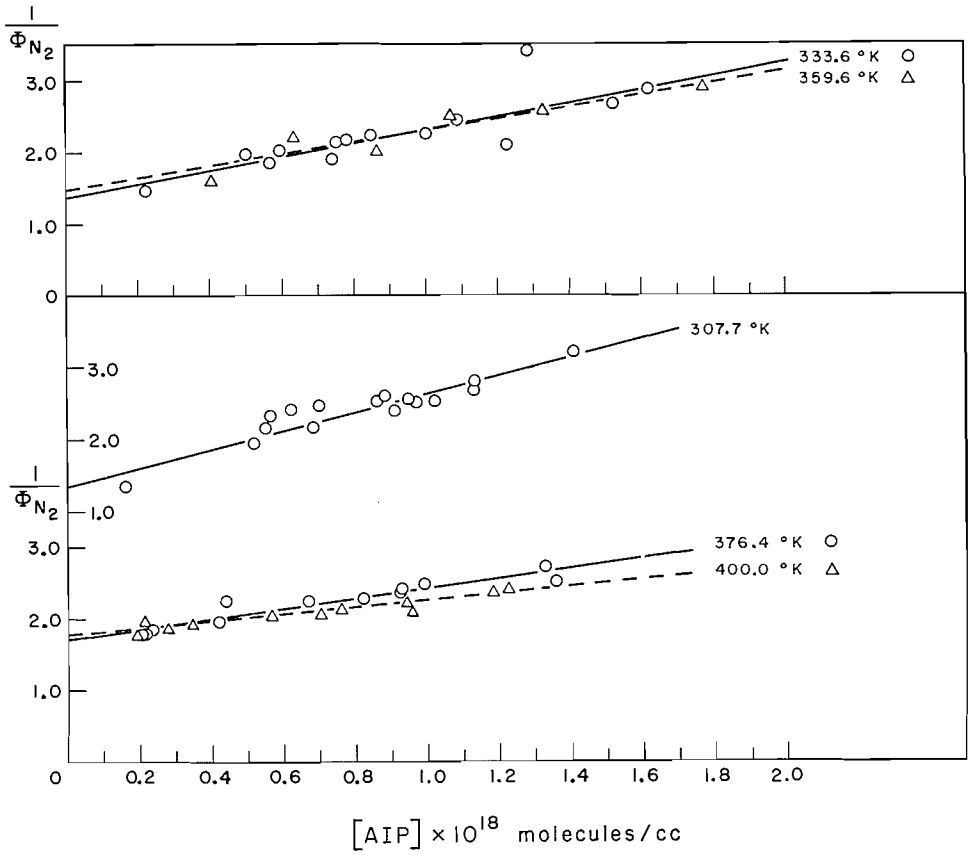


FIG. 1. Plots of expression [I].

TABLE I

[AIP] 10^{-18} molecules per cc per sec	I_a 10^{-12} quanta per cc per sec	Φ_{N_2}	$R_{C_6H_{14}}$ 10^{-12} molecules per cc per sec	$R_{C_3H_6}/R_{C_6H_{14}}$	$R_{C_5}/R_{C_6H_{14}}$
		Temp. 307.7° K (hydrocarbons not determined)			
0.166	1.78	0.733			
0.521	6.75	0.508			
0.557	10.36	0.459			
0.566	11.65	0.427			
0.625	8.18	0.361			
0.687	8.66	0.328			
0.706	12.49	0.488			
0.866	15.80	0.394			
0.882	12.67	0.385			
0.913	15.85	0.416			
0.953	16.88	0.391			
0.976	16.27	0.392			
1.033	16.81	0.392			
1.132	15.20	0.371			
1.136	15.56	0.354			
1.411	20.09	0.312			
		Temp. 333.6° K			
0.225	3.85	0.679	1.671	0.515	1.121
0.501	9.28	0.510	—	—	—
0.569	10.35	0.537	3.497	0.536	1.175
0.597	11.75	0.491	—	—	—
0.743	15.25	0.524	—	—	—
0.756	13.46	0.467	—	—	—
0.783	14.54	0.459	—	—	—
0.850	15.90	0.446	4.400	0.531	1.198
1.006	18.37	0.443	—	—	—
1.090	19.67	0.403	—	—	—
1.228	20.81	0.473	—	—	—
1.285	23.25	0.329	5.098	0.560	1.279
1.522	24.20	0.374	—	—	—
1.619	27.76	0.345	5.957	0.557	1.357
		Temp. 359.6° K			
0.405	8.19	0.592	2.869	0.534	1.240
0.636	12.98	0.453	3.348	0.548	1.329
0.865	15.86	0.499	4.560	0.539	1.308
1.072	20.06	0.399	4.281	0.557	1.443
1.324	22.94	0.384	4.582	0.553	1.497
1.773	26.07	0.341	—	—	—
		Temp. 376.4° K			
0.210	3.72	0.560	1.153	0.530	1.266
0.216	3.84	0.557	—	—	—
0.239	4.14	0.543	—	—	—
0.423	8.02	0.512	2.310	0.598	1.373
0.443	8.97	0.445	2.046	0.595	1.481
0.454	—	—	2.123	0.589	1.462
0.674	12.46	0.445	—	—	—
0.827	15.38	0.436	3.436	0.541	1.467
0.924	16.27	0.424	3.238	0.572	1.711
0.936	17.05	0.414	—	—	—
0.995	18.65	0.402	—	—	—
1.331	22.68	0.369	3.634	0.595	1.901
1.363	22.54	0.399	4.114	0.581	1.736
		Temp. 400.0° K			
0.193	4.07	0.557	1.272	0.545	1.325
0.214	4.84	0.512	—	—	—
0.280	7.16	0.534	2.072	0.509	1.375
0.348	7.07	0.518	1.890	0.552	1.464
0.569	10.86	0.488	—	—	—
0.706	13.41	0.480	2.882	0.604	1.800
0.760	15.58	0.466	3.236	0.534	1.838
0.946	17.66	0.443	3.404	0.531	1.936
0.959	18.47	0.475	4.022	0.508	1.810
1.185	21.42	0.421	—	—	—
1.224	21.79	0.415	—	—	—

Can. J. Chem. Downloaded from www.nrcresearchpress.com by 210.87.254.6 on 09/05/12
For personal use only.

(9). Values for k_2/k_1 were obtained from the slopes of the lines in Fig. 1, and are given in Table II. The related Arrhenius plot, Fig. 3, indicates that $E_1-E_2 = (2.28\pm0.35)$ kcal/

TABLE II

T, °K	(k_2/k_1) 10^{18}	S.D.	Inter.	S.D.	(k_i/k_1)
307.2	1.28	0.13	1.35	0.11	0.35
333.6	0.93	0.14	1.38	0.14	0.38
359.6	0.86	0.15	1.46	0.17	0.46
376.4	0.707	0.075	1.715	0.061	0.715
400.0	0.500	0.050	1.753	0.031	0.753

mole and $A_2/A_1 = (3.2\pm1.9)\ 10^{-20}$ (molecule/cc)$^{-1}$.

The mechanism proposed above differs from that of Durham and Steacie (1) in the inclusion of reaction [6]. Neglecting this reaction leads to

[II] $$1/\Phi_{N_2} = 1+(k_2/k_1)\,[\mathrm{AIP}],$$

a relation which is not supported by the experimental data.

There is the possibility of a reduction in the quantum yield of nitrogen through an activated molecule of sufficient complexity, such as the AIP* molecule, whose large number of internal degrees of freedom would be able to contain the activating energy for a considerable time. Thus a certain portion of these activated molecules could reach the walls of the reaction vessel and there be deactivated. This process would entail including the following reaction in the mechanism:

$$\mathrm{AIP}^* + \mathrm{wall} \rightarrow \mathrm{AIP}, \qquad k_w \qquad [7]$$

which in turn would lead to

[III] $$1/\Phi_{N_2} = 1+(k_2/k_1)[\mathrm{AIP}]+k_i/k_1+k_w/k_1\,[\mathrm{AIP}],$$

where [AIP] is included in the denominator of the last term to take into account the variation of diffusion with pressure. Including this reaction, therefore, would require non-linearity in Fig. 1, the deviation from linearity depending on the ratio k_w/k_1, but in any case being most pronounced at low [AIP]. It is just in this region that the measurements become less accurate due to the small amount of light absorption. However, from [III] it can be shown that

[IV] $$[\mathrm{AIP}]/\Phi_{N_2} = k_2/k_1\,[\mathrm{AIP}]^2+(1+k_i/k_1)[\mathrm{AIP}]+k_w/k_1.$$

A plot of $[\mathrm{AIP}]/\Phi_{N_2}$ against [AIP] should therefore be parabolic with an intercept equal to k_w/k_1. The experimental data has been treated statistically using the least squares method for a quadratic parabola (11). For example, the data at 400° K (Fig. 2) are best described by the following expression:

$$[\mathrm{AIP}]/\Phi_{N_2} = (0.66\pm0.12)\ 10^{-18}[\mathrm{AIP}]^2+(1.549\pm0.058)[\mathrm{AIP}]+(0.045\pm0.70)\ 10^{-18}.$$

The uncertainties given are the statistical probable errors (12). Both from this and from the calculation of correlation coefficients it is clear that the data are best represented when wall deactivation is excluded. Under the present experimental conditions of pressure range and surface-to-volume ratio, wall deactivation may, therefore, be neglected.

As the amounts by which the intercepts in Fig. 1 are in excess of unity equals k_i/k_1 it is possible to obtain $E_i - E_1$ by the usual Arrhenius plot. Considering the standard deviation of these intercepts as given in Table II, it is obvious that this determination will not be highly accurate (Fig. 3). The best line calculated by weighing each point according

Can. J. Chem. Downloaded from www.nrcresearchpress.com by 210.87.254.6 on 09/05/12
For personal use only.

Can. J. Chem. Downloaded from www.nrcresearchpress.com by 210.87.254.6 on 09/05/12
For personal use only.

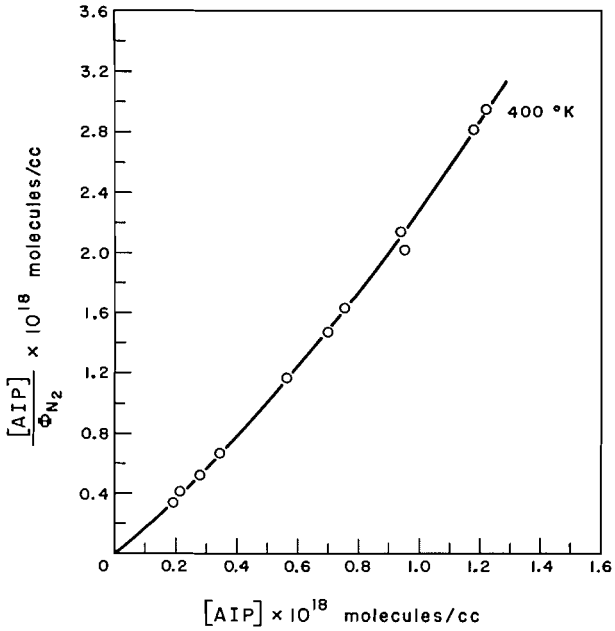


FIG. 2. Test for wall deactivation, expression [III].

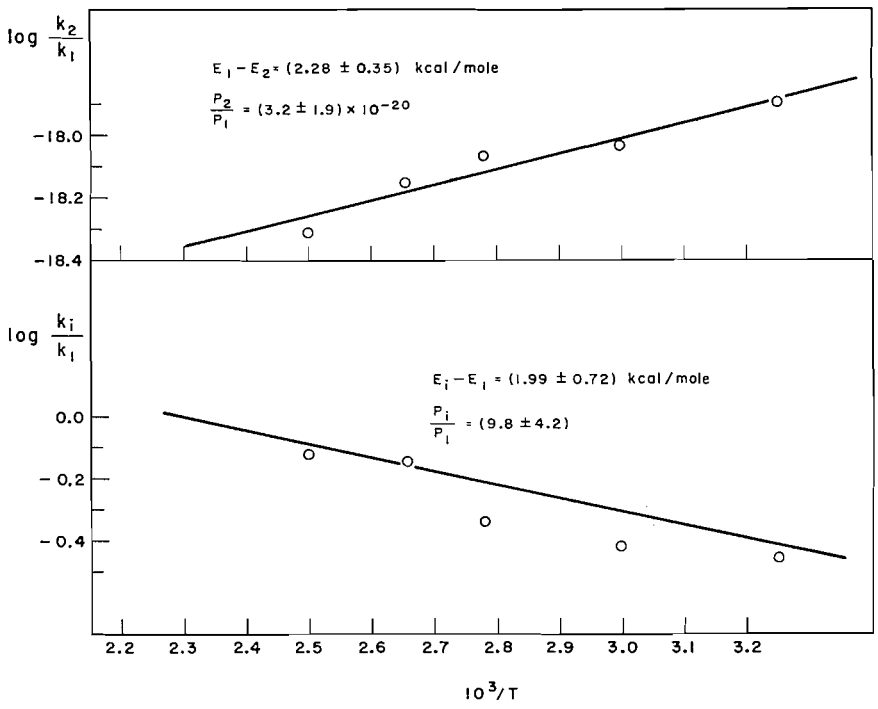


FIG. 3. Arrhenius plots of the ratio of rates of deactivation to decomposition and internal conversion to decomposition.

to its standard deviation (12) gives the values $E_1-E_1 = (1.99\pm0.72)$ kcal/mole and $P_1/P_1 = (9.8\pm4.2)$. This is believed to be the first case reported in which $E_1 > E_{\text{decomp}}$.

In an attempt to specify further the physical nature of the internal conversion reaction, luminescence measurements were made. No luminescence was discernible with 3660 Å incident radiation when a sensitive photomultiplier (IP 21) instrument normally used in studying the fluorescence of ketones was employed. As a logical extension of the theory of Franck and Livingston (13) it might be suggested that internal conversion of the excitation energy in the case of azoisopropane occurs through isomerization to a cis ground state when starting from trans ground state molecules. Fischer (14) has shown that *trans*-azobenzene in toluene solution, when irradiated with 3650 Å light until equilibrium has been obtained, consists of 91% of the cis form. The activation energy of this isomerization in various solvents, as determined by Hartley (15) and by Halpern, Brady, and Winkler (16), lies in the range 28.8 to 24.7 kcal/mole. As in the cis–trans isomerization of azobenzene, considerable resonance stabilization is possible of the unpaired electrons in the activated complex, a situation which does not exist in the case of azoisopropane, the activation energy for the cis–trans isomerization of the latter compound will undoubtedly be even higher. Since the energy supplied in the form of radiation is equivalent to only 78 kcal the resultant cis form will not contain sufficient energy to decompose unless it absorbs another quantum. If this were the only route to decomposition the quantum yield of nitrogen would be 0.5. The fact that this is not the case, both higher and lower values being observed, justifies the inclusion of the other steps in the primary process.

The large radical created in reaction [5] through abstraction from the parent compound was also generated in darkness through the thermal decomposition of di-*tertiary*-butyl peroxide at 127° C (17) in the presence of azoisopropane. Though methane was formed in the required manner, no nitrogen could be detected. Thus a chain reaction is not anticipated in the photolysis and the quantum yields discussed in the section on primary processes are not subject to correction for the possible further decomposition of the azoalkyl radical.

Secondary Processes

The preceding mechanism also leads to the following relations:

$$[V] \qquad R_{C_3H_6}/R_{C_6H_{14}} = k_3/k_4,$$

$$[VI] \qquad \frac{R_{C_3H_8}+R_{C_3H_6}}{R_{C_6H_{14}}} = \frac{R_{C_3}}{R_{C_6H_{14}}} = \frac{2k_3}{k_4}+\frac{k_5}{k_4^{\frac{1}{2}}}\frac{[\text{AIP}]}{R^{\frac{1}{2}}_{C_6H_{14}}},$$

$$[VII] \qquad \frac{R_{C_3H_8}-R_{C_3H_6}}{R_{C_6H_{14}}} = \frac{\Delta R_{C_3}}{R_{C_6H_{14}}} = \frac{k_5}{k_4^{\frac{1}{2}}}\frac{[\text{AIP}]}{R^{\frac{1}{2}}_{C_6H_{14}}}.$$

The various quantities necessary to test these expressions have been calculated from the experimental data and are given in Table I.

The ratio of k_3/k_4, as calculated for each individual run, is given in Table I. These values are compared with the values obtained from expression [VI] using Fig. 4 and Table III. From Table I it is seen that $R_{C_3H_6}/R_{C_6H_{14}}$ has a slight tendency to increase with increasing [AIP]. This tendency is, however, not very pronounced and seems in fact to have disappeared at the highest temperature employed. Further though there would

Can. J. Chem. Downloaded from www.nrcresearchpress.com by 210.87.254.6 on 09/05/12
For personal use only.

Can. J. Chem. Downloaded from www.nrcresearchpress.com by 210.87.254.6 on 09/05/12
For personal use only.

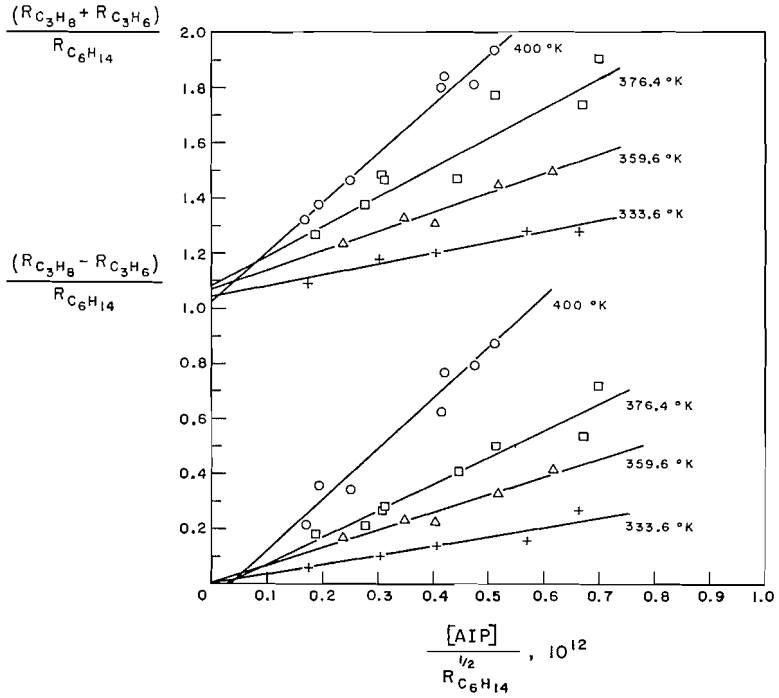


FIG. 4. Plots of the expressions [VI] and [VII].

TABLE III

Rate constants of secondary processes
(Units entering constants are molecules, cc, and sec)

	Equation [VII]				Equation [VI]					
T, °K	$(k_5/k_4^{\frac{1}{2}})\,10^{12}$	S.D. × 10^{12}	Inter.	S.D.	$(k_5/k_4^{\frac{1}{2}})\,10^{12}$	S.D. × 10^{12}	k_3/k_4	S.D.	Average $\frac{R_{C_3H_6}}{R_{C_6H_{14}}}$	S.D.
333.6	0.335	0.032	−0.0020	0.015	0.389	0.054	0.520	0.013	0.532	0.018
359.6	0.633	0.053	−0.0052	0.035	0.690	0.095	0.535	0.021	0.546	0.010
376.4	0.950	0.046	−0.0220	0.046	1.07	0.14	0.540	0.033	0.575	0.026
400.0	1.82	0.057	−0.069	0.057	1.78	0.12	0.511	0.022	0.540	0.033

at first seem to be an increase of $R_{C_3H_6}/R_{C_6H_{14}}$ with temperature, this is invalidated by the results at 127° C. Therefore within experimental error it is considered that k_3/k_4 is constant. Identical conclusions must be drawn from the results obtained using equation [VI]. It may be noted that constancy has also been found for this ratio of rates in the case of azoethane to 150° C (9) and in the case of diisopropyl ketone to 192° C (2). Since k_3/k_4 is independent of temperature, $E_3-E_4 = 0$. The actual numerical value of k_3/k_4 agrees well with the data of Heller and Gordon (2) and Robb and Boddy (4). The value reported by Kerr and Trotman-Dickenson (3) for this ratio of rates is, however, slightly higher.

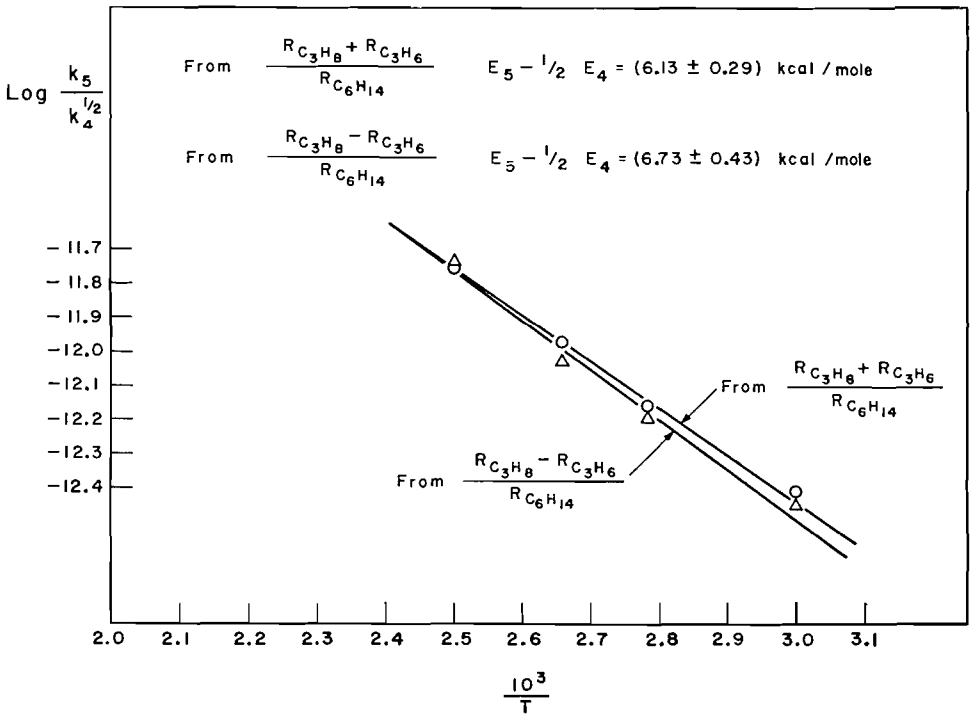


FIG. 5. Arrhenius plots relevant to the expressions [VI] and [VII]. ○ from expression [VI] and △ from expression [VII].

The ratio $k_5/k_4^{\frac{1}{2}}$ has also been obtained from both [VI] and [VII] (Table III). The Arrhenius plot for both cases is given in Fig. 5 and leads to

$$E_5-\tfrac{1}{2}E_4 = (6.12\pm0.29)\ \text{kcal/mole},$$

$$P_5\sigma_5^2/P_4^{\frac{1}{2}}\sigma_4 = 0.369\ 10^{-10}.$$

Assuming (10) that $\sigma_5 = 3$ Å and $\sigma_4 = 2.1$ Å leads to

$$P_5/P_4^{\frac{1}{2}} = 0.85\ 10^{-3}$$

when equation [VI] is used. If equation [VII] is employed it is found that

$$E_5-\tfrac{1}{2}E_4 = (6.73\pm0.43)\ \text{kcal/mole},$$

$$P_5\sigma_5^2/P_4^{\frac{1}{2}}\sigma_4 = 0.774\ 10^{-10} \rightarrow P_5/P_4^{\frac{1}{2}} = 1.8\ 10^{-3}.$$

These results are in good agreement with those of Heller and Gordon (2).

The experimental data in Table I show a decrease in the mass balance, i.e. $\{\frac{1}{2}(C_3H_6 + C_3H_8) + C_6H_{14}\}/N_2$, with increasing temperature. As no new compounds are found in the first two fractions removed in the runs at higher temperature it must be concluded that these new compounds are of high molecular weight and constitute part of the "liquid products". No positive identification of these new products could be made by mass spectrometry though it was noted that (*sec*-Pr)$_2$NN(*sec*-Pr)$_2$ would, among other compounds, be consistent with the observed spectrum.

Can. J. Chem. Downloaded from www.nrcresearchpress.com by 210.87.254.6 on 09/05/12
For personal use only.

ACKNOWLEDGMENT

The authors are indebted to Mrs. R. H. Riem for the mass spectrometric analyses.

REFERENCES

1. R. W. DURHAM and E. W. R. STEACIE. Can. J. Chem. **31**, 377 (1953).
2. C. A. HELLER and A. S. GORDON. J. Phys. Chem. **60**, 1315 (1956).
3. J. A. KERR and A. F. TROTMAN-DICKENSON. Trans. Faraday Soc. **55**, 921 (1959).
4. P. J. BODDY and J. C. ROBB. Proc. Roy. Soc. (London), A, **249**, 547 (1959).
5. D. E. MCELCHEREN, M. H. J. WIJNEN, and E. W. R. STEACIE. Can. J. Chem. **36**, 321 (1958).
6. H. KASHA. J. Opt. Soc. Am. **38**, 929 (1948).
7. M. H. JONES and E. W. R. STEACIE. J. Chem. Phys. **21**, 1018 (1953).
8. C. R. YOKLEY and R. E. FERGUSON. Combustion and Flame, **2**, 117 (1958).
9. H. CERFONTAIN and K. O. KUTSCHKE. Can. J. Chem. **36**, 344 (1958).
10. J. L. WEINIGER and O. K. RICE. J. Am. Chem. Soc. **74**, 6216 (1952).
11. A. G. WORTHING and J. GEFFNER. Treatment of experimental data. John Wiley & Sons, Inc., New York. 1943.
12. D. BRUNT. The combination of observations. 2nd ed. Cambridge University Press. Cambridge, England. 1931.
13. J. FRANCK and R. LIVINGSTON. J. Chem. Phys. **9**, 184 (1941).
14. E. FISCHER. J. Chem. Phys. **23**, 1369 (1955).
15. G. S. HARTLEY. Nature, **140**, 281 (1937).
16. J. HALPERN, G. W. BRADY, and C. A. WINKLER. Can. J. Research, B, **28**, 140 (1950).
17. A. R. BLAKE and K. O. KUTSCHKE. Can. J. Chem. **37**, 1462 (1959).

Can. J. Chem. Downloaded from www.nrcresearchpress.com by 210.87.254.6 on 09/05/12
For personal use only.

Can. J. Chem. Downloaded from www.nrcresearchpress.com by 210.87.254.40 on 09/05/12
For personal use only.

THE OXIDATION OF MANGANATE BY PERIODATE[1]

M. W. Lister and Y. Yoshino

ABSTRACT

The reaction between periodate and manganate ions in alkaline solution has been examined, and at 35° C the rate is given by the equation, time being measured in minutes,

$$\text{rate} = 107[MnO_4^{--}]^2(1+167[H_3IO_6^{--}])(1+0.111[OH^-]^{-1}).$$

It is proposed that the main reaction mechanism is

$$2MnO_4^{--} \underset{k_2}{\overset{k_1}{\rightleftharpoons}} MnO_4^- + MnO_4^{-3}, \quad \text{(i)}$$

$$MnO_4^{-3} + H_3IO_6^{--} \xrightarrow{k_3} MnO_4^- + IO_3^- + 3OH^-. \quad \text{(ii)}$$

Hence $k_1 = 107$ (g-molecule/l.)$^{-1}$ min^{-1} at 35° C, and it was found that the activation energy is about 13.9 kcal/g-molecule. Data of Carrington and Symonds (2), combined with the value for k_1, make $k_2 = 2.8\times10^6$ (g-molecule/l.)$^{-1}$ min^{-1}. Added permanganate ions slow up the reaction; this is ascribed to the reverse of reaction (i) competing with reaction (ii). This gives a value for k_3 of 2×10^7 (g-molecule/l.)$^{-1}$ min^{-1}; this is so large a rate constant as to make it probable that the hypomanganate ions are hydrolyzed. The effect of hydroxide concentration on the rate is ascribed to partial hydrolysis of manganate ions. The observed results would require the ionization constant of $HMnO_4^-$ to be 7×10^{-11}.

In a recent paper (1) the present writers prepared several complex manganese periodates, such as $Na_7H_4Mn(IO_6)_3.17H_2O$, containing tetravalent manganese. These were shown to decompose in solution to give manganate ions as the first product, and finally permanganate ions. The mechanism of the decomposition of the complex salt was investigated, and shown to go through a partial breaking up of the complex to simpler ions. The present paper reports an examination of the second stage of this reaction, that is, the oxidation of manganate to permanganate. Apart from its connection with the behavior of manganato-periodates, this reaction is of interest because it involves a change of two in the oxidation state of the iodine, and of one in the oxidation state of the manganese. Thus we might expect either a termolecular reaction, or a mechanism which avoided this. In the latter case, the reaction would have to go through an intermediate containing either iodine or manganese in a usual valency. As it turned out, the main route seemed to be through hypomanganate ions, containing the relatively rare pentavalent manganese. There is also evidence for a termolecular reaction.

The over-all reaction is

$$2MnO_4^{--} + H_3IO_6^{--} \rightarrow 2MnO_4^- + IO_3^- + 3OH^-.$$

EXPERIMENTAL METHOD

The reaction was followed by mixing known amounts of stock solutions of sodium manganate, sodium periodate, and sodium hydroxide, previously brought to the required temperature. The mixture was kept in a thermostat, and the extent of reaction was found by measuring the optical density of a sample.

The sodium manganate was prepared by boiling sodium permanganate in concentrated sodium hydroxide solution, as described by Carrington and Symonds (2). Sodium periodate was prepared by oxidation of a weakly alkaline sodium iodate solution by means of sodium hypochlorite at about 80° C; the fairly insoluble sodium periodate,

[1]*Manuscript received August 25, 1960.*
Contribution from the Department of Chemistry, University of Toronto, Toronto, Ontario.

$Na_3H_2IO_6$, crystallized out, and was filtered off and thoroughly washed with distilled water.

The initial concentration of manganate in the runs was between 1.6×10^{-4} M and 6×10^{-4} M, and the initial concentration of periodate between 3×10^{-4} M and 13×10^{-4} M. Sodium hydroxide was present in sufficient excess for its concentration not to change appreciably during the runs; many runs were in 0.1 M sodium hydroxide.

The optical density was measured on a Beckmann DU spectrophotometer, with a 1-cm cell. The wavelength used was 610 mμ, which is at the absorption maximum for manganate ions. Measurements on several solutions gave a value of 1530 for the extinction coefficient of sodium manganate, and 207 for sodium permanganate (2, 3). The concentrations of the solutions were calculated assuming that only these two ions contributed to the optical density, and that all the manganese was present as one or other ion. This was supported by the fact that the solutions showed no signs of any precipitate of manganese dioxide. It was checked that the total oxidizing power of the solutions, as measured by the amount of iodine liberated by adding potassium iodide and sulphuric acid, did not change during the reaction; and finally it was checked that iodate caused no oxidation of manganate. Thus there is no evidence of any side reactions.

RESULTS

It was found that for all runs a plot of the inverse of the manganate concentration against time was linear, as in a second-order reaction. Accordingly the results are shown in the figures as graphs of this sort. The initial concentrations and temperatures are given in Table I. The ionic strengths of the solutions were close to 0.1, except for the

TABLE I

Initial concentrations

Run	Temp., °C	$[MnO_4^{--}]\times10^{-4}$ M	$[H_3IO_6^{--}]\times10^{-4}$ M	$[OH^-]$, M	$d[MnO_4^{--}]^{-1}/dt$, (g-molecule/l.)$^{-1}$ min^{-1}
2	35	2.83	7.85	0.099	277
3	35	1.69	7.85	0.100	280
4	35	3.38	12.56	0.0985	290
5	35	3.38	3.14	0.0965	254
6	35	3.38	7.85	0.100	271
7	35	3.38	7.85	0.100	284
8	40	3.38	7.85	0.100	383
9	45	3.38	7.85	0.100	520
10	25	3.38	7.85	0.100	118
11	35	3.38	12.56	0.100	294
12	35	3.38	3.14	0.100	254
13	35	3.38	3.14	0.022	729
14	35	3.38	3.14	0.049	394
15	35	3.38	0	0.049	9
16	35	3.38	3.14	0.0091	1485
17	35	3.38	0	0.050	7
18	35	3.45	7.85	0.050	465
19	25	3.45	7.85	0.050	209
20	45	3.45	7.85	0.050	1010
21	45	3.45	7.85	0.100	535
22	25	3.45	7.85	0.100	125
23	25	3.34	7.85	0.200	113
24	35	3.34	7.85	0.200	224
25	45	3.34	7.85	0.200	435
26*	35	3.34	7.85	0.100	222
27*	35	3.34	7.85	0.100	137

*Potassium permanganate was added to these solutions. In run 26 $[KMnO_4] = 10.8\times10^{-4}$ M, in run 27 $[KMnO_4] = 54.0\times10^{-4}$ M initially.

Can. J. Chem. Downloaded from www.nrcresearchpress.com by 210.87.254.40 on 09/05/12
For personal use only.

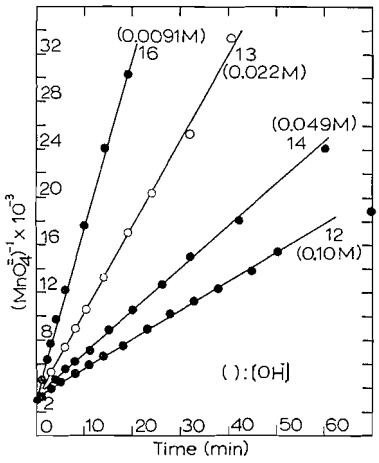


FIG. 1. Effect of hydroxide concentration on rate.

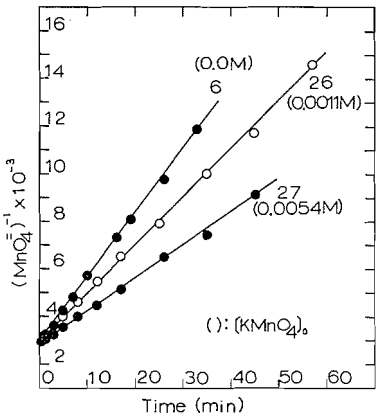


FIG. 2. Effect of permanganate concentration on rate.

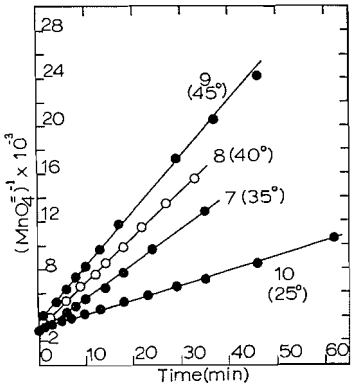


FIG. 3. Effect of temperature on rate.

three runs in 0.2 M sodium hydroxide, where the ionic strength was slightly above 0.2.

There are two comments to make on these graphs. Firstly the points at the time of mixing were calculated from the volumes of stock solution put in, the stock solution being standardized by adding potassium iodide and acid, and titrating with thiosulphate. These are plotted at $t = 0$, and the next point, usually at $t = 1$ minute, represents the first measurement of optical density. These first two points were always in reasonable agreement. The second comment is that the final points fall off somewhat from a second-order plot, though by this time the manganate concentration was usually less than 25% of its initial value. The best straight lines were drawn through the experimental points obtained before this falling off became apparent, and the slopes of these lines are given in the last column of Table I, headed "$d[MnO_4^{--}]^{-1}/dt$". Time is measured in minutes.

DISCUSSION OF RESULTS

Attention may first be drawn to runs 15 and 17 in which no periodate was present. These runs show that the disproportionation of manganate is much slower than the

Can. J. Chem. Downloaded from www.nrcresearchpress.com by 210.87.254.40 on 09/05/12
For personal use only.

oxidation by periodate. In these runs a precipitate of manganese dioxide appeared, while in no run with periodate present was any precipitate observed. Although the rate of disproportionation is about 5% of the rate in the slowest runs with periodate, no correction was made for this in the calculations, because the absence of any sign of manganese dioxide made it doubtful if the disproportionation to manganese dioxide and permanganate was in fact occurring. The reason for this will appear later when the mechanism of the reaction with periodate is discussed.

Turning now to the main series of runs, the first point, of course, is that the rate is proportional to $[MnO_4^{--}]^2$. Secondly, when rates at different periodate concentrations are compared, it is seen that this has only a moderate effect on the rate. In runs at 35° C and 0.1 M sodium hydroxide, the average values of $d[MnO_4^{--}]^{-1}/dt$ at various periodate concentrations were:

$[H_3IO_6^{--}]$	12.56	7.85	3.14×10^{-4} M
$d[MnO_4^{--}]^{-1}/dt$	292	278	254

Over this range, the results approximately follow the equation

$$\text{rate} = [MnO_4^{--}]^2(241+4.0\times10^4[H_3IO_6^{--}]).$$

Although the term in periodate looks large, its contribution was fairly small.

The effect of hydroxide concentration can be seen from the runs at 35° C and 7.85×10^{-4} M periodate, and an ionic strength of 0.1.

$[OH^-]$	0.100	0.049	0.022	0.0091 M
$d[MnO_4^{--}]^{-1}/dt$	254	394	729	1485

If $[OH^-]^{-1}$ is plotted against $d[MnO_4^{--}]^{-1}/dt$, the first three results fall on a straight line, and the fourth is near the line, but a little low. The straight line has the equation

$$d[MnO_4^{--}]^{-1}/dt = 121+13.4[OH^-]^{-1}.$$

Combining these two equations, the total equation is

$$\text{(A)} \qquad \text{rate} = 107[MnO_4^{--}]^2(1+167[H_3IO_6^{--}])(1+0.111[OH^-]^{-1}).$$

This is for 35° C. It is evident that this could be written in terms of hydrogen ions,

$$\text{rate} = 107[MnO_4^{--}]^2(1+167[H_3IO_6^{--}])(1+4.83\times10^{12}[H^+]).$$

The mechanism which could give this equation must involve more than one reaction. However, at high hydroxide concentrations, the main part of the reaction is simply a second-order reaction in manganate ions. The most obvious suggestion is that the reaction goes through hypomanganate ions:

$$2MnO_4^{--} \underset{k_2}{\overset{k_1}{\rightleftharpoons}} MnO_4^- + MnO_4^{---}, \qquad \text{(i)}$$

$$MnO_4^{---} + H_3IO_6^{--} \xrightarrow{k_3} MnO_4^- + IO_3^- + 3OH^-. \qquad \text{(ii)}$$

The scheme has the advantage that each stage is a simple bimolecular reaction. For the reaction to depend on the manganate concentration alone, it would be necessary for reaction (ii) to go much faster than the reverse of (i), so that all hypomanganate is oxidized to permanganate. Otherwise the permanganate formed during the run would cause a continuous extra decrease in the rate, which is not found until the reaction is

Can. J. Chem. Downloaded from www.nrcresearchpress.com by 210.87.254.40 on 09/05/12
For personal use only.

nearly over. If this is the correct mechanism, then k_1, the rate constant of reaction (i) going to the right, is 107 (g-molecule/l.)$^{-1}$ min^{-1} at 35° C, from equation (A) above.

Carrington and Symonds (2) calculate that ΔF^0 for reaction (i) is 6.2 kcal at 25° C. This makes the equilibrium constant of reaction (i) 2.85×10^{-5} at 25° C. ΔH^0 is 5.5 kcal, so the equilibrium constant is 3.85×10^{-5} at 35° C. Hence k_2, the rate constant of reaction (i) going to the left, is 2.8×10^{6} (g-molecule/l.)$^{-1}$ min^{-1} at 35° C.

The dependence on $[OH^-]$ or $[H^+]$ probably means that the sodium manganate is partially hydrolyzed. One might expect this to give $Mn_2O_7^{--}$ ions, by analogy with the behavior of chromate, but this would require a dependence on the square of $[H^+]$; the first power of $[H^+]$ in the equation shows that the hydrolyzed species is $HMnO_4^-$, which then must react thus:

$$HMnO_4^- + MnO_4^{--} \overset{k_4}{\rightleftharpoons} MnO_4^- + HMnO_4^{--}. \qquad \text{(iii)}$$

On this hypothesis, if k_a is the ionization constant of $HMnO_4^-$ (to give H^+ and MnO_4^{--}), and k_4 is the rate constant of reaction (iii) going to the right, then it is easily found that the contribution of reaction (iii) to the rate is

$$k_4[MnO_4^{--}]^2\left\{\frac{[H^+]k_a}{(k_a+[H^+])^2}\right\}$$

where $[MnO_4^{--}]$ here means the total manganate present. The contribution of reaction (i) becomes

$$k_1[MnO_4^{--}]^2\left\{\frac{k_a^{\,2}}{(k_a+[H^+])^2}\right\};$$

so that the total equation is

$$\text{rate} = [MnO_4^{--}]^2\left\{\frac{k_1+k_4[H^+]/k_a}{(1+[H^+]/k_a)^2}\right\}.$$

Evidently if $[H^+]$ is low, and k_4 not too small, this will give an equation for the rate of the type actually found: by comparison, $k_4/k_1.k_a = 4.83\times10^{12}$. The slight decrease of the rate in 0.0091 M sodium hydroxide below what is calculated is presumably due to the term $(1+[H^+]/k_a)^2$; this explanation would require k_a to be 7×10^{-11}. This is perhaps a somewhat small value for k_a; for instance, the bichromate ion, $HCrO_4^-$, has an ionization constant of 3.2×10^{-7} (4). This value of k_a gives 340 for the ratio k_4/k_1, so that k_4 is 3.6×10^{4} (g-molecule/l.)$^{-1}$ min^{-1} at 35° C. This ratio is not unreasonable as MnO_4^{--} and $HMnO_4^-$ will repel each other less than two MnO_4^{--} ions.

The graphs of $[MnO_4^{--}]^{-1}$ against time cease to be linear towards the end of the reaction. It can be calculated that this is not due to the decrease in periodate concentration, which would cause only a very small decrease in the rate. Another possible explanation is that reaction (ii) is reversible, and that the equilibrium lies far from complete conversion to permanganate. Latimer (4) gives −0.564 volt for the standard potential of the half reaction: $MnO_4^{--} \rightarrow MnO_4^- + e^-$, and a rather doubtful −0.7 volt for $IO_3^- + 3OH^- \rightarrow H_3IO_6^{--} + 2e^-$. If this value of −0.7 volt is right, then the equilibrium lies at almost complete conversion to permanganate. A check on this was made by mixing potassium permanganate with a relatively large concentration of sodium iodate (and sodium hydroxide) and examining the spectrum of the mixture to see whether any manganate ions were formed. A small concentration of manganate ions did appear,

Can. J. Chem. Downloaded from www.nrcresearchpress.com by 210.87.254.40 on 09/05/12
For personal use only.

and a rough measurement showed that the equilibrium constant of reaction (ii) is at least 25 or larger (this is with the permanganate on top). Hence in concentrations of sodium hydroxide below 0.1 M, the equilibrium mixture will be almost entirely permanganate. It was calculated that, in a typical run such as run 6, at equilibrium 0.4% or less of the manganese would be present as manganate.

A more plausible explanation is that as the permanganate increases in concentration and periodate decreases, the reverse of reaction (i) starts to compete with reaction (ii). This suggestion was tested in runs 26 and 27, when appreciable amounts of permanganate were added initially, and it was found that the permanganate reduced the rate of reaction. If ordinary kinetic considerations are applied to these reactions, it is found that the concentration should follow the equation

$$\text{(B)} \qquad k_1 t - (\theta - \theta_0) = a\left[\frac{(2+2y_0\theta_0)(\theta-\theta_0)}{2b-1} - \frac{2\theta_0(2b+y_0\theta_0)}{(2b-1)^2}\ln\frac{\theta(2b-1)+\theta_0}{2b\theta_0}\right]$$

where $\theta = [MnO_4^{--}]^{-1}$, initially θ_0,
$a = k_2/k_3$,
b = initial value of the ratio $[H_3IO_6^{--}]/[MnO_4^{--}]$,
y_0 = initial $[MnO_4^{-}]$.

In the earlier runs, $y_0 = 0$. If k_2 is zero, this equation reduces to the usual second-order equation; and it is found that for moderate values of a, a plot of θ against t only deviates to any great extent from a straight line when the reaction is nearly over. This is in agreement with experiment, as the experimental points followed a second-order equation for a considerable time. The above equation gives

$$\left(\frac{d\theta}{dt}\right)_0 = \frac{k_1}{1+ay_0/[H_3IO_6^{--}]_0}$$

where $(d\theta/dt)_0$ is the initial value of $d\theta/dt$, and $[H_3IO_6^{--}]_0$ is the initial periodate concentration. Hence with no added permanganate, $(d\theta/dt)_0 = k_1$, as was assumed above. The value of a can be found (i) from the initial slopes, $(d\theta/dt)_0$, in runs 26 or 27, or (ii) by applying the full equation to the later points in runs with no added permanganate. The first method is obviously more accurate, but the values of a found by the second are in rough agreement.

For run 26, the initial $d\theta/dt$ is about 222, for conditions where $d\theta/dt$ without added permanganate is 278. The ratio $[MnO_4^{-}]/[H_3IO_6^{--}]$ is initially 1.38. This makes $a = 0.18$. In run 27, the initial $d\theta/dt$ is 137, with $[MnO_4^{-}]/[H_3IO_6^{--}]$ initially 6.88. This makes $a = 0.15$. Applying the second method above to the earlier runs gives slightly smaller values of a, mostly between 0.1 and 0.15. Hence the value of k_2/k_3 at 35° C is evidently about 0.15. From the value of k_2 obtained above, it follows that k_3 is about 2×10^7 (g-molecule/l.)$^{-1}$ min^{-1} at 35° C. This is a relatively large rate constant, and is surprisingly large if the reaction is one between MnO_4^{--} and $H_3IO_6^{--}$, because of the electrostatic repulsion of the ions. There seems to be no doubt that the periodate is mainly $H_3IO_6^{--}$ in these solutions, as Crouthamel, Hayes, and Martin (5) find pk_2 to be 8.36 and $pk_3 = 15$, for periodic acid. Hence at the concentrations of sodium hydroxide used in these experiments the periodate must be predominantly $H_3IO_6^{--}$. This is in agreement with the phase diagram for sodium hydroxide, periodic acid, and water, as determined by Hill (6). However, although the periodate ion is $H_3IO_6^{--}$, it is possible that the hypomanganate is hydrolyzed to ions of lower charge, $HMnO_4^{--}$ or $H_2MnO_4^{-}$.

Can. J. Chem. Downloaded from www.nrcresearchpress.com by 210.87.254.40 on 09/05/12
For personal use only.

There are no values for the ionization constants of hypomanganic acid, and the most that can be said is that the present results provide some evidence for partial hydrolysis of hypomanganate ions in 0.1 M sodium hydroxide. The reaction might consist of hydrogen atom transfer from $H_2MnO_4^-$ to $H_3IO_6^{--}$.

The experimental rate equation (A) above contained a term in $[H_3IO_6^{--}]$, which suggests that part of the reaction is termolecular. However, it is necessary to be sure that this is not an indirect result of the varying success of the competition between the k_2 and k_3 reactions. Obviously a high periodate concentration will favor reaction (ii), with rate constant k_3. This will not affect the initial slope for $[MnO_4^{--}]^{-1}$ plotted against t, but as in practice the slope has to be obtained over a number of points, the periodate concentration may alter the slope in effect; in equation (B) this would be due to different values of b. It is found that if equation (B) is plotted, it gives very nearly a straight line for a considerable distance, after which the values of θ fall below the straight line. Over the range of θ used in the experiments (about 3,000 to 15,000) the curvature is slight, but the mean slope is altered by the value of b. If the slope is taken as unity for $b = 1$, it is 1.05 for $b = 2$, and 1.07 for $b = 4$. However, over this range of b (or periodate concentration) the relative observed slopes are about 1.067 for $b = 2$ and 1.16 for $b = 4$. The conclusion must therefore be that there is a direct effect due to periodate, apart from its alteration of the relative rates of the k_2 and k_3 reactions, that is, that there is a termolecular reaction, at least to a small extent.

The temperature dependence of the slope, $d[MnO_4^{--}]^{-1}/dt$, needs some comment. For the same values of $[OH^-]$ and $[H_3IO_6^{--}]$, the usual plot of $\log(d[MnO_4^{--}]^{-1}/dt)$ against $1/T$ gives nearly straight lines. The activation energies so obtained are: $[OH^-] = 0.05$ M, $E = 14.8$ kcal/g-molecule; $[OH^-] = 0.1$ M, $E = 13.9$ kcal/g-molecule; and $[OH^-] = 0.2$ M, $E = 12.7$ kcal/g-molecule. If the value of 13.9 kcal/g-molecule is taken to apply to k_1 deduced above, and if $k_1 = Ae^{-E/RT}$, then $\log A = 11.9$ (time measured in minutes). This is an unremarkable value. This activation energy may also be compared with that obtained (7) for the interchange of radioactive manganese between manganate and permanganate ions: here $E = 10.5$ kcal. As might be expected, this is somewhat less than the value for the reaction between two manganates, which involves the transfer of an electron between two doubly charged ions. If ΔH^0 is 5.5 kcal, then the activation energy for $MnO_4^{-3} + MnO_4^- \rightarrow 2MnO_4^{--}$ is only 8.4 kcal; however, the hypomanganate ion may be partially hydrolyzed, which would vitiate any arguments concerned with the size of the charges on the ions. The activation energy found above drifts to slightly lower values as the hydroxide concentration increases. The difference is not large, but the cause is at present obscure, as the change is in the opposite direction from what would be expected from the rate constants. The change is too large, and the rate constants too consistent, to ascribe this to experimental error.

REFERENCES

1. M. W. Lister and Y. Yoshino. Can. J. Chem. **38**, 1291 (1960).
2. A. Carrington and M. C. R. Symonds. J. Chem. Soc. 3373 (1956).
3. G. Zimmerman. J. Chem. Phys. **23**, 825 (1955).
4. W. M. Latimer. Oxidation potentials. 2nd ed. Prentice Hall, New York. 1952. p. 249.
5. C. E. Crouthamel, A. M. Hayes, and D. S. Martin. J. Am. Chem. Soc. **73**, 81 (1951).
6. A. E. Hill. J. Am. Chem. Soc. **50**, 2678 (1928).
7. J. C. Shepherd and A. C. Wahl. J. Am. Chem. Soc. **79**, 1020 (1957).

Can. J. Chem. Downloaded from www.nrcresearchpress.com by 210.87.254.40 on 09/05/12
For personal use only.

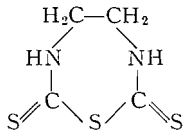
SOME OBSERVATIONS ON THE STRUCTURE OF ETHYLENETHIURAM MONOSULPHIDE[1]

G. D. THORN

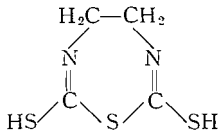
ABSTRACT

An attempt has been made to answer several apparent objections to the structure ethylenethiuram monosulphide assigned to the monomeric material of formula $C_4H_6N_2S_3$ obtained by air oxidation of disodium ethylenebisdithiocarbamate. Comparison of the ultraviolet and infrared absorption spectra, potentiometric titrations, and biological assays of the compound and several heterocyclic and other compounds containing the N–C–S grouping has eliminated two possible alternative structures containing thiadiazolidine and dithiazolidine ring systems and has led to the conclusion that the original assignment of structure was correct.

Vigorous aeration of dilute aqueous solutions of disodium ethylenebisdithiocarbamate (nabam) results in the formation of a yellow insoluble fungicidal material consisting mainly of a polymer $(C_4H_6N_2S_3)_n$, together with up to 20% of the corresponding monomer and varying amounts of elemental sulphur (1, 2). The compound $C_4H_6N_2S_3$ has been assigned the structure ethylenethiuram monosulphide (hexahydro-1,3,6-thiadiazepine-2,7-dithione) (IA), which can be written also as the enethiol (IB). Interpretation of the infrared spectrum of the compound favored the latter structure. The strong band at 1610 cm^{-1} was taken as indicative of C=N (3); the bands attributable to the thioamide group (4, 5) are absent, and there is no evidence of absorption in the N—H stretching region.

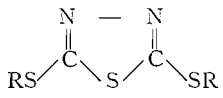


IA



IB

A number of objections can be raised to the formulation of the compound $C_4H_6N_2S_3$ as structure I. From a study of its infrared spectrum, two points can be made. Firstly, there is the lack of SH absorption in the 2600–2550 cm^{-1} region, and secondly, the observation that 2,5-di(methylmercapto)-1,3,4-thiadiazole (II, R = CH_3) does not display the "C=N absorption" in the 1650–1500 cm^{-1} region (6). From a chemical



II

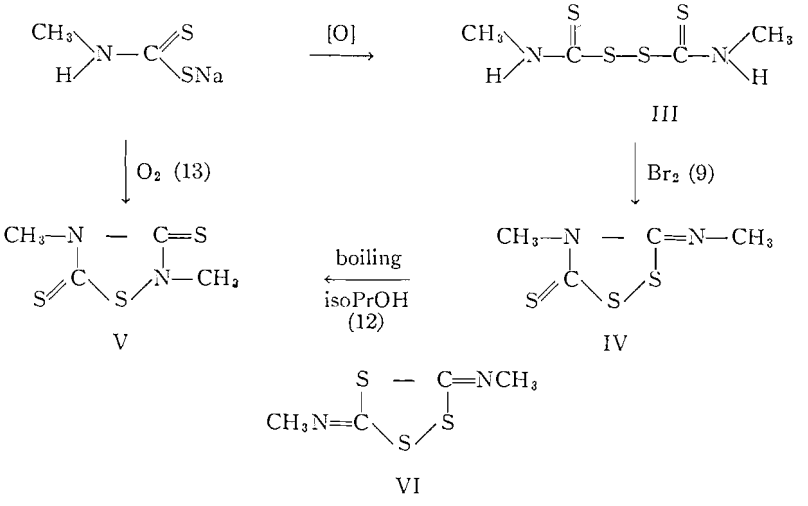
standpoint, the formation of mono-addition products with HCl and $HClO_4$ (2) and with carbon disulphide* is suggestive of unequivalent nitrogens in the structure. Also, the

[1]*Manuscript received June 3, 1960.*
Contribution No. 175, Pesticide Research Institute, Canada Department of Agriculture, University Sub Post Office, London, Ontario.

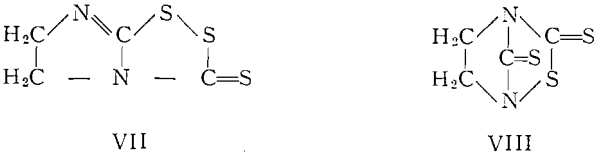
**The formation of an ethylenethiuram monosulphide – carbon disulphide complex has been recognized by Dr. G. J. M. van der Kerk and by Dr. I. A. M. Ford (personal communications) and by Kirby and Frick (7), but to our knowledge, analytical data have not been published.*

only other thiuram monosulphide derived from a primary amine which has been reported in the literature is in the recent work by D'Angeli and Iliceto (8), who described N,N'-dimethylthiuram monosulphide. This material is highly unstable either in solution or in the solid form, in contrast with the much more stable material designated ethylenethiuram monosulphide. Accordingly, further evidence was sought either to support the ethylenethiuram monosulphide structure, or perhaps to suggest that an entirely different structure might well be assigned to fit the data more adequately. The results of these investigations are reported in this paper.

Two compounds of interest in this study which are obtainable by oxidation of sodium methyldithiocarbamate or the intermediate dimethylthiuram disulphide (III) are 4-methyl-5-methylimino-1,2,4-dithiazolidine-3-thione (IV) and 2,4-dimethyl-1,2,4-thiadiazolidine-3,5-dithione (V). These compounds were first prepared by Freund and coworkers (9, 10) and the assignments of structure by Hantzsch and Wolvekamp (11) confirmed by means of infrared absorption spectra by Bradsher *et al.* (12). Freund and Asbrand (10) had given structure VI to what is now considered to be the thiadiazolidine (V), but Bradsher *et al.* (12) discounted this assignment because of lack of C=N absorption in the 1660–1610 cm^{-1} region. It might be noted again that the thiadiazole (II) does not exhibit absorption in this region, but this point alone cannot be used as evidence for structure VI, as the compound exhibits "thioureide" absorption in the 1450 cm^{-1} region.



Since Benghiat *et al.* (13) have shown that the thiadiazolidine (V) can be obtained merely by conveying wet sodium methyldithiocarbamate in air through a pneumatic conveying drier, it is conceivable that disodium ethylenebisdithiocarbamate on aeration might yield, instead of a thiuram monosulphide (I), structures analogous to IV and V, namely VII and VIII, respectively.

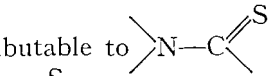
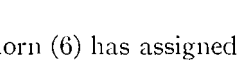
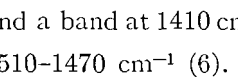


Compound VII especially answers several of the objections raised to the thiuram monosulphide structure designation. It was therefore considered important to make chemical and biological comparisons of ethylenethiuram monosulphide* with 4-methyl-5-methylimino-1,2,4-dithiazolidine-3-thione (IV) and 2,4-dimethyl-1,2,4-thiadiazolidine-3,5-dithione (V).

Ultraviolet Absorption Spectra

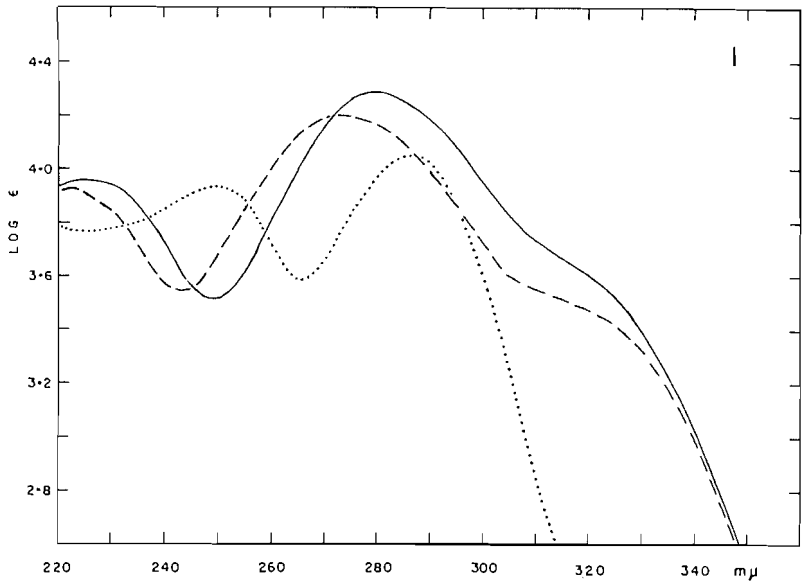
The similarity in ultraviolet absorption spectra of ethylenethiuram monosulphide and of tetramethylthiuram monosulphide was used by Thorn and Ludwig (2) as part of the evidence in favor of the thiuram monosulphide structure for the former compound. However, making further comparisons shows a possible fallacy in this argument. Figures 1 and 2 give the ultraviolet absorption spectra (ethanol solution) of several of the compounds in question. For ethylenethiuram monosulphide, the peaks are at 280 mμ, ϵ = 19,600, and at 227.5 mμ, ϵ = 8800; for tetramethylthiuram monosulphide the maxima are at 280 mμ, ϵ = 16,300, and at 210 mμ, ϵ = 17,000; and for dimethylthiuram monosulphide maximum absorption is at 287 mμ, ϵ = 11,300,† and at 250 mμ, ϵ = 8700.† On the other hand, 4-methyl-5-methylimino-1,2,4-dithiazolidine-3-thione (IV) also shows an ultraviolet absorption spectrum (Fig. 1) very similar to that of ethylenethiuram monosulphide, with peaks at 274 mμ, ϵ = 16,000, and at 223 mμ, ϵ = 8250. Compound V, 2,4-dimethyl-1,2,4-thiadiazolidine-3,5-dithione, displays a different absorption to that of the above compounds (Fig. 2). Thus, on the basis of ultraviolet absorption, no decision can be made between a thiuram monosulphide or a dithiazolidine structure for "ethylenethiuram monosulphide".

Infrared Absorption Spectra

Table I summarizes the important absorption bands in the infrared region 2000–900 cm^{-1} of ethylenethiuram monosulphide and a number of other compounds containing the N–C–S linkage. The ethylenethiuram monosulphide structure is a more plausible assignment than that of a dithiazolidine structure (VII), based on the following observations. Methyl-methylimino-dithiazolidine-thione (IV) shows absorption at 1650 cm^{-1}, assignable to $\nu_{C=N}$ (3), at 1470 cm^{-1}, attributable to  (6) and at 1430 cm^{-1}, which Thorn (6) has assigned to the  grouping. Ethylenethiuram monosulphide also shows $\nu_{C=N}$ absorption, at 1615 cm^{-1}, and a band at 1410 cm^{-1} () but no thioureide absorption in the region of 1510–1470 cm^{-1} (6). The lack of C=N absorption in the region of 1600 cm^{-1} in the spectrum of 2,5-dimercapto-1,3,4-thiadiazole (II, R = H) can be accounted for by the pseudoaromatic character of the compound (14). Likewise, in 2,5-di(methylmercapto)-1,3,4-thiadiazole (II, R = CH_3), this band is missing. (In this latter compound the structure is rigidly held in the enethiol form, whereas in II, R = H, the thione–thiol tautomeric structure has been assigned (6).) On the basis of our interpretation of the infrared spectra, then, the assignment of the ethylenethiuram monosulphide structure originally proposed (2) can be taken as correct, the only unexplainable feature being the lack of SH absorption in the 2600–2550 cm^{-1} region.

*Although the remarks above raise doubt as to the actual structure, the name ethylenethiuram monosulphide will be used throughout this discussion for the sake of convenience.

†These values are approximate, owing to the instability of dimethylthiuram monosulphide.



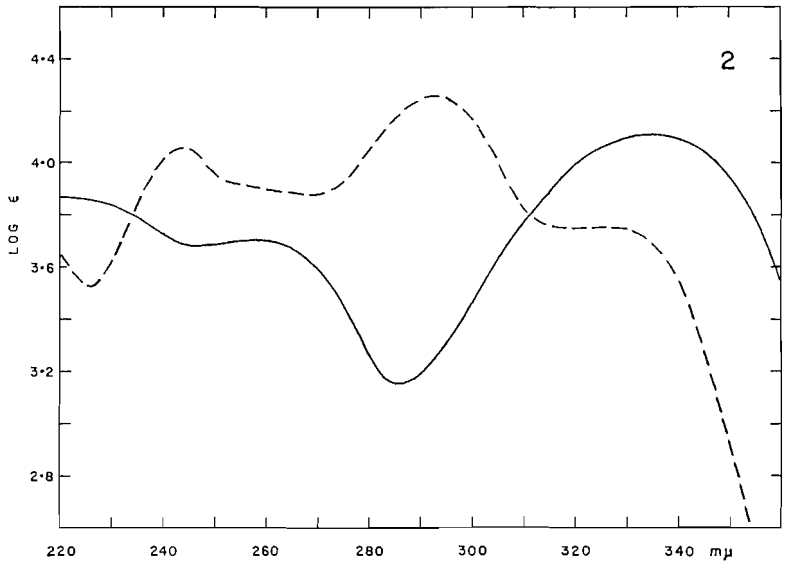


FIG. 1. Ultraviolet absorption spectra. ——— Ethylenethiuram monosulphide. – – – 4-Methyl-5-methylimino-1,2,4-dithiazolidine-3-thione. ····· Dimethylthiuram monosulphide.
FIG. 2. Ultraviolet absorption spectra. ——— 2,5-Dimercapto-1,3,4-thiadiazole. – – – 2,4-Dimethyl-1,2,4-thiadiazolidine-3,5-dithione.

In this connection, thiourea also displays a strong band at 1615 cm^{-1}, assignable to $\nu_{C=N}$ vibration, but shows no absorption band in the region 2600–2550 cm^{-1} given by Bellamy (15) as assignable to ν_{SH} vibration.

Potentiometric Studies

The apparent lack of SH according to the infrared spectrum in ethylenethiuram

TABLE I

Principal absorption bands of several compounds containing the $\rangle N—C\overset{S}{\langle}$ grouping, in the region 2000–900 cm^{-1}

Compound	Solvent	Absorption bands, cm^{-1}												
Ethylenethiuram monosulphide	$CHCl_3$	1615				1410		1325	1300m			1085		980
Dimethylthiuram monosulphide	Nujol	1572m	1535m	1473	1428w		1385	1350		1155		1045		912
Dimethylthiuram disulphide	$CHCl_3$		1525		1430m			1360		1165		1040		920
Tetramethylthiuram monosulphide	$CHCl_3$		1505		1450w	1410w	1385		1245w	1150		1050m	1005	965
4-Methyl-5-methylimino-1,2,4-dithiazolidine-3-thione	$CHCl_3$	1650		1470	1430	1410	1385		1278	1145w	1112	1057w	1010w	955
2,4-Dimethyl-1,2,4-thiadiazolidine-3,5-dithione	$CHCl_3$			1450	1425		1375		1300	1165		1095	1030	
Ethylenethiuram monosulphide – CS_2 complex	KBr	1605m		1485	1435w	1420			1280	1195	1135	1085		970
Thiourea	Nujol	1615		1475		1415						1085		
N,N-Dimethyl dimethylthiocarbamylsulphenamide	$CHCl_3$		1500		1445w	1410w	1382		1255	1150		1050m	995	980

monosulphide prompted potentiometric titrations to determine the presence or absence of weakly acid hydrogen in the compound in question. Harlow *et al.* (16) have shown the feasibility of potentiometric titration of very weak acids using tetrabutylammonium hydroxide as titrant in non-aqueous media. Structurally, 4-methyl-5-methylimino-1,2,4-dithiazolidine-3-thione (IV) and 2,4-dimethyl-1,2,4-thiadiazolidine-3,5-dithione (V) should show no consumption of alkali. The other compounds tested, i.e., ethylenethiuram monosulphide, dimethylthiuram mono- and di-sulphide, and 3,5-dimercapto-1,3,4-thiadiazole (II, R = H) should each show two inflection points in its titration curve. The results of these titrations, using tetrabutylammonium hydroxide in isopropyl alcohol as titrant and acetonitrile as solvent, are given in Figs. 3 and 4. Pyridine was also used as solvent in a parallel series of titrations, but, except in the case of dimercaptothiadiazole, no greater resolution was obtained. Cundiff and Markunas (17) have demonstrated the possibility of titrating potentiometrically organic dibasic acids whose ionization constants (K_1 and K_2) are close together, and of obtaining two sharp inflections in the titration curve. As can be seen in Figs. 3 and 4, two inflections were obtained with

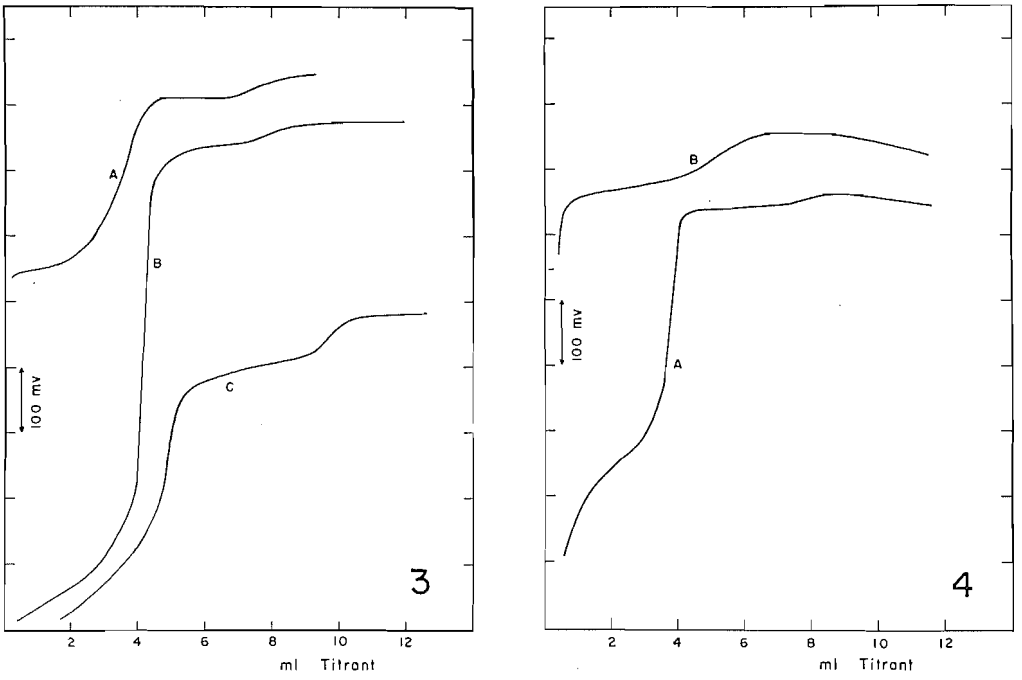


FIG. 3. Potentiometric titration curves. (A) Ethylenethiuram monosulphide. (B) Dimethylthiuram disulphide. (C) 2,5-Dimercapto-1,3,4-thiadiazole.
FIG. 4. Potentiometric titration curves. (A) Dimethylthiuram monosulphide. (B) 2,4-Dimethyl-1,2,4-thiadiazolidine-3,5-dithione.

all the above-mentioned compounds, except for IV and V. With ethylenethiuram monosulphide and dimethylthiuram disulphide, the inflections occurred at about 85% of equivalence, and with dimethylthiuram monosulphide, the inflections were at about 60–65% of equivalence. The discrepancy shown by dimethylthiuram monosulphide is not surprising in the light of the work of D'Angeli and Iliceto (8), who showed the instability of this compound in neutral solution and also the formation of molecular amounts

of sodium methyldithiocarbamate and methylisothiocyanate when the thiuram monosulphide was treated with an equivalent of sodium hydroxide. Similar decompositions probably occurred with ethylenethiuram monosulphide and dimethylthiuram disulphide during the titrations. It had been shown in earlier work (18) that ethylenethiuram monosulphide is converted to ethylenethiourea on treatment with alcoholic potassium hydroxide.

One unexpected result arising from these potentiometric titrations was the occurrence of a single weak inflection in the titration curve of dimethylthiadiazolidinedithione (V), at 80% of one equivalent of alkali. As expected, however, methyl-methylimino-dithiazolidine-thione (IV), on the other hand, gave no "titration curve".

Biological Studies

Ethylenethiuram monosulphide, 4-methyl-5-methylimino-1,2,4-dithiazolidine-3-thione (IV), 2,4-dimethyl-1,2,4-thiadiazolidine-3,5-dithione (V), and 2,5-dimercapto-1,3,4-thiadiazole were tested for biological activity by the A.P.S.-recommended spore drop method (19) using *Monilinia fructicola* as test organism. Dimethylthiuram monosulphide was not assayed in view of its instability. The dosage response data are shown in Fig. 5, plotted on logarithmic probability grid. These data were subjected to probit analysis, and $Y = a+bx$, the linear regression equation of toxicity probit values on the dose metameter, determined for each toxicant according to Finney (20). From these equations not only is the median lethal dosage, $m = (5-a)/b$, obtainable, but also the spread in distribution of tolerance, σ^2, a second expression of the effectiveness of the toxicant. The variance, σ^2, is equal to the reciprocal of the square of the slope, b, of the regression line. Toxicants whose physiological effects are similar often have approximately equal variances for any given organism, even though they may display substantial differences in their median lethal dosages. In other words, the slope of the regression line is considered a criterion of mechanism of fungicidal action (21, 22). If two fungicidal compounds yield different dosage response slopes, a different mechanism of action is inferred. Parallel slopes are given by members of homologous series.

The regression line equations for ethylenethiuram monosulphide (I), 4-methyl-5-methylimino-1,2,4-dithiazolidine-3-thione (IV), and 2,4-dimethyl-1,2,4-thiadiazolidine-3,5-dithione (V) were calculated to be: $Y_{\mathrm{I}} = 4.26+8.65 \log \lambda$, $Y_{\mathrm{IV}} = 3.45+0.12 \lambda$, and $Y_{\mathrm{V}} = 4.78+0.024 \lambda$. It will be noted that whereas I gives the more usual linear log-dosage response (20), a linear regression line is given by compounds IV and V according to the Parker–Rhodes equation (21). In most toxicity tests, the logarithm of λ is normally distributed, but occasionally λ itself has been found to be normally distributed. No explanation has as yet been advanced for this variation. The widely different values of b for the three compounds are thus indicative of differing chemical structure. This biological evidence complements the physicochemical evidence, presented above, that the structure of ethylenethiuram monosulphide is *not* given by VII, an analogue of the iminodithiazolidinethione (IV), but is in all likelihood structure (IB) as originally suggested (1, 2). It has been shown earlier (23) that ethylenethiuram monosulphide and 2,5-dimercapto-1;3,4-thiadiazole displayed regression lines of the same slope, differing in position, suggesting a similarity in structure.

Still unexplained is the formation of mono-addition compounds of ethylenethiuram monosulphide with HCl, $HClO_4$, and CS_2. The precipitation of these 1:1 compounds from solution as they are formed, together with electromeric influence through the

conjugated system to the second enethiol grouping, may be sufficient explanation for this apparent anomaly in structure.

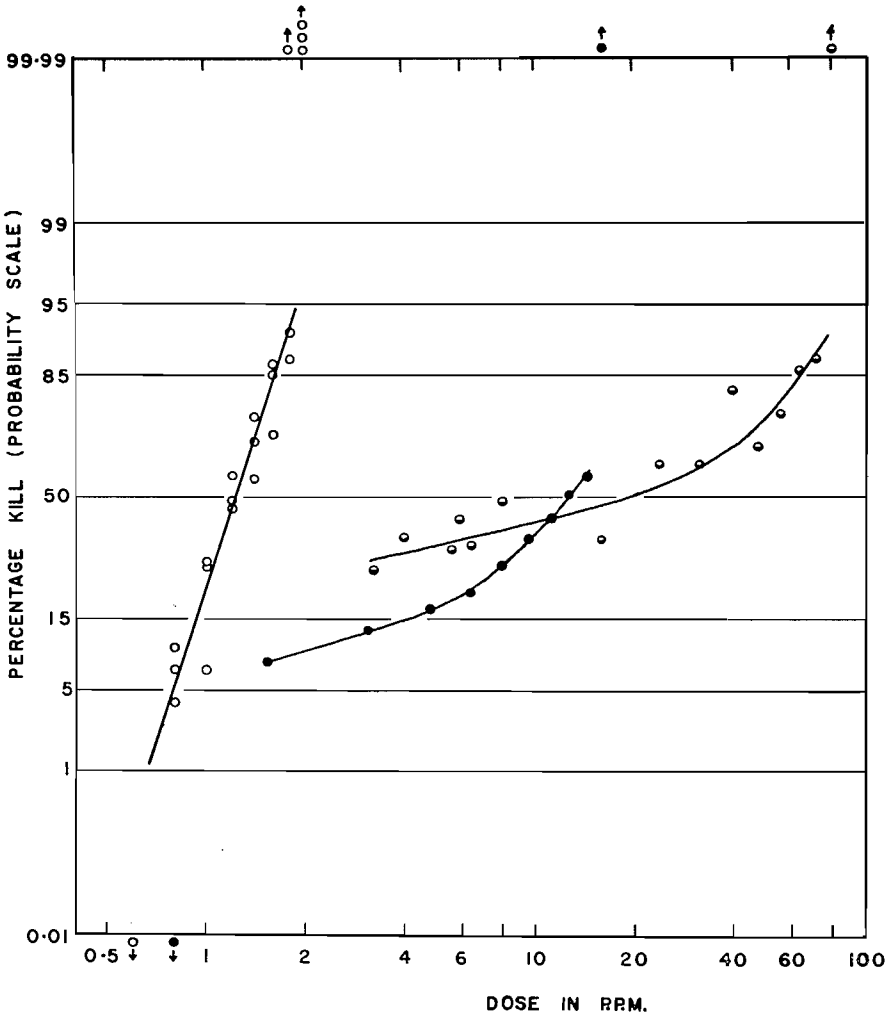


FIG. 5. An in vitro comparison of the fungicidal activities of ethylenethiuram monosulphide (○), 4-methyl-5-methylimino-1,2,4-dithiazolidine-3-thione (●), and 2,4-dimethyl-1,2,4-thiadiazolidine-3,5-dithione (◒).

EXPERIMENTAL

Ultraviolet absorption spectra were obtained in ethanol solution, using the Beckman DK-1 spectrophotometer. Infrared spectra were obtained with the Perkin–Elmer model 21, with NaCl optics, in chloroform solution or in Nujol[R] mull. Potentiometric titrations were performed with the aid of the Radiometer Titrator, type TTT1 with standard plug-type calomel and glass electrodes. The sample, 0.100 g, dissolved in 50 ml acetonitrile or pyridine, was stirred magnetically under a blanket of nitrogen, and the e.m.f. measured with increments of titrant. The titrant, approximately 0.2 *N* tetrabutyl-

ammonium hydroxide in methanol, was prepared according to the method of Harlow *et al.* (16) and standardized potentiometrically against benzoic acid.

Ethylenethiuram monosulphide (I) was isolated from the mixture resulting from air oxidation of disodium ethylenebisdithiocarbamate (24) by extraction with chloroform, addition of concentrated HCl to precipitate the ethylenethiuram monosulphide hydrochloride (2), filtration and suspension of the hydrochloride in chloroform, and addition of sodium hydroxide solution to convert the insoluble salt to ethylenethiuram monosulphide. The yellow chloroform solution was filtered, dried with anhydrous sodium sulphate, and evaporated to dryness to yield the thiuram monosulphide free of elemental sulphur, m.p. 120–123°. Crystallization from chloroform–ethanol gave material of melting point 125–126°.

2,5-Dimercapto- and *2,5-di(methylmercapto)-1,3,4-thiadiazole* (II) were prepared according to Thorn and Ludwig (21) and Thorn (6), respectively.

4-Methyl-5-methylimino-1,2,4-dithiazolidine-3-thione (IV) was obtained according to the method of Freund and Asbrand (10) by the action of bromine on ammonium methyldithiocarbamate. Crystallization from ethanol gave pale yellow material of melting point 84° (lit. (10), m.p. 86°). Calc. for $C_4H_6N_2S_3$: S, 53.9; N, 15.7%. Found: S, 53.7; N, 15.6%. *2,4-Dimethyl-1,2,4-thiadiazolidine-3,5-dithione* (V), obtained by rearrangement of IV with alcoholic ammonia (10), melted at 122–123° (lit. (12) gives 123–124°). Calc. for $C_4H_6N_2S_3$: S, 53.9; N, 15.7%. Found: S, 54.0; N, 15.5%.

Dimethylthiuram monosulphide was prepared by the reaction of equimolar amounts of methyl isothiocyanate and aqueous sodium methyldithiocarbamate (8). Addition of glacial acetic acid yielded colorless crystals of melting point 77–78° (lit. (8), m.p. 78–80°). Calc. for $C_4H_8N_2S_3$: S, 53.3; N, 15.5%. Found: S, 52.9; N, 15.6%.

The *ethylenethiuram monosulphide – carbon disulphide addition complex* was obtained by dissolving ethylenethiuram monosulphide in carbon disulphide. The brick-red complex, which precipitates within a few minutes, loses CS_2 upon heating above 100°, and melts at 125–126°. Calc. for $C_5H_6N_2S_5$: S, 63.0%. Found: S, 62.9%.

ACKNOWLEDGMENTS

The author is grateful for the discussions with Robert W. White and expresses his thanks to Marilyn Coleman for technical assistance, to Dorle Bongart for the microanalyses, and to C. H. Unwin for the biological assays.

REFERENCES

1. R. A. Ludwig and G. D. Thorn. Plant Disease Reptr. **37**, 127 (1953).
2. G. D. Thorn and R. A. Ludwig. Can. J. Chem. **32**, 872 (1954).
3. M. G. Ettlinger. J. Am. Chem. Soc. **72**, 4699 (1950).
4. H. M. Randall, R. G. Fowler, N. Fuson, and J. R. Dangl. Infrared determination of organic structures. D. Van Nostrand Co. Inc., New York. 1949. p. 66.
5. D. T. Elmore. J. Chem. Soc. 3489 (1958).
6. G. D. Thorn. Can. J. Chem. **38**, 1439 (1960).
7. A. H. M. Kirby and E. L. Frick. Ann. Rept. East Malling Res. Station. 1956. p. 146.
8. F. D'Angeli and A. Iliceto. Gazz. chim. ital. **89**, 2095 (1959).
9. M. Freund. Ann. **285**, 154 (1895).
10. M. Freund and E. Asbrand. Ann. **285**, 166 (1895).
11. A. Hantzsch and M. Wolvekamp. Ann. **331**, 278 (1904).
12. C. K. Bradsher, F. C. Brown, E. F. Sinclair, and S. T. Webster. J. Am. Chem. Soc. **80**, 414 (1958).
13. I. Benghiat, J. B. Bowers, G. E. Lukes, and S. L. Giolito. To Stauffer Chemical Co. U.S. Patent No. 2,863,803 (December 9, 1958).
14. R. Zahradník. Collection Czechoslov. Chem. Commun. **24**, 3193 (1959).
15. L. J. Bellamy. The infrared spectra of complex molecules. Methuen & Co. Ltd., London. 1954.

16. G. A. HARLOW, C. M. NOBLE, and G. E. A. WYLD. Anal. Chem. **28**, 787 (1956).
17. R. H. CUNDIFF and P. C. MARKUNAS. Anal. Chem. **28**, 792 (1956).
18. G. D. THORN and R. A. LUDWIG. Unpublished data.
19. THE AMERICAN PHYTOPATHOLOGICAL SOCIETY. Committee on Standardization of Fungicidal Tests. Phytopathology, **33**, 627 (1943).
20. D. J. FINNEY. Probit analysis. Cambridge University Press, Cambridge. 1952.
21. A. F. PARKER-RHODES. Ann. Appl. Biol. **29**, 126 (1942).
22. J. G. HORSFALL. Principles of fungicidal action. Chronica Botanica Co., Waltham, Mass. 1956.
23. G. D. THORN and R. A. LUDWIG. Can. J. Botany, **36**, 389 (1958).
24. R. A. LUDWIG and G. D. THORN. Can. J. Botany, **36**, 473 (1958).

EXOTHERMIC REACTIONS DUE TO ANNEALING OF DEFECTS IN OXIDE LATTICES: STUDY OF THE DECOMPOSITION OF CARBONATES[1]

C. N. R. Rao,[2] S. R. Yoganarasimhan, and M. P. Lewis[3]

ABSTRACT

Small exothermic reaction peaks are observed in the differential thermal curves of carbonates. The heat evolution is probably due to the removal of internal crystal defects in the metastable oxide lattices.

Can. J. Chem. Downloaded from www.nrcresearchpress.com by 210.87.254.5 on 09/05/12
For personal use only.

Recently, Rao and Pitzer (1) have reported that when magnesium and calcium hydroxides are heated just beyond their decomposition temperatures, there is some evolution of heat of the order of 300 to 400 calories per mole. This exothermic reaction was explained as due to the removal of internal crystal defects in the metastable oxide lattices formed just after the decomposition of the hydroxides. The possibility that the reduction in surface area of the oxides also contributed to the heat evolution was not excluded. We have now studied the decomposition of a few carbonates to see if similar exothermic reactions are observed in the oxides obtained by their decomposition. Differential thermal analysis and X-ray diffraction analysis have been employed for the study.

EXPERIMENTAL

The differential thermal analysis was carried out using a high-sensitivity apparatus described by Pask and Warner (2). A constant heating rate of 12 degrees per minute was employed in all the runs. The reaction temperatures reported here are constant only for a given set of experimental conditions.

The carbonates studied are $MgCO_3$, $CaCO_3$, $CdCO_3$, $ZnCO_3$, and Ag_2CO_3. All the carbonates were obtained commercially. The X-ray diffraction patterns were taken using a Rich Seifert X-ray unit or a North American Philips diffractometer fitted with a Geiger counter recording device.

RESULTS AND DISCUSSION

Typical differential thermal analysis curves are shown in Fig. 1. All the carbonates first showed large endothermic reaction peaks due to their decomposition to the corresponding oxides and carbon dioxide; immediately following these were observed small exothermic reaction peaks. The exothermic reactions were irreversible and occurred at temperatures usually 40–80° higher than the decomposition temperatures of the carbonates (Table I). It was made certain by X-ray analysis that the carbonates had completely decomposed to the oxides before the exothermic reaction. There was no change in crystal structure or parameters of the oxides after the exothermic reaction. Thus, the heat evolution could not have resulted from a crystal structure transformation. However, marked decrease in X-ray line widths were noticed in samples heated just past the exothermic reaction temperature indicating greater crystallinity in the samples. The

[1]*Manuscript received August 29, 1960.*
Contribution from the Department of Inorganic and Physical Chemistry, Indian Institute of Science, Bangalore, India.
[2]*To whom all the correspondence should be addressed at: Department of Inorganic and Physical Chemistry, Indian Institute of Science, Bangalore-12, India.*
[3]*Department of Ceramic Engineering, University of California, Berkeley, California, U.S.A.*

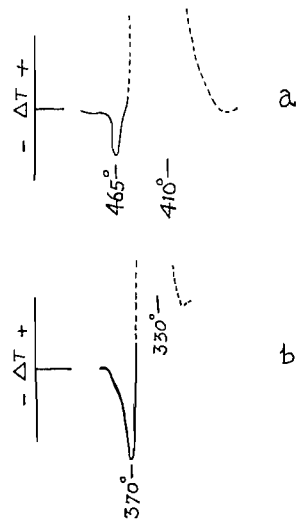


FIG. 1. Differential thermal analysis curves. (*a*) $MgCO_3$, (*b*) $ZnCO_3$. The dotted peaks correspond to the decomposition of the carbonates.

results reported in this communication on carbonates are similar to those observed in the decomposition of magnesium and calcium hydroxides (1).

The heats of the exothermic reactions were estimated by comparing the peak areas with the peak area for the α–β inversion of quartz (4.3 calories per gram). The heats thus estimated and the reaction temperatures for the different oxides are given in Table I. The values of ΔH are good to within $\pm 25\%$.

TABLE I

Carbonate	Endothermic reaction (decomposition) peak temperature, °C	Exothermic reaction peak temperature, °C	Estimated ΔH of the exothermic reaction, cal/mole of oxide
$MgCO_3$	410	465	360
$CaCO_3$	1015	1090	230
$ZnCO_3$	330	370	1000
$CdCO_3$	510	570	640
Ag_2CO_3	180	210	200

It is interesting to note that the heat evolution is very sharp and occurs over a short range of temperature in all the cases. It is known that the surface areas of oxides decrease with increase in temperature (3); but there is no reason why reduction in surface should result in a sharp evolution of heat over a short temperature range. When differential thermal analysis of oxides was extended to high temperatures where considerable reduction in surface area occurred, sharp exothermic reaction peaks were not noticed. The more important contribution to the heat evolution may be from the removal of internal crystal defects in the metastable oxide lattices. It is understandable that when a compound, say a hydroxide or carbonate, decomposes, it first gives a metastable or active oxide associated with a high degree of lattice disorder. This metastable oxide, when heated to a slightly higher temperature, goes into an ordered lattice. The decrease in the X-ray line widths apparently results from the annealing of these defects in the metastable oxide lattices. Such an interpretation of the decrease in X-ray line widths

Can. J. Chem. Downloaded from www.nrcresearchpress.com by 210.87.254.5 on 09/05/12
For personal use only.

Can. J. Chem. Downloaded from www.nrcresearchpress.com by 210.87.254.5 on 09/05/12
For personal use only.

is by no means new. It is therefore suggested that the observed evolution of heat mainly results from the disorder → order reaction (metastable oxide* → crystalline oxide) in the oxide lattice.

Exothermic reactions associated with large heats have been observed in the differential thermal analysis of hydrates of chromic and ferric hydroxides (4, 5) and titanium peroxide gel (6). The exothermic reactions are found just after the endothermic peaks due to the decomposition of the hydrate or the peroxide. It has been shown that the exothermic reactions in these cases result from the crystallization of the oxides from the amorphous state. The small exothermic reactions reported in this communication and elsewhere (1) may be similar to these crystallization reactions differing only in the magnitude of heat evolution. One may thus visualize the so-called disorder → order reaction in metastable oxide lattices as a crystallization process.

The formation of a metastable or active calcium oxide (CaO*) during decomposition of calcium carbonate has been proposed by Hyatt *et al.* (7) on the basis of their kinetic studies. These active CaO* groups are supposed to act as bridges between layers of well-crystallized cubic CaO and the decomposing $CaCO_3$. Razouk and Mikhail (8) have observed that the rate of crystallization of magnesium oxide obtained from the decomposition of magnesium hydroxide or carbonate at 500° is rather slow. This is probably reasonable. If the initial formation of a metastable MgO* similar to the CaO* proposed by Hyatt *et al.* (7) is postulated, the results of Razouk and Mikhail can be explained. Razouk and Mikhail have reported that some of the lines of the parent compound persist in the X-ray pattern of the oxides obtained by decomposition at 500° C. However, when the oxide was hydrated and then dehydrated at the same temperature only the pattern of the oxide was obtained. This indicates that Razouk and Mikhail have affected the crystallization of magnesium oxide by prolonged heating at 500° C, which would naturally render the process of rehydration difficult. If they had carried out their experiments at a slightly higher temperature, i.e. a temperature high enough for the exothermic disorder → order reaction of the metastable oxide, they would have probably obtained highly crystalline magnesium oxide in the first instance itself.

The crystalline and finely divided samples of magnesium oxide (9) and calcium oxide (10) have been reported to show large differences in their heat contents (~900 and 500 calories per mole respectively). The heat capacity of finely divided magnesium oxide is also found to be higher than that of crystalline magnesium oxide (9). The crystalline oxides were inevitably prepared by the decomposition of the hydroxides at high temperatures whereas the finely divided samples were prepared by decomposition at relatively low temperatures. On the basis of the investigations on the decomposition of carbonates and hydroxides (1), it is suggested that at least the major part of these heat content differences may be explained on the basis of the disorder → order reaction in oxides. A small irreversible exothermic reaction peak (ca. $\Delta H \sim -100$ calories per mole) has been noticed around 200° in the differential thermal analysis curve of silver oxide prepared by the dehydration of the freshly precipitated oxide (11). It is interesting to note that the oxide obtained by the decomposition of silver carbonate* also exhibits an irreversible exothermic reaction of the same magnitude (Table I). An irreversible heat evolution of about 300 calories per mole has been observed by Kobayashi (12) in the range 100–200° C during his measurements of the heat capacity of silver oxide. Kobayashi suggested

**The differential thermal analysis of curve Ag_2CO_3 first shows an endothermic peak due to decomposition of the carbonate to the oxide (Ag_2O^*) and CO_2 and then a small exothermic reaction peak around 210° C ($Ag_2O^* \rightarrow Ag_2O$, cryst.) followed by another endothermic peak due to the dissociation of Ag_2O.*

that the heat "originates in the melting of the *freezing in* of the crystal imperfections". Such "stabilization" of the silver oxide lattice at higher temperatures has successfully explained the discrepancies in the thermodynamics of the dissociation of silver carbonate (13). It therefore appears likely that the evolution of heat in the differential thermal analysis curves of silver oxide arises from the annealing of crystal defects.

ACKNOWLEDGMENTS

The authors are thankful to Professor M. R. A. Rao for his interest in the work. One of the authors (S. R. Yoganarasimhan) is thankful to the University Grants Commission of India for the award of a research scholarship.

REFERENCES

1. C. N. R. Rao and K. S. Pitzer. J. Phys. Chem. **64**, 282 (1960).
2. J. A. Pask and M. F. Warner. Am. Ceram. Soc. Bull. **33**, 168 (1954).
3. R. I. Razouk and R. Sh. Mikhail. J. Phys. Chem. **63**, 1050 (1959).
4. S. K. Bhattacharya, V. S. Ramachandran, and J. C. Ghosh. Advances in Catalysis, **9**, 114 (1957).
5. C. N. R. Rao and A. Mountwala. Unpublished results.
6. C. N. R. Rao and S. R. Yoganarasimhan. Unpublished results.
7. E. P. Hyatt, I. B. Cutler, and M. E. Wadsworth. J. Am. Ceram. Soc. **41**, 70 (1958).
8. R. I. Razouk and R. Sh. Mikhail. J. Phys. Chem. **62**, 920 (1958).
9. W. F. Giauque. J. Am. Chem. Soc. **71**, 3192 (1949).
10. K. Kobayashi. Sci. Repts. Tôhoku Univ. **34**, 153 (1950).
11. K. S. Pitzer, R. E. Gerkin, L. V. Gregor, and C. N. R. Rao. Symposium on Chem. Thermodynamics. Intern. Union of Pure and Appl. Chem. Wattens, Austria. 1959.
12. K. Kobayashi. Sci. Repts. Tôhoku Univ. **35**, 173 (1951).
13. K. Kobayashi. Sci. Repts. Tôhoku Univ. **35**, 283 (1951).

Can. J. Chem. Downloaded from www.nrcresearchpress.com by 210.87.254.5 on 09/05/12
For personal use only.

Can. J. Chem. Downloaded from www.nrcresearchpress.com by 210.87.254.6 on 09/05/12
For personal use only.

REDUCTION OF MONOHALOGENATED NITROBENZENES WITH HYDRAZINE AND RANEY NICKEL

A CONVENIENT PREPARATION OF HALOGENATED ANILINES[1]

B. E. Leggetter and R. K. Brown

ABSTRACT

The isomeric fluoro-, chloro-, bromo-, and iodo-nitrobenzenes can be converted to the corresponding halogenated anilines in good yield by refluxing methanolic hydrazine hydrate in the presence of Raney nickel.

INTRODUCTION

The reduction of alcoholic solutions of substituted nitrobenzenes with hydrazine hydrate in the presence of Raney nickel provides a facile and convenient method for the preparation of aromatic amines. This method has in recent years been applied successfully not only to the reduction of nitro compounds directly to amines without affecting most functional groups (1, 2) or destroying heat sensitive amines (3) but also to the conversion of nitro compounds to intermediate azoxy and hydrazo derivatives (4, 5, 6) and of nitriles to the hydrazones of the corresponding aldehydes (7). Palladized charcoal (8–12), ruthenium on charcoal (11, 12), and platinum (8) have been used in place of Raney nickel quite successfully in hydrazine reductions. Copper and iron powder have also been employed though with inferior results (13).

The present work was undertaken in order to provide a convenient method for the preparation of halogenated anilines, particularly the iodo derivatives, via reduction of the corresponding nitro compounds.

Whilst previous methods of preparation of halogenated anilines by reduction of the nitro precursors with reagents such as stannous chloride and hydrochloric acid (14, 15), tin and hydrochloric acid (16), iron and hydrochloric acid (15, 17, 18), or hydrogen and a nickel catalyst (19, 20, 21) and rhodium on alumina (22) have given fair to good yields in the case of fluoro-, chloro-, and bromonitro-benzenes, the same methods applied to the iodonitrobenzenes caused considerable displacement of the iodine atom and generally gave very low yields of the halogenated amines. Baeyer (14), however, has reported good yields of *o*-iodoaniline from the low-temperature reduction of *o*-iodonitrobenzene with stannous chloride and hydrochloric acid. The same reagents were used to prepare the para and meta isomers from their nitro precursors but no yields were given although it was stated that because increased temperatures were necessary to effect reduction of the *p*-iodonitrobenzene the yield of the *p*-iodoaniline was low (14). We have found that when *m*-bromonitrobenzene was reduced with Raney nickel and hydrogen at low pressure and at room temperature much aniline was produced (23).

RESULTS AND DISCUSSION

A summary of the results of this work is presented in the accompanying table. The melting points and boiling points are recorded for convenience along with reported constants.

[1]*Manuscript received August 4, 1960.*
Contribution from the Department of Chemistry, University of Alberta, Edmonton, Alberta. Taken from the thesis to be submitted by B. E. Leggetter to the Graduate School of the University of Alberta in partial fulfillment of the requirements for the Degree of Doctor of Philosophy.

The reduction of methanolic solutions of iodonitrobenzenes to iodoanilines with freshly prepared Raney nickel and hydrazine hydrate proceeds smoothly in reasonably good yields (64 to 87%) with little or no displacement of the iodine atom. The results are even better when the fluoro (80 to 90%), chloro (95%), and bromo (80 to 90%) analogues are involved. A study of the reaction conditions showed that the reduction is best accom-

TABLE I

Reduction of halogenated nitrobenzenes with Raney nickel and hydrazine ($R = C_6H_4NO_2$)

Compound	% yield of halogenated amine	Reduction method	Melting point or boiling point		
			Observed	Literature	
o-F-R	80	A	45°/2 mm	58°/11 mm	(15)
m-F-R	90	A	50°/2 mm	187°/760 mm	(25)
p-F-R	86	A	50°/2 mm	187°/767 mm	(15)
o-Cl-R	95	A	201°/700 mm	207°/760 mm	(26)
m-Cl-R	96	A	224°/700 mm	230°/760 mm	(26)
p-Cl-R	95	A	70–71°	69–70°	(26)
o-Br-R	90	A	27–28° (88°/8 mm)	32° (229°/760)	(27)
m-Br-R	82	A	14–15° (124°/12 mm)	17° (130°/12 mm)	(16)
p-Br-R	80	A	65–66°	66°	(27)
o-I-R	64	B	57–59°	60–61°	(14)
m-I-R	73	B	22–24° (128°/8 mm)	25° (145°/15 mm)	(27)
p-I-R	87	B	64–65°	67–68°	(14)

plished at elevated temperatures. Complete reduction of the nitro group to the amine occurs at the temperature of boiling methanol whereas reduction in methanolic solution at 25° was found to give in some cases only partially reduced products such as the azoxy or hydrazobenzene even though excess reducing agent is present. Furthermore, unless a large ratio of solvent to nitro compound is used, some products tend to precipitate as the less soluble intermediate compound. Furst and Moore (6) have also reported the formation of intermediate reduction products, the azoxybenzene and hydrazobenzene (but no azobenzene) particularly when a lower proportion of hydrazine to nitro compound is used, or when small volumes of solvent are employed. In addition, the quality of the Raney nickel catalyst has been shown by these authors to influence the extent of reduction (4).

In our work gradual addition of the hydrazine hydrate to a refluxing methanolic solution of the nitro compound to which Raney nickel had been added approximated the conditions of limited amount of reducing agent reported by Furst and Moore (6) and, especially when smaller amounts of solvent were employed, tended to produce intermediate reduction products as contaminants. Generally, best results were obtained when an excess of solvent was involved (solvent:solute $\approx$ 10:1 by weight) and the reducing agent (hydrazine:nitro compound $\approx$ 2:1) was always kept in excess by slow addition of the nitro compound to the refluxing alcoholic solution of hydrazine hydrate containing a small amount of Raney nickel. This modified procedure (method A in the experimental section) was found to be superior for the fluoro, chloro, and bromo analogues but gave somewhat lower yields than did the original method (method B in the experimental section) in the case of the iodo compounds. Attempts to reduce *m*-iodonitrobenzene to *m*-iodoaniline at 25° gave 3,3′-diiodoazobenzene rather than the expected *m*-iodoaniline.

Can. J. Chem. Downloaded from www.nrcresearchpress.com by 210.87.254.6 on 09/05/12
For personal use only.

Can. J. Chem. Downloaded from www.nrcresearchpress.com by 210.87.254.6 on 09/05/12
For personal use only.

EXPERIMENTAL

The methods of reduction employed for these experiments are shown in the following two examples. Commercially available reagent grade samples of the halogenated nitrobenzenes were used while the Raney nickel catalyst was prepared by published directions (24).

o-Bromoaniline by Method A

A methanolic solution of *o*-bromonitrobenzene (20.2 g, 0.1 mole) was added dropwise to a refluxing solution of hydrazine hydrate (64% hydrazine in water) (15.0 g, 0.3 mole) in methanol (70 ml) to which about 1 gram of Raney nickel had been added. The rate of addition of the *o*-bromonitrobenzene solution was such that the evolution of gases from the reaction mixture did not become too vigorous; generally about 10–15 minutes were required for this step. At the end of the addition, the solution was refluxed for 10 minutes by which time the characteristic yellow color of the nitro compound had disappeared. The Raney nickel was then separated by filtration. Evaporation of the solvent and purification of the product by steam distillation gave 15.5 g of material boiling at 88°/8 mm.

The following anilines were also prepared by this method, the percentage yields obtained being reported in the table: *o*-, *m*-, and *p*-fluoroaniline, *o*-, *m*-, and *p*-chloroaniline, and *o*-, *m*-, and *p*-bromoaniline.

m-Iodoaniline by Method B

A solution of *m*-iodonitrobenzene (13.0 g, 0.052 mole) in methanol (150 ml), containing 1 g of Raney nickel catalyst, was refluxed while hydrazine hydrate was added dropwise at such a rate that the evolution of gas did not become too vigorous. The addition of the hydrazine was discontinued when the reaction solution became colorless indicating complete reduction. Steam distillation of the residual oil obtained after removal of the solvent gave the required product, which was further purified by distillation under reduced pressure, b.p. 128°/5 mm, m.p. 22–24°; yield, 8.3 g (73%).

o-Iodo- and *p*-iodo-aniline were prepared by the above methods. Yields and physical constants are reported in the table.

ACKNOWLEDGMENTS

The authors wish to thank the National Research Council of Canada for financial assistance throughout the course of this work. One of us (B. E. L.) wishes to thank the National Research Council for support during the summer months.

REFERENCES

1. D. Balcom and A. Furst. J. Am. Chem. Soc. **75**, 4334 (1953).
2. L. M. Litvnenko and A. P. Grekov. Zhur. Obshcheĭ Khim. **27**, 234 (1957); Chem. Abstr. **51**, 12866 (1957).
3. R. K. Brown and N. A. Nelson. J. Am. Chem. Soc. **76**, 5149 (1954).
4. R. E. Moore and A. Furst. J. Org. Chem. **23**, 1504 (1958).
5. P. M. G. Bavin. Can. J. Chem. **36**, 238 (1958).
6. A. Furst and R. E. Moore. J. Am. Chem. Soc. **79**, 5492 (1957).
7. S. Pietra and C. Trinchera. Gazz. chim. ital. **86**, 1045 (1956); Chem. Abstr. **52**, 3721 (1958).
8. L. P. Kuhn. J. Am. Chem. Soc. **73**, 1510 (1951).
9. S. Pietra. Ann. chim. (Rome), **45**, 850 (1955); Chem. Abstr. **50**, 10668 (1956).
10. M. J. S. Dewar and T. Mole. J. Chem. Soc. 2556 (1956).
11. S. Pietra. Ann. chim. (Rome), **47**, 410 (1957); Chem. Abstr. **51**, 15438 (1957).
12. S. Pietra and M. Ris. Ann. chim. (Rome), **48**, 299 (1958); Chem. Abstr. **52**, 18277 (1958).
13. S. Kubota, K. Nara, and S. Onishi. J. Pharm. Soc. Japan, **76**, 801 (1956); Chem. Abstr. **51**, 1086 (1957).
14. A. Baeyer. Ber. **38**, 2760 (1905).

15. G. SHIEMAN and R. PILLARSKY. Ber. **62**, 3035 (1929).
16. S. NATELSON and S. P. GOTTFRIED. J. Am. Chem. Soc. **61**, 1001 (1939).
17. S. E. HAZLET and C. A. DORNFELD. J. Am. Chem. Soc. **66**, 1781 (1944).
18. D. W. MATHIESON and G. NEWBURY. J. Chem. Soc. 1133 (1949).
19. C. F. WINANS. J. Am. Chem. Soc. **61**, 3564 (1939).
20. F. BENINGTON, E. V. SHOOP, and R. H. POIRIER. J. Org. Chem. **18**, 1506 (1953).
21. N. M. LÖFGREN, B. J. LUNDQUIST, and S. LINDSTRÖM. Acta Chem. Scand. **9**, 1079 (1955).
22. Unpublished results.
23. U.S.P. 2,772,313; Chem. Abstr. **51**, 10570 (1957).
24. ORGANIC SYNTHESES. Coll. Vol. III. John Wiley and Sons, Inc., New York, 1955. p. 181.
25. C. K. INGOLD and C. C. N. VASS. J. Chem. Soc. 421 (1928).
26. F. BEILSTEIN and A. KURBATOW. Ann. **176**, 27 (1875).
27. J. M. HEILBRON. Dictionary of organic compounds. Eyre and Spottiswoode, London. 1934.

Can. J. Chem. Downloaded from www.nrcresearchpress.com by 210.87.254.6 on 09/05/12
For personal use only.

Can. J. Chem. Downloaded from www.nrcresearchpress.com by 210.87.254.105 on 09/05/12
For personal use only.

A SYSTEM OF MOLECULAR THERMOCHEMISTRY FOR ORGANIC GASES AND LIQUIDS

PART II. EXTENSION TO COMPOUNDS CONTAINING SULPHUR AND OXYGEN[1]

EDWARD G. LOVERING AND KEITH J. LAIDLER

ABSTRACT

The system of bond and group energies described in Part I has been extended and applied to certain compounds containing sulphur and oxygen. The substances treated are the alkanethiols, the thiaalkanes, and the dithiaalkanes. The bond additivity scheme enables reliable values for heats of formation, combustion, atomization, and vaporization to be calculated for these compounds.

A similar treatment has been applied to the data for alcohols, ethers, and alkyl peroxides.

INTRODUCTION

In Part I of this series (1) a scheme of bond and group energies, suitable for the reliable calculation of heats of formation, combustion, and atomization of organic compounds, was developed. The method was applied in some detail to the paraffins, olefins, and acetylenes. For other compounds adequate data for homologous series were not available, and only approximate group contributions could be obtained. A method whereby the scheme could be extended to substituted homologous series, when sufficient reliable data became available, was also given. During the past few years excellent data have become available for alkanethiols (R—S—H), thiaalkanes (R—S—R), and dithiaalkanes (R—S—S—R), and in the present paper the scheme is applied to these. A few recent data are also available for certain alcohols, ethers, and peroxides, and the scheme has been extended to cover these compounds also.

The previous paper also provided a scheme for the calculation of heats of vaporization, and it is applied in the present work to the sulphur compounds mentioned above.

HEATS OF FORMATION, COMBUSTION, AND ATOMIZATION

The heat of atomization is the energy required to dissociate 1 mole of a compound, in the gaseous state, into its constituent atoms in their ground states. The heats of atomization given in this paper are calculated with the aid of the following relationships, which apply at 25.0° C:

$$\begin{aligned} \text{C (graphite)} &= \text{C(g, }^3\text{P)} \quad -171.7 \text{ kcal},\\ \tfrac{1}{2}\text{H}_2\text{ (g)} &= \text{H(g)} \quad -52.09 \text{ kcal},\\ \tfrac{1}{2}\text{O}_2\text{ (g)} &= \text{O(g)} \quad -59.16 \text{ kcal},\\ \text{S (rhombic)} &= \text{S(g, }^3\text{P)} \quad -57 \text{ kcal}. \end{aligned}$$

The choice of the first three values was discussed in Part I. The value for the heat of sublimation of rhombic sulphur has not been firmly established. Cottrell (2) has recently reviewed the chemical and spectroscopic evidence, on the basis of which he favors the value of 57 kcal. We have chosen to use this value in the present paper.

Based upon the above relations, the heat of atomization, Q_a, of compounds containing carbon, hydrogen, sulphur, and oxygen is obtained through the equation

$$[1] \qquad Q_a = Q_f + 171.7\, n_C + 52.09\, n_H + 57\, n_S + 59.16\, n_O.$$

[1]*Manuscript received August 8, 1960.*
Contribution from the Department of Chemistry, University of Ottawa, Ottawa, Ontario.

Here Q_f ($= -\Delta H_f$) is the heat (evolved) of formation of the gaseous compound at 25° C and n_C, n_H, n_S, and n_O are the numbers of carbon, hydrogen, sulphur, and oxygen atoms, respectively.

The relationship between Q_a and the heat of combustion, Q_c, depends upon the combustion products. If these are carbon dioxide, water, and rhombic sulphur, then

$$[2] \qquad Q_a = -Q_c + 265.75\ n_C + 86.25\ n_H + 57\ n_S + 59.16\ n_O.$$

This equation is based upon heat of formation values for carbon dioxide and liquid water of 94.05 and 68.32 kilocalories per mole, respectively (3).

In view of the relationships between heats of combustion, formation, and atomization it is necessary to obtain a scheme for only one of them. In the following section this is done for heats of atomization.

EMPIRICAL SCHEMES FOR SULPHUR-CONTAINING COMPOUNDS

Heats of Atomization

The strength of all C—C bonds, denoted by c_1, and of the primary (p), secondary (s), and tertiary (t) C—H bonds is assumed to be the same as given in Part I, except in the case of C—H bonds when there is a sulphur atom bound to the carbon. These bonds, the bond symbol, and the bond strength are given in Table I.

TABLE I

Paraffin bond strengths

Bond	Symbol	Bond energy, kcal
C—C	c_1	85.40
C—H (primary)	p	98.47
C—H (secondary)	s	97.65
C—H (tertiary)	t	96.80

It is assumed that the presence of a C—S bond will affect the bond strength of hydrogen atoms bound to that carbon atom. These C—H bonds can be primary, secondary, or tertiary, and their strengths are denoted by p_s, s_s, or t_s respectively. It is further assumed that the S—C bond does not affect any other C—H bonds. Three types of bond directly involving sulphur atoms are considered. These are the S—H bond, of energy sh, the S—C bond, of energy sc, and the S—S bond, of energy ss. It is assumed that these bonds have the same energy in each of the three classes of sulphur compounds considered (alkanethiols, thiaalkanes, and dithiaalkanes).

Six quantities, sh, sc, ss, p_s, s_s, and t_s, must be determined from the experimental data. This has been done by a standard least-squares procedure, carried out on the IBM 650 computer through the courtesy of the staff of the Computing Center of the University of Ottawa. In this way the values given in Table II were obtained.

TABLE II

The bond strengths for sulphur compounds

$sh = 81.90$	$p_s = 98.14$
$sc = 66.36$	$s_s = 97.63$
$ss = 54.46$	$t_s = 97.14$

Can. J. Chem. Downloaded from www.nrcresearchpress.com by 210.87.254.105 on 09/05/12
For personal use only.

Heats of atomization calculated from these values, together with those in Table I, are compared with the experimental heats of atomization for various compounds in Table III. The heats of formation of the gaseous compounds at 25° C are also given in Table III.

TABLE III

Sulphur compounds: heats of atomization

Compound	Bonds	Q_f(obs.), kcal/mole	Q_a(obs.), kcal/mole	Q_a(calc.), kcal/mole	Q(obs.) − Q(calc.)	Ref.
Ethanethiol C_2H_6S	$sh+sc+2s_s+3p+c_1$	11.03	724.0	724.3	−0.3	4
2-Thiapropane C_2H_6S	$2sc+6p_s$	8.98	721.9	721.6	0.3	4
2,3-Dithiabutane $C_2H_6S_2$	$2sc+ss+6p_s$	5.75	775.7	776.0	−0.3	14
1-Propanethiol C_3H_8S	$sh+sc+2s_s+3p+2s+2c_1$	16.04	1004.9	1005.0	−0.1	12
2-Propanethiol C_3H_8S	$sh+sc+t_s+6p+2c_1$	18.04	1006.9	1007.0	−0.1	13
2-Thiabutane C_3H_8S	$2sc+3p_s+2s_s+3p+c_1$	14.07	1002.9	1003.2	−0.3	17
1-Butanethiol $C_4H_{10}S$	$sh+sc+2s_s+3p+4s+3c_1$	20.87	1285.6	1285.7	−0.1	5, 6
2-Butanethiol $C_4H_{10}S$	$sh+sc+t_s+6p+2s+3c_1$	22.97	1287.7	1287.7	0	5, 7
2-Methyl-1-propanethiol $C_4H_{10}S$	$sh+sc+2s_s+6p+t+3c_1$	23.06	1287.8	1287.7	0.1	5, 8
2-Methyl-2-propanethiol $C_4H_{10}S$	$sh+sc+9p+3c_1$	25.99	1290.7	1290.7	0	9
3-Thiapentane $C_4H_{10}S$	$2sc+4s_s+6p+2c_1$	19.77	1284.5	1284.9	−0.4	5, 15
2-Thiapentane $C_4H_{10}S$	$2sc+3p_s+2s_s+3p+2s+2c_1$	19.36	1284.1	1283.9	0.2	5, 6
3-Methyl-2-thiabutane $C_4H_{10}S$	$2sc+3p_s+t_s+6p+2c_1$	21.43	1286.1	1285.9	0.2	5, 16
3,4-Dithiahexane $C_4H_{10}S_2$	$2sc+ss+4s_s+6p+2c_1$	17.42	1339.1	1339.3	−0.2	14
1-Pentanethiol $C_5H_{12}S$	$sh+sc+2s_s+3p+6s+4c_1$	26.29	1566.9	1566.4	0.5	10, 11
4,5-Dithiaoctane $C_6H_{14}S_2$	$2sc+ss+4s_s+6p+4s+4c_1$	27.77	1901.2	1900.7	0.5	14
5-Thianonane $C_8H_{18}S$	$2sc+4s_s+6p+8s+6c_1$	40.3*	2408.5	2407.7	0.8	11

*T = 20° C; this compound was not included in the least-squares calculation.

The S—H, S—C, and S—S bond energies have also been given by Sunner (11). Since these are based upon heats of sublimation of graphite and rhombic sulphur of 138 and 66.3 kilocalories per mole, respectively, they are not directly comparable to the bond energies derived in this paper.

Heats of Vaporization

In Part I a scheme was developed which related the heat of vaporization (ΔH_v) to bond contributions. This scheme may now be extended to the sulphur compounds. The bond terms are the same as those used for the heats of atomization; they were evaluated by the least-squares procedure in the computer, and are given in Table IV. As in the

TABLE IV

Bond contributions to the heat of vaporization of sulphur compounds

sh = 2.209	p_s = 0.877
sc = 0.735	s_s = 1.002
ss = 2.349	t_s = 1.117

previous treatment, all C—C bonds are assumed to make a contribution of zero. The C—H contributions when there is no sulphur atom bound to the carbon are, as given in Part I,

$$p = 0.494 \text{ kcal/mole},$$
$$s = 0.579 \text{ kcal/mole},$$
$$t = 0.518 \text{ kcal/mole}.$$

Table V gives the experimental and calculated heats of vaporization, and the difference between them for each compound. The source of the heat of vaporization data is given in Table III.

Can. J. Chem. Downloaded from www.nrcresearchpress.com by 210.87.254.105 on 09/05/12
For personal use only.

Can. J. Chem. Downloaded from www.nrcresearchpress.com by 210.87.254.105 on 09/05/12
For personal use only.

TABLE V
Heats of vaporization of sulphur compounds

Compound	ΔH_v(obs.), kcal/mole	ΔH_v(calc.), kcal/mole	ΔH_v(obs.) − ΔH_v(calc.)
Ethanethiol	6.58	6.68	−0.10
2-Thiapropane	6.66	6.73	−0.07
2,3-Dithiabutane	9.18	9.08	0.10
1-Propanethiol	7.65	7.59	0.06
2-Propanethiol	7.08	7.03	0.05
2-Thiabutane	7.61	7.59	0.02
1-Butanethiol	8.74	8.75	−0.01
2-Butanethiol	8.13	8.18	−0.05
2-Methyl-1-propanethiol	8.30	8.43	−0.13
2-Methyl-2-propanethiol	7.39	7.39	0.00
3-Thiapentane	8.57	8.44	0.13
2-Thiapentane	8.67	8.74	−0.07
3-Methyl-2-thiabutane	8.18	8.18	0.00
3,4-Dithiahexane	10.86	10.79	0.07
1-Pentanethiol	9.83	9.90	−0.07
4,5-Dithiaoctane	12.94	13.11	−0.17
5-Thianonane	12.4	13.1	−0.7

HEAT OF ATOMIZATION CONTRIBUTIONS FOR COMPOUNDS CONTAINING OXYGEN

The data available for the oxygen analogues of the above sulphur compounds are not as plentiful, and in most cases they are not as reliable. The manner of treatment is the same as for the sulphur compounds: thus C—H bonds are assumed to be affected by the presence of oxygen only when the oxygen is attached to the same carbon atom, and all other interactions are neglected. The C—H bonds evaluated, with an oxygen bound to the carbon, and the symbols used to denote their energies are: the C—H primary, p_o; the C—H secondary, s_o; and the C—H tertiary, t_o. The bonds involving oxygen directly are the O—H bond, *oh*; the O—C bond, *oc*; and the O—O bond, *oo*. The bond energy terms were evaluated by putting the least-squares method in the computer. The bond energies are given in Table VI. The bonds involved, the heats of formation, and the experimental and calculated heats of atomization are given in Table VII.

TABLE VI
The bond strengths for oxygen compounds

oh = 109.79	p_o = 96.24
oc = 90.99	s_o = 95.42
oo = 47.72	t_o = 94.54

TABLE VII
Oxygen compounds: heats of atomization

Compound	Bonds	Q_f(obs.) (g, 25° C), kcal/mole	Q_a(obs.), kcal/mole	Q_a(calc.), kcal/mole	Q_a(obs.) − Q_a(calc.)	Ref.
Ethanol C_2H_6O	$oh+oc+2s_o+3p+c_1$	56.24	771.3	772.4	−1.1	3
Methyl ether C_2H_6O	$2oc+6p_o$	44.3	759.4	759.4	0.0	3
2-Propanol C_3H_8O	$oh+oc+t_o+6p+2c_1$	65.96*	1056.9	1056.9	0.0	19
1-Butanol $C_4H_{10}O$	$oh+oc+2s_o+3p+4s+3c_1$	67.84†	1334.7	1333.8	0.9	20
2-Methyl-2-propanol $C_4H_{10}O$	$oh+oc+9p+3c_1$	77.0	1343.9	1343.2	0.7	21
Diethyl peroxide $C_4H_{10}O_2$	$2oc+oo+4s_o+6sp+2c_1$	47.3	1373.3	1373.0	0.3	22
Diisopropyl ether $C_6H_{14}O$	$2oc+2t_o+12p+4c_1$	75.68†	1894.3	1894.3	0.0	19
2-Ethyl-1-hexanol $C_8H_{18}O$	$oh+oc+2s_o+6p+8s+t+7c_1$	87.43†	2457.8	2458.2	−0.4	20
Di(*tert*-butyl) peroxide $C_8H_{18}O_2$	$2oc+oo+18p+6c_1$	84.7	2514.2	2514.6	−0.4	21

*ΔH_f (l, 25° C) was given in the reference; ΔH_f (g, 25° C) was calculated from ΔH_f (l) and vapor pressure data (19).

†ΔH_f (l, 25° C) was given in the reference; ΔH_f (g, 25° C) was calculated from ΔH_f (l) and ΔH_v as calculated by the method given in Part I.

HEATS OF FORMATION AND COMBUSTION

Using the method described in Part I, bond contributions have been evaluated for the heats of formation and combustion of the gaseous and liquid compounds: these are given in Table VIII. For sulphur compounds, the products of combustion are taken to be water,

TABLE VIII

Bond contributions to heats of atomization, formation, and combustion of sulphur- and oxygen-containing liquids and gases

		Q_a		Q_f		Q_0	
Bond	Symbol	Gas	Liquid	Gas	Liquid	Gas	Liquid
C—C	c_1	85.40	85.40	−0.45	−0.45	47.48	47.48
C—H	p	98.47	98.96	3.45	3.94	54.22	53.73
C—H	s	97.65	98.23	2.63	3.21	55.04	54.46
C—H	t	96.80	97.32	1.78	2.30	55.89	55.37
S—H	sh	81.90	84.11	1.31	3.52	32.85	30.64
S—C	sc	66.36	67.10	−5.07	−4.33	28.58	27.84
S—S	ss	54.46	56.81	−2.34	0.01	2.34	0
C—H	p_s	98.14	99.02	3.12	4.00	54.55	53.67
C—H	s_s	97.63	98.63	2.61	3.61	55.06	54.06
C—H	t_s	97.14	98.26	2.12	3.24	55.55	54.43
O—H	oh	109.79		28.12		6.04	
O—C	oc	90.99		18.48		5.03	
O—O	oo	47.72		−11.44		11.44	
C—H	p_o	96.24		1.22		56.45	
C—H	s_o	95.42		0.40		57.27	
C—H	t_o	94.54		−0.48		58.15	

carbon dioxide, and rhombic sulphur. In practice the combustion products are carbon dioxide, and an aqueous sulphuric acid solution.

DISCUSSION

The differences between the experimental and calculated heats of formation indicate that the scheme is more successful with the sulphur compounds than with the oxygen compounds. This is probably because the experimental data are more accurate in the case of the former than the latter. The authors feel that the relatively poor agreement between the experimental and calculated heats of atomization of the oxygen compounds points out the need for more accurate heat of formation data on the various homologous series.

ACKNOWLEDGMENT

This work was supported by the Defence Research Board under Grant No. 1028-28.

REFERENCES

1. K. J. LAIDLER. Can. J. Chem. **34**, 626 (1956).
2. T. L. COTTRELL. The strengths of chemical bonds. Butterworths Scientific Publications, London. 1958.
3. U.S. NATIONAL BUREAU OF STANDARDS. Selected values of chemical thermodynamic properties. Ser. I. Washington. 1952.
4. J. P. MCCULLOUGH, W. N. HUBBARD, F. R. FROW, I. A. HOSSENLOPP, and G. WADDINGTON. J. Am. Chem. Soc. **79**, 561 (1957).
5. W. N. HUBBARD, W. D. GOOD, and G. WADDINGTON. J. Phys. Chem. **62**, 614 (1958).
6. D. W. SCOTT, H. L. FINKE, W. N. HUBBARD, J. P. MCCULLOUGH, G. D. OLIVER, M. E. GROSS, C. KATZ, K. D. WILLIAMSON, G. WADDINGTON, and H. M. HUFFMAN. J. Am. Chem. Soc. **79**, 1062 (1957).
7. J. P. MCCULLOUGH, H. L. FINKE, D. W. SCOTT, R. E. PENNINGTON, M. E. GROSS, J. F. MESSERLY, and G. WADDINGTON. J. Am. Chem. Soc. **80**, 4786 (1958).
8. D. W. SCOTT, J. P. MCCULLOUGH, J. F. MESSERLY, R. E. PENNINGTON, I. A. HOSSENLOPP, H. L. FINKE, and G. WADDINGTON. J. Am. Chem. Soc. **80**, 55 (1958).

Can. J. Chem. Downloaded from www.nrcresearchpress.com by 210.87.254.105 on 09/05/12
For personal use only.

9. J. P. McCULLOUGH, D. W. SCOTT, H. L. FINKE, W. N. HUBBARD, M. E. GROSS, C. KATZ, R. E. PENNINGTON, J. F. MESSERLY, and G. WADDINGTON. J. Am. Chem. Soc. **75**, 1818 (1953).
10. W. N. HUBBARD, C. KATZ, and G. WADDINGTON. J. Phys. Chem. **58**, 142 (1954).
11. S. SUNNER. Acta Chem. Scand. **9**, 837 (1955).
12. R. E. PENNINGTON, D. W. SCOTT, H. L. FINKE, J. P. McCULLOUGH, J. F. MESSERLY, I. A. HOSSENLOPP, and G. WADDINGTON. J. Am. Chem. Soc. **78**, 3266 (1956).
13. J. P. McCULLOUGH, H. L. FINKE, D. W. SCOTT, M. E. GROSS, J. F. MESSERLY, R. E. PENNINGTON, and G. WADDINGTON. J. Am. Chem. Soc. **76**, 4796 (1954).
14. W. D. SCOTT and J. P. McCULLOUGH. J. Am. Chem. Soc. **80**, 3547 (1958).
15. W. D. SCOTT, H. L. FINKE, W. N. HUBBARD, J. P. McCULLOUGH, G. D. OLIVER, M. E. GROSS, C. KATZ, K. D. WILLIAMSON, G. WADDINGTON, and H. M. HUFFMAN. J. Am. Chem. Soc. **74**, 4656 (1952).
16. J. P. McCULLOUGH, H. L. FINKE, J. F. MESSERLY, R. E. PENNINGTON, I. A. HOSSENLOPP, and G. WADDINGTON. J. Am. Chem. Soc. **77**, 6119 (1955).
17. D. W. SCOTT, G. B. GUTHRIE, J. P. McCULLOUGH, and G. WADDINGTON. J. Chem. & Eng. Data Ser. **4**, No. 3, 246 (1958).
18. K. D. WILLIAMSON and R. H. HARRISON. J. Chem. Phys. **26**, 1409 (1957).
19. G. S. PARKS and K. E. MANCHESTER. I.U.P.A.C. Sub-Commission on Experimental Thermochemistry. Thermochemical Bull. No. 2, March, 1956; the value is quoted with the kind permission of Professor G. S. Parks.
20. J. TJEBBES. Acta Chem. Scand. **14**, 180 (1960).
21. J. H. RALEY, F. F. RUST, and W. E. VAUGHAN. J. Am. Chem. Soc. **70**, 88 (1948).
22. R. E. REBBERT and K. J. LAIDLER. J. Chem. Phys. **20**, 574 (1952).

Can. J. Chem. Downloaded from www.nrcresearchpress.com by 210.87.254.105 on 09/05/12
For personal use only.

ABOUT THE PRIMARY ACT OF PHOTOCHEMICAL DECOMPOSITION REACTIONS OF MONOSUBSTITUTED COBALTIHEXAMINE IONS[1]

Z. SIMON

ABSTRACT

We will discuss the primary act of photochemical decomposition of $Co(NH_3)_5X^{n+}$ ions in aqueous solution. The potential energy surfaces are plotted correlating the complex ion's energy levels with those of the decomposition products. For this purpose spectral and kinetic data are used, as well as Wigner–Witmer correlation rules. The potential energy surfaces and certain rules regarding the radiationless transitions between them permit us to draw certain qualitative conclusions concerning these decompositions. Our conclusions seem to be confirmed by available experimental data.

INTRODUCTION

In order to describe the primary act of photochemical reactions, the potential energy surfaces of the molecules in their ground states and in electronically excited states, as well as the transition rates between the surfaces, should be known. Shuler (1) and Higuki (2) have discussed the photochemical decompositions of certain relatively simple molecules. They obtained the necessary surfaces by correlating the energy levels of the molecule and of the decomposition products, using the Wigner–Witmer correlation rules (3, 4). Linhard and Weigel (4*a*) have discussed the photochemical decomposition of the $Co(NH_3)_5X^{n+}$ ions based on ideas similar to those expressed in this article, without, however, taking into consideration the symmetry properties of the ions and the radiationless transitions.

In our paper we apply these correlation rules to more complicated molecules, namely to $Co(NH_3)_5X^{++}$ ions. We attach greater importance to the radiationless transitions than other authors and we use symmetry properties of the wave functions and the nuclear vibration co-ordinates. We proceed in the following manner: the decomposition of the molecule excited by light takes place following one of these processes:

1. The potential-energy surface for the excited state is unstable with respect to a vibrational co-ordinate along which the molecule is dissociated.

2. The electronic excitation energy is converted into vibrational energy of the ground state.

(*a*) If the vibration of a single valence bond is strongly enough excited, the molecule will immediately dissociate (predissociation).

(*b*) If a vibration which does not lead to direct dissociation is excited, the molecule will become vibrationally "overheated" and will either dissociate thermally or cool down without dissociation.

Should process 1 or 2 (*a*) take place, the quantum yield of the decomposition is about 1. Should process 2(*b*) take place, the quantum yield is small (ϕ smaller than about 0.01) for complex molecules as shown by Zimmermann (5) for the MnO_4^- ion. The correlation rules show whether process 1 or 2 takes place and indicate the decomposition products. If process 2 takes place, considerations regarding the radiationless transitions show whether it is a direct decomposition ($\phi \cong 1$) or a decomposition by the mechanism of the "hot" (i.e. containing excess vibrational energy) molecule ($\phi \lesssim 0.01$).

[1]*Manuscript received February 4, 1960.*
(Splaiul Independentei NR89, Bucuresti, R.P. Romina.)

Can. J. Chem. Vol. 38 (1960)

Can. J. Chem. Downloaded from www.nrcresearchpress.com by 210.87.254.105 on 09/05/12
For personal use only.

Experimentally, it has been established that $Co(NH_3)_5X^{++}$ ions irradiated in aqueous solution undergo aquation and oxidation–reduction decomposition. Photochemical and thermal aquation reactions follow, according to Adamson and Sporer (6), Basolo and Pearson (7), an S_N1 mechanism with the primary act,

$$Co(NH_3)_5X^{++}(aq.) \rightarrow Co(NH_3)_5^{+++}(aq.) + X^-(aq.). \quad [1]$$

The primary act of the oxidation–reduction decomposition is also a unimolecular decomposition (6),

$$Co(NH_3)_5X^{++}(aq.) \rightarrow Co(NH_3)_5^{++}(aq.) + X(aq.). \quad [2]$$

The quantum yields ϕ for irradiation with $\lambda = 370$ mμ and $\lambda = 550$ mμ, according to Adamson (6*a*), are given in Table I.

TABLE I

Experimental photochemical data (aqueous solutions 0.01*M*; 25° C) (6*a*)

Ion	ϕ and the nature of the reaction						Thermal aquation rate, k, min^{-1}
	370 mμ			550 mμ			
$Co(NH_3)_6^{+++}$	$<2\times10^{-3}$			$<2\times10^{-3}$			
$Co(NH_3)_5SO_4^+$	About 10^{-3}						7×10^{-5}
$Co(NH_3)_5F^{++}$	Small						4×10^{-6}
$Co(NH_3)_5Cl^{++}$	0.011	100%	A	1.5×10^{-3}	100%	A	1×10^{-4}
		Tr	R		Tr	R	
$Co(NH_3)_5Br^{++}$	0.21	50%	A	1.3×10^{-3}	100%	A	4×10^{-4}
		50%	R		Tr	R	
$Co(NH_3)_5NO_2^{++}$	1.0	35%	A				$<1\times10^{-6}$
		65%	R				
$Co(NH_3)_5SCN^{++}$	0.045	30%	A	6.7×10^{-4}	80%	A	2×10^{-7}
		70%	R		20%	R	
$Co(NH_3)_5N_3^{++}$	0.44	<1%	A	0.011	<1%	A	$<1\times10^{-6}$
		100%	R		100%	R	
$Co(NH_3)_5J^{++}$	0.66	<1%	A	0.10	<1%	A	5×10^{-4}
		100%	R		100%	R	

NOTE: A = aquation decomposition. R = oxidation–reduction decomposition. Tr = traces.

CORRELATION DIAGRAMS AND DECOMPOSITION PRODUCTS

The energy levels of $Co(NH_3)_5X^{++}$ ions were determined by using the spectral data of Nakamoto *et al.* (8) (and from tables (13)). The small differences of energy between the levels corresponding to the same spectral band are those calculated by Nakamoto *et al.* according to the simple molecular orbital method.

The energies for the ground states of the aquation reaction products (the right-hand equation [1] have been assumed equal to the activation energies for the thermal aquation reactions, that is about 1.1 ev (25 kcal/mole) for $X^{-1} = Cl^-$, Br^-, SCN^-, J^- and 1.5 ev (34 kcal/mole) for the aquation of the $Co(NH_3)_6^{+++}$ ion (7).

In order to calculate the energies of the ground states of oxidation–reduction decomposition products (the right-hand equation [2]), as sufficient data are not available to us, we will proceed as follows, based upon the observation of oxidation–reduction reaction traces at 370 mμ. We assume the energy of the ground state of $Co(NH_3)_5^{++}$ (aq.) + Cl (aq.) products should be 3.5 ev (a little more than the energy corresponding to 370 mμ), the corresponding energy of the $Co(NH_3)_5^{++}$ (aq.) + X (aq.) products being 3.5 ev plus the difference of energy ΔE_x between the process Cl^- (aq.) $\rightarrow$ Cl (aq.) + e and the processes:

Can. J. Chem. Downloaded from www.nrcresearchpress.com by 210.87.254.105 on 09/05/12
For personal use only.

$$Br^- \text{ (aq.)} \rightarrow Br \text{ (aq.)} + e \qquad \Delta E_{Br} = -0.5 \text{ ev}$$

$$J^- \text{ (aq.)} \rightarrow J \text{ (aq.)} + e \qquad \Delta E_{J} = -1.0 \text{ ev}$$

$$NH_3 \text{ (aq.)} \rightarrow NH_3^+\text{(aq.)} + e \qquad \Delta E_{NH_3} = +1.5 \text{ ev}$$

The values for ΔE_x were taken from (8) and thermochemical data (9).

A not very reliable, approximate, estimate of the difference between the energies of the products $Co(NH_3)_5^{++} + Cl$ and $Co(NH_3)_5^{+++} + Cl^-$ can be obtained identifying this difference with the enthalpy $\Delta H = \Delta H_2 - \Delta H_1 + \Delta H_3$ of the reactions:

$$Co(NH_3)_6^{++} \text{ (aq.)} \rightleftarrows Co(NH_3)_6^{+++} \text{ (aq.)} + e \qquad \Delta H_1$$

$$Cl^- \text{ (aq.)} \rightleftarrows \tfrac{1}{2}Cl_2\text{(g.)} + e \qquad \Delta H_2$$

$$\tfrac{1}{2}Cl_2\text{(g.)} \rightleftarrows Cl \text{ (aq.)} \qquad \Delta H_3$$

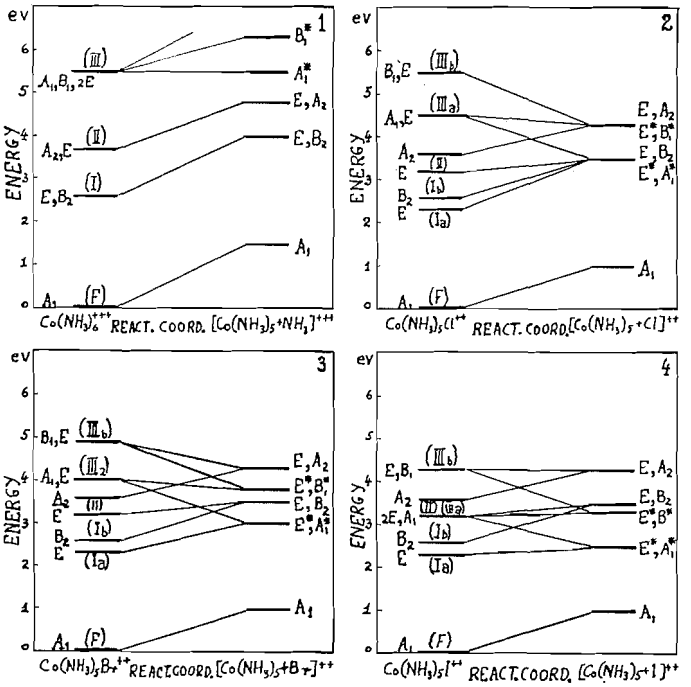
$\Delta H_2 - \Delta H_1 = 1.36 - 0.16 = 1.2$ ev (9) respectively Lamb and Larson (14), $\Delta H_3 \cong 1.2$ ev (9).

Thus $\Delta H \cong 2.4$ ev and the energy of the $Co(NH_3)_5^{++} + Cl$ products would be approximately $2.4 + 1.1 = 3.5$ ev. The value is perhaps an upper limit, as $Co(NH_3)_6^{+++}$ is more stable than $Co(NH_3)_6^{++}$ towards the dissociation of a NH_3 group.

We supposed that the energies of the first excited states of the $Co(NH_3)_5^{+++}$ are approximately equal to the excitation energies corresponding to the crystalline field bands in the $Co(NH_3)_5X^{n+}$ ions. This hypothesis appears plausible from the point of view of the crystalline field theory and from the fact that the position of the ligand field bands is approximately the same in the $Co(NH_3)_6^{+++}$, $Co(NH_3)_5Cl^{++}$, etc. ions (about 2.5 ev and 3.3 ev (8)). It also agrees with the result of the calculation based on the simple molecular orbital method (used for the excited energy levels of the aquation and oxidation-reduction decomposition products). The excited states of the halogen ions and of the NH_3 groups have not been taken into consideration because they have a very high energy. The position of the excited levels of the oxidation–reduction decomposition is less important (at least for not too short wave lengths) for the interpretation of the correlation diagrams because the energy of the ground state is high enough.

In Figs. 1, 2, 3, and 4 the energy levels of some complex ions have been listed on the left and the levels of the decomposition products on the right. The capital letters beside the energy levels represent electronic states having energy equal or approximately equal to that indicated by the level. The identification of the electronic states of complex ions with the energy levels observed spectroscopically was performed by taking into account the order of the molecular orbital energy levels calculated by Nakamoto *et al.* (8) and the degree of their occupation. The states of the oxidation–reduction decomposition products are starred. The capital letters show the species of the C_{4v} point group to which the respective electronic states belong. The states of the $Co(NH_3)_6^{+++}$ ion are recorded considering the resolution of the species belonging to the O_h point group to those of the C_{4v} point group. According to Nakamoto (8), the states marked in E(I), E(II), B_2, and A_2 which derive from the electronic configuration $(1e_g)^4(1a_{1g})^2(1f_{1u})^6(2f_{2g})^5(2e_g)$ belong to the two energy levels which correspond to the first two absorption bands of the $Co(NH_3)_6^{+++}$ ion. The attribution of these two states to the two energy levels is arbitrary. This does not affect the interpretation of the correlation diagrams, if the states of the dissociation products with which these states can be correlated are higher than the two first levels of the $Co(NH_3)_6^{+++}$ ion. This is the case if the first excited

Can. J. Chem. Downloaded from www.nrcresearchpress.com by 210.87.254.105 on 09/05/12
For personal use only.



FIGS. 1–4. Correlation diagrams for the $Co(NH_3)_6^{+++}$, $Co(NH_3)_5Cl^{++}$, $Co(NH_3)_5Br^{++}$, and $Co(NH_3)_5J^{++}$ ions.

state of the $Co(NH_3)_5^{+++}$ ion has approximately the same energy as in the $Co(NH_3)_6^{+++}$ ion; the reasons for this situation were discussed above.

In every case the energy of the complex ion's ground state was taken as origin in the scale of energies.

The energy levels of the complex ions are correlated with those of the aquation reaction products and of the oxidation–reduction decomposition products using the Wigner–Witmer correlation rules (3, 4). In the course of the decomposition (the elimination of X or X^-), the symmetry of the system remains C_{4v}. Although we are concerned with polyatomic molecules, we shall assume that only one vibrational co-ordinate varies. Thus, only the surfaces of different species of the molecular point group can intersect each other. In the case of the decomposition of the $Co(NH_3)_5X^{++}$ ions, no new valence bonds are formed, so that we assume that the electronic energy of different states changes continuously with respect to the reaction co-ordinate.*

Levels III from ultraviolet ($\lambda \gtrsim 300$ mμ) correlate with lower levels of the ionic and oxidation–reduction decomposition products. That is why in ultraviolet the quantum yield for the redox and aquation reactions should approach 1 (or be even greater if

If the energy levels were known more exactly, it would be useful to correlate first the "crystalline field (the Co^{+3}) states" of the reactants with those of the ionic decomposition products and the "charge transfer (the Co^{+2}) states" with those of the redox decomposition products. Afterwards, taking into account the configuration interaction which appears between some Co^{+3} and Co^{+2} states, a correlation diagram would be obtained which respects the Wigner–Witmer non-crossing rules and also indicates intermediate maxima on potential-energy curves. For example, the E(II) state of $Co(NH_3)_5Cl^{++}$ would correlate with the state E at about 4.3 ev of the ionic decomposition products; configuration interaction with the E(IIIa) (which without Cl correlates with the E level at 3.5 ev) state would produce the correlation with an E* level at about 3.5 ev, producing also a maxima on the E(II)–E* potential curve.*

Can. J. Chem. Downloaded from www.nrcresearchpress.com by 210.87.254.105 on 09/05/12
For personal use only.

chain reactions are involved). The decomposition should take place by process 1. The I and II levels of the near ultraviolet and visible spectrum usually correlate with higher states of the decomposition products. For this reason, the decomposition at 370 mμ and 550 mμ for which ϕ was measured will take place via process 2. Figures 1, 2, 3, 4 show that the oxidation–reduction decomposition is favored by the increase in oxidizability of X^- in the series NH_3, Cl^-, Br^-, J^-. For instance, the level I (corresponding to the first crystalline field band) of $Co(NH_3)_5Cl^{++}$ correlate with higher levels of the decomposition products. For $Co(NH_3)_5J^{++}$ the first excited level $E(I)$ already correlates with level E^* of the oxidation–reduction decomposition products which is approximately isoenergetic. The correlation diagrams show that the complex ions in their ground state may only undergo aquation reaction. The data in Table I confirm the favoring of the oxidation–reduction decomposition passing from $Co(NH_3)_6^{+++}$ to $Co(NH_3)_5J^{++}$. The complex ions in Table I are placed, according to Adamson, approximately in the ascending order of oxidizability of X^-.

RADIATIONLESS TRANSITIONS. QUANTUM YIELDS

When we plotted the correlation diagrams we considered the singlet states alone. The neglect of the triplet states is justified by the following three circumstances: Nakamoto (8) succeeded in interpreting the absorption spectra of these complexes on the ground of only their singlet states. According to Kasha (10) the radiationless transitions between excited singlet states are much more rapid than those between singlet and triplet states. In some previous papers (11), we have shown that radiationless singlet–singlet transitions can occur with a high probability (corresponding to a rate of approximately 10^{10} sec^{-1}) if the interaction between the movement of the electrons and that of the nuclei is strong enough and the anharmonicity of the nuclear movement great enough. The interaction energy W_{AB}, which produces the transition between the potential-energy surfaces A and B, is equal to

$$[3] \qquad W_{AB} = \frac{h^2}{2\pi^2 M} \int \phi_A^* \frac{\partial \phi_B}{\partial r}\, dr \int X_A^* \frac{\partial X_B}{\partial r}\, dx.$$

X_A and X_B are electronic wave functions; ϕ_A and ϕ_B are vibrational wave functions in the Born–Oppenheimer approximation; x stands for electronic co-ordinates, r the vibrational (nuclear) ones, and M is the corresponding reduced nuclear mass. Formula [3] is obtained by a method of first approximation in relation to the Born–Oppenheimer approximation (11) (see likewise Hellmann (12)). In our case we have diluted aqueous non-fluorescent solutions (7). That is why we do not consider the possibility of intermolecular energy transfer between the complex ions and we shall assume that the radiationless transitions have a high rate ($> 10^{10}$ sec^{-1}) unless they are forbidden by symmetry considerations.

In this way, we can explain the low quantum yields for the aquations at $\lambda = 550$ mμ (see Table I) and also at 370 mμ for $Co(NH_3)_5Cl^{++}$ and the preceding ions. The correlation diagrams show that the decomposition in this case will take place according to process 2. Let us show that process 2(a) is prevented for reasons of symmetry, so that the decomposition actually takes place according to process 2(b), for which we must expect $\phi \gtrsim 0.01$. The dissociation of particle X in $Co(NH_3)_5X^{++}$ does not change the symmetry of the system, therefore the vibrational co-ordinate r and also $\partial/\partial r$ belong to the A_1 species. The electronic function of the ground state also belongs to A_1 species. In order that integral $\int X_A^*(\partial X_B/\partial r)dx$ should not vanish, the electronic wave function

Can. J. Chem. Downloaded from www.nrcresearchpress.com by 210.87.254.105 on 09/05/12
For personal use only.

X_B of the excited state must also belong to the A_1 species (independent of the vibrational wave functions ϕ_A and ϕ_B, which are not implied in this integral). As may be seen in Nakamoto's work (8), it is only by absorption in the relative distant ultraviolet that such a state can be obtained.

It remains to be explained why aquation is not produced by the elimination of the NH_3 molecule. The activation energy for the elimination of NH_3, at least from $Co(NH_3)_6^{+++}$, is greater than for the elimination of halogen (1.5 ev instead of 1.1 ev (7)). According to Zimmermann's arguments, this fact explains why NH_3 is eliminated with greater difficulty than X^- in the case of process 2(*b*). But process 2(*a*) is no longer prevented for reasons of symmetry, because the elimination of NH_3 considerably modifies the symmetry of the complex. For the ions under consideration, however, the five or six Co–NH_3 valency vibrations interact strongly. That is why the elimination of NH_3 can only be achieved by the simultaneous excitation of the five or six corresponding normal vibrations. The interaction energy W_{AB} (formula [3]) is also proportional to the integral $\int \phi_A^* (\partial \phi_B / \partial r) dr$. In this integral the derivative is only once performed with respect to a single normal vibrational co-ordinate. There remain as factors four or five overlap integrals amid a vibration function corresponding to a low vibrational quantum number (from ϕ_A) and a function for a high quantum number (from ϕ_B). We have shown that such overlap integrals are small (11). Therefore, the electronic excitation energy will be converted into the energy of a vibration that leads to the formation of a "hot" molecule (process 2(*b*)).

CONCLUSIONS

We applied the Wigner–Witmer correlation rules to discuss the photochemical decomposition of certain molecules more complex than those to which these rules have so far been applied. We discussed in greater detail than in other papers of this kind the radiationless transitions between different potential-energy surfaces. Theoretical considerations suggest the following mechanism for the photochemical decomposition of the $Co(NH_3)_5X^{++}$ ions:

(*a*) Through excitation with fairly short wave-length light ($\lambda \lesssim 220$ mμ for $Co(NH_3)_6^{+++}$, $\lambda \lesssim 350$ mμ for $Co(NH_3)_5Br^{++}$) unstable states with respect to the dissociation of atom X or of ion X^- (or rather NH_3^+ and NH_3) are obtained. Both aquation and oxidation–reduction decomposition should take place with a large total quantum yield ($\phi \cong 1$).

(*b*) Through excitation with longer wave-length light only ionic dissociation (followed by aquation) occurs according to the "hot" molecule mechanism. Hence the quantum yield is low. As we indicated above, the most stable of the ions is $Co(NH_3)_6^{+++}$.

The experimental data of Adamson (6*a*) (Table I) agree with this mechanism, which, however, differs from that suggested by Adamson and Sporer (6). They assume the same initial stage for all the wave lengths—an internal oxidation–reduction reaction—the final transformation of the ion depending on the subsequent stages.

Their mechanism also explains the photochemical decomposition characteristics of the complex ions, but according to the correlation diagrams by the excitation with $\lambda = 550$ mμ the energy is in many cases insufficient for redox decomposition. It is true that the value assumed for the ground state of the $Co(NH_3)_5^{++} + Cl$ (and therefore also for $Co(NH_3)_5^{++} + X$) is not too reliable. If, however, the redox decomposition products separate with an energy excess of 0.5 ev or more, considering the activation energy of

Can. J. Chem. Downloaded from www.nrcresearchpress.com by 210.87.254.105 on 09/05/12
For personal use only.

diffusion in water (which is about 0.15 ev) it seems improbable that the cage effect of the solvent should be capable of providing the recombination of the dissociated particles, as stated by Adamson and Sporer (6).

ACKNOWLEDGMENTS

We are indebted to Dr. Léo Marion, who was so kind to give us the opportunity of seeing the preprint of a paper by Adamson (6*a*) (from the Discussion meeting of the Faraday Society, April 1960).

REFERENCES

1. K. E. SHULER. J. Chem. Phys. **21**, 624 (1953).
2. K. HIGUKI. Bull. Chem. Soc. Japan, **30**, 382 (1957).
3. J. NEUMANN and E. WIGNER. Physik. Z. **30**, 467 (1929).
4. K. J. LAIDLER. The chemical kinetics of excited states. Oxford at the Clarendon Press. 1955. p. 21.
4*a*. M. LINHARD and M. WEIGEL. Z. anorg. Chem. **266**, 49 (1951).
5. G. ZIMMERMANN. J. Chem. Phys. **23**, 825 (1955).
6. A. ADAMSON and A. SPORER. J. Am. Chem. Soc. **80**, 3865 (1958).
6*a*. A. W. ADAMSON. Discussions Faraday Soc. (1960).
7. F. BASOLO and R. G. PEARSON. Mechanisms of inorganic reactions. John Wiley & Sons, Inc., New York. 1958. Chap. 3.
8. K. NAKAMOTO, J. FUJITA, M. KOBAYASHI, and R. TSUCHIDA. J. Chem. Phys. **27**, 439 (1957).
9. A. F. KAPUSTINSSKI. Termiceskie Konstanty neorganiceskich beskestv. izd. Akad. Nauk S.S.S.R. Moskov, Leningrad. 1949. Tables.
10. M. KASHA. Discussions Faraday Soc. **9**, 14 (1950).
11. Z. SIMON. Studii şi cercetări de fizică, **9**, 469 (1958); **10**, 291, 317 (1959).
12. H. HELLMANN. Einführung in die Quantenchemie Deuticke, Leipzig, Wien. 1937. Chap. VIII.
13. LANDOLT-BÖRNSTEIN. Tabellen Bd. I. 3 Teil: Molekeln 2. Springer-Verlag, Berlin. 1951.
14. A. B. LAMB and A. T. LARSON. J. Am. Chem. Soc. **42**, 2024 (1920).

Can. J. Chem. Downloaded from www.nrcresearchpress.com by 210.87.254.105 on 09/05/12
For personal use only.

Can. J. Chem. Downloaded from www.nrcresearchpress.com by 210.87.254.42 on 09/05/12
For personal use only.

CONSTITUTION OF AN ARABINOGALACTAN FROM MAPLE SAP[1]

G. A. Adams and C. T. Bishop

ABSTRACT

An arabinogalactan ($[\alpha]_D^{25}$ −41°) has been isolated from maple sap in yields varying between 7.5 and 17.0 mg per 100 ml of sap. The polysaccharide was electrophoretically homogeneous and contained D-galactose, L-arabinose, and rhamnose in a molar ratio of 51:44:5. Methylation and hydrolysis of the polysaccharide yielded the following *O*-methyl ethers which were analyzed by gas–liquid partition chromatography: 2,3,5-tri-*O*-methyl-L-arabinose (4 moles); 2,5-di-*O*-methyl-L-arabinose (2 moles); 2,4-di-*O*-methyl-D-galactose (4 moles); 2,4,6-tri-*O*-methyl-D-galactose (7 moles); 2,3,4-tri-*O*-methyl-L-rhamnose (1 mole). A possible structure for the polysaccharide is proposed and discussed in relation to other arabinogalactans.

One of the reasons for studying non-cellulosic wood polysaccharides is that a knowledge of their structures may help in elucidating the modes of formation and the physiological roles of these materials in the plant. In recent years there have been reports of the synthesis of polymeric carbohydrates by transglycosidation reactions catalyzed by enzymes extracted from plants (1, 2, 3). It seemed possible that a physiologically active material like wood sap might be rich in products of transglycosidation reactions and that it would be interesting to see, by correlation of structures, if such products bore any significance as precursors in the formation of non-cellulosic wood polysaccharides. Maple wood was chosen for this study because of its high production of sap and because the non-cellulosic polysaccharides of this wood had already been examined (4, 5).

A previous publication (6) described the isolation of a polysaccharide from maple sap, some of its properties, identification of the component monosaccharides, and showed that it was a true sap constituent and not of bacterial or fungal origin. The present report describes methylation studies on the maple sap polysaccharide and compares the main structural features with those of other arabinogalactans.

The polysaccharide, isolated from the non-dialyzable sap constituents by precipitation with ethanol, contained D-galactose, L-arabinose, and rhamnose and showed one large pand one small component on electrophoresis (6). One repetition of the fractional precipitation with ethanol (7) yielded the larger component in a form which gave a single sharp peak ($\mu = 9.36 \times 10^{-5}$ cm^2 volt^{-1} sec^{-1}) on free-boundary electrophoresis in borate buffer (8). The relative amounts of constituent monosaccharides reported previously (6) were found to be inaccurate because of variations in reactivity of the different sugars with silver nitrate in the method used (9). The monosaccharide composition was therefore redetermined by a new method: the polysaccharide was hydrolyzed and the reducing sugars were converted to their glycosides which were then methylated completely by the Kuhn (10) procedure. The resulting mixture of fully methylated methyl glycosides was then analyzed by gas–liquid partition chromatography (11, 12) giving the separation shown in Fig. 1. Areas under the six peaks were measured and those arising from a single monosaccharide were totalled giving a molar ratio of galactose:arabinose:rhamnose of 51:44:5. It was possible to use this method here because each of the fully methylated monosaccharides was completely separated in both furanoside and pyranoside ring forms. It is interesting to note that considerable amounts of the furanoside forms of D-galactose and L-arabinose were present although the methanolysis was carried out under conditions that are generally considered to yield primarily pyranosides.

[1]*Manuscript received August 30, 1960.*
Contribution from the Division of Applied Biology, National Research Council, Ottawa, Canada. Presented at a meeting of the Royal Society of Canada, Kingston, June 7, 1960.
Issued as N.R.C. No. 6015.

Can. J. Chem. Downloaded from www.nrcresearchpress.com by 210.87.254.42 on 09/05/12
For personal use only.

The polysaccharide was methylated to completion and hydrolyzed by formic acid (13). Paper chromatographic examination of this hydrolyzate revealed the presence of three components having the same mobilities as 2,3,5-tri-*O*-methyl arabinose; 2,4,6-tri-*O*-methyl galactose; and 2,4-di-*O*-methyl galactose. The mixture of *O*-methyl ethers was converted to methyl glycosides and examined by gas–liquid partition chromatography to give the separation shown in Fig. 2. Identities of the compounds listed were established by comparison of their retention volumes on the gas–liquid partition chromatogram with authentic samples and by their isolation as crystalline derivatives. The shoulder on peak 2, Fig. 2, was identified as methyl 2,3,4-tri-*O*-methyl α-L-(?)-rhamnopyranoside

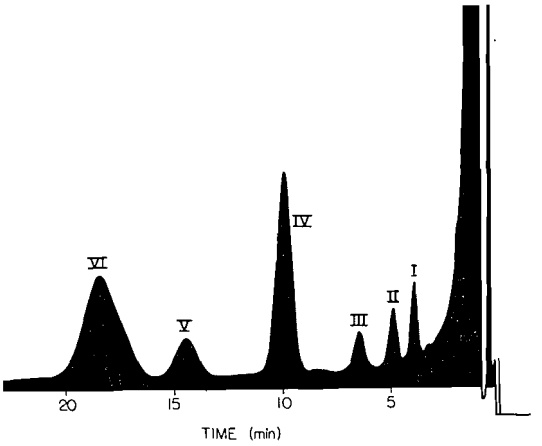


FIG. 1. Separation of fully methylated methyl glycosides of sugars present in maple sap arabinogalactan. Conditions: butanediol succinate polyester liquid phase, 150° C, 150 ml argon/minute.

(I) Methyl 2,3,4-tri-*O*-methyl-α-L-rhamnopyranoside.
(II) and (III) Methyl 2,3,5-tri-*O*-methyl-α-β-L-arabofuranoside.
(IV) Methyl 2,3,4-tri-*O*-methyl-α-β-L-arabopyranoside.
(V) Methyl 2,3,5,6-tetra-*O*-methyl-α-β-D-galactofuranoside.
(VI) Methyl 2,3,4,6-tetra-*O*-methyl-α-β-D-galactopyranoside.

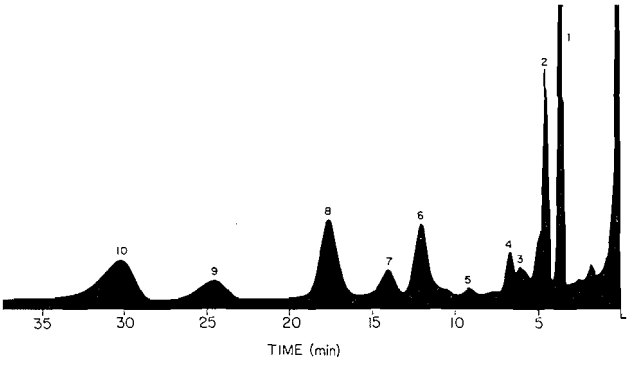


FIG. 2. Separation of methanolysis products from fully methylated maple sap arabinogalactan. Conditions: Apiezon M liquid phase, 150° C, 170 ml argon/minute.

(1) Methyl 2,3,5-tri-*O*-methyl-α-β-L-arabofuranoside.
(2) Methyl 2,5-di-*O*-methyl-α-β-L-arabofuranoside.
(3), (4), (5), and (6) Not identified positively.
(7) Methyl 2,4,6-tri-*O*-methyl-β-D-galactopyranoside.
(8) Methyl 2,4,6-tri-*O*-methyl-α-D-galactopyranoside.
(9) Methyl 2,4,-di-*O*-methyl-β-D-galactopyranoside.
(10) Methyl 2,4-di-*O*-methyl-α-D-galactopyranoside.

by separation of the mixture on butanediol succinate polyester liquid phase (see, for example, Fig. 1). This procedure also permitted the quantitative estimation of the rhamnose component. The amounts of the rhamnose moiety obtained here and in the preliminary study (6) were not sufficient for measurement of specific rotation. Its assignment as the normally occurring L-enantiomorph must therefore be regarded as tentative, although probably correct.

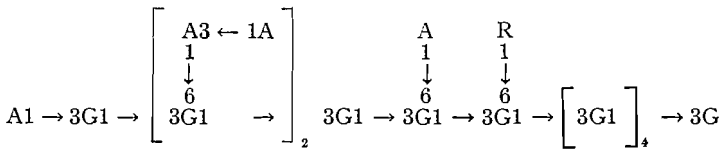
The components giving peaks 3, 4, 5, and 6 could not be identified positively. Peaks 3 and 4 (together, about 7% of the total mixture) had retention volumes in the range predicted for di-*O*-methyl pentoses but were different from glycosides of 2,3-, 2,4-, and 2,5-di-*O*-methyl-L-arabinose on the gas–liquid chromatogram. These peaks could represent glycosides of 3,4- and 3,5-di-*O*-methyl-L-arabinose or could be the separated anomeric glycosides of one of these isomers; however, lack of authentic samples prevented further investigation of these components. The component represented by peak 5 constituted less than 1% of the total mixture and was therefore regarded as of doubtful structural significance. Component 6 was different, on the gas–liquid chromatogram, from glycosides of all available *O*-methyl ethers of L-arabinose and D-galactose. When the mixture was run on a polar liquid phase (butanediol succinate polyester) component 6 had a much higher retention volume indicative of the presence of hydroxyl or other polar groups (12). In an attempt to isolate component 6 the mixture of glycosides was hydrolyzed by aqueous hydrochloric acid and separated into three fractions by preparative paper chromatography. These three fractions were then methanolyzed and examined by gas–liquid partition chromatography. No trace of component 6 could be found in these fractions or in methanolyzates of eluates from blank areas of the paper chromatograms. It must therefore be concluded that component 6 was an acid-labile artifact produced during the formic acid hydrolysis of the methylated polysaccharide. Such an artifact could be either a formate ester or an anhydro sugar and the former is favored because of the polar characteristics mentioned above. Quantitative estimation of those components in Fig. 2 that were identified gave a molar ratio of galactose:arabinose:rhamnose of 61:33:6 (see Fig. 3). This is low in arabinose when compared with the composition of the original polysaccharide (galactose:arabinose:rhamnose 51:44:5) and indicated that component 6 was probably an arabinose derivative. When the disappearance of component 6 after acid hydrolysis was observed some of the other components had already been isolated as crystalline compounds and it was not possible to reconstitute the mixture to see which component had increased at the expense of component 6. No new compounds were found after the disappearance of component 6 so it must have been a derivative of one of the other compounds in the mixture. It should be mentioned that components 3–6 inclusive were not detectable by paper chromatography and, indeed, the 2,5-di-*O*-methyl-L-arabinose may have been missed because of the difficulty in separating it from tri-*O*-methyl-D-galactose by that technique. The detection of unknown components is to be expected in the application of gas–liquid partition chromatography to this field; their identification will depend on the accumulation of pure standards and on improved gas–liquid chromatographic procedures that will permit their isolation.

Despite the presence of some unidentified methyl ethers the identification and estimation of the major components in the methanolysis products revealed the gross structural features of the polysaccharide. Figure 3 shows the molar ratio of the methyl ethers that were identified and a structure that would give those results. This structure is not proposed as unique or complete for the arabinogalactan from maple sap but simply serves

Can. J. Chem. Downloaded from www.nrcresearchpress.com by 210.87.254.42 on 09/05/12
For personal use only.

to illustrate those structural features that are known. Thus the predominant *O*-methyl ether was 2,4,6-tri-*O*-methyl-D-galactose which must have arisen from 1 → 3 linked D-galactose units as illustrated. The 2,4-di-*O*-methyl-D-galactose represented the only branch points found and originated from D-galactose units substituted in positions 1, 3, and 6. The 2,5-di-*O*-methyl-L-arabinose arose from chain-forming units joined through positions 1 and 3 and, because arabinose but not galactose was released by partial hydrolysis of the polysaccharide (6), these units could not have been interposed between galactose units but must have been joined to other arabinose residues as shown in Fig. 3. The 2,3,5-tri-*O*-methyl-L-arabinose and 2,3,4-tri-*O*-methyl-L-(?)-rhamnose repre-

	Moles
2,3,5-Tri-*O*-methyl-L-arabinose	4
2,5-Di-*O*-methyl-L-arabinose	2
2,4-Di-*O*-methyl-D-galactose	4
2,4,6-Tri-*O*-methyl-D-galactose	7
2,3,4-Tri-*O*-methyl-L-rhamnose	1



A = arabofuranose
G = galactopyranose
R = rhamnopyranose

FIG. 3. Molar ratio of methylated sugars and a possible structure for the arabinogalactan.

sented terminal, non-reducing units. Of course, the galactan portion of the molecule need not be straight as shown but could consist of a branch-on-branch structure of 1 → 3 linked chains joined by 1 → 6 linkages.

It is clear from the foregoing evidence that the polysaccharides in maple sap bear no structural relation to the non-cellulosic polysaccharides of the wood which are predominantly acidic xylans (4, 5). The possibility exists that the arabinogalactans found in aqueous extracts of numerous woods (14) might be of sap origin rather than components of the plant tissue. An attempt to obtain further evidence on this point by examination of the sap from a tamarack tree which is rich in arabinogalactan was frustrated by a lack of sap flow. However, an examination of the structures reported for various arabinogalactans reveals some differences in the galactan portions of the molecules. In most of the water-soluble arabinogalactans from woods the *unbranched* portion of the galactan chain is formed by 1 → 6 linkages and gives rise to 2,3,4-tri-*O*-methyl-D-galactose after methylation and hydrolysis (14). On the other hand, in the more complex group of polysaccharides which form the plant gums, the unbranched portion of the galactan chain is usually formed by 1 → 3 linkages giving rise to 2,4,6-tri-*O*-methyl-D-galactose after methylation and hydrolysis (15). In this respect, and in having rhamnose as an integral part of its structure, the arabinogalactan from maple sap resembles more closely the plant gums than the water-soluble arabinogalactans of coniferous woods.

Can. J. Chem. Downloaded from www.nrcresearchpress.com by 210.87.254.42 on 09/05/12
For personal use only.

Can. J. Chem. Downloaded from www.nrcresearchpress.com by 210.87.254.42 on 09/05/12
For personal use only.

EXPERIMENTAL

Paper chromatograms were run by the descending method using the following solvent systems (v/v ratio):

(A) 2-butanone:water, azeotrope;
(B) *n*-butanol:ethanol:water, 9:3:3;
(C) *n*-butanol:ethanol:water, 40:11:19.

Reducing sugars were detected on chromatograms by the *p*-anisidine hydrochloride spray reagent (16). Evaporations were carried out at 35° C or less under diminished pressure and specific rotations are equilibrium values unless stated otherwise. Melting points are corrected.

Gas–liquid partition chromatography was done as previously described (12). The Pye argon chromatograph was used for the qualitative and quantitative estimations. Samples isolated by gas–liquid partition chromatography were collected from the effluent gas stream after separation on a modified (11) Podbielniack "Chromacon" (series 9475-3V).

Isolation of Polysaccharide, Electrophoresis, and Estimation of Constituent Sugars

The isolation and yields of polysaccharide from maple sap were described previously (6). The crude polysaccharide which contained a large and a small component as shown by electrophoresis was refractionated from aqueous solution by gradient addition of ethanol (7). A portion (150 mg) of the main fraction (precipitated at an ethanol concentration of 65%) was dissolved in 0.05 *M* borate buffer (15 ml) and dialyzed through cellophane against 3 liters of the buffer. The solution of polysaccharide was then subjected to electrophoresis in a Tiselius-type Spinco Model-H apparatus and showed a single, sharp, peak with $\mu = 9.36 \times 10^{-5}$ cm^2 volt^{-1} sec^{-1}.

A sample (50 mg) of the polysaccharide was hydrolyzed by *N* sulphuric acid (2 ml) at 100° C in a sealed tube. Since no uronic acids were found in the previous investigation (6) the acid was neutralized by Amberlite IR-45 (OH) exchange resin and the filtrate was evaporated to dryness. The dried residue was refluxed with 4% methanolic hydrogen chloride for 20 hours, acid was neutralized with silver carbonate, and silver salts were filtered. The mixture of methyl glycosides obtained by evaporation of the filtrate was methylated by being shaken for 20 hours with silver oxide (200 mg) and methyl iodide (2 ml) in dimethylformamide (10 ml) (10). The silver salts were allowed to settle out and the clear supernatant was examined directly by gas–liquid partition chromatography to give the separation shown in Fig. 1. Areas under the peaks originating from a single monosaccharide were added together and the resulting three areas gave a molar ratio of galactose:arabinose:rhamnose of 51:44:5. Methyl α-D-glucopyranoside when methylated under the same conditions showed no partially methylated products detectable by gas–liquid partition chromatography or, after hydrolysis, by paper chromatography.

Methylation of Arabinogalactan

The polysaccharide (3.0 g) was methylated five times with 30% aqueous sodium hydroxide and dimethyl sulphate (17). The reaction mixture was extracted continuously with chloroform for 3 days and the extract was dried (anhydrous sodium sulphate) and evaporated to yield the partially methylated polysaccharide (2.08 g, methoxyl 34.7%; calc. methoxyl 41.3%). This product was methylated twice in tetrahydrofuran with solid sodium hydroxide and dimethyl sulphate (18) to yield a product having no hydroxyl absorption at 3500–3600 cm^{-1}. Precipitation from chloroform by addition of petroleum

ether (b.p. 30–60° C) yielded the fully methylated polysaccharide as a cream-colored powder, 1.47 g, $[\alpha]_D^{25} = -93°$ (*c*, 2% in chloroform), methoxyl = 40.7%.

Hydrolysis of Methylated Arabinogalactan

The fully methylated polysaccharide was hydrolyzed by formic acid according to the procedure of Jones and Wilkie (13). Paper chromatography of the hydrolyzate revealed three components with the following R_g values in solvents A and B respectively: component 1—1.01, 0.97; component 2—0.54, 0.82; component 3—0.22, 0.61. These values and the color reactions with the *p*-anisidine spray reagent were the same as those given by authentic samples of 2,3,5-tri-*O*-methyl-L-arabinose (component 1), 2,4,6-tri-*O*-methyl-D-galactose (component 2), and 2,4-di-*O*-methyl-D-galactose (component 3).

To obtain a quantitative estimate of the above components the mixture was refluxed for 20 hours with 4% methanolic hydrogen chloride and the methyl glycosides were analyzed by gas–liquid partition chromatography (11, 12). Figure 2 shows the separation obtained on a liquid phase of Apiezon M; separation on butanediol succinate polyester gave complete resolution of the shoulder on peak 2, which had the same retention volume as methyl-2,3,4-tri-*O*-methyl α-L-rhamnopyranoside, and permitted its quantitative estimation. The molar ratio of identified components (Fig. 3) was obtained by measurement of areas under the peaks on the gas–liquid partition chromatograms. These separations also provided additional evidence for the identities of the components which had the same retention volumes as authentic specimens.

In an attempt to isolate component 6, Fig. 2, the mixture of glycosides was hydrolyzed by *N* hydrochloric acid at 97° C for 24 hours. The hydrolyzate was neutralized by Amberlite IR-45 (OH) exchange resin and chromatographed on paper sheets in solvent C to give three fractions which were eluted from the papers and refluxed with 4% methanolic hydrogen chloride for 20 hours. Examination of the methanolyzates by gas–liquid partition chromatography showed that fraction 1 (R_g 0.9) contained only 2,3,5-tri-*O*-methyl-L-arabinose; fraction 2 (R_g 0.8) contained 2,4,6-tri-*O*-methyl-D-galactose and 2,5-di-*O*-methyl-L-arabinose; and fraction 3 (R_g 0.6) contained only 2,4-di-*O*-methyl-D-galactose. No component corresponding to peak 6, Fig. 2, was found in methanolyzates of eluates from blank areas of these chromatograms.

Identification of O-Methyl Ethers

2,3,5-Tri-O-methyl-L-arabinose

A sample of the mixed anomeric methyl glycosides of this component was collected from the effluent gas stream of the gas–liquid partition chromatogram. Hydrolysis, bromine oxidation, lactonization, and reaction with methanolic ammonia yielded 2,3,5-tri-*O*-methyl-L-arabonamide (19), which was crystallized from ethyl acetate:petroleum ether (b.p. 30–60° C) to a melting point of 134–136° C, $[\alpha]_D^{27} = +18°$ (*c*, 0.35% in methanol).

2,4,6-Tri-O-methyl-D-galactose

The anomeric glycosides were collected separately from the gas–liquid partition chromatogram. The faster-moving component (peak 7, Fig. 2) was crystallized from petroleum ether (b.p. 30–60° C) as fine needles, m.p. 108–109° C, $[\alpha]_D^{25} = -44°$ (*c*, 0.25% in methanol). The slower-moving component (peak 8, Fig. 2) was crystallized from petroleum ether (b.p. 65–110° C) to a melting point of 65–68° C, $[\alpha]_D^{25} = +149°$ (*c*, 0.45% in methanol). Bell and Williamson (20) report a melting point of 111–112° C, $[\alpha]_D^{25} = -40.9°$ (in chloroform), for methyl 2,4,6-tri-*O*-methyl-β-D-galactopyranoside and a melting point of 73–74° C, $[\alpha]_D^{25} = +163.9°$ (in chloroform), for the α-anomer.

Can. J. Chem. Downloaded from www.nrcresearchpress.com by 210.87.254.42 on 09/05/12
For personal use only.

The two crystalline fractions were combined and hydrolyzed to yield a sirupy reducing sugar which could not be crystallized. The crystalline anilide derivative had a melting point of 160–165° C raised to 178–179° C by recrystallization from methanol:ether, $[\alpha]_D^{25} = +35°$ (*c*, 1% in methanol). These are in good agreement with the reported values of melting point 179° C, $[\alpha]_D^{25}$ +38° (in acetone) for *N*-phenyl-2,4,6-tri-*O*-methyl-D-galactosylamine (21).

*2,4-Di-O-methyl-*D*-galactose*

The anomeric glycosides of this component (peaks 9 and 10, Fig. 2) were collected separately from the gas–liquid partition chromatogram. The faster-moving component crystallized in the collecting tube and was found to be methyl 2,4-di-*O*-methyl-β-D-galactopyranoside, m.p. 168–170° C (22). The slower-moving component was recrystallized twice from petroleum ether (b.p. 30–60° C) to yield methyl 2,4-di-*O*-methyl-α-D-galactopyranoside, m.p. 106.5–108° C (22).

Another sample of this component was isolated from preparative paper chromatograms as the reducing sugar, m.p. 98–100° C, $[\alpha]_D^{26} = +85°$ (*c*, 1% in water). These values agree with those reported for 2,4-di-*O*-methyl-D-galactose monohydrate (22).

*2,5-Di-O-methyl-*L*-arabinose*

The fraction from preparative paper chromatograms that contained 2,4,6-tri-*O*-methyl-D-galactose and 2,5-di-*O*-methyl-L-arabinose was rechromatographed on paper sheets in solvent A to yield a chromatographically pure sample of 2,5-di-*O*-methyl-L-arabinose. Bromine oxidation, lactonization, and reaction with methanolic ammonia yielded crystalline 2,5-di-*O*-methyl-L-arabonamide (23), m.p. and mixed m.p. 132° C.

ACKNOWLEDGMENTS

The authors would like to thank Mr. F. P. Cooper, Mr. W. R. Rowsome, and Mr. A. E. Castagne for technical assistance. Grateful acknowledgment is made of the donation of *O*-methyl-L-arabinoses by Dr. G. O. Aspinall, University of Edinburgh, Edinburgh, Scotland; Dr. H. O. Bouveng, Institutionen för Träkemi, Kungl. Tekniska Högskolan, Stockholm, Sweden; Dr. G. G. S. Dutton, University of British Columbia, Vancouver, British Columbia; Dr. J. K. N. Jones, Queen's University, Kingston, Ontario.

REFERENCES

1. W. A. M. Duncan and D. J. Manners. Biochem. J. **69**, 343 (1958).
2. F. B. Anderson and D. J. Manners. Biochem. J. **71**, 407 (1959).
3. W. A. M. Duncan, D. J. Manners, and J. L. Thompson. Biochem. J. **73**, 295 (1959).
4. L. G. Neubauer and C. B. Purves. Can. J. Chem. **35**, 388 (1957).
5. T. E. Timell. Can. J. Chem. **37**, 893 (1959).
6. G. A. Adams, C. T. Bishop, and I. J. McDonald. Can. J. Biochem. and Physiol. **37**, 507 (1959).
7. R. L. Whistler and K. W. Kirby. J. Am. Chem. Soc. **78**, 1755 (1956).
8. D. H. Northcote. Biochem. J. **58**, 353 (1954).
9. S. M. Martin. Chem. & Ind. (London), 823 (1957).
10. R. Kuhn, H. Trischmann, and I. Löw. Angew. Chem. **67**, 32 (1955).
11. A. G. McInnes, D. H. Ball, F. P. Cooper, and C. T. Bishop. J. Chromatog. **1**, 556 (1958).
12. C. T. Bishop and F. P. Cooper. Can. J. Chem. **38**, 388 (1960).
13. J. K. N. Jones and K. C. B. Wilkie. Can. J. Biochem. and Physiol. **37**, 377 (1959).
14. G. O. Aspinall. Advances in Carbohydrate Chem. **14**, 429 (1959).
15. F. Smith and R. Montgomery. Chemistry of plant gums and mucilages. Reinhold Publishing Corp., New York. 1959.
16. L. Hough, J. K. N. Jones, and W. H. Wadman. J. Chem. Soc. 1702 (1950).
17. W. N. Haworth. J. Chem. Soc. **107**, 8 (1915).
18. E. L. Falconer and G. A. Adams. Can. J. Chem. **34**, 338 (1956).
19. R. W. Humphreys, J. Pryde, and E. T. Waters. J. Chem. Soc. 1298 (1931).
20. D. J. Bell and S. Williamson. J. Chem. Soc. 1196 (1938).
21. E. L. Hirst and J. K. N. Jones. J. Chem. Soc. 1482 (1939).
22. F. Smith. J. Chem. Soc. 1724 (1939).
23. F. Smith. J. Chem. Soc. 1035 (1940).

Can. J. Chem. Downloaded from www.nrcresearchpress.com by 210.87.254.42 on 09/05/12
For personal use only.

Can. J. Chem. Downloaded from www.nrcresearchpress.com by 210.87.254.40 on 09/05/12
For personal use only.

THE POLYOXYPHENOLS OF WESTERN RED CEDAR (THUJA PLICATA DONN)

II. DEGRADATION STUDIES ON PLICATIC ACID, A POSSIBLE LIGNAN ACID[1]

J. A. F. GARDNER, B. F. MACDONALD, AND HAROLD MACLEAN

ABSTRACT

Plicatic acid, $C_{20}H_{22}O_{10}$, a polyoxyphenol from western red cedar heartwood, described in a previous paper, has been further characterized by preparation and analysis of additional crystalline derivatives. Crystalline trimethyl and triethyl ethers have been oxidized by alkaline permanganate. The trimethyl ether yielded 3,4,5-trimethoxybenzioc acid, 4,5-dimethoxyphthalic acid (*m*-hemipinic acid), a pentamethoxy anthraquinone, and a pentamethoxy *o*-benzoylbenzoic acid which decarboxylated to 3,4,5,3′,4′-pentamethoxy benzophenone. Correspondingly, the triethyl ether gave 3,4-diethoxy-5-methoxybenzoic and 4-ethoxy-5-methoxyphthalic acids, a mixture of pentaalkoxy anthraquinones and a pentaalkoxy *o*-benzoylbenzoic acid which decarboxylated to 3,3′,4-triethoxy-4′,5-dimethoxy benzophenone identified by cleavage to 3-ethoxy-4-methoxybenzoic and 3,4-diethoxy-5-methoxybenzoic acids. These results fix the positions of the two methoxyl, three phenolic hydroxyls, and mode of linkage of the two benzene rings. Further evidence is provided indicating plicatic acid is probably a lignan of the 4-aryltetrahydronaphthalene series.

In a previous paper (1), the isolation and properties of plicatic acid, a reactive polyoxyphenolic amorphous acid, occurring in the aqueous extractive of western red cedar, were described. Analysis of crystalline derivatives, methylation results, color tests, and spectra indicated it to be an *n*-propylphenol dimer, $C_{20}H_{22}O_{10}$, probably a lignan acid, in which one phenyl ring was 4-hydroxy-3-methoxyphenyl and the other was 3,4-dihydroxy-5-methoxyphenyl, but the mode of linkage was unknown. Thus the formula was given provisionally as $C_6H_3(OH)(OCH_3).C_5H_4(OH)_3(COOH).C_6H_2(OH)_2(OCH_3)$. This paper describes the alkaline permanganate oxidation of the crystalline trimethyl and triethyl ethers which establishes the aromatic substitution and indicates that plicatic acid is a lignan of the aryltetrahydronaphthalene series.

Alkaline permanganate oxidation of plicatic acid trimethyl ether (II*a*) gave a 15% yield of a crystalline colorless pentamethoxy keto-acid, $C_{19}H_{20}O_8$, m.p. 225.5–226°; smaller quantities of a neutral brilliant yellow crystalline substance, $C_{19}H_{18}O_7$, m.p. 209–210°, which gave qualitative tests and had spectral characteristics of an anthraquinone; 3,4,5-trimethoxybenzoic acid (V*a*); and 4,5-dimethoxyphthalic acid (IV*a*). The latter two acids were not isolated but their presence in the oxidation mixture was shown by paper chromatographic comparison with synthetic samples.

The pentamethoxy keto-acid decarboxylated to a benzophenone shown to be 3,4,5,3′,4′-pentamethoxybenzophenone by comparison with a synthetic sample. With concentrated sulphuric acid, the keto-acid readily gave a yellow anthraquinone. The infrared absorption spectrum of the acid was typical of the lactol form of a γ keto-acid (2) showing an alcoholic, but no acidic, hydroxyl band. These results indicate it to be an *o*-benzoylbenzoic acid, either 2,3,4-trimethoxy-6-(3′,4′-dimethoxybenzoyl)-benzoic acid or 3,4-dimethoxy-6-(3′,4′,5′-trimethoxybenzoyl)-benzoic acid (III*a*), either of which would give the same benzophenone (VIII*a*) on decarboxylation. Since Chatterjee and Chakravarti (3) had reported the isolation of an *o*-benzoylbenzoic acid of formula III*a* of much lower melting

[1]*Manuscript received July 14, 1960.*
Contribution from the Vancouver Laboratory, Forest Products Laboratories of Canada, a Division of the Forestry Branch, Department of Northern Affairs and National Resources, Ottawa, Canada. Paper presented in part at the Northwest Regional Meeting, American Chemical Society, Seattle, Washington, June 18–19, 1959, and at the I.U.P.A.C. Symposium on the Chemistry of Natural Products, Australia, August 15–25, 1960.

point, 210–211°, by the permanganate oxidation of the lignan, sikkimotoxin, and since plicatic acid gave some vanillin on alkaline nitrobenzene oxidation, the former was considered first. However, this possibility was eliminated when neither veratric acid nor 3,4,5-trimethoxyphthalic could be detected in the other oxidation products. The presence of 3,4,5-trimethoxybenzoic acid (V*a*) and 4,5-dimethoxyphthalic acid (IV*a*) as shown by paper chromatography required formula III*a*. It was concluded that Chatterjee and Chakravarti's compound, m.p. 210–211° from boiling water and dilute ethanol, must have been a mixture of the keto-acid (III*a*) and its lactol form (III*c*).

In the present work, the acid when purified by repeated recrystallization, was obtained in the lactol form (III*c*), m.p. 225.5–226°, as shown by the infrared absorption spectra. However, acidification of a dilute alkaline solution of the lactol gave a crystalline product, m.p. 180–185° depending on the rate of heating, which on the basis of its infrared absorption was the keto-acid (III*a*), i.e., a strong acidic hydroxyl band, no alcoholic hydroxyl band, and a shift of the carbonyl band to the benzoic acid region. This material was rapidly transformed on the melting point stage to the lactol form. The lactol nature was confirmed by the formation of a neutral crystalline acetate whose infrared absorption spectrum was clearly characteristic of a pseudoacetate, showing one broad enhanced carbonyl absorption band at 1758 cm^{-1} (2).

The anthraquinone obtained in nearly quantitative yield from the *o*-benzoylbenzoic acid by ring closure with concentrated sulphuric acid was found to be identical with that obtained as one of the permanganate oxidation products of plicatic acid trimethyl ether. Inspection of formula III*a* shows that ring closure of this substituted *o*-benzoylbenzoic acid, at either the 2′ or 6′ position, would give only one anthraquinone, namely, 1,2,3,6,7-pentamethoxy anthraquinone (VI).

Formation of the products III*a*, IV*a*, and V*a* proves that the position of aromatic substitutions in plicatic acid is as shown in formula I. To confirm the relative positions of the phenolic hydroxyl and methoxyl groups, which had been indicated by color tests and vanillin formation (1), the permanganate oxidation products at 100° of plicatic acid triethyl ether were examined. A crystalline monomeric acid was obtained which was shown to be 3,4-diethoxy-5-methoxybenzoic acid (V*b*) by comparison with a synthetic sample. The presence in the oxidation products of 4-ethoxy-5-methoxyphthalic acid (IV*b*) was demonstrated by paper chromatography in three solvent systems using a synthetic reference sample.

A neutral brilliant yellow crystalline product, giving qualitative tests for an anthraquinone, was also obtained in small yield. In contrast to the readily purified sharply melting anthraquinone obtained in the oxidation of plicatic acid trimethyl ether, the product in this case appeared to be a mixture since, after repeated recrystallizations, it melted over a wide range. This result was to be expected since, in the case of the ethylated derivatives, two anthraquinones, VII*a* and VII*b*, should result in approximately equal yield from ortho ring closure of the triethoxy-dimethoxy-*o*-benzoylbenzoic acid (III*b*).

The formation of 3,4-diethoxy-5-methoxybenzoic proves ring C to be 3,4-dihydroxy-5-methoxyphenyl and the formation of the 4-ethoxy-5-methoxyphthalic acid indicates the substitution pattern on ring A as shown in formula I for plicatic acid. Alkaline permanganate oxidation of the triethyl ether at lower temperature yielded mainly the ethylated keto-acid 4-ethoxy-3-methoxy-6-(3′,4′-diethoxy-5′-methoxybenzoyl)-benzoic acid (III*b*) which underwent conversion from its keto form III*b* to the lactol form III*d* near the melting point similar to the methylated derivative previously obtained. Decarboxylation gave the corresponding benzophenone, 3,3′,4-triethoxy-4′,5-dimethoxy benzo-

Can. J. Chem. Downloaded from www.nrcresearchpress.com by 210.87.254.40 on 09/05/12
For personal use only.

phenone, which on cleavage with potassium *t*-butoxide yielded 3-ethoxy-4-methoxybenzoic acid (IX) and 3,4-diethoxy-5-methoxybenzoic acid (V*b*). The formation of these latter products fixes with certainty the position of the hydroxyl group on ring A, as shown in Fig. 1, formula I.

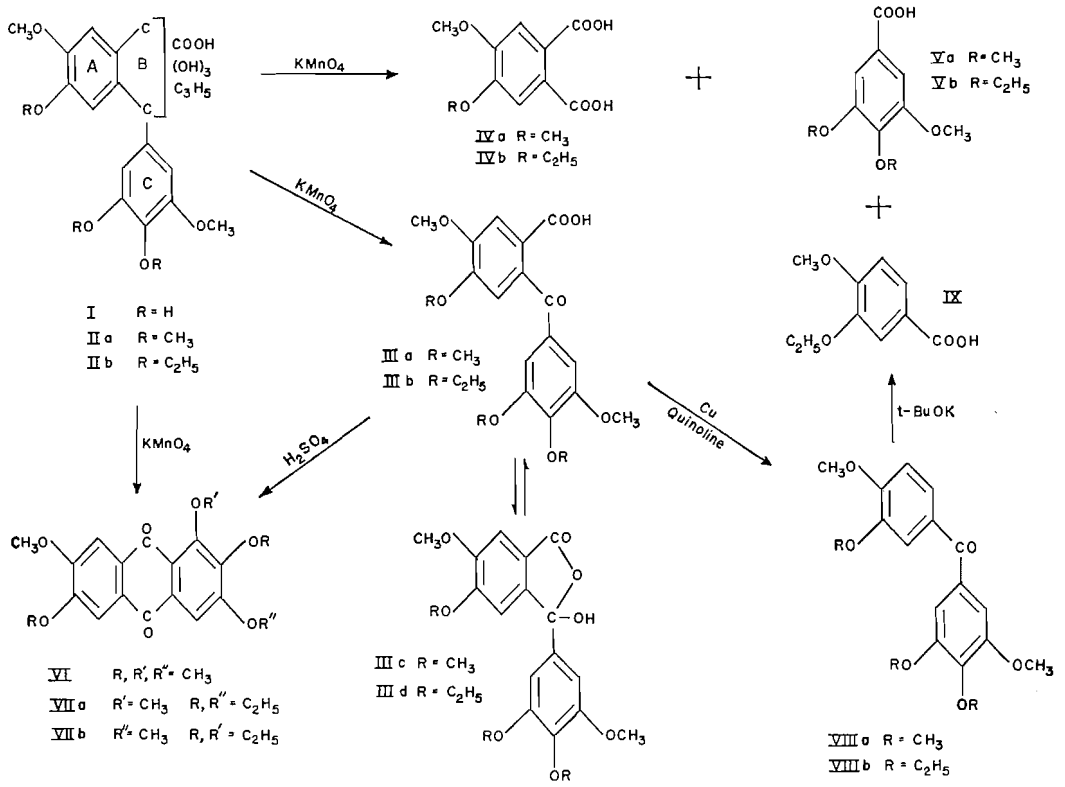


FIG. 1. Oxidation of methyl and ethyl ethers of plicatic acid.

The yield of vanillin (4%) obtained by alkaline nitrobenzene oxidation of plicatic acid (I) is in the same low range as that obtained from two other lignans, conidendrin and iso-olivil, 1 and 3% respectively (4). In the case of plicatic acid, since the C ring is a pyrogallol derivative, the vanillin formed must arise from the A ring via cleavage of an ortho-formylbenzophenone or decarboxylation of 6-carboxyvanillin. The vanillin from conidendrin and iso-olivil is probably derived similarly. This mode of vanillin formation is of interest in connection with alkaline nitrobenzene oxidation studies on lignins since a part of the vanillin formed could be so derived. While there is no evidence for the presence in lignin *in situ* of 3-methoxy-4-hydroxyphenylpropane structural units linked to the next through the 6-position, Richtzenhain (5) suggested the presence of such linkages in lignins isolated by acidic procedures to explain the formation of *m*-hemipinic acid by oxidation after methylation.

The presence of a monomethylated pyrogallol nucleus in plicatic acid explains the positive Mäule test, although this test is usually considered indicative of the dimethylated (syringyl) derivative. In contrast to the dimethylated (syringyl) derivatives, which occur widely in deciduous extractives and lignin, monomethylated derivatives of pyrogallol

Can. J. Chem. Downloaded from www.nrcresearchpress.com by 210.87.254.40 on 09/05/12
For personal use only.

are very rare in all plant products, none having been reported in wood components heretofore. It will be of considerable interest to determine whether products of additional methylation, i.e., syringyl derivatives, are also present in the western red cedar phenols.

In view of the easy formation of the tropolone derivative purpurogallin from pyrogallol, the occurrence of pyrogallol derivatives as well as tropolones in western red cedar is of interest in considering possible modes of biogenesis of the latter substances.

The oxidation products obtained herein together with the formation of γ lactones by plicatic acid and its trimethyl ether (1) are consistent with plicatic acid being a lignan of the 4-aryltetrahydronaphthalene series. Experimental proof of this and the pattern of hydroxylation on the saturated ring is in progress.

EXPERIMENTAL

Plicatic Acid Trimethyl Ether (IIa)

Plicatic acid (20 g) in water (40 ml) was treated with dimethyl sulphate (28 ml) and 20% sodium hydroxide dropwise at reflux for 2 hours under nitrogen while maintaining the pH at 9–10. After addition of the dimethyl sulphate, sodium hydroxide (50%) was added to raise the pH to 14. On cooling of the solution, the sodium salt precipitated and was separated on the centrifuge. The precipitated salt was dissolved in a minimum of distilled water, the solution acidified to pH 7 with sulphuric acid, extracted with chloroform to remove tarry residues, filtered, and further acidified to pH 2 to precipitate the free acid product. After filtration an additional crop was obtained by partial evaporation of the filtrate. Crude yield, 14.79 g (74%). The product was recrystallized from boiling water using decolorizing charcoal. Yield, 10.52 g (53%). Anal. Calc. for $C_{23}H_{28}O_{10}$: neutral equivalent, 464; OCH_3, 33.4. Found: neutral equivalent, 467; OCH_3, 32.7.

On rapid heating, the product melted with foaming between 210° and 218° depending on the rate of heating. It slowly recrystallized on the melting point stage and remelted at 253–255°. On slow heating, the product underwent a change in crystal structure between 220° and 245° and melted at 253–255°. The gas evolved during this conversion was shown to be water vapor and the new product proved to be plicatic acid trimethyl ether lactone, previously prepared from plicatic acid trimethyl ether methyl ester through loss of methanol (1), by mixed fusion and comparison of infrared spectra.

3,4-Dimethoxy-6-(3′,4′,5′-trimethoxybenzoyl)-benzoic Acid (IIIa)

Plicatic acid trimethyl ether (IIa) (4.56 g) was dissolved in 4% sodium hydroxide (100 ml) on a steam bath and 4% potassium permanganate (511 ml) slowly added with stirring in 10-ml portions until 400 ml had been added, and then in smaller portions to a 15-minute end point. The manganese dioxide together with the small yellowish precipitate which floated on the reaction mixture was filtered out (precipitate A) and washed with hot water (200 ml). After the pink filtrate had been decolorized with a few drops of bisulphite solution and acidified to pH 2 with hydrochloric acid, cooling precipitated pale yellow crystals. Filtration (filtrate B) and recrystallization from methanol–water (1:2) gave colorless needles. Yield, 0.679 g (15%). Anal. Calc. for $C_{19}H_{20}O_8$: C, 60.78; H, 5.10; OCH_3, 41.28; neutral equivalent, 375.4; mol. wt., 375.4. Found: C, 60.86; H, 5.09; OCH_3, 41.00; neutral equivalent, 371.3; mol. wt. (isothermal distillation), 388. The product gave a positive test with 2,4-dinitrophenylhydrazine. Heating rapidly gave partial melting at 180–185° followed by recrystallization and remelting at 218–220°, m.p. after five recrystallizations 225.5–226°. Infrared absorption spectrum was characteristic of the lactol of a keto-acid. ν_{max}^{KBr} 3340, 1702, 1668, 1582, 1322, 1128, 997, 765.

Can. J. Chem. Downloaded from www.nrcresearchpress.com by 210.87.254.40 on 09/05/12
For personal use only.

Acidification of a dilute alkaline solution and vacuum drying at room temperature produced the pure keto-acid form (III*a*), m.p. 184–185°. ν_{max}^{KBr} no hydroxyl band, 2600, 1668, 1648, 1580, 1502, 1460, 1410, 1322, 1280, 1120, 1003, 772.

When treated with concentrated sulphuric acid, the product gave a brilliant purple color transformed in a few minutes warming to brown. Dilution of the brown mixture with water and neutralization precipitated a bright yellow crystalline substance, m.p. 207–208° from methanol, showing no mixed melting point depression with 1,2,3,6,7-pentamethoxy anthraquinone (VI) (see below).

Treatment with diazomethane in methanol–ether gave a crystalline monomethyl ester, m.p. 147–147.5°, showing no absorption bands for the hydroxyl group in the infrared spectrum. Anal. Calc. for $C_{20}H_{22}O_8$: OCH_3, 47.64; mol. wt., 390. Found: OCH_3, 46.87; mol. wt. (Rast), 390.

Refluxing with acetic anhydride in pyridine gave a crystalline acetate, insoluble in bicarbonate solution, m.p. 118–119° from methanol. The infrared absorption spectrum showed no hydroxyl band and had one broad intense carbonyl band at 1758 cm^{-1} typical of a lactol acetate (2).

1,2,3,6,7-Pentamethoxy Anthraquinone (VI)

"Precipitate A" after drying was triturated with chloroform (4×50 ml). The solution was then dried over sodium sulphate and evaporated to yield a brilliant yellow powder (0.154 g, 3% yield), melting point after two recrystallizations from methanol, 209–210°. This compound when heated with sodium hydrosulphite in alkali gave a red solution which precipitated the yellow starting material on air oxidation. The red solution on further reduction with zinc and alkali gave a pale yellow precipitate. These positive qualitative tests for anthraquinone structure were supported by formation of the same substance by ring closure of the keto-acid (III*a*) and by the absorption spectra. The ultraviolet absorption in methanol exhibited an intense maximum at 285 mμ ($\log \epsilon = 4.81$). The infrared absorption (KBr pellet) showed one weak and one very strong band attributable to the carbonyls at 1740 cm^{-1} and 1662 cm^{-1}, respectively, comparable to those of anthraquinone at 1740 cm^{-1} and 1665 cm^{-1}. Anal. Calc. for 1,2,3,6,7-pentamethoxy anthraquinone, $C_{19}H_{18}O_7$: C, 63.67; H, 5.06; OCH_3, 43.24; mol. wt., 358. Found: C, 63.56; H, 4.97; OCH_3, 42.80; mol. wt. (Rast), 360.

Identification of 3,4,5-Trimethoxybenzoic Acid (Va) and 4,5-Dimethoxyphthalic Acid (IVa)

"Filtrate B" was extracted with ether (3×100 ml) and the ether solution extracted with sodium bicarbonate (3×25 ml). The mixed acids were isolated by acidification of the bicarbonate solution, extraction into ether, and solvent removal to yield a light tan solid (135 mg, 3% yield). This material was compared by descending paper chromatography on Whatman No. 1 using two solvents, *n*-propanol:26% ammonia (3:2) (6) and *n*-butanol:2% ammonia (1:1) using reference samples of 3,4,5-trimethoxybenzoic acid and 4,5-dimethoxyphthalic acid (7). Spots at R_f's 0.79 and 0.29 and at 0.30 and 0.036 in the two solvents systems respectively, identical with those of the reference samples, were present. Detection was made first with short ultraviolet light which shows the acids as dark spots, then by spraying with universal indicator (B.D.H.). Since 4,5-dimethoxyphthalic acid (*m*-hemipinic acid) and 3,4-dimethoxyphthalic acid (hemipinic acid) (7) have very similar R_f's in these solvents, the oxidation product was also run in benzene:acetic acid:water (125:72:3) over a period of 16 hours, the solvent being allowed to run off the paper. The synthetic 4,5-dimethoxyphthalic and the oxidation product ran $15\frac{1}{4}$ inches while the 3,4-dimethoxyphthalic acid ran 17 inches. These acids

Can. J. Chem. Downloaded from www.nrcresearchpress.com by 210.87.254.40 on 09/05/12
For personal use only.

were detected with short ultraviolet light as dark spots. No spots corresponding to synthetic veratric and 3,4,5-trimethoxyphthalic acid (8) were detected.

3,4,5,3′,4′-Pentamethoxy Benzophenone (VIIIa)

3,4,5,3′,4′-Pentamethoxy benzophenone was prepared by dissolving the keto-acid (III*a*) (275 mg) and its copper salt (25 mg) as catalyst (9) in quinoline (7 ml) and refluxing for ½ hour. Metallic copper settled out on cooling. The reaction mixture was diluted with ether (20 ml) and filtered. The filtrate was washed with 2 *N* hydrochloric acid (5×10 ml) until nearly colorless, then with 5% sodium hydroxide (2×10 ml) to remove the trace yellow color, dried over sodium sulphate, and evaporated to colorless crystals. Yield, 123 mg (45%). Recrystallization from methanol:water gave colorless platelets, m.p. 120.5–121°, oxime, m.p. 149.5–150°. Mixed melting point with synthetic samples (10, 11) 123.5° and 148.5–149.5°, respectively, showed no depression and the infrared absorption spectra of the benzophenones were identical. ν_{max}^{KBr} 1632, 1582, 1518, 1466, 1415, 1326, 1268, 1125, 770.

Plicatic Acid Triethyl Ether (IIb)

Plicatic acid (28.1 g) in water (25 ml) was treated with diethyl sulphate (30 ml) and 20% sodium hydroxide dropwise at reflux for 3 hours under nitrogen while maintaining the pH at 9–10. After addition of the diethyl sulphate, sodium hydroxide (10 ml, 20%) was added and the reaction mixture refluxed for an additional hour. On cooling, the reaction mixture solidified. After stirring and centrifuging several times, the supernatant liquor was decanted, the precipitated sodium salt acidified, and the free acid taken up in chloroform. The chloroform solution was extracted with sodium bicarbonate solution, the bicarbonate solution acidified, and the precipitated product recrystallized from methanol:water (1:1), m.p. 113–114°. Yield, 10.74 g (38%). As this compound lactonized very readily at 140°, excessive heating during recrystallization and drying was avoided. Stable gels were formed by cooling benzene solutions. Calc. for $C_{26}H_{34}O_{10}$: alkoxyl as methoxyl, 30.6%; neutral equivalent, 506. Found: alkoxyl as methoxyl, 30.2%; neutral equivalent, 509.

Permanganate Oxidation of Plicatic Acid Triethyl Ether (IIb) at 100°

Oxidation of this ether (6.2 g) was similar to that of the trimethyl ether with the exception that 5% potassium hydroxide and 5% potassium permanganate were used and the solution kept boiling throughout the addition of the potassium permanganate (864 ml). Due to the more drastic oxidation conditions no ethyl-substituted *o*-benzoylbenzoic acid was obtained. The monomeric acids were obtained as a yellow plastic solid. Yield, 0.334 g (5.4%).

As in the case of oxidation of the trimethyl ether, brilliant yellow crystals precipitated from the boiling alkaline reaction mixture. Yield, 0.143 g (2%). Qualitative tests for anthraquinone structure were positive. A mixture of anthraquinones was suspected since two recrystallizations gave no change in the melting point range of 150–167°.

Isolation of 3,4-Diethoxy-5-methoxybenzoic Acid (Vb)

A portion of the mixed acids (0.09 g) was fractionated by column chromatography on silicic acid using the technique of Hathaway (6). Evaporation of the first fraction gave a crystalline product, m.p. 112–113°, from ethanol:water (1:1) identical with, by mixed melting point and infrared absorption spectrum, a reference sample synthesized from 5-hydroxy vanillin (12) by ethylation with diethyl sulphate followed by oxidation with cold 1% permanganate (13).

Can. J. Chem. Downloaded from www.nrcresearchpress.com by 210.87.254.40 on 09/05/12
For personal use only.

Can. J. Chem. Downloaded from www.nrcresearchpress.com by 210.87.254.40 on 09/05/12
For personal use only.

Detection of 4-Ethoxy-5-methoxyphthalic Acid (IVb)

A sample of the mixed acids was examined by descending paper chromatography in three solvent systems, *n*-propanol:26% ammonia (3:2), *n*-butanol:2% ammonia (1:1) and benzene:acetic acid:water (125:72:3). In each case, spots at R_f's identical with those of a synthetic sample of 4-ethoxy-5-methoxyphthalic acid were obtained. In the first two, the spots (R_f's 0.51 and 0.045 respectively) were detected first by short ultraviolet light and then by spraying with universal indicator (B.D.H.). In the last, the solvent was allowed to run off the paper to give 14 inches of migration by the acid and detection was by short ultraviolet light.

The reference sample of 4-ethoxy-5-methoxyphthalic acid (melting point of ethylimide, 204°) was obtained by the permanganate oxidation (13) of 4-ethoxy-5-methoxyphthalide synthesized from the ethyl ether of vanillic acid using the method of King and King (14).

4-Ethoxy-3-methoxy-6-(3',4'-diethoxy-5'-methoxybenzoyl)-benzoic Acid (IIIb)

Permanganate oxidation of plicatic acid triethyl ether (II*b*) at 50–55° was analogous to the previous oxidation for the trimethyl ether (II*a*). At this temperature only a trivial amount of the corresponding anthraquinones (VII*a* and VII*b*) was obtained. The main product was similarly a keto-acid, 4-ethoxy-3-methoxy-6-(3',4'-diethoxy-5'-methoxybenzoyl)-benzoic acid (III*b*) (8% yield). Anal. Calc. for $C_{22}H_{26}O_8$: neutral equivalent, 418. Found: 416. Heating rapidly gave a partial melting at 120–124° followed by recrystallization and remelting at 136–137°. Infrared absorption spectrum of the original material before melting was that of the keto-acid (III*b*). ν_{max}^{KBr} no hydroxyl band, 2600, 1670–1660 (doublet), 1580, 1500, 1418, 1320, 1270. After melting at 136–137° the spectrum was mainly that of the lactol (III*d*) contaminated with some of the keto-acid. ν_{max}^{KBr} 3250, 2600, 1705, 1680, 1580, 1500, 1418, 1320, 1270, 1120, 766.

3,3',4-Triethoxy-4',5-dimethoxy Benzophenone (VIIIb)

3,3',4-Triethoxy-4',5-dimethoxy benzophenone was prepared from the keto-acid (III*b*) in an analogous manner to the fully methylated benzophenone (VIII*a*). Yield, 68% of theoretical. Recrystallization from methanol:water (2:1) gave colorless needles, m.p. 96–96.5°. The infrared spectrogram was free of acid hydroxyl and acid carbonyl bands showing only the expected diaryl ketone carbonyl. ν_{max}^{KBr} 1640, 1580, 1518, 1420, 1322, 1262, 1122, 1023, 776.

Cleavage of 3,3',4-Triethoxy-4',5-dimethoxy Benzophenone (VIIIb)

In accordance with the procedure of Swan (15), potassium wire (30 mg, 0.00075 mole) was converted to potassium tertiary butoxide. A solution of the benzophenone (90.3 mg, 0.000242 mole) and water (4.8 microliters, 0.000265 mole) in anhydrous dioxane (5 ml) was added and refluxed at 90° for 18 hours under anhydrous conditions. The solvent was evaporated under reduced pressure, the residue dissolved in water, and extracted with ether (2×10 ml) to remove unreacted benzophenone and the neutral products. On acidification with HCl, the acids precipitated as colorless solids (36 mg, 80% yield). The mixed acids (30 mg) were separated by dissolving in acetone and streaking across a 9-in. wide No. 17 Whatman chromatographic paper. Development was with butanol – 2% ammonia (1:1) solvent and detection by short ultraviolet light. The spots were excised and Soxhlet extracted with acetone. After removal of the acetone under reduced pressure, the separated acids were taken up in bicarbonate, filtered, and precipitated with HCl. Yields were 3-ethoxy-4-methoxybenzoic acid (IX), 13 mg, m.p. 167.5–168° (R_f = 0.32

in butanol – 2% ammonia), and 3,4-diethoxy-5-methoxybenzoic acid (V*b*), 9 mg, m.p. 113–114° (R_f = 0.51 in butanol – 2% ammonia), identical with authentic samples by mixed melting point and infrared spectrogram.

REFERENCES

1. J. A. F. GARDNER, G. M. BARTON, and H. MACLEAN. Can. J. Chem. **37**, 1703 (1959).
2. J. F. GROVE and H. A. WILLIS. J. Chem. Soc. 877 (1951).
3. R. CHATTERJEE and S. C. CHAKRAVARTI. J. Am. Pharm. Assoc. Sci. Ed. **41**, No. 8, 415 (1952).
4. B. LEOPOLD and I. L. MALMSTROM. Acta Chem. Scand. **5**, 936 (1951).
5. H. RICHTZENHAIN. Svensk Papperstidn. **53**, 644 (1950).
6. D. E. HATHWAY. J. Chem. Soc. 520 (1958).
7. G. A. EDWARDS, W. H. PERKIN, JR., and F. W. STOYLE. J. Chem. Soc. **127**, 195 (1925).
8. R. L. ALIMCHANDANI and A. N. MELDRUM. J. Chem. Soc. **117**, 964 (1920).
9. LOUIS F. FIESER. Experiments in organic chemistry. 2nd ed. D. C. Heath & Co., New York. 1941. p. 199.
10. W. H. PERKIN, JR. and CARL WEIZMANN. J. Chem. Soc. **89**, 1649 (1906).
11. W. H. PERKIN, JR. and J. NAYLOR. J. Chem. Soc. **89**, 1664 (1906).
12. W. BRADLEY, R. ROBINSON, and G. SCHWARZENBACH. J. Chem. Soc. 793 (1930).
13. R. H. F. MANSKE, A. E. LEDINGHAM, and H. L. HOLMES. Can. J. Chem. **23**, 100 (1945).
14. F. E. KING and T. J. KING. J. Chem. Soc. 726 (1942).
15. G. A. SWAN. J. Chem. Soc. 1408 (1948).

Can. J. Chem. Downloaded from www.nrcresearchpress.com by 210.87.254.40 on 09/05/12
For personal use only.

Can. J. Chem. Downloaded from www.nrcresearchpress.com by 210.87.254.42 on 09/05/12
For personal use only.

PROTON MAGNETIC RESONANCE ABSORPTION IN ANHYDROUS SODIUM STEARATE[1]

R. F. GRANT[2] AND B. A. DUNELL

ABSTRACT

The proton magnetic resonance absorption in anhydrous sodium stearate has been investigated over the temperature range −182° C to 200° C. An abrupt change in the line width and the second moment has been observed between 113° C and 114° C, which corresponds to a known phase transition. The results suggest that at temperatures below 114° C the motion of the hydrocarbon-chain portion of the sodium stearate molecule is chiefly one of oscillation or rotation about the chain longitudinal axis. The hydrocarbon chains may be free to move about other axes at temperatures above 114° C, although the molecule as a whole retains a fixed position in the crystal lattice.

INTRODUCTION

The various mesomorphic phase transitions in sodium salts of long-chain fatty acids have been extensively studied by several physical methods (1). X-Ray, infrared, and nuclear magnetic resonance studies have indicated that the lower temperature transitions may represent the onset of rapid reorientation in the paraffin-chain part of the sodium soap molecule (2, 3, 4). Of particular interest are the phase transitions curd–supercurd at 89–92° C, supercurd–subwaxy at 110–117° C, and subwaxy–waxy at 125–135° C (4). The following is a proton magnetic resonance investigation of these transitions in sodium stearate, and is an extension and correction of the work in a previous communication (4).

EXPERIMENTAL

The sodium stearate was prepared from Eastman Kodak white label stearic acid, f.p. 68.1° C, which had been purified by repeated crystallization at −20° in acetone (5). The purified acid, f.p. 69.2° C, was dissolved in hot ethanol and titrated to a phenolphthalein end point with an aqueous ethanol solution of sodium hydroxide. The sodium stearate precipitate was filtered, dried in air, and melted under vacuum to remove residual solvents and to render it anhydrous (6). This compact, fused soap was remelted under vacuum in sample tubes; dry nitrogen was admitted to the system and the tubes were sealed off.

The nuclear magnetic resonance spectrometer and the methods of temperature control have been described previously (7). The temperature of the sample was measured with a thermocouple inserted in a well in the side of the sample tube. The line width was taken as the separation in gauss between points of maximum and minimum slope. The second moments of the resonance lines were obtained from the experimental derivative curves (8) by numerical integration and were corrected for the effects of modulation (9).

RESULTS

The proton magnetic resonance line widths, measured from −68° C to 130° C, are given by the open circles in Fig. 1. The line width was also measured at −182° C where it is 16.1 gauss. Particularly notable is the extensive decrease in the line width at temperatures above 30° C, and the abrupt change from a width of 2.8 gauss at 113° C to a width determined by the field homogeneity at 114° C. This abrupt narrowing coincides with

[1]*Manuscript received August 29, 1960.*
Contribution from the Department of Chemistry, University of British Columbia, Vancouver 8, B.C.
[2]*Holder of National Research Council Studentships. Present address: Division of Applied Chemistry, National Research Council of Canada, Ottawa.*

the supercurd–subwaxy phase transition. In all these measurements it was found necessary to maintain a given temperature for at least 2 hours before the proton magnetic resonance absorption was recorded. In most cases the temperature was maintained for about 4 hours, and above 100° C, in the vicinity of the phase transition, temperatures were held constant for about 12 hours. The filled circles in Fig. 1 represent one continuous experiment in which each temperature was maintained for only 30 minutes before the resonance

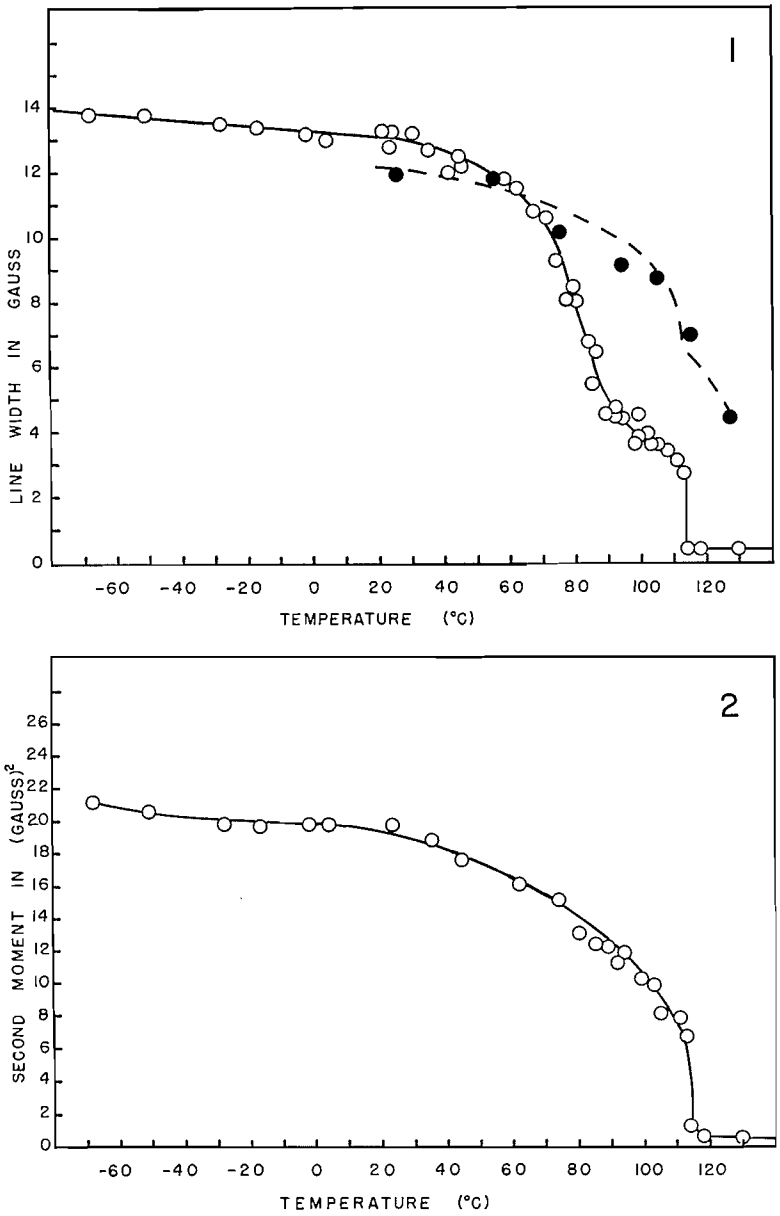


FIG. 1. Line width of sodium stearate as a function of temperature. Open circles, line width from samples at thermal equilibrium; filled circles, line width from samples not at thermal equilibrium; dashed line, line width from previous study.

FIG. 2. Second moment of sodium stearate as a function of temperature.

Can. J. Chem. Downloaded from www.nrcresearchpress.com by 210.87.254.42 on 09/05/12
For personal use only.

absorption was measured. These points fall closely along the discontinuous line in Fig. 1, which represents the course of the results in the original magnetic resonance studies on sodium stearate (4). It seems evident, therefore, that this previous work (4) reported a situation where thermal equilibrium had not been properly established although the line-width changes were reproducible.

The second moment of the proton magnetic resonance absorption in sodium stearate at $-182°$ C was found to be 28.0 ± 1.5 gauss^2. The behavior of the second moment over the temperature range $-68°$ C to 130° C is shown in Fig. 2. Like the line width, the second moment begins to decrease rapidly above about 30° C and changes abruptly from 6.7 gauss^2 to 1.2 gauss^2 as the temperature is raised through the supercurd–subwaxy transition. Above 114° C the second moment decreases even more: it is 0.6 gauss^2 at 118° C and 0.4 gauss^2 at 130° C, near the subwaxy–waxy transition temperature. Although the line width is very narrow above 114° C, the second moment does not approach zero because of small wings on the resonance absorption line. These wings decrease in amplitude and width as the temperature is raised, and there is some evidence for them up to 200° C; however, the amplitude becomes so small that it is difficult to determine a reliable second moment.

DISCUSSION

The X-ray diffraction analysis of most solid fatty acid salts shows that they have a layer structure in which the carboxyl ion ends lie in parallel sheets. Two such sheets form a double layer, and both individual sheets and the double layer are held together by positive ions. The long paraffin chains stick out parallel to each other from both sides of this electrically balanced double layer, with their longitudinal axes slightly inclined to it. Reliable and reproducible results are difficult to obtain from X-ray studies of sodium stearate and details of the molecular arrangement in the unit cell have not been determined (10). However, the unit cell cross section of sodium stearate (11) is almost identical with that of silver stearate (12), whose triclinic structure has been fairly well defined. Infrared studies have suggested that the higher sodium soaps also have a triclinic structure (3). In view of these similarities it seems reasonable to assume that the arrangement of sodium stearate molecules in the crystal lattice is very much the same as the arrangement of the silver stearate molecules. In the paraffin-chain portion, the carbon atoms are arranged in the zigzag configuration and it has been assumed that the bond angles are tetrahedral throughout. The carbon—hydrogen bond length is taken as 1.094 Å, and the carbon—carbon distance is 1.54 Å (13). On the basis of this knowledge of the structure of the sodium stearate unit cell, the second moment, S, of the proton magnetic resonance can be calculated (14).

For a polycrystalline sample the expression for the second moment S of the proton magnetic resonance in an assembly of protons and sodium nuclei is

$$[1] \qquad S = \frac{716}{N} \sum_{j>k} r_{jk}^{-6} + \frac{55}{N} \sum_{j,f} r_{jf}^{-6},$$

where N is the number of protons whose interactions are considered, r_{jk} is the distance between any two protons j and k, and r_{jf} is the distance between any proton j and sodium nucleus f. The contribution of the second part of equation [1] is very small for sodium stearate. The intramolecular second moment for sodium stearate was found to be 18.9 gauss^2 and the intermolecular second moment was 9.4 gauss^2 for a total of 28.3 gauss^2.

Can. J. Chem. Downloaded from www.nrcresearchpress.com by 210.87.254.42 on 09/05/12
For personal use only.

This compares quite well with the experimental value of 28.0 ± 1.5 gauss^2 found at $-183°$ C and it is assumed that molecular motion at frequencies comparable to or greater than the resonance line width is absent (15).

According to the theory of Gutowsky and Pake (16), both the width and second moment of the resonance absorption line should decrease when molecular reorientation becomes sufficiently rapid. A more recent treatment of the theory has shown that molecular motion should cause a change in the line shape such that the second moment remains constant at its rigid lattice value (17); as the line width narrows due to the motion, the tails of the line become extended. However, experimentally observed second moments usually decrease as the line width decreases, in agreement with the earlier theory (16). This is because the amplitude of the extended tail part of the resonance absorption line is comparable to the amplitude of the spectrometer noise, hence it is not observed when the experimental line is obtained. This seems to be the case with sodium stearate; the second moment and line width behave in roughly the same way with changing temperature and no extended tails were detected on the resonance absorption line with the spectrometer signal-to-noise ratio of 30.

Since the molecules in solid sodium stearate are arranged side by side as in a bundle of rods, one of the most likely forms of motion would be a rotation or oscillation about the longitudinal axis of the paraffin chain. The reduction in the intramolecular second moment due to the complete reorientation of the sodium stearate molecules about their longitudinal axes can be calculated by means of the treatment of Gutowsky and Pake (16). Also for some kinds of motion likely in solid long-chain paraffins, Andrew (18) has found that the intra- and inter-molecular contributions are reduced by about the same factor. Hence the total second moment for reorientation about the longitudinal axes of sodium stearate molecules is about 8.1 gauss^2. This corresponds to the experimental second moment found around 110° C or just prior to the supercurd–subwaxy transition as shown in Fig. 2. The second moment expected for torsional oscillation of the paraffin chains about their long axes in solid sodium stearate is given by the graph in Fig. 3. This was calculated by means of equation [2] originally derived by Andrew (18).

$$[2] \qquad \rho = 1 - \tfrac{3}{4}[(1 - J_0^2(\alpha)) \sin^2 2\gamma + (1 - J_0^2(2\alpha)) \sin^4 \gamma].$$

Here ρ is the ratio of the second moments for the oscillating and rigid cases, α is the angular amplitude of oscillation, γ is the angle between the internuclear vector and the axis of reorientation, and J_0 is a Bessel function.

The model of a paraffin chain undergoing torsional oscillation or complete reorientation about its longitudinal axis seems sufficient to account for most of the experimental results below 113° C. So far, however, the possible effect of the ionic layer formed at the carboxyl ends in solid sodium stearate has been ignored. It would seem reasonable to suppose that the portion of the paraffin chain nearest the strongly bonded ionic layer would be able to undergo torsional oscillation to a somewhat lesser extent than the portions of the chain farthest away from the ionic layer. Moreover, it has been shown that such a twisting about the longitudinal axis of the paraffin chain may require less energy of activation than is required in the case where the whole chain must be lifted over the potential barrier at the same time (19). A rigid ionic layer may also prevent the complete reorientation of the chain predicted for a second moment of about 8 gauss^2. However, this value could also be accounted for by a twisting chain that is also free to oscillate slightly in a direction perpendicular to the chain axis.

The very narrow line width which occurs between 113° C and 114° C is usually taken

Can. J. Chem. Downloaded from www.nrcresearchpress.com by 210.87.254.42 on 09/05/12
For personal use only.

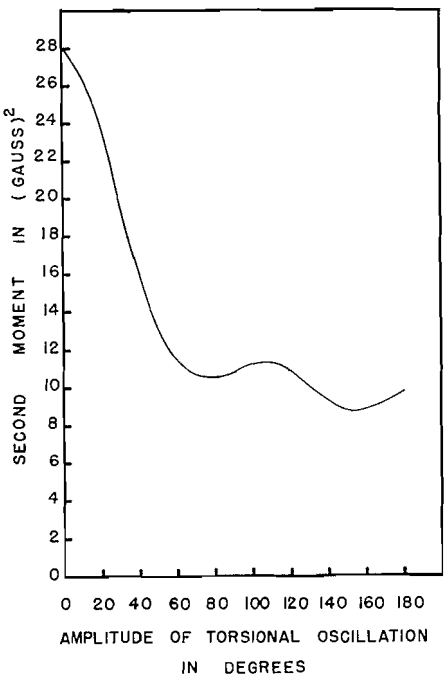


FIG. 3. Calculated effect of torsional oscillation on the second moment of sodium stearate.

to indicate that the whole molecule is reorienting about more than one axis (15). If molecular reorientation is isotropic, the intramolecular contribution to the second moment should average to zero. However, so long as the centers of mass of the molecules remain fixed, the intermolecular contributions will not average to zero and a small but finite second moment should be observed (20). The supercurd to subwaxy transition between 113° C and 114° C in sodium stearate appears to involve a change from rotation or twisting about the longitudinal axis of the paraffin chain to a condition where reorientation may be possible about other axes. Yet the second moment of 1.2 gauss² at 114° C suggests that the sodium stearate molecules are still fixed in the crystal lattice. This seems to agree with the conclusions drawn from recent X-ray studies on sodium stearate (2). Above the supercurd–subwaxy transition the lattice structure consists of a set of parallel ribbons, indefinite in length and packed in a rectangular array. The sodium carboxylate ends of the molecules fit into the ribbon and the hydrocarbon chains, in a liquid-like state (3), fill up the rest of the lattice.

The correlation frequency ν_c of the motion responsible for narrowing proton magnetic resonance absorption lines may be calculated (16) by means of the following equation:

$$[3] \qquad \nu_c = 4260\Delta H/\tan\left[(\pi/2)(\Delta H^2-B^2)/(A^2-B^2)\right].$$

Here ΔH is the line width in the line-narrowing region, B is the line width at temperatures above this region, and A is the line width below it. For sodium stearate B is taken as 2.8 gauss, which is the line width at 113° C just prior to the supercurd–subwaxy transition and A is 16.1 gauss, which is considered to be the rigid lattice line width at −182° C. The second moments, previously discussed, indicated that only motion about the molecular longitudinal axis is likely between these limits. It is assumed that for a

Can. J. Chem. Downloaded from www.nrcresearchpress.com by 210.87.254.42 on 09/05/12
For personal use only.

given temperature this motion can be described by a single correlation frequency which varies with temperature T as

$$\nu_c = \nu_0 \exp (V/RT), \quad [4]$$

where V is analogous to an activation energy for the motion and R is the gas constant. The correlation frequencies from sodium stearate line widths, shown in Fig. 4, gave two

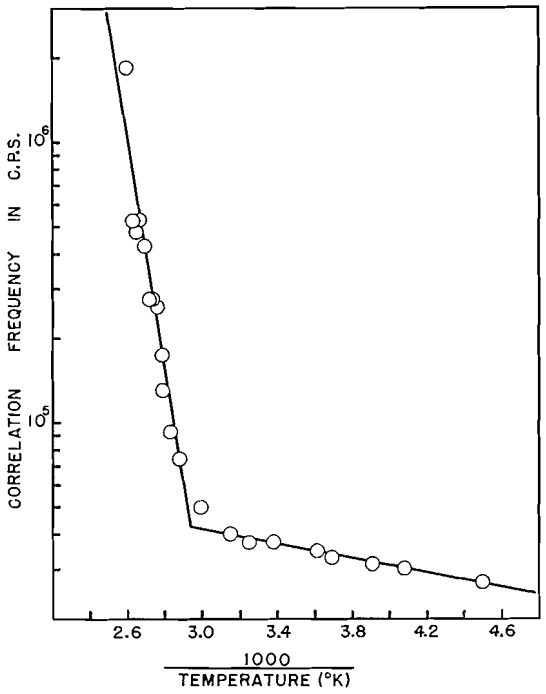


FIG. 4. Correlation frequency for sodium stearate as a function of inverse temperature.

activation energies: below about 65° C, V was 0.8 kcal/mole, and above 65° C, V was 19.2 kcal/mole. Finding two activation energies by this method may not be unusual, for a similar situation has been reported for polyethylene (21). For the small activation energy at low temperatures in polyethylene a small-amplitude torsional oscillation has been postulated, while at high temperatures the large activation energy is ascribed to rotational and translational modes of large amplitude (21). The case for sodium stearate may be similar, although the known crystal structure would not be expected to allow large translational modes below the supercurd–subwaxy transition. The activation energy of 19.2 kcal/mole seems to be of the right magnitude for a violent twisting or rotation of the paraffin chains (19) which leads to a radical change in the crystal structure.

ACKNOWLEDGMENTS

We thank the National Research Council for a studentship awarded to one of us (R. F. G.) and for a grant-in-aid of the research. We are also indebted to Professor C. A. McDowell for his interest in this problem.

Can. J. Chem. Downloaded from www.nrcresearchpress.com by 210.87.254.42 on 09/05/12
For personal use only.

REFERENCES

1. G. H. BROWN and W. G. SHAW. Chem. Revs. **57**, 1049 (1957).
2. A. SKOULIOS and V. LUZZOTI. Nature (London), **183**, 1310 (1959).
3. D. CHAPMAN. J. Chem. Soc. 784 (1958).
4. R. F. GRANT, N. HEDGECOCK, and B. A. DUNELL. Can. J. Chem. **34**, 1514 (1956).
5. J. B. BROWN and D. K. KOLB. Progress in the chemistry of fats and other lipids. Vol. 3. Pergamon Press, Ltd., London. 1955. p. 58.
6. G. STAINSBY, R. FARNAND, and I. E. PUDDINGTON. Can. J. Chem. **28**, 838 (1951).
7. R. F. GRANT and B. A. DUNELL. Can. J. Chem. **38**, 359 (1960).
8. G. E. PAKE and E. M. PURCELL. Phys. Rev. **74**, 1184 (1948).
9. E. R. ANDREW. Phys. Rev. **91**, 425 (1953).
10. A. STOSICK. J. Chem. Phys. **18**, 1035 (1950).
11. G. KOKOTAILO. Thesis, Temple University. 1955.
12. V. VAND, A. AITKEN, and R. K. CAMPBELL. Acta Cryst. **2**, 398 (1949).
13. L. PAULING. The nature of the chemical bond. Cornell University Press, Ithaca. 1948. p. 189.
14. J. H. VAN VLECK. Phys. Rev. **74**, 1168 (1948).
15. N. BLOEMBERGEN, E. M. PURCELL, and R. V. POUND. Phys. Rev. **73**, 679 (1948).
16. H. S. GUTOWSKY and G. E. PAKE. J. Chem. Phys. **18**, 162 (1950).
17. E. R. ANDREW and R. A. NEWING. Proc. Phys. Soc. (London), A, **72**, 959 (1958).
18. E. R. ANDREW. J. Chem. Phys. **18**, 607 (1950).
19. H. FRÖHLICH. Theory of dielectrics. 2nd ed. Oxford University Press, 1958. p. 128.
20. E. R. ANDREW. Nuclear magnetic resonance. Cambridge University Press. 1956. p. 173.
21. D. W. MCCALL and W. P. SLICHTER. J. Polymer Sci. **27**, 171 (1957).

Can. J. Chem. Downloaded from www.nrcresearchpress.com by 210.87.254.42 on 09/05/12
For personal use only.

Can. J. Chem. Downloaded from www.nrcresearchpress.com by 210.87.254.42 on 09/05/12
For personal use only.

CONSTITUTION OF AN ACIDIC XYLAN FROM TAMARACK (LARIX LARICINA)[1]

G. A. ADAMS

ABSTRACT

An acidic xylan isolated from tamarack wood contained arabinose, xylose, and uronic acid (1:17:3) and was homogeneous on examination by electrophoresis and sedimentation. Molecular weight estimations by four different methods showed a degree of polymerization of 20. Methylation and periodate oxidation showed that the xylan consisted of ca. 16 β-D-xylopyranose units joined by 1 → 4 glycosidic bonds with the possible occurrence of one 1 → 3 linkage. To this unbranched structure were attached as side branches, three single units of 4-*O*-methyl-D-glucuronic acid through C_2 and one unit of L-arabofuranose through C_3.

INTRODUCTION

The many xylans that have been isolated from land plants have all shown the same basic structure (1, 2, 3, 4). Variations in the xylans from individual species are provided by differences in the nature and number of single-unit side chains which are attached to the xylan chain and these differences have been summarized for a number of species of wood (4).

Xylans from softwoods have not been studied as extensively as those from hardwoods mainly because of the difficulty of separating them from glucomannans and other hemicelluloses. However, improved methods of fractionation will now permit this separation and the present paper reports the isolation and structure of an acidic xylan from tamarack.

The starting material was holocellulose prepared by chlorite delignification of extractive-free tamarack wood. Extraction with dilute alkali yielded a mixture of hemicelluloses from which the acidic xylan was separated by copper complexing. Evidence for the homogeneity of the purified hemicellulose was provided by single symmetrical peaks shown in the electrophoretic and sedimentation patterns (Fig. 1).

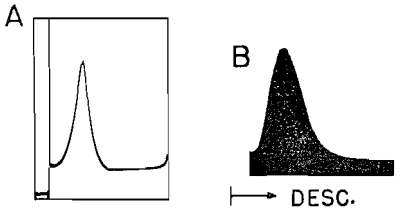


FIG. 1. (A) Sedimentation pattern of tamarack acidic xylan. (B) Electrophoresis pattern of tamarack acidic xylan.

The yield of purified hemicellulose, $[\alpha]_D$ −35°, was 1% (based on extractive-free wood) and arabinose, xylose, and uronic acid were present in a molar ratio of 1:17:3. There was a trace of rhamnose in the xylan hydrolyzate but no structural significance could be assigned to this sugar.

Hydrolysis of the hemicellulose yielded an aldobiouronic acid as the main acidic

[1]*Manuscript received August 30, 1960.*
Contribution from the Division of Applied Biology, National Research Council, Ottawa 2, Canada. Presented before Symposium on Carbohydrate Chemistry, Royal Society of Canada, Section III, June meeting, 1960, Queen's University, Kingston, Ontario.
Issued as N.R.C. No. 6023.

Can. J. Chem. Downloaded from www.nrcresearchpress.com by 210.87.254.42 on 09/05/12
For personal use only.

product. Acetylation of the methyl ester methyl glycoside of the acid yielded a crystalline acetate (1) which established the identity of the original aldobiouronic acid as 2-*O*-(4-*O*-methyl-α-D-glucopyranosyl uronic acid)-D-xylopyranose. The hemicellulose was methylated and fractionated to give one main fraction. Methanolysis and hydrolysis yielded the following products: (1) methylated aldobiouronic acid (3.0 moles); (2) 2-*O*-methyl-D-xylose (1.0 mole); (3) 3-*O*-methyl-D-xylose (trace); (4) 2,3-di-*O*-methyl-D-xylose (10 moles); (5) 2,4-di-*O*-methyl-D-xylose (1.0 mole); (6) 2,3,4-tri-*O*-methyl-D-xylose (1.0 mole); (7) 2,3,5-tri-*O*-methyl-L-arabinose (0.90 mole).

Isolation of crystalline methyl-2-*O*-(2,3,4-tri-*O*-methyl-D-glucopyranosyl)-3-*O*-methyl-β-D-xyloside (2) from reduction of component 1 confirmed the earlier identification of the aldobiouronic acid and showed that the uronic acid was attached to C_2 of a xylose unit in the main chain.

The 2-*O*-methyl-D-xylose (component 2) represented branch points in the xylan chain and was found in the same molar amount as 2,3,5-tri-*O*-methyl-L-arabinose (component 7). It is probable, therefore, that the 2-*O*-methyl-D-xylose arose from those units in the xylan chain that carried single-unit L-arabofuranose side chains linked through C_3. The 3-*O*-methyl-D-xylose (component 3) probably arose from a slight amount of hydrolysis of the partially methylated aldobiouronic acid.

The 2,3-di-*O*-methyl-D-xylose (component 4) represented the main structural feature of the xylan, i.e. D-xylopyranose units joined in a straight chain by glycosidic bonds through C_1 and C_4. The presence of 1 mole of 2,4-di-*O*-methyl-D-xylose (component 5) could be accounted for by either a $1 \rightarrow 3$ linkage in the main chain or by incomplete methylation. It was unlikely that this component represented a non-reducing terminal xylose unit substituted at C_3 by an arabofuranose residue because all of the latter was accommodated by attachment to C_3 of xylose units in the chain. Xylans of red algae have been shown to contain $1 \rightarrow 3$ and $1 \rightarrow 4$ linkages (6) and there is evidence for $1 \rightarrow 2$ linkages in some of the xylans of aspen wood (7). On the other hand, Croon and Timell (8) have shown that C_3 is less reactive than C_2 in xylans and hence may not be completely methylated. Attempts to resolve this question by enzymic degradation of the tamarack xylan are now in progress.

The 2,3,4-tri-*O*-methyl-D-xylose (component 6) represented nonreducing terminal units and the amount found indicated a degree of polymerization (D.P.) of 20. The 2,3,5-tri-*O*-methyl-L-arabinose (component 7) was the only -*O*-methyl ether of arabinose present in the mixture and showed that all the residues of this sugar were attached as single-unit side chains. The ease with which the arabinose units were removed from the original hemicellulose by mild acid hydrolysis also confirmed that they were in the furanose form and attached as terminal groups. It has not been proved that these single arabofuranose units were attached directly to the main xylan chain with no xylose units interposed. However, this point has been established in other araboxylans by two different methods (9, 10) and it is very likely that the present araboxylan is similar.

From the foregoing evidence it was clear that the arabomethoxyglucuronoxylan consisted of 16 β-D-xylopyranose units linked $\beta 1 \rightarrow 4$ with the possible occurrence of one $\beta 1 \rightarrow 3$ linkage. To this unbranched structure were attached, as single-unit side chains, three 4-*O*-methyl-D-glucuronic acid units through C_2 and one L-arabofuranose unit through C_3.

Such a molecule would consume 0.85 mole of periodate and yield 0.15 mole of formic acid per monomer unit and the experimental values of 0.87 mole of periodate and 0.15 mole of formic were in agreement with these calculations. The D.P. of the polysaccharides

was 19–20 based on formic acid production by periodate oxidation and 20 on the basis of nonreducing terminal D-xylose units in the methylated products. The values are in reasonable agreement with those given by viscosity (D.P. 20–22) and by the method of vapor pressure lowering (11, 12) (D.P. 16). On the basis of this agreement between four methods of molecular weight estimation the molecule is considered to contain about 20 sugar units. This value is small in comparison with the D.P. values reported for xylans which range from 85–220 (13, 4). The xylan under examination was less than 10% of the original crude hemicellulose and represents a molecular species which is about equivalent in size to the repeating unit of other softwood xylans (14, 15). It seems probable that the xylans from one wood species exist in a wide range of molecular sizes. It has already been shown that xylans from one wood source have differences in chemical composition (16).

The structure of the arabomethoxyglucuronoxylan from tamarack is similar, in general, to that of other xylans isolated from coniferous woods. While the xylan of loblolly pine (16) and Norway spruce (17) do not contain L-arabinose units, those of European larch (18), Sitka spruce (15), and western hemlock (14) all contain small amounts of arabinose. The proportions of 4-*O*-methyl-D-glucuronic acid, L-arabinose, and D-xylose are almost the same in Sitka spruce (15), western hemlock (14), and tamarack.

EXPERIMENTAL

All specific rotations are equilibrium values unless otherwise stated, melting points are corrected, and all evaporations were done at 35° C or less.

Paper Chromatography

Chromatographic separations were carried out using the following solvent systems (v/v ratios): (*a*) pyridine:ethyl acetate:water (2:1:2); (*b*) methyl ethyl ketone:water (2:1); (*c*) ethanol:benzene:water (47:200:15); (*d*) *n*-butanol:ethanol:water (40:11:19); (*e*) ethyl acetate:acetic acid:formic acid:water (18:3:1:4). Separations were made by the descending technique on Whatman No. 1 filter paper. Sugars were located on the paper by *p*-anisidine hydrochloride spray reagent (19).

Preparation of the Hemicellulose

A tamarack (*Larix laricina*) log, 47 years old, was converted to shavings, and then ground in a Wiley mill. The wood particles were thoroughly extracted successively with benzene:ethanol (2:1), ethanol, and water. From the aqueous solution an arabogalactan was recovered in about 6% yield; its constitution has been determined and was the subject of an earlier publication (20).

The water-extracted residue was converted to chlorite holocellulose (21) and was extracted with sodium hydroxide solution (1%) at room temperature for three successive 24-hour periods. The alkaline solutions and washings were combined, neutralized with acetic acid, concentrated at 25° C under reduced pressure, and the salts removed by dialysis in running water. The crude hemicellulose was recovered by freeze-drying, and the yield was 12.9% (extractive-free wood basis). Hydrolysis of the hemicellulose in *N* sulphuric acid for 12 hours at 100° C and chromatographic examination of the hydrolyzate ($[\alpha]_D^{25}$ +22°) showed the presence of xylose, arabinose, rhamnose, mannose, glucose, galactose, and a uronic acid. The number of sugars in the hydrolyzate indicated that more than one polysaccharide was present. Further evidence of heterogeneity was provided by electrophoretic examination in a Tiselius-type apparatus in borate buffer which showed two main peaks and indications of additional minor components.

Can. J. Chem. Downloaded from www.nrcresearchpress.com by 210.87.254.42 on 09/05/12
For personal use only.

Fractionation of the Hemicellulose

The crude polysaccharide (53 g) was dissolved, with stirring, in water (5 l.) and the insoluble material (fraction 1) was removed by centrifuging. A solution of 7% copper acetate solution (142 ml) was added to the supernatant and the precipitate which formed was removed by centrifuging (fraction 2). Addition of ethanol gave a series of fractions (No. 3 – No. 8) which were centrifuged off, freed of copper by acidification and dialysis, and recovered by freeze-drying. The results are shown in Table I.

TABLE I

Fractionation of hemicellulose
(53.14 g in 5 liters of water)

Fraction No.	Precipitating agent	Yield, g	Sugars present*				
			Xyl.	Arab.	Gal.	Glu.	Rham.
1	—	8.50	x	x	x	Tr.	Tr.
2	7% Copper acetate (143 ml)	3.41	x	x	x	Tr.	Tr.
3	Ethanol (570 ml)	22.91	x	x	x	Tr.	Tr.
4	Ethanol (142 ml)	1.22	x	x	x	Tr.	Tr.
5	Ethanol (199 ml)	2.01	x	x			Tr.
6	Ethanol (241 ml)	1.32	x	x			Tr.
7	Ethanol (285 ml)	1.24	x	x	Tr.		Tr.
8	Ethanol (570 ml)	1.72	x	x	x		Tr.
9	—	2.96	x	x	x		Tr.

*All fractions contain uronic acids.

On the basis of these results fractions No. 4 and No. 7 were combined and refractionated. The purified material was then combined with fractions No. 5 and No. 6. The last trace of copper was removed from the hemicellulose by passage of its aqueous solution over Amberlite IR-120.

The yield of purified xylan was 8.0% of the original crude hemicellulose. Analysis gave an arabinose:xylose:uronic acid ratio of 1:17:3; methoxyl, 2.9%; nitrogen, nil; and $[\alpha]_D^{25}$ −34.8° (*c*, 1.03% in water). The sugar mixture obtained on acid hydrolysis had $[\alpha]_D^{25}$ +24°.

Graded Hydrolysis

Hemicellulose (51 mg) was heated on a boiling-water bath with 5 ml of hydrochloric acid (0.01 *N*). At 30-minute intervals the hydrolyzate was examined chromatographically in solvent (*a*). In 3.5 hours the arabinose had been removed from the hemicellulose along with only a minor amount of xylose. The degraded hemicellulose was recovered with ethanol. Hydrolysis with *N* sulphuric acid and chromatographic examination of the hydrolyzate showed mainly xylose, some uronic acids, and only traces of arabinose.

Periodate Oxidation

Tamarack hemicellulose (100 mg duplicate samples) was dissolved in water (50 ml) and oxidized by 0.1 *M* sodium metaperiodate (50 ml) in the dark at 16° C. Analysis for periodate consumption and formic acid production (22) gave the following results.

Time, hours	24	48	72	120
Formic acid, moles per anhydropentose unit	0.14	0.145	0.15	0.16
Periodate consumption, per anhydropentose unit	0.54	0.61	0.86	0.87

Can. J. Chem. Downloaded from www.nrcresearchpress.com by 210.87.254.42 on 09/05/12
For personal use only.

In a separate experiment, the hemicellulose (50 mg) was oxidized for 120 hours as previously described. The excess periodate was destroyed by ethylene glycol and the solution was dialyzed. The oxidized hemicellulose was recovered by freeze-drying and then hydrolyzed with *N* sulphuric acid. Chromatographic examination of the hydrolyzate showed only xylose to be present; the amount was approximately 25% of that originally present in the hemicellulose.

Preparation of Uronic Acids from the Xylan

Xylan (100 g) was stirred overnight in 0.5 *N* sulphuric acid at room temperature and then heated at 100° C for 8 hours. After neutralization of the acid, the neutral sugars and uronic acids were separated on a column of Dowex 1-X[4] (HCO_3^-) and the uronic acids recovered by elution with *N* formic acid by procedures already described (23). Chromatographic examination in solvent (*e*) showed the presence of four components with R_x values (movement relative to xylose) as follows: 0.29, 0.42, 0.70, and 1.30 (fractions 1, 2, 3, and 4). Fraction 4 was chromatographically identical with 4-*O*-methyl-D-glucuronic acid.

The uronic acid fractions (2.1 g) were separated on a cellulose column (27×2.5 cm) using solvent (*e*). Fraction No. 3 was mixed with some of fraction No. 4 and was purified by reseparating on sheets of Whatman No. 1 filter paper using solvent (*e*). The acids were eluted with water and concentrated *in vacuo*. Hydrolysis of fraction No. 3 with *N* sulphuric acid for 20 hours at 100° C yielded xylose and 4-*O*-methyl-D-glucuronic acid.

Identification of 2-O-(4-O-Methyl-α-D-glucopyranosyluronic acid)-D-xylopyranose

The aldobiouronic acid (fraction No. 3) was a slightly yellowish solid, $[\alpha]_D^{25}$ +98° (*c*, 1.0% in water). Anal. Calc. for $C_{12}H_{20}O_{11}$: OCH_3, 9.1%. Found: OCH_3, 9.0%. The acid (57 mg) was converted to methyl 2-*O*-[methyl-(4-*O*-methyl-α-D-glucopyranosyl)uronate]-D-xylopyranoside by heating with 2.5% methanolic hydrogen chloride (3 ml) for 8 hours. The methyl ester methyl glycoside was acetylated according to Timell (24). The acetylated product was recovered and crystallized from ethyl ether, yield 30.7 mg. Recrystallization three times from ethyl ether yielded crystalline methyl-2-*O*-[methyl-(2,3-di-*O*-acetyl-4-*O*-methyl-α-D-glucopyranosyl)uronate]-3,4-di-*O*-acetyl-D-xylopyranoside, m.p. 201–203°, $[\alpha]_D^{25}$ +106° (*c*, 1.0% in chloroform). Anal. Calc. for $C_{22}H_{32}O_{15}$: OCH_3, 17.3%. Found: OCH_3, 17.2%. These values are in good agreement with the reported values (24).

Methylation of the Xylan

The xylan (6.1 g) was methylated five times with dimethyl sulphate (65 ml) and 45% sodium hydroxide (120 ml) and the product was isolated from the reaction mixture by continuous extraction with chloroform after acidification. Material that was not extracted by chloroform was recovered from the aqueous solution by dialysis and freeze-drying. The combined products (6.2 g) showed a definite hydroxyl absorption at 3500–3600 cm^{-1}. Four methylations with Purdies reagents (methyl iodide, 60 ml, and silver oxide, 10 g) yielded the fully methylated xylan (5.28 g) showing no hydroxyl absorption at 3500-3600 cm^{-1}; $[\alpha]_D^{25}$ −30° (*c*, 1% in chloroform); methoxyl, 39.23% (calculated methoxyl, 40.83%). Fractionation of this material by mixtures of chloroform:petroleum ether gave one main fraction constituting 94% of the mixture and having the same analytical values as given above.

Hydrolysis of Methylated Xylan

The fully methylated xylan (4.9 g) was heated in 8% methanolic hydrogen chloride at 80° C for 16 hours. Acid was removed by silver carbonate and the filtrate was evaporated by a stream of air at room temperature. The residue was heated at 65° C for 2

Can. J. Chem. Downloaded from www.nrcresearchpress.com by 210.87.254.42 on 09/05/12
For personal use only.

hours with a saturated solution of barium hydroxide to convert the uronosides to their barium salts. Methylated glucosides (3.78 g) were recovered from this solution by extraction with chloroform and methylated uronic acids (1.53 g) were isolated by evaporation of the aqueous residue after removal of the barium ions by Amberlite IR-120.

Methyl glucosides of the neutral sugars were analyzed by gas–liquid partition chromatography (25, 26) giving the quantitative data cited in the discussion. The procedure also provided additional evidence for the identities of the components by comparison of their relative retention volumes with those of authentic samples. To obtain sufficient amounts of the methylated sugars for complete identification the mixture of glycosides was hydrolyzed by 88% formic acid at 97° C for 24 hours. The mixture of sugars (2.43 g) recovered from the hydrolyzate after neutralization with Amberlite IR-4B(OH) showed the following components on paper chromatography in solvents (*b*) and (*c*): 2,3,5-tri-*O*-methyl-L-arabinose, R_g 1.07, R_g 1.02; 2,3,4-tri-*O*-methyl-D-xylose, R_g 1.03, R_g 0.89; 2,3-di-*O*-methyl-D-xylose, R_g 0.69, R_g 0.25; 2,4-di-*O*-methyl-D-xylose, R_g 0.55, R_g 0.25; 2-*O*-methyl-D-xylose, R_g 0.26, R_g 0.04; 3-*O*-methyl-D-xylose, R_g 0.27, R_g 0.08. An attempt to resolve this mixture by chromatography on a cellulose column using solvent (*b*) was unsuccessful, all fractions obtained being mixtures of two or more components. Separations were therefore carried out on paper sheets (Whatman No. 3 MM with Whatman No. I wicks) using solvents (*b*), (*c*), and (*d*).

Identification of Methylated Sugars

2,3,5-Tri-O-methyl-L-arabinose

The sugar was dissolved in water, clarified with charcoal, and dried to constant weight (134 mg), $[\alpha]_D^{25}$ −33° (*c*, 1% in water), and OMe, 48.0% (calculated for $C_8H_{16}O_5$: OMe, 48.4%). Chromatographic examination in solvents (*b*) and (*c*) showed that the sugar had a rate of movement identical with that of authentic 2,3,5-tri-*O*-methyl-L-arabinose. A portion of the sugar (70 mg) was oxidized with bromine to yield 2,3,5-tri-*O*-methyl-L-arabonic acid. Distillation (bath temperature, 120–145° C at 0.020 mm) lactonized the acid, which on treatment with methanolic ammonia, yielded 2,3,5-tri-*O*-methyl arabonamide in crystalline form. Recrystallization from methanol – petroleum ether solution yielded pure crystals, m.p. 136° C, $[\alpha]_D^{25}$ −18° (*c*, 1% in water); these values agree closely with those reported for this compound (27).

2,3,4-Tri-O-methyl-D-xylose

Chromatographic examination in solvents (*b*) and (*c*) showed the syrup to be 2,3,4-tri-*O*-methyl-D-xylose units with a trace of the trimethyl arabinose. The syrup was dissolved in ether and a few drops of petroleum ether added; on seeding with 2,3,4-tri-*O*-methyl-D-xylose, crystallization occurred. Recrystallization from the same solvent yielded crystals having a melting point of 88–89° C, $[\alpha]_D^{25}$ +20° (*c*, 1.0 in water). Anal. calc. for $C_8H_{16}O_5$: OMe, 48.4%. Found: OMe, 48.2%.

2,3-Di-O-methyl-D-xylose

The syrup (1492 mg) had $[\alpha]_D^{25}$ +23° (*c*, 1.1% in water) and OMe, 34.5%. Calculated for $C_7H_{14}O_5$: OMe, 34.8%. Chromatographic examination in solvents (*b*) and (*c*) showed that it moved at the same rate as 2,3-di-*O*-methyl-D-xylose. On cooling an ethyl ether solution of the sugar, crystals were obtained which on recrystallization from the same solvent had a melting point of 91–92° (undepressed with an authentic sample). The anilide was formed by refluxing aniline (200 mg) with the sugar (300 mg) in methanol (5 ml) for 2.5 hours. The crystalline anilide was recrystallized twice from ethyl acetate and had a melting point of 123–124° (undepressed with an authentic sample of 2,3-di-*O*-methyl-N-phenyl-D-xylosylamine.

Can. J. Chem. Downloaded from www.nrcresearchpress.com by 210.87.254.42 on 09/05/12
For personal use only.

2-O-Methyl-D-xylose

The syrup (139 mg) had the same rate of movement on paper in solvents (*b*) and (*c*) as 2-*O*-methyl-D-xylose. After clarification with charcoal in 50% methanol, the syrup crystallized partially. Recrystallization from methanol – petroleum ether solution yielded 2-mono-*O*-methyl-D-xylose, m.p. 132–133°, $[\alpha]_D^{25}$ +34° (*c*, 1% in water).

3-O-Methyl-D-xylose

Electrophoresis of this sugar on paper strips in borate buffer (pH 9.2), with known references differentiated it from 2-*O*-methyl-D-xylose, which moves only slightly compared with the rapid migration of the 3-*O*-methyl sugar. The amounts recovered were too small to permit other identification.

Methylated Aldobiouronic Acid

The methylated aldobiouronic acid (1.53 g) which had been separated from the neutral glycosides was converted to the methyl ester methyl glycoside by refluxing for 6 hours with 4% methanolic hydrogen chloride. This product was then reduced with lithium aluminum hydride in ether solution to yield methyl 2-*O*-(2,3,4-tri-*O*-methyl-D-glucopyranosyl)-3-*O*-methyl-β-D-xyloside, which crystallized partially on standing. Recrystallization from ethyl acetate yielded a product with a melting point of 166–168° and $[\alpha]_D^{25}$ +80° (*c*, 1.05% in water) in good agreement with the reported values (14). Anal. Calc. for $C_{16}H_{20}O_{10}$: C, 50.25%; H, 7.91%; OMe, 40.6%. Found: C, 50.10%; H, 8.01%; OMe, 40.2%.

Electrophoresis

Hemicellulose (150 mg) was dissolved in 0.05 *M* borate buffer and dialyzed against the buffer at 4° C for 24 hours. The electrophoretic separation was made in a Spinco apparatus Model H for 270 minutes; the acidic xylan moved as a single symmetrical peak with mobility (μ) = 5.65×10^{-5} cm^2 v^{-1} sec^{-1}. The diagram is shown in Fig. 1.

Sedimentation

Hemicellulose (2%) in 0.05 *M* borate buffer was centrifuged in a Model E Spinco ultracentrifuge. The rotor speed was 59,780 r.p.m. and the photograph was taken on attaining full speed (after 8 minutes). The pattern shows one sharp peak (Fig. 1).

Molecular Weight

Two physical methods of estimating molecular weight were used.

Viscosity.—Viscosity measurements were made on cupriethylenediamine solutions of the hemicellulose at concentrations of 0.08, 0.04, 0.02, 0.01, and 0.005%. Flow times were measured in an Ostwald-Cannon-Fenske type viscometer in a bath maintained at 20°± 0.02° C. The value for intrinsic viscosity [η] was substituted in the equation D.P. = K [η], where value of K = 212 (13), D.P. value = 20–22.

Vapor Pressure.—The method used was that developed by Sirianni and Puddington (11). The methylated hemicellulose was dissolved in benzene and the difference in vapor pressure between the pure solvent and the solution was measured at concentrations of 5.20, 3.72, 3.01, 2.56, 2.11, 1.90, 1.06% (g/100 g solution). The molecular weight at infinite concentrations was calculated according to Raoult's law. A straight line was fitted through the experimental points and extrapolated to infinite dilution. The observed molecular weight (number average) was 2900, therefore D.P. = 16.

Can. J. Chem. Downloaded from www.nrcresearchpress.com by 210.87.254.42 on 09/05/12
For personal use only.

ACKNOWLEDGMENTS

The author wishes to thank Mr. W. R. Rowsome for valuable technical assistance throughout the course of this investigation. Thanks are also due Dr. T. E. Timell for a sample of methyl-2-*O*-[methyl-(2,3-di-*O*-acetyl-4-*O*-methyl-α-D-glucopyranosyl)uronate]-3,4-di-*O*-acetyl-D-xylopyranoside.

REFERENCES

1. R. L. WHISTLER. Advances in Carbohydrate Chem. **5**, 269 (1950).
2. R. L. WHISTLER and C. L. SMART. Polysaccharide chemistry. Academic Press Inc., New York. 1953. p. 134.
3. W. J. POLGLASE. Advances in Carbohydrate Chem. **10**, 299 (1955).
4. G. O. ASPINALL. Advances in Carbohydrate Chem. **14**, 446 (1959).
5. T. E. TIMELL, C. P. T. GLAUDEMANS, and J. K. GILLHAM. Pulp Paper Mag. Can. **59**, 243 (1958).
6. E. G. V. PERCIVAL and S. K. CHANDA. Nature, **166**, 787 (1950).
7. J. K. N. JONES, E. MERLER, and K. E. WISE. Can. J. Chem. **35**, 634 (1957).
8. I. CROON and T. E. TIMELL. Can. J. Chem. **38**, 720 (1960).
9. C. T. BISHOP. J. Am. Chem. Soc. **78**, 2840 (1956).
10. G. O. ASPINALL and R. J. FERRIER. J. Chem. Soc. 4188 (1957).
11. A. F. SIRIANNI and I. E. PUDDINGTON. Can. J. Chem. **33**, 755 (1955).
12. R. TREMBLAY, A. F. SIRIANNI, and I. E. PUDDINGTON. Can. J. Chem. **36**, 725 (1958).
13. C. P. T. GLAUDEMANS and T. E. TIMELL. Svensk Papperstidn. **61**, 1 (1958).
14. G. G. S. DUTTON and F. SMITH. J. Am. Chem. Soc. **78**, 3744 (1956).
15. G. G. S. DUTTON and K. HUNT. J. Am. Chem. Soc. **82**, 1682 (1960).
16. J. K. N. JONES and T. J. PAINTER. J. Chem. Soc. 573 (1959).
17. G. O. ASPINALL and M. CARTER. J. Chem. Soc. 3744 (1956).
18. G. O. ASPINALL and J. E. MCKAY. J. Chem. Soc. 1059 (1958).
19. L. HOUGH, J. K. N. JONES, and W. H. WADMAN. J. Chem. Soc. 1702 (1950).
20. G. A. ADAMS. Can. J. Chem. **38**, 280 (1960).
21. L. E. WISE, M. MURPHY, and A. A. D'ADDIECO. Paper Trade J. **122**, 35 (1946).
22. S. K. CHANDA, E. L. HIRST, and E. G. V. PERCIVAL. J. Chem. Soc. 1240 (1951).
23. H. C. SRIVASTAVA and G. A. ADAMS. J. Am. Chem. Soc. **81**, 2409 (1959).
24. T. E. TIMELL. Can. J. Chem. **37**, 827 (1959).
25. A. G. MCINNES, D. H. BALL, F. P. COOPER, and C. T. BISHOP. J. Chromatog. **1**, 556 (1958).
26. C. T. BISHOP and F. P. COOPER. Can. J. Chem. **38**, 388 (1960).
27. R. W. HUMPHREYS, J. PRYDE, and E. T. WATERS. J. Chem. Soc. 1298 (1931).

Can. J. Chem. Downloaded from www.nrcresearchpress.com by 210.87.254.42 on 09/05/12
For personal use only.

Can. J. Chem. Downloaded from www.nrcresearchpress.com by 210.87.254.42 on 09/05/12
For personal use only.

PYRAZOLINES. PART II[1]

DONALD E. MCGREER, WING WAI, AND GEORGE CARMICHAEL

ABSTRACT

Product analysis has been carried out on the pyrolysis reaction in the liquid and vapor phase of 4- and 5-methyl-3-carbomethoxy-Δ^2-pyrazolines and 3-methyl-3-carbomethoxy-Δ^1-pyrazoline. The proportion of cyclopropane product was found to be greater than earlier reports had indicated and was higher for the vapor-phase pyrolysis than for the liquid-phase reaction. Vapor-phase pyrolysis of Δ^2-pyrazolines was found to require a catalyst, such as potassium hydrogen phosphate, which is believed to make possible the transformation of the Δ^2-pyrazoline into the pyrolyzable Δ^1-pyrazoline.

The pyrolysis of carbalkoxypyrazolines and related compounds has been shown to be a useful synthetic method for the preparation of derivatives of cyclopropane only in a limited number of cases. The method is particularly useful when there are carbalkoxy groups in the pyrazoline nucleus at positions 3 and 4 (1–5) and when there is an alkyl substituent and carbalkoxy substituent at the 3 position (1, 6, 7). For example, von Auwers (1) reported that 3-methyl-3-carbomethoxypyrazoline gave a product which contained 63% of methyl 1-methylcyclopropanecarboxylate and that 3,4-dicarbomethoxy-4-methylpyrazoline gave methyl 1-methylcyclopropane-1,2-dicarboxylate as the sole product. In general it has also been found that 3-carbomethoxypyrazolines with alkyl substitution at the 4 or 5 positions yield no cyclopropane product.

Recently we reported (8) that 3-carbomethoxy-Δ^2-pyrazoline yields a product which contains 32% of methyl cyclopropanecarboxylate. In a continuation of this work the 4- and 5-methyl-3-carbomethoxy-Δ^2-pyrazolines and 3-methyl-3-carbomethoxy-Δ^1-pyrazoline have been found to yield products containing cyclopropane derivatives. Upon further investigation of the pyrolysis reaction we have found that the proportion of cyclopropane derivative in the product is increased considerably when the pyrolysis is carried out in the vapor phase. For example, under these conditions 3-carbomethoxy-Δ^2-pyrazoline yields a product which contains 62% of methyl cyclopropanecarboxylate, an increase of 30% over the liquid-phase reaction.

The results of the pyrolysis of the three isomeric methyl-3-carbomethoxypyrazolines is shown in Table I and illustrated in Chart I. The liquid-phase pyrolyses were carried out by heating the pyrazoline in a distillation apparatus to a temperature at which nitrogen evolution was rapid and distillation of the product occurred as it was formed. The vapor-phase pyrolyses were carried out by dropping the liquid pyrazoline on beads or other packing material in a vertical tube heated to about 200° and connected to a vacuum system which maintained a pressure of 2 to 5 mm in the tube. The Δ^1-pyrazoline readily pyrolyzed when a glass bead packing was used but the Δ^2-pyrazolines were unchanged even with the beads at 500° unless the tube was charged with a catalyst (potassium hydrogen phosphate was used) to promote transformation of the Δ^2-pyrazoline to the Δ^1-form. This observation may be taken as further evidence that it is the Δ^1-form of the pyrazoline which pyrolyzes and not the Δ^2-form. Jones (9) and Beech *et al.* (10) have also obtained strong evidence in support of this postulate.

It is not possible to determine with certainty whether pyrolysis in the tube is occurring in the vapor phase or on the surface of the packing material. The catalyst, potassium

[1]*Manuscript received August 22, 1960.*
Contribution from the Department of Chemistry, University of British Columbia, Vancouver, British Columbia.

TABLE I
Product analysis from pyrazoline pyrolyses

Substituent in 3-carbomethoxy-pyrazoline	Phase	Proportion of components in the product in %				
		Cyclo-propane	α,β-Unsaturated ester		β,γ-Unsaturated ester	
			cis	trans	cis	trans
None	Liquid	32	30	31	7	
	Vapor	62	20	12	6	
3-Methyl	Liquid	65	15	15	5*	
	Vapor	85	7	4	4	
4-Methyl	Liquid	4	88		8	
	Vapor	26	62		12	
5-Methyl	Liquid	29	23*	43*	—	5
	Vapor	74†	12	10	—	4

*These compounds have not been previously reported and are tentatively identified from their N.M.R. and infrared spectra.
†Chromatography through a dinonyl phthalate or Ucon Polar column did not effect separation of the cis and trans esters. Infrared analysis of the acid obtained from the ester by hydrolysis indicated it to be 40% cis and 60% trans.

hydrogen phosphate, when added to the liquid-phase pyrolysis of 3-carbomethoxy-Δ^2-pyrazoline gives a lower yield of product which has approximately the same composition as the normal liquid-phase pyrolysis product. Because of this fact and since the boiling points of the pyrazolines at 2.5 mm are below the temperature at which pyrolysis occurs it is assumed that the pyrolysis takes place in the vapor phase. Further studies are now underway to determine the effect of catalyst, temperature, and pressure on the vapor-phase pyrolysis and to develop the method as a synthetic route to cyclopropane derivatives.

The pyrazolines used in the pyrolysis studies were prepared by the addition of diazomethane to the appropriate α,β-unsaturated ester. 3-Methyl-3-carbomethoxy-Δ^1-pyrazoline is a colorless liquid whereas the 4- and 5-methyl and the unsubstituted 3-carbomethoxypyrazolines are low-melting colorless solids which readily become straw-colored in the presence of air. The latter three are assigned the Δ^2-structure resulting from conjugation of the double bond with the ester carbonyl on the basis of their infrared spectra, which show N—H stretch and a conjugated carbonyl absorption.

The products from the pyrazoline pyrolyses were isolated by vapor chromatography and were identified from their physical properties. Three of these products (methyl 2-methyl-3-butenoate and methyl *cis*- and *trans*-2-pentenoate) have not previously been reported and the structures are tentatively assigned from the analysis, N.M.R., and infrared data and from the fact that each occur in equilibrium studies on known isomeric olefins. The evidence for these assignments is given in the experimental section.

The composition of the olefin portion of the pyrolysis product is in general not an equilibrium mixture as can be seen by a comparison of the equilibrium results in Table II with the pyrolysis results in Table I. The equilibrium values were determined by heating olefin samples at 250° for 2 weeks. The equilibrium was reached in each case by starting with two isomeric olefins and the equilibrium mixtures were analyzed by vapor chromatography. In general the olefin product from the pyrolysis reaction is richer in the *cis*-α,β-unsaturated olefin than is the equilibrium mixture and in many cases the cis-to-trans ratio approaches 1. A ratio of about 1 would be expected if both olefins were formed from the same high-energy intermediate for which the transition state to each olefin would be approximated by the intermediate rather than the product (11).

Can. J. Chem. Downloaded from www.nrcresearchpress.com by 210.87.254.42 on 09/05/12
For personal use only.

TABLE II

Equilibrium composition in % after equilibration at 250° C

	α,β-Unsaturated ester		β,γ-Unsaturated ester	
Initial olefin	cis	trans	cis	trans
Methyl *trans*-crotonate (8)	12	83	5	
Methyl *cis*-crotonate (8)	12	84	4	
Methyl tiglate	14	84	2	
Methyl 2-methyl-3-butenoate	14	82	4	
Methyl senecioate	84		16	
Methyl 3-methyl-3-butenoate	86		13	
Methyl *trans*-2-pentenoate	7	47	—*	46
Methyl *cis*-2-pentenoate	7	48	—*	45

*A new peak appeared in the chromatogram having one-half the area of the *cis*-2-pentenoate but was not identified.

The percentage of β,γ-unsaturated ester formed in the various reactions studied thus far seems remarkably constant and does not seem to be dependent on the relative stability of α,β- and β,γ-unsaturated products. This may mean that the β,γ-unsaturated product is also formed from the same intermediate from which the other products are formed and possibly by a proton migration (12).

The change in product composition between the liquid-phase reaction and the vapor-phase reaction is quite interesting and may make the vapor-phase reaction a feasible method for the preparation of a number of cyclopropane derivatives not readily available at the present time. The effect of the phase on the reaction may indicate that at least part of the olefin product in the liquid phase is formed by a bimolecular process which is reduced in favor of unimolecular processes in the high dilution of the vapor phase. It is therefore possible that high dilution in a solvent may also be useful for the preparation of cyclopropane derivatives where reaction in the vapor phase is not possible.

EXPERIMENTAL

Melting points and boiling points are uncorrected. Most boiling points were determined by the micro inverted capillary method. Infrared spectra were measured with a Perkin–Elmer Model 21 spectrometer using sodium chloride optics. N.M.R. spectra were recorded on a 40 Mc/s Varian spectrophotometer with field stabilizer VK 3506 and the methylene chloride used as an external standard was observed to have a value of 4.60 τ. The vapor chromatograph unit was an Aerograph model A-100-C.

Methyl-3-carbomethoxypyrazolines

The pyrazolines were prepared from diazomethane plus methyl methacrylate, diazomethane plus methyl crotonate, and diazoethane plus methyl acrylate. Ether solutions of the diazoalkane were prepared from the corresponding nitrosourea by treatment with 40% potassium hydroxide and were dried over potassium hydroxide but were not distilled. The α,β-unsaturated ester was added slowly to the ether solution until the color of the diazoalkane disappeared. The reaction to form the 4-methyl derivative took several hours but the 3- and 5-methylpyrazolines formed almost immediately at room temperature. These pyrazolines have been reported previously (1) but the following physical constants were not included in the report. The yields given are based on the reagent used in lowest molar quantity indicated in parentheses after the yield.

3-Methyl-3-carbomethoxy-Δ^1-pyrazoline: b.p. 89°/1.5 mm, yield 57% (nitrosourea).

Can. J. Chem. Downloaded from www.nrcresearchpress.com by 210.87.254.42 on 09/05/12
For personal use only.

The infrared spectrum (10% in chloroform) showed no absorption due to N—H or C=N. The ester carbonyl appeared at 1734 cm^{-1}.

4-Methyl-3-carbomethoxypyrazoline: b.p. 98/1.2 mm, m.p. 26–27°, yield 35% (nitrosourea). The infrared spectrum (10% in chloroform) had bands at 3400, 1705, and 1566 cm^{-1} assigned to the N—H, C=O, and C=N functions (13).

5-Methyl-3-carbomethoxypyrazoline: b.p. 96°/1 mm, m.p. 37–38°, yield 77% (methylacrylate). The infrared spectrum (10% in chloroform) had bands at 3420, 1706, and 1568 cm^{-1} assigned to the N—H, C=O, and C=N functions (13).

Pyrolysis of 3-Methyl-3-carbomethoxy-Δ^1-pyrazoline

3-Methyl-3-carbomethoxy-Δ^1-pyrazoline (10 g, 0.07 mole) was heated in a distillation apparatus in an oil bath. At a bath temperature of 110° pyrolysis was indicated by the evolution of a gas and at 150° it became vigorous. Distillation yielded 7.0 g (88%) of a colorless product boiling up to 141°. Four components were isolated by vapor chromatography and were identified as indicated below where boiling point, refractive index, retention time in the vapor chromatogram using a 10-ft Ucon Polar column of 0.25-in. diameter with a helium flow rate of 67 cc/minute, and percentage of the total product determined by the weights of paper cuts of the peaks are given. In all chromatographic analyses it is assumed that the thermal conductivities of the components are close enough to each other compared to helium to be assumed equal.

Methyl tiglate: b.p. 137–139°, n_D^{24} 1.4353 (lit. (14) b.p. 139.4–139.6°, n_D^{20} 1.4370), 29.1 minutes, 15%.

Methyl angelate: b.p. 127–128°, n_D^{20} 1.4320 (lit. (14) b.p. 127.6–127.8°, n_D^{20} 1.4321), 19.5 minutes, 15%.

Methyl 1-methylcyclopropanecarboxylate: b.p. 122.5–123° (lit. (15) b.p. 121–123°), n_D^{24} 1.4198, 17.9 minutes, 65%.

Methyl 2-methyl-3-butenoate: b.p. 115–116°, n_D^{24} 1.4091, 13.3 minutes, 5%. Calc. for $C_6H_{10}O_2$: C, 63.11; H, 8.84. Found: C, 62.81; H, 8.79. The physical constants for the isomer methyl α-ethylacrylate are b.p. 122–123° and n_D^{20} 1.4243 (14). The structure was confirmed from the infrared spectrum (10% in carbon tetrachloride), which showed absorption at 1740 cm^{-1} and 1640 cm^{-1} indicative of a non-conjugated ester and a carbon–carbon double bond (16). The N.M.R. spectrum (0.20 ml per ml of carbon tetrachloride) had a complex multiplet in the olefin hydrogen region with peaks at 4.14, 4.36, 4.57, 4.82, 4.89, 5.22, and 5.27 τ. Other peaks were due to the ester methyl, 6.42 (singlet), the tertiary hydrogen, 6.88 (quartet with $J \simeq 7$ c.p.s.), and the alkyl methyl, 8.83 (doublet with $J \simeq 7.2$ c.p.s.) (17).

Vapor-Phase Pyrolysis of 3-Methyl-3-carbomethoxy-Δ^1-pyrazoline

The lower portion of a 50 cm × 25 mm tube was placed in a vertical position in a tube furnace 25 cm in length and heated to 200°. The tube was filled to 35 cm from its lower end with $\frac{5}{8}$ in. diameter pyrex beads. The portion of the tube above the furnace was heated to 100° with a heating coil. The tube was fitted at the top with a pressure-equalized dropping funnel and at the bottom with two traps in series connected to a vacuum system. The traps were cooled with acetone – Dry Ice mixtures.

Two grams of 3-methyl-3-carbomethoxypyrazoline, b.p. 89°/1.5 mm, was added dropwise to the pyrolysis tube held at a pressure of 2 to 5 mm. The pyrolysis product was analyzed by vapor chromatography as in the analysis of the liquid-phase pyrolysis product and was found to contain 4% of methyl 2-methyl-3-butenoate, 85% of methyl 1-methylcyclopropanecarboxylate, 7% of methyl angelate, and 4% of methyl tiglate.

Can. J. Chem. Downloaded from www.nrcresearchpress.com by 210.87.254.42 on 09/05/12
For personal use only.

Isomerization Studies on Methyl Tiglate and Methyl 2-Methyl-3-butenoate

Ampoules containing 100 mg of methyl tiglate and methyl 2-methyl-3-butenoate isolated from the pyrolysis mixture were heated in a furnace at 250° for 2 weeks. The samples were analyzed by vapor chromatography in the same manner as the product from the pyrolysis of 3-methyl-3-carbomethoxypyrazoline and was found to contain from methyl tiglate and methyl 2-methyl-3-butenoate, respectively, methyl 2-methyl-3-butenoate 2%, 4%; methyl angelate 14%, 14%; and methyl tiglate 84%, 82%. The only new peak which might possibly be due to the isomer methyl α-ethylacrylate was a peak at 11.7 minutes, which showed a maximum area of 0.5 that of the methyl 2-methyl-3-butenoate. Analysis with a dinonyl phthalate column failed to show any new peaks.

Vapor-Phase Pyrolysis of 3-Carbomethoxy-Δ^2-pyrazoline

The apparatus used was identical with that used for the pyrolysis of 3-methyl-3-carbomethoxy-Δ^1-pyrazoline except that the pyrolysis tube above the furnace was heated with heating tape to 90° and the 15-cm portion of the tube in the center of the tube furnace was packed with potassium hydrogen phosphate. Pyrolysis of a 2-g sample yielded a colorless product which was shown by vapor chromatographic analysis (8) to contain methyl vinylacetate 6%, methyl *cis*-crotonate 20%, methyl cyclopropanecarboxylate 62%, and methyl *trans*-crotonate 12%.

Pyrolysis of 3-Carbomethoxypyrazoline in the Presence of Potassium Hydrogen Phosphate

In a distillation apparatus was placed 5.2 g of 3-carbomethoxy-Δ^2-pyrazoline and 1.5 g of potassium hydrogen phosphate and the mixture was heated in an oil bath to 190°. Analysis of the distillate (1.8 g, 44%) (8) showed methyl vinylacetate 6%, methyl cyclopropanecarboxylate 27%, methyl *cis*-crotonate 35%, and methyl *trans*-crotonate 32%.

Pyrolysis of 4-Methyl-3-carbomethoxy-Δ^2-pyrazoline

4-Methyl-3-carbomethoxy-Δ^2-pyrazoline (23 g, 0.15 mole) was pyrolyzed in a distillation apparatus at 190° in a similar manner to that described for 3-methyl-3-carbomethoxy-Δ^1-pyrazoline to give 15 g (80%) of a colorless product boiling up to 138°. Three components were isolated by vapor chromatography and identified as indicated below where boiling point, refractive index, retention time in the vapor chromatogram using a 10-ft Ucon Polar column of 0.25-in. diameter with a helium flow rate of 67 cc/minute, and percentage of the total product are given.

Methyl senecioate: b.p. 136°, n_D^{24} 1.4368, 31.2 minutes, 88%. This sample was identical in all respects with an authentic sample prepared by the procedure of Wagner (18).

Methyl 3-methyl-3-butenoate: b.p. 125°, n_D^{23} 1.4171 (lit. (18) b.p. 41°/27 mm, n_D^{20} 1.4168), 21.2 minutes, 8%.

Methyl 2-methylcyclopropanecarboxylate: —, n_D^{23} 1.4220, 26.8 minutes, 4%. The infrared and N.M.R. spectra of this compound were identical with those of the sample isolated from the pyrolysis of 5-methyl-3-carbomethoxypyrazoline.

Vapor-Phase Pyrolysis of 4-Methyl-3-carbomethoxy-Δ^2-pyrazoline

The pyrolysis was carried out at 225° by the procedure described for the vapor-phase pyrolysis of 3-carbomethoxy-Δ^2-pyrazoline. Under these conditions 10% of the pyrazoline was not pyrolyzed and was frozen out of the product. Analysis of the product by vapor chromatography showed that the product contained methyl senecioate 62%, methyl 2-methylcyclopropanecarboxylate 26%, and methyl 3-methyl-3-butenoate 12%.

Isomerization Studies on Methyl Senecioate and Methyl 3-Methyl-3-butenoate

Samples of methyl senecioate and methyl 3-methyl-3-butenoate were heated at 250°

Can. J. Chem. Downloaded from www.nrcresearchpress.com by 210.87.254.42 on 09/05/12
For personal use only.

for 2 weeks. Analysis of the product showed, respectively, methyl senecioate 84%, 87%; and methyl 3-methyl-3-butenoate 16%, 13%.

Pyrolysis of 5-Methyl-3-carbomethoxy-Δ^2-pyrazoline

5-Methyl-3-carbomethoxy-Δ^2-pyrazoline (5.0 g, 0.33 mole) was pyrolyzed in a distillation apparatus at 190° in a similar manner to that described for 3-methyl-3-carbomethoxy-Δ^1-pyrazoline to give 3.0 g (80%) of a colorless liquid boiling up to 142°. Four components were isolated and identified as indicated below where boiling point, refractive index, retention time in the vapor chromatogram using a 10-ft Ucon Polar column at 100° with a helium flow rate of 45 cc/minute, and percentage of the total product are given.

Methyl *trans*-2-pentenoate: b.p. 142°, n_D^{21} 1.4315, 37.2 minutes, 43%. Calc. for $C_6H_{10}O_2$: C, 63.11; H, 8.84. Found: C, 62.90; H, 8.91. The infrared spectrum (10% in carbon tetrachloride) showed bands at 1712, 1662, and 981 cm^{-1} characteristic of a *trans*-α,β-unsaturated ester (16). The N.M.R. spectrum (0.5 g per cc of carbon tetrachloride) showed vinyl hydrogen signals at 3.16 τ (sextet with $J_{trans} \simeq 16$ c.p.s. and $J_{CH_2} \simeq 6.4$ c.p.s.) and 4.41 τ (doublet), ester methyl hydrogens at 6.50 τ (singlet), methylene hydrogens at 7.78 τ (multiplet), and alkyl methyl hydrogens at 9.05 τ (triplet $J \simeq 7.2$ c.p.s.). These data are consistent with the *trans*-α,β-unsaturated structure assigned to this compound (17).

Methyl *cis*-2-pentenoate: b.p. 128°, n_D^{20} 1.4281, 23.6 minutes, 23%. Calc. for $C_6H_{10}O_2$: C, 63.11; H, 8.84. Found: C, 62.91; H, 9.14. The infrared spectrum (10% in carbon tetrachloride) showed bands at 1723 and 1643 cm^{-1} characteristic of an α,β-unsaturated ester (16). The N.M.R. spectrum (0.5 g per cc of carbon tetrachloride) was similar to that of the trans ester except for the value of the vinyl splitting constant, which was smaller in magnitude. Signals were found at 3.89 τ (sextet $J_{cis} \simeq 11.6$ c.p.s. and $J_{CH_2} \simeq 6.8$ c.p.s.), 4.46 τ (doublet), 6.55 τ (singlet), 7.56 τ (multiplet), and 9.23 τ (triplet $J \simeq 7.2$). These data are consistent with the *cis*-α,β-unsaturated structure assigned to this compound (17).

Methyl 2-methylcyclopropanecarboxylate: b.p. 130°, n_D^{20} 1.4228, 27.2 minutes, 29%. Calc. for $C_6H_{10}O_2$: C, 63.11; H, 8.84. Found: C, 63.28; H, 8.76. Hydrolysis with 10% sodium hydroxide of a 2-g sample obtained from a large-scale pyrolysis run, from which the olefin product was removed by oxidation with potassium permanganate, gave 1 g of 2-methylcyclopropanecarboxylic acid, b.p. 190–191° (lit. (19) b.p. 190–191°), n_D^{26} 1.4381. The infrared spectrum (10% in carbon disulphide) showed bands at 1174 cm^{-1} and 1013 cm^{-1} characteristic of the cis and trans acids, respectively, as well as the other prominent bands reported for these acids (20). The mixture was analyzed by the baseline method of Heigl (21) using the bands at 1174 and 1013 cm^{-1} and the spectra of the pure cis and trans acids kindly provided by D. E. Applequist and A. H. Peterson and was found to be 40% cis and 60% trans.

Methyl *trans*-3-pentenoate: b.p. 137°, n_D^{21} 1.4220 (lit. (22) b.p. 128°/625 mm, n_D^{20} 1.4217), 30.4 minutes, 5%. No reason can be found for the discrepancy in the boiling point. A sample isolated from the isomerization mixture (see below) had a boiling point of 136°. The infrared spectrum (10% in carbon tetrachloride) showed bands at 1740 and 970 cm^{-1} characteristic of a trans olefin and an ester but no bands were found in the 1600 to 1700 cm^{-1} region possibly due to the symmetry of the double bond (16). The N.M.R. spectrum (0.3 g per cc of carbon tetrachloride) showed bands at 4.62 τ (multiplet), 6.46 τ (singlet), 7.12 τ (broad), and 8.50 τ (broad) as would be expected for the assigned

Can. J. Chem. Downloaded from www.nrcresearchpress.com by 210.87.254.42 on 09/05/12
For personal use only.

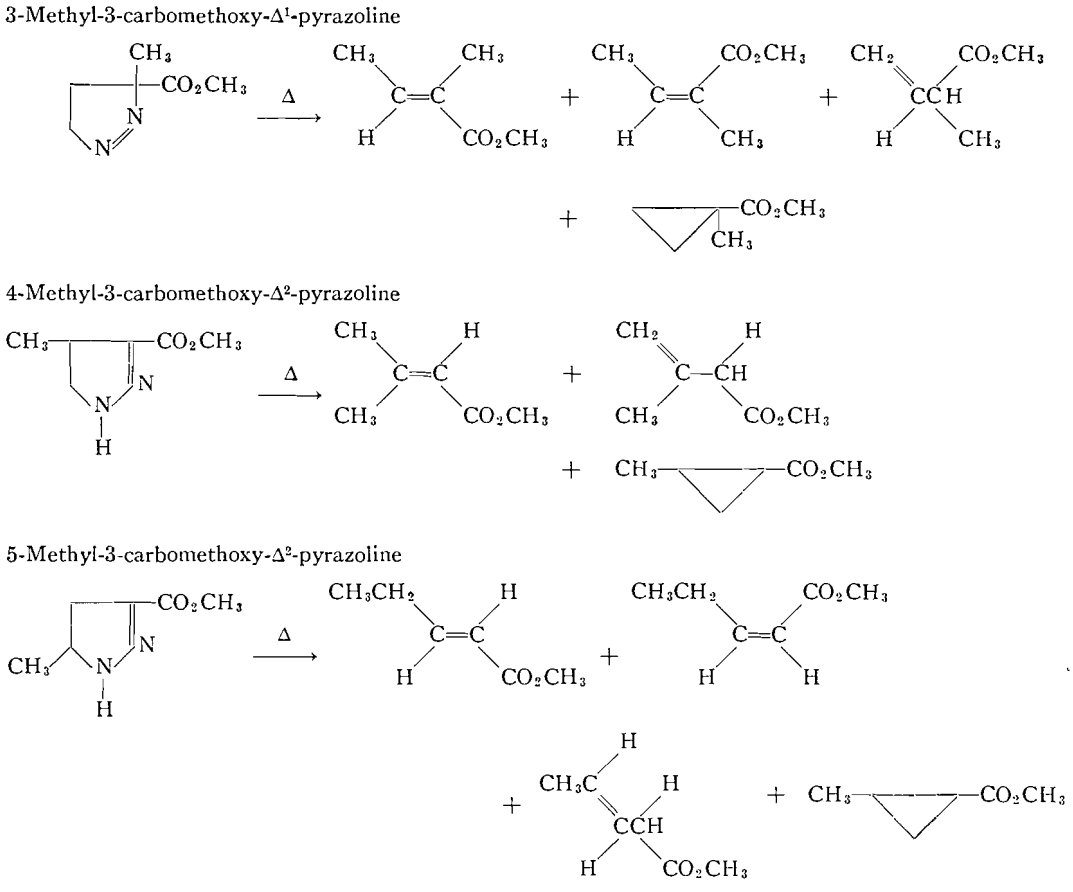


CHART I.

structure with broadening of the signals due to the large amount of long-range splitting possible (23).

Vapor-Phase Pyrolysis of 5-Methyl-3-carbomethoxy-Δ²-pyrazoline

The pyrolysis was carried out at 225° by the procedure described for the vapor-phase pyrolysis of 3-carbomethoxy-Δ²-pyrazoline. Analysis of the product showed the presence of methyl *trans*-2-pentenoate 10%, methyl *cis*-2-pentenoate 12%, methyl 2-methylcyclopropanecarboxylate 74%, and methyl *trans*-3-pentenoate 4%.

Isomerization Studies on Methyl trans-2-Pentenoate and Methyl cis-2-Pentenoate

Samples of methyl *trans*-2-pentenoate and methyl *cis*-2-pentenoate were heated at 250° for 2 weeks. Analysis of the product showed, respectively, methyl *cis*-2-pentenoate 7%, 7%; methyl *trans*-2-pentenoate 47%, 48%; and methyl *trans*-3-pentenoate 46%, 45%. In addition to these components a peak which had not previously been observed appeared in the chromatogram at 20.8 minutes. This peak was approximately one half of the area of that for methyl *cis*-2-pentenoate and might possibly be due to methyl *cis*-3-pentenoate. No new peaks were found when a dinonyl phthalate column was used.

Can. J. Chem. Downloaded from www.nrcresearchpress.com by 210.87.254.42 on 09/05/12
For personal use only.

ACKNOWLEDGMENTS

The authors gratefully appreciate the support received for this work from the National Research Council of Canada and from the President's Committee on Research of the University of British Columbia.

Thanks are also extended to Mr. J. Hochglaube and Mr. K. Wong for synthetic work and to Mrs. M. Zell for determining the infrared spectra.

REFERENCES

1. K. VON AUWERS and F. KONIG. Ann. **496**, 252 (1932).
2. H. STAUDINGER, E. ANTHES, and F. PFENNINGER. Ber. **49**, 1928 (1916).
3. L. J. SMITH and K. L. HOWARD. J. Am. Chem. Soc. **65**, 159 (1943).
4. P. C. GUHA and D. K. SANKARAN. Ber. **70**, 1688 (1937).
5. W. M. JONES. J. Am. Chem. Soc. **81**, 5155 (1959).
6. D. GOTKIS and J. B. CLOKE. J. Am. Chem. Soc. **56**, 2710 (1934).
7. P. C. GUHA and D. K. SANKARAN. Ber. **71**, 2673 (1938).
8. D. E. MCGREER. J. Org. Chem. **25**, 852 (1960).
9. W. M. JONES. J. Am. Chem. Soc. **82**, 3136 (1960).
10. S. G. BEECH, J. H. TURNBULL, and W. WILSON. J. Chem. Soc. 4686 (1952).
11. G. S. HAMMOND. J. Am. Chem. Soc. **77**, 334 (1955).
12. W. G. YOUNG, L. J. ANDREWS, S. L. LINDENBAUM, and S. J. CRISTOL. J. Am. Chem. Soc. **66**, 810 (1944).
13. J. A. MOORE. J. Org. Chem. **20**, 1607 (1955).
14. M. NASTER and A. GAVRILOFF. Bull. soc. chim. Belges, **42**, 519 (1933).
15. M. KOHN and A. MENDELEWITSCH. Monatsh. **42**, 227 (1921).
16. L. J. BELLAMY. The infra-red spectra of complex molecules. Methuen & Co., Ltd., London. 1958. pp. 34, 175.
17. L. M. JACKMAN. Applications of nuclear magnetic resonance spectroscopy in organic chemistry. Pergamon Press, New York. 1959. pp. 50, 85.
18. R. B. WAGNER. J. Am. Chem. Soc. **71**, 3214 (1949).
19. R. MARBURG. Ann. **294**, 111 (1897).
20. D. E. APPLEQUIST and A. H. PETERSON. J. Am. Chem. Soc. **82**, 2372 (1960). The authors are deeply indebted to D. E. Applequist and A. H. Peterson for providing copies of these spectra.
21. J. J. HEIGL, M. F. BELL, and J. U. WHITE. Anal. Chem. **19**, 293 (1947).
22. H. L. GOERING, S. J. CRISTOL, and K. DITTMAR. J. Am. Chem. Soc. **70**, 3314 (1948).
23. R. R. FRASER. Can. J. Chem. **38**, 549 (1960).

Can. J. Chem. Downloaded from www.nrcresearchpress.com by 210.87.254.42 on 09/05/12
For personal use only.

Can. J. Chem. Downloaded from www.nrcresearchpress.com by 210.87.254.6 on 09/05/12
For personal use only.

THE KINETICS OF THE TERTIARY-AMINE-CATALYZED REACTION OF ORGANIC ISOCYANATES WITH THIOLS[1]

YOSHIO IWAKURA AND HISAO OKADA

ABSTRACT

The kinetics of the reactions of isocyanates with thiols in the presence of tertiary amines were examined. The rate of the reaction was of the first order with respect to the concentration of isocyanate, thiol, and tertiary amine. The catalytic action of tertiary amines decreased in the order of triethylenediamine, triethylamine, diethylcyclohexylamine, tributylamine, N-methylmorpholine, pyridine, and quinoline. The relative rate of the reaction of phenyl isocyanate with thiols decreased in the order of phenylmethanethiol, 1,4-butanedithiol, 1-butanethiol, 1-dodecanethiol, and thiophenol. The reaction took place more smoothly in strong ionizing solvents. These facts can be explained by the reaction mechanism indicated by the equations [6] to [8].

INTRODUCTION

The kinetics of the reactions of phenyl isocyanate in the presence of triethylamine with 1-butanethiol, 1-dodecanethiol, and 2-methylpropane-2-thiol in toluene solution at 25° have been investigated by Dyer and Glenn (1). Their work revealed the strong catalytic effect of triethylamine in the reaction, but did not elucidate the mechanism of the reaction. In the absence of a catalyst, the reaction of organic isocyanates with thiols proceeds at high temperatures (2, 3, 4). In the presence of triethylamine, however, the reaction proceeds very smoothly even at room temperature. In the presence of diethylcyclohexylamine, aromatic isocyanates react preferentially with the thiol group rather than the hydroxyl group in 2-mercaptoethanol (5).

In the present work, the catalytic effect of tertiary amines in the reaction between isocyanates and thiols has been kinetically studied and a reaction mechanism has been proposed. The results are compared with similar data from the reactions of isocyanates with alcohols (6, 7) and with carboxylic acids (8).

RESULTS AND DISCUSSION

It has been reported that, in the reaction of phenyl isocyanate with 1-butanethiol in the presence of triethylamine in toluene solution at 25°, the catalytic action was of the first order with respect to concentration of the amine; the reaction approximately followed the second-order kinetics during the early stages of the reaction (1).

The reaction of phenyl isocyanate in the presence of 0.0050 mole/liter of tributylamine catalyst with various initial concentrations of 1-dodecanethiol in benzene solution at 35° was examined kinetically and the results obtained are plotted in Fig. 1. The rate constants calculated for a second-order reaction are almost constant over the full course of the reaction and do not vary according to the initial concentration of 1-dodecanethiol. This indicates that the reaction followed second-order kinetics. Figure 1 and other data are summarized in Table I.

The reaction velocity of organic isocyanate with thiol in the presence of tertiary amine

[1]*Manuscript received April 21, 1960.*
Contribution from the Research Laboratory of Resources Utilization, Tokyo Institute of Technology, Ookayama, Meguro-Ku, Tokyo, Japan.

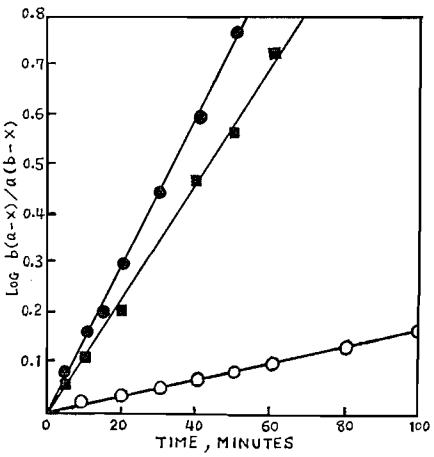


FIG. 1. Representative second-order rate plots for the reaction of phenyl isocyanate with 1-dodecanethiol in the presence of 0.0050 mole/liter tributylamine in toluene at 35°.
Ordinate: variables in the equation [12].
Initial concentration: b = C_6H_5NCO = 0.1250 mole/liter.
a = $C_{12}H_{25}SH$ = 0.1498 mole/liter ○.
$C_{12}H_{25}SH$ = 0.2995 mole/liter ■.
$C_{12}H_{25}SH$ = 0.3603 mole/liter ●.

TABLE I

The reaction of phenyl isocyanate with thiols at 35±0.02°
(Initial concentration: [C_6H_5NCO] = 0.1250 mole/liter)

Thiol	Initial concn. of thiol (mole/liter)	Solvent	Tertiary amine	Concn. of tertiary amine (mole/liter)	Second-order rate constant (liter mole^{-1} min^{-1})
n-$C_{12}H_{25}SH$	0.1498	Benzene	Tributylamine	0.0050	0.154
"	0.2995	"	"	0.0050	0.153
"	0.3603	"	"	0.0050	0.144
n-C_4H_9SH	0.0750	p-Dioxane	N-Methylmorpholine	0.010	0.0456
"	0.1250	"	"	0.010	0.0518
"	0.2500	"	"	0.010	0.0466
"	0.3750	"	"	0.010	0.0441
n-$C_{12}H_{25}SH$	0.1250	Dibutyl ether	Tributylamine	0.0025	0.0309
"	0.3750	"	"	0.0025	0.0255

is of the first order with respect to the concentration of isocyanate, thiol, and tertiary amine, and is shown to follow equation [1]:

$$[1] \qquad -d[\text{R—NCO}]/dt = k[\text{R—NCO}][\text{R—SH}][\text{R}_3\text{N}].$$

If [R_3N] is regarded as constant through a run, equation [2] is applicable, where k' is k[R_3N]:

$$[2] \qquad -d[\text{R—NCO}]/dt = k'[\text{R—NCO}][\text{R—SH}].$$

To compare the catalytic effects of tertiary amines in the reaction of phenyl isocyanate with 1-butanethiol, the rates of reaction catalyzed by seven tertiary amines were studied in toluene solution at 30°. In the absence of a catalyst, the reaction proceeded very

Can. J. Chem. Downloaded from www.nrcresearchpress.com by 210.87.254.6 on 09/05/12
For personal use only.

slowly and the rate constant was regarded as almost zero, that is, k_0 was negligible in the equation [3],

$$[3] \qquad k_{obs} = k_0 + k_c[R_3N],$$

where k_{obs} is the second-order rate constant observed. The results obtained are listed in Table II.

TABLE II

The reaction of phenyl isocyanate with 1-butanethiol in toluene solution at 30°
(Initial concentration: $[C_6H_5NCO] = [n\text{-}C_4H_9SH] = 0.1250$ mole/liter)

Tertiary amine	pK_a	Concn. of tertiary amine (mole/liter)	Second-order rate constant (liter mole^{-1} min^{-1})	Catalytic coefficient, k_c
Triethylenediamine	8.60	0.000468	0.0365	77.9
Triethylamine	10.78	0.0050	0.345	68.6
"		0.0025	0.174	
Diethylcyclohexylamine		0.00994	0.375	39.6
"		0.00497	0.178	
Tributylamine	9.93	0.0050	0.0754	15.6
"		0.0025	0.0364	
N-Methylmorpholine	9.29	0.10	Too fast	1.08
"		0.010	0.0108	
Pyridine	5.23	0.10	0.00314	
"		0.010	Too slow	0.0314
N,N-Dimethylaniline	5.00	0.10	—	0.0

N,N-Dimethylaniline did not show any catalytic effect. This phenomenon confirms evidences obtained for the reaction of phenyl isocyanate with methyl alcohol (6*a*), the polymerization reaction of isocyanates (9), and the reaction of diisocyanates with polyols (10). The plot of $[R_3N]$ against k_{obs} gave a straight line, showing that the catalytic effect was directly proportional to the concentration of tertiary amines. The catalytic coefficient k_c in the equation [3] was calculated from this slope for each of the tertiary amines used; the value obtained are listed in the fifth column in Table II. The catalytic coefficients fall almost in the same order as the basicity of the tertiary amines with the exception of triethylenediamine. With such strongly basic tertiary amines as triethylamine, diethylcyclohexylamine, and tributylamine the catalytic coefficients for the reaction of phenyl isocyanate with 1-butanethiol are larger than for the reaction of phenyl isocyanate with ethanol in dibutyl ether (6), but with weakly basic tertiary amines the opposite is true, that is, the coefficients for the reaction with alcohol are larger. This possibly explains the difference in reactivity of the hydroxyl and the thiol group of 2-mercaptoethanol in the presence of diethylcyclohexylamine (5). Triethylenediamine was much more effective catalytically than would be expected from its basicity, but this effect was less than that in the reaction between phenyl isocyanate and alcohol (11, 12).

The reactions of phenyl isocyanate with a large excess of 1-dodecanethiol in toluene at various temperatures were kinetically examined. The second-order rate constants and the apparent energies of activation calculated from the Arrhenius equation are listed in Table III with respect to the seven tertiary amines.

The reactions between phenyl isocyanate and 1-butanethiol in the presence of tertiary amines were studied in various solvents; the results obtained are listed in Table IV. The rate constants of the reaction increased in the order of benzene, toluene, dibutyl ether, dioxane, methyl ethyl ketone, and nitrobenzene. This solvent effect increased with increasing ionizing power of the solvents and was contrary to the result of the reaction

Can. J. Chem. Downloaded from www.nrcresearchpress.com by 210.87.254.6 on 09/05/12
For personal use only.

TABLE III

The reaction of phenyl isocyanate (0.1 mole/liter) with a large excess of 1-dodecanethiol (2 g) in toluene solution

Tertiary amine	Second-order rate constant (liter mole^{-1} sec^{-1}) 20°	30°	40°	Apparent energies of activation (cal/mole)
Triethylenediamine	—	—	1.07	—
Triethylamine	0.765	0.877	1.03	2500
Diethylcyclohexylamine	0.617	0.704	0.811	2500
Tributylamine	0.363	0.406	0.470	2600
N-Methylmorpholine	0.0165	0.0201	0.0246	3600
Pyridine	0.000299	0.000427	—	5800
Quinoline	0.000232	0.000319	—	5800

TABLE IV

The reaction of phenyl isocyanate with 1-butanethiol in various solvents (Initial concentration: [C_6H_5NCO] = [n-C_4H_9SH] = 0.1250 mole/liter)

Solvent	Tertiary amine	Concn. of tertiary amine (mole/liter)	Second-order rate constant (liter mole^{-1} min^{-1})	Reaction temperature (±0.02°)
Toluene	Triethylamine	0.0050	0.345	30
"	"	0.0025	0.174	"
p-Dioxane	"	0.0053	1.68	"
"	"	0.0026	0.826	"
Methyl ethyl ketone	"	0.0025	1.17	"
Nitrobenzene	"	0.0025	2.27	"
Methyl ethyl ketone	Pyridine	0.050	0.0158	35
Nitrobenzene	"	0.050	0.0169	"

of organic isocyanates with alcohols (7). This indicates that the rate-controlling step is represented by equation [8] and that the attack of the thiols on the complex-2 is accelerated by ionization of the thiols. In a powerful ionizing solvent, that is, a solvent having a greater dielectric constant, the thiols undergo ionization to a greater degree and gain more acidic character.

The reactions of phenyl isocyanate with different thiols in toluene at 30°, in the presence of triethylamine or diethylcyclohexylamine, was examined. The results obtained are listed in Table V. The reactivity of the thiols increased in the order of thiophenol,

TABLE V

The reaction of phenyl isocyanate with thiols in toluene solution at 30° (Initial concentration: [C_6H_5NCO] = [R—SH] = 0.1250 mole/liter)

Thiol	pK_a*	Catalyzed with diethylcyclohexylamine (0.0050 mole/liter)	Catalyzed with triethylamine (0.0050 mole/liter)
1-Dodecanethiol	13.8	0.162	0.306
1-Butanethiol	12.4	0.178	0.345
Phenylmethanethiol	11.8	2.6	3.1
Thiophenol	8.3	Too slow	Too slow
1,4-Butanedithiol	—	—	0.92

NOTE: Unit of second-order rate constant, liter mole^{-1} min^{-1}.
*Compt. rend. **232**, 2428 (1951).

1-dodecanethiol, 1-butanethiol, 1,4-butanedithiol, and phenylmethanethiol. No satisfactory explanation can be suggested at this time for the low activity of thiophenol.

Can. J. Chem. Downloaded from www.nrcresearchpress.com by 210.87.254.6 on 09/05/12
For personal use only.

In order to compare the reactivity of aromatic and aliphatic isocyanates and to examine the catalytic effect of tertiary amines on the two types, the kinetics of the reaction of ethyl isocyanate with 1-butanethiol in the presence of triethylamine in toluene at 30° were studied. The rate constants were 0.0422 liter mole^{-1} min^{-1} for 0.050 mole/liter and 0.0219 liter mole^{-1} min^{-1} for 0.025 mole/liter of triethylamine. The catalytic coefficients of triethylamine were 68.6 for phenyl isocyanate and 0.86 for ethyl isocyanate in their reaction with 1-butanethiol.

The work of Baker and Gaunt (6) indicates that the probable mechanism of the catalyzed reaction of phenyl isocyanate and alcohol follows the path shown by formulae [4], [5]:

$$\begin{cases} \text{R—NCO} + \text{R}_3\text{N} \rightleftharpoons \begin{pmatrix} \text{R—N=C=O} \\ \vdots \\ \text{R}_3\text{N} \end{pmatrix} \text{(complex)} & [4] \\ \text{complex} + \text{R—OH} \rightarrow \text{RNHCO}_2\text{R} + \text{R}_3\text{N}. & [5] \end{cases}$$

In equation [5], the active hydrogen-containing compound attacks the complex consisting of isocyanate and tertiary amine. In this case the rate of reaction is controlled by the acidity of the active hydrogen compound. Thiols are more acidic than alcohols; therefore, the catalytic coefficient of strongly basic tertiary amines in the reaction of isocyanate with thiol is larger than in the reaction with alcohol. With very weakly basic tertiary amines, however, the catalytic coefficient does not agree with the above presumption. From previously published (13) spectroscopic evidence of interaction between tertiary amines and thiols and from the experimental results given above, the probable mechanism of the catalyzed reaction of isocyanate and thiol seems to follow the kinetic scheme outlined below:

$$\begin{cases} \text{R—SH} + \text{R}_3\text{N} \overset{k_1}{\underset{k_2}{\rightleftharpoons}} \underset{\text{complex-1}}{(\text{R—SH---NR}_3)} & [6] \\ \text{complex-1} + \text{R—N=C=O} \overset{k_3}{\underset{k_4}{\rightleftharpoons}} \underset{\text{complex-2}}{\begin{pmatrix} \text{complex-1} \\ \vdots \\ \text{R—N=C=O} \end{pmatrix}} & [7] \\ \text{complex-2} + \text{R—SH} \overset{k_5}{\rightarrow} \text{RNHCOSR} + \text{R}_3\text{N} + \text{R—SH}. & [8] \end{cases}$$

Assuming a steady-state concentration of the complex, the following kinetic equation is obtained:

$$[9] \qquad \frac{d[\text{RNHCOSR}]}{dt} = \frac{k_1 k_3 k_5 [\text{R}_3\text{N}][\text{R—NCO}][\text{R—SH}]^2}{(k_2 + k_3[\text{R—NCO}])(k_4 + k_5[\text{R—SH}])}.$$

In this equation, if

$$[10] \qquad k_2 \gg k_3[\text{R—NCO}], \qquad k_4 \ll k_5[\text{R—SH}]$$

are effective, the equation [9] stands for the equation [1].

EXPERIMENTAL

Procedures

The reaction vessel used was a long-necked, round-bottomed flask of approximately 50-ml capacity. A thiol – tertiary amine solution was prepared using a volumetric flask at a specified reaction temperature. Two milliliters of the thiol – tertiary amine solution

Can. J. Chem. Downloaded from www.nrcresearchpress.com by 210.87.254.6 on 09/05/12
For personal use only.

Can. J. Chem. Downloaded from www.nrcresearchpress.com by 210.87.254.6 on 09/05/12
For personal use only.

was pipetted into the reaction vessel. The isocyanate solution was prepared by the same method as the thiol – tertiary amine solution. A kinetic run was initiated by adding 2 ml of the isocyanate solution into the reaction vessel. To the reaction mixture in each of the reaction vessels (seven or eight) 10 ml of dibutylamine–acetone solution was periodically added and allowed to stand for about 15 minutes to react completely the remaining isocyanate in the vessel. Reaction rates were determined by following the disappearance of the isocyanate group by a modified Stagg method (14). Unreacted dibutylamine in a reaction vessel was then titrated with 0.05 N hydrochloric acid – ethanol solution, using a semimicroburette and bromophenol blue as the indicator. Blank titration of dibutylamine and tertiary amine was also carried out and normality of the isocyanate solution was determined. In the case of a reaction with a large excess of thiol, 1 ml of tertiary amine solution and about 2 g of 1-dodecanethiol were mixed and 2 ml of isocyanate solution was added. Reproducibility of the experiments was good and agreement of duplicate runs was $\pm 2\%$.

Data were calculated and plotted according to the usual second-order reaction rate equation for reactants either at equal or at different initial concentration,

$$kt = \frac{x}{a(a-x)}, \qquad [11]$$

$$kt = \frac{2.303}{a-b} \log \frac{b(a-x)}{a(b-x)}, \qquad [12]$$

where a and b are initial concentration of isocyanate and thiol and x is concentration reacted at time t. In the case of a large excess of thiol, calculations were carried out using the first-order reaction rate equation. Representative rate plots are given in Fig. 1. Rate constants were determined from the slope of the best straight line drawn through the points of the plot (by the method of least squares).

In the literature (1) the autocatalytic effect of the product in this kind of reaction was described, but, in this present study, the autocatalytic phenomenon was not examined in detail. In the reaction catalyzed with a very weakly basic tertiary amine, however, very weak autocatalytic acceleration effect on the reaction was observed.

Materials

Diethylcyclohexylamine was prepared from hexylamine and ethyl iodide by a method described in the literature (15) and distilled, b.p. 185–192°. Triethylenediamine was recrystallized from ether, m.p. 156–157°. Other tertiary amines were dried over potassium hydroxide and fractionally distilled: b.p. triethylamine, 87–89°; tributylamine, 98–99°/19 mm; pyridine, 115.5°; N-methylmorpholine, 114°; N,N-dimethylaniline, 93°/29 mm; quinoline, 112°/14 mm. Commercial thiophenol was distilled, b.p. 68°/20 mm. Other thiols were synthesized starting from the corresponding alcohol or bromide and dried over calcium oxide and fractionally distilled under nitrogen atmosphere prior to use: b.p. 1-butanethiol, 95–99°; 1,4-butanedithiol, 96°/28 mm; 1-dodecanethiol, 116.5–117°/3 mm; phenylmethanethiol, 118°/29 mm. Commercial phenyl isocyanate and synthesized ethyl isocyanate were distilled before use: b.p. phenyl isocyanate, 164–165°; ethyl isocyanate, 60°. Toluene (16), dibutyl ether (6*a*), benzene (17), and dioxane (18) were purified by distillation from sodium. Nitrobenzene was dried over phosphorus pentoxide and distilled. Methyl ethyl ketone was dried over anhydrous potassium carbonate, refluxed for 2 days with a small amount of phenyl isocyanate, and fractionally distilled. Acetone, dibutylamine, and ethanol were used after distillation.

REFERENCES

1. E. DYER and J. F. GLENN. J. Am. Chem. Soc. **79**, 366 (1957).
2. H. L. SNAPE. Ber. **18**, 2432 (1885).
3. H. GOLDSCHMIDT and A. MEISSLER. Ber. **23**, 272 (1890).
4. S. PETERSEN. Ann. **562**, 205 (1949).
5. J. F. SMITH and E. C. FRIEDRICH. J. Am. Chem. Soc. **81**, 161 (1959).
6. (*a*) J. W. BAKER and J. B. HOLDSWORTH. J. Chem. Soc. 713 (1947).
   (*b*) J. W. BAKER and J. GAUNT. J. Chem. Soc. 9, 19, 24, 27 (1949).
7. S. EPHRAIN, A. E. WOODWARD, and R. B. MESROBIAN. J. Am. Chem. Soc. **80**, 1326 (1958).
8. S. OZAKI and S. SHIMADA. Nippon Kagaku Zasshi, **80**, 430 (1959).
9. R. G. ARNOLD, J. A. NELSON, and J. J. VERBANC. Chem. Revs. **57**, 57 (1957).
10. J. H. SAUNDERS *et al.* Ind. Eng. Chem. **46**, 1498 (1954).
11. A. FARKAS, G. A. MILLS, W. E. ERNER, and J. B. MAERKER. Ind. Eng. Chem. **51**, 1299 (1959).
12. A. FARKAS and K. G. FLYNN. J. Am. Chem. Soc. **82**, 642 (1960).
13. W. GORDY and S. C. STANFORD. J. Am. Chem. Soc. **62**, 497 (1940).
14. H. E. STAGG. Analyst, **71**, 557 (1946).
15. A. SKITA and H. ROLFES. Ber. **53**, 1252 (1920).
16. L. F. FIESER. Experiments in organic chemistry. D. C. Heath & Co. 1955. p. 292.
17. L. F. FIESER. Experiments in organic chemistry. D. C. Heath & Co. 1955. p. 282.
18. L. F. FIESER. Experiments in organic chemistry. D. C. Heath & Co. 1955. p. 284.

Can. J. Chem. Downloaded from www.nrcresearchpress.com by 210.87.254.6 on 09/05/12
For personal use only.

Can. J. Chem. Downloaded from www.nrcresearchpress.com by 210.87.254.42 on 09/05/12
For personal use only.

THE LOCATION OF XANTHATE GROUPS IN PARTIALLY SUBSTITUTED STARCH XANTHATES[1]

E. G. ADAMEK[2] AND C. B. PURVES

ABSTRACT

The rate of xanthation of starch with carbon disulphide in 17.8% potassium hydroxide at 23° was followed by converting the potassium salts to the *S*-methyl xanthate esters, and analyzing the latter for sulphur. These esters were tritylated without changing the xanthate D.S., and unity minus the trityl D.S. was assumed to represent xanthate D.S. in the primary alcohol positions of the starch. About 62% of the xanthate groups occupied secondary positions after 100 minutes of xanthation, but after 3350 minutes about 58% of the surviving xanthate groups were primary.

A sodium chlorite – pyridine – lactic acid mixture reduced the sulphur content of a fully acetylated starch *S*-methyl xanthate by about nine-tenths with little loss of acetyl groups, but the residual sulphur could not be eliminated and the resulting starch acetate could not be completely reacetylated or tosylated. The location of the hydroxyl groups in this acetate thus could not be studied by the tosylation–iodination method.

INTRODUCTION

A previous article (1) described attempts to discover the distribution of xanthate groups among the 2-, 3-, and 6-positions of cellulose sodium xanthates whose average degree of substitution (D.S.) ranged from 0.66 to 0.41. The xanthate salts were converted to the much more stable *S*-methyl esters, and the latter to completely substituted acetates, without significant loss in xanthate D.S. Attempts to dexanthate this acetate at 0° with chlorine dioxide buffered to pH 4.5, however, occasioned small losses in acetyl groups, and about one-tenth of the original sulphur content remained associated in an unknown chemical state with the dexanthated cellulose acetate. Fractional precipitation or dialysis of this acetate failed to remove the residual sulphur compounds. This failure diminished the reliability of the subsequent work, which consisted of determining distribution of unsubstituted hydroxyl groups in the dexanthated cellulose acetate (and hence of xanthate groups in the original cellulose xanthate) by the tosylation–iodination procedure. The present research was begun with a repetition of the above series of reactions with starch, since it was reasonable to hope that the great difference in the colloidal state of cellulose and starch might facilitate the study, particularly in the dexanthation step. A search of the literature (2) revealed a few articles and patents on the preparation and uses of starch sodium xanthates, but none on the distribution of the xanthate groups.

Since the primary object of the work was to explore possible methods of determining this distribution, it did not seem necessary to separate the original starch into the amylose and amylopectin components. The error caused by any incompleteness, or loss of acetyl groups, in dexanthation was reduced by starting with a starch potassium xanthate of relatively high D.S. (near unity). As expected (2), this product could be converted to the fully acetylated *S*-methyl ester with little or no change in the xanthate D.S. Subsequent attempts to remove the *S*-methyl xanthate groups selectively by aqueous chlorine dioxide, as used in the parallel work with cellulose *S*-methyl xanthates (1), resulted in poor yields of a starch acetate markedly deficient in acetyl groups and retaining 2.4, 4.6% of sulphur as residual sulphur compounds. About 20 attempts, briefly outlined

[1]*Manuscript received September 1, 1960.*
Contribution from the Division of Industrial and Cellulose Chemistry, McGill University, Montreal, Que., and from the Wood Chemistry Division, Pulp and Paper Research Institute of Canada, Montreal, Que. Abstracted from a Ph.D. thesis submitted by E. G. A. to the University in February, 1959.
[2]*Present address: Du Pont of Canada, Limited, Maitland, Ontario.*

in the Experimental portion, were made to find a more selective method of dexanthation. Hydrogen peroxide or peracetic acid in buffered aqueous solution, or sodium persulphate–sodium chlorite in aqueous pyridine, degraded the starch acetate to water-soluble products on those occasions when they reduced the sulphur content substantially. The *S*-methyl xanthate group, unlike the primary tosyl group, was not eliminated by heating with sodium iodide in a ketone solvent.

Sanyal and his co-workers (3), however, had dexanthated a cellulose *S*-methyl xanthate acetate with sodium chlorite in 90% acetic acid, and it seemed worth while to explore the use of nearly anhydrous systems in which chlorine dioxide was liberated from sodium chlorite. Alkali chlorites were known to be reduced in aqueous solution by aldehydes (4), carbohydrates (5), formic acid, oxalic acid, citric acid (6, 7), and acetic anhydride (4), the action in at least the latter case appearing to be catalytic. Trial showed that formic acid or acetic anhydride, but not formaldehyde, in a glacial acetic acid – sodium acetate medium removed most of the *S*-methyl xanthate groups from the acetylated starch derivative. Since these additives might have altered the acyl substitution, they were replaced by lactic acid as the reducing or catalytic agent for the chlorite, and in its final form the method removed about 90% of the sulphur content of the starting material with the loss of only about 6% of the acetyl groups.

After dexanthation, the residual sulphur compounds in the resulting starch acetate were not removed by mercuric chloride. One of these dexanthated acetates was extracted with pyridine, in which 33% dissolved, but both the soluble portion and the undissolved gel retained the original sulphur content. Since the starch contained 33% of amylose, it was possible that the fractionation followed the amylose–amylopectin ratio rather than any difference in substitution. Such experiments, together with similar negative results in the cellulose field (1, 3) strengthened the view that the residual sulphur was part of groupings that were chemically combined with, rather than tenaciously adsorbed on, the residual starch acetate. The groups in question were probably thioesters, because complete deacetylation with sodium methylate yielded a nearly sulphur-free starch; further acetylation, provided the catalyst was sulphuric acid, also greatly reduced the sulphur content. The simplest, but not necessarily the correct, explanation was that the supposed thioesters were monothiocarbonates of the —O—CO—SCH_3 type formed as a by-product in the dexanthation. If so, the monothiocarbonate group was fairly stable toward chlorine dioxide or chlorite, and was hydrolyzed at a rate comparable to that of acetyl groups.

Repeated attempts were then made to reacetylate the dexanthated starch acetates to the maximum theoretical substitution of 3.0, but customary methods of acetylation, even if successful with the original starch *S*-methyl xanthate or repeated two or three times, yielded products of D.S. 2.0 to 2.4. Pacsu and Mullen (8) previously noted the resistance of starch itself to complete acylation, but successfully overcame it by first swelling the starch in aqueous pyridine. Their method increased the D.S. to only 2.6 in the present case and to 2.8 after a second identical acetylation. As might be expected from these negative results, the sulphur content of the dexanthated starch acetate increased by only 1.9% when tosylated under conditions that produced extensive substitution with the similar cellulose derivative. The tosylation–iodination method of locating *S*-methyl xanthate groups in starch was thus inapplicable and other methods had to be investigated.

An attempt was made to hydrolyze starch *S*-methyl xanthate to the corresponding mixture of glucose *S*-methyl xanthates, and to identify the latter by paper chromatog-

Can. J. Chem. Downloaded from www.nrcresearchpress.com by 210.87.254.42 on 09/05/12
For personal use only.

raphy with butanol–water as eluent. Although this hydrolysis required much less drastic conditions than those required in the parallel hydrolysis of cellulose *S*-methyl xanthate (3) the result was the same; the two spots of R_F 0.56 and 0.70 derived from glucose 6-*S*-methyl xanthate were evident, but the 2- and 3-derivatives had failed to survive the hydrolysis. Neither a dextrinizing nor a saccharifying enzyme preparation produced glucose from starch *S*-methyl xanthate, although starch itself was readily degraded, even in presence of the xanthate.

Preliminary experiments then showed that starch and starch *S*-methyl xanthates, like cellulose (9) and cellulose *S*-methyl xanthates (1), could be successfully condensed with triphenylmethyl chloride (trityl chloride) in pyridine. The determination of the trityl group in the starch *S*-methyl xanthates was by weighing the triphenylmethyl carbinol produced by acid hydrolysis (9), but the earlier uncertainties originating in the formation of colloidal sulphur and traces of mercaptans (1) were overcome by correcting the weight of the crude carbinol for its sulphur content. In the final work, starch was xanthated by the "emulsion" technique while dispersed in aqueous potassium hydroxide, and samples of the starch potassium xanthate, isolated at various times by precipitation into methanol, were promptly converted to the pure *S*-methyl xanthates. These xanthate esters were then tritylated, over-all yields from the potassium salts being in all cases close to theoretical, and the D.S. of the products with respect to both trityl and *S*-methyl xanthate groups was determined by analysis. Comparison of the data (Table I, columns

TABLE I

Tritylation of starch *S*-methyl xanthates

Starch *S*-methyl xanthate[a]			Tritylated starch xanthate[b]				Trityl carbinol
Xanthation, minutes	% S	D.S. xanthate	% S	% Trityl	D.S. xanthate	D.S. trityl[c]	% S
10	6.3	0.17	2.5	56.0	0.16	0.92	0.20
20	9.4	0.28	4.1	54.0	0.25	0.89	0.41
40	16.4	0.54	8.9	45.9	0.54	0.73	2.1
60	21.1	0.76	11.7	43.6	0.74	0.73	1.6
75	24.0	0.92	14.5	40.0	0.92	0.67	5.3
105	26.8	1.09	17.2	35.2	1.07	0.58	10.2
170[d]	26.8	1.09	19.0	29.8	1.10	0.46	14.0
250	29.3	1.26	22.7	23.1	1.27	0.34	22.5
330	28.6	1.21	20.7	27.1	1.19	0.41	15.9
740	23.4	0.89	16.3	32.0	0.91	0.47	13.9
1940	19.0	0.66	12.0	38.5	0.68	0.57	8.0
3350	18.3	0.63	10.3	42.1	0.60	0.65	3.7

[a]Starch, 30 g, shaken at 23° with 350 ml of aqueous 17.8% potassium hydroxide and 150 ml of carbon disulphide. Aliquots, 50 ml, withdrawn at times stated and products promptly converted to the *S*-methyl xanthates.

[b]Tritylations with excess trityl chloride in pyridine at 70° for 3 days.

[c]Corrected for sulphur content noted in right-hand column.

[d]Residual xanthation slurry (*a*), 150 ml, diluted with 50 ml of carbon disulphide and 100 ml of 17.8% potassium hydroxide. Aliquots, 60 ml, taken at times stated.

3 and 6) showed that none of the *S*-methyl xanthate groups were lost during tritylation, and that the accuracy of the analytical work (D.S. $\pm$0.03) was satisfactory. By assuming that the trityl group selectively and completely substituted the primary alcohol positions left unoccupied by the *S*-methyl xanthate group, the substitution of the latter in the 6-position of the starch was calculated as unity minus the trityl D.S. given in column 7. The primary *S*-methyl xanthate D.S. thus being known, the average substitution in the

Can. J. Chem. Downloaded from www.nrcresearchpress.com by 210.87.254.42 on 09/05/12
For personal use only.

secondary 2- and 3-positions of the starch was found by difference from the total xanthate substitution (column 3 or 6).

When the rates of xanthation were plotted against time (Fig. 1), the plot for secondary

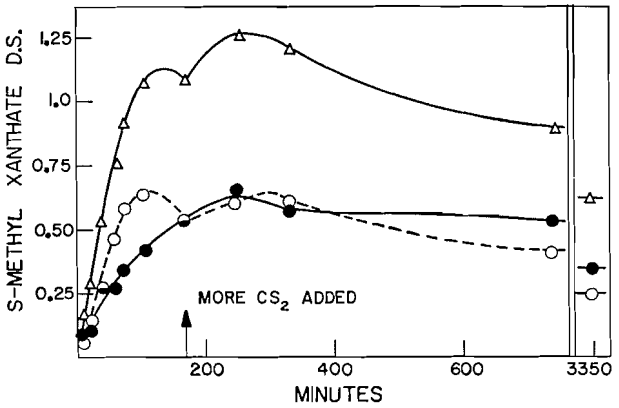


FIG. 1. Rate of xanthation of starch (see Table I, footnotes *a* and *d*). Total substitution, △; primary substitution, ●; secondary substitution, ○.

S-methyl xanthate D.S. (open circles) went through a maximum near 100 minutes which was reflected in the plot for total D.S. (triangles) but not in that for primary D.S. (filled circles), which continued to increase. About 38% of the substitution was in the primary, and 62% in the secondary, positions at this maximum. It was also evident from the shape of the plots that xanthation proceeded more rapidly in the secondary positions. When the maximum near 100 minutes was past, the addition of more carbon disulphide and alkali to the xanthating mixture produced higher maxima in all three plots after 250 to 300 minutes, and in this period the amounts of primary and secondary xanthation were almost the same. Thereafter, the substitution in the secondary positions declined more rapidly than that in the first; the plots crossed, and after 3350 minutes, when the experiment was terminated, almost 60% of the surviving xanthate groups occupied primary positions in the starch macromolecule. The course of the xanthation of starch was thus similar to that of cellulose, which was discussed in the previous publication (1) and which has now been studied in much greater detail by Philipp and Liu (10).

EXPERIMENTAL

Materials and Analytical Methods

The wheat starch used was a defatted, purified sample kindly supplied by Dr. K. M. Gaver of Ogilvie Flour Mills Limited, Montreal, Quebec. Preparation of the purified starch potassium xanthates, of D.S. near unity, and from them the corresponding *S*-methyl esters, were as previously described (2). All products were dried by solvent-exchange into ether and then *in vacuo* over phosphorus pentoxide at room temperature.

Analyses for sulphur by the Parr semimicro bomb method, for ash, and for acetyl groups by distillation with 30% chromic acid, were as previously described (1, 2). The method for acetyl was the most reliable found, but the results tended to be slightly high. In the analyses of tritylated starch *S*-methyl xanthate for trityl content by the method of Hearon and his collaborators (9), a 0.5-g sample was digested in 10 ml of concentrated sulphuric acid for 2 hours at room temperature. Dilution of the resulting clear, brown solution with 100 ml of water, which was added with cooling and shaking

Can. J. Chem. Downloaded from www.nrcresearchpress.com by 210.87.254.42 on 09/05/12
For personal use only.

as a fine stream, caused the precipitation of the crude triphenyl carbinol. After being allowed to settle overnight, the slurry could be conveniently filtered in a tared porous crucible. The residue was washed several times with water, was dried *in vacuo* over phosphorus pentoxide, and was weighed. The sulphur content of the triphenyl carbinol was determined and the weight of carbinol corrected accordingly. If the corrected weight was a, and the original sample weight was b, then % trityl = $24{,}300a/260b$.

If x and y represented the D.S. of trityl and *S*-methyl xanthate groups, respectively, in starch, their values were found by solving the simultaneous equations:

$$\% \text{ trityl} = 24300x/(162+242x+90y),$$
$$\% S = 6400y/(162+242x+90y).$$

The corresponding equations for *S*-methyl xanthates and their acetates were reported previously (1).

Acetylated Starch S-Methyl Xanthate

As noted previously (2), the acetylation of the *S*-methyl xanthate with sulphuric acid as catalyst gave a white, completely substituted product but occasioned a small loss in the xanthate D.S. Several acetylations with pyridine – acetic anhydride showed that no loss of *S*-methyl xanthate groups occurred, but that acetylations at 55° or 95° for 20 to 30 hours yielded a total D.S. of about 2.9. Prolonged acetylations of the above kind gave brown products, and one particularly dark sample contained 0.56% of nitrogen. This amount corresponded to the presence of 3.2% of pyridine, but extraction with cold *N* hydrochloric acid for 2 days at 5° failed to alter the sulphur and acetyl analyses significantly. The following method illustrated the final procedure.

Twenty grams of starch *S*-methyl xanthate (D.S. 1.20), 240 ml of pyridine, and 120 ml of acetic anhydride were heated together under gentle reflux (112°) for 45 minutes, with exclusion of moisture. After cooling, the turbid reaction mixture was poured slowly into 2 liters of vigorously stirred ice water. The resulting precipitate was recovered on a filter of coarse sintered glass; was washed several times with water, methanol, and ether in succession; was ground in a mortar; and was subjected once more to the washing sequence. When dried, the product was a white powder which was dispersible in chloroform and trichloroethylene but not to clear solutions. Yield, 23.6 g or 93% of theory. Found: S, 23.0; acetyl, 21.5%. Calculated for starch substituted to D.S. 1.25 with *S*-methyl xanthate and to D.S. 1.74 with acetyl groups: S, 23.0; acetyl, 21.5%. The total substitution was thus 2.99. When chloroform solutions of such products were examined in a Perkin–Elmer Model 21 double-beam spectrophotometer, the characteristic stretching frequencies of unsubstituted hydroxyl groups between wave numbers 3100 cm^{-1} and 3600 cm^{-1} were absent.

Attempted Dexanthations of Starch S-Methyl Xanthate Acetate

(*a*) Three grams of the above *S*-methyl xanthate acetate, 3 g of sodium iodide, 150 ml of acetonyl acetone, and 20 ml of allyl alcohol to remove any free iodine that formed were heated for 2 hours at 98° under reflux. The product, recovered by filtration, retained almost the original amount of sulphur. Yield, 2.9 g with S, 22.6%.

(*b*) The original *S*-methyl xanthate acetate, 1.5 g, dispersed in 40 ml of glacial acetic acid containing an excess of sodium acetate, was shaken with 12 ml of aqueous 30% hydrogen peroxide for 20 hours at room temperature. After dilution with 250 ml of water, the suspension was filtered and the product isolated. Yield, 1.1 g. Found: S, 7.3; acetyl, 24.4%. A repetition of this dexanthation caused the loss of more than half of the product

Can. J. Chem. Downloaded from www.nrcresearchpress.com by 210.87.254.42 on 09/05/12
For personal use only.

in the liquors. The remainder had S, 0.8%. Dexanthation with hydrogen peroxide at 5° proceeded very slowly, and hardly at all with peracetic acid in buffered acetic acid at room temperature during 16 hours at 23°.

(*c*) A highly viscous dispersion of 1.5 g of the *S*-methyl xanthate acetate in 28 ml of pyridine was mixed with 60 ml of water containing sodium persulphate, 14 g, and sodium chlorite, 14 g. The mixture was heated under reflux for 45 minutes, but no starch acetate separated when it was poured into water, presumably because the product was highly degraded.

(*d*) Two grams of another starch *S*-methyl xanthate acetate (S, 18.8; acetyl, 25.5%), dispersed in 25 ml of chloroform, was transferred into a black-painted flask containing 20 ml of glacial acetic acid, 20 ml of acetic anhydride, and 10 g of sodium acetate. The mixture was cooled to 0° before 10 g of powdered sodium chlorite and then 10 ml of water were added; the initial reaction was vigorous, and the stopper of the flask was kept loose to permit large volumes of chlorine dioxide gas to escape. After being kept near 0° for 30 minutes, the flask and contents were tightly stoppered and shaken mechanically for 22 hours at room temperature. After recovery by precipitation into water saturated with sodium acetate, the product was washed and dried. Yield, 1.6 g. Found: S, 2.6; acetyl, 31.1%. The analysis showed that 90% of the *S*-methyl xanthate and 8.5% of the acetyl groups had been removed.

The replacement of the acetic anhydride, acetic acid, and sodium acetate in the above experiment with 30 ml of pyridine and 21 ml of anhydrous formic acid caused the loss of 92% of the *S*-methyl xanthate and no loss of acetyl groups.

(*e*) Another starch *S*-methyl xanthate acetate (with S, 24.1; acetyl, 20.3%; D.S. 1.22 and 1.65) was used in the last seven dexanthations, each of which was restricted to an 8-g scale to reduce the risk of chlorine dioxide exploding in the apparatus used. The sample, 8 g, dispersed in 60 ml of chloroform, was contained in a wide-necked, black-painted 350-ml jar equipped with a glass stopper. A mixture of 40 ml of pyridine and 30 ml of 85 to 90% lactic acid was added, and the whole was cooled to 0°. The addition of 15 g of powdered sodium chlorite caused a vigorous evolution of chlorine dioxide gas and the stopper was kept loose. When the initial reaction had been completed at 0°, the jar was stoppered and shaken mechanically at room temperature for 1 hour. The mixture, still yellow-green in color, was then poured with stirring into 1.5 liters of diethyl ether. The soft precipitate was recovered and kneaded several times with ether, and then with small amounts of water, alternated with grinding in a mortar. After drying in the air, and further washings with ether, the white product was dried *in vacuo*. Found: S, 3.0; acetyl, 28.4% (D.S. 0.11, 1.58). In this case 91% of the *S*-methyl xanthate and 4% of the acetyl groups had been lost; in other cases the losses ranged as high as 93% and 10%, respectively. A repetition of the dexanthation gave a product with S, about 0.4% with the loss of 15% of the acetyl groups.

Examination of the Dexanthated Starch S-Methyl Xanthate Acetate

(*a*) A 0.4-g sample (S, 6.5; acetyl, 29.3%) was extracted at room temperature with 10-ml volumes of pyridine, which were separated from a swollen, gelatinous portion on the centrifuge. The extraction was repeated until, after the fifth, a drop of the supernatant liquor yielded no precipitate when diluted with ether. The combined extracts were then poured into much ether and the precipitate washed with water and ether and dried. Yield, 0.13 g or 33%. Found: S, 6.2; acetyl, 28.8%. The gel insoluble in pyridine was recovered in the same way. Yield, 0.21 g or 53%. Found: S, 6.4; acetyl, 28.8%.

Can. J. Chem. Downloaded from www.nrcresearchpress.com by 210.87.254.42 on 09/05/12
For personal use only.

(*b*) The above dexanthated starch *S*-methyl xanthate, 1.7 g, was deacetylated by being heated under reflux for 20 minutes with 100 ml of anhydrous methanol in which 1 g of sodium had been dissolved. After recovery on a filter, the product was ground in a mortar and deacetylated again in the same way. After washing in dilute acetic acid, methanol, and ether, the product weighed 1.3 g. Found: S, 0.29%. This sulphur content was not changed when an aqueous suspension was dialyzed through "Cellophane" against water for 55 hours.

(*c*) Another sample, 0.5 g, of dexanthated starch *S*-methyl xanthate acetate (with S, 2.0%; acetyl, 34.4%) was kept at 80° for 10 minutes while suspended in 20 ml of glacial acetic acid containing 1 g of mercuric acetate. The mixture was kept near 20° for 24 hours before being poured into water to isolate the product, which agreed with the original sample in yield and sulphur content.

(*d*) A sample, 0.8 g, of the composition noted in (*c*) was dispersed in 15 ml of dry pyridine to which 4.3 g of pure *p*-toluenesulphonyl chloride was added. The product was isolated after being kept near 20° for 24 hours, a period long enough to tosylate a similar cellulose derivative extensively (1). Found: S, 3.9%. The starch acetate thus resisted tosylation.

(*e*) Acetylation of similar dexanthated starch *S*-methyl xanthate acetates with pyridine and acetic anhydride, under conditions that led to the complete acetylation of the original starch *S*-methyl xanthate (see above) diminished the sulphur content somewhat but failed to raise the total substitution above 2.4, even when the acetylation was repeated. The use of sulphuric acid as the catalyst, of chloroacetic acid as impeller with magnesium perchlorate as catalyst (11), or of acetyl chloride in pyridine (12) gave no better results, although these methods gave complete, or almost complete, substitution with cellulose. Dexanthated starch *S*-methyl xanthates that had never been dried did not acetylate more completely than other samples. Although still unsatisfactory, the best method of acetylation found was that of Pacsu and Mullen (8). Two grams of a sample (with S, 2.3%; acetyl, 33.0%) was soaked in 30% aqueous pyridine, which was then replaced by 30 ml of anhydrous pyridine by distillation of the pyridine–water azeotrope. Acetic anhydride, 30 ml, was then added and the mixture kept at 115° for 1 hour. Found for the nearly white product: S, 1.9; acetyl, 39.4%, corresponding to D.S. 0.08, 2.52, respectively. The total D.S. was thus only 2.6.

Tritylation of Starch S-Methyl Xanthate

The procedure for tritylating cellulose (9) was slightly modified. In a typical experiment the pure, dry starch *S*-methyl xanthate, 2.5 g, was dispersed in 30 ml of pyridine contained in a flask fitted with a reflux condenser and protected from atmospheric moisture. The flask and contents were heated at 70° for 3 days, since it was found that some dexanthation occurred when a higher temperature (106°) was used for 20 hours. After being cooled, the light brown liquor was poured with stirring into 500 ml of ice and water, and the resulting precipitate was recovered on a filter of sintered glass. The product was washed with water, methanol, and ether, was ground in a mortar, washed again in the same sequence, and dried. Yields were close to those calculated from the content of *S*-methyl xanthate and trityl groups.

REFERENCES

1. E. P. Swan and C. B. Purves. Can. J. Chem. **35**, 1522 (1957).
2. E. G. Adamek and C. B. Purves. Can. J. Chem. **35**, 960 (1957).
3. A. K. Sanyal, E. L. Falconer, D. L. Vincent, and C. B. Purves. Can. J. Chem. **35**, 1164 (1957).
4. J. W. Mellor. Comprehensive treatise on inorganic and theoretical chemistry. Suppl. II, Part I. Longmans, Green & Co., Inc., New York. 1956. p. 523.

Can. J. Chem. Downloaded from www.nrcresearchpress.com by 210.87.254.42 on 09/05/12
For personal use only.

5. W. BECHER. Brit. Patent No. 345,190(1929); Chem. Abstr. **26**, 264 (1932).
6. E. STOSSEL and E. ZERNER. U.S. Patent No. 2,338,268(1944); Chem. Abstr. **38**, 3786 (1944).
7. C. A. HAMPEL. Brit. Patent No. 561,229(1944); Chem. Abstr. **39**, 5057 (1945).
8. E. PACSU and J. W. MULLEN. J. Am. Chem. Soc. **63**, 1487 (1941).
9. W. M. HEARON, G. D. HIATT, and C. R. FORDYCE. J. Am. Chem. Soc. **65**, 2449 (1943).
10. B. PHILIPP and K. T. LIU. Faserforsch. u. Textiltech. **10**, 555 (1959).
11. H. T. CLARK and C. J. MALM. U.S. Patent No. 1,880,808 (1932); Chem. Abstr. **27**, 600 (1933).
12. C. J. MALM, J. W. MENCH, D. L. KENDALL, and G. D. HIATT. Ind. Eng. Chem. **43**, 684 (1951).

Can. J. Chem. Downloaded from www.nrcresearchpress.com by 210.87.254.42 on 09/05/12
For personal use only.

Can. J. Chem. Downloaded from www.nrcresearchpress.com by 210.87.254.40 on 09/05/12
For personal use only.

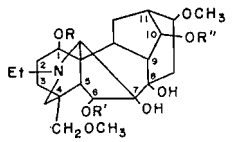
REACTIONS OF OXODELCOSINE AND INTERRELATION OF DELCOSINE AND DELSOLINE[1]

VINKO SKARIĆ[2] AND LÉO MARION

ABSTRACT

The oxidation of diacetyldelcosine produces a lactam which, after hydrolysis of the acetyl groups, can be oxidized further to a diketo-lactam in which one of the keto groups is in a five- and the other in a six-membered ring. This result leads to an alteration of the previously suggested structure of delcosine. The new structure suggests a close relationship between delcosine and delsoline which is confirmed by the methylation of the former. The reaction is selective and gives rise to a monomethyldelcosine identical in every way with delsoline. Reduction of the diketo-lactam (didehydro-oxodelcosine) with sodium borohydride gives oxodelcosine. Dehydro-oxodelcosine is also described, and its oxidation with lead tetraacetate as well as that of oxodelcosine lead to the formation of keto-products which lend supporting evidence for the structure assigned to delcosine.

Delcosine, an alkaloid isolated from *Delphinium consolida* L., has been investigated previously. The results then obtained (1) are best interpreted by assuming that the alkaloid possesses the same carbon–nitrogen skeleton as lycoctonine (2), and have led to the suggestion of tentative structure I (R = CH_3, R′ = R″ = H) for delcosine.



I

Although in this formula R″ = H has been established and the presence of a ditertiary vicinal glycol has been demonstrated chemically (3), the evidence for R′ = H is very meager and rests only on the interpretation of the formation of a carbinolamine ether (1) which requires the presence of a hydroxyl in the vicinity of the nitrogen. The work now described was designed to establish the nature of the substituents R and R′ in I.

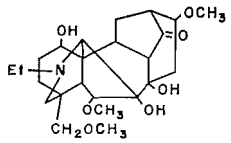
It has already been shown that the oxidation of delcosine ($C_{24}H_{39}O_7N$) with chromic acid in acetic acid gives rise to dehydrodelcosine (II) in which the keto group forms part of a five-membered ring (1). When diacetyldelcosine (4) is oxidized with potassium permanganate, or with chromic acid – pyridine complex (Sarett's method), a lactam, diacetyl-oxodelcosine (III), m.p. 103–108° ($C_{28}H_{41}O_{10}N$), is obtained, which on hydrolysis, produces the neutral product, oxodelcosine (IV) ($C_{24}H_{37}O_8N$), m.p. 245–246°. Oxodelcosine (IV) in glacial acetic acid is oxidized by sodium dichromate to a diketone, didehydro-oxodelcosine (V) ($C_{24}H_{33}O_8N$), m.p. 211–212°, which in the infrared shows absorption bands at 1757 cm^{-1} (five-membered cyclic ketone), 1720 cm^{-1} (six-membered cyclic ketone), and 1653 cm^{-1} (six-membered lactam). The product V, which is also obtainable by direct oxidation of delcosine with Sarett's reagent, is converted back to oxodelcosine (IV) by reduction with sodium borohydride.

This result confirms that the nitrogen forms part of a six-membered ring, but indicates that contrary to the original assumption only one of the two secondary hydroxyl groups

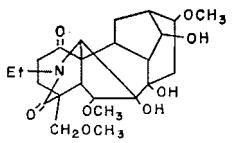
[1]*Manuscript received August 16, 1960.*
Contribution from the Division of Pure Chemistry, National Research Council, Ottawa, Canada.
Issued as N.R.C. No. 6026.
[2]*National Research Council of Canada Postdoctorate Fellow 1957–1959. Present address: Rudjer Boscović Institute, Zagreb, Yugoslavia.*

present in delcosine is on a five-membered ring, while the other is on a six-membered ring. The substituents, therefore, cannot be as represented in structure I (R = CH_3, R′ = R″ = H) since, were R′ = H, both keto groups in V should have been in five-membered rings. To account for this experimental result and the formation of the carbinolamine ether previously described (1), which requires that one hydroxyl group be in close proximity to the nitrogen, it is necessary to alter the suggested structure of delcosine to I (R = R″ = H, R′ = CH_3). This new structure has already been reported in a preliminary communication (5).

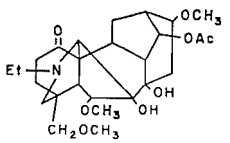
The fact that one of the two secondary hydroxyl groups is attached to a six-membered ring is confirmed by the oxidation with Sarett's reagent of monoacetyldelcosine (4), which gives rise to a monoacetyldehydro-oxodelcosine (VI) ($C_{26}H_{37}O_9N$), m.p. 107–110°, hydrolyzed by potassium hydroxide to dehydro-oxodelcosine (VII) ($C_{24}H_{35}O_8N$), m.p. 228–229°, in which the keto group, according to the infrared spectrum (1719 cm^{-1}), is in a six-membered ring. The formation of VII from monoacetyldelcosine also establishes



II



VII



VI

that it is the secondary hydroxyl group attached to the five-membered ring that is more readily and preferentially acetylated. Hence, compound II should be designated 10-dehydrodelcosine, whereas compound VII is 1-dehydro-oxodelcosine.

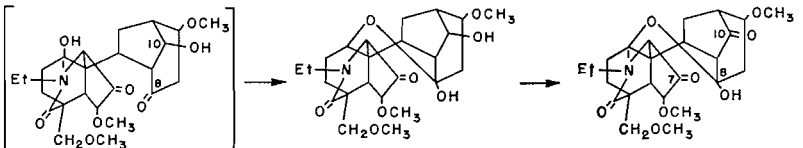
If structure I (R = R″ = H, R′ = CH_3) be the correct one, then delcosine must be very closely related to delsoline, which has been assigned structure I (R = H, R′ = R″ = CH_3) (6). In order to ascertain this point, delcosine was methylated by means of sodium hydride and methyliodide in dioxane according to the method used by Carmack *et al.* (7) in establishing the relationship of deltaline, delphaline, and lycoctonine. The product obtained after chromatography on alumina melted at 215–216°, undepressed on admixture with delsoline, and its optical rotation, infrared spectrum, and Debye–Scherrer diagram were all identical with the corresponding physical constants of delsoline. The methylation was therefore selective and affected only the secondary hydroxyl located on the five-membered ring which is also the hydroxyl that is the more readily acetylated.

The selective methylation of delcosine occurred only if the reaction was allowed to proceed at room temperature. When the reaction mixture was heated under reflux, the methylation was no longer selective and the product was di-*O*,*O*-methyldelcosine, $C_{26}H_{43}O_7N$, m.p. 203–206°.

The oxidation with periodic acid of the carbinolamine ether, anhydro-hydroxydelcosine, indicating the presence of a vicinal glycol in delcosine, has been reported previously (3). The action of lead tetraacetate on oxodelcosine has now been investigated. Preliminary studies showed that 1 mole of the oxidizing agent is consumed in 1 hour. In this oxidation oxodelcosine is converted to a compound VIII ($C_{24}H_{35}O_8N$), m.p. 191–193°, which in the infrared shows two absorption bands (3408 and 3360 cm^{-1}) in the hydroxyl region, a band at 1763 cm^{-1} attributable to a five-membered cyclic ketone, and one at 1654 cm^{-1} due to the lactam carbonyl. This oxidation indicating a vicinal glycol should give rise to a dicarbonyl derivative. The absence of an absorption band in the infrared region

Can. J. Chem. Downloaded from www.nrcresearchpress.com by 210.87.254.40 on 09/05/12
For personal use only.

1700–1720 cm^{-1} shows that the expected six-membered cyclic ketone carbonyl is not present, and consequently that it must have become masked by a secondary reaction. On the other hand, the further oxidation of VIII with Sarett's reagent gives rise to a compound IX ($C_{24}H_{33}O_8N$), m.p. 209–210°, which in the infrared contains only one hydroxyl band (3320 cm^{-1}) and two five-membered cyclic ketone carbonyls (1766, 1758 cm^{-1}) as well as the lactam carbonyl (1657 cm^{-1}). Hence, of the two hydroxyl groups present in VIII, only one (on a five-membered ring) is secondary. These results are explainable

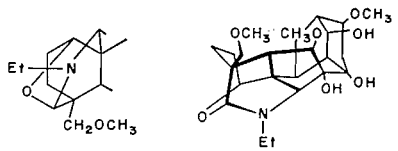


VIII IX

if in the secodiketone originally formed in the reaction, the carbonyl at 8 is assumed to have condensed with the secondary hydroxyl at 1 to form a hemiketal. There would result a tertiary hydroxyl at 8, and in the further oxidation of VIII to IX only the hydroxyl at 10 could be converted to a keto group.

In support of this interpretation, 1,10-didehydro-oxodelcosine (V), in which no secondary hydroxyl group is present, is oxidized by lead tetraacetate to 1,10-didehydroseco-oxodelcosine diketone (X) ($C_{24}H_{31}O_8N$), m.p. 175–177°, which according to its infrared absorption spectrum contains no hydroxyls. Further, 1-dehydro-oxodelcosine (VII), in which the hydroxyl at 1 is no longer present, is oxidized by lead tetraacetate to 1-dehydro-seco-oxodelcosine diketone (XI) ($C_{24}H_{33}O_8N$), m.p. 181–183°. In the infrared XI shows a hydroxyl band at 3344 cm^{-1}, one five-membered cyclic ketone (1776 cm^{-1}), two six-membered cyclic ketones (1712; 1688 cm^{-1}), and a lactam carbonyl (1655 cm^{-1}). Hence, in the absence of a secondary hydroxyl in ring A (position 1) no hemiketal is formed in the secodiketones.

Every one of the reactions of delcosine reported so far is accommodated by the new structure I (R = R″ = H, R′ = CH_3) assigned to the alkaloid, including the formation



XII

of the carbinolamine ether previously described (1). Notwithstanding a recently expressed view that the structure XII assigned to the carbinolamine ether (anhydrohydroxy-delcosine) is geometrically impossible (8), this structure when built with Courtauld models is remarkably strainless. It involves boat conformations for ring A and the nitrogen-bearing ring, and in this structure the ethyl group attached to the nitrogen is much less hindered than in delcosine itself. Consequently, the above statement of Büchi (8) does not appear to constitute a very serious argument.

It had been suggested previously (4) that the alkaloid delphamine (9) was very probably identical with delcosine. Due to the courtesy of Drs. L. S. Chetverikova and A. D. Kuzovkov, who sent us a sample of delphamine for comparison, this has been confirmed. The two bases have the same melting point, which is not depressed on admixture, and the infrared spectra and X-ray powder diagrams of both are identical.

Can. J. Chem. Downloaded from www.nrcresearchpress.com by 210.87.254.40 on 09/05/12
For personal use only.

As already reported by Ochiai, Okamoto, and Kaneko (10), their Takaobase-I has been found to be identical with delcosine. Through the kindness of Professor Ochiai, we have been able to compare their Shimoburobase-II with 10-dehydrodelcosine and find that the melting points of the bases and their mixture, their infrared spectra, and their X-ray powder diagrams are identical.

The alkaloids lucaconine and monoacetyllucaconine have been described in the literature (11) and some degradative work on the former has been recorded recently (12) as well as a corrected formula (13), which is the same as that of delcosine. The physical and chemical properties of lucaconine and its derivatives are so strikingly similar to those of delcosine and its corresponding derivatives that it is most probable that the two bases are identical and that monoacetyllucaconine is identical with monoacetyldelcosine.

EXPERIMENTAL

The physical constants were determined as follows: the melting points, uncorrected, were taken on a Kofler hot stage; optical rotations were measured in chloroform unless otherwise stated; the ultraviolet spectra were measured in 95% ethanol on a Beckman DU spectrophotometer, and the infrared absorption spectra were recorded on a Perkin–Elmer double-beam instrument Model 21B. The infrared absorption bands are reported in wave numbers followed by a number in parentheses which designates the percentage absorption. The neutral alumina used for adsorption chromatography was standardized according to Brockmann.

Diacetyloxodelcosine (III)

Diacetyldelcosine prepared as previously described (4) (200 mg) was dissolved in acetone (4 ml) containing water (0.15 ml) and acetic acid (0.1 ml) and the solution heated under reflux. To the refluxing solution powdered potassium permanganate (220 mg) was added portionwise with agitation over a period of 2 hours. The reaction mixture was then kept at room temperature overnight. Sulphur dioxide was bubbled in the solution, which was subsequently filtered and evaporated under reduced pressure to a syrup. The syrup was partitioned between 0.5 *N* sulphuric acid and chloroform and the chloroform solution washed with 4% aqueous sodium carbonate. The chloroform extract was dried, evaporated under reduced pressure, and the microcrystalline residue (169 mg) fractionally recrystallized from ether–hexane. The middle fractions (80.3 mg) were recrystallized from hexane from which diacetyloxodelcosine separated as colorless microcrystals, m.p. 103–105°. $[\alpha]_D^{25}$ +24.6±1.4° (*c*, 0.71). Found: C, 60.95; H, 7.42. Calc. for $C_{28}H_{41}O_{10}N$: C, 60.96; H, 7.49%. Infrared (nujol mull): 3454(50), 1738(92), 1644(84), 1245(95) cm^{-1}.

Diacetyloxodelcosine is also obtained in 65% yield from diacetyldelcosine by oxidation with chromic anhydride – pyridine complex.

Oxodelcosine (IV)

Diacetyloxodelcosine (54.0 mg) was refluxed for 2 hours with 5% potassium hydroxide in (1:1) aqueous methanol. After it was cooled, the solution was evaporated to a syrup under reduced pressure, water was added, and the product extracted with chloroform. The chloroform extract was washed with 0.5 *N* sulphuric acid, washed with water, dried, and evaporated under reduced pressure. The residue (47.9 mg) was crystallized from ether, m.p. 236–245°, dissolved in benzene, and chromatographed on alumina (activity II). Elution of the column with chloroform gave oxodelcosine, which crystallized from

Can. J. Chem. Downloaded from www.nrcresearchpress.com by 210.87.254.40 on 09/05/12
For personal use only.

a mixture of acetone, ether, and hexane as colorless prisms, m.p. 245–246.5, $[\alpha]_D^{23}$ +44.3 ±0.6° (*c*, 1.83). Found: C, 61.75; H, 7.93. Calc. for $C_{24}H_{37}O_8N$: C, 61.65; H, 7.98%. Ultraviolet spectrum: shoulder λ_{max} 210 mμ, log ε 3.8. Infrared spectrum (nujol mull): 3446(72), 3406(69), 1649(93), 1622(56) cm^{-1}; (chloroform solution): 3608(17), 3468(43), 1638(86) cm^{-1}.

1,10-Didehydro-oxodelcosine (V)

(*a*) *From oxodelcosine.*—To a solution of oxodelcosine (200 mg) in glacial acetic acid (15 ml), sodium dichromate (100 mg) dissolved in glacial acetic acid (15 ml) was added dropwise. The solution was set aside for 1 hour at room temperature. Sulphur dioxide was bubbled into the reaction mixture to destroy excess reagent and the solvent was removed under reduced pressure, leaving a residue which was partitioned between 0.5 *N* sulphuric acid and chloroform. The chloroform layer was washed with 4% sodium carbonate, dried, and evaporated under reduced pressure. The residue was crystallized from acetone–ether–hexane (wt. 136.3 mg, m.p. 202–208°), dissolved in benzene, and chromatographed on alumina (activity II–III) and eluted with benzene. Didehydro-oxodelcosine (88.3 mg) obtained from the eluate was recrystallized from benzene–hexane, m.p. 208–211°. Further elution with methanol gave another 46.5 mg of the product, m.p. 202–206°. On recrystallization from benzene–hexane the product was obtained as colorless prisms, m.p. 211–212°, $[\alpha]_D^{21}$ +135±0.9° (*c*, 1.11). Found: C, 62.35; H, 7.12. Calc. for $C_{24}H_{33}O_8N$: C, 62.19; H, 7.18%. Ultraviolet spectrum: λ_{max} 297 mμ, log ε 2.07, λ_{min} 267 mμ, log ε 1.63. Infrared spectrum (nujol mull): 3446(69), 1757(90), 1720(80), 1653(92) cm^{-1}; (chloroform solution): 3540(25), 3476(27), 1761(81), 1721(72), 1643(89) cm^{-1}.

(*b*) *From delcosine.*—Chromic anhydride (1.5 g) was added gradually with stirring to dry, freshly distilled pyridine (15 ml) previously cooled to 0°. The yellow complex began to precipitate and the mixture was allowed to warm to room temperature. A solution of delcosine (0.5 g) in pyridine (10 ml) was then added and the mixture allowed to stand at room temperature for 20 hours in a stoppered flask. The solvent was distilled off under reduced pressure, and, to the residue, cracked ice and 0.5 *N* sulphuric acid were added. Sulphur dioxide was bubbled into the solution which was then extracted with chloroform. The extract was washed with 0.5 *N* sulphuric acid, with 4% aqueous sodium carbonate, and with water. The didehydro-oxodelcosine recovered from the chloroform solution was purified as described above, m.p. 209–211°, wt. 233.9 mg.

Reduction of Didehydro-oxodelcosine

To a solution of didehydro-oxodelcosine (100 mg) in 80% methanol (25 ml), sodium borohydride (600 mg) was added and the mixture was kept at room temperature for 2 hours. The solvent was evaporated, 0.5 *N* sulphuric acid added to the residue and the mixture was extracted with chloroform. The extract was washed with 4% aqueous sodium carbonate and evaporated under reduced pressure. The residue was crystallized from ether (wt., 88 mg) and purified by chromatography in chloroform on neutral alumina and recrystallization from acetone–hexane, m.p. 241–243°, $[\alpha]_D^{23}$ +43.6±0.8°. The infrared spectrum (in chloroform solution) was superimposable on that of oxodelcosine.

10-Monoacetyl-1-dehydro-oxodelcosine (VI)

Monoacetyldelcosine (4) (190 mg) in pyridine (3.6 ml) was oxidized with chromic oxide – pyridine complex. The complex was prepared in the usual way from chromic anhydride (360 mg) and pyridine (3.6 ml). The product was isolated exactly as described above. The monoacetyldehydro-oxodelcosine thus obtained and crystallized from

Can. J. Chem. Downloaded from www.nrcresearchpress.com by 210.87.254.40 on 09/05/12
For personal use only.

hexane consisted of microcrystals, m.p. 107–110°, $[\alpha]_D^{26}$ +94.6±1.3° (*c*, 0.74). Found: C, 62.01; H, 7.68. Calc. for $C_{26}H_{37}O_9N$: C, 61.52; H, 7.35%. Ultraviolet spectrum: λ_{max} 298 mμ, log ε 1.873 and shoulder at λ 214 mμ, log ε 3.382. Infrared spectrum (nujol mull): 3436(53), 1738(86), 1721(78), 1645(86), 1253(86) cm^{-1}; (in chloroform solution): 3520(18), 3440(25), 1732(75), 1723(79), 1645(81), 1248(84) cm^{-1}.

1-Dehydro-oxodelcosine (VII)

Monoacetyldehydro-oxodelcosine (186 mg) was saponified by refluxing for 2 hours with 5% potassium hydroxide in 1:1 methanol–water. The solution was evaporated to a syrup under reduced pressure, water was added, and the mixture was extracted with chloroform. The extract was washed with 0.5 *N* sulphuric acid, dried, and evaporated under reduced pressure. The residue (137 mg) was dissolved in benzene and chromatographed on a column of alumina of activity IV. The column was eluted with benzene and the eluate yielded a fraction of the product (86 mg), m.p. 221–225°, and a less pure fraction (43 mg), m.p. 208–216°. The first fraction was crystallized twice from acetone–hexane from which it separated in long, colorless needles, m.p. 228–229°, $[\alpha]_D^{23}$ +120±0.9° (*c*, 1.08). Found: C, 61.83; H, 7.45. Calc. for $C_{24}H_{35}O_8N$: C, 61.92; H, 7.58%. Ultraviolet spectrum: λ_{max} 297 mμ, log ε 1.937 and shoulder at λ 211 mμ, log ε 3.479, λ_{min} 267 mμ, log ε 1.565. Infrared spectrum (nujol mull): 3476(34), 3358(64), 1719(53), 1633(91) cm^{-1}.

Di-O,O-Methyldelcosine

To a solution of delcosine (76 mg) in dioxane (6 ml), sodium hydride (80 mg) and methyliodide (2 ml) were added, and the mixture kept overnight at room temperature. It was then refluxed for 8 hours. After it had cooled the reaction mixture was filtered and the filtrate evaporated to dryness under reduced pressure. The residual product (quantitative yield) was crystallized from acetone–ether (49 mg), m.p. 203–206°, $[\alpha]_D^{24}$ +48.6±1.3° (*c*, 0.74). Found: C, 65.00; H, 9.06; OCH_3, 31.60. Calc. for $C_{26}H_{43}O_7N$: C, 64.84; H, 9.00; $5OCH_3$, 32.21%.

O-Methyldelcosine (Delsoline)

To a solution of delcosine (45.4 mg) in dioxane (2 ml), sodium hydride (30 mg) and methyliodide (0.5 ml) were added and the mixture was allowed to stand at room temperature for 21 hours in a flask protected by a calcium chloride tube. After this period the mixture was filtered through a hyflo-supercel column and the filtrate was evaporated to dryness under reduced pressure. The residue, which was crystalline, was recrystallized from benzene–hexane, m.p. 213–216°, wt. 42 mg. It was dissolved in benzene, chromatographed on a column of alumina grade IV (370 mg), and eluted with benzene. The benzene eluate yielded 26 mg of base and further elution with methanol yielded another 11 mg. Recrystallization of the product in benzene–hexane gave colorless prisms, m.p. 215–216°, undepressed on admixture with an authentic sample of delsoline. Its optical activity, $[\alpha]_D^{22}$ +53.4±0.5° (*c*, 2.04), was the same as that of delsoline, $[\alpha]_D^{27}$ +53.5±0.5° (*c*, 2.11). Found: C, 64.43; H, 8.79. Calc. for $C_{25}H_{41}O_7N$: C, 64.22; H, 8.84%. The infrared spectrum of the product was superimposable on that of delsoline, and its Debye–Scherrer powder diagram was identical with that of delsoline.

Internal Hemiketal of Seco-oxodelcosine Diketone (VIII)

Oxodelcosine (75 mg) was dissolved in a saturated solution of lead tetraacetate in glacial acetic acid (50 ml) and the solution was kept in the dark for 2 hours at room temperature. Excess lead tetraacetate was reduced with sulphur dioxide, water was

Can. J. Chem. Downloaded from www.nrcresearchpress.com by 210.87.254.40 on 09/05/12
For personal use only.

added, and the mixture was cooled for 1 hour. The precipitate was filtered off and the filtrate evaporated under reduced pressure to dryness. Sulphuric acid (0.5 *N*) was added to the residue and the mixture extracted with chloroform. The extract was washed with 4% aqueous sodium carbonate, dried, and evaporated. The neutral residue was crystallized in acetone–hexane, wt. 50 mg, m.p. 183–186°. Several recrystallizations from dichloromethane–ether yielded colorless prisms, m.p. 191–193°, $[\alpha]_D^{24}$ +1.5±0.8° (*c*, 0.65). Found: C, 62.06; H, 7.42. Calc. for $C_{24}H_{35}O_8N$: C, 61.92; H, 7.58%. Ultraviolet spectrum: λ_{max} 215 mμ, log ε 3.72, λ_{max} 322 mμ, log ε 2.40, λ_{min} 275 mμ, log ε 1.86. Infrared spectrum (nujol mull): 3408(55), 3360(52), 1763(84), 1654(93) cm^{-1}.

Internal Hemiketal of 10-Dehydroseco-oxodelcosine Diketone (IX)

To dried, freshly distilled pyridine (2.2 ml) cooled to 0°, chromic anhydride (116 mg) was added portionwise with shaking. The mixture from which a yellow complex had separated was allowed to warm to room temperature and to it was added a solution of the hemiketal of seco-oxodelcosine diketone (58 mg) in pyridine (1.2 ml). The reaction flask was stoppered and allowed to stand at room temperature for 20 hours. The solvent was then removed under reduced pressure and to the residue ice and 0.5 *N* sulphuric acid were added. Excess oxidizing agent was destroyed with sulphur dioxide and the solution was extracted with chloroform. The extract was washed with 0.5 *N* sulphuric acid, with 4% aqueous sodium carbonate, dried, and evaporated. The neutral residue crystallized on trituration with ether (wt. 31 mg) and was recrystallized from benzene–hexane from which it separated as colorless needles, m.p. 209–210°, $[\alpha]_D^{26}$ +13.7±1.0° (*c*, 1.1). Found: C, 62.33; H, 7.19. Calc. for $C_{24}H_{33}O_8N$: C, 62.19; H, 7.18%. Ultraviolet spectrum: λ_{max} 319 mμ, log ε 2.52, shoulder λ 213 mμ, log ε 3.80, λ_{min} 270 mμ, log ε 2.11. Infrared spectrum: 3320(56), 1766(86), 1758(78), 1657(90) cm^{-1}.

1,10-Didehydroseco-oxodelcosine Diketone (X)

Didehydro-oxodelcosine (75 mg) was dissolved in a saturated solution of lead tetraacetate in glacial acetic acid (50 ml) containing water (2.5 ml) and kept at room temperature in the dark for 3 hours. Sulphur dioxide was bubbled through the solution and the precipitate filtered off after the mixture had been cooled. The filtrate was evaporated to dryness under reduced pressure, 0.5 *N* sulphuric acid was added to the residue, and the mixture was extracted with chloroform. After it was washed with acid and sodium carbonate as described above, the extract yielded a product which crystallized on trituration with ether, wt. 46 mg, m.p. 161–167°. Recrystallization from benzene–ether gave colorless plates, m.p. 175–177°, $[\alpha]_D^{27}$ +77.4±1.0 (*c*, 1.2). Found: C, 62.34; H, 6.75. Calc. for $C_{24}H_{31}O_8N$: C, 62.45; H, 6.77%. Ultraviolet spectrum: λ_{max} 312 mμ, log ε 2.29, λ_{min} 272 mμ, log ε 1.98. Infrared spectrum (nujol mull): 1780(84), 1764(77), 1717(89), 1652(87) cm^{-1}; (in chloroform solution): 1776(89), 1722(85), 1658(84) cm^{-1}.

1-Dehydroseco-oxodelcosine Diketone (XI)

1-Dehydro-oxodelcosine (49 mg) was oxidized with a saturated solution of lead tetraacetate in glacial acetic acid (35 ml) and water (1.8 ml). The solution was kept for 1.5 hours in the dark at room temperature and the product isolated exactly as described above, wt. 30 mg. After recrystallization from benzene–ether the product consisted of colorless hexagonal prisms, m.p. 181–183°, $[\alpha]_D^{28}$ +57.1±2.1° (*c*, 0.28). Found: C, 62.36; H, 6.90. Calc. for $C_{24}H_{33}O_8N$: C, 62.19; H, 7.18%. Ultraviolet spectrum: λ_{max} 323 mμ, log ε 2.36, λ_{min} 274 mμ, log ε 1.87. Infrared spectrum (nujol mull): 3344(55), 1776(70), 1712(73), 1688(81), 1655(92) cm^{-1}.

Can. J. Chem. Downloaded from www.nrcresearchpress.com by 210.87.254.40 on 09/05/12
For personal use only.

ACKNOWLEDGMENTS

We acknowledge with thanks our indebtedness to Mr. R. Lauzon for recording the infrared spectra and to Dr. Maria Przybylska for preparing the X-ray powder diagrams. We also thank Professor E. Ochiai, Dr. L. S. Chetverikova, and Dr. A. D. Kuzovkov for their kindness in sending us samples of Shimoburobase-II and delphamine respectively.

REFERENCES

1. R. Anet, D. W. Clayton, and L. Marion. Can. J. Chem. **35**, 397 (1957).
2. M. Przybylska and L. Marion. Can. J. Chem. **34**, 185 (1956).
3. R. Anet and L. Marion. Can. J. Chem. **36**, 766 (1958).
4. W. I. Taylor, W. E. Walles, and L. Marion. Can. J. Chem. **32**, 780 (1954).
5. V. Skarić and L. Marion. J. Am. Chem. Soc. **80**, 4434 (1958).
6. F. Sparatore, R. Greenhalgh, and L. Marion. Tetrahedron, **4**, 157 (1958).
7. M. Carmack, J. P. Ferris, J. Harvey, Jr., P. L. Magat, E. W. Martin, and D. W. Mayo. J. Am. Chem. Soc. **80**, 497 (1958).
8. F. W. Bachelor, R. F. C. Brown, and G. Büchi. Tetrahedron Letters, **10**, 1 (1960).
9. M. S. Rabinovich and R. Konovalova. J. Gen. Chem. U.S.S.R. **12**, 321, 329 (1942).
10. E. Ochiai, T. Okamoto, and M. Kaneko. Chem. and Pharm. Bull. **6**, 730 (1958).
11. T. Amiya and T. Shima. Bull. Chem. Soc. Japan, **31**, 1083 (1958).
12. S. Furusawa. Bull. Chem. Soc. Japan, **32**, 399 (1959).
13. H. Suginome and S. Furusawa. Bull. Chem. Soc. Japan, **32**, 354 (1959).

Can. J. Chem. Downloaded from www.nrcresearchpress.com by 210.87.254.40 on 09/05/12
For personal use only.

Can. J. Chem. Downloaded from www.nrcresearchpress.com by 210.87.254.5 on 09/05/12
For personal use only.

THE ORTON REARRANGEMENT IN APROTIC SOLVENTS

SOME OBSERVATIONS ON THE REACTIONS OF *p*-SUBSTITUTED N-BROMOACYLANILIDES IN CHLOROBENZENE AND TRICHLOROACETIC ACID[1]

J. M. W. Scott[2]

ABSTRACT

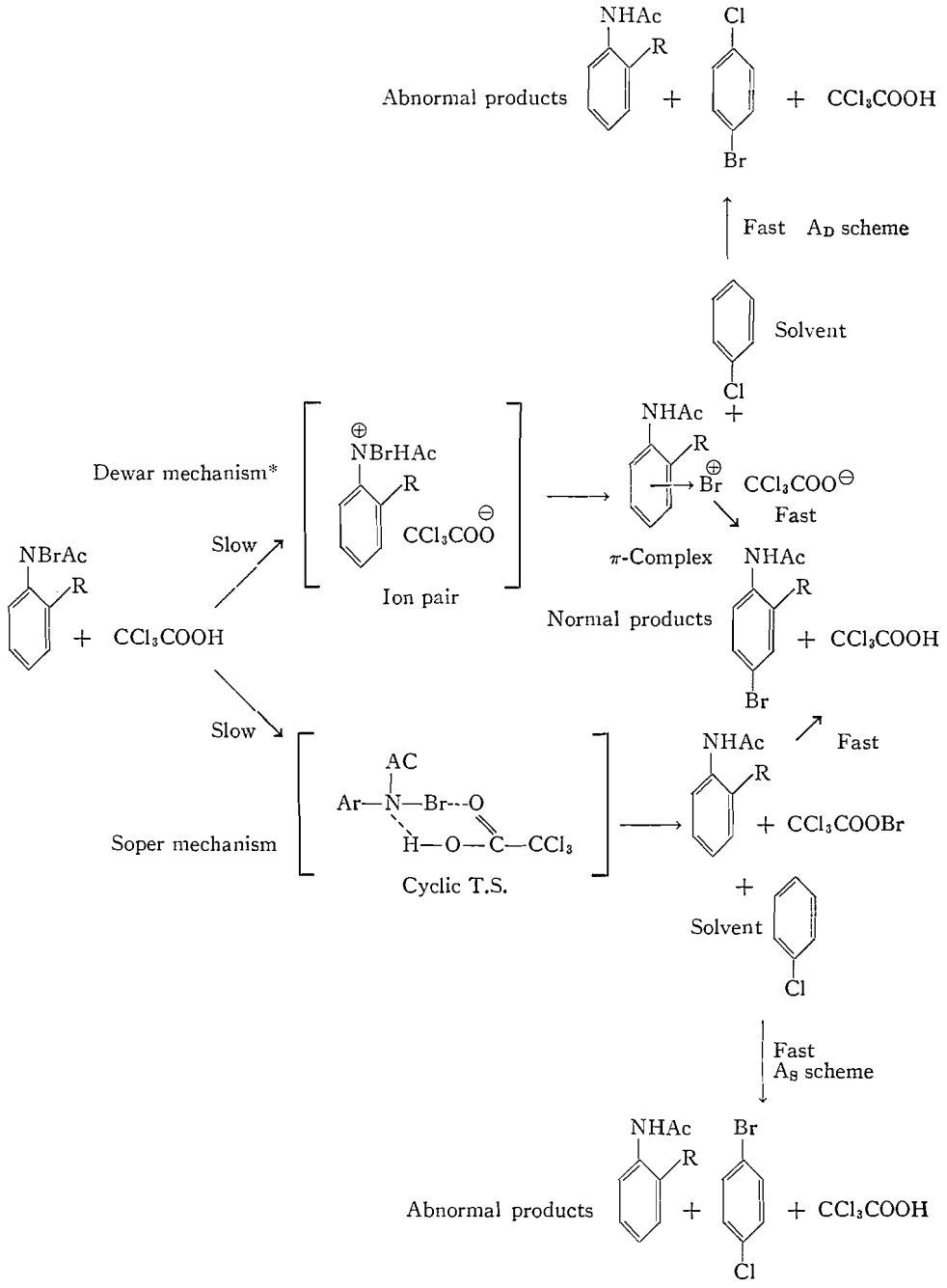
The qualitative and kinetic behavior of a series of *p*-substituted N-bromoacylanilides when treated with trichloroacetic acid in chlorobenzene has been studied. The abnormal reaction which was previously demonstrated for the *o*-nitro derivative has been shown to occur with the *p*-isomer. The mechanisms of the normal and abnormal reactions are discussed. Some derivatives of 4-fluoro-3-bromoaniline are described.

Recently interest in the Orton rearrangement has been revived with a view to substantiating the 'π-complex' mechanism originally proposed by Dewar (1). In one of a series of publications (2) evidence for the production of an intermediate (acetyl hypobromite) was reported which appeared to support the alternative mechanism proposed by Soper (3). A closer examination of the experimental conditions under which this intermediate was produced has revealed that the intermediate was due to a slight trace of impurity in the reaction media (4). Although a further attack on the problem has been made using tracer techniques some aspects of the problem of the mechanism remained unsolved (5).*

One of the most interesting facts which the previous work revealed, and one with which this paper is particularly concerned, was the failure of N-bromo-2-nitroacetanilide to rearrange when treated with trichloroacetic acid in chlorobenzene (6). The bromine migrated to the solvent to give *p*-bromochlorobenzene. There are several mechanistic alternatives for this migration and it is of interest to assess their relative merits, and examine any implications they may have with respect to the normal rearrangement.

The rate-determining step for the rearrangement is considered to be a proton transfer and there is much evidence to support this (7–9). On the Dewar mechanism this yields an ion pair which rapidly and irreversibly forms a 'π-complex'. On the Soper mechanism it has been proposed (2) that the proton transfer is accompanied by a concerted attack of the carbonyl oxygen on the bromine atom to give a cyclic transition state which subsequently breaks down into the anilide and the acid hypohalite. These alternatives are represented schematically for both the 'normal (N)' and 'abnormal (A)' reactions:

[1]*Manuscript received July 8, 1960.*
Contribution from Queen Mary College, University of London and Services Electronics Research Laboratories, Harlow, Essex, England.
[2]*Present address: American Cyanamid Co., 1937 West Main St., Stamford, Conn., U.S.A.*
**When the present investigation was started the Dewar and Soper mechanisms were the only schemes available which were capable of explaining the experimental facts. Although the subsequent investigations described in reference 4 show that the approach outlined here is oversimplified, we feel that this is the best way of presenting our data.*

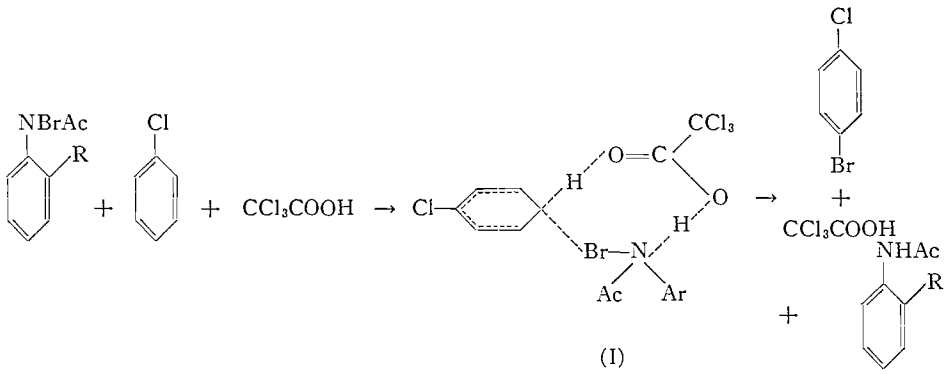


**It is possible that the stages* N-*bromoanilide + acid → ion pair → π-complex may be concerted.*

On the A_D scheme the 'π-complex' acts as a brominating agent, the reactivity of the bromine being enhanced in the particular instance R = NO_2 by the electron-withdrawing properties of the nitro substituent. A similar explanation has been advanced by Dewar to account for the intermolecular transfer observed by Soper *et al.* (3) when N-bromo-

Can. J. Chem. Downloaded from www.nrcresearchpress.com by 210.87.254.5 on 09/05/12
For personal use only.

acetanilide was treated with acetic acid in phenetole and anisole. On the Soper scheme the A_S reaction results from the competition for the bromine in the second bimolecular step between the anilide and the solvent. In the case R = NO_2 although the anilide may possibly have a more reactive *p*-position than the solvent, this is offset by the high concentration of the latter. The preceding discussion demonstrates that both mechanisms will superficially account for the observed experimental facts for both the A and N reactions. However, the possibility of other transition states for the A reaction must be considered. Two other schemes may be invoked in the case of R = NO_2. The first of these consists of a termolecular reaction:



(I)

Some evidence for such transition states has been obtained when N-bromoacetanilide is 'rearranged' in the presence of anisole, i.e.

$$\text{rate} = k[\text{anisole}]^n[\text{N-bromoacetanilide}]\,[\text{acid}].$$

However, the order (*n*) with respect to anisole shows a complex behavior with variation in the anisole concentration (4), which precludes any simple formulation of transition states such as I.

The transition state (I) bears obvious analogy to that proposed for the N_S reaction, the ring now being effectively six-membered instead of five. It would bear some resemblance to the transition state for the A_D fast reaction since the same molecules must be involved. Finally it may be envisaged that the bromine, the ion pair, or π-complex stage, forms some type of internal complex with the *o*-nitro group. This could then brominate the solvent. This hypothesis may be safely discarded since it has been demonstrated (see below) that the *p*-nitro compound behaves similarly and in this case the possibility of such an intermediate is very unlikely.

The problem, at this stage, appears to be reduced to deciding between the termolecular scheme on one hand and Dewar and Soper schemes on the other, since the latter appear almost indistinguishable experimentally. This was approached in the following manner. If the transition states leading to the A and N reactions are identical the rate of reaction for a series of *p*-substituted N-bromoacylanilides should presumably be related by the equation $\log k = x \log K_b +$ constant where K_b is the dissociation constant of the amine corresponding to the N-bromoacylanilide and *x* is a constant. If the abnormal reaction involves a termolecular transition state, this should not obey equation [1]. The use of equation [1] implies the use of a single catalyzing acid to compare the rates.

The above discussion shows that the investigation of the series of compounds R = NO_2, Cl, F, Br, Me, Ph, and H might be expected to aid in the elucidation of the problem and the result of such investigations is reported below.

Can. J. Chem. Downloaded from www.nrcresearchpress.com by 210.87.254.5 on 09/05/12
For personal use only.

Can. J. Chem. Downloaded from www.nrcresearchpress.com by 210.87.254.5 on 09/05/12
For personal use only.

EXPERIMENTAL

Materials

Acetanilides

p-Nitro-, *p*-bromo-, *p*-methyl- and *p*-chloro-acetanilides were purchased commercially and purified where necessary. *p*-Aminobiphenyl was purchased commercially and acylated with acetyl chloride in dry pyridine (10). *p*-Fluoroacetanilide was prepared by the route described for the *o*-isomer (6).

N-Bromo-4-fluoroacetanilide

p-Fluoroacetanilide (2.2 g) in chloroform (150 ml) was vigorously stirred (30 minutes) with a solution of sodium hypobromite prepared by dissolving bromine (5 ml) in 0.5 *N* NaOH (500 ml) also containing potassium bicarbonate (4 g). The chloroform layer was then washed with dilute potassium bicarbonate solution and dried over anhydrous sodium sulphate. Removal of the chloroform under reduced pressure and treatment with light petroleum (b.p. 40–60°) yielded a pale yellow solid which crystallized in plates from benzene and light petroleum (b.p. 40–60°), m.p. 95–97° (decomp.). (Active bromine 34.5, 34.6. C_8H_7NOBrF requires Br, 34.4%.)

N-Bromo-4-nitro-, chloro-, and bromo-acetanilides all previously characterized were prepared in the same way as the 2-fluoro derivative. The 4-nitro compound could not be obtained pure.

N-Bromo-p-acetaminobiphenyl

This compound was prepared by the same route as was used for the *o*-isomer (6). It crystallized from chloroform and light petroleum (b.p. 40–60°) yellow prisms, m.p. ca. 83° (decomp.). (Active bromine 27.3, 27.2. $C_{14}H_{13}NOBr$ requires Br, 27.5%.) N-Bromo-4-methylacetanilide was prepared by the dioxane method (6). It had previously been characterized and was found to be extremely labile.

3-Bromo-4-fluorotoluene

2-Bromo-*p*-toluidine hydrochloride (10 g) was suspended in hydrofluoroboric acid solution (10.3 g, 42% w/w) and cooled to 0°. Sodium nitrite (4 g) in the minimum of water was added dropwise with vigorous stirring, maintaining the temperature of the solution below 10°. After a further 30 minutes the diazonium salt was collected, washed with several small portions of ether, and dried over phosphorus pentoxide in a vacuum desiccator (11.8 g, 73.5%). The dry diazonium salt was decomposed in 30- to 50-g portions, the reaction being moderated by an equal weight of dry sand. The product was washed with dilute alkali and steam distilled. It was dried over calcium chloride and distilled under reduced pressure, b.p. 69–70°/11 mm (76.7 g, 43%). Found: C, 45.2; H, 3.5. C_7H_6BrF requires C, 44.5; H, 3.2%.

3-Bromo-4-fluorobenzoic Acid

3-Bromo-4-fluorotoluene (30 g) was oxidized with aqueous potassium permanganate (50 g). (For details see reference 2.) The product crystallized from aqueous alcohol in needles (10 g), m.p. 137°. Found: equivalent, 219; C, 38.7; H, 1.8. $C_7H_4O_2BrF$ requires equivalent, 219; C, 38.4; H, 1.8%. K_D (uncorr.) = 1.38×10^{-5} in 50/50 absolute ethanol water by volume, T = 21–22°.

3-Bromo-4-fluorobenzoyl Chloride

3-Bromo-4-fluorobenzoic acid (5 g) was boiled with thionyl chloride for 1 hour. The excess thionyl chloride was removed under reduced pressure and the residue distilled, b.p. 110–112°/11 mm. The distillate solidified giving colorless blades which were crystallized from light petroleum (b.p. 40–60°), m.p. 43–45°. Found: solvolysable Cl, 14.9. $C_7H_3O_2ClBrF$ requires Cl, 14.9%).

3-Bromo-4-fluorobenzamide crystallized in fine needles from anisole and light petroleum (b.p. 100–120°), m.p. 133° C. Found: C, 38.8; H, 2.3; N, 6.4. C_7H_5NOBrF requires C, 38.6; H, 2.3; N, 6.4%.

3-Bromo-4-fluorobenzanilide crystallized in needles from toluene, m.p. 148–149°. Found: C, 53.4; H, 3.3; N, 4.9. $C_{13}H_9NOBrF$ requires C, 53.1; H, 3.1; N, 4.8%.

3-Bromo-4-fluorobenz-p-toluidide crystallized in needles from toluene, m.p. 153–155°. Found: C, 54.3; H, 3.7; N, 4.7. $C_{14}H_{11}NOBrF$ requires C, 54.6; H, 3.6; N, 4.6%.

3-Bromo-4-fluoroaniline

3-Bromo-4-fluorobenzoic acid (6.6 g) in chloroform (200 ml) was treated with hydrazoic acid (2 moles) and concentrated sulphuric acid (40 ml) at 50–55° C on a steam bath. Working up in the usual fashion gave an amine (2 g, 36%) distilling at 124°/11 mm.

The *3-bromo-4-fluoroacetanilide* crystallized from toluene in prisms, m.p. 114°. Found: C, 41.4; H, 2.9; N, 6.1. C_8H_7NOBrF requires C, 41.4; H, 3.0; N, 6.0%.

The *3-bromo-4-fluoroformanilide* crystallized in needles from benzene – light petroleum (b.p. 40–60°), m.p. 91–92°. Found: C, 38.6; H, 2.1; N, 6.3%. C_7H_5NOBrF requires C, 38.6; H, 2.3; N, 6.4%.

The *N-benzoyl-3-bromo-4-fluoroaniline* crystallized from aqueous alcohol in plates, m.p. 125–127°. Found: C, 54.3; H, 2.8; N, 5.0. $C_{13}H_9NOBrF$ requires C, 53.1; H, 3.1; N, 4.8%.

Rearrangements

These were all carried out in a solution of 0.617 *N* A.R. trichloroacetic acid in chlorobenzene, the solution being prepared as described in the section dealing with the kinetic data. The rearranging solutions of the N-bromoamide and acid were left in the dark until they displayed negligible oxidizing properties towards acid potassium iodide solution. The N-bromoacylanilides were pure samples unless otherwise stated.

(*a*) *N-Bromo-p-methylacetanilide* (16 g) on treatment with the acid solution (ca. 30 ml) gave on removal of acid and the bulk of solvent a gummy product (11.8 g, 73.5%). Chromatography of a portion of the product on alumina from benzene/light petroleum (b.p. 60–80°) yielded a compound which crystallized from the same solvent in fine white needles, m.p. 117° C (lit. 2-bromo-4-methyl acetanilide 117° C). Because of the tarry nature of the product this reaction was not studied kinetically.

(*b*) *N-Bromo-p-acetaminobiphenyl* (5 g) on treatment with acid solution (ca. 10 ml) yielded a clean product (4.67 g, 81.4%), m.p. 139–142° C. C, 58.5; H, 4.1; N, 5.00; Br, 26.9. Calc. for $C_{14}H_{12}NOBr$: C, 58.0; H, 4.2; N, 4.8; Br, 27.5%. Hydrolysis of the product yielded an amine crystallizing in needles from light petroleum (b.p. 40–80°), m.p. 66–68° (lit. for 2-bromo-*p*-aminobiphenyl 66° C).

(*c*) *N-Bromo-4-bromoacetanilide* (10.35 g) on treatment with acid solution (ca. 20 ml) yielded a very clean product (9.6 g, 92.7%), m.p. 145–147° (lit. for 2,4-dibromoacetanilide 146° C).

(*d*) *N-Bromo-4-chloroacetanilide* (9.97 g) on treatment with acid solution yielded a very clean product (8.39 g, 84%), m.p. 134–136° (lit. for 2-bromo-4-chloroacetanilide 135°). Hydrolysis of product yielded an amine which crystallized in needles from light petroleum, b.p. 40–60°, m.p. 65–67° (lit. for 2-bromo-4-chloroaniline 69°).

(*e*) *N-Bromo-4-fluoroacetanilide* (1 g) on treatment with acid (2 ml) gave a clean product which appeared to be a mixture of the ring-brominated product and anilide formed possibly by loss of bromine to the solvent. Separation of the product was not achieved.

Can. J. Chem. Downloaded from www.nrcresearchpress.com by 210.87.254.5 on 09/05/12
For personal use only.

(*f*) *N-Bromo-4-nitroacetanilide* (10.84 g), 90.9% pure, when treated with acid yielded *p*-bromochlorobenzene (3.5 g, 50%), m.p. 64–67° C (lit. 67° C), and unchanged anilide (4.28 g, 72.2%), m.p. 215° C (lit. 215° C).

Kinetic Experiments

The kinetic experiments were mainly carried out as previously described (2) but with certain modifications. All the glass apparatus used was carefully washed with distilled water and dried in a vacuum oven.*

Chlorobenzene

Chlorobenzene was treated as previously (2) and then distilled twice from an all-glass apparatus with liberal rejection of initial and tail fractions. Its physical properties were essentially the same as those previously reported.

Solutions of Trichloroacetic Acid

A suitable weight of trichloroacetic acid (A.R. grade) was introduced into a 250-ml flask which was then attached to a vacuum line. The flask was then warmed (ca. 50° C) and pumped for about 2 hours. Air was then admitted through the silica-gel drying train, followed by a suitable volume of purified chlorobenzene. The solutions so prepared were standardized as before (2).

Solutions of the N-Bromoacylanilides

These were prepared and stored as previously described (2). The purity of each sample was >97% except in the case of N-bromo-4-nitroacetanilide, which could be obtained only ca. 90% pure. In consequence the purity of the sample was determined and the weight of the impure sample required to give a solution of the desired strength calculated. The solutions thus prepared eventually precipitated unchanged 4-nitroacetanilide (obviously the main impurity) and this was removed by filtration. The precipitation of the anilide was not due to any reaction of the N-bromo-4-nitroacetanilide with the solvent since the oxidative power of the solutions towards acid potassium iodide solution remained constant over a period of months.

Comparison of Rates

The meaningful comparison of rate constants between the various N-bromoacylanilides is rather uncertain for the following reasons.

(*a*) The reaction is not strictly first-order with respect to the N-bromoacylanilide, the first-order constants showing a variation with the initial concentration (C_1) of the N-bromo compound (see references 2 and 8).

(*b*) The variation of the first-order rate constants with the concentration (C_a) of the catalyzing acid is complex (see Bell (7)).

The following procedure was adopted. The first-order rate constants (k) for each N-bromoacylanilide were determined for three values of C_1 and three values of C_a giving nine rate constants at 45° C. A second-order rate constant k_m for each compound was evaluated from these results in the following rather arbitrary manner.

Within the range C_a 0.2 *M*–0.1 *M*, k is approximately linear in C_a. The measured rates were consequently reduced to unit acid concentration to give nine values of a quantity k_u. Bell and Levinge (8) have shown that the variation of k with C_1 can be represented by an equation of the form

$$1/k = A + BC_1$$

where A and B are empirically determined constants. Thus three k_u values for a given

**The spurious production of an intermediate previously reported was almost certainly due to traces of acetone in the reacting system; in consequence the use of acetone for washing glassware was completely avoided.*

Can. J. Chem. Downloaded from www.nrcresearchpress.com by 210.87.254.5 on 09/05/12
For personal use only.

value of C_a were fitted to the above equation by the method of least squares and a value of k_u for $C_i = 0.01\ N$ was determined from the above equation. This procedure was repeated on the k_u values from the remaining two C_a values giving in all, three values of k_u at $C_i = 0.01\ N$. The mean of these three values of k_u was defined as k_m and was expressed with a standard deviation.

This procedure for treating the reported rate data was found satisfactory for the 4-nitro-, 4-chloro-, 4-bromo-, and 4-fluoro-N-bromoacylanilides. One rate constant for the N-bromo-4-bromoacetanilide ($C_i = 0.0309\ N$; $C_a = 0.199\ M$, see Table I below) failed

TABLE I

Rate data for N-bromo-4-bromoacetanilide

C_i	0.046 N	0.0309 N	0.00939 N	0.01 N
C_a	$k\times10^4$ sec^{-1}	$k\times10^4$ sec^{-1}	$k\times10^4$ sec^{-1}	$k_u\times10^4$ sec^{-1} mole^{-1}l.
0.199 M	1.75	1.66	2.00	10.8
0.150 M	1.36	1.41	1.56	10.6
0.102 M	0.89	0.975	1.17	11.3

$k_m = 10.9\pm0.5\times10^{-4}$ sec^{-1} mole^{-1}l.

to conform to the general pattern observed and the rates of the N-bromo-4-phenylacetanilide showing a curious minimal reactivity at the intermediate N-bromoamide concentration. In consequence the rate constants for the latter compound are reported without the evaluation of k_m. The anomalous behavior of the odd N-bromo-4-bromoacetanilide rate constant and all the N-bromo-4-phenylacetanilide rate constants do not invalidate the general conclusions which we wish to make in this instance.

TABLE II

Rate data for N-bromo-4-chloroacetanilide

C_i	0.046 N	0.0279 N	0.00961 N	0.01 N
C_a	$k\times10^4$ sec^{-1}	$k\times10^4$ sec^{-1}	$k\times10^4$ sec^{-1}	$k_u\times10^4$ sec^{-1} mole^{-1}l.
0.199 M	1.66	1.80	2.00	9.94
0.150 M	1.31	1.44	1.60	10.6
0.102 M	0.89	0.953	1.19	11.2

$k_m = 10.6\pm0.6\times10^{-4}$ sec^{-1} mole^{-1}l.

TABLE III

Rate data for N-bromo-4-fluoroacetanilide

C_i	0.0464 N	0.0281 N	0.0110 N	0.01 N
C_a	$k\times10^4$ sec^{-1}	$k\times10^4$ sec^{-1}	$k\times10^4$ sec^{-1}	$k_u\times10^4$ sec^{-1} mole^{-1}l.
0.199 M	1.75	1.88	1.95	9.65
0.150 M	1.34	1.39	1.56	9.96
0.102 M	0.891	0.986	1.08	10.3

$k_m = 9.97\pm0.5\times10^{-4}$ sec^{-1} mole^{-1}l.

TABLE IV

Rate data for N-bromo-4-nitroacetanilide

C_i	0.0500 N	0.0289 N	0.0104 N	0.01 N
C_a	$k\times10^4$ sec^{-1}	$k\times10^4$ sec^{-1}	$k\times10^4$ sec^{-1}	$k_u\times10^4$ sec^{-1} mole^{-1}l.
0.199 M	1.45	1.51	1.55	7.95
0.150 M	1.11	1.16	1.27	8.74
0.102 M	0.78	0.83	0.88	8.97

$k_m = 8.55\pm0.5\times10^{-4}$ sec^{-1} mole^{-1}l.

Can. J. Chem. Downloaded from www.nrcresearchpress.com by 210.87.254.5 on 09/05/12
For personal use only.

TABLE V

Rate data for N-bromo-4-phenylacetanilide

C_i	0.0445 N	0.0273 N	0.00922 N
C_a	$k\times10^4$ sec^{-1}	$k\times10^4$ sec^{-1}	$k\times10^4$ sec^{-2}
0.199 M	3.23	2.77	3.38
0.150 M	2.31	2.14	2.67
0.102 M	1.36	1.31	1.67

TABLE VI

Rate constants and pK_b values of the related amines

	pK_b (amine)	k_m, sec^{-1} mole^{-1}l. $\times10^4$
N-Bromoacetanilide*	9.39	11.3±0.8
N-Bromo-4-nitroacetanilide	12.95	8.55±0.5
N-Bromo-4-fluoroacetanilide	9.48	9.97±0.5
N-Bromo-4-chloroacetanilide	10.19	10.6±0.6
N-Bromo-4-bromoacetanilide	10.09	10.9±0.5

*The calculation of the rate constant for N-bromoacetanilide at 45° C was made in the following way. The first-order rate constants (C_i = 0.01 N) reported by Bell (7) at 15° C are linear in C_a over a range 0.07 M–0.2 M. Values of k at 15° C C_a = 0.102 M, 0.150 M, and 0.199 M were thus interpolated from Bell's results, and from these, three values of k_u calculated. Using these values in conjunction with the Arrhenius equation (E_a = 11.8 kcal) three values of k_u at 45° C were calculated. These were then averaged and the mean value indentified with k_m as in the previous treatment. It should be noted that Bell's rate constants must be multiplied by a factor 2.3026/3600 to bring them to the units used in this paper.

DISCUSSION

The examination of the reaction products which preceded the kinetic studies revealed that the reactions of the 4-substituted N-bromoacylanilides were similar to those of the corresponding 2-substituted compounds. The 4-nitro compound was again exceptional, the bromine being transferred to the solvent to give 4-nitroacetanilide and 4-bromochlorobenzene. The products from the rearrangement of N-bromo-4-fluoroacetanilide also appeared complex and possibly contain 2- and 3-bromo-4-fluoroacetanilides, 4-fluoroacetanilide, and 4-bromo-chlorobenzene. An unambiguous synthesis of 3-bromo-4-fluoroacetanilide was devised with the hope that both 2- and 3-bromo-4-fluoroacetanilides could be characterized. However, the complexity of the products from the rearrangement of N-bromo-4-fluoroacetanilide (which it was hoped would yield 2-bromo-4-fluoroacetanilide as the sole product) prevented this project from being completely realized.

The recent work of Dewar and Couzens (4, 5) show that the premises on which the kinetic work was based are vastly oversimplified. It now appears that the Dewar and Soper formulations as originally postulated are insufficient to account for the observed complexities of the reacting system. However, two useful points appear to emerge from the present investigation.

(*a*) There is a rough correlation between log k_m and the logarithm of the dissociation constant of the parent amine (Table IV and Fig. 1). The slope of this line is very small, i.e. the reaction is very insensitive to substituent effects.

(*b*) Although the 2- or 4-substituted nitro group and possibly the 4-fluoro group induce the reaction to give different products, this does not appear to alter the nature of the rate-determining step, i.e. the differentiation in products occurs subsequent to the rate-determining step.

Can. J. Chem. Downloaded from www.nrcresearchpress.com by 210.87.254.5 on 09/05/12
For personal use only.

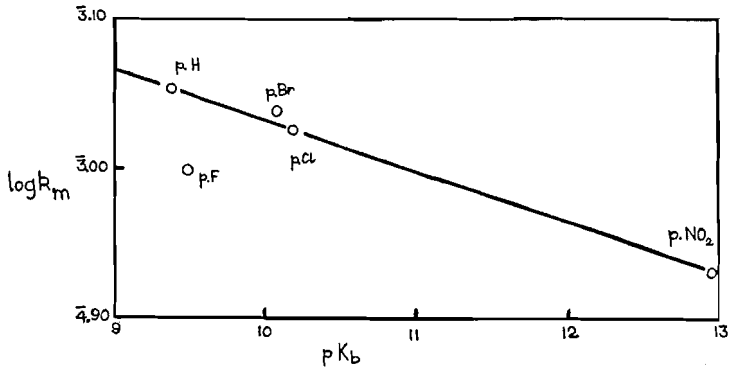


FIG. 1. Correlation between log k_m and pK_b for a series of *p*-substituted N-bromoacylanilides.

The author wishes to acknowledge assistance from Mr. D. Allardyce during the investigation and some useful criticisms from Dr. R. F. Garwood.

REFERENCES

1. M. J. S. DEWAR. Electronic theory of organic chemistry. Oxford University Press. 1949. p. 225.
2. M. J. S. DEWAR and J. M. W. SCOTT. J. Chem. Soc. 2676 (1957).
3. C. G. ISRAEL, A. W. N. TUCK, and F. G. SOPER. J. Chem. Soc. 547 (1945).
4. P. J. COUZENS. Ph.D. Thesis, London. 1959.
5. M. J. S. DEWAR. Kekule Symposium. International Union of Pure and Applied Chemistry, Organic Chemistry Section. Butterworth Scientific Publications, London. 1957. p. 179.
6. M. J. S. DEWAR and J. M. W. SCOTT. J. Chem. Soc. 1445 (1957).
7. R. P. BELL. Proc. Roy. Soc. (London), A, **143**, 377 (1934).
8. R. P. BELL. Proc. Roy. Soc. (London), A, **151**, 211 (1935).
9. R. P. BELL. J. Chem. Soc. 1154 (1936).
10. H. A. SCARBOROUGH and W. A. WATERS. J. Chem. Soc. 89 (1927).

Can. J. Chem. Downloaded from www.nrcresearchpress.com by 210.87.254.5 on 09/05/12
For personal use only.

Can. J. Chem. Downloaded from www.nrcresearchpress.com by 210.87.254.5 on 09/05/12
For personal use only.

POTASSIUM DERIVATIVES OF FLUORENE AS INTERMEDIATES IN THE PREPARATION OF C_9-SUBSTITUTED FLUORENES

II. COMPARATIVE REACTIVITIES OF THE ALKALI METALS, LITHIUM, SODIUM, AND POTASSIUM, WITH FLUORENE IN GLYCOL DIMETHYL ETHER, GLYCOL DIETHYL ETHER, TETRAHYDROFURAN, AND DIOXANE[1]

G. W. H. Scherf and R. K. Brown

ABSTRACT

In the solvents 1,2-dimethoxyethane (DME), 1,2-diethoxyethane (DEE), tetrahydrofuran (THF), and dioxane, potassium reacts much more readily with fluorene than does sodium or lithium. Lithium is generally more reactive than is sodium. The order of effectiveness of the ethers is DME > DEE ≈ THF > dioxane. Although practically no reaction of these metals with fluorene occurs in toluene, the addition of small amounts of these ethers to toluene does accelerate such reaction. All three organometallic compounds are soluble in refluxing and cold (22°) DME, THF, and DEE except the 9-fluorenyllithium, which precipitates largely from cold DEE. The results are explained in terms of the relative electropositivities of the metals, their size, and the structure of the ethers. It is suggested that these ethers actually participate in the formation of the organometallic compound from the metal.

Sodamide and lithium amide react as readily as or more readily than the metals with fluorene in DME to produce the organometallic compounds.

Diphenylmethane and triphenylmethane react reasonably well with potassium in DME, but too slowly with lithium and sodium to be useful.

INTRODUCTION

It was recently reported (1) that 9-fluorenylpotassium could be prepared by the direct action of potassium with fluorene in dioxane solvent. The organometallic compound was a reddish-brown precipitate singularly free of tarry impurities and quite useful for the synthesis of 9-substituted fluorenes. The simplicity of preparation led us to study the scope of this reaction in greater detail.

In a preliminary examination of the effects of solvents on the preparation of 9-fluorenylpotassium (2), it was found, in agreement with general information already established in the literature (3), that dioxane, dialkyl, alkylaryl, or diaryl ethers as well as tertiary amines promoted the reaction of potassium with fluorene. Generally no reaction was observed in hydrocarbon solvents. The tertiary amines proved to be either less effective than the ethers or themselves reacted with the organometallic substance formed.

Since, of all the pure ethers examined, dioxane was the most effective, and because addition of ethers to the normally ineffective hydrocarbons to the extent of 20% gave reactions of the metal with fluorene in the case of dioxane but not for dialkyl or arylalkyl ethers, it was suggested that the presence of *two* ether oxygen atoms in a single molecule, suitably situated as in the unstable boat form of dioxane, and/or sterically less hindered oxygen atoms (4) might be responsible for the preferred reaction found for dioxane. This viewpoint, augmented by the reports that certain ethers such as those of ethylene glycol (5, 6) dissolve small amounts of potassium metal at low temperatures to form blue, electrically conducting solutions, while dialkyl ethers do not, led to the investigation of the comparative efficiencies of ethers of ethylene glycol, as well as tetrahydrofuran as solvents for the reaction of the alkali metals, lithium, sodium, and potassium, with fluorene. This paper presents the results of experiments in this direction.

[1]*Manuscript received May 19, 1960.*

Contribution from the Department of Chemistry, University of Alberta, Edmonton, Alberta, from the thesis of G. W. H. Scherf to be submitted to the Graduate School of the University of Alberta, in partial fulfillment of the requirements for the degree of Doctor of Philosophy.

Can. J. Chem. Downloaded from www.nrcresearchpress.com by 210.87.254.5 on 09/05/12
For personal use only.

Gilman and Gorsich (7) have reported that lithium does react directly with fluorene and with cyclopentadiene in tetrahydrofuran to form the corresponding 9-fluorenyllithium and cyclopentadienyl lithium. Recently a paper by Normant and Angelo (8) described the metalation of a number of hydrocarbons with reactive hydrogen atoms in tetrahydrofuran, primarily with sodium but in some examples with lithium or potassium, using as the intermediate metalating agent the product arising from the combination of the metal with naphthalene. The mixture of naphthalene, tetrahydrofuran, metal, and active hydrogen compound gave metalation of a number of hydrocarbons which previously had reacted very slowly or failed to react at all with metallic sodium. The use of amines and of special ethers such as dimethyl ether and 1,2-dimethoxyethane to facilitate the addition of alkali metals to hydrocarbons such as naphthalene, biphenyl, etc., and the utility of these addition compounds to prepare alkali metal salts of active hydrogen-containing hydrocarbons had been pointed out previously by Scott *et al.* (9). However, the presence of naphthalene and the dihydronaphthalene by-product complicated isolation and purification. The results of our work show that in the case of fluorene, the hydrocarbon under examination in this laboratory, the addition of naphthalene is an unnecessary factor in the reaction of alkali metals with fluorene to form the organometallic compound and hydrogen.

RESULTS AND DISCUSSION

For the comparative studies, equivalent amounts of metal and fluorene were used in the appropriate solvent. The particular quantities upon which time and extent of reaction are quoted were 0.05 mole of fluorene, 0.05 gram-atom of the metal, and 50 ml of the solvent. Reactions were protected by nitrogen atmosphere and anhydrous conditions were employed at all times. The results are compiled in the accompanying table for convenience. The metals lithium, sodium, and potassium were studied while the solvents examined were 1,2-dimethoxyethane (DME), 1,2-diethoxyethane (DEE), and tetrahydrofuran (THF). The results in these solvents are compared with those obtained for dioxane in the previous work (2). For those cases where the metal remained solid under the conditions employed, we did attempt to use pieces of roughly similar size, about 1 mm^3. Solid pieces of sodium, especially at higher temperatures, had a strong tendency to stick together, hence presenting a smaller surface area to the reagent than was originally obtained. Molten sodium did not show this property. A similar behavior for potassium was not found, probably due to the greater rate of reaction with fluorene at the surface preventing adhesion of metal particles. Lithium particles did not stick together at all.

The extent of metalation was estimated by methylation of the salt by addition of methyl iodide, and, after isolation of the product, measurement of the amount of mono- and di-methylfluorene and of unchanged fluorene by infrared spectroscopy (1).

From the results shown in Table I, and from previous work (2), it is seen that, generally, hydrocarbon–ether mixtures are less effective solvents for the reaction of these alkali metals with fluorene than are the pure ethers, and also cause precipitation of the product even from the hot solutions. However, a mixture of 20% DME in *heptane* not only gave nearly complete metalation with potassium in 3 hours, but showed no precipitation of the organometal. Instead, during the reaction, there was observed the formation of a nearly colorless upper layer composed of heptane, unreacted fluorene, and some DME, and a dark-red lower layer containing 9-fluorenylpotassium and DME contaminated with some heptane. The formation of this lower layer apparently approximated the conditions for DME only as solvent and would account for the greater extent of reaction.

TABLE I

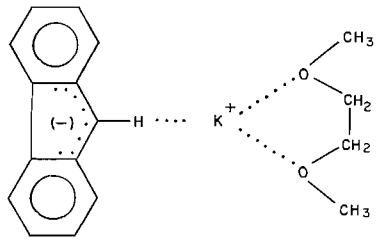
Solvent	Metal	Temperature	Observation	Extent of Metalation
Dioxane (98°/700 mm)	Li	Reflux	Little reaction in 4 hours	<5%
	Na	Reflux	Little reaction in 4 hours	<5%
	K	Reflux	Complete in 4 hours. Product largely insoluble hot	80–90%
	K	22°	Some reaction in 12 hours. Product largely insoluble hot	~30%
DME (85°/700 mm)	Li	22°	Small pieces. Complete reaction in ~5 hours. Product soluble R.T.	~80–90%
		Reflux	Small pieces. Complete reaction in ~5 hours. Product soluble R.T.	~80–90%
	Na	22°	Small pieces. Complete reaction in ~8 hours. Product soluble R.T.	~80–90%
		Reflux	Small pieces. Complete reaction in ~10 hours. Product soluble R.T.	~80–90%
	K	22°	Complete in 2 hours. Product soluble R.T.	~90–95%
		Reflux	Complete within 1 hour. Product soluble R.T.	~90–95%
DEE (118°/700 mm)	Li	22°	About 20% unreacted after 50 hours. Product largely insoluble R.T.	—
		Reflux	Complete in 5–6 hours. Product soluble in hot, insoluble R.T.	70–80%
	Na	22°	Incomplete in 50 hours	—
		Reflux	Nearly complete in 30 hours. Product largely soluble R.T.	70–80%
	K	22°	Complete in ~3 hours. Product soluble R.T.	~70–80%
		Reflux	Complete in ~2 hours. Product soluble R.T.	~70–80%
THF (65°/700 mm)	Li	22°	Little reaction in 4 hours. Complete in 50 hours. Product soluble R.T.	~80%
		Reflux	Complete in 7–8 hours. Product soluble R.T.	~80%
	Na	22°	Incomplete in 50 hours. Product soluble R.T.	—
		Reflux	Incomplete in 48 hours. Product soluble R.T.	—
	K	22°	Complete in ~2½ hours. Product soluble R.T.	—
		Reflux	Complete in 1 hour. Product soluble R.T.	~70%
Toluene +20% dioxane	K	Reflux	In 5 hours incomplete. Product largely insoluble hot	40–50%
Toluene +20% DME	K	Reflux	Complete in 2 hours. Product largely insoluble hot	60–70%
Toluene +20% DEE	K	Reflux	Nearly complete in 4 hours. Product largely insoluble hot	60–70%
Toluene +20% THF	K	Reflux	Incomplete in 4 hours. Product largely insoluble hot	~50–60%
Toluene +1% dioxane	K	Reflux	In 4 hours, very little reaction	—
Toluene +1% DME	K	Reflux	In 4 hours, red solution + some precipitate	~10–15%
Toluene	K	Reflux	In 4 hours very little reaction	~ 2–3%
Dioxane +10% DME	Li	Reflux	Complete in 10 hours. Product soluble at R.T.	~90%
	Na	Reflux	Incomplete in 24 hours. Product soluble at R.T.	~50%
	K	Reflux	Complete in 2 hours. Product largely soluble at R.T.	~90%
Heptane +20% DME	K	Reflux	Complete in 3 hours. Two layers. Product soluble R.T.	~90%

NOTE: R.T. = room temperature (22°).
In all solvents, solutions of the potassium salt were very dark red, those of the sodium or lithium salts were quite light red (those of the lithium salt somewhat lighter than those of the sodium salt).

The same separation into two layers, with the formation of no precipitate, was observed when a solution of 9-fluorenyl-potassium (-sodium or -lithium) in DME only was diluted with heptane. A similar dilution of a dioxane *solution* of 9-fluorenylpotassium caused the precipitation of most of the salt and when this salt was washed three times with hexane,

Can. J. Chem. Downloaded from www.nrcresearchpress.com by 210.87.254.5 on 09/05/12
For personal use only.

it was apparently free of dioxane since no ether–oxygen band was discernible in the infrared spectrum of a Nujol mull of the salt. However frequent, heptane washes of the dark-red layer obtained from the heptane diluted DME solutions failed to yield any solid precipitate or to remove the ether from the organometal. It is quite clear that with DME as solvent or cosolvent the diluting aliphatic hydrocarbon competed with the metalated fluorene for the ether far less effectively than did the hexane versus 9-fluorenylpotassium for dioxane, no doubt due to the stronger association of the DME with the organometallic compound. Diethyl ether, a solvent more compatible with DME, and also capable of dissolving the 9-fluorenylpotassium only to a limited extent, did cause a precipitation of an oily solid which, however, could not be completely freed from ether. Toluene, however, added to a DME solution of 9-fluorenylpotassium slowly precipitated a portion of the red salt. In contrast, a DME solution of 9-fluorenyl*lithium* poured into excess diethyl ether caused much precipitation of solid 9-fluorenyllithium which was readily freed from ether by hexane washes, showing that the greater polar character of the potassium–carbon bond intensifies the association of the type shown below.



That the lithium salt remains quite soluble in DME is most likely due to the small size of the lithium atom which compensates largely for the lower polarity of the lithium–carbon bond. The lithium atom thus can approach the two oxygen atoms of the glycol ether more closely than can potassium or sodium and because of this close approach will develop more polar character and hence a stronger association of the type shown above. A similar structure has been suggested by Wittig (11) to explain the difficultly soluble molecular complex between phenyllithium and 1,2-dimethoxyethane.

The larger sodium and potassium ions must then depend primarily upon the original polar character of the metal–carbon bond (somewhat augmented upon approach to the ether) for their degree of association with the ether. On the basis of only the original polarity of the metal–carbon bond, the sodium salt should then associate with DME less firmly than does the potassium compound but more so than does the lithium compound. One might therefore expect that small steric factors should affect the degree of proximity of the lithium atom to the ether oxygens, therefore the degree of polarization of the lithium–carbon bond by the glycol ether and hence the strength of association, more than would be the case for the sodium or potassium analogues.

Some evidence for this is given in the results found for the solubilities of the organometallic compounds in DEE. The 9-fluorenyllithium is quite soluble in hot DEE but precipitates largely from the cold solution (at R.T.). On the other hand, both the potassium and sodium compounds remain almost completely soluble in DEE at room temperature. The larger steric interference of the ethyl group in DEE thus hinders close approach of the lithium to the two oxygen atoms. This small difference is of great significance in the association of 9-fluorenyllithium with the glycol ethers, but not as critical with the more ionic sodium and potassium compounds.

Can. J. Chem. Downloaded from www.nrcresearchpress.com by 210.87.254.5 on 09/05/12
For personal use only.

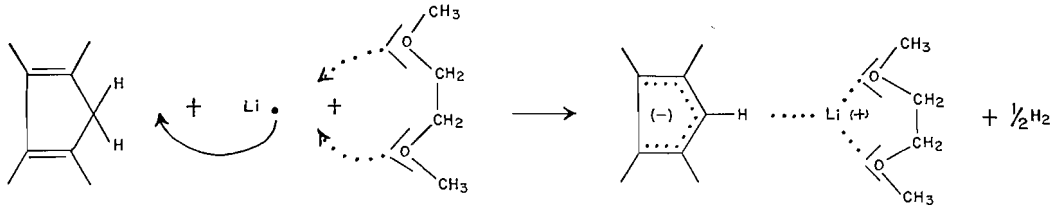
Can. J. Chem. Downloaded from www.nrcresearchpress.com by 210.87.254.5 on 09/05/12
For personal use only.

It is noteworthy that the red-orange solid 9-fluorenyllithium (obtained from DEE as above) dissolved readily in dioxane. Diethyl ether dissolved only a small amount of the lithium salt while toluene failed to dissolve any of it.

It is furthermore quite clear that for the preparation of the lithium, sodium, or potassium salts of fluorene, the solvents of choice are, in order of effectiveness, DME > DEE ≈ THF > dioxane > dialkyl ethers.* In all cases, potassium reacts much more vigorously with fluorene than does sodium or lithium, as expected on the basis of the difference in electropositivity between potassium and the other two metals. The presence of two favorably situated oxygen atoms such as found in the ethers of ethylene glycol promotes this reaction. The larger bulk of the ethyl group over that of the methyl group (in DEE vs. DME) is thus expected to, and does, offer steric hindrance to co-ordination. Ferguson (4), in his discussion of solubility of ethers in water, points out that the methyl groups of diethyl ether partially shield the oxygen atom from facile approach by water, thus accounting for the much greater water solubility of dimethyl ether, tetrahydrofuran, and dioxane over that of diethyl ether. That THF is a better solvent for the metalation reaction than is dioxane is also expected since the co-ordinating electrons of the oxygen atom in the former are exposed to a greater extent than they are in the latter molecule, a fact which is readily discerned by consideration of the models of these two molecules.

That the reactivity of lithium is similar to and sometimes greater than that of sodium,† although its electropositivity is less, is quite likely due to its smaller size, which permits closer approach to the favorably located and exposed oxygen atoms in DME, DEE, and THF.

The observation that the solid, dioxane-free 9-fluorenylpotassium, suspended in heptane, is quite definitely deeply colored, and that even the very reactive molten potassium shows no coloration of the bright surface of the metal, when it is refluxed with fluorene in heptane, but upon addition of dioxane a reaction does occur (2) indicates that the ether not only hastens metalation by removing the product from the surface of the metal but also actually participates in the formation of the organometallic compound. Further support for this point of view is given by the fact that ether-free 9-fluorenyllithium, made in DEE, dissolves readily in dioxane but that the reaction of lithium and fluorene in dioxane was found to be very slow, the refluxing solvent in 15 hours developing only a slight color. Removal of the product from the surface of the metal cannot therefore be the controlling factor in this case. A concerted reaction of the type suggested below is thus indicated.



Generally, increased temperature facilitates metalation. Thus in tetrahydrofuran, DEE, and dioxane, both sodium and lithium react faster at reflux temperature than at room temperature while potassium does so in these three solvents *and* in DME. The

*Dimethyl ether, no doubt, is an exception since it has been shown to co-ordinate readily with water due to the lower steric effect of the methyl groups (4, 9).

†W. Schlenk and E. Bergmann (Ann. **463**, 1 (1928)) have found that lithium metal in ether suspension adds more readily to hydrocarbons, such as biphenyl and naphthalene, than does sodium.

similarity of the reaction of sodium at room temperature and at the boiling point in DME may be accounted for by the tendency of the warmed solid metal to agglomerate. However, though lithium reacts about equally well in DME at room temperature and at reflux temperature, the explanation offered for the behavior of sodium cannot apply. This similar time of reaction of lithium at high and low temperatures has been observed in several repetitions of the same experiment. It might be that the increasing rate of reaction due to elevation of temperature does occur but is offset by the increased thermal agitation of the molecule which hinders the attainment of the favorable conformation of the ether and hence the simultaneous close approach to the two oxygen atoms required for the reaction with lithium.

Reaction of Fluorene with Lithium Amide and Sodium Amide in DME

In DME, both lithium amide and sodium amide react quite readily with fluorene. 9-Fluorenylsodium of good quality can thus be prepared more rapidly using sodamide rather than metallic sodium. In 3 hours, 0.05 mole of a good grade of sodamide reacted completely with an equivalent amount of fluorene in refluxing DME as compared with 10 hours required for reaction of 0.05 mole of sodium under the same conditions. Extent of the reaction was again measured by methylation. The lithium amide used was a technical grade, but it reacted completely in 5 hours yielding about 60% metalation. The clear solutions of the organometallic compounds in DME obtained in this manner possessed a deeper red color than those obtained by the direct action of the metal with fluorene. This may be due to the presence of ammonia since the addition of dry gaseous ammonia to 9-fluorenylsodium prepared from sodium reacting with fluorene in DME actually caused intensification of color.

Reaction of Triphenylmethane and Diphenylmethane with Lithium, Sodium, or Potassium in DME as the Solvent

Triphenylmethane was found to react with potassium, showing the red color characteristic of the metal salt after 30 minutes of reflux, and being completely consumed in 10 hours. Reaction with benzyl chloride gave the expected 1,1,1,2-tetraphenylethane in good yield.

Both sodium and lithium under the same conditions reacted very slowly with triphenylmethane and in a period of 100 hours had reacted only to the extent of about 10% as judged by the weight of the unreacted metal.

Diphenylmethane after 3 days' reflux in DME had consumed nearly all the potassium. However, lithium under the same conditions in 30 hours showed only a slight accumulation of red solid on the surface of the metal but no solution of the product.

EXPERIMENTAL

Details for the comparative reactions of the metals in the various solvents and isolation and estimation of products followed published directions (1). In all cases, 0.05 mole of fluorene, 0.05 mole of metal, and 50 ml of purified, dry solvent were used. A constant stream of pure, dry nitrogen supplied a protective atmosphere for the reactions.

The solvents were generally commercially available reagent grade materials but were further purified by distillation from potassium. Only a technical grade of 1,2-diethoxyethane was available. This was treated carefully with metallic potassium, over which the liquid stood for 24 hours. Distillation from the metal gave a glycol ether of good quality.

Can. J. Chem. Downloaded from www.nrcresearchpress.com by 210.87.254.5 on 09/05/12
For personal use only.

Metalation of Triphenylmethane

Triphenylmethane (12.2 g, 0.05 mole) and potassium (1.95 g, 0.05 mole) were refluxed in 50 ml 1,2-dimethoxyethane. The solution showed a red color after 30 minutes and in 10 hours all the metal was consumed. To the deep-red solution, containing the completely dissolved triphenylmethylpotassium was added 6.3 g (0.05 mole) of benzyl chloride. The solution, which decolorized rapidly, was then diluted with 150 ml of water, extracted with ether, and the ether extracts dried ($CaCl_2$). Removal of the ether gave a yellow solid which was triturated with pentane to remove unreacted triphenylmethane. Colorless 1,1,1,2-tetraphenylethane requiring no further purification was obtained in good yield, m.p. 140° uncorr., lit. 140–142° (12).

When sodium replaced potassium in a similar experiment a light-red color developed only after 12 to 15 hours of reflux. The small pieces of sodium had formed a single spherical piece of metal. After 100 hours of reflux, 90% of the metal (by weight) remained unreacted. Lithium showed red coloration of the surface of the metal in 5 hours, but gave only 10% reaction of the metal after 100 hours reflux.

Metalation of Diphenylmethane

Details for the reaction between diphenylmethane and potassium followed those described for the triphenylmethane. Evidence of the reaction, via appearance of a red color in the solution, occurred within 3 hours. In 3 days, nearly all the potassium had disappeared giving a product quite soluble in DME. Treatment of the salt with benzyl chloride gave 1,1,2-triphenylethane, m.p. 53°, lit. 54° (13).

Lithium, under the same conditions, formed only a small amount of red precipitate on the metal surface but no change occurred after 30 hours of reflux.

ACKNOWLEDGMENTS

The authors wish to express their appreciation to the National Research Council of Canada for funds which permitted the pursuit of this problem. One of us (G.S.) wishes to thank the National Research Council of Canada for summer student financial support.

REFERENCES

1. G. W. H. Scherf and R. K. Brown. Can. J. Chem. **38**, 697 (1960).
2. Unpublished work.
3. M. S. Kharasch and O. Reinmut. Grignard reactions of non-metallic substances. Prentice-Hall, Inc., New York. 1954.
4. L. M. Ferguson. J. Am. Chem. Soc. **77**, 5288 (1955).
5. J. L. Down, J. Lewis, B. Moore, and G. Wilkinson. J. Chem. Soc. 3767 (1959).
6. F. Cafasso and B. R. Sundheim. J. Chem. Phys. **31**, 809 (1959).
7. H. Gilman and R. D. Gorsich. J. Org. Chem. **23**, 550 (1958).
8. H. Normant and B. Angello. Bull. soc. chim. France, 354 (1960).
9. N. D. Scott, J. F. Walker, and V. L. Hansley. J. Am. Chem. Soc. **58**, 2442 (1936).
10. S. Searles and M. Tamres. J. Am. Chem. Soc. **73**, 3704 (1951).
11. G. Wittig. Naturwiss. **30**, 696 (1942).
12. J. Schmidlin and H. H. Hodgson. Ber. **41**, 435 (1908).
13. A. Klages and S. Heilmann. Ber. **37**, 1455 (1904).

Can. J. Chem. Downloaded from www.nrcresearchpress.com by 210.87.254.5 on 09/05/12
For personal use only.

Can. J. Chem. Downloaded from www.nrcresearchpress.com by 210.87.254.40 on 09/05/12
For personal use only.

THE MECHANISM OF THE CARBONYL ELIMINATION REACTION OF BENZYL NITRATE

KINETIC ISOTOPE EFFECTS AND DEUTERIUM EXCHANGE[1]

ERWIN BUNCEL[2] AND A. N. BOURNS

ABSTRACT

The carbonyl elimination reaction ($E_{CO}2$) of benzyl nitrate has been investigated with the object of distinguishing between the concerted and carbanion mechanisms. A deuterium exchange experiment resulted in a very small amount of deuterium pickup. The nitrogen isotope effect, k_{14}/k_{15}, associated with formation of the nitrite ion was found to be 1.0196 $\pm$0.0007 at 30° C. The two results taken together exclude the formation of a carbanion intermediate but are consistent with a concerted mechanism.

Benzyl-α-d_2 nitrate has been prepared and the rate of its carbonyl elimination reaction compared with that of the undeuterated compound. The deuterium isotope effect was 5.04$\pm$0.25 at 60° C. The significance of the magnitude of the nitrogen and deuterium isotope effects and of their interrelationship with the Hammett reaction constant *rho* is discussed in terms of the nature of the transition state and a comparison is made with other $E2$ elimination reactions.

Nitrate esters have been extensively studied during the last decade and are the subject of a recent review article (1). Several types of reaction have been observed with nucleophilic reagents (2, 3). The reaction followed in a given system depends on the structure of the nitrate, the nature of the nucleophilic reagent, and the solvent, and often two or more of the reactions take place simultaneously.

1. Substitution on carbon:

$$RCH_2—CH_2—O—NO_2 + Y^- \longrightarrow RCH_2CH_2—Y + NO_3^-.$$

2. Substitution on nitrogen:

$$RCH_2—CH_2—O—NO_2 + Y^- \longrightarrow RCH_2CH_2O^- + Y—NO_2.$$

3. β-Hydrogen elimination:

$$RCH_2—CH_2—O—NO_2 + Y^- \longrightarrow RCH{=}CH_2 + NO_3^- + YH.$$

4. α-Hydrogen elimination:

$$RCH_2—CH_2—O—NO_2 + Y^- \longrightarrow RCH_2CH{=}O + NO_2^- + YH.$$

The substitution reaction on carbon has been shown (2) to follow either the S_N1 or the S_N2 mechanism, the factors determining the course of reaction being analogous to those for alkyl halides. For example, in 90% ethanol the rate of reaction of *tert*-butyl nitrate is first order, being independent of the hydroxide ion concentration, while for ethyl nitrate the rate is second order, being proportional to both the nitrate and the hydroxide ion concentrations. Evidence for substitution on nitrogen (reaction 2) is based on oxygen-18 studies of the position of bond fission in the hydrolysis of *n*-butyl and *n*-octyl nitrate (4) and on stereochemical studies in the hydrolysis of optically active 2-octyl nitrate (5). This reaction differs from the others in that it results in the nitration of the base, and this property has been utilized as a synthetic method for the nitration of amines and active methylene groups (6, 7). The β-hydrogen elimination of

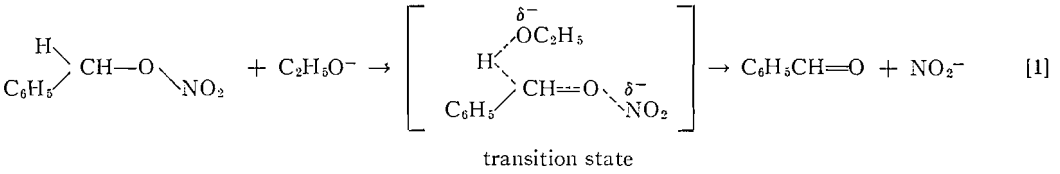
[1]*Manuscript received August 16, 1960.*
Contribution from the Burke Chemical Laboratories, Hamilton College, McMaster University, Hamilton, Ontario.
[2]*National Research Council of Canada Postdoctorate Fellow 1958–60.*

alkyl nitrates (reaction 3) has also been shown to proceed by the unimolecular or bimolecular mechanisms (2) and often occurs concurrently with substitution on carbon.

Whereas the first three types of reaction cited have counterparts in the reactions of carboxylic esters or alkyl halides, the α-hydrogen elimination finds no direct analogy in the reactions of these compounds. It has been named a carbonyl elimination reaction (2) and has been designated $E_{CO}2$ since it always shows the characteristics of a typical bimolecular reaction, viz., a strong base is necessary to remove the α-hydrogen atom and the reaction has never been observed under solvolytic conditions. From a thorough study Baker and Heggs concluded that the $E_{CO}2$ reaction is strongly facilitated by increased acidity of the eliminated hydrogen and by substituent groups which can conjugate with the forming carbonyl bond (8). The importance of these factors in determining the rates of the $E_{CO}2$ reaction and the yields of aldehyde product is demonstrated by the following data, obtained in 90% aqueous ethanol at 60° C (8): ethyl nitrate, 0.2×10^{-5} l. mole^{-1} sec^{-1}, 2%; *p*-methylbenzyl nitrate, 3×10^{-3} l. mole^{-1} sec^{-1}, 54%; benzyl nitrate, 8×10^{-3} l. mole^{-1} sec^{-1}, 87%; and *p*-nitrobenzyl nitrate, 3×10^{2} l. mole^{-1} sec^{-1}, 100%. The Hammett reaction constant ρ for *m*- and *p*-substituted benzyl nitrates has the high positive value of +3.40.

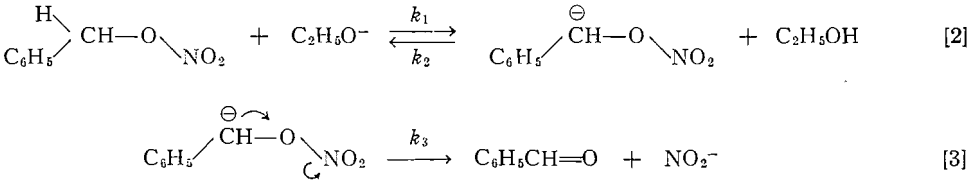
By analogy with other elimination reactions, two mechanisms must be considered for the carbonyl elimination reaction of organic nitrates.

Concerted mechanism



transition state

Two-step mechanism



In the concerted mechanism the removal of hydrogen by base is synchronous with formation of the carbon–oxygen double bond and separation of nitrite ion. This is analogous to the *E*2 mechanism observed in olefin-forming eliminations of alkyl halides, ammonium and sulphonium salts (9). The alternative possibility is a two-step process in which the base first removes the hydrogen to form a carbanion intermediate which subsequently eliminates the nitrite ion with formation of aldehyde. This corresponds to the *E*1*cb* mechanism suggested by Ingold as a possible path in olefin-forming eliminations, and may be designated $E_{CO}1cb$ (8). Cristol has proposed that the *E*1*cb* mechanism does indeed occur in cyclic systems where the eliminated groups have cis orientations (10, 11).

The carbonyl elimination reaction is one in which the carbanion mechanism is expected to be "inherently probable" (8), and a particularly favorable system should be that of

Can. J. Chem. Downloaded from www.nrcresearchpress.com by 210.87.254.40 on 09/05/12
For personal use only.

benzyl nitrate. The high positive value for the Hammett reaction constant ρ, +3.40, obtained for *m*- and *p*-substituted benzyl nitrates, and the fact that the σ^* value (12) for the para-nitro group must be used for a linear relationship to hold between log k and σ clearly show that the transition state of the reaction has a high degree of carbanion character. Further, the strongly electron-attracting nitrate group will have an appreciable effect on the acidity of the eliminated hydrogen, and this would be expected to promote reaction by a carbanion mechanism.[3]

The present investigation was undertaken with the object of establishing which of the two possible mechanisms, the concerted or the two-step, is being followed in the carbonyl elimination reaction of benzyl nitrate.

Deuterium Exchange Test

An established method for detecting a carbanion intermediate in an elimination reaction is the deuterium exchange test of Skell and Hauser (14). The reaction between substrate and base is carried out in hydroxyl-deuterated solvent (the solvent being the conjugate acid of the base) to partial completion and the unreacted substrate is isolated and examined for its deuterium content. If a true carbanion intermediate is present then the reverse of the first stage will result in deuterium pickup by the substrate.

An appreciable pickup of deuterium by the substrate would unquestionably prove that a carbanion intermediate is formed. The absence of deuterium pickup, however, would not necessarily exclude the intervention of a carbanion intermediate, since the rate at which the carbanion decomposes to product could be so much greater than its rate of return to reactant by combination with solvent (i.e., $k_3 \gg k_2$) as to preclude the observation of deuterium in the recovered substrate by the available experimental methods.

A deuterium exchange test was carried out with benzyl nitrate and ethoxide ion in anhydrous 99% ethanol-1-*d*. The reaction was interrupted at about 40% completion by the addition of *p*-toluenesulphonic acid. The unchanged benzyl nitrate was recovered and purified by fractional distillation. It was analyzed for deuterium by combustion to water and measurement of the O–D absorption at 2500 cm^{-1} (15). The purest sample of benzyl nitrate isolated, as judged by the identity of its infrared spectrum with authentic benzyl nitrate, analyzed for a deuterium content of 0.007 ± 0.003 atom% excess of deuterium. The significance of such a small deuterium content is open to more than one explanation. It could result from the actual presence of $C_6H_5CHDONO_2$ (0.05 mole% excess) formed by the reaction of a carbanion intermediate with deutero-ethanol. In this case the observed deuterium enrichment would require that for every one carbanion that reverts to reactant 1200 decompose to product (see Experimental), i.e., $k_3/k_2 = 1200$, where k_3 includes the concentration of solvent deutero-ethanol.[4] An alternative explanation, however, is that this very small deuterium enrichment is caused by the presence of some deuterium-containing contaminant.[5]

In past studies of elimination reactions the interpretation given to the observation of a very small deuterium enrichment in the recovered reactant has varied. Some workers

[3]*Cristol found that in a cis dehydrochlorination the replacement of a chlorine substituent by the strongly electron-attracting p-toluenesulphonyl group increased the rate of reaction by a factor of about 10^{10} (13).*

[4]*Because of a possible isotope effect associated with the reaction of deutero-ethanol with carbanion, the k_3/k_2 ratio in undeuterated ethanol may differ somewhat from this figure (16).*

[5]*Some enrichment will undoubtedly arise from a kinetic isotope effect involving the reactant, which originally has the natural isotopic abundance of deuterium. It can be shown, however, that this factor could account for no more than a quarter of the observed enrichment.*

Can. J. Chem. Downloaded from www.nrcresearchpress.com by 210.87.254.40 on 09/05/12
For personal use only.

have taken the result to mean the absence of exchange and have inferred that a concerted mechanism is being followed (14), while others have concluded that the enrichment is evidence in support of a carbanion intermediate (10).

Kinetic Nitrogen Isotope Effect

In previous applications of the deuterium exchange test the ambiguity presented by an apparent very small deuterium pickup could not be resolved. It has been possible to resolve this problem in the present reaction system by an evaluation of the kinetic nitrogen isotope effect. In the concerted process (equation [1]) the O—NO_2 bond is broken in the rate-determining step and this should result in a nitrogen isotope effect of considerable magnitude, i.e., of the order of 1–3% (*vide infra*). In the carbanion mechanism with $k_3 \gg k_2$, which is the only possibility for a carbanion mechanism permitted by the results of the deuterium study, the rate-determining step is the formation of the carbanion in which the bonds associated with nitrogen are still intact. In this case there should be no nitrogen isotope effect, or at the most an isotope effect of a few tenths of a per cent.

A kinetic nitrogen isotope effect study was undertaken with benzyl nitrate of normal isotopic composition. The procedure consisted of allowing reaction between benzyl nitrate and ethoxide ion to proceed to 10% completion and comparing the nitrogen isotopic composition of the formed nitrite ion with that of the starting benzyl nitrate. Since a simultaneous substitution reaction results in displacement of nitrate ion, a separation of the nitrate ion formed in the carbonyl elimination reaction was required.[6] This separation was achieved by selective reduction of the nitrite and nitrate ion to ammonia (17). The ammonia was subsequently oxidized to nitrogen (18), which was analyzed by mass spectrometry. The total nitrite and nitrate ion obtained from the 100% reaction was similarly converted to nitrogen and analyzed by mass spectrometry. The results of these experiments are shown in Table I.

TABLE I

N^{14}/N^{15} ratios in $E_{CO}2$ reaction of benzyl nitrate at 30° C

Expt. No.	Extent of reaction	N^{14}/N^{15}	
		$NO_2^- + NO_3^-$	NO_2^-
1	100	265.58	
2	100	265.78	
3	100	265.46	
4	100	265.66	
5	100	265.62	
6	10		270.52
7	10		270.54
8	10		270.66
9	10		270.42
10	10		270.74
Mean N^{14}/N^{15} ratios*		265.62±.12	270.58±.12

*The limits shown are the standard deviations.

The kinetic isotope effect, calculated from these isotopic ratios and the known extent of reaction (19), is

$$k^{14}/k^{15} = 1.0196 \pm 0.0007.$$

[6]*Experiments using nitrogen-15 enriched nitrate ion established the absence of isotopic exchange between nitrite and nitrate ions under the reaction conditions and in the subsequent separation procedure. Details of this work will be published elsewhere.*

Can. J. Chem. Downloaded from www.nrcresearchpress.com by 210.87.254.40 on 09/05/12
For personal use only.

This isotope effect, which is one of the largest observed for nitrogen in a rate process unequivocally establishes that the O—N bond is undergoing rupture in the rate-determining step. Since the observation of no significant deuterium exchange has ruled out a carbanion mechanism in which the step involving O—N bond rupture is rate determining, it follows that only a concerted process is consistent with the results of both the nitrogen isotope effect and the deuterium exchange studies.

Although the results of this investigation clearly exclude the carbanion mechanism for the reaction of benzyl nitrate the possibility still exists for reaction by this mechanism with reactants in which structural features would provide greater stability to a carbanion. Systems of this type are under investigation.

It was convenient to determine the nitrogen isotope effect in the competing substitution reaction forming nitrate ion since this had been converted to ammonia in the process of separating it from the elimination product. The isotopic ratio for the nitrogen of nitrate ion (combined products of experiments 6–10) was 265.52, which is identical, within the limit of measurement, with the mean value obtained for the product of 100% reaction. This observation of a zero isotope effect is consistent with a nucleophilic substitution of ethoxide ion on carbon with displacement of nitrate ion.

Hydrogen–Deuterium Isotope Effect

To gain greater insight into the nature of the transition state of the carbonyl elimination reaction the hydrogen–deuterium isotope effect for the reaction has also been determined. This was measured by separately evaluating the specific reaction constants for $C_6H_5CH_2ONO_2$ and $C_6H_5CD_2ONO_2$. Benzyl-α-d_2 nitrate was prepared by the lithium aluminum deuteride reduction of ethyl benzoate to benzyl-α-d_2 alcohol which was converted to benzyl-α-d_2 chloride and to benzyl-α-d_2 nitrate by usual procedures. The kinetics were conducted in anhydrous ethanol. The total rate was followed by acid–base titration and the rate constants for the carbonyl elimination reaction, $k_{E_{CO^2}}$, and for the substitution reaction, k_{S_N2}, were evaluated from the relative yields of nitrite and nitrate ions. These yields remained constant throughout the reaction, demonstrating that the two ions were formed by reactions of the same kinetic order. The rate data are shown in Table II. It is seen that the carbonyl elimination reaction shows an isotope effect of 5.0 at 60° C. From the data given in Table II one may also calculate a k_H/k_D ratio of 1.16 for the substitution reaction. No significance, however, is attached to the difference between this value and unity because of the rather large percentage error in the determination of the small amount of nitrate ion.

TABLE II

Hydrogen–deuterium isotope effect at 60.2° C

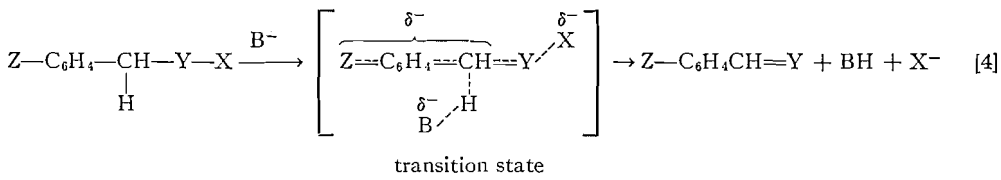
	$C_6H_5CH_2ONO_2$	$C_6H_5CD_2ONO_2$
% $E_{CO}2$	88.7	64.4
% S_N2	11.3	35.6
10^3 k_{total}*	13.9	3.79
10^3 $k_{E_{CO^2}}$	12.3	2.44
10^3 k_{S_N2}	1.57	1.35
$(k_H/k_D)_{E_{CO^2}}$ = (12.3/2.44) = 5.04±0.25†		

*k in l. mole^{-1} sec^{-1}.
†Estimated uncertainty based upon variation in yields of nitrite ion and rate constant values.

Can. J. Chem. Downloaded from www.nrcresearchpress.com by 210.87.254.40 on 09/05/12
For personal use only.

Nature of the Transition State in the $E_{CO}2$ Reaction

Information concerning charge distribution and extent of bond rupture in the transition state of a bimolecular elimination reaction of the type



transition state

is provided by three quantities: (*a*) the deuterium isotope effect, (*b*) the isotope effect associated with the leaving group X, and (*c*) the Hammett ρ value. A large k_H/k_D value implies a large degree of carbon–hydrogen bond stretching with the release to the rest of the molecule of the electron pair associated with this bond. The resulting negative charge may reside largely on the carbon atom and its attached aryl group, in which case the transition state may be described as having a high degree of carbanion character and the reaction will be characterized by a large positive Hammett ρ, or the charge may reside in part or in whole on the leaving group X. Other factors being equal, the greater the extent to which this charge is accommodated in the transition state by the leaving group the more highly concerted the reaction, the larger the isotope effect associated with X, and the smaller the ρ value.

The k_H/k_D value of 5.0 at 60° C for the $E_{CO}2$ reaction of benzyl nitrate (X = NO_2, Y = O, and Z = H in equation [4]) is large, being only slightly smaller than that calculated (ca. 5.6) for the complete loss of the carbon–hydrogen bond stretching frequency in the transition state (16). The ρ value, +3.4, for the $E_{CO}2$ reaction of substituted benzyl nitrates is large also; indeed, it is larger than the ρ values observed in other bimolecular elimination reactions involving ethoxide ion (20), and is one of the largest found for a rate process (12). To a considerable extent, then, the negative charge which is developed as a result of the large carbon–hydrogen bond stretching resides on the benzyl carbon, and the transition state, therefore, may be described as having a high degree of carbanion character.

That the oxygen–nitrogen bond is also considerably weakened in the transition state of the $E_{CO}2$ reaction of benzyl nitrate is evident from the magnitude of the nitrogen isotope effect, 2.0% at 30° C. Although this value is considerably smaller than the 3.8%[7] calculated on the assumption of complete oxygen–nitrogen bond rupture in the transition state, it is significantly greater than the nitrogen isotope effect of 1.3% found in this laboratory (24) for the *E*2 Hofmann elimination reaction of β-phenylethyltrimethylammonium bromide (X = $\overset{+}{N}(CH_3)_3$, Y = CH_2, and Z = H in equation [4]) with ethoxide ion at the same temperature. Since the deuterium effect is also larger, 5.0 at 60° C compared with 3.0 at 50° C observed by Saunders for the Hofmann reaction (25), it would appear that rupture of both C—H and Y—X bonds is more fully developed in the transition state of the carbonyl elimination reaction. On the other hand, the transition state for the $E_{CO}2$ reaction must have considerably more carbanion character than that of the bimolecular elimination with ethoxide ion of the structurally related β-phenylethyl bromide (X = Br, Y = CH_2, and Z = H in equation [4]). The deuterium

[7]*This value is obtained from the Bigeleisen expression (21) using 860.6 cm^{-1} for the stretching vibration of the* O—NO_2 *bond (22) in evaluating the free-energy term and the Slater theorem for the effective mass term. Using the mass fragment method of evaluating the mass term (23), the calculated effect is 2.8%.*

Can. J. Chem. Downloaded from www.nrcresearchpress.com by 210.87.254.40 on 09/05/12
For personal use only.

isotope effect for this dehydrobromination reaction has the abnormally large value of 7.1 at 30° C (25), while the ρ value for the reaction of substituted β-phenylethyl bromides is only +2.18 (20), compared with the +3.4 found for the $E_{CO}2$ reaction of the benzyl nitrates. More of the negative charge developed in the transition state must, therefore, reside on the bromine atom in the halide reaction than on the nitro group in the carbonyl elimination, and carbon–bromine bond rupture must have progressed further than oxygen–nitrogen bond rupture.

From these considerations it would appear that with respect to the extent to which bonds have been weakened, the transition state for the carbonyl elimination of benzyl nitrate is intermediate between the transition states for the $E2$ reaction of β-phenylethyltrimethylammonium ion and of β-phenylethylbromide.

EXPERIMENTAL

Materials

Benzyl nitrate.—This was prepared from benzyl chloride and silver nitrate in acetonitrile (26). The product, purified by fractional distillation from silver nitrate and calcium carbonate, was obtained in 75% yield (b.p. 45°/0.5 mm, n_D^{20} 1.5209).

Benzyl-α-d_2 nitrate.—The steps involved in the synthesis of benzyl-α-d_2 nitrate were: (1) reduction of ethyl benzoate to benzyl-α-d_2 alcohol with lithium aluminum deuteride; (2) conversion of benzyl-α-d_2 alcohol to benzyl-α-d_2 chloride with zinc chloride and hydrochloric acid; and (3) reaction of benzyl-α-d_2 chloride with silver nitrate in acetonitrile. The over-all yield of benzyl-α-d_2 nitrate (b.p. 45°/0.5 mm, n_D^{20} 1.5203) was 62%. A N.M.R. analysis[8] showed that the product was 99% $C_6H_5CD_2ONO_2$.

Benzyl-α-d_2 alcohol.—Ethyl benzoate (28.5 g, 0.190 mole) was reacted for 4 hours with lithium aluminum deuteride (3.94 g, 0.099 mole) in 400 ml ether which had been distilled from lithium aluminum hydride, and the complex was then decomposed with 10% sulphuric acid. The product, recovered by ether extraction, was treated with aqueous alcoholic sodium hydroxide to hydrolyze any unreacted ethyl benzoate. After removal of ethanol and extraction with ether, distillation yielded benzyl-α-d_2 alcohol (b.p. 76°/5 mm, n_D^{20} 1.5398) in 84% yield.

Benzyl-α-d_2 chloride.—Benzyl-α-d_2 alcohol (17.4 g, 0.158 mole) was added during 1 hour to 77 g of a stirred solution of hydrochloric acid and zinc chloride (Lucas' reagent (27)) at 0° C. Stirring was continued for 1 hour at 0° C and 2 hours at room temperature. The reaction mixture separated into two layers and was extracted with a 1:1 mixture of ether and petroleum ether. Distillation yielded benzyl-α-d_2 chloride (b.p. 64°/12 mm) in 86% yield.

Deuterium Exchange Experiment

Ethanol-1-*d* was prepared by the action of 99.4% deuterium oxide on sodium ethoxide, prepared from molecular sodium (28) under strictly anhydrous conditions in a nitrogen atmosphere. The product was shown by N.M.R.[8] to be at least 99% deuterated on the hydroxyl group. A solution of sodium ethoxide in the deutero-ethanol (ca. 0.5 *M*) was prepared by dissolution of sodium metal and was standardized by titration with acid. Fifty milliliters of the ethoxide solution was added to an equimolar quantity of benzyl nitrate and reaction was allowed to proceed at 30° C to an appropriate extent of completion when it was quenched by addition of *p*-toluenesulphonic acid. Solvent was removed under reduced pressure and the residue was taken up in ether and washed

[8]*N.M.R. analyses were performed by Dr. R. J. Gillespie.*

Can. J. Chem. Downloaded from www.nrcresearchpress.com by 210.87.254.40 on 09/05/12
For personal use only.

with ice-cold water. The extent of reaction was determined by an acid–base titration of the aqueous washings. The ethereal solution was evaporated and treated with three 25-ml quantities of methanol, each of which was removed by distillation through a Vigreux column. The purpose of this methanol treatment was to remove last traces of deutero-ethanol and to exchange any hydroxyl-deuterated benzyl alcohol which may have been formed by hydrolysis following the quenching. The product of this treatment was fractionally distilled through a 15-cm tantalum spiral column. Deuterium analysis was carried out by combustion of the recovered benzyl nitrate and measurement of the O—D absorption at 2500 cm^{-1} in the water formed (15).

In the first exchange experiment, carried to 44% completion, two fractions of benzyl nitrate were collected, both of which showed some contamination with benzaldehyde, as shown by a carbonyl absorption in the infrared spectra, although the higher boiling fraction was the purer. The analysis results for the two fractions were 0.029 ± 0.006 and 0.015 ± 0.003 atom% excess deuterium, respectively. In a second exchange experiment, carried to 37% completion, the recovered material was more carefully purified and a fraction which was almost completely carbonyl-free was obtained. This fraction was found to contain 0.007 ± 0.003 atom% excess deuterium.

On the basis of the carbanion intermediate mechanism one can calculate the k_3/k_2 ratio corresponding to a deuterium pickup of 0.007 atom%. Assuming that only one hydrogen in the benzyl nitrate exchanges, the following can be derived from equations [2] and [3]. (The rate constant for the reverse step in equation [2] will here also be denoted by k_2 even though it now applies to the reaction of carbanion with deutero-ethanol.)

$$\frac{d}{dt}[C_6H_5CHDONO_2] = k_2[C_6H_5\overset{\ominus}{C}HONO_2][C_2H_5OD] \qquad [5]$$

$$\frac{d}{dt}[\text{product}] = k_3[C_6H_5\overset{\ominus}{C}HONO_2] \qquad [6]$$

Dividing equations [5] and [6] and integrating one obtains

$$\frac{[C_6H_5CHDONO_2]}{[C_6H_5CHDONO_2]+[C_6H_5CH_2ONO_2]} = \frac{k_2[C_2H_5OD]}{k_3} \times \frac{[\text{product}]}{[C_6H_5CHDONO_2]+[C_6H_5CH_2ONO_2]}. \qquad [7]$$

Substituting $[(0.007\times7)/100] = 0.00049$ for the mole fraction excess of $C_6H_5CHDONO_2$ in the benzyl nitrate recovered after 37% reaction, it follows that

$$\frac{k_3}{k_2[C_2H_5OD]} = \frac{37}{63\times0.00049} = 1200.$$

Kinetic Measurements with $C_6H_5CH_2ONO_2$ *and* $C_6H_5CD_2ONO_2$

A solution of benzyl nitrate (0.04–0.05 *M*) and sodium ethoxide (0.05–0.08 *M*) in anhydrous ethanol was prepared by the addition of standard sodium ethoxide solution to a weighed amount of the nitrate and was maintained in a constant temperature bath to $\pm0.03°$ C. At suitable intervals of time aliquots of 2 ml each were removed and added to 15 ml of ice-cold water for quenching the reaction. Following titration with standard acid the unreacted nitrate ester was extracted with petroleum ether. The aqueous extract was analyzed for nitrite and nitrate ions by a modification of the method described by Varner *et al.* (17). This method is based on the differential rates of reduction

Can. J. Chem. Downloaded from www.nrcresearchpress.com by 210.87.254.40 on 09/05/12
For personal use only.

Can. J. Chem. Downloaded from www.nrcresearchpress.com by 210.87.254.40 on 09/05/12
For personal use only.

of nitrite and nitrate to ammonia. While nitrite ion is rapidly reduced by ferrous hydroxide alone, the presence of a silver ion catalyst is required for the reduction of nitrate ion.

The solution containing nitrite and nitrate was placed in a Kjeldahl-type distillation apparatus constructed with a double splash-head. A 40% aqueous sodium hydroxide solution (15 ml) was added and steam was passed through until all the ethanol had distilled over. This initial removal of ethanol was found to be necessary for quantitative reduction. A 20% aqueous solution of ferrous sulphate (5 ml) was added and steam distillation continued for 3 minutes during which time the nitrite ion was reduced to ammonia which was collected in 5% boric acid solution. The nitrate ion was then reduced on the addition of a saturated silver sulphate solution (5 ml) and the ammonia formed was distilled during 5 minutes into a fresh receiver containing boric acid solution. The ammonia from the reductions was titrated with 0.01 *N* sulphuric acid using methyl red–methylene blue indicator. A complete analysis involving the reduction of both nitrite and nitrate was performed without interruption of steam distillation.

The over-all rate constant for the reaction was calculated from the usual second-order plot using the data from the acid–base titrations. At least two kinetic runs were performed with each compound at a given temperature, and rate constants agreed within ±2%. The nitrite and nitrate analyses were performed for at least five points in each kinetic run. The yields of nitrite and nitrate ion were reproducible within ±1% absolute and the mean values were used to calculate the rate constants of the component $E_{CO}2$ and S_N2 reactions.

Nitrogen Isotope Effect

The kinetic nitrogen isotope effect in the $E_{CO}2$ reaction was obtained by comparing the nitrogen isotopic abundance in the nitrite ion formed in reactions carried out to some small known extent of completion with the isotopic abundance in the starting compound. The latter was obtained by measuring the isotopic abundance in the combined nitrite and nitrate ion product formed in reactions allowed to proceed to completion.

Benzyl nitrate (0.05 *M*) and sodium ethoxide (0.05 *M*) in 50 ml of anhydrous ethanol were allowed to react at 30° C for a length of time corresponding to 10% reaction. The solution was then added to a mixture of ice-cold petroleum ether and 0.1 *N* aqueous sodium bicarbonate (5% excess over the remaining ethoxide) and the two layers were separated. The bicarbonate served to neutralize excess ethoxide which otherwise would react with the small amount of benzyl nitrate not removed in the petroleum ether. (Neutralization with 0.1 *N* sulphuric acid resulted in some loss of nitrite and nitrate ion, possibly by reaction of nitrous acid with ethanol.) The aqueous ethanol solution was concentrated to a small volume on a rotary evaporator and the last trace of benzyl nitrate was extracted with petroleum ether. Nitrite and nitrate ion were separately reduced, following the procedure described in the previous section, and the ammonia absorbed in 0.01 *N* sulphuric acid. The extent of reaction was calculated from the total yield of ammonia obtained in the reductions. The solution of ammonium sulphate obtained from the reduction of nitrite ion was concentrated to about 3 ml and transferred to a high-vacuum system where it was oxidized by means of sodium hypobromite solution (18) to nitrogen gas for mass spectrometric analysis. The nitrogen was purified by continuous circulation over copper and copper oxide, both at 750° C, and through a trap cooled in liquid nitrogen.[9] Sufficient ammonium sulphate was present to give on oxidation 2 ml of nitrogen at atmospheric pressure.

[9]*Details of the purification procedure will appear in a subsequent publication.*

Since the amount of nitrogen which would be formed from the nitrate ion produced in a single experiment would be much too small for mass spectrometric analysis, the ammonium sulphate solutions from all the nitrate ion reductions were combined and oxidized to give a single nitrogen sample for analysis.

The nitrogen isotopic abundance in the starting benzyl nitrate was determined as follows. Benzyl nitrate (0.04–0.05 *M*) was completely hydrolyzed by sodium ethoxide (0.05–0.10 *M*) in anhydrous ethanol at 60° C. An aliquot of 5 ml was then removed and the nitrite and nitrate reduced to ammonia by the method described in the section on Kinetic Measurements, except that no titration of ethoxide was performed and the ammonia from nitrite and nitrate was collected in the same acid solution. The ammonium sulphate solution was oxidized to nitrogen and the latter was measured mass spectrometrically as described previously. From two separate reactions carried out to completion a total of five nitrogen samples was prepared.

The mass spectrometric analysis was carried out using a 90° sector type instrument, similar to the one described by Wanless and Thode (29). It was capable of measuring *relative* isotopic abundance ratios, $N^{14}-N^{14}/N^{14}-N^{15}$, to $\pm 0.02\%$.

The kinetic isotope effect was calculated from the expression (19)

$$k_{14}/k_{15} = \frac{\ln(1-f)}{\ln(1-rf)}$$

where

$$r = \frac{(N^{14}/N^{15})_{\text{reactant}}}{(N^{14}/N^{15})_{NO_2^-}}$$

and $f = 0.09$, the mole fraction of reactant which has undergone decomposition to nitrite ion.[10]

REFERENCES

1. R. Boschan, R. T. Merrow, and R. W. Van Dolah. Chem. Revs. **55**, 485 (1955).
2. J. W. Baker and D. M. Easty. J. Chem. Soc. 1193, 1208 (1952).
3. G. W. H. Cheeseman. J. Chem. Soc. 115 (1957).
4. M. Anbar, I. Dostrovsky, D. Samuel, and A. D. Yoffe. J. Chem. Soc. 3603 (1954).
5. S. J. Cristol, B. Franzus, and A. Shadan. J. Am. Chem. Soc. **77**, 2512 (1955).
6. W. D. Emmons and J. P. Freeman. J. Am. Chem. Soc. **77**, 4387, 4391 (1955).
7. H. Feuer and C. Savides. J. Am. Chem. Soc. **81**, 5826 (1959).
8. J. W. Baker and T. G. Heggs. J. Chem. Soc. 616 (1955).
9. C. K. Ingold. Structure and mechanism in organic chemistry. Cornell University Press, Ithaca, N.Y. 1953. Chap. VIII.
10. S. J. Cristol and D. D. Fix. J. Am. Chem. Soc. **75**, 2647 (1953).
11. S. J. Cristol and E. F. Hoegger. J. Am. Chem. Soc. **79**, 3438 (1957).
12. H. H. Jaffé. Chem. Revs. **53**, 191 (1953).
13. S. J. Cristol and R. P. Arganbright. J. Am. Chem. Soc. **79**, 3441 (1957).
14. P. S. Skell and C. R. Hauser. J. Am. Chem. Soc. **67**, 1661 (1945).
15. N. R. Jones and M. A. MacKenzie. Talanta, **3**, 356 (1960).
16. K. B. Wiberg. Chem. Revs. **55**, 713 (1955).
17. J. E. Varner, W. A. Bulen, S. Vanecko, and R. C. Burrell. Anal. Chem. **25**, 1528 (1953).
18. D. Rittenberg. *In* Preparation and measurement of isotopic tracers. J. W. Edwards. Ann Arbor, Michigan. 1946. p. 31.
19. W. H. Stevens and R. W. Attree. Can. J. Research, B, **27**, 807 (1949).
20. C. H. DePuy and C. A. Bishop. J. Am. Chem. Soc. **82**, 2532 (1960).
21. J. Bigeleisen. J. Chem. Phys. **17**, 675 (1949).
22. J. F. Brown. J. Am. Chem. Soc. **77**, 6341 (1955).
23. J. Bigeleisen and M. Wolfsberg. Advances in Chem. Phys. **1**, 15 (1958).
24. G. Ayrey. Private communication.
25. W. H. Saunders and D. H. Edison. J. Am. Chem. Soc. **82**, 138 (1960).
26. A. F. Ferris, K. W. McLean, I. G. Marks, and W. D. Emmons. J. Am. Chem. Soc. **75**, 4078 (1953).
27. A. I. Vogel. Practical organic chemistry. 3rd ed. Longmans, Toronto. 1956. p. 261.
28. A. I. Vogel. Practical organic chemistry. 3rd ed. Longmans, Toronto. 1956. p. 193.
29. R. K. Wanless and H. G. Thode. J. Sci. Instr. **30**, 395 (1953).

[10]*The error introduced by neglecting in the calculation of the isotope effect the 0.01 mole fraction of reactant which has produced nitrate ion without isotopic fractionation is insignificantly small.*

Can. J. Chem. Downloaded from www.nrcresearchpress.com by 210.87.254.40 on 09/05/12
For personal use only.

Can. J. Chem. Downloaded from www.nrcresearchpress.com by 210.87.254.6 on 09/05/12
For personal use only.

LES SPECTRES INFRAROUGES DE L'ACIDE SULFURIQUE ET DES OLÉUMS[1]

PAUL A. GIGUÈRE ET RODRIGUE SAVOIE

RÉSUMÉ

On a mesuré les spectres infrarouges, entre 2 et 30 μ, de l'acide sulfurique et de ses solutions aqueuses à diverses concentrations de même que celui de l'acide deutéré, D_2SO_4. On a aussi mesuré à l'état solide les spectres de l'acide pur et de ses hydrates à une, deux et quatre molécules d'eau. Les fréquences observées ont pu être attribuées aux différents modes de vibration de la molécule H_2SO_4. Les résultats confirment et complètent ceux déjà obtenus par d'autres méthodes quant à la nature et l'abondance relative des diverses espèces ioniques (y compris H_3O^+) et moléculaires présentes dans ces solutions. En particulier, on a vérifié l'auto-dissociation de H_2SO_4 pur et l'ionisation incomplète de l'eau, même dans l'acide très concentré. Enfin on a étudié de la même façon les spectres des oléums contenant jusqu'à 70% de l'anhydride SO_3. En augmentant la concentration de ce dernier, on voit apparaître graduellement les bandes de $H_2S_2O_7$, $H_2S_3O_{10}$ et enfin SO_3.

INTRODUCTION

Les spectres moléculaires de l'acide sulfurique et de ses solutions offrent un intérêt particulier en ce qu'ils permettent d'identifier les diverses espèces, ioniques et autres, présentes dans ces systèmes relativement complexes. D'autres méthodes physico-chimiques, surtout colligatives et partant moins sélectives, en particulier la conductivité électrique, la cryoscopie (voir les importants travaux de Gillespie, dans la revue récente (1)), la calorimétrie (2) et la résonance nucléo-magnétique (3), ont déjà servi à élucider la question. Quant aux spectres, seul l'effet Raman avait été étudié jusqu'ici surtout par Chédin (4) et plus récemment par Millen (5) et Young (6). Dans l'infrarouge, le caractère extrêmement corrosif et la grande absorptivité des solutions d'acide sulfurique présentaient des difficultés qui n'ont pu être surmontées que dernièrement grâce à l'invention du chlorure d'argent de qualité optique. C'est par ce moyen que Marcus et Fresco (7) ont obtenu un premier spectre infrarouge de l'acide pur au cours d'un travail sur les mélanges nitrifiants, et que dans ce laboratoire nous avons précédemment étudié les solutions diluées d'acide sulfurique (8) afin de mettre en évidence le spectre de l'ion H_3O^+. Il nous a semblé utile de compléter ce travail par une analyse systématique des spectres infrarouges de l'acide liquide et de ses solutions aqueuses, de même que ceux des hydrates à une, deux et quatre molécules d'eau à l'état solide. Comme prolongement naturel de ce travail nous avons été conduits à mesurer pour la première fois l'absorption infrarouge des oléums à des concentrations allant jusqu'à 70%. Rappelons que par convention le titre $X\%$ d'un oléum signifie une composition pondérale de X parties d'anhydride sulfurique SO_3 et $(100-X)$ parties d'acide sulfurique pur.

MÉTHODE EXPÉRIMENTALE

Pour l'étude des spectres entre 3500 et 500 cm^{-1} on préparait les échantillons simplement en pressant une goutte de solution de concentration appropriée entre deux disques de chlorure d'argent fraîchement polis au moyen d'une grande lime douce trempée dans l'eau. L'épaisseur des films ainsi obtenus est évaluée à quelque 10 μ d'après la quantité d'acide employée et la surface recouverte. Comme le chlorure d'argent commence à absorber vers 500 cm^{-1}, il a fallu utiliser du côté des basses fréquences des plaques d'iodure de césium protégées par un mince film de polyéthylène. En effet, ce matériau est à la

[1]*Manuscrit reçu le 31 août 1960.*
Contribution du Département de Chimie, Université Laval, Québec, Qué.

Can. J. Chem. Downloaded from www.nrcresearchpress.com by 210.87.254.6 on 09/05/12
For personal use only.

fois résistant à l'acide sulfurique et assez transparent dans l'infrarouge moyen, sauf pour une forte bande d'absorption vers 730 cm^{-1}; par contre il s'est révélé inutilisable avec les oléums. Il en fut de même du Teflon qui, bien que non attaqué par le liquide, semblait perméable aux vapeurs corrosives. En fait, aucun des matériaux couramment utilisés pour l'infrarouge n'a permis d'observer les spectres d'absorption des oléums dans la région des basses fréquences au delà de 450 cm^{-1}.

Pour l'étude des solides, on s'est servi d'une cellule de type conventionnel (9) dans laquelle les films de liquide pressé entre deux plaques de chlorure d'argent étaient refroidis, sous vide, à l'aide de mélanges d'acétone et de neige carbonique. Après une première solidification du film, on laissait remonter la température (mesurée avec un thermocouple) jusqu'à 4° ou 5° au-dessous du point de fusion de l'hydrate en question; puis on refroidissait de nouveau, et très lentement. Cette opération était répétée plusieurs fois afin d'obtenir un solide cristallin et non pas vitreux. Toutefois, si l'on en juge par l'allure des bandes, il n'est pas certain que ce but aît été atteint entièrement.

L'acide sulfurique commercial (96%) fut employé tel quel, soit pur, soit additionné d'eau distillée ou d'oléum à 23% suivant le cas. Ce dernier (General Chemical Co.) était d'abord distillé dans un appareil en Pyrex assemblé par rodages et comprenant une colonne Vigreux mais sans réfrigérant. Pour obtenir des concentrations supérieures à 23%, on faisait barboter à froid dans cet oléum des vapeurs provenant de la distillation d'un autre échantillon du même oléum. De cette façon, on a pu atteindre progressivement un titre de quelque 70%. Tous les échantillons étudiés au cours de ce travail étaient liquides à température ordinaire, sauf celui à 28.5% qui cristallisa partiellement au bout de quelques semaines. Une étude préliminaire de l'absorption infrarouge des vapeurs blanches dégagées par les oléums a montré les bandes de l'acide sulfurique et celles, beaucoup plus faibles, de l'anhydride SO_3. Le titre des oléums fut déterminé par alcalimétrie selon la méthode usuelle. L'échantillon de D_2SO_4 fut obtenu en faisant absorber très lentement dans un peu d'eau lourde (à 99% de D_2O), refroidie dans la glace, des vapeurs d'anhydride sulfurique provenant de la distillation d'oléum commercial. Par titrations et dilutions successives, on a réussi à atteindre exactement la concentration $100 \pm 0.2\%$ de D_2SO_4.

Pour enregistrer les spectres, on s'est servi alternativement d'un spectrophotomètre Beckman (modèle IR-4) à double faisceau, et d'un appareil Perkin–Elmer (modèle 112-C) avec prismes de chlorure de sodium et de bromure de césium. Afin de diminuer l'absorption par le gaz carbonique et l'humidité, on faisait circuler un courant d'azote sec à travers l'appareil avant et pendant les mesures.

DISCUSSION DES RÉSULTATS

Les fréquences au maximum des diverses bandes d'absorption sont énumérées dans les Tableaux I, II, III et IV; quelques spectres infrarouges sont reproduits dans les Figures 1 et 2. Pour faciliter la discussion, on considérera successivement les solutions aqueuses, l'acide sulfurique pur, les hydrates solides et enfin les oléums.

(A) Les solutions liquides

Dans les solutions diluées l'espèce moléculaire la plus abondante H_2O cause une forte absorption dans les régions de 3400 cm^{-1} (ν_3), 1650 cm^{-1} (ν_2) et 730 cm^{-1} (ν_R). Les deux premières sont encore nettement visibles dans les solutions à environ 80% (Fig. 1, A); c'est là une confirmation directe de la déduction de Gillespie (10), basée sur des données cryoscopiques, à l'effet que l'ionisation de l'eau est incomplète dans l'acide sulfurique même aux fortes concentrations. Fait remarquable, l'addition de H_2SO_4 affecte à peine

la fréquence de libration ν_R de l'eau, contrairement aux électrolytes du type KCl qui l'abaissent considérablement (8). La différence vient de ce que ces électrolytes affaiblissent la structure de l'eau liquide en diminuant le nombre de liaisons hydrogène. Dans

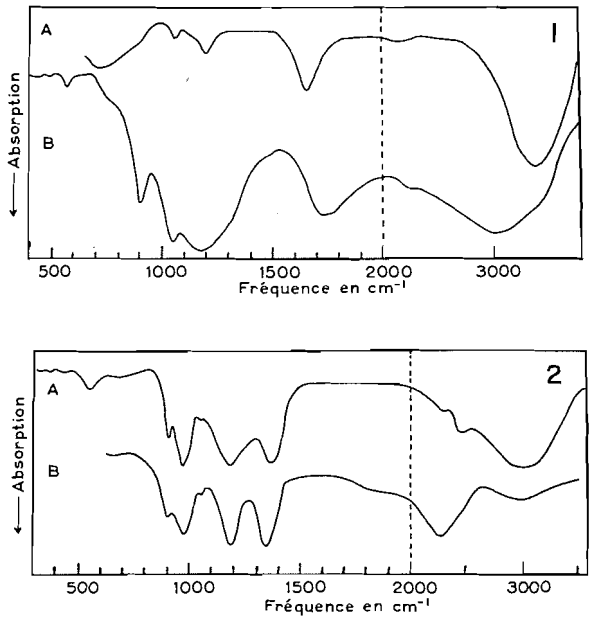


FIG. 1. Spectres infrarouges des solutions aqueuses d'acide sulfurique. (A) 8.5% H_2SO_4; (B) 78.5% H_2SO_4.

FIG. 2. Spectre d'absorption infrarouge de l'acide sulfurique (A) et deutérosulfurique (B).

TABLEAU I

Fréquences (en cm^{-1}) des bandes d'absorption dans les spectres infrarouges de l'acide sulfurique et de ses solutions aqueuses

8.5%	25.5%	46%	78.5%	90.5%	95.5%	100% H_2SO_4
—	—	—	—	332	332	332 f
—	—	—	—	372	372	372 f
—	—	—	—	420	420	420 f
445	445	442	444 f	—	—	—
500	500	500	500 f	—	—	—
—	—	—	549	549	549	549 F
584	584	584	584 F	584	584	—
—	—	—	—	(675)	(675)	675 ff
720 m	720 mf	—	—	—	—	—
—	—	—	740 f	735 f	740 f	?
890 ff	890 m	895 m	907 F	907 F	907 F	907 F
—	—	—	967 ff	966 F	967 F	967 FF
1052 f	1052 F	1050 FF	1050 FF	1052 m	1052 m	1050 f
1100 ff	—	—	—	—	—	—
—	—	—	1155 f	1160 m	1165 m	1170 FF
1205 m	1195 F	1192 FF	1190 FF	(1190)	(1190)	—
—	—	?	?	?	(1240)	(1240)
—	(1350)	(1350)	(1350)	1355 F	1365 F	1368 FF
1655 F	1650 F	1655 m	1650 ff	—	—	—
(1750)	1750 f	1750 m	1740 F	(1710)	(1700)	—
2150 ff	—	—	—	—	—	—
—	—	—	2250 f	2225 m	2250 m	2250 f
—	—	2450 ff	2450 ff	2450 f	2450 m	2450 m
—	—	(2910)	(2950)	2950 F	2970 FF	2970 FF
3400 FF	3400 FF	3400 F	(3400)	—	—	—

SYMBOLES: ff = très faible; f = faible; m = moyenne; F = forte; FF = très forte. Les fréquences entre parenthèses indiquent des bandes incertaines (épaules, etc.).

Can. J. Chem. Downloaded from www.nrcresearchpress.com by 210.87.254.6 on 09/05/12
For personal use only.

Can. J. Chem. Downloaded from www.nrcresearchpress.com by 210.87.254.6 on 09/05/12
For personal use only.

TABLEAU II

Fréquences (en cm^{-1}) des bandes Raman et infrarouges de H_2SO_4 et HSO_4^-

	Raman	Infrarouge
H_2SO_4	—	332±10
	395	372±10
	430	420±10
	560	549±5
	917	907±5
	972	967±5
	1140	1170±10
	—	1240±25
	1370	1365±5
	—	2450±50
	—	2970±50
HSO_4^-	595	584±5
	895	890±8
	1036	1052±5

TABLEAU III

Fréquences (en cm^{-1}) des principales bandes dans le spectre infrarouge de l'acide sulfurique et de ses hydrates à l'état solide

H_2SO_4	$H_2SO_4.H_2O$	$H_2SO_4.2H_2O$	$H_2SO_4.4H_2O$
?	732 F	(735)	735 ff
—	890 F	900 F	890 F
910 FF	—	—	—
980 F	—	—	—
1030 f	1046 FF	1045 FF	1045 FF
—	—	—	1100
—	1142	1153 FF	1160 FF
1165 F	1180	—	—
1225 m	—	—	—
—	1240 F	—	—
1375	—	(1320) f	(1340) f
—	—	—	1650 F
—	1730 F	1710 F	1750 F
2150 f	2125 F	2050 ?	—
2400 F	?	2400 m	(2500)
—	2775 FF	2700 f	—
2980 FF	—	2950 F	3000 m
—	—	—	3350 F

TABLEAU IV

Spectres infrarouges des oléums (Les fréquences sont données en cm^{-1})

6.5%	12.5%	23%	28.5%	46.5%	51%	69% SO_3
(472)	(475)	472 f	472 f	472 f	476 f	476 f
—	—	—	510 f	513 f	510 f	516 f
—	?	538 mf	538 F	538 F	538 F	540 FF
550 F	555 F	555 F	550 F	552 f	552 f	—
618 ff	618 f	619 mf	618 m	619 mF	620 F	618 F
?	655 f	640 mf	640 mf	640 mF	635 mf	640 mf
—	—	—	688 ff	688 ff	688 f	688 f
732 f	732 mf	732 m	732 m	732 mF	730 mF	728 mF
806 f	807 mf	809 FF	808 FF	806 FF	806 FF	806 FF
907 F	908 mF	906 m	905 mf	(905)	(905)	—
970 FF	970 FF	969 FF	969 FF	969 FF	965 FF	965 FF
—	—	—	—	1075 ff	1075 ff	1075 f
1180 FF	1185 FF	1190 FF	1190 FF	1190 FF	1200 FF	1200 FF
1365 FF	1365 FF	1370 FF	1370 FF	1370 FF	1370 FF	1370 FF
—	—	1430 f	1430 mf	1430 m	1430 m	1430 m
2250 f	2250 f	2200 f	2200 f	2200 mf	2200 mf	2200 mf
2450 F	2450 F	2425 F	2425 F	2425 F	2424 F	2425 F
2970 FF	2970 FF	3000 FF	3000 FF	3000 FF	3000 FF	3000 FF

Can. J. Chem. Downloaded from www.nrcresearchpress.com by 210.87.254.6 on 09/05/12
For personal use only.

l'acide sulfurique, au contraire, on a en moyenne le même nombre de liaisons hydrogène (soit quatre) par molecule (ou ion).

Viennent ensuite les espèces ioniques: d'abord H_3O^+ dont les bandes caractéristiques à 1750 et 1200 cm^{-1} (8) augmentent d'intensité avec la concentration jusqu'à un maximum vers 80% d'acide (Tableau I). Il en est de même de l'ion bisulfate HSO_4^- pour lequel Young et ses collaborateurs (5) ont établi avec précision les fluctuations de concentration en se basant sur l'intensité des bandes Raman. Plusieurs des bandes de l'anion HSO_4^- se confondent avec celles de la molécule H_2SO_4 comme on pouvait le prévoir; les trois plus caractéristiques, à 584, 890 et 1052 cm^{-1}, ont leur équivalent en Raman (Tableau II). Les deux ions H_3O^+ et HSO_4^- sont donc les plus abondants dans les solutions aqueuses d'acide sulfurique. À noter que la bande à 1050 cm^{-1} est encore perceptible dans le spectre de H_2SO_4 pur, une autre confirmation expérimentale de l'auto-dissociation déjà démontrée par la cryoscopie et la conductivité électrique (1). Les spectres Raman ne permettent pas de vérifier ce point, pas plus d'ailleurs que mettre en évidence l'ion H_3O^+ (11).

Quant à l'anion sulfate SO_4^{--} sa concentration maximum (moins de la moitié de celle de l'ion bisulfate) se trouve entre 40 et 60% d'acide, toujours d'après les spectres Raman (5). C'est de cette façon que varie l'intensité des deux bandes à 445 et 500 cm^{-1} que nous attribuons pour cette raison aux modes de déformation asymétrique de l'ion sulfate. Dans les spectres infrarouges des sulfates ioniques cristallins (12) ces fréquences sont notablement plus élevées, soit environ 600–650 cm^{-1}. Le décalage observé dans les solutions d'acide provient peut-être de l'hydratation des ions. Par ailleurs la bande très faible à 1100 cm^{-1} dans la solution la plus diluée, et qui va se perdre dans la forte absorption vers 1050 cm^{-1} aux grandes concentrations d'acide, provient également de l'anion sulfate (12). Elle est due à la vibration de valence S—O asymétrique; la fréquence symétrique correspondante est 982 cm^{-1} en Raman (13).

Au delà de 80% d'acide, une douzaine de bandes appartenant à la molécule H_2SO_4 (Tableau II) émergent graduellement alors que celles de l'ion bisulfate s'affaiblissent. Au moins trois de ces bandes (i.e. à 907, 1365 et 2950 cm^{-1}) sont communes à l'acide et à l'anion comme le prouvent les variations d'intensité avec la composition. Le problème de la constitution des solutions très concentrées (au-dessus de 80%) d'acide sulfurique n'est pas entièrement élucidé. Dans l'acide pur, outre l'auto-dissociation déjà mentionnée,

$$2H_2SO_4 \rightleftarrows HSO_4^- + H_3SO_4^+; \qquad [1]$$

une seconde, moins importante, est censée exister (1), soit

$$2H_2SO_4 \rightleftarrows H_3O^+ + HS_2O_7^-. \qquad [2]$$

Cependant les ions ainsi produits sont si peu abondants qu'on ne saurait les déceler par spectroscopie, sauf dans les cas les plus favorables (telle la bande de HSO_4^- à 1050 cm^{-1} citée plus haut). Ainsi il est à prévoir que le spectre du cation $H_3SO_4^+$ diffère assez peu de celui de la molécule H_2SO_4. Les seuls indices qu'on pourrait lui attribuer dans les présents spectres, en se basant sur le critère intensité, sont deux bandes très diffuses, l'une vers 740 cm^{-1} et l'autre à 2250 cm^{-1}. La première, en particulier, a une fréquence appropriée pour un mode de balancement (wagging) des hydrogènes. Par contre, la seconde fréquence à 2250 cm^{-1} semble un peu trop basse pour une vibration de valence O—H; elle doit plutôt appartenir à quelque combinaison ou harmonique des bandes plus fortes de H_2SO_4.

Par ailleurs, diverses propriétés physiques (14) conduisent à postuler l'existence d'un ion solvaté $H_3O^+(H_2SO_4)$ dans les solutions très concentrées (au-delà de 90%). La présence

des bandes caractéristiques de l'ion hydroxonium dans les solutions à plus de 95% d'acide renforce cette hypothèse au détriment d'une autre mise récemment de l'avant par Young et Walrafen (15) et qui fait appel à une espèce nouvelle $H_5SO_5^+$. En effet, tout laisse prévoir que ce cation hypothétique aurait une structure, et partant un spectre de vibration nettement différents de ceux des espèces H_2SO_4, $H_3SO_4^+$ et HSO_4^-.

(B) Les vibrations normales de H_2SO_4

Dans les travaux antérieurs sur le spectre moléculaire de l'acide sulfurique on ne s'est pas préoccupé d'attribuer les fréquences des bandes observées aux divers modes de vibration de la molécule. La diffraction aux rayons-X (16) a confirmé la structure la plus probable, soit un arrangement quasi-tétraédral des oxygènes autour du soufre, les deux hydrogènes étant normalement situés dans le plan Z (Fig. 3). La molécule appartient

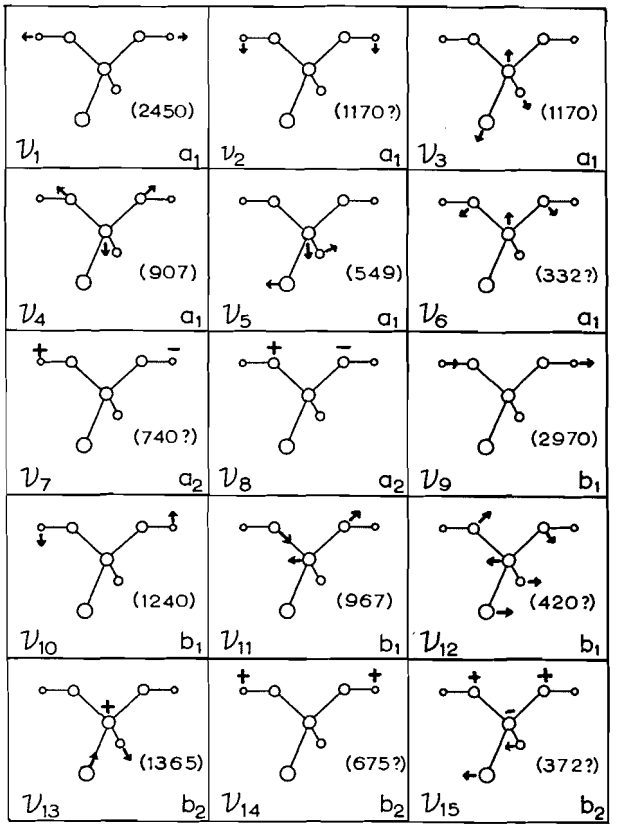


FIG. 3. Modes de vibration de la molécule H_2SO_4. Les nombres entre parenthèses indiquent les fréquences en cm^{-1}.

donc au groupe de symétrie C_{2v} et la théorie (17) prévoit que ses 15 vibrations normales sont réparties en deux classes: soit 8 symétriques par rapport à l'axe (dont 6 du type a_1 et 2 du type a_2) et 7 asymétriques (dont 4 du type b_1 et 3 du type b_2). Les vibrations de type a_2 étant inactives en infrarouge, on observera donc au maximum 13 vibrations fondamentales, du moins pour la molécule à l'état libre. Pour fins d'identification on peut séparer les vibrations en deux groupes de 6 et 9 respectivement, suivant qu'elles font intervenir directement ou non les atomes d'hydrogène. On a représenté sur la Fig. 3

Can. J. Chem. Downloaded from www.nrcresearchpress.com by 210.87.254.6 on 09/05/12
For personal use only.

Can. J. Chem. Downloaded from www.nrcresearchpress.com by 210.87.254.6 on 09/05/12
For personal use only.

ces divers modes de vibration de la molécule H_2SO_4 avec la fréquence probable de chacune. Les vibrations de valence O—H, ν_1 et ν_9, se retrouvent ici presque exactement aux mêmes fréquences que dans le cas de l'acide sélénieux (18); elles sont décalées à 1860 et 2280 cm^{-1} dans D_2SO_4. Ces fréquences relativement basses confirment l'existence de fortes liaisons hydrogène dans l'acide sulfurique et ses solutions. D'autre part, les vibrations de déformation $\angle$SOH sont difficiles à identifier parce qu'elles tombent dans une région de forte absorption due aux bandes de valence S—O. Pour la même raison, les décalages isotopiques dans D_2SO_4 sont de peu d'utilité ici. Cependant, en comparant minutieusement les spectres des deux molécules on peut déceler dans le cas de H_2SO_4 un léger excédent d'absorption vers 1240 cm^{-1} qui doit provenir d'une bande de déformation $\angle$SOH. Etant donné sa faible intensité, il s'agit peut-être de la vibration asymétrique ν_{10} qui affecte assez peu le moment polaire de la molécule. Si cette explication est valide, il est alors possible que la vibration symétrique correspondante soit comprise dans la forte bande à 1170 cm^{-1} (ν_3) qui effectivement semble encore plus large pour H_2SO_4 que pour D_2SO_4. Dans les solutions aqueuses d'acide sélénieux, on ne trouve qu'une seule bande intense de déformation $\angle$SeOH à 1236 cm^{-1}. Enfin, le seul des deux modes de balancement (wagging) des hydrogènes qui soit actif en infrarouge, ν_{14} n'a pas lui non plus été identifié avec certitude dans les présents spectres. Par analogie avec diverses molécules, en particulier des alcools et des acides organiques, on peut prévoir pour ce mode une fréquence de l'ordre de 650 à 700 cm^{-1}. La bande assez floue à 675 cm^{-1} conviendrait bien à cet égard, quoique son intensité semble un peu faible. Dans l'anion HSO_4^- ce mouvement de l'unique hydrogène se traduit par une bande à 584 cm^{-1}.

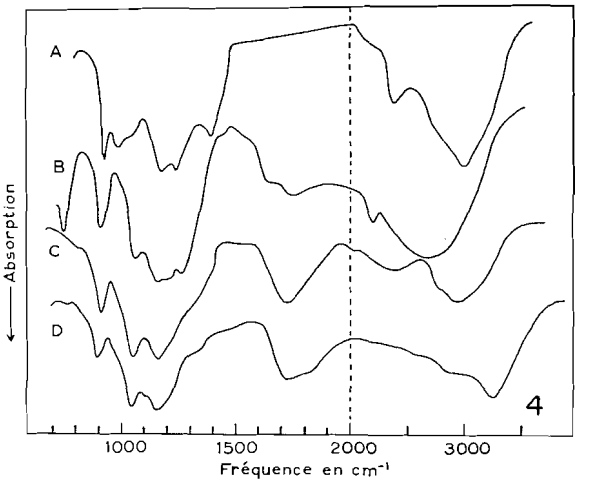
Pour sa part le groupe SO_4 dans l'acide sulfurique possède neuf vibrations caractéristiques non dégénérées. Du côté des hautes fréquences on rencontre d'abord les vibrations de valence double S=O, ν_3 à 1170 et ν_{13} à 1365 cm^{-1}, soit presque exactement les mêmes valeurs que dans SO_2. Les distances interatomiques sont aussi identiques, 1.42 Å (19). Les deux vibrations de valence simple S—O ont des fréquences sensiblement plus basses, ν_4 à 907 et ν_{11} à 967 cm^{-1}, en accord avec les longueurs plus grandes, 1.52–1.55 Å, de ces liaisons. Dans l'anion HSO_4^- les fréquences correspondantes se trouvent à 895 et 1052 cm^{-1} respectivement. Quant aux diverses fréquences de déformation, nous avons essayé de les identifier par comparaison avec la molécule SO_2F_2 déjà étudiée par spectroscopie infrarouge (20) et centimétrique (21). Outre que la symétrie est la même dans les deux cas, les masses et les distances diffèrent assez peu. Ainsi, on retrouve dans les deux spectres une bande à environ 550 cm^{-1} attribuable au mode de déformation commun $\angle$OSO. Des trois autres bandes qui restent dans le spectre de H_2SO_4 à 420, 372 et 332 cm^{-1}, on serait porté a priori à assigner la première au mode de déformation $\angle$OSO impliquant les groupements hydroxyles (ν_6) étant donné les liaisons hydrogène qui doivent en augmenter la fréquence. Cependant, seules les deux faibles bandes à 420 et 372 cm^{-1} ont leur équivalent dans le spectre Raman (Tableau II). Vu la similitude des deux modes de balancement ν_{12} et ν_{15}, il semble plus logique de leur attribuer les deux premières bandes, ce qui laisse la dernière à 332 cm^{-1} pour ν_6. Toutefois, cette interprétation n'est que provisoire.

(C) Les hydrates solides

Lors de la solidification, les bandes infrarouges de l'acide sulfurique et de ses solutions aqueuses deviennent plus nettes et plus minces comme c'est généralement le cas. Par comparaison avec celui du liquide (Fig. 2, A) on note les particularités suivantes dans le spectre de l'acide pur à l'état solide (Fig. 4, A). Les deux bandes à 910 et 1050 cm^{-1}

caractéristiques de l'ion bisulfate sont nettement plus intenses, confirmant par là que l'auto-dissociation est plus forte à l'état solide. Par ailleurs, la bande de déformation $\angle$SOH à 1225 cm^{-1} est maintenant très distincte de la bande de valence S=O à 1165 cm^{-1}. L'harmonique de cette dernière fréquence se retrouve sans doute dans la bande très diffuse à 2150 cm^{-1}, de même que la combinaison des deux fondamentales à 1365 et 910 cm^{-1}.

Le monohydrate $H_2SO_4 \cdot H_2O$ montre un spectre (Fig. 4, B) entièrement différent de ceux *non seulement* de l'acide *pur mais encore* des solutions liquides de composition voisine (comp. Fig. 1, B). Notons en passant que le monohydrate contient 84.5% de H_2SO_4, le dihydrate, 73.15% et le tétrahydrate, 57.7%. L'effet Raman (11) et la résonance nucléo-magnétique (22) ont donné pour ce solide des résultats compatibles avec



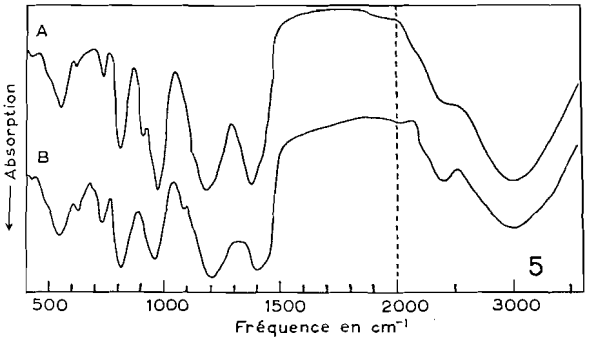


FIG. 4. Spectres de l'acide sulfurique et de ses hydrates à l'état solide. (A) H_2SO_4; (B) monohydrate (C) dihydrate; (D) tétrahydrate.
FIG. 5. Spectres infrarouges entre 2 et 25 μ des oléums. (A) 23% SO_3; (B) 69% SO_3.

la structure ionique $(H_3O^+)(HSO_4^-)$. Effectivement, la majorité des bandes rapportées ici (Tableau III) peuvent s'interpréter sans ambiguité d'après ces deux ions, à savoir celles de H_3O^+ à 732, 1142, 1730 et 2125 cm^{-1} (23) et celles de HSO_4^- à 890, 1046 et 1240 cm^{-1} (12). Cependant, la bande à 732 cm^{-1} constitue ici une énigme en ce qu'elle est beaucoup trop intense pour provenir uniquement de l'ion hydroxonium. En effet,

Can. J. Chem. Downloaded from www.nrcresearchpress.com by 210.87.254.6 on 09/05/12
For personal use only.

elle est à peine visible dans les deux autres hydrates (Fig. 4, C et D). Nous nous proposons d'étudier cette question plus en détail. Dans les spectres du dihydrate toute trace d'acide non-ionisé a disparu et les bandes de H_2O sont bien évidentes. Enfin dans le cas du tétrahydrate la bande de l'ion sulfate à 1100 cm^{-1} se détache nettement de celle de l'ion bisulfate à 1045 cm^{-1} contrairement au cas des solutions liquides.

(D) Les oléums

Les spectres Raman des oléums à diverses concentrations sont déjà bien connus à la suite des travaux originaux de Chédin (4) et de ceux plus récents de Millen (5). Ce dernier a attribué les bandes observées à des acides supérieurs tels $H_2S_2O_7$, $H_2S_3O_{10}$, etc. dont l'existence avait été révélée par les mesures cryoscopiques de Gillespie (24). Les présents résultats (Tableau IV) confirment en général cette interprétation. Ainsi la bande d'absorption à 907 cm^{-1}, caractéristique de H_2SO_4, s'affaiblit graduellement lors de l'addition de SO_3 et finit par disparaître dans les oléums à environ 45%, composition correspondant à l'acide disulfurique $H_2S_2O_7$. Quant aux autres bandes de H_2SO_4 à 550, 970, 1170 et 1368 cm^{-1}, ainsi que les bandes de valence OH vers 3–4 μ, si elles semblent garder la même intensité à toutes concentrations, c'est qu'elles sont communes aux acides supérieurs et leurs ions, comme on pouvait le prévoir. Dans la plupart des cas on observe un léger déplacement du maximum de ces bandes suivant la concentration. En fait, seules quelques-unes des bandes rapportées ici peuvent servir à identifier sans ambiguité l'une quelconque des espèces moléculaires ou ioniques présentes dans les oléums.

En se basant sur des considérations de structure on doit s'attendre à des vibrations caractéristiques du "pont" S—O—S présent dans tous les acides supérieurs de formule générale $H_2SO_4 \cdot (SO_3)_n$. Aussi attribuons-nous aux vibrations de valence de ce groupe les deux bandes à 732 et 806 cm^{-1} qui sont de fréquence et d'intensité relative appropriées. Comme la première seule apparaît en Raman, elle doit correspondre à la vibration symétrique S—O. En ceci, notre interprétation diffère de celle de Millen (5) qui considère cette bande comme un diagnostic sûr de la molécule $H_2S_2O_7$ à l'exclusion des acides supérieurs. En fait, nos spectres infrarouges ne montrent aucune diminution appréciable d'intensité des deux bandes à 732 et 806 cm^{-1} pour des concentrations supérieures à 45% (i.e. $H_2S_2O_7$) ce qui concorde bien avec l'explication que nous proposons ici. Les autres bandes, qui d'après la distribution d'intensité pourraient être assignées à la molécule $H_2S_2O_7$, se trouvent à 618 et 640–655 cm^{-1}; cette dernière appartient peut-être à l'anion $HS_2O_7^-$ sur la concentration duquel on ne possède pas de données précises.

Quant à l'acide trisulfurique $H_2S_3O_{10}$ qui, selon les mesures cryoscopiques de Gillespie (24) existe aux concentrations supérieures à 30%, on peut lui attribuer avec assez de certitude les deux bandes à 688 et 1430 cm^{-1}. Dans les spectres Raman on observe à 480 cm^{-1} une bande qui semble bien provenir de cet acide, du moins si l'on s'en rapporte à son intensité. Son équivalent (à 472 cm^{-1}) dans les présents spectres ne montre pas le même profil d'intensité, mais ceci provient sans doute de difficultés expérimentales (lumière diffractée, etc.) dans cette région située à la limite utile de notre instrument.

Par ailleurs, nous n'avons pu déceler dans les spectres des oléums, même les plus concentrés, d'indices certains de l'acide tétrasulfurique $H_2S_4O_{13}$. Des deux fréquences Raman attribuées par Millen à cet acide, la première à 245 cm^{-1} tombe loin en dehors de la région étudiée ici et la seconde à 688 cm^{-1} apparaît déjà à 28% dans nos spectres, d'où l'attribution à $H_2S_3O_{10}$ ci-haut. Enfin, la faible bande à 1075 cm^{-1} dans les oléums

Can. J. Chem. Downloaded from www.nrcresearchpress.com by 210.87.254.6 on 09/05/12
For personal use only.

à plus de 45% de SO_3 révèle la présence de cette dernière molécule comme l'a démontré Chédin (4) à partir des spectres Raman. Selon toute apparence, l'anhydride SO_3 se trouve ici à l'état de monomère puisque les bandes caractéristiques du polymère S_3O_9 (25), en particulier celle à 860 cm^{-1}, n'apparaissent pas dans les spectres infrarouges des oléums même à 70%. Notons en terminant que, pas plus que pour les solutions aqueuses d'acide sulfurique, nous n'avons pu trouver dans les spectres des oléums d'évidence positive pour l'espèce $H_3SO_4^+$ bien que, d'après la stoéchiométrie, ce cation doive exister dans ce milieu.

REMERCIEMENTS

Les auteurs désirent remercier le Conseil National des Recherches du Canada pour l'aide financière qui leur a permis d'exécuter ce travail.

SUMMARY

The infrared absorption spectra from 2 to 30 μ have been measured for sulphuric acid, its aqueous solutions at various concentrations, the solid acid and its three hydrates, and finally the deuterated acid D_2SO_4. The results confirm and extend our knowledge as to the nature and relative abundance of the ionic and molecular species present in these systems. In particular, direct evidence was found for the self-dissociation of the pure acid as well as for the incomplete ionization of water even in very concentrated sulphuric acid. It was possible to assign most of the observed frequencies to the various vibrational modes of the H_2SO_4 molecule. Likewise the infrared spectra of oleums in concentrations up to 70% have been studied, and the higher acids, $H_2S_2O_7$ and $H_2S_3O_{10}$, have been identified.

BIBLIOGRAPHIE

1. R. J. GILLESPIE. Revs. Pure and Appl. Chem. (Australia), **9**, 1 (1959).
2. B. J. KIRKBRIDE et P. A. H. WYATT. Trans. Faraday Soc. **54**, 483 (1958).
3. G. C. HOOD et C. A. REILLY. J. Chem. Phys. **27**, 1126 (1957).
4. J. CHÉDIN. Compt. rend. **201**, 724 (1935); Ann. chim. (Paris), **8**(11), 432 (1937).
5. D. J. MILLEN. J. Chem. Soc. 2589 (1950).
6. T. F. YOUNG, L. F. MARANVILLE et H. M. SMITH. The structure of electrolytic solutions. *Edité par* W. J. Hamer. John Wiley & Sons, New York. 1959. Chap. 4.
7. R. A. MARCUS et J. M. FRESCO. J. Chem. Phys. **27**, 564 (1957).
8. M. FALK et P. A. GIGUÈRE. Can. J. Chem. **35**, 1195 (1957).
9. E. L. WAGNER et D. F. HORNIG. J. Chem. Phys. **18**, 296 (1950).
10. R. J. GILLESPIE. J. Chem. Soc. 2493 (1950).
11. D. J. MILLEN et E. G. VAAL. J. Chem. Soc. 2913 (1956).
12. F. A. MILLER et C. H. WILKINS. Anal. Chem. **24**, 1253 (1952).
13. L. A. WOODWARD et R. G. HORNER. Proc. Roy. Soc. (London), A, **144**, 129 (1934).
14. P. A. H. WYATT. Trans. Faraday Soc. **56**, 490 (1960).
15. T. F. YOUNG et G. E. WALRAFEN. Communication à la 136ième réunion de l'American Chemical Society, Atlantic City, N.J., Septembre, 1959.
16. R. PASCARD. Compt. rend. **240**, 2162 (1955).
17. G. HERZBERG. Infrared and Raman spectra of polyatomic molecules. D. Van Nostrand Co., Inc., New York. 1945.
18. M. FALK and P. A. GIGUÈRE. Can. J. Chem. **36**, 1680 (1958).
19. L. E. SUTTON (*Editeur*). Tables of interatomic distances. Special Publication No. 11, The Chemical Society, London. 1958.
20. W. D. PERKINS et M. K. WILSON. J. Chem. Phys. **20**, 1791 (1952).
21. R. M. FRISTROM. J. Chem. Phys. **20**, 1 (1952).
22. R. E. RICHARDS et J. A. S. SMITH. Trans. Faraday Soc. **47**, 1261 (1951).
23. C. C. FERRISO et D. F. HORNIG. J. Chem. Phys. **23**, 1464 (1955).
24. R. J. GILLESPIE. J. Chem. Soc. 2516 (1950).
25. H. GERDING et J. LECOMTE. Physica, **6**, 737 (1939).

Can. J. Chem. Downloaded from www.nrcresearchpress.com by 210.87.254.6 on 09/05/12
For personal use only.

Can. J. Chem. Downloaded from www.nrcresearchpress.com by 210.87.254.5 on 09/05/12
For personal use only.

THE COPPER/ARSENIC SYSTEM AND THE COPPER ARSENIDE MINERALS[1]

R. D. Heyding and G. J. G. Despault

ABSTRACT

In addition to the α solid solution of arsenic in copper, three intermediate phases exist in the copper/arsenic system. The ϵ phase, stable only below ca. 340° C, has the hexagonal $A3$ (D^4_{6h}, $P6_3/mmc$) structure with $a = 2.588$, $c = 4.226$ Å, and the approximate formula Cu_8As. The compound $Cu_{3-x}As$, with $0 \leqslant x \leqslant 0.3$, is trigonal ($D^4_{3d}$, $P\bar{3}c1$) with $a = 7.132$, $c = 7.304$ Å at $x = 0$. This compound has no polymorphic forms between 200° C and the melting point. The arsenic-rich compound $Cu_{5-u}As_2$, with $0 \leqslant u \leqslant 0.1$, melts incongruently at about 700° C, and decomposes at 300° C to arsenic and Cu_3As. The structure has not been determined, but the powder diffraction pattern is recorded. The solubility of copper in arsenic appears to be negligible.

It is suggested that the mineral α domeykite is a high-pressure phase, and that the mineral algodonite is a high-pressure modification of the ϵ phase. The mineral β domeykite is isostructural with Cu_3As.

According to the phase diagram (1), two compounds are formed in the binary copper/arsenic system. The first of these, Cu_3As, has been synthesized by Katoh (2) and the structure determined by Steenberg (3). It is trigonal (D^4_{3d}, $P\bar{3}c1$), and exists over a short composition range. A transition on the copper-rich side of Cu_3As at 380° C has been interpreted by Hansen (1) as the transformation of Cu_3As into a polymorphic low-temperature form, although Steenberg was unable to prepare Cu_3As with other than the trigonal structure mentioned above. Bolfa *et al.* (4) have reported the formation of a phase at relatively high pressure which is isostructural with the mineral *domeykite*, but the diffraction pattern and unit cell dimensions were not recorded.

Although the exact composition of the second compound in the binary phase diagram is not known, Hansen has assumed the formula to be Cu_5As_2, and has attributed the transitions at 700° and 300° C on the arsenic-rich side of Cu_3As to incongruent melting and peritectoid decomposition of this compound.

Recently, Schubert *et al.* (5) have reported the synthesis of a compound Cu_9As which does not appear on Hansen's phase diagram. It has the hexagonal close-packed $A3$ structure, and is stable only below 400° C.

The present study was undertaken to confirm the composition of the phase reported by Schubert, to search for transitions in Cu_3As, and to investigate the composition and structure of the arsenic-rich compound.

EXPERIMENTAL

Twenty-four alloys containing 2.5 to 36 at.% As in copper were prepared by heating the elements in sealed evacuated pyrex, vycor, or quartz tubes in the usual manner. The copper was prepared by reduction of powdered copper oxide with purified hydrogen. Spectroscopic analysis indicated impurity limits (in p.p.m.) of: Ag, 5–10; Fe, 5; Ni, 5; Si, 3; and Mg, 2. ASARCO metallic arsenic of 99.999% spectroscopic purity was sublimed prior to use to remove traces of oxide and to facilitate crushing.

Alloys containing less than 20 at.% As were melted and quenched, annealed at 680° C, and cooled slowly to room temperature. Filings of the specimens were placed in quartz

[1]*Manuscript received September 1, 1960.*
Contribution of the Division of Applied Chemistry, National Research Council, Ottawa, Canada.
Issued as N.R.C. No. 6013.

X-ray capillaries which were in turn sealed under vacuum in larger vycor or pyrex capillaries for heat treatment. Alloys containing more than 20 at.% As were readily crushed by mortar and pestle, and subsequent heat treatment was conducted on bulk powders.

Some of the copper-rich alloys were annealed at moderate pressures and temperatures by heating open capillaries or tubes in a steel bomb under argon at 1500 to 2500 p.s.i.

X-Ray diffraction patterns were obtained in Norelco 11.46-cm Debye–Scherrer cameras using CuK_α radiation.

RESULTS AND DISCUSSION

The Copper-rich Region: The ϵ Phase

Diffraction patterns of alloys containing less than 25% As quenched from temperatures between 350° and 660° C showed only patterns of the α solid solution, or the α solid solution and Cu_3As. The unit cell dimension of the saturated α phase in equilibrium with Cu_3As was found to be 3.647 ± 0.001 Å, in good agreement with Mertz and Mathewson's value of 3.6483 Å (6).

A third phase appeared in alloys quenched or cooled slowly from 300° C with a corresponding decrease in intensities of the patterns of the α phase and Cu_3As. This phase was never obtained pure, even after cold-working and prolonged annealing. It has the approximate composition Cu_8As, and is isostructural with the compound Cu_9As recorded by Schubert, with hexagonal unit cell dimensions $a = 2.588 \pm 0.001$, $c = 4.226 \pm 0.001$ Å, $c/a = 1.633$. This $A3$, Mg-type structure (D^4_{6h}, $P6_3/mmc$) is also found in the ϵ phases of the Cu/Sb, Ag/As, and Ag/Sb systems (1, 7), and by analogy, should be referred to as the ϵ phase. Like the other ϵ phases, decomposition occurs at relatively moderate temperatures. Our inability to prepare a uniphase specimen may have been due either to a sluggish transformation or to the existence of a lower stability limit such as that observed in the Ag/As system, or both. In either event, the unit cell dimensions are not sensitive to total alloy compositions, and consequently the homogeneity range appears to be quite narrow under normal conditions.

The mineral *algodonite* is obviously isostructural with the ϵ phase, although compositions reported for the mineral range from Cu_7As (8) to Cu_4As (3). The diffraction pattern given by Peacock (9) for algodonite with the composition Cu_6As is identical with that of the ϵ phase, with minor variations in intensities of some of the reflections. One might expect the homogeneity limit of this close-packed phase to alter under pressure at the expense of the Cu_3As phase, and indeed, we have found that even at 2500 p.s.i. appreciable quantities of the ϵ phase (with slightly altered lattice parameters) appear in alloys of the composition Cu_4As. The variation in composition of the mineral, and the apparent discrepancy between composition of mineral and synthetic specimens can be attributed to differences in ambient pressures during formation of the phase.

The transition at 380° C in the phase diagram is, as far as we are able to estimate, 30 to 80° C higher than the temperature at which the peritectoid decomposition of the phase occurred in our alloys. There is some uncertainty in the figure given in the diagram, since it is based on an inflection in the solubility limit of arsenic in copper. It is not likely that the transition would be observed by differential thermal analysis unless the alloys were cold-worked before analysis.

The Compound Cu_3As

In alloys containing 22 to 27 at.% As, hexagonal Cu_3As or Cu_3As and the second phase appropriate to the two-phase region (α solid solution or the ϵ phase) were the only phases observed regardless of formation temperature or heat treatment between

Can. J. Chem. Downloaded from www.nrcresearchpress.com by 210.87.254.5 on 09/05/12
For personal use only.

200° and 660° C. The unit cell dimensions and the analyses of homogeneous alloys at the copper- and arsenic-rich limits, quenched from 560° C, are:

As, (at.%)	Composition	a (Å)	c (Å)	c/a
24.92	$Cu_{3.01}As$	7.132	7.304	1.024
26.87	$Cu_{2.72}As$	7.113	7.272	1.022

These dimensions are in excellent agreement with Katoh's values for the terminal alloys (2), but the limits are somewhat richer in arsenic than those proposed by Katoh.

The mineral *β domeykite*, also with the formula Cu_3As, is isostructural with this phase, with unit cell dimensions of $a = 7.10$ kX and $c = 7.25$ kX (8).

There was no indication of a polymorphic transformation in Cu_3As within 2- to 3-week annealing periods at temperatures below 400° C. Moreover, an alloy prepared by heating the elements at 200° C for 2 months exhibited only the pattern of Cu_3As, although traces of unreacted copper and arsenic were visible under the microscope. We conclude that this phase exists only in the trigonal form described by Steenberg.

The Arsenic-rich Phase

Alloys containing 27 to 36 at.% As exhibited the diffraction patterns of Cu_3As and arsenic when quenched from 700° C or annealed and cooled slowly to room temperature from 280° C. A new phase was observed in alloys quenched from intermediate temperatures, with arsenic the second phase in alloys containing greater than 30 at.% As. Hansen's interpretation of the transformations at 700° and 300° C, incongruent melting and peritectoid decomposition of the arsenic-rich phase, is confirmed.

The decomposition at 300° C is rapid, and quenching was invariably attended by deposition of an arsenic mirror on the wall of the ampoule. Analysis of an alloy quenched from 550° C when in equilibrium with metallic arsenic at 450° C indicated a maximum copper content corresponding to $Cu_{2.5}As$ and a minimum content corresponding to $Cu_{2.45}As$.

The first 33 lines of the rather complicated diffraction pattern are recorded in Table I. The compound does not appear to be isostructural with any of the transition metal

TABLE I

Powder diffraction pattern of $Cu_{5-u}As_2$*

I†	d (Å)	hkl‡	I†	d (Å)	hkl‡
1	5.30	110	3	1.694	114
13	3.30	201	3	1.673	420
2	3.23	102	1	1.576	332
1	2.87	112	9	1.493	{500} {430}
7	2.65	220			
1	2.56	202	7	1.445	413
6	2.47	221	2	1.431	314
21	2.43	212	4	1.395	105
3	2.35	310	11	1.373	115
13	2.16	113	7	1.343	324
100	2.075	320	13	1.324	440
90	2.022	302	2	1.313	215
100	1.991	321	4	1.295	522
17	1.960	312	13	1.197	523
11	1.925	213	13	1.177	{602} {325}
13	1.780	004			
13	1.737	{322} {104}	4	1.158	116
			33	1.146	504

*Uncertainty in composition: $0 \leqslant u \leqslant 0.1$.

†Intensities by visual comparison with density wedge.

‡Tentative tetragonal cell, $a = 7.48$ Å, $c = 7.12$ Å. Observed density 7.88 g/cc, $Z = 4$.

Can. J. Chem. Downloaded from www.nrcresearchpress.com by 210.87.254.5 on 09/05/12
For personal use only.

or copper family chalcogenides or phosphogenides of approximately the same composition, although there is some superficial similarity to $Ni_{2.5}As$ (10) and $Ni_{2-2.5}Sb$ (11). The pattern can be indexed on a tetragonal cell with $a = 7.48$ Å, $c = 7.12$ Å, but this analysis must be regarded as provisional.

The Copper/Arsenic Minerals Algodonite and Domeykite

Three copper/arsenic minerals are recognized: hexagonal algodonite mentioned previously, the trigonal Cu_3As mineral called β domeykite by Paděra (8) and 'artificial domeykite' by Katoh (2) and Steenberg (3), and the cubic Cu_3As mineral called α domeykite by Paděra and domeykite or mineral domeykite by Katoh and Steenberg. The uncertainty in composition of the phases these minerals represent and the misinterpretation of the transformations they undergo has led to some confusion in the literature not only with respect to the minerals but with respect to the phase diagram as well.

The cubic mineral α domeykite decomposes at 225° C with the formation of algodonite and trigonal Cu_3As.* The composition of cubic α domeykite corresponds to Cu_3As, and Steenberg has argued that if cubic α domeykite and trigonal β domeykite are both Cu_3As, the transition at 225° cannot be explained unless algodonite is also, ideally, Cu_3As. This interpretation has been the basis for the assumption in subsequent literature that Cu_3As has two or three modifications. We have found no such modifications. Moreover, Pearson (7) has observed that cubic α domeykite is isostructural with $Cu_{15}Si_4$, and has suggested that the correct formula is $Cu_{15}As_4$ rather than Cu_2As. Finally, algodonite itself decomposes to trigonal β domeykite and the α solid solution at 250° C (3, 12), an impossible transformation unless algodonite lies between the solid solution and Cu_3As in the phase diagram.

We attempted to repeat the synthesis of the high-pressure Cu_3As phase described by Bolfa (4) without success, probably because the pressures we could attain were too low. It is unfortunate that Bolfa and his co-workers did not give the diffraction pattern of their product, but we must assume that it was identical with the mineral they used for comparison, and that the mineral was indeed cubic α domeykite.

With this assumption, the relationship of the minerals to the binary phase diagram can be explained quite simply. Cubic α domeykite is a high-pressure phase, probably with the formula $Cu_{15}As_4$, which decomposes on heating to trigonal Cu_3As (which is identical with trigonal β domeykite) and the ϵ phase. Algodonite is a high-pressure modification of the ϵ phase with variable composition, which decomposes at 250° C, somewhat below the normal transition temperature, with the formation of the α solid solution and trigonal Cu_3As. Neither of the high-pressure phases, algodonite and α domeykite, will appear on the normal phase diagram, and there is no reason to expect that the compound Cu_3As exists other than with the trigonal lattice.

As a result of this investigation we submit that three modifications are required in the phase diagram shown and described in Hansen:

1. The transition at 380° C, on the copper-rich side of Cu_3As represents the peritectoid decomposition of the ϵ phase rather than a polymorphic transition in Cu_3As. The ϵ phase has very narrow homogeneity limits at about Cu_8As.

2. The homogeneity limits of Cu_3As at 560° C are $Cu_{3.0}As$ and $Cu_{2.7}As$, somewhat richer in arsenic than indicated in the diagram.

**The description in Hansen of cubic α domeykite as a high-temperature phase is obviously a misprint.*

Can. J. Chem. Downloaded from www.nrcresearchpress.com by 210.87.254.5 on 09/05/12
For personal use only.

3. The composition of the arsenic-rich phase can be represented by the expression $Cu_{5-u}As_2$ in which u, the uncertainty, is within the limits $0 \rightarrow 0.1$. We have found no evidence to indicate that a compound richer in arsenic is formed at normal pressure.

ACKNOWLEDGMENTS

We are indebted to Mrs. T. M. Dolan for assistance in obtaining Debye–Scherrer patterns, and to Mr. P. Tymchuk and Mr. G. R. Duval for analysis of reactants and products.

REFERENCES

1. M. HANSEN. Constitution of binary alloys. 2nd ed. McGraw-Hill. 1958. p. 160 et seq.
2. N. KATOH. Z. Krist, **76**, 228 (1930).
3. B. STEENBERG. Arkiv. Kemi, Mineral Geol. A, **12**, No. 26, 1 (1936–38).
4. J. BOLFA, R. PASTANT, and M. ROUBAULT. Compt. rend. **230**, 103 (1950).
5. K. SCHUBERT, H. BREIMER, W. BURKHARDT, E. GUNZEL, R. HAUFLER, H. L. LUKAS, H. VELTER, J. WEGST, and M. WILKENS. Naturwiss. **44**, 229 (1957).
6. J. C. MERTZ and C. H. MATHEWSON. Trans. Am. Inst. Mining Met. Engrs. **124**, 59 (1937).
7. W. B. PEARSON. Handbook of lattice spacing and structures of metals and alloys. Pergamon. 1958.
8. K. PADĚRA. Rozpravy České Akad. **61** (4), 22 (1951); Structure Reports, **16**, 23 (1952).
9. M. A. PEACOCK. X-Ray Powder Data File, Card 9-429.
10. R. D. HEYDING and L. D. CALVERT. Can. J. Chem. **35**, 1205 (1957).
11. U. FURST and F. HALLA. Z. physik. Chem. (Leipzig), B, **40**, 285 (1938).
12. C. PALACHE, H. BERMAN, and C. FRONDEL. Dana's system of mineralogy. Vol. 1. 7th ed. John Wiley & Sons. 1952. p. 170 et seq.

Can. J. Chem. Downloaded from www.nrcresearchpress.com by 210.87.254.5 on 09/05/12
For personal use only.

Can. J. Chem. Downloaded from www.nrcresearchpress.com by 210.87.254.6 on 09/05/12
For personal use only.

A METHOD FOR ADIABATIC COMPRESSION OF GASES UNDER CONTROLLED CONDITIONS[1]

G. D. GRAHAM[2] AND O. MAASS[3]

ABSTRACT

A preliminary account is given of an experimental technique by means of which the specific heats of gases may be measured at high temperatures and pressures. With the transducer employed consistent results were obtained up to 7000 p.s.i. and it is proposed to incorporate a transducer having a much higher pressure range where it is estimated that temperatures up to 10,000° K can be recorded.

INTRODUCTION

In a number of research directions it is of considerable interest to determine the properties of gases at high temperatures. In this paper an experimental procedure is described where the ratio of specific heats can be determined at temperatures above 1000° K.

This paper must be considered as a preliminary one in which the method of approach is described in some detail, and where measurements have been carried out as yet only to the relatively low temperature of 3000° K. By using the term low temperature it is implied that with the incorporation of a transducer which is adaptable to higher pressure measurements than the one used so far it is hoped that it will be possible to get useful information up to temperatures at least as high as 10,000° K. The procedure to be described involves the application of a high pressure impinging on one end of a double-headed piston which causes the other piston head to compress the gas under examination suddenly and under controlled conditions.

To make this possible the use of a double diaphragm is incorporated. This can be ruptured in such a way by an impinging pressure which exerts its full force on the upper piston head. This makes it possible to have an immediate and controlled impinging pressure to a high degree of accuracy whereby insuring reproducible results.

To recapitulate, the device to be described enables one to compress a gas to a predetermined volume with a high degree of accuracy and in a small fraction of a second.

The incorporation of a transducer which is adaptable to higher pressure measurements involving higher temperatures should make it possible to approach the main objective, namely to go to the high temperature mentioned above. This is under immediate consideration but it is thought that publication of the experimental procedure is warranted.

Before going on to a description of what has been accomplished so far, it may be pointed out that a transducer has been procured which will enable pressure measurements to be made up to 150,000 p.s.i. It is claimed by the manufacturer that this transducer can make reproducible measurements at this pressure but has been found to give non-reproducible results in the range below 10,000 p.s.i.

EXPERIMENTAL

The experimental procedure which is to be described may seem somewhat complicated and it is to be hoped that the diagrammatic sketch of the apparatus (Fig. 1) may help to elucidate this.

[1]*Manuscript received July 18, 1960.*
Contribution from the Division of Pure Chemistry, National Research Council, Ottawa, Canada. Issued as N.R.C. No. 6051.
[2]*Present address: National Aeronautical Establishment.*
[3]*Present address: Department of Chemistry, McGill University, Montreal, Que.*

Can. J. Chem. Downloaded from www.nrcresearchpress.com by 210.87.254.6 on 09/05/12
For personal use only.

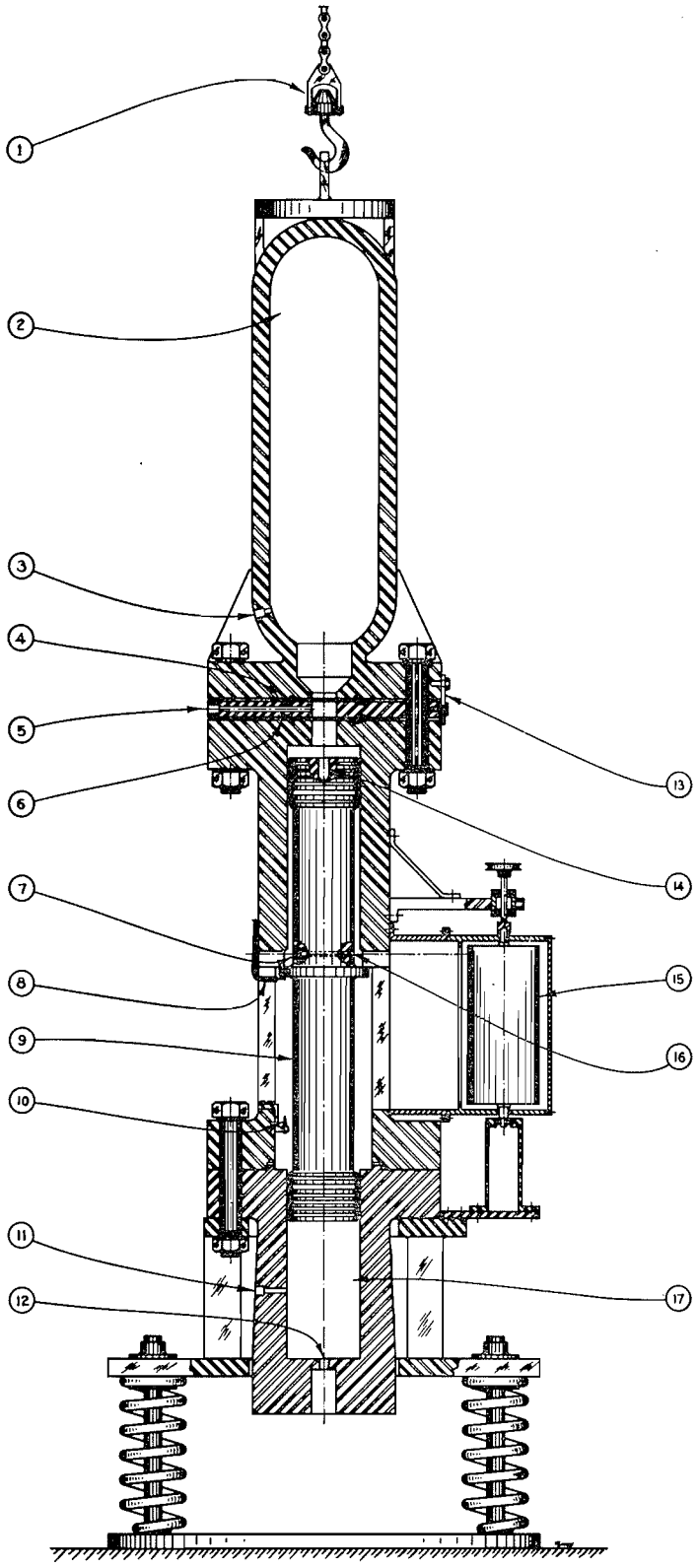


FIG. 1.

A gas of known volume is to be compressed suddenly and this to be done under controlled conditions in such a small fraction of time that adiabatic conditions prevail. This will be described under Apparatus, Measurements, and Procedure.

APPARATUS

The entire apparatus is mounted on eight automobile springs (Fig. 1). The gas under examination is contained in compression chamber (17)* which may be evacuated and filled through inlet (11). The chamber was forged from stainless steel No. 410 and was designed to withstand pressures of at least 150,000 p.s.i. The internal dimensions are 6 in. diameter and 16 in. high with a surface finish of 32 microns. In the bottom of the chamber is a threaded cavity (12) into which a suitable transducer can be flush mounted.

The double-headed piston (9) is of forged aluminum alloy weighing approximately 100 pounds and is fitted at both ends with five aircraft piston rings. Although the rings were fitted so as to have zero gap, as an added precaution against leakage, a rubber "O" ring was fitted to the bottom end in place of one of the piston rings. At its middle as shown in Fig. 1 the piston is flanged; this acts as a stop when the piston is raised into firing position and as a reference point in volume measurements. To facilitate dismantling and assembling there is a threaded hole (14) in the upper end of the piston into which a hoisting device may be inserted.

The upper end of the piston travels in a cylinder which was forged from stainless steel No. 410. To enable volume measurements to be carried out two openings were cut on opposite sides in the lower half of this cylinder. Both the compression chamber and cylinder are held securely together by means of sixteen 1 in. diameter bolts.

The air reservoir (2), which has a volume of 2 cubic feet, contains the propelling gas and is filled through inlet (3) from compressed air cylinders. This reservoir pressure is later on referred to as the impinging pressure.

Between the cylinder and air reservoir the firing assembly is located. This consists of two identical brass disks separated by a 1-in. thick, washer-shaped, steel plate. The volume so formed between the disks is known as the compensating chamber and has a volume of approximately 50 cc which is insignificant to the volume pressure changes which take place. Compressed air may be fed into this chamber through inlet (5). To insure a rigid and leakproof seal, "O" rings (6) are situated on both faces of each disk. The air reservoir, firing assembly, and cylinder are fastened together with sixteen 1 in. diameter bolts. Either disk will burst instantaneously if subjected to a force somewhat above its breaking pressure. Knowing the approximate breaking pressure of the disks, it is possible to contain a pressure in the air reservoir greater than the breaking pressure of the upper disk by admitting a balancing pressure to the compensating chamber. For example, if the desired impinging pressure is 200 p.s.i. one would select disks having a breaking pressure of approximately 150 p.s.i. plus or minus 15 p.s.i. In this case the compensating chamber may be pressurized to 100 p.s.i. and concurrently the air reservoir to 200 p.s.i. without fear of rupture of either disk. Release of the compensating pressure by bleeding through a valve will result in the bursting of the upper disk whereupon the 200 p.s.i. pressure will burst the lower disk, thus exerting the full force of the impinging pressure on the piston. It may be pointed out here that it is important to know the impinging pressure accurately so as to be able to reproduce and vary these impinging pressures. If only one disk is used it would be almost impossible to reproduce the impinging pressure because such a disk might have a variation in its breaking pressure of

**Throughout the paper, numbers in parentheses refer to circled numbers in Fig. 1.*

Can. J. Chem. Downloaded from www.nrcresearchpress.com by 210.87.254.6 on 09/05/12
For personal use only.

possibly 20%. Furthermore in the investigation underway it was of considerable interest to be in a position to vary the impinging pressure by relatively small amounts. By having perfect metal disks that would break at say 95.0 p.s.i., 100.0 p.s.i., or 105.0 p.s.i. in a reproducible way enabling only one disk to be used would entail considerable cost in procuring such disks. With the double-disk procedure reproducible impinging pressures can be obtained at say 95 p.s.i., 100 p.s.i., or 105 p.s.i. or any other arbitrary pressure within small variations using the same sheet of foil from which the disks are cut. It also makes it possible to initiate the experiment with relative ease. The impinging pressure in the range used to date can be determined to within 0.5% by use of a pressure gauge with 1 p.s.i. per division markings.

MEASUREMENTS PROCEDURE

The maximum pressure attained in the initial compression is measured by means of a transducer. The choice of transducer is governed by the pressure range being investigated. For the work to date an Endevco No. 5000 piezoelectric gauge having a pressure range of 0 to 2500 p.s.i. has been used. The signal from the transducer is fed through a high-impedance (500-megohm) amplifier and then into a Hughes Memoscope Model No. 104. The peak height of the trace observed in the memoscope is measured by means of a cathetometer and from a previous calibration of the transducer this is converted to a pressure. A permanent record of the trace is obtained by photographing with a polaroid Land camera (see Fig. 2).

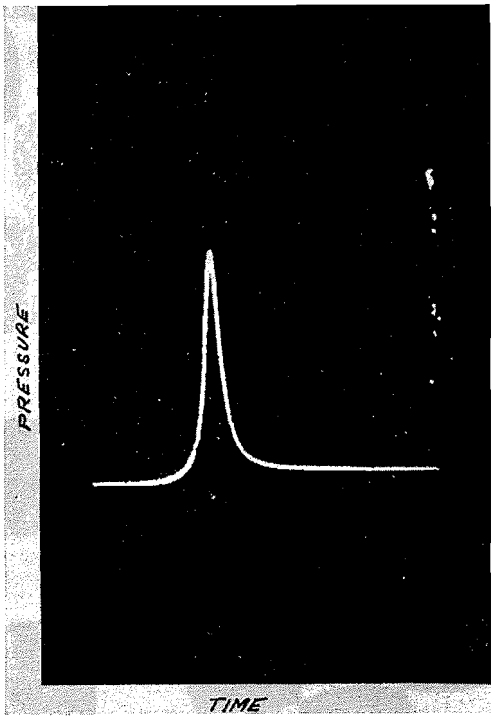


FIG. 2.

The volume at maximum pressure is measured by means of a small lead pyramid (10) which is attached by means of a screw to a small platform. When the piston is propelled downward the flange on the piston body strikes the lead. The depression of the lead is

Can. J. Chem. Downloaded from www.nrcresearchpress.com by 210.87.254.6 on 09/05/12
For personal use only.

then measured and the volume calculated. The accuracy of these volume measurements were confirmed by placing a lead pyramid directly under the piston during a run. This pyramid was then measured and it was found that the calculated volume based on the measurement of the outside pyramid was in agreement within 0.1%.

The drum camera (15), which records the oscillations of the piston, is mounted on the side of the apparatus at one of the openings. A variable speed motor drives the drum at any desired speed and by means of a zirconium arc lamp (7) inserted in the piston a light beam is pinpointed on the camera through lens (16). A manually operated shutter is opened just before the piston is propelled and closed after the oscillations have ceased. In Fig. 3 a photographic copy of a typical drum camera trace is shown. It is believed that considerable data can be obtained from such a trace.

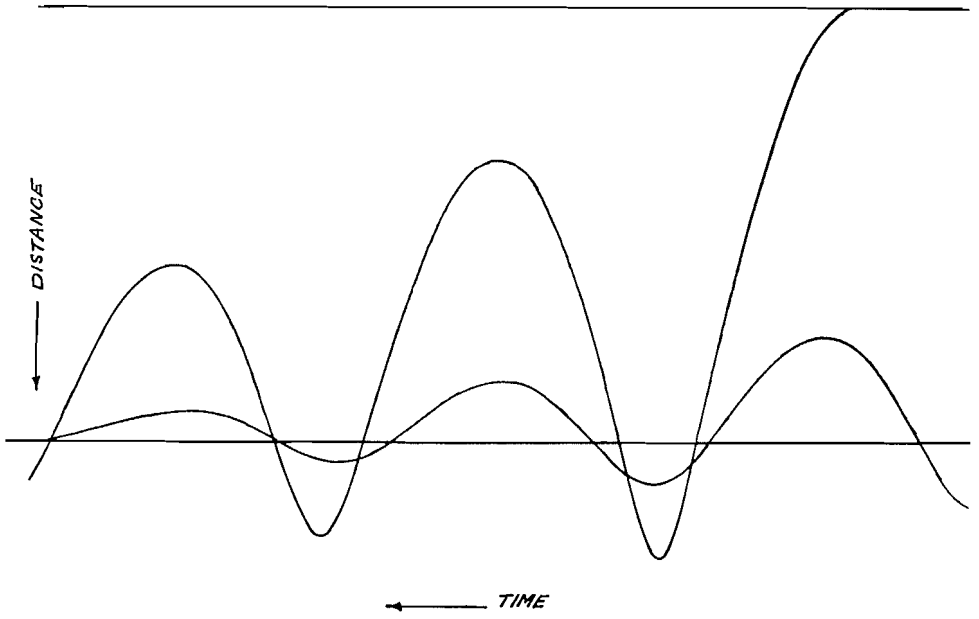


FIG. 3.

PROCEDURE

In Fig. 1 the apparatus is shown ready for an experiment. The propelling gas is fed into the cylinder and at the same time into the compensating chamber between the shims through inlet (5). When the desired pressures have been reached the valves are closed. The shutter on the drum camera (15) is opened and the compensating pressure is bled off through inlet (5). The disks break, as explained above, propelling the piston downward compressing the gas under observation in compression chamber (17). As the piston starts to move down it triggers the memoscope sweep by means of trigger (8).

To reload for the next experiment the piston is raised by opening inlet (11) and evacuating the reservoir above the piston. The bolts holding the upper sections are loosened and hooks (13) (there are three hooks spaced 120° apart) are set in place. By means of hoist (1) the air reservoir and steel plate are raised enabling the lower brass shim (6) to be replaced. The hoist is then lowered and the three hooks removed. The air reservoir is now hoisted alone and the upper shim (4) replaced. The air reservoir is again lowered and

Can. J. Chem. Downloaded from www.nrcresearchpress.com by 210.87.254.6 on 09/05/12
For personal use only.

the bolts tightened. The drum camera is reloaded and the lead volume indicator replaced. The piston is then held securely in position (by means of a wooden block placed between the piston flange and the lower edge of the opening) and the compression chamber (17) is evacuated. The gas under test is then fed into the chamber at atmospheric pressure and inlet (11) is closed. The wooden block holding the piston is removed and the apparatus is now ready for another experiment.

RESULTS

It is recognized that using ideal gas laws to make any calculations is not justified; nevertheless to make certain approximations is a reasonable approach. Having done this the following data is tabulated in Table I. The results of many experiments are summarized

TABLE I

Gas	Impinging pressure, p.s.i.	Temperature, °K	Pressure, p.s.i.	Ratio specific heats
Argon	140	1690	1280	1.630
	150	1790	1470	1.632
	170	1930	1984	1.634
	200	2000	2572	1.610
	450	3100	7203	1.603
Nitrogen	100	600	397	1.270
	110	675	544	1.290
	150	850	911	1.320
	190	1380	985	1.344
	200	1450	1029	1.354
Carbon dioxide	100	650	1411	1.203
	130	700	1500	1.224
	150	875	2675	1.258
	180	1000	4778	1.305
	200	1325	5880	1.327

as far as argon is concerned and the wide pressure and temperature range show how constant the specific heats remain. The results for nitrogen and carbon dioxide are consistent.

None of the results tabulated should be taken as establishing data which approach the accuracy of those previously established by others. It may be stated again that the purpose of this paper is to describe an experimental technique which is useful for exploring a higher-temperature region which has not yet been adequately explored.

REMARKS

There are a number of side issues for which this equipment can be usefully employed because a relatively large (5 liters) initial volume of gas can be used.

For example, it can be used to compress adiabatically a gas which undergoes chemical decomposition at high temperatures and under controlled conditions. The resulting products can be withdrawn for analysis and, as can be readily seen, a wide range of temperatures can be covered.

Can. J. Chem. Downloaded from www.nrcresearchpress.com by 210.87.254.6 on 09/05/12
For personal use only.

Can. J. Chem. Downloaded from www.nrcresearchpress.com by 210.87.254.105 on 09/05/12
For personal use only.

THE DETERMINATION OF ZIRCONIUM WITH BENZOYLPHENYLHYDROXYLAMINE[1]

D. E. RYAN

ABSTRACT

Zirconium is completely precipitated by benzoylphenylhydroxylamine from 0.5 *N* acid solutions. The complex formed in sulphuric acid solutions has a constant composition, $Zr(C_{13}H_{10}O_2N)_4$, and is used for the direct weighing of zirconium; the factor is 0.0970. The product precipitated from hydrochloric acid solutions must be ignited to the oxide. The reaction is sensitive, 1 p.p.m. of zirconium being detectable, and quantitative determination of 0.2 mg is possible. Thorium and the rare earths do not interfere.

INTRODUCTION

Benzoylphenylhydroxylamine (BPHA),* where the benzoyl group has replaced the nitroso group in cupferron, has become an important reagent in the past 10 years. It has been used for the determination of iron, copper, aluminum, and titanium (1); for tin (2); for vanadium (3, 4); and for tantalum and niobium (5, 6, 7). It is recommended as superior to cupferron, when applicable, because it is more sensitive to hydrogen ion concentration, is much more stable to heat and light, and forms complexes that can, in some instances, be dried at 110° C (1, 2). BPHA has been stated to form a complex of definite composition with zirconium (8) that does not decompose at 110° C. Since only a few reagents, from the many precipitants available for zirconium, are suitable for direct weighing and as BPHA yields no precipitates with thorium or trivalent rare earths in acid solution, a detailed investigation into its possibilities for the determination of zirconium was considered worth while.

EXPERIMENTAL

From hydrochloric acid solutions of zirconium a flocculent white precipitate is obtained on adding a solution of BPHA; the precipitate becomes granular on digestion upon the steam bath and filters easily. No zirconium was detected by alizarin in filtrates from solutions containing 5% of concentrated hydrochloric acid. Under these conditions the following ions are not precipitated by the reagent: Cu^{++}, Al^{+++}, Bi^{+++}, Cd^{++}, Cr^{+++}, Pb^{++}, Mg^{++}, Mn^{++}, Ni^{++}, Zn^{++}, UO_2^{++}, Th^{++++}, Y^{+++}, Ce^{+++}, Sm^{+++}, La^{+++}, Pr^{+++}, Gd^{+++}, Nd^{+++}, and Dy^{+++}. The soluble 1:1 purple complex (9) is formed in ferric iron solutions whereas tin, vanadium V, cerium IV, and titanium react to give the usual precipitates.

Zirconium is readily precipitated by BPHA in sulphate solutions and precipitation is quantitative in 0.5 *N* sulphuric acid. BPHA fails to precipitate zirconium from solutions containing fluoride.

The compound precipitated from sulphate solutions contains, found after drying at 110° C and ignition to the oxide, 9.71% zirconium. $(C_{13}H_{11}O_2N)_4Zr$, in which four molecules of BPHA are combined with one atom of zirconium, has a zirconium content of 9.70%. This complex is stable to several hours' drying at 130° C but at 160° C some decomposition occurs, the compound becoming buff rather than white in color.

[1]*Manuscript received June 15, 1960.*
Contribution from the Department of Chemistry, Dalhousie University, Halifax, Nova Scotia, with financial assistance from the National Research Council, Ottawa, Canada.
**Hereafter designated by BPHA.*

Reagents

N-*Benzoylphenylhydroxylamine.*—The reagent was prepared as previously described (2) and recrystallized from hot water; the compound can be purchased from leading chemical supply houses. A solution was prepared by dissolving 4 g in 100 ml of 95% ethyl alcohol.

Standard zirconium solutions.—The zirconium solutions were prepared from Matthey specpure zirconium oxychloride and zirconium sulphate. The chloride solutions, even in 5% hydrochloric acid, were found to be unstable over a convenient period of time and fresh solutions were prepared for each series of determinations. The sulphate solutions, in 2% sulphuric acid, caused no such difficulty. The zirconium content was determined gravimetrically by means of cupferron and mandelic acid.

Procedure

1. Ignition to the Oxide

Varying amounts of acid were added to samples of the zirconium standards and the solutions diluted to 150–200 ml. Reagent, in excess of the theoretical quantity required for the zirconium present, was added and the solutions digested for half an hour on the steam bath. After the samples were cooled to room temperature, they were filtered through Whatman No. 42 filter paper, washed with a saturated aqueous reagent solution, and ignited to the oxide. The results are shown in Table I.

TABLE I

Precipitation of zirconium by benzoylphenylhydroxylamine and subsequent weighing as the oxide

No.	Zr taken, mg	Zr found, mg	Conditions
1	2.70*	2.72	Solution 1% in concentrated HCl
2	2.70*	2.75	Solution 3% in concentrated HCl
3	2.70*	2.71	Solution 5% in concentrated HCl
4	2.70*	2.36	Solution 7% in concentrated HCl
5	8.42	8.42	Solution 5% in concentrated HCl
6	11.55	11.55	"
7	11.55	11.53	"
8	17.90	17.90	"
9	21.80	21.75	"
10	8.42	8.42	Solution 1.5% in concentrated H_2SO_4
11	8.42	8.31	Solution 2% in concentrated H_2SO_4
12	8.42	5.45	Solution 5% in concentrated H_2SO_4
13	8.42	5.50	Solution 10% in concentrated HCl
14	8.42	8.41	As sample No. 5 but 10 mg Th present
15	8.42	8.45	As sample No. 5 but 50 mg Th present
16	8.42	8.44	As sample No. 5 but 70 mg rare earths present
17	8.42	8.51	As sample No. 5 but 10 mg Ce^{++++} present reduced with H_2O_2
18	8.42	8.54	As sample No. 5 but 10 mg Ti^{++++} present complexed with H_2O_2

*These results were obtained independently by a member of this laboratory.

These results show that precipitation of zirconium by BPHA is quantitative in solutions containing up to 5% of concentrated hydrochloric acid and 1.5% of concentrated sulphuric acid (approximately 0.5 to 0.6 *N* in hydrogen ions); precipitation is incomplete at higher acidities. Thorium and the trivalent rare earths do not interfere. The interference of titanic and ceric ions is largely removed in one precipitation by complexing the titanium or reducing the cerium with hydrogen peroxide.

Attempts to remove interference of quinquevalent vanadium by complexing with hydrogen peroxide were unsuccessful; the result obtained for 8.42 mg of zirconium taken

Can. J. Chem. Downloaded from www.nrcresearchpress.com by 210.87.254.105 on 09/05/12
For personal use only.

was 9.91 mg in the presence of 10 mg of vanadium. In the presence of 20 mg of iron, the result was 0.5 mg higher than for the 8.42 mg of zirconium taken on a single precipitation.

THE DIRECT WEIGHING OF ZIRCONIUM COMPLEXES

Complexes that are capable of direct weighing eliminate the necessity of ignition to an oxide and permit, by virtue of their favorable factor, smaller quantities of metal ions to be determined more accurately. For zirconium, where one must invariably consider hafnium and its similar chemical behavior, there is the additional advantage that formation of such complexes permits the ready determination of the hafnium-to-zirconium ratio.

Of the many precipitants available for zirconium only 8-hydroxyquinoline, mandelic acid and its derivatives, and, more recently, tartrazine have been recommended as forming precipitates suitable for direct weighing. Balanescu (10) found that zirconium precipitates with 8-hydroxyquinoline could be dried at 140° C if precipitated from nitrate solutions buffered with acetate; precipitates varying in composition were obtained in chloride solutions.

There has been some disagreement regarding the mandelic acid derivatives. Oesper and Klingenberg (11) claimed good results on drying at 110° C for the *p*-bromo derivative whereas Belcher *et al.* (12) stated that consistent but low results were found with this same compound. Astanina and Ostroumov (13) found that mandelic acid gave zirconium precipitates that could be dried at 110° provided the final solutions were 20% by volume in concentrated hydrochloric acid; Hahn and Baginsky (14) reported also that complexes of constant composition were precipitated by mandelic acid from strong hydrochloric acid solutions and stated that low results in less acid solutions were due to basic salts; similar results have been found in this laboratory.

Tartrazine (15) has been recently recommended for the direct weighing of zirconium. The zirconium is precipitated at 80° C from chloride or nitrate solutions at pH 1; the factor used was for a compound with the formula Zr_3 (tartrazine)$(OOH)_3$. In view of the ease of hydrolysis of zirconium solutions and the failure to obtain precipitates of constant composition by well-known reagents under these conditions, further confirmation on the usefulness of this reagent is necessary.

The zirconium precipitates obtained with benzoylphenylhydroxylamine from 5% hydrochloric acid solutions are stable but are not of a constant composition; as expected, compounds precipitated from chloride solutions of zirconium at this acidity are not suitable for direct weighing. From sulphuric acid solutions, however, complexes having the composition $(C_{13}H_{11}O_2N)_4Zr$ are obtained and precipitation is complete at acidities up to 0.5 *N*; apparently the sulphate complexes of zirconium prevent the formation of unwelcome basic salts and permit compounds of unvarying composition to be precipitated. Mandelic acid, used subsequently in these solutions, gives also zirconium complexes suitable for direct weighing.

Procedure

2. Direct Weighing of Zirconium Complex with Benzoylphenylhydroxylamine

Samples of zirconium sulphate standard solution were diluted to 100–150 ml and the solutions made not more than 0.5 *N* in sulphuric acid. Reagent, in slight excess (not more than 40 mg for every 100 ml of solution) of the theoretical quantity required for the zirconium present, was added dropwise with stirring and the solutions digested on the steam bath for an hour. The samples, after cooling, were filtered through porous-

Can. J. Chem. Downloaded from www.nrcresearchpress.com by 210.87.254.105 on 09/05/12
For personal use only.

based porcelain crucibles and washed with cold water. The precipitates were then washed with two or three 5-ml aliquots of hot water (80° C) and dried at 110° C. The weight of the complex was multiplied by the theoretical factor 0.0970 to obtain the weight of zirconium. Results are shown in Table II.

TABLE II

Direct weighing of zirconium complex with benzoylphenylhydroxylamine

No.	Zr taken, mg	Zr found, mg	Remarks
1	8.38	8.36	—
2	8.41	8.42	—
3	8.41	8.41	—
4	8.41	8.45	—
5	8.41	8.38	Solution 0.7 *N* in H_2SO_4; 7.84 mg found after usual digestion period but an additional 0.54 mg precipitated from filtrate after standing overnight
6	16.76	16.75	—
7	16.82	16.85	—
8	25.23	25.23	—
9	0.85	0.70	Solution volume 50 ml; usual digestion period before filtering
10	0.51	0.51	As sample No. 9 but digested overnight
11	0.17	0.15	As sample No. 9 but digested overnight

The results show that benzoylphenylhydroxylamine is a suitable reagent for the direct weighing of zirconium when applied to dilute sulphuric acid solutions. Complete precipitation of the zirconium is possible from 0.7 *N* H_2SO_4 solutions, but at acidities greater than 0.5 *N* an overlong digestion period is necessary. Results 9, 10, and 11 show that a prolonged digestion period is required for solutions containing very small amounts of zirconium.

From 5% hydrochloric acid, although precipitation is complete, the weights of complex obtained are low and the compositions vary with the amount of zirconium present in solution; for 8.42 mg of zirconium, in one instance, the weight of complex found was 0.0845 g (theoretical 0.0868) and for 21.05 mg of zirconium was 0.2063 g (theoretical 0.2170). Since degree of hydrolysis in zirconium solutions is dependent on time, temperature, and acid present, these results are undoubtedly due to simultaneous precipitation of varying amounts of basic salts; a distinct cloudiness, for example, develops on heating 5% hydrochloric acid solutions of zirconium oxychloride for less than an hour on the hot plate.

From sulphuric acid solutions, zirconium complexes suitable for direct weighing are also precipitated by mandelic acid. A typical result obtained for 8.41 mg taken was 8.42 mg, the weight of mandelic acid complex (precipitated from 0.5 *N* sulphuric acid solution) being 0.0643 g.

Mandelic acid and its derivatives, although undoubtedly the most useful of the organic reagents used for zirconium, have been criticized (16) because of their non-sensitivity and the large amounts of reagent thus required for each precipitation. It is worth while noting, therefore, that benzoylphenylhydroxylamine detects as little as 0.1 mg of zirconium in 100 ml of solution and quantitative precipitation of 0.2 mg is possible.

This work was carried out at the Imperial College of Science and Technology, London, England, and was supported by a travel grant from the National Research Council.

Can. J. Chem. Downloaded from www.nrcresearchpress.com by 210.87.254.105 on 09/05/12
For personal use only.

REFERENCES

1. S. C. SHOME. Analyst, **75**, 27 (1950).
2. D. E. RYAN and G. D. LUTWICK. Can. J. Chem. **31**, 9 (1953).
3. S. C. SHOME. Anal. Chem. **23**, 1186 (1951).
4. D. E. RYAN. Analyst, **85**, 569 (1960).
5. R. W. MOSHIER and J. E. SCHWARBERG. Anal. Chem. **29**, 947 (1957).
6. A. K. MAJUMDAR and A. K. MUKHERJEE. Anal. Chim. Acta, **19**, 23 (1958).
7. F. J. LANGMHYR and T. HONGSLO. Anal. Chim. Acta, **22**, 301 (1960).
8. G. D. LUTWICK and D. E. RYAN. Can. J. Chem. **32**, 949 (1954).
9. C. A. ARMOUR and D. E. RYAN. Can. J. Chem. **35**, 1454 (1957).
10. G. BALANESCU. Z. anal. Chem. **101**, 101 (1935).
11. R. E. OESPER and J. J. KLINGENBERG. Anal. Chem. **21**, 1509 (1949).
12. R. BELCHER, A. SYKES, and J. C. TATLOW. Anal. Chim. Acta, **10**, 34 (1954).
13. A. A. ASTANINA, and E. A. OSTROUMOV. J. Anal. Chem. U.S.S.R. **6**, 27 (1951).
14. R. B. HAHN and E. S. BAGINSKY. Anal. Chim. Acta, **14**, 45 (1956).
15. GH. BAIULESCU and L. TURCU. Anal. Chim. Acta, **21**, 33 (1959).
16. P. S. MARTY and BH. S. V. R. RAO. Z. anal. Chem. **141**, 93 (1954).

Can. J. Chem. Downloaded from www.nrcresearchpress.com by 210.87.254.105 on 09/05/12
For personal use only.

Can. J. Chem. Downloaded from www.nrcresearchpress.com by 210.87.254.42 on 09/05/12
For personal use only.

THE APPLICATION OF THE HAMMETT EQUATION TO ORTHO-SUBSTITUTED BENZENE REACTION SERIES[1]

MARVIN CHARTON

ABSTRACT

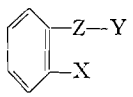
The Hammett equation is directly applicable to ortho-substituted benzene reaction series in which reaction site and benzene ring are separated by some group Z, apparently due to the absence of steric effects in these series. The σ_p values are used in the correlations. Fourteen ortho-substituted benzene reaction series have been correlated. The electrical effect of a substituent in the ortho position is found to be about 0.75 times its effect in the para position. The effect of the side-chain Z in the transmission of substituent effects is $OCH_2 > SCH_2 > CH{=}CH > SeCH_2 > CH_2CH_2$.

INTRODUCTION

Linear free-energy relationships have been shown to be of great value for the correlation of reaction rates, equilibria, and physical properties with variations in structure. The Hammett equation,

$$\log(K_X/K_H) = \rho\sigma_X, \qquad [1]$$

has been widely applied to meta- and para-substituted benzene reaction series (2, 3) and to olefins (4, 5) and acetylenes (6). In modified form, it has been applied to aliphatic and to ortho-substituted benzene reaction series (7). Direct application of the Hammett equation to ortho-substituted benzene derivatives is unsuccessful, due to steric effects. Taft (7) has been able to correlate a few ortho-substituted benzene reaction series by an approach which is dependent upon the elimination of the steric effect in the evaluation of the substituent constants. Mammalis and Rydon (8) have suggested that substituent constants for ortho substituents be defined from reaction series in which the reaction site is not adjacent to the substituent. It has been suggested by a number of authors that the inductive and resonance effects of an ortho substituent are similar to those of the same substituent in the para position. It is of interest to compare the σ_o^* substituent constants obtained by Taft (7), by elimination of steric effects, with the σ_p substituent constants. Considering the degree of uncertainty in the values of substituent constants, they are almost identical. These results suggested the possibility of direct application of the Hammett equation, using the σ_p substituent constants, to ortho-substituted benzene reaction series in which the reaction site is not directly attached to the ring (I). As the reaction site and substituent are not adjacent in such reaction series, hydrogen bonding and other secondary bonding interactions between them cannot occur, and no hindrance to the attack of reagent should exist. The literature was searched for reaction series of this type. Fourteen such reaction series have been examined, seven involving equilibrium data and seven involving rate data. The correlations were made by the method described by Jaffé.



(I)

[1]*Manuscript received March 28, 1960.*
Contribution from the Department of Chemistry, Pratt Institute, Brooklyn 5, New York.

RESULTS AND DISCUSSION

Data and Correlations

The data used in the correlations are given in Table I. The substituent constants used are those given by Jaffé (3) and by McDaniel and Brown (9) except for the carbomethoxy group, which was taken from Charton and Meislich (4). A statistical factor of 1/2 was used in reaction series 12 for methyl phthalate to account for the presence of two potential reaction sites. The results of the correlation are shown in Table II; Figs. 1 and 2 are typical curves.

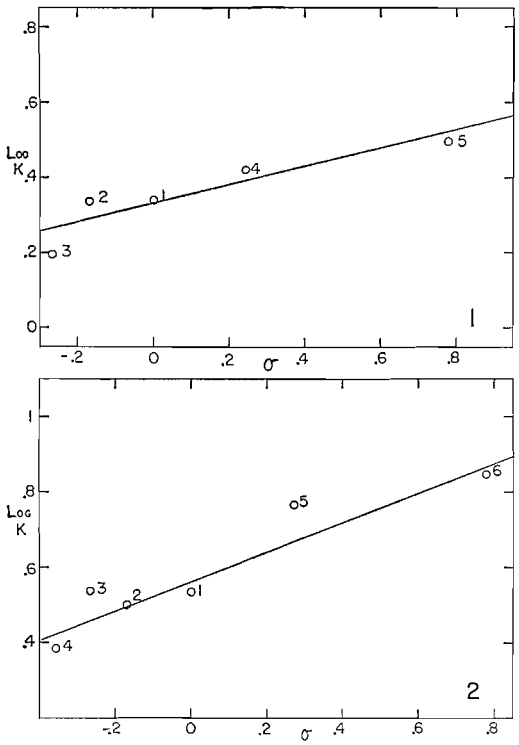


FIG. 1. Hammett equation plot of log $10^5 K$ vs. σ for 3-(2′-substituted)phenyl propanoic acids. The substituents are: 1, H; 2, Me; 3, MeO; 4, Cl; 5, NO_2.

FIG. 2. Hammett equation plot of log $10^5 K$ vs. σ for *trans*-2-substituted cinnamic acids. The substituents are: 1, H; 2, Me; 3, OMe; 4, OH; 5, Cl; 6, NO_2.

The results of the correlations are as good as those generally obtained for meta- and para-substituted benzene reaction series. Of the 14 reaction series examined, six show fair correlation ($0.90 \leqq r \leqq 0.95$), five show good correlation ($0.95 \leqq r \leqq 0.99$), and three show excellent correlation ($0.99 \leqq r$), according to the empirical scale proposed by Jaffé (3, 18). Jaffé (3) has pointed out that the correlation coefficients decrease with decreasing absolute values of ρ. Of the six reaction series which had fair correlation, the value of ρ_0 (19) was less than 0.400 in five (20).

Structural Requirements for Correlation

Apparently, the side-chain Z must consist of at least two atoms, for satisfactory correlation to result. No satisfactory correlation is obtained in the case of the ionization constants of 2-substituted phenylacetic acids, however, although the available data (for

Can. J. Chem. Downloaded from www.nrcresearchpress.com by 210.87.254.42 on 09/05/12
For personal use only.

X = H, Cl, Br, I, NO_2) is insufficient to support a conclusive statement. Examination of the Stuart–Briegleb models for this reaction series, and for others in which the side chain is a methylene group indicates the possibility of considerable interaction between the substituent and the reaction site.

TABLE I

Rate and equilibrium data

1. Ionization constants of 3-(2-substituted)phenyl propanoic acids in water at 25° C

Subst.	H	Me	MeO	Cl	NO_2	Ref.
$10^5 K$	2.19	2.17	1.57	2.65	3.13	10*a*, 10*b*

2. Ionization constants of *trans*-2-substituted cinnamic acids in water at 25° C

Subst.	H	Me	MeO	OH	Cl	NO_2	Ref.
$10^5 K$	3.65	3.165	3.45	2.44	5.83	7.07	10*c*

3. Ionization constants of 2-substituted propiolic acids in 35% dioxane–water at 25° C

Subst.	H	Cl	NO_2	OMe	Ref.
$10^4 K$	5.8	8.3	15.0	4.3	11

4. Ionization constants of 2-substituted phenoxyacetic acids in water

Subst.	MeO	Me	Cl	NO_2	Ref.
$10^4 K$	5.8	6.8	10.2	15.8	12

5. Ionization constants of 2-substituted phenylthioacetic acids in water

Subst.	MeO	Me	Cl	NO_2	Ref.
$10^4 K$	1.8	2.8	3.0	5.5	12

6. Ionization constants of 2-substituted phenylselenoacetic acids in water

Subst.	MeO	Me	Cl	NO_2	Ref.
$10^4 K$	1.4	1.5	2.3	3.2	12

7. Ionization constants of 2-substituted benzohydroxamic acids in 0.1 *M* KNO_3 at 30° C

Subst.	H	MeO	NH_2	Me_2N	NO_2	Ref.
$10^9 K$	15.9	12.6	10.0	8.91	63.1	13*a*

8. Rates of acid-catalyzed esterification of 2-substituted propiolic acids in methanol at 35° C

Subst.	H	Cl	NO_2	OMe	Ref.
$10^4 k$	5.3	4.8	4.1	7.3	11

9. Rates of acid-catalyzed esterification of 2-substituted propiolic acids in methanol at 35° C

Subst.	H	Cl	NO_2	OMe	Ref.
$10^4 k$	11.7	11.2	9.3	16.3	11

10. Rates of alkaline hydrolysis of 2-substituted cinnamic acid ethyl esters in 87.83% aqueous ethanol at 30° C

Subst.	H	OMe	F	Cl	Br	I	NO_2	Ref.
$10^2 k$	10.6	3.99	2.48	21.1	32.5	2.67	84.1	14*a*, 14*b*

11. Rates of reaction of 2-substituted benzohydroxamic acids with sarin in water at 30.5° C

Subst.	H	OMe	NH_2	Me_2N	NO_2	Ref.
k	2.61	21.1	35.3	37.5	7.4	13*a*

12. Rates of reaction of 2-substituted methyl benzoates with trimethylamine

Subst.	H	Me	Cl	CO_2Me	NO_2	Ref.
$10^2 k$	1.609	1.66	7.27	12.43	33	16

13. Rates of alkaline fission of 2-substituted benzoyloxymethyl dimethyl sulphinium iodides

Subst.	H	Me	OMe	Cl	NO_2	Ref.
k	356.5	314.1	291.1	673	1242	8

14. Rates of rearrangement of N-2-substituted benzyl-N-phenacyl-N,N-dimethyl quaternary ammonium halides at 16.4° C

Subst.	Me	OMe	Cl	Br	I	NO_2	Ref.
k	1.58	1.63	36.7	49.1	83.0	1070	15, 17

NOTE: Units of k are (*a*) l. mole^{-1} sec^{-1}; (*b*) l. mole^{-1} min^{-1}; (*c*) l. mole^{-1} hr^{-1}.

The Effect of Side Chain on Transmission of Substituent Effect

A comparison of the ρ_o values obtained from the correlation of ortho-substituted benzene reaction series with the ρ values for the corresponding meta- and/or para-substituted benzene reaction series may be used to determine variation in transmission

Can. J. Chem. Downloaded from www.nrcresearchpress.com by 210.87.254.42 on 09/05/12
For personal use only.

of substituent effects through different side chains. The ratio of the $\rho_{o,Z}$ value for some side-chain Z to that for the CH_2CH_2 side chain, ρ_{o,Z^0}, for a given reaction under identical reaction conditions, provides a method of making such comparisons (3). Those values of ρ, r, s, n, and $-\log K$ for the corresponding meta- and/or para-substituted reaction series which are available are given in Table II.

Thus,

$$[2] \qquad \rho_{oZ}/\rho_{oZ^0} = q_o, \qquad \rho_Z/\rho_{Z^0} = q.$$

Values of q_o obtained from reaction series 1, 2, 4, 5, and 6 are shown in Table II. The values for the OCH_2, SCH_2, and $SeCH_2$ groups are of about the same order of magnitude as that for the CH=CH group, and increase in order of increasing electronegativity of the group VI element. This might be explained in the case of the SCH_2 and $SeCH_2$ groups by hyperconjugation and an expansion of the S or Se valence shell from an octet to a decet, but such an explanation is, of course, not possible for the OCH_2 group, which exhibits the greatest transmission of the substituent effect.

The values of q for the corresponding meta- and/or para-substituted reaction series are also given in Table II. It is notable that although the distance between the reaction site and the substituent is greater for meta- and para-substituted compounds than it is for ortho-substituted compounds, it appears that the effect of the substituent is not transmitted to the reaction site to as great an extent in the ortho-substituted reaction series as it is in the meta- and para-substituted reaction series. Transmission through the side chain from the limited data available appears to be about 1.5 times as effective for meta- and para-substituted compounds as for ortho-substituted compounds. This might be due to some distortion of the bond angle in the ortho-substituted reaction series which decreases the overlap of the p orbitals in O, S, and Se, or the π orbital of the CH=CH group, with the π orbital of the ring.

The Magnitude of the Electrical Effect of an Ortho Substituent

In the absence of steric effects and secondary bonding,

$$[3] \qquad \sigma_{oX} = C\sigma_{pX}.$$

The correlations made in this paper have used the Hammett equation in the following form,

$$[4] \qquad \log(K_{oX}/K_H) = \rho_o\sigma_{pX}.$$

If the substituent constants for ortho substituents were available, then assuming steric effects are nonexistent, ortho-, meta-, and para-substituted benzene reaction series would be included in a single correlation with the same value for ρ. Thus

$$[5] \qquad \log(K_{o,m,p\ X}/K_H) = \rho\sigma_{o,m,p\ X}$$

or considering only ortho substitution,

$$[5a] \qquad \log(K_{oX}/K_H) = \rho\sigma_{oX}.$$

To a good first approximation, steric effects will not exist in ortho-substituted benzene reaction series of type I, and therefore use of equation 5*a* is justified for these reaction series. It is, of course, not applicable to ortho-substituted benzene reaction series in which the substituent and reaction site are directly attached to the ring.

Can. J. Chem. Downloaded from www.nrcresearchpress.com by 210.87.254.42 on 09/05/12
For personal use only.

TABLE II

Reaction series[a]	ρ_o[b]	r_o[c]	s_o[d]	$-\log K_{H_o}$	n_o[e]	ρ	r	s	n	$-\log K_H$ calc.	Ref.[f]	Z	q_o	q	q_o/q
1	0.243	0.905	0.055	4.669	5	0.212	0.979	0.016	8	4.551	3	CH_2CH_2	1	1	—
2	0.389	0.940	0.0661	4.413	6	0.466	0.977	0.040	9	4.447	3	CH=CH	1.60	2.20	1.38
3	0.524	0.997	0.019	3.223	4	—	—	—	7	—	11	—	—	—	—
4	0.408	0.994	0.0245	3.107	4	—	—	—	—	—	[g]	OCH_2	1.68	—	—
5	0.395	0.943	0.0824	3.576	4	0.561	0.922	0.139	5	1.644	[g]	SCH_2	1.63	2.65	1.63
6	0.351	0.990	0.0282	3.752	4	0.419	0.930	0.209	5	1.873	[g]	$SeCH_2$	1.44	1.98	1.38
7	0.576	0.977	0.0839	7.704	5	0.977	0.999	0.016	6	8.773	13*b*	—	—	—	—
8	−0.221	0.928	0.0485	3.239	4	−0.44	—	—	7	—	11	—	—	—	—
9	−0.211	0.924	0.0474	2.887	4	−0.44	—	—	7	—	11	—	—	—	—
10	1.211	0.941	0.153	0.911	7	1.329	0.996	0.046	15	2.752	3	—	—	—	—
11	−0.467	0.954	0.0986	−1.416	5	−0.762	0.996	0.035	6	−1.328	13*b*	—	—	—	—
12	1.394	0.955	0.185	1.634	5	—	—	—	—	—	—	—	—	—	—
13	0.636	0.984	0.0557	−1.968	5	0.768	0.987	0.050	—	—	8	—	—	—	—
14	2.376	0.962	0.266	2.823	6	—	—	—	—	—	—	—	—	—	—

[a]These numbers refer to Table I.
[b]The subscript "o" designates values for ortho-substituted reaction series, other values are for meta- and/or para-substituted reaction series.
[c]Correlation coefficient.
[d]Standard deviation.
[e]Number of compounds in series.
[f]References are for ρ, r, s, n, and log K_H calc. taken from the literature.
[g]Calculated from data of ref. 12.

Can. J. Chem. Downloaded from www.nrcresearchpress.com by 210.87.254.42 on 09/05/12
For personal use only.

From equations 2, 4, and 5*a*, equation 6 is obtained

$$C = \rho_o/\rho \qquad [6]$$

where C represents approximately the electrical effects of a substituent in the ortho position as compared with its electrical effects in the para position. Actually, C is subject to variations in ρ_o due to phenomena such as a bulk effect between the ortho substituent and the side-chain Z which may cause decreased orbital overlap in unsaturated side chains, and to variations in solvation as compared with meta- and para-substituted benzene reaction series. Values of C obtained from those reactions series for which both ρ_o and ρ are available are shown in Table II. Although the values of C vary considerably, they are all of the same order of magnitude, and in view of the uncertainties inherent in ρ values, the variation found is reasonable. The magnitude of $\bar{C}$ shows that the electrical effects of a substituent in the ortho and in the para positions are of the same order of magnitude.

TABLE III

Reaction series C		Reaction series C	
1	1.147	7	0.590
2	0.835	8	0.500
3	0.646	9	0.480
5	0.704	10	0.913
6	0.838	11	0.613
$\bar{C} = 0.736$		13	0.830

SUMMARY

On the basis of the above results, ortho-substituted benzene reaction series in which substituent and reaction site are not adjacent, can be correlated directly by the Hammett equation using the σ_p substituent constants. Ortho substituents in such reaction series have the same type of electrical effects as para substituents. These effects are about the same order of magnitude for ortho as for para substituents. Steric effects are largely absent for these reaction series.

REFERENCES

1. M. CHARTON. Abstracts, 134th Meeting of the American Chemical Society, Chicago, Ill. September, 1958. p. 9P.
2. L. P. HAMMETT. Physical organic chemistry. McGraw-Hill Book Co., Inc., New York. 1940. pp. 118–123, 173.
3. H. H. JAFFÉ. Chem. Revs. **53**, 191 (1953).
4. M. CHARTON and H. MEISLICH. J. Am. Chem. Soc. **80**, 5940 (1958).
5. M. CHARTON. Abstracts, 132nd Meeting of the American Chemical Society, New York. September, 1957. p. 78P.
6. M. CHARTON. Unpublished results.
7. R. W. TAFT. *In* Steric effects in organic chemistry. *Edited by* M. S. NEWMAN. John Wiley & Sons Inc., New York. 1957. p. 556.
8. P. MAMMALIS and H. N. RYDON. J. Chem. Soc. 1049 (1955).
9. D. H. MCDANIEL and H. C. BROWN. J. Org. Chem. **23**, 420 (1958).
10*a*. J. F. J. DIPPY and R. H. LEWIS. J. Chem. Soc. 1008 (1937).
10*b*. J. F. J. DIPPY and J. E. PAGE. J. Chem. Soc. 357 (1938).
10*c*. J. F. J. DIPPY and R. H. LEWIS. J. Chem. Soc. 1426 (1937).
11. M. S. NEWMAN and S. H. MERRILL. J. Am. Chem. Soc. 77, 5552 (1955).
12. O. BEHAGEL and M. ROLLMANN. Chem. Ber. **62**, 2693 (1929).
13*a*. M. A. STOLBERG and W. A. MOSHER. J. Am. Chem. Soc. **79**, 2618 (1957).
13*b*. R. SWIDLER, R. E. PLAPINGER, and G. M. STEINBERG. J. Am. Chem. Soc. **81**, 3271 (1959).
14*a*. K. KINDLER. Ann. **452**, 90 (1927).
14*b*. K. KINDLER. Ann, **464**, 278 (1928).
15. T. THOMSON and T. S. STEVENS. J. Chem Soc. 55 (1932)

Can. J. Chem. Downloaded from www.nrcresearchpress.com by 210.87.254.42 on 09/05/12
For personal use only.

16. L. P. HAMMETT and H. PFLUGER. J. Am. Chem. Soc. **55**, 4079 (1933).
17. T. THOMSON and T. S. STEVENS. J. Chem. Soc. 55 (1932), reported that 12–15% of a by-product which could not be further characterized was found in this reaction. They claimed to have developed an analytical method which allowed determination of both rearrangement products and unreacted starting material without interference from the by-product. For a further discussion of the results of these authors see J. H. BREWSTER and M. W. KLINE. J. Am. Chem. Soc. **74**, 5179 (1952).
18. It has also been suggested that for $r \geqslant 0.90$ correlation is very poor, for $r \geqslant 0.95$ correlation is fair.
19. ρ_o will be used to denote rho for the ortho-substituted benzene reaction series obtained by correlation with σ_p values. ρ will be used to denote rho for the meta- and/or para-substituted benzene reaction series obtained by correlation with the appropriate σ_m or σ_p constants.
20. One of the referees has pointed out that Wepster has shown one group ortho to a bulky substituent to be sufficient to appreciably decrease resonance interaction between the substituent and the benzene ring (B. M. WEPSTER. Progress in stereochemistry. Vol. II. Butterworth Scientific Publications, London. 1958. p. 99). This is a likely cause of the poorer results obtained in some of the correlations.

Can. J. Chem. Downloaded from www.nrcresearchpress.com by 210.87.254.42 on 09/05/12
For personal use only.

Can. J. Chem. Downloaded from www.nrcresearchpress.com by 210.87.254.5 on 09/05/12
For personal use only.

CONJUGATED FATTY ACIDS OF TRAGOPOGON AND CALENDULA SEED OILS[1]

MARY J. CHISHOLM AND C. Y. HOPKINS

ABSTRACT

The seed oil of *Tragopogon porrifolius* L. was found to contain about 4% of conjugated diene hydroxy fatty acids, identified as 9-hydroxy-10,12- and 13-hydroxy-9,11-octadecadienoic acids. On dehydration, the products were 8,10,12- and 9,11,13-octadecatrienoic acids. The diene acids were *cis,trans* or *trans,cis* and the triene acids were judged to be all-*trans*.

The conjugated triene acid of *Calendula officinalis* L. seed oil was isolated and identified as *trans*,8:*trans*,10:*cis*,12-octadecatrienoic acid by spectral analysis, by the structure of the maleic anhydride adduct, and by identification of degradation products. All-*trans*-8,10,12-octadecatrienoic acid was found to react with maleic anhydride at both the 8,11 and 10,13 positions.

INTRODUCTION

During the isolation of an epoxy fatty acid from the seed oil of *Tragopogon porrifolius* L. (family Compositae) (1) it was observed that a small proportion of an unsaturated acid of unusual characteristics was also present. It amounted to about 4% of the total fatty acids and had a conjugated diene linkage. On heating with glacial acetic acid it was converted to a conjugated triene acid. Both the diene and triene acids were unstable. Their structures were determined as described below, each proving to be a mixture of two position isomers.

The diene acids were found to have a hydroxy group and were identified as 9-hydroxy-10,12-octadecadienoic acid and 13-hydroxy-9,11-octadecadienoic acid. The triene acids were identified as 8,10,12- and 9,11,13-octadecatrienoic acids.

A naturally occurring triene acid was isolated from the seed oil of *Calendula officinalis* L. (family Compositae) and shown to be *trans*,8:*trans*,10:*cis*,12-octadecatrienoic acid. The isomerized form (all-*trans*) of this acid had been prepared previously by McLean and Clark from the same species (2). The configuration of the natural acid (*trans, trans,cis*) is opposite to that of α-eleostearic acid (*cis,trans,trans*).

Shortly after this work was completed, Morris, Holman, and Fontell reported the occurrence of two hydroxy diene acids in the seed oils of certain other species, apparently identical with the hydroxy acids described herein (3). Their evidence, based on spectral data and thin-layer chromatography, is in agreement with ours, which is based on spectral data and chemical degradative results. All of the results lead to the conclusion that the substances are 9-hydroxy-10,12- and 13-hydroxy-9,11-octadecadienoic acids.

RESULTS AND DISCUSSION

Conjugated Acids of Tragopogon Oil

The oil had ultraviolet absorption characteristic of diene conjugation, indicating the presence of about 4% of a diene acid, based on the total fatty acids. There was no appreciable triene absorption. After saponification in the cold and removal of unsaponifiable matter, the fatty acids were partitioned between petroleum ether and aqueous ethanol (1 volume H_2O: 4 volumes EtOH). The alcoholic portion contained both diene acid and epoxy acid in about equal amounts. Further partitioning and crystallization from acetone

[1]*Manuscript received September 1, 1960.*
Contribution from the Division of Pure Chemistry, National Research Council, Ottawa, Canada.
Issued as N.R.C. No. 6017.

at low temperature yielded a concentrate consisting mainly of conjugated diene acid (ultraviolet max. 233 mμ). It had infrared absorption at 3580 cm^{-1}, indicating an hydroxyl group, and two peaks of nearly equal intensity at 945 and 980 cm^{-1}, characteristic of a conjugated *cis,trans* or *trans,cis* diene (4).

The substance was subjected to oxidative splitting by periodate–permanganate (5) and the acidic products were converted to methyl esters, avoiding loss of volatile components (6). The mixture of methyl esters was examined by gas chromatography. Peaks corresponding to hexanoate and azelate were observed, indicating unsaturated centers at the 12,13 and 9,10 positions, respectively. Since these could not both be present in one conjugated diene acid, it is concluded that the substance was a mixture of two acids, one being $\Delta^{9,11}$ and the other $\Delta^{10,12}$. Neither heptanoic nor sebacic esters appeared, hence the hydroxyl group must have been attached to the terminal fragment in the 9,11 acid and to the carboxyl fragment in the 10,12 acid (III, I).

Boiling the hydroxy diene acid mixture with glacial acetic acid gave a solid acid (or acids), shown by spectral analysis to have a conjugated triene structure and no hydroxyl group. This substance absorbed 3 moles of hydrogen to give stearic acid, hence it had a straight chain of 18 carbon atoms. The triene acid was split by periodate–permanganate and the fragments were shown by gas chromatography to consist of valeric, hexanoic, suberic, and azelaic acids. The substance was therefore a mixture of two octadecatrienoic acids (II and IV) having double bonds in the 8,10,12 and 9,11,13 positions, respectively.

$$CH_3(CH_2)_4CH{=}CHCH{=}CHCH(CH_2)_7COOH \quad (I)$$
$$\qquad\qquad\qquad\qquad\quad \downarrow \qquad\quad |$$
$$\qquad\qquad\qquad\qquad\quad \downarrow \qquad\quad OH$$
$$CH_3(CH_2)_4CH{=}CHCH{=}CHCH{=}CH(CH_2)_6\,COOH \quad (II)$$
$$CH_3(CH_2)_4CHCH{=}CHCH{=}CH(CH_2)_7COOH \quad (III)$$
$$\qquad\qquad |\qquad\quad \downarrow$$
$$\qquad\quad OH \qquad\quad \downarrow$$
$$CH_3(CH_2)_3CH{=}CHCH{=}CHCH{=}CH(CH_2)_7COOH \quad (IV)$$

This result confirms the positions of the two double bonds in the diene acids as reported above (10,12 and 9,11). It also provides evidence for the location of the hydroxyl group. Thus, in the 10,12-diene acid, the hydroxyl group must be attached to carbon 8 or 9 to produce an 8,10,12-triene. Because of the ease with which dehydration takes place, it is almost certain that the hydroxyl is at position 9, where it is activated by the adjacent double bond (I). By similar reasoning, the 9,11-diene acid is considered to have the hydroxyl at position 13 (III), giving the 9,11,13-triene on dehydration. 9-Hydroxy-10,12-octadecadienoic is evidently a geometric isomer of dimorphecolic acid, discovered by Smith and co-workers (7), in which the double bonds are *trans,trans*, and which underwent dehydration with the same readiness.

Confirmation of the position of the hydroxyl group was obtained by hydrogenating the mixture of hydroxy diene acids. The product melted at 65–66° and appeared to be a mixture of monohydroxystearic acids. Oxidative splitting by solid permanganate in acetic acid was performed first on a model substance, 12-hydroxystearic acid. The fragments therefrom, identified by gas chromatography, were hexanoic, heptanoic, undecanedioic, and dodecanedioic acids. Thus splitting took place at two positions, 11,12 and 12,13. Minor proportions of azelaic and sebacic acids were also produced. Applying this procedure to the hydrogenated acids gave four monobasic acids, pentanoic, hexanoic, nonanoic, and decanoic (Table I), hence the original hydroxyl group must have been on the 13th

Can. J. Chem. Downloaded from www.nrcresearchpress.com by 210.87.254.5 on 09/05/12
For personal use only.

TABLE I

Oxidative splitting of hydrogenated acids

$CH_3(CH_2)_4\underset{\underset{OH}{\vert}}{CH}(CH_2)_{11}COOH \xrightarrow{O}$	$CH_3(CH_2)_3COOH$	$HOOC(CH_2)_{11}COOH$
	$CH_3(CH_2)_4COOH$	$HOOC(CH_2)_{10}COOH$
$CH_3(CH_2)_8\underset{\underset{OH}{\vert}}{CH}(CH_2)_7COOH \xrightarrow{O}$	$CH_3(CH_2)_7COOH$	$HOOC(CH_2)_7COOH$
	$CH_3(CH_2)_8COOH$	$HOOC(CH_2)_6COOH$

carbon atom in one acid (III) and on the 9th carbon atom in the other (I). There were minor amounts of heptanoic and octanoic acids. One pair of the corresponding dibasic acids was identified, viz. suberic and azelaic, both in substantial amount. The C_{12} and C_{13} dibasic acids were in smaller amount, apparently having been partially degraded by the oxidizing agent, as occurred in the oxidation of 12-hydroxystearic acid.

The two hydroxy diene acids appeared to be present in about equal amounts in the original oil. This was determined from the relative amounts of the respective fragments of the oxidized hydroxy diene acids and of the oxidized triene acids, estimated from the gas chromatograms.

The possible presence of 11-hydroxy-9,13-octadecadienoic acid was considered but was judged unlikely. Oxidation of the hydrogenated hydroxy acids gave no sebacic acid, one of the expected products from 11-hydroxystearic acid.

The concentrate of the hydroxy diene acids had infrared maxima of nearly equal intensity at 945 and 980 cm^{-1} (Fig. 1). By analogy with the spectra of the simple conjugated diene acids (4), this is strong evidence that both hydroxy acids are mainly, if not entirely, *cis,trans* or *trans,cis* in configuration. The mixture of the two triene acids obtained on dehydration, however, had a single strong infrared band at 990 cm^{-1} and no other maxima in the 900–1000 cm^{-1} region. It is concluded that these acids are all *trans*. Since the diene acids had one *trans* bond and dehydration may be expected to produce a second *trans* bond, the original *cis* bond must have isomerized spontaneously to *trans* during the dehydration to give the all-*trans* triene product. The all-*trans* structure was confirmed when an attempt to isomerize it by iodine in pentane produced no change in melting point or other properties.

Conjugated Acid of Calendula Oil

Saponification of calendula oil and crystallization of the acids from acetone at low temperature yielded a conjugated triene acid, $C_{18}H_{30}O_2$, as determined by elementary analysis and ultraviolet absorption. It gave stearic acid on hydrogenation. Oxidative splitting of the triene acid gave hexanoic and suberic acids, identified by gas chromatography. The double bonds must have been, therefore, at positions 8, 10, and 12 (V).

The infrared spectrum prepared from a solid film of the acid had a very strong peak at 990 cm^{-1} and a medium strong band at 940–975 cm^{-1}. The solution spectrum, in CS_2, had maxima at 987 (vs), 955 (m), and 920 cm^{-1} (m). This type of spectrum suggests a grouping of two *trans* and one *cis* bond, although it is not exactly the same as that of α-eleostearic acid (8). The ultraviolet spectrum showed maxima at 262, 272, and 283 mμ, also indicative of two *trans* and one *cis* bond in conjugation, by analogy with α-eleostearic acid (8, 9).

Can. J. Chem. Downloaded from www.nrcresearchpress.com by 210.87.254.5 on 09/05/12
For personal use only.

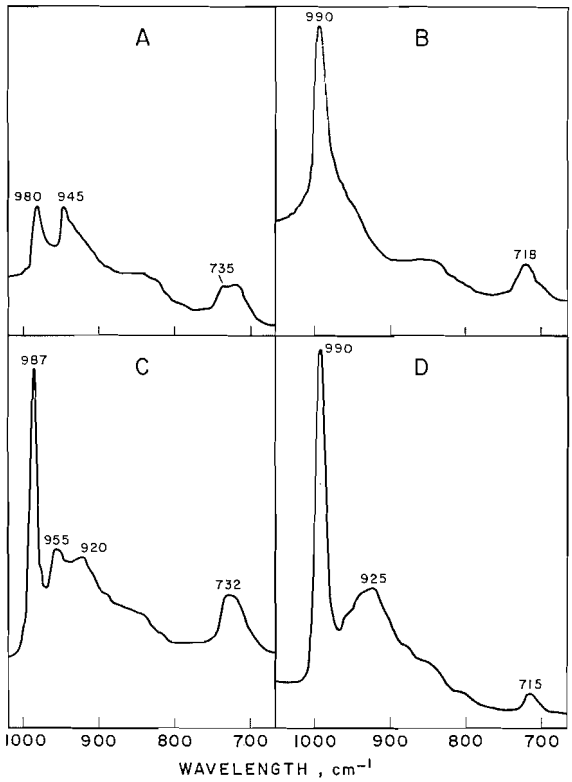


FIG. 1. Infrared spectra, between 700 and 1000 cm^{-1}, determined in CS_2 solution. A, concentrate of hydroxy diene acids from tragopogon; B, methyl esters of triene acids obtained by dehydration of the hydroxy diene acids; C, triene acid from calendula; D, all-*trans* isomer of triene acid from calendula.

The acid reacted readily with maleic anhydride and the adduct was easily purified, showing the presence of two adjacent *trans* double bonds. On splitting the adduct by permanganate–periodate, only one straight chain acid was obtained as a major product. It was identified by gas chromatography as hexanoic acid. There was only a trace of suberic acid. Thus the adduct must have been formed by reaction at the 8 and 11 positions, leaving the 12,13 double bond free (VI).

$$CH_3(CH_2)_4\,CH{=}\overset{c}{C}HCH{=}\overset{t}{C}HCH{=}\overset{t}{C}H(CH_2)_6\,COOH \qquad \text{(V)}$$

maleic anhydride

$$CH_3(CH_2)_4\,CH{=}CHCHCH{=}CHCH\,(CH_2)_6\,COOH \qquad \text{(VI)}$$

The infrared spectrum of the adduct (VI) had no peak in the region 950–975 cm^{-1} and hence no *trans* exocyclic double bond. The 12,13 double bond was therefore *cis* and the original acid was *trans*,8:*trans*,10:*cis*,12-octadecatrienoic acid. The reasoning is similar to that employed by Paschke and co-workers in determining the configuration

Can. J. Chem. Downloaded from www.nrcresearchpress.com by 210.87.254.5 on 09/05/12
For personal use only.

of the eleostearic acids (10). The maleic anhydride adduct of all-*trans*-8,10,12-octadecatrienoic acid was prepared for comparison. Its infrared spectrum had a peak at 963 cm^{-1} (*trans* exocyclic double bond).

The *trans*,8:*trans*,10:*cis*,12 acid, m.p. 40–40.5°, was readily converted to the all-*trans* form, m.p. 77–78°, by treatment with iodine in pentane. The infrared spectrum (CS_2 solution) had a strong single peak at 990 cm^{-1}, indicative of the all-*trans* structure, and very little absorption in the vicinity of 950 cm^{-1}. An all-*trans* conjugated triene acid may be expected to react with maleic anhydride in two ways. Thus, Bickford and coworkers found evidence that addition occurs to β-eleostearic acid at both the 9,12 and 11,14 positions (11). In the present work, proof was obtained that two different adducts are formed in the reaction of all-*trans*-8,10,12-octadecatrienoic acid with maleic anhydride. The reaction product was oxidized by permanganate–periodate and the fragments were examined by gas chromatography. Both hexanoic acid and suberic acid were found in substantial amounts, showing that addition of maleic anhydride had occurred at the 10,13 as well as the 8,11 positions, forming two separate adducts.

The name calendic acid is proposed for *trans*,8: *trans*,10: *cis*,12-octadecatrienoic acid.

EXPERIMENTAL

Methods

Infrared spectral data were obtained with a Perkin–Elmer Model 21 infrared spectrophotometer with sodium chloride prism. Samples were in carbon disulphide solution unless stated otherwise. Ultraviolet measurements were made in cyclohexane or isooctane solution. Gas–liquid chromatography of methyl esters was conducted at various column temperatures from 70° to 170°, according to the chain length of the sample. The detector was a thermistor type of thermal conductivity cell. Column length was 1 meter, helium flow rate 95 ml/min, and inlet pressure 7 to 12 p.s.i., depending on the column temperature. Identification of the various esters was made by comparing the emergence time with that of a standard sample of the same ester under the same conditions on the same day.

Tragopogon oil

Seed of *Tragopogon porrifolius* L. was purchased from a commercial seed house. It was of the current year's stock. The seed (450 g) was ground and extracted with petroleum ether by stirring with successive lots of the solvent at room temperature. The solvent was removed at 25–30° under nitrogen. The oil had ultraviolet absorption maximum at 233 mμ, $E^{1\%}_{1\,cm}$ 47.5, equivalent to 4.0% conjugated octadecadienoic acid based on the total fatty acids. There was no measurable absorption at 268 mμ (conjugated triene).

The oil (83 g) was saponified at room temperature (25°) by letting it stand for 18 hours with a solution of 25 g of potassium hydroxide in 500 ml of ethanol. The unsaponifiable matter was removed by extraction and the fatty acids were partitioned between petroleum ether and ethanol:water (4 volumes EtOH:1 volume H_2O). The partitioning was carried out in three stages and the products recovered from the alcohol portions were analyzed for conjugated diene by ultraviolet absorption and for oxirane oxygen by Swern's method (12) with the following results:

Portion	Wt. of acids, g	Conjugated diene acid, %	Oxirane oxygen, %
1	7.0	32.0	2.1
2	7.2	8.7	1.2
3	4.4		0.7

Can. J. Chem. Downloaded from www.nrcresearchpress.com by 210.87.254.5 on 09/05/12
For personal use only.

The acids from the first portion were estimated to contain 32% conjugated diene acid and 37% epoxy acid, assuming that both are of chain length C_{18}. This mixture was treated further by solvent partition and the alcohol-soluble portion, on crystallization from acetone at −70°, yielded an oil (0.34 g) which was a concentrate of the conjugated diene acid. It had ultraviolet maximum 233 mμ and $E^{1\%}_{1cm}$ 561.

Identification of Diene Acids

The concentrate had an infrared peak at 3580 cm^{-1} (OH) and two peaks of equal intensity at 945 and 980 (conjugated *cis,trans* double bonds). Oxidative splitting by permanganate–periodate (5) and examination of the esterified fragments by gas chromatography (6) showed that they were hexanoate and azelate. There was no heptanoate or sebacate. There was some evidence of other compounds at longer emergence times, possibly fragments carrying the hydroxy group.

On hydrogenation of the diene acid concentrate (1.0 g) with Adams catalyst in ethyl acetate and successive crystallizations from ethyl acetate and from hexane, the product (0.33 g) melted at 65–66° and was evidently a mixture of monohydroxystearic acids. Calculated for $C_{18}H_{36}O_3$: C, 71.95; H, 12.08. Found: C, 71.83; H, 11.70. Infrared maximum, 3600 cm^{-1} (OH). Oxidative splitting of the hydrogenated product by solid permanganate in glacial acetic acid at 50° (13) gave a mixture of monobasic and dibasic acids which was esterified and submitted to gas chromatography. A similar oxidation of 12-hydroxystearic acid gave two monobasic acids, hexanoic and heptanoic, and two dibasic acids, undecanedioic and dodecanedioic, along with minor proportions of azelaic and sebacic acids. The monobasic acids obtained from the oxidation of the hydrogenated diene acids were chromatographed (as methyl esters) at 55°, 70°, and 93°. They were mainly pentanoic (15%), hexanoic (22%), nonanoic (25%), and decanoic (28%), with smaller amounts of heptanoic (5%), and octanoic acids (5%). Suberic and azelaic acids were observed in substantial amount (as esters) when chromatographed at 175°. There were also dodecanedioic and tridecanedioic acids, in smaller proportions, along with pimelic and undecanedioic. There was little or no sebacic acid.

Dehydration to Triene Acids

The mixed hydroxy diene acids were dehydrated as follows. The concentrate (3.4 g) was refluxed with glacial acetic acid (17 ml) for 4 hours, the acetic acid was removed under reduced pressure and the residue was heated for 1 hour with 35 ml of *N* alcoholic KOH. The crude acids were crystallized from 15 ml of acetone at −35°, giving 0.9 g of glistening plates, m.p. 58–60°. Further crystallization from ethyl acetate raised the melting point to 60–61° but no higher. (Found: C, 77.69; H, 10.65. Octadecatrienoic acid, $C_{18}H_{30}O_2$, requires C, 77.65; H, 10.85.) The substance had ultraviolet absorption maxima at 260, 269, 280 mμ (all-*trans* conjugated triene). The infrared spectrum (solid film) had a single strong peak at 985–995 cm^{-1}, also characteristic of the all-*trans* form. There was no OH peak. The spectrum of the methyl ester (in CS_2) showed a similar all-*trans* band at 990 cm^{-1}. When hydrogenated in methanol with Adams catalyst, the acid (0.37 g) absorbed 3.06 moles of hydrogen, and the product was stearic acid (0.34 g), m.p. and mixed m.p. 69–70°, equivalent weight 284.9 (calc. 284.4).

A portion of the triene acid was oxidized by periodate–permanganate (5) and the products were converted to methyl esters (6) for identification by gas chromatography. Valerate and hexanoate were identified at 80°, in approximately equal amounts (53:47). Suberate and azelate were observed at 170°. A larger portion was oxidized by the procedure of McLean and Clark (2). Azelaic acid, m.p. and mixed m.p. 104–105°, was

Can. J. Chem. Downloaded from www.nrcresearchpress.com by 210.87.254.5 on 09/05/12
For personal use only.

isolated with some difficulty by crystallizing the mixture of products. It was judged that more than one dibasic acid was present.

An attempt to isomerize the triene acids by iodine in hexane solution produced no change in melting point.

CALENDULA OIL

trans,8:trans,10:cis,12-Octadecatrienoic Acid (Calendic Acid)

Seed of *Calendula officinalis* L. was purchased from a commercial seed house. It was ground and the oil was extracted with petroleum ether in a Soxhlet. Ten grams of the oil was saponified by heating for 1 hour with 6% alcoholic potassium hydroxide under nitrogen. The unsaponifiable matter was removed and the fatty acids were crystallized fractionally from acetone at temperatures from 0° to −40°, giving 2.5 g of an acid, m.p. 40–40.5°. The acid was highly unstable in air, becoming sticky in a few minutes if exposed at room temperature. It was kept under nitrogen at the temperature of solid carbon dioxide. Calculated for $C_{18}H_{30}O_2$: C, 77.65; H, 10.85. Found: C, 77.97; H, 10.92. Ultraviolet maxima at 262, 272, and 283 mμ. Infrared maxima (solid film) at 990 (vs), 940–975 (m), and 740 (m); (in CS_2) at 987 (vs), 955 (m), 920 (m), and 732 cm^{-1} (m).

Hydrogenation with Adams catalyst in methanol gave stearic acid, m.p. and mixed m.p. 69.5–70°. The triene acid was oxidized by permanganate–periodate (5) and the products were examined as methyl esters by gas chromatography (6). Peaks corresponding to hexanoate and suberate were observed. There were no other peaks.

The triene acid was heated with maleic anhydride in benzene for 1 hour, forming an adduct, m.p. 73–74° after several crystallizations from ether:petroleum ether (1:5). Calculated for $C_{22}H_{32}O_5$: C, 70.18; H. 8.57. Found: C, 70.18; H, 8.55. The infrared spectrum showed no peak or shoulder in the region of 950–975 cm^{-1}. The adduct was oxidized by permanganate–periodate and the fission products were converted to methyl esters and chromatographed. There was a large peak identified by its emergence time as hexanoate and a very small peak identified as suberate.

The content of conjugated triene acid in the oil was estimated to be 47%.

All-trans-8,10,12-Octadecatrienoic Acid

On treatment with iodine in pentane, the triene acid (2.5 g), m.p. 40–40.5°, was quickly converted to the all-*trans* isomer which melted at 77–78° after crystallization from ethanol at 0° (1.9 g). Infrared maximum 990 cm^{-1} (vs); ultraviolet maxima 259, 269, and 280 mμ. McLean and Clark reported ultraviolet maxima 258, 268, and 280 mμ (2). The maleic anhydride adduct was prepared. It was more difficult to purify than that from the unisomerized acid and melted no higher than 70–71° (McLean and Clark, 71°). The yield was 1.5 g from 1.9 g of the *trans* acid. In admixture with the adduct from the unisomerized acid it melted at 56–58°. Its infrared spectrum showed a small but distinct peak at 963 cm^{-1}. The adduct was oxidized by permanganate–periodate and the fragments were identified by gas chromatography as hexanoate and suberate, both in considerable amount.

ACKNOWLEDGMENTS

The authors are indebted to Mr. R. Lauzon for determination of infrared spectra and to Mr. H. Seguin for C and H analyses.

Can. J. Chem. Downloaded from www.nrcresearchpress.com by 210.87.254.5 on 09/05/12
For personal use only.

REFERENCES

1. M. J. Chisholm and C. Y. Hopkins. Chem. & Ind. (London), 1154 (1959).
2. John McLean and A. H. Clark. J. Chem. Soc. 777 (1956).
3. L. J. Morris, R. T. Holman, and K. Fontell. J. Am. Oil Chemists' Soc. **37**, 323 (1960).
4. J. R. Chipault and J. M. Hawkins. J. Am. Oil Chemists' Soc. **36**, 535 (1959).
5. R. U. Lemieux and E. von Rudloff. Can. J. Chem. **33**, 1701 (1955).
6. M. J. Chisholm and C. Y. Hopkins. Can. J. Chem. **38**, 805 (1960).
7. C. R. Smith, Jr., T. L. Wilson, E. H. Melvin, and I. A. Wolff. J. Am. Chem. Soc. **82**, 1417 (1960).
8. L. Crombie and A. G. Jacklin. J. Chem. Soc. 1632 (1957).
9. F. D. Gunstone. Chemistry of fats and fatty acids. Chapman and Hall Ltd., London. 1958. p. 25.
10. R. F. Paschke, W. Tolberg, and D. H. Wheeler. J. Am. Oil Chemists' Soc. **30**, 97 (1953).
11. W. G. Bickford, E. F. DuPre, C. H. Mack, and R. T. O'Connor. J. Am. Oil Chemists' Soc. **30**, 376 (1953).
12. D. Swern, T. W. Findley, G. N. Billen, and J. T. Scanlan. Anal. Chem. **19**, 414 (1947).
13. K. E. Bharucha and F. D. Gunstone. J. Chem. Soc. 613 (1957).

Can. J. Chem. Downloaded from www.nrcresearchpress.com by 210.87.254.5 on 09/05/12
For personal use only.

Can. J. Chem. Downloaded from www.nrcresearchpress.com by 210.87.254.105 on 09/05/12
For personal use only.

STRUCTURAL AND SOLVENT EFFECTS ON THE $n \rightarrow \pi^*(^1U \leftarrow {}^1A)$ TRANSITIONS IN ALIPHATIC CARBONYL DERIVATIVES: EVIDENCE FOR HYPERCONJUGATION IN THE ELECTRONICALLY EXCITED STATES OF MOLECULES[1]

C. N. R. Rao,[2] G. K. Goldman,[3] and A. Balasubramanian

ABSTRACT

The $n \rightarrow \pi^*$ transition of the carbonyl group has been studied in solvents of varying degree of polarity and hydrogen-bonding ability, in a number of aliphatic carbonyl derivatives. Evidence for hyperconjugation of the alkyl groups in the electronically excited states of molecules has been presented.

INTRODUCTION

The long-wavelength low-intensity absorption between 2600 and 3000 Å in carbonyl compounds has been shown (1, 2) to be due to a singlet–singlet symmetry forbidden transition* arising from the excitation of an electron from a nonbonding orbital(n orbital) to an antibonding orbital (π^* orbital). Empirical criteria which permit distinctions between the pure π-electron transitions and the $n \rightarrow \pi^*$ transitions have been formulated (3, 4, 5). The solvent effects on $n \rightarrow \pi^*$ transitions have been characterized (4) and, in general, the transition energies are found to increase with the increase in the polarity of the solvent. We have now studied the substituent and solvent effects on the $n \rightarrow \pi^*$ transitions in aliphatic carbonyl derivatives with the purpose of understanding the nature of alkyl group interaction in the electronically excited states of molecules† since it has not been possible to evaluate the contributions from the inductive and the hyperconjugation effects from the earlier studies (6).

EXPERIMENTAL

All the solutes and solvents were subjected to suitable purification and fractionation before use. Particular care was taken in distilling trifluoromethylacetone from phosphorus pentoxide just before running the spectrum, since it readily forms the hydrate.

The ultraviolet absorption spectra were recorded using a Cary Model 11 recording spectrophotometer and a Hilger spectrophotometer, H700. The absorption maxima have been recorded in cm^{-1} (ν') and the intensities in terms of the molar extinction coefficients (ϵ).

RESULTS AND DISCUSSION

The $n \rightarrow \pi^*$ transition frequencies and intensities of some aliphatic carbonyl derivatives are summarized in Table I. The results are in general agreement with the earlier work (6). The results satisfy all the necessary criteria (3, 4, 5) proposed for $n \rightarrow \pi^*$ transitions. In Fig. 1 the $n \rightarrow \pi^*$ bands of acetaldehyde and methyl *i*-propyl ketone are reproduced.

[1]*Manuscript received May 24, 1960.*
Contribution from the Department of Inorganic and Physical Chemistry, Indian Institute of Science, and the Department of Chemistry, Purdue University, Lafayette, Indiana.
[2]*To whom all the correspondence should be addressed at the Department of Inorganic and Physical Chemistry, Indian Institute of Science, Bangalore-12, India.*
[3]*Department of Chemistry, Purdue University, Lafayette, Indiana, U.S.A.*
*According to the recent notation, this transition is given the label $^1U \leftarrow {}^1A$. See J. R. Platt, J. Opt. Soc. Am. **43**, 252 (1953).*
†*A preliminary communication has been published. See C. N. R. Rao, J. Ramachandran, and G. K. Goldman, Tetrahedron Letters, **2**, 1 (1960).*

TABLE I

The $n \rightarrow \pi^*$ transition of the carbonyl group in aliphatic carbonyl derivatives (RCOR′)

			Solvent					
			Heptane		Methanol		Water	
No.	R	R′	ν', cm^{-1}	ϵ_{max}	ν', cm^{-1}	ϵ_{max}	ν', cm^{-1}	ϵ_{max}
1	CH_3	H	34,360*	10.2	35,088	—	36,036	—
2	CH_3	CH_3	36,133	11.8	37,037	15.4	37,809	16.8
3	CH_3	C_2H_5	36,036	15.3	36,765	17.8	37,523	18.6
4	CH_3	i-C_3H_7	35,242	17.3	35,971	20.1	36,663	24.7
5	CH_3	t-C_4H_9	34,965	18.3	35,461	23.7	36,101	—
6	CH_3	CF_3	36,036	40.0	—	—	—	—
7	CH_3	$CH_2CH_2COCH_3$†	36,430	15.1	—	—	37,736	20.6
8	C_2H_5	C_2H_5	35,842	16.4	36,630	19.2	37,037	—
9	i-C_3H_7	i-C_3H_7	34,722	21.7	35,273	25.5	35,714	—
10	CH_3	n-C_3H_7	35,842	—	36,563	—	36,900	—
11	n-C_3H_7	n-C_3H_7	35,399	—	—	—	36,496	—
12	CH_3	i-C_4H_9	35,398	—	35,907	—	36,900	—
13	i-C_4H_9	i-C_4H_9	35,211	—	—	—	—	—
14	t-C_4H_9	t-C_4H_9	33,445	19.8	34,014	24.1	—	—
15	CH_3	n-C_5H_{11}	35,650	—	36,298	—	37,174	—
16	CH_3	n-C_6H_{13}	35,778	—	36,363	—	—	—

*Center of the nearly symmetric band system.

†Acetylacetone does not exhibit the $n \rightarrow \pi^*$ transition in this region. It gives a band around 37,175 cm^{-1} in heptane, which shows solvent red shift (4). This is because of the aromatic nature resulting from enolization.

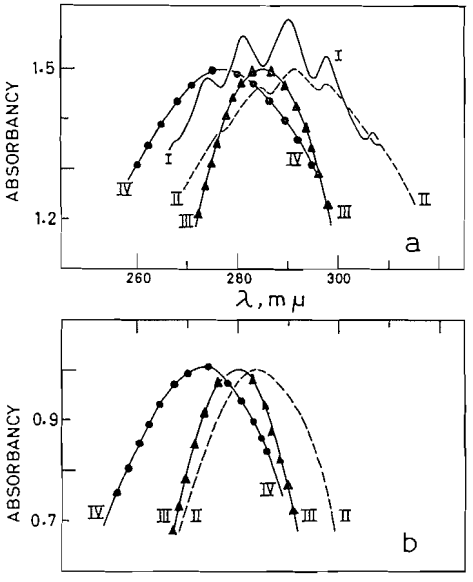


FIG. 1. The $n \rightarrow \pi^*$ transition of the carbonyl group of (*a*) acetaldehyde, (*b*) methyl *i*-propyl ketone: I, in gas phase; II, in heptane solution; III, in methanol solution; and IV, in water solution.

Acetaldehyde shows vibrational fine structure in heptane just as it does in gas phase except that there is a slight bathochromic shift in the former case. The fine structure is not seen in the spectrum taken in methanol or water. Ketones do not show any recognizable fine structure even in heptane solutions. However, all the carbonyl derivatives do show increasing $n \rightarrow \pi^*$ transition energies with the increasing polarity or hydrogen-bonding ability of the solvents.

Can. J. Chem. Downloaded from www.nrcresearchpress.com by 210.87.254.105 on 09/05/12
For personal use only.

Can. J. Chem. Downloaded from www.nrcresearchpress.com by 210.87.254.105 on 09/05/12
For personal use only.

The intensities of the $n \rightarrow \pi^*$ bands in all the derivatives studied are seen to be weak. The ϵ value for acetone is not much different from that of acetaldehyde, even though the two molecules differ in symmetry (C_{2v} and C_s). Similarly, methyl ethyl ketone and acetone exhibit nearly comparable intensities. The intensity of the forbidden $n \rightarrow \pi^*$ transition in all these molecules is undoubtedly derived in the same manner. Thus, all the aldehydes and saturated ketones seem to retain the C_{2v} symmetry characteristics of the formaldehyde molecule. The intensity-borrowing mechanism of the $n \rightarrow \pi^*$ transition in formaldehyde has been shown (5) to be due to the vibrationally induced mixing of the electronic states. The out-of-plane vibration, ν_6, is considered responsible for the intensity of the $n \rightarrow \pi^*$ transition in formaldehyde. The mode of motion responsible for the intensity of the transition in acetone should then be ν_6, in which the two carbon atoms and the oxygen atom bonded to the central carbon atom are displaced out of the plane of symmetry in one direction and the central carbon in the opposite direction. Among the saturated aliphatic ketones, the $n \rightarrow \pi^*$ transition intensity is least in acetone and it is slightly greater in other cases. It can be seen from the data in Table I that the $n \rightarrow \pi^*$ transition intensity increases with the increasing polarity or hydrogen-bonding ability of the solvent.

It has been generalized (5, 7, 8) that electron-donating substituents shift the $n \rightarrow \pi^*$ transition to shorter wavelengths due to the increase in the energy of the excited state caused by the accumulation of electronic charge in a localized region. In the $n \rightarrow \pi^*$ transition of the carbonyl group, the electronic charge is transferred from oxygen to carbon. Electron-donating groups like —Cl, —OCH_3, etc., when attached to the carbon atom, produce large intramolecular blue shifts of the transition. Interestingly enough, aliphatic carbonyl compounds (RCOR′ where R = CH_3), with R′ as CH_3, C_2H_5, i-C_3H_7, and t-C_4H_9, exhibit the $n \rightarrow \pi^*$ transitions at 36133, 36036, 35242, and 34965 cm^{-1}, respectively, in a hydrocarbon solvent. Such a trend cannot be explained in terms of inductive effect alone because acetaldehyde (R′ = H) and trifluoromethylacetone (R′ = CF_3) show the transition at 34360 and 36036 cm^{-1}, respectively, in heptane. There is no proportionality between the $n \rightarrow \pi^*$ frequencies and the polar effects of groups in these carbonyl derivatives, as can be seen from Fig. 2(a), where ν' is plotted against Taft's aliphatic polar substituent constants (9), $\Sigma\sigma^*$. However, the infrared carbonyl stretching frequencies in aliphatic ketones bear a linear relation to $\Sigma\sigma^*$ of groups (10, 11) showing that there may be no hyperconjugative effect of alkyl groups in the ground electronic states of molecules. In fact, it has been fairly well accepted nowadays that hyperconjugation may not play a prominent role in the electronic ground states of molecules (12). If one assumes that there is some contribution by the resonance interaction of the alkyl groups in the electronically excited states of molecules, one may be able to explain the observed $n \rightarrow \pi^*$ frequencies in the aliphatic carbonyl derivatives. The frequency is highest in acetone (where both R and R′ are methyl groups), just what one would expect if there were electron donation by C—H hyperconjugation.

Kreevoy and Taft (13) applied the linear inductive energy relationship to study the nature of the electronic interaction of alkyl groups in the acid-catalyzed rates of hydrolysis of diethyl acetals and ketals. Assuming that only C—H hyperconjugation was operative in addition to the inductive effect, they proposed the relation

$$\text{(i)} \qquad \log (k/k_0) = (\Sigma\sigma^*)\rho^* + \Delta n h$$

where Δn is the difference in the number of α-hydrogens actually available for C—H

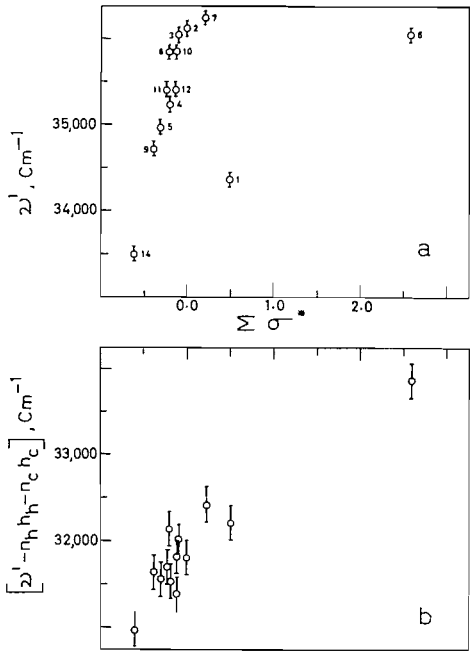


FIG. 2. (*a*) Plot of the $n \rightarrow \pi^*$ transition frequencies (ν') in aliphatic carbonyl derivatives against the polar substituent constants of Taft, $\Sigma\sigma^*$.
(*b*) Plot of $(\nu' - n_h h_h - n_c h_c)$ against $\Sigma\sigma^*$. The maximum limits of uncertainty on the frequencies have been shown.

hyperconjugation compared with the maximum number of six and h is the hyperconjugation constant. A similar treatment of the $n \rightarrow \pi^*$ frequencies of aliphatic carbonyl derivatives, taking into consideration only the inductive and C—H hyperconjugative effects of alkyl groups, was carried out by employing the equation

(ii) $$\nu' = \nu_0' + (\Sigma\sigma^*)\rho^* + n_h h_h$$

where ν' is the observed $n \rightarrow \pi^*$ frequency in cm^{-1}, n_h is the number of α-hydrogens available for C—H hyperconjugation, and h_h is the hyperconjugation constant. The value of h_h was estimated to be 385 cm^{-1} (in heptane solution) by solving simultaneous equations. The plot of $(\nu' - 385\ n_h)$ versus $\Sigma\sigma^*$ showed considerable scatter of the points. The standard deviation of the points was found to be 348 cm^{-1} and the correlation coefficient was 0.557. In view of the rather poor correlation obtained, it was decided to consider possible contribution by the C—C hyperconjugation of the alkyl groups.

Taft and Lewis (14) have recently proposed a modified treatment which takes into account both C—H and C—C hyperconjugation. The quantitative relation between the measured reactivity effects and the sum of the inductive and the hyperconjugation effects has been expressed as

(iii) $$\log (k/k_0) = (\Sigma\sigma^*)\rho^* + R$$

and $R = n_n h_n + n_c h_c$, where n_h and n_c are the number of α-C—H and α-C—C bonds of the alkyl group and h_n and h_c are the C—H and C—C hyperconjugation constants. The quantity $[\log(k/k_0) - R]$ should then depend only on the polar effects of groups.

Can. J. Chem. Downloaded from www.nrcresearchpress.com by 210.87.254.105 on 09/05/12
For personal use only.

Can. J. Chem. Downloaded from www.nrcresearchpress.com by 210.87.254.105 on 09/05/12
For personal use only.

Such a relation has been found to explain quantitatively the reaction rate data in several alkyl-substituted systems (14, 15). The effects of alkyl groups on the transition energies of the 0–0 bands of gaseous benzene spectra were also found to follow equation (iii). The $n \rightarrow \pi^*$ transition frequencies in Table I may be treated similarly, by employing the equation

$$\text{(iv)} \qquad \nu' = \nu_0' + (\Sigma\sigma^*)\rho^* + n_h h_n + n_c h_c.$$

By assuming a linear relation between the points for acetaldehyde and trifluoromethylacetone in Fig. 2(*a*), the constants h_h and h_c were found to be approximately 720 and 410 cm^{-1}, respectively, for the data in heptane. An approximate proportionality is found between $(\nu' - 720\, n_h - 410\, n_c)$ and $\Sigma\sigma^*$ as shown in Fig. 2(*b*). The standard deviation of the points and the correlation coefficient are 276 cm^{-1} and 0.920, respectively.

It is seen that the correlation coefficient for equation (iv) is much greater than for equation (ii).* Thus, it appears that the contributions from the inductive and the C—H and C—C hyperconjugative effects are necessary to explain the $n \rightarrow \pi^*$ transition frequencies of aliphatic carbonyl derivatives. The ratio h_h/h_c is seen to be about 1.75, which is greater than the value of 1.3 generally found in aromatic systems (14). Apparently, the contribution from C—H hyperconjugation, compared with C—C hyperconjugation, is much greater in the aliphatic systems than in the aromatic systems.

The $n \rightarrow \pi^*$ frequencies of acetone, methyl ethyl ketone, methyl *i*-propyl ketone, and methyl *t*-butyl ketone in heptane solution are in the Baker-Nathan order, i.e., $CH_3 > C_2H_5 > i\text{-}C_3H_7 > t\text{-}C_4H_9$. The same trend is maintained in solvents of varying degree of polarity or/and hydrogen-bonding ability, as can be seen from Fig. 3. There is no indication of an inversion of this order with the change in solvents as observed by Schubert *et al.* (16) in *p*-alkylacetophenones and *p*-alkylnitrobenzenes. The results of Schubert

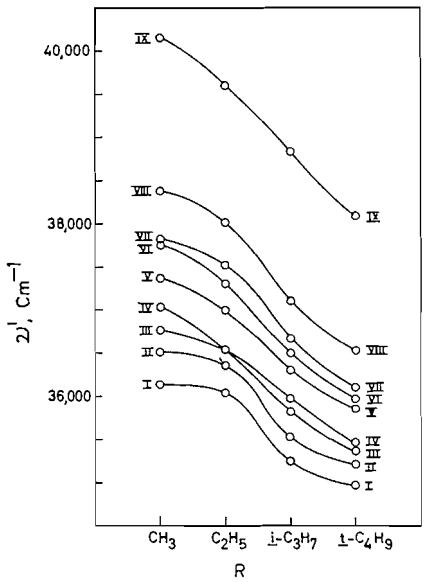


FIG. 3. Solvent effects on the $n \rightarrow \pi^*$ transition frequencies of CH_3COR: I, heptane; II, acetonitrile; III, *i*-propanol; IV, methanol; V, acetic acid; VI, 2,2,2-trifluoroethanol; VII, water; VIII, 30% perchloric acid; and IX, 60% perchloric acid.

**The authors are thankful to the referee for suggesting the statistical analyses of the relations.*

et al. (16) may be explained (14) as due to possible errors in fixing the positions of the 0–0 bands and also due to the uncertainty in the mechanism of the substituent effects on the transition. In general, it may be said that the effect of alkyl groups on the near ultraviolet absorption spectra of aromatic systems is not consistent. The evidence for hyperconjugation in the excited states of molecules presented in this study seems to be quite reasonable because (*a*) the molecules studied are aliphatic and so no other type of resonance interaction can occur, (*b*) the infrared carbonyl stretching frequencies in these molecules are proportional to Taft's aliphatic polar parameters of groups, thus indicating that hyperconjugation may be unimportant in the ground electronic states, (*c*) the $n \rightarrow \pi^*$ transition is very sensitive to change in structure and solvent, and (*d*) similar trends of the $n \rightarrow \pi^*$ frequencies are found in solvents of varying degree of polarity or/and hydrogen bonding.

All the carbonyl derivatives show increasing solvent blue shifts* with the increasing polarity or/and hydrogen-bonding ability of the solvent.† In the series of ketones, RCOR′ (with R = CH_3), the solvent blue shift is maximum in acetone (where R′ is also a methyl group) in all the solvents studied. The significance of this observed effect is not completely clear.†

ACKNOWLEDGMENTS

The authors are thankful to Mr. J. Ramachandran and Mr. S. R. Yoganarasimhan for their kind assistance. They are indebted to Professor M. R. A. Rao for his keen interest in the work. One of us (A. Balasubramanian) is grateful to the authorities of the Indian Institute of Science for the award of a research scholarship.

REFERENCES

1. R. S. MULLIKEN. J. Chem. Phys. **3**, 564 (1935).
2. H. L. MCMURRY. J. Chem. Phys. **9**, 231 (1941).
3. M. KASHA. Discussions Faraday Soc. No. 9, 14 (1950).
4. H. MCCONNELL. J. Chem. Phys. **20**, 700 (1952).
5. J. W. SIDMAN. Chem. Revs. **58**, 689 (1958).
6. P. MARONI. Ann. chim. (Paris), **2** (13), 757 (1957).
7. A. BURAWOY. J. Chem. Soc. 1177 (1939).
8. S. NAGAKURA. Bull. Chem. Soc. Japan, **25**, 164 (1952).
9. R. W. TAFT, JR. *In* Steric effects in organic chemistry. *Edited by* M. S. Newman. John Wiley & Sons, Inc., New York. 1956. Chap. 13.
10. C. N. R. RAO, G. K. GOLDMAN, and C. LURIE. J. Phys. Chem. **63**, 1311 (1959).
11. H. W. THOMPSON and D. A. JAMESON. Spectrochim. Acta, **13**, 236 (1958).
12. C. N. R. RAO. Current Sci. (India), **28**, 231 (1959); Nature, **187**, 913 (1960).
13. M. M. KREEVOY and R. W. TAFT, JR. J. Am. Chem. Soc. **77**, 5590 (1955).
14. R. W. TAFT, JR. and I. C. LEWIS. Tetrahedron, **5**, 210 (1959).
15. J. W. BAKER. Tetrahedron, **5**, 135 (1959).
16. W. M. SCHUBERT, J. ROBINS, and J. L. HAUN. J. Am. Chem. Soc. **79**, 910 (1957).

*Blue shift $\Delta\nu' = \nu'_{\text{solvent}} - \nu'_{\text{heptane}}$.

†*A detailed analysis of the solvent effects on the $n \rightarrow \pi^*$ transition of the carbonyl group is now in progress in this laboratory and will be published in the near future.*

Can. J. Chem. Downloaded from www.nrcresearchpress.com by 210.87.254.105 on 09/05/12
For personal use only.

CATALYZED RECOMBINATION OF NITROGEN ATOMS, AND THE POSSIBLE PRESENCE OF A SECOND ACTIVE SPECIES IN ACTIVE NITROGEN[1]

ROGER KELLY[2] AND C. A. WINKLER

ABSTRACT

The reactions of ethylene, ethane, and ammonia with active nitrogen have been studied over the pressure range 0.3 to 4 mm *using an unheated reaction vessel.* The object was to determine why each reactant shows, as is well-known, a smaller extent of reaction at lower temperatures than would be predicted from the atom concentration. It was concluded that ethylene probably brought about *homogeneous catalyzed recombination*, i.e. the process $N + C_2H_4 \rightleftarrows N \cdot C_2H_4$, followed by $N + N \cdot C_2H_4 \rightarrow N_2 + C_2H_4$. The over-all third-order rate constant appeared to be very large, about 1.8×10^{-28} cc^2 molecule^{-2} sec^{-1}. The behavior of ammonia was quite different from that of ethylene and it was, in fact, possible to show that the extent of reaction was not governed by the instantaneous atom concentration at all. The results can be explained qualitatively, however, if it is assumed that excited molecules formed in the course of homogeneous atom decay constitute a second active species in active nitrogen. This view serves also to explain the failure in such work as that of Kistiakowsky *et al.* to observe ammonia destruction or excited molecules when especially low atom concentrations are used. The few experiments involving ethane were sufficient to show that the reactivity was low for a different reason than with ethylene.

In a previous study (1), active nitrogen was produced in a condensed discharge at pressures between 0.3 and 4 mm and under conditions of approximately complete initial dissociation. It was then allowed to flow rapidly through a "decay tube" to a reaction vessel, where the limiting (i.e. maximum) rate of HCN production from ethylene or ethane at 350° C was assumed to measure the flowrate of residual N atoms. Information on the rate constants for N atom decay was thus obtained. The present experiments have been conducted along similar lines, the same apparatus being used; however, the "activity" of the active nitrogen has been derived *with the reaction vessel unheated.* Measurements were made of HCN production from ethylene and ethane, and also of the decomposition of ammonia.

Ethylene and ethane are of particular interest at lower temperatures since they are typical of several substances with which the extents of reaction at all temperatures approach well-defined limiting values as the flowrate of reactant is increased, yet these values are significantly temperature dependent and, except at the highest temperatures, are substantially less than might be expected from the available N atom concentration (2, 3, 1). An explanation for such behavior has been given by Forst *et al.* (4), who suggested that N atom reactions might be accompanied by extensive recombination of the atoms catalyzed by the *reactant.* (Such a process is not eliminated by increasing the flowrate of reactant provided it is of the same order in reactant as the main reaction. On the other hand, ordinary homogeneous and surface decay, as well as recombination catalyzed by a *product*, would necessarily be swamped in the presence of a large excess of reactant, and would therefore have no effect whatsoever on a limiting reactivity.) By contrast, the destruction of ammonia by active nitrogen, while occurring to only a small extent, appears to be unaffected by moderate changes in temperature, is quite rapid (5),

[1]*Manuscript received April 13, 1960.*
Contribution from the Upper Atmosphere Chemistry Research Group, the Physical Chemistry Laboratory, McGill University, Montreal, Que., with financial assistance from Imperial Oil Limited, Sarnia, Ontario, and the National Research Council of Canada, Ottawa, Canada.
[2]*Holder of National Research Council Studentships 1956–57, 1957–58. Present address: Atomic Energy of Canada Limited, Chalk River, Ontario.*

is accompanied by only partial quenching of the afterglow (6, 7), and apparently does not involve N atoms in the rate-controlling step (6, 8).[3] The behavior of ammonia is therefore, at least superficially, not consistent with a combination of N atom attack plus catalyzed recombination and has, in fact, seemed to require an alternative explanation in which it is assumed that an active species other than the N atom is present in active nitrogen (see, for example, 5, 9, 10).

It will be the object of the present work to determine whether the depressed reactivity of each substance studied can be better explained in terms of catalyzed recombination or a second active species.

EXPERIMENTAL

The apparatus was identical with that described earlier (Fig. 1 of reference 1), except that a decay tube (volume = 281 cc) was used only in series 1 to 3. In series 4 and 5 the decay tube was removed altogether. The reaction vessel was then connected directly to the discharge tube at a point *near the end of one electrode* and with the usual constriction present at the entrance to the reaction vessel (Fig. 1). Nitrogen was admitted

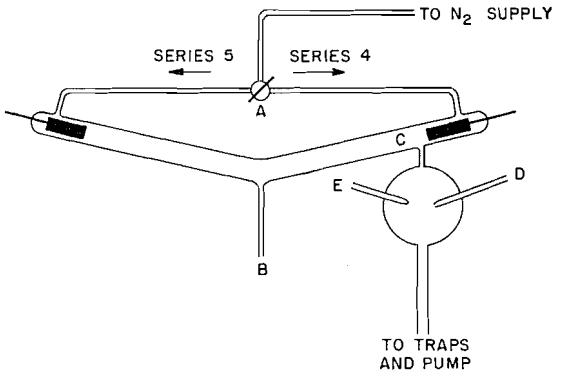


FIG. 1. Arrangement of the discharge tube and reaction vessel in series 4 and 5. (A) is a stopcock, according to the position of which the nitrogen enters the discharge tube either at the right electrode (series 4) or at the left (series 5). (B) is a constricted outlet from the discharge tube which served *in series 4* to set up a slight flow of gas *away* from the outlet to the reaction vessel, and thereby to minimize the diffusion of active nitrogen from region (C) into the reaction vessel. (D) is the reactant jet and (E) the thermocouple well. Further details of the apparatus are the same as in Fig. 1 of reference 1.

to the discharge tube either at the end to which the reaction vessel was sealed (series 4), or at the opposite end (series 5). The polarity of the electrodes was shown not to affect the results (cf. p. 2334 of reference 11).

In all experiments the system was poisoned with Na_2HPO_4 since this poison, in contrast to HPO_3, is unreactive towards ammonia. The electrical circuit and analytical procedures were as described previously (1) and, as before, the reactant flowrates were sufficiently high that the extents of reaction were at their limiting values for the temperatures used.

Whether or not complete initial dissociation was achieved is of no consequence to the arguments to follow.

[3]*The conclusion that* N *atoms do not participate in the rate-controlling step follows from the observations that, when ammonia is added to active nitrogen of microwave origin in amounts as great as 10 times the atom concentration, neither the atom concentration itself (6) nor the ability of the active nitrogen to destroy* NO *(8) is affected.*

THEORY

If the reactivity towards active nitrogen shown by a substance were depressed due to the fact that the substance catalyzed the recombination of the N atoms, then it should be possible to account for the details of the reaction by means of some combination of elementary N atom reactions. The possible elementary reactions include, firstly, those which lead to product formation:

$$[1] \qquad N + M \underset{k_{-1}}{\overset{k_1}{\rightleftharpoons}} NM,$$

followed by one of

$$[2] \qquad NM \xrightarrow{k_2} n(\text{HCN, CNCl, NH, etc.}) + p_2(\text{reactive fragments}), \quad \text{(cf. 10, 12, 13)}$$

$$\left.\begin{aligned} [3] \qquad & N + NM \xrightarrow{k_3} N_2 + M^*, \quad M^* \rightarrow p_3(\text{reactive fragments}), \\ [4] \qquad & NM + NM \xrightarrow{k_4} N_2 + M + M^*, \quad M^* \rightarrow p_4(\text{reactive fragments}). \end{aligned}\right\} \text{(cf. 2, 10, 12, 14)}$$

Here M is the reactant, M* is an unspecified excited state of M, n is the number of molecules of HCN, etc., formed in the primary step of [2] (*one*, except in special cases, as when M is a cyanide), and p_2, p_3, and p_4 are the numbers of N atoms lost in rapid secondary reactions involving fragments of M. The values of p_2, etc. are not necessarily integral (cf. footnote 4).

Next there are reactions leading solely to recombination:

$$[5] \qquad N + NM \xrightarrow{k_5} N_2^* + M, \qquad \text{(cf. 4)}$$

$$[6] \qquad NM + NM \xrightarrow{k_6} N_2^* + 2M,$$

$$[7] \qquad NM + \text{surface} \xrightarrow{k_7} N\cdot\text{surface} + M,$$

where N_2^* represents an excited state of N_2. In principle, the M on the right side of [5], [6], and [7] might be excited; however, if so, it is assumed to revert to the ground state.

As mentioned previously, ordinary homogeneous and surface decay, as well as recombination catalyzed by a product, need not be considered provided the experiments are confined to conditions when the reactant is in excess.

If a low extent of reaction were due, not to catalyzed recombination, but to the fact that the reaction was initiated by a species other than the N atom, it is obviously true that experimental results would be consistent with no combination of elementary N atom reactions. However, a far simpler way of demonstrating the involvement of a second active species would be to show that the reactivity of a substance could be varied significantly by some act affecting the active nitrogen prior to its entry into the reaction vessel, yet which leaves the atom concentration within the reaction vessel essentially unchanged.

RESULTS AND DISCUSSION

The following abbreviation will be used henceforth: $[N]_a \equiv$ "apparent atom concentration" = reactivity.

Ethylene

In Figure 2 are shown the HCN production from ethylene as a function of pressure

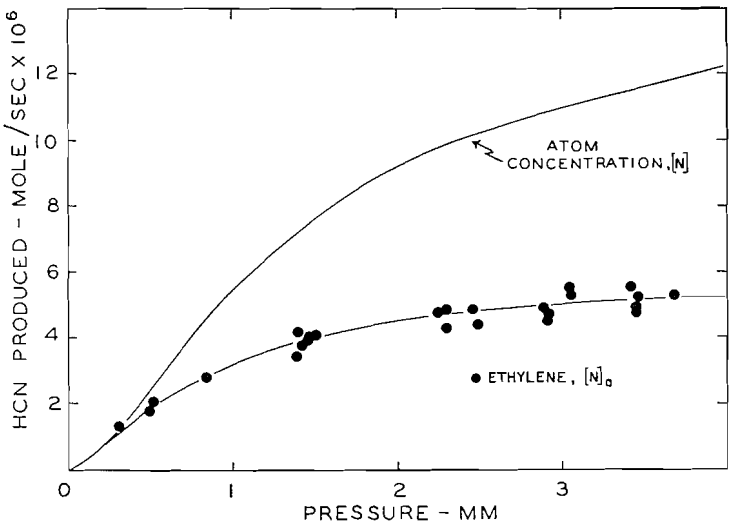


FIG. 2. Series 1. HCN production from ethylene as a function of pressure with both the decay tube and reaction vessel unheated. The reaction temperature varied between 55 and 85° C, depending on the pressure.

with both the decay tube and reaction vessel unheated (*series 1*), together with the corresponding atom concentrations, obtained by reacting ethylene or ethane at 350° C (identical with series 5 of reference 1). The reaction temperature varied from 55 to 85° C, depending on the pressure. The afterglow was completely extinguished in all the experiments of the series.

If the reactivity of ethylene at a given temperature is defined in terms of the HCN production, i.e. $[N]_a = [HCN]$, it follows from Fig. 2 that at the temperature used in the present work $[N]_a < [N]$. This is true in spite of the fact that the suggested mechanism for the ethylene reaction requires that $[N]_a = [N]$ (15, cf. 16). To determine whether the depression of the reactivity is due to catalyzed recombination or to a second active species, it will be noted that $[N]_a \rightarrow [N]$ as $[N] \rightarrow 0$. In other words, taking into consideration that, when the reactant is present in excess, the applicable elementary reactions will have the same order in M, the ethylene reaction appears to involve a combination of reactions [1] and [2] with *one or both* of [3] and [5]. The adequacy of these reactions may be tested by comparing the observed and predicted relations between $[N]_a$ and [N]. The predicted relations will be derived assuming (i) that the reactant M is in excess, (ii) that the NM complexes exist in steady-state (cf. footnote 5), and (iii) that reactions between N atoms and fragments of M give rise to HCN. Then, for the combination

[1] + [2] + ([3] and/or [5]), where $p_3 = 0$, one has

$$d[N]/dt = -(1+p_2)k_2[NM]-2(k_3+k_5)[N][NM],$$

$$d[N]_a/dt = d[HCN]/dt = (n+p_2)k_2[NM].$$

Hence, proceeding as in reference 4,

$$[8] \qquad [N]_a = \frac{(n+p_2)k_2}{2(k_3+k_5)} \ln\left\{1+\frac{2(k_3+k_5)[N]}{(1+p_2)k_2}\right\}.$$

Similarly, for a combination [1] + [2] + [3], where $p_3 > 0$, one has

$$[9] \qquad [N]_a = \frac{p_3[N]}{2+p_3} + \frac{k_2[2(n+p_2)+(n-1)p_3]}{(2+p_3)^2k_3} \ln\left\{1+\frac{(2+p_3)k_3[N]}{(1+p_2)k_2}\right\}.$$

For the ethylene reaction $n = 1$, while p_3 will lie somewhere between 0 and 2. The experimental data should therefore be consistent either (i) with equation [8] ($n = 1$), (ii) with equation [9] ($n = 1$, $p_3 = 2$), or (iii) with some intermediate type of behavior. It is seen in Table I that equation [8] is by itself sufficient to correlate the data. One thus concludes that the ethylene reaction can be adequately explained in terms of a combination of reactions [1] and [2] with [3] and/or [5], where $p_3 \rightarrow 0$, the last two processes being varieties of what may be called *homogeneous catalyzed recombination*. It is not necessary to introduce a second active species.

TABLE I

HCN production from ethylene in the region 55 to 85° C

Pressure (mm)	$[N]_a$ = [HCN]* (mm)	[N]* (mm)	Predicted values of $[N]_a$ when $(k_3+k_5)/(1+p_2)k_2 = 8$ mm^{-1} or 2.8×10^{-16} cc molecule^{-1} (using equation [8] with $n = 1$)†	Predicted values of $[N]_a$ when $k_3/(1+p_2)k_2 = 32$ mm^{-1} (using equation [9] with $n = 1$ and $p_3 = 2$)†
0.5	.042	.054	.039	.035
1.0	.061	.103	.061	.062
1.5	.072	.139	.073	.081
2.0	.079	.164	.080	.094
3.0	.088	.190	.087	.108
4.0	.093	.210	.092	.118

*The experimental values of $[N]_a$ and [N], as given in Fig. 2, have been converted from *micromole sec*$^{-1}$ to *millimeter* using the factors given in Table I of reference 1. A slight error is associated with this change of units, since the conversion factors do not take into account the presence of the reactant and products. When referring to Table I of reference 1, the following change should be made in the heading of column 2: delete "$\times10^6$".

†The values assigned to the constants $(k_3+k_5)/(1+p_2)k_2$ and $k_3/(1+p_2)k_2$ have been chosen by trial and error so as to give the best fit to the data at 1 mm pressure.

The conclusion that $p_3 \rightarrow 0$, i.e. that the reactive fragments formed in reaction [3] do not consume an appreciable quantity of N atoms, may seem surprising. However, it is in accord with the work of Dunford *et al.* (17), where there was indication that ethylene which is excited by a process like [3] tends to revert to the ground state rather than to C_2H_2 or CH_2.

Several interesting rate constants can be obtained from the ratio $(k_3+k_5)/(1+p_2)k_2$ as given in Table I. Assuming that $p_2 = 1$,[4] and combining the above ratio with the over-all second-order rate constant for HCN production from ethylene as estimated by Milton and Dunford (18), i.e. $k_2k_1/k_{-1} \approx 1.6\times10^{-13}$ cc molecule^{-1} sec^{-1} at 40° C, one obtains the over-all third-order rate constant for N atom recombination catalyzed by

[4]*One* CH_3 *is believed to form in the ethylene reaction along with each primary* HCN *(15). The value* $p_2 = 1$ *therefore corresponds to complete conversion of the* CH_3 *to secondary* HCN, *so that a value slightly less than 1 might be more consistent with the recovery of small amounts of methane and ethane.*

ethylene, namely $2(k_3+k_5)k_1/k_{-1} \approx 1.8\times10^{-28}$ cc^2 molecule^{-2} sec^{-1}.[5] Combining the ratio with *upper* limits for (k_3+k_5) and k_1, as derived from the collision frequencies, one obtains the values $1/k_2 \geqslant 1\times10^{-6}$ sec for the lifetime of the $N\cdot C_2H_4$ complex with respect to decomposition into $HCN + CH_3$, and $1/k_{-1} \geqslant 5\times10^{-10}$ sec for the lifetime with respect to dissociation into $N + C_2H_4$. (In calculating (k_3+k_5) and k_1, the values $\sigma_N = 3\times10^{-8}$ cm and $\sigma_{C_2H_4} = \sigma_{N\cdot C_2H_4} = 5\times10^{-8}$ cm were used, and a temperature of 70° C was assumed.)

The value obtained for the rate constant of N atom recombination catalyzed by ethylene is compared with certain related constants in Table II. It is seen that the catalyzed

TABLE II

Comparison of third-order processes involving N atoms

Process*	Temperature (°C)	Third-order rate constant (cc^2 molecule^{-2} sec$^{-1}\times10^{33}$)	Lifetime of the relevant bimolecular complex with respect to dissociation (sec)	Reference
Homogeneous catalyzed recombination in the presence of C_2H_4	55 to 85	180,000	$\geqslant5\times10^{-10}$ (i.e. $1/k_{-1}$)	Present
Homogeneous catalyzed recombination in the presence of CH_3CN	70	700	$\geqslant2\times10^{-12}$ (i.e. $1/k_{-1}$)	4†
Collision rate $\times2$ (using $\sigma = 3\times10^{-8}$ cm)	70	40	$\sim4\times10^{-13}$	—
Homogeneous decay	Ambient	15 to 33	?	8, 19, 20
	~55	3 to 5‡	?	1, 21

*Though surface decay is not a third-order process, it is interesting to note that, as shown on p. 73 of reference 1, this process is perhaps an order of magnitude *more* efficient than homogeneous decay, and therefore much *less* efficient than the particular examples of catalyzed recombination.

†The rate constants in Table I of reference 4 have been extrapolated to 70° C in a plot of log k vs $1/T$. The value of $1/k_{-1}$ was then found as in the present work. The lifetime of the $N\cdot CH_3CN$ complex with respect to *reaction* (i.e. $1/k_2$) is not included in Table II; its value is $\geqslant4\times10^{-6}$ sec, which is comparable to the value for $N\cdot C_2H_4$ as given in the text.

‡The range of values 1.3 to 2.4 was given in reference 1; however, a recalculation of the results of reference 1 using improved values for the time of decay gives 3 to 5 (21).

recombination is particularly rapid, and, as would be expected, that the rapidity is associated with a relatively long-lived NM complex.

It is obvious that the preceding treatment of the ethylene reaction is valid only in so far as the elementary processes considered (equations [1] to [7]) represent all that are relevant.

Ethane and Ammonia

The production of HCN from ethane and the destruction of ammonia were next investigated, the reaction vessel being unheated and the decay tube either unheated (*series 2*), at 400° C (*series 3*), or removed altogether as shown in Fig. 1 (*series 4 and 5*). The results, together with the corresponding atom concentrations estimated from the reactions of ethylene or ethane at 350° C (for series 2 and 3 identical with series 5 and 6 of reference 1), are shown in Figs. 3A, 3B, and 3C. The afterglow was weakened, but not extinguished, in the presence of ammonia.

In marked contrast to ethylene, the extents of reaction of ethane and ammonia at lower temperatures, i.e. $[N]_a$, remain substantially less than the atom concentration in

[5] *The over-all rate constants for* HCN *production and catalyzed recombination take on the simple forms given only (i) if the* NM *complexes are in steady-state, i.e.* $k_{-1} \gg k_1[M]$ *(cf. equation [44] of reference 4), and (ii) if* $k_{-1} \gg (k_2+(k_3+k_5)[N])$. *That these inequalities are reasonable is borne out by the values actually obtained for the various constants.*

the limit $[N] \rightarrow 0$. The very low ammonia reactivity in the experiments of series 4 is perhaps especially to be noted. The low reactivities of ethane and ammonia are therefore clearly due to some effect other than the combination [1] + [2] + ([3] and/or [5]) as with ethylene. Considering ammonia alone, all other combinations of elementary reactions can be eliminated on the basis of the fact that the reactivity of ammonia can be varied over wide limits by acts affecting the active nitrogen prior to its entry into the reaction vessel, yet which in certain cases leave the atom concentration within the reaction vessel essentially unchanged. For example, in series 2 at 1 mm pressure, $[N] = 5.4$ micromole sec^{-1} and $[N]_a = 0.50$; in series 5, on the other hand, though the value of $[N]$ at 1 mm was nearly the same (4.6), the value of $[N]_a$ was very low (0.00).

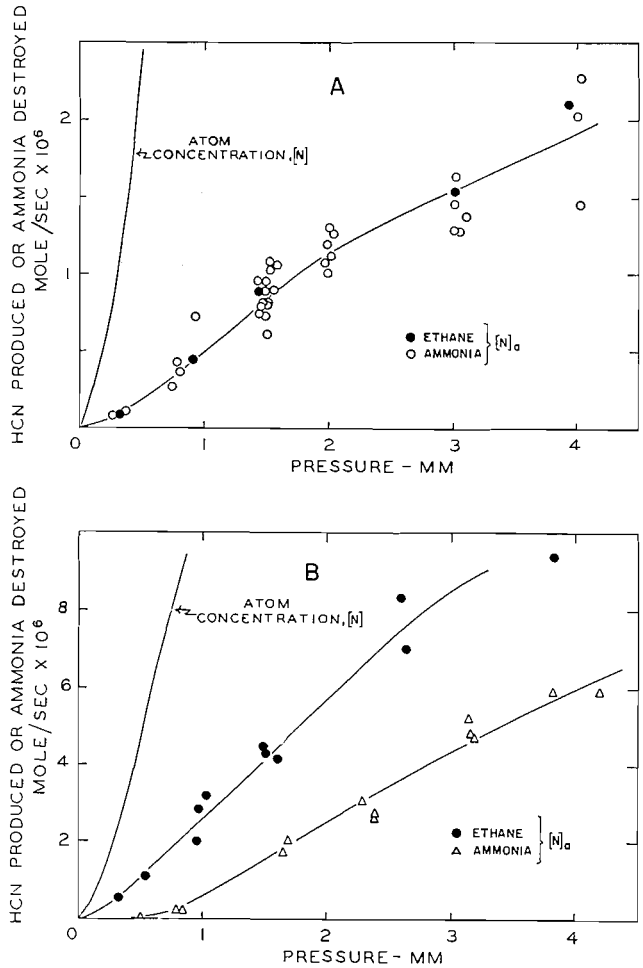


FIG. 3. (A) Series 2. HCN production from ethane and ammonia destruction as functions of pressure with both the decay tube and reaction vessel unheated. Temperature of reaction vessel = 40 to 70° C.

(B) Series 3. HCN production from ethane and ammonia destruction as functions of pressure with the reaction vessel unheated, as before, but the decay tube at 400° C. The reactivity of ethane is probably spuriously high due to the proximity of the hot decay tube. Temperature of reaction vessel = 50 to 130° C.

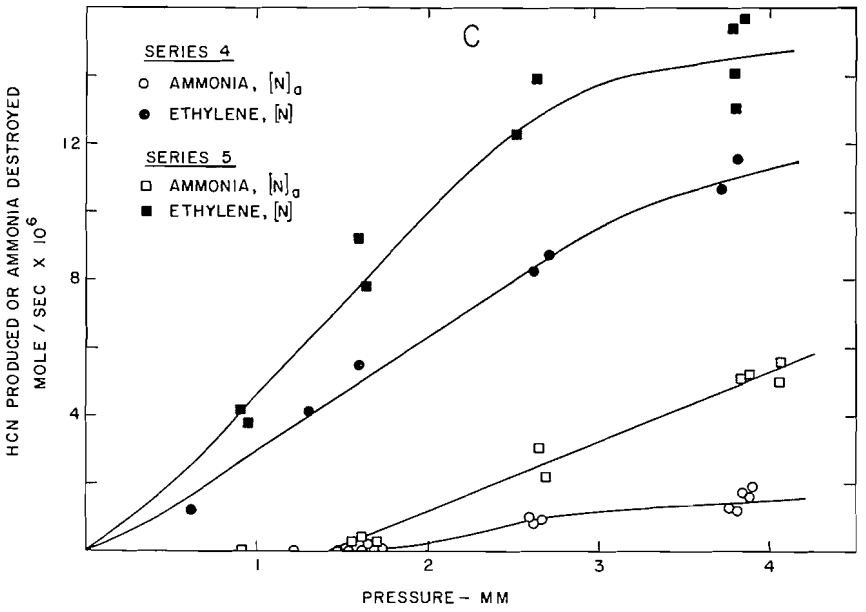


FIG. 3. (C) Series 4 and 5. Ammonia destruction as a function of pressure with the reaction vessel attached directly to the discharge tube near an electrode. In series 4 the nitrogen entered the discharge tube at the end to which the reaction vessel was attached, while in series 5 it entered at the opposite end. The reaction vessel was unheated, the temperature being 55 to 100° C in series 4, and 60 to 150° C in series 5.

The failure of the ammonia reactivity to be governed by the instantaneous atom concentration is strong evidence that an active species other than the N atom initiates the ammonia reaction, a conclusion in essential agreement with previous work (see introductory section). Whether the ethane reaction involves a second active species, or merely a combination of elementary reactions different from those involved with ethylene, cannot be determined from the present data. In particular a better control of temperature is needed since, while the ammonia reaction is virtually independent of temperature in the region of interest (5), the ethane reaction is not. H atom attack might also serve to complicate the ethane reaction (3).

An indication of the mode of formation of the species which reacts with ammonia can be obtained from series 4. In this series, the reaction vessel was attached directly to the discharge tube *near the point of entry of the nitrogen*, so that the active nitrogen formed in the proximity of a metal electrode. The atom concentration therefore fell rapidly from the high value necessarily existing at the instant of each flash. Accordingly, the observation in series 4 that the ratio $[N]_a/[N]$ was lower at a given pressure than in any other series, and also lower than in the work of references 5, 22, and 23, implies that the second active species is formed by homogeneous atom decay.

A species formed by homogeneous atom decay is necessarily an excited molecule.

It is not possible, with the information available, to determine whether the reactivity of ammonia can be predicted quantitatively in terms of a second active species; however, the fact that the species is formed by a *multiorder* mode of atom decay is certainly consistent with the trend that is revealed by examining the data in Figs. 3A, 3B, and 3C for the ratio $[N]_a/[N]$ to increase as [N] is increased. A similar trend was observed in references 22 and 23, in both of which a condensed discharge was used as in the present

work. A multiorder origin for the second active species also serves to explain the observations that, when a microwave discharge is used so that the atom concentration is very low even in the discharge tube, little or no ammonia destruction is found (6, 8), and excited molecules are not observed by mass spectrometry (11, 24).

The observation of Kaufman and Kelso (25) that, under conditions similar to those where essentially *no* ammonia destruction is observed (6, 8), certain thermal effects appear to be caused by excited molecules would seem at first sight contradictory to the present work. Note, however, that Dressler (26) has observed ground-state nitrogen in the first vibrational level as a component of active nitrogen. Provided this species were formed in the discharge process, it would be expected to persist even at the very low atom concentrations of reference 25; moreover, though the species would be comparatively inert chemically, it could lead to simple thermal effects.

The subject of the identity of the species reacting with ammonia will be considered in a subsequent paper.

REFERENCES

1. R. KELLY and C. A. WINKLER. Can. J. Chem. **37**, 62 (1959).
2. D. M. WILES and C. A. WINKLER. Can. J. Chem. **35**, 1298 (1957).
3. P. A. GARTAGANIS and C. A. WINKLER. Can. J. Chem. **34**, 1457 (1956).
4. W. FORST, H. G. V. EVANS, and C. A. WINKLER. J. Phys. Chem. **61**, 320 (1957).
5. G. R. FREEMAN and C. A. WINKLER. J. Phys. Chem. **59**, 371 (1955).
6. G. B. KISTIAKOWSKY and G. G. VOLPI. J. Chem. Phys. **28**, 665 (1958).
7. K. D. BAYES and G. B. KISTIAKOWSKY. J. Chem. Phys. **32**, 992 (1960).
8. J. T. HERRON, J. L. FRANKLIN, P. BRADT, and V. H. DIBELER. J. Chem. Phys. **30**, 879 (1959).
9. H. G. V. EVANS and C. A. WINKLER. Can. J. Chem. **34**, 1217 (1956).
10. H. G. V. EVANS, G. R. FREEMAN, and C. A. WINKLER. Can. J. Chem. **34**, 1271 (1956).
11. D. S. JACKSON and H. I. SCHIFF. J. Chem. Phys. **23**, 2333 (1955).
12. S. E. SOBERING and C. A. WINKLER. Can. J. Chem. **36**, 1223 (1958).
13. H. B. DUNFORD and B. E. MELANSON. Can. J. Chem. **37**, 641 (1959).
14. R. A. WESTBURY and C. A. WINKLER. Can. J. Chem. **38**, 334 (1960).
15. J. VERSTEEG and C. A. WINKLER. J. Chem. Phys. **31**, 1 (1953).
16. J. T. HERRON, J. L. FRANKLIN, and P. BRADT. Can. J. Chem. **37**, 579 (1959).
17. H. B. DUNFORD, H. G. V. EVANS, and C. A. WINKLER. Can. J. Chem. **34**, 1074 (1956).
18. E. R. V. MILTON and H. B. DUNFORD. J. Chem. Phys. To be published.
19. P. HARTECK, R. R. REEVES, and G. MANNELLA. J. Chem. Phys. **29**, 608 (1958).
20. T. WENTINK, J. O. SULLIVAN, and K. L. WRAY. J. Chem. Phys. **29**, 231 (1958).
21. R. A. BACK, W. DUTTON, and C. A. WINKLER. Can. J. Chem. **37**, 2059 (1959).
22. D. A. ARMSTRONG and C. A. WINKLER. J. Phys. Chem. **60**, 1100 (1956).
23. G. J. VERBEKE and C. A. WINKLER. J. Phys. Chem. **64**, 319 (1960).
24. J. BERKOWITZ, W. A. CHUPKA, and G. B. KISTIAKOWSKY. J. Chem. Phys. **25**, 457 (1956).
25. F. KAUFMAN and J. R. KELSO. J. Chem. Phys. **28**, 510 (1958).
26. K. DRESSLER. J. Chem. Phys. **30**, 1621 (1959).

Can. J. Chem. Downloaded from www.nrcresearchpress.com by 210.87.254.42 on 09/05/12
For personal use only.

NOTES

INDOLYL-3-ACETALDOXIME

A. Ahmad, I. Eelnurme, and Ian D. Spenser

In connection with our work on the biosynthesis of indolyl-3-acetonitrile (1) we have prepared and characterized indolyl-3-acetaldoxime, which had been postulated (2) as the biological precursor of indolyl-3-acetonitrile, but does not appear to have been described.

EXPERIMENTAL

Indolyl-3-acetaldoxime

The sodium bisulphite adduct of indolyl-3-acetaldehyde (3) (1.310 g, 0.005 mole) was suspended in water and the pH of the mixture was adjusted to pH 8 by addition of 5% Na_2CO_3 solution. A solution of hydroxylamine hydrochloride (0.380 g, 0.0055 mole) in water, similarly adjusted to pH 8, was added, the mixture was stirred for a few minutes, filtered, and kept at 5°. After 12 hours the product (0.450 g, 52%), melting at 127–128° was filtered off. Recrystallization from chloroform gave indolyl-3-acetaldoxime as silvery plates, melting at 140–141°. (Found: C, 68.8; H, 5.9; N, 15.9. $C_{10}H_{10}N_2O$ requires: C, 69.0; H, 5.8; N, 16.1%.) Infrared absorption in Nujol (cm^{-1}): 3385 (s), 3220 (s), 1642 (m). Ultraviolet absorption (λ_{max}, $m\mu$ (log ϵ)) in ethanol: 220(4.58), 275 (shoulder) (3.83), 281(3.85), 290(3.77).

Conversion of Indolyl-3-acetaldoxime to Indolyl-3-acetonitrile

The oxime (0.210 g, 0.0012 mole) was dissolved in 5 ml acetic anhydride and allowed to stand 18 hours at room temperature. The dark mixture was treated with excess 10% NaOH solution and extracted with ether. The ether extract was dried (Na_2CO_3) and concentrated, and the residual oil was distilled at 100–110° and 2.10^{-3} mm yielding indolyl-3-acetonitrile as an oil (0.055 g, 30%) whose infrared absorption was identical with that of an authentic specimen (1). The oil crystallized on seeding with authentic indolyl-3-acetonitrile, melting point 34–36°.

The same product was obtained when $POCl_3$ was used in place of acetic anhydride.

Reduction of Indolyl-3-acetaldoxime to Tryptamine

A solution of the oxime (0.250 g, 0.00144 mole) in dry ether was added dropwise to a boiling suspension of $LiAlH_4$ in ether. After complete addition the mixture was refluxed for 1 hour, allowed to cool, decomposed by pouring into water, and acidified with 2 *M* H_2SO_4 until a clear solution was obtained, which was extracted with ether. The aqueous layer was made alkaline with 10% NaOH and some LiOH was filtered off. The filtrate was repeatedly extracted and the precipitate washed with ether. The combined ether extracts and washings were dried (NaOH), the solvent evaporated, and the oily residue distilled at 105–110° and 5.10^{-3} mm yielding tryptamine (0.132 g, 57%), melting at 116–118°, identical with an authentic specimen in melting point, mixed melting point, and infrared absorption.

1. A. Ahmad and I. D. Spenser. Can. J. Chem. **38**, 1625 (1960).
2. W. N. Dannenburg and J. L. Liverman. Plant Physiol. **32**, 263 (1957).
3. R. A. Gray. Arch. Biochem. Biophys. **81**, 480 (1959).

Received August 16, 1960.
Department of Chemistry,
McMaster University,
Hamilton, Ontario.

STRETCHING VIBRATIONS OF THE FREE $\overset{+}{N}H_3$ GROUP

P. CHEVALIER AND C. SANDORFY

The usual method of measuring vibrational frequencies of free X–H groups i.e. taking the spectra of dilute solutions in a non-polar solvent cannot be applied to the case of the protonated amino group because of the insolubility of amine salts in such solvents. Even if they were soluble the hydrogen bonds which are of the $\overset{+}{N}$—H— — — halogen$^-$ type would probably still prevail.

The only possibility seems to be, therefore, to prepare salts with bulky anions where steric hindrance would prevent the formation of hydrogen bonds. This method was applied by Nakamoto, Margoshes, and Rundle (1) and by Nakanishi, Goto, and Ohashi (2), who used the tetraphenylborate anion. They obtained $\overset{+}{N}H_3$ stretching bands which lie around 3100 cm^{-1} for methyl and ethyl amine salts.

There is some doubt, however, whether these bands can be considered as "free" $\overset{+}{N}H_3$ stretching bands. First, the half-width of these bands as found by us is between 30 and 40 cm^{-1} while, for example, the half-width of the free OH band in phenol is about 15 cm^{-1}. Secondly, we have observed (3) that perchloric acid salts of amines have $\overset{+}{N}H_3$ stretching bands in the same frequency range but they are broad. It seems to be likely therefore that the bonds described by the above-mentioned authors correspond actually to weakly hydrogen-bonded $\overset{+}{N}H_3$ groups and the really free $\overset{+}{N}H_3$ groups give bands at higher frequencies.

Whether the $\overset{+}{N}H_3$ groups are "free" or hydrogen-bonded seems to depend, even in the case of tetraphenylborates, on the particular spacial requirements in the given crystal.

Here are some of the frequencies and half-widths related to cases where the $\overset{+}{N}H_3$ group appears to be "free" in a very good approximation:

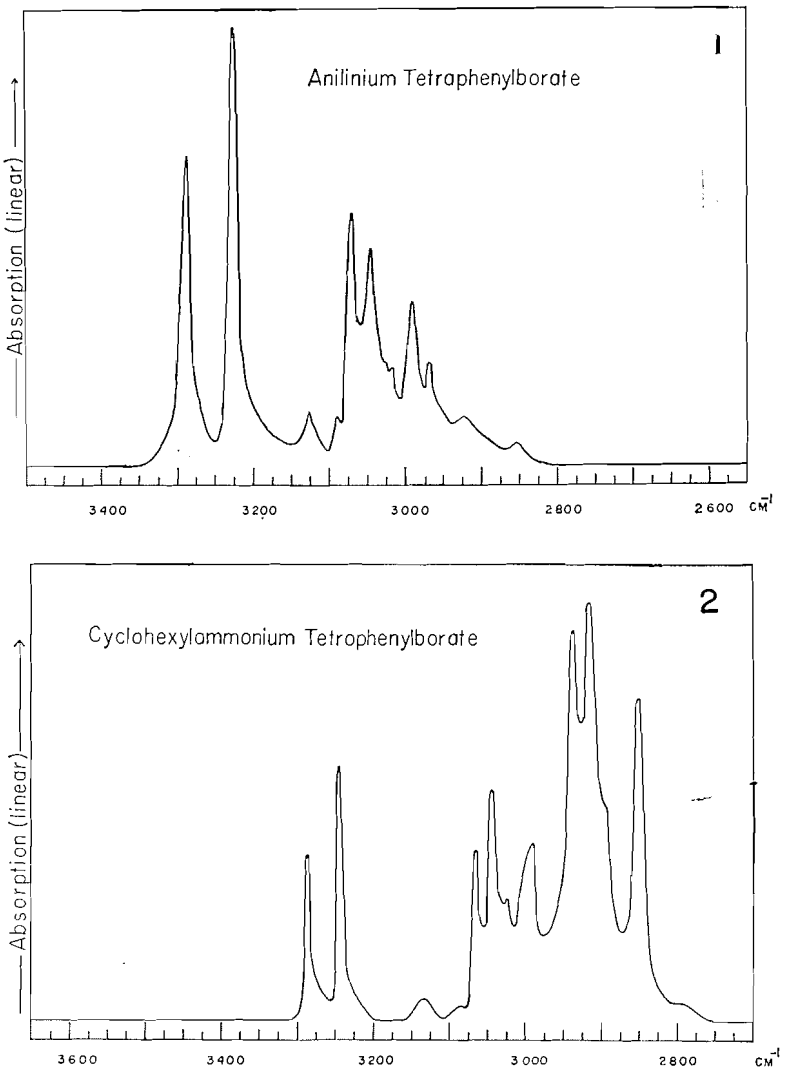
Anilinium tetraphenylborate	3286 cm^{-1}	3225 cm^{-1}
	11 cm^{-1}	12 cm^{-1}
α-Naphthylammonium tetraphenylborate	3313 cm^{-1}	3260 cm^{-1}
	12 cm^{-1}	13 cm^{-1}
β-Naphthylammonium tetraphenylborate	3313 cm^{-1}	3260 cm^{-1}
	14 cm^{-1}	16 cm^{-1}
Cyclohexylammonium tetraphenylborate	3286 cm^{-1}	3246 cm^{-1}
	9 cm^{-1}	11 cm^{-1}

Figure 1 gives the spectrum of the anilinium salt, and Fig. 2 the one of the cyclohexylammonium salt (dried in vacuum at 105° C). They were measured in fluorocarbon oil mulls.

Since this work was started Kynaston, Larcombe, and Turner (4) reported the spectra of a number of tetrachloroborates and a few tetrafluoroborates. They found the bands pertaining to the free $\overset{+}{N}H_3$ group in the case of methylammonium tetrafluoroborate to

Can. J. Chem. Downloaded from www.nrcresearchpress.com by 210.87.254.40 on 09/05/12
For personal use only.

Can. J. Chem. Downloaded from www.nrcresearchpress.com by 210.87.254.40 on 09/05/12
For personal use only.



FIGS. 1 AND 2.

lie at 3282 and 3223 cm^{-1}. As may be inferred from their data, weak hydrogen bonds occur in all the other compounds.

From our data it is possible to measure the shift from the "free" bands to the bands in hydrochlorides.

Taking the arithmetic means of the two free $\overset{+}{N}H_3$ frequencies and the "center of gravity" of the broad composite hydrochloride bands (see 5 and 6) we obtain the following values:

Cyclohexylammonium	3266–2980 = 286 cm^{-1}
Anilinium	3256–2810 = 446 cm^{-1}
α-Naphthylammonium	3286–2810 = 476 cm^{-1}
β-Naphthylammonium	3286–2850 = 436 cm^{-1}

These values indicate medium strong hydrogen bonding in the hydrochlorides.

It is of interest to mention in this respect that Côté and Thompson (7) found 3332 cm^{-1} for the frequency of the triply degenerate stretching vibration of the ammonium ion in NH_4BF_4 where it very probably does not form hydrogen bonds and that Wagner and Hornig (8) found the corresponding band of the hydrogen-bonded ion at 3086 cm^{-1} in NH_4Cl.

Work is going on in this laboratory in order to prepare tetraphenylborates of many more primary, secondary, and tertiary amines. The results and further discussion will be given later.

We acknowledge a stimulating conversation with Professor D. F. Hornig.

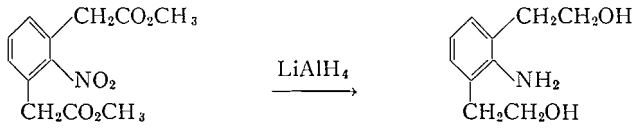
1. K. Nakamoto, M. Margoshes, and R. E. Rundle. J. Am. Chem. Soc. **77**, 6480 (1955).
2. K. Nakanishi, T. Goto, and M. Ohashi. Bull. Chem. Soc. Japan, **30**, 403 (1957).
3. C. Brissette. M.Sc. Thesis, Université de Montréal, Montréal, Qué. 1959.
4. W. Kynaston, B. E. Larcombe, and H. S. Turner. J. Chem. Soc. 1774 (1960).
5. B. Chenon and C. Sandorfy. Can. J. Chem. **36**, 1181 (1958).
6. C. Brissette and C. Sandorfy. Can. J. Chem. **38**, 34 (1960).
7. G. L. Côté and H. W. Thompson. Proc. Roy. Soc. A, **210**, 217 (1951).
8. E. L. Wagner and D. F. Hornig. J. Chem. Phys. **18**, 296 (1950).

Received July 4, 1960.
Département de Chimie,
Université de Montréal,
Montréal, Qué.

LITHIUM ALUMINUM HYDRIDE REDUCTION OF STERICALLY HINDERED AROMATIC NITRO COMPOUNDS

F. A. L. Anet and J. M. Muchowski

In connection with another research problem it became necessary to prepare 2,6-di-(2-hydroxyethyl)-aniline (II). When 2,6-di(methoxycarbonylmethyl)-nitrobenzene (I) was subjected to lithium aluminum hydride reduction none of the azo compound was obtained; instead the desired amino di-alcohol was isolated in 54% yield. This reduction



I II

was unexpected as it has been reported (1–5) that aromatic nitro compounds on lithium aluminum hydride reduction give rise to the corresponding azo compounds exclusively. Indeed, the immediate appearance of a red "azo" color on treatment of an ether solution of lithium aluminum hydride with an aromatic nitro compound has been suggested as a sensitive test for such compounds (1, 6, 7).

To test the generality of the reaction several mono- and di-ortho substituted nitro benzenes were reduced (see Table I). Obviously, the increase in amine formation parallels

Can. J. Chem. Downloaded from www.nrcresearchpress.com by 210.87.254.40 on 09/05/12
For personal use only.

These values indicate medium strong hydrogen bonding in the hydrochlorides.

It is of interest to mention in this respect that Côté and Thompson (7) found 3332 cm^{-1} for the frequency of the triply degenerate stretching vibration of the ammonium ion in NH_4BF_4 where it very probably does not form hydrogen bonds and that Wagner and Hornig (8) found the corresponding band of the hydrogen-bonded ion at 3086 cm^{-1} in NH_4Cl.

Work is going on in this laboratory in order to prepare tetraphenylborates of many more primary, secondary, and tertiary amines. The results and further discussion will be given later.

We acknowledge a stimulating conversation with Professor D. F. Hornig.

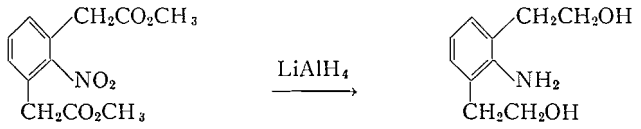
1. K. Nakamoto, M. Margoshes, and R. E. Rundle. J. Am. Chem. Soc. **77**, 6480 (1955).
2. K. Nakanishi, T. Goto, and M. Ohashi. Bull. Chem. Soc. Japan, **30**, 403 (1957).
3. C. Brissette. M.Sc. Thesis, Université de Montréal, Montréal, Qué. 1959.
4. W. Kynaston, B. E. Larcombe, and H. S. Turner. J. Chem. Soc. 1774 (1960).
5. B. Chenon and C. Sandorfy. Can. J. Chem. **36**, 1181 (1958).
6. C. Brissette and C. Sandorfy. Can. J. Chem. **38**, 34 (1960).
7. G. L. Côté and H. W. Thompson. Proc. Roy. Soc. A, **210**, 217 (1951).
8. E. L. Wagner and D. F. Hornig. J. Chem. Phys. **18**, 296 (1950).

Received July 4, 1960.
Département de Chimie,
Université de Montréal,
Montréal, Qué.

LITHIUM ALUMINUM HYDRIDE REDUCTION OF STERICALLY HINDERED AROMATIC NITRO COMPOUNDS

F. A. L. Anet and J. M. Muchowski

In connection with another research problem it became necessary to prepare 2,6-di-(2-hydroxyethyl)-aniline (II). When 2,6-di(methoxycarbonylmethyl)-nitrobenzene (I) was subjected to lithium aluminum hydride reduction none of the azo compound was obtained; instead the desired amino di-alcohol was isolated in 54% yield. This reduction



I II

was unexpected as it has been reported (1–5) that aromatic nitro compounds on lithium aluminum hydride reduction give rise to the corresponding azo compounds exclusively. Indeed, the immediate appearance of a red "azo" color on treatment of an ether solution of lithium aluminum hydride with an aromatic nitro compound has been suggested as a sensitive test for such compounds (1, 6, 7).

To test the generality of the reaction several mono- and di-ortho substituted nitro benzenes were reduced (see Table I). Obviously, the increase in amine formation parallels

Can. J. Chem. Downloaded from www.nrcresearchpress.com by 210.87.254.42 on 09/05/12
For personal use only.

TABLE I

Reduction products of aromatic nitro compounds with lithium aluminum hydride

Nitro compound	Azo derivative		Amine		
	% Yield	M.p., °C	% Yield	M.p., °C	Picrate, m.p., °C
Nitrobenzene	73.5	67–68[a]	—	—	
o-Nitrotoluene	30.9	53–54[a]	25.5	—	213[a]
o-Nitro-β-phenylethanol	41.2	138–139[b]	30.9	—	181.5–183.5[c]
1,3-Dimethyl-2-nitrobenzene	20.9	44.5–45[d]	53.1	—	184.5–186[a]
Nitromesitylene	10.7	73–75[e]	61.2	—	189–190[a]
2,6-Di(methoxycarbonyl)-nitrobenzene	—	—	44.4	120–121[f]	—
2,6-Di(methoxycarbonylmethyl)-nitrobenzene[g]	—	—	54.4	101–102[h]	—

[a]These melting points are in agreement with those stated in "A textbook of practical organic chemistry", *edited by* A. I. Vogel. Longmans, Green and Co. Ltd., London. 1948.

[b]Recrystallized from ethanol – petroleum ether (b.p. 80–100°). Calc. for $C_{16}H_{13}O_2N_2$: C, 71.09; H, 6.71%. Found: C, 71.33; H, 6.70%.

[c]Recrystallized from ethanol. Calc. for $C_8H_{11}ON$, $C_6H_3O_7N_3$: C, 45.90; H, 3.85%. Found: C, 46.19; H, 3.97%.

[d]J. T. Edward (J. Chem. Soc. 222 (1956)) reported m.p. 46–47°.

[e]P. Grammaticakis (Bull. Soc. chim. France, 951 (1951)) reported m.p. 75°.

[f]Recrystallized from ethanol – petroleum ether (b.p. 80–100°). Calc. for $C_8H_{11}O_2N$: C, 62.72; H, 7.24%. Found: C, 63.13; H, 7.22%.

[g]F. A. L. Anet and E. Nishizawa (unpublished work) give m.p. 144–145°.

[h]Recrystallized from ethanol – petroleum ether (b.p. 80–100°). Calc. for $C_{10}H_{15}O_2N$: C, 66.27; H, 8.34%. Found: C, 65.96; H, 8.33%.

increasing steric hindrance around the nitro group. The formation of azo compounds is known to take place by the condensation of the nitroso compound and the hydroxylamine or the amine (10) and these reactions would be expected to be sensitive to steric hindrance. The 2,6-disubstituted nitrobenzenes investigated gave mainly the amine. On the other hand, Nystrom and Brown (1) report a 71% yield of azomesitylene, while in our hands 61% mesidine and 11% azomesitylene were obtained on reduction of nitromesitylene, even under conditions identical with those given by these workers.

It appears that such anomalous reductions are not completely unknown. Ried and Müller (8) obtained 4,4′-diaminoazobenzene by lithium aluminum hydride reduction of 4,4′-dinitroazobenzene. Adams *et al.* (9) were unable to reduce 3-chloro-2-nitroanisole to the azo derivative. They do not, however, mention what, if any, product was isolated. Wiberg and Jahn (11) have reported the formation of *p*-toluidine from *p*-nitrotoluene by reduction with lithium aluminum hydride, but only in presence of aluminum chloride. In the absence of aluminum chloride *p*-azotoluene was the main product.

EXPERIMENTAL

Melting points and boiling points are uncorrected.

The lithium aluminum hydride reductions were carried out in one of two ways depending on the solubility of the starting material in ether.

(i) When the nitro compound was ether soluble, its ether solution was added in a dropwise manner to a suspension of a half-molar excess of the hydride in anhydrous ether. When the addition was complete, the mixture was boiled under reflux for 6 hours. Amines formed were extracted with 10% hydrochloric acid and identified as their picrates (melting points and mixed melting points). The azo compounds were crystallized from the appropriate solvent and identified by comparing their properties with those given in the literature.

Can. J. Chem. Downloaded from www.nrcresearchpress.com by 210.87.254.42 on 09/05/12
For personal use only.

(ii) If the nitro compounds* were only slightly soluble in ether, they were introduced to the hydride suspension (over a period of 24 hours) by the Soxhlet extractor technique. No azo compounds were formed in these cases and the amines were isolated by filtration of the organic layer, evaporation to dryness, and crystallization of the solid residue from the appropriate solvent system.

ACKNOWLEDGMENT

We wish to thank the National Research Council of Canada for the award of a studentship to one of us (J.M.M.).

1. R. NYSTROM and W. G. BROWN. J. Am. Chem. Soc. **70**, 3738 (1948).
2. G. M. BADGER, J. H. SAIDLER, and B. THOMSON. J. Chem. Soc. 3207 (1951).
3. N. G. GAYLORD and J. A. SNYDER. Rec. trav. chim. **72**, 1007 (1953).
4. T. W. CAMPBELL, W. A. MCALLISTER, and M. T. ROGERS. J. Am. Chem. Soc. **75**, 864 (1953).
5. W. THEILACKER and F. BAXMANN. Ann. **581**, 117 (1953).
6. H. GILMAN and TH. N. GOREAU. J. Am. Chem. Soc. **73**, 2939 (1951).
7. L. S. NELSON and D. E. LASKOWSKI. Anal. Chem. **23**, 1495 (1951).
8. W. RIED and F. MÜLLER. Ber. **85**, 470 (1952).
9. R. ADAMS, R. HOLMES, and J. W. WAY. J. Am. Chem. Soc. **75**, 5901 (1953).
10. N. V. SIDGEWICK. The organic chemistry of nitrogen. Oxford University Press, Oxford. 1937. p. 436.
11. E. WIBERG and A. JAHN. Z. Naturforsch. **76**, 581 (1952).

RECEIVED AUGUST 2, 1960.
DEPARTMENT OF CHEMISTRY,
UNIVERSITY OF OTTAWA,
OTTAWA, ONTARIO.

*2,6-Di(methoxycarbonyl)-nitrobenzene and 2,6-di(methoxycarbonylmethyl)-nitrobenzene.

NOTE ON THE THERMAL NEUTRON CAPTURE CROSS SECTION OF Cs^{133}*

A. P. BAERG† AND R. M. BARTHOLOMEW

During the course of recent investigations relating to the detection efficiency of 4π beta proportional counters for Cs^{134m} (1) it was noted that in the neutron irradiation of Cs^{133} the amount of Cs^{134m} produced is several orders of magnitude greater than would be estimated from the 17-millibarn cross section quoted for this reaction (2). The $Cs^{133}(n,\gamma)$ Cs^{134m} cross section was therefore re-examined. At the same time it was possible to check the cross section for the reactions leading to the ground state.

Irradiations

Samples of about 500 μg each of CsCl, together with cobalt wire neutron flux monitors (0.0127 cm diameter) (3), were irradiated in an empty fuel rod position of the NRX reactor. The CsCl was prepared by weighing a solution of known concentration into quartz tubes. These samples were evaporated to dryness in the tubes, which were then sealed for irradiation. Two samples in iron capsules were irradiated for 3 hours each and two others, in 0.076-cm cadmium-lined iron capsules, for a period of 16.5 hours each. The reactor power remained constant during any one irradiation and to within a few per cent throughout these irradiations.

Purification and Counting

The irradiated quartz capsules were crushed under a solution 9 N in hydrochloric acid

*Issued as A.E.C.L. No. 1110.
†Present address: National Research Council, Ottawa, Ontario.

Can. J. Chem. Downloaded from www.nrcresearchpress.com by 210.87.254.42 on 09/05/12
For personal use only.

(ii) If the nitro compounds* were only slightly soluble in ether, they were introduced to the hydride suspension (over a period of 24 hours) by the Soxhlet extractor technique. No azo compounds were formed in these cases and the amines were isolated by filtration of the organic layer, evaporation to dryness, and crystallization of the solid residue from the appropriate solvent system.

ACKNOWLEDGMENT

We wish to thank the National Research Council of Canada for the award of a studentship to one of us (J.M.M.).

1. R. NYSTROM and W. G. BROWN. J. Am. Chem. Soc. **70**, 3738 (1948).
2. G. M. BADGER, J. H. SAIDLER, and B. THOMSON. J. Chem. Soc. 3207 (1951).
3. N. G. GAYLORD and J. A. SNYDER. Rec. trav. chim. **72**, 1007 (1953).
4. T. W. CAMPBELL, W. A. MCALLISTER, and M. T. ROGERS. J. Am. Chem. Soc. **75**, 864 (1953).
5. W. THEILACKER and F. BAXMANN. Ann. **581**, 117 (1953).
6. H. GILMAN and TH. N. GOREAU. J. Am. Chem. Soc. **73**, 2939 (1951).
7. L. S. NELSON and D. E. LASKOWSKI. Anal. Chem. **23**, 1495 (1951).
8. W. RIED and F. MÜLLER. Ber. **85**, 470 (1952).
9. R. ADAMS, R. HOLMES, and J. W. WAY. J. Am. Chem. Soc. **75**, 5901 (1953).
10. N. V. SIDGEWICK. The organic chemistry of nitrogen. Oxford University Press, Oxford. 1937. p. 436.
11. E. WIBERG and A. JAHN. Z. Naturforsch. **76**, 581 (1952).

RECEIVED AUGUST 2, 1960.
DEPARTMENT OF CHEMISTRY,
UNIVERSITY OF OTTAWA,
OTTAWA, ONTARIO.

*2,6-Di(methoxycarbonyl)-nitrobenzene and 2,6-di(methoxycarbonylmethyl)-nitrobenzene.

NOTE ON THE THERMAL NEUTRON CAPTURE CROSS SECTION OF Cs^{133}*

A. P. BAERG† AND R. M. BARTHOLOMEW

During the course of recent investigations relating to the detection efficiency of 4π beta proportional counters for Cs^{134m} (1) it was noted that in the neutron irradiation of Cs^{133} the amount of Cs^{134m} produced is several orders of magnitude greater than would be estimated from the 17-millibarn cross section quoted for this reaction (2). The $Cs^{133}(n,\gamma)$ Cs^{134m} cross section was therefore re-examined. At the same time it was possible to check the cross section for the reactions leading to the ground state.

Irradiations

Samples of about 500 μg each of CsCl, together with cobalt wire neutron flux monitors (0.0127 cm diameter) (3), were irradiated in an empty fuel rod position of the NRX reactor. The CsCl was prepared by weighing a solution of known concentration into quartz tubes. These samples were evaporated to dryness in the tubes, which were then sealed for irradiation. Two samples in iron capsules were irradiated for 3 hours each and two others, in 0.076-cm cadmium-lined iron capsules, for a period of 16.5 hours each. The reactor power remained constant during any one irradiation and to within a few per cent throughout these irradiations.

Purification and Counting

The irradiated quartz capsules were crushed under a solution 9 N in hydrochloric acid

*Issued as A.E.C.L. No. 1110.
†Present address: National Research Council, Ottawa, Ontario.

Can. J. Chem. Downloaded from www.nrcresearchpress.com by 210.87.254.105 on 09/05/12
For personal use only.

and the resulting solution of cesium was then passed through a Dowex A-1 anion exchange column to remove particulate silica. The effluent was evaporated to dryness and the cesium further purified by elution from a Dowex-50 cation resin column (1). Quantitative recovery of the cesium, to within 1/10%, throughout the purification was ensured by suitable monitoring. Weighed aliquots of the cesium solution from the cation resin column were mounted and dried on thin plastic, gold-coated films (4) for counting.

Special precautions were taken to ensure that the cesium was pure and, in particular, free of 2.6-hour Si^{31} from the quartz irradiation capsules. In each experiment, portions of the purified cesium solution were taken for precipitation of the cesium as silicotungstate (5). This cesium was then extracted several times with an amyl acetate solution of sodium tetraphenyl boron (see reference 1). This extraction, though very inefficient for macro amounts of cesium, provided ample activity for study. The decay characteristics of this specially purified material were carefully compared with those of the samples used for the cross-section measurements. The beta decay of all samples showed a half-life of 2.91±0.01 hours (1) after subtraction of the 2.19-year Cs^{134} contribution (less than 1%).

The cobalt wire flux monitors were dissolved, and weighed aliquots dried on plastic films for counting.

All samples were counted with a 4π beta–gamma coincidence counter similar to that described by Campion (6). The method used for determining the detection efficiency of the 4π beta counter for Cs^{134m} is described in reference 1. In the counting of Cs^{134}, the gamma rays in the energy range 0.47 to 1.17 Mev were counted in coincidence with the beta radiations to arrive at the absolute disintegration rates.

Calculations and Results

The distintegration rates observed, referred to the end of the irradiations, are given in Table I together with irradiation times and the cadmium ratios (i.e. the ratio of observed

TABLE I

Experimental data

Irradiation	Irradiation time, hours	Counting rate at end of irradiation d.p.s./μg of target element		
		Co^{60}	Cs^{134m}	Cs^{134}
1. Uncovered	3	1.091×10^{3}	5.50×10^{5}	1.308×10^{3}
2. Uncovered	3	1.075×10^{3}	5.40×10^{5}	1.318×10^{3}
3. Cadmium-covered	16.5	1.882×10^{2}	2.55×10^{5}	2.052×10^{3}
4. Cadmium-covered	16.5	1.892×10^{2}	2.44×10^{5}	1.971×10^{3}
Cadmium ratio (average)		20.26±0.5	4.19±0.12	3.59±0.09

rates of reaction without and with cadmium filter). The half-life values used to calculate the reaction rates are given in Table II. Self-shielding correction factors of 1.04 and 1.62, respectively, for uncovered and cadmium-covered irradiations were also applied to the cobalt data (7).

The cross-sections were calculated using the convention described by Westcott (8) (see also reference 9). A very brief outline only is given here to indicate the method which was used.

The measured reaction rate, R, is equated to the product of the effective cross section, $\hat{\sigma}$, and the conventional flux, nv_0, where n is the neturon density and v_0 is 2200 m/sec.

[1] $$R = \hat{\sigma} n v_0.$$

Can. J. Chem. Downloaded from www.nrcresearchpress.com by 210.87.254.105 on 09/05/12
For personal use only.

TABLE II

Values of parameters used in calculations of cross sections

Co^{59} self-shielding correction factor, cadmium-covered	1.62 (7)
Co^{59} self-shielding correction factor, uncovered	1.04 (7)
Half-life of Co^{60}	5.28 years (2)
Half-life of Cs^{134m}	2.91 hours (1)
Half-life of Cs^{134}	2.19 years (10)
Co^{59} 2200 m/sec cross section	36.68 barns (2)
Co^{59} resonance integral, RI	75 barns (13)
$r\sqrt{T/T_0}$ (measured for irradiation position used)	0.0223±0.0004

The effective cross section is defined by

$$\hat{\sigma} = \sigma_0(g+rs) \qquad [2]$$

where σ_0 is the 2200 m/sec cross section, r is a measure of the relative density of epithermal neutrons, and g and s are factors which depend on the departure of the cross sections from the $1/v$ law. In the present experiment it is assumed that $g = 1$ and the factor s is written as $\sqrt{(T/T_0)}s_0$; thus

$$\hat{\sigma} = \sigma_0\left(1+r\sqrt{\frac{T}{T_0}}s_0\right) \qquad [3]$$

where T is the neturon temperature and T_0 is 293.6° K corresponding to 2200 m/sec neutrons. The term $r\sqrt{T/T_0}$, which is a constant of the reactor for the irradiation position used, is then related to the cadmium ratio, R_{Cd}, and s_0 as follows:

$$r\sqrt{\frac{T}{T_0}} = \frac{1}{R_{Cd}\{s_0+(1/K)\}-s_0}. \qquad [4]$$

Here K is a function of the cadmium cross section and the thickness of filter used, having the value 2.2 in the present experiment (8). The factor s_0, in turn, is given by

$$s_0 = \sqrt{\frac{4}{\pi}}\left(\frac{RI}{\sigma_0}\right)-\frac{1}{K} \qquad [5]$$

where RI is the resonance integral, evaluated above the cadmium cutoff and includes the $1/v$ part above this energy.

The conventional flux, nv_0, is first obtained in the following way from the cobalt data. The factor s_0 is calculated from the known values of RI and σ_0 for cobalt (Table II). The factor $r\sqrt{T/T_0}$ is obtained from equation 4 using the measured cadmium ratio for cobalt and the calculated value of s_0. Then the effective cross section for cobalt (equation 3) is used in equation 1 to get the conventional flux, nv_0.

The effective cross section for cesium was obtained from equation 1 using the observed reaction rate and the conventional flux, nv_0 from the cobalt data. The factor s_0 for cesium is calculated (equation 4) from the observed cadmium ratio and the already known value of $r\sqrt{T/T_0}$. The 2200 m/sec cross section, σ_0, then follows from equation 3 and the resonance integral, RI, from equation 5.

The average cross-section values obtained in this way are given in Table III. The errors quoted are based on an estimated combined uncertainty of 1% in the determination of distintegration rates and a 2% uncertainty in the relative neutron fluxes for the cadmium-covered and uncovered irradiations. Possible errors associated with the parameters listed in Table II (except for $r\sqrt{T/T_0}$) have not been included.

Can. J. Chem. Downloaded from www.nrcresearchpress.com by 210.87.254.105 on 09/05/12
For personal use only.

TABLE III

Cross sections calculated from experimental data and the parameters of Table II

Reaction	$Co^{59}(n, \gamma)Co^{60}$	$Cs^{133}(n, \gamma)Cs^{134m}$	All reactions leading to the ground state
Effective cross section, $\hat{\sigma}$ (barns)	38.19±0.04	3.67±0.07	41.6±0.9
2200 m/sec cross section, σ_0 (barns)	—	2.82±0.07	30.4±0.8
Resonance integral, *RI* (barns)	—	34.4±1.9	461±25

The value obtained in this work for σ_0 (2.82±0.07 barns) for the production of Cs^{134m} is very much greater than that (17 millibarns) quoted in reference 2.

The effective cross section for the reactions leading to the ground state Cs^{134} (41.6 ±0.9 barns) is found to be in good agreement with those obtained by Bidinosti *et al.* (40 barns) (11) and Brown *et al.* (40.9±4.1 barns, which was also measured in a vacant fuel rod position in the NRX reactor) (12). The value obtained for σ_0 is in good agreement with 30±1 barns reported in BNL-325 (2) but differs by somewhat more than the combined errors from the value obtained by Brown. The difference would appear to be accountable to the inherent difficulties in measuring cadmium ratios and uncertainties in neutron energy spectra (see discussion by Brown (12)).

1. A. P. Baerg, R. M. Bartholomew, and R. H. Betts. Can. J. Chem. **38**, 2147 (1960).
2. D. J. Hughes and R. T. Schwartz. Brookhaven National Laboratory Report, BNL-325, 2nd ed.
3. R. E. Jervis. Atomic Energy of Canada Ltd. Report CRDC-730 (1957).
4. B. D. Pate and L. Yaffe. Can. J. Chem. **33**, 15 (1955).
5. R. M. Bartholomew and A. P. Baerg. Can. J. Chem. **34**, 201 (1956).
6. P. J. Campion. Intern. J. Appl. Radiation and Isotopes, **4**, 232 (1959).
7. T. A. Eastwood. Private communication.
8. C. H. Westcott, W. H. Walker, and T. K. Alexander. Intern. Conf. on the Peaceful Uses of Atomic Energy. 2nd Conf. Geneva, 1958. Paper P/202.
9. T. A. Eastwood, A. P. Baerg, C. B. Bigham, F. Brown, M. S. Cabell, W. E. Grummitt, J. C. Roy, L. P. Roy, and R. P. Schuman. Intern. Conf. on the Peaceful Uses of Atomic Energy. 2nd Conf. Geneva, 1958. Paper P/203.
10. W. F. Merritt, P. J. Campion, and R. C. Hawkings. Can. J. Phys. **35**, 16 (1957).
11. D. R. Bidinosti, H. R. Fickel, and R. H. Tomlinson. Intern. Conf. on the Peaceful Uses of Atomic Energy. 2nd Conf. Geneva, 1958. Paper P/201.
12. F. Brown, P. J. Campion, and B. H. Oliver. Can. J. Phys. 1960.
13. F. J. Johnston, J. Halperin, and R. W. Stoughton. Reactor Science, **11**, 95 (1960).

Received July 13, 1960.
Research Chemistry Branch,
Chemistry and Metallurgy Division,
Atomic Energy of Canada Limited,
Chalk River, Ontario.

ISOLATION OF HYPERIN FROM RED-OSIER DOGWOOD (CORNUS STOLONIFERA MICHX.)*

G. V. Nair and E. von Rudloff

In continuation of a systematic search for flavonoid and phenolic compounds in Prairie plants, red-osier dogwood (*Cornus stolonifera* Michx.) was investigated. The members of the *Cornus* family vary from herbs to fairly large trees. *C. stolonifera*, also known as *Svida stolonifera* (Michx.) Rydb., is a medium-sized shrub with characteristic bright red

*Issued as N.R.C. No. 6007.

Can. J. Chem. Downloaded from www.nrcresearchpress.com by 210.87.254.105 on 09/05/12
For personal use only.

TABLE III

Cross sections calculated from experimental data and the parameters of Table II

Reaction	$Co^{59}(n, \gamma)Co^{60}$	$Cs^{133}(n, \gamma)Cs^{134m}$	All reactions leading to the ground state
Effective cross section, $\hat{\sigma}$ (barns)	38.19±0.04	3.67±0.07	41.6±0.9
2200 m/sec cross section, σ_0 (barns)	—	2.82±0.07	30.4±0.8
Resonance integral, *RI* (barns)	—	34.4±1.9	461±25

The value obtained in this work for σ_0 (2.82±0.07 barns) for the production of Cs^{134m} is very much greater than that (17 millibarns) quoted in reference 2.

The effective cross section for the reactions leading to the ground state Cs^{134} (41.6 ±0.9 barns) is found to be in good agreement with those obtained by Bidinosti *et al.* (40 barns) (11) and Brown *et al.* (40.9±4.1 barns, which was also measured in a vacant fuel rod position in the NRX reactor) (12). The value obtained for σ_0 is in good agreement with 30±1 barns reported in BNL-325 (2) but differs by somewhat more than the combined errors from the value obtained by Brown. The difference would appear to be accountable to the inherent difficulties in measuring cadmium ratios and uncertainties in neutron energy spectra (see discussion by Brown (12)).

1. A. P. Baerg, R. M. Bartholomew, and R. H. Betts. Can. J. Chem. **38**, 2147 (1960).
2. D. J. Hughes and R. T. Schwartz. Brookhaven National Laboratory Report, BNL-325, 2nd ed.
3. R. E. Jervis. Atomic Energy of Canada Ltd. Report CRDC-730 (1957).
4. B. D. Pate and L. Yaffe. Can. J. Chem. **33**, 15 (1955).
5. R. M. Bartholomew and A. P. Baerg. Can. J. Chem. **34**, 201 (1956).
6. P. J. Campion. Intern. J. Appl. Radiation and Isotopes, 4, 232 (1959).
7. T. A. Eastwood. Private communication.
8. C. H. Westcott, W. H. Walker, and T. K. Alexander. Intern. Conf. on the Peaceful Uses of Atomic Energy. 2nd Conf. Geneva, 1958. Paper P/202.
9. T. A. Eastwood, A. P. Baerg, C. B. Bigham, F. Brown, M. S. Cabell, W. E. Grummitt, J. C. Roy, L. P. Roy, and R. P. Schuman. Intern. Conf. on the Peaceful Uses of Atomic Energy. 2nd Conf. Geneva, 1958. Paper P/203.
10. W. F. Merritt, P. J. Campion, and R. C. Hawkings. Can. J. Phys. **35**, 16 (1957).
11. D. R. Bidinosti, H. R. Fickel, and R. H. Tomlinson. Intern. Conf. on the Peaceful Uses of Atomic Energy. 2nd Conf. Geneva, 1958. Paper P/201.
12. F. Brown, P. J. Campion, and B. H. Oliver. Can. J. Phys. 1960.
13. F. J. Johnston, J. Halperin, and R. W. Stoughton. Reactor Science, **11**, 95 (1960).

Received July 13, 1960.
Research Chemistry Branch,
Chemistry and Metallurgy Division,
Atomic Energy of Canada Limited,
Chalk River, Ontario.

ISOLATION OF HYPERIN FROM RED-OSIER DOGWOOD (CORNUS STOLONIFERA MICHX.)*

G. V. Nair and E. von Rudloff

In continuation of a systematic search for flavonoid and phenolic compounds in Prairie plants, red-osier dogwood (*Cornus stolonifera* Michx.) was investigated. The members of the *Cornus* family vary from herbs to fairly large trees. *C. stolonifera*, also known as *Svida stolonifera* (Michx.) Rydb., is a medium-sized shrub with characteristic bright red

*Issued as N.R.C. No. 6007.

Can. J. Chem. Downloaded from www.nrcresearchpress.com by 210.87.254.42 on 09/05/12
For personal use only.

twigs and branches. It is common throughout the Prairie provinces. Wall *et al.* (1), in a general survey of steroids, flavones, and tannins in plants, report that an extract of the whole plant gave a positive test only for tannins. In the current study, the leaves and stems of plants from the Saskatoon district were found to be devoid of flavonoid compounds, but a positive color reaction was obtained with an alcoholic extract of the red stem bark.

About 10% of the air-dried stem bark was ethanol-soluble. This extract was solvent fractionated and the chloroform-insoluble portion was chromatographed on a cellulose powder column. One of the products obtained (0.075% yield, based on the weight of bark) was a flavone glycoside, m.p. 238° C, $[\alpha]_D$ −19.7°, identified as hyperin (quercetin-3-galactoside) by mixed melting point. Hyperin was isolated for the first time by Jerzmanowska (2) from the herb *Hypericum perforatum* L.

In addition to hyperin, the alcohol extract contained fumaric acid, tannins, and a mixture of long-chain fatty acids. The latter mixture was resolved by gas–liquid chromatography (3) and found to consist of *n*-C_{24}- (66.7%), *n*-C_{26}- (22.8%), and *n*-C_{28}-carboxylic acids. In one experiment, when fresh bark was extracted at once, these fatty acids were obtained only after saponification, showing that hydrolysis may occur during storage of the plant.

EXPERIMENTAL

Melting points were determined on a Leitz hot-stage microscope, and infrared spectra were recorded with a Perkin–Elmer Model 21 double-beam spectrophotometer. Gas–liquid chromatography was carried out on a Beckman GC-2 chromatograph, using the technique previously described (4).

Air-dried stem bark (1000 g) of dogwood was extracted with ethanol (5 l.) in the cold. The solvent was evaporated, leaving a brownish-red sirupy residue (102 g). This material was extracted with chloroform to remove chlorophyll, waxes, etc. (22 g). An aliquot (16.5 g) of the chloroform-insoluble residue was chromatographed on a 60×7 cm cellulose powder column, using 15% acetic acid as solvent. Aliquots of 20 ml were collected and fractions 33 to 40 on evaporation gave a solid material (150 mg) which gave a pink color reaction when treated with magnesium and dilute hydrochloric acid. The material was crystallized from dilute alcohol, m.p. 238° C, $[\alpha]_D$ −19.7° (*c*, 3.9 H_2O–acetone 1:1). Found: C, 51.87%; H, 4.70%. Calculated for $C_{21}H_{20}O_{12}\cdot 2H_2O$: C, 52.43%; H, 4.87%. The infrared absorption spectrum corresponded to that of a flavone glycoside. The glycoside (20 mg) was hydrolyzed with dilute sulphuric acid and the aglycone and sugar portions were worked up in the usual manner. Paper chromatography showed these to correspond to quercetin and galactose respectively. The glycoside had the same R_f value (0.32, using 15% acetic acid) as hyperin, and its melting point was undepressed in admixture with an authentic specimen of hyperin.

Fractions 41–43 in the cellulose powder fractionation contained the bulk of the material (12.5 g) and appeared to be mainly tannin-like. On rechromatographing on cellulose powder, using ethyl acetate:ethanol:acetic acid (41:2:1 v/v) as eluent, a small amount of fumaric acid (characterized by mixed melting point and its infrared spectrum) was obtained.

The chloroform-soluble portion was dried and chlorophyll was removed by extraction with petrol (b.p. 40–60° C) in the cold. The insoluble residue was chromatographed on a silicic acid column, using petrol:benzene (1:1) as eluent. The only crystalline material isolated was a mixture of fatty acids, m.p. 78–79° C. Similar material was also found in

Can. J. Chem. Downloaded from www.nrcresearchpress.com by 210.87.254.42 on 09/05/12
For personal use only.

the petrol-soluble portion. The mixture was methylated with diazomethane and small aliquots (1 μl) were analyzed by gas–liquid chromatography on a silicone column (18×1/4 in.) at 240° C (3, 4). Three peaks corresponding to n-C_{24}, n-C_{26}, and n-C_{28} methyl ester were recorded in the proportion of 6.7:2.3:1.

We are grateful to Miss I. M. Gaffney and Mr. M. Mazurek for recording the infrared spectra and microanalyses.

1. M. E. Wall, C. S. Fenske, J. W. Garvin, J. J. Willaman, Q. Jones, B. G. Schubert, and H. S. Gentry. J. Am. Pharm. Assoc. **48**, 695 (1959).
2. Z. Jerzmanowska. Wiadomości farm. **64**, 527 (1937); cf. Chem. Abstr. **33**, 7299[8] (1939).
3. B. M. Craig and N. L. Murty. Can. J. Chem. **36**, 1297 (1958).
4. G. V. Nair and E. von Rudloff. Can. J. Chem. **37**, 1608 (1959).

Received September 6, 1960.
National Research Council of Canada,
Prairie Regional Laboratory,
Saskatoon, Saskatchewan.

Can. J. Chem. Downloaded from www.nrcresearchpress.com by 210.87.254.42 on 09/05/12
For personal use only.